ENCYCLOPEDIA OF
Biological Chemistry

Editors
William J. Lennarz
M. Daniel Lane

ABC Transporters

André Goffeau, Benoît De Hertogh and Philippe V. Baret
Université Catholique de Louvain, Louvain-la-Neuve, Belgium

The ABC proteins constitute the largest family of proteins. They are present in all living species from *Archaea* to *Homo sapiens*. They make up to 4% of the full genome complement of bacteria such as *Escherichia coli* or *Bacillus subtilis*. Each eukaryote genome contains several dozens of members (over 100 in the plant *Arabidopsis thaliana*). They are recognized by a consensus ATP-binding region of approximately 100 amino acids which include the two Walker A and B motifs encompassing a linker or C region (Figure 1). The ABC proteins catalyze a wide variety of physiological functions, most (but not all) of which being related to transport. This article describes the major physiological and biochemical functions as well as the structural properties of some of the best-known ABC transporters using examples from the yeast *Saccharomyces cerevisiae* and *Homo sapiens*.

Topology

Most, but not all, ABC proteins are ABC transporters. Each of those molecules contains, or is associated to, one or two cytoplasmic ATP-binding domains named nucleotide binding domains (NBDs) (Figure 1) and one or two transmembrane domains (TMDs) (Figure 2). Each TMD comprises usually six α-helix spans. Association of one TMD to one NBD results in a half-size ABC transporter; however, they are believed to function as homo- or heterodimers so that the minimal functional organization of an ABC transporter is considered to be TMD–NBD–TMD–NBD or NBD–TMD–NBD–TMD. In eukaryotes, two TMDs and two NBDs are often associated in one single molecule called full-sized ABC transporter. The topological relation between NBD(s) and TMDs is variable (Figure 2). In bacteria two NBDs often associate with two TMDs either as four single subunits encoded by the same operon or in various combinations of fused subunits. Association of other proteins may occur. The most prominent associated bacterial protein is the periplasmic solute-binding receptor, which in gram-negative bacteria is found in the periplasm, and in gram-positive bacteria is present often as a lipoprotein, bound to the external membrane surface via electrostatic interactions (Figure 3). The three domains of the bacterial ABC uptake transporters: namely the periplasmic binding receptor, the cytoplasmic NDB, and the membrane TMD are believed to have arisen from a common ancestral ABC transporter in which these three proteins were already present. However, during evolution, the sequence of the periplasmic solute-binding receptors diverges more rapidly than that of the TMDs, while that of NBDs is the least divergent. Thus, all NBDs are homologous, but this is not true for the TMDs or the receptors. Nevertheless, the phylogenetic clustering patterns in bacterial ABC from different species are generally the same for all three types of proteins, despite their variable rate of evolution.

The topology of some eukaryotic ABC effluxers can be complex as additional TM spans occur in some systems (Figure 3) as well as extra cytoplasmic domains of presumed regulatory function.

Phylogeny

The different families of ABC proteins transport a wide variety of substrates against their concentration gradient using the energy of ATP hydrolysis carried out by NBD. In bacteria, the transported substrates are either imported in or exported out of the cell. In eukaryotes, only extracytoplasmic exporters (transporting substrates either out of the cell or into organelles) are known up to now. Within the ABC superfamily, 61 phylogenetic families have been identified so far. These families generally correlate with substrate specificity. Their classification based both on functional and phylogenetic criteria has been carried out within the transporter classification (TC) system developed by Milton Saier in San Diego. The TC system has recently been endorsed by The International Union of the Biochemical and Molecular Biology Societies. In the TC system, prokaryotic ABC influx porters comprise 22 phylogenetic families including histidine permease, the first ABC transporter to be cloned and sequenced in the laboratory of Giovanna Ames in 1982. Another famous example is the MalEFGK operon classified in TC as a maltooligosaccharide porter within "the carbohydrate uptake transporter-1 (CUT1) family," and given the TC digit 3.A.1.1. In this operon, MalE is the receptor, MalF

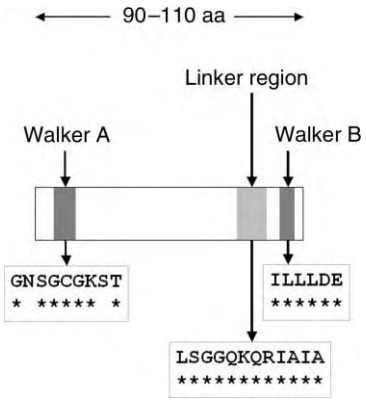

FIGURE 1 The consensus ATP-binding region of a typical ABC protein is made of approximately 100 amino acids (aa), including both Walker A and B motifs and the linker C region.

and MalG are distinct TMD subunits, and MalK is a double NBD.

The prokaryotic effluxers comprise 27 families including the multidrug exporter LmrA from the gram-positive *Lactococcus lactis* well studied by Will Koning and belonging to "the drug exporter-2 family" (3.A.1.117).

The eukaryotic ABCs can be grouped in only 12 efflux families including the famous MDR1 also named Pgp (permease-glycoprotein), discovered in 1986 by Ira Pastan, Michael Gottesman and colleagues, and shown to be involved in MDR of chemiotreated tumor cells. In the TC system, this ABC exporter is classified in "the multidrug resistance exporter family" (3.A.1.201).

The TC system is redundant with the Human Genome Organization (HUGO) classification adopted by the scientific community working on mammalian objects (mouse or man). The 45 human or mouse ABC proteins, comprising efflux transporters and

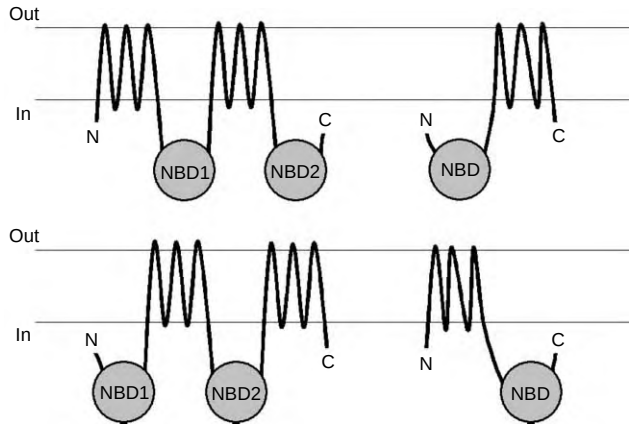

FIGURE 2 Example of topological relations between NBDs and transmembrane spans in full-sized and half-sized ABC transporters.

nontransporter proteins, have been classified in seven families named ABCA to ABCG according to topological and phylogenetical criteria that are less stringent than those used by TC. In its present form, the HUGO nomenclature and classification are difficult to use for identification of novel ABC from non-mammalian species. For instance, the *Saccharomyces cerevisiae* genome contains 32 ABC genes among which 22 (16 full-size and six small-size) are associated to transmembrane domains in four different topologies. Its largest family is the full-sized Pdr5p-like family identified in 1996 by Anabelle Decottignies and André Goffeau and shown later to be present in all fungi and plants. This family is not detected in the animal kingdom. Conversely, the large human and mouse ABCA subfamily is not represented in yeast genomes. There is a necessity to adopt a consistent classification system, which combines the TC and HUGO nomenclatures.

Function and Diseases

The immense variety of substrates transported in bacteria is reflected by the identification of 49 phylogenetic ABC families including 22 influx protein complexes and 27 efflux transporter systems. As they belong to Archaea, gram-negative and gram-positive plasma membranes that are widely different in organization and composition, the number and nature of proteins associated to given ABC transporters are variable and their transport mechanisms may be partly different. In bacterial and Archaea ABC, the variety of substrates: sugars, amino acids, lipids, ions, polysaccharides, peptides, proteins, toxins, drugs, antibiotics, xenobiotics and other metabolites is reflected by the divergence of the periplasmic sensor and that of the TMD, which must control both specificity of substrate and part of the coupling mechanism.

Even if all eukaryotic ABC transporters are effluxers that comprise subunits in which each TMD is fused to a NBD, some of them are not directly involved in moving substrates. For instance, in the cystic fibrosis transmembrane regulator CFTR, and in the sulfonylurea receptor SUR, the hydrolysis of ATP appears to be linked to the regulation of opening and closing of ion channels carried by the ABC protein itself or other proteins (Figure 3B). The conservation of NBD in all ABC transporters, however, suggests that a basic coupling mechanism exists for efflux and influx whatever the transported substrate. Moreover, distantly related proteins exist which utilize an NBD to drive diverse nontransport processes such as DNA repair or protein-elongation or regulation of RNAse activities.

The 32 yeast ABC proteins are in principle easy to study, as sensitive genetic tools are available. However, only a few successful cases of overexpressions and

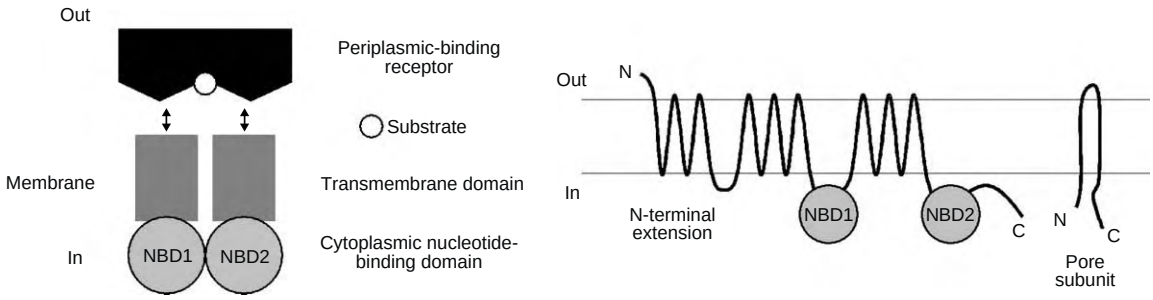

FIGURE 3 Example of proteins associated to bacterial and mammalian ABC transporters.

in vitro UTPase or ATPase measurements of purified ABCs have been reported. Only one purified yeast ABC transporter, the pleiotropic drug resistance effluxer Pdr5p, has been submitted to structural studies.

The biochemical study of human ABC transporters is often more advanced than that of the yeasts. The Pgp protein responsible for multiple drug resistance (MDR) in human cells is especially well studied. One strong impetus for the study of mammalian ABC transporters is their involvement in diseases. Many mendelian diseases and complex genetic disorders are caused by ABC transporters including cystic fibrosis, adrenoleukodystrophy, Stargardt disease, Tangier disease, immune deficiencies, progressive familial intrahepatic cholestasis, Dublin–Johnson syndrome, Pseudoxanthoma elasticum, persistent hyperinsulinemic hypoglycemia of infancy due to focal adenomatous hyperplasia, X-linked sideroblastosis and anemia, age-related macular degeneration, familial hypoapoproteinemia, Fundus flavimaculatis, Retinitis pigmentosum, cone rod dystrophy etc. Cell lines isolated from diseased tissues allow molecular study of the involved ABC transporter. Moreover, a variety of drug-resistant cell lines is available from MDR or MDR-related protein (MRP) tissues. Basic studies of human ABC transporters would greatly benefit from heterologous expression of human ABC transporter genes in yeast or other cells, but this technology is far from being satisfactory yet. Meanwhile, knockout technology in the mouse may be needed to begin to understand the molecular and physiological functions of the mammalian transporters.

Structure and Biochemical Mechanism

In 1998, the first high-resolution structure of a NBD, that from the histidine ABC importer HisP, was reported. Five years later, about six related structures were available and a consensus view emerged. NBDs are organized as dimers and two molecules of ATP are bound at their interface. Each nucleotide-binding site comprises a Walker A motif from monomer 1 and the C motif from monomer 2. This results from a "head-to-tail" arrangement of the two interacting monomers. This is supported by biochemical arguments and is coherent with the cooperative hydrolysis for ATP hydrolysis observed with MalK.

More recently, three structures of complete dimeric ABC transporters comprising both NDB and TMD were obtained: that of the presumed phospholipid flippase MsbA from *E. coli* and *Vibrio cholera* and that of the vitamin B12 importer BtuCD from *E. coli*. The structures obtained were dissimilar, which may not be too surprising taking into account the different conditions used, the different numbers of TM spans and the different functions (import or export) of the proteins analyzed. No generalization can be made, for instance, on the angle between the TM spans and the membrane plane or on the identification of the interaction domains between the TM spans. The nature of communication between the NBD and TMD is variable and carried out either through the long and complex so-called intracellular domain named ICD in MsbA, or through a short L-shaped linker between the transmembrane spans 6 and 7 in BtuCD. The nature, the size, the orientation, and the location of the so-called chamber (or water channel, or pore, or cone) presumed to be involved in substrate binding are also variable. No consensus interaction points between the NBDs (open or closed conformation) were observed. Obviously, more structures are needed on several transporters carrying out similar functions, such as drug efflux, for instance, to clarify these issues and to reach a consensus interpretation of the basic structural elements involved in the transport and in the coupling mechanism.

In contrast, recent analyses at the electron microscopy level of a bacteria (BmrA or YccV from *Bacillus subtilis*) and a yeast (Pdr5p) drug efflux ABC transporter came to a remarkably coherent set of conclusions. In both cases, the basic structural unit seems to comprise four joining NBDs (that corresponds to two full-size Pdr5p or four half-size BmrA), which are

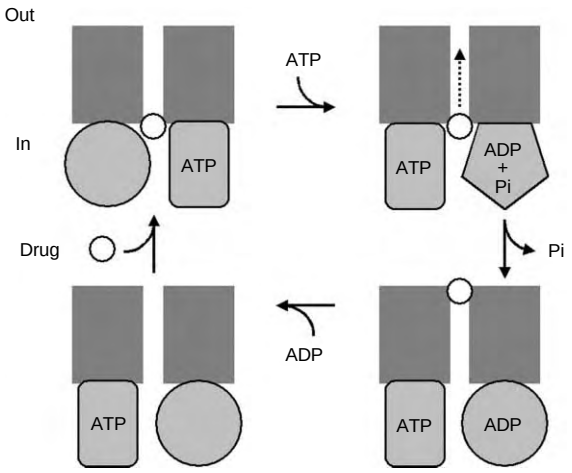

FIGURE 4 The alternating catalytic sites hypothesis for P-glycoprotein, according to Alan Senior. The NBDs have three ligands and four states: free, ATP bound, ADP + Pi bound, and ADP bound. They alternate in such a way that two ATPs never bind simultaneously. The binding of one ATP to one NBD induces hydrolysis at the other ATP. The drug is transported out during Pi release.

related to the TMDs through four distinct stalks. Each NBD is oriented at a fixed 90° angle relative to its neighbor NBDs. This raises the possibility of concerted rotation movements of the NBDs implying a certain flexibility of the stalks. No intramolecular or no intramembrane pores were observed even though there is room (or chamber) between the four stalks that join together at their NBDs tips.

These latter observations are difficult to reconcile with the mechanism of alternating sites established for the drug exporters, the human Pgp and the bacterial LmrA (Figure 4). In these cases the monomeric NBDs are similar and both are able to hydrolyze ATP. Hydrolysis of ATP at one NBD is believed to be responsible for drug release outside. Upon release of ADP and Pi, the other NBDs bind and then hydrolyze ATP while the drug is taken up inside. However, the simplest version of this "two-cylinder" mechanism cannot function when the two NBDs partners are not equivalent in a dimeric arrangement as it is the cases of yeast Pdr5p and human CFTR, where one of the two NBDs from a full-sized ABC molecule might be unable to hydrolyze ATP.

The Substrate Specificity of the ABC Multidrug Exporters

One of the most intriguing contemporary biochemical problems is the characterization of the interactions of the TMDs with their transported substrate. The most extraordinary feature in this context is the apparent lack of specificity of the yeast Pdr5p and human Pgp that transports hundreds of different chemicals, apparently contradicting the famous key/slot concept described in all enzymology textbooks. It must be recognized that the identification of presumed ABC substrates are often based on indirect data such as resistance or sensitivity of mutants or drug-induced transcription profiles. These measurements should in principle be corroborated by direct transport measurements, which are often difficult to obtain.

Regarding specificity of transport, one of the best-studied yeast transporters is Pdr5p through the capacity of its deleted mutants to gain growth sensitivity to an amazing variety of xenobiotics. From a large screen of several hundreds of toxic compounds, no chemical determinants for transported substrate specificity could be identified among a wide range of compounds including the fungicides anilinopyrimidines, benzimidazoles, benzenedicarbonitriles, dithiocarbamates, guanidines, imidothiazoles, polyenes, pyrimidynyl carbinols, and strobilurine analogues, the urea derivative and anilide herbicides, a wide collection of flavonoids and steroids, several membrane lipids resembling detergents, and newly synthesized lysosomotropic aminoesters. However, it could be concluded that Pdr5p shows considerable substrate overlap with members of the same ABC phylogenetic family or even with yeast drug effluxers from other families such as Snq2p or Yor1p. This was demonstrated by the numerous cases showing full sensitivity only in double or triple mutants. The most promiscuous substrates were: itraconazole, miconazole, nystatin, antimycin, nigericidin, and tetradodecylammonium bromide, which are transported by at least three distinct yeast ABC transporters. In contrast many substrates show relative specificity for a given pleiotropic drug resistance exporter. Prominent examples include cycloheximide, benomyl, fluxilazole, nuarimal, and soraphen for Pdr5p. From a first large scale screen it was concluded that Pdr5p's most efficient substrates were valinomycin, the antifungal azoles and rhodamine 6G. These compounds are inhibiting the growth of a sensitive PDR5 deletant at concentrations below the micromolar range. Up to now, the most potent competitive inhibitor of binding of rhodamine 6G to the yeast Pdr5p is the oestradiol derivative RU 49953, which exhibits a K_i of 23 nM.

Other recent systematic screens have provided more precise chemical information on the determinants of Pdr5p specificity. From such studies it was concluded that Pdr5p is capable of transporting substrates that neither ionize nor have electron pair donors and that are much simpler in structure than those handled by the human Pgp. The substrate optimum surface volume is about 200Å^3. Analysis of the interactions between imidazole derivatives, organotin and other compounds argues, that, as also established for Pgp, the Pdr5p comprises at least two substrate-binding sites. One site

might use only hydrophobic binding interactions. Some substrates may bind to two sites, others associate more specifically to only one site. However, the Pdr5p substrates-binding sites, behave differently from those of Pgp. This concept of overlapping substrate-binding sites may reconcile many previous observations concerning the substrate broad specificity of Pdr5p and Pgp, which up to now appeared contradictory.

Conclusion

The present frontiers in the study of ABC transporters are challenging. The evolutionary history of this large ubiquitous family has to be unraveled. Additional atomic structures have to be produced. Better heterologous overexpression systems have to be developed to allow further biochemical studies. Specific inhibitors of drug (and other) ABC exporters have to be screened for. The physiological mechanisms of ABC-linked diseases have to be further studied in mouse knockouts. Systems prone to specific inhibition of ABC transporters expression by interfering RNA have to be explored. Genetic therapy has to be developed.

See Also the Following Article

MDR Membrane Proteins

Glossary

human genome organization (HUGO) An international association that comprises scientists involved in all aspects of the sequence of the human genome and its analysis.

linker C Small amino acids sequence signature involved in ATP binding of ABC proteins.

Pdr5p The major yeast ABC transporter, involved in pleiotropic drug resistance.

Pgp The first ABC transporter (glycoprotein) shown to be involved in mammalian multidrug resistance.

transmembrane span and transmembrane domain (TMS and TMD) The existence of the transmembrane span is predicted by frequency of hydrophobic residues in a reading window of about 17 amino acids. In ABC transporters, the transmembrane domains usually comprises six continuous transmembrane spans.

transporter classification (TC) Classification of over 800 transporters families, developed by Milton Saier (UCSD), based on a combination of mechanistic and phylogenetic criteria.

Walker A and B Small consensus of amino acid sequences involved in ATP binding.

Further Reading

Dean, M. (2002). *The Human ATP-Binding Cassette (ABC) Transporter Superfamily.* Monograph Bethesda (MD), NCBI, National Library of Medicine (US).

Decottignies, A., and Goffeau, A. (1997). Complete inventory of the yeast ABC proteins. *Nat. Genet.* **15**, 137–145.

Gottesman, M. M., and Ambudkar, S. V. (2001). Overview: ABC transporters and human disease. *J. Bioenerg. Biomembr.* **33**, 438–453.

Hipfner, D. R., Deeley, R. G., and Cole, S. P. C. (1999). Structural mechanistic and clinical aspects of MRP1. *Biochim. Biophys. Acta* **1461**, 359–376.

Martinoia, E., Klein, M., Geisler, M., Bovet, L., Forestier, C., Kolukisaoglu, U., Muller-Rober, B., and Schulz, B. (2002). Plant ABC transporters: more than just detoxifiers. *Planta* **214**, 345–355.

Schmitt, L., and Tampé, R. (2002). Structure and mechanism of ABC transporters. *Curr. Opin. Struct. Biol.* **12**, 754–760.

Senior, A. E., al-Shawi, M. K., and Urbatsch, I. L. (1995). The catalytic cycle of P-glycoprotein. *FEBS Lett.* **27**, 285–289.

Biography

André Goffeau is Emeritus Professor at the Université Catholique de Louvain (Belgium), Department of Physiological Chemistry. He investigates the P-type ATPases and the ABC transporters in *S. cerevisiae*. He has initiated and organized the sequencing of the yeast genome. He is interested in the phylogenetic classification of yeast membrane proteins.

Benoît De Hertogh is Ingénieur Agronome at the Université Catholique de Louvain (Belgium), Department of Quantitative Genetics. He is completing a Ph.D. thesis on population genetics on the genetical basis of fertility in livestock. He is interested in comparative genomics of membrane proteins.

Philippe V. Baret is Associate Professor at the Université Catholique de Louvain (Belgium), Department of Quantitative Genetics. He is modeling the relationship between genes and phenotypes, with a peculiar interest in quantitative trait loci mapping and cladistic approaches.

Abscisic Acid (ABA)

Ramanjulu Sunkar and Jian-Kang Zhu
University of Arizona, Tucson, Arizona, USA

Plants perceive a variety of environmental and endogenous signals, which elicit appropriate responses with altered metabolism, growth, and development. Phytohormones are signaling molecules, present in trace quantities and are tightly controlled by various biosynthetic, catabolic, and conjugation pathways. Changes in hormone concentration determine a wide range of plant responses, some of which involve interactions with environmental factors. One such important phytohormone is abscisic acid (ABA), a sesquiterpenoid (15-carbon) which is partly produced in chloroplasts and other plastids. A low basal level of ABA is required for normal growth and development of plants. However, a dramatic and rapid increase in ABA levels occurs due to *de novo* synthesis in vegetative parts of the plants exposed to osmotic stress, as well as in developing seeds during maturation. Elevated levels of ABA play a central role in promoting stomatal closure, dehydration tolerance, leaf senescence, seed dormancy and maturation, and coordinated growth of roots and shoots. ABA apparently acts as a signal of reduced water availability. This is manifested at the physiological level, by controlling germination, stomatal movements, and growth. At the molecular level, ABA-dependent changes in gene expression and posttranslational modifications underpin these physiological processes.

Mutants As Tools for Studying ABA Biosynthesis and Signaling

Mutant plants with altered biosynthesis, perception, or responses have been crucial in identification of various components involved in ABA biosynthesis and signaling. The genetic screens and selections that have been used include production of nondormant seeds, loss or gain of sensitivity to ABA during germination, seedling or root growth, and altered expression of reporter genes. These approaches have yielded three classes of ABA mutants: ABA-deficient, -hypersensitive, and -insensitive mutants. The characteristic feature of ABA-deficient mutants is a wilty phenotype largely due to impaired stomatal closure (impaired ABA biosynthesis in *aba1/los6*, *vp14*, *aba2*, and *aba3/los5* mutants; *ABA1*, *VP14*, *ABA2*, and ABA3 encode enzymes of ABA biosynthetic pathway, zeaxanthin epoxidase (ZEP), *9-cis* epoxycarotenoid dioxygenase (NCED), short-chain alcohol dehydrogenase/reductase (SDR), and molybdenum cofactor sulfurase (MoCoSu) respectively). Hypersensitive mutants display enhanced sensitivity to ABA, resulting in diminished germination rates at low ABA concentrations and reduced water loss due to enhanced ABA-induced stomatal closure (*Arabidopsis era1, sad1, abh1, hyl1, rop10, and fiery1*). The *ERA1* gene encodes a protein farnesyltransferase; *HYL1*, *SAD1*, and *ABH1* genes encode different types of RNA-binding proteins; *ROP10* encodes a small G protein; and *FIERY1* encodes an inositol polyphosphate 1-phosphatase. In addition to these mutants, silencing of the calcium sensor SCaBP5 and protein kinase PKS3 resulted in ABA hypersensitivity. ABA-insensitive mutants including *abi1*, *abi2*, *abi3*, *abi4*, *abi5*, and *rcn1* from *Arabidopsis*, and *vp1* (orthologue of *abi3*) from maize have been identified. This class of mutants display loss of ABA sensitivity, leading to nondormancy or vivipary. The genes *ABI1* and *ABI2* encode homologous-type 2C protein phosphatases; *RCN1* encodes a 2A-type protein phosphatase; *ABI3/VP1* encodes a B3 type of transcriptional activator; *ABI4* encodes an AP2-type transcription factor; and *ABI5* encodes a b-ZIP transcription factor.

ABA Biosynthesis

Osmotic stress induction of ABA accumulation is a complex signaling process from the initial water-stress perception, intracellular signal transduction, to gene expression or activation of the enzymes involved in the ABA biosynthesis. The chain of events from the perception of osmotic stress to the gene activation leading to ABA biosynthesis is unknown. Presumably, it involves reactive oxygen species (ROS)/calcium signaling and protein phosphorylation cascades. Significant progress has been made in recent years in cloning the genes encoding enzymes involved in ABA biosynthesis (Figure 1). Some of these genes in *Arabidopsis* are encoded by members of multi-gene families (NCED, abscisic aldehyde oxidase) while others are represented by single gene (ZEP, SDR, MoCoSu). Several of these genes appear to be transcriptionally activated by osmotic stress and ABA.

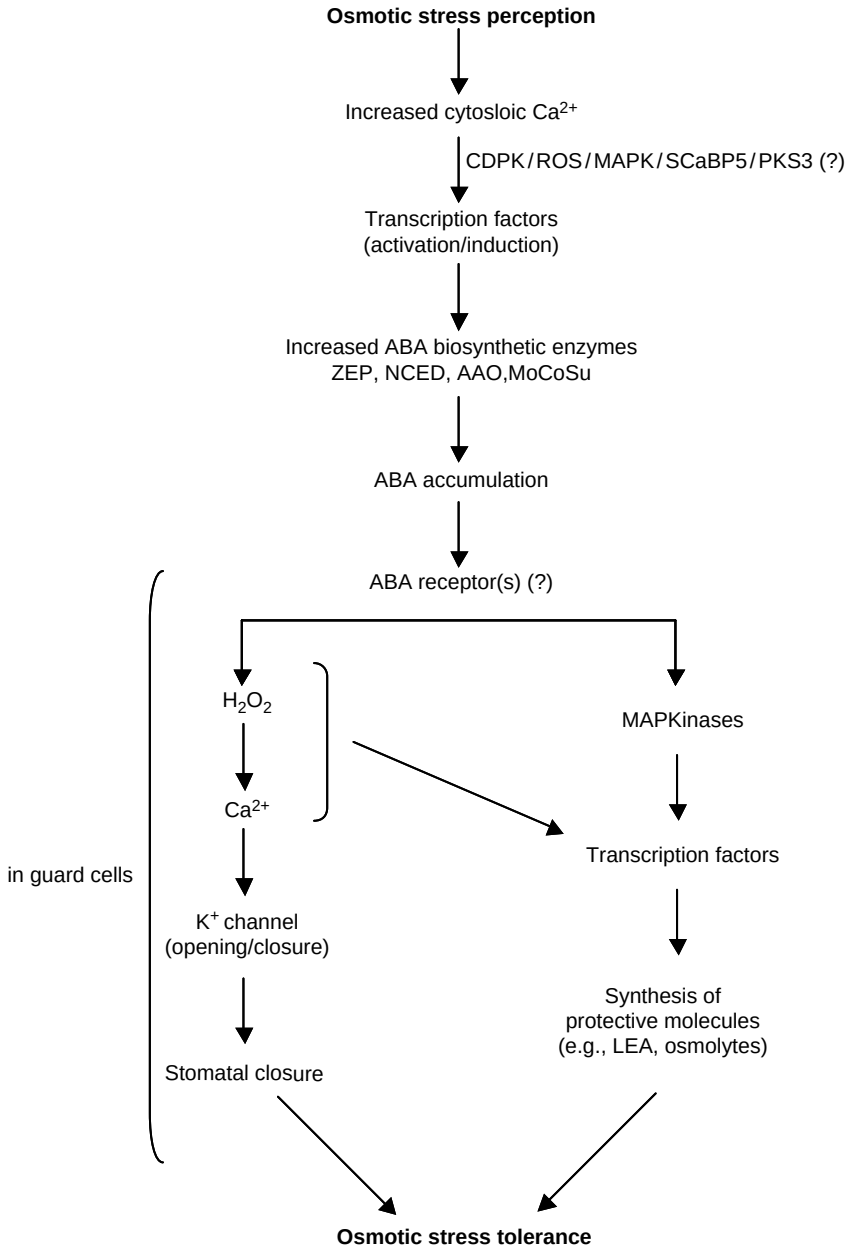

FIGURE 1 An overview of osmotic stress-induced biosynthesis of ABA and ABA mediated signaling leading to stomatal closure in guard cells and the regulation of gene expression in plants.

ABA biosynthesis in seeds is similar to that in the vegetative tissues. However, the regulation of ABA biosynthesis in developing seeds is not clear since these aspects were mainly investigated in vegetative tissues.

Role of ABA in Seed Development and Maturation

Seed development represents an important part of the plant's life cycle as the success of seedling establishment to a large extent is determined by the physiological and biochemical properties of the seed. Plant hormones, particularly ABA and gibberellic acid (GA), play antagonistic roles and are important regulators of seed maturation, germination, and postgerminative growth. ABA mediates several important functions in developing seeds such as seed maturation, synthesis of storage proteins, synthesis of late embryogenesis abundant (LEA) proteins, and initiation of seed dormancy, whereas GA is required to break dormancy and to trigger germination. It seems that two peaks of ABA accumulation coordinate these processes in developing seeds. The first peak of ABA is relatively large and occurs

about halfway during seed development (~10 days after pollination) and plays a role in the synthesis of storage proteins. The second peak is relatively weaker compared to the first peak and seems to be important for the synthesis of LEA proteins and for initiation of seed dormancy. During maturation, seeds lose up to 90% of their water content and are still viable. This ability to tolerate extreme dehydration is achieved by ABA-dependent accumulation of LEA proteins and compatible solutes such as sugars. LEA proteins appear to be important for desiccation tolerance by maintaining the structural integrity of membranes and proteins and controlling water exchange. Transcripts encoding either storage proteins or LEA proteins can be precociously induced by ABA in cultured embryos suggesting that endogenous ABA is indeed responsible for these processes. The analysis of promoter sequences for storage proteins and LEA genes corroborated with the ABA responsiveness of *cis*-elements and tissue specificity. Embryo enters a quiescent state (dormancy) at this stage which is also maintained by ABA.

ABA Signaling in Developing Seeds

ABA signaling components mediating seed dormancy and germination have been inferred from genetic analysis. The best known components involved in ABA signaling in seeds are PP2C-like phosphatases (ABI1 and ABI2) and transcription factors (ABI3, ABI4, and ABI5) and a farnesyltransferase (ERA1). *ABI1* and *ABI2* encode homologous type 2C serine/threonine protein phosphatases. The ABA signaling pathway appears to be negatively regulated by these phosphatases. *ABI3*, *ABI4,* and *ABI5* encode transcription factors of the B3, AP2, and b-ZIP domain families respectively and regulate the expression of ABA-inducible genes in seeds as well as in vegetative tissues. The *ABI3* gene encodes a transcriptional activator with homology to the seed-specific VP1 protein from maize. ABI3 plays a central role in the establishment of desiccation tolerance and dormancy during embryogenesis. ABI3 activates down stream genes and thus is a major player in ABA signaling. VP1 activates expression of ABA-inducible genes through the G-box promoter element. Interestingly, VP1 does not appear to bind to the element directly. Rather, VP1 regulation is likely mediated by protein–protein interactions with G-box-binding factors. In support of this model, the rice TRAB1 b-ZIP protein was shown to interact with rice VP1 in the yeast two-hybrid system. The *Arabidopsis* ABI5 is homologous to TRAB1 and similarly interacts with ABI3. Coexpression of ABI5 and ABI3 transcription factors, which interact physically, synergistically activate several promoters in the presence of ABA. ABI5 plays a role in protecting germinating embryos from drought. ABI5 accumulation, stability, and activity are regulated by ABA during germination. These findings suggest complex interactions of ABI3 and ABI5 in ABA signaling.

ABA as Mediator of Osmotic Stress Tolerance

ABA has dual roles during osmotic stress: (1) a rapid response in guard cells leading to stomatal closure and (2) a slower response of reprogramming gene expression patterns (Figure 1). Both roles are critical for water-stress tolerance.

Stomatal Closure Meditated by ABA

Guard cells, which flank stomatal pores, integrate and respond appropriately to changes in water levels mediated by ABA. ABA-deficient and ABA-insensitive mutants are prone to wilting and cannot withstand water-deficit conditions due to their inability to close stomata, while hypersensitive mutants exhibit opposite responses. ABA-induced stomatal closure is vital for plants to limit transpirational water loss during periods of drought. Investigations on ABA-induced stomatal movements have led to the identification of several components acting downstream of ABA. These include protein kinases and phosphatases, phospholipase C and D, slow anion channels, K^+ channels, G proteins, sphingosine-1-phosphate, syntaxin, cyclic ADP ribose (cADPR), ROS, and free calcium ions in the guard cell cytosol. However, a complete picture is yet to emerge and there are several missing links.

Stomatal opening and closure are coordinated by regulation of the relative activities of the inward- and outward-rectifying channels and anion channels. ABA-induced stomatal closure is mediated by a reduction in the turgor pressure of guard cells, which requires an efflux of K^+ and Cl^-, sucrose removal, and the conversion of malate to osmotically inactive starch. Therefore, opening or closing of guard cell ion channels determine the status of stomatal aperture.

Second Messengers (ROS and Ca^{2+})

Recent studies have established a role for H_2O_2 in ABA signaling through its influence on Ca^{2+} channels in guard cells. ABA stimulates H_2O_2 production in guard cells. The plasma membrane NADPH oxidase complex, which consists of many components, seems to be responsible for H_2O_2 generation. H_2O_2 triggered by ABA plays a vital role as signal mediator for the activation of downstream events including the opening

of Ca^{2+} channels, leading to increases in the cytosolic Ca^{2+} level. It appears that Ca^{2+} plays a very important role in ABA-mediated stomatal closure. ABA-induced changes in cytosolic Ca^{2+} concentration have been attributed to both Ca^{2+} release from internal stores and Ca^{2+} influx from external stores. Downstream to ABA, inositol triphosphate (IP3), cADPR, and possibly inositol hexakisphosphate (IP6) are also implicated in increasing cytosolic Ca^{2+} levels. The highly localized calcium oscillations in the cytoplasm then control various processes leading to ion efflux and stomatal closure. These include inhibition of inward rectifying K^+ channels and activation of outward rectifying K^+ channels in guard cells, reducing influx and increasing efflux of K^+ in guard cells, cation and anion channels in the plasma membrane, changes in the cytoskeleton, and movement of water through water channels in the tonoplast and plasma membrane. The activities of all these cellular structures need to be coordinated during ABA-induced stomatal closure.

ABA responses in guard cells require a specific cytosolic calcium signature. Guard cell cytosolic calcium oscillations with defined frequency and amplitude result in stomatal closure. In contrast, steady and sustained cytosolic calcium increases without oscillations fail to confer stomatal closure, suggesting that excessive, nonoscillating cytosolic calcium may interfere with or inhibit ABA responses. Hence in addition to calcium sensors as positive regulators of downstream ABA signaling, there may be calcium-sensing systems that regulate ABA responses negatively. Consistent with this hypothesis, a calcium sensor protein, SCaBP5, and a protein kinase, PKS3, involved in ABA signaling have been identified recently. *Arabidopsis* loss-of-function mutations in either of these genes resulted in ABA hypersensitivity during seed germination, vegetative growth, and stomatal closure.

Protein Phosphatases

Phosphorylation events are central to ABA signaling. The *abi1-1* and *abi2-1* mutations confer ABA insensitivity in seed germination, vegetative growth, and the expression of certain ABA-regulated genes. The fact that ABI1 and ABI2 are protein phosphatases suggests involvement of protein phosphorylation/dephosphorylation in regulating ABA signaling. Protein phosphatase genes *ABI1* and *ABI2* encoding type-2C protein phosphatases are up-regulated by ABA. These phosphatases, in general, are implicated in negative regulation of ABA signaling.

Kinases

Protein kinases that are specifically activated by ABA offer better understanding of the ABA signaling in plant cells. PKABA1 (abscisic acid-responsive protein kinase) from wheat, open stomata 1 (OST1) from *Arabidopsis*, and abscisic acid-activated protein kinase (AAPK) from fava bean are ABA-activated serine-threonine protein kinases. Both AAPK and OST1 display ABA-dependent autophosphorylation. Mutations in the *OST1* gene suppressed ABA-induced ROS production, which is important for stomatal closure, suggesting that OST1 is an important component acting upstream of ROS generation in ABA signaling. Dissection of guard cell signaling events identified a target for AAPK. AAPK activates AKIP1, which is highly similar to a single-stranded RNA-binding protein that binds heterogenous nuclear RNA (HnRNA). HnRNA-binding proteins are a class of proteins involved in transcriptional, posttranscriptional, and translational control of gene expression. AKIP1 is phosphorylated by AAPK and the phosphorylation activates AKIP1 and increases its affinity for a dehydrin (LEA-type) mRNA.

Kinases that act as negative regulators of ABA signaling have been identified. Silencing of PKS3 caused ABA hypersensitivity in seed germination, stomatal closing, and gene expression, suggesting that this protein acts as negative regulator that specifically modulates ABA signal transduction. These findings highlight the existence of ABA-dependent kinases that function both in guard cell signaling and in gene expression.

Farnesyltransferase

Farnesyltransferases influence protein structure or localization through mechanisms other than phosphorylation. Protein farnesylation, a posttranslational modification process, mediates the COOH-terminal lipidation of specific cellular proteins such as Ras and other G proteins. Deletion of the *Arabidopsis* farnesyltransferase gene *ERA1* or application of farnesyltransferase inhibitors resulted in ABA hypersensitivity of guard cell anion channel activation and of stomatal closing.

Cytoskeleton

ABA-induced stomatal closure requires a reorganization of the actin cytoskeleton of guard cells. A link for such an action has been demonstrated between ABA and actin through AtRac1. AtRac1 (*Arabidopsis* Rho-related small guanosine triphosphatase, GTPase) has been identified as a central component in ABA-mediated stomatal closure. In animals and yeast, Rho GTPases are key regulators of the actin cytoskeleton. GTPases are inactivated by ABA treatment leading to the disruption of guard cell actin organization. ABA-induced increase in cytosolic Ca^{2+} and the cytoskeleton reorganization seems to be another link in this pathway, suggesting that the ABA-induced increases in cytosolic

Ca^{2+} regulate cytoskeletal reorganization, in addition to ion channels.

RNA-Associated Proteins and ABA Signaling

Accumulation of some of the ABA-inducible proteins is also dependent on posttranscriptional regulation. RNA processing proteins may contribute to this level of regulation. Isolation of three ABA hypersensitive mutants *abh1*, *hyl1*, and *sad1* all encode RNA-associated proteins implicating that RNA processing modulates ABA signal transduction. The *hyl1* mutant shows ABA hypersensitivity during seed germination. The *HYL1* gene is ABA-regulated and encodes a nuclear dsRNA-binding protein. Mutation in this gene alters the plant responses to several exogenous hormones. The *abh1* mutation confers ABA hypersensitivity in seed germination, stomatal closure, and ABA-induced guard cell calcium increases. ABH1, an mRNA cap-binding protein, is a negative regulator of ABA responses including stomatal closure. The *sad1* mutant is not only hypersensitive to ABA but also to drought, unlike *abh1* and *hyl1* which are drought tolerant. *SAD1* encodes an Sm-like SnRNP protein required for mRNA splicing, export, and degradation. Similarly, AKIP1 is another RNA-binding protein that belongs to this group of proteins involved in ABA signaling. How these proteins execute their role in the ABA pathway is unknown but the findings provide a strong link between RNA processing and ABA signaling.

ABA-Induced Modulation of Gene Expression

The synthesis of endogenous ABA increases in response to osmotic stress, which in turn induces numerous stress-associated genes involved in the accumulation of osmoprotectants and LEA proteins, protein turnover, stress signaling pathways, and transcriptional regulation. ABA accumulated in response to osmotic stress is likely to be sensed by a receptor protein (sensor), albeit the identity and the location of such a component is yet unknown. The components of ABA signaling involved in transcriptional and posttranscriptional regulation have been less understood as compared to the guard cell signaling. MAPK cascade is an extensively used pathway in eukaryotic signaling. ABA signaling in plants may also use an MAPK pathway. MAPKs (AtMPK3 and AtMPK6) that are activated by ABA are known in plants. These MAPKs receive signals from the ANP1 family of MAPKKKs through MAPKKs (AtMKK4 and AtMKK5). However, a functional link between ABA and MAPK pathway is unknown, although ABA-dependent phosphatidic acid generated by phospholipase D may be responsible for the activation of the MAPK pathway. In addition to the MAPK pathway, CDPKs may also be involved in transmitting the ABA signal to the transcriptional machinery.

Transcription Factors

Several classes of transcription factors emerged as targets of ABA signaling events and comprise members of the basic leucine zipper proteins (b-ZIP), AP2, Myb, Myc (basic helix-loop-helix, b-HLH), and homeodomain-containing leucine zipper proteins (HD-ZIP). Several of the genes that encode transcription factors or DNA-binding proteins are regulated by ABA, suggesting that a cascade of transcription factors may mediate stimulus-dependent gene expression in ABA responses.

b-ZIP ABFs/AREBs and ABI5 belong to a family of basic leucine zipper class of transcription factors that bind to ABA responsive *cis*-acting elements (ABREs) and confer ABA responsive gene expression. ABF/AREB proteins respond at the transcriptional and posttranscriptional levels to drought and salt stress and appear to be specifically phosphorylated in response to ABA, mediated through ABA-activated protein kinase. ABF3 and ABF4/AREB2 overexpression in transgenic *Arabidopsis* plants resulted in ABA hypersensitivity, enhanced drought tolerance accompanied with decreased transpiration, suggesting that ABF3 and ABF4 are involved in stomatal closure mediated by ABA. Promoters of both *ABF3* and *ABF4* were found to be most active in roots and guard cells, consistent with their roles in stomatal regulation and water-stress response. Some of the target genes for b-ZIPs are LEA, and other ABA-dependent genes.

MYB and MYC Regulation of expression of many ABA-inducible genes has been postulated to involve the ABRE *cis*-elements in their promoter regions. However, the RD22 promoter does not contain any typical ABRE consensus sequence but still is activated by ABA, suggesting the possible involvement of other regulatory elements responding to ABA other than the ABRE-b-ZIP regulatory module. The *Rd22* promoter contains MYC- and MYB-binding elements responsible for drought and ABA activation. The transcription factors that bind these elements, AtMYB2 and AtMYC2 are able to induce *RD22* gene expression in response to drought and ABA. Consistent with their roles, transgenic plants overexpressing AtMYC2 and/or AtMYB2 are hypersensitive to ABA. Hypersensitivity to ABA was enhanced in transgenics when both genes are overexpressed together. On the other hand, knockout mutant in *AtMYC2* showed insensitivity to ABA.

HD-ZIP A number of HD-ZIP proteins have been suggested to be dependent on ABA signaling for their transcriptional regulation. *Arabidopsis* HD-ZIPs, *ATHB5*, *ATHB6*, *ATHB7*, and *ATHB12* are induced

by the exogenous application of ABA or abiotic stresses that cause ABA accumulation, indicating that these transcription factors form part of the ABA signaling. The target genes induced by HD-ZIPs are unknown.

ABRE (Abscisic Acid Responsive Elements)

Exploration on more downstream elements of ABA signaling in stress responses, especially drought and cold tolerance, identified ABREs in promoters of ABA-induced genes. In most cases, the ABREs contain a core ACGT motif, the most common of those is designated the G-box (CACGTG) that is recognized by b-ZIP transcription factors. The ABRE functions efficiently when two copies are located tandemly or when it is associated with a coupling element. *Cis*-elements called coupling elements which are active in combination with an ABRE but not alone have also been identified. In the promoters of barley genes *HVA22* and *HVA1*, the coupling elements CE1 and CE3 (ACGCGTGTCCTG) are necessary for activation by ABA. Dissection of these promoters defined ABA responsive complexes (ABRCs) consisting of a coupling element and an ABRE capable of conferring ABA inducible transcription.

See Also the Following Articles

Calcium Signaling: Cell Cycle • Mitogen-Activated Protein Kinase Family • Photosynthetic Carbon Dioxide Fixation • Protein Kinase B • Protein Kinase C Family • Protein Tyrosine Phosphatases • Small GTPases

Glossary

abscisic acid Terpenoid compound, one of the plant hormones.

phytohormone Compound that is synthesized by a plant which regulates growth, differentiation, or other specific physiological processes.

seed dormancy A resting condition of the nongerminating seed with reduced metabolic rate.

stomata Microscopic pores surrounded by two crescent-shaped epidermal guard cells.

water-stress tolerance Ability to tolerate water-stress conditions.

Further Reading

Busk, P. K., and Pages, M. (1998). Regulation of abscisic acid-induced transcription. *Plant Mol. Biol.* **37**, 425–435.

Federoff, N. V. (2002). Cross-talk in abscisic acid signaling. *Science's STKE* — http://www.Stke.org/cgi/content/full/sigtrans;2002/140/re10.

Finkelstein, R. R., and Rock, C. D. (2002). Abscisic acid biosynthesis and signaling. In *The Arabidopsis Book* (C. R. Somerville and E. M. Mayerowitz, eds.) American Society of Plant Biologists, Rockville, MD.

Ingram, J., and Bartels, D. (1996). The molecular basis of dehydration tolerance in plants. *Annu. Rev. Plant Physiol. Plant Mol. Biol.* **47**, 377–403.

Schroeder, J. I., Kwak, J. M., and Allen, G. J. (2001). Guard cell abscisic acid signaling and engineering drought hardiness in plants. *Nature* **410**, 327–330.

Xiong, L., and Zhu, J.-K. (2003). Regulation of abscisic acid biosynthesis. *Plant Physiol.* **133**, 29–36.

Zhu, J.-K. (2002). Salt and drought stress signal transduction in plants. *Annu. Rev. Plant Biol.* **53**, 247–273.

Biography

R. Sunkar is a Postdoctoral fellow at the University of California, Riverside.

Jian-Kang Zhu is the Director of The Institute for Integrative Genome Biology at the University of California, Riverside. His principal research interest is abiotic stress signaling and tolerance in plants. He holds a Ph.D. from Purdue University and received his postdoctoral training at the Rockefeller University.

Actin Assembly/Disassembly

Henry N. Higgs
Dartmouth Medical School, Hanover, New Hampshire, USA

Actin is a monomeric protein that polymerizes into helical filaments. Apart from its role in muscle cells as a scaffold for myosin-based contraction, actin's function often depends on its ability to assemble into filaments from monomers rapidly, and to disassemble equally rapidly. Actin alone can polymerize *in vitro*, but both the kinetics and equilibria of polymerization are controlled in cells by specific actin-binding proteins that serve to modify the assembly/disassembly cycle inherent to actin itself. Some actin-binding proteins of particular importance are sequestering proteins, profilin, capping protein, and ADF/cofilin.

Actin Structure

Actin Monomer Structures

Actin is a 43 kDa (375 amino acid) globular monomer, which binds a nucleotide (ATP or ADP in cells) in a deep cleft between two halves of the protein (Figure 1A). The affinity of actin for nucleotide is greatly increased by divalent cation. Due to its relative cytosolic abundance (100s of μM), Mg^{2+} is the main actin-bound divalent cation in cells, but other cations, especially Ca^{2+}, are used for special purposes *in vitro*.

Actin Isoforms and Model Systems

Mammals contain six highly conserved actin isoforms, with at least 93% amino acid identity (Table I). Actin from non-mammals is similarly conserved, with budding yeast 88% and *Acanthamoeba castellani* 95% identical to human non-muscle β-actin. Bacteria contain several proteins with some properties similar to actin, Mbl, and Mreb.

Much of the biochemical data on actin assembly/disassembly is derived from studies of vertebrate muscle actin. Seminal studies on actin biochemistry were begun by Straub and Feuer during World War II using rabbit muscle actin. The sole actin isoform of budding yeast has also been a model, due to the combination of biochemistry and genetics in this system.

The highly similar sequences of actins from diverse species suggest that results in these model systems will be close approximations for most actins. However, specific biochemical properties can vary between actins, such as affinities for some actin-binding proteins.

Individual cells can possess multiple actin isoforms simultaneously. Mammalian non-muscle cells often contain both β- and γ-actin. The reasons behind this diversity are not well understood, but differential subcellular localization has been observed. Some unicellular organisms possess multiple actin isoforms. For instance, Dictyostelium has ~20 actin genes.

Actin Filaments

Actin filaments are right-handed double helices, with ~13 monomers per turn (Figure 1B). Each monomer adds ~2.7Å to the filament, so there are ~370 monomers per μm. All monomers are oriented in the same direction along the helix, making the filament polar. Due to the filament's arrow-like appearance when coated with myosin, the two ends are often called "barbed" and "pointed", respectively. The nucleotide-binding cleft faces the pointed end. Some refer to the barbed and pointed ends as "+" and "−," respectively.

Actin Dynamics

General Concepts in Actin Assembly/Disassembly

Under polymerizing conditions, actin monomers spontaneously polymerize into filaments, without need of other proteins. Polymerization from monomers can be broken down to two processes: nucleation, whereby actin monomers assemble to form a trimeric nucleus; and elongation, whereby additional monomers add to this nucleus (Figure 2). Nucleation is highly unfavorable, with equilibrium dissociation constants in the mM range. Consequently, a major control point for cellular actin assembly is enhancement of nucleation rate. Elongation occurs rapidly at the barbed end, (diffusion-limited on-rate) and tenfold more slowly at the pointed end. For reasons explained later, at pointed end elongation rarely occurs in cells, and we will only consider barbed end elongation in this chapter.

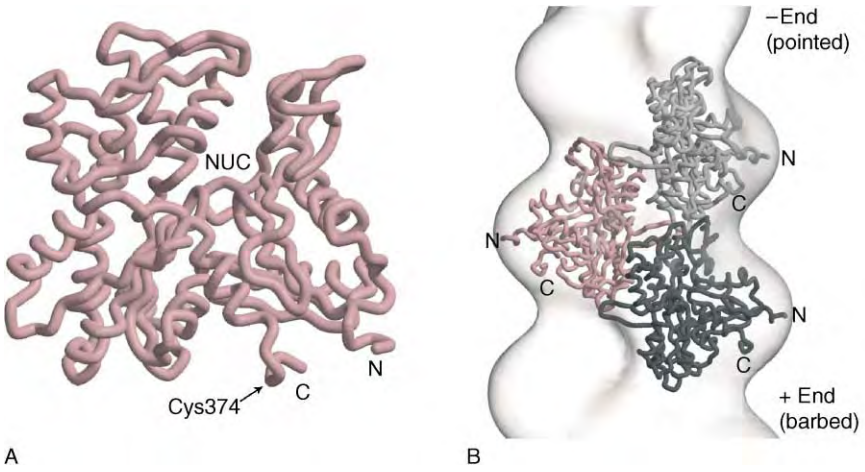

FIGURE 1 Structure of actin monomers and filaments. (A) Ribbon diagram of actin monomer backbone, oriented with the surface at the pointed end facing upwards. NUC = nucleotide/divalent cation-binding pocket. N and C termini are indicated, as well as cysteine374, which is labeled by pyrene-iodoacetimide. (B) Atomic model of three actin monomers fit into a three-dimensional reconstruction of an actin filament obtained by electron microscopy and image analysis. Both A and B are modified from images provided by Dorit Hanein and Niels Volkmann.

While both Mg-ATP and Mg-ADP monomers can nucleate and elongate, Mg-ATP monomers do both faster. Upon adding to filaments, monomers are referred to as "subunits."

Monomers hydrolyze ATP extremely slowly. Upon adding to a filament, the hydrolysis rate increases to $\sim 0.3\ \text{sec}^{-1}$. With a reasonable concentration of ATP-actin monomers, ATP hydrolysis occurs more slowly than elongation, which occurs at $10\ \mu\text{M}^{-1}\ \text{sec}^{-1}$. Thus, a "cap" of ATP-subunits builds up at the barbed end. Furthermore, the inorganic phosphate (Pi) hydrolysis product remains bound to the subunit for a considerable time before dissociating, while the ADP product remains tightly bound while the subunit remains on the filament.

TABLE I

Actin Isoforms

Species	Isoform	% identity[a]	GI #
Human	Non-muscle β	100	113270
Human	Non-muscle γ	98	113278
Human	Skeletal muscle	93	113287
Human	Cardiac	94	113272
Human	Smooth muscle α	94	113266
Human	Smooth muscle γ	93	113279
Rabbit	Skeletal muscle	93	71611
Chicken	Skeletal muscle	93	71613
Drosophila	Muscle 88F	95	2113792
Budding yeast	Sole Isoform	88	2262056
Acanthamoeba	[b]	95	71630

[a] To human non-muscle β.
[b] Number of actin isoforms unknown.

At steady state, three regions exist on an actin filament: ATP-subunits at the barbed end; ADP-Pi-subunits in the middle; and ADP-subunits toward the pointed end. As discussed later, Pi release is crucial to actin disassembly.

Subunits disassociate from both ends of a filament, and do so more rapidly from the barbed end than from the pointed end. ADP-subunits release from the barbed end faster than ATP-subunits. Once released from the filament, the monomer slowly exchanges its ADP with ATP, assuming an excess of ATP in solution.

Thus, actin assembly/disassembly occurs in a cycle (Figure 2). Nucleation occurs slowly, but filaments elongate rapidly once formed. Since barbed end elongation is tenfold faster than pointed end elongation, and since ATP hydrolysis occurs slowly, ADP-subunits are at higher concentration toward the pointed end. Subunits dissociate from both ends, and do so faster from the barbed end in both the ATP-and ADP-bound states. However, since monomer association is much more rapid at the barbed end, more net growth occurs at this end. Released ADP-monomers exchange ATP for ADP slowly (half-time ~ 50 s).

Through this cycle, equilibrium between assembly and disassembly is reached, in which the concentrations of actin in filaments and as monomers become constant. When ATP is in constant supply (and assuming an excess of Mg^{2+} over Ca^{2+}), the equilibrium monomer concentration is $\sim 0.1\ \mu\text{M}$ under polymerizing conditions. This monomer concentration, the "critical concentration," is always found in solution at equilibrium under these conditions. The concentration of actin in filaments is the excess above $0.1\ \mu\text{M}$. In other words, given $4\ \mu\text{M}$ actin under polymerizing conditions, $3.9\ \mu\text{M}$ will be in

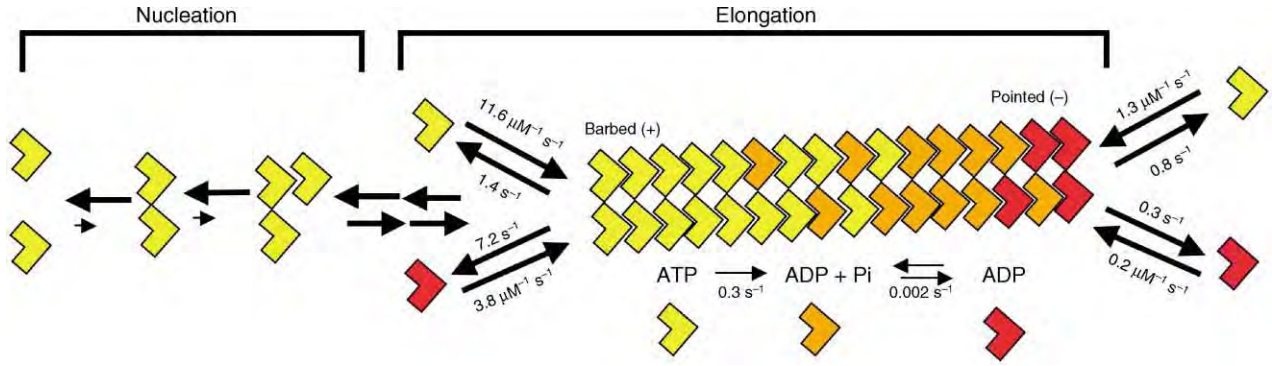

FIGURE 2 Assembly/disassembly of actin alone. Nucleation is highly unfavorable, signified by the large back arrows in the dimerization and trimerization steps. Once a tetramer is formed, the filament is more stable and monomers add to and disassemble from each end with the indicated kinetic constants (Pollard (1986) *J. Cell Biol*, **103**, 2747–2754). Subunits hydrolyze bound ATP slowly upon addition to filaments, and release the Pi product even more slowly, creating sectors of the filament enriched in ATP-actin (yellow), ADP-Pi-actin (orange), and ADP-actin (red). Upon release from the filament, the ADP on the monomer exchanges slowly with ATP.

filaments and 0.1 μM as monomers. With 100 μM actin, 99.9 μM is in filaments, 0.1 μM as monomers. At or below 0.1 μM, there are no filaments. Even at equilibrium, monomers constantly add to and release from both ends.

Polymerization Conditions

Three buffer conditions strongly affect actin's propensity to polymerize: ionic strength, the divalent cation present, and pH. Increased ionic strength increases elongation rate. The reason for this effect is not well understood, but thought to be due to masking of charge repulsion between the highly anionic actin monomers. The ionic effect reaches a maximum at around the equivalent of 50 mM KCl, and higher concentrations slow polymerization, probably due to inhibition of specific inter-monomer charge interactions in the filament. As for divalent cation, Mg-actin is better than Ca-actin at polymerizing, due to differences in monomer conformation. For pH, higher pH inhibits polymerization, likely due to increasing the net negative charge of actin, hence increasing charge repulsion between monomers.

Effects of Actin-Binding Proteins

Actin-binding proteins are widely expressed in eukaryotes, generally at concentrations that exert a significant effect on cellular actin assembly/disassembly. Each protein alters one or more aspects of actin's assembly/disassembly cycle. The basic biochemical functions of these proteins are discussed in this section and illustrated in Figure 3, while their coordinated cellular effects are described in the next section.

Sequestering Proteins

Sequestering proteins, present in most eukaryotic cells, bind actin monomers and prevent their addition to either end of filaments (Figure 3). Metazoan cells often contain the small protein, thymosin (5 kDa), the most well-characterized isoform being thymosin β4. Yeast do not have thymosins, but do express twinfilin, which can sequester. Twinifilin is present in mammals and other organisms as well.

Profilin

Profilin is a 13 kDa protein that binds actin monomers, preferring ATP-actin over ADP-actin about fivefold. Profilin binding has three consequences for actin (Figure 3). First, profilin strongly inhibits spontaneous nucleation. Second, profilin prevents monomer addition to pointed ends. Third, profilin serves as a nucleotide exchange factor for actin, increasing exchange of ATP or ADP at least fivefold, though by some accounts its effect is much greater. A common misconception is that profilin is a sequestering protein. Profilin-bound actin can add to barbed ends at a rate comparable to that of free monomer. An additional feature of profilin is that it binds stretches of polyproline found in many cytoskeletal proteins (e.g., VASP, formins, WASp/Scar/WAVE family proteins, vinculin), binding such proteins and an actin monomer simultaneously.

Capping Proteins

Capping protein is a heterodimer of 30 kDa subunits that binds filament barbed ends, preventing monomer addition (Figure 3). With barbed ends capped,

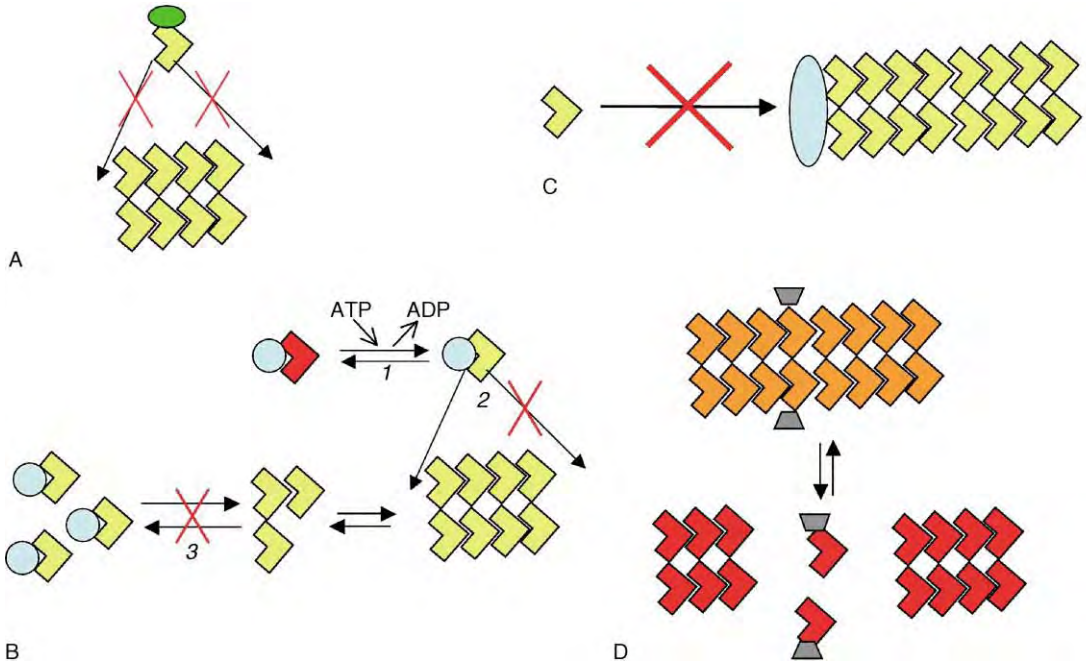

FIGURE 3 Effects of actin-binding proteins on actin dynamics. (A) Sequestering proteins (green oval) bind actin monomers and prevent addition to either end of the filament. (B) Profilin (light blue circle) binds monomers and has three effects: (1) acceleration of nucleotide exchange on monomers; (2) prevention of monomer addition to pointed ends; and (3) inhibition of spontaneous nucleation. (C) capping proteins (light blue oval) bind filament barbed ends and prevent monomer addition. (D) ADF/cofilin (gray trapezoid) binds ADP-subunits on filaments and promotes Pi release from other subunits. ADF/cofilin also severs filaments. These two activities result in accelerated filament depolymerization.

the critical concentration of actin shifts to 0.7 μM, the critical concentration of the pointed end. Capping protein's high affinity ($K_d < 1$ nM) and slow off-rate (half-life of capped barbed end is 30 min) cause a stable block to barbed end elongation. Members of the gelsolin family also cap barbed ends, in addition to severing filaments.

ADF/Cofilin

ADF/cofilin is a 15 kDa protein that binds both filaments and monomers, with a 40-fold preference for the ADP-bound state over ATP- or ADP-Pi states in both cases. Mammals contain two isoforms, ADF and cofilin. ADF/cofilin binding to filaments is cooperative, and accelerates Pi release from other subunits on the filament at least 20-fold. ADF/cofilin also severs filaments. ADF/cofilin is often referred to as a depolymerization factor, because its binding to filaments accelerates depolymerization. The mechanism of depolymerization acceleration probably involves both acceleration of Pi release (increasing subunit off-rate from filaments) and severing (creating more ends for depolymerization). However, ADF/cofilin does not prevent polymerization, as ADF/cofilin-bound monomers can still add to filaments.

Cellular Aspects of Actin Assembly/Disassembly

In mammalian cells, actin concentration is in the 50–200 μM range. Since the critical concentration is 0.1 μM, one would expect the vast majority of actin to be in filaments. However, the ratio of polymerized:unpolymerized actin is often around 1:1 in unactivated cells, while activated cells can reach close to 100% polymerized actin. The 1:1 ratio is maintained largely by the proteins discussed. Many mammalian cells contain more thymosin than actin, as well as a high concentration of profilin (e.g., Neutrophils have ~200 μM actin, 400 μM thymosin, and 100 μM profilin). Despite its lower concentration, profilin binds ATP-actin more tightly than thymosin (K_d of 0.2 μM vs >10 μM), so that monomers distribute between the two proteins. The rapid off-rates of monomers from these proteins (at or above five per second) allow rapid equilibration. Almost all monomers are bound to one protein or the other, leaving ~0.5 μM free actin monomer in cells. This low free monomer concentration virtually eliminates spontaneous nucleation in cytoplasm. Another consequence of these two proteins is that pointed end elongation is effectively suppressed, since thymosin prevents elongation from both ends and profilin prevents pointed

end elongation. For this reason, cellular filaments only elongate from barbed ends (except under specific conditions in muscle cells).

Cellular actin filaments are created by specific nucleation factors. Examples of such factors are Arp2/3 complex and formins. Both nucleation factors are tightly regulated. Thus, cells control the when and where of filament formation.

Mammalian cells contain ~1 μM capping protein, and its high affinity for barbed ends means that new filaments are capped rapidly (~1 s after formation). Capping protein is inhibited by bound polyphosphoinositides, which can promote cellular filament elongation. Some proteins can also inhibit capping protein by competing for barbed end binding, specifically VASP and formins. By controlling capping, cells control filament elongation.

The mechanisms by which cellular filaments disassemble are not understood fully, since off-rates from pointed ends can not explain the rapidity of disassembly in many circumstances. Filament networks 100s of nm thick can disassemble in seconds. ADF/cofilin clearly has a central role in this process, probably both by catalyzing Pi release from filaments and by severing filaments to create new ends for depolymerization. There is, however, evidence that ADF/cofilin may contribute to filament assembly upon initiation of cell motility, perhaps by severing to create new ends capable of elongating and supporting Arp2/3 complex-based nucleation.

The coordinated action of these proteins results in a cycle of assembly/disassembly in cells (Figure 4). Monomers shift from thymosin to profilin, then add to the barbed end. The filament-bound monomer hydrolyzes its ATP and retains ADP and Pi. ADF/cofilin binding to the filament accelerates Pi release and causes filament severing. Monomers dissociate from the pointed end and remain bound to ADF/cofilin. Monomeric ADP-actin exchanges between ADF/cofilin, thymosin, and profilin. Even though ADF/cofilin binds more tightly than profilin to ADP-actin, profilin is at higher concentration (100 versus ~20 μM), and the rapid off-rate from ADF/cofilin enables equilibration. Profilin catalyzes recharging of ATP onto its bound monomer, enabling re-addition of that monomer to the barbed end. Capping protein terminates barbed end elongation except under specific circumstances.

Profilin's ability to bind proline-rich sequences in VASP and formins may have interesting consequences. Both proteins are postulated to reside close to barbed ends of particular filaments and to compete for barbed end binding with capping protein. Binding of profilin-actin at these areas may enable preferential elongation of these filaments even in the presence of capping protein.

The above description is probably accurate for most eukaryotes, including mammals, other vertebrates and multicellular animals, and protozoa. Fungi such as *Saccharomyces cerevisiae* (budding yeast) are somewhat different, containing lower actin and profilin concentrations (5–10 μM for each) and no thymosin. A yeast sequestering protein, twinfilin, is present at unknown concentration. Unlike in vertebrates, most yeast actin (>90%) is polymerized. Yeast contain ADF/cofilin, capping protein, Arp2/3 complex and formins.

Actin assembly/disassembly in plants is poorly understood. Plants contain all the discussed proteins except thymosin. Plant profilin does not catalyze nucleotide exchange.

Other proteins, less well characterized at present, may play significant roles in actin assembly/disassembly.

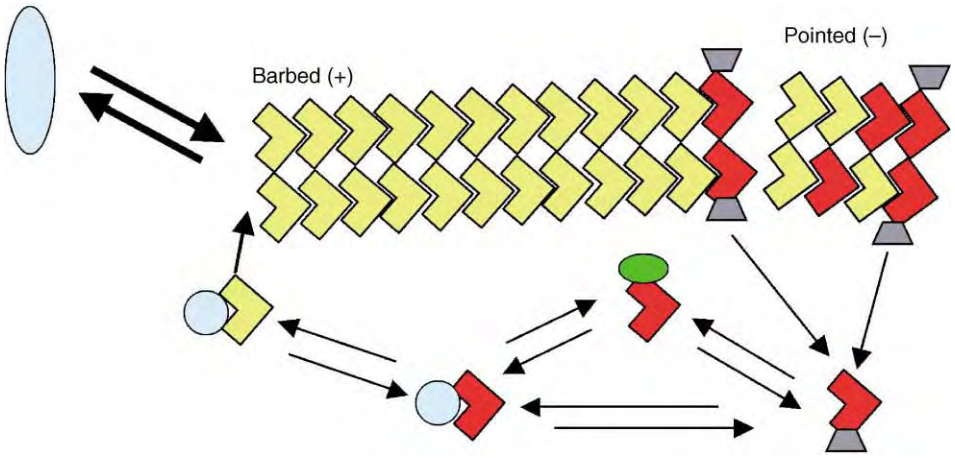

FIGURE 4 Concerted effects of actin-binding proteins in the assembly/disassembly cycle. Profilin-bound ATP-actin adds to the filament barbed end, then hydrolyzes its ATP slowly. ADF/cofilin binding accelerates Pi release along the filament, and severs the filament. ADF/cofilin-bound ADP-subunits release from filament ends. Profilin, thymosin, and ADF/cofilin compete for binding ADP-monomers. Profilin-bound ADP-monomers exchange ADP for ATP, enhancing their ability to assemble onto barbed ends.

TABLE II

Small Molecule Reagents Used in Actin Research

Reagent	Biochemical effect	Cellular effect	Cell-permeant?
Latrunculin A	Sequesters monomer	Depolymerization	Yes
Cytochalasins	Cap barbed ends	Depolymerization	Yes
Swinholide A	Sequesters dimers, severs filaments	Depolymerization	Yes
Phalloidin	Binds filaments	Prevent depolymerization	No
Jasplakinolide	Binds filaments	Prevent depolymerization	Yes

Srv2/CAP complex may accelerate ADF/cofilin-mediated filament depolymerization and monomer recycling. Aip1 may associate with ADF/cofilin and cap barbed ends.

Reagents Used in Actin Research

Small Molecules Affecting Actin Dynamics

Table II presents a catalogue of the reagents commonly used in actin research. While this table is simplistic, the effects of some reagents are not, and care must be taken to avoid artifacts. An example is the cytochalasins, a group of compounds commonly used to depolymerize cellular actin. This effect is attributed to the barbed end capping activity of cytochalasins. With barbed ends capped, filaments depolymerize from pointed ends since profilin and thymosin prohibit pointed end elongation. However, at higher concentrations, cytochalasins can have other effects, such as causing ATP hydrolysis on actin monomers through non-productive dimer formation. Use of concentrations below 1 μM largely suppress this secondary effect. In addition, cytochalasin B binds and inhibits a plasma membrane glucose transporter. Despite this property, cytochalasin B is sometimes used in preference to cytochalasin D, because the tenfold lower affinity of cytochalasin B for barbed ends enables more rapid wash-out during cellular recovery experiments.

Latrunculins (isomers A and B) can cause a similar cellular effect to cytochalasins (depolymerizing filaments), but by a different mechanism (sequestering monomers). In neither case do these compounds actively depolymerize filaments. What they do is block polymerization, leaving only depolymerization to occur by the normal cellular mechanisms.

Swinholide A binds/severs filaments, and binds/sequesters dimers, again causing cellular actin depolymerization. This compound has not been widely used in actin cell biology.

Two compounds stabilize filaments: phalloidin and jasplakinolide. Phalloidin is much better characterized. In the presence of phalloidin, the off-rate from barbed and pointed ends drops to near zero, and the critical concentration essentially becomes zero. Phalloidin also slows Pi release significantly. Phalloidin can be labeled with many compounds, including fluorophores, enabling localization of actin filaments in permeabilized cells. TRITC-phalloidin is especially useful, since its fluorescence increases 20-fold upon binding filaments. Since phalloidin is not cell-permeable, jasplakinolide is used for live cell studies. For either compound, concentrations equal to those of actin are necessary to block depolymerization fully, because they bind stoichiometrically along the filament.

See Also the Following Articles

Actin-Capping and -Severing Proteins • Actin-Related Proteins • Cell Migration • Focal Adhesions • Phosphatidylinositol Bisphosphate and Trisphosphate

Glossary

capping protein In theory, any protein that binds either barbed or pointed end of actin filament and prevents monomer addition to that end. In practice, used to mean barbed end capping protein, and often heterodimeric capping protein in particular.

critical concentration The concentration of monomers in a solution of actin at equilibrium between monomers and filaments. Under polymerizing conditions, the critical concentration with both the barbed and pointed ends free is ~0.1 μM. When the barbed end is capped, the critical concentration rises to 0.5–0.7 μM.

sequestering protein Protein that binds actin monomer and prevents addition to either end of the filament. Neither profilin nor cofilin are sequestering proteins.

Further Reading

Amos, L. A., van den Ent, F., and Lowe, J. (2004). Structural/functional homology between the bacterial and eukaryotic cytoskeletons. *Curr. Op. Cell Biol.* **16**, 24–31.

Carlier, M. F., and Pantaloni, D. (1997). Control of actin dynamics in cell motility. *J. Mol. Biol.* **269**, 459–467.

Condeelis, J. (2001). How is actin polymerization nucleated *in vivo*? *Trends Cell Biol.* **11**, 288–293.

Cooper, J. A., and Schafer, D. A. (2000). Control of actin assembly and disassembly at filament ends. *Curr. Opin. Cell Biol.* **12**, 97–103.

Goddette, D. W., and Frieden, C. (1986). Actin polymerization. The mechanism of action of cytochalasin D. *J. Biol. Chem.* **261**, 15974–15980.

Kreis, T., and Vale, R. (eds.) (1999). *Guidebook to Cytoskeletal and Motor Proteins*, 2nd edition. Oxford University Press, New York.

MacLean-Fletcher, S., and Pollard, T. D. (1980). Identification of a factor in conventional muscle actin preparations which inhibits actin filament self-association. *Biochem. Biophys. Res. Commun.* **96**, 18–27.

Pollard, T. D. (1984). Purification of ADP-actin. *J. Cell Biol.* **99**, 769–777.

Pollard, T. D., Blanchoin, L., and Mullins, R. D. (2000). Molecular mechanisms controlling actin filament dynamics in nonmuscle cells. *Ann. Rev. Biophys. Biomol. Struct.* **29**, 545–576.

Spudich, J. A., and Watt, S. (1971). The regulation of rabbit skeletal muscle contraction. *J. Biol. Chem.* **246**, 4866–4871.

Straub, F. B., and Feuer, G. (1950). Adenosine triphosphoate. The functional group of actin. *Biochim. Biophys. Acta.* **4**, 455–470.

Biography

Henry Higgs is an Assistant Professor of Biochemistry at Dartmouth Medical School. His principal research interest is to determine how cells produce so many different surface protrusions. Since most of these structures depend on actin filaments, he utilizes a great deal of time in research about actin assembly. He holds a Ph.D. in Biochemistry from the University of Washington, and did postdoctoral research at the Salk Institute. Dr. Higgs is a Pew Biomedical Science Scholar.

Actin-Capping and -Severing Proteins

Sankar Maiti and James R. Bamburg
Colorado State University, Fort Collins, Colorado, USA

Actin is one of the major components of the cytoskeleton, a network of protein filaments that organizes the cytoplasm of eukaryotic cells. Actin filaments (F-actin), in the form of a right-handed double-stranded helix, are formed by assembly of globular (G-actin) monomer subunits in a head to tail orientation that gives the filaments a molecular polarity. Based on the orientation of an arrowhead pattern on F-actin decorated with a fragment of the muscle motor protein myosin, one end of the filament is called the barbed end and the other the pointed end. Spatial and temporal regulation of actin-filament assembly, disassembly, and stability in cells drives most aspects of cell motility, cell shape, and the interaction of a cell with its neighbors or surrounding matrix. Actin-capping and -severing proteins are special classes of actin-binding proteins (ABP) that regulate the assembly dynamics of actin filaments. Actin-capping proteins are classified into two groups, the barbed-end-capping proteins and the pointed-end-capping proteins. Depending on their binding affinity and off-rate constants, capping proteins slow down or stop the growth and/or depolymerization of filaments at the end to which they bind. Their interaction with actin may promote nucleation of new filaments, increase branching of filaments, and/or enhance filament depolymerization. Actin-severing proteins bind to the side of actin filaments and enhance fragmentation. Some severing proteins also become barbed-end-capping proteins (e.g., gelsolin) whereas others (e.g., ADF/cofilin) can provide both free barbed and pointed ends that can influence actin dynamics.

Actin

Actin is a major cytoskeletal protein in virtually all eukaryotic cells, usually comprising $>1\%$ of cellular protein. In muscle cells where it was first identified, F-actin is the major component of the thin filaments of the contractile apparatus where the myosin motor head groups of the thick filament walk along the actin thin filaments in an energy-dependent process, causing contraction. Mammals have six actin genes, each expressing a different isoform, but the structure of the 42.5 kDa actin monomer is highly conserved across phyla. G-actin has four quasi-subdomains at the center of which is bound an essential adenine nucleotide, either adenosine triphosphate (ATP) or adenosine diphosphate (ADP). As is the case with most molecular self-assembly systems, actin assembly is driven by a positive entropy change that arises from the displacement of water as the subunits come together. Following assembly, bound ATP is hydrolyzed to ADP through an ADP + Pi intermediate. Nucleotide hydrolysis provides the energy input required for actin filaments to maintain equilibrium binding constants for monomers that differ at the barbed and pointed ends. The concentration of monomer required to maintain the filament end is called the critical concentration, and is lower for the barbed end than for the pointed end. Thus, as monomer assembles into filaments and the monomer concentration decreases, the critical concentration of the pointed end is reached first. Monomers still add to the barbed end, leading to monomer loss from the pointed end. This phenomenon is called treadmilling. At steady state there is consumption of energy through ATP hydrolysis that drives the treadmilling of the actin subunits (Figure 1). In some cells this may account for up to 50% of the total ATP consumption. Tropomyosin, a short helical filamentous ABP, binds along the side of actin filaments and covers 5–7 actin subunits. Binding of tropomyosin usually aids in the formation of stable actin filaments, in part because they can inhibit the severing and depolymerizing activity of other ABPs. Dimers of actin are not stable and tend to dissociate but with addition of another monomer, the trimeric actin acts as a nucleus for filament formation. In the cell, spontaneous nucleation of filaments is kept at a minimum by the presence of actin monomer sequestering proteins. Thus, nucleation is a highly regulated event and may be initiated in the cell by three mechanisms: (1) the activation of certain actin binding proteins that help form trimeric nuclei; (2) the removal of capping proteins from the filament barbed ends; and (3) the severing of existing filaments to provide new barbed ends for filament elongation. The sites of nucleation and directionality of actin-filament growth is important for the development of cell polarity and cell migration and is regulated, in part, by the localized activity of capping and severing proteins.

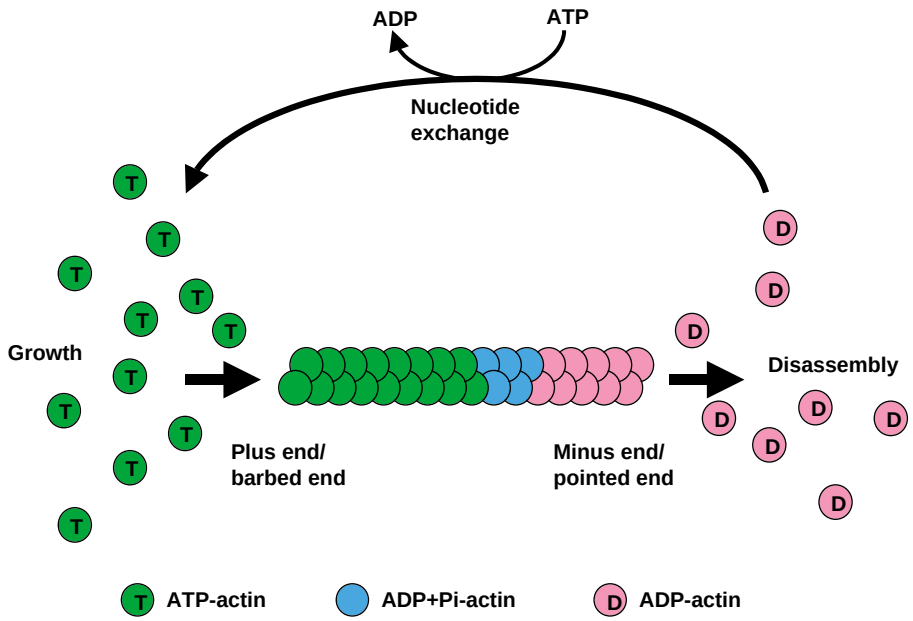

FIGURE 1 Dynamics of actin filaments at steady-state demonstrating treadmilling. ATP-actin adds onto the barbed end, nucleotide hydrolysis occurs and the inorganic phosphate dissociates leaving ADP-actin subunits to dissociate from the pointed end. Nucleotide exchange of ATP for ADP occurs on the monomer, giving rise to more ATP-actin for filament growth.

Actin Dynamics at the Leading Edge

Various cell membrane protrusions and inversions, especially lamellipodia, filopodia (microspikes), phagocytic cups, and upward ruffles are distinct morphologies of cells and are important for cell function, motility, and organismal development. These leading edge phenomena are based on actin-filament reorganization. In extending lamellipodia and filopodia, polarized arrays of actin filaments turn over very rapidly, with filament barbed ends facing toward the plasma membrane. The pointed ends of the filaments rapidly depolymerize at the rear of these arrays. In extending lamellipodia, the actin-filament growth is regulated mainly by Ena/VASP, capping protein, and Arp2/3 complex. The Arp2/3 complex causes branching of growing actin filaments and the barbed-end-capping protein limits the growth of newly assembled filaments to maintain short rigid filaments that can serve to push the membrane forward in the broad lamellipodium. Ena/VASP proteins bind to the barbed ends of growing actin filaments and inhibit the binding of Arp2/3 complex and capping protein, leading to the formation of longer and unbranched actin filaments, such as those found in the finger-like filopodial extensions (microspikes). This antagonism in barbed-end binding between Ena/VASP and Arp2/3 complex and capping protein, can help explain the often rapid conversion between lamellipodial and filopodial type of membrane protrusions seen at the leading edge of many migrating cells, especially within the growing tip of neurons, called the growth cone (Figure 2).

Pointed-End Binding and Branching

Arp2 and Arp3 are two actin-related proteins that form part of a seven-subunit complex known as the Arp2/3 complex, ubiquitous in eukaryotes. The Arp2/3 complex is required for generating the 70° branched actin filaments observed at the leading edge of expanding cell membranes in lamellipodia. There are several possible mechanisms for generating this type of filament array. The Arp2/3 complex may capture the pointed ends of actin filaments created by severing pre-existing

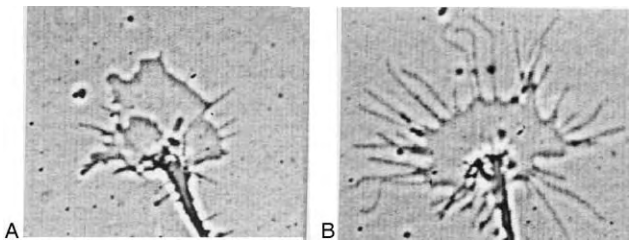

FIGURE 2 A typical dorsal root ganglion neuronal growth cone. Phase contrast picture in A shows growth cone exhibiting lamellipodial growth. Within a few minutes after reducing the osmolarity of the growth medium, the growth cone exhibits many long and active filopodia (B). Panel width = 44 μm.

filaments and then associate with the side of another pre-existing filament to create a branch point. Alternatively, Arp2/3 complex may bind at the barbed end of a growing filament to create a branch point. The Arp2/3 complex requires activation to become a potent nucleator of actin-filament growth. Activation can occur through the binding of members of the Wiskott–Aldrich syndrome protein (WASP) family, some of which are activated by signaling through G protein-coupled receptors. Arp2/3 complex can also be activated by other mechanisms. The active Arp2/3 complex can bind an actin monomer and initiate the nucleation of a new filament at an angle of ~70° to the mother filament. This branched actin-filament network, called the dendritic brush, generates the force needed for cell protrusion at the leading edge (Figure 3). To maintain proper stiffness and maintain the best angle for membrane expansion, the filaments are not allowed to grow very long before their barbed ends are capped by capping protein. The branching of filaments is inhibited by the binding of at least some forms of tropomyosin, which prevent Arp2/3 binding, and branching is also inhibited by proteins in the Ena/VASP family. The binding of tropomyosin and Ena/VASP proteins also inhibits binding of some barbed-end capping proteins, allowing filaments to grow into long parallel bundles, such as those that form filopodia.

Evolutionary and Structural Relationships between Some Severing and Severing/ Barbed-End-Capping Proteins

The present sequence, structural, and biochemical data suggest that many of the actin-binding proteins have evolved through gene duplication or mutation of DNA sequences encoding a small number of protein motifs. Variants of a single 15 kDa molecular module have evolved, which interact with both G-actin and F-actin with severing and capping functions that may be regulated by calcium and/or by specific phospholipids. Proteins in the ADF/cofilin family are single domain, bind both G-actin and F-actin, have pH-dependent actin-filament severing activity, and are found in all eukaryotes. Twinfilin is a 40 kDa protein with two ADF-homology

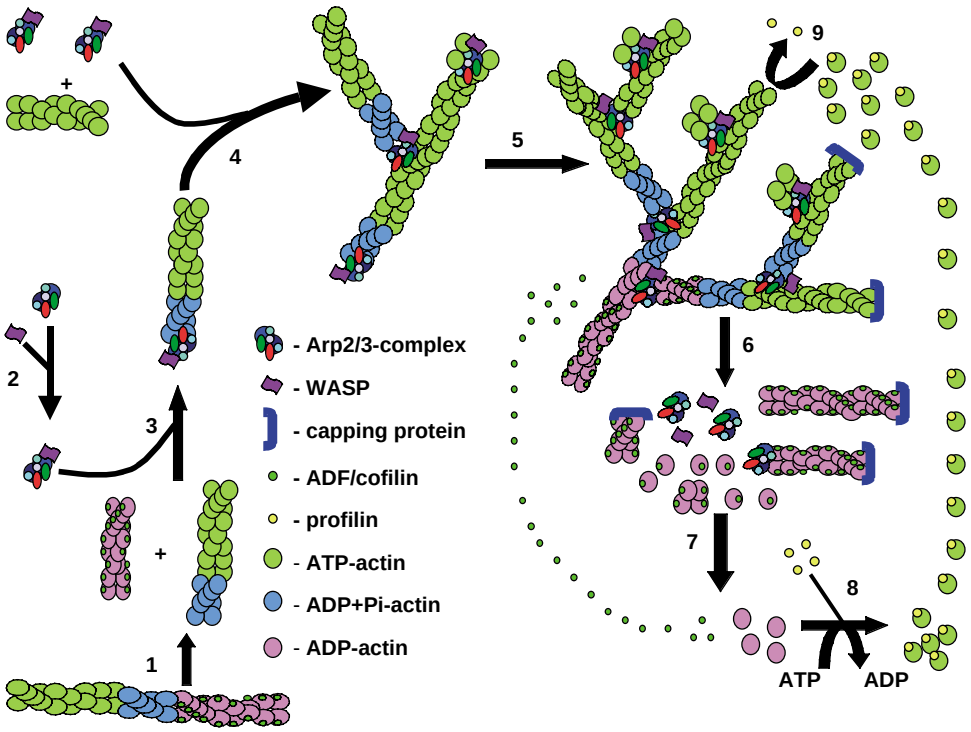

FIGURE 3 Schematic of actin-filament dynamics at the leading edge of a cell. (1) Severing of actin filament is one mechanism to create new barbed ends. (2) Activation of Arp2/3 complex by WASP can cause *de novo* nucleation of filaments, but active Arp2/3 complex may also be captured by pointed ends of severed filaments (3). (4) Arp2/3 complex either nucleates from the side or ends of actin filaments or when bound to actin, is captured along the side of a filament to create the 70° branches. Further growth of barbed ends with rapid capping and nucleation of new branches leads to complex networks of actin filaments (5). (6) ADF/cofilin-mediated severing and depolymerization of the filament arrays occurs when subunits become ADP-actin. Release of ADF/cofilin (7) and enhanced nucleotide exchange by profilin (8) provide profilin–actin complex that serves as a monomer pool for filament growth (9).

(ADF-H) domains connected by a small linker region. Twinfilin is found across the phyla. Unlike ADF/cofilin, twinfilin does not interact with F-actin and does not promote filament disassembly, but acts as an actin monomer sequestering protein thereby preventing spontaneous actin-filament assembly. CapG, severin, and fragmin contain three structural repeats of the 15 kDa ADF-H domain, and have barbed-end-capping and -severing activity. Presumed duplication of the three repeat-containing proteins gives rise to proteins with six ADF-H repeats, such as gelsolin, villin, and adseverin/scinderin, which are more complicated regulators of actin dynamics. Functions of all of the members of the three repeat and six repeat families are regulated by calcium and specific membrane phospholipids, and are commonly known as the gelsolin family of actin-filament-capping and -severing proteins. Although ADF/cofilins and some gelsolin family members show little or no sequence homology, structurally they display similar overall folding and secondary/tertiary structural elements suggesting both divergent and convergent evolutionary mechanisms may have given rise to these structurally related molecules.

The Three Segment Proteins: CapG, Severin, and Fragmin

CapG, severin, and fragmin are gelsolin family proteins containing three ADF-H segments. The first segment (S1) binds to G-actin and has the capping function whereas segments 2 and 3 (S2, S3) bind to F-actin. CapG is a 39 kDa barbed-end-capping protein, the name reflecting its capping function and structural similarity to gelsolin, though only half its size. CapG is highly expressed in macrophages and was initially known as macrophage-capping protein, gCap39 or Mbh1. CapG has a structure similar to severin and fragmin, but does not sever actin filaments as does severin and fragmin. CapG caps barbed ends of actin filaments at micromolar concentrations of Ca^{2+}, but it dissociates from barbed ends when Ca^{2+} levels return to their normal nanomolar levels, whereas gelsolin remains bound to the barbed ends under the same conditions. CapG is important for the actin-based motility of macrophages. Phosphatidylinositol-4,5-bisphosphate (PIP_2) binds to CapG thereby inhibiting its binding to F-actin. The actin monomer sequestering protein profilin is also able to dissociate CapG from actin-filament barbed ends when profilin is present at high concentration ($>10\ \mu M$).

CapG is also found within the nucleus as well as the cytoplasm, but its function there is unknown. Although CapG lacks a nuclear export signal, which is present in severin and fragmin, CapG does not contain any known nuclear localization signal. Thus, the method by which it is translocated into the nucleus is also unknown. Severin and fragmin, found in the slime moulds *Dictyostelium* and *Physarum* respectively, are structurally similar to CapG, but they also bind to the side of and sever F-actin as well as cap the barbed ends of the severed filaments. They have two Ca^{2+}-binding sites and can be thought of as small versions of gelsolin.

The Six Segment Proteins: Gelsolin, Villin, and Adseverin/Scinderin

Gelsolin, villin, and adseverin/scinderin contain six ADF-H repeats and are F-actin barbed-end-capping and -severing proteins. The N-terminal half of these proteins, with three repeats similar to CapG, severin, and fragmin, is able to bind two actin monomers and sever actin filaments. The C-terminal half is able to bind to a single actin monomer at elevated Ca^{2+} concentration.

Gelsolin, with a mass of 80 kDa, is expressed in all eukaryotes. The name arose from its ability to rapidly dissolve an actin gel and convert it into a soluble form. The N-terminal half of gelsolin contains two Ca^{2+}-binding sites, one of which is high affinity, in the submicromolar range. Gelsolin severs actin filaments at Ca^{2+} concentrations $>10^{-5}$ M. The severing mechanism probably involves the binding of gelsolin along the side of the filament and intercalation between actin subunits during the normal bending of the actin. After severing filaments, gelsolin remains bound to the barbed end of one new filament (Figure 4) and produces a new pointed end. At Ca^{2+} concentrations in the submicromolar range, gelsolin acts to cap barbed ends of actin filaments. An extracellular (secreted) isoform of gelsolin with molecular mass 83 kDa, called serum gelsolin, circulates in blood where it severs and caps actin filaments released from lysed cells. The resulting monomers of actin are then sequestered by vitamin D-binding protein, a potent monomer-binding protein and ultimately removed from circulation by liver. This mechanism prevents accumulation of actin filaments in the blood, which could potentially block circulation in capillaries.

Gelsolin binding to F-actin is inhibited by tropomyosin in two ways. Tropomyosin binding to F-actin induces a cooperative conformational change in actin filaments resulting in dissociation of gelsolin. Secondly, tropomyosin can directly bind gelsolin and thereby dissociate gelsolin from actin–gelsolin complex. Dissociation of gelsolin by tropomyosin from a gelsolin capped actin filament leads to formation of long filaments from smaller gelsolin-actin complexes, even from gelsolin–actin heterodimers, heterotrimers, and heterotetramers. PIP_2 can bind directly to gelsolin and dissociate gelsolin

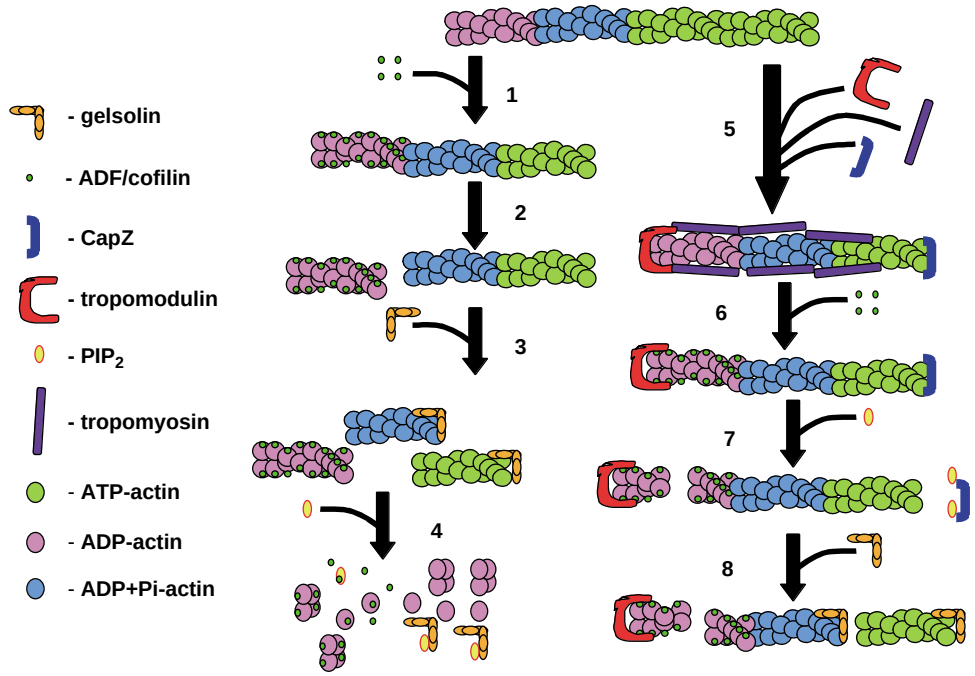

FIGURE 4 Diagrams showing actin-filament capping and severing by different types of molecules. (1) ADF/cofilin bind with highest affinity and cooperatively to ADP-actin and (2) sever actin filaments as well as enhancing monomer off-rates from the pointed ends (not shown). (5) Stable filaments generated by tropomodulin binding to pointed ends, CapZ binding to barbed ends and tropomyosin binding along filament length. ADF/cofilin competes for F-actin binding with some tropomyosins (6) and can lead to severing and exposure of new pointed ends (7). (4 and 7) PIP_2 regulates the binding of capping proteins, dissociating both gelsolin and CapZ from barbed ends of actin filaments. (3 and 8) Actin-filament capping and severing by gelsolin.

that is already bound to the barbed end of an actin filament to yield a free barbed end for growth. Gelsolin can be proteolytically cleaved by caspase-3 during apoptosis. The short amino-terminal cleavage (residues 1–352) fragment does not need Ca^{2+} for severing existing actin filaments and contributing to the progression of apoptosis.

Villin, a gelsolin family member with molecular mass of 92.5 kDa, controls actin assembly in the microvilli of epithelial cells. Villin has the unique property of being able to bundle actin filaments through an 8 kDa F-actin-binding module known as the villin headpiece. The activity of villin is highly regulated by Ca^{2+}. At submicromolar Ca^{2+} concentrations, villin bundles actin filaments whereas at micromolar Ca^{2+} concentrations it caps barbed ends of actin filaments and at >100 μM Ca^{2+} it severs F-actin. As with gelsolin, the activity of villin is regulated by both PIP_2 and Ca^{2+}. In addition, villin is regulated by phosphorylation on tyrosine in intestinal epithelial cells, a requirement for regulating the interaction of actin filaments with apical ion channels in the epithelial cells. Deletion of the villin gene in mice leads to accumulation of actin filaments within the epithelial cells making them prone to injury.

Adseverin, also known as Scinderin, is only expressed in secretory cells. It has slightly different temperature and Ca^{2+} sensitivity from gelsolin, but its functions appear to be very similar. During cell stimulation by Ca^{2+}, adseverin is activated and disassembles cortical F-actin to allow secretory vesicle exocitosis. As with gelsolin, adseverin binds to and is regulated by PIP_2.

The Single Domain ADF/Cofilin Family

Cell motility and morphogenesis require high rates of turnover of actin filaments, ~100–150-fold faster than occurs for purified actin *in vitro*. The ADF/cofilins are 13–19 kDa proteins containing a single ADF-H domain and are required for this high rate of actin-filament dynamics. They have been isolated or identified by genomic or cDNA analysis from more than 20 different animals, higher plants, fungi, yeasts, and protists. The lethality of the loss of the ADF/cofilin gene in organisms that express only a single gene for this family (e.g., yeast), demonstrates the essential nature of these proteins. Mammals have three separate genes for these proteins: ADF, the ubiquitous cofilin 1 and the muscle-specific cofilin 2. Within any given species, the three proteins are ~70% identical. In an ADF null mouse, cofilin 1 expression is up-regulated to compensate for the loss of ADF and the animals are viable. The only major defect observed is that the mice become blind due to corneal

thickening, even though cofilin 1 is up-regulated in the cornea. This finding, along with differences in the quantitative behavior of the three proteins *in vitro*, suggests that each isoform has some unique tissue specific function. Many ADF/cofilins have nuclear localization sequences, but the protein is usually cytosolic. However, it can be targeted to the nucleus, along with cytoplasmic actin, under certain conditions, although its function there is not known. ADF/cofilins enhance filament turnover (dynamize filaments) in two ways. They can bind cooperatively along the filament, stabilizing a "twisted" form of the actin that is more readily fragmented (severed), creating more filament ends that can either enhance depolymerization, if the environment is an actin monomer sequestering one, or nucleate filament elongation, if the pool of assembly competent monomer is sufficient to sustain growth. If F-actin is severed by ADF/cofilin at the leading edge of cells where active Arp2/3 complex is present, the Arp2/3 complex can capture the pointed ends of the newly severed filaments and bind them along the side of existing filaments to create the highly branched network.

The ADF/cofilin proteins also enhance the rate of subunit loss from the pointed end of filaments. ADF/cofilins bind ADP-actin subunits or monomer with higher affinity than they bind to ATP-actin. Thus, within an actin filament, ADF/cofilin binding is preferentially toward the pointed end, the desired region for filament turnover in cells (Figures 3 and 4). ADF/cofilin activity is regulated by pH: pH $>$ 7.3 favors severing and depolymerization whereas pH $<$ 7.1 favors F-actin binding. ADF/cofilin-mediated F-actin severing is inhibited by tropomyosin, several isoforms of which compete with ADF/cofilin for binding to F-actin. Actin binding, and thus ADF/cofilin activity, is inhibited by phosphorylation at a highly conserved serine residue (ser 3 in mammalian ADF and cofilin). Two related kinases, the LIM kinases and TES kinases, each with two members, phosphorylate ADF/cofilins. The removal of the phosphate from Ser3 may be through the general phosphatases, but a more specific phosphatase called slingshot appears to be the major ADF/cofilin phosphatase for regulated dephosphorylation (activation). Both the kinase and phosphatase pathways are regulated by upstream signaling events through which extracellular signals affect actin dynamics.

Actin-interacting protein 1 (Aip1) is an actin filament-capping protein with a molecular mass of ~65 kDa. *In vitro*, Aip-1 binds to F-actin weakly or not at all in the absence of ADF/cofilin, but caps the barbed end of filaments severed by ADF/cofilin in the presence of ADF/cofilin. Aip1 activity inhibits annealing of the ADF/cofilin severed filaments, maintaining a higher filament number, and blocks the growth at the filament barbed ends. In the nematode *Caenorhabditis elegans*, which expresses two forms of ADF/cofilin, the ubiquitous unc60A and the muscle specific unc60B, only the weaker F-actin-binding/severing species unc60B is able to form a high affinity complex with Aip-1 (unc78). Thus, Aip1 enhances the apparent severing activity of the weaker ADF/cofilin and gives this family of proteins the ability to function much like the severing and capping proteins discussed earlier.

Other Capping Proteins

There are several capping proteins that appear to be structurally unrelated to those with ADF-H domains. In general these proteins bind weakly to actin monomer but often bind strongly to dimer and thus they can stabilize the dimer and enhance nucleation of filament growth. They have high affinity for the filament ends to which they bind and they usually bind in a 1:1 stoichiometry with the filament (Figures 3 and 4). The main function of capping is to restrict the polymerization/depolymerization, thereby controlling the filament length *in vivo*. As mentioned before, limiting the growth of actin filaments at the leading edge of migrating cells is important for actin-assembly driven membrane protrusion (lamellipodial growth). Pointed-end-capping proteins are important for filament branching, regulating filament turnover, and cross-linking of actin filaments to other components of the cytoskeleton.

Barbed-End-Capping Proteins

CapZ

The most abundant barbed-end-capping protein is CapZ. In striated muscle cells, CapZ binds to actin filaments at the Z-disk, where CapZ also interacts with α-actinin, an actin cross-linking protein, to anchor the thin filaments from the neighboring sarcomere, the contractile unit of skeletal muscle. Nonsarcomeric isoforms of CapZ are localized at the site of membrane actin contact. Cap Z also interacts with two other regulators of actin dynamics, the actin-monomer-binding protein, twinfilin, and with CARMIL, a protein named for its service as a CapZ, Arp2/3 and myosin-I-linker. CapZ is a heterodimer composed of α- and β-subunits, which are 32 and 31 kDa, respectively. Each subunit has two isoforms. Both subunits are structurally similar, and assemble tightly to form a dimer with pseudo twofold rotational symmetry. The C-terminal ends of each subunit are flexible, hydrophobic, mobile in nature, and necessary for actin binding. This flexibility explains how CapZ can tightly bind two actin subunits or the barbed end of the double-stranded F-actin. Cells have capping protein in 1:1 molar ratio with actin filaments and 1:100 to 1:150 with respect to total actin subunits. *In vivo*, the capping activity is regulated by

PIP_2, which binds directly to CapZ inhibiting its capping activity. The generation of PIP_2 in platelets in response to thrombin, uncaps actin-filament barbed ends allowing localized filament growth needed for the shape changes of platelets associated with blood clot retraction.

Tensin

Tensin, a large focal adhesion molecule with a mass of ~ 200 kDa, caps the barbed ends of actin filaments within the focal adhesions of fibroblasts and muscle. Tensin interacts with other molecules within the focal adhesion. Tensin is very susceptible to proteolysis, especially by the calcium-activated calpain-II. Full-length recombinant tensin shows complete capping activity whereas "insertin," most likely a proteolytic fragment of tensin, only partially caps F-actin.

Pointed-End-Capping Proteins

Tropomodulin

Tropomodulin is a unique pointed-end-capping protein first discovered as an actin-tropomyosin-binding protein (Figure 4). The name tropomodulin was given, because it binds actin filaments tightly in the presence of tropomyosin. Human skeletal muscle tropomodulin is 40.5 kDa, but a related protein named leiomodin is 64 kDa and is found in smooth and cardiac muscle. Tropomodulin caps the pointed end of actin filaments in striated muscle, playing an important role in the assembly of the sarcomere. In striated muscle, tropomodulin is present in a 1:1 molar ratio with respect to actin filaments. The N-terminal half of tropomodulin is rod shaped and binds to the N-terminal part of tropomyosin. The C-terminal half of tropomodulin is responsible for capping the pointed end of F-actin. Although tropomodulin binds to actin filaments tightly, it does not bind to actin monomer. Binding affinity to the pointed end of F-actin is threefold higher in the presence of muscle tropomyosin. Tropomodulin is found in nonmuscle cells and it binds with differing affinities to F-actin containing different isoforms of tropomyosin, suggesting it might play a role in modulating filament turnover through regulating the dynamics at filament pointed ends, where ADF/cofilins function to enhance turnover. However, its cellular role is not well defined.

Spectrin/Band 4.1

Spectrin/band 4.1 acts as an F-actin pointed-end-capping complex *in vitro*. The proteins are expressed in a wide variety of tissues in multiple isoforms. Spectrin/band 4.1-actin complex was first isolated from red blood cell (erythrocyte) membranes, where actin filaments are short and of uniform length. Both ends of these filaments are capped, the pointed end with spectrin/band 4.1, but the nature of the barbed-end-capping protein is not known. Spectrin binds to some transmembrane proteins as well as to actin, forming a cortical cytoskeleton in erythrocytes.

See Also the Following Articles

Actin Assembly/Disassembly • Actin-Related Proteins • Rho GTPases and Actin Cytoskeleton Dynamics

Glossary

actin depolymerizing factor (ADF)/cofilin Related actin-binding proteins that increase the turnover of actin filaments *in vivo* through severing and enhancing the off-rate of subunits from the pointed ends of F-actin. The ADF-H domain is used to build larger versions of related proteins that can sever and cap filaments.

Arp2/3 complex A complex of two actin related proteins, Arp2 and Arp3, with five other proteins that can nucleate the growth of new actin filaments and cause branching of filaments at the leading edge of a migrating cell.

Ena/VASP Enabled/Vasodilator-stimulated phosphoprotein, a family of actin-binding proteins that bind to but do not cap the growing barbed end of actin filaments, reducing branching and aiding in growth of long filaments.

F-actin The dynamic filamentous cytoskeletal structures, composed of subunits of actin monomer (G-actin), that organize the cytoplasm to maintain the shape of eukaryotic cells.

filament capping The binding of a protein at the end of an actin filament to stop filament growth or depolymerization.

filament severing The process whereby a protein binds along the side of an actin filament and severs the filament into smaller pieces.

filament treadmilling The dynamic process in which actin filaments elongate at their barbed (plus) end by addition of subunits and at the same time disassemble at their pointed (minus) end with loss of subunits.

filopodia Finger-like protrusions with sensory capability that extend from the cell membrane and contain a bundle of parallel cross-linked actin filaments with uniform polarity.

lamellipodia Flat web-shaped membrane protrusions containing highly branched actin filaments, seen at the leading edge of many migrating cells.

WASP Wiscott–Aldrich syndrome protein, a family of actin-binding protein involved in actin-filament nucleation.

Further Reading

Bamburg, J. R. (1999). Proteins of the ADF/cofilin family: Essential regulators of actin dynamics. *Annu. Rev. Cell. Biol.* **15**, 185–230.

Carlier, M. F., Le Clainche, C., Wiesner, S., and Pantaloni, D. (2003). Actin-based motility: From molecules to movement. *Bioessays* **25**, 336–345.

Dos Remedios, C. G., Chhabra, D., Kekic, M., Dedova, I. V., Tsubakihara, M., Berry, D. A., and Nosworthy, N. J. (2003). Actin binding proteins: Regulation of cytoskeletal microfilaments. *Physiol. Rev.* **83**, 433–473.

Kwiatkowski, A. V., Gertler, F. B., and Loureiro, J. J. (2003). Function and regulation of Ena/VASP proteins. *Trends Cell Biol.* **13**, 386–392.

Pollard, T. D., and Borisy, G. G. (2003). Cellular motility driven by assembly and disassembly of actin filaments. *Cell* **112**, 453–465.

Puius, Y. A., Mahoney, N. M., and Almo, S. C. (1998). The modular structure of actin-regulatory proteins. *Curr. Opin. Cell Biol.* **10**, 23–34.

Schafer, D. A., and Cooper, J. A. (1995). Control of actin assembly at filament ends. *Annu. Rev. Cell Dev. Biol.* **11**, 497–518.

Biography

Dr. James R. Bamburg is a Professor of Biochemistry and Molecular Biology and Director of the Molecular, Cellular and Integrative Neuroscience Program at Colorado State University, Fort Collins, Colorado. His principal research interest is the neuronal cytoskeleton and its regulation by assembly modulatory proteins. He holds a Ph.D. degree from the University of Wisconsin, Madison and did postdoctoral research at Stanford University. He has had visiting scientific appointments at the Laboratory of Molecular Biology, Cambridge, UK; Woods Hole Marine Biology Laboratory, Massachusetts; Cell Biophysics Unit, Kings College, London; University of Otago, Dunedin, New Zealand; University of Sydney, Australia; Ludwig Institute, University of California, San Diego, California. He has authored over 100 papers, most dealing with aspects of actin-filament dynamics in neuronal systems.

Dr. Sankar Maiti received his Ph.D. in 2003 from Punjab University where he performed molecular studies on mechanism of protein folding and protein thermostability. He worked as a research fellow in the Institute of Microbial Technology in Chandigarh, India and is currently a postdoctoral fellow in the laboratory of Dr. Bamburg.

Actin-Related Proteins

R. Dyche Mullins
University of California, San Francisco, California, USA

Actin-related proteins (Arps) are a class of proteins found in all eukaryotes and many species of bacteria and archaea. Arps are defined by their degree of similarity to actin (conventional actin), a ubiquitous, eukaryotic cytoskeletal protein. All Arps are built around a common structural fold. This "actin fold" binds and hydrolyzes ATP. In most Arps, ATP hydrolysis is converted into a conformational change that regulates assembly and/or function of multiprotein complexes. Conventional actin assembles into two-stranded helical filaments that form structural scaffolds used to organize the intracellular space and to drive cell division, shape change, and cell locomotion. Eukaryotic Arps fall into ten groups (Figure 1 and Table I) that can be loosely grouped into two categories: (1) cytoskeleton-associated Arps (Arp1, Arp2, Arp3, and Arp10) that regulate the assembly and function of the actin and microtubule cytoskeletons; and (2) chromatin-associated Arps (Arp4–Arp9) that regulate the structure and function of eukaryotic chromatin. Prokaryotic Arps were discovered only recently and their functions are not well understood. The best-characterized prokaryotic Arps (MreB, Mbl, and the plasmid-encoded protein, ParM) polymerize into filaments required for proper cell shape and DNA segregation. The primary sequences of prokaryotic Arps are highly divergent from those of the eukaryotic Arps but we include them in this discussion based on the similarity of their biochemical activities and cellular functions to conventional actin and the eukaryotic Arps. The presence of Arps in chromatin-remodeling complexes and the importance of prokaryotic Arps in DNA segregation suggest that their role in the handling of DNA is as ancient and well conserved as their more well-known cytoskeletal functions.

The Actin Fold

There is little or no conservation of surface-exposed residues among Arps. This reflects the fact that the proteins in this family have different binding partners and cellular functions (Figure 1 and Table 1). All Arps, however, share a common structural fold. The core of the protein is formed from two globular domains (domain I and domain II) connected by a flexible hinge (Figure 2B). The interface between the two domains forms an ATP-binding pocket. Five highly conserved sequences – three ATP-binding loops and two connecting helices – line this pocket and define the "actin fold." These sequences are an adenosine-binding loop (adenosine), two phosphate binding loops (phosphate 1 and phosphate 2), and two connecting domains (connect 1 and connect 2). These sequences are conserved in actin, the Arps, and all other members of the actin superfamily (which includes proteins like hexokinase and HSP70) and they are always arranged in the following order: phosphate 1, connect 1, phosphate 2, adenosine, and connect 2 (Figure 2A). The ATP-binding loops are distributed between the two domains of the protein. Phosphate 1 is located in domain I and both phosphate 2 and adenosine are in domain II (Figure 2B). When all three loops interact with ATP the two domains are tightly associated. Hydrolysis of the gamma phosphate of ATP weakens binding to the phosphate 1 domain and causes the two domains of the protein to swing apart around the hinge formed by connect 1 and connect 2. Complete loss of nucleotide results in further opening of the protein around the hinge. In some members of the actin superfamily the binding of ATP to a nucleotide-free protein causes the domains to rotate by 30° around the hinge region (Figure 2C). The shift from closed to open conformation is used by Arps to regulate their interactions with other proteins.

Prokaryotic Arps

An actin cytoskeleton is thought to be a prerequisite for the establishment and maintenance of intracellular compartments and organelles and until recently actin was thought to be a strictly eukaryotic protein. Recent work, however, has identified actin-like proteins in prokaryotes. The first two prokaryotic actin-like proteins, MreB and Mbl, were discovered in *B. subtilis*. These proteins have very limited primary sequence similarity to conventional actin but, remarkably, they fold into three-dimensional structures very similar to actin and, like conventional actin, they polymerize into two-stranded filaments in a manner that depends on

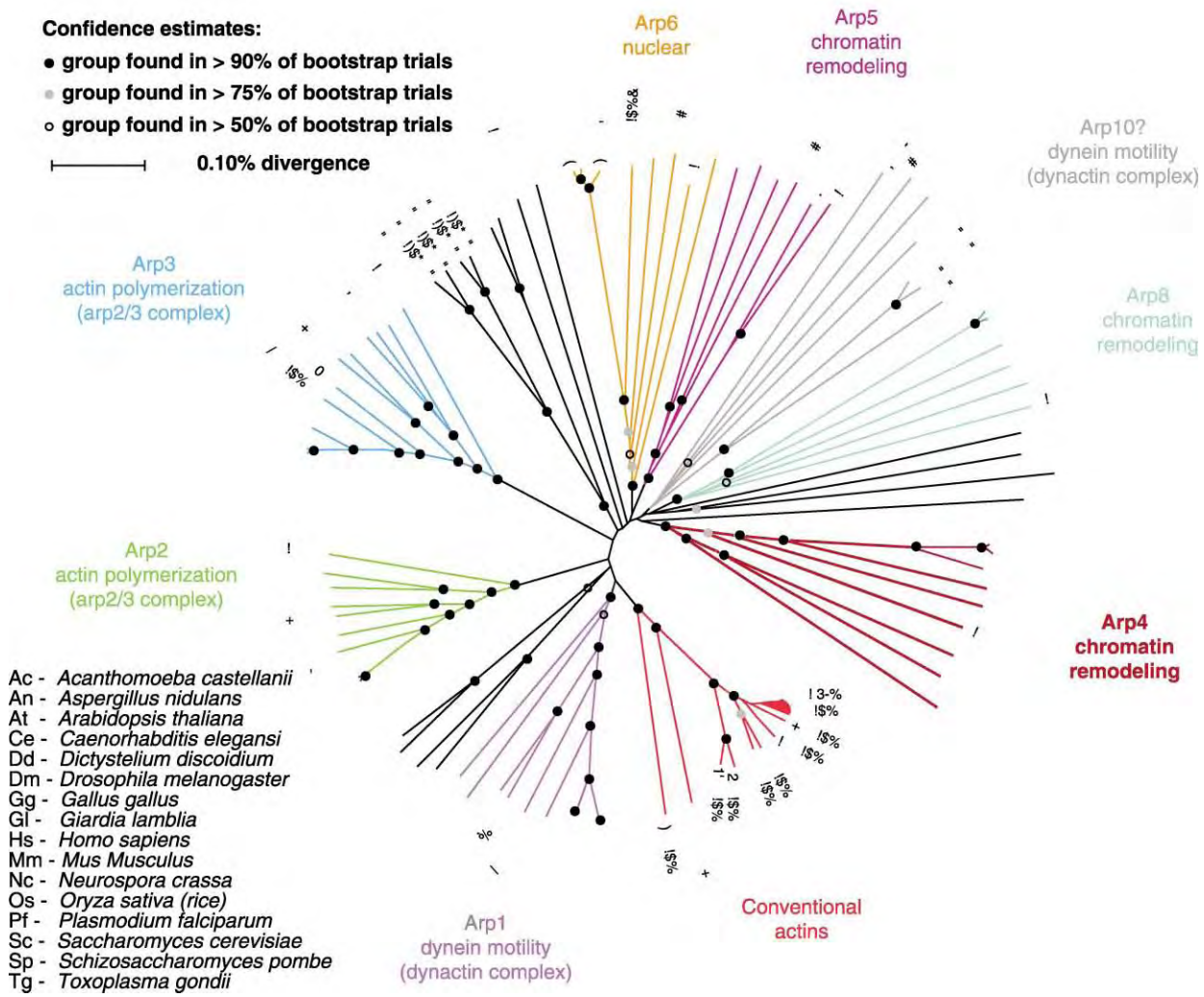

FIGURE 1 The eukaryotic Arp family is composed of ten, highly conserved members. Members fall broadly into two categories: cytoskeletal Arps (conventional actin, Arp1, Arp2, Arp3, and Arp10) and nuclear Arps (Arp4, Arp5, Arp6, Arp7, Arp8, and Arp9). The diagram is an unrooted phylogenetic tree of the actin superfamily. (Reprinted from *J. Cell Sci.* **202**(115), 2619–2622.) (Calculated by Clustal X Thompson J. D., Gibson, T. J., Plewniak, F., Jeanmougin, F., and Higgins, D. G. (1997) *Nucl. Acids Res.* **25**, 4876–4882.

ATP and salt. At present not much is known about the cellular roles of MreB and Mbl, but they do appear to form filaments *in vivo* that are required for proper positioning of the cell-wall synthesis machinery and proper shape determination of rod-shaped bacteria. In addition, MreB and Mbl are required for proper segregation of bacterial DNA during cell division. These are the types of functions performed by polymeric cytoskeletal elements in eukaryotes so it is fair to say that MreB and Mbl form a bona fide bacterial cytoskeleton.

Another remarkable prokaryotic actin-like protein is encoded by the *parM* locus of the low-copy drug resistance plasmid, R100. The R100 plasmid is stably maintained at one copy per cell in bacterial populations because it accurately segregates one copy each into daughter cells during each cell division. Three plasmid loci are required for this accurate segregation: ParR, *parM*, and ParC. ParR encodes a DNA-binding protein that binds tightly to the ParC locus. *parM* encodes an actin-like protein that assembles into two-stranded filaments in an ATP-dependent manner. The ParR protein bound to the ParC locus appears to nucleate formation of *parM* filaments, which drive plasmid segregation. This simple three-piece system may form a structure functionally equivalent to a mitotic spindle and may represent the minimal system for segregating DNA. Unlike conventional actin filaments in which ATP hydrolysis regulates interaction with depolymerizing factors (Figure 3B), ATP binding and hydrolysis directly control assembly and disassembly of ParM filaments. ATP-bound monomers polymerize into filaments.

TABLE I

Cellular Localization, Function and Multi-Protein Complexes of Eukaryotic Arps

Arp	Sequence similarity to actin	Cellular localization	Function	Multi-protein complexes
Actin	100% ident. 100% simil.	Cell cortex, leading edge, stress fibers, endosomes, vesicles, nucleus	Cell shape and motility, intracellular trafficking, chromatin remodeling (?), histone acetylation (?)	Actin filaments, INO80, BAF, and NuA4 complexes
Arp1	45% ident. 68% simil.	Golgi apparatus, transport vesicles, centrosomes, cell cortex	Dynein-driven intracellular movements	Dynactin complex
Arp2	45% ident. 69% simil.	Cell cortex, leading edge, some motile endosomes	Actin filament nucleation and crosslinking	Arp2/3 complex
Arp3	39% ident. 60% simil.	Cell cortex, leading edge, some motile endosomes	Actin filament nucleation and crosslinking	Arp2/3 complex
Arp4	30% ident. 53% simil.	Nucleus	Histone acetylation, chromatin remodeling, control of transcription	NuA4 and INO80 complexes
Arp5	26% ident. 51% simil.	Nucleus	Chromatin remodeling, control of transcription	INO80 complex
Arp6	24% ident. 46% simil.	Nucleus	Unknown	Unknown
Arp7	22% ident. 44% simil.	Nucleus	Chromatin remodeling, control of transcription	Swi/Snf and RSC complexes
Arp8	21% ident. 44% simil.	Nucleus	Chromatin remodeling, control of transcription	INO8 complex
Arp9	17% ident. 40% simil.	Nucleus	Chromatin remodeling, control of transcription	Swi/Snf and RSC complexes
Arp10	17% ident. 38% simil.	Golgi apparatus, transport vesicles, centrosomes, cell cortex	Dynein-driven intracellular movements	Dynactin complex

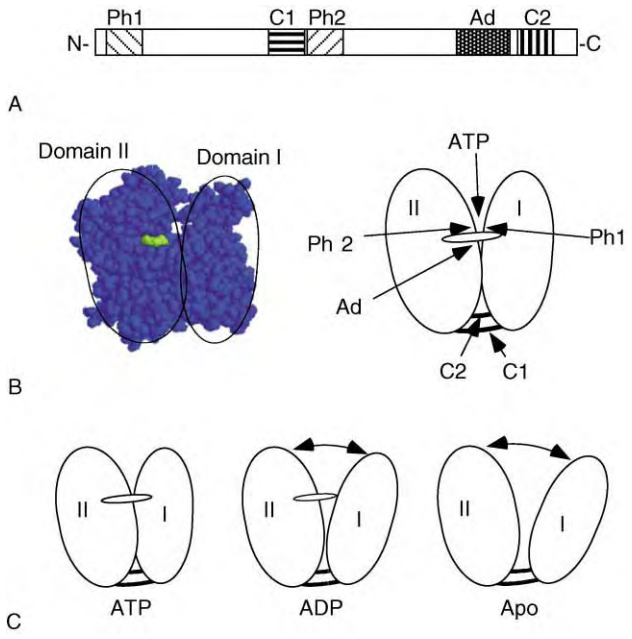

FIGURE 2 Organization and structure of Arps and the conformational changes driven by ATP binding and hydrolysis. (A) Organization of conserved sequences that define the ATP-binding pocket of the actin fold. Ph1 and Ph2: phosphate-binding loops. C1 and C2: connecting domains. Ad: adenosine-binding domain. The order of these sequences is the same in the primary amino acid sequence of all actin related proteins. (B) Atomic structure and domain organization of an actin monomer. The atomic structure of actin (left) is shown with a bound ATP molecule (green) and with ellipses identifying the two large domains – domain I and domain II – that define the ATP-binding pocket. The phosphate- and adenosine-binding sequences line the interface between domain I and domain II and interact with the ATP molecule (right). The connecting sequences (C1 and C2) link the two protein domains and act as a hinge. (C) Nucleotide-dependent conformational changes in the actin fold. ATP binding holds the domain I and domain II tightly together (ATP, left). Hydrolysis of the γ-phosphate of ATP to form ADP weakens the interaction with one of the phosphate-binding loops (Ph1) and causes the cleft between the domains to open (ADP, center). Loss of nucleotide from the binding pocket causes the cleft to open even further (Apo, right). Actin-related proteins use this conformational change to regulate their interactions with other proteins.

Within the filament, monomers hydrolyze ATP to ADP. ADP-bound filaments then rapidly disassemble (Figure 3A).

Eukrayotic Arps

Cytoskeletal Arps

We will briefly discuss conventional actin, which is well described in a separate article on actin dynamics in this encyclopedia. Arp1 and Arp10 are part of a dynein-activating (dynactin) complex that regulates activity of the microtubule motor protein dynein. Arp2 and Arp3 are subunits of the Arp2/3 complex – a protein complex that nucleates formation of new actin filaments in response to upstream signaling events (see Table I).

Conventional Actin

Actin is one of the most abundant and highly conserved proteins in eukaryotes. In motile cells actin is typically the most abundant cellular protein and is present at concentrations of 100–200 μM (or 5–10% of total cellular protein). Protozoans, such as budding and fission yeast and slime molds, generally express one isoform of actin. Metazoans typically express multiple, tissue-specific isoforms. Humans express at least six isoforms of actin: two striated muscle isoforms (α-skeletal and α-cardiac), two smooth muscle isoforms (α-smooth muscle and α-enteric), and two widely expressed cytoplasmic isoforms (β-cytoplasmic and γ-cytoplasmic). The α-skeletal and α-cardiac striated muscle isoforms are expressed specifically in muscle tissues where they form arrays of "thin" filaments that interdigitate with "thick" filaments composed of the motor protein myosin. Sliding of the thick and thin filaments past each other drives contraction of the muscle tissue. The thin filaments in muscle tissues are very stable structures whose architecture does not change much over time. The smooth muscle actins form less organized filament arrays involved in contraction of vascular and enteric smooth muscle. The cytoplasmic β- and γ-isoforms are the most widely expressed and form much more dynamic cytoskeletal structures. The β-isoform is ubiquitously expressed and is responsible for building the contractile ring that divides cells at the end of mitosis and for most actin-based intracellular traffic. The assembly of β-cytoplasmic actin also drives cell spreading and the amoeboid, or crawling, motility of many cell types, including those of the nervous and immune systems. The β-isoform is most closely related to protozoan actins. The γ-cytoplasmic isoform is expressed in many different cell types but it is much less abundant than β-cytoplasmic actin. The specific function of γ-actin is unknown.

The defining property of conventional actin is its self-assembly into helical polymeric filaments. Monomeric actin binds ATP with high (nanomolar) affinity but does not hydrolyze it. The transition from monomer to polymer stimulates the hydrolysis of ATP. Hydrolysis is not required for polymerization but rather for depolymerization. Cleavage of the γ-phosphate and its subsequent dissociation trigger a conformational change that enables binding of actin depolymerizing factors such as ADF or cofilin (Figure 3B).

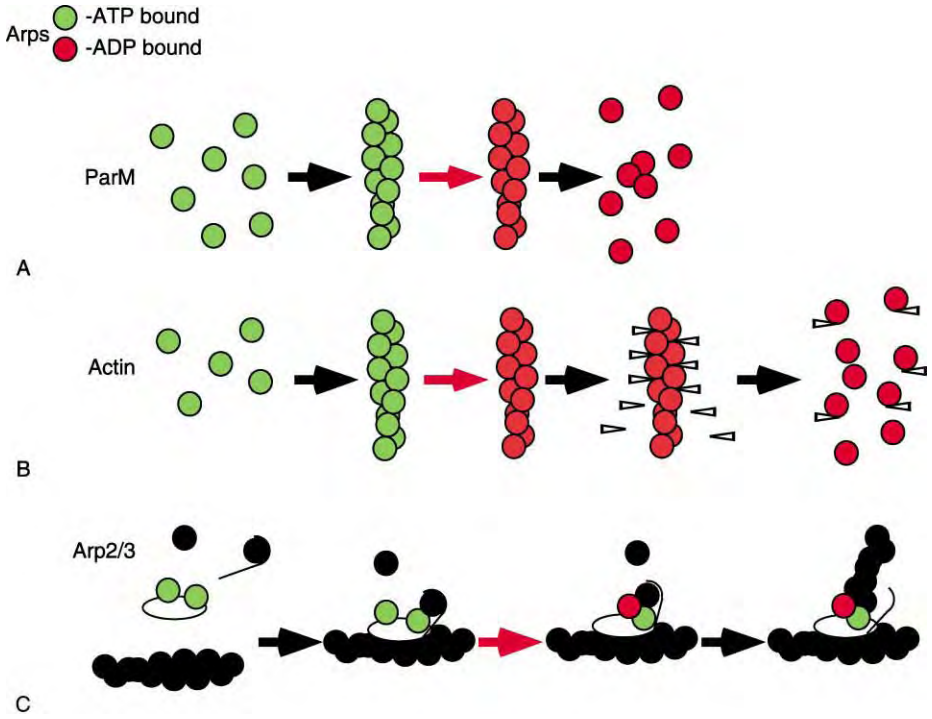

FIGURE 3 Regulation of actin and Arp function by ATP hydrolysis. The relationship between ATP hydrolysis and protein–protein interactions is best understood in the cytoskeletal Arps. (A) When bound to ATP the plasmid-encoded Arp, ParM (green circles), polymerizes into actin like filaments. Polymerization induces hydrolysis of bound ATP (red arrow); and the ADP ParM filaments (red circles) undergo a conformational change that causes them to rapidly fall apart. (B) Conventional actin and Arp1 (green circles) polymerize into similar two-stranded helical filaments. Polymerization induces ATP hydrolysis on both proteins (red arrow) but the filaments do not spontaneously disassemble. In the case of conventional actin, a conformational change in the ADP filament structure (red circles) promotes binding of actin depolymerization factors (white wedges), which drive filament disassembly. (C) As part of the Arp2/3 complex, Arp2 and Arp3 bind ATP (green circles are ATP-bound Arp2 and Arp3) and nucleate formation of new actin filaments. The nucleation reaction requires monomeric actin and a pre-formed actin filament (black circles) and an Arp2/3 activator (black hook). Assembly of these cofactors induces ATP hydrolysis on Arp2 and promotes a conformational change in the Arp2/3 complex that converts it into a filament nucleus.

Arp1

Arp1 is most closely related to conventional actin and, like actin, it assembles into a filamentous polymer. Arp1 forms part of a large (1.2 MDa) protein complex that modulates the activity of the microtubule motor protein dynein. Within the dynactin complex, ~10 Arp1 molecules assemble to form a short (37 nm), actin-like filament. This short filament functions as a scaffold that connects dynein motors to cargo vesicles. The Arp1 filaments bind an isoform of the actin-binding protein spectrin that is specific for the Golgi apparatus and for Golgi-derived vesicles. Arp1 and Golgi spectrin are thought to assemble into a membrane-associated meshwork that surrounds vesicles like a cargo net and allows dynein motors to move them around inside the cell.

In vitro, purified Arp1 polymerizes into short filaments indistinguishable from conventional actin filaments. Arp1 hydrolyzes ATP upon polymerization but this does not have a dramatic effect on filament stability *in vitro*. Like actin, Arp1 may hydrolyze ATP to modulate its affinity for an accessory factor required for filament disassembly (Figure 3B).

Arp2 and Arp3

Arp2 and Arp3 are both subunits of a seven-member protein complex, called the Arp2/3 complex that is an essential regulator of the actin cytoskeleton. The Arp2/3 complex nucleates formation of new actin filaments in response to activation of intracellular signaling systems. It also cross-links actin filaments into mechanically rigid networks so that, in general, it functions to convert intracellular signals into cytoskeletal structures. Within the complex the Arp2 and Arp3 subunits are thought to form a heterodimer with a surface that mimics the fast-growing, barbed end of an actin filament. This surface forms a template to initiate

actin filament formation. In the crystal structure of the complex Arp2 and Arp3 are separated by a large (40Å) cleft and formation of an actin-like Arp2–Arp3 dimer would require a significant conformational change. This conformational change may require ATP hydrolysis on one of the Arps (Figure 3C). Binding of ATP to Arp2/3 is required for actin nucleation and neither ADP nor nonhydrolyzable ATP analogues support Arp2/3-dependent actin filament nucleation. Further study is required to understand the connection between ATP hydrolysis and conformational changes on the Arp2/3 complex.

Chromatin-Associated Arps

Several Arps are associated with eukaryotic chromatin and with chromatin-remodeling complexes. In budding yeast, Arp4, Arp5, Arp7, Arp8, and Arp9 are subunits of ATP-dependent chromatin remodeling complexes. Very little is known about the molecular mechanisms of their activity, but presumably ATPase-driven conformational changes in the Arp subunits regulate the overall structure and activity of these complexes. All of these complexes contain two or four Arp subunits so it is possible that they function as heterodimers and that their interaction is regulated in a manner similar to that of the Arp2/3 complex described earlier.

Arp4

Arp4 is involved in chromatin remodeling and transcriptional activation. In budding yeast, Arp4 is a subunit of both the NuA4 histone acetyl-transferase complex and the INO80 chromatin-remodeling complex. The NuA4 complex acetylates histones H4 and H2A. Acetylation increases accessibility of the DNA within the nucleosome and recruits other chromatin remodeling enzymes to the region. Human cells contain a similar histone acetyl-transferase complex, called Tip60. This complex also contains an Arp4-type subunit in addition to at least one monomer of conventional actin. The INO80 complex contains Arp4 as well as Arp5, Arp8, and conventional actin. The precise role of Arp4 in these complexes is unknown but yeast Arp4 mutants exhibit phenotypes similar to mutants missing the catalytic acetylase subunit of NuA4, suggesting that it plays an integral role in the function of the NuA4 complex. Arp4 has also been shown to bind directly to histones. Its ATPase activity has not been well studied but Arp4 may use ATP binding and hydrolysis to regulate the interaction between chromatin remodeling complexes and DNA-bound histones.

Arp5 and Arp8

Arp5 and Arp8 (along with Arp4 and conventional actin) are members of the INO80 chromatin-remodeling complex. INO80 is a large (2 MDa) protein complex that plays a role in transcription of several important yeast genes including pho5, an essential regulator of phosphate metabolism. The total number of yeast genes that require INO80 activity for transcription is not known. Arp8 has been shown to bind directly to histones H3 and H4 so it may be directly involved in moving histones around on the DNA. Arp8 is also required for the incorporation of both Arp4 and conventional actin into the complex so it may play an important structural or scaffolding role.

Arp7 and Arp9

Arp7 and Arp9 associate tightly to form a heterodimer and dimerization appears to be important to their cellular function. In budding yeast, the Arp7/Arp9 dimer is an essential part of both the Swi/Snf and RSC chromatin remodeling complexes. Like the INO80 complex, these large complexes drive DNA and histone rearrangements necessary for transcription. Swi/Snf activity is required for transcription of ~5% of yeast genes while RSC activity is more globally important. As with the other chromatin-associated Arps, the precise functions of Arp7 and Arp9 are unknown. Loss of the RSC complex is lethal. The loss of either Arp7 or Arp9 causes severe growth defects *in vivo* but does not significantly impair RSC activity *in vitro*. So *in vivo* the Arp7/Arp9 dimer may act to correctly target or regulate the RSC complex.

Chromatin-Associated Conventional Actin

The large majority of cellular actin is cytoplasmic and generally actin is considered as a cytoskeletal protein whose function is limited to the cytoplasm. In many species, however, chromatin-remodeling complexes contain one or more tightly associated monomers of conventional actin. In addition to Arp4, the NuA4 complex contains a subunit of conventional actin. Also, the yeast INO80 complex and the mammalian BAF complex (a chromatin-remodeling complex similar to the budding yeast swi/snf) contain tightly associated actin monomers. The role of conventional actin in chromatin structure and remodeling is mysterious. It has been speculated that actin assembly in the nucleus could drive large-scale changes in chromatin architecture in the way that actin assembly in the cytoplasm drives

large-scale plasma membrane movements. It is also possible that short actin filaments form an essential scaffold for the assembly and function of chromatin organizing factors.

Arps of Unknown Function

We know almost nothing about the function of Arp6. In budding yeast Arp6 is localized to the nucleus so it may be part of a chromatin-remodeling complex or it may play a role in determining nuclear architecture.

See Also the Following Articles

Actin Assembly/Disassembly • Actin-Capping and -Severing Proteins • Chromatin Remodeling • Chromatin: Physical Organization • Nuclear Organization, Chromatin Structure, and Gene Silencing

Glossary

actin Ubiquitous, eukaryotic cytoskeletal protein. Actin monomers assemble into filaments that are used to organize the intracellular space and to define the shape and mechanical properties of eukaryotic cells.

ATP Adenosine triphosphate. It is the major energy currency of living cells. The removal or hydrolysis of phosphates from ATP releases energy that individual proteins can use to do work.

chromatin DNA that has been packaged and compacted by specialized proteins, called histones. The packaged DNA must be partially unpackaged (by chromatin remodeling complexes) to allow transcription of genes.

cytoskeleton A network of protein polymers that organize the intracellular space; transport intracellular cargos; determine cell shape; and drive cell locomotion. The three most important eukaryotic cytoskeletal polymers are actin filaments, microtubules, and intermediate filaments.

eukaryote A cell with a nucleus and other membrane-bound organelles.

histones DNA packaging proteins. In compacted chromatin DNA is wound around histones like thread around a spool.

primary sequence The sequence of amino acids that comprise a protein. Usually given from amino to carboxy terminus.

prokaryote A simple cell, such as a bacterium, that lacks a nucleus and other intracellular compartments.

Further Reading

Bork, P., Sander, C., and Valencia, A. (1992). An ATPase domain common to prokaryotic cell cycle proteins, sugar kinases, actin, and hsp70 heat shock proteins. *Proc. Natl Acad. Sci. USA* **89**, 7290–7294.

Boyer, L. A., and Peterson, C. L. (2000). Actin-related proteins (Arps): Conformational switches for chromatin-remodeling machines? *Bioessays* **22**(7), 666–672.

Carballido-Lopez, R., and Errington, J. (2003). A dynamic bacterial cytoskeleton. *Trends Cell Biol.* **13**(11), 577–583.

Goodson, H. V., and Hawse, W. F. (2002). Molecular evolution of the actin family. *J. Cell Sci.* **115**(Pt 13), 2619–2622.

Herman, I. M. (1993). Actin isoforms. *Curr. Opin. Cell Biol.* **5**(1), 48–55.

Olave, I. A., Reck-Peterson, S. L., and Crabtree, G. R. (2002). Nuclear actin and actin-related proteins in chromatin remodeling. *Annu. Rev. Biochem.* **71**, 755–781.

Pollard, T., Blanchoin, L., and Mullins, R. D. (2000). Molecular mechanisms controlling actin filament dynamics in nonmuscle cells. *Annu. Rev. Biophys. Biomol. Struct.* **29**, 545–576.

Sterner, D. E., and Berger, S. L. (2000). Acetylation of histones and transcription-related factors. *Microbiol. Mol. Biol. Rev.* **64**(2), 435–459.

Thompson, J. D., Gibson, T. J., Plewniak, F., Jeanmougin, F., and Higgins, D. G. (1997). *Nucl. Acids Res.* **25**, 4876–4882.

Biography

R. Dyche Mullins is an Assistant Professor of Cellular and Molecular Pharmacology at the University of California Medical School, San Francisco. As an undergraduate, graduate student, and Postdoctoral Fellow he studied Electrical Engineering, Mathematics, and Biochemistry. His research goal is to understand how interactions between signaling molecules and structural molecules determine the architecture of living cells.

Adenosine Receptors

Lauren J. Murphree and Joel Linden
University of Virginia, Charlottesville, Virginia, USA

Adenosine is a purine nucleoside that serves as a link between energy metabolism and cell signaling. Adenosine is a physiologic regulator of all cell types that binds to G protein coupled receptors (GPCRs) that exist as four subtypes (A_1, A_{2A}, A_{2B}, and A_3). The receptor-mediated actions of adenosine have been extensively studied in the central nervous system, cardiac muscle, blood vessels, gastrointestinal tract, kidneys, lung, liver, immune system, and other tissues. In light of the clear therapeutic potential of selective adenosine receptor subtype-selective agonists or antagonists, new therapeutic candidates are being intensely pursued by the pharmaceutical industry. Naturally occurring xanthines are nonselective antagonists of adenosine receptors. One such compound, caffeine, is the most widely used psychotropic drug in the world.

Adenosine

Formation

Adenosine is a purine nucleoside that is formed within cells from the breakdown of adenosine monophosphate (AMP), which, in turn, is formed from adenosine triphosphate (ATP) and adenosine diphosphate (ADP) in the course of utilizing energy for cellular functions. Adenine nucleotides released from nerves, mast cells, platelets, endothelial cells, and dying cells also can be dephosphorylated in the extracellular space by ecto-nucleotidases. Increased energy utilization or hypoxia enhances the cellular formation of AMP, which is dephosphorylated by a 5′-nucleotidase in the rate-limiting step for adenosine production. The signaling molecule cyclic AMP (cAMP) can also be a source of AMP for adenosine production. Under resting conditions, a sizable fraction of adenosine is formed by the hydrolysis of *S*-adenosyl-homocysteine.

Location

Adenosine is produced in either the intracellular or extracellular spaces and can be transported across cell membranes in either direction by a family of nucleoside transporters that allow for equilibration of adenosine concentrations by facilitated diffusion or sodium-dependent active transport.

Regulation of Production

Production of adenosine is increased during periods of high metabolic activity or ischemia, when there is increased cellular demand for ATP or decreased delivery of oxygen. Adenosine also is derived from adenine nucleotides released from nerves, platelets, mast cells, or other cells. In the brain, adenosine release has been observed experimentally following various manipulations (e.g., hypoxia, ischemia, hypoglycemia, seizures, electrical stimulation, prolonged wakefulness, and application of free radicals). Changes in extracellular levels of adenosine of up to 100-fold have been observed following oxidative or ischemic stress.

Breakdown of Adenosine

Adenosine is eliminated by metabolic transformation to inosine by adenosine deaminase. It can also be phosphorylated to form AMP by adenosine kinase with a phosphate group donated by ATP, but this enzyme is inhibited in metabolically stressed cells.

Receptor Structure

Adenosine receptors (ARs) belong to a class of integral membrane proteins known as GPCRs. Members of this class of proteins have seven membrane-spanning α-helices with an extracellular amino terminus and an intracellular carboxy-terminal tail. All four subtypes are asparagine-linked glycoproteins and all but the A_{2A} receptor have palmitoylation sites near the C terminus.

Sequence Similarity

In the mammalian species thus far investigated, differences in protein sequence between species for each receptor subtype are generally much smaller than the differences between subtypes within a given species. For example, cloned mammalian A_1 receptors are 90–95% identical, but rat adenosine receptors have

similarities of ~60–80% across subtypes. The A_3 receptors are an exception to this rule, as they vary by as much as 30% across mammalian species.

Gene Structure

All four subtypes of adenosine receptors appear to have a similar genomic structure involving two coding exons separated by a single intron located in the region corresponding to the second intracellular loop (between transmembrane regions 3 and 4). The A_1 receptor, which is the most well studied, can be transcribed from two different and mutually exclusive promoters. Transcription from these promoters, located approximately 600 bp apart, appears to be differentially regulated. Table I lists some properties of the four AR subtypes.

Protein Structure

The most precise structural information for proteins has been obtained from X-ray diffraction of protein crystals. GPCRs, like most integral membrane proteins, have proven to be difficult to crystallize due in part to their large size and association with membrane lipids. Thus, most structural information about adenosine receptors has been derived through comparison with the known structures of the related proteins bacteriorhodopsin and mammalian rhodopsin. By comparing the amino acid sequence of an adenosine receptor with the structure of mammalian rhodopsin, researchers have developed models that aid in understanding receptor–ligand interactions. When combined with studies with mutated receptors and pharmacological data, the sites of interactions between the receptors and ligands appear to occur in helices 3, 5, 6, and 7.

Receptor Physiology and Localization

Adenosine receptor subtypes are differentially distributed throughout the body, allowing for adenosine to initiate a wide variety of physiologic responses. The A_1 and A_{2A} ARs have proven to be the easiest to study because of the available pharmacological tools (e.g., radioligands) and their high affinity for adenosine. Consequently, much more is known about the location and physiology of these receptors than about those of the A_{2B} and A_3 receptors, which were more recently discovered and have a lower affinity for the natural ligand.

A_1 Receptors

Adenosine acting through A_1 ARs has a diverse array of physiological actions. The A_1 AR is widely distributed (it is found in, e.g., liver, kidney, adipose tissue, lung, pancreas, and testis) but has been most extensively studied as a regulator of the central nervous system (CNS) and the cardiovascular system.

A_1 ARs in the CNS

In the CNS, A_1 ARs are located in many brain regions (especially the cortex, cerebellum, and hippocampus) and in the dorsal horn of the spinal cord. These receptors are important for regulating sleep and the excitability of neurons. The concept of adenosine as a regulator of sleep follows in part from the fact that caffeine, a naturally occurring AR antagonist, promotes wakefulness. Experimental evidence shows that adenosine concentrations in the brain rise during waking hours but decrease during subsequent recovery sleep. In addition, administration of A_1 agonists to brain *in vivo* promotes sleep and reduces arousal. A_1 ARs are also important for modulating the excitability of neurons. Adenosine acting at A_1 ARs causes an inhibition of synaptic activity by decreasing the neuron's ability to respond to excitatory molecules (i.e., neuropeptides and glutamate).

A_1 ARs in the Cardiovascular System

A_1 ARs are particularly important in the cardiovascular system and are expressed in the heart. Their effects are generally anti-adrenergic, leading to a decrease in heart

TABLE I

Properties of Human Adenosine Receptor Subtypes

Adenosine receptor subtype	Length (aa)	Protein Accession No.	GenBank Accession No.	GenBank Accession No. (mouse)	Chromosomal location
A_1	326	P30542	S45235	U05671	1q32.1
A_{2A}	410	P29274	S46950	U05672	22q11.2
A_{2B}	328	P29275	X68487	U05673	17p11.2–p12
A_3	318	P33765	L22607	L20331	1p13.3

rate and blood pressure. One of the most interesting physiological roles of A_1 ARs is in the phenomenon of ischemic preconditioning in the heart. During periods of low oxygen supply (ischemia), adenosine is released and activates A_1 ARs. This activation begins a cascade of events that protects the heart against a subsequent ischemic event (e.g., infarction and arrhythmia). A_1 receptors are also found on sympathetic nerve terminals, where they act to inhibit the release of norepinephrine.

A_{2A} ARs

A_{2A} ARs are highly expressed by cells in the striatum and olfactory tubercles of the brain, by cells in the spleen and thymus, and by cells in certain blood vessels and immune cells. Lower levels of expression occur in the heart and lung. Like the A_1 AR, the most widely studied effects of the A_{2A} AR are in the CNS and the cardiovascular system.

A_{2A} ARs in the CNS

A_{2A} ARs are highly expressed on small spiny neurons of the striatum, which also express D_2 dopamine receptors. The activities of A_{2A} ARs and D_2 dopamine receptors are antagonistic. Although A_{2A} receptors are coupled to G_s proteins in many tissues, in the striatum there is evidence to suggest that they signal through the related G protein, G_{olf}. Work using mice lacking the A_{2A} AR showed that these receptors also stimulate sensory nerve activity, are involved in mediating pain, and mediate the motor stimulant effects of caffeine.

A_{2A} ARs in the Cardiovascular System

In the cardiovascular system, the A_{2A} receptor plays two important roles: regulation of blood flow and inhibition of inflammatory cells. Activation of A_{2A} ARs is an important physiological mechanism for coupling energy demand to blood flow. When cells are using large amounts of energy (ATP), they produce adenosine. The adenosine binds to A_{2A} receptors on vascular smooth muscle and causes vasodilation, allowing more blood (and the nutrients it contains) to reach the tissue. A_{2A} ARs also play an autoregulatory role during the process of inflammation. Activation of this receptor causes an array of responses that are generally anti-inflammatory, including inhibition of neutrophil, monocyte, platelet, and T cell activation. A_{2A} ARs also protect against ischemic damage through a mechanism involving its anti-inflammatory properties, which is different from the ischemic preconditioning effects of the A_1 AR.

A_{2B} ARs

The A_{2B} AR is closely related to the A_{2A} AR, though with a much lower affinity for adenosine. This receptor is widely distributed. The epithelium of the cecum, colon, and bladder have high levels of expression of A_{2B}. Intermediate levels of expression exist in the lung, blood vessels, and eye, and low levels of expression occur in many tissues (e.g., adipose tissue, adrenal gland, brain, and kidney). The physiological role of the A_{2B} AR is not well characterized, but most researchers agree that it is involved in the relaxation of vascular smooth muscle and in the inhibition of monocyte and macrophage function, effects that are similar to those of the A_{2A} AR. The A_{2B} receptor stimulates fluid and chloride secretion from epithelial cells in the infected gut in response to AMP release from neutrophils, leading to diarrhea. The A_{2B} AR also seems to be involved in the stimulation of mast cell degranulation (a pro-inflammatory event) in some species, including humans.

A_3 ARs

Investigation of the physiology and localization of the A_3 AR has been ongoing since the receptor was cloned in 1991 by Meyerhof and co-workers, but characterization has proven to be difficult since there is great variability in its expression and function among species. It is expressed at low levels in the thyroid, brain, liver, kidney, heart, and intestine across species. Rats express high levels in testis and mast cells. In some species (including rats), activation of the A_3 AR enhances the release of mast cell mediators. A preconditioning effect similar to that caused by the A_1 AR can also result from A_3 activation in some species.

Signaling Downstream of Adenosine Receptors

Adenosine receptors, like all GPCRs, transmit signals to the cell interior by activating intracellular heterotrimeric GTP-binding proteins (G proteins) that consist of α-, β-, and γ-subunits. Activation of these receptors causes the α-subunit to exchange its bound GDP molecule for GTP and become active. The α-subunit then dissociates from the $\beta\gamma$ dimer and both can then activate downstream effectors.

The four adenosine receptor subtypes exert their varying effects by coupling to different G proteins, which are summarized in Table II. G protein α-subunits control the intracellular levels of many second messengers (e.g., cAMP and inositol triphosphate), which, in turn, activate downstream signaling pathways typical of G proteins. For example, A_1 and A_3 receptors generally

TABLE II

G Protein Coupling of Adenosine Receptors

AR Subtype	G protein	Second messengers
A_1	$G_{i/o}$	Decrease in cAMP
		Increase in IP_3/DAG via PLC
		Activation of PLA2 and PLD
A_{2A}	G_s	Increase in cAMP
	G_{olf}	Increase in cAMP
	$G_{15/16}$	Increase in IP_3
A_{2B}	G_s	Increase in cAMP
	$G_{q/11}$	Increase in IP_3/DAG via PLC
A_3	G_i	Decrease in cAMP
	$G_{q/11}$	Increase in IP_3/DAG via PLC

Note. DAG, diacylglycerol; IP_3, inositol triphosphate, PLC, phospholipase C; PLD, phospholipase D.

couple to G_i, which inhibits adenylyl cyclase, causing a decrease in intracellular cAMP, whereas A_{2A} and A_{2B} couple to G_s, which stimulates cAMP production. In some cells, A_{2B} receptors also are coupled to the calcium-mobilizing G protein, G_q.

Other Ligands

Because of their interesting properties, adenosine receptors are important pharmacological targets. There are several naturally occurring ligands in addition to adenosine, including caffeine, theophylline, and inosine. Inosine is a product of adenosine metabolism, occurs naturally in the body, and can activate A_3 receptors at high concentrations that occur in ischemic or inflamed tissues. Caffeine and theophylline are AR antagonists commonly found in coffee and tea.

Many investigators have developed synthetic ligands for adenosine receptors (see Figure 1). It has been particularly challenging to produce ligands that are selective for a given AR subtype, given the high degree of homology between the receptors. Selective compounds are desirable both as tools for understanding receptor functions and as potential drugs. All of the agonist ligands thus far developed are based on the structure of adenosine (an adenine base attached to a ribose moiety). Adenosine is rapidly metabolized. In human, it has a half-life in blood of only 2 s. Modification of this molecule at three different sites has led to agonists with increased longevity, improved selectivity, and nanomolar potency. Some of the most subtype-selective compounds that have been developed are shown in Figure 1.

Caffeine provided a lead compound for the development of xanthine AR antagonists. It belongs to a class of compounds called methylxanthines. Modification of the basic molecule produced high-affinity compounds, some of which show high potency and receptor-subtype selectivity (e.g., MRS1754 in Figure 1). Nonxanthine antagonists (e.g., ZM241385 in Figure 1) were developed later and many appear promising for use in therapeutic applications.

An additional class of ligands for adenosine receptors is known as allosteric enhancers, which were first identified by Bruns and Fergus in 1990. The prototype of the class is PD81723, which binds to the A_1 receptor at an allosteric site that is distinct from the adenosine-binding site, known as the orthosteric site. The binding of PD81723 and related allosteric enhancers increases agonist-binding affinity for the A_1 AR and amplifies the functional effect of the agonist. Allosteric enhancers seem to stabilize the conformation state of receptors that activate G proteins.

Therapeutic Possibilities

Adenosine is used clinically to treat certain tachycardias and to dilate coronary arteries to help in the diagnosis of coronary artery disease. There is great interest in developing more selective drugs that selectively activate or block specific adenosine receptor subtypes and that have a longer duration of action than adenosine.

A_1 Receptors

A_1 ARs are an attractive pharmacological target because of their ability to simulate ischemic preconditioning. Theoretically, an A_1 agonist could protect the heart (and other tissues) from a future ischemic episode, such as myocardial infarction. A_1 ARs are also attractive targets for anti-nociceptive agents because of their effects in the CNS. A_1 antagonists are undergoing clinical trials as diuretics for use in patients with congestive heart failure. A_1 agonists are being developed to reduce heart rate in certain arrhythmias.

A_{2A} Receptors

Both agonists and antagonists of the A_{2A} AR are being investigated for clinical use. Short-acting A_{2A} agonists may be useful for imaging coronary artery disease since they simulate the effect of exercise and dilate the coronary vasculature. Longer acting A_{2A} agonists may be useful for their anti-inflammatory properties in the treatment of asthma, sepsis, or ischemia–reperfusion injury. A_{2A} antagonists may be helpful in the treatment of CNS diseases, such as Parkinson's disease and schizophrenia.

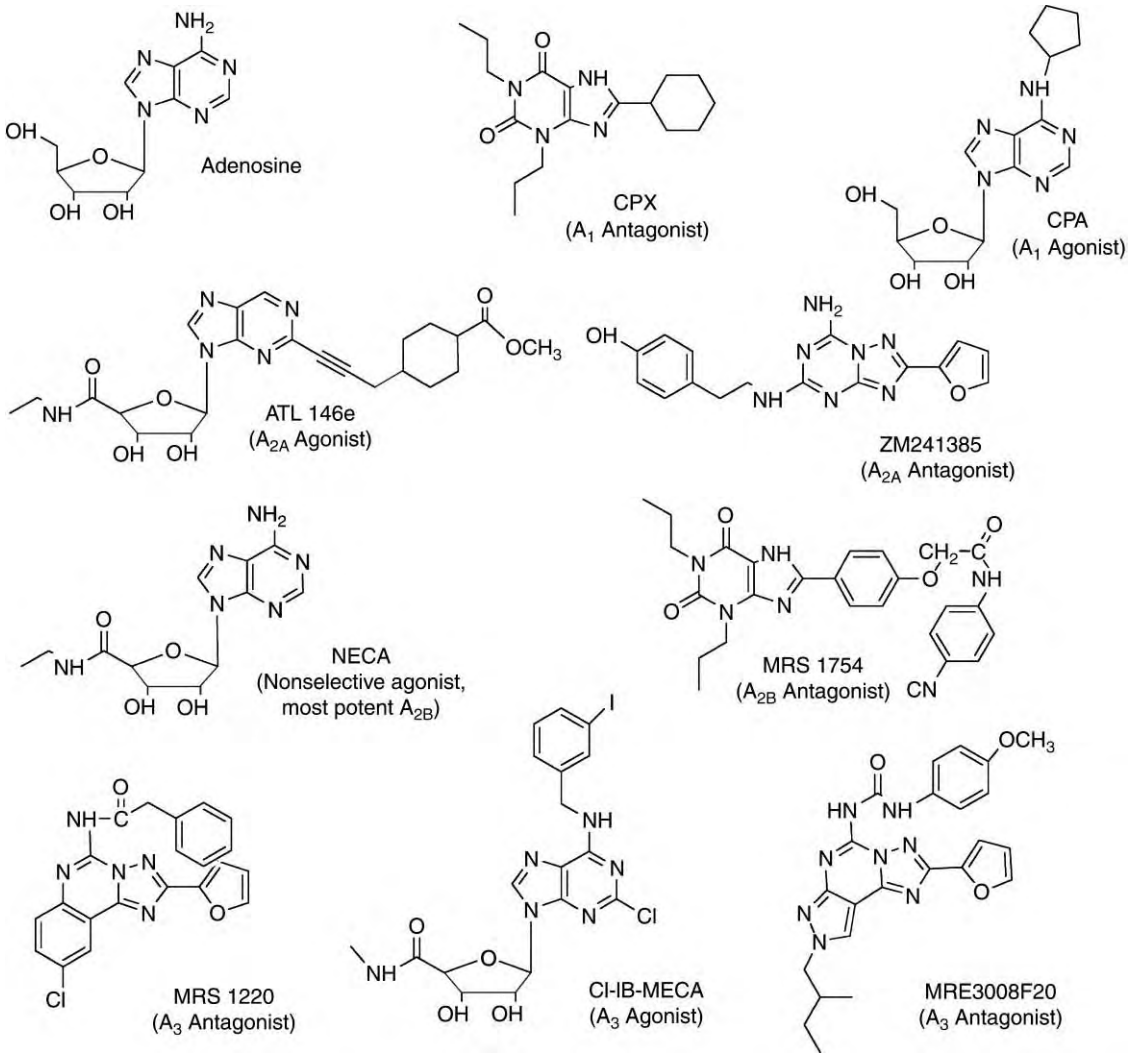

FIGURE 1 Adenosine receptor ligands.

A_{2B} Receptors

Antagonists of the A_{2B} AR are being developed as potential treatments for asthma since enprofylline and theophylline are used to prevent bronchoconstriction in asthmatics and are effective at concentrations that would indicate that the A_{2B} AR is its target. There is also some evidence to suggest that A_{2B} blockade may enhance the effects of insulin in liver and skeletal muscle and hence these compounds may be useful for the treatment of diabetes. Blockade of A_{2B} receptors may be useful for inhibiting angiogenesis.

A_3 Receptors

Some researchers have proposed the use of A_3 agonists as an adjuvant to chemotherapy since some compounds in this category have an anti-proliferative effect on tumor cells. However, some of these effects appear not to be receptor-mediated.

See Also the Following Articles

Adenylyl Cyclases • Allosteric Regulation • Diabetes • G Protein-Coupled Receptor Kinases and Arrestins • G Protein Signaling Regulators • Inositol Phosphate Kinases and Phosphatases • Insulin- and Glucagon-Secreting Cells of the Pancreas

Glossary

agonist A ligand that binds to a receptor and causes activation, mimicking the effect of the endogenous ligand.

antagonist A ligand that binds to its receptor and inhibits its activity.

ligand A chemical or biological substance that binds to a receptor.

receptor A recognition site (usually a macromolecule, such as a protein) for a ligand that mediates the ligand's physiological effects.

Further Reading

Dunwiddie, T. V., and Masino, S. A. (2001). The role and regulation of adenosine in the central nervous system. *Annu. Rev. Neurosci.* **24**, 31–55.

Fredholm, B. B., Arslan, G., Halldner, L., Kull, B., Schulte, G., and Wasserman, W. (2000). Structure and function of adenosine receptors and their genes. *Naunyn-Schmiedeberg Arch. Pharmacol.* **362**, 364–374.

Fredholm, B. B., Izerman, A. P., Jocobson, K. A., Klotz, K. N., and Linden, J. (2001). International Union of Pharmacology. XXV. Nomenclature and classification of adenosine receptors. *Pharmacol. Rev.* **53**, 527–552.

Klotz, K.-N. (2000). Adenosine receptors and their ligands. *Naunyn-Schmiedeberg Arch. Pharmacol.* **362**, 382–391.

Linden, J. (2001). Molecular approach to adenosine receptors: Receptor-mediated mechanisms of tissue protection. *Annu. Rev. Pharmacol. Toxicol.* **41**, 775–787.

Biography

Dr. Joel Linden is a Professor of Medicine and Molecular Physiology and Biological Physics at the University of Virginia in Charlottesville. His principal research interests involve the study of adenosine and adenosine receptor signaling. He holds a Ph.D. from the University of Virginia. Dr. Linden is also a consultant to for Adenosine Therapeutics, LLC, which is developing adenosine receptor agonists and antagonists for potential therapeutic use.

Adenylyl Cyclases

Ronald Taussig
University of Texas Southwestern Medical Center, Dallas, Texas, USA

Adenylyl cyclases are enzymes that synthesize the intracellular second messenger, cyclic AMP (cAMP), which in turn triggers a cascade of biochemical changes that regulate a number of important cellular processes. These cAMP-regulated cellular processes play an important role in the control of a number of metabolic processes including the regulation of blood glucose homeostasis, learning and memory, and cell growth.

The Hormone-Regulated Adenylyl Cyclase System

In order to function and survive, cells must respond to a multitude of signals present in their environment. These include chemical messengers released from local or distant parts of the body (such as circulating hormones and neurotransmitters) and external stimuli (such as light and odorants). Typically, these chemical messengers do not cross the cell membrane, but rather transduce their signal to the interior of the cell utilizing a "hand-off' mechanism occurring at the plasma membrane. In this process, the stimulus or "first messenger" acts at the membrane to regulate the activity of an enzyme that synthesizes (or degrades) an intracellular "second messenger" that can in turn regulate downstream intracellular metabolic enzymes (Figure 1). Cyclic AMP (cAMP), which is synthesized by adenylyl cyclases, was the first of these second messengers identified, and this mechanism has subsequently shown to be utilized as a common biological strategy to regulate cellular behaviors.

Regulation of intracellular cAMP concentrations is principally controlled at the level of its synthesis, through the hormonal regulation of adenylyl cyclase, the enzyme responsible for the conversion of ATP into cAMP. The adenylyl cyclase system is comprised of three components: heptahelical G protein-coupled receptors for a variety of hormones, neurotransmitters, and odorants; heterotrimeric G proteins; and the catalytic entity itself. Nine isoforms of membrane-bound adenylyl cyclases and a single soluble form have been identified in man. The nine membrane-bound isoforms are subjected to hormonal regulation that is mediated by G proteins of the G_s, G_i subclasses. Most importantly, adenylyl cyclase isoforms have the ability to integrate the multitude of hormonal inputs relayed by these pathways to ultimately control intracellular cAMP levels.

Discovery

The identification of cAMP resulted from studies aimed at elucidating the biochemical mechanism underlying the breakdown of glycogen in liver cells that is triggered by the hormone glucagon. In his Nobel prize winning discoveries, Earl Sutherland demonstrated that the process involved two distinct stages, a binding of the hormone at the membrane that activated adenylyl cyclase and subsequently generated the second messenger cAMP, and the activation within the cell of the downstream enzymatic process. The later discoveries that the receptor and the adenylyl cyclase were two distinct entities, and the subsequent identification of a third component (the intervening heterotrimeric G protein) have provided our modern day model of the hormone-regulated adenylyl cyclase system. Almost three decades following the discovery of cAMP, the genetic material encoding the first adenylyl cyclase was isolated, which further exposed the complexity of this signaling system.

Members of the Family

Our current knowledge of the structure and function of the mammalian adenylyl cyclase family has reached a new understanding following the application of molecular approaches. Ten distinct genes encoding the soluble and membrane-bound adenylyl cyclases have been identified (Table I). These genes are broadly distributed on different chromosomes throughout the human genome. Further diversity of adenylyl cyclases is provided by alternatively spliced mRNAs derived from transcripts of some of the family members.

These ten genes are differentially expressed in various tissues in mammalian species. All isoforms of adenylyl

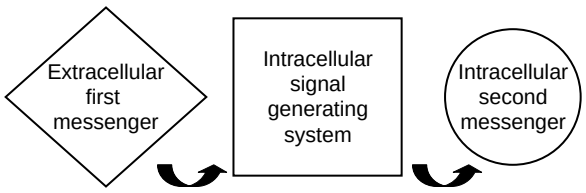

(a) Adrenaline	Adenylyl cyclase	Cyclic AMP
(b) Bradykinin	Phospholipase C	Diacylglycerol
(c) Bradykinin	Phospholipase C	Inositol trisphosphate
(d) Opiates	Calcium channels	Calcium
(e) Light	Phosphodiesterase	Cyclic GMP

FIGURE 1 Schematic diagram of second messenger systems. The diagram above the line outlines the progression of cell signaling from the extracellular signal (first messenger) to the generation of intracellular second messengers. The lettered subheadings below the line outline specific examples of intracellular second messengers, their extracellular signals, and the cellular proteins that mediate the changes in the levels of the second messengers. Arrows indicate the direction of the flow of information.

cyclase appear to be expressed in the brain; however, expression of each isoform is limited to specific regions of the central nervous system. Additionally, some adenylyl cyclase appears to be rather widely distributed in most tissues of the body (e.g., types 4, 6, and 7). All adenylyl cyclases have roughly the same size and contain between 1064 and 1610 amino acid residues. The deduced amino acid sequence of all identified adenylyl cyclase isoforms predicts a complex topology within the membrane (Figure 2). The noted exception is the soluble adenylyl cyclase (SAC), which is localized to the intracellular compartment and exhibits regulation quite distinct from the membrane-bound forms. This isoform is more related to an ancestral form found in bacteria than to the other types.

Based on the similarities of their amino acid sequences, and patterns of regulation by G protein pathways, the membrane-bound adenylyl cyclases can be grouped into subfamilies. The first group, comprised of the types 1 and 8, are characterized by their stimulation by calmodulin. The types 2, 4, and 7 adenylyl cyclases form the second group; characteristic of these isoforms is their stimulation by G protein $\beta\gamma$-subunits. Types 5 and 6, which are the two most related isoforms constitute the last group and are characterized by their inhibition by calcium. The type 9 is the largest and most diverse of the adenylyl cyclase isoforms, and like the type 3 enzyme, does not belong to any of the three groups outlined above.

Regulation of Adenylyl Cyclase Activity by G Proteins and Calcium

There are multiple classes of heterotrimeric G proteins that regulate adenylyl cyclases, either in a stimulatory (G_s family), or inhibitory (G_i family) manner. The two G protein families are normally coupled to distinct receptor subtypes. The $\beta\gamma$-subunits also regulate adenylyl cyclase activity, but in a manner specific to an adenylyl cyclase isoform. Additionally, calcium ions are very strong modulators of some isoforms of adenylyl cyclase; thus, G proteins that regulate calcium entry through voltage-dependent Ca^{2+} channels may also regulate adenylyl cyclase activity.

Hormonal activation of AC occurs primarily through receptors coupled to the stimulatory G protein G_s. G_s is the most widely distributed activator of all mammalian membrane-bound AC isoforms. All membrane-bound forms of adenylyl cyclases are regulated by G_s through the interaction of adenylyl cyclase with the Gα-subunit that is released from the $\beta\gamma$-subunits upon activation by a hormone-bound stimulating receptor (Figure 3A).

Members of the G_i family inhibit adenylyl cyclase activity through the binding of the alpha subunit to the cyclase, but this regulation exhibits selectivity for a

TABLE I

Localization and Expression of the Adenylyl Cyclase Gene Family

AC isoform	Length (amino acids)	Location (chromosome)	Sites of expression (tissue)
AC1	1135	7	Brain, adrenal medulla
AC2	1090	5	Brain, skeletal muscle, lung, heart
AC3	1144	2	Olfactory epithelium, brain
AC4	1064	14	Widely distributed
AC5	1184	3	Heart, brain, kidney, liver, lung, uterus
AC6	1165	12	Ubiquitous
AC7	1099	16	Ubiquitous (highly expressed in brain)
AC8	1248	8	Brain, lung, (some in testes, adrenal, uterus, heart)
AC9	1353	16	Brain, skeletal muscle, lung, heart
SAC	1610	1	Testes

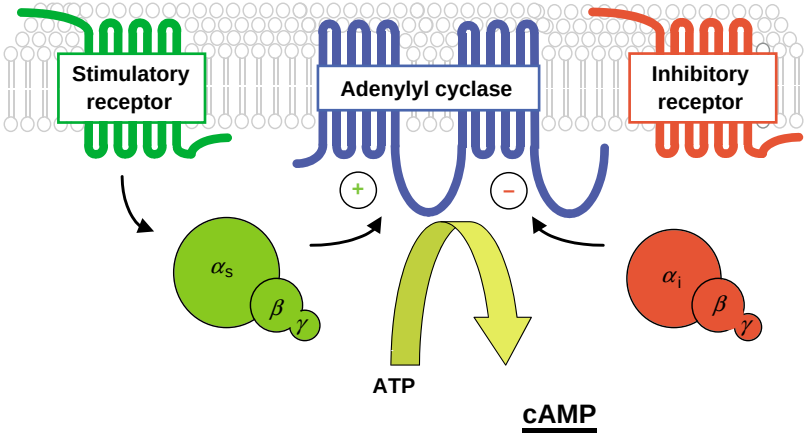

FIGURE 2 Schematic view of plasma membrane components that participate in the hormone-regulated adenylyl cyclase system. A prototypic adenylyl cyclase is shown. G protein-coupled receptors that enhance or inhibit adenylyl cyclase activity are shown in green and red respectively. All receptors of this family have a similar predicted structure and span the plasma membrane seven times. These receptors couple to their corresponding heterotrimeric G proteins (composed of an α-, β-, and γ-subunits); G_s (green) and G_i (red) couple to stimulatory and inhibitory receptors respectively. Adenylyl cyclase (shown in blue) is predicted to span the plasma membrane twelve times, and projects its active site towards the cytoplasmic side of the membrane. The result of extracellular messengers binding to the receptors results in the regulation of the conversion of ATP into cAMP by the enzyme adenylyl cyclase.

subset of adenylyl cyclase isoforms (Figure 3B). All three G_i family members (G_{i1}, G_{i2}, G_{i3}) inhibit types 1, 5, 6, and 8; the remaining cyclase isoforms are insensitive to this inhibitory input. Interestingly, this mode of inhibition is not through direct competition with G_s binding to the cyclase, and a number of experimental approaches demonstrate that $G_i\alpha$ exerts its effects at a site, symmetrical to the G_s binding site, and located on the side opposite the cyclase molecule.

As illustrated in Figure 3C, activation of inhibitory receptors leads to the release of G protein $\beta\gamma$-subunits which can exert profound regulation of adenylyl cyclase activity. Like regulation by the G_i α-subunit, this regulation is isoform specific. However, an added complication is that the $\beta\gamma$-subunits can either activate or inhibit the activity – types 2, 4, and 7 are activated whereas types 1 and 8 are inhibited.

Regulation of adenylyl cyclase activity by calcium is still more complex (Figure 4). At physiological intracellular calcium concentrations the types 3, 5, and 6 adenylyl cyclases are inhibited by calcium. For the types 5 and 6, this appears to be due to a direct effect of calcium on the adenylyl cyclase. Stimulation of adenylyl cyclase activity by calcium has been demonstrated for the types 1 and 8 isoforms, but this form of regulation requires calmodulin, a calcium-binding protein that regulates the activity of many cellular enzymes. Indeed, one of these calmodulin-regulated enzymes is a protein kinase, that mediates the inhibitory effects that were observed for the type 3 adenylyl cyclase.

Physiological Roles of Adenylyl Cyclases

The hormonal activation of adenylyl cyclases and the subsequent regulation of intracellular cAMP impacts on a wide array of cellular processes (Table II). These roles include diverse processes underlying regulation of blood sugar levels, regulation of heart function, water retention as well as higher brain functions of learning and memory. However, while much is known at the biochemical level regarding the regulation of the many adenylyl cyclase isoforms, the precise physiological roles of each isoform are less well known. A further complication is that each cell of our body expresses more than one isoform of adenylyl cyclase. Nevertheless, investigators have begun

FIGURE 3 Schematic representation of the isoform-specific regulation of adenylyl cyclases by G protein subunits. (A) Regulation of adenylyl cyclases by $G_s\alpha$. Upon activation of stimulatory receptors, the heterotrimeric G protein, G_s undergoes subunit dissociation whereby the $\beta\gamma$-subunits are released from the α-subunit. The α-subunit subsequently binds to the adenylyl cyclase and increases its catalytic activity, resulting in an increase in intracellular cAMP levels (+). (B) Regulation of adenylyl cyclases by $G_i\alpha$. Upon activation of inhibitory receptors, the heterotrimeric G protein, G_i undergoes subunit dissociation whereby the $\beta\gamma$-subunits are released from the α-subunit. The α-subunit subsequently binds to the adenylyl cyclase and decreases its catalytic activity, resulting in a decrease in intracellular cAMP levels (−). Specific isoforms of adenylyl cyclase that are responsive to G_i inhibition are noted. (C) Dual regulation of adenylyl cyclases by G-protein $\beta\gamma$-subunits. $\beta\gamma$-subunits released from G_i heterotrimers can either positively (+) or negatively (−) regulate adenylyl cyclases. Specific isoforms of adenylyl cyclase that are responsive to these 2 types of regulation are noted.

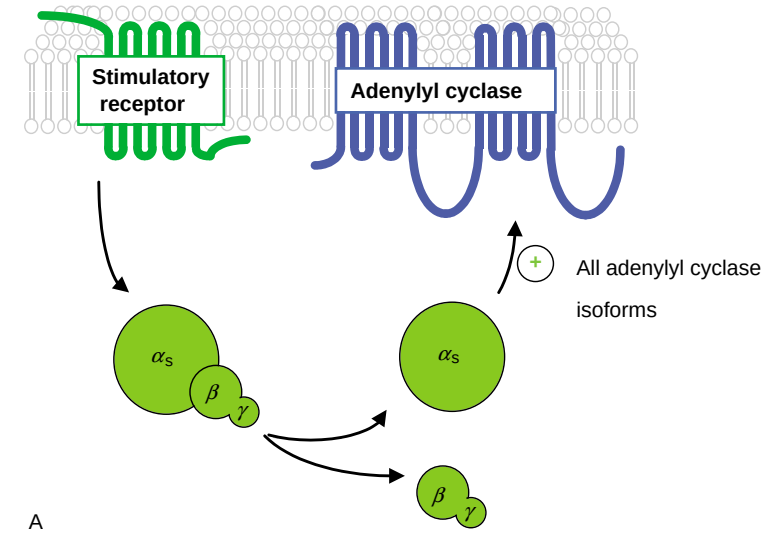
Stimulatory receptor
Adenylyl cyclase
All adenylyl cyclase isoforms
α_s
β
γ
α_s
β
γ

A

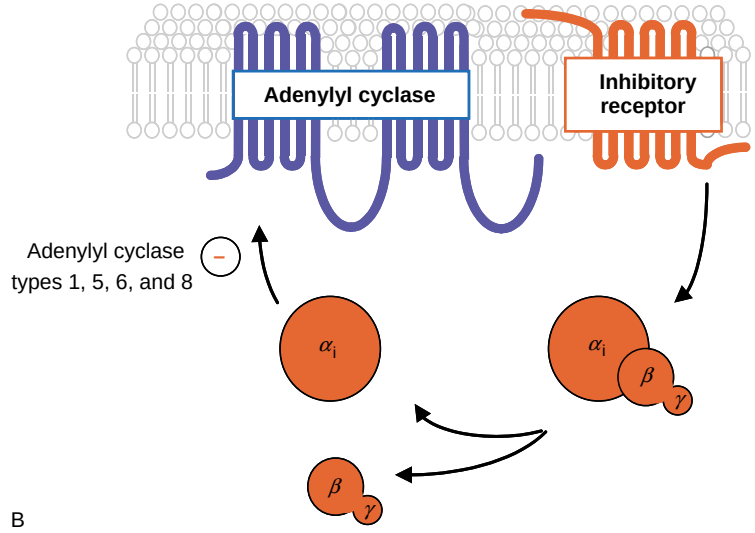
Adenylyl cyclase
Inhibitory receptor
Adenylyl cyclase types 1, 5, 6, and 8
α_i
α_i
β
γ
β
γ

B

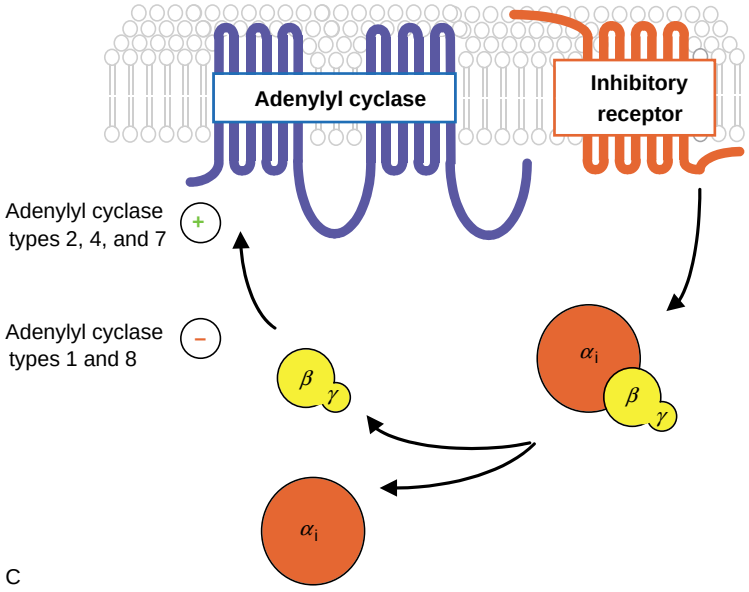
Adenylyl cyclase
Inhibitory receptor
Adenylyl cyclase types 2, 4, and 7
Adenylyl cyclase types 1 and 8
β
γ
α_i
β
γ
α_i

C

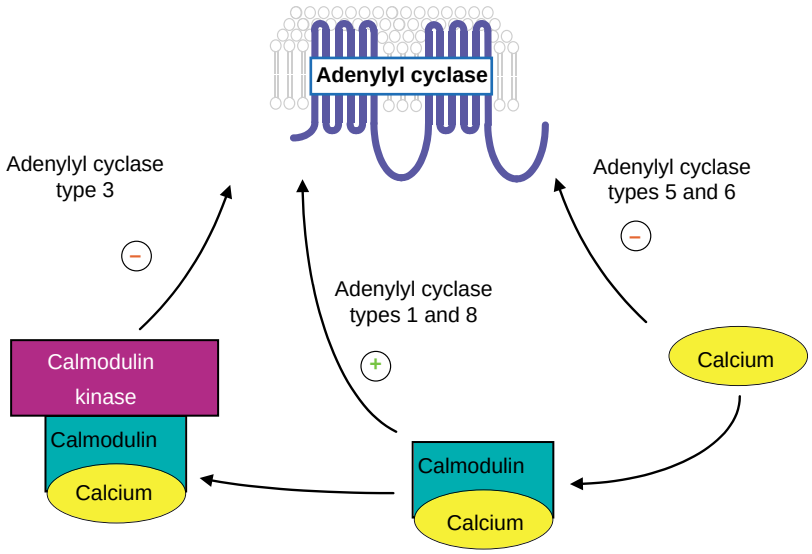

FIGURE 4 Schematic representation of the isoform-specific regulation of adenylyl cyclases by calcium. Increases in intracellular calcium can regulate the activities of adenylyl cyclases by at least three mechanisms. Calcium can directly bind to and inhibit AC 5 and 6. Calcium bound to calmodulin can bind directly to and activate AC 1 and 8, or can bind and activate a calmodulin-regulated kinase that can subsequently inhibit AC3.

to examine the specific roles of each adenylyl cyclase isoform through the use of mouse strains that are genetically altered by the removal of a particular adenylyl cyclase gene from the mouse genome. Such studies emphasize the involvement of cAMP signaling pathways in pattern formation of the brain and provide definitive evidence for roles of the types 1 and 8 adenylyl cyclases in higher brain function. Similar approaches have revealed a role for the type 3 cyclase in regulation of smooth muscle proliferation in the aorta and recently, a role of the type 5 cyclase in heart function.

A number of studies have uncovered both sporadic and inherited mutations in components of the adenylyl cyclase system associated, or in some cases, shown to be causal to certain human diseases. Mutations causing constitutively active receptors (resulting in elevated intracellular cAMP levels due to constant stimulation of adenylyl cyclase via $G_{s\alpha}$) have been found in patients with familial male precocious puberty/testotoxicosis (LH receptor), hyperfunctioning thyroid adenomas and nonautoimmune autosomal dominant hyperthyroidism (thyroid-stimulating hormone receptor), and Jansen-type metaphyseal chondrodysplasia (parathyroid hormone receptor). Similarly, diseases associated with constitutively activated G proteins ($G_{s\alpha}$) were also identified in patients with endocrine tumors, McCune–Albright syndrome, and testitoxicosis. However, to date no mutations associated with these diseases have been found in the adenylyl cyclase component of this system, but these investigations are ongoing. Here again, a major complication of these studies is the presence of multiple adenylyl cyclase isoforms that are present in each of the cell types.

See Also the Following Articles

Adenosine Receptors • Adrenergic Receptors • Cyclic GMP Phosphodiesterases • Cyclic Nucleotide

TABLE II

Examples of Physiological Effects Mediated by Adenylyl Cyclases

Extracellular signal (hormone or chemical)	Tissue	Isoform (if known)	Effect
Adrenaline	Heart	AC5 and 6	Increased rate and force of contraction
Adrenaline glucagon	Liver	Unknown	Breakdown of glucagon into glucose
Neurotransmitters (e.g., serotonin, dopamine)	Brain	Many	Learning, memory, synaptic transmission
Chemical odorants	Olfactory epithelium	AC3	Odorant sensation
Antidiuretic hormone	Kidney	Unknown	Regulation of water retention
Prostaglandin	Arteries	AC3	Inhibition of smooth muscle cell proliferation
Bicarbonate	Testes	SAC	Fertilization (sperm acrosome reaction)

Phosphodiesterases • G_i Family of Heterotrimeric G Proteins • G_s Family of Heterotrimeric G Proteins • Phospholipase C

Glossary

G protein A heterotrimeric protein composed of an α-, β-, and γ-subunit that binds and hydrolyzes GTP and transduces signals from outside to the inside of the cell.

receptor A protein that resides in the plasma membrane and specifically recognizes an extracellular signal and upon binding of this signal, transmits information to the cell interior.

second messenger A small molecule that is synthesized by a cellular protein and conveys the information within the cell that an extracellular signal has been received.

signal transduction The process of transmitting information from the outside to the inside of a cell, resulting in a change in cellular behavior.

Further Reading

Hanoune, J., and Defer, N. (2001). Regulation and role of adenylyl cyclase isoforms. *Annu. Rev. Pharmacol. Toxicol.* **41**, 145–174.

Johnston, C. A., and Watts, V. J. (2003). Sensitization of adenylate cyclase: A general mechanism of neuroadaptation to persistent activation of G alpha(i/o)-coupled receptors? *Life Sci.* **73**, 2913–2925.

Sunahara, R. K., and Taussig, R. (2002). Isoforms of mammalian adenylyl cyclase: Multiplicities of signaling. *Mol. Interv.* **2**, 168–184.

Tesmer, J. J., and Sprang, S. R. (1998). The structure, catalytic mechanism and regulation of adenylyl cyclase. *Curr. Opin. Struct. Biol.* **8**, 713–719.

Wuttke, M. S., Buck, J., and Levin, L. R. (2001). Bicarbonate-regulated soluble adenylyl cyclase. *JOP* **2**, 154–158.

Biography

Dr. Ronald Taussig is an Associate Professor in the Department of Pharmacology at the University of Texas Southwestern Medical Center at Dallas. He received a Ph.D. in biology from Stanford University. His principal research interests focus on signaling by heterotrimeric G proteins and the hormone-regulated adenylyl cyclase system. Dr. Taussig is also the Associate Director of the Alliance for Cellular Signaling, a multi-institutional collaboration whose goal is to study and model G protein-mediated and related signaling systems in mouse macrophages.

Adrenergic Receptors

David B. Bylund
University of Nebraska Medical Center, Omaha, Nebraska, USA

Adrenergic receptors (adrenoceptors) mediate the central and peripheral actions of the neurotransmitter norepinephrine (noradrenaline) and the hormone epinephrine (adrenaline); they are widely distributed throughout the body. There are three major adrenergic receptor types: alpha-1, alpha-2, and beta. Each of these three receptor types is further divided into three subtypes. Adrenergic receptors are seven-transmembrane receptors, which consist of a single polypeptide chain with seven hydrophobic regions that are thought to form alpha helical structures that span or transverse the membrane. Because the mechanism of action of adrenergic receptors includes the activation of guanine nucleotide regulatory binding proteins (G proteins), they are also called G protein-coupled receptors.

Epinephrine and Norepinephrine

Norepinephrine (noradrenaline) is a neurotransmitter in both the peripheral and central nervous systems. Epinephrine (adrenaline) is a hormone released from the adrenal gland. Norepinephrine and epinephrine are catecholamines, because they have both the catechol moiety (two hydroxyl groups on a benzene ring) and an amine (NH_2). Both of these catecholamine messengers play important roles in the regulation of diverse physiological systems by acting through adrenergic receptors. Stimulation of adrenergic receptors by catecholamines released in response to activation of the sympathetic autonomic nervous system results in a variety of effects such as increased heart rate, regulation of vascular tone, and bronchodilatation. In the central nervous system, adrenergic receptors are involved in many functions including memory, learning, alertness, and the response to stress.

Norepinephrine is synthesized starting with the amino acid tyrosine, which is obtained from the diet and can also be synthesized from phenylalanine. Tyrosine is converted to dihydroxyphenylalanine (DOPA) by the enzyme tyrosine hydroxylase, and DOPA in turn is converted to dopamine. Dopamine is then converted to norepinephrine by the enzyme dopamine beta-hydroxylase. In the adrenal medulla and in a few brain regions, norepinephrine is converted to epinephrine by the enzyme phenylethanolamine N-methyltransferase. The major mechanism by which the effects of norepinephrine are terminated is re-uptake back into the nerve terminal by a high affinity norepinephrine transporter. Epinephrine, as well as norepinephrine are metabolized to inactive products. Norepinephrine is metabolized by the enzymes monoamine oxidase (MAO) and catechol-O-methyltransferase (COMT) to 3-methoxy-4-hydroxyphenylglycol (MHPG) and 3-methoxy-4-hydroxymandelic acid (VMA). The major metabolite found in the blood and urine is MHPG. Epinephrine is similarly metabolized by MAO and COMT to VMA.

Classification and Mechanism of Action of Adrenergic Receptors

Adrenergic receptors were originally divided into two major types, alpha and beta, based on their pharmacological characteristics (i.e., rank order potency of agonists). Subsequently, the beta adrenergic receptors were subdivided into beta-1 and beta-2 subtypes; more recently, a beta-3 has been defined. The alpha adrenergic receptors were first subdivided into postsynaptic (alpha-1) and presynaptic (alpha-2) subtypes. After it was realized that not all alpha receptors with alpha-2 pharmacological characteristics were presynaptic, the pharmacological definition was used. The current classification scheme is based on three major types: alpha-1, alpha-2, and beta. Each of these three receptor types is further divided into three subtypes as shown in Figure 1: alpha-1A, alpha-1B, alpha-1D; alpha-2A, alpha-2B, alpha-2C; beta-1, beta-2, beta-3.

The binding of an agonist to an adrenergic receptor induces (or stabilizes) a conformational change that allows the receptor to interact with and activate a G protein. The activated receptor facilitates the exchange of GDP for GTP, leading to the dissociation of the α and $\beta\gamma$_ subunits of the G protein, which in turn stimulate or inhibit the activity various effectors. It is important to note that each of the three types of adrenergic receptors couples to a distinct class

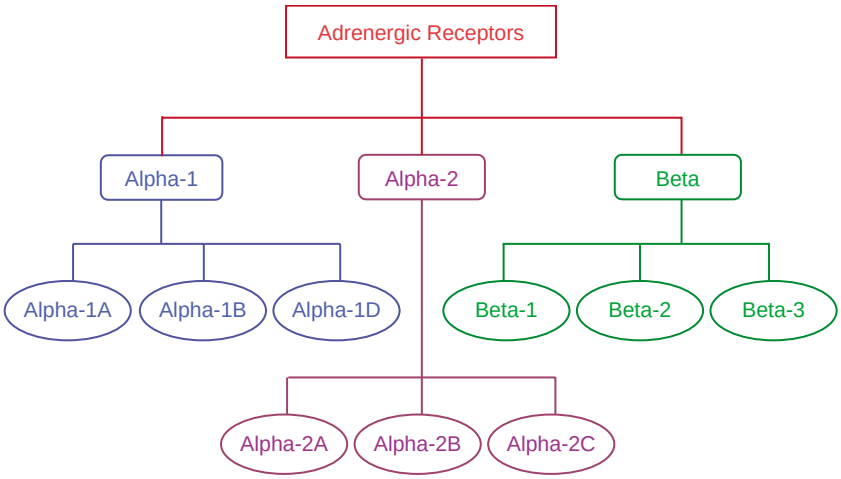

FIGURE 1 The classification scheme for adrenergic receptors.

of G proteins: alpha-1 to G_q; alpha-2 to $G_{i/o}$ and beta to G_s. In addition to G proteins, adrenergic receptors interact with other signaling proteins and pathways such as those involving tyrosine kinases.

Alpha-1 Adrenergic Receptors

Three genetic and four pharmacological alpha-1 adrenergic receptor subtypes have been defined. The alpha-1A and alpha-1B subtypes were initially defined based on their differential affinity for adrenergic agents, such as WB4101 and phentolamine, and on their differential sensitivities to the site-directed alkylating agent chloroethylclonidine. The alpha-1B subtype was subsequently cloned from the hamster and the alpha-1A was cloned from bovine brain, although it was originally called the alpha-1c adrenergic receptor. A third subtype, alpha-1D adrenergic receptor, was subsequently cloned from the rat cerebral cortex, although this clone was originally called the alpha-1a subtype by some investigators. A fourth pharmacological subtype, the alpha-1L, has been identified in vascular tissues from several species, but it may represent a conformational state of the alpha-1A receptor. The current classification scheme includes the alpha-1A, the alpha-1B and the alpha-1D, but there is no alpha-1C (Figure 1).

Pharmacological and Molecular Characteristics of Alpha-1 Adrenergic Receptors

In addition to norepinephrine and epinephrine, alpha-1 receptors are activated by various agonists such as phenylephrine (Neosynephrine) and methoxamine (Vasoxyl). These agonists are relative selective for alpha-1 receptors and have low affinity for alpha-2 and beta receptors. In contrast, they have similar affinities for the three alpha-1 subtypes and are thus nonsubtype selectively agonists. Similarly, antagonists including prazosin (Minipress) and tamsulosin (Flomax) are relatively selective for alpha-1 receptors and block alpha-2 and beta receptors only at high concentrations. Several other antagonists such as phentolamine (Regitine) and phenoxybenzamine (Dibenzyline) block both alpha-1 and alpha-2 adrenergic receptors with similar affinities. Alpha-1A selective antagonists include 5-methylurapidil and niguldipine, whereas cirazoline appears to be a selective alpha-1A agonist.

The alpha-1 adrenergic receptors are single polypeptide chains of 446 to 572 amino acid residues that span the membrane seven times, with the amino terminal being extracellular and the carboxy terminal intracellular. Thus, there are three intracellular loops and three extracellular loops. In contrast to the alpha-2 receptors, but similar to the beta receptors, the alpha-1 receptors have a long carboxy terminal tail (137–179) amino acid residues) and a short third intracellular loop (68–73 amino acid residues). The amino terminal of the alpha-1A and alpha-1B subtypes have three (alpha-1A) or four (alpha-1B) consensus sites for N-linked glycosylation. The carboxy terminal tails of all three subtypes are potentially palmitolyated, thus anchoring the tail to the membrane and forming a small fourth intracellular loop. The carboxy terminal tails also have multiple sites of phosphorylation that are thought to be important in the desensitization, recycling, and down-regulation of the receptor.

The human alpha-1 adrenergic receptor genes consist of two exons and a single large intron of at least 20 kilobases in the region corresponding to the sixth transmembrane domain. No splice variants are known

for the alpha-1B and alpha-1D subtypes. In contrast, at least 10 splice variants of human alpha-1A subtype have been reported, but only 4 produce full-length receptors.

Alpha-2 Adrenergic Receptors

Three genetic and four pharmacological alpha-2 adrenergic receptor subtypes have also been defined (Figure 1). The alpha-2A and alpha-2B subtypes were initially defined based on their differential affinity for adrenergic agents such as prazosin and oxymetazoline. These subtypes were subsequently cloned from human, rat, and mouse. A third subtype, alpha-2C, was originally identified in an opossum kidney cell line and has also been cloned from several species. A fourth pharmacological subtype, the alpha-2D, has been identified in the rat, mouse, and cow. This pharmacological subtype is a species orthologue of the human alpha-2A subtype, and thus it is not considered to be a separate genetic subtype.

Pharmacological and Molecular Characteristics of Alpha-2 Adrenergic Receptors

In addition to norepinephrine and epinephrine, alpha-2 receptors are activated by clonidine (Catapres) and brimonidine (Alphagan). These agonists are relatively selective for alpha-2 receptors and have lower affinity at alpha-1 and beta receptors. Similarly, the antagonist yohimibine is relatively selective for alpha-2 receptors and blocks alpha-1 and beta receptors only at higher concentrations. Antagonists that are at least somewhat selective for one of the alpha-2 subtypes include BRL44408 for the alpha-2A, prazosin and ARC-239 for the alpha-2B (note, however, that these two agents have much higher affinities for alpha-1 receptors), and rauwolscine for the alpha-2C subtype. Ozymetazoline is a partial agonist that has a higher affinity for the alpha-2A subtype when compared to the alpha-2B and alpha-2C subtypes.

The alpha-2 adrenergic receptors are single polypeptide chains of 450 to 462 amino acid residues. In contrast to the alpha-1 and beta receptors, the alpha-2 receptors tend to have long third intracellular loops (148–179 amino acid residues) and a short carboxy terminal tail (20–21 amino acid residues). The amino terminal of the alpha-2A and alpha-2C subtypes have two consensus sites for N-linked glycosylation, and the carboxy terminal tails of all three subtypes are potentially palmitolyated. The third intracellular loops have multiple sites of phosphorylation, which are thought to be important in the desensitization, recycling, and down-regulation of the receptor. The alpha-2 adrenergic receptor genes do not contain introns, and thus there are no splice variants.

Beta Adrenergic Receptors

Three beta adrenergic receptor subtypes have been identified. The beta-1 adrenergic receptor, the dominant receptor in heart and adipose tissue, is equally sensitive to epinephrine and norepinephrine, whereas the beta-2 adrenergic receptor, responsible for relaxation of vascular, uterine, and airway smooth muscle, is less sensitive to norepinephrine as compared to epinephrine. The beta-3 receptor is insensitive to the commonly used beta-adrenergic receptor antagonists and was previously referred to as the "atypical" beta adrenergic receptor. A beta-4 receptor has been postulated; however, definitive evidence of its existence is lacking, and it is now thought to be a "state" of the beta-1 adrenergic receptor.

Pharmacological and Molecular Characteristics of Beta Adrenergic Receptors

Isoproterenol (Isuprel) is the prototypic nonsubtype selective beta agonist that has no activity at alpha-1 and alpha-2 receptors except at high concentrations. Epinephrine is 10- to 100-fold more potent at the beta-2 receptor as compared to the beta-1 subtype, whereas norepinephrine is more potent than epinephrine at the beta-3 subtype. Many beta-2 selective agonists, such as terbutaline (Brethine) and salmeterol (Serevent), have been developed for the treatment of asthma. Due to their subtype selectivity, they have a lower incidence of side effects mediated by the beta-1 receptor. Propranolol (Inderal) is the prototypic nonsubtype selective beta antagonist that has equal affinities at the beta-1 and beta-2 subtypes. Other nonselective beta adrenergic antagonists include timolol (Blocadren), pindolol (Visken, which is actually a weak partial agonist), and carvedilol (Coreg), which is also an alpha-1 antagonist. Several beta-1 selective antagonists have been developed, such as metoprolol (Lopressor) and esmolol (Brevibloc).

The beta adrenergic receptors are single polypeptide chains of 408 to 477. In contrast to the alpha-2 receptors, but similar to the alpha-1 receptors, the beta receptors tend to have longer carboxy terminal tails (61–97 amino acid residues) and shorter third intracellular loops (54–80 aa). The amino terminal of the beta receptors have one or two consensus sites for N-linked glycosylation, and the carboxy terminal tails of all three subtypes are potentially palmitoylated. The carboxy terminal tails also have multiple sites of phosphorylation which are thought to be important in

the desensitization, recycling, and down-regulation of the receptor.

The beta-1 and beta-2 adrenergic receptor genes do not contain introns, thus they have no splice variants. In contrast, the beta-3 receptor has one intron, resulting in two splice variants. However, no functional differences have been found between the two splice variants.

Regulation of Adrenergic Receptors

The processes involved in desensitization and down-regulation have been extensively investigated for the beta-2 adrenergic receptor. The other adrenergic receptors, as well as many other G protein-coupled receptors, appear to behave in a similar manner. Initial uncoupling of the beta-2 receptor from the G protein after agonist binding is mediated by phosphorylation of specific residues in the carboxyl tail of the receptor. The phosphorylated beta-2 receptor serves as a substrate for the binding of β-arrestin, which not only uncouples the receptor from the signal transduction process but also serves as an adapter protein that mediates the binding of additional signaling proteins and entry into the internalization pathway. The mechanisms of beta-2 adrenergic receptor down-regulation appear to involve both an increase in the rate of degradation of the receptor as well as a decrease in the levels of beta receptor mRNA (8).

Adrenergic Receptor Signal Transduction Pathways

The alpha-1 adrenergic receptors activate the $G_{q/11}$ family of G proteins leading to the dissociation of the α and $\beta\gamma$ subunits and the subsequent stimulation of the enzyme phospholipase C. This enzyme hydrolyzes phosphatidylinositol 1,2-biphosphate in the membrane producing inositol trisphosphate (IP_3) and diacylglycerol. These molecules act as second messengers mediating intracellular Ca^{++} release via the IP_3 receptor and activating protein kinase C. Other signaling pathways that have also been shown to be activated by alpha-1 receptors include Ca^{++} influx via voltage-dependent and independent calcium channels, arachidonic acid release, and activation of phospholipase A_2, phospholipase D activation, and mitogen-activated protein kinase.

The alpha-2 adrenergic receptors activate the $G_{i/o}$ family of G proteins and alter (classically inhibit) the activity of the enzyme adenylyl cyclase, which in turn, decreases the concentration of the second messenger cyclic AMP. In addition, the stimulation of alpha-2 receptors can regulate several other effector systems including the activation of K^+ channels, inhibition or activation of Ca^{++} channels, and activation of phospholipase A_2, phospholipase C, and Na^+/H^+ exchange.

The beta adrenergic receptors activate the G_s family of G proteins and activate adenylyl cyclase, thus increasing in cyclic AMP concentrations. Beta adrenergic receptors interact with many other signaling proteins, including the phosphoprotein EBP50 (ezrinradixin-moesin-binding phosphoprotein-50), the Na^+/H^+ exchanger regulatory factor, and with CNrasGEF.

Adrenergic Receptor Polymorphisms

Polymorphisms have been identified in some of the alpha-2 and beta adrenergic receptor subtypes, which may have important clinical implications. A common polymorphism has been identified in the third intracellular loop of the alpha-2B receptor, which consists of a deletion of three glutamate residues (301–303); the deletion is a risk factor for acute coronary events, but not hypertension. This deletion results in a loss of short-term agonist-induced desensitization. A common polymorphism has been identified in the third intracellular loop of alpha-2C subtype, which consists of a deletion of four amino acid residues (322–325); the deletion results in an impaired coupling to several effectors.

The gene encoding the human beta-1 adrenergic receptor is quite polymorphic with 18 single nucleotide polymorphisms (SNPs), 7 of which cause amino acid substitutions. A total of 13 polymorphisms in the beta-2 adrenergic receptor gene and its transcriptional regulator upstream peptide have been identified. Three closely linked polymorphisms, two coding region at amino acid positions 16 and 27 and one in the upstream peptide, are common in the general Caucasian population. The glycine-16 receptor exhibits enhanced down-regulation *in vitro* after agonist exposure. In contrast, arginine-16 receptors are more resistant to down-regulation. Some studies have suggested a relationship among these polymorphisms, airway responsiveness (e.g., asthma) and the responsiveness to beta adrenergic agonists.

A tryptophan-64 to arginine polymorphism has been identified in the beta-3 adrenergic receptor. The allele frequency is approximately 30% in the Japanese population, higher in Pima Indians, and lower in Caucasians. Type 2 diabetic patients with this mutation showed a significantly younger onset-age of diabetes and an increased tendency to obesity, hyperinsulinemia, and hypertension.

See Also the Following Articles

Adenylyl Cyclases • Diabetes • Dopamine Receptors • G Protein-Coupled Receptor Kinases and Arrestins • Inositol Phosphate Kinases and Phosphatases • Phosphatidylinositol Bisphosphate and Trisphosphate • Phospholipase A_2 • Phospholipase C • Phospholipase D

Glossary

agonist Compound that binds to a receptor and activates it, thus causing a biological response.

antagonist Compound that binds to a receptor but does not activate it. It can block or inhibit the activation caused by an agonist.

desensitization Decrease in response of a tissue to a neurotransmitter or agonist drug following repeated administration.

down-regulation Decrease in the number or density of receptor binding sites following chronic agonist treatment.

partial agonist Agonist that has less than full efficacy in activating its receptor.

polymorphism Variability in DNA sequence that occurs with an allele frequency of greater than 1% in the population.

Further Reading

Bylund, D. B. (1988). Subtypes of α_2-adrenoceptors: Pharmacological and molecular biological evidence converge. *Trends Pharmacol. Sci.* **9**, 356–361.

Bylund, D. B. (2003). Norepinephrine. In *Encyclopedia of the Neurological Sciences* (M. J. Aminoff and R. B. Daroff, eds.) Vol. 3, pp. 638–640. Academic Press, San Diego.

Bylund, D. B., Eikenberg, D. C., Hieble, J. P., Langer, S. Z., Lefkowitz, R. J., Minneman, K. P., Molinoff, P. B., Ruffolo, R. R., and Trendelenburg, A. U. (1994). IV. International Union of Pharmacology nomenclature of adrenoceptors. *Pharmacol. Rev.* **46**, 121–136.

Cooper, J. R., Bloom, F. E., and Roth, R. H. (2003). *The Biochemical Basis of Neuropharmacology.* 8th edition, Oxford University Press, New York, pp. 181–223.

Ferguson, S. S. G. (2001). Evolving concepts in G protein-coupled receptor endocytosis: The role in receptor desensitization and signaling. *Pharmacol. Rev.* **53**, 1–24.

Hieble, J. P., Bylund, D. B., Clarke, D. E., Eikenburg, D. C., Langer, S. Z., Lefkowitz, R. J., Minneman, K. P., and Ruffolo, R. R. (1995). International Union of Pharmacology X. Recommendation for nomenclature of alpha-1 adrenoceptors: Consensus update. *Pharmacol. Rev.* **47**, 267–270.

Rockman, H. A., Koch, W. J., and Lefkowitz, R. J. (2002). Seven-transmembrane-spanning receptors and heart function. *Nature* **415**, 206–212.

Small, K. M., McGraw, D. W., and Liggett, S. B. (2003). Pharmacology and physiology of human adrenergic receptor polymorphisms. *Annu. Rev. Pharmacol. Toxicol.* **43**, 381–411.

Biography

David B. Bylund is a professor and former chair of the Department of Pharmacology at the University of Nebraska Medical Center in Omaha, Nebraska. His main research interests are related to the regulation of adrenergic receptors and their role in mental disorders. He received his Ph.D. from the University of California at Davis and was a postdoctoral fellow at Johns Hopkins University. He was President of the American Society for Pharmacology and Experimental Therapeutics for 2003–2004.

Affinity Chromatography

Pedro Cuatrecasas
University of California, San Diego, California, USA

Meir Wilchek
Weizmann Institute of Science, Rehovot, Israel

Affinity chromatography (AC) is a variant of liquid chromatography in which biospecific and reversible interactions between biologically active or structurally unique and complementary molecules are used for the selective extraction, separation, purification, analysis, or tagging of specific macromolecules or cell components from crude biological samples. AC was first introduced as a procedure for purifying enzymes and proteins more than 30 years ago. AC is based on the principles of molecular recognition, and today it is one of the most powerful techniques available for purifying physiologically or structurally interacting proteins. In addition to the multitude of proteins purified by AC, the method has also been an indispensable tool for studying many biological processes, such as the mechanism of action of enzymes and hormones, protein–protein or cell–cell interactions, and others encountered in genetic engineering. The emergence of many related methodologies, which are based on molecular recognition (or biorecognition), has impacted virtually all fields of research in the biological sciences.

The Key Steps in AC

The first step involves the preparation of a matrix support (resin) material to which a unique "ligand" (typically a small molecule such as an enzyme inhibitor or substrate) is attached (coupled) irreversibly. This is accomplished by chemical activation of the inert resin followed by the irreversible attachment of the ligand (Figure 1). Such a derivatized resin is then used for purification of a biologically active compound by AC following a three-step process as illustrated in Figure 2. These steps are (1) adsorption or reversible attachment of the protein (or macromolecule) to be purified from the mixture to the resin, (2) thorough washing of this resin, and (3) then elution or removal of the protein from the resin. Generally, the used resin can be thoroughly washed and cleaned (regenerated) and used again for the same purpose.

Why and Where AC Works

Biological macromolecules such as enzymes, polynucleotides (like DNA and RNA), antibodies, receptors, and structural proteins normally interact with chemically different but highly specific molecules by virtue of conformationally unique active sites (such as in enzymes, for substrate binding and catalysis) or binding recognition sites (as for antigens, hormones, and oligonucleotides). If one of these partners of the interacting pair (e.g., enzyme inhibitor) is immobilized on a polymeric carrier, it can be used to attract and isolate the complementary partner (e.g., the enzyme) by simply passing a cell extract containing the latter through a chromatography column packed with the immobilized molecule. Molecules without appreciable affinity for the immobilized ligand will pass unretarded through the column, whereas those capable of binding to the ligand will be retained (adsorbed). Since this binding on the column is based on reversible interactions, the adsorbed component, which is chemically and physically free in solution, will upon continued passage of buffer through the column eventually also come off the column, depending on the strength of the interaction (i.e., affinity). The affinity will depend on factors such as the intrinsic affinity, the effective concentration of covalently bound ligand, temperature, and the composition of the buffer (e.g., pH and salt concentrations). Since the adsorption process is based on the principles of classical bimolecular interactions, a very important factor is also the concentration of the interacting molecule in the solute. The concentration of this component increases progressively as more sample is run through the column, thus effectively increasing its retention on the matrix support during the process of applying the sample through the column. After washing the column, the desired biomolecule adsorbed to the column can be removed (eluted) by varying the buffer conditions.

The distinguishing feature of AC over all other techniques used in purifying macromolecules is the

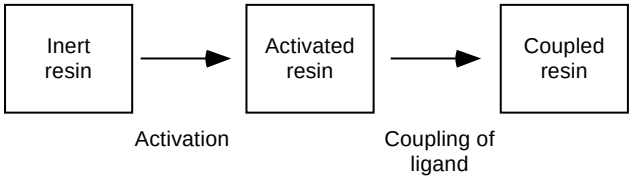

FIGURE 1 Schematic representation of the process of activation and immobilization of a specific ligand to a surface (resin) for the preparation of specific AC resins (solid supports). For the use of this resin in a purification procedure, see Figure 2.

fundamental dependence on the biological, or functional, rather than on the physicochemical (e.g., size, charge, shape, and hydrophobicity) properties of the molecule to be purified. Virtually all interacting systems consisting of two or more (e.g., when cofactors, metal ions, are essential for complex formation) components are suitable targets for affinity purification. Some of the classes of compounds which have been isolated by AC are described in Table I.

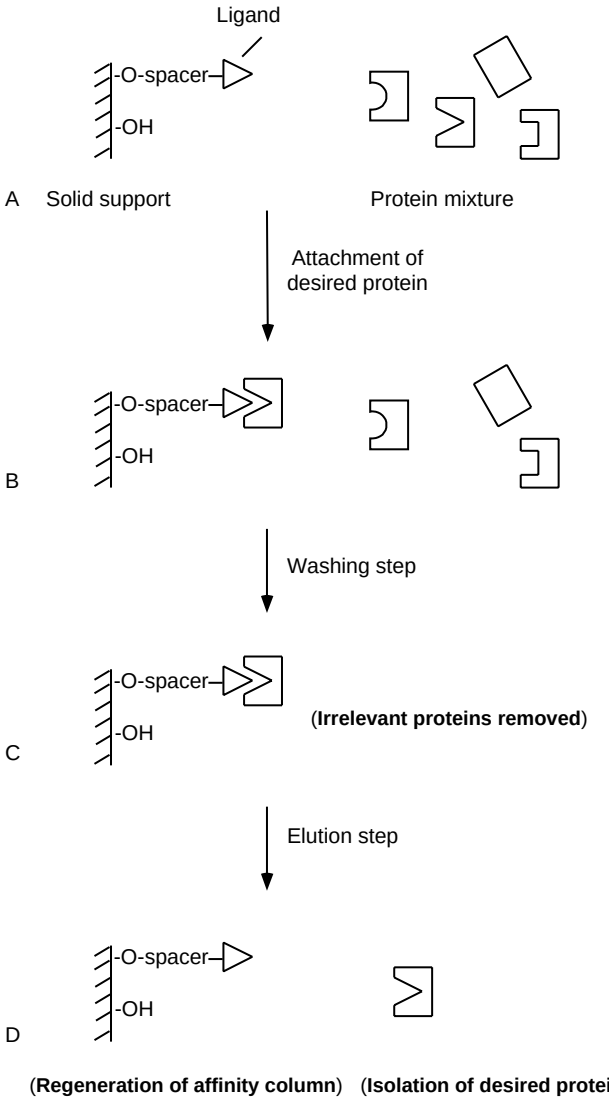

FIGURE 2 AC involves reversible attachment of a protein to a ligand. (A) The ligand is irreversibly attached to a solid support via a spacer arm; (B) Selective adsorption of a protein from a mixture of proteins; (C) The unadsorbed contaminating proteins are washed away; (D) The desired protein is eluted and recovered from the affinity matrix.

TABLE I

Some Molecular and Cellular Entities Purified by AC

Antibodies and antigens
Bacteria
Cells
Dehydrogenases
Enzymes and inhibitors
Genetically engineered proteins
Hormone-binding proteins
Lectins and glycoproteins
Receptors (soluble and membrane bound)
Regulatory enzymes
RNA and DNA (genes)
Transaminases
Viruses and phages
Vitamin-binding proteins

The Procedures Used in AC

Solid Carriers or Matrix Materials Used

Historically, nearly all of the applications of AC were performed under conditions of low pressure, using beaded particles of a size between 50 and 400 μm. A large number of macro-particle support materials for AC are commercially available. By far, the most popular support has been and continues to be agarose. Its success can be attributed not just to its inherently good qualities for AC, but also to its introduction in the initial discovery and its rapid acceptance and widespread use by the research community. Indeed, a literature survey has shown that agarose is used 90% of the time as a solid phase matrix for AC. A number of other supports have also been used successfully in applications of AC. Among these are cross-linked cellulose, trisacryl, Fractogel TSK, and silica (glass beads).

Activation of and Coupling to Carriers

There are many methods that can be used for the immobilization of ligands to polymeric support materials (carriers). A few of the more representative of these will be described briefly here. The most frequently used method (Figure 3) is the cyanogen bromide activation of agarose that leads to a highly reactive

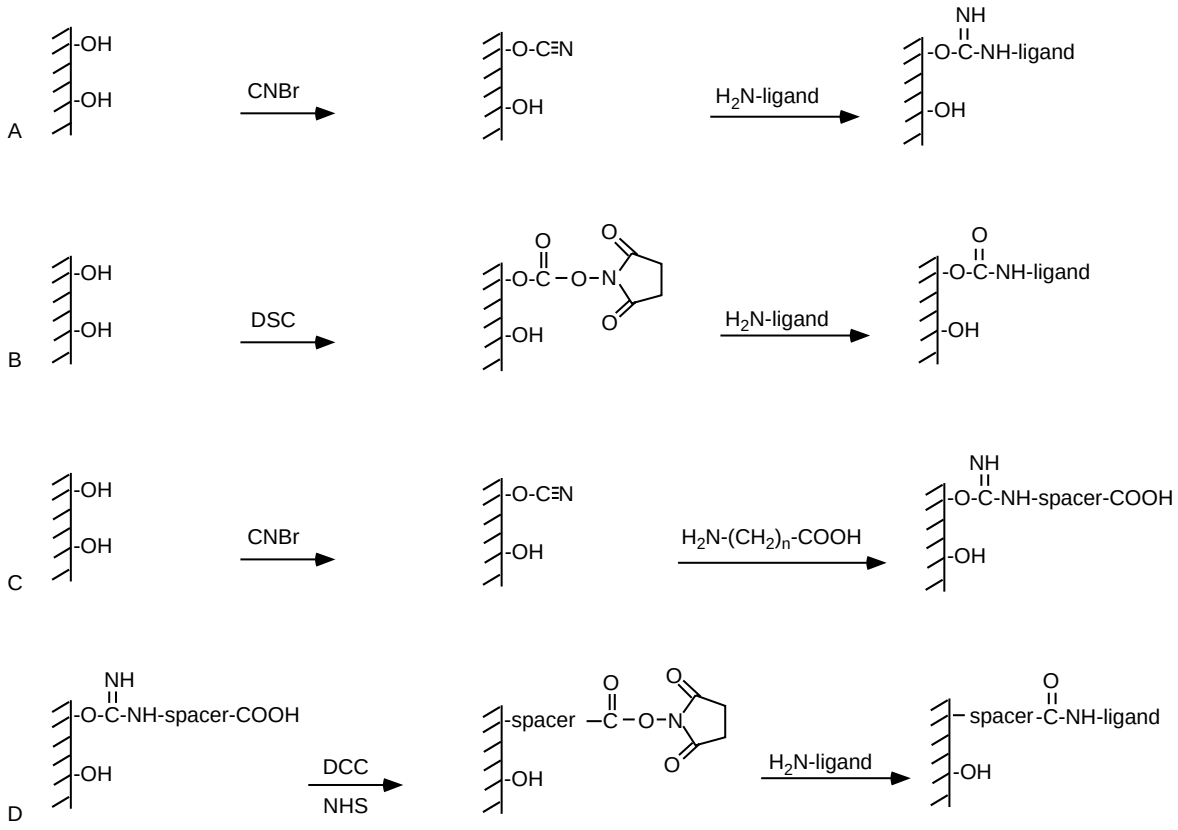

FIGURE 3 Immobilization of ligands to different activated resins. (A) Cyanate ester, obtained by activation with cyanogen bromide (CNBr), leading to isourea derivative; (B) *N*-hydroxysuccinimide carbonate obtained by activation with *N′N*-disuccinimidyl carbonate (DSC) giving a carbonate derivative; (C) Introduction of a spacer arm using *ω*-amino acids as the spacer resulting in a terminal carboxyl group; (D) Activation of carboxyl groups with dicyclohexylcarbodiimide (DCC) and *N*-hydroxysuccinimide (NHS) yielding a stable amide derivative.

cyanate ester (the activated resin is commercially available). Subsequent coupling of ligands to the activated matrix results in isourea linkages.

Since the earliest days of AC, active esters, in particular *N*-hydroxy-succinimide (NHS) esters, have also been used for immobilizing ligands (Figure 3). The preparation of active esters for subsequent coupling with primary amino group containing ligands requires a matrix that contains carboxylic acid groups. Such matrices can be prepared by activating the hydroxyl groups of agarose with various reagents, including cyanogen bromide and activated carbonates (Figure 3). Successive reaction occurs readily with ligands containing ω-amino acids of various size, depending on the length of the "spacer arm" required. The NHS ester is prepared by mixing the carboxylic matrix with dicyclohexylcarbodiimide and NHS. The covalent attachment via the amino groups of ligands proceeds spontaneously in aqueous solution, resulting in stable amide bonds.

Another method for activating polysaccharide-based polymeric supports like agarose, which contain hydroxyl groups, is the use of *N′N′*-disuccinimidyl carbonate (DSC), which forms highly reactive carbonate derivatives (Figure 3). These derivatives react with nucleophiles under mild, physiological conditions (pH 7.4), and the procedure results in a stable carbamate linkage of the coupled ligand.

Adsorption

An important step in AC is the selective extraction (adsorption) of the desired macromolecule by its unique binding to the immobilized ligand, thus removing it from the crude mixture in which it was present. The macromolecule, whether an enzyme, antibody, receptor, hormone, or growth factor, is selectively bound to the immobilized specific ligand, which can be a small synthetic or natural molecule, protein, peptide, polynucleotide, nucleotide, polysaccharide, carbohydrate, lipid, or vitamin. Functionally, such ligands may be substrate analogs or inhibitors, antibodies, antigens, coenzymes, or cofactors. The adsorption should be performed under the most favorable conditions for the interaction, including buffer pH, ionic strength, and special ions, as well as temperature. Molecules not possessing appreciable affinity for the immobilized counterpart will pass unretarded through the column.

Elution

After thoroughly washing the column (usually with adsorption buffer) the desired biomolecule can be eluted by using a buffer containing high concentrations of the same ligand (or a related one, such as a substrate instead of an inhibitor) that was used in the immobilized state. It may be necessary to stop the flow of the column for a period of time, and/or to adjust the temperature, to facilitate the ligand exchange and thus dissociation. Alternatively, the buffer composition can be changed such that the complex will no longer be stable. The buffer conditions usually changed are pH, ionic strength, metal chelators, and organic solvents. The conditions used must not result in irreversible denaturation and inactivation of the eluted macromolecule. If the macromolecule can totally recover its structure and function after total unfolding, effective and complete elution can be achieved with 6 M urea or guanidine (followed by dialysis of the eluate).

Techniques that Stem from AC

The broad scope of the basic concepts of AC has led to a wide variety of related applications. This has generated various subspecialty adaptations, many of which are now recognized by their own nomenclature, and some of which are covered by their own chapters in this volume. Here, we list some of these (Table II), and briefly discuss a few of the more exciting and recent examples.

TABLE II

Various Techniques Derived from Affinity Chromatography

Affinity capillary electrophoresis
Affinity electrophoresis
Affinity partitioning
Affinity precipitation
Affinity repulsion chromatography
Affinity tag chromatography
Avidin-biotin immobilized system
Covalent affinity chromatography
Dye-ligand affinity chromatography
High performance affinity chromatography
Hydrophobic chromatography
Immunoaffinity chromatography
Lectin affinity chromatography
Library-derived affinity ligands
Membrane-based affinity chromatography
Metal–chelate affinity chromatography
Molecular imprinting affinity
Perfusion affinity
Receptor affinity chromatography
Tandem affinity purification (TAP)
Thiophilic chromatography
Weak affinity chromatography

Immunoaffinity Chromatography (IAC)

Among the most popular of these affinity-derived technologies is IAC on antibody columns to purify antigens. The growth of IAC has been ignited by the advancements over the past decade or two in the fields of molecular biology and biotechnology. Great need has existed for purifying pharmacologically active proteins for which ligands of small molecular weight are not available. Also, antibodies can now be produced against virtually any compound. Immobilized antibodies have also been used to remove toxic components from blood by hemoperfusion through affinity resins, and for a variety of applications of solid phase radio- or fluoroimmunoassay. In the biotechnology industry, IAC is providing methods for the large scale preparation of monoclonal antibodies.

AC and DNA Recombinant Techniques

Recent advances in molecular biology permit determination of the amino acid sequences of proteins by genetic approaches. Thus, large scale isolation of the protein from its native source is often unnecessary, except of course to determine posttranscriptional modifications. Since today most proteins are produced by recombinant technology and genetic engineering, the means for their purification is usually pre-engineered by introducing a biologically active tagging element into the gene itself. Such elements include various temporary "affinity tags" or "affinity tails" such as the His-Tag, which can be purified by metal-chelate AC. FLA–TM-peptide, which consists of eight amino acids, includes both an antigenic site and an enterokinase cleavage site. This affinity tag is used to purify a fusion protein on an immunoaffinity column, and the native protein is recovered by enterokinase cleavage. Fusion proteins can also be produced containing other large proteins such as glutathione transferase, protein A, maltose-binding proteins, cellulose-binding domains, and biotinylated sequences, all of which can serve as targets for purifying the fused proteins on specific ligand affinity columns.

IAC represents a valuable complement, especially when specific ligands that are suitable for immobilization and AC are not available. Today, because of the routine use of recombinant technologies and IAC, pure proteins are so readily obtained that often their function or ligand specificity are the major unknown factors.

We have seen a shift in the challenge toward the "discovery of the ligand," whether the ligand is the naturally occurring species (e.g., what is the substrate, the hormone, or vitamin for this protein), or synthetic. This search can sometimes be achieved using either a phage display library or a combinatorial library to

screen for molecules that may display specific binding. Such a molecule, if found, can then also be used as an affinity ligand for AC. Discovery of ligands can provide insight into the unknown function of genetically coded proteins and serve as useful tools for the purification of proteins or for the discovery of novel medicinal drugs.

AC and Proteomics: Tandem Affinity Purification (TAP)

In proteomics, the study of protein–protein interactions, especially those occurring in multiprotein cellular complexes, is one of the major challenges. When mass spectrometry (MS) is used, fast and reliable methods of protein purification are necessary. The method perhaps most suitable is affinity purification based on the fusion with tags to the target protein (Tandem Affinity Purification, TAP). The TAP procedures use two different tags for more effective purification on two different affinity columns. These procedures have advantages over other approaches since all of the directly and indirectly interacting components of a protein complex of the expressed protein can be identified and purified in a single experiment. It is claimed that the TAP biphase method will be useful to characterize large, multiprotein complexes, as shown recently in studies of the functional organization of the yeast proteome. In fact, the TAP approach may represent the first real *in vivo* use of affinity purification. This system, however, is not totally without potential problems and it is important to also monitor expression levels to avoid artifacts. Other precautions include the use of immunochemistry to ensure proper cellular localization of the proteins. Another major application of TAP proteins is that they may be used in searching for interacting proteins in discrete cellular domains.

AC and Biochips

Molecular biosensors based on the affinity concepts described here have evolved over the years in remarkable ways. Recently, a number of technologies have appeared that marry AC between solid phase technologies and sensitive analytic procedures. These include protein and antibody microarrays, mass spectrometric immunoassays, surface-enhanced laser desorption–ionization spectrometry, and surface plasma resonance (SPR). In SPR, a protein, antibody, DNA, or other large macromolecule is attached to a derivatized surface (i.e., glass or metal), creating a biochip. A complex mixture of macromolecules can then be passed over the chip surface and the retained molecules can be detected using various techniques. In some cases, detection is simply a matter of positional location on an ordered array using fluorescent markers; in other cases, the retentates on the chip are desorbed and ionized by lasers. Ionized components, then, are analyzed using time-of-flight or other mass spectrometry techniques. Still in others, mass changes consequent to macromolecular interactions are detected directly using changes in the surface refractive index (by SPR).

The SPR biosensor approach also provides some other unique characteristics. These include (1) access to on- and off-rate analyses of molecular interactions and (2) analyses, in real time, of the interaction dynamics. In addition, SPR has been combined with matrix assisted time-of-flight mass spectrometry to yield a two-dimensional quantitative and qualitative analysis technique. Together, these methods provide a means to detect subtle variations in hundreds of thousands of macromolecules, including single nucleotide polymorphisms in DNA and amino acid changes, or posttranslational modifications of peptides and proteins.

See Also the Following Articles

Affinity Tags for Protein Purification • Oligosaccharide Analysis by Mass Spectrometry • Recombination-Dependent DNA Replication

Glossary

affinity tags Molecules, like vitamins, peptides, amino acids, proteins, fluorophores or inhibitors, which are incorporated structurally into a protein (often by genetic approaches) to subsequently use with affinity resins to purify (as in AC), or otherwise detect the presence of, or to quantitate, the macromolecule that is thus tagged.

chromatography A technique used to separate mixtures of substances on the basis of differences in the ability to adsorb or attach to two different media, one being mobile, which is a moving fluid, and the other being stationary, which is a porous solid or gel, or a liquid coated on a solid support. Substances are carried along by the mobile phase at different rates, depending on their solubility (in a liquid mobile phase) or vapor pressure (in a gas mobile phase) and their avidity for the solid support. Examples are adsorption, column, gas, gas–liquid, gas–solid, gel filtration, high performance liquid, ion exchange, molecular exclusion, partition, thin layer, and affinity (AC).

ligands Molecules that bind with specificity and affinity to active sites or special binding sites of macromolecules, as substrates to an enzyme or a hormones to a receptor.

resin The solid (stationary) or adsorbent in the chromatographic procedure to which molecules are attached covalently for use in AC. Referred to synonymously as solid support, matrix, polymeric support (insoluble), or carrier.

spacer arms or extension arms Linear molecules, like amino acids, diamines or polyethylene glycol (PEG), that are attached irreversibly to the resin and to which specific ligands are then attached covalently for the purpose of allowing macromolecules to interact with the ligand with less potential steric hindrance by the resin.

Further Reading

Bailon, P., Ehrlich, G. K., Funk, W. J., and Berthold, W. (eds.) (2000). *Affinity Chromatography*. Humana Press, Totowa, NJ.

Cuatrecasas, P. (1972). Affinity chromatography of macromolecules. In *Advances in Enzymology* (A. Meister ed.) Vol. 36, Wiley, New York.

Cuatrecasas, P. (1970). Protein purification by affinity chromatography. Derivatizations of agarose and, polyacrylamide beads. *J. Biol. Chem.* **245**, 3059–3065.

Cuatrecasas, P., and Anfinsen, C. B. (1971). Affinity chromatography. *Ann. Rev. Biochem.* **40**, 259–278.

Cuatrecasas, P., Wilchek, M., and Anfinsen, C. B. (1968). Selective enzyme purification by affinity chromatography. *Proc. Natl Acad. Sci.* **61**, 636–643.

Jacoby, W., and Wilchek, M. (eds.) (1974). *Methods in Enzymology*, Vol. 34, Academic Press, New York.

Matejtschuk, P. (ed.) (1997). *Affinity Separations*. Oxford University Press, New York.

Phillips, T. M., and Dickens, B. F. (2000). *Affinity and Immunoaffinity Purification Techniques*. Eaton, Boston.

Biography

Pedro Cuatrecasas is adjunct professor of Pharmacology and of Medicine at the University of California, San Diego. He received an M.D. from the Washington University School of Medicine, St. Louis. During more than twenty years, he was in charge of research and development at Burroughs Wellcome Co., Glaxo Inc., and Parke Davis/Warner Lambert Co. His research interests have included drug discovery, protein chemistry, hormone action, receptor chemistry and signal transduction.

Meir Wilchek is a professor at the Weizmann Institute of Science in Rehovot, Israel. He received his Ph.D. from the same institute and has been a frequent Visiting Scholar at the National Institute of Health, Bethesda, Maryland. His entire career has been devoted to the study of the biorecognition or "affinity" phenomenon, particularly the application of biorecognition for various purposes.

Cuatrecasas and Wilchek were the first to describe AC, over 30 years ago; they elucidated the basic principles, described the chemical procedures, and explored and suggested applications of these and related technologies.

Affinity Tags for Protein Purification

Joseph J. Falke and John A. Corbin
University of Colorado, Boulder, Colorado, USA

Selective immobilization of proteins greatly facilitates their purification, as well as their biochemical and biophysical characterization. When genetically fused to a target protein, a protein affinity tag provides a powerful tool to selectively capture and immobilize that target, in some cases providing single-step purification. Affinity tags consist of proteins or peptides with distinct amino acid sequences that are capable of a reversible, high affinity binding interaction with a specific partner molecule. The binding partner is linked to a large macroscopic particle or surface that renders it immobile, and thus it is readily amenable to manipulation. The highly specific interaction between the affinity tag and its cognate partner serves as the basis for selective capture of the target protein.

Applications of Affinity Tags

Affinity tags have proven to be tremendously effective tools for a wide variety of applications, and they are now incorporated as a standard feature to reduce the number of steps in purification protocols developed for recombinant proteins. In addition, affinity tags have become indispensable in the immobilization of proteins for display on a surface, where the tag ensures that the fusion protein of interest is oriented with its functional regions exposed to docking with other macromolecules. Affinity tags are also used to detect and quantitate target proteins and to analyze protein–protein or protein–ligand interactions. Related technologies are developing rapidly, including bioreactors for multistep enzymatic reactions and bioadsorbants for extraction or degradation of toxic contaminants.

Construction of a Fusion Protein

An affinity-tagged fusion protein typically consists of a single polypeptide chain with one or more affinity tags coupled to the C- or N-terminus of the target protein or inserted into a loop region. The coupling is via a peptide linker, usually up to 15 amino acids in length. If desired, the linker can contain a specific protease site for affinity tag removal. The use of multiple tags is increasingly common and endows the target protein with two or more unique molecular handles.

Selection Criteria for an Affinity Tag

Construction of a fusion protein begins with the selection of an affinity tag that is appropriate for the protein of interest (see below). The selection criteria include the size of the affinity tag, the organism that will be used to express the fusion protein, conditions for the immobilization or purification of the fusion protein, and the influence of the affinity tag on the structural and functional characterization of the target protein.

Affinity-Fusion Gene Constructs

To incorporate the selected affinity tag, a suitable expression plasmid vector is chosen and recombinant DNA techniques are used to insert the target gene next to the affinity tag gene. Numerous vectors are commercially available that code for a selected affinity tag and a linker peptide, the latter often containing an imbedded protease recognition sequence. Additionally, an inducible promoter is present to enhance and regulate fusion protein expression, and a multiple cloning site region is included to facilitate insertion of the target gene with the fusion site at the C- or N-terminus as desired. In some cases, the coding region for a signal peptide is included to promote the secretion of the fusion protein into a specific cellular compartment or into the extracellular medium. Newly developed vectors fuse two different tags to each terminus of a target protein, thereby allowing two-step isolation schemes with enhanced purity and ensuring that only fully intact forms of the fusion protein are isolated.

Linker Peptide Composition

The composition of the linker peptide can have a substantial impact on the function and utility of the fusion protein; therefore, a number of factors are considered during linker design. Typically, the linker is at least 5–10 residues long to allow free tumbling of

the fusion and target proteins relative to one another, thereby preventing unwanted steric hindrance to binding events. For linkers containing a proteolytic cleavage site (typically for enterokinase, factor Xa, thrombin, or tobacco etch virus (TEV)), inclusion of 5–10 flanking amino acids at both ends of the site ensures adequate accessibility to protease. Finally, the linker amino acid composition must be selected to minimize susceptibility to host organism proteases.

Overview of Fusion Protein Production and Immobilization

Purification of a recombinant fusion protein begins with the introduction of the expression plasmid into the host cell, followed by cell growth and induction of the fusion promoter. The host cells are lysed and the resulting lysate, containing the affinity-tagged protein, is incubated with a solid phase support to which the binding partner is coupled. Following binding of the tag to its immobilized partner, the support is washed to remove unbound components, yielding specific isolation of the tagged protein. If desired, the tagged protein can be released by either disrupting its interaction with the binding partner or by proteolysis of the linker region. Isolation and immobilization procedures often need to be optimized for each new affinity-tagged protein and expression host.

Features and Types of Affinity Tag Systems

The large number of affinity tags currently available offers a diverse spectrum of biochemical properties that can be exploited for protein immobilization in a variety of contexts. Affinity tags range in size from short peptides less than 1 kDa to proteins as large as 120 kDa, and they can be classified into general categories based on their binding partner interaction such as protein–ligand, polyamino acid–matrix, antigen–antibody, and protein–protein. New types of tags based on novel binding partner interactions continue to emerge at a rapid pace.

When choosing an affinity tag for a specific application, several features are considered. A subset of affinity tags possess the useful property of binding to their partner even under denaturing conditions. The ability to immobilize a tagged protein under denaturing conditions is a great advantage when the fusion protein is expressed in an insoluble or non-native form. Other tags utilize a binding partner interaction that is easily disrupted under mild conditions, thereby facilitating the recovery of target protein with full biological activity. Affinity tag size can also impact target protein function and structural integrity. Small tags generally have less impact on protein structure and function and often need not be removed, while large tags can be perturbing and thus are typically removed prior to structural and functional studies. On the other hand, certain large tags can significantly enhance the solubility of a fusion protein expressed at high levels; therefore, they are appropriate choices for the isolation of poorly soluble target proteins. Finally, when a target protein is toxic to the expression host, affinity tags that promote the aggregation of fusion protein into insoluble aggregates known as inclusion bodies are used. Key features of representative affinity tags are discussed below, and Table I presents a more comprehensive list.

Protein–Ligand Interaction Affinity Tags

Enzymes and small molecule-binding proteins are designed to bind their ligands with high specificity, thus many highly effective affinity tag systems are based on ligand-binding interactions. One of these is the widely utilized glutathione S-transferase (GST) tag (26 kDa) that binds with high specificity and low affinity ($K_D \sim 180\ \mu M$) to its substrate glutathione. Although the affinity of the GST tag for its ligand is low, commercially available immobilized glutathione matrices provide high local ligand concentrations that ensure adequate retention of the fusion protein. GST-tagged proteins are typically isolated from crude cell lysates by their interaction with immobilized glutathione on beads then eluted by competitive displacement with free, reduced glutathione. The low ligand affinity enables elution under mild, nondenaturing conditions. The GST tag often increases fusion protein solubility and stability, and it is ideally suited for overexpression of recombinant proteins in their native state. Often, the GST tag is proteolytically removed at the end of the purification due to its large size and tendency to form dimers. In other applications, the GST tag is retained and used to couple the target protein to a bead or surface for biochemical or biophysical studies.

Another family of affinity tags that relies on protein–ligand interactions are the cellulose-binding domains (CelBD). CelBDs are small, highly stable protein modules consisting of between 33 and 180 amino acids (3–20 kDa) that bind to different forms of cellulose or chitin with a broad range of affinities ($K_D \sim 0.01$ to $400\ \mu M$). CelBD fusions can be constructed with affinity tags inserted internally or linked to either the C- or N-terminus of the protein of interest. Over 180 different CelBDs have been identified, providing a spectrum of polysaccharide specificities, binding affinities, and targeting properties. Certain CelBDs bind

cellulose essentially irreversibly, making them ideal for protein immobilization, while other CelBDs exhibit easily reversible binding. Denaturing conditions or proteolysis are often needed to elute irreversible CelBDs, while reversible CelBDs can be eluted under mild conditions such as the use of a competitive ligand (cellbiose or ethylene glycol) or desorption with water. Finally, CelBDs can be selected that target the fusion protein for secretion or inclusion body formation.

The 51 amino acid chitin-binding domain (ChiBD) is derived from *Bacillus circulans* chitinase and exhibits high affinity, essentially irreversible binding to its ligand chitin, a natural carbohydrate polymer. ChiBD fusion proteins are immobilized under physiological conditions by adsorption to chitin coupled to a solid phase material. ChiBD fusion proteins often have an intein element incorporated into the linker region in place of a proteolytic recognition sequence. When remobilization of the fusion protein is desired, the intein element is activated and undergoes self-cleavage, resulting in the release of the target protein, while the intein-ChiBD region is retained on the solid phase. Similar inteins will probably soon be incorporated into the linkers of other affinity tags. Several other protein–ligand affinity tag systems are currently in use, each having unique advantages. For example, the 40 kDa maltose binding protein (MalBP) is a large tag that often increases fusion protein solubility. MalBP binds to cross-linked amylose with moderate affinity ($K_D \sim$ micromolar range), permitting MalBP tagged fusion proteins to be immobilized in a reversible fashion. The full length MalBP tag directs a fusion protein to the oxidizing *E. coli* periplasm, where MalBP is a native protein and where the fusion protein may benefit from disulfide bond formation. Alternatively, removal of the MalBP leader peptide yields retention of the fusion protein in the cytosol, where the greater volume can allow higher expression levels.

Polyamino Acid–Matrix Interaction Affinity Tags

Immobilized-metal affinity chromatography (IMAC) is a common technique used to purify recombinant proteins fused to a short peptide affinity tag. IMAC, which can be carried out under denaturing or nondenaturing conditions, relies on the interaction between multiple electron donors on the affinity tag with a transition metal ion (Co^{2+}, Ni^{2+}, Cu^{2+}, Zn^{2+}) chelated to a solid phase support. The affinity tag is typically polyhistidine, ranging 6 to 12 residues in length fused to the N- or C-terminus of the target, where "6-His" is most common and the electron donor is the histidine imidazole ring. Recently, an affinity tag based on a natural peptide derived from the N-terminus of chicken lactate dehydrogenase has also been utilized. This HAT-tag contains 6 histidine residues interspersed within a 19-residue polypeptide (KDHLI HNVHK EEHAH AHNK) that binds to specifically Co^{2+}-carboxymethylaspartate and has a lower net charge than polyhistidine tags. The most widely employed metal chelator is iminodiacetic (IDA), while nitrilotriacetic acid (NTA) and carboxymethylated aspartic acid (trade name TALON) are also popular. The chelator is generally covalently coupled to polymer beads, or ferromagnetic beads for magnetic isolation. Adsorption of IMAC tagged proteins is normally performed at neutral to slightly basic pH to ensure that the histidine imidazole groups are not protonated. Mild elution conditions include ligand exchange with imidazole, extraction of the metal ion by a strong chelator like EDTA, or proteolytic elution. Low pH will also elute, but it can sometimes denature the target protein. IMAC is not recommended for target proteins possessing a metal center, since the metal can be stripped by the binding partner chelators.

The Arg-tag is another example of a small polyamino acid affinity tag, in this case designed to raise the isoelectric point of the fusion protein to enhance its binding to a cation exchange matrix. Mild elution conditions are generally a NaCl gradient at alkaline pH. This tag also binds to flat mica sheets, which may enable a variety of new applications.

Antibody–Epitope Interaction Affinity Tags

Recombinant DNA technology has been employed to create peptide epitopes that bind well-characterized antibodies. This process is known as epitope tagging and is complementary to a more traditional approach where a novel antibody is generated for an existing epitope. Both approaches have been exploited to develop affinity tag systems based on the binding interaction between a peptide epitope and its specific antibody partner. In some cases, several antibodies with different properties are available for a given epitope. Proteins fused to peptide epitope affinity tags can be captured by immunoaffinity interactions via immobilized monoclonal antibodies. Typical epitope tags range from 6 to 30 residues in length, are highly charged, and have little effect on protein structure–function. They can be fused at either the C- or N-terminus, or even inserted within the protein of interest. Epitope tag expression vectors are commercially available for mammalian, insect, yeast, and bacterial host cells and provide a variety of tags including c-myc, FLAG, HA, T7, V5, VSV-G, recA, Protein C, Protein A, and Protein Z. Some of these are optimized for immobilization while others are primarily used for protein detection. The importance of epitope tags is illustrated by their many applications including analysis of *in vivo* protein expression,

TABLE I

Commonly Used Affinity Tags and Their Features

						Nondenaturing		
Category of tag	**Name of tag**	**Number of residues in tag**	**Size of tag (kDa)**	**Location of tag**	**Immobile phase binding partner**	**Immobilization conditions**	**Affinity tag elution conditions (eluent)**	**Expression host[a]**
Protein–ligand interactions	Glutathione S-transferase	211	26	N-Term, C-Term	Glutathione	Yes	Yes (10 mM Reduced Glutathione)	B, Y, I, M
	Cellulose-binding domains	27–189	3–20	N-Term, C-Term, Internal	Cellulose and other cellulosics	Yes	Yes (water) or No (Guanidinium HCL)	B, Y, I, M
	Maltose-binding protein	396	40	N-Term, C-Term	Cross-linked amylose	Yes	Yes (10 mM Maltose)	B
	Chitin-binding domain	51	5.6	N-Term, C-Term	Chitin	Yes	No	B
Polyamino acid–matrix interactions	Polyhistidine	6–12	0.8–1.7	N-Term, C-Term, Internal	Metal chelate	Yes or No (Denaturants)	Yes (Imidazole) or No (Low pH)	B, Y, I, M, P
	Polyarginine	5–15	0.8–2.4	C-Term	Cation-exchange resin	Yes	Yes (NaCl gradient at alkaline pH)	B, P
Antibody–epitope interactions	Hemagglutinin (HA)	9	1.1	N-Term, C-Term	IgG	Yes	No (Low pH)	Y, M
	T7	11	1.1	N-Term	IgG	Yes	No (Low pH)	B, Y, M, P, I
	Synthetic protein A (Z domain)	58	7	N-Term	IgG	Yes	No (Low pH)	B, Y, I, M, P

	FLAG	8	1.0	N-Term, C-Term	mAb M1 and mAb M2	Yes	Yes (EDTA)	B, Y, I, M, P
	c-myc	11	1.2	N-Term, C-Term	IgG	Yes	Yes (free c-myc epitope)	B, Y, I, M, P
Protein–protein interactions	Biotin	~20–100	~2–11	N-Term, C-Term	Modified avidin or streptavidin	Yes	Yes (20 mM Biotin)	B, I, M
	Calmodulin-binding peptide	26	3	N-Term, C-Term	Calmodulin	Yes (+Ca^{2+})	Yes (+EGTA)	B
	Strep-tag II	8	1.1	N-Term, C-Term, Internal	Strep-tactin	Yes	Yes (desthiobiotin)	B, Y, I, M, P
	Streptavidin-binding peptide	38	4	C-Term	Streptavidin	Yes	Yes (biotin)	B
	Thioredoxin	109	11.7	N-Term, C-Term	Phenylarsine oxide-agarose	Yes	Yes (β-mercaptoethanol)	B
	His-patch thioredoxin	109	11.7	N-Term, C-Term	Metal chelate	Yes or no	Yes (Imidazole) or No (Low pH)	B
	S-tag	15	1.8	N-Term, C-Term	S-protein	Yes	Yes (2 M Sodium Thiocyanate)	B, I, M

[a] B = bacteria; Y = yeast; I = insect; M = mammalian; P = plant.

subcellular localization of gene products, determination of protein topology, cellular trafficking studies, and the investigation of protein–protein interactions. They are also important in protein purification and immobilization.

Antibody-binding partners are covalently coupled to agarose chromatography resins or magnetic glass beads. Immobilized antibodies tend to be less stable than many other affinity-binding partners due to their need for native structure. Elution under mild native conditions can be achieved by competitive displacement with free epitope, by proteolysis, or by exposure of the Ca^{2+} dependent FLAG-tag to EDTA.

Protein–Protein Interaction Affinity Tags

Several high-affinity and high-specificity protein–protein interactions identified in biological systems have been adapted for use as affinity tags. *In vivo* biotinylation enzymatically couples biotin, a small molecule vitamin, to a protein acceptor domain. The resulting modified protein provides an interesting example of a natural affinity tag. A number of well-characterized protein sequences are enzymatically biotinylated *in vivo*. These natural peptides of approximately 100 residues have been used as fusion tags that direct *in vivo* biotinylation of a fusion protein in a site-specific manner. Additionally, shorter synthetic peptides (approximately 20 residues) known as biotin acceptor peptides (BAPs) have been developed for use as biotin affinity tags.

The high-affinity, specific interaction between biotin and either avidin or streptavidin ($K_D \sim 10^{-15}$ M) serves as the basis for immobilization. Biotin-tagged fusion proteins are typically captured by binding to monomeric avidin or streptavidin coupled to a chromatography matrix or other surface. Elution with free biotin requires harsh conditions that can be detrimental to the target protein, but proteolytic elution can be carried out under mild conditions. Alternatively, the biotin-tag fusion can be immobilized to modified forms of avidin or streptavidin that exhibit lower biotin affinity. Elution can then be conducted under nondenaturing conditions by competitive displacement with free biotin or alkaline pH.

Other examples of protein–protein affinity tags include the Strep-tag, the calmodulin-binding peptide (CalBP), and the S-tag. The Strep-tag is a nine amino acid peptide that was developed as an artificial ligand for streptavidin. Further refinements to these molecules yielded the eight amino acid peptide Strep-tag II and a mutant form of streptavidin called Strep-Tactin capable of moderate-affinity binding ($K_D \sim 1$ μM). Strep-tag fusion proteins are bound to streptavidin under physiological conditions and are efficiently displaced by free biotin or a biotin derivative. The mild conditions used for binding and elution enable Strep-fusions to be utilized in their native state. This small, stable, and nonperturbing tag is ideal for many applications in which a small tag is required, and for applications where detection of the fusion protein on a Western blot or by ELISA is desired. Moreover, since the Strep-tag is not itself a metalloprotein and its elution does not require metal chelators, it is well suited for metalloprotein applications.

The 26 amino acid calmodulin-binding peptide (CalBP) was derived from the C-terminus of skeletal muscle light-chain kinase. The CalBP binds to calmodulin with high affinity ($K_D \sim 1$ nM) in the presence of low $CaCl_2$ concentrations (≥ 0.2 mM). The binding partner, calmodulin, is commercially available linked to chromatography resins that are used to immobilize CalBP fusions. CalBP fusion proteins are eluted under mild conditions by a Ca^{2+} chelating agent such as EGTA. CalBP fusions are primarily expressed in *E. coli* that lacks calmodulin family members and thus possesses no sequences evolved to bind to calmodulin. Eukaryotic cells are not recommended for expression of CalBP-tagged proteins due to their large number of endogenous proteins (approximately 30) that bind to calmodulin.

The S-tag protein fusion system consists of the S-peptide and its binding partner the S-protein, both derived from RNAase A. The S-tag binds to the S-protein with moderate affinity ($K_D \sim 100$ nM), resulting in a strong interaction that is influenced by pH, temperature, and ionic strength. A unique feature of the S-tag system is that ribonucleolytic activity is restored when the S-peptide is bound to the 103 amino acid S-protein. This enzymatic activity is exploited to measure the molar concentration of the S-tag fusion protein down to 20 fM in a highly sensitive and rapid assay. S-protein-based reagents have been developed to probe SDS-PAGE blots for S-tag fusions employing colorimetric or chemiluminescent detection of the target protein down to nanogram quantities.

See Also the Following Articles

Affinity Chromatography • Two-Hybrid Protein–Protein Interactions

Glossary

epitope tag Short polypeptide fused to a protein of interest so that it will be recognized as a high-affinity binding target by a specific, well-characterized antibody.

fusion protein Polypeptide made from a recombinant gene consisting of two or more gene fragments fused together.

immobilized metal-affinity chromatography (IMAC) A type of affinity chromatography based on the specific interaction between a metal chelate stationary phase and a metal-binding peptide fused to a protein of interest.

Further Reading

Bornhorst, J., and Falke, J. (2000). Purification of proteins using polyhistidine affinity tags. *Methods Enzymol.* **326**, 245–254.

Jarvic, J., and Telmer, C. (1998). Epitope tagging. *Annu. Rev. Genet.* **32**, 601–618.

Nilsson, J., Ståhl, S., Lundeberg, J., Uhlén, M., and Per-Åke, N. (1997). Affinity fusion strategies for detection, purification, and immobilization of recombinant proteins. *Protein Expr. Purif.* **11**, 1–16.

Sheibani, N. (1999). Prokaryotic gene fusion expression systems and their use in structural and functional studies of proteins. *Prep. Biochem. Biotechnol.* **29**, 77–90.

Terpe, K. (2003). Overview of tag protein fusions: From molecular and biochemical fundamentals to commercial systems. *Appl. Microbiol. Biotechnol.* **60**, 523–533.

Biography

Joseph J. Falke is Professor of Chemistry and Biochemistry, and Chair of the Molecular Biophysics Program, at the University of Colorado, Boulder. His research interests are in the area of signal transduction, in particular the mechanisms of cellular chemotaxis pathways in bacterial and eukaryotic systems. He holds a Ph.D. in chemistry from the California Institute of Technology and carried out his postdoctoral research at the University of California, Berkeley. His laboratory has made fundamental discoveries regarding the molecular mechanisms of receptors and signaling proteins involved in chemical sensing.

John A. Corbin is a Postdoctoral Fellow in the Falke Laboratory at the University of Colorado, Boulder. He holds a Ph.D. in biology from the University of California, Santa Cruz. His research interests are in the general areas of protein structure, function, and mechanism.

A-Kinase Anchoring Proteins

Lorene K. Langeberg and John D. Scott
Howard Hughes Medical Institute, Vollum Institute, Oregon Health and Sciences University, Portland, Oregon, USA

The precise transmission of information from a plasma membrane receptor to the downstream target inside the cell is essential for the control of dynamic cellular functions. It has been proposed that the coordination of signaling pathways inside cells is achieved, in part, by the localization of signaling enzymes such as kinases and phosphatases near their intended protein substrates. The organization of these enzymes into signaling scaffolds facilitates the phosphorylation state of specific proteins at appropriate time and place.

Protein Phosphorylation

Protein phosphorylation is a predominant form of covalent modification of proteins inside cells. This bidirectional process, catalysed by protein kinases and reversed by phosphoprotein phosphatases, provides a flexible means of influencing the proteins that control cellular metabolism, transcription, division, and movement. The utility of this regulatory mechanism is underscored by evidence that ~30% of intracellular proteins are phosphoproteins.

Protein Kinase A

One well-studied "protein phosphorylation pathway" is regulated by the second messenger cAMP. When extracellular messengers bind to heptahelical receptors on the surface of the cell and recruit heterotrimeric G proteins to activate adenylyl cyclases on the inner face of the plasma membrane cAMP synthesis is triggered. This newly synthesized "second messenger" then diffuses to its sites of action. Although cAMP can modulate a few classes of signaling molecules, the predominant intracellular receptors are cAMP dependent protein kinases (PKA). The PKA holoenzyme is composed of two catalytic (C) subunits that are held in an inactive state by association with a regulatory (R) subunit dimer. The C subunits are expressed from three genes; Cα, Cβ, and Cγ, whereas the R subunits are transcribed from four genes; RIα, RIβ, RIIα, and RIIβ. The type I PKA (composed of RI dimers) is predominantly cytoplasmic and is most highly expressed in the immune system, whereas type II PKA (composed of RII dimers) associates with cellular structures and organelles and is abundant in the heart and brain.

Phosphorylation Specificity

One unresolved issue in cAMP signaling is the question of how this commonly used pathway is able to selectively regulate so many different cellular processes. For that reason, the mechanism by which PKA discriminates among its substrates is a topic of considerable interest. One hypothesis proposes that specific pools of the kinase are compartmentalized within the cell and are activated in close proximity to particular substrates. This can only occur if there is a means to both (1) selectively control the level of subcellular pools of cAMP and (2) maintain PKA in these environments. It has been proposed that a balance between adenylyl cyclase and phosphodiesterase activities leads to the establishment of intracellular gradients of cAMP. An equally important component of this model requires "scaffolding" proteins called "A-kinase anchoring proteins" that keep the kinase in close proximity to its substrates. This article will discuss the compartmentalization of the protein kinase A and other enzymes through their association with A-kinase anchoring proteins (AKAPs).

The PKA Anchoring Hypothesis

The first AKAPs that were identified remained tightly associated with the type II R subunits during purification from tissues and were therefore designated "RII-binding proteins". Over 30 AKAPs have now been identified and are recognized as a family of diverse proteins that are classified on the basis of their interaction with the PKA inside cells. It has also become apparent that most AKAPs share some other common properties (Figure 1). These include a common R subunit binding sequence (Figure 1A), localization regions that target the PKA/AKAP complex to precise intracellular environments (Figure 1B) and binding sites for other enzymes to form

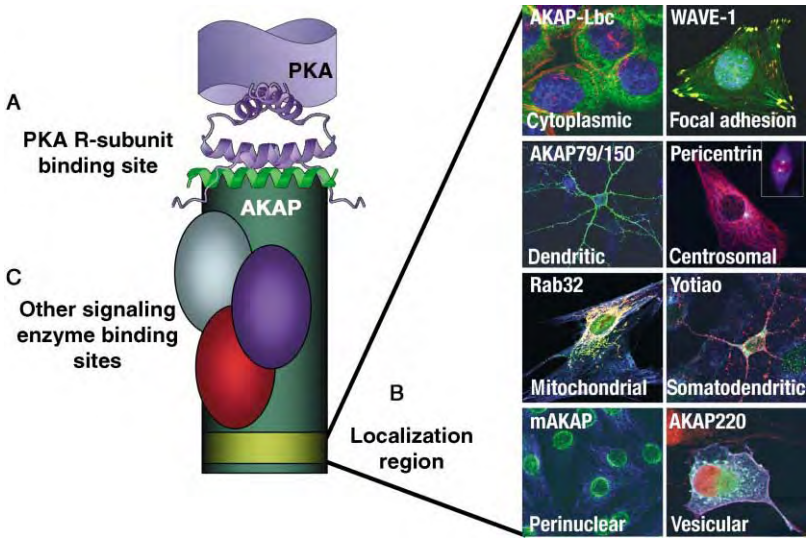

FIGURE 1 Properties of A-kinase anchoring proteins. (A) A common identifying characteristic of AKAPs is a protein–protein interaction site that binds to protein kinase A. The amphipathic helix of the AKAP (green) tightly associates with the regulatory subunit amino terminal dimer of PKA (purple). (B) The localization region of the AKAP (yellow) is responsible for the precise subcellular targeting of the scaffold. Here we show the subcellular staining pattern for eight different AKAPs (in green, or yellow and white when colocalized with other stained proteins) found at distinct locations within the cell. (C) Multiple signaling enzymes associate with an AKAP via protein–protein interactions, nucleating a unique signaling complex for efficient signal transmission.

signaling complexes (Figure 1C). Each property is discussed here.

Protein Kinase A Binding

RII Subunit Binding Sequences

Most AKAPs contain a short sequence that forms a binding site for the R subunit dimmer and was first recognized in the human thyroid anchoring protein, AKAP-Lbc. The region likely forms an amphipathic helix that slots into a binding pocket formed by the amino terminal regions of RII. This view is supported by evidence that a 24-amino acid peptide encompassing this region, called Ht31, binds RII with low nanomolar affinity. Cellular delivery of this peptide antagonizes PKA anchoring and has become a standard means to delineate a role for AKAPs in the coordination of cAMP-responsive events. Recently, a new and improved anchoring inhibitor peptide has been developed from a comprehensive analysis of 10 AKAP sequences. This 17-amino acid peptide, called "AKAP-is", selectively binds RII with subnanomolar affinity, efficiently disrupts PKA anchoring inside cells, and functions to block cAMP signaling to glutamate receptor ion channels in cells.

RI Subunit Binding

Although most AKAPs associate with the type II PKA, it is now clear that some anchoring proteins also target the type I kinase. Yeast two-hybrid screening and affinity purification techniques have identified anchoring proteins that can interact with either RI or RII (designated dual function AKAPs) and, in a few instances, RI selective AKAPs have been reported. Apparently, RI anchoring also proceeds through an amphipathic helix although other determinants may contribute to the compartmentalization of the type I PKA holoenzyme. Recently, a single nucleotide polymorphism (SNP) that causes a valine to isoleucine mutation in the anchoring helix of D-AKAP-2 has been shown to increase RI-binding affinity threefold. Although the functional ramifications of this valine to isoleucine change are unclear it is more prevalent in the aging population. Detailed structural analyses will be necessary to define the differences between type I and type II PKA anchoring.

Anchoring Protein Targeting Regions

While protein–protein interactions are responsible for the precise orientation of the kinase toward its substrates, it appears that protein–lipid interactions target the AKAP–PKA complex to the correct intracellular membranes and organelles. In the brain for example, repeat sequences that bind negatively charged phospholipids tether an AKAP called AKAP79/150 to the inner surface of synaptic membranes. In addition, protein–protein interactions with SAP97, an adapter protein that binds to the cytoplasmic tail of the AMPA

receptor ion channel, places the AKAP79/150-PKA complex in the vicinity of substrates. This elaborate molecular bridging facilitates the PKA phosphorylation of serine 845 in the cytoplasmic tail of GluR1. Serine 845 is an important regulatory site on the channel that is modified during chemically induced long term potentiation (LTP). The AKAP79/150 complex also includes the phosphatase PP2B which functions to dephosphorylate serine 845 leading to attenuation of GluR1 channels. In fact, peptide disruption of the PP2B-AKAP79/150 interaction prevents efficient dephosphorylation of the channel and suggests that targeting of the phosphatase with its substrate is necessary for modulation of channel activity. In a similar manner myristoylation and palmitoylation signals facilitate the protein–lipid tethering of another AKAP, AKAP15/18 in close proximity to PKA substrates such as calcium channels and sodium channels. AKAP15/18 may also be cross-linked to the α_1-subunit of the L type Ca^{2+} channel via a modified leucine zipper motif.

There are instances where multiple AKAPs mediate PKA targeting to the same organelle. Three anchoring proteins (D-AKAP-1/AKAP149, D-AKAP-2, and Rab32) anchor PKA at mitochondria, two AKAPs (AKAP350-450/CG-NAP and pericentrin) tether the kinase to centrosomes whereas Ezrin, WAVE-1 and AKAP-Lbc tether PKA to distinct areas of the actin cytoskeleton. One explanation for these apparent redundancies may be the need to always maintain an anchored pool of PKA at certain sites. Alternatively, each compartment specific AKAP may direct the kinase to different microenvironments where specific substrates reside. Thus, compartmentalization of PKA is likely to be a more finely organized process than was initially appreciated.

Scaffolding Complexes

Multiple Enzyme Pathways

Perhaps the most important feature of AKAPs is their ability to simultaneously interact with several signaling proteins (Figure 1C). By localizing PKA with enzymes such as protein phosphatases, phosphodiesterases, G proteins, and other protein kinases, AKAPs provide focal points for the integration and processing of distinct intracellular signals. The notion was first proposed for the AKAP79/150 family, which maintains PKA, protein kinase C (PKC) and the phosphatase PP2B at the synaptic membrane. Subsequently, it has been shown that most, if not all, AKAPs nucleate signaling protein networks. For example, Yotiao, AKAP220, and AKAP149, tether protein phosphatase 1 to oppose the action of anchored kinases. This creates an environment where protein phosphorylation is only favored when kinase activity is sufficiently stimulated to overcome these basal dephosphorylation events. One variation on this theme occurs when signal termination enzymes that act upstream of protein kinases are recruited to AKAP signaling complexes. For example, AKAP450 and mAKAP co-localize a cAMP-metabolizing enzyme, the phosphodiesterase PDE4D3, with PKA. This creates a local environment where PDE activity reduces cAMP levels in the vicinity of the kinase. Presumably, these signaling complexes not only contribute to the formation of intracellular gradients of cAMP but also confer temporal control on PKA activation by generating pulses of kinase activity.

Parallel Signaling Pathways

Other AKAP complexes are known to participate in the parallel processing of distinct intracellular signals. In the brain WAVE-1 is a scaffolding protein that principally functions to relay signals from the plasma membrane via the small molecular weight GTPase Rac to the Arp2/3 complex, a group of seven related proteins that nucleate actin polymerization and branching to facilitate remodeling events in the cytoskeleton. However, WAVE-1 also anchors PKA and binds to the Abelson tyrosine kinase (Abl). Proteomic approaches have identified additional binding partners that are positive and negative regulators of WAVE-1 function and substrates for either kinase. Thus WAVE-1 is capable of recruiting different combinations of signaling enzymes to the neuronal cytoskeleton for control of distinct protein phosphorylation and actin-remodeling events. This multifaceted role is reflected in the complex phenotype of WAVE-1 knockout mice which exhibit abnormalities in their brain morphology as well as behavioral defects that may be linked to altered signaling in the cerebellum or hippocampus.

Alternatively Spliced Scaffolds

The AKAP350/450/CG-NAP/Yotiao family arise from alternative splicing of a single gene on chromosome 7q21. At least four anchoring proteins that are targeted to three distinct subcellular locations are transcribed from this gene. Initially a cDNA was isolated that encodes a 350 kDa protein believed to be a high molecular weight AKAP previously identified in centrosomal fractions. Around the same time variants encoding AKAP450 and CG-NAP were identified. The latter protein was named CG-NAP on the basis of its detection in centrosomal and Golgi fractions. Detailed analysis of CG-NAP has identified additional binding partners that include protein phosphatase 2A, the Rho-dependent-protein kinase PKN and the protein kinase C epsilon isoform. Functional studies propose that enzymes in this signaling complex may participate in membrane trafficking, microtubule nucleation and/or cell cycle progression.

Yotiao, the shortest splice variant in this family is targeted to synaptic sites where it anchors PKA and the type 1 protein phosphatase PP1 to regulate the phosphorylation state of NMDA receptor ion channels. Tonic PP1 activity negatively regulates NMDA receptors by favoring the dephosphorylated state. However, upon PKA activation the PP1 activity is overcome and the channel is phosphorylated resulting in increased NMDA receptor currents. More recently a requirement for yotiao targeting of PKA and PP1 to GABA(A) receptors at inhibitory synapses has been demonstrated in the dopaminergic regulation of cognitive processes. Thus, AKAP350/450, CG-NAP and yotiao organize PKA and a plethora of signaling enzymes in a variety of subcellular locations. Transcriptional regulation is undoubtedly a critical determinant for location and composition of each signaling complex maintained by these AKAP gene products.

Understanding the Function of Scaffolds

An emerging area of investigation is the genetic manipulation of AKAPs. Although several anchoring proteins have been identified in genetically tractable organisms including *C. elegans*, *D. melanogaster*, and *D. rerio* (zebrafish) the most significant advances have come from the characterization of genetically modified mice. Genetic disruption of the MAP2 gene causes a redistribution of the PKA holoenzyme in neurons that limits certain cAMP responsive phosphorylation events and causes reduction in dendrite length. In a similar manner disruption of the WAVE-1 gene has apparent effects on brain morphology and effects complex neuronal behaviors including coordination, balance, learning, and memory. These observations complement previous evidence that ablation of PKA subunit genes alters hippocampal-based forms of learning and memory.

Traditionally, these anchoring molecules were thought to exclusively control cAMP responsive events. However AKAP-mediated compartmentalization of other signaling enzymes may be an equally important function. Recent reports have implicated AKAP350/CG-NAP, AKAP220 and WAVE-1 networks in the control of Rho kinase signaling, glycogen synthase kinase 3 action and Rac mediated actin remodeling respectively. As the detailed dissection of these AKAP signaling complexes progresses it seems probable that their role in the coordination of both cAMP dependent and independent signaling events will become more evident.

See Also the Following Articles

Cyclic Nucleotide-Dependent Protein Kinases • Cyclic Nucleotide Phosphodiesterases • Glycogen Synthase Kinase-3 • Protein Kinase C Family

Glossary

cytoskeleton The complex network of actin microtubules and microfilaments in the cytoplasm that provide structure to the cytoplasm of the cell and plays an important role in cell movement and maintaining the characteristic shape of the cells.

phosphorylation/dephosphorylation The activation of an enzyme by the addition of a phosphate group to the enzyme or the inactivation of an enzyme by the removal of a phosphate group from the enzyme.

protein kinase The enzyme that catalyzes the transfer of phosphate from ATP to the hydroxyl side chains of a protein causing changes in the function of the protein.

protein phosphatase An enzyme that catalyzes the removal of phosphate from a phosphorylated protein, thereby causing changes in the function of the protein.

receptor Proteins located either on the cell surface or within the cytoplasm that bind ligand, initiating signal transduction and cellular activity.

scaffold A protein that serves as a platform to bring together a unique assortment of signaling enzymes for the efficient transmission of intracellular messages.

Further Reading

Bauman, A. L., and Scott, J. D. (2002). Kinase- and phosphatase-anchoring proteins: Harnessing the dynamic duo. *Nat. Cell Biol.* **4**(8), E203–E206.

Cohen, P. (2000). The regulation of protein function by multisite phosphorylation – A 25 year update. *Trends Biochem. Sci.* **25**(12), 596–601.

Colledge, M., and Scott, J. D. (1999). AKAPs: From structure to function. *Trends Cell Biol.* **9**(6), 216–221.

Hunter, T. (1995). Protein kinases and phosphatases: The yin and yang of protein phosphorylation and signaling. *Cell* **80**, 225–236. (January 27).

Pawson, T., and Nash, P. (2000). Protein–protein interactions define specificity in signal transduction. *Genes Dev.* **14**(9), 1027–1047.

Pawson, T., and Scott, J. D. (1997). Signaling through scaffold, anchoring, and adaptor proteins. *Science* **278**, 2075–2080.

Scott, J. D., and Pawson, T. (2000). Cell communication: The inside story. *Sci. Am.* **282**(6), 72–79.

Skalhegg, B. S., and Tasken, K. (2000). Specificity in the cAMP/PKA signaling pathway. Differential expression, regulation, and subcellular localization of subunits of PKA. *Front Biosci.* **5**, D678–D693.

Biography

Lorene K. Langeberg earned her B.A. from the University of Colorado at Boulder followed by work with Jon Lindstrom at The Salk Institute. She moved to John Scott's laboratory at the Vollum Institute in 1992 and is currently a Research Specialist with the Howard Hughes Medical Institute.

John D. Scott received his Ph.D. in Biochemistry from the University of Aberdeen prior to postdoctoral work with Edwin Krebs at the University of Washington. In 1990 he joined the faculty at the Vollum Institute at Oregon Health and Science University where he is now a Senior Scientist and an Investigator with the Howard Hughes Medical Institute.

Allosteric Regulation

Barry S. Cooperman
University of Pennsylvania, Philadelphia, Pennsylvania, USA

Allosteric regulation refers to the process for modulating the activity of a protein by the binding of a ligand, called an effector, to a site topographically distinct from the site of the protein, called the "active site," in which the activity characterizing the protein is carried out, whether catalytic (in the case of enzymes) or binding (in the case of receptors) in nature. The word allosteric, Greek for "other site," was coined to emphasize this distinctness. The modulation of protein activity is accomplished by the reversible alteration of the protein conformation that accompanies effector binding. Effectors that increase activity are called activators, while those that decrease activity are called inhibitors. For the purposes of this article we will use the term substrate to indicate a ligand bound to the active site of either an enzyme or a receptor that undergoes the characteristic activity of the protein.

Allosterism and Cooperativity

Allosteric regulation has been found to be extensive in proteins, particularly in enzymes at key branch points of metabolism and in receptors that must be sensitive to small variation in signals. Although a monomeric protein having one subunit can display allosteric regulation, the great majority of proteins regulated in this manner have multiple subunits, with changes in activity arising from changes in subunit–subunit contacts. A characteristic feature of these regulatory proteins is the occurrence of cooperative interactions for both the substrate and the regulatory ligand. This property renders their function dependent upon threshold concentrations of ligand.

Cooperative Binding of O_2 to Hemoglobin

Cooperativity may be defined as any process in which an initial event affects subsequent similar events. It was initially identified with the sigmoid plot for the binding of four molecules of O_2 to hemoglobin (Hb) (Figure 1), a pseudotetrameric protein that gives red blood cells their color. A similar cooperativity of substrate binding occurs in many allosteric enzymes, leading to sigmoid plots of enzyme activity versus substrate concentration. Hb has the subunit composition $\alpha_2\beta_2$, in which the α- and β-subunits are nearly identical to one another, with each containing a heme group to which O_2 binds. The sigmoid plot was explained by the concept that the first molecule of O_2 bound makes it easier for subsequent molecules to bind, and so is an example of positive cooperativity. In fact, if the Hb-binding curve is fitted to four successive binding constants, the affinity for the fourth O_2 bound is calculated to be 100–1000 times as high as the first O_2 bound. In contrast, O_2 binding to myoglobin (Mb), a monomeric protein found in vertebrate muscle with no possibility for site-site interaction, follows a rectangular hyperbola plot.

An essential feature of the positive cooperativity, shown in Figure 1 for Hb, is that it sharpens the responsiveness of a system to a change in substrate (or effector) concentration. Thus, to go from 10% to 90%, O_2 saturation of Mb requires an 81-fold change in O_2 concentration, whereas the corresponding change for O_2 saturation of Hb requires only a fourfold change. Such responsiveness is obviously desirable in a protein whose activity must be highly regulated.

The Hill *n*, a Measure of Cooperativity

The Hill plot linearizes saturation data over the major portion of the saturation curve (typically 10–90% saturation) yielding a slope, called the Hill n and denoted n_H, which provides a convenient empirical measure of cooperativity. If we define the saturation function Y_S as the fraction of all binding sites containing a bound ligand (i.e., $0 \leq Y_S \leq 1$) then the Hill plot is obtained by plotting $\log(Y_S/(1 - Y_S))$ versus $\log [S]$ (when enzyme activity is measured, $\log(v/(V_{max} - v))$ versus $\log [S]$ is plotted instead). The value of n_H is one for a noncooperative saturation function (e.g., O_2 binding to Mb). Positive cooperativity is defined by an $n_H > 1$, with an upper limit of n, the number of identical subunits, for a cooperative saturation function. For a tetramer, an n_H equal to its upper limit of 4 would correspond to the situation where there were only two protein species in solution, one with no ligands bound

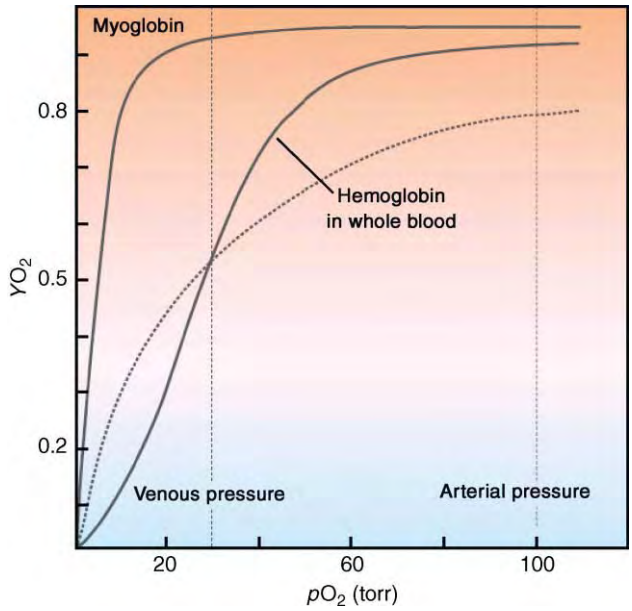

FIGURE 1 The O_2 binding curves for Hb (cooperative) and Mb (noncooperative). The dashed line represents a noncooperative curve for O_2 binding having the same value as Hb for the O_2 pressure (pO_2) required for half-saturation ($YO_2 = 0.5$). Adapted from Voet, D., Voet J. G., and Pratt, C. W. (2002) *Fundamentals of Biochemistry*. Wiley, New York.

and with ligands bound to all four sites. For Hb, a strongly cooperative tetramer, the n_H value is near 3 under physiological conditions. Some allosteric proteins have $n_H < 1$, i.e., have negative cooperativity. In contrast to positive cooperativity, negative cooperativity gives a less sensitive response over a broad range of stimulus and might be important, for example, in the response of growth or general metabolism to changes in hormone concentration.

One caveat to the use of n_H values evaluated from enzyme activity studies is that hysteresis or ligand-induced slow transitions that have the same timescale as the catalytic cycle can give rise to apparent cooperativity, even for monomeric enzymes. In addition, n_H values of < 1, whether determined by binding or enzyme activity studies, can arise from sample heterogeneity, rather than from true negative cooperativity.

Two-State Models to Explain Cooperativity in Allosteric Proteins

Two models were proposed in the 1960s to explain not only the cooperative binding of O_2 to Hb, and of substrate binding to allosteric proteins in general, but also the effects of allosteric effector molecules on substrate binding. Each of the models posits that the identical subunits within the protein can exist in two states, T and R, with the R state having higher activity for substrate. Here some definitions are in order before proceeding further. O_2 binding to hemoglobin is an example of a "positive homotropic effect," since the initial binding of O_2 increases the affinity for subsequent O_2 molecules. On the other hand, addition of the allosteric inhibitor 2,3-diphosphoglycerate reduces O_2 affinity for Hb, providing an example of a "negative heterotropic effect." In a similar fashion, an allosteric activator which increases substrate affinity gives rise to a positive heterotropic effect, whereas a negative homotropic effect is seen when initial binding of substrate decreases the affinity for subsequent substrate molecules.

The first model, proposed by Monod, Wyman, and Changeux in 1965, and known as the MWC (or symmetry) model hypothesizes that: (1) allosteric regulatory proteins, in general, are oligomers made up of a finite number of identical subunits that occupy equivalent positions and, as a consequence, possess at least one axis of rotational symmetry; (2) the allosteric oligomers can exist in two freely interconvertible and discrete conformational states (T or R) that differ in the energy of their intersubunit interactions, but in which molecular symmetry is conserved, so that all subunits are either in the T state or the R state; (3) in the absence of ligand, the pre-existing conformational equilibrium is characterized by an allosteric constant $L = (T_n)/(R_n)$, where n is equal to the number of identical subunits; and (4) ligand affinities for the active and allosteric sites carried by the oligomers may differ between the two states, allowing ligand binding to preferentially stabilize the state for which it exhibits a higher affinity. Such modulation of the conformational equilibrium by ligand binding suffices to generate positive homotropic effects and both positive and negative heterotropic effects.

The second model, proposed by Koshland, Nemethy, and Filmer in 1966, and known as the KNF (or sequential) model, hypothesizes that in the absence of ligand the protein exists in a single state, that ligand binding induces a conformational change only in the subunit to which it binds, and that cooperative interactions arise through the influence of such conformational changes on intersubunit interaction. The KNF model embodies the notion of "induced fit," whereby the binding of substrate to an active site causes conformational changes of active site residues that are necessary for the protein's function. Since conformational change only occurs on ligand binding, partially saturated protein contains a mixture of R and T states, so that the symmetry of the oligomeric protein is not preserved during the binding process.

Both the MWC and KNF models are limiting cases of the more general scheme of a two-state model, as shown for the case of substrate binding to a tetrameric protein in Figure 2. In the MWC model only species corresponding to the left-most ($T_nS_i, i = 0 - n$) and right-most

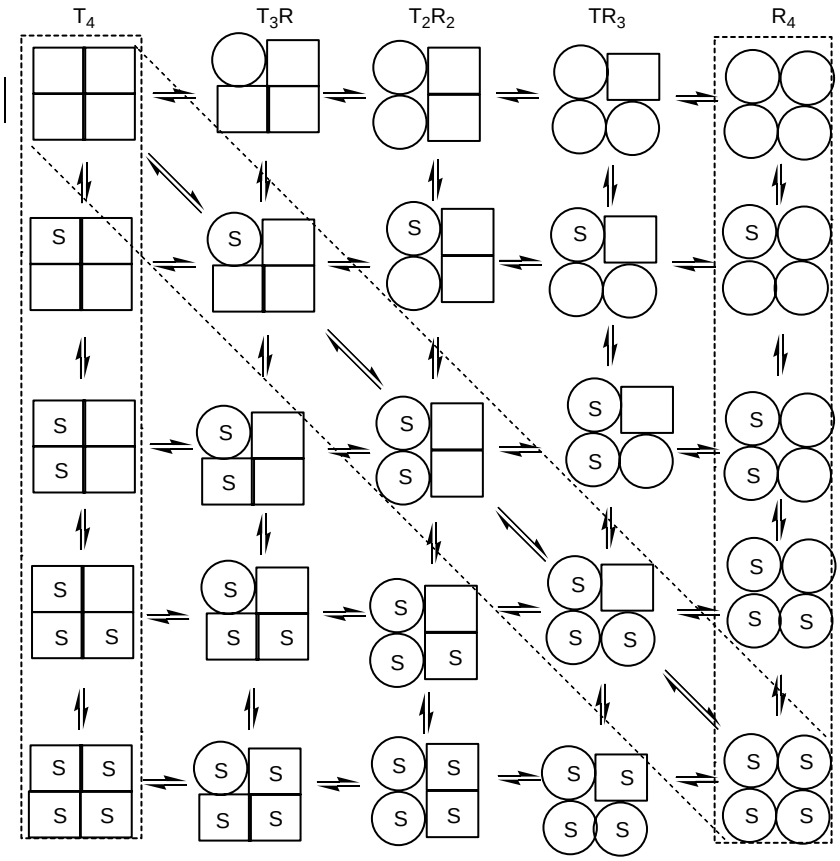

FIGURE 2 The general two-state model for substrate binding to an allosteric tetrameric protein. The columns on the left and right show the species included in the MWC model. The diagonal from upper left to lower right shows the species included in the KNF model.

($R_nS_i, i = 0 - n$) columns are considered, because it is posited that hybrid states containing both R- and T-subunits are inherently unstable and do not accumulate. In contrast, in the KNF model only species lying along the diagonal connecting T_n to R_nS_n (i.e., $T_{n-i}R_iS_i, i = 0 - n$) are considered, because of the requirement that conformational change only results from substrate binding.

Either limiting model generates the sigmoidal saturation curve for substrate binding to an allosteric protein using just three parameters. For the MWC model these are L, the allosteric constant, and K_T and K_R, the dissociation constants for S binding to the T and R states, respectively. In the KNF model the three parameters are K_SK_t (as a product), K_{RT}, and K_{RR}, where K_S is the binding constant for substrate to the R state, K_t is the equilibrium constant for changing a single, isolated, subunit from the T to the R conformation (= [R]/[T]) and K_{RT} and K_{RR} measure the relative strength of associations of $R-T$ and $R-R$ intersubunit contacts, respectively, versus the strength of association of $T-T$ intersubunit contact. In the two models, allosteric effectors exert their heterotropic effects by altering the apparent conformational equilibrium constant (L' or K_t') in each model, with inhibitors, which bind T state preferentially, increasing L' or decreasing K_t' and activators, which bind R state preferentially, decreasing L' or increasing K_t'.

Because of their relative simplicities, both the MWC and KNF models provide useful frameworks for the analysis of allosteric proteins, although, in detail, each enzyme studied may show deviations. In some cases one model may be preferred over the other. Thus, the MWC model does not account for negative homotropic effects ($n_H < 1$), whereas such effects can arise in the KNF model when K_{RT} is substantially greater than either K_{TT} or K_{RR}. On the other hand, the MWC predicts that the state function R, which measures the fraction of all subunits in the R state, will, in general, increase more rapidly as a function of substrate concentration than the saturation function Y_S, since the binding of one substrate molecule can shift all the subunits in T_n to the R_n conformation. In contrast, the KNF model demands that R is always equal to Y_S. Experimental examples have been found for both negative homotropic cooperativity and for $R \neq Y_S$. Detailed examination of structural or energetic changes on partial ligand binding have been used to differentiate between the two models.

Extensions and Modifications of Two-State Models

When ligand binding induces a change in the oligomeric state of the protein, cooperativity can result as a direct consequence of ligand binding preferentially to either the associated or dissociated form. If, for example, substrate binding favors a higher state of oligomerization, then higher enzyme concentrations will enhance activity but depress cooperativity, and, at constant enzyme concentration, allosteric ligands that favor association will be activators while those that favor dissociation will be inhibitors. The equations to account for this type of behavior are similar in form to those generated by either the MWC or KNF models, but with the addition of terms that are dependent on protein concentration.

Thus far, we have considered allosteric proteins in which the substrate and effector molecules have different affinities for the *R* and *T* states. These are the so-called *K* (binding constant) systems. In pure *K* allosteric enzymes, the *T* and *R* states have identical V_{max} values. However, allosteric enzymes can also be regulated by *V* (velocity) systems. In pure *V* allosteric enzymes, the *R* and *T* states have identical affinity for substrate but different V_{max} values. In both *K* and *V* enzymes an effector functions by binding preferentially to the *R* or *T* state. For *K* systems, such binding results in altered affinity and cooperativity of substrate binding. In *V* sytems, effector binding results in altered V_{max} values, and there is no cooperativity in substrate binding.

Structures of Allosteric Proteins

High-resolution structures have been determined for a number of allosteric enzymes in both the *R* and *T* states, permitting some generalizations to be made and allowing critical consideration of the MWC and KNF models. One common finding is that ligand-binding sites, both active site and regulatory, are located at subunit interfaces. Such placement provides an exquisite means of communicating cooperative and/or allosteric effects between subunits in an oligomeric enzyme, since sites at the interface are likely to respond to the changes in subunit interactions that are critical for allosteric regulation. For similar reasons, a second common location for ligand binding is at the interface of two domains within same subunit. Placement of the active site at either interface has as a consequence that even modest conformational changes can cause significant changes in the size and shape of the active site, thus altering the protein's activity. Allosteric binding sites also tend to be located in low-stability regions of the protein. The binding of an effector stabilizes both the region itself and specific contacts the region makes with adjacent regions, requiring the movements of polypeptide backbone and side chains, and, in particular, the alteration of salt bridges and hydrogen bonds at subunit interfaces. These movements provide a mechanism for transmission of signals to the active site and to other allosteric sites over distances of tens of angstroms. Other common features are: (1) small but critical movements at the active site; (2) the rotation of subunits with respect to one another around a cyclic axis; (3) only two modes of subunit:subunit docking, consistent with the MWC model of concerted transition; and (4) a more highly constrained and extensive subunit interface in the less active *T*-state than in the *R*-state.

Examples of Allosteric Proteins Other than Hemoglobin

Aspartate Transcarbamoylase (ATCase)

ATCase catalyzes a key step of pyrimidine biosynthesis, the condensation of carbamoyl phosphate with aspartate to form N-carbamoylaspartate. The *Escherichia coli* enzyme has been extensively studied. CTP is an allosteric inhibitor representing a classic case of feedback inhibition whereby the end product of a biosynthetic pathway inhibits an enzyme catalyzing a reaction at the beginning of the pathway. ATP is an allosteric activator, and together CTP and ATP act on ATCase to coordinate the rates of purine and pyrimidine nucleotide biosynthesis. The enzyme has the subunit composition c_6r_6, where *c* and *r* are catalytic and regulatory subunits, respectively. The *c* subunits are arranged as two c_3 s, which are complexed with three r_2 s. In the absence of *r* subunits, the *c* subunits are catalytically active, and are unaffected by ATP or CTP, which bind only to the *r* subunit. Crystal structures have shown that the c_6r_6 holoenzyme exists in two conformations, with CTP preferentially binding to the inactive *T*-state and ATP to the active *R*-state. Interestingly, ATP and CTP bind competitively to the same allosteric site in the *r* subunit. CTP binding induces a contraction in r_2, which in turn, via interactions at the $r-c$ interface, results in the c_3 s moving together by 0.5Å. This movement causes a perturbation of the active site and a loss in catalytic activity. In contrast, ATP binding results in the c_3 s moving apart by 0.4Å.

Ribonucleotide Reductase (RR)

RRs form a family of allosterically regulated enzymes that catalyze the conversion of ribonucleotides to deoxyribonucleotides and are essential for *de novo* DNA biosynthesis. Their allosteric regulation is designed to match the flux of the four deoxynucleotides produced with the base composition of the organism's DNA.

Class Ia RRs are the most widespread in nature. They accept the four common nucleoside diphosphates (NDPs) as substrates, with enzymatic activity dependent upon the formation of a heterocomplex between subunit R1, which contains the active site and three allosteric sites (the s-, a-, and h-sites), and subunit R2, which contains a stable tyrosyl-free radical that is necessary for NDP reduction at the active site. The substrate specificity of RR is determined by the allosteric ligand occupying the s-site. ATP and dATP stimulate the reduction of CDP and UDP, dTTP stimulates the reduction of GDP and dGTP stimulates the reduction of ADP. The s-site is located at the interface between R1 monomers, such that effector binding drives formation of $R1_2$. The regulation of total enzyme activity is controlled by ATP and dATP, chiefly at the level of changes in oligomerization state. Both bind to the a-site, located at the interface between two $R1_2$ s, driving formation of $R1_4$, which exists in two conformations, $R1_{4a}$ and $R1_{4b}$, with the latter predominating at equilibrium, while only ATP binds to the h-site, which drives formation of $R1_6$. Only the $R2_2$ complexes of $R1_2$, $R1_{4a}$, and $R1_6$ are enzymatically active. dATP is a universal inhibitor of RR activity due to its induction of $R1_{4b}$ formation whereas ATP is a universal activator because it induces $R1_6$ formation. Class II RRs, which are only found in bacteria, are considerably simpler, comprising only a monomeric protein containing an active site, an s-site and a B_{12} cofactor. Interestingly, the active site and s-site have the same relative orientations as in Class Ia, with the s-site located at an interdomain interface.

GroEL

E. coli GroEL is an example of a chaperonin, which mediates protein folding in an MgATP-dependent manner. GroEL consists of 14 identical subunits that form two heptameric rings. Cooperativity in ATP binding and hydrolysis by chaperonins reflects the switching of rings between protein-binding and protein-release states and is important for regulation of their reaction cycle. GroEL displays two levels of allostery: one within each ring and the second between the two rings. In the first level of allostery, each heptameric ring is in equilibrium between T and R states that interconvert in a concerted manner, in accordance with the MWC model. In the absence of ligands, GroEL is predominantly in the T_7T_7 state. In the presence of low concentrations of ATP ($<100\ \mu$M), the equilibrium is shifted toward the T_7R_7 state, displaying positive cooperativity in ATP binding and hydrolysis. A further shift in the equilibrium from the T_7R_7 state to the R_7R_7 state ($L2 = [RR]/[TR]$) takes place only at higher ATP concentrations because of inter-ring negative cooperativity. This second level of allostery is better described by the KNF model.

Cell-Surface Receptors Involved in Signal Transduction

Membrane receptors for transmitters, peptides, and pharmacological agents are central to signal transduction. They selectively recognize chemical effectors (neuronal or hormonal) and allosterically transduce binding recognition into biological action though the activation of ligand-gated ion channels (LGICs) and/or G-protein-coupled receptors (GPCRs). Various features of membrane receptors for neurotransmitters are well accommodated by the MWC model. These receptor proteins are typically heterooligomers and exhibit transmembrane polarity. In general, the regulatory site to which the neurotransmitter binds is exposed to the synaptic side of the membrane while the biologically active site is either a transmembrane ion channel, a G protein-binding site, or a kinase-catalytic site facing the cytoplasm. Interactions between the two classes of sites are mediated by a transmembrane allosteric transition. Signal transduction or activation is mediated by a concerted cooperative transition between a silent resting state and an active state. Agonists stabilize the active state and competitive antagonists the silent state, and partial agonists may bind nonexclusively to both. These receptors can also undergo a cascade of slower, discrete allosteric transitions, which include refractory regulatory states that result in the desensitization or potentiation of the physiological response.

See Also the Following Articles

Chaperonins • Ligand-Operated Membrane Channels: Calcium (Glutamate) • Ligand-Operated Membrane Channels: GABA • Pyrimidine Biosynthesis

Glossary

allosteric effector A molecule binding to a protein site other than the active site, which can either increase or decrease the activity of the protein.

heterotropic cooperativity The effect of an allosteric effector on protein activity toward a substrate.

homotropic cooperativity The effect of initial substrate binding on subsequent substrate binding.

KNF and MWC models Thermodynamic models that account for the cooperativity displayed by allosteric enzymes.

Further Reading

Changeux, J.-P., and Edelstein, S. J. (1998). Allosteric receptors after 30 years. *Neuron* **21**, 959–980.

Cooperman, B. S., and Kashlan, O. B. (2003). A comprehensive model for the allosteric regulation of class in ribonucleotide reductases. *Adv. Enzyme Regulation* **43**, 167–182.

Eaton, W. A. E., Henry, E. R., Hofrichter, J., and Mozzarelli, A. (1999). Is cooperative oxygen binding by hemoglobin really understood? *Nature Struct. Biol.* **6**, 351–358.

Fersht, A. (1999). *Structure and Mechanism in Protein Science*. WH Freeman, New York.

Horovitz, A. (2001). Review: Allostery in chaperonins. *Journal of Structural Biology* **135**, 104–114.

Koshland, D. E., Jr., Nemethy, G., and Filmer, D. (1966). *Biochemistry* **5**, 365–385.

Luque, I., and Freire, E. (2000). Structural stability of binding sites: Consequences for binding affinity and allosteric effects. *PROTEINS: Structure, Function, and Genetics* **41**(suppl 4), 63–71.

Monod, J., Wyman, J., and Changeux, J. P. (1965). *J. Mol. Biol.* **12**, 88–118.

Neet, K. E. (1995). Cooperativity in enzyme function: Equilibrium and kinetic aspects. *Methods of Enzymology* **249**, 519–567.

Voet, D., and Voet, J. G. (2004). *Biochemistry*, 3rd edition, Vol. 1, Wiley, New York.

Voet, D., Voet, J. G., and Pratt, C. W. (2002). *Fundamentals of Biochemistry*. Wiley, New York.

Biography

Dr. Barry S. Cooperman is a Professor of Chemistry at the University of Pennsylvania, where he previously also served as Vice Provost for Research. His broad interests are in the fields of biological and bioorganic chemistry, with a special focus on the mechanisms of action of ribosomes, ribonucleotide reductase, and serpins, and has published numerous articles in these fields. He holds a Ph.D. from Harvard University and was a postdoctoral fellow with Jacques Monod at the Institut Pasteur.

Alternative Splicing: Regulation of Fibroblast Growth Factor Receptor (FGFR)

Mariano A. Garcia-Blanco
Duke University Medical Center, Durham, North Carolina, USA

Most stable biological programs and many dynamic biological responses rely on the quantitative and qualitative regulation of gene expression. Such regulation can be accomplished by rearranging the gene, controlling transcription of the primary RNAs, regulating the processing of these primary transcripts into mature RNA species, modulating the stability and distribution of these mature RNAs, and finally, in some cases, manipulating the synthesis and stability of the protein products templated by messenger RNAs. Among these steps in the information flow of gene expression, this article focuses on the regulation of RNA processing and, in particular, alternative splicing. Alternative splicing is the process by which a single species of primary transcript undergoes differential removal of introns to yield different mature RNAs. Alternative splicing, which affects gene products from the majority of protein-coding genes, is likely one of the major engines of proteome diversity.

Premessenger RNA Splicing

The initial RNA products of transcription by RNA polymerase II (RNAPII), primary transcripts, are large molecules (averaging 30,000 nucleotides) that are divided into exons and introns. Exons, which usually average 300 nucleotides in length, are retained in mature RNAs, whereas introns, which average over 3000 nucleotides, are removed from the primary transcripts by RNA splicing. RNA splicing occurs in the nucleus and appears to be coupled to the synthesis of primary transcripts by RNAPII. RNA splicing is catalyzed by the spliceosome, an RNA-based macromolecular enzyme that recognizes and defines the exons and introns and precisely removes the latter and rejoins the exons (Figure 1). The definition of exons and introns is governed by conserved cis-acting elements: the 5′ splice site (also known as the donor site) demarcating the 5′-end of an intron and the 3′ splice site (also known as the acceptor site), a tripartite element marking the 3′-end of an intron. It should be noted that although the definition focuses on introns, all internal exons (e.g., exon M in Figure 1D) are defined by a 3′- splice site upstream and a 5′- splice site downstream.

Alternative Splicing

There are four types of alternative splicing events in which splice site choice solely determines the sequence of mature RNAs (Figures 1A–D). In rare cases, an intron is removed or retained to give two very different RNAs (A). The use of two or more alternative 5′ splice sites (B) or 3′ splice sites (C) can lead to RNA isoforms. Finally, inclusion or skipping of one or more exons is a common form of alternative splicing (D). In addition, alternative splicing of transcripts initiated at different transcription start sites leads to mature RNAs with different first exons (E). The 3′ terminal exons can also vary by coupling alternative splicing with alternative polyadenylation (F). This entry describes a slightly more complex form of the decision to skip or include an exon (D), which is observed among transcripts encoding the fibroblast growth factor receptor-2 (FGFR2).

Alternative Splicing of FGF-R2 Transcripts

The extracellular region of FGF-R2 has three immunoglobulin-like (Ig) domains and the third Ig domain determines ligand-binding specificity. This third domain comes in two forms, which differ only in the sequence of the C-terminal half of the domain. One form, predominant in cells of epithelial origin, is encoded by sequences within exons 7 and 8 (IIIb), while the other IgIII domain isoform, which is expressed in fibroblasts, is encoded by sequences within exons 7 and 9 (IIIc) (Figure 2). Alternative splicing of the same FGF-R2 primary transcript, via the mutually exclusive use of exons 8 (IIIb) or 9 (IIIc), leads to the production of FGF-R2

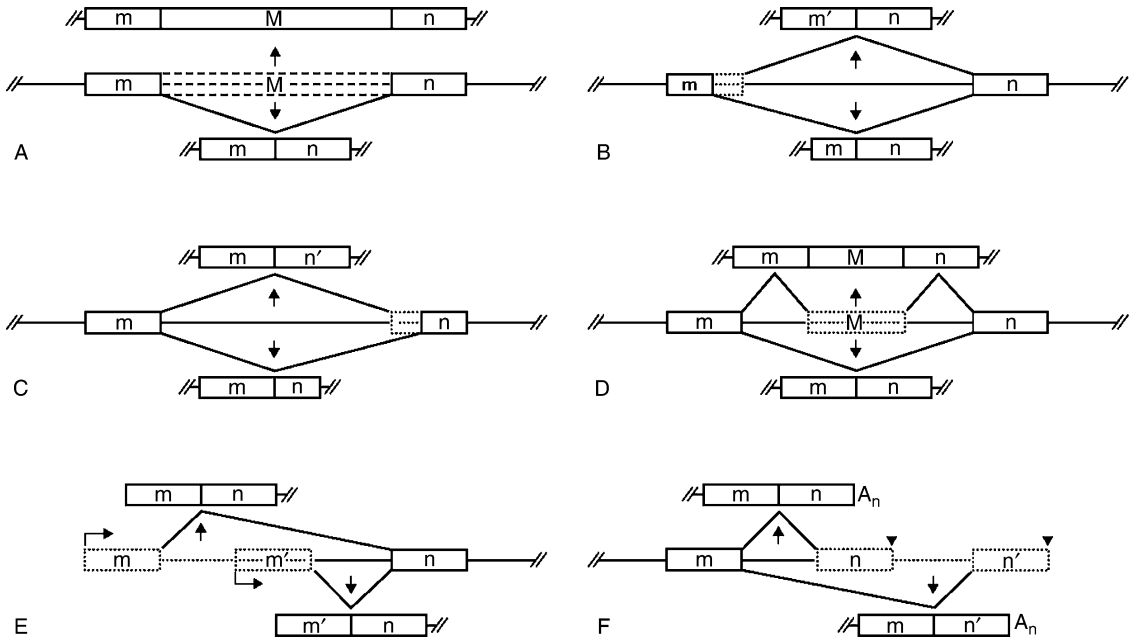

FIGURE 1 Forms of alternative splicing. (A–D) Cases in which transcript diversity is provided solely by alternative splicing. (E) A case in which alternative transcription-initiation sites coupled with alternative splicing leads to diversity of products. (F) A case in which alternative splicing and alternative 3′-end formation lead to diverse transcripts.

(IIIb) or FGF-R2 (IIIc). The importance of this alternative splicing is suggested by the following: (1) FGF-R2 (IIIb) and FGF-R2 (IIIc) bind different FGFs; (2) the expression of two isoforms is tightly regulated in different cell types; (3) the targeted disruption of exon 8 (IIIb) or exon 9 (IIIc) in transgenic animals leads to nonoverlapping defects in organogenesis and development, which are not compatible with viability; and finally (4) several genetic disorders in humans have been mapped to mutations in IgIII of FGF-R2. The regulation of the mutually exclusive use of exons IIIb or IIIc is mediated by cis-acting elements within the primary transcript and trans-acting factors, which must differ in different cell types.

Regulatory Elements and Factors

The cis-acting regulatory elements that control alternative splicing can be divided generally into four categories: exonic splicing enhancers, exonic splicing silencers, intronic activators of splicing, and intronic splicing silencers. These cis-elements mediate their function by interacting, directly or indirectly, with trans-acting activators or repressors of splicing.

Exonic Splicing Enhancers

Exonic splicing enhancers (ESEs) are cis-acting elements that activate the definition of an otherwise weak

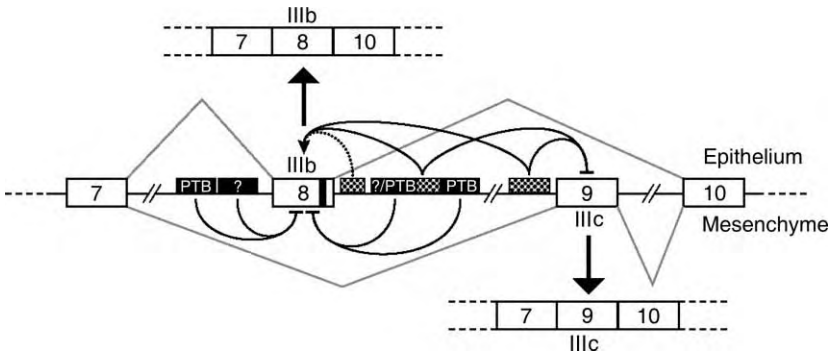

FIGURE 2 Multiple layers of combinatorial interactions result in tissue-specific alternative spliced transcripts: the example of fibroblast growth factor receptor-2. A schematic of exons 7–10 and introns 7–9 of FGF-R2 transcripts is shown indicating that in mesenchymal cells a layer of negative regulation, which includes weak splices bordering exon 8, an exonic splicing silencer (black bar in exon 8), and flanking intronic splicing silencers (black rectangles) silence exon 8 and lead to the choice of exon 9. In epithelial cells, however, a second layer of regulation combines activation of exon 8 by intronic activators of splicing (stippled rectangles) with repression of exon 9 (stippled rectangles) to ensure the use of exon 8.

exon, promoting its inclusion into mature transcripts. Several families of ESEs have been recognized, and the most common are characterized by purine-rich sequences (consensus) and mediate their action via members of the SR protein family (e.g., SC35). Although ESEs have been implicated in regulated splicing, they appear to have a role in defining many constitutive exons. The FGF-R2 IgIII alternative splicing unit does not have obvious ESEs (Figure 2).

Exonic Splicing Silencers

Exon definition can be repressed by exonic splicing silencers (ESSs). The best-characterized ESSs bind hnRNP A1, a protein originally described as an abundant heterogeneous nuclear RNA-binding protein. HnRNP A1 binding at ESSs can suppress inclusion of a weak exon, as has been noted for exon IIIb of FGF-R2 transcripts (Figure 2). HnRNP A1 and SR proteins can play counterbalancing roles in exon definition and their relative levels may determine tissue-specific alternative splicing outcomes.

Intronic Activators of Splicing

Intronic activators of splicing (IASs), which can provide constitutive or regulated enhancements of exon definition, can selectively activate weak exons. Exon IIIb definition requires IAS1, which is a long U-rich element found immediately downstream of the exon. IAS1 binds the Tia-1 (huNam8p) protein that provides ancillary activation of exon IIIb. This activation critically requires two other IASs, IAS2 and IAS3, which mediate epithelial cell-specific inclusion of the exon. Portions of IAS2 and IAS3 directly interact, forcing a double-stranded RNA stem that is required for activation (Figure 2). IAS2 and IAS3 are part of more complex elements that also mediate repression of exon IIIc in epithelial cells and are thus termed intronic splicing activators and repressors of splicing (ISARs) (Figure 2). The coordinated cell-type activation of exon IIIb and repression of exon IIIc results in the epithelial pattern of FGF-R2 splicing.

Intronic Splicing Silencers

Intronic splicing silencers (ISSs) inhibit exon definition by directly occluding cis-elements within canonical splice sites or by creating zones of silence around exons. Many times, ISSs are found flanking exons subject to silencing; this is the case for exon IIIb. Two bipartite silencers, upstream and downstream of exon IIIb, are required for repression of this exon in fibroblasts. Both ISSs mediate their action via the polypyrimidine tract binding protein (PTB), another member of the hnRNP protein family, and other unidentified factors (Figure 2). The actions of the ISSs dominate in fibroblasts; however, in epithelial cells IASs antagonize the silencers. Silencing of introns, possibly in combination with a lack of ESEs, can be important to prevent inappropriate inclusion of pseudo exons, which have canonical splice sites with proper spacing but are not used as exons. These pseudo exons can serve as silent reservoirs of genetic information.

Layers of Regulation

The alternative splicing of FGF-R2 exons IIIb and IIIc provide examples of ESSs, IAS, and ISS, and in addition reveal several general features of regulated alternative splicing units. First, regulation is mediated by the superimposition of several layers of control, starting with weakening of the canonical splice sites bordering regulated exons, followed by global silencing mediated

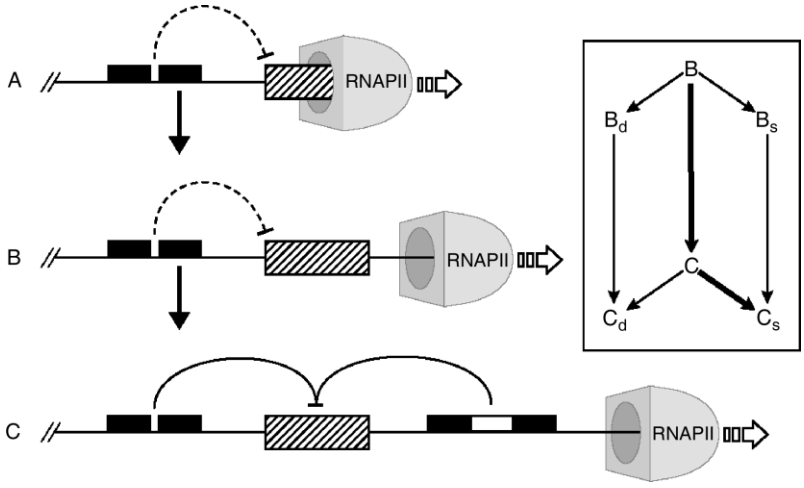

FIGURE 3 A dynamic view of exon silencing. In many exons, for example, for exon 8 (IIIb) of FGF-R2 transcripts, flanking ISSs are required for silencing. (B) During the synthesis of the transcript there is a time when the exon is fully accessible to the splicing apparatus but either is not defined or is defined reversibly. (C) Synthesis of the downstream ISS leads to full repression. The inset proposes the view that the rate of synthesis (B → C) is faster than the rate of exon definition (B → B_d).

by non-cell-type-specific ESS and ISS, and finally capped by cell-type-specific ISAR elements. Second, the layers of regulation involve antagonistic interactions between activators and repressors of exon definition. Third, each individual layer is determined by a combination of cis-elements and factors. Fourth, a general principle that is far from being understood mechanistically, regulation must be coupled with transcription of RNAPII.

A Dynamic View of Alternative Splicing

Most schematics of alternative splicing (including Figure 2) present a static splicing substrate. Although useful, this static view must give way to a more realistic representation. A dynamic representation of the silencing of exon IIIb is presented in Figure 3. This schematic focuses on the potential to define the exon, which can only proceed once the exon is synthesized and accessible to the splicing machinery (Figure 3B). Exon definition ($B \rightarrow B_d$) must be slow relative to the rate of transcript synthesis ($B \rightarrow C$). Upon the appearance of the downstream ISS full silencing can ensue (Figure 3C).

See Also the Following Articles

Fibroblast Growth Factor Receptors and Cancer-Associated Perturbations • Pre-tRNA and Pre-rRNA Processing in Bacteria • RNA Polymerase II and Basal Transcription Factors in Eukaryotes • RNA Polymerase II Structure in Eukaryotes • RNA Polymerase Reaction in Bacteria • RNA Polymerase Structure, Bacterial

Glossary

alternative splicing The process by which a single species of primary transcript undergoes differential removal of introns to yield different mature RNAs. Alternative splicing, which affects gene products from the majority of protein-coding genes, is probably one of the major engines of proteome diversity.

exon A block of sequence within the primary transcript that is retained in the mature transcript after splicing. Internal exons average 145 nucleotides in length among protein-coding transcripts.

intron A block of sequence, which averages ~3000 nucleotides in length but can be larger than 100,000 nucleotides, that is removed during splicing.

RNA splicing One of the processes by which primary transcripts (RNAs) are converted into mature transcripts. During RNA splicing, introns are removed and exons are precisely ligated together.

Further Reading

Berget, S. M. (1995). Exon recognition in vertebrate splicing. *J. Biol. Chem.* **270**, 2411–2414.

Black, D. L. (2000). Protein diversity from alternative splicing: A challenge for bioinformatics and post-genome biology. *Cell* **103**, 367–370.

Fairbrother, W. G., Yeh, R. F., Sharp, P. A., and Burge, C. B. (2002). Predictive identification of exonic splicing enhancers in human genes. *Science* **297**, 1007–1013.

Garcia-Blanco, M. A., Lindsey, L. A., and Ghosh, S. (2001). The phosphoryl transfer reactions in pre-messenger RNA splicing. In *RNA* (D. Söll, S. Nishimura and P. Moore, eds.), pp. 109–123. Pergamon Press, San Diego, CA.

Goldstrohm, A. C., Greenleaf, A., and Garcia-Blanco, M. A. (2001). Co-transcriptional splicing of pre-messenger RNAs: Considerations for the mechanism of alternative splicing.*Gene* **277**, 31–47.

Maniatis, T., and Tasic, B. (2002). Alternative pre-mRNA splicing and proteome expansion in metazoans. *Nature* **418**, 236–243.

Biography

Dr. Mariano A. Garcia-Blanco is Professor of Molecular Genetics and Microbiology, Professor of Medicine at Duke University Medical Center, and Co-director of the Duke Center for RNA Biology. His principal research interest is in the field of gene expression, specifically the interactions that connect transcription with pre-mRNA processing and the regulation of alternative splicing. He holds M.D. and Ph.D. from Yale University.

Alternative Splicing: Regulation of Sex Determination in *Drosophila melanogaster*

Jill K. M. Penn, Patricia Graham and Paul Schedl
Princeton University, Princeton, New Jersey, USA

Alternative splicing is a regulatory process that produces multiple mRNA transcripts from pre-mRNAs transcribed from a single gene. The net effect of alternative splicing is that diverse proteins can be manufactured from a limited amount of DNA. Often a cell contains distinct ratios of alternatively spliced mRNAs and, consequently, distinct ratios of protein isoforms. The ratio of isoforms can vary among different cell types and different stages of development. Conversely, alternative splicing can contribute to cell identity by producing tissue- or stage-specific mRNAs rather than distinct ratios. One example of this exists in *Drosophila melanogaster*, in which alternative splicing is responsible for sex-specific protein expression that functions to maintain sexual identity. Intriguingly, *Drosophila* sexual development is governed by alternative splicing at multiple levels of the regulatory hierarchy.

The Sex Determination Hierarchy in *Drosophila melanogaster*

Sexual Choice, Memory, and Differentiation

The X chromosome/autosome ratio (X/A ratio) determines the choice of sexual identity early in embryogenesis by setting the activity state of the master regulatory switch gene *Sex-lethal* (*Sxl*). An X/A ratio of 1.0 specifies female identity by turning *Sxl* on, whereas an X/A ratio of 0.5 specifies male identity by keeping *Sxl* off (Figure 1). Once *Sxl* is activated in 2X/2A animals, it functions to maintain the female determined state through a positive autoregulatory feedback loop in which Sxl protein promotes its own expression and to orchestrate female development by directing the expression of several regulatory cascades in the female mode. In 1X/2A animals, male identity is remembered by the absence of Sxl protein, while male development is specified by the expression of these same regulatory cascades in the default mode. Although the initial choice of sexual identity is controlled at the level of transcription, many of the key regulatory steps for both memory and differentiation depend on sex-specific alternative splicing.

Details of the Hierarchy

Although *Sxl* is on in females and off in males, the gene is transcribed in both sexes from a promoter, *Sxl-Pm*, which is active from the cellular blastoderm stage onwards. The critical difference between the sexes is that all *Sxl* mRNAs in males have an additional exon, exon 3, which is spliced out of the *Sxl* mRNAs in females (Figure 2A). This male-specific exon has multiple in-frame stop codons that prematurely truncate the *Sxl* open reading frame that begins at an AUG codon in exon 2. Consequently, male mRNAs do not encode functional proteins. In contrast, female *Sxl* mRNAs encode proteins that have two RNA recognition motif (RRM)-type RNA-binding domains. These proteins positively autoregulate their own synthesis by directing the splicing machinery to join exon 2 to exon 4, skipping the male-specific exon 3 (Figure 2A). Because female splicing never occurs in the absence of Sxl protein, the X/A ratio must activate the *Sxl* autoregulatory feedback loop in female embryos by a mechanism that bypasses this requirement. This is accomplished by turning on a special promoter, *Sxl-Pe*, in precellular blastoderm 2X/2A, but not 1X/2A embryos. The Sxl proteins encoded by the *Sxl-Pe* mRNAs set the autoregulatory feedback loop in motion in 2X/2A embryos by directing the female-specific splicing of the first *Sxl-Pm* transcripts. Because *Sxl-Pe* is not activated in 1X/2A embryos, the *Sxl-Pm* transcripts are spliced in the default male pattern.

The regulatory target for *Sxl* in the somatic sexual differentiation pathway is *transformer* (*tra*). The second exon of the *tra* pre-mRNA has two 3′ splice sites, the upstream default splice site and the downstream female-specific site (Figure 2B). Sxl protein turns *tra* on in

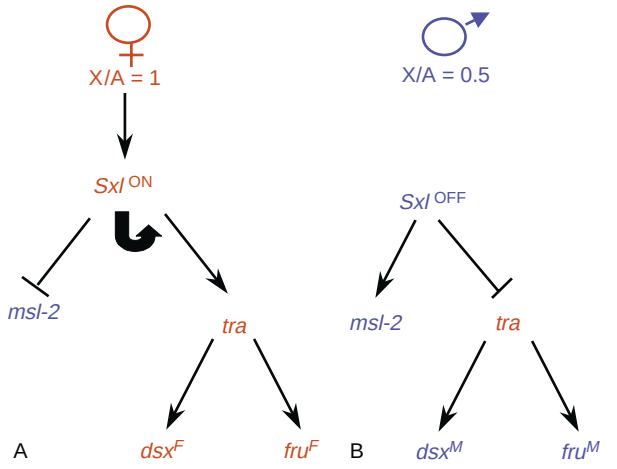

FIGURE 1 Sex determination hierarchy in *Drosophila melanogaster*. (A) Female regulatory cascade showing that *Sex-lethal* is the master regulator of sex determination because it receives the initial signal that chooses sexual identity, maintains sexual identity by a positive autoregulatory feedback loop, and regulates sexual differentiation through downstream target genes. (B) Male regulatory cascade showing the opposite events leading to male development.

females by promoting splicing to the downstream 3′ splice site of exon 2. This produces an mRNA that has an open reading frame that encodes a functional Tra protein. When Sxl protein is absent, as in males, the default 3′ splice site is used. Because there is an in-frame stop codon just downstream of the default 3′ splice site, the male *tra* mRNA does not encode a functional protein and *tra* is off.

Like *Sxl*, *tra* promotes female differentiation by regulating splicing. The two known targets of Tra, *double-sex (dsx)* and *fruitless (fru)*, encode transcription factors. In the case of *dsx*, *tra* controls the production of sex-specific isoforms that have a common N-terminal DNA-binding domain, but different C-terminal activation domains. In females Tra promotes the joining of the 5′ splice site of exon 3 to the 3′ splice site of exon 4 (Figure 2D). In males, where Tra is absent, splicing is to the default 3′ splice site of exon 5. Although Tra regulates *dsx* pre-mRNA splicing by controlling the use of alternative 3′ splice sites, it regulates *fru* pre-mRNA splicing by controlling the use of alternative 5′ splice sites. As illustrated in Figure 2E, a default upstream 5′ splice site in exon 2 is used in males, whereas in females, in which Tra is present, the splicing machinery skips this 5′ splice site and uses instead a 5′ splice spite located some 1500 bp further downstream. Although both the male and female mRNAs are predicted to encode functional protein, the female-specific mRNA does not appear to be translated.

In addition to controlling somatic sexual differentiation, *Sxl* regulates dosage compensation. To make up for the difference in dose of X-linked gene products in the two sexes, transcription from the X chromosome is hyperactivated in males by the male-specific lethal (MSL) dosage-compensation system. *Sxl* turns off the dosage compensation system in females by negatively regulating one of its components, *msl-2*. Interestingly, Sxl regulates *msl-2* by blocking the alternative splicing of an intron in the 5′-UTR and by inhibiting the translation of the message (Figure 2C).

Alternative Splicing Regulation by *Sxl*

tra: A Simple Blockage Model?

The regulation of *tra* splicing by *Sxl* is much simpler than autoregulation in that it only involves a choice between alternative 3′ splice sites (Figure 2B), and it will be considered first. In principle, Sxl could promote the use of the downstream female-specific 3′ splice site in the *tra* pre-mRNA by preventing the splicing machinery from using the upstream default 3′ splice site. Alternatively, it could activate the downstream 3′ splice site. Sosnowski *et al*. tested these models by making deletion constructs that were missing one of the two alternative 3′ splice sites of exon 2. Deletion of the default 3′ splice site led to use of the downstream female-specific 3′ splice site not only in females, but also in males in which Sxl protein is absent. This finding is inconsistent with a simple activation model because in this model Sxl protein would be required to use the downstream site even when the upstream site is missing. Deletion of the downstream 3′ splice site did not interfere with splicing in males, but led to an increased amount of unspliced mRNA in females. This result is consistent with a simple blocking model because when an alternative 3′ splice site is not present, Sxl protein still inhibits the use of the default 3′ splice site, leading to an increase in unspliced mRNA.

Biochemical studies suggest that Sxl blocks the use of the default 3′ splice site by competing with the generic splicing factor U2AF^{50}. U2AF^{50} normally binds to polypyrimidine tracts where it facilitates spliceosome assembly by interacting with the U2 small nuclear ribonucleoparticle (snRNP). Although U2AF^{50} can bind to the polypyrimidine tracts of both the default 3′ and female-specific splice site, it binds with much higher affinity to the default polypyrimidine tract. The default polypyrimidine tract is unusual in that it contains two polyuridine (poly U) runs. Poly U is the recognition sequence for the Sxl protein and mutations in the *tra* poly U runs that eliminate Sxl protein binding *in vitro* prevent *Sxl* from regulating splicing *in vivo*. Thus, the classic model of *tra* splicing is that the Sxl protein outcompetes U2AF^{50} for binding to the polypyrimidine tract of the default 3′ splice site, forcing U2AF^{50} to bind to and activate the weaker, downstream 3′ splice site.

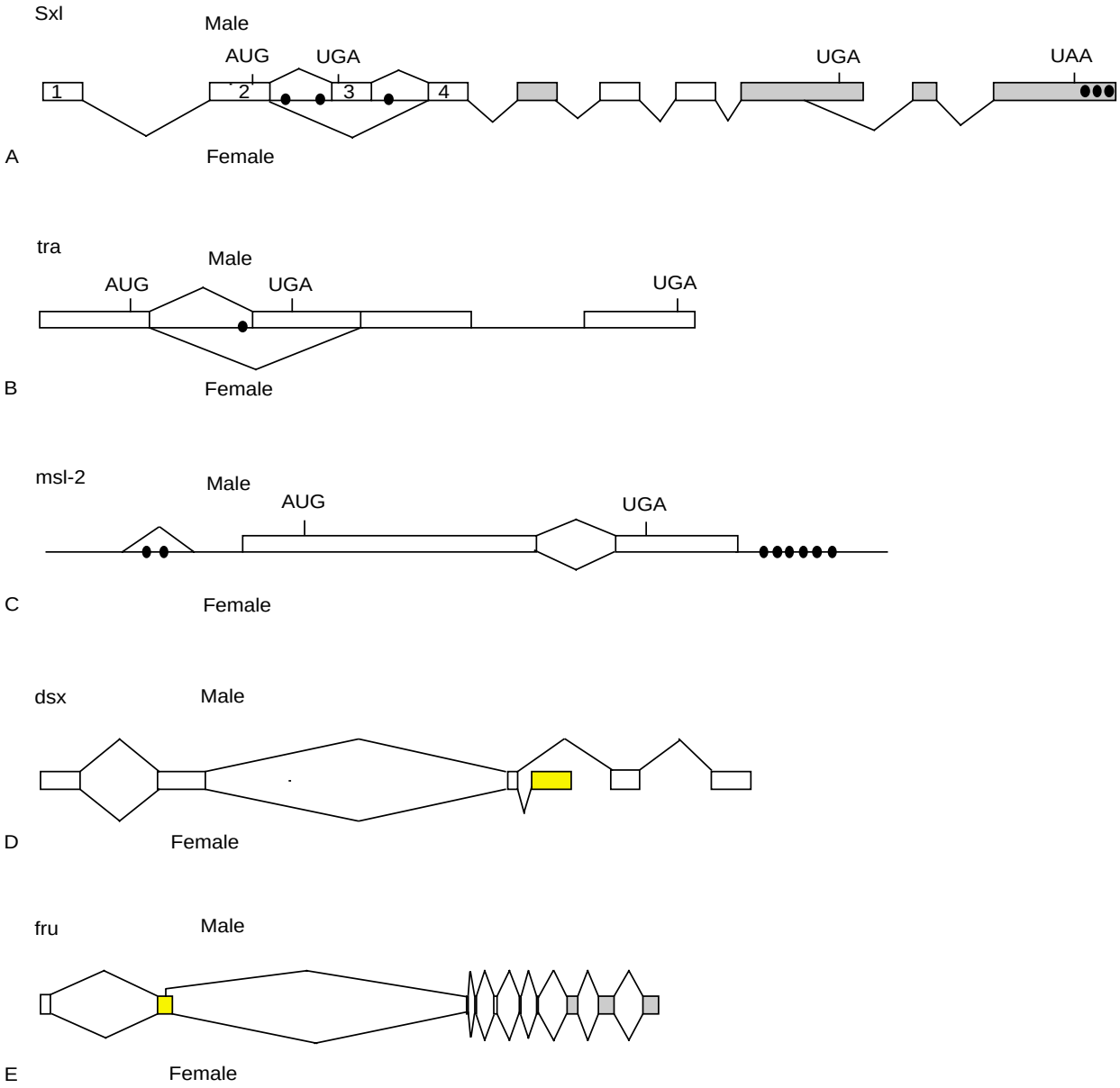

FIGURE 2 Sex-specific alternative splicing. The sex-specific splicing patterns for (A) Sxl, (B) tra, (C) msl-2, (D) dsx, and (E) fru. The male splicing pattern is shown above the gene, and the female pattern is below. Ovals indicate Sxl binding sites. Yellow exons in dsx and fru contain RE and PRE binding sites. Sxl and fru have multiple promoters, and some regions of these genes undergo non-sex-specific splicing (gray). The establishment promoter of Sxl, controlled by the X/A ratio, is not sex-specifically spliced. For fru, only transcripts from promoters that are alternatively spliced in a sex-specific manner are indicated.

Consistent with this model, when the N terminus of Sxl protein is replaced with the U2AF activation domain, the hybrid Sxl protein binds to poly U sites and activates splicing to the default 3′ splice site.

Because a protein consisting of only the two Sxl RRM domains can bind to the default polypyrimidine tract with higher affinity than U2AF[50], this competition model predicts that only the RNA-binding domain of the Sxl protein should be necessary to direct female-specific splicing of *tra*. Indeed, this is the case in *in vitro* splicing reactions. However, a Sxl protein containing the RNA-binding domains, but lacking the first 40 amino acids is unable to regulate *tra* splicing *in vivo* in transgenic animals. One explanation for this discrepancy is that the binding of Sxl to the poly U runs in the default polypyrimidine tract must be stabilized *in vivo* by protein–protein interactions involving the N-terminal domain. However, this reasoning would not explain why a protein consisting of the N-terminal 100 amino acids of Sxl fused to β-galactosidase (N-βgal) is able to weakly promote female-specific splicing of *tra* when expressed in male flies.

This N-βgal fusion protein does not have the two Sxl RNA binding domains and consequently cannot directly compete with U2AF^{50} for binding to the polypyrimidine tract of the default 3′ splice site. Taken together, these findings suggest that in addition to competing with U2AF^{50} for binding to the default polypyrimidine tract, Sxl may play a more active role in directing the splicing machinery to use the downstream female-specific 3′ splice site. As described later, Sxl is known to associate with a number of components of the splicing machinery *in vivo*, including U2AF. Potentially such interactions could provide a mechanism for directing assembly of a functional spliceosome on the weak downstream splice site.

Sxl Autoregulation

Although autoregulation is also thought to involve some type of blockage mechanism, it must be more complicated than *tra* splicing because Sxl has to regulate the use of both the 3′ and 5′ splice sites of the male exon (Figure 2A). Like *tra*, the polypyrimidine tract at the 3′ splice site of the *Sxl* male exon has a poly U run that is recognized by Sxl protein. However, because mutations in this poly U run have no effect on the splicing of *Sxl* pre-mRNAs in either tissue culture cells or transgenic animals, one can rule out a mechanism in which Sxl directs female splicing by binding to the polypyrimidine tract of the male exon and directly occluding U2AF or other generic splicing factors.

In fact, splicing regulation does not seem to pivot on controlling the use of the male exon 3′ splice site. When the male exon 5′ splice site is deleted, placing the 3′ splice sites of the male exon and exon 4 in direct competition, the male exon 3′ splice site is skipped in *both* sexes and exon 2 is spliced exclusively to exon 4. A different result is obtained when the 5′ splice sites of exon 2 and the male exon are placed in competition by deleting the male exon 3′ splice site. In males, a new male exon is generated using a cryptic 3′ splice site in the second intron and the normal male exon 5′ splice site. This deletion mutant transcript is also appropriately regulated by Sxl in females where exon 2 is spliced directly to exon 4, skipping the cryptic male exon. Other findings also argue that controlling the use of the male exon 5′ splice site is likely to be more important than controlling the 3′ splice site.

One mechanism to make the 5′ splice site of the male exon preeminent is to perturb the functioning of the male exon 3′ splice site. The male exon is unusual in that it has two 3′ splice site AGs, located 18 nucleotides apart, that compete with one another and reduce the efficiency of splicing. Use of the male exon in a heterologous context can be improved by mutating the upstream AG so that it can no longer be used. In the context of *Sxl*, inactivating the upstream AG compromises the ability of Sxl to block the inclusion of the male exon, presumably because the male exon 3′ splice site now functions much more efficiently. Finally, Lallena *et al.* have recently shown that the downstream AG is recognized by U2AF, whereas the upstream AG is recognized by the splicing factor SPF45. As would be predicted, if SPF45 is important for splicing to the upstream AG, reducing the activity of SPF45 in tissue culture cells (with RNAi) substantially increases the use of the downstream 3′-AG. The consequent improvement in efficiency of splicing of exon 2 to the male exon 3′ splice site compromises the ability of Sxl to block the inclusion of the male exon.

How does Sxl regulate the male exon 3′ and 5′ splice sites? It turns out that there are multiple poly U runs that are critical for regulation, located some 200 bp from the male exon. The deletion of the upstream or downstream poly U runs greatly compromises, but does not completely abolish, regulation by Sxl, whereas regulation is eliminated when both are deleted. Because the critical poly U runs are located far from the regulated splice sites, it is thought Sxl exerts its effect on male exon splicing indirectly through interactions with other components of the splicing machinery. Consistent with this idea, a number of proteins have been found in complexes with Sxl, and mutations in the genes encoding these proteins show genetic interactions with *Sxl*. The best characterized of these is *sans-fille* (*snf*), which encodes the *Drosophila* homologue of the mammalian U1 and U2 snRNP proteins U1A and U2B′. Although recombinant Sxl and Snf interact directly with one another *in vitro*, the immunoprecipitable complexes between Snf and Sxl seen in nuclear extracts are RNase-sensitive and do not include the U1 and U2 snRNPs unless the extracts are cross-linked prior to immunoprecipitation. Cline *et al.* proposed a snRNP-independent function for Snf in regulating *Sxl* splicing because they found that increasing the levels of *snf*, but not other genes encoding U1 or U2 snRNP proteins, could promote *Sxl* autoregulation under conditions of limiting Sxl protein. However, recent genetic experiments by Nagengast *et al.* show that Sxl interacts with the Snf protein associated with U1 snRNPs. The same study has also shown that Sxl can form an RNA-independent complex with the U1 snRNP protein U170K, and genetic interactions indicate that this protein–protein interaction is important for autoregulation.

The association of Sxl with two U1 snRNP proteins suggests that Sxl may prevent splicing between the male exon and exon 4 by blocking the assembly of a functional U1 complex at the male exon 5′ splice site. However, this would not explain how Sxl prevents exon 2 from splicing to the male exon 3′ splice site(s). An understanding of the role of Sxl in this context is becoming clearer from studies done with U2AF.

In nuclear extracts, Sxl can form a complex with U2AF^{50} and U2AF^{38}, and *Sxl* mutations interact genetically with U2AF^{38}. Naggengast *et al.* suggest that one mechanism Sxl might use to block splicing between exon 2 and the male exon would be through interactions with the U2AF heterodimer. Because U2AF recognizes the downstream AG in the male exon 3′ splice site, some other mechanism might be required to block the use of the upstream AG.

Genetic and molecular studies indicate that genes encoding two additional trans-acting factors, *fl(2)d* and *virilizer* (*vir*), are necessary for regulating the female-specific splicing of *Sxl* (and of *tra*), although how these proteins function is unclear. *fl(2)d* is homologous to *wilm*'s *tumor associated protein* (*wtap*) and encodes a protein present in human spliceosomes. In *Drosophila*, the Fl(2)d protein can form an RNA-independent complex with Sxl, and the two proteins are able to interact directly *in vitro*. Interestingly, Fl(2)d is able to form an RNA-independent complex with Snf, which would be consistent with Fl(2)d functioning with the U1 or U2 snRNP because Snf is a component of both. *vir*, on the other hand, is not homologous to any known gene involved in splicing, but Vir protein has been shown to be in a complex with Fl(2)d, suggesting that Vir might function in splicing regulation.

Alternative Splicing Regulation by Tra

Tra Protein

Tra protein is an arginine/serine domain containing splicing regulator (SR) protein. SR proteins generally function to activate splice sites, but there are examples of SR proteins that are able to block splice sites instead. In *Drosophila*, female-specific Tra protein functions with sex-nonspecific Tra-2 protein to activate splice sites in *dsx* and *fru* pre-mRNAs.

Regulation of *DSX* and *FRU*

In males, the default splicing machinery joins the 5′ splice site of *dsx* exon 3 to the 3′ splice site of exon 5. When Tra is present in females, it promotes splicing of exon 3 to exon 4 by activating the 3′ splice site of exon 4. Exon 4 contains six 13-nt repeat elements (RE) and one purine-rich element (PRE) (located between RE #5 and RE #6) that are necessary for efficient use of the female-specific splice site. When these elements are deleted, *dsx* is spliced in the male pattern irrespective of whether Tra protein is present. Conversely, when these elements are placed downstream of a heterologous 3′ splice site they can activate the splice site when Tra is present. *In vitro* experiments indicate that Tra and Tra-2, together with the SR protein RBP1, associate with the 13-nt REs, whereas the SR proteins dSRp30 and b52/dSRp55 function at the PRE. It is thought Tra and Tra-2 plus the various SR proteins form an enhancer complex in exon 4. Because Tra and Tra-2 interact with U2AF^{38}, this suggests a model in which the enhancer complexes assembled in exon 4 recruit U2AF^{38} and subsequently U2AF^{50} to the 3′ splice site.

This model is complicated by the fact that the *fru* transcript contains three similar Tra/Tra-2 binding sites within exon 2, which are necessary for activating a female-specific 5′ splice site. This is difficult to reconcile with the U2AF recruitment model because recruiting U2AF is not useful for activating a 5′ splice site. Moreover, when the six REs and the PRE within exon 4 of *dsx* are replaced with the Tra/Tra-2 binding sites found in the *fru* transcript, activation of the female-specific 3′ splice site still occurs. One explanation for this result is that recruitment of general splicing regulators by Tra, Tra-2, and other SR proteins might be context dependent. Tra, Tra-2, and specific SR proteins might be able to recruit different proteins to activate either a 3′ or a 5′ splice site. Which component of the splicing machinery is recruited may be determined by additional proteins specific to each transcript that bind to sites other than the REs and/or PREs. Alternatively, the U2AF recruitment model might be entirely incorrect and Tra and Tra-2 might use a similar mechanism to activate both 5′ and 3′ splice sites.

Alternative Splicing and Sex Determination in Other Species

Sex-lethal is produced in a sex-specific manner within the genus *Drosophila*, but in every other dipteran examined outside of this genus, *Sex-lethal* is not expressed sex-specifically nor does it appear to have a role in sex determination. By contrast, some of the downstream genes seem to maintain their role in sex determination. In *Ceratitis capitata*, *tra* seems to act as the master regulator of sex determination. *Cctra* appears to receive the initial sex-determination signal and subsequently regulates not only the necessary downstream gene(s) in the hierarchy of sexual development, but also maintains its own expression via alternative splicing. Further down the hierarchy, the gene *dsx* is much more evolutionarily conserved. In both *Megaselia scalaris* and *C. capitata*, *dsx* is structurally conserved and sex-specifically alternatively spliced. Intriguingly, the *dsx* homologue in *Caenorhabditis elegans*, *male abnormal 3* (*mab-3*), also controls sexual cell fate, thus extending the conservation beyond dipteran insects.

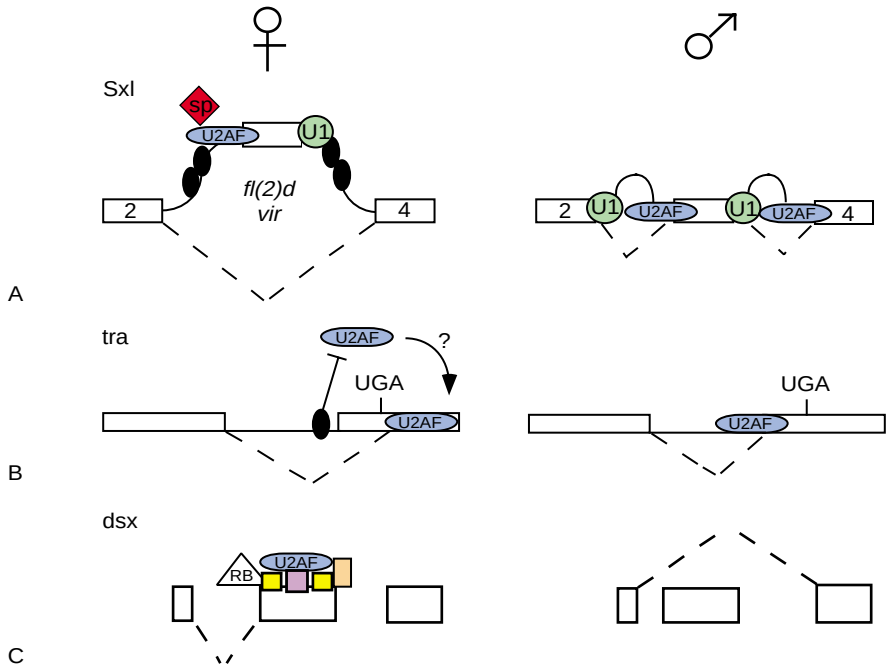

FIGURE 3 Models for regulation of alternative splicing. Splicing patterns for (A) Sxl, (B) tra, and (C) dsx mRNAs in females (left column) and males (right column). Black ovals, Sxl; green circles, Ul snRNP (including snf and U170K); red diamond, spF45; yellow squares, tra/tra2; orange rectangle, dSRp30; purple square, b52/dSRp55; white triangle, RBP1. (A) To regulate splicing of its own mRNA, Sxl may bind to components of U2AF at the male 3′ splice site and components of the U1snRNP at the male 5′ splice site, thereby preventing these splice sites from being used. When no Sxl protein is present, the male exon splice sites are available. (B) To regulate tra splicing, Sxl competes with U2AF for binding to the poly(U) tract near the upstream 3′ splice site, forcing U2AF to use the weaker downstream site. Sxl may also activate the downstream 3′ splice site. When there is no Sxl, U2AF uses the stronger site. (C) Tra/tra-2 bound with the RE and PRE elements in exon 4 of doublesex may form a complex with other factors to activate the upstream 3′ splice site. When the complex is not present, the downstream site is used.

Summary

Drosophila sex determination is a powerful and practical system in which to examine the mechanisms of alternative splicing. Studies done thus far indicate that within the *Drosophila* sex determination hierarchy are examples of several different mechanisms that control alternative splicing. *Sxl* autoregulation is controlled by blocking both the 3′ and 5′ splice sites of an exon, while female-specific *tra* expression is achieved by blocking the stronger 3′ splice site (Figure 3). Splice site activation is used for female-specific *dsx* and *fru* expression. However, a 3′ splice site is activated in *dsx*, whereas a 5′ splice site is activated in *fru*. Each of the various alternative splicing events is unique, but some of the proteins regulating these splicing reactions are shared. Sxl protein probably interacts with Fl(2)d and Vir to direct female-specific splicing of both *Sxl* and *tra*. Likewise, Tra and Tra-2 interact at similar consensus binding sites in the exons of *dsx* and *fru* pre-mRNAs. Further studies will hopefully elucidate which combinations of protein–protein interactions allow the same trans-acting factors to regulate two different alternative splicing events.

See Also the Following Articles

Chromosome Organization and Structure, Overview • Spliceosome

Glossary

dosage compensation A process that equalizes the amount of gene products when opposite sexes have different numbers of sex chromosomes.

small nuclear ribonucleoparticle (snRNP) A complex composed of proteins and snRNA (small nuclear RNA) that functions in the splicing reaction.

spliceosome A large complex composed of proteins and snRNPs that assembles on pre-mRNAs and catalyzes the splicing reaction.

splicing regulator (SR) proteins Proteins containing one or more arginine–serine (RS)-rich domains that often activate weak splice sites by protein–protein interactions.

Further Reading

Cline, T. W., and Meyer, B. J. (1996). Vive la difference: Males vs females in flies vs worms. *Annu. Rev. Genet.* **30**, 637–702.

Cline, T. W. (1999). Functioning of the *Drosophila* integral U1/U2 protein Snf independent of U1 and U2 small nuclear ribonucleoprotein particles is revealed by *snf+* gene dosage effects. *Proc. Natl. Acad. Sci. U.S.A.* **96**, 14451–14458.

Deshpande, G., Samuels, M. E., and Schedl, P. (1996). *Sex-lethal* interacts with splicing factors in vitro and in vivo. *Mol. Cell. Biol.* **16**, 5036–5047.

Deshpande, G., Calhoun, G., and Schedl, P. (1999). The N-terminal domain of Sxl protein disrupts *Sxl* autoregulation in females and promotes female-specific splicing of *tra* in males. *Development* **126**, 2841–2853.

Graham, P., Penn, J. K. M., and Schedl, P. (2002). Masters change, slaves remain. *Bioessays* **25**, 1–4.

Horabin, J., and Schedl, P. (1993). Sex-lethal autoregulation requires multiple cis-acting elements upstream and downstream of the male exon and appears to depend largely on controlling the use of the male exon 5′ splice site. *Mol. Cell. Biol.* **13**, 7734–7746.

Lallena, M. J., Chalmers, K. J., Llamazares, S., Lamond, A. I., and Valcarcel, J. (2002). Splicing regulation at the second catalytic step by Sex-lethal involves 3′ splice site recognition by SPF45. *Cell* **109**, 285–296.

Nagengast, A. A., Stitzinger, S. M., Tseng, C., Mount, S. M., and Salz, H. K. (2003). *Sex-lethal* splicing autoregulation in vivo: Interactions between SEX-LETHAL, the U1 snRNP and U2AF underlie male exon skipping. *Development* **130**, 463–471.

Schutt, C., and Nothiger, R. (2000). Structure, function and evolution of sex-determining systems in Dipteran insects. *Development* **127**, 667–677.

Sosnowski, B. A., Belote, J. M., and McKeown, M. (1989). Sex-specific alternative splicing of RNA from the *transformer* gene results from sequence-dependent splice site blockage. *Cell* **58**, 449–459.

Yanowitz, J., Deshpande, G., Calhoun, G., and Schedl, P. (1999). An N-terminal truncation uncouples sex transforming and dosage compensation functions of *Sex-lethal*. *Mol. Cell. Biol.* **19**, 3018–3028.

Biography

Jill Penn is a graduate student at Princeton University. She received her B.S. in Engineering Chemistry from Oakland University in Rochester, Michigan.

Patricia Graham is a post doctoral Fellow at Princeton University. She received her Ph.D. from the University of Wisconsin-Madison.

Dr. Paul Schedl is a Professor in the Department of Molecular Biology at Princeton University. He holds a Ph.D. degree from Stanford University and received his postdoctoral training at Biozentrun in Switzerland.

Amine Oxidases

Giovanni Floris
University of Cagliari, Cagliari, Italy

Alessandro Finazzi Agrò
University of Rome "Tor Vergata," Rome, Italy

Amine oxidases (AOs), a widespread class of enzymes, are present in all living systems, where they control the level of very active compounds, i.e., mono-, di-, and polyamines. The oxidation of these compounds may generate other biologically active substances, like aldehydes, ammonia, and hydrogen peroxide, which either directly or indirectly influence cells and tissues. Hydrogen peroxide, which is always formed in the reactions catalyzed by AOs, is more and more considered either a crucial substrate for important biochemical processes or a signal and a defense molecule, rather than a noxious waste product.

Classification

The oxidative deamination of mono-, di-, and polyamines is catalyzed by a number of AOs that exhibit different patterns of substrate specificity and inhibitor sensitivity and also differ in their action mechanism. Amine oxidases have been divided into two main categories, depending on the nature of the cofactor involved. One class is characterized by the presence of flavin adenine dinucleotide (FAD) as the redox cofactor. The enzymes belonging to this class are further subdivided into monoamine oxidases (MAO A and MAO B) and polyamine oxidases (PAOs). The second class is represented by enzymes having a tightly bound Cu^{II} ion and a carbonyl-type group identified as 6-hydroxydopa quinone (2,4,5-trihydroxyphenethylamine quinone; TPQ) at the active site (Figures 1A and 1B). TPQ is derived from the oxidation of a tyrosyl residue in a posttranslational event. It has been proposed that the bound copper itself catalyzes the process of TPQ formation by the initial insertion of an oxygen atom into the tyrosine ring to generate dihydroxyphenylalanine (Scheme 1).

Distribution, Reaction Mechanism, and Physiological Roles

FAD-Containing Monoamine Oxidases

MAO A and MAO B [amine:oxygen oxidoreductase (deaminating); EC 1.4.3.4] have subunits of M_r of 59.7 and 58 kDa, respectively. The crystal structure of human MAO B shows that FAD is covalently bound through the flavin C8α-position to a cysteine (Cys397) side chain (Figure 1C). MAOs are ubiquitous in the cells of most mammalian species, the notable exception being erythrocytes, and are tightly associated with the mitochondrial outer membrane, although both MAOs have been also found in the microsomal fraction. The distribution of MAOs has been studied principally in the brain: MAO A is found in catecholaminergic neurons, whereas MAO B is abundant in serotonergic and histaminergic neurons and glial cells. Moreover, some tissues mainly contain MAO A (human placenta and bovine tyroid), and other tissues contain predominantly MAO B (human platelets and bovine liver and kidney).

MAOs oxidize primary amino group of arylalkyl amines to form an imine product with the concomitant reduction of flavin to $FADH_2$. The imine is then hydrolyzed to the corresponding aldehyde and ammonia, and $FADH_2$ is oxidized back to FAD by oxygen with the formation of hydrogen peroxide. MAO A oxidizes preferentially dopamine, noradrenaline, and serotonin and is sensitive to the irreversible inhibitor clorgyline. MAO B oxidizes preferentially benzylamine and phenylethylamine and has a higher affinity for the inhibitor deprenyl. Adrenaline, kynuramine, tyramine, and tryptamine are substrates for both enzymes.

MAO A and B have been implicated in apoptosis, immunosuppression, cytotoxicity, cell growth and proliferation. These enzymes play a protective role in the body by preventing the entry of amines at the renal and intestinal levels or by oxidizing them in blood. In fact, liver MAOs are involved in controlling the blood level of pressor amines. MAO A can oxidize circulating serotonin thus preventing its effects on the heart and vascular system. Both MAO A and MAO B have important roles in the metabolism of neurotransmitters and other biogenic amines in the brain and are implicated in a large number of neurological and psychiatric disorders. The loss of dopaminergic neurons in the substantia nigra, which causes Parkinson's disease, has been associated

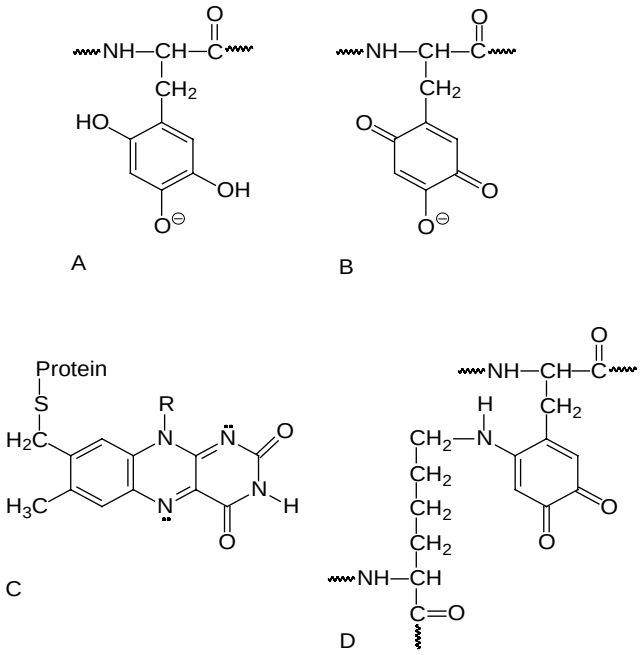

FIGURE 1 Structure of the (A) reduced and (B) oxidized form of TPQ; (C) FAD covalently bound in MAO B; (D) lysine tyrosylquinone.

with an increased dopamine oxidation by MAO B producing high amounts of oxygen radicals responsible for oxidative damage of nigrostriatal neurons. Therefore, the pharmacological regulation of MAO activity has been shown to be important in the treatment of depression and Parkinson's disease.

FAD-Containing Polyamine Oxidases

FAD-containing polyamine oxidases (PAOs) are monomeric enzymes with a M_r ranging from 53 to 63 kDa, with 1 mol of FAD per mol of protein. The prosthetic FAD is noncovalently bound to the protein.

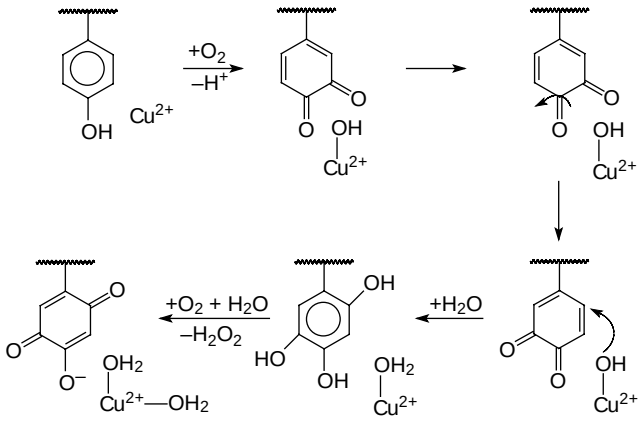

SCHEME 1 Postulated pathway for the biogenesis of TPQ from tyrosine.

PAOs [N^1-acetylspermidine:oxidoreductase (deaminating); E.C. 1.5.3.11] are intracellular enzymes mainly found in vertebrates and plants. PAOs with characteristics similar to vertebrate enzymes are present in yeasts and amoebae, whereas bacteria and protozoans contain enzymes similar to those of plants. Plant PAOs have been isolated and characterized, particularly from the Gramineae oat, maize, barley, wheat, and rye. The enzyme from maize seedlings has been crystallized.

The mechanism by which PAOs catalyze the oxidation of polyamines is still unknown, but the catalytic mechanism can be divided into two half-reactions: (1) flavin reduction upon polyamine oxidation followed by (2) flavin reoxidation by molecular oxygen. Polyamine oxidases catalyze the oxidation of polyamines at the secondary amino group yielding different products according to the organism considered. Mammalian PAOs oxidize preferentially acetyl spermine and acetyl spermidine: spermidine and putrescine are respectively formed as reaction products, together with 3-aminopropanal and hydrogen peroxide. Oxidation of spermine by plant PAOs gives 1,3-diaminopropane, hydrogen peroxide, and 1-(3-aminopropyl)-4-aminobutanal. The latter spontaneously cyclizes to 1-(3-aminopropyl)pyrrolinium that undergoes further spontaneous rearrangements to 1,5-diazobicyclo[4.3.0.]nonane (Scheme 2). The oxidation of spermidine by plant PAOs gives 1,3-diaminopropane, hydrogen peroxide, and 4-aminobutanal that yields 1-pyrroline by spontaneous cyclization. Contrary to the reaction of MAOs and copper/TPQ AOs, the oxidation of polyamines by PAOs does not release ammonia.

PAOs play an important role in the regulation of intracellular polyamine level, and seem to be important for homeostasis and cell survival.

Cu/TPQ Amine Oxidases

Copper/TPQ-containing amine oxidases [amine:oxygen oxidoreductase (deaminating) (copper containing); EC 1.4.3.6] are homodimers in which each subunit (M_r 70–90 kDa) contains a tightly bound type II copper ion and a quinone (TPQ). Copper/TPQ AOs catalyze the oxidative deamination of primary amino groups of mono-, di-, and polyamines, abstracting two electrons from amines and transferring them to molecular oxygen, to form the corresponding aldehyde, ammonia and hydrogen peroxide. Again, the catalytic mechanism can be divided into two half-reactions: (1) enzyme reduction at the quinone moiety (TPQ → $TPQH_2$) by substrate followed by (2) reoxidation by molecular oxygen:

$$E_{ox} + R{-}CH_2{-}NH_3^+ \rightarrow E_{red}{-}NH_3^+ + R{-}CHO \quad (1)$$

$$E_{red}{-}NH_3^+ + O_2 + H_2O \rightarrow E_{ox} + NH_4^+ + H_2O_2 \quad (2)$$

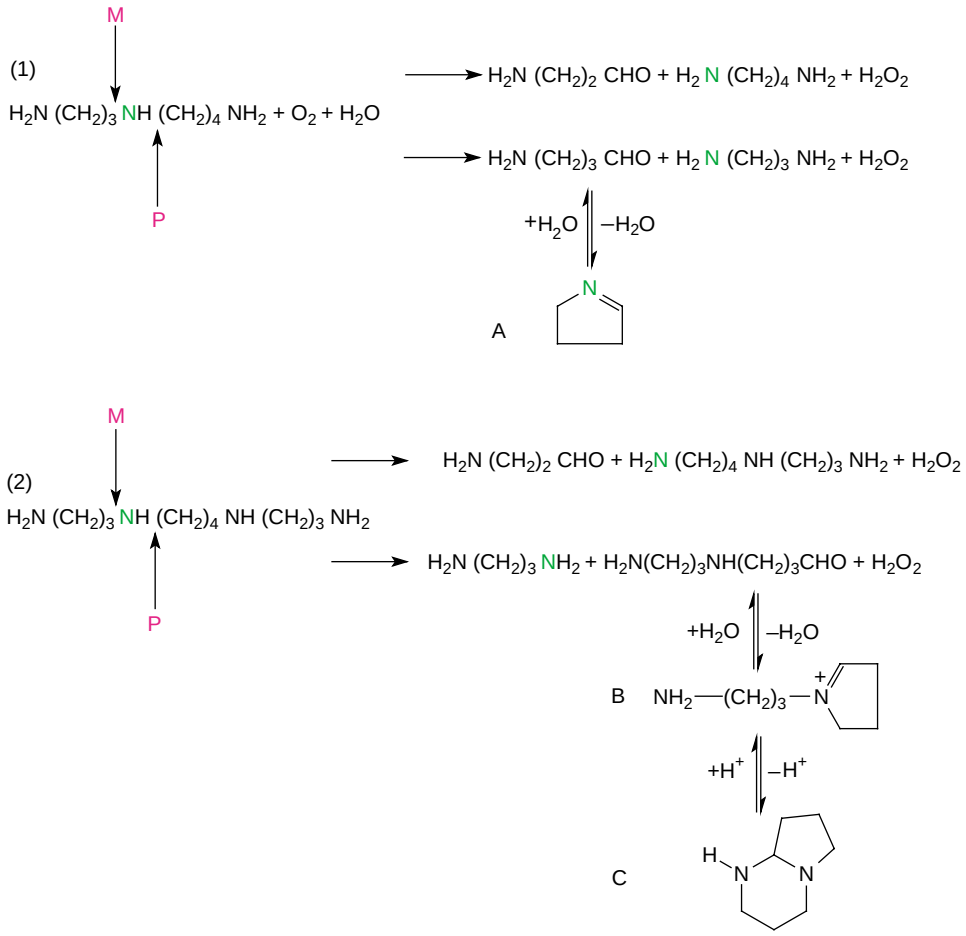

SCHEME 2 Reaction catalyzed by mammalian (M) and plant (P) PAOs. (1) Spermidine; (2) Spermine; (A) 1-pyrroline; (B) 1-(3-aminopropyl)- pyrrolinium; and (C) 1,5-diazobicyclo[4.3.0.]nonane.

Within the class of Cu/TPQ amine oxidases are included:

(i) The intracellular amine oxidases, also called diamine oxidases (DAOs), are ubiquitous enzymes occurring in microorganisms (fungi and bacteria), plants, and mammals. Some DAOs have been crystallized from bacteria, the yeast *Hansenula polymorpha*, and from pea seedlings. The crystal structure shows that the copper atom is coordinated by three histidine side chains and two water molecules, laying at approximately 6Å distance from TPQ (Figure 2). Plant DAOs from various species have been purified to homogeneity and characterized, the best known and studied being those from lentil (*Lens esculenta*) and pea (*Pisum sativum*) and from latex of the shrub *Euphorbia characias*. In mammals, the best known enzymes are those from pig kidney and intestine, and from human placenta. DAOs prefer short aliphatic diamines like putrescine (1,4 diaminobutane) and cadaverine (1,5 diaminopentane) as substrates.

The role of DAOs is difficult to define, because this class includes several enzymes with different localizations and substrates. Bacteria and yeasts can utilize amines as nitrogen and carbon sources through the reaction with amine oxidase. Plant DAOs have an important role in cell growth by regulating the intracellular di- and polyamine levels, and the aldehyde products might have a key role in the biosynthesis of some alkaloids. The function of amine

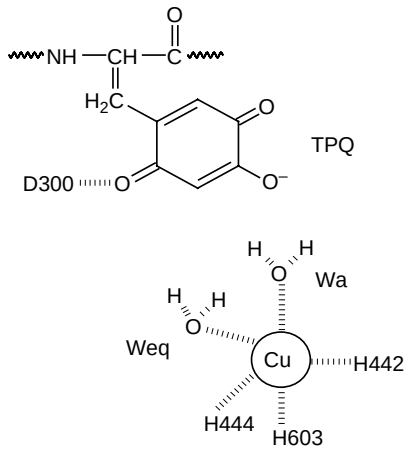

FIGURE 2 Structural arrangement of the copper center and TPQ in the active site of pea seedling amine oxidase. D300 is the base required for the catalytic mechanism.

oxidases in mammals is even more diverse and elusive. Amine oxidase activity is found in many tissues, the highest levels being in decidual cells of placenta, in kidney tubular epithelial cells, and in intestinal epithelial cells. These localizations may suggest a general barrier function for this enzyme in preventing the entrance of extracellular diamines and polyamines into circulation. Furthermore, these enzymes may keep under control the endogenous histamine, which may be responsible for several pathological conditions like allergy, peptic ulcer, and anaphylactic reactions. Several observations point to a relationship between amine oxidase activity and growth, both in normal and tumoral tissues possibly correlated with cell proliferation and differentiation. DAOs have also been proposed as immune response modulators. It has been demonstrated that human placental diamine oxidase is identical to the amiloride-binding protein and thus in some way is involved in the regulation of epithelial ion transport.

(ii) The mammalian extracellular plasma soluble and intracellular tissue-bound amine oxidases are able to metabolize mono-, di-, and polyamines, even though *in vitro* they are preferentially active toward nonphysiological amines like benzylamine. Plasma soluble AOs are generally termed either plasma and serum AOs or benzylamine oxidases (BzAOs). Tissue-bound AOs are often indicated as semicarbazide-sensitive amine oxidases (SSAOs), somewhat misleading since all Cu/TPQ AOs, at variance with FAD-dependent enzymes, are inhibited by semicarbazide and other carbonyl reagents. There has been considerable disagreement whether the extracellular plasma AO were a product of a different gene or a cleavage product of a tissue-bound amine oxidase. The better known examples of BzAOs are those from bovine, swine, and equine plasma. Intracellular SSAOs are widely distributed: smooth muscle cells of vascular tissue of all mammalian species are a good source of these enzymes, which have been also detected in uterus, ureter and vas deferens, in ox dental pulp, in human umbilical artery, in rat adipocytes, and chondrocytes.

The increased BzAO activity in blood serum of pregnant women supports the possibility that this enzyme has a protective role against the polyamines released from the fetoplacental unit. SSAOs have been also shown to be a new class of DNA-binding proteins: in the presence of polyamines they bind DNA and oxidize DNA-bound polyamines. Structural similarity between SSAOs and VAP-1, a protein involved in cellular adhesion, has been observed. SSAOs seem to be involved in the regulation of glucose metabolism (via the H_2O_2 produced?) and in the regulation of leukocyte trafficking in endothelial cells.

(iii) The extracellular matrix-bound lysyl oxidase has the best-defined role: it catalyzes maturation and aging of collagen and elastin, by oxidizing the ε-aminogroups of their lysyl residues, allowing the formation of cross-links essential for the structure of these proteins. Lysyl oxidase differs from other members of the group because lysine tyrosyl quinone (Figure 1D) rather than TPQ is the redox cofactor. The genetic or acquired decrease of lysyl oxidase activity is accompanied by severe pathological conditions like the formation of aneurisms in arteries.

Concluding Remarks

In the past few years, evidence has accumulated about the physiological relevance of hydrogen peroxide, which is generated in the catabolism of mono-, di-, and polyamines by all amine oxidases. This reactive oxygen species is toxic at high concentration. However, at lower concentrations it regulates cell number during embryonic development as well as the proliferation and adhesive properties of endothelial and smooth muscle cells. Hydrogen peroxide appears to be involved in the impairment of cell growth and proliferation, in the regulation of many genes and transcription factors, and in the transduction of cellular signals in many living species. In plants, hydrogen peroxide might be utilized by peroxidases in crucial physiological events, such as in development, in the polymerization of lignin and suberin precursors, and in the catabolism of indoleacetic acid, in response to wounding or to pathogen invasion.

See Also the Following Articles

Flavins • Quinones

Glossary

amines Hydrocarbon compounds bearing an amine group. They are called primary, secondary, or tertiary when nitrogen binds two, one, or zero hydrogen atoms.

oxidases Enzymes that oxidize substrates using molecular oxygen.

polyamines Hydrocarbon compounds bearing both primary and secondary amino groups (e.g., spermine and sperimidine) strongly interacting with nucleic acids involved in many important cellular functions.

primary amines Metabolically derived from amino acids by decarboxylation. Primary amines often show potent pharmacological or hormonal activity (e.g., histamine, serotonin, GABA, and noradrenaline).

Further Reading

Binda, C., Mattevi, A., and Edmondson, D. E. (2002). Structure–function relationship in flavoenzyme-dependent amine oxidation. *J. Biol. Chem.* **277**, 23973–23976.

Federico, R., and Angelini, R. (1991). Polyamine catabolism in plants. In *Biochemistry and Physiology of Polyamines in Plants* (R. D. Slocum and H. E. Flores, eds.) pp. 41–56. CRC Press, Boca Raton, FL.

Girmen, A. S., Baenziger, J., Hotamisligil, G. S., Konradi, C., Shalish, C., Sullivan, J. L., and Breakefield, X. O. (1992). Relationship

between platelet monoamine oxidase B activity and alleles at the MAOB locus. *J. Neurochem.* **59**, 2063–2066.

Jalkanen, S., and Salmi, M. (2001). Cell surface monoamine oxidases: Enzymes in search of a function. New EMBO Member's Review. *The EMBO Journal* **20**, 3893–3901.

Janes, S. M., Mu, D., Wemmer, D., Smith, A. J., Kaur, S., Maltby, D., Burlingame, A. L., and Klinman, J. P. (1990). A new redox cofactor in eukaryotic enzymes: 6-hydroxydopa at the active site of bovine serum amine oxidase. *Science* **248**, 981–987.

Lyes, G. A. (1995). Substrate-specificity of mammalian tissue–bound semicarbazide–sensitive amine oxidase. In *Progress in Brain Research* (P. M. Yu, K. F. Tipton and A. A. Boulton, eds.) Vol. 106, pp. 293–303. Elsevier Science BV, Amsterdam.

Medda, R., Padiglia, A., Bellelli, A., Pedersen, J. Z., Finazzi Agrò, A., and Floris, G. (1999). Cu^{I}-semiquinone radical species in plant copperamine oxidases. *FEBS Lett.* **453**, 15.

Mondovì, B. (1985). *Structure and Functions of Amine Oxidases*. CRC Press, Boca Raton, FL.

Mure, M., Mills, S. A., and Klinman, J. P. (2002). Current topics. Catalytic mechanism of the Topa quinone containing copper amine oxidases. *Biochemistry* **41**, 9269–9278.

Shish, J. C., Chen, K., and Ridd, M. J. (1999). Monoamine oxidase: From genes to behavior. *Annu. Rev. Neurosci.* **22**, 197–217.

Tipton, K. F., and Strolin Benedetti, M. (2002). Amine oxidase and the metabolism of xenobiotics. In *Enzyme Systems That Metabolise Drugs and Other Xenobiotics* (C. Ioannides, ed.) pp. 95–146. Wiley & Sons, New York.

Wilce, M. C. J., Dooley, D. M., Freeman, H. C., Guss, J. M., Matsunami, H., McIntire, W. S., Ruggiero, C. E., Tanizawa, K., and Yamaguchi, H. (1997). Crystal structure of the copper-containing amine oxidase from *Arthrobacter globiformis* in the holo and apo forms: implication for the biogenesis of topaquinone. *Biochemistry* **36**, 16116–16133.

Biography

Alessandro Finazzi Agrò is full Professor of Enzymology, Faculty of Medicine, at the University of Rome "Tor Vergata," Italy. He is currently Rector of the same University. For the past 35 years he has been studying copper proteins and copper enzymes with respect to their biochemical, physiological, and pathological roles.

Giovanni Floris is full Professor of Biochemistry and Molecular Biology, Faculty of Science, at the University of Cagliari, Italy. He is working on the purification and characterization of enzymatic proteins, particularly on plant copper/TPQ amine oxidases.

Amino Acid Metabolism

Luc Cynober
Hôtel-Dieu Hospital and Paris 5 University, Paris, France

Amino acids are major macronutrients involved in (1) protein synthesis, (2) energy requirements, and (3) specific functions either directly (as mediators) or through their metabolism into mediators or hormones. This article describes amino acid metabolism with special emphasis on tissue-specific metabolism, inter-organ exchanges, and regulation.

Structure, Functions, and Classification of Amino Acids

Amino acids (AAs) are defined as organic molecules possessing an amino moiety located at α-position to a carboxylic group. AAs therefore have the following general formula:

$$R-\alpha CH\begin{<}NH_2\\COOH\end{>}$$

where R may be an aliphatic or a cyclic structure.

Note that proline is considered as an AA even though its $-NH_2$ group is part of a heterocycle. Also, taurine is considered as an AA even though it has a sulfur moiety instead of an amino group in the α-position.

AAs can be classified in three different ways (Table I):

- *Chemical Classification* This classification is based on structure and identifies different chemical families of AAs: aliphatic (subdivided into several subgroups – see Table I for details), aromatic, heterocyclic, etc.
- *Metabolic Classification* Although in theory most AAs can be precursors of glucose, *in vivo*, because most AAs preferentially use other metabolic pathways, only alanine (ALA), glutamine (GLN), and to a lesser extent proline (PRO) and glycine (GLY) contribute significantly to gluconeogenesis.

Certain AAs can be precursors of ketone bodies (ketogenic AAs). Again, *in vivo*, only leucine (LEU) contributes significantly to ketogenesis.

Finally, some AAs can be both glucogenic and ketogenic: isoleucine (ILE) and phenylalanine (PHE).

- *Nutritional Classification* This is based on what AAs the human body can or cannot synthesize. The former are named nonessential AAs (NEAAs) and the latter essential AAs (EAAs). There are nine EAAs (Table I). Note that some NEAAs can become EAAs in specific situations, e.g., arginine (ARG) during growth, tyrosine (TYR) during renal failure, or GLN in trauma patients.

Intestinal Absorption of AAs

Digestion of proteins (beyond the scope of this chapter) releases a mixture of free AAs and short-chain peptides. Nitrogen is absorbed mainly in the jejunum and the ileum in the form of free AAs and di- and tripeptides. It is now well recognized that the latter have a kinetic advantage for uptake. To date, two peptide transporters have been cloned, PEPT-1 and PEPT-2.

AAs are taken up by systems that are rather different from those found in other cells and also from those located at the basolateral side of enterocytes. The groups of transporters are relatively specific to:

- neutral AAs,
- imino acids,
- dibasic AAs + cysteine (CYS), and
- dicarboxylic AAs.

Intestinal Metabolism

It was long thought that the gut had a single function, namely, taking up AAs from the lumen for transport in the bloodstream.

In fact, the intestine avidly consumes some AAs for its energy requirements: GLU and GLN are used to the same extent as glucose by enterocytes, producing α-ketoglutarate, which is oxidized in the Krebs cycle. After a balanced meal, at least 30% of GLU + GLN is used by enterocytes, and as a consequence ammonia is released in the portal vein. Interestingly, when GLN is taken up at the luminal side of enterocytes, its uptake at the basolateral side decreases. The reverse is true in the postabsorptive state, so that the supply of GLN to enterocytes remains roughly constant.

TABLE I

Classifications of Amino Acids.

Aliphatic	Aromatic
• Short-chain	***Phenylalanine***
Glycine	**Tyrosine**
Alanine	Heterocyclic
• Alcohol	*Tryptophan*
Threonine	Dibasic
Serine	**Arginine**
• Branched-chain	*Histidine*
Leucine	*Lysine*
Isoleucine	Diacid
Valine	**Glutamate**
• Sulfur	**Glutamine**
Methionine	**Aspartate**
Cysteine	**Asparagine**
Imino acid	
Proline	

Only AAS engaged in protein bonds are presented. Note that there are numerous other AAs: (1) intermediary metabolites: ornithine, citrulline; and (2) posttranscriptionally formed: hydroxyproline, γ-carboxyGLU acid – (a) in italics: essentials AAs; (b) in bold type: gluconeogenic AAs; and (c) underlined; ketogenic AAs.

Also, the turnover of enterocytes is very rapid, causing a strong requirement for purine and pyrimidine precursors (e.g., GLN).

Cellular Transport of AAs

Once AAs appear in the circulation, cellular transport is a critical step in AA metabolism, since it is a prerequisite for any further metabolism. In certain cases this step may even be rate limiting or rate controlling for metabolic pathways.

The systems of transport have long been classified according to their preferred substrates, their dependency towards sodium, their sensitivity to pH, and their ability to transport nonmetabolizable analogues. Based on these criteria a large number of transport systems have been identified. The most ubiquitous are system A (A for ALA-preferring), system ASC (ALA-, serine (SER-) and CYS-preferring), system L (LEU-preferring), y + (ARG being the main substrate), N (for the transport of GLN and histidine (HIS)), etc. With progress in molecular biology methods, a number of transporters have been cloned, allowing a new classification. Not surprisingly, the number of transport systems was found to be greater. For example, for ARG, four transporters have been cloned (CAT-1, CAT-2A, CAT-2B, and CAT-3) with different cell localizations, properties, and affinities for the different cationic AAs.

The organs that are most contributive to AA metabolism are the liver and muscle.

TABLE II

Some Amino Acid Functions

Function	Amino acid	Example
Constituent of proteins	20 AAs	
Hormone precursor	Phenylalanine	Tyroxine
	Tyrosine	Cathecholamines
	Tryptophan	Serotonin
Mediators	Glutamate	Glutamate, GABA
	Glutamine	Glutamine
	Arginine	Nitric oxide
Binding of calcium	Glutamate	γ-carboxyglutamate
Collagen structure	Proline	hydroxyproline

GABA: γ-aminobutyric acid.

Liver Metabolism

The liver holds a central place in the metabolism of AAs because it is responsible for the synthesis of most circulating proteins, transforms AAs as energy sources (i.e., glucose and ketone bodies) for other tissues, and eliminates surplus nitrogen.

AAs supplied via the portal vein after a meal are heavily metabolized (~50%). The carbon chain is oxidized or forms glucose, which is saved as glycogen, while the N-moiety (ies) is (are) removed in ureagenesis.

The reason for this process is that whereas the intestinal absorption of AAs is not limiting (95–99% of nitrogen is absorbed in a large range of protein intake), the brain must be protected against excessive AA exposure because several of them are neurotoxic or are the precursors of potent neuromediators (see Table II). Thus, the liver acts as a filter, limiting the amount of AAs released in the general circulation. Notable exceptions are the branched-chain AAs (BCAAs; VAL, ILE, LEU), which are almost nonmetabolized in the liver: BCAAs form ~22% of AAs in food proteins but almost 50% of AAs reaching the general circulation.

The biochemical explanation for this effect is that hepatocytes do not contain BCAA transaminase, which mediates the first step of BCAA metabolism. The physiological reason may be related to the fact that LEU plays a critical role in the stimulation of muscle protein synthesis in the postprandial phase.

In the postabsorptive state, with glycogen exhaustion, gluconeogenesis increases to maintain glucose homeostasis. As stated above, ALA is the main gluconeogenic

substrate among AAs: in healthy humans starved for 8 h, 30% of perfused ALA is metabolized into glucose, and, in these conditions, 11% of glucose formed by the liver comes from ALA. When the starvation time is increased, and in situations of hyperglucagonemia (e.g., during response to injury such as burn, trauma, or sepsis), the contribution of ALA to gluconeogenesis increases like those of other AAs, in particular GLN. In these situations, most AAs taken up by the liver come from the muscles.

During starvation, another metabolic pathway is activated: ketogenesis is mainly supported by free fatty acid metabolism, but one AA, LEU, is also contributive. This may seem paradoxical because, as stated above, hepatocytes do not express BCAA-T. However, hepatocytes express all the other enzymes required for ketone body (KB) production, in particular the highly regulated enzyme branched-chain keto-acid-dehydrogenase (BCKA-dh). Thus, as described below, the production of KB from LEU is a typical example of the importance of inter-organ exchanges in AA metabolism.

Muscle Metabolism

Muscles contain ~50% of the proteins in the human body and the largest pool of free AAs (i.e., 87 g in a male weighing 70 kg; by comparison the plasma pool is only 1.2 g).

Therefore, muscles can be considered as a reserve of AAs, either directly (i.e., as free AAs) or indirectly (i.e., in the form of proteins).

After a meal, arterio-venous measurements indicate that all AAs are taken up by the muscles to support protein synthesis.

At the postabsorptive state, all but one (GLU) are released by the muscles. It is noteworthy that ALA + GLN together represent 60% of the total AAs released by muscle, whereas they form less than 20% of protein content. This underlies the fact that most ALA and GLN comes from *de novo* synthesis in the muscle. The carbon chain required for ALA synthesis comes from anaerobic degradation of glucose, and the amino moiety comes from transamination with GLU. The resulting α-KG is retransaminated by BCAA-T releasing BCKAs from BCAAs (Figure 1). Ultimately, 18% of the glucose taken up by muscle is metabolized into ALA and 12.5% of the nitrogen contained in circulating ALA comes from LEU. For GLN, the carbon chain comes from GLU and GLU comes both from transamination and from the bloodstream. The ammonia required for the amidation of GLU comes from oxidative deamination of AAs and from the degradation of purine bases (Figure 1).

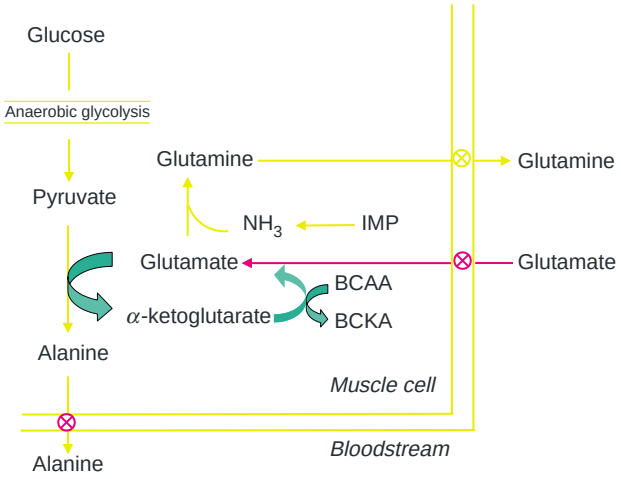

FIGURE 1 *De novo* synthesis of alanine and glutamine in muscles at the postabsorptive state. IMP, inosin monophosphate; BCAA, branched-chain amino acid; BCKA, branched-chain keto acid.

Inter-Organ Exchanges

Every tissue or organ possesses enzymatic equipment that is specific both qualitatively and quantitatively. Correspondingly, each tissue plays a specific role in nitrogen homeostasis. This explains the importance of inter-organ exchanges, each organ contributing as a provider of those AAs that others are unable (or not sufficiently able) to produce. The inter-organ exchanges are highly dependent on the feeding state (i.e., postprandial versus postabsorptive).

At the postprandial state, as mentioned above, there is major AA splanchnic sequestration. AAs appearing in the general circulation are taken up by peripheral tissues, especially muscles.

At the postabsorptive state, the body must use its stores to generate the energy required. Lipolysis and glycogenolysis are contributive to this process. However, the glycogen stores are limited and as fasting progresses, the glucose supply becomes more and more dependent on gluconeogenesis. This process implies the transfer to the liver of gluconeogenic AAs such as ALA and GLN. As described earlier in this article, the nitrogen moiety ultimately comes from BCAAs. This fact has two consequences:

1. Since BCAAs are essential AAs (i.e., no possibility of synthesis in humans), their sole source is protein breakdown. Hence gluconeogenesis in the liver results in net protein breakdown in muscle.
2. Branched-chain keto acids (BCKAs) resulting from BCAA transamination are poorly metabolized in muscles (except in severe catabolic situations where BCKA-dh is activated by proinflammatory cytokines)

and therefore released in the bloodstream. They are then taken up by the liver, where two of them (α-ketoisocaproate and α-ketomethylvalerate) contribute to ketogenesis.

Gluconeogenic AAs taken up by the liver are readily transformed into glucose and this is favored by increased glucagon levels and decreased insulin secretion. Of course, synthesis of one molecule of glucose from one molecule of AA requires the removal of the N-residues. This is the job of ureagenesis. This process has an important consequence: each molecule of glucose produced in this pathway leads to the irreversible loss of (at least) one N-residue from net muscle proteolysis. This explains why in conditions of prolonged food restriction or when energy demand increases (e.g., in injury), a characteristic sign of metabolic adaptation is loss of muscle mass.

Glucose produced by the liver is taken up by glucose-dependent tissues. In the muscle, glucose is largely used anaerobically, leading to further generation of alanine, producing an alanine–glucose–alanine cycle also called the Cahill cycle.

At the whole-body level, this cycle makes no sense energetically because anaerobic glucose consumption generates little ATP and gluconeogenesis consumes at least the same amount of ATP. However, reasoning at the tissue level casts a different light: in the postabsorptive state the liver is rich in energy owing to β-oxidation of free fatty acids from lipolysis in adipose tissue, whereas muscle is somewhat depleted in energy. Therefore, the Cahill cycle corresponds ultimately to the transfer of energy from an organ that is energy-rich (the liver) to a tissue that demands energy (muscle) at the cost of net protein breakdown.

Final Products of AA Metabolism, Elimination of Surplus Nitrogen

N-metabolic products of AAs are mostly excreted in urine. Only an average 7 mg kg^{-1} body weight in males and 8 mg kg^{-1} in females is removed daily in other ways: shed skin (5 mg kg^{-1}), nasal secretions, shed hair, menstrual losses, etc.

Elimination of nitrogen cannot be carried out directly as ammonia because this substance is toxic for the central nervous system at plasma concentrations above 50 μmol l^{-1}. Yet the equivalent of a mole of NH_3 has to be cleared every day. For this reason, in humans, the main form of nitrogen elimination is urea, a water-soluble nontoxic compound synthesized by the liver.

However, not all the ammonia must be converted into urea, because ammonia plays a key role in acid–base homeostasis, in particular in the kidney.

Ureagenesis

The urea cycle is partly cytoplasmic and partly mitochondrial. Only the liver possesses all the enzymes required to synthesize urea from ammonia, and this pathway is strictly located in periportal hepatocytes.

Five enzymes are involved: carbamoylphosphate synthase (CPS), ornithine carbamoyltransferase (OCT), arginosuccinate synthase, arginosuccinate lyase, and arginase.

Ureagenesis is governed by three different types of regulation:

1. Regulation by the availability of precursors: the rate of flux of AAs towards the liver is a key regulator of ureagenesis; the more AAs the liver takes up, the higher is the rate of ureagenesis. AAs may come from food in the postprandial phase or from muscles in the post-absorptive phase. Conversely, during prolonged starvation, urea production declines simply because the muscle efflux of AAs decreases. All the AAs are not equally ureogenic: GLN, ALA, and ARG are the most contributive.
   - GLN is hydrolyzed into GLU and ammonia by glutaminase present in large amounts in periportal hepatocytes. This reaction forms a ureagenesis amplification loop because the product of the reaction (ammonia) has the unusual property of activating glutaminase. The accumulation of GLU, the other product of the reaction, allows the synthesis of N-acetylglutamate, the regulatory role of which is described next.
   - ALA is transaminated into PYR and in parallel α-ketoglutarate gives rise to GLU. This GLU forms a pool distinct from those described above: a second transamination reaction turns oxaloacetate into aspartate, which provides the second nitrogen donor in ureagenesis.
   - ARG is very ureagenic because (1) it is the direct precursor of urea and (2) it plays a key role in the allosteric regulation of ureagenesis.
2. Allosteric regulation: role of N-acetylglutamate. This substance plays a key role in ureagenesis regulation because it is the allosteric regulator of CPS, the enzyme controlling the entry of ammonia into the cycle. N-acetylglutamate synthesis is catalyzed by N-acetylglutamate synthase, which is strongly activated by ARG. Hence the flux of substrates (GLN, NH_3, and ARG) and the allosteric regulation of CPS act synergistically to modulate ureagenesis both upstream and downstream.

3. *Hormonal Regulation* This regulation operates at two levels:

- On substrate availability: cortisol increases proteolysis and muscle efflux of AAs; glucagon promotes their transport into hepatocytes and further metabolism into ureagenesis and gluconeogenesis.
- On the activity of enzymes.

Ammoniagenesis

This pathway is located in kidney tubular cells and is 80% supported by GLN. The first step is mediated by type I phosphodependent glutaminase, an enzyme activated by acidosis; GLU can then be transaminated into α-ketoglutarate or deaminated by GLU dehydrogenase. This last reaction is strongly activated by acidosis, further increasing the flux of NH_3. NH_3 passes freely into the lumen, where it combines with protons to form the ammonium ion, which cannot return to cells.

The one-way flux of NH_3 means that during acidosis (i.e., high amount of H^+ in the lumen) the intra-cellular NH_3 level is low, derepressing GLU-dh. In turn, this favors GLU metabolism and low GLU derepresses glutaminase. Hence it appears that ammoniagenesis is an adaptative pathway that plays a fundamental role in metabolic acidosis.

Relationship between Ureagenesis and Ammoniagenesis: A Contribution to Acid–Base Homeostasis

The observations described above underline the unique role of GLN as a donor of nitrogen for both ureagenesis and ammoniagenesis. However, heavy consumption of GLN in ureagenesis is not compatible with an increased demand by the kidney in acidosis. A balance between these two almost exclusive processes is achieved, thanks to an anatomical detail – the liver contains two different hepatocyte populations:

- Periportal hepatocytes (93% of the total), which possess a glutaminase activity and enzymes of the urea cycle.
- Perivenous hepatocytes, which form only 7% of the total but have a metabolic activity 100 times higher. These cells possess GLN synthase activity.

Hence catabolism and synthesis of GLN are two processes that occur simultaneously in the liver, but at a different rates according to the situation.

- Physiologically, most of the GLN from the portal vein is taken up by periportal hepatocytes, and the liver is a net consumer of GLN.
- In acidosis, hepatic glutaminase is inhibited (note: acidosis activates kidney glutaminase and inhibits the liver isoform). Consequently, GLN remains available for amino acid metabolism.

Hormonal Control of Amino Acid Metabolism

Physiologically as well as in disease, hormones play a key role in the control of AA metabolism, with a balance between anabolic and catabolic hormones.

Anabolic Hormones

1. *Insulin* Insulin exerts actions at every level of AA metabolism:
   (a) It increases the cell transport of numerous AAs, especially in muscle and liver.
   (b) It favors net protein anabolism by decreasing protein breakdown.
   (c) It decreases gluconeogenesis both by decreasing the availability of precursors and by inhibiting key enzymes of this pathway.

2. *Growth Hormone (GH)* GH stimulates protein synthesis.

Catabolic Hormones

1. *Glucagon* Like insulin, glucagon activates the A system of AA transport, but unlike insulin, glucagon favors the use of AAs in gluconeogenesis.

In addition, glucagon favors proteolysis (through macro-autophagy) in the liver.

2. *Cortisol* Cortisol induces hyper-amino-acidemia because although it increases hepatic, intestinal and renal uptake of AAs, it increases their muscle release even more strongly. In addition, cortisol favors net protein breakdown. Hence in a stress situation, cortisol and glucagon have a synergistic action (Figure 2) leading to a unidirectional flux of nitrogen from the muscle to the liver.

3. *Cytokines* Physiologically, their role is minor. However, in disease, proinflammatory cytokines (e.g., tumor necrosis factor α, interleukins 1 and 6) are overproduced and act synergistically with glucagon and cortisol on AA metabolism.

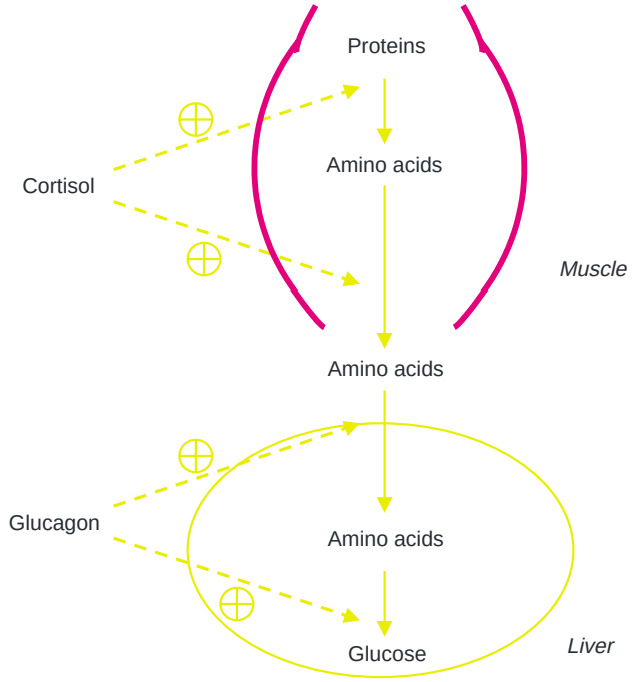

FIGURE 2 Cortisol and glucagon act synergistically to drive AAs from muscle to the liver.

See Also the Following Articles

Glucagon Family of Peptides and their Receptors • Gluconeogenesis • Glycogen Metabolism • G_q Family • Insulin- and Glucagon- Secreting Cells of the Pancreas • Ketogenesis • Steroid/Thyroid Hormone Receptors • Urea Cycle, Inborn Defects of

Glossary

ammoniagenesis *De novo* ammonia synthesis from amino acids. The main precursor is glutamine and this process occurs mainly in the kidney. Ammoniagenesis plays a key role in acid–base homeostasis.

enterocyte A cell that ensures the transport of nutrients from the gut lumen to the bloodstream and protects the internal milieu from invasion by bacteria and others.

essential amino acid An amino acid that cannot be synthesized by humans; hence, their provision is strictly dependent upon alimentation.

gluconeogenesis Glucose synthesis from nonglucidic precursors. Main substrates are AAs (mainly alanine, glutamine, and proline), lactate, pyruvate, and glycerol. Gluconeogenesis occurs during fasting mainly in the liver and also in the kidney.

ketogenesis Synthesis of ketone bodies. Fatty acids are the main substrates. Some AAs are also involved, especially leucine. Ketogenesis occurs specifically in the liver.

ureagenesis Synthesis of urea from ammonia or from ammonia derived from amino acids. Ureagenesis allows removal of amino acid in excess and/or the incorporation of the carbon moiety of AAs into glucose (i.e., gluconeogenesis). Ureagenesis is located in the liver.

Further Reading

Cynober, L. A. (2002). Plasma amino acid levels with a note on membrane transport: Characteristics, regulation, and metabolic significance. *Nutrition* **18**, 761–766.

Cynober, L. (ed.) (2004). *Metabolic and Therapeutic Aspects of Amino Acids in Clinical Nutrition*. 746p. CRC Press, Boca Raton.

Felig, P. (1975). Amino acid metabolism in man. *Annu. Rev. Biochem.* **44**, 933–955.

Harper, A. E., Miller, R. H., and Block, K. P. (1984). Branched-chain amino acid metabolism. *Annu. Rev. Nutr.* **4**, 409–454.

Haussinger, D. (1990). Nitrogen metabolism in liver: Structural and functional organization and physiological relevance. *Biochem. J.* **267**, 281–290.

Husson, A., Brasse-Lagnel, C., Fairand, A., Renouf, S., and Lavoinne, A. (2003). Argininosuccinate synthetase from the urea cycle to the citrulline-NO cycle. *Eur. J. Biochem.* **270**, 1887–1899.

Meijer, A. J., Lamers, W. H., and Chamuleau, R. A. (1990). Nitrogen metabolism and ornithine cycle function. *Physiol. Rev.* **70**, 701–748.

Millward, D. J. (1990). The hormonal control of protein turnover. *Clin. Nutr.* **9**, 115–126.

Biography

Luc A. Cynober is Head of the Department of Clinical Biochemistry, Hôtel-Dieu Hospital, Paris, and Professor of Nutrition and Head of the Biological Nutrition Laboratory at the School of Pharmacy, University Paris 5. He holds a Pharm.D. and a Ph.D. from Paris XI University. Dr. Cynober is editor of *Current Opinion in Clinical Nutrition and Metabolic Care* and has chaired since 2001 the French-Speaking Society of Enteral and Parenteral Nutrition. His major research interests relate to amino acid metabolism and therapy in critical illness and aging.

Aminopeptidases

Ralph A. Bradshaw
University of California, Irvine, California, USA

Aminopeptidases, which are widely distributed in nature, are one of the two major subclasses of the exopeptidases, proteolytic enzymes that remove amino acids from the termini of peptides and proteins (the other being the carboxypeptidases). As the name indicates, the aminopeptidases attack their substrates exclusively from the amino terminal end. Most remove one amino acid at a time, but a small group cleaves two or three residues at a time; these are known as dipeptidyl and tripeptidyl aminopeptidases, respectively. A few enzymes such as acylaminoacyl-peptidase and pyroglutamyl-peptidase remove derivatized amino acids, but generally aminopeptidases require an unmodified or free amino group.

General Description

Properties

Aminopeptidases occur in both soluble and membrane-bound forms and can be found in various cellular compartments as well as in the extracellular environment. The majority are metalloenzymes; that is, they minimally require a metal cofactor at the catalytic site for activity, which is usually zinc ion but can be a number of other metal ions, including Fe^{2+}, Mn^{2+}, and Co^{2+}. There are subclasses containing one and two metal ions. In some cases, the physiological relevant metal is uncertain. There are a few aminopeptidases, particularly of the dipeptidyl- and tripeptidyl-peptidase type, that are classified as serine or cysteine proteases. Aminopeptidases can be processive, meaning that they will continue to degrade the substrate until they reach an unfavorable residue (or combination of residues), and nonprocessive. The latter are usually highly specific for an amino acid type and do not further degrade the substrate after the initial susceptible residue is removed.

Functions

The physiologic functions of aminopeptidases can be divided into three main categories: processing/maturation, activation, and degradation. The enzymes involved in the first two areas usually are highly specific, are nonprocessive, and tailor the N terminus of proteins or peptides either co- or posttranslationally to induce activity or to allow for subsequent modifications that will, in turn, affect activity. Degradation (including inactivation) can also use specific enzymes, particularly where individual bioactive peptides are targeted, but most often involves nonspecific enzymes that participate in protein turnover by the reduction of small peptides, arising from proteosomal cleavage of targeted proteins, to amino acids or by the extracellular degradation of peptides arising from a number of sources.

N-Terminal Cotranslational Processing

One of the best understood functions of aminopeptidases is their role in N-terminal cotranslational processing. Protein synthesis that is directed by the genetic material is universally initiated by the amino acid methionine (in prokaryotes, N-formyl methionine), but the majority of the protein mass in organisms does not reflect this event; that is, most proteins (at least those commonly studied to date) do not have an N-terminal methionine residue. Extracellular proteins that are exported through the endoplasmic reticulum and proteins imported into mitochondria (as well as related organelles such as chloroplasts) lose their respective signal peptides (usually ~20–25 amino acids), including the initiator methionine, through the action of specific signal peptidases, which are endopeptidases. The removal of the initiator methionine from intracellular proteins is accomplished through the action of a specific class of aminopeptidases (clan MG of the metallopeptidases) designated methionine aminopeptidases (MetAPs). All living organisms apparently have at least one form of this enzyme, and they require this activity for vitality. There are several reasons for this: (1) methionine is a relatively scarce amino acid and failure to return a large percentage of the methionine used in the initiation process for reuse (in a variety of activities) leads to a starvation condition that is ultimately lethal; (2) many proteins are subsequently modified on the α-amino group of the newly exposed residue (but can also occur on methionine residues that are not removed) that in many cases is a requirement for their further function; and (3) a few proteins use the newly exposed penultimate residue as a

part of their active structure. The reason that methionine is not removed from all N termini is apparently due to its role as a protecting group against degradation by the N-end rule pathway.

MetAP Specificity

The substrate profile of the MetAPs, despite other distinguishing physical characteristics, is highly conserved over all living organisms, suggesting that it is a very ancient enzyme. Briefly, susceptible substrates have the seven smallest amino acids (glycine, alanine, serine, threonine, cysteine, proline, and valine) in the adjacent (penultimate) position to the methionine. In yeast, a little over one-half of the open reading frames (ORFs) are predicted to code for proteins with these N-terminal sequences, but in terms of mass the percentage of soluble proteins is much higher, perhaps as high as 80%. Because essentially all exported and transmembrane proteins (which may account for as much as one-third of the total protein in a cell) and most of the proteins imported into the mitochondrion also lose their N termini through cleavage of their signal peptides, which are in turn degraded to amino acids, there is a very high degree of recyclization of initiator methionine.

Properties of MetAPs

Structural Organization

The basic catalytic domain, first defined by X-ray analyses of the *E. coli* enzyme, is ~30 kDa in mass and contains two metal ions at the active site. It has an internal symmetry (described as a pita bread fold) suggestive of an early gene duplication event. This structure appears, with only minor variations, to be found in all eubacteria and represents the type 1 isoform. Archaebacteria contain a different but related (homologous) form of MetAP, principally characterized by an insertion of approximately 65 residues, that forms an extra highly helical domain on the surface of the protein. It is designated type 2. Eukaryotes contain both types and in addition each contains an amino terminal extension. The N-terminal segment of the type 1 enzyme contains zinc-finger domains that are thought to act as a tether to tie this enzyme to the ribosome. The corresponding segment of the eukaryotic type 2 proteins is marked by extended stretches of polyacidic and basic amino acids. The function of this domain is unknown. The overall organization of the MetAP family is shown in Figure 1.

Metal Use

These enzymes were initially characterized as using two Co^{2+}, based on early experiments with the eubacterial MetAPs. Subsequently, it was shown that multiple metals could be used in many of the forms, particularly the *E. coli* enzyme, which is active with Fe^{2+}, Zn^{2+}, Ni^{2+}, and Mn^{2+}, in addition to Co^{2+}. It is possible that, depending on availability, the eubacterial enzymes may use different metals. In recent studies in eukaryotes, Mn^{2+} has emerged as the preferred candidate for the type 2 enzyme, whereas Zn^{2+} remains the most likely metal cofactor for the type 1 enzymes under physiological conditions. Although early studies suggested that the MetAPs used a bivalent metal structure, they can clearly function with only a single metal ion present.

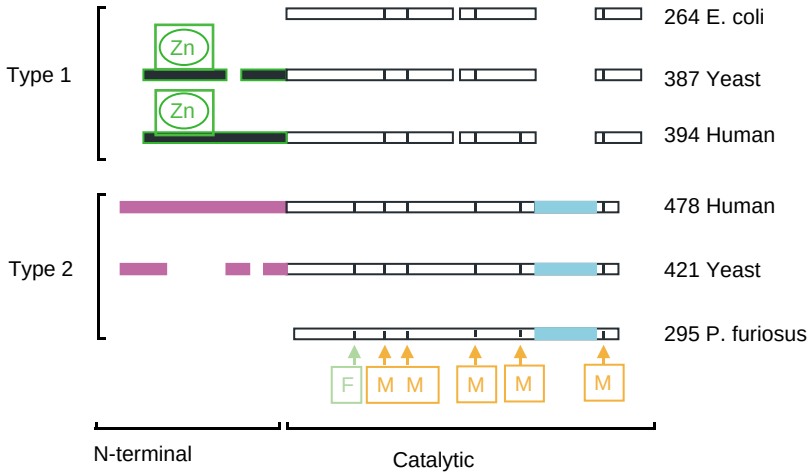

FIGURE 1 Schematic presentation of the structural organization of the MetAP family. Separate domains are indicated by color (magenta, N-terminal extension characteristic of MetAP2s; brown, N-terminal extension with putative Zn-binding domains characteristic of MetAP1s; light blue, catalytic domain insert characteristic of MetAP2s) and are presented approximately to scale. Major deletions (and insertions) deduced from sequence and structural comparisons are indicated as gaps. M denotes the site of a metal ligand; F indicates the location of the histidine modified in type 2 enzymes. The number of residues for each protein is given in the column at the right. Reproduced with permission from Bradshaw and Yi, 2002, *Essays in Biochemistry*, Vol. 38, pp. 65–77. © the Biochemical Society.

In all cases, the metal ions are bound through five amino acid side chains and these are well preserved in all the isoforms in both prokaryotes and eukaryotes.

Roles of the MetAP Isoforms

The substrate specificity of all of the isoforms is generally the same as just described and is heavily predicated on the nature of the penultimate residue. Substrate length, in *in vitro* studies, does have some effect but it is unclear whether this is of significance *in vivo*. Similarly, different metal ions could also affect substrate selection, but this has not been systematically demonstrated. Null mutations (manipulations that prevent the expression of a gene) in yeast demonstrate some measure of redundancy because cells will survive with one or the other of the isoforms but not when both are eliminated. Deletion of the single gene in prokaryotes is also lethal. Nonetheless, there is both direct and indirect evidence to support the view that the two isoforms have different cellular functions. MetAP1 is thought to function as the main processing enzyme and be physically associated with the ribosome in a position to hydrolyze the methionine from germane nascent chains during protein synthesis. MetAP2 is thought to be a soluble enzyme and to probably provide secondary processing for substrates that improperly escape the action of MetAP1. However, it is clearly involved in other activities as well. This is illustrated by a class of irreversible chemical inhibitors that are highly selective for MetAP2, which cause cell-cycle arrest in endothelial cells (but not cell death) resulting in anti-angiogenesis. These potential drugs are being refined for use in treating tumors. Presumably this inhibition results from the failure of MetAP2 to process a select protein or subset of proteins involved in mitosis of these cells, but their nature is unknown. Downstream sequences probably are responsible for rendering these select targets susceptible to MetAP2 but not MetAP1. MetAP2 also functions to inhibit the phosphorylation of eIF2α and thereby promote translation. This activity is entirely distinct from its catalytic one and is not connected to its cell-cycle functions because the inhibited protein is still fully functional as a phosphorylation inhibitor. It is thus one of many proteins known to have dual (and often unrelated) functions.

See Also the Following Articles

Amino Acid Metabolism • Metalloproteases • N-End Rule • Proteasomes, Overview • Protein Import into Mitochondria • Zinc Fingers

Glossary

anti-angiogenesis The process by which blood vessel formation is inhibited. Disruption of this activity is an effective way to prevent tissue proliferation, as is encountered in tumor growth.

carboxypeptidase One of two major classes of exopeptidases. They cleave protein and peptide substrates sequentially from the carboxyl terminal end.

endopeptidase One of two major classes of proteolytic enzymes (the other being exopeptidases) that cleave peptide and protein substrates at internal peptide bonds.

N-end rule pathway An intracellular pathway in which selected N termini of proteins are recognized by a specific part of the ubiquitin tagging machinery of the cell, leading to their degradation via proteosomal cleavage.

open reading frames (ORFs) Genome sequences that can be continuously interpreted in an unbroken protein sequence. They generally, but not always, correspond to true structural genes.

proteosome An intracellular suborganelle (or protein machine) composed of multiple subunits organized in a stack of four 7-membered rings. The subunits of the inner rings are proteolytic enzymes that degrade target proteins into short peptides, which are then either further broken down into free amino acids by exopeptidases action or (in the immune system) presented as cell surface antigens to elicit an antibody response. When associated with additional subunits that recognize appropriately marked proteins, it is the principal entity responsible for intracellular protein turnover.

zinc-finger domains Short amino acid sequences that contain four appropriately spaced residues capable of binding a zinc ion through their side chains. This structure, usually predictable from sequence alignments, is often involved in binding to both protein and nucleic acid partners.

Further Reading

Barrett, A. J., Rawlings, N. D., and Woessner, J. F. (eds.) (1998). *Handbook of Proteolytic Enzymes*. Academic Press, London.

Bradshaw, R. A., Hope, C. J., Yi, E., and Walker, K. W. (2001). Co- and posttranslational processing: The removal of methionine. *Enzymes* **22**, 387–420.

Bradshaw, R. A., and Yi, E. (2002). Methionine aminopeptidase and angiogenesis. *Essays Biochem.* **38**, 65–78.

Lowther, W. T., and Matthews, B. W. (2000). Structure and function of the methionine aminopeptidases. *Biochim. Biophys. Acta* **1477**, 157–167.

Taylor, A. (ed.) (1996). *Aminopeptidases*. R.G. Landes Co., Austin, TX.

Biography

Dr. Ralph A. Bradshaw is a Professor of Physiology and Biophysics at the University of California, Irvine. His principal research interests are in protein chemistry and proteomics, with a focus on N-terminal processing of proteins and protein turnover and on signal transduction by growth factors and their receptors. He received his Ph.D. degree from Duke University and was a researcher and faculty member at Indiana University, University of Washington, and Washington University.

Amyloid

Ronald Wetzel
University of Tennessee, Knoxville, Tennessee, USA

Amyloid is an aggregated protein structure consisting of unbranched microscopic fibrils often found in dense tissue deposits and associated with a variety of human diseases, including a number of significant neurodegenerative disorders. In its broadest usage, the term amyloid does not pertain to a specific protein molecule or sequence, but rather to a general folding pattern, or folding motif, that appears to be accessible to many, if not all, polypeptide chains. Although the three-dimensional structures of these proteins in their native states can vary enormously, the abnormal amyloid structures that they form exhibit a characteristic folding pattern, called a "cross-β" structure, that differs from that of the native state structure.

Introduction

Amyloid formation thus involves a protein misfolding reaction. Amyloid fibrils are generally very stable and quite insoluble in native, aqueous buffer. In a way, amyloid is a foreign substance composed of self-proteins, but it is not easily recognized and removed as a foreign substance by the immune system, for reasons that are not well understood. In some disease states involving amyloid deposition, the amyloid deposit is directly involved in the disease mechanism, whereas in other cases its mechanistic role is less clear. In some microorganisms, specific proteins and protein domains appear to have evolved for the purpose of making amyloid fibrils that play an important, positive role in the cell. In most cases, however, amyloid is a pathogenic structure, formed by accident under conditions of molecular, cellular, or organismic stress, from proteins that evolved to fold and function in quite different structural states. The recognition that proteins not known to be involved in amyloid disease can be induced to form amyloid fibrils, through exposure to certain nonnative conditions *in vitro*, has led to a picture of the amyloid motif as a general default structure in protein folding accessible to many, if not all, polypeptide sequences. Notwithstanding the predominant usage described above, the word "amyloid" is also occasionally found as part of the names of specific proteins. These proteins tend to be associated in some way with the amyloid phenomenon, either as proteins capable of making amyloid fibrils [such as serum amyloid A, islet amyloid polypeptide, and β-amyloid (also known as Aβ)] or as proteins that interact with amyloid fibrils (such as serum amyloid P component).

History

Waxy masses found at autopsy in the liver and spleen have been observed in humans since the 17th century. In 1854, Virchow reported that an iodine stain thought to be specific for starch generated a positive test on such material and therefore classified these structures as amyloid (starch-like). Although 5 years later Friedreich and Kekule demonstrated that these deposits contained negligible carbohydrate, the name amyloid has been retained. In 1922, Bennhold introduced the use of the dye Congo red to stain tissue amyloid deposits. After the dye binds, it exhibits an apple-green birefringence when examined by polarized microscopy that sharply distinguishes amyloid from other tissue components (Figure 1). Ever since, Congo red has been the primary method by which pathologists identify amyloid deposits in tissue samples. In 1927, Divry showed that the cores of senile plaques, the cortical structures that Alzheimer linked with early-onset senile dementia in his classic 1906 paper, exhibit the Congo red birefringence characteristic of amyloid. Amyloid plaques are recognized as one of the pathological hallmarks of Alzheimer's disease (AD) and it is believed that some aggregated form of the main protein component of the amyloid fibrils in these plaques plays a direct role in AD etiology. Although it had long been recognized that the main chemical component of amyloid fibrils is protein, it was not until the pioneering work of the Glenner and Benditt groups in the early 1970s that it was realized that amyloid fibrils are predominantly composed of *specific* protein sequences rather than a broad mixture of protein molecules. Glenner showed that amyloid extracted from primary amyloidosis patients contained the immunoglobulin light chain molecule, and Benditt found that amyloid from tissues of chronic inflammation patients consisted of a new protein called amyloid A. Other clinically distinct forms of amyloid

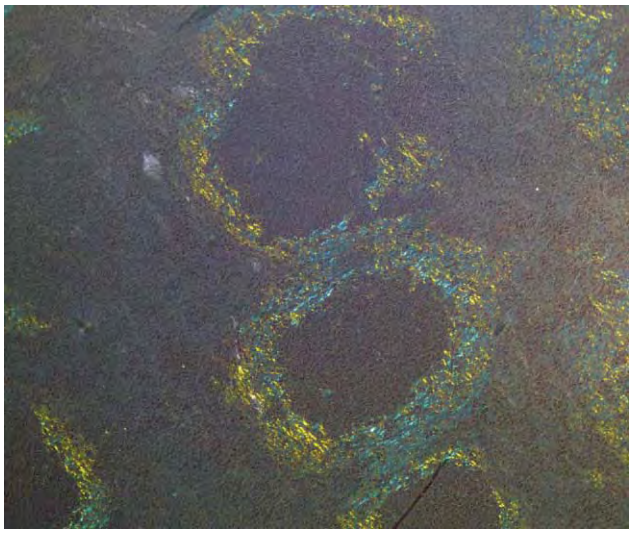

FIGURE 1 Rings of amyloid detected by Congo red staining and polarized microscopy in the spleen of a mouse with serum amyloid A amyloidosis. Courtesy of Professor Jonathan Wall, University of Tennessee.

were soon thereafter shown to have different characteristic protein constituents. In the mid-1980s, Glenner isolated and characterized by amino acid sequencing the previously unknown peptide Aβ as the principal component of AD amyloid fibrils. By the end of the 20th century, many naturally occurring amyloid proteins had been characterized and the list continues to grow with the development of more sensitive means of analysis.

Amyloid Diseases

Range of Amyloid-Related Diseases

Table I lists some of the over 30 human disease states in which amyloid fibrils have been observed, as characterized by the principal organ involved and the principal protein component of each. Amyloid diseases can occur both in the brain and in the rest of the body. The systemic amyloid diseases tend, as a general rule, to involve large deposits of amyloid that in extreme cases dramatically increase the size of the affected organ. In these cases, the toxicity of the amyloid deposit may be largely due to the mass of deposited material and its ability to disrupt normal tissue structure and function. In some peripheral amyloid diseases, the amyloid deposits are localized to a particular tissue. Such is the case in pancreatic amyloid, which is found in over 90% of adult-onset (type 2) diabetes patients (despite this high incidence, the pathogenic role of amyloid deposition in diabetes is not yet known). In contrast, in other amyloidoses, protein deposits can be found in a variety of tissues. Amyloid is also observed in a number of brain diseases. In AD, extracellular amyloid deposits are found in the cerebral cortex, usually embedded with fragments of neuronal processes and surrounded by activated glial cells. In Huntington's disease, amyloid deposits are found in both the cytoplasm and the nucleoplasm of particular neurons in the cortex and elsewhere. In Parkinson's disease, large neuronal deposits called Lewy bodies are rich in the protein α-synuclein. In each of these brain diseases, the mechanistic role of protein deposits has not yet been established.

TABLE I

Major Polypeptide Components of Pathogenic Amyloid Deposits in Humans

Polypeptide	Major disease states
Transthyretin	Heart, kidney, peripheral neuropathy
Serum amyloid A	Kidney, peripheral neuropathy
Immunoglobulin light chain	Kidney, heart
Immunoglobulin heavy chain	Spleen
β_2-Microglobulin	Carpal tunnel syndrome, osteoarthropathies
Lysozyme	Nonnaturopathic visceral amyloid
Islet amyloid polypeptide	Diabetic pancreatic islet cells
Fibrinogen α-chain	Kidney
Apolipoprotein A1	Peripheral neuropathy, liver
Atrial natriuretic peptide	Heart
Amyloid β-protein (Aβ)	Brain (Alzheimer's disease, cerebral amyloid angiopathy)
α-Synuclein	Brain (Parkinson's disease)
huntingtin polyglutamine sequence	Brain (Huntington's disease)
Prion protein (PrP)	Brain (Creutzfeldt–Jakob disease, mad cow disease)
Cystatin C	Brain (cerebral amyloid angiopathy)
Gelsolin	Brain (cerebral amyloid angiopathy)
ABri	Brain (familial British dementia)

Physiological Factors in Amyloid Formation

Although much remains to be learned about the events that trigger amyloid deposition, it is clear that a variety of factors are involved. Some well-established factors are molecular aspects of the proteins themselves. Since the rates of aggregation reactions, such as amyloid formation, depend on concentration, dramatic increases in the amount of the "amyloidogenic" precursor protein can initiate amyloid formation. This is the case for the protein serum amyloid A, which increases in concentration in response to infection and, when persistently elevated, can deposit as amyloid. Similarly, the reason Down's syndrome patients invariably develop AD may be because the extra chromosome associated with the

disease contains the gene for the amyloid β-protein precursor (APP), the protein from which the main plaque component Aβ is generated. The presence of a third active copy of the APP gene in cells results in increased levels of Aβ, which in turn serves to initiate, or "nucleate," fibril formation. One of the unsolved mysteries of amyloid disease is how nucleation of amyloid growth occurs in most disease states. When studied *in vitro*, proteins responsible for amyloid disease often require extremely high, nonphysiological concentrations for nucleation and growth of amyloid fibrils. This indicates that there are unknown specific structures and/or environments in the body that facilitate nucleation. Amyloid plaques typically contain other proteins in addition to the main fibril component and one role of some of these proteins may be to contribute to amyloid formation by helping to stabilize the fibrils and protect them from normal degradative mechanisms. Amyloid diseases are often age-related, leading to the speculation that sporadic amyloid deposition may be a not uncommon occurrence that is held in check in the young and healthy but which advances when normal surveillance mechanisms break down in the aged. This may account for the finding that, in the inherited amyloidosis associated with mutant forms of amyloidogenic precursor proteins, the diseases generally occur later in life, despite the fact that the proteins are expressed from birth.

Prions and Amyloid Enhancement Factor

In one group of amyloid-related brain diseases, a group including Creutzfeldt–Jakob disease, mad cow disease, and the sheep disease scrapie, the conditions can be transmitted by ingestion of "prion" particles, misfolded versions of a normal cellular protein, from the nervous system tissue of a previous victim. Although it is not firmly established that the actual prion particle or state is itself an amyloid fibril, the ability of prion infectivity levels to be amplified in the body bears an intriguing resemblance to the ability of amyloid fibrils to amplify themselves from a pool of precursor protein, through seeding. All mammals express a version of the prion precursor protein, PrP, which has a normal function and does not normally lead to disease. Except in rare instances of sporadic and genetic forms of the disease, prion-associated diseases are observed only when the animal has been exposed to exogenously supplied prion particles, which appear to act *in vivo* as seeds or templates for the propagation of new prions from the normal PrP pool. This scenario is reminiscent of the phenomenon that serum amyloid A amyloidosis can be accelerated in experimental animals by administration of an agent called amyloid enhancement factor (AEF). AEF extracted from the amyloidotic spleen of a mouse and injected intravenously into new mice can induce the rapid development of amyloid deposits compared to untreated controls. Biochemical studies are consistent with AEF being essentially composed of amyloid fibrils, although the presence of an important minor component is difficult to rule out. A possible strong connection between the AEF and prion phenomena has been suggested by experiments showing that AEF, as well as pure amyloid fibrils created *in vitro*, can induce amyloid disease in mice when placed in their drinking water. Thus, although most amyloid diseases are not considered to be transmissible, the results in this experimental system suggest that various amyloid fibrils might be capable of behaving as prions in some circumstances.

Toxicity of Amyloid Fibrils

Although in some peripheral conditions, amyloid can cause life-threatening disease by accumulating in such high mass that normal tissue structure and function are disrupted, in other cases, particularly in the neurodegenerative diseases, the accumulated mass of amyloid is very low compared to the surrounding cell mass. In these cases, the mechanism(s) by which amyloid fibrils cause cell death or cell dystrophy is not at all clear. Whether there is a uniform toxic mechanism in all diseases or different mechanisms for different diseases is also unknown. Toxicity mechanisms under investigation include the following: (1) collateral damage caused by immune responses to an amyloid deposit; (2) membrane depolarization resulting from channels created by amyloid fibril assembly intermediates inserted into membranes; (3) recruitment of other proteins into growing aggregates, which has the effect of denying the cell the activity of the recruited protein(s); (4) disruption or overwhelming of the normal cellular apparatus for breakdown and elimination of misfolded proteins, such as the ubiquitin – proteasome system and the molecular chaperones.

Evolved Amyloid

As far as is known, most protein sequences in evolution were selected for their abilities to efficiently access functional, folded states, while being either unselected, or selected against, with respect to the ability to make amyloid fibrils. Thus, in most cases where amyloid forms, the amyloid can be viewed as an accidental, environmentally induced structure never intended by nature. There are several examples, however, of proteins whose ability to make amyloid fibrils in microbial cells is beneficial to the organism. Yeast prions, for example, function through their ability to form and seed amyloid fibrils and in doing so they modulate the levels of the soluble form of the prion protein in the cell, the fluctuations in which play metabolic and ultimately regulatory roles. In another example, a complex system

of proteins in *Escherichia coli* is responsible for producing an extracellular amyloid fibril that plays a role in cell adhesion. The existence of functional, beneficial amyloid might be viewed as an example of nature's ability to exploit to advantage the novel properties of the products of evolution.

Amyloid Proteins

Range of Amyloid Proteins

Amyloid fibrils composed of different proteins share a number of common structural features, despite the fact that these proteins, in their native states, vary widely in structure, cellular locations, and properties. For example, the amyloid protein transthyretin is a tetramer of subunits with a total molecular weight of 55 kDa. In contrast, small peptides of approximately 40 amino acid residues, such as Aβ and islet amyloid polypeptide (IAPP), and fragments of IAPP as short as pentapeptides, are also capable of amyloid fibril formation. Proteins can grow into amyloid fibrils regardless of the nature of their normal folding patterns. In their native states, α-synuclein exhibits no stable structure in solution, transthyretin is dominated by β-sheet, lysozyme is a mixed α-helix/β-sheet protein, and serum amyloid A is essentially fully α-helical, yet all are capable of forming amyloid fibrils. Most of the peripheral amyloidoses involve secreted proteins, whereas the nine different proteins responsible for nine expanded polyglutamine diseases – including Huntington's disease – are cellular proteins (which, in turn, are found in a variety of subcellular locations). Most amyloid proteins contain significant percentages of hydrophobic residues, but polyglutamine consists entirely of the relatively polar amino acid glutamine. One of the few patterns shared among amyloidogenic protein regions is the infrequent occurrence of proline residues, which strongly disfavor β-sheet – the dominant secondary structural feature of the amyloid fibril.

Molecular Factors in Amyloid Formation

Until the early 1990s, the unusually insoluble, fibrous, quasi-crystalline amyloid fibril was generally viewed as a structural form in which the subunit building block was essentially the native state of the amyloidogenic precursor protein, in a model analogous to structural models for aggregated sickle cell hemoglobin. A significant advance in the understanding of amyloidosis was the demonstration in the mid-1990s that amyloid formation is strongly enhanced when the folded state of a protein is destabilized by mutation or by the solution environment, indicating that fibril structure involves nonnative states. These studies were later extended to show that denaturing conditions can induce amyloid formation even in some proteins not known to be pathogenic. It is clear that misfolding, i.e., the rearrangement of the complex folded shape of a protein molecule, is central to amyloid formation. Thus, protein stability – the resistance of the folded conformation to misfolding/unfolding – is an important factor in determining susceptibility to amyloid formation. Extreme environments in the body, such as acidic cell compartments, may, in some cases, facilitate protein unfolding and therefore promote amyloid formation. Proteolytic removal of a portion of a protein by an endogenous protease can also be a destabilizing factor leading to amyloid formation. Notably, mutations that alter the primary structure of proteins can affect protein stability. In fact, many of the amyloid diseases involve amino acid substitutions in an amyloid precursor protein. The most common example is familial amyloidosis, caused by a variety of single point mutations in the protein transthyretin. In addition, noninheritable, specific amino acid changes in immunoglobulin light chains are linked to a high risk of amyloidosis. Amino acid changes can contribute to the efficiency of amyloid formation not only by modifying the stability of the native state of the precursor protein, but also by modifying the stability of the amyloid fibril itself; an example of the latter is the ability of proline residues to destabilize amyloid structure.

Amyloid Assembly

The manner in which amyloid fibrils grow can be considered in terms of the kinetics of the process or in terms of the structures of assembly intermediates. Kinetically, amyloid fibril formation *in vitro* typically exhibits a lag time of hours to days, followed by a rapid growth phase. In many such cases, the lag phase can be abbreviated or eliminated if a small amount of fibril is provided as seed at the start of the reaction. Such behavior has been interpreted as evidence that fibril growth takes place by nucleated growth polymerization, a mechanism of colloidal assembly in which the initiation of aggregate growth depends on the sporadic generation of a highly unstable, highly organized nucleus state. However, it is far from clear how amyloid growth is initiated *in vivo* and it is possible, even likely, that other molecules or structures are involved, which would make the *in vivo* mechanism more akin to what in physics is referred to as heterogeneous nucleation. *In vitro*, after the nucleation (or seeding) phase has occurred, growth continues predominantly via the elongation of existing fibrils and it has been argued that this is a more realistic view of how amyloid develops *in vivo*. A number of assembly intermediates have been detected when amyloid growth is studied *in vitro*. Whether or not any of these can be considered

to be true kinetic nuclei, some of these structures may have relevance *in vivo*. Amyloid growth from monomeric proteins seems to proceed via the formation of successively larger, more complex structures, from small globular aggregates to short curvilinear filaments to isolated straight and unbranched fibrils to bundles of fibrils. The early assembly intermediates in this progression appear to be more cytotoxic than the mature fibrils, leading to the speculation that assembly intermediates are the real culprits in disease pathogenesis. Little is known, however, about whether and how these intermediates might be formed in the body and how they might kill cells.

Amyloid Structure

Amyloid ultrastructure as revealed by electron microscopy (Figure 2) or atomic force microscopy shows fibrils to be relatively straight and unbranched, with diameters in the range of 80–160Å. Fibrils have a characteristic twist, being composed of two to six protofilaments of diameter 30–40Å. X-ray fiber diffraction studies reveal that fibrils and their constituent protofilaments are rich in a type of β-sheet structure known as cross-β. In this conformational structure type, the extended chain elements of the β-sheet are perpendicular to the fibril axis and the hydrogen bonds between the strands are parallel to the fibril axis. Beyond this level of resolution, little is known about the detailed protein folding of the amyloid motif because of imposing technical barriers to their study by the standard methods of X-ray crystallography and solution-phase nuclear magnetic resonance spectroscopy. Nevertheless, a number of structural models have been proposed and important insights continue to be obtained through lower resolution studies. The structure of the amyloid folding motif is important for a number of reasons, only one of which is their association with a variety of human diseases. It is clear that misfolded, aggregated proteins are formed routinely in the cell due to fundamental inefficiencies in the protein folding process; understanding amyloid structure may help elucidate how the cell manages to recognize and eliminate the products of folding mishaps. Mapping amyloid structure and assembly will also contribute to understanding of this previously ignored aspect of the protein folding reaction – unproductive side products. Finally, better structural information may allow a rational design approach to the development of anti-amyloid therapeutics.

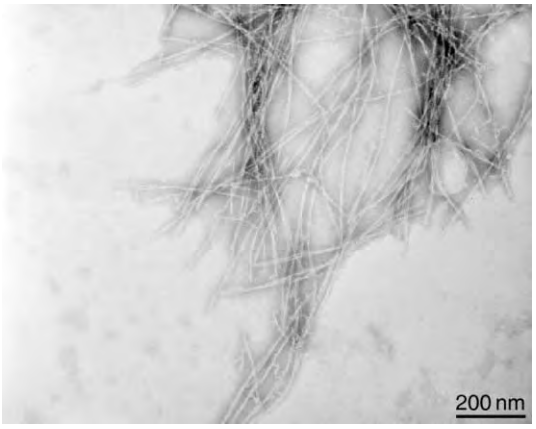

FIGURE 2 An electron micrograph of an amyloid fibril grown in the laboratory from the Alzheimer's disease peptide Aβ. Courtesy of Professors Indu Kheterpal and John Dunlap, University of Tennessee.

See Also the Following Articles

Cell Death by Apoptosis and Necrosis • Chaperones, Molecular • Prions and Epigenetic Inheritance • Prions, Overview • Proteasomes, Overview • Ubiquitin System

Glossary

folding motif The three-dimensional shape pattern exhibited by a folded protein, consisting of the secondary structural units (e.g., α-helix, β-strands) accessed by different elements of the primary sequence, and how those secondary structural units interact with one another in space. Although there are tens of thousands of protein sequences coded within the human genome, it is believed that the three-dimensional structures of these proteins will ultimately be described by perhaps only a few hundred folding motifs.

glial cells Nonneuronal, accessory cells in the brain that are responsible for maintaining brain structure and development and for fighting infection.

membrane depolarization Loss of chemical potential across a membrane.

molecular chaperones Enzymatic protein assemblies that are responsible for detecting, reversing, and, where necessary, eliminating failed products of protein folding, such as misfolded and aggregated proteins.

nuclear magnetic resonance A type of spectroscopy in which the unique covalent and noncovalent environments of atoms in molecules in solution can be assessed, allowing for construction of a high-resolution structural model of the three-dimensional relationships between atoms.

ubiquitin–proteasome system A complex pathway of enzymes responsible for marking and destroying proteins that are no longer required by the cell due to their being obsolete or defective. Such proteins are first marked by the attachment of the small protein ubiquitin, at which point they are recognized and destroyed by the proteasome, a large protein machine consisting of proteases and other enzyme activities.

X-ray crystallography A technique for determining at high resolution the spatial relationships between atoms in a molecule in the solid state, by the detailed diffraction pattern generated when a molecular crystal is exposed to X-ray beams.

X-ray fiber diffraction An intermediate-resolution version of X-ray diffraction analysis, not requiring a crystalline form, in which repeated patterns of a structure can be recognized from a limited diffraction pattern.

Further Reading

Dobson, C. M. (2001). The structural basis of protein folding and its links with human disease. *Philos. Trans. R. Soc. London B Biol. Sci.* **356**, 133–145.

Falk, R. H., Comenzo, R. L., and Skinner, M. (1997). The systemic amyloidoses. *N. Engl. J. Med.* **337**, 898–909.

Kelly, J. W. (1998). The alternative conformations of amyloidogenic proteins and their multi-step assembly pathways. *Curr. Opin. Struct. Biol.* **8**, 101–106.

Lindquist, S. (1997). Mad cows meet psi-chotic yeast: The expansion of the prion hypothesis. *Cell* **89**, 495–498.

Martin, J. B. (1999). Molecular basis of the neurodegenerative disorders. *N. Engl. J. Med.* **340**, 1970–1980. [Published erratum appears in *N. Engl. J. Med.* (1999). **341**, 1407].

Selkoe, D. J. (1999). Translating cell biology into therapeutic advances in Alzheimer's disease. *Nature* **399**, A23–A31.

Sipe, J. D., and Cohen, A. S. (2000). Review: History of the amyloid fibril. *J. Struct. Biol.* **130**, 88–98.

Wetzel, R. (1994). Mutations and off-pathway aggregation. *Trends Biotechnol.* **12**, 193–198.

Biography

Dr. Ronald Wetzel is a Professor of Medicine in the Graduate School of Medicine at the University of Tennessee in Knoxville. He obtained a Ph.D. in physical organic chemistry from the University of California, Berkeley, and completed postdoctoral studies at the Max–Planck Institute for Experimental Medicine and at Yale University. He participated in the development of the modern biotechnology industry as an early employee at Genentech, Inc. Dr. Wetzel's major research focus is in the structures and assembly mechanisms of misfolded proteins and protein aggregates, in how they contribute to human disease, and in developing therapeutic interventions for these diseases.

Anaplerosis

Raymond R. Russell, III
Yale University School of Medicine, New Haven, Connecticut, USA

Heinrich Taegtmeyer
University of Texas-Houston Medical School, Houston, Texas, USA

The word anaplerosis (from the Greek, meaning "to fill up") was coined in the 1960s by Sir Hans Kornberg to describe metabolic processes that replenish intermediates in a biochemical cycle. Anaplerotic pathways are present in both eukaryotic and prokaryotic organisms. This article discusses anaplerosis as it relates to the citric acid cycle in mammalian tissues with reference to organ function. Metabolic cycles are essential for the efficient transfer of energy in the cell. In organs such as the heart and skeletal muscle, a series of moiety-conserved cycles connects the circulation with the cycling of crossbridges in the contractile elements of sarcomeres. Here we focus on anaplerotic mechanisms that maintain the intermediates of one of the most important metabolic cycles.

Introduction

Steady-state concentrations of intermediates in a metabolic pathway depend on their rates of synthesis and degradation. Substrates entering the citric acid cycle as citrate (via the condensation of acetyl-CoA with oxaloacetate) do not cause a net change in the citric acid cycle pool size. The two carbons of acetyl-CoA are lost as CO_2 in the isocitrate and the α-ketoglutarate dehydrogenase reactions. In contrast, anaplerosis supplies compounds to the citric acid cycle through reactions other than those catalyzed by citrate synthase. These compounds replenish carbon intermediates lost primarily as amino acids (glutamate or aspartate) or as oxaloacetate. The role of anaplerosis in the citric acid cycle is twofold. First, as intermediates are drained away during synthetic processes such as gluconeogenesis, glyceroneogenesis, and amino acid synthesis, anaplerosis replaces them, allowing citric acid cycle flux to proceed without impairment. This functional aspect of anaplerosis is especially important in the liver and renal cortex. Second, anaplerosis facilitates energy production in organs with high rates of energy turnover, such as the heart and skeletal muscle. The citric acid cycle operates in two spans, and flux is regulated by the α-ketoglutarate dehydrogenase reaction. Under normoxic conditions, faster energy turnover leads to an increase in the pool size of citric acid cycle intermediates. However, under hypoxic conditions, flux through a portion of the citric acid cycle provides anaerobic energy by substrate level phosphorylation.

Anaplerotic Pathways

Substrates for Anaplerosis

As a key component of all living cells, the citric acid cycle is highly organized and must be able to respond to constant changes in its environment. It is thought to be tied into a distributive system of energy transformation; however, this distributive control theory is difficult to prove experimentally, even though regulation of anaplerotic flux through a variety of pathways is part of this response (Figure 1).

The primary substrates for anaplerosis are pyruvate and alanine, although glutamate can be a physiologically significant substrate as well. In addition, the branched-chain amino acids valine and isoleucine, as well as odd-chain fatty acids and their degradation product, propionate, serve as anaplerotic substrates.

Entry at Malate and Oxaloacetate

A major anaplerotic substrate in the heart is pyruvate. Although most pyruvate is oxidatively decarboxylated and enters the citric acid cycle as acetyl-CoA, a portion is also carboxylated and enters the C4 pool of the citric acid cycle. This reaction is catalyzed by either pyruvate carboxylase (forming oxaloacetate) or by NADP-dependent malic enzyme (forming malate). Even though the NADP-dependent malic enzyme reaction is reversible, the reaction in the direction of malate production is slow and unlikely to play a significant role in anaplerosis. Aspartate can also enter the citric acid cycle as a C4 intermediate. It is transaminated with α-ketoglutarate via aspartic aminotransferase to form oxaloacetate and

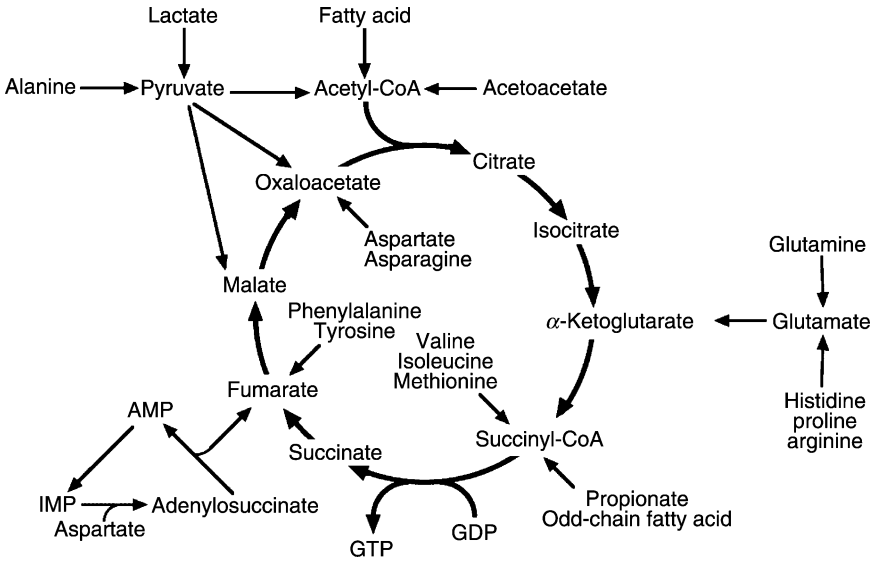

FIGURE 1 Summary of anaplerotic pathways leading to the citric acid cycle.

glutamate. In this reaction, anaplerosis balances the loss of α-ketoglutarate; however, the exact stoichiometry of these reactions has not yet been determined.

Entry via α-Ketoglutarate

In heart muscle (which has the highest rate of oxygen consumption of all mammalian organs), α-ketoglutarate dehydrogenase activity correlates with the rate of oxygen consumption. Therefore, it is likely that α-ketoglutarate dehydrogenase is rate limiting for citric acid cycle flux. Indeed, isotopomer analysis of glutamate enrichment from acetyl-CoA is a lap counter for measuring citric acid cycle flux. A fundamental assumption is that α-ketoglutarate leaves the cycle as glutamate. This reaction is readily reversible by mass action when α-ketoglutarate is formed from glutamate via transamination with pyruvate (forming alanine) or oxaloacetate (forming aspartate). Furthermore, in skeletal muscle glutamate is converted to α-ketoglutarate and NH_4^+ by glutamate dehydrogenase. This enzyme shows no activity in heart muscle.

Entry via Succinyl-CoA

The citric acid cycle intermediate succinyl-CoA plays an important role in fatty acid and amino acid metabolism because it is the entry point of odd-chain fatty acids, propionate, and the branched-chain amino acids valine and isoleucine into the citric acid cycle. Substrate entry as α-ketoglutarate or succinyl-CoA, in contrast to other anaplerotic pathways, is associated with the generation of high-energy phosphates. The reaction catalyzed by succinyl-CoA synthetase is reversed and leads to substrate-level phosphorylation of GDP to GTP. This energy-producing pathway becomes important in myocardial ischemia when ATP generation by oxidative phosphorylation is inhibited.

Entry via Fumarate

In addition to the amino acids phenylalanine and tyrosine entering as fumarate, the purine nucleotide cycle enriches the citric acid cycle based on the net reaction:

$$\text{aspartate} + \text{GTP} \rightarrow \text{fumarate} + NH_3 + \text{GDP} + P_i$$

Previous work has demonstrated that flux through the purine nucleotide cycle increases in skeletal muscle during intense exercise. This increased flux has two effects: First, it can maintain the pool of adenine nucleotides, and second, it can increase the citric acid cycle pool size via anaplerosis. Both of these effects are expected to improve energy metabolism in exercising muscle.

Exit of Intermediates: Balancing Anaplerosis

By definition, under steady-state conditions, substrates entering the citric acid cycle via anaplerotic pathways are balanced by removing an equivalent amount of citric acid cycle intermediates via pathways that maintain a constant citric acid cycle pool size. These pathways have been termed cataplerotic, although the term is a misnomer; instead, the word drainage seems more appropriate. Drainage pathways generally involve removing the citric acid cycle intermediates oxaloacetate

(as aspartate via transamination or as phosphoenolpyruvate via decarboxylation by phosphoenolpyruvate carboxykinase), citrate, or α-ketoglutarate (via transamination to glutamate). Although these drainage pathways are usually thought of as means to balance anaplerotic pathways, they play critical roles in renal gluconeogenesis and enterocyte energy production from glutamine (see later discussion).

Measuring Anaplerosis

Changes in Citric Acid Cycle Pool Size

There are two principal methods of assessing anaplerosis based on changes in citric acid cycle pool size. The amount of citric acid cycle pool intermediates can be measured enzymatically or resolved with high-performance liquid chromatography. Although both methods can reliably assess changes in the citric acid pool size, they do not provide an insight into the pathways involved in anaplerosis nor do they determine relative rates of enrichment. Furthermore, because anaplerosis is usually balanced by the exit of intermediates, changes in citric acid pool size are generally negligible.

Simply determining changes in citric acid cycle pool size provides no information on the rates of anaplerosis or on specific anaplerotic reactions. Using substrates labeled with tracer ^{14}C and measuring incorporation into specific positions in citric acid cycle intermediates is more revealing. This method can not only determine rates of anaplerosis, but also characterize the pathways involved in the process. However, the method is laborious and prone to error. It requires the sequential enzymatic degradation of intermediates and quantitation of the release of the ^{14}C label. It has been replaced by ^{13}C-nuclear magnetic resonance (NMR) spectroscopy or mass spectroscopy.

^{13}C-Nuclear Magnetic Resonance-Mass Spectroscopy

^{13}C-NMR spectroscopy is used to assess quantitatively the relative contributions of various substrates to the citric acid cycle. This method determines the anaplerotic enrichment of citric acid cycle intermediates such as the radiotracer method already discussed, but without digesting the carbon skeleton. ^{13}C-labeled compounds enter the carbon skeleton of citric acid cycle intermediates at specific positions through anaplerotic pathways or through the dilution of ^{13}C by the entry of unlabeled anaplerotic substrates. The enrichment of ^{13}C at those positions is then assessed, indicating citric acid cycle intermediate enrichment. The method is illustrated in Figure 2, in which the enrichment of the carbon skeleton

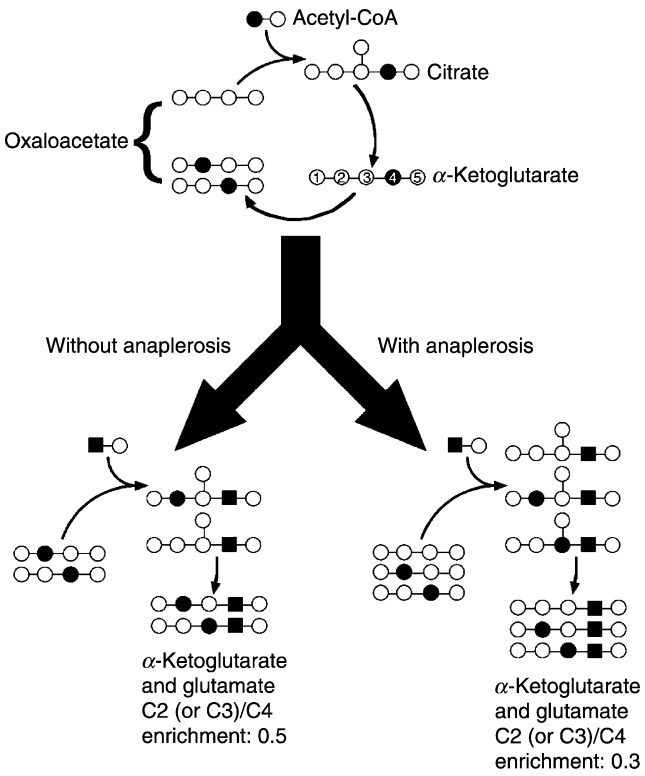

FIGURE 2 Fundamental concept of assessing anaplerotic flux using ^{13}C-NMR spectroscopy as described by Malloy *et al.* (1988). The black circles represent ^{13}C that enters the citric acid cycle pool via the first turn of the citric acid cycle. The black squares represent ^{13}C that enters the citric acid cycle pool via the second turn of the citric acid cycle.

of α-ketoglutarate (and glutamate) at the C2, C3, and C4 positions is used to quantify anaplerosis. Investigators have used the following strategy. Using [2-^{13}C]acetyl-CoA as a substrate and conditions in which there is no anaplerotic flux, one can assume that there is no dilution of the ^{13}C label in the C2 or C3 position of α-ketoglutarate. The label in these positions is generated from the randomization of the C4-position carbon in the first turn of the citric acid cycle. Therefore, the sum of the ^{13}C enrichments of the C2 and C3 carbons will be equal to the enrichment of the C4 carbon of glutamate. In contrast, with anaplerotic activity, the labeled C2 and C3 carbons will be diluted by ^{12}C arising from anaplerotic substrates, and the sum of the enrichments of the labeled C2 and C3 carbons will be less than the enrichment of the C4 carbon of glutamate.

Expression and Activity of Proteins Regulating Anaplerosis

Using the methods outlined, studies have focused on changes in enrichment of citric acid cycle intermediates to assess the activity of anaplerotic pathways and

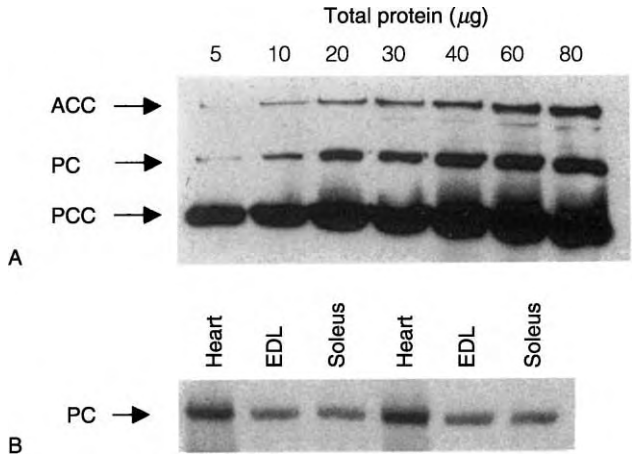

FIGURE 3 Expression of the biotin-containing carboxylases, acetyl-CoA (ACC), pyruvate carboxylase (PC), and propionyl-CoA carboxylase (PCC) in heart muscle based on (A) streptavidin blotting and (B) pyruvate carboxylase expression in rat heart and skeletal muscle. Reprinted from Gibala *et al.* (2000), *Acta Physiol. Scand.* **168**, 657–665, Scandinavian Physiological Society.

explain changes in flux in terms of mass action and allosteric regulation of key enzymes. Although this is most likely the case with acute changes in anaplerotic flux, changes in the expression and activity of enzymes responsible for anaplerosis should be taken into account when studying chronic processes such as pressure-overload-induced hypertrophy, heart failure, or diabetes. In streptozocin-treated diabetic rats, transcript levels of enzymes in anaplerosis in heart and skeletal muscle are down-regulated (Figure 3). Changes in transcript levels are paralleled by similar changes in protein expression. Although, the *in vitro* activities of the anaplerotic enzymes involved in the carboxylation of substrates (e.g., pyruvate carboxylase) can be measured by determining the incorporation of ^{14}C from $H^{14}CO_3^{-1}$, it is not known whether changes in expression correlate with changes in activity.

Changes in Anaplerosis in Response to Environmental Stress: Workload, Nutritional Status, and Disease

Ultimately, any metabolic process has functional consequences, and anaplerotic pathways are no exception. Anaplerotic pathways play important roles in regulating a wide variety of organ responses to conditions of metabolic stress ranging from exercise to inborn errors of metabolism.

Anaplerosis in Skeletal Muscle during Exercise

The transition from rest to moderate or intense exercise is associated with large increases in skeletal muscle ATP turnover, implying increases in citric acid cycle flux (up to 100-fold increases). Although, citric acid cycle intermediates increase only three- to fourfold, these relatively small increases in the citric acid cycle pool size (via anaplerosis) can reflect dramatic increases in citric acid cycle flux. It has been suggested that the increases allow skeletal muscle to adapt to the energetic demands of exercise, but, interestingly, there is no appreciable change in citric acid cycle pool size at lower levels of exercise. The majority of changes in individual intermediates occur in the second span of the citric acid cycle (i.e., from succinate to oxaloacetate) because the primary source of enrichment during acute exercise appears to be flux through the reaction catalyzed by alanine aminotransferase. This reaction results in entry of glutamate as α-ketoglutarate; however, pyruvate carboxylase and malic enzyme may contribute minor amounts to citric acid cycle enrichment in exercising muscle.

Glutamine Metabolism by the Small Intestine

Glutamine is a source of energy for a number of specialized tissues, including the small intestine. When glutamine is taken up by the small intestine, it enters the citric acid cycle as α-ketoglutarate and leaves the cycle through oxidation as CO_2. More specifically, α-ketoglutarate is converted to malate by citric acid cycle reactions and malate may be transported out of the mitochondria. In the cytosol, malate is converted to oxaloacetate. As in the liver and heart, the malate-aspartate shuttle is bidirectional. It can transport electrons from extramitochondrial NADH into the mitochondria or from intramitochondrial NADH to the cytosol.

Renal Ammonia Formation during Starvation

During starvation, when protein breakdown, renal gluconeogenesis, and hepatic ketogenesis increase, the rate of renal ammoniagenesis also increases. Ammonia is generated from amino acids, including glutamine, released by skeletal muscle. Glutamine is converted to α-ketoglutarate in renal cells; α-ketoglutarate is metabolized to malate; and malate is transported out of the mitochondria, oxidized to oxaloacetate and to phosphoenolpyruvate, and ultimately used for gluconeogenesis. Although different from glutamine oxidation by

enterocytes, this series of reactions also reflects the balance that is generally observed between anaplerotic and drainage pathways.

Ischemia and Substrate-Level Phosphorylation

Early studies assessing cardiac metabolism by measuring arteriovenous differences in amino acid concentrations revealed that, in patients with coronary artery disease and myocardial ischemia, the heart avidly takes up glutamate and releases alanine. This finding led to the hypothesis that the anaplerotic substrate glutamate enters the citric acid cycle as α-ketoglutarate via transamination with pyruvate (thereby forming the alanine that is released). Subsequently, the α-ketoglutarate is metabolized to succinate with the concomitant substrate-level phosphorylation of GDP to form GTP (Figure 4A). In this way, a span of the citric acid cycle can generate high-energy phosphates in the absence of sufficient oxygen for full citric acid cycle operation. Translational research based on this anaplerotic pathway has led to the development of glutamate-enriched solutions that increase anaerobic energy production of the heart during coronary artery bypass surgery.

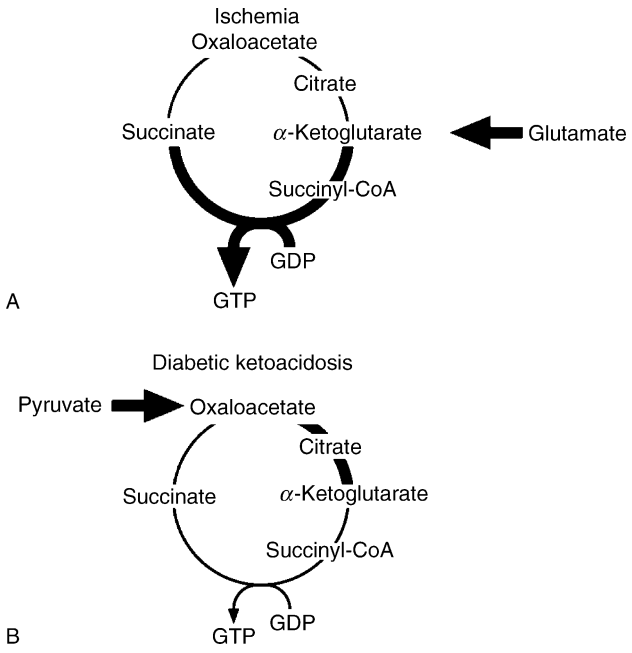

FIGURE 4 Role of anaplerosis in improving myocardial energetics in the setting of (A) ischemia and (B) diabetic ketoacidosis. Under both conditions, loss of cofactors (NAD^+/FAD^+ for ischemia, CoASH for diabetic ketoacidosis) inhibits full citric acid cycle activity. Anaplerotic pathways allow the citric acid cycle to work in spans, thereby increasing the production of high-energy phosphates. Adapted from Taegtmeyer and Passmore (1985).

Diabetes and Ketone Body Metabolism

Citric acid cycle pool size increases in the hearts of rats with experimentally induced diabetes, suggesting enrichment by anaplerotic pathways. We have suggested that an increase in anaplerotic flux, which primarily occurs through pyruvate carboxylation (via malic enzyme), plays an important role in maintaining flux through the second span of the citric acid cycle. Acutely, the metabolic derangement of ketoacidosis that occurs with diabetes inhibits flux through α-ketoglutarate dehydrogenase by sequestration of coenzyme A (CoASH). This phenomenon is associated with contractile dysfunction of the heart that can be readily reversed by the addition of glucose, lactate, or pyruvate (all of which are anaplerotic substrates). The effects of pyruvate are mediated by enrichment of malate in the citric acid cycle pool, which occurs by carboxylation of pyruvate to form malate and oxaloacetate through the actions of malic enzyme and pyruvate carboxylase, respectively (Figure 4B). The citric acid cycle is thereby able to operate once again in a span that can generate reducing equivalents to support oxidative phosphorylation of ADP to form the ATP necessary to drive the contractile machinery of the heart.

Long-Chain Fatty Acid Oxidation Defects and Myopathies

The inability to oxidize long-chain fatty acids due to deficiencies in activity of carnitine palmitoyltransferase-1 or the enzymes involved in β-oxidation is associated with contractile dysfunction due to skeletal and heart muscle damage. One proposed mechanism for the decrease in contractile activity is decreased citric acid cycle flux due to loss of intermediates from damaged myocytes. Based on this hypothesis, a recent trial treated patients with defects in long-chain fatty acid oxidation with odd-chain triglycerides (which can increase the citric acid cycle pool size by entering as succinyl-CoA) and tested the hypothesis that an increase in citric acid cycle pool size may improve muscle function. The study demonstrated beneficial effects, such as reversing left-ventricular dysfunction, decreasing muscle breakdown, and decreasing weakness.

Summary and Perspective

Efficient energy transfer in the mammalian cell is linked to a series of moiety-conserved cycles, including the citric acid cycle. Changes in the cell's environment lead to depletion and replenishment (anaplerosis) of citric acid cycle intermediates. The multiple pathways of

anaplerosis use a variety of substrates, including carbohydrates, odd-chain fatty acids, and amino acids. These pathways reflect a system of redundancy that is important for the functional survival of the cell.

See Also the Following Articles

ATP Synthesis: Mitochondrial Cyanide-Resistant Terminal Oxidases • Cytochrome *c* • Cytochrome Oxidases, Bacterial • Respiratory Chain and ATP Synthase • Uncoupling Proteins

Glossary

anaplerosis The entry of substrates into the citric acid cycle as intermediates other than acetyl-CoA, thereby increasing the citric acid cycle pool size.

carboxylation The introduction of a carboxyl group into a compound.

***β*-oxidation** The oxidative metabolism of fatty acids through a cycle of reactions that removes successive two-carbon units (acetyl-CoA) from the fatty acid.

Further Reading

Gibala, M. J., Young, M. E., and Taegtmeyer, H. (2000). Anaplerosis of the citric acid cycle: Role in energy metabolism of heart and skeletal muscle. *Acta Physiol. Scand.* **168**, 657–665.

Kornberg, H. (1966). Anaplerotic sequences and their role in metabolism. *Essays Biochem.* **2**, 1–31.

Malloy, C., Sherry, A., and Jeffrey, F. (1988). Evaluation of carbon flux and substrate selection through alternate pathways involving the citric acid cycle of the heart by ^{13}C-NMR spectroscopy. *J. Biol. Chem.* **263**, 6964–6971.

Martini, W. Z., Stanley, W. C., Huang, H., Rosiers, C. D., Hoppel, C. L., and Brunengraber, H. (2003). Quantitative assessment of anaplerosis from propionate in pig heart *in vivo*. *Am. J. Physiol.* **284**, E351–E356.

Owen, O. E., Kalhan, S. C., and Hanson, R. W. (2002). The key role of anaplerosis and cataplerosis for citric acid cycle function. *J. Biol. Chem.* **277**(34), 30409–30412.

Panchal, A. R., Comte, B., Huang, H., Kerwin, T., Darvish, A., Des Rosiers, C., Brunengraber, H., and Stanley, W. C. (2000). Partitioning of pyruvate between oxidation and anaplerosis in swine hearts. *Am. J. Physiol.* **279**(5), H2390–H2398.

Roe, C. R., Sweetman, L., Roe, D. S., David, F., and Brunengraber, H. (2002). Treatment of cardiomyopathy and rhabdomyolysis in long-chain fat oxidation disorders using an anaplerotic odd-chain triglyceride. *J. Clin. Invest.* **110**, 259–269.

Russell, R., and Taegtmeyer, H. (1991a). Changes in citric acid cycle flux and anaplerosis antedate the functional decline in isolated rat hearts utilizing acetoacetate. *J. Clin. Invest.* **87**, 384–390.

Russell, R., and Taegtmeyer, H. (1991b). Pyruvate carboxylation prevents the decline in contractile function of rat hearts oxidizing acetoacetate. *Am. J. Physiol.* **261**, H1756–H1762.

Taegtmeyer, H., and Passmore, J. M. (1985). Defective energy metabolism of the heart in diabetes. *Lancet* **1**, 139–141.

Vincent, G., Comte, B., Poirier, M., and DesRosiers, C. (2000). Citrate release by perfused rat hearts: A window on mitochondrial cataplerosis. *Am. J. Physiol.* **278**(5), E846–E856.

Biography

Raymond R. Russell III is an Assistant Professor of Medicine (Cardiology) at Yale University School of Medicine. His laboratory investigates mechanisms of non-insulin-mediated glucose uptake, uncoupling proteins, and metabolic regulation in the heart. He received both his M.D. and his Ph.D. from the University of Texas Health Science Center at Houston in 1991 and served his residency and fellowship at Yale.

Heinrich Taegtmeyer is a Professor at the University of Texas-Houston Medical School, a cardiologist, and a biochemist. His research interests focus on the logic of cardiac metabolism. He received his M.D. from the University of Freiburg in Breisgau, Germany; was a resident on the Harvard Medical Service at the Boston City Hospital; and was a cardiology fellow at the Peter Bent Brigham Hospital. From 1978 to 1981 he studied in the Metabolic Research Laboratory at the University of Oxford (England), under the late Sir Hans Krebs and Regnal Hems, where he earned his D.Phil.

Angiotensin Receptors

Tadashi Inagami
Vanderbilt University, Nashville, Tennessee, USA

Angiotensin (Ang), initially considered as a major pressor substance, is now recognized to mediate numerous physiological and pathophysiological functions. Over the past 70 years, four different active forms of angiotensins, Ang II, Ang III, Ang IV, and Ang (1-7), have been identified. The complexity of their action was multiplied by subtypes of their respective receptors, AT_{1A}, AT_{1B}, and AT_2 for Ang II, AT_4 for Ang IV, and Ang (1-7) receptors (Table I). Each subtype of the receptors shows more than one signaling mechanism. This article presents an overview of the formation and structure, and the receptors of Ang's and representative signaling pathways that play very colorful regulatory functions, which cover wide areas such as vasoconstriction, vasorelaxation cardiovascular hypertrophy and remodeling, atherosclerosis, thrombosis, stimulation of mineralocorticoid synthesis and release, facilitation of sympathetic outflow, renal electrolyte metabolism, control of central nervous system in water drinking behavior, blood pressure regulation, memory retention, growth inhibition apoptosis, tissue differentiation, arachidonic acid and prostaglandin formation, and regulation of insulin signals.

Angiotensins (Ang) Structure and Formation

Angiotensin I

All angiotensins are derived from the amino terminus of the ~65 kDa prohormone angiotensinogen via a series of proteolytic cleavage by a variety of proteinases and peptidases. The enzyme that initiates this process is renin. This aspartyl protease is active in pH 6–7, reacts exclusively with angiotensinogen, and cleaves only one singular leucyl peptide bond of the prohormone between residues 10 and 11 generating the decapeptide Ang I (Figure 1). Ang I is hormonally inactive, thus it is prohormone as it has no specific receptor to transmit its signal. The physiological, significance of Ang I appears to confer the high degree of specificity to the angiotensin generating system in plasma or intracellular system in which there are numerous proteins.

Angiotensin II

The inactive Ang I is activated to the active Ang II by the metallo-endopeptidase, angiotensin I converting enzyme (ACE), which is identical to kininase II. This enzyme was the target for the first most successful drugs for the treatment of renin-dependent hypertension, with a minimum of side effects and complications. Starting with captopril, a series of long acting ACE inhibitors were synthesized and were found to almost completely block Ang II formation. Ang II has two subtypes of receptors, AT_1 and AT_2. The heptapeptide Ang III is the product of amino terminal cleavage of Ang II by aminopeptidases. Although Ang III is prominent in the neuronal system, it shares receptors, AT_1 and AT_2, with Ang II. The amino acid sequence of rat AT_1 and AT_2 are shown in Figure 2.

Ang (1-7)

Ang (1-7) can be formed mainly by the removal of carboxyl terminal tripeptide from Ang I or of a carboxypeptidase from Ang II. It has been shown to activate phospholipase A_2 to release arachidonic acid from phospholipids leading to the formation of prostaglandins.

Ang IV

Ang IV is the hexapeptide Ang (3-8). It was reported to stimulate the production of plasminogen activator inhibitor to stabilize blood clots and to promote atherosclerosis. Other roles in the brain have been reported.

Whereas receptors for Ang II, Ang III, and Ang (1-7) are G-protein coupled receptors, the receptor isolated and cloned from the adrenal membranes is a single transmembrane type.

Angiotensin Receptor

Ang I Binding Protein

Despite the ubiquitous distribution of Ang I binding proteins, no physiological function was found for it.

TABLE I

Angiotensin Receptors

Angiotensins	Receptors	G-proteins coupled
Ang II	AT_{1a}	$G_{q/11}$, G_i, $G_{12/13}$
	AT_{1b}	$G_{q/11}$, G_i, $G_{12/13}$
	AT_2	G_i
Ang III	The same as Ang II	The same as AT_1 and AT_2
Ang (1-7)	*Mas* oncogene product	?
Ang IV	AT_4/IRAM	Single transmembrane receptor

ANG II RECEPTORS

Receptor Subtypes

Synthesis of a series of variants of Ang II revealed the presence of an Ang II receptor, confirming the earlier finding that there are two types of Ang II receptors, one resistant to dithiothreitol and the other sensitive to the treatment. Inactive variants of Ang II were synthesized to obtain Ang II receptor antagonists. These inhibitor peptides also showed the importance of Arg^2, Tyr^4, and Arg^8 for type 1 Ang II receptors. Particularly, replacement of Phe^8 to Ile, Thr, or Ala (saralisine) greatly reduced Ang II receptor signals such as Ca^{2+} response although binding is not significantly affected. However, these peptidic analogs were partial agonists. These peptidic inhibitors did not distinguish two different receptors, AT_1 and AT_2. We had to wait until the syntheses of nonpeptide inhibitors to obtain indications for the presence of at least two receptor subtypes for Ang II that differ in biochemical and physiological responses, localization, and ontogeny.

Direct proof for the two major receptor subtypes AT_1 and AT_2 were provided by expression cloning of their cDNAs from rat and bovine tissues. Rodents were found to have three genes: AT_{1a}, AT_{1b}, and AT_2. It is likely that birds, reptiles, and amphibians may also have more than one type of receptor. Rat or mouse murine AT_{1a} and AT_{1b} share a 98% amino acid sequence identity through their respective genes and are located in different chromosomes. They can be distinguished only by Northern blot analysis or *in situ* hybridization of 3′ noncoding sequences, where a sizeable difference occurs in nucleotide sequences. In contrast, AT_1 and AT_2 share only 34% amino acid sequence homology. Noteworthy is the localization of the AT_2 gene in the X chromosome throughout species.

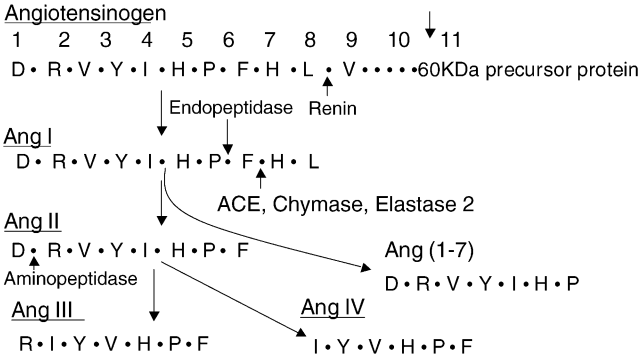

FIGURE 1 Angiotensinogen and generation.

AT_1 Receptor Signaling

Most of the signal responses considered earlier as Ang II actions seem to be mediated by AT_1. These responses are smooth muscle contraction and hypertension, mineralocorticoid synthesis, tyrosine hydroxylase gene expression in adrenal and central and peripheal adrenergic facilitation, stimulation of cellular hypertrophy, mitogenesis and migration, plasminogen activator synthesis, stimulation of fibrosis, renal sodium retentions, centrally regulated dipsogenesis, and hypertension. The major AT_1 signaling pathways are mediated by the Gq/11 mediated phospholipase β_1 activation via cellular $[Ca^{2+}]$ increase and protein kinase activation. However, AT_1 can also couple to Gi, $G_{12/13}$.

It is now well accepted that AT_1 can also activate pathways that involve tyrosine kinase activation such as epidermal growth factor (EGF) receptor through Ca^{2+}-stimulated heparin binding-EGF, and consequent activation of Ras, ERK 1/2 which will further result in $p70^{s6k}$ and phosphatidyl inositol-3-kinase and activation of immediate early gene pathways. AT1 also activates the JAK-STAT system, Src family kinases, tyrosine phosphatase SHP-2, PLC-δ, JNK, and p38 MAP kinase. Accumulating lines of evidence seem to support that some of these tyrosine kinase pathways do not involve G-proteins based on results of mutagenesis studies that eliminate key residues required for interaction of cytoplasmic loops of AT_1.

Importantly, many of the tyrosine kinase activation steps are activated by the reactive oxygen species (ROS), such as superoxide anion and hydrogen peroxide. The formation of super oxide anion is mediated by NAD(P)H oxidase, which is also activated by Ang II. Important recent additions to the knowledge of Ang II mediated smooth muscle contraction is sensitized by the Rho–Rho kinase system. This information is of particular significance for the mechanism of hypertension. On the other hand, cardiovascular hypertrophy and remodeling of resistance vessels are another important aspect for cardiac failure and diminished vascular compliance and hypertension.

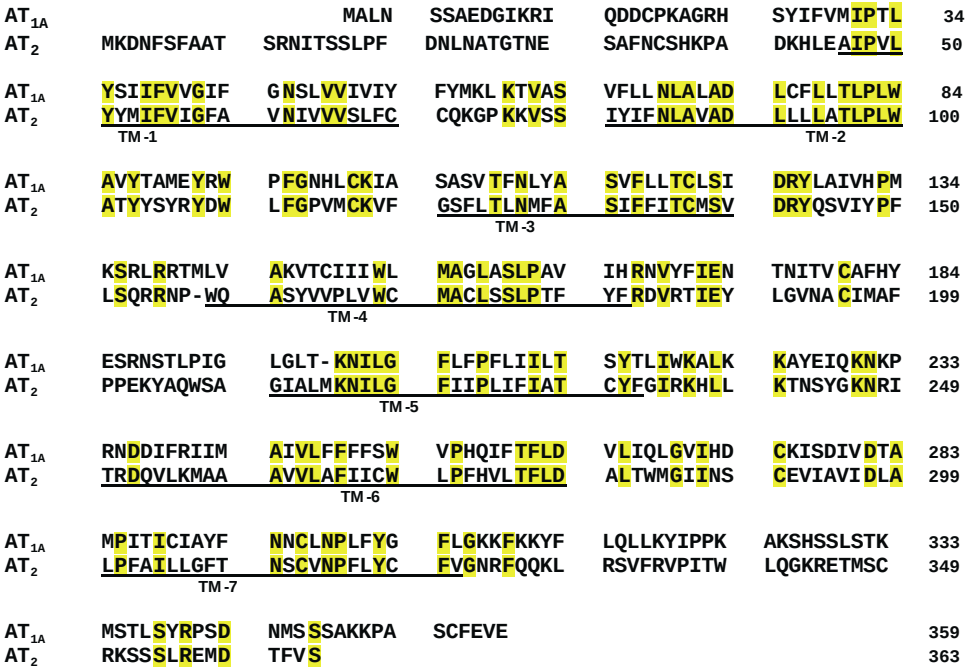

FIGURE 2 Rat angiotensin receptor AT_{1A} and AT_2.

AT_2 Receptor Signaling

Studies on AT_2 signaling, particularly using cultured cells, were not straightforward because of rapid disappearance of AT_2 receptor during repeated passage of cells and exposure to growth medium. Interpretation of results was also difficult because of rapid ontogenic change in AT_2 expression, particularly postnatal decline and increase under stress, during tissue repair or inflammation. *In vivo* studies eliminate many of these difficulties. Thus, *in vivo* studies of loss-of-function studies of AT_2 in the kidney, vasculature, heart, and brain particularly adrenal and colon, where AT_2 remains expressed in adults, are producing substantive results.

In vitro Studies on AT_2 Receptor Signals

Although AT_2 (the AT_2 receptor) is labile in cells in growth culture medium, some cells, such as PC12w, N1E115, and R3T3, maintain AT_2 expression but not AT_1 over several generations. Ang II stimulation resulted in growth inhibition via either MAP kinase phosphatase or the tyrosine phosphatase SHP1 even inducing apoptosis, but not all AT_2 expressing tissues or cells undergo apoptosis. Ovarian atretic cells express AT_2 prominently, yet Ang II treatment failed to induce apoptosis. AT_2 expressed in neuronal cells activate Ser/Thr phosphatase PP2A via a Gi-coupled mechanism and was reported to open delayed rectifier K^+ channel, a hyperpolarizing mechanism. Its growth inhibitory mechanism on endothelial cells was shown to involve the following sequence of events:

Lowering pH → Release of cycloplasmic kallikrein → generation of bradykinin → activation of NOS

This can explain relaxation or dilation of resistance arteries *ex vivo* by AT_2 and its reversal by its specific synthetic inhibitor PD123319 or PD123177 and relaxation by AT_2 partial agonists CGP24112. Although AT_2 was shown to bind specifically with Giα2 or Giα3, not all of these growth suppressing or cGMP mediated signals were inhibited by pertussis toxin.

In vivo Studies on AT_2 Signals

AT_2 gene deleted mice and AT_2 inhibitor treated mice were shown to slowly retain Na and show impaired natriuresis and markedly diminished urinary cGMP, presumably by the mechanism analogous to endothelial cells discussed above. These observations seem to indicate that the signals mediated presumably by inhibition of phosphatases work in the direction opposite to the growth-stimulating signal of AT_1. However, paradoxical observation exists in which AT_1 and AT_2 function in parallel. An increasing number of publications reported that chronic infusion of the AT_2-specific blocker PD123319 was able to inhibit chronic Ang II-induced aortic smooth muscle hypertrophy and fibrosis despite continuously elevated blood pressure. Despite a short half-lifetime of PD123319 *in vivo*, chronic infusion by osmotic mini-pump suppressed

the Ang II-infused aortic hypertrophy. AT_2 gene deleted mice also showed marked resistance against left ventricular hypertrophy induced by pressure overload or chronic Ang II infusion. Another example of parallel phenotypic effect of AT_1 and AT_2 was found in stimulation of tyrosine hydroxylase by both AT_1 and AT_2 in adrenal chromaffin cells *in vivo*.

Since all of the paradoxical results were obtained under well-controlled conditions, signaling mechanism specific tissues were investigated. It was found that the AT_2 binds a zinc finger protein and serves as a transporter to deliver the zinc finger protein to the nucleus, which activated transcription of phosphatidyl inositol 3-kinase p85α subunit (p85αPI3K). This triggers a subsequent cardiac hypertrophic pathway. These results indicate that the AT_2 mediated cardiac hypertrophy uses signals distinct from that which are activated by AT_1. The parallel phenotypic results were due to tissue specific expression of the zinc finger protein in the heart but not in the kidney, where the AT_2 signal depends on the kallikrein-NOS-cGMP mechanism. In contrast, the cardiac tissue uses a more direct activation mechanism of nuclear transcription of p85αPI3K. The p85PI3K activation has been shown to induce a variety of cardiac hypertrophy mechanisms.

Major Physiologic Roles and Morphogenesis of AT_1 and AT_2

Targeted gene deletion of AT_{1A}, AT_{1B}, or angiotensinogen in mice showed that angiotensin II has a profound effect on the maintenance of blood pressure, dual deletion of AT_{1A}, AT_{1B} resulted in hypotension by 45–50 mmHg and no pressor response to Ang II infusion. AT_{1B} was responsible for only 10% of the pressor effect. Interestingly, these animals showed profound defects in the renal papillary and medullary formation suggesting defects in Na reabsorption, an idea in agreement with the poly urea and increased Na excretion. These animals were stunted and it was difficult to keep them alive without daily saline injection. AT_2 gene deletion did not cause overt physical deficiency. However, closer examination revealed that AT_2 deficient mice show high frequency (28% penetrance) of uretero-renal pelvis ligation that is closely analogous to a human neonatal disease called Kakkut syndrome. Connection to the ureter of the renal pelvis is the last step of the kidney morphogenesis and AT_2 concentration is seen in the renal pelvis at this stage in a normal fetus.

Recently, Srivastava's group reported a very intriguing observation in which they identified families with severe mental retardation and traced their gene defect to the absence or "mis sense" mutation of AT_2 gene on the X chromosome. Thus, AT_2 function is not only limited to the renal, adrenal, and cardiovascular system, but brain function also depends on AT_2. Indeed AT_2 gene deficient mice show a pattern of fearful behavior.

Angiotensin (1-7)

Functions

Ferrario and his associate reported physiological functions of Ang (1-7). Since the heptapeptide seemed to be generated by one step of carboxypeptidase, it was not clear whether it was a part of Ang II function. However, it was shown that Ang (1-7) is generated from Ang I by an endopeptidase. Since the affinity of the heptapeptide binding to the brain plasma membrane was in the nanomolar range, it seemed to have a physiological significance. Its specific action was shown as arachidonate release and prostaglandin synthesis. Its systemic presence and function were also demonstrated. Decisive evidence of Ang (1-7) as a hormonal peptide came as the receptor was identified.

Ang (1-7) Receptor

In 1988, Hunley *et al.* presented the hypothesis that *Mas* oncogene product was the Ang II receptor. This hypothesis failed to meet the test of many investigators. AT_1 and AT_2 were cloned soon afterward as unmistakable Ang II receptors. However, the *Mas* oncogene story made a full circle recently when Santos, Walther, and their collaborators showed that the *Mas* oncogene product expressed in COS7 cells binds Ang (1-7) with a nanomolar K_D value and releases prostaglandins in an abstract form. It has a structural feature of a seven transmembrane domain receptor. Further details are awaited.

Ang IV

Harding *et al.* showed that the hexapeptide Ang IV binds to receptors in a variety of tissues and increases blood flow. Recently, Xie, Mendelsohn, and their collaborators purified Ang IV receptor from adrenal plasma membrane and succeeded in cloning the cDNA. They found that it is identical with insulin-regulated amino peptidase (IRAP) with a single transmembrane domain. Its possible interaction with insulin is of potential interest as an interface between angiotensin and insulin. However, Ang IV is not the only ligand that binds the extracellular domain. LVV hemorphin, a segment of hemoglobin, was also reported to be a binding ligand. AT_4 is expressed heavily in the hippocampus and signals to stimulate acetylcholine. Its potential role in memory retention is of great interest in relation to a possible regulatory role of this aminopeptidase.

Ang II also was shown to be involved in the regulation of long-term potentiation (LTP). Thus, the roles of angiotensin are not limited to the control of blood pressure, water drinking, and dipsogenesis in the hypothalamus and brain stem. AT_4 expressed in hippocampus, AT_2 expressed in central amygdala nucleus, and Ang II stimulation of LTP points to roles of angiotensins in normal cortical function.

AT_3

We reported non-AT_1-non AT_2 Ang II receptors in neuro 2A cells were expressed at room temperature, but not at 37 °C. Therefore, we consider it as a likely product of mycoplasm that infected the neuro 2A cell line we used. Thus, at present AT_3 is not of mammalian origin.

See Also the Following Articles

Epidermal Growth Factor Receptor Family • JAK-STAT Signaling Paradigm • Src Family of Protein Tyrosine Kinases

Glossary

angiotensin II Peptide hormone derived from angiotensinogen.
cardiovascular effects Effects on the heart and blood vessels.
receptor Hormone binding protein.
receptor signal Reaction emitted from the receptor upon hormone binding.

Further Reading

Berk, B. C., and Corson, M. A. (1997). Angiotensin II signal transduction in vascular smooth muscle, role of tyrosine kinase. *Circ. Res.* **80**, 607–616.

deGasparo, M., Catt, K. J., Inagami, T., and Harding, J. (2000). The angiotensin II receptors. *Pharmacol. Rev.* **52**, 639–672.

Eguchi, S., and Inagami, T. (2000). Signal transduction of angiotensin II type 1 receptor through receptor tyrosine kinase. *Regul. Pept.* **91**, 13–20.

Ferrario, C. M., and Iyar, S. M. (1998). Angiotensin (1-7): A bioactive fragment of the renin–angiotensin system. *Regul. Pept.* **78**, 13–18.

Gallinat, S., Busche, S., Raizada, M. K., and Sumners, C. (2000). The angiotensin II type 2 receptor: An enigma with multiple variations. *Am. J. Physiol.* **278**, E357–E374.

Horiuchi, M., Akishita, M., and Dzau, V. J. (1999). Recent progress in angiotensin II type 2 receptor research in the cardiovascular system. *Hypertension* **33**, 613–621.

Inagami, T. (1999). Molecular biology and signaling of angiotensin receptors: An overview. *J. Am. Soc. Nephrology* **10**, 52–57.

Matsubara, H. (1998). Pathophysiological roles of angiotensin II type 2 receptor in cardiovascular and renal diseases. *Circ. Res.* **83**, 1182–1191.

Timmermans, P. B. M. W. M., Wong, P. C., Chiu, A. T., Herblin, W. F., Carini, D. J., Lee, R. J., Wexler, R. R., Saye, J. A. M., and Smith, R. D. (1993). Angiotensin receptor and angiotensin II antagonists. *Pharmacol. Rev.* **45**, 205–251.

Touyz, R. M., and Schiffrin, E. (2000). Signal transduction mechanisms mediating the physiological and pathological actions of angiotensin II in vascular smooth muscle cells. *Pharmacol. Rev.* **52**, 639–672.

Wright, J. W., Krebs, L. T., Stobb, J. W., and Harding, J. W. (1995). The angiotensin IV system: Functional implication. *Front. Neuroendocrinol.* **16**, 23–52.

Biography

Tadashi Inagami obtained his B.S. from Kyoto University, Kyoto, Japan in 1953, and his Ph.D. in Chemistry from Yale University in 1958. After his postdoctoral training, he joined the Vanderbilt University School of Medicine and has been on the faculty of the Department of Biochemistry since 1966. He assumed the Stanford Moore Professorship in 1992. His research has centered on the biochemistry of vasoactive substances including renin, angiotensin receptor and signaling on intracellular angiotensin generation, cellular hypertrophy signals in vascular smooth muscle cells, and cardiac myocytes.

ara Operon

Robert F. Schleif
The Johns Hopkins University, Baltimore, Maryland, USA

The arabinose operon in the bacterium *Escherichia coli* enables uptake and catabolism of the pentose sugar L-arabinose as the cell's sole source of carbon and energy. In the presence of arabinose, the synthesis of the proteins required for these activities is increased up to 300-fold under the control of the operon's arabinose sensor and regulatory protein, AraC. Expression of the arabinose genes is also subject to catabolite repression, and the catabolite repression protein, CRP, as well as the AraC protein, both bind in the promoter regions of the arabinose gene clusters to regulate expression. In the absence of arabinose, AraC protein binds to two half-sites at the ara p_{BAD} promoter and forms a DNA loop that represses expression. The widespread phenomenon of DNA looping was discovered in the arabinose system. In the presence of arabinose, the loop opens and AraC protein acts positively to assist the binding of RNA polymerase to the p_{BAD} promoter and also speeds the conversion of bound RNA polymerase into the transcriptionally active open complex.

Genetics and Physiology

The pathway for the catabolism of L-arabinose in *Escherichia coli* includes two uptake systems and three enzymes for the conversion of arabinose into D-xylulose-5-phosphate (Figure 1). The *araE* gene codes for a low-affinity arabinose symport protein that couples arabinose uptake to proton uptake. The *araF, araG,* and *araH* genes code for three components of a high-affinity transport system that uses ATP as the source of energy. The products of the *araA*, *araB*, and *araD* genes catalyze the isomerization of L-arabinose to L-ribulose, its phosphorylation to L-ribulose-5-phosphate, and its epimerization to D-xylulose-5-phosphate, which then enters the pentose phosphate pathway and whose enzymes are not subject to direct regulation by arabinose. Expression of the *araA, B, D, E, F, G,* and *H* genes as well as a gene of unknown function, *araJ*, is under control of the *araC* gene product. Expression of the *ara* genes is also under control of the catabolite repression protein, CRP. Thus, expression is low in growth medium containing glucose. Arabinose stimulates increased initiation of *ara* operon messenger within 3 s of its addition to a growing culture.

Transcription Regulation Mechanisms

In the absence of arabinose, the dimeric AraC protein binds to the $araO_2$ and $araI_1$ half-sites, which are 210 bp apart, and forms a DNA loop (Figure 2). The presence of the DNA loop interferes with the binding of RNA polymerase to the p_{BAD} and p_C promoters. Upon the addition of arabinose, AraC protein prefers to bind to the adjacent I_1 and I_2 half-sites. Occupancy of the I_2 half-site stimulates the binding of RNA polymerase to its adjacent binding site and assists RNA polymerase in making the transition to an open complex capable of initiating transcription. Protein–protein contacts important for binding and open complex formation are made between the C-terminal domain of the α-subunit of RNA polymerase and activation region three of CRP as well as the two DNA binding domains of AraC. Contacts likely are also made between the DNA-binding domain of the AraC subunit bound to I_2 and the σ-subunit of RNA polymerase.

Control of DNA Looping

AraC protein shifts from the state of preferring to loop DNA (when arabinose is absent) to the state of preferring to bind to adjacent DNA half-sites (when arabinose is present). The mechanism by which arabinose brings about this change in DNA-binding properties is called the light switch mechanism. In the absence of arabinose, an arm of 18 residues extends from the dimerization-arabinose-binding domain of AraC and binds to the backside of the DNA-binding domain. This arm interaction, plus the covalent connection between the dimerization-arabinose-binding domain and the DNA-binding domain, holds the DNA-binding domains of AraC protein in such an orientation with respect to each other that they are well positioned for DNA looping between O_2 and I_1. Binding to the adjacent I_1 and I_2 half-sites would require extensive bending of the protein and breaking of at least one of the two arm-DNA-binding domain interactions.

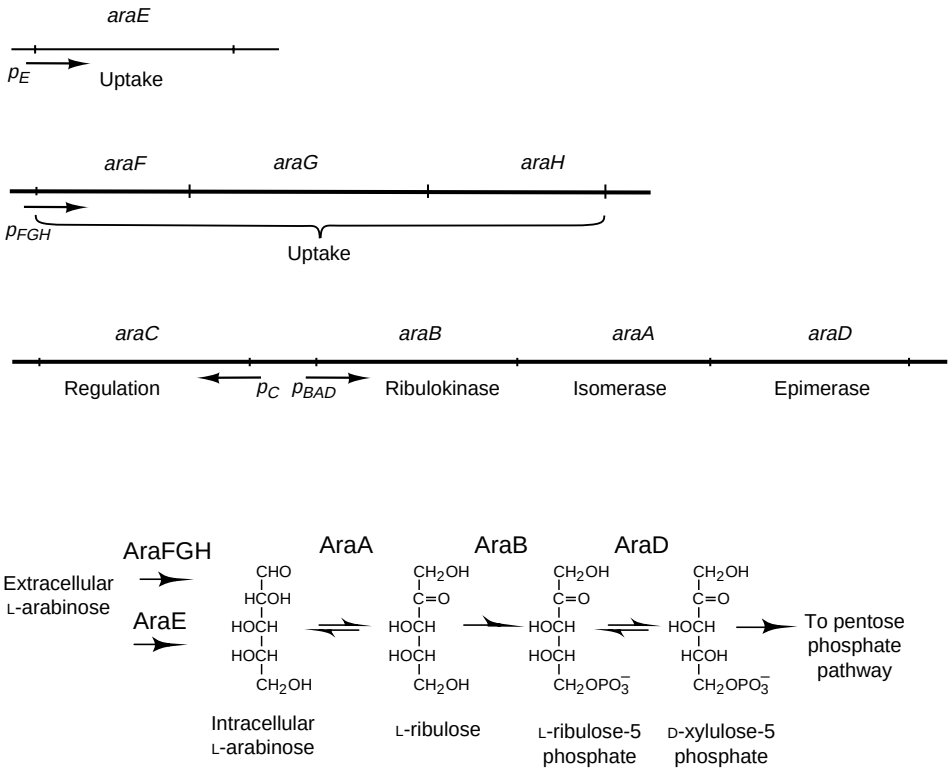

FIGURE 1 Structure of the *ara* gene clusters in *E. coli* that code for the proteins required for arabinose uptake and catabolism, the catabolic pathway, and the enzymes involved.

When arabinose binds to the dimerization-arabinose-binding domain, the arm prefers to bind over the arabinose rather than to the DNA-binding domain. Thus, the DNA-binding domains are freed from the arm-induced constraints, and they can easily position themselves for binding to the direct repeat half-sites I_1 and I_2. In this situation, it is energetically more favorable for the protein to bind to these half-sites rather than to form a DNA loop. Thus, the DNA-binding domain that formerly had been bound to O_2 repositions to I_2, and induction ensues.

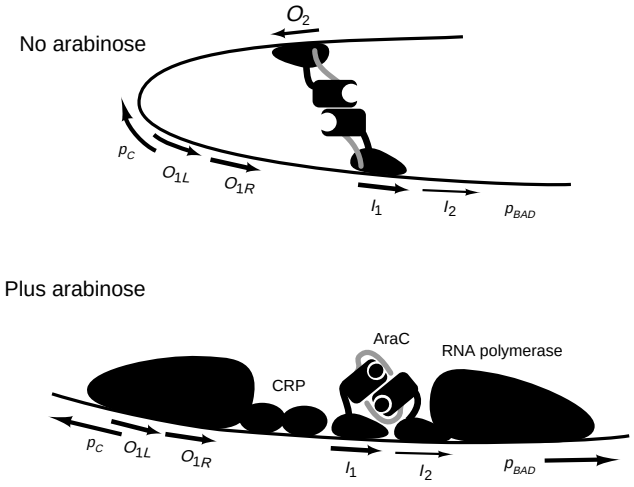

FIGURE 2 The regulatory region between the *araC* and *araBAD* genes containing the promoters p_{BAD} and p_C. In the absence of arabinose, AraC forms a loop between the O_2 and I_1 half-sites. In the presence of arabinose, AraC binds to the adjacent I_1 and I_2 half-sites. The N-terminal arm of AraC is indicated in gray. The p_C promoter is considerably less active than the p_{BAD} promoter. Its activity is further depressed by the binding of AraC to the O_{1L} and O_{1R} half-sites.

The Discovery and Demonstration of DNA Looping

Ellis Englesberg, who initiated genetic studies of the arabinose operon, isolated a deletion extending from outside the *araCBAD* region through at least part of the *araC* gene and into the promoter region. The deletion has the peculiar property that the remaining p_{BAD} promoter can still be fully induced even though the promoter has lost the ability to be repressed by AraC. This property suggested that a site that is required for repression lies upstream from all the sites required for induction. Indeed, an extensive deletion analysis by Schleif confirmed the existence of such repression from upstream and indicated that the upstream site is several hundred nucleotides ahead of all the sites required for induction. The site was definitively identified after the development of genetic engineering technology. *In vivo* footprinting showed

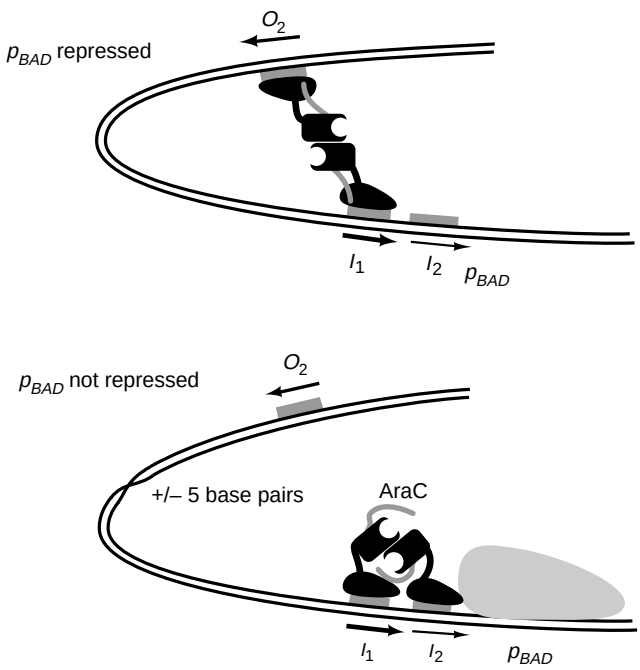

FIGURE 3 Helical twist experiment showing the involvement of the O_2 half-site in repression of p_{BAD}. Introduction of 5 bp of DNA between O_2 and I_1 rotates O_2 to the backside of the DNA and prevents loop formation. In this situation, a small fraction of AraC, even though arabinose is absent, binds at I_1–I_2 and somewhat stimulates the activity of p_{BAD}.

that both the upstream half-site, *ara*O_2, and the *ara*I_1 half-site are occupied by AraC and that mutations in either half-site abolish binding at both half-sites. Introduction of 5 bp of DNA between *ara*O_2 and *ara*I_1 blocks DNA looping and repression by AraC, but still allows induction of p_{BAD} in the presence of arabinose (Figure 3). A 5 bp insertion rotates the O_2 half-site half a turn around the helical DNA with respect to the I_1 half-site so that O_2 the half-site no longer faces toward I_1 and loop formation is not possible. The expression pattern of many additional spacing strains that were generated by inserting and deleting DNA between the half-sites reveals a cyclical pattern of repression with a period of 11.1 bp, thus measuring the helical twist of DNA *in vivo*. DNA looping in the *ara* system has also been demonstrated and studied *in vitro* with gel electrophoresis.

Related Systems

A number of bacteria – e.g., *Salmonella typhimurium, Citrobacter freundii,* and *Erwinia chrysanthemi* – contain genes with greater than 95% sequence identity to AraC, and thus it can be inferred that they contain arabinose operons that are controlled like that in *E. coli*. *Bacilus subtilis* can utilize arabinose as a source of carbon and energy, but its arabinose operon genes are negatively regulated.

At the amino acid sequence level, no close homologues are yet known to the dimerization domain of AraC. Its structure is known to consist of a jelly roll motif that binds arabinose and a coiled-coil motif that dimerizes the protein. Several homologues – including the rhamnose operon regulators, RhaR and RhaS, and the melibiose operon regulator, MelR – are likely however to possess related structures. Many sequence homologues exist to the DNA-binding domain of AraC. Typically, the level of sequence homology between two members of this family, called the AraC/XylS family, is ~20%. Because these family members are gene regulators and generally act positively, they can be inferred to possess similar structure. The structures of MarA and Rob, two proteins in the family, have been determined. Each consists of two helix–turn–helix motifs joined by a long α-helix. This provides an explanation of how each of the two DNA-binding motifs that are found in each DNA-binding domain of the dimeric AraC, contact 17 bp half-sites. For AraC these half-sites are in a direct repeat orientation. The half-sites of RhaR and RhaS, however, are in inverted orientation, illustrating how flexibly the dimerization and DNA-binding domains may be connected in this family.

History and Historical Significance

Genetic analysis of the arabinose operon was begun by Ellis Englesberg. His studies were among the first to suggest that a regulatory protein could act positively to turn on expression of a gene rather than act negatively to turn off expression as had been shown for the *lac* and lambda phage repressors. His genetic analyses also indicated that AraC protein acted negatively and that at least some of the DNA sequence required for this repression lay upstream of all the sites required for induction of expression. Subsequent genetic analysis by Schleif confirmed this result, and revealed DNA looping as the explanation. Further work by Schleif discovered the light switch mechanism by which arabinose controls the preference of AraC to loop in the absence of arabinose and to bind to adjacent DNA half-sites in the presence of arabinose.

The demonstration of positive regulation by AraC was one of the first indications of the wide diversity of regulatory mechanisms that are utilized in nature. Positive regulation is now known to occur in a great many regulation systems, both prokaryotic and eukaryotic. Similarly, DNA looping is widespread in nature. The discovery of DNA looping came at a convenient time to provide an explanation for action-at-a-distance phenomena, e.g., the way in which enhancers in eukaryotic cells can affect gene expression.

See Also the Following Articles

RNA Polymerase Reaction in Bacteria • RNA Polymerase Structure, Bacterial • T7 RNA Polymerase

Glossary

CRP or **CAP** A positive regulator of many genes in *E. coli* that is active only in the presence of cyclic AMP.

DNA looping The binding of a protein or a complex of proteins to two well-separated DNA sites.

light switch Name of the mechanism by which AraC responds to arabinose. In one position of its N-terminal arm of 18 amino acids AraC prefers to form DNA loops, and in the other position of the arm the protein prefers to activate transcription.

open complex RNA polymerase bound at a promoter possessing a melted structure of ~14 bases centered at the site at which transcription will begin. RNA polymerase first binds to double stranded DNA in a closed complex, which then opens.

positive regulation The regulation mode of a gene that requires the presence and activity of a protein in addition to RNA polymerase for its expression.

Further Reading

Dunn, T., Hahn, S., Ogden, S., and Schleif, R. (1984). An operator at −280 base pairs that is required for repression of *araBAD* operon promoter: Addition of DNA helical turns between the operator and promoter cyclically hinders repression. *Proc. Natl. Acad. Sci. USA* **81**, 5017–5020.

Englesberg, E., Irr, J., Power, J., and Lee, N. (1965). Positive control of enzyme synthesis by gene C in the L-arabinose system. *J. Bact.* **90**, 946–957.

Greenblatt, J., and Schleif, R. (1971). Arabinose C protein: Regulation of the arabinose operon *in vitro*. *Nat. New Biol.* **233**, 166–170.

Hirsh, J., and Schleif, R. (1973). On the mechanism of action of L-arabinose C gene activator and lactose repressor. *J. Mol. Biol.* **80**, 433–444.

Lobell, R., and Schleif, R. (1990). DNA looping and unlooping by AraC protein. *Science* **250**, 528–532.

Martin, K., Huo, L., and Schleif, R. (1986). The DNA loop model for *ara* repression: AraC protein occupies the proposed loop sites *in vivo* and repression-negative mutations lie in these same sites. *Proc. Natl Acad. Sci. USA* **83**, 3654–3658.

Saviola, B., Seabold, R., and Schleif, R. (1998). Arm-domain interactions in AraC. *J. Mol. Biol.* **278**, 539–548.

Zhang, X., Reeder, T., and Schleif, R. (1996). Transcription activation parameters at *ara* p_{BAD}. *J. Mol. Biol.* **258**, 14–24.

Biography

Robert Schleif is a Professor in the Biology and Biophysics Departments at Johns Hopkins University. His principal research interests are in understanding the fundamental mechanisms that govern the action of proteins, particularly those involved with regulation of gene activity. His laboratory discovered the phenomenon of DNA looping and the light switch mechanism.

ARF Family

Gustavo Pacheco-Rodriguez, Joel Moss and Martha Vaughan
National Institutes of Health, Bethesda, Maryland, USA

ARFs or ADP-ribosylation factors are highly conserved 20-kDa guanine nucleotide-binding proteins found in all eukaryotic cells from *Giardia*, the most primitive existing eukaryote, to primates. No ARFs have been found in prokaryotes, which likewise have a paucity of intracellular organelles. ARFs have critical roles in multiple cellular functions, such as protein secretion, cytoskeletal rearrangements, and signal transduction. Vesicular trafficking in eukaryotes is required for intracellular communication and cargo transportation among organelles. Membrane trafficking involves the formation, translocation, and fusion of vesicles of defined structure and composition, initiated at specific sites on intracellular membranes. Vesicles are constructed and dismantled in a step-wise fashion, beginning with initiation at the donor membrane, formation of the membrane bud, assembly of vesicle cargo, and finally, fission to release the vesicle, followed by its transport, tethering at its destination, uncoating, and fusion with the target membrane. The investigation of ARF actions has contributed significantly to understanding many of those events at a molecular level. Although information regarding the function of ARF6 in actin cytoskeleton and membrane dynamics has expanded rapidly in recent years, the mechanisms of trafficking in endoplasmic reticulum and Golgi compartments are probably still better understood and in more detail.

Molecular Characteristics of ARFs

ARFs were first identified, purified, and characterized because of their ability to enhance the cholera toxin-catalyzed ADP-ribosylation of Gαs, the GTP-binding protein activator of adenylyl cyclase. ARF action in cells requires its controlled alternation between the inactive GDP-bound and active GTP-bound forms. This property allows ARFs to regulate enzyme activities and to participate in the formation and transformation of multi-molecular complexes that effect intracellular transport and cytoskeletal rearrangements.

Mammalian ARFs have been grouped in three classes, with ARF1, 2, and 3 in class I, ARF4 and 5 in class II, and ARF6 in class III. Grouping was based on molecular size, amino acid sequence, and gene structure. The yeast *Saccharomyces cerevisiae* has one class III and two class I ARFs. ARF amino acid sequences are highly conserved among species with $>65\%$ identity among human, yeast, and *Giardia* ARFs. All ARFs contain the stereotypical sequences and specific amino acids that function in GTP binding and hydrolysis. One of the hallmarks of these molecules is the presence of the Rossman fold, a $\beta-\alpha-\beta$ structure responsible for nucleotide binding. The availability of high-resolution structures of ARFs allowed identification of other regions, such as the internal β-sheet that distinguishes ARFs from other subfamilies of GTPases. The ARF structure also determines the specificity of its interactions with other molecules, and thereby its function. ARF structure differs from those of all other ca. 20-kDa GTPases in having an N-terminal extension that ends with an N-myristoylated glycine. The fatty acid modification, plus the added amphipathic helix at the N-terminus of the ARF protein, facilitates its membrane association through interaction with phospholipids as well as proteins.

ARF-Related Proteins

In both structure and function, ARFs resemble the several subfamilies of ca. 20-kDa Ras-like GTPases that include Rho, Rac, Rab, and Rap. Each of these proteins, like the ARFs, has special, specific functions in cells. It is notable, however, that many of their actions, effects, and mechanisms of regulation are similar and may even appear to overlap. Perhaps this is because all of these GTPases function by interacting with numerous other molecules, simultaneously or sequentially, in a manner that depends on whether GDP or GTP is bound, to modify their activities or effects.

Among the ARF-related proteins, are ARF-like proteins or ARLs that appear to be more diverse in function and, as a group, differ more in structure than do the ARFs. The 181 amino acid sequences of human ARF1 and ARL1 are, however, 56% identical. There is also ARP (ARF-related protein) and the intriguing 64-kDa ARD1 (ARF domain protein 1), with an 18-kDa ARF domain at the C-terminus.

ARF Actions

With GTP bound, all of the ARFs are activators of the cholera toxin ADP-ribosyltransferase, which is secreted by *Vibrio cholerae*. They also activate the very similar *Escherichia coli* heat-labile enterotoxin (LT) that causes travelers' diarrhea. Allosteric activation of the cholera toxin A subunit (CTA), which is the ADP-ribosyltransferase enzyme, has been well established *in vitro*. The role of ARF in CTA action on cells however, is less clear. The capacity to activate CTA and LT distinguishes ARFs from other GTPases, including the ARF-like proteins or ARLs. The biochemical and/or catalytic behavior of ARFs can be markedly influenced by their interaction with specific phospholipids.

ARF-GTP can also activate mammalian phospholipase D (PLD) and phosphatidylinositol kinases that metabolize phospholipids critical in cell signaling. PLD-catalyzed hydrolysis of phosphatidylcholine produces phosphatidic acid, a molecule that alters the physical properties of membranes and can also activate specific receptors to initiate signaling. Phosphorylation of phosphatidylinositol 4-phosphate by an ARF-activated kinase likewise contributes to the modification of membrane composition and thus the molecular interactions that can be vitally important in properly controlling cell functions.

The shape of the ARF molecule differs dramatically depending on whether GDP or GTP is bound. Activation of ARF by GTP binding results from movement of the N-terminal helix with its N-myristoylated glycine away from a position close to the surface of the ARF molecule, where it resides when GDP is bound. This facilitates its interaction with other molecules and means that ARF-GTP binds membranes more effectively than does ARF-GDP (Figure 1). Membrane-bound active ARF then recruits adaptor and coat proteins to initiate vesicle formation. ARF function in vesicular trafficking probably involves interactions with phospholipids, as well as with proteins, whether they result in the activation of an enzyme like phospholipase D or in the generation of a vesicle when ARF-GTP becomes membrane-bound to begin the assembly of proteins that will become vesicle coat and cargo. Among the three types of coated vesicles, the COPI- and clathrin-coated structures require ARFs (probably class I ARFs) for formation.

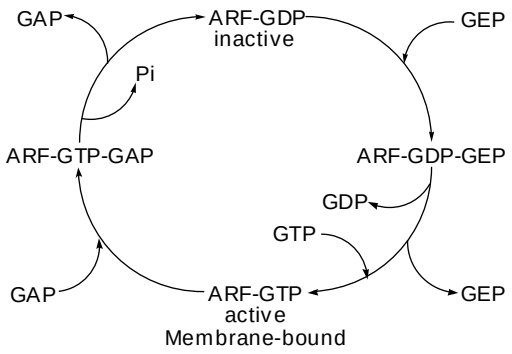

FIGURE 1 Cycle of ARF activation and inactivation mediated, respectively, by GEPs and GAPs. ARF is active in the GTP-bound form, which is produced by GEP-catalyzed replacement of bound GDP with GTP. Active ARF-GTP associates with membranes, to which it recruits adaptor and coat protein molecules. GAP-accelerated hydrolysis of ARF-bound GTP yields inactive ARF-GDP, which has a lower affinity for membranes and therefore dissociates from them.

Regulators of ARF Activity

Activation of ARF requires the replacement of bound GDP by GTP, which under physiological conditions occurs very slowly. ARF activation is regulated, therefore, by guanine nucleotide-exchange proteins, or GEPs, which accelerate the replacement process (Figure 1). The turn-off results from hydrolysis of bound GTP, the rate of which is undetectable until ARF-GTP interacts with a GTPase-activating protein or GAP to generate inactive ARF-GDP (Figure 1).

Several families of ARF GEPs with complex regulatory properties that parallel their critical functions have been described. All ARF GEP molecules are characterized by the presence of a ~190-amino acid Sec7 domain, which contains specific sites for ARF binding; also present are residues (i.e., glutamic acid) that act catalytically to accelerate the release of bound GDP and thereby the binding of GTP, which is present at higher concentration in cells than is GDP. Families of GEPs are distinguished by overall molecular size and structural elements outside of the Sec7 domain, as well as by sensitivity to inhibition by brefeldin A (BFA), a fungal fatty acid metabolite. BFA, which was first used experimentally as an inhibitor of viral replication, was later shown to inhibit protein secretion and certain pathways of intracellular membrane trafficking. BFA-inhibited GEPs include mammalian BIG1 and BIG2, yeast Gea1, Gea2, and Sec7, and the *Arabadopsis* GNOM protein.

Among the BFA-insensitive GEPs, the ca. 47-kDa cytohesin family appears to be the most numerous, with four human genes. These molecules contain a central Sec7 domain responsible for ARF activation, followed by a pleckstrin homolog (PH) domain, which binds phosphatidylinositol phosphates with notable specificity; it thereby influences intracellular localization of the protein. The cytohesins are also of interest as cell adhesion molecules. Before its role in ARF activation was recognized, cytohesin-1 had been identified and cloned because of its function in adhesion of lymphocytes to the extracellular matrix. The multiplicity of GEPs (as well as ARFs) complicates delineation of their individual physiological functions, just as the diversity

and complexity of their structures emphasizes the crucial importance to the cell of accurate and timely integration of signals from multiple sources.

There are also several families of GAPs that regulate ARF inactivation, which is just as critical as activation for maintenance of the ARF cyclical function. These proteins contain characteristic zinc-finger structures that are responsible for acceleration of ARF GTPase activity via a critical arginine residue. The diverse GAPs, like the GEP molecules, contain additional structural domains specialized for different functions and interactions, e.g., with cytoskeletal molecules. Three types of ARF GAPs have been recognized: ARF GAP type, GIT type, and ASAP type. Molecules of the last type contain multiple domains, including PH, ankyrin, proline-rich, and SH3. The multiple domains of these proteins enable them to localize at specific intracellular sites and to interact with numerous other molecules with reciprocal effects on function.

See Also the Following Articles

Phosphatidylinositol Bisphosphate and Trisphosphate • Phospholipase D • Ran GTPase • Rho GTPases and Actin Cytoskeleton Dynamics • Small GTPases

Glossary

domain The element of protein molecular structure, with or without known function, that is conserved among different proteins and/or organisms.

GAP GTPase-activating protein that accelerates hydrolysis of GTPase-bound GTP to generate inactive ARF-GDP.

GEP Guanine nucleotide-exchange protein that acclerates replacement of GTPase-bound GDP by GTP.

GTPase Protein that catalyzes hydrolysis of guanine nucleoside triphosphate (GTP) to yield inorganic phosphate and guanine nucleoside diphosphate (GDP).

vesicle Membrane-enclosed intracellular structure, 100 to 200 nm in diameter, with or without visible coat structure, that can be a vehicle for the transport of molecules to support many kinds of cell functions, e.g., secretion, endocytosis, migration, and proliferation.

Further Reading

Antonny, B., and Schekman, R. (2001). ER export: Public transportation by the COPII coach. *Curr. Opin. Cell Biol.* **13**, 438–443.

Bonifacino, J. S., and Lippincott-Schwartz, J. (2003). Coat proteins: Shaping membrane transport. *Nat. Rev. Mol. Cell. Biol.* **4**, 409–414.

Donaldson, J. G., and Jackson, C. L. (2000). Regulators and effectors of the ARF GTPases. *Curr. Opin. Cell Biol.* **12**, 475–482.

Moss, J., and Vaughan, M. (1998). Molecules in the ARF orbit. *J. Biol. Chem.* **273**(34), 21431–21437.

Moss, J., and Vaughan, M. (2002). Cytohesin 1 in 2001. *Arch. Biochem. Biophys.* **397**, 156–161.

Pacheco-Rodriguez, G., Morinaga, N., Noda, M., Moss, J., and Vaughan, M. (2004). Activation of Cholera Toxin and *E. coli* Heat-labile Enterotoxin (LT) by ARF, in press.

Pelham, H. R., and Rothman, J. E. (2000). The debate about transport in the Golgi – Two sides of the same coin? *Cell* **102**, 713–719.

Randazzo, P. A., Nie, Z., Miura, K., and Hsu, V. W. (2000). Molecular aspects of the cellular activities of ADP-ribosylation factors. *Sci. STKE* **21**, 1–15.

Rothman, J. E. (2002). The machinery and principles of vesicle transport in the cell. *Nat. Med.* **8**, 1059–1062.

Biography

Gustavo Pacheco-Rodriguez, Ph.D., Joel Moss, M.D., Ph.D., and Martha Vaughan, M.D. are members of the Pulmonary-Critical Care Medicine Branch of the National Heart, Lung, and Blood Institute in Bethesda, Maryland. Their research interests include biochemical and molecular mechanisms of ARF function in signal transduction and vesicular trafficking.

Aspartic Proteases

Ben M. Dunn
University of Florida College of Medicine, Gainesville, Florida, USA

Aspartic proteases are one of the four classes of proteolytic enzymes, which cut other proteins into smaller pieces. Proteolytic enzymes are also known as peptidases, because they cleave peptide bonds, and as proteinases, because they cleave proteins. The four classes include serine-, cysteine-, and metallo-proteases, in addition to the aspartic proteases. Each of these classes derives their name from the amino acid residue or functional group in the case of the metallopeptidases, which serves as the critical part of the catalytic mechanism. In the aspartic proteases, it is actually two aspartic acids that make up the catalytic machinery of the enzyme. The carboxylate groups of these two aspartic acid residues assist in proton transfers from a water molecule that acts as the nucleophile, to attack the peptide bond of the peptide or protein to be cleaved. Aspartic proteases are found in all forms of life and play important roles in some disease processes.

The Spectrum of Aspartic Proteases in Biology

Historically, aspartic peptidases were first found in the digestive tract of many animals. Pepsin is found in the stomach of most animals with an acidic phase of digestion. A related enzyme, gastricisin, is also present in the stomach and in some animals it is the dominant enzyme. Chymosin, a similar enzyme from the fourth stomach of the calf, is responsible for clotting milk when the young animal suckles from its mother. This helps retain the semisolid form of milk proteins in the digestive track for further processing. The presence of an activity was inferred in ancient times when milk was placed in a sack made from the stomach of an animal so that the milk could be transported on long journeys. The travelers found the milk had clotted and realized that something from the stomach lining was causing this to happen. Chymosin is now used to initiate the production of cheese. In some countries, farmers discovered that certain flowering plants also contained a substance that caused milk to clot and these flowers are used in what is termed artisanal cheese making. Other plant enzymes may be involved in digestion of stored seed protein to provide nourishment for a growing seedling. In the world of fungi, many aspartic peptidases have been found. For example, the common bakers yeast, *Saccharomyces cerevisiae*, contains several enzymes in an intracellular organelle called the food vacuole; one of these enzymes is yeast proteinase A.

Due to the progress of genome sequencing projects from 1990 to the present, sequence information is now available for 354 members of the aspartic protease family. They can be related by sequence identities as seen in Figure 1. Representative examples are given for enzymes from animals, plants, fungi, protozoa, insects, and worms. Furthermore, within one organism, different members of the family play different roles. As an example, humans have two enzymes in the stomach that are involved in the digestion of protein in the diet. In addition, an enzyme in the bloodstream, renin, is involved in regulation of blood pressure by converting a precursor molecule, angiotensinogen to angiotensin I. Subsequent conversion of angiotensin I to angiotensin II has a large effect upon blood pressure, as the latter molecule causes constriction of blood vessels and increases in blood pressure. Within cells, several aspartic proteases are found to play important roles. Cathepsin D in the lysosomes of cells acts to activate other enzymes, prohormones, and growth factors. Cathepsin E, which is found mainly in cells of the lymphoid system, seems to have a function in the response of cells to immunological stimuli. Memapsin, also known as BACE, is involved in the conversion of the β-amyloid precursor protein to a form that can aggregate and cause fibrils that are found in Alzheimer's disease. Several enzymes known as napsins have recently been discovered in humans. Their function is unknown at this point in time. In the genomes of the plant, *Arabidopsis thaliana*, the nematode, *Caenorhabditis elegans*, and the fruit fly, *Drosophila melanogaster,* a similar pattern of multiple potential functions has emerged, as multiple sequences with identities to the aspartic protease family have also been identified.

Structure

Pepsin from the stomach of the pig was one of the first proteins to be crystallized; however, the

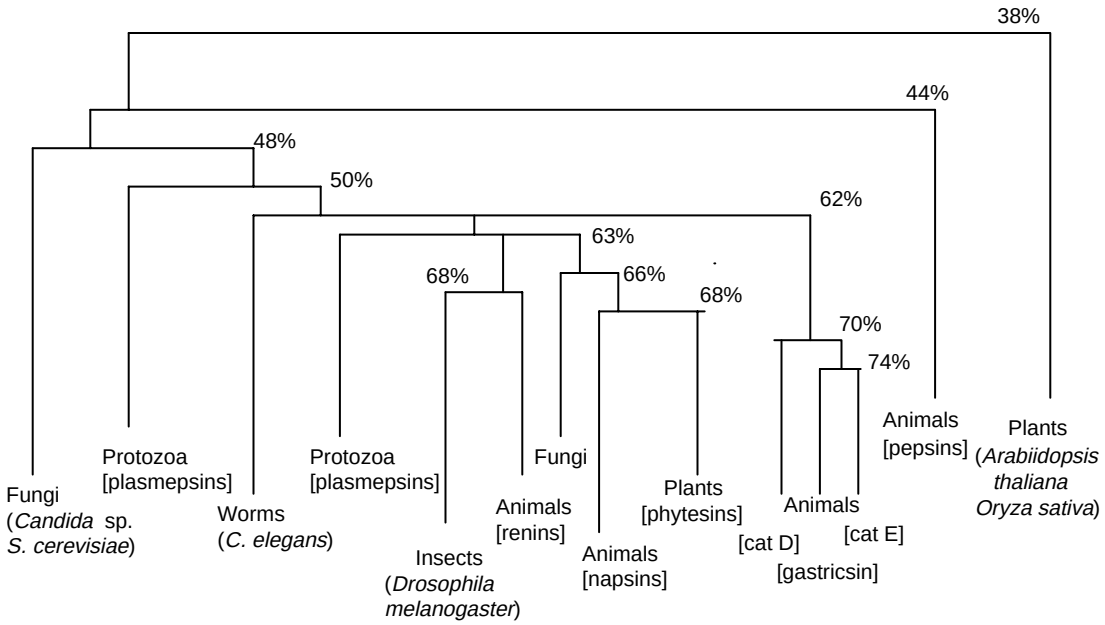

FIGURE 1 Diagrammatic representation of the relationship among several major classes of aspartic proteinases. The number at the top of each division point is the percentage identity between all species below the line. Organism names are given in italics inside parentheses and specific enzyme names are given inside square brackets. Note that different organisms are seen in different points in the diagram. This is due to the fact that different enzymes within one species play different functional roles.

three-dimensional structure of three fungal enzymes were reported before the structure of pig pepsin was solved. Since the 1970s several hundred structures have been solved by X-ray diffraction. At this point in time, we can state with certainty that all proteins that have sequence homology over 40% with the aspartic protease family will have the same overall structure.

Overall Structure

The structure of a typical aspartic protease is shown in Figure 2 in several views. The structure can be divided in two ways. First, there is a twofold axis of symmetry down the middle of the protein as seen in Figure 2A. The first ~165 amino acids of the protein (the N-terminal domain) are an independent folding unit that is mostly

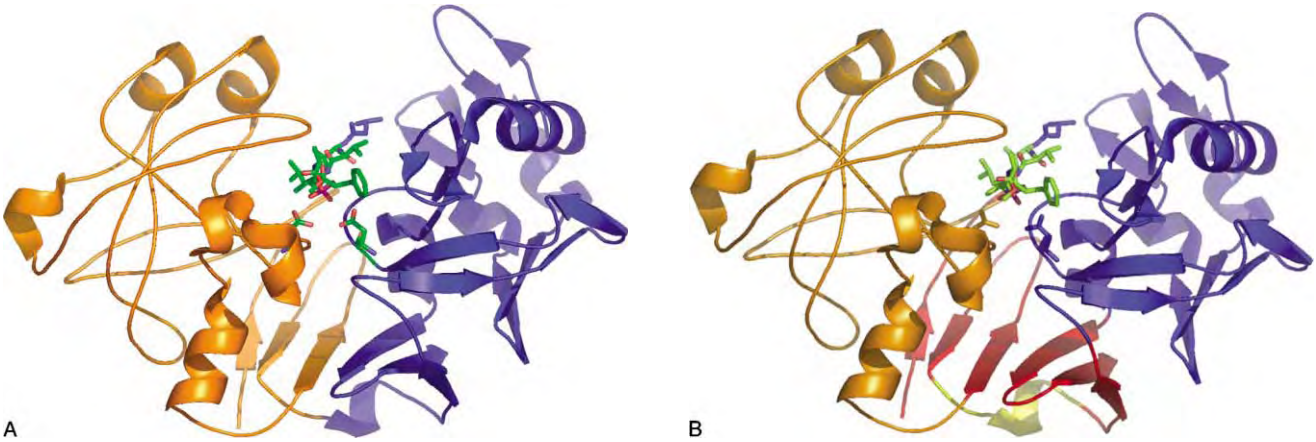

FIGURE 2 Representation of the three-dimensional structure of a typical aspartic protease. The flat arrows represent β-strand structure and the spiral shapes represent α-helices. These elements are from the backbone only and do not show the complete structure of the protein. (A) View of the enzyme looking end-on into the active site cleft at the top. In this representation, the N-terminal domain is colored orange and the C-terminal domain is colored blue. The two catalytic aspartic acid residues are shown in sticks at the bottom of the active site cleft. Above these amino acids one can see an inhibitor molecule bound in the active site. (B) Same orientation as A, with the N-terminal domain colored orange, the C-terminal domain colored blue, and the β-sheet at the bottom of the molecule colored red. A small connecting loop between the first three strands of the red β-sheet and the second three strands is colored yellow.

composed of β-strands and very little α-helical structure. The last ~165 amino acids (the C-terminal domain) are also an independent folding unit with exactly the same folding pattern. The active site cleft is located between the two domains and on one side of the molecule. Each domain contributes to the surface of the cleft, which binds substrates for cleavage or inhibitors that block cleavage. The two halves of the enzymes are believed to have arisen by a gene duplication event before divergence into the different forms shown in Figure 1. A second way to analyze the structure has the same division as described above, but also considers the β-sheet shown at the bottom of Figure 2B as an independent unit comprised of β-strands from each of the two domains. In either analysis, all the known structures are highly similar in structure. Some variation is seen in the relative orientation of the two (or three) domains with respect to each other. In addition, some variability is provided by the length of some of the β-hairpin loops that impinge on the active-site cleft. This provides diversity in the active site binding characteristics of each enzyme, which could be involved in the specific function of each member of the family.

Catalytic Residues

Each of the two domains (N-terminal and C-terminal) provides one aspartic acid, and these two amino acids are located in the 3D structure at the bottom of the active site cleft, and the carboxylic acid functional group of each of the aspartic acid side chains are within 3–5Å. In the enzyme without bound ligands, a water molecule is hydrogen bonded to the two aspartic acid residues and is the nucleophile that attacks the peptide bond of a substrate held within the active site cleft.

Flap Structure

Another significant feature of all aspartic proteases is a β-hairpin that hangs over the active site cleft. This is frequently referred to as the "flap" and movement of this is important in the binding of substrates and inhibitors in the active site. Amino acid differences on the flap, when comparing different members of the family, are important in the different activities exhibited by the enzymes.

Proenzyme Structure

Most aspartic proteases are synthesized within cells as inactive precursors known as zymogens or proenzymes. In all known cases, this involves an N-terminal extension of between 35 and 125 amino acids. In cases where the 3D structure has been determined for some of the proenzyme forms, the extra amino acid sequence acts to either block the active site cleft or to pull the two domains apart from one another, in either case this prevents activity. For many cases, conversion from the proenzyme to the mature enzyme form is self-catalyzed and occurs when the proenzyme moves from a neutral pH condition to a compartment of lower pH. Removal of the N-terminal extension results in a decrease in molecular weight of between 4 and 15 kDa. In a few known cases, the conversion requires a second enzyme.

Diseases

Efforts to understand the structure and function of aspartic proteases have been stimulated by the discovery that many disease processes involve the activity of these enzymes.

Hypertension

As mentioned above, renin is involved in a cascade of reactions that leads to elevation of blood pressure. While this is a normal function that can increase blood pressure in times of activity of an individual, when the levels of renin activity are slightly out of balance, the effects can be dangerous to health. Studies in animals have shown conclusively that giving a selective renin inhibitor, i.e., a compound that will bind to and block the activity of renin without affecting the other aspartic proteases of the human body, has a dramatic effect on blood pressure levels. This area of investigation was extremely important to the study of the whole field of aspartic proteases, as it allowed scientists to develop the tools and strategies to develop selective inhibitors. This has paid dividends in the development of antiviral inhibitors as well as in programs searching for inhibitors against many other family members.

Cancer

High levels of cathepsin D have been observed in areas surrounding tumors in both humans and animals. This has led to the hypothesis that cathepsin D is involved in the invasiveness of cancer cells. However, cathepsin D activity is normally highest at pH values well below that of tissue. Cathepsin D exhibits its activity in the lysosome, where the pH level is believed to be less than 6. In addition, cathepsin D is released when cells break open, so that the excess levels seen in necrotic tissues may be due to cellular decay. Furthermore, in some conditions, excess levels of cathepsin D are due to overloads of the secretory pathway so that the proenzyme form of cathepsin D is released rather than the mature form. Cathepsin D or the proenzyme form may act as a growth factor to stimulate the growth of cancerous cells.

AIDS

An aspartic protease is part of the causative agent for AIDS, human immunodeficiency virus. This protease acts to cut apart a viral polyprotein so that new virus particles can assemble. The HIV protease was the second target against which new antiviral drugs were developed. These compounds have had a major impact on therapy for AIDS.

Malaria

The malaria parasite, *Plasmodium falciparum*, lives during part of its complicated life cycle within human erythrocytes where it degrades hemoglobin for two reasons: one, to provide nutrients in the form of free amino acids for new protein synthesis, and, two, to create space for growth of the parasitic cell. Digestion of hemoglobin is initiated by the action of aspartic proteases. Following the sequencing of the *P. falciparum* genome, it is now known that ten different aspartic protease genes are present. Four of these are expressed and the proteins are located within a special organelle, the food vacuole. This organelle is equivalent to the lysosome of mammalian cells and a similar vacuole of *S. cerevisiae*. Complete digestion of hemoglobin requires the coordinated activity of cysteine proteases and metallo-proteases as well as the aspartic proteases. Inhibitors of aspartic proteases are able to kill the parasite in culture studies.

Fungal Infections

A number of fungi are known to cause diseases in humans and in plants. For example, *Candida albicans* is a common commensal organism, living within the human body but kept in check by a healthy immune system. In situations where the immune system is compromised, due to chemotherapy for cancer or immune suppression to avoid transplant rejection or due to suppression by diseases such as AIDS, *C. albicans* can become a life-threatening systemic infection. The fungus is also known to have a number of aspartic proteases, including several that are secreted into the extracellular environment surrounding the fungal cells. These enzymes are believed to assist in providing nutrients to the fungus by digesting proteins found in the surrounding environment. Some of these secreted enzymes may work to aid in the invasiveness of the fungus as the infection spreads.

Alzheimer's Disease

The newest target for drug discovery is the β-secretase or memapsin. This enzyme acts to cleave the β-amyloid precursor protein at a specific bond, generating a fragment that can become, with further modification by the so-called gamma secretase, a peptide that forms amyloid fibrils. This condition leads to neurofibrilary plaques in the brain, which are a hallmark of Alzheimer's disease. Due to the unique specificity of memapsin, development of specific inhibitors is possible and new therapies for this condition may develop in the next few years.

Inhibitors

Naturally Occurring Inhibitors

Unlike the serine protease family, naturally occurring inhibitors of aspartic proteases are relatively rare. A few have been described in detail and structural information obtained. By investigating the mechanism of inhibition of these protein inhibitors, it is hoped that new insights into inhibitor design will be found.

Pepstatin

Culture filtrates of the organism *Streptomyces* have been found to contain many interesting compounds. Pepstatin, discovered around 1970, was found to strongly inhibit pepsin and other members of the aspartic protease family. This compound is a relatively nonspecific inhibitor, as it seems to block most members of the aspartic protease class. Pepstatin contains an unusual amino acid, 3-hydroxy-4-amino-6-methylheptanoic acid. The 3-OH group binds to the two catalytic aspartic acids to form a transition-state analogue, which provides very tight binding. Because all aspartic proteases have the identical catalytic mechanism, pepstatin is an excellent inhibitor. This compound has been used in many studies of the 3D structure of members of the aspartic protease family and, thus provides convenient comparisons between these enzymes. Many synthetic inhibitors, mentioned below, utilize the same concept in the design of selective inhibitors.

PI-3 Pepsin Inhibitor of *Ascaris*

The nematode, *Ascaris lumbriocoides*, lives within the human digestive tract for a significant part of the life cycle. The digestive tract contains many proteolytic enzymes, including aspartic proteases. The nematode produces several proteins, each of which is able to bind to and inhibit a specific host enzyme. Several inhibitors have been purified to homogeneity, including PI-3. From a purification of the aspartic protease inhibitors, the third fraction had the highest activity in assays of the ability to inhibit pepsin, thus leading to the designation, PI-3. PI-3 is a protein of 149 amino acid residues. It inhibits pepsins and gastricsins from humans and pigs, and has been shown to inhibit the

cathepsin E from humans. The structure of PI-3 in complex with porcine pepsin has been determined and it was found that the inhibitor is a rigid protein, which makes contact with pepsin at two points, using a total of about 13 out of the 149 residues. The structure of the inhibitor does not change when interacting with pepsin.

IA-3 Yeast Protease Inhibitor of *S. cerevisiae*

The yeast *S. cerevisiae* synthesizes a 68-residue protein called IA-3, which is a strong and selective inhibitor of yeast proteinase A. The 3D structure of the complex between the two proteins shows that the inhibitor forms a near-perfect α-helix between amino acids 2 and 34 when it binds to the enzyme, while the inhibitor when free in solution has little or no organized structure. The IA-3 inhibitor does not inhibit any other member of the aspartic protease class that have been tested so far and, in fact, is cleaved by several of the other enzymes. The transition from an unstructured protein to a tightly folded one is a unique aspect of this inhibitor. This is an example of an "intrinsically unstructured protein."

Synthetic Inhibitors

Due to the importance of aspartic proteases in several disease processes, strong efforts have gone into the design and testing of compounds that could become new drugs for treatment of disease. In many cases, the observations that pepstatin was a potent inhibitor gave the initial clue to inhibitor design. Thus, the presence of a hydroxyl group within the structure of a new compound is frequently coupled with the variation in the amino acid sequence (for peptide-like compounds), or in the structural groups (for non-peptide compounds) to create a selective inhibitor. Other variations on the central hydroxyl group include replacements for the peptide bond such as –CH2NH–, –PO2–CH2–, and –CHOH–CHOH–. These replacements have proven effective in the development of new inhibitors.

See Also the Following Articles

Aminopeptidases • Amyloid • Angiotensin Receptors • HIV Protease • Metalloproteases • Secretases

Glossary

active site A portion of a protein where the catalytic amino acids or associated groups are located and where a binding site for substrate exists.

chemotherapy Use of compounds to kill disease-causing cells in the human body.

hemoglobin The oxygen carrying molecule of the bloodstream found in red blood cells.

inhibitor A molecule that binds to the active site of an enzyme to block the catalytic activity.

proteolytic enzyme A protein that has the ability to digest other proteins by cleaving peptide bonds to produce smaller fragments.

substrate A molecule acted upon by an enzyme to cause a chemical change.

three-dimensional structure The detailed arrangement of atoms in space for a molecule, usually determined by X-ray crystallography.

transition state analogue A molecule with a chemical structure that resembles the geometry of the state between a substrate and the products of a reaction.

zymogen A precursor form of an enzyme, usually larger in size due to the addition of extra amino acid residues; also known as a proenzyme.

Further Reading

Dunn, B. M. (ed.) (1999). *Proteases of Infectious Agents*. Academic Press, San Diego.

Dunn, B. M. (2002). Structure and mechanism of the pepsin-like family of aspartic peptidases. *Chem. Rev.* **102**, 4431–4458.

James, M. N. G. (ed.) (1998). *Aspartic Proteinases: Retroviral and Cellular Enzymes*. Plenum, New York.

MEROPS—The Peptidase Database. http://merops.sanger.ac.uk.

Biography

Ben M. Dunn is Distinguished Professor of Biochemistry and Molecular Biology at the University of Florida College of Medicine. He began his career at Florida after earning a B.S. in chemistry at Delaware in 1967 and a Ph.D. at the University of California, Santa Barbara in bioorganic chemistry, two years of postdoctoral work in protein chemistry, and one year as a staff fellow at the NIH. His laboratory studies the enzymatic function of proteases, using kinetics and biophysical techniques including X-ray crystallography.

ATP Synthesis in Plant Mitochondria: Substrates, Inhibitors, Uncouplers

Kathleen L. Soole and R. Ian Menz
Flinders University, Adelaide, Australia

Adenosine triphosphate (ATP) is the energy carrier of the cell and in eukaryotic cells is synthesized via photosynthesis and respiration. Within respiration there is a low level of ATP synthesis associated with glycolysis in the cytoplasm; however, the majority of ATP is synthesized via oxidative phosphorylation which occurs within mitochondria, specifically via the operation of an electron transport chain (ETC) in the inner mitochondrial membrane. In mammals, flux through the respiratory pathway is tightly regulated by the ATP/ADP ratio or adenylate energy charge of the cell. Plants, unlike mammals, must synthesize all of their cellular components. In plants, the presence of a nonphosphorylating pathway in the mitochondrial ETC and an uncoupler protein in the inner membrane overcomes this restriction by adenylate control. In plants, respiration is not only important for energy production but also has a major role in biosynthesis and anabolic reactions.

Mitochondrial Electron Transport Chain in Plants

Sucrose and starch are converted to metabolites that feed into the early steps of glycolysis which occurs in the cytoplasm. The end products of glycolysis in plants can be either pyruvate or malate, the latter being formed by the action of PEP carboxylase and malate dehydrogenase, which together bypass pyruvate kinase. Once within the mitochondrial matrix, pyruvate is metabolized by pyruvate dehydrogenase and the enzymes of the citric acid cycle. Being a substrate for mitochondrial malate dehydrogenase, malate can either feed into the citric acid cycle or be metabolized to pyruvate via NAD-malic enzyme. There must be a balance between these processes, since because of the poor forward equilibrium of malate dehydrogenase, the accumulation of oxaloacetate would prevent further malate metabolism. The net result of these reactions is the production of NADH and $FADH_2$ (via succinate dehydrogenase). During a turn of the citric acid cycle, 1 ATP is produced directly by substrate level phosphorylation, not GTP as in mammalian mitochondria. Matrix NADH is oxidized by the ETC and more ATP produced via oxidative phosphorylation.

Oxidative phosphorylation occurs via the interaction of large lipo-protein complexes of the (ETC) and smaller mobile electron carriers found in the inner mitochondrial membrane (Figure 1). NADH is oxidized by complex I, which donates its electrons to a mobile lipophilic electron carrier, ubiquinone. Complex II or succinate dehydrogenase also donates electrons to the ubiquinone pool. Reduced ubiquinone (or ubiquinol) is oxidized by complex III via the Q-cycle and reduces the mobile peripheral protein cytochrome *c*. By interacting with complex IV (cytochrome oxidase), the electrons carried by cytochrome *c* are donated to the terminal electron acceptor, oxygen. During these electron transfer events, protons are translocated from the matrix side of the inner membrane to the inter-membrane space at complexes I, III, and IV, thus establishing the proton motive force (pmf or $\Delta\mu_{H+}$). If ADP is bound to the F_oF_1-ATPase in the inner membrane, then protons pass through this complex and the energy within the pmf is used to synthesize ATP. Once ATP is synthesized, it is then exported out of the matrix in exchange for another ADP via the adenine nucleotide translocase. Thus, the flow of electrons and hence oxygen consumption is tightly under control of cellular ADP levels. This is called acceptor or adenylate control.

In plant mitochondria, additional protein complexes are found associated with this ETC. They are distinct from complexes I–IV in that they participate in the transfer of electrons from NADH to oxygen, but do not contribute to the pmf. These enzymes are the alternative or nonphosphorylating NAD(P)H dehydrogenases (NDE and NDI), which donate electrons to the ubiquinone pool and the alternative oxidase (AOX), which accepts electrons from reduced ubiquinone (Figure 1).

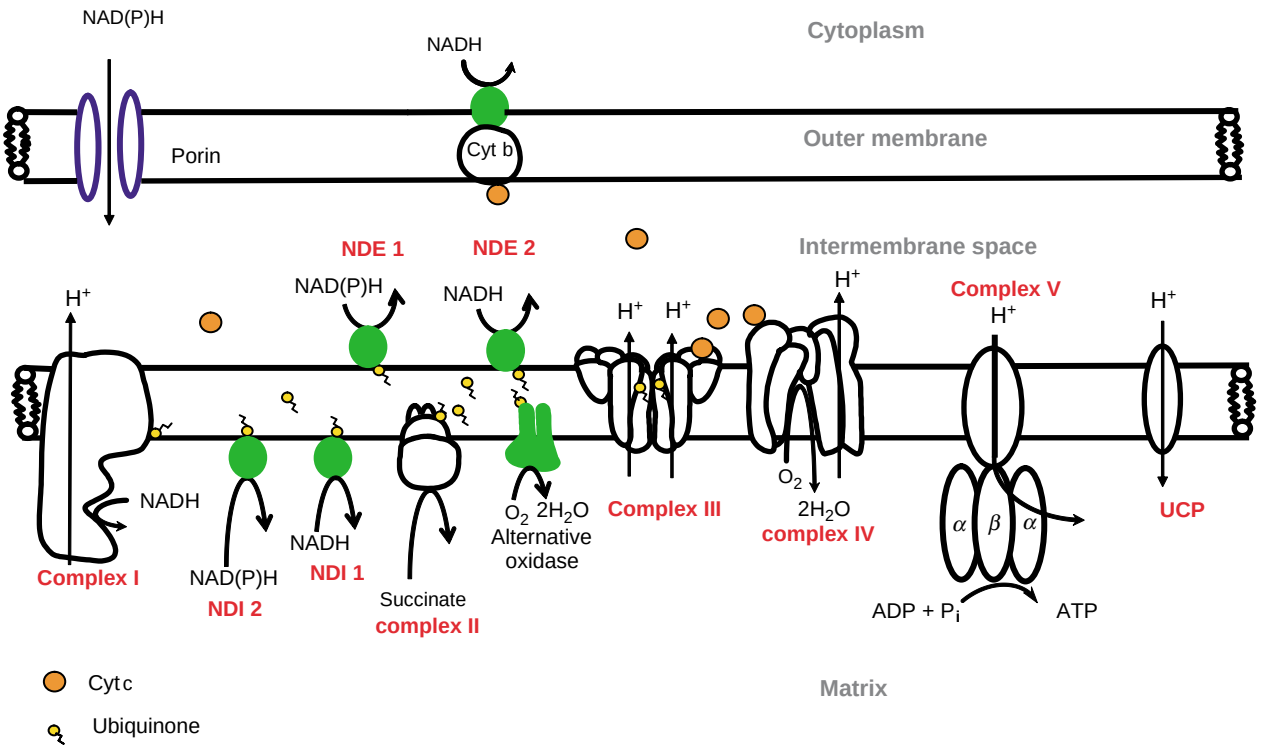

FIGURE 1 A schematic representation of the routes of NAD(P)H oxidation and the electron transport chain (ETC) of plant mitochondria. NDI refers to internal matrix-facing nonphosphorylating NAD(P)H dehydrogenase, and NDE refers to external cytosolic nonphosphorylating NAD(P)H dehydrogenase. UCP refers to the uncoupling protein. Reproduced from Rasmusson *et al.* (2004) *Annual Review of Plant Biology*, Volume 55.

Evidence for the alternative nonphosphorylating NAD(P)H dehydrogenases comes from the ability of isolated plant mitochondria to oxidize externally supplied NAD(P)H, which cannot pass through the inner membrane. The external cytosolic-facing NAD(P)H dehydrogenase (NDE) feeds directly into the ubiquinone pool, as external NAD(P)H oxidation has an ADP/O ratio equivalent to succinate of less than 2.0. Matrix NADH oxidation in plants has a component which is insensitive to inhibition by the complex I inhibitor, rotenone. This oxidation is catalyzed by NDI. The rotenone-insensitive alternative matrix NADH oxidation has an ADP/O ratio also similar to succinate indicating that NDI also feeds electrons into the ubiquinone pool, bypassing proton pumping at complex I. The alternative oxidase is a cyanide and antimycin A-resistant ubiquinol oxidase that catalyses the reduction of oxygen to water with electrons from ubiquinol and thus bypasses the proton pumps at complexes III and IV.

Thus, it is possible to have electron transport/transfer with no ATP synthesis in plant mitochondria. Therefore, due to the bypasses that exist around key regulatory sites in glycolysis, plant respiration can be totally independent of respiratory control, which gives plants great metabolic flexibility. This flexibility, which results in the loss of adenylate control of respiration by the energy status of the cell can theoretically allow the release of biosynthetic intermediates from the respiratory pathway, independent of energy charge of the cell. This role of the nonphosphorylating pathway is hypothesized and has not been clearly demonstrated *in vivo*.

Substrates for ATP Synthesis

The plant mitochondrial ETC can oxidize matrix NADH and NADPH to a much lesser extent. The source of this NADH is from pyruvate dehydrogenase and citric acid cycle, and plants have the full complement of these enzymes in addition to other unique enzymes. The presence of matrix pools of NADPH is indicative of the mitochondria's anabolic role. NADP-dependent enzymes involved in folate and thymidylate synthesis such as NADP-dihydrofolate reductase and methylene tetrahydrofolate dehydrogenase have been found in plant mitochondria and their continued operation requires the turnover of the NADPH generated via NDI2. Apart from NAD-dependent isocitrate dehydrogenase, there is also another NADP-dependent form in the matrix, however its role in plant metabolism is not yet clear. Additionally, via the action of a soluble

transhydrogenase detected recently in pea leaf matrix, the mitochondrial oxidation of any strictly NAD-linked substrates such as pyruvate would also be able to produce NADPH.

Another unique enzyme found in plant mitochondria is glycine decarboxylase, which generates NADH in the matrix, is part of photorespiratory cycle and is important in photosynthetic metabolism. It is accepted that the mitochondrial ETC operates in the light, and that ATP synthesis in the light is not exclusively generated from photosynthesis. Evidence indicates that glycine oxidation is linked to a nonphosphorylating NADH dehydrogenase, such as NDI. Recently it has been shown that NDI is regulated at the transcriptional level by light, at least in potato leaf, suggesting a link between nonphosphorylating enzymes and photorespiratory metabolism.

Plant mitochondria also have the capacity to oxidize cytosolic NADH and NADPH via the enzymes NDE1 and NDE2. Thus, ATP synthesis can also occur from the recycling of cytosolic NAD(P)H.

Inhibitors of ATP Synthesis

There are a multitude of inhibitors that act on specific components of the ETC and the use of many of these has been invaluable in elucidating the composition of the respiratory chain in different species (Table I).

The two most common and specific complex I inhibitors are rotenone and piericidin A, both inhibitors block electron flow between the final iron–sulfur center and ubiquinone. However, they display different inhibition kinetics and it is postulated that the transfer of electrons to quinone may involve more than one quinone-binding site, similar to those observed in complex III. Many other inhibitors of mammalian complex I have been discovered, such as aurachin A and B, thiangazole, phenoxan, and aureothin, and many are likely to inhibit plant complex I; however, their efficacy and specificity has not been demonstrated.

Relatively few inhibitors of plant complex II have been described (Table I), the most widely used is the competitive substrate inhibitor malonate; however, several new complex II inhibitors that are potential fungicides or pesticides have been reported recently.

The two most significant specific complex III inhibitors are antimycin A and myxothiazol, which are specific to the N-side and P-side quinone-binding sites, respectively, and have been important for developing models of the Q-cycle which is involved in proton translocation by complex III.

Complex IV is inhibited by a variety of competitive inhibitors of the oxygen-binding site, such as cyanide and azide. The most interesting of these is the rapid

TABLE I

Specific Inhibitors of Plant Respiratory Enzymes

Respiratory protein	Inhibitor	Site/mode of action
Complex I	Rotenone	Blocks between FeS
	Piericidin A	cluster N2 to quinone
Complex II	Malonate	Competitive substrate
	Thenoyltrifluoroacetone (TTFA)	Blocks FeS cluster S3
Complex III	Antimycin A	Quinone binding (N side)
	Myxathiazol	Quinone binding (P side)
	Stigamatellin	Quinone binding (P side)
Complex IV	Cyanide	Competitive inhibitors of
	Azide	O_2 binding site
	Nitric oxide	
Complex V	Oligomycin	Binds to OSCP-subunit
	Venturicidin	Proton translocation
		(c-subunit)
NDE1 (external NAD(P)H)	DPI	
	Calcium chelators	
NDE2 (external NADH)	Calcium chelators	
NDI1 (internal NADH)		
NDI2 (internal NAD(P)H)	Calcium chelator	
	DPI	
Alternative oxidase	*n*-Propylgallate	
	SHAM	

and reversible inhibition by nitric oxide, which may play an important role in regulation of oxidative phosphorylation.

There are several chemical inhibitors of ATP synthase (Table I), the most prominent being oligomycin, which is a specific inhibitor of F-type ATP synthases found in a variety of organisms. Apart from the chemical inhibitors, there are also inhibitor proteins, which play a role in regulating the activity *in vivo*. The most characterized is the mammalian inhibitor protein (IF1), whose conformation and inhibitory activity changes in response to pH. Proteins with low homology to IF1 have been found in plants, and although they can inhibit ATP synthetase activity, they do not appear to be regulated by pH. More recently, a class of phosphoserine/phosphothreonine-binding proteins, called the 14-3-3′s, have been identified in plant mitochondria and shown to regulate the ATP synthetase activity.

There are several inhibitors of the alternative NAD(P)H dehydrogenases, while a few show differential selectivity between the various alternative NAD(P)H dehydrogenases many of these such as platanetin, IACA (7-iodo-acridone-4-carboxylic acid), dicumarol, hydroxyflavaones, and sulphydryl reagents can inhibit all of the alternative NAD(P)H dehydrogenases. Interestingly, many of these were originally reported as specific inhibitors of particular alternative NAD(P)H activities. The most effective selective inhibitors are calcium chelators such as EGTA, which are potent inhibitors of the external and NADPH utilizing enzymes, which have a calcium requirement, and DPI (diphenyleneiodonium) which is more effective at inhibiting NADPH utilizing enzymes compared to NADH utilizing enzymes (Table I). SHAM (salicylhydroxamic acid) and *n*-propylgallate are the most prominent inhibitors of the alternative oxidase, the latter being more specific as SHAM can also effect other enzymes of oxidative metabolism such as peroxidases, lipoxygenase, and xanthine oxidases.

Uncouplers of ATP Synthesis

Chemical Uncouplers

Oxidative phosphorylation in plants is sensitive to chemical uncouplers such as dinitro phenol (DNP) and carbonyl cyanide *p*-(trifluoromethoxy)phenylhydrazone (FCCP) which dissipate the $\Delta\mu_{H+}$ by carrying proteins across the inner membrane, thus equilibrating the proton gradient. In heterotrophically grown tobacco suspensions cells, cellular respiration is increased by the addition of the uncoupler, FCCP, therefore under these conditions respiration is substrate limited.

Nonphosphorylating Respiration

Plants have the capacity to uncouple respiration and ATP synthesis using naturally occurring enzymes such as the alternative NDE and NDI, and AOX. Therefore, the level of "coupled" respiration will be dependent on the level and activity of these alternative ETC enzymes.

Alternative NAD(P)H Dehydrogenases

In plants, complex I has a much better affinity for NADH than NDI. This suggests that the latter route of electron flow will only be active when the matrix concentration of NADH is high. This has been clearly demonstrated in tissues like potato, which lose NAD from their mitochondrial matrix during longterm storage. In NAD-depleted mitochondria, the rate of electron flow through NDI was markedly reduced, i.e., malate oxidation in isolated mitochondria was totally sensitive to rotenone; however, this could be overcome if the mitochondria were reloaded with NAD from the bathing media. NAD enters via a specific transporter on the inner membrane. It is not clear if this level of regulation occurs *in vivo*. One of the NDI enzymes that uses NADPH as a substrate is calcium-dependent and could be regulated via matrix calcium levels. One question is whether, these alternative pathways operate as overflow for complex I or operate simultaneously during respiration *in vivo*. In a mutant where expression of one of the NDI enzymes was eliminated, the total respiration was reduced, which suggests that NDI contributes to respiration in presence of ADP along with complex I. Both the NDE enzymes are dependent on calcium for maximal activity. It has been suggested that electron flow through the NDE can be regulated by alteration of the local calcium concentration which can be facilitated by polyamines which occur naturally in plant cells, e.g., spermine and spermidine.

Alternative Oxidase

For many years, it was thought that the AOX acted as an overflow, only being used when there was an excess of reduced ubiquinone and the cytochrome pathway (via complexes III and IV) was saturated. It is now known that this is not the case, and that AOX and cytochrome pathway can operate simultaneously. Thus, the level of ATP synthesis will rely on the regulation of AOX. AOX can be regulated at both the transcriptional and posttranslational level. AOX exists as a monomer or dimer, with the monomeric form being most active. Further, AOX is activated by organics acids such as pyruvate. Pyruvate is the end product of glycolysis and thus this activation can act as a positive feed-forward mechanism of control when glycolytic flux is high. AOX is induced upon inhibition of the complexes III and/or IV

and also under various environmental stresses. It is thought that the expression of AOX is an attempt by the plant to have a flexible control of ATP synthesis and to maintain growth rate homeostasis. It is also thought to be part of the cell's defense against oxidative stress, as increased flux through the ETC would prevent the accumulation of high-energy electrons in the respiratory pathway, which could react with oxygen to form harmful, reactive oxygen species.

Uncoupling Protein

In addition to AOX, plants also have uncoupling protein (UCP), which mediates proton re-uptake across the inner membrane (Figure 1). This activity is activated by free fatty acids and inhibited by pyridine nucleotides. UCP is active during respiration in the presence of excess ADP when the free fatty acid concentration is $\sim 4\ \mu M$, and thus can divert energy from oxidative phosphorylation, impacting on the capacity for ATP synthesis. There is a reciprocal regulation between UCP and AOX as free fatty acids inhibit AOX activity. However a precise understanding of the integration and regulation of nonphosphorylating respiratory pathway, UCP and ATP synthase remains a major research challenge.

See Also the Following Articles

ATP Synthesis: Mitochondrial Cyanide-Resistant Terminal Oxidases • Cytochrome *c* • Cytochrome Oxidases, Bacterial • Respiratory Chain and ATP Synthase • Uncoupling Proteins

Glossary

alternative oxidase A ubiquinol oxidase located in the inner mitochondrial membrane, which accepts electrons from reduced ubiquinone and reduces oxygen to water. During this process, no protons are translocated across the inner mitochondrial membrane.

nonphosphorylating NAD(P)H dehydrogenase(s) Enzymes that accept electrons from NADH or NADPH and reduce ubiquinone, a mobile lipophilic electron carrier in the inner mitochondrial membrane with no consequent proton translocation across the membrane.

nonphosphorylating pathway A route of electron transfer with no concomitant translocation of protons across the inner mitochondrial membrane, hence this route of electron flow does not contribute to the proton motive force.

proton motive force Refers to the proton gradient that is established across the inner mitochondrial membrane during electron transfer through complexes I, II, and IV. Often referred to as $\Delta\mu_{H+}$ or pmf.

Further Reading

Jarmuszkiewicz, W. (2001). Uncoupling proteins in mitochondria of plants and some microorganisms. *Acta Biochim. Polon.* **48**(1), 145–155.

Joseph-Horne, T., Hollomon, D. W., and Wood, P. M. (2001). Fungal respiration: A fusion of standard and alternative components. *Biochim. Biophys. Acta* **1504**, 179–195.

Moore, A. L., Albury, M. S., Crichton, P., and Affourtit, C. (2002). Function of the alternative oxidase: Is it still a scavenger? *Trends. Plant Sci.* **7**(11), 478–481.

Rasmusson, A. R., Soole, K. L., and Elthon, T. E. (2004). Alternative NAD(P)H dehydrogenases in plant mitochondria. *Annu. Rev. Plant Biol.* **54**, 23–39.

Scheffler, I. E. (2001). Mitochondria make a come back. *Adv. Drug Deliv. Rev.* **49**, 3–36.

Biography

Dr. Kathleen L. Soole is a Senior Lecturer in the School of Biological Sciences at Flinders University, South Australia. Her principal research interests are in the roles that the nonphosphorylating pathways play in plant mitochondria, plant growth, and stress adaptation. She holds a Ph.D. from the University of Adelaide in South Australia and gained her postdoctoral training at the University of Newcastle-upon-Tyne, England. She has recently identified the gene in Arabidopsis that encodes the protein responsible for matrix nonphosphorylating NADH oxidation in Arabidopsis.

Dr. R. Ian Menz is a Biotechnology Lecturer in the School of Biological Sciences at Flinders University, South Australia. His research interests include the function and structural biology of respiratory proteins. He holds a Ph.D. from the Australian National University, Canberra, Australia. He worked on the structural biology of ATP synthase as a postdoctoral fellow with Sir John E. Walker at the Medical Research Council, Laboratory of Molecular Biology, Cambridge, England.

ATP Synthesis: Mitochondrial Cyanide-Resistant Terminal Oxidases

James N. Siedow
Duke University, Durham, North Carolina, USA

Mitochondria from all higher plants, most algae, many fungi, and some protozoa contain a second terminal oxidase in their electron transfer chain in addition to cytochrome *c* oxidase, the standard terminal oxidase found in all mitochondria. Functionally, this "alternative" oxidase is a ubiquinol oxidase, receiving electrons from reduced ubiquinone and transferring them to oxygen, which is reduced to water. Electron flow from reduced ubiquinone to cytochrome *c* oxidase includes two sites for transporting protons across the inner mitochondrial membrane to form a proton gradient across the membrane that drives ATP formation. Electron flow through the alternative oxidase involves no proton translocation and therefore wastes all the free energy released during electron transfer that would otherwise be conserved in the proton gradient to produce ATP. The role of such an energetically wasteful pathway has yet to be fully elucidated, but in plants it appears to be associated with response to a variety of stresses, possibly acting to prevent over-reduction of the quinone pool and the subsequent formation of harmful reactive oxygen species.

The Uniqueness of Plant Mitochondria

Plant mitochondria, like those of all other eukaryotes, contain a standard set of protein complexes that make up the electron transport chain in the inner mitochondrial membrane, complexes I–IV (Figure 1). This electron transfer chain functions as the third stage of aerobic respiration, whereby reductants (NADH, $FADH_2$) generated by operation of the TCA cycle in the mitochondrial matrix are oxidized and the resulting electrons transferred to molecular oxygen. The free energy released during electron transfer is used to translocate protons across the inner membrane from the mitochondrial matrix to the intermembrane space at complexes I, III, and IV, forming an electrochemical proton gradient across the inner membrane. Another inner membrane protein complex (complex V, ATP synthase) provides a path for protons to move back into the matrix and, in the process, couples the energy stored in the proton gradient to the synthesis of ATP from ADP and Pi. The terminal reaction of the electron transfer chain is the reduction of O_2 to H_2O by complex IV, cytochrome *c* oxidase. This standard electron transfer pathway is frequently termed the "cytochrome" (cyt) pathway because of the cytochromes present in complexes III and IV and cytochrome *c*. Specific inhibitors of each of the mitochondrial complexes are known. For example, rotenone inhibits complex I, antimycin A inhibits complex III, and cyanide inhibits cyt *c* oxidase.

In addition to the standard cyt pathway, mitochondria in plants contain a variety of additional electron transport proteins that impart flexibility to the system because they can operate without being coupled to ATP synthesis (Figure 1). On the electron input side of the ubiquinone pool are two sets of NAD(P)H dehydrogenases. One pair of dehydrogenases is found on the outside of the inner mitochondrial membrane, allowing mitochondria to oxidize cytoplasmic NADH or NADPH. A second set exists on the inner surface of the inner membrane and oxidizes matrix-derived NAD(P)H. These dehydrogenases do not contribute to proton gradient formation during electron transfer and therefore are able to operate unconstrained by it, unlike proton-pumping components such as complex I whose activity will be impaired as the proton gradient increases. These dehydrogenases are also insensitive to complex I inhibitors such as rotenone. Electrons derived from the oxidation of NAD(P)H by all these dehydrogenases are transferred to the common pool of ubiquinone that also serves as the electron sink for complexes I and II (Figure 1).

Cyanide-Resistant Respiration

Plant mitochondria also have an additional electron transport branch downstream of the ubiquinone pool due to the presence of a second terminal oxidase in addition to cyt *c* oxidase. This "alternative oxidase"

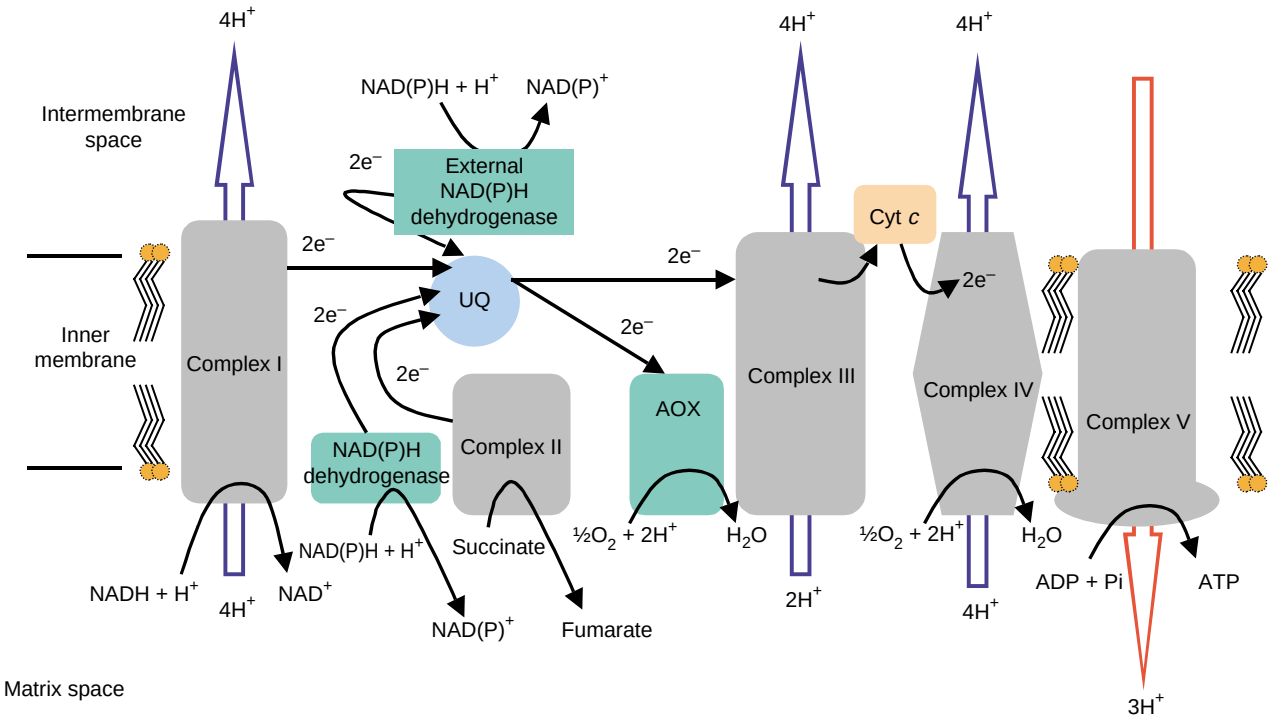

FIGURE 1 Schematic representation of the plant mitochondrial electron transfer chain.

(AOX) is a ubiquinol:oxygen oxidoreductase that accepts electrons from reduced ubiquinone and subsequently reduces O_2 to H_2O (Figure 1). AOX activity is resistant to cyanide and other inhibitors of cyt *c* oxidase but is specifically inhibited by salicylhydroxamic acid (SHAM) and n-alkyl gallate which do not affect the cyt pathway. An important feature distinguishes the two oxidase pathways. Electron flux downstream of the ubiquinone pool through the cyt pathway drives proton gradient formation at complexes III and IV, but no proton gradient formation occurs during operation of the alternative pathway. Thus, AOX would appear to be a wasteful enzyme from an energetic standpoint, eliminating a primary mitochondrial function during aerobic respiration, coupling the oxidation of reductants generated during the operation of glycolysis and the TCA cycle to the synthesis of ATP. Apart from its apparent absence in any metazoan (animal), AOX occurs widely among eukaryotic organisms. AOX has been found in all plants examined to date, but it is also present in most eukaryotic algae, many fungi, and a number of protozoa, including the bloodstream form of the organism responsible for African sleeping sickness, *Trypanosoma bruceii*.

Contemporary understanding of AOX can be traced to the development of an antibody against the plant AOX in 1989. The availability of this antibody led to the first isolation of a plant AOX gene and now dozens of AOX sequences from plants and fungi, and several protozoa and algae are present in gene databases. AOX is nuclear encoded and in plants, it occurs as a small gene family (e.g., five genes in *Arabidopsis*, three in soybean), that produces proteins from 32–35 kDa (~285 amino acids). More recently, characterization of the gene associated with a mutation leading to a defect in chloroplast biogenesis, IMMUTANS, identified a chloroplast protein having sequence similarity to AOX. IMMUTANS also functions as a quinol oxidase, leading to its general characterization as a "plastid terminal oxidase" (PTOX), and it has been shown to participate in a desaturation step during carotenoid biosynthesis in chloroplasts. As prokaryotic genome sequencing has progressed, AOX and PTOX homologues of unknown function have now been identified in an α-proteobacterium and several cyanobacteria, respectively. Phylogenetic analyses of the bacterial and eukaryotic sequences suggest that AOX and PTOX arose from a common prokaryotic ancestor, but the two activities diverged prior to the endosymbiotic events that gave rise to mitochondria and chloroplasts.

AOX Structure

AOX is integral inner membrane protein, but attempts to purify and characterize it have been hampered by the marked instability of the protein following its

solubilization from the membrane and the lack of any apparent visible (>350 nm) absorption spectrum or EPR spectral features in either its oxidized or reduced states. The observation that iron was required for induction of AOX activity in the fungus *Hansenula anomala* originally led to the suggestion that the active site contained iron. AOX sequence analyses later revealed the presence of conserved iron-binding motifs found in members of the family of diiron carboxylate proteins that include the R2 subunit of ribonucleotide reductase and the hydroxylase subunit of methane monooxygenase. This led to the initial development of a model of the AOX active site that contained a four-helical bundle forming a hydroxo-bridged diiron-binding site. The suggestion of a hydroxo-bridged iron center accounted for the absence of any visible absorbance, analogous to the diiron center in methane monooxygenase. Recently, an EPR signal associated with a mixed valence Fe(II)/Fe(III) hydroxo-bridged binuclear iron center has been reported for an *Arabidopsis thaliana* AOX expressed in *Escherichia coli*, providing direct spectral evidence for the diiron carboxylate nature of the AOX (and, by analogy, PTOX) active site.

Over time, the AOX structural model has been refined. As currently envisioned (Figure 2A), the C-terminal two-thirds of the AOX protein comprises a four-helical bundle that makes up the diiron-binding scaffold. Two short hydrophobic helical regions anchor the protein in the inner leaflet of the bilayer, with the bulk of the protein protruding into the mitochondrial matrix. This C-terminal region is relatively conserved among all AOXs, showing 85-90% sequence similarity among plants and over 55% similarity between plants and fungi.

While the C-terminal two-thirds of the AOX protein is responsible for forming the catalytic diiron site, the structure of the N-terminal third of the protein is unknown. When plant and fungal amino acid sequences in this region are compared, there is considerable sequence conservation within each organism type but marked sequence variability between them. Within the N-terminal third of the plant AOX, there is a highly conserved block of ~38 amino acids that includes a regulatory cysteine (*cf.* below). Fungal sequences initially align with plant sequences right after this block. From that point on, the plant and fungal sequences are highly similar with two exceptions: (1) an insertion of 20–25 amino acids unique to fungi just before the first of the four iron-binding helical regions and (2) an extension of the fungal C terminus 20–50 amino acids beyond that found in plants. AOX sequences in protozoa are more similar to the fungal AOX than they are to that of plants.

In plants, chemical cross-linking studies have established that AOX exists in the membrane as a dimer consisting of two AOX monomers (Figure 2B). However, the fundamental unit of catalytic activity based on radiation–inactivation analysis is the monomer. Consistent with the latter observation, AOXs dimers are not universal; cross-linking studies with AOX in both fungi and protozoa have established that they both exist in the membrane as monomers.

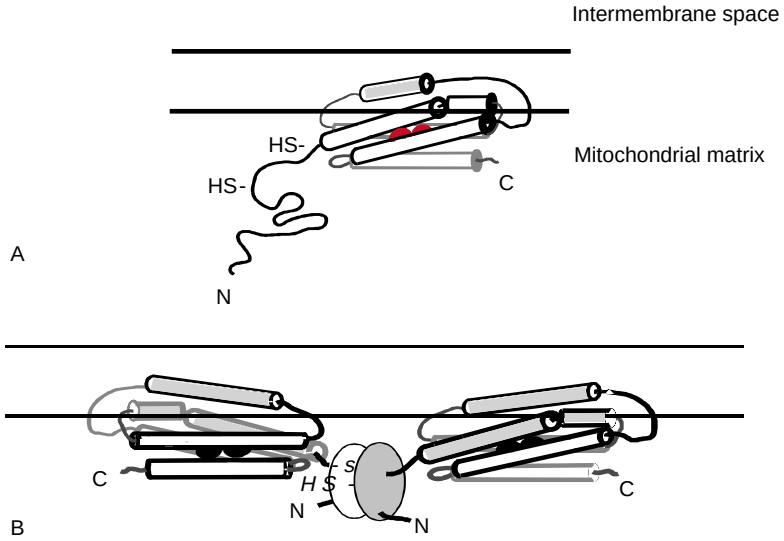

FIGURE 2 Diagrammatic representation of the structure of the AOX. (A) AOX monomer, (B) dimeric AOX structure found in plants. The two red spheres in (A) represent the diiron center (shown in black in (B)). The inner mitochondrial membrane is delimited by the set of parallel horizontal lines.

Biochemical Regulation of AOX Activity

While the N-terminal third of the AOX protein is less well characterized structurally than the remainder of the protein, this region has been found to confer regulatory features on the plant AOX. The plant AOX homodimer can exist in two forms, an oxidized state where the two monomeric subunits are covalently linked by an intermolecular disulfide bond and a reduced state where the AOX remains dimeric but the disulfide is reduced to its component sulfhydryls (Figure 3). In the oxidized state, AOX is inactive. When the disulfide is reduced, AOX remains inactive but has the ability to become activated in the presence of an α-keto acid, such as pyruvate (Figure 3). In the absence of α-keto acids, AOX has essentially no activity. AOX is activated by α-keto acids through reaction with a cysteine residue to form a thiohemiacetal. Site-directed mutagenesis of AOX has established that a single cysteine residue (termed CysI, the more N-terminal of two highly conserved cysteines located in the N-terminal region (Figure 2A)) is responsible for both the inactivating disulfide bond and interaction with α-keto acids to form the thiohemiacetal that activates AOX (Figure 3). As noted previously, CysI appears in the middle of a conserved block of amino acids in plant AOXs. Given the close proximity of the two regulatory CysIs on adjacent AOX monomers it appears that AOX activation following α-keto acid binding results from a conformational change brought about by charge repulsion between the resulting two proximal negative charges.

The regulatory features outlined above provide a facile mechanism for activating AOX under conditions when electron flow through the standard cyt pathway is restricted. Under such conditions, electron transfer would slow down leading to a buildup of reductant in the mitochondrial matrix. The more reduced environment in the matrix would bring about the reduction of the AOX regulatory disulfide, possibly via reduced thioredoxin, which is found in the mitochondrial matrix. As electron transfer becomes limiting, TCA cycle activity would become restricted causing pyruvate concentrations to increase, activating the AOX through a feed-forward regulatory system.

Biochemical regulation of AOX activity in fungi and protozoa is not as well characterized as in plants, but purine nucleotides, particularly GMP, AMP, and ADP, are known to markedly stimulate AOX activity in fungi and protozoa. No stimulation of alternative oxidase activity by α-keto acids has been seen in fungi.

Physiological Role(s) of AOX

The fact that the alternative pathway wastes much of the free energy released during aerobic respiration must be related to its metabolic role. AOX has been found in all higher plants but there is only one instance where its role is clearly established, thermogenesis during flowering in certain members of the plant family Araceae (aroids). Just prior to pollen release, high levels of mitochondria found in club-like structures on the floral inflorescence undergo very high rates of respiration, heating up the inflorescence and volatilizing aromatic compounds that serve to attract pollinating insects. Mitochondria from this thermogenic tissue have extremely high levels of AOX, allowing the high rates of respiration without having to synthesize and use comparable amounts of ATP.

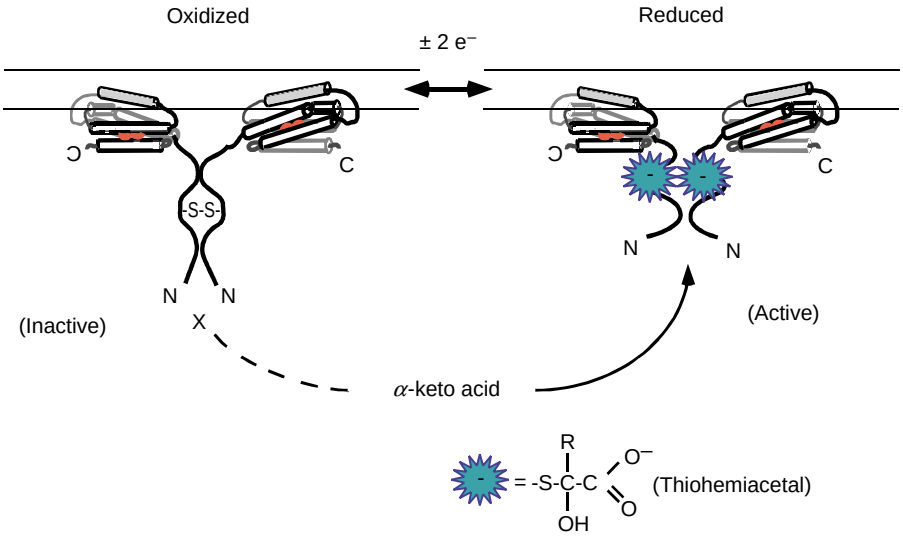

FIGURE 3 Biochemical regulation of plant AOX by the combined effects of reduction/oxidation of the redox active sulfhydryl/disulfide bond and reaction with α-keto acids to form an activating thiohemiacetal.

Most plant tissues do not respire at rates sufficient to support even modest thermogenesis, so that cannot represent its primary function in the vast majority of plant tissues. Because AOX is not involved in proton gradient generation, its activity is independent of the size of the gradient, unlike the cyt pathway, whose activity will be impaired as the proton gradient increases. Therefore, the AOX is in a position to use mitochondrial and cytoplasmic reductant in excess of that needed to maintain ATP synthesis, or when either ATP synthesis or the cyt pathway is impaired. Recognition of this fact originally served as the basis for the suggestion that the alternative pathway only operated when the activity of the cyt pathway was saturated, the so-called "energy overflow" hypothesis. Subsequent studies have established that the alternative pathway can compete with the cyt pathway for electrons from the ubiquinone pool when the cyt pathway is not saturated. This eliminated the overflow hypothesis in is purest form, but not from the standpoint of the alternative pathway helping to regulate mitochondrial electron flow and, as such maintain mitochondrial redox homeostasis.

One outcome of the ability of the alternative pathway to use excess mitochondrial reductant, resulting either from increased input to the ubiquinone pool or decreased use by the cyt pathway, is amelioration of the formation of reactive oxygen species (ROS; superoxide, hydrogen peroxide, hydroxyl radical) by the mitochondrial ubiquinone pool upon over-reduction. Operation of the alternative pathway has been shown to decrease both the reduction state of the ubiquinone pool in roots, and the formation of ROS in plant culture cells. The ability of AOX to decrease mitochondrial ROS formation is the basis of a hypothesis suggesting that AOX plays a role in plant response to environmental stresses. In several circumstances where increased mitochondrial ROS levels are predicted, including chilling stress, post-hypoxia-induced reperfusion injury, and reduced Pi availability, AOX gene expression and protein levels are observed to increase markedly.

Similarly, enhanced AOX gene expression and protein formation have been found to accompany oxidative stresses in fungi, including treatment with hydrogen peroxide. A survey of the appearance of the alternative pathway among yeasts found it was only present in so-called "Crabtree negative" yeast, that lack the presence of alcoholic fermentation as an option to the cyt pathway consistent with the concept of the alternative pathway serving as a mechanism for eliminating excess reducing equivalents in these organisms.

See Also the Following Articles

ATP Synthesis in Plant Mitochondria: Substrates, Inhibitors, Uncouplers • Cytochrome *c* • Free Radicals, Sources and Targets of: Mitochondria • Mitochondrial Membranes, Structural Organization • Mitochondrial Outer Membrane and the VDAC Channel

Glossary

aerobic respiration The biochemical process whereby reduced organic compounds are completely oxidized in three stages, glycolysis, the TCA cycle, and oxidative phosphorylation with the free energy released used to drive the synthesis of ATP.

alternative pathway The mitochondrial electron transfer pathway that goes via a cyanide-resistant, alternative oxidase (AOX) and transfers electrons from the ubiquinone pool to molecular oxygen without storing any of the released free energy in the form of a proton gradient.

cytochrome (cyt) pathway The mitochondrial electron transfer pathway that goes from the ubiquinone pool to molecular oxygen via Complex III and Complex IV (cytochrome *c* oxidase) and is coupled at each complex to the transport of protons across the membrane to produce a proton gradient that subsequently drives the synthesis of ATP.

diiron carboxylate protein Any member of a large family of proteins that contain a diiron active site formed by a four-helix bundle, two helices of which provide ligands to the two iron atoms via an E–X–X–H sequence motif, and two of which, each provide a single carboxylate ligand (i.e., Glu or Asp) to the irons. Family members include the R2 subunit of ribonucleotide reductase and the hydroxylase subunit of methane monooxygenase.

reactive oxygen species (ROS) Any of several highly reactive chemical species that can be formed following the reduction of molecular oxygen (O_2), including superoxide anion ($O_2^{\cdot -}$) hydrogen peroxide (H_2O_2) and hydroxyl radical ($OH^{\cdot}$).

Further Reading

Berthold, D. A., and Stenmark, P. (2003). Membrane-bound diiron carboxylate proteins. *Annu. Rev. Plant Biol.* **54**, 497–517.

Finnegan, P. M., Soole, K. L., and Umbach, A. L. (2004). Alternative mitochondrial electron transport proteins in higher plants. In *Advances in Photosynthesis and Respiration* (D. A. Day, A. H. Millar and J. Whelan, eds.), in press.

Moller, I. M. (2001). Plant mitochondria and oxidative stress: Electron transport, NADPH turnover and metabolism of reactive oxygen species. *Annu. Rev. Plant Physiol. Plant Mol. Biol.* **52**, 561–591.

Moore, A. L., and Siedow, J. N. (1991). The regulation and nature of the cyanide-resistant alternative oxidase of plant mitochondria. *Biochim. Biophys. Acta* **1059**, 121–140.

Moore, A. L., Albury, M. S., Crichton, P. G., and Affourtit, C. (2002). Function of the alternative oxidase: Is it still a scavenger? *Trends Plant Sci.* **7**, 478–481.

Peltier, G., and Cournac, L. (2002). Chlororespiration. *Annu. Rev. Plant Biol.* **53**, 523–550.

Siedow, J. N., and Umbach, A. L. (2000). The mitochondrial cyanide-resistant oxidase: Structural conservation amid regulatory diversity. *Biochim. Biophys. Acta* **1459**, 423–439.

Vanlerberghe, G. C., and McIntosh, L. (1997). Alternative oxidase: From gene to function. *Annu. Rev. Plant Physiol. Plant Mol. Biol.* **48**, 703–734.

Biography

James N. Siedow is a Professor in the Department of Biology at Duke University. His research interests are in oxidative processes in plants. He received his Ph.D. from Indiana University and was a Postdoctoral Fellow at Rice University. He has served as an Associate Editor of *Plant Physiology* and *Plant Molecular Biology* and on the Editorial Board of the *Journal of Biological Chemistry* and is a Fellow of the American Association for the Advancement of Science.

Autophagy in Fungi and Mammals

Daniel J. Klionsky and Ju Guan
University of Michigan, Ann Arbor, Michigan, USA

Autophagy refers to the processes by which portions of the cytoplasm are sequestered by membranes and transported into hydrolytic compartments to be degraded. This process occurs by two modes. During macroautophagy, double- or multiple-membrane vesicles, called autophagosomes, form in the cytoplasm. Upon completion, the autophagosome outer membrane fuses with the lysosome/vacuole or endosome. Subsequently the inner membrane and the enclosed cytoplasmic materials are degraded by hydrolases. Microautophagy entails the direct uptake of cytoplasm by invaginations or arm-like extensions of the lysosomal/vacuolar membrane. Autophagy is one of the major mechanisms for degradation and recycling of macromolecules. It is highly regulated by both physiological and environmental cues.

Autophagy in Mammals

Macroautophagy in Mammals

The phenomenon of macroautophagy has been observed in virtually all eukaryotic cell types. Mammalian hepatic tissues and cell cultures have been extensively studied, and in these macroautophagy accounts for the majority of macromolecular recycling once it is induced by hormonal or other signals. The content of the autophagosomes is indistinguishable from its surrounding cytoplasm and often includes recognizable structures such as mitochondria and ribosomes, suggesting that the sequestration is nonselective. There also exists evidence for selective sequestration of certain structures such as peroxisomes, particularly when these organelles are specifically induced to proliferate before the onset of autophagy. Based on morphological and immunocytochemical studies, macroautophagy proceeds through distinct steps of autophagosome formation and maturation (Figure 1). Each of these steps requires ATP.

Formation of Autophagosomes

The autophagosomes are distinct from most other intracellular vesicles in that double or multiple delimiting membranes are employed. In addition, formation of these vesicles topologically converts the sequestered cytoplasm to a lumenal or extracellular space. Although the membrane source of the sequestering vesicle has been extensively investigated, the origin is still not known. The autophagosomal membrane may be directly derived from other organelles. Immunostaining of the autophagosomal membrane identified organelle markers of the smooth endoplasmic reticulum (ER), a ribosome-free region of rough ER or the Golgi complex. However, the autophagosomal membranes are extremely poor in proteins, indicating that they do not have protein profiles typical of most endomembranes. Accordingly, it has been proposed that a novel organelle or membrane is dedicated to generating the initial sequestering membrane, termed the phagophore.

Maturation of the Phagophore

The maturation of phagophores into autophagosomes proceeds in a stepwise manner. For example, early phagophores may retain protein markers from the membrane of origin. These proteins may be lost and others acquired as the phagophore matures. Upon completion, which is marked by closure of the phagophore membrane, the cytosolic vesicle is termed an autophagosome. The autophagosomes fuse with lysosomes to acquire degradative enzymes. As a result of fusion, the inner autophagosomal membrane is released into the lysosome lumen, where it is broken down to expose the sequestered cytoplasm to the lysosomal hydrolases. The cytoplasmic cargo is subsequently degraded and recycled for use by the cell. A population of autophagosomes may fuse with endosomes to give rise to amphisomes, an intermediate compartment named for its dual role in both macroautophagy and endocytosis. The amphisome ultimately fuses with a lysosome to allow the degradation of its cargo.

Regulation of Macroautophagy in Mammals

The regulatory mechanism of macroautophagy is rather complex. Hormones and metabolites may activate or inhibit autophagy in different tissues. The intracellular signaling pathway has been studied mainly by using reagents that can alter the rates of autophagic protein degradation. It is very likely that the cellular responses to

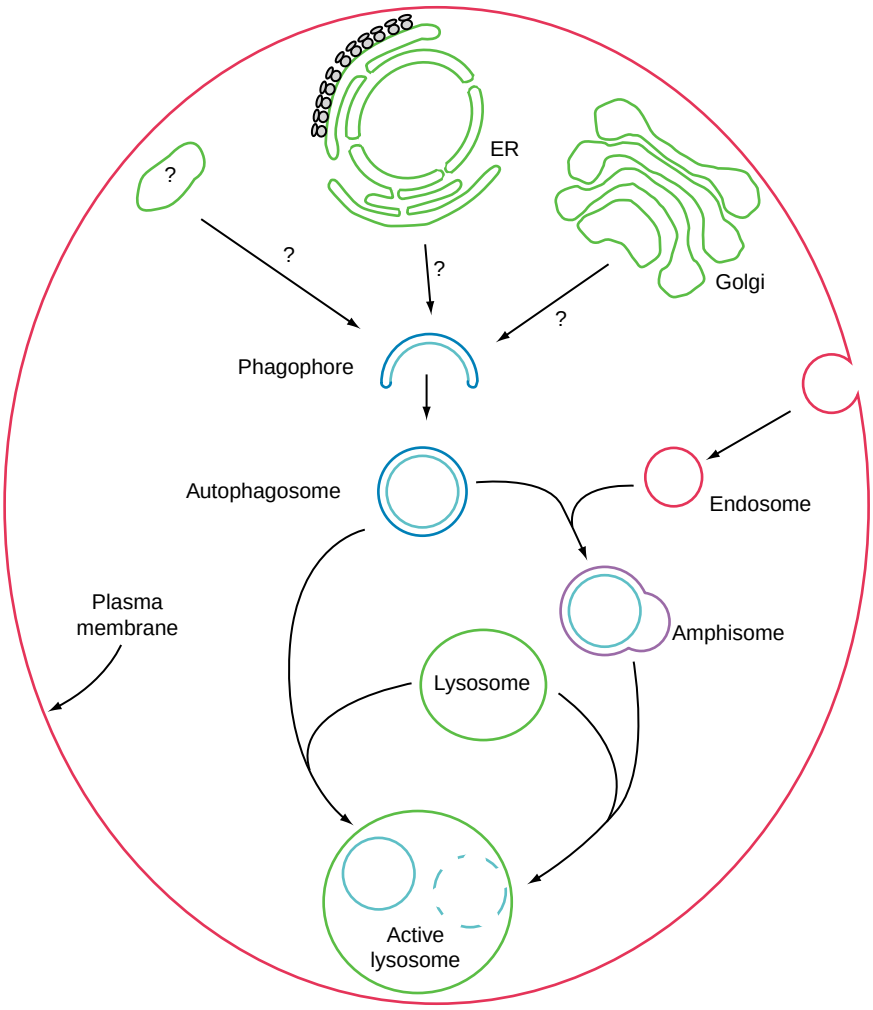

FIGURE 1 Macroautophagy in mammals. The initial sequestering membrane is termed the phagophore. Upon closure, the resulting double-membrane cytosolic vesicle is called an autophagosome. The origin of the phagophore or autophagosomal membrane is not known, but may include the endoplasmic reticulum, the Golgi complex, or a novel compartment. The autophagosome may fuse with an endosome to form an amphisome. The autophagosome or amphisome ultimately fuses with a lysosome, releasing the inner vesicle that is broken down to allow degradation and recycling of the vesicle contents.

these reagents are pleiotropic. Various proteins have been identified that play a role in regulating macroautophagy, including a phosphatidylinositol 3-kinase, heterotrimeric G proteins, protein kinases, and phosphatases. The inhibition of membrane fusion and cytoskeletal functions affects the final stages of cargo delivery. Table I lists some of the factors and chemicals that affect macroautophagy.

Microautophagy in Mammals

Microautophagy refers to the direct import of cytoplasmic materials by lysosomal membrane protrusions or invaginations. It is less well characterized in terms of its mechanisms and its contribution to overall protein degradation. In mammals, lysosomes with appendages or intralysosomal vesicles have been observed *in vivo*. Isolated lysosomes have shown the ability to uptake and degrade proteins or incorporate electron-dense markers into intralysosomal vesicles. Microautophagy is also induced by environmental cues such as nutrient deprivation.

Autophagy in Fungi

Macroautophagy in Yeast

Budding Yeast as a Model for Macroautophagy

During the last decade, autophagy has been studied using the budding yeast *Saccharomyces cerevisiae* as a model system. Nitrogen or carbon starvation induces the formation of cytoplasmic autophagosomes that have the characteristic double delimiting membranes. Similar to

TABLE I

Inhibitors of Macroautophagy in Mammals

Compounds	Effects on autophagy	Mechanism/targets
Physiological effectors		
Amino acids	Decrease	Charged tRNA, surface receptors
Anabolic hormones (insulin, IGF, EGF)	Decrease	Signaling
Catabolic factors/hormones (cyclic AMP, glucocorticoids)	Increase	Signaling
Pharmacological agents		
Okadaic acid	Decrease	Serine/threonine protein phosphatases
Wortmannin, LY294002, 3-methyladenine	Decrease	Phosphatidylinositol 3-kinase
Cycloheximide	Decrease	Ribosome
Cytochalasin B	Decrease	Microfilaments
Colchicine, vinblastine	Decrease	Microtubules

the findings in mammalian cells, yeast autophagosomal membranes are also protein-poor, as revealed by freeze-fracture electron microscopy studies. Once formed in the cytoplasm, the outer autophagosomal membrane will fuse with the vacuole (equivalent to the mammalian lysosome) membrane, leaving the inner vesicle, called the autophagic body, in the vacuolar lumen. The autophagic bodies are subsequently degraded by vacuolar hydrolases (Figure 2).

Autophagic mutants (*apg*) were isolated that failed to accumulate autophagic bodies when their vacuolar degradation was blocked by a protease inhibitor or by their decreased viability upon nitrogen starvation. An independent group of autophagic mutants (*aut*) were isolated by their inability to degrade a cytoplasmic enzyme under autophagy-inducing conditions.

The Cytoplasm to Vacuole Targeting Pathway and its Overlap with Macroautophagy

The cytoplasm to vacuole targeting (Cvt) pathway was discovered as the biosynthetic targeting pathway of a vacuolar resident enzyme, aminopeptidase I (Ape1). Precursor Ape1 (prApe1) is synthesized in the cytosol. It rapidly assembles into a dodecamer and remains in an oligomerized form during its course of transport into the vacuole (Figure 2). Cleavage of the N-terminal propeptide of prApe1 by vacuolar proteases gives rise to the mature, active form of the protein (mApe1). A group of *cvt* mutants were isolated that specifically block prApe1 maturation.

Genetic analysis revealed that the *apg* and *aut* mutants overlap with the *cvt* mutants that are defective in prApe1 targeting. Recently, a unified nomenclature has been adopted and the corresponding genes have all been termed autophagy-related (*ATG*). Morphological and biochemical studies further confirmed that prApe1 is transported to the vacuole using a vesicular mode similar to that of macroautophagy. Precursor Ape1 exists in the cytoplasm as a morphological structure that can be detected by electron microscopy. This structure, which consists of multiple prApe1 dodecamers bound to receptor proteins, is called the Cvt complex. Under vegetative growth conditions, the Cvt complex is specifically enwrapped by double-membrane Cvt vesicles. When autophagy is induced, the Cvt complex becomes a preferential cargo of autophagosomes. Thus, uptake of prApe1 represents a type of specific autophagy. Another hydrolase, α-mannosidase, is also targeted to the vacuole via the Cvt and autophagy pathways. The parallel studies of the Cvt pathway complement the analysis of autophagy by providing a specific cargo and the opportunity to study selective uptake mechanisms of autophagy.

Molecular Mechanism of the Cvt and Autophagic Pathways in Yeast

The molecular machinery was identified by cloning the genes that complement the *atg* mutants. Additional components were found by other approaches, including two-hybrid studies and the identification of homologues to pexophagy genes (see later discussion). Table II lists the Atg proteins and their proposed roles in these pathways. The molecular mechanism for the Cvt pathway and macroautophagy is briefly outlined next.

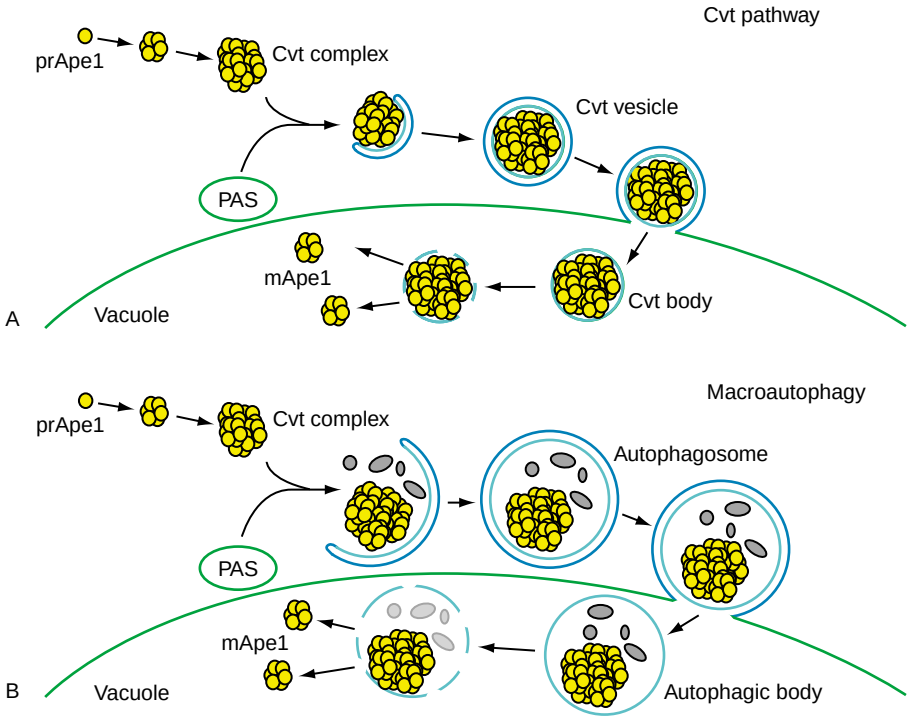

FIGURE 2 Cytoplasm to vacuole targeting (Cvt) pathway and macroautophagy in yeast. (A) Cvt pathway. Precursor Ape1 (prApe1) forms a dodecamer that assembles into a higher-order Cvt complex. Recruitment of the Cvt complex to the PAS leads to the formation of a Cvt vesicle. The completed Cvt vesicle fuses with the vacuolar membrane and releases the inner vesicle (Cvt body) into the vacuole lumen. Breakdown of the Cvt body allows the maturation of Ape1 (mApe1). (B) Macroautophagy. Under starvation conditions, the PAS is activated by specific signals resulting in the formation of autophagosomes. The Cvt complex is enclosed along with bulk cytoplasm inside autophagosomes. The inclusion of the Cvt complex is a specific process resulting from the action of receptor and adaptor proteins. Fusion between autophagosomes and the vacuole membrane and the subsequent breakdown of the inner membrane (autophagic body) release the cytoplasmic contents into the vacuole lumen for degradation and recycling or, in the case of the Cvt complex, maturation of precursor aminopeptidase I.

TABLE II

Proteins Involved in Autophagy and the Cvt Pathway

Function	Proteins	Molecular characteristics
Organization of the PAS	Atg6, Atg14	Phosphatidylinositol 3-kinase interacting proteins
	Atg9	Transmembrane protein
Localized on PAS; may control initiation of vesicle formation	Atg1, Atg11, Atg13, Atg17, Atg20, Atg24	Kinase or phosphorylated proteins PX domain proteins bind phosphatidylinositol(3)P
Localized on PAS; vesicle formation	Atg5, Atg8, Atg12, Atg16	Form conjugates or complexes conjugated to phosphatidylethanolamine
Conjugating proteins; catalyze formation of Atg12-Atg5 or Atg8-PE	Atg7, Atg3, Atg10, Atg4	E1 enzyme E2 enzymes Protease
Receptor protein of the Cvt complex	Atg19	Interacts with Atg11 and Atg8 to mediate specific enclosure of cargo
Degradation of intravacuolar vesicles	Atg15, Atg22	Lipase homologue Permease homologue
Others	Atg2, Atg18, Atg21, Atg23, Vps51	Proteins involved in vesicle formation, signaling and/or membrane retrieval

A Novel Organelle for De Novo Vesicle Formation *In vivo* fluorescence microscopy studies have colocalized the autophagosomal membrane marker protein Atg8 with several other Atg proteins on a perivacuolar structure. This structure is physiologically functional and appears to play a pivotal role in autophagosome formation; therefore, it has been termed the pre-autophagosomal structure (PAS). Localized on the PAS are two conjugates: Atg12, covalently linked to Atg5, and Atg8, covalently attached to phosphatidylethanolamine (Atg8-PE). These conjugates may directly participate in the generation of autophagosomes. Formation of the Atg12-Atg5 and Atg8-PE conjugates involves ubiquitin-like cascades. Recruitment of Atg12-Atg5 and Atg8 to the PAS depends on the function of the transmembrane protein Atg9 and an autophagy-specific phosphatidylinositol 3-kinase complex, underlying the key role of specific lipids in autophagosome formation.

Regulation of Autophagy The Cvt pathway operates under vegetative conditions, whereas autophagy is induced by starvation. Atg1 is localized at the PAS and is important in signaling Cvt vesicle or autophagosome formation, possibly via its differential association with other proteins such as Atg11 and Atg13. In particular, the Atg1-Atg13 interaction is regulated by the TOR (target of rapamycin) kinase. TOR also regulates autophagy at the transcriptional level.

Mechanism for Cargo Selection in the Cvt Pathway and Autophagy The Cvt complex is selectively sequestered by Cvt vesicles or autophagosomes. Atg19, a structural component of the Cvt complex, mediates the recruitment of the oligomerized prApe1 cargo and its recognition by the PAS though protein-protein interactions with Atg11 and Atg8. This may provide a prototype for other selective autophagic targeting pathways.

Fusion and Breakdown The fusion between the Cvt vesicles or autophagosomes and the vacuole membrane is probably similar to vacuole homotypic fusion and requires docking or tethering factors in addition to SNARE and Rab proteins. The breakdown of the inner vesicles requires the action of specific components such as the Atg15 lipase in addition to other vacuolar hydrolases.

Microautophagy and Selective Organelle Degradation in Yeasts

Nonselective Microautophagy

The morphological features of microautophagy have been observed in yeasts. Microautophagic vacuole invagination was also reconstituted *in vitro*. Interestingly, the molecular components of macroautophagy, the Atg proteins, were implicated to function at least partly in microautophagy as well.

Selective Autophagy of Peroxisomes in Methylotrophic Yeasts

Selective degradation of peroxisomes by autophagic mechanisms has been well demonstrated in methylotrophic yeasts. Peroxisomes are necessary for using methanol and are induced when methanol is the sole carbon source. Upon shift of culture medium to preferred carbon sources, superfluous peroxisomes are targeted to the vacuole via either a macro- or microautophagic mode, depending on nutrient conditions. The selective degradation of peroxisomes is termed pexophagy. The proteins involved in glucose-induced selective microautophagy of peroxisomes (Gsa proteins) are generally found to be homologous to the Atg proteins. This finding suggests that macro- and microautophagy may be more closely related at the molecular level than they appear to be morphologically. Alternatively, the Atg proteins may play a unique role in micropexophagy.

Autophagy, from Yeasts to Mammals

Most of the Atg proteins are conserved in higher eukaryotes, suggesting that the mechanism for autophagy is similar in yeasts and mammals. A few mammalian autophagy proteins have been directly demonstrated to function in macroautophagy. Future studies with mammalian cells may further benefit from the molecular model provided by yeast systems. On the other hand, abnormalities in autophagy have been connected with various human diseases such as Parkinson's disease and certain types of cancer. The importance of autophagy in developmental or pathological macromolecular turnover has yet to be directly demonstrated in higher eukaryotes, but promises to be an exciting area of future research.

See Also the Following Articles

Aminopeptidases • G_i Family of Heterotrimeric G Proteins • *N*-Linked Glycan Processing Glucosidases and Mannosidases • Peroxisomes • Phosphatidylinositol Bisphosphate and Trisphosphate • Vacuoles

Glossary

autophagy A process in which the cell undergoes membrane rearrangements to sequester a portion of cytoplasm, deliver it to a degradative organelle, and recycle the macromolecular constituents.

cytoplasm to vacuole targeting (Cvt) pathway A biosynthetic pathway that transports resident hydrolases to the vacuole through a specific autophagy-like process.

lysosome A degradative organelle in mammals that compartmentalizes a range of hydrolytic enzymes and maintains a reduced pH.

macroautophagy An autophagic process involving the formation of a double- or multiple-membrane cytosolic vesicle of nonlysosomal or nonvacuolar origin.

microautophagy An autophagic process involving direct uptake of cytoplasm at the lysosome or vacuole by protrusion, invagination, or septation of the sequestering organelle membrane.

pexophagy A selective type of autophagy involving the sequestration and degradation of peroxisomes.

vacuole A degradative organelle in fungi that compartmentalizes a range of hydrolytic enzymes and maintains a reduced pH.

Further Reading

Blommaart, E. F. C., Luiken, J. J. F. P., and Meijer, A. J. (1997). Autophagic proteolysis: Control and specificity. *Histochem. J.* **29**, 365–385.

Codogno, P., Ogier-Denis, E., and Houri, J.-J. (1997). Signal transduction pathways in macroautophagy. *Cell. Signaling* **9**, 125–130.

Dunn, Jr. W. A. (1994). Autophagy and related mechanisms of lysosome-mediated protein degradation. *Trends Cell Biol.* **4**, 139–143.

Glaumann, H., and Ballard, J. F. (eds.) (1987). *Lysosomes: Their Role in Protein Breakdown*. Academic Press, London.

Kim, J., and Klionsky, D. J. (2000). Autophagy, cytoplasm-to-vacuole targeting pathway, and pexophagy in yeast and mammalian cells. *Annu. Rev. Biochem.* **69**, 303–342.

Klionsky, D. J. (2004). *Autophagy*. Landes Bioscience, Georgetown, TX.

Klionsky, D. J., and Emr, S. D. (2000). Autophagy as a regulated pathway of cellular degradation. *Science* **290**, 1717–1721.

Klionsky, D. J., and Ohsumi, Y. (1999). Vacuolar import of proteins and organelles from the cytoplasm. *Annu. Rev. Cell Dev. Biol.* **15**, 1–32.

Noda, T., Suzuki, K., and Ohsumi, Y. (2002). Yeast autophagosomes: De novo formation of a membrane structure. *Trends Cell Biol.* **12**, 231–235.

Seglen, P. O., Berg, T. O., Blankson, H., Fengsrud, M., Holen, I., and Stromhaug, P. E. (1996). Structural aspects of autophagy. *Adv. Exp. Med. Biol.* **389**, 103–111.

Biography

Daniel J. Klionsky is the Abram Sager Collegiate Professor of Life Sciences in the Life Sciences Institute and is a professor in the Departments of Molecular, Cellular, and Developmental Biology and of Biological Chemistry at the University of Michigan, Ann Arbor. His principal research interest is the regulated targeting of proteins and organelles from the cytoplasm into the vacuole using the budding yeast as a model system. He holds a Ph.D. from Stanford University and received his postdoctoral training at the California Institute of Technology. He is a fellow of the John Simon Guggenheim Memorial Foundation and a recipient of the National Science Foundation Director's Award for Distinguished Teaching Scholars.

Ju Guan was a graduate research student in the Klionsky laboratory until 2002. She is currently a postdoctoral research scholar at the University of Michigan, Ann Arbor.

B_{12}-Containing Enzymes

Vahe Bandarian* **and Rowena G. Matthews**
University of Michigan, Ann Arbor, Michigan, USA

Vitamin B_{12}, or cobalamin, was isolated from liver extracts over 50 years ago as a red crystalline metabolite that cured pernicious anemia in humans. The X-ray crystal structure of the cofactor and various derivatives subsequently showed that it has an elaborate organometallic structure. Cobalamin is widely distributed in nature and biochemical studies have shown that it facilitates enzymatic transformations that involve methyl group transfer and radical-mediated rearrangements. The biosynthesis of cobalamin, the molecular mechanisms of the transformations that are catalyzed by cobalamin-dependent enzymes, and the inherent chemical flexibility in this organometallic cofactor that permit it to participate in these disparate reactions, have fascinated chemists and biochemists for decades. This entry highlights the chemical transformations that are catalyzed by cobalamin-dependent enzymes.

The Cobalamin Cofactor

The central feature of the cobalamin cofactor (Figure 1A) is a cobalt atom with octahedral geometry, which is centered in the corrin macrocycle by coordination to pyrrole nitrogens from the corrin in the four equatorial coordination positions of the metal ion. A nitrogen atom that is donated by a dimethylbenzimidazole moiety, which in turn is ligated to the corrin ring, coordinates the cobalt from the lower axial position. In some eubacteria and Archaea, the dimethylbenzimidazole substituent of the cobalamin is replaced by other compounds (e.g., *p*-cresol); such cofactors are referred to as corrinoids. The macrocycle is further adorned by methyl, acetamide, and propionamide side chains. The upper axial position of the cobalt ion is occupied by an alkyl substituent specific to the type of reaction catalyzed by the protein.

The upper face of the cobalamin is where the chemistry takes place in all cobalamin-dependent enzymes. The chemical versatility of cobalamin and corrinoids lies in the carbon–cobalt bond of the cofactor, which is susceptible to cleavage by heterolytic or homolytic pathways (see Figure 1B). The upper coordination position of the cobalamin, in the enzymes that catalyze methyl group transfer, is transiently occupied by a methyl group en route from a donor molecule to an acceptor molecule. In these enzymes, the cobalamin serves both as a nucleophile, accepting the methyl group from the donor, and as a leaving group, donating the methyl group to an acceptor molecule. By contrast, enzymes that catalyze radical-mediated transformations require that the cobalamin have 5′-deoxyadenosine coordinated to the cobalt on the upper face of the corrin. In these enzymes, the organometallic bond between the 5′-methylene of the deoxyadenosyl moiety and the cobalt is severed homolytically to generate a 5′-deoxyadenosyl radical, which initiates the radical cascades that lead to formation of product.

The identity of the ligand that occupies the lower axial coordination position of protein-bound cobalamin may differ significantly from that in solution. In some proteins, in addition to the network of interactions with the side chains of the corrin, the imidazole side chain of a histidine residue substitutes for the dimethylbenzimidazole of the cofactor and donates a nitrogen ligand to the cobalt. This latter form of binding is referred to as a base-off binding mode. Most of the proteins that bind the cobalamin in the base-off mode also contain a DxHxxG sequence that contains the histidine residue that donates the lower axial imidazole ligand. In other proteins, binding of cobalamin to the protein backbone is accomplished by extensive interactions with the corrin and its side chains, and the dimethylbenzimidazole remains coordinated to the cobalt atom. This is referred to as base-on binding of the cofactor.

The cobalamin cofactor can exist in three oxidation states, and each form of the cobalamin exhibits distinct ultraviolet (UV)-visible spectra that allow one to follow the course of the catalytic cycle. For instance, the cobalt in alkyl cobalamins, such as adenosylcobalamin or methylcobalamin, is in the +3 oxidation state (formally, the alkyl ligand is considered to be the anion R^-). Homolysis of the cobalamin to generate a deoxyadenosyl radical is accompanied by the formation of a reduced cobalamin, cob(II)alamin, in which the cobalt is in the +2 oxidation state, and reformation of the C–Co bond of the cofactor oxidizes the cobalt to the +3 state. Therefore, adenosylcobalamin-dependent proteins cycle

*Current address: University of Arizona, Tucson, Arizona.

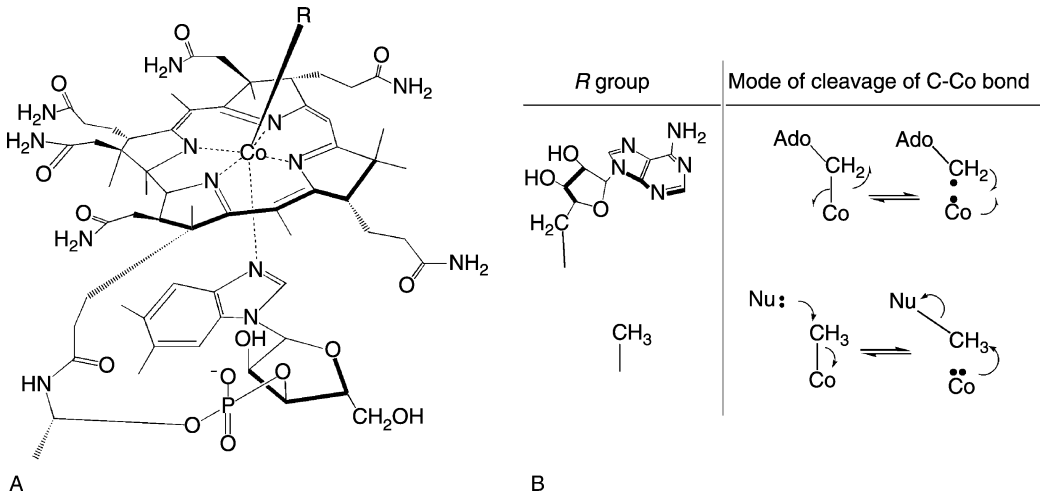

FIGURE 1 Structure and reactivity of alkylcobalamins. (A) The upper coordination position of cobalamin can be occupied by 5′-deoxyadenosine or by a methyl group. (B) Homolysis of the C–Co bond in adenosylcobalamin-dependent enzymes generates a 5′-deoxyadenosyl radical and cob(II)alamin. By comparison, the cofactor is transiently methylated in enzymes that catalyze group transfer reactions.

between the +3 and +2 oxidation states during the course of the catalytic cycle. By contrast, upon nucleophilic displacement of methyl group from the cobalamin during group transfer chemistry, the cobalamin cycles between the +3 oxidation state in the methylcobalamin form and the +1 state upon loss of the alkyl group. Remethylation of the cobalamin reoxidizes the cobalamin to the +3 oxidation state.

In this entry we summarize the reactions that are catalyzed by cobalamin-requiring enzymes, first highlighting the reactions in which cobalamin serves as a source of the highly reactive 5′-deoxyadenosyl radical and then discussing the reactions that involve methyl transfer chemistry.

Reactions Catalyzed by Cobalamin-Dependent Enzymes

Radical-Mediated Rearrangement Reactions

The enzymes that catalyze radical-mediated transformation exploit the inherent weakness of the carbon-cobalt bond of adenosylcobalamin (bond dissociation energy ~ 30 kcal mol^{-1}) to form the highly reactive 5′-deoxyadenosyl radical. Binding of the cobalamin to these enzymes accelerates the rate of homolysis of the C–Co bond $\geq 10^{12}$-fold. Homolysis of the carbon–cobalt bond is triggered by the presence of the substrate or by an allosteric effector. Presumably, the binding energy derived from substrate/effector-enzyme interactions is essential to elicit the conformational changes that are required to facilitate homolysis of the relatively weak organometallic bond. The 5′-deoxyadenosyl radical is a primary radical and readily abstracts a hydrogen atom from the substrate or from a residue on the protein. Therefore, a hallmark of catalysis by the enzymes in this group is formation of radical intermediates. Figure 2 shows the general catalytic cycles for these enzymes.

Adenosylcobalamin-dependent enzymes can be divided into four groups based on the details of the catalytic transformations (Table I). The reactions catalyzed by enzymes in each group are discussed next.

Migration and Elimination Reactions

The enzymes in this group participate in the fermentation of short-chain organic compounds such as ethanolamine, glycerol, 1,2-propanediol, and 1,2-ethanediol. The reactions catalyzed by these enzymes are formally the interchange of a hydrogen atom on one carbon with a group X (= OH or NH_3) at the adjacent position. The catalytic mechanism of these enzymes is quite similar to the mechanism of the carbon skeleton mutase enzymes discussed later. These two groups, in fact, differ only in that the mutases retain the rearranged substituent.

The catalytic mechanisms of ethanolamine ammonia-lyase and diol dehydratase have been studied extensively and a generalized mechanism for these enzymes is shown in Figure 2A. As with all cobalamin-dependent enzymes, the carbon–cobalt bond of the cofactor is homolyzed to generate 5′-deoxyadenosyl radical and cob(II)alamin in the first step of the catalytic reaction. The deoxyadenosyl radical abstracts a hydrogen atom from the substrate (S–H) to generate a substrate-like radical (S·) $\sim$ 9–12Å away from the cob(II)alamin. The rearrangement of S· to a product-like radical (P·) followed by return of a hydrogen atom from the 5′-deoxyadenosine results in the formation of the enol form of the product (P–H). The deoxyadenosyl radical recombines with cob(II)alamin to regenerate

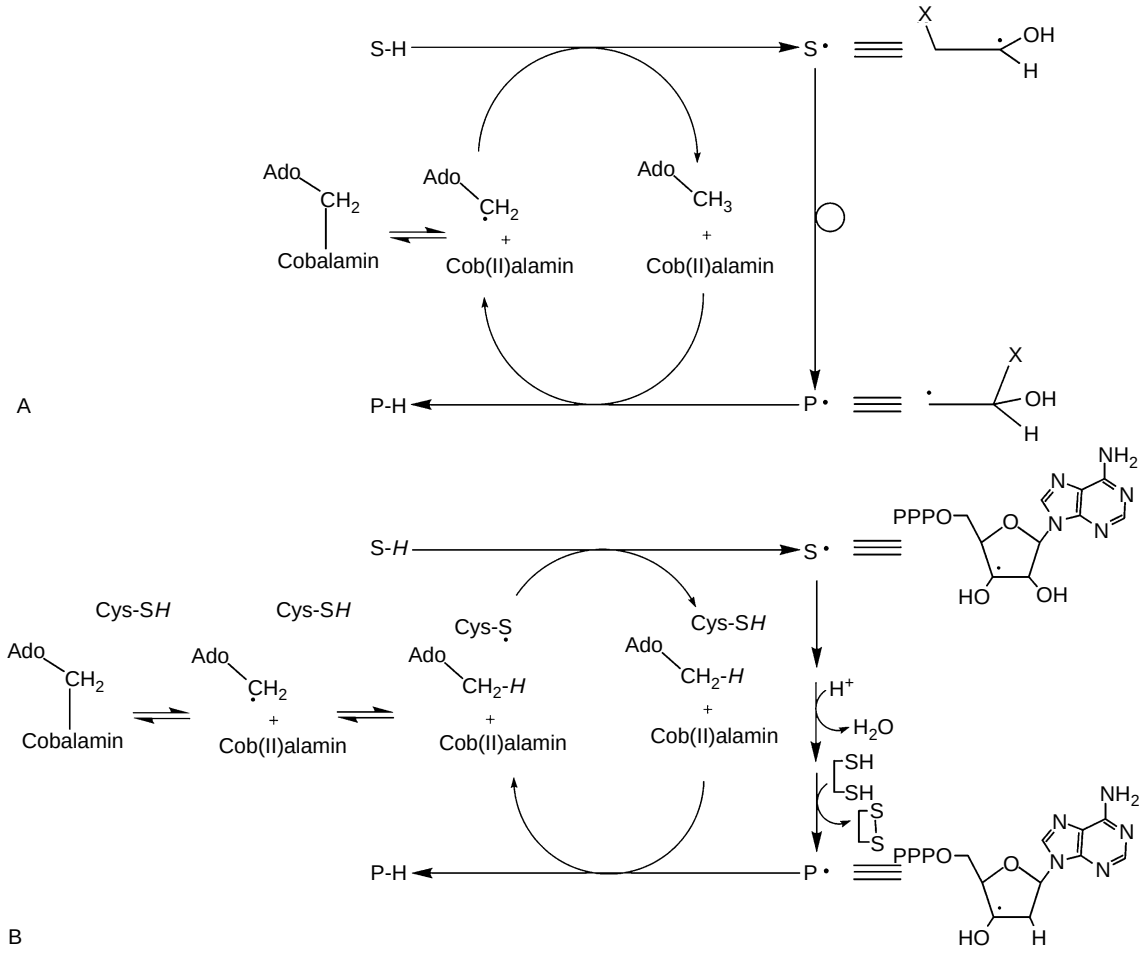

FIGURE 2 Generalized reaction cycles for enzymes that catalyze radical-mediated rearrangements. (A) The catalytic cycles for enzymes that catalyze rearrangements and eliminations, carbon skeleton rearrangements, and PLP-dependent aminomutase reactions. The structures on the right are examples of the intermediates that would be expected in the conversion of ethanolamine acetaldehyde and ammonia by ethanolamine ammonia-lyase. (B) The catalytic cycle of ribonucleotide triphosphate reductase differs from the cycle in (A) in that the 5′-deoxyadenosyl radical abstracts a hydrogen atom from an active site cysteine thiol to generate a thiyl radical that subsequently generates a substrate-based radical species. The structures on the right show some of the reaction intermediates that form in the course of conversion of ATP to dATP.

adenosylcobalamin. The initial *gem*-diol or *gem*-amino alcohol that is formed in the course of these transformations subsequently eliminates water or ammonia, respectively, to generate the corresponding aldehydes.

Diol and glycerol dehydratases have the best characterized structures in this group. Few sequence similarities exist between the diol and glycerol dehydratases and ethanolamine ammonia-lyase, despite the similarities in the reactions that they catalyze. Nevertheless, members of these groups of enzymes appear to retain coordination of the cobalamin to dimethylbenzimidazole.

Diol dehydratase and glycerol dehydratase are rapidly inactivated in the course of their catalytic cycle by side reactions that lead the formation of tightly bound inactive cofactor at the active site of these enzymes. The gene clusters that code for the structural genes for these proteins also contain open reading frames whose products have been shown to catalyze the ATP- and Mg^{2+}-dependent exchange of inactive cofactor with cofactor from solution. The generality of the reactivation mechanism remains to be determined.

Carbon Skeleton Rearrangement Reactions

As with the enzymes that catalyze rearrangement and elimination, the enzymes in this group catalyze the interchange of a hydrogen atom on one atom with an alkyl group on the adjacent carbon atom (see Table I). The reactions catalyzed by these enzymes differ from the others in several respects. First, the migrating alkyl group is not eliminated from the product. Second, the mutase reactions are *reversible*. Two significant structural differences have also been noted between these enzymes. First, spectroscopic and structural studies have shown that cobalamin binds in the base-off conformation and that the histidine residue that donates the imidazole ligand is conserved in the members of

TABLE I

Adenosylcobalamin-Dependent Radical-Mediated Transformations

Group 1	Rearrangement/Elimination reactions	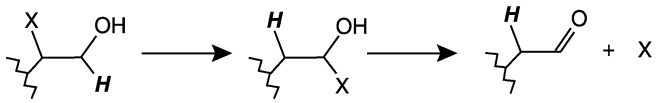
	Diol dehydratase	1,2-propanediol → propionaldehyde + water
		ethylene glycol → acetaldehyde + water
	Glycerol dehydratase	glycerol → 3-hydroxypropionaldehyde
	Ethanolamine ammonialyase	ethanolamine → acetaldehyde + ammonia
Group 2	Carbon skeleton mutases	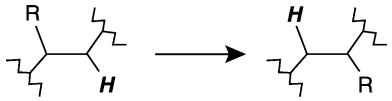
	Methylmalonyl-CoA mutase	(2*R*)-methylmalonyl-CoA ⇔ succinyl-CoA
	Isobutyryl-CoA mutase	isobutyryl-CoA ⇔ *n*-butyryl-CoA
	Glutamate mutase	*S*-glutamate ⇔ (2*S*,3*S*)-3-methylaspartate
	2-Methyleneglutarate mutase	2-methyleneglutarate ⇔ (*R*)-3-methylitaconate
Group 3	PLP-dependent aminomutases	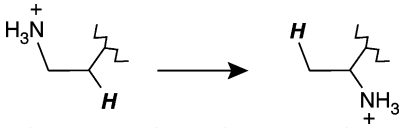
	Lysine 5,6-aminomutase	D-lysine ⇔ 2,5-diaminohexanoic acid
		L-β-lysine ⇔ 3,5-diaminohexanoic acid
	D-Ornithine 4,5-aminomutase	D-ornithine ⇔ (2*R*,4*S*)-diaminopentanoate
Group 4	Ribonucleotide reduction	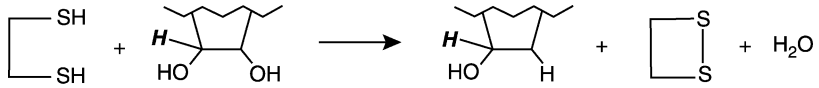
	Ribonucleotide triphosphate reductase	ribonucleotide triphosphate → deoxyribonucleotide triphosphate

the group. Second, the substrate-based radicals that are formed in the course of the reaction reside ~6Å away from the cob(II)alamin. However, despite these differences, the 5′-deoxyadenosyl radical is involved in generating a substrate-based radical and the catalytic cycle of these enzymes resembles that of the enzymes that catalyze rearrangement and elimination reactions (see Figure 2A).

PLP-Dependent Aminomutase Reactions

Pyridoxal 5′-phosphate (PLP)-dependent aminomutases catalyze the interchange of a hydrogen atom with an amino group on the adjacent carbon atom. These enzymes (see Table I) have been purified from several strict anaerobes that catabolize lysine or ornithine to organic acids and ammonia. The salient features of the generic aminomutase mechanism are the formation of a Schiff base linkage between the substrate and PLP and the use of 5′-deoxyadenosyl radical to initiate catalysis. In these enzymes, the PLP may assist in the intramolecular migration of the amino group. In addition to the presence of PLP, these enzymes differ from the enzymes that catalyze migration and elimination reactions in that aminomutases catalyze a reversible interchange of a hydrogen atom with the amino group on the adjacent carbon atom and the cofactor binds in a base-off configuration. Despite these differences, the catalytic cycle shown in Figure 2A applies to these enzymes as well.

Ribonucleotide Triphosphate Reductase Reaction

Ribonucleotide reductases catalyze the conversion of nucleotides to deoxynucleotides in all organisms. The prominent role of these enzymes in nucleotide metabolism has made them attractive targets of antiviral and antitumor therapies. Ribonucleotide reductase can synthesize all four DNA bases from the corresponding nucleosides; however, the activity of the enzymes from all sources is allosterically regulated by the ratio of the deoxyribonucleotides and nucleotides. Four classes

of reductases have been described. Although the overall reactions catalyzed by all of these enzymes are identical, they differ in two respects. First, some use nucleoside diphosphates as substrates, whereas others prefer nucleotide triphosphates. Second, these enzymes differ in the source of the species that initiates the radical turnover cascade. In fact, ribonucleotide reductases have been categorized into four classes based on the free-radical initiators. Only one of these, the class II ribonucleotide triphosphate reductase, is adenosylcobalamin-dependent. However, the catalytic transformations that ensue following the formation of the substrate radical are remarkably similar. The ribonucleotide triphosphate-specific enzyme from *Lactobacillus leichmannii* is the best-characterized example of adenosylcobalamin-dependent reductases.

The mechanistic details of the ribonucleotide reduction differ significantly from the paradigms that have been discussed in the previous sections for the group migration and elimination, aminomutase, and carbon skeleton mutase enzymes. First, ribonucleotide reductases contain a pair of active-site cysteine residues that are oxidized in the course of the reaction and must undergo reduction between each catalytic cycle. Second, a cysteine on the protein forms a thiyl radical that is directly involved in the reaction. Figure 2B shows a general catalytic cycle for the adenosylcobalamin-dependent ribonucleotide reductase, highlighting the differences between this enzyme and other radical-mediated rearrangement reactions. The carbon–cobalt bond of the cofactor is homolyzed by the protein in the presence of allosteric effector; the resulting 5′-deoxyadenosyl radical abstracts a hydrogen atom from an active-site cysteine residue to generate a thiyl radical, which in turn abstracts a hydrogen atom from C3′ of the substrate. In the course of reduction of the substrate to the product, a pair of active-site thiols is oxidized and the active-site thiyl radical is reformed. Reformation of the cofactor and reduction of the active-site thiols prepare the active site for subsequent turnover.

Methyl Transfer Reactions

Enzymes that catalyze cobalamin-dependent methyl transfer reactions use the potential for heterolytic cleavage of the carbon-cobalt bond of the cofactor (see Figure 1B). The cofactor in these enzymes serves both as a nucleophile and as a leaving group, undergoing transient methylation in the course of the reaction. Although the identities of the donor and acceptor molecules vary among the family of cobalamin-dependent methyl transferase enzymes (Figure 3), the overall catalytic cycles of these enzymes are similar. In this section, we consider methionine synthase as a prototype of the cobalamin-dependent methyltransferases, highlighting the similarities and differences among the members of the methyl transferase family of enzymes.

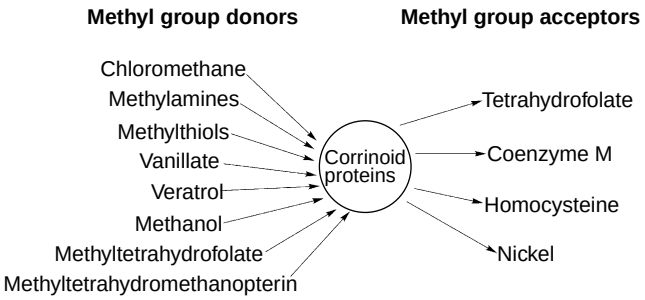

FIGURE 3 Diversity of methyl group donors and acceptors in cobalamin-dependent methyltransferase enzymes.

Cobalamin-Dependent Methionine Synthase

Cobalamin-dependent methionine synthase is found in mammals and in *Caenorhabditis elegans*, but not in insects or in plants, which neither produce nor transport cobalamin. It is also found in many prokaryotes, including *Escherichia coli*, but not in Archaea. The enzyme catalyzes the transfer of a methyl group from the tertiary amine methyltetrahydrofolate to the thiol of homocysteine, and the cobalamin cofactor serves as an intermediary in the methyl transfer. A catalytic cycle for methionine synthase is shown in Figure 4.

Methionine synthase is a large monomeric protein (1227 amino acid residues in the enzyme from *E. coli*) containing four discrete modules. The N-terminal module binds and activates homocysteine; the thiol of homocysteine coordinates to a catalytically essential zinc metal ion in this module. The next module in the sequence binds and activates methyltetrahydrofolate. Each of these substrate-binding modules communicates with the third module in the sequence, the B_{12}-binding module, to transfer methyl groups to and from the base-off cofactor. The C-terminal module is required for activation of methionine synthase when the cob(I)alamin cofactor becomes oxidized during turnover (~1 in 2000 turnovers results in oxidation *in vitro*). Activation of the inactive cob(II)alamin form of the cofactor requires both a methyl donor and an electron donor. The methyl donor is *S*-adenosyl-L-methionine. In *E. coli* the electron donor is reduced flavodoxin, and in mammals it is methionine synthase reductase, a protein containing a domain with homology to flavodoxin. To allow methyl transfer during reductive activation, the C-terminal domain must also access the cobalamin; a structure of a fragment of methionine synthase in this conformation has recently been determined.

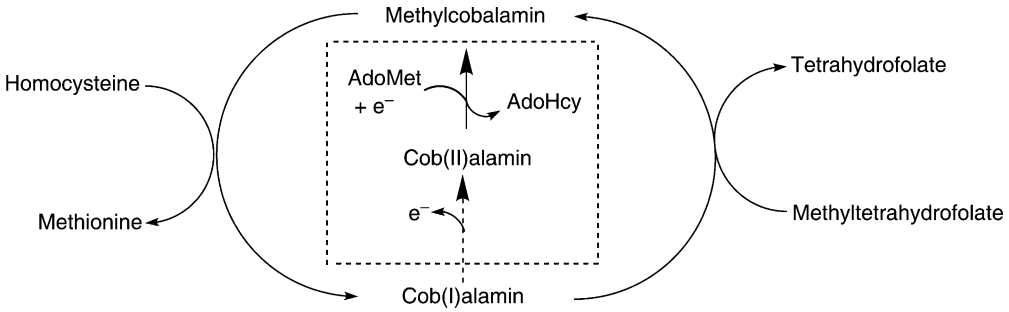

FIGURE 4 Catalytic cycle of cobalamin-dependent methionine synthase. The dashed box shows the reactivation of the oxidized cofactor by reductive methylation.

Methyl Transferases Involved in Methanogenesis and Acetogenesis

Although cobalamin-dependent methionine synthase is the only B_{12}-dependent methyl transferase in eubacteria and eukaryotes, a large number of enzymes catalyzing similar methyl transfers that employ corrinoid cofactors have been identified in Archaea and acetogenic eubacteria. The diversity in the methyl group donor-acceptor pairs is illustrated in Figure 3. In general, in methanogens, corrinoid-dependent enzymes are involved in the formation of methylcoenzyme M, the methyl thioether that provides the methyl group destined to form methane in methanogenesis. The methyl donors in these reactions include methyltetrahydromethanopterin, which is chemically similar to methyltetrahydrofolate. The methyl group of methyltetrahydromethanopterin is formed by the reduction of carbon dioxide using reducing equivalents derived from molecular hydrogen. Some methanogens can also use simple compounds such as methylamines, methanol, or methylsulfides as the source of methyl groups for methanogenesis. In contrast to cobalamin-dependent methionine synthase, in which a single protein catalyzes methyl transfer from methyltetrahydrofolate to cobalamin and from methylcobalamin to homocysteine, most of these methanogenic methyl transferase reactions require three separate proteins, a corrinoid-containing protein, a methyltransferase that transfers methyl groups from the donor molecule to the corrinoid protein, and a second methyltransferase that transfers methyl groups from the methylcorrinoid protein to the acceptor.

Eubacterial acetogenesis also involves corrinoid-dependent methyl transferases. In these organisms, carbon dioxide and hydrogen are used to generate acetyl CoA. The methyl group of acetyl CoA is generated by reduction of carbon dioxide using reducing equivalents from molecular hydrogen, as in methanogens, and is transferred to a corrinoid cofactor that serves as the direct methyl donor to the enzyme responsible for the synthesis of acetyl CoA from a methyl group and carbon dioxide. Additional acetogenic substrates include vanillate, veratrol, and halogenated aryl or alkene compounds. The precise nature of the chemistry that is promoted by cobalamin with the last substrates remains to be elucidated.

See Also the Following Articles

DNA Methyltransferases, Bacterial • DNA Methyltransferases: Eubacterial GATC • Pyridoxal Phosphate

Glossary

B_{12} A complex organometallic cofactor, also called cobalamin, that is used by enzymes that catalyze group transfer or radical-mediated rearrangement reactions.

cofactor A compound that is noncovalently associated with an enzyme and is required for the catalytic activity.

radical A species that contains an unpaired electron.

Further Reading

Banerjee, R. (ed.) (1999). *Chemistry and Biochemistry of B_{12}*. John Wiley & Sons, Inc., New York.

Dolphin, D. (ed.) (1982). *B_{12}*, Vol. 2, John Wiley & Sons, New York.

Hay, B. P., and Finke, R. G. (1987). Thermolysis of the Co–C bond in adenosylcorrins. 3. Quantification of the axial base effect in adenosylcobalamin by the synthesis and thermolysis of axial base-free adenosylcobinamide: Insights into the energetics of enzyme-assisted cobalt-carbon bond homolysis. *J. Am. Chem. Soc.* **109**, 8012–8018.

Licht, S., and Stubbe, J. (1999). Mechanistic investigations of ribonucleotide reductases. In *Comprehensive Natural Products Chemistry, Enzyme and Enzyme Mechanisms, Proteins, and Aspects of NO Chemistry*, (C. D. Poulter, ed.) Vol. 5, pp. 163–204. Elsevier Science Ltd., Oxford, U.K.

Marsh, E. N., and Drennan, C. L. (2001). Adenosylcobalamin-dependent isomerases: New insights into structure and mechanism. *Curr. Opin. Chem. Biol.* **5**, 499–505.

Sintchak, M. D., Arjara, G., Kellogg, B. A., Stubbe, J., and Drennan, C. L. (2002). The crystal structure of class II ribonucleotide reductase reveals how an allosterically regulated monomer mimics a dimer. *Nat. Struct. Biol.* **9**, 293–300.

Thauer, R. K. (1998). Biochemistry of methanogenesis: A tribute to Marjory Stephenson. 1998 Marjory Stephenson Prize Lecture. *Microbiology* **144**, 2377–2406.

Toraya, T. (2000). The structure and the mechanism of action of coenzyme B_{12}-dependent diol dehydratases. *J. Mol. Cat. B* **10**, 87–106.

Biography

Vahe Bandarian is a postdoctoral fellow at the University of Michigan at Ann Arbor. His research interest is the mechanism of action of adenosylcobalamin-dependent enzymes. He holds a Ph.D. in biochemistry from the University of Wisconsin-Madison and is a recipient of a 2002 Burroughs Wellcome Career Award in Biomedical Sciences.

Rowena G. Matthews is the G. Robert Greenberg Distinguished University Professor of Biological Chemistry and Senior Research Scientist at the Life Sciences Institute of the University of Michigan. Research in her laboratory focuses on the role of vitamins, especially folic acid and vitamin B_{12}, in biochemical reactions, and on the regulation of folic acid-dependent metabolism. She received her Ph.D. from the University of Michigan and her B.A. from Radcliffe College, Cambridge, MA. Dr Matthews is a Fellow of the American Association for the Advancement of Science and of the National Academy of Sciences and has served on the Advisory Council of the National Institute of General Medical Sciences.

Bax and Bcl2 Cell Death Enhancers and Inhibitors

David L. Vaux
The Walter and Eliza Hall Institute, Parkville, Victoria, Australia

Apoptosis, the physiological cell death mechanism used by metazoans to remove unwanted cells, is controlled by a family of pro- and anti-apoptotic proteins that bear varying degrees of similarity to a protein called Bcl2. Some members of this family, such as Bcl2 itself, stop cells from activating their suicide mechanism, whereas other members of this family, such as Bax, activate the cell death process.

Identification of Bcl2 as a Cell Death Inhibitor

A gene at the site of chromosomal translocations associated with the common lymphoid cancer follicular lymphoma was designated Bcl2 for B-cell leukemia/lymphoma gene number 2. Rather than promoting cell growth and proliferation like most cancer genes, Bcl2 does not stimulate cells to divide but prevents them from activating their endogenous apoptotic cell suicide mechanism. The association of activation of the apoptosis inhibitor Bcl2 with lymphoma was the first evidence that cell death is required to avoid the development of cancer.

Genetics of Cell Death in *Caenorhabditis elegans*

Although Bcl2 was the first component of the apoptosis mechanism to be recognized at the molecular level in any organism, genetic analysis of programmed cell death in the nematode *C. elegans* revealed that in worms developmental cell death is controlled and implemented by a specific genetic program. Programmed cell death in *C. elegans* fails to occur in *egl-1*, *ced-4*, and *ced-3* loss of function mutants, as well as in *ced-9* gain of function mutants, implying that *egl-1*, *ced-4*, and *ced-3* encode killer proteins and that *ced-9* encodes a survival protein. The expression of human Bcl2 in the worm, and the cloning and sequencing of *ced-9*, showed that they are structurally and functionally homologous. In the worm CED-9 prevents cell death by preventing the adaptor CED-4 from activating the protease CED-3, and in mammalian cells Bcl2 stops apoptosis by indirectly preventing activation of CED-3-like proteases, termed caspases.

Bcl2 Function

Exactly how Bcl2 prevents apoptosis is unresolved, but there are two main models. In one, Bcl2 acts like CED-9 does in the worm, namely by preventing a mammalian CED-4-like adaptor molecule from activating the caspases. In the other, Bcl2 stops the release of pro-apoptotic proteins from the mitochondria that are sufficient to cause cell death and lead to the further activation of caspases.

Three Classes of Bcl2 Family Members

Several mammalian proteins have been identified that resemble Bcl2 and bear one or more Bcl2 homology domains, designated BH1-4. These proteins fall into three groups. The first group, to which belong Bcl-x, Bcl-w, and Mcl-1, for example, like Bcl2, is anti-apoptotic and carries three or more of the BH domains. Bax and Bak are members of the second group, which is pro-apoptotic and bears BH domains 1, 2, and 3. The third group of the Bcl2 family is also pro-apoptotic, but carries only the BH3 domain and is therefore often referred to as BH3-only proteins. This class includes proteins such as Bim, Bid, Bad, Bmf, Bik, Hrk, Noxa, and Puma, as well as the *C. elegans* protein EGL-1 (see Figure 1).

Structure of Bcl2 Family Proteins

Structural studies have shown that Bcl2, Bcl-x, Bcl-w, Bax, and Bid adopt similar three-dimensional folds,

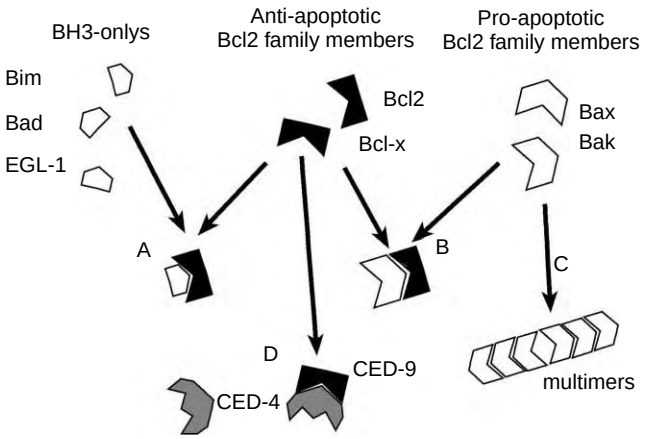

FIGURE 1 Interactions between Bcl2 family members. (A) Following death signals, BH3-only proteins (e.g., Bim, Bad, Bid, Noxa, Bik, and EGL-1) become activated and can bind strongly to anti-apoptotic family members (e.g., Bcl2, Bcl-x, Bcl-w, and CED-9). (B) In some circumstances anti-apoptotic family members can associate with Bax and Bak. (C) Apoptosis has been associated with movement of Bax to the mitochondria and the formation of multimers of pro-apoptotic Bax and Bak. (D) In *C. elegans*, the anti-apoptotic protein CED-9 can bind to and inhibit the caspase activator CED-4. CED-4 is liberated if enough of the BH3-only protein EGL-1 is present.

composed almost entirely of α-helixes. On the surface is a groove formed from parts of BH1, 2, and 3 that can be occupied either by the carboxy terminus of the protein itself or by the BH3 domain of another Bcl2 family member. Binding of the pro-apoptotic, BH3-only protein EGL-1 via its BH3 domain to the *C. elegans* cell death inhibitor CED-9 blocks its anti-apoptotic activity. In mammals, BH3-only proteins are believed to promote apoptosis by analogous interactions with other mammalian Bcl2 family members. For example, Bak can bind to Bcl-x in an interaction whereby the BH3 domain of Bak binds into the groove on the surface of Bcl-x (Figure 1).

BH3-Only Family Members

The BH3-only proteins from mammals (Bim, Bad, Bid, Hrk, Bmf, Noxa, Puma, etc.) and *C. elegans* (EGL-1) transduce pro-apoptotic signals to the core cell death machinery by binding, via their BH3 domains, to anti-apoptotic members of the Bcl2 family.

To give a pro-apoptotic signal, the BH3-only proteins can be activated in a wide variety of ways. Some are regulated transcriptionally by proteins such as p53. Others are under posttranslational control. For example, Bid is activated by proteolytic cleavage, Bad is activated by dephosphorylation, and Bim and Bmf are activated when released from sequestration by components of the cell's cytoskeleton. In this way, pro-apoptotic signals from various parts of the cell can be integrated into a common cell death effector mechanism.

Bax and Bak

Bax and Bak are pro-apoptotic proteins that bear BH1-3 domains. The deletion of genes for either Bax or Bak results in a very mild phenotype in mice, but the deletion of both has very dramatic effects, suggesting that there is a requirement for Bax or Bak for cell death in many circumstances but that the presence of one can compensate for absence of the other. Most mice lacking both Bax and Bak die perinatally. Those that do survive have persistent interdigital webs, imperforate vaginas, and accumulate excess neurons and blood cells. The fact that lymphocytes from these animals retain full sensitivity to cell death stimulated by the ligation of the tumor necrosis factor (TNF) receptor family member Fas shows that in these cells apoptosis can be activated by two independent pathways, only one of which is regulated by Bcl2 family members.

How Bax and Bak function is not certain. Cells lacking Bax and Bak are resistant to apoptosis caused by the overexpression of BH3-only proteins, and BH3-only proteins have been reported to bind to Bax and Bak, but the interactions appear to be weak and may not occur *in vivo*. Apoptosis is associated with the translocation of Bax from the cytosol to the mitochondria and the formation of multimers of Bax and Bak that can be detected by cross-linking (Figure 1). Some believe that these multimers can act as channels in the mitochondrial membranes allowing release of proteins such as cytochrome c and Smac/Diablo.

Role of the Mitochondria

In almost all cases, apoptosis is associated with the release of proteins such as cytochrome c and Smac/Diablo from the mitochondria. It has not yet been resolved whether this is necessary or sufficient for cell death. Some groups believe that Bcl2 prevents apoptosis by stopping the release of these mitochondrial proteins, whereas Bax and Bak cause apoptosis by enabling their release. Based on comparisons of their 3D structure with that of diphtheria toxin, it has been proposed that Bcl2, Bcl-xl, Bax, and Bak form or regulate channels in the mitochondrial outer membrane through which the proteins leave the mitochondria. The BH3-only proteins somehow cause Bax and Bak to form these channels. According to this model, cells subsequently die either because of the loss of mitochondrial function or because cytochrome c activates the CED-4 homologue Apaf-1, which in turn activates the caspases.

Other groups believe that Bcl2 inhibits, whereas Bax promotes, the activation of caspases that are sufficient to cause apoptosis independently of the mitochondria. According to this model, these caspases also cause

secondary damage to the mitochondria, resulting in the release of proteins such as cytochrome c and Smac/Diablo that accelerate the death process.

Roles of Bcl2 Family Members *in vivo*

To determine their essential functions, many of the genes for Bcl2 family members have been deleted in mice. The deletion of Bcl-x results in death in early embryogenesis. Mice lacking Bcl2 genes are healthy at birth but grow poorly, turn gray, and usually die of renal failure caused by cysts in their kidneys. White blood cells from these mice are very sensitive to apoptotic stimuli.

Although mice lacking Bax or Bak have no major abnormalities, mice lacking both these pro-apoptotic proteins accumulate large numbers of white blood cells and have extra neurons. Cells from these mice are resistant to apoptosis triggered by BH3-only proteins, but not that triggered by members of the TNF family of receptors.

Mice lacking genes for Bim have excess white blood cells, and these are resistant to some cell-death-inducing drugs but not others. The fact that mice lacking genes for both Bim and Bcl2 have different phenotypes from those missing one or the other indicates that, although Bim can be inhibited by Bcl2, it can also act independently of Bcl2 and, conversely, although Bcl2 can be inhibited by Bim, it can also act independently of Bim.

Therapeutic Implications

The association of Bcl2 with follicular lymphoma and the ability of antiapoptotic Bcl2 family members to inhibit chemotherapy-induced apoptosis have led to speculation that antagonizing anti-apoptotic Bcl2 family members or reducing their levels will promote the death of cancer cells. Consequently, trials are underway to use antisense against Bcl2 and to test novel drugs that mimic BH3-only proteins against a variety of cancers.

See Also the Following Articles

Caspases and Cell Death • Cell Death by Apoptosis and Necrosis • Cytochrome *c*

Glossary

apoptosis A physiological form of cell death with a characteristic morphology whose mechanism is shared by metazoans.

Bcl2 family proteins Proteins that have a structural similarity to the apoptosis inhibitory protein Bcl2.

BH domains Bcl2 homology domains; there are four, BH1-4.

BH3-only proteins A group of pro-apoptotic proteins that have the BH3 domain but no other BH domains.

caspases Cysteine proteases with aspartic acid specificity that are related to the *C. elegans* caspase CED-3 that is essential for programmed cell death in the worm.

***ced* genes** Genes that implement programmed cell death in the worm *C. elegans*.

Further Reading

Adams, J. M., and Cory, S. (2001). Life-or-death decisions by the Bcl-2 protein family. *Trends Biochem. Sci.* **26**, 61–66.

Huang, D. C. S., and Strasser, A. (2000). BH3-only proteins – essential initiators of apoptotic cell death. *Cell* **103**, 839–842.

Lindsten, T., Ross, A. J., King, A., Zong, W. X., Rathmell, J. C., Shiels, H. A., Ulrich, E., Waymire, K. G., Mahar, P., Frauwirth, K., Chen, Y., Wei, M., Eng, V. M., Adelman, D. M., Simon, M. C., Ma, A., Golden, J. A., Evan, G., Korsmeyer, S. J., MacGregor, G. R., Thompson, C. B. (2000). The combined functions of proapoptotic Bcl-2 family members Bak and Bax are essential for normal development of multiple tissues. *Mol. Cell* **6**, 1389–1399.

Metzstein, M. M., Stanfield, G. M., and Horvitz, H. R. (1998). Genetics of programmed cell death in *C. elegans* – past, present and future. *Trends Genetics* **14**, 410–416.

Sattler, M., Liang, H., Nettesheim, D., Meadows, R. P., Harlan, J. E., Eberstadt, M., Yoon, H. S., Shuker, S. B., Chang, B. S., Minn, A. J., Thompson, C. B., and Fesik, S. W. (1997). Structure of bcl-x(l)-bak peptide complex – recognition between regulators of apoptosis. *Science* **275**, 983–986.

Vaux, D. L., Cory, S., and Adams, J. M. (1988). Bcl-2 gene promotes haemopoietic cell survival and cooperates with c-myc to immortalize pre-B cells. *Nature* **335**, 440–442.

Vaux, D. L., Weissman, I. L., and Kim, S. K. (1992). Prevention of programmed cell death in *Caenorhabditis elegans* by human bcl-2. *Science* **258**, 1955–1957.

Biography

David L. Vaux is a Laboratory Head at the Walter and Eliza Hall Institute in Melbourne, Australia. His principal research interest is the molecular biology of apoptosis. He holds an M.D. and a Ph.D. from Melbourne University and received postdoctoral training at Stanford University. He was the first to recognize that Bcl2 was an inhibitor of cell death, and he linked apoptosis in mammals to programmed cell death in the worm.

B-Cell Antigen Receptor

Thomas M. Yankee and Edward A. Clark
University of Washington, Seattle, Washington, USA

B-cell functions in the immune system are dependent on their ability to recognize foreign antigens and to discriminate between foreign antigens and self-antigens. The complex of proteins responsible for the identification of foreign antigens is the B-cell antigen receptor (BCR) complex. Signals originating with the BCR can lead to a variety of cell fates, depending on the developmental stage of the B-cell and the concentration and avidity of the antigen. B-cell precursors in the bone marrow require BCR signals for survival. Once a competent signaling complex is formed, the BCR is tested to ensure that it does not react with self-antigens. If the BCR is ligated by self-antigens, it must either change its specificity or undergo cell death. Later in B-cell development, basal BCR signaling is required for the survival and homeostatic maintenance of the B-cell pool. BCR stimulation of mature B-cells initiates an immune response, characterized by the proliferation and differentiation of B-cells into either antibody-producing plasma cells or memory B-cells. Hence, a competent BCR that recognizes foreign antigens and not self-antigens is critical for the development and maintenance of B-cells and for the initiation of humoral immune responses.

Structure of the B-Cell Antigen Receptor

The BCR complex contains a membrane-bound immunoglobulin (mIg). mIg can be one of five isotypes: IgM, IgD, IgA, IgG, or IgE. The isotype of mIg expressed on a given B-cell varies with the stage of development and activation. Immature and transitional B-cells express mIgM, whereas mature resting B-cells express mostly mIgD and some mIgM. Cells that have been activated undergo a process called isotype class-switching and may then express mIgG, mIgA, or mIgE in addition to soluble IgG, IgA, or IgE. The process of isotype class-switching results in the activation of other hematopoietic cells. Each molecule of mIgM contains two heavy-chain (H) and two light-chain (L) proteins, that is H_2L_2 (Figure 1). Disulfide bonds link the heavy chains to one another and each heavy chain is disulfide-bonded to a light chain. At the membrane proximal end of the heavy chain is a transmembrane domain followed by a short intracellular domain. mIgM and mIgD contain only three intracellular residues that anchor the protein in the membrane. Other classes of mIg contain slightly longer intracellular domains and appear to mediate functions only present in B-cells that express mIgG, mIgA, or mIgE.

The short intracellular domains of mIgM and mIgD alone cannot generate a signal; mIg-associated accessory proteins fulfill this function. There are two such accessory molecules, Igα (also called CD79a) and Igβ (CD79b). The interaction between mIg and Igα/Igβ depends on the transmembrane domains of each protein. The transmembrane domains of mIg, Igα, and Igβ are α-helices and contain both polar and nonpolar regions. The polar regions are critical for protein–protein interactions among the BCR components. mIg contains polar residues on both sides of the α-helix. One side is conserved among all Ig isotypes and the other side is isotype specific. The residues that are isotype specific allow for oligomerization of the BCR complex. The degree of oligomerization varies with each Ig isotype. The side of the molecule that is conserved among all isotypes participates in the association between mIg and Igα/Igβ.

Like mIg, the transmembrane domain of Igα contains polar residues on both sides of the α-helix. In contrast, Igβ contains polar residues on only one side of the α-helix. Thus, a favored model for the structure of the BCR complex is that Igα bridges mIg and Igβ (Figure 1). According to this model, when the BCR complex is assembled, the polar residues within the transmembrane domains are masked by protein–protein interactions. This is essential for the surface expression and stability of the BCR.

B-Cell Antigen Receptor Diversity

In order to contribute to protective immunity to a range of pathogens, B-cells must be able to recognize a vast array of antigens. The diversity of the Ig repertoire is accomplished using three factors: combinatorial diversity, junctional diversity, and somatic hypermutation. Combinatorial diversity occurs through the

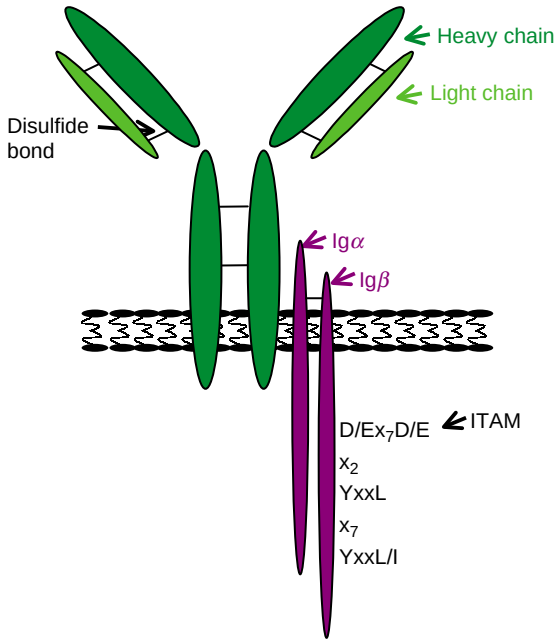

FIGURE 1 The structure of the BCR. The BCR consists of two heavy chains disulfide-bonded to one another. Each heavy chain is disulfide-bonded to a light chain. Igα and Igβ are also disulfide-linked. mIg and Igα/Igβ are noncovalently coupled. Also shown is the ITAM motif on Igβ; Igα and Igβ each have one ITAM motif.

recombination of sets of heavy- and light-chain gene segments. Three gene segments, variable (V_H), diversity (D_H), and joining (J_H), recombine to form the variable region of the heavy chain. There are many V_H gene segments, D_H gene segments, and J_H gene segments. Thus, sets of different segments recombine to form a range of different VDJ_H genes. The light chain undergoes a similar process of recombination. To generate the light chain, two gene loci, κ and λ, undergo recombination. Here, V_L and J_L gene segments recombine and result in VJ_L. The combination of heavy-chain rearrangement and light-chain rearrangement results in substantial BCR diversity.

Junctional diversity also arises from the recombination of the gene segments. When a V_H gene segment recombines, nucleotides may be added or subtracted. This results in the addition or loss of amino acids or a shift in the reading frame of the new gene. The third mechanism by which diversity is introduced to the BCR repertoire is through somatic hypermutation (discussed later).

B-Cell Antigen Receptor Signaling

Ligation of the BCR complex triggers a series of events that ultimately affects the fate of the cell. A B-cell stimulated through the antigen receptor may proliferate, differentiate, or undergo apoptosis. B-cells are also very efficient antigen-presenting cells. BCR signaling is essential for antigen internalization and processing after the BCR binds and captures antigen.

Antibody–Antigen Interactions

Antigens interact with the variable regions of mIg. Within the variable region, there are framework regions interspersed with three hypervariable regions, the areas that contain the most variability. The framework regions, folded as β-sheets, provide much of the antibody structure. The hypervariable regions are located on one edge of the β-sheets. To provide even greater repertoire diversity, the hypervariable regions of the heavy and light chain are within close proximity to one another and together create the antigen-binding site. Haptens and other small antigens bind the antibody in the grooves between the hypervariable regions of the heavy and light chains. Interactions between the BCR and larger antigens may extend into the framework region. The interactions between the antibodies and antigens are noncovalent in nature. These interactions may consist of electrostatic interactions, van der Waals interactions, hydrophobic interactions, and hydrogen bonding.

Early Signaling Events

Igα and Igβ each contains tyrosine residues that are phosphorylated following BCR engagement. Two of the tyrosine phosphorylation sites on Igα and Igβ are located within immunoreceptor tyrosine-based activated motifs (ITAMs) (Figure 1). These regions contain six conserved residues in the specific configuration, D/ExxxxxxxD/ExxYxxLxxxxxxxYxxL/I. The spacing between the tyrosine residues in the ITAM results in these residues being positioned on the same side of an α-helix, facilitating the interactions with downstream SH2-domain-containing signaling molecules. (SH2 domains are motifs that bind phosphotyrosine and the surrounding residues.)

In addition to the ITAM tyrosine residues, Igα and Igβ contain other residues that become phosphorylated. Non-ITAM tyrosine residues may also recruit SH2-domain-containing signaling proteins. Serine/threonine phosphorylation of Igα may negatively regulate phosphorylation of the ITAM tyrosine residues and, therefore, may negatively regulate downstream signaling.

Three families of protein tyrosine kinases (PTKs) play key roles in the initiation of BCR signaling (Figure 2). These kinases are Src-family PTKs, such as Lyn; the Syk/ZAP-70-family PTKs, such as Syk; and the Tec-family PTKs, such as Btk. Following BCR ligation, Lyn becomes activated and phosphorylates the ITAM tyrosines. The phosphorylated ITAM becomes the docking sites for Syk, which has two tandem SH2 domains.

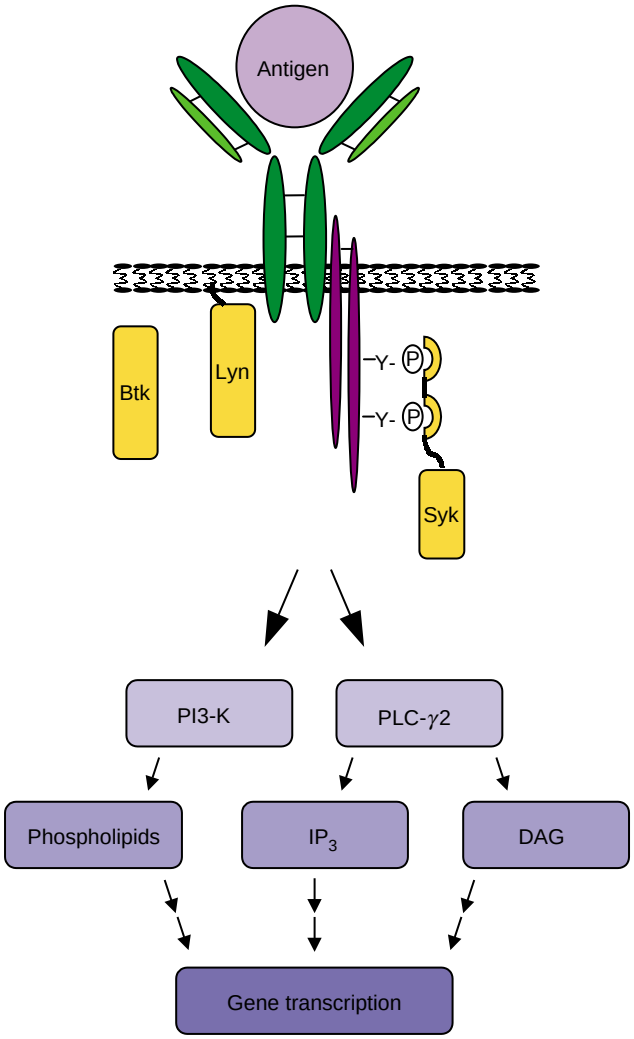

FIGURE 2 BCR-mediated signaling events. Following antigen binding to the BCR complex, tyrosine residues on Igα and Igβ become phosphorylated and bound by the tandem SH2 domains of the Syk. Lyn is also activated. The activation of these two PTKs trigger many downstream signaling cascades, including the activation of PI3-K and PLC-γ2.

The binding of the SH2 domains of Syk to the phospho-ITAM contributes to its activation. Syk can also become activated in the absence of Src-family PTKs. A small amount of Syk is constitutively associated with the BCR complex. Cross-linking the BCR leads to the clustering of Syk, which then may transautophosphorylate and become activated. Activation of Syk and Lyn, then, leads to the activation of Btk. The combination of Syk, Lyn, and Btk activity is necessary for optimal signaling through the BCR.

Downstream Signaling Events

The activation of Syk-, Src-, and Tec-family PTKs trigger a number of downstream signaling pathways (Figure 2). For example, phosphatidylinositol 3′-kinase (PI3-K) and phospholipase C-γ2 (PLC-γ2) are two enzymes that generate second messengers in BCR signaling. PI3-K is a lipid kinase important for the recruitment and activation of PH-domain-containing proteins. (PH domains are motifs that bind phospholipids.) PLC-γ2 generates inositol-1,4,5-triphosphate (IP_3) and diacylglycerol (DAG), second messengers critical for calcium influx and protein kinase C activation. The activation of these signaling pathways, along with many other pathways, leads to gene transcription and cell-fate decisions.

In addition to gene transcription, BCR signaling is also critical for antigen internalization and processing. When the BCR binds an antigen, the BCR complex is internalized. The antigen is then processed and presented on the cell surface in order to activate antigen-specific T cells.

The B-Cell Antigen Receptor and the Immune Response

When antigen and other immune cells activate a B-cell, a complex series of events takes place that can result in proliferation, somatic hypermutation, isotype class-switching, and differentiation. The BCR on mature naïve B-cells may be able to recognize more than one antigen. This multispecific nature of the BCR results in relatively low affinity to any specific antigen. Somatic hypermutation is a process by which high-affinity BCRs are generated. Under some conditions following BCR ligation, a somatic hypermutation program is induced. During somatic hypermutation mutations are introduced into the V segment of the heavy- and light-chain genes. After somatic hypermutation, B-cells expressing BCRs with high affinity are selected for further expansion. In this way, the immune system creates B-cells that have produced high affinity antibodies tailor-made for specific pathogens.

The other major changes in the BCR following B-cell activation include isotype class-switching. The genomic organization of mIg is the recombined variable region followed by the constant genes of μ, ∂, γ3, γ1, γ2b, γ2a, ε, and α in mice and μ, ∂, γ3, γ1 α1, γ2, γ4, ε, and α2 in humans. Following the activation of the B-cell through certain key receptors such as CD40, DNA recombination can occur so that the V_H joins a C_H segment of another isotype. This process is a guided repetitive DNA sequence preceding each constant domain known as a switch region. The precise mechanism of class-switching is unknown, but probably involves DNA recombination between homologous repeats in the switch regions of different constant genes.

The result of somatic hypermutation and class-switching is the generation of highly specific antibodies of an isotype that generates an effective immune response.

In particular, the constant regions of the antibody bind specific receptors on other immune cells. For example, the constant region of IgGγ1 and IgGγ3 bind Fcγ receptors on macrophages and neutrophils leading to phagocytosis of the antigen, whereas the constant region of IgE binds Fcε receptors on mast cells and basophils leading to the secretion of inflammatory agents.

Membrane-bound forms of IgG, IgA, and IgE may function differently than mIgM and mIgD. Cross-linking mIgG leads to the proliferation and antibody secretion of mIgG-expressing B-cells. Although mIgG and mIgM activate similar downstream signaling pathways, mIgG cross-linking triggers a much more robust response than does mIgM cross-linking. This may be due to the fact that mIgG is resistant to down-regulation by certain B-cell co-receptors, such as CD22. The mechanism for this resistance may be related to differences in the intracellular domains between mIgM and mIgG.

Summary

The BCR complex is a critical component of the humoral immune response. The BCR repertoire must be diverse enough to recognize an incredible number of foreign antigens, but must also avoid targeting self-antigens. Ligation of the BCR triggers a complex series of events that include the activation of PTKs, the phosphorylation of Igα and Igβ, and the initiation of multiple signaling cascades. These signaling pathways lead to cell-fate decisions, antigen presentation, and an immune response.

See Also the Following Articles

Diacylglycerol Kinases and Phosphatidic Acid Phosphatases • Inositol Phosphate Kinases and Phosphatases • Phosphatidylinositol Bisphosphate and Trisphosphate • Protein Tyrosine Phosphatases • Src Family of Protein Tyrosine Kinases

Glossary

antibody A protein that is produced in response to immune challenge and binds specifically to a particular antigen.

antigen A molecule that specifically binds an antibody.

avidity The sum of the binding strengths of all points of interaction between an antigen and an immunoglobulin.

humoral immune response The antibody-mediated response to a specific antigen.

immunoglobulin A protein complex with a characteristic structure of heavy and light chains.

isotype A class of immunoglobulin as determined by the constant region.

somatic hypermutation The process by which mutations are introduced into the heavy- and light-chain genes.

Further Reading

Cyster, J. (1997). Signaling thresholds and interclonal competition in preimmune B-cell selection. *Immunol. Rev.* **156**, 87–101.

Janeway, C., Travers, P., Walport, M., and Schlomchick, M. (2001). *Immunobiology: The Immune System in Health and Disease*. Garland Publishing, New York.

Matsuuchi, L., and Gold, M. (2001). New views on BCR structure and function. *Curr. Opinion Immunol.* **13**, 270–277.

Melchers, F., ten Boekel, E., Seidl, T., Kong, X., Yamagami, T., Onishi, K., Shimizu, T., Rolink, A., and Andersson, J. (2000). Repertoire selection by pre-B-cell receptors and B-cell receptors, and genetic control of b-cell development from immature to mature B-cells. *Immunol. Rev.* **175**, 33–46.

Niiro, H., and Clark, E. (2002). Regulation of B-cell fate by antigen receptor signals. *Nat. Rev. Immunol.* **2**, 945–956.

Reth, M. (1992). Antigen receptors on B-lymphocytes. *Annu. Rev. Immunol.* **10**, 97–121.

Yankee, T., and Clark, E. (2000). Signaling through the B-cell antigen receptor in developing B-cells. *Rev. Immunogenet.* **2**, 185–203.

Biography

Dr. Thomas M. Yankee is a Senior Fellow in the Department of Microbiology at the University of Washington, Seattle. His principal interest is the regulation of cell fate in B- and T-lymphocytes. He holds a Pharm.D. degree from the University of Illinois and a Ph.D. degree from Purdue University.

Dr. Edward A. Clark is a Professor of Microbiology and Immunology at the University of Washington, Seattle. His principal interest is the regulation of B-cells and dendritic cells during immune responses. He holds a Ph.D. degree from the University of California, Los Angeles. He has helped to discover and characterize a number of receptors and signaling molecules in B-lymphocytes such as CD40, CD80, and Syk.

Bile Salts and their Metabolism

Ulrich Beuers and Thomas Pusl
University of Munich, Munich, Germany

Bile salts originate from conversion of cholesterol in the liver, a major pathway for elimination of cholesterol from the body. Bile salts together with phospholipids and cholesterol are the major organic solutes in bile and are the key driving force of bile formation being actively secreted into bile canaliculi across the apical membranes of hepatocytes. Bile salts undergo an efficient enterohepatic circulation. Their structure is amphipathic with a hydrophobic and hydrophilic side allowing them to interact with both lipids and the aqueous environment. Molecular self-aggregation occurs, by means of micelle formation, above a critical micellar concentration. Bile salt micelles can solubilize other lipophilic molecules such as cholesterol, phospholipids, and monoglycerides to form mixed micelles, acting as carriers for these lipids in bile and in the intestine. Such micelle formation promotes absorption of dietary lipids and fat-soluble vitamins in the small intestine. Bile salts may become cytotoxic when their intracellular concentrations increase beyond physiological levels due to impairment of bile secretion as observed in a variety of pathological conditions, particularly cholestatic liver diseases. Therefore, bile salt homeostasis is tightly regulated. Bile salts have recently been shown to represent potent intracellular signaling molecules that activate nuclear receptors and modulate cytosolic signaling cascades, thereby regulating their own metabolism and transport.

Bile Salt Synthesis and its Regulation

Bile salts consist of a steroid nucleus with its hydroxyl or other substituents and an aliphatic side chain of variable length. They are synthesized in pericentral hepatocytes from cholesterol by different pathways, which involve up to 17 enzymes located in the endoplasmatic reticulum, mitochondria, cytosol, and peroxisomes (Figure 1). The rate-limiting step of the classic bile salt biosynthetic pathway, also known as the "neutral" pathway, is 7α-hydroxylation of cholesterol by a microsomal cytochrome P-450 monooxygenase (CYP7A1). End products of the complex biosynthetic steps are the two major human primary bile salts, cholate (C; 3α,7α,12α-trihydroxy-5β-cholanoate) and chenodeoxycholate (CDC; 3α,7α-dihydroxy-5β-cholanoate). These primary bile salts undergo further modifications during enterohepatic cycling by bacterial enzymes in the distal intestine which lead to dehydroxylation at C-7 of C or CDC to form the secondary bile salts, deoxycholate (DC; 3α,12α-dihydroxy-5β-cholanoate) and lithocholate (LC; 3α-hydroxy-5β-cholanoate), respectively, or to epimerization of the hydroxy group at C-7 of CDC to form ursodeoxycholate (UDC; 3α,7β-dihydroxy-5β-cholanoate). A second pathway (commonly referred to as the "alternative" or "acidic" pathway) is initiated by the mitochondrial enzyme sterol 27-hydroxylase (CYP27A1), which allows for the conversion of cholesterol to both 27-hydroxycholesterol and 3β-hydroxy-5-cholestenoic acid. Although CYP27A1 is expressed also in peripheral tissues such as macrophages and vascular endothelium, the liver remains the sole site for complete bile salt formation. The acidic pathway provides a mechanism by which excess oxidized cholesterol generated in peripheral tissues can be removed through conversion to bile salts. The relative contribution of CYP7A1 and CYP27A1 to overall bile salt synthesis is unclear, but CYP7A1 has been estimated to account for 75% (mice) to 90–95% (human) of total bile salt synthesis. Cholesterol 25-hydroxylase and cholesterol 24-hydroxylase (CYP46A1) may also initiate bile salt synthesis *in vitro*, but their contribution to bile salt formation *in vivo* may be limited.

Bile salt synthesis is highly regulated and subject to feedforward and feedback control whereby bile salts down-regulate their own synthesis and oxysterols up-regulate bile salt synthesis, mainly by regulating CYP7A1 gene transcription (Figure 2). Promoter analyses of the CYP7A1 gene have identified two bile acid response elements, which are highly conserved among different species, contain hexameric repeats of an AGGTCA sequence, and are binding sites for nuclear hormone receptors. Nuclear hormone receptors are ligand-activated transcription factors with a highly conserved DNA-binding domain (DBD) in the N-terminal region and a moderately conserved ligand-binding domain (LBD) in the C-terminal region. Upon ligand binding to the LBD, nuclear receptors undergo conformational changes that allow dissociation of corepressors and recruitment of coactivator proteins to

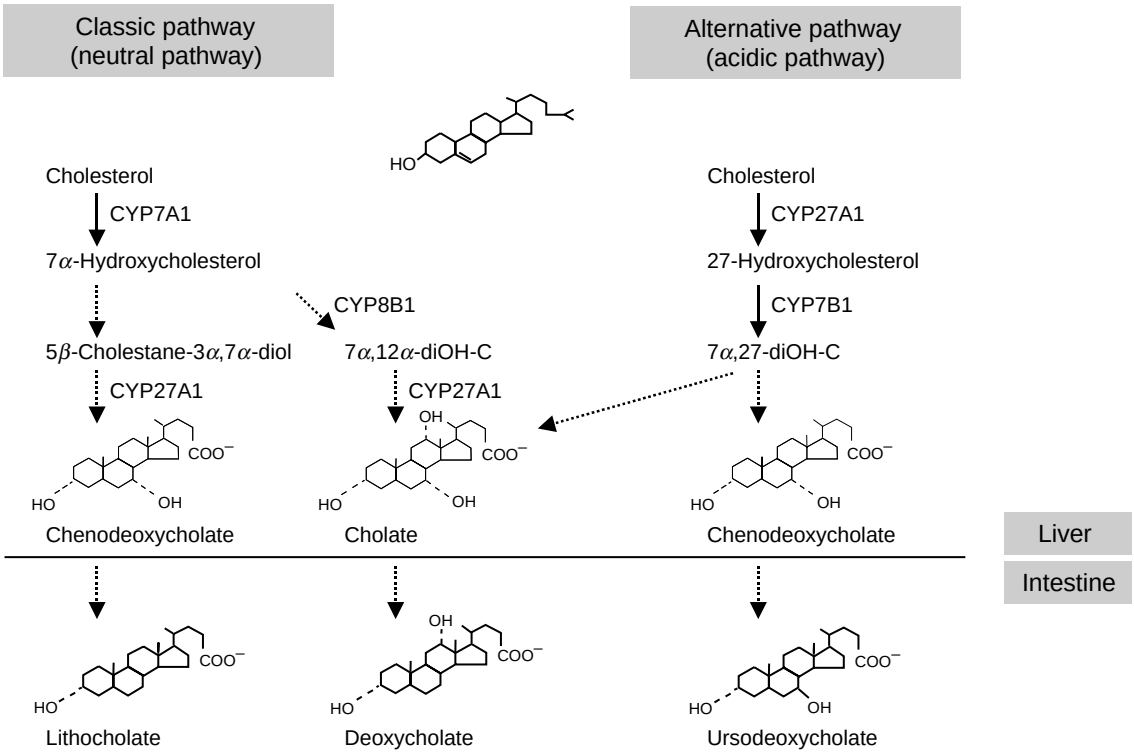

FIGURE 1 Major bile salt biosynthetic pathways in the liver. The initial and rate-determining step of the classic ("neutral") pathway is the conversion of cholesterol to 7α-hydroxycholesterol by microsomal cholesterol 7α-hydroxylase (CYP7A1) leading to formation of cholate and chenodeoxycholate. The initial step of the alternative ("acidic") pathway is the conversion of cholesterol to 27-hydroxycholesterol by mitochondrial sterol 27-hydroxylase (CYP27A1) leading to formation mainly of chenodeoxycholate. These primary bile salts undergo further structural modifications by bacterial enzymes during enterohepatic cycling resulting in the formation of the secondary and tertiary bile salts, deoxycholate, lithocholate, and ursodeoxycholate. Only major biosynthetic steps are shown. CYP7B1, oxysterol 7α-hydroxylase; CYP8B1, sterol 12α-hydroxylase; 7α,27-diOH-C, 7α,27-dihydroxycholesterol; 7α,12α-diOH-C, 7α,12α-dihydroxy-4-cholestene-3-one.

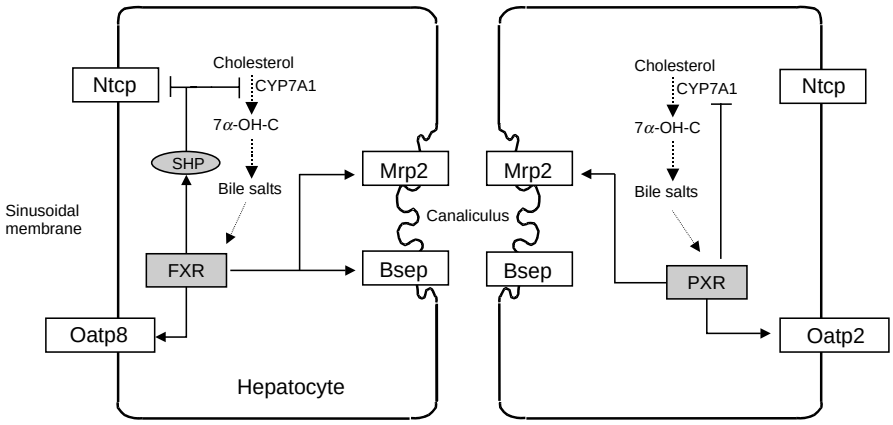

FIGURE 2 Regulation of bile salt transport and metabolism by nuclear bile salt receptors in hepatocytes. The transport of bile salts is vectorial in liver. Bile salts are taken up by the Ntcp and Oatp in the sinusoidal membrane of hepatocytes and are excreted into bile via the Bsep and the conjugate export pump (Mrp2) located in the canalicular membrane. The FXR acts as a bile salt sensor and represses the transcription of cholesterol 7α-hydroxylase (CYP7A1) and Ntcp genes via up-regulation of small heterodimer partner-1 (SHP-1), thereby inhibiting bile salt synthesis and uptake. FXR also stimulates expression of Bsep, Mrp2, and Oatp8. PXR represses bile salt synthesis by down-regulation of transcription of CYP7A1. PXR also stimulates the expression of Mrp2 and Oatp2. 7α-OH-C, 7α-hydroxycholesterol ($\rightarrow$ activation; $\dashv$ repression).

activate the expression of target genes. The nuclear hormone receptor superfamily includes receptors for steroid and thyroid hormones, retinoids and vitamin A and D, as well as different so-called orphan receptors, whose ligands were initially unknown. Analyses of orphan receptor expression patterns in enterohepatic tissue have identified bile salts, including CDC and C, as the endogenous ligands of farnesoid X receptor (FXR). In the liver, bile salt activation of FXR represses CYP7A1 transcription by an indirect mechanism involving nuclear receptors small heterodimer partner (SHP) and liver receptor homologue 1 (LRH1). Activation of pregnane X receptor (PXR), a promiscuous bile salt receptor, also results in repression of CYP7A1. The liver X receptor α (LXRα), abundantly expressed in the liver and bound by oxysterol ligands, has been shown to mediate the feedforward cholesterol catabolism to bile acids by up-regulation of CYP7A1. Nuclear hormone receptor-independent pathways may also be involved in bile salt feedback inhibition of gene transcription based on protein kinase C (PKC) and mitogen-activated protein kinase (MAPK) signaling pathways as well as bile-salt-induced release of inflammatory cytokines.

Bile Salt Transport and its Regulation

After their biosynthesis and conjugation mainly to glycine and taurine in hepatocytes, bile salts are secreted into bile and reach the intestinal lumen. More than 95% of intestinal conjugated bile salts are actively reabsorbed mainly from the distal ileum by an apical sodium-dependent bile salt transporter (Asbt) and reach the liver via the portal vein, the majority being bound to albumin. Hepatic extraction followed by resecretion into bile completes the enterohepatic circulation of bile salts. In humans, the normal bile salt pool size averages 3–4 g recirculating 5–10 times each day. The hepatocyte plays a key role in the vectorial transport of bile salts from portal vein to the bile canaliculus, with distinct bile salt transport systems at its basolateral (sinusoidal) and apical (canalicular) plasma membranes (Figure 2). Functional impairment of bile salt transport at any level of the hepatocyte may be an important cause of cholestasis, a syndrome characterized by a reduction in bile flow and retention of biliary constituents in serum, liver, and other organs leading to biochemical, morphological, and clinical alterations.

Hepatocellular uptake of bile salts at the basolateral membrane is the first step in hepatic bile salt transport, and is predominantly mediated by the Na^+-taurocholate-cotransporting polypeptide (Ntcp) and to a lesser extent by the organic anion transporting protein (Oatp) family. The 362-amino acid Ntcp with a molecular mass of 50 kDa has been cloned from human liver and mediates secondary active transport of bile salts, using an inwardly directed sodium gradient generated by Na^+-K^+-ATPase and the intracellular negative electrical potential generated in part by a potassium channel. Members of the Oatp family mediate sodium-independent uptake of organic anions and mainly unconjugated bile salts. Tissue distribution of Oatps is not restricted to the liver, where they are exclusively located in the basolateral membrane of the hepatocyte.

Little is known about the intrahepatocellular transport of bile salts. Cytosolic proteins such as a 36 kDa bile salt binding protein in human liver are considered to play a major role in the intracellular trafficking of bile salts, but rapid diffusion may also contribute to bile salt trafficking across the cell. In addition, bile salt partitioning into organelles may be observed when the intracellular bile salt load is increasing.

Under physiologic conditions, bile salt levels in the hepatocyte remain low, indicating the existence of efficient secretory mechanisms. Canalicular excretion of bile salts is predominantly achieved by the ATP-dependent bile salt export pump (Bsep), which transports monovalent bile salts against a steep gradient (up to 1000-fold) across the apical liver cell membrane into the canaliculus. This 60 kDa protein is a member of a large family of ATP-binding cassette (ABC) transporters. Mutations in the Bsep gene may lead to progressive familial intrahepatic cholestasis type 2 (PFIC 2) in childhood, a disorder with markedly elevated serum bile salt levels and low content of bile salts in bile, which carries a dismal prognosis. The conjugate export pump (multidrug resistance-associated protein 2, Mrp2) is another ABC-type transporter that has been shown to be capable of transporting divalent sulfated and glucuronidated bile salts.

In experimental animal models of cholestasis induced by application of endotoxin (model for inflammatory cholestasis), ethinyloestradiol (cholestasis of pregnancy), alpha-naphtylisocyanate (vanishing bile duct syndrome), and common bile duct ligation (extrahepatic biliary obstruction), most of the hepatic transporters are down-regulated. Recent findings of up-regulation of basolateral bile salt transporters in cholestasis such as Mrp3 and Mrp4 may provide an escape route for bile salts out of the hepatocyte when apical transport is defective. Cholestasis is also associated with retrieval of canalicular transporters to pericanalicular vesicles. Thus, the function of most hepatobiliary transport systems is presumed to decrease after exposure to cholestatic injury.

Active transport of bile salts across the canalicular membrane represents the rate-limiting step in overall transport from blood to bile and is under both short-term and long-term regulation by posttranscriptional and transcriptional mechanisms, respectively. On the

transcriptional level, hepatic transporters have been shown to be regulated by nuclear receptors (Figure 2). FXR up-regulates Bsep expression in the canalicular membrane of the hepatocyte. An FXR-dependent transactivation has also been demonstrated for the Mrp2 and Oatp8 gene promoter. PXR stimulates expression of Mrp2 and Oatp2. Short-term regulation on the post-transcriptional level occurs via signaling cascades which may involve cytosolic free calcium, adenosine 3,5-cyclic monophosphate (cAMP), phosphatidylinositol 3-kinases, PKC isoforms, and different MAP kinases.

Bile Salts in Therapy

UDC is a hydrophilic bile salt that is increasingly used for the treatment of various cholestatic disorders. It is normally present in human bile at a low concentration of about 3% of total bile salts. It is the major bile salt in black bear's bile, which has been used in Chinese traditional medicine for the treatment of liver diseases. First reports on the beneficial effects of UDC in patients with liver diseases came from Japan in the 1970s. A number of controlled trials on the use of UDC in primary biliary cirrhosis (PBC) and primary sclerosing cholangitis (PSC) have been published in the Western literature since the early 1990s. UDC improves serum liver tests and may delay disease progression to cirrhosis and prolong transplant-free survival in PBC. In PSC, UDC improves serum liver tests and surrogate prognostic markers, but effects on disease progression must further be evaluated. Anticholestatic effects of UDC have also been reported in a number of other cholestatic conditions. After oral administration of unconjugated UDC, 30–60% of the dose is absorbed by nonionic diffusion mainly in the small intestine and to a small extent in the colon and undergoes efficient hepatic uptake and conjugation with glycine and to a lesser extent with taurine. A daily dose of 13–15 mg kg^{-1} UDC causes an enrichment of ~40–50% in biliary bile salts of patients with PBC. The mechanisms underlying the beneficial effects of UDC in cholestatic disorders are increasingly being unraveled. Experimental evidence suggests three major mechanisms of actions: (1) protection of cholangiocytes against cytotoxicity of hydrophobic bile salts, resulting from modulation of the composition of mixed phospholipid-rich micelles, reduction of bile salt cytotoxicity of bile, and possibly, decrease of the concentration of hydrophobic bile salts in the cholangiocytes; (2) stimulation of hepatobiliary secretion, putatively via Ca^{2+}- and PKC-dependent mechanisms and/or activation of p38MAPK and extracellular signal-regulated kinases (Erk) resulting in vesicular insertion of transporter molecules (e.g., bile salt export pump, Bsep, and conjugate export pump, Mrp2) into the canalicular membrane of the hepatocyte and, possibly, activation of the inserted carriers; (3) protection of hepatocytes against bile-salt-induced apoptosis, involving inhibition of the mitochondrial membrane permeability transition (MMPT), and possibly, stimulation of a survival pathway.

See Also the Following Articles

Biliary Cirrhosis, Primary • Cytochrome P-450 • Mitogen-Activated Protein Kinase Family • Protein Kinase C Family • P-Type Pumps: Na^+/K^+ Pump

Glossary

bile salts Family of organic anions with a steroid nucleus formed by enzymatic conversion of cholesterol (major human bile salts: cholate, chenodeoxycholate, deoxycholate, lithocholate, ursodeoxycholate).

bile salt transporters Membrane carrier proteins mediating the transport of bile salts across cell membranes, among which the Na^+-taurocholate-cotransporting polypeptide (Ntcp) at the basolateral hepatocyte membrane, the Bsep at the apical hepatocyte membrane, and the Asbt at the apical membrane of ileocytes represent key carriers for maintenance of an effective enterohepatic circulation of bile salts.

nuclear hormone receptors Ligand-activated transcription factors regulating gene expression by interaction with specific DNA sequences. Bile salts have so far been identified to act as physiological ligands of the farnesoid X receptor (FXR), the pregnane X receptor (PXR), and the vitamin D receptor (VDR), thereby modulating their own metabolism and transport.

Further Reading

Bouscarel, B., Kroll, S. D., and Fromm, H. (1999). Signal transduction and hepatocellular bile acid transport: Cross talk between bile acids and second messengers. *Gastroenterology* **117**, 433–452.

Chiang, J. Y. L. (2002). Bile acid regulation of gene expression: Roles of nuclear hormone receptors. *Endocrine Rev.* **23**, 443–463.

Fuchs, M., and Stange, E. F. (1999). Metabolism of bile acids. In *Oxford Textbook of Clinical Hepatology* (J. Bircher, J. P. Benhamou, N. McIntyre, M. Rizzetto and J. Rodés, eds.) 2nd edition, pp. 223–256. Oxford University Press, New York.

Meier, P. J., and Stieger, B. (2002). Bile salt transporters. *Annu. Rev. Physiol.* **64**, 653–661.

Paumgartner, G., and Beuers, U. (2002). Ursodeoxycholic acid in cholestatic liver disease: Mechanisms of action and therapeutic use revisited. *Hepatology* **36**, 525–531.

Paumgartner, G., Keppler, D., Leuschner, U., and Stiehl, A. (eds.) (2003). *Bile Acids: From Genomics to Disease and Therapy.* Kluwer, Dordrecht, Boston, London.

Russell, D. W. (2003). The enzymes, regulation and genetics of bile acid synthesis. *Annu. Rev. Biochem.* **72**, 137–174.

Trauner, M., and Boyer, J. L. (2003). Bile salt transporters: Molecular characterization, function and regulation. *Physiol. Rev.* **83**, 633–671.

Biography

Ulrich Beuers is a Professor in the Department of Internal Medicine II, University of Munich, Germany. His principal research

interest is in the field of bile acids and cholestasis with a focus on bile acid-induced modulation of signaling and secretion in liver cells and treatment of chronic cholestatic liver diseases. He holds an M.D. from the University of Freiburg and received his postdoctoral training at the Universities of Göttingen (Department of Biochemistry), Munich (Department of Internal Medicine II), and the Yale University, New Haven (Section of Digestive Diseases).

Thomas Pusl is a resident in the Department of Internal Medicine II, University of Munich, Germany. His special research interests include mechanisms and effects of calcium signals in liver, and mechanisms underlying cholestasis and treatment of chronic cholestatic liver diseases. He holds an M.D. from the University of Munich and received his postdoctoral training at the University of Munich (Department of Internal Medicine II), and the Yale University, New Haven (Section of Digestive Diseases).

Biliary Cirrhosis, Primary

Marshall M. Kaplan
Tufts-New England Medical Center and Tufts University School of Medicine, Boston, Massachusetts, USA

Primary biliary cirrhosis (PBC) is a chronic cholestatic liver disease that is characterized by a continuing destruction of interlobular bile ducts, progressive fibrosis, and the eventual development of cirrhosis and liver failure. In contrast to patients seen more than a decade ago, most of whom had symptoms of fatigue, pruritus (itching), or jaundice, more than 60% of PBC patients who are diagnosed now are asymptomatic. Asymptomatic patients live longer than symptomatic ones. However, most asymptomatic patients eventually develop symptoms and their survival is reduced compared to an age- and sex-matched healthy population. There is general agreement that all patients with PBC should be treated but no agreement about the best treatment or even whether any treatment prolongs survival free of liver transplantation. Most physicians initiate treatment with ursodeoxycholic acid (UDCA), the only treatment for PBC approved by the U.S. Food and Drug Administrations (FDA). Some, including the author, believe that the addition of colchicine and/or methotrexate to those who fail to respond fully to UDCA provides an added benefit.

Epidemiology

Primary biliary cirrhosis (PBC) was once considered a rare disease. However, increased awareness of PBC has led to earlier and more frequent diagnoses. In some series, it accounted for almost 2% of deaths due to cirrhosis. In a study from England, there was an annual incidence of 5.8 cases per million population and a point prevalence of 54 cases per million. The prevalence in the United States is at least that high. Estimates place the number between 50,000 to 100,000 patients. The etiology is unknown, but may be related to altered immunoregulation. The lack of concordance of PBC in identical twins suggests that some triggering event is required to initiate PBC in a genetically susceptible individual. PBC is much more likely to occur in families of patients with an index case compared to the general population. A number of environmental causes have been implicated in the pathogenesis of PBC, including bacteria and viruses. Some of the most compelling evidence for an environmental factor has been derived from an epidemiological study that demonstrated significant geographic clustering of PBC cases in urban areas in northeast England.

Etiology

Autoantibodies and Antimitochondrial Antibody

Ninety to 95% of patients with PBC are women, a sex distribution similar to that for other autoimmune diseases such as systemic lupus. There is an increased incidence of autoantibodies including antimitochondrial antibody, antinuclear antibody, and antimicrosomal antibody. Antimitochondrial antibody (AMA) is detected in 95% of patients with PBC. The major autoantibody found in PBC patients has been called anti-M2. It is directed principally against the dihydrolipoamide acyltransferase component (E2) of the branched keto-acid dehydrogenase and pyruvate dehydrogenase complexes on the inner mitochondrial membrane. Other antimitochondrial antibodies that have been described in PBC, anti-M4, anti-M8, and anti-M9, are most likely artifacts and were not found in a study that employed highly purified human mitochondrial proteins as antigens. The relationship between antimitochondrial antibodies and immunologic bile duct injury is not clear. The mitochondrial antigens are not tissuespecific, and their intracellular location should reduce their immunogenicity. Repeated studies have shown that there is no correlation between the presence or titer of AMA and the severity or course of PBC.

Mitochondrial Antigens and the Cellular Immune System

Although there is little evidence that AMA plays a direct role in the pathogenesis of PBC, an interaction between the mitochondrial antigens and the cellular immune system appears to be important. The E2 antigens stimulate interleukin-2 production by peripheral blood mononuclear cells and by T cells cloned from liver biopsies of PBC patients. E2 antigens are recognized by both helper and cytotoxic T cells in PBC and cytotoxic

T cells appear to mediate bile duct epithelial cell necrosis. The mitochondrial antigens are aberrantly expressed on the luminal surface of biliary epithelial cells from PBC patients, but not in control subjects or patients with primary sclerosing cholangitis. These antigens are expressed in bile duct epithelial cells before two other antigens that are also required for T-lymphocyte-mediated cell destruction, human leukocyte antigen (HLA) class II antigens, and the cellular recognition factor, BB1/B7. This chronology suggests that aberrant expression of the E-2 autoantigen on the surface of biliary epithelial cells initiates lymphocytic destruction of bile ducts, the characteristic lesion in PBC.

Association with Other Autoimmune Diseases

There is an increased association of PBC with other autoimmune diseases, such as thyroiditis, rheumatoid arthritis, calcinosis cutis, Raynaud's phenomenon, esophageal dysmotility, sclerodactylyl and telangiectasia (CREST) syndrome, Raynaud's disease and Sjögren's syndrome. Although circulating immune complexes have been demonstrated in some PBC patients, it is unlikely that they play a role in pathogenesis. Only a small percentage of PBC patients have immune complexes. Some PBC patients have an IgM that can fix complement in the absence of demonstrable antigen binding and will give false positive results with many of the assays used to detect immune complexes.

Pathophysiology

The signs and symptoms of PBC are due to long-standing cholestasis. There is a gradual destruction of small intrahepatic bile ducts that results in a decreased number of functioning bile ducts within the liver. This, in turn, causes retention within the liver of substances that are normally secreted or excreted into bile, such as bile acids, bilirubin, and copper. The increased concentration of some of these substances (e.g., bile acids) causes further damage to liver cells. Other substances regurgitate from the liver into the blood and soft tissues and cause symptoms such as pruritus. The identity of the substance or substances that cause pruritus is unknown. It is not any of the naturally occurring primary and secondary bile acids. Most data suggest that it is some substance that is secreted into bile and that binds tightly to cholestyramine, a nonabsorbed, quaternary ammonium resin. Possible pruritogens include the naturally occurring opioids. Serum levels of endogenous opioids (endorphins and encephalins) are increased in PBC, and opioid antagonists will relieve itching in some patients. The striking hyperlipidemia and xanthoma formations in some PBC patients are also a consequence of longstanding cholestasis. The impaired secretion of bile in patients with clinically advanced PBC causes a diminished concentration of bile acids within the intestinal lumen. The bile acid concentration may fall below the critical micellar concentration and thus be inadequate for complete digestion and absorption of neutral triglycerides in the diet. This causes the striking fat malabsorption seen in some jaundiced PBC patients, as well as malabsorption of the fat-soluble vitamins A, D, E, and K. Some PBC patients with Sicca syndrome also have pancreatic insufficiency. The pathogenesis of the osteopenic bone disease that occurs in at least 25% of PBC patients is still unclear. Some data suggest that high concentrations of serum bilirubin may impede osteoblast function. The clinically important bone disorder is osteoporosis, not osteomalacia, as was once believed.

Pathology

PBC is characterized by portal inflammation, the destruction of interlobular bile ducts, progressive fibrosis, and the eventual development of cirrhosis. PBC is divided into four histologic stages, I to IV. The disease is believed to progress from stage I to stage IV. However, the liver is not affected uniformly in PBC. One biopsy specimen may demonstrate lesions ranging from normal to stage IV. By convention, the histologic stage is the highest stage seen in a biopsy. There are two widely used staging systems, those of Scheuer and Ludwig, both well-known liver pathologists. In the Scheuer classification, stage I is defined by the presence of florid, asymmetric destructive bile duct lesions within portal triads (Figure 1). These lesions are irregularly scattered throughout the portal triads and are often seen only on large surgical biopsies of the liver. The damaged bile ducts are often surrounded by dense collections of lymphocytes, histiocytes, plasma cells eosinophils, and occasionally true giant cells, a pathologic lesion that is called a granuloma (Figure 1A). In the Ludwig classification, stage I is defined by the localization of inflammation to the portal triads. In stage II in the Scheuer classification, there are reduced numbers of normal bile ducts within some portal triads and increased numbers of poorly formed bile ducts with irregularly shaped lumens in others, a lesion called atypical bile duct hyperplasia (Figure 2). There is also mononuclear cell inflammation in portal triads and the beginning of portal fibrosis. In stage II in the Ludwig classification, the inflammation and fibrosis extends beyond portal triads and into the surrounding parenchyma. A diminished number of bile ducts in an otherwise unremarkable-appearing needle biopsy of the liver

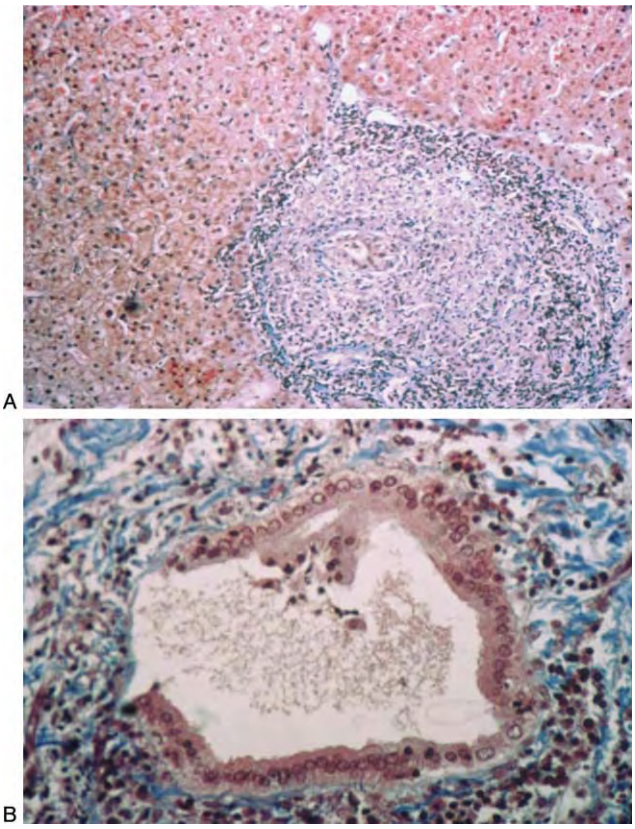

FIGURE 1 (A) Stage I florid bile duct lesion in primary biliary cirrhosis. A damaged bile duct is at the center of a granuloma (masson trichrome, ×124). (B) Stage I florid bile duct lesion in primary biliary cirrhosis. Epithelial cells have been dislodged from one quadrant of a bile duct (masson trichrome, ×310).

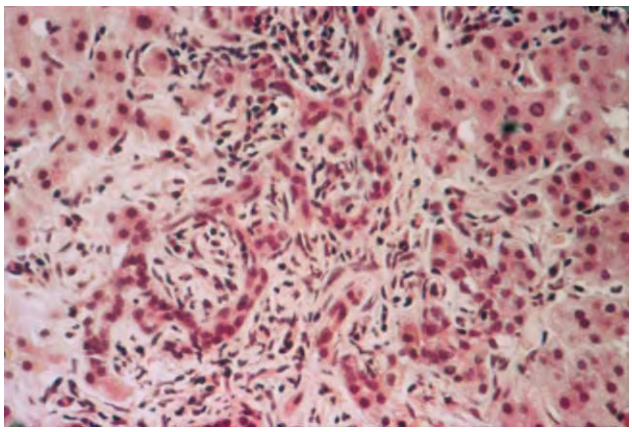

FIGURE 2 Stage II primary biliary cirrhosis. Atypical bile duct hyperplasia. Bile ducts are tortuous. None is cut in cross section, and there are no visible bile duct lumens (hematoxylin and eosin, ×310).

should alert one to the possibility of PBC. In stage III in both classifications, fibrous septa now extend beyond triads and form portal-to-portal bridges (Figure 3). The portal triads are otherwise similar to those in stage II. Stage IV represents the end stage of the

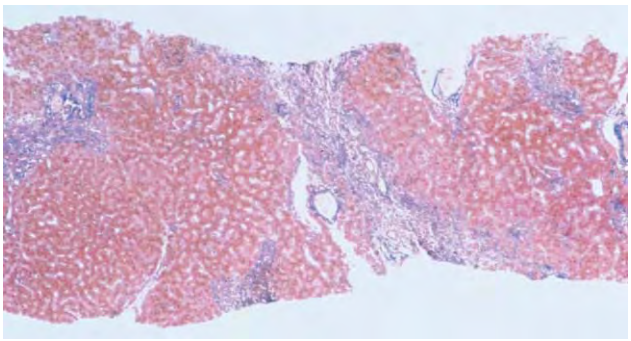

FIGURE 3 Stage III primary biliary cirrhosis. Adjacent portal triads are linked by septae that contain mononuclear inflammatory cells and scar tissue (masson trichrome, ×310).

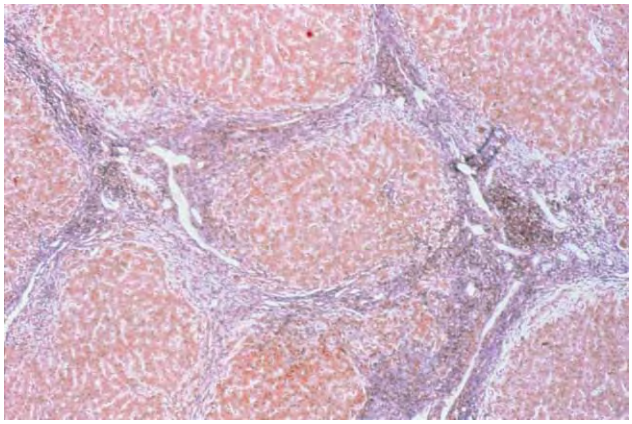

FIGURE 4 Stage IV primary biliary cirrhosis. Cirrhotic liver removed at the time of liver transplantation performed because of end-stage primary biliary cirrhosis. Nodule formation is evident and there are no visible bile ducts (masson trichrome, ×54).

lesion, frank cirrhosis, and regenerative nodules. It may be difficult to distinguish this late lesion from other types of cirrhosis. A paucity of normal bile ducts in areas of scarring suggests PBC (Figure 4).

Clinical Findings

The earliest and most common complaint is fatigue. Fatigue, however, is nonspecific and is found in many diseases. The earliest specific complaint in PBC is pruritus, usually worse at bedtime. In some patients, the pruritus begins during the third trimester of pregnancy and persists after delivery. Physical examination may reveal hepatomegaly and increased skin pigmentation. The pigment is melanin, not bilirubin, at this early stage. Excoriations, caused by intense itching and an uncontrollable urge to scratch, may be widespread. Jaundice usually presents later in the course of the disease. Kayser-Fleischer rings have been observed in a few PBC patients with long-standing jaundice.

Unexplained weight loss may also occur. Rarely, patients with PBC may go undetected until late in the course of the disease when they present with severe jaundice, ascites, or bleeding from esophageal varices. During the course of the disease, some jaundiced patients may develop malabsorption and complain of nocturnal diarrhea; frothy, bulky stools; or weight loss in the face of a voracious appetite and increased caloric intake. Fewer than 5% of patients will develop xanthomas (a cutaneous tumor composed of lipid-laden foam cells), but xanthelasmas (a planar xanthoma of the eyelids) are common. Bone pain may occur in PBC patients with osteoporosis, as well as spontaneous collapses of vertebral bodies and hairline fractures of the ribs. Fractures of the long bones are less common.

Laboratory Tests

Liver function tests reveal a cholestatic pattern. The serum alkaline phosphatase and gamma glutamyl transpeptidase (GGT) are often strikingly elevated. The serum aminotransferases are less elevated and may be normal early in the course of PBC. Serum albumin and prothrombin times are characteristically normal early in the course of the disease. whereas IgM levels are often elevated. The elevated alkaline phosphatase is usually of liver origin. 5′-Nucleotidase and GGT levels parallel the alkaline phosphatase. The serum bilirubin is normal early in the course of the disease, but becomes elevated in most patients as the disease progresses. Both direct and indirect fractions are increased. Despite strikingly high serum cholesterol values, occasionally 800–1600 mg/dl, atherosclerosis is uncommon, most likely because serum high-density lipoprotein (HDL) cholesterol levels are also elevated. Antimitochondrial antibody is positive in 95% of patients. Serum ceruloplasmin is elevated, in contrast to Wilson's disease, another disorder with increased retention of copper within the liver. There is an increased incidence of hypothyroidism in PBC that is not always reflected by routine tests of thyroid function. Elevated thyroid-stimulating hormone (TSH) levels will usually identify such individuals.

Diagnosis

The combination of a disproportionately elevated alkaline phosphatase and a positive AMA is sufficient evidence to make a diagnosis of PBC as long as the liver biopsy is consistent with this diagnosis. It is prudent to demonstrate that the bile ducts are patent. Ultrasonography is usually adequate for this purpose. Endoscopic cholangiography (ERCP) is recommended if there is a suspicion of bile duct obstruction on imaging tests or if the AMA is negative in a patient with inflammatory bowel disease. The ERCP is done in this setting to detect primary sclerosing cholangitis. A percutaneous needle biopsy of the liver will confirm the diagnosis, allow histologic staging, and provide a baseline for follow-up biopsies that are done to evaluate the efficacy of medical treatment.

Treatment

Treatment of Symptoms

Pruritus

The nonabsorbed resin, cholestyramine, 4–8 g twice daily with meals, will relieve pruritus in most patients. Commonly prescribed anti-itch medicines such as antihistamines are only helpful early in the course of PBC when itching is not severe. Rifampin, 150 mg twice daily, will control itching in most patients who fail to respond to cholestyramine. Opioid antagonists, such as naloxone and naltrexone, may be effective in the small number of PBC patients who fail to respond to ammonium resins and rifampin.

Malabsorption

Some patients with PBC and the Sicca syndrome may have concomitant pancreatic insufficiency. This can be treated with pancreatic enzyme preparations given orally. Malabsorption of fat-soluble vitamins is irregular and unpredictable, but deficiencies of vitamins A, D, E, and K may occur in patients who are chronically jaundiced. Patients with low levels of a specific vitamin should be given supplements of it orally.

Anemia and Osteoporosis

PBC patients may develop iron-deficiency anemia. This often reflects unrecognized gastrointestinal (GI) blood loss. Upper endoscopy is indicated to detect esophageal varices or congestive gastropathy. There is no proven effective medical treatment for the osteoporosis other than liver transplantation. Because bisphosphates are an effective treatment for osteoporosis in postmenopausal women and prevent steroid-induced osteoporosis, they are often used in PBC.

Treatment of the Underlying Disease Process

PBC, if untreated, is a progressive disease that eventually ends in liver failure and the need for liver transplantation. The median survival for symptomatic patients without treatment is approximately 7–10 years. Patients who are asymptomatic at the time of diagnosis have a longer life expectancy than symptomatic patients.

Medical Treatment

Ursodeoxycholic acid (UDCA), 12–15 mg/kg body weight daily, is the only drug approved by the FDA for the treatment of the PBC. It improves serum bilirubin, alkaline phosphatase, alanine aminotransferase (ALT), aspartate aminotransferase (AST), and IgM levels in most patients. It also decreases pruritus and prolongs the time before clinical deterioration and referral for liver transplantation. It is safe and well tolerated. Colchicine 0.6 mg twice daily and/or methotrexate, 0.25 mg/kg body weight per week in three divided doses, have been effective in the author's experience when given to patients who do not respond adequately to UDCA. Combination therapy (UDCA plus colchicine and/or methotrexate) is still under study. At this time, there is still debate about the effectiveness of medical treatment, although the author's experience suggests that medical treatment is effective in most patients, particularly those with precirrhotic PBC. Initiating treatment early in the course of PBC is important because medical therapy is less likely to help once cirrhosis and portal hypertension develop. Liver transplantation is the only effective treatment in patients with clinically advanced disease. The author's current approach is based on the observation that the response to medical treatment in PBC varies among patients. Treatment is initiated with UDCA. Colchicine is added if patients have not responded adequately to UDCA after 1 year. Methotrexate is added if patients have not responded fully to the combination of UDCA and colchicine after another year. An adequate response to treatment consists of the resolution of pruritus, a decrease in serum alkaline phosphatase to values that are $<50\%$ above normal, and improvement in liver histology of at least two points on the necroinflammatory scale. Methotrexate is discontinued after 1 year if patients fail to respond to it. They are maintained on UDCA and colchicine.

Liver Transplantation

Liver transplantation has improved the survival of PBC patients with cirrhosis and liver failure. Patients who are candidates for liver transplantation are those with cirrhosis and (1) persistent jaundice that is unresponsive to medical treatment, (2) fluid retention, (3) bleeding from esophageal varices, (4) hepatic encephalopathy, or any combination of these four. One-year survival after liver transplantation is greater than 90% in most transplant centers. Survival thereafter resembles a control population matched for age and sex. Recurrence of PBC after liver transplantation is uncommon, but has been seen in a small percentage of patients. It has responded to treatment with ursodiol and colchicine in the author's experience.

See Also the Following Articles

Bile Salts and their Metabolism • Mitochondrial Auto-Antibodies

Glossary

cholestasis A liver disorder in which bile flow is impeded. Clinical signs of cholestasis are a disproportionate increase in the serum alkaline phosphatase or gamma glutamyl transpeptidase compared to the serum alanine aminotransferase or aspartate aminotransferase. The symptom most characteristic of cholestasis is pruritus.

hepatic encephalopathy A disturbance in consciousness that occurs in patients with advanced liver disease. Manifestations can range from subtle changes in personality to frank coma.

micellar Pertaining to a colloid particle formed by the aggregation of small molecules. Micelles in bile contain bile acids, phospholipids, and cholesterol.

mitochondria Organelles important in energy metabolism that are found in nucleated cells throughout the body.

necroinflammatory scale A method of evaluating liver biopsies quantitatively. Scores from 0 to 4 are given for lesions, such as portal inflammation, periportal inflammation, lobular inflammation, bile duct necrosis, and fibrosis, and added together to give a final score.

Further Reading

Bonis, P. A. L., and Kaplan, M. (1999). Methotrexate in primary biliary cirrhosis unresponsive to ursodeoxycholic acid: An observational study in 10 patients. *Gastroenterology* **117**, 395–399.

Goulis, J., Leandro, G., and Burroughs, A. K., *et al.* (1999). Randomised controlled trials of ursodeoxycholic-acid therapy for primary biliary cirrhosis: A meta-analysis. *Lancet* **354**, 1053–1060.

Hendrickse, M., Rigney, E., Giaffer, M., *et al.* (1999). Low-dose methotrexate is ineffective in primary biliary cirrhosis: Long-term results of a placebo-controlled trial. *Gastroenterology* **117**, 400–407.

Jorgensen, R. A., Dickson, E. R., Hofmann, A. F., Rossi, S. S., and Lindor, K. D. (1995). Characterisation of patients with a complete biochemical response to ursodeoxycholic acid. *Gut* **36**, 935–938.

Kaplan, M. M. (1996). Primary biliary cirrhosis [review]. *N. Engl. J. Med.* **335**, 1570–1578.

Kaplan, M. M., DeLellis, R., and Wolfe, H. (1997). Sustained biochemical and histological remission of primary biliary cirrhosis in response to medical treatment. *Ann. Int. Med.* **126**, 682–688.

Kaplan, M. M., Schmid, C., Provenzale, D., Dickstein, G., and McKusick, A. (1999). A prospective trial of colchicine and methotrexate in the treatment of primary biliary cirrhosis. *Gastroenterology* **117**, 1–9.

Pares, A., Caballeris, L., Rodes, J., *et al.* (2000). Long-term effects of ursodeoxycholic acid in primary biliiary cirrhosis: Results of a double-blind controlled multicentric trial. *J. Hepatol.* **32**, 561–566.

Poupon, R. E., Lindor, K. D., Cauch-Dudek, K., Dickson, E. R., Poupon, R., and Heathcote, E. J. (1997). Combined analysis of randomized controlled trials of ursodeoxycholic acid in primary biliary cirrhosis. *Gastroenterology* **113**, 884–890.

Poupon, R. E., Poupon, R., and Balkau, B. (1994). Ursodiol for the long-term treatment of primary biliary cirrhosis. *N. Engl. J. Med.* **330**, 1342–1347.

Vuoristo, M., Farkkila, M., Karvonen, A. L., *et al.* (1995). A placebo-controlled trial of primary biliary cirrhosis treatment with colchicine and ursodeoxycholic acid. *Gastroenterology* **108**, 1470–1478.

Biography

Marshall M. Kaplan is the former Chief of the Division of Gastroenterology at Tufts-New England Medical Center and is a Professor of Medicine at Tufts University School of Medicine. His research interests are the etiology and treatment of chronic-cholestatic liver disease. He received his M.D. and M.A.C.P. degrees from Harvard Medical School and the American College of Physicians. He was an associate editor of the *New England Journal of Medicine* from 1993 until 2001, served as Chairman of the Subspecialty Board in Gastroenterology of the American Board of Internal Medicine, and was awarded a mastership by the American College of Physicians.

Bioenergetics: General Definition of Principles

David G. Nicholls
Buck Institute for Age Research, Novato, California, USA

"Bioenergetics" is the study of the molecular mechanisms by which energy, made available by catabolic metabolic pathways or by light capture in photosynthesis, is transformed and made available for cellular processes of growth, motility, and survival. Traditionally, the field has largely focused on studies of bacteria, mitochondria, and chloroplasts, although the principles, largely involving the generation and utilization of ion gradients across membranes, are much more generally applicable.

Thermodynamics

Two factors are required for a biochemical reaction to occur spontaneously: the process should involve an increase in the entropy of the system and its surroundings and there should be a mechanism, usually enzymatic, to lower the energy barrier sufficiently to allow the transformation to occur at a significant rate. The entropy difference is the realm of thermodynamics, whereas the energy barrier helps to define the rate of the process.

The simplest thermodynamics deals with the limiting case of isolated systems that exchange neither material nor energy across their boundaries and therefore have no influence on their surroundings. Closed systems exchange energy but not material with their surroundings, whereas real biological systems are open, i.e., exchanging both energy and material (substrates, products). The treatment of open systems is complex and requires non-equilibrium thermodynamics; however, the equilibrium thermodynamics of closed systems can be used to obtain important information, such as the conditions under which a given reaction would be at equilibrium and the extent to which the actual reaction in the cell is displaced from equilibrium. Although equilibrium thermodynamics gives no information as to the rate of a reaction, it can unequivocally exclude any process that is energetically impossible.

Gibbs Free Energy

The entropic driving force is equally valid for closed and isolated systems; however, analysis is complicated by the effects of the energy transfer across the boundaries of the system affecting the entropy of the surroundings. The Gibbs free energy change, ΔG, is a function that, under conditions of constant temperature and pressure, corrects for the entropy change in the surroundings and enables equilibrium to be calculated just using parameters for the system itself. Gibbs energy changes are used not only to study a reaction in solution, but also to quantify reduction–oxidation (redox) reactions occurring, for example, in the mitochondrial respiratory chain, to calculate the available energy in an ion gradient, and to compare the energy available from absorption of light quanta in photosynthesis.

A basic understanding of bioenergetics is considerably helped by the use of simple analogies. Figure 1 shows schematically the *content* of Gibbs energy (G) in a closed system when the reaction A = B is displaced on either side of equilibrium. The slope of the parabola at any point represents the Gibbs energy *change* (ΔG). The bottom of the parabola represents the equilibrium condition: the content of Gibbs free energy is at a minimum and the tangent to the slope, ΔG, is zero. Equilibrium is the lowest energy state and a small conversion of substrate to product at equilibrium causes no free energy change. The left side of the parabola represents reaction conditions that have not yet proceeded as far as equilibrium. The slope ΔG is negative, which indicates that the reaction can proceed spontaneously (as long as a pathway exists). The further from equilibrium, the greater the slope; i.e., the Gibbs energy change becomes more negative and more energy is available from a conversion of substrate to product at those concentrations. Beyond the equilibrium point, the slope is "uphill." Reactions cannot proceed beyond equilibrium without some independent energy input.

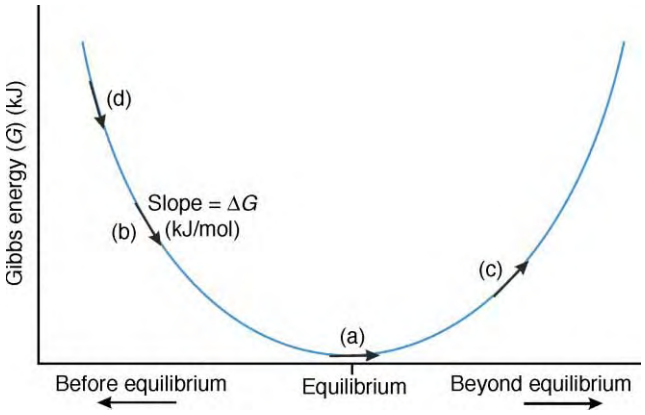

FIGURE 1 Schematic representation of Gibbs energy in relation to displacement from equilibrium. (a) Gibbs energy (G) is at a minimum at equilibrium and Gibbs energy change (ΔG), given by the slope of the parabola, is zero. (b) Before equilibrium, the slope (ΔG) is negative and the reaction can proceed spontaneously. (c) Beyond equilibrium, the slope is "uphill" and an additional energy input would be required. (d) The further the reaction is displaced from equilibrium, the greater the slope; i.e., ΔG becomes more negative. Adapted from Nicholls, D. G., and Ferguson, S. J. *Bioenergetics* 3 Copyright 2002, with permission from Elsevier.

The Gibbs free energy change can be quantified as a function of the displacement from equilibrium

$$\Delta G(\text{kJ/mol}) = -2.3RT\log_{10}\left(\frac{K}{\Gamma}\right), \qquad (1)$$

where R is the gas constant, T is the absolute temperature, K is the equilibrium constant under the conditions of the determination, and Γ is the mass-action ratio of the concentrations of substrates and products measured in the cell or assay mixture. Put more simply, ΔG changes by approximately 5.7 kJ/mol for each 10-fold displacement from equilibrium. Note that this equation corresponds to the more familiar form that involves standard free energy, e.g.,

$$\Delta G = \Delta G^0 + 2.3RT\log_{10}\left(\frac{[C]^c[D]^d}{[A]^a[B]^b}\right), \qquad (2)$$

but is more logical and symmetrical, emphasizing displacement from equilibrium, rather than the frequently misused abstract concept of standard free energy.

ATP

ATP synthesis from ADP and phosphate (P_i) and the reverse hydrolysis reaction are the dominant reactions in the distribution and utilization, respectively, of Gibbs free energy in the cell. The ATP synthesis reaction is held up to 10^{10}-fold beyond its equilibrium and thus requires an input of Gibbs free energy of approximately $10 \times 5.7 = 57$ kJ/mol. Conversely, the hydrolysis of 1 mol of ATP can yield up to 57 kJ/mol. There is no magic property associated with ATP (such as the myth of the "high-energy" bond) that fits it for this universal role, except that the equilibrium constant of the reaction is such that a sufficient concentration of ADP remains in a functioning cell to bind to the ATP synthase (see below).

The ATP synthesis reaction is usually expressed in short-hand form, ignoring water, ionization, pH, and chelating ions such as Mg^{2+}; i.e.,

$$\text{ADP} + \text{P}_\text{i} = \text{ATP}$$

This may only be used as the basis for thermodynamic calculations if the equilibrium constant is known under *exactly* identical conditions, in which case the common factors cancel out of the ratio Γ/K in Eq. (1).

Redox Potentials

Redox reactions are those that involve coordinate oxidation of one substrate and the reduction of another. An example of a redox reaction occurring in the cytoplasm is that catalyzed by lactate dehydrogenase:

$$\text{Pyruvate} + \text{NADH} + \text{H}^+ = \text{Lactate} + \text{NAD}^+. \qquad (3)$$

Redox reactions can be considered hypothetically as the sum of two linked half-reactions:

$$\text{NADH} = \text{NAD}^+ + \text{H}^+ + 2e^- \qquad (4)$$

and

$$\text{Pyruvate} + 2\text{H}^+ + 2e^- = \text{Lactate}. \qquad (5)$$

All biological redox reactions can be considered to involve primary electron transfer, although in many cases the increased negative charge on the reduced component leads to the subsequent binding of one or more protons; thus, ubiquinone reduction to ubiquinol in the respiratory chain involves the addition of two electrons followed by two protons, whereas NAD^+ reduction to NADH requires the addition of two electrons followed by one proton [Eq. (5)].

A reduced/oxidized pair, such as NADH/NAD^+, is a redox couple and the equilibrium of the half-reaction can be defined in terms of its half-reduction redox potential (the potential at which the concentrations of oxidized and reduced species are equal). A redox couple with a more negative redox potential will tend to oxidize one with a more positive potential. Zero is defined as the potential of a $\frac{1}{2}H_2/H^+$ couple at pH 0 when H_2 is 1 atm. Important half-reduction potentials include those for NADPH/$NADP^+$ and NADH/NAD^+ (both -320 mV), fumarate/succinate ($+30$ mV), ubiquinol/ubiquinone ($+60$ mV), and reduced/oxidized cytochrome c ($+220$ mV). The important $H_2O/\frac{1}{2}O_2$ couple has a redox potential

of + 820 mV when O_2 is present at 1 atm and water is 55 *M*.

Redox potentials are not constants, but vary with the state of reduction of the couple. The redox potential of a one-electron reduction couple becomes 60 mV more negative for each 10-fold increase in the reduced/oxidized ratio. Thus, although the *standard* hydrogen electrode at pH 0 has a redox potential of zero, at pH 7 when the proton concentration is only 10^{-7} *M*, the redox potential is −420 mV. Two electron reductions change by 30 mV per decade; thus, the NADH/NAD^+ couple in mitochondria is typically 10% reduced and thus has a redox potential of approximately −320 + 30 = −290 mV, whereas the NADPH/$NADP^+$ pool is at least 90% reduced and so operates at approximately −350 mV.

Although the historical origin of redox potentials (in electrochemistry) may obscure the relationship, redox changes are governed by Gibbs free energy principles; indeed, the ΔG associated with the difference in redox potential between two couples can be simply calculated as

$$\Delta G = -nF\Delta E_h, \qquad (6)$$

where n is the number of electrons transferred and F is the Faraday constant (0.965 kJ/mol/mV). As a rough rule of thumb, a "mole" of electrons falling through a potential of 1 V makes 100 kJ of Gibbs free energy available, and 2 mol of electrons passing from NADH to O_2 through the respiratory chain corresponds to a ΔG of −224 kJ. Note that this is compatible with the formation of approximately 3 mol of ATP.

Ion Electrochemical Potential Differences

The concept of Gibbs free energy as displacement from equilibrium can be extended to gradients of ions and solutes across biological membranes. Two components must be considered: that due to a difference in concentration between the two aqueous compartments and (if the species is charged) that due to the difference in electrical potential between the compartments (usually termed the membrane potential, not to be confused with any surface charge on the membrane itself). The Gibbs free energy is simply the sum of the two components (hence "electrochemical"),

$$\Delta G(\text{kJ mol}^{-1}) = -mF\Delta\psi + 2.3RT\log_{10}\frac{[X^{m+}]_B}{[X^{m+}]_A}, \qquad (7)$$

where m is the charge on the ion, $\Delta\psi$ is the membrane potential in millivolts, and X^{m+} is the concentration of the ion in compartment A or B.

The ion of most interest in bioenergetics is the proton. The equation for the proton electrochemical gradient ($\Delta\mu_{H^+}$) is rather simple, due to the logarithmic nature of pH:

$$\Delta\mu_{H^+}(\text{kJ/mol}) = -F\Delta\psi + 2.3RT\Delta\text{pH}. \qquad (8)$$

The mitochondrial convention is that ΔpH is the pH outside *minus* that in the matrix and is usually negative.

The proton electrochemical gradient is usually expressed in units of voltage. This "proton-motive force," Δp, is defined as:

$$\Delta p(\text{mV}) = -(\Delta\mu_{H^+})/F = \Delta\psi - 60\Delta\text{pH}. \qquad (9)$$

Photons

The Gibbs free energy available from a single photon is equal to Planck's constant times frequency, i.e., $h\nu$, where ν is the frequency of the radiation. A mole (Avagadro's number) of photons corresponds to a ΔG of 120,000/λ kJ/mol, where λ is the wavelength in nanometers. For 600 nm red light, this corresponds to 200 kJ/mol. Note that the absorption of such a photon would theoretically be capable of lowering (making more negative) the potential of an electron by 2 V.

The Thermodynamics of Bioenergetic Interconversions

The bioenergetic processes occurring in mitochondria involve the sequential conversion of redox energy into proton-motive force and of proton-motive force into the Gibbs free energy of the ATP pool. Since each is based on Gibbs free energy, the interconversion is very simple. Consider a respiratory chain complex that transfers two electrons through a redox span of ΔE_h mV. If the complex pumps n protons against a proton-motive force of Δp mV, equilibrium would be reached when $n\Delta p = 2\Delta E_h$. For the complex to work in the forward direction, therefore, $n\Delta p = 2\Delta E_h$. Roughly speaking, the forward rate of the complex is proportional to the disequilibrium for small displacements, which is why respiration accelerates when the proton gradient is lowered.

The equilibrium condition for the ATP synthase, where Δp is expressed in kilojoules per mole and Δp is expressed in millivolts, requires the Faraday constant, $\Delta G_{ATP} = mF\Delta p$, where m represents the number of protons required to generate 1 mol of ATP. Since the ATP synthase is reversible, it can operate in the forward direction (ATP synthesis) when $\Delta G_{ATP} < mF\Delta p$ and in the reverse direction (ATP hydrolysis) when $G_{ATP} > mF\Delta p$.

Mitochondrial Respiration Rate: The Proton Circuit

A simple but immensely powerful aid to understanding the relationships between proton-motive force, respiration, and proton re-entry pathways is to use a simple electrical analogy (Figure 2). Because there is a fixed stoichiometry between electron flow (and hence respiration) and proton translocation, and because protons must re-enter the mitochondrial matrix at exactly the same rate that they are pumped out, the "proton current," J_{H^+}, circulating around the "proton circuit" will equal the rate of respiration times the H^+/O (protons pumped divided by oxygen utilized) stoichiometry of the respiratory chain.

Because the current and potential (Δp) in the proton circuit are known, Ohm's law can be used to calculate the resistance (or its reciprocal, i.e., the conductance, $C_M H^+$) of the inner membrane to proton re-entry:

$$C_M H^+ = J_{H^+}/\Delta p \qquad (10)$$

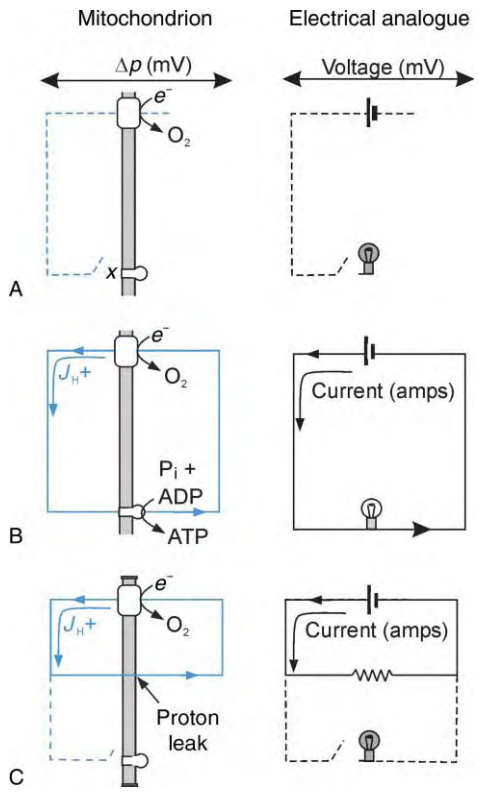

FIGURE 2 The analogy between the proton circuit and a simple electrical circuit. (A) Open circuit. Zero current (no respiration), potential (Δp) maximal. (B) Circuits completed, current flows (respiration). Useful work done (ATP synthesized). Potential (Δp) less than maximal. (C) Short-circuit introduced; energy dissipated, potential low, respiration maximal. Adapted from Nicholls, D. G., and Ferguson, S. J. *Bioenergetics* 3 Copyright 2002, with permission from Elsevier.

Two major components of proton conductance are that which occurs through the ATP synthase, which is tightly coupled to the rate of ATP synthesis, and an endogenous proton leak possessed by all mitochondria. One specialized tissue, brown adipose tissue, possesses an additional controllable proton leak catalyzed by an uncoupling protein that allows respiration, and heat production, to occur without concomitant ATP synthesis.

See Also the Following Articles

ATP Synthesis in Plant Mitochondria: Substrates, Inhibitors, Uncouplers • Chloroplast Redox Poise and Signaling • Energy Transduction in Anaerobic Prokaryotes • Membrane-Associated Energy Transduction in Bacteria and Archaea

Glossary

electrochemical gradient The driving force inherent in an ion gradient across a membrane, made up of two components: the membrane potential and the ion concentration gradient.

Gibbs free energy A thermodynamic term that expresses the extent to which a process is displaced from equilibrium and hence defines its capacity to do work.

proton circuit The closed cycle comprising protons pumped across, e.g., the mitochondrial inner membrane and re-entering via the ATP synthase or a leak pathway.

proton conductance The conductance of a membrane to protons calculated by applying Ohm's law to the proton circuit.

redox couple A reduced/oxidized pair, such as $NADH/NAD^+$.

redox potential A thermodynamic measure of the tendency of a redox couple to gain or lose electrons.

Further Reading

Cramer, W. A., and Soriano, G. M. (2003). Thermodynamics of energy transduction in biological membranes. *In Biophysics Textbook Online*. Available at http://www.biophysics.org/btol/. Biophysical Society.

Nelson, D. L., Cox, M. M., and Lehninger, A. L. (2000). *Principles of Biochemistry*. 3rd edition, Worth, New York.

Nicholls, D. G., and Ferguson, S. J. (2002). *Bioenergetics 3*. Academic Press, London.

Biography

Dr. David Nicholls is at the Buck Institute for Age Research in Novato, California. His principal research interest is in mitochondrial bioenergetics, with a focus on mitochondrial function/dysfunction in neurons and the relationship to neurodegenerative disease. He holds a Ph.D. from the University of Bristol. He has published articles on brown fat and uncoupling proteins, mitochondrial calcium transport and bioenergetics, and transmitter release of isolated nerve terminals and is co-author of the textbook *Bioenergetics 3*.

Biotin

Steven W. Polyak and Anne Chapman-Smith
The University of Adelaide, Adelaide, Australia

Biotin, or Vitamin H, is a member of the water-soluble class of vitamins. It has been appreciated for some time that biotin is an essential cofactor for a family of enzymes known as the biotin-dependent enzymes. These enzymes are found in all living organisms and catalyze several important metabolic reactions. The cofactor actively participates in the binding and transfer of carbon dioxide between metabolites. Biotin is specifically attached to these enzymes through the activity of another ubiquitous enzyme, biotin protein ligase (BPL). In bacteria, this protein also behaves as a transcriptional repressor of the biotin biosynthetic operon, where biotin itself is an integral component required for DNA binding.

Historical Perspective

At the end of the nineteenth century it was observed that extracts from liver and meat could serve as effective treatments for skin lesions induced by a diet of raw egg. Earlier studies had identified a heat stable factor in the same extracts that was also required for yeast growth. In 1935 Kogl and Tannis isolated this factor from egg yolk and called it biotin. The essential growth factor present in the meat extracts, which had become known as Vitamin H (*Haut*, German = skin), was found to be identical to biotin. Later, it was discovered that avidin, a biotin-binding glycoprotein, was the toxic component of raw eggs. The structure of biotin was determined in 1942 and confirmed by chemical synthesis and X-ray analysis.

During the 1950s it became evident that biotin is involved as a cofactor for a class of enzymes that catalyze a variety of carboxyl transfer reactions. It was first demonstrated that β-methylcrotonoyl-CoA carboxylase, a biotin-requiring enzyme that catalyzes a step in the degradation of leucine, was capable of carboxylating free biotin. It soon became apparent that, in the cell, biotin functions as a cofactor only when bound to protein and that biotin is covalently attached to the ε-amino group of a specific lysine residue of propionyl CoA carboxylase. Subsequently, it was demonstrated for other biotin enzymes that the biotin prosthetic group is attached in the same way.

Biotin

Biotin, a member of the water-soluble B-complex group of vitamins, is synthesized by higher plants and most fungi and bacteria. Humans, other mammals, and birds cannot synthesize biotin *de novo* and therefore must obtain this essential micronutrient from material synthesized by intestinal microflora and from dietary sources. In mammals, absorption of biotin occurs in the small intestine. Other important sites that play a role in normal biotin physiology include the liver (the principal site of biotin utilization), the kidney (the site of reabsorption of filtered biotin), and the placenta (the site of transport of biotin from the maternal circulation to the developing embryo). Biotin obtained from dietary sources exists in both free and protein-bound forms. Protein-bound biotin is digested by gastrointestinal proteases and peptidases to biocytin and biotin-containing short peptides. Biotin present in these compounds is recycled through the action of biotinidase to release free biotin.

Biotin Enzymes

Biotin enzymes are a family of enzymes ubiquitously found throughout nature. It appears that all organisms contain acetyl coA carboxylase, reflecting the essential role this enzyme plays in the synthesis of fatty acids required for membrane biogenesis. While some organisms, such as bacteria, possess only one biotin enzyme, other organisms have multiple biotin enzymes. For example, mammalian cells express pyruvate carboxylase, propionyl-CoA carboxylase, and methylcrotonyl-CoA carboxylase in addition to two isoforms of acetyl-CoA carboxylase. These enzymes catalyze key metabolic reactions in gluconeogenesis and amino acid metabolism, in addition to fatty acid metabolism.

The members of this enzyme family utilize biotin as a mobile carboxyl carrier in a conserved reaction

mechanism that requires three domains: a biotin carboxylase domain, a transcarboxylase domain, and a biotin domain containing the covalently attached biotin moiety. As shown in Figure 1, these enzymes catalyze reactions in two partial reactions carried out at spatially separate sites on the protein where biotin itself carries a carboxyl group between the two sites. Biotin enzymes can be divided into three classes depending on the nature of the original donor and final carboxyl acceptor. These are the carboxylases (Class I), decarboxylases (Class II), and transcarboxylases (Class III). All eukaryotic enzymes belong to Class I, while prokaryotes contain enzymes from all three classes

The mechanism of biotin carboxylation in the Class I enzymes has been extensively investigated. Experiments on propionyl CoA carboxylase and pyruvate carboxylase showed that the source of CO_2 in the reaction is bicarbonate and the reaction is dependent upon the presence of ATP:

$$\text{MgATP} + \text{HCO}_3^- + \text{Enz-biotin} \rightleftharpoons \text{MgADP} + \text{Pi} + \text{Enz-biotin-CO}_2^- \quad (1)$$

At the first partial reaction site, biotin is carboxylated at the 1′-nitrogen probably after the formation of a very labile enzyme-bound carboxyphosphate intermediate that donates the activated carboxyl group to biotin. Although no direct evidence of this reaction mechanism has been reported, several observations suggest this as the most likely scheme. Most notable are the similarities between the biotin enzymes and carbamoyl phosphate synthetase; an enzyme known to utilize a carboxyphosphate intermediate.

Subsequently, in the second partial reaction, the transfer of the carboxyl group from carboxybiotin to the acceptor molecule occurs. It has been proposed that the decarboxylation of carboxybiotin proceeds along a pathway where CO_2 and the enolate of biotin are formed. Following protonation, carboxylated biotin can again be formed at the first reaction site under physiological conditions:

$$\text{Enz-biotin-CO}_2 + \text{acceptor metabolite} \rightleftharpoons \text{Enzyme–biotin} + \text{Carboxylated acceptor} \quad (2)$$

The Class II decarboxylases differ from the Class I carboxylases in that the reactions are ATP-independent. The decarboxylases of anaerobic prokaryotes all catalyze decarboxylation of a specific β-keto acid or acyl-CoA coupled to sodium ion export against a concentration gradient. Thus, this class of enzyme serves as an important energy transducer that does not require ATP. There is only one known member belonging to the Class III biotin enzymes: *Propionibacterium freudenreichii subsp. shermanii* transcarboxylase (TC). TC catalyzes the formation of methylmalonyl-CoA from propionyl-CoA using oxaloacetate as a carboxyl donor, and it exists as a multimeric complex composed of 30 polypeptides of three different types.

Biotin Domains

The biotin prosthetic group is covalently attached via the ε-amino group of one specific lysine residue within the biotin enzymes. This biotin-accepting lysine is found in a tetrapeptide sequence, Ala–Met–Lys–Met, which is extremely conserved among all biotin enzymes (Figure 2). Additionally, the primary structure surrounding the target lysine residue shows a high degree of homology between a wide range of enzymes and species (Figure 2). Deletion studies have revealed that 30–35 amino acid residues either side of biocytin are necessary to specify biotinylation. Collectively, these structures, able to incorporate biotin *in vivo*, are termed *biotin domains*. The removal of determinants necessary to define the structure of a biotin domain by truncation or mutation results in a molecule that is unable to be biotinylated.

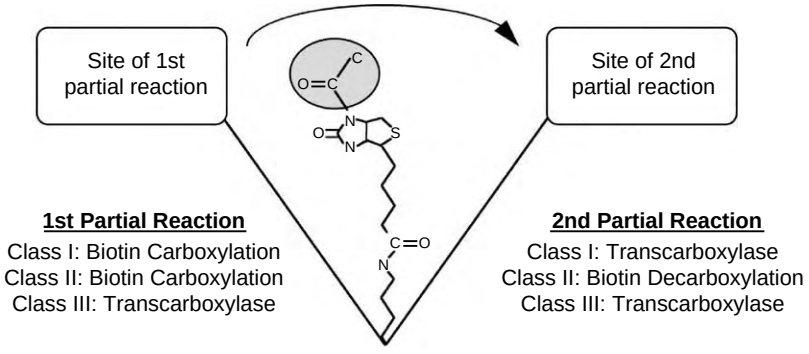

FIGURE 1 Biotin mediated carboxyl transfer between reaction subsites of biotin enzymes. The biotin group attached to the target lysine is shown located in the cleft of the biotin enzyme. The carboxylate anion, complexed to the biotin, is shown in the shaded circle. The arrow represents movement of the mobile cofactor between the two partial reaction subsites during catalysis. The reactions performed at the separate subsites are indicated for the three classes of biotin enzymes.

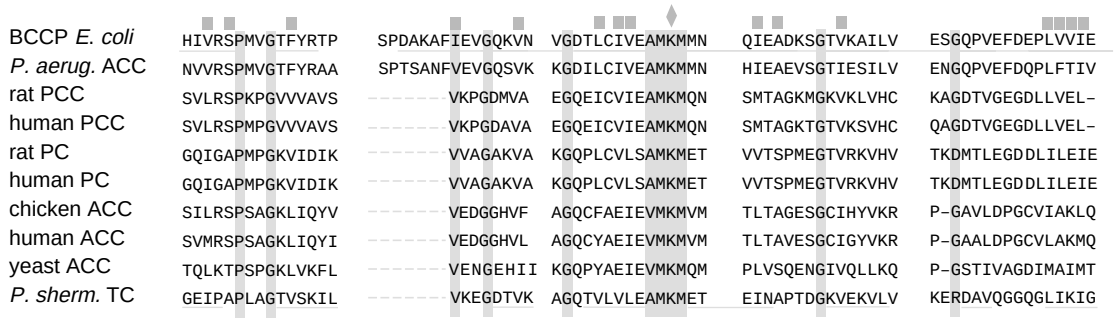

FIGURE 2 Sequence alignment of the biotin domains of biotin carboxylases from diverse organisms. Residues forming β-strands in the three-dimensional structures of *Escherichia coli* biotin carboxyl carrier protein (BCCP) and *Propionibacterium freudenreichii subsp. shermanii* transcarboxylase (TC) are underlined, and hydrophobic core residues are indicated by (■). The biotinylated lysine is marked (◆). Shading indicates residues very highly conserved in all biotin domains for which sequence data is available. Reproduced with permission from Chapman-Smith and Cronan (1999), *J. Nutr.* 129, 447S–484S.

The biotin domain participates in a number of heterologous protein:protein interactions in the cell. First, it serves as a substrate in the biotinylation reaction. Here, the biotin prosthetic group is covalently attached to the biotin domain through the enzymatic action of biotin protein ligase (BPL). Subtle conformational changes to the biotin domain that occur upon biotinylation are thought to signal dissociation of the two proteins and yield the biotinylated product. The biotinylated or holo biotin domain is then free to interact with each of the two partial reaction sites in the carboxylase, shuttling carboxyl groups between substrates in the enzyme complex.

The formation of multimeric protein complexes, characteristic of all biotin enzymes, is not necessary for substrate recognition by BPLs. Enzymatic biotinylation experiments, performed using the biotin accepting subunit of the *P. shermanii* TC or the biotin carboxyl carrier protein (BCCP) of *E. coli* acetyl CoA carboxylase, have shown that these domains function equally well as BPL substrates as do the intact or multimeric protein complex. Therefore, the information required for association with BPL is present within the structured biotin domain. BPLs from various sources have been found to recognize and biotinylate acceptor proteins from very different sources.

In 1966, McAllister and Coon first showed that extracts containing BPLs from rabbit liver, yeast, and *P. shermanii* were able to activate enzyme substrates from rabbit and bacteria via the attachment of the biotin prosthetic group. Evidence of cross species recognition *in vivo* was demonstrated when the 1.3S subunit of TC was recombinantly expressed in *E. coli* and shown to be a substrate for the *E. coli* BPL. Truncation analysis of the 1.3S TC subunit revealed that the minimum amount of information required to specify biotinylation was present in the 75 C-terminal amino acid residues. This minimal peptide, fused to β-galactosidase, was biotinylated *in vivo* by the BPL from *E. coli*. Similarly, the C-terminal 87 amino acid residue of BCCP (BCCP-87) was shown to be a stable protein that can function as a substrate for *E. coli*, insect, yeast, and human BPLs. Together, these studies suggest that all biotin domains fold into an essentially common tertiary structure recognized by all members of the BPL enzyme family.

Biotin Domain Structure

The structures of two biotin domains have been determined: that of the *E. coli* BCCP-87 (Figure 3) and the 1.3S subunit of *P. shermanii* transcarboxylase. These proteins are structurally related to the lipoyl domains of 2-oxo acid dehydrogenase multienzyme complexes, which also undergo an analogous posttranslational modification. These domains form a flattened β-barrel structure comprising two 4-stranded β-sheets with the N- and C-terminal residues close together at one end of the structure. At the other end of the molecule, the biotinyl- or lipoyl-accepting lysine resides on a highly exposed, tight hairpin loop between β-strands four and five. The structure of the domain is stabilized by a core of hydrophobic residues, which are important structural determinants. Conserved glycine residues (Figure 2) occupy β-turns linking the β-strands.

BCCP-87 contains a seven amino acid insertion common to prokaryotic acetyl-CoA carboxylases but not present in other biotin domains. This region of the peptide adopts a "thumb" structure between the β2 and β3 strands and, interestingly, forms direct contacts with the biotin moiety in both the crystal and solution structures. The significance of this interaction is not understood, but structural studies on the 1.3S subunit of TC, which is a "thumbless" biotin domain, have revealed that biotin also interacts with the protein. Residues in the N-terminal region of the TC subunit, independent of the biotin domain, functionally compensate for the thumb structure by binding to biotin only when the cofactor is in its carboxylated state.

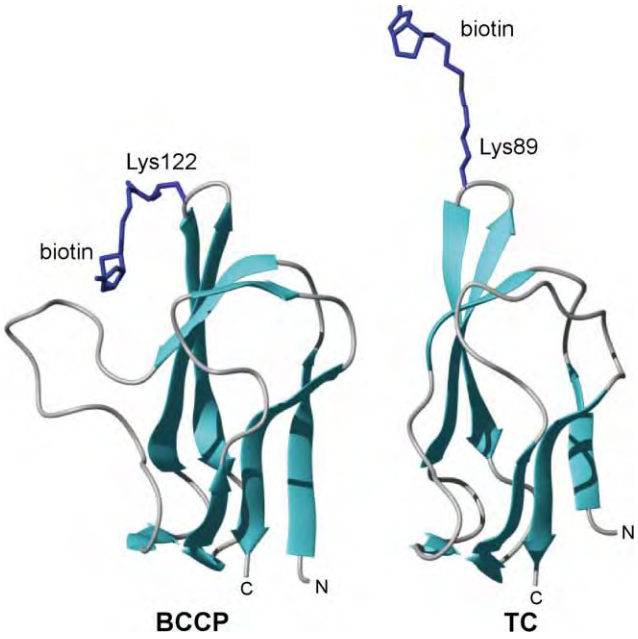

FIGURE 3 Three-dimensional structures of two biotin domains. The structures of the biotin domains from the biotin carboxyl carrier protein (BCCP) of (left) *Escherichia coli* acetyl CoA carboxylase and (right) the 1.3S subunit of *Propionibacterium freudenreichii subsp. shermanii* transcarboxylase (TC) have been determined. The holo forms of the two proteins with the biotin moiety specifically attached to the target lysine residues at position 122 and 89, respectively, are depicted. Solid arrows represent the β-strands in the fold. The amino (N) and carboxyl (C) termini of the domain are indicated. The molecules have been orientated to highlight the interaction of biotin with the "thumb" structure in BCCP.

Therefore, it is possible that the mechanism employed by the biotin-enzymes may involve non-covalent interactions between the protein and the prosthetic group.

Biotin Ligase

Reaction Mechanism

All BPLs catalyze biotinylation through the same reaction mechanism:

$$\text{Biotin} + \text{MgATP} \rightleftharpoons \text{Biotinyl-5}'\text{-AMP} + \text{PPi} \quad (3)$$

$$\text{Biotinyl-5}'\text{-AMP} + \text{apo-protein} \rightarrow \text{biotinylated protein} + \text{AMP} \quad (4)$$

In the first partial reaction, BPLs bind biotin and ATP in an ordered manner (depending on the species) to form an enzyme:biotinyl-5′-AMP complex or holo-BPL. At this stage, the carboxyl group of inert biotin is activated by the addition of an adenylate group forming the intermediate biotinyl-5′-AMP. In the second partial reaction, holo-BPL complexes with an apo-biotin domain. Nucleophilic attack upon the activated biotin by the amine group of the biotin-accepting lysine residue results in the transfer of biotin from the adenylate onto the biotin domain with AMP acting as the leaving group. This two-step process is analogous to the tRNA synthetase catalyzed linkage of amino acids to the 3′ hydroxyl group of tRNAs.

E. coli Biotin Ligase, BirA

The best characterized BPL is the 35.3 kDa protein BirA from *E. coli*. This protein is a bifunctional molecule which, in addition to biotin protein ligase activity, acts as the transcriptional repressor of the biotin biosynthetic operon. By combining regulation of biotin synthesis and metabolism through the actions of a single protein, bacteria have evolved an exceptional mechanism for maintaining biotin homeostasis. Recent structural studies of BirA, together with enzymatic and genetic studies, have provided powerful insights into BirA action. The crystal structure of BirA shows that the protein is composed of three domains: a DNA binding N-terminal domain, a central catalytic domain, and a C-terminal domain (Figure 4). The central domain contains several poorly defined loops that become more ordered upon binding of biotin or biotinyl-5′-AMP.

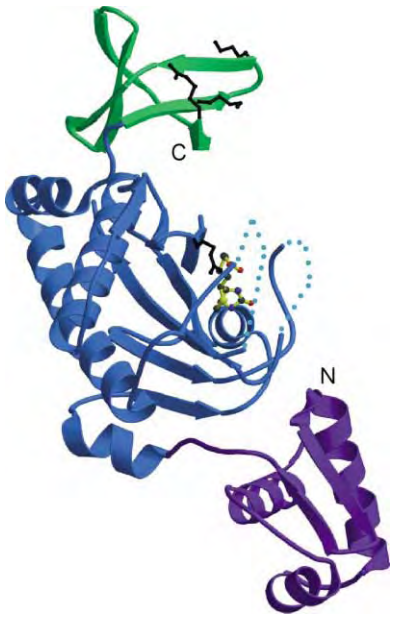

FIGURE 4 The three-dimensional structure of BirA. The diagram shows the structure of *Escherichia coli* biotin protein ligase, BirA, determined by X-ray crystallography. This figure highlights the three functional domains in the bifunctional protein. The N-terminal domain (N), shown in purple, contains a helix-loop-helix fold to facilitate DNA binding. The central catalytic domain (shown in blue) is depicted with biotin (ball and stick representation) bound at the active site. Dots represent the unstructured loops around the active site that become ordered during the reaction. The function of the C-terminal (C) domain (shown in green) is not fully understood. Modified with permission from Chapman-Smith *et al.* (2001), *Protein Sci.* 10, 2608–2617.

Ordering of these loops in the complex results in the generation of an extended β-sheet which is required for the interaction with other proteins. Thus, when complexed with biotinyl-5′-AMP, BirA is competent to participate in one of two competing interactions: either with apo-BCCP or with the 40 base pair operator sequence within the biotin synthesis operon. In the presence of apo-BCCP, monomeric BirA preferentially interacts with this protein substrate and catalyzes biotinylation. In the absence of apo-BCCP, the BirA complex forms the homodimer structure required for DNA binding and thus functions as a transcriptional repressor. Therefore, when *E. coli* needs to produce additional active acetyl-CoA carboxylase, its biotin biosynthetic pathway can be derepressed by the expression of apo-BCCP, thereby allowing the bacteria to balance its nutritional requirements.

See Also the Following Articles

Biotinylation of Proteins • Pyruvate Carboxylation, Transamination and Gluconeogenesis

Glossary

biocytin Biotinylated lysine which is formed between the carboxyl group of biotin and the epsilon amino group on the side chain of lysine.

biotin A small, water soluble vitamin belonging to the B-complex group; it is also known as vitamin H.

biotinidase A mammalian enzyme that can hydrolyze biotin from either biocytin or short biotin-containing peptides thus facilitating recycling of the vitamin.

biotin protein ligase The enzyme [E.C. 6.3.4.15] responsible for covalent attachment of a biotin moiety onto a biotin-enzyme; it is also known as the biotin inducible repressor (BirA) in some prokaryotes and holocarboxylase synthetase in mammalian cells.

Further Reading

Athappilly, F. K., and Hendrickson, W. A. (1995). Structure of the biotinyl domain of acetyl-coenzyme A carboxylase determined by MAD phasing. *Structure* **3**, 1407–1419.

Attwood, P. V. (1995). The structure and the mechanism of action of pyruvate carboxylase. *Int. J. Biochem. Cell Biol.* **27**(3), 231–249.

Attwood, P. V., and Wallace, J. C. (2002). Chemical and catalytic mechanisms of carboxyl transfer reactions in biotin-dependent enzymes. *Acc. Chem. Res.* **35**(2), 113–120.

Chapman-Smith, A., and Cronan, J. E., Jr. (1999). The enzymatic biotinylation of proteins: A post-translational modification of exceptional specificity. *Trends Biol. Sci.* **24**, 359–363.

McMahon, R. J. (2002). Biotin in metabolism and molecular biology. *Annu. Rev. Nutr.* **22**, 221–239.

Pacheco-Alvarez, D., Solorzano-Vargas, R. S., and Del Rio, A. L. (2002). Biotin in metabolism and its relationship to human disease. *Arch. Med. Res.* **33**(5), 439–447.

Reddy, D. V., Shenoy, B. C., Carey, P. R., and Sonnichsen, F. D. (2000). High resolution solution structure of the 1.3S subunit of transcarboxylase from *Propionibacterium shermanii*. *Biochemistry* **39**, 2509–2516.

Roberts, E. L., Shu, N., Howard, M. J., Broodhurst, R. W., Chapman-Smith, A., Wallace, J. C., Morris, T., Cronan, J. E., Jr. and Perham, R. N. (1999). Solution structures of Apo and Holo biotinyl domains from acetyl coenzyme A carboxylase of *Escherichia coli* determined by triple-resonance nuclear magnetic resonance spectroscopy. *Biochemistry* **38**, 5045–5053.

Weaver, L., Kwon, K., Beckett, D., and Matthews, B. W. (2001). Competing protein: Protein interactions are proposed to control the biological switch of the *E. coli* biotin repressor. *Protein Sci.* **10**, 2618–2622.

Wilson, K. P., Shewchuk, L. M., Brennan, R. G., Otsuka, A. J., and Matthews, B. W. (1992). *Escherichia coli* biotin holoenzyme synthetase/*bio* repressor crystal structure delineates the biotin- and DNA-binding domains. *Proc. Natl. Acad. Sci. U. S. A.* **89**, 9257–9261.

Biography

Steven Polyak completed his graduate studies on biotin protein ligase at The University of Adelaide, Australia, in 1999 before commencing a postdoctoral position at The Hanson Institute. He returned to The University of Adelaide in 2001, where he continues to investigate the protein structure and relationships of BPL.

Anne Chapman-Smith completed a Ph.D. working on pyruvate carboxylase in the early 1980s. Since 1990, she has studied the structure and function of the biotin domains of the biotin carboxylases and their interaction with biotin ligase at the University of Adelaide and the University of Illinois at Urbana – Champaign.

Biotinylation of Proteins

Ronald A. Kohanski
The Johns Hopkins University, Baltimore, Maryland, USA

The biotinylation of proteins is the covalent coupling of biotin to an amino acid or carbohydrate moiety of the protein. Biotinylation occurs in a specific group of proteins known as carboxylases. These are enzymes that are important in several metabolic pathways, including amino acid metabolism, fatty acid biosynthesis, and gluconeogenesis. Each of these carboxylases is biotinylated on a single lysyl residue through the action of a biotin:protein ligase, and are found in all organisms (bacteria, plants, and animals). Biotinylation of proteins is also done by *in vitro* chemical synthesis, whereby biotin can be covalently coupled to any reactive functional group on the protein, and is not necessarily restricted to a single amino acid residue.

Analytical and Clinical Applications

Chemically biotinylated proteins are important tools in cell biology, and biochemistry, and have clinical applications. The uses of chemically biotinylated proteins have evolved from the strong interaction between biotin (and its derivatives) and avidin or streptavidin. The medical importance of biotinylated proteins is twofold: (1) life-threatening diseases result from failure to produce adequate levels of endogenous biotinylated proteins. These diseases are particularly serious in newborns and early childhood and (2) the diagnosis and treatment of tumors has been greatly facilitated by chemically biotinylated proteins. As an analytical reagent in cell biology and biochemistry, chemical biotinylation of proteins is in widespread use not only primarily for protein detection and assay, but also for purification. These are considered in greater detail in this article.

Biosynthesis and Degradation of Natively Biotinylated Proteins

The biotinylated proteins native to cells are the biotin-dependent carboxylases: acetyl CoA carboxylase, beta-methylcrotonyl CoA carboxylase, proprionyl CoA carboxylase, and pyruvate carboxylase. The first is a cytosolic protein and the latter three are in the mitochondria. In bacteria, the biotinylated protein is biotin carboxyl carrier protein which is a subunit of bacterial carboxylases. The biosynthesis of naturally biotinylated proteins occurs in two steps. Biotin is activated by reaction with adenosine triphosphate (ATP), releasing pyrophosphate and biotinyl $5'$-adenosine monophosphate. The hydrolysis of pyrophosphate makes this step essentially irreversible under physiological conditions. The transfer of biotin to an ε-amino group of a specific lysyl residue in the acceptor protein is catalyzed by holocarboxylase synthetase (HS) in eukaryotes, and biotin protein ligase (BPL) in bacteria. The specific lysyl residue that is biotinylated is found within a highly conserved structural motif of the apoprotein – the biotin domain – that ranges in length from 67 to 85 amino acids. The biotin domain is an independently folding motif with a core structure of eight β-strands forming two apposing antiparallel β-sheets. Conservation of the catalytic portions of the HS/BPL enzymes and of the biotin domains are so high across evolution that bacterial BPL can recognize and biotinylate mammalian biotin domains, and mammalian HS can recognize and biotinylate bacterial biotin domains. The consensus amino acid sequence surrounding the acceptor lysyl residue is Glu-Ala-Met-Lys-Met, but only the Met-Lys-Met residues are invariant. The conservation of the methionyl residues appears to be dictated by evolutionary pressure to retain a catalytically active carboxylase rather than a recognition site for the synthetase, since Thr or Val can be substituted for these Met residues with little loss of biotinylation but more significant losses in catalytic efficiency of the biotinylated product. In general, it appears that conservation of the β-sheet structure of the biotin domain is as critical for recognition by the ligase as the consensus sequence, but the latter is governed by the need to conserve optimal enzymatic activity in the biotinylated proteins. Thus the two aspects controlling specificity of protein biotinylation are: first, recognition by the ligase and second, enzymatic activity of the biotinylated protein. Biotinylated proteins are degraded by cellular proteases and the biotinylated lysyl residue (biocytin) is the product of that degradation. Biotinidase is the enzyme that cleaves biocytin to biotin and lysine.

Medical Importance of Biotinylated Proteins

Diseases caused by deficiencies in the biotin-dependent carboxylases fall into two general categories based on whether biotin administration is an effective treatment. Those not treatable with biotin are due to genetic lesions in the biotin-dependent carboxylases (OMIM 200350, 210200, 232050, 232000, and 266150 which are described at the National Institutes of Health website http://www.ncbi.nlm.nih.gov/omim), whereas those treatable with biotin are the result of genetic lesions in the synthetase (multiple carboxylase deficiency; OMIM 253270) or biotinidase (OMIM 25360). Clinically the synthetase and biotinidase deficiencies are distinguished by the early (up to three months post-partum) versus late onset of symptoms, respectively. Mutations in holocarboxylase generally cause a raised Michaelis constant for biotin. Thus the treatment with pharmacological doses of biotin is probably successful because the enzyme only requires higher concentrations of biotin for efficient biotinylation of the apoprotein carboxylases. The success of biotin administration when biotinidase is lost indicates the biological importance of recycling biotin from biocytin to maintain sufficient levels of carboxylase activity. The other clinically significant aspect of biotinidase is its ability to degrade radiolabeled biotin derivatives, which are used in conjunction with biotinylated antibodies to image and/or treat tumors.

Chemical Synthesis of Biotinylated Proteins

The usual goal of protein biotinylation is to detect the modified protein with avidin, where the avidin is itself linked to a reporter group (a radionuclide, chromophore, fluorophore, or an enzyme). The detection of biotinylated proteins has been important in Western blots in order to determine the expression of proteins in diverse cells exposed to different stimuli or growth conditions, for the immunocytochemical and immunohistochemical localization of proteins within subcellular compartments or in tissues, and for the identification and tracking of surface-biotinylated proteins. In addition, the immobilized avidin (and derivatives) can be used for affinity capture and purification of biotinylated proteins, or in the capture of receptors using biotinylated ligands. Biotinylation of proteins can be achieved through covalent attachment of a biotin derivative to any freely reactive functional group on a protein. The most commonly used sites include primary amines (α- or ε-amino groups of the N-terminal or lysyl residues, respectively, as illustrated in Figure 1B), thiol

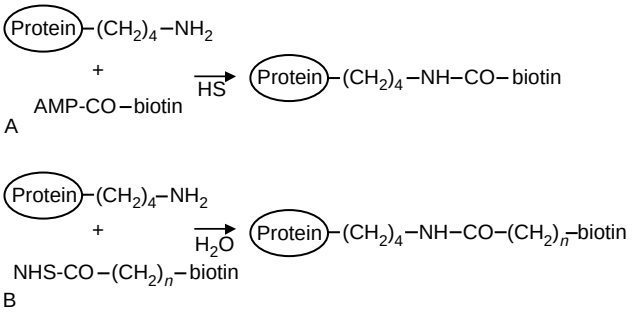

FIGURE 1 Biotinylation of proteins by enzymatic and chemical reactions. (A) The transfer of biotin from AMP to the ε-amino group of a lysyl residue in a protein, catalyzed by holocarboxylase synthetase (HS) forming an amide linkage. (B) The transfer of biotin, with a hydrocarbon spacer of "n" methylene groups from an N-hydroxysuccinimide ester (NHS) to an ε-amino group of a protein in water.

groups (of cysteinyl residues), and carbohydrate groups. The reactive derivatives of biotin for these reactions use N-hydroxysuccinmide esters, iodoacetyl, or disulfide derivatives of biotin, and hydrazide derivatives of biotin, respectively. The critical factor in the useful biotinylation of proteins is allowing avidin to bind the biotinyl group after conjugation. This requires sufficient distance between the surface of the biotinylated protein and avidin, since biotin is bound in a fairly deep pocket in avidin. This problem was solved by Klaus Hofmann, who found that an ε aminocaproyl group offered a sufficiently long spacer group for this purpose, as illustrated in Figure 1. The use of sulfo-N-hydroxysuccinimidyl-esters (sulfo-NHSH esters) for biotin derivitization introduced by James Staros further simplified the use of biotin derivatives because it increased the water-solubility and amine-specificity of the reactive ester. Importantly, the sulfo-NHS esters cannot cross cell membranes, and this permits the selective labeling of cell surface proteins through biotinylation of their extracellular domains.

Clinical Application of Biotinylated Antibodies

Clinically, biotinylated antibodies are in current use for the detection and treatment of tumors, with success in many cases. The multistep procedure can be summarized as follows: biotinylated antibodies against a tumor-specific antigen are introduced into circulation. Binding to the antigen concentrates the biotinylated antibody at the site of the tumor. Avidin or strepavidin is introduced, which binds the pretargeted antibody. Because these are tetramers, at least one biotin-binding site is expected to remain unoccupied in the avidin:biotinylated antibody complex.

A biotin derivative that chelates a radionuclide is then introduced, which is trapped by the open biotin-binding sites on avidin at the site of the tumor. This protocol can be used to visualize the tumor *in vivo* by immunoscintigraphy or positron emission tomography. With the appropriate radionuclide, radiotherapy of the tumor is also achievable. In such protocols, circulating biotinidase plays a counter-productive role, since it can and does break down biocytin analogues. Thus knowledge of the "biotin cycle" of endogenously biotinylated proteins has been important in the clinical application of chemically synthesized biotinylated proteins.

See Also the Following Articles

Biotin • Pyruvate Carboxylation, Transamination and Gluconeogenesis

Glossary

avidin A protein that binds "avidly" to biotin ($K_d < 10^{-15}$ M) and is found in egg whites. A related bacterial protein is streptavidin, from *Streptomyces avidinii*.

biocytin A biotin derivative formed between biotin and lysine. It is formed by the catabolism of carboxylases, and is itself degraded to biotin and lysine by the enzyme biotinidase.

biotin A water-soluble vitamin that is used by carboxylases for transfer of CO_2 groups in biosynthesis. It is bound tightly by the proteins avidin and streptavidin.

Further Reading

Boerman, O. C., van Schaijk, F. G., Oyen, W. J. G., and Corstens, F. H. M. (2003). Pretargeted radioimmunotherapy of cancer: Progress step by step. *J. Nucl. Med.* **124**, 400–411.

Luna, E. J. (2001). Biotinylation of proteins in solution and on cell surfaces. In *Current Protocols in Protein Science* (J. E. Coligan, B. M. Dunn, H. L. Ploegh, D. W. Speicher and P. T. Wingfield, eds.) 1st edition, Vol 3, supplement 6, pp. 3.6.1–3.6.15. Wiley, New York.

Wilchek, M., and Bayer, E. A. (eds.) (1990). Avidin-biotin technology. In *Methods in Enzymology*, Vol 184. Academic Press, San Diego, CA.

Wilchek, M., and Bayer, E. A. (eds.) (1999). (Strept) Avidin-biotin system. In *Biomolecular Engineering*, Vol 16.

Wolf, B. (2001). Disorders of biotin metabolism. In *The Metabolic and Molecular Bases of Inherited Disease* (C. R. Scriver, A. L. Beaudet, W. S. Sly and D. Valle, eds.) 8th edition, Vol 3, pp. 3935–3962. McGraw-Hill, New York.

Biography

Ronald Kohanski received his Ph.D. in Biochemistry in 1981 at the University of Chicago. He was a member of the Department of Biochemistry at the Mount Sinai School of Medicine in New York, from 1986 to 2002, and is currently on the faculty at Johns Hopkins University, in the Department of Pediatrics.

Bradykinin Receptors

Ronald M. Burch
AlgoRx Pharmaceuticals, Inc., Cranbury, New Jersey, USA

Bradykinin is an inflammatory nonapeptide, whose generation in tissues and body fluids elicits numerous physiological effects including vasodilation, edema, smooth muscle contraction, as well as pain and hyperalgesia, by stimulating A- and C-neurons. Bradykinin contributes to inflammatory responses in acute and chronic diseases including allergic reactions, arthritis, asthma, sepsis, viral rhinitis, and inflammatory bowel diseases.

Overview

Most G protein agonists are hormones or neurotransmitters synthesized intracellularly and stored in secretory granules prior to release. In contrast, bradykinin is a member of the kallikrein–kininogen–kinin system, a complex of two substrates (kininogens) activated by two enzymes (kallikreins) to produce four inflammatory mediators (kinins) that bind to two bradykinin receptors (Figure 1). The substrates, high molecular weight (HMW) kininogen and low molecular weight (LMW) kininogen, are α_2 macroglobulins produced by alternative splicing of the same mRNA. HMW kininogen circulates in blood in a 1:1 complex with plasma prekallikrein. Upon tissue injury, factor XII, a component of the coagulation cascade, cleaves plasma prekallikrein to activate it. Plasma kallikrein acts on HMW kininogen to release bradykinin (plasma kallikrein also activates LMW kininogen to produce bradykinin). Tissue kallikrein is synthesized by many types of epithelial cells and secretory cells. Thus, unlike plasma kallikrein, it acts locally. Tissue kallikrein acts only on LMW kininogen and cleaves it one residue to the amino terminus of the site of cleavage of plasma kallikrein to produce a decapeptide, kallidin (or Lys-bradykinin). Bradykinin and kallidin are equipotent agonists of bradykinin B2 receptors and are usually referred to generically as bradykinin or kinins. It should be noted that bradykinin and kallidin are chemically heterogeneous since the proline residues within the peptides may be partially hydroxylated.

Kinins are metabolized further by a variety of enzymes, most of which inactivate them. The major inactivating enzyme is kininase II, especially prevalent in the lungs and in vascular beds, and its activity is largely responsible for the very short half-life of the kinins, about 15 seconds. Kininase II removes the carboxyterminal dipeptide from both bradykinin and kallidin. Kininase II is also known as an angiotensin-converting enzyme because it converts angiotensin I into the vasoconstrictor angiotensin II. Of importance to the present discussion, another enzyme, kininase I, removes the carboxyterminal Arg from bradykinin and kallidin to produce the other two inflammatory mediators, the bradykinin B1 receptor agonists desArg^9-bradykinin and desArg^{10}-kallidin, respectively. Like the agonists of B2 receptors, bradykinin and kallidin, the desArg metabolites have similar potency as agonists of B1 receptors.

Nearly all tissues express B2 receptors, and bradykinin-induced activation of B2 receptors is implicated in many disease states. B1 receptors are expressed in only a few tissues under normal conditions and only in very small numbers. Several disease states are associated with rapid induction of B1 receptors in specific tissues.

B1 Receptor

The existence of a B1 receptor activated by what had been considered an inactive bradykinin metabolite, desArg^9-bradykinin, was a provocative proposal. This receptor was not found in normal tissues, but was found to be induced during incubation of tissues *in vitro*. Identification of a synthetic B1 receptor antagonist, desArg^9, Leu^8-bradykinin, added credence to the existence of a physiologic receptor. Later, induction of B1 receptors was found pharmacologically to be associated with specific disease processes *in vivo*, and in 1994, the existence of the B1 receptor was conclusively confirmed with the cloning of the receptor protein.

B1 receptors have been implicated in hyperalgesia, plasma extravasation, white blood cell activation and accumulation, and in the control of blood pressure. However, it seems certain that complete understanding of the roles of this inducible receptor in pathophysiology is not at hand. B1 receptors from several species have been cloned. They are typical G protein-coupled

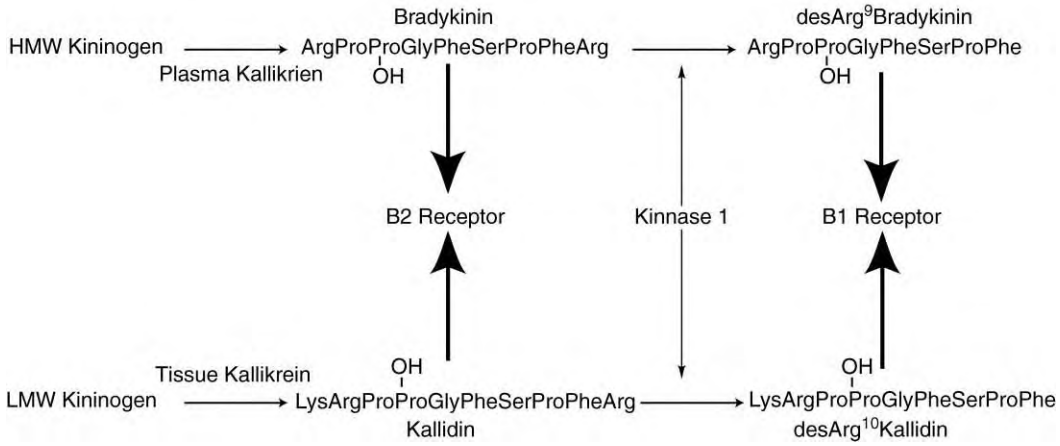

FIGURE 1 Formation of endogenous bradykinin receptor ligands. Bradykinin and kallidin bind to B2 receptors, whereas, desArg^9-bradykinin and desArg^{10}-kallidin bind to B1 receptors. Both bradykinin and kallidin may contain some proline residues that are hydroxylated. If hydroxylated, the most common residue is Pro^3 in bradykinin and Pro^4 in kallidin (shown hydroxylated in the figure).

receptors in sequence. The human receptor has a predicted sequence of 353 amino acids and is only 36% homologous to B2 receptors. The B1 receptor activates phosphatidylinositol-specific phospholipase C and possibly phospholipase A_2.

The B1 receptor gene is composed of three exons. The entire coding region for the receptor is contained within the third exon. A variety of polymorphisms have been identified. One, a G/C single nucleotide polymorphism in the promoter region has been associated with disease. Expression of the C allele is higher than the G allele, and patients with the G allele have greater incidence of inflammatory bowel disease and end-stage renal disease.

B1 Receptor Regulation

Most G protein-coupled receptors are internalized quickly after the binding of their ligands. B1 receptors, however, are not internalized following binding of desArg-kinins. This results in very prolonged activation of signal transduction, which translates into rather few receptors per cell being necessary for biological activity when compared to many other G protein-coupled receptors. Ligand binding studies in a variety of tissues reveal only hundreds to a few thousand B1 receptors per cell, whereas most G protein-coupled receptors, including B2 receptors, are found in the tens of thousands per cell.

In contrast to prolonged phosphatidylinositol turnover, B1 receptor-mediated arachidonic acid release and prostaglandin synthesis is short-lived, which is similar to B2 receptors. The mechanism for this differential desensitization is unknown, but it may be linked to sequestered pools of arachidonate-containing phospholipids or phosphorylation of an intracellular binding site for a transduction protein.

B1 receptors have been shown by immunoprecipitation studies to couple to $G\alpha q$ and $G\alpha i$. These G proteins commonly couple receptors to phosphatylinositol-specific phospholipase C and elevation of intracellular free calcium activity. Activation of B1 receptors leads to elevation of intracellular free calcium activity by increasing calcium entry into the cell; this is in contrast to the B2 receptor which acts primarily to release bound intracellular calcium.

Regulation of B1 Receptor Induction

Unlike many G protein-coupled receptors, the primary regulation of the B1 receptor number appears to occur by transcriptional induction. Biological studies have found that B1 receptor expression is induced by a variety of cytokines including endotoxin, interleukin 1β, and tumor necrosis factor. The specific domains affected by these stimulating ligands have not been identified, but activation of B1 receptor transcription has been correlated to activation of the transcription factor NF-κB.

The regulation of the B1 receptor gene has also been shown to be regulated by stabilization of mRNA. Interleukin 1 treatment of cells has been demonstrated to double the half-life of B1 receptor mRNA. In addition, protein synthesis inhibitors increase B1 receptor gene stability, suggesting the existence of a short-lived protein that causes destabilization. This protein may interact with the 3′ untranslated region, since experimentally altering the 3′ untranslated region results in B1 receptor mRNA's with varying half-lives.

B1 Receptor Knockout Animals

B1 receptor knockout mice have been reported to develop normally and to have normal blood pressure. In contrast, when inflammatory stimuli are applied, a dramatic reduction in accumulation and apoptosis of neutrophils have been reported, as well as hypoalgesia; this is consistent with pharmacological evidence presented in the past.

B2 Receptors

B2 receptors mediate bronchoconstriction, local blood flow regulation, hypotension, acute inflammatory reactions, pain, and hyperalgesia. B2 receptors from several species have been cloned. Like B1 receptors, they are typical G protein-coupled receptors in sequence. The human receptor has a predicted sequence of 364 amino acids. Both B1 and B2 receptors are found on chromosome 14 in humans, only about 12 kb apart. Like B1 receptors, B2 receptors activate phosphotidylinositol-specific phospholipase C. In addition, in most tissues, B2 receptor activation results in the production of prostaglandins and other arachidonic acid metabolites.

The B2 receptor gene is composed of three exons, of which exon 2 and exon 3 provide the coding region for the receptor. Bradykinin has been implicated in hypertension for decades. To date, nearly 80 single nucleotide polymorphisms have been identified for the B2 receptor. The promoter region for the B2 receptor contains a single nucleotide polymorphism, T/C. The C allele has been demonstrated to be an independent risk factor for essential hypertension in several ethnic groups. Several other alleles have been reported and were found to be differentially associated with several disease states. Expansion of these observations promises the potential to define the role of bradykinin in a variety of physiologic and pathophysiologic states.

B2 Receptor Regulation

In contrast to the B1 receptor, B2 receptor number does not seem to be significantly regulated by inducible gene expression. Instead, B2 receptors are constitutively expressed, as is the case for many G protein-coupled receptors. Activation of the B2 receptor by binding of bradykinin results in rapid internalization of the receptor protein by endocytosis, occurring within a few minutes. Internalization results in cessation of the biological activity of the receptor. Thus, activation of a particular B2 receptor results in a transient increase in intracellular calcium activity and transient prostaglandin release. Receptors are recycled intracellularly, with stripping of bradykinin and the return of a reactivated B2 receptor to the cell surface where it may be reactivated. Most G protein-coupled receptors are internalized following attachment to arrestin and dynamin-dependent clathrin-coated vesicles. In contrast, the B2 receptor becomes associated with caveolae.

B2 Signal Transduction

B2 receptors have been demonstrated to activate all of the signal transduction mechanisms described for G protein-coupled receptors (Figure 2). Any given cell type supports only a few of the transduction pathways, and these are primarily controlled by the specific G proteins expressed by the given cell type. B2 receptors have been shown by immunoprecipitation studies to couple to Gαq, which mediates interaction with phosphatidylinositol-specific phospholipase C. B2 receptors have also been shown by immunoprecipitation to couple to Gαi. G protein depletion studies have suggested that Gαi(2) and Gαi(3) couple B2 receptors to arachidonic acid release, presumably through the activation of phospholipase A_2. In contrast to B1 receptors, activation of B2 receptors results in increased intracellular calcium activity from the release of calcium from intracellular stores.

B2 Receptor Knockout Animals

Studies with B2 receptor knockout mice have shown that the animals develop normally. However, one study found that when animals are fed a high-salt diet, severe hypertension occurs. It has also been reported that the

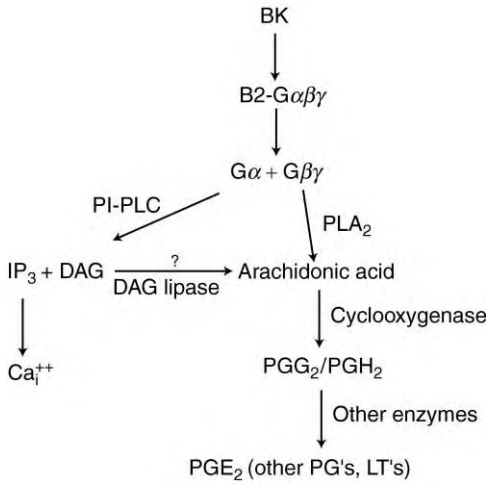

FIGURE 2 Signal transduction elicited by B2 receptors: BK, bradykinin or kallidin; PLA_2, phospholipase A_2; IP_3, inositol trisphosphate; DAG, diacylglycerol; PG, prostaglandin; LT, leukotriene. Not shown is phospholipase D, which in some cells provides a shuttle for arachidonic acid to appropriate subtrates for hormone-sensitive phosphlipase A_2. In most cells, bradykinin does not directly alter cAMP concentration; often, this occurs as a consequence of PGE_2 binding to its receptor.

renin–angiotensin system was abnormal (the kallikrein–kinin system and the renin–angiotensin system are antagonistic hemodynamic regulatory systems that play important roles in blood pressure homeostasis) and abnormal renal development occurred. A variety of cardiac defects have also been reported as well as chronically elevated heart rate.

Other Bradykinin Receptors

Many pharmacologic studies using bradykinin analogs have yielded data suggestive of additional bradykinin receptors, or at least heterogeneity of bradykinin receptors. For example, in smooth muscle preparations there is evidence for expression of different B2-like receptors expressed by the smooth muscle and the neuronal endings in the smooth muscle. Similarly, "B3" receptors have been reported in trachea, and "B4" and "B5" receptors have been reported in opossum esophagus. A criticism of all of these studies is the use of rather weak bradykinin analogs, with dissociation constants of several nM, compared to pM dissociation constant for bradykinin itself. No genetic evidence for additional receptors beyond B1 and B2 has been obtained to date.

Bradykinin Receptor Antagonists in Clinical Medicine

While highly potent peptide antagonists for B1 receptors have been described, none to date have been evaluated in clinical trials. In contrast, several peptide antagonists for B2 receptors have been evaluated as anti-inflammatory agents, including NPC 567 and Hoe 140. In addition, several nonpeptide antagonists of B2 receptors have been described. An issue that has slowed clinical development of such antagonists is the observation that bradykinin appears to play an important role in coronary artery function. It has been suggested that antagonism of B2 receptors in patients with coronary artery disease may have deleterious effects during ischemic events, perhaps even triggering myocardial infarction.

See Also the Following Articles

Angiotensin Receptors • G Protein-Coupled Receptor Kinases and Arrestins • Inositol Phosphate Kinases and Phosphatases • Phospholipase A_2 • Prostaglandins and Leukotrienes

Glossary

angiotensin Peptide produced by the action of the enzyme renin on the protein angiotensinogen.

G protein Trimeric complex of α, β, and γ subunits. Activation of a G protein-coupled receptor results in dissociation of the Gα subunit, which in turn activates signaling proteins such as adenylyl cyclase, certain ion channels, and phospholipases. The activity of the Gα subunit is terminated by endogenous GTPase activity, followed by reassociation of the Gα with G$\beta\gamma$ subunit.

ischemia Loss of blood flow with resultant metabolic insufficiency of a tissue bed.

myocardial infarction Death of heart muscle following prolonged, complete ischemia.

prostaglandin Autocoid (local hormone) produced by the action of cyclooxygenase 1 or cyclooxygenase 2 on arachidonic acid. A variety of prostaglandins may be produced, each with specific biological actions elicited by binding to cell-surface receptors.

single nucleotide polymorphism Difference at a specific place in a DNA sequence of a single nucleotide. The two gene variants are alleles.

Further Reading

Ausitn, C. E., Faussner, A., Robinson, H. E., Chakravarty, S., Kyle, D. J., Bathon, J. M., and Proud, D. (1997). Stable expression of the human kinin B1 receptor in chinese hamster ovary cells. *J. Biol. Chem.* **272**, 11420–11425.

Burch, R. M. (ed.) (1991). *Bradykinin Antagonists. Basic and Clinical Research*. Dekker, New York.

Burch, R. M., and Kyle, D. J. (1992). Recent developments in the understanding of bradykinin receptors. *Life Sci* **50**, 829–838.

Marceau, F., and Bachvarov, D. R. (1998). Kinin receptors. *Clin. Rev. Allergy Immunol* **16**, 385–401.

Prado, G. N., Taylor, L., Zhou, X., Ricupero, D., Mierke, D. F., and Polgar, P. (2002). Mechanisms regulating the expression, self-maintenance, and signaling-function of the bradykinin B2 and B1 receptors. *J. Cell. Physiol* **193**, 275–286.

Regoli, D., and Barabe, J. (1980). *Pharmacol. Rev.* **32**, 1–46.

Biography

Ronald M. Burch is President and Chief Executive Officer of AlgoRx Pharmaceuticals, Inc. His primary research interests are in the mechanisms of pain transmission and immunotherapeutics, both are areas in which bradykinin play roles. He holds a Ph.D. in pharmacology and M.D., both obtained from the Medical University of South Carolina.

Branched-Chain α-Ketoacids

David T. Chuang
University of Texas Southwestern Medical Center, Dallas, Texas, USA

The branched-chain α-ketoacids (BCKAs) comprise α-keto-isocaproate (KIC), α-keto-β-methylisovalerate (KMV), and α-ketoisovalerate (KIV) that are derived from branched-chain amino acids (BCAAs) leucine, isoleucine, and valine, respectively, through reversible transamination. The oxidative decarboxylation of these three BCKAs is catalyzed by a single branched-chain α-ketoacid dehydrogenase (BCKD) complex to give rise to various branched-chain acyl-CoAs (reaction [1]).

$$\text{R–CO–COOH} + \text{CoA-SH} + \text{NAD}^+ \rightarrow \text{R–CO–S–CoA} + \text{CO}_2\uparrow + \text{NADH} + \text{H}^+ \quad [1]$$

In patients with the inherited Maple Syrup Urine Disease (MSUD), the activity of the BCKD complex is deficient. This metabolic block results in the accumulation of BCAAs and BCKAs. Clinical manifestations include neonatal or later onset of often-fatal ketoacidosis, encephalopathy and other acute and chronic neurological dysfunction as well as mental retardation in survivors. A distinct phenotype is the strong maple syrup odor in the urine of patients, and hence the name of the disease. There are currently five clinical phenotypes associated with MSUD: classic, intermediate, intermittent, thiamin-responsive and E3-deficient. The prevalence of MSUD is one in 185 000 live births worldwide.

Degradative Pathways of BCAAs

The oxidation of BCAAs leucine, isoleucine, and valine begins with the transport of these amino acids into cells through the Na^+-independent L transporter in the plasma membrane. In the cell, the BCAAs undergo the first transamination step catalyzed by BCAA aminotransferases (BCATs), which are either cytosolic or mitochondrial, to produce BCKAs (Figure 1). The second step, i.e., the oxidative decarboxylation of BCKAs catalyzed by the mammalian BCKD complex, occurs exclusively in mitochondria. The reaction products of KIC, KMV, and KIV are isovaleryl-CoA, α-methylbutyryl-CoA, and isobutyryl-CoA, respectively. These branched-chain acyl-CoAs subsequently undergo the third step, i.e., dehydrogenation by specific acyl-CoA dehydrogenases. The dehydrogenation of isovaleryl-CoA is catalyzed by isovaleryl-CoA dehydrogenase; and of α-methylbutyryl-CoA as well as isobutyryl-CoA is carried out by α-methyl branched-chain acyl-CoA dehydrogenase. After these three steps, the degradative pathways for each of BCKAs diverge. Leucine yields acetyl-CoA and acetoacetate as end products, and is therefore a ketogenic amino acid. Valine produces succinyl-CoA, and is accordingly glucogenic. Succinyl-CoA enters the Krebs cycle, and is eventually converted to glucose by gluconeogenesis. Isoleucine is both ketogenic and glucogenic since it is metabolized to acetyl-CoA and succinyl-CoA.

Interorgan Relationships

Oxidation of BCAAs involves extensive interplay of metabolites between muscle and liver in the rat. This is due to the nonuniform distribution of BCATs and the BCKD complex among organs and tissues. In rat skeletal muscle, BCAT activity is high, but the BCKD complex activity is low. A reverse situation exists in rat liver with respect to levels of the two enzyme activities. Both rat liver and heart degrade BCKAs at high rates, but in hepatectomized rats leucine oxidation is decreased. This led to the prevailing view, based on the rat model, that the primary role of muscle is transamination of BCAAs, which provides the major source of circulating BCKAs. BCKAs are transported to liver, kidney, and heart, where they are oxidized. However, the interorgan shuttling of BCAA metabolites may not occur in humans. It was shown recently that the BCKD complex activity in human liver is similar to that in skeletal muscle. The results confirm an earlier observation that BCKD complex activity in human liver and kidney was markedly lower than in the rat counterparts, but activity in skeletal muscle was similar between two species. The human liver exhibits twice as high BCAT activity as human skeletal muscle. This finding suggests that human liver is capable of oxidizing BCAAs *in situ* and does not depend on BCAT activity in skeletal muscle for the conversion of BCAAs to BCKAs. Since skeletal muscle comprises 40% of the body mass, this tissue is likely the major site for BCAA oxidation in humans.

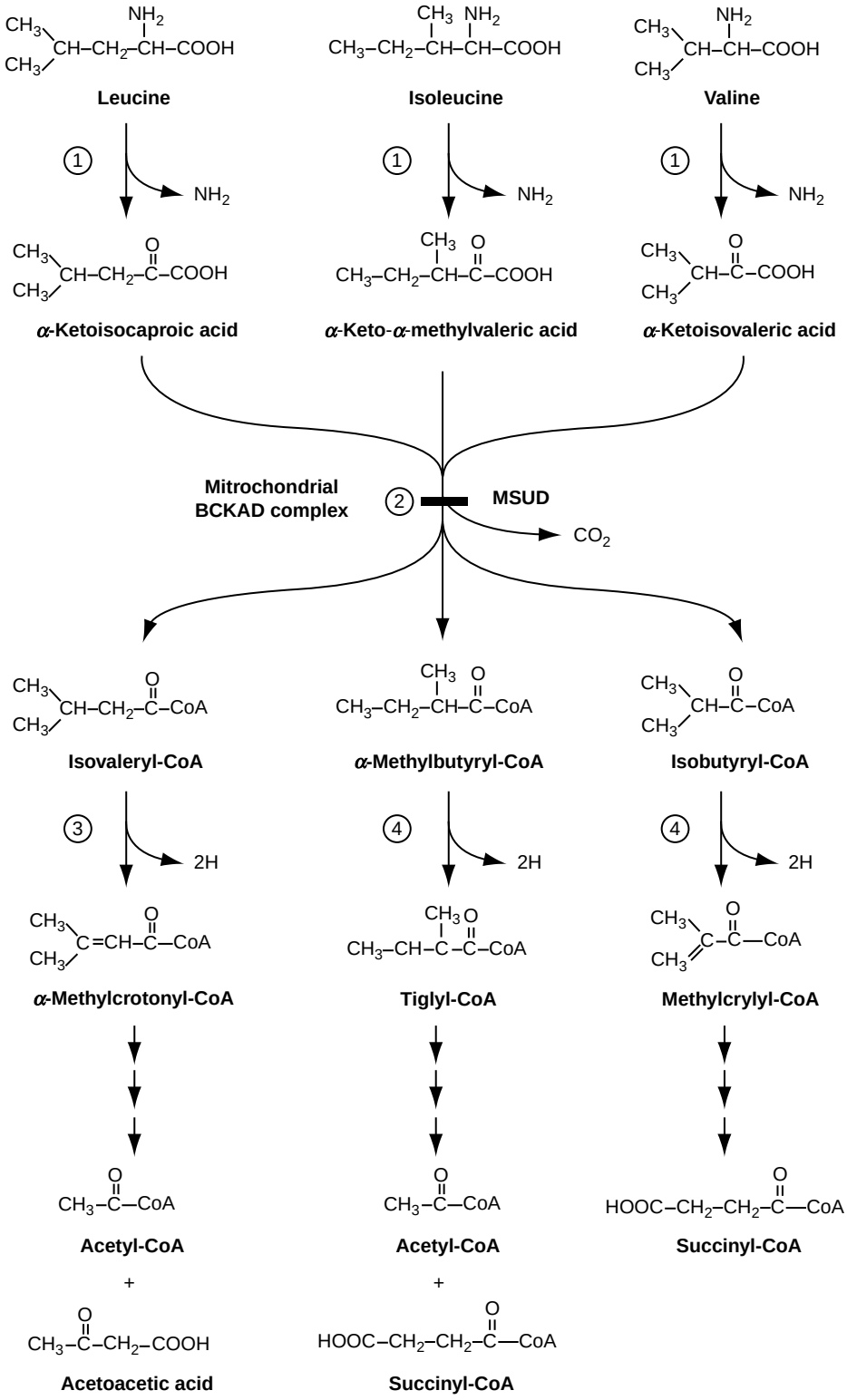

FIGURE 1 Catabolic pathways for the branched-chain amino acids (BCAAs) leucine, isoleucine, and valine. The first three common reactions are catalyzed by the following enzymes: reversible transamination by BCAA aminotransferases (1), oxidative decarboxylation of BCKAs and esterification of CoASH by the single mitochondrial branched-chain α-ketoacid dehydrogenase (BCKD) complex (2) and dehydrogenation by isovaleryl-CoA dehydrogenase (3) or α-methyl branched-chain acyl-CoA dehydrogenase (4). After these steps the degradation pathway for each amino acid diverges. As end products, leucine yields acetyl-CoA and acetoacetic acid; isoleucine produces acetyl-CoA and succinyl-CoA; and valine is converted exclusively to succinyl-CoA. The solid horizontal bar (center) depicts the metabolic block imposed by Maple Syrup Urine Disease mutations in the BCKD complex.

Regulation of BCAA and BCKA Oxidation

The oxidation of BCAAs and BCKAs is tightly regulated but exhibits tissue-specific patterns. The plasma concentrations of BCAAs and BCKAs are elevated in starvation and in clinical conditions such as diabetes mellitus, obesity, and MSUD. Paradoxically, BCAA oxidation is accelerated in muscles from fasted and diabetic rats. Epinephrine (10^{-5}–10^{-6} M) and glucagon (2×10^{-8}–5×10^{-9} M) were shown to also stimulate BCAA oxidation in the heart and hemidiaphragms of rats. Insulin decreases the oxidation of BCKAs in striated muscle of fed rats, whereas the same hormone increases oxidative decarboxylation of the ketoacids during starvation. Clofibrate administration augments BCAA oxidation in muscle, but inhibits their degradation in liver. Carnitine, ketone bodies, hexanoate, and octanoate increase the oxidation of leucine by skeletal muscle, while pyruvate and decanoate exert inhibitory effects. The metabolism of KIC in isolated rat hepatocytes is inhibited by fatty acids, KIV, KMV, and pyruvate. The mechanism of regulation for BCAA and BCKA oxidation was not fully elucidated in the above earlier studies. However, it has now become clear that these controls are through alteration in activity state or the degree of de-phosphorylation of the BCKD complex.

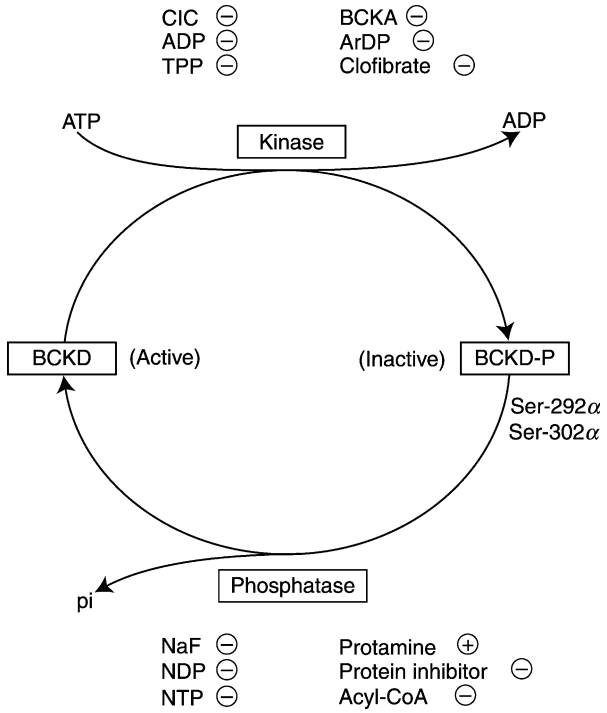

FIGURE 2 Regulation of the BCKD complex by the phosphorylation–dephosphorylation cycle. Phosphorylation at Ser-292 and Ser-302 of the E1α subunit by BCKD kinase in the presence of ATP results in the inactivation of the BCKD complex. Removal of the phosphate group on E1 converts the BCKD complex back to the active form. Inhibitors (−) and activators (+) for each enzyme are shown. CIC, α-chloroisocaproate; ArDP, arylidene pyruvate; NDP, nucleoside diphosphate; NTP, nucleoside triphosphate.

The Macromolecular Organization of the BCKD Complex

The mammalian BCKD complex is a member of the highly conserved α-ketoacid dehydrogenase complexes comprising pyruvate dehydrogenase complex (PDC), α-ketoglutarate dehydrogenase complex (α-KGDC), and the BCKD complex with similar structure and function. The mammalian BCKD multi-enzyme complex consists of three catalytic components: a heterotetrameric ($\alpha_2\beta_2$) branched-chain α-ketoacid decarboxylase or E1, a homo-24 meric dihydrolipoyl transacylase or E2, and a homodimeric dihydrolipoamide dehydrogenase or E3. The E1 and E2 components are specific for the BCKD complex, whereas the E3 component is common among the three α-ketoacid dehydrogenase complexes. In addition, the mammalian BCKD complex contains two regulatory enzymes: the specific kinase and the specific phosphatase that regulate activity of the BCKD complex through phosphorylation (inactivation)/dephosphorylation (activation) cycles (Figure 2). The six subunits with their cofactors and prosthetic groups that make up the mammalian BCKD complex are shown in Table I. Three-dimensional structures for the E1 and kinase components and the lipoyl-bearing and subunit-binding domains of the E2 component of the mammalian BCKD complex have been determined. The BCKD complex is organized around a cubic E2 core, to which 12 copies of E1, up to six copies of E3, and unknown numbers of the kinase and the phosphatase are attached through ionic interactions (Figure 3). The molecular mass of the BCKD multienzyme complex is estimated to be 4×10^6 Da. The purified bovine E1–E2 subcomplex has a sedimentation coefficient ($S_{20,w}$) of 40 S. The E3 component has low affinity for the E2 core, and was mostly lost during purification of the mammalian BCKD complex.

The reaction steps catalyzed by the three enzyme components are also shown in Figure 3. The E1 component catalyzes a thiamin diphosphate (ThDP)-mediated decarboxylation of the α-ketoacids and the subsequent reduction of the lipoyl moiety, which is covalently bound to E2. The reduced lipoyl moiety and the lipoyl domain serve as a "swinging arm" to transfer the acyl group from E1 to CoA giving rise to acyl-CoA. Finally, the E3-component with tightly bound flavin adenine dinucleotide (FAD) reoxidizes the dihydrolipoyl residue of E2 with NAD^+ as the ultimate electron

TABLE I

Component Enzymes and Subunit Composition of the Mammalian Branched-Chain α-Ketoacid Dehydrogenase (BCKD) Complex

Component	Molecular mass (Da)	Prosthetic group (P) and cofactor (C)
BCKA decarboxylase (E1)	1.7×10^5 ($\alpha_2\beta_2$)	ThDP (C)
α-Subunit	46 500	Mg^{2+} (C)
β-Subunit	37 200	K^+
Dihydrolipoyl transacylase (E2)	1.1×10^6 (α_{24})	Lipoic acid (P)
Subunit	46 518[a]	
Dihydrolipoyl dehydrogenase (E3)	1.1×10^5 (α_2)	FAD (C)
Subunit	55 000	
BCKD kinase	1.8×10^5 (α_4)	Mg^{2+} (C)
Subunit	43 000	
BCKD phosphatase	4.6×10^5 (?)	None
Subunit	33 000	

BCKA, branched-chain α-ketoacid; ThDP, thiamin diphosphate.
[a]Calculated from the amino acid composition deduced from a bovine E2 cDNA. The E2-subnit migrates anomalously as a 52 kDa species in SDS-PAGE.

acceptor. The net or overall reaction is the production of a branched-chain acyl-CoA, CO_2 and NADH from a α-ketoacid, CoA and NAD^+ (see reaction [1]).

Dietary and Hormonal Regulation of the BCKD Complex

The regulation of BCKA oxidation was shown to be at the BCKD complex step by using inhibitors such as oleate and palmitoyl carnitine. The mammalian BCKD complex is predominantly regulated by the reversible phosphorylation of the Ser-292 and Ser-302 residues in the E1α subunit. The activity state of the BCKD complex in different tissues is the ratio of the actual activity of a partially de-phosphorylated form to the maximal activity of the fully de-phosphorylated form. Thus, the activity state represents the percentage of the total BCKD complex that is active in a given tissue or cell type. Recent studies showed that the activity state of the BCKD complex in human tissues is 40% in heart, 26% in skeletal muscle, 28% in liver, and only 14% in kidney. Rats fed with low-protein diets show a reduction in the activity state, but not the amount, of the BCKD complex in hepatocytes, compared to chow-fed rats. The decrease in activity state inversely correlates with an increase in the amounts of the BCKD kinase protein and mRNA in rat liver. Starvation, exercise, and diabetes stimulate the activity of the BCKD complex in skeletal muscle by increasing the proportion of active or de-phosphorylated enzyme. Recently, it was shown that glucocorticoids cause a marked reduction in the BCKD kinase mRNA level in rat hepatoma cells and rat liver with a concomitant increase in the activity state of the BCKD complex. Glucocorticoids and acidification also significantly increase the activity state of the BCKD complex in pig kidney cells expressing the hormone receptor.

Brain Neuropathology of BCKAs

The BCAAs, in particular leucine, are rapidly transported into the brain and actively metabolized. It was proposed that a leucine–glutamate cycle which plays an important role in maintaining a steady supply of glutamate, a major excitatory neurotransmitter for inter-neuronal communication. The BCAAs are nitrogen donors for glutamate synthesis in astrocytes, a major site of BCAA transamination. The amino group is transferred to α-ketoglutarate to yield glutamate. This amino acid, in turn, is converted to glutamine. ^{15}N-labeled BCAA studies showed that at least one-third of the amino groups of brain glutamate are derived from BCAAs. The BCKAs may be released from astrocytes to the extracellular fluid and taken up by neurons. Although neurons can oxidize KIC, it is preferentially reaminated to leucine. The flux of the reverse transamination in rat cortical synaptosomes is several times greater than the rate of nitrogen transfer from leucine to glutamate. This is in contrast to the flux in astrocytes which is mainly for glutamate synthesis. In the leucine oxidative pathway, acetoacetyl-CoA is generated for ketone synthesis or for cleavage to acetyl-CoA to enter the tricarboxylic acid cycle.

In the classic form of MSUD, the excess BCAAs and BCKAs are likely to interfere with the neuronal and astrocytic metabolism. BCKAs accumulated in MSUD compromise brain energy metabolism by blocking the respiratory chain and inhibiting creatine kinase activity. Perfusion by microdialysis with leucine and KIV has created a microenvironment similar to that found in MSUD. The infusion of leucine resulted in an increase of large neutral amino acids in the extra-cellular space, thereby a decreased concentration in neurons. The infusion of KIC caused an 11-fold increase in leucine and two- to threefold increase in other large neutral amino acids in the extracellular space. This pattern is consistent with active transamination of KIC to leucine. These changes could affect biosynthesis of serotonin and catecholamines, and alter the homeostasis of the leucine/glutamate cycle and the glutamate/glutamine cycle in brain.

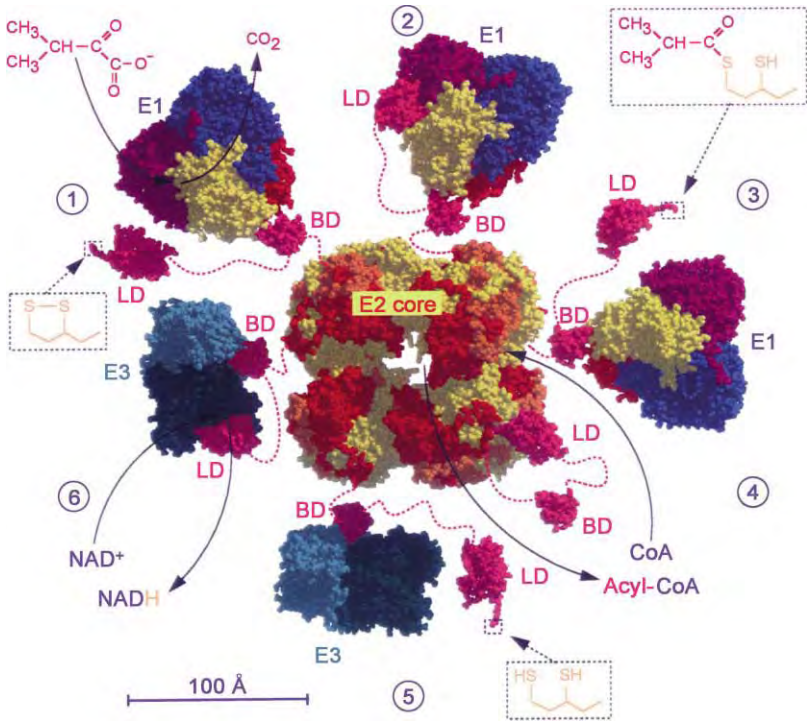

FIGURE 3 Model for structural organization and individual component reactions of the BCKD complex. The macromolecular structure (4×10^6 Da in size) is organized about a cubic transacylase (E2) core (based on the structure of *Azotobacter* pyruvate dehydrogenase E2), to which a decarboxylase (E1) (based upon *Pseudomonas* BCKD E1 structure), a dehydrogenase (E3) (according to the structure of *Azotobacter* pyruvate dehydrogenase E3) are attached through ionic interactions. E2 of the BCKD complex contains 24 identical subunits with each polypeptide made up of three folded domains: lipoyl (LD), E1/E3-binding (BD), and the E2 core domains that are linked by flexible regions (represented by dotted lines). E1 $\alpha_2\beta_2$ heterotetramers or E3 homodimers are attached to BD. The BCKD kinase and BCKD phosphatase (not shown) bind to LD. E1 catalyzes the ThDP-mediated oxidative decarboxylation of α-ketoacids. The ThDP-hydroxyacylidene moiety is transferred to a reduced lipoyl prosthetic group (in the box) on LD. The flexible LD carries S-acyldihydrolipoamide to the active site in the E2 core to generate acyl-CoA. The reduced lipoyl moiety on LD is oxidized by E3 on BD with the concomitant reduction of NAD^+. The sum of the above component reactions is the oxidative decarboxylation of BCKAs (reaction [1] in the text).

See Also the Following Articles

Amino Acid Metabolism • Pyruvate Carboxylation, Transamination and Gluconeogenesis • Pyruvate Dehydrogenase

Glossary

activity state The ratio of the actual (partially de-phosphorylated) activity to the maximal (fully de-phosphorylated) activity of the mammalian mitochondrial branched-chain α-ketoacid (BCKD) complex. The activity state represents % of the total BCKD complex that is active in a tissue under defined physiological conditions.

ketoacidosis A clinical condition associated with the accumulation of the branched-chain α-ketoacids derived from branched-chain amino acids leucine, isoleucine and valine present in dietary proteins. This pathological state is presented by patients with the Maple Syrup Urine Disease caused by congenital defects in the BCKD complex.

oxidative decarboxylation The removal of a CO_2 group from a molecule by a decarboxylase/dehydrogenase with a concomitant transfer of electrons from the substrate to a biological electron acceptor. For the branched-chain α-ketoacids, this reaction is catalyzed by the BCKD complex coupled with the reduction of NAD^+.

phosphorylation The posttranslational modification of a protein or enzyme molecule by a specific kinase, in which the γ-phosphoryl group from ATP is incorporated into a serine, threonine or tyrosine residue of the protein/enzyme as a means to regulate its biological activity.

transamination A reversible enzymatic reaction that converts an amino acid into a corresponding α-ketoacid. For branched-chain amino acids, this reaction is carried out by the distinct isozymes of branched-chain aminotransferase both in the cytoplasm and the mitochondrion.

Further Reading

Chuang, D. T., and Shih, V. E. (2001). Maple syrup urine disease (Branched-chain ketoaciduria). In *The Metabolic and Molecular Bases of Inherited Disease* (C. R. Scriver, A. L. Beaudet, W. S. Sly and D. Valle, eds.) 8th edition, pp. 1971–2006. McGraw-Hill, New York.

Harper, A. E., Miller, R. H., and Block, K. P. (1984). Branched-chain amino acid metabolism. *Annu. Rev. Nutr.* **4**, 409–454.

Harris, R. A., Hawes, J. W., Popou, K. M., Zhao, Y., Shimomura, Y., Sato, J., Jaskiewicz, J., and Hurley, T. D. (1997). Studies on the regulation of the mitochondrial α-ketoacid dehydro-

genase complexes and their kinases. *Adv. Enzyme Regul.* **37**, 271–293.

Perham, R. N. (2000). Swinging arms and swinging domains in multifunctional enzymes: Catalytic machines for multistep reactions. *Annu. Rev. Biochem.* **69**, 961–1004.

Reed, L. J., Damuni, Z., and Merryfield, M. L. (1985). Regulation of mammalian pyruvate and branched-chain α-keto acid dehydrogenase complexes by phosphorylation–dephosphorylation. *Curr. Topics Cell. Regul.* **27**, 41–49.

Yudkoff, M. (1997). Brain metabolism of branched-chain aminoacids. *Glia* **21**, 92–98.

Biography

David T. Chuang is a professor in the Department of biochemistry at the University of Texas Southwestern Medical Center in Dallas. His principal research interests are in the structure/function and molecular genetics of the human branched-chain α-ketoacid dehydrogenase (BCKD) complex. His laboratory determined three-dimensional structures for components and domains of the human BCKD complex, and characterized mutations in the BCKD genes of patients with the inherited Maple Syrup Urine Disease.

Brassinosteroids

Steven D. Clouse
North Carolina State University, Raleigh, North Carolina, USA

Brassinosteroids (BRs) are endogenous plant growth-promoting hormones that function at low concentrations to influence cellular expansion and proliferation, while interacting with other plant hormones and environmental factors to regulate the overall form and function of the plant. BRs are found throughout the plant kingdom in seeds, pollen, and young vegetative tissue, and the examination of the phenotype of mutants affected in BR biosynthesis or signaling provides genetic evidence that BRs are essential for normal organ elongation, vascular differentiation, male fertility, timing of senescence, leaf development, and responses to light. BRs are unique among plant hormones in their close structural similarity to vertebrate and invertebrate steroid hormones, which have well-known roles in regulating embryonic and postembryonic development and adult homeostasis in mammals and insects.

Brassinosteroid Structure and Natural Occurrence

BRs have been identified throughout the plant kingdom as naturally occurring compounds in monocot and dicot angiosperms, gymnosperms, algae, and pteridophytes. At least 40 free BRs and four conjugates have been rigorously characterized from plant tissue by a variety of biochemical approaches.

Discovery and Chemical Structure of Brassinolide

The discovery of brassinolide, the most active natural BR currently identified, was preceded by three decades of experiments at the United States Department of Agriculture (USDA) in which organic extracts of pollen from over 60 species were applied to a variety of crop plants to identify new compounds with growth-promoting properties. An extract from *Brassica napus* pollen was extremely potent in promoting cell elongation and division in bean second internodes and enhanced overall growth of radishes, leafy vegetables, and potatoes when young seedlings were sprayed in greenhouse experiments. USDA researchers identified the active component of the *B. napus* extract in 1979 and named the novel compound brassinolide. It was determined by single-crystal X-ray analysis to be a polyhydroxylated derivative of 5α-cholestane, namely (22*R*,23*R*,24*S*)-2α,3α,22,23-tetrahydroxy-24-methyl-B-homo-7-oxa-5α-cholestan-6-one (Figure 1).

Other BRs differ from brassinolide by variations at C-2 and C-3, the presence of a ketone or de-oxo function instead of a lactone at C-6, various substitutions at C-24, and the stereochemistry of the hydroxyl groups in the side chain. Known BR conjugates include glycosylated, myristylated, and laurylated derivatives of the hydroxyls at C-2 and C-3 or in the side chain. Many BRs are biosynthetic precursors or metabolic products of brassinolide, although some of these BRs are believed to have independent biological activity in specific plants.

Endogenous Levels of BRs in the Plant Kingdom

Endogenous levels of BRs vary according to plant organ type, tissue age, and species, with pollen and immature seeds containing the highest levels, followed by young growing shoots. Pollen and immature seeds generally show BR levels of 1–100 ng g^{-1} fw; shoots and leaves typically have lower amounts, 0.01–0.1 ng g^{-1} fw. BRs are isolated from plant tissues by organic solvent extraction followed by reverse-phase high-performance liquid chromatography (HPLC). Accurate quantification of endogenous levels involves spiking with deuterated forms of the BR of interest followed by gas chromatography–mass spectrometry with selected ion monitoring (GC–MS–SIM) analysis of derivatized BR samples.

Brassinosteroid Biosynthesis

The BR biosynthetic pathway can be divided into general sterol synthesis (cycloartenol to campesterol) and the BR-specific pathway from campesterol to brassinolide. Details of the pathway have been obtained by following the fate of labeled intermediates fed to cell-suspension cultures and whole plants, and by measuring

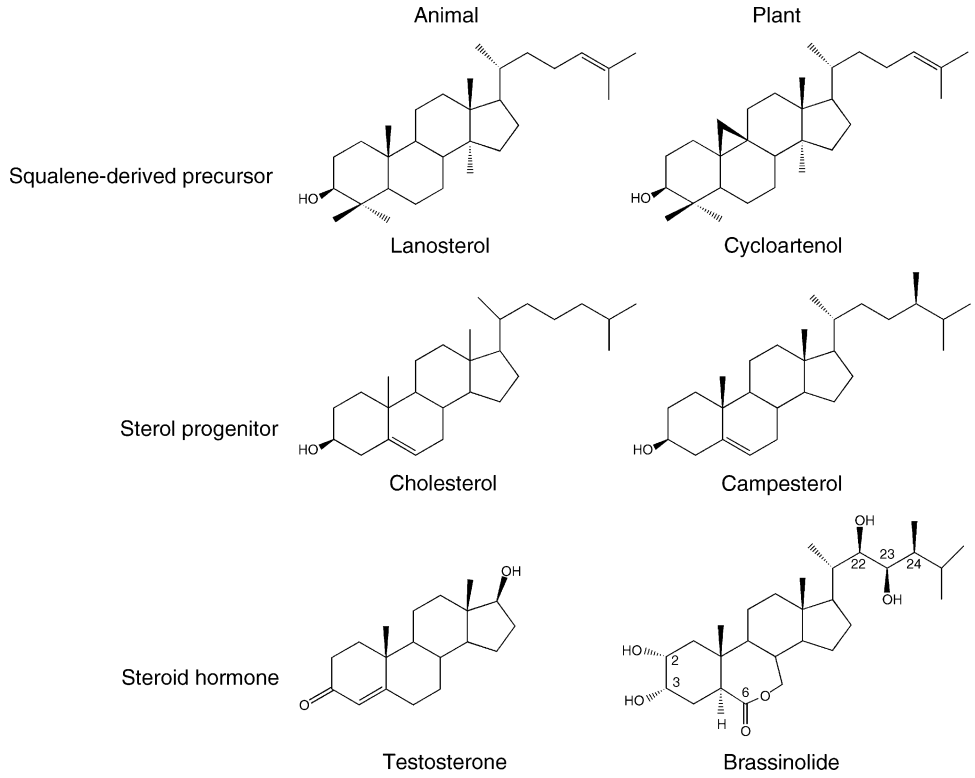

FIGURE 1 Structure of brassinolide and its sterol progenitor is compared with the animal steroid hormone testosterone and its sterol progenitor.

endogenous sterol and BR levels in biosynthetic mutants blocked at various steps of the pathway.

Mevalonic Acid to Cycloartenol

Like animal steroids, BRs are products of the isoprenoid biosynthetic pathway beginning with acetyl-CoA and proceeding through intermediates such as mevalonate, isopentenyl pyrophosphate, farnesyl pyrophosphate, and squalene-2,3-epoxide. It appears that the biosynthetic steps from mevalonate to squalene-2,3-epoxide are conserved among the phyla, but in animals and fungi squalene-2,3-epoxide is converted to lanosterol, the precursor of cholesterol, whereas in plants it is converted to cycloartenol, the progenitor of the plant sterols campesterol, stigmasterol, and sitosterol (Figure 1).

Cycloartenol to Campesterol

The conversion of cycloartenol to campesterol begins with C-24 alkylation of the side chain catalyzed by the enzyme sterol methyl transferase 1 (SMT1) in the presence of S-adenosylmethionine. The product, 24-methylenecycloartenol, is converted to 24-methylenelophenol in a series of steps including a C-14 sterol reductase and a Δ^7–Δ^8 sterol isomerase, encoded in *Arabidopsis* by the *FACKEL* and *HYDRA1* genes, respectively. Mutants in the *SMT1*, *FACKEL*, and *HYDRA1* genes show dwarfism and severe defects in embryogenesis and vascular development that are not rescued by BR treatment, possibly because the early sterol pathway may produce a non-BR signaling molecule that is critical for these developmental processes.

The conversion of 24-methylenelophenol to campesterol involves a Δ^7-C-5-desaturase, encoded by *DWARF7* (*DWF7*); a Δ^7-sterol reductase, encoded by *DWARF5* (*DWF5*); and a C-24 sterol reductase, encoded by *DWARF1* (*DWF1*). *Arabidopsis dwf7*, *dwf5*, and *dwf1* mutants are intermediate dwarfs with altered vascular development and have reduced BR levels. These developmental defects can be rescued by treatment with exogenous BRs.

Campesterol to Brassinolide

Four reactions lead from campesterol to campestanol via reduction of the C-5 double bond (Figure 2). One of these steps requires a 5α-steroid reductase (encoded by the *DE-ETIOLATED2*, *DET2*, gene) that is an orthologue of the mammalian enzyme that catalyzes the NADPH-dependent reduction of testosterone to dihydrotestosterone. From campestanol, two biosynthetic routes are possible: early C-6 oxidation, in which a ketone is introduced at C-6 before the hydroxylation of the side chain, and late C-6 oxidation, in which the side chain is

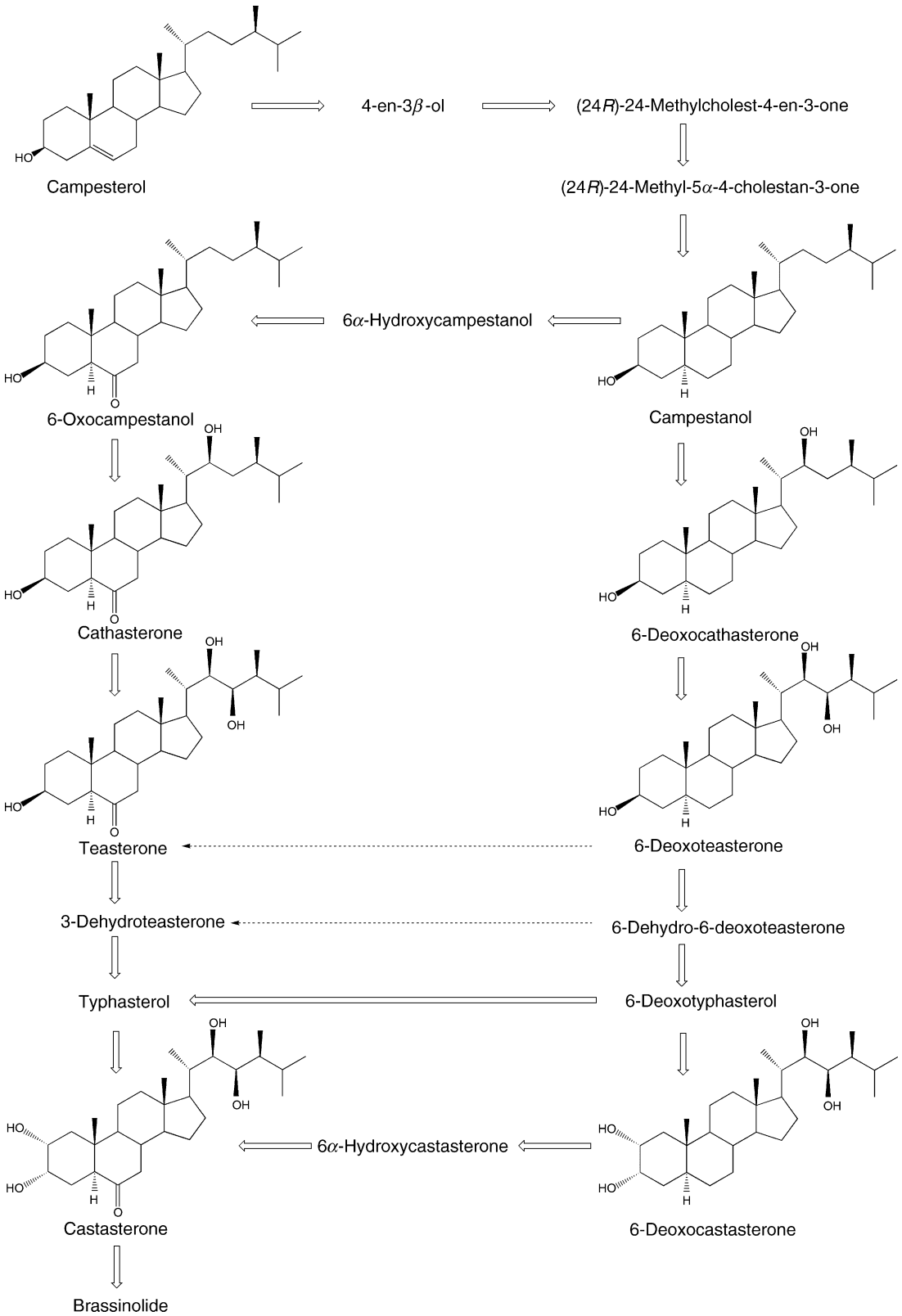

FIGURE 2 Biosynthetic pathway leading from the plant sterol campesterol to brassinolide. From campestanol, two alternative pathways exist, early C-6 oxidation (left) and late C-6 oxidation (right). Several points of interconnection are possible between the two pathways.

modified first and the ketone is introduced in the penultimate step. Many plants, including *Arabidopsis*, have both pathways functional, whereas others, such as tomato, appear to use only late C-6 oxidation. Hydroxylation of the side chain in either pathway occurs via successive steps involving the cytochrome P-450 steroid hydroxylases DWARF4 (DWF4) and CONSTITUTIVE PHOTOMORPHISM AND DWARFISM (CPD).

The *det2*, *dwf4*, and *cpd* mutants of *Arabidopsis* are extremely dwarf in stature; have dark-green, rounded, and downward-curling leaves; and exhibit a prolonged life span with reduced fertility and altered vascular development. In the dark, these mutants show some of the features of light-grown plants, including shortened hypocotyls and open cotyledons. All these phenotypic alterations can be rescued to wild type by exogenous application of brassinolide or BR intermediates downstream of the biosynthetic block caused by the mutant.

Brassinosteroid Physiology

BRs have a dramatic positive effect on stem elongation, promoting epicotyl, hypocotyl, and peduncle elongation in dicots and enhancing coleoptile and mesocotyl growth in monocots. Exogenous BRs also stimulate tracheary element differentiation and numerous studies *in vivo* suggest that endogenous BRs are essential for normal vascular development. In many systems, BRs increase rates of cell division, particularly under conditions of limiting auxin and cytokinin. BRs also promote seed germination, accelerate senescence, cause hyperpolarization of membranes, stimulate ATPase activity, and alter the orientation of cortical microtubules. In addition to effects on growth, BRs also mediate the effects of abiotic and biotic stresses, including salt and drought stress, temperature extremes, and pathogen attack.

Brassinosteroid Signal Transduction

Recently it has been shown that animal steroids can be recognized by cell-surface receptors. However, the classic signaling pathway for these hormones involves binding the steroid to an intracellular receptor consisting of a variable N-terminal domain, a highly conserved DNA-binding domain with two zinc-fingers, and a multifunctional domain that mediates ligand-binding, dimerization, and ligand-dependent transcriptional activation. The completed genome sequence of *Arabidopsis thaliana* indicates that plants do not contain members of this superfamily of intracellular steroid receptors, suggesting that cell-surface recognition is the primary, if not only, form of plant steroid perception. Thus, plant and animal steroid hormones share many structural and functional features, but differ in their primary signaling pathways.

Receptor Kinases and BR Perception

The best characterized component of BR signal transduction is *BRASSINOSTEROID INSENSITIVE 1* (*BRI1*), a single genetic locus in *Arabidopsis* encoding a leucine-rich repeat receptor kinase. Homologous genes have been identified in rice, tomato, and pea. Numerous *bri1* mutant alleles have been identified by various genetic screens, most of which exhibit the extreme dwarfism and other phenotypic characteristics of severe BR-deficient mutants. In contrast to the biosynthetic mutants, *bri1* mutants cannot be rescued by BR treatment, consistent with their role in signal transduction.

The BRI1 protein consists of a putative signal peptide followed by the extracellular domain proper including a leucine zipper and 25 leucine-rich repeats that are flanked by short sequences containing paired cysteines. A 70-amino-acid island that is critical for biological function is embedded between repeats 21 and 22. Downstream of the extracellular domain lies a short hydrophobic single-pass transmembrane domain, followed by the juxtamembrane region and the cytoplasmic Ser-Thr kinase domain. Binding studies with radiolabeled brassinolide and microsomal fractions of wild-type, mutant, and transgenic *Arabidopsis* plants clearly shows that BRI1 is an essential component of the BR receptor complex. Whether it binds BR directly or in association with other sterol-binding proteins is currently unclear.

The mechanism of action of many animal receptor kinases involves ligand-mediated homo- or heterodimerization of the receptor followed by autophosphorylation of the intracellular kinase domain. This activation of the kinase results in the recognition and phosphorylation of downstream signaling components, leading ultimately to the regulation of specific gene expression. Plant receptor kinases appear to follow the same general paradigm of receptor kinase action, and mutational analysis shows that both a functional extracellular domain and an active cytoplasmic kinase are essential for BRI1 function.

With respect to BRI1 and BR signaling, recent evidence suggests that heterodimerization with another leucine-rich repeat receptor kinase may play an important role. BAK1 (BRI1 associated receptor kinase 1) shares similar structural organization to BRI except that it has only five leucine-rich repeats in its extracellular domain and lacks the 70-amino-acid island of BRI1. BAK1 is expressed in all tissues of the plant, similar to the global expression pattern of BRI1, and confocal laser

microscopy of transgenic plants expressing fusion proteins shows plasma membrane localization for both BRI1 and BAK1. Direct physical interaction between BRI1 and BAK1 was confirmed in yeast cells and *Arabidopsis* plants by co-immunoprecipitation experiments and genetic studies strongly suggest that BAK1 plays an important role in BR signaling.

Downstream Components

Both BRI1 and BAK1 have been shown to possess kinase activity *in vitro*, and they can autophosphorylate themselves and transphosphorylate one another. Other *in vitro* substrates of the BRI1 kinase have been identified, but no *in vivo* cytoplasmic substrates of either BRI1 or BAK1 have been characterized thus far. An element further downstream from BRI1/BAK1 is the BIN2 (brassinosteroid insensitive 2) kinase, a negative regulator of BR signal transduction. BIN2, which is homologous to insect and mammalian shaggy-like kinases involved in the Wingless/Wnt signaling pathways, most likely acts by phosphorylating two related cytoplasmic proteins, BZR1 and BES1. Phosphorylation by BIN2 targets BZR1 and BES1 for proteasome-mediated degradation. In the presence of BR, BIN2 activity is apparently inhibited and the nonphosphorylated forms of BZR1 and BES1 accumulate and move to the nucleus where they interact with unknown transcription factors to regulate the expression of specific genes involved in the BR response. Our current knowledge of BR signal transduction is summarized in Figure 3.

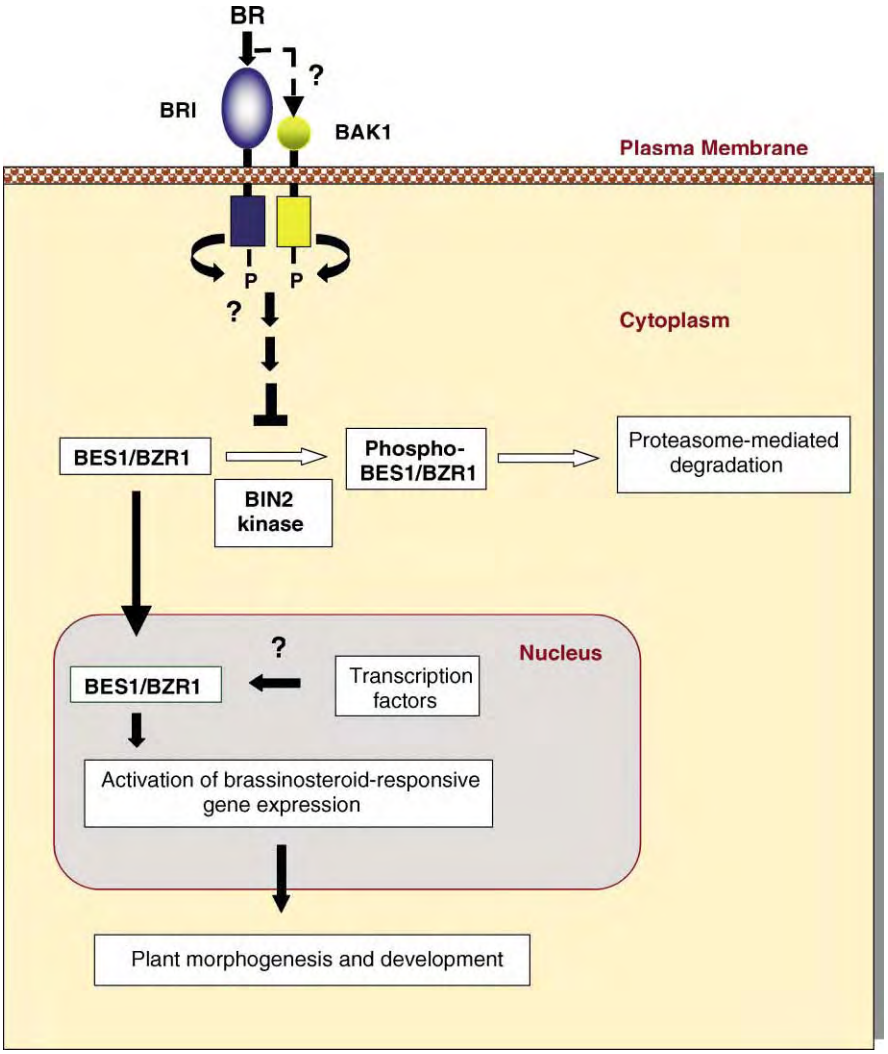

FIGURE 3 A model for BR signal transduction in *Arabidopsis*. BR binds to BRI1 or the BRI1/BAK1 heterodimer and initiates a signaling cascade that inactivates the BIN2 kinase. This allows accumulation and nuclear localization of the unphosphorylated forms of the positive regulators BES1 and BZR1. Question marks indicate proposed but uncharacterized steps. Adapted from *Molecular Cell*, Vol. 10, S. D. Clouse, Brassinosteroid Signal Transduction, pp. 973–982, Copyright 2002, with permission from Elsevier.

See Also the Following Articles

Cholesterol Synthesis • G Protein-Coupled Receptor Kinases and Arrestins

Glossary

brassinolide The most active brassinosteroid. It affects cell elongation and division at nanomolar levels. A unique polyhydroxylated steroid with a C-6, C-7 lactone.

gas chromatography–mass spectrometry with selected ion monitoring (GC–MS–SIM) Technique used with deuterated standards to determine endogenous levels of brassinosteroids in plants.

receptor kinase A signal-transduction protein with multiple domains, including an extracellular ligand-binding domain, a membrane-anchoring region, and an intracellular kinase. Numerous receptor kinases occur in various cell types in both plants and animals.

Further Reading

Altmann, T. (1999). Molecular physiology of brassinosteroids revealed by the analysis of mutants. *Planta* **208**, 1–11.

Bishop, G. J., and Koncz, C. (2002). Brassinosteroids and plant steroid hormone signaling. *Plant Cell* **14**, S97–S110.

Clouse, S. D. (2002). Brassinosteroid signal transduction: Clarifying the pathway from ligand perception to gene expression. *Mol. Cell* **10**, 973–982.

Clouse, S. D., and Sasse, J. M. (1998). Brassinosteroids: Essential regulators of plant growth and development. *Annu. Rev. Plant Physiol. Plant Mol. Biol.* **49**, 427–451.

Sakurai, A., Yokota, T., and Clouse, S. D. (eds.) (1999). *Brassinosteroids: Steroidal Plant Hormones*. Springer, Tokyo.

Biography

Steven D. Clouse is a Professor in the Department of Horticultural Science at North Carolina State University in Raleigh. His principal research interests are brassinosteroid signal transduction and the regulation of gene expression by plant steroids. He holds a Ph.D. from the University of California, Davis and received his postdoctoral training at the Salk Institute for Biological Studies in La Jolla, California. His group cloned some of the first BR-regulated genes and was the first to identify the *bri*1 mutant, which is the focus of much current BR signal transduction research.

Cadherin Signaling

David B. Sacks and Jonathan M.G. Higgins
Brigham and Women's Hospital and Harvard Medical School, Boston, Massachusetts, USA

The associations of cells with one another regulate many cellular processes. Adherens junctions are specialized adhesive structures between cells that are formed by cadherin-dependent interactions. Cadherins are a family of Ca^{2+}-dependent intercellular adhesion molecules linked to the cytoskeleton. Cadherins are also signaling molecules that convey information from the environment to the interior of the cell. In addition, signals from inside the cell can modulate adhesion through cadherins. These forms of cadherin signaling, together with their ability to support adhesion, allow cadherins to participate in coordinating many aspects of cellular organization.

The Cadherin Family

The cadherin superfamily includes six main subfamilies. These are type-I (or classical) cadherins, type-II (atypical) cadherins, desmocollins, desmogleins, protocadherins, and Flamingo cadherins.

Classical and Atypical Cadherins

Classical cadherins like E-, N-, and P-cadherin are components of adherens junctions between cells. The most highly characterized is E-cadherin, which is predominantly expressed in epithelium. The classical cadherins are single-span transmembrane proteins with a highly conserved carboxy-terminal cytoplasmic domain and five extracellular domains, termed cadherin repeats. Ca^{2+} binding to the extracellular domain induces homophilic adhesion with cadherin molecules on adjacent cells. The cytoplasmic tail of cadherin associates with the actin cytoskeleton via proteins called catenins. Cadherin binds β-catenin or γ-catenin (also termed plakoglobin), which in turn bind to α-catenin (Figure 1). The interaction of α-catenin with the actin cytoskeleton strengthens the intercellular adherens junction. Another catenin, termed $p120^{ctn}$, also binds to the cadherin tail in the cytoplasm. The closely related atypical cadherins have similar properties.

Desmosomal Cadherins

Desmocollins and desmogleins are components of desmosomes, which are sites of cell–cell adhesion in tissues subjected to mechanical strain (e.g., epidermis and the myocardium). The overall structure of these desmosomal cadherins resembles that of the classical cadherins, but their cytoplasmic tails are linked to the intermediate filaments of the cytoskeleton.

Protocadherins

The protocadherin family members have as many as seven extracellular Ca^{2+}-binding domains, a transmembrane region and divergent cytoplasmic domains. They appear to participate in development, and may have a particularly important role in the central nervous system.

Other Cadherins

Other cadherins range from those with seven transmembrane segments (such as Flamingo) to T-cadherin, which lacks both transmembrane and cytoplasmic regions.

Functions of Cadherin Signaling

Originally described exclusively as cell adhesion proteins, cadherins have been shown to influence multiple aspects of cell behavior. Indeed, cadherins can transmit signals across the cellular membrane into the interior to modulate cell function. While many members of the cadherin family are likely to share this capacity, to date only members of the classical and atypical cadherin families have been studied in detail and they will be the focus of this article.

Signaling Triggered by Cell–Cell Contact

Signaling can be triggered when cadherins attach to other cadherins on adjacent cells, allowing information about the external environment to be conveyed into the cell. For example, most normal cells grown in culture dishes will reproduce until they form a single continuous layer. A process known as "contact inhibition" then prevents further cell division. Cadherin–cadherin junctions

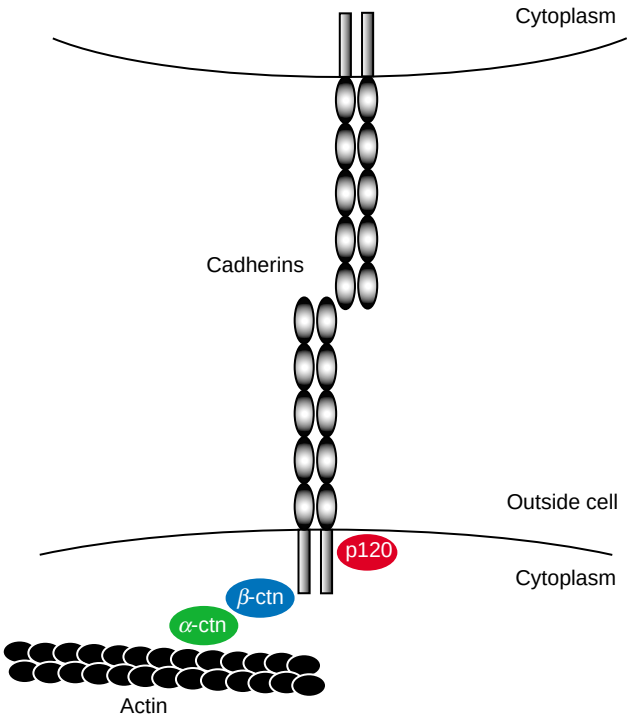

FIGURE 1 Schematic model of a cadherin-mediated adherens junction. Cadherins on adjacent cells interact with one another to provide intercellular adhesion. The terminal portion of the cytoplasmic tail of cadherin binds to β-catenin (β-ctn) or γ-catenin (not shown), which in turn binds to α-catenin (α-ctn). The interaction of α-catenin with the actin cytoskeleton stabilizes the adherens junction. Another catenin, $p120^{ctn}$ (p120), interacts with the cytoplasmic portion of the cadherin tail near the cell membrane.

between cells produce a signal that leads to contact inhibition and renders the cells insensitive to the stimulatory effects of growth factors. Signals generated by interactions between cadherins are also implicated in the formation of desmosomal cell junctions, nerve outgrowth, establishment of cell polarity, cytoskeletal organization, tissue formation, cell differentiation, cell movement, and regulation of gene expression.

Influence of Cadherin Level on Signaling

The amount of cadherin present on the cell surface may influence the signals generated. For example, expression of high levels of E-cadherin can inhibit cell motility and cell division and induce cell polarity. These effects have led to the description of E-cadherin as a tumor suppressor. In fact, loss of functional E-cadherin is often associated with epithelial tumor progression and invasion. Regulation of E-cadherin gene transcription alters the total amount of E-cadherin protein in cells during morphogenic processes such as hair follicle development. The level of E-cadherin on the cell surface also can be specifically regulated. These changes are likely to modulate not only the adhesive properties of the cell, but also the signals that the cell receives through contacts with other cells. In some cases, alterations in the level of cadherin may regulate cellular function even in the absence of cadherin–cadherin interactions between cells.

Different Signaling Properties of Various Cadherins

It is notable that the different types of cadherins induce different changes in cell behavior. For example, while E-cadherin usually reduces the motility of a cell, the presence of N-cadherin or cadherin-11 has the opposite effect, enhancing the ability of cells to crawl over surfaces and invade tissue. It is clear that the various cadherins trigger different signaling pathways. These differences are likely to play a critical role in the regulated changes in cell behavior that occur during early animal development ("embryogenesis"). A striking example of this sort of change occurs when cells undergo "epithelial–mesenchymal transitions." This process occurs during tissue remodeling when relatively sedentary epithelial cells with stable adherens junctions transform into more motile and invasive mesenchymal cells in order to migrate and form new tissue structures. These events are frequently accompanied by a switch in cadherin expression, for example, from E-cadherin to N-cadherin. Similar changes occur during malignant transformation. Most human cancers arise from epithelial cells. These cells normally express E-cadherin. In many cases, expression of functional E-cadherin is lost during malignant transformation, and anomalous expression of N-cadherin or cadherin-11 occurs. These changes may contribute to the increased growth rate, and increased migratory and invasive capacity of cancer cells.

Inside-Out Cadherin Signaling

It is also apparent that the adhesiveness of cell surface cadherins can be modulated from within the cell in the absence of changes in the level of cadherin expression. Therefore, cadherins are able to transduce both "outside-in" and "inside-out" signals. Feedback between these two types of signals is critical to allow the correct formation and disassembly of cadherin–cadherin junctions during morphogenesis and for the continuous remodeling of adherens junctions that occurs even in sedentary cells.

Mechanisms of Cadherin Signaling

Considerable progress has been made in describing cadherin signaling. Classical and atypical cadherins

interact with several signaling molecules, but the molecular mechanisms that constitute the signaling pathways are not completely understood. Three major signaling pathways have been described.

Rho Family GTPase Signaling

An important target of cadherin signaling is the cytoskeleton. This dynamic scaffold of rod-like actin must be rearranged to allow cells to form junctions with other cells and for cells to move. Members of the Rho family of small GTPases are vital regulators of these events, and they are activated in response to the formation of cadherin-mediated cell junctions. Changes in the activity of the Rho family GTPases also lead to alterations in the adhesive capacity of cadherins. Thus, communication between cadherin and Rho GTPases is bidirectional. In general, GTPases serve as switches that are "on" when bound to GTP and "off" when the bound GTP is hydrolyzed to GDP. The best-characterized members of the Rho family are Cdc42, Rac1, and RhoA.

Cdc42 induces the formation of filopodia or microspikes, small finger-like projections from the cell that are needed for the first steps of adherens junction formation by cadherins. Cdc42 is activated upon the assembly of E-cadherin-mediated cell junctions (Figure 2). This mechanism perhaps allows E-cadherin to initiate signals that in turn further stimulate adherens junction formation. Cdc42 also activates the so-called PAR/atypical protein kinase (aPKC) complex and thereby stimulates cell polarity and tight junction formation.

Rac1 is activated rapidly in response to cadherin binding. Active Rac1 stimulates remodeling of the actin cytoskeleton that leads to the formation of cell membrane protrusions known as lamellipodia. This change in morphology may help extend the contact zone between cells, enhancing formation of stable adherens junctions. Activated Cdc42 or Rac1 can also influence the function of a protein known as IQGAP1. High levels of IQGAP1 in a cell decrease E-cadherin-mediated adhesion, perhaps by binding β-catenin, thus displacing α-catenin from the E-cadherin–β-catenin complex.

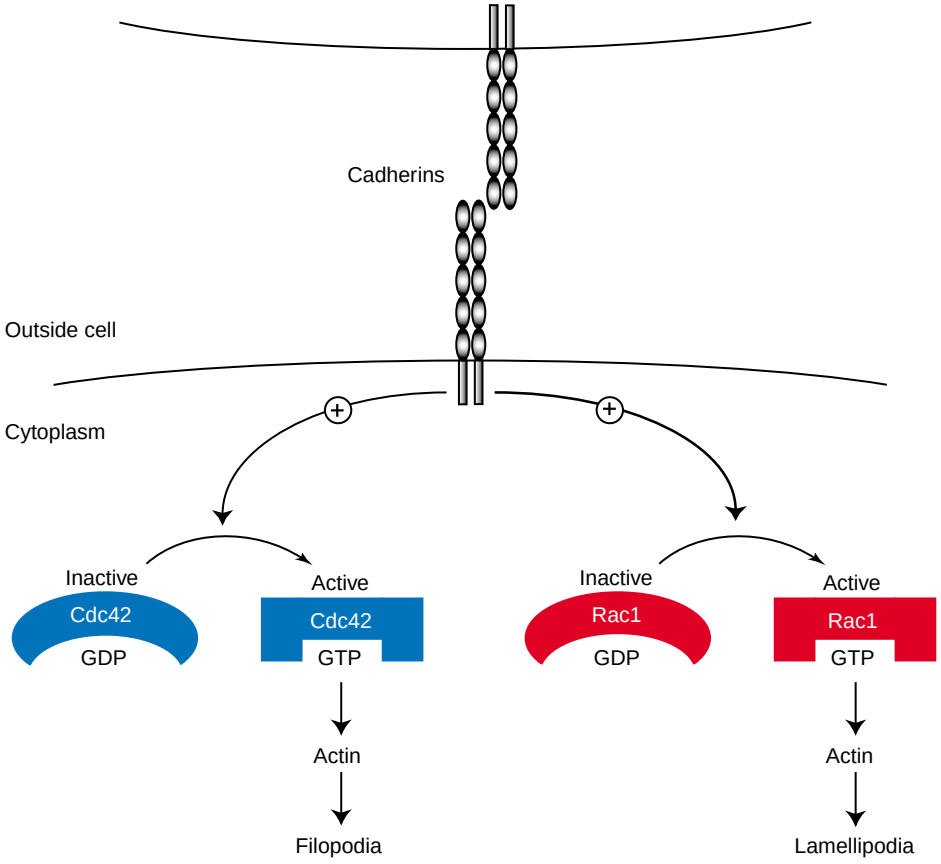

FIGURE 2 Cadherin-mediated adhesion activates Rho family GTPases. The formation of cadherin contacts between cells leads to the activation of Cdc42 and Rac1 (i.e., generation of GTP-bound forms). In the active state, Cdc42 and Rac1 cause alterations in the actin cytoskeleton that lead to the generation of finger-like filopodia and membrane ruffles known as lamellipodia, respectively. These events lead to changes in both the ability of cells to adhere to their surroundings and in cell migration, and can increase the stability of the cadherin-mediated junctions themselves.

Activated Cdc42 or Rac1 can bind to IQGAP1 and counteract this activity, thereby increasing the adhesive capacity of cadherins.

Activation of RhoA leads to the formation of stress fibers. Active RhoA influences E-cadherin function and appears necessary for maintenance of adherens junctions. Moreover, cadherin signals can modulate the activity of RhoA. Thus, cadherin can regulate the actin cytoskeleton by multiple mechanisms.

The transition from the off to the on state of GTPases can be brought about by guanine nucleotide exchange factors (GEFs) that cause the displacement of GDP from the GTPase, and replacement with GTP. Conversely, GTPase activating proteins (GAPs) enhance the conversion of GTP to GDP, so inactivating the GTPase. It is likely that cadherin-mediated adhesion leads to the activation of GEFs, or perhaps the inactivation of GAPs, for Cdc42 and Rac1. RhoA may be regulated by direct interactions with $p120^{ctn}$.

Wnt/β-Catenin Signaling

In addition to linking the cytoplasmic tails of cadherins to the actin cytoskeleton (see Figure 1), β-catenin is an important component of a signaling pathway involved in both normal development and cancer. Normally, β-catenin molecules not attached to cadherins are degraded in the cytoplasm. When cells are exposed to an extracellular growth factor known as Wnt, β-catenin is protected from degradation and accumulates in the nucleus (Figure 3). There, in association with the TCF/LEF family of DNA-binding proteins, β-catenin activates the transcription of genes that stimulate cell proliferation. Thus, the extent to which β-catenin is "soaked up" by binding to

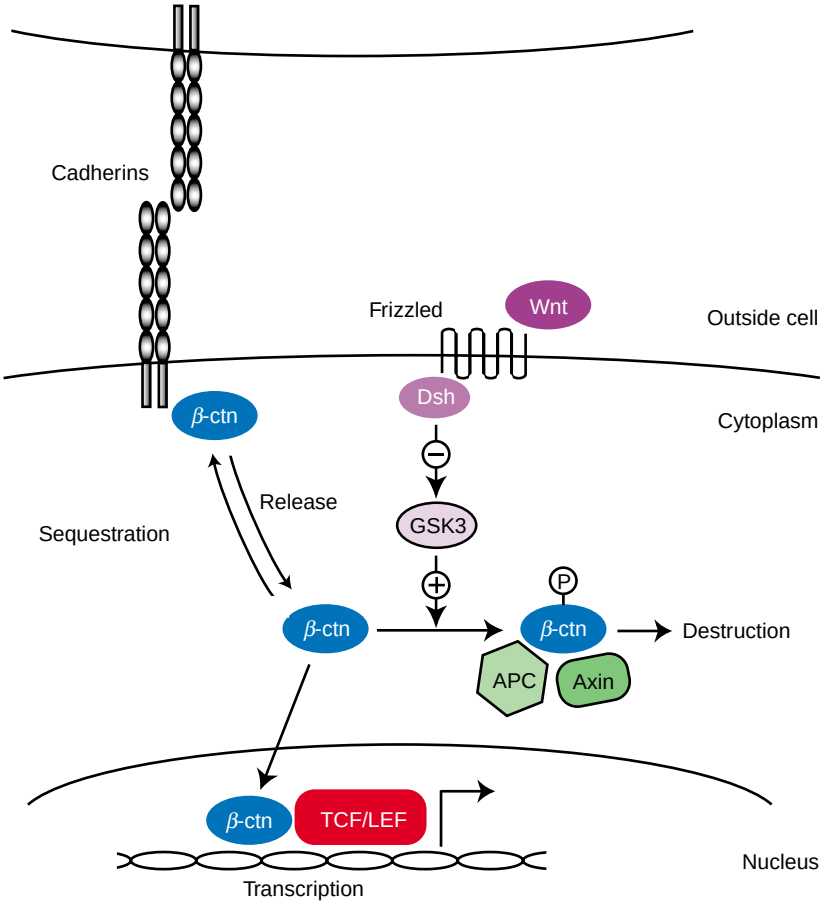

FIGURE 3 Cadherins modulate Wnt/β-catenin signaling. In addition to its role as a component of adherens junctions, β-catenin (β-ctn) increases the activity of the TCF/LEF transcription factor in the nucleus. The extent to which β-catenin accumulates in the nucleus depends in part upon the level of free β-catenin in the cytoplasm. The amount of free β-catenin is normally low due to its phosphorylation by glycogen synthase kinase-3 (GSK3), binding to adenomatous polyposis coli (APC) and Axin proteins, and subsequent destruction (P indicates the added phosphate group). GSK3 activity is decreased by Disheveled (Dsh) when the growth factor Wnt binds to its receptor frizzled on the cell surface. Therefore, Wnt can reduce degradation of β-catenin and increase the amount of β-catenin in the nucleus, thereby promoting transcription. In contrast, the formation of cadherin–cadherin junctions, or an increase in the amount of cadherin, can lead to the sequestration of β-catenin due to its interaction with cadherin tails. In this way, cadherins are thought to decrease the amount of nuclear β-catenin, and act in opposition to Wnt signals.

cadherins can potentially modulate the signal generated by activation of the Wnt pathway. High expression levels of E-cadherin can substantially reduce the amount of free β-catenin, and lower the cellular response to Wnt. In the absence of Wnt, increased adherens junction formation recruits β-catenin, decreasing the nuclear pool of β-catenin, and attenuating β-catenin-mediated transcription. Conversely, disruption of cell–cell adhesion may release β-catenin, thereby enhancing transcription. It is noteworthy that mutations of proteins that regulate turnover of β-catenin have been found in several human cancers.

Phosphorylation and Dephosphorylation

The phosphorylation of proteins (i.e., addition of phosphate groups) by kinase enzymes is a common mechanism for regulating numerous cellular processes. Although the cadherins themselves do not have kinase activity, a number of examples of cross talk have been observed between cadherins and growth factor receptors that contain intrinsic tyrosine kinases (Figure 4). For example, N-cadherin interacts with the fibroblast growth factor receptor FGFR1 and can boost the phosphorylation cascade triggered by binding of fibroblast growth factor-2 to FGFR1. Analogous interactions may occur between E-cadherin and the epidermal growth factor receptor, as well as VE-cadherin and the vascular endothelial growth factor receptor-2. In this way, cadherins can modulate changes in the survival, proliferation and motility of cells in response to a variety of growth factors.

Conversely, phosphorylation can modulate inside-out signals to regulate cadherin activity. The association between growth factor receptor tyrosine kinases and cadherins allows growth factors to promote the phosphorylation of several adherens junction proteins (Figure 4). A number of non-receptor kinases, including Src, also can phosphorylate junction components. Phosphorylation of β-catenin on tyrosine residues is believed to induce dissociation of β-catenin from cadherins and decrease adherens junction stability. Phosphorylation of the cadherins themselves, and of γ-catenin and $p120^{ctn}$, also modulates adherens junction assembly. In particular, the interaction of $p120^{ctn}$ with the cytoplasmic domain of cadherins appears to be an important regulator of cadherin activity, perhaps by influencing the clustering of cadherins in the cell membrane. Cadherins are also found in a complex with selected protein phosphatases. These enzymes, which are activated by cadherins, dephosphorylate (i.e., remove phosphate from) β-catenin, allowing reversible regulation of cadherin adhesive capacity (Figure 4).

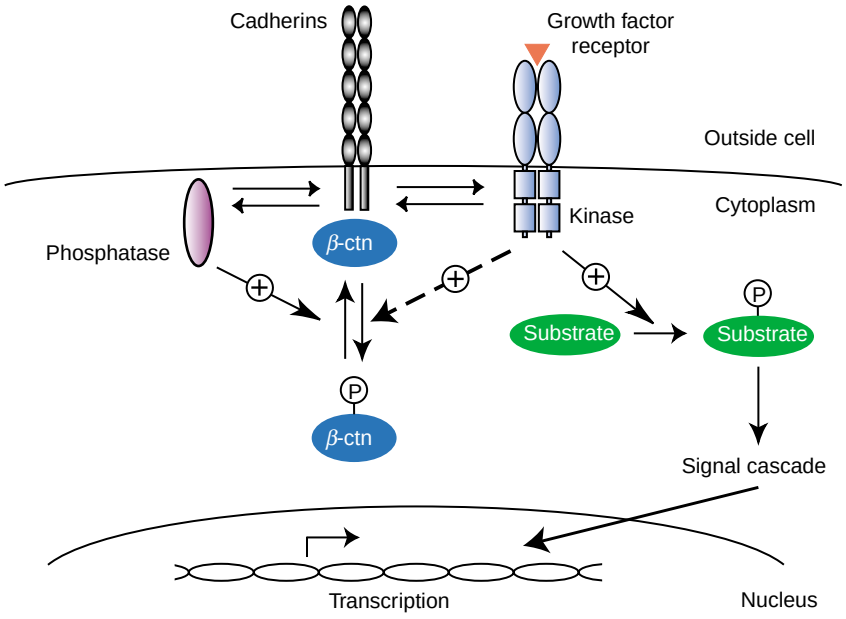

FIGURE 4 Cadherin crosstalk with kinases and phosphatases. Cadherins interact with a number of growth factor receptors that have intrinsic kinase activity. By this mechanism, cadherins can modulate the signaling cascades triggered by growth factors that lead, for example, to the activation of gene transcription. In addition, activation of receptor kinases can promote the phosphorylation on tyrosine residues of β-catenin (dotted line; P indicates the added phosphate group), its dissociation from cadherin tails, and disassembly of the adherens junction (not shown). Cadherins are also found in a complex with a number of protein phosphatases that can dephosphorylate β-catenin. In this way, cadherins can modulate the reversible phosphorylation of adherens junction components that alter the activity of cadherin itself.

See Also the Following Articles

Cadherin-Mediated Cell–Cell Adhesion • Rho GTPases and Actin Cytoskeleton Dynamics

Glossary

adherens junction Cadherin-dependent adhesive structures linked to the actin cytoskeleton that mediate attachment of cells to one another.

cadherins Family of homophilic adhesion molecules that mediate Ca^{2+}-dependent cell–cell adhesion.

catenins Family of proteins comprising α-, β-, γ-, and p120 catenin, that attach to the cytoplasmic tails of cadherins.

homophilic The preference of a molecule for interactions with identical molecules.

Rho family GTPases Family of regulatory proteins that act as molecular switches, alternating between active and inactive forms.

Further Reading

Ben-Ze'ev, A., Shtutman, M., and Zhurinsky, J. (2000). The integration of cell adhesion with gene expression: The role of beta-catenin. *Exp. Cell Res.* **261**, 75–82.

Bracke, M. E., Van Roy, F. M., and Mareel, M. M. (1996). The E-cadherin/catenin complex in invasion and metastasis. *Curr. Top Microbiol. Immunol.* **213**, 123–161.

Braga, V. M. (2002). Cell–cell adhesion and signalling. *Curr. Opin. Cell Biol.* **14**, 546–556.

Christofori, G., and Semb, H. (1999). The role of the cell-adhesion molecule E-cadherin as a tumour-suppressor gene. *Trends Biochem. Sci.* **24**, 73–76.

Gumbiner, B. M. (2000). Regulation of cadherin adhesive activity. *J. Cell Biol.* **148**, 399–403.

Perez-Moreno, M., Jamora, C., and Fuchs, E. (2003). Sticky business: Orchestrating cellular signals at adherens junctions. *Cell* **112**, 535–548.

Polakis, P. (2000). Wnt signaling and cancer. *Genes Dev.* **14**, 1837–1851.

Biography

David B. Sacks is an Associate Professor in the Department of Pathology at Brigham and Women's Hospital and Harvard Medical School. His principal research interest is in the field of signal transduction, with a focus on Ca^{2+} and calmodulin signaling. He holds an M.B.Ch.B from the University of Cape Town (South Africa) and received his postdoctoral training at Washington University.

Jonathan M. G. Higgins is an Assistant Professor in the Division of Rheumatology, Immunology, and Allergy at Brigham and Women's Hospital, Harvard Medical School. He holds a D.Phil. from the University of Oxford.

Cadherin-Mediated Cell–Cell Adhesion

Frauke Drees and W. James Nelson
Stanford University, Stanford, California, USA

Cell–cell adhesion is the process of establishment and maintenance of contacts between adjacent cells in tissues and organs of multicellular organisms. Cadherins comprise a superfamily of transmembrane glycoproteins that mediate calcium-dependent cell–cell adhesion and are found in all metazoans. Cadherins are involved in a wide variety of biological processes including development, tissue morphogenesis, and tumor metastasis. The cadherin family consists of four major subfamilies: classical cadherins, desmosomal cadherins, protocadherins, and atypical cadherins. Members of the cadherin superfamily share a conserved extracellular, calcium-binding domain (CD repeat) involved in specifying cell–cell adhesion, but the number (5–34) and arrangement of these domains differ between subfamily members.

Cadherin Subfamilies

Classical Cadherins

Classical cadherins comprise a small subfamily of proteins with the simplest, prototypic organization of cadherins: an extracellular domain comprising five EC repeats, a single transmembrane domain, and a conserved cytoplasmic domain that binds specific cytosolic proteins that link cadherins to the actin cytoskeleton. They are also the best understood of all cadherins in terms of structure, mechanism of adhesion, and function. Generally, classical cadherins are expressed in specific tissues, from which they were originally named (e.g., epithelia, E-cadherin; nervous system, N-cadherin; placenta, P-cadherin) although it is now recognized that each is broadly expressed in most tissues. Classical cadherins have been implicated in a variety of developmental processes, particularly in cell sorting during tissue remodeling. They are the major components of adherens junctions, an ultrastructurally defined adhesion site between opposing cells; note that other adhesion proteins such as nectin, a member of the immunoglobulin superfamily of adhesion proteins, have also been shown to localize and contribute to the formation and maintenance of adherens junctions. Classical cadherins mostly form homotypic adhesions between the same type of cadherin on adjacent cells (e.g., E–E, N–N, P–P).

Desmosomal Cadherins

Desmosomal cadherins, termed desmocollin and desmoglein, are found in desmosomes, a structure morphologically distinct from the adherens junction. Desmosomal cadherins have five EC domains, a single transmembrane domain, and a cytoplasmic domain that interacts with cytosolic proteins different from those that bind classical cadherins that link desmosomal cadherins to the intermediate filament network. Desmosomes and desmosomal cadherins are typically found in tissues that have to withstand high mechanical stress, such as epithelia, and are well conserved throughout most higher metazoans, but are absent in flies and worms. There are three subtypes of desmocollins and desmogleins, which are expressed in a tissue- and differentiation-specific manner. Desmosomal cadherins form heterotypic interactions, in contrast to the homotypic interactions of classical cadherins. Desmosomal cadherins can initiate and maintain cell–cell adhesion in the absence of classical cadherins, but adherens junctions containing classical cadherins are generally assembled before desmosomes in development.

Protocadherins

Protocadherins constitute the largest cadherin subfamily, but its members are far less well characterized than either classical or desmosomal cadherins. Protocadherins are highly expressed in the mammalian brain and nervous system. Genomically, they are organized in three large gene clusters with a very large number of exons encoding "variable" extracellular domains, and three exons encoding "constant" intracellular domains; combinations of extracellular and intracellular domains can be assembled to potentially generate thousands of different protocadherins. This has prompted speculation that protocadherin genes might reorganize in a manner

similar to that of immunoglobulins (hence the analogy to immunoglobulin "variable" and "constant" domains), and their resulting diversity might contribute to specifying cell–cell connections during development of the nervous system. This is substantiated by the fact that protocadherins show distinct spatio-temporal expression patterns during brain development. However, a clear role for protocadherins in cell–cell adhesion has not yet been demonstrated.

Atypical Cadherins

Atypical cadherins comprise the fat-like cadherins (e.g., fat, dachsous, two related proteins expressed in *Drosophila*), cadherins with a seven-pass transmembrane domain (e.g., flamingo), protein kinase cadherins, Dcad102F-like cadherins, and T-cadherin. Fat-like cadherins are a heterogeneous subfamily of proteins with very large extracellular domains that contain up to 34 EC repeats, in addition to EGF and laminin-G domains. They have a single transmembrane domain, and the cytoplasmic domains of fat and dachsous have predicted binding sites for cytoplasmic proteins that bind classical cadherins. The seven-pass transmembrane cadherins, such as flamingo, were first identified in *Drosophila*. The extracellular domain contains eight or nine EC domains and EGFR- and laminin-like domains, and mediates homotypic cell–cell adhesion. Amino acid sequence analysis predicts seven transmembrane domains, which show similarity to G protein-coupled receptors (GPCR). The cytoplasmic domain is different from those of classical and fat-like cadherins, and interacting cytosolic proteins have not been found, but due to their similarity to GPCR, flamingo-like cadherins have been implicated in cell signaling pathways. In *Drosophila*, flamingo-like cadherins are required for establishment of planar cell polarity. T-cadherin differs from all other cadherins because it lacks transmembrane or cytosplasmic domains, but instead associates with the membrane via a glycophosphidylinositol-anchor that inserts directly into the outer leaflet of the plasma membrane lipid bilayer. T-cadherin can mediate calcium-dependent cell–cell adhesion, but does not cluster in cell–cell contacts. T-cadherin has been implicated in signaling events and might constitute a negative guidance cue for neurons in the nervous system. Little is known about the other members of this subfamily, protein kinase cadherins, and Dcad102F-like cadherins.

Regulation of Cadherin Adhesion: Role of the Extracellular Domain

Although it is broadly accepted that the main role of cadherins is to mediate adhesion between cells, the exact mechanism of how the adhesive contact forms is not fully resolved. Analysis of this problem has focused primarily on the classical cadherins: N- and E-cadherin. Classical cadherins are believed to form two types of dimers, lateral or *cis*-dimers between two cadherin molecules on the same cell, and *trans*-dimers between cadherins on opposite cells (Figure 1).

Mechanisms of Cadherin Specificity in Cell Sorting

Specificity of adhesion appears to be determined in two ways. Early cell-sorting experiments showed that when two cell lines expressing N- and E-cadherin were mixed the cells sorted out and formed separate aggregates each of which expressed the same cadherin. In this case, homotypic *trans* adhesion between extracellular domains of the same cadherins appears to mediate adhesion specificity. The specificity for homotypic recognition is thought to be encoded in the EC1 extracellular domain, because when the EC1 domain of N-cadherin is swapped onto EC domains 2–5 of E-cadherin for example, the resulting chimeric protein sorts like N-cadherin in the experiments described earlier. More recent experiments showed that cells also sort from each other in aggregates formed between cells expressing different levels of the same cadherin. Thus, cell sorting may also be mediated by differences in adhesion strength that is proportional to the amount of cadherin expressed. The exact mechanism involved in adhesion specificity remains to be elucidated, but it will probably be a combination of spatio-temporal expression patterns of different cadherins, as well as differences in adhesive properties (strengths) between different cadherins.

Extracellular Domain Structure (*cis*- and *trans*-Dimers)

These early studies indicated that the outermost, N-terminal cadherin domain (EC1) is important in adhesion of E- and N-cadherin, and that a specific tripeptide, histidine–alanine–valine (HAV), and a conserved trytophan residue at position 2 (W2) in EC1 formed cadherin-binding motifs. Short peptides comprising the HAV sequence block adhesion in cell aggregation assays, and mutations of W2 also decrease adhesion. Both the EC1 domain and the EC1–EC2 domain of E- and N-cadherin have been crystallized. The crystal structures reveal that EC domains comprise an immunoglobulin-like fold with a seven-strand β-sheet, and that 6 Ca^{2+}-ions associate with residues in the linker region between EC1 and EC2. Calcium binding stabilizes the extracellular domain into a rigid bent rod-like structure that is resistant to proteolytic

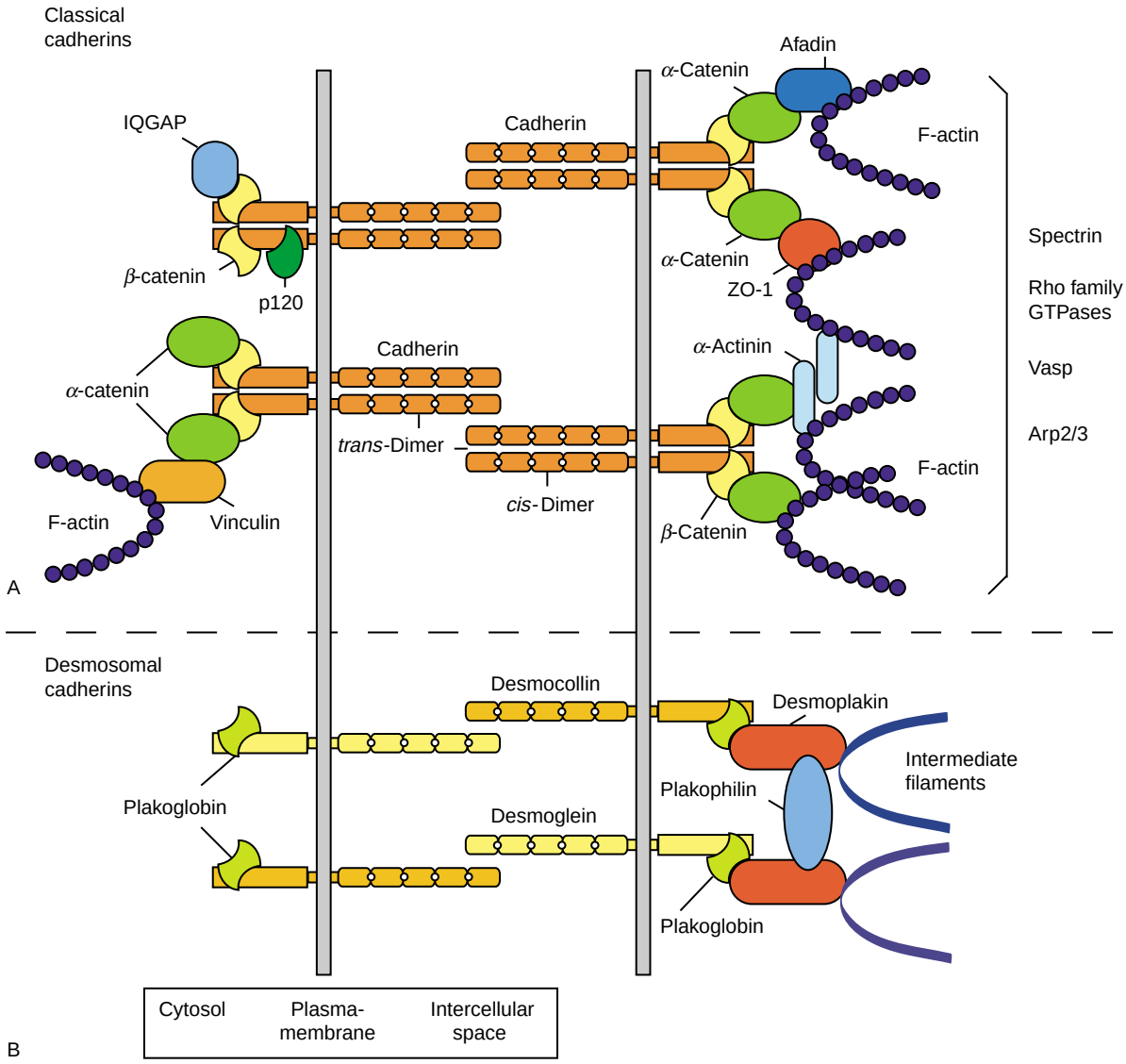

FIGURE 1 Schematic model of the linkage of protein–protein interactions between cadherins and cytoplasmic proteins. (A) Classical cadherins form *cis*- and *trans*-dimers to mediate Ca^{2+}-dependent adhesion. The cytoplasmic domain interacts directly with p120 and β-catenin. β-catenin in turn binds α-catenin, which links the complex to the actin cytoskeleton both directly through interaction with actin filaments and indirectly through the actin-binding proteins vinculin, ZO-1, α-actinin, and afadin. Other actin-associated proteins such as Rho-family GTPases, Vasp, Arp2/3, and spectrin have been shown to localize at adherens junctions, but the molecular nature of their interactions is less well defined. IQGAP binds β-catenin and has been suggested to negatively regulate adhesion by causing α-catenin to dissociate from β-catenin. (B) The desmosomal cadherins, desmocollin and desmoglein, form heterodimers and are linked to the intermediate filament network through interaction with plakoglobin, desmoplakin, and plakophilin.

cleavage, which may explain why cadherin adhesion is dependent on extracellular Ca^{2+}. Several models have been proposed for *cis*- and *trans*-dimerization. Mechanisms involved in *cis*-dimerization are poorly understood. Early models favored *trans*-dimerization through interaction between two opposing EC1 domains, but biophysical studies argue for *trans*-interaction involving contact between several EC domains. Further analysis of cadherin extracellular domains and their interactions will be required to resolve the mechanism of interaction and adhesion.

Regulation of Cadherin Adhesion: Role of the Cytoplasmic Domain

Linkage To β-Catenin Family Members

Classical and desmosomal cadherins are linked to the cytoskeleton via their intracellular domains through a class of cytosolic proteins collectively called catenins: β-catenin, plakoglobin (γ-catenin), and p120 (Figure 1). There are different binding sites on the cadherin

cytoplasmic domain for p120 catenin, and β-catenin and plakoglobin. p120 interacts directly with the juxtamembrane region of the cadherin intracellular domain, but its role in adhesion is not clearly defined; it may negatively modify adhesive strength of cadherin interaction, or regulate cadherin clustering. β-catenin and plakoglobin bind a conserved C-terminal domain of classical cadherins in a mutually exclusive manner and, in turn, interact with α-catenin to link the complex to the actin cytoskeleton (Figure 1). Desmosomal cadherins also bind plakoglobin, but not β-catenin; plakoglobin in turn binds cytosolic proteins termed plakophillin and desmoplakin that link desmosomal cadherins to the intermediate filament cytoskeleton (Figure 1). How different catenins specifically bind to different members of the cadherin superfamily is poorly understood, but it may be dependent on structural recognition between different β-catenin family members and the cytoplasmic domain of different cadherin subtypes.

Linkage to the Cytoskeleton

When cells initiate cell–cell contact, additional proteins are rapidly recruited to the cadherin-β-catenin/plakoglobin-α-catenin complex, which results in clustering of cadherins and strengthening of cell–cell adhesion. α-catenin binds directly to actin filaments, but also interacts with several actin-binding proteins including α-actinin, vinculin, ZO-1, and afadin (Figure 1). Afadin also binds the transmembrane adhesion protein nectin, which is localized with cadherins to the adherens junction, thereby interlinking the cadherin and nectin adhesion complexes. Other proteins such as VASP, IQGAP, fodrin, and members of the Rho family of small GTPases are localized to cadherin-based adhesion junctions and these proteins may further regulate actin assembly and organization at sites on the plasma membrane involved in cadherin-mediated adhesion (Figure 1). The importance of these cytosolic proteins to cell–cell adhesion is illustrated by the fact that α-catenin-deficient tumor cell lines or cell lines expressing E-cadherin lacking the intracellular domain adhere very poorly despite the expression of E-cadherin and other adherens junction proteins. Reintroduction of α-catenin causes these cells to form fully developed adhesion junctions.

Regulation by Phosphorylation

Cadherin complex assembly and disassembly is a highly regulated process. Both cadherin and β-catenin can be phosphorylated on serine/threonine and tyrosine residues, which modifies their binding affinity for each other. Serine/threonine phosphorylation by casein kinase II increases the binding affinities between cadherin/β-catenin and β-catenin/α-catenin, thereby stabilizing the cadherin/catenin complex and strengthening adhesion. Conversely, tyrosine-phosphorylation of either cadherin or β-catenin appears to destabilize the adhesion complex and weaken adhesion.

Functions in Signaling

In addition to the role as linkers between cadherins and the cytoskeleton, β-catenin, plakoglobin and p120 function as co-activators of gene transcription with members of the LEF/Tcf family of transcription factors in the Wnt/*wingless* pathway. Whether functions of β-catenin in the cytoplasm (cell–cell adhesion) and nucleus (gene expression) are interchangeable or separate is not known.

Roles of Cadherins in Cell and Tissue Morphogenesis

Classical cadherins are essential for embryonic development and have long been implicated in cell sorting, and in tissue formation and integrity. As noted above, two cell populations expressing different types, or protein levels of cadherins form separate aggregates when mixed together, and in development cell populations sort from one another by the same mechanism. To obtain evidence of morphogenic roles of cadherin in development, several cadherin genes have been deleted (Table I). E-cadherin knockout mice exhibit the most severe phenotype with very early lethality due to inability of pre-implantation embryos to fully compact and to develop into blastocysts. The N-cadherin knockout results in embryonic death at embryonic days 9–10 due to heart defects and malformation of the neural tube. In contrast, P-cadherin knockout mice are viable and fertile with only slight abnormalities in mammary glands. This demonstrates that while specific cadherins are important in development and morphogensis, some cadherins can be substituted by another. While the phenotype of the E- and N-cadherin knockout mice can be explained by adhesion defects, it is an open question as to whether there are defects in induction of tissue differentiation due to lack of a specific cadherin. In this context it is noteworthy that embryonic stem (ES) cells derived from E-cadherin −/− embryos form different tissues depending upon which cadherin is used to rescue cell–cell adhesion. When injected subcutaneously into mice, wild-type ES cells form benign teratomas that are highly differentiated and show a variety of tissue subtypes. By contrast, the E-cadherin null ES cells formed teratomas with no organized tissue structures. Interestingly, null cells rescued with overexpressed E-cadherin formed teratomas of almost exclusively epithelia, whereas overexpression of N-cadherin in the

TABLE I

Effects of Gene Deletions of Selected Cadherins and Adherens Junction Components on Mouse Development

Gene/protein	Subfamily	Genetic defect	Phenotype
E-cadherin	Classical cadherin	Knockout, deletion of extracellular Ca^{2+}-binding and adhesion motif	Embryonic lethal at time of implantation, embryonic compaction occurs, probably due to maternally deposited E-cadherin, but embryos fail to form trophectoderm or blastocyst cavity.
N-cadherin	Classical cadherin	Knockout	Embryonic lethal E9–10, major heart defects and malformed neural tube and somites.
P-cadherin	Classical cadherin	Knockout	Viable and fertile, despite high expression of P-cadherin in placenta. Virgin P-cadherin-null females exhibit precocious differentiation of mammary gland. Hyperplasia and dysplasia of mammary epithelium with age.
R-cadherin	Classical cadherin	Knockout	Viable and fertile, dilated proximal kidney tubules, defects in development of ureteric bud- and metanephric-mesenchymal-derived cells during nephrogenesis.
Cadherin-6	Classical cadherin	Targeted gene disruption (deletion of membrane targeting sequence)	Viable and fertile, transition of fraction of mesenchymal aggregates into epithelial structures in nephrogenesis is delayed.
β-Catenin	AJ component	Knockout	Embryonic lethal E7–9, at day 7 cells detach from ectodermal cell layer, the three germlayers and amniotic folds fail to form, and epithelial organization of ectoderm is completely lost.
Desmocollin Dsc1	Desmosomal cadherin	Knockout	Normal at birth, epidermal fragility and barrier defects, hyperproliferation and abnormal differentiation of epidermis, hair loss, hair follicle degeneration, mice develop ulcerating lesions resembling chronic dermatitis.
Desmoglein Dsg3	Desmosomal cadherin	Knockout	Normal at birth, disintegration of epidermis (Acantholysis), hair loss, runting (probably due to oral lesions). Phenotype resembles pemphigus vulgaris (caused by autoantibodies against Dsg3).
Desmoplakin	Desmosome component	Knockout	Embryonic lethal E6.5 due to defects in extra-embryonic tissues and failure of egg-cylinder expansion, abnormal desmosomes. Animals rescued with wild-type chimeras in extra-embryonic tissue die at E10 with major defects in heart muscle, neuro-, and skin epithelium.
Plakoglobin	Desmosome component	Knockout	Embryonic lethal E10.5–15 due to heart failure. Reduction in number and size of desmosomes and abnormal structure. Some genetic backgrounds delayed embryonic lethality, epidermal blistering.

ES cells led to the formation of neuroepithelia and cartilage in the teratomas.

A crucial and reoccurring step during development and tissue morphogenesis is the role of cell–cell adhesion in the structural and functional polarization of cells. One example is the development of polarized epithelial cells. Cadherin-mediated cell–cell adhesion between simple epithelial cells generates a cell monolayer that separates two biological compartments and regulates homeostasis by vectorial transport of ions and solutes between those compartments. This function requires cells to generate and maintain two functionally and structurally distinct plasma membrane domains, termed apical and basal-lateral, which face these different compartments. Cell–cell adhesion initiates structural and biochemical asymmetries at the cell membrane, through assembly of cytoskeleton and vesicle docking complexes that initiate formation of the (basal-) lateral membrane domain. Studies in *Drosophila* have shown that cadherins play additional roles in establishing planar polarity of ommatidia in the eye and wing hairs (fat-like cadherins), and a role for cadherins in migration has been proposed in oocyte border cell migration.

Consequences of Disruption of Cadherin Functions: Disease States and Cancer

Loss of cell–cell adhesion, changes in cytoskeletal organization, and aberrant adhesion-mediated signaling are hallmarks of malignant transformation, tumors, and cancer. Disruption of cell–cell adhesion might contribute to increased proliferation and migration of tumor cells, thereby leading to invasion of surrounding tissue and metastasis. Alterations of cadherin-mediated cell–cell adhesion arise mainly through three mechanisms: loss of adhesion complex function, most commonly through inactivation of E-cadherin or α-catenin expression or function; aberrant cadherin function due to "cadherin switching"; and changes in cell signaling through cadherins or catenins (Table I).

First, inactivating mutations in the E-cadherin gene CDH1 are frequently found in certain carcinomas such as gastric or breast lobular carcinomas, and germ-line mutations in CDH1 strongly predispose individuals to gastric cancer. Loss of E-cadherin expression requires inactivation of both CDH1 alleles, as would be expected for a tumor suppressor gene, and reintroduction of E-cadherin into tumor cell lines can reverse transformation from an invasive to a benign, epithelial tumor cell phenotype in culture. In addition to genetic mutation or gene deletion, down-regulation of E-cadherin at the transcriptional level has been observed in certain tumors, for example through DNA hypermethylation of the CDH1 promoter and/or up-regulation of transcriptional repressors of E-cadherin.

Second, up-regulation of nonepithelial cadherins, such as N-cadherin and cadherin-11, either with or without loss of E-cadherin, may contribute to the transformation and invasiveness of tumor cells. This change in cadherin expression pattern is termed "cadherin switch" and has been found in primary tumors. In tissue cancer cell lines, it causes an epithelial to fibroblast-like transition of cellular phenotype.

Third, alterations in cell signaling pathways through cadherins or catenins contribute to cancer formation. Mutations in β-catenin generally inhibit β-catenin degradation and thereby inappropriately activate the Wnt signaling pathway. In addition, tyrosine phosphorylation of E-cadherin and β-catenin destabilizes the adhesion complex and, therefore, changes in this signaling pathway, for example by activation of tyrosine kinases, might contribute to tumor cell invasiveness by decreasing the amount of cell–cell adhesion.

Mutations in desmosomal cadherins and other protein components of desmosomes, such as plakoglobin or plakophilin, give rise to specific diseases of the skin and, in some cases, heart defects, thereby illustrating the importance of desmosomal adhesion in tissues exposed to high mechanical stress. Patients with the skin conditions Darier–White and Hailey–Hailey disease suffer from defects in keratinocyte adhesion due to breakdown of desmosomal adhesion. In the blistering diseases pemphigus vulgaris and pemphigus foliaceus, which affect skin and mucous cell membranes, auto-immune antibodies against desmoglein 1 and 3, respectively, interact with the extracellular domain of these cadherins, thereby functionally blocking adhesion and leading to the disassembly of desmosomes in the skin.

In summary, the cadherin superfamily of adhesion proteins plays important roles in development, and cellular reorganization and polarization, and abnormalities in cadherins and associated proteins are characteristic of disease states and cancer. While cadherins are known to regulate calcium-dependent cell–cell adhesion, and many associated proteins that link cadherins to the cytoskeleton have been identified, there remain many unanswered questions about the way cadherins form cell–cell contacts, regulate assembly of the cytoskeleton, and determine cell differentiation.

See Also the Following Articles

Actin Assembly/Disassembly • Actin-Related Proteins • Cadherin Signaling • Rho GTPases and Actin Cytoskeleton Dynamics

Glossary

adaptor proteins Cytosolic proteins that link protein complexes together and allow for regulation of physiological responses. In the example of cell adhesion proteins, adaptor proteins (catenins) provide the linkage between cell adhesion transmembrane proteins and the cytoskeleton.

cell–cell adhesion Process of establishment and maintenance of contacts between adjacent cells in tissues and organs of multicellular organisms.

cell–cell adhesion molecules Transmembrane glycoproteins that mediate cell–cell binding. There are three major protein families: selectins, immunoglobulin superfamily, and cadherins.

cell–cell junctions Specialized regions on the cell surface by which cells are joined to each other. Tight junctions in epithelial cell layers form a ribbon-like seal between compartments. Gap junctions are protein-lined channels between two cells that allow diffusion of small molecules from one cell to the next. Adherens junctions and desmosomes are dense protein plaques connected to cytoskeletal networks that link two adjacent cells together.

cytoskeleton Network of fibrous proteins found in the cytosol of eukaryotic cells that provides structural support for the cell, determines cell shape and motility, and allows directional movement of organelles and vesicles inside the cell. There are three major classes of cytoskeletal filaments: actin microfilaments, microtubules, and intermediate filaments.

Further Reading

Braga, V. M. M. (2002). Cell–cell adhesion and signaling. *Curr. Opin. Cell Biol.* **14**, 546–556.

Fukata, M., and Kaibuchi, K. (2001). Rho-family GTPases in cadherin-mediated cell–cell adhesion. *Nat. Rev. Mol. Cell Biol.* **2**, 887–897.

Hajra, K. M., and Fearon, E. R. (2002). Cadherin and catenin alterations in human cancer. *Genes, Chromosomes Cancer* **34**, 255–268.

Jamora, C., and Fuchs, E. (2002). Intercellular adhesion, signaling and the cytoskeleton. *Nat. Cell Biol.* **4**, 101–108.

Koch, A. W., Bozic, D., Pertz, O., and Engel, J. (1999). Homophilic adhesion by cadherins. *Curr. Opin. Struct. Biol.* **9**, 275–281.

Steinberg, M. S. (1996). Adhesion in development: An historical overview. *Dev. Biol.* **180**, 377–388.

Takeichi, M. (1995). Morphogenetic roles of classic cadherins. *Curr. Opin. Cell Biol.* **7**, 619–627.

Tepass, U., Truong, K., Godt, D., Ikura, M., and Pfeifer, S. (2000). Cadherins in embryonic and neural morphogenesis. *Nat. Rev. Mol. Cell Biol.* **1**, 91–100.

Vleminckx, K., and Kemler, R. (1999). Cadherins and tissue formation: integrating adhesion and signaling. *BioEssays* **21**, 211–220.

Biography

W. James Nelson is the Rudy J. and Daphne Donohue Munzer Professor in the School of Medicine, Professor of Molecular and Cellular Physiology, and Biological Sciences (by courtesy). Professor Nelson's research focuses on basic cellular mechanisms involved in generating cell asymmetry, particularly in epithelia and neurons. His research has uncovered a hierarchy of cellular events initiated by cell–cell adhesion that leads to cellular remodeling and the generation of structurally and functionally polarized cells.

Calcitonin Gene-Related Peptide and Adrenomedullin Receptors

Debbie L. Hay, Alex C. Conner and David R. Poyner
Aston University, Birmingham, UK

Calcitonin gene-related peptide (CGRP) and adrenomedullin are abundant, related peptides that share many biological actions. Most prominently, both are very potent vasodilators. CGRP is a neurotransmitter in sensory neurons and adrenomedullin is a hormone that is locally released from tissues including vascular endothelium and smooth muscle. Together with calcitonin and amylin, they form a peptide family. For some time, there was considerable controversy about the nature of the receptors for this family. It has been established that they define a new paradigm among G protein coupled receptors (GPCRs), in that they are heterodimers of a seven-transmembrane-spanning protein that resembles a classical GPCR and a member of the single-transmembrane-spanning receptor activity-modifying protein (RAMP) family. Although there is still much to be learned, this discovery has clarified the pharmacology of these peptides and may have implications for other GPCRs.

The Pharmacology of CGRP and Adrenomedullin

The Structure of CGRP and Adrenomedullin

The primary sequences of CGRP and adrenomedullin (Figure 1) share a low level of homology but the secondary structure of these peptides is conserved. For both peptides, an amino-terminal ring is important for receptor activation; peptides that lack this structure ($CGRP_{8-37}$ and $adrenomedullin_{22-52}$) are antagonists.

The Pharmacology of Endogenous CGRP and Adrenomedullin Receptors

CGRP Receptor-Selective Drugs and their Pharmacological Properties

There are few high-affinity, selective drugs that can be used to define CGRP and adrenomedullin receptors. For CGRP, the only widely available antagonist is $CGRP_{8-37}$. This has only limited selectivity. A number of high-affinity nonpeptide antagonists have been developed. The most interesting of these appears to be BIBN4096BS (Figure 2), which shows marked selectivity for primate over rodent CGRP receptors and has very little affinity for non-CGRP receptors. Largely on the basis of work with $CGRP_{8-37}$, it has been suggested that CGRP receptors should be divided into two subtypes. $CGRP_1$ receptors have a high affinity for $CGRP_{8-37}$ ($pA_2 > 7$); $CGRP_2$ receptors have a lower affinity for this antagonist. A number of linear CGRP analogues have been suggested to be $CGRP_1$-selective agonists, but their usefulness has been questioned.

The $CGRP_1/CGRP_2$ classification has proved controversial. $CGRP_{8-37}$ reveals marked heterogeneity in receptors that respond to CGRP in assays of physiological function. However, this is not apparent in radioligand-binding studies. The heterogeneity may reflect the existence of bona fide receptor subtypes, it may be due to cross-reactivity of CGRP at receptors for other peptides, or it may be caused by other factors,

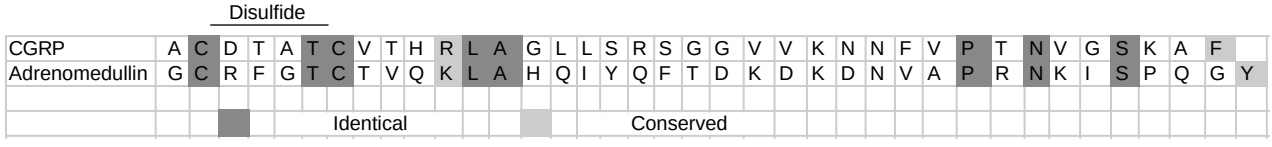

FIGURE 1 A comparison of the structure of human CGRP and $adrenomedullin_{15-52}$. Note the disulfide bond in both peptides, indicated by a bar over the sequences. The first 14 amino acids of adrenomedullin are not required for biological activity and are not shown.

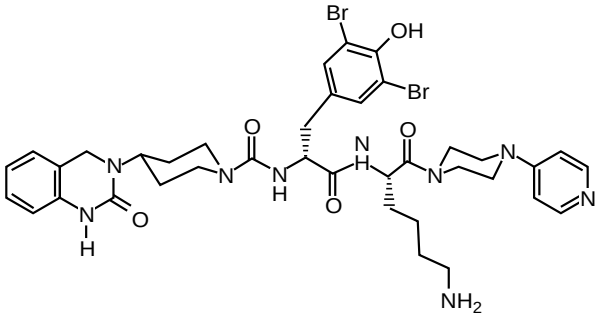

FIGURE 2 The structure of BIBN4096BS.

such as differential peptidase activity. The issue is likely to be resolved with progress in the molecular characterization of CGRP receptors hand-in-hand with the development of CGRP antagonists.

Adrenomedullin-Selective Drugs and their Pharmacological Properties

The only adrenomedullin antagonist that has been widely used is adrenomedullin$_{22-52}$. This is not particularly potent ($pA_2 \sim 7$) and does not antagonize all adrenomedullin-mediated responses. Nonetheless, it has proved useful in some circumstances in defining adrenomedullin receptors.

The Molecular Structure of CGRP and Adrenomedullin Receptors

CRLR and RAMPs

CGRP and adrenomedullin receptors display a very unusual molecular architecture. Both are composed of a common seven-transmembrane-spanning protein called calcitonin receptor-like receptor (CRLR or CL; Figure 3). This is a member of the B-family of GPCRs (related to other receptors, such as those for secretin and calcitonin). Human CRLR is 461 amino acids long and has 55.5% sequence identity with the human calcitonin receptor. It has three potential glycosylation sites, although only two appear to be utilized in the mature protein. By itself, CRLR does not function as a receptor for any peptide. However, when associated in a dimer with a RAMP, it functions as a high-affinity receptor for either CGRP or adrenomedullin. The RAMPs are a family of three proteins (Figure 4), each with an extracellular amino terminus of approximately 100 amino acids, a single transmembrane section, and a very short carboxy terminus of approximately 10 amino acids.

CRLR/RAMP1; A CGRP$_1$ Receptor

CRLR and RAMP1 associate intracellularly and this facilitates their transport to the cell surface. There, the heterodimer functions as a CGRP$_1$ receptor, with a high affinity for CGRP, CGRP$_{8-37}$, and BIBN4096BS. The complex binds adrenomedullin with an approximately 10-fold lower affinity than CGRP. Little is known about the mechanism of ligand binding and receptor activation. CGRP can cross-link to both CRLR and RAMP1, showing that both components create the peptide-binding site. However, it is not clear whether CGRP has specific contacts with both proteins or whether RAMP1 indirectly contributes to the ligand-binding site by modifying the structure of CRLR. Based on studies with other members of the B-family of G protein coupled receptors, it is likely that CGRP makes contacts with both the extracellular domain of CRLR/RAMP1 and the membrane–extracellular loop interfaces of CRLR. The selectivity of BIBN4096BS for primate over rodent CGRP receptors is due to a single amino acid at position 74 in RAMP1; this is tryptophan in humans and lysine in rats.

CRLR/RAMP2 and CRLR/RAMP3 are Adrenomedullin Receptors

The heterodimers formed by RAMP2 and RAMP3 with CRLR produce adrenomedullin receptors. Their formation is very similar to that of the CRLR/RAMP1 complex; in the absence of CRLR, they are not expressed at the cell surface. It was initially thought that RAMP2 might work by modulating the glycosylation state of CRLR. However, it is now thought that adrenomedullin and CGRP both bind to the fully glycosylated form of CRLR. As with the CRLR/RAMP1 complex, there is little detailed information on mechanisms of adrenomedullin binding to either the CRLR/RAMP2 or the CRLR/RAMP3 complexes. Both complexes exhibit higher affinity for adrenomedullin than CGRP. It has been proposed that the CRLR/RAMP2 complex should be designated as the AM$_1$ receptor and the CRLR/RAMP3 complex as the AM$_2$ receptor. The CRLR/RAMP2 complex has high affinities for adrenomedullin and adrenomedullin$_{22-52}$ but low affinity for CGRP. The CRLR/RAMP3 complex has not been extensively characterized but has high affinity for adrenomedullin and an intermediate affinity for CGRP, leading to the suggestion that it may function as a mixed adrenomedullin/CGRP receptor.

Cellular Signaling and RCP

The CRLR/RAMP complexes all couple to stimulation of adenylate cyclase production via the G protein known as G_s. However, as is the case with many related GPCRs,

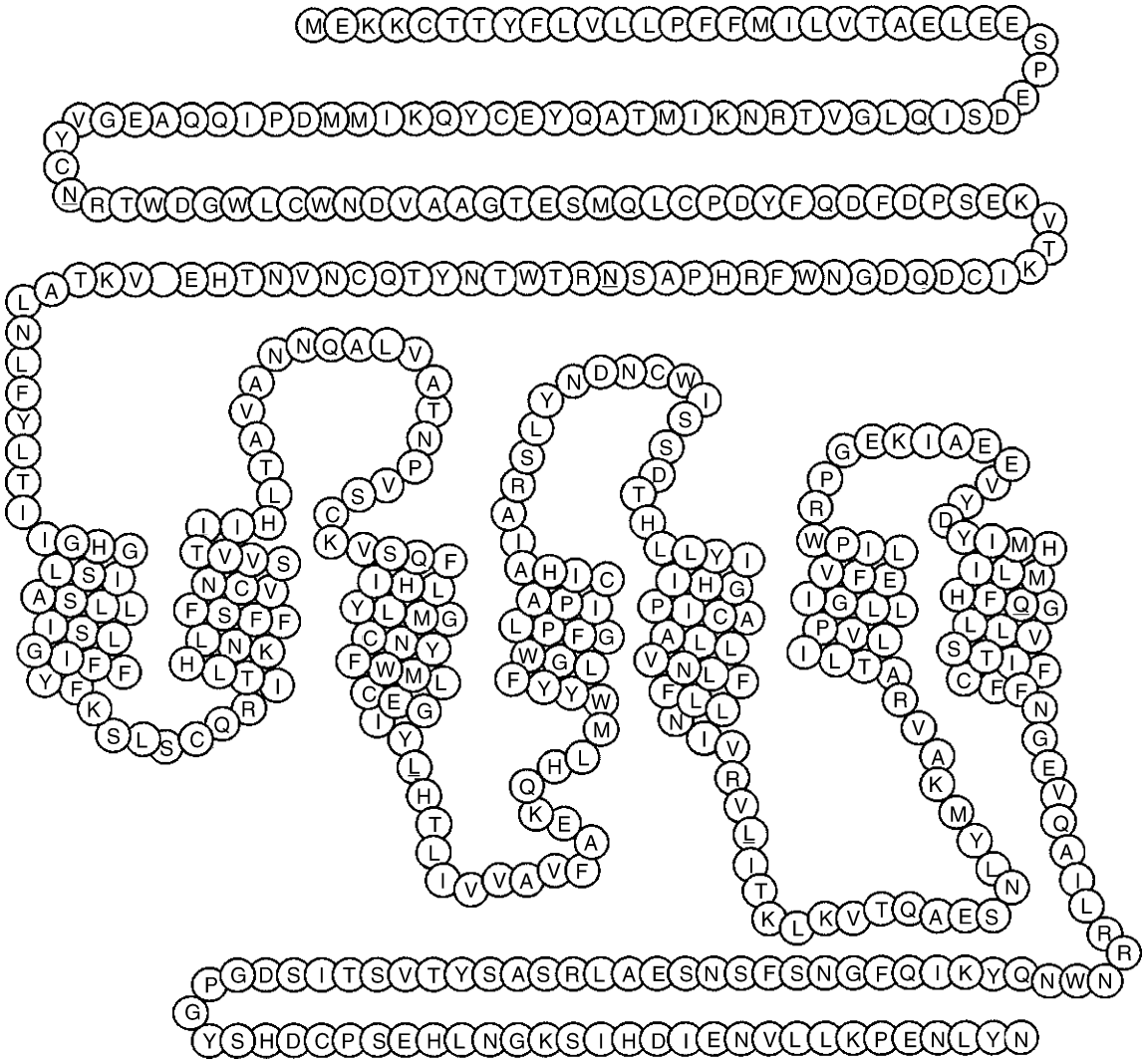

FIGURE 3 The structure of human CRLR, showing the postulated seven-transmembrane helices. The residues that are likely glycosylation sites on the amino terminus are underlined.

```
RAMP3   -------------METGALRRPQLLPLLLLLCG---------------GCPRAGGCNETG
RAMP2   MASLRVERAGGPRLPRTRVGRPAAVRLLLLLGAVLNPHEALAQPLPTTGTPGSEGGTVKN
RMAP1   -------------MARALCRLPRRGLWLLLAHH----------------LFMTTACQEAN
                                 *     ***

RAMP3   MLERL-PLCGKAFADMMGKVDVWKWCNLSEFIVYYESFTNCTEMEANVVGCYWPNPLAQG
RAMP2   YETAV-QFCWNHYKDQMDPIEK-DWCDWAMISRPYSTLRDCLEHFAELFDLGFPNPLAER
RAMP1   YGALLRELCLTQFQVDMEAVGETLWCDWGRTIRSYRELADCTWHMAEKLGCFWPNAEVDR
                 *       *       **        *     *    *       **

RAMP3   FITGIHRQFFSNCTVDRVHLEDPPDEVLIPLIVIPVVLTVAMAGLVVWRSKRTDTLL
RAMP2   IIFETHQIHFANCSLVQPTFSDPPEDVLLAMIIAPICLIPFLITLVVWRSKDSEAQA
RAMP1   FFLAVHGRYFRSCPISGRAVRDPPGSILYPFIVVPITVTLLVTALVVWQSKRTEGIV
             *   *   *        ***   *   *  *          **** **
                                      TM domain
```

FIGURE 4 Alignment of human RAMPs 1, 2, and 3. * Single, fully conserved residue. Underlined italic residues at the start of the sequence represent signal peptides. Underlined boldface residues are potential glycosylation sites.

coupling to G_i/G_o and the G_q family of G proteins (leading to changes in ion channel activity and elevation of intracellular calcium) has also been reported.

A novel protein called receptor component protein (RCP) is reportedly essential for coupling the CRLR/RAMP complexes to stimulation of G_s. Immunoprecipitation studies suggest that RCP is physically associated with the CRLR/RAMP heterodimer. It has been reported that inhibiting RCP expression disrupts signaling mediated via CRLR/RAMP complexes. RCP is very widely distributed in cell lines but a broader role has not yet been demonstrated.

Other Receptors that Respond to CGRP and Adrenomedullin

There is pharmacological evidence for heterogeneity among endogenous receptors for both CGRP and adrenomedullin. However, the molecular basis for this remains unclear. Adrenomedullin receptor heterogeneity may be explained at least in part by CRLR/RAMP2 and CRLR/RAMP3 dimers. As the CRLR/RAMP3 complex shows appreciable affinity for CGRP, it may also contribute to the appearance of $CGRP_2$-like pharmacology. RAMPs can also dimerize with calcitonin receptors. These complexes are usually considered to be amylin receptors; however, the RAMP1-containing dimer shows an appreciable affinity for CGRP. In addition, the presence of completely novel receptors for CGRP and adrenomedullin cannot be excluded.

The Distribution and Physiology of CGRP and Adrenomedullin Receptors

The Distribution of Binding Sites for CGRP and Adrenomedullin

CGRP-binding sites are present in both the central nervous system (CNS) and peripheral tissues. In some of the earlier literature, there was confusion due to cross-labeling of what would now be considered amylin receptors. Specific CGRP receptors show the potency order: CGRP > adrenomedullin > amylin. In the rat CNS, the highest densities of CGRP binding are in the nucleus accumbens, caudate putamen, amygdaloid body, pontine nuclei, cerebellum, spinal cord, and inferior olive. In the periphery, CGRP receptors are particularly associated with the cardiovascular system, on blood vessels and in the atria. There are high densities of these receptors in the spleen. However, receptors are also found on nonvascular cells, for example, in the vas deferens and secretory cells in the gastrointestinal tract. In tissues, adrenomedullin receptors show a high level of specificity for adrenomedullin over CGRP or other peptides. Binding in the CNS is highest in the spinal cord, but moderate to low levels are seen in many other brain regions. In the periphery, it is closely associated with the cardiovascular system, with very high levels in the heart and lungs.

Distribution of RAMPs and CRLR

Almost all information on the distribution of CRLR and RAMPs comes from mRNA measurements. Generally, there is fair agreement between the distribution of RAMPs and CRLR and binding sites for CGRP and adrenomedullin. Often RAMP2 appears to be more abundant than RAMP1, with RAMP3 being expressed at the lowest levels. However, there are many exceptions; RAMP1 is the most abundant transcript in the brain and the pancreas and RAMP3 predominates in liver. There are some anomalies; the nucleus accumbens has strong CGRP binding and RAMP1 expression but little CRLR; by contrast, the frontal cortex has very little binding for CGRP, adrenomedullin, or amylin, but has high levels of RAMP expression. It is unclear whether this reflects problems of inferring protein expression from mRNA abundance or whether it indicates additional complexity in the field. There is some preliminary evidence that RAMPs can associate with other receptors in addition to those for calcitonin and CRLR.

Changes in Expression of CGRP and Adrenomedullin Receptors

There is good evidence for changes in CGRP and adrenomedullin receptors during various (patho)physiological processes. For example, adjuvant-induced arthritis in rats leads to a decrease in CGRP binding in the spinal cord. Changes in CRLR and RAMP expression have also been noted in disease. In a mouse model of sepsis, CRLR mRNA and RAMP2 mRNA show large decreases but RAMP3 expression increases in the lung. In a rat model of ischemic heart failure, RAMP2 expression is increased in the ventricles.

The Pathophysiology of CGRP and Adrenomedullin Receptors

Changes in receptor expression suggest that both CGRP and adrenomedullin receptors are of importance during normal physiological processes and also in disease. Although receptor knockout models have not yet been described, mice in which the gene for adrenomedullin has been inactivated die *in utero*, showing gross defects in their cardiovascular systems. Heterozygote knockout mice, in which adrenomedullin

production has been reduced, show an elevated blood pressure. Thus, adrenomedullin appears to be vital for normal operation of the cardiovascular system. Similar studies on αCGRP-deficient mice have produced less dramatic effects, although some workers have noted an increased blood pressure, decreased pain sensitivity, and reduced hypersensitivity to antigens in airways. The data are consistent with roles for CGRP in the cardiovascular system and also as an inflammatory mediator, involved in pain perception and the activation of cells of the immune system. Adrenomedullin and CGRP receptors are potentially important therapeutic targets in cardiovascular and inflammatory diseases.

See Also the Following Articles

Calcitonin Receptor • G Protein-Coupled Receptor Kinases and Arrestins

Glossary

agonist A drug that activates a receptor.

antagonist A drug that blocks the action of an agonist at a receptor.

glycosylation The attachment of sugars to a protein.

pA_2 The negative logarithm of the antagonist concentration that causes a twofold shift in the agonist dose–response curve. It is a measure of antagonist affinity.

Further Reading

Brain, S. D., Poyner, D. R., and Hill, R. G. (2002). Calcitonin gene-related peptide (CGRP) receptors: A headache to study, but will antagonists prove therapeutic in migraine? *Trends Pharmacol. Sci.* **23**, 51–53.

Hinson, J. P., Kapas, S., and Smith, D. M. (2000). Adrenomedullin, a multifunctional regulatory peptide. *Endocr. Rev.* **21**, 138–167.

Juaneda, C., Dumont, Y., and Quirion, R. (2000). The molecular pharmacology of CGRP and related peptide receptor subtypes. *Trends Pharmacol. Sci.* **21**, 432–438.

Poyner, D. R., Marshall, I., and Brain, S. D. (2000). *The CGRP Family; CGRP, Amylin and Adrenomedullin*. Eurekah.com, Landes Biosciences, TX.

Poyner, D. R., Sexton, P. M., Marshall, I., Smith, D. M., Quirion, R., Born, W., Muff, R., Fischer, J. A., and Foord, S. M. (2002). International Union of Pharmacology XXXII. The mammalian CGRP, adrenomedullin, amylin and calcitonin receptors. *Pharmacol. Rev.* **54**, 233–246.

Sexton, P. M., Albiston, A., Morfis, M., and Tilakaratne, N. (2001). Receptor activity modifying proteins. *Cell Signal.* **13**, 73–83.

Biography

David Poyner is a Senior Lecturer in Pharmacology at Aston University. Debbie Hay and Alex Conner are postdoctoral fellows at the same institute. The Aston group has been researching the pharmacology of CGRP and adrenomedullin for over 10 years and in that time has produced over 40 publications in these fields.

Calcitonin Receptor

Samia I. Girgis, Niloufar Moradi-Bidhendi, Lucia Mancini and Iain MacIntyre
Imperial College and William Harvey Research Institute, London, UK

The calcitonin receptor (CTR) is a cell-surface receptor on which the peptide hormone calcitonin binds with high affinity to exert its bio-effects. Calcitonin (CT) has a wide range of effects, the most obvious of which is its effect on bone. CT is a powerful inhibitor of bone resorption. It directly inhibits the activity of the osteoclast (special bone cell responsible for bone resorption). CT receptors are widely distributed and CT has a much broader range of biological activities, including the effects on the central nervous system (CNS), gastrointestinal tract, and vascular and immune systems. Peptides that are structurally similar to CT, known as the CT peptide family bind with lower affinities to the CT receptors. The CTR has seven transmembrane-domains, and belongs to the G protein-coupled family of receptors (GPCRs).

Calcitonin Peptide Family

The calcitonin family of peptides comprises five known members, which are structurally similar (Figure 1). They have some overlapping biological effects due to cross-reactivity at each other's receptors. The CT peptide family includes calcitonin, two calcitonin gene-related peptides, amylin, and adrenomedullin, which are discussed next.

Calcitonin

Calcitonin (CT) is a peptide hormone secreted mainly by special type of cells within the thyroid gland in mammals, called C cells. CT was first identified as a calcium-lowering factor. This calcium-lowering effect of CT is mainly due to inhibition of osteoclast activity, and to a lesser extent to increasing calcium excretion by the kidney. As mentioned previously, CT also has a wide range of biological activities, including its analgesic effect, suppression of gastric acid secretion, and appetite.

Two Calcitonin Gene-Related Peptides (CGRP 1 and CGRP 2)

These are neuropeptides widely distributed throughout the CNS and in peripheral nerves associated with the cardiovascular system. The tissue distribution suggests a role in the transmission of sensory impulses and in the regulation of vascular tone. Both are very potent vasodilators.

Amylin

This is found in secretory granules in β-cells of the pancreas (cells that secrete insulin) and is co-secreted with insulin in response to a high blood glucose, e.g., after a meal. Amylin is a potent inhibitor of gastric emptying and food intake. It also opposes the metabolic actions of insulin in skeletal muscle.

Adrenomedullin (ADM)

This is produced predominantly by the vascular endothelium. It is a potent vasodilator.

The CT Receptor (CTR)

Distribution

Calcitonin receptors (CTRs) are widely distributed. They are particularly numerous in osteoclasts, where there are $\sim$1.3 million receptors per cell. They are found in lower amounts in the CNS, in areas involved in the control of appetite, pain perception, and lactation, e.g., hypothalamus and pituitary. CTRs are also found in peripheral tissues, e.g., in cells of the distal nephron of the kidney, testes, placenta, lung, prostate, and lymphocytes. Receptors for CT have been identified in some human cancer cells, including those of lung, breast, bone, and prostate.

Protein Structure

The CTR was initially cloned from a pig kidney cell line. Analysis of the predicted 482 amino acid sequence demonstrated seven hydrophobic regions that could generate transmembrane (TM)-spanning domains. The CTR is a member of a subset of the G protein-coupled receptors (GPCRs) family termed GPCR$_B$. Members of this family typically recognize regulatory peptides, including parathyroid hormone (PTH), glucagon, and secretin.

Human CGRPα	A **C** D T A T **C** V T H R L A G L L S R S G G V V K N N F V P T N V G S K A F-**amide**
Human CGRPβ	A **C** N T A T **C** V T H R L A G L L S R S G G M V K S N F V P T N V G S K A F- **amide**
Human AMY	K **C** N T A T **C** A T Q R L A N F L V H S S N N F G A I L S S T N V G S N T Y -**amide**
Human ADM	Y R Q S M N N F Q G L R S F G **C** R F G T **C** T V Q K L A H Q I Y Q F T D K D K D N V A P R S K I S P Q G Y -**amide**
Human CT	**C** G N L S T **C** M L G T Y T Q D F N K F H T F P Q T A I G V G A P -**amide**

FIGURE 1 The CT peptide family. The peptides share a six/seven amino acid ring structure, formed by a disulphide bridge at or close to the N terminus. The peptides also have C-terminal amides, which are essential for full biological activity. (This material is from Calcitonin Gene-related Peptide (CGRP), Girgis, S. I., and MacIntyre, I. (2002). In *Encyclopedia of Molecular Medicine* (T.E. Creighton ed.), Vol. 5, John Wiley & Sons Inc.

This family of receptors is characterized by seven TM segments connected by three extracellular and three intracellular loops (Figure 2). They all have an extracellular amino (N)-terminal sequence and an intracellular carboxy(C)-terminal sequence. The extended extracellular N-terminal region contains multiple potential glycosylation sites and conserved cysteine residues. Glycosylation is important for recognition and high-affinity binding of CT. While the TM domain sequences are conserved (40–60% identical), the N-terminal domains are generally less than 25% identical. The N-terminal domain fulfills the role for ligand binding and receptor specificity.

Multiple Forms

The human CTR gene is localized to chromosome 7. The CTR gene has a complex structural organization with several CTR protein isoforms derived from alternative splicing of transcripts from a single gene. These isoforms are functionally distinct in terms of ligand-binding specificity and signal transduction pathway utilization, and tissue distribution. In humans at least five splice variants have been described whereas two splice variants have been identified in rodents (C1a and C1b), which differ by the presence or absence of an additional 37 amino acids in the second extracellular domain. The C1a is more widely distributed and is the predominant isoform found in osteoclasts. C1b isoform is primarily localized in the central nervous system.

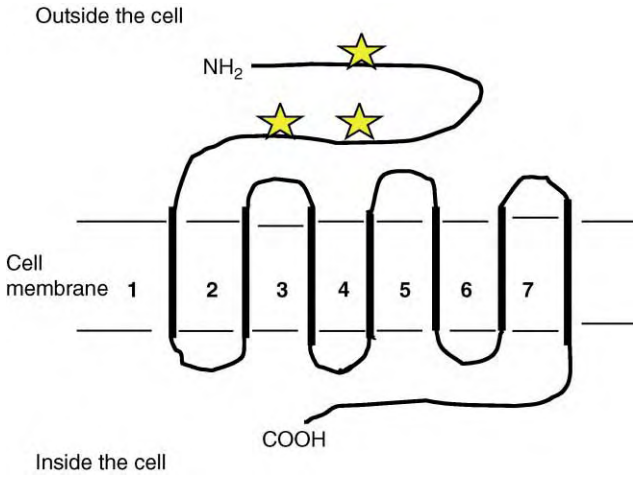

FIGURE 2 Schematic representation of the porcine CTR. Seven transmembrane regions span the cell membrane, and are connected by three extracellular and three intracellular loops. The amino-terminal extracellular loop contains three glycosylation sites (indicated by stars) and is involved with CT recognition and binding. The intracellular domain is involved with G protein coupling.

Signaling

The CTR is coupled to multiple signal pathways through interaction with different members of the heterotrimeric G protein family. These are a family of plasma membrane regulatory proteins that many activated receptors interact with and alter. The main signal pathways are the adenylate cyclase/cAMP/protein kinase A and the phosphoinositide-dependent phospholipase C (PLC) pathway, which are discussed next.

The Adenylate Cyclase/cAMP/Protein Kinase A

The binding of CT to its receptor induces conformational change in the receptor that allows it to bind to an adjacent membrane G-protein, known as G_s (the subscript s denotes stimulation). The binding causes the G_s protein to activate the membrane enzyme called adenylate cyclase. The activated adenylate cyclase, whose catalytic site is on the cytosolic site of the plasma membrane, then catalyses the conversion of cytosolic ATP to cyclic 3′,5′ adenosine monophosphate (cAMP). Cyclic AMP can diffuse throughout the cell to trigger the sequence of events leading to the cell's ultimate response to CT.

The Phosphoinositide-Dependent Phospholipase C (PLC) Pathway

The PLC pathway results in both an increase in intracellular Ca^{2+} and protein kinase C (PKC) activation via G_q protein. Both cAMP and intracellular Ca^{2+} are important second messengers for mediating the actions of CT on the osteoclast.

While adenylate cyclase, PLC and PLD are established effectors for CTR, recently CTR mediated activation of the mitogen-activated protein kinase (MAPK) pathway has been described. MAPKs are a group of serine/threonine protein kinases that are activated by several distinct classes of cell surface receptors including G-protein coupled receptors and tyrosine kinases.

Regulation

Regulation of the level or affinity of cell-surface receptors is a key component in the response to either endogenous or administered agents. The CTR is subject to both homologous (CT-induced) and heterologous regulation. Although CT effectively inhibits osteoclast-mediated bone resorption after acute administration, continuous exposure to CT results in a loss of responsiveness due to receptor down-regulation. Continuous treatment of osteoclast-like cells with CT results in the decrease in steady state levels of CTR mRNA and down-regulation of CTR binding.

It is also known that glucocorticoids stimulate CTR expression.

CTR-Like Receptor (CTRLR)

This receptor has a significant sequence homology (55%) with the CTR and share similarities in general structure and length. The CTRLR is expressed in a variety of tissues, being most prevalent in the brain, and in high densities in the pulmonary and cardiovascular system (especially in blood vessels). It is also expressed

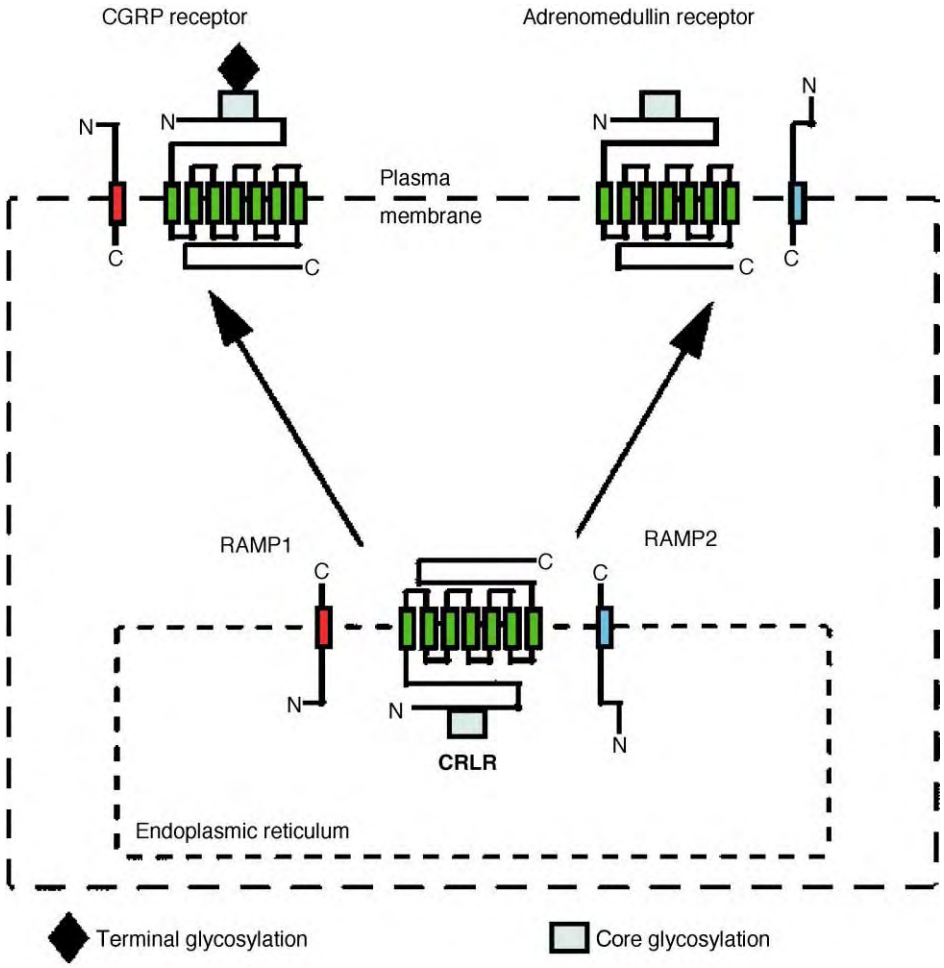

FIGURE 3 The role of RAMPs 1 and 2 and CRLR in generating CGRP or ADM receptors. (Reproduced from McLatchie L.M., Fraser, N.J., Main, M.J., Wise, A., Brown, J., Thompson, N., Solari, R., Lee, M.G., and Foord, S.M. (1998). RAMPs regulate the transport and ligand specificity of the CRLR. *Nature* (*Lond.*) **393**, 333–339.)

in the adrenal and pituitary glands, exocrine pancreas, kidney, and bone. Surprisingly, it does not bind with high affinity to any of the members of the CT peptide family. It requires other cell membrane proteins called receptor activity-modifying proteins (RAMPs) to modify its affinity for the different peptide of the CT peptide family (Figure 3).

RAMPs are single TM proteins. There are three members: RAMP1, RAMP2, and RAMP3. RAMP I acts to modify the glycosylation of CTRLR, enhance the transport of the receptor protein to the cell surface and potentially contribute to the cell surface phenotype of the receptor. RAMP I-transported CTRLR is a CGRP receptor. RAMP 2 and 3 also enhance the transport of CTRLR to the cell surface, but do not alter the pattern of glycosylation of the receptor. RAMP 2 or 3-CTRLR is an ADM receptor (Figure 3). They also act to modify the affinity of the CTR for the different peptide ligands of the CT peptide family.

See Also the Following Articles

Calcitonin Gene-Related Peptide and Adrenomedullin Receptors • Phospholipase C

Glossary

affinity The strength with which a chemical messenger binds to its receptor.

calcitonin (CT) A small peptide hormone and a potent inhibitor of bone resorption.

down-regulation A decrease in receptor number resulting from prolonged exposure to high concentration of the message.

G proteins A family of plasma membrane regulatory proteins that many activated receptors interact with and alter.

osteoclast A large multinucleated bone cell that can destroy bone.

phospholipase C Enzyme that catalyzes the breakdown of a plasma membrane phospholipid known as phosphatidyl-inositol bisphosphate (PIP_2) to inositol triphosphate (IP_3) and diacylglycerol (DAG).

protein kinases Enzymes that phosphorylate other proteins by transferring to them a phosphate group from ATP. Introduction of a phosphate group alters the activity of the protein, often itself an enzyme.

receptor-activity-modifying proteins (RAMPs) Single transmembrane-domain proteins that alter the phenotype of the calcitonin receptor-like receptor.

second messengers Substances that serve as the relay from the plasma membrane to the biochemical machinery inside the cell.

Further Reading

Christopouos, G., Perry, K. J., Morfis, M., Tilakaratne, N., Gao, Y., Fraser, N. J., Main, M. J., Foord, S. M., and Sexton, P. M. (1999). Multiple Amylin receptors arise from receptor activity – modifying protein interaction with the Calcitonin receptor gene product. *Am. Soc. Pharm. Exp. Ther.* **56**, 235–242.

Galson, D. L., and Goldring, S. R. (2002). Structure and molecular biology of the calcitonin receptor. In *Principle of Bone Biology*, (J. P. Bilezikian, L. G. Raisz, and G. A. Rodan, eds.) 2nd edition, Vol 1, pp. 603–617. Academic Press, California.

McLatchie, L. M., Fraser, N. J., Main, M. J., Wise, A., Brown, J., Thompson, N., Solari, R., Lee, M. G., and Foord, S. M. (1998). RAMPs regulate the transport and ligand specificity of the calcitonin receptor-like receptor. *Nature (Lond.)* **393**, 333–339.

Pondel, M. (2000). Calcitonin and calcitonin receptors: Bone and beyond. *Int. J. Exp. Pathol.* **81**, 405–422.

Poyner, D. R., Sexton, P. M., Marshall, I., Smith, D. M., Quirion, R., Born, W., Muff, R., Fischer, J. A., and Foord, S. M. (2002). International union of pharmacology: XXXII. The mammalian calcitonin gene-related peptides, adrenomedullin, amylin, and calcitonin receptors. *Pharmacol. Rev.* **54**, 233–246.

Sexton, P. M., Findlay, D. M., and Martin, T. J. (1999). Calcitonin. *Curr. Med. Chem.* **6**, 1067–1093.

Biography

Samia I. Girgis is a Senior Lecturer in the Department of Metabolic Medicine at Imperial College London, Hammersmith Campus, and an Honorary Consultant Chemical Pathologist at the Hammersmith Hospitals NHS Trust. For many years, her research interest has been concerned with the calcitonin gene peptide family. This included the isolation, characterization and measurement of these peptides. Her recent research interest has focused on biochemical markers of bone metabolism, their potential role in diagnosis and monitoring of patients with metabolic bone diseases.

Niloufar Moradi-Bidhendi is a Post-doctoral Research Assistant in the William Harvey Research Insitute. In 2001 she was awarded a Ph.D. on "The Interrelation of Nitric Oxide and 17ß-Oestradiol in Bone Cells." Her research interests have focused mainly on bone metabolism although her more recent studies have included work on the role of nitric oxide in wound healing.

Lucia Mancini is a Post-doctoral Research Assistant in the William Harvey Research Institute. In 2000 she was awarded a Ph.D. on "Nitric Oxide Regulation of Bone Metabolism." She is currently working in the Centre of Biochemical Pharmacology on a project examining the effect of calcitonin on the regulation of the RANK/OPG system.

Iain MacIntyre is Director of Research in the William Harvey Research Institute. After qualifying in medicine in Glasgow he trained in biochemistry as a demonstrator in Professor Hans Krebs' laboratory in Sheffield and thereafter he became Director of the Endocrine Unit at Hammersmith. His research interests have always centered on calcium and after the co-discovery of calcitonin and the definition of the thyroid as its gland of origin, he contributed many research papers on the chemistry, physiology, and clinical relevance of calcitonin. His more recent interests have focused on nitric oxide and its interaction with estrogen.

Calcium Buffering Proteins: Calbindin

Willi Hunziker
Frimorfo SA, Fribourg, Switzerland

Igor Bendik
DSM Nutritional Products, Kaiseraugst, Switzerland

The calbindins, calbindin D-9k and calbindin D-28k, belong to a large family of intracellular Ca^{2+}-binding proteins of more than 300 members classified in 45 distinct EF-hand subfamilies. Their names relate to their early discovery based on calcium binding and vitamin-D responsive expression. The calbindins are mainly localized in the cytosolic compartment of the cells and exert their action after binding ionized calcium (Ca^{2+}). Calcium ions are important biological regulators that trigger a wide array of processes. Therefore, the handling of Ca^{2+}, i.e., the Ca^{2+}-absorption, -transport, -buffering, -storage, -distribution, -signaling, and -sensing are fundamental for higher life. Functionally, the large family of EF-hand calcium-binding proteins can be classified into (1) calcium-sensing proteins, which propagate a cellular signal, (2) calcium transport proteins which are involved in the cellular calcium transport, and (3) calcium buffer proteins, that are believed to buffer the intracellular free calcium, to prevent it from damaging the cells. The calbindins are believed to be involved in some of these essential processes but their exact physiological function remains still to be determined.

Calbindin D-9k

History

Originally, calbindin D-9k and calbindin D-28k have been identified during the study of vitamin-D-dependent calcium absorption. In 1966 Wassermann and Taylor reported an intracellular vitamin D-dependent calcium-binding protein in the chicken intestine. One year later, Kallfelz and colleagues observed that this 28 kDa protein was not present in the mammalian intestine, but instead they identified a vitamin D-regulated 9 kDa intestinal calcium-binding protein that was later on called calbindin D-9k. Calbindin D-9k seems to be an evolutionary younger protein, since it does not seem to exist in birds. In mammals calbindins D-9k and D-28k have a dissimilar tissue distribution. Calbindin D-9k is highly abundant in the small intestine, whereas calbindin D-28k is absent, but it is predominant in brain and kidney. Vitamin D-induced calbindin expression is only observed in organs involved in Ca^{2+} homeostasis like intestine and kidney, in the brain calbindin D28 is present independent of vitamin D.

After its identification in 1967 calbindin D-9k was initially called calcium-binding protein 9 kDa, CaBP9k, or intestinal calcium binding protein (ICBP). Five years later the first polyclonal antibodies were generated that allowed localization and tissue distribution studies of calbindin D-9k. In 1983 the rat cDNA clone of calbindin D-9k was isolated, whereas the human counterpart was identified later in 1993. The calbindin D-9k protein is characteristic for mammals but seems to be absent in birds. It consists of two calcium-binding domains and is more closely related to S100 proteins than to calbindin D-28k. Members of the S100 protein family, a subfamily of intracellular Ca^{2+}-binding protein family, are typically small, acidic proteins containing two Ca^{2+}-binding sites. Each member of the S100 protein family has a unique spatial and temporal expression pattern. The structural relatedness seems not to coincide with its location and function.

Distribution and Localization

Calbindin D-9k is only found in mammals where it is highly abundant in the small intestine, and at lower levels also in placenta, uterus, kidney, yolk sac, fallopian tube, lung, cartilage, bone, and teeth. In the intestine the highest calbindin D-9k concentration is found in the cytoplasma of duodenal villus enterocytes. The expression levels in juvenile tissues are substantially higher than in adult ones. Antisera raised against intestinal calbindin D-9k from one species generally do not crossreact with calbindin D-9k from other species. This is likely due to the lower amino acid sequence conservation of calbindin D9 in evolution as compared to that of calbindin D28.

Gene and Sequence

The human calbindin D-9k is a heatstable and acidic ($pI = 4.52$) protein consisting of 79 amino acid (9016 Da). The human protein has an amino acid sequence identity of 78% and 74% to that of the rat and that of the mouse, respectively. The first cDNA clone was identified in 1983 by differential *in situ* ybridization in the rat system. The structural organization of the calbindin D-9k gene was determined five years later. The chromosomal location was assigned to Xp22.2 and the gene name was defined to CALB3. The CALB3 gene is a small gene of 5.5 kb comprising three exons, the coding region is contained in the exons two and three, which code for the two Ca^{2+}-binding sites, respectively.

Calcium Binding

The X-ray structure of the Ca^{2+}-binding sites of calbindin D-9k was first resolved for the bovine protein. Calbindin D9-k contains two helix-loop-helix structures of 29 and 31 amino acids called EF-hands, each binding one Ca^{2+} ion. These EF-hand structures are similar to those found in the S100 proteins and thus, calbindin 9k is considered to be a member of the S-100 protein family. Characteristic for the S100 protein family members is the atypical second EF-hand with a 14 amino-acid loop, which is different to the prototype EF-hand having a loop of 12 amino acids. Calbindin D-9k reportedly binds Ca^{2+} without a significant change in conformation. The equilibrium binding constant for calbindin D-9k is in the high nanomolar range.

Regulation

Calbindin D-9k is believed to play an important role in the Ca^{2+} absorption by transporting and/or buffering cytoplastic Ca^{2+}. Vitamin D plays a pivotal role in this regulation. The hormonally active metabolite of vitamin D, $1,25(OH)_2D_3$ (calcitriol), rapidly induces calbindin D-9k synthesis in the mammalian intestine. Calcitriol regulates the expression of calbindin D-9k not only at the transcriptional but also at the translational level. For transcriptional regulation calcitriol binds the nuclear vitamin D receptor (VDR), which is a DNA-binding protein that belongs to steroid receptor superfamily. The liganded VDR recognizes a specific VDR-response element in the promoter of the calbindin D-9k gene and activates its expression. A similar regulation of expression is believed to take place in the kidney, placenta, bone, and teeth. In the uterus calbindin D-9k is regulated by estradiol but not by vitamin D. Expression of calbindin D-9k is undetectable in the uterus in the absence of estradiol. If estradiol is present, it binds to the estrogen receptor and activates expression of the calbindin D-9k gene in a mechanism similar to that described above for vitamin D. In the lung calbindin D-9k is expressed independent of vitamin D and estradiol.

Summary and Outlook

Calbindin D-9k is a calcium-binding protein with two calcium-binding domains which belongs to the S-100 EF-hand protein family. It has a characteristic tissue distribution in mammals and does not seem to exist in birds. Its expression is regulated by calcitriol, the active metabolite of vitamin D, mainly in intestine and kidney, whereas it is regulated by estrogens in the uterus. It is thought to be involved in the transport of calcium. To our knowledge, gene knockout mice have thus far not yet been generated and no human genetic disease based on a calbindin D-9k defect has been described, both of which would allow to gain further insight on the function of this protein.

Calbindin D-28k

History

In the chicken intestinal mucosa Wassermann and co-workers identified a vitamin D-inducible 28 kDa protein that makes up from 1% to 3% of all cytosolic proteins. This protein was referred to vitamin D-dependent calcium-binding protein or CaBP. Heat treatment to 80°C did not result in significant alterations of its immunological, electrophoretical, or calcium-binding properties. As a matter of fact, a heating step was used in some of the early calbindin D-28k purification protocols. It took 20 years from its original discovery until the calbindin D-28k cDNA was cloned and sequenced. The amino acid sequence implied a 6 EF-domain structure of which two domains have lost their Ca^{2+}-binding function. This finding confirmed previous observations that calbindin D-28k binds 3–4 moles of Ca^{2+}. Calbindin D-28k shares only minimal sequence homology with calbindin D-9k and the S-100 family, but is rather closely related to calretinin, another 6 EF-hand domain calcium-binding protein expressed mainly in neuronal tissues. Calbindin D-28k is highly conserved during evolution suggestive of an important physiological function that allows only little sequence divergence. The exact physiological function, however, remains still unclear.

Distribution and Localization

Calbindin D-28k is expressed in brain, kidney, bone, pancreas, and less in some other tissues (pituitary gland, salivary gland, adrenal gland, stomach, thymus, bladder, ovary, heart, liver). The expression level between tissues varies from 0.1% to 1.5% of the total soluble protein. Calbindin D-28k is expressed in specific

regions throughout the central nervous system. The highest calbindin D-28k levels are present in the cerebellar Purkinje cells where it is located in the cell bodies, axons, and dendrites, but not or to a much lesser extent in the adjacent granular cell layer. Furthermore, calbindin D-28k is localized in specific cells of the sensory pathways in mammalian cochlear and vestibular hair cells in the inner ear, as well as in the basilar papilla of the chick cochlea. Calbindin D-28k concentrations of up to 2 mM were reported to be present in the auditory neurons. In the kidney, calbindin D-28k is exclusively localized in the tubular regions of the distal nephron (distal convoluted tubule, the connecting tubule, and the cortical collecting tubule), where reabsorption of calcium is known to occur. Calbindin D-28k is also found to be expressed in the insulin-producing B cells of the avian and mammalian pancreas.

Calbindin D-28k is expressed in the avian but not in the mammalian intestine, where it is found by immunocytochemical techniques to be present in the intestinal absorptive cells whereas globlet cells are negative. The subcellular distribution of calbindin D-28k was determined in chick duodenum by electron microscopy using the protein A-gold technique. Calbindin D-28k was found in the cytosol and the nuclear euchromatin of the intestinal absorptive cells, but not in the mitochondria, the lysosomes, or the cysternal spaces of the rough endoplasmic reticulum nor in the Golgi apparatus.

An antiserum raised to chick intestinal calbindin D28 was found to also crossreact with calbindin D-28k from other species. The antiserum revealed the presence of calbindin D-28k in intestinal homogenates of duck, robin, and Japanese quail and with a protein in the duodenum of reptiles but not fishes and amphibia. Similarly, calbindin D-28k was also identified in the kidney and brain of amphibia, reptiles, birds, and mammals and also in the nervous system of fish and several mollusks. Since calbindin D-28k is found in fish brain but not in fish intestine and kidney, one might speculate that it was originally a neuronal protein.

Gene and Sequence

The rigid structure of calbindin D-28k is acidic ($pI = 4.54$) and contains 261 amino acids (30 025 Da). The chicken cDNA sequence was the first to be cloned (1986). The deduced amino acid sequence of this calbindin D-28k cDNA revealed surprisingly the presence of six EF-hand domains. Of these predicted six EF-hand domains only four were considered to be functional due to mutations within the conserved calcium coordination sites in the loop regions of domains 2 and 6. A protein sequence comparison of calbindin D-28k showed a high degree of conservation over all species. The human calbindin D-28k gene was localized to the human chromosome 8q21.3–q22.1 and the gene name was annotated to CALB1. CALB1 spans 24 kb interspersed by 10 introns and 11 exons.

Calcium Binding

EF-hand proteins play a crucial role to guide and sustain the calcium signal. The designation "EF hand" is derived from the structural orientation of the two α-helices (E and F) that form together with the calcium-binding loop of 12 amino acids the highly conserved metal-binding consensus sequence. The loop contains five oxygen-containing amino acids at defined positions that are important for coordinating the calcium ion. Da Silva and Reinach proposed to classify the EF-hand members into proteins with regulatory roles called Ca^{2+} sensor proteins and those involved in Ca^{2+} buffer and transport were entitled Ca^{2+} buffer proteins. The Ca^{2+}-binding affinities of EF-hand proteins have a wide equilibrium constant range ($K_d = 10^{-4}$–10^{-9} M). This large binding range is coded in the amino acid sequence, in particular within the 12-residues consensus loop that directly coordinates the Ca^{2+} ion. The four EF-hands domains of calbindin D-28k bind calcium with high affinity. The binding is Ca^{2+}-specific with marginal Ca^{2+}/Mg^{2+} antagonism. Therefore, under resting intracellular calcium concentrations (<100 nM) the calcium-binding sites of calbindin D-28k are largely empty and are thus immediately available for a fast buffering of nerve stimulation evoked Ca^{2+} transients. Two K_d values have been determined calbindin D-28k. The first $K_d(1)$ value ranges from 175 to 237 nM and the second $K_d(2)$ ranges from 411 to 513 nM, respectively. Ca^{2+} binding seemingly causes a conformational change in the molecule, which could trigger an interaction with another protein, thereby propagating a calcium signal.

Knockout Animals

The evaluation of the physiological role of calbindin D-28k has been facilitated by the recent generation of mouse strains deficient in this protein. Calbindin D-28k-nullmutant (−/−) mice are viable and appeared phenotypically normal in their general development. There was no evidence of any major changes in the histology neither of their nervous system nor of any other organ. However, calbindin D-28k knockout mice showed a distinct motor coordination problem that could not be overcome by continuous learning. These animals lack the calbindin D-28k in the Purkinje cells of the cerebellum, a center for motor coordination. This result points towards a critical physiological role of calbindin D-28k in controlling Purkinje cell-dependent motor behavior.

Due to its presence in Purkinje cells calbindin D-28k was also thought to be associated with other neurological disorders such as ataxia. Patients with spinocerebellar ataxia type 1 (SCA1) show a decreased calbindin D-28k staining in Purkinje cells and an aggregation of ataxin-1 in the nucleus, leading eventually to Purkinje cell death. A similar decrease in calbindin D-28 staining of Purkinje cells was found in transgenic mice overexpressing mutant ataxin-1, an animal model for SCA1. Calbindin D-28k knockout mice on the other hand did not show any Purkinje cell loss, suggesting that the lowered calbindin D-28k levels in SCA1 patients are unlikely the cause but rather the consequence of the Purkinje cell damage due to the high ataxin-1 levels. The fact that the Purkinje cells and other calbindin D-28k positive neurons of wild type mice also survive in the calbindin knockout mice, shows that the lack of calbindin D-28k is not per se detrimental to these cells. Thus, this finding argues against a general calcium-mediated excitotoxicity preventive role of calbindin D-28k. The functional data available thus far suggests that in the cerebellum calbindin D-28k plays a role in motor coordination. To our knowledge, no human genetic disease is known where the root cause is a calbindin D-28k gene defect.

Regulation

Calbindin D-28k has a unique tissue-specific expression pattern indicating a highly specialized function. Calbindin D-28k is regulated in a vitamin D-dependent fashion in kidney and pancreas, whereas its presence in the specific brain regions is independent of the vitamin D status. There are, however, reports showing a brain region-specific regulation by gluccocorticoids, by sex steroids and by nerve growth factor.

The initial finding that calbindin D-28k is induced by vitamin D in tissues involved in calcium transport, suggested that calbindin D28 might have an important role in vitamin D regulated calcium absorption. The intestine, the kidney, and the bone are target organs for the biologically active form of vitamin D, the 1α, 25-dihydroxyvitamin D3, that is known to regulate the calcium demand of the body. The active vitamin D metabolite regulates the expression of calbindin D-28k in these tissues by the steroid hormone mechanism of action as described earlier for calbindin D-9k.

Summary and Outlook

The fact that antibodies to chicken calbindin D-28k crossreact with calbindin D-28k of evolutionary far-diverged species suggest a high conservation of this protein in evolution. This finding is further evidenced by sequence comparison among the different species. The four intact and the two degenerated EF-hands show similarly a high degree of conservation, suggesting, apart from Ca^{2+}-binding, an additional functional conservation pressure. Such an additional function could be triggered by protein–protein interaction in a Ca^{2+}-dependent manner. Indeed, there is increasing evidence that similar to calmodulin, also calbindin D-28k could act as calcium sensor, undergoing a conformational change upon Ca^{2+}-binding. Such a conformational change could unmask new domains and allow calbindin D-28k to interact with other yet to be identified intracellular effectors thereby propagating the Ca^{2+}-signal.

Another intriguing question regarding calbindin D-28k function is the partial substitution during evolution by calbindin D-9k. In mammals calbindin D-9k substitutes for calbindin D-28k in the intestine and in part in the kidney. This raises the intriguing hypothesis that in the evolutionary older species calbindin D28k could have a dual function, one for calcium absorption in the intestine (vitamin D dependent), the other as calcium sensor in neurons (vitamin D-independent). With the evolution of mammals, the calcium absorption function apparently was delegated the "newly invented" calbindin D-9k.

See Also the Following Articles

Calcium-Binding Proteins: Cytosolic (Annexins, Gelsolins, C_2-Domain Proteins) • Calcium Buffering Proteins: ER Luminal Proteins • Calcium Sensing Receptor • Calcium Signaling: Cell Cycle • Calcium Transport in Mitochondria • Vitamin D • Vitamin D Receptor

Glossary

EF-hand calcium-binding site A specific protein sequence constisting of two α-helices connected by a sequence of 12–14 amino acids that constitute a high affinity calcium-binding site (K_d in the nM range). Depending on the protein sequence, the binding site is either specific for calcium (e.g., calbindin) or can also accept magnesium (e.g., parvalbumin).

gene family A number of closely related genes that arose by a series of gene duplications during evolution. Gene families can have from only very few up to several hundred members. The EF-hand family of calcium-binding proteins has more than 300 members grouped in several subfamilies.

Further Reading

Bouillon, R., Van Cromphaut, S., and Carmeliet, G. (2003). Intestinal calcium absorption: Molecular vitamin D mediated mechanisms. *J. Cell Biochem.* **88**, 332–339.

Hemmingsen, C. (2000). Regulation of renal calbindin-D28k. *Pharmacol. Toxicol.* **87**(suppl. 3), 5–30.

Schwaller, B., Meyer, M., and Schiffmann, S. (2002). "New" functions for "old" proteins: The role of the calcium-binding proteins

calbindin D-28k, calretinin and parvalbumin, in cerebellar physiologycalbindin D-28k, calretinin and parvalbumin, in cerebellar physiology. Studies with knockout mice. *Cerebellum* **1**, 241–258.

Biography

Willi Hunziker holds a DVM degree from the University of Zürich, Switzerland. He did postdoctoral fellowships at Baylor College of Medicine in Houston, TX and at University California in Riverside. After heading an R&D department at Big Pharma, he is currently CEO of Frimorfo, a Swiss Biotech Service Company (www.frimorfo.com). His research interests are calcium metabolism and regulation of gene expression by steroids, retinoic acid, and vitamin D.

Igor Bendik obtained his Ph.D. from the University of Basel, Switzerland. During his Ph.D. thesis he was interested in calbindin D-28k and the vitamin D receptor. At the Burnham Institute in La Jolla, California, he expanded his knowledge on nuclear receptors. Back in Basel he was a group leader in the medical faculty working on tumor suppressor genes. He is currently employed by DSM, a company active in life sciences, performance materials, and industrial chemicals.

Calcium Buffering Proteins: ER Luminal Proteins

Jody Groenendyk and Marek Michalak
University of Alberta, Edmonton, Alberta, Canada

Ca^{2+} buffering endoplasmic reticulum (ER) proteins are ER resident proteins that bind Ca^{2+} with a high capacity. They play an important role in the maintenance of resting free Ca^{2+} concentration in the lumen of ER and subsequently in the modulation of cellular Ca^{2+} homeostasis. This is critical because Ca^{2+} is a universal intracellular signaling molecule, which controls numerous developmental and cellular pathways. Changes in Ca^{2+} concentration affect processes as diverse as learning and memory, secretion, contraction and relaxation, membrane excitability, cell motility, cytoplasmic and mitochondrial metabolism, protein and lipid synthesis, cell cycle, apoptosis, organellar trafficking, and protein folding and quality control. Therefore, it is of the utmost importance that Ca^{2+} homeostasis is tightly regulated in all cells. This is accomplished by a variety of Ca^{2+} transporting, binding, and buffering proteins, which are found in many cellular compartments.

The Endoplasmic Reticulum and Ca^{2+} Homeostasis

The ER is one of the most important intracellular Ca^{2+} buffering and storage organelles. In response to a variety of external stimuli, Ca^{2+} is released from the lumen of the ER into the cytosol, via the inositol-1,4,5-triphosphate receptor ($InsP_3R$) and/or the ryanodine receptor (RyR) Ca^{2+} channels. Some Ca^{2+} also enters the cytosol from the extracellular environment, via Ca^{2+} channels in the plasma membrane. Most of the released Ca^{2+} is taken up back into the lumen of the ER via the sarcoplasmic–endoplasmic-reticulum Ca^{2+}-ATPase (SERCA). Some of the Ca^{2+} is also removed from the cytosol by the plasma membrane Ca^{2+}-ATPase and the Na^{+}–Ca^{2+} exchanger. Within the ER, Ca^{2+} is bound to and buffered by high concentrations of luminal Ca^{2+} binding proteins.

Ca^{2+} Buffering in the ER Lumen

In total, the lumen of the ER contains 1–3 mM Ca^{2+}, a concentration similar to that in the extracellular space. A small portion of this ER lumenal Ca^{2+} is not buffered by Ca^{2+} binding to proteins and is considered free. Resting free Ca^{2+} concentrations in the ER vary from 100 to 400 μM, while those in the cytosol are in the nanomolar range. The actual resting free Ca^{2+} concentration in the ER is determined by the balance between the rates of Ca^{2+} uptake and Ca^{2+} leak and by the extent of buffering by the resident Ca^{2+} binding proteins.

Most Ca^{2+} in the lumen of the ER is bound to the Ca^{2+} binding molecular chaperones that are resident there. These proteins maintain specific concentration gradients of Ca^{2+} in the ER and localize Ca^{2+} to the sites of release. They also directly affect both the Ca^{2+} storage capacity of the ER and the free Ca^{2+} concentration under resting conditions and after cellular stimulation. Table I shows a list of ER proteins that are involved in buffering Ca^{2+} in the ER lumen. There are two major classes of ER Ca^{2+} binding proteins. Class I, the larger of the two, represents proteins which bind Ca^{2+} with relatively high capacity and low affinity. These proteins contain a large proportion of acidic amino acid residues that are involved in the high capacity and low affinity Ca^{2+} binding. Their Ca^{2+} binding capacity varies from as little as 2 moles of Ca^{2+} per mole of protein to as much as 50 moles of Ca^{2+} per mole of protein. The high capacity Ca^{2+} binding sites have a relatively low affinity for Ca^{2+} ($K_d = 1–2$ mM), which parallels the relatively high content of Ca^{2+} in the ER lumen. These Ca binding proteins are responsible for Ca^{2+} storage in the lumen of the ER/sarcoplasmic reticulum (SR), and they effectively determine the capacity of these intracellular organelles for Ca^{2+}. In contrast, class II represents Ca^{2+} binding proteins in the lumen of the ER that bind Ca^{2+} with relatively high affinity and low capacity. The function of these high affinity binding sites is not obvious, given the high concentrations of Ca^{2+} in the lumen of the ER. It is thought that they might play a structural role, or that they might be responsible for the regulation/maintenance of specific protein–protein interactions. Several of the class II proteins contain a classic EF-hand

TABLE I

Ca^{2+} Binding Proteins of the Endoplasmic Reticulum Lumen

Protein name	Ca^{2+} binding (mole/mole of protein)
CLASS I proteins (high capacity and low affinity Ca^{2+} proteins)	
Calreticulin	25
Grp 94/endoplasmin	10
Grp 78/BiP	binds Ca^{2+}
PDI family	
PDI	20
ERp72	12
ERCalcistorin/PDI	20
P5	binds Ca^{2+}
ERp57	not investigated
ERp44	not investigated
ERp29	not investigated
Calsequestrin	50
CLASS II proteins (contain EF-hand Ca^{2+} binding motifs and bind 6–7 moles of Ca^{2+}/mole of protein with high affinity)	
Reticulocalbin	
Cab45	
Calumenin	
ERC55	
Crocalbin/CBP-50	

Ca^{2+} binding site, previously identified in many cytoplasmic proteins that bind Ca^{2+} with high affinity.

A characteristic common to proteins in both classes is that they contain an N-terminal signal sequence that targets them to the lumen of the ER. They also terminate with a KDEL-like amino acid sequence that is responsible for their continual retrieval back to the ER lumen. Finally, most of the proteins resident in the lumen of the ER are multifunctional, regardless of their Ca^{2+} binding properties. They are involved in maintaining Ca^{2+} homeostasis and they assist in both protein folding and assembly, and lipid synthesis and transport.

Class I Ca^{2+} Binding Proteins in the ER Lumen

The class I ER luminal proteins are those that bind Ca^{2+} with high capacity and low affinity. In most of these proteins, specific regions of the amino acid sequence contain a high proportion of acidic residues, and it is these acidic residues that are involved in the high capacity Ca^{2+} binding. The following ER proteins belong to class I: calreticulin, Grp94, BiP, the PDI-family, and calsequestrin.

Calreticulin

Calreticulin (46 kDa) is a major Ca^{2+} storage protein in the ER lumen, which contains both high affinity/low capacity *and* low affinity/high capacity Ca^{2+} binding sites. Specifically, it binds up to 25 moles of Ca^{2+} per mole of protein with $K_d = 1$ mM (low affinity) and 1 mole of Ca^{2+} per mole of protein with a $K_d = 1\ \mu M$ (high affinity). Calreticulin, one of the most extensively studied ER luminal proteins, is responsible for binding approximately 50% of the Ca^{2+} stored in the lumen of the ER. As observed for other ER luminal proteins, the expression of calreticulin is up-regulated by stress, Ca^{2+} depletion, and metabolic starvation. The overexpression of calreticulin in the ER significantly affects the ER Ca^{2+} storage capacity, Ca^{2+} uptake via SERCA, and release via $InsP_3$ receptor, indicating an important role for calreticulin in ER Ca^{2+} buffering.

Calreticulin is composed of three structural and functional domains. The N-domain has the most conserved amino acid sequence and binds both Zn^{2+} and ATP. In conjunction with the central, P-domain of the protein, it enables calreticulin's chaperone function. The central, P-domain of the protein is very rich in proline residues and contains several repeated amino acid sequences. It forms a highly unusual hairpin-like structure that involves the entire proline-rich region, and it is stabilized by a three-strand antiparallel B-sheet that is formed by the amino acid repeat sequences. The P-domain binds Ca^{2+} with high affinity and low capacity. It also interacts with other ER chaperones and their substrates. The carboxyl-terminal C-domain of calreticulin contains a large number of acidic amino acid residues, and it is responsible for the high capacity Ca^{2+} binding behavior of calreticulin.

In addition to binding and buffering Ca^{2+} in the lumen of ER, calreticulin also plays a significant role as a molecular chaperone with a specificity for glycosylated proteins. Specifically, calreticulin binds N-linked, monoglucosylated carbohydrates on newly synthesized proteins. In conjunction with calnexin, an integral membrane protein and also a chaperone in the ER, calreticulin facilitates protein folding and oligomerization, and it supports quality control in protein folding processes. As components of the calreticulin/calnexin cycle, calreticulin might prefer secretory proteins and calnexin integral membrane proteins. Calreticulin and calnexin both form heterodimeric complexes with ERp57 and other chaperones. The formation of these chaperone–chaperone and chaperone–substrate interactions is regulated by changes in Ca^{2+} concentration in the lumen of the ER.

Grp94 (Glucose-Regulated Protein)

Grp94 (94 kDa) is another major Ca^{2+} binding protein, and one of the most abundant proteins in the lumen

of the ER. It binds 8–10 mol of Ca^{2+} per mol of protein with low affinity ($K_d = \sim 600\ \mu M$). Like calreticulin, Grp94 contains an acidic C-terminal region that comprises the low affinity Ca^{2+} binding site. Because of their relatively high capacity for Ca^{2+} binding and their abundance, Grp94 and calreticulin are the most significant Ca^{2+} binding/buffering proteins in the ER lumen. The expression of Grp94 is up-regulated upon glucose starvation, hence its name (glucose-regulated protein). It binds ATP, but has only very low ATPase activity. It also functions as a molecular chaperone but binds to limited numbers of nascent proteins, most of them advanced folding intermediates or misfolded proteins that have been previously associated with other chaperones; it has a relatively low affinity for early folding intermediates. It appears that Grp94 is a chaperone specific for advanced intermediates in protein biosynthesis and that it works downstream of, or in conjunction with, other chaperones. Ca^{2+} binding to Grp94 may play a role in the *in vivo* interactions of the protein with other chaperones and with its substrates.

BiP (Immunoglobulin Binding Protein)

BiP is a 78-kDa ER chaperone that binds immunoglobulins. It is a monomeric protein with two distinct functional domains, an ATP-binding domain and a peptide-binding domain. While it has a relatively low capacity for binding Ca^{2+} (1–2 mole of Ca^{2+} per mole of protein), it contributes possibly as much as 25% of the total Ca^{2+} storage capacity of the ER, and its elevated expression causes an appreciable increase in ER Ca^{2+} storage capacity. BiP assists in the folding of newly synthesized polypeptides by binding to exposed hydrophobic side chains and subsequently coordinating the formation of their correct tertiary and quaternary structure. BiP binds ATP and has high ATPase activity essential for its chaperone function. Its association with nascent polypeptides is stabilized by the high concentrations of Ca^{2+} in the ER lumen and likely involves Ca^{2+} binding. The expression of BiP is up-regulated by a variety of stress conditions, including ER Ca^{2+} depletion.

The Protein Disulfide Isomerase (PDI) Family of Proteins

Several members of the protein disulfide isomerase (PDI) family are well-characterized. Each is folded similarly to thioredoxin, with a "typical" sequence of α helices and β strands. PDI proteins also contain one or more active sites (typically two), again similar to that of thioredoxin. The main function of the PDI family of proteins is to catalyze the oxidation of disulfide bonds and to isomerize incorrectly formed disulfide bonds in newly synthesized polypeptides. Recent studies indicate that some members of this family (PDI, ERp72, and ERcalcistorin/PDI) also contribute to Ca^{2+} buffering in the ER lumen.

PDI

PDI is a 58-kDa Ca^{2+}-binding chaperone. It binds 19 mol of Ca^{2+} per mol of protein with low affinity ($K_d = 2–5$ mM). The C-terminus of the protein contains numerous pairs of acidic residues that form the low affinity, high capacity Ca^{2+} binding sites. PDI is an abundant and widely distributed ER luminal protein. Its major function is to catalyze disulfide bond formation in newly synthesized proteins and, importantly, high concentrations of Ca^{2+} augment this activity. PDI contains a typical thioredoxin active site, which contains two cysteines separated by two other amino acid residues (the CXXC motif).

ERp72

ERp72 is a 72-kDa member of the PDI family that binds 12 mol of Ca^{2+} per mol protein with low affinity. Its amino acid sequence includes an acidic C-terminus that is involved in the high capacity Ca^{2+} binding. ERp72 contains 3 thioredoxin-like active sites and has PDI-like activity. The expression of ERp72 is induced under stress conditions, including ER Ca^{2+} depletion.

ERcalcistorin/PDI

ERcalcistorin/PDI, a 58-kDa protein, also has high Ca^{2+} binding capacity and low affinity. ERcalcistorin/PDI binds 23 mol of Ca^{2+} per mol of protein with low affinity ($K_d = \sim 1$ mM). Like other class I ER Ca^{2+} binding proteins, the high-capacity Ca^{2+} binding sites in ERcalcistorin/PDI are localized to a C-terminal stretch of acidic amino acid residues. As noted previously for members of the PDI family, high concentrations of Ca^{2+} augment the protein's isomerase activity. ERcalcistorin/PDI has 55% amino acid sequence identity to PDI, and it shows PDI-like chaperone activity.

Other PDI Family Members

Other members of the PDI family have also been identified. While information regarding their Ca^{2+} binding properties is limited, it has been established that they play a role in protein folding and posttranslational modification. P5, a 44-kDa polypeptide also known as CaBP1, contains two internal thioredoxin-like domains and a C-terminal KDEL retention/retrieval signal. While it does bind Ca^{2+}, it is unclear what role it plays in Ca^{2+} buffering in the ER lumen. ERp57, a 57-kDa protein, carries out disulfide bond exchange

in conjunction/complex with calreticulin or calnexin. Ca^{2+} binding to this protein has not been investigated. PDIR has the three CXXC motifs typically found in proteins within the PDI superfamily that are responsible for their oxidoreductase activity. PDIR is preferentially expressed in cells that actively secrete proteins, and its expression is stress-inducible. PDIp is a PDI-like protein expressed specifically in the pancreas. ERp44 and ERp29 are two other proteins of PDI family each containing a single thioredoxin-fold domain but no thioredoxin-like active site.

Calsequestrin

Calsequestrin is a high-capacity Ca^{2+} binding protein found in the SR of cardiac and skeletal muscle. It binds 40–50 moles of Ca^{2+} per mole of protein with low affinity ($K_d = \sim 1–2$ mM). Small quantities of calsequestrin are also present in the ER of smooth muscle and the cerebellum. There are two isoforms of calsequestrin that are encoded by distinct genes: a 55-kDa cardiac form and 63-kDa skeletal muscle form. These proteins have very similar amino acid sequences with a C-terminal stretch containing over 100 acidic amino acids that are involved in the high-capacity Ca^{2+} binding. Calsequestrin is localized to the terminal cisternae of the SR, where it acts as a Ca^{2+} buffer. It lowers the concentration of free Ca^{2+} inside the SR, thereby decreasing the concentration gradient against which the Ca^{2+}-ATPase must work as it transports Ca^{2+} from the cytosol back into the SR. During the initiation of muscle contraction, Ca^{2+} is released from the terminal cisternae of the SR into the cytosol via the ryanodine receptor. Ca^{2+}-induced conformational changes in calsequestrin affect the junctional face of these membrane proteins and this, in turn, regulates the opening and closing of the Ca^{2+} channel. Interestingly, the crystal structure of calsequestrin shows that it contains three similar domains that contain a thioredoxin-like region. The thioredoxin-like fold may, therefore, be a common structural feature of ER/SR luminal proteins.

Class II Ca^{2+} Binding Proteins in the ER Lumen

Class II Ca^{2+} binding proteins in the ER lumen are those that bind Ca^{2+} with high affinity ($K_d = 1\ \mu M$ or less). Much less is known about this class of Ca^{2+} binding proteins, which includes: reticulocalbin, Cab45, calumenin, ERC-55/TCBP-49/E6BP, crocalbin/CBP-50, and calreticulin. Calreticulin's structure, function, and Ca^{2+} binding properties have been discussed already, with the class I ER proteins. The class II Ca^{2+} binding proteins have also been found in the Golgi and may, therefore, play an important role in the secretory pathway. With the exception of calreticulin, they all contain six or seven EF-hand type, high-affinity Ca^{2+} binding sites, and they are considered to be members of the reticulocalbin family. This family is a new subset of the EF-hand superfamily of proteins. The function of the high-affinity Ca^{2+} binding sites in these proteins is not clear, but they may be involved in Ca^{2+}-dependent processes. They may also play an important structural role in the proteins.

Reticulocalbin is a 44-kDa protein that contains six EF-hand motifs. The difference between the amino acid sequences of these domains and EF-hand consensus sequences suggests that some of the domains may have lost their Ca^{2+}-binding capability. Cab45 is a 45-kDa, ubiquitously expressed protein. It contains six EF-hand Ca^{2+} binding motifs. In contrast to reticulocalbin and ERC-55, which are soluble components of the ER, Cab45 is localized to the Golgi. Cab45 is the first calcium-binding protein that has been localized to the lumen of the Golgi, a post-ER compartment. Calumenin is a 39-kDa member of the reticulocalbin family. It is highly homologous to other family members, including reticulocalbin, Cab45, and ERC55. It is localized to the lumen of the ER and has a KDEL-like (HDEF) ER retrieval signal. ERC-55 (55 kDa) comprises an amino-terminal signal sequence followed by six copies of the EF-hand Ca^{2+} binding motif.

The Functional Significance of Ca^{2+} Buffering in the ER

There are many Ca^{2+}-binding proteins in the ER lumen that both bind and buffer Ca^{2+} and that also assist in protein folding and posttranslational modification. Ca^{2+} buffering within the ER lumen is an essential component of proper cellular Ca^{2+} homeostasis. Furthermore, it has a profound effect on other ER functions including protein and lipid synthesis and stress response. For example, reduction of Ca^{2+} concentration in the ER leads to the accumulation of misfolded proteins, increased expression of ER chaperones, and ER to nucleus/ER to plasma membrane signaling, which inhibits protein synthesis and facilitates protein degradation. Overall, disruption of ER Ca^{2+} homeostasis has profound effects on intracellular communication and cell growth, resulting in organellar diseases, and it has detrimental effects at cellular and systemic levels.

See Also the Following Articles

Calcium-Binding Proteins: Cytosolic (Annexins, Gelsolins, C_2-Domain Proteins) • Calcium-Modulated Proteins (EF-hand) • Chaperones, Molecular

Glossary

calreticulin Multifunctional Ca^{2+} binding/buffering ER resident chaperone. The protein is responsible for the buffering of over 50% of ER luminal Ca^{2+} and for assisting in the folding of newly synthesized glycoproteins.

chaperones Molecules that bind to misfolded proteins and assist in their folding and posttranslational modification.

endoplasmic reticulum Intracellular organelle involved in many cellular functions including modulation of Ca^{2+} homeostasis, protein synthesis and modification, and lipid synthesis.

protein disulfide isomerase Belonging to a family of proteins containing thioredoxin, they modify and catalyze the formation of disulfide bonds in newly synthesized proteins.

Further Reading

Baumann, O., and Walz, B. (2001). Endoplasmic reticulum of animal cells and its organization into structural and functional domains. *Int. Rev. Cytol.* **205**, 149–214.

Eggleton, P., and Michalak, M. (2003). *Calreticulin in Health and Disease*. R. G. Landes Co., Austin, Texas.

Molinari, M., and Helenius, A. (2000). Chaperone selection during glycoprotein translocation into the endoplasmic reticulum. *Science* **288**, 331–333.

Noiva, R. (1999). Protein disulfide isomerase: The multifunctional redox chaperone of the endoplasmic reticulum. *Sem. Cell Dev. Biol.* **10**, 481–493.

Biography

Jody Groenendyk is a graduate student in the Department of Pediatrics, Faculty of Medicine, and the University of Alberta. For several years she has been involved in studies on Ca^{2+} and buffering proteins for the ER. She is supported by the Alberta Heritage Foundation for Medical Research and by the Canadian Institutes for Health Research.

Marek Michalak is a Professor of Biochemistry at the University of Alberta, Edmonton, Alberta. He obtained his Ph.D. at the Nencki Institute for Experimental Biology, Warsaw, Poland. Michalak's laboratory has been studying ER luminal proteins for almost 20 years. The major focus of this work is on Ca^{2+} buffering and chaperone protein, with a special emphasis on calreticulin. He has published over 150 papers in the area of ER Ca^{2+} binding chaperones. He has authored and edited books on the structure and function of calreticulin and calnexin.

Calcium Oscillations

Marisa Brini
University of Padova and Venetian Institute of Molecular Medicine (VIMM), Padova, Italy

Cellular signaling mechanisms are designed to transmit information from the cell surface to specific targets within the cell. Usually, the information is transmitted by intracellular messengers, of which the calcium ion, Ca^{2+}, is one of the most important. Generally, extracellular stimuli are converted in a transient increase in the cytosolic Ca^{2+} concentration, $[Ca^{2+}]_c$, which, in turn, activates cellular functions. The specificity of the activated signal is guaranteed by the complex spatial and temporal organization of the changes in Ca^{2+} concentration, which increases the versatility of this messenger. Different cell types use distinct Ca^{2+} signals, as appropriate to their physiology. The ability to use Ca^{2+} in different modes helps cells to vary the amplitude, frequency, kinetics, and localization of the signal. It is now recognized that periodic $[Ca^{2+}]_c$ changes (i.e., oscillations) probably represent the typical response of cells to physiological agonists concentrations.

General Considerations

It has been known since the 1950s that the periodic opening of plasma-membrane Ca^{2+} channels, such as induced, for example, by the rhythmic changes of the plasma membrane potential of the heart or by burst of action potential in neurons, can produce fluctuations in cytosolic $[Ca^{2+}]$. The idea that $[Ca^{2+}]_c$ oscillations may also occur in nonexcitable cells has emerged much later, thanks to seminal observations by Cobbold and coworkers in the mid-1980s on the fertilization of oocytes and on hormone-stimulated hepatocytes. Surprisingly, these oscillations were not dependent on the periodic opening and closing of plasma membrane Ca^{2+} channels, but rather on cycles of Ca^{2+} release and uptake from the intracellular compartment sensitive to the second messengers inositol (1,4,5)-trisphosphate ($InsP_3$), which is the endoplasmic reticulum. Later, Ca^{2+} oscillations were observed in other animal as well as plant cells, even if many of these cells do not have an obvious oscillatory biological function.

A question that immediately arises is the reason for the transmission of the Ca^{2+} signal by oscillations rather than by a stationary change in Ca^{2+} concentration. It is generally assumed that the oscillatory behavior has physiological advantages. This is so because the elevation of Ca^{2+} concentration over a long period is known to be lethal to the cell: the oscillatory behavior would prevent this negative effect, while still permitting optimal activation of Ca^{2+} sensing enzymes. The oscillatory regime would also prevent long-lasting receptor desensitization thus increasing the sensitivity of sensing enzymes to Ca^{2+}, i.e., $[Ca^{2+}]$ would be permitted to periodically exceed the threshold for enzyme activation, even its level would remain below the threshold. Another advantage is the wide range of temporal and spatial aspects that oscillations can assume, allowing different signals to be transmitted within cells and from cell to cell.

Usually, Ca^{2+} oscillations are characterized by rather constant amplitude and by a variable frequency, which ranges from 5 to 60 s depending to the cell type, and on the nature and the strength of the stimulus (Figure 1). These characteristics have led to the concept of frequency-modulated Ca^{2+} signaling, which reflects the ability of cells to interpret changes in the frequency of the oscillations.

Mechanism of $[Ca^{2+}]_c$ Oscillations

The mechanism of Ca^{2+} oscillation has received much experimental and theoretical attention, but is still largely debated. A first distinction considers the origin of the Ca^{2+} spikes, for which two major mechanisms exist: one is linked to the periodic opening of plasma membrane channels and another to cycles of Ca^{2+} release and uptake from intracellular stores (Figure 2). However, this distinction is incomplete since very often the contributions of intracellular Ca^{2+} release and of extracellular Ca^{2+} influx cannot be clearly separated. An obvious example is that of cardiac myocytes, where the periodic contraction of the cells is directly promoted by the release of Ca^{2+} from the sarcoplasmic reticulum (SR), which is triggered by localized influx of Ca^{2+} through plasma-membrane voltage-operated Ca^{2+} channels (VOCs), a process known as Ca^{2+}-induced Ca^{2+} release (CIRC).

In excitable cells such as neurons, heart, and neuroendocrine cells, the transient $[Ca^{2+}]$ elevation is

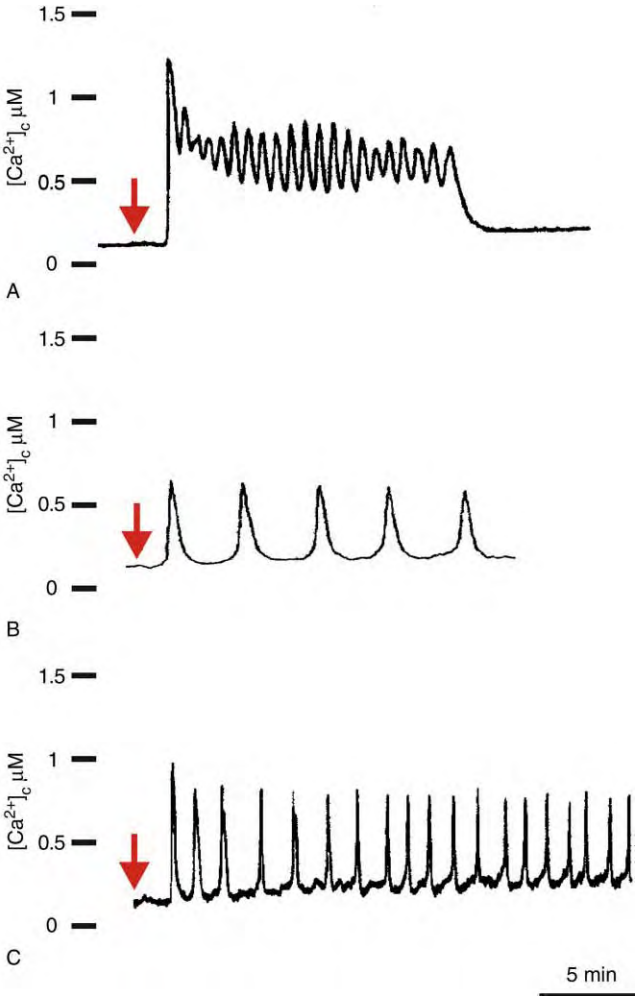

FIGURE 1 Examples of different oscillatory pathways. A, parotid gland; B, hepatocyte; C, endothelial cell. The pattern of oscillations may vary with respect to amplitude and period. The red arrow indicates agonist stimulation.

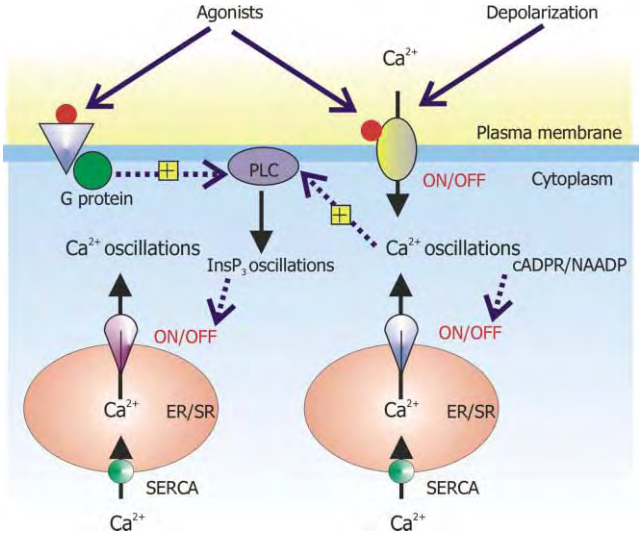

FIGURE 2 Signaling pathways that participate in the generation of Ca^{2+} oscillations. Three models are proposed. In excitable cells Ca^{2+} oscillations are evoked by rhythmic oscillatory changes in membrane potential. In nonexcitable cells they are induced either by the oscillatory production of $InsP_3$, or following the oscillatory inactivation of $InsP_3$ receptors (ON/OFF). ER/SR, endoplasmic/sarcoplasmic reticulum; PLC, phospholipase C; SERCA, sarco/endoplasmic reticulum calcium ATPase; $InsP_3$, inositol 1,4,5-trisphosphate; cADPR, cyclic ADP-ribose; NAADP, nicotinic acid adenine dinucleotide phosphate.

due to Ca^{2+} entry through voltage-operated Ca^{2+} channels or receptor-operated Ca^{2+} channels (ROCs) activated in response to neurotransmitters. In these cells the oscillatory behavior is secondary to the oscillatory nature of the trigger itself. For example, cortical and cerebellar neurons in primary cultures exhibit spontaneous oscillations that occur in synchrony with adjacent neurons and are dependent on synaptic activity, i.e., changes of membrane potential.

In nonexcitable cells the predominant mechanism of $[Ca^{2+}]_c$ elevation is through the activation of plasma membrane receptors coupled to G proteins and the phosphoinositide pathway. Activation of membrane phospholipase C (PLC) generates the second messenger $InsP_3$ from phosphatidylinositol 4,5-bisphosphate, mobilizing Ca^{2+} from stores, associated with the endoplasmic or sarcoplasmic reticulum. The pattern of the Ca^{2+} signals is often complex but $InsP_3$-linked agonists frequently give rise to repetitive $[Ca^{2+}]_c$ transients.

Other molecules (i.e., cyclic ADP-ribose, cADPR, and nicotinic acid adenine dinucleotide phosphate, NAADP) have recently also been shown to mobilize Ca^{2+} from internal stores generating Ca^{2+} oscillations. Studies using Ca^{2+} indicator dyes targeted to the lumen of intracellular stores of intact cells have shown that agonist-induced cytosolic Ca^{2+} oscillations are accompanied by inverse oscillations of stored Ca^{2+}.

Recent works suggest at least two possible mechanisms for the generation of oscillatory Ca^{2+} signals: either an oscillatory production of $InsP_3$ or oscillatory inactivation of $InsP_3$ receptors. Both mechanisms appear to operate in different cell types, the common denominator being the positive and negative feedback by Ca^{2+} on the release system, e.g., in hormone-stimulated hepatocytes, oscillations are driven by the cycling of the $InsP_3$ channels between a fully open and a largely closed state, rather than by oscillations in $InsP_3$. Similarly, in pancreatic acinar cells, the pulsatile calcium release does not depend on fluctuations in $InsP_3$ concentration, but in kidney epithelial cells spatiotemporal changes in the concentration of $InsP_3$ appear to be synchronous with Ca^{2+} oscillations, and intracellular $InsP_3$ waves accompany Ca^{2+} waves.

The fluctuations in $InsP_3$ may be controlled by Ca^{2+} itself through the regulation of PLC activity or through

regulatory proteins which act directly on G proteins, thus affecting the downstream $InsP_3$ production. Alternatively, the activity of the $InsP_3$-sensitive Ca^{2+} channels may be controlled by Ca^{2+} itself both at the cytosolic and the luminal side, and, possibly, by kinase-mediated phosphorylation/dephosphorylation cycles. Thus, low concentrations of cytosolic Ca^{2+} increase the open probability of the channels, whereas higher concentrations favor their closure, generating the oscillatory Ca^{2+}-signaling pattern.

Role and Functional Significance of $[Ca^{2+}]_c$ Oscillations

Ca^{2+} oscillations have been implicated in the control of different cell processes, among them oocyte activation and fertilization, growth-cone migration and tuning, axonal growth of cortical neurons, neuronal-cell migration, development of neurotransmitter phenotypes, formation of nodules in plant root hairs, developmental of muscle, release of cytokines from renal epithelial cells, and disassembly of adhesive structures during cell migration (Figure 3).

Numerous experimental protocols modulate the amplitude and the frequency of Ca^{2+} spikes in living cells. In general, cells choose the shape of Ca^{2+} signals according to the type of process that must be activated: single Ca^{2+} transients are used to activate processes such as muscle contraction, repetitive signals are used when information must be relayed over long time periods, as in fertilization and in the triggering of the developmental program. Furthermore, oscillations can be directed to discrete subcellular domains to generate large local $[Ca^{2+}]_c$ increases required to couple $[Ca^{2+}]_c$ to secretion and to mitochondrial metabolism. They can also propagate through entire cells, or even through coupled cells to coordinate the activities in intact tissues and organs.

The most obvious mechanism for the regulating of specific functions would seem to be modulation of the amplitude of Ca^{2+} signals. However, the efficiency of the activating stimulus is frequently related to the frequency rather than to the amplitude of the $[Ca^{2+}]_c$ oscillations.

A particularly illustrative example of decoding of the Ca^{2+} signal through the frequency of the oscillations is the Ca^{2+}-regulated gene expression.

Dolmetsch and colleagues have recently reported that Ca^{2+} oscillations in T-lymphocytes reduce the effective Ca^{2+}-threshold for activating some transcription factors, more effectively than the sustained Ca^{2+} increase. The efficacy is encoded by the oscillation frequency: rapid oscillations stimulate three transcription factors (NF-AT, Oct/OAP, and NF-κB), while lower-frequency oscillations only activate NF-κB. Thus, Ca^{2+}-modulated gene transcription is a frequency-sensitive process. Another elegant example of the correlation between the frequency of the $[Ca^{2+}]$ spikes and cellular function is the translation of repetitive cytosolic Ca^{2+} spiking through mitochondrial Ca^{2+} oscillations in primary cultures of rat hepatocytes in the final and sustained elevation of NAD(P)H production. This coupling allows the coordination of mitochondrial ATP production, linked to the sustained activation of mitochondrial Ca^{2+}-sensitive dehydrogenases, with the level of energy demand, at the same time avoiding the deleterious effects of the prolonged increase in $[Ca^{2+}]$.

In polarized cells, such as those of pancreatic acini, the receptor-evoked Ca^{2+} signal initiates at the apical pole, generating agonist-specific Ca^{2+} oscillation patterns. Acetylcholine stimulation evokes repetitive local spikes, which remain confined to the secretory apical pole. Cholecystokin instead induces local Ca^{2+} spikes

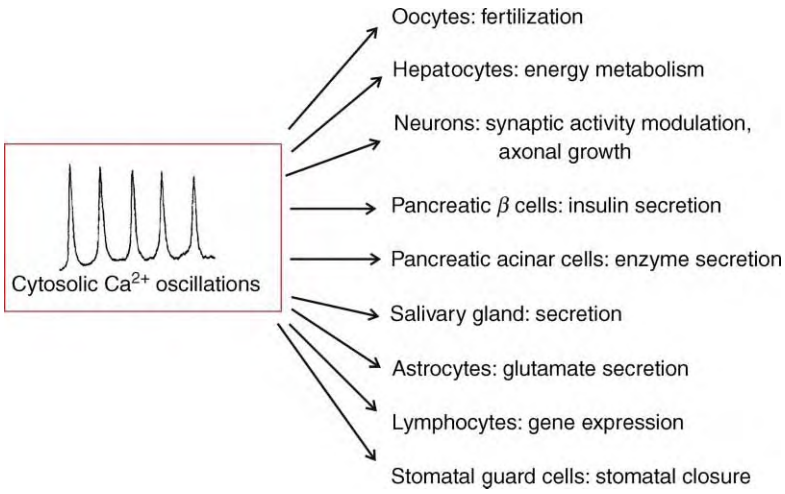

FIGURE 3 Scheme of the main cellular events modulated by the oscillatory behavior of Ca^{2+} signal.

that end in longer-lasting Ca^{2+} transients that spread to the whole cell.

Last but not least, in considering the functional significance of Ca^{2+} oscillations it is necessary to empathize their role in the central nervous system. In neurons, the sequential openings of plasma membrane Ca^{2+} channels lead to rhythmic Ca^{2+} spikes that, in turn, are linked to synaptic communication within and among neuronal circuitries, i.e., by inducing the release of neurotransmitters. A peculiar role has recently been attributed to the spontaneous and synchronous Ca^{2+} oscillations that occur independently from synaptic activity in developing neurons, such as those in rat visual cortex. It was suggested that these oscillations could propagate through different cells and determine a common developmental pattern of cells from the same domain.

A sophisticated example of the role of Ca^{2+} oscillation in the coordination of the activity of neuronal circuits has been described in glial astrocytes, a cell type of the central nervous system, which plays a number of important functions. Very recently, it has been proposed that they work as detectors of synaptic activity: by changing the frequency of Ca^{2+} oscillations evoked by the synaptic release of glutamate, these astrocytes acquire the ability to discriminate between different levels and patterns of synaptic activity.

How Are $[Ca^{2+}]_c$ Oscillations Decoded?

Although the frequency of Ca^{2+} oscillations seems critical for the induction of selective cellular functions, the mechanisms by which the cell decodes the oscillatory signal remain unclear.

In 1998 De Koninck and Schulman showed that the oscillation frequency modulates the activity of Ca^{2+}-calmodulin Kinase II (CaMKII) *in vitro*. This enzyme is tuned to respond optimally to Ca^{2+} oscillations with high frequency. The multimeric structure of the enzyme, coupled to its autophosphorylation properties, has led to the suggestion that it can act as a frequency decoder of $[Ca^{2+}]_c$ oscillations. The enzyme is now considered of special importance to the nervous system, where it regulates the process of memory formation and storage.

More recently, the advent of the green fluorescent protein (GFP) technology has shown that protein kinase C (PKC), one of the most important enzymes in cell signaling, undergoes an oscillatory plasma membrane association in phase with receptor-mediated oscillations in $[Ca^{2+}]_c$. Each $[Ca^{2+}]_c$ oscillation induces the transient membrane association of PKC leading to a transient burst of PKC substrate phosphorylation. It was suggested that the detachment of PKC from the membrane, which occurs as Ca^{2+} returns to the basal level between oscillations, results in a pause of PKC activity, allowing substrate dephosphorylation. In this respect, the Ca^{2+}-mediated regulation of PKC differs from that of CaMKII, since the latter does not fully deactivate between spikes as the frequency of $[Ca^{2+}]_c$ oscillations increases.

See Also the Following Articles

Calcium Signaling: Cell Cycle • Ligand-Operated Membrane Channels: Calcium (Glutamate) • Phosphatidylinositol Bisphosphate and Trisphosphate • Phospholipase C • Store-Operated Membrane Channels: Calcium • Voltage-Sensitive Ca^{2+} Channels

Glossary

G protein Protein associated to specific hormone receptor of the plasma membrane and responsible for the conversion of extracellular signals in intracellular messages.

inositol (1,4,5)-trisphosphate ($InsP_3$) Diffusible cytosolic messenger which induces the release of Ca^{2+} from intracellular stores (the endo/sarcoplasmic reticulum) by opening $InsP_3$-sensitive Ca^{2+} channels.

membrane potential Electrical gradient across the plasma membrane (and other membranes as well).

NAD(P)H Nicotinamide adenine dinucleotide, acceptor of the reducing equivalent produced in the oxidation of most metabolites. It is a small organic molecule, which participates as a coenzyme in enzymatic reactions.

neurotransmitters Chemical messengers by which neurons communicate with each other.

Further Reading

Berridge, M. J. (1990). Calcium oscillations. *J. Biol. Chem.* **265**, 9583–9586.

Berridge, M. J., and Dupont, G. (1994). Spatial and temporal signalling by calcium. *Curr. Opin. Cell Biol.* **6**, 267–274.

Carafoli, E., Santella, L., Branca, D., and Brini, M. (2001). Generation, control, and processing of cellular calcium signals. *Crit. Rev. Biochem. Mol. Biol.* **36**, 107–260.

Petersen, O. H., Petersen, C. C., and Kasai, H. (1994). Calcium and hormone action. *Annu. Rev. Physiol.* **56**, 297–319.

Thomas, A. P., St. Bird, G. J., Hajnóczky, G., Robb-Gaspers, L. D., and Putney, J. W., Jr. (1996). Spatial and temporal aspects of cellular calcium signalling. *FASEB J.* **10**, 1505–1517.

Biography

Marisa Brini is an Assistant Professor of Biochemistry at the University of Padova. Her main interest is in the study of calcium signaling defects occurring in human genetic diseases and/or transgenic animal models (malignant hyperthermia, mitochondrial disorders, and various cardiopathies) in which the homeostasis of Ca^{2+} in muscle is altered.

Calcium Sensing Receptor

Jacob Tfelt-Hansen and Edward M. Brown
Brigham and Women's Hospital, Harvard University, Boston, Massachusetts, USA

The calcium sensing receptor (CaR) is a membrane-bound, G protein-coupled receptor that is expressed in all tissues that regulate extracellular calcium homeostasis – the parathyroid glands, thyroidal C cells, bone, kidney, and intestine. The CaR senses the level of calcium in the blood and acts, therefore, as the body's thermostat for calcium (or calciostat). When the level of calcium changes by even a few percent from its normal level, the CaR senses this change and then modulates the functions of the cells expressing it so as to restore the level of blood calcium to normal. The CaR-mediated regulation of the secretion of parathyroid hormone plays a particularly important role in calcium homeostasis because it directly or indirectly modulates the functions of all tissues involved in regulating blood calcium.

Background

The body maintains the level of extracellular calcium (Ca_o^{2+}) within a narrow range (1.1–1.3 mM) because both high and low levels of Ca_o^{2+} are dangerous and can be life-threatening. Very small changes in Ca_o^{2+}, on the order of a few percent, lead to immediate physiological responses that restore the level of Ca_o^{2+} to normal. These fast responses are essential because rapid changes in Ca_o^{2+} are more dangerous than those that develop more slowly. The calcium sensing receptor (CaR), which was cloned almost a decade ago, plays a central role in this delicate homeostatic system. The CaR acts like a thermostat, but instead of measuring changes in temperature it measures alterations in the level of Ca_o^{2+}, thereby functioning as a calciostat. This means that the CaR tells the chief cells of the parathyroid glands the exact level of Ca_o^{2+}. The CaR is a seven-transmembrane-domain receptor that is coupled to G proteins – called a G protein-coupled receptor (GPCR). The importance of the CaR is illustrated by the diseases caused by naturally occurring mutations in it that lead to either loss of function or gain of function. Heterozygous (one-allele) loss-of-function mutations give rise to familial hypocalciuric hypercalcemia (FHH, also called familial benign hypocalciuric hypercalcemia, FBHH), in which most patients have asymptomatic hypercalcemia. The homozygous variant of inactivating CaR mutations, in contrast, is a much more severe, potentially fatal disease if left untreated; it is called neonatal severe primary hyperparathyroidism (NSHPT). The mouse model of FHH (e.g., heterozygous knockout of the CaR gene) has a phenotype comparable to that of the human condition, suggesting that the number of receptors on the cell surface is the determining factor for the clinical expression of the disease. Gain-of-function mutations give rise to autosomal-dominant hypoparathyroidism (ADH). Most patients with this condition have asymptomatic hypocalcemia. Although the principal role for the CaR is in calcium homeostasis, other functions of the receptor have been elucidated in the wide variety of cell types expressing it. The CaR can modulate the cell cycle, regulate ion channels, and control peptide secretion. This entry provides a broad overview of the CaR's biochemical features, a discussion of its functions in normal and pathophysiologic states, and a discussion of new drugs that have been developed that target the CaR.

Biochemical Features of the CaR

The CaR is a seven-transmembrane-domain GPCR whose gene is located on chromosome 3q. Other receptors in the superfamily of GPCRs that are related structurally to the CaR include the $GABA_B$ and metabotropic glutamate receptors (mGluRs), which recognize gamma aminobutyric acid (GABA) and glutamate, respectively, as their ligands, as well as putative pheromone and odorant receptors.

Structure

The human CaR has a very large N-terminal extracellular domain (ECD) of 612 amino acids (Figure 1). The ECD contains binding sites for calcium and is thought to have a bilobed venus flytrap structure that closes upon binding its principal physiological ligand, extracellular calcium ions. The binding of Ca_o^{2+} is very weak compared to many other receptors. These weak forces between the ECD and Ca_o^{2+} are crucial for the receptor to act as a calciostat. The CaR has a central core of

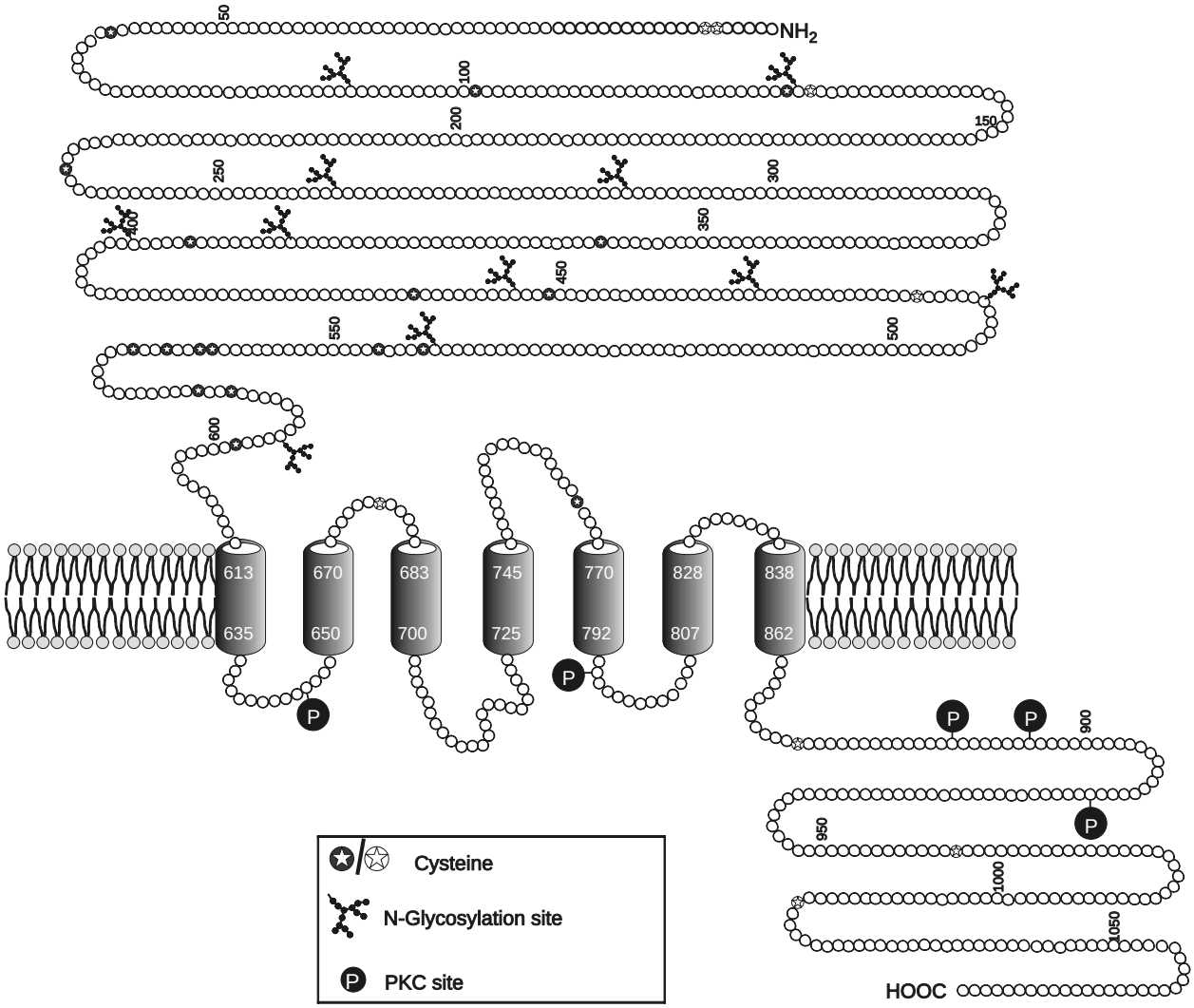

FIGURE 1 Representation of the predicted topological features of the human extracellular Ca^{2+} sensing receptor. The extracellular domain contains 612 amino acids, and the transmembrane domains and intracellular C tail each contain approximately 200 amino acids. Also shown are the PKC sites, N-glycosylation sites, and cysteine residues conserved with the metatropic glutamate receptors.

250 amino acids with seven transmembrane domains (TMDs), which is characteristic of the GPCRs. The TMDs serve as the target for newly developed drugs (discussed later). The intracellular carboxy (C) terminus of the receptor consists of 216 amino acids and has an important role, along with the CaR's intracellular loops, in the transduction of the Ca_o^{2+} signal to inside the cell.

N-Glycosylation with Carbohydrates is Crucial for Cell Surface Expression

The CaR has several N-linked glycosylation sites that are important for its expression on the cell surface. Western blotting of the CaR shows several bands between 120 and 200 kDa. A minor band at 120 kDa represents the nonglycosylated CaR, whereas major bands at 140 and 160 kDa correspond to the immature, high mannose and mature, fully N-glycosylated forms of the CaR, respectively. If the degree of glycosylation of the receptor is reduced to a significant extent by site-directed mutagenesis of its N-linked glycosylation sites, less of the receptor reaches the cell surface.

CaR Functions as a Dimer on the Cell Surface

Additional immunoreactive bands observed on Western blot analysis of the CaR at >200 kDa represent CaR dimers or even larger species. The dimer is the major form of CaR on the cell surface and is thought to be the active form of the receptor. Two monomers of the CaR are linked covalently by two disulfide bonds between cysteine residues 129 and 131 as well as by noncovalent interactions. The disulfide bonds constrain the receptor

in its inactive form; disrupting them produces a receptor that responds to lower than normal levels of Ca_o^{2+}. Moreover, heterodimerization of a normal CaR monomer with a monomer harboring an FHH mutation can interfere with the function of the wild-type CaR monomer, documenting that there are functional interactions between the monomers of the dimeric CaR.

Amino Acids in Intracellular Loops are Pivotal for Activation of Intracellular Signaling by the CaR

Amino acids in intracellular loops 2 and 3 are key players in determining selective coupling of the CaR to G proteins. For example, two amino acids residues within intracellular loop 2 and eight residues in intracellular loop 3 have been shown to be important for the G protein-dependent activation of phospholipase C (PLC) – one of the major intracellular signaling pathways used by the CaR.

The C Tail of the CaR is Important for its Function

The amino acid sequence of the proximal portion of the C tail of the CaR is highly conserved among species, suggesting its functional importance. In addition, naturally occurring mutations in the C tail have been shown to cause the diseases mentioned earlier (e.g., FHH and ADH). Furthermore, certain truncation and deletion mutations of the receptor's C tail up-regulate the expression of the receptor on the cell surface, thereby causing gain of function. Other truncations have been shown to cause loss of function, demonstrating that there are discrete elements within the C tail that modulate both the cell surface expression and function of the receptor.

Functionally Important Mutations in the CaR as Experiments in Nature

Approximately 100 naturally occurring mutations have so far been described that cause either a loss of function of the CaR in FHH and NSHPT or a gain of function in ADH. Deletion, nonsense, insertion, missense, truncations, and splice-site mutations have been described throughout the whole CaR gene. They have not only proven the physiological importance of the CaR in Ca_o^{2+} homeostasis, but have also provided an important source of information about the structure-function relationships of the receptor, as noted previously.

Agonists of the CaR

As previously mentioned, the CaR can detect very small changes in the level of $Ca_{o,}^{2+}$ on the order of a few percent. The receptor's principal physiological agonist, Ca_o^{2+}, regulates its activity at millimolar concentrations, implying an extremely low affinity compared with those of other receptors for their respective agonists. Calcium has been shown to interact with the ECD of the CaR. This has been established elegantly through the creation of a chimeric receptor containing the ECD of the CaR and the TMDs and C tail of an mGluR. The chimeric receptor responds to Ca_o^{2+} but not to glutamate. The CaR's Hill coefficient is typically 3–4, implying the presence of several binding sites for Ca_o^{2+}, but the steepness of the physiological response of the parathyroid glands to Ca^{2+} is even more extreme. Suppression of parathyroid hormone (PTH) release *in vitro* is minimal at 0.75 mM and maximal at ~2 mM. Unlike many receptors, the CaR is resistant to desensitization; this optimizes the CaR's capacity for continuous surveillance of extracellular Ca^{2+} levels. Although Ca_o^{2+} is the major ligand for the CaR, a variety of other agonists have been identified. Mg^{2+}(another biologically important divalent cation whose extracellular level is maintained within a narrow range) has been shown, like Ca_o^{2+}, to inhibit PTH secretion. Although this effect seems to be at supraphysiological levels, magnesium's action on the CaR in the kidney may regulate its renal reabsorption and contribute to Mg_o^{2+} homeostasis. Other well-established agonists acting on the ECD are gadalinium, neomycin, and spermine; all exhibit positive cooperativity with regard to their interactions with calcium in activating the receptor. These three agonists, as well as Mg_o^{2+}, are defined as type 1 agonists, which bind to the ECD and activate the CaR regardless of whether Ca_o^{2+} is present. Type 2 agonists, in contrast, are allosteric activators that require calcium to exert their effects. Certain L-amino acids, particularly aromatic amino acids, have been shown to be type 2 agonists, binding to a site within the ECD of the CaR. It is possible that they function in this manner in the gut, where the CaR is widely distributed, enabling the CaR to act, in effect, as a nutrient receptor. The CaR also senses ionic strength, as illustrated by the fact that exposing dispersed bovine parathyroid cells to a 40-mM increment in NaCl shifts the EC_{50} for high Ca_o^{2+}-evoked inhibition of PTH release by at least 0.5 mM. Ionic strength may exert physiologically relevant actions on the CaR in select regions of the gastrointestinal (GI) tract and kidney, where the levels of ionic strength can vary greatly.

Intracellular Signaling Pathways Used by the CaR

CaR agonists activate phospholipases C, A_2, and D in parathyroid as well as in CaR-transfected but not in nontransfected human embryonic kidney (HEK293) cells. The high Ca_o^{2+}-evoked, transient rise in the cytosolic calcium concentration (Ca_i^{2+}) in bovine parathyroid and CaR-transfected HEK293 cells is mediated

by activation of PLC and the resultant inositol triphosphate (IP_3)-mediated release of Ca^{2+} from intracellular stores. In parathyroid and CaR-transfected HEK293 cells, the activation of PLC is insensitive to pertussis toxin and probably involves $G\alpha_{q/11}$. In contrast, the CaR-mediated increase in inositol phosphates observed in the mouse pituitary AtT-20 cell line is sensitive to pertussis toxin, showing that the CaR can also activate PLC through pertussis toxin-sensitive G proteins (i.e., $G\alpha_i$). The CaR also stimulates the p42/44 mitogen-activated protein kinases (MAPKs) by a pathway that involves cytoplasmic tyrosine kinases (e.g., c-Src) and inhibits adenylate cyclase via $G\alpha_i$ in parathyroid and some kidney cells. In other cells, the CaR inhibits the accumulation of cAMP by increasing Ca_i^{2+}, which then inhibits the activity of a Ca^{2+}-inhibitable isoform of adenylate cyclase.

Feedback Regulation of the CaR by Protein Kinase C

The CaR has two protein kinase A (PKA) and five protein kinase C (PKC) phosphorylation sites within its intracellular domains. Phosphorylation of these PKC sites, especially the one located at threonine 888, inhibits the receptor's coupling to PLC, one of the CaR's principal intracellular signaling pathways. This serves as a negative feedback loop because PKC is activated downstream of PLC.

The Importance of the CaR in Calcium Homeostasis

The level of calcium is regulated by three calciotropic hormones: PTH, calcitonin (CT), and $1,25(OH)_2$ vitamin D_3. There is an inverse sigmoidal relationship between PTH, a key calcium-elevating hormone, and Ca_o^{2+} (Figure 2), whereas there is a positive relationship between Ca_o^{2+} and CT, the calcium-lowering hormone, both of which are mediated by the CaR. These features confer on the CaR the role of the gatekeeper to normal calcium homeostasis. The additional Ca_o^{2+}-elevating hormone, $1,25(OH)_2$ vitamin D_3, like PTH, displays an inverse relationship with Ca_o^{2+}, although whether this is CaR-mediated is currently unknown. In addition to the effects of the CaR on calciotropic hormone production and secretion, the receptor also directly modulates the function of target tissues for PTH, especially the kidney and perhaps in bone and intestine. In this way, Ca_o^{2+} functions as a first messenger, serving as the body's major Ca_o^{2+}-lowering hormone (described later).

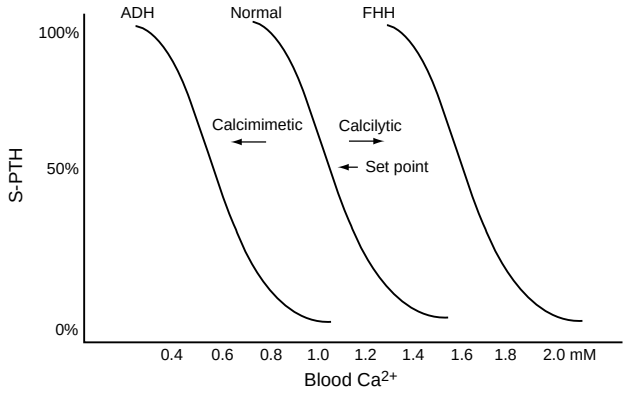

FIGURE 2 Sigmoidal relationship between the blood Ca^{2+} and serum PTH (S-PTH) levels in normal individuals (eucalcemia), in autosomal dominant hypoparathyroidism (ADH) (hypocalcemia), and in familial hypocalciuric hypercalcemia (FHH). The arrows represent the effects of calcimimetics (shifting the set point to the left) and calcilytics (shifting the set point to the right). Set point is defined as the calcium level that produces one-half of the maximal inhibition of the PTH secretion.

CaR in Hypercalcemia

The responses of the CaR to hypercalcemia provide an accurate picture of its role in calcium homeostasis. An increase in Ca_o^{2+} is sensed by the chief cells in the parathyroid gland, which within seconds lowers the rate of PTH secretion. The impact of this reduction in PTH secretion and in the direct actions of Ca_o^{2+} on cellular function occur in several target tissues.

Bone

The high Ca_o^{2+}-elicited lowering of PTH decreases the rate of release of calcium ions from bone – an action mediated through its action on the PTH receptor (PTHR) on the osteoblast. The production of $1,25(OH)_2$ vitamin D_3 is likewise inhibited by hypercalcemia – and this fall in $1,25(OH)_2$ vitamin D_3 also reduces bone resorption. High Ca_o^{2+}, by itself, also exerts negative effects on osteoclast formation and function and increases osteoblast activity, thereby reducing the net release of calcium from bone. Taken together, the effects of PTH, $1,25(OH)_2$ vitamin D_3, and Ca_o^{2+} on bone all lower the level of blood calcium.

Kidney and Intestine

The high Ca_o^{2+}-elicited decrease in the circulating level of PTH also promotes rapid excretion of calcium by the kidney. This action is thought to take place through a reduction in the PTH-induced stimulation of calcium reabsorption in the thick ascending limb of the loop of Henle as well as the distal convoluted tubule. However, high Ca_o^{2+} also directly inhibits calcium reabsorption by virtue of the presence of the CaR on the basolateral

surface of the epithelial cells of the thick ascending limb, where the receptor antagonizes the stimulatory action of PTH on calcium reabsorption. Both the high Ca_o^{2+}-elicited decrease in PTH and the direct inhibitory action of high Ca_o^{2+} on the 1-hydroxylation of 25-hydroxy-vitamin D_3 inhibit the production of $1,25(OH)_2$ vitamin D_3, thereby reducing the absorption of Ca_o^{2+} by the intestine. All these effects of hypercalcemia on the kidney reduce the level of Ca_o^{2+} toward normal. When combined with the effects of a reduction in PTH and an increase in Ca_o^{2+} on bone, the Ca_o^{2+} homeostatic system provides an elegant mechanism for maintaining near constancy of Ca_o^{2+}.

Nonhomeostatic Functions of the CaR

Although the physiological role of the CaR in cells that do not participate in mineral ion homeostasis still remain to be fully defined, studies of the CaR's functions in these diverse cell types have widened the range of functions that the CaR is known to regulate. These CaR-modulated processes include (1) secretion of peptides, for example, ACTH, gastrin, insulin, growth hormone, and PTHrP; (2) ion channel/transporter activity, for example, aquaporin-2 water channels, nonselective cation channels, voltage-dependent Ca^{2+} channels, and calcium-activated potassium (K^+) and other K^+ channels; (3) gene expression, for example, of the vitamin D receptor and the CaR; (4) proliferation of colonic and ovarian surface epithelial cells, fibroblasts, and keratinocytes; (5) differentiation of keratinocytes, goblet cells, and mammary epithelial cells; (6) apoptosis of fibroblasts, HEK-293 cells stably transfected with the CaR, and prostate cancer cells; and (7) chemotaxis of preosteoblastic cells and macrophages. Thus Ca_o^{2+} may serve as an extracellular messenger regulating diverse cellular functions, not only in cells directly involved in Ca_o^{2+} homeostasis but also in the variety of additional cell types expressing the CaR that play no apparent role in this process.

Pharmaceutical Aspects

The CaR has become a drug target as a consequence of its central role in calcium homeostasis and the evidence given earlier that it contributes to hyper- and hypocalcemic states. There are two classes of drugs acting on the CaR. One group activates the receptor; these drugs are called calcimimetics. The other group inhibits the effect of Ca_o^{2+} on the CaR; these agents are called calcilytics.

Calcimimetics

Calcimimetics are type 2 activators that bind to the receptor's TMDs and potentiate the action of Ca_o^{2+} on the CaR. NPS R-568 and AMG073 are two such agents that shift the curve for Ca_o^{2+}-regulated changes in Ca_i^{2+} and PTH release to the left without affecting the maximal or minimal responses (Figure 2). Ongoing clinical trials suggest that calcimimetics may prove to be useful in the treatment of hyperparathyroidism, such as in the secondary hyperparathyroidism that occurs in end-stage renal disease.

Calcilytics

This group of agents has the opposite effect, inhibiting the receptor and thereby stimulating PTH secretion (Figure 2). This class of drugs could potentially be useful in the treatment of osteoporosis by providing brief pulses of endogenous PTH secretion. The resultant transient increase in PTH mimics that caused by the once-daily administration of exogenous PTH, which is known to exert anabolic actions on bone and has recently been approved for use in the treatment of osteoporosis.

See Also the Following Articles

Calcium, Biological Fitness of • Mitogen-Activated Protein Kinase Family • Phospholipase A_2 • Phospholipase C • Phospholipase D • Protein Kinase C Family

Glossary

autosomal dominant hypoparathyroidism (ADH) A generally benign form of hypocalcemia caused by gain-of-function mutations in the CaR.

calcilytic An inhibitor of the CaR.

calcimetic The allosteric activator of the CaR.

calcium sensing receptor (CaR) A G protein-coupled receptor maintaining the near constancy of extracellular calcium.

familial hypocalciuric hypercalcemia (FHH) A benign form of hypercalcemia caused by loss of function in the CaR.

neonatal severe primary hyperparathyroidism (NSHPT) An autosomal recessive disease with loss of function of both alleles of the CaR.

Further Reading

Brown, E. M. (2001). Physiology of calcium homeostasis. In *The Parathyroids* (J. P. Bilezikian, R. Marcus and M. A. Levine, eds.), pp. 167–183. Academic Press, San Diego, CA.

Brown, E. M., Gamba, G., Riccardi, D., Lombardi, M., Butters, R., Kifor, O., Sun, A., Hediger, M. A., Lytton, J., and Hebert, S. C. (1993). Cloning and characterization of an extracellular $Ca^{(2+)}$-sensing receptor from bovine parathyroid. *Nature* **366**, 575–580.

Brown, E. M., and MacLeod, R. J. (2001). Extracellular calcium sensing and extracellular calcium signaling. *Physiol. Rev.* **81**, 239–297.

Tfelt-Hansen, J., Yano, S., Brown, E. M., and Chattopadhyay, N. (2002). The role of the calcium-sensing receptor in human pathophysiology. *Curr. Med. Chem.-Immunol. Endocrinol. Metab. Agents* **2**, 175–193.

Biography

Jacob Tfelt-Hansen is a Postdoctoral Fellow at Harvard University. His research interests are calcium homeostasis and the non-calcium-homeostatic effects of the CaR. He received his M.D. degree from Copenhagen University, Denmark.

Edward M. Brown is a Professor of Medicine at Harvard Medical School and Brigham and Women's Hospitals. He has worked in the field of calcium homeostasis for nearly 30 years. He received his M.D. degree from Harvard University in 1972. He led the team that cloned the CaR and also played a key role in the identification and characterization of inactivating and activating mutations in the CaR.

Calcium Signaling: Calmodulin-Dependent Phosphatase

Claude Klee, Hao Ren and Shipeng Li
National Cancer Institute, Bethesda, Maryland, USA

Calcineurin (also called protein phosphatase-2B) is a eukaryotic protein phosphatase whose activity is dependent on Ca^{2+} and calmodulin. Ten years ago, the identification of calcineurin as the target of the immunosuppressive drugs, cyclosporin A (CsA) and tacrolimus (FK506), revealed the key role of calcineurin in the transduction pathway from the plasma membrane to the nucleus leading to T cell activation. Since then, the inhibition of calcineurin by FK506 and CsA complexes with their respective binding proteins, FKBP12 and cyclophilin A (CyPA), together with the overexpression of a truncated derivative of calcineurin, not dependent on Ca^{2+} or calmodulin (CaM), have been widely used to probe the involvement of calcineurin in the regulation of cellular processes. These are as diverse as gene expression, ion homeostasis, muscle differentiation, embryogenesis, secretion, and neurological functions. Alteration of calcineurin activity has been implicated in the pathogenesis of many diseases such as cardiac hypertrophy, congenital heart diseases, and immunological and neurological disorders.

Subunit Structure and Isoforms

Calcineurin is a heterodimer of a 58–64 kDa catalytic subunit, calcineurin A (CnA), tightly bound to a 19 kDa Ca^{2+}-binding regulatory subunit, calcineurin B (CnB). This subunit structure, unique among protein phosphatases, is conserved in all eukaryotes. Three mammalian isoforms (α, β, γ) of CnA have been identified at the mRNA level. The corresponding human genes (PPP3CA, PPP3CB, PPP3CC) are located on human chromosomes 4, 10, and 8 respectively. Additional isoforms, products of alternative splicing, have only been detected at the mRNA level. Two mammalian isoforms of CnB, CnB1, and CnB2 (expressed only in testis), are the products of two genes (PPP3R1 located on chromosome 2, and PPP3R2). Although expressed in most, if not all tissues, calcineurin is particularly abundant in the brain where the α-isoform of CnA is predominant. The β-isoform is broadly distributed whereas the γ-isoform is expressed specifically in the testis. Calcineurin has been identified in many other eukaryotes including plants, fungi, and the budding yeast, *Saccharomyces cerevisiae*. Another calmodulin-stimulated protein phosphatase with a CnB-like structure covalently bound to the catalytic subunit has been identified in *Drosophila melanogaster*'s retina.

Structure

The domain structure of calcineurin is well conserved. In all species the catalytic domain located in the N-terminal two-thirds of CnA, is followed by a CnB-binding domain. The C-terminal regulatory domain is composed of CaM-binding and autoinhibitory subdomains. In the absence of CaM the native protein is inactive. The catalytic and CnB-binding domains, severed from the regulatory domain by limited proteolysis, constitute the Ca^{2+}-independent, truncated, form of calcineurin routinely used in overexpression experiments. CnB is an "EF-hand" Ca^{2+}-binding protein of the CaM family. It binds four Ca^{2+}, two with high affinity ($K_d < 10^{-7}$ M) and two with moderate affinity ($K_d \geq 10^{-6}$M). The N-terminal glycine of CnB is myristoylated. This perfectly conserved posttranslational modification of CnB, apparently not involved in membrane association or required for enzymatic activity, may serve as a stabilizing structural element.

The crystal structure of the recombinant α-isoform of human calcineurin as expressed in *E. coli* is illustrated in Figure 1A. The architecture of the catalytic domain is similar to those of protein phosphatases-1 and -2A. It consists of a β-sandwich surrounded on one side by seven α-helices and on the other by a mixed α/β structure. The catalytic site contains a Fe^{3+}–Zn^{2+} binuclear metal center. The catalytic domain extends into a five-turn amphipathic α-helix whose top face is covered by a 33Å groove formed by the N- and C-terminal lobes and the C-terminal strand of CnB. A short helical segment, corresponding to the autoinhibitory domain, blocks the catalytic center. With the exception of this segment, the C-terminal regulatory domain is not visible in the electron density map, and is flexible and highly sensitive to proteolysis, in the absence of CaM. The crystal

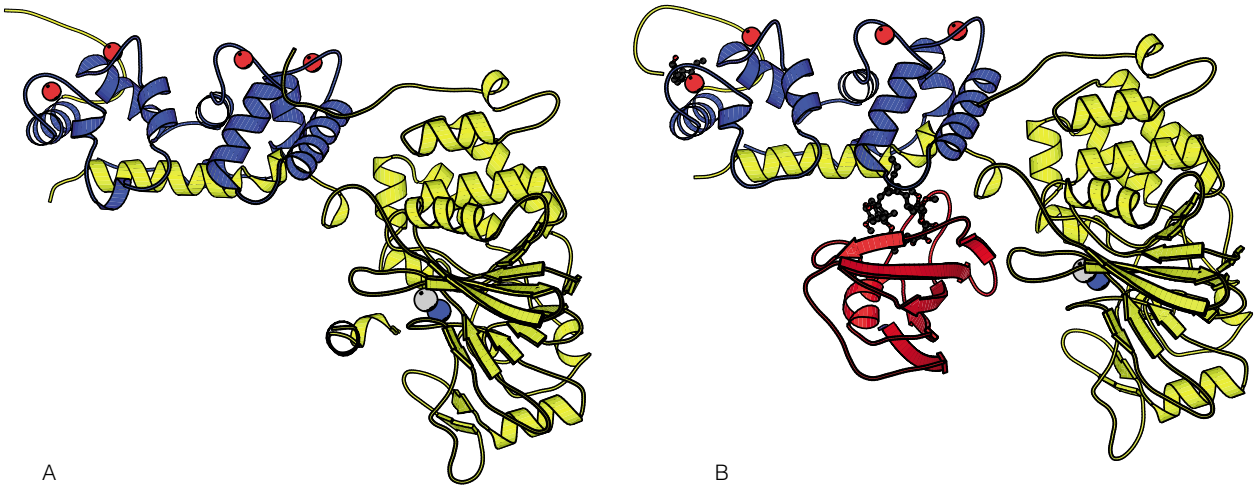

FIGURE 1 Ribbon representation of the crystal structure of calcineurin. (A) Human recombinant α-calcineurin [PDB code 1AUI, Kissinger, C. R., Parge, H. E. *et al.* (1995). *Nature* **378**, 641–644]. (B) Truncated calcineurin complexed with FKBP12-FK506 [PDB code 1TCO Griffith, J. P., Kim, J. L. Kim, E. E., Sintchak, M. D., Thomson, J. A., Fitzgibbon, M. J., Fleming, M. A., Caron, P. R., Hsiao, K., and Navia, M. A. (1995). X-ray structure of calcineurin inhibited by the immunophilin-immunosuppressant FKBP12-FK506 complex. *Cell* **11**, 507–522. CnA is shown in yellow, CnB in blue. Iron and zinc are shown as light gray and blue spheres respectively. The four calcium bound to CnB are shown as red spheres. FKBP12 is shown in red.

structure of the proteolytic derivative of calcineurin, lacking the regulatory domain, when bound to FK506/FKBP12, is similar to that of the full-length protein (Figure 1B). The bottom face of the CnB-binding helix of CnA and CnB form the site of interaction with the FKBP–FK506 and CsA–CyP complexes. The key role of CnB in forming the drug-binding site provides a molecular basis for the specificity of FK506 and CsA as calcineurin inhibitors.

Enzymatic Properties

Ca^{2+}/Calmodulin-Dependent Stimulation and Inactivation

Calcineurin is a protein phosphatase with a binuclear iron–zinc active center. The purified enzyme, partially depleted of its metal cofactors, is activated by 0.1 mM Mn^{2+} or 6 mM Mg^{2+}. Purified calcineurin, that has retained stoichiometric amounts of Fe^{3+} and Zn^{2+}, is inactive and not activated by exogenous metal ions. Activation requires treatment under anaerobic conditions with the reducing agent, ascorbate, which converts Fe^{3+} to Fe^{2+}. The phosphatase activity of calcineurin is also dependent on the presence of Ca^{2+} and calmodulin. A small activation is observed upon addition of Ca^{2+} ($K_{act} = 0.5\ \mu M$). Supplementation with CaM results in a 50–100-fold increase of the V_{max} without affecting the value of the K_m. The highly cooperative stimulation of the enzyme by CaM (Hill coefficient of 2.5–3) allows calcineurin to respond to narrow Ca^{2+} thresholds following cell stimulation. Because of its high affinity for CaM ($K_{act} < 10^{-10}$ M) the activation of calcineurin in response to a Ca^{2+} signal can precede the activation of all known CaM-regulated kinases.

Enzymatic Assays

A 19-residue synthetic peptide containing the phosphorylation site of the RII subunit of cAMP-dependent protein kinase (PKA) and *p*-nitrophenylphosphate are used routinely to measure the phosphatase activity of calcineurin. In crude tissue extracts calcineurin activity is distinguished from that of other neutral serine–threonine protein phosphatases by its (1) Ca^{2+} dependence; (2) inhibition by CaM-binding peptides and inhibitors; (3) resistance to the inhibitors of protein phosphatases-1 and -2A (Inhibitor-1, DARPP32, Inhibitor-2, okadaic acid, microcystin, and calyculin); and (4) specific inhibition by FK506 (but not rapamycin) and CsA in the presence of saturating amounts of their respective binding proteins, FKBP12 and CyPA. The *p*-nitrophosphatase activity of calcineurin, which is stimulated by FK506 and CsA, cannot be used to measure calcineurin activity in crude extracts. Unlike protein phosphatase-2C, which requires Mg^{2+} for activity, calcineurin that has retained its natural metal cofactors does not require Mg^{2+}.

Substrate Specificity

Calcineurin is a dual protein phosphatase. It dephosphorylates both phosphoseryl/threonyl and phosphotyrosyl peptides. Peptides with a basic residue on the

N-terminal side of the phosphorylated amino acid and lacking acidic residues on the C-terminal side are preferentially dephosphorylated by calcineurin. The substrate specificity of calcineurin also depends on an extended N-terminal stretch. In addition to the recognition of the sequence surrounding the phosphorylated residues, the presence of docking domains greatly decrease the K_m values. A major substrate of calcineurin, the transcription factor NFAT (Nuclear Factor of Activated T cells), contains two such domains responsible for its Ca^{2+}-dependent and phosphorylation-independent anchoring to calcineurin. The anchoring of NFAT allows its dephosphorylation, despite its low intracellular concentration, and the nuclear cotranslocation of calcineurin and NFAT.

Regulation

Ca^{2+} Regulation

Two structurally similar but functionally different Ca^{2+}-binding proteins, CaM and CnB mediate the Ca^{2+} regulation of calcineurin. CnB is tightly bound to CnA even in the absence of Ca^{2+}, and plays both structural and functional roles. It is required to confer enzymatic activity to the catalytic subunit. The recombinant α- and β-isoforms of CnA expressed in bacteria and SF9 cells require CnB for activity. Ca^{2+}-binding to CnB is required for the interaction of calcineurin with immunosuppressive drugs bound to their binding proteins.

Ca^{2+}-dependent binding of CaM to calcineurin induces a conformational change of the regulatory domain accompanied by the displacement of the autoinhibitoy domain. The resulting exposure of the catalytic center allows substrate binding and results in activation of the phosphatase activity. Prolonged exposure of the catalytic center facilitates the oxidation of Fe^{2+} and results in inactivation of calcineurin that is prevented by superoxide dismutase and reversed by ascorbate. Thus, CaM can both activate and inactivate calcineurin depending of the length of the Ca^{2+} signal. The calmodulin-dependent oxidation of Fe^{2+} and inactivation of calcineurin is a potential mechanism to regulate its activity during oxidative stress.

Endogenous Regulatory Proteins

Endogenous protein inhibitors or activators, whose expression varies from tissue to tissue, can also modulate the activity of calcineurin activity *in vivo*. A family of 22–24 kDa proteins, identified in both yeast (RCn1p) and mammalian cells (calsuppressins, MCPs), act as feedback inhibitors of calcineurin. The mammalian proteins, whose expression is up-regulated by a calcineurin/NFAT-dependent mechanism, are identical to the proteins encoded in the Down's syndrome Critical Region 1 gene, ZAK1–4, DSCRIL1, and DSCRIL. These inhibitory proteins inhibit both calcineurin expression and activity. They interact with calcineurin in the absence of Ca^{2+} through a highly conserved ISPP × SPP motif, similar to the SP motifs of NFAT, and inhibit calcineurin activity *in vitro* as well as NFAT activation *in vivo*.

A 240 kDa nuclear protein, Cain/Cabin1 has been identified as a non-competitive inhibitor of calcineurin. Binding of Cabin1 to calcineurin requires Ca^{2+} and protein kinase C activation and is inhibited by FK506/FKBP, suggesting that it binds at the drug interaction site. A basic domain in the C terminus of Cabin1 has been identified as the calcineurin-binding site. A third group of proteins, including the PKA scaffold protein, AKAP79 in brain, and calsarcins in skeletal and cardiac muscles may serve to anchor calcineurin to its sites of action. They all inhibit calcineurin activity but their mechanism of action is not yet fully understood.

Functions

Regulation of Gene Expression

The elucidation of the Ca^{2+}/calcineurin/NFAT pathway of T cell activation opened the way to uncover the important role of calcineurin in the regulation of gene expression in many other cell types. As illustrated on Figure 2, in T cells, when Ca^{2+} is released from the inositol trisphosphate (IP_3)-sensitive stores following occupancy of the T cell receptor, calcineurin is activated and dephosphorylates the transcription factor NFAT. Dephosphorylation of NFAT is accompanied by the exposure of a nuclear localization signal and NFAT is translocated to the nucleus. Calcineurin, anchored to NFAT through an anchoring domain (P × I × IT), is translocated to the nucleus as well. Dephosphorylation of NFAT not only results in its nuclear translocation but also in an enhancement of its DNA binding and transcriptional activity. This is also dependent on the activation of the Ras/protein kinase C (PKC) pathway. Nuclear export depends on NFAT rephosphorylation upon removal of Ca^{2+} and calcineurin inactivation. Several kinases, including glycogen synthase kinase 3 (GSK3) and casein kinase 1 have been implicated in this process.

Four NFAT isoforms (NFAT1–4) are expressed in many tissues. These isoforms share a highly conserved regulatory domain composed of two calcineurin-binding motifs, multiple phosphorylation sites, and a nuclear localization signal. The two motifs bind calcineurin with an affinity in the micro molar range. In skeletal

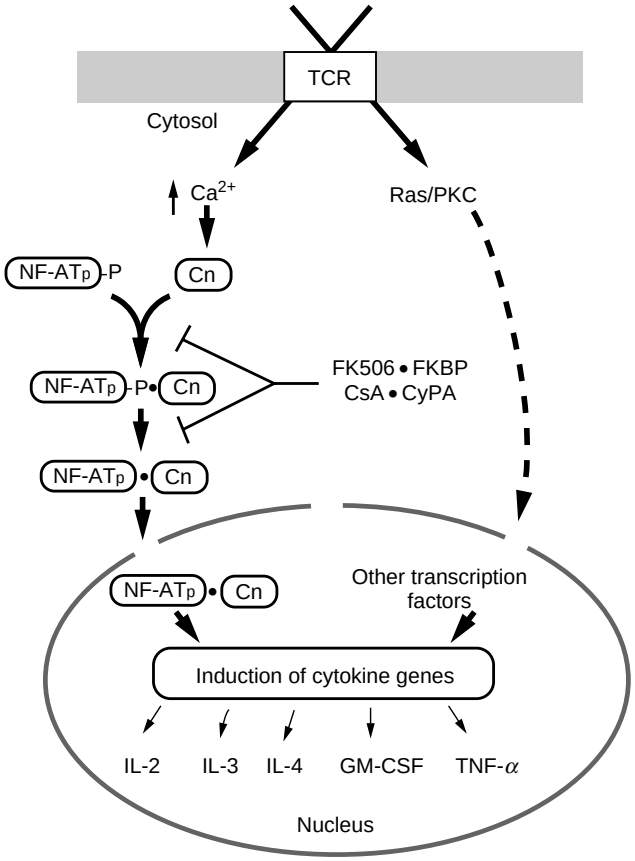

FIGURE 2 Calcineurin-mediated signal transduction from the T cell receptor to the nucleus leading to the induction of the cytokine genes (IL-2, -3, -4), granulocyte-macrophage stimulating factor (GM-CFS), and tumor necrosis factor (TNF-α). Gene activation requires the concomitant activation of the Ras/protein kinase C (PKC) pathway. [Reproduced from Klee, C. B., Wang, X., and Ren, H. (1999). Calcium-regulated protein dephosphorylation. In *Calcium as a Cellular Regulator* (Carafoli and Klee, eds.) with permission of Oxford University Press, Inc.]

muscle calcineurin-mediated dephosphorylation of the transcription factors, NFAT-3 and the myogenic enhancing factor (MEF2) plays a critical role in the switch from fast-to-slow oxidative fibers induced by sustained tonic contraction. In the heart, the calcineurin-mediated activation of NFAT3 and MEF2D, in conjunction with the cardiac specific transcription factor GATA4, has been implicated in the development of cardiac hypertrophy in response to stress. Transgenic mice lacking the β-isoform of calcineurin (the predominant isoform in heart) have impaired ability to develop cardiac hypertrophy in response to hypertrophic agonists while severe hypertrophy and cardiac heart failure is induced by overexpression of constitutively active calcineurin. The calcineurin/NFAT pathway is also essential for the development of heart valves and the vascular developmental pattern during embryogenesis. In the brain, Ca^{2+} homeostasis is itself regulated by calcineurin. Activation of NFAT increases the expression of the IP_3 receptors, the plasma membrane Ca^{2+} pumps and the Ca^{2+} exchanger. The increasing number of genes whose expression is induced by NFAT suggests a potential role of calcineurin in the regulation of gene expression during cell differentiation and apoptosis. The importance of calcineurin in the regulation of these cellular processes and its involvement in the pathogenesis of many diseases based on overexpression and knock out models is well documented. To fully assess the contribution of calcineurin in the transduction of so many diverse signals, we must understand how different pathways interact with each other.

In budding yeast, the calcineurin-mediated dephosphorylation of a transcription factor (Crz1p/Tcn1p) plays a major role in the regulation of genes involved in ion homeostasis. The mechanism is similar to NFAT-mediated transcriptional control in mammalian cells. In yeast, genetic analysis adds strong support to the physiological significance of this calcineurin signaling pathway in response to exposure to abnormal concentrations of ions or prolonged exposure to mating pheromones. It not only illustrates the important role of calcineurin in the regulation of gene expression but also reveals the participation of many other factors in this complex signaling pathway.

Neuronal Functions

Calcineurin is 1% of the total protein and broadly distributed in brain. There are few neuronal functions which are not modulated by calcineurin. A major role of calcineurin in brain is to trigger a protein phosphatase cascade initiated by the dephosphorylation of two other major substrates of calcineurin, the endogenous inhibitors of protein phosphatase-1, Inhibitor-1, and DARPP32. This cascade counteracts the stimulatory effects of cAMP and Ca^{2+}-regulated kinases. It explains the antagonistic effects of Ca^{2+} release induced by glutamate binding to the NMDA receptor and dopamine binding to some dopamine receptors in striatal neurons. Whether it activates protein phosphatase-1, or dephosphorytes an increasing number of specific substrates, calcineurin has been implicated in the regulation of neuronal processes as diverse as the expression and activity of ion channels, the synthesis of nitric oxide, the release of neurotransmitters, synaptic vesicle recycling, and neurite outgrowth. Calcineurin inhibitors and transgenic animals lacking the calcineurin genes or overexpressing the constitutive form of calcineurin have been widely used to study the involvement of calcineurin in the storage of long and short memory. How calcineurin and other protein kinases and phosphatases affect learning and memory remains one of the most challenging problems in neurobiology.

See Also the Following Articles

Calcium/Calmodulin-Dependent Protein Kinase II • Protein Kinase C Family

Glossary

calmodulin A unique member of a class of calcium-binding proteins that acts as sensors of changes in intracellular concentration of calcium induced by external signals. It modulates the activity of a large number of enzymes involved in the regulation of cellular processes, particularly those involved in protein phosphorylation.

EF-hand Structural motif composed of 30 contiguous amino acids forming two helices joined by a Ca^{2+}-binding loop.

immunosuppressive drugs (FK506 and CsA) Fungal natural products used to prevent organ rejection after organ transplant operations and treatment of autoimmune diseases.

NFAT Broadly distributed transcription factor originally identified as a nuclear factor of activated T cells required for the coordinated induction of several cytokine genes.

Further Reading

Aramburu, J., Rao, A., and Klee, C. B. (2000). Calcineurin: From structure to function. *Curr. Top. Cell. Regul.* **36**, 237–295.

Barford, D., Da, A. K., and Egloff, M.-P. (1998). The structure and mechanism of protein phosphatases: Insights into catalysis and regulation. *Annu. Rev. Biophys. Biomol. Struct.* **27**, 133–164.

Bito, H., Deisseroth, K., and Tsien, R. W. (1996). CREB phosphorylation and dephosphorylation: A Ca^{2+}-and stimulus duration-dependent switch for hippocampal gene expression. *Cell* **87**, 1203–1214.

Cyert, M. S. (2001). Genetic analysis of calmodulin and its targets in *Saccharomyces cerevisiae*. *Annu. Rev. Genet.* **35**, 647–672.

Fienberg, A. A., Hiroi, N., Mennelstein, P. G., Song, W., Snyder, G. L., Nishi, A., Cheramy, A., O'Callaghan, J. P., Miller, D. B., Cole, D. G., Corbett, R., Haile, C. N., Cooper, D. C., Onn, S. P., Grace, A. A., Ouimet, C. C., White, F. J., Hyman, S. E., Surmeier, D. J., Girault, J., Nestler, E. J., and Greengard, P. (1998). DARPP-32: Regulator of the efficacy of dopaminergic neurotransmission. *Science* **281**, 838–842.

Graef, I. A., Chen, F., Chen, L., Kuo, A., and Crabtree, G. (2001). Signals transduced by Ca^{2+}/calcineurin and N-F-ATc3/c4 pattern the developing vasculature. *Cell* **105**, 863–875.

Griffith, J. P., Kim, J. L. Kim, E. E., Sintchak, M. D., Thomson, J. A., Fitzgibbon, M. J., Fleming, M. A., Caron, P. R., Hsiao, K., and Navia, M. A. (1995). X-ray structure of calcineurin inhibited by the immunophilin-immunosuppressant FKBP12-FK506 complex. *Cell* **11**, 507–522.

Kandel, E. R. (2001). The molecular biology of memory storage: a dialogue between genes and synapses. *Science* **294**, 1030–1038.

Kissinger, C. R., Parge, H. E. *et al.* (1995). *Nature* **378**, 641–644.

Klee, C. B., Wang, X., and Ren, H. (1999). Calcium-regulated protein dephosphorylation. In *Calcium as a Cellular Regulator.* (C. Carafoli, C. Klee, eds.) pp. 344–370. Oxford University Press, New York.

Malleret, G., Haditsch, U., Genoux, D., Jones, M. W., Bliss, T. V., Vanhoose, A. M., Weitlauf, C., Kandel, E. R., Winder, D. G., and Mansuy, I. M. (2001). Reversible enhancement of leaming, memory, and long-term potentiation by genetic inhibition of calcineurin. *Cell* **104**, 675–686.

McKinsey, T. A., Zhang, C. L., and Olson, R. N. (2002). Signaling chromatin to make muscle. *Curr. Opin. Cell Biol.* **14**, 763–772.

Schreiber, S. L., Liu, J. L., Albers, M. W., Rosen, M. K., Standaert, R. F., Wandless, T. J., and Somer, P. K. (1992). Molecular recognition of immunophilins and immunophilinligand complexes. *Tetrahydron* **48**, 2545–2558.

Winder, D. G., and Sweatt, J. D. (2001). Roles of serine/threonine phosphataes in hippocampal synaptic plasticity. *Nat. Rev. Neurosci.* **2**, 41–474.

Biography

Claude B. Klee is Scientist Emeritus in the Laboratory of Biochemistry at the National Cancer Institute in Bethesda, MD. Her principal research interest is in Ca^{2+} signaling with emphasis on the mechanism of action of calmodulin using as a model system the activation of the calmodulin-dependent protein phosphatase, calcineurin. She holds an M.D. from the University of Marseille, France, and is a member of the Institute of Medicine and the American Association of Arts and Sciences.

Hao Ren and Shipeng Li are long time associates of Dr. Klee. They developed in her laboratory the procedures to express human calcineurin in bacteria, and to characterize the enzymatic activity and calcium regulation of the recombinant proteins.

Calcium Signaling: Cell Cycle

Luigia Santella
Stazione Zoologica "Anton Dohrn," Naples, Italy

Because calcium controls the most important cellular functions, it is not surprising that it should also have a role in a process as vital as the ability of cells to divide and multiply. Eukaryotes from yeasts to humans have similar division cycles, which are carefully regulated and coordinated with both cell growth and DNA replication to ensure the formation of a progeny of cells containing intact genomes. This is made possible by the existence of a system of checkpoints and feedback controls that prevent the entry of cells into the next phase of the cycle if the preceding phase has not been successfully completed.

A large number of regulatory elements have a function in the various stages of the cell cycle, among them, a variety of kinases, phosphatases, proteases, and a number of second messengers that control them. Among second messengers that have a role in the regulation of the cycle, calcium is a relatively late entry, but is now attracting increasing attention. This short article will offer a succinct survey of its role, paying attention to the meiotic cycle as well. For more detailed information, readers may consult a number of comprehensive reviews that deal with the general topic of cell-cycle regulation.

The Mitotic Cycle

The cell division is conventionally subdivided into four stages: G_1, S, G_2, and M. The M phase usually ends with the formation of two daughter cells (cytokinesis) (Figure 1). The G_1 phase corresponds to the interval gap that starts at the completion of mitosis and extends to the initiation of DNA synthesis. During this phase, the cell grows continuously and synthesizes the histones necessary for the new chromatin. G_1 is also the phase in which the cell responds to external signals by becoming committed irreversibly to enter the replicative process. This occurs at a point of no return called the restriction point (R) (in yeast it is named start). When proliferating cells are deprived of the appropriate medium they exit from the cycle after having reached the G_1 phase and enter a quiescent state termed G_0 in which they stop growing. DNA replication occurs in the S phase. The G_2 phase is the time-gap between the completion of DNA synthesis and the beginning of chromosome condensation. During G_2 phase, mRNAs and proteins are synthesized in preparation for the M phase (M), which consists of four steps: prophase, metaphase, anaphase, and telophase. The beginning of prophase is marked by the appearance of condensed chromosomes with the two sister chromatids. During prophase, in addition to chromosome condensation, changes leading to the development of the mitotic spindle also occur in the cytoplasm. The centrosomes, which had duplicated during interphase and which serve as the two poles of the mitotic spindle, separate and move to opposite sides of the nucleus. The breakdown of the nuclear envelope then allows spindle microtubules to attach to the kinetochores of chromosomes. At the metaphase stage the chromosomes align in the center of the spindle, and the sister chromatids separate, to move to opposite poles of the spindle during the anaphase stage. Chromosomes decondensation and nuclear envelope reformation take place during telophase, after which cytokinesis yields two interphase daughter cells.

Cell-Cycle Regulators

The central actor in the initiation and progression of the cell cycle is a well-conserved family of serine/threonine protein kinases (CDKs), which become activated by associating with cyclins. This binding is strictly necessary for CDKs activity and cyclin protein levels are tightly controlled during the cell cycle. Various cyclins become synthesized and degraded at specific phases of the cycle. In mammalian cells, three cyclins (C, D1, and E) that are essential for entering S phase are synthesized during the G_1 phase. The D-cyclins, which control the restriction point R, form complexes with CDK4 and CDK6, and are regulated by external signals, such as growth factors, anti-mitogenic factors, etc. Cyclin E is synthesized late in G_1 and once the active complex CDK2/cyclin E is formed the active kinase triggers the onset of DNA replication. Cyclin A and B, that are essential for M-phase entry, are synthesized during G_2. At the end of M phase, the ubiquitin-dependent proteasome pathway, which is required to inactivate CDK1 and to allow cells to enter G_1, degrades mitotic cyclins. However, it has been claimed that one of the cylins (D1) is processed by calpain.

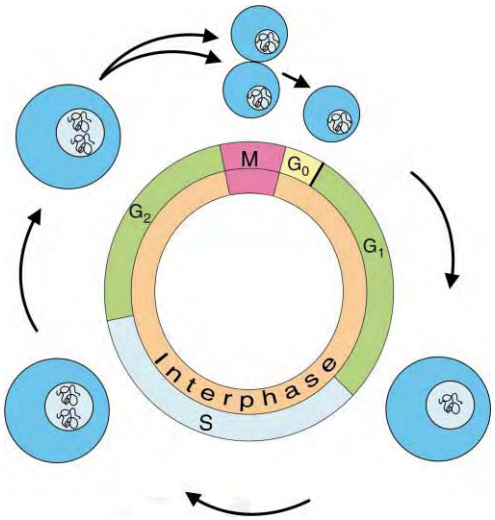

FIGURE 1 Cell-cycle phases. The cell grows throughout interphase, which includes G_1, S, and G_2. Once the cell has passed through the restriction point, it is committed to proceed through S and the rest of the cycle. If growth factors are not available during G_1, the cell stops growing and protein synthesis becomes depressed. S phase is the period during which DNA replication occurs. During G_2 mRNAs and proteins are synthesized in preparation for the mitosis (M) that ends with the two daughter cells.

Calcium and Mitosis

Although the mechanisms responsible for the activation of the cell-cycle kinases are still incompletely understood, increasing evidence now strongly suggest that changes in intracellular calcium may have an important role. During the early embryonic cell cycle in the sea urchin, cyclic increases in inositol 1,4,5-trisphosphate trigger the release of Ca^{2+} from intracellular stores that generate mitotic events. Blocking of the calcium increase prevents the dissolution of the nuclear envelope and stops mitosis. Calcium transients are associated with chromosome movement during anaphase in plants and mammalian cells. Calcium and the principal decoder of its signal, the calcium-binding protein, calmodulin (CaM), are intimately connected to the events of the cycle. Anti-CaM drugs block the G_1–S transition and the onset of DNA replication. The CaM level increases as the cell progress into mitosis, correlating nicely with the detection of CaM in the mitotic apparatus in yeast. Local activation of CaM occurs near the nuclear envelope just before its breakdown and the onset of anaphase. CaM is also involved in the phosphorylation of the retinoblastoma protein, the product of the Rb1 tumor suppressor gene (which is responsible for a rare inherited childhood eye tumor) that modulates a set of regulatory proteins that promote cell proliferation. The retinoblastoma protein is one of the key regulators that control R in G_1, past which the cells become irreversibly committed to enter S phase. The multifunctional Ca^{2+}/CaM-dependent protein kinase II (Ca^{2+}/CaMKII) is a potential transducer of the effect of CaM on cell-cycle progression. Inhibition of the G_2/M transition, and thus of the nuclear envelope breakdown, occurs upon injection of a Ca^{2+}/CaMKII specific peptide inhibitor or of Ca^{2+}/CaMKII antibodies. The involvement of Ca^{2+}/CaMKII at mitosis and meiosis entry is due to the activation of a Cdc25, a phosphatase that is a Ca^{2+}/CaMKII substrate that dephosphorylates and which activates, the M-phase promoting factor (MPF). The kinase induces multiple nuclear and cytoplasmic changes at the onset of the M phase by activating other protein kinases, and by phosphorylating structural proteins such as histone H1, nuclear lamins, proteins of the endoplasmic reticulum (ER) and Golgi membranes, and microtubule and actin-associated proteins. Once the metaphase spindle has been formed the cell proceeds to initiate anaphase and complete meiosis. Progression from metaphase to anaphase is triggered by the activation of an ubiquitin-mediated proteolysis system (proteasome) that degrades cyclin B and thereby inactivates MPF. In turn, phosphorylation of the proteasome by activated Ca^{2+}/CaMKII promotes cyclin degradation. As mentioned Ca^{2+} may also intervene in the degradation of cyclins by activating the Ca^{2+}-dependent protease calpain, that has been shown to degrade cyclin D1.

The Meiotic Cycle

Oocyte Prophase and Metaphase Arrest

Oocytes have long been used to study the meiotic cycle. In the gonads their growth is arrested at a specific phase of the meiotic cycle (prophase I). Following growth, a hormonal signal causes oocytes to mature. During maturation oocytes undergo a number of morphological, electrical, and biochemical changes that are a necessary preparation for successful fertilization. At the onset of maturation, the envelope of the germinal vesicle (nucleus) of prophase I-arrested oocytes disassembles (GVBD), the nucleoplasm mixes with the cytoplasm and the ER undergoes a structural reorganization that will ensure a normal Ca^{2+} response at fertilization: data indicate that MPF plays an important role in the restructurating of the ER. In addition to the dissolution of the nuclear envelope, resumption of meiosis entails the condensation of chromatin and the extrusion of the first polar body. The latter results from an unequal cell division that leaves most of the cytoplasm with half of the DNA. Following the release of the first polar body, oocytes enter the second mitosis of the meiotic cycle with the

extrusion of the second polar body and the formation of the pronucleus.

Although the pathway leading to the release from prophase I differs significantly among species, its ultimate common goal is to activate MPF. The experiments that have contributed to the identification of MPF as the agent responsible for the mitotic and meiotic cycle regulation have been performed on frog and starfish oocytes. Arrested oocytes could be induced to enter the M phase of meiosis by microinjecting cytoplasm from oocytes that had been hormonally stimulated, i.e., the cytoplasmic factor generated in hormone-treated oocytes was evidently sufficient to trigger the transition from G_2 to M in oocytes that had not been exposed to the hormone.

Calcium and Meiosis

Abundant evidence links the meiotic division cycle to calcium. For example, prophase I arrested starfish oocytes release calcium in the cytoplasm and in the nucleus following the resumption of meiosis promoted by the maturation-inducing hormone 1-methyladenine. A role of calcium during maturation is indicated by the inhibition of meiosis progression by the injection of CaM antagonists or of CaM antibodies directly into the oocytes nucleus. MPF activation could thus occur in the nuclear compartment, and could be linked to the Ca^{2+}/CaMKII-dependent stimulation of the Cdc25 phosphatase, which dephosphorylates two inhibitory (Th-14 and Tyr-15) MPF sites. In line with this, both MPF and Cdc25 have been shown to migrate to the nucleus once the re-initiation of meiosis has started. In some species in which fertilization triggers the release from prophase I, oocytes complete meiosis and enter mitosis directly without arrest. However, in most species in which hormonal stimuli rather than fertilization trigger the release from prophase I, the oocytes become arrested again at either metaphase I, metaphase II, or the pronucleus stage (depending on the species), until fertilization (Figure 2). For instance, *Xenopus* oocytes become arrested for a second time after maturation at the metaphase of the second meiotic division: The cytoplasmic activity that causes metaphase II arrest is termed the cytostatic factor. Injection of cytoplasm from metaphase-arrested oocytes that contains the cytostatic factor into a dividing blastomere results in the arrest of the recipient at metaphase. A serine/threonine kinase termed Mos was first identified as an essential component of the cytostatic factor. Mos is specifically synthesized in oocytes at about the time of completion of meiosis I and is responsible for the maintenance of MPF activity during the metaphase II arrest. Mos can readily arrest a dividing blastomere, and its

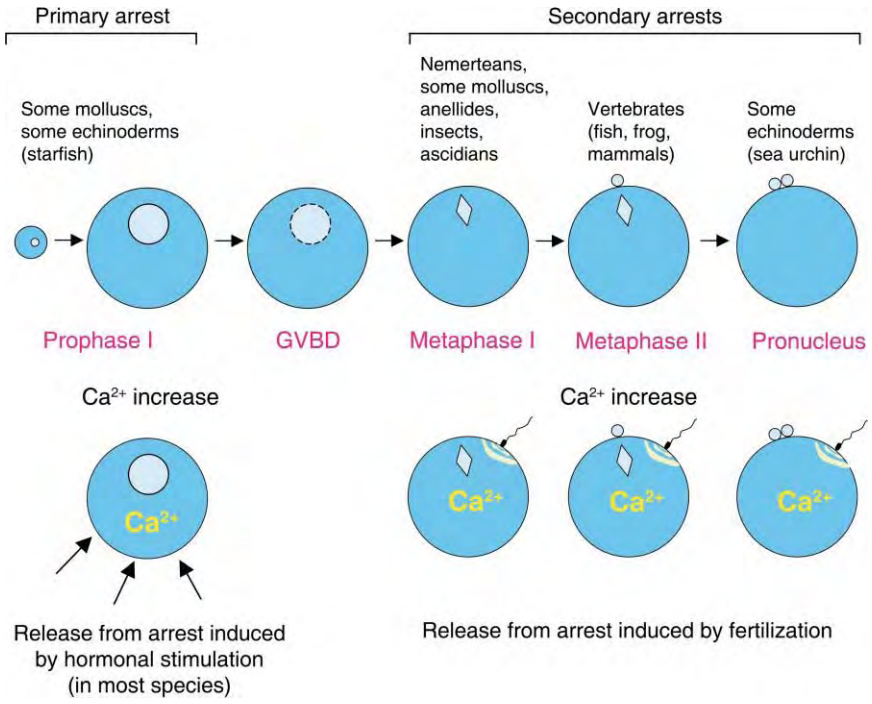

FIGURE 2 Release from meiotic arrest in different animal oocytes. In most species prophase I-arrested oocytes at the germinal vesicle (nucleus) stage (GV) re-initiate the meiotic cycle following the intracellular Ca^{2+} increase induced by hormonal stimulation. In a minority of species, however, fertilization may induce the release from prophase I arrest in the absence of hormonal stimulation. Then, in the species in which the release is induced by the hormone, a secondary arrest may occur (however, not in starfish oocytes) at metaphase I and II that is released by the intracellular Ca^{2+} increase promoted by sperm entry at fertilization.

immunodepletion removes cytostatic factor activity. The release of the secondary arrest is promoted by the entry of the sperm at fertilization and by the associated Ca^{2+} wave produced by the emptying of the intracellular stores. The Ca^{2+} increase inactivates both the cytostatic factor and the MPF, inactivation of MPF occurring through the ubiquitin-dependent proteolysis of the regulatory cyclin B. At variance with the oocytes in which the entry of the sperm induces a single Ca^{2+} transient (a Ca^{2+} wave), e.g., those of *Xenopus*, sea urchin, and starfish, in other oocytes species fertilization triggers, instead, repetitive Ca^{2+} transients. This occurs in nemertean, ascidian, and mammalian oocytes, which become fertilized at metaphase I and II when MPF activity is very high. In these species, Ca^{2+} fails to inactivate MPF, whose activity remains high and might actually regulate the Ca^{2+} oscillations induced by the sperm.

See Also the Following Articles

Cell Cycle: Mitotic Checkpoint • Homologous Recombination in Meiosis • Meiosis • Metaphase Chromosome • Mitosis • The Neuronal Calcium Signal in Activity-Dependent Transcription

Glossary

endoplasmic reticulum (ER) A cytoplasmic network of membrane-enclosed tubules and cisternae extending from the nuclear envelope through the cytoplasm that regulates the intracellular Ca^{2+} levels.

germinal vesicle The large nucleus of fully grown, prophase I-arrested oocytes.

inositol 1,4,5-trisphosphate An intracellular second messenger produced by the hydrolysis of membrane phospholipid through the activation of a specific phospholipase following interaction of first messengers with specific plasma membrane receptors.

M-phase promoting factor (MPF) A cyclin-dependent kinase complex formed by the catalytic subunit of the protein kinase CDK1, and a regulatory subunit, cyclin B.

Further Reading

Carafoli, E., Santella, L., Branca, D., and Brini, M. (2001). Generation, control, and processing of cellular calcium signals. *Crit. Rev. Biochem. Mol. Biol.* **36**, 107–260.

Carroll, J. (2001). The initiation and regulation of Ca^{2+} signalling at fertilization in mammals. *Semin. Cell Dev. Biol.* **12**, 37–43.

Means, A. R. (1994). Calcium, calmodulin and cell cycle regulation. *FEBS Lett.* **347**, 1–4.

Runft, L. L., Jaffe, L. A., and Mehlmann, L. (2002). Egg activation at fertilization: Where it all begins? *Dev. Biol.* **245**, 237–254.

Santella, L. (1998). The role of calcium in the cell cycle: Facts and hypotheses. *Biochem. Biophys. Res. Commun.* **244**, 317–324.

Stricker, S. A. (1999). Comparative biology of calcium signaling during fertilization and egg activation in animals. *Dev. Biol.* **211**, 157–176.

Whitaker, M., and Patel, R. (1990). Calcium and cell cycle control. *Development* **108**, 525–542.

Biography

Luigia Santella is a Senior Scientist in the Laboratory of Cell Biology of the Stazione Zoologica "A. Dohrn", Naples, Italy. Her principal research interest is the spatio-temporal dynamics of Ca^{2+} signaling during the cell cycle and fertilization in invertebrate marine animals. She has also contributed to the clarification of the role of the actin cytoskeleton in modulating the intracellular Ca^{2+} increase.

Calcium Signaling: Motility (Actomyosin–Troponin System)

Takeyuki Wakabayashi
Teikyo University, Utsunomiya, Japan

Setsuro Ebashi
National Institute for Physiological Sciences, Myodaiji, Japan

Muscle contraction is regulated by the level of intracellular Ca^{2+}. In skeletal or cardiac muscles of vertebrate, Ca^{2+} regulation is mediated at the level of thin filaments, which consist of troponin, tropomyosin, and actin. Because actin filaments themselves are Ca^{2+}-insensitive, troponin and tropomyosin, which form a Ca^{2+}-sensitive switch, are required. When the cytosolic Ca^{2+} concentration increases to a micromolar level, Ca^{2+} binds to troponin and triggers a series of conformational changes in the thin filaments that lead to a sliding interaction between actin-containing thin filaments and myosin-containing thick filaments.

Structure of Thin Filaments and their Components

Thin filaments are based on a helical arrangement of actin monomers (F-actin), which can be thought of as two strands of globular actin monomers (G-actin) twisted around one another, staggered by ~27.3Å (2.73 nm) (Figure 1). One crossover (half pitch) containing approximately 13 monomers is ~360Å in length. Actin can be divided into the outer domain (subdomains 1 and 2) and the inner domain (subdomains 3 and 4) (Figure 1B). The inner domain is nearer to the helix axis. Myosin binds mainly to the subdomain 1.

In the generally accepted model of the thin filament, tropomyosin molecules are located in the two grooves of actin. Troponin binds to each of tropomyosin molecules as shown schematically in Figure 1A. The native thin filaments also contain nebulin molecules (not shown in Figure 1). One tropomyosin–troponin unit corresponds to exactly seven actin monomers, and the troponin molecules on the opposite strands are staggered with respect to one another by 27.3Å. This had been assumed for the sake of simplicity, but was recently shown to actually be the case. Tropomyosin is a rod-shaped coiled-coil dimer (~400Å, M_r ~35,000 × 2). Tropomyosin molecules form continuous ropes by longitudinal association through head-to-tail contact. Troponin consists of three subunits: troponin-T (TnT, M_r~31,000) binds to tropomyosin, troponin-I (TnI, M_r~21,000) binds to actin and inhibits the actin-activated myosin ATPase, and troponin-C (TnC, M_r ~ 18,000) binds calcium ions and neutralizes the inhibitory activity of TnI. Troponin, therefore, can bind to both tropomyosin and actin (Figure 2). Troponin can be dissociated into its three subunits in the presence of urea and Ca^{2+}-chelating reagents and can be reassembled by removing urea.

Tropomyosin Shift and Steric Blocking Model

The thin filament model shown in Figure 1A suggests that Ca^{2+}-induced changes of troponin can be transmitted to actin monomers through tropomyosin. The simplest hypothesis in calcium regulation has been the steric blocking model, in which the azimuthal position of tropomyosin on actin filaments is considered to be critical.

The increase in the second-actin-layer line intensity of the X-ray diffraction pattern from living muscle and the concomitant decrease in the third-actin-layer line intensity take place during the activation of muscle contraction. These changes in X-ray intensity can be explained if tropomyosins are located near the grooves of the actin double strands in the contracting state but dislocated more from the grooves due to the influence of Ca^{2+}-deprived troponin. If the tropomyosins in the off-groove position are located where they block sterically the myosin-binding sites of actin but the tropomyosins in the in-groove position do not, the tropomyosin shift can explain why tropomyosin is required for Ca^{2+}-regulation: Tropomyosin transmits the Ca^{2+}-induced changes in one troponin to the seven actin monomers. Three-dimensional image reconstruction from electron micrographs showed more directly the changes in thin filament

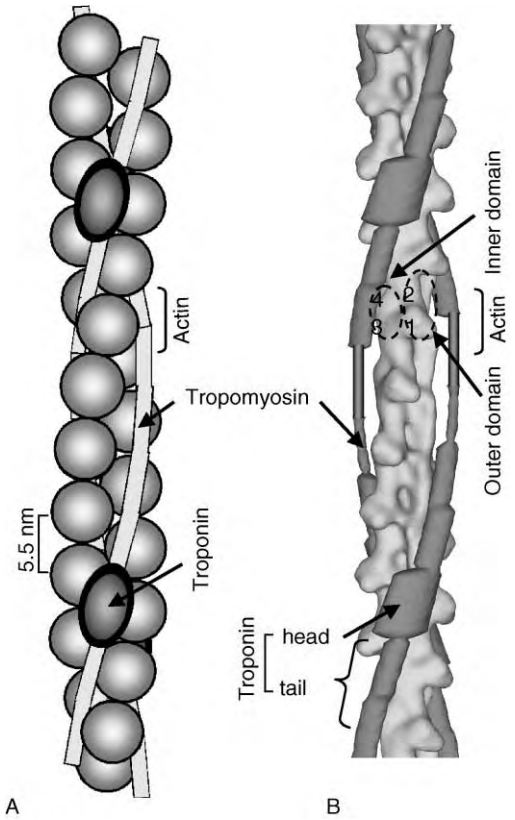

FIGURE 1 (A) Schematic illustration of a thin filament based on the model shown in (B). One tropomyosin molecule binds seven actin monomers and one troponin. The model in (B) is a composite illustration – the actin part is based on the atomic model of actin, and the troponin and tropomyosin part is based on the three-dimensionally reconstituted image of the actin–tropomyosin–troponin complex (reconstituted thin filament). Smoothing along the actin helix was applied to the tropomyosin and troponin part to simplify it. The four subdomains of actin are indicated by numerals, and the approximate location of the head and tail domains of troponin are indicated. Tropomyosin is ~400Å in length. Reprinted from Narita, A., Yasunaga, T., Ishikawa, T., Mayanagi, K., and Wakabayashi, T. (2001). Ca^{2+}-induced switching of troponin and tropomyosin on actin filaments as revealed by electron cryomicroscopy. *J. Mol. Biol.* **308**, 241–261, copyright 2001, with permission from Elsevier.

structure – the addition of TnT–TnI complex (which inhibits actin–myosin interaction irrespective of Ca^{2+} concentration) to the actin–tropomyosin complex induces the tropomyosin shift. It was later shown that the three-dimensional images of reconstituted thin filaments containing actin, tropomyosin, and troponin were changed by the addition of Ca^{2+}, and the structural changes were interpreted to be the result of the tropomyosin shift induced by Ca^{2+}. The addition of TnI–TnC complex (without TnT) to the actin–tropomyosin complex also induces the tropomyosin shift in a Ca^{2+}-dependent manner. There are indications that troponin movement and conformational changes of actin are also involved in Ca^{2+} regulation, and the changes in the X-ray diffraction pattern therefore could be explained solely by the shift of troponin instead of tropomyosin. The positions of tropomyosin determined by modeling or helical image reconstruction are therefore not unambiguous and are biased by changes in the other components of thin filament, especially troponin, as described next.

Three-State Model for Ca^{2+} Regulation

Biochemical studies showed that the simple steric blocking model, which proposes that only the position of tropomyosin is responsible for Ca^{2+} regulation, is an oversimplification. The binding of the myosin head (subfragment-1, S1) to the reconstituted thin filaments (actin–tropomyosin–troponin complex) is cooperative irrespective of Ca^{2+} concentration and the Ca^{2+} binding to troponin alone is not sufficient for the full activation of actin-activated myosin ATPase.

The cooperative/allosteric model, or three-state model, emphasizes the importance of conformational changes in actin. At low Ca^{2+} concentrations, the thin filament is in a blocked state, in which myosin cannot bind to actin. There are two states at high Ca^{2+} concentrations: an open state (called R state in the allosteric model), in which myosin bound with ADP-phosphate can interact with actin weakly and the weak binding can be converted to a strong binding by releasing phosphate; and a closed state (called T state in the allosteric model), in which myosin with bound ADP-phosphate can bind to actin but no phosphate release step can follow. Thus, the transition to the strong binding of myosin with bound ADP or nucleotide-free myosin does not occur in a closed state. These three states are illustrated in Figure 3. Moreover, the closed state is favored against the open state, with an allosteric constant L (the ratio of T state to R state, or closed/open) of ~10. The open state is achieved fully only when the concentration of the myosin head is high enough to shift the allosteric equilibrium from a closed state (T state) toward an open state (R state). When the positions of tropomyosin are determined by electron microscopy in the absence of the myosin head (S1), the position at low Ca^{2+} and high Ca^{2+} concentrations should represent the position at a blocked and a closed state, respectively. The biochemical studies showed that the thin filament is only ~67% blocked even in the absence of Ca^{2+}.

Molecular Organization of Troponin and its Ca^{2+}-Induced Changes

Troponin is a target protein of Ca^{2+} signaling and its Ca^{2+}-induced changes are important to understanding

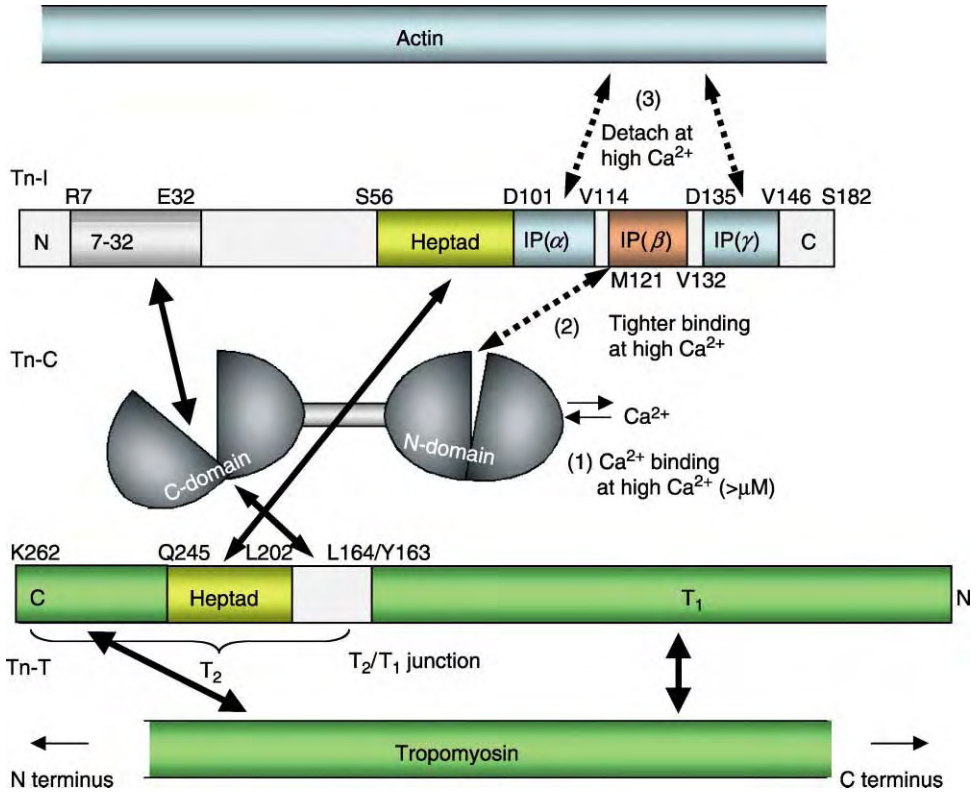

FIGURE 2 The three steps of Ca^{2+}-induced changes in interactions among actin, troponin subunits, and tropomyosin. The interactions indicated by dashed arrows are Ca^{2+}-sensitive, whereas those indicated by solid arrows are Ca^{2+}-insensitive and constitutive. The numbering shown is for chicken skeletal troponin; skeletal TnI differs from cardiac TnI by ~30 due to the insertion in the N-terminal region of cardiac TnI.

how the muscle contraction is triggered. Such changes have been revealed by ultracentrifugation, X-ray scattering, neutron scattering, circular dichroism, infrared and ultraviolet spectroscopy, fluorescence resonance energy transfer, and chemical cross-linking.

TnC is dumbbell-shaped with two globular domains connected by a long helix. Each domain possesses two EF-hand helix–loop–helix Ca^{2+}-binding motifs. The N-terminal domain (N domain in Figure 2) of TnC from skeletal muscle binds two Ca^{2+} specifically but with lower affinity (with a dissociation constant, K_d, of a few micromolars), whereas the C-terminal domain (C domain in Figure 2) binds either Ca^{2+} or Mg^{2+} (two Ca^{2+}/Mg^{2+} sites) with higher affinity ($K_d \sim 0.01$ μM). Only one of the EF-hand motifs in the N domain of cardiac TnC binds Ca^{2+}. The metal-binding sites of the C domain are occupied always by either Ca^{2+} or Mg^{2+}, and the hydrophobic pocket of the C domain is always exposed and binds the N-terminal region (the residues 7–32) of TnI. The corresponding hydrophobic pocket of the N domain becomes open only at high Ca^{2+} (step 1 in the Figure 2).

TnT binds to tropomyosin. Many isoforms have been isolated for TnT. TnT can be divided into TnT_1 and TnT_2 by chymotryptic cleavage at the carboxyl side of Tyr158 (chicken skeletal TnT), which follows two seryl residues (S156 and S157). TnT_1 and the C-terminal region of TnT_2 bind to tropomyosin. TnT_2 also binds to the C domain of TnC. The primary structures of TnI and TnT show the heptad-repeat pattern – in a heptad the first and the fourth residues are almost always hydrophobic. Two such regions (the residues 56–101 of TnI and 202–245 of TnT) associate and form a coiled coil. Thus, TnT_2 binds to tropomyosin, TnI, and TnC.

TnI binds to actin and inhibits the actin-activated ATPase. Its inhibitory activity is neutralized by Ca^{2+}-loaded TnC. The residues 97–117 and the peptide corresponding to the residues 96–116 were shown to be responsible for the inhibitory activity and are called the inhibitory region, which approximately corresponds to IP(α) in Figure 2, and the inhibitory peptide (IP), respectively. The numbering shown in Figure 2 is for skeletal troponin, which differs from cardiac TnI by ~30 due to the insertion at the N-terminal region of cardiac TnI. The minimum sequence necessary for inhibition (but not sufficient for full inhibition) is residues 104–115 (GKFKRPPLRRVR), which approximately corresponds to IP(α). There are two other regions with a homologous

sequence, called IP(β) and IP(γ) (Figure 2). The region near residues 117–127, which forms a helix according to the prediction of the secondary structure and the preliminary report of the crystal structure of the cardiac TnT_2–TnI–TnC complex at high Ca^{2+} concentrations, follows the inhibitory region and is identified as the target of the hydrophobic pocket in the N domain of TnC; it is called the second TnC-binding site and corresponds approximately to region IP(β).

When Ca^{2+} binds to the N domain of TnC and the hydrophobic pocket becomes open (step 1 in Figure 2), the association between the second TnC binding site of TnI and the N domain of TnC becomes tighter (step 2 in Figure 2). Then, the inhibitory regions IP(α) and IP(γ) detach from actin (step 3 in Figure 3). This detachment step is key for triggering the activation of muscle contraction. Thus, the N domain of TnC, the C-terminal region of TnI, and actin make up the regulatory machinery. Actin is therefore not just a *target* of Ca^{2+} regulation but is an important *component* of the Ca^{2+} switch.

Ca^{2+}-Induced Troponin Shift on the Thin Filaments

The first event of muscle contraction is the binding of Ca^{2+} to TnC and the detachment of TnI from actin, which is followed by the changes in the location of troponin on the thin filaments. Several parts of TnI have been known to change their positions on the thin filaments. Recent electron cryomicroscopic work shows that troponin changes its shape and shifts toward the inner domain of actin during activation (Figure 3A–B).

The region near Cys117 between the IP(α) and IP(β) of TnI and the region near Cys133 between the IP(β) and IP(γ) are nearer to the C terminus of actin at low Ca^{2+} concentrations. The details of the troponin shift, however, have been difficult to visualize because troponin does not follow the helical symmetry of actin filament. In 2001, the location of troponin was visualized by the three-dimensional reconstruction from electron cryomicrographs of thin filaments using single-particle analysis. The troponin head (Figure 1B) is gourd-shaped and at high Ca^{2+} concentrations it is located over the inner domain of actin (Figure 3B), whereas at low Ca^{2+} concentrations it is shifted by ~30Å toward the outer domain and bifurcated, with a troponin arm (Figure 3B) covering the N- and C-terminal regions of actin in subdomain 1 (Figure 1B). The troponin arm disappears at high Ca^{2+} concentrations. This might be the consequence of the detachment of the IP(α) and IP(γ) of TnI from actin. According to the analysis of the data from fluorescence resonance energy transfer experiments, the position of the C domain of TnC seems to change more than that of the N domain. Presumably, the association between the troponin arm and subdomain 1 of actin pulls the C domain of TnC toward ubdomain 1 at low Ca^{2+} concentrations. At high Ca^{2+} concentrations, however, such interactions disappear and the C domain of TnC returns to its original position over the inner domain of actin.

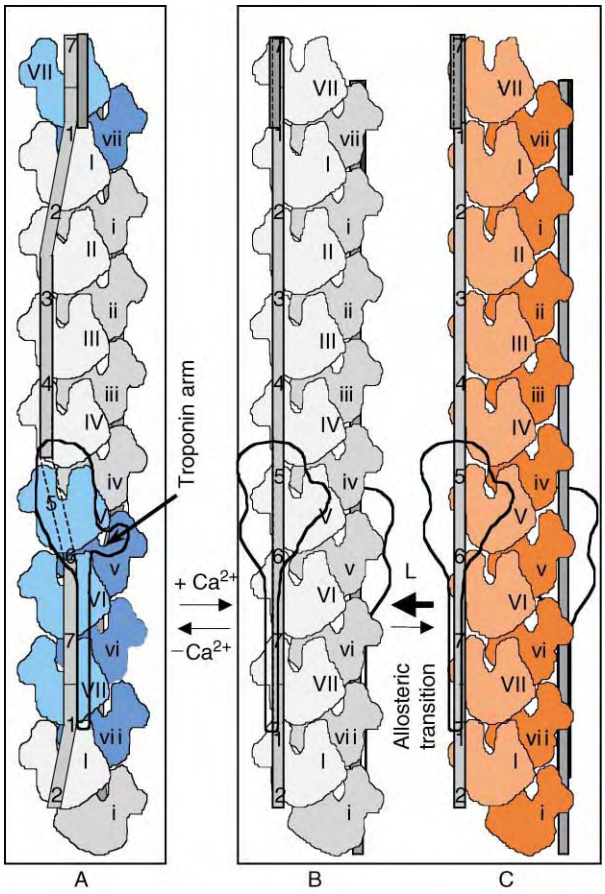

FIGURE 3 A model for Ca^{2+} regulation. (A) blocked state (T * state); (B) closed state (T state); (C) open state (R state). For simplicity, the two strands of actin are shown untwisted, so that they are parallel, and in different colors. The uppercase roman numerals label the outer domain of actin, and the lowercase ones label the backside of the inner domain. The arabic numerals label the seven segments of tropomyosin, with the segment 5 being the binding site of a troponin head. At high Ca^{2+} concentrations, there are two states, with the T or closed state (B) ~10 times higher in population than the R or open state (C) (L =~10). Myosin favors the transition from the T state to the R state (actin colored orange; myosin can bind and release phosphate to fully support contraction). At low Ca^{2+} concentrations (A), a troponin arm emerges and tropomyosin shifts differentially. Only the actin colored blue is blocked (myosin cannot bind); the actin colored gray is in a closed state (myosin can bind weakly and cannot release bound phosphate). Reprinted from Narita, A., Yasunaga, T., Ishikawa, T., Mayanagi, K., and Wakabayashi, T. (2001). Ca^{2+}-induced switching of troponin and tropomyosin on actin filaments as revealed by electron cryo-microscopy. *J. Mol. Biol.*, **308**, 241–261, copyright 2001, with permission from Elsevier.

Ca^{2+}-Induced Tropomyosin Shift

Since the Ca^{2+}-induced tropomyosin shift was first proposed, there has been controversy over the locations of tropomyosin, which were determined by assuming helical symmetry. It was found that the thin filaments deviate from helical symmetry; the extent is greater at low Ca^{2+} concentrations than at high Ca^{2+} concentrations. Thus, the locations of tropomyosin were determined by three-dimensional reconstruction without assuming such symmetry.

Tropomyosin follows a smoothly curved path in crystals and in thin filament at high Ca^{2+} concentrations (Figure 1B). At low Ca^{2+} concentrations, however, tropomyosin does not seem to follow a smooth path; it shifts differentially (Figure 3A) at the N-terminal half and the C-terminal third. There is evidence suggesting that the C-terminal third of tropomyosin may not always be in a rigid coiled-coil conformation and is sensitive to the changes in environment (e.g., the changes in troponin). The X-ray crystallographic studies showed that residues 160–220 of tropomyosin are mobile and that its mobility increases at higher temperatures, with the N-terminal half being immobile and almost insensitive to temperature. The region around residue 220 of tropomyosin shows low scores for coiled-coil structure, and the secondary structure prediction of sequence 214–218 of tropomyosin is ambivalent.

The myosin-binding site is located mainly in subdomain 1 in the outer domain of actin. At low Ca^{2+} concentrations, the myosin-binding sites of three actin monomers (colored blue in Figure 3A) out of seven are blocked by the C-terminal third of tropomyosin or troponin. The myosin-binding sites of the remaining four actin monomers (colored gray in Figure 3A), however, are not blocked because the N-terminal half of tropomyosin does not shift much. This is consistent with the biochemical study that found that the thin filament is only 67% blocked even at low Ca^{2+} concentrations. Thus, the simple steric blocking hypothesis is only partially correct.

Molecular Mechanism of Ca^{2+} Regulation

The relationship between the three states of actin and the location of tropomyosin is presented in Figure 3. When tropomyosin is located on the outer domain, actin monomers are in a blocked state. When tropomyosin is located on the inner domain, there are two states of actin monomers.

Figure 3A–B illustrates the three-dimensional structure of the thin filaments reconstructed from electron cryomicrographs. For clarity, the double helix of thin filament has been untwisted so that two strands are parallel and the strands are colored. The uppercase roman numerals label the outer domains of actin, and lowercase ones label the back side of the inner domains. Arabic numerals label the seven segments of tropomyosin, with segment 5 as the binding site of a troponin head.

At high Ca^{2+} concentrations (Figure 3B), the troponin head looks gourd-shaped and is located over the inner domain of actin (subdomains 3 and 4). Tropomyosin is also located entirely over the inner domain of actin, allowing greater access of myosin to the outer domain, where the myosin-binding site of actin is located, for the generation of force. Thus, all actin monomers are in a closed state (colored gray in Figure 3B).

At low Ca^{2+} concentrations, however, the troponin head shifts toward the outer domain and bifurcates, with a troponin arm covering the N- and C-terminal regions in subdomain 1 of actin. The C-terminal third of tropomyosin also shifts, together with a troponin tail, toward the outer domain of actin and the myosin-binding sites are blocked (colored blue in Figure 3A), but the N-terminal half of tropomyosin shifts only small amount and these myosin-binding sites are still accessible in a closed state (colored gray in Figure 3A). Thus, the myosin-binding sites of only three actin monomers are blocked by tropomyosin and troponin at low Ca^{2+} concentrations.

According to the three-state model, tropomyosin should shift further toward the inner domain of actin to achieve full activation of actin-activated myosin ATPase (Figure 3C). The mutagenesis introduced in residue 230 in subdomain 4 of actin facilitates the actin activation of myosin ATPase in the presence of tropomyosin, with the activation by pure actin being unchanged. Such mutagenesis increases the accessibility of the hydrophobic pocket in subdomain 4 of actin. It is conceivable that tropomyosin shifts further to bind to the exposed hydrophobic pocket to achieve an open state (colored orange).

This model predicts that the full activation of contraction is a two-step process: (1) a Ca^{2+}-dependent transition from a blocked state (T^* state) to a closed state (T state) and (2) a Ca^{2+}-independent allosteric transition from a closed state (T state) to an open state (R state), facilitated by the binding of myosin to actin. The model also explains why complete relaxation is difficult to achieve in skeletal and cardiac muscles – not all the myosin-binding sites of actin monomers are blocked at low Ca^{2+} concentrations. This may be on purpose; unlike smooth muscles, striated muscles must be always on standby. Ca^{2+} regulation appears to be the result of the delicate balance of interactions among calcium ions, troponin, actin, tropomyosin, myosin, and nucleotides. Such delicateness is consistent with the large number of

reports of mutations that cause familial hypertrophic myocardiopathy.

See Also the Following Articles

Actin Assembly/Disassembly • Meiosis • Rho GTPases and Actin Cytoskeleton Dynamics

Glossary

actin A globular protein (G-actin, $M_r \sim 42,000$) that forms filaments (F-actin) that bind tropomyosin and troponin. Actin filaments activate myosin ATPase, which supplies the free energy for contraction. The folding pattern of actin is homologous to RNase H.

myosin (Myosin II) A motor protein, for example, ATPase, which is activated by an actin filament by approximately 100 times. Myosin consists of two head domains and a tail domain. Tail domains assemble to form thick filaments. A head domain (subfragment 1) can bind to actin and hydrolyze ATP. The myosin head, kinesin, and ras protein share a common folding pattern.

thin filament A structure formed by F-actin, tropomyosin, and troponin; native thin filaments also contain nebulin. At high Ca^{2+} concentrations, thin filaments interact with myosin-containing thick filaments to generate force.

tropomyosin A fibrous protein ($\sim$400Å, $M_r \sim 35,000 \times 2$) that polymerizes in a head-to-tail manner. When the myosin concentration is low, tropomyosin inhibits actin-activated myosin ATPase. Tropomyosin and troponin are essential for Ca^{2+} regulation.

troponin A protein complex formed from troponin-T (TnT, $M_r \sim 31,000$, tropomyosin-binding), troponin-I (TnI, $M_r \sim 21,000$, inhibitory), and troponin-C (TnC, $M_r \sim 18,000$, Ca^{2+}-binding). TnT can be divided into TnT_1 and TnT_2. TnT_2, TnI, and TnC form a troponin head, from which a troponin arm emerges at low Ca^{2+} concentrations. TnT_1 forms a tail domain.

Further Reading

Ebashi, S., and Endo, M. (1968). Ca ion and muscle contraction. *Progr. Biophys. Mol. Biol.* **18**, 123–183.

Farah, C. S., and Reinach, F. C. (1995). The troponin complex and regulation of muscle contraction. *FASEB J.* **9**, 755–767.

Huxley, H. E. (1972). Structural changes in the actin- and myosin-containing filaments during contraction. *Cold Spring Harbor Symp. Quant. Biol.* **37**, 361–376.

Maytum, R., Lehrer, S. S., and Geeves, M. A. (1999). Cooperativity and switching within the three-state model of muscle regulation. *Biochemistry* **38**, 1102–1110.

Narita, A., Yasunaga, T., Ishikawa, T., Mayanagi, K., and Wakabayashi, T. (2001). Ca^{2+}-induced switching of troponin and tropomyosin on actin filaments as revealed by electron cryo-microscopy. *J. Mol. Biol.* **308**, 241–261.

Squire, J. M., and Morris, E. P. (1998). A new look at thin filament regulation in vertebrate skeletal muscle. *FASEB J.* **12**, 761–771.

Biography

Dr. Setsuro Ebashi is a Professor Emeritus of the University of Tokyo and a former director of the National Institute of Physiological Sciences. His research interest is the regulatory mechanism of muscle contraction. He holds an M.D and a Ph.D. from the University of Tokyo. He discovered the relaxation induced by Ca^{2+}-uptake by sarcoplasmic microsomes, discovered Ca^{2+} regulation of muscle contraction, and isolated troponin.

Dr. Takeyuki Wakabayashi is a Professor of Teikyo University and a Professor Emeritus of the University of Tokyo. His interest is the structural basis of Ca^{2+} regulation of muscle contraction. He holds an M.D. and a Ph.D. from the University of Tokyo. He determined the three-dimensional location of troponin on thin filaments, the myosin-binding site of actin, and the ATP-binding site of myosin; and he showed the differential tropomyosin shift by Ca^{2+}.

Calcium Signaling: NO Synthase

Zhi-Qiang Wang and Dennis J. Stuehr
The Lerner Research Institute, Cleveland Clinic Foundation, Cleveland, Ohio, USA

Nitric oxide (NO) is an important signal and effector molecule in animal physiology. NO is generated from L-arginine by the NO synthases (NOSs). Three NOSs have been characterized in animals: neuronal NOS (nNOS, type I), cytokine-inducible NOS (iNOS, type II), and endothelial NOS (eNOS, type III). Importantly, the activities of all three depend on their binding calmodulin (CaM). CaM binds reversibly to eNOS and nNOS in response to elevated Ca^{2+} concentrations and so their activities are regulated by intracellular Ca^{2+}. In contrast, iNOS binds CaM independent of Ca^{2+} concentrations and is therefore continuously active after it is expressed. Because it is unusual for a redox enzyme like NOS to be controlled by a Ca^{2+} binding protein, the NOS–CaM interaction has provided new insight into some aspects of protein structure and function.

NO Synthases

To become active each NOS enzyme must assemble into a dimer of two subunits. Each subunit in the NOS dimer contains a N-terminal "oxygenase domain" that binds iron protoporphyrin IX (heme), the cofactor 6R-tetrahydrobiopterin (H_4B), and the substrate Arg, and a C-terminal "reductase domain" that binds FMN, FAD, and NADPH. Between oxygenase and reductase domains there is a 20–25 amino acid CaM binding motif (Figure 1).

NO synthesis depends on electron transfer to the heme, and this process only occurs when CaM is bound. In a CaM-bound NOS dimer, the electrons from NADPH load into the FAD and FMN groups in one subunit, and then transfer from the FMN to the heme that is located in the partner subunit (Figure 1). In general, CaM activates electron transfer in NOS at two points: electron transfer into the flavins (intradomain) and between the FMN and heme (interdomain). Intradomain transfer is associated with enhanced catalysis by the NOS reductase domain, as measured by rates of NADPH-dependent ferricyanide or cytochrome c (Cyt c) reduction. CaM activation of the interdomain electron transfer in NOS results in reduction of the ferric heme iron, which is a prerequisite for oxygen binding to the heme and for NO synthesis.

Calmodulin Interactions with Ca^{2+} and with NOS

CaM is a small Ca^{2+} binding protein (molecular weight 17 kDa) consisting of two similar globular domains (called lobes) that each contain two E–F hands. An E–F hand includes a N-terminal helix (E helix), a centrally located Ca^{2+} coordinating loop, and a C-terminal helix (F helix). Upon Ca^{2+} binding, CaM is able to bind to and activate more than 30 target enzymes, enabling it to regulate numerous second messengers and cell functions. Binding and full activation of target proteins by CaM typically requires occupancy of all four Ca^{2+} binding sites in CaM. The carboxy-terminal lobe contains two high affinity Ca^{2+} binding sites, while the amino-terminal lobe contains two sites with lower Ca^{2+} affinity. Conformational changes that occur in CaM after it binds Ca^{2+} expose its hydrophobic surface residues in order to form critical van der Waals interactions with the hydrophobic face of the target peptide recognition site.

CaM binds to each NOS subunit in a 1:1 stoichiometry with reasonably high affinity. Binding affinity studies with peptides that correspond to NOS CaM recognition sequences show that the three NOSs display different affinities toward CaM with the general order being iNOS $\gg$ nNOS $\approx$ eNOS. The iNOS peptide binds well to CaM both in the presence and absence of Ca^{2+}, but eNOS and nNOS peptides bind to the CaM only in the presence of Ca^{2+}.

Each lobe of CaM binds to NOS independently and displays different affinities toward NOS. The CaM–nNOS interaction has been investigated using CaM mutants and plant CaM proteins. nNOS displays a high degree of structural specificity toward CaM domains 1, 3, and possibly 4 regarding activation of heme reduction and NO synthesis. The CaM–nNOS interactions are particularly important for electron transfer and involve the latch region of CaM (formed by CaM domains 1 and 3) and a methionine residue in domain 4. These regions of CaM appear to interact with as yet unknown regions on nNOS that are distinct from its CaM binding sequence. Ca^{2+} dissociation from

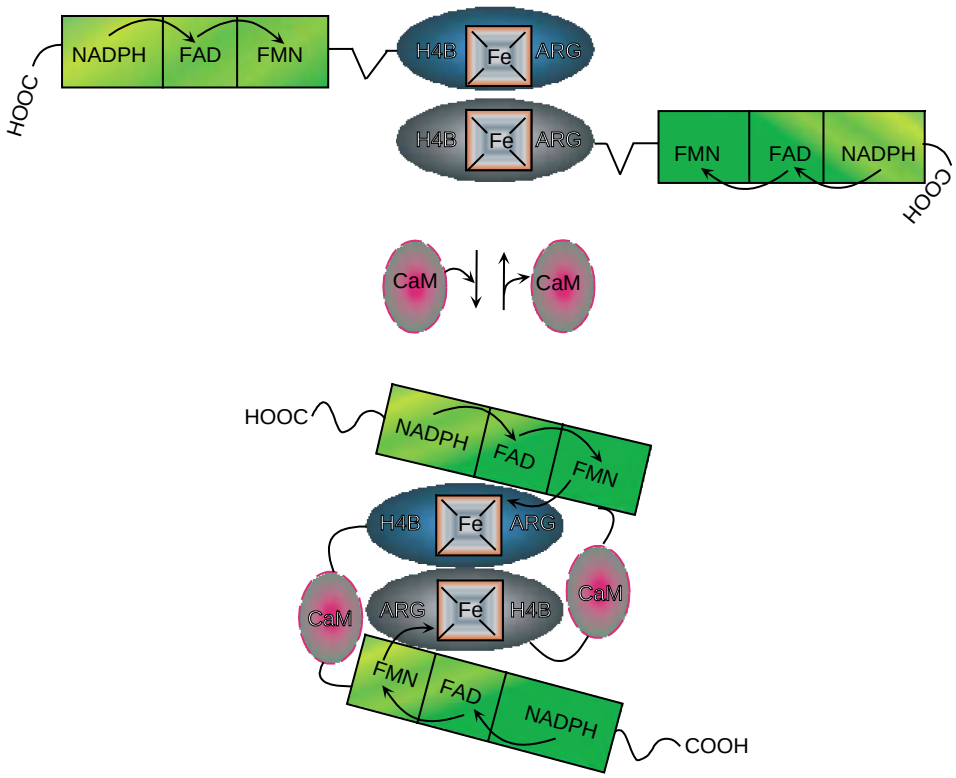

FIGURE 1 CaM-induced electron transfer in nNOS. CaM binding in response to elevated Ca^{2+} concentrations enables electron transfer between FMN and the heme located in adjacent subunits of the NOS dimer.

NOS-bound CaM has also been investigated. It occurs in two sequential steps: rapid Ca^{2+} dissociation from the N-terminal lobe occurs first and corresponds with inactivation of NO synthesis, followed by a slower Ca^{2+} dissociation from the C-terminal lobe, which leads to the dissociation of CaM from NOS.

Conformational changes occur in the NOS CaM binding peptides when they bind CaM. Typically, the peptides acquire an α-helical conformation upon interaction with Ca^{2+} bound CaM. A CaM-induced conformational change in the NOS reductase domain also occurs as indicated by changes in protein and flavin fluorescence and by a change in the trypsin proteolysis pattern.

A crystallographic structure of Ca^{2+}-loaded CaM bound to a 20-residue peptide corresponding to the eNOS CaM recognition sequence is available. The structure revealed that the α-helical eNOS peptide binds to CaM in an antiparallel orientation through extensive hydrophobic interactions: the N-terminal and C-terminal lobes of CaM wrap around the bound peptide, interacting with the C- and N-terminal halves of the peptide, respectively. Specific CaM residues in the latch region and domain 4 were positioned in a manner consistent with their importance as determined by mutagenesis studies. The crystal structure also suggested a basis for tighter CaM binding in iNOS: because iNOS contains a greater number of hydrophobic residues within its corresponding CaM recognition sequence, it was argued that these would support more extensive van der Waals contacts with CaM and minimize unfavorable solvent exposure of hydrophobic residues in order to favor tighter association between CaM and the iNOS CaM recognition sequence.

Ca^{2+}/CaM Regulation of NOS

How Ca^{2+}/CaM regulates NO synthesis and heme reduction in NOS is not entirely clear. CaM binding does not appear to change the thermodynamic driving force for electron transfer in NOS and instead may control the electron transfer primarily via structural rearrangement. CaM binding likely induces a relatively large conformational rearrangement which then enables the FMN subdomain to get close enough to the NOS oxygenase domain heme to make electron transfer between them more efficient.

Some cellular proteins that bind to NOS can regulate its response to Ca^{2+}/CaM. These include caveolins, dynamin, the bradykinin β-2 receptor, and heat shock protein-90. In addition, several different structural elements that are present in NOS regulate its interaction and response to Ca^{2+}/CaM (Table I, Figure 2). These

TABLE I

NOS Structural Elements Involved in Its Ca^{2+}/CaM Response

NOS structural element	Role
CaM binding site	Binds CaM to NOS; is inhibitory in the absence of CaM
Autoinhibitory loop	Impacts Ca^{2+} concentration response, represses NOS activity in absence of CaM, also required for full CaM response
C terminal extension	Impacts Ca^{2+} concentration response, represses NOS activities in absence of CaM, also required for full CaM response
Amino acid 484–726 in the FMN subdomain of iNOS	Required for Ca^{2+}-independent CaM-binding to iNOS
CD2 loop in reductase domain of eNOS	Impacts Ca^{2+} concentration response, represses NOS activities in absence of CaM
Phe1395 in FNR subdomain of nNOS	Helps to repress NOS activities in absence of CaM, also required for CaM to fully relieve the repression
Phosphorylation sites in eNOS	
S1179	Phosphorylation impacts Ca^{2+} concentration response and increases enzyme activity
T497	Dephosphorylation increases enzyme activity
S635	Phosphorylation may impact enzyme activity
S617	Phosphorylation impacts Ca^{2+} concentration response, no change in enzyme activity

include the canonical CaM binding site in each NOS and at least four other structural elements within the reductase domain. Initially, it was imagined that the CaM interaction with each NOS isoform might depend solely on its CaM recognition sequence. However, subsequent studies showed that other sequence elements are important. For example, substitution of the eNOS CaM-binding sequence by that of iNOS, and vice versa, yielded proteins whose Ca^{2+} dependence were intermediate between those of iNOS and eNOS. Other studies showed that both eNOS and nNOS, after having their CaM binding sequences replaced with the corresponding sequence from iNOS, still required added Ca^{2+} for full CaM binding and activity. Other more specific deletion studies have identified short regions within the iNOS and eNOS reductase domains that modulate the NOS Ca^{2+} requirement and CaM affinity in a positive or negative manner (Table I). Finally, there are several amino acids that can undergo phosphorylation within the NOS reductase domains and CaM binding sites (Figure 2). Phosphorylation at these individual or combined sites in NOS alters the CaM response with regard to its Ca^{2+} concentration requirement and may also alter the maximal level of enzyme activation that is achieved.

One regulatory element that is unique to NOS is the autoinhibitory loop insert (Figure 2). Constitutive NOSs (for example, eNOS and nNOS) contain a 40–50 amino acid insert in their FMN binding module that is not shared with iNOS or with other related flavoproteins. Similar autoinhibitory loops have been reported in a number of CaM-dependent enzymes, including CaM-dependent protein kinase II, smooth muscle myosin light chain kinase, and calcineurin. Peptides based on the eNOS insert sequence inhibited NOS enzymatic activity by altering their CaM binding. Subsequent studies showed that deleting the insert in eNOS or nNOS decreased their EC_{50} for Ca^{2+}, confirming that the insert was inhibitory (i.e., causes the enzyme to require a higher Ca^{2+} concentration to enable its CaM response). Deletion of the autoinhibitory peptide also enables some NO synthesis in the absence of CaM and increases the intrinsic catalytic activity of CaM-bound eNOS. Thus, the insert contributes to the Ca^{2+}-dependence of the constitutive NOS, and also regulates the electron transfer between its FMN and heme centers.

How the autoinhibitory insert participates in Ca^{2+}/CaM regulation is still unclear. One model has the insert docking on a site in NOSs that impedes both CaM binding and the structural rearrangement that is expected to be required for enzymatic activation. Upon binding, the Ca^{2+}/CaM, a conformational change that displaces the autoinhibitory insert from its docking site would then relieve the inhibitory effect and facilitate activation of the enzyme. A two-stage model seems reasonable to explain the Ca^{2+}/CaM activation in NOSs: CaM binding is largely determined by the recognition sequence and some other interactions with the enzyme. However, activation of the enzyme is fully dependent on a movement of the autoinhibitory insert, which could only be affected by the Ca^{2+}-saturated CaM. The conformational change induced by Ca^{2+}/CaM is passed on to the autoinhibitory insert, and this in turn presumably enables the enzyme reductase and oxygenase domains to adopt

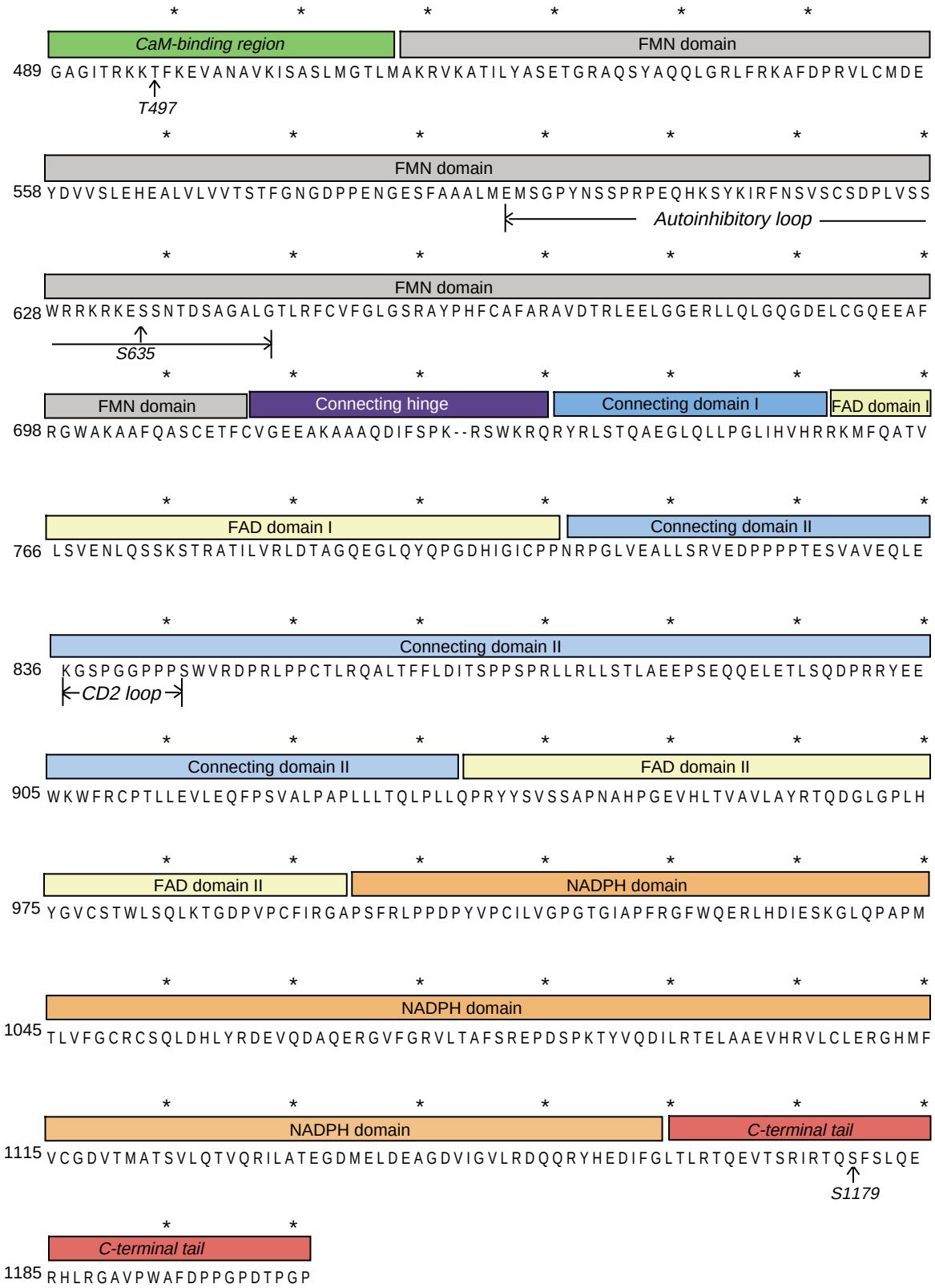

FIGURE 2 Sequence of eNOS CaM binding site and reductase domain. Colored rectangles indicate subdomains that make up the reductase domain. Structural elements and phosphorylation sites that impact Ca^{2+}/CaM regulation of NOS are noted in italics.

conformations that lead to productive electron transfer between the FMN and heme redox centers.

Another regulatory element that is unique to NOS is the C-terminal extension. The protein sequences of NOS reductase domains closely resemble that of NADPH-cytochrome P450 reductase (CPR). However, all NOS isoforms have an additional 20–40 residue extension in their C terminus, forming a "tail" that is absent in CPR. Deletion of 33 or 42 C-terminal residues from nNOS or eNOS speeds electron transfer into the flavins, implying that the C-terminal extension is a negative regulator. Another NOS mutant with a partial deletion of the C-terminal extension (Δ27 eNOS) exhibited a lower Ca^{2+} concentration response and an increase in some of its catalytic activities. Importantly, there is an Akt-dependent phosphorylation site located in the C-terminal tail of the constitutive NOS enzymes that modulates their regulation by Ca^{2+}/CaM (Figure 2). Phosphorylation at this site relieves some of the repression attributed to the C-terminal tail in the absence of CaM. It also lowers the Ca^{2+} concentration that is required for CaM binding and increases the NO synthesis activity of eNOS (but not of nNOS). When the autoinhibitory loop is present (as in nNOS and eNOS), the C-terminal tail is also needed to enable full activation in response to Ca^{2+}/CaM. This indicates that it functions as a positive regulatory element under this circumstance.

Ca^{2+}/CaM regulation of NOS may involve the two regulatory elements in the following manner. In the absence of CaM, the C-terminal extension helps to cover the NADPH-FAD and FMN subdomain interfaces, and this inhibits (but does not completely prevent) the FMN subdomain from transferring electrons to redox partners like cytochrome c or the NOS heme. This repression by the C-terminal tail requires that the enzyme NADPH binding site be occupied. Under this condition, the autoinhibitory insert is positioned in a way that antagonizes CaM binding and prevents the FMN subdomain from interacting productively with the NOS oxygenase domain. Upon CaM binding, the autoinhibitory loop swings away and this conformational change enables interactions between the FMN subdomain and the oxygenase domain that are productive for electron transfer to the heme. Specific interactions between the C-terminal extension and the autoinhibitory insert are likely to occur within the CaM-bound NOS. Such interactions between the two regulatory elements are likely to enable full activation of electron transfer by Ca^{2+}/CaM. Thus, the autoinhibitory loop and C-terminal tail repress enzyme function in the absence of CaM, and help to positively modulate function when Ca^{2+}/CaM is bound. Other structural elements that are present in the NOS reductase domain (Table I) along with protein phosphorylation events also help to regulate Ca^{2+}/CaM binding and to tune its activation of enzyme catalysis.

See Also the Following Articles

Calcium/Calmodulin-Dependent Protein Kinases • Calcium/Calmodulin-Dependent Protein Kinase II • Cytochrome *c* • Flavins • Heme Proteins • Heme Synthesis • Ligand-Operated Membrane Channels: Calcium (Glutamate) • Nitric Oxide Signaling • Pteridines

Glossary

calmodulin Calcium binding protein that binds to target enzymes in a Ca^{2+}-dependent manner and activates their function.

nitric oxide Diatomic free radical that is generated from L-arginine by the NO synthases and is widely active in numerous processes in biology.

reductase domain Flavoprotein domain of NO synthases that contains bound FAD and FMN and is responsible for transferring electrons from NADPH to the heme group in NO synthase.

Further Reading

Abu-Soud, H. M., and Stuehr, D. J. (1993). Nitric oxide synthases reveal a role for calmodulin in controlling electron transfer. *Proc. Natl. Acad. Sci. U.S.A.* **90**, 10769–10772.

Aoyagi, M., Arvai, A. S., Tainer, J. A., and Getzoff, E. D. (2003). Structural basis for endothelial nitric oxide synthase binding to calmodulin. *EMBO J.* **22**, 766–775.

Hemmens, B., and Mayer, B. (1998). Enzymology of nitric oxide synthases. *Methods Mol. Biol.* **100**, 1–32.

James, P., Vorherr, T., and Carafoli, E. (1995). Calmodulin-binding domains: Just two faced or multi-faceted? *Trends Biochem. Sci.* **20**, 38–42.

Nishida, C. R., Knudsen, G., Straub, W., and Ortiz de Montellano, P. R. (2002). Electron supply and catalytic oxidation of nitrogen by cytochrome P450 and nitric oxide synthase. *Drug. Metab. Rev.* **34**, 479–501.

Persechini, A., White, H. D., and Gansz, K. J. (1996). Different mechanisms for Ca^{2+} dissociation from complexes of calmodulin with nitric oxide synthase or myosin light chain kinase. *J. Biol. Chem.* **271**, 62–67.

Roman, L. J., Martasek, P., and Masters, B. S. (2002). Intrinsic and extrinsic modulation of nitric oxide synthase activity. *Chem. Rev.* **102**, 1179–1190.

Biography

Zhi-Qiang Wang is a Research Associate in the Department of Immunology at the Lerner Research Institute, Cleveland Clinic Foundation, in Ohio. She holds a Ph.D. from Fudan University (People's Republic of China) and served as a postdoctoral fellow at the Cleveland Clinic. Her principal research interests are the structure and function relationships of enzymes.

Dennis Stuehr is a Professor of Molecular Medicine and a member of the Department of Immunology at the Lerner Research Institute, Cleveland Clinic, in Cleveland, Ohio. He holds a Ph.D. from the Massachusetts Institute of Technology and received his postdoctoral training at Cornell University Medical School.

Calcium Transport in Mitochondria

Rosario Rizzuto
University of Ferrara, Ferrara, Italy

Marisa Brini
University of Padova and Venetian Institute of Molecular Medicine (VIMM), Padova, Italy

Mitochondria have long been known to accumulate Ca^{2+} down the electrical gradient established by the respiratory chain. Recent work has shown that, despite the low affinity of their Ca^{2+} transporters, Ca^{2+} uptake into mitochondria always follows the stimulation of cells with agonists causing an increase of cytoplasmic Ca^{2+} concentration. This process can modulate cellular events as diverse as aerobic metabolism, cytoplasmic diffusion of Ca^{2+} signals, and induction of apoptotic cell death.

The Origins and the Fundamental Principles

Studies of Ca^{2+} transport in isolated mitochondria began in the 1960s when evidence was provided that isolated, respiring mitochondria accumulate Ca^{2+} in the presence of inorganic phosphate. Ca^{2+} uptake was inhibited by respiratory chain blockers, but not by the ATP synthesis inhibitor oligomycin, and during Ca^{2+} uptake no ADP phosphorylation took place. In the presence of ATP no respiratory chain activity was necessary. Thus, the process of Ca^{2+} uptake was regarded as an alternative pathway to ADP phosphorylation for the use of the respiratory chain energy. In this scenario, mitochondria were thought as large stores of Ca^{2+}, which could be accumulated together with inorganic phosphate and precipitate in the matrix, leaving the matrix Ca^{2+} concentration virtually unchanged.

The general picture became clearer when the chemiosmotic theory solved the mechanism allowing mitochondria to store the energy obtained from metabolite breakdown and couple it to ATP synthesis. Indeed, the concept that the respiratory chain establishes a gradient ($\Delta\mu_H$), given by the Nernst equation $\Delta\mu_H = zF\Delta\psi + RT\ln[H^+]_i/[H^+]_o$, has major implications for Ca^{2+} transport and distribution. The gradient, composed of an electrical potential ($\Delta\psi$) and a concentration ratio (ΔpH), results by pumping protons across the ion-impermeable inner membrane. In actively respiring mitochondria, considering the buffering capacity mostly provided by weak acids, the gradient is supposed to be maintained mostly in the form of electrical gradient across the inner membrane ($\sim$180 mV). This implies a strong thermodynamic force in favor of the accumulation of cations (in the case of a divalent cation, such as Ca^{2+}, thermodynamic equilibrium is attained when in the matrix the concentration is $\sim 10^6$ higher than in the inter-membrane space). Based on these simple considerations, much attention was focused in the 1960s and 1970s on the capacity of mitochondria to accumulate Ca^{2+}, and on the biochemical and thermodynamic properties of this transport. Through the contribution of numerous laboratories and a large body of experimental work carried out in isolated, respiring mitochondria, these organelles were shown to possess separate accumulation and release pathways for the cation along with defined characteristics. Accumulation was shown to depend on the activity of an electrogenic "uniporter," which transports Ca^{2+} down the electrical gradient established by the respiratory chain. Inhibition of the respiratory chain or collapse of the electrical gradient (e.g., by the use of a protonophore) abolishes the capacity of mitochondria to accumulate Ca^{2+}. Ca^{2+} uptake is also directly inhibited by the compound Ruthenium Red (or its recently identified subcomponent Ru360) or lanthanides. Unfortunately, none of the inhibitors is highly specific, thus no selective tool has aided the purification of the transporter. Indeed, through the years this as well as the other mitochondrial Ca^{2+} transporters were not purified, and thus, despite the renewed interest, no molecular information on this process is available. As for the release pathways, two sets of exchangers have been shown to extrude Ca^{2+} from mitochondria: a Na^+/Ca^{2+} exchanger, mostly expressed in excitable cells (muscle and brain) and a H^+/Ca^{2+} exchanger, that represents the prevailing route in most other tissues. Both exchangers (although with different K_d) are inhibited by verapamil, diltiazem and other Ca^{2+} channel blockers.

More recently, much attention has been drawn to the potential role of a large-conductance channel, commonly referred to as the permeability transition pore (PTP). It is supposed to be a multiprotein complex (the putatively essential components being the voltage dependent anion channel, VDAC, of the outer membrane, the adenine nucleotide transporter, ANT, of the inner membrane and cyclophilin D) activated by various pathophysiological conditions (e.g., Ca^{2+} increases in the mitochondrial matrix and oxidation of critical cysteins). However, its role in mitochondrial Ca^{2+} homeostasis still remains elusive: it appears to play no role in Ca^{2+} efflux (as expected, considering that, unless an almost complete collapse of the electrical gradient occurs, the driving force is for Ca^{2+} accumulation, not release) and there is no clear evidence for its participation in mitochondrial Ca^{2+} uptake.

The Middle Ages

In the 1980s mitochondrial participation in intracellular Ca^{2+} homeostasis rapidly lost support, as the focus in calcium signaling was largely diverted to the endoplasmic reticulum (ER). In these years, the chain of events that couples the stimulation of plasma membrane receptors to the induction of a rise in cytoplasmic Ca^{2+} concentration was clarified, and it became clear that the ER and not mitochondria, were the main sites of action. Indeed, stimulation of receptors coupled through a G_q protein to the activation of phospholipase C induces the hydrolysis of the plasma membrane phospholipid phosphatidylinositol 4,5bisphosphate (PIP2) into diacylglycerol (DAG) and inositol 1,4,5trisphosphate (IP3). IP3 diffuses into the cytosol and interacts with Ca^{2+}-permeant channels of the ER membrane, causing their opening and the release of Ca^{2+} into the cytoplasm. The ER (and its specialized version of muscle cells, the sarcoplasmic reticulum, SR) was shown to be endowed with a molecular repertoire allowing it to act as a highly reactive intracellular Ca^{2+} store: pumps (that accumulate Ca^{2+} at the expense of ATP hydrolysis, and maintain a standing gradient between the lumen and the cytosol), low-affinity Ca^{2+} binding proteins (that increase the net amount of cation that can be accumulated, but promptly make it available when the concentration in the lumen decreases), and channels (opening, with different mechanisms, after stimulation of plasma membrane receptors).

What was left for mitochondria? In principle, given the large thermodynamic force for Ca^{2+} accumulation, they could take up most of the Ca^{2+} released by the ER. However, in the same years the availability of powerful and versatile Ca^{2+} indicators, the intracellularly trappable fluorescent dyes (e.g., quin2, fura-2, etc.) allowed for the careful estimation of cytosolic Ca^{2+} concentration ($[Ca^{2+}]_c$) of living cells and further reduced the possible roles of mitochondria. Indeed, these indicators showed that both at rest (0.1 μM) and upon stimulation (1–3 μM) the $[Ca^{2+}]_c$ is well below the affinity of the mitochondrial uniporter, and thus very little Ca^{2+} is supposed to be accumulated in mitochondria during the brief pulse of a physiological stimulation. Thus, the general consensus incorporating this series of information was that mitochondria acted as a low-affinity sink that could accumulate large Ca^{2+} loads, but only if the cell was exposed to challenges (most likely pathological events) that induced sustained, large $[Ca^{2+}]_c$ increases. In other words, mitochondria were mostly intended as salvage mechanisms against deleterious Ca^{2+} overloads.

The Renaissance

In this situation, the only opportunity for mitochondria to reobtain credit in the calcium field was to directly demonstrate in intact, living cells changes in mitochondrial $[Ca^{2+}]$ occurring in physiological conditions. This became possible in the early 1990s when novel experimental tools allowed to specifically measure the Ca^{2+} concentration in the mitochondrial matrix ($[Ca^{2+}]_m$): positively charged fluorescent indicators, which are largely accumulated in the mitochondria and molecularly engineered chimeras of the Ca^{2+}-sensitive photoprotein aequorin that include mitochondrial targeting sequences, and are thus exclusively localized in the mitochondrial matrix. Using these probes, it was possible to demonstrate that, in a variety of cell systems (ranging from epithelial cells to skeletal and cardiac myocytes, from hepatocytes to neurons), the $[Ca^{2+}]_c$ rises evoked by physiological stimulations are always paralleled by rapid $[Ca^{2+}]_m$ increases, which reach values well above those of the bulk cytosol (up to ~500 μM in chromaffin cells). The obvious discrepancy between this prompt response and the low affinity of the calcium uniporter was reconciled by the demonstration that mitochondria are exposed to microdomains of high $[Ca^{2+}]$ that largely exceed the values reported in the bulk cytosol and meet the low affinity of the uniporter. This is achieved through a close interaction between the mitochondria and the ER, the intracellular Ca^{2+} store, which could be directly demonstrated using targeted chimeras of a fluorescent recombinant protein (GFP) and a high-resolution imaging system. A consequence of this morphological arrangement is the capacity of mitochondria to "sense" the microenvironment at the mouth of the IP3-sensitive channel (and/or the plasma membrane Ca^{2+} channels), and thus the high $[Ca^{2+}]_c$ generated by their opening upon cell stimulation (Figure 1).

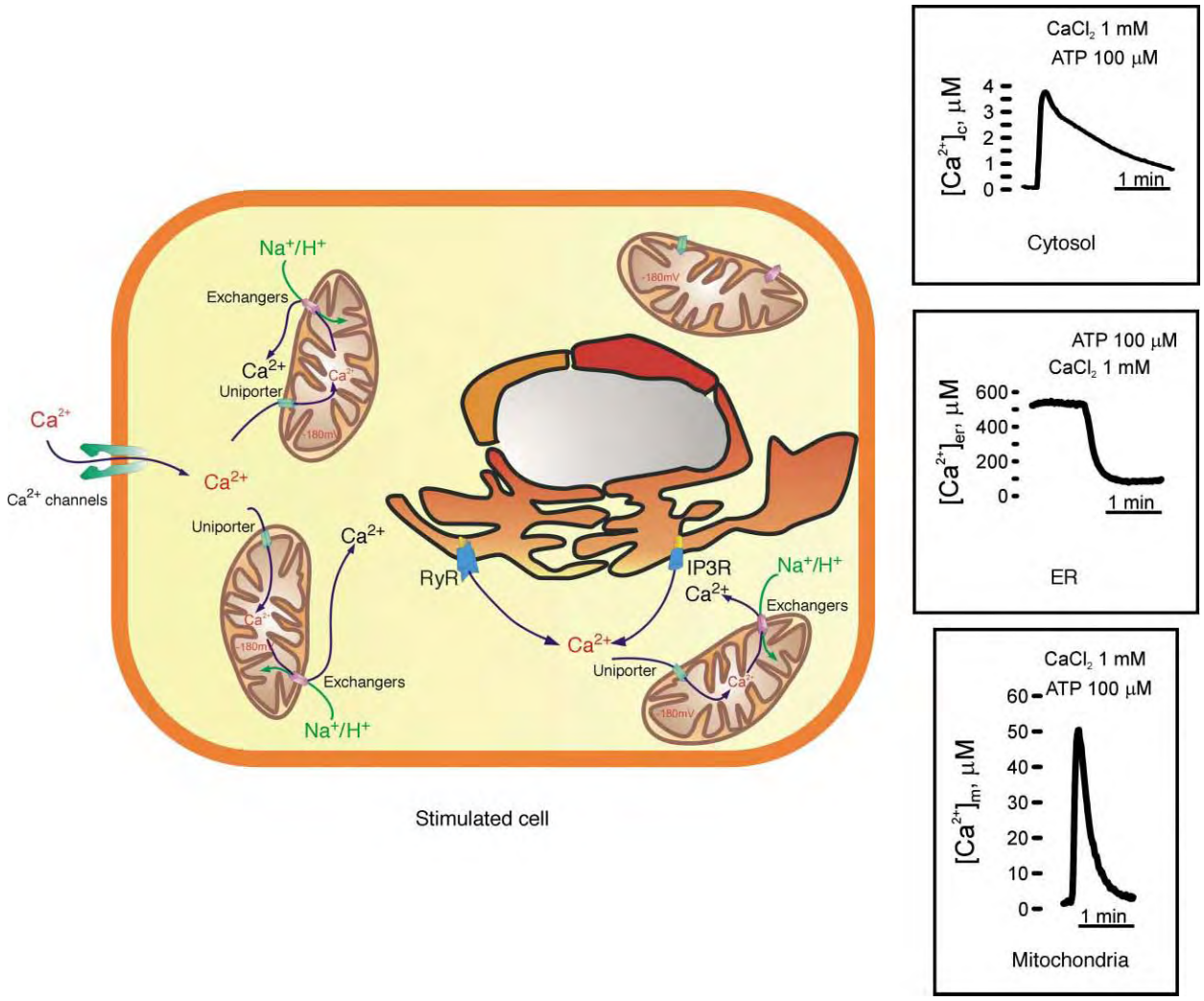

FIGURE 1 Mitochondrial Ca^{2+} transport. Cell stimulation induces the opening of plasma membrane Ca^{2+} channels and ER Ca^{2+} channels (IP3R and RyR), which, in turn, generates "hot spots" of Ca^{2+} concentration. Mitochondria located in the Ca^{2+} channels proximity could rapidly take up Ca^{2+} since their low-affinity uniporter could experience high local Ca^{2+} concentrations. The three traces represent measurements of $[Ca^{2+}]$ in the three cellular compartments shown, performed with suitably targeted aequorin.

One (or Many) Roles?

What is the functional significance of the re-evaluated mitochondrial Ca^{2+} transport? An obvious answer again stems from biochemical work by Denton, McCormack and Hansford in the 1960s, who could demonstrate that three key metabolic enzymes (the pyruvate, α-ketoglutarate and isocitrate dehydrogenases) are activated by Ca^{2+}, by different mechanisms: in the case of pyruvate dehydrogenase through a Ca^{2+}-dependent dephosphorylation step, and in the latter two cases through the direct binding of Ca^{2+} to the enzyme complex. Thus, the extension of a Ca^{2+} signal originated in the cytoplasm to the mitochondria would serve the purpose of transmitting an activatory signal to the energy powerhouse of the cell. In conjunction with the triggering of energy-consuming processes in the cytosol (contraction, secretion, etc.), mitochondrial dehydrogenases are stimulated, thus adapting aerobic metabolism to the increased needs of an active cell. Using the luciferase-based probe for ATP, it was possible to demonstrate that a rise in mitochondrial ATP levels parallels the $[Ca^{2+}]_m$ increase evoked by cell stimulation, and strictly depends on the $[Ca^{2+}]_m$ rise; if the latter is prevented by the use of Ca^{2+} chelators, such as 1,2-Bis(2-aminophenoxy) ethane-N, N, N′, N′-tetracetic acid (BAPTA), the [ATP] rise does not occur.

However, recent work by different groups has clarified that the role of mitochondrial Ca^{2+} uptake is not limited to the control of organelle function, but has a direct impact on the Ca^{2+} signals evoked by agonist stimulation in the cytosol. Two different mechanisms concur in this effect. The first occurs in the microdomains where mitochondria and ER get in

close contact. Here, the efficiency of mitochondrial Ca^{2+} accumulation accounts for the rapid clearing of the high $[Ca^{2+}]$ at the mouth of the release channel of the ER, and thus reduces the (positive or negative) feedback effect of the cation on the channel itself. Such a mechanism has been shown in a variety of experimental systems ranging from Xenopus oocytes (in which the diffusion properties of Ca^{2+} waves correlates with the energization state of mitochondria) to mammalian cells such as hepatocytes and glial cells, where it was demonstrated that the kinetics of Ca^{2+} release from the ER, and thus the spatio-temporal properties of the $[Ca^{2+}]_c$ rise are influenced by the process of mitochondrial Ca^{2+} uptake.

The second mechanism by which mitochondrial Ca^{2+} uptake affects cytosolic Ca^{2+} signals has been demonstrated in pancreatic acinar cells, which are endowed with a defined polarized morphology and the occurrence of cellular Ca^{2+} signals with different cellular locations and physiological consequences.

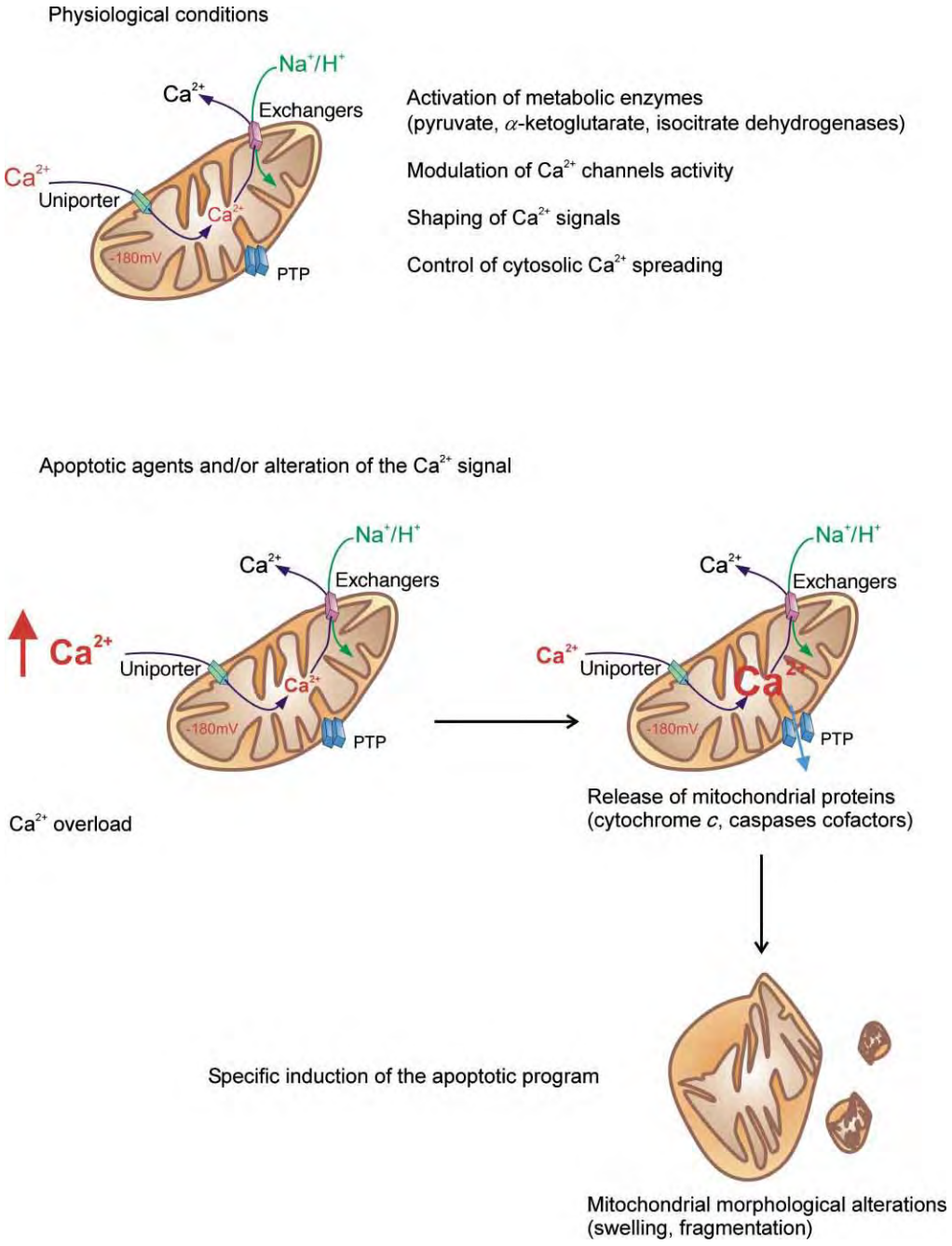

FIGURE 2 Physiological and pathological role of mitochondrial Ca^{2+} signaling.

At lower doses of agonists (e.g., colecystokinin) the $[Ca^{2+}]_c$ rise is restricted to the apical pole and causes granule secretion, at higher doses the $[Ca^{2+}]_c$ rise extends to the basal pole (where the nucleus is located), thus causing activation of gene expression and long-term alterations of cell function. The restriction mechanism was shown to be dependent on Ca^{2+} uptake by mitochondria clustered below the apical region that act as a "firewall" preventing the spread of the $[Ca^{2+}]_c$ rise. When the mitochondrial "belt" is overwhelmed (e.g., upon intense stimulation, or when the Ca^{2+} uptake capacity of mitochondria is experimentally impaired), then the Ca^{2+} signal can freely diffuse to the rest of the cell.

Finally, in the past years a more "dangerous" role for mitochondrial Ca^{2+} uptake has emerged. Work from various labs has revealed that the alteration of the Ca^{2+} signal reaching the mitochondria and/or the combined action of apoptotic agents or pathological conditions (e.g., oxidative stress) can induce a profound alteration of organelle structure and function. As a consequence, proteins normally retained in the organelle (such as an important component of the respiratory chain, cytochrome *c*, as well as newly discovered proteins, such as AIF and Smac/Diablo) are released into the cytoplasm, where they activate effector caspases and drive cells to apoptotic cell death. Different effects have been described: in hepatocytes, upon treatment with suboptimal doses of the lipid mediator of apoptosis ceramide, the repetitive spiking of cytoplasmic Ca^{2+} concentration ($[Ca^{2+}]_c$) rather than triggering the activation of matrix dehydrogenases (and thus the stimulation of aerobic metabolism), causes the opening of the permeability transition pore, the swelling of mitochondria, and the release of cytochrome *c*. Thus, a mechanism of "coincidence detection" of physiological agonists and apoptotic stimuli allows the specific induction of the apoptotic program (the mitochondria acting as the site where this "differential decoding" is operated). In addition, apoptotic stimuli can induce the impairment of the Ca^{2+} clearing mechanism of the cell (the plasma membrane Ca^{2+}-ATPase) thus potentiating Ca^{2+} loading. In this scenario, it can be easily understood how the partial depletion of Ca^{2+} from the ER, induced by the oncogene Bcl-2, has a protective effect toward some apoptotic stimuli (those involving mitochondria in the signaling pathway). Both in neurons and in hepatic cells it was observed that apoptotic signals cause mitochondrial Ca^{2+} overload, thus resulting in apoptotic morphological and functional alterations. A general scheme of the physiological role of mitochondrial Ca^{2+} signaling, and the potential alterations occurring in pathological conditions (modifying the final outcome) is summarized in Figure 2.

Conclusions

Recent work has greatly re-evaluated mitochondrial Ca^{2+} homeostasis as a key event not only for the maintenance of ion balance within the organelle (avoiding deleterious short-circuitry of the chemiosmotic machinery), but also as a control mechanism for physiological and pathological processes occurring in mitochondria, or activated by mitochondrial factors. Thus, both in basic and applied research there is an expanding interest on this topic, that contrasts with the paucity of molecular information. Neither the transporters nor the regulatory elements (and the crosstalk with other signaling routes) have been characterized, leaving a stimulating challenge (and much work to do) for scientists joining the field.

See Also the Following Articles

ATP Synthesis in Plant Mitochondria: Substrates, Inhibitors, Uncouplers • Calcium Signaling: Cell Cycle • Cell Death by Apoptosis and Necrosis • ER/SR Calcium Pump: Function • ER/SR Calcium Pump: Structure • Membrane Transporters: Na^+Ca^{2+} Exchangers • Phosphatidylinositol Bisphosphate and Trisphosphate • Voltage-Sensitive Ca^{2+} Channels

Glossary

apoptosis A type of cell death, characterized by specific morphological changes (i.e., chromatin condensation, DNA damage, and shrinkage of the cells) and utilized by organisms to regulate the growth and the development of tissues, organs, etc. Also called "programmed cell death."

ATP Adenosine trisphosphate, the biochemical molecule utilized by the cells as energy source.

caspases Family of proteins responsible for the degradation of specific proteins that contain recognizing sequences. Their activation leads to signals of programmed cell death.

G protein Protein associated to specific hormone receptor of the plasma membrane and responsible for the conversion of extracellular signals in intracellular messages.

respiratory chain A series of multisubunits proteins located in the inner mitochondrial membrane responsible for the electron and proton transfer necessary to generate the electrochemical gradient used for ATP production.

Further Reading

Carafoli, E. (2003). Historical review: Mitochondria and calcium: Ups and downs of unusual relationship. *Trends Biochem. Sci.* **28**, 175–181.

Carafoli, E., Santella, L., Branca, D., and Brini, M. (2001). Generation, control, and processing of cellular calcium signals. *Crit. Rev. Biochem. Mol. Biol.* **36**, 107–260.

Duchen, M. R. (1999). Contributions of mitochondria to animal physiology: From homeostatic sensor to calcium signalling and cell death. *J. Physiol.* **16**, 1–17.

Green, D., and Kroemer, G. (1998). The central executioners of apoptosis: Caspases or mitochondria? *Trends Cell. Biol.* **8**, 267–271.

MacCormack, J. G., Halestrap, A. P., and Denton, R. M. (1990). Role of calcium ions in regulation of mammalian intramitochondrial metabolism. *Physiol. Rev.* **70**, 391–425.

Rizzuto, R., Brini, M., Murgia, M., and Pozzan, T. (1993). Microdomains of high Ca^{2+} close to inositol-triphosphate sensitive channels are sensed by neighbouring mitochondria. *Science* **262**, 744–747.

Rizzuto, R., Bernardi, P., and Pozzan, T. (2000). Mitochondria as all-round players of the calcium game. *J. Physiol.* **529**, 37–47.

Biography

Rosario Rizzuto is a Professor of General Pathology at the University of Ferrara. He developed a new method for measuring Ca^{2+} concentration in specific cell domains, based on the targeting of the Ca^{2+}-sensitive photoprotein aequorin. His research interest is the role of calcium ions as intracellular second messengers with special emphasis on the mechanism and functional role of mitochondrial Ca^{2+} homeostasis.

Marisa Brini is Assistant Professor of Biochemistry at the University of Padova. Her main interest is the study of calcium signaling defects occurring in human genetic diseases and/or transgenic models affecting the homeostasis machinery of muscle. These include malignant hyperthermia, mitochondrial disorders, and cardiopathies due to mutations in the Ca^{2+} ATPase modulator phospholamban.

Calcium Waves

Lionel F. Jaffe
Marine Biological Laboratory, Woods Hole, Massachusetts, USA

Calcicum waves are actively propagated increases in intracellular calcium that carry signals within all organisms above the bacterial level. They occur in four main classes with characteristic speeds that vary over a range of a billionfold. Fast calcium waves move at 10 to 30 micrometers per second along endoplasmic reticula and include fertilization waves and brain injury waves. Slow calcium waves move at 0.1 to 1 micrometer per second and are surface contraction waves such as those that cleave dividing cells. Ultrafast calcium waves move at 10 to 40 centimeters per second along cell membranes and are electrical ones which underlie calcium action potentials in nerves and muscles. Ultraslow calcium waves move at 0.1 to 10 nanometers per second during development and include waves of DNA replication and of floret formation. Their mechanism is unknown.

Fast Calcium Waves

History, Roles, and Visualization

Calcium waves occur in four main classes with characteristic speeds that vary over a range of a billionfold. This speed spectrum is shown in Figure 1.

Calcium waves were discovered in 1978 by Gilkey *et al.* as the giant 10 μ/s fast wave or tsunami that crosses a medaka fish egg as it is fertilized and serves to start its development or activate it. This was done by injecting the eggs with the chemiluminescent calcium reporter, aequorin, and observing the wave of luminescence with an ultralow light imaging system (Figure 2). The American, Ernest Just first grasped the significance of fertilization waves and first measured their speeds accurately (in sea urchin eggs) in 1919. Just believed that such waves were restricted to the cell cortex, but they are now known to traverse the whole cytoplasm including the nucleus. The role and speed of such fertilization waves through medaka eggs was discovered by Tok-io Yamamoto during the Second World War in Japan. Moreover, he correctly predicted that they would prove to be calcium waves. Whereas sea urchin and fish eggs are activated by a single fast calcium wave, many other eggs – including human ones – can only be fully activated by a long series of fast calcium waves that start every few minutes. Aequorins still provide the best way to visualize calcium waves because these reporters are nondisturbing and provide quantitative information over a far larger dynamic range than the more widely used fluorescent indicators. Other roles of fast calcium waves include the control of contraction within muscle cells isolated from whole hearts, the control of contraction within isolated uterine muscle cells, the control of spreading depression or convulsion in the injured brain, the control of neuroglial waves in various vertebrate retinas, and the control of secretion in isolated rat livers.

Among brain injury waves are those that propagate migraine attacks and stroke. As early as 1941, the propagation of fast waves through the visual cortex of the brain during migraine attacks was inferred by Karl Lashley from the wave of visual blurring that sometimes accompanies migraine attacks.

Mechanisms

The initiation of fast calcium waves is best understood during fertilization. The interaction of eggs and sperm starts when contact of the sperm with the jelly coat around the egg induces a flow of calcium ions into the sperm from the medium. The influx ceases only when the sperm dies of calcium poisoning approximately 1 hour later. When the gametes fuse, this influx is diverted into the egg to help initiate a calcium wave. In most creatures, initiation is also speeded up by small molecules (sometimes called second messengers), such as nicotinic acid adenine dinucleotide phosphate (NAADP) or nitric oxide, that diffuse into the egg along with calcium ions.

Fast calcium waves are propagated within cells by a reaction–diffusion cycle or cycles that travel along the endoplasmic reticulum (ER). In the best understood of these cycles, the only reaction is one that opens calcium channels within the ER membrane. Calcium ions then move through such a channel from the lumen of the ER to the region just outside it. There they diffuse along the outside of the ER to other calcium channels a few microns away so as to induce their own release; a reaction called calcium-induced calcium release (CICR). In this way, a fast calcium wave is relayed from channel to channel so as to traverse a cell. Successful relay also requires a high enough level of channel sensitizers.

FIGURE 1 Main classes of natural calcium waves based on speeds at room temperature. Fast waves through active cells refers to all such waves in this speed class except for the slightly slower ones that activate eggs and are marked f. Fast waves are reaction–diffusion waves propagated by the short-range diffusion of calcium ions between relay points in the endoplasmic reticulum (ER). Slow waves are a second coherent class of calcium waves and seem to be stretch propagated. Ultrafast waves are electrically propagated waves or action potentials that are primarily dependent on an influx of calcium, rather than sodium, ions. Ultraslow waves are developmental. Reproduced with permission from L.F. Jaffe (1999). *BioEssays* **21**, 657–677. Copyright 1999, John Wiley & Sons.

In various cells these include cyclic AMP (cAMP), inositol trisphosphate (IP_3), cyclic adenosine 5′-diphosphate-ribose (cADPR), as well as NAADP. One way that fast calcium waves are carried between cells is by the diffusion of calcium ions through minute cytoplasmic bridges called gap junctions. Reaction–diffusion waves can also be seen in dishes containing a complex mixture of nonbiological chemicals such as the brominated ones that support the Bielozov–Zhabotinsky (BZ) reaction.

However, they may also be propagated along the interiors or lumens of ER strands by a reaction–diffusion cycle in which calcium induces its own release from a luminal calcium-binding protein such as a calsequestrin, a calreticulin, or a calcistorin/PDI. The two cycles mutually reinforce one another like the riders of a tandem bicycle; this is called a tandem wave mechanism.

Slow Calcium Waves

History, Roles, and Visualization

Slow calcium waves (like fast ones) were discovered in medaka fish eggs with the aid of aequorin. They were seen as two successive waves, both of which move at 0.5 μm/s within the forming second furrow of the cleaving medaka egg. The first of these accompanies elongation of the second furrow, whereas the second accompanies the subsequent, sequential apposition, or zipping together, of the newly formed blastomeres. This discovery was made in 1991 and the results of calcium buffer injections into Xenopus eggs (which likewise exhibit slow calcium waves during cleavage) soon showed that these waves do more than accompany furrowing. They are needed for it to start, to continue, and to remain. Moreover, by 1998, 30 apparently similar slow surface contraction waves had been recognized. An especially vivid one is the repeated gross contractile waves that traverse the barnacle egg from pole to pole before its first mitotic division. Its discoverers called these barnacle egg waves peristaltic in the plausible belief that they serve to drive morphogens to the vegetal pole via intracellular peristalsis. Another remarkable one is the surface contraction wave that accompanies primary neural induction in the axolotl egg.

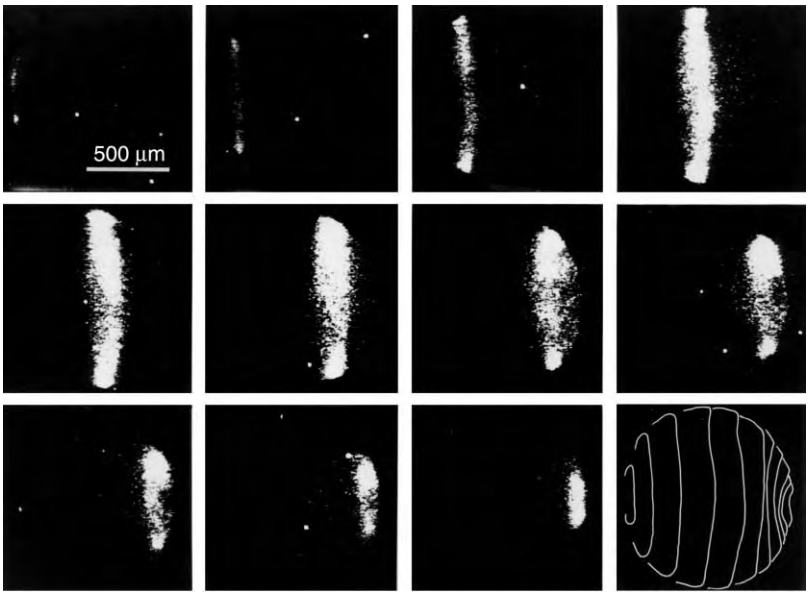

FIGURE 2 A free calcium wave propagating across a sperm-activated medaka egg. Successive photographs are 10 seconds apart. The last frame is a tracing showing the leading edges of the 11 illustrated wave fronts. Reproduced from Gilkey, J. C., Jaffe, L. F., Ridgway, E. B., and Reynolds, G. T. (1978). A free calcium wave traverses the activating egg of the medaka, *Oryzias latipes*. *J. Cell Biol.* **76**, 448–466, by copyright permission of the Rockefeller University Press.

Mechanisms

Slow calcium waves are thought to be propagated mechanically. Local surface contraction opens stretch-activated calcium channels in the subsurface ER of nearby regions. This releases calcium ions, which induces contraction in these nearby regions and thereby relays the wave. If the initial contraction is along a line, then the wave spreads along a line as in a cleavage furrow; however, if the initial contraction acts to shrink a small disk, then the wave spreads over the entire surface, as in the precleavage surface contraction waves of axolotl eggs.

Ultrafast Calcium Waves

Action potentials are electrical waves that are propagated by voltage-gated ion channels in the plasma membranes of nerve, muscle, and other cells. In the best-understood action potentials, sodium ions flow in through these ion channels to extend the electrical field along a cell; however, in another important class of action potentials, calcium ions flow in; these are called calcium action potentials or ultrafast calcium waves. The speeds of calcium action potentials have been measured along neurons within systems that range from jellyfish up to guinea pig brains, along muscles that range from moth hearts up to guinea pig hearts and even along an insectivorous plant. Unlike sodium action potentials, whose speeds vary over a thousandfold range, calcium action potential speeds vary over a range of approximately 10–40 cm/s (at 20°C) and thus over only a fourfold range. Moreover, unlike the speeds of sodium action potentials, the speeds of calcium ones are unrelated to cell diameter.

Why do calcium action potentials, or ultrafast calcium waves, have such a limited range of speeds? Perhaps evolution has driven them to be the fastest waves of calcium influx that avoid subsurface poisoning of the cell.

Ultraslow Calcium Waves

Ultraslow calcium waves are the least understood class of calcium waves. They include waves of formation of the morphogenetic furrow in developing Drosophila eyes, of floret formation in sunflowers, of DNA replication in certain protozoa, and of growth-cone-like bulges along certain growing mammalian brain neurons, as well as, perhaps, waves of cell division in rat lenses as they heal after a wound. The propagation mechanism of ultraslow calcium waves is completely unknown.

See Also the Following Articles

Calcium, Biological Fitness of • Calcium Buffering Proteins: ER Luminal Proteins • Chemiluminescence and Bioluminescence • Phosphatidylinositol-3-Phosphate

Glossary

aequorins Small chemiluminescent proteins that emit blue–green light when they react with calcium ions. They were first isolated from jellyfish and are used to measure and image calcium ions within living cells.

endoplasmic reticulum (ER) A network of thin tubes and flat sacs that pervades eukaryotic cells.

spreading depression A phenomenon found in the central nervous system that underlies migraine headaches and epileptic seizures (sometimes called Leão's SD). It involves a complex of intense changes that transiently inhibit cell function.

Further Reading

Fluck, R. A., Miller, A. L., and Jaffe, L. F. (1991). Slow calcium waves accompany cytokinesis in medaka fish eggs. *J. Cell Biol.* **115**, 1259–1265.

Gilkey, J. C., Jaffe, L. F., Ridgway, E. B., and Reynolds, G. T. (1978). A free calcium wave traverses the activating egg of the medaka, *Oryzias latipes*. *J. Cell Biol.* **76**, 448–466.

Jaffe, L. F. (1993). Classes and mechanisms of calcium waves. *Cell Calcium* **14**, 736–745.

Jaffe, L. F. (1999). Organization of early development by calcium patterns. *BioEssays* **21**, 657–677.

Jaffe, L. F. (2002). On the conservation of fast calcium wave speeds. *Cell Calcium* **32**, 217–229.

Jaffe, L.F. (2003). The propagation speeds of calcium action potentials are remarkably invariant. *Biol. Cell (Pans)* **95**, 343–355.

Jaffe, L. F., and Créton, R. (1998). On the conservation of calcium wave speeds. *Cell Calcium* **24**, 1–8.

Biography

Lionel F. Jaffe is a Senior Scientist at the Marine Biological Laboratory in Woods Hole and at Brown University. His principal research interest is in the broad field of developmental physiology, including calcium waves and calcium gradients, electrical field and polarized light effects, and interactions via chemiluminescent signals. He holds a Ph.D. from the California Institute of Technology.

Calcium, Biological Fitness of

Robert J. P. Williams
University of Oxford, Oxford, UK

Calcium has a special cation, Ca^{2+}, in cellular activity. It is rejected by all cell cytoplasm either to the outside of cells or to the inside of resides. From these stores it is released by events outside eukaryote cells to the cytoplasm and organells were it activates many processes. Thus calcium is the dominant messenger, relaying information concerning the environment to activities such as contraction of muscles, release of digestive jucies from the pancreas, to hormone release from glands. It is also the major cation in organizing external protein structures and in formation of biological mineral – shells and bones.

Calcium: The Element and its Ion, Ca^{2+}

Calcium, atomic number 20 lies in group 2 in the third row of the periodic table and before the first row of transition metals. It resides below magnesium and above strontium and then barium in its group. It has low ionization potentials, giving a rather large calcium ion, Ca^{2+} (radius 1.0Å), which is a rather poor Lewis acid and hence a somewhat poor acid catalyst. However, it can bind quite strongly to certain anion centers. Within its group, the chemistry of the Ca^{2+} ion has close resemblance to that of the larger strontium ion, Sr^{2+}, but differs markedly from the smaller magnesium ion, Mg^{2+}, which is a better Lewis acid.

Calcium, like magnesium, is an abundant element in the universe and on Earth, and its salts are quite soluble in water. Hence, calcium is available in the sea, 10^{-2} M, compared to magnesium at 5×10^{-2} M, whereas in fresh water it, like magnesium, is often as high as 10^{-3} M. It is against these background levels in water, especially in the sea, that life evolved.

The calcium ion has three major mass isotopes, 40, 42, and 44, which can be used to follow the reactions of its ions. It can also be followed in biological systems through association with fluorescent organic dyestuffs.

The Aqueous Calcium Ion

The free aqueous calcium ion has a variable fluctuating number of water molecules around it, exceeding six but not exceeding nine. This loose hydration sphere is common to all cations of a radius greater than 0.8Å. In this way the calcium ion differs from the magnesium ion, radius 0.6Å, which has a fixed, rather rigid coordination of six water molecules. The differences in structure are reflected in the rates of exchange of the water molecules from their respective coordination spheres, that of magnesium being rather slow, $10^6\ s^{-1}$ and that of calcium being close to the diffusion limit of $10^9\ s^{-1}$.

Insoluble Salts

The binding of calcium, a large ion, is less than that of magnesium when the in-coming anion is small (e.g., fluoride or hydroxide) and these magnesium salts tend to be the more insoluble. However, larger groups, which include the vast majority of anions (e.g., carbonate, sulfate, and phosphate anions), are more readily accommodated around the larger calcium ion. Hence, we observe that the vast majority of calcium salts are more insoluble than the corresponding magnesium salts. This becomes a feature in organisms, where we find calcium carbonate in shells and calcium phosphate in bones, whereas in plants calcium oxalate is often precipitated. Aberrant precipitation causes stones in animal organs. Among minerals, calcium and magnesium often occur together, as, for example, in dolomite.

Soluble Complex Ions and their Binding Strengths

Calcium ions do not bind strongly to simple anions in water at pH 7. Thus, complexes with carbonate, sulfate, hydroxide, and phosphate are not of great importance in organisms. However, binding to ligands with several donor atoms can be strong because despite their bulkiness they can be fitted around the large calcium ion. By contrast, the Mg^{2+} ion fails to bind strongly, so these chelating ligands selectively bind calcium relative to magnesium by at least a thousandfold. Typical examples are proteins both inside cells and in external circulating fluids. The use of the calcium buffer (ethylene tetra-acetate (EGTA)) depends on this quite strong

binding to calcium but weak binding to magnesium at pH 7.

Structures of Calcium Salts and Complexes

The structures of many calcium salts have been determined, and the extremes of their variation are shown even within the allotropic forms of its carbonates. Whereas calcite has a six-coordinate lattice, aragonite has a nine-coordinate structure. These salts have no water of crystallization and both are found in shells. More frequently, when calcium ions are bound to bulky chelating organic ligands in solution, calcium has seven near-neighbors, but the distances from the metal ion to the nearest ligand atom are very irregular, from 2.2 to 3.0Å. Bound to saccharides or proteins, the ion has this structure, but it fluctuates. It is usual for one or two water molecules to remain bound. The binding ligand atoms are invariably oxygen from such centers as oxyanions, carboxylates, alcohols, carbonyls, and ethers.

Rates of Exchange

The rate of loss of water molecules from around Ca^{2+}, $10^9\ s^{-1}$, is the rate at which ligands can bind, k_{on}. The rate of leaving is related to the ligand binding constant, $K = k_{on}/k_{off}$, so for $K = 10^6\ M^{-1}$ the leaving rate is $10^3\ s^{-1}$. This binding constant is close to that found for several proteins inside cells. The combination of such a protein (e.g., calmodulin) with calcium then provides a response time of $10^3\ s^{-1}$, as is seen in fast muscle cells. It is the rates of exchange together with the *selective* binding constants that make calcium an incomparable messenger in aqueous solution.

Biological Salts and Ligand Complexes

The major insoluble calcium salts found in organisms are the fluoride (in krill), carbonates (in shells in at least three allotropic forms), phosphates (in bone), and oxalates (in many plants). There are variable amounts of other metal ions and anions in these salts, so their exact nature is far from simple; for example, bone, hydroxy apatite, does not have an ideal stoichiometric formula and easily incorporates other elements including magnesium and fluoride. The apatite structure is somewhat different in bones of different organisms and even in the teeth and bones of one species (e.g., humans). Calcite is also found in the ears of animals, with a balance function.

In cellular complexes, calcium is bound, seven-coordinate, to oxygen (O-) donor groups of proteins and polysaccharides through both side chain and main chain atoms (e.g., $-OH$, $>CO$, CO_2^-, ether, and SO_4^{2-}). There is little or no binding to DNA or RNA in cells, in marked contrast to the essential function of magnesium in the structures of these nucleotides. The selective binding arises from the differences in concentration and binding ability.

Concentrations and Selectivity of Binding in Organisms

The ability of calcium ions to precipitate many organic anions including DNA required that one primary necessity of the original life forms, prokaryotes, was the rejection of calcium. Consequently, all organisms hold Ca^{2+} concentrations at 10^{-6} M or below in their cytoplasm using calcium outward pumps. Magnesium ions do not precipitate organic anions and are found at 10^{-3} M in all cell cytoplasms. Hence, for Ca^{2+} to bind selectively inside cells, its binding constant must be close to $10^6\ M^{-1}$, whereas that of Mg^{2+} has to be less than $10^3\ M^{-1}$. This selectivity between the two ions is found for many cytoplasmic messenger proteins, for example, calmodulin, troponin and S-100. Meanwhile, Ca^{2+} fails to bind to such molecules as ATP and DNA, $K = 10^4$, but Mg^{2+} can bind with the same binding constant. Outside cells, both Mg^{2+} and Ca^{2+} are $> 10^{-3}$ M and in eukaryotes the cell vesicles hold Ca^{2+} at this concentration also. Ca^{2+} can again bind selectively if its binding constant to proteins or now saccharides is $\geqslant 10^3\ M^{-1}$, whereas that of Mg^{2+} is less than $10^2\ M^{-1}$, because both ions are present outside cells at 10^{-3} M. These constants are found for some coat, blood-clotting, and immune-response proteins and for some vesicle proteins. Note that in higher organisms the free Ca^{2+} concentration in external fluids and vesicles is extremely well controlled and in the extracellular fluid of humans is nearly in equilibrium with the precipitated bone. The further requirement for a messenger activity, that the rate of exchange to the internal proteins be fast, at least $10^3\ s^{-1}$ for calcium, is also met.

Consider now a cytoplasmic concentration in a resting cell of Ca^{2+} of 10^{-7} M and an external or vesicle concentration of 10^{-3} M. Any influx of Ca^{2+} to the cytoplasm from outside through channels will increase Ca^{2+} to 10^{-6} M, which will trigger activity through cytoplasmic protein binding. On closing the channel, the outward pumps will restore rest conditions quickly. The calcium ion is therefore able to act as a pulsed messenger. Hence, the combination of sufficiency of binding, of selectivity, of concentration control, and of rates of on/off reactions give optimal messenger character to this elementary ion. No other ion or molecule could be better.

Overall Functional Fitness of Calcium Ions in Evolution

The properties of the calcium ion, its fast on/off reactions reflecting the structural flexibility of its coordination sphere and its quite strong binding to selected organic ligands, have made it an extremely valuable partner to organic chemicals in almost all forms of life. In the most primitive forms of life, this value is seen in protective external constructs (walls) and mineralization, but also in the use of bound calcium in external digestive catalytic enzymes. These functions are found in all other organisms but the most striking feature of the use of calcium appeared at the time the eukaryotes developed from the prokaryotes. At that time, the problem of coordinating activities of different compartments (vesicles) and the need for an increasing recognition of the environment became critical for the survival of the large eukaryote cells. Cooperation between compartments and sensing required the rapid transfer of information between cellular compartments and from the outside environment, and there is no better possible mode of communication in cellular biology than that which can be derived from the happy coincidental values of the high availability with concentration control and the response properties of the calcium ion. Hence, it was an evolutionary requirement that led to a messenger system in which the calcium ion was the best of all available carriers (Table I). The protein receptors in the cytoplasm acted as mechanical triggers of action, changing conformation upon binding calcium. They include all muscle responses (troponins), fertilizations, many metabolic responses (calmodulins), genetic activations (possibly S-100 and other proteins), and immune responses (calcineurin). The necessary refinement of the homeostasis of the calcium concentrations increased all the way up to humans and included the control over both the internal cytoplasmic and the external circulating fluid concentrations. In the external fluids, there arose various novel functions that used the calcium ion, including further immune responses and blood-clotting controls in addition to digestive actions. Finally, we must remember that the messenger system from outside to inside the cell

TABLE I

Calcium-Controlled Events in Cells

Activity	Controlled events or systems
Photosynthesis	Dioxygen release
Oxidative phosphorylation	Dehydrogenases
Receptor responses	Nerve synapse; IP_3-linked reactions
Contractile devices	Muscle triggering (actomyosin); cell filament controls (tubulins)
Phosphorylation	Activation of kinases, e.g., in fertilization
Metabolism	Numerous enzymes inside cells
Membrane/filament organization	Annexin-like proteins modulate tension
Cell division	S-100 proteins, immune system
Cell death (apotosis)	Internal proteases
Hormone/transmitter release	Homeostasis
Binding to membranes	C2 domains of enzymes
Cross-linking	Outside cells
Enzyme-activation	Outside cells; in membranes

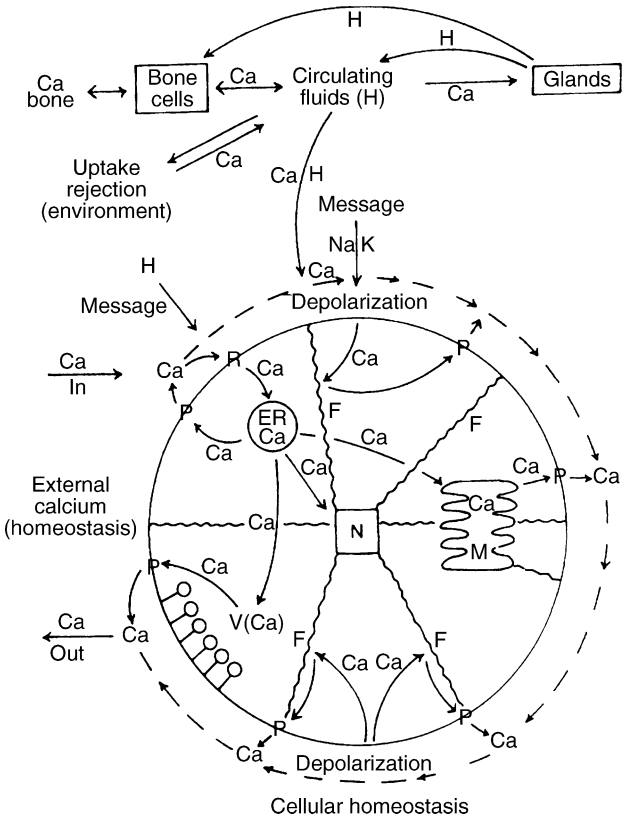

FIGURE 1 The generalized way in which calcium ions act as a messenger in advanced animal cells. The top of the figure shows the connection between the calcium in the external fluids, bone, and glands and uptake and rejection systems (e.g., the epithelial cells of digestion and the rejection cells of the kidney). H is a hormone. Calcium ions from the circulating fluids together with hormones and Na/K nerve messages activate a large range of cells. The calcium entry is controlled by channels R responding to perturbations. On entering the cell, calcium can release further calcium from vesicles such as the endoplasmic reticulum (ER). The calcium in the cytoplasm can act directly on filaments (F), on mitochondria (M) (or chloroplasts), through transcription factors on the nucleus (N), and on vesicles (V). The vesicles act to release transmitters, hormones, or enzymes. The calcium is removed by pumps (P). The bottom of the diagram shows the effect of general depolarization rather than specific channel activation. This allows calcium entry by electrically operated channels, as, for example, at nerve synapses of the heart.

was augmented by the further responses, releases due to calcium pulses of chemicals, which caused release from internal vesicles and organelles to both the cytoplasm and the external fluids. Thus, the pulsed calcium ion input to the mitochondria and chloroplasts stimulates the release of energy (ATP) to the cytoplasm, and the release of this ion from vesicles to the external fluids stimulates the release not only of enzymes (e.g., for digestion, general to many organisms) but also of hormones and synaptic messengers, leading to overall homeostatic control. Hence, calcium signaling is central to a huge variety of communication modes leading up to and including synaptic action in the brain. In this homeostasis, we must not forget the buffer action of the bone. The overall fitness of calcium for a multitude of functions is very clear (see Figure 1).

See Also the Following Articles

Calcium Oscillations • Calcium Signaling: Calmodulin-Dependent Phosphatase • Calcium Signaling: Cell Cycle • Calcium Transport in Mitochondria • Calcium Waves • ER/SR Calcium Pump: Function • ER/SR Calcium Pump: Structure • Ligand-Operated Membrane Channels: Calcium (Glutamate) • Plasma Membrane Calcium Pump: Structure and Function • Store-Operated Membrane Channels: Calcium

Glossary

biological minerals Shells and bones.
calcium complexes Soluble combinations of calcium with ligands.
calcium ion properties Ion size, ionization potential, and fast exchange.
fitness The Darwinian concept of being valuable for a biological function.
messenger function of calcium Calcium moving between internal compartments of a cell or between external and internal zones.
organelles Mitochondria or chloroplasts. They differ from vesicles in having residual DNA/RNA synthetic systems, although both organelles and vesicles are compartments separated by membranes from the cytoplasm.

Further Reading

Carafoli, E., and Klee, C. (eds.) (1999). *Calcium as a Cellular Regulator.* Oxford University Press, New York.
Carafoli, E., and Krebs, J. (eds.) (2000). *Calcium Homeostasis*. Springer Verlag, Berlin.
Fraústo da Silva, J. J. R., and Williams, R. J. P. (2001). Chapters 10 and 20. *The Biological Chemistry of the Elements*. Oxford University Press, Oxford.
Pochet, R. (ed.) (2000). *Calcium: The Molecular Basis of Calcium Action in Biology and Medicine*. Kluwer Academic Press, Dordrecht, The Netherlands.
Vogel, H. J. (ed.) (2002). *Calcium-Binding Protocols*, Vols. 1–2, Humana Press, Totowa, N.J.

Biography

Robert J. P. Williams is Emeritus Professor at Oxford University, having been a Royal Society Research Professor there for many years. He holds an M.A., D.Phil. (Oxford), F.R.S. (London), Hon. D.Sc. (East Anglia, Leicester, Keele) and is a Fellow of the Academies of the Czech Republic, Belgium, Sweden and Portugal. His research interests are in bio-energetics and the roles of inorganic ions in organisms. He has received many honors: four honorary doctorates and more than ten medals from chemical and biochemical societies. He is an academy member of four national bodies. His founding contribution was to biological inorganic chemistry including the development of the protein chemistries of elements such as Ca, Fe, Cu, Zn, Co, and Mg; he also proposed the use of protons as intermediates in bio-energetics. He is the author of four leading books in these areas.

Calcium/Calmodulin-Dependent Protein Kinase II

Andy Hudmon
Yale University, New Haven, Connecticut, USA

Howard Schulman
Mountain View, California, USA

Calcium/calmodulin-dependent protein kinase II (CaMKII) is a multifunctional serine/threonine (Ser/Thr) protein kinase involved with a diverse array of cellular functions. From metabolism and cytoskeletal organization to gene expression and the cell cycle, CaMKII phosphorylation of key substrates transduces a transient rise in free calcium (Ca^{2+}) induced by neurotransmitters, hormones, or other signaling molecules, into complex cellular functions. CaMKII is particularly important in the nervous system, where neurogenetics (knockouts, knockins, and transgenics) have directly implicated it in behavior and learning/memory. It is strategically localized in both pre- and postsynaptic compartments, where it regulates Ca^{2+}-dependent processes central to neuronal communication, including neurotransmitter synthesis and release and ion flux through voltage and ligand-gated channels. In addition, CaMKII possesses autoregulatory properties that may enable it to function as a "molecular switch" to translate neuronal activity into specific alterations in synaptic connectivity, such as long-term potentiation (LTP), a cellular correlate of learning and memory. Autophosphorylation can be considered as a form of molecular memory, as it generates a form of persistent activity (autonomous) that is temporally uncoupled from the Ca^{2+} signal. This autoregulation also enables CaMKII to function as a Ca^{2+} spike integrator – the ability to generate graded levels of autonomous activity that is differentially sensitive to the frequency of Ca^{2+} transients. Thus, its direct action on neuronal substrates and its complex autoregulation enables CaMKII to function as a cognitive kinase with both short- and long-term consequences on complex behaviors, such as learning and memory.

Neuronal CaMKII: Localization and Substrates

CaMKII is highly concentrated in the nervous system. At roughly 1–2% of the total protein in the brain, it is the predominant Ca^{2+}/calmodulin (Ca^{2+}/CaM) regulated kinase in the central nervous system. CaMKII has a diverse intracellular localization, including the postsynaptic density (PSD), a cytoskeletal specialization replete with signaling molecules (e.g., ligand and voltage gated receptors, kinases, phosphatases, and anchoring and structural proteins) that lies immediately across the presynaptic terminal below the postsynaptic membrane. Biochemical cascades at the PSD regulated by CaMKII are likely central to the function of this highly specialized signaling network for the following reasons: (1) CaMKII constitutes a significant fraction of the total PSD protein, (2) it is recruited to the PSD in an activity-dependent manner, (3) it anchors to multiple PSD proteins (e.g., densin-180, α-actinin, and NMDA-receptors), and (4) it regulates the activity of multiple PSD proteins through phosphorylation. One prominent PSD substrate of CaMKII is the GluR1 subunit of the AMPA-subtype of glutamate receptor. CaMKII phosphorylation of a specific serine (Ser^{831}) in this channel increases its conductance by favoring the open probability of its high conductance state. CaMKII was also shown by Malinow and his colleagues to regulate the targeting or insertion of AMPA-receptors into the PSD. Although both effects may underlie long-term potentiation, CaMKII regulation of AMPA receptor function and targeting has obvious implications for postsynaptic function; further studies will be required to determine how the 28 CaMKII substrates in the PSD recently identified using mass spectrometry contribute to PSD structure and function.

In addition to the postsynaptic compartment of neurons, CaMKII is also present in the presynaptic compartment, where it regulates neurotransmitter synthesis, neurotransmitter vesicle availability and release by its phosphorylation of vesicle proteins (e.g., Synapsin I) cytoskeletal regulating proteins (e.g., MAP2), membrane channels (e.g., calcium channels), and other enzymes (e.g., Tyrosine Hydroxlyase). CaMKII is also present in the nucleus, where it phosphorylates key

substrates (e.g., CREB) involved in the regulation of gene transcription and long-term changes in neuronal function. Thus, CaMKII is strategically positioned throughout the neuron to transduce and coordinate a host of calcium mobilizing stimuli into the appropriate alterations in neuronal function (see Figure 1).

Activation, Autoregulation, and Structure of CaMKII

CaMKII is composed of a family of highly conserved isoforms (α, β, γ and δ that are encoded by unique genes and differentially expressed throughout the body (see Figure 1). Although the δ and γ isoforms are ubiqitous, the α and β isoforms are brain specific. The molecular weights of these subunits range from 54 to 72 kDa, with α-isoform being the smallest subunit at 54 kDa. This size difference is due primarily to domain insertions in the region between the regulatory and association domains, because each of these genes encode protein products possessing a catalytic, regulatory, and association domain. A proto-typical α-subunit of CaMKII, illustrating the relative positions of these domains, is shown in Figure 2. Like all protein kinases, the catalytic domain serves to bind substrates and catalyze the phosphotransferase reaction from Mg^{2+}/ATP to the protein substrate.

CaMKII is coupled to the Ca^{2+} stimulus via CaM, a small dumbbell-shaped protein that, following Ca^{2+} binding, is competent to bind and activate multiple target proteins, including CaMKII. The autoregulatory domain is composed of a CaM binding domain and a region that resembles a protein substrate. This pseudo-substrate and the surrounding sequence of the regulatory domain (including the CaM binding domain) interacts with the catalytic domain to inhibit kinase activity in the absence of Ca^{2+}/CaM. C-terminal to the autoregulatory domain, the association domain produces the supramolecular association of kinase subunits into a multimeric complex, termed the holoenzyme.

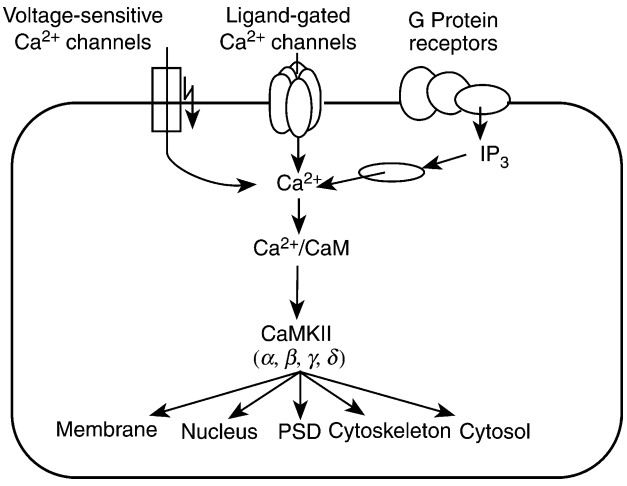

FIGURE 1 A variety of extracellular signals (e.g., depolarization, neurotransmitters, and hormones) function to elevate intracelular Ca^{2+} levels through the action of ligand and voltage-gated channels and IP_3 operated intracellular stores. Activation of CaMKII (α, β, γ, and δ isoforms) throughout the neuron via Ca^{2+}/CaM leads to phosphorylation of substrates at the membrane, cytoskeleton, postsynaptic density (PSD), nucleus, and in the cytosol. Adapted with permission from *Annu. Rev. Biochem.* **71**, 473–510 by Annual Reviews.

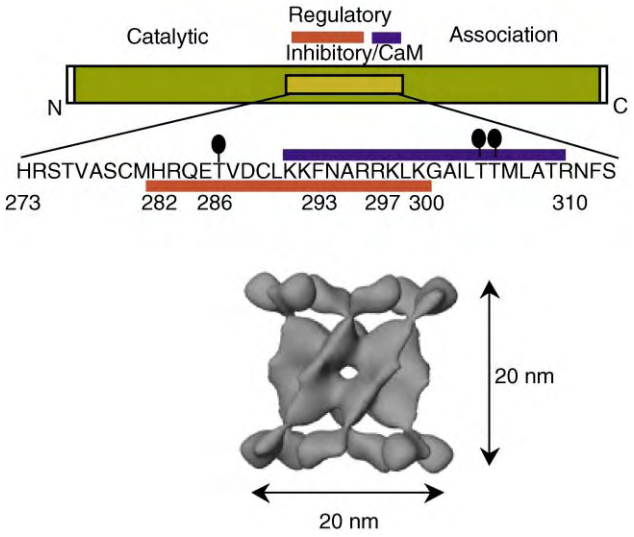

FIGURE 2 Linear diagram of α-CaMKII illustrating the catalytic, regulatory, and association domains. Like all kinases, the catalytic domain is composed of both an ATP and a protein substrate binding region. Adjacent to the catalytic domain is an autoregulatory region (shown in yellow): a bifunctional sequence that serves to inhibit kinase activity through an inhibitory region (red) and to activate the kinase via the calmodulin binding domain (blue). The association domain drives subunit multimerization and holoenzyme assembly. A computer assisted reconstruction of α-CaMKII obtained from images produced using transmission electron microscopy indicates a dodecameric structure, with 12 catalytic heads radiating out form the top and bottom of the central core.

A computer-assisted reconstruction of α-CaMKII obtained from images using transmission electron microscopy indicated that the catalytic heads extend from the gear-shaped central core via delicate stalk in a dodecameric (12 subunits) arrangement (Figure 2). The structure of the core hub-like assembly was recently resolved in a crystal obtained from a truncated form of CaMKII. In this structure, the association domain appeared as a tetradecameric structure (14 subunits) with extensive contacts between neighboring subunits in a head-to-head orientation. Variance in the number of subunits forming the holoenzyme may be expected, as native CaMKII isolated from forebrain varies greatly in its apparent molecular weight (450–650 kDa). In addition, CaMKII isolated from brain may be homo- and heteromeric in its isoform composition.

The isoform composition of the holoenzyme may afford CaMKII with the properties and regulation unique to each isoform. For example, in addition to the α and β isoforms being differentially expressed throughout the brain and during development, recent evidence indicates that neuronal activity favors the expression of the α-isoform whereas, a lack of activity favors the β-isoform. One functional consequence of altering the subunit composition is in its regulation of the subcellular localization of CaMKII. For example, unlike the α-isoform, the β-isoform possesses an F-actin binding domain that targets this isoform to cytoskeletal structures, where it participates in regulating the sprouting and stability of neuronal dendrites.

The Structure/Function of CaMKII Autophosphorylation

In addition to phosphorylating protein substrates throughout the cell (see Figure 1), CaMKII is a substrate for its own catalytic activity via *auto*phosphorylation reactions. CaMKII undergoes both Ca^{2+}/CaM-dependent as well as Ca^{2+}/CaM-independent forms of autophosphorylation. These modes of autophosphorylation occur at distinct sites within different regions of the autoregulatory domain and, importantly, have both been implicated in both the cellular correlates of learning and memory (i.e., LTP), as well as the behavior itself.

Ca^{2+}/CaM-Dependent Autophosphorylation

Following CaM activation, autophosphorylation may occur at Thr^{286} (Thr^{287} of the β, γ and δ), a phosphoamino acceptor that resides just N-terminal to the pseudo substrate anchor and CaM binding domain (see Figure 2). Autophosphorylation at Thr^{286} is not necessary for enzyme activation, because nonphosphorylatable amino acids (e.g., Ala) substituted at position 286 are similar to wild-type enzyme in regards to both CaM activation and substrate phosphorylation. The autophosphorylation reaction is dominated by an intraholenzyme inter-subunit reaction that requires CaM bound to both the subunit acting as kinase as well as the subunit behaving as substrate (Figure 3). Three functional consequences associated with Thr^{286} autophosphorylation are (a) the generation of

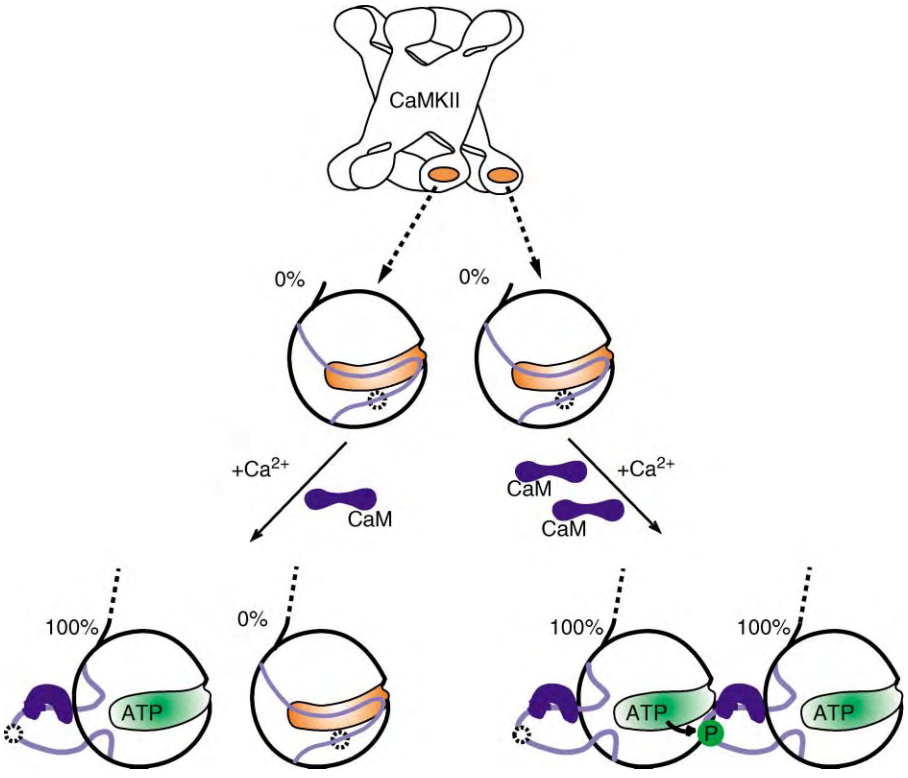

FIGURE 3 Autophosphorylation requires coincident Ca^{2+}/CaM binding between neighboring subunits within CaMKII. Catalytic/regulatory regions are depicted from subunits within the same holoenzyme (i.e., intraholoenzyme) and CaM is depicted as the purple dumbbell. Ca^{2+}/CaM binding displaces the autoinhibitory domain to activate subunits within the holoenzyme. Coincident binding of Ca^{2+}/CaM exposes the autonomy site (Thr^{286}), represented as a dashed circle, of one subunit for phosphorylation by an active neighboring subunit in an intersubunit reaction. Adapted with permission from *Annu. Rev. Biochem.* **71**, 473–510 by Annual Reviews.

autonomous activity, (b) an increase in the binding affinity of CaM (CaM trapping) and (c) exposure of a site on the catalytic domain that functions as a binding site to anchor CaMKII to its substrates.

Autonomous Activity

Autonomous activity (Ca^{2+}/CaM-independent activity) has intrigued neurobiologists and enzymologists since its discovery almost 20 years ago in the marine mollusc, *Aplysia californica* – a well-characterized animal model for studying the molecular mechanisms of learning and memory. Autonomous activity can be described as the "residual" activity attributed to an autophosphorylated subunit after CaM dissociation. At the structural level, the mechanism of autonomous activity is likely attributed to the negative charges associated with phospho-Thr^{286} preventing reassociation and inactivation of the catalytic domain by the autoregulatory domain following CaM dissociation.

CaM Trapping

Among the various CaM target proteins reported, CaMKII possesses a relatively low binding affinity for CaM (K_d 15 nM). However, following autophosphorylation, the CaM binding affinity is decreased by over a 1000-fold (K_d 20 pM), thus attaining one of the highest CaM binding affinities reported to date. The autophosphorylation of Thr^{286} is thought to indirectly produce CaM trapping, because a peptide designed from the Ca^{2+}/CaM binding domain of CaMKII (290–309) possesses high affinity Ca^{2+}/CaM binding, even though Thr^{286} is not contained within the peptide sequence (see Figure 2). This is mechanistically consistent with steric constraints or an inaccessibility of the binding site for Ca^{2+}/CaM in the nonautophosphorylated state. In support of the peptide binding studies, mutant cycle analysis studies designed to delineate the amino acid contacts responsible for high affinity binding between CaM and CaMKII supports a model for CaM trapping whereby Thr^{286} autophosphorylation exposes amino acids (Phe^{293} and Arg^{294}) within the N-terminal part of the CaM target sequence to thermodynamically stabilize and expose the target sequence for optimal Ca^{2+}/CaM binding.

Substrate Anchoring

The subcellular targeting of multifunctional kinases (e.g., CaMKII, cAMP-dependent protein kinase, and protein kinase C), is thought to be an integral component in generating the kinetics of the phosphorylation reaction and substrate specificity. Ca^{2+}/CaM binding and autophosphorylation of Thr^{286} exposes a binding site on CaMKII to permit anchor proteins and substrates to directly associate with the enzyme. Protein targeting may also afford new modes of regulation for CaMKII. For example, CaMKII targeting to the NR2B subunit of the NMDA-type glutamate receptor requires Ca^{2+}/CaM to induce binding. However, once the interaction is formed, the enzyme is active and remains bound *even* in the absence of Ca^{2+}/CaM and Thr^{286} autophosphorylation. Binding of the NR2B subunit to the catalytic domain may act as a wedge to prevent the autoregulatory domain from reforming its contacts subsequent to CaM dissociation.

Autophosphorylation at Thr^{305}/Thr^{306}

Ca^{2+}/CaM-independent autophosphorylation occurs at amino acids Thr^{305}/Thr^{306} with the CaM binding domain. Often referred to as inhibitory or "burst" autophosphorylation, Ca^{2+}/CaM-independent autophosphorylation is initiated once Ca^{2+}/CaM dissociates from a kinase phosphorylated at Thr^{286}. Autophosphorylation within the CaM binding domain (Thr^{305} or Thr^{306}) disrupts CaM from rebinding to this subunit. Autophosphorylation in the Ca^{2+}/CaM binding domain has also been reported in the basal state (autoinhibited), a process that appears to occur by an intrasubunit mechanism and is likely a result of this regions proximity to the substrate binding pocket on the catalytic domain. Basal autophosphorylation preferentially occurs at Thr^{306}, and like burst autophosphorylation, it functions to block Ca^{2+}/CaM binding.

Autophosphorylation as an Index of Neuronal Activity

In neurons, like in other excitable cells, Ca^{2+} signaling is a balance between homeostatic mechanisms (e.g., Ca^{2+} binding proteins and membrane extrusion pumps) designed to maintain and buffer the intracellular free Ca^{2+} concentration at roughly 20,000-fold below extracellular levels and a transient rise in free Ca^{2+} induced by hormones, neurotransmitters, or other signaling molecules. Autonomous activity is a form of persistent activity that is temporarily uncoupled from Ca^{2+} signaling. In addition to possessing the capacity to potentiate its activity beyond the Ca^{2+} transient, CaMKII is also capable of translating the temporal dynamics (e.g., frequency) of Ca^{2+} signaling. Immobilized CaMKII subjected to Ca^{2+}/CaM pulsed at varying frequencies by a high pressure computer controlled valve assembly generates distinct graded levels of autonomous activity *in vitro*. Two factors identified in computer simulations as key for frequency decoding are the effective cooperativity in the Thr^{286} autophosphorylation reaction and the availability of CaM for this reaction. In cells, CaM is thought to be largely bound to a variety of cellular proteins and presumably not available to maximally activate all of its targets. CaMKII

activation and autophosphorylation are particularly sensitive to limiting CaM levels as its relatively high affinity for CaM would predict that a transient rise in Ca^{2+} would lead to only a few of the subunits in each holoenzyme being activated (Figure 4). Under these conditions, a minority of activated subunits would actually undergo Thr^{286} autophosphorylation and trap CaM due to the requirement of coincident CaM binding for the autophosphorylation reaction. Higher Ca^{2+} spike frequencies produce shorter Ca^{2+} spike intervals that increase the CaM remaining associated between Ca^{2+} transients and the probability of autophosphorylation. Because autophosphorylation further prolongs CaM association, a feed-forward process ensues at a threshold level of autophosphorylation to produce the nonlinear Ca^{2+} spike frequency function for CaMKII activation/autophosphorylation illustrated in Figure 4. The frequency response function of CaMKII could also be influenced by autophosphorylation within the CaM binding domain, because inhibitory autophosphorylation could function to limit activated/autonomous subunits from subsequently competing with nonactivated subunits for the available free CaM.

CaMKII in LTP and Learning and Memory

Neuronal information in the brain is propagated and encoded through synaptic activity and multiple lines of evidence indicate that CaMKII is necessary and sufficient to induce long-lasting changes in synaptic efficacy, such as long-term potentiation (LTP). LTP is a long-lasting enhancement in the strength of neurotransmission that is believed to represent a cellular correlate of learning. Synaptic stimulation protocols that produce LTP in the hippocampus also produce long-lasting changes in the activation and autophosphorylation of CaMKII. Importantly, peptide inhibitors of CaMKII are potent inhibitors of LTP induction and viral introduction of a

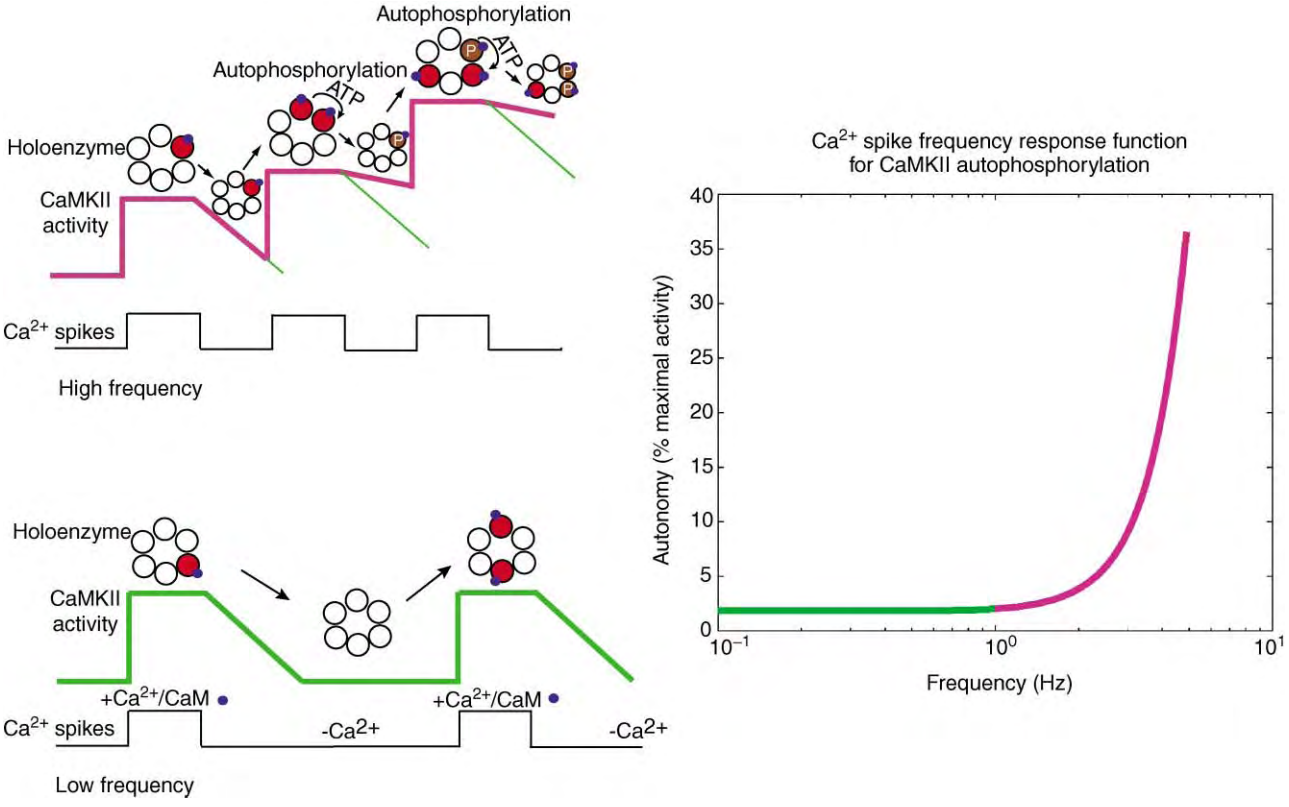

FIGURE 4 (Left) The role of coincident CaM binding, autophosphorylation, and CaM trapping in Ca^{2+} spike frequency detection. Inactive subunits within CaMKII (holoenzymes are shown as 6 mers for simplicity) are represented by open circles. Ca^{2+}/CaM (blue circle) binding activates a given subunit (shown in red) and coincident Ca^{2+}/CaM binding results in autophosphorylation and CaM trapping ("P" inside a filled dark red circle). During low frequency Ca^{2+} spikes, CaM completely dissociates between Ca^{2+} spikes, effectively producing "naïve" CaMKII subunits at each inner spike interval. However, at high Ca^{2+} spike frequencies, CaM does not completely dissociate between Ca^{2+} spikes; this increases the probability that coincident CaM binding, autophosphorylation, and CaM trapping may occur – a process that effectively increases the probability that a neighboring subunit will also bind Ca^{2+}/CaM during successive spikes to produce the nonlinear increase in autonomous activity illustrated by a computer simulation encompassing the biophysical and enzymatic characteristics of CaMKII (Right). Adapted with permission from *Biochem. J.* **364**, 593–611 © the Biochemical Society.

constitutively active form of CaMKII occludes LTP generated by the high frequency stimulation protocols typically used to induce LTP. In addition to being implicated in synaptic plasticity, the activity and autophosphorylation of CaMKII are also important for learning and memory.

In the field of neuroscience as in other areas of biology, genetic approaches in flies, worms, and mice have greatly advanced our understanding of the molecular mechanisms involved in behavior and learning. Although we will focus on the role of CaMKII in mammalian learning, disrupting the activity of CaMKII induces behavioral or cognitive defects in *all* of these organisms. The genetic deletion in the α-isoform of CaMKII was a pioneering study aimed at understanding the role of CaMKII in mammalian learning and memory. These CaMKII knockout mice displayed deficits in hippocampal LTP and possessed severe learning impairments in spatial learning tasks, such as the Morris Water Maze. These knockout mice directly implicated CaMKII and hippocampal LTP in mammalian learning and memory.

The use of knockin genetics permitted researchers to introduce mutant forms of CaMKII into both wild-type and knockout mice. This technology permitting further dissection of the role of CaMKII in learning, as mutant mice could be created that had altered autoregulatory properties without ablating kinase activity. A knockin mouse in which Thr^{286} (α-isoform) was mutated to Ala^{286} to prevent autophosphorylation displayed deficient LTP and spatial learning, directly implicating Thr^{286} autophosphorylation in synaptic plasticity and learning. Recent knockin technology has also permitted temporal control of transgene expression with inducible promoters. In experiments with a transgenic mouse in which Thr^{286} was replaced with a charged residue (e.g., Asp^{286}) in order to mimic an autophosphorylated state of the enzyme, enhanced LTP at low levels of transgene expression and deficient LTP at higher levels occurred, suggesting complex interactions between the level of activated CaMKII and its function in regulating synaptic strength. Autophosphorylation within the CaM-binding domain (Thr^{305}/Thr^{306}) has also been implicated in regulating CaMKII targeting and function. Knockin mice that cannot undergo inhibitory autophosphorylation (Ala^{305}/Ala^{306}) have increased levels of CaMKII in the PSD and a lower threshold for LTP. Mimicking inhibitory autophosphorylation (Asp^{305}/Asp^{306}) lowers the CaMKII content in the PSD and blocks LTP induction and hippocampal learning. Finally, in addition to CaMKII autophosphoryation regulating synaptic plasticity and behavior, a knockin mouse with an intact coding region for α-CaMKII yet possessing an altered mRNA targeting was created. Disrupting mRNA localization into dendrites was found to impair LTP and learning, suggesting that local translation and delivery of CaMKII to its site of action at the synapse is important for synaptic plasticity learning.

The Tao of Neuronal CaMKII

The function of CaMKII in synaptic plasticity and learning and memory appears to be tightly linked to its unique structure and autoregulation. The multimeric structure of CaMKII permits different isoforms to associate into a macromolecular signaling complex to provide specific targeting information essential for its subcellular localization as well as an intersubunit autophosphorylation reaction. Key autoregulatory features following autophosphorylation include the ability to (1) reduce its Ca^{2+}/CaM dependence following dissociation of CaM (autonomous activity), (2) increase its affinity for Ca^{2+}/CaM by over 1000-fold (CaM trapping), (3) enable activity-dependent substrate targeting, and (4) enable it to function as a Ca^{2+} spike frequency detector. Thus, the designation of a kinase as a cognitive kinase (i.e., based on its requirement in learning and memory) possesses a double meaning for CaMKII. Because of this enzyme's complex autoregulation and autophosphorylation, CaMKII activity may directly function as a molecular representation of synaptic activity: a molecular memory that is expressed as a persistent form of activity temporarily uncoupled from the Ca^{2+} stimulus. Thus, the role of CaMKII in transducing synaptic activity into the complex neuronal changes associated with learning appears to be an intimate dance between its autoregulation and its capacity to phosphorylate key protein substrates integral to neuronal function.

See Also the Following Articles

Protein Kinase C Family • Voltage-Sensitive Ca^{2+} Channels

Glossary

Ca^{2+} transient A temporary rise in the intracellular levels of free Ca^{2+} ($\approx$100 nM to 1 μM) induced by a variety of extracellular signals (hormones, neurotransmitters, and depolarization) that may vary in its localization, duration, frequency, and amplitude.

hippocampus Part of the limbic system of the brain that is involved in spatial learning; because of its laminar architecture, it is routinely used for electrophysiological studies designed to evaluate synaptic connectivity and plasticity.

long-term potentiation A long-lasting increase in synaptic strength that could function to strengthen synaptic connectivity; it is considered to represent a cellular correlate of learning and memory.

Morris water maze An apparatus that is routinely used to assess spatial learning and memory in rodents. In this task, a mouse is placed in a large tub of an opaque liquid and assayed both for its ability to find a visible platform as well as a submerged

platform – tasks that evaluate the general function and ability to learn the task as well as its spatial learning, respectively.

pre- and postsynaptic elements of neurons Components of typical neuronal synapse: the presynaptic terminal releases neurotransmitter that diffuses across a synaptic cleft to bind and activate ligand-gated channels along the postsynaptic specialization.

pseudosubstrate A component of the autoregulatory domain that binds to the substrate binding pocket on the catalytic domain to prevent kinase activity in the absence of calmodulin.

Further Reading

Griffith, L. C. (1997). Drosophila melanogastor as a model system for the study of the function of calcium/calmodulin-dependent protein kinase II in synaptic plasticity. *Invert. Neurosci.* **3**, 93–103.

Hudmon, A., and Schulman, H. (2002). Neuronal Ca^{2+}/calmodulin-dependent protein kinase II: The role of structure and autoregulation in cellular function. *Annu. Rev. Biochem.* **71**, 473–510.

Kennedy, M. B. (2000). Signal-processing machines at the postsynaptic density. *Science* **290**, 243–257.

Lisman, J., Schulman, H., and Cline, H. (2002). The molecular basis of CaMKII function in synaptic and behavioral memory. *Nature Rev. Neurosci.* **3**, 175–190.

Miller, S., Yasuda, M., Coats, J. K., Jones, Y., Martone, M. E., and Mayford, M. (2002). Disruption of dendritic translation of CaMKIIα impairs stabilization of synaptic plasticity and memory consolidation. *Neuron* **36**, 507–519.

Shen, K., Teruel, M. N., Connor, J. H., Shenolikar, S., and Meyer, T. (2000). *Molecular memory by reversible translocation of calcium/calmodulin-dependent protein kinase II. Nature* **3**, 881–886.

Silva, A. J. (2003). Molecular and cellular cognitive studies of the role of synaptic plasticity in learning and memory. *J. Neurobiol.* **54**(1), 224–327.

Soderling, T. R. (2000). CaM-Kinases: Modulators of synaptic plasticity. *Curr. Opin. Neurobiol.* **10**, 375–380.

Biography

Andy Hudmon is currently a research scientist at the PVA-EPVA Center for Neuroscience and Regeneration Research in the Department of Neurology at Yale University where he is studying the calcium-dependent regulation of voltage gated sodium channels in models of pain and spinal cord trauma. As a postdoctoral fellow in the laboratory of Dr. Howard Schulman at Stanford University, he studied the targeting and function of the multi-functional Ca^{2+}-calmodulin-dependent protein kinase II in regulating voltage-gated calcium channels in the heart and nervous system. He received his M.S. in physiology at Auburn University in the laboratory of Dr. Jim Sartin, and he holds a Ph.D. from the University of Texas Health Science Center at Houston, where he trained in the laboratory of Dr. Neal Waxham.

Howard Schulman is a Professor in the Department of Neurobiology at Stanford University and currently is Vice President of research at Surromed (MountainView, CA). His principle research interest is in how the structure/regulation of protein kinases decode and translate the calcium signal during neuronal function and plasticity. He holds a Ph.D from Harvard University, where he trained under Dr. Eugene Kennedy. Dr. Schulman received his postdoctoral training in the laboratory of Dr. Paul Greengard at Yale University.

Calcium/Calmodulin-Dependent Protein Kinases

J. Robison and Roger J. Colbran
Vanderbilt University, Nashville, Tennessee, USA

The Ca^{2+}/calmodulin-dependent protein kinase (CaMK) enzyme family is activated by increases in intracellular calcium ions (Ca^{2+}) and transfers phosphates from ATP to specific serine or threonine residues in other proteins. Family members vary in expression level, subcellular location, and substrate specificity. They are essential for signal transduction in all cells and modulate a variety of physiological processes including learning and memory, metabolism, gene transcription, and motor function.

Ca^{2+} Signaling

Modulation of the concentration of Ca^{2+} is used as an intracellular signal to allow hormones and neurotransmitters to control numerous processes in virtually all cell types. In general, cells have a resting Ca^{2+} concentration of 50–100 n*M*, but this concentration can "spike" above 1 μ*M* in an activated cell. Interestingly, these changes in Ca^{2+} concentration can activate extremely disparate signaling cascades not only in different cell types but also in different areas of the same cell. For instance, Ca^{2+} elevation in the nucleus of a neuron activates gene transcription, whereas a similar elevation at the synapse causes neurotransmitter release. These responses are possible because of the hundreds of different molecules that are directly or indirectly responsive to Ca^{2+}, the numerous mechanisms for increasing Ca^{2+}, and the variation in duration, frequency, amplitude, and localization of Ca^{2+} spikes. Ca^{2+} can enter the cell through channels in the membrane or be released from internal stores. The resulting Ca^{2+} spikes can occur on the millisecond level in neurons or be separated by days in the mitotic cell and modulate diverse enzymes and/or alterations in the shape of structural molecules. Many of the intracellular effects of Ca^{2+} are mediated by calmodulin, a small protein that undergoes dramatic conformational changes when bound to Ca^{2+} ions. Among the many enzymes activated by Ca^{2+}/calmodulin (Figure 1), members of the CaMK family mediate diverse physiological responses in most, if not all, cell types.

Protein kinases are enzymes that catalyze the addition of phosphates onto specific residues in target proteins, thereby regulating them in some way. Substrate proteins include other enzymes, gene transcription factors, scaffolding proteins, receptors, and many other cellular proteins. Thus, kinases can regulate such diverse cellular events as intercellular signaling, cell motility and shape, cell cycle, metabolic pathways, and gene transcription. In addition, kinases themselves may be regulated by intracellular signals, including Ca^{2+} acting via calmodulin. Most cells contain multiple representatives from the diverse family of CaMKs (Figure 2). Generally, CaMKs contain an autoinhibitory domain (AID) that interferes with catalysis by blocking or disrupting the catalytic site. This inhibition is relieved by the binding of Ca^{2+}/calmodulin to a domain that overlaps the AID (Figure 2), thus activating the kinase.

CaMKs phosphorylate specific serine or threonine residues in substrate proteins based in part on the surrounding amino acid sequence. Each of the kinases favors target serines or threonines in specific consensus sequences, although their substrate specificities can overlap. For instance, Ca^{2+}/calmodulin-dependent protein kinase II (CaMKII) and Ca^{2+}/calmodulin-dependent protein kinase IV (CaMKIV) recognize the consensus sequences Hyd-X-Arg-NB-X-Ser/Thr-Hyd and Hyd-X-Arg-X-X-Ser/Thr-X (where Hyd is a hydrophobic residue, NB is a nonbasic residue, and X is any residue), respectively; however, some peptide substrates that fit both of these sequences are phosphorylated by the two kinases with similar affinity. In addition, the catalytic domains of most CaMKs contain acidic residues that are important for interaction with the basic residues in their specific substrates (exceptions are noted below). Based on their substrate specificity, CaMKs can be divided into two general groups: those with narrow substrate specificity and those with broad substrate specificity.

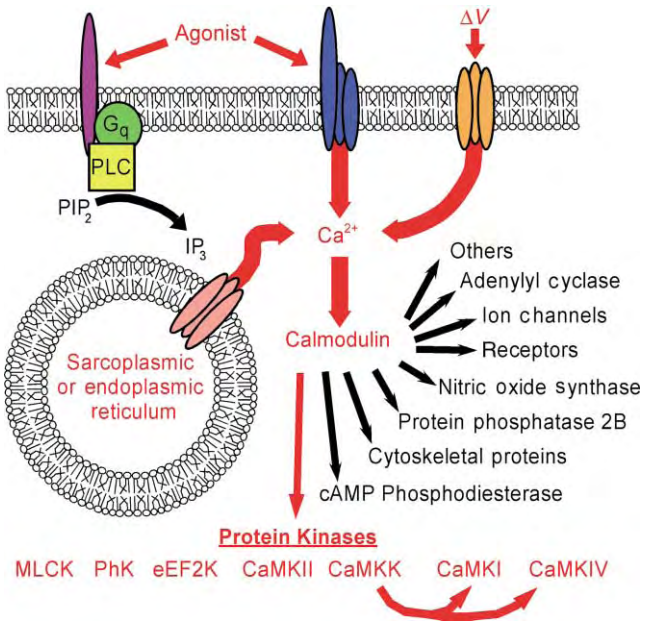

FIGURE 1 Modulation and effects of intracellular Ca^{2+}. Ca^{2+} enters cells via ligand-gated (blue) or voltage-gated (orange) Ca^{2+} channels in the plasma membrane or can be released from sarcoplasmic or endoplasmic reticulum stores via inositol 1,4,5-triphosphate (IP_3 (pink)) receptors and/or ryanodine receptors (not shown). IP_3 is generated from phosphatidyl-inositol 4,5-bisphosphate (PIP_2) by phospholipase C (PLC), which is activated by ligand binding to specific G_q protein coupled receptors (magenta) in the plasma membrane. Cytosolic Ca^{2+} is rapidly extruded from the cell or taken up by the intracellular stores (not shown). The combined actions of these pathways result in spatially localized and transient changes in intracellular Ca^{2+}. The ubiquitous Ca^{2+}-binding protein calmodulin senses the changes in Ca^{2+} and mediates the activation of multiple intracellular enzymes and other processes, including the family of CaMKs.

Narrow-Specificity Ca^{2+}/Calmodulin-Dependent Protein Kinases

Myosin Light Chain Kinase

Myosin is the only known *in vivo* substrate of myosin light chain kinase (MLCK), which is found in all vertebrate muscle cells and many nonmuscle tissues. Distinct genes encode two MLCK isoforms. Skeletal muscle MLCK (SkMLCK) is found only in skeletal muscle and contains a catalytic core, an AID, a calmodulin-binding domain, and a short N-terminal extension. The smooth muscle MLCK (SmMLCK), which is expressed in multiple tissues, also contains an actin-binding domain, a fibronectin domain, a PEVK repeat, and a number of immunoglobulin domains that can be varied by alternative splicing. MLCK is normally activated by Ca^{2+} release from the sarcoplasmic reticulum (SR) or endoplasmic reticulum and phosphorylates the regulatory light chain of the molecular motor myosin II, which is sufficient to initiate contraction in smooth muscle or to potentiate the force and speed of contraction in skeletal muscle. Although both forms of MLCK are tightly regulated by calmodulin binding, SmMLCK can be further regulated by phosphorylation. Many kinases, including CaMKII, cyclic AMP-dependent protein kinase (PKA), cyclic GMP-dependent protein kinase, p21-activated kinase, and protein kinase C, can phosphorylate SmMLCK *in vitro* at two serine residues in the calmodulin-binding domain and thus decrease the affinity for calmodulin. In addition,

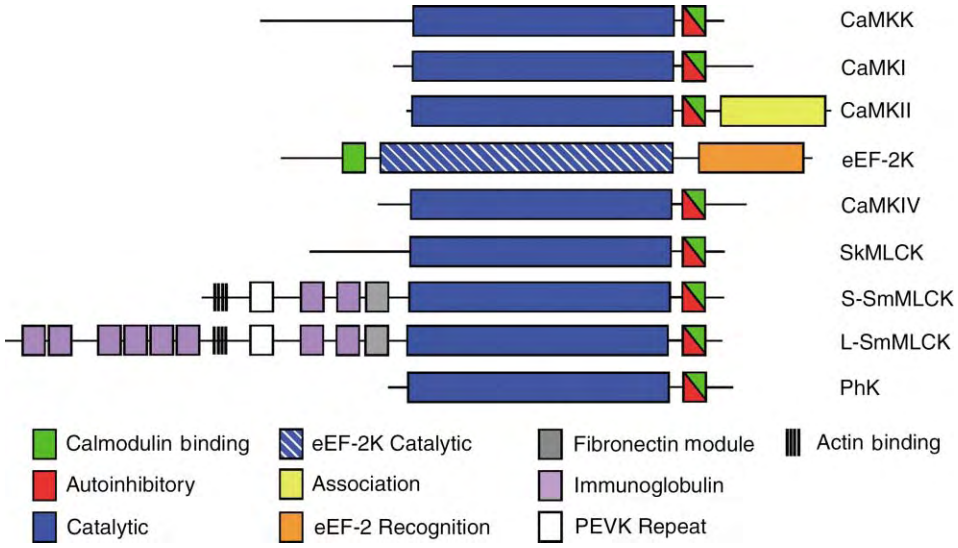

FIGURE 2 Schematic representation of CaMK domain structures. The key depicts various domains. The kinase domain of eEF-2K, formerly known as CaMKIII, bears no homology to those of the other CaMKs and thus is represented with white hatching. Most family members have multiple isoforms (not shown). Modified from Soderling, T. R., and Stull, J. T. (2001). Structure and regulation of calcium/calmodulin-dependent protein kinases. *Chem. Rev.* **101**, 2341–2351.

two sites outside the catalytic and regulatory regions of SmMLCK can be phosphorylated by members of the mitogen-activated protein kinase family, resulting in an increase in V_{max} but no change in K_{CaM}. SmMLCK, but not SkMLCK, is targeted to actin/myosin filaments through interaction with actin subunits.

Phosphorylase Kinase

Phosphorylase kinase (PhK) phosphorylates and activates glycogen phosphorylase, thus accelerating glycogen degradation. Splice variations and gene duplications result in multiple isoforms, many of which are tissue-specific. Isoforms of PhK are found in muscle, brain, heart, liver, intestines, and many other cell types. The highly abundant liver and muscle enzymes contribute to blood-glucose homeostasis and provide an energy source to facilitate muscle contraction, respectively. Four catalytic γ-subunits form a 1.3 mDa holoenzyme complex with α, β, and δ regulatory subunits, each of which is present at four copies per holoenzyme. The three regulatory subunits inhibit the phosphotransferase activity of the catalytic subunit. The δ-subunit is in fact calmodulin, which, unusually, is stably associated with the holoenzyme even at low Ca^{2+} concentrations. Ca^{2+} binding to δ partially activates PhK and phosphorylation of the α- and β-subunits by PKA potentiates activation. Binding of additional Ca^{2+}/calmodulin molecules, or Ca^{2+}-bound troponin C, to the holoenzyme maximally activates PhK. PhK associates with a protein termed PTG (protein targeted to glycogen) in muscle, which may facilitate phosphorylation of glycogen phosphorylase *b*, which is also associated with glycogen. PhK also interacts with other proteins in a tissue-specific manner, such as tubulin in rat brain lysates, and is found in membrane preparations from various tissue types.

Eukaryotic Elongation Factor 2 Kinase

The ubiquitous 90 kDa eukaryotic elongation factor 2 kinase (eEF-2K), also known as CaMKIII, phosphorylates Thr-56 in eEF-2, a protein elongation factor that promotes ribosomal translocation along mRNA during translation. Since eEF-2 is inactivated by this phosphorylation, eEF-2K was initially proposed as a link to reduced global protein synthesis following Ca^{2+} elevation. The eEF-2K contains a calmodulin-binding domain and an eEF-2 recognition domain. However, the catalytic domain of eEF-2K bears no homology to conventional kinases and is a member of the α-kinase family. Regulation of eEF-2K is both subtle and complex. In the presence of Ca^{2+} and calmodulin, autophosphorylation of eEF-2K occurs at several serine residues and confers a partially Ca^{2+}-independent activity. In addition, phosphorylation by a variety of kinases *in vitro* can both up- and down-regulate eEF-2K activity. Phosphorylation by PKA confers Ca^{2+} independence. Thus, stimulation of β-adrenergic receptors and subsequent cyclic AMP elevation causes eEF-2K activation and inhibition of protein synthesis in cultured mammalian cells. In addition, studies suggest that slight drops in cellular pH (such as those caused by hypoxia and ischemia) cause activation of eEF-2K. In combination, these data suggest that this kinase may not be a simple, direct link between Ca^{2+} and translation, but rather may function to integrate multiple intracellular signals.

Broad-Specificity Ca^{2+}/Calmodulin-Dependent Protein Kinases

Ca^{2+}/Calmodulin-Dependent Protein Kinase I

Ca^{2+}/Calmodulin-dependent protein kinase I (CaMKI) is a ubiquitous cytoplasmic enzyme enriched in brain, liver, and intestine. Three isoforms of the kinase, α, β, and γ, have been reported and are products of separate genes, each of which may be alternately spliced. CaMKI is an approximately 42 kDa monomer and its catalytic domain shows sequence and structural homologies with those of other serine/threonine kinases. A kinase originally termed CaMKV has been shown to be a splice variant of CaMKI. Goldberg *et al*. crystallized CaMKI, demonstrating that the AID binds and distorts the ATP-binding pocket in the basal state. Binding of Ca^{2+}/calmodulin presumably disrupts these interactions. This is the only known structure of a CaMK. A threonine residue in the catalytic domain (activation loop) of CaMKI is then phosphorylated by an upstream kinase, Ca^{2+}/calmodulin-dependent protein kinase kinase (CaMKK), resulting in a 10- to 20-fold increase in CaMKI catalytic activity without conferring Ca^{2+}/calmodulin independence. However, this phosphorylation can occur only when both CaMKK and CaMKI are bound by Ca^{2+}/calmodulin, perhaps permitting synergism in kinase activation. CaMKI phosphorylates synapsin I and cAMP Response Element Binding protein (CREB) *in vitro* and expression of truncated forms of CaMKI activates CREB-dependent gene transcription. However, the physiological substrates and roles of CaMKI remain elusive.

Ca^{2+}/Calmodulin-Dependent Protein Kinase II

CaMKII is a ubiquitous kinase that has been implicated in the regulation of diverse physiological processes, such

as gene transcription, neuronal plasticity, exocytosis, and metabolism. Four separate genes encode the α-, β-, γ-, and δ-isoforms of CaMKII. Each isoform is subjected to alternative mRNA splicing, resulting in over 20 known variants of the kinase, many of which have specific cellular and tissue distributions. In addition to catalytic, AID, and calmodulin-binding domains, most CaMKII isoforms contain a C-terminal association domain that facilitates the formation of a holoenzyme structure. The α-isoform forms a double hexameric ring-shaped holoenzyme and other isoforms appear to form similar multimeric holoenzymes, which may contain multiple isoforms or splice variants. The holoenzyme structure of CaMKII facilitates complex regulatory properties. Each subunit is independently activated by Ca^{2+}/calmodulin binding. When adjacent subunits in a holoenzyme bind Ca^{2+}/calmodulin, there is a trans-autophosphorylation at Thr-286, resulting in Ca^{2+} independence and also a 1000-fold increase in affinity for calmodulin. The kinase can be inactivated only by the actions of cellular protein phosphatases. Additional autophosphorylation at Thr-305 and Thr-306 in the calmodulin-binding domain occurs in the absence of Ca^{2+}/calmodulin. Thr-305/Thr-306 phosphorylation interferes with calmodulin binding, blocking Ca^{2+}/ calmodulin-dependent activation.

The number of subunits in a holoenzyme that become active and autophosphorylated at Thr-286 is directly related to the Ca^{2+} concentration. Thus, CaMKII is able to "decode" the frequency and amplitude of Ca^{2+} spikes. This unique capacity has been proposed to play an important role in prolonged signaling after transient changes in Ca^{2+}, such as may be involved in learning and memory. Consistent with this idea, transgenic mice in which the CaMKIIα gene has been mutated such that the kinase cannot autophosphorylate at Thr-286 are deficient in spatial learning tasks.

CaMKII can be found in the cytosol, in the nucleus, and associated with various organelles or membranes, depending on the cell type examined. The identity of CaMKII splice variants expressed is believed to play a role in modulating subcellular localization, although few specific examples have been documented. For example, one variant of CaMKIIδ contains a nuclear localization sequence and has been shown to regulate gene transcription in cardiac myocytes. Variable subcellular localization can also be attributed in part to the large number of proteins with which CaMKII may associate, including several neuronal proteins (e.g., *N*-methyl-D-aspartate (NMDA) receptor, α-actinin, synapsin I, and densin-180) and contractile/motor proteins (e.g., actin and myosin V). Binding of CaMKII to these proteins may position the kinase close to Ca^{2+} sources, and/or close to specific substrates, and may modulate its availability to cellular phosphatases, thereby affecting the rate of inactivation. One splice variant of the CaMKIIα gene (αKAP) functions as a CaMKII anchoring protein. αKAP lacks a catalytic domain but forms hetero-multimers with the conventional isoforms through an intact association domain and associates with the SR in muscle via an N-terminal hydrophobic region.

At last count, CaMKII phosphorylates at least 50 distinct proteins *in vitro* and many of these are likely to be physiologically relevant. However, relatively few of these have been formally shown to be phosphorylated in intact cells under physiologically relevant conditions. One of the best characterized substrates is the neuronal L-alpha-amino-3-hydroxy-5-methylisoxazole-4-propionate (AMPA)-type glutamate receptor; phosphorylation of this receptor at Ser-831 by CaMKII plays an important role in the regulation of synaptic transmission. In neuronal presynaptic terminals, phosphorylation of synapsin 1 by CaMKII modulates synaptic vesicle movement. In the heart, CaMKII plays a critical role in feedback regulation of Ca^{2+} dynamics by regulating Ca^{2+} entry via L-type voltage-gated Ca^{2+} channels, by phosphorylating ryanodine receptors to regulate SR Ca^{2+} release, and by phosphorylating phospholamban at Thr-17, thereby regulating SR Ca^{2+} uptake via the Ca^{2+}-ATPase.

Ca^{2+}/Calmodulin-Dependent Protein Kinase IV

αCaMKIV is a monomeric kinase expressed largely in neuronal tissues, testes, and T cells, whereas the βCaMKIV splice variant is differentially expressed in the cerebellum during development. Like CaMKI, CaMKIV is initially activated by calmodulin binding and is further activated when phosphorylated by CaMKK in its activation loop. However, combined with a subsequent N-terminal autophosphorylation, the activation by CaMKK eventually leads to Ca^{2+}-independent activity of CaMKIV. An additional autophosphorylation at Ser-332 of the calmodulin-binding domain prevents further Ca^{2+}/calmodulin binding in a manner analogous to CaMKII autophosphorylation at Thr-305 and Thr-306. CaMKIV contains a nuclear localization sequence and it is thought to be responsible for Ca^{2+}-dependent phosphorylation of a variety of transcription factors (e.g., CREB, serum response factor, and myocyte enhancer factor 2 (MEF2)) and regulatory factors, such as the CREB-binding protein. In the cytosol, CaMKIV phosphorylates oncoprotein 18, preventing its association with tubulin. Protein phosphatase 2A (PP2A), a ubiquitous multimeric protein phosphatase, associates with and dephosphorylates CaMKIV, forming a

self-regulating complex that may be a prototype for phosphatase–kinase cross-talk in cell signaling.

Ca^{2+}/Calmodulin-Dependent Protein Kinase Kinase

CaMKK, originally characterized as an "activating factor" from brain extracts, can dramatically increase the activity of CaMKI and CaMKIV when incubated in the presence of Ca^{2+}/calmodulin, Mg^{2+}, and ATP. Two isoforms (α and β) of CaMKK have been cloned and their domain organization and function are similar to those of other Ca^{2+}/calmodulin-dependent kinases. However, CaMKK is unique in its method of substrate recognition, lacking acidic residues to recognize basic residues near its preferred phosphorylation sites. Instead, this kinase contains an arginine- and proline-rich (RP) insert that is important for phosphorylation of CaMKI and CaMKIV and Ca^{2+}/calmodulin must be bound to both CaMKK and the substrate (CaMKI or CaMKIV) for phosphorylation to occur. CaMKK also phosphorylates protein kinase B both *in vitro* and in cultured cells, although this does not require the RP domain. Regulation of CaMKK also occurs via other kinases, such as PKA, which phosphorylates CaMKK in its calmodulin-binding domain, resulting in the inhibition of Ca^{2+}/calmodulin-induced activity.

Summary

Repetitive transient changes in Ca^{2+} concentration in every mammalian cell are sensed by a number of different Ca^{2+}/calmodulin-dependent protein kinases. Although many of these kinases share a great deal of functional homology, there are diverse regulatory nuances. Moreover, some of these kinases phosphorylate a number of different substrates, whereas others have only one principal substrate. The specific response of individual cells to changes in intracellular Ca^{2+} concentration likely depends on the subset and specific isoforms of Ca^{2+}/calmodulin-dependent kinases expressed in that cell. For example, in hippocampal neurons, synaptic activity increases Ca^{2+} levels in dendritic regions. In the short term, dendritic Ca^{2+} locally activates CaMKII, which phosphorylates pre-existing synaptic glutamate receptors. However, over a longer time frame, Ca^{2+} signals the activation of nuclear CaMKIV and thus the transcription of specific genes. It is the

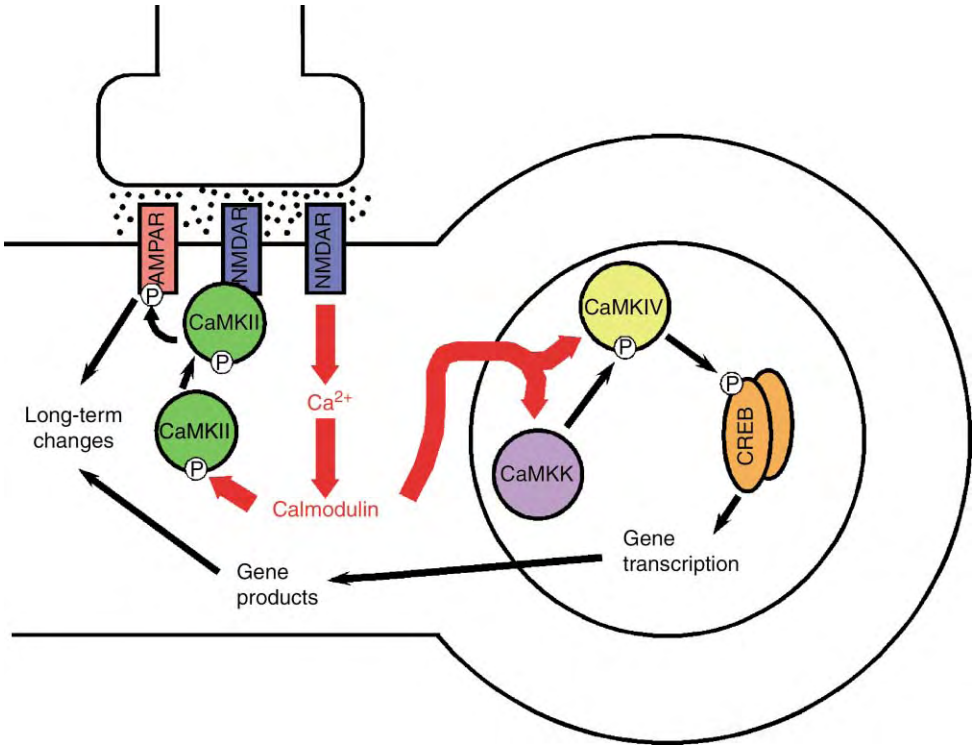

FIGURE 3 Modulation of neuronal function by activation of CaMKII and CaMKIV. Glutamate release from presynaptic terminals activates NMDA- (blue) and AMPA- (red) type glutamate receptors on the postsynaptic neuron. The NMDA receptor (NMDAR) is a ligand-gated Ca^{2+} channel. The elevated local intracellular Ca^{2+} in the dendrites activates CaMKII, which phosphorylates AMPA-type glutamate receptors, potentiating synaptic transmission. Ca^{2+} elevation via NMDA- and voltage-gated Ca^{2+} channels (not shown) also signals to the nucleus to activate CaMKK and CaMKIV, driving the transcription of specific genes. The dual CaMKII and CaMKIV signals combine to promote long-term changes in synaptic function. AMPAR, AMPA receptor.

combined actions of CaMKII and CaMKIV that result in long-lasting changes in the synaptic response of these neurons that may underlie learning and memory (Figure 3). However, much work remains to be performed in identifying substrates and physiological roles of the various Ca^{2+}/calmodulin-dependent protein kinases in other cells and tissues.

See Also the Following Articles

Calcium/Calmodulin-Dependent Protein Kinase II • Calcium Signaling: Cell Cycle • Mitochondrial Membranes, Structural Organization • Protein Kinase C Family

Glossary

autoinhibitory domain (AID) The region of a Ca^{2+}/calmodulin-dependent protein kinase that binds and inhibits the catalytic domain. Inhibition is relieved by interaction with calmodulin and in some cases is prevented by subsequent autophosphorylation.

calmodulin A small cytosolic protein that binds four Ca^{2+} ions and subsequently associates with and modulates many important proteins, including some protein kinases.

catalytic domain The region of an enzyme responsible for activity; in protein kinases, this domain transfers the γ-phosphate from ATP to the target residue.

protein kinase An enzyme that transfers the terminal (γ) phosphate from ATP to a serine, threonine, or tyrosine residue of a substrate protein.

protein phosphatase An enzyme that hydrolyzes a phosphate group from a serine, threonine, or tyrosine residue of a phosphoprotein substrate.

Further Reading

Berridge, M. J., Lipp, P., and Bootman, M. D. (2000). The versatility and universality of calcium signaling. *Nature Rev.* **1**, 11–20.

Braun, A. P., and Schulman, H. (1995). The multifunctional calcium/calmodulin-dependent protein kinase: From form to function. *Annu. Rev. Phyiol.* **57**, 417–445.

Brushia, R. J., and Walsh, D. A. (1999). Phosphorylase kinase: The complexity of its regulation is reflected in the complexity of its structure. *Front. Biosci.* **4**, 618–641.

Goldberg, J., Nairn, A. C., and Kuriyan, J. (1996). Structural basis for the autoinhibition of calcium/calmodulin-dependent protein kinase I. *Cell* **84**, 875–887.

Hook, S. S., and Means, A. (2001). Ca^{2+}/CaM-dependent kinases: From activation to function. *Annu. Rev. Pharmacol. Toxicol.* **41**, 471–505.

Kamm, K. E., and Stull, J. T. (2001). Dedicated myosin light chain kinases with diverse cellular functions. *J. Biol. Chem.* **276**, 4527–4530.

Lisman, J., Schulman, H., and Cline, H. (2002). The molecular basis of CaMKII function in synaptic and behavioural memory. *Nature Rev. Neurosci.* **3**, 175–190.

Pavur, K. S., Petrov, A. N., and Ryanazov, A. G. (2000). Mapping the functional domains of elongation factor-2 kinase. *Biochemistry* **39**, 12216–12224.

Proud, C. G., and Denton, R. M. (1997). Molecular mechanisms for the control of translation by insulin. *Biochem. J.* **328**, 329–341.

Soderling, T. R., and Stull, J. T. (2001). Structure and regulation of calcium/calmodulin-dependent protein kinases. *Chem. Rev.* **101**, 2341–2351.

Biography

A. J. Robison is a graduate student in the Molecular Physiology and Biophysics Department at Vanderbilt University. He received a B.S. in biology with honors from Rhodes College in 1999. He is studying the subcellular anchoring of neuronal CaMKII in the laboratory of Dr. Roger Colbran.

Roger. J. Colbran is an Associate Professor of Molecular Physiology and Biophysics, a member of the Center for Molecular Neuroscience, and an Investigator at the John F. Kennedy Center for Research on Human Development at Vanderbilt University. He earned a Ph.D. from the University of Newcastle upon Tyne (United Kingdom) and received postdoctoral training at Vanderbilt University. His principal research interest is in understanding calcium-dependent signaling events in neurons, especially as this relates to the regulation of synaptic transmission, and in cardiomyocytes.

Calcium-Binding Proteins: Cytosolic (Annexins, Gelsolins, C_2-Domain Proteins)

Joachim Krebs
Swiss Federal Institute of Technology, Zurich, Switzerland

Calcium is one of the most common elements on Earth, and it is the fifth most abundant element of the human body. Inside cells, calcium is a very versatile second messenger involved in the regulation of a variety of different cellular processes. This pivotal role of calcium is made possible due to the binding of Ca^{2+} to a great variety of different calcium-binding proteins. Next to the well-studied family of the so-called EF-hand containing proteins, a number of other calcium-binding proteins became known in recent years. These proteins are composed of a number of repeat units containing a variety of different Ca^{2+}-binding sites. The families of annexins, gelsolins, and C_2-domain containing proteins described in this article bind to different membranous or cytoskeletal structures in a Ca^{2+}-dependent manner, and are involved in a number of different cellular functions.

Annexins

The family of intracellular Ca^{2+}-binding proteins called annexins is soluble, amphipathic proteins that bind to membranes containing negatively charged phospholipids in a Ca^{2+}-dependent manner. They are called annexins since they bring or hold together different cellular structures, in particular membranes. The close to 200 different annexin proteins known to date are widespread in the animal and plant kingdoms, and have been claimed to be involved in a variety of cellular functions such as interaction with the cytoskeleton, membrane fusion, anticoagulation, signal transduction, or phospholipase inhibition. The primary structure of the annexins contains four or eight (annexin VI) conserved repeat units of ~75 amino acids in length, the protein core, which are separated by intervening sequences of variable length. These repeat units probably originated from gene duplications, a view which is corroborated by the evolutionary conservation of the intron–exon boundary positions. Most annexins containing four repeat units are comprised of 12–15 exons resulting in a quite variable amino-terminal part of the different annexins. Most alternative splicing sites have been located within exons encoding the variable amino-terminal parts of annexins. Since these parts are also the locations containing motifs for binding partners or for post-translational modifications, thus alternative splicing may contribute to the regulation of annexin function.

After the first determination of an annexin crystal structure (annexin V) by Huber and his co-workers, a number of additional annexin structures from different sources (including those from lower eukaryotes and plants) have been reported. From these structures it can be concluded that the conserved repeat units are packed into an α-helical disk, as first described for annexin V, which is almost entirely α-helical. It consists of five α-helices bundled into a right-handed super-helix. On the basis of this structure it was proposed that annexin V functions as a calcium channel, and some experiments using an *in vitro* reconstituted system seem to support a voltage-gated mechanism. This property is connected with the structure of the annexin core, which is shared by most annexins. Meanwhile, for most annexins a Ca^{2+} channel activity has been demonstrated in artificial bilayer systems, but never *in vivo*; therefore, the physiological relevance of these observations is questionable.

In contrast to the EF-hand containing Ca^{2+}-binding proteins, the ligands coordinating calcium in the annexins are not adjacent in sequence. Several calcium-binding sites seem to exist in annexins, two invariably in repeats II and IV, one in either repeat I or III, but annexins may contain as many as 10–12 Ca^{2+}-binding sites along the membrane-binding surface of the protein. The sites with the highest Ca^{2+} affinity are structurally related to the Ca^{2+}- and phospholipid-binding site of phospholipase A_2. The calcium ion is heptacoordinated with ligands organized in a pentagonal bipyramidal arrangement with ligating oxygens provided mainly from peptide carbonyls and water molecules, together with a single side-chain oxygen from a distant part of the sequence. Replacement of this latter

"capping" residue, which is usually acidic, with alanine precludes Ca^{2+} binding at the site. Once bound to membranes, many annexins oligomerize to form highly ordered two-dimensional arrays that have been shown to strongly influence *in vitro* membrane properties, e.g., increased rigidity.

An interesting feature is the role of Trp185 in the Ca^{2+}-binding site of repeat III of annexin V (see Figure 1). As suggested by Seaton and others, a Ca^{2+}-dependent exposure of Trp185, which is buried within the protein core in the absence of calcium, may facilitate the interaction between annexin V and the phospholipid bilayer. This view has been supported by fluorescence data and by mutagenesis experiments in which replacement of Trp185 by alanine decreased the annexin V membrane-binding affinity.

Annexins have long been known as targets for post-translational modifications. In fact, annexin II was originally isolated as a major substrate of the *src*-encoded protein kinase, and annexin I was long known to be phosphorylated by the tyrosine kinase activity of the epidermal growth factor (EGF) receptor, suggesting that annexins I and II could be used as coupling factors between growth factor receptors and their cellular targets, since these phosphorylations alter the Ca^{2+}-dependent binding of annexin I and II to membranes. In addition to the phosphorylation by different tyrosine kinases, also serine/threonine kinases have been identified to phosphorylate annexins. As a result, annexin phosphorylation often leads to an altered susceptibility towards proteolysis. On the other hand, phosphorylation of annexin II by different kinases interferes with its ability to form stable heterotetrameric complexes with p11, a member of the S100 family (S100A10), since these phosphorylation sites are located – like in the other annexins – within the variable amino-terminal domain, which comprises also binding motifs to interact with other proteins. Due to the binding of p11 (S100A10) the Ca^{2+}-sensitivity of the complex is increased by 3 orders of magnitude, and enables the heterotetrameric complex to bind simultaneously to two different membrane surfaces through the two annexin II cores. Next to the interaction between annexin II and S100A10 (p11) two other complexes between an annexin and an EF-hand containing protein of the S100 family may exist, i.e., interactions between annexin XI and S100A6 and annexin I and S100A11, respectively, but in contrast to annexin II/S100A10 the existence of the latter complexes *in vivo* has not been described to date.

In spite of extended studies in many laboratories over the years, the precise function of individual annexins is not yet understood. The accumulated data suggest that due to the many ways that annexins interact with different membranes in a Ca^{2+}-dependent manner, annexins may participate in Ca^{2+} signaling as effectors, mediators or even as regulators, but to clarify their biological activities unambiguously, this has to await further experiments. However, *in vivo* experiments from knockout and transgenic mice are beginning to shed some light on annexin function.

Gelsolin

Gelsolin belongs to the superfamily of actin-binding proteins (ABPs) expressed in all eukaryotes. It is a multifunctional protein-binding actin in a Ca^{2+}-dependent

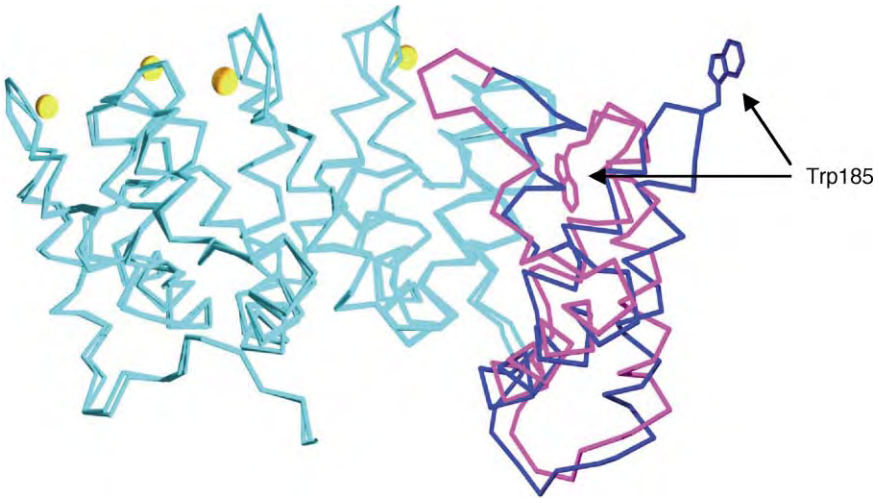

FIGURE 1 Superposition of α-carbon backbones of annexin V in the Ca^{2+}-free and the Ca^{2+}-bound form. Domains 1, 2, and 4 are light green, both in the Ca^{2+}-free and in the Ca^{2+}-bound form. Domain 3 is shown in magenta (Ca^{2+}-free, trp185 buried) and in blue (Ca^{2+}-bound, trp185 exposed). (Courtesy of Barbara Seaton.)

manner, and is composed of up to six repeats of 120–150 amino acids. To the gelsolin family belong proteins such as villin, adseverin, CapG, flil, and others. Villin, for example, is a six gelsolin-domain ABP regulating actin assembly in microvilli, whereas CapG is a smaller, three-domain gelsolin analogue that responds to Ca^{2+} and phosphatidylinositol-(4,5)-diphosphate under conditions where gelsolin is ineffective.

Alternative transcription initiation and selective RNA processing produces two isoforms of gelsolin from the same gene. One isoform of 80 kDa is located intracellular, whereas the other extracellular, slightly larger (83 kDa) protein is derived by alternative splicing, which results in a short amino-terminal elongation of the protein. The intracellular gelsolin is involved in cell motility regulating actin function, whereas extracellular gelsolin can act as an actin-scavenging system to prevent the polymerization of actin released after cell death.

Gelsolin consists of six repeat units (G1–6). The units are organized in two clusters of similar architecture, and are connected by a flexible linker of ~50 amino acids that may be cleaved by caspase-3, thereby cleaving the actin-binding domain of gelsolin from its calcium-binding domain. Caspase-3 cleavage and separation of subdomains of gelsolin coincides with plasma membrane blebbing, one of the characteristics of apoptosis. Apoptosis could also be induced by the overexpression of the amino-terminal half of gelsolin, whereas neutrophils of gelsolin-null mice have a delayed onset of apoptosis.

The structure of gelsolin in the absence of Ca^{2+} has been determined at 2.5Å resolution by Robinson and his co-workers (Figure 2). The amino-terminal half can bind to two actin monomers independent of calcium, whereas the carboxy-terminal half binds a single actin in a Ca^{2+}-dependent manner.

A detailed mechanism for the regulation of gelsolin activity by Ca^{2+} has recently been proposed. This was made possible by comparing the Ca^{2+}-free structure of nonactive gelsolin (Figure 2) with the recently solved structure of the active form of Ca^{2+}-bound gelsolin complexed to actin (see Figure 3). In this latter structure consisting of the C-terminal half of gelsolin, i.e., G4–6, bound to monomeric actin two classes of Ca^{2+}-binding sites have been identified: type-1 sites bind calcium in a coordination sphere shared by actin and gelsolin, whereas type-2 sites are identified only in gelsolin, i.e., located within G5 and G6. Due to conservation of the ligating residues within all gelsolin repeats, type-2 Ca^{2+}-binding sites should exist in all six domains of gelsolin. In total, gelsolin should be able to bind eight calcium ions in the active gelsolin–actin complex, i.e., two in type-1 sites and six in type 2.

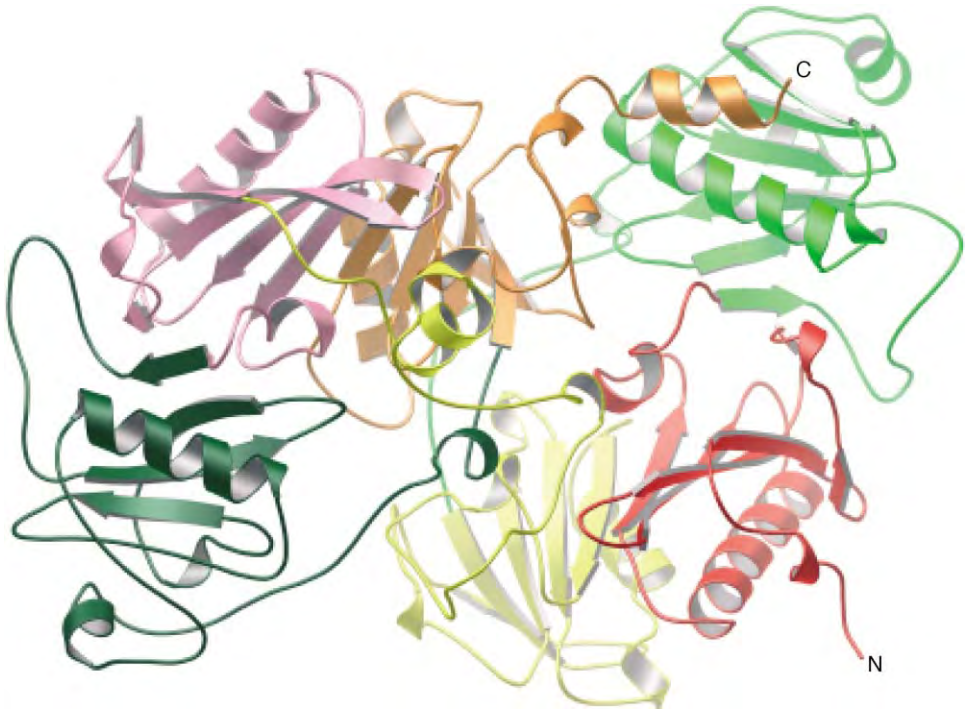

FIGURE 2 A ribbon diagram of the structure of gelsolin in the absence of calcium. The following color code for the different segments (G1–6) has been used: G1 (containing the amino terminus) red; G2, light green; G3, yellow; G4, magenta; G5, dark green; G6, (containing the carboxy terminus) gold. (Reproduced from Burtnick, L. D., Koepf, E. K., Grimes, J., Jones, E. Y., Stuart, D. I., McLaughlin, P. J., and Robinson, R. C. (1997). The crystal structure of plasma gelsolin: Implications for actin severing, capping and nucleation. *Cell* **90**, 661–670, with permission from Elsevier.)

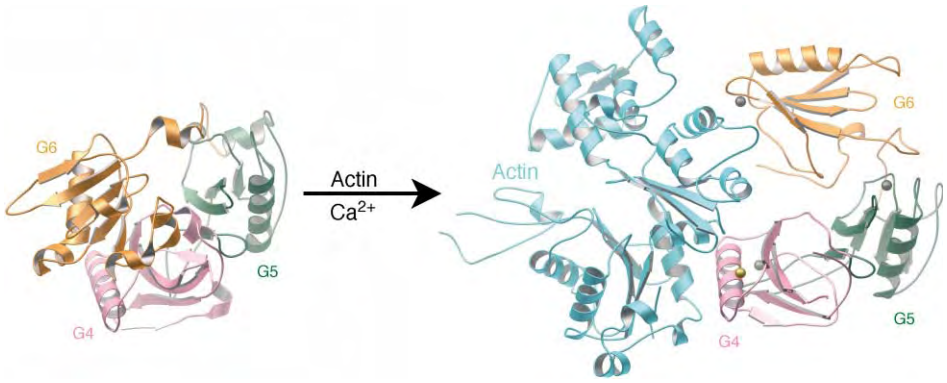

FIGURE 3 Ribbon diagram of gelsolin domains G4–G6 demonstrating the influence of binding Ca^{2+} and actin (shown in cyan) on the conformational changes of the protein. The same color code as in Figure 2 is used for domains G4–G6. The left-hand panel shows G4–G6 in a Ca^{2+}-free conformation (see Figure 2), whereas the right hand panel depicts the actin and Ca^{2+}-bound form of G4–6. (Reproduced from Choe, H., Burtnick, L. D., Mejillano, M., Yin, H. L., Robinson, R. C., and Choe, S. (2002). The calcium activation of gelsolin: Insights from the 3Å structure of the G4–G6/actin complex. *J. Mol. Biol.* **324**, 691–702, with permission from Elsevier.)

The latter are proposed to facilitate structural rearrangements within gelsolin as part of the activation and actin-binding process.

In the absence of Ca^{2+} the six repeat units of gelsolin provide a very compact globular structure, thus blocking the actin-binding helices of the appropriate sub-domains. Therefore, in a first step, this compact globular arrangement of the six sub-domains has to be opened up. As suggested by H. Choe and co-workers in 2002, binding of Ca^{2+} first to G6 should induce a conformational rearrangement in which G6 is flipped over G5 to tear apart the continuous β-sheet core of G4 and G6, thereby unmasking the actin-binding site on G4, and hence permit binding to actin strands (see Figure 3). Similar events should also occur in the N-terminal half of gelsolin, i.e., Ca^{2+}-binding to G3, flipping over G2 to open up the actin-binding site of G1. Finally, to tighten up the gelsolin–actin complex, Ca^{2+} binds to the two type-1 sites shared between actin and gelsolin, which might explain the very high affinity of gelsolin to actin (K_d 50 nM).

Gelsolin-null mice show normal embryonic development, but suffer subtle changes. This suggests the need of gelsolin for cell motility during processes such as hemostasis leading to reduced platelet function, inflammation leading to delayed neutrophil migration, or during wound healing, which would lead to reduced movement of fibroblasts. In this context it is interesting to note that it was demonstrated that during development of zebrafish embryos gelsolin is required for dorsoventral patterning. Inhibition of gelsolin expression that starts to be expressed already at the two-cell stage resulted in ventralized phenotypes, some of which lacked brain or eyes. These phenotypes could be rescued by injecting zebrafish gelsolin mRNA or even by injecting human gelsolin protein. These data indicate that gelsolin may have at least two separate functions: a structural role for the cytoskeletal/cell motility apparatus, and a regulatory role during development.

C_2-Domain Proteins

Interaction of proteins, intracellularly or extracellularly, often occurs via different binding modules or domains such as SH2, SH3, WW, PDZ, or C_2-domains. These modules are formed by folding domains consisting of 100–150 residues with different binding properties, that is, SH2-domains interact with phosphotyrosine-containing sequences, SH3- and WW-domains with proline-rich sequences, PDZ-domains with C-terminal sequences to link multiprotein complexes to the cytoskeleton, and C_2-domains with phospholipids, some in a Ca^{2+}-dependent, some in a Ca^{2+}-independent, manner. C_2-domains consist of about 120–130 amino acid residues. They were first identified in protein kinase C. More than 100 C_2-domain containing proteins can now be identified in current data banks.

Most proteins containing C_2-domains are linked either to signal transduction pathways or are involved in membrane traffic. The former proteins either generate lipid second messengers (e.g., phospholipase A2, phospholipase C, or phosphatidylinositol-3-kinase), phosphorylate proteins (e.g., protein kinase C), or ligate ubiquitin (e.g., Nedd4). Those proteins involved in membrane traffic include, for instance, the Rab-binding proteins rabphilin and RIM, which are involved in regulating the exocytosis of secretory vesicles. However, the best-characterized protein of

this category is synaptotagmin, which will be discussed in more detail.

Synaptotagmin I is a transmembrane protein belonging to a family of more than ten members which contain two C_2-domains, C_2A and C_2B, comprising most of the cytoplasmic region of synaptotagmins. The C_2-domains contain Ca^{2+}-binding domains of non-EF-hand character. Synaptotagmin I is found in synaptic vesicles, and is believed to act as the major Ca^{2+}-sensor of exocytosis and neurotransmitter release. Important in this respect is the Ca^{2+}-dependent binding of synaptotagmin to syntaxin, a member of the SNARE family of membrane proteins, involved in vesicle transport mechanisms.

C_2-domains have been suggested to be responsible for binding to membranes in response to Ca^{2+}. Sudhof and his co-workers determined the first structure of a C_2-domain, the C_2A-domain of synaptotagmin I (see Figure 4). The C_2-domain consists of a β-sandwich of two four-stranded β-sheets (Figure 4A). The eight β-strands are connected by three loops at the top that bind Ca^{2+} in the form of a cluster, primarily through oxygen of aspartate side chains serving as bidentate ligands, and by four loops at the bottom lacking

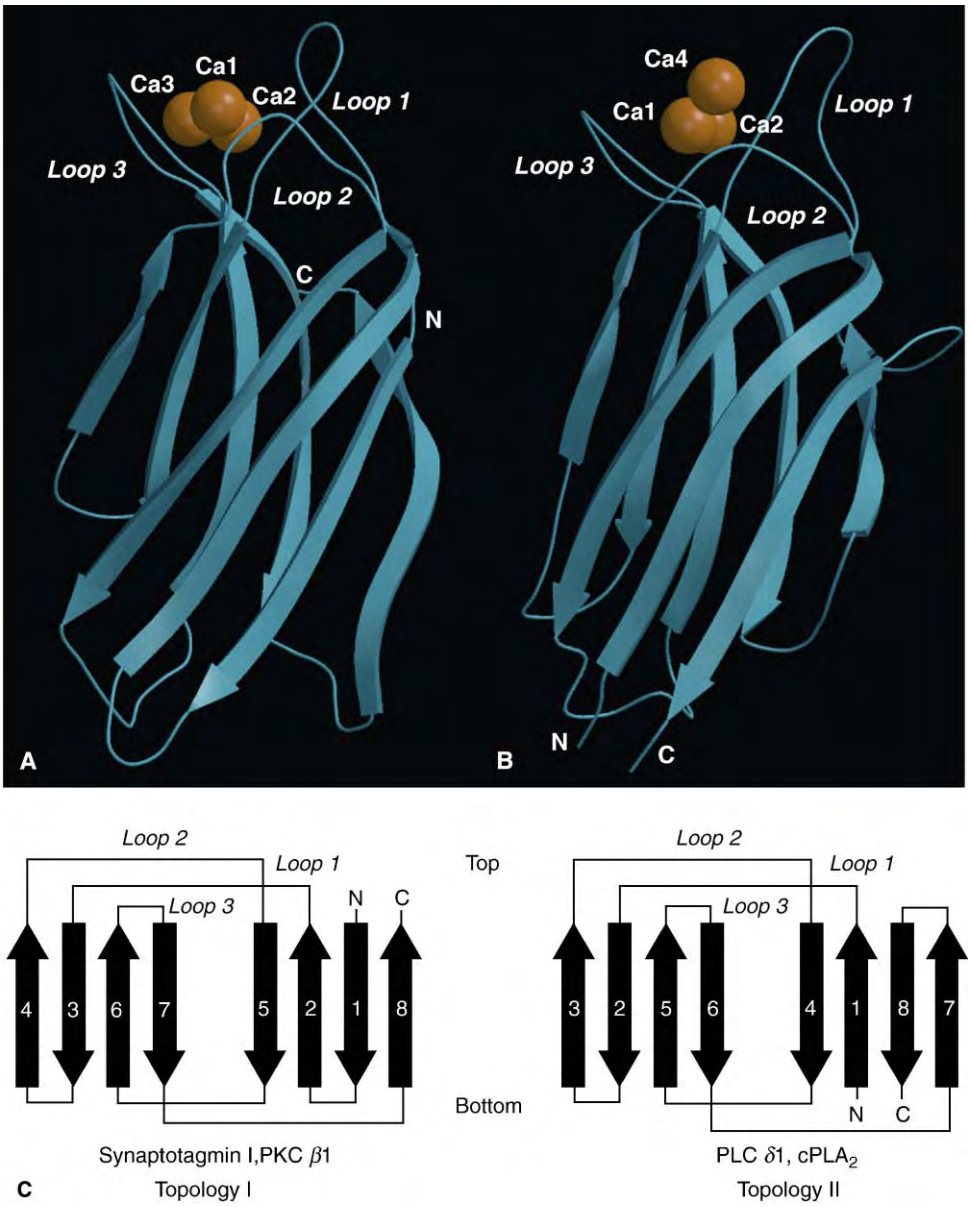

FIGURE 4 Ribbon diagrams of the structures of the C_2A-domain of synaptotagmin I (A) and of the C_2-domain of phospholipase Cδ1(B). (C) A schematic drawing of the β-strand topologies of the two structures. The locations of the Ca^{2+} clusters (orange) are indicated. (Reproduced from Rizo, J., and Südhof, T. C. (1998). C_2-domains, structure and function of a universal Ca^{2+}-binding domain. *J. Biol. Chem.* **273**, 15879–15882, with permission of the American Society for Biochemistry & Molecular Biology.)

Ca^{2+}-binding sites. In contrast to Ca^{2+}-binding to EF-hand type of sites, which causes substantial conformational changes, Ca^{2+}-binding to sites of C_2-domains leads to structural stabilization rather than backbone rearrangements.

Structural determination of other C_2-domains revealed similar designs, but significant differences in the topology of the arrangement of the β-strands (see Figure 4C). It could be shown that the structure of the C_2-domain of protein kinase Cβ is very similar to synaptotagmin I (topology I), whereas the topological arrangement of the structure of the C_2-domain of phospholipase Cδ is significantly different (topology II) (see Figure 4C). Phospholipase Cδ contains several protein modules including EF-hand Ca^{2+}-binding domains, which provides evidence for the existence of proteins containing EF-hand and non-EF-hand Ca^{2+}-binding sites.

An interesting finding concerning important functional differences between Ca^{2+}-binding sites of C_2A- and C_2B-domains of synaptotagmin has recently been reported. It has been shown that by mutating an aspartate essential for Ca^{2+}-binding to the C_2A-domain into an asparagine, this domain lost its Ca^{2+}-dependent binding to phospholipids or to syntaxin. However, introducing such a mutated synaptotagmin into the germline of *Drosophila* lacking synaptotagmin I that were severely impaired in neurotransmitter release, the mutated synaptotagmin I could fully rescue this defect, indicating that Ca^{2+}-binding to the C_2A-domain of synaptotagmin is not essential for neurotransmitter release. However, by replacing an aspartate for asparagine essential for Ca^{2+}-binding in the C_2B-domain, this mutated protein could not rescue such a defect in a similar set of experiments suggesting a significant functional difference in Ca^{2+}-binding between the C_2A- and C_2B-domains of synaptotagmin I.

In another C_2-domain containing protein, Nedd4, it was demonstrated that binding of Ca^{2+} to the C_2-domain was responsible not only for the localization of the protein but also for part of its function. Nedd4, the neuronal precursor cell-expressed developmentally down-regulated four protein, is a multimodular ubiquitin protein ligase. This enzyme is involved in controlling the turnover of membrane proteins. It was shown that localization of Nedd4 to the apical region of polarized epithelial cells was dependent on the Ca^{2+}-binding to its C_2-domain. Here an important target of Nedd4 is the Na^+-channel (ENaC), which plays a critical role in Na^+ homeostasis of epithelial cells. However, the C_2-domain of Nedd4 was not required to inhibit EnaC. On the other hand, it was shown that Nedd4 lacking its C_2-domain was still able to ligate ubiquitin to appropriate membrane protein targets such as Gap1, the general amino acid permease, but subsequent internalization by endocytosis, a prerequisite for the downregulation of membrane receptor proteins, was impaired.

See Also the Following Articles

Actin-Capping and -Severing Proteins • Calcium-Modulated Proteins (EF-Hand) • Phospholipase A_2 • Phospholipase C • Ribozyme Structural Elements: Group I Introns

Glossary

actin A eukaryotic protein that has the capability to form thin helical filaments.

alternative splicing Alternate usage of particular exons to create isoforms of a given protein.

amphipathic proteins Proteins composed of helices containing both hydrophobic and hydrophilic amino acid residues.

apoptosis Apoptosis (or programmed cell death) is derived from a Greek word describing the shedding of leaves from trees. During apoptosis, the cell responds to specific physiological or developmental signals undergoing a regulated, well-programmed series of events which will lead to its death and its removal from the organism.

cytoskeleton Complement of actin filaments, microtubules, and intermediate filaments forming a network in the cytoplasm.

EF-hand proteins Term coined by R.H. Kretsinger to describe the helix–loop–helix calcium-binding domains of specific proteins. The highly conserved motif (first described on the basis of the crystal structure of parvalbumin containing six helices, A–F) in which certain amino acids are invariant consists of two helices enclosing the Ca^{2+}-binding loop. As a model, the forefinger and the thumb of the right hand can resemble the two helices (e.g., E and F of the second Ca^{2+}-binding domain of parvalbumin) and the bent midfinger the enclosed loop, hence the EF-hand.

exon Segments of a eukaryotic gene preserved in the mature messenger RNA.

intron Segments of a gene transcribed into the precursor RNA but excised by RNA splicing before the mature RNA is exported from the nucleus into the cytoplasm.

post-translational modification Enzymatic modification such as acetylation, phosphorylation, myristoylation, or ubiquitination of proteins regulate their activity, topology, or degradation.

second messenger Intracellular small molecules (e.g., cyclic nucleotides or inositol polyphosphates) or ions such as Ca^{2+} or gases such as NO, indispensable for the transduction of signals converting extracellular stimuli – e.g., raised by hormones (= primary messengers) – into intracellular responses.

splicing Removal of introns from the precursor messenger RNA and joining of exons in mature messenger RNA; positions of boundaries between introns and exons are often conserved in homologous proteins of different species.

Further Reading

Burtnick, L. D., Koepf, E. K., Grimes, J., Jones, E. Y., Stuart, D. I., McLaughlin, P. J., and Robinson, R. C. (1997). The crystal structure of plasma gelsolin: Implications for actin severing, capping and nucleation. *Cell* **90**, 661–670.

Choe, H., Burtnick, L. D., Mejillano, M., Yin, H. L., Robinson, R. C., and Choe, S. (2002). The calcium activation of gelsolin: Insights

from the 3Å structure of the G4–G6/actin complex. *J. Mol. Biol.* **324**, 691–702.

Concha, N. O., Head, J. F., Kaetzel, M. A., Dedman, J. R., and Seaton, B. A. (1993). Rat annexin V crystal structure: Ca^{2+}-induced conformational changes. *Science* **261**, 1321–1324.

Dos Remedios, C. G., Chhabra, D., Kekic, M., Dedova, I. V., Tsubakihara, M., Berry, D. A., and Nosworthy, N. J. (2003). Actin binding proteins: Regulation of cytoskeletal microfilaments. *Physiol. Rev.* **83**, 433–473.

Gerke, V., and Moss, S. E. (2002). Annexins: from structure to function. *Physiol. Rev.* **82**, 331–371.

Huber, R., Römisch, J., and Paques, E. P. (1990). The crystal and molecular structure of human annexin V, an anticoagulant calcium, membrane binding protein. *EMBO J.* **9**, 3867–3874.

Pallanck, L. (2003). A tale of two C_2-domains. *TINS* **26**, 2–4.

Rizo, J., and Südhof, T. C. (1998). C_2-domains, structure and function of a universal Ca^{2+}-binding domain. *J. Biol. Chem.* **273**, 15879–15882.

Swairjo, M. A., and Seaton, B. A. (1994). Annexin structure and membrane interactions: A molecular perspective. *Annu. Rev. Biophys. Biomol. Struct.* **23**, 193–213.

Biography

Joachim Krebs has been working in the field of calcium-binding and calcium-transporting proteins for many years. After receiving his Ph.D. from the University of Tuebingen, Germany, he spent 2 years as a postdoctoral fellow at the Institute of Inorganic Chemistry of the University of Oxford, UK, before joining the Institute of Biochemistry at the Swiss Federal Institute of Technology (ETH) in Zurich, Switzerland. He has authored, co-authored, and edited numerous articles in international journals and books in the field of calcium biochemistry.

Calcium-Modulated Proteins (EF-Hand)

Robert H. Kretsinger
University of Virginia, Charlottesville, Virginia, USA

Many different proteins – extracellular, membrane, and intracellular – bind calcium more or less selectively. Those calcium binding proteins in the cytosol or bound to membranes facing the cytosol are inferred to be calcium modulated. That is, when the cell is quiescent, the concentration of free calcium ion is less than 10^{-7} M (pCa > 7) and the calcium-modulated protein is in the apo- or magnesi-form. Following stimulus, the concentration of calcium rises (pCa < 5.5), and the protein binds calcium. The attendant change in structure is involved in the transduction of the information of a pulse or wave of Ca^{2+} ions to an ultimate target enzyme or structure. Most of these calcium-modulated proteins contain from 2 to 12 copies of the EF-hand domain. There are other proteins in the cytosol that bind calcium and appear to be modulated by calcium; these include the annexins, proteins that contain one or several C2 domains, such as protein kinases C or synaptotagmin, and calcium pumps.

Calcium Coordination

Many of the functional characteristics of calcium and of calcium-modulated proteins can be rationalized from the geometry of calcium coordination.

Pentagonal Bipyramid

In proteins, the Ca^{2+} ion (atomic radius 0.99Å) is usually bound by seven oxygen atoms in an approximately pentagonal bipyramid conformation at average Ca–O distance 2.3 ± 0.3Å; the oxygen atoms have some lateral flexibility. The Mg^{2+} ion (atomic radius 0.65Å) is usually coordinated by six oxygen atoms at the vertices of an octahedron with Mg–O, 2.0Å; these oxygens are in tight van der Waals contact with one another. Although many small molecules bind magnesium with greater affinity than they bind calcium, most intra- and extra-cellular proteins bind calcium with much greater affinity than they bind magnesium.

Kinetics of Calcium and Magnesium Binding

The dissociation constant is the ratio of the off rate to the on rate: K_d (M) = k_{off} (s^{-1})/k_{on} ($M^{-1}s^{-1}$). The rate limiting dehydration of $Ca(H_2O)_7^{2+}$ is fast, $\sim 10^{8.0}\ s^{-1}$; while that of $Mg(H_2O)_6^{2+}$ is slow, $\sim 10^{4.6}\ s^{-1}$. This reflects the loose pentagonal bipyramidal vs the tight octahedral packing of the oxygen ligands. The cation must be (partially) dehydrated before it can bind to the protein. These rates are extremely important for modeling the flux of Ca^{2+} ions through the cytosol and the attendant binding of proteins. The increase in affinity of most proteins for calcium relative to magnesium derives primarily from this difference in k_{on} (e.g., see Table I).

Temporal Buffering

It is intriguing that most EF-hand proteins bind calcium ~10,000 times more strongly than they bind magnesium. This reflects strong evolutionary selection and cannot yet be mimicked by protein designers. The cytosolic concentration of the free Ca^{2+} ion is $\sim 10^{-7.2}$ M and that of the Mg^{2+} ion is $\sim 10^{-2.8}$; in contrast, both pCa_{out} and pMg_{out} are ~ 2.8. This means that a cytosolic protein, such as parvalbumin, that binds calcium with high affinity, e.g., $pK_d(Ca^{2+})$ ~8.0, will also bind magnesium with relatively high affinity, e.g., $pK_d(Mg^{2+})$ ~4.1, and, in the resting cell, will be in the magnesium state. In contrast, lower affinity sites, such as EF-hands 1&2 of troponin C have lower affinities for divalent cations, $pK_d(Ca^{2+}) \sim 6.5$ and $pK_d(Mg^{2+}) \sim 2.3$, and are apo in the resting state. This leads to the counterintuitive situation in which a pulse of messenger calcium first binds to the weaker apo sites in domains 1 and 2 of troponin C, misleadingly referred to as calcium specific. The Ca^{2+} ion, whose concentration during the pulse reaches $10^{-6.0}$ M, can bind to the apo site only after the Mg^{2+} ion diffuses off the strong site of parvalbumin. Parvalbumin, with higher affinity for divalent cations, binds calcium after the weaker

TABLE I

	K_d (M)	k_{off} (s^{-1})	k_{on} ($M^{-1}s^{-1}$)
Parvalbumin/Ca^{2+}	$10^{-8.0}$	$10^{0.0}$	$10^{8.0}$
Parvalbumin/Mg^{2+}	$10^{-4.1}$	$10^{0.5}$	$10^{4.6}$
Troponin C (domains 1&2)/Ca^{2+}	$10^{-6.5}$	$10^{1.5}$	$10^{8.0}$
Troponin C (domains 1&2)/Mg^{2+}	$10^{-2.3}$	$10^{2.3}$	$10^{4.6}$

troponin C and thereby helps to relax the muscle and prevent tetany. Such temporal buffering surely plays a significant role in the propagation and transduction of calcium waves observed in many cell types. The information encoded in the frequencies, durations, and amplitudes of calcium waves and spikes might be decoded by a corresponding matching of k_{off} and k_{on} rates for calcium and for magnesium in calcium-modulated proteins.

EF-Hand Containing Proteins

The structure of the EF-hand provides insight into its evolution and function.

Structure of the EF-Hand

The canonical EF-hand (Figure 1) consists of α-helix E, (forefinger, residues 1–10), a loop around the Ca^{2+} ion (clenched middle finger, 10–21), and α-helix F (thumb, 19–29). Residue 1 is often Glu; the insides of the helices (palmer surfaces) usually have hydrophobic residues that contact the insides of the other EF-hand of the pair (Figure 2). The side chains of five residues, approximating the vertices of an octahedron (X, residue 10; Y, 12; Z, 14; $-X$, 18; and $-Z$ 21), provide oxygen atoms to coordinate Ca^{2+}; residue 16 at $-Y$ bonds to Ca^{2+} with its carbonyl oxygen. The positions of these ligands within the loop are often referred to as 1, 3, 5, 7, 9, and 12. The Ca^{2+} ion is actually 7 coordinate in a pentagonal bipyramid with major axis, X, $-X$. There are five oxygen atoms in the Y, Z plane; since, the $-Z$ ligand (residue 21, usually Glu) coordinates Ca^{2+} with both oxygen atoms of its carboxylate group. A Gly at 15 permits a tight bend; residue 17 has a hydrophobic side chain that attaches the loop to the hydrophobic core of the pair of EF-hands.

Several variations to this canonical calcium coordination scheme have been inferred from amino acid sequence and confirmed in crystal structures of other EF-hand proteins. Nearly one-third of all known EF-hands do not bind calcium; those with no indels

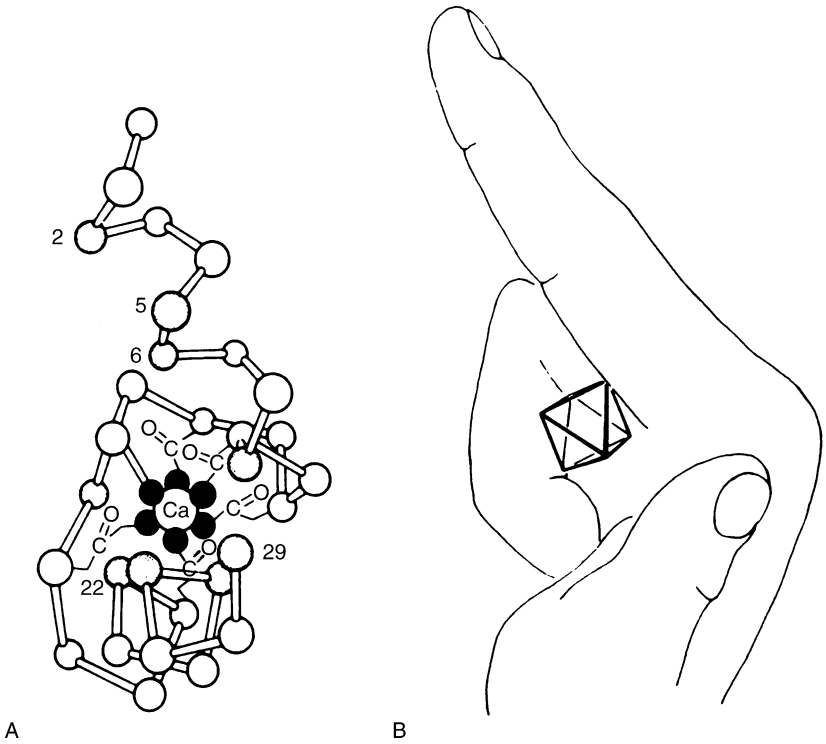

FIGURE 1 The EF-hand. (A) The spheres represent α-carbons. Residues 2, 5, 6, and 9 of helix E and residues 22, 25, 26, and 29 of helix F are usually hydrophobic and face the hydrophobic surface of the other EF-hand of the pair. Five residues—10, 12, 14, 18, and 21—coordinate the Ca^{2+} ion with an oxygen from a side chain. Residue 21 is usually Glu and contributes both oxygen atoms of its carboxylate to the pentagonal bipyramid coordination of calcium. Residue 16 coordinates with its carbonyl oxygen. (B) Helix E, the loop around the Ca^{2+} ion, and helix F are represented by the forefinger, clenched middle finger, and thumb.

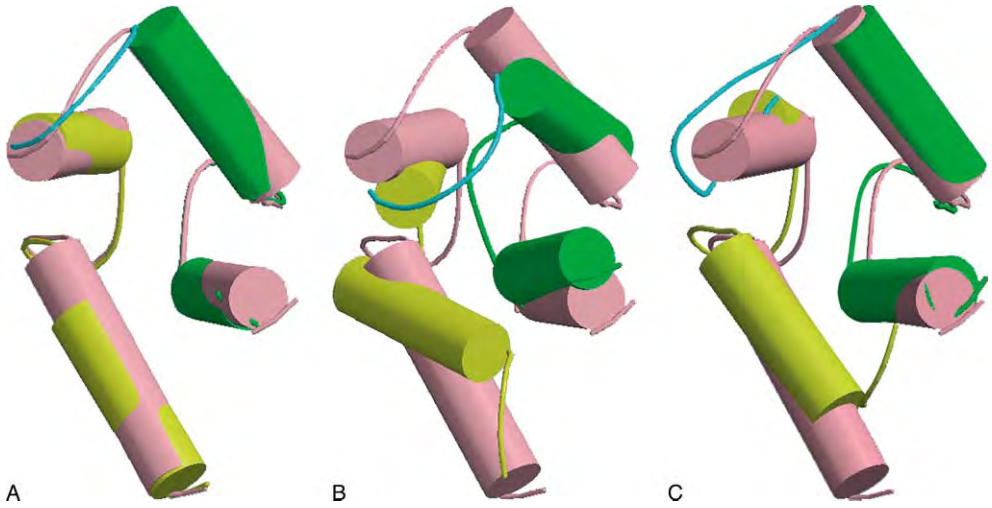

FIGURE 2 Conformations of pairs of EF-hands. Calmodulin consists of two pairs (1&2 and 3&4) of EF-hands. A flexible tether, seven residues long, connects helix F2 to helix E3. In the crystal structure, F2, the tether, and E3 form a single continuous helix. Calmodulin is widely distributed and interacts with at least 30 different target proteins. Furthermore, calmodulin's four EF-hands are all canonical; hence, it serves as a reference point for many evaluations and comparisons. (A) The backbone of the pair calmodulin-3&4 in its dicalci form is shown as a cylinder when it is α-helical and as a strand elsewhere. It is viewed down its approximate twofold axis and is shown in light salmon color; the calcium binding loops are far from the viewer. Dicalci-parvalbumin-CD&EF (CD, yellow; linker, light blue; EF, green) is superimposed on dicalci-calmodulin-3&4; their conformations are very similar. (B) Apo-calmodulin-3&4 (yellow, blue, green) is superimposed on dicalci-calmodulin-3&4 (salmon); the binding of calcium opens the cleft between the two helices of each EF-hand and between the two EF-hands of the pair. This is supposedly a necessary step permitting calmodulin to interact with its numerous targets. The structure of apo-parvalbumin is not known. (C) Dicalci-calmodulin-3&4 (yellow, light blue, and green) as complexed with the target peptide from myosin light chain kinase (not shown) is superimposed on dicalci-calmodulin-3&4 (salmon). Both the 3&4 and the 1&2 pairs of calmodulin undergo little additional change in conformation to bind their targets. The binding of a target peptide facilitates binding of calcium and vice versa. (Courtesy of Hiroshi Kawasaki, Yokohama City University, Yokohama, Japan.)

(insertions or deletions), have a non-oxygen-containing side chain substituted at position 10, 12, 14, 18, or 21. Other EF-hands have indels; most notable is EF-hand 1 of the S-100 subfamily (Table II), in which several carbonyl oxygens, instead of side chain oxygens, coordinate Ca^{2+}.

Evolution of the EF-Hand Family

All members of a protein homolog family are inferred to have evolved from a common precursor domain in a single ancestral organism. The most parsimonious interpretation is that all of the EF-hand domains listed in Table II are homologs; however, the statistics are weak since the domains are only 30 residues long. We employ other criteria, such as the fact that nearly all EF-hands occur in pairs (Figure 2) and that in nearly all EF-hand proteins at least one of the EF-hands binds calcium. Many domains have been suggested to resemble the EF-hand. They are not included in Table II unless they have passed a Hidden Markov Model test based on unambiguous EF-hands of known structure. Most EF-hand containing proteins have been found in eukaryotes; however, there are several examples in eubacteria. EF-hand proteins, e.g., calmodulin, have been found in all eukaryotes subject to thorough investigation. This distribution might reflect an origin in the bacterium that gave rise to eukaryotic cells; other bacteria may have lost their EF-hands. Or, the precursor EF-hand may have arisen in an early eukaryote and been transferred to a few bacteria by some sort of transduction or transformation.

Distribution of EF-Hand Domains

Most of the calcium-modulated proteins contain 2 to 12 tandem copies of the EF-hand domain. EF-hands occur in pairs and are related by an approximate twofold axis of rotation (Figure 2). Although about one-third of all EF-hands are known or inferred not to bind calcium, usually at least one EF-hand domain in any protein does bind calcium with $pK_d(Ca^{2+}) \sim 7.0$. The protein, such as archetypical calmodulin, is in the apo or magnesium form prior to stimulation of the cell; following a rise in $[Ca^{2+}]_{cyt}$, the competent EF-hand binds calcium with attendant change in conformation of itself and probably of the paired EF-hand of the two-domain lobe. If the protein is hetero-chimeric with a non-EF-hand catalytic portion, the change in conformation of the EF-hand region activates the enzyme. If the EF-hand protein itself is not catalytic, the change in conformation causes the EF-hand protein to activate a target enzyme or structural protein.

The characteristics of 77 distinct EF-hand proteins are summarized in Table II. The functions of only 26 of

TABLE II

EF-Hand Containing Proteins

Name	Animal Plant Fungi Protist	Func.	Struct.	1 (7	2 8	3 9	4 10	5 11	6 12)
CTER									
CAM	calmodulin	APFP	+X	+	+	+	+/−		
TNC	troponin C	A…	+X	+/−	+	+/−	+		
ELC	essential light chain, myosin	A.F.	+X	a/−	+/−	+/−	+/−		
RLC	regulatory light chain	A.FP	+X	+	−	−	−		
TPNV	troponin, nonvertebrate	A…	+?	−	+	+/−	+		
CLAT	CAM-like leaf (*Arabidopsis*)	P..	??	+	+	+	+****		
SQUD	squidulin (*Loligo*)	A…	+?	+	+	+	+		
CDC	CDC31 & caltractin	APFP	??	+	+/−	+/−	+		
CAL	cal1 (*Caenorhabditis*)	A…	??	+	+	+	+		
CAST	CAST	.P..	??	***+	−	+	+		
CPV									
CLNB	calcineurin B	A.F.	+X	+	+	+	+		
P22	p22	A…	??	+	−	+	+		
VIS	visinin & recoverin	A…	+X	−	+	+	−		
CALS	calsenilin (*Homo*)	A…	??	***−	−	+	+		
DREM	DRE antag. modul. (*Homo*)	A…	+?	***−/?	+/?	+	+		
CMPK	CAM dep prot kinase (*Lilium*)	.P..	+?	***+	+	+	+		
SOS3	Ca sens homo (*Arabidopsis*)	.P..	+?	−	−	−	−		
Pairings									
RTC	reticulocalbin (*Mus*)	A…	??	+	?/+	?/+	+	+	+
SCF	DNA supercoil fact (*Bombyx*)	A…	??	***+	−	+	+	+	+
CALP	calpain	A…	+X	***+	+	−	−	−	
SORC	sorcin/grancyclin	A.F.	+X	***+	+	−	−	−	
S100	S100	A…	?X	b/−	+				
ICBP	intestinal Ca binding protein	A…	?X	b/−	+				
HYFL	trichohylin profilag	A…	??	b/?	+***				
DGK	diacylglycerol kinase	A…	+?	***+	+***				
NUBN	nucleobindin & NEFA	A…	??	***+	+***				
CRGP	CAM rel gene product (*Homo*)	A…	??	+	+				
ACTN	α-actinin	A.F.	+X	***+/−	+/−				
FDRN	α-spectrin & α-fodrin	A…	+?	***−	−				
GPD	Glycerol-P-dehydrogenase	A…	+?	***−	+				
AIF1	allograft inflammatory factor	A…	??	***+	+/?				
BM40	osteonectin, SPARK	A…	?X	***c	+				
QR1	QR1 & SC1	A…	??	−	+				
Self									
EF12	Ca Binding prot of nematodes	A…	??	***+	+	+	−	+	+
				+	+	+	+	+	+
LPS	*L. pictus* SPEC resembl prot	A…	??	+	+	+	+	+	+
				+	−				
CLBN	calbindin 28 kDa, calretinin	A…	??	+	+/−	+	+	+	−
EP15	EP15	A…	+X	***−	−***	−	+***	+	−***
TCBP	Tetrahymena CaBP	…P	??	−	+	+	+		
P26	p260lf (*Rana*)	A…	??	−	−***	−	−		
PLC	phopholipase C	A.F.	+X	***−	−	−	−***		
CBP	CBP1, CBP2 (*Dictyostelium*)	..F.	??	+	+	+	+		
Miscellaneous									
PFS	surface protein (*Plasmodium*)	…P	??	***+	+	+	+	+	−***
CLSM	calsymin	bact	??	+	−	+	−	+	−

continues

TABLE II

Continued

Name	Animal Plant Fungi Protist	Func.	Struct.	1 (7	2 8	3 9	4 10	5 11	6 12)
UEBP	URE3-BP	A…	+?	+	+	+	−?	−?	
CDPK	Ca dependent protein kinase	.P..	+?	*** +	+	+	+		
PFPK	protein kinase (*Plasmodium*)	…P	+?	*** +	+	+	+		
SPEC	*Strongylocentrotus* CaBP	A…	??	+/−	+	+	+/−		
TPP	p24 thyroid protein	A…	??	+	+	+	?		
1F8	1F8 & TB17 & calflagin	…P	??	+	+	+	+		
SARC	sarcoplasm Ca bind prot	A…	?X	+	+/−	+	+/−		
AEQ	aequorin & luciferin BP	A…	+X	+	*−*	+	+		
PPTS	protein phosphatase	A…	+?	*** −	*−*	+	+		
H32	HRA32 (*Phaseolus*)	.P..	??	+	+	+	+		
EFH5	EFH5	…P	??	−	+/−	+/−	−		
CVP	Ca vector prot (*Branch.*)	A…	?X	−	−	+	+		
PMAT	memb. assoc. (*Arabidopsis*)	.P..	??	*** +	+	+	+		
LAV	LAV1 (*Physarum*)	..F.	??	*** +	+	+	+		
CMSE	CaBP (*Saccharopolyspora*)	bact	??	+/−	+/−	+/−	+/−		
MSV	MSV097 (*Entomopoxvirinae*)	virus	??	+	+	−	–		
PARV	parvalbumin	A…	?X	del	−	+	+		
BCBP	brain calcium binding protein	A…	??	+/−	−	+	+		
CSCJ	S. coelicolor CBP	bact	??	+	+	−	+		
DYSN	dystrophin	A…	+X	*** −	−	−	−		
FIMB	fimbrin	A.F.	+?	+/−	+/−***				
GRP	ras guan releasing prot (*Rattus*)	A…	??	*** +/?	+/?***				
PKD	PKD2L/polycystin	A…	??	*** −	+***				
RYR	ryanodine receptor/Ca release	A…	+?	*** −	+***				
CBL	proto-oncogene Cbl	A…	+X	*** −	d***				
CIB	Ca & integrin binding protein	A…	??	*** +	+				
SENS	calsensin (*Haemopsis*)	A…	??	+	+				
GRV	groovin (*Drosophila*)	A…	??	+	+				
BET4	calcium bind. pollen allergen	.P..	?X	+	+				
CSCD	S. coelicolor CBP	bact	??	+	+				
CBCC	C. crescentus CBP	bact	??	+	+				
ACHE	acetylcholine esterase	A…	+X	*** −	−				
NCAB	neuronal CaBP	A…	??	+	−***				
SWPN	swiprosin	A…	??	*** −	+***				

Note. The 77 known EF-hand homolog subfamilies are described in several groups: CTER, those that are congruent with calmodulin, troponin C, essential, and regulatory light chains; CPV, those that are congruent with calcineurin B, p22, and visinin (recoverin); Pairings, those closely related between or among themselves but not closely related to other subfamilies; Self, those (some of) whose EF-hands are most closely related to other EF-hands within the same subfamily; and Miscellaneous, those whose domains do not show a strong and consistent pattern of similarity with other EF-hand subfamilies. The first domain of (pre)parvalbumin is inferred to have been deleted; hence, its domains are listed as 2(AB), 3(CD), and 4(EF). In congruent subfamilies, all of the EF-hands 1 (or *n*) resemble one another more closely than they resemble other EF-hands within their own protein. For 26 subfamilies, only one sequence is available; this is indicated by inclusion of genus name in parentheses or as part of the name of that subfamily. APFP refers to whether the protein is found in Animals, Plants, Fungi, and/or Protists. Five subfamilies are found in prokaryotes (bact) and one in a virus. The Func/Struct columns indicate whether a function is known + or not ? and whether a crystal structure is available X or not ?. The symbol *** before the first EF-hand column or after the last column indicates a protein with the non-EF-hand domain(s) to either the N-side or C-side of the EF-hands. For P26 and for EP15 *** indicates another domain between EF-hands 1 & 2 and EF-hands 3 & 4. Thirty-four, including the nine enzymes, of the 77 subfamilies are hetero-chimeric. For AEQ and PPTS, **−*** indicates that domain is not recognizable as an EF-hand by analysis of its sequence; however, its proximity to an otherwise unpaired EF-hand suggests that it may be an EF-hand and is inferred not to bind calcium. For each EF-hand is indicated whether calcium binding is observed (or inferred from sequence) + or not −. For some EF-hands there are instances of both binding and not binding calcium +/−. There are four examples—a, b, c, and d—of noncanonical EF-hand loops that bind calcium. Some loops inferred not to bind calcium may provide additional examples of noncanonical calcium binding loops. EF12 has 12 and LPS has 8 EF-hands; for ease of formatting EF-hands, 7 and on are listed under EF-hands 1 and on. Of the 77 distinct EF-hand proteins 56 have been found in animals. The functions of only 27 of the 77 are known. Nine of these are enzymes and have been demonstrated or inferred to be activated by the binding of calcium. Many, but certainly not all, of the remaining 50 function in the information transduction pathway summarized for calcium modulated proteins, such as calmodulin.

the 77 are known. Nine of these are enzymes and have been demonstrated or inferred to be activated by the binding of calcium. Many, but certainly not all, of the remaining 51 function in information transduction pathways as summarized for calcium-modulated proteins, such as calmodulin. However, others such as intestinal calcium binding protein, probably facilitate the diffusion of calcium through the cytosol; parvalbumin appears to function as a temporal buffer. Thirty-one, including the nine enzymes, of the 77 subfamilies are hetero-chimeric. In addition to their EF-hands, they contain other domains of different evolutionary origin and conformation. It is not unusual for a basic protein domain to find many uses, often spliced together with other domains; however, the EF-hand is one of the most widely distributed domains in eukaryotes, perhaps reflecting the range and subtlety of calcium signaling. The downstream regulation element antagonist modulator (DREAM) upon binding calcium dissociates from a DNA binding regulatory element that otherwise functions as a gene silencer. Whether this might provide a precedent for long-term potentiation remains to be seen.

Calmodulin

Calmodulin is probably present in all cells of all eukaryotes. It consists of four EF-hands and is highly conserved in amino acid sequence. The second (F2) α-helix of domain 2, the eight residue linker between domains 2 and 3 and the first (E3) α-helix of domain 3 form a single continuous α-helix ~28 residues long, thereby giving calmodulin a dumbbell shape as seen both in the crystal and in solution. Upon binding calcium, the relative orientations of the four helices in both lobes change, thereby exposing hydrophobic regions and permitting the interaction of calmodulin with target enzymes and structural proteins. Over 30 calmodulin targets have been reported. The structures of calmodulin complexed with α-helical regions of several targets, such as myosin light chain kinase (MLCK), reveal what appears to be a general pattern for the interactions of four domain EF-hand proteins, such as calmodulin, troponin C, and the essential and regulatory light chains of myosin, with their respective targets. MLCK is self-inhibited by its own peptide 796–813; limited proteolysis removes this peptide. The 1–795 MLCK is then constitutively active. *In vivo*, calmodulin binds calcium, undergoes a change in conformation, binds α-helix 796–813 of MLCK, and thereby removes the self inhibition of MLCK. Calmodulin assumes a near spherical shape when complexed with its target, as opposed to the elongated dumbbell shape of uncomplexed calmodulin. The eight-residue linker is flexible, permitting calmodulin to assume a broad range of conformations. Among these conformations are some that grasp the MLCK target peptide; other conformations fit other targets.

See Also the Following Articles

Calcium-Binding Proteins: Cytosolic (Annexins, Gelsolins, C_2-Domain Proteins) • Calcium Signaling: Motility (Actomyosin–Troponin System) • ER/SR Calcium Pump: Function • ER/SR Calcium Pump: Structure • Plasma-Membrane Calcium Pump: Structure and Function

Glossary

calcium-modulated protein Calcium binding protein found in the cytosol whose structure changes with binding and release of Ca^{2+} ions associated with a pulse of messenger calcium.

calmodulin Protein consisting of two pairs of EF-hands. It is found in nearly all cells of all eukaryotes and interacts with some 30 different target enzymes or structural proteins.

EF-hand Domain of 30 amino acids consisting of an α-helix, a loop around a Ca^{2+} ion, and a second α-helix.

transduction Process of changing energy and/or information from one modality to another.

Further Reading

Berridge, M. (2001). The versatility and complexity of calcium signalling. In *Novartis Foundation Symposium*, Vol. 239, pp. 52–67. Novartis Foundation, London.

Gerke, V., and Moss, S. E. (2002). Annexins: From structure to function. *Physiol. Rev.* **82**, 331–371.

Nakayama, S., Kawasaki, H., and Kretsinger, R. H. (2000). Evolution of EF-hand proteins. *Topics Biol. Inorg. Chem.* **3**, 29–58.

Schuster, S., Marhl, M., and Hofer, T. (2002). Modelling of simple and complex calcium oscillations—From single-cell responses to intercellular signalling. *Eur. J. Biochem.* **269**, 1333–1355.

Sudhof, T. C. (2002). Synaptotagmins: Why so many? *J. Biol. Chem.* **277**, 7629–7632.

Toyoshima, C., and Nomura, H. (2002). Structural changes in the calcium pump accompanying the dissociation of calcium. *Nature* **418**, 605–611.

Biography

Robert Kretsinger is Professor of Biology at the University of Virgina, Charlottesville, Virginia. He received his Ph.D. in biophysics from the Massachusetts Institute of Technology and carried out his post-doctoral training at the Medical Research Council Laboratory of Molecular Biology in Cambridge, England. He determined the first crystal structure of an EF-hand protein, parvalbumin, in 1970, and he has continued his research in various aspects of protein structure, evolution, and structure prediction.

Calpain

Hiroyuki Sorimachi and Yasuko Ono
University of Tokyo, Tokyo, Japan

Calpain (Clan CA, family C02, EC 3.4.22.17) is a ubiquitous intracellular Ca^{2+}-dependent cysteine protease that displays limited proteolytic activity at neutral pH. Calpain acts by proteolytically processing, rather than digesting, substrates to transform and modulate their structures and activities. Thus, calpain is viewed as a representative "modulator protease" that governs various cellular functions such as signal transduction and cell morphogenesis. Calpain belongs to the papain superfamily and constitutes one of the three distinct kingdoms, i.e., calpain-, papain-, and bleomycin-hydrolase-sub-superfamilies. The human genome has 14 genes that encode a calpain-like protease domain. These generate diverse types of calpain homologues possessing combinations of several functional domains such as a Ca^{2+}-binding domain (C2-type and EF-hand-type) and a Zn-finger domain. Furthermore, calpain homologues are increasingly being found in other organisms including insect, nematode, trypanosome, plant, fungus, yeast, and even some bacteria, thus constituting a superfamily possessing versatile functions. The importance of the physiological roles of calpains is reflected by the fact that particular defects in calpain functionality cause a variety of deficiencies in many different organisms. These include muscular dystrophies, diabetes and tumorigenesis in humans, embryonic lethality in mice, neurogenesis deficiency in flies, incomplete sex determination in nematodes, defects in aleurone cell development in maize, and alkaline/osmotic stress susceptibility in yeast.

History and Nomenclature

Calpain was described as early as 1964. After several "re-identifications," calpain, which was called CANP (calcium activated neutral protease) at that time, was finally purified into homogeneity in 1978. Both names, "calpain" and "CANP," were unified as calpain in 1991. In 1984, the cDNA for the catalytic subunit of calpain was cloned for the first time, revealing that calpain is a chimeric molecule consisting of a cysteine protease and a calmodulin-like Ca^{2+}-binding module. In the two decades following this event, hundreds of calpain-related molecules, including its endogenous specific inhibitor protein, calpastatin, have been identified through the use of cDNA cloning and genome/EST projects.

Two major ubiquitous calpains are found in mammals, μ- and m-calpains. Since most of the studies carried out concerned μ- and m-calpains, they are referred to as the "conventional" calpains. As the names suggest, μ-calpain and m-calpain are activated by μM and mM levels of Ca^{2+} *in vitro*, respectively. They are both hetero-dimers and consist of a common calpain small regulatory subunit (30K, ca. 28 kDa) and large distinct μ- and m-calpain catalytic subunit (μCL and mCL, respectively, ca. 80 kDa), which have ca. 60% amino acid identity. Fourteen human calpain homologues have been numbered as in the case of caspases as shown in Table I and Figure 1. As an example, μCL is now called "calpain 1," i.e., μ-calpain is a hetero-dimer consisting of a 30K subunit and calpain 1. To avoid unnecessary confusions, however, the original name and the gene product name are adopted in this section, e.g., μCL/CAPN1, mCL/CAPN2, p94/CAPN3, 30K/CAPNS1, hTRA-3/CAPN5.

Structure and Function of Conventional Calpains

In general, potential substrates for calpain are very limited and specific. Most oligopeptides investigated are poor substrates for calpain. Although casein is not an *in vivo* substrate of calpain, it is a very good *in vitro* substrate and is used to assay calpain activity. Although the rules governing substrate specificity remain unclear, calpain is thought to recognize a large scope of 3D substrate structures rather than a particular primary amino acid sequence. For example, protein kinases, phosphatases, phospholipases, cytoskeletal proteins, membrane proteins, cytokines, transcription factors, lens proteins, and calmodulin-binding proteins are just some of the proteins suggested to be *in vivo* substrates. There has been no report suggesting differences in substrate specificity between μ- and m-calpains.

Calpain has a very specific proteinaceous inhibitor *in vivo* called calpastatin. Calpastatin has four repeats of an inhibitor unit, each of which inhibits calpain. Both μ- and m-calpains possess similar susceptibility

TABLE I

Human Calpain Related Genes[a]

Gene	Chr.	Originally described names(s) of the gene product	Other name(s) used	Name in number	Domains				Expression	Note
					Protease activity[b]	C2-like	5EF-hands	C2 (T)		
The large subunits										
CAPN1	**11q12-13.1**	μCANP[c]/calpain-I large subunit	μ-calpain large subunit(μCL), μ80K	Calpain 1	+	+	+	−	ubiquitous	+30K/CAPNS1 = μ-calpain
CAPN2	**1q32-41**	mCANP/calpain-II large subunit	m-calpain large subunit (mCL), m80K	Calpain 2	+	+	+	−	ubiquitous except for mammalian erythrocytes	+30K/CAPNS1 = m-calpain
		p94	calpain 3, nCL-1	Calpain 3a	+	+	+	−	skeletal muscle	binds to connectin/titin termination codon in the human
CAPN3	**15q15**	Lp82, Lp85, etc.	—	Calpain 3b, 3c etc.	+	+	+	−	lens, retina	first exon
CAPN5	**11q14**	calpain 5, hTRA-3	nCL-3	Calpain 5	+	+	−	+	testis, brain	nematode TRA-3 homologue
CAPN6	**Xq23**	calpain 6	calpamodulin, CANPX	Calpain 6	−	+	−	+	placenta, embryonic muscles	nematode TRA-3 homologue, but no Cys at the active site
CAPN7	**3p24**	calpain 7, PalBH	—	Calpain 7	n.d.	+	−	−	ubiquitous	Aspergillus PalB homologue
		nCL-2	—	Calpain 8a	+	+	+	−	stomach	
CAPN8	**1q32-41**	nCL-2′	—	Calpain 8b	+	−	−	−	stomach	Ca^{2+}-dependent
CAPN9	**1q42.1-43**	nCL-4	—	Calpain 9	+	+	+	−	digestive tracts	30K is required for activity
CAPN10	**2q37.3**	calpain 10a–h	—	Calpain 10a–h	n.d.				ubiquitous	SNP is related to NIDDM
CAPN11	**6p12**	calpain 11	—	Calpain 11	n.d.				testis	
CAPN12	**19q13**	calpain 12a–c	—	Calpain 12a–c	n.d.	+	+	−	hair follicle	
CAPN13	**2p21-22**	calpain 13	—	Calpain 13	n.d.	+	+	−	ubiquitous	mRNA not detected
CAPN14	**2p21-22**	calpain 14	—	Calpain 14 n.d.	n.d.	+	−	−	n.d.	
CAPN15	**16p13.3**	SOLH	—	Calpain 15	n.d.	−	−	−	ubiquitous	drosophila SOL homologue
The small subunits										
CAPNS1	**19q13**	CANP/calpain small subunit	30K, ccs1	CAPNS1	–	−	+	−	ubiquitous	regulatory subunit for μCL and mCL
CAPNS2	**16q13**	CAPNS2	30K-2, ccs2	CAPNS2	−	−	+	−	ubiquitous	intron less gene
The calpain inhibitor										
CAST	**5q15-21**	CANP inhibitor/ calpastatin	—	–	−	−	−	−	ubiquitous	specific inhibitor for μ-, m-calpains, and nCL-4

[a] Human disease and results of knock-out mice were taken together.

[b] (+) indicates that it was experimentally shown to have protease activity, and (−) in calpain 6 means that it has no active site cysteine residue.

[c] Abbreviations: n.d., not yet determined; CANP, Ca^{2+}-activated neutral protease; nCL, novel calpain large subunit; LGMD2A, limb-girdle muscular dystrophy type 2A; TRA-3, transform genotypic hermaphrodites; PalB, phosphatase mutants: loss in activity at alkaline pH but normal or increased activity at acidic pH; PalBH, PalB homologue; SNP, single nucleotide polymorphism; NIDDM, non-insulin-dependent diabetes mellitus; SOL, small optic lobes; SOLH, SOL homologue; ALG-2, apoptosis-linked gene-2; PDCD6, programmed cell death 6.

[d] The corresponding mammalian gene does not exist.

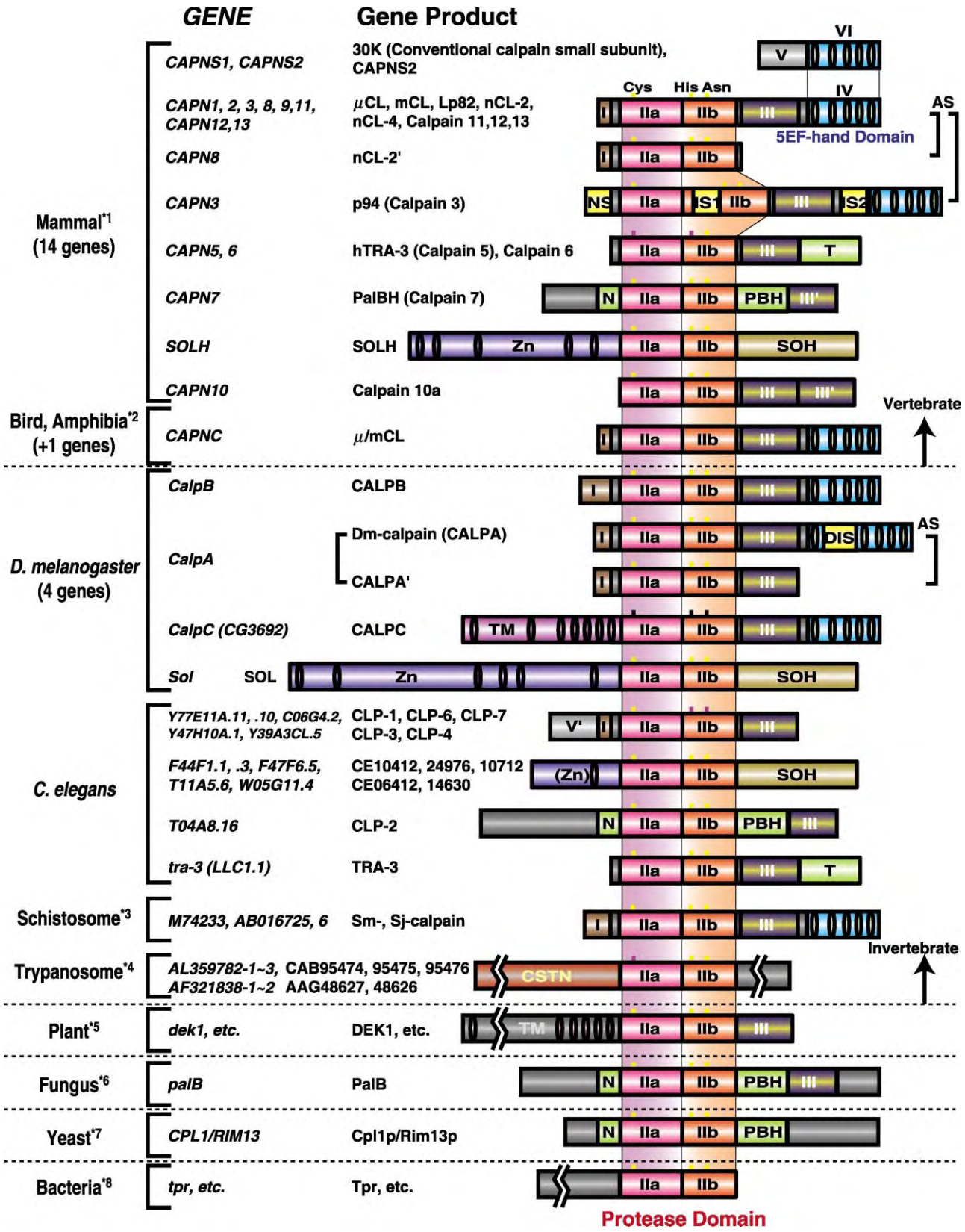

FIGURE 1 Schematic structures of calpain. Calpain homologues have been identified in Mammals (*1: human, mouse, rat, rabbit, porcine, bovine, ovine), birds (*2: chicken and quail), amphibians (*2: *X. laevis*), flies, nematodes, schistosomes (*3: *S. mansoni* and *S. japonicum*), trypanosomes (*4: *Leishmania major* and *Trypanosoma brucei*), plants (*5: *A. thaliana*, maize, rice, and loblolly pine), fungi (*6: *A. oryzae* and *E. nidulans*), yeasts (*7: *S. cerevisiae*, *Y. lipolytica*, and *C. alabicans*) and bacteria (*8: *Porphyromonas gingivalis*, *Cyanobacterium Anabaena*, etc.). I,

to calpastatin. μ- and m-calpains are ubiquitously expressed in mammalian and avian cells. Thus, their function is thought to be fundamental and essential. Many functions including the regulation of signal transduction systems, cell motility and apoptosis have been suggested, although they have not yet been completely clarified. *CAPN1* knock-out mice showed almost no phenotype, while *CAPNS1* knock-out mice resulted in embryonic lethality, indicating the indispensable roles of conventional calpains and, at the same time, differentiating between μ- and m-calpain functionality.

As shown in Figure 1, the catalytic and regulatory subunits of conventional calpains can be divided into 4 and 2 domains, respectively. The N-terminus of domain I of the large subunit is autolyzed upon activation by Ca^{2+}. This results in a lower requirement for Ca^{2+} and the dissociation of both subunits. Therefore, autolysis is involved in the regulation of calpain activity and specificity.

Three-D structural studies revealed that the protease domain in the absence of Ca^{2+} is divided into two subdomains—domains IIa and IIb, which are folded into one domain upon Ca^{2+} binding. This domain is highly conserved among calpain family members, suggesting the functional importance of this domain (Figure 1). Surprisingly, only the protease domain of μ- and m-calpains showed Ca^{2+}-dependent protease activity. This is supported by the 3D structural studies of the protease domain in the presence of Ca^{2+} that showed Ca^{2+} bound to domains IIa and IIb. Thus, the whole calpain molecule mediates Ca^{2+}-dependency since all of the domains IIa, IIb, III, IV, and VI bind at least one Ca^{2+} with varying affinities.

The 3D structure of domain III consists of 8 antiparallel β-strands (β-sandwich structure), a structure very similar to TNF-α and the C2-domains found in several Ca^{2+}-regulated proteins such as PKCs and synaptotagmins. Although the primary structure of domain III is highly conserved in calpain homologues, it has no similarity to any other proteins including TNF-α and C2-domains. This domain actually binds Ca^{2+}, and may play an important role in the Ca^{2+}-dependent membrane translocation of calpains.

Domain IV is very similar to domain VI of the small subunit, and each contains 5 EF-hand motifs. Thus, these domains are referred to as 5-EF-hand, or penta EF-hand (PEF) domains. *In vitro* experiments together with 3D structural studies showed that only the first, second, and third EF-hands bind Ca^{2+}. The fifth EF-hand motif is involved in the dimerization of both subunits.

Domain V of the calpain regulatory subunit contains clusters of Gly making it hydrophobic. This domain is thought to interact with membrane and/or membrane proteins through hydrophobic interactions. Most of this domain is cut off by autolysis, indicating no involvement of this region in protease activity. In humans, the *CAPNS2* gene encodes a regulatory subunit homologue, whose physiological roles remain unclear.

Calpain Superfamily and Its Members

Classifications

As for calpain homologues other than conventional calpains, domains other than the protease domain are not necessarily conserved amongst homologues (Figure 1). Amino acid sequence identities of the protease domains vary, depending on the molecules, from less than 30% to more than 75%. Several kinds of domains, putatively originated from independent genes, exist in both N- and C-terminal parts of the protease domain. These include C2 and C2-like domains, a 5-EF-hand domain, a transmembrane domain, as well as conserved domains with unknown functions (SOH, PBH, etc). These features, together with the organization of mammalian calpain genes, strongly suggest that calpain molecules are the result of the combination of the gene for the ancestral calpain-type cysteine protease with genes encoding other functions.

These calpain homologues can be divided into two categories. The first group consists of molecules having domains II, III, and IV (the protease domain), and the C2-like and 5-EF-hand Ca^{2+}-binding domains. In other words, these group members have a "typical" structure highly similar to conventional calpain catalytic subunits. Beside mammalian μCL/CAPN1 and mCL/CAPN2, typical calpains include p94/CAPN3, nCL-2/CAPN8, nCL-4/CAPN9, CAPN11, and CAPN12. Chicken and *Xenopus laevis* are reported to additionally have μ/mCL. In invertebrates, only five typical calpains have been identified thus far. Three are found in *Drosophila melanogaster* as Dm-calpain (CALPA), CALPB, and CG-3692. *Schistosome mansoni* and

the N-terminal domain with little homology; IIa and IIb, the protease subdomains containing the active site Cys and His residues, respectively; III, the C2-like Ca2 + -binding domain; IV and VI, the 5-EF-hand Ca2 + -binding domain; V, Gly-rich hydrophobic domain; NS, IS1 and IS2, p94-specific sequences; T, TRA-3 subfamily-specific C2 domain; PBH, PalB subfamily homology domain; N, PalB subfamily N-terminal conserved domain; Zn, Zn-finger motif containing domain; SOH, SOL subfamily homology domain; DIS, CALPA-specific insertion sequence; TM, transmembrane domain; CSTN, the domain weakly similar to calpastatin.

S. japonicum also have at least one typical calpain (Sm-, and Sj-calpain). No typical calpain homologues have been found in *Caenorhabtisis elegans*, plants, fungi, trypanosomes, and *Saccharomyces cerevisiae*.

The second group contains various molecules that have the protease domain but do not have domains III or IV. Instead, some possess an extra domain(s) distinct from the known domains I to VI. Thus, these molecules are "atypical" calpain homologues. These atypical calpains are thought to have somewhat different functions compared with those of typical calpains. Atypical calpains include the TRA-3, SOL, and PalB subfamilies, the alternative splicing products of *Capn8* (nCL-2′) and *CalpA*, and others.

In addition to the structural features, independent classification is possible according to the localization of the expression. In mammals, μCL/CAPN1, mCL/CAPN2, PalBH/CAPN7, CAPN10, and CAPN13 are ubiquitously expressed, whereas p94/CAPN3, nCL-2/CAPN8, nCL-4/CAPN9, hTRA-3/CAPN5, CAPN6, 10, 11, and 12 are predominantly expressed in specific organs (Table I).

Structure and Functions of Calpain Superfamily Members

Skeletal Muscle-Specific Calpain, p94/CAPN3

p94/CANP3, the first tissue-specific calpain found in 1989, is ca. 60% identical to the large subunits of μ- and m-calpains, and has a conserved domain structure (Figure 1). Given that p94/CAPN3 contains three specific regions, NS, IS1, and IS2, it is often referred to as "calpain 3."

mRNA for p94/CAPN3 is expressed predominantly in skeletal muscle, and the amount expressed is approximately 10 times larger than that of conventional calpain. p94/CAPN3 possesses several unique properties. For example, p94/CAPN3 protein undergoes extremely rapid autolysis (half-life *in vitro* is less than 10 minutes), and this autolysis is obviated by deletion of the p94-specific region, IS1 or IS2. Specific inhibitors of μ- and m-calpains such as calpastatin, E-64, and leupeptin have no effect on autolysis. Furthermore, p94/CAPN3 possesses a nuclear localization signal-like sequence in IS2 and is localized in the nucleus in addition to the cytosol. p94/CAPN3 binds to gigantic muscle protein, connectin/titin, specifically through IS2. The protease activity of p94/CAPN3 should be regulated *in vivo*; however, the mechanism remains unclear. Connectin/titin is a candidate as a suppressor of p94/CAPN3 proteolytic activity.

Some alternative splicing products (Lp82) of *CAPN3* are specifically expressed in lenses. Lp82 showed Ca^{2+}-dependent protease activity against βA3 and αB crystallins. The activity is inhibited by E-64, but not by calpastatin. Some other splicing variants are expressed in embryonic skeletal muscles, although the physiological functions of these variants remain clear.

In 1995, mutations in *CAPN3* were shown to be responsible for limb-girdle muscular dystrophy type 2A (LGMD2A). Positions of the mutation found in the LGMD2A patients were distributed widely within *CAPN3*, with more than half of the mutations being missense mutations. No "hot point" was found, making its diagnosis very difficult. A primary cause of LGMD2A is a defect in protease activity, and not structural property, of p94.

nCL-2 and nCL-2′ (CAPN8)

nCL-2 and nCL-2′ are alternative splicing products of *CAPN8*, with and without C2-like and 5-EF-hand domains, respectively. They are predominantly expressed in the stomach. nCL-2 is highly similar to mCL/CAPN2 along the whole molecule (ca. 62% identical). Moreover, *CAPN8* and *CAPN2* are closely located, and their transcripts have overlap, i.e., complementary sequences. Recombinant nCL-2 and nCL-2′ proteins were expressed in *E. coli* and showed Ca^{2+}-dependent caseinolytic activities. *X. laevis* possesses an nCL-2 orthologue, xCL-2, the disruption of which causes severe developmental defects.

nCL-4/CAPN9

nCL-4/CAPN9 is a typical calpain homologue that is predominantly expressed in the digestive tract. It possesses overall similarity to μCL/CAPN1 and mCL/CAPN2, and requires 30K/CAPNS1 for its activity. Recombinant human nCL-4 + 30K protein showed Ca^{2+}-dependent caseinolytic activity, which was inhibited by calpastatin and other cysteine protease inhibitors, as in the case of conventional calpains. Involvement of nCL-4 in anti-tumorigenesis was reported in human gastric cancer and NIH3T3 transformation.

TRA-3 and Its Orthologues (TRA-3 Subfamily)

TRA-3 is involved in the sex determination cascade of *C. elegans*. Although enzymatic characterization of the purified enzyme has not yet been reported, protease activity of TRA-3 is Ca^{2+}-dependent and necessary for female development in XX hermaphrodites through the processing of TRA-2A membrane protein. Mammals possess two orthologues of TRA-3, hTRA-3/CAPN5, and CAPN6, whose amino acid sequences are more than 30% identical to that of TRA-3. The T domain, which is conserved in all three molecules, has weak similarity to the C2-domain. Surprisingly, CAPN6 apparently has no

active site residues (active site Cys is substituted with Lys), strongly suggesting that CAPN6 has no proteolytic activity.

Cpl1p, PalB, and its Orthologues (PalB Subfamily)

Cpl1p is the only calpain homologue found in *S. cerevisiae* and is considered both structurally and functionally to be the orthologue of Aspergillus PalB, which plays important roles in the adaptation of fungi to alkaline conditions. *CPL1*, also referred to as *RIM13*, is involved in both the alkaline adaptation and sporulation process of yeast through its processing activity. Rim101p and the Aspergillus orthologue PacC, are probable *in vivo* substrates for Cpl1p and PalB, respectively. Several other yeasts also have a Cpl1p orthologue. Cpl1p, PalB, and their orthologues share a somewhat conserved domain, the PalB homology domain (PBH). Mammals have one orthologue, PalBH/CAPN7, whose physiological functions are unknown.

Calpain 10/CAPN10

This homologue was identified by reverse genetics of non-insulin-dependent diabetes mellitus (NIDDM, type 2 diabetes). The single nucleotide polymorphism (SNP) in intron 3 of *CAPN10* is statistically related to a risk of NIDDM. This SNP probably affects transcription levels of *CAPN10*. *CAPN10* generates several alternative splicing products. The longest, CAPN10a, has two C2-like domains moderately and weakly similar to that of domain III. The physiological functions of calpain 10/CAPN10 are unclear.

SOL and its Orthologues (SOL Subfamily)

The Drosophila gene responsible for a defect in neuronal cells (small optic lobes) was positionally cloned and shown to encode a calpain homologue with several Zn-finger motifs located at the N-terminus. Mammals possess one orthologue, SOLH/CAPN15, while *C. elegans* has several. They share a conserved C-terminal structure called the SOL homology domain (SOH).

DEK1 and its Orthologues (DEK1 Subfamily)

The maize *defective kernel 1* gene required for aleurone cell development in the endosperm of maize grains revealed that it encodes a plant calpain homologue with 21 transmembrane regions located at the N-terminus and a C2-like domain, significantly similar to domain III, located at the C-terminus. Rice, Arabidopsis, and loblolly pine have very conserved orthologues (above 70% identity), and the whole genome sequence of Arabidopsis has revealed that DEK1 is the only calpain homologue in the genome. The structure and function of the DEK1 subfamily members are quite intriguing, and investigations have just begun.

Other Calpain Homologues

As described with the TRA-3 subfamily, some of the calpain homologues possess substituted residues in one of the very conserved active site residues, Cys, His, and Asn. Besides CAPN6 and Drosophila CG3692, some of the *C. elegans* homologues, and all of the trypanosome homologues, do not possess one or more of the active site residues. These molecules are thought not to possess Cys protease activity. Some of the *C. elegans* calpain homologues possess Gly-rich sequences, which is a characteristic of domain V of the calpain regulatory subunits (CAPNS1 and CAPNS2). Trypanosome calpains have N-terminal domains weakly similar to calpastatin. The physiological significance of these structural features has yet to be determined.

See Also the Following Articles

Calcium-Binding Proteins: Cytosolic (Annexins, Gelsolins, C_2-Domain Proteins) • Cysteine Proteases • Zinc Fingers

Glossary

C2 domain Common Ca^{2+}-binding structure composed of 8 antiparallel β-strand structures.

calpain homepage Calpain-related reagents are now available from several companies, which are summarized on the calpain homepage (http://ag.arizona.edu/calpains/reagents.html).

cysteine protease Peptide bond hydrolyzing enzyme whose active site is composed of a catalytically active Cys residue.

EF-hand motif Common Ca^{2+}-binding motif composed of 2 α-helices (E- and F-helices) and a Ca^{2+}-binding loop between.

LGMD2A Information on pathogenic mutations of LGMD2A is available in the Human Gene Mutation Database (http://archive.uwcm.ac.uk/uwcm/mg/search/119751.html).

muscular dystrophy Progressive deterioration of muscle tissue and resultant weakness caused by a defect of the number of muscle genes such as dystrophin, sarcoglycan, merosin, laminin, and calpain.

Further Reading

Glading, A., Lauffenburger, D. A., and Wells, A. (2002). Cutting to the chase: Calpain proteases in cell motility. *Trends Cell. Biol.* **12**, 46–54.

Goll, D. E., Thompson, V. F., Li, H., Wei, W., and Cong, J. (2003). The calpain system. *Physiol. Rev.* **83**, 731–801.

Huang, Y., and Wang, K. K. (2001). The calpain family and human disease. *Trends Mol. Med.* **7**, 355–362.

Khorchid, A., and Ikura, M. (2002). How calpain is activated by calcium. *Nat. Struct. Biol.* **9**, 239–241.

Maki, M., Kitaura, Y., Satoh, H., Ohkouchi, S., and Shibata, H. (2002). Structures, functions and molecular evolution of the

penta-EF-hand Ca^{2+}-binding proteins. *Biochim. Biophys. Acta.* **1600**, 51–60.

Margis, R., and Margis-Pinheiro, M. (2003). Phytocalpains: Orthologous calcium-dependent cysteine proteinases. *Trends Plant Sci.* **8**, 58–62.

Ono, Y., Sorimachi, H., and Suzuki, K. (1999). New aspect of the research on limb-girdle muscular dystrophy 2A: A molecular biologic and biochemical approach to pathology. *Trends Cardiovasc. Med.* **9**, 114–118.

Sorimachi, H., and Suzuki, K. (2001). The structure of calpain. *J. Biochem.* **129**, 653–664.

Sorimachi, H., Ishiura, S., and Suzuki, K. (1997). Structure and physiological function of calpains. *Biochem. J.* **328**, 721–732.

Suzuki, K., Hata, S., Kawabata, Y., and Sorimachi, H. (2002). Structure activation, and biology of calpain. *Diabetes* **53**, S12–18.

Biography

Hiroyuki Sorimachi is a Department Head of the Department of Enzymatic Regulation for Cell Functions, The Tokyo Metropolitan Institute of Medical Science (Rinshoken).

Yasuko Ono is a Chief Researcher in the Department of Enzymatic Regulation for Cell Functions, The Tokyo Metropolitan Institute of Medical Science (Rinshoken), devoting herself to the study of the role of calpains and the related molecules in muscle functions.

Carbohydrate Chains: Enzymatic and Chemical Synthesis

Thomas J. Tolbert and Chi-Huey Wong
Scripps Research Institute, La Jolla, California, USA

Carbohydrate chains play many important roles in biology, covering the surfaces of cells, mediating cell–cell recognition events, and forming major classes of biologically active molecules. Though carbohydrate chains are very important in biology, their study is frequently problematical because *in vivo* biosynthesis of carbohydrate chains often produces heterogeneous mixtures that are hard to purify in sufficient quantities for biochemical and structural studies. The *in vitro* enzymatic and chemical synthesis of carbohydrate chains offers another route to these interesting biomolecules that allows sufficient quantities of homogeneous oligosaccharides to be produced for biological studies.

Difficulties in the Synthesis of Carbohydrate Chains

The synthesis of oligosaccharides can present several technical difficulties that do not occur in the synthesis of other biopolymers. Unlike nucleic acids and proteins, the linkage between each subunit, i.e., sugar, of a carbohydrate chain forms a chiral center at the sugar's anomeric carbon that has two possible configurations, termed the α- or β-anomer (Figure 1B). Each time a sugar is joined to a carbohydrate chain through a glycosidic linkage, the stereochemistry of the bond that is formed must be controlled or directed in some manner to insure that the correct anomer is produced. In addition, carbohydrate chains are not just simple linear chains as DNA and proteins are, but can also be branched chains with increased complexity. Glycosidic linkages can be formed through each hydroxyl of a sugar, and when multiple hydroxyls on a single sugar form glycosidic linkages, branched oligosaccharide structures result. Distinguishing between the different hydroxyl moieties on sugars is another difficulty of carbohydrate chain synthesis. Each sugar of a carbohydrate chain can have several hydroxyl moieties that are nearly equivalent in chemical reactivity, making them difficult to differentiate from one another and adding several steps to most chemical syntheses. To overcome these difficulties, several enzymatic and chemical methods have been developed.

Enzymatic Synthesis of Oligosaccharides

Enzymes have frequently been employed to synthesize carbohydrate chains, because they offer a few technical advantages over traditional organic synthesis. Enzymes generally do not require protecting groups to select the correct chemical moiety on their substrates, and in carbohydrate chain synthesis this is a great advantage. The many nearly chemically equivalent hydroxyl moieties of sugars make selective chemical protection of sugar hydroxyls a laborious task. The use of enzymes in carbohydrate chain synthesis can eliminate the need for both selective hydroxyl protection before forming the glycosidic linkage, and removal of the protecting groups after forming the glycosidic linkage, greatly reducing the number of steps required for synthesis of an oligosaccharide. Another advantage of the use of enzymes in carbohydrate chain synthesis is the stereoselectivity of glycosidic bond-forming enzymes, which often produce a single anomer during the formation of a glycosidic bond. In contrast, chemical methods frequently produce mixtures of anomers during glycosidic bond formation, which must be purified from one another after formation of the glycosidic bond. Though enzymatic synthesis of oligosaccharides has many advantages, it is often limited by the availability of specific enzymes needed to form certain types of carbohydrate structures, but with the increased number of enzymes being discovered by genomic research this should improve in the future. Two classes of enzymes that have been used to form carbohydrate chains will be discussed further below, glycosidases and glycotransferases.

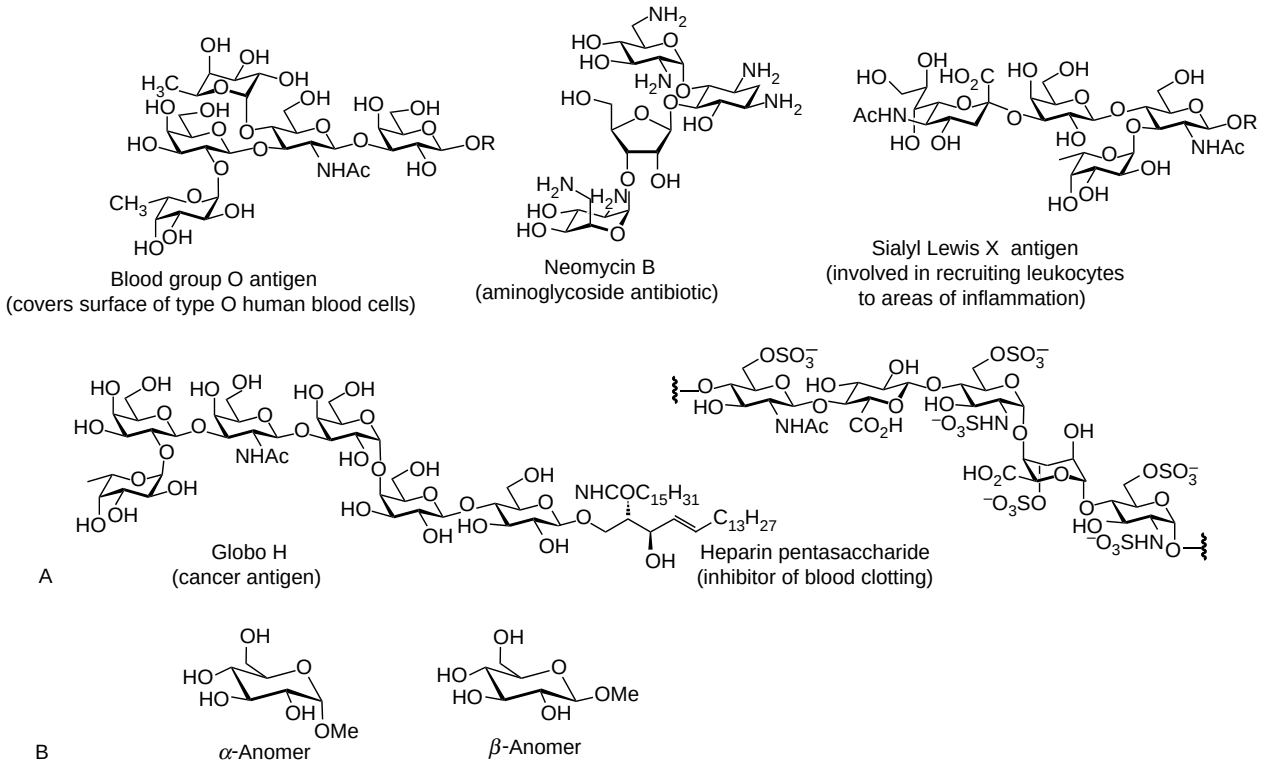

FIGURE 1 Carbohydrate chains: (A) some biologically important oligosaccharides and (B) 1-O-methyl-glucopyranosides, α- and β-anomers.

Carbohydrate Chain Synthesis Utilizing Glycosidases

Glycosidases are enzymes that normally break glycosidic bonds during glycoprocessing or catabolism of oligosaccharides, but by placing glycosidases under certain controlled reaction conditions they can be utilized to form, rather than break, glycosidic bonds. Most often, glycosidases are used to form glycosidic bonds in transglycosylation reactions, where a glycosidic bond is broken in a glycosyl donor glycoside, and a new glycosidic bond is formed with a glycosyl acceptor (Figure 2A). Several approaches can be utilized to favor formation of the desired glycosidic bond, including the use of activated glycosyl donors such as *p*-nitrophenyl glycosides, elevated concentrations of glycosyl donors and acceptors, organic cosolvents, and the use of mutated glycosidases with reduced hydrolysis activity. The use of glycosidases to form glycosidic bonds generally results in low to medium yields ranging from 20% to 40%, although yields as high as 90% have been reported using mutated glycosidases. Glycosidase catalyzed synthesis generally has good stereoselectivity, forming a single α- or β-anomer, but sometimes has low regioselectivity for the different hydroxyls on the acceptor sugar resulting in multiple products being formed. Though glycosidase reactions can suffer from low yield and low regioselectivity, there is a wide range of glycosidases available to catalyze the formation of many different types of glycosidic linkages.

Carbohydrate Chain Synthesis Utilizing Glycotransferases

Glycotransferases are enzymes that catalyze the transfer of activated monosaccharide donors to carbohydrates during the biosynthesis of oligosaccharides. They are very useful in synthesizing oligosaccharides *in vitro* because they exhibit high regioselectivity and stereoselectivity in the formation of glycosidic bonds. Glycotransferases that utilize nucleotide sugars as activated monosaccharide donors have been used most often in the *in vitro* synthesis of carbohydrate chains (Figure 2B). A wide variety of oligosaccharide structures can be produced using the available glycotransferases and activated nucleotide sugars such as UDP-glucose (UDP-Glc), UDP-N-acetylglucosamine (UDP-GlcNAc), UDP-galactose (UDP-Gal), UDP-N-acetylgalactosamine (UDP-GalNAc), UDP-glucuronic acid (UDP-GlcUA), GDP-mannose (GDP-Man), GDP-fucose (GDP-Fuc), and CMP-sialic acid (CMP-NeuAc). Generally, each glycotransferase is selective for a specific

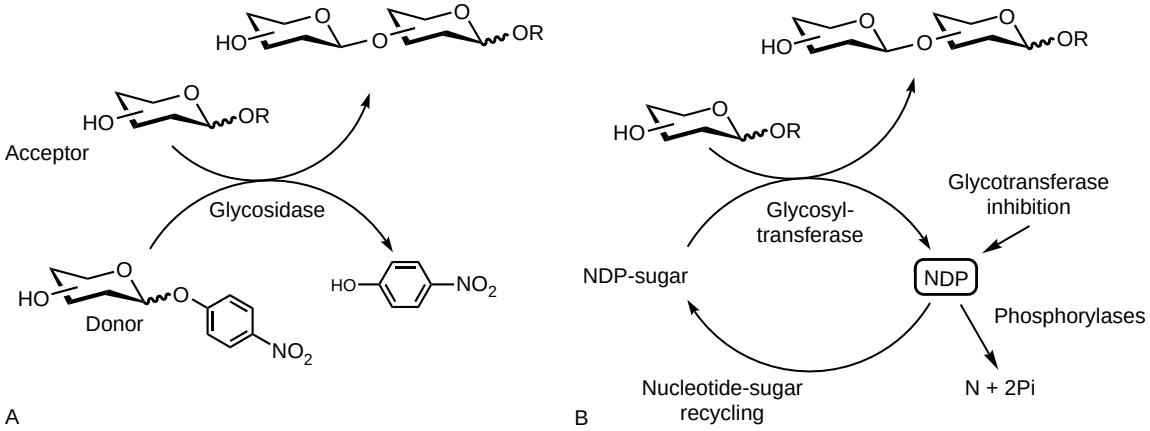

FIGURE 2 Enzymatic synthesis of oligosaccharides using: (A) glycosidases and (B) glycotransferases.

nucleotide-sugar donor, and also has specificity for certain oligosaccharide structures in its substrates. Because of this it is often difficult to make unnatural oligosaccharides using glycotransferases, but in some cases relaxed substrate and nucleotide-sugar specificity has been utilized to make unnatural carbohydrate chains. Formation of oligosaccharides with glycotransferases requires the substrate oligosaccharide, manganese, the nucleotide-sugar donor, and the glycotransferase itself in an appropriate buffer. Glycotransferase-catalyzed synthesis of carbohydrate chains usually results in high yields, approaching 100%, but the enzymatic reaction can suffer from product inhibition that has to be overcome to achieve those high yields. The use of glycotransferases in oligosaccharide synthesis is limited by the high cost of nucleotide sugars and the availability of glycotransferases that form certain oligosaccharide structures. Sugar-nucleotide recycling alleviates some of the former problem while genomic sequencing and research has started to alleviate some of the latter problem.

Product Inhibition in Glycotransferase Reactions

Though glycotransferases can be used to form oligosaccharides in nearly 100% yield, they suffer from product inhibition from the nucleoside diphosphates and nucleoside monophosphates that are produced as the activated nucleotide-sugar donors are transferred to the growing carbohydrate chain. This product inhibition can drastically slow the enzymatic reaction and also reduce the yield of product, and so it is desirable to remove the nucleotide by-products of the glycotransferase reactions. Two approaches can be used to overcome product inhibition in glycotransferase reactions use of phosphorylases and nucleotide-sugar recycling (Figure 2B).

Reduction of Glycotransferase Inhibition with Phosphorylases Nucleoside diphosphates and monophosphates can be converted into nucleosides, which do not inhibit glycotransferases, using phosphorylases. This is a very simple method, which requires only one or two additional enzymes to be added to the glycotransferase reaction. Unfortunately this method requires a stoichiometric amount of nucleotide-sugar donor for formation of the desired oligosaccharide, which can be quite costly on larger scales since nucleotide sugars are generally very expensive.

Reduction of Glycotransferase Inhibition with Nucleotide-Sugar Recycling Another method to remove nucleotide by-products of glycotransferase reactions is to regenerate the nucleotide-sugar donors from the nucleotide by-products using an enzymatic recycling reaction. This method of overcoming product inhibition is somewhat more complicated than using phosphorylases, requiring several additional enzymes for the nucleotide-sugar recycling reaction, but it allows a catalytic amount of nucleotide-sugar donor to be used in the glycotransferase reaction. Since nucleotide-sugars are generally expensive, this method is desirable for larger-scale glycotransferase reactions.

Chemical Synthesis of Oligosaccharides

Chemical synthesis of oligosaccharides is often the method of choice for constructing carbohydrate chains because chemical methods are flexible, can be used to produce both natural and unnatural oligosaccharides, and are also not limited by the availability of specific enzymes. Formation of glycosidic bonds by chemical methods usually relies upon activation of a leaving group on the anomeric carbon of a glycosyl donor with a

Lewis acid, which once activated will react with a free hydroxyl upon a glycosyl acceptor (Figure 3A). A wide variety of glycosyl leaving groups have been utilized for carbohydrate chain synthesis some of which are shown in Figure 3B.

Control of Stereochemistry in Chemical Glycosidic Bond Formation

Control of the stereochemistry of the anomeric linkage in the products of glycosylation reactions can be very complex, and many factors including types of protecting groups on the sugars, solvent, temperature, and leaving groups can be used to influence the α/β ratio of the products formed in glycosylation reactions. In general, the anomeric effect, stabilization of axial orientation over equatorial orientation of electron withdrawing groups attached to the C1 of pyranose sugars, can be utilized to produce α-linked glucosides and galactosides. Participation of protecting groups of the 2-OH, such as acetate, and the use of polar solvents in glycosylation reactions can direct products toward β-linked glucosides and galactosides through dioxocarbenium or solvent intermediates (Figure 3A). Sometimes it is difficult to obtain the desired anomer using chemical synthesis, as in the case of sialic acid glycosides, where the natural sialic acid linkage is exclusively the α-anomer, but the β-anomer is obtained from most chemical glycosylation reactions. Controlling the anomeric outcome of chemical glycosylation reactions can still be a difficult problem, and requires several approaches for different types of glycosidic linkages and sugars.

Protection of Sugar Hydroxyls in Chemical Carbohydrate Synthesis

Chemical oligosaccharide synthesis relies heavily upon sugar protecting groups to both distinguish between sugar hydroxyls with similar chemical reactivity and also to control the stereochemical outcome, either α or β, of glycosylation reactions. Because of this, chemical oligosaccharide synthesis typically requires a large amount of protecting group manipulations. Normally, protecting groups must be placed on hydroxyls that are not going to be used to form glycosidic linkages to prevent them from reacting in glycosylation reactions. In addition, the synthesis of carbohydrate chains longer than two sugars requires sugar subunits that can act both as glycosyl donors and acceptors, and this usually requires selective protection and deprotection of the hydroxyls that are to form glycosidic linkages. Selective protection of sugar subunits for glycosylation reactions often requires many chemical steps to produce each selectively protected subunit for the synthesis of an oligosaccharide, and this is one factor that can contribute to the large number of steps required for chemical oligosaccharide syntheses. Some protecting groups commonly used in chemical carbohydrate chain synthesis include benzyl ethers, *p*-methoxybenzyl ethers, *tert*-butyl-diphenylsilyl ethers, *tert*-butyl-dimethylsilyl ethers, allyl ethers, acetate esters, benzoate esters, levulinoyl esters, and dimethyl acetals.

Solution Phase Chemical Oligosaccharide Synthesis

In conventional solution-phase oligosaccharide synthesis, a donor sugar is activated by a Lewis acid at the anomeric carbon, and then reacted with an acceptor

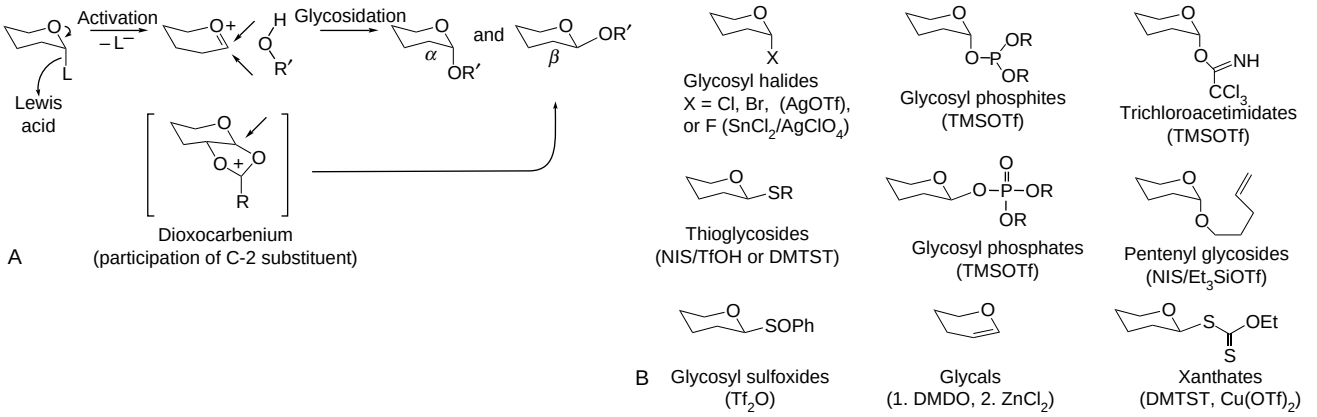

FIGURE 3 Chemical glycosylation reactions. (A) Mechanism of glycosylation. (B) Some commonly used glycosylation leaving groups and the reagents used to activator them (in parentheses). Abbreviations: L, leaving group; R, variable group; TMSOTf, trimethylsilyl triflate; NIS, N-iodosuccinimide; TfOH, triflic acid; Et_3SiOTf, triethylsilyl triflate; Tf_2O, triflic anhydride; DMDO, 3,3-dimethyldioxirane; DMTST, dimethylthiosulfonium triflate.

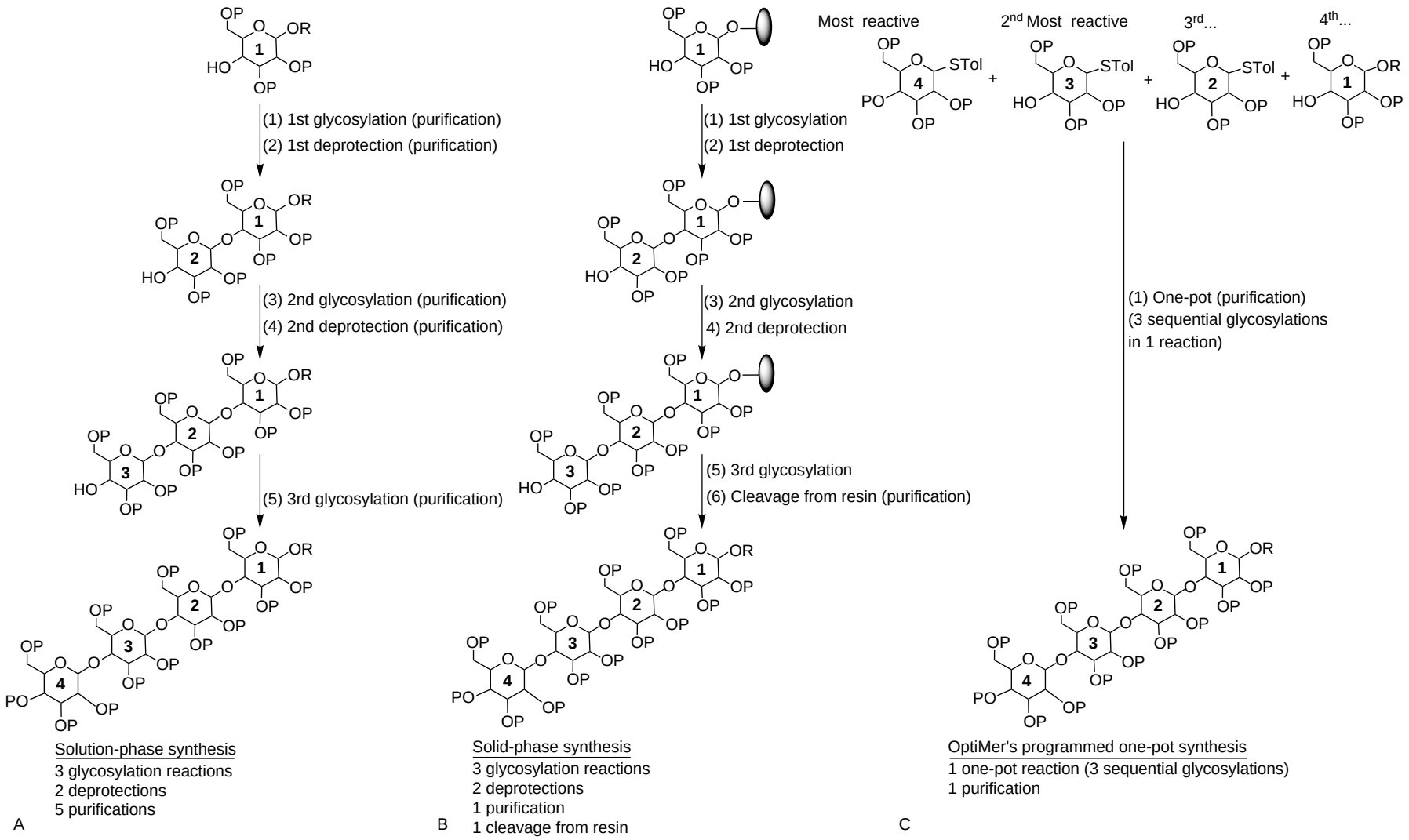

FIGURE 4 Chemical synthesis of oligosaccharides: (A) solution-phase synthesis, (B) solid-phase synthesis, and (C) OptiMer's programmed one-pot synthesis.

sugar that contains a free hydroxyl. Once the glycosidic bond has been formed, the product disaccharide must be purified away from other glycosylation reaction reagents and side products, and then selectively deprotected to unmask a single hydroxyl so that it can then act as a glycosyl acceptor in the next glycosylation reaction (Figure 4A). Purification is often necessary after each glycosylation and deprotection step in the preparation of an oligosaccharide by solution phase synthesis. When combined with the number of steps necessary to produce selectively protected sugar subunits, the number of chemical steps and purifications necessary to construct even small oligosaccharides can be very large.

Automated Oligosaccharide Synthesis

Because of the large amount of work necessary to construct even relatively small oligosaccharides by solution-phase synthesis, many approaches toward automating oligosaccharide synthesis have been developed in hopes of minimizing the number of chemical steps and purifications required to synthesize oligosaccharides. Two approaches to automated oligosaccharide synthesis will be discussed below: solid-phase oligosaccharide synthesis and programmable one-pot oligosaccharide synthesis.

Solid-Phase Chemical Oligosaccharide Synthesis

In solid-phase oligosaccharide synthesis, either the glycosyl donor or acceptor of a glycosylation reaction is attached to the solid phase. The advantage of this is that large excesses of the other components of the glycosylation reaction can be used to increase the rate of the reaction and insure that it goes to completion, and then rinsed away by simple filtration. This has the potential of increasing the yield of glycosylation reactions and also eliminates many of the laborious purification steps that are necessary in solution-phase oligosaccharide synthesis (Figure 4B). Unfortunately there are many technical difficulties that must be overcome to successfully apply solid-phase synthesis to the production of oligosaccharides. Solid supports that function well with many solvents must be selected, since a wide variety of solvents are used to affect the outcome of glycosylation reactions. Linkers must be developed that are not sterically hindering for glycosylation reactions, stable to glycosylation conditions, and easily cleaved after the oligosaccharide has been synthesized. Strategies for protecting sugar monomers that allow highly flexible and selective deprotection of sugar hydroxyl groups in the presence of many other protected hydroxyls must be worked out. Since the reaction conditions of glycosidic bond formation can vary widely depending on oligosaccharide structure and the types of glycosidic linkages to be formed, there has been great difficulty in developing broadly applicable general methods for solid-phase oligosaccharide synthesis. Nevertheless, there have been many notable examples of successful solid-phase syntheses including the synthesis of a dodecasaccharide by both the Nicolaou and Seeberger groups.

Programmable One-Pot Oligosaccharide Synthesis

One-pot reaction approaches that involve conducting several sequential glycosylation reactions in one reaction flask have been developed to facilitate automated oligosaccharide synthesis. The one-pot approach relies upon using a reactivity profile of protected sugars to determine what sequence of sugars to add to glycosylation reactions to obtain the desired products. Protected sugars are added to one-pot reactions in the order of most reactive to least reactive, thereby controlling the order of glycosidic bond formation during the synthesis of carbohydrate chains (Figure 4C). Since it has been shown that the types of protecting groups and type of anomeric activating groups used on sugars can greatly alter the speed at which a sugar will react in a glycosylation reaction, a wide range of reactivities can be obtained for a single type of sugar, allowing wide flexibility in oligosaccharide synthesis using this approach. The one-pot approach greatly reduces the number of steps necessary to construct oligosaccharides and eliminates several tedious purifications by combining multiple glycosylation reactions into a single one-pot reaction. The one-pot approach also minimizes protecting group manipulations, eliminating protecting group manipulations after construction of the building blocks. A large number of *p*-methylphenyl thioglycosides have been synthesized and had their reactivities measured to facilitate the use of this strategy. A computer program, OptiMer, has been developed that uses these *p*-methylphenyl thioglycosides as a set of building blocks to choose from to build oligosaccharides. When a carbohydrate chain structure is entered as input, the OptiMer program will calculate the best set of reactants for the construction of that carbohydrate chain. Because the programmable one-pot strategy requires a minimum of protecting group manipulations and has a large library of building blocks, a wide range of oligosaccharide structures can be synthesized rapidly using this method.

See Also the Following Articles

Enzyme Reaction Mechanisms: Stereochemistry • Oligosaccharide Chains: Free, *N*-Linked, *O*-Linked

Glossary

anomeric carbon The carbon of a cyclic sugar which forms a hemiacetal or hemiketal. In the linear form of the sugar, the carbon that will become the anomeric carbon when the sugar cyclizes is the carbonyl carbon.

anomeric effect The stabilization of axial orientation over equatorial orientation of electron withdrawing groups attached to the C1 of pyranose sugars.

anomers The pair of diastereomers, termed the α- or β-anomer, that results when a linear sugar forms a cyclic hemiacetal or hemiketal.

glycosidic linkage The linkage formed between the anomeric carbon of a sugar and an alcohol.

Further Reading

Koeller, K. M., and Wong, C.-H. (2000). Synthesis of complex carbohydrates and glycoconjugates: Enzyme-based and programmable one-pot strategies. *Chem. Rev.* **100**, 4465–4493.

Nicolaou, K. C., Watanabe, N., Li, J., Pastor, J., and Winssinger, N. (1998). Solid-phase synthesis of oligosaccharides: Construction of a dodecasaccharide. *Angew. Chem. Int. Ed.* **37**, 1559.

Plante, O. J., Palmacci, E. R., and Seeberger, P. H. (2001). Automated solid-phase synthesis of oligosaccharides. *Science* **291**, 1523.

Sears, P., and Wong, C.-H. (2001). Toward automated synthesis of oligosaccharides and glycoproteins. *Science* **291**, 2344–2350.

Seeberger, P. H., and Haase, W.-C. (2000). Solid-phase oligosaccharide synthesis and combinatorial carbohydrate libraries. *Chem. Rev.* **100**, 4349–4393.

Varki, A., Cummings, R., Esko, J., Freeze, H., Hart, G., and Marth, J. (eds.) (1999). *Essentials of Glycobiology.* Cold Spring Harbor Laboratory Press, Cold Spring Harbor.

Wong, C.-H., Halcomb, R. L., Ichikawa, Y., and Kajimoto, T. (1995). Enzymes in organic synthesis: Application to the problems of carbohydrate recognition: Part 1. *Angew. Chem. Int. Ed.* **34**, 412–432.

Wong, C.-H., Halcomb, R. L., Ichikawa, Y., and Kajimoto, T. (1995). Enzymes in organic synthesis: Application to the problems of carbohydrate recognition: Part 2. *Angew. Chem. Int. Ed.* **34**, 521–546.

Zhang, Z., Ollman, I. R., Ye, X.-S., Wischnot, R., Baasov, T., and Wong, C.-H. (1999). Programmable one-pot digosaccharide synthesis. *J. Am. Chem. Soc.* **121**, 734.

Biography

Thomas J. Tolbert is an Assistant Professor at Indiana University. His principal research interests lie in the use of chemical and enzymatic synthesis to solve biological problems. He holds a Ph.D. in Biochemistry from MIT, and a B.S. degree in chemistry from Purdue University.

Chi-Huey Wong is Professor and Ernest W. Hahn Chair in Chemistry at the Scripps Research Institute and also a Member of the Skaggs Insitute for Chemical Biology. His principal research interests are in the areas of bioorganic and synthetic chemistry and biocatalysis, with particular focus on development of new chemoenzymatic methods to tackle major problems in carbohydrate-mediated biological recognitions. He received his B.S. and M.S. degrees from National Taiwan University, and Ph.D. in Chemistry from Massachusetts Institute of Technology. He is a Member of the National Academy of Sciences.

Carnitine and β-Oxidation

Janos Kerner and Charles L. Hoppel
Case Western Reserve University School of Medicine, Louis Stokes VA Medical Center, Cleveland, Ohio, USA

Carnitine is derived from the essential amino acids lysine and methionine. It is ubiquitous in nature, found in especially high concentration in muscle tissue of higher organisms. It functions as a transport vehicle for activated fatty acids of different chain length through membranes within the cell. This transport function is best characterized in mitochondrial oxidation of long-chain fatty acids. This latter process, also known as mitochondrial β-oxidation, represents the repetitive oxidative cleavage of long-chain fatty acids into two-carbon units, acetyl-CoA. Acetyl-CoA is then either further oxidized for energy production (all tissues) or used to synthesize ketone bodies (liver) as metabolic fuel for peripheral tissues.

Carnitine Biosynthesis and Homeostasis

The first clue about the physiological function of carnitine (Figure 1) came from studies in the mealworm, *Tenebrio molitor*, that suggested that carnitine plays a vital function in fat catabolism. However, carnitine is not a vitamin for higher animals; the daily need is met by endogenous synthesis and dietary intake, mostly from meat products. For endogenous synthesis, the ultimate precursors are the essential amino acids lysine and methionine. Protein-bound lysine is methylated to trimethyllysine using S-adenosylmethionine; following liberation by proteolysis, the free trimethyllysine is converted (mostly in muscle) by a series of reactions to butyrobetaine, the ultimate carnitine precursor. Although most tissues are capable of synthesizing butyrobetaine, the hydroxylation of butyrobetaine to carnitine is restricted to the liver (and to a lesser extent to the kidney and brain). Following release of carnitine from the liver into the plasma, carnitine is taken up by other tissues in a carrier-mediated transport process (Figure 2).

The body distribution of carnitine is determined by a series of systems that transport carnitine into cells against a concentration gradient, an independent efflux process, and an exchange mechanism in a tissue-specific fashion. Under physiological conditions, plasma carnitine concentration is maintained within a narrow range, predominantly by renal clearance, which is determined by the kinetic properties of carnitine transport system in the brush border.

Functions of Carnitine

In higher animals, the only reaction carnitine undergoes is a reversible transesterification with acyl-CoAs catalyzed by carnitine acyltransferases of differing chain length specificity (carnitine acetyl-, octanoyl-, and palmitoyltransferases) (Figure 3).

All known functions of carnitine are based on the reversible transesterification with acyl-CoA esters. The physiologically most important and therefore best studied metabolic pathway in which carnitine plays a significant role is the mitochondrial oxidation of long-chain fatty acids.

Mitochondrial β-Oxidation

Cellular Uptake and Activation of Long-Chain Fatty Acids

Long-chain fatty acids represent a main energy source for many organs, especially for muscle (heart and skeletal) and liver. Since most tissues contain only small amounts of storage lipids, for energy production they depend on a continuous supply of fatty acids, mostly from adipose tissue. Following mobilization by lipolysis in adipose tissue and transport in the blood bound to albumin, fatty acids are taken up by the tissues in a process mediated by transport proteins present in the plasma membrane. Once within the cell, free fatty acids are bound to fatty acid binding proteins, which are present in the cytosol in large amounts. Depending on the tissue and its metabolic demand, fatty acids are converted to triglycerides and stored, secreted as very-low-density lipoproteins (liver), or oxidized in the mitochondria for energy production. Before being directed into storage or oxidation, fatty acids first are activated to acyl-CoA esters. This reaction is catalyzed by long-chain acyl-CoA synthetase, an enzyme present in abundance both in microsomes and in mitochondria. In mitochondria, long-chain acyl-CoA synthetase is

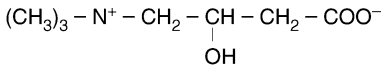

FIGURE 1 Structure of L-carnitine (4-N-trimethylammonio-3-hydroxybutanoate).

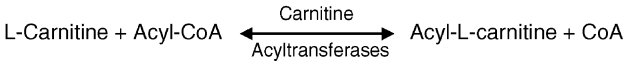

FIGURE 3 Reversible transesterification of carnitine catalyzed by carnitine acyltransferases with different chain-lengths specificity.

associated with the mitochondrial outer membrane and appears to be a transmembrane protein with its active site exposed to the cytosol. This orientation of long-chain acyl-CoA synthetase gives rise to cytosolic production of long-chain acyl-CoAs, which for their further β-oxidation must cross both mitochondrial boundary membranes. Although the impermeability of the inner membrane to metabolites is well known, it is now recognized that the outer membrane is not freely permeable to solutes as previously thought. A potential route for long-chain acyl-CoAs to cross the outer membrane is the voltage-dependent, anion-selective channel (VDAC), also called mitochondrial porin, which occurs at high density in the mitochondrial outer membrane and regulates the permeability of this membrane to ions and metabolites (Figure 4).

Mitochondrial Uptake of Activated Fatty Acids: The Mitochondrial Carnitine System

The mitochondrial carnitine system plays an obligatory role in β-oxidation of long-chain fatty acids by providing a means for their transport into the mitochondrial matrix. This transport system consists of the malonyl-CoA sensitive carnitine palmitoyltransferase-I (CPT-I) localized in the mitochondrial outer membrane, the carnitine:acylcarnitine translocase, an integral inner membrane protein, and carnitine palmitoyltransferase-II (CPT-II) localized on the matrix side of the inner membrane. In the schema depicted in Figure 4, the catalytic site of CPT-I faces the intermembrane space. In an alternative model, the catalytic site of CPT-I faces the cytosol. In this scenario, the carnitine esters must cross both mitochondrial membranes. In either case, transesterification of long-chain acyl-CoA esters to their carnitine esters by CPT-I commits activated fatty acids to oxidation in the mitochondrial matrix.

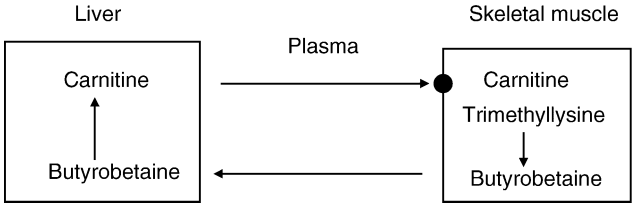

FIGURE 2 Interorgan relationship in carnitine biosynthesis.

CPT-I, by virtue of its inhibition by malonyl-CoA, represents a key regulatory site controlling the flux through β-oxidation. Consistent with its central role in mitochondrial fatty acid oxidation, the enzyme exists in at least two isoforms with significantly different kinetic and regulatory properties. The liver type displays a higher affinity for carnitine and a lower affinity for the physiological inhibitor, malonyl-CoA, as opposed to the muscle isoform. Long-term regulation of both isoforms is accomplished at the transcriptional level. Short-term or acute regulation is achieved via changes in tissue malonyl-CoA concentration, and for the liver isoform also via changes in the enzyme's sensitivity to malonyl-CoA inhibition.

The long-chain acylcarnitines formed by CPT-I in the mitochondrial outer membrane enter the mitochondrial matrix in exchange for free carnitine catalyzed by the carnitine:acylcarnitine translocase, an integral inner membrane protein. The carnitine:acylcarnitine translocase catalyzes a homologous/heterologous carnitine exchange (in addition to the slow unidirectional carnitine transport) and displays increasing affinity for carnitine esters with increasing acyl chain length. Experimental data suggest the existence of a single transporter protein with a substrate specificity ranging

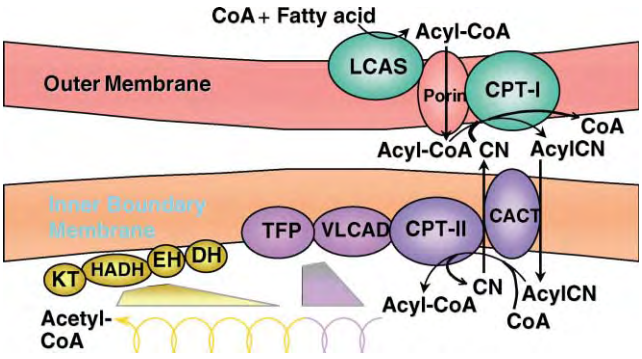

FIGURE 4 Schematic depiction of the carnitine-dependent transport of activated fatty acids into the mitochondrial matrix and of their oxidative chain shortening via the β-oxidation pathway. CACT, carnitine:acylcarnitine translocase; CN, carnitine; CPT-I, malonyl-CoA sensitive carnitine palmitoyltransferase; CPT-II, malonyl-CoA insensitive carnitine palmitoyltransferase; DH, acyl-CoA dehydrogenase; EH, enoyl-CoA hydratase; HADH, 3-hydroxyacyl-CoA dehydrogenase; KT, 3-ketoacyl-CoA thiolase; LCAS, long-chain acyl-CoA synthetase; TFP, trifunctional protein; VLCAD, very-long-chain acyl-CoA dehydrogenase.

from free carnitine to long-chain carnitine esters. This is in contrast to the known substrate specificity of the mitochondrial carnitine acyltransferases (carnitine palmitoyl- and acetyltransferase) and implies that in addition to its role in mitochondrial fatty acid oxidation, the same transporter also is engaged in other functions involving membrane transport of acyl groups.

Following the translocation of long-chain acylcarnitines by carnitine:acylcarnitine translocase into the mitochondrial matrix, the carnitine esters are reconverted to their respective CoA esters by CPT-II, thus completing the carnitine-dependent uptake of activated fatty acids. Within the matrix, CPT-II is anchored to the inner membrane as a peripheral membrane protein. The enzyme has been isolated in catalytically active form from a variety of tissues, and its physical, kinetic, and immunological properties have been determined. CPT-II is the product of a single gene and is expressed as the same protein in all tissues within the body. It is not inhibited by malonyl-CoA, either in its native environment (membrane-bound) or when isolated.

Pathway of Mitochondrial β-Oxidation

In the fatty acid oxidation cycle, the activated long-chain fatty acid undergoes a consecutive oxidative chain shortening. Each cycle of this sequence of four reactions results in the removal of two-carbon atoms from the fatty acyl residue in the form of acetyl-CoA (Figures 4 and 5) and two reducing equivalents (FADH and NADH). Thus, the complete oxidation of palmitoyl-CoA requires seven cycles, yielding eight acetyl-CoAs and seven FADH and NADH. Acetyl-CoA is then further oxidized in the tricarboxylic acid cycle to CO_2 and reducing equivalents, each acetyl-CoA yielding three NADH and one FADH. The reoxidation of these reducing equivalents in the electron transport chain then produces ATP. The complete oxidation of 1 mole palmitic acid thus results in the formation of 131 moles ATP. On a molar basis, this is 3.6 times more ATP generated (on a weight basis, 2.5 times more) compared to an equivalent amount of glucose.

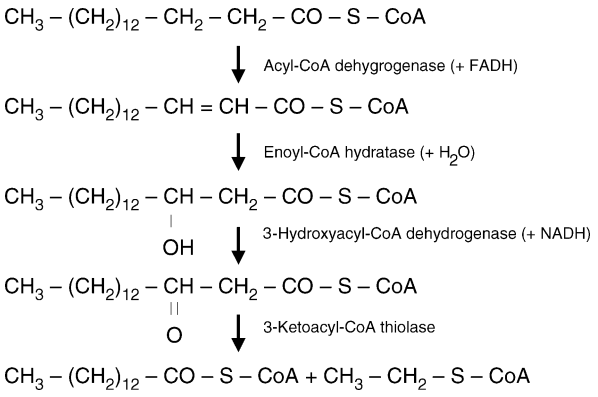

FIGURE 5 Reactions of mitochondrial β-oxidation of saturated long-chain acyl-CoAs.

The first of the four reactions in mitochondrial β-oxidation of activated long-chain fatty acids is catalyzed by the acyl-CoA dehydrogenases, a group of enzymes with differing but somewhat overlapping chain-length specificity (very-long-chain, long-chain, medium-chain, and short-chain), resulting in the formation of 2-*trans*-enoyl-CoA. They are composed of four identical subunits, each of which contains a non-covalently bound flavin adenine dinucleotide (FAD). The enzyme is reoxidized via the electron-transferring flavoprotein and then in the electron transport chain by electron-transferring flavoprotein:ubiquinone oxidoreductase.

The second step of β-oxidation is catalyzed by 2-enoyl-CoA hydratases converting 2-*trans*-enoyl-CoA to 3-hydroxyacyl-CoA. This reaction is catalyzed by the membrane-bound long-chain trifunctional protein TFP, formerly known as the long-chain enoyl-CoA hydratase. The TFP is composed of two nonidentical subunits, the α and β subunits, present in a 1:1 molar ratio. The enzyme comprises the catalytic activities of 2-enoyl-CoA hydratase and 3-hydroxyacyl-CoA dehydrogenase (α subunit) and 3-ketoacyl-CoA thiolase (β subunit). The soluble short-chain specific form, also known as crotonase, catalyzes the hydration of short-chain 2-enoyl-CoAs.

The third reaction is catalyzed by 3-hydroxyacyl-CoA dehydrogenases. At least two 3-hydroxyacyl-CoA dehydrogenase activities are found in the mitochondria. In addition to the TFP, there also is a short-chain specific form. The latter is composed of two identical subunits. Both activities require NAD as a cofactor. The NADH formed is then reoxidized by complex I of the electron transport chain.

The last reaction of the β-oxidation spiral is the thiolytic cleavage of 3-ketoacyl-CoA catalyzed by 3-ketoacyl-CoA thiolases. The general acyl-CoA thiolase and the long-chain 3-ketoacyl thiolase of the TFP have overlapping substrate specificities. The reaction is greatly in favor of product formation. There also is a third thiolase enzyme present in mitochondria called acetyl-CoA acetyltransferase or acetoacetyl-CoA thiolase. This enzyme is specific for acetoacetyl-CoA and 2-methylacetoacetyl-CoA and probably is involved in branched-chain amino acid metabolism, in ketogenesis, and in ketone body utilization.

The oxidation of (poly)unsaturated fatty acids requires auxiliary enzymes for their complete β-oxidation. Most unsaturated fatty acids have their double bonds in *cis* configuration with the first double bond between carbon atoms 9 and 10. Additional double bonds, if any, occur at three-carbon intervals.

Several cycles of β-oxidation yield a chain-shortened acyl-CoA with a *cis* double bond in 3, 4 position that is not a substrate for enoyl-CoA hydratase. Isomerization catalyzed by 2,3-enoyl-CoA isomerase leads to 2-*trans*-enoyl-CoA, which can undergo further β-oxidation, yielding after two additional cycles *trans*-2, *cis*-4-dienoyl-CoA, which also is a poor substrate for enoyl-CoA hydratase. The *cis*-4 double bond is reduced by the enzyme 2,4-dienoyl-CoA reductase, producing *trans*-3-enoyl-CoA, which is isomerized to *trans*-2-enoyl-CoA by 2,3-enoyl-CoA isomerase.

The rate of β-oxidation is adjusted to physiological needs and is subject to control in which substrate supply is important. The reaction catalyzed by CPT-I committing activated fatty acids toward oxidation in the mitochondria often is considered rate limiting. The regulatory property that imparts such control to this otherwise near-equilibrium reaction is the inhibition of CPT-I by malonyl-CoA. The muscle isoform of CPT-I is extremely sensitive to inhibition by malonyl-CoA, and it is thought that in heart and skeletal muscle, CPT-I is regulated only by changes in tissue malonyl-CoA concentrations. The liver isoform of CPT-I is much less sensitive to malonyl-CoA inhibition, and in liver the entry of activated fatty acids into the mitochondria is controlled by changes in the enzyme's sensitivity to malonyl-CoA as well as by changes in hepatic malonyl-CoA concentrations.

Although the mitochondrial uptake of long-chain activated fatty acids is absolutely carnitine dependent, the efficiency of the system is such that under physiological conditions, tissue carnitine concentrations seemingly have no significant impact on this process.

The control of β-oxidation flux by the redox state of NAD/NADH and FAD/FADH (ETF/$ETFH_2$) as well as by the acetyl-CoA/CoA ratio is important under some conditions.

Regulation of Mitochondrial Acyl-CoA/CoA Ratio

β-oxidation is not the only pathway in which carnitine plays a role as a carrier of activated acyl groups. In conjunction with carnitine acetyltransferase and carnitine:acylcarnitine translocase, carnitine forms an effective shuttle system for acetyl groups out of the mitochondria, thus preventing sequestration of intramitochondrial free CoA. This acetyl-CoA buffer function allows CoA-dependent reactions such as pyruvate oxidation to proceed unimpaired. The CoA buffer function is not restricted to acetyl-CoA. Under normal physiological conditions, long-chain fatty acid movement is directed into the mitochondrial matrix. However, the carnitine:acylcarnitine translocase and CPT-II/carnitine acetyltransferase system can under certain conditions operate in the reverse direction, e.g., removing activated short-, medium-, and long-chain acyl groups from the matrix. This buffering has been demonstrated with isolated mitochondria as well as with cultured fibroblasts and lymphocytes from patients with defects in mitochondrial fatty acid oxidation. The accumulation of cellular acyl-CoAs as a result of an inborn error of fatty acid metabolism leads to a corresponding increase in acylcarnitines in the cell. In contrast to the acyl-CoAs, the acylcarnitines can be transported across the plasma membrane into the blood. The identification of these acylcarnitines in blood thus is a signpost for the metabolic defect.

See Also the Following Articles

Coenzyme A • Fatty Acid Oxidation • Fatty Acid Receptors • Fatty Acid Synthesis and its Regulation

Glossary

carnitine A water-soluble, small molecular weight compound derived from the essential amino acids lysine and methionine; involved in reversible transesterification reactions with acyl-CoAs of different chain length. It serves as a general transport vehicle for activated fatty acids.

coenzyme A (CoA) A cosubstrate of all acylcarnitine transferases catalyzing the reversible transesterification as well as of numerous other enzymes central to energy metabolism.

mitochondria Eukaryotic organelles surrounded by an inner and an outer membrane; they are the sites of energy production.

β-oxidation A series of enzyme reactions within the mitochondria, called the mitochondrial matrix, in which fatty acid chains are progressively shortened by the removal of two-carbon units as acetyl-CoA.

Further Reading

Eaton, S. (2002). Control of mitochondrial β-oxidation flux. *Prog. Lipid Res.* **41**, 197–239.

Fraenkel, G., and Friedman, S. (1957). Carnitine. In *Vitamins and Hormones* (Harris, R. S., Marian, G. F. and Thiman, K. V., eds.) Vol. 15, pp. 73–118. Academic Press, New York.

Guzman, M., and Geelen, M. J. H. (1993). Regulation of fatty acid oxidation in mammalian liver. *Biochim. Biophys. Acta* **1167**, 227–241.

Kerner, J., and Hoppel, C. (1998). Genetic disorders of carnitine metabolism and their nutritional management. *Annu. Rev. Nutr.* **18**, 179–206.

Kerner, J., and Hoppel, C. (2000). Fatty acid import into mitochondria. *Biochim. Biophys. Acta* **1486**, 1–17.

McGarry, J. D., and Foster, D. W. (1980). Regulation of hepatic fatty acid oxidation and ketone production. *Ann. Rev. Biochem.* **49**, 395–420.

McGarry, J. D., and Brown, N. F. (1997). The mitochondrial carnitine palmitoyltransferase system. *Eur. J. Biochem.* **244**, 1–14.

Vaz, F. M., and Wanders, R. J. A. (2002). Carnitine biosynthesis in mammals. *Biochem. J.* **361**, 417–429.

Zammit, V. A. (1999). Carnitine acyltransferases: Functional significance of subcellular distribution and membrane topology. *Prog. Lipid Res.* **38**, 199–224.

Biography

Charles L. Hoppel graduated from Gonzaga University and St. Louis University School of Medicine. He is Professor of Pharmacology, Medicine and Oncology at Case Western Reserve University, Co-Director of the Center for Inherited Disorders of Energy Metabolism at CWRU, and Associate Director, Research in the Geriatric Research, Education, and Clinical Center at the Louis Stokes VA Medical Center, Cleveland. His research interests are in mitochondrial structure and function, mitochondrial fatty acid oxidation, and regulation of carnitine palmitoyltransferase-I.

Janos Kerner graduated from Humboldt University in Berlin and held a faculty position in the Department of Biochemistry at Medical University of Pecs (Hungary) until 1994. He was a visiting faculty member in the Department of Biochemistry at Michigan State University and joined the faculty in the Department of Nutrition at Case Western Reserve University in 1995. His research interest is in mitochondrial fatty acid oxidation and its regulation.

Caspases and Cell Death

Don W. Nicholson
Merck Frosst Centre for Therapeutic Research, Pointe Claire-Dorval, Quebec, Canada

Pierluigi Nicotera
MRC Toxicology Unit, Leicester University, Leicester, UK

Gerry Melino
MRC Toxicology Unit, Leicester University, Leicester, UK

Caspases are cysteine proteases involved in cell death. The name "caspase" is derived from *c*ysteinyl aspartate-specific protease, i.e., proteases which cleave after an aspartate. The caspase family is comprised of 13 proteins in humans, seven in *D. melanogaster*, and a single protein in *C. elegans*. All caspases consist of three structural domains: a prodomain, a large subunit, and a small subunit. The prodomain is important for the regulation of the enzymatic activation of caspases; the active enzyme consists of the small and large subunits together. To obtain an enzymatically active enzyme, the three subunits must be proteolytically cleaved, which is effected by other endoproteases, normally also a caspase. This article discusses caspases in the context of cell death.

History and Classification

Caspases were first identified in 1989 by Sleath and Schmidt as a protease required for the activation of interleukin-1β. In 1993, the group of Bob Horvitz discovered that the cell death gene ced-3 is a protease belonging to the same family. In 1999, the first human genetic disease caused by mutation of a caspase (type 10) was identified by Michael Lenardo.

Phylogenetic analyses, and also studies of substrate specificity, indicate that caspases can be subdivided into three different groups. Figure 1 reports the present classification of the human caspases.

Group 1 includes caspases 1, 4, 5, and 12, which are involved in inflammation. The prototype of this group is caspase 1, previously known as interleukin conversion enzyme 1β, or ICE. Its enzymatic activity was identified in 1989, but the enzyme was only purified and cloned in 1992, the same year in which Lois Miller identified the first inhibitor, the viral protein CrmA. Caspase 1, or ICE, controls the maturation of IL-1β, actively participating in the inflammatory response. Site P4 of the substrate is preferentially a hydrophobic residue.

Group 2 includes caspases 2, 3, and 7, shown by a star in Figure 1. The prototype of this group is caspase 3, the homologue of ced-3 in *C. elegans*. Group 2 caspases are directly involved in apoptosis in the terminal effector phases. Group 2 caspases have a very small prodomain, indicating a simple regulation of their enzymatic activation. These caspases are in general activated directly by another caspase, in a cascade of enzymatic amplification. Site P4 of the substrate is preferentially an Asp (D) residue. Site P3 of the substrate is preferentially a Glu (E) residue. Therefore, this subfamily preferentially cleaves substrates with the sequence DExD.

Group 3 consists of caspases 6, 8, 9, and 10. These caspases have a very large prodomain, and therefore a complex mechanism of activation. In fact, these caspases need molecular adaptors to be enzymatically activated, in contrast to group 2 caspases. Caspases 8 and 10 are part of the signal transduction mechanism of apoptosis receptors such as CD95; in this case, the adaptor molecule is FADD. Caspase 9 is activated in the apoptosome, and the necessary adaptor molecule is Apaf-1. Site P4 of the substrate is preferentially an aliphatic residue.

Structure and Active Site

As already mentioned, caspases consist of three structural domains: a prodomain, a large subunit (also named as p20), and a small subunit (called p10).

The enzyme is constituted of the small and large subunits (p20/p10, ~30 kDa). In fact, the active site is mostly in the p20 subunit: it can be further classified into four different subsites, S4 to S1. The S1 subsite, which attacks the carboxyl group of the polypeptide side chain in P1 (the site of cleavage is Asp-D), is composed of p20 as well as p10 subunits. Similarly, the site for recognition and positioning of the substrate (S4–S1) is furnished by both p20 and p10, even though the residues mostly

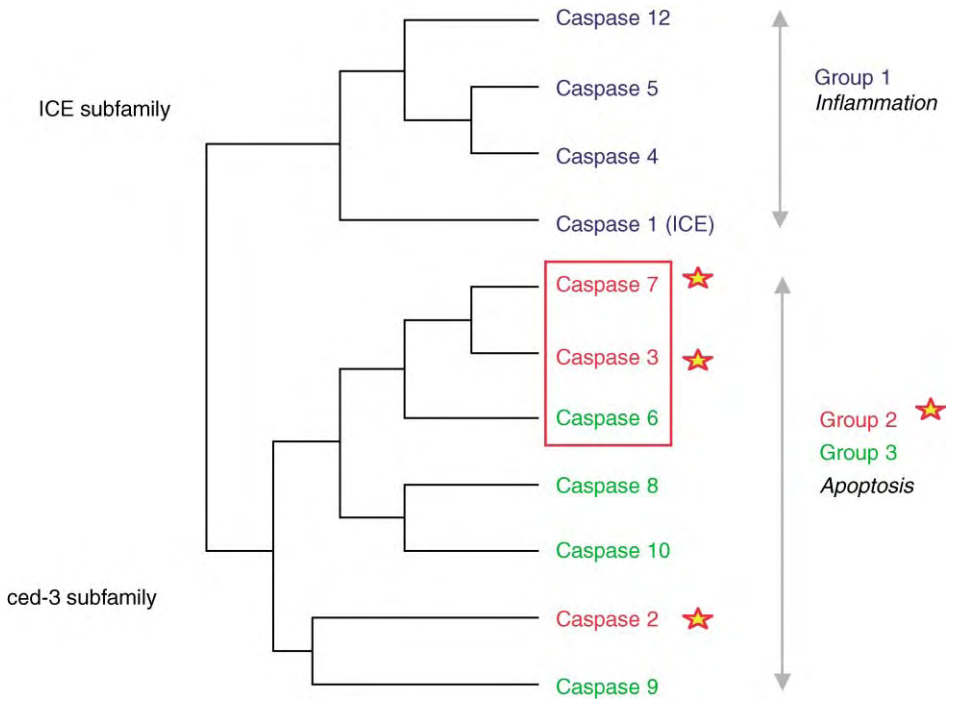

FIGURE 1 The human caspases family. Classification of the human caspases. According to the phylogenic tree, caspases are subdivided in two major subfamilies, ICE and ced-3. The former are involved in inflammation, and the latter in apoptosis. The caspases with a very short prodomains (<30 a.a.) are boxed (types 3, 6, 7); all the other enzymes have long prodromains (>10 kDa) subject to complex regulation. The enzymes can be divided according to their proteolytic specificity into group 1, involved in cytokine maturation, group 2, involved in the final effector phase of apoptosis (indicated by a star), and group 3, involved in the upstream regulation of apoptosis. At least two gene clusters have been identified, consistent with some caspases arising from tandem gene duplication. Caspase 13 is an error of sequencing; caspase 12 is mutated into a nonfunctional enzyme in up to 90% of the human population; caspase 11 is involved in neuronal death; caspase 14 is involved in skin differentiation. Please note that caspases are not indicated in the scheme. Modified from Nicholson, D. W. (2000). From bench to clinic with apoptosis-based therapeutic agents. *Nature* **407**, 810–816.

responsible for specificity (S4) are contained in p10 (Figure 2).

Caspases enzymatically function as dimers of two identical molecules bound to each other. Figure 2 shows a very schematic view of the dimer formation.

Each monomer (p20/p10) is formed by a compact cylinder dominated by six β-sheets and five α-helices distributed on the opposite site of the plane formed by the β-sheets. The dimer (p20/p10)2 contains two (p20/p10) units aligned head to tail, which therefore position their respective active sites on opposite sides of the molecule. While there are two active sites, their cooperation has never been observed. The orientation of the molecule indicates a specific mechanism of activation, well regulated with security systems (a "safety catch").

Substrate Recognition

The substrate recognition site of the caspase is indicated as S4–S1, at which the substrate is bound at residues P4–P1 (Figure 3). This recognition guarantees an absolute specificity. The S4–S1 substrate recognition site varies in each caspase, even if S1 is absolutely constant and highly tight. This is responsible for the absolute specificity to bind Asp (D) as the substrate residue P4. In fact, Asp is physically constrained and held by a hydrogen bond with Arg179, Gln283, and Arg341 (the numbers refer to caspase 3). The dimensions of the S1 subsite are reduced to a minimum and are therefore responsible for the lack of tolerance for P1 (Arg). Bond sites P2 and P3 (subsites S2 and S3) are more tolerant, less specific, and more heterogeneous in the various caspases. Therefore, the substrate (or the inhibitor) positions itself within the S1–S4 site, creating interactions as hydrogen bonds with Ser339 and Arg341 (conserved in practically all of the caspases). The P4 (S4) binding site is the major determinant of specificity.

Mechanism of Action

Caspases are cysteine proteases and, therefore, possess a catalytic triad, which includes a cysteine (active site) in the vicinity of a histidine. The third component of the classical catalytic triad typical of cysteine proteases is

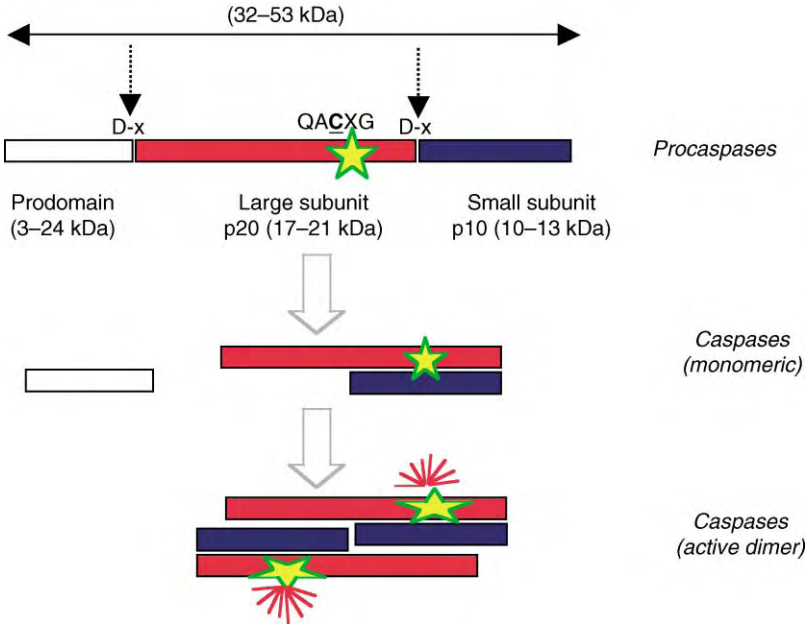

FIGURE 2 Structural organization and activation of caspases. The caspases are produced as proenzymes (32–53 kDa), including a prodomain (3–24 kDa), the large subunit (17–21 kDa) containing the active site, and the small subunit (10–13 kDa). To become enzymatically active, these three components must be proteolytically cleaved (D-x site), a phenomemon that is regulated by the prodomain itself; this allows the assembly of the large and small subunits, with the dimerization into a functional enzyme.

not constant in caspases, and its function can be substituted by different groups in different components of the family. For example, if we consider caspase 3, subsequent to substrate binding, the catalysis can take place with the catalytic diad Cys285 and His237. In fact, the third element of the cysteine protease triad is substituted by an ossianionic bond formed with Gly238 and Cys285 (conserved in all caspases).

Sequence of Action

While the regulatory caspases of the death receptor (types 8 and 10) or of the apoptosome (type 9) participate in signal transmission, the effector caspases (types 3, 6 and 7) determine the death of the cell. Effector caspases are diverse, and are not activated in parallel, but in a sequential manner, resulting in an amplification cascade of proteolytic cleavage (vaguely similar to the cascade of proteolytic activation and amplification of the complement system, or blood coagulation). These cascades have the effect of augmenting the signal.

In the apoptosome, the first caspase to be activated is caspase 9. This in turn activates caspases 3 and 7. Caspase 3 is also able to proteolytically activate caspase 9, therefore creating a reciprocating loop of potentiation.

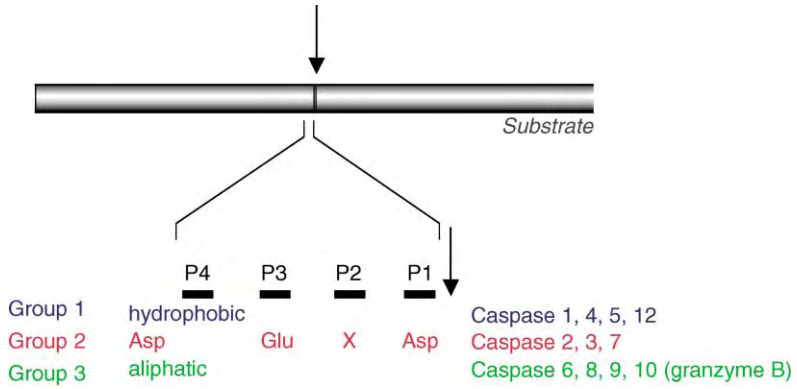

FIGURE 3 Caspase proteolytic specificity. The caspases recognize a tetrapeptide motif corresponding to the four residues P4–P3–P2–P1. While the positions at P3 and P1 seem to be obligatory, the position P4 allows the classification of three subfamilies (Figure 5). This property has facilitated the identification of group-specific inhibitors.

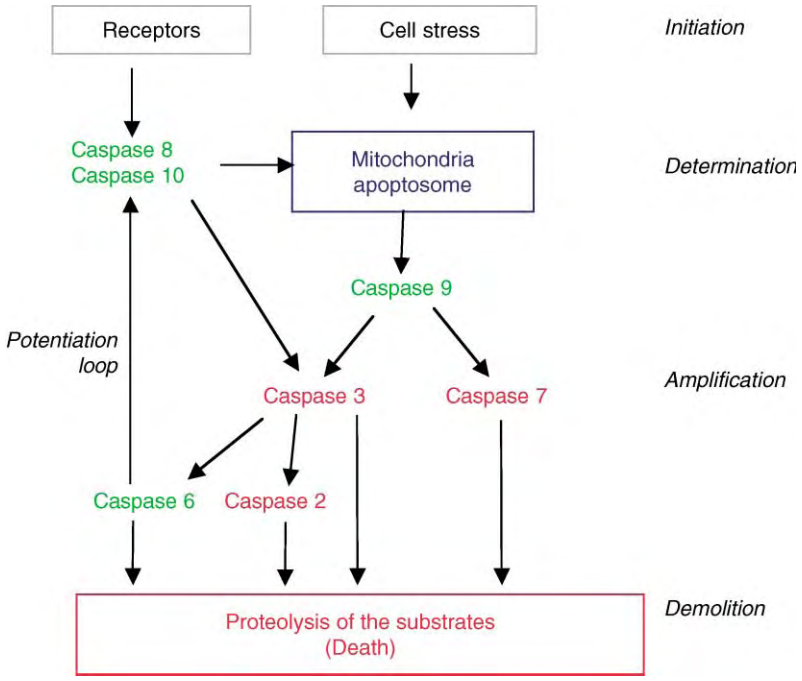

FIGURE 4 Sequential activation of caspases. In general, caspases with a long prodomain are involved in the upstream regulation and activation of the apoptotic pathway; they require a tight regulation and activation; furthermore, they cleave very specific substrates. Caspases with a short prodomain are involved in the amplification of the effector cascade, thus they have a very simple, fast, and direct activation, and they also have many substrates, inactivation of which finally kills the cell. Caspase 6 seems to be able to reactivate the upstream regulatory caspases, creating a feedback forward potentiation loop that strongly enhances the amplification of the death signal. Color code is in keeping with Figure 4. Modified from Slee, E. A., Adrian, C., and Martin, S. J. (1999). Serial killers: Ordering caspase activation events in apoptosis. *Cell Death Diff.* **6**, 1067–1074.

Caspase 3 proteolytically activates caspases 6 and 2. At this point, caspases 3, 7, 6, and 2 are highly activated and work to proteolytically cleave their intracellular substrates and determine cell death itself. A diagram of this order of activation is depicted in Figure 4.

Caspase 6 can also proteolytically activate the apical regulatory caspases 8 and 10, therefore creating a further loop of potentiation, which further enhances the death receptor signals. Figures 5–7 show the caspase activation, the apoptic pathway in humans, and the regulation of the apical regulatory caspases.

Schematically we can redefine the molecular phases of apoptosis in the following manner: (1) "initiation," activation of death receptors (caspases 8 and 10), (2) "determination," activation of the apoptosome (caspase 9), (3) "amplification," increase in the type and number of active caspases (caspases 3, 7, 6, and 2) and apical reactivation loop (caspases 8 and 10), and (4) "demolition," proteolytic cleavage of over 250 different substrates which determine the death of the cell (Figure 4).

Substrates during Apoptosis

Experimental studies indicate that over 700 different polypeptides can be generated during apoptosis. Up to

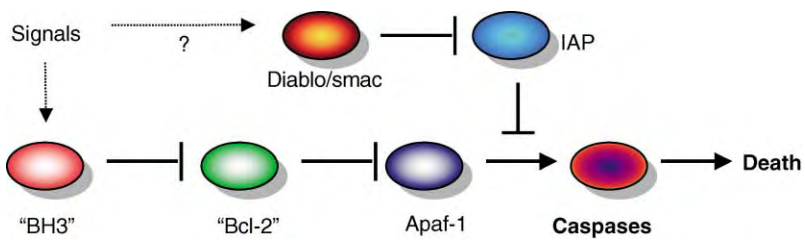

FIGURE 5 Caspases and cell death. Caspases are the proteolytic enzymes responsible for cell death. They are activated by an adaptor molecule (apaf-1), which in turn are controlled by the Bcl-2 family, and in particular by the "BH3-only" subfamily and the Bcl2-subfamily. The final stages of activation of the caspase can be regulated by a different pathway, the IAPs. This simple scheme is conserved in evolution from *C. elegans* and *D. melanogaster.*

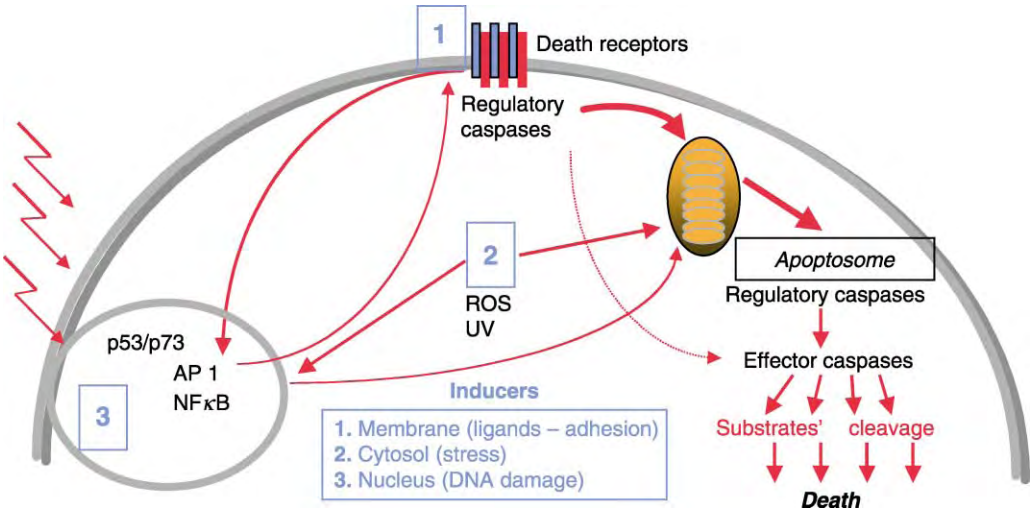

FIGURE 6 The apoptotic pathways in humans. In mammalian cells, apoptosis can de triggered at three different levels, as indicated. The signal converges to the apoptosome were the final effector phase occurs. Caspases are involved both in the upstream regulatory phase, and in the final terminal phase. The regulation at the level of the death receptor, and of the apoptosome is shown in greater detail in Figure 7.

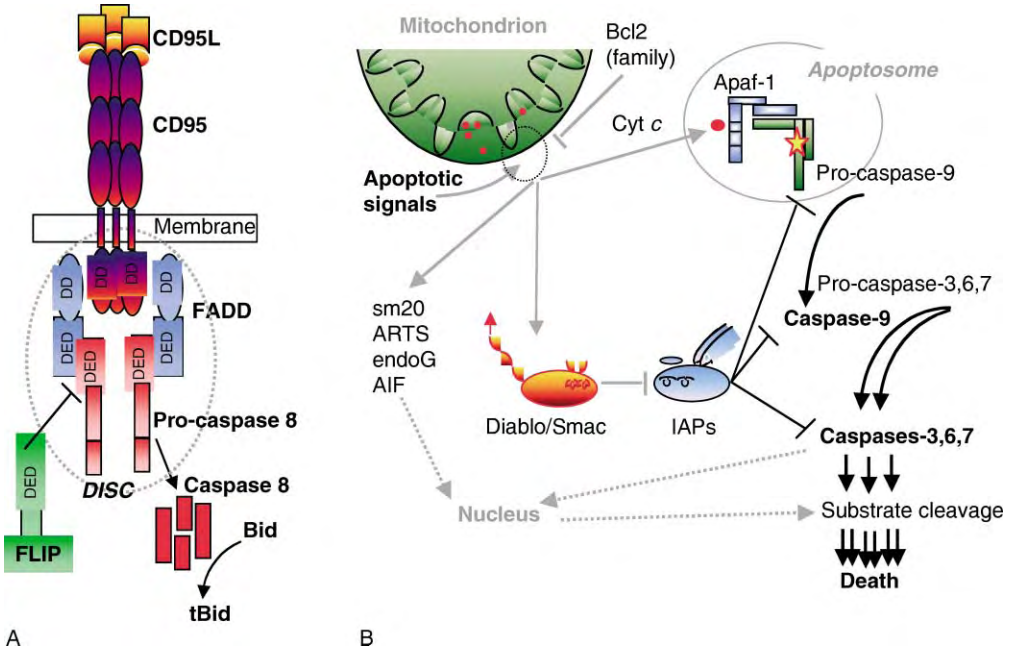

FIGURE 7 Regulation of the apical regulatory caspases. The general scheme is reported as Figure 6. (A) Formation of the death inducing signaling complex (DISC), following the activation of a death receptor such as CD95 (also called Fas or APO-1). Three molecules of ligand (CD95L) bind three molecules of receptor (CD95), allowing the recruitment of the adaptor molecule FADD via their death domain (DD). In turn FADD, via its death effector domain (DED), recruits and activates caspase 8, which cleaves the specific substrate Bid. Truncated Bid (tBid) is in fact the molecular signal that propagates the death signal to the mitochondria and the apoptosome. This mechanism can be inhibited by the molecule FLIP, via its DED. (B) When activated by apoptotic signals (e.g., by tBid), mitochondria release several molecules, as indicated. In particular, cytochrome *c* goes to the apoptosome (formed by cytochrome *c*, Apaf-1, pro-caspase 9, and dATP), and allows the activation of caspase 9. This in turns activates several molecules of downstream effector caspases (types 3, 6, 7), and consequently the cleavage of many cellular substrates results in cell death. Still at its terminal stage, cell death can be inhibited by specific inhibitory proteins (IAPs), but another mitochondria-released protein, Diablo/Smac, can remove the protection by IAPs. The cascade of proteolytic amplification created by caspase 9 (apical regulatory caspase) and caspases 3, 6, and 7 (downstream effector caspases) is extremely powerful.

2003, according to Schultze Ostoff, over 250 proteins have been found to be cleaved by caspases during the execution of apoptosis.

Table I indicates some of the principal substrates. The proteolytic cleavage of these substrates clearly renders the cell incapable of performing its proper functions.

Inhibitors

For practical reasons we distinguish pharmacological (Table II) and natural (Table III) inhibitors of caspases.

TABLE I

Caspase Substrates

DxxD site	*non-DxxD Site*
DNA-PKs	STAT1
PARP	Sp-1
Rad 51	SRP p72
Acinus	NFκB
CAD/DFF45	PITSLRE kinases
DNA-RTC140	PAK-2
Rb	p59 fyn
mdm2/HDM	CaMK-IV
p21-waf1/cip	p28 Bap31
NuMA	Actin
ATM	Gas2
U1-70KsnRNP	Lamin A and B
hnRNP-C1/C2	Bcl-XI
SREB	Bid
IκB-alfa	APP-beta
D4-GDI	Pro-IL-16
cPLA2	Pro-caspases
PKC-delta, -theta, -zeta	
MEKK-1	
Mst1	
PRK2	*Unknown site*
PP2A	wee1
FAK	CDC27
Fodrine (all)	SAF-A/hnRNP-U
Gelsolin	hnRNP-A1
Keratin-18	Ras GAP
LAP2	Raf 1
Nup153	Akt 1
Rabaptin-5	Cbl e Cbl-b
APC	PKN
Hsp90	Catenin-beta, -gamma
UbqCE NEDD4	Kinectin
Bcl 2	Caplastatin
Presenilin 2	Ataxin-3
Huntigtin	AMPA receptors
SBMA-AR	p27 kip1
Atrofin-1	MCM3

The substrates of caspases can have single cleavage site (e.g., DQTD in Gelsonin), nested multiple sties (e.g., DEVDGVD in PARP), redundant clustered sites (e.g., DSLD-(X13)-DEED-(X16)-DLND-(X32)-DGTD in Huntigtin), or distal multiple sites (e.g., DEPD and DAVD in ICAD).

TABLE II

Peptide Inhibitors of Caspases

	zVAD-fmk	aDEVD-cho	aYVAD-cho
Caspase 1	2	15	1
Caspase 2	2400	1700	>10 000
Caspase 3	40	1	>10 000
Caspase 4	130	130	360
Caspase 5	5	200	160
Caspase 6	100	30	>10 000
Caspase 7	40	2	>10 000
Caspase 8	2	1	350
Caspase 9	4	60	1000
Caspase 10		10	400

Inhibition constant (Ki, nM) shown is t1/2 at 1 μM in seconds.

Modified from Ekert, P. G., Silke, J., and Vaux, D. L. (1999). Caspase inhibitors. *Cell Death Diff.* **6**, 1081–1086.

The understanding of the molecular mechanism of catalysis and of the properties of the sites P4–P1 of the substrate were the basis for designating pharmacological inhibitors, both of polypeptide type and of low molecular weight compounds. The electrophylic groups, which interact irreversibly with the catalytic Cys are aldehydes, nitriles, and ketones, of which the latter are much more stable than the others *in vivo* and therefore are most easily applied to pharmaceutics. Caspase inhibitors are all constituted according to the following schema: [tetrapeptide]-C-CH2-X. Here X signifies a –Cl or –F (fluoro- or chloro-methyl ketone, fmk), -N2 (diazomethylketone), or –OCOR (acyloxymethylketone). The peptide portion (stabilized), determines the specific selectivity of the various caspases. Thus, zVAD-fmk is a nonspecific inhibitor of almost all of the caspases. DEVD-fmk, on the other hand, is specifically selective for effector caspases such as caspases 3, 6, and 7. Table II gives an idea of the specific inhibitors for different caspases.

In 1991, Lois Miller first identified a natural inhibitor of apoptosis, before even the discovery of caspases. The protein p35 produced by baculovirus (*Autographa californica*) is a potent and selective inhibitor of caspases. Subsequently, numerous other viral caspase inhibitors were identified, such as cytokine response modifier A (CrmA). Inhibition of caspases by these specific proteins is one of the important pathways among which viruses regulate apoptosis.

Numerous cellular proteins exist with actions similar to those of these viral caspase inhibitors. They are called IAPs (inhibitors of apoptosis). Table III shows the different viral and human IAPs with their relative inhibitory effects on each caspase.

All of the proteins which inhibit caspases, whether viral or cellular, are characterized by structural domains

TABLE III

Natural Caspase Inhibitors

	Viral			Cellular					
	crmA	p35	OpIAP	XIAP	cIAP1	cIAP2	Survivin	NAIPPI9	GBI
Caspase 1	0.01	9	Inib	NI	NI	NI			NI
Caspase 2	>10 000	Inib	Inib						
Caspase 3	1 600	0.1	NI	0.7	100	35	Inib	NI	
Caspase 4	1								
Caspase 5	0.1								
Caspase 6	110	0.4		NI	NI	NI			
Caspase 7	>10 000	2		0.2	40	30	Inib	NI	
Caspase 8	0.8	0.5		NI	NI	NI	NI		NI
Caspase 9	2			Inib	Inib	Inib			
Caspase 10	17	7							
Granzyme B	NI	NI							Inib

Inhibition constant (Ki, nM) shown is t1/2 at 1 μM in seconds. NI = noninhibitory, Inib = inhibitory.

Modified from Ekert, P. G., Silke, J., and Vaux, D. L. (1999). Caspase inhibitors. *Cell Death Diff.* **6**, 1081–1086.

called BIR (baculovirus IAP repeat), consequently all IAP proteins are also called BIR proteins (BIRp). On the other hand, the contrary does not hold: there are BIR proteins which do not show IAP activity. This fact is due to the prokaryotic origin of BIR proteins, which are multifunctional. Many BIR proteins in humans (e.g., survivin) are passenger proteins in the mitotic spindle and are implicated in cell division.

Caspase Knockouts

The creation of transgenic mice lacking specific caspases has been accomplished for most caspases. Table IV displays the phenotypes for these mice. Because caspases play a determining role in apoptosis, sometimes specifically, sometimes redundantly, the phenotypes are extremely diverse, as indicated by the table.

The role of caspases in the receptor mechanism is indicated by the caspase 8 knockout.

The similarity of the phenotypes of the knockouts of caspases 3, 9, and Apaf-1 indicate the presence of a very important mechanism in the apoptosome by which the amplification of the caspase cascade is initiated and regulated.

TABLE IV

Caspase Knockouts

	Development	Apoptotic phenotype
Caspase 1	Normal	Inflammation (CD95?)
Caspase 2	Normal	Germinal cells (stem cells?)
Caspase 3	Lethal PN	Neural
Caspase 6	Normal	
Caspase 7	Lethal E	
Caspase 8	Lethal E	Death receptors (CD95, TNF, DR3)
Caspase 9	Lethal E	Neural
Caspase 11	Normal	Thymocytes, neural (CD95?)

Often, the severity of the phenotype depends on the genetic background of the animals, as, for example, described in caspase 3.

E = embrionically lethal; PN = perinatally lethal.

Pathological Implications

The execution of apoptosis is dependent on the activation of caspases, and as a result, caspases play a determining role in all pathologies of excessive apoptosis. For example, caspases play a crucial role in the *in vivo* activation of death described in myocardial infarction and in cerebral ischemia, conditions in which cell death occurs both by apoptosis as well as by necrosis.

Caspases can also play an aberrant role in regulatory processes determining the major propensity or vulnerability of cells to lethal insults. Examples are the possible role played by caspases in triplet diseases such as Huntington's and in neurodegeneration like in Alzheimer's disease.

In the case of Huntington's disease, low level of intracellular activation of caspase 3 liberates an amino terminal fragment of the protein Huntington (four DxxD sites in a cluster), containing the Glu expansion, facilitating a pathological aggregation. In turn, this

aggregate sensitizes more caspase 3, forming a vicious cycle of activation and aggregation of poly-Glu. The cell, thus sensitized, facilitates the activation of caspase 8 (from the CD95 receptor, or directly by an effector caspase, or even stimulated indirectly by the poly-Glu aggregate), determining the death of the cell. This sensitization can also occur extremely slowly (years).

In Alzheimer's disease, caspase 3 alters the normal processing of the amyloid β-precursor protein (APP), removing the carboxy terminal. APP, deprived of the intramolecular reinternalization signal, proceeds down a route of degradation that results in the formation of the amyloid beta (Aβ) peptide, which can in turn favor the activation of apoptosis by means not yet clearly understood.

In either case, caspase 3 seems to augment the baseline levels (threshold?) of activation of cell death, rendering the cell more sensitive to death, and participating therefore in the pathogenetic mechanisms of these important illnesses.

Therapeutic Outlook

Selective peptide inhibitors of different caspases (Table II) have been successfully developed, even though they show serious problems penetrating the cell membrane, as well as having electrophyllic promiscuity and stability in solution, which makes them susceptible to attacks by biological nucleophiles, such as catepsin. Because of this, they are not easily adaptable to clinical use; this has allowed scientists to obtain many interesting *in vitro* results. More recently, Merck (like Smith Kline Beecham, BASF, Idun/Novartis, and Vertex) has in advanced stages of development, new classes of low molecular weight nonpeptide inhibitors. These show a much higher potency and specificity, opening new therapeutic perspectives. Nonpeptide inhibitors like "isatins" attain potencies 100–1000 times greater than the class of zVAD-fmk, with substantial improvements *in vivo*. These studies are still in early stages, and we hope that the near future will tell as the best clinical application for this new class of drugs.

See Also the Following Articles

Amyloid • Bax and Bcl2 Cell Death Enhancers and Inhibitors • Cell Death by Apoptosis and Necrosis

Glossary

apoptosis The physiological mechanism of programmed cell death mediated by caspases (cysteine proteases), regulated by the Bcl-2 family of proteins, and triggered from the membrane (death receptors, adhesion), cytosolic stress, or nuclear signals (DNA damage). Excessive or defective apoptosis is involved in diseases such as ischemia, AIDS, neurodegeneration, autoimmunity, and cancer.

apoptosome Multiprotein complex of 700 kDa molecular weight formed by procaspase-9, apaf-1, dATP, and cytochrome *c*. It proteolytically activates caspase-9, leading to the activation of downstream-effector caspases, and subsequently death of the cell.

BIR Baculovirus IAP Repeat. A protein-structural domain, conserved in both mammalian and viral proteins, able to react with the apoptosome or with the active caspases. It characterizes the IAP proteins.

caspase Cysteinyl *asp*artate-specific prote*ase*, cysteine proteases which cleave after an aspartate (D). The family includes 13 enzymes involved either in programmed cell death (apoptosis) or in inflammation.

death receptors Cell membrane receptors (e.g., CD95, TRAIL-R, TNF) belonging to the TNF (tumor necrosis factor) superfamily, able to activate apoptosis via the formation of a DISC when bound by their specific ligands (e.g., CD95L, TRAIL, TNF). Essential in regulating immune responses.

DISC Death initiation signaling complex. Multiprotein complex beneath the cell membrane activated by trimeric death receptors (e.g., CD95, TRAIL-R, TNF). It includes the receptor, adaptor molecules, procaspases (caspases 8 and 10), and their related substrates (e.g., Bid) that signal to the mitochondria-apoptosome to activate the caspases, and therefore kill the cell by apoptosis.

IAP *I*nhibitors of *ap*optosis. Mammalian or viral proteins able to inhibit the activation of the apoptosome or the active caspases. They are characterized by structural domains called BIR; consequently all IAP proteins are also called BIR proteins (BIRp).

Further Reading

Black, R. A., Kronheim, S. R., and Sleath, P. R. (1989). Activation of interleukin 1β by a co-induced protease. *FEBS Lett.* **247**, 386–390.

Ekert, P. G., Silke, J., and Vaux, D. L. (1999). Caspase inhibitors. *Cell Death Diff.* **6**, 1081–1086.

Fischer, U., Laenicke, R. U., and Schultze-Ostoff, K. (2003). Many cuts to ruin: A comprehensive update of caspase substrates. *Cell Death Diff.* **10**, 76–100.

Kostura, M. J., Tocci, M. J., Limjuco, G., Chin, J., Cameron, P., Hillman, A. G., Chartrain, N. A., and Schmidt, J. A. (1989). Identification of a monocyte specific pre-interleukin 1β convertase activity. *PNAS-USA* **86**, 5227–5231.

Melino, G. (2001). The Syren's song (Concept: Apoptosis). *Nature* **412**, 23.

Nicholson, D. W. (1999). Caspase structure, proteolytic substrates, and function during apoptotic cell death. *Cell Death Diff.* **6**, 1028–1042.

Nicholson, D. W. (2000). From bench to clinic with apoptosis-based therapeutic agents. *Nature* **407**, 810–816.

Slee, E. A., Adrian, C., and Martin, S. J. (1999). Serial killers: Ordering caspase activation events in apoptosis. *Cell Death Diff.* **6**, 1067–1074.

Wang, J., Zheng, L., Lobito, A., Chan, F. K.-M., Dale, J., Sneller, M., Yao, X., Puck, J. M., Strauss, S. E., and Lenardo, M. J. (1999). Inherited human caspase 10 mutations underlie defective lymphocyte and dendritic cell apoptosis in autoimmune lymphoproliferative syndrome type II. *Cell* **98**, 47–58.

Yuan, J., Shaham, S., Ledoux, S., Ellis, H. M., and Horvitz, H. R. (1993). The *C. elegans* cell death genes ced-3 encodes a protein similar to mammalian interleukin 1β-converting enzyme. *Cell* **75**, 641–652.

Zheng, T. S., Hunot, S., Kuida, K., and Flavell, R. A. (1999). Caspase knockouts: Matter of life and death. *Cell Death Diff.* **6**, 1043–1053.

Biography

Gerry Melino is Editor in Chief of the journal *Cell Death Differentiation* (www.nature.com/cdd) as well as group leader at the Medical Research Council, Toxicology Unit in Leicester, UK, and Professor at the University of Rome "Tor Vergata." His research is mainly focused on the p53 family and in particular on p73 and p63.

Pierluigi Nicotera is the Director of the Medical Research Council, Toxicology Unit in Leicester, UK, and his research interest is on neurodegeneration and neurotoxicology.

Don W. Nicholson is Vice President of Merck, responsible for the San Diego (California, USA) research site dedicated to neurodegeneration. He is a major contributor to the enzymology of caspases, and to drug development of low molecular weight inhibitors of caspases.

Cell Cycle Controls in G_1 and G_0

Wenge Shi and Steven F. Dowdy
University of California, San Diego School of Medicine, La Jolla, California, USA

The cell cycle is the process by which one cell becomes two. Somatic cell division involves cell growth (increase in cellular components, such as ribosomes, membranes, organelles) throughout the cell cycle, faithful replication of its DNA during the S phase of the cell cycle, and precise distribution of DNA between daughter cells during the mitosis (M) phase. In addition, with the exception of early embryonic cell divisions, two gap phases, Gap 1 (G_1) and Gap 2 (G_2), are separated by S phase. As multicellular eukaryote organisms regulate cell division tightly to maintain tissue homeostasis, the most important regulatory decision is made during exiting of the resting state so called the G_0 phase and G_1 phase of the cell cycle before cells become committed to initiate DNA synthesis and complete the cell cycle.

G_1 and G_0 Phase of the Cell Cycle

The majority of cells in adult metazoans are permanently withdrawn from the cell cycle in a terminally differentiated state. Only small numbers of cells, such as hematopoietic and epithelial early progenitor cells, are actively proliferating. Other cells are reversibly withdrawn from the cell cycle and remain in a quiescent stage or the G_0 phase of the cell cycle. Upon proper stimulation, these cells can re-enter the cell cycle. For example, highly differentiated hepatocytes in adult liver are present in the G_0 resting phase and rarely replicate normally. However, in response to acute liver injury or distress, these G_0 hepatocytes can be stimulated to re-enter the cell cycle and regenerate the liver. Similarly, primary peripheral blood lymphocytes (T and B cells), which are present in the G_0 phase, can re-enter the cell cycle and start clonal expansion when presented with the appropriate antigen. These examples serve to demonstrate that certain cell types may enter and exit the cell cycle pending the appropriate stimulus, whereas the vast majority of cells in a matured metazoan have permanently exited the cell cycle.

The most important decision for cell cycle progression is made during the G_1 phase. In G_0 phase, cells respond to extracellular signals by entering the G_1 phase of the cell cycle. However, prior to transiting into the late G_1 phase, they must traverse the growth factor-dependent restriction point. This is a critical regulatory phase of the cell cycle where a cell becomes committed to enter S phase and finish the remaining cell cycle. In contrast to normal cells, tumor cells are often less growth factor-dependent and fail to respond to growth inhibitory signals. Consequently, tumor cells select for genetic mutations that disrupt the important decisions performed at the restriction point and this is, in fact, one of the hallmarks of cancer.

Regulators of G_0 Exit and G_1–S Progression

One of the key negative regulators of the restriction point and early G_1 to G_0 cell cycle exit is the retinoblastoma tumor suppressor protein (pRb) and two closely related family members, p107 and p130. Murine embryonic fibroblasts (MEF) deficient for all three pocket proteins fail to respond to G_1 phase arrest signals following contact inhibition, serum starvation, or DNA damage. The antiproliferation function of the pocket proteins depends, at least in part, on their interaction with E2F/DP transcriptional factors, which regulate the expression of key genes required for DNA synthesis, DNA repair, DNA-damage checkpoint, apoptosis, and mitosis. Direct interactions of pRb family members with E2F/DP complexes and the recruitment of chromatin-modifying enzyme complexes, such as histone deacetylases (HDAC), polycomb group proteins, the SWI/SNF complex, and histone methyl transferases, to E2F-reponsive genes results in inhibition of target gene expression.

Distinct pRb family member–E2F repressor complexes exist in different cell cycle phases. As an example, during the G_0 phase, p130 and p107 interact with E2F4 and E2F5, whereas pRb remains unbound. E2F4 and E2F5 are expressed constitutively and are involved in E2F-dependent gene repression during cell cycle exit and terminal differentiation. It is also reported that E2F6, the sole E2F family protein that does not interact with the pocket proteins, mediates gene repression with polycomb group proteins in the G_0 phase. Further studies are

needed to resolve the contributions of E2F6 versus E2F4 and E2F5 for maintaining quiescence. In contrast, during early G_1 phase, pRb interacts with E2F1, E2F2, and E2F3, the so-called "activator E2Fs." When the cell passes through the restriction point, pRb becomes inactivated by hyperphosphorylation, releasing E2Fs 1–3 and promoting the activation of E2F-responsive genes for cellular proliferation. Not surprisingly, MEFs deficient for these E2F1, E2F2, and E2F3 exhibit impaired E2F-responsive gene induction in response to serum and significant proliferative defects.

pRb undergoes cell-cycle-specific phosphorylation through the G_1 and S phases of the cell cycle and subsequent dephosphorylation during mitosis. Hypophosphorylated (low level of phosphorylation) pRb is the active, transcriptional repressing form of pRb and can simultaneously bind to both E2F and HDAC. Hypophosphorylated pRb is also selectively bound and inactivated by DNA tumor virus oncogenes, SV40 large T antigen, adenovirus E1A protein, and human papillomavirus (HPV) E7 protein.

pRb is physiologically regulated by a group of serine/threonine-specific protein kinases called cyclin-dependent kinases (Cdks). Specifically, cyclin D:Cdk4/6 and cyclin E:Cdk2 kinases are responsible for phosphorylating pRb during the G_1 phase of the cell cycle. However, cyclin D and cyclin E are regulated differently and play distinct roles in the cell cycle regulation of pRb (Figure 1). D-type cyclins are not expressed in G_0 cells. However, cyclin D levels increase after stimulation of growth factors as a result of increased transcription mediated by Myc and Ras/MEK/MAPK signaling pathway and increased stability mediated by the PI(3)K/Akt signaling. In cycling cells, cyclin D levels and associated kinase activity remain relatively constant. Therefore, the D-type cyclins control cell cycle entrance and exit by linking the mitogenic pathway to the core cell cycle machinery.

Unlike cyclin D, the expression of cyclin E is mitogen-independent and dependent on the action of E2Fs after the hyperphosphorylation and inactivation of pRb at the late G_1 phase of the cell cycle. However, because pRb represses cyclin E expression, questions remain as to how cyclin E gene expression and cyclin–Cdk2 activity is initially turned on. Once cyclin E levels reach a critical threshold, its levels can be further increased as a result of a positive feedback loop. Active cyclin E:Cdk2 increases degradation of $p27^{Kip1}$ by phosphorylation, which leads to more inactive pRb, free E2F for activation of cyclin E transcription and hence, more active cyclin E:Cdk2.

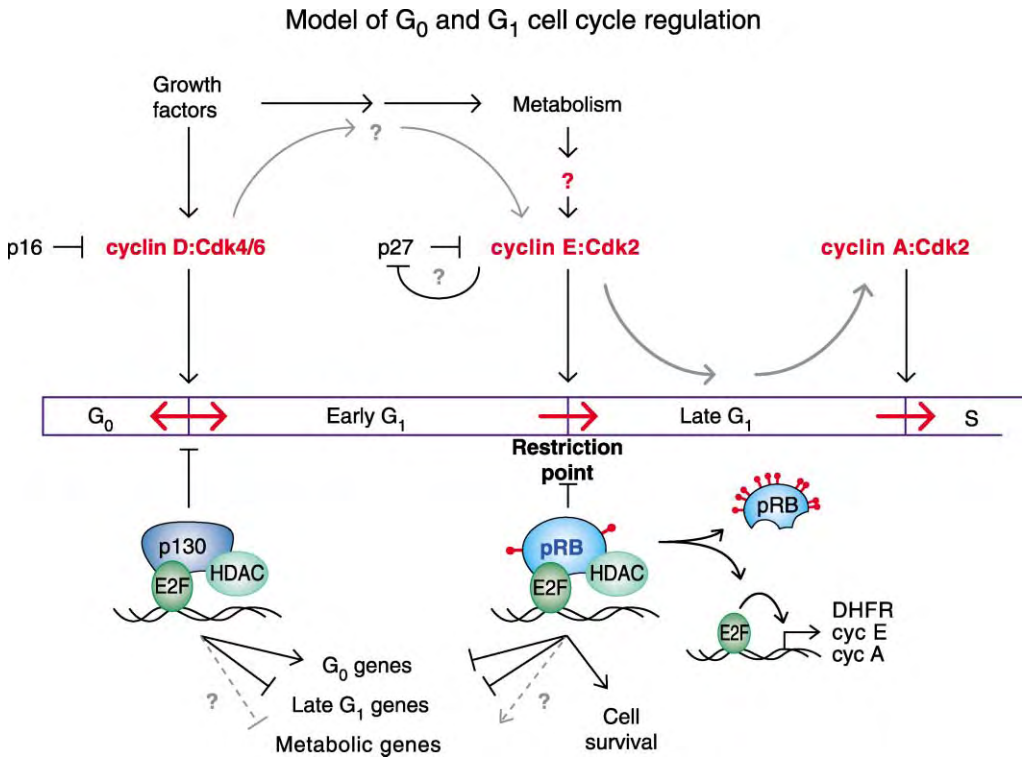

FIGURE 1 Model of G_0 and G_1 cell cycle progression. Activation of cyclin D:Cdk4/6 kinases by growth factor stimulation of G_0 cells results in increased metabolism or growth and switching of p130:E2F complexes to pRb:E2F complexes. By an unknown mechanism increased metabolism and cell mass leads to activation of cyclin E:Cdk2 complexes at the restriction point resulting in hyperphosphorylation (inactivation) of pRb, release of E2Fs, and activation of late-G_1-specific genes involved in DNA synthesis and late G_1 cell cycle regulation. Activation of cyclin A:Cdk2 complexes initiates DNA synthesis.

Several mechanisms may contribute to this process. First, $p27^{Kip1}$ in the cyclin E–Cdk2 complex may be sequestered by increased cyclin D–Cdk4/6 complexes. Second, growth factor-activated PI(3)K/Akt pathway may cause the phosphorylation and relocation of the family of forkhead transcription factors into cytosol, which leads to a decrease in the transcription of $p27^{Kip1}$. Furthermore, $p27^{Kip1}$ can be phosphorylated directly by Akt and relocate into cytosol.

The consequence of cyclin D-dependent and cyclin E-dependent kinase activity on pRb also results in differential regulation. It is apparent that cyclin D-dependent kinases are not sufficient for disrupting the pRb-E2F–HDAC complex. Indeed, this is most dramatically supported by the detection of functional pRb–HDAC–E2F complex in $p16^{INK4a}$-deficient cancer cells with deregulated and active cyclin D-dependent kinases. Furthermore, in T cells entering the cell cycle, E2F4 associates with pRb only after cyclin D kinase activity is turned on. In contrast, cyclin E-dependent kinase activity and hyperphosphorylation of pRb are required for disrupting E2F–pRb and HDAC–pRb interactions. Moreover, in addition to pRb family members, cyclin E-dependent kinase phosphorylates target proteins involved in chromatin remodeling, DNA synthesis, centromere functions, further triggering the cell to traverse across the restriction point into late G_1 and S phase.

Cell Growth Regulation

The other aspect of cell cycle regulation is the increase in cell mass or cell growth. In general, cells must grow to a minimum size to be able to divide and generate two daughter cells equal in size to the starting mother cell. Premature entry into S phase results in smaller daughter cells. Therefore, it has been realized, but not well understood, that generally with the exception of some developmental programs, such as early embryonic cell division and endo-reduplication, cell division and cell growth must be coordinated. Although cell growth is often reflected by an increase in cell size, cell growth needs to be defined as an increase in cell mass, or more precisely, the underlying global RNA and protein synthesis capacity, and additional macromolecule synthesis and storage.

How mitotic cells coordinate cell growth and division remains an open question. Some of the key regulators involved in cell cycle regulation also control cell growth. For example, the Myc transcription factor has long been implicated in cell growth regulation in both *Drosophila* and mammalian cells. Besides the gene products involved in cell cycle regulation, such as cyclin D2, Cdk4, cdc25, cyclin E, and cyclin A, many Myc-target gene products are involved in ribosome biosynthesis, protein synthesis, and specific metabolic pathways. Another example of a key cell cycle regulator is pRb. In addition to regulating E2F-dependent gene transcription, pRb can also repress RNA polymerase I- and III-dependent transcription that are responsible for the synthesis of rRNA, various small RNAs such as 5S rRNA, and tRNA. This regulation is mediated by direct interaction of pRb with the upstream-binding factor (UBF) and with the TF-IIIB coactivator, respectively.

On the other hand, cell growth may influence cell division. Understanding of cell growth regulation comes from studying immune suppressant rapamycin. Treatment of both yeast cells and mammalian cells with rapamycin delays cell growth and proliferation. In budding yeast, signaling of the target of rapamycin (TOR), a protein kinase, coordinates nutrient availability, such as carbon source and nitrogen, with cell growth and proliferation. It turns out that the yeast G_1/S cyclin Cln3 is both translationally and post-translationally regulated in response to nutrient levels. Cell division occurs when cells reach a certain size. In metazoans, the situation is more complex since nutrient levels are maintained by tissue homeostasis. Not only does mammalian TOR (mTOR) signaling coordinate protein synthesis with glucose and amino acid availability (linked to nutrient sensing signaling pathways), but it also mediates hormonal and mitogenic factor responses. mTOR lies downstream of PI(3) kinase/Akt, although it is currently unclear that they belong to a linear signaling cascade.

PI(3)K/Akt may also activate further downstream targets through tumor suppressor tuberous sclerosis (TSC) complexes. It turns out that the mTOR pathway in conjunction with signaling through the PI(3)K pathway regulates the translational initiation and elongation, ribosome biosynthesis, amino acid import and metabolism. One of the important targets in ribosome synthesis regulated by the PI(3)K/Akt/mTOR pathway is S6 kinase, which phosphorylates ribosomal protein S6. In *Drosophila*, S6 is associated with body size and cell growth. S6 phosphorylation is required for the translation of a group of mRNAs with a 5′ terminal oligopyrimidine tract (5′TOP), including ribosomal protein mRNAs and mRNAs encoding for translation machinery. In addition, the Akt/mTOR pathway regulates protein translation by phosphorylating and inactivating the translation initiation factor 4E-binding protein (4E-BP1). As a result, PI(3)K/Akt and mTOR are linked to translation initiation by regulating the eukaryotic translation initiation factor 4E (eIF-4E), which enhances the translation of essential genes for cell cycle regulation, including cyclin D and $p27^{Kip1}$. Future studies will ultimately resolve how cell growth signaling impinges on and is incorporated into the cell cycle regulatory machinery.

Future Perspectives

There has been an increased understanding of signal transduction and cell division. A lot of focus has been on protein post-translational modification and gene expression regulation. However, until recently, the importance of cell growth has not been fully appreciated. Clearly there is cross-talk between cell growth and cell cycle regulation. Future studies should fill in the gaps in our understanding of cell growth, cell cycle progression, and their subsequent contributions to neoplastic transformation.

See Also the Following Articles

Cell Cycle: Control of Entry and Progression Through S Phase • Cell Cycle: Mitotic Checkpoint • Metaphase Chromosome • RNA Polymerase Structure, Bacterial • RNA Polymerase Reaction in Bacteria • RNA Polymerase I and RNA Polymerase III in Eukaryotes

Glossary

Cdk inhibitors (CKI) There are two families of CKI: the Ink4 family proteins (inhibitors of Cdk4: p15INK4b, p16INK4a, p18INK4c, and p19INK4d), which specifically bind monomeric Cdk4 and Cdk6 to inhibit cyclin D-dependent kinase activity and the Cip/Kip family (p21WAF1, p27Kip1, and p57Kip2) that specifically binds and inhibits cyclin:Cdk complexes (cyclin D:Cdk4/6; cyclin E:Cdk2; cyclin A:Cdk2).

cyclin-dependent kinases (Cdk) Key activators of the cell cycle. A group of serine/threonine-specific protein kinase complexes composed of a cyclin regulatory subunit and a Cdk catalytic subunit. Activation of the kinase requires cyclin binding to Cdk.

restriction point A key cell cycle transition between the early G_1 mitogen-dependent phase into the late G_1 mitogen-independent phase prior to initiation of DNA synthesis in S phase.

Further Reading

Abraham, R. T. (2002). Identification of TOR signaling complexes: More TORC for the cell growth engine. *Cell* **111**, 9–12.

Ho, A., and Dowdy, S. F. (2002). Regulation of G1 cell-cycle progression by oncogenes and tumor suppressor genes. *Curr. Opin. Genet. Dev.* **12**(1), 47–52.

Malumbres, M., and Barbacid, M. (2001). To cycle or not to cycle: A critical decision in cancer. *Nat. Rev. Cancer* **1**, 222–231.

Saucedo, L., and Edgar, B. (2002). Why size matters: Altering cell size. *Curr. Opin. Genet. Dev.* **12**(5), 556–565.

Stevaux, O., and Dyson, N. J. (2002). A revised picture of the E2F transcriptional network and RB function. *Curr. Opin. Cell Biol.* **14**, 684–691.

Biography

Wenge Shi is a postdoctoral Fellow at the Howard Hughes Medical Institute, UCSD School of Medicine. He received his Ph.D. from the University of Wisconsin at Madison.

Steven Dowdy is an Associate Investigator of the Howard Hughes Medical Institute and an Associate Professor of Cellular and Molecular Medicine at UCSD School of Medicine. He received his Ph.D. from the University of California, Irvine and did his postdoctoral fellowship at the Whitehead Institute for Biomedical Research at the Massachusetts Institute of Technology.

Cell Cycle: Control of Entry and Progression Through S Phase

Susan L. Forsburg
University of Southern California, Los Angeles, California, USA

The process of DNA synthesis during S phase requires regulation at multiple levels to ensure that DNA replication is coordinated with overall cell-cycle progression. There are numerous mechanisms to ensure that S phase occurs in a timely and regulated fashion. These ensure the onset of replication occurs in response to the appropriate signals, and they also prevent the re-replication of the genome in a single cell cycle. Much of this regulation occurs by controlling the activation of DNA synthesis at individual origins of replication.

The study of S phase and its many levels of control is continuing in many laboratories. This work has benefited from genetic systems such as the yeasts *S. cerevisiae* and *S. pombe*, and the fruit fly *Drosophila*. Biochemical studies primarily in *Xenopus* extracts complement early work that reconstituted the replication apparatus using viral systems and human cells. Given this long and distinguished history, there are inevitably different names for the conserved proteins involved. A listing of the equivalents that are most relevant to this article is provided (Table I).

Initiation and Elongation of DNA Replication Origins

The major control of DNA replication occurs at initiation, by regulating assembly and activation at the origins of replication of the multiple proteins of the prereplication complex (preRC). Following initiation, the enzymes of the DNA synthesis machinery take over and extend replication forks to duplicate the genome.

Origins

DNA synthesis begins at replication origins. Generally, there are many replication origins in each chromosome, to facilitate the timely duplication of the genome. In a few species, the origin is defined by a consensus sequence in the DNA. More commonly, origins are defined by general features of the sequence rather than a linear consensus, and are typically A/T rich and easily unwound. In some cases, origins appear to be distributed not by sequence, but by some sort of spacing mechanism. Not all origins are activated at the same time: while some regions of the genome may undergo initiation early in S phase, others are activated late. Despite these differences, the proteins responsible for replication initiation at individual origins are remarkably similar amongst species.

Assembly of the preRC

The preRC is assembled by sequential binding of conserved proteins (Figure 1). This occurs at the end of M phase in cycling cells. First, the six proteins of the origin recognition complex (ORC) bind DNA near what will become the initiation site in the replication origin. Next, Cdc6 (called Cdc18 in fission yeast) and Cdt1 bind. These are followed by the six-membered mini-chromosome maintenance (MCM) complex (Mcm2–7). Biochemical studies suggest that once the MCM complex is loaded, the other preRC components are no longer essential for origin initiation. The assembled preRC is now poised for initiation of the origin. The triggers that activate initiation will be discussed later.

Initiation

Initiation at each origin requires assembly of another set of proteins. It begins with the binding of a protein called Cdc45, which is required for association of the single-stranded DNA-binding protein RPA. This is the essential first step that leads to assembly of primase and DNA polymerase α, the initiating polymerase.

Studies suggest that the MCM complex is not only an assembly factor, but plays an active role in elongation. A subset of MCM proteins has *in vitro* helicase activity, and there is some evidence that the MCM proteins are associated with the replication fork. The current model suggests that the MCMs provide an unwinding activity required for replication fork elongation. Curiously, MCMs are extremely abundant proteins, far outnumbering the replication origins, and it remains to be determined why the cell requires so many of them.

TABLE I

Names of Replication Proteins in Multiple Systems. The same Protein may have Synonyms even in one Species (Indicated by a Slash)

S. cerevisiae	*S. pombe*	Metazoans	Product
Cdc7	Hsk1	Cdc7	DDK kinase
Cdc28	Cdc2	Cdk2 and Cdk4	S phase CDK
Cdc6	Cdc18	Cdc6	Activator
Mcm2–7	Mcm2–7	Mcm2–7	MCM complex members
Orc1–6	Orp1–6	Orc1–6	ORC
Cdc45	Sna41	Cdc45	Initiation factor
RPA	RPA	RPA	Replication protein A: single-strand DNA-binding protein
Dpb11	Rad4/Cut5	TopBP1/Mus101	Possible assembly factor?
Tah1	Cdt1	Cdt1/Dup	pre-RC factor
No homologue[a]	No homologue[a]	Geminin	Cdt1 inhibitor
Mec1	Rad3	ATR	ATM-related kinase
Chk1	Chk1	Chk1	Damage checkpoint kinase
Rad53	Cds1	Chk2	Replication checkpoint kinase
Drc 1, S1d2	Drc1	No homologue[a]	Dpb11 associated factor
Sld3	Sld3	No homologue[a]	Cdc45 associated factor
RFC	RFC	RFC	Replication factor C: PCNA clamp loader
Cdc17/Pol1	Swi7/Pol1	Polα	DNA pol α
Cdc2/Pol3	Cdc6/Pol3	Pol δ	DNA pol δ
Pol 2	Cdc20/Pol2	Pol ε	DNA pol ε
Cdc44	Pcn1	PCNA	Clamp
Cdc9	Cdc17	Ligase	Ligase
Mcm10	Cdc23	Mcm10	Initiation factor
Sic 1[b]	Rum 1[b]	P27[b]	Non-homologous CKIs

[a] Homologue not (yet) identified.
[b] Not related by sequence.

Elongation

As the leading strand is elongated, a polymerase switch occurs, and the highly processive DNA polymerase δ assumes the job of DNA synthesis. It is locked into place by a clamp called PCNA, which is loaded onto the DNA by a clamp-loader called RFC. Replication proceeds bi-directionally from the origin, with each leading strand generating a replication fork structure. While DNA polymerase δ elongates the leading strand, the opposite lagging strand is synthesized in a series of short fragments by DNA polymerase α. These Okazaki fragments are joined together by a group of processing enzymes including DNA ligase, to create a single continuous strand. Processive DNA replication may be interrupted if the polymerase encounters lesions in the template, or if it runs out of nucleotide precursors. Checkpoint mechanisms that protect the integrity of the replication fork in these conditions will be discussed below.

Little is known about the resolution of two colliding replication forks from adjacent origins, or the termination of replication. However, studies show that the MCM proteins are dislodged from the chromatin as S phase progresses, and by the conclusion of DNA synthesis they are no longer DNA associated.

Regulation of Origin Firing by Kinases

Activation of DNA synthesis at the assembled preRC requires the activity of at least two kinases: a cyclin dependent kinase (CDK), and a related kinase called Cdc7 (DDK). Investigators are still examining the molecular effect of these kinases, but a general model for their function has been determined (Figure 1).

Cdc7 (DDK)

The Cdc7 kinase is essential for initiation of DNA replication. It acts at individual replication origins to initiate DNA synthesis. Its activity requires binding to a regulated subunit, originally identified as Dbf4, which is required for the catalytic Cdc7 subunit to recognize its substrates and targets it to the preRC. Dbf4 is regulated

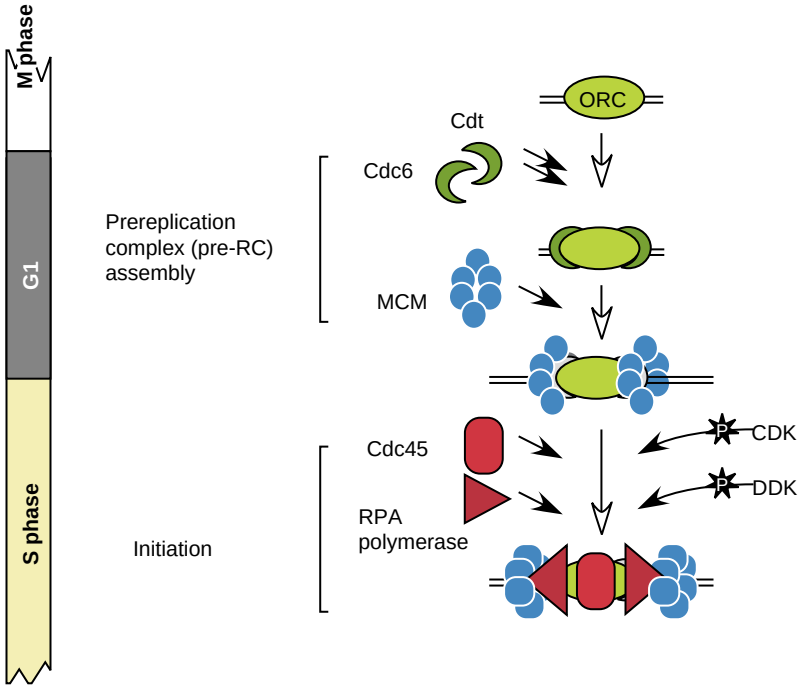

FIGURE 1 Ordered assembly of the prereplication complex (pre-RC) occurs during late M and G1 phase. Initiation at individual replication origins occurs during S phase. Kinase activity is indicated by stars and results in recruitment of DNA synthesis factors. Positive effects, arrow; Negative effects, bars.

both transcriptionally and posttranslationally, and restricts kinase activity to the S phase of the cell cycle. The Cdc7 kinase is sometimes called a DDK, or Dbf4-dependent kinase, in recognition of its similarity to CDKs. *In vitro* data indicate that Cdc7 kinase can phosphorylate components of the preRC and initiation proteins, including MCM proteins, Cdc45, and DNA polymerase α.

A change-of-function mutation in *S. cerevisiae MCM5* was isolated that completely bypasses the requirement for Cdc7 kinase. This led to the suggestion that phosphorylation of the MCM complex by Cdc7 results in a conformational change in the complex that allows Cdc45 to bind to the origin. As described above, Cdc45 binding is a prerequisite for assembly of RPA and primase, and is thought to be limiting for replication. This model has not been confirmed biochemically, but is consistent with genetic data.

Cyclin-Dependent Kinase

CDKs are the engine of the cell cycle, and their oscillation controls multiple events. In yeasts, a single kinase subunit switches cyclin partners during the cell cycle to provide substrate specificity. In metazoans, multiple kinases combine with multiple cyclins to achieve the same specificity. Studies *in vitro* and *in vivo* investigating replication proteins show that CDK phosphorylates ORC, MCMs, RPA, and DNA polymerase α. CDKs play both positive and negative roles in the regulation of DNA replication: while initiation clearly requires CDK activity, the kinase is also required to prevent reinitiation of origins within the same cell cycle (Figure 2).

Recent data from several systems provide an intriguing suggestion that the positive role of CDK in replication initiation operates in a pathway parallel to MCM assembly. In the two yeasts, a conserved protein called Dpb11 (Rad4) interacts with Drc1, which is a known CDK substrate. If Drc1 is not phosphorylated, it cannot bind to Dpb11. Data from *Xenopus* suggest that the Xmus101 protein (related to Dpb11) is required for Cdc45 binding. Together, these studies suggest that two components are required for Cdc45 binding: Cdc7 activation of the preRC, and CDK activation of the Dpb11 pathway. This model is speculative. However, it provides an attractive fail-safe mechanism for the cell to ensure that multiple signals are integrated before it fires a single replication origin, which would significantly reduce the chance of aberrant initiation.

Coupling Replication to the Cell-Cycle Engine

Activation and inhibition of replication from individual origins is controlled at multiple levels that ultimately depend upon the oscillation of CDK activity during the cell cycle. This oscillation reflects the control of

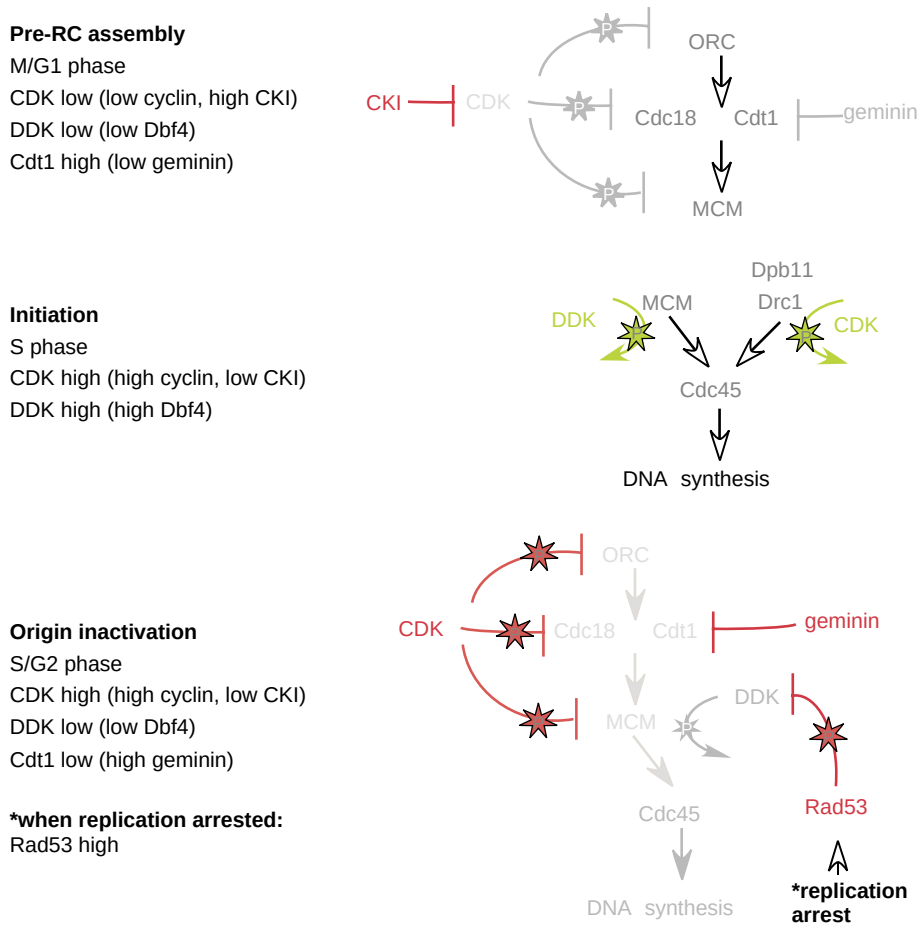

FIGURE 2 Positive and negative regulation of S phase initiation prevents re-replication. The pre-RC is assembled on origins when CDK activity is low, and reassembly is prevented when CDK activity is high. Origins only fire when both CDK and DDK are active on pre-RCs. Fluctuation in the levels or activity of cyclins, cyclin kinase inhibitors (CKI), Dbf4 protein, and geminin contribute to this regulation. Under conditions when defects in replication block synthesis, Rad53 checkpoint kinase is activated to prevent further origin firing and to protect the structure of active replication forks. Gray text/arrows indicates inactivated pathway components.

the individual cyclins. The DDK subunit Dbf4 is also subject to this regulation (Figure 2).

CDK Inhibitors and Proteolysis

CDK activity is regulated at multiple levels including phosphorylation. Most obviously, association of the kinase with transiently produced cyclin proteins provides temporal specificity (Figure 2). The cyclins are targeted for destruction by specific ubiquitination complexes at various points in the cell cycle. The Dbf4 subunit of the DDK in yeasts (and probably in larger cells) also oscillates in the cell cycle. It is regulated transcriptionally, and is also a target for ubiquitination during M phase, which restricts its activity to the S phase of the cell cycle. Thus, destruction of proteins in M phase helps maintain the timing of events in S phase.

Specific inhibitor molecules expressed during G1 also modulate CDK activity prior to S phase. These are usually specific to particular cyclin forms of the CDK. These inhibitors keep kinase activity repressed, which allows assembly of a preRC. As cells proceed towards S phase, the increasing levels of cyclin lead to increasing CDK activity which ultimately overcomes the inhibitor. The accumulating CDK phosphorylates its inhibitor, leading to its ubiquitination by an S-phase specific complex that targets the inhibitor for destruction. Although this same general pattern describes most cell types, surprisingly the individual CDK inhibitor molecules in different species such as *S. cerevisiae* Sic1, *S. pombe* Rum1 and human Kip1 are highly diverged, and show no primary sequence homology.

In mammals, Cyclin D/CDK4 phosphorylates and inactivates the Rb protein. Active Rb inhibits E2F, a component of the S-phase-inducing transcription factor; thus Rb needs to be inactivated before S phase can initiate. Because Rb inhibits entry into S phase and the cell cycle, its loss can lead to dysregulation of cell-cycle progression, so it is not surprising that Rb was originally identified as a tumor suppressor.

Activation of the preRC: Once and Only Once

The negative role of CDKs in preventing reinitiation of DNA replication is dramatically illustrated in fission yeast, in which overproduction of the CDK inhibitor Rum1 results in cells repeating S phase many times, without an intervening mitosis. The CDK is inhibited so it cannot promote mitosis, or prevent reinitiation of replication origins; however, the S-phase-promoting form of the CDK remains active.

The targets of the CDK for this inhibitory activity include several factors at the replication origin. Data suggest that the ORC complex is a CDK target that prevents re-replication. Similarly, Cdc6 protein is tightly regulated so that it is only present in the nucleus at the time of preRC assembly (between mitosis and S phase). It is a CDK substrate, and depending on the system, is either degraded, or exported from the nucleus, in response to phosphorylation. In metazoans, Cdt1 associates with an inhibitor molecule called geminin, which itself is degraded during mitosis to free active Cdt1. Thus, active forms of Cdc6 and Cdt1 are only present at the time of preRC assembly to allow MCM loading. This provides one way to ensure that origins cannot be reactivated in a single cell cycle.

The MCM complex, although present throughout the cell cycle, can only bind at the origin in the presence of Cdc6 and Cdt1. The MCM complex is dislodged during replication, and some subunits are phosphorylated by CDK. In the yeast *S. cerevisiae*, this phosphorylation results in the active export of MCMs from the nucleus as S phase proceeds. The dislodged proteins remain in the nucleus in other species, but are unable to bind the chromatin. The MCMs cannot regain access to the origin (or in *Saccharomyces*, the nucleus) until CDK levels fall at the end of mitosis, and Cdc6 and Cdt1 are active again in the next G1 phase.

This sequential requirement for origin binding allows tight cell-cycle regulation of initiation. Low CDK activity allows pre-RC assembly. High CDK activity allows origin firing, but prevents reassembly of initiation factors. The CDKs thus play a dual role by both promoting initiation and preventing re-replication at individual origins.

Genome Integrity during S Phase

The assembly and elongation of a replication fork involves nicks and unwinding, generating fragile regions in the chromosome that may be prone to breakage. Replication does not proceed all in one piece, but involves pauses and stops along the way. Thus, the cell must have a sensitive quality control mechanism to prevent damage from occurring, and to respond appropriately if it does occur. The response prevents mitosis (by inhibiting the mitotic CDK), and repairs the damage (by activating repair proteins). Components of the replication checkpoint pathways are responsible for processing these signals and generating the correct response. Proteins required for repair via recombination are also likely to be important components for quality control during DNA replication.

Data suggest that the Rad53/Cds1/Chk2 kinase is a crucial component of the response to replication defects in all eukaryotes. In a few species, cells can survive loss of this kinase, but even these survivors show genome instability and sensitivity to damaging agents when it is missing. Some experiments suggest that the Rad53/Cds1/Chk2 kinase regulates the timing of origin activation even in normal cells, by inhibiting DDK activity. But its best-understood function is in response to replication arrest early in S phase. The kinase maintains the structure of the assembled replication fork and promotes repair, by phosphorylation of substrates in the recombination-repair pathway. It also prevents initiation from late origins during replication arrest by inhibiting DDK activity.

Regulating Chromosome Structure during S Phase

The events of S phase are intimately linked to chromosome structure. Although the mechanism is not clear, it is known that cohesion between sister chromatids is established during S phase, as the sister chromatids are generated. Cohesion is essential for proper segregation of the chromosomes during mitosis. It prevents chromosome loss, contributes to centromere structure, and helps orient the chromatids to the opposite spindles. Whether the passing replication fork activates the cohesin proteins, or they are activated by the S-phase kinases, remains to be determined.

Chromatin assembly is also affected during S phase. The cell must assemble its newly duplicated DNA into nucleosomes and higher-order chromatin structures. The mechanisms for this are also not well understood, but are likely to involve conserved protein complexes activated during DNA replication. Chromatin structure may in turn regulate S-phase timing. Recent studies suggest that modification of histones by acetylation may help determine the timing of firing for individual origins.

Conclusions

Events during S phase have profound effects on chromosome biology throughout the cell cycle. The replication fork has an enormous capacity to remodel chromatin.

In addition, activation of specific kinases only during S phase can provide a temporal link between DNA replication and modification of other proteins. Clearly, investigators are only beginning to trace these links. The study of S-phase regulation of multiple chromosome events will expand for years to come.

See Also the Following Articles

DNA Ligases: Mechanism and Functions • DNA Ligases: Structures • DNA Replication Fork, Bacterial • DNA Replication: Initiation in Bacteria • Recombination-Dependent DNA Replication

Glossary

CDK Cyclin-dependent kinase, a family of kinases that requires binding to a regulatory subunit called a cyclin to be active against exogenous substrates.

CKI Cyclin-kinase inhibitor.

DDK DBF4-dependent kinase Cdc7, required for replication initiation.

origin Site of replication initiation in the genome; usually intergenic, but often has no defining sequence.

preRC Prereplication complex assembled before origin firing comprises ORC, Cdc6, Cdt1, and MCM proteins.

Further Reading

Bell, S. P., and Dutta, A. (2002). DNA replication in eukaryotic cells. *Annu. Rev. Biochem.* **71**, 333–374.

Diffley, J. F., and Labib, K. (2002). The chromosome replication cycle. *J. Cell Sci.* **115**, 869–872.

Kelly, T. J., and Brown, G. W. (2000). Regulation of chromosome replication. *Annu. Rev. Biochem.* **69**, 829–880.

Lei, M., and Tye, B. (2001). Initiating DNA synthesis: From recruiting to activating the MCM complex. *J. Cell Sci.* **114**, 1447–1454.

Takisawa, H., Mimura, S., and Kubota, Y. (2000). Eukaryotic DNA replication: From pre-replication complex to initiation complex. *Curr. Opin. Cell Biol.* **12**, 690–696.

Biography

Susan L. Forsburg is an Associate Professor of Molecular and Computational Biology at the University of Southern California in Los Angeles. Her research investigates the initiation of DNA replication and regulation of chromosome dynamics in the fission yeast *Schizosaccharomyces pombe*. Prior to joining USC in 2004 she was on the facility at the Salk Institute in La Jolla, California. She received her Ph.D. from MIT, and carried out postdoctoral training at the Imperial Cancer Research Fund at Oxford University.

Cell Cycle: DNA Damage Checkpoints

Jean Y. J. Wang
University of California, San Diego, La Jolla, California, USA

DNA damage activates cell cycle checkpoints to prevent replication and segregation of damaged genome. DNA damage also inhibits cellular differentiation, activates apoptosis, and induces premature senescence. Defects in these checkpoint responses to DNA damage contribute to tumor progression, resistance to radiation/chemotherapy, and the development of degenerative diseases.

Overview

The orderly progression through a cell division cycle is controlled by a series of checkpoints. Two fundamental checkpoints, i.e., replication checkpoint and spindle checkpoint, operate in every round of cell cycle (Table I). The replication checkpoint monitors progress of DNA replication; it prevents entry into mitosis until replication is completed. The spindle checkpoint monitors attachment of chromosomes to the mitotic spindles; it prevents segregation of sister chromatids until they are properly aligned on the metaphase plate. Under normal physiological conditions of abundant energy and nutrients, these checkpoints are experimentally invisible. Perturbation in the cellular environment can prolong the operation of these two checkpoints and/or activate additional checkpoints, leading to an observed inhibition of cell cycle progression.

This article discusses three distinct cell cycle checkpoints activated by DNA damage: the G1/S checkpoint, the intra-S checkpoint and the G2/M checkpoint (Figure 1). The G1/S checkpoint inhibits S-phase entry in G1 cells that have not yet committed to DNA replication. The intra-S checkpoint prevents initiation of DNA replication at origins that have not yet been activated. The G2/M checkpoint inhibits entry into mitosis. DNA damage also delays differentiation, activates programmed cell death, or induces premature senescence (Figure 2). The inhibition of cell cycle progression or differentiation is reversible, allowing resumption of cell proliferation and differentiation after DNA repair. Apoptosis and premature senescence are irreversible, most likely triggered by the accumulation of persistent lesions in the genomic DNA.

Cell Cycle Checkpoints Activated by DNA Damage

G2/M Checkpoint

The G2/M checkpoint is activated by a variety of DNA lesions, including base modification, cross-linking, and strand break. The sister chromatids in G2 cells are advantageous to DNA repair. Thus, G2 arrest serves two important purposes: to promote the repair of DNA lesions and to prevent mitotic catastrophe caused by segregating damaged DNA. The G2/M checkpoint causes G2 arrest by blocking mitosis (Table I).

Inhibition of Mitosis

In all eukaryotic cells, mitosis requires the cyclin-dependent protein complex of Cdc2/M-cyclin (also known as MPF). This MPF complex is formed throughout S and G2, but held in a latent state through phosphorylation of a threonine and a tyrosine in the N-terminal ATP-binding lobe of Cdc2. The G2/M checkpoint prevents dephosphorylation of Cdc2, holding MPF in the inactive state, and thereby prolongs G2 phase of the cell cycle (Figure 1).

DNA damage maintains the inhibitory phosphorylation of Cdc2 by several mechanisms. Dephosphorylation of Cdc2 at the two inhibitory sites requires a dual specificity phosphatase encoded by the highly conserved Cdc25 gene. DNA damage causes an inhibition of Cdc25 phosphatase through the Chk1 kinase, which is also conserved in all eukaryotes. Chk1 phosphorylates Cdc25 to inhibit its activity and its access to MPF. Sequestration of phosphorylated Cdc25 requires the adaptor protein 14-3-3, another function that is conserved through evolution. The Cdc25 phosphatase is further controlled by DNA damage

TABLE I

Summary of Cell Cycle Checkpoints

Checkpoint	Trigger	Target of inhibition
Replication checkpoint	Cell cycle intrinsic	MPF
Spindle checkpoint	Cell cycle intrinsic	Sister chromatin separation
G2/M checkpoint	DNA lesions	MPF (Sister chromatin separation)
Intra-S checkpoint	DNA lesions (stalled replication forks)	Origins of replication
G1/S checkpoint	DNA lesions	SPF

through the inhibition of polo-like kinase 1 (Plk1), which activates Cdc25. DNA damage also maintains the activity of Wee1, the conserved kinase that phosphorylates Cdc2 at the inhibitory tyrosine site. Therefore, DNA damage targets several regulators of MPF to keep it in the latent state and thereby blocking the entry into mitosis.

Replication Block Also Inhibits Mitosis

The cell cycle intrinsic replication checkpoint also controls the activity of MPF (Table I). Experimentally, replication checkpoint function is measured by the inhibition of MPF under conditions when DNA replication is blocked. Hydroxyurea (HU), an inhibitor of nucleotide biosynthesis, is commonly used to reveal the replication checkpoint. In the fission yeast, HU-induced inhibition of MPF requires Cds1 kinase, another checkpoint protein conserved in all eukaryotes. The budding yeast contains two Cds1-related kinases: RAD53 and DUN1. The mammalian homologue of Cds1 is commonly known as the Chk2 kinase. Similar to Chk1, Cds1 (Chk2) kinase also inhibits Cdc25 to keep MPF in the inactive state. DNA damage-induced G2 arrest is therefore triggered by a mechanism that overlaps in part with the cell-cycle-intrinsic replication checkpoint.

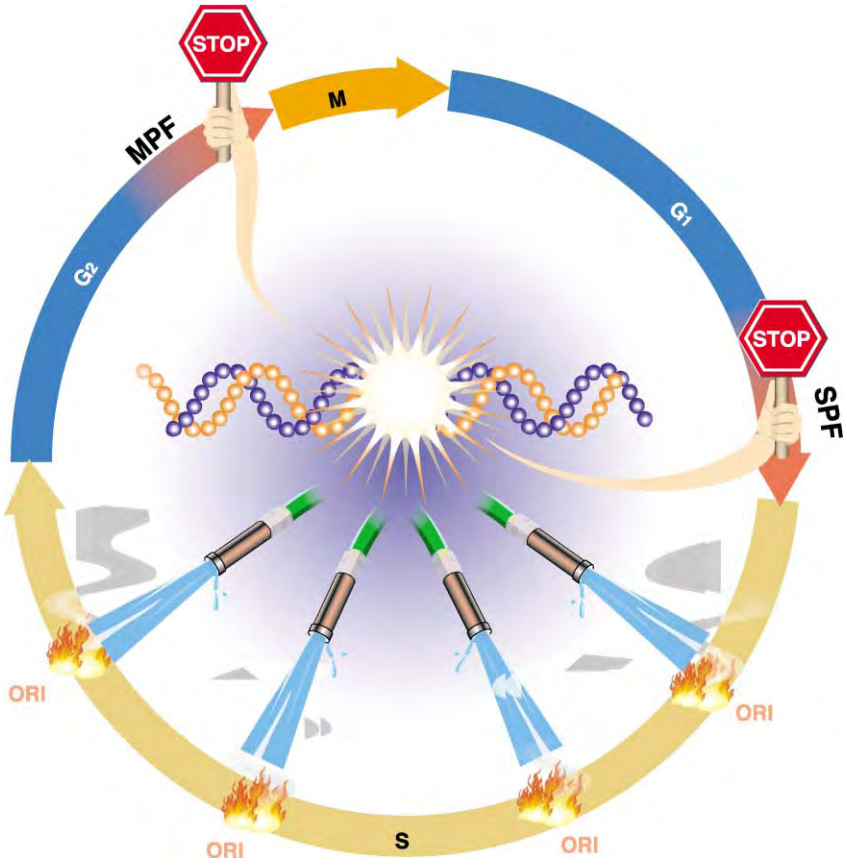

FIGURE 1 DNA damage checkpoints. DNA lesions activate three distinct cell cycle checkpoints. The G1/S checkpoint prevents G1 cells from entering S phase by inhibiting the function of S-phase-promoting factor (SPF). The intra-S checkpoint inhibits the origins of replications (ORI). The G2/M checkpoint prevents G2 cells from entering M phase by maintaining the M-phase-promoting factor (MPF) in its latent, inactive state.

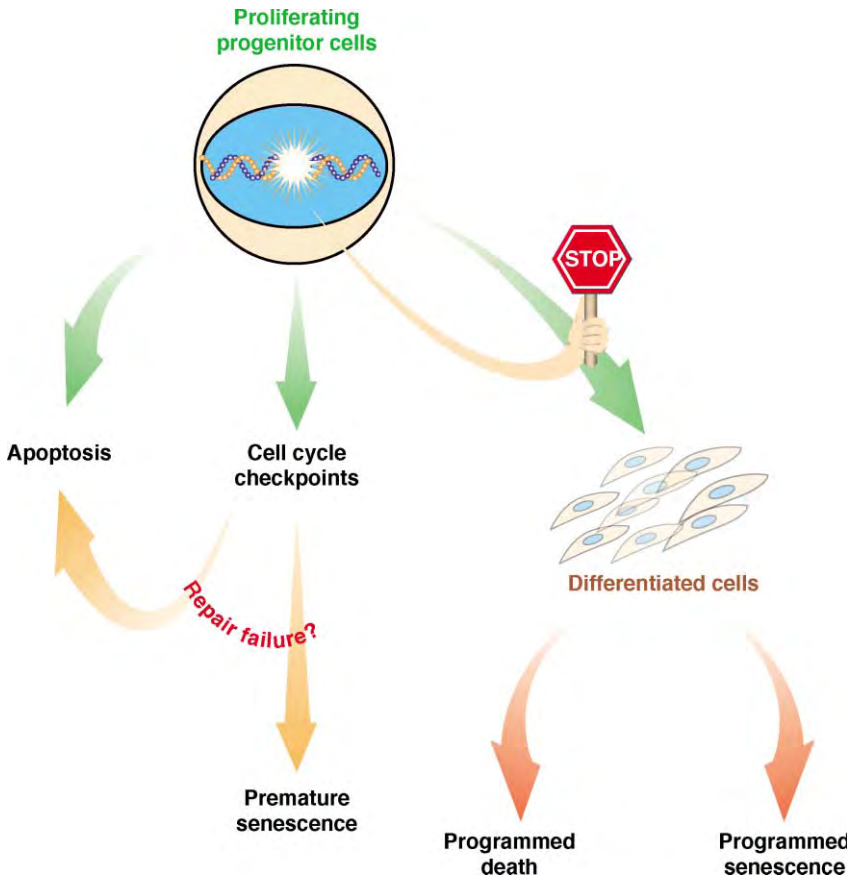

FIGURE 2 DNA damage responses. Cell cycle checkpoints are among several different cellular responses to DNA damage. In some cell types, DNA damage triggers a rapid death response, through the activation of the cellular suicide program (apoptosis). DNA damage also halts differentiation, preventing the global reprogramming of gene expression until lesions are repaired. Death and senescence are preprogrammed for different types of terminally differentiated cells. Interestingly, DNA damage can also cause death or senescence as a delayed response that is likely to be triggered by failure in DNA repair. The choice between apoptosis or premature senescence is not determined by the damage alone, but also dependent on cell type and developmental lineage.

Overlapping Function of Chk1 and Chk2 Kinases in Blocking Mitosis

In fission yeast, Chk1 is required for DNA damage to cause G2 arrest; whereas Cds1 is required to prevent premature mitosis when replication is blocked. In the budding yeast, RAD53 is required for both the replication checkpoint and the damage-induced G2/M checkpoint. Unlike the fission yeast, the budding yeast does not arrest in G2 following DNA damage. Instead, the budding yeast arrests at the metaphase–anaphase transition, unable to separate sister chromatids. Thus, DNA damage activates a G2/M-phase checkpoint that overlaps in part with the spindle checkpoint in the budding yeast. Whether DNA damage also maintains the cohesion of sister chromatids in other eukaryotic cells awaits further investigation. In mammalian cells, current results suggest Chk1 and Chk2 to have redundant and overlapping functions in DNA damage-induced G2 arrest. In mouse embryonic stem (ES) cells, elimination of Chk1 but not Chk2 causes mitotic catastrophe, suggesting Chk1 to have an essential role in preventing premature mitosis in every round of the ES cell cycle.

Intra-S Checkpoint

The intra-S checkpoint is activated by DNA lesions that impede the progress of replication forks. The eukaryotic genomes are divided into replicons, each with an origin of replication. During G1 phase, origins become licensed for replication. Not all of the licensed origins are activated at the onset of S phase. Instead, they are activated in stages; some of them activated early, others late in S phase. When ongoing replication forks are stalled due to DNA lesions, intra-S checkpoint is activated to prevent initiation at licensed origins that have not yet been activated (Table I). Stalled replication, as discussed above, also prevents the activation of MPF; this is known as the replication checkpoint. Therefore, stalled replication forks can cause the inhibition of

replication origins (intra-S checkpoint), or the inhibition of MPF (replication checkpoint) (Table I).

Intra-S Checkpoint Defect in *Ataxia telangiectasia*

In mammalian cells, defect in the intra-S checkpoint was first described decades ago as radiation-resistant DNA synthesis (RDS) in cells isolated from patients suffering from the genetic disease *Ataxia telangiectasia* (AT). Exposure of normal human fibroblasts to ionizing radiation causes a transient inhibition of DNA synthesis due to the inhibition of replication origins. Thus, ionizing radiation (IR), which generates single-stranded and double-stranded breaks, can activate the intra-S checkpoint. Fibroblasts from AT patients continue to synthesize DNA irrespective of IR, i.e., exhibiting the phenotype of RDS. Therefore, RDS results from a defect in the intra-S checkpoint; and *ATM*, the gene mutated in AT, is required for IR to activate the intra-S checkpoint in mammalian cells.

Inhibition of Replication Origins

The target of inhibition by the intra-S checkpoint is the licensed origins of replication. Licensing of replication is a complicated process involving the orderly assembly of a large protein complex called the pre-RC (replication complex) during G1. The pre-RC is then converted to pre-IC (initiation complex) in late G1. Activation of the pre-IC initiates the onset of S phase. The formation and activation of pre-IC requires two types of protein kinase complexes: the Cdk/S-cyclin complex and the Cdc7/Dbf4 kinase complex, both are conserved through evolution. In the budding yeast, inhibition of late origins during S phase requires the RAD53 kinase and involves the inhibition of Cdc7/Dbf4. In mammalian cells, the IR-induced and ATM-dependent intra-S checkpoint requires the Chk2 kinase, which phosphorylates Cdc25A to promote its degradation. Mammalian cells contain three Cdc25 genes: *A*, *B*, and *C*. Cdc25C dephosphorylates and activates the Cdc2/M-cyclin complex (MPF), whereas Cdc25A dephosphorylates and activates the Cdk/S-cyclin complex (S-phase-promoting factor, SPF). Degradation of Cdc25A, therefore, interferes with the formation and activation of pre-IC, leading to the inhibition of replication initiation. Whether the mammalian Cdc7/Dfb4 complex is also a target of the mammalian intra-S checkpoint remains to be determined. The Cdk/S-cyclin and Cdc7/Dbf4 kinases may not be the only targets of the intra-S checkpoint. Ongoing studies in the yeast model system have suggested several intra-S checkpoint pathways. Therefore, molecular mechanisms of intra-S checkpoint have yet to be fully elucidated.

G1/S Checkpoint

The G1/S checkpoint is activated by DNA damage in cells that have not yet initiated replication, and its function is to prevent the onset of S phase. The G1/S checkpoint inhibits Cdk/G1–cyclin to prolong the G1 phase. The G1/S checkpoint also inhibits Cdk/S–cyclin to prevent the onset of S phase, thus arresting cells in G1.

The p53-Dependent G1 Arrest

The most well-known mechanism for DNA damaged-induced G1 arrest is that mediated by the tumor-suppressor protein p53 in mammalian cells. DNA damage stabilizes the p53 protein and activates its transcription function. One of the p53 target genes is p21Cip1, a heat-stable inhibitor of Cdk/cyclin. The p53-dependent up-regulation of p21Cip1 causes inhibition of Cdk2/cyclin-E and Cdk2/cyclin-A to block S-phase entry. This p53-mediated G1 arrest is a slower response, because up-regulation of p21Cip1 requires transcription and new protein synthesis. The p53 gene is conserved in metazoan. However, the *Drosophila* p53 does not stimulate the expression of p21Cip1. Therefore, the p53/p21Cip1 pathway is not a conserved mechanism for DNA damage to cause G1 arrest.

The p53 protein belongs to a family of transcription factors with similar DNA binding specificity. The other two members, p63 and p73, are also activated by DNA damage. Together, this family of transcription factors may induce G1-arrest, premature senescence, or apoptosis in damaged cells (Figure 2). Premature senescence describes the phenotype of long-term arrest in G1, S, or G2. This long-term arrested state requires the RB-family of pocket proteins, which repress the expression of E2F-regulated cell cycle genes. DNA damage-induced apoptosis requires the functions of p53 and its related p63 and p73 proteins. The current model proposes that this family of transcription factors regulates the expression of pro-apoptotic proteins to induce cell death. At present, we do not understand how a damaged cell chooses between premature senescence and apoptosis through p53-family proteins. Choice between these two irreversible cell fates appears to be determined by cell types and developmental lineage.

Inhibition of S-Phase Entry

The up-regulation of p21Cip1 is not the only way to inhibit G1/S transition by DNA damage. In late G1 cells, Cdk2 is in complex with cyclin-E, and Cdk2/cyclin-E is required for the initiation of DNA replication. DNA damage can cause the inhibition of Cdk2/cyclin-E by two mechanisms: the up-regulation of p21Cip1 and the degradation of Cdc25A. As discussed above,

degradation of Cdc25A contributes to the inhibition of pre-IC in S phase cells. The inhibition of pre-IC can also cause G1 arrest if it occurs prior to the onset of S phase. Current evidence suggests that p21Cip1 only prevents the onset of S phase but does not contribute to the intra-S checkpoint. The degradation of Cdc25A, however, can inhibit S-phase entry and origin activation within the S phase.

Delay in G1 Progression

In the budding yeast, a short-lived G1 delay is observed in response to DNA damage. This G1 delay requires RAD53 and involves the inhibition of G1-cyclin (yeast CLN) expression. The mammalian G1-cyclins are the D-type cyclins, which form complex with Cdk4 or Cdk6. Degradation of cyclin D1 has been observed in response to DNA damage. The D-type cyclins promote G1 progression but they are dispensable for DNA replication. Loss of D-type cyclins alone is not likely to block S-phase entry, but may contribute to a delay in G1 progression.

DNA Damage Signal Transduction

The G1/S, intra-S, and G2/M checkpoints are terms to describe the distinctive effects of DNA damage on the cell cycle. These descriptive terms, however, do not imply distinctive molecular mechanisms. As discussed above, these cell-cycle effects can result from a common biochemical mechanism. For example, negative regulation of Cdc25 phosphatase can inhibit the onset of DNA replication in G1, prevent origin firing in S phase, or arrest cells in G2. Indeed, current evidence suggests DNA damage checkpoints are the effects of a common signal transduction network, the core of which is conserved in all eukaryotic cells. The conserved core components of this DNA damage-signaling network are listed in Table II. This list is far from complete, because the workings of this network are still under investigation.

The 9–1–1 Complex

Functioning at the top of the conserved signaling network is a PCNA-like protein complex composed of three proteins forming a heterotrimer that resembles the PCNA homotrimeric DNA-clamp. This PCNA-like complex is conserved from yeast to man. Based on the fission yeast gene names (RAD9, Rad1, Hus1), a unifying term has recently been coined to describe this trimer as the 9–1–1 complex. The 9–1–1 complex is loaded onto DNA by a protein (fission yeast Rad17) that resembles a subunit of the RFC (replication factor C). The normal RFC loads PCNA at the origin of replication. Rad17 is a component of a special RFC that loads the 9–1–1 complex onto damaged DNA. Together, Rad17-RFC and 9–1–1 function as a sensor of DNA damage. The 9–1–1 complex may provide a molecular platform for the assembly of DNA damage signaling complex.

TABLE II

Conserved Core Components in DNA Damage Signal Transduction

Name	Biochemical activity	Role in DNA damage signaling
Rad17-RFC	Loading the 9–1–1 clamp onto damaged DNA	Sensor
9–1–1	Heterotrimeric DNA clamp	Sensor
ATR, ATM, MEC1 (*S.c.*), Rad3 (*S.p.*)	Protein kinase of the PI3-kinase superfamily	Master switch
BRCA1, p53-BP1, MDC1, RAD9 (*S.c.*), Crb2 (*S.p.*)	Varied	Adaptor
Chk1	Protein kinase	Effector
Chk2, RAD53 (*S.c.*), Cds1 (*S.p.*)	Protein kinase with FHA domain	Effector

S.c.: Saccharomyces cerivisiae; *S.p.: Schizosaccharomyces pombe*.

Protein Kinase of the PI3K Family

The master switch in DNA damage signaling is a protein kinase of the PI3-kinase superfamily. In the budding yeast, *mec1* gene encodes this master protein kinase. In the fission yeast, *rad3* encodes a similar master protein kinase. In mammalian cells, ATR is likely to be the functional homologue of the yeast MEC1, Rad3 protein kinase. The MEC1, Rad3, and ATR kinase each associates with an accessory factor, encoded by the budding yeast Ddc2, fission yeast Rad23 and mammalian ATRIP, respectively. The MEC1/Ddc2, Rad3/Rad26 or ATR/ATRIP complex each associates with damaged DNA, in parallel with the Rad17-RFC/9–1–1 sensor. The MEC1, Rad3 and ATR kinase then phosphorylate downstream effectors to propagate the damage signals.

In mammalian cells, the ATM kinase, another member of the PI3K-family, also plays an important role in DNA damage signaling. As discussed above, ATM is required for IR to activate the intra-S checkpoint. *ATM* is not an essential gene. *Atm*-knockout mice are born, and they exhibit many of the phenotypes of AT patients. By contrast, *ATR* is essential for life. *Atr*-knockout causes early embryonic lethality in mice. Conditional knockout of *Atr* causes lethality

within one round of cell cycle, suggesting ATR to control cell cycle intrinsic regulatory processes.

Chk1 and Chk2 Kinases

Downstream of the master switch kinase is a network of substrates with varying degree of evolutionary conservation. The most highly conserved substrates with essential functions in DNA damage signaling are the Chk1 and Chk2 kinases. The fission yeast Chk1 is required for DNA damage to prevent the activation of MPF. This function is conserved for the metazoan Chk1 kinase. The mammalian Chk2 is homologous to the fission yeast Cds1, and the budding yeast RAD53 and Dun1. The Chk2-family of kinases is distinguished by the FHA domain, which is not found in Chk1. The FHA domain preferentially interacts with peptides that contain a phospho-threonine residue. The FHA domain in Chk2 mediates phosphorylation-dependent protein-protein interaction and plays a critical role in the regulation of Chk2 kinase activity. The Chk1 and Chk2 kinases are directly phosphorylated by ATR/ATM kinases in mammalian cells. Phosphorylation is necessary, although not sufficient, for activation of the Chk1 and Chk2 kinase activity.

BRCT-Containing Adaptor Proteins

The master switch kinase also phosphorylates another class of proteins, which have been postulated to function as "adaptors" in DNA damage signal transduction. The founding member of this class of adaptor proteins is the budding yeast RAD9 gene product. The RAD9 protein contains a pair of BRCT domains at its C terminus. RAD9 is phosphorylated by the PI3 kinase; and phosphorylated RAD9 has an essential role in activating RAD53 kinase. In the fission yeast, Crb2 contains a pair of BRCT domains at its C terminus and it is required for DNA damage to activate Chk1 kinase. In mammalian cells, at least three proteins have exhibited structural and functional characteristics similar to RAD9. These are BRCA1 (breast cancer associated 1), p53-BP1, and MDC1 (also known as Kiaa0170). Each of these three proteins are phosphorylated in response to DNA damage and each plays important roles in activating DNA repair or cell cycle checkpoints. Whether these BRCT proteins have specific or redundant functions in DNA damage signal transduction is presently unknown.

Other Transducers

DNA damage signal transduction involves many more proteins than those summarized in Table II. A number of downstream effectors in this signal transduction network are not conserved through evolution and not included in Table II. A good example is the p53 tumor-suppressor protein. As discussed earlier, p53 is conserved in metazoan. The conserved biological effect of p53 is to activate apoptosis in response to DNA damage. In vertebrates, p53 can additionally activate p21Cip1 to cause G1 arrest. The conserved core of the DNA damage signal transduction network, therefore, recruits non-conserved effectors to tailor the biological responses. If so, studies of the conserved core alone may not elucidate all the damage response pathways. Instead, each response to DNA damage may have to be investigated in an appropriate experimental system to identify the specific downstream effectors for that biological response.

See Also the Following Articles

DNA Base Excision Repair • DNA Damage: Alkylation • DNA Mismatch Repair and the DNA Damage Response • Mitosis

Glossary

ATM A large-molecular-weight protein encoded by the gene that is mutated in the human disease AT. AT patients suffer from cerebella degeneration, extreme sensitivity to ionizing radiation, increased cancer risk, and sterility. *Atm*-knockout mice exhibit most of the AT phenotypes, except cerebella degeneration. ATM contains a PI3-kinase homology domain and its function is required for IR to activate the DNA damage checkpoints.

ATR ATM and Rad3 related, a protein with a PI3-kinase homology domain. ATR has an essential function in mammalian cells, and is required for the activation of replication, G2/M, and intra-S checkpoints.

BRCT A modular protein–protein interaction domain conserved through evolution and found in proteins required for checkpoint activation or DNA repair.

Cdk Cyclin-dependent protein kinase. Cdk forms complex with and is activated by cyclin. Cdk1 is also known as Cdc2 kinase.

Chk1 Checkpoint kinase-1, first identified in the fission yeast and conserved through evolution. DNA damage activates Chk1 to maintain MPF in the latent, inactive state. Chk1 is not an essential gene in yeasts, but Chk1-knockout mouse ES cells die from mitotic catastrophe.

Chk2 Checkpoint kinase-2, first identified in the fission yeast as the Cds1 kinase and conserved through evolution. The budding yeast contains two Chk2-like kinases: RAD53 and DUN-1. Germline mutation of the *CHK2* gene is found in a fraction of patients with the Li–Fraumeni cancer syndrome, which can also result from germline mutation of the p53 tumor-suppressor gene.

Cyclins Activators of cyclin-dependent kinases. Cyclins are expressed and degraded periodically through the cell cycle.

FHA A modular protein–protein interaction domain conserved through evolution. FHA domain binds peptides with phosphorylated-threonine. However, binding to unphosphorylated peptide can also occur. FHA domain is found in a variety of proteins with diverse functions, including those involved in DNA damage signal transduction.

MPF M-phase-promoting factor, a protein kinase composed of a catalytic subunit Cdc2 and a regulatory subunit, M-phase cyclin.

premature senescence A prolonged growth arrest induced by DNA damage. The arrest can occur in G1, S, or G2 and is mediated by the repression of cell cycle genes.

SPF S-phase promoting factor. In the context of this article, SPF denotes the function of Cdk2, activated by the mammalian E-type or A-type cyclins.

Further Reading

Bork, P., Hofmann, K., Bucher, P., Neuwald, A. E., Attschul, S. F., and Koonin, E. U. (1997). A superfamily of conserved domains in DNA damage-responsive cell cycle checkpoint proteins. *Faseb J.* **11**, 68–76.

Durocher, D., and Jackson, S. P. (2002). The FHA domain. *FEBS Lett.* **513**, 58–66.

Melo, J., and Toczyski, D. (2002). A unified view of the DNA-damage checkpoint. *Curr. Opin. Cell. Biol.* **14**, 237–245.

Nyberg, K. A., Michelson, R. J., Putnam, C. W., and Weinert, T. A. (2002). Toward maintaining the genome: DNA damage and replication checkpoints. *Annu. Rev. Genet.* **36**, 617–656.

Rouse, J., and Jackson, S. P. (2002). Interfaces between the detection, signaling, and repair of DNA damage. *Science* **297**, 547–551.

Yang, A., Kaghad, M., Caput, D., and McKeon, F. (2002). On the shoulders of giants: p63, p73 and the rise of p53. *Trends Genet.* **18**, 90–95.

Zhou, B. B., and Elledge, S. J. (2000). The DNA damage response: Putting checkpoints in perspective. *Nature* **408**, 433–439.

Biography

Jean Y. J. Wang is a Professor in the Division of Biological Sciences at the University of California, San Diego. Her principal research interest is to understand mammalian cell growth control. Her research has been focused on elucidating the role of retinoblastoma tumor suppressor protein, Abl tyrosine kinase and p73 in regulating differentiation and apoptosis. She holds a Ph.D. in biochemistry from the University of California, Berkeley. She was also a postdoctoral fellow at the Massachusetts Institute of Technology Cancer Center.

Cell Cycle: Mitotic Checkpoint

Tim J. Yen
Fox Chase Cancer Center, Philadelphia, Pennsylvania, USA

The mitotic checkpoint is a fail-safe mechanism that evolved to ensure that cells with even a single unaligned chromosome do not exit mitosis to produce aneuploid cells. The mitotic checkpoint solves a inherent problem that arises because of the stochastic nature by which chromosomes attach to the spindle. At the onset of mitosis, chromosomes are randomly distributed throughout the cell so that not all chromosomes will achieve alignment at the spindle equator at the same time. Chromosomes located in the center of the spindle will rapidly establish bipolar attachments due to their higher frequency of encounters with microtubules. By contrast, chromosomes located near a pole will rapidly attach to that pole but attachment to the opposite pole will take more time given the lower frequency that it will find the rare microtubule that originates from the opposite pole. As the kinetochore is the structure on chromosomes that establishes connections with spindle microtubules, the checkpoint monitors this site to determine if chromosomes are properly attached to the spindle and whether it has achieved alignment.

The goal of this article is to discuss current models that explain how the checkpoint monitors kinetochore functions and how a localized defect that is restricted in space can alter the global biochemical status of a cell.

The Mitotic Checkpoint Monitors Kinetochores

The checkpoint is able to sense the status of chromosome alignment by monitoring microtubule occupancy and tension (or the lack thereof) at kinetochores. Once a defect is detected, the kinetochore generates an inhibitory signal to block the onset of anaphase. Early studies showed that a single unattached kinetochore is sufficient to arrest cells in mitosis. Thus, the mitotic checkpoint functions much like a signal transduction cascade where a defective kinetochore generates a signal that must be amplified throughout the cell to inhibit its targets. The discovery of the molecular components of the mitotic checkpoint has shed considerable light into how the mechanical activities at the kinetochore can regulate mitotic progression.

Molecular Components of the Mitotic Checkpoint

The mitotic checkpoint is specified by six evolutionarily conserved genes, BUB1, BUB3, MAD1, MAD2, MAD3, and MPS1. All of these genes are essential as inactivation of any single gene prevents cells from delaying mitosis in the presence of unaligned chromosomes. BUB1 and MPS1 are protein kinases, while the biochemical activities of the remaining proteins are unknown. It appears that MAD3 in metazoans has evolved into BUBR1, a third protein kinase of the mitotic checkpoint. It is interesting that BUBR1 may have co-evolved with CENP-E, a kinetochore motor whose activity is thought to be monitored by BUBR1 and is also only present in metazoans. With the identification of checkpoint genes, the outstanding question is how their gene products interact at the molecular and biochemical levels to specify the signaling pathway that links a defective kinetochore to inhibition of the anaphase promoting complex (APC).

Monitoring Microtubule Occupancy and Tension at Kinetochores

The discovery that mitotic checkpoint proteins preferentially localize to unattached kinetochores suggested their roles in monitoring kinetochore activities and generating the "wait anaphase" signal. In this regard, the role of the MAD2 checkpoint protein at kinetochores has been extensively characterized. Quantitative studies have shown that the staining intensity of MAD2 at unattached kinetochores can be nearly 100-fold higher than that detected at kinetochores that are fully saturated with microtubules. In contrast, the intensity of BUB1 and BUBR1 staining varies only three- to fivefold between unattached and attached kinetochores. It is now evident that MAD2 localization is sensitive to microtubule attachments rather that kinetochore tension. When microtubule dynamics is suppressed by drugs (taxol or low concentrations of nocodazole or vinblastine) or low temperature, kinetochores are fully attached with microtubules, but no tension develops. As MAD2 is

not detected at these kinetochores, the conclusion was that MAD2 monitors microtubule attachment, but not the tension. These studies therefore reinforced an early notion that kinetochore tension is monitored by the checkpoint.

How tension is monitored by the checkpoint is not fully understood but it clearly involves aurora B/Ipl1, a protein kinase that is situated between sister kinetochores where tension is developed. Recent studies in yeast and mammalian cells showed that aurora B/Ipl1 is required for cells to arrest in mitosis when their kinetochores fail to establish tension despite being saturated with microtubules. Thus, aurora B was found to be essential for cells to arrest in the presence of taxol, a drug that suppresses microtubule dynamics and thus prevents kinetochores from developing tension. Despite this data, aurora-B/Ipl1 does not behave like the other checkpoint proteins, as it is not required for cells to arrest in mitosis in response to the loss of microtubule attachments. Aurora B/Ipl may therefore provide tension-sensing checkpoint functions.

AuroraB/Ipl1 has been proposed to be part of a mechanism that ensures that improperly attached kinetochores are provided the opportunity to establish proper connections to the spindle. The need for a self-correcting mechanism is evident because of the error-prone nature by which kinetochores establish microtubule connections. Merotelic and syntelic attachments are conditions where both kinetochores are connected to the same pole or when one kinetochore is attached to opposite poles, respectively. As kinetochores with merotelic and syntelic attachments are fully saturated with microtubules, a checkpoint that is only sensitive to microtubule occupancy at kinetochores will fail to detect these aberrant connections. AuroraB/Ipl is thought to monitor merotelic and syntelic attachments as these abnormal connections accumulated when this kinase was inactivated. Aurora B/Ipl1 is thought to resolve merotelic and syntelic attachments by stimulating the release of microtubules from these kinetochores and thus promoting new rounds of interactions. Given this scenario, it is possible that kinetochores lacking tension do not directly activate the checkpoint but do so as a result of microtubule detachments that is stimulated by aurora B kinase. This could explain why, in taxol arrested cells, there is on average one kinetochore that exhibits MAD2 staining. It may be possible that this is sufficient to arrest these cells in mitosis.

The mechanism by which aurora B promotes microtubule release from kinetochores has not been clarified but is likely mediated through MCAK, an unconventional kinesin-like protein that colocalizes with aurora B and functions to depolymerize microtubules.

The Mitotic Checkpoint Monitors a Kinetochore Motor

CENP-E is a kinesin-like protein that binds to kinetochores at the onset of mitosis where it plays a critical role in establishing microtubule attachments. The link between CENP-E and the mitotic checkpoint was first established when cells whose kinetochores were depleted of CENP-E were found to arrest in mitosis. Cells defective for CENP-E functions characteristically accumulate a few chromosomes with monopolar attachments while the majority establish bipolar connections. The inability of monopolar chromosomes to establish bipolar connections is thought to reflect the importance of CENP-E in allowing kinetochores to capture the rare microtubules that emanate from the opposite pole. On the other hand, chromosomes that are positioned near the middle of the cell can establish bipolar attachments because the higher-frequency encounters with microtubules from both poles can compensate for the loss of CENP-E. Quantitative EM analysis showed that the bipolar attached kinetochores lack tension despite attaining near normal numbers of microtubule attachments. In contrast, the kinetochores of the monopolar chromosomes established very few microtubule connections. The defects of the monopolar versus the bipolar attached chromosomes are viewed differently by the mitotic checkpoint. Consistent with its role in detecting microtubule attachments, MAD2 accumulated at kinetochores of the monopolar chromosomes, while it was undetectable at kinetochores of the bipolar chromosomes. These findings clearly show that the mitotic delay induced by the loss of CENP-E may be due to loss of microtubule attachments and tension.

The precise role of CENP-E in the mitotic checkpoint has been somewhat controversial. Studies in human cells suggested that it was not essential for the checkpoint as cells were able to arrest in the absence of CENP-E. In contrast, *Xenopus* egg extracts depleted of CENP-E and hepatocytes derived from CENP-E null mice failed to delay mitosis in the presence of unaligned chromosomes. The difference in response however is most likely a function of whether the assembly of checkpoint proteins to kinetochores is dependent on CENP-E. In egg extracts, the localization of a number of checkpoint proteins to kinetochores was absolutely dependent on CENP-E. Thus, the failure of egg extracts to delay mitosis in the absence of CENP-E can be ascribed to the absence of checkpoint proteins at unattached kinetochores. This contrasts with human cells where checkpoint proteins present at kinetochores that were depleted of CENP-E. However, quantitative analysis showed that in mouse and human cells, CENP-E did affect the assembly of checkpoint proteins at kinetochores. In both species, kinetochores depleted of CENP-E had approximately two- to fourfold lower levels of

MAD1, MAD2, and BUBR1 than normal. However, this did not resolve why mouse cells failed to arrest in mitosis in the absence of CENP-E while human cells arrested. The discrepancy could be resolved if we take into account the fact that far fewer monopolar chromosomes accumulated in CENP-E depleted mouse cells than in human cells (two versus eight). Given that the reduction in the amount of checkpoint proteins at these kinetochores likely compromised their ability to generate the "wait anaphase" signal, the combined output from all of the unattached kinetochores in mouse cells may not reach a threshold level that is required to sustain a prolonged arrest. In human cells, this threshold may be achieved as a result of the higher numbers of unattached kinetochores. Indeed, both mouse and human cells depleted of CENP-E were able to arrest in mitosis if the number of unattached kinetochores were increased by using drugs that inhibit spindle formation.

The mechanism by which CENP-E function is monitored by the checkpoint is believed to be mediated by the BUBR1 kinase. This connection was uncovered when hBUBR1 was identified in a yeast two-hybrid screen for proteins that interacted with CENP-E. This interaction was subsequently validated when CENP-E and hBUBR1 were found to form a complex in cells. This finding coupled to the fact that hBUBR1 is an essential checkpoint protein suggested that hBUBR1 might act as a mechanosensor to monitor the activities of CENP-E at kinetochores (Figure 1). Consistent with this, hBUBR1 was found to be required for cells to arrest in mitosis when CENP-E functions were inhibited. The mechanism by which hBUBR1 monitors CENP-E activity remains to be clarified but the working hypothesis is that hBUBR1 kinase activity is sensitive to interactions between CENP-E and microtubules. In the absence of microtubule interactions, CENP-E assumes a conformation that stimulates hBUBR1 to generate the "wait anaphase" signal. When CENP-E is interacting productively with microtubules, hBUBR1 is then silenced. Recent *in vitro* data showed that both *Xenopus* and human CENP-E can directly bind to BUBR1 and this binding stimulated its kinase activity. As microtubules were not present in these reactions, it is possible that the interaction reflected the "checkpoint on" state. Addition of a CENP-E antibody to the CENP-E:BUBR1 complex inhibited kinase activity without disrupting the complex. The interpretation of this finding was that antibody binding altered the conformation of CENP-E so that it was unable to stimulate BUBR1 kinase activity. Thus, kinase activity of BUBR1 may be regulated allosterically by different conformational states of CENP-E. Although this model may indeed apply to the situation *in vivo*, the exact details of the mechanism remain to be clarified. For example, the *in vitro* dependence of BUBR1 kinase activity on CENP-E does not account for how cells that are depleted of CENP-E arrest in mitosis.

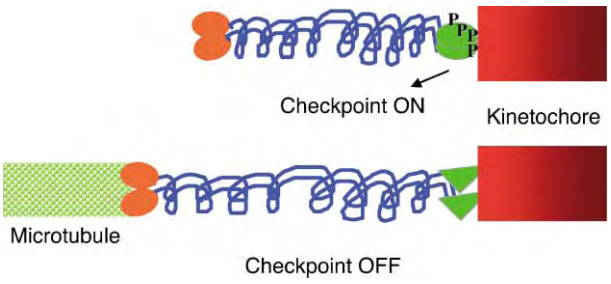

FIGURE 1 BUBR1 kinase acts as a mechanosensor that monitors CENP-E at kinetochores. BUBR1 kinase (green) interacts near the carboxy-terminus of CENP-E where it is postulated to monitor the microtubule binding status of CENP-E. In the absence of microtubule attachments, BUBR1 is phosphorylated and activated (green oval) so that it generates the "wait anaphase" signal. When CENP-E is properly attached to microtubules, it undergoes a conformational change that inhibits BUBR1 kinase (green triangles) and thus extinguishes the "wait anaphase" signal.

Inhibition of Mitotic Exit by the Checkpoint

Checkpoint proteins are functionally complex as they participate in multiple steps along the checkpoint signaling pathway. A confluence of genetic and biochemical studies showed that the target of the checkpoint is the APC, an E3 ubiquitin ligase that promotes the degradation of substrates that inhibit the onset of anaphase.

Sequestration Model

Studies in budding and fission yeast identified checkpoint defective alleles of CDC20/Slp1, a protein that was shown biochemically to activate the APC by recruiting substrates to it. These CDC20 and Slp1 mutants were unable to bind to MAD2 and thus supported *in vitro* data that MAD2 can inhibit the ubiquitin ligase activity of CDC20-dependent APC. These findings coupled with the *in vivo* observation that MAD2 exhibited a rapid rate of turnover at unattached kinetochores led to a model that described how MAD2 might act as the diffusible wait anaphase signal. In this Sequestration Model, unattached kinetochores are thought to catalytically convert MAD2 into an "activated" state which upon release from kinetochores binds to CDC20 and sequesters it from the APC (Figure 2). The existence of an activated MAD2 initially gained support when it was discovered that recombinant MAD2 existed as monomers and oligomers (di- and tetramers), but the oligomeric form was more potent at inhibiting APC than the monomeric form *in vitro*. However, the existence of a

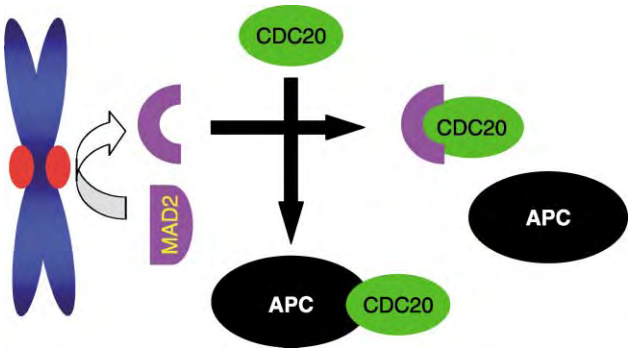

FIGURE 2 Sequestration model. The MAD2 checkpoint protein (purple semicircle) transiently binds to unattached kinetochores (red ovals) where they are converted to a form that upon dissociation will bind to CDC20. CDC20 when associated with MAD2 is incapable of activating the APC. In this model, the pool of MAD2 that is released from kinetochores acts as the "wait anaphase" signal by indirectly preventing the activation of APC.

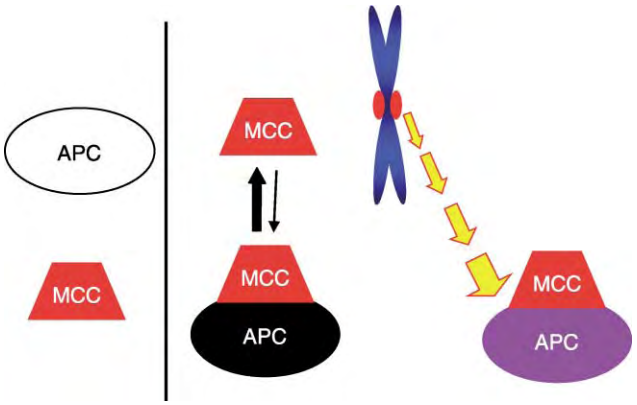

FIGURE 3 Direct inhibition model. BUBR1, Bub3, CDC20, and MAD2 form the MCC that does not depend on kinetochores and exists throughout the cell cycle. The MCC exhibits little affinity for the interphase form of the APC (white oval). Upon entry into mitosis, the APC is rapidly activated by modifications (black oval) that if unchecked will prematurely drive cells out of mitosis. A preformed pool of MCC binds and inhibits the APC. The interaction between MCC and the mitotic APC is by necessity unstable. The role of unattached kinetochores (red ovals) is to generate a signal transduction cascade that targets and sensitizes the APC (purple) to prolonged inhibition by the MCC.

MAD2 oligomer *in vivo* has been elusive. Furthermore, MAD2 mutants that failed to form tetramers *in vitro* were found to be well tolerated in yeast. These data suggest that if an activated MAD2 does exist *in vivo*, it is unlikely to be a tetramer. Regardless, the biochemical fate of the MAD2 that is released from kinetochores is unknown. Thus, it remains open as to whether turnover of MAD2 at kinetochores is functionally significant for the checkpoint.

A similar model has been proposed for how BUBR1 inhibits the APC. As with MAD2, recombinant BUBR1 was found to also bind CDC20 *in vitro*. Not surprisingly, BUBR1 was found to block CDC20-dependent activation of the APC *in vitro*. This result led to the proposal that BUBR1 may act in parallel with MAD2 to inhibit the APC *in vivo*. The caveat of these studies was that the experimental design for the BUBR1 assays employed the interphase form of the APC, which is not the *in vivo* substrate for the mitotic checkpoint. The rationale for this approach was that the activity of the interphase APC was dependent on the addition of exogenous CDC20. This assay was limited in the sense that it was designed to identify factors that inhibited CDC20. The caveat of these studies was further highlighted when recombinant BUBR1 failed to inactivate mitotic APC, which should be the physiologically relevant substrate of the mitotic checkpoint.

Direct Inhibitor Model

The Direct Inhibitor model differs from the sequestration model in that the APC is directly inhibited by checkpoint proteins and posits that unattached kinetochore sensitize the APC to its inhibitor (rather than generating a factor that sequesters an activator of the APC) (Figure 3). This model was proposed as a result of the discovery of the mitotic checkpoint complex (MCC), a factor that was identified in cell extracts that inhibited mitotic APC *in vitro*. The MCC was originally identified in Hela cells, where it was found to consist of near stoichiometric amounts of hBUBR1, hBUB3, CDC20, and MAD2. The interesting finding was that the MAD2 that was present in the MCC represented a very small fraction ($<5\%$) of the total pool of MAD2. Despite the presence of a large pool of monomeric MAD2, this pool was not found to inhibit the mitotic APC. Furthermore, MCC was more than 3000-fold more potent inhibitor of the APC than recombinant MAD2 (which was used in all the previous studies). The large difference in the inhibitory activities suggests that Hela cells do not express sufficient amounts of monomeric MAD2 to inhibit the APC. The mechanism by which MCC inhibited APC activity is not clear but is likely to depend on its ability to bind to the APC. When purified from cells, APC that was associated with MCC was found to be inactive, while APC that lacked MCC was highly active. Based on these findings, the MCC was proposed to be primary checkpoint inhibitor of the APC in mitotically arrested cells.

Although MCC was identified in mitotic Hela cells, it was subsequently found to be present and active throughout the cell cycle. Importantly, only APC that was isolated from mitotic cells was sensitive to inhibition by the MCC. How MCC distinguishes between interphase APC from mitotic APC is not

known but is most likely due to mitosis-specific modifications. Indeed, MCC appeared to preferentially bind to APC whose CDC27 subunit was mitotically phosphorylated. It is currently unknown if MCC directly interacts with CDC27 or through other APC subunits that undergo mitotic modifications. Regardless, the existence of MCC in interphase was unexpected, given that kinetochores, which are the sites thought to generate the inhibitor of the APC, are not fully formed until cells are in mitosis.

The importance of MCC in interphase becomes evident when one considers that the APC is rapidly activated at the onset of mitosis. A pre-formed pool of inhibitor provides the cell with a rapid way to inactivate APC. The inhibition of the APC by the MCC must be reversible so that cells can exit mitosis once the checkpoint is extinguished. Indeed, the interaction between MCC and the APC/C appears to be quite labile as APC activity in lysates prepared from mitotically arrested Hela cells cannot remain suppressed as ubiquitin ligase activity is reproducibly reactivated after a 10–15 min lag. This lag, however, could be extended if the extracts were supplemented with chromosomes (which provide the unattached kinetochores). Further studies using partially purified components showed that chromosomes did not enhance the inhibitory activity of MCC or the stimulating activity of CDC20, the likely target of kinetochores appears to be the APC/C.

The discovery of the MCC has led to a view that is fundamentally different from the predominant view that MAD2 cycles through kinetochores to bind and sequester CDC20 from the APC. In the "Direct Inhibitor model" the MCC acts independently of kinetochores to inhibit the APC. However, the interaction between MCC and APC is not stable unless unattached kinetochores are present. The role of unattached kinetochores is to sensitize the APC to prolonged inhibition by the MCC. The mechanism of APC sensitization is purely speculative. It is envisioned that unattached kinetochores initiate a kinase cascade that phosphorylates critical APC subunits that are required for MCC interactions. One expectation is that the modifications that sensitize APC to MCC inhibition must also be labile so that when the signaling cascade from kinetochores is extinguished, the APC will be de-sensitized. If unattached kinetochores generate a kinase cascade, it may target additional components besides the APC. One potential target is CDC20, as recent studies in *Xenopus* showed that phosphorylated CDC20 was unable to activate the APC.

The existence of the MCC has been confirmed in other species including *Xenopus* and yeast. Interestingly, MCC formation in budding yeast was also found to be independent of kinetochores. In the light of this finding, the molecular basis for the checkpoint-defective CDC20 mutants should be reinterpreted. The original interpretation was that these CDC20 mutants failed to be sequestered from the APC because they were unable to bind MAD2. From the perspective of the MCC, the checkpoint phenotype of these CDC20 mutants may result from their inability to assemble a functional MCC.

Dual Roles for Mitotic Checkpoint Proteins

The discovery that the MCC contains proteins that are also localized at kinetochores suggested that they might play dual roles in the checkpoint. These proteins participate in monitoring kinetochore defects and then generating the "wait anaphase" signal. The same proteins can act independently of the kinetochore by being part of the MCC that directly inhibits the APC.

Checkpoint Proteins can have Dual Functions

Until recently, it was technically not possible to design experiments that directly test if checkpoint proteins can serve dual functions. The solution came when it was discovered that the assembly of MAD2 onto kinetochores depended on hNuf2 and CENP-I. When kinetochores in Hela cells were depleted of hNuf2, they failed to assemble the checkpoint proteins, MPS1, MAD1 and MAD2. Similarly, kinetochores depleted of CENP-I failed to bind MAD1 and MAD2 (MPS1 was not investigated). In both cases, cells defective for hNuf2 or CENP-I functions failed to align chromosomes properly. Despite the lack of detectable MAD2 at kinetochores, the cells were able to delay mitotic exit. More surprisingly, this delay was still dependent on MAD2 as simultaneous depletion of MAD2 and hNuf2 by siRNA prevented accumulation of mitotic cells. Similarly, mitotic cells depleted of CENP-I rapidly exited mitosis when they were injected with MAD2 antibodies, while those injected with nonimmune antibodies remained in mitosis. These results are fully consistent with the idea that there are two functional pools of MAD2. The one that is present at kinetochores is involved in generating the "wait anaphase" signal, while the other pool acts independently of kinetochores. These studies indicate that the kinetochore-bound MAD2 is not essential. The characteristics of the kinetochore-independent pool of MAD2 are highly reminiscent of MCC, which is postulated to directly inhibit APC activity.

Aside from MAD2, there is also evidence to suggest that MPS1 and BUBR1 functions in a kinetochore-dependent and kinetochore-independent manner. MPS1 was one of the checkpoint proteins that was depleted

from kinetochores that lacked hNuf2. While hNuf2-depleted cells were shown to delay mitosis, cells directly lacking MPS1 failed to arrest in mitosis in response to microtubule poisons. The difference in outcomes is best explained if MPS1 possessed two distinct functions. As MPS1 is not associated with the MCC, its kinetochore-independent function remains uncertain.

Early studies of the human BUBR1 kinase showed that its kinase activity was essential for the mitotic checkpoint. Nevertheless, hBUBR1 purified from interphase cells as part of the MCC exhibits no detectable kinase activity, yet is fully capable of inhibiting APC. Likewise, *in vitro* studies showed that inhibition of the CDC20-dependent APC activity by recombinant BUBR1 can also be independent of its kinase activity. The apparent contradictory findings could be resolved by postulating that kinase activity of BUBR1 was required for the kinetochore while kinase activity was not required for its kinetochore-independent role as the MCC. This hypothesis has now been confirmed that were conducted in *Xenopus* egg extracts by BUBR1 depletion and add-back experiments. When extracts depleted of BUBR1 are reprogrammed with a kinase-dead mutant, they are no longer able to activate their checkpoint. Interestingly, if the BUBR1 (wild type or mutant) was supplemented to 20% of the endogenous level, it is sufficient to saturate all the kinetochores to levels seen in normal kinetochores. However, the presence of BUBR1 at kinetochores is still insufficient to activate the checkpoint unless the cytosolic pool of BUBR1 is also restored. This suggests that BUBR1 might provide two separable functions in the checkpoint. Whether the cytosolic BUBR1 acts by sequestering CDC20 or as part of the MCC is not clear. The finding that either wild-type or kinase-dead BUBR1 can restore the checkpoint to kinetochores that had assembled BUBR1 wild-type kinase but not the mutant supports the idea that its kinase activity was essential at kinetochores but not in the cytosol.

"Wait Anaphase" Output Regulated by Checkpoint Proteins

Studies of hNuf2 and CENP-I led to the remarkable finding that MPS1, MAD1, and MAD2 do not appear to play an essential role at the kinetochore. How do kinetochores that lack MPS1, MAD2, and MAD2 maintain the checkpoint? This is most likely achieved in part by BUBR1 and BUB1 whose levels were not noticeably depleted. However, these proteins by themselves do not appear to be sufficient to generate a robust "wait anaphase" signal from unattached kinetochores. Cells defective for CENP-I accumulate a few monopolar chromosomes, while most chromosomes appear aligned (similar to loss of CENP-E). These cells are unable to sustain a prolonged mitotic arrest because the unattached kinetochores cannot generate sufficient amounts of "wait anaphase" signal to sustain a prolonged arrest. Consistent with this explanation, if the total number of unattached kinetochores was increased by disrupting the spindle with microtubule poisons, the collective output from a large number of unattached kinetochores must reach a critical threshold that is required for cells to arrest in mitosis. The caveat of this interpretation is that, after nocodazole treatment, kinetochores depleted of CENP-I exhibited detectable MAD2, although it was 20-fold lower than the level that is present at in-control cells. Nocodazole-treated Hela cells easily contain more than 20 unattached kinetochores (Karyotype > 60 chromosomes) and should therefore be able to generate a threshold level that can normally be achieved by a single unattached kinetochore.

See Also the Following Articles

Cell Cycle: Control of Entry and Progression Through S Phase • Cell Cycle: DNA Damage Checkpoints • Chromosome Organization and Structure, Overview • Mitosis

Glossary

anaphase promoting complex (APC) A multisubunit E3 ubiquitin ligase that promotes the proteolytic degradation of substrates such as cyclin B and securin in order for cells to exit mitosis.

kinetochore A macromolecular complex that is assembled at centromeres near the onset of mitosis that is essential for chromosomes to attach to the spindle.

kinetochore tension The force that is developed between sister kinetochores because of opposing poleward forces that attempt to separate them.

monopolar and bipolar States of attachment of chromosomes to either a single pole or to both poles of a spindle.

"wait anaphase" signal An inhibitory signal generated from unattached kinetochores that diffuses throughout the cell to block the onset of anaphase.

Further Reading

Chan, G. K., Jablonski, S. A., Sudakin, V., Hittle, J. C., and Yen, T. J. (1999). Human BUBR1 is a mitotic checkpoint kinase that monitors CENP-E functions at kinetochores and binds the cyclosome. *APCJ. Cell. Biol.* **146**, 941–954.

Fang, G., Yu, H., and Kirschner, M. W. (1998). Direct binding of CDC20 protein family members activates the anaphase- promoting complex in mitosis and G1. *Mol. Cell* **2**, 163–171.

Hauf, S., Cole, R. W., La Terra, S., Zimmer, C., Schnopp, G., Walter, R., Heckel, A., von Meel, J., Riedel, C. L., and Peters, J. M. (2003). The small molecule Hesperadin reveals a role for Aurora B in correcting kinetochore-microtubule attachment and in maintaining the spindle assembly checkpoint. *J. Cell Biol.* **161**, 281–294.

Hunter, A. W., Caplour, M., Coy, D. L., Honceck, W. O., Diez, S., Wordeman, L., and Howard, J. (2003). The kinesin-related protein MCAK is a microtubule depolymerase that forms an ATP-hydrolyzing complex at microtubule ends. *Mol. Cell* **11**, 445–457.

Liu, S. T., *et al.* (2003). Human CENP-I specifies localization of CENP-F, MAD1 and MAD2 to kinetochores and is essential for mitosis. *Nat. Cell Biol.* **5**, 341–345.

Mao, Y., Abrieu, A., and Cleveland, D. W. (2003). Activating and silencing the mitotic checkpoint through CENP-E-dependent activation/inactivation of BubR1. *Cell* **114**, 87–98.

Martin-Lluesma, S., Stucke, V. M., and Nigg, E. A. (2002). Role of Hec1 in spindle checkpoint signaling and kinetochore recruitment of Mad1/Mad2. *Science* **297**, 2267–2270.

McEwen, B. F., Chan, G. K. T., Zubrowski, B., Savoian, M. S., Sauer, M. T., and Yen, T. J. (2001). CENP-E is essential for reliable bioriented spindle attachment, but chromosome alignment can be achieved via redundant mechanisms in mammalian cells. *Mol. Biol. Cell.* **12**, 2776–2789.

Sudakin, V., Chan, G. K. T., and Yen, T. J. (2001). Checkpoint inhibition of the APC/C in Hela cells is mediated by a complex of BUBR1, BUB3, CDC20, MAD2. *J. Cell Biol.* **154**, 925–936.

Weaver, B. A., Bonday, Z. Q., Putkey, F. R., Kops, G. J. P. L., Silk, A. S., and Cleveland, D. W (2003). Centromere-associated protein-E is essential for the mammalian mitotic checkpoint to prevent aneuploidy due to single chromosome loss. *J. Cell Biol.* **162**, 551–563.

Biography

Tim Yen is a senior member at the Fox Chase Cancer Center in Philadelphia, Pennsylvania. His major research interest is to characterize the molecular and biochemical composition of the kinetochore as a means to understand the mechanism of chromosome segregation in mammalian cells. He obtained his Ph.D. at the University of California at Santa Barbara and trained as a Postdoctoral Fellow at the Department of Biological Chemistry at the Johns Hopkins University School of Medicine. He was a Lucille Markey Scholar and a Scholar of the Leukemia and Lymphoma Society.

Cell Death by Apoptosis and Necrosis

Pierluigi Nicotera
MRC Toxicology Unit, Leicester University, Leicester, UK

Various genetically encoded programs involved in the signaling, initiation, and execution of cell death decide cells' fate during development and adult life. These programs can execute physiological cell death during development or tissue turnover, but are also involved in the inappropriate elimination of cells under pathological conditions. Because balanced cell turnover is essential for life, defects in cell elimination can also result in disease, the foremost example being cancer. In many circumstances, both physiological cell death and cell death in pathological settings have similar morphological and biochemical characteristics. Perhaps the best characterized biochemical and morphological changes during a cell death program are those defined as apoptosis. Apoptosis is characterized by condensation and fragmentation of the nucleus with shrinkage of the cytoplasm and exposure of surface molecules that facilitate recognition of the dying cells by phagocytes. However, other types of cell death are present and are strictly regulated *in vivo*, including cell lysis/necrosis or autophagy. Imbalance in cellular calcium regulation has been involved in both apoptotic and non-apoptotic cell death. Calcium can be a signal for cell death or simply a downstream consequence of the activation of the death machinery.

Ca^{2+} as a Signal for Cell Death

A sustained Ca^{2+} overload, such as that resulting from dysfunction of the main routes of Ca^{2+} entry or efflux or from the irreversible loss of intracellular buffering capacity, can be lethal. The idea that Ca^{2+} may be cytotoxic dates back to A. Fleckenstein's suggestion in 1968 that excessive entry of Ca^{2+} into myocytes could be the underlying mechanism of cardiac pathology following ischemia. Subsequent studies showed that agonist stimulation or cytotoxic agents could cause lethal Ca^{2+} entry into cells. Cellular Ca^{2+} overload involves multiple intra- and extracellular routes, most of which are also used for physiological signaling, which implies that not only alterations of the normal Ca^{2+} homeostasis but also changes in Ca^{2+} signaling can have adverse effects. The following have been shown in a large number of experimental paradigms: (1) Direct sustained elevation of $[Ca^{2+}]_i$ (e.g., by exposure of cells to ionophores or to conditions that cause prolonged gating of inward-directed channels) causes cell death. (2) A $[Ca^{2+}]_i$ elevation precedes cell death induced by pathophysiological stimuli. (3) Prevention of $[Ca^{2+}]_i$ elevation during such experiments can inhibit cell death. (4) Alterations of Ca^{2+}-signaling pathways (e.g., potentiation or inhibition of Ca^{2+} currents) can result in cytotoxicity.

Executors of Ca^{2+} Death Signals

Intracellular Ca^{2+} signals can set off cell demise via Ca^{2+}-dependent processes, change the mode of cell death from apoptosis to necrosis, or synergize with elements of the apoptotic death program. In particular, Ca^{2+}-activated proteases (calpains) can synergize with caspases and amplify apoptotic death routines, while modulators of apoptosis such as members of the Bcl-2 protein family can modulate Ca^{2+} compartmentalization. Hydrolytic enzymes, which include calpains, various DNAses, and lipases, are the best-characterized effectors of cell death directly mediated by calcium overload. Calpains are Ca^{2+}-activated cysteine proteases that have been implicated in toxic cell death in the liver and in excitotoxic neuronal death. Calcium-dependent DNAses can be responsible for DNA degradation, although the nature of the Ca^{2+}-dependent enzyme(s) responsible for the typical oligonucleosomal DNA cleavage has remained elusive. Among lipases, the Ca^{2+}-dependent phospholipase A_2 (PLA_2) has been implicated in neurotoxicity. Its activation results in the release of arachidonic acid and related polyunsaturated fatty acids, which are further metabolized by lipoxygenases or cyclooxygenases with concomitant generation of reactive oxygen species (ROS). In addition, PLA_2 activation generates lysophosphatids that alter the membrane structure, which may facilitate Ca^{2+} influx and Ca^{2+} release from internal stores.

Ca^{2+}, Excitotoxicity, and Death During Brain Ischemia

Excitotoxicity is a phenomenon typically encountered in neurons or myocytes following receptor stimulation by excitatory amino acids that exceeds the physiological range with respect to duration or intensity. Typical excitotoxic stimulators are capsaicin, acetylcholine, or – most important in the central nervous system – glutamate. Direct injection of glutamate is selectively neurotoxic *in vivo*. Also, inhibition of excess synaptic activity by inhibitors of glutamate receptor subtypes (mainly N-methyl-D-aspartate, or NMDA) protects neurons from hypoxia. Generally, excitotoxicity is induced by conditions favoring glutamate accumulation in the extracellular space. Typical conditions leading to increased extracellular glutamate concentration are depolarization of neurons, energy depletion due to hypoglycemia or hypoxia, or defects in the glutamate reuptake systems.

Overall, three different lines of evidence suggest the key role of Ca^{2+} in excitotoxicity: (1) There is an obvious increase in intracellular Ca^{2+} concentration ($[Ca^{2+}]_i$) in both *in vivo* and *in vitro* models of excitotoxic cell death. This has been observed in ischemic brain and in brain slices exposed to NMDA agonists or anoxia. In addition, glutamate-stimulated Ca^{2+} influx in cultured neurons has been shown by the Ca^{45} technique, and increased $[Ca^{2+}]_i$ after NMDA stimulation has been observed repeatedly using fluorescent probes. (2) Prevention of Ca^{2+} entry into the cell by removal of extracellular Ca^{2+} depletion of NMDA or by pharmacological inhibition of glutamate receptors or voltage-dependent Ca^{2+} channels prevents neuronal death in many paradigms of excitotoxicity. (3) Prevention of neurotoxicity by inhibition of downstream effects of Ca^{2+} overload strongly suggests a causal role of Ca^{2+} in excitotoxicity. Intracellular Ca^{2+} chelators can prevent ischemic damage *in vivo* and excitotoxic neuronal damage *in vitro*. Also, inhibition of effectors of Ca^{2+} toxicity such as calmodulin, calcineurin, and bNOS protects neurons from the toxicity of excitatory amino acids. On the other hand, there could potentially be other routes for Ca^{2+} entry under excitotoxic conditions.

Using a model of hypoxia (oxygen/glucose deprivation, or OGD), a new lethal pathway that involves the activation of a cation conductance (I_{OGD}) has recently been unveiled. This leads to neuronal Ca^{2+} overload in the absence of excitotoxic stimulation. I_{OGD} requires the TRMP7 ion channel protein, a member of the TRP (transient receptor potential) cation channel super family. Gating of TRMP7 occurs because of the generation of an excess of reactive oxygen/nitrogen species in anoxic neurons. Because gating TRMP7 allows Ca^{2+} entry into the neuron and Ca^{2+} can stimulate further radical production, a vicious loop leading to sustained Ca^{2+} overload is established in the absence of NMDA-R stimulation by excess glutamate.

In addition to excessive entry of Ca^{2+} trough membrane channels, mitochondrial Ca^{2+} sequestration and subsequent release play a central role in ischemia- or glutamate-mediated cell death. Nevertheless, mitochondrial Ca^{2+} release and increased Ca^{2+} influx into neurons cannot fully account for the irreversible build-up of intracellular Ca^{2+} after excitotoxic stimulation. The bulk increase in cellular Ca^{2+} should be rectified over time, unless cellular Ca^{2+} extrusion is inhibited. Inhibition of cellular Ca^{2+} efflux from cells is sufficient to trigger cell death in non-neuronal cells, and in neurons may be brought about by oxidative damage downstream of mitochondrial dysfunction. Recent work shows that calpains can cleave the plasma membrane Na^+/Ca^{2+} exchanger (NCX) in brain ischemia and in cerebellar granule neurons exposed to glutamate. Calpain-mediated NCX proteolysis is necessary for the delayed excitotoxic Ca^{2+} deregulation leading to neuronal death (for a schematic summary of excitotoxicity, see Figure 1).

Apoptosis, Necrosis, and Other Ca^{2+}-Dependent Forms of Cell Death in Brain Ischemia

Neuronal demise and neurological dysfunction in brain ischemia are clearly due to several components. Apoptosis and necrosis, in their classical definition, are two fundamentally different modes of cell death. Whereas apoptosis is characterized by a preservation of membrane integrity until the cell is phagocytosed, this is not the case in necrosis/lysis of cells. The duration and extent of Ca^{2+} influx may determine if neurons survive, die by apoptosis, or undergo necrotic lysis. Very low $[Ca^{2+}]_i$ or the prolonged inhibition of Ca^{2+} influx may be neurotoxic. A continuous moderate increase in $[Ca^{2+}]_i$, such as that produced by a sustained slow influx, may cause apoptosis, whereas an exceedingly high influx causes rapid cell lysis. For example, stimulation of cortical neurons with high concentrations of NMDA results in necrosis, whereas exposure to low concentrations causes apoptosis. Accordingly, neuronal death in experimental stroke models is predominantly necrotic in the ischemic core, but apoptosis occurs in the less severely compromised penumbra or border regions. The same applies to several other neuropathological conditions in which apoptosis and necrosis have been observed to occur simultaneously. One sensor that switches neurons toward one of the two fates is the ability of cells to generate ATP. A complete de-energization of the cell (e.g., failure of all mitochondria and of glycolysis) does not allow the

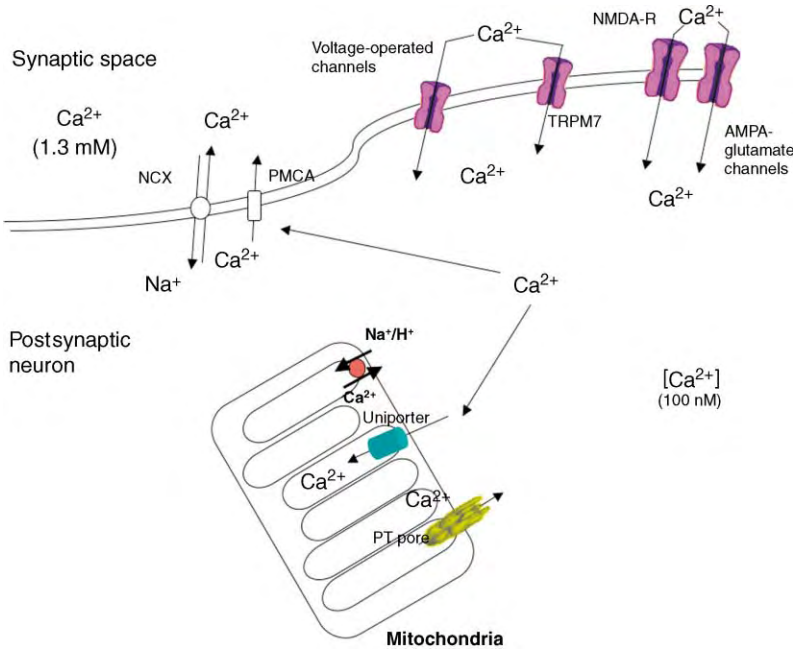

FIGURE 1 The term neuronal excitotoxicity defines as consequences of excessive stimulation of postsynaptic glutamate receptors. Excess glutamate in the synapse causes gating of AMPA and NMDA receptors. The former allows entry of Na^+ and Ca^{2+} into the neuron. Na^+ hyperpolarizes the plasma membrane and removes the Mg^{2+} block from the NMDA receptor (the NMDA receptor is normally "plugged" by Mg^{2+}). The NMDA receptor is then gated to Ca^{2+} that flows into the neuron. Additional routes for Ca^{2+} entry involve the TRPM7 cation channel and voltage-operated Ca^{2+} channels. Ca^{2+} accumulates in mitochondria as amorphous calcium phosphate. When the buffering capacity of mitochondria is overwhelmed, Ca^{2+} is released in a process known as permeability transition (PT). Efflux of Ca^{2+} from the neuron is operated by the NCX and the PMCA. When mitochondria release their Ca^{2+} and the efflux systems are unable to extrude the excess intracellular Ca^{2+}, Ca^{2+} overload becomes irreversible and causes neuronal demise.

ordered sequence of changes required for the apoptotic demise. In such a case, other processes result in rapid, uncontrolled cell lysis/necrosis. Therefore, under conditions of Ca^{2+} overload, apoptosis ensues when sufficient energy production (ATP) is available to execute the death program. The main ATP-requiring step for the execution of apoptosis is the formation of the apoptosome protein complex between cytochrome c released from damaged mitochondria, the cytosolic protein APAF-1, and procaspases. Either ATP or dATP is required to promote the functional activation and assembly of this complex, which then leads to caspase activation and cell breakdown.

Ca^{2+} Signals as Subroutines of the Apoptotic Program

The role of Ca^{2+} in apoptosis signaling was initially suggested by studies in thymocytes and lymphocytes showing that sustained Ca^{2+} increases could trigger the DNA fragmentation typical of apoptosis and all the other features of the apoptotic demise. Ca^{2+} may be central in the unfolding of the apoptotic program at different stages. Ca^{2+}-mediated mitochondrial permeability transition is recognized as one important mechanism for cytochrome c release and caspase activation. In addition, ER-mitochondrial Ca^{2+} fluxes are modulated by the Bcl-2 protein family, and caspase-mediated cleavage of Ca^{2+} transporters then results in further disruption of ER Ca^{2+} handling, with subsequent mitochondrial Ca^{2+} overload and permeability transition. Ample evidence has documented crosstalk among calpains, caspases, and other protease families, which alters the downstream effects of these families on cellular Ca^{2+} fluxes. Finally, Ca^{2+}-regulated processes are also involved in the ultimate fate of dying cells, their clearing by phagocytes due to Ca^{2+}-dependent exposure of surface recognition molecules and secondary lysis. The latter can be brought about by caspase-dependent cleavage of the plasma membrane Ca^{2+} ATPase (PMCA), which results in a secondary Ca^{2+} overload and the activation of Ca^{2+}-dependent mechanisms causing cell lysis.

See Also the Following Articles

Autophagy in Fungi and Mammals • Bax and Bcl2 Cell Death Enhancers and Inhibitors • Calpain • Caspases and Cell Death • Plasma-Membrane Calcium Pump: Structure and Function

Glossary

calpains A family of Ca^{2+}-activated proteases that mediates some of the physiological effects of Ca^{2+} signals but that can also mediate cell death. Substrates include cytoskeletal proteins, other proteases, and Ca^{2+} transport proteins.

caspases Cysteine aspartases that are activated during inflammatory processes and in apoptosis.

NCX The sodium–calcium exchanger that operates the transport of these two ions depending on their electrochemical gradients.

plasma membrane Ca^{2+} pump ATPase (PMCA) Transmembrane Ca^{2+} pump that uses ATP to pump Ca^{2+} out of cells.

Further Reading

Aarts, M., Iihara, K., Wei, W.-L., Xiong, Z.-G., Arundine, M., Cerwinski, W., MacDonald, J. F., and Tymianski, M. (2003). A key role for TRPM7 channels in anoxic neuronal death. *Cell* **115**, 863–877.

Ankarcrona, M. D. J., Bonfoco, E., Zhivotovsky, B., Orrenius, S., Lipton, S. A., and Nicotera, P. (1995). Glutamate-induced neuronal death: A succession of necrosis or apoptosis depending on mitochondrial function. *Neuron* **14**, 961–973.

Han, B. H., Xu, D., Choi, J., Han, Y., Xanthoudakis, S., Roy, S., Tam, J., Vaillancourt, J., Colucci, J., Siman, R., *et al.* (2002). Selective, reversible caspase-3 inhibitor is neuroprotective and reveals distinct pathways of cell death after neonatal hypoxic-ischemic brain injury. *J. Biol. Chem.* **277**, 30128–30136.

Lee, J. M., Zipfel, G. J., and Choi, D. W. (1999). The changing landscape of ischaemic brain injury mechanisms. *Nature* **399**, A7–14.

Lipton, S. A. (1996). Similarity of neuronal cell injury and death in AIDS dementia and focal cerebral ischemia: Potential treatment with NMDA open-channel blockers and nitric oxide-related species. *Brain Pathol.* **6**, 507–517.

Orrenius, S., Zhivotovsky, B., and Nicotera, P. (2003). Regulation of cell death: The calcium apoptosis link. *Nat. Rev. Mol. Cell. Biol.* **4**, 552–565.

Scorrano, L., Oakes, S. A., Opferman, J. T., Cheng, E. H., Sorcinelli, M. D., Pozzan, T., and Korsmeyer, S. J. (2003). BAX and BAK regulation of endoplasmic reticulum Ca^{2+}: A control point for apoptosis. *Science* **300**, 135–139.

Biography

Pierluigi Nicotera is Professor of Neuroscience and Professor of Toxicology at the University of Leicester, where he is also the Director of the UK Medical Research Council Toxicology Unit. His main research interest is in the mechanisms of cell injury and death in disease and toxic conditions. His research has contributed to the understanding of the mechanisms in which Ca^{2+} can cause cell dysfunction and death in neurons and non-neuronal cells.

Cell Migration

J. Victor Small and Emmanuel Vignal
Austrian Academy of Sciences, Salzburg, Austria

The morphogenesis of multicellular organisms involves the extensive migration of cells from primordial sites to locations destined for specific tissue development. Among the most dramatic are the movements of cells of the neural crest, which travel from the neural tube to distant sites where they differentiate into diverse cell lineages. The fusion of epithelial layers, such as those which occur during closure of the neural tube, entails coordinated cell migration. In the adult, wound closure and tissue repair depends on the migration of surrounding cells to effect the regeneration process. In defense against foreign organisms, cells of the immune system are mobilized and migrate to the sites of inflammation to engage with the enemy. In another context, cell migration contributes to the dissemination of malignant cells in the spread of cancer. Understanding cell migration has therefore much to do with life and death, which concerns all.

Metazoan cells migrate by a crawling mechanism that entails continuous changes in shape. Crawling, in turn, requires traction and this is provided by the development of transient points of anchorage with the connective tissue scaffold and with other cells. In both processes, shape change and traction, the intracellular polymer framework of the cell, the so-called cytoskeleton, plays a central role. Changes in the cytoskeleton framework are influenced, in turn, by the chemical and mechanical properties of the surrounding matrix, so there is an active crosstalk between the two. Most of what is known about the mechanisms of cell migration comes from studies of cells moving on planar surfaces *in vitro* and from investigations of the test tube properties of cytoskeleton polymers and their associated proteins. However, parallel studies indicate that the basic principles derived from these approaches apply also to cell movement in a tissue environment.

The Cytoskeleton

The cytoskeleton is composed of three distinct, but interlinked networks of polymers, composed of actin, tubulin, and proteins of the intermediate filament family, together with many associated proteins. The term cytoskeleton is a misnomer, because the cytoplasmic filament networks that make it up are in a state of continuous turnover and rearrangement. Cell migration is driven primarily by the programmed turnover of the actin cytoskeleton, but microtubules exert an important influence on polarization and guidance, which is required for directional motility. Intermediate filaments do not appear to play an important role in cell motility, but a subtle modulatory role cannot yet be excluded.

The Actin Cytoskeleton

The actin cytoskeleton is composed of actin filaments organized in networks and bundles: the salient features of the actin cytoskeleton in a fibroblast are illustrated in Figures 1 and 2. The cell periphery is delimited by either bundles of actin filaments, running parallel to the cell edge, or by dense actin meshworks (Figure 2A) that are commonly punctuated by small, radial actin bundles, termed microspikes or filopodia (Figure 2B). The actin meshworks (Figure 2) are the structural component of the sheet-like lamella regions at the cell periphery called lamellipodia (or ruffles, when they fold upwards. Figure 3). The body of the cell is pervaded by a loose network of actin filaments, a proportion of which are organized into prominent bundles, called stress fibers. According to cell type, the ratio of peripheral actin meshworks to stress fibers differs and as a general rule, cells that migrate faster have fewer stress fiber bundles in the body of the cell. The different organizations of actin filaments that make up the subcompartments of the actin cytoskeleton are signaled via pathways involving different members of the Rho family of small GTPases: Rho for stress fibers, Rac for lamellipodia, and Cdc42 for filopodia.

One important feature of the actin cytoskeleton is its linkage to the cell membrane, which explains its pivotal influence on cell form. Major sites of linkage occur at the termini of the stress fiber bundles, which in turn correspond to sites of adhesion of the cell to the extracellular matrix. Because of their focal nature, these sites are called focal adhesions (Figure 2C). They comprise more than 50 structural, adaptor, and signaling proteins that form and regulate the linkage of the actin cytoskeleton, via transmembrane receptors of the integrin family, to the extracellular matrix. The precursors of these anchorage sites are assembled in

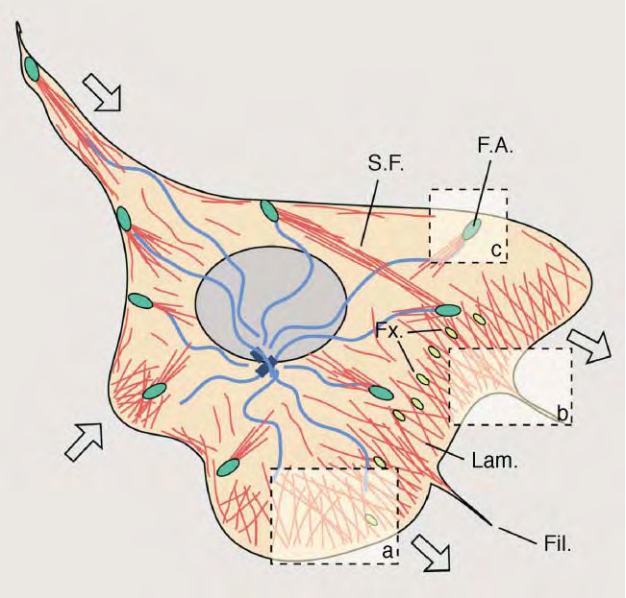

FIGURE 1 General features of the actin cytoskeleton of a migrating cell. Actin filaments are in red. Protrusion of the cell is driven by the formation of sheet-like meshworks (lamellipodia, Lam) and rod-like projections (filopodia, Fil). Early adhesions form beneath protrusions as focal complexes (Fx) and can mature into larger, focal adhesions (FA) at the termini of actin bundles, called stress fibers (SF). The polarization of the cell is reflected in a polarization of the adhesion pattern, with stationary focal complexes and focal adhesions at the front and sliding focal adhesions at the rear. Microtubules (blue) interact with adhesions and influence their turnover. Details of the boxed areas are provided in Figure 2.

association with lamellipodia and filopodia at the cell periphery and are called focal complexes (Figure 1).

Phases of Movement

In general terms, the mode of translocation of a cell can be divided into three phases: (1) protrusion of a cell front; (2) the development of adhesion to the substrate for the purpose of traction; and (3) retraction of the cell rear.

Protrusion

In the first step of movement, the cell protrudes lamellipodia and filopodia: sheet-like and rod-like processes $\sim$0.2 μm thick and several microns in length (Figures 3 and 4). The rate of protrusion varies from $\sim$2–15 μm min^{-1}. Protrusion is based on the unidirectional polymerization of actin, whereby actin monomers are inserted at the tips of actin filaments where they abut the cell membrane at the leading front (Figures 2A and 2B). Complexes of proteins are recruited at these membrane sites that signal and drive actin polymerization, downstream from Rac and Cdc42. Additional proteins are responsible for cross-linking the formed actin filaments into meshworks (lamellipodia) and bundles (filopodia) and for disassembling actin filaments at the base of lamellipodia and filopodia to provide building blocks for further protrusion. Protrusion therefore involves a regulated "treadmilling" of actin monomers from the front to the rear of lamellipodia and filopodia. This produces a "retrograde flow" of actin which is accompanied by a retrograde flow of associated material in protruding zones. The mechanisms underlying the delivery of actin and other components to the front of lamellipodia, to support polymerization and retrograde flow have yet to be clarified, but likely involve the engagement of myosin motor molecules. In their role as protruding organelles, lamellipodia and filopodia are major sites of actin filament generation in a motile cell and contribute filaments also to the cytoskeleton network that spans the cell.

Adhesion

In addition to their role in protrusion, lamellipodia and filopodia initiate adhesion to the extracellular matrix. This involves the recognition of matrix ligands on the outside and the accumulation of integrins and proteins of the adhesion machinery to form specific focal points, the focal complexes (Figure 1). The accumulation of proteins in focal complexes is likely to be linked to the cycling of proteins through lamellipodia and filopodia by retrograde flow.

Focal complexes do not move relative to the substrate and can experience one of two fates. They either exist transitorily for a few minutes and disperse, or they enlarge and differentiate into larger anchorage sites at the ends of stress fiber bundles, the focal adhesions. The transition from focal complexes to focal adhesions is linked to a switch in signaling from Rac/Cdc42 to Rho and to the engagement of muscle-type myosin with actin to form contractile bundles.

The regulation of adhesion formation and turnover is a complex process that involves both enzymatic and mechano-sensory pathways. Both focal complexes and focal adhesions are enriched in tyrosine kinases as well as their substrates and changes in their activities modulate adhesion complex turnover. Focal adhesion formation and maintenance depends also on mechanical stress in the actin cytoskeleton. This is illustrated dramatically by their disappearance when cells are treated with drugs that inhibit the interaction between muscle type myosin and actin. Mechano-sensory mechanisms therefore play a role in regulating adhesion dynamics, most likely through mechanically induced

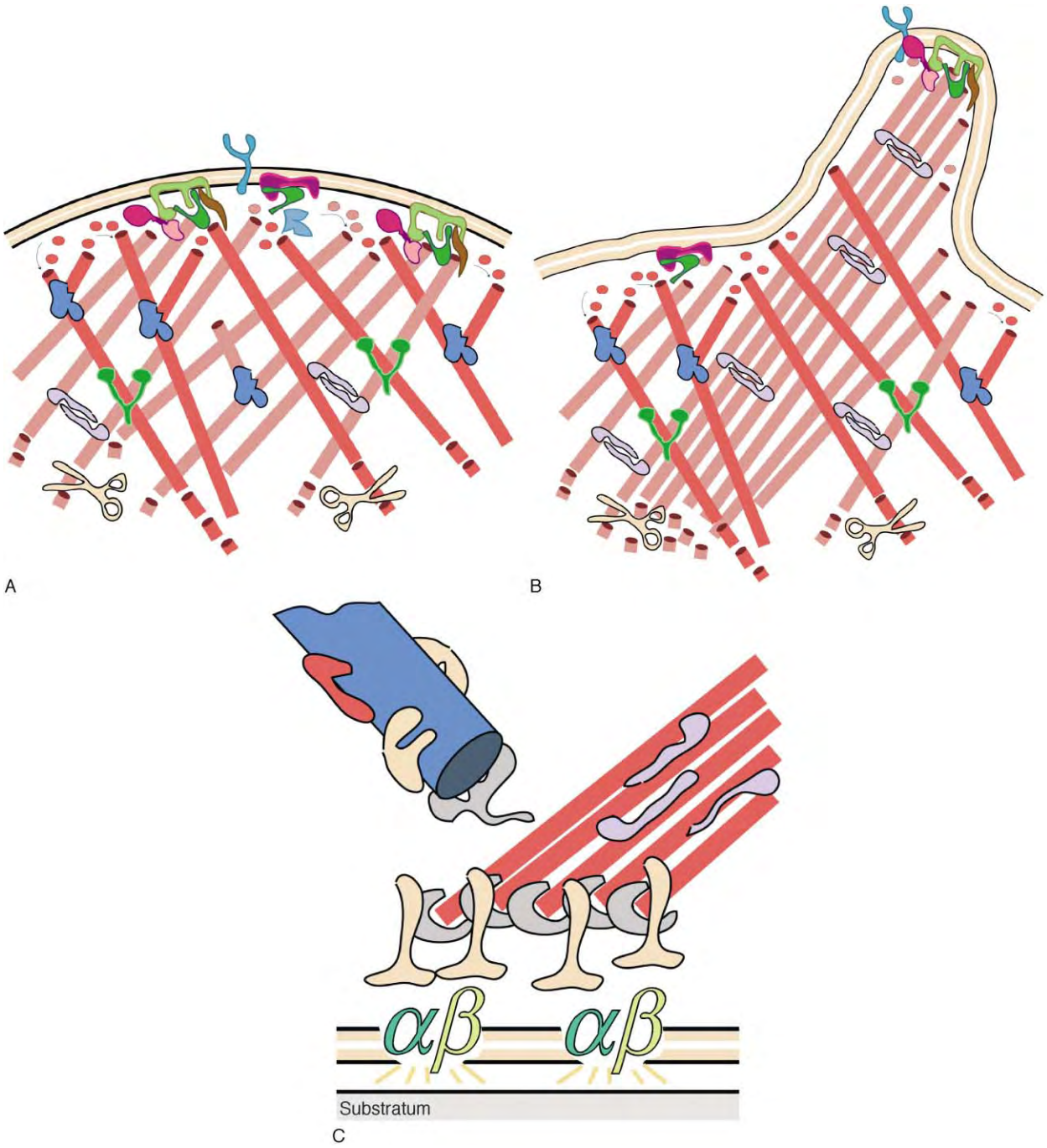

FIGURE 2 Schematic details of the boxed areas in Figure 1. Lamellipodia (A) are formed by the generation of an actin meshwork through the initiation of actin polymerization and the addition of actin monomers (red dots) at the cell membrane. Protein complexes recruited to the membrane control the polymerization process in response to signaling stimuli. Other actin-binding proteins serve to cross-link the actin network. Turnover of the lamellipodium components occurs through the depolymerization of most of the actin filaments towards the base of the lamelipodium by destabilizing and severing factors (scissors). Filopodia (B) are formed by the bundling of lamellipodia filaments, by additional proteins (antiparallel bars), followed by extension via actin polymerization at the tip. Focal adhesions (C) are sites of linkage of actin filament stress fiber bundles to the extracellular matrix via transmembrane matrix receptors called integrins ($\alpha\beta$). A complex of at least 50 structural, adaptor, and signaling proteins are recruited to these sites. The actin filaments are bundled by the cooperation of myosin and actin cross-linking proteins. Microtubules (blue cylinder) polymerize into focal adhesions and impart signals via associated proteins, that promote adhesion turnover.

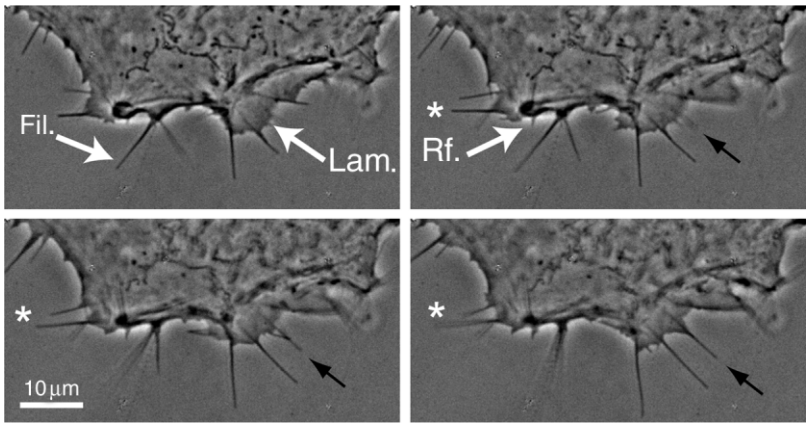

FIGURE 3 Lamellipodia (Lam.) and filopodia (Fil.) in a living fibroblast. Figure shows a sequence of video frames (20 s apart) of the periphery of a living goldfish fibroblast seen in phase contrast optics. These cells show a high incidence of filopodia. The white asterisk indicates a filopodium situated close to the ruffling region that lifted upwards during the sequence. The black arrow indicates the position of a protruding filopodium. These images were kindly supplied by Dr. Irina Kaverina.

conformational changes of specific proteins in adhesion sites.

Adhesion Asymmetry and Polarization

For a cell to move it must develop an advancing front and a retracting tail (Figure 4). This polarization process is reflected in an asymmetry of the pattern of adhesions developed with the extracellular matrix. It is interesting to consider how this asymmetry is established as it is relevant to the question of how polarization is determined.

As long as a cell edge protrudes, focal complexes are created in newly won territory under lamellipodia and filopodia and a proportion differentiates into focal adhesions. In general, however, lamellipodia and filopodia do not protrude in a persistent manner. Instead, forward advancement is the net result of repetitive protrusion and retraction events. Retraction involves the withdrawal of lamellipodia or filopodia, or their backfolding, as ruffles. When this occurs, focal complexes dissolve, or convert into focal adhesions that tether the retracted cell edge.

In the above context, polarization can be considered the result of regional changes in the ratio of protrusion and retraction events at the cell edge. Thus, at the advancing front of a migrating cell the duration of protrusion exceeds that of retraction. Elsewhere, at the rear and flanks, protrusion can occur, but retraction dominates. In the simplest terms, the front edge of a migrating cell is accordingly populated by focal complexes and the rear edge by focal adhesions. In many cases, focal adhesions are also formed behind the front edge and contribute to traction. This asymmetry of adhesion site development is the hallmark of a polarized cell.

Traction and Retraction

An important difference between focal adhesions at the front and rear of migrating cells is that those at the front remain fixed relative to the substrate, whereas those at the retracting rear and flanks can slide. Studies of fibroblasts moving on flexible substrates show that the anterior focal adhesions exert more stress per unit area on the substrate than those at the rear. The anterior adhesions therefore provide anchorage points for the actin cytoskeleton that support the retraction of the trailing cell body. Retraction itself is driven by the interaction of myosin with the actin filaments of the cytoplasmic network.

Microtubules and Cell Guidance

When fibroblasts are treated with drugs that dissassemble microtubules they become depolarized and extend protrusions in all directions. At the same time, tension in the actin cytoskeleton increases and focal adhesions grow in size. These changes are linked to an increase in the activity of Rho. Microtubules are therefore required for polarization and they exert their influence on polarity via a cross-talk with the actin cytoskeleton. The cross-talk takes place between the tips of microtubules and the focal adhesion sites at the ends of actin bundles (Figures 1 and 2C).

Microtubules grow from the centrosome towards the cell periphery, but not in a continuous manner. Instead, they exhibit alternating periods of polymerization and depolymerization in a mode referred to as

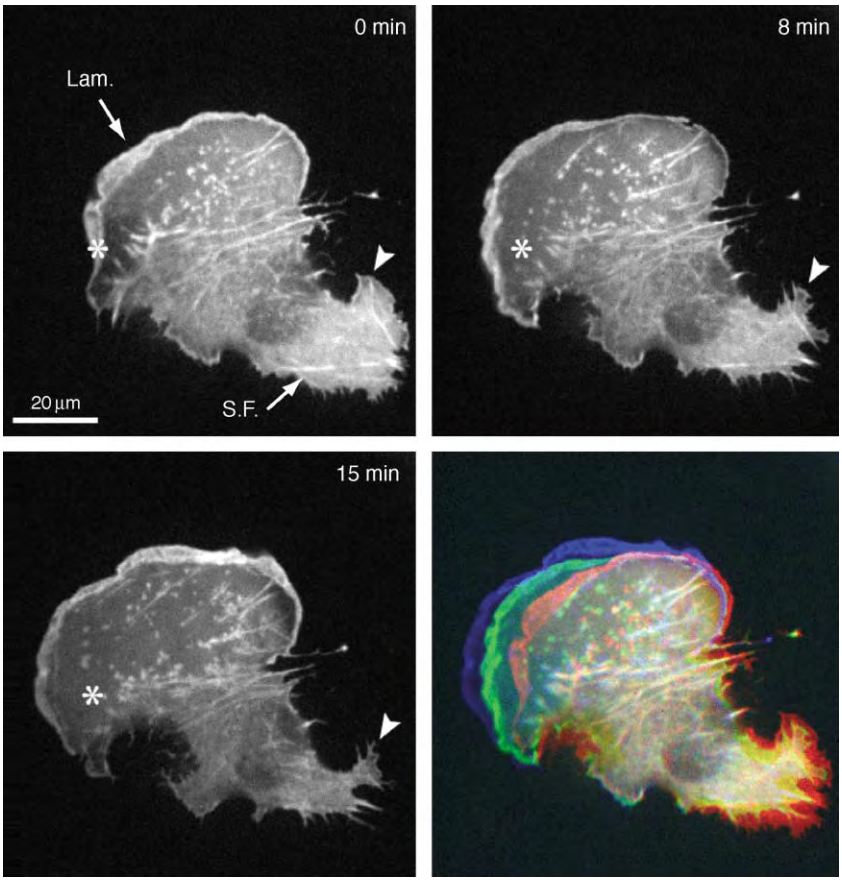

FIGURE 4 A motile melanoma cell, showing a protruding front and a retracting rear. The cell was transfected with GFP-actin and images were recorded by fluorescence optics. The protruding front is marked by a prominent lamellipodium (Lam.). When moving on laminin these cells show few filopodia. The extent of protrusion and retraction during the video sequence is indicated by reference to the fixed points marked by an asterisk and the arrowhead as well as by the color overlay of the frames. Retraction is mediated by the shortening of actin stress fiber bundles that connect to the cell rear (e.g., S.F.).

"dynamic instability." When they reach the cell periphery, microtubules target focal adhesions and this targeting can occur in a repetitive manner. Targeting is more frequent at retracting cell edges and is correlated with the dispersal of focal adhesions or with their release from the substrate. Microtubules bind various molecules including Rho family exchange factors that have an influence on the turnover of the actin cytoskeleton. Some of these associate with proteins concentrated at the growing tips of microtubules. Microtubules then serve as transmission elements to target potential regulators of actin cytoskeleton turnover to focal adhesions. Transmission most likely involves the engagement of microtubule motors to deliver the regulators to the microtubule tip.

Microtubules and Contractility

The global effect of microtubules is to reduce cell contractility. At the level of focal adhesions, microtubules appear to mediate the localized relaxation of actomyosin interactions at the ends of stress fibers, to promote focal adhesion disassembly. This occurs in a feedback mode, whereby an increase in mechanical stress at adhesion sites signals the polymerization of microtubules into them. The influence of microtubules on cell polarity can be explained by their modulation of focal adhesion turnover, in a spatially defined manner involving a mechano-sensory feedback on microtubule dynamics.

The dependence of a cell on microtubules to maintain polarity is linked to the extent of formation of focal adhesions. Very motile cells, such as neutrophils do not form stress fibers and typical focal adhesions and are less dependent on microtubules for directional locomotion. Likewise, fish epidermal keratocytes exhibit focal complexes, but lack focal adhesions and can also migrate without microtubules. Some cells appear to have the inherent ability to segregate protruding and contractile domains. But most cells are unable to maintain this segregation without the modulatory input of microtubules.

Migration *in vivo*

Cells migrating in tissues exhibit both filopodia and lamellipodia. These thin protrusive extensions are ideal for exploring and penetrating tissue spaces. They are also well suited for intercalating between cells, such as during the migration of leukocytes across endothelial layers. Stress fibers, as seen in cultured cells, are not obvious features of cells moving in a three-dimensional environment. However, inhibition of the Rho pathway – which signals contractility – inhibits the migration of primordial cells during embryogenesis and prevents tail retraction during the transendothelial migration of monocytes. Migration *in vivo* therefore involves protrusion of lamellipodia and filopodia signaled by Rac and Cdc42 as well as retraction signaled by Rho. The closure of epithelial layers during embryogenesis is likewise dependent on protrusion and retraction events, whereby the contractility of actin bundles parallel to the epithelial boundary contributes to closure in a zipper-like mode.

Further factors important for cell migration have not been discussed here. These include the cues initiating migration at an appropriate timepoint and the gradients of chemotactic factors that define the destinations of migrating cells. Needless to say, these must impinge on the network of pathways that signal to the locomotion machinery.

See Also the Following Articles

Actin Assembly/Disassembly • Centromeres • Centrosomes and Microtubule Nucleation • Focal Adhesions • Integrin Signaling

Glossary

actin filament A filament of ~8 nm in diameter, made up from two helical strands of actin monomers.

filopodia Bundles of unipolar actin filaments, ~0.2 μm in diameter, that protrude from the cell edge, normally in association with lamellipodia and ruffles. Filopodia and lamellipodia are interconvertible assemblies of actin filaments.

focal adhesions Longer-lived adhesion foci that link to contractile actin bundles (stress fibers) in the actin cytoskeleton. Both focal complexes and focal adhesions harbor more than 50 proteins, involved in structural and signaling activities.

focal complex A site of early adhesion to the extracellular matrix, formed beneath a lamellipodium or a filopodium. Focal complexes can either form and dissolve, within 1–2 mins, or they can mature into focal adhesions.

integrins A family of transmembrane receptor molecules that cluster at adhesion foci to link the matrix on the outside to the actin cytoskeleton on the inside.

lamellipodia Thin, membrane-bound leaflets of cytoplasm, 0.2–0.3 μm thick and up to several microns wide that are protruded at the cell edge, close to and parallel to the substrate. They are composed of unipolar networks of actin filaments.

Rho (Ras homology) proteins A subfamily of small GTPases whose roles include signaling to the actin cytoskeleton.

ruffles Manifestations of lamellipodia, protruding upward from the dorsal cell surface, and migrating generally rearwards over it. Lamellipodia can also fold upwards and rearwards to form ruffles.

Further Reading

Bray, D. (2000). *Cell Movements, from Molecules to Motility.* Garland, New York.

Geiger, B., Bershadsky, A., Pankov, R., and Yamada, K. M. (2001). Transmembrane extracellular matrix–cytoskeleton crosstalk. *Nat. Rev. Mol. Cell Biol.* **2**, 793–805.

Kaverina, I., Krylyshkina, O., and Small, J. V. (2002). Regulation of substrate adhesion dynamics during cell motility. *Int. J. Biochem. Cell Biol.* **34**, 746–761.

Martin, P. (1997). Wound healing – aiming for perfect skin regeneration. *Science* **276**, 75–81.

Martin, P., and Wood, W. (2002). Epithelial fusions in the embryo. *Curr. Opin. Cell Biol.* **14**, 569–574.

Montell, D. J. (2003). Border-cell migration: the race is on. *Nat. Rev. Mol. Cell Biol.* **4**, 13–24.

Small, J. V., Geiger, B., Kaverina, I., and Bershadsky, A. (2002). How do microtubules guide migrating cells. *Nature Rev. Mol. Cell Biol.* **3**, 957–964.

Trinkaus, J. P. (1984). *Cells into Organs*. Prentice-Hall. Englewood Cliffs, NJ, USA.

Webb, D. J., Parsons, J. T., and Horwitz, A. F. (2002). Adhesion assembly, disassembly and turnover in migrating cells – over and over and over again. *Nat. Cell Biol.* **4**, E97–E100.

Biography

Victor Small graduated from King's College in London in 1969 with a Ph.D. in Biophysics. From 1970 to 1977 he held a lectureship position in Aarhus University, Denmark where he began work on contractile systems and the cytoskeleton. Since 1977, he has headed the Department of Cell Biology of the Institute of Molecular Biology of the Austrian Academy of Sciences in Salzburg. His laboratory explores live cell microscopy in studies of the cytoskeleton and the mechanisms underlying cell motility.

Emmanuel Vignal is a postdoctoral Fellow at the Institute of Molecular Biology in Salzburg. He graduated in 2001 with a Ph.D. in Cell Biology from the University of Montpellier in France. His current work focuses on the molecular mechanisms of lamellipodia protrusion.

Cell–Matrix Interactions

Janet A. Askari and Martin J. Humphries
The Wellcome Trust Centre for Cell–Matrix Research, School of Biological Sciences, University of Manchester, Manchester, UK

The extracellular matrix (ECM) is a network of macromolecules that underlies all epithelia and endothelia and that surrounds all connective tissue cells. The ECM provides mechanical support and also profoundly influences the behavior and differentiation state of cells in contact with it. The main receptors mediating the interaction of cells with ECM proteins are known as integrins, referring to their function of integrating the cell's exterior with its interior. Following ligand binding, the cytoplasmic domains of integrins connect to the cytoskeleton and trigger the assembly of signaling complexes. Conversely, the binding of intracellular cytoplasmic components influences cell adhesiveness by altering integrin conformation. Thus, a large variety of complex signaling events can be transduced by integrins in a bidirectional manner across the cell membrane. These events serve to modulate and coordinate many aspects of cell behavior, such as proliferation, survival, shape, polarity, motility, gene expression, and differentiation, that are required for such fundamental processes as development, tissue morphogenesis, and wound healing within multicellular organisms. Integrins are also implicated in several disease processes such as inflammation, thrombosis, and cancer metastasis, whereas mutations in integrin genes lead to deficiencies in leucocyte adhesion, myopathy, and blistering skin diseases.

The Extracellular Matrix

Main Components

The extracellular matrix (ECM) components are diverse in composition, but they generally comprise a mixture of fibrillar proteins, polysaccharides, and glycoproteins synthesized, secreted, and organized by neighboring cells. Collagens, fibronectin, and laminins are the principal components involved in cell–matrix interactions; other components, such as vitronectin, thrombospondin, and osteopontin, although less abundant, are also important adhesive molecules.

Over 20 different collagens exist in mammals, but the most abundant exist as helical molecules that assemble into fibrils and provide tensile strength for many tissues. The ECM also contains a large number of glycoproteins, the best studied of which is fibronectin, a dimeric molecule that also forms insoluble fibrils. The laminins are heterotrimeric glycoproteins that fold into cruciform-shaped molecules and are important components of basement membranes. Fibrinogen and von Willebrand factor are also considered to be matrix proteins because they function as major adhesive molecules in blood, but they can also pass into extravascular fluid and influence cell function.

Adhesive Motifs

Although matrix proteins are large molecules, their major integrin recognition sites are very short peptide motifs of only three to six amino acids. The best known and most widespread of these adhesive motifs is arginine–glycine–aspartic acid (RGD, using the single-letter amino acid nomenclature). This motif was first discovered in 1984 by Pierschbacher and Ruoslahti in the center of fibronectin (FN), but it is also present and functional in vitronectin, von Willebrand factor, and thrombospondin. The crystal structure of the area of FN containing this motif has been solved and shows the tripeptide extending out as a loop from the surface of the protein. Similar short peptide motifs are present in other matrix proteins (see Table I). A constant feature of the motifs is the presence of an acidic residue, either aspartic or glutamic acid, which is an absolute requirement for the adhesive activity of the proteins in which they reside. As yet, no corresponding motif has been determined in laminin; however, integrin binding has been localized to distinct regions within the molecule.

In FN, a second region of the molecule, termed the synergy site, has been shown to work in concert with the RGD motif and to enhance integrin-binding affinity. Part of the synergy site is a pentapeptide proline–histidine–serine–arginine–asparagine (PHSRN). Although they probably exist, no synergy sequences have as yet been defined for other matrix proteins.

TABLE I

Adhesive Sequences in Matrix Proteins and their Integrin Receptors[a]

Matrix protein	Adhesive sequence	Integrin receptor
Collagens	GFOGER	$\alpha1\beta1$, $\alpha2\beta1$, $\alpha10\beta1$, $\alpha11\beta1$
Fibronectin	RGD	$\alpha5\beta1$, $\alpha V\beta3$, $\alpha8\beta1$, $\alpha V\beta1$, $\alpha V\beta6$, $\alpha IIb\beta3$
	LDV	$\alpha4\beta1$, $\alpha4\beta7$
	REDV	$\alpha4\beta1$
Laminins	E1′ fragment	$\alpha1\beta1$, $\alpha2\beta1$, $\alpha10\beta1$
	E8 fragment	$\alpha3\beta1$, $\alpha6\beta1$, $\alpha7\beta1$, $\alpha6\beta4$
Vitronectin	RGD	$\alpha V\beta3$, $\alpha IIb\beta3$, $\alpha V\beta5$, $\alpha V\beta1$ $\alpha V\beta8$
Fibrinogen	RGD	$\alpha V\beta3$
	KQAGDV	$\alpha IIb\beta3$
von Willebrand factor	RGD	$\alpha IIb\beta3$, $\alpha V\beta3$

[a] GFOGER, glycine–phenylalanine–hydroxyproline–glycine–glutamic acid–arginine; KQAGDV, lysine–glutamine–alanine–glycine–aspartic acid–valine; LDV, leucine–aspartic acid–valine; REDV, arginine–glutamic acid–aspartic acid–valine; RGD, arginine–glycine–aspartic acid.

Integrins

Structure

Integrins are noncovalently linked dimers consisting of an α- and a β-subunit, and the 18 α- and 8 β-subunits that have been identified in humans combine to form 24 different receptors. Integrin homologues are present in organisms ranging from sponges to humans, indicating their central role in metazoan evolution. Integrins possess large extracellular domains, approximately 1200 amino acids in α-subunits and 800 in β-subunits, a transmembrane domain, and short cytoplasmic regions of 50 residues or less. The exception to this rule is the $\beta4$-subunit, which has a cytoplasmic domain of over 1000 amino acid residues. In addition, half of all α-subunits contain an extra 200 residue module toward their N terminus (see Table II), which has homology with the von Willebrand factor A-domain and is referred to as the α A- or I- (for inserted) domain. Several α A-domains have been crystallized and all adopt a Rossmann fold characterized by central β-sheets surrounded by α-helices. A conserved motif, the metal-ion-dependent adhesion site (MIDAS), which includes the sequence aspartic acid–any residue–serine–any residue–serine (DxSxS), coordinates a divalent metal cation at the top of the domain. The N terminus of the β-subunit also contains an A-domain with a MIDAS motif. Electron micrographs show the integrin dimer to have a globular head 8–12 nm in diameter that constitutes the ligand-binding domain from which two stalks 2 nm thick and 14–20 nm in length project; the distal regions of these contain hydrophobic sequences representing the transmembrane domains.

TABLE II

Properties of Integrins[a]

Integrin	Alternative names	Matrix ligands
With an A-domain		
$\alpha1\beta1$	VLA 1, CD49a/CD29	CO, LM
$\alpha2\beta1$	VLA 2, GPIaIIa, CD49b/CD29	CO, LM
$\alpha10\beta1$		CO, LM
$\alpha11\beta1$		CO
$\alpha D\beta2$	CD11d/CD18	[b]
$\alpha L\beta2$	LFA-1, CD11a/CD18	[b]
$\alpha M\beta2$	Mac1, CD11b/CD18	FG
$\alpha X\beta2$	p150,95, CD11c/CD18	FG
$\alpha E\beta7$	$\alpha_{IEL}\beta7$, HML-1 antigen, CD103(αE)	[b]
Without an A-domain		
$\alpha3\beta1$	VLA 3, CD49c/CD29	LM
$\alpha4\beta1$	VLA 4, CD49d/CD29	FN, OP
$\alpha5\beta1$	VLA 5, FNR, CD49e/CD29	FN, OP
$\alpha6\beta1$	VLA 6, CD49f/CD29	LM
$\alpha7\beta1$		LM
$\alpha8\beta1$		FN, TN, NN
$\alpha9\beta1$		TN, OP
$\alpha V\beta1$	CD51/CD29	FN, VN
$\alpha IIb\beta3$	GPIIbIIIa, CD41/CD61	FN, FG, VN, vWF, Tsp
$\alpha V\beta3$	VNR, CD51/CD61	VN, FG, FN, vWF, Tsp
$\alpha V\beta5$		VN
$\alpha V\beta6$		FN
$\alpha V\beta8$		VN
$\alpha6\beta4$	CD49f/CD104	LM
$\alpha4\beta7$	LPAM-1	FN

[a] CO, collagen; FG, fibrinogen; FN, fibronectin; LM, laminin; NN, nephronectin; OP, osteopontin; TN, tenascin; Tsp, thrombospondin; VN, vitronectin; vWF, von Willebrand factor.
[b] Involved in cell–cell interactions only.

Those α-subunits that do not contain A-domains undergo posttranslational cleavage into a light and heavy chain held together by a disulfide bond, the exception being $\alpha4$, which is cleaved at a more central position to yield fragments of 70 and 80 kDa. In addition, several integrin subunits, $\alpha3$, $\alpha6$, $\alpha7$, $\beta1$, $\beta3$, $\beta4$, and $\beta5$, are subject to alternative splicing mainly in their cytoplasmic domains, yielding isoforms that are differentially expressed in specific patterns. This splicing serves to increase the cell–matrix interaction repertoire and hone the temporal and spatial adhesive responses of cells.

The field of integrin research was advanced enormously by the publication of the crystal structure of the extracellular domain of $\alpha V\beta3$ in 2001 by a group led by Arnaout. This structure shows that the globular head of

the integrin is made up of a seven-bladed β-propeller contributed by the α-subunit and the A-domain from the β-subunit together with an immunoglobulin fold, termed the hybrid domain, made up of polypeptide sequences from either side of the β A-domain. The integrin stalks are folded into three β-sandwich domains in the α and four epidermal growth factor (EGF)-like repeats in the β-subunit. The β-subunit also has an N-terminal plexin–semaphorin–integrin (PSI) domain and a novel cystatin-like fold just before the transmembrane region. An arginine residue, R261, in the β3-subunit A-domain extends into the core of the α-subunit propeller, where it is held in place by aromatic residues and is the main area of subunit association.

Ligand Binding

All interactions between integrins and matrix proteins are dependent on divalent cations, whereas the ligand-binding specificity of integrin molecules is determined by the particular α–β combination. Some matrix proteins (e.g., FN) can bind to several integrins, or, conversely, one integrin can recognize ligands of diverse structure; for example, $\alpha2\beta1$ binds to both laminin and collagen. In general, each integrin has a specific nonredundant function, which is emphasized by the distinct phenotypes of knockout mice.

The integrin dimers can be broadly divided into three families consisting of the $\beta1$, $\beta2/\beta7$, and $\beta3/\alpha$V integrins. $\beta1$ associates with 12 α-subunits and can be further divided into RGD-, collagen-, or laminin-binding and the related $\alpha4/\alpha9$ integrins that recognise both matrix and vascular ligands. $\beta2/\beta7$ integrins are restricted to leukocytes and mediate cell–cell rather than cell–matrix interactions, although some recognize fibrinogen. The $\beta3/\alpha$V family members are all RGD receptors and comprise αIIb$\beta3$, an important receptor on platelets, and the remaining β-subunits, which all associate with αV. It is the collagen receptors and leukocyte-specific integrins that contain α A-domains.

In non-α A-domain-containing integrins, both the α- and β-subunits are required for ligand binding. An integrin–ligand complex crystal structure showed that RGD peptide binds at the α–β interface, with its arginine residue contacting the α-subunit propeller and its aspartate helping to coordinate the divalent cation at the MIDAS site via a carboxyl linkage, which in the presence of ligand is occupied. Two further cations are present in the ligand-bound structure, one at a site adjacent to the MIDAS (termed ADMIDAS) and the other at a site in close proximity, termed the ligand-induced metal-binding site (LIMBS). Isolated recombinant α A-domains are able to bind peptide and macromolecular ligands with the same affinity as intact dimer. A crystal structure of the A-domain of $\alpha2$ in complex with a triple-helical collagenous peptide containing the glycine–phenylalanine–hydroxyproline–glycine–glutamic acid–arginine (GFOGER) motif also shows the carboxyl from an acidic residue, in this case glutamate, from the ligand directly completing the coordination sphere of the metal ion in the MIDAS. This explains the absolute requirement for either aspartic or glutamic acid in matrix adhesive proteins and the dependence on divalent cations for integrin–ligand interactions.

Cation Modulation

The binding of ligand to integrin cannot take place without a divalent cation, which directly contacts a carboxyl group from the ligand. However, cations also play an important role in the regulation of integrin affinity. Integrin αV$\beta3$ contains six cation-binding sites in the unliganded crystal structure and eight in the presence of cyclic RGD peptide, at least three of which are affected by ligand binding. In general, integrin–ligand binding is stimulated by magnesium and manganese ions and inhibited by calcium ions. However, this situation is complicated by the fact that the binding of one cation can affect the binding of another at a different site. In addition, several cation-binding sites within an individual integrin can influence ligand binding. The physiological relevance of cation modulation of integrin affinity has yet to be resolved.

Activation and Signaling

Focal Adhesions

When cells attach and spread on a matrix ligand, there is an initial clustering of integrins in the membrane, followed by an accumulation of cytoskeletal and signaling molecules into dynamic structures known as focal adhesions or focal contacts. These structures represent the anchor points of the cell where integrins link the cell to both the underlying matrix and the intracellular actin filaments of the cytoskeleton. The contacts appear as dense plaques, often located near the cell periphery, and provide both a scaffold and a means whereby cells can generate traction during migration. More important, focal adhesions also serve as nucleation points for the recruitment of not only structural proteins such as vinculin, talin, and paxillin, but also many signaling and adaptor molecules able to trigger a cascade of phosphorylation events that can activate numerous downstream targets.

Conformational Changes

Many integrins are not constitutively active, and adhesion of cells to matrix proteins needs to be strictly

controlled and regulated in response to environmental changes. Integrins exist in at least three states, inactive, active, and ligand-bound; the switching of integrins from an inactive to an active state involves conformational changes not only in the ligand-binding pocket, but also across the whole of the extracellular domain and in the cytoplasmic face. Thus, the activation of the ligand-binding domain in the head and the binding of ligand are coupled via long-range conformational changes to signaling events in the cytoplasm. Conversely, intracellular events effect changes in the cytoplasmic domains that are translated in the opposite direction to the integrin head, allowing activation and ligand binding. This bidirectional communication is termed outside-in and inside-out signaling.

Cytoplasmic Domains

The short cytoplasmic domains of integrins play a vital role in integrin function because they control the activation states of integrins and are required to maintain integrins in an inactive state. They are also the sites of interaction with, and linkage to, both cytoskeletal and signaling molecules when clustered in focal adhesions. Interactions between the α and β tails occur by a salt bridge and hydrophobic and electrostatic contacts in the α-helical, membrane-proximal region of both domains, and it is likely that this association is lost on integrin activation, allowing the tails to separate and effector molecules to bind. The β-subunit tail is the principal site for binding of cytoplasmic molecules, whereas the α-subunit plays a more regulatory role in controlling activation.

Many proteins are intimately associated with integrins in focal adhesions, but direct interaction has only been proven for the binding of the structural protein talin to the $\beta 3$ cytoplasmic domain. The site of interaction is a conserved asparagine–proline–any residue–tyrosine (NPxY) motif in the $\beta 3$ tail with a phosphotyrosine-binding-like (PTB) subdomain of talin. This interaction may be the prototype for protein interactions with integrin β tails through PTB domains.

Signaling by Integrins

Integrin-mediated signaling can be broadly divided into two categories, direct and collaborative. In the first, ligation and clustering of integrins are the only stimuli and adhesion to ECM proteins activates cytoplasmic tyrosine kinases, for example, focal adhesion kinase (FAK) and serine/threonine kinases such as those in the mitogen-activated protein kinase (MAPK) cascade. Direct signaling also induces ionic transients (e.g. Ca^{2+}, Na^{+}/H^{+}) and stimulates lipid metabolism. In collaborative signaling, integrin–ECM adhesion modulates signaling initiated by other types of receptors, such as receptor tyrosine kinases (RTK) and G protein-coupled receptors, allowing cells to integrate positional information concerning matrix contacts with information about the availability of soluble growth or differentiation factors that are also located in the ECM. Cells that are deprived of anchorage to the ECM eventually die by a specialized form of programmed cell death (apoptosis) known as anoikis. Cell–matrix interactions via integrins are thus essential for cell survival. Integrins also directly affect the organization of the cytoskeleton, and consequently cell motility, by activating the Rho GTPases, a branch of the Ras GTPase superfamily, particularly CDC42, Rac1, and RhoA. Rho promotes the formation and maintenance of actin stress fibers, whereas Rac and CDC42 regulate structures such as lamellipodia and filopodia, respectively.

It is worth remembering that each signaling pathway mentioned influences others at some point, so signaling within a cell is better considered as a series of networks rather than a direct path. Thus, integrins are able to modulate, either directly or indirectly, every signaling pathway within the cell, a fact that emphasizes the importance of cell–matrix interactions on all aspects of cell behavior.

See Also the Following Articles

Focal Adhesions • Integrin Signaling • Rho GTPases and Actin Cytoskeleton Dynamics

Glossary

extracellular matrix (ECM) A network of proteins and polysaccharides underlying and surrounding cells.

focal adhesions Points of anchorage of the cell to the underlying matrix allowing communication between the inside and outside of the cell via integrins.

integrins A family of $\alpha\beta$ heterodimeric cell surface receptors for extracellular matrix proteins.

inside-out signaling The modulation of integrin–ligand binding activity by intracellular events, leading to integrin clustering and conformational changes.

outside-in signaling The modulation of cell phenotype or behavior by extracellular events such as ligand binding.

Further Reading

Humphries, M. J., McEwan, P. A., Barton, S. J., Buckley, P. A., Bella, J., and Mould, P. A. (2003). Integrin structure: Heady advances in ligand binding, but activation still makes the knees wobble. *Trends Biochem. Sci.* **28**, 313–320.

Hynes, R. O. (2002). Integrins: Bidirectional, allosteric signaling machines. *Cell* **110**, 673–687.

Xiong, J-P., Stehle, T., Diefenbach, B., Zhang, R., Dunker, R., Scott, D. L., Joachimiak, A., Goodman, S. L., and Arnaout, M. A. (2001). Crystal structure of the extracellular segment of integrin $\alpha V\beta 3$. *Science* **294**, 339–345.

BIOGRAPHY

Janet Askari is a researcher in the Wellcome Trust Centre for Cell–Matrix Research at the University of Manchester, U.K., with an interest in mechanisms of signal transduction by integrins. She received a B.Sc. (Hons) Microbiology from the University of Kent in 1976.

Martin Humphries is Professor of Biochemistry, a Wellcome Trust Principal Research Fellow, and Director of the Wellcome Trust Centre for Cell–Matrix Research at the University of Manchester, U.K. His interests center on integrin structure, mechanisms of integrin priming and activation, and coordination of adhesion-dependent signaling. He received a B.Sc. (Hons) Biochemistry from the University of Manchester in 1980 and a Ph.D. in Biochemistry from the University of Manchester in 1983.

Centromeres

Beth A. Sullivan
Boston University School of Medicine, Boston, Massachusetts, USA

The centromere is a specialized mixture of DNA and proteins, and ensures chromosome inheritance and genome stability. As a chromosomal locus, the centromere is the minimal DNA or chromatin element that promotes formation of the proteinaceous kinetochore complex and coordinates chromosome movement in mitosis and meiosis. The centromere also synchronizes aspects of chromosome structure, such as heterochromatin formation, sister chromatid cohesion, and chromosome condensation. It is a multidomain locus, recruiting a variety of proteins with distinct functions.

Organization of the Centromere Region

Cytologically, centromeres have been defined by the visible primary constriction on metaphase chromosomes. This chromosomal locus is structurally complex, and contributes to various processes that ensure chromosome stability. The centromere region can be broadly classified into two major domains that encode kinetochore and heterochromatin functions. The kinetochore and heterochromatin are assembled independently, but each is equally important for complete centromere function and for ensuring chromosome and genome stability. The centromere/kinetochore domain comprises both DNA and proteins involved in chromatin assembly and structural aspects of the kinetochore. The heterochromatin domain is located adjacent to, or flanks, centromeric chromatin. Studies in various organisms have shown that heterochromatin is equally important for centromere function and chromosome inheritance as the kinetochore domain.

Kinetochore Domain

At metaphase, the kinetochore, a proteinaceous multidomain structure, is assembled on the outer surface of the centromere, promoting attachment of the chromosome to spindle microtubules and movement during anaphase.

The Inner Kinetochore

The inner kinetochore is the region most intimately associated with centromeric DNA and/or chromatin. Many structural proteins that bind centromeric DNA or contribute to specialized chromatin structure are located here (Table I). The inner kinetochore contains constitutive proteins that serve as the foundation for the kinetochore, often termed the prekinetochore. CENP-A, a centromere-specific histone H3 variant that replaces H3 in centromeric nucleosomes, is located here and serves as an initiatory signal for kinetochore assembly by recruiting other inner and outer kinetochore proteins.

The Outer Kinetochore

The outer kinetochore region contains primarily microtubule-associated and chromosomal motor proteins that are involved in chromosome congression to the midzone at metaphase or engage spindle microtubules and move chromosomes to spindle poles in anaphase. In addition, the outer kinetochore contains surveillance or checkpoint proteins that monitor kinetochore attachments to the spindle and regulate the transition from metaphase to anaphase.

The Central Domain

The centromeric region that spans the interior of the centromere and connects sister kinetochores comprise the interior central domain. Centromeric DNA-binding proteins are concentrated here, as well as cohesion and condensation proteins and transiently associated proteins (chromosomal passengers) that co-ordinate chromosome segregation and cytokinesis.

Heterochromatin Domain

Heterochromatin is cytologically dense material that is typically found at centromeres and telomeres. It mostly consists of repetitive DNA sequences and is relatively "gene poor." Its most notable property is its ability to silence euchromatic gene expression. Centromeres in yeast, fruit flies, and mammals are flanked by heterochromatin, indicating that its repetitive composition

TABLE I

Homologous Centromere Region Proteins in Different Species

Location	Function	*S. cerevisiae*	*S. pombe*	*C. elegans*	*D. melanogaster*	*H. sapiens*
Kinetochore	Centromere specific histone	Cse4p	Cnp1	HCP-3	CID	CENP-A
	Centromeric chromatin architecture		Mis6 Mis12 Mal2 Sim4			CENP-I
	Inner plate: structure and DNA binding	Mif2p	Cnp3	HCP-4		CENP-C CENP-G CENP-H
	Outer plate: chromosome congression and movement	CBF1, CBF3		HCP-1,2	Cenpmeta Cenpana Zw10 Rod	CENP-E CENP-F ZW10 ROD
Heterochromatin	Histone H3 methyltransferase		Clr4		Su(var)3-9	SUVAR39H1
	Heterochromatin formation		Swi6 Chp1 Rik1		Su(var)2-5/HP1 HP2	HP1
	Sister chromatid cohesion	Scc1/Mcd1, Scc3 Pds5	Rad21/Scc1 Mis4,6,12	SCC-1/COH-2 SCC-3 EVL-14/PDS-5	dRad21/Scc1	RAD21/SCC1

or dense chromatin structure may represent an important, conserved function in centromere structure and function. Heterochromatin assembly is linked to chromatin regulation, occurring in a pathway that initiates with methylation of histone H3 at amino acid residue lysine 9 in order to recruit heterochromatin proteins (HPs), such as HP1 (heterochromatin protein 1). Once heterochromatin is established, cohesion and condensation proteins accumulate between sister kinetochores and chromatids. Mutations in HPs or certain histone modifying enzymes lead to chromosome mis-segregation and mitotic defects, indicating that heterochromatin contributes significantly to chromosome stability and segregation.

Specification of Centromere Identity and Function

The Centromere as DNA

How are the distinct kinetochore and heterochromatin domains assembled at centromeric regions? A well-debated question in centromere biology has been the role of primary DNA sequence in centromere identity and assembly. In a few organisms specific DNA sequences are required for centromeric protein binding, while in other organisms, centromere-specific DNA sequences have not been found. In addition, epigenetic mechanisms often determine centromere identity. In short, a centromere is established, and it is consistently maintained at a genomic region, but the site of formation is not determined by the underlying sequence itself. Recent studies indicate that RNA as well participates in centromere assembly.

Point Centromeres

Centromeres in the budding yeast *Saccharomyces cerevisiae* are the best studied and understood. *S. cerevisiae* centromeres are encoded by three distinct DNA elements (CDE I, II, and III) within a 125 bp region (Figure 1). Two elements (CDE I and III) are absolutely conserved and required to recruit centromere and kinetochore proteins. The centromeric histone CENP-A (Cse4p) is recruited to CDE II, the centromeric element that varies in sequence, but not size, from chromosome to chromosome. The small size of budding yeast centromeres, as well as the strict reliance on DNA–protein interactions for assembly, have resulted in detailed molecular maps and models of centromere assembly that are lacking in larger eukaryotes.

Regional Centromeres

Centromeres in fission yeast, *Schizosaccharomyces pombe*, and in flies, worms, mammals, and plants are monocentric, forming on a limited, specific region of the chromosome (Figure 1). These centromeres are comprised of multiple subunits encoding kilobase or megabase-sized genomic regions. Unlike in budding yeast, centromeric DNA sequences are not obviously conserved, and centromere identity and assembly depend largely on epigenetic factors.

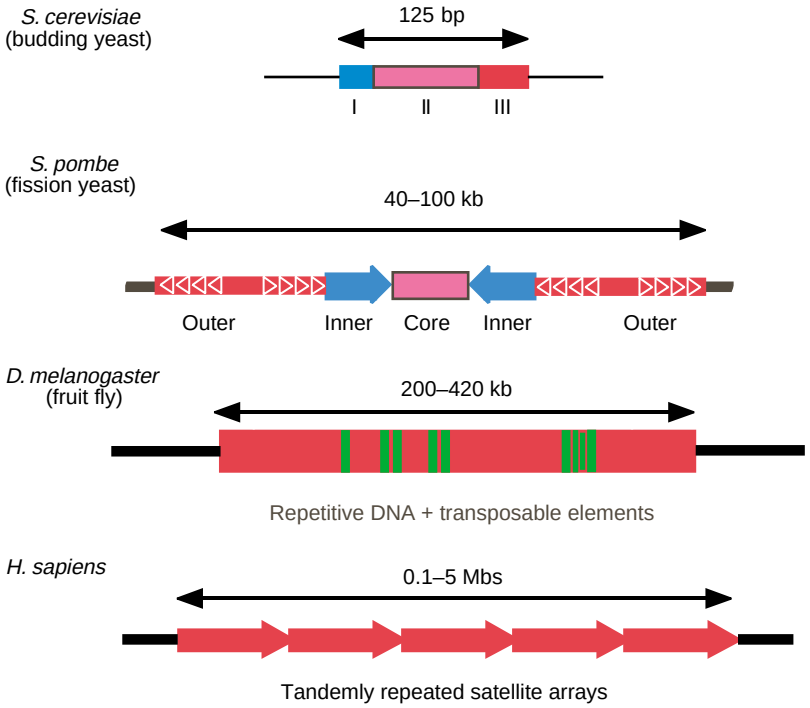

FIGURE 1 Centromeric structure in various eukaryotes. Schematic diagram of eukaryotic centromeres. The DNA sequence of centromeres differs between species, but the organization of the centromere and the presence of centromere proteins is conserved. Budding yeast (*S. cerevisiae*) centromeres are 125 bp and are composed of three distinct elements, two of which are conserved (I and III). *S. pombe* (fission yeast) centromeres contain a unique central core flanked by inverted inner and outer repeats. *Drosophila* centromeres extend for 200–420 kb and contain repetitive DNA (red boxes) that is interspersed with transposable elements (green lines). Human centromeres consist of tandemly repeated alpha-satellite DNA arranged into higher order repeats that extend over several megabases.

Schizosaccharomyces pombe The three centromeres in fission yeast consist of unconserved central core sequences flanked by inverted arrays of inner and outer repeats. Both the central core and portions of the inner repeats are required for establishment and maintenance of centromere function and for recruitment of CENP-A (Cnp1) and other centromeric proteins. The outer repeats are essential for assembly of centric heterochromatin through histone modifications and noncoding RNAs.

Multisubunit Centromeres: Flies, Humans, and Plants Metazoan and plant centromeres are large, often ranging in size from a few hundred kb to 5 Mb. They primarily consist of thousands of copies of satellite DNA, often arranged in tandem (mammals and plants). In flies and plants, these repeats are often interspersed with transposable elements. In humans, *de novo* centromere assembly via artificial chromosomes has been most efficiently achieved when centromeric satellites (alpha-satellite DNA) are introduced into cells. However, not all human alpha-satellite DNAs form centromere *de novo*, indicating that other sequences or factors are required to assemble and maintain human centromeres.

Holocentric Chromosomes In the nematode *Caenorhabditis elegans*, crayfish, and some insects, the holocentric chromosomes assemble centromeres along their lengths. *C. elegans* centromeres are the best-studied holocentrics. Most of the known eukaryotic centromere and kinetochore proteins have been identified in worms and the order of assembly, with CENP-A (CeCenp-A or HCP-3) at the top of the assembly pathway, are conserved. Proteins are recruited into distinct foci at prophase, but by metaphase, these foci spread evenly into "ribbons" along the poleward face of the chromosome arms. The distribution of centromere and kinetochore proteins into inner and outer kinetochore regions is conserved in *C. elegans*.

The Centromere as Chromatin

Chromatin is an important regulator of gene expression and compartmentalization of the genome in interphase. Establishment of distinct chromatin domains (kinetochore, heterochromatin) is necessary for complete centromere function, thus chromatin may be a more important determinant of centromere function than DNA sequence.

Epigenetic Centromeres

The simple presence of centromeric DNA in a cell or a chromosome does not necessarily correlate with centromere function. Besides the obvious lack of sequence conservation at eukaryotic centromeres, additional evidence exists to argue the role of underlying DNA sequence in centromere assembly. First at normal mammalian centromeres, only a fraction of the arrays actually participate in centromere assembly. In humans, the kinetochore domain typically comprises one-half to two-thirds of the satellite DNA found at eukaryotic centromeres. The remainder of the satellite DNA is involved in forming heterochromatin and cohesion. Secondly, naturally occurring or engineered dicentric chromosomes that contain two regions of centromeric DNA are stably transmitted in flies and humans only after inactivation of one centromere. Finally, neocentromeres are formed in flies and humans on stable marker chromosomes that completely lack centromeric sequences. None of the neocentromeres share sequence homology and even those that are derived from similar genomic regions assemble centromere, kinetochore, and heterochromatin proteins on different sequences.

Specification by CENP-A

All centromeres are associated with the centromere-specific histone CENP-A. CENP-A is required to recruit all other centromere and kinetochore proteins, with the exception of HP1, making it is a strong candidate for a protein that specifies and maintains the site of kinetochore assembly. Unlike replication-dependent histones, CENP-A is dispersed in a semiconservative manner, thus providing the scaffold on which new CENP-A can be loaded and the centromere can be maintained irrespective of underlying DNA sequence. The organization of

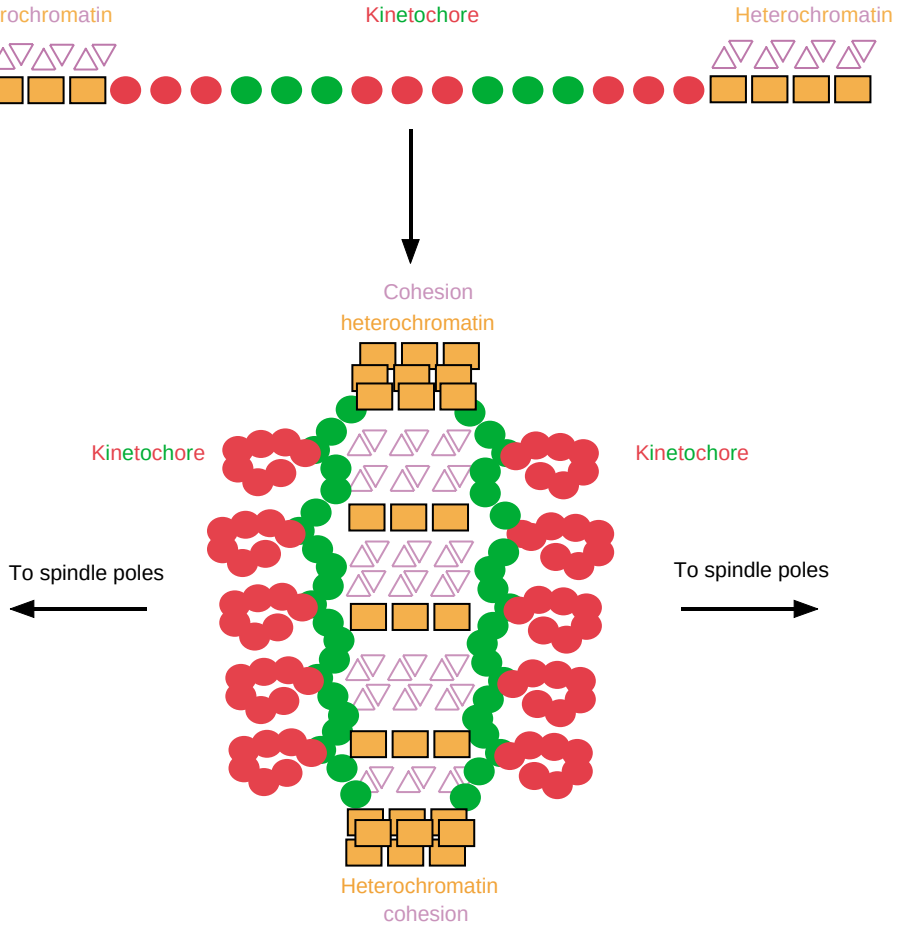

FIGURE 2 Unique organization of centromeric chromatin creates proper structure of the centromere region. In 2D, CENP-A (red circles) and H3 (green circles) nucleosomes within centromeric chromatin are interspersed, forming the foundation of the kinetochore domain, which is flanked by heterochromatic proteins (squares) and cohesion proteins (triangles). In metaphase (3D), the blocks of CENP-A and H3 nucleosomes may be arranged in a spiral, orienting CENP-A nucleosomes to the poleward face of the chromosome, presumably to bi-orient the chromosome and facilitate recruitment and interactions with other kinetochore proteins. H3 nucleosomes are sequestered to the region between sister kinetochores, where heterochromatin and cohesion proteins are recruited. Flanking heterochromatin that is assembled between sister kinetochores may be as important as CENP-A:H3 interspersion for ensuring that CENP-A opposes spindle poles.

centromeric chromatin may further facilitate its maintenance and/or function. In two dimensions (2D), centromeric chromatin in flies and humans contains interspersed subunits of CENP-A and H3 nucleosomes (Figure 2). CENP-A subunits coalesce to form a three-dimensional (3D) interface that promotes recruitment of additional kinetochore proteins, biorientation of chromatids to opposite spindle poles, and attachments to microtubules. Conversely, the H3 subdomains are oriented toward the interior of the chromosome to establish a platform for recruiting cohesion and condensation proteins. The unique interspersion of CENP-A and H3 nucleosomes is important for centromere function, since depletion of CENP-A by RNA interference (RNAi) or in CENP-A mutants alters the ratio of CENP-A:H3 and leads to chromosome segregation defects and mitotic arrest.

The Centromere as RNA

One of the most exciting discoveries in the past few years has been the involvement of double-stranded RNA (dsRNA) in specifying chromosomal, and particularly centromere, function. Although originally considered "junk DNA," the arrays of repeats that surround active centromeres have been shown to be functionally significant. In particular, noncoding, antiparallel RNAs are transcribed from the outer centromeric repeats in *S. pombe*. These transcripts are typically unstable and are normally processed by RNAi machinery that mediates the formation of heterochromatin. Full-length double-stranded transcripts from the repeats are reduced into small interfering RNAs (siRNAs) by the protein Dicer, a member of the RNA-induced silencing complex (RISC). The siRNAs then initiate methylation of histone H3 at lysine 9 that subsequently recruits heterochromatin proteins. The siRNAs are only required for establishment, but not maintenance of heterochromatin, and although noncoding RNAs from regions that contain CENP-A have not been identified, it is tempting to speculate that kinetochore-specific transcripts might initiate *de novo* centromere assembly that is then maintained by retention of CENP-A and/or other proteins through many rounds of replication and division.

See Also the Following Articles

Chromatin Remodeling • Chromatin: Physical Organization • Chromosome Organization and Structure, Overview • Metaphase Chromosome • Nuclear Organization, Chromatin Structure, and Gene Silencing • Nucleoid Organization of Bacterial Chromosomes

Glossary

epigenetic Referring to or describing any heritable influence on chromosome or gene function that is not correlated with, or dependent on, a change in DNA sequence.

heterochromatin Cytologically defined regions of the genome that contain repetitive DNA (satellite DNA, transposable elements). A defining feature of heterochromatin is the ability to silence gene expression.

kinetochore The proteinaceous structure on each chromosome that is responsible for chromosomal attachment to and movement along spindle microtubules.

RNA interference A cellular defense mechanism for specific gene silencing that is induced by double-stranded RNAs that are processed into 21–23 nucleotide small interfering RNAs (siRNAs), causing degradation of homologous endogenous mRNA.

Further Reading

Choo, K. H. A. (1997). *The Centromere*. Oxford University Press, New York.

Cleveland, D. W., Mao, Y., and Sullivan, K. F. (2003). Centromeres and kinetochores: From epigenetics to mitotic checkpoint signaling. *Cell* **112**, 407–421.

Karpen, G. H., and Allshire, R. C. (1997). The case for epigenetic effects of centromere identity and function. *Trends Genet.* **13**, 489–496.

Martienssen, R. A. (2003). Maintenance of heterochromatin by RNA interference of tandem repeats. *Nat. Genet.* **35**, 213–214.

Mellone, B. G., and Allshire, R. C. (2003). Stretching it: Putting the CEN(P-A) in centromere. *Curr. Opin. Genet. Dev.* **13**, 191–198.

Sharp, J. A., and Kaufman, P. D. (2003). Chromatin proteins are determinants of centromere function. *Curr. Top. Microbiol. Immunol.* **274**, 23–52.

Sullivan, B. A., Blower, M. D., and Karpen, G. H. (2001). Determining centromere identity: Cyclical stories and forking paths. *Nat. Rev. Genet.* **2**, 584–596.

Sullivan, K. F. (2001). A solid foundation: Functional specialization of centromeric chromatin. *Curr. Opin. Genet. Dev.* **11**, 182–188.

Biography

Dr. Beth Sullivan is an Assistant Professor in the Department of Genetics and Genomics at Boston University School of Medicine. Her research interests are in eukaryotic centromere structure and function, including organization and regulation of centromeric chromatin. She holds a Ph.D. from the University of Maryland, Baltimore and received postdoctoral training at Case Western Reserve University (Cleveland) and The Salk Institute (La Jolla). Her laboratory focuses on developing new cytological and cell biology techniques to facilitate comparative studies of centromere organization in mammals and *Drosophila*.

Centrosomes and Microtubule Nucleation

Reiko Nakajima, Ming-Ying Tsai and Yixian Zheng
Carnegie Institution of Washington and Howard Hughes Medical Institute, Baltimore, Maryland, USA

In animal cells, the microtubule network consisting of the centrosome and the filamentous microtubule array is required for intracellular trafficking, intracellular organization, and cell division. The timely assembly and organization of different microtubule arrays is critical for executing all functions of microtubules. Centrosome-mediated microtubule nucleation plays an important role in the formation of a functional microtubule network.

Microtubules

Structure of Microtubules

Microtubules are assembled from dimers of α- and β-tubulins that share significant ($\sim$50%) amino acid identity. Each tubulin has a molecular mass of $\sim$50 000 Da and binds to one molecule of GTP. Since the GTP-binding pocket of α-tubulin is covered by β-tubulin in a tubulin dimer, only the GTP in β-tubulin can be exchanged and hydrolyzed. The tubulin dimers, often referred to as tubulin(s), polymerize in a head-to-tail fashion to form protofilaments that associate laterally into hollow cylindrical microtubules with diameters of $\sim$25 nm (Figure 1). The microtubule polymer exhibits a distinct polarity with a fast-growing plus end and a slow-growing minus end. Studies have shown that the plus and minus ends of microtubules terminate with β-tubulins and α-tubulins, respectively.

Microtubule Polymerization

Microtubule polymerization begins with a slow nucleation step where several tubulins come together to form a microtubule "seed" or "nucleus." The rate of microtubule nucleation is proportional to the nth power of tubulin concentration, where n is the number of tubulins in a microtubule seed. Following nucleation, microtubule elongation by adding tubulins to the seeds occurs at a rate that is proportional to tubulin concentration. Therefore, microtubule nucleation is kinetically less favored than microtubule elongation. Once formed, the microtubule polymer exhibits a stochastic growth and shrinkage behavior termed "dynamic instability," which is defined by the rates of elongation and shrinkage as well as by the frequencies of transition from growth to shrinkage and from shrinkage to growth. Therefore, microtubule formation is governed by both the microtubule nucleation rate and by the various parameters of microtubule dynamic instability. These intrinsic features of microtubule polymers are exploited in living cells to achieve proper microtubule organization in response to various cellular signals.

Centrosomes

Structure of the Centrosome

The centrosome provides a major microtubule-nucleating and -organizing site in animal cells. Electron micrographs reveal that a centrosome consists of a pair of centrioles and an electron-dense pericentriolar material (PCM). Each centriole is barrel-shaped with nine triplet microtubules making up the barrel wall (Figure 2). Studies have shown that the two centrioles in a centrosome are linked by filamentous structures. An interesting feature of the centriole pair is that they are arranged in angles of varying degrees with respect to each other. The bottom of one centriole always faces the wall at one end of the second centriole that has additional appendages at the other end of the wall (Figure 2). Compared to the structure of centrioles, the structure of the PCM is less defined. With low-resolution electron microscopy, the PCM appears unstructured. Recent high-resolution electron tomography studies suggest that the PCM is made of filamentous matrices. Although the detailed organization of the centrosome matrix remains largely unknown, a number of centrosome proteins that have the potential to form a filamentous-matrix structure have been identified.

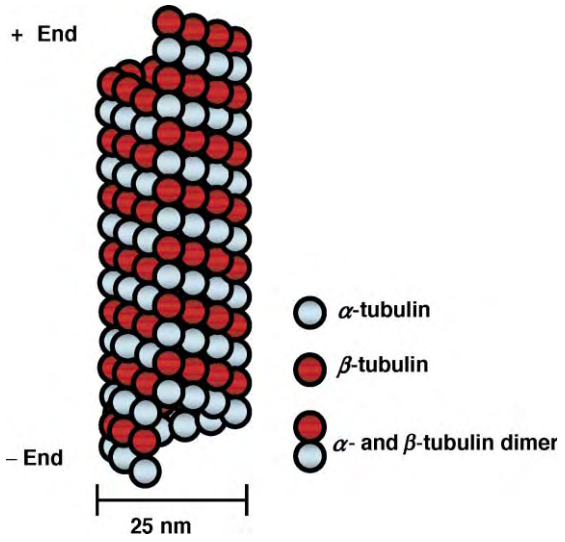

FIGURE 1 Microtubules are assembled from α- and β-tubulin heterodimers. The dimers interact with each other in a head-to-tail fashion to form linear protofilaments that associate with each other laterally to form a hollow cylindrical microtubule with a diameter of 25 nm. The plus and minus ends of the microtubule are indicated.

Centrosome Duplication

Unlike many other cellular organelles, a cell contains either one or two centrosomes depending on the cell-cycle stage. In G1 phase, there is only one centrosome per cell, which duplicates itself in S phase when the nuclear DNA is replicated. Centrosome duplication is characterized by the growth of a new centriole from the side of each of the existing centrioles, which results in two pairs of centrioles. Following centriole duplication, the PCM is partitioned between the two centriole pairs, giving rise to two centrosomes in G2 phase. As the cell cycle progresses into mitosis, the two centrosomes are further separated from each other and each centrosome participates in the organization of the bipolar mitotic spindle. At the end of a cell cycle, cell division results in two new cells each consisting of a single centrosome. Since bipolar spindle assembly is essential for equal chromosome segregation, the single duplication of the centrosome in each cell cycle is important for proper cell division. Recent studies show that the cyclin-dependent protein kinase, CDK2, drives centrosome duplication in S phase. However, the duplication process and the mechanism that ensures only one round of centrosome duplication per cell cycle are not well understood.

The PCM Harbors Microtubule Nucleating and Organizing Activity

The centrosome was first recognized as a microtubule-nucleating and -organizing center over 100 years ago. Studies in the 1990s have now established that a protein complex called the γ-tubulin ring complex (γTuRC), which resides in the PCM, is responsible for microtubule nucleation. Hundreds of γTuRCs at the PCM nucleate the growth of plus ends of microtubules. The minus ends of these microtubules often associate with the PCM through interactions with γTuRC and/or with other PCM proteins (Figure 2), though the detailed mechanism of this association is not clear. The ability of the centrosome to associate with numerous nucleated microtubules gives rise to an organized microtubule array, which is essential for many aspects of microtubule functions.

Microtubule Nucleation

γTuRC

In addition to α- and β-tubulins, eukaryotic cells possess a third tubulin called γ-tubulin. Unlike α- and β-tubulins, γ-tubulin associates with nontubulin proteins to form protein complexes that can nucleate microtubule assembly. γ-Tubulin is a major component of the γTuRC that has been purified and studied in *Xenopus* eggs, *Drosophila* embryos, and human tissue culture cells. In all cases, γTuRC appears as an open-ring structure with a diameter of ~25 nm consisting of approximately seven proteins. The best-characterized *Drosophila* γTuRC consists of at least seven proteins: γ-tubulin, Dgp71WD, Dgrips75, 84, 91, 128, and 163. Dgrip84, Dgrip91, and γ-tubulin, which are the most abundant proteins in *Drosophila* γTuRC, have homologues in all organisms examined to date. Some of the remaining less abundant components of *Drosophila* γTuRC also have homologues in other animal cells. Therefore, the structure and organization of *Drosophila* γTuRC are likely to represent general features of γTuRC in animal cells.

In *Drosophila* γTuRC, γ-tubulin interacts directly with Dgrip84 and Dgrip91 to form a γ-tubulin small complex (γTuSC) consisting of two molecules of γ-tubulin and one molecule each of Dgrip84 and Dgrip91. Multiple γTuSCs are assembled into one γTuRC. Although a detailed structural model of γTuRC is not available, a number of studies strongly suggest that γTuRC consists of a ring and a cap that covers one face of the ring (Figure 3). The ring is primarily made of γTuSCs, whereas some or all of the less abundant γTuRC components (Dgp71WD, Dgrips75, 128, and 163) makes up the cap. The uncapped side of the γTuRC ends with a ring of γ-tubulins that directly interacts with tubulin to mediate microtubule nucleation (Figure 4).

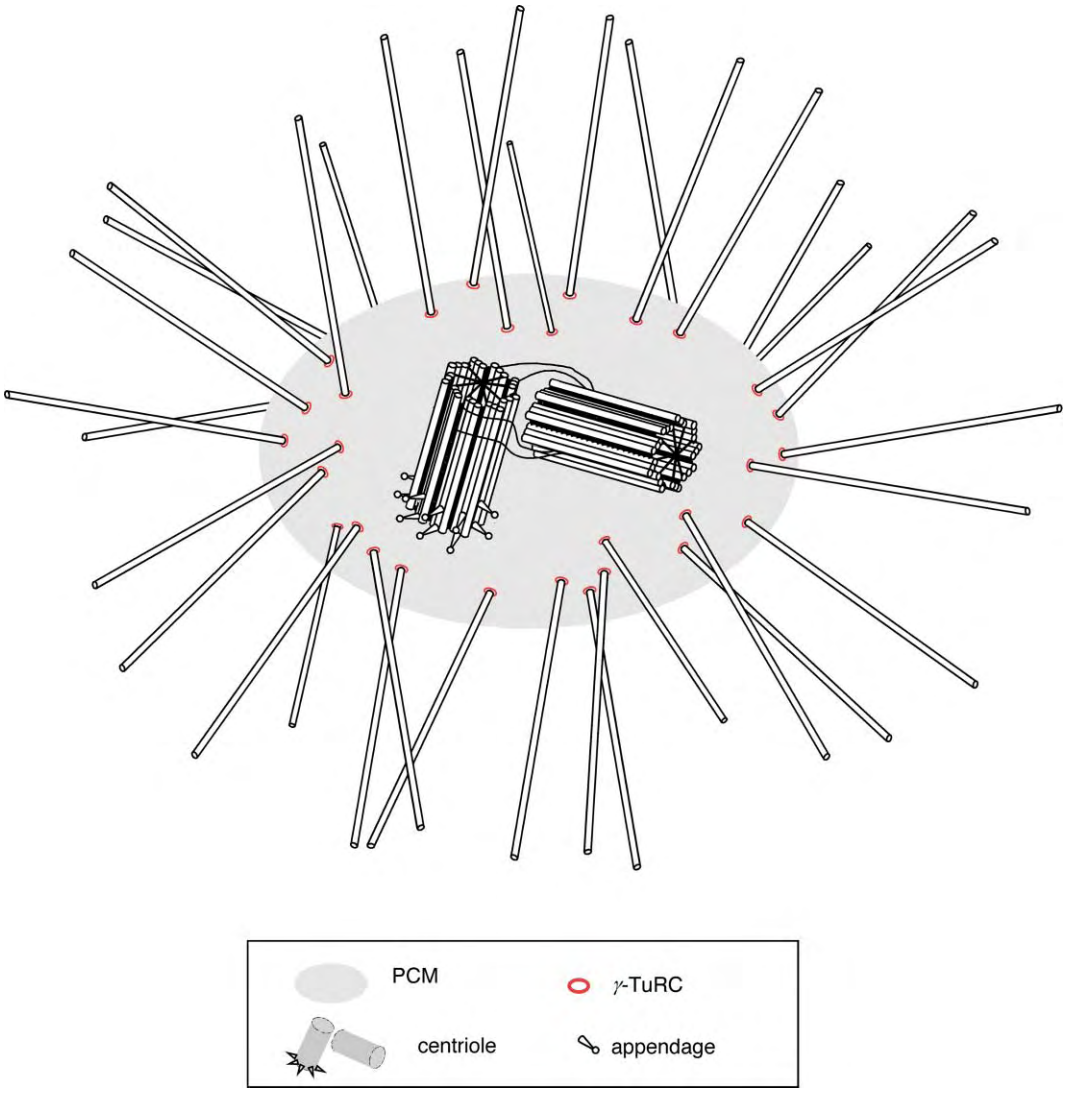

FIGURE 2 The centrosome contains a pair of centrioles and a PCM. The centrioles are connected to each other and one of them has appendages. Microtubules are nucleated from γTuRCs that are associated with the PCM.

Models of γTuRC-Mediated Microtubule Nucleation

The purified γTuRC can stimulate microtubule nucleation from purified tubulin *in vitro*. Although the detailed mechanism of γTuRC-mediated microtubule nucleation remains to be elucidated, two models have been proposed. Both models suggest that the presence of multiple γ-tubulins in the γTuRC allow simultaneous interactions with multiple tubulins during microtubule nucleation, thereby lowering the kinetic barrier of microtubule nucleation. However, the two models are completely different in terms of how the γTuRC may interact with its nucleated microtubules.

The so-called template nucleation model suggests that the γ-tubulin ring of the γTuRC acts as a template during microtubule nucleation (Figure 4). The newly formed microtubule is capped by the γTuRC at its minus end. Consistent with this model, a number of studies suggest that γTuRC-nucleated microtubules are capped at their minus ends. The other drastically different model—the protofilament model—suggests that the γTuRC ring opens up during microtubule nucleation with the multiple γ-tubulins acting as a protofilament to stimulate or stabilize the formation of microtubule seeds (Figure 4). Further high-resolution studies focusing on the interaction between the γTuRC and the microtubule minus ends are required to unequivocally discriminate between the two models of γTuRC-mediated microtubule nucleation.

γTuRC-Mediated Microtubule Nucleation *in vivo*

In living cells, about half of the γTuRC is recruited to the centrosome where it mediates centrosome

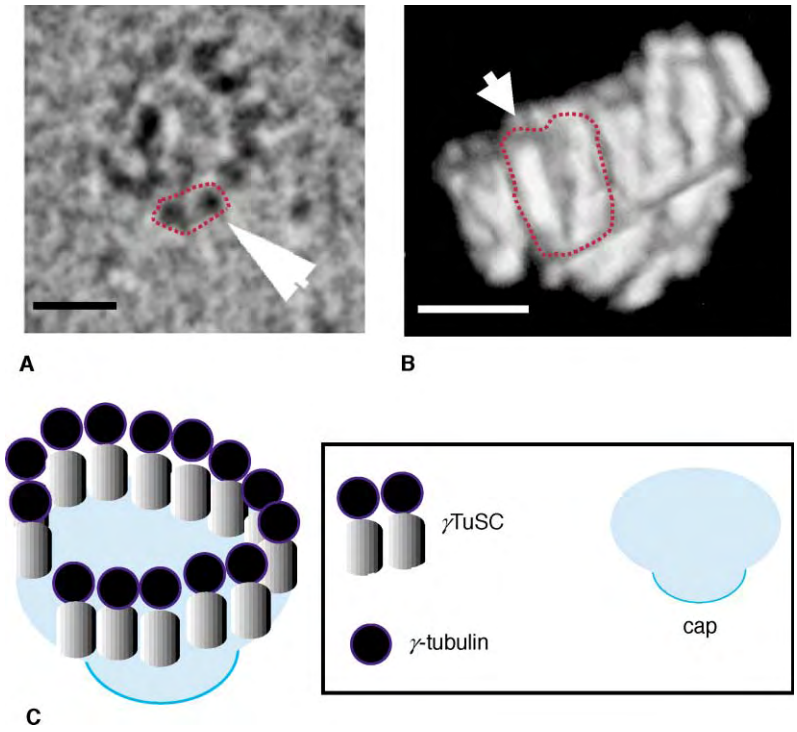

FIGURE 3 The structure of the γTuRC. (A) Cryo-electron micrograph of a γTuRC in cross section. Approximately 13 subunits make up the ring. Arrow points to two subunits that may correspond to one γTuSC. The apparent internal structure may correspond to the cap. Reproduced from *J. Cell Biol.* **144**, 721–733, with permission. (B) Three-dimensional structure of a γTuRC reconstructed from negative staining samples. This side view of γTuRC shows the cap that covers one face of the ring. Arrow points to the structure that may correspond to one γTuSC. Reproduced from Moritz, M., Braunfeld, M. B., Guenebaut, V., Heuser, J., and Agard, D. A. (2000). Structure of the gamma-tubulin ring complex: A template for microtubule nucleation. *Nat. Cell Biol.* **2**, 365–370 with permision of Nature Publishing Group. (C) Schematic diagram of the γTuRC. The ring is primarily made of γTuSCs. Scale bars, 10 μm.

microtubule nucleation. Since centrosomes provide the major microtubule nucleating activity in dividing cells, it is not clear whether the other half of the γTuRC in the cytoplasm also participates in microtubule nucleation. One possibility is that the cytoplasmic γTuRC does not nucleate microtubules because it is associated with an inhibitor. Alternatively, centrosomal recruitment of γTuRC may greatly enhance its microtubule-nucleating activity. In this case, even though the cytoplasmic pool of γTuRC can nucleate microtubules, the centrosomal γTuRC provides the major source of microtubule-nucleating activity.

The cytoplasmic pool of γTuRC serves as a reserve for additional centrosome recruitment of γTuRC that occurs at the onset of mitosis. This recruitment of additional γTuRC contributes toward the enhanced microtubule-nucleating activity of the centrosome, which is important for efficient spindle assembly in mitosis. Interestingly, a fraction of the γTuRC also associates with the mitotic spindle in mitosis. It is possible that this pool of γTuRC plays a role in spindle assembly and function.

Other Microtubule Nucleators

By definition, any proteins that facilitate the formation of microtubule seeds during microtubule nucleation can function as microtubule nucleators. Before the discovery of γ-tubulin and γTuRC, microtubule-associated proteins (MAPs) were considered as prime candidates for microtubule nucleators. MAPs may nucleate microtubules by binding and stabilizing tubulin oligomers formed during microtubule seed formation. Interestingly, some MAPs, such as XMAP215, are found at the centrosome in animal cells. Further study is required to determine whether or how the centrosomally localized MAPs mediate microtubule nucleation *in vivo*.

Centrosome Abnormalities in Cancer

A number of studies have shown that abnormalities in centrosome shape, nucleating capacity, and number exist in cells derived from many tumor tissues. These centrosome anomalies can disrupt bipolar spindle assembly in mitosis, resulting in the formation of either monopolar or multipolar spindles and chromosome mis-segregation. Since aneuploidy – the gain or loss of chromosomes due to chromosome mis-segregation – is linked to genomic instability in human cancers, centrosome abnormalities have been implicated in causing aneuploidy and tumorigenesis.

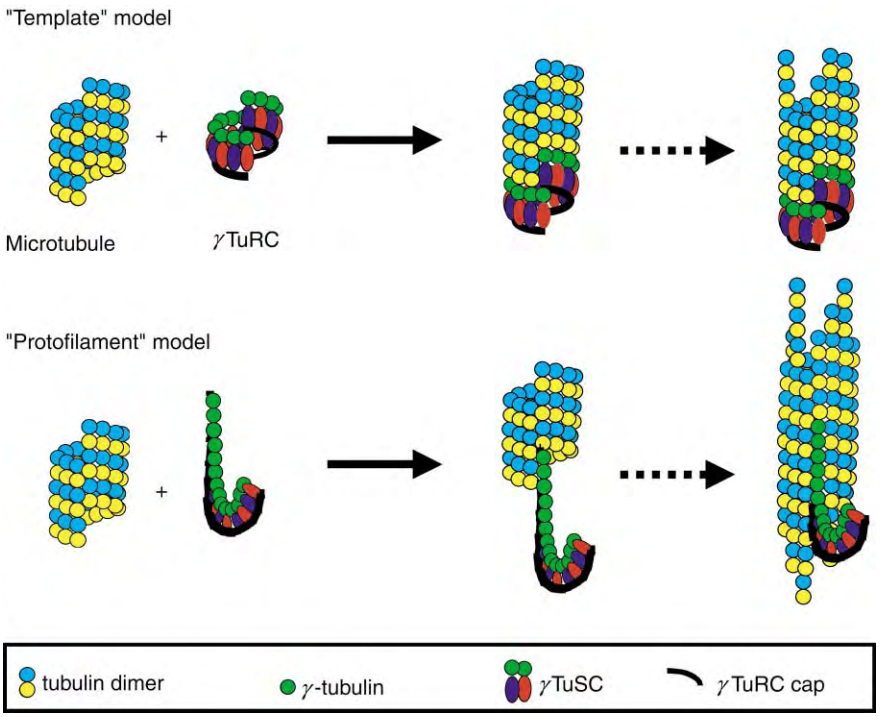

FIGURE 4 Microtubule nucleation by the γTuRC. In the "template model" of microtubule nucleation, the γTuRC caps the minus ends of microtubules after nucleation. In the "protofilament model" of microtubule nucleation, the γTuRC undergoes a large structural change, resulting in the formation of protofilament-like γ-tubulins that nucleate microtubules. For simplicity, the cap of the γTuRC is represented as a line in the γTuRC drawings. (Reproduced from Wiese, C., and Zheng, Y. (2000). A new function for the γ-tubulin ring complex as a microtubule minus-end cap. *Nat. Cell Biol.* **2**, 358–364 with permission of Nature Publishing Group.)

See Also the Following Articles

Chromosome Organization and Structure, Overview • Microtubule-Associated Proteins • Nucleoid Organization of Bacterial Chromosomes • Tubulin and its Isoforms

Glossary

aneuploidy The state of the cell that has gained or lost a whole chromosome.

bipolar spindle A microtubule-based structure assembled during cell division, required for equal segregation of chromosomes into two daughter cells.

chromosome mis-segregation Inappropriate chromosome segregation that leads to gain or loss of chromosomes.

genomic instability The loss, gain, or rearrangement of chromosomes.

tumorigenesis Processes that lead to the development of cancer.

Further Reading

Anderson, S. S. L. (1999). Molecular characterization of the centrosome. *Int. Rev. Cytol.* **187**, 51–109.

Desai, A., and Mitchison, T. J. (1997). Microtubule polymerization dynamics. *Annu. Rev. Cell Develop. Biol.* **13**, 83–117.

Keating, T. J., and Borisy, G. G. (2000). Immunostructural evidence for the template mechanism of microtubule nucleation. *Nat. Cell Biol.* **2**, 352–357.

Moritz, M., Braunfeld, M. B., Sedat, J. W., Alberts, B., and Agard, D. A. (1995). Microtubule nucleation by gamma-tubulin-containing rings in the centrosome. *Nature* **378**, 638–640.

Moritz, M., Braunfeld, M. B., Guenebaut, V., Heuser, J., and Agard, D. A. (2000). Structure of the gamma-tubulin ring complex: A template for microtubule nucleation. *Nat. Cell Biol.* **2**, 365–370.

Nigg, E. (2002). Centrosome aberrations: Cause or consequence of cancer progression? *Nat. Rev.* **2**, 1–11.

Oakley, B. R., Oakley, C. E., Yoon, Y., and Jung, M. K. (1990). γ-Tubulin is a component of the spindle pole body that is essential for microtubule function in *Aspergillus nidulans*. *Cell* **61**, 1289–1301.

Oegema, K., Wiese, C., Martin, O., Milligan, R., Iwamatsu, A., Mitchison, T., and Zheng, Y. (1999). Characterization of two related *Drosophila* γ-tubulin complexes that differ in their ability to nucleate microtubules. *J. Cell Biol.* **144**, 721–733.

Wiese, C., and Zheng, Y. (2000). A new function for the γ-tubulin ring complex as a microtubule minus-end cap. *Nat. Cell Biol.* **2**, 358–364.

Zheng, Y., Wong, M. L., Alberts, B., and Mitchison, T. (1995). Nucleation of microtubule assembly by a gamma-tubulin-containing ring complex. *Nature* **378**, 578–583.

Biography

Yixian Zheng is a staff member and assistant investigator of the Carnegie Institution of Washington and the Howard Hughes Medical Institute, respectively. She holds a B. S. from Sichuan University (P. R. China) and a D.Phil. from the Ohio State University. Her research includes microtubule nucleation and mitotic spindle morphogenesis.

Reiko Nakajima holds a B.S. from Tokyo University and a D.Phil. from Osaka University, while Ming-Ying Tsai holds a B.S. from National Yang Ming Medical School and a D.Phil. from University of Southwestern Medical Center. Both are currently postdoctoral fellows in Yixian Zheng's group studying different aspects of spindle morphogenesis.

c-*fes* Proto-Oncogene

Thomas E. Smithgall
University of Pittsburgh, Pittsburgh, Pennsylvania, USA

Robert I. Glazer
Georgetown University, Washington, DC, USA

The human c-*fes* proto-oncogene (Fes) encodes a protein-tyrosine kinase distinct from c-Src, c-Abl, and other non-receptor tyrosine kinases. Originally identified as the cellular homologue of avian (v-Fps) and feline (v-Fes) transforming retroviral oncoproteins, Fes is strongly expressed in myeloid hematopoietic cells where it may play a direct role in myeloid differentiation. The Fes promoter exhibits strong myeloid lineage specificity for directing transgene expression in animals. Fes is also expressed in endothelial and epithelial cells where it is involved in migration and cell survival, respectively. Structurally, Fes consists of a unique N-terminal region, a central SH2 domain, and a C-terminal kinase domain. Within the unique region are two coiled-coil oligomerization domains that regulate kinase activity. Fes is linked to growth, differentiation, and survival signaling through Ras and other small G proteins, STAT transcription factors, and phosphatidylinositol 3-kinase. Fes phosphorylates cell adhesion-related substrates in macrophages and promotes myelomonocytic differentiation. Fes is also involved in endothelial cell migration in response to angiogenic factors, neuron differentiation, and is up-regulated in the mammary gland during pregnancy. Although Fes had not been directly implicated in human disease, it can suppress the transforming activity of Bcr-Abl, the transforming oncoprotein associated with chronic myelogenous leukemia (CML).

Structure and Regulation

Human c-*fes* is located on chromosome 15 at position 15q26.1 and is comprised of 19 exons, the first of which is noncoding. The product of the *fes* gene is a 93 kDa protein-tyrosine kinase with three distinct structural regions (Figure 1). These include a long N-terminal unique region, a central Src homology 2 (SH2) domain, and a C-terminal kinase domain. Absent are an SH3 domain and signal sequences for lipid modification, such as an N-terminal myristoylation site associated with Src, Abl, and other nonreceptor tyrosine kinase families. Fes tyrosine kinase activity can be readily demonstrated *in vitro*, however, unlike its transforming viral counterparts, Fes kinase activity is tightly regulated in cells. As described, recent evidence suggests that the unique N-terminal region plays an important role in negative regulation.

N-Terminal Region

One unusual feature of Fes is that its active form exists as a large oligomeric complex. Oligomerization requires the N-terminal region and promotes Fes autophosphorylation by a *trans* mechanism, a key step in the activation of the kinase domain. Analysis of the unique region using COILS, a computer algorithm that searches for the heptad repeat pattern associated with coiled-coil domains, reveals the presence of at least two regions with a high probability of forming coiled-coil structures. The presence of two N-terminal coiled-coil-forming sequences suggests several mechanisms for the regulation of Fes tyrosine kinase activity. One possibility is that a cellular protein binds to the coiled-coil regions and suppresses oligomerization. Alternatively, the two coiled coils may interact in an intramolecular fashion, thus preventing the formation of the active oligomer. A recent study has shown that Fes activity is repressed following ectopic expression in yeast, suggesting that the kinase naturally adopts the inactive conformation without the need for mammalian host cell factors. Deletion or mutagenesis of the more N-terminal coiled-coil domain releases the tyrosine kinase and biological activities of Fes in living cells, consistent with a critical role for this domain in negative regulation. In contrast, deletion of the more C-terminal coiled-coil domain impairs the kinase activity and biological function of active Fes mutants, suggesting a more dominant role in maintenance of the active state or recruitment of signaling partners.

In addition to its role in the regulation of kinase activity, the unique N-terminal region of Fes also contributes to the recruitment of signaling partners. One example is the breakpoint-cluster region protein (Bcr), which was originally discovered in the context of the Bcr-Abl oncoprotein associated with chronic

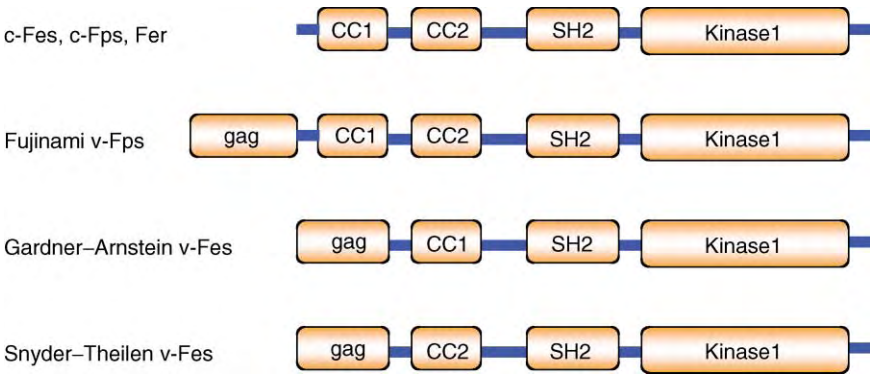

FIGURE 1 Primary structure of the c-Fes protein-tyrosine kinase. Fes consists of a unique N-terminal region, a central SH2 domain, and a C-terminal kinase domain. Two coiled-coil oligomerization motifs (CC1 and CC2) are located in the unique region.

myelogenous leukemia (CML). Bcr is a multidomain signaling protein with an N-terminal Ser/Thr kinase domain, a central region with homology to the Dbl family of guanine nucleotide exchange factors, and a C-terminal GTPase-activating domain for Rho-related small GTPases. Bcr-Fes interaction involves the unique N-terminal region and SH2 domain of Fes and the N-terminal kinase domain of Bcr. Bcr is strongly phosphorylated by Fes both *in vitro* and *in vivo* on a cluster of sites localized to the N-terminal domain. Expression of this Bcr region suppresses Fes-induced neurite outgrowth in rat PC12 cells, suggesting that Bcr may couple Fes to Rho family small GTPases in neuronal cells (C. Laurent and T. Smithgall, unpublished data). Fes also interacts with Bcr-Abl through the Bcr-derived portion of the protein. This interaction may contribute to Fes-induced suppression of transformation signaling by Bcr-Abl.

SH2 Domain

SH2 domains are signaling modules that mediate protein–protein interactions during tyrosine kinase signal transduction. By binding with high affinity and specificity to short, tyrosine-phosphorylated target sequences, SH2 domains mediate the assembly of multiprotein complexes in response to tyrosine kinase activation. Although the role of SH2 domains in the recruitment of effector proteins to autophosphorylated growth factor receptors is well known, SH2 domains were first identified within the sequences of nonreceptor tyrosine kinases. In fact, the SH2 domain of the Fes-related oncoprotein v-Fps was among the first to be described, and was shown to be required for full catalytic activity and to influence host range. Later work established a function for the SH2 domain in v-Fps-induced phosphorylation of transformation-related substrates. More recent studies reveal a similar dual role for the human Fes SH2 domain in the regulation of kinase activity and biological function. Deletion of the SH2 domain greatly reduces Fes kinase activity both in terms of substrate phosphorylation as well as autophosphorylation *in vitro*. The SH2 region also contributes to substrate recognition in macrophages.

Kinase Domain

The Fes catalytic domain is localized to the C-terminal region of the protein and exhibits structural features typical of tyrosine kinases. These include a conserved lysine in the ATP-binding pocket (Lys 590) and a major site of tyrosine autophosphorylation (Tyr 713). Mutagenesis of Tyr 713 to Phe greatly reduces catalytic activity both *in vitro* and *in vivo*, suggesting that autophosphorylation is required for kinase activation. Substitution of Lys 590 with Glu or Arg completely abolishes kinase activity. *Trans* or autophosphorylation of Tyr 811 is likely associated with recruitment of other SH2 proteins but not with kinase regulation.

Biological Functions

Myeloid Differentiation

Early studies describing Fes expression patterns noted a striking correlation with terminal differentiation of myeloid hematopoietic cells. Fes expression is absent in myeloid leukemia cell lines resistant to myeloid differentiation inducers or selected for differentiation resistance, while expression increases following induction of differentiation with a variety of agents. Other work demonstrates a strong connection between Fes and the induction of myeloid differentiation. Chicken bone marrow cells infected with Fujinami sarcoma virus, which carries the fes-related oncogene, v-fps, undergo macrophage differentiation in the absence of macrophage colony-stimulating factor. Recent studies show

that expression of activated c-Fes mutants is sufficient to induce differentiation of myeloid leukemia cells along the macrophage lineage. Consistent with these observations, Fes activation is linked to a number of hematopoietic cytokines. Fes associates with the IL-4, IL-3, GM-CSF, and erythropoietin receptors. Kinase-inactive Fes blocks IL-4-induced phosphorylation of the insulin receptor substrate-2 and recruitment of phosphatidylinositol 3-kinase (PI3-K) in hematopoietic cells.

Evidence supporting a requirement for Fes in myeloid differentiation also comes from antisense experiments. Suppression of Fes expression in HL-60 promyelocytic leukemia cells using antisense oligonucleotides blocks the myeloid differentiation response to phorbol esters and other chemical inducers. However, targeted disruption of Fes in mice has yielded contradictory findings with respect to its role in hematopoiesis. Replacement of the *fes* alleles with a kinase-defective K588R mutant Fes did not show any remarkable effect on hematopoiesis, although STAT3 and STAT5A phosphorylation in response to GM-CSF was markedly reduced. In contrast to these findings, homozygous deletion of Fes led to a runted appearance, abnormal myeloid proliferation, but increased STAT3 activation in response to GM-CSF and IL-6. These apparently contradictory results can be explained by the competition of kinase-dead Fes with Jak2 for STAT3 resulting in a lower degree of STAT3 activation, whereas the complete absence of Fes produces less competition with Jak2 for STAT3 resulting in STAT3 hyperactivation.

Is Fes a Tumor Suppressor?

Other work shows that Fes-induced differentiation may overcome signals for transformation in certain forms of leukemia. The first demonstration of this phenomenon involved transfer of the c-*fes* gene into the human cell line K-562, resulting in growth suppression and differentiation to macrophage-like cells. K-562 cells were established from the blast crisis phase of CML and exhibit no detectable Fes expression. Because they are CML derived, K-562 cells exhibit the Philadelphia chromosome translocation and express p210 Bcr-Abl, the oncogenic tyrosine kinase, that initiates the disease process. Thus, the Fes signal for differentiation is dominant to the Bcr-Abl signal for growth and survival. Fes can also suppress Bcr-Abl-induced transformation of murine myeloid leukemia cells to cytokine independence, providing further support for the idea that Fes may delay the progression of CML.

Angiogenesis

In addition to its role in hematopoiesis, Fes may contribute directly to differentiation and development of the vascular endothelium. Expression of constitutively active Myr-Fes in transgenic mice under the control of the general SV40 promoter induced hypervascularity, which progressed to multifocal hemangiomas. This study also demonstrated expression of endogenous Fes in primary human vascular endothelial cells at levels comparable to those detected in myeloid cells. Consistent with these findings are the observations that Fes is activated by the angiogenic growth factors FGF-2 and angiopoietin-2 in capillary endothelial cells, and that overexpression of Fes is sufficient to induce formation of tube-like structures and chemotaxis in this cell type.

Downstream Signaling Pathways

Major signaling pathways linked to Fes are briefly summarized here (Figure 2).

Small G Proteins

Ras and other small *GTPases* are critical intermediates in most tyrosine kinase signal transduction pathways, and Fes is no exception. Activation of Ras and the related small GTPases Rac and Cdc42 are required for fibroblast transformation by Fes oncogenes. Dominant-negative mutants of all three small G proteins inhibit fibroblast colony-forming activity by Myr-Fes and v-Fps, and transformation correlates with constitutive activation of both the Erk and Jnk serine/threonine kinase pathways downstream. Sustained Erk activation is sufficient to induce myeloid differentiation of K-562 cells, suggesting that Fes-induced differentiation in these cells may be due in part to activation of the Ras/Erk pathway.

The activation and termination of small GTPase signaling are regulated by protein factors (guanine nucleotide exchange factors (GEFs) and GTPase-activating proteins (GAPs), respectively) that link small GTPases with upstream tyrosine kinases, including Fes and its transforming viral homologues. Transformation of fibroblasts by v-Fps has been shown to induce tyrosine phosphorylation of p120 Ras GAP, and similar results have been observed *in vitro* with purified Fes and GAP proteins. Fibroblast transformation by v-Fps also correlates with tyrosine phosphorylation of Shc, an adaptor protein that serves as an intermediate between tyrosine kinases and the Ras GEF complex, Grb-2/Sos. As mentioned above, endogenous Bcr is also strongly tyrosine-phosphorylated in fibroblasts transformed by v-Fps. Tyrosine phosphorylation of Bcr in v-*fps*-transformed cells induces its association with Grb-2/Sos via the Grb-2 SH2 domain. Like Shc, Bcr may serve as an intermediate between Fes and the activation of Ras downstream. In addition, tyrosine phosphorylation of

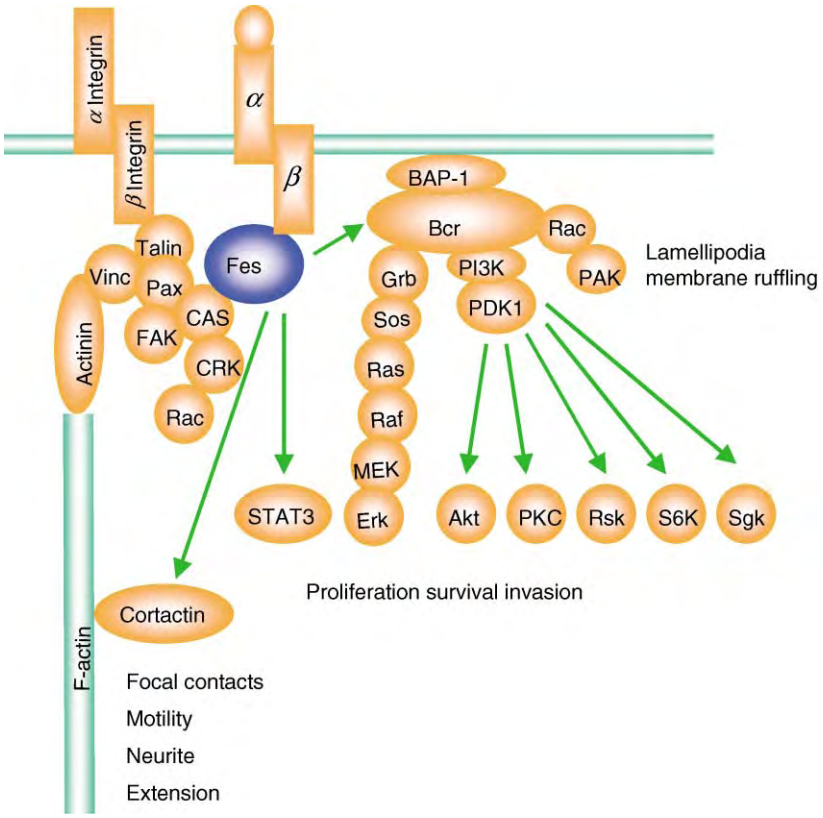

FIGURE 2 Fes signaling pathways involved in cell motility, proliferation, survival, and differentiation.

Bcr may modulate either its GEF or GAP activities toward Rac and other GTPases.

STAT Signaling

STATs are transcription factors with SH2 domains that are activated by tyrosine phosphorylation, often in response to cytokine stimulation. Although kinases of the Jak family are most often associated with STAT activation, a growing body of evidence indicates that Fes and other tyrosine kinases can induce STAT activation as well. For example, STAT3 DNA-binding activity is strongly activated following co-expression with Fes in Sf-9 insect cells, which lack endogenous Jak kinases. In addition, macrophages from homozygous knockout mice in which both *fes* alleles have been deleted hyperactivates STAT3 in response to GM-CSF. STAT3 has been strongly implicated in myeloid differentiation, making it tempting to speculate that Fes may signal to differentiation-related genes through a STAT3-dependent pathway.

PI3-K Pathway

PI3-K phosphorylates phosphoinositol lipids at the 3′ position, leading to the generation of second messengers such as phosphatidylinositol-3,4,5-trisphosphate (PIP_3). PI3-K is a heterodimer consisting of 85 kDa regulatory (p85) and 110 kDa catalytic (p110) subunits, and interacts with tyrosine phosphorylated target proteins through SH2 domains found in the p85 subunit. Several reports have linked Fes to the activation of PI3-K signaling. Early work demonstrated elevated PI3-K activity in chicken embryo fibroblasts transformed by v-Fps as well as other transforming tyrosine kinases. More recently, IL-4 was shown to induce the association of endogenous Fes with PI3-K in IL-2-dependent T-cell lines. The SH2 domain of p85 forms a stable complex with Fes, suggesting a possible mechanism for factor-induced complex formation. The PI3-K pathway is often associated with survival signaling, and activation of this pathway by Fes may contribute to macrophage survival, perhaps through association with the Crk substrate, CAS (Figure 2). Interestingly, the protein-serine kinase immediately downstream to PI3-K, 3-phosphoinositide-dependent protein kinase-1 (PDK1) (Figure 2), coimmunoprecipitates with Fes, and is phosphorylated on tyrosine (Zeng and Glazer, unpublished data). This suggests a mechanism by which Fes can mediate the activation of other downstream signaling pathways such as $p70^{S6K}$. Activation of PI3-K is also essential to Fes-induced neurite extension in PC12 cells, where it may serve to couple Fes to Rac activation in this system.

Other Substrates

Most of the substrates reported for Fes have been identified using fibroblast transformation as a model system. However, overexpression of Fes in a macrophage cell line, which represents a physiological context, led to the phosphorylation of proteins related to integrin-mediated responses including adhesion and cell-cell contact. Interestingly, phosphorylation of Shc and other proteins associated with mitogenic responses have not been observed. A role for Fes in cell adhesion is further suggested by the interaction of the Fps SH2 domain with cortactin (Figure 2), which is also phosphorylated by Fes. These results suggest a mechanism for the localization of Fes with focal adhesions.

Transcriptional Regulation of Fes

Transgene expression directed by the 13 kb genomic Fes locus reproduced the myeloid-specific expression pattern of the endogenous gene. The Fes promoter sequence spanning + 28 to +2523 (within exon 1 to intron 3) directed myeloid-specific expression of a heterologous gene in transgenic mice. Myeloid-specific expression has been attributed to a tissue-specific repressor at + 441 to +454, a Fes-specific transcription factor (FEF) binding to a *cis*-acting element at − 9 to − 4 and to transcription factors Sp1, PU.1, and Spi-1 binding to elements within the − 425 to +75 promoter sequence. Although these studies account for the myeloid-selective expression of Fes, they do not address Fes expression in other tissues, such as endothelial and epithelial cells, and its transient expression in embryonic tissues, such as the brain. Fes up-regulation occurs during neuronal differentiation and accelerates neurite outgrowth in PC12 cells. Fes also associates with and activates semaphorin3A that is associated with axonal guidance and neuronal outgrowth, further suggesting a role for Fes in brain development and differentiation.

Conclusions

The c-*fes* proto-oncogene encodes a unique cytoplasmic tyrosine kinase involved in myelopoiesis, angiogenesis, CML progression and likely survival in mammary epithelial cells. Although the SH2 and kinase domains found in Fes share homology with other tyrosine kinase families, the N-terminal region is structurally distinct. The presence of coiled-coil oligomerization domains within the N-terminal region suggests a mode of kinase regulation and substrate recruitment that is unique to this tyrosine kinase family. Fes is associated with terminal differentiation in myeloid cells, as opposed to other tyrosine kinases that serve a predominant role in proliferation and survival. Work implicating Fes in the regulation of vascular endothelial cell migration suggests a role in tumor angiogenesis, and Fes may also serve a role in regulating cell survival and apoptosis during mammary gland differentiation, as well as neuronal differentiation.

See Also the Following Articles

Fibroblast Growth Factor Receptors and Cancer Associated Perturbations • Hematopoetin Receptors • Inositol Phosphate Kinases and Phosphatases • JAK-STAT Signaling Paradigm • Ras Family • Small GTPases • Src Family of Protein Tyrosine Kinases • Syk Family of Protein Tyrosine Kinases • Tec/Btk Family Tyrosine Kinases

Glossary

GM-CSF Granulocyte/macrophage-colony stimulating factor.

promoter The DNA sequence upstream to the transcription initiation site that directs expression of the gene.

STAT (signal transducers and activators of transcription) Transcription factors originally identified as mediating the transcriptional effects of interferon.

Further Reading

Glazer, R. I., Smithgall, T. E., Yu, G., and Borellini, G. (1991). The role of the c-*fes* proto-oncogene protein-tyrosine kinase in myeloid differentiation. In *Advances in Regulation of Cell Growth* (J. Mond, J. C. Cambier and A. Weiss, eds.) Vol. 2, pp. 41–60. Raven Press, New York.

Greer, P. (2002). Closing in on the biological functions of FPS/FES and FER. *Nat. Rev. Mol. Cell Biol.* **3**, 278–289.

Kuriyan, J., and Cowburn, D. (1997). Modular peptide recognition domains in eukaryotic signaling. *Annu. Rev. Biophys. Biomol. Struct.* **26**, 259–288.

Pawson (1988). Non-catalytic domains of a cytoplasmic protein-tyrosine kinases: regulatory elements in signal transduction. *Oncogene* **3**, 491–495.

Sawyers, C. L. (1999). Chronic myeloid leukemia. *N. Engl. J. Med.* **340**, 1330–1340.

Scheijen, B., and Griffin, J. D. (2002). Tyrosine kinase oncogenes in normal hematopoiesis and hematological disease. *Oncogene* **21**, 3314–3333.

Smithgall, T. E. (1998). Signal transduction pathways regulating hematopoietic differentiation. *Pharmacol. Rev.* **50**, 1–19.

Smithgall, T. E., Rogers, J., Peters, K. L., Li, J., Briggs, S. D., Lionberger, J. M., Cheng, H., Shibata, A., Scholtz, B., Schreiner, S., and Dunham, N. (1998). The c-Fes family of protein-tyrosine kinases. *Crit. Rev. Oncogenesis* **9**, 43–62.

Takashima Y., Delfino, F. J., Engen, J. R., Superti-Furga, G., and Smithgall, T. E. (2003). Regulation of c-Fes tyrosine kinase activity

by coiled-coil and SH2 domains: analysis with *Saccharomyces cerevisiae*. *Biochemistry* **42**, 3567–3574.

Yu, G., Smithgall, T. E., and Glazer, R. I. (1989). K562 leukemia cells transfected with the human c-fes gene acquire the ability to undergo myeloid differentiation. *J. Biol. Chem.* **264**, 10276–10281.

BIOGRAPHY

Thomas E. Smithgall is a professor in the Department of Molecular Genetics and Biochemistry at the University of Pittsburgh School of Medicine. His principal research interests are in the structural organization and signaling mechanisms of cytoplasmic protein-tyrosine kinases. He holds a Ph.D. from the University of Pennsylvania and received his postdoctoral training at the National Cancer Institute, NIH with Dr. Robert I. Glazer.

Robert I. Glazer is a professor in the Department of Oncology at Georgetown University School of Medicine. His principal research interests are in the signal transduction pathways mediate by protein kinases involved in transformation. He holds a Ph.D. from Indiana University and received his postdoctoral training at Yale University with Dr. Alan C. Sartorelli.

Chaperones for Metalloproteins

Valeria C. Culotta and Edward Luk
Johns Hopkins University Bloomberg School of Public Health, Baltimore, Maryland, USA

Metal ions are not only essential co-factors for enzymes, but are also potentially toxic to cells. Therefore, the passage of metals inside a cell must be tightly regulated. A family of proteins has been identified that functions in the intracellular trafficking of copper ions to enzymes that require the metal for activity. These copper carriers are known as copper chaperones or metallochaperones. This article will highlight recent findings regarding the mechanism of copper chaperones.

Historical Background

Chaperones for metalloproteins are a small family of molecules that have evolved specifically to insert metal ion cofactors into enzymes or other proteins that rely on metals for function. All living cells, from bacteria to humans, harbor numerous metalloproteins that require metal ions such as zinc, copper, manganese, or iron to function. These metals either can serve in a structural role to help maintain the proper conformation of a protein or can actually carry out the chemistry that represents the protein or enzyme's catalytic function. Generally, each metalloprotein is only active with one particular metal ion type and, if fortuitously loaded with the wrong metal, the function of the protein is inhibited. Therefore, it is paramount that the right metal be delivered to the right metalloprotein and also that it be delivered at the right time. How this occurs in a regulated fashion eluded biochemists until the late 1990s, when a new paradigm for metal ion homeostasis emerged. It was discovered that many metalloproteins actually coexist with accessory molecules that ensure the acquisition of the proper metal ion. These accessory proteins have been termed metallochaperones or chaperones for metalloproteins. The term chaperone, first coined by Tom O'Halloran in 1997, was derived from Webster's definition of chaperone, "one delegated to ensure proper behavior." In this case, the one delegated is the metallochaperone, which ensures the proper behavior of the potentially promiscuous metal ion.

The Concept of Metal Trafficking

There are a number of barriers that a metal ion must cross before it reaches its metalloprotein target inside the cell. First, the metal existing in the extracellular environment must traverse the plasma membrane. Metals by themselves cannot penetrate lipid bilayers and therefore rely on metal-transporter molecules to direct their movement across membranes. A variety of membrane transporters exist at the cell surface that act in the specific uptake of metals such as copper, zinc, iron, and manganese. Once inside the cell, some metal ions are delivered directly to proteins in soluble compartments (i.e., the cytosol); however, many metalloproteins reside in membranous organelles such as the mitochondria or secretory pathway, and as such the metal needs to cross a second membrane barrier. This again is accomplished by metal transporters that help translocate the ion across the lipid bilayer. Finally, at a site proximal to the metalloprotein target, the metal cargo is carried by a highly specific metal chaperone that helps insert the metal into the proper site of the metalloprotein. In essence, a metal ion does not freely move about the cell but rather is carried through a well-defined pathway involving the combined action of metal transporters and metal chaperones. This process of moving metals through defined pathways is commonly referred to as metal trafficking, and there are many such highways for the trafficking of metals to metalloproteins.

Why the Need for Metal Trafficking?

The cell devotes a great deal of effort to ensure a highly regimented fate of a metal ion. Why not instead have the metal freely diffusible in the cell? Metalloproteins typically exhibit a very high affinity for their cofactor and are inherently able to self-activate with metals in a test-tube setting. However, the availability of metals inside cells is very limited. Although metals are essential for life, metals are also notoriously toxic and can cause much cellular damage. Therefore, all organisms have

evolved with a series of metal detoxification pathways that act to sequester metals and prevent them from reacting at biological sites. A classic example is the metal-binding metallothionein protein that acts as a sponge for these ions and precludes metals from accumulating in their free ionic form. In measurements that have been made in yeast and bacteria, not a single atom of copper or zinc is freely available in the cytoplasm of the cell, in spite of the micromolar quantities of metal that are accumulated. Intracellular metalloproteins therefore have the challenge of acquiring their cognate metal cofactor in an environment that is essentially a vacuum for metals. To overcome this dilemma, the metal ion chaperones spare a few ions from the metal detoxification pathways and ensure the safe delivery of metals to the active site of metalloproteins. Whereas proteins such as metallothioneins act to protect the *cell from the metal*, the metal chaperones act to protect the *metal from the cell*.

Copper Metalloproteins as Models for Metal Trafficking

Much of what is currently known about metal chaperones and metal trafficking pathways stems from studies on copper. Because copper is a redox-active metal ion that can readily donate or accept electrons, it serves as an excellent catalytic cofactor for enzymes involved in oxygen chemistry. Compared to metalloproteins that bind iron or zinc, copper-containing enzymes are relatively few in number. However, an abundance of information is available on the metal-trafficking pathways relevant to this small subset of metalloenzymes.

In eukaryotes, copper is generally taken up into cells via a cell surface transporter, CTR1. This transporter was originally discovered in 1994 by Andrew Dancis through elegant genetic studies in yeast, and the human homologue was subsequently isolated by J. Gitschier in 1997. Following entry into the cell via CTR1, the copper ion can be shuttled through one of many distinct trafficking pathways, depending on its destination or fate. The copper is either subject to detoxification (a dead-end fate) or is selected for use by copper-containing enzymes. Three such utilization pathways for copper have been identified, and these specifically supply the metal to copper proteins in the Golgi, the cytosol, and the mitochondria (Figure 1).

There are a variety of enzymes that acquire copper in the Golgi compartment, and these are copper proteins destined for the cell surface or for export outside the cell. Examples include multicopper oxidases needed for iron transport (i.e., human ceruloplasmin), extracellular superoxide dismutases for anti-oxidant defense

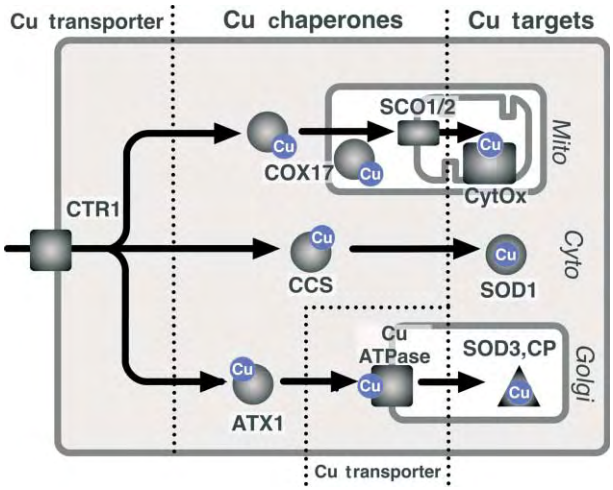

FIGURE 1 Three metal-trafficking pathways involving copper in a typical eukaryotic cell. Copper is first taken up by the cell surface CTR1 copper transporter. The metal can then be delivered in one pathway involving cytosolic ATX1, which carries the copper to the P type copper-transporting ATPase. This transporter in turn pumps copper into the lumen of the Golgi for the activation of a variety of copper enzymes in the secretory pathway, such as extacellular superoxide dismutase (SOD3) and ceruloplasm (CP). A second pathway involves copper carried by CCS to the copper-zinc superoxide dimustase (SOD1) in the cytosol (Cyto). The third pathway involves a relay system of copper delivery to cytochrome oxidase (CytOx) in the mitochondria involving COX17 (both cytosolic and mitochondrial) and mitochondrial SCO1 and SCO2 proteins. Grouped within dotted lines are molecules designated as cell surface and intracellular copper transporters, copper chaperones, and targets for copper delivery.

(SOD3), enzymes for connective-tissue formation (lysyl oxidase), enzymes for pigment formation (tyrosinase), and enzymes for neuronal function (peptidly amidating enzyme and dopamine β-hydroxylase). Prior to reaching their location at the cell surface or extracellular milieu, all these enzymes pass through a specific compartment of the Golgi, where they are activated with copper.

A second copper-trafficking pathway in the cell delivers copper to the cytoplasm, where the ion activates a single enzyme, a cytosolic copper- and zinc-containing superoxide dismutase (SOD1). SOD1 functions to protect the cell against oxidative damage. The third copper-trafficking pathway delivers the metal to the mitochondria. Here a copper-containing oxidase (cytochrome oxidase) resides that functions as the terminal electron acceptor during cellular respiration.

These three pathways involve separate factors for transmembrane metal transport and metal ion chaperoning, and they are discussed independently next.

Delivering Copper to the Golgi: Pathways Involving the ATX1 Copper Chaperone

In order for copper to gain access to enzymes that pass through the Golgi, the metal must traverse the

Golgi membrane. This is accomplished through the action of a specialized copper transporter, called P type ATPase, that uses the energy of ATP hydrolysis to drive the transmembrane translocation of copper from the cytoplasma into the lumen of the Golgi. Humans express two such copper transporters, known as the Wilson or Menkes disease proteins. As the names imply, these molecules have been associated with inherited diseases of copper transport. Copper-transporting ATPase molecules are found in virtually every eukaryotic cell, and they all contain a series of two to six short copper-binding protein domains that capture copper in the cytosol for translocation into the Golgi. How does the metal find these domains if there is no free copper in the cytosol? This is achieved through the action of a small copper-binding copper chaperone known as ATX1 (also called ATOX1).

ATX1 was originally identified in 1995 by V. Culotta as a potential anti-oxidant protein in yeast that guards against oxidative damage, hence the name ATX1. However, subsequent studies revealed that the major function of this molecule was to carry copper from the cytosol to the copper-transporting ATPase in the Golgi. Interesting, the polypeptide sequence of ATX1 is very similar to its recipient of copper delivery, the copper-binding domains of the Cu ATPase in the Golgi. ATX1 and these domains of the transporter bind copper via a single copper-binding site CXXC (where C = cysteine, a sulfur-containing amino acid, and X = any amino acid). With the same copper site present in the donor (ATX1) and recipient (Cu ATPase) molecules for copper transfer, copper is able to move from one site to the other by a facile exchange of sulfur ligands. This mechanism, originally proposed by O'Halloran, Culotta, and Penner-Hahn in 1997, was the first description of a copper-transfer reaction involving a copper chaperone.

The Copper-Trafficking Pathway Involving the CCS Copper Chaperone for SOD1

The SOD1 enzyme is a copper- and zinc-containing superoxide dismutase that protects cells against oxidative damage by scavenging toxic superoxide anion radicals. This is a highly abundant copper enzyme that is ubiquitously expressed among eukaryotes, and in some cells SOD1 represents as much as 1% of the total cellular protein. It is the copper at the active site that carries out enzyme catalysis, whereas the zinc serves more of a structural role.

Although SOD1 has been found in numerous cellular compartments, the bulk ($\geq$95%) of the enzyme is cytosolic, and so there is no intracellular membrane barrier for copper delivery to SOD1. However, due to the absence of free cytsolic copper, SOD1 is highly dependent on its metal chaperone for acquiring its copper.

The copper chaperone for SOD1 (CCS) was first identified by Culotta and Gitlin in 1997. As is the case with ATX1, CCS was discovered by genetic studies in the baker's yeast *Saccharomyces cerevisiae*, but this protein is well conserved throughout eukaryotes. Unlike ATX1, which is a simple one-domain protein, CCS is a complex molecule consisting of three domains that serve separable functions in the copper-transfer process. At the extreme amino terminus, CCS has a short domain that exhibits extensive homology to ATX1, including the CXXC copper site. However, this site is not needed for copper transfer to SOD1 but rather appears to be involved in capturing copper under conditions of copper starvation. A large middle portion of CCS exhibits strong homology to SOD1, but is missing the SOD1 copper site. This homology allows CCS to dock with SOD1 by the formation of a transient heterodimer. SOD1 is normally a homodimer consisting of two identical molecules, and the formation of a heterodimer with CCS is the prerequisite to copper transfer. Finally, at the extreme carboxyl terminus of CCS lies a very short copper-binding domain containing a CXC copper site essential for mediating copper insertion into SOD1.

The mechanism of copper transfer from CCS to SOD1 is far more complicated than that described for ATX1. With ATX1, the donor and recipient for copper transfer bind the metal in the same manner. However, copper transfer by CCS is accompanied by a large change in metal coordination chemistry. Copper binds to CCS in the reduced Cu(I) form via sulfhydral ligands from cysteines in domain III and possibly in domain I as well. Yet in SOD1, copper is oxidized to the cupric Cu(II) state and is coordinated in an all-nitrogen environment. The mechanism by which transfer occurs with this drastic change in metal coordination is just now being elucidated. Oxidation of the copper ion is certainly involved, and oxygen or superoxide itself could be the driving force, as recently proposed by O'Halloran and colleagues.

Delivery of Copper to Mitochondrial Cytochrome Oxidase

Cytochrome oxidase is a very large multisubunit enzyme that represents the terminal electron acceptor in the respiratory chain of the mitochondria. Two subunits of the enzyme contain harbor copper sites that are employed for electron-transfer reactions:

The Cu_A site in subunit 2 of cytochrome oxidase contains two copper ions, whereas subunit 1 of the

enzyme harbors a single copper atom. The Cu_A site acquires its metal via two sets of accessory proteins in the mitochondria: COX17 and SCOI/SCOII. Less is known regarding the assembly of the copper site in subunit 2, but it appears to require separate accessory factors. For the purposes of this review, we focus on assembly of the Cu_A site.

As with ATX1 and CCS, all the accessory proteins for metal insertion into the Cu_A site of cytochrome oxidase were originally discovered by genetic studies in the baker's yeast. Much of this work was pioneered by Moira Glerum and Alexander Tzagaloff in 1996.

COX17 is a cysteine-rich soluble copper-binding protein. Because COX17 exists in both the cytoplasm and the mitochondrial intermembrane space, it was proposed as the shuttle for copper ions between these cellular compartments. However, this function has not been confirmed and it is possible that COX17 only operates in the mitochondria to bring copper to the second set of accessory proteins for the Cu_A site of cytochrome oxidase: SCO1 and SCO2.

The SCO proteins are two very homologous molecules that lie in the inner membrane of the mitochondria. These proteins are believed to capture copper from COX17 and then transfer the metal to the Cu_A site of cytochrome oxidase. The SCO proteins clearly play an essential role in the assembly of cytochrome oxidase and in cellular respiration. A deletion of *SCO1* and also *COX17* in yeast results in a cell that is respiratory deficient. And in humans, mutations in *SCO2* have been associated with a fatal disease in infants, hypertrophic cardioencephalomyopathy.

Perspectives

Virtually all that is known regarding specific metal-trafficking pathways and metal ion chaperones has stemmed from studies in copper. However, it is highly likely that analogous pathways will exist for other metals as well. Metal ions such as iron, manganese, and even zinc are known to be toxic but essential nutrients. Therefore, it is critical that cells maintain these ions under strict guidance and regulation to ensure their proper incorporation into cognate metalloproteins while minimizing deleterious reactivity with other biological sites in the cell.

See Also the Following Articles

Chaperones, Molecular • Cytochrome Oxidases, Bacterial

Glossary

ATX1 A copper chaperone for the copper-transporting P type ATPase in the Golgi.

CCS A copper chaperone for the largely cytosolic copper-zinc superoxide dismutase.

copper COX17 A copper-carrying molecule for the mitochondria.

metal chaperone A molecule that binds a specific metal and helps insert this ion into the metal-binding site of a metalloprotein.

metalloprotein A protein that binds a specific metal ion and requires that metal ion for proper function.

metal transporter A transmembrane protein responsible for the translocation of metal ions across a lipid bilayer.

SCO A copper-carrying molecule, possibly the copper chaperone or copper insertion factor for cytochrome oxidase.

transporting P type ATPase A membrane transporter for copper that uses energy derived from ATP hydrolysis to drive copper transport.

Further Reading

Culotta, V. C., and Gitlin, J. (2001). Disorders of copper transport. In *Molecular and Metabolic Basis of Inherited Disease*. (C. R. Scriver, A. L. Beaudet, W. S. Sly and D. Valle, eds.) 8th edition, Vol. 2, pp. 3105–3126. McGraw-Hill, New York.

O'Halloran, T. V., and Culotta, V. C. (2000). Metallochaperones: An intracellular shuttle service for metal ions. *J. Biol. Chem.* **275**, 25057–25060.

Outten, C. E., and O'Halloran, T. V. (2001). Femtomolar sensitivity of metalloregulatory proteins controlling zinc homeostasis. *Science* **292**, 2488–2492.

Pufhal, R. A., Singer, C. P., Pearison, K. L., Lin, S. J., Schmidt, P. J., Culotta, V., Penner-Hahn, J. E., and O'Halloran, T. V. (1997). Metal ion chaperone function of the soluble Cu(I) receptor Atx1. *Science* **278**, 853–856.

Rae, T., Schmidt, P., Pufhal, B., Culotta, V. C., and O'Halloran, T. V. (1999). Undetectable intracellular free copper: The requirement of a copper chaperone for superoxide dismutase. *Science* **284**, 805–808.

Biography

Valeria Culotta is a professor of environmental health sciences at the Johns Hopkins University Bloomberg School of Public Health in Baltimore, MD. She received her Ph.D. from the Johns Hopkins University Medical School and conducted her postdoctoral training at the National Institutes of Health. Her laboratory focuses on metal ion homeostasis and metal chaperones using baker's yeast as a genetic model system.

Edward Luk is a Ph.D. student in the Department of Biochemistry and Molecular Biology, Johns Hopkins University. His research interests are yeast genetics and metal ion biology.

Chaperones, Molecular

Sue Wickner and Joel R. Hoskins
National Cancer Institute, National Institutes of Health, Bethesda, Maryland, USA

A new concept in molecular biology that has evolved over the past 15 years is that proteins fold with assistance from other proteins, collectively referred to as molecular chaperones. All organisms, from bacteria to humans, possess several classes of molecular chaperones that are highly conserved throughout evolution. In general, molecular chaperones are proteins that bind to unfolded or misfolded proteins and facilitate protein remodeling without being part of the final complex themselves. Typically, they catalyze protein folding or unfolding in energy-dependent reactions. Chaperones participate in many cellular processes, including DNA replication, regulation of gene expression, protein synthesis, cell division, protection and recovery from stress conditions, membrane translocation, and protein degradation. There are four major classes of energy-dependent molecular chaperones: (1) GroEL or Hsp60, (2) DnaK or Hsp70, (3) Hsp90, and (4) Clp or Hsp100. All of these chaperones act in some situations in conjunction with cochaperones or accessory proteins. For example, DnaK acts with DnaJ/Hsp40 and GrpE, GroEL acts with GroES/Hsp10, Hsp90 associates with numerous partner proteins, and Clp proteins associate with proteases and other specificity factors to regulate protein degradation. This entry focuses on the role of Clp/Hsp100, Hsp90, and DnaK/Hsp70 chaperones in protein quality control. Another article in this encyclopedia will cover GroEL/Hsp60.

Protein Quality Control in the Cell

Molecular chaperones play a critical role in protein quality control during the course of cell growth as well as during stress conditions (Figure 1). Normal protein synthesis produces nascent unfolded proteins. Although some nascent polypeptides are able to fold spontaneously into their native conformation as they emerge from the ribosome (1 in Figure 1), others require the action of molecular chaperones, including members of the DnaK/Hsp70 and GroEL/Hsp60 families, to facilitate folding (2 in Figure 1). Unfolded and misfolded proteins also arise in cells as a result of environmental stresses, such as heat shock, or pathologic conditions, such as inflammation, tissue damage, infection, and genetic diseases involving mutant proteins. Molecular chaperones are able to refold and reactivate some misfolded proteins (2 in Figure 1). Other irreversibly misfolded proteins are recognized by proteases, such as Lon and Clp proteases in prokaryotes and the proteasome in eukaryotes. These multicomponent proteases use associated chaperones to unfold and deliver damaged proteins to the protease for degradation (3 in Figure 1). Finally, proteins that are neither refolded nor degraded form insoluble aggregates in the cell (4 in Figure 1). Aggregates are not always an end product, but can be dissolved by molecular chaperones. For example, the combined action of Clp/Hsp100 chaperones and DnaK/Hsp70 chaperones and cochaperones can carry out this function. Thus, chaperones play a critical role in protein quality control during both normal growth and cell stress by assisting proteins with functional potential to become properly folded and by ensuring that irreversibly damaged proteins are degraded.

Clp/Hsp100 Chaperones

Clp ATPases, like the other chaperone families, are highly conserved and have been identified in many diverse organisms, including bacteria, archaea, yeast, plants, insects, and humans. They were first identified as molecular chaperones by S. Lindquist and colleagues and by S. Wickner and colleagues. Many organisms have multiple family members. For example, *Escherichia coli* has four Clp ATPases: ClpA, ClpB, ClpX, and HslU.

The Clp ATPase family is broadly divided into two classes. Class I Clp ATPases contain two nucleotide-binding domains, such as ClpA and ClpB in *E. coli*, Hsp104 in *Saccharomyces cerevisiae,*ClpC in plants, and ClpE in *Bacillus subtilis*. Class II Clp proteins contain one nucleotide-binding domain, such as ClpX in *E. coli*, yeast, plants, mice, and humans. Although the two ATP-binding domains of Class I differ from one another, they are highly conserved in all members of the class. The single ATP-binding domain of Class II Clp ATPases shares significant homology to the second ATP-binding domain of Class I. The Clp ATPases are members of the AAA^+ superfamily of ATPases (*A*TPases *a*ssociated with a variety of cellular *a*ctivities). The key feature of the superfamily is a

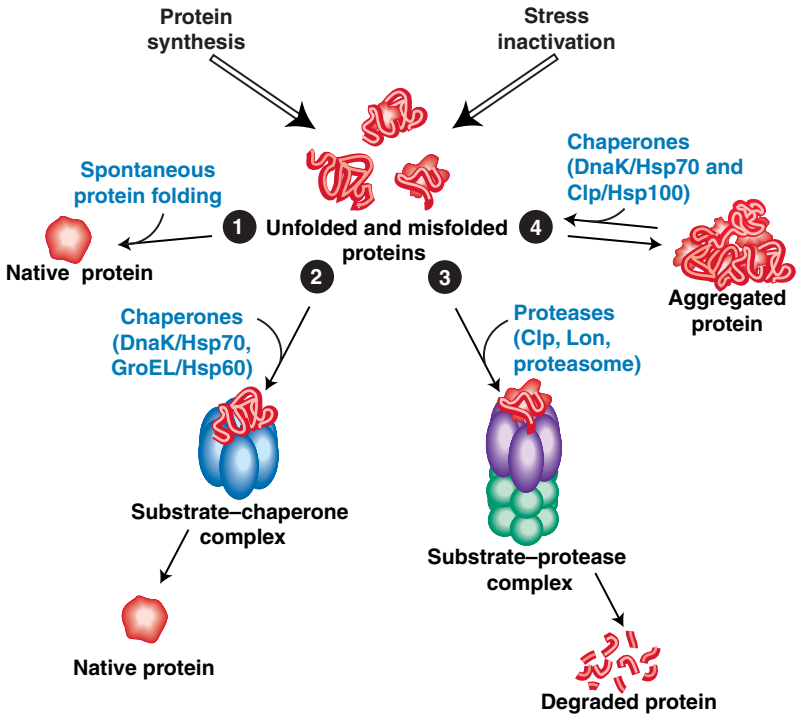

FIGURE 1 Interplay of molecular chaperones and proteases in the cell. See text for description. Substrate proteins are shown in red; an ATP-dependent chaperone, such as GroEL, is shown in blue; a Clp chaperone is purple and is associated with a compartmentalized protease shown in green.

highly conserved ATP-binding module. Another feature is a protein recognition domain located C-terminally to the ATPase domain, referred to as the sensor-2 domain. Many AAA^+ ATPases, including many Clp ATPases, are components of molecular machines that function in a large number of diverse cellular processes.

Clp ATPases act as classical ATP-dependent chaperones. For example, ClpA performs ATP-dependent chaperone functions *in vitro* that mimic those of the DnaK/Hsp70 chaperone system. It catalyzes the remodeling of dimers of the plasmid P1 replication initiator protein into monomers. In an analogous reaction, ClpX dissociates the dimeric initiator protein of plasmid RK2 into monomers *in vitro*. ClpX participates in DNA transposition and replication of bacteriophage Mu by mediating the disassembly of MuA transposase tetramers from Mu DNA after recombination. Similar to other chaperones, both ClpA and ClpX prevent heat inactivation of proteins *in vitro*. Many of the Clp ATPases, such as ClpB, Hsp104, ClpX, and HslU, are induced by heat shock, suggesting that one of their *in vivo* roles is to prevent heat denaturation and to promote reactivation of heat-damaged proteins. Mutants in Hsp104 and ClpB are unable to grow at high temperatures, and *in vitro* Hsp104 and ClpB act in conjunction with their respective Hsp70 chaperone and cochaperones to resolubilize aggregates formed during exposure to high temperature or denaturants.

Some Clp chaperones associate with proteolytic partners, forming ATP-dependent proteases. The founding member of the Clp ATPase family, ClpA, was first identified as the ATPase component of a two-component ATP-dependent protease (referred to as ClpAP or protease Ti). ClpP, the proteolytic component, is unrelated to the Clp ATPases but is a member of a large family of serine proteases. By itself ClpP can degrade only short peptides, but when present as a complex with ClpA or ClpX it can degrade large proteins. Similarly, *E. coli* HslU associates with HslV, a proteolytic component, forming HslUV protease, and *B. subtilis* ClpE associates with ClpP of *B. subtilis*, forming ClpEP protease.

In view of the fact that Clp chaperones and proteases are generally not essential for growth, there is very likely an overlap in the functions carried out by the various cellular chaperones and proteases.

Structure of Clp ATPases and Their Associated Proteases

The structures of the Clp ATPases that have been determined, including ClpA, ClpB, ClpX, and HslU, are very similar. Both electron microscopic and X-ray crystallographic studies show that Clp ATPases

self-assemble into oligomeric rings in the presence of ATP. The Clp ATPases that are known to be components of degradation machinery form stable complexes with their corresponding proteolytic component. The structure of one Clp ATPase, *Haemophilus influenzae* HslU, has been solved alone and in a complex with its proteolytic component, HslV, by McKay and colleagues (Figure 2). The HslUV structure shows that a hexameric ring of HslU ATPase binds to each axial end of the HslV proteolytic core. The proteolytic core is made up of two stacked rings of six identical subunits. The junction of the two stacked rings forms a chamber with the proteolytic active sites lining the interior chamber. With this molecular architecture, the active sites of the protease are sequestered from the cytoplasm. The structure of HslV is similar to other compartmentalized proteases, including the 20S proteolytic core of the proteasome and ClpP. The cavities formed by HslV, and also by ClpP, can accommodate unfolded proteins of roughly 30–40 kDa. Access to the proteolytic chamber appears to be through narrow pores at either end of the stacked rings; these small pores are only large enough to allow short polypeptides or unfolded proteins entry into the proteolytic chamber without major conformational changes. The pores of HslV are covered at one or both ends by the HslU ATPase rings, indicating the role of the Clp chaperone in regulating entry to the protease cavity. ClpAP and ClpXP have similar structures. The archaebacterial and eukaryotic 26S proteasomes are also similar to Clp proteases, in that regulatory ATPase components cover the pores of the 20S proteolytic core, indicating a common mechanism of action despite little sequence similarity between the analogous components.

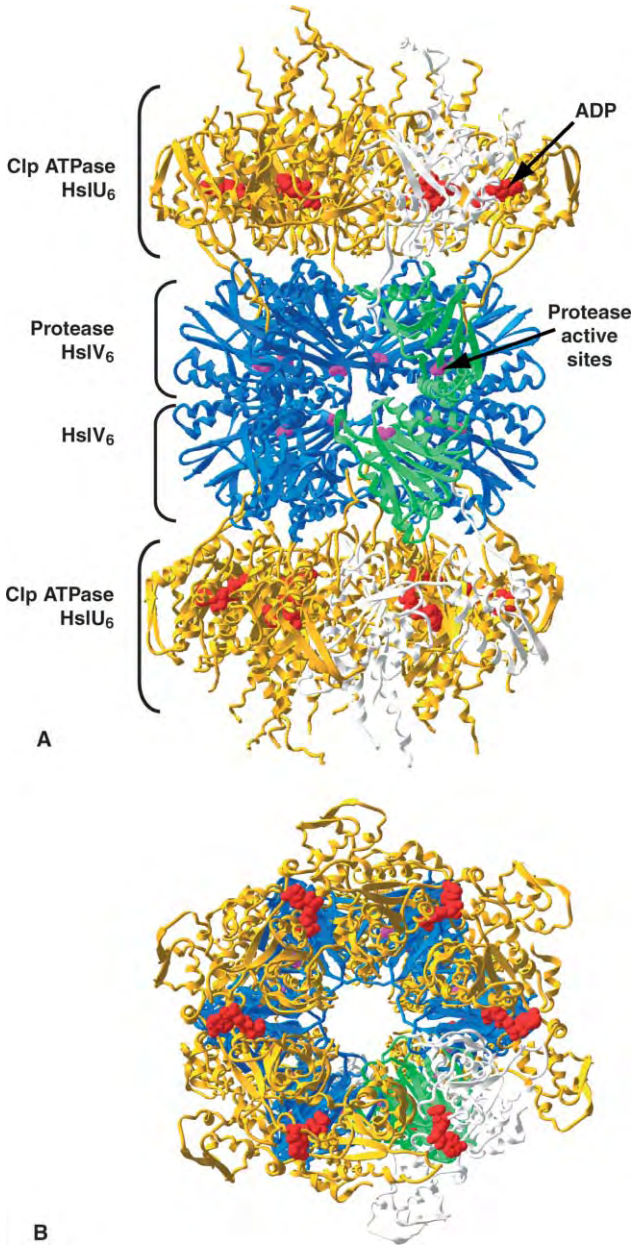

FIGURE 2 Model of the crystal structure of a Clp ATPase, HslU, associated with a proteolytic component, HslV. (A) Side view. (B) Top view. HslU is represented in yellow, with one subunit per hexamer shown in white and ADP shown in red. HslV is represented in blue, with one subunit per hexamer shown in green and serine active sites shown in magenta. The crystal structure was solved by Sousa, M. C., Trame, C. B., Tsuruta, H., Wilbanks, S. M., Reddy, V. S., and McKay, D. B. (2000). Crystal and solution structures of an HslUV protease-chaperone complex. *Cell* **103**, 633–643.

Mechanism of Action of Clp Chaperones and Proteases

The mechanism of action of Clp chaperones and Clp proteases is emerging from structural and biochemical data. Clp ATPases bind substrates that have Clp-specific recognition signals (1 in Figure 3). The recognition signals are approximately 10 amino acids and are typically found very near the N or C terminus of the protein. The various Clp ATPases recognize different motifs and thus act on separate but sometimes overlapping sets of substrates. As first shown by A. L. Horwich and colleagues, Clp ATPases catalyze ATP-dependent unfolding of bound substrates (2 in Figure 3). When Clp ATPases function as chaperones, they bind and unfold the substrate and then release the unfolded protein (3 in Figure 3). The released protein either refolds spontaneously (4 in Figure 3) or is rebound by Clp or another chaperone to undergo another cycle of unfolding. Multimeric complexes and aggregates can also be substrates for Clp chaperones. In these cases, the process of unfolding and release by the combined action of a Clp chaperone and the DnaK/Hsp70 chaperone system results in disassociation of the complex or aggregate.

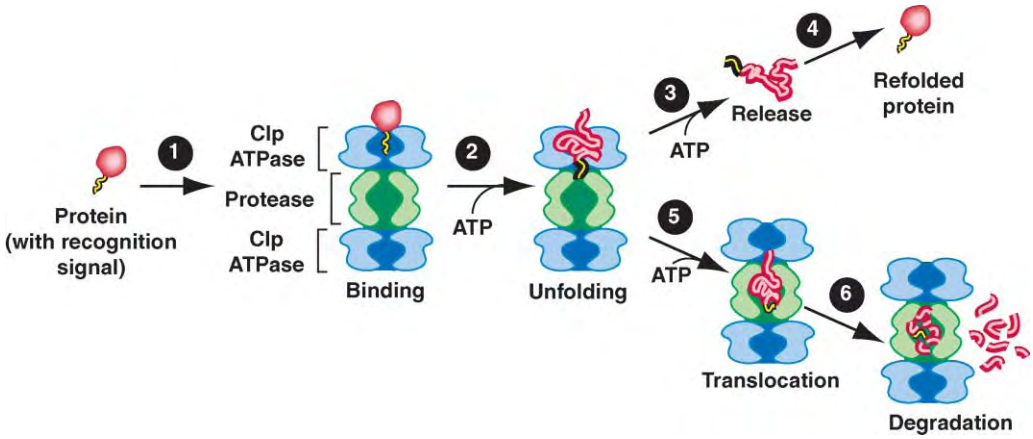

FIGURE 3 Model of the mechanism of protein unfolding by Clp chaperones and degradation by Clp proteases. See text for description. A lateral cross section of a Clp chaperone is shown in blue, associated with a proteolytic core shown in green. A substrate protein is shown in red, with a recognition signal shown in yellow.

When Clp ATPases function as regulatory components of proteases, they specifically bind and unfold substrates (1 and 2 in Figure 3), but rather than releasing the unfolded substrate, the unfolded protein is translocated to the cavity of the protease in an ATP-dependent reaction (5 in Figure 3). The unfolded protein is threaded processively into the proteolytic cavity starting with the end containing the recognition signal. Degradation occurs in the proteolytic cavity (6 in Figure 3).

Clp Specificity Factors or Cofactors

The activity of Clp ATPases is modulated in some situations by proteins that act as specificity factors. Specificity factors interact simultaneously with a substrate and a Clp ATPase. In this way they deliver otherwise unrecognizable substrates to a protease for degradation. There are examples of specificity factors that interact with ClpA, ClpX, and eukaryotic Clp homologues.

DnaK/Hsp70

The most extensively studied DnaK/Hsp70 family member is the *E. coli* homologue DnaK. DnaK and its homologues consist of two domains, an amino-terminal ATPase domain and a carboxy-terminal peptide-binding domain. The structures of the ATPase domain and the peptide-binding domain have been solved separately (Figure 4). Because the structure of full-length DnaK has not yet been determined, it is still unknown how the two domains interact at the molecular level. Unlike GroEL and Clp chaperones, DnaK does not assemble into a multisubunit structure with a central cavity to accommodate substrates undergoing remodeling.

DnaK/Hsp70 chaperones act in conjunction with cochaperones. One cochaperone that is essential for DnaK/Hsp70 activity is DnaJ/Hsp40. DnaJ binds hydrophobic regions in substrate polypeptides and in addition interacts with DnaK. Another cochaperone is GrpE, a protein that stimulates nucleotide exchange by DnaK.

The current model for the mechanism of reactivation of heat-inactivated proteins by the DnaK chaperone system is that ATP-bound DnaK binds and releases heat-denatured polypeptides rapidly, through interactions with exposed hydrophobic region. DnaJ stimulates hydrolysis of ATP bound to DnaK, forming the ADP-bound state of DnaK, which stabilizes the DnaK–substrate interaction. GrpE binds to the ATPase domain of DnaK and induces nucleotide exchange. Conformational changes in DnaK accompanying ADP/ATP exchange force the release of the substrate and DnaJ. When released from DnaK, the substrate is likely in a partially unfolded conformation and either refolds spontaneously or is rebound by other chaperones or proteases.

Hsp90 Chaperones

Hsp90 has been most extensively studied in eukaryotes, although there is a bacterial homologue, HtpG. The Hsp90 chaperone system is the most complex of the molecular chaperones in that it includes the Hsp70 chaperone system and a large number of cofactors. Hsp90 has an amino-terminal ATPase domain and a carboxy-terminal dimerization domain. The amino-terminal domain has been crystallized with

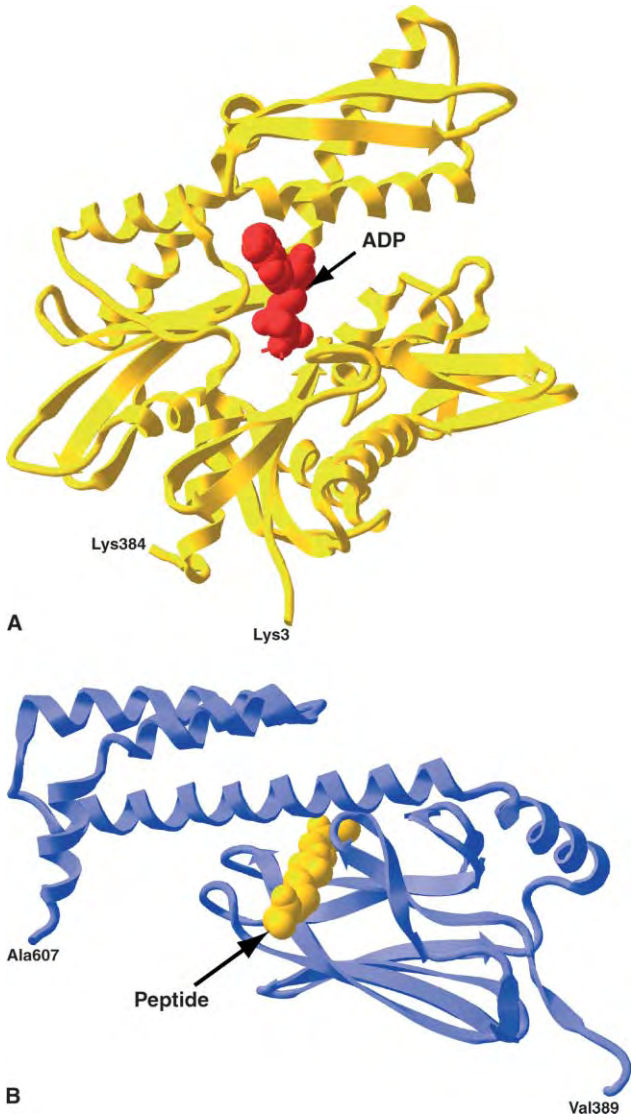

FIGURE 4 Model of the crystal structure of a DnaK/Hsp70 chaperone. (A) Structure of the nucleotide-binding domain of a DnaK homologue, Hsc70, with bound ADP (shown in red). The structure was solved by Flaherty, K. M., Deluca-Flaherty, C., and McKay, D. B. (1990) *Nature* **346**, 623–628. (B) Structure of the peptide-binding domain of DnaK with a bound peptide (shown in yellow). The structure was solved by Zhu, X., Zhao, X., Burkholder, W. F., Gragerov, A., Ogata, C. M., Gottesman, M. E., and Hendrickson, W. A. (1996). Structural analysis of substrate binding by the molecular chaperone DnaK. *Science* **272**, 1606–1614.

bound ATP (Figure 5). The mechanism of action of the Hsp90 system is less well characterized, but very likely it functions in a fashion similar to the other energy-dependent chaperones by remodeling substrate proteins through ATP-induced conformational changes. Hsp90 appears to be important for the folding of some proteins that are involved in key regulatory processes. It does not appear to play a major role in the de novo folding of proteins.

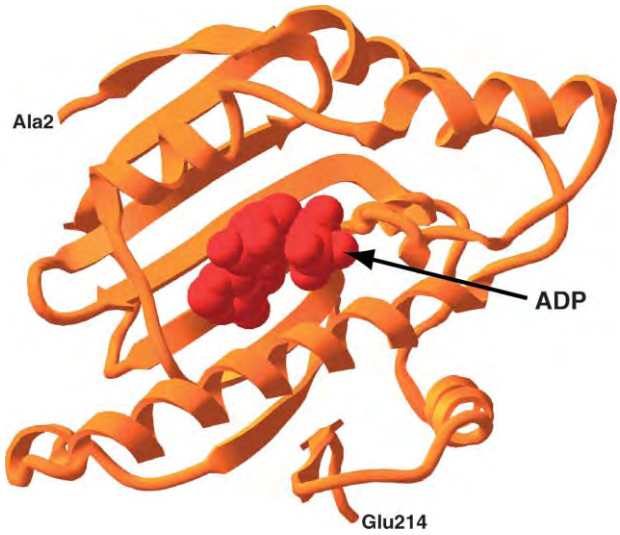

FIGURE 5 Model of the crystal structure of the ATPase domain of Hsp90 with bound ADP (shown in red). The structure was solved by Prodromou, C., Roe, S. M., O'Brien, R., Ladbury, J. E., Piper, P. W., and Pearl, L. H. (1997) Identification and structural characterization of the ATP/ADP-binding site in the Hsp90 molecular chaperone. *Cell* **90**, 65–75.

Summary

In summary, chaperones and proteases function together to determine the fate of proteins by facilitating the kinetic partitioning of substrates between pathways leading to reactivation, degradation, or, when quality control fails, aggregation.

See Also the Following Articles

Chaperones for Metalloproteins • Chaperonins • Endoplasmic Reticulum-Associated Protein Degradation • Heat/Stress Responses • Protein Folding and Assembly • Unfolded Protein Responses

Glossary

AAA$^+$ ATPases A large family of ATPases (AAA is derived from *A*TPases *a*ssociated with a variety of cellular *a*ctivities) characterized by a highly conserved 230–250 amino acid motif.

Clp/Hsp100 chaperones A large family of homologous ATPases that facilitate protein unfolding, some of which are induced by heat shock and are roughly 100 kDa in size.

molecular chaperones Specialized proteins that bind nonnative states of other proteins and assist them to reach a functional native conformation, in most cases through the expenditure of ATP.

Further Reading

Bukau, B., and Horwich, A. L. (1998). The Hsp70 and Hsp60 chaperone machines. *Cell* **92**, 351–366.

Dougan, D. A., Mogk, A., Zeth, K., Turgay, K., and Bukau, B. (2002). AAA^{+}proteins and substrate recognition, it all depends on their partner in crime. *FEBS Lett.* **529**, 6–10.

Fink, A. L. (1999). Chaperone-mediated protein folding. *Physiol. Rev.* **79**, 425–449.

Gottesman, S., Wickner, S., and Maurizi, M. (1997). Protein quality control: Triage by chaperones and proteases. *Genes Dev.* **11**, 815–823.

Horwich, A. L. (2001). *Advances in Protein Chemistry, Vol. 59. Academic Press, San Diego.*

Horwich, A. L., Weber-Ban, E. U., and Finley, D. (1999). Chaperone rings in protein folding and degradation. *Proc. Natl Acad. Sci. USA* **96**, 11033–11040.

Hoskins, J. R., Sharma, S., Sathyanarayana, B. K., and Wickner, S. (2001). Clp ATPases and their role in protein unfolding and degradation. *Adv. Protein Chem.* **59**, 413–429.

Patel, S., and Latterich, M. (1998). The AAA team: Related ATPases with diverse functions. *Trends Cell Biol.* **8**, 65–71.

Wickner, S., Maurizi, M. R., and Gottesman, S. (1999). Posttranslational quality control: Folding, refolding, and degrading proteins. *Science* **286**, 1888–1893.

Biography

Sue Wickner is a Scientist in the Laboratory of Molecular Biology at the National Cancer Institute in Maryland. She received her Ph.D. from Albert Einstein College of Medicine and her postdoctoral training at the National Institutes of Health. Her principal research interests are in molecular chaperones and their role in proteolysis. Her more recent work helped to demonstrate that Clp ATPases are a class of ATP-dependent molecular chaperones and demonstrated that molecular chaperones act directly in protein degradation. She is a member of the National Academy of Sciences and the American Academy of Arts and Sciences and is a fellow of the American Association for the Advancement of Sciences.

Joel Hoskins received his B.S. from Catholic University and his M.S. from Johns Hopkins University. He is currently a Senior Research-Associate in the Laboratory of Molecular Biology in the NCI and has collaborated with Dr. Wickner on studies of molecular chaperones for 15 years.

Chaperonins

Arthur L. Horwich, Wayne A. Fenton and George W. Farr
Howard Hughes Medical Institute and Yale School of Medicine, New Haven, Connecticut, USA

Chaperonins are large ring assemblies that provide essential assistance in folding to the native state of a large variety of proteins through an ATP-driven mechanism. Substrate proteins acted on by these machines include many newly translated proteins in the cytosol of eubacteria, archaebacteria, and eukaryotes, and newly imported proteins inside eukaryotic mitochondria and chloroplasts. Chaperonins in many of these compartments are heat-shock proteins that help to restore native conformation under stress conditions. For example, in archaebacteria and eubacteria, a high basal abundance of ~1% of soluble protein can be increased by heat shock to more than 10%.

Two Classes of Chaperonin

Two classes of chaperonin have been distinguished, based on evolutionary and structural considerations (Table I). One class, termed type I, includes GroEL, Hsp60, and ribulose bis-phosphate carboxylase/oxygenase (rubisco)-binding protein. These reside in the bacterial cytoplasm and endosymbiotically related mitochondria and chloroplasts, respectively. Type I chaperonins function through cooperation with distinct co-chaperonins, e.g., GroES, Hsp10, and Cpn10 respectively. Co-chaperonins also form ring structures and dynamically associate coaxially with chaperonin rings, functioning as "lid" structures that encapsulate a protein substrate during folding in the central cavity. The other class of chaperonins, termed type II, includes TF55 (thermophilic factor 55) and the thermosome in archaebacteria and the eukaryotic cytosolic chaperonin, known as chaperonin containing TCP1 (CCT). This class differs architecturally from type I in containing a built-in lid structure.

Overall Mechanism

Both classes of chaperonin function by the same general mechanism, a sequence of steps involving substrate protein binding, substrate folding in an encapsulated cavity, and release into the bulk solution (Figure 1). An open ring binds non-native protein in its central cavity through interactions between the cavity lining and exposed surfaces of the substrate protein, preventing misfolding and aggregation. In the case of type I chaperonins, this interaction occurs between the hydrophobic cavity lining of the chaperonin (Figure 2C) and exposed hydrophobic surfaces of the non-native protein, surfaces that will become buried to the interior of the substrate protein in the native state. Upon binding ATP and co-chaperonin in the case of type I, or ATP alone in the case of type II, large rigid body changes occur in the subunits of the ring, which dislocate its binding surface away from the central cavity, ejecting polypeptide into the cavity where it commences folding (Figure 1). Associated with the same movements, the cavity becomes encapsulated, in the case of type I chaperonins by binding co-chaperonin (Figure 2A) and in the case of type II chaperonins by the movement of protrusions comprising the built-in lid structure over the mouth of the cavity. Such encapsulation produces an environment in which polypeptide folds in isolation, prevented from forming any multimolecular interactions that could lead to aggregation. The enclosed chamber may also contribute to productive folding via a change in its wall character. In the case of type I chaperonins, there is a switch from the hydrophobic character of an open polypeptide-accepting ring to the hydrophilic character of the folding-active ring (Figure 2C). This switch presumably favors exposure in the folding polypeptide of hydrophilic surfaces and burial of hydrophobic ones, properties of the native state. Additionally, encapsulation in a confined space may also contribute to efficient folding, preventing population of a variety of extended off-pathway conformations.

Subsequent to the step of folding in an encapsulated space, shown to be the longest phase of the chaperonin reaction, hydrolysis of ATP permits release of the substrate protein from the central cavity into the bulk solution (Figure 1). For many substrate proteins, multiple rounds of binding to an open ring and folding inside the encapsulated cavity, followed by release into the bulk solution, are required to achieve the native state, with each round likely comprising an "all-or-none" trial at reaching the native state.

TABLE I

Characteristics of Chaperonins

Chaperonin	Cellular compartment	Co-chaperonin	Subunits/ring	Subunit composition	Substrate proteins
Type I					
Hsp60	Mitochondrial matrix	Hsp10	7	Homo-oligomer	Many imported proteins
Rubisco binding protein	Chloroplast stroma	Cpn10	8	α, β	Rubisco small subunit, other imported proteins
GroEL	Eubacterial cytoplasm	GroES	7	Homo-oligomer	Many cytoplasmic proteins, including λ phage components
Type II					
TF55	Archaebacterial cytoplasm	None	9	α, β	Unknown
Thermosome	Archaebacterial cytoplasm	None	8	α, β	Unknown
CCT (TRiC)	Eukaryotic cytosol	None	8	α, ε, ζ, β, γ, θ, δ, η	Actin, tubulin, cyclin E, G_α-transducin, VHL

Those molecules failing, at the point of release into the bulk solution, to reach native form or a state that is committed to reaching native form in the bulk solution, are subject to an unfolding action upon rebinding to a chaperonin ring that likely returns them to the original non-native ensemble of states, enabling a fresh trial at folding.

The sum of these actions is the provision of kinetic assistance to the process of protein folding, effectively smoothing an energy landscape. That is, while the primary amino acid sequence of the substrate polypeptide provides all the information necessary to specifying a characteristic native conformation that typically lies at the energetic minimum, as articulated by Anfinsen and co-workers, during folding under physiologic conditions, there can be production of conformations that are kinetically trapped, preventing a protein from reaching the native state on a physiologic timescale. Chaperonins function in this context as biological catalysts that prevent or reverse formation of such misfolded species, thus enhancing the rate of folding *in vivo*.

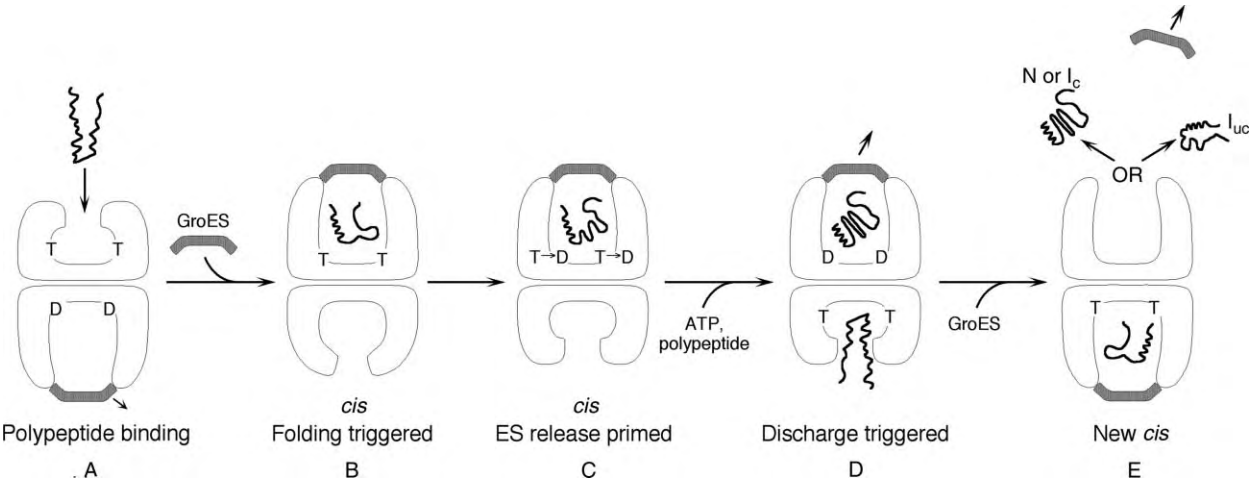

FIGURE 1 The ATP-driven folding cycle of GroEL–GroES. Asymmetric GroEL–GroES–ADP complexes (A) are the most likely polypeptide-acceptor state *in vivo*. In the presence of ATP, GroES binds to the open ring, simultaneously discharging the substrate polypeptide from its binding sites and encapsulating it in the folding chamber (B). Folding proceeds in this sequestered environment, the longest step of the reaction cycle (~10 s), until ATP hydrolysis occurs (C). This weakens the GroES association and permits ATP and polypeptide to bind to the opposite ring (D). This discharges the ligands from the folding chamber and simultaneously establishes a new folding chamber in the opposite ring (E). Thus, the two rings of GroEL alternate asymmetrically between binding-active and folding-active states. The discharged polypeptides in (E) are in several possible states: N (native) or I_c, a state committed to becoming native without further chaperonin action; or I_{uc}, a non-native intermediate state that must rebind to chaperonin for another trial at folding. For many GroEL substrates, any given round of folding only produces a few percent of N or I_c states; most of the population must be rebound for another attempt. In a cellular context, I_{uc} states can also partition to other chaperone pathways or to degradative pathways. This latter option is vital for removing potential chaperonin substrates that are damaged or mutated such that they cannot fold.

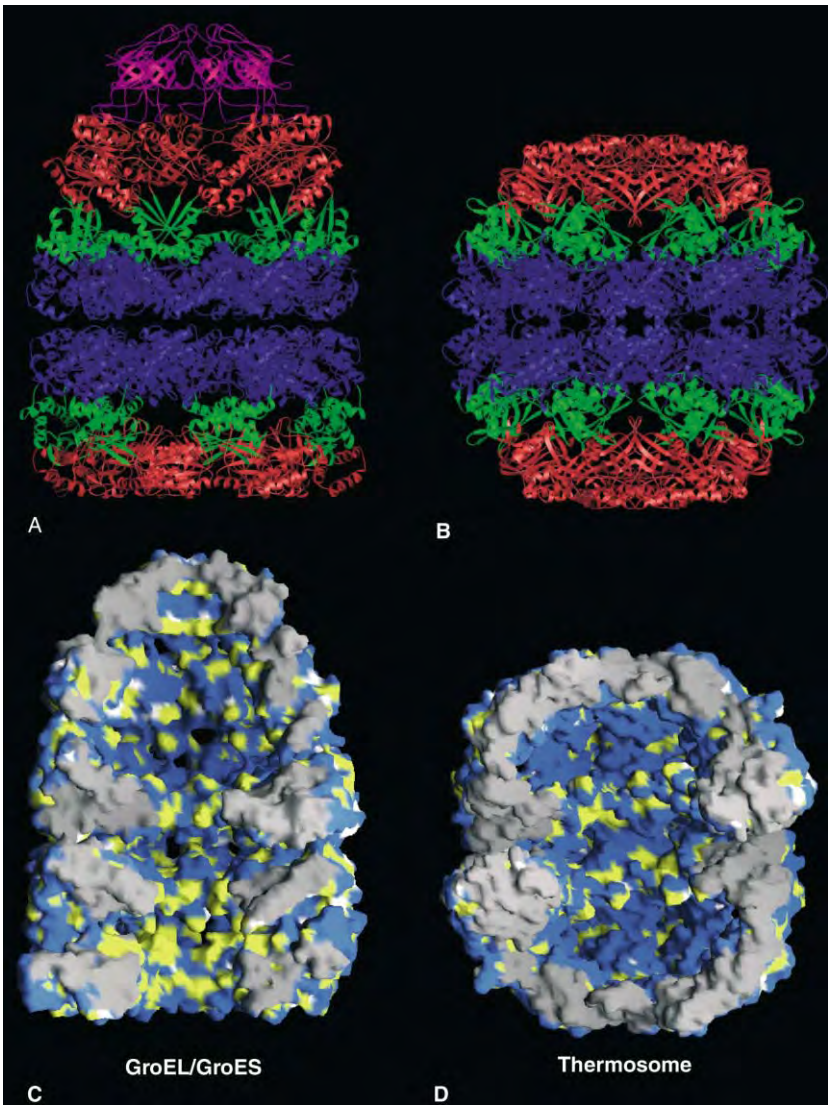

FIGURE 2 Architecture of chaperonins. Structural models of a type I chaperonin, GroEL from *E. coli*, complexed with its co-chaperonin GroES (A, C) and structural models of a type II chaperonin, the thermosome from *T. acidophilum* (B, D). (A, B) Ribbon diagrams showing the domains of each chaperonin: equatorial, blue; intermediate, green; apical, red. In (A), GroES is colored magenta. (C, D) Space-filling models presented as cutaway views to show the interior cavities of the chaperonins, with surfaces colored according to hydrophobicity of the amino acid side chains: yellow, hydrophobic; blue, hydrophilic. Gray represents cutaway interface between subunits. Note the relative hydrophobicity of the lower (trans) ring of the GroEL/GroES, its polypeptide binding surface, as compared to the upper, GroES bound ring, relatively hydrophilic in character. Note also the absence of exposed hydrophobic surface in the type II complex.

Architecture

Chaperonins are generally composed of two rings, stacked back-to-back, that function out of phase with respect to each other during the reaction cycle, such that only one ring is folding-active at a time. Each ring is composed of radially arranged identical or nearly identical subunits, each folded into three domains (Figure 2A, B). The "equatorial" domains, at the waistline of the cylinder, each contain an ATP-binding pocket. The collective of these domains comprises the stable base of the assembly, with the domains forming tight contacts with each other both side-by-side within a ring and across the ring–ring interface. The "apical" domains, at the end portion of the cylinder, are mobile, hinged at their bottom aspect, and contain the polypeptide-binding site at the inside surface. For type I chaperonins, this same binding surface, hydrophobic in character, is the one that associates with the co-chaperonin following rigid body elevation and twisting of the domains directed by ATP binding to the ring. These apical movements, captured by cryoEM and X-ray analyses of *E. coli* GroEL–GroES, amount to elevation by 60° and clockwise twist of 90°. They serve to dislocate the hydrophobic polypeptide-binding surface away from the central cavity, driving

polypeptide release into the cavity. Simultaneously, they enable GroES binding via interaction through its mobile loop segments, which extend down from each of the seven GroES subunits to contact the hydrophobic surface of each of the dislocated apical domains. This interaction is itself hydrophobic in character, mediated by an isoleucine-valine-leucine edge of the β-hairpin loop extended from GroES, which interacts with a portion of the hydrophobic binding surface of GroEL. This association of GroES with GroEL, and of other chaperonin–co-chaperonin pairs, results in encapsulation of the central cavity. For type II chaperonins, the apical domains each contain an insertion of residues, relative to type I, that comprises a protrusion, the collective of which function as a lid. The protrusions are marginated to the cavity wall of an open ring, but then are pointed centrally to collectively form a lid upon ATP binding. For both classes of chaperonin, the apical domains are covalently connected to the corresponding stable equatorial domains via a slender "intermediate" domain, which is hinged at both its top (apical) and bottom (equatorial) aspects (Figure 2A, B). This domain almost certainly contributes to transmitting the signal of ATP binding into the rigid body movements of the apical domains, and it also supplies a highly conserved aspartate residue that functions as a base in the mechanism of ATP hydrolysis: upon downward rotation of the intermediate domain attendant to ATP binding, the aspartate swings into the equatorial nucleotide pocket and activates water to attack the gamma phosphate of ATP.

The variations within different kingdoms on the basic theme of chaperonin architecture are interesting to contemplate and not fully understood (Table I). For example, an exception to the double-ring architecture is the mammalian mitochondrial chaperonin, which can be isolated as a single ring. Evidence has suggested that it may remain as a single ring throughout the nucleotide cycle, implying that it does not use the same allosteric ejection mechanism as the other chaperonins, which employ ATP binding on the opposite ring as a signal for release. The number of subunits per chaperonin ring also varies, with the bacterial and mitochondrial (type I) chaperonins containing seven subunits per ring, the chloroplast chaperonin containing eight subunits per ring, archaebacterial (type II) chaperonins containing eight or nine subunits per ring, and the eukaryotic cytosolic chaperonin (CCT) containing eight subunits per ring. Clearly, the volume of the central cavity, as well as the angle of adjacent subunits with respect to each other, is affected by the number of subunits per ring. Notably, because substrate proteins likely co-evolved with the machines that assist their folding, there could be stringency with respect to subunit number and ring size.

The hetero-oligomeric nature of some of the chaperonins also remains to be fully understood. For example, while GroEL and Hsp60 (type I) are homo-oligomers, the thermosome in archaebacteria (type II) contains eight-membered rings that are composed of α–β heterodimers in which the two subunits differ in amino acid sequence, principally in their apical domains. Most extreme is the eukaryotic cytosolic CCT chaperonin (type II), which contains eight different subunits per ring, arranged in a characteristic order. Here also, apical domain sequences are the most varied among the subunits (but any given subunit is well conserved across species lines, for example, from yeast to man). Studies of two major substrate proteins assisted by CCT, actin and tubulin, suggest that specific apical domains that are positioned at opposite aspects of the ring are involved in binding these proteins. Thus, it would seem that binding affinity for particular substrate proteins can comprise an evolutionary force directing apical domain evolution and hetero-oligomeric composition. Indeed, the overall character of the cavity wall of type I and II chaperonins seems to differ (Figure 2C, D). Rings of type I chaperonins present a hydrophobic cavity surface in the open state, with highly conserved hydrophobic residues positioned on a tier of three structures, two horizontally configured α-helices and an underlying extended segment, that form the cavity-facing aspect of the apical domains (Figure 2C, bottom ring). By contrast, type II chaperonins present a surface, corresponding to these same secondary structures, that is not obviously hydrophobic – in fact, some of the residues that are hydrophobic and conserved in type I chaperonins are instead hydrophilic in type II (Figure 2D). Yet type II chaperonins harbor hydrophobic residues on their protrusions, and the potential role of these residues, as well as those lining the cavity wall, in substrate binding remains to be addressed.

Polypeptide Binding by Type I Chaperonins

As mentioned, the step of polypeptide binding appears to be associated with capturing non-native states before they can irreversibly misfold and aggregate, and the step of binding, via exposed hydrophobic surfaces at least in the case of GroEL, appears to be associated with an action of unfolding. Such an action may be either a passive one, in which less folded states are preferred, with mass action shifting an ensemble of states in equilibrium with each other toward the less-folded ones, or unfolding may be catalyzed, where the polypeptide, bound by multiple apical domains simultaneously, is effectively unfolded. Either or both mechanisms could

be operative, but the net result for many canonical GroEL substrate proteins is a stably bound state that is weakly structured, e.g., very susceptible to exogenously added proteases and highly exchangeable in hydrogen/deuterium isotope exchange experiments. In the case of GroEL, crystallographic studies of peptides associated with the chaperonin apical domain have captured the peptides bound horizontally in the groove between the two α-helices of the apical domain, forming hydrophobic contacts with those residues projected from the helices. Additional NMR studies reveal that other peptides are capable of forming α-helices when they become associated with GroEL. Thus, it appears that at least some secondary structural elements can be preserved through the step of binding by chaperonin, but tertiary structure is unstable.

The Nucleotide Cycle

The progression through the chaperonin reaction is driven by ATP binding and hydrolysis. This has been best studied in the case of the GroEL–GroES reaction (Figure 1). Here, ATP binds cooperatively to the seven equatorial sites within a ring but anti-cooperatively with respect to the opposite ring. Because GroES binding requires initial ATP occupancy of a ring, the GroEL–GroES complexes formed are asymmetric in character. The normal acceptor state for non-native polypeptide is an open ring of an asymmetric GroEL–GroES–ADP complex (Figure 1A). Once bound with polypeptide, a GroEL ring is converted to its folding-active state by the binding of ATP and GroES (Figure 1B). These produce the large rigid body domain movements associated with ejection of polypeptide into the central cavity and attendant folding. These steps can occur in the setting of a GroEL mutant unable to hydrolyze ATP and also in the presence of ADP–metal complexes such as ADP–beryllium fluoride (an ATP ground-state analogue) or ADP–aluminum fluoride (a transition-state analogue). In all of these cases, polypeptide proceeds to the native state inside a very stable GroES-encapsulated cavity. That is, the energy of ATP/GroES binding is sufficient to trigger the rigid body conformational changes that lead to ejection into the central cavity and productive folding. Thus, it is ATP binding, not hydrolysis, that is crucial for triggering folding.

The folding-active complex has a long half-life ($\sim$10 s for GroEL–GroES–ATP), after which ATP hydrolysis occurs (Figure 1C). This event does not interfere with folding but serves rather to weaken the stability of the GroEL–GroES complex. This "primes" the complex for discharge of its ligands, GroES, polypeptide, and ADP, effected by ATP binding to the opposite ring (Figure 1D). In sum, then, the GroEL–GroES machine functions asymmetrically, with only one ring folding-active at a time (and the other, opposite an ATP–GroES-occupied ring, empty of polypeptide and nucleotide until ATP hydrolysis occurs). The machine oscillates back and forth using one round of binding seven ATPs to simultaneously nucleate one folding-active ring and discharge the opposite ring that has completed its folding cycle (Figure 1E). It seems likely, given recent studies of CCT and archaebacterial chaperonins, that the same asymmetric cycle pertains there as well, with the apical protrusions mimicking the behavior of GroES with respect to the open or encapsulated state of a ring.

Substrate Proteins

In general, small proteins (fewer than 100–150 amino acids) fold very rapidly and thus do not appear to require chaperonin assistance *in vivo*. Many larger proteins fold slowly, however, and are potential substrates for chaperonin-assisted folding. The actual *in vivo* substrates of chaperonins vary widely depending on chaperonin-type and subcellular compartment (Table I). GroEL in the bacterial cytoplasm is estimated to fold 10–30% of newly synthesized proteins, with particular preference for those between 20 and 60 kDa in size. Mitochondrial Hsp60 and the chloroplast rubisco-binding protein appear to be required for folding a potentially larger percentage of proteins newly translocated into these organelles. In the case of mitochondria, several large proteins, too large to be encapsulated inside the Hsp60 cavity, have been identified that require both Hsp60 and Hsp10. In the case of the yeast mitochondrial Krebs cycle enzyme, aconitase, studies with GroEL–GroES have resolved a *trans*-acting mechanism in which the polypeptide, unable to be encapsulated by GroES in *cis*, is productively released from the open ring by binding of ATP and GroES in *trans*.

The natural substrate specificity of archaebacterial (type II) chaperonins has not been defined, in part because these species have not been amenable to genetic manipulation. On the other hand, CCT, the type II chaperonin of the eukaryotic cytosol, may have a narrower substrate specificity than the other cytosolic chaperonins. Actin and tubulin are major substrates, yet additional cytosolic polypeptides have been shown to require CCT for efficient folding, including G_α transducin, cyclin E, and the von Hippel–Lindau tumor suppressor protein. For several of these substrates, evidence has emerged to suggest that they may be recognized in non-native form via exposed hydrophobic surfaces, as with type I chaperonins, yet the sites of binding on CCT itself remain to be identified.

See Also the Following Articles

Chaperones for Metalloproteins • Chaperones, Molecular • Cytochrome Oxidases, Bacterial

Glossary

ATP Adenosine triphosphate, the major energy metabolite in cells.

cryoEM An electron microscopy (EM) technique that involves rapid freezing of droplets of a protein solution to form a glass, which is then analyzed without further fixation or staining; as a result, the images closely represent the structural state of the protein in solution.

energy landscape The representation of the energetics of protein folding as a three-dimensional surface with hills and valleys (local energetic maxima and minima) to reflect the complexity of multiple interconnected pathways to the native state for the ensemble of non-native and intermediate folding states; this is in contrast to a two-dimensional reaction coordinate diagram used for simpler reactions.

hydrophilic/hydrophobic A description of the relative polarity of amino acid side chains in terms of their affinity for an aqueous environment. Hydrophilic side chains are polar, including ones with charged groups (e.g., lysine and aspartic acid) and ones with hydroxyl or amide groups (e.g., serine and asparagine). Hydrophobic side chains are non-polar, including aliphatic and aromatic groups (e.g., leucine and phenylalanine).

rubisco Ribulose bis-phosphate carboxylase/oxygenase, a major protein in the photosynthetic pathway.

Further Reading

Cowan, N. J., and Lewis, S. A. (2001). Type II chaperonins, prefoldin, and the tubulin-specific chaperones. *Adv. Protein Chem.* **59**, 73–104.

Ellis, J. (ed.) (1996). *The Chaperonins*. Academic Press, San Diego.

Fenton, W. A., and Horwich, A. L. (2003). Chaperonin-mediated protein folding: Fate of substrate polypeptide. *Quar. Rev. Biophys.* **36**, 229–256.

Sigler, P. B., Xu, Z., Rye, H. S., Burston, S. G., Fenton, W. A., and Horwich, A. L. (1998). Structure and function in GroEL-mediated protein folding. *Annu. Rev. Biochem.* **67**, 581–608.

Biography

Arthur Horwich is Professor of Genetics at Yale School of Medicine and an Investigator in the Howard Hughes Medical Institute. His research interests are in the general areas of cellular protein folding, unfolding, and misfolding. He holds an M.D. from Brown University and carried out postdoctoral research at the Salk Institute and Yale University. He is a member of the National Academy of Sciences.

Wayne Fenton is a Research Scientist in Genetics at Yale University School of Medicine. His general interests are in the mechanisms of protein folding and unfolding. He received a Ph.D. from Brandeis University and carried out postdoctoral work at Yale University.

George Farr is an Associate Research Scientist in the Howard Hughes Medical Institute. His research interest is in chaperonin-assisted protein folding. He received a Ph.D. from Case Western Reserve University and carried out postdoctoral work at Case Western and Yale University.

Chemiluminescence and Bioluminescence

Thomas O. Baldwin
University of Arizona, Tucson, Arizona, USA

Chemiluminescence and bioluminescence are terms that refer to the same physical process of light emission without heat. Bioluminescence is the process by which a living system or components isolated from a living system, such as a firefly tail, carries out a series of reactions that result in emission of light. Chemiluminescence is the same kind of process, but involving molecules that are not of biological origin. Chemiluminescence should be distinguished from incandescence, which occurs at high temperatures. Both bioluminescence and chemiluminescence are well known to the public, and both hold great fascination for all observers. Light without heat has intrigued people since the beginning of recorded history, and surely before.

Fluorescence: The Underlying Property

Fluorescence is a characteristic common to molecules formed as a result of chemiluminescent and bioluminescent reactions. At normal ambient temperatures, the vast majority of molecules exist in what is known as the ground state. However, under certain conditions, such as absorption of light energy, a molecule may be converted into an excited state. For fluorescent molecules, the excited state can return to the ground state by emitting energy as light. Virtually all molecules are fluorescent to some extent, but most emit such a small amount of light that sensitive instruments are required to detect it. A graphic description of fluorescence is shown in Figure 1.

In the case of fluorescence, the energy input is the absorption of light. The chemical characteristics of a molecule will determine which wavelengths (color) of light it will absorb. As in the ground state, the excited state will have multiple vibrational modes at discrete energy levels. At normal ambient temperatures, most of the molecules will be in the lowest vibrational energy level, so following absorption of the input energy, the molecules will relax to the lowest vibrational level of that excited state. Excited states tend to be very unstable, with lifetimes in the nanosecond to picosecond range. There are many ways for a molecule to return to the ground state. In solution, the excited molecules may collide with other molecules in solution and impart energy through the collisions, thereby increasing the vibrational and translational energies of the other molecules while itself returning to the ground state. Alternatively, some molecules, referred to as fluorescent molecules, have the ability to return to ground state by emission of light. Note that the emitted light will be of a lower energy (red-shifted in the spectrum) relative to that of the input energy due to the relaxation of the excited state. This effect is known as the Stokes shift.

Chemiluminescence: Fluorescence from a Chemical Reaction

In the case of chemiluminescence, the input energy is derived from the making and breaking of bonds that occur during a chemical reaction. Other than that important detail, fluorescence and chemiluminescence result from the same fundamental characteristics of the molecules involved. For a reaction to be chemiluminescent, one of the products must be fluorescent, and the chemical step that results in generation of the fluorescent product must be of sufficiently high energy to result in formation of the excited state. Therefore, the efficiency of light emission from a chemiluminescent reaction is the product of the efficiencies of each step. That is, the chemiluminescent quantum yield, Φ_{CL}, or the yield of photons per molecule of reactant consumed in the reaction, is given by the equation

$$\Phi_{CL} = \Phi_R \cdot \Phi_{CE} \cdot \Phi_F$$

All of these efficiencies have values between 0 and 1. The reaction yield, Φ_R, is the chemical yield of the correct products, rather than the products of side reactions, which may not be fluorescent, and is typically near 1. The chemical excitation yield, Φ_{CE}, is the fraction of the fluorescent product molecules that are produced in the excited state, rather than the ground state.

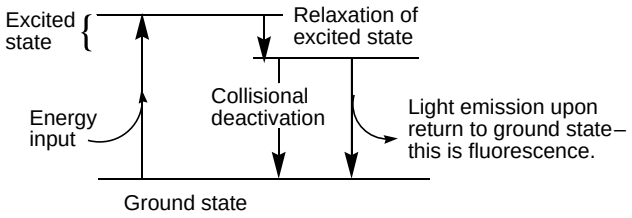

FIGURE 1 Diagram showing the processes of generation of the excited state and return of the excited state to the ground state.

To be considered a chemiluminescent reaction, this value should be 10^{-3} or greater. Finally, the fluorescence quantum yield, Φ_F, is the proportion of those molecules that are produced in the excited state that return to the ground state by emission of light rather than by collisional quenching or some other process, as depicted in Figure 1. The fluorescence quantum yield is typically 0.1 or greater. Conditions that impact any of these three factors will impact the overall yield of light from the reaction.

In some cases, product molecules are produced with exceptionally high chemical yield in the excited state, but the product is itself nonfluorescent (very low Φ_F). In these cases, the yield of luminescence can be increased dramatically by addition of a highly fluorescent molecule to the reaction, which can, by a process called energy transfer, accept the energy from the excited product to become excited itself. The overall chemiluminescence quantum yield in such cases becomes

$$\Phi_{CL} = \Phi_R \cdot \Phi_{CE} \cdot \Phi_F \cdot \Phi_{ET},$$

where Φ_{ET} is the efficiency of energy transfer from the primary excited state produced in the chemical reaction to the acceptor, which then emits with the efficiency given by Φ_F. The chemiluminescence quantum yields in some sensitized chemiluminescent reactions can be very high indeed, approaching 1.

Much research has been reported on the chemiluminescence properties of a wide array of peroxides, especially the cyclic peroxides such as the dioxetanes. Tetramethyldioxetane will decompose to yield 2 molecules of acetone, one in the singlet excited state and the other in the triplet (Figure 2). Of course, acetone is nonfluorescent, so the decomposition reaction is essentially dark. However, if 9,10-dibromoanthracene or 9,10-diphenylanthracene is added to the reaction, intense light emission is detected as a result of the energy transfer from the excited state acetone product to the fluorescent dye, DBA or DPA.

These and related technologies have found wide use in the form of chemiluminescence-based diagnostics and other applications. Perhaps one of the best known applications is the "light-stick" technology used by campers and hikers, and for fun and safety during Halloween. The light stick consists of a sealed, flexible plastic tube containing a solution of oxalic phthalate ester and a sealed glass vial containing a solution of hydrogen peroxide. Bending of the plastic tube will cause the glass vial to break, mixing the two solutions. The hydrogen peroxide will oxidize the ester, yielding 2 molecules of phenol and 1 molecule of 1,2-dioxetane-3,4-dione. The dioxetane will decompose to yield 2 molecules of carbon dioxide in the excited state. By including a dye sensitizer in the solution, the energy of the excited state carbon dioxide will result in light emission (see Figure 3). The color of the light emitted is determined by the fluorescence properties of the dye used in the light stick and can range from blue to red. Examples of dyes used are shown in Figure 3. One characteristic common to most fluorescent compounds and demonstrated in these examples is a system of conjugated double bonds.

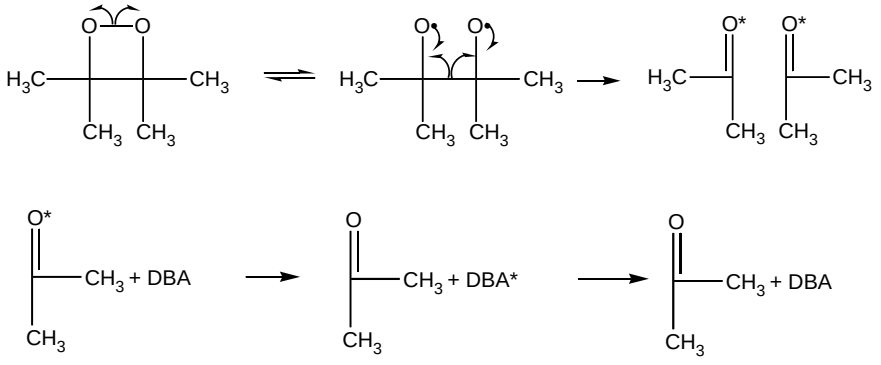

FIGURE 2 Chemiluminescent decomposition of tetramethyldioxetane. The first step of the reaction is the hemolytic cleavage of the oxygen–oxygen bond, followed by hemolytic cleavage of the carbon–carbon bond to yield the diradical, which recombines to form acetone in the excited state. In the absence of the dye 9,10-dibromoanthracene, the reaction is dark. However, the dye can accept the energy from the excited state carbonyl to yield the excited state of the dye, which returns to ground state with the emission of light.

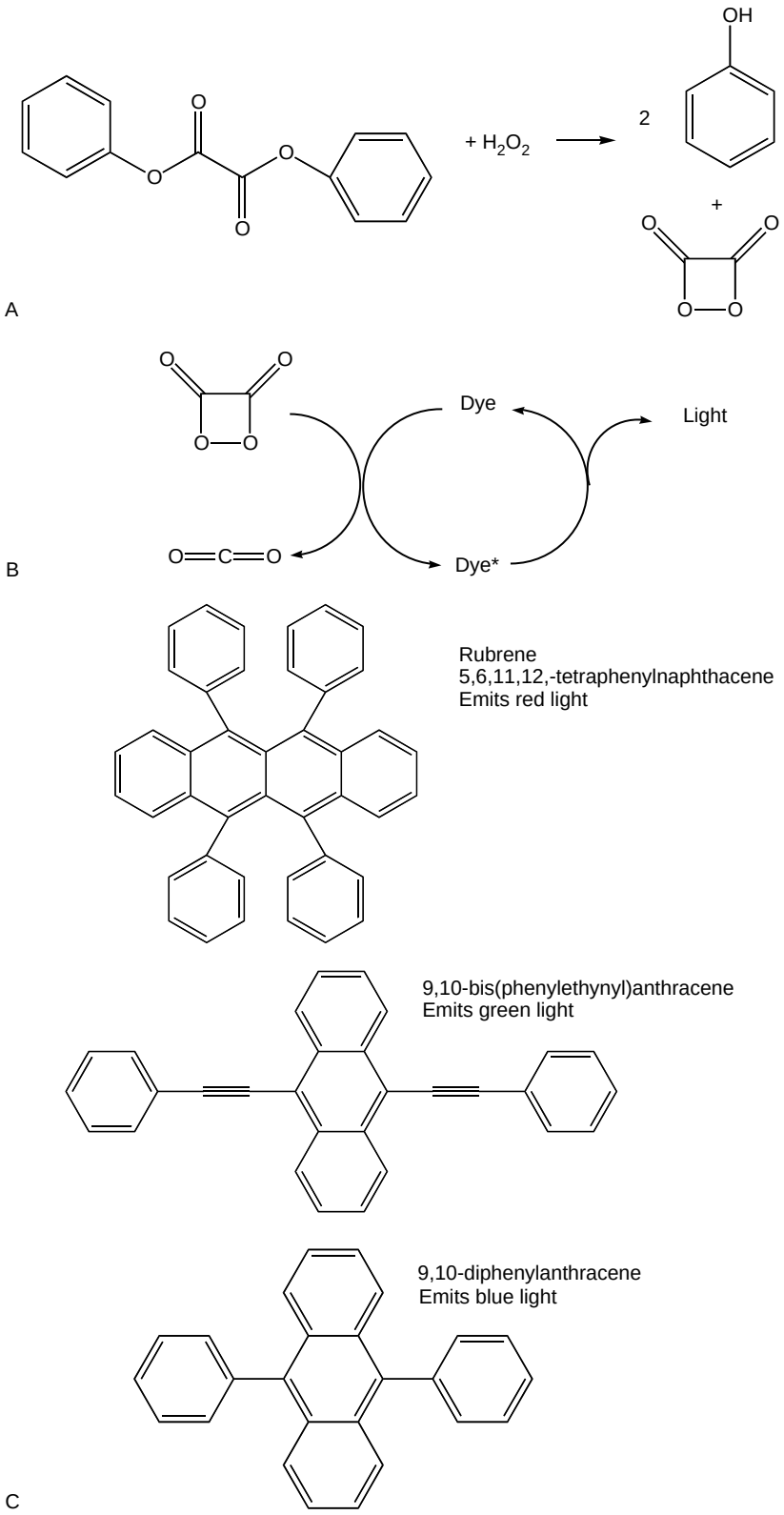

FIGURE 3 The chemistry of the light stick. The reaction that occurs in a light stick upon breaking the glass ampule and allowing the two solutions to mix is shown in panel A. The oxalic phthalate ester is oxidized to yield 2 molecules of phenol and 1 molecule of the dioxetane. In panel B, the dioxetane decomposes by the same mechanism shown in Figure 2 to yield 2 molecules of carbon dioxide. The excited state carbon dioxide transfers energy to the dye to yield the excited state of the dye, which in turn emits light. The color of the light is determined by the chemistry of the dye. Three examples are shown in panel C, spanning the spectrum from red to blue.

Bioluminescence: Chemiluminescence from a Biological Source

Bioluminescence reactions, unlike chemiluminescence, require an enzymatic catalyst for the reaction to occur. These enzymes are generically referred to as luciferases. Even though they have the same name, they catalyze vastly different reactions. For comparison, other groups of enzymes that have a common name, such as proteases, all catalyze the same kind of reactions. Proteases all hydrolyze peptide bonds, but luciferases catalyze reactions on completely different substrates, and they have no evolutionary relationship. Firefly luciferase, bacterial luciferase, and Renilla luciferase catalyze different reactions, having in common only the fact that light is emitted from a product of the reaction. It is therefore very important when discussing bioluminescence to stipulate the biological source of the enzyme.

There are many examples of bioluminescence that resemble the nonbiological chemiluminescence reactions described previously. For example, the reaction that occurs in the tail of the firefly is very similar to that of the light stick, but unlike the light stick, the firefly reaction requires the participation of an enzyme, firefly luciferase. As with chemiluminescent reactions, the firefly luciferase-catalyzed reaction has found numerous practical applications, primarily due to the involvement of ATP in the reaction (Figure 4). Many of these applications involve accurate and sensitive analysis of ATP levels within samples. The role of the ATP is to activate the carboxyl group of the firefly luciferin, the substrate for the luciferase-catalyzed reaction. As a result of this adenylation reaction, the luciferyl adenylate is now poised to react with molecular oxygen, eliminating AMP and forming the dioxetanone intermediate (Figure 5). The dioxetanone ring then decomposes by a mechanism similar to that shown in Figure 2, ultimately yielding CO_2 and the excited state of the product oxyluciferin, which emits light as it returns to ground state.

Different species of firefly emit light of different colors, but they all appear to use the same substrate luciferin, and there appear to be no energy transfer systems involved. At present, the detailed mechanism by which the insects emit light of different color is unknown, but it surely has to do with the details of the interactions of the excited state with the luciferase enzyme, since the enzymes are slightly different between the species. The color of the light emitted ranges from green to red, and the quantum yield of these reactions approaches 1.

Unlike firefly luciferase, which is a single polypeptide and employs ATP and a special substrate firefly luciferase, bacterial luciferase is a heterodimer ($\alpha\beta$) consisting of two similar but nonidentical polypeptides. In bacterial luciferase there is a single active center on the α subunit, but both subunits are required for the high quantum yield reaction. The substrates for the bacterial luciferase reaction are reduced flavin mononucleotide, molecular oxygen, and a long-chain saturated aldehyde. The enzyme formally is a flavin monooxygenase, catalyzing the cleavage of molecular oxygen and inserting 1 atom of oxygen into a substrate and the other into water. The mechanism of light emission in the bacterial luciferase-catalyzed reaction is still under debate, but there is general agreement regarding most of the reaction. In the first step of the reaction, reduced flavin mononucleotide ($FMNH_2$) reacts with O_2 to yield a reduced flavin peroxide (step 1, Figure 6). In the second step, the peroxide reacts with the aldehyde substrate to form the tetrahedral intermediate shown in Figure 6, step 2. There is general agreement in the field that this tetrahedral intermediate forms in the reaction, but how the intermediate decomposes to yield the excited state is under debate. One possible mechanism is shown in step 3 of Figure 6.

The identity of the emitter in the bacterial bioluminescence has been difficult to identify unambiguously because the product of the reaction, oxidized flavin mononucleotide, although fluorescent in solution, is nonfluorescent when bound to the luciferase. Various lines of evidence suggest that the emitter in the reaction is the flavin pseudobase shown in step 3 of Figure 6. The primary excited state, however, must be some other molecule, possibly the excited carbonyl shown in step 4 of Figure 6. In some species of bioluminescent bacteria, light emission from the living bacteria is significantly blue-shifted from that from the purified luciferase enzyme. It has been shown that the blue light comes from another protein, the lumazine protein, which becomes excited through some form of interaction with the luciferase during the reaction. This is an example of an energy transfer process in a bioluminescence

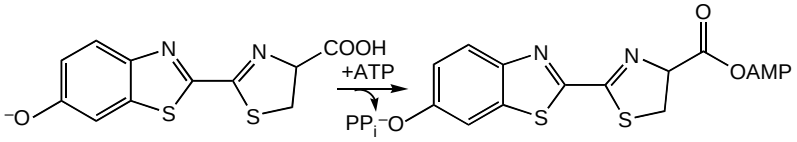

FIGURE 4 Proposed mechanism of the firefly luciferase reaction. The luciferin reacts with ATP to form the luciferyl adenylate, thus preparing the molecule for reaction with oxygen.

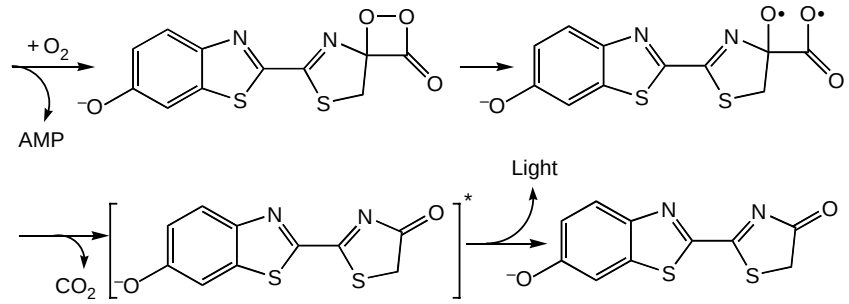

FIGURE 5 Proposed mechanism of the firefly luciferase-catalyzed reaction. The luciferyl adenylate (Figure 4) reacts with molecular oxygen, eliminating the AMP and forming the cyclic peroxide dioxetanone structure. The dioxetanone then decomposes by homolytic cleavage of the O–O and C–C bonds, liberating CO_2 and yielding the excited state of the oxyluciferin. Light emission occurs as the excited state returns to ground state.

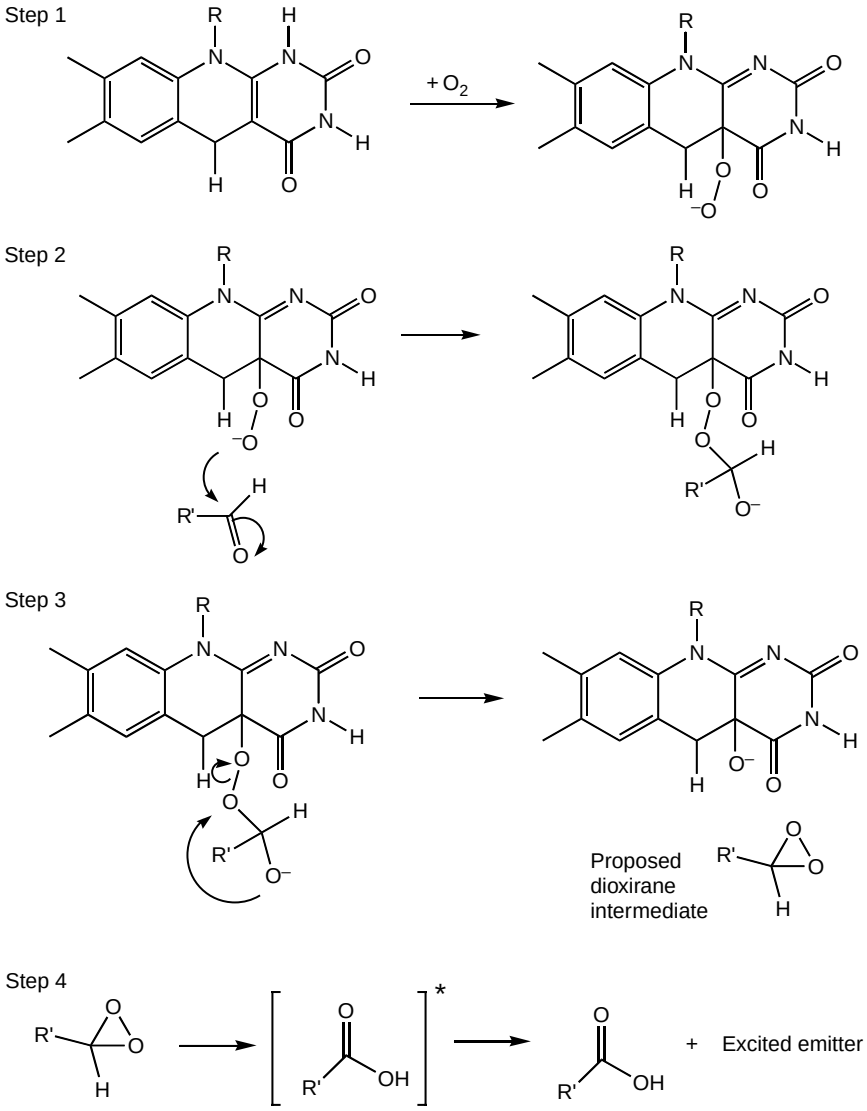

FIGURE 6 Proposed mechanism of the bacterial luciferase-catalyzed reaction, as described in the text.

system, similar to the chemiluminescent examples described in Figure 3. But for the energy transfer to be efficient, it must occur in an energetically downhill direction. That is, the primary excited state must have an energy level higher than the excited flavin, which emits at a longer wavelength (lower energy) than does the lumazine protein. It is this fact, among others, that leads to the belief that the primary excited state in this reaction is likely to be an excited carbonyl, rather than the excited flavin. In the absence of the lumazine protein, energy transfer can occur to the flavin with emission from the excited flavin.

Another example of energy transfer in the bacterial bioluminescence system is from a yellow-emitting strain of *Vibrio fischeri*. These bacteria have a luciferase that emits blue-green light, similar to other bacterial luciferases, but *in vivo* and at temperatures of 20°C or lower, the color of the light emitted is bright yellow. This color shift is the result of a yellow fluorescence protein that has a highly fluorescent oxidized flavin mononucleotide chromophore. It is interesting that the lumazine protein, which causes a blue shift, and the yellow fluorescence protein appear to be homologous and carry out similar functions of energy transfer but do so with different chromophores.

There are many other examples of bioluminescent and chemiluminescent reactions, many of which have found important and valuable uses. The green fluorescent protein that was isolated from jellyfish is a very important tool in the study of protein trafficking and other molecular imaging applications. In immunoassays, chemiluminescent and bioluminescent reactions offer sensitivity, but without the hazards of radioactive labels. In recent years, work in the field has become primarily focused on applications of the technology; by comparison, very little effort is being directed at a basic understanding of the mechanisms of the processes involved. As should be apparent from this brief overview, much remains to be learned.

See Also the Following Article

Flavins

Glossary

bioluminescence The light that results from a chemiluminescent reaction in a living organism or from components of a living system, such as firefly tails.

chemiluminescence The light that is emitted from certain chemical reactions without the production of significant heat.

flavin mononucleotide Riboflavin-5′-phosphate, the 5′-phosphate derivative of vitamin B_2.

flavin monooxygenase An enzyme that employs a flavin coenzyme to split the two atoms of molecular oxygen apart, depositing one in an organic substrate as a hydroxyl group and the other in water.

fluorescence The phenomenon of light emission that occurs from certain molecules as they return to the ground state from the lowest excited singlet excited state. Population of the singlet excited state is the result of absorption of energy from incident light.

luciferase An enzyme that catalyzes a reaction that emits visible light with high efficiency. Luciferases are exceptionally diverse, many with no evolutionary relationship to the others.

Further Reading

Baldwin, T. O. (1996). Firefly luciferase: The structure is known, but the mystery remains. *Structure* 4, 223–228.

Baldwin, T. O., and Ziegler, M. M. (1992). The biochemistry and molecular biology of bacterial bioluminescence. In *Chemistry and Biochemistry of Flavoenzymes*, Vol III, (F. Müller, ed.) pp. 467–530. CRC Press, Boca Raton, FL.

Harvey, E. N. (1952). *Bioluminescence*. Academic Press, New York.

Harvey, N. E. (1957). *A History of Luminescence from the Earliest Times to 1900*. American Philosophical Society, New York.

Lakowicz, J. R. (1999). *Principles of Fluorescence Spectroscopy*. Kluwer Academic/Plenum Publishers, New York.

Ziegler, M. M., and Baldwin, T. O. (eds.) (2000). *Bioluminescence and Chemiluminescence Part C. Methods in Enzymology*, Vol 305. Academic Press, New York.

Biography

Thomas O. Baldwin received his graduate education at the University of Texas at Austin in the laboratory of Professor Austen Riggs. He then did postdoctoral studies at Harvard University, where he began his studies of the structure and function of bacterial luciferase. He has been on the faculty of biochemistry at the University of Illinois and Texas A&M University. In 1999, he moved to the University of Arizona, where he is professor and head of biochemistry and molecular biophysics and Founding Director of the Institute for Biomedical Science and Biotechnology.

Chemiosmotic Theory

Keith D. Garlid
Portland State University, Portland, Oregon, USA

Mitochondria transform the chemical energy derived from food and body stores into ATP by a process called oxidative phosphorylation. The chemiosmotic theory begins by describing the mechanism of coupling between substrate oxidation and phosphorylation. It goes on to describe the membrane properties that are required in order for mitochondria to provide ATP to the cell and, indeed, to survive within the cell. The chemiosmotic theory was presented as a hypothesis far in advance of experimental evidence, and it stands as a monument to the scientific method. For this extraordinary achievement, Peter Mitchell was awarded the Nobel prize in chemistry in 1978.

Basic Chemiosmotic Theory

Mitochondrial Structure

Mitochondria are small, vesicular organelles. The internal aqueous compartment is called the *matrix*, which contains the enzymes of the Krebs tricarboxylic acid cycle. The matrix is enclosed by a highly folded, insulating membrane called the inner membrane, which contains the enzymic machinery of oxidative phosphorylation. The inner membrane is separated from the cytosol by a more permeable outer membrane, and the aqueous compartment between the inner and outer membranes is called the intermembrane space.

The Four Postulates

Peter Mitchell proposed that nature uses protonic batteries to drive ATP synthesis and that biological energy conservation is essentially a problem in membrane transport, as diagrammed in Figure 1. The chemiosmotic theory consists of four postulates.

1. The inner membrane contains electron transport enzymes which are vectorially oriented so that the energy of electron transport drives ejection of protons outward across the membrane. The energy of substrate oxidation is thereby converted to and stored as a proton electrochemical potential gradient, called the protonmotive force.

2. The inner membrane contains a reversible, proton-translocating ATPase, which is also vectorially oriented so that the energy of ATP hydrolysis will drive protons outward across the inner membrane. The ATPase is reversible, so that protons driven inward through the enzyme by the redox-generated protonmotive force will cause ATP synthesis.

3. The inner membrane must have a low diffusive permeability to ions in general and to protons in particular. Otherwise, ion leaks would short-circuit the protonmotive batteries, and ATP would not be synthesized.

4. The inner membrane was postulated to contain exchange carriers in which anion entry is effectively coupled to proton entry. This provides a thermodynamically favorable pathway for substrate anions to reach enzymes within the electronegative matrix. The membrane was also postulated to contain exchange carriers in which cation exit is coupled to proton entry. This provides a thermodynamically favorable pathway for removal of cations that entered the matrix by diffusion down the very large electrical gradient caused by outward proton pumping.

First Postulate – Respiration and the Electron Transport System

Electron Transport

NADH and succinate arising from the tricarboxylic acid cycle are oxidized by the electron transport chain as diagrammed in Figure 2. The structure–function of the electron transport enzymes is discussed in other articles.

Protonmotive Force

Electron transport through complexes I, III, and IV is coupled to electrogenic proton ejection across the inner membrane. The protonmotive force (Δp) is the free energy per mol required to move protons outward across the membrane. It is simply the sum of the work done against the electrical force and the work done against the

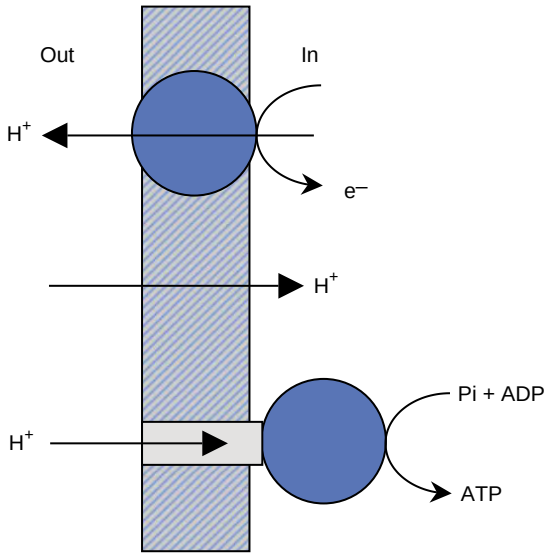

FIGURE 1 Coupling of electron transport with ATP synthesis. The chemiosmotic theory states that vectorial enzymes of electron transport and ATP synthesis are coupled "indirectly" via the protonmotive force across the inner membrane of mitochondria. In order for oxidative phosphorylation to be coupled by this mechanism, the membrane must have a low permeability to protons (postulate 4).

proton concentration difference. Δp is defined as the electrochemical proton gradient divided by the Faraday constant ($\Delta\mu_{H+}/F$); therefore

$$\Delta p = Z\Delta\text{pH} - \Delta\psi \qquad (1)$$

where $Z \equiv (RT\ \ln 10)/F = 59$ mV at 25 °C, and $\Delta\psi$ is the membrane potential (inside minus outside). $\Delta\psi$ and ΔpH can be estimated from equilibrium distributions of cationic dyes and weak acids, respectively. It is customary in bioenergetics to drop the negative signs of $\Delta\psi$ and Δp. Commonly observed values in isolated, nonphosphorylating mitochondria are 190 mV for $\Delta\psi$, 0.3 units for ΔpH, resulting in a Δp of ~208 mV.

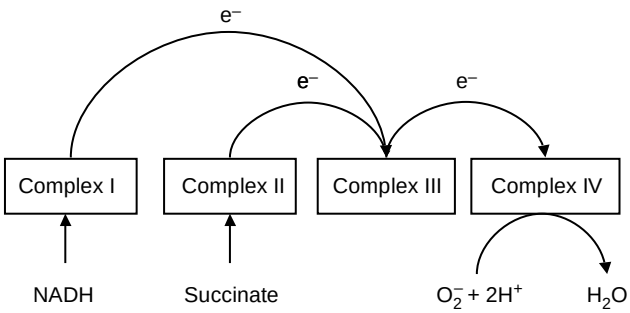

FIGURE 2 Electron transport chain in mitochondria. Complex I (NADH-coenzyme Q reductase) and complex II (succinate coenzyme Q reductase) feed electrons into coenzyme Q at complex III (coenzyme Q cytochrome c reductase), then onto cytochrome c, which delivers them to complex IV (cytochrome *c* oxidase). At complex IV, molecular oxygen is reduced by the electrons to water. Electrogenic proton ejection occurs via complexes I, III, and IV.

Stoichiometries

In the final step of electron transport, the dioxygen molecule (O_2) is reduced to water by four electrons ($e^-/O = 2$). When a pair of electrons moves from NADH to oxygen, it is estimated that ten protons are ejected across the inner membrane ($H^+/O = 10$).

Respiratory Control

Respiration can readily be measured as oxygen uptake by isolated mitochondria. The typical traces in Figure 3 illustrate the principle of respiratory control, which is that respiration increases if the proton back-flux across the inner membrane is facilitated, either through the ATP synthase or by proton-translocating drugs or proteins.

The Protonmotive Circuit

The chemiosmotic theory identifies the electron transport system (ETS) as a protonmotive cell, the behavior of which is identical to the well-known behavior of electromotive circuits, such as is shown in Figure 4. We note four salient aspects of this circuit: (1) The electron current is measured as respiration, as shown in Figure 3. (2) The current is determined entirely by the external resistances, and the battery will deliver increased current only when R_e or R_{ATP} are decreased.

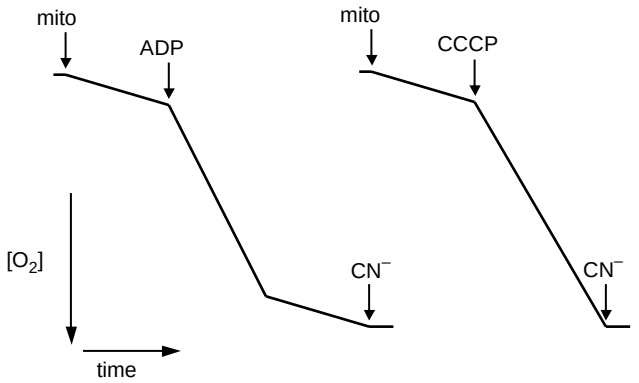

FIGURE 3 Respiratory control in mitochondria. Mitochondria are added to a closed vessel containing an oxygen electrode and a medium containing phosphate and substrates to support respiration. A slow rate of oxygen consumption is observed, which is due primarily to proton leak across the inner membrane. When ADP is added, respiration accelerates until most of the ADP is consumed, after which it returns to the control rate. The protonophore CCCP accelerates respiration by catalyzing proton back-flux across the inner membrane. Respiration is stopped by addition of cyanide, which inhibits cytochrome *c* oxidase.

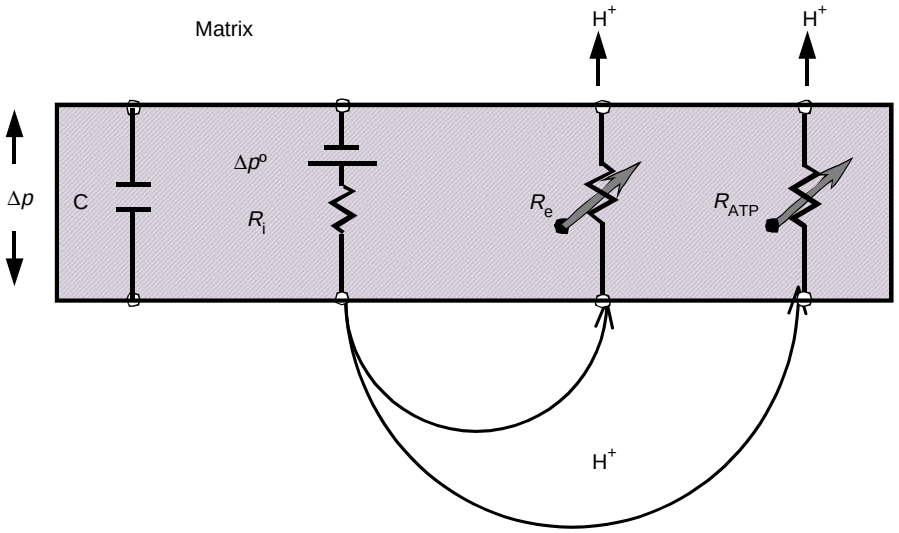

FIGURE 4 Circuit diagram of the mitochondrial electron transport sytem (ETS). In the diagram, the battery symbol corresponds to the ETS, connected across the membrane through an internal resistance, R_i. C is the capacitance of the membrane. Δp^o corresponds to the free energy drop when two electrons pass from the input redox couple to oxygen. R_e is the sum of cation and proton leak resistances and those of the futile cation cycles necessary to regulate mitochondrial physiology. Proton back-flux through the ATP synthase is designated by the element containing R_{ATP}. If conductance through both of these back-flux pathways were zero, there would be no respiration, no proton pumping, and Δp would equal Δp^o, the open-circuit voltage.

(3) The battery will respond the same whether current is drawn through R_e or R_{ATP}. (4) As increasing current is drawn from the battery, the voltage will decrease, due to the internal resistance, R_i. Thus, respiration is "driven" by the free energy contained in the redox drop, and it is "controlled" by the proton back-flux through leak pathways and the ATP synthase.

Behavior of the Protonmotive Circuit

The experiment in Figure 5 shows how Δp varies when electron current is progressively increased by adding a protonophore that decreases external resistance (R_e) to H^+ ions. The resulting increase in respiration causes Δp to fall gradually until the V_{max} of the ETS is reached. What is being measured in such experiments is evident from the circuit diagram of Figure 4:

$$\Delta p = \Delta p^o - R_i \times V_O \qquad (2)$$

where V_O is the respiration rate. The slope, R_i, is the internal resistance of the ETS, representing the weighted sum of frictional coefficients of the reactions leading to proton ejection. The intercept is Δp^o, the theoretical open-circuit voltage of the system, whose value is given by

$$\Delta p^o = (2/n_H)\Delta E \qquad (3)$$

where n_H is the H^+/O stoichiometry, and ΔE is the redox span being studied. The total redox potential, ΔE, for a pair of electrons moving from NADH/NAD^+ to oxygen is ~1.16 V. Therefore, if n_H is 10, $\Delta p^o = 232$ mV. Decreasing R_e to increase proton back-flux may be achieved by ionophores, by uncoupling protein, or by futile Ca^{2+} or K^+ cycling. Decreasing R_{ATP} to increase proton back-flux may be achieved by adding ADP and

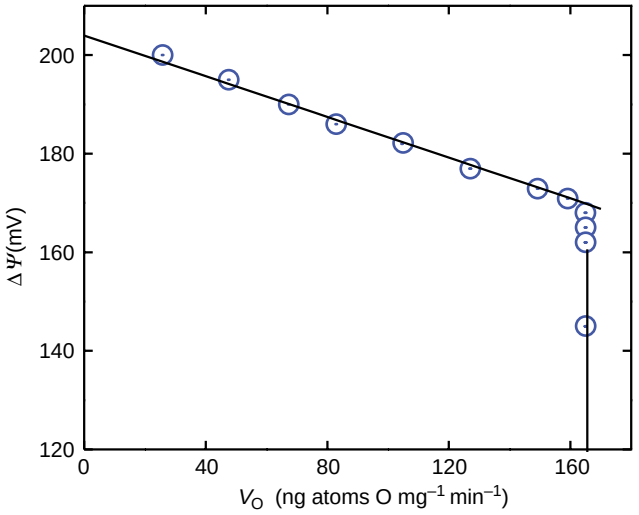

FIGURE 5 Dependence of protonmotive force on electron transport rate. Membrane potential ($\Delta\psi$) of rat liver mitochondria is plotted versus respiration rate (V_o), which was varied by adding the protonophoretic uncoupler, CCCP. Respiration was measured using a standard Clark electrode. $\Delta\psi$ was determined from the distribution of tetraphenylphosphonium cation. The slope of the curve, R_i, is 0.35, the intercept is 210 mV, and V_{max} is ~160 ng atom O min^{-1} mg^{-1}. These are typical values for rat liver mitochondria respiring on succinate. The pH gradient was 0.3 and assumed to be invariant with increased respiration. Therefore, Δp^o is ~228 mV.

phosphate so that current is drawn via the ATP synthase. Careful measurements show that all methods of increasing respiration yield points that fall on the same battery curve as illustrated in Figure 5.

Second Postulate – The ATP Synthase

Δp formed by the ETS is used to drive ATP synthesis via a remarkable series of steps. First, a proton binds to one of the 10–14 C subunits of the F_0 complex. This induces a conformational change that causes the C ring to rotate, after which the bound proton is released into a channel that carries it into the matrix. In this fashion, Δp is transduced into a rotary mechanical force. The rotation of the C ring, in turn, drives the rotation of the attached γ-subunit, and rotation of γ induces conformational changes in the catalytic sites of the three β-subunits of the F_1 head group of the ATP synthase. These catalytic sites exist in three different conformations, corresponding to the three faces presented by the end of the γ subunit. If one proton is associated with each step of the cycle as it occurs on F_1, then the H^+/ATP stoichiometry would be 3 for ATP synthesis. On the other hand, if a complete revolution of the C ring is required for ATP synthesis, and if there are 12 C subunits in F_0, then the stoichiometry would be 4.

Third Postulate – Ion Leaks and the Permeability Barrier

Notwithstanding the low diffusive permeability of the inner membrane, cation, and proton leaks occur at significant rates, and they are physiologically important. Inward K^+ leak causes matrix swelling, and inward proton leak contributes to the basal metabolic rate. Moreover, nature has engineered the uncoupling proteins to increase proton leak under certain physiological circumstances.

Ion Leaks in Mitochondria

Diffusive transport of ions obeys the same laws that govern transport of nonelectrolytes across thin membranes. The rate is proportional to the concentration difference, and the proportionality constant (the permeability coefficient) is a function of the energy barrier that must be crossed during transport. The ionic charge adds a new complexity that derives from the long-range effects of the electric field on the local free energy of the diffusing ions. An ion diffusing across the inner membrane of mitochondria must cross an energy barrier whose maximum is located at the center of the membrane, and only those ions having sufficient energy to reach this peak will cross to the energy well on the opposite side. Net flux will therefore be proportional to the differential probability of getting to this peak from either side. This probability is given by the Boltzmann function, $\exp(-\Delta\mu_p/RT)$, where $\Delta\mu_p \equiv \mu_p - \mu_{aq}$ is the Gibbs energy of the ion at the peak (p) relative to its value in the aqueous energy well at the surface of the membrane (aq). These considerations lead to the following expression for diffusive flux of cations across thin biomembranes:

$$J = fxP(C_1 e^{u/2} - C_2 e^{-u/2}) \tag{4}$$

where u is the reduced voltage ($zF\Delta\psi/RT$), C_1 and C_2 are bulk aqueous concentrations, f is the surface partition coefficient (energy well/bulk), and P is the permeability constant, given by

$$P \equiv k e^{-\Delta\mu_p^{\circ}RT} \tag{5}$$

The factor 1/2 in the exponents of eqn. (4) arises from the fact that the maximum energy barrier is found at the midpoint of the membrane.

The second term in eqn. (4) represents back-flux of cations from the matrix and becomes negligible at the high values of $\Delta\psi$ maintained by mitochondria under physiological conditions. Thus, eqn. (4) reduces to a simple exponential function of $\Delta\psi$:

$$J = fPC_1 e^{u/2} \tag{6}$$

Eqn. (6) emphasizes the point that ion flux at high potentials is not affected by the concentration gradient across the membrane. Figure 6A contains data showing that proton leak is in good agreement with eqn. (6), and the flux–voltage plots in Figure 6B show that diffusion of TEA^+ (tetraethylammonium ion) and H^+ (hydronium ion) across the inner membrane behave identically with respect to their voltage-dependence.

Uncoupling Proteins

Uncoupling proteins (UCPs) are the exception that proves the rule of the inner membrane permeability barrier. Nature devised the UCPs to intentionally short-circuit the inner membrane in order to dissipate energy and generate heat instead of ATP. UCP1 is expressed solely in brown adipose tissue, where it plays a major role in providing heat to hibernating animals and mammalian newborns. The human genome contains at least three additional UCPs, designated UCP2–4. UCP2 is ubiquitously expressed in mammalian tissues; UCP3 is expressed primarily in glycolytic skeletal muscle in humans; and UCP4 is expressed in brain. The roles of UCP in non-thermogenic tissue are uncertain but may involve reduction of mitochondrial production of reactive oxygen species.

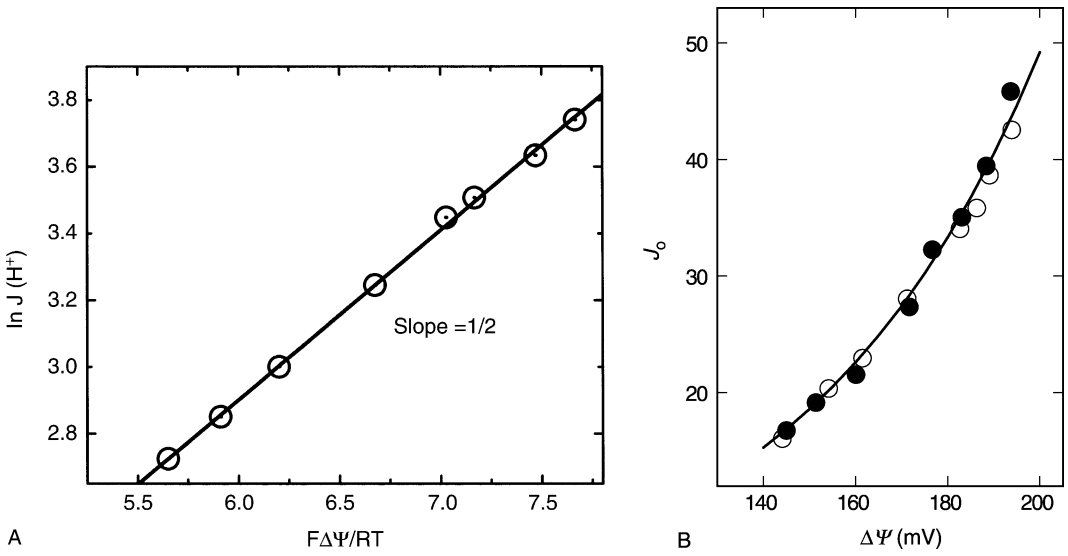

FIGURE 6 Proton and cation diffusion across the inner membrane. (A) Proton flux. The semilogarithmic plot shows that H^+ leak is exponential with voltage, and the slope of ln J_H vs. $F\Delta\psi/RT$ is 1/2, in agreement with eqn. (6). The intercept of such plots gives $J_o \equiv fP[C]_o$, where $[C]_o$ is the aqueous concentration, and f and P are defined in the text. (B) Tetraethylammonium (TEA^+) and H^+ flux. Fluxes were normalized to their respective values of J_o and plotted vs. $\Delta\psi$. Note that the rate-limiting step of crossing the energy barrier is identical for TEA^+ and H^+ (H^+ probably crosses as hydronium ion).

The transport functions and regulation of UCP1–3 have been characterized using recombinant proteins expressed in *E. coli* and reconstituted into liposomes for flux measurements. The purified UCP proteins are qualitatively identical with respect to transport function and regulation. They catalyze electrophoretic flux of protons and alkylsulfonates, and proton flux exhibits an obligatory requirement for fatty acids. Fatty acid-dependent proton transport by UCP1–3 is inhibited by purine nucleotides, including ATP. The mechanism by which UCPs catalyze proton back-flux is somewhat controversial. It is thought that they act as fatty acid anion flipases, causing the outward movement of the fatty acid anion head group across the inner membrane. Once on the outer surface, the fatty acid picks up a proton and then flip-flops rapidly back into the matrix. Thus, UCP does not conduct protons, per se; rather, it enables fatty acids to behave as cycling protonophores, as shown in Figure 7.

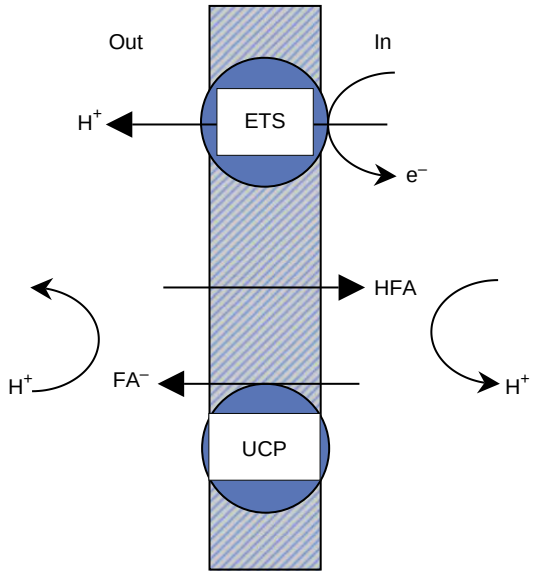

FIGURE 7 Mitochondrial uncoupling protein (UCP). UCP contains a weak binding site for anions near the center of the membrane. This constitutes an energy well for anions and provides a low-resistance pathway for normally impermeant anions to cross the membrane. The physiological substrates of UCP are anions of free fatty acids (FA). The FA head groups are located at the acylglycerol linkages of the phospholipid bilayer. When the FA is at the surface of UCP, the negative membrane potential drives the head group to the energy well at the center of the membrane. The FA then "flip-flops" and the head group is driven to the opposite surface. Here, it diffuses away from the protein and picks up a proton. The protonated FA (HFA) head group freely diffuses across the membrane, during which the FA flip-flops again, and delivers a proton to the other side. Thus, UCP is a FA anion flipase, and its role is to enable FA to behave as cycling protonophores.

Fourth Postulate – Ion Carriers and Channels

With astute physiological insight, Mitchell recognized that solving the problem of energy transduction gave rise to another. The high transmembrane electrical potential required for ATP synthesis would prevent anions, including the substrates of the tricarboxylic acid cycle, from entering the matrix. It would also promote cation uptake, with consequent osmotic swelling and

lysis. Thus, the fourth postulate was born out of physiological necessity.

Anion Exchange Carriers

Because ATP is synthesized in the matrix, ADP and phosphate must be imported and ATP must be exported across the inner membrane. As shown in Figure 8, nucleotides are exchanged on the ATP/ADP translocase (ANT) in a process involving outward movement of one negative charge. The phosphate carrier catalyzes electroneutral P_i/H^+ symport or P_i/OH^- antiport, with the net result that it transports phosphoric acid.

The inner membrane also contains a variety of anion exchange carriers, which are designed to deliver substrates to the tricarboxylic acid cycle. The anion exchange carriers catalyze 1:1 electroneutral exchange of anions, and they are arranged in a cascade in which phosphate and malate are key intermediates. In liver mitochondria, the dicarboxylic acid exchanger catalyzes malate/phosphate exchange, and the tricarboxylic acid exchanger catalyzes malate/citrate exchange. In this way, both di- and tricarboxylic acids are linked to the phosphate carrier. Since the phosphate carrier effectively transports fully protonated phosphate, the net result is that di- and tricarboxylic acids also behave as if they were fully protonated, and they are distributed across the membrane as if they were transported as fully protonated acids:

$$(A-)_{in}/(A-)_{out} = 10^{z\,\Delta pH} \qquad (7)$$

where z is the valence of the acid.

The Sodium–Calcium Cycle

The mitochondrial Ca^{2+} cycle consists of three separate transporters and is diagrammed in Figure 9. Ca^{2+} is taken up by the Ca^{2+} channel at the expense of two ejected protons. In spite of the enormous gradient for electrophoretic Ca^{2+} uptake, free mitochondrial [Ca^{2+}] is comparable to cytosolic [Ca^{2+}] *in vivo*. This disequilibrium is maintained in heart mitochondria by an electrophoretic Na^+/Ca^{2+} antiporter, which exchanges 3 Na^+ per Ca^{2+}. The three Na^+ ions taken up are then ejected by the electroneutral Na^+/H^+ antiporter, which holds Na^+ close to equilibrium with the pH gradient.

The physiological role of the mitochondrial Ca^{2+} cycle is to regulate matrix Ca^{2+} activity in response to signals from the cytosol. As a second messenger, Ca^{2+} signals need to increase cellular work. Because increased work requires a higher rate of ATP production, this

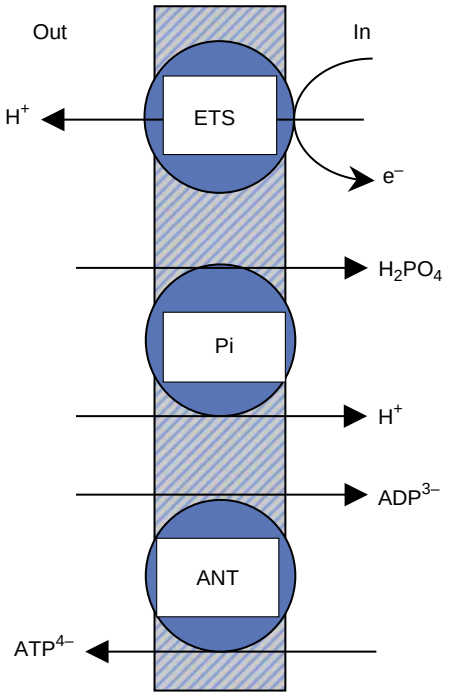

FIGURE 8 Mitochondrial transport of inorganic phosphate, ADP, and ATP. The phosphate carrier (Pi) catalyzes electroneutral transport, and the adenine nucleotide translocase (ANT) catalyzes electrophoretic exchange of ADP and ATP. Uptake of Pi and ADP and expulsion of ATP use one electrogenically ejected proton.

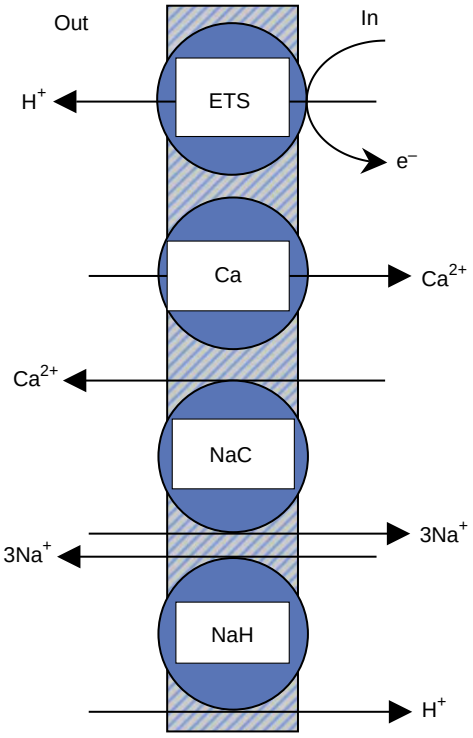

FIGURE 9 The mitochondrial Ca^{2+} cycle. Ca^{2+} enters the matrix via the electrophoretic Ca^{2+} channel and is ejected by the electrophoretic Na^+/Ca^{2+} antiporter (NaC), utilizing three ejected protons per Ca^{2+} taken up. The Na^+ is then expelled by the electroneutral Na^+/H^+ antiporter (NaH).

message must be relayed to the mitochondrial matrix. Intramitochondrial Ca^{2+} is required to activate the phosphorylase that converts pyruvate dehydrogenase to its active form, and α-ketoglutarate dehydrogenase is allosterically activated by matrix Ca^{2+} in the physiological range.

The Potassium Cycle

The mitochondrial K^+ cycle consists of electrophoretic K^+ influx and electroneutral K^+ efflux across the inner membrane, as diagrammed in Figure 10. Mitochondria must regulate net K^+ flux to zero in the steady state; otherwise, inward K^+ diffusion would cause the matrix to swell and eventually lyse. This regulation is provided by the K^+/H^+ antiporter, which ejects exactly the amount of K^+ that is taken in. Regulation of the K^+/H^+ antiporter is mediated by reversible binding of Mg^{2+} and H^+ to the K^+/H^+ antiporter on its matrix side. The activity of these ions decreases with uptake of K^+ salts, causing a graded, compensatory activation of K^+ efflux in response to increases in matrix volume.

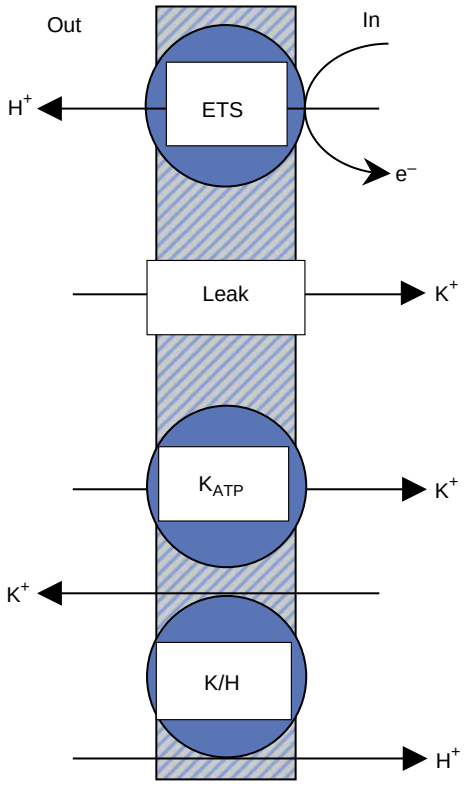

FIGURE 10 The mitochondrial K^+ cycle. Electrogenic proton ejection drives K^+ uptake by diffusive leak. In addition, the inner membrane contains a KATP channel, which is highly regulated by nucleotides, CoA esters, and pharmacological agents. Net K^+ flux is regulated to zero in the steady state. Compensatory K^+ efflux is provided by the electroneutral K^+/H^+ antiporter, which is regulated by matrix Mg^{2+} and H^+ and is exquisitely sensitive to changes in matrix volume.

The primary role of the K^+/H^+ antiporter is to provide "volume homeostasis" to mitochondria in order to maintain the vesicular integrity necessary for oxidative phosphorylation.

The mitochondrial K_{ATP} channel (mitoK_{ATP}) also plays an important role in volume homeostasis. When mitoK_{ATP} is open, the added K^+ conductance is thought to compensate for the lower driving force for K^+ influx (lower $\Delta\psi$) in ischemia and in high ATP-consuming states of the cell. MitoK_{ATP} is regulated by a rich variety of metabolic and pharmacological ligands. It is inhibited with high affinity by ATP, long-chain acyl-CoA esters, the antidiabetic sulfonylurea, glyburide, and 5-hydroxydecanoate. The ATP-inhibited channel is opened with high affinity by guanine nucleotides and K^+ channel openers such as cromakalim and diazoxide. There is indirect evidence that mitoK_{ATP} is opened *in vivo* by phosphorylation. MitoK_{ATP} has been found to play a pivotal role in protecting heart and brain from ischemic stress. Thus, opening mitoK_{ATP}, either with K_{ATP} channel openers or with endogenous signals, confers significant protection against ischemia–reperfusion injury.

See Also the Following Articles

ATP Synthesis in Plant Mitochondria: Substrates, Inhibitors, Uncouplers • ATP Synthesis: Mitochondrial Cyanide-Resistant Terminal Oxidases • F1–F0 AT Synthase • Mitochondrial Channels • Mitochondrial Membranes, Structural Organization • Respiratory Chain and ATP Synthase • Tricarboxylic Acid Cycle • Uncoupling Proteins

Glossary

electrogenic transport Ion transport (and net charge movement) that requires chemical energy to move an ion across the membrane against its electrochemical potential gradient. Electrogenic transport in mitochondria is limited to proton transport by the electron transport system and by the ATP synthase, when ATP is being hydrolyzed.

electrophoretic transport Ion transport (and net charge movement) driven by the ion electrochemical potential gradient. In mitochondria, this includes diffusion and transport by ion channels and ionophores such as valinomycin.

ionophore A chemical compound that conducts ions across membranes. Examples include valinomycin, CCCP, and nigericin.

protonophore An ionophore that conducts protons (H^+ ions) across membranes. Examples include dinitrophenol and CCCP (carbonyl cyanide *m*-chlorophenylhydrazone).

Further Reading

Garlid, K. D., and Paucek, P. (2003). Mitochondrial potassium transport: The K+ cycle. *Biochim. Biophys. Acta* **1606**, 23–41.

Garlid, K. D., Beavis, A. D., and Ratkje, S. K. (1989). On the nature of ion leaks in energy-transducing membranes. *Biochim. Biophys. Acta* **976**, 109–120.

Garlid, K. D., Dos Santos, P., Xie, Z., Costa, A. D., and Paucek, P. (2003). Mitochondrial potassium transport: the role of the mitochondrial ATP-sensitive K+ channel in cardiac function and cardioprotection. *Biochim. Biophys. Acta* **1606**, 1–21.

Hansford, R. G. (1994). Physiological role of mitochondrial Ca^{2+} transport. *J. Bioenerg. Biomembr.* **26**, 495–508.

Mitchell, P. (1966). Chemiosmotic coupling in oxidative and photosynthetic phosphorylation. *Biol. Rev. Camb. Philos. Soc.* **41**, 445–502.

Nicholls, D. G., and Ferguson, S. J. (2000). *Bioenergetics 3*. Academic Press, London.

BIOGRAPHY

Keith D. Garlid is a Professor of Biology at Portland State University, in Portland, Oregon. He holds an M.D. from Johns Hopkins University, and a Doctor tecnicae degree from the Norwegian Institute of Technology. His principal research interests are in mitochondrial physiology and bioenergetics. He has published extensively on the mitochondrial uncoupling proteins and on the mitochondrial potassium cycle. His paper showing that the mitochondrial ATP-sensitive K^+ channel is the receptor for drugs that protect the heart from ischemia–reperfusion injury has had a major impact on ischemia research.

Chemokine Receptors

Ann Richmond and Guo-Huang Fan
Department of Veterans Affairs, VA Medical Center, Nashville, Tennessee, USA and Vanderbilt University School of Medicine, Nashville, Tennessee, USA

Chemokine receptors are seven-transmembrane proteins expressed on neutrophils, lymphocytes, dendritic cells, and many other cell types. They function to mediate migration of leukocytes to the sites of injury and infection in response to a gradient concentration of chemokines, a group of small proteins that specifically bind the chemokine receptors. Chemokine receptors belong to the G protein-coupled seven-transmembrane receptor superfamily, which has more than 600 members that use the heterotrimeric G proteins to initiate signals. Eighteen chemokine receptors have been identified and cloned so far, and these receptors have been classified into four subfamilies (CXC, CC, CX3C, and C) based on the chemokine subclass specificity. In addition to the mediation of migration of leukocytes to the inflammatory sites (chemotaxis), chemokine receptors play a role in leukocyte homing, HIV entry, angiogenesis, tumor growth and metastasis, development, and inflammation of the central nervous system.

Ligands

The ligands that bind and activate chemokine receptors are chemokines or chemoattractant cytokines. Approximately 50 chemokines have been identified so far, and these chemokines are classified into four (CXC, CC, C, and CX3C) subfamilies based on their primary amino acid sequences (Table I). The CXC subfamily has six members, which have one amino acid (X) interrupting the first two of their four conserved cysteine residues. The CC subfamily has 10 members, which have no intervening amino acid between the first two of their four cysteine residues. In both the CXC and CC subfamilies, disulfide bonds are formed between the first and third cysteines and between the second and fourth cysteines to establish a stable tertiary structure with the molecular mass of 7–9 kDa. The C subfamily has two members, which are 16 kDa in molecular size. The CX3C subfamily has only one member (CX3L1), which has three intervening amino acids between the N-terminal cysteines, with a molecular mass of 38 kDa, larger than any other known chemokine. Chemokines have two main sites of interaction with their receptors, the flexible N-terminal region and the conformationally rigid loop that follows the second cysteine. Chemokines dock onto receptors by means of the loop region, and this contact is necessary to facilitate the binding of the N-terminal region to the receptor that results in receptor activation. Chemokines possess heparin-binding capacity at their C-terminal end, which enables them to bind to glycosaminoglycans and other negatively charged sugar moieties on cell surfaces and matrix glycoproteins. This property may result in the adsorption of chemokines onto the endothelial cell lining of the blood vessels, connective tissues, and cell matrices. Thus, chemokines immobilized on tissue or matrix surfaces may induce haptotactic migration of target cells.

Structure

The chemokine receptors generally are composed of 340–370 amino acid residues and have 25–80% identity. These receptors share a common putative structural topology composed of seven hydrophobic transmembrane domains, an N terminus outside the cell surface, three extracellular and three intracellular loops, and a C terminus in the cytoplasmic compartment. The poorly conserved N-terminal domains together with a second binding site in the extracellular loops determine the specificity for ligand binding. The sequence DRYLAIVHA, or a variation of it, in the second intracellular loop and the third intracellular loop is required for G protein coupling. A cysteine residue in each of the four extracellular domains is required for the disulfide-bond formation that is critical for cell surface expression. The C terminus of the receptors contains a number of serine and threonine residues that, upon phosphorylation, are involved in signaling and receptor desensitization. A leucine–leucine or isoleucine–leucine motif in the C terminus is required for the receptor internalization (Figure 1). Some chemokine receptors such as CCR2, CCR5, and CXCR4 form homodimers, which may be needed for signal transduction.

TABLE I

Chemokine Receptor Family[a]

Name	Main agonists	Main functions
CXCR1	CXCL8	Neutrophil migration; innate immunity; acute inflammation
CXCR2	CXCL1–3, CXCL5–8	Neutrophil migration; innate immunity; acute inflammation; angiogenesis
CXCR3	CXCL9–11	T-cell migration; adaptive immunity; Th1 inflammation
CXCR4	CXCL12	B-cell lymphopoiesis; bone marrow myelopoiesis; central nervous system and vascular development; HIV infection
CXCR5	CXCL13	B-cell trafficking; lymphoid development
CXCR6	CXCL16	T-cell migration
CCR1	CCL3, CCL5, CCL7, CCL8, CCL13–16, CCL23	T-cell and monocyte migration; innate and adaptive immunity; inflammation
CCR2	CCL2, CCL7, CCL8, CCL13	T-cell and monocyte migration; innate and adaptive immunity; Th1 inflammation
CCR3	CCL5, CCL7, CCL8, CCL11, CCL13, CCL15, CCL24, CCL26	Eosinophil, basophil, and T-cell migration; allergic inflammation
CCR4	CCL17, CCL22	T-cell and monocyte migration; allergic inflammation
CCR5	CCL3, CCL4, CCL5, CCL8, CCL14	T-cell and monocyte migration; innate and adaptive immunity; HIV infection
CCR6	CCL20	Dendritic cell migration
CCR7	CCL19, CCL21	T-cell and dendritic cell migration; lymphoid development; primary immune response
CCR8	CCL1, CCL4, CCL17	T-cell trafficking
CCR9	CCL25	T-cell homing to gut
CCR10	CCL26–28	T-cell homing to skin
CX3CR1	CX3CL1	T-cell and NK cell trafficking and adhesion; innate and adaptive immunity; Th1 inflammation
XCR1	XCL1–2	T-cell trafficking

[a] Modified from Murphy, P. M., Baggiolini, M., Charo, I. F., Hébert, C. A., Horuk, R., Matsushima, K., Miller, L. H., Oppenheim, J. J., and Powe, C. A. (2000). International Union of Pharmacology, XXII. Nomenclature for chemokine receptors. *Pharmacol. Rev.* **52**, 145–176, National Institutes of Health.

Consequence of Receptor–Ligand Interaction

Signal Transduction

Ligand binding to chemokine receptors initiates a cascade of intracellular events (Figure 2). The first step is the conformational change of the chemokine receptors, inducing the exchange in the α-subunit of the G proteins from the GDP to GTP bound state dissociating the α from the β and γ G protein subunits. The G$\beta\gamma$ subunits activate phospholipase C β2 (PLCβ2), which hydrolyzes phosphatidylinositol 4,5-bisphosphate [(4,5)P2] to produce inositol trisphosphate (IP3) and diacylglycerol (DAG). IP3 mediates Ca^{2+} release from the intracellular stores. DAG activates protein kinase C (PKC), which phosphorylates a number of effector molecules. The activation of isotypes of PLC and hydrolysis of PIP2 vary among chemokine receptors and from cell type to cell type, which may account for the divergent cellular responses to a given chemokine. Another important signaling pathway of chemokine receptors is the activation of phosphoinositide 3-kinases (PI3K), which convert the plasma membrane lipid PI (4,5)P2 to phosphatidylinositol-3,4,5-trisphosphate [PI(3,4,5)P3], resulting in the phosphorylation and activation of the serine-threonine kinase Akt (PKB). An additional part of the signals that evoke the motility response involves activation of the rho GTPase family including rho, rac, and cdc42, which can feed into the activation of P^{21} activated Kinase (PAK), Wiskott-Aldrich syndrome protein (WASP), and Arp2/3 to mediate actin cytoskeletal changes. Chemokines also induce tyrosine phosphorylation of p130 Cas, focal adhesion Kinase (FAK), and members of the src family in several cell types. Through activation of the ras, raf, MAPK cascade and through activation of the NF-κB cascade, transcription factors are activated and gene expression is affected. The signaling pathways of chemokine receptors play a role in cell growth, cell migration, cell survival, and superoxide production.

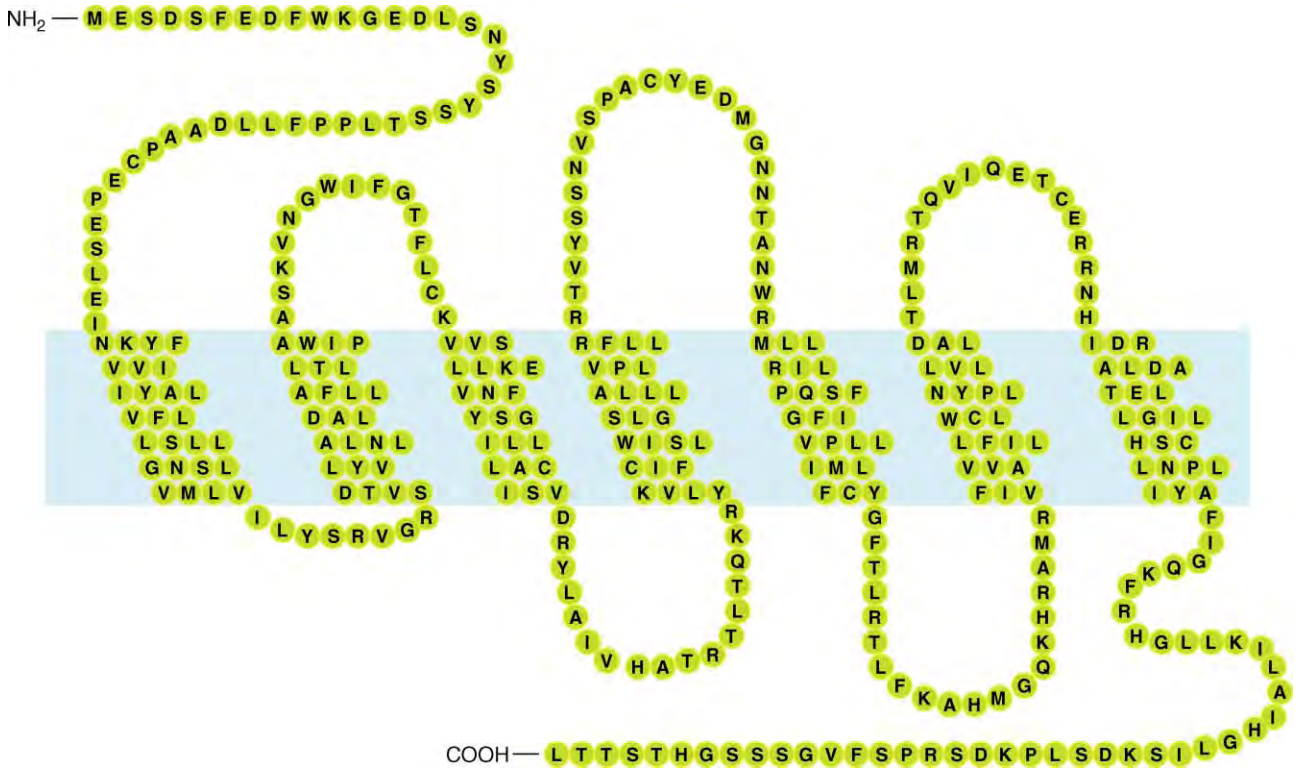

FIGURE 1 Proposed conformation of the chemokine receptor CXCR2. This receptor is a seven-transmembrane G protein-coupled receptor. The free amino terminus provides ligand binding specificity. The third extracellular loop participates in ligand binding, whereas the third intracellular loop is thought to be the site of G protein coupling. The serine residues in the carboxyl terminus are phosphorylation sites.

Desensitization

The ligand-induced activation of chemokine receptors is transient. The functional response of chemokine receptors is rapidly reduced following repeated stimulation by chemokines. This process is called desensitization. Agonist-dependent (homologous) desensitization occurs when a receptor binds chemokine and is phosphorylated by a G protein receptor-coupled receptor kinase (GRK). The phosphorylated receptor recruits β-arrestin, an adaptor protein that uncouples the receptor with G proteins, thus retaining the receptor in a desensitized state, resulting in attenuation in the cell excitability (Figure 3). This mechanism plays a major role in determining the duration of leukocyte trafficking, migration, or sequestration in certain situations (see later discussion). Chemokine receptors can also be phosphorylated by a kinase, such as PKC, activated by a different signaling cascade. This is called heterologous desensitization. For example, the chemokine receptor CXCR1 or CXCR2 can be phosphorylated and desensitized through the activation of formyl peptide receptors by the tripeptide formyl-methionyl-leucyl-phenylalanine (fMLP). The importance of this phenomenon in inflammation and leukocyte trafficking is not completely clear, but the capacity for heterologous desensitization appears to be different among chemokine receptors, suggesting a hierarchy of chemokines.

Internalization

After agonist occupancy, chemokine receptors are rapidly translocated from the cell membrane to the cytoplasm. This process is called receptor internalization. Chemokine receptors generally undergo internalization through clathrin-coated pits, a complex process that involves clathrin and adaptor proteins such as β-arrestins and adaptin-2. After pinching off from the cell membrane through a dynamin-dependent process, the clathrin-coated vesicles containing the internalized receptors fuse with early endosomal compartments. When there is a low pH value in the early endosomes, the receptors become dephosphorylated by a specific serine/threonine protein phosphatase such as protein phosphatase 2A. The dephosphorylated receptors are either transported to recycling endosomes and subsequently reexpressed on the cell surface after removal of the extracellular ligand or delivered to late endosomes and lysosomes for degradation in the continued presence of a high concentration of ligands. The intracellular trafficking processes are regulated by a number of molecules including the Ras-like GTPases (Rabs) (Figure 3). Such trafficking may be important for

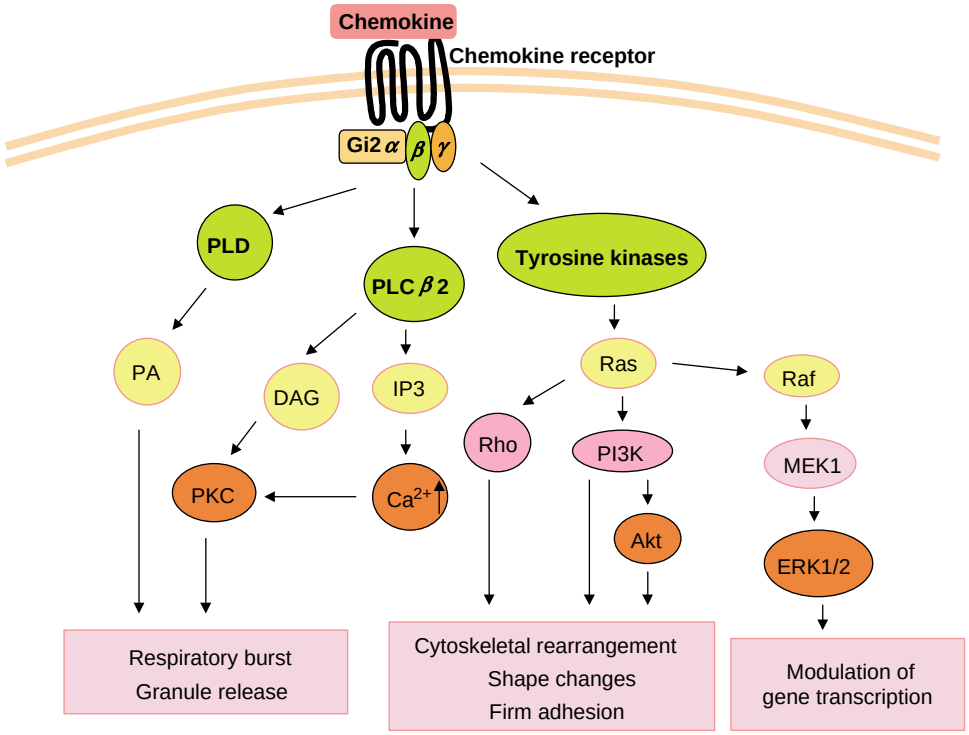

FIGURE 2 The major intracellular signaling events induced by a chemokine binding to its receptor and activating responses in a neutrophil. Stimulation of a chemokine receptor by its ligand results in a conformational change of the receptor and activation of the coupled G proteins. The Gα (proteins coupled with chemokine receptors are generally the inhibitory Gα proteins (Gαi). The β- and γ-subunits of the G protein activate phospholipase C (PLCβ2), which cleave PIP3 to produce diacylglycerol (DAG) and inositol triphosphate (IP3). IP3 initiates mobilization of the intracellular free Ca^{2+} and DAG activates PKC, which is required for the respiratory burst and granule release. Stimulation of chemokine receptors also results in activation of tyrosine kinases, which trigger several signaling pathways, including mitogen-activated protein kinase (MAPK) pathway, phosphotidylinositol 3-kinase (PI3K)/protein kinase B (Akt) pathway, as well as Rho signaling pathway. These pathways are required for cell movement and gene transcription. In addition, stimulation of chemokine receptors results in activation of phospholipase D (PLD), which produces phosphatidic acid (PA), which plays a role in respiratory burst and granule release. ERK1/2, extracellular signal-regulated kinases 1 and 2; MEK, mitogen-activated protein kinase kinase; Ras and Rho, small G proteins.

both transmission and termination of the receptor signals and may play an important role in mediating cell chemotaxis (see later discussion).

Multiple Roles

Chemotaxis

Neutrophils, lymphocytes, and other immune cells migrate to the sites of injury and infection. This process, which is called chemotaxis, occurs through the dynamic response of chemokine receptors expressed on these cells to the gradient concentrations of chemokines produced in the inflammatory sites. Chemokine receptor signaling leading to the establishment of cell polarity, cytoskeletal rearrangement, and interaction with the extracellular matrix plays an essential role in this complex process. In addition, the desensitization and internalization of chemokine receptors play a regulatory role. For example, human immature dendritic cells derived from monocytes express the inflammatory chemokine receptors CXCR1, CCR1, CCR2, CCR5, and CCR7, which allow these cells to follow chemotactic gradients to inflammatory sites. Once there, dendritic cells process antigen and become exposed to the maturation-stimulating cytokines. Maturing dendritic cells express large amounts of chemokines such as CCL3, CCL4, CCL5, CCL8, and CCL10. One consequence of this increased chemokine expression is the down-regulation of chemokine receptors on maturing dendritic cells, particularly CCR1 and CCR5, by receptor desensitization and internalization. The second consequence of this up-regulation of chemokines is that it strengthens the original chemotactic gradient, further boosting recruitment of immature dendritic cells, monocytes, and lymphocytes.

HIV Entry

Human immunodeficiency virus (HIV) is the causative agent of acquired immune deficiency syndrome (AIDS). Type 1 HIV (HIV-1) uses chemokine receptor as a coreceptor together with CD4 to enter the CD4-positive (CD4+) target cells. The main cells targeted by HIV-1 are

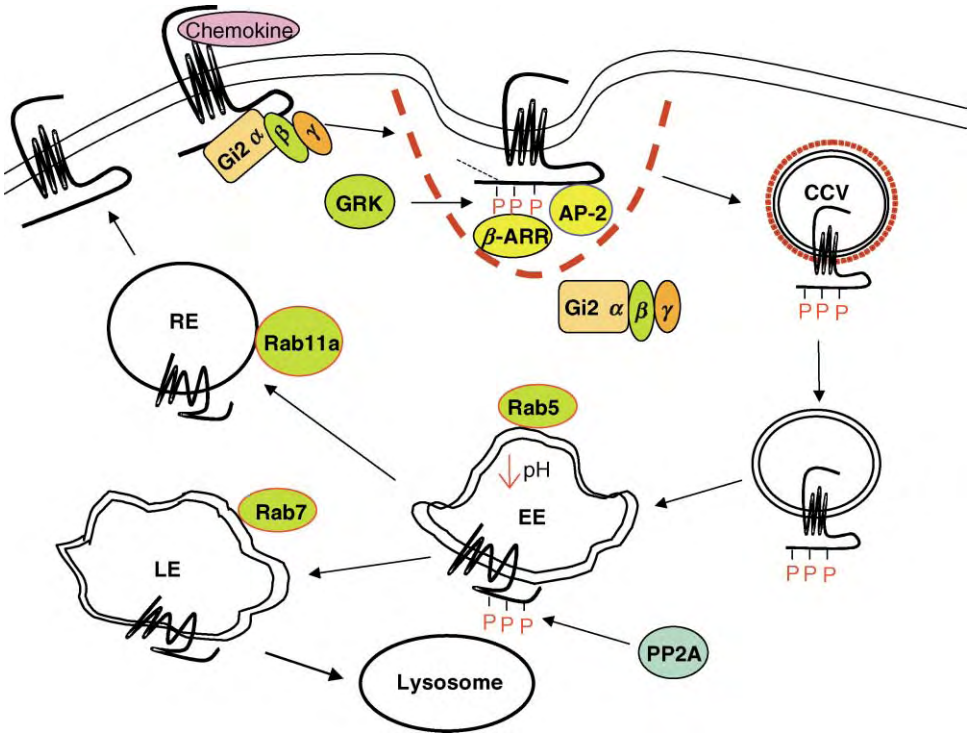

FIGURE 3 Homologous desensitization and intracellular trafficking of chemokine receptors. In response to chemokine stimulation, the receptor undergoes homologous desensitization, in which phosphorylation by a G protein-coupled receptor kinase leads to uncoupling of G proteins, binding of β-arrestins, and subsequent internalization of the receptor through clathrin-coated pits. After pinching off from the membrane, the clathrin-coated vesicles fuse to early endosomes, where the chemokine receptors are dephosphorylated by protein phosphatase 2A, and the receptors are transported to late endosomes and lysosomes for degradation. However, after removal of the extracellular ligands, the receptors are transported from early endosomes to recycling endosomes so as to re-express on the cell surface. β-ARR, β-arrestin; AP2, adaptin 2; CCV, clathrin-coated vesicle; EE, early endosome; GRK, G protein-coupled receptor kinase; LE, late endosome; P, phosphate; PP2A, protein phosphatase 2A; Rab5, Rab11a, Rab7, small GTPases that regulate receptor trafficking; RE, recycling endosome.

T lymphocytes (T cells), macrophages, and probably dendritic cells. The chemokine receptors CXCR4 and CCR5 are the major coreceptors for T-cell line-tropic and macrophage-tropic HIV-1 strains, respectively, although many other chemokine and orphan receptors have also been identified as potential coreceptors for HIV-1. The fusion of the viral envelope and the lymphocyte is as follows. The envelope glycoprotein on the surface of virus particles comprising a trimer of three gp120 and three transmembrane gp41 molecules binds to CD4 and triggers a structural change, which exposes a binding site for a coreceptor. Further structural rearrangements are initiated when the coreceptor is bound. These changes occur predominantly in gp41 and are sufficient to trigger fusion of viral and cellular membranes and entry of the virion core into the cytoplasm.

Angiogenesis

Angiogenesis is the formation of new blood vessels from pre-existing microvasculature. It is a biological process that is critical to both physiological and pathological processes such as wound healing and tumor growth. Angiogenesis is regulated by an opposing balance of angiogenic and angiostatic factors. The CXC chemokines are a family of cytokines unique in their ability to behave in a disparate manner in the regulation of angiogenesis. The N terminus of the majority of the CXC chemokines contains three amino acid residues (Glu-Leu-Arg; the ELR motif). This motif, in general, determines whether these chemokines promote angiogenesis. Members that contain the ELR motif (ELR+), such as CXCL1 and CXCL8, are potent promoters of angiogenesis. In contrast, members that are inducible by interferons and lack the ELR motif (ELR−), such as CXCL10, are potent inhibitors of angiogenesis. ELR-CXC chemokines bind to CXCR2 and a few to CXCR1, whereas non-ELR-CXC chemokines bind to CXCR3, CXCR4, CXCR5, and CXCR6. The mechanisms for the differential regulation of angiogenesis by chemokines and chemokine receptors are under investigation.

Tumor Growth and Metastasis

Many cancer cells such as melanomas express a number of chemokines, including CXCL8, CXCL1-3, CCL5,

and CCL2, which have been implicated in tumor growth and progression. Recent studies have demonstrated organ-specific patterns of melanoma metastasis that correlate with their expression of specific chemokine receptors, including CXCR4, CCR7, and CCR10. The chemokine receptors CXCR4 and CCR7 are also found on breast cancer cells and their ligands are highly expressed at sites associated with breast cancer metastases. Other models in which CXCR4 has been suggested to play a role in metastasis are ovarian, prostate, and lung cancers. It is thus postulated that chemokine receptors and their ligand pairs may play a role in the migration of tumor cells from their primary site via the circulation to the preferential sites of metastases.

Central Nervous System

In addition to their well-established role in the immune system, chemokine receptors also play a role in the development and inflammation of the central nervous system (CNS). Certain chemokine receptors such as CXCR2, CXCR4, CCR1, and CCR5 are constitutively expressed in both developing and adult brains, and the role played by these proteins in the normal brain is the object of intense study. Chemokines are involved in brain development and in the maintenance of normal brain homeostasis; these proteins play a role in the migration, differentiation, and proliferation of glial and neuronal cells. For example, the chemokine receptor CXCR4 is essential for life during development, and this receptor has a fundamental role in neuron migration during cerebellar formation. In the CNS, chemokines play an essential role in neuroinflammation as mediators of leukocyte infiltration and glial cell activation. Their overexpression has been implicated in several neurological disorders, such as multiple sclerosis, trauma, stroke, Alzheimer's disease, tumor progression, and AIDS-associated dementia.

See Also the Following Articles

G Protein-Coupled Receptor Kinases and Arrestins • Phosphatidylinositol Bisphosphate and Trisphosphate • Phosphoinositide 3-Kinase • Phospholipase C • Protein Kinase C Family • Ras Family

Glossary

angiogenesis The growth of new vasculature from pre-existing blood vessels.

chemotaxis Directed migration of leukocytes toward to an inflammatory site.

coreceptor Any of certain chemokine receptors that are used together with CD4 by human immunodeficient virus to enter the target cells.

desensitization Attenuation of the functional response of chemokine receptors to their ligands following repeated ligand stimulation.

internalization Translocation of chemokine receptors from the cell membrane to the cytoplasmic compartments.

metastasis The migration of cancer cells to sites distant from the primary tumor.

Further Reading

Bajetto, A., Bonavia, R., Barbero, S., and Schettini, G. (2002). Characterization of chemokines and their receptors in the central nervous system: Physiopathological implications. *J. Neurochem.* **82**, 1311–1329.

Belperio, J. A., Keane, M. P., Arenberg, D. A., Addison, C. L., Ehlert, J. E., Burdick, M. D., and Strieter, R. M. (2000). CXC chemokines in angiogenesis. *J. Leukoc. Biol.* **68**, 1–8.

Dhawan, P., and Richmond, A. (2002). Role of CXCL1 in tumorigenesis of melanoma. *J. Leukoc. Biol.* **72**, 9–18.

Murphy, P. M., Baggiolini, M., Charo, I. F., Hébert, C. A., Horuk, R., Matsushima, K., Miller, L. H., Oppenheim, J. J., and Powe, C. A. (2000). International Union of Pharmacology, XXII. Nomenclature for chemokine receptors. *Pharmacol. Rev.* **52**, 145–176.

Olson, T. S., and Ley, K. (2002). Chemokines and chemokine receptors in leukocyte trafficking. *Am. J. Physiol. Regul. Integr. Comp. Physiol.* **283**, R7–R28.

Richmond, A. (2002). NF-kappa B, chemokine gene transcription and tumour growth. *Nat. Rev. Immunol.* **2**, 664–674.

Wang, J-M., Deng, X., Gong, W., and Su, S. (1998). Chemokines and their role in tumor growth and metastasis. *J. Immunol. Methods* **220**, 1–17.

Biography

Ann Richmond is a Professor in the Department of Cancer Biology at Vanderbilt University School of Medicine and a Senior Career Scientist in the Department of Veterans Affairs at Nashville Campus. Her research interests include chemokine receptor signal transduction, desensitization, and trafficking; transcriptional regulation of chemokines; and biological roles of chemokines in tumorigenesis, angiogenesis, and wound healing. She received her Ph.D. from Emory University and her postdoctoral training in the Division of Endocrinology at Emory University. During that time, she and her colleagues characterized one of the first chemokines, which is now known as CXCL1.

Guo-Huang Fan is a Research Assistant Professor in the Department of Cancer Biology at Vanderbilt University and an Assistant Professor in the Department of Pharmacology at Meharry Medical College. His research interests are signaling and trafficking of chemokine receptors. He received his Ph.D. from Shanghai Second Medical University and his postdoctoral training at the Chinese Academy of Sciences, University of Wuerzburg, and Vanderbilt University.

Chemolithotrophy

Alan B. Hooper
University of Minnesota, St. Paul, Minnesota, USA

The chemolithotrophic bacteria are defined by their ability to utilize inorganic or one-carbon molecules as a growth-supporting reductant. Oxidation of the growth-supporting reductant initiates a chain of redox electron-transfer reactions ending with reduction of a terminal electron acceptor such as oxygen and resulting in the generation of ATP. Alternatively, the reducing equivalents from the growth-supporting substrate are used in biosynthetic reductive reactions leading to cellular components.

Bioenergetics

Oxidation of the Growth-Supporting Substrate Drives Synthesis of Adenosine Triphosphate (ATP)

In all organisms a source of energy is required to drive biosynthesis, mechanical work, and pumping of molecules across a membrane against a gradient. Within cells this "energy" is commonly manifest as ATP since the hydrolysis of its terminal phosphoric anhydride bond can drive an otherwise thermodynamically unfavorable reaction when the two reactions are functionally coupled by an enzyme. The rephosphorylation of the resulting adenosine diphosphate (ADP) is most often catalyzed by a remarkable ATP synthase, an enzyme that is able to use the potential energy of a steady-state transmembrane gradient of protons. As the protons are relayed through the protein and across the membrane, the process is coupled to the synthesis of ATP. In turn, maintenance of the proton gradient requires the continuous turnover of a "low potential" half reaction (the oxidation of the growth-supporting reducing substrate). The continuation of the latter oxidative reaction is dependent on a "high potential" half reaction by which a growth-supporting *oxidant* substrate (a terminal electron acceptor) is reduced by electrons originating from the growth supporting reductant. A series of enzymes and electron transfer proteins are arranged in the membrane so that the process results in the net transfer of protons to the external side against a proton gradient.

The Variety of Terminal Electron Acceptors Used by Bacteria

Many bacteria are able to use one or more of the half-reactions shown in Table I as an electron sink supporting the continuity of the energy-generating reactions (i.e., the substrate molecules of Table I are terminal electron acceptors). The name of the enzyme is given for half-reactions: (1a–1g) are half-reactions; (1h–1k) are identified as processes. Because of its high redox potential, half-reaction 1a is preferred by bacteria. The other terminal electron acceptors are used when oxygen is absent (i.e., in anoxic or anaerobic rather than oxic or aerobic environments). Note that the reduction of protons in half-reaction 1f requires a low-potential reductant. Half-reactions 1f and 1g are employed in anaerobic fermentation by organotrophs. Line 1h is a multistep process carried out by the methane-generating bacteria. In line 1i, each step involves two electrons. The sulfur-reducing bacteria vary in the steps they are able to use. The reactions in this table are steps in the cycling of carbon, hydrogen, nitrogen, sulfur, and metals in nature.

Reductant for Biosynthesis

Biosynthetic reactions often require an electron or hydrogen donor molecule with a low enough potential to drive reductive reactions. This is often the reduced form of nicotinamide adenine dinucleotide (NADH). Hence, a second role of the growth-supporting reductant is the reduction of NAD^+; $NAD^+ + 2e^- + H^+ \rightarrow$ NADH.

Lithotrophy

Categories of Growth Based on the Nature of the Growth-Supporting Reductant

Organisms for which the growth-supporting reductant is a reduced carbon molecule such as glucose are called *chemoorganotrophs*. The sum of many reactions, including dehydrogenations, in the pathway of aerobic

TABLE I

Reductive Reactions Employed by Bacteria[a]

Half reaction	Name of enzyme or process
Aerobic conditions	
a. $O_2 + 4e^- + 4H^+ \rightarrow 2H_2O$	cytochrome oxidase
Anaerobic conditions	
b. $NO_3^- + 2e^- + 2H^+ \rightarrow NO_2^- + H_2O$	nitrate reductase
c. $NO_2^- + 2e^- + 2H^+ \rightarrow NO + H_2O$	nitrite reductase
d. $2NO + 2e^- + 2H^+ \rightarrow N_2O + H_2O$	nitric oxide reductase
e. $N_2O + 2e^- + 2H^+ \rightarrow N_2 + H_2O$	nitrous oxide reductase
f. $2H^+ + 2e^- \rightarrow H_2$	hydrogenase
g. $CH_3CHO^- + 4e^- + 4H^+ \rightarrow CH_3CH_2OH + H_2O$	aldehyde dehydrogenase
h. $CO_2 + 8e^- + 8H^+ \rightarrow CH_4 + 2H_2O$	methanogenesis
i. $SO_4^{2-} \rightarrow SO_3^{2-} \rightarrow S_4O_6^{2-} \rightarrow S_2O_3^{2-} \rightarrow S^0 \rightarrow S^{2-}$	reduction of sulfate
j. $Fe^{3+} + e^- \rightarrow Fe^{2+}$	
k. $Mn^{4+} + 2e^- \rightarrow Mn^{2+}$	

[a] The substrates of these reactions are terminal electron acceptors.

glucose oxidation is $C_6H_{12}O_6 + 6H_2O \rightarrow 6CO_2 + 24H^+ + 24e^-$.

Organisms defined as *phototrophs* are able to photochemically activate an internal substituent of a membrane protein thus converting it to a lower potential reductant. Reoxidation of the latter drives the creation of the proton gradient. Electrons are then recycled back to the center of photochemical reduction. Phototrophs require an external source of reductant (e.g., H_2O) only for reduction of NAD for use in biosynthetic reactions.

Bacteria that are specialized to use inorganic or one-carbon compounds as their growth-supporting reductant are called *chemolithotrophs*. Bacteria that are only able to grow in this manner are *obligate* chemolithotrophs; *facultative* chemolithotrophs have the activities necessary for chemoorganotrophic or chemolithotrophic growth.

The reducing half-reactions of the major chemolithotrophic growth-supporting substrates are listed in Tables II–V. In the majority of chemolithotrophic bacteria the oxidation of the growth-supporting reductant is coupled to reduction of oxygen (Table I, line a). The overall reactions supporting ATP synthesis for aerobic bacteria which oxidize ammonia, methane, sulfur, hydrogen, or ferric ion, respectively, are as follows:

$$NH_3 + 1.5O_2 \rightarrow NO_2^- + H_2O + H^+$$

$$CH_4 + 2O_2 \rightarrow CO_2 + 2H_2O$$

$$S^0 + 3O_2 \rightarrow SO_4^{2-} + 2H^+ + 2H_2O$$

$$2H_2 + O_2 \rightarrow 2H_2O$$

$$4Fe^{2+} + 4H^+ + O_2 \rightarrow 4Fe^{3+} + 2H_2O$$

Bacteria that use a substrate half-reaction with a sufficiently low redox potential can grow anaerobically using terminal electron acceptors other than oxygen:

$$4H_2 + HCO_3^- + H^+ \rightarrow CH_4 + 3H_2O$$

$$4H_2 + SO_4^{2-} + 2H^+ \rightarrow H_2S + 4H_2O$$

$$5S_2O_3^{2-} + 8NO_3^- + H_2O \rightarrow 10SO_4^{2-} + 4N_2 + 2H^+$$

Examples of Half-Reactions of the Growth-Supporting Reductant in the Chemolithotrophic Bacteria

Nitrifying Bacteria

The half-reactions of the nitrifying bacteria represent the oxidative arm of the nitrogen cycle. Two enzymes are involved in the ammonia-oxidizers and one enzyme is involved in the nitrite oxidizers, respectively (see Table II). A recently discovered anaerobic chemolithotroph generates energy in a series of ANAMMOX

TABLE II

Oxidation of the Growth-Supporting Reductant in the Nitrifying Bacteria

Half reaction	Name of enzyme
Ammonia oxidizers	
overall growth-supporting half-reaction	
a. $NH_3 + O_2 \rightarrow HNO_2 + H_2O + 2H^+ + 2e^-$	
enzyme steps	
b. $NH_3 + O_2 + 2H^+ + 2e^- \rightarrow NH_2OH$	ammonia monooxygenase
c. $NH_2OH + H_2O \rightarrow HNO_2 + 4e^- + 4H^+$	hydroxylamine oxidoreductase
Nitrite oxidizers	
d. $HNO_2 + H_2O \rightarrow HNO_3 + 2H^+ + 2e^-$	nitrite oxidoreductase
Anaerobic conversion of ammonia to dinitrogen (ANAMMOX bacterium)	
overall reaction supporting energy conservation	
e. $HNO_2 + NH_3 \rightarrow N_2 + 2H_2O$	
enzyme steps	
f. $NO_2^- + 4e^- + 4H^+ \rightarrow NH_2OH + H_2O$	(hypothetical)
g. $NH_2OH + NH_3 \rightarrow N_2H_2 + H_2O$	(hypothetical)
h. $N_2H_4 \rightarrow N_2 + 4e^- + 4H$	hydroxylamine oxidoreductase

TABLE III

Oxidation of the Growth-Supporting Reductant in the Hydrogen-, Methane-, and Carbon Monoxide-Oxidizing Bacteria

Half reaction	Name of enzyme or process
Hydrogen-oxidizing bacteria	
a. $H_2 \rightarrow 2H^+ + 2e^-$	hydrogenase
Methanotrophic bacteria	
overall growth-supporting half-reaction:	
b. $CH_4 + 2O_2 \rightarrow CO_2 + 4H^+ + 4e^- + 2H_2O$	
enzyme steps	
c. $CH_4 + O_2 + 2H^+ + 2e^- \rightarrow CH_3OH + H_2O$	methane monooxygenase
d. $CH_3OH \rightarrow CH_2O + 2H^+ + 2e^-$	methanol dehydrogenase
e. $CH_2O + H_2O \rightarrow H_2CO_2 + 2H^+ + 2e^-$	formate dehydrogenase
f. $H_2CO_2 + H_2O \rightarrow H_2CO_3 + 2H^+ + 2e^-$	formate dehydrogenase
g. $H_2CO_3 \rightarrow CO_2 + H_2O$	carbonic anhydrase
Carboxydobacteria	
h. $CO + H_2O \rightarrow CO_2 + 2H^+ + 2e^-$	CO dehydrogenase

reactions involving ammonia and nitrite with hydrazine as an intermediate and dinitrogen as the end product.

Hydrogen-, Methane-, and Carbon Monoxide-Oxidizing Bacteria

Hydrogenase (Table I, line f) of hydrogen-oxidizing bacteria oxidizes hydrogen to protons. The aerobic oxidation of methane by the methanotrophic bacteria (Table III, line b) involves an electron consuming monooxygenase (line c) and successive methanol-, formaldehyde-, and formate- dehydrogenases (lines d–f). The conversion of carbonic acid to CO_2 can be spontaneous or enzyme-catalyzed (line g). In the carboxydobacteria, carbon monoxide reductase catalyzes the net extraction of two electrons and two protons to produce carbon dioxide from carbon monoxide and water.

TABLE IV

Oxidation of the Growth-Supporting Reductant in the Sulfur Oxidizing Bacteria

Half reaction
Overall growth-supporting half-reactions
a. $H_2S + 4H_2O \rightarrow SO_4^{2-} + 10H^+ + 8e^-$
b. $S_2O_3^{2-} + 5H_2O \rightarrow 2SO_4^{2-} + 10H^+ + 8e^-$
c. $S^0 + 4H_2O \rightarrow SO_4^{2-} + 8H^+ + 6e^-$
d. $SO_3^{2-} + H_2O \rightarrow SO_4^{2-} + 2H^+ + 2e^-$
Enzymatic steps observed within sulfur oxidizing pathways
e. $H_2S \rightarrow S^0 + 2H^+ + 2e^-$
f. $2S^0 + 3H_2O \rightarrow S_2O_3^{2-} + 6H^+ + 4e^-$
g. $2S_2O_3^{2-} \rightarrow S_4O_6^{2-} + 2e^-$
h. $S_4O_6^{2-} + 6H_2O \rightarrow 4SO_3^{2-} + 12H^+ + 12e^-$
i. $SO_3^{2-} + H_2O \rightarrow SO_4^{2-} + 2H^+ + 2e^-$

TABLE V

Oxidation of the Growth-Supporting Reductant in the Metal Oxidizing Bacteria

Half reaction
a. $Fe^{II} \rightarrow Fe^{III} + e^-$
b. $Mn^{II} \rightarrow Mn^{III} + e^-$
c. $Cu^{I} \rightarrow Cu^{II} + e^-$
d. $Sn^{II} \rightarrow Sn^{III} + e^-$
e. $Fe^0 \rightarrow Fe^{II} + 2e^-$

Sulfur Oxidizing Bacteria

Depending on the specific bacterium, oxidation of a variety of reduced sulfur compounds are used to support growth. Some examples of the half-reactions are shown in Table IV, lines a–d. The enzymatic steps used within the respective pathways are listed in Table IV, lines e–i. Some bacteria utilize the adenosine phosphosulfate (APS) pathway for synthesis of ATP coupled to the oxidation of sulfite.

Metal-Oxidizing Bacteria

The half reactions shown in Table V, lines a–d are carried out by *Thiobacillus ferrooxidans*. A metalloenzyme catalyzes the oxidation of ferrous iron to ferric ion which hydrolyzes to form an orange precipitate: $Fe^{3+} + 3H_2O \rightarrow Fe(OH)_3 + 3H^+$. Metallic Fe^0 can be oxidized by methanogenic bacteria coupled to the reduction of CO_2 to methane (Table I, line h).

Basic Mechanisms of Energy-Transduction and ATP Synthesis in Chemolithotrophs

Generation of the Electrochemical Gradient and ATP Synthesis

Some generalizations regarding location of the enzymes catalyzing the oxidation of substrate, generation of a proton gradient and synthesis of ATP are illustrated in

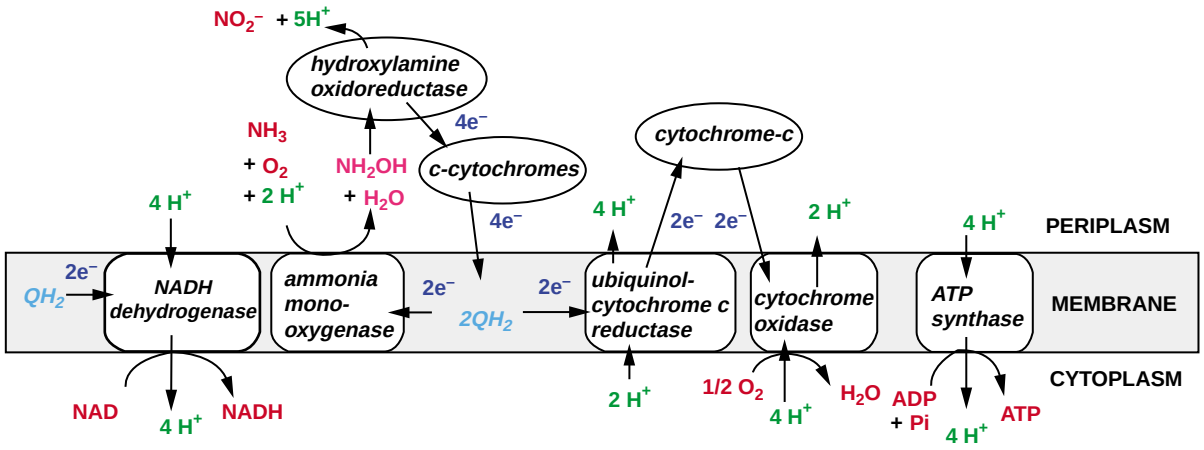

FIGURE 1 Catalysis of the oxidation of ammonia to nitrite coupled to generation of ATP and NADH in the chemolithotrophic bacterium, *Nitrosomonas europaea*. The four enzymes in the center of the figure create a proton gradient that is employed by the enzymes on the left and right to make NADH and ATP, respectively. Electrons from hydroxylamine oxidoreductase are relayed by heme-containing electron-transferring proteins, "cytochromes" in which Fe cycles between Fe^{2+} and Fe^{3+}, to reduce a quinone to a quinol (QH_2). The quinol is reoxidized either by ammonia monooxygenase or by an electron-transfer chain including a proton-pumping ubiquinol–cytochrome c reductase, a cytochrome- c and a proton-pumping cytochrome oxidase. The proton-pumping NADH-dehydrogenase functions in reverse to form NADH as shown in the figure. ATP synthase catalyzes the proton-gradient-driven phosphorylation of ADP. The periplasm is the region outside the cell membrane; the cytoplasm is inside the cell membrane. The membrane itself is impermeable to protons. Substrates and final products are shown in red (the intermediate hydroxylamine is pink). Protons are shown in green. Electrons are shown in blue and quinone is in light blue. Enzymes and cytochromes are italicized and circled.

the oxidation of ammonia to nitrite by the nitrifying bacterium *Nitrosomonas*, an obligate chemolithoautotroph (Figure 1). Although ammonia is the substrate required for growth, it is the oxidation of hydroxylamine that generates low-potential electrons for energy conversion and reductive biosynthetic reactions. Four electrons are transferred from hydroxylamine oxidoreductase (Table II, line c) to an electron-transfer chain made up of two heme-containing proteins (cytochromes) to two quinone molecules in the membrane. Two electrons from the reoxidation of one quinol are utilized by ammonia monooxygenase to regenerate a molecule of hydroxylamine, i.e., to "re-prime the pump." The two electrons (per hydroxylamine oxidized) from the second quinol may reduce dioxygen in a pathway that involves the two membrane enzymes ubiquinol cytochrome c reductase and cytochrome c oxidase, each of which couple the reaction to the transport of protons against a gradient to the outside (the "periplasm" of the bacterial cell). In this way a steady-state electrochemical potential (outside positive) is maintained across the membrane and "drives" ATP synthesis.

Substrate-Level Phosphorylation of ADP

In one chemolithotroph, a sulfite oxidizing bacterium, the net phosphorylation of ADP occurs by a substrate-level process that is independent of the membrane electrochemical gradient. The key reaction involves the simultaneous dehydrogenation of sulfite and reaction with adenosine monophosphate (AMP) to form the anhydride of phosphoric and sulfuric groups in the product, adenosine phosphosulfate (APS).

$$SO_3^{2-} + AMP \rightarrow APS + 2e^-$$

Phosphate can then displace sulfate to form ADP and the subsequent dismutation of two molecules of ADP provides an ATP.

$$APS + P_i \rightarrow ADP + SO_4^{2-}$$

$$2ADP \rightarrow ATP + AMP$$

Release and Uptake of Protons in Chemolithotrophic Reactions

In the reducing half-reactions of the major chemolithotrophic growth-supporting reductants (Tables II–V) the energetically fruitful reactions are, in effect, dehydrogenases where the products are free protons and electrons transferred to a metal redox center. The protons originate from the substrate (in the oxidation of ethanol, formaldehyde, H_2, N_2H_2, H_2S), H_2O (in the oxidation of CO, nitrite, S^0, SO_3^{2-}) or both (in the oxidation of NH_2OH). In all cases where location of the enzyme has been determined, the proton-yielding reactions are found in the periplasm and thus contribute to maintenance of the positive charge on the outer side of the membrane. Correspondingly, almost all terminal electron acceptor reactions (Table I) consume protons and are located on the internal side of

the membrane thus contributing to the maintenance of the negative charge on that side. This is illustrated in the location of hydroxylamine dehydrogenation and oxygen reduction in *Nitrosomonas* (Figure 1).

Production of NADH by Chemolithotrophic Bacteria

With many chemolithotrophs, the potential of the half reaction that drives metabolism (in the case of *Nitrosomonas*, the dehydrogenation of hydroxylamine) is not low enough to reduce NAD^+ directly. The reduction of NAD^+ is catalyzed by an enzyme which, in chemoorganotrophs, dehydrogenates NADH, reduces quinone, and pumps protons to the outside of the cell. However, in the case of *Nitrosomonas* (Figure 1) and other chemolithotrophs, the reaction runs in the reverse direction; thermodynamically, the steady-state gradient of protons drives the reduction of NAD^+ by quinol. This process is not needed in bacteria such as the hydrogen oxidizers in which the growth-supporting reductive half reaction ($H_2 \rightarrow 2H^+ + 2e^-$) has a low enough potential to reduce NAD^+ directly.

Carbon Source for Chemolithotrophic Bacteria

The carbon source for most chemolithotrophic bacteria is CO_2. This mode of growth is called *autotrophic*, i.e., the organisms are chemolithoautotrophs. Most chemolithotrophs are *obligate* autotrophs, meaning that they can only grow having synthesized all or most of their reduced carbon compounds from CO_2. This contrasts with heterotrophic organisms, which can fulfill all their need for carbon compounds with previously fixed carbons such as sugars. *Facultative* autotrophs are able to alter their content of biosynthetic enzymes to catalyze either the autotrophic or heterotrophic mode of life. The most common pathway of carbon dioxide fixation in the chemolithoautotrophs is the Calvin Cycle starting with the reaction of ribulose bis phosphate carboxylase:

$$\text{ribulose 1,5 bis phosphate} + CO_2 \rightarrow 2,3\text{-phosphoglycerate}$$

Considering the reduction of 3-phosphoglycerate and the regeneration of ribulose 1,5 bis phosphate in the Calvin cycle, approximately 12 molecules of NADH and 18 of ATP are required per hexose synthesized from CO_2. Remarkably, the obligate chemolithoautotrophs contain the enzymes for biosynthesis of all cellular constituents. Furthermore, they have genes for enzymes for the uptake, metabolism, and incorporation of carbon from extremely few carbon compounds other than CO_2. This is illustrated nicely by analysis of the genes present and absent in the genome of *Nitrosomonas*.

Growth Yields of Chemolithoautotrophs

Given the required expenditure of energy (in effect, low potential electrons from the substrate) to drive the synthesis of ATP and the reduction of NAD, which are then used in biosynthetic reactions, the yield of biomass per mole of substrate oxidized is usually much lower in the chemolithoautotrophs than with heterotrophic organotrophs. Profiting from their unique catalytic capabilities, chemolithotrophs grow slowly and live frugally with a highly selective diet of a thin soup of inorganic compounds or small carbon molecules.

Ecology

The chemolithotrophs represent the oxidative segment of the biological cycles of inorganic compounds such as hydrogen, nitrogen, sulfur, and metal ions. The vast majority of these steps occur aerobically. Most of the reduced substrates for chemolithotrophs are generated by the terminal electron accepting reactions of anaerobic organisms (Table I). For example, hydrogen from reduction of protons by organotrophic bacteria in cattle rumen (Table I, line f) is oxidized by chemolithotrophic hydrogen-oxidizing bacteria using the conversion of carbon dioxide to methane as the terminal electron acceptor half-reaction (line h). Methane released from ruminants finds its way to an oxic (aerobic) environment, where it is oxidized by the methanotrophic bacteria (Table III, line b). The chemolithotrophs and the anaerobes are sometimes found at oxic/anoxic (aerobic/anaerobic) interfaces, where the respective oxidative and reductive reactions provide a cycle to the advantage of both types of organism.

There are many examples of economically significant effects of chemolithotrophic activity. The production of sulfuric acid by the sulfur-oxidizing bacteria facilitates corrosion of metals and the acidification of mine drainage is attributed to the iron oxidizing bacteria.

Other major natural sources of the reduced compounds include volcanic activity and atmospheric activity such as lightning. Anthropogenic sources of reduced compounds include agricultural waste and residential waste water, combustion of fossil fuels, industrial processes, and mining operations. Significantly, the annual production of ammonia from dinitrogen by industry now exceeds the flux from all other biological and nonbiological sources.

See Also the Following Article

Respiratory Processes in Anoxygenic and Oxygenic Phototrophs

Glossary

autotrophy A mode of bacterial growth in which carbon dioxide is the source of all or most of the carbon for biosynthesis. These bacteria are *autotrophic*. Autotrophy contrasts with heterotrophy, a mode of growth where organic carbon compounds can provide all carbon for biosynthesis.

chemolithotrophy A mode of bacterial growth in which the reductive substrate for energy generation and for biosynthesis is an inorganic or a single carbon compound. These bacteria are *chemolithotrophic*. Chemolithotrophy contrasts with organotrophy or phototrophy in which the energy generation occurs by the oxidation of organic molecule or absorption of light, respectively.

growth-supporting reductant A compound whose oxidation can be coupled biologically to the conservation of energy in forms of general use to cellular activities: as an electrochemical gradient, as a phosphate anhydride bond in ATP, or as the low-potential reductant, reduced nicotinamide adenine dinucleotide.

oxic environment An environment containing dioxygen (O_2). The word *aerobic* is also used. Oxic contrasts with anoxic (or anaerobic), which applies to environments in which oxygen is absent.

terminal electron acceptor A compound whose reduction can be coupled to the stoichiometric oxidation of the growth-supporting reductant and conservation of energy in cells.

Further Reading

Chain, P., Lamerdin, J., Larimer, F., Regala, W., Lao, V., Land, M., Hauser, L., Hooper, A., Klotz, M., Norton, J., Sayavedra-Soto, L., Arciero, D., Hommes, N., Whittaker, M., and Arp, D (2003). Complete genome sequence of the ammonia oxidizing bacterium and obligate chemolithoautotroph *Nitrosomonas europaea*. *J. Bacteriol.* **185**, 2759–2773.

Hooper, A. B., and DiSpirito, A. A. (1985). In bacteria which grow on simple reductants, generation of a proton gradient involves extracytoplasmic oxidation of substrate. *Microbiol. Rev.* **49**, 140–157.

Hooper, A. B., Arciero, D. M., Bergmann, D., and Hendrich, M. P (2003). The oxidation of ammonia as an energy source in bacteria in respiration. In *Archaea and Bacteria, Volume 2: Diversity of Procaryotic Respiratory Systems* (D. Zannoni, ed.), in press. Kluwer Scientific, The Netherlands.

Lengeler, J. W., Drews, G., and Schlegel, H. G. (1999). *Biology of the Prokaryotes*. Blackwell Science, Oxford, U.K.

White, D. (2000). *The Physiology and Biochemistry of Prokaryotes*. Oxford University Press, New York.

Biography

Alan Bacon Hooper is a Professor in the Department of Biochemistry, Molecular Biology and Biophysics at the University of Minnesota. His research interest is in the biochemistry of the ammonia oxidizing chemolithotrophic bacteria. He earned his B.A. from Oberlin College and his Ph.D. from Johns Hopkins University. He joined the University of Minnesota faculty in 1963. He currently teaches biochemistry and a course on Biology, Ethics, and Public Policy.

Chemotactic Peptide/Complement Receptors

Eric R. Prossnitz and Larry A. Sklar
University of New Mexico, Albuquerque, New Mexico, USA

A critical aspect in the normal function of many cell types is their ability to migrate in response to soluble ligands or chemoattractants. Directional migration, where the cell seeks out the highest concentration of chemoattractant, is referred to as chemotaxis. This is of paramount importance in the immune system where a large collection of G protein-coupled receptors (GPCRs) exists to coordinate the complex interactions of immune cells. These receptors can be divided into two families, the chemotactic or chemoattractant GPCRs that respond to a wide variety of endogenous as well as exogenous ligands and the chemokine GPCRs that respond to the structurally conserved family of endogenous peptide chemokines. The chemotactic GPCRs respond to ligands as varied as oligopeptides, such as bacterially derived N-formylated peptides; proteins, such as complement components; and lipids, such as leukotrienes and platelet-activating factor.

Leukocytes and the Immune System

The immune system is responsible for numerous activities in the body including defense against pathogens (bacterial, viral, and parasitic), removal of dead and cancerous cells as well as the rejection of foreign cells. Leukocytes, or white blood cells, which represent the principal cells of the immune system, are produced as progenitor cells in the bone marrow and mature in various sites throughout the body, including the spleen, thymus, and lymph nodes. Leukocytes can be divided into five broad categories: neutrophils (highly mobile phagocytic cells), basophils (allergy mediators through histamine release), eosinophils (parasitic killing and allergy), lymphocytes (B cells, which produce antibodies and T cells, which effect cell-mediated immunity), and monocytes/macrophages (tissue-specific phagocytic cells). These cells differentially participate in two types of immune responses: innate immunity, an inherent and rapid response of neutrophils, macrophages, and natural killer lymphocytes to foreign materials; and acquired immunity, a selective "trained" response involving lymphocytes requiring prior exposure to the agent. An additional noncellular defensive mechanism, the complement system consisting of at least 20–30 distinct serum proteins, destroys foreign cells through membrane lysis of antibody-targeted cells. Two of the smaller bioactive fragments released by proteolysis from the C3 and C5 components, C3a and C5a, are known as anaphylatoxins and play a major role in inflammation. Immune cells for the most part circulate in the vascular and lymphatic systems, although tissue resident cells such as macrophages are essential to proper immune function. In almost any immune response, however, leukocytes must migrate to the site of damage/infection from the blood. This is a complex multistep process involving inflammatory mediators (such as histamine) that induce vasodilation and increased vascular permeability, activation of adhesion molecules on capillary lining endothelial cells to slow leukocytes and release of chemoattractants to activate leukocytes resulting in firm adhesion to endothelial cells. The concentration gradients of chemoattractants induce the leukocyte to transverse the endothelium and migrate through the tissue to the peak concentration of chemoattractant at the site of inflammation or infection. Having arrived at this site, neutrophils, for example, phagocytose bacteria, generate superoxide radicals and release granules containing degradative proteases. Most of these responses are initiated and regulated by a family of cell surface receptors that bind inflammatory mediators.

Receptors

The largest family of proteins in the human genome is the GPCR superfamily consisting of at least 600 members. GPCRs exhibit a highly conserved structure, consisting of seven transmembrane segments with the amino terminus on the cell exterior and the carboxy terminus in the cytoplasm. The chemoattractant family of receptors consists of proteins with ~350 amino acids. The transmembrane regions consist primarily of α-helices arranged in a bundle. Despite this conserved

structure, there is substantial sequence diversity between members of this receptor family. Binding of small ligands, such as chemotactic peptides, occurs deep within the receptor in the plane of the membrane. Ligand binding and receptor activation result in a conformational change that activates heterotrimeric G proteins, which further stimulate a wide variety of effector proteins. Following activation, GPCRs undergo phosphorylation, resulting in desensitization and internalization, which in turn can lead to receptor degradation or recycling back to the cell surface.

Chemotactic Peptide Receptors

Though identified as a neutrophil receptor for formyl peptides in the 1970s, it was not until 1990 that the FPR gene was isolated, representing the first chemoattractant or chemokine receptor to be cloned. Two human homologues were subsequently identified and designated FPRL1 and FPRL2. Of these, only the former responds, though poorly, to formyl peptides. Although the FPR is expressed predominantly in neutrophils, it also appears to be expressed in monocytes, dendritic cells, hepatocytes, endothelial cells, and the nervous system. FPRL1 and FPRL2 are expressed in some of the same cell types as well as unique sites. Although the human FPR gene family consists of only three members, the number varies considerably in other species, with six members in the murine gene family for example. Thus, distinct evolutionary pressures seem to dictate the repertoire of formyl peptide receptors in a given organism.

The role of the FPR in antimicrobial defense has recently been directly demonstrated in knockout mice lacking mFPR1, the homologue of the human FPR. Although such mice appear normal under unstressed conditions, they demonstrate a lack of neutrophil responses to fMLF challenge as well as an increased susceptibility to infection with *Listeria monocytogenes*. Furthermore, in humans, two variant alleles of the FPR representing single point mutations that disrupt normal function are associated with localized juvenile periodontitis, a result of periodontal bacterial infection. It is perhaps surprising that such defects do not lead to more serious conditions.

Complement Receptors

C5a Receptor

At the same time that formylated peptides were being characterized as chemoattractants, proinflammatory peptides derived from the complement system were similarly being studied. Two receptors have been identified that respond to the cleavage products of the complement components C3 and C5. The C5a receptor is similar in size to the FPR and closely related phylogenetically. Interestingly, there exists little interspecies homology in the extracellular regions of the C5a receptor, despite apparent contact sites with C5a and interspecies activation (C5a from one species activating the receptor from another species). Antibodies against peptides representing the amino terminus of the receptor and amino-terminal truncations of the receptor block C5a binding. As the antibodies do not block activation of the receptor by synthetic C5a carboxy terminal peptides, the amino terminus of the receptor may represent a secondary noneffector binding site and not the primary effector site. Mutagenesis studies suggest a critical role for a number of aspartic acid residues in the amino terminus. Recent evidence is consistent with C5a receptor dimerization, a phenomenon now demonstrated for many GPCRs with unclear functional consequences. Studies of genetically engineered mice lacking the C5a receptor demonstrated that this receptor plays a critical role in clearing pulmonary pseudomonas infections, with mice succumbing to pneumonia despite a marked neutrophil influx.

C3a Receptor

The C3a receptor is unusual in that it possesses a second extracellular loop of some 175 amino acids compared to about 30 amino acids for most GPCRs including the C5a and FPRs. Deletion analysis of this loop suggests that it plays a role in C3a binding and receptor activation, although as much as two-thirds of the loop can be deleted without affecting activity. It is thought that the second extracellular loop may replace the function of the amino terminus of the C5a receptor in providing a secondary noneffector binding site. Recent studies with C3a receptor knockout mice suggest a role for the receptor in allergic airway diseases such as asthma.

Ligands

Chemotactic Peptide Receptors

The first leukocyte chemotactic factors to be defined structurally were the N-formyl peptides. These consist of short oligopeptides consisting of 3–6 hydrophobic amino acids with the amino terminal residue being formylated. Such peptides are not synthesized by eukaryotic cells *per se*. There are only two sources of N-formylated peptides in nature: one endogenous to eukaryotic cells, mitochondria, and the other exogenous, bacteria. Each of these sources initiates protein synthesis with an N-formyl methionine tRNA. This suggests an ideal targeting mechanism for leukocytes to sense bacterial infection or cell damage through the release of peptides containing N-formyl-methionyl peptides.

The first chemoattractant peptide was isolated from bacterial lysates and was identified in 1976 as N-formyl-methionyl-leucyl-phenylalanine (fMLP or fMLF). This agonist is capable of eliciting the full complement of leukocyte functions from chemotaxis to degranulation to superoxide production at concentrations ranging from pM to nM. The FPR is the primary receptor responsible for cellular stimulation in these concentration ranges, whereas FPRL1 responds to fMLF at μM concentrations. Both the FPR and FPRL1 have recently been shown to be activated by a diverse collection of endogenous as well as exogenous peptides. These include non-formylated peptides from exogenous sources such as Helicobacter pylori and HIV-1 envelope proteins as well as endogenous host-derived proteins such as serum amyloid A and peptides from annexin I, amyloid precursor protein and prion protein among others. Lipoxin A4, a lipid metabolite, has also been reported to activate FPRL1. The biological relevance of these agonists remains to be determined. Finally, a number of non-formylated high-affinity peptide agonists for the FPR and FPRL1 have been isolated from peptide libraries. A number of antagonists have also been identified including Boc-FLFLF, cyclosporine H (a fungal metabolite), and deoxycholic acid (a bile acid).

Complement Receptors

C5a

The anaphylatoxin C5a, the most potent plasma-derived chemotactic factor, is a 74 amino acid peptide/protein released from the α-chain of C5 by either the classical or alternative pathway C5 convertases. Structurally, the protein consists of four antiparallel α-helices held together by disulfide bonds and an 11-amino acid carboxy terminal tail. Unlike the small formyl peptides, C5a appears to interact with its receptor at two sites. The α-helical bundle interacts with the receptor's amino-terminal domain whereas the tail appears to insert itself into the transmembrane bundle of the receptor, thereby activating the receptor. Synthetic peptides representing the carboxy-terminal 10-amino acids are full agonists, though with potencies 1000–10 000 lower than C5a itself. The sequence Gln–Leu–Gly–Arg is a highly conserved effector sequence in C5a from numerous species. Substitution of residues within this region can greatly augment potency. Removal of the final arginine residue in C5a results in greatly decreased potency, ranging from 1000-fold decrease for spasmogenic activity to tenfold for chemotactic activity.

C3a

Less is known regarding the interactions between C3a and its receptor. C3a is a 77-amino acid protein released from the α-chain of C3 by either the classical or alternative pathway C3 convertases. C3a and C5a, despite having common genetic ancestry, have markedly different sequences. Only 13-amino acid positions have been totally conserved between C3a, C5a, and the related C4a molecules from numerous species analyzed. Six of these residues represent immutable cysteine residues that direct folding of the protein. Again, the carboxy-terminal sequence seems to define molecular action as the terminal sequence Leu–Gly–Leu–Ala–Arg is conserved in all known C3a molecules. C3a appears to interact both with portions of the large second extracellular loop of the receptor as well as charged residues at the transmembrane boundaries of this loop. For both the C5a and C3a receptors, insertion of the carboxy terminus of the anaphylatoxin into a binding pocket formed by the transmembrane helices of the receptor appears essential to receptor activation.

G Proteins

Following ligand binding and the commensurate activation of the receptor, GPCRs interact with G proteins initiating a vast array of intracellular signaling (Figure 1). Of the four major G protein subfamilies (G_s, G_i, G_q, and $G_{12/13}$), chemoattractant/complement receptors activate primarily the G_i family of G proteins. This is demonstrated by the inhibition of virtually all chemoattractant receptor-mediated cell activation by pertussis toxin, a bacterial toxin that inactivates G_i (and closely related G_o) α-subunits of G proteins. G proteins consist of three subunits: the guanine nucleotide-binding α-subunit, and the nondissociable membrane-associated $\beta\gamma$-subunit dimer. Receptor activation catalyzes the exchange of GDP for GTP on the α-subunit followed by activation of the α- and $\beta\gamma$-subunits. Hydrolysis of the bound GTP by the intrinsic activity of the G_α protein, accelerated by a family of regulators of G protein signaling (RGS) proteins, inactivates the protein and allows reassembly of the inactive $\alpha\beta\gamma$ heterotrimer.

Effector Proteins

Chemoattractant-mediated G protein activation leads to a plethora of downstream signaling events. Although G_i proteins are generally considered to inhibit adenylyl cyclase activity, in the case of most chemoattractant and chemokine receptors, G_i activation leads to $G_{\beta\gamma}$-mediated activation of phospholipase Cβ2, resulting in the production of inositol trisphosphate (IP3) and diacyl glycerol (DAG). IP3 generation results in the release of calcium from intracellular endoplasmic reticulum stores, often followed by the influx of

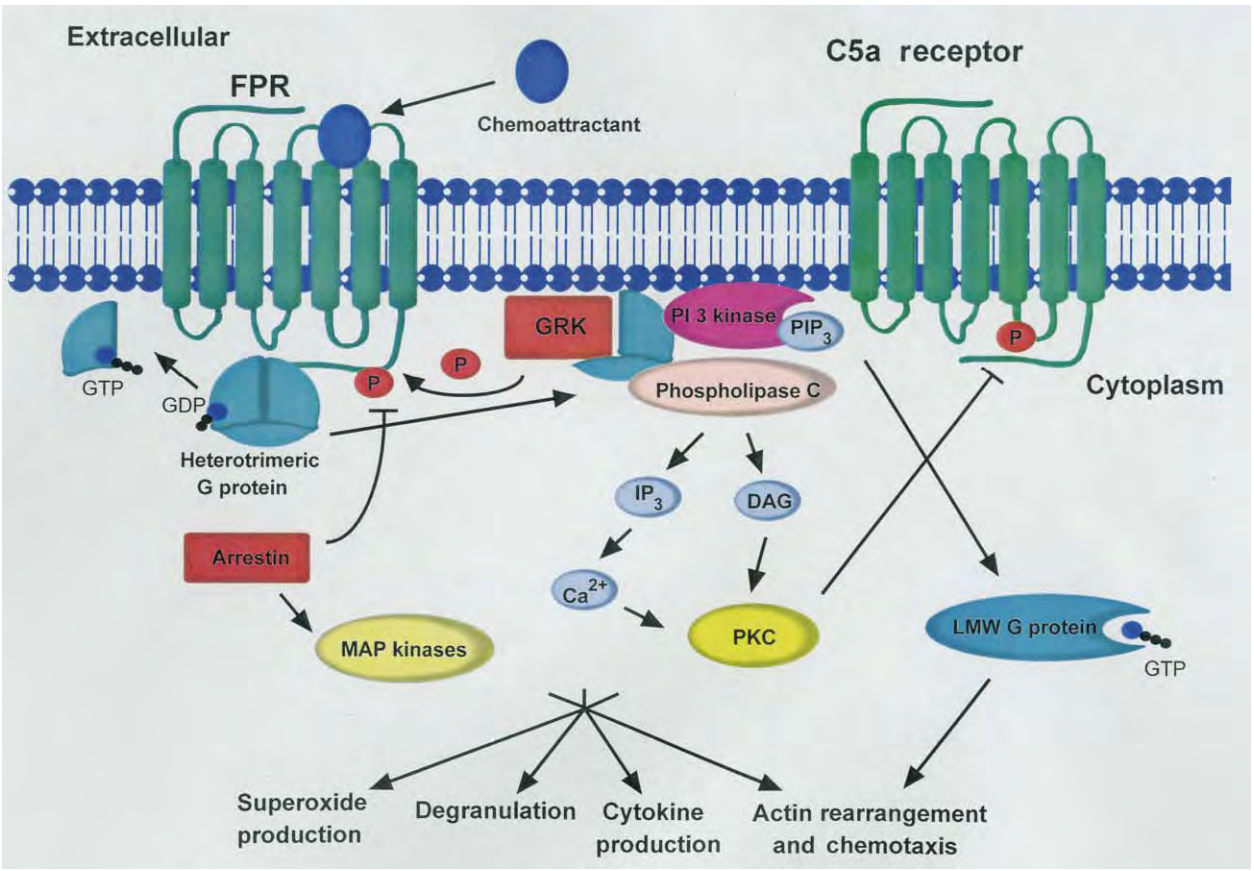

FIGURE 1 Signaling and regulation of chemoattractant/complement receptors in leukocytes. Binding of a chemoattractant (agonist) results in a conformational change in the FPR, which activates G proteins. Dissociation of GDP from the α-subunit is followed by GTP binding and dissociation of the α-subunit from the $\beta\gamma$-subunits, both of which can stimulate downstream effectors. The $\beta\gamma$-subunits provide a docking site for G protein-coupled receptor kinases (GRKs), which phosphorylate (P) the ligand-bound, activated receptor. $\beta\gamma$-subunits also activate phospholipases, which generate diacyl glycerol (DAG) and inositol trisphosphate (IP_3) and phosphatidylinositol-3 kinase (PI_3 kinase), which generates phosphatidyl inositol trisphosphate (PIP_3). PIP_3 is an activator of numerous pathways including those culminating in low molecular weight (LMW) monomeric G proteins of the Ras superfamily that regulate actin assembly and ultimately chemotaxis. IP_3 production results in the release of Ca^{2+} from intracellular stores, and together with DAG activates protein kinase C (PKC). PKC is capable of phosphorylating many proteins including complement receptors, such as the C5a receptor, resulting in their heterologous desenstization. Desensitization of the FPR occurs through the binding of arrestin to GRK-phosphorylated receptors. In addition to preventing further signaling through heterotrimeric G proteins, arrestins serve as scaffolds for multiple MAP kinases, resulting in their localized activation. Together, these and many additional pathways produce cellular responses including superoxide generation, degranulation, chemotactic cell movement and transcriptional activation resulting in cytokine production.

calcium from the extracellular environment through ion channels. The calcium and DAG in turn activate protein kinase C (PKC). Receptor-mediated phospholipase A_2 activation results in the generation of arachidonic acid and subsequently prostaglandins and leukotrienes. Phosphatidylinositol 3-kinase (PI3K) also plays a critical role in leukocyte activation and chemotaxis in particular. MAP kinase family members ERK, p38, and Jnk have all been shown to be essential to cellular activation events. The low-molecular-weight monomeric G proteins Rac and Rap, as well as their associated regulatory proteins and downstream effectors, are important mediators of actin assembly/chemotaxis and superoxide production.

Receptor Regulation

The dysregulated activation of leukocytes is a serious contributing factor to numerous chronic inflammatory diseases such as arthritis and reperfusion injury in ischaemic tissues following myocardial thrombosis and stroke. Activated chemoattractant/complement receptors are rapidly phosphorylated following ligand binding and receptor activation. This can be mediated either by G protein-coupled receptor kinases (GRKs) that are specific for the active state of GPCRs or by second messenger kinases such as protein kinase A and protein kinase C that phosphorylate active and inactive receptors. The latter provides a mechanism

(termed heterologous desensitization) by which GPCRs such as the FPR, which has no PKC phosphorylation sites, can desensitize the C5a receptor, which is phosphorylated by PKC, leading to decreased G protein coupling (see Figure 1). Since any inflammatory process is likely to lead to the generation of multiple simultaneous chemoattractant signals, these regulatory mechanisms create a hierarchy of chemotactic responsiveness to different ligands. GRK phosphorylation of chemoattractant receptors, which occurs within the carboxy terminus of the receptor at sites distinct from PKC sites, leads to binding of arrestins and receptor internalization. Arrestin binding further uncouples receptors from G proteins by physically preventing access of G proteins to the receptor (termed homologous desensitization). For many GPCRs, arrestin binding also mediates interactions with clathrin and adapter proteins such as AP-2 initiating receptor translocation to clathrin-coated pits and subsequent internalization. Contrary to this paradigm, the FPR has recently been shown to internalize in an arrestin-independent manner. However, arrestin is required for recycling of the FPR. Arrestins have also been shown to play an important role in the scaffolding of numerous intracellular signaling cascades including Src and MAP kinases. This mechanism is believed to provide both spatial and temporal regulation of the downstream effectors.

Drug Discovery and Receptor Technology

GPCRs represent ~50% of the targets of drugs on the market today. In particular, the family of chemokine/chemoattractant receptors is a highly sought after target as the receptors are involved in immune disorders such as chronic inflammation and asthma, cancer, and many more disease states. The formyl peptide receptor, in particular, has served as an important model for the real-time analysis of ligand-receptor interactions based on the detection of fluorescent peptide ligands by solution fluorescence, flow cytometry, and microscopy. These ligands and receptors have provided the basis for developing subsecond kinetic resolution of molecular assemblies and disassemblies by flow cytometry as well as small volume, high throughput flow cytometric platforms for screening. These approaches are now being extended to other molecular classes.

See Also the Following Articles

Chemokine Receptors • Chemotactic Peptide/Complement Receptors • G Protein Signaling Regulators • G Protein-Coupled Receptor Kinases and Arrestins • G_i Family of Heterotrimeric G Proteins • Protein Kinase C Family

Glossary

chemokine A family of structurally related 70–90 aminoacid-long glycoproteins that exhibit potent chemotactic and stimulatory properties on leukocytes.

complement system A series of ~30 components that include proteolytic pro-enzymes, non-enzymatic components that form functional complexes, regulators, and receptors. The proteolytic pro-enzymes become sequentially activated. C5a and C3a are terminal non-enzymatic cleavage products.

G protein A protein that binds and is regulated by guanine nucleotides. Heterotrimeric members of this family couple to GPCRs. Low-molecular-weight monomeric members of the family are activated downstream of heterotrimeric G proteins.

G protein-coupled receptor (GPCR) Transmembrane receptor containing seven membrane-spanning helices that activates cells through coupling to heterotrimeric G proteins.

Further Reading

Cicchetti, G., Allen, P. G., and Glogauer, M. (2002). Chemotactic signaling pathways in neutrophils: From receptor to actin assembly. *Crit. Rev. Oral Biol. Med.* **13**, 220–228.

Ember, J. A., and Hugli, T. E. (1997). Complement factors and their receptors. *Immunopharmacology* **38**, 3–15.

Haribabu, B., Richardson, R. M., Verghese, M. W., Barr, A. J., Zhelev, D. V., and Snyderman, R. (2000). Function and regulation of chemoattractant receptors. *Immunol. Res.* **22**, 271–279.

Le, Y., Murphy, P. M., and Wang, J. M. (2002). Formyl-peptide receptors revisited. *Trends Immunol.* **23**, 541–548.

Prossnitz, E. R., and Ye, R. D. (1997). The N-formyl peptide receptor: A model for the study of chemoattractant receptor structure and function. *Pharmacol. Ther.* **74**, 73–102.

Sklar, L. A., Edwards, B. S., Graves, S. W., Nolan, J. P., and Prossnitz, E. R. (2002). Flow cytometric analysis of ligand-receptor interactions and molecular assemblies. *Ann. Rev. Biophys. Biomol. Struct.* **31**, 97–119.

Biography

Dr. Eric R. Prossnitz is Associate Professor of Cell Biology and Physiology at the University of New Mexico Health Sciences Center. His principal research interest is in the broad field of G protein-coupled receptor activation and regulation, utilizing the N-formyl peptide receptor of leukocytes as a model system. He holds a Ph.D. from the University of California at Berkeley and received his postdoctoral training at the Scripps Research Institute.

Dr. Larry A. Sklar is Regents' Professor of Pathology at the University of New Mexico Health Sciences Center. His principal interests are in signal transduction and cell adhesion molecular assemblies. He holds a Ph.D. from Stanford University and received postdoctoral training at the Baylor College of Medicine.

Chlorophylls and Carotenoids

Hugo Scheer
Universität München, Munich, Germany

The green (Greek "chloros") of leaves (Greek "phyllos") is a mixture of two water-insoluble pigment classes: chlorophylls, mainly the blue chlorophyll (Chl) *a*, and carotenoids, mainly *β*-carotene. Both pigment classes cooperate in photosynthesis to safely capture light provided by the Sun, as the primary energy source for life on Earth. Chlorophylls are responsible for light harvesting and its transduction to an electrochemical potential across the photosynthetic membrane which ultimately serves to reduce atmospheric carbon dioxide to carbohydrates. Thus, the energy of the fleeting photons is stored in increasingly longer-lived products: first Chl excited states are generated with lifetimes in the order of several nanoseconds (10^{-9} s), then a membrane potential which is stable for seconds, then high-energy products such as ATP and NADH that live for minutes or even hours, and eventually storage products like starch.

The carotenoids can act, too, as light-harvesting pigments, in regions where Chl has only little absorption. Their major and indispensable function is, however, to safely drain excess excitation energy from the chlorophylls and convert it into heat. Photons are by biological standards a high-energy source which is potentially highly toxic (sunburn). The combination of chlorophylls with carotenoids allows photosynthetic organisms a careful balance between tapping and competing for this source, and being killed by an overdose. Photosynthesis based on these two pigments has therefore conquered nearly all habitats on earth where light is available. It has produced the atmospheric oxygen we breathe, and fixes $\sim 10^{11}$ ton of carbon annually. The greening and degreening of the vegetation is probably the most obvious life-process on Earth, visible clearly from outer space. The widespread occurrence of photosynthesis is paralleled by considerable variations of the photosynthetic apparatus, including the pigments. It is this variety, but also the basic similarities among the different chlorophylls and carotenoids, respectively, which will be dealt with in this article.

Chlorophylls

Structures

The basic structure of chlorophylls is the porphyrin macrocycle. It is comprised of four pyrrole rings containing each four carbons and one nitrogen, which are joined via one-carbon bridges to an aromatic macrocycle (Figure 1). The four nitrogens face inward, creating a hole which is ideal for binding metal ions. In the chlorophylls, this central metal is almost always magnesium (Mg). While many of the peripheral substituents vary among the different structures, all chlorophylls contain an additional five-membered ring E and, with the exception of some Chl *c*, the C-17 propionic acid side chain is esterified by a long-chain alcohol, usually the C_{20} terpenoid alcohol, phytol. The chlorophylls can further be classified by the degree of unsaturation of the macrocylus, into the fully unsaturated true porphyrins, the chlorins with an unsaturated ring D and the bacteriochlorins in which ring B is unsaturated, too.

Spectroscopy

The spectral properties of chlorophylls are described by the four-orbital model: chlorophylls have four major absorptions termed Q_Y, Q_X, B_Y, and B_X, in the near ultraviolet (NUV), visible (Vis), and near infrared (NIR) spectral regions. The type of spectrum is mainly determined by the degree of unsaturation of the tetrapyrrole macrocycle (Figure 2): in the fully unsaturated Chl *c* containing a porphyrin macrocyclic system, the B-bands around 400 nm overlap, the Q_Y-band around 620 nm is weak, and Q_X-band is visible only with special techniques. In chlorin-type chlorophylls (Chl *a, b, d,* BChl *c, d, e*), the B-bands are reduced in intensity, the Q_X-band increased to near equal intensity and redshifted to $\sim$660 nm. In the bacteriochlorin-type chlorophylls (BChl *a, b, g*), the B-bands are blueshifted to $<$400 nm and well separated, the Q_y-band is even more increased in intensity and redshifted to $\sim$780 nm, and in these pigments the Q_y-band also has gained in intensity and becomes visible around 570 nm. By these characteristics, the chlorophyll type can be readily determined from the spectra, and often also other details like substitution pattern, ligation to the central metal (e.g., by the protein), or aggregation.

Chlorophylls dissolved in organic solvents have long-lived excited states (10^{-8} s). They are therefore highly fluorescent, and there is significant intersystem

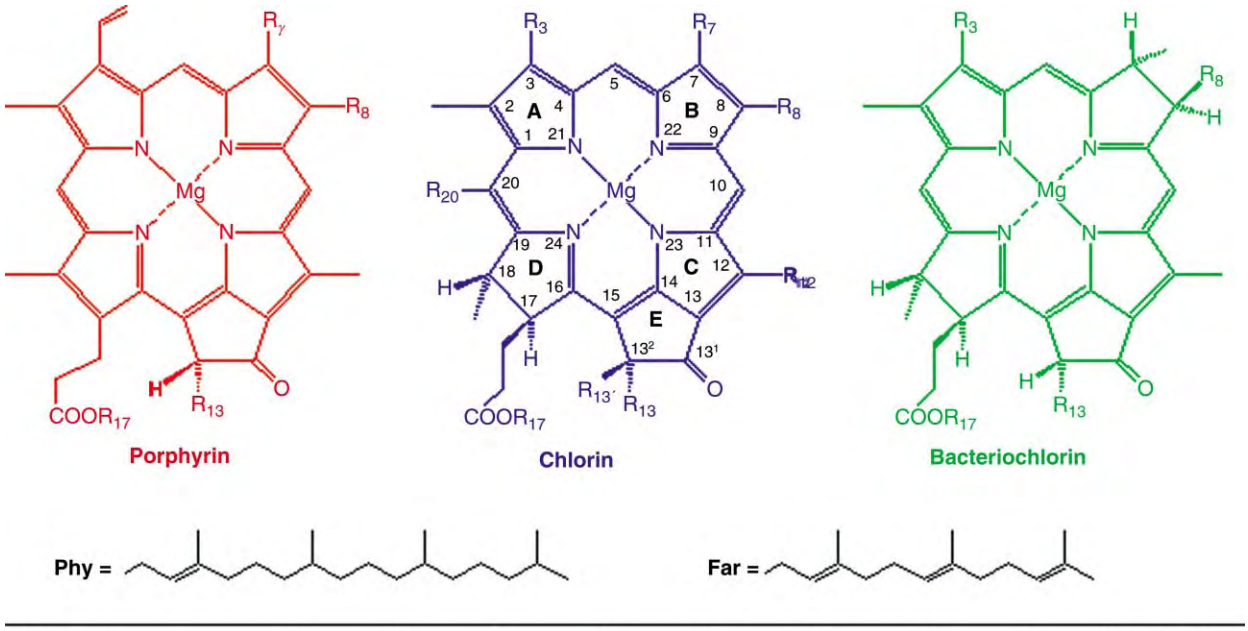

Pigment	R_3	R_7	R_8	R_{12}	$R_{13'}$	R_{13}	R_{17}	R_{20}	Macrocycle
Chl *a*	C_2H_3	CH_3	C_2H_5	CH_3	H	$COOCH_3$	Phy	H	Chlorin
Chl *b*	C_2H_3	CHO	C_2H_5	CH_3	H	$COOCH_3$	Phy	H	Chlorin
Chl *d*	CHO	CH_3	C_2H_5	CH_3	H	$COOCH_3$	Phy	H	Chlorin
Phe *a*	C_2H_3	CH_3	C_2H_5	CH_3	H	$COOCH_3$	Phy	H	Chlorin
BChl *c*	$CHOH\text{-}CH_3$	CH_3	C_2H_5	CH_3/C_2H_5	H	H	Far + others	CH_3	Chlorin
BChl *d*	$CHOH\text{-}CH_3$	CH_3	C_2H_5	CH_3/C_2H_5	H	H	Far + others	H	Chlorin
BChl *e*	$CHOH\text{-}CH_3$	CH_3	C_2H_5	CH_3/C_2H_5	H	H	Far + others	CH_3	Chlorin
BChl *a*	$CO\text{-}CH_3$	CH_3	C_2H_5	CH_3	H	$COOCH_3$	Phy + others	H	Bacteriochlorin
BChl *b*	$CO\text{-}CH_3$	CH_3	$=CH\text{-}CH_2$	CH_3	H	$COOCH_3$	Phy + others	H	Bacteriochlorin
BChl *g*	$CO\text{-}CH_3$	CHO	$=CH\text{-}CH_2$	CH_3	H	$COOCH_3$	Phy + others	H	Bacteriochlorin
Chl(ide) c_1	C_2H_3	CH_3	C_2H_5	CH_3	H	$COOCH_3$	H[a,b1]	H	Porphyrin
Chl(ide) c_2	C_2H_3	CH_3	C_2H_3	CH_3	H	$COOCH_3$	H[a,b1]	H	Porphyrin
Chl(ide) c_3	C_2H_3	$COOCH_3$	C_2H_5	CH_3	H	$COOCH_3$	H[a,b1]	H	Porphyrin
[8-Vinyl]-PChlide *a*	C_2H_3	CH_3	C_2H_3	CH_3	H	$COOCH_3$	H[a,b1]	H	Porphyrin

a) Sometimes esterified, b) Acrylic side chain at c-17^1-17^2 double bond)

FIGURE 1 Structures of common chlorophylls. In particular, reaction centers contain a series of specialized chlorophylls which are being dealt with in a recent survey by M. Kobayashi and co-workers in 1999.

crossing to the triplet state, giving rise to phosphorescence and, more significantly, under aerobic conditions to the generation of highly reactive oxygen species (ROS) like singlet oxygen. Chlorophyll solutions therefore bleach rapidly by attack of the pigment by these ROS, and chlorophylls injected into animals lead to severe "sunburn" and destruction of tissue. This effect is used in photodynamic therapy (PDT) of cancer.

In chlorophyll aggregates, there is generally a pronounced redshift of the Q_Y-band, and the excited state lifetimes (and thereby fluorescence and phosphorescence) are drastically reduced due to rapid conversion of the excitation energy into heat by internal conversion (IC). These effects are summarized under the term "concentration quenching" and probably due to the presence of "traps" in the large aggregates in which the excitation is highly delocalized over many pigment molecules.

Aggregation is also observed in photosynthetic pigment–protein complexes, where it is considered a major organizing force. In addition, there is a general redshift of all bands brought about by the protein environment. There is, however, a very distinct difference to aggregates: while excitation energy is mainly transformed to heat in the latter, this loss is avoided in the pigment protein complexes. Isolated light harvesting complexes (LHC), which contain the vast majority ($\geq 99\%$) of chlorophylls, therefore show, under moderate light intensities, high fluorescence. The avoidance of concentration quenching in these aggregates is in fact one of the major, mechanistically still unresolved tricks of efficient photosynthesis. In the reaction centers

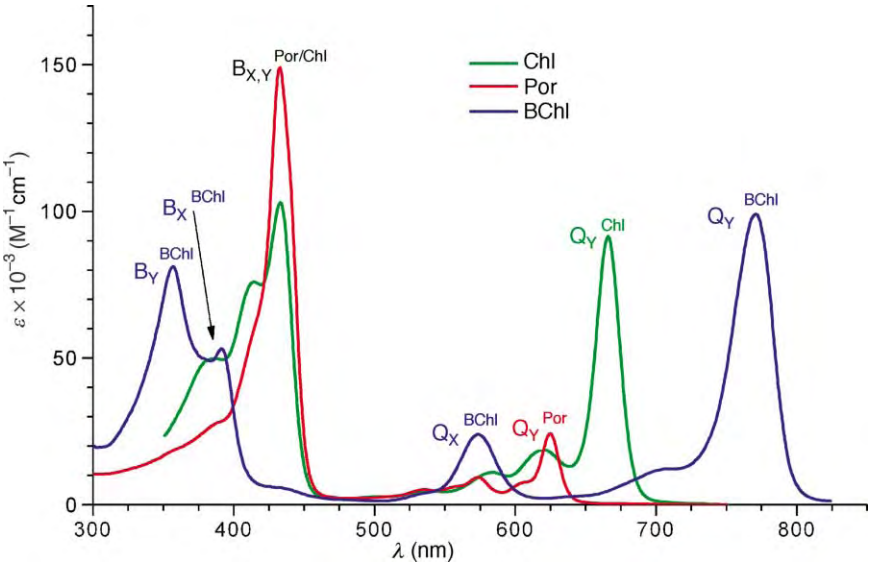

FIGURE 2 Type spectra of the three chlorophyll classes: porphyrins (Por), chlorins (Chl), and bacteriochlorins (BChl).

(RCs), the lifetime is short, but here the excitation energy is used to create, with quantum efficiencies near 100%, a charge separation across the photosynthetic membrane which is otherwise an insulator, thus creating a long-lived membrane potential. This energy transduction process is at the heart of photosynthesis, and the high-resolution crystal structures of RC together with extensive spectroscopy at high time-resolution have provided a general picture on how this process is working. In the photosynthetic apparatus, LHC containing >99% of the chlorophylls are coupled to RC, such that now the excitation energy of the former is efficiently transferred to the latter. By this means, the absorption is increased by orders of magnitude, and different numbers and types of LHC can be combined to adapt to the prevailing light conditions. Since the amount of protein is much less in LHC than in RC, the biosynthetic expenses for such a coupled system are at the same time strongly reduced.

Occurrence and Functions

The majority of chlorophylls, both in terms of structure diversity and quantity, serve as light-harvesting pigments. Taken together, they absorb light across most of the spectral range from 350 to 1020 nm, with a gap only in the region from 500 to 600 nm where carotenoids and biliproteins add to light harvesting. No organism contains all types of chlorophylls, however, so different organisms occupy different spectral niches, and the pigmentation is an important taxonomic criterion. Due to the more demanding energetics, oxygenic organisms (plants, algae, cyanobacteria) can only use light <730 nm, while the anoxygenic photosynthetic bacteria have specialized in the NIR with extremes like the purple bacterium, *Blastochloris viridis*; reaching 1020 nm. RCs contain chlorophylls, too, including besides the bulk pigments some specialized derivatives. They form a chain of pigments across the membrane, over which in a stepwise fashion electrons are transferred from the primary donor, a pair of chlorophylls located on the periplasmic side of the membrane, to the acceptors on the cytoplasmic side. It should be mentioned that some chlorophyll-like pigments perform other functions in nature: certain deep-sea fish use chlorophylls as visual pigments, and in the marine worm, *Bonella viridis*, a chlorophyll-derivative acts as a sex determinant.

Chemical Properties

Chlorophylls are large, aromatic molecules with a central hole fit to complex many metals. They are basically planar, but not rigid, and deviations from planarity are observed in most structures of chlorophyll proteins. While the macrocyclic system is quite stable, the functional groups and the central Mg render the chlorophylls quite labile. Under acidic conditions, the central Mg is lost rapidly, and the long-chain alcohol residue hydrolyzed. The central Mg is also readily replaced by other, more stable metals like Zn, Ni, Ag, Cu. Under alkaline conditions, the isocyclic ring is modified extensively. The macrocycle can be opened at the methine bridges, both (photo)chemically and enzymatically.

After binding to the tetrapyrrole, the central Mg still has free valences, which are important for aggregation, and in particular for interactions with the natural protein environment. By interactions with suitable amino acids (e.g., histidin, methionin, glutamate) they can be positioned properly for efficient energy or electron transfer. In the LHC of green bacteria, the chlorosomes, the coordinating properties of the central Mg and the ligation of special peripheral substituents

combine to form large aggregates of bacteriochlorophylls *c*, *d*, and *e* nearly devoid of protein.

Metabolism

The formation of chlorophylls can be separated in stages. The first is the synthesis of 5-aminolevulinic acid (ALA), the basic building block of all tetrapyrroles. In most organisms it is formed from glutamic acid, involving an intermediate (Glu-tRNA^{glu}) which is otherwise only involved in protein synthesis. Some photosynthetic bacteria (purple bacteria) use, like man, the alternative C_{4+1}-pathway in which succinyl coenzyme A is condensed with glycin. The second stage is ubiquitous in all organisms and for all natural tetrapyrroles. The two ALA first react to yield a pyrrol (porphobilinogen), a five membered ring containing one nitrogen atom. Four such pyrroles then condense to a linear tetrapyrrole, and then cyclize in a remarkable reaction in which one of the pyrroles is flipped. The resulting cyclic tetrapyrrole is transformed by a series of decarboxylation and oxidation reactions to protoporphyrin. It is noteworthy that the latter is the first colored product in the synthesis, and highly phototoxic like most porphyrins. The organisms therefore avoid, over large stretches of biosynthesis, the formation of such potentially harmful precursors. They also regulate precisely the amount of ALA in order to avoid any overproduction of protoporphyrin, and any deregulation of this process, as any alteration of the biosynthesis can result in severe damage and often death. The last stage of the pathway is the insertion of Mg, which is thermodynamically unfavorable and energy requiring, and the formation of the isocyclic ring from the propionic acid side chain at C-13. While the synthesis of Chl *c* is practically complete at this stage, all other chlorophylls require further modifications, viz., the reduction of ring D (chlorins) and B (bacteriochlorins), modifications at the periphery, and the condensation of the C-17 propionic acid with the long-chain alcohol derived from the isoprenoid pathway.

Chlorophyll degradation has been studied in some detail for Chl *a* and *b*, it involves the (light independent) ring-opening to the much less phototoxic open-chain tetrapyrroles (bilins). Very little is known on the degradation of the other pigments.

Applications

Unmodified chlorophylls are too labile for most practical use, but some derivatives are used as dyes for cosmetics and food (Cu-chlorophyllin), and in photodynamic tumor therapy (chlorins, bacteriochlorins). The "chlorophyll" used, e.g., in certain health care is a complex mixture of degradation products. The best source for Chl *a* is the cyanobacterium *Spirulina platensis*, which is available commercially. Chl *a*/*b* mixtures can be obtained from all green plants. All other chlorophylls are less readily accessible, thereby limiting their applications.

Carotenoids

Structures

Carotenoids much more widespread and not confined to photosynthetic organisms, and structurally and functionally more diverse than chlorophylls. There are currently more than 800 natural carotenoids known, each of which can form several *cis–trans* isomers and be further modified. Chemically, most carotenoids are tetraterpenes: two C_{20}-units (originally geranyl-geraniol) are joined tail-to-tail to a chain of 32 carbon atoms bearing eight methyl side chains. Often, this basic carbon C_{40}-skeleton is either retained, or only slightly modified, e.g., by cyclization at one or both ends (Figure 3). However, much more extensive modifications are possible, including isomerization and rearrangement of the double bonds, the introduction of oxygen-containing functional groups, and their glycosylation or acylation. This modification seems to be particularly far-reaching in carotenoids dedicated to light harvesting, as exemplified by peridinin; a highly modified C_{37} pigment from algae.

Spectroscopy

The rod-shaped carotenoids show the typical absorption spectra of linear polyenes, which are characterized by some unusual features. (1) The lowest energy $S_0 > S_1$ transition located in the red to NIR spectral range, is extremely weak (optically forbidden) in most carotenoids, and has been accurately determined only in few pigments by special techniques. (2) The most intense absorption, responsible for the yellow-orange color of most carotenoids, is a series of closely spaced, sometimes overlapping bands in the 400–550 nm range. With an increasing number of conjugated double bonds, this absorption is shifted, in an asymptotic fashion, to the red. The sub-bands are generally well resolved, but can be broadened to a degree that they appear only as a single, somewhat structured band. (2) There is at least one other transition between these two bands, which again is forbidden and therefore very weak. (4) *cis*-Carotenoids show an additional, typical band 100–150 nm to the blue of the main absorption (see Figure 4 for type spectra). Although the "forbidden" bands do not contribute to absorption, they are fundamentally important for the biological functions of carotenoids. The states responsible for them can be reached indirectly, e.g., after absorption into the energy-rich major absorption band and IC, or by energy transfer from neighboring pigments like chlorophylls,

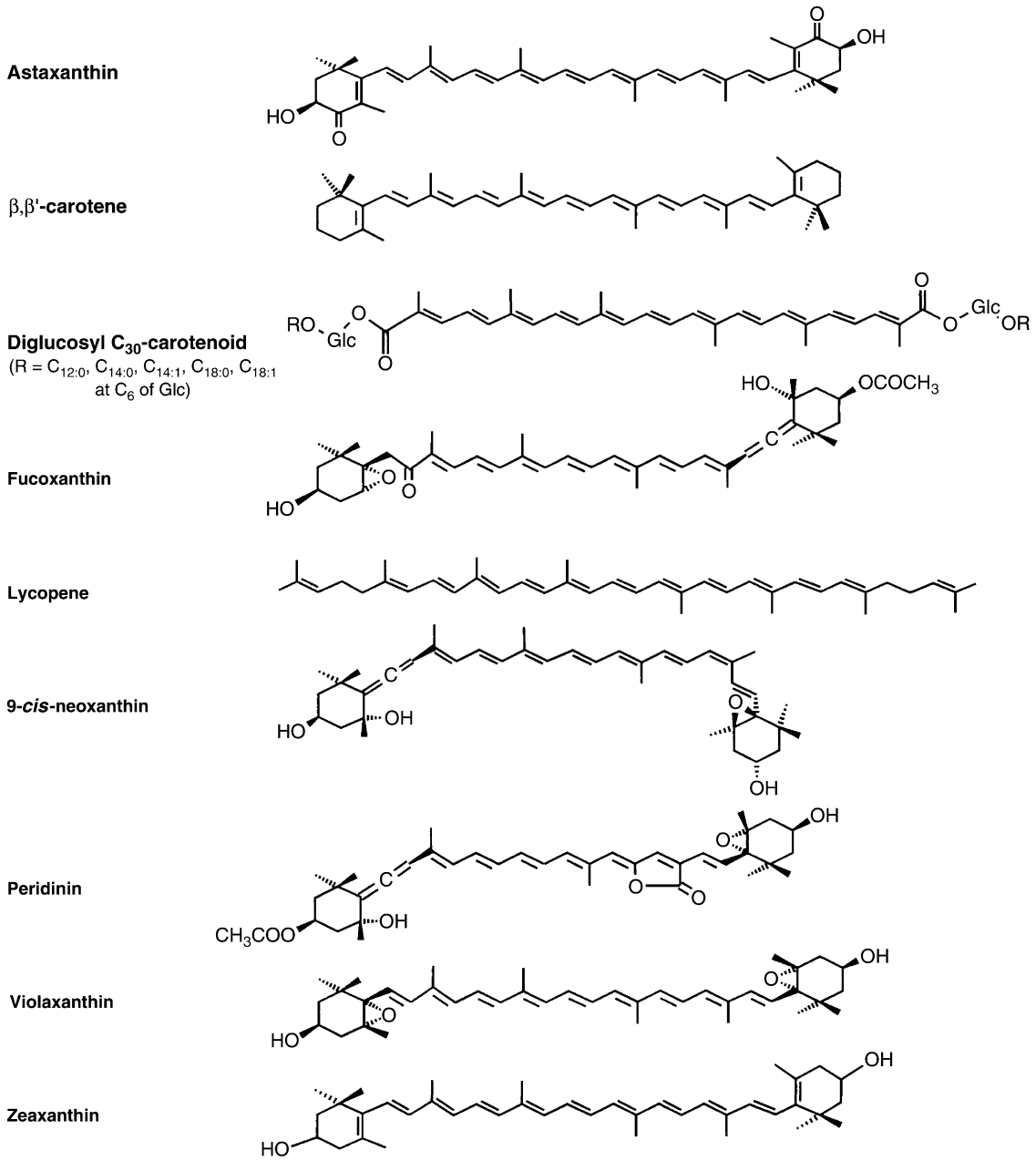

FIGURE 3 Example of carotenoid structures.

and they thereby contribute to energy transfer and dissipation.

Most carotenoids show extremely rapid IC from all excited states, and therefore negligible fluorescence, with lifetimes in the range of only a few picoseconds. Carotenoids have unusually low-lying triplet states, many of them even below the energy of singlet oxygen (1250 nm). Again, they can be reached only indirectly, mainly via energy transfer from triplets (e.g., of chlorophylls) or from singlet oxygen. Since the latter are highly cytotoxic, this property is functionally very important, too, because it is the basis for the protective effects of carotenoids.

The spectral properties of carotenoids can be modified considerably by interactions with the protein. A spectacular case is the color change of astaxanthin from orange to green when it is bound in the crustacean protein, α-crustaxanthin, and its reversion when the protein is denatured by boiling.

Occurrence and Functions

Carotenoids are almost ubiquitous in living organisms, even though animals including man can not synthesize them but have to rely on dietary supplies.

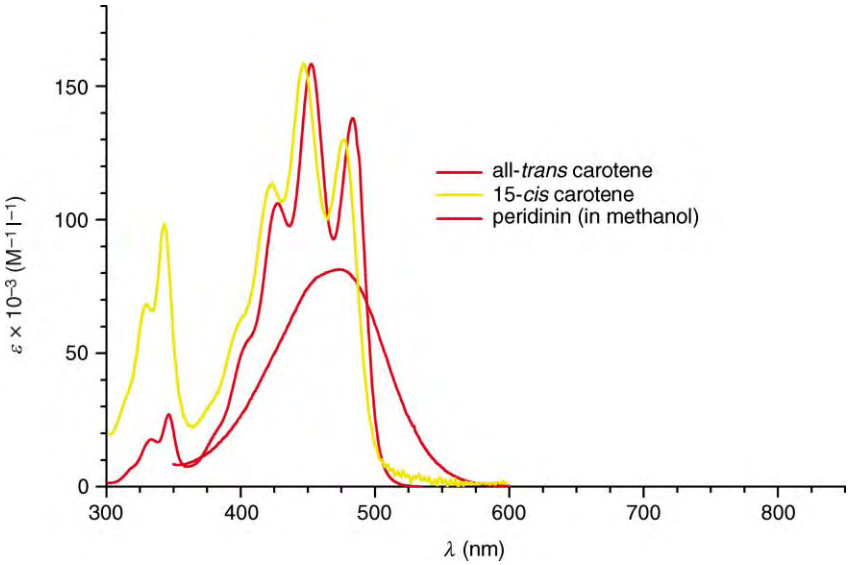

FIGURE 4 Type spectra of carotenoids.

Their functions are as diverse as their structures. In photosynthesis, their essential function is the protection of the photosynthetic apparatus under conditions of light overload. Whenever the RC cannot follow the energy input from the LHC, the long-lived excited states of the chlorophylls pose a deadly danger to these organisms due the formation of ROS. This is prevented by carotenoids at several levels. They can accept excess energy via their low-lying "forbidden" states, they can quench chlorophyll triplets by triplet energy transfer to the low-lying carotenoid triplets, and they can quench ROS by energy transfer, e.g., from singlet oxygen, or addition of ROS to the double bond system. All these processes require very close distances between donor and acceptor, which is nicely corroborated by X-ray structures of photosynthetic complexes. Specialized carotenoids are found in contact to chlorophylls in the RC and in all chlorophyll-containing LHC. In the latter, they seem to be positioned strategically at critical sites where the energy is funneled to the RC.

Since ROS are also important in the attack of infectious agents by the immune system, bacteria synthesize carotenoids for their protection, and many of the more virulent forms are deeply colored by carotenoids.

Carotenoids also protect from light, simply by their function as light filters, removing NUV and blue light by virtue of their high absorption in these spectral regions, and their capacity to rapidly degrade the excitation energy to heat by IC. Certain algae tolerant to extreme light stress contain droplets of pure carotenoids. And many non-photosynthetic organisms synthesize carotenoids when subjected to increasing light intensities. As nonphototoxic pigments, carotenoids often function as "safe" dyes in nature. Examples are the colors of flowers used for attracting insects, or of crustaceans to blend into the marine background.

In spite of their general protective function, carotenoids have also been adapted by photosynthetic organisms for light harvesting in the "green gap" (470–600 nm) where chlorophylls absorb only poorly, in particular in microalgae and phototrophic bacteria which cannot outgrow their competitors. Two factors are important to this function. One is the development of carotenoids in which the excited state lifetime is somewhat increased, and therefore IC reduced. The two most abundant carotenoids, fucoxanthin and peridinin, show this very nicely with lifetimes reaching more than 100 ps. The second factor is to position the carotenoids in contact with chlorophylls, thereby speeding up energy transfer sufficiently to be effective within the short excited state lifetimes (electron exchange mechanism). Since the direction of energy transfer depends on the relative energies of the excited states, they have to be properly ordered: for light harvesting, the carotenoid excited state needs to be above that of the neighboring chlorophyll; for protection it needs to be below. There is evidence that plants and some algae use, in the so-called violaxanthin cycle, subtle structural modifications in order to manipulate the excited state energies of carotenoids, thereby converting a light harvesting into a protecting pigment, and vice versa, in response to the light supply.

Last but not least are carotenoids precursors for certain important metabolites. Only two examples are stated. (1) Retinal, the chromophore of the visual pigment rhodopsin, is derived from carotene. Since the latter cannot be synthesized by animals, they need it supplied as provitamin A. Retinal derivatives are also required for other regulatory functions.

(2) Certain fragrances of roses have also been shown not to be synthesized directly, but rather to be breakdown products of the flowers' carotenoids.

Chemical Properties

Due to their hydrocarbon skeleton, almost all are insoluble in water and well soluble in nonpolar solvents. The conjugated double-bond system is chemically moderately stable. It is subject to rearrangements, in particular in the light, and to additions, for example, of oxygen. The chemical properties of the more highly modified carotenoids are determined by their particular functional groups.

Metabolism

Carotenoids, like all terpenoids, are products of the isopentenyl-pyrophosphate metabolism. This intermediate can be synthesized either by the mevalonate pathway from acetyl-coenzyme A, or via the more recently discovered deoxyxylulose pathway. While still under study, the latter seems to be the pathway leading to carotenoids in most photosynthetic organisms. One of the resulting C_5-units (dimethylallyl-pyrophosphate) is condensed sequentially by prenyl transferases in a head-to-tail fashion with three isomeric C_5-units (isopentenyl-pyrophosphate) to yield geranylgeranyl-pyrophosphate (GGPP), an important branching point in terpenoid metabolism. GGPP is, for example, directly or indirectly, the substrate for esterifying the C-17 propionic acid side chain of most chlorophylls, thereby linking the tetrapyrrole- and terpenoid pathways. The biosynthesis directed to carotenoids begins with a tail-to-tail condensation of two molecules of GGPP by the dedicated enzyme phytoene synthase. Having only three conjugated double bonds, the resulting phytoene is still uncolored. Dehydrogenation by desaturases via phytofluene to lycopene is common to most carotenoids currently known. C_{30} carotenoids are derived from condensation of two C_{15}-units (farnesol-pyrphosphate) in an otherwise very similar reaction sequence. A wide variety of enzymes, many of them still poorly characterized, is responsible for further structural modifications. They include cyclases to form the end rings characteristic of many carotenoids, oxygenases to introduce OH groups, isomerases and (de)hydrogenases to modify the double-bond system, and many more follow-up enzymes allowing for the structural variety of carotenoids.

Applications

The most frequent applications of carotenoids, which are of considerable economic importance, are as food colorants, as dietary supplies, and as sun screens in cosmetics. Food is frequently colored indirectly, e.g., by supplying carotenoids or carotenoid-rich algae in the feedings of fish (salmon) or poultry (chicken eggs). Provitamin A (β-carotene) is supplied directly but also indirectly, e.g., as milk supplement. Industry scale synthetic methods have been developed, natural sources are algae such as *Hematococcus*, plants such as carrots, and genetically manipulated bacteria.

See Also the Following Articles

Chloroplast-Redox Poise and Signaling • Chloroplasts • The Cytochrome b_6f Complex • Light-Harvesting Complex (LHC) I and II: Pigments and Proteins • Photosynthesis • Photosynthetic Carbon Dioxide Fixation

Glossary

absorption The process of interaction of a molecule with a photon to produce an excited state.

excited states More precisely, electronically excited states; there are usually generated by light absorption in molecules containing a large number of conjugated double bonds. Singlet and triplet states are distinguished by their lifetimes. If the ground state is a singlet, as in practically all dyes, excited singlet states are short lived (10^{-12}–10^{-8} s), and the lowest triplet states are long-lived (up to milliseconds). If the ground state is a triplet, one of the rare cases being molecular oxygen, the lowest excited singlet state is long lived.

fluorescence It is the spontaneous decay of an excited state to the ground state with the concomitant emission of the energy in the form of a photon. Together with phosphorescence, which is distinguished from fluorescence mainly by its longer timescale ($>10^{-6}$ versus $<10^{-8}$ s), they are often summarized as luminescence.

internal conversion The spontaneous decay of an excited state to the ground state with the concomitant release of the energy in small packages as heat. It is a so-called loss channel, because the heat is (generally) of no use in biology, but is, by the same token, important in light protection, e.g., by preventing photosensitized generation of reactive oxygen species.

isoprenoids These are compounds derived from the branched C_5-unit, isoprene. Besides carotenoids, important natural isoprenoids are the steroids, gibberellins (plant hormones), mono-, sesqui-, and diterpenes (fragrances and flavors), and polymers like rubber.

photodynamic therapy (PDT) This is the diagnostic and therapeutic application, for example in treatment of cancer, which relies on photosensitizing dyes, light, and oxygen to selectively attack cells, virus, tissue, or organs.

photosensitization The process of indirectly generating reactive oxygen species by triplet energy transfer. A sensitizing dye is excited by light to the singlet state. This reacts spontaneously to a long-lived triplet state, capable of generating reactive oxygen species by several mechanisms.

photosynthesis The natural process of plants, algae and certain bacteria by which (sun)light is converted to biochemical energy (carbohydrates), which is eventually the primary source for life on Earth.

reactive oxygen species (ROS) These species comprise several highly aggressive and cytotoxic chemicals derived from oxygen and often produced by action of light, including singlet oxygen, superoxide, peroxide, and hydroxyl radicals.

tertrapyrroles These are compounds comprised of four pyrrole rings. In natural tetrapyrroles, they are linked either directly or by single carbon bridges, and they can by linked in a linear (bile pigments) or a cyclic fashion (hemes, chlorophylls, vitamin B_{12}).

Further Reading

Britton, G., Liaaen-Jensen, S., and Pfander, H. (eds.) (1995). *Carotenoids*. Birkhäuser, Basel.

Deisenhofer, J., and Norris, J. R. (eds.) (1993). *The Photosynthetic Reaction Center.* Academic Press, New York.

Frank, H. A., Young, A. J., Britton, G., and Cogdell, R. J. (eds.) (1999). *The Photochemistry of Carotenoids*. Kluwer, Dordrecht.

Green, B., and Parson, W. W. (eds.) (2003). *Light-Harvesting Antennas in Photosynthesis*. Kluwer, Dordrecht.

Hörtensteiner, S., Wüthrich, K. L., Matile, P., Ongania, K., and Kräutler, B. (1998). The key step in chlorophyll breakdown in higher plants. *J. Biol. Chem.* **273**, 15335–15339.

http://photoscience.la.asu.edu/photosyn/photoweb/default.html (photosynthesis at all levels).

http://www.carotenoidsociety.org/ (carotenoids).

http://www.photosynthesisresearch.org (photosynthesis).

http://terra.nasa.gov/Gallery/ (images of the Earth).

Kobayashi, M., Akiyama, M., Watanabe, T., and Kano, H. (1999). Exotic chlorophylls as key components of photosynthesis. *Curr. Top. Plant Biol.* **1**, 17–35.

Eisenreich, W., Rohdich, F., and Bacher, A., (2001). Deoxyxylulose phosphate pathway to terpenoids. *Trends Plant Sci.* **6**, 78–84.

Moser, J. G. (ed.) (1998). *Photodynamic Tumor Therapy: 2nd and 3rd Generation Photosensitizers*. OPA, Amsterdam.

Scheer, H. (ed.) (1991). *Chlorophylls*. CRC Press, Boca Raton, USA.

Vernon, L. P., and Seely, G. R. (eds.) (1966). *The Chlorophylls*. Academic Press, New York.

Biography

Hugo Scheer studied chemistry in Braunschweig, Germany. After graduation he spent 3 years with J. J. Katz and J. R. Norris at Argonne National Laboratory, USA, and then went in 1975 to the Universität München, Germany, where he became Professor of Plant Biochemistry. His research interest is in chlorophylls and plant biliproteins, with a focus on their functions, on pigment–protein interactions, and on their use as probes in protein dynamics and in photodynamic therapy of cancer.

Chloroplast Redox Poise and Signaling

John F. Allen
Lund University, Lund, Sweden

Chloroplasts are membrane-bound compartments (organelles) in plant and algal cells. Chloroplasts perform all of the component reactions of photosynthesis, including absorption of light energy by chlorophyll; conversion of that energy into chemical potential; electron transfer; synthesis of ATP; and assimilation of carbon dioxide to give carbohydrates. Primary steps in photosynthesis are light-driven redox (reduction–oxidation) reactions; transfer of electrons or hydrogen atoms. These redox reactions function safely and efficiently only within a narrow range of degrees of reduction of their reactants and products. In electron transport pathways, each intermediate must be capable of acting as both an acceptor and a donor, and must therefore be present in both its oxidized and its reduced form. An optimal state of redox poise is achieved by a variety of regulatory mechanisms, operating on different stages of gene expression. Redox signaling occurs when a signal of redox imbalance initiates a change that corrects that imbalance, restoring poise. The response may be within or between cells, and may concern chloroplast or nuclear gene expression. Chloroplast redox signaling utilizes the chloroplast genome and apparatus of gene expression. Redox signaling may require, and be the reason for, both chloroplast and mitochondrial genomes.

The Redox Chemistry of Photosynthesis

Redox Reactions and Photosynthesis

A redox reaction involves an electron or hydrogen atom donor, and an electron or hydrogen atom acceptor. During the course of the redox reaction, as the electron or hydrogen atom is transferred, the donor reduces the acceptor, and the acceptor oxidizes the donor. Thus, an electron (or hydrogen) donor is a chemical reductant, and an electron (or hydrogen) acceptor is a chemical oxidant. The direction of electron (or hydrogen) transfer between two chemical species is determined by their relative activities and also by their relative electrochemical potentials, or redox potentials, as given by the Nernst equation. A species with a lower redox potential will tend to act as a reductant, or donor, when coupled in a redox reaction with a species with a higher redox potential, acting as the oxidant, or acceptor.

In photosynthesis, light-driven electron transport may be cyclic, or linear (also known as "noncyclic"). Linear electron transport requires an electron donor and an electron acceptor. In many bacteria the donor is an organic compound, or an inorganic reductant such as H_2S or H_2. In cyanobacteria and chloroplasts, the donor is water, and oxygen is released as a by-product. The electron acceptor is $NADP^+$. Together with ATP produced by photosynthetic phosphorylation, NADPH represents stored energy, which may be used to drive carbon dioxide assimilation and processes including synthesis (e.g., protein synthesis) and transport.

van Niel and Bacteria

Photosynthesis occurs in bacteria, and in most plants and algae. Even in eukaryotes, photosynthesis is localized in chloroplasts, which are bacterial in origin. The microbiologist Cornelius van Niel, working in Stanford, California, showed that photosynthetic bacteria use light as a source of energy to cause hydrogen atom transfer to carbon dioxide, from any one of a range of weak reducing agents, collectively designated "H_2A" in a reaction described by the van Niel equation:

$$2H_2A + CO_2 \xrightarrow{\text{light}} CH_2O + 2A + H_2O$$

In the special case of oxygenic photosynthesis in plant and algal chloroplasts and in cyanobacteria, the weak reducing agent (H_2A) is water (H_2O), and the van Niel equation then becomes:

$$2H_2O + CO_2 \xrightarrow{\text{light}} CH_2O + O_2 + H_2O$$

The Hill Reaction

Independently, Robert (Robin) Hill, in Cambridge, showed that chloroplasts isolated from leaves

produce oxygen in the light, provided a suitable electron acceptor, or "Hill oxidant" is available ("A," below):

$$2H_2O + 2A \xrightarrow{\text{light, chloroplasts}} 2AH_2 + O_2$$

Assimilation of CO_2 by reoxidation of AH_2 will give "complete" photosynthesis, and its overall formulation is identical to a simplified version of the oxygenic version of the van Niel equation:

$$H_2O + CO_2 \xrightarrow{\text{light, chloroplasts}} CH_2O + O_2$$

Reaction Centers

How does light drive electron or hydrogen atom transfer? Louis Duysens, in Leiden, and others demonstrated light-induced oxidation of chlorophyll (Chl) at photosynthetic reaction centers, and it became clear that some chlorophyll molecules themselves undergo photo-oxidation after absorbing a quantum of light and reaching an excited state (Chl^*). Photosynthetic electron transport is initiated when the chlorophyll excited state decays to a ground state by passing an electron on to an acceptor (A), and by taking one from a donor (D):

$$DChlA \xrightarrow{\text{light}} DChl^*A \rightarrow DChl^+A^- \rightarrow D^+ChlA^-$$

The Z-Scheme and Two Photosystems

In 1960, Robert Hill and Fay Bendall proposed a "Z-scheme" for photosynthetic electron transport, in which two separate photosystems, termed I and II, each with a core reaction center, act as intermediates in the chloroplast electron transport chain. The two photosystems are connected, in series, by electron carriers (Figure 1).

Chloroplast Function

Intrinsic to internal membranes called thylakoids, chloroplasts contain chlorophyll and other pigments (such as carotenoids) that harvest and convert light energy, an electron transport chain that intersects with light-harvesting pigments at photosynthetic reaction centers, and an ATPase that couples electron transport with synthesis of ATP. The soluble phase of the chloroplast usually contains the enzymes and intermediates of the Benson–Calvin cycle of assimilation of carbon dioxide. In development, chloroplasts originate from plastids in parallel with nonphotosynthetic plastids with other specific functions in metabolism. Although most plastid proteins are imported from the cytosol, as precursors, all plastids also contain DNA, RNA, ribosomes, and a genetic system, which is responsible for synthesis of some of their components.

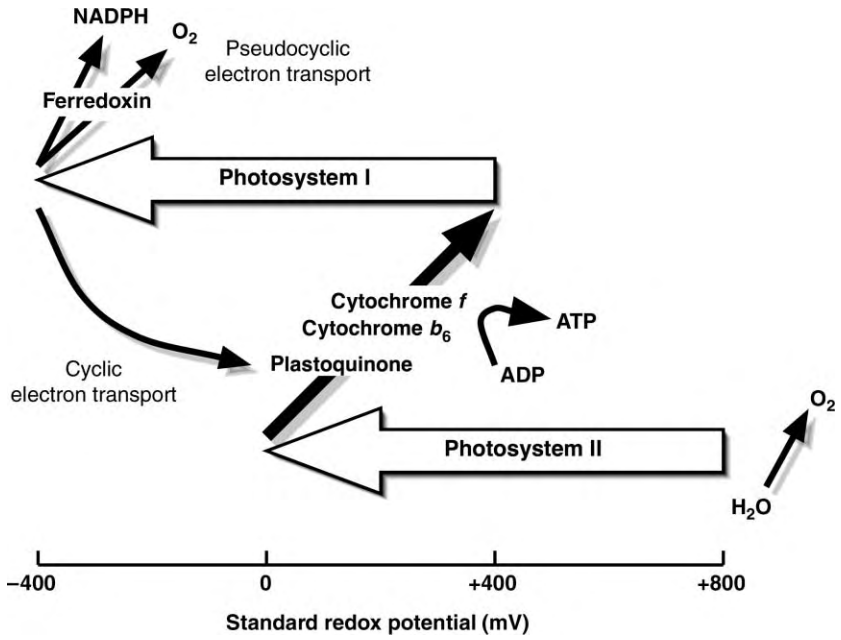

FIGURE 1 The two-light reaction model, or "Z-scheme," for photosynthetic, noncyclic electron transport and photophosphorylation (ATP synthesis) in chloroplasts. Noncyclic electron transport involves photosystems I and II, which are connected in series. The cyclic and pseudocyclic pathways are superimposed on the noncyclic pathway.

Chloroplasts, in particular, still bear a striking resemblance to prokaryotic cyanobacteria, from which all plastids evolved.

Photophosphorylation

In 1954, F. R. (Bob) Whatley, Mary Belle Allen, and Daniel I. Arnon, in Berkeley, California showed that isolated chloroplasts carry out ATP synthesis in the light, a process also demonstrated for isolated bacterial membranes by Albert Frenkel:

$$ADP + P_i \xrightarrow{\text{light, chloroplasts}} ATP + H_2O$$

Cyclic

The original chloroplast photophosphorylation of Whatley, Allen, and Arnon was not accompanied by net redox changes, and is coupled to cyclic electron transport. In the Z-scheme, this cyclic electron transport drives cyclic photophosphorylation, and requires photosystem I alone (Figure 1), although photosystem II activity and other factors greatly affect its onset.

Noncyclic

The Arnon group later showed that ATP synthesis is also coupled to the Hill reaction, and the yield of ATP occurs in a fixed stoichiometry with reduction of a Hill oxidant. There is thus a distinction between cyclic and noncyclic photophosphorylation. After 1960 it was realized that noncyclic photophosphorylation normally requires both photosystems I and II (Figure 1).

Pseudocyclic

In 1952, Alan Mehler discovered that molecular oxygen will act as a Hill oxidant. Noncyclic electron transport (Figure 1) with oxygen as the terminal acceptor is coupled to ATP synthesis, and requires photosystems I and II. However, oxygen is both consumed and produced in this reaction, no net oxidation–reduction is observed, and so the ATP synthesis resembles cyclic one, and is known as pseudocyclic phosphorylation.

Kinetics and Maintenance of Redox Poise

The interplay between noncyclic, pseudocyclic and true cyclic photosphosphorylation first gave rise to the concept of "redox poise" in chloroplast photosynthesis. If the photosystem I of the Z-scheme (Figure 1) is the same for all three forms of phosphorylation, then there is competition between paths of electron transport.

An optimal state for cyclic electron tranport is one of maximal "redox poise," when the total pool of each component gives a redox state that is 50% oxidized and 50% reduced. The rapid, primary photochemical reactions at photosynthetic reaction centers use light energy to move electrons in the direction opposite to that predicted by their redox potentials: the donor has a much higher redox potential than the acceptor, and light is therefore used to generate a redox couple that is far from redox equilibrium. Secondary electron transport nevertheless moves the electrons in the predicted direction, towards equilibrium. "Redox poise" can then still be applied to linear or noncyclic electron transport, and especially to any of its components. When applied to noncyclic electron transport, "redox poise" indicates a position of optimal redox state where the activities of components are such that their effective redox potentials favor physiologically useful electron transfer. Two extreme departures from redox poise exist in the form of states of over-reduction and over-oxidation (Figure 1). A cyclic chain is said to be over-reduced when all components are in their reduced forms; there are no electron acceptors. The same chain is said to be overoxidized when all components are in their oxidized forms; there are no electrons to cycle. When applied to noncyclic electron transport, "over-reduced" and "overoxidized" can be applied to indicate the preponderence of one or other redox state, giving the tendency of a component to engage in redox chemistry with donors or acceptors that are presumed to be nonphysiological, especially where reactive and toxic chemical species are produced in consequence. Oxygen, for example, readily accepts electrons from most components of the photosynthetic chain, a product is the superoxide anion radical, and redox poise may ensure that the "correct" electron transfer competes kinetically with reduction of oxygen.

Cyclic Electron Transport and Photophosphorylation

As first identified by Whatley and Bruce Grant, the onset of cyclic photophosphorylation is delayed, sometimes indefinitely, under anaerobic conditions. The delay can be avoided by addition of an inhibitor of electron transport in photosystem II, or by choice of a wavelength of illumination that is selective for photosystem I. It was concluded that the cyclic chain can become over-reduced when photosystem II is active, and no electron acceptor is available. Over-reduction could also be reversed, and redox poise restored, if a pulse of an oxidant, such as potassium ferricyanide or oxygen, is added to remove excess electrons from the cyclic chain.

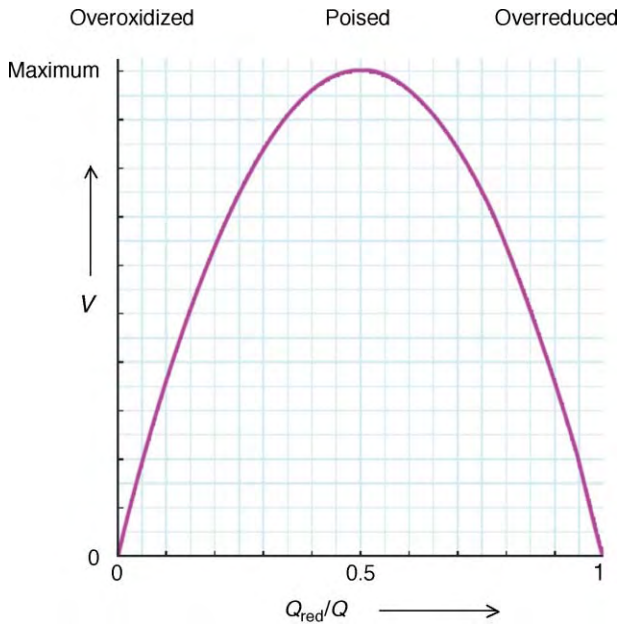

FIGURE 2 The ideal rate, v, of cyclic electron transport as a function of the redox ratio of one of its components, Q. Q must be present in both its oxidized and reduced forms: in cyclic electron flow, Q must be both a donor and acceptor of electrons.

In contrast, under aerobic conditions, Grant and Whatley found that the photosystem II inhibitor, just like a choice of wavelength specific to photosystem I, actually inhibits photosystem I-cyclic photophosphorylation. This is explained by the ability of oxygen to accept electrons from photosystem I, so that, in the absence of photosystem II activity, the cyclic chain becomes drained of electrons, or overoxidized (see Figure 2).

Photosystem 1 Cyclic Electron Flow

The contribution of cyclic photophosphorylation to photosynthesis (Figure 1) depends on maintaining redox poise, and avoiding over-reduction and overoxidation (Figure 2). There is evidence that oxygen acts as a poising oxidant under physiological conditions. Ulrich Heber and colleagues in Wurzburg showed that intact, functional chloroplasts are held in an indefinite lag phase under anaerobic conditions. However, if a pulse of oxygen is given at any time, sufficient ATP is produced to start the Benson–Calvin pathway, and regeneration of the electron acceptor $NADP^+$ then allows whole-chain electron transport to generate oxygen, maintaining a poised cyclic chain, ATP synthesis, and complete photosynthesis. *In vivo*, down-regulation of photosystem II may also counteract over-reduction, and chloroplast NAD(P)H dehydrogenase activity may counteract overoxidation.

The Q-Cycle

In the electron transport chain between photosystems I and II, the cytochrome b_6f complex catalyzes a cycle of electrons through two cytochromes b, involving intermediate states of the two-electron carrier plastoquinone. Redox poise is likely to be essential in the Q-cycle, where the plastosemiquinone participates in one-electron transfer with cytochrome b, despite its tendency to transfer its single electron to oxygen, generating superoxide.

Noncyclic Electron Transport

In intact chloroplasts, continued operation of noncyclic electron transport seems to depend on production of some additional ATP by cyclic electron transport. The ATP is required to drive the Benson–Calvin cycle, and therefore for regeneration of the physiological electron acceptor, $NADP^+$. Insufficient ATP therefore "stalls" photosynthesis by causing over-reduction of the cyclic chain.

Oxygen and Poise

Oxygen is an effective electron acceptor for noncyclic electron transport, and also acts as a poising oxidant for cyclic electron transport. However, the products of oxygen reduction are superoxide and hydrogen peroxide. Reduction of oxygen by the iron–sulfur protein and electron transport intermediate, ferredoxin, may proceed by a physiologically safe route of two one-electron transfers, and also lead to creation of "antioxidant" defenses against the toxicity of reactive oxygen species.

Posttranslational Modification of Pre-Existing Proteins

Regulatory devices that maintain redox poise also extend to gene expression at different levels. Feedback control loops involving components of electron transfer chains and stages in gene expression are seen in all bioenergetic systems. Close association between bioenergetic coupling membranes and genes for their protein components is conspicuous in chloroplasts and mitochondria. The need for direct redox signaling has been proposed as the primary reason for the persistence, in evolution, of chloroplast and mitochondrial genomes.

State Transitions

Control of gene expression by posttranslational modification underpins a well-known process, namely, state transitions. Photosystems I and II have different

light-harvesting pigment systems, and different absorption and action spectra. Thus, any randomly chosen wavelength of light is likely to favor either photosystem I or photosytem II. Yet their connection in series requires a fixed ratio of rates of electron transport through their reaction centers, 1:1 for noncyclic electron transport alone, but incrementally more (estimated at 20%) to photosystem I to account for additional, cyclic electron transport. Cecilia Bonaventura and Jack Myers in Austin, Texas, and Norio Murata in Tokyo independently showed that different unicellular algae redistribute absorbed excitation energy between photosystems I and II, as if to achieve balanced delivery of energy to the two reaction centers. Light delivered to one reaction center whose rate is limited by another will be wasted as heat or fluorescence. Redistribution therefore achieves maximal efficiency despite changing wavelengths of light that otherwise favor one photosystem or the other. Photosystem II works effectively at wavelengths up to ~660–670 nm; photosystem I can utilize light beyond this "red drop" in photosynthetic yield. A beam of light with a spectrum centered at, say, 700 nm, will be selective for photosystem I, and is termed "light 1." A beam centered below 660 nm will drive both photosystems, but is required for photosystem II, and is termed "light 2." Switching beams from light 2 to light 1, or superimposing light 1 onto light 2, induces a change in the light-harvesting apparatus, redistributing energy to photosystem II at the expense of photosystem I. The state arrived at is called the "light 1 state" or "state 1." Conversely, switching from light 1 to light 2 induces a "light 2 state," or "state 2."

Chloroplast Protein Phosphorylation

John Bennett at Warwick University discovered chloroplast protein phosphorylation and showed that one conspicuous phosphoprotein was a light-harvesting chlorophyll *a*/*b*-binding protein forming part of chloroplast light-harvesting complex II (LHC II). LHC II is an intrinsic membrane protein which becomes phosphorylated on a threonine residue by the action of a membrane-associated LHC II kinase.

Plastoquinone Redox Control of the LHC II Kinase

The LHC II kinase was originally thought to be activated by light. However, in Urbana, Illinois, in a collaboration with Bennett, John F. Allen and Charles J. Arntzen showed that LHC II becomes phosphorylated in darkness, provided the electron carrier plastoquinone is chemically reduced. The apparent light activation is sufficiently explained as redox-activation, with electrons being supplied to plastoquinone from photosystem II. In addition, LHC II phosphorylation is accompanied by changes in chlorophyll fluorescence and in electron transport, demonstrating that absorbed light energy simultaneously became redistributed to photosystem I at the expense of photosystem II.

Distribution of Absorbed Excitation Energy

The state-2 transition, an apparently purposeful response increasing efficiency of energy conversion, is the result of activation of the LHC II kinase by reduced plastoquinone. In light 1, the state-1 transition results from oxidation of plastoquinone by photosystem I: the LHC II kinase becomes inactivated, a light- and redox-dependent phospho-LHC II phosphatase catalyzes dephosphorylation of phospho-LHC II, and light energy absorbed by chlorophyll molecules of LHC II is returned to photosystem II, at the expense of photosystem I (Figure 3). Phosphorylation affects the three-dimensional structure of LHC II, and the movement of LHC II between photosystems I and II proceeds because its two structural forms differ in their capacity to bind and interact functionally with the two photosystems – a change in molecular recognition. An LHC II kinase has been identified by Jean–David Rochaix and co-workers in Geneva.

Thioredoxin

A number of enzymes of the Benson–Calvin cycle, and the coupling ATPase of chloroplast membranes, are activated by the reduced form of a soluble iron–sulfur protein, thioredoxin. This example of chloroplast redox signaling was discovered by Robert (Bob) Buchanan and co-workers in Berkeley, California. Thioredoxin accepts electron from ferredoxin, an electron carrier on the acceptor side of photosystem I, and light activation therefore depends on the activity of both photosystems. The function of thioredoxin redox signaling seems to be to ensure that CO_2 assimilation and ATP synthesis are inactivated in darkness, so that energy stored in photosynthesis is not subsequently dissipated.

Posttranscriptional Control

Within chloroplasts, reduced thioredoxin also activates ribosomal translation and processing of RNA, and has been studied for the *psbA* gene product (the D1 reaction center apoprotein of photosystem II) by Steven Mayfield at the Scripps Institute in San Diego, California.

Transcriptional Control

Redox and other signal transduction pathways in bacteria often exert parallel effects at posttranslational

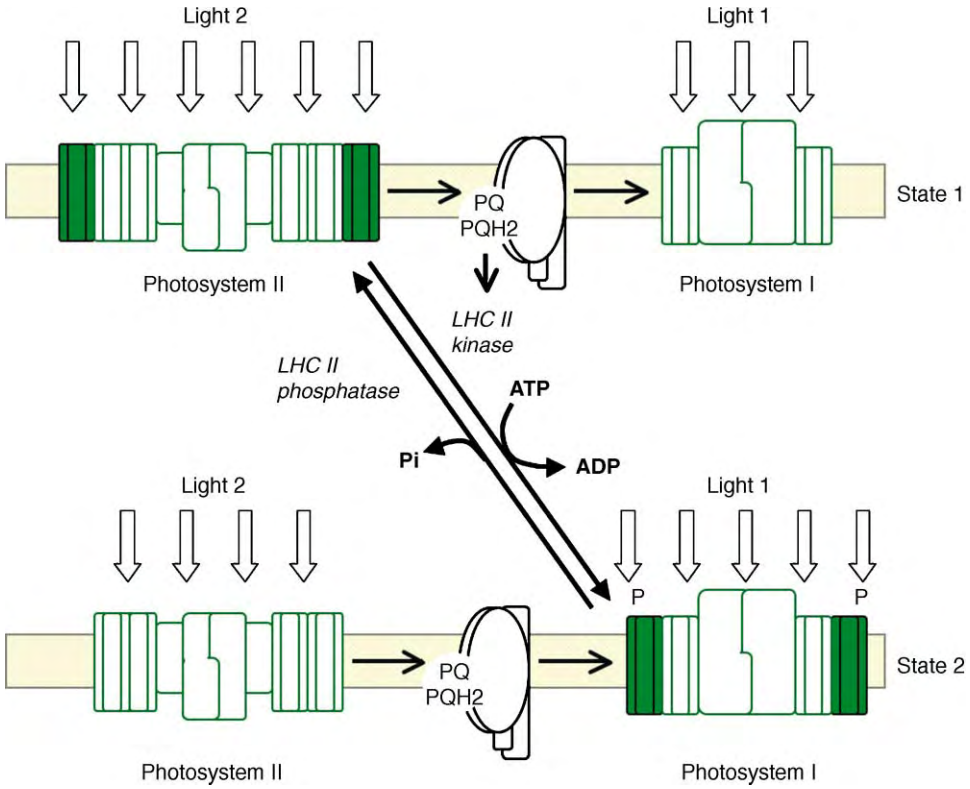

FIGURE 3 Plastoquinone redox control of LHC II kinase activity and its role in balancing distribution of excitation energy between photosystems I and II.

and transcriptional levels of gene expression. Chloroplasts are no exception.

Chloroplast Genes

Thomas Pfannschmidt and John F. Allen, working at Lund University, showed that transcription of chloroplast genes for reaction center apoproteins is regulated by the redox state of plastoquinone. As with phosphorylation of LHC II, the direction of control is functionally intelligible. Reduced plastoquinone is a signal that photosystem I is rate-limiting and photosystem II activity is in excess. Reduction of plastoquinone turns off transcription of photosystem II reaction center genes, and turns on transcription of photosystem I reaction center genes. Conversely, oxidized plastoquinone is a signal of imbalance with photosystem II rate-limiting, and photosystem I in excess: oxidized plastoquinone turns off photosystem I transcription, and turns on photosystem II transcription. Thus, the stoichiometry of photosystems I and II will tend to adjust itself to match changes in the prevailing light regime, as well as changes in metabolic demand for ATP relative to NADPH. Plastoquinone redox control of reaction center gene transcription maintains redox poise of plastoquinone (Figure 4) and of other components linked to it, including components of the cyclic electron transport pathway of photosystem I (Figure 1).

Nuclear Genes

Redox signals from the chloroplast also affect transcription of nuclear genes. In the case of light 1–light 2 effects and redox control at the level of plastoquinone, nuclear genes for photosystems I and II are regulated in the same functionally intelligible way, suggesting a backup which serves the same goal of maintaining redox poise within the chloroplast.

Mechanisms and Evolutionary Implications

Mechanisms and components in chloroplast redox signaling are not fully resolved, especially as regards transcription and translation. Based on bacterial redox signaling, candidate pathways are proposed as follows, and preliminary evidence is consistent with these.

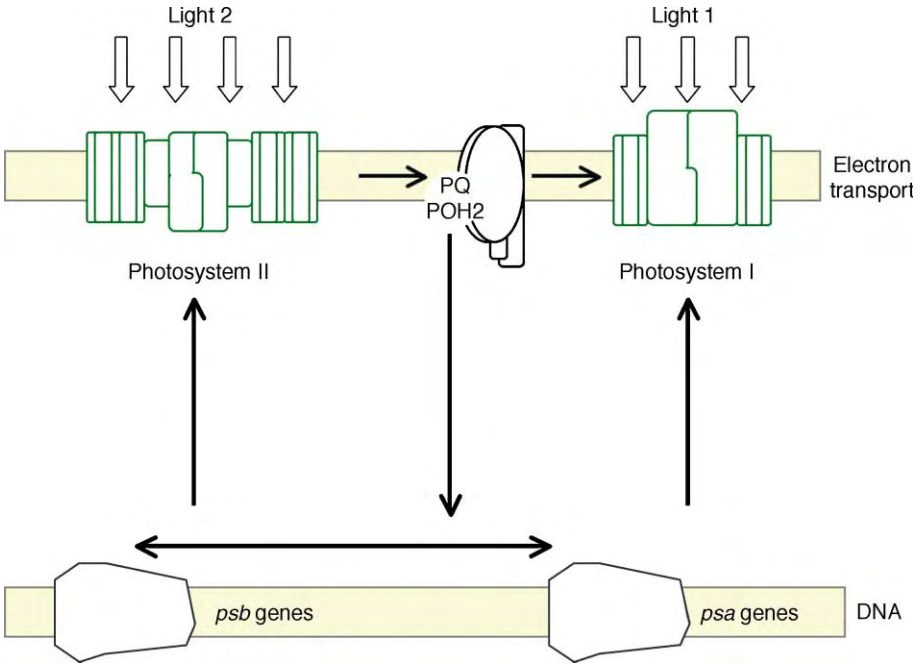

FIGURE 4 Plastoquinone redox control of chloroplast photosynthetic reaction center gene transcription and its role in adjusting the stoichiometry of photosystem I to photosystem II.

Two-Component Systems

A bacterial two-component redox regulatory pathway utilizes a membrane-intrinsic histidine sensor kinase which becomes phosphorylated when ubiquinone in the respiratory chain is reduced. The phosphate from the sensor is then transferred to an aspartate of a soluble response regulator. The response regulator is a sequence-specific DNA-binding protein, and the effect is to switch on transcription of genes for proteins required for anaerobic respiration. This aerobic respiratory control (Arc) system senses redox state. Photosynthetic bacteria, including cyanobacteria, possess cognate systems. Chloroplast genomes of some eukaryotic, red and brown algae have genes for similar components (sensors and response regulators), and green algae and plants have nuclear genes for these components, including transit sequences required for chloroplast import.

FNR and Redox Activators

At the level of thioredoxin, accepting electrons from ferredoxins, bacteria have DNA-binding iron–sulfur proteins. The best-studied example is "fumarate and nitrate reductase" of *Escherichia coli* (FNR: by coincidence, the abbreviation also for ferredoxin–NADP reductase of photosystem I). Since reduced ferredoxin sends redox signals to gene expression, it is likely that a cognate redox activator system is involved.

Redox Signaling and the Function of Cytoplasmic Genomes

Redox signaling is unique neither to chloroplasts nor to photosynthesis. Close coupling between primary redox chemistry and gene expression is seen in bacteria and chloroplasts, with some preliminary evidence also in mitochondria. Inspection of the genes contained in chloroplast and mitochondrial DNA reveals no clear correlation with the hydrophobicity of the gene product, as sometimes supposed. Rather, the core, membrane-intrinsic proteins of primary electron transfer are always encoded in chloroplasts and mitochondria, and synthesized on organelle ribosomes. This rule is especially clear for chloroplast reaction center genes, whose transcription is known to be controlled by the redox state of the plastoquinone pool. It has been proposed that retention, in evolution, of chloroplast and mitochondrial genetic systems gives a co-location of gene with gene product, and that this co-location is essential for redox regulation. Chloroplast redox poise and signaling therefore have important implications for cell evolution, and may account for the distribution of genes between nucleus and cytoplasm in eukaryotic cells.

See Also the Following Articles

Chlorophylls and Carotenoids • Chloroplasts • Ferredoxin • Ferredoxin-NADP$^+$ Reductase • Photosynthesis

Glossary

chloroplast (from Greek for "green box") A subcellular organelle of plants and algae. Chloroplasts are the location for the process of photosynthesis in eukaryotes.

photosynthesis The capture of light energy and its utilization to produce reduced carbon compounds whose subsequent oxidation in respiration releases the free energy originally obtained from light.

poise A state of balance. "Redox poise" in electron transport occurs when each electron-carrying intermediate is present in both its oxidized state and its reduced state, in order for that component both to accept and to donate electrons or hydrogen atoms.

redox An adjective derived from "reduction–oxidation," and describing a class of chemical reactions that involve transfer of electrons or hydrogen atoms.

redox signaling Coupling between biological electron transfer and gene expression. Regulatory control is exerted in both directions.

Further Reading

Allen, J. F. (1992). Protein phosphorylation in regulation of photosynthesis. *Biochim. Biophys. Acta* **1098**(3), 275–335.

Allen, J. F. (2002). Photosynthesis of ATP-electrons, proton pumps, rotors, and poise. *Cell* **110**(3), 273–276.

Allen, J. F. (2003). The function of genomes in bioenergetic organelles. *Philos. Trans. Roy. Soc. London Series B-Biological Sci.* **358**(1429), 19–38.

Allen, J. F. (2004). Chromosome b6f: Structure for signalling and vectorial metabolism. *Trends Plant Sci.* **9**(3), 130–137.

Bauer, C. E., Elsen, S., and Bird, T. H. (1999). Mechanisms for redox control of gene expression. *Annu. Rev. Microbiol.* **53**, 495–523.

Blankenship, R. E. (2002). *Molecular Mechanisms of Photosynthesis*. Blackwell Science, Oxford.

Heathcote, P., Fyfe, P. K. and Jones, M. R. (2002). Reaction centres: The structure and evolution of biological solar power. *Trends Biochem. Sci.* **27**(2), 79–87.

Pfannschmidt, T. (2003). Chloroplast redox signals: How photosynthesis controls its own genes. *Trends Plant Sci.* **8**(1), 33–41.

Race, H. L., Herrmann, R. G. and Martin, W. (1999). Why have organelles retained genomes? *Trends Genet.* **15**(9), 364–370.

Wollman, F. A. (2001). State transitions reveal the dynamics and flexibility of the photosynthetic apparatus. *EMBO J.* **20**(14), 3623–3630.

Biography

John F. Allen is Professor of Plant Cell Biology in Lund University, Sweden. He was educated in Newport, Monmouthshire, UK, and then at King's College in London University, obtaining his Ph.D. with David O. Hall. Dr. Allen carried out postdoctoral work in Oxford and Warwick Universities and in the University of Illinois at Urbana, subsequently working in Leeds University, and, on sabbatical, in University of California, Berkeley. He was Professor of Plant Physiology in Oslo for two years before moving to his present position in 1992. Allen demonstrated superoxide production by isolated chloroplasts and, later, plastoquinone redox control of chloroplast protein phosphorylation. His work on redox regulation of photosynthesis contributed to his theory that chloroplast and mitochondrial genomes allow genetic control of redox poise.

Chloroplasts

Nicoletta Rascio
University of Padova, Padova, Italy

Chloroplasts are the organelles specialized in carrying out the photosynthetic process, which uses light energy to synthesize organic compounds: for this reason they are common to all photoautotrophic eukaryotes.

Besides the biosynthetic pathways directly related to photosynthesis, such as synthesis of pigments (chlorophylls and carotenoids), conversion of CO_2 to carbohydrates and reduction and organization of sulfur and nitrogen, several other metabolic pathways occur in chloroplasts. These organelles produce or participate in the production of a series of essential compounds required by other cell compartments. For instance, they are the primary site of biosynthesis of fatty acids, isoprenoids, tetrapyrroles, and aminoacids, as well as of purines, pirimidines, and pentoses necessary for nucleic acid build-up. Thus, chloroplasts, in addition to photosynthesis, play other essential roles in sustaining the metabolism of the cell and the whole plant. The complexity and variety of chloroplast activities can arise from the fact that this, which is now a cell organelle, was originally an organism.

Chloroplast Origin

The chloroplast originated from a cyanobacterium-like prokaryotic ancestor with oxygenic photosynthesis, which was engulfed by a heterotroph proeukaryote. This endosymbiotic event, which took place about 1 billion years ago, was of enormous importance, since it triggered the evolution of photosynthetic eukaryotes and even led, as a consequence, to the expansion of the heterotroph forms of life on the Earth.

During the evolutionary route which changed it into the chloroplast, the cyanobacterium-like ancestor underwent substantial modifications. A significant event was the transfer of most prokaryotic DNA to the host cell nucleus. The genome of a present chloroplast, actually, codes for ~100 proteins, while the DNA of a free-living cyanobacterium, like *Synecocystis*, whose entire sequence is known, encodes more than 3000 proteins. The massive "endosymbiotic gene transfer" possibly occurred to avoid the mutagenic load for organelle genes due to free radicals produced by photosynthetic light reactions, and to escape the accumulation of deleterious mutations caused by the genetic isolation of the organelle DNA in the host cells (the so-called Muller's ratchet).

This transfer of genetic information made it necessary for the chloroplast to recover the proteins encoded in the nucleus and this was achieved by inserting in the nuclear genes a presequence coding for a transit peptide which targeted the choroplast proteins and redirected them to the organelle.

Another essential change undergone by the evolving chloroplast concerned the photosynthetic light-harvesting pigments. With the exception of some algal groups (Rhodophytes and Cryptophytes), the original phycobiliproteins were replaced by chlorophyll forms, in particular by chlorophyll *b* in green organisms.

Chloroplast Organization

Algae and lower plants have chloroplasts which can vary considerably in shape and size, whereas in higher plants these organelles are commonly lens-shaped and measure ~5–10 μm.

Envelope

The chloroplast (Figure 1) is enclosed by a pair of concentric membranes forming the "envelope." The inner envelope membrane is highly selective and contains numerous carriers which regulate the flows of metabolites and ions between chloroplast and the cytosol. The most abundant is the phosphate translocator, which plays a major role in supplying the cell with the products of photosynthesis. The inner membrane also supports some enzymes of biosynthetic pathways, like those of carotenoids, tetrapyrroles, and fatty acids. The outer envelope membrane contains a nonspecific porine-like protein, which allows ions and metabolites of up to ~10 kDa to pass. It is essentially involved in recognizing the cytosol-synthesized chloroplastic proteins which must be transferred into the organelle. This translocation occurs through two multiproteic complexes, one of them inserted in the outer membrane (translocation outer complex, TOC), the other in the inner membrane (translocation inner complex, TIC) of the envelope.

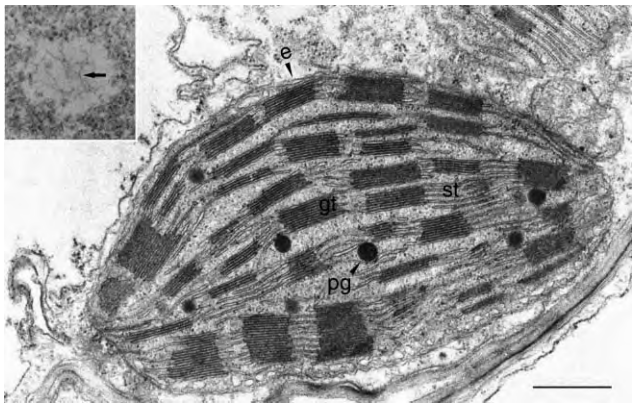

FIGURE 1 Transmission electron microscope (TEM) micrograph of a chloroplast from a mesophyll cell in a maize leaf. Note the envelope (e) the inner membrane system formed by stacked granal thylakoids (gt) and single stromal thylakoids (st). Some plastoglobules (pg) are present in the stroma which look finely granular due to the presence of 70S ribosomes. (bar = 1 μm). The insert shows the region of a chloroplast stroma with DNA microfibrils (arrow).

Stroma

The chloroplast internal milieu, called "stroma", looks finely granular due to the presence of 70S ribosomes. It contains prokaryotic DNA (Figure 1), RNA and the entire protein synthesis machinery allowing the organelle to translate its own genetic information. In the stroma are also inserted the soluble enzymes engaged in the numerous biosynthetic pathways. The ribulose-1, 5-bisphosphate carboxylase/oxygenase (Rubisco), which catalyzes CO_2 fixation in the first reaction of the Calvin–Benson cycle, is the most abundant enzyme, and is even the most abundant protein in the world. Small roundish inclusions, named plastoglobules, made up of plastoquinones, carotenoids, and proteins, are common in the stroma, where also starch grains of photosynthetic origin can occasionally accumulate.

Thylakoid System

Within the chloroplast a membrane system, the "thylakoid system", is present, which contains the multiproteic complexes involved in the light reactions of photosynthesis. The inner membrane system of the chloroplast (Figure 1) consists of coupled lamellae (thylakoid membranes) separated by a narrow intermembrane space. They form flattened cisternae or saccules (thylakoids), intercommunicating to constitute a continuous and closed membrane system, whose internal space (lumen) is totally isolated from the stromal environment.

A feature common to the green plant chloroplasts (Figures 2A and 2B) is the stacking of thylakoids (granal thylakoids) one upon the other to make piles of saccules named "grana" (singular: granum), which are interconnected by single unstacked thylakoids running in the stroma (stromal thylakoids). This kind of organization, which gives rise to a huge surface area of thylakoid membranes, acquires functional significance, taking into account that, as stated above, these membranes support the complexes carrying out the photosynthetic light reactions and the correlated electron transport and ATP synthesis (precisely: photosystem I (PSI), photosystem II (PSII), the cytochrome b_6f complex (Cyt b_6f), and the ATP synthase). These components are diversely and specifically located in the thylakoid membranes (Figure 3). Most of PSII resides in the approached regions of stacked thylakoids (partitions), while PSI and the ATP synthase only occur in the stromal thylakoids and in all the unstacked regions of granal thylakoids (end granal membranes and margins). Finally, the Cyt b_6f is rather homogeneously distributed in the thylakoid system.

A peculiarity of chloroplast membranes, which distinguishes them from the other cell membranes, is the great abundance of glycolipids, represented by two neutral galactolipids, the monogalactosyldiacylglycerol

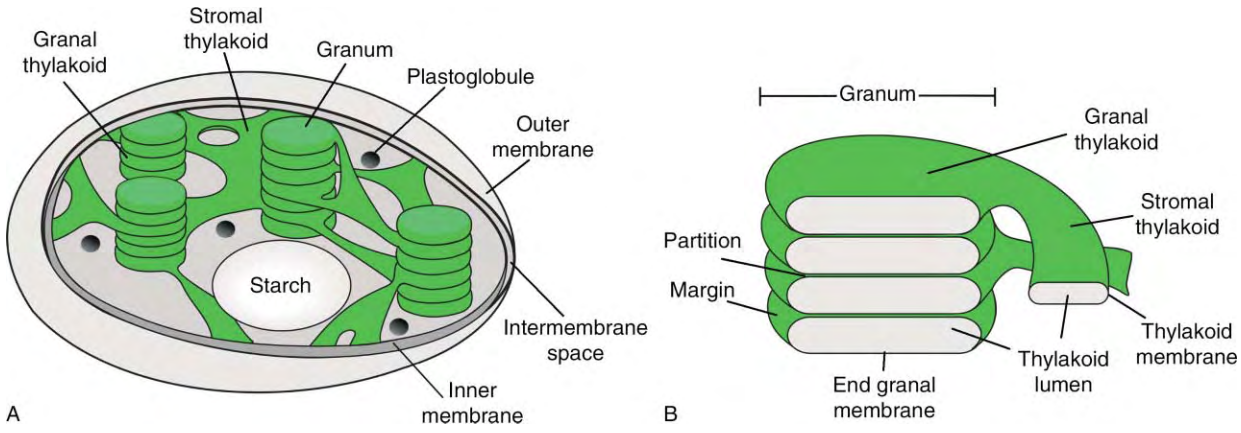

FIGURE 2 (A) Three-dimensional scheme of a chloroplast. (B) Particulars of the thylakoid system organization.

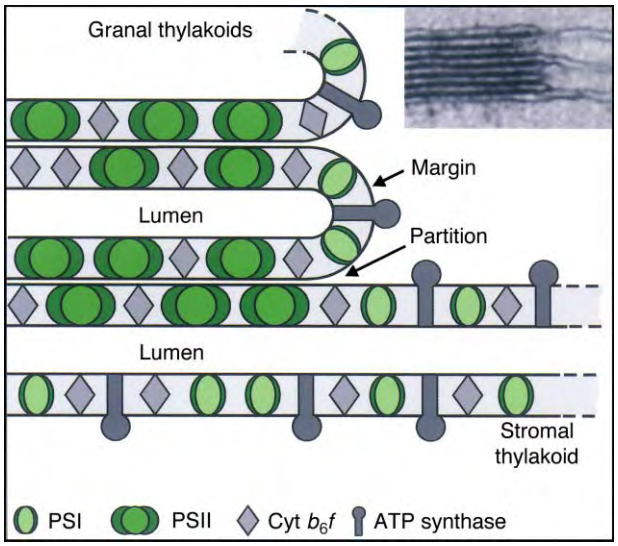

FIGURE 3 Distribution of the multiproteic complexes in the thylakoid membranes.

(MGDG) and the digalactosyldiacylglycerol (DGDG), which account for 70% of the entire acyl-lipid moiety, and by the anionic sulfolipid sulfoquinovosildyacylglycerol (SQDG). Phosphatidylglycerol (PG) is the only phospholipid present in the membranes. A feature of all thylakoid lipids is the high concentration of polyunsaturated fatty acids, which maintain membrane fluidity in spite of the high protein/lipid ratio. Nonpolar lipids, like plastoquinones, phylloquinones, and tocopherols are inserted in the hydrophobic region of the membrane matrix. Plastoquinone-9, a component of the photosynthetic electron transport chain, is particularly abundant.

Chloroplast Biogenesis

In higher plants chloroplasts develop from proplastids, which are small undifferentiated organelles present in the meristematic cells. Chloroplast differentiation involves the synthesis of pigments, proteins, and lipids and the structural and functional organization of the whole thylakoid system, as well as the acquisition of the enzymatic components carrying out the numerous metabolic pathways of the mature organelle. These events are accompanied by the increase in the developing chloroplast size and the rise of the organelle number in the cells. Proplastids and young chloroplasts, indeed, can divide through a process of "binary fission" similar to that occurring in bacteria. The chloroplast division is independent of cell division, being part of the developmental program which defines the final number of photosynthetic organelles in the mature green cell.

The dependence on both nuclear and own genetic information makes chloroplast biogenesis a quite complex process requiring the coordinated expression of genes located in the two cellular compartments. This takes place through environmental cues, the most important of which is light, and through endogenous nucleus–chloroplast signaling. The nucleus exerts a preeminent role in controlling the chloroplast gene expression. However, also chloroplast-to-nucleus signaling pathways exist that greatly affect the transcription of nuclear genes encoding photosynthesis-related proteins. This kind of "retrograde" informational flow is triggered by different chloroplast-generated signals, involving, for instance, chlorophyll precursors or the plastoquinone redox state, and serves to correlate the nuclear gene expression with the chloroplast developmental stage and the organelle functionality, but also to achieve a swift photosystem adjustment in response to qualitative and quantitative light changes in the plant growth environment.

Light and Chloroplast Differentiation

In lower vascular plants as well as in most gymnosperms the events leading to chloroplast differentiation can occur both in light and in darkness. On the contrary, in the angiosperms, light is a key factor for chloroplast biogenesis and the build-up of the thylakoid system. In these more evolved plants, light, by phytochrome mediation, induces the expression of different nuclear genes (photo-genes) coding for essential chloroplast components. Light, for instance, is required for the transcription of the *Cab* genes encoding numerous chlorophyll *a/b*-binding proteins. Moreover, chlorophyll is not produced in the dark because one of the final steps of its biosynthetic pathway, precisely the protochlorophyllide (Pchlide) to chlorophyllide (Chlide) reduction, is carried out by the enzyme Pchlide oxidoreductase (POR) which, in flowering plants, has become light dependent. As a consequence, in dark-grown (etiolated) seedlings of angiosperms, peculiar organelles, named "etioplasts," originate from proplastids in cells that would become green in the presence of light.

Etioplasts

Etioplasts, which are the chloroplast counterparts in darkness, can be formed in nature during the first phase of plantlet growth, before the emergence from soil. An inner membrane system very different from the thylakoid develops in etioplasts (Figure 4). Most membranes have a tubular arrangement and aggregate in a tridimensional semicrystalline network of interconnected tubules, defined "prolamellar body," from which some lamellar membranes (prothylakoids) extend. The prolamellar body membranes contain the

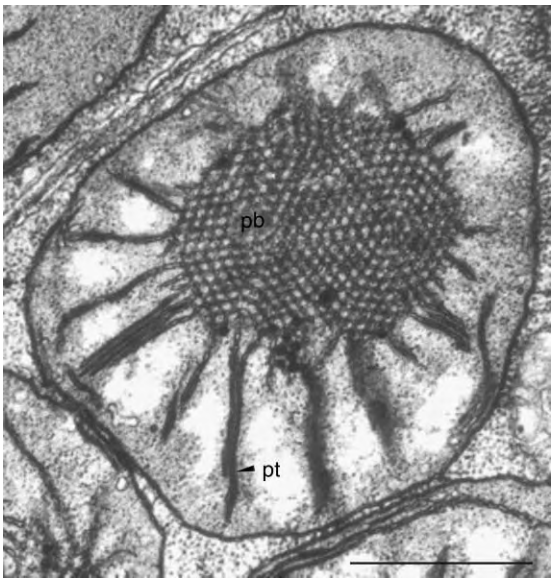

FIGURE 4 TEM micrograph of an etioplast from a dark-grown bean cotyledon. The inner tubular membranes are arranged in a semicrystalline prolamellar body (pb) from which lamellar prothylakoids (pt) extend (bar = 1 μm).

POR associated with Pchlide and NADPH to form a stable "ternary complex," and are particularly rich in MGDG, which favors the tubular arrangement due to its cone- shaped molecular configuration.

Etioplasts exposed to light convert to chloroplasts. The first event of this greening process is the Pchlide reduction that the photo-activated POR carries out by using the NADPH of the ternary complex. Successively the etioplast membranes rearrange to form primary thylakoids and then a massive synthesis *de novo* of chlorophylls and membranes leads to the formation of the well organized and photosynthetically competent chloroplast.

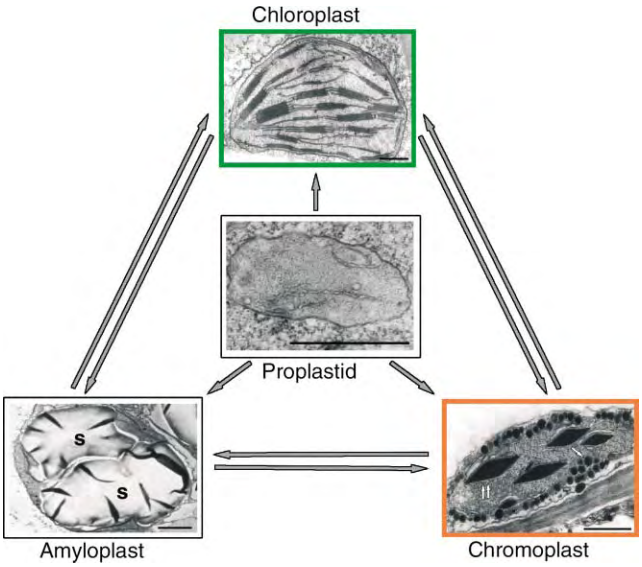

FIGURE 5 The cyclic model of plastid interconversions. The amyloplast from a cell of *Raphanus* hypocotyl contains large starch grains (s). Globular (arrow) and crystalline (double arrow) carotenoid masses are inserted in the chromoplast from a cell of *Ranunculus* petal. Chloroplast and proplastid are from a mesophyll cell and a basal meristem cell of a maize leaf, respectively (bars = 1 μm).

Plastids

The chloroplast belongs to the organellar class of plastids. In lower photoautotroph organisms, like algae, which do not possess cell types with very distinct functions, the photosynthetic chloroplast has remained the sole kind of plastid. On the contrary, in terrestrial plants, which evolved highly specialized tissues and organs, different kinds of plastids with specific structures and functions arose from the original chloroplast. In these plants the class of plastids, besides the green chloroplasts, includes uncolored amyloplasts, whose function is to store large amounts of starch (Figure 5) and yellow-red-brown chromoplasts which synthesize a lot of carotenoids (Figure 5) and have attractive functions. Apart from the lack of thylakoids, these non-photosynthesizing plastids share common characteristics with the chloroplasts, like the envelope membranes, the prokaryotic DNA and the 70S ribosomes. Furthermore, they maintain several biosynthetic pathways carried out by enzymes inserted in the stroma or bound to the envelope, such as those of fatty acids and terpenoids.

All the plastids can differentiate from proplastids. However, the possibility also exists that a plastid derives from the conversion of another kind of plastid, according to the "cyclic model" (Figure 5) proposed already by Schimper at the end of 1800. These reversible plastid interconversions depend on cell developmental programs as well as on endogenous (hormones and nutrients) or environmental (light and temperature) signals. Only the chromoplasts (named gerontoplasts) derived from chloroplast degeneration during a green tissue senescence cannot undergo further conversion.

See Also the Following Articles

Chlorophylls and Carotenoids • Chloroplast Redox Poise and Signaling • Cytochrome b_6f Complex

Glossary

binary fission Mechanism, similar to that occurring in bacteria, by which the chloroplast divides independently from the cell division.
envelope Pair of concentric membranes enclosing the chloroplast.
etioplast Organelle which is the counterpart of chloroplast and develops in dark-grown seedlings of flowering plants.

prolamellar body Tridimensional semicrystalline aggregate of the etioplast tubular membranes.

thylakoids Flattened cisternae or saccules intercommunicating, which form the closed inner membrane system of chloroplast.

Further Reading

Cornah, J., Terry, M. J., and Smith, A. G. (2003). Green or red: What stops the traffic in the tetrapyrrole pathway. *Trends Plant Sci.* **5**, 224–230.

Goldschmidt-Clermont, M. (1998). Coordination of nuclear and chloroplast gene expression in plant cells. *Internat. Rev. Cytol.* **177**, 115–179.

Jarvis, P. (2003). Intracellular signalling: The language of the chloroplast. *Curr. Biol.* **13**, R314–R316.

Kleinig, H. (1989). The role of plastids in isoprenoid biosynthesis. *Annu. Rev. Plant Physiol. Plant Mol. Biol.* **40**, 39–59.

Martin, W., and Herrmann, R. G. (1998). Gene transfer from organelles to the nucleus: How much, what happens, and why? *Plant Physiol.* **118**, 9–17.

McFadden, G. I. (1999). Endosymbiosis and evolution of the plant cell. *Curr. Opin. Plant Biol.* **2**, 513–519.

Ohlrogge, J., and Browse, J. (1995). Lipid biosynthesis. *Plant Cell* **7**, 957–970.

Sundqvist, C., and Dahlin, C. (1997). With chlorophyll pigments from prolamellar bodies to light-harvesting complexes. *Physiol. Plant.* **199**, 748–759.

Willows, R. D. (2003). Biosynthesis of chlorophylls from protoporphyrin IX. *Net. Prod. Rep.* **20**, 327–341.

Biography

Nicoletta Rascio is a Professor of plant physiology at the Department of Biology of the University of Padova (Italy). Her principal research interest is in the biogenesis, organization, and functionality of the photosynthetic apparatus in algae and higher plants at the ultrastructural, molecular, biochemical, and physiological level, in normal and stressful environmental conditions. In this field she has published more than 100 papers in mainstream journals.

Cholesterol Synthesis

Peter A. Edwards
University of California Los Angeles, Los Angeles, California, USA

Cholesterol is a critical component of eukaryotic cell membranes and a precursor of steroid hormones, oxysterols, and bile acids that have important roles in cell signaling and/or lipid absorption. In addition, intermediates in the cholesterol biosynthetic pathway are diverted to the synthesis of diverse polyisoprenoids that have important functions in the cell. Thus, it is not surprising that the cholesterol biosynthetic pathway is highly regulated. Drugs, collectively called statins, that inhibit the rate-limiting enzyme of cholesterol synthesis, have been shown to both reduce plasma LDL cholesterol levels and impair the progression of atherosclerosis and coronary artery disease.

Properties of Cholesterol

Cholesterol is a cyclic hydrocarbon that can be esterified with a fatty acid to form a cholesteryl ester. Both cholesterol and cholesteryl esters are lipids and are essentially insoluble in aqueous solution but soluble in organic solvents. Excess cholesterol esters are stored as lipid droplets within the cytosol. Such droplets are prevalent in steroidogenic tissues where they serve as precursors of the steroid hormones. In eukaroyotic cells, cholesterol is "solubilized" as a result of its interaction with either membrane phospholipids or with phospholipids and bile acid micelles in the gall bladder. In blood, cholesterol and cholesterol esters are "solubilized" within lipoprotein complexes. These lipoproteins, that include low density lipoprotein (LDL), very low density lipoprotein (VLDL), chylomicrons and high density lipoprotein (HDL), function to transport insoluble lipids around the body.

Functions of Cholesterol

Membrane Structure

Cholesterol is absent from prokaryotic cells. However, cholesterol plays an essential structural role in maintaining the fluidity of eukaryotic cell membranes. Cholesterol is not equally distributed in all membranes; the membranes of mitochondria, peroxisomes, and endoplasmic reticulum are cholesterol-poor, whereas the plasma membrane is enriched in the sterol. However, the concentration of cholesterol varies significantly even within the plasma membrane; it is highly enriched in two specialized areas termed lipid rafts and caveolae. Since many receptors are localized to these cholesterol- and sphingomyelin-rich domains, it has been suggested that lipid rafts and caveolae function as "signaling gateways" into the cell. The myelin sheath that surrounds nerves has the highest cholesterol concentration.

Precursor of Signaling Molecules

As shown in Figure 1, cholesterol is a precursor of bile acids, steroid hormones, and oxysterols (oxidized cholesterol). These cholesterol metabolites function to activate specific nuclear receptors that control many metabolic and developmental processes. In addition, intermediates in the cholesterol biosynthetic pathway are themselves precursors for other critical pathways. For example, 7-dehydrocholesterol is a precursor of vitamin D, and farnesyl diphosphate is a precursor of geranylgeranyl diphosphate, ubiquinone, Heme a, and dolichols (Figure 1). Although beyond the scope of this article, it is now clear that modification (prenylation) of many proteins by either farnesyl diphosphate or geranylgeranyl diphosphate is critical for cell survival. Thus, hypolipidemic drugs (e.g., statins) that inhibit HMG-CoA reductase activity must be used at doses that result in partial, not total, inhibition of the pathway.

Sources of Cellular Cholesterol

Diet and Lipoproteins

Insects are cholesterol auxotrophs and must obtain all their cholesterol from the diet. In contrast, other eukaryotes obtain cholesterol from two sources; the diet and endogenous synthesis. Mammals absorb 40–50% of the cholesterol in their diet and transport it to the liver and other tissues in lipoproteins. The plasma lipoproteins bind to cell surface receptors prior to the delivery of the lipid cargo to the cell. Such receptors include the LDL receptor, SR-B1, SR-A, and CD36.

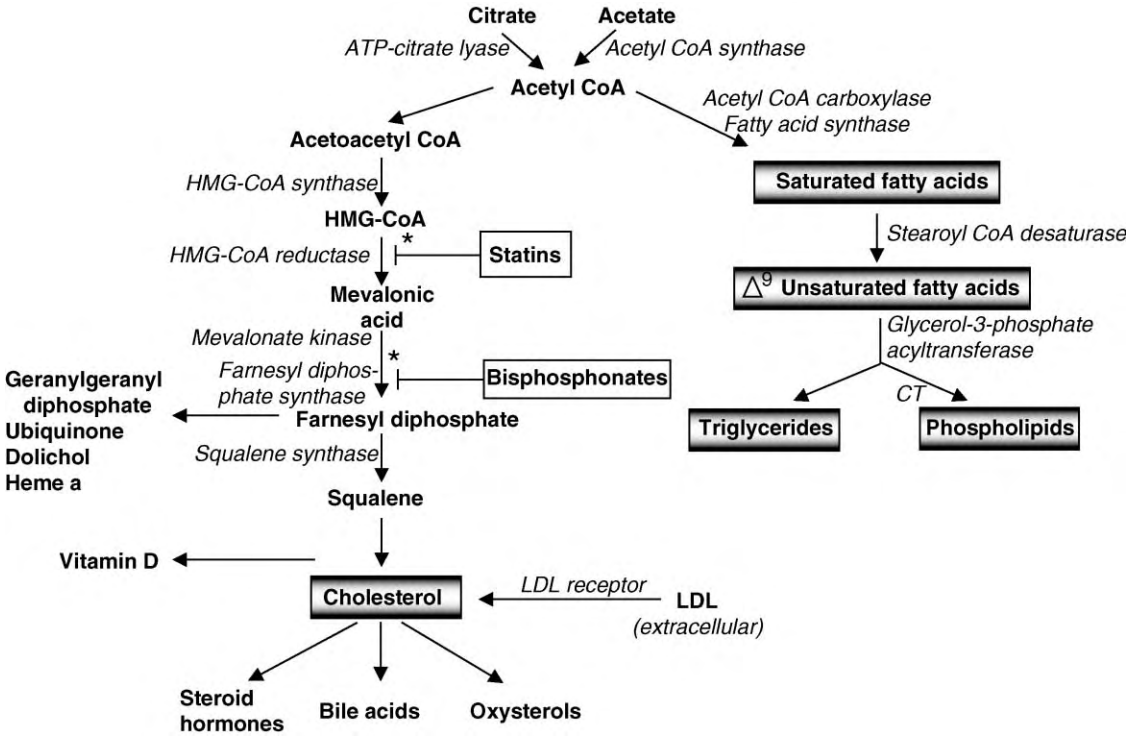

FIGURE 1 The cholesterol and fatty acid biosynthetic pathways are regulated by SREBPs. A few of the intermediates and enzymes of the cholesterol and fatty acid synthetic pathways are shown. Genes that are preferentially regulated by SREBP-2 (left side) or SREBP-1c (right side) are italicized. The inhibition of HMG-CoA reductase or farnesyl diphosphate synthase by statins and bisphosphonates, respectively, is indicated by *, many intermediates and enzymes have been omitted for simplicity, such as CT, CTP, phosphocholine cytidyltransferase.

The LDL receptor is expressed on the surface of most cells and plays a particularly important role in cholesterol homeostasis. This transmembrane protein binds cholesterol-rich LDL and facilitates the delivery of cholesterol into the cell via specialized areas on the cell surface called clathrin-coated pits. However, virtually all mammalian cells also synthesize cholesterol (Figure 1).

Cholesterol Synthesis

There are many reviews on the biosynthesis of cholesterol, possibly in part because work in this area has been extensive and has led to numerous Nobel prizes. All mammalian cells, with the exception of mature red blood cells, utilize more than 30 enzymes to convert the 2 carbon acetate to the 27 carbon cholesterol via isoprenoid intermediates (Figure 1). The rate-limiting enzyme in this pathway, HMG-CoA reductase, is the target for many hypolipidemic drugs (Figures 1 and 2). Together, the cholesterol biosynthetic pathway and the LDL receptor pathway provide sufficient cholesterol necessary for cell growth and division. These two pathways are coordinately controlled by an exquisite mechanism that "senses" cellular cholesterol levels. The mechanism involves the generation of three functionally active transcription factors termed sterol regulatory element binding proteins (SREBPs).

Transcriptional Control of Cholesterol Synthesis

There are two SREBP genes, SREBP-1 and SREBP-2. The SREBP-2 gene produces one protein that preferentially activates genes involved in cholesterol homeostasis. In contrast, two proteins, SREBP-1a and SREBP-1c are produced from the SREBP-1 gene. SREBP-1c preferentially activates genes involved in fatty acid synthesis. SREBP-1a activates both pathways but is expressed at relatively low levels. Newly synthesized SREBP proteins contain two transmembrane domains that form a hairpin-like structure and anchor the proteins in the endoplasmic reticulum, outside the nucleus (Figure 2). If these proteins are anchored to membranes outside the nucleus, how can they function as transcription factors in the nucleus?

The answer came from a series of elegant studies initiated in the laboratory of Goldstein and Brown in Dallas. They showed that generation of nuclear-localized SREBPs requires additional proteins named Insig-1, Insig-2, SCAP, the site 1 protease (S1P), and the site 2 protease (S2P) (Figure 2). The roles of these proteins vary; SCAP functions both as a cholesterol sensor and as an escort protein to transport SREBP to the Golgi where two proteases cleave SREBPs to release the soluble amino terminal fragment. The process is also regulated by the two Insig proteins, which function to

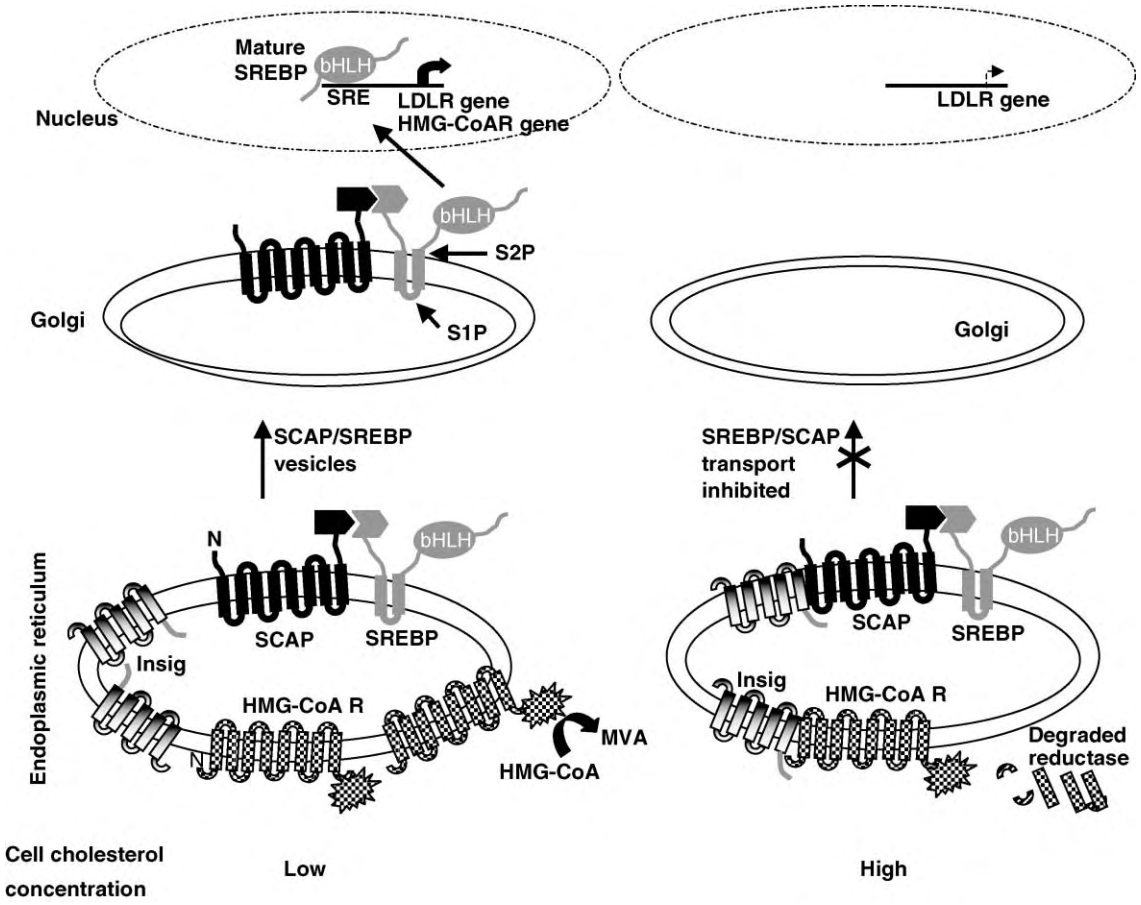

FIGURE 2 Mechanisms involved in the nuclear targeting of SREBP-2 and the altered stability of HMG-CoA reductase. The left side represents conditions where the cholesterol concentration in the cell is low. Under these conditions, SREBP-2 is targeted first to the Golgi and then to the nucleus where it activates many SREBP-2 target genes. For simplicity, only the LDL receptor and HMG-CoA reductase (HMG-CoA R) genes are shown. HMG-CoA reductase protein also accumulates in the endoplasmic reticulum where it catalyzes the reduction of HMG-CoA to mevalonic acid (MVA). The right side represents conditions where cellular cholesterol levels are higher than normal. Under these cholesterol-enriched conditions, Insig complexes with SCAP/SREBP and inhibits the maturation and nuclear localization of SREBP-2. In addition, the rate of degradation of HMG-CoA reductase is increased. The degradation is preceded by the formation of an Insig/HMG-CoA reductase complex. Details are given in the text.

control the release of SCAP/SREBP from the endoplasmic reticulum (Figure 2). In brief, when cells become "cholesterol-poor," for example, after addition of a drug that inhibits cholesterol synthesis, a SCAP/SREBP-2 heterodimeric complex is transported in vesicles that bud from the endoplasmic reticulum and then fuse with the Golgi (Figure 2). The Golgi contains two resident proteases, S1P and S2P, that sequentially cleave the newly arrived SREBP-2 protein; first S1P cleaves SREBP into two parts by cleaving the hairpin loop in the lumen of the Golgi, then S2P cleaves the protein at a second site to release a soluble amino-terminal domain (Figure 2). This soluble amino-terminal fragment, containing a basic helix-loop-helix-leucine zipper transactivation domain (bHLH), migrates into the nucleus where it binds to specific DNA sequences termed sterol responsive elements (SREs) and activates transcription. SREs have been identified in the promoters of many genes involved in cholesterol and fatty acid and lipid synthesis. Such genes include HMG-CoA reductase, HMG-CoA synthase, farnesyl diphosphate synthase, squalene synthase, and the LDL receptor (Figure 1). In summary, a transient decrease in cellular cholesterol levels leads to increased levels of transcriptionally active SREBP-2 in the nucleus and activation of genes involved in cholesterol synthesis and uptake of LDL. The net result is a rapid return of the cellular sterol levels to normal.

In contrast, when cells accumulate cholesterol, the SCAP/SREBP heterodimer complexes with another protein called Insig. Since Insig is a resident protein of the endoplasmic reticulum, the Insig/SCAP/SREBP-2 complex remains localized to this membrane (Figure 2). Consequently, transport of SREBP-2 to the Golgi and subsequent cleavage and nuclear localization of the protein is impaired. As a result, transcription of genes encoding the LDL receptor and cholesterogenic

genes is low. Such changes in gene expression will prevent or reduce subsequent cholesterol accumulation in the cell.

Although beyond the scope of this review, SREBPs, especially SREBP-1c, also activate genes involved in the synthesis of saturated and unsaturated fatty acids, triglycerides, and phospholipids (Figure 1).

Regulated Degradation of HMG-CoA Reductase

HMG-CoA reductase catalyses the NADPH-dependent reduction of HMG-CoA to mevalonic acid (MVA in Figure 2). It is considered to be the rate-limiting enzyme of the cholesterol biosynthetic pathway. Thus, changes in the activity of the enzyme are paralleled by changes in cholesterol synthesis. The activity of the enzyme is regulated by changes in transcription, translation (mechanism unknown) and protein stability.

HMG-CoA reductase contains two domains; an eight transmembrane spanning region that localizes the protein to the endoplasmic reticulum and a carboxy-terminal domain that projects into the cytosol and contains all the catalytic activity (Figure 2). The half-life (a measure of protein stability) of the enzyme varies at least tenfold, depending on the concentration of cholesterol and isoprenoids in the cell. When cellular cholesterol levels are low the enzyme is relatively stable (half-life $\sim$10 h). Thus, active HMG-CoA reductase enzyme accumulates in the endoplasmic reticulum in response to (1) a slow rate of degradation of the protein and (2) increased transcription and enzyme synthesis (Figure 2). Since HMG-CoA reductase is the rate-limiting enzyme, the net result is increased cholesterol synthesis.

However, when cellular cholesterol levels increase, the rate of degradation of HMG-CoA reductase protein is enhanced $\geq$10-fold (half-life $<$45 min) by a process that requires both a sterol and an unidentified non-sterol derived from farnesyl diphosphate (Figure 1). Recent studies have shown that Insig-1 forms a complex with the transmembrane domains of HMG-CoA reductase prior to the ubiquination and degradation of the enzyme in proteosomes (Figure 2).

Thus, Insig appears to have a dual role in cholesterol-enriched cells; it interacts with HMG-CoA reductase to promote degradation of the enzyme, and with SCAP to retain SREBP-2 in the endoplasmic reticulum (Figure 2). It seems likely that these interactions may depend on the partially conserved "sterol-sensing domains" identified in both HMG-CoA reductase and SCAP. In summary, cholesterol-loaded cells have low levels of HMG-CoA reductase protein (and hence low rates of cholesterol synthesis) because (1) the enzyme is rapidly degraded and (2) transcription of the gene is low as a result of the retention of SREBP-2 in the endoplasmic reticulum (Figure 2, right side). Such changes will minimize subsequent cholesterol accumulation in the cell.

Effect of Mutations in the Cholesterol Synthetic Pathway

Mutations in the cholesterol synthetic pathway are rare because they are usually incompatible with life. Mutations in genes encoding mevalonic kinase (an early enzyme in the pathway) and 7-dehydrocholesterol (a late enzyme in the pathway) result in mevalonic acid urea and Smith–Lemli–Opitz syndrome, respectively. It should be emphasized that patients with mevalonic acid urea have residual mevalonic acid kinase activity, sufficient to provide isprenoid intermediates that are necessary for cell survival. Indeed, a complete blockage of early steps in cholesterol biosynthesis leads to embryonic death. Patients with mutations in genes that result in impaired cholesterol synthesis exhibit various neurological dysfunctions. Such observations only emphasize the importance of cholesterol to the neurological system.

Inhibitors of Cholesterol Synthesis; Treatment for Hyperlipidemia and Osteoporosis

Statins

Elevated LDL cholesterol levels (hypercholesterolemia) are relatively common in the West. Hypercholesterolemia is associated with the development of atherosclerosis, coronary heart disease, myocardial infarction and increased mortality. One class of drugs, referred to collectively as statins, have proven to be extremely effective in lowering plasma LDL levels and in reducing the progression of atherosclerosis and clinically associated problems.

Mevinolin is a fungal metabolite that is structurally related to HMG-CoA. It was originally discovered in 1976 by Akira Endo in Japan and shown to be a potent competitive inhibitor of HMG-CoA reductase; it binds to the enzyme with a $K_i \sim 10^{-9}$ M, compared to a K_m of $\sim 10^{-6}$ M for the natural substrate HMG-CoA. Subsequent studies by many investigators led to the identification of a number of natural and synthetic compounds that also inhibit the enzymatic activity of HMG-CoA reductase. These drugs are collectively known as statins. When taken orally, these drugs are absorbed and targeted to the liver where they bind and partially inhibit HMG-CoA reductase and cholesterol synthesis. The liver cells "sense" this decrease in newly synthesized cholesterol and respond by enhancing the cleavage and nuclear localization of SREBP-2 (Figure 2). As a result, expression of a number of genes, including the LDL receptor and HMG-CoA reductase are increased. The increased expression of the LDL receptor

protein on the hepatocyte cell surface results in increased clearance of cholesterol-rich LDL from the plasma into the liver. This is the molecular basis for the clinical effects of the drug. Fortunately, the liver does not become loaded with lipid because it converts the LDL-derived cholesterol to bile acids and excretes the latter in the bile. In summary, oral administration of statins results in an increased rate of removal of LDL from the blood and a 30–50% decline in blood LDL cholesterol levels. Such a change has been shown to reduce both the progression of coronary atherosclerosis and the incidence of myocardial infarction and death.

A number of epidemiological studies have recently reported that statins also reduce osteoporosis and improve the status of patients with Alzeimers. However, at the current time, these latter conclusions are highly controversial and additional studies will be necessary to determine whether these drugs have such additional benefits.

Bisphosphonates

Bisphosphonates are potent inhibitors of bone resorption and are used widely to treat osteoporosis. After absorption, these drugs are targeted to bone, where they are taken up by osteoclasts, the bone-resorping cells. The bisphosphonates inhibit farnesyl diphosphate synthase and isoprenoid synthesis (Figure 1). As a result, the osteoclasts undergo apoptosis and bone resorption is attenuated.

See Also the Following Articles

Fatty Acid Oxidation • Fatty Acid Synthesis and its Regulation • LipoProteins, HDL/LDL

Glossary

HMG-CoA reductase 3-Hydroxy-3-methylglutaryl coenzyme A reductase, the rate-limiting enzyme of cholesterol biosynthesis.

SCAP SREBP cleavage activating protein. SCAP is required for the transport of SREBP from the endoplasmic reticulum to the Golgi.

SREBP Sterol regulatory element binding protein, a transcription factor that is proteolytically processed before entering the nucleus and binding to a *cis* element on the DNA, termed sterol regulatory element (SRE).

statins A class of drugs that inhibit the activity of HMG-CoA reductase.

Further Reading

Horton, J. D., Goldstein, J. L., and Brown, M. S. (2002). SREBPs: Activators of the complete program of cholesterol and fatty acid synthesis in the liver. *J. Clin. Invest.* **109**, 1125–1131.

Osborne, T. F. (2001). CREating a SCAP-less liver keeps SREBPs pinned in the ER membrane and prevents increased lipid synthesis in response to low cholesterol and high insulin. *Genes Dev.* **15**, 1873–1878.

Porter, F. D. (2002). Malformation syndromes due to inborn errors of cholesterol synthesis. *J. Clin. Invest.* **110**, 715–724.

Sever, N., Yang, T., Brown, M. S., Goldstein, J. L., and Debose-Boyd, R. A. (2003). Accelerated degradation of HMG CoA reductase mediated by binding of Insig-1 to its sterol-sensing domain. *Mol. Cell* **11**, 25–33.

Tobert, J. A. (2003). Lovastatin and beyond: The history of the HMG-CoA reductase inhibitors. *Nat. Rev.* **2**, 517–526.

Biography

Dr. Peter Edwards is a Professor of both Biological Chemistry and Medicine at UCLA. His principal interests are centered on the roles of oxysterols and bile acids as agonists of two nuclear receptors, LXR and FXR. He holds a Ph.D. from the University of Liverpool, United Kingdom and received postdoctoral training at Stanford University. His group has purified/cloned and studied the regulation of a number of enzymes involved in cholesterol and isoprenoid biosynthesis.

Chromatin Remodeling

Eric Kallin and Yi Zhang
University of North Carolina, Chapel Hill, North Carolina, USA

A cell's ability to regulate gene expression has been directly linked to DNA packaging within the nucleus. The active process involved in the alteration of DNA packaging has been termed chromatin remodeling. Several types of enzyme complexes have been identified which are capable of altering the packaging state and thus affecting gene expression. To date, three distinct chromatin-remodeling mechanisms, including ATP-dependent nucleosome remodeling, covalent modification of histones, and histone variant incorporation, have been identified and each has been linked to gene expression by regulating chromatin dynamics. This article will briefly describe these three mechanisms as well as explain their relationship with gene expression.

Chromatin Basics

Researchers have known that certain proteins, called histones, were closely associated with DNA even before DNA was identified as the genetic material. When DNA was identified as the genetic material, it was thought that the histones only functioned as scaffolding for the wrapping of DNA so that the long stretch of DNA (3.2 cm long for human) can be contained within the cell nucleus (with a diameter of 4×10^{-3} cm). The first breakthrough in the studies of the role of histones in organizing DNA was made by Roger Kornberg in 1974. He found that core histones exist as defined octamers that are associated with DNA at nearly even intervals similar to that of "beads on a string." The basic repeating unit of chromatin, called the nucleosome, includes two copies of each of the four core histones, H2A, H2B, H3, and H4. Further biochemical analysis has shown that each histone octamer is encircled almost twice by DNA of 146 bp. Large numbers of noncovalent bonds form between the DNA and the histone proteins resulting in a stable complex. A fifth histone protein, called H1, binds to the linker DNA of two adjacent nucleosomes to maintain the higher-order chromatin structure.

The function of a given cell is largely determined by the sets of genes that it expresses. Cells control their gene expression mainly at the transcriptional level which involves binding of specific transcription factors to DNA elements located at the promoter regions of a given gene. Compacting of DNA into chromatin impedes access to transcription factors thus stopping gene expression. Therefore, regulation of chromatin structure and nucleosome placement along the DNA strand has a significant impact on gene expression. Studies in the past 10 years have revealed at least two groups of enzymes capable of modulating chromatin structure. The first group involves factors utilizing the energy derived from ATP hydrolysis to "remodel or relocate nucleosomes." The second group involves enzymes that covalently modify core histone proteins. Recent studies also indicate that substitution of regular histones with their variants also affects chromatin structure.

ATP-Dependent Nucleosome Remodeling

ATP-dependent nucleosome remodeling refers to the use of energy derived from ATP hydrolysis to fuel a reaction that results in the translocation of a nucleosome to another portion of the DNA molecule. If a nucleosome is positioned in such a way that an important regulatory DNA element is blocked from transcription factor binding, relocating that nucleosome to another portion of DNA could expose the binding site and result in gene expression. ATP-dependent nucleosome-remodeling factors usually exist in multiprotein complexes. A common feature of these protein complexes is that they all contain a subunit capable of hydrolyzing ATP. Based on the ATPase subunit, the known remodeling factors have been grouped into three families.

Remodeling Enzymes

SWI/SNF Family

The SWI/SNF family of proteins was first identified in budding yeast by genetic screens to identify genes that are involved in mating type switch (SWI) and sucrose nonfermenting (SNF). Sequence analysis revealed that *SNF2* and *SWI2* encode the same protein which is

the founding member of an ATPase family. Biochemical and genetic studies led to the identification of an 11-subunit complex, named the SWI/SNF complex, capable of increasing the accessibility of nucleosomal DNA by transcription factors. Components of this complex have been linked to ATPase activity (Snf2), nonspecific-DNA-binding activity (Swi1), and nuclear-structure binding (Arp7 and Arp9). A highly related complex called remodels structure of chromatin (RSC) has also been identified in budding yeast. The ATPase subunit of RSC has been named Sth1 and is homologous to Snf2 of the SWI/SNF complex. In comparison with the SWI/SNF complex, RSC is a much more abundant complex. Genes that encode components of the RSC complex are essential for yeast survival. Protein complexes homologous to the yeast SWI/SNF complex have been identified in other multicellular organisms such as *Drosophila* and human.

ISWI Family

Using a functional assay that measures activities capable of disrupting regular nucleosome spacing, Carl Wu and colleagues purified the nucleosome remodeling factor (NURF) complex from *Drosophila* embryo extracts. The complex is composed of four subunits, including the ATPase, imitation switch (ISW) I. In addition to NURF, ISWI was also found to be present in two other *Drosophila* remodeling factors, ACF (ATP-utilizing chromatin assembly and remodeling factor) and CHRAC (chromatin accessibility complex). Although ISWI by itself is able to remodel nucleosomes *in vitro*, it functions in one of the three complexes *in vivo*. At least three homologous complexes containing the ISWI homologue hSNF2h have been identified in humans and two complexes containing the ATPase ISW1 and ISW2 have been identified in budding yeast.

Mi-2 Family

Mi-2 was initially identified as a nuclear autoantigen in patients with dermatomyositis. Two forms, Mi-2α (or CHD3) and Mi-2β (or CHD4), which are 72% identical at the amino acid level, exist in human cells. They both belong to the chromo-helicase-DNA-binding (CHD) protein family, which includes at least four human family members. In addition to the conserved SWI2/SNF2 helicase/ATPase domain present in the ATPase subunit of other nucleosome remodeling factors, the Mi-2 proteins also include two plant homeodomain (PHD) zinc-fingers, two chromo domains, and an HMG-like domain. Biochemical studies indicate that Mi-2 proteins exist in a protein complex named NuRD that possesses both nucleosome remodeling and histone deacetylase activities. Both HDAC1 and HDAC2 (histone deacetylase 1 and 2) are components of the NuRD complex. They interact with the PHD fingers of the Mi-2 protein. Recent studies indicate that the NuRD complex can associate with the methyl-CpG-binding protein MBD2 to form the MeCP1 complex. Thus, the NuRD complex links nucleosome remodeling and histone deacetylation to DNA methylation-mediated gene silencing. Although NuRD-specific subunits were not found in the budding yeast, homologues of Mi-2 and MTA2 proteins exist in *Drosophila* and *Caenorhabditis elegans*. Therefore, it is likely that the functional counterpart of NuRD was evolutionarily conserved in multicellular organisms.

Remodeling Mechanisms

Although all of the remodeling complexes identified so far have a component that possesses ATPase activity, the properties of their respective ATPases appear different. While the SWI2/SNF2 protein and SWI/SNF complexes exhibit DNA-stimulated ATPase activity, the ATPase activity of ISWI alone or in complex is only stimulated by nucleosomes. Moreover, SWI/SNF complexes seem to induce much more dramatic structural changes in nucleosomes than the ISWI complexes. These differences suggest that different remodeling factors may use different remodeling mechanisms. Based on the observation that in the presence of SWI/SNF and ATP, mononucleosomes can generate a novel nucleosome dimer species which has loosened histone–DNA contacts, an interconversion model was proposed to explain how the human SWI/SNF complex works. It is believed that interconversion between the two nucleosome states occurs constantly (Figure 1A). The SWI/SNF complex simply lowers the energy required for this interconversion. An alternative "octamer transfer" model was proposed to explain the mechanism of the RSC function (Figure 1B). The basis for this model was the observation that RSC can completely disrupt histone–DNA contact and transfer the histone octamer to another molecule of DNA. As explained above, histones associate with DNA through a collection of noncovalent interactions. Given the large energy requirement for breaking the histone–DNA interactions, the "octamer transfer" model appears unlikely. Therefore, a third "octamer sliding" model (Figure 1C) was proposed for NURF and CHRAC. In contrast to RSC, NURF and CHRAC increase the mobility of histone octamers along DNA without affecting the integrity of the octamer. The basis of this model is that both NURF and CHRAC can promote nucleosome redistribution to one favored position. Whether any of the models are correct *in vivo* remains to be determined.

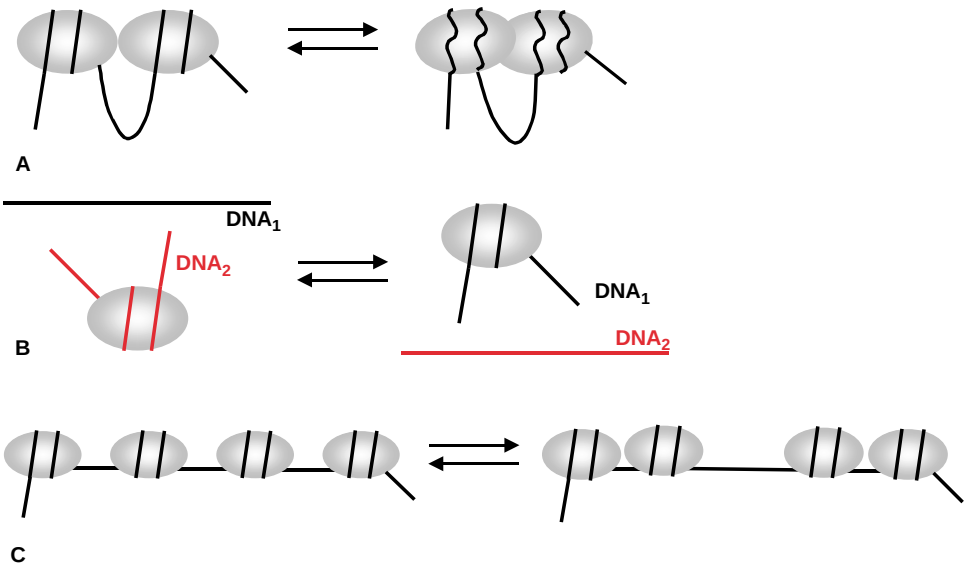

FIGURE 1 Schematic representation of the proposed ATP-dependent remodeling mechanisms. (A) Interconversion model (nucleosome destabilization model). (B) Octamer transfer model showing a histone octamer being transferred from one molecule of DNA to another. (C) Octamer sliding model showing the regularly spaced nucleosomes are disrupted. All three models would result in segments of DNA becoming more accessible to additional protein complexes.

Targeting of Activity

The above-described remodeling factors were first thought to bind and randomly scan DNA for nucleosome targets. However, this view changed when the BRG1 remodeling complex was found to interact with the glucocorticoid receptor, a sequence-specific DNA-binding transcription factor. Recruitment of a remodeling factor by a sequence-specific transcription factor could result in localized nucleosome remodeling and transcriptional activation. Similarly, the methyl-CpG-binding protein MBD2 could recruit the NuRD complex to patches of methylated DNA resulting in targeted remodeling, histone deacetylation, and consequently repression of methylated promoters. A third targeting strategy has developed in SWI/SNF through its ARP7/9 subunits. These proteins have distinct domains that can bind to actin and actin-related proteins which in turn target the protein complex to specific chromatin domains. A common feature of these strategies is to bring the remodeling complex into close proximity with DNA promoter sequences to achieve precise control of gene expression.

Covalent Modifications

As an important component of the nucleosome, each core histone is composed of a structured, three-helix domain called the histone fold and two unstructured tails. Although the histone tails are dispensable for the formation of the nucleosome, they are required for nucleosome–nucleosome interaction. The core histone tails are susceptible to a variety of covalent modifications, including acetylation, phosphorylation, methylation, and ubiquitination (Figure 2). Although these modifications were identified in the early 1960s, their function was not understood until very recently. The identification of the first nuclear histone acetyltransferase (HAT) by David Allis and colleagues has led to intensive studies on the function of these histone modifications. As a result, enzymes responsible for each of the modifications have been identified and the functions of these modifications, particularly in transcriptional regulation, are beginning to be dissected.

Acetylation

Since the discovery of histone acetylation by Allfrey and colleagues in 1964, many studies on this modification have been performed. As a result, this modification is the best-studied histone modification that has a direct effect on gene regulation. In contrast to the N-terminal α-acetylation on many proteins, histone acetylation occurs on the ε-amino group of specific lysine residues in the N-terminal tails. Acetylation involves the transfer of an acetyl group from acetyl-CoA onto the ε-amino group of lysine residues, which neutralizes the positive charge of the histone tails and decreases their affinity for DNA. Deacetylation, on the other hand, involves the removal of the acetyl group, thus introducing a positive charge on the histone tails. Enzymes that catalyze the acetylation process are referred to as histone acetyltransferases (HATs). Enzymes that

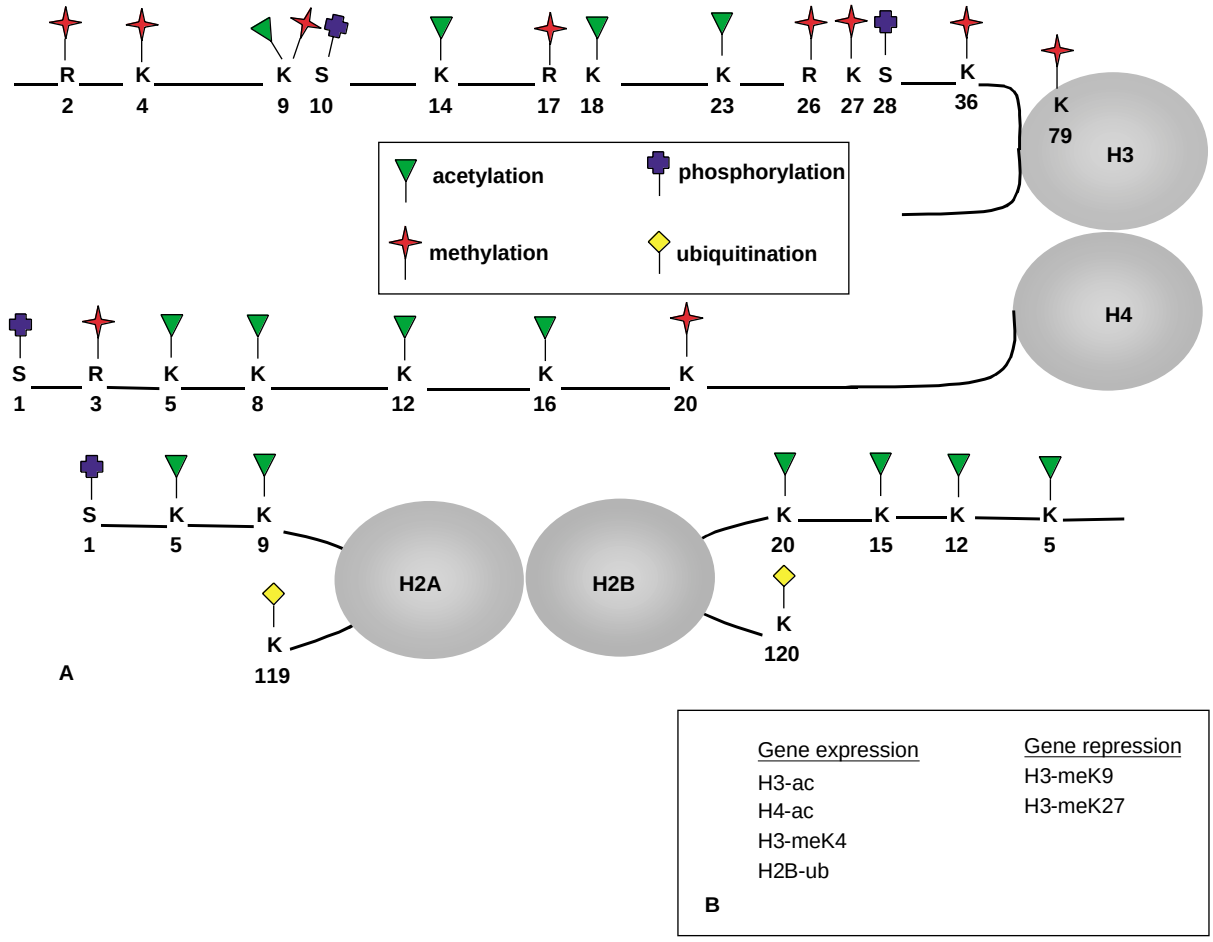

FIGURE 2 (A) Sites of known core histone post-translational modifications. (B) List of general gene expression patterns relating to histone modifications.

catalyze the reverse process are called histone deacetylases (HDACs).

Numerous HATs and HDACs have been identified and several of these enzymes are conserved across the eukaryotic spectra. While a number of the HATs, such as Gcn5, p300, and PCAF, function as transcriptional coactivators; several HDACs function as transcriptional corepressor. In general, histone acetylation leads to the relaxation of chromatin structure and thus correlates with gene activation. In contrast, histone deacetylation leads to condensation of chromatin structure and thus correlates with gene repression. Therefore, histones in the actively transcribed chromatin region, the euchromatin, are hyperacetylated while histones in the silenced chromatin region, the heterochromatin, are hypoacetylated. It has been shown that the enzymatic activities of both HATs and HDACs are important in transcriptional regulation, as inactivation of the enzymatic activity by mutagenesis of the catalytic site impairs both the enzymatic activity and their transcriptional activity. It is believed that histone acetylation levels affect higher-order chromatin structure. Therefore, acetylation likely impacts transcription by affecting the accessibility of transcription factors to their cognate DNA.

Methylation

First described in 1964, histones have long been known to be a substrate for methylation. Early studies using metabolic labeling followed by sequencing of bulk histones have shown that several lysine residues, including lysines 4, 9, 27, 36, and 79 of H3 and lysine 20 of H4, are the preferred sites of methylation. Recent studies indicate that histone methylation can also occur on arginine residues, including arginine 17 of H3 and arginine 3 of H4 (Figure 2). Arginine can be either mono- or dimethylated, with the latter in symmetric or asymmetric configurations. Proteins that catalyze histone arginine methylation belong to the protein arginine methyltransferases (PRMT) family. PRMT1 and PRMT4 catalyze H4-R3 and H3-R17 methylation, respectively. Accumulating evidence indicates that histone arginine methylation plays an important role in nuclear hormone-mediated transcriptional activation.

Although histone arginine methyltransferases were discovered before histone lysine methyltransferases, the latter have recently attracted more attention. Since the discovery of the first lysine methyltransferase SUV39H1, many histone methyltransferases (HMTases) that target to different lysine residues on histone H3 and histone H4 have been discovered. A common feature of these histone lysine methyltransferases is that they all contain an evolutionarily conserved SET domain, a motif shared in the *Drosophila* PEV (*p*osition *e*ffect *v*ariegation) suppressor Su(var)3-9, the *Polycomb*-group protein E(z), and the *trithorax*-group protein Trx. Recent studies, however, have uncovered that lysine 79 of histone H3, located in the globular domain, is also methylated in diverse species from yeast to human. Surprisingly, the responsible enzymes, DOT1 and its homologues, do not contain a SET domain. Thus, lysine methylation can be catalyzed by proteins with or without a SET domain.

Unlike histone acetylation which usually results in gene activation, the effect of histone methylation on transcription is site dependent. While H3-K4 methylation correlates with gene activation, methylation on H3-K9 and H3-K27 usually causes gene silencing. Recent studies indicate that even on the same site, the outcome of methylation may be different depending on whether it is a mono-, di-, or trimethylation. These site-specific or methylation state-specific effects may reflect the fact that different modifications are recognized and interpreted by different protein modules, such as the chromadomain and bromodomain, as suggested by the "histone code" hypothesis. Studies in the past three years have revealed that this modification has significant effects on multiple biological processes ranging from heterochromatin formation and transcriptional regulation to genomic imprinting, X-chromosome inactivation, and DNA methylation. How this modification results in such a diverse effect is currently unknown.

Phosphorylation

Both the linker histone H1 and core histones undergo phosphorylation on specific serine and threonine residues (Figure 2). Phosphorylation of histones is cell-cycle dependent with the highest level of phosphorylation occurring in M phase. H1 phosphorylation occurs on both N-terminal and C-terminal domains and is linked to transcription. For example, inactivation of the MMTV promoter correlates with H1 dephosphorylation while reactivation of the promoter correlates with H1 rephosphorylation.

Recent studies indicate that phosphorylation of serines 10 and 28 of H3 are tightly regulated and are implicated in the establishment of transcriptional competence of immediate early-response genes. For example, induction of early-response genes, such as c-*fos* and c-*jun*, is concurrent with H3 phosphorylation. Both the MAP (mitogen-activated protein kinase) pathway and the stress-activated p38 pathway are involved in this process. At least two kinases, the ERKs-activated Rsk-2 kinase and the related Msk-1 (MAP- and stress-activated kinase 1), are responsible for the rapid H3 phosphorylation. Although phosphorylation of histones correlates with transcriptional activation of a small set of immediate-early genes that are rapidly turned on and off in response to extracellular signals, the bulk of histone phosphorylation occurs in M phase when genes are silenced. Recent studies indicate that mitotic histone phosphorylation correlates with chromosome condensation and is mediated by the Ipl1 and Aurora kinases.

In addition to transcription regulation, histone phosphorylation is also linked to other cellular processes such as DNA damage and apoptosis. For example, H2A.X, an H2A variant in mammalian cells, has been shown to be rapidly phosphorylated on S139 upon exposure to ionizing radiation. Interestingly, the phosphorylated form of H2A.X is localized to mega-base regions of DNA that flank sites of double-strand breaks, suggesting that this modification may function to facilitate access of repair machinery to damaged DNA. Recent studies on H2B indicate that H2B-S14 phosphorylation is tightly associated with apoptotic chromatin and that the caspase-cleaved Mst1 (mammalian sterile twenty) kinase is responsible for this modification.

Ubiquitination

In addition to the modifications discussed above, histones and their variants can also be reversibly ubiquitinated. Unlike other modifications which result in the addition of relatively small moieties, ubiquitin is a highly conserved 76 amino acid protein. Ubiquitination occurs on the ε-amino group of specific lysine residues (H2A-K119 and H2B-K120). In higher eukaryotic cells, about 10% of H2A and 2% of H2B are ubiquitinated. While mono-ubiquitination is the major form of H2B ubiquitination, polyubiquitination, where ubiquitin molecules join to each other by isopeptide bonds, has been reported for H2A.

H2B ubiquitination has long been linked to transcriptionally active genes. It is possible that actively transcribing genes have an open chromatin structure exposing the C terminus of H2B to the enzymes catalyzing the addition of ubiquitin. Studies in the budding yeast have identified Rad6 as an H2B ubiquitination enzyme. Recent studies also indicate that methylation on H3-K4 and H3-K79 in budding yeast is dependent on Rad6 and H2B ubiquitination suggesting that different modifications have "crosstalk." It is believed that ubiquitination may serve as a signal for

the recruitment of other histone-modifying enzymes, such as histone methyltransferases. However, whether this is the case awaits demonstration.

Modification Crosstalk and the "Histone Code" Hypothesis

In addition to the crosstalk between histone methylation and ubiquitination mentioned above, crosstalk also has been shown among other modifications. For example, H3-K9 methylation and H3-S10 phosphorylation inhibit each other. H3-S10 phosphorylation, on the other hand, appears to act synergistically with H3-K14 acetylation. Moreover, it has been demonstrated that methylation on H3-K9 by SUV39H1 inhibits subsequent histone acetylation by p300, while methylation on H3-K4 by SET7 facilitates subsequent histone methylation by p300. Given that histone acetylation is linked to gene expression, the differential effects of histone methylation on subsequent acetylation provide an explanation as to why methylation on different lysine residues results in different outcomes on gene expression.

Based on the observed cross-talks, David Allis and Bryan Turner have proposed a "histone code" hypothesis. This hypothesis predicts that a pre-existing modification affects subsequent modifications on histone tails and that these modifications serve as markers for the recruitment of different proteins or protein complexes to regulate diverse chromatin functions, such as gene expression, DNA replication, and chromosome segregation. The best available evidence supporting this hypothesis is derived from the identification of protein modules that recognize specific modifications on histones. For example, the bromodomain, a motif present in many chromatin-related proteins, can specifically bind to acetylated

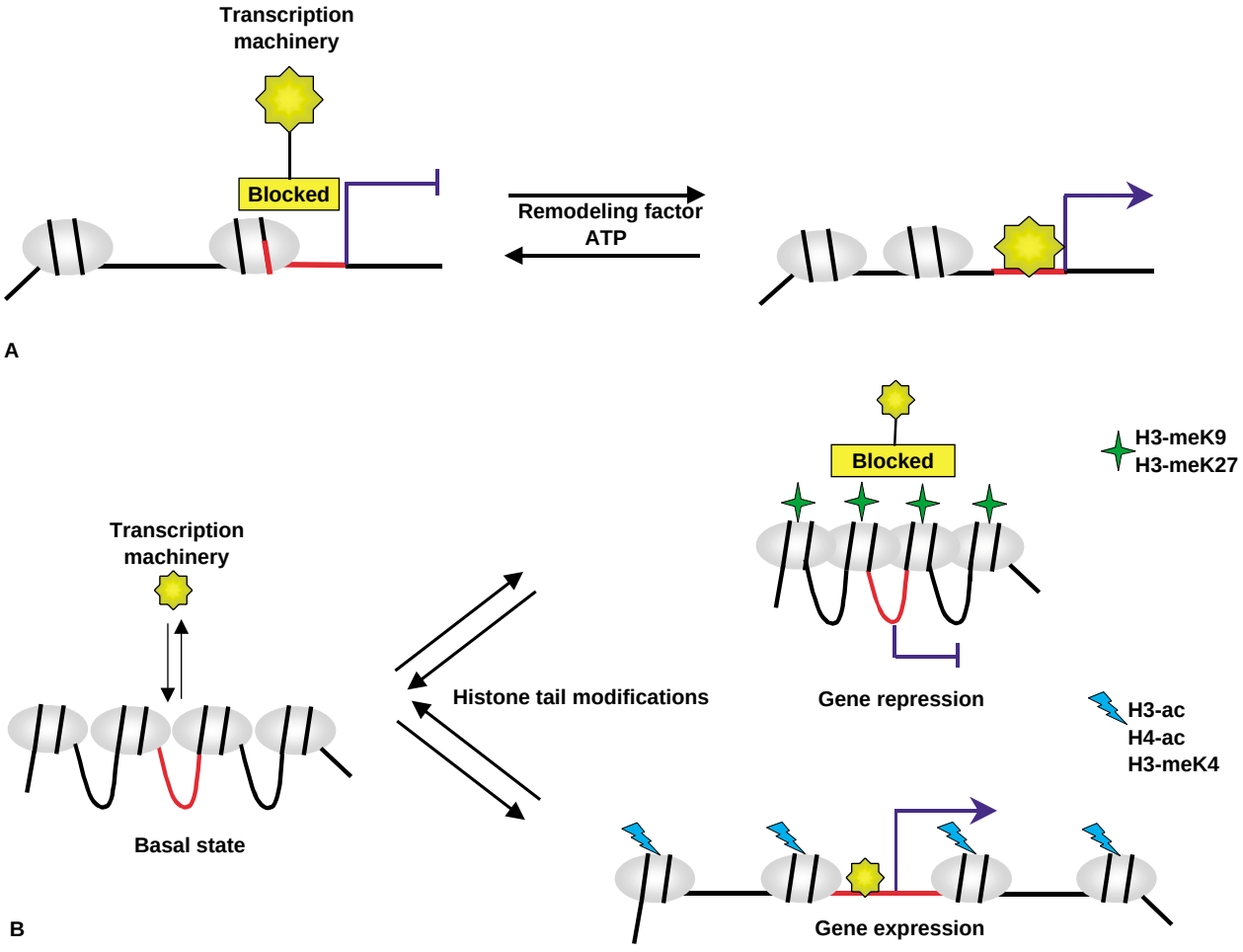

FIGURE 3 General mechanisms of chromatin remodeling and histone modification in relation to gene expression. Sunburst represents transcriptional machinery and associated factors, red lines represent gene promoter regions, stars and lightning bolts represent different histone tail modifications. (A) ATP-dependent chromatin remodeling can lead to blocked promoters becoming accessible to transcription stimulating complexes. (B) Histone tail modifications can lead to gene repression or expression depending on the modification.

lysine residues. Similarly, chromodomain, a motif also present in many chromatin-related proteins, can specifically bind to methylated lysine residues. It is believed that the unique set of covalent modifications present on a given nucleosome serves as a "landing pad" for the recruitment of additional proteins that "read" or "interpret" the "histone code" to decide the outcome. Defining the "histone code" and identifying protein modules that read the code remain a challenge for the people in the chromatin and transcription field.

Histone Variants

A discussion of chromatin and gene expression would not be complete without mention of histone variants. Several variations of "conventional" histone proteins have been identified in all eukaryotes from yeast to man. These variations on the histone proteins are usually found complexed in the octamer with the "normal" versions of the other histone proteins within defined regions of DNA. A well-documented H3 variant called CENP-A has been found to mark centromeres in all eukaryotic organisms studied thus far. Centromeric chromosomal regions have very few genes and are compacted into repressed heterochromatin. In contrast, the H2A variant called H2A.Z has been found to associate with inducible promoters. These are thought to play a role in the signal transduction pathways necessary for the expression of inducible genes. In addition, another H2A variant, H2A.X has been found to be specifically enriched in the proximity of double-strand break.

Putting it All Together

While compacting DNA into a manageable structure is important for cell integrity, it also creates the problem of restricting the access of important regulators from DNA elements. To circumvent this potentially dangerous problem, the cell has developed a rather complex scaffold of histone proteins that can be altered and modified to expose important regions of the DNA. Covalent modifications of histone tails can serve to disrupt higher-order chromatin structure returning DNA to a "beads on a string" state. ATP-dependent nucleosome remodeling machinery can reveal DNA sequences masked by nucleosome interaction to important regulatory proteins, and variant histones can serve to mark complete functional domains within the chromosome (such as repressed centromeric regions) as active or inactive transcriptional regions. Studies in the past 10 years have changed our view of chromatin from a static structure to a dynamic regulatory machine that impacts all aspects of biological processes involving DNA (Figure 3). A combination of all the regulatory systems that a cell uses to modulate chromatin structure is the basis on which the complexity and diversity of life is built.

See Also the Following Articles

Actin-Related Proteins • Centromeres • Chromatin: Physical Organization • Chromosome Organization and Structure, Overview • DNA Replication: Eukaryotic Origins and the Origin Recognition Complex • Metaphase Chromosome • Nuclear Organization, Chromatin Structure, and Gene Silencing • Ubiquitin System

Glossary

bromodomain A distinct protein domain that is found in chromatin-related proteins in a variety of organisms from mammals to yeast. Bromodomain binds specifically to acetylated lysine residues on histone proteins.

chromatin Name given to the DNA–protein complex present in the nucleus of eukaryotic cells.

chromodomain The chromatin-organization-modifier domain, a conserved region of ~60 amino acids, originally identified in *Drosophila* modifiers of variegation. Recent studies indicate that this domain binds specifically to methylated lysine residues on histone proteins.

nucleosome The repeating unit of chromatin composed of DNA wrapped around a histone octamer consisted of two copies each of H2A, H2B, H3, and H4.

Further Reading

Becker, P. B., and Horz, W. (2002). ATP-dependent nucleosome remodeling. *Annu. Rev. Biochem.* **71**, 247–273.

Cheung, P., Allis, C. D., and Sassone-Corsi, P. (2000). Signaling to chromatin through histone modifications. *Cell* **103**, 263–271.

Kornberg, R. D., and Lorch, Y. (1999). Twenty-five years of the nucleosome, fundamental particle of the eukaryotic chromosome. *Cell* **98**, 285–294.

Moore, S. C., Jason, L., and Ausio, J. (2002). Elusive structural role of ubiquitinated histones. *Biochem. Cell Biol.* **80**, 311–319.

Roth, S. Y., Denu, J. M., and Allis, C. D. (2001). Histone acetyltransferases. *Annu. Rev. Biochem.* **70**, 81–120.

Strahl, B. D., and Allis, C. D. (2000). The language of covalent histone modifications. *Nature* **403**, 41–45.

Zhang, Y., and Reinberg, D. (2001). Transcription regulation by histone methylation: Interplay between different covalent modifications of the core histone tails. *Genes Dev.* **15**, 2343–2360.

Biography

Eric M. Kallin is a graduate student in the curriculum in Genetics and Molecular Biology at the University of North Carolina at Chapel Hill. He received his B.S. in Biochemistry at the State University of New York at Geneseo. His current research, understanding the role of epigenetic modifications in cell lineage commitment, is being carried out in the laboratory of Dr. Yi Zhang.

Yi Zhang is an assistant Professor of the Department of Biochemistry and Biophysics and a member of the Lineberger Comprehensive Cancer Center at the University of North Carolina at Chapel Hill. His research interest centers on the role of chromatin remodeling and histone tail modification in gene expression and cell lineage commitment. He obtained his Ph.D. from Florida State University in 1995. He made seminal discoveries that link nucleosome remodeling to histone tail modification. His laboratory at UNC has been responsible for the discovery of a number of novel histone methyltransferases.

Chromatin: Physical Organization

Christopher L. Woodcock
University of Massachusetts, Amherst, Massachusetts, USA

The term chromatin was coined by cytologists to designate the brightly staining portions of nuclei exposed to basic dyes. Although this terminology is still in effect, in the context of biological chemistry, chromatin usually refers to the complex of DNA and protein that is present in the interphase nucleus, and can be isolated for study *in vitro*. As with all biological systems, the physical organization of chromatin results from the intrinsic biochemical properties of the components as influenced by the composition of the aqueous medium. Since chromatin organization plays a critical role in many aspects of gene regulation, there is much interest in understanding the basic principles involved. Here, the current status of this challenging task is discussed in terms of the major components of chromatin, their interactions, and the complex, dynamic "biopolymer" that results.

A crude analysis of isolated chromatin reveals a 1:1 ratio of DNA and histones, small, highly conserved basic proteins. Four species of histone (H2A, H2B, H3, and H4) contribute two copies each to the histone core of the nucleosome, a disk-shaped structure 11 nm in diameter and 6 nm in height, while histone H1 binds to the exterior of the nucleosome. Other proteins bound to DNA in chromatin are collectively known as "non-histone chromatin proteins" (NHCPs), and include both structural and enzymatic components. Thus, at the simplest level, the physical organization of chromatin consists of very long linear arrays (one for each chromosome) of nucleosomes arranged in a beads-on-a-string conformation, together with bound NHCPs. This "primary structure" is variously folded and compacted, and (in the interphase nucleus) occupies a distinct volume or "territory" with little or no intermixing with other chromosome territories. Prior to cell division, a complex series of events transforms interphase chromatin into the familiar linear metaphase chromosomes. It is clear that the arrays of nucleosomes are exposed to a wide range of local and global factors that influence the degree of chromatin compaction, and the challenge has been to understand the impact of these factors on the physical organization. There is strong evidence that features of chromatin organization such as compaction level are related to mechanisms of differential gene expression. Further, some aspects of chromatin organization are important in epigenetic inheritance, whereby properties such as differential gene silencing or activation are inherited not as differences in DNA sequence, but as specific chromatin structures and their components.

Global factors that influence the physical organization of chromatin include the ionic milieu of the nucleus, especially the concentrations of monovalent and divalent cations, and polycations such as polyamines. The combination of charge shielding and charge neutralization that results from exposure of chromatin to cations *in vitro* results in stronger intra-chromatin interactions (as the self-repulsive properties of DNA are negated) and greater compaction. Indeed, at the concentration of cations thought to be present in the living nucleus, chromatin *in vitro* tends to aggregate and essentially precipitate. Modulating the effects of cations are local variations in nucleosomes (histone variants, histone modifications), DNA modifications (chiefly cytosine methylation), and bound NHCPs (often related to histone modifications). Thus, the chromatin template has the potential to assume a continuum of compaction levels, and it is this context that its physical organization has to be viewed. In this article, the principal variables that can influence the structure and function of a given portion of the genome are outlined, after which the question of physical organization is discussed.

Variables that may Influence Chromatin Physical Organization

Posttranslational Modifications of Core Histones

The presence of a large variety of core histone modifications has been known for many years, but its role in chromatin was very poorly understood. Recently, however, evidence has grown that the pattern of histone modifications on an individual nucleosome or array of nucleosomes encodes information that is essential in determining a variety of functional states. Many modifications occur on the N termini of the core histones which project from the nucleosome and are

unstructured in the sense that they are not detected in nucleosome crystals by X-ray analysis. Some, such as acetylation and methylation of lysine residues result in the net loss of a positive charge, and may in itself result in a change in chromatin conformation. However, it is clear that the functional implications of histone modification result from far more complex effects than alterations in charge balance.

For example, H4 acetylation can occur at one or more of four lysines in the N terminus, and these modifications alone, and in combination, carry important functional signals. The net acetylation pattern is the result of the balance between histone acetylase (HAT) enzymes and deacetylase (HDAC) enzymes. Both HATs and HDACs tend to occur in large complexes that may contain proteins that serve to target the enzymatic activity to the appropriate gene(s). Specific acetylation patterns also occur on newly synthesized chromatin, and are erased after deposition as nucleosomes close to the replication fork.

Another key set of histone modifications involves the methylation of lysines on histone H3. Here, another level of complexity arises because the methyl transferases may deposit one, two, or three methyl groups, and the number of methyl groups provides another signal. Certain methylation patterns are important in providing binding sites for a group of NHCPs known as heterochromatin protein 1 (HP1). HP1 tends to accumulate on transcriptionally silent chromatin and appears to be involved in the down-regulation of genes.

Variants of Core Histones

Typically, higher organisms have several genes for each of the core histones, some of which may be identical in sequence, while others vary in amino acid sequence. The majority of core histone genes are transcribed only during DNA replication, and are incorporated into nucleosomes in the wake of the replication fork. Others are synthesized constitutively, and incorporated into nucleosomes only at the relatively rare event of displacement of a complete histone octamer. An interesting example is provided by the replication coupled H3 and the H3.3 variant which can be deposited in both replication-coupled and replication-independent pathways, and which differ at only four amino acid positions. Single amino acid changes of H3 toward H3.3 allow replication independent deposition. H3.3 accumulates modifications that favor transcription, while H3 accumulates lysine methylations, a mark of "inactive chromatin." Although H3 is by far the most abundant variant in higher organisms, it is likely to have evolved from H3.3, which is the only H3 isoform in yeast. Another H3 variant which is highly conserved evolutionarily occurs only in centromeric chromatin.

Histone H1

Histone H1, also known as "linker histone," plays a dominant role in establishing the compaction state of an array of nucleosomes, as well as influencing the conformation. H1 has three domains: a central globular domain that binds near the entry/exit site of linker DNA on the nucleosome, and extended N and C termini. The C terminus is particularly rich in the basic amino acids lysine and arginine, and thus has a strong propensity to bind DNA. H1 binding protects an extra $\sim$20 bp of nucleosomal DNA from nuclease digestion, a protection conferred by the globular region alone. There is a general correlation between the amount of H1 in chromatin, and its ability to be transcribed, and most models of transcriptional regulation call for the displacement of H1. The silencing effect of H1 could be due to the "sealing" of two turns of nucleosomal DNA, thus preventing the unwrapping needed for RNA polymerase, or to the H1-induced physical compaction of arrays of nucleosomes or most likely to a combination of both.

Like the core histones, there are several variants of H1 in most higher organisms, but little is known about their individual properties. Genetic manipulations of mice that knock out one or two variants produce no observable phenotype, and the remaining variants are up-regulated to compensate for the loss. The loss of additional variants leads to a depletion in total H1 and eventually embryonic lethality. However, in H1-depleted nuclei, there is no general derepression of transcription, as predicted by the simple model that H1 loss should create "open" and permissive chromatin.

NHCPs

A two-dimensional gel of the proteins bound to the chromatin of an active nucleus reveals hundreds of spots, and it is clear that there are many other proteins present in low abundance that are revealed only after staining with specific antibodies. To date, relatively few of these NHCPs have been studied in detail, and most of these are either abundant in the nucleus, or came to researchers' attention through functional studies of specific genes or classes of genes. Most NHCPs can be eluted from chromatin by treatment with 0.3–0.4 M monovalent ions (usually NaCl), in contrast to H1 which requires 0.5–0.6 M NaCl and the core histones which elute between 0.8 and 2.0 M salt. There is some evidence that the few proteins that remain bound in 2.0 M salt contribute to a nuclear skeleton (karyoskeleton, nuclear matrix), which provides structural integrity to the nucleus, and has an important dynamic role in its spatial organization as well as replication and transcription. However, despite much effort, it has not been possible to reveal an *in vivo* karyoskeleton analogous to the cytoskeleton, and the possibility that

the residual proteins in salt-extracted (and usually DNase-treated) nuclei represent an aggregation phenomenon has not been excluded. The finding that the most abundant nuclear matrix proteins are associated with the peripheral nuclear lamina or are part of the RNA transcript processing machinery has reinforced these concerns.

The ubiquitous and abundant (typically 1 per 10–15 nucleosomes) high mobility group (HMG) proteins elute from nuclei in 0.3–0.4 M salt, and were originally grouped together on the basis of their solubility properties and rapid mobility in gels. A new nomenclature based on the presence of conserved domains or "boxes" distinguishes three classes. Members of the HMG-B group share the "HMG-box" functional domain, which contains three α-helices and, when bound to double-stranded DNA, induces a bend of $\sim 90°$. In contrast, the HMG-N family of proteins bind to nucleosomes via a nucleosome binding domain (NBD), resulting in a change of conformation, and the stimulation of transcription and replication. Finally, the HMG-A family members contain three "A–T hook" motifs that bind preferentially to the minor groove of DNA rich in AT sequences. HMG-A proteins appear to participate in a wide range of chromatin-based processes and are often up-regulated in cancerous cells. The lack of sequence specificity of all the HMG proteins suggests that they are targeted to the appropriate sites by interactions with other nuclear proteins, and evidence is accumulating for many such interactions.

The HP1 family of NHCPs, known to play a role in epigenetic inheritance, is also conserved across a wide range of eukaryotes, with three isoforms, α, β, and γ found in mammalian nuclei. HP1 (as well as several other important NHCPs) molecules share a "chromo" domain which binds not to DNA but to the methylated form of lysine 9 on histone H3. HP1 also interacts with numerous other proteins, including an enzyme that methylates H3. This illustrates the complex interactions and feedback loops that are probably widespread in the nucleus.

The protein families discussed above are certainly only a small subset of the repertoire of NHCPs, but perhaps representative of the different modes of action, which range from modifying chromatin "architecture" to acting as targets for other proteins. Most NHCPs are not stably bound to chromatin, but are remarkably mobile within the nucleus.

Levels of Physical Organization

The large number of variables in chromatin composition have the potential to influence its global and local physical organization, especially the degree of compaction, and the related level of transcriptional competence (higher compaction correlates with reduced transcription). A useful approach is to consider chromatin compaction in terms of hierarchical levels of folding, using a nomenclature based on that devised for proteins (Table I). For chromatin, it is necessary to distinguish between "local" structures that may be confined to specific genes, portions of genes, or groups of genes, and "global" structures that are nucleus wide.

Global Primary Structures – The Nucleosome Repeat Length (NRL)

While the length of DNA incorporated into the nucleosome is fixed at 146 bp, the length of "linker" DNA between nucleosomes is variable. At the level of the whole nucleus, each cell type in an organism has a characteristic average NRL, most mammalian cells having NRLs between 175 and 195 bp. The longest

TABLE I

Hierarchical Classification Scheme for Chromatin Physical Organization

Level of chromatin physical organization	Examples of global features	Examples of local features
Primary – the linear arrangement of nucleosomes on DNA	The nucleosome repeat length	Preferred locations of nucleosomes and features such as DNase hypersensitive sites on a specific DNA sequence.
Secondary – structures formed by interactions of nucleosomes	The "30 nm" chromatin fiber	3D architecture of nucleosomes and regulatory proteins on a specific DNA sequence.
Tertiary – structures formed by interactions between secondary structures	Thicker fibers seen in nuclei and postulated to be composed of 30 nm fibers	Long-distance contacts possibly involving locus control regions, enhancers and promoters, or looped chromatin domains.
Quaternary and above – structures formed by interactions between tertiary structures etc.	No unambiguous examples – see text	Interphase chromosome territories; metaphase chromosomes

NRLs, measured to date, ~240 bp are in echinoderm sperm (which have unusual core and H1 histones), and the shortest, ~165 bp, derived from yeast (*Saccharomyces cerevisiae*), which lack a typical histone H1.

Local Primary Structures

Overlaying the global NRL for a given nucleus, and the general rule that nucleosomes are randomly deposited, there are many instances where nucleosomes on particular genes and gene-regulatory sequences may be positioned with base-pair precision, and the local NRL may differ from the global NRL. This local positioning often contributes to transcriptional regulation. For example, a nucleosome positioned on a promoter sequence may block the binding of proteins and protein complexes that are required for transcription initiation. Relieving such a transcriptional block may be achieved by a nucleosome "remodeling" process. Other cases are known where a specific DNA sequence is normally nucleosome free. These sites, which are most common in gene-regulatory sequences and are probably occupied by NHCPs *in vivo*, may be detected by their hypersensitivity to nucleases.

Specialized DNA sequences may have a characteristic NRL that differs from the global value. The long stretches of gene-free chromatin at the ends (telomeres) of chromosomes, which consist of tandem repeats of TTAGGG typically have a shorter NRL than bulk chromatin.

Local primary structures may also be influenced by cytosine methylation of CpG dinucleotides, followed by binding of methylated DNA-binding proteins (MBDs). Some MBDs have binding sites for HDAC complexes, leading to local histone deacetylation and hence transcriptional silencing, and there is evidence that MBDs may promote chromatin compaction.

Global Secondary Structures – The "30 nm" Chromatin Fiber

If chromatin is isolated from nuclei and observed by electron or atomic force microscopy, it is seen to have a conformation highly dependent on the ionic strength of the medium – at low ionic strength (5–25 mM Na^+), the linear array of nucleosomes is clearly seen, while at higher ionic strengths, increasing compaction occurs, leading to the formation of an irregular fiber ~30 nm in diameter. This reversible transformation, which is dependent on H1, can also be monitored by changes in physical properties such as sedimentation velocity. Much research effort has been expended on determining the physical organization of the 30 nm fiber, and several different models have been proposed. The most widely discussed are solenoidal structures in which the linker DNA continues the superhelix established in the nucleosome, creating a "stack-of-coins" which subsequently coils into a 30 nm diameter fiber, and zigzag structures in which the linker DNA remains more or less straight and compaction results from the accordion-like compression of the zigzag. Among recent results supporting a zigzag arrangement are computer models derived from force-extension curves of individual chromatin fibers (Figure 1), which bear a striking similarity to native chromatin fibers imaged in the hydrated form (Figure 2). The physical irregularity of native chromatin fibers, which probably results largely from the local variations in NRL has contributed to the ongoing controversy. The ability to reconstitute artificial chromatin with regularly spaced nucleosomes may finally provide an unequivocal answer to the structure of the 30 nm fiber.

Local Secondary Structures

There is much evidence that local chromatin secondary structures play a large role in chromatin function by promoting or repressing transcription, but little is known of the precise physical organization of these local structures. In some instances, it has been demonstrated that a stretch of chromatin may accumulate many copies of NHCP that acts as a transcriptional silencer (e.g., HP1), but the difficulty of isolating single gene chromatin for observation precludes rapid progress.

Tertiary and Higher Level Features

Although it is often assumed that native chromatin exists as a series of hierarchical structures above the 30 nm chromatin fiber (and such illustrations are common in textbooks), there is very little solid supporting data. Methods used to examine isolated 30 nm fibers fail to reveal tertiary or higher levels of folding as the ionic

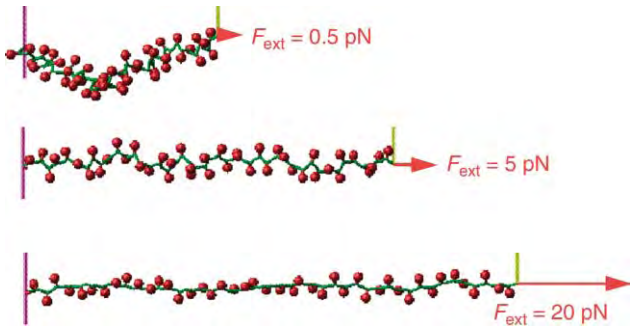

FIGURE 1 Computer models of chromatin secondary structure at different levels of extension (F_{ext}) based on force-extension data derived from pulling single chromatin fibers. Nucleosome core particles are represented by red spheres, and linker DNA by green rods. Modified from Katritch, V., Bustamante, C., and Olson, W. K. (2000). Pulling a single chromatin fiber: Computer simulations of direct physical manipulations. *J. Mol. Biol.* **295**, 29–40.

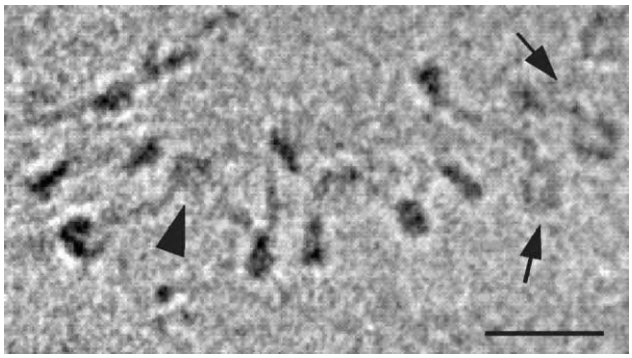

FIGURE 2 Chromatin fiber observed in the frozen hydrated state in 20 mM NaCl. Many of the nucleosomes are viewed edge-on and appear as dark ovals. Arrowheads point to two nucleosome showing the circular enface profile. The zigzag secondary structure bears a strong resemblance to the model in Figure 1. Scale is 30 nm. From Bednar, J., Horowitz, R. A., Grigoryev, S. A., Carruthers, L. M., Hansen, J. C., and Woodcock, C. L. (1998). Nucleosomes, linker DNA, and linker histone form a unique structural motif that directs the higher-order folding and compaction of chromatin. *Proc. Natl Acad. Sci. USA* **95**, 14173–14178.

strength is increased toward the "physiological" level. Rather, chromatin tends to aggregate. Examination of thin sections of nuclei in the electron microscope reveals many different "fiber" diameters ranging up to 240 nm, with no clear hierarchical arrangement. Indeed, only under rather specialized conditions and with inactive nuclei can 30 nm fibers be routinely observed in sections. Whether this lack of order *in situ* is due to problems of adequate structural preservation, or simply to a very unstructured and dynamic native organization remains to be seen.

Chromatin Dynamics

Recent work has revealed that living nuclei are remarkably dynamic. While the nucleosome core histones are long lived and stably incorporated, histone H1 binds to chromatin with a half-life of a few minutes, and most NHCPs have half-lives of a few seconds. Modeling of chromatin fibers based on thermodynamic principals indicates a constant fluctuation in local compaction. Also, individual clusters of genes may change dramatically in compaction state and even location in the nucleus when transcription is stimulated. These observations reinforce the concept of the living nucleus as a highly dynamic entity, both in terms of genetic activity and physical organization.

See Also the Following Articles:

Chromatin Remodeling • Metaphase Chromosome • Nuclear Organization, Chromatin Structure, and Gene Silencing

Glossary

chromatin Generic term used for (1) material in the nucleus that stains strongly with basophilic dyes and (2) the complex of DNA and chromatin that may be extracted from nuclei for *in vitro* study.

histone Family of highly conserved, small basic proteins which constitute the principal protein components of chromatin.

histone modification Covalent addition of one or more chemical groups to a specific amino acid in a histone. Modifications include acetylation, methylation, phosphorylation, poly-ADP ribosylation, and ubiquitination.

histone variant A histone molecule derived from a different gene and having specific amino acid differences from the "canonical" histone type.

nonhistone chromatin proteins Generic term for proteins other than histones that may be bound to chromatin.

nucleosome The complete repeat unit consisting of a nucleosome core particle and the linker DNA that continues to the next nucleosome core particle, often with histone H1.

nucleosome core particle The disc-shaped (11 nm diameter, 6 nm high) complex of 146 bp of DNA and octamer of histones H2A, H2B, H3, and H4 that is the fundamental structural unit of chromatin. The X-ray structure of the core particle has been solved.

Further Reading

Allis, C. D. and Jenuwein, T. (2001). Translating the histone code. *Science* **293**, 1074–1080.

Bednar, J., Horowitz, R. A., Grigoryev, S. A., Carruthers, L. M., Hansen, J. C., and Woodcock, C. L. (1998). Nucleosomes, linker DNA, and linker histone form a unique structural motif that directs the higher-order folding and compaction of chromatin. *Proc. Natl Acad. Sci. USA* **95**, 14173–14178.

Bustin, M. (2001). Chromatin folding and activation by HMGN chromosomal proteins. *Trends Biochem. Sci.* **26**, 431–438.

Katritch, V., Bustamante, C., and Olson, W. K. (2000). Pulling a single chromatin fiber: Computer simulations of direct physical manipulations. *J. Mol. Biol.* **295**, 29–40.

Misteli, T. (2001). Protein dynamics: implications for nuclear structure and function. *Science* **291**, 843–847.

Singh, P. B., and Georgatos, S. D. (2003). HP1: Facts, open questions, and speculation. *J. Struct. Biol.* **140**, 10–16.

Van Holde, K. E. (1988). *Chromatin*. Springer-Verlag, New York.

Wolffe, A. (1998). *Chromatin Structure and Function*, 3rd edition. Academic Press, San Diego, London.

Woodcock, C. L., and Dimitrov, S. (2001). Higher-order structure of chromatin and chromosomes. *Curr. Opin. Genet. Develop.* **11**, 130–135.

Biography

Christopher L. Woodcock received his bachelors and doctoral degrees at University College London, and pursued postdoctoral research at the University of Chicago and Harvard University before joining the University of Massachusetts Amherst in 1972, where he is now Gilbert Woodside Professor of biology and Chair of the biology department. His interest in chromatin organization began in the early 1970s at the inception of nucleosome model of chromatin, and he has focused his research largely on the physical organization of nucleosomal arrays using direct visualization by electron microscopy as the major analytical tool.

Chromosome Organization and Structure, Overview

Elena Gracheva and Sarah C. R. Elgin
Washington University, St. Louis, Missouri, USA

A chromosome is the packaged form of a single linear double-helical DNA molecule. The genome of a eukaryotic organism consists of from 1 to over 200 chromosomes. Chromosomes are located in the nucleus of the cell and exist in the form of chromatin, a complex between the DNA, the histones (small, highly basic proteins), nonhistone chromosomal proteins (both enzymatic complexes and structural components), and a small amount of RNA (both nascent transcripts and structural components). The numbers and sizes of chromosomes vary considerably between species (*Drosophila* has four chromosomes per haploid cell, human has 23, etc.). As cells enter mitosis, the chromatin is condensed into readily observed, rod-shaped structures, the metaphase chromosomes; a complex process, as described below, is required to package the linear DNA molecule in this form, typically achieving 10,000-fold compactness. Metaphase chromosomes were one of the first subcellular structures observed by cell biologists of the 19th century. Chromosomes were subsequently identified as the vehicle for transmission of genetic information during cell division. As the daughter cells return to interphase, the nucleus reforms, and the chromosomes are decondensed and distributed within the nucleus. The level of DNA packing is much lower during interphase, but is of critical importance in the regulation of gene expression.

All genetic information – genes, regulatory elements and signals for structural organization – is arranged linearly along chromosomes. The chromosomes provide not only the means for inheritance, but also the template for transcription, the process of "reading out" the information required by the cell. Different and specific expression profiles are needed for each cell type and stage of development. A full understanding of the mechanisms used in the global regulation of gene expression will not be achieved until the relationships between the linear content of each chromosome, its local and higher-order packaging, or chromatin structure, and the three-dimensional arrangement of the chromosomes in the nucleus have been defined.

The Structure of Chromatin

The nucleotide sequence of DNA represents the primary level of chromosome organization. When a DNA molecule is packaged into chromatin, the latter does not behave as a uniform fiber. The chromosome conformation is affected by regulatory and structural features. These sequence elements include promoter proximal elements that control the activity of individual genes, locus control regions that impact a cluster of genes, and boundary elements that potentially regulate the activity of large (10–100 kb) chromosomal domains. In addition to the unique sequences that code for genes, eukaryotic genomes include a high percentage of repetitious DNA, both tandem arrays of short-repeating motifs (often identified as "satellite" DNA because of its different density) and dispersed relics of transposable elements, retroviruses, and the like. Some of the repetitious DNA is utilized in the generation of special chromosome structures such as the centromere, the site of microtubule attachment during mitosis, and the telomeres, structures that protect the ends of the DNA molecules.

The discovery of nucleosomes, repeating subunits based on DNA folding around an octamer of histones, provided a molecular description of the fundamental unit of chromatin folding and accounted for the first six- to sevenfold linear compaction of the DNA. The octamer, containing two molecules each of the core histones H2A, H2B, H3, and H4 (a tetramer of $[H3 + H4]_2$ plus two dimers of [H2A + H2B]) with 147 bp of DNA wrapped around it in 1 2/3 left-handed turns, makes up the core particle. The high-resolution 2.8 Å structure reveals the details of histone organization within the nucleosome (Figure 1). The C-terminal two-thirds of the histone molecules, folded in a "handshake" motif, form the core of the nucleosome, while their amino-terminal tails extend outwards and are potentially involved in further interactions with DNA, with other proteins, and between adjacent nucleosomes. Typically 170 bp of DNA follows a bent path round the histone core, held strongly by electrostatic bonds between the basic amino acids of the histones and the phosphates of the DNA. The segments of DNA that link adjacent nucleosome core particles ("linker" DNA) are bound by linker histones (H1 and its variants) or

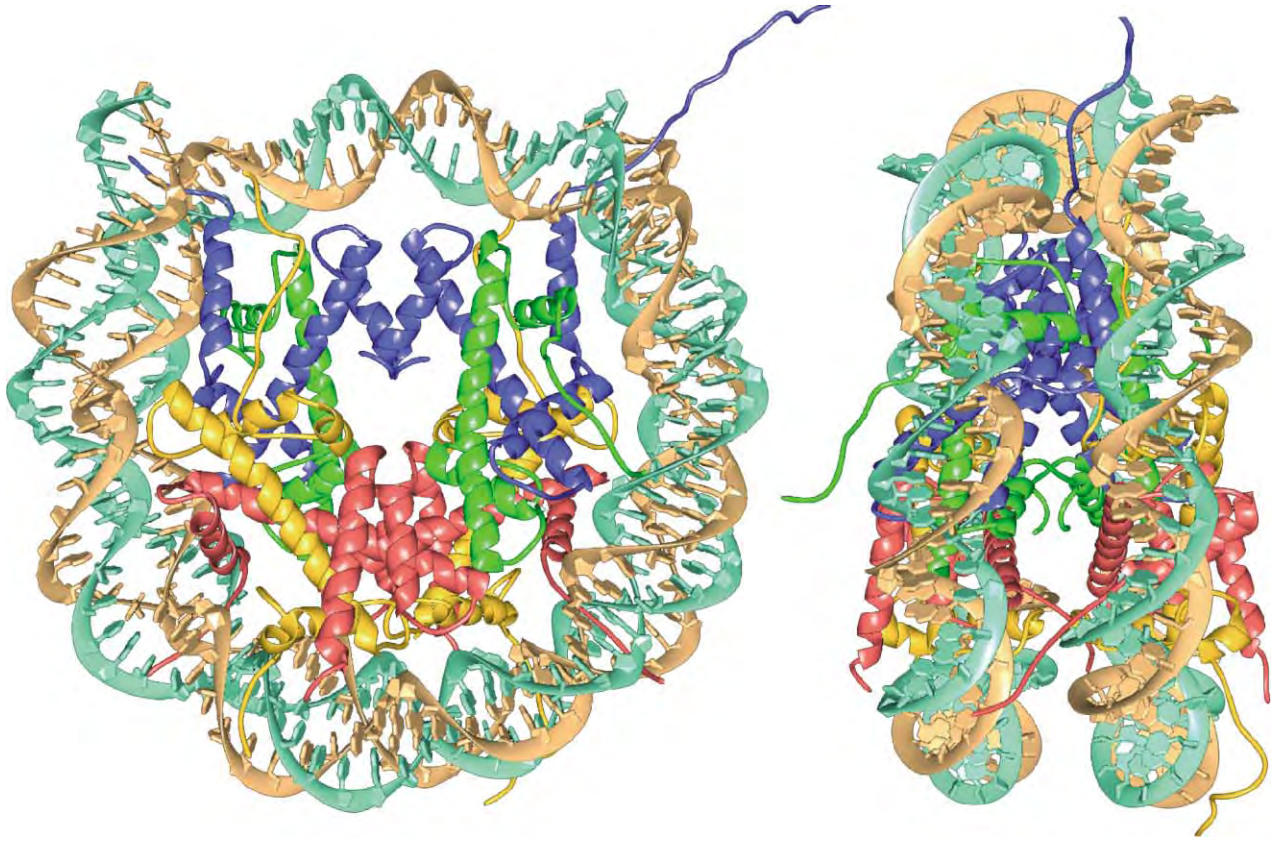

FIGURE 1 The structure of the nucleosome core particle. Brown and green ribbon traces represent the double-stranded 146 bp fragment of DNA. H2A molecules are shown in yellow, H2B in red, H3 in blue, and H4 in green. (Reprinted from Luger, K., Mader, A. W., Richmond, R. K., Sargent, D. F., and Richmond, T. J. (1997). Crystal structure of the nucleosome core particle at 2.8Å resolution. *Nature* **389**(6648), 251–260.)

HMG proteins. These proteins contribute to the further folding of the chromatin fiber, playing a role in the condensation of the 10 nm fiber to form a 30 nm fiber (Figure 2).

The arrangement of nucleosomes within the 30 nm fiber remains largely unknown. A widely utilized model, derived primarily from physical measurements and diffraction studies, is based on a solenoid, in which the nucleosomal fiber is wound in a regular helix, with about six nucleosomes per turn. The linker histones face inwards and help to stabilize the solenoid. However, new single-molecule methods, using microscopy to study single chromatin fibers, suggest a different picture. Both atomic force microscopy (AFM) and cryo-electron microscopy (EM) images show a chromatin fiber that appears as an irregular helix, with a fluctuating zigzag secondary structure. These images do not support the notion of regular solenoids. Comparative studies suggest that the linker DNA with the associated linker histone generates a specific orientation that directs the higher-order folding and compaction of chromatin along the 30 nm fiber axis in an accordion-like manner (Figure 2B).

The 30 nm fiber is thought to be the basic form of much of the chromatin during interphase. However, a subfraction of the chromatin remains condensed, and darkly staining (heteropycnotic), as the cell returns from metaphase to interphase. This condensed fraction is referred to as "heterochromatin," while the more diffuse material is labeled "euchromatin."

Heterochromatic domains contain a high proportion of repetitious DNA sequences (satellite DNA, retrotransposons, and other transposable element relics), have a low gene density, are replicated late in S phase, and show little or no meiotic recombination. Genes normally resident in euchromatin become inactive when placed in or near a heterochromatic environment by rearrangement or transposition. The factors that define specific chromosomal domains as preferred sites of heterochromatin assembly are not well understood, but it appears likely that heterochromatin formation is linked to the presence of repeated DNA sequences. Heterochromatic regions show a more regular nucleosome array (more even spacing) than euchromatic regions; however, the precise nature of the difference in packaging between heterochromatin and euchromatin remains unknown.

Chromatin structure is intimately involved in the regulation of chromosome activities: replication, transcription, and repair. The packaging of a DNA

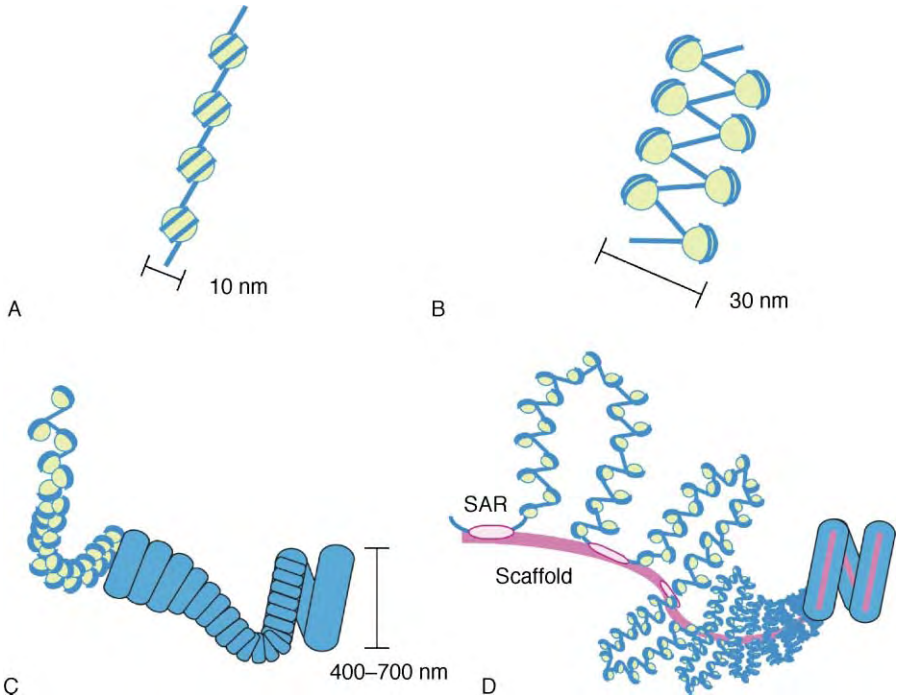

FIGURE 2 Hierarchical levels of chromatin organization. (A) Structure of the 10 nm nucleosome fiber. Histone octamers are shown as yellow circles, the blue line designates double-stranded DNA wrapped around an octamer. (B) Possible structure of the 30 nm chromatin fiber based on a three-dimensional zigzag arrangement. (C) Formation of higher-order chromatin structure by coiling into thicker (400–700 nm) chromatin fibers. (D) Organization of the chromatin into loops radiating out from a scaffold (magenta). Pink ovals represent SAR elements. (Reprinted from Swedlow, J. R., and Hirano, T. (2003). The making of the mitotic chromosome: Modern insights into classical questions. *Molecul. Cell.* **11**(3), 557–569.)

protein-binding motif with histones in a nucleosome often renders that signal invisible to the protein. For example, packaging of a TATA box sequence into a nucleosome blocks initiation of transcription; assembly of a restriction site into a nucleosome blocks cleavage by that restriction enzyme. Thus, it is no surprise that chromatin needs to undergo significant structural change, or "remodeling," to enable the cellular machines that perform various functions to gain access to their template, the double-helical DNA. The challenge to understand chromatin structure and dynamics, and to link chromatin structure to function, is enormous. Current research has highlighted the role of postsynthetic modifications of both the histones and the DNA in "marking" different structural states and providing appropriate signals to the cellular machines.

The core histone proteins are highly conserved; in the most extreme example, there are only two amino acid changes between the sequences of histone H4 from plants and animals. While the globular carboxy-terminal domains make up the nucleosome core, the flexible amino-terminal tails protrude outward from the core structure. These basic tails function as acceptors for a variety of posttranslational modifications, including acetylation, methylation, and ubiquitination of lysine (K) residues, phosphorylation of serine (S) and threonine (T) residues, and methylation of arginine (R) residues. Several studies have shown that histone modifications can be cooperative or conflicting, one modification facilitating or blocking another. The combination of histone modifications present determines the chromatin status of small and large regions of the genome and mediates its functional activity. In particular, histone acetylation is associated with gene expression, while deacetylation, with methylation of histone H3 on lysines 9 and/or 27, is associated with silencing. These patterns can be altered by multiple extracellular and intracellular stimuli that signal to the nucleus. In fact, recent studies have shown that many proteins characterized as activators or silencers of transcription work by causing or facilitating a change in the modification state of the histones at a given locus. Thus, chromatin itself has been proposed to serve as a signaling platform and to function as a genomic integrator of various signaling pathways. Covalent modifications of histone tails are believed to act in concert to establish the "histone code" essential for assembly of the desired chromatin state.

In addition to the proteins that package DNA, there are also sets of proteins that interact with specific sequences to control gene expression, interacting with promoters, enhancers, locus control regions, etc. While some such proteins can recognize DNA sequences in a nucleosome, many cannot. Both targeted alterations in histone modification and the remodeling of nucleosomes

are often required to allow these latter proteins to function. The order of the required operations for activation of transcription varies at different loci.

Other nonhistone proteins contribute to structural elements such as insulators and/or boundary complexes. Insulators define a region of regulatory activity by blocking enhancer/promoter interactions, while boundaries (or barriers) limit the spread of heterochromatin into a euchromatic domain. The arrangement of these genomic features contributes to the functional design of a locus and region. Unfortunately, it has not yet been possible to relate boundary elements, defined by their functional role described above, with the structural elements that anchor loops of DNA, as seen by electron microscopy, or with the protein scaffold that constrains the DNA in supercoiled domains of 10–100 kb. A better understanding of this level of organization will be essential to develop an understanding of how chromosomes function.

The Role of Spatial Organization of the Genome in the Nucleus

The next level of chromosome organization must take into account the three-dimensional arrangement of the chromosomes within the cell nucleus. Approaches to microscopy that allow us to examine the nucleus in three dimensions have shown that individual chromosomes occupy defined subdomains within the nucleus. This organization involves the interaction of different factors bound to specific sites in the chromosomes with regions of the nuclear envelope; the protein-facilitated juxtaposition of chromosome sites to form stable connections between distant sequences, with intervening loops of the chromatin fiber; and the possible interaction of certain DNA regions (MARs, or matrix attachment regions) with some nonchromatin elements of internal nuclear structure. Recently, there has been increasing evidence that both actin and myosin, found inside the nucleus, might have an impact on its internal structure. Unfortunately, our understanding of this higher-level packaging is very meager compared to our knowledge of the primary levels of organization. Nonetheless, such packaging can be thought of as the culmination of the hierarchy of chromatin structures that functionally connect the linear genomic sequence to the mechanisms for information processing inside the cell nucleus.

The Mitotic Chromosome

Substantial differences in the organization of chromosomes occur during mitosis. The most obvious difference is that the chromosome structure is more compact and the shape much better defined than in interphase chromosomes. This more stable structure has offered some advantages for examining the organization and packaging of the single DNA molecule of a chromatid. Several biochemical and structural studies have argued for the partitioning of the genome into a series of defined units (domains) containing 10–100 kb of DNA. Early EM studies suggested the presence of a chromosome scaffold from which loops of chromatin radiate. The scaffold might be considered as either an axial core, presumably made up of DNA and/or protein, or a loose network of DNA/protein complexes whose regulated assembly controls the higher-order structure of the chromosome. In general, scaffold models presume interactions between specific protein factors and *cis*-acting DNA sequences (SARs, or scaffold attachment regions) that determine the limits of the domains. In most models, two neighboring elements, separated by up to 100 kb of DNA, bind to the scaffold forming a loop. Experimentally, a group of very AT-rich sequences has been identified as potential SARs, based on the association of these sequences with the protein scaffold remaining after histones have been extracted from chromosomes. Using fluorescence *in situ* hybridization (FISH), SARs were visualized as a long queue running the length of the chromosome that alternately followed a fairly linear or tightly coiled path. These images were highly variable. Helically folded mitotic chromosomes have been visualized under certain conditions, suggesting that the highest order of folding is a helical winding of the chromosome arm.

However, *cis*-acting elements affecting chromosome architecture have not been identified by genetic criteria, nor have the proposed SARs (identified by biochemical assay) been mapped successfully in relation to cytological preparations. Recently, biophysical approaches for quantifying the elastic properties of mitotic chromosomes have provided important insights into their structure. The mechanical integrity of mitotic chromosomes appears to be maintained by links between chromatin fibers, not by a proteinaceous axial core. Isolation of whole chromosomes and reconstitution of mitotic chromosomes has identified topoisomerase IIa, a five-subunit complex termed condensin, chromokinesin, and the chromatin remodeling ATPase ISWI as major constituents. All presumably contribute to the change from the interphase form to the condensed mitotic chromosome. ATPases are very abundant in mitotic chromosome fractions. Probably these enzymes provide the energy for the aforementioned complexes to induce the local and global conformational changes in chromosomes required to support condensation, and microtubule-dependent movement of assembled chromosomes to opposite poles prior to cell division.

The centromere, observed in all higher eukaryote chromosomes, is a well-known landmark. It takes the form of a distinct primary constriction where the sister chromatids are held together until separated. The constricted region comprises a differentiated chromatin structure onto which microtubules bind to provide proper chromosome movements during the processes of mitosis and meiosis. The centromere in higher eukaryotes is generally made up of massive regions of repetitious sequences. Many observations suggest that there is no specific DNA sequence that is required for centromere formation, strongly implicating an epigenetic mechanism. Five mammalian CENP proteins (CENtromere Proteins) – CENP-A, CENP-B, CENP-C, CENP-G, and CENP-H – are unique and essential to the centromere. Three of these proteins – CENP-A, CENP-B, and CENP-C – have demonstrated DNA-binding activity and are potential candidates for marking the site. CENP-A is a histone H3-like protein that is conserved in mammals and other organisms; it is present only in the nucleosomes of active centromeric regions, where its presence triggers kinetochore formation. A mechanism for centromerization is not identified at present. Most of the chromatin properties of centromeres are not unique. For example, hypoacetylation of histones, a high level of DNA methylation and late replication, are also characteristic features of noncentromeric heterochromatin. The most attractive candidate for the centromeric mark is CENP-A, but the mechanism for incorporation of CENP-A into only one site per chromosome remains a puzzle.

The ends of eukaryotic chromosomes are organized into telomeres, nucleoprotein structures essential for maintaining the integrity of the genome, the so-called "guardians of the chromosome." Telomeric DNA in the majority of eukaryotes is made up of tandem repeats of short guanine-rich sequences. In some cases (e.g., in *Drosophila*), a subset of transposable elements is maintained at the chromosome ends and guanine-rich repeats are not observed. The telomeres show a very special pattern of chromatin fiber organization, distinct from the rest of the genome. The G-rich sequences can form a quadruple helix. *In vivo*, telomeres are not necessarily linear, but can form looped foldback structures, stabilized by protein components. Many of the key proteins in the telomere have been identified, although their functions are still poorly understood.

Summary

A chromosome, then, can be considered to be a single, double helical DNA molecule, running from one telomere through the centromere to the other telomere. Multiple origins of replication, and many genes, are typically found distributed along the length of the DNA molecule. The DNA is packaged first in a nucleosome array, subsequently in a 30 nm fiber, and finally in higher-order structures. This packaging contributes to gene regulation both at the level of individual genes, and at the level of large domains.

See Also the Following Articles

Chromatin: Physical Organization • Chromatin Remodeling • Nuclear Organization, Chromatin Structure, and Gene Silencing • Nucleoid Organization of Bacterial Chromosomes • Metaphase Chromosome

Glossary

chromatin The highly dynamic complex of DNA, histones, and nonhistone proteins from which the eukaryotic chromosome is built; it is generally used in reference to the interphase form and can refer to the sum of all chromosomes.

chromosome Structural unit of the genetic material in eukaryotes. It consists of one double-stranded DNA molecule, packaged as interphase chromatin or a metaphase chromosome. Eukaryotes have from 1 to over 200 chromosomes, depending on the species.

nucleosome Fundamental repeating subunit of the chromatin fiber, consisting of a core histone octamer (made up of two molecules each of H2A, H2B, H3, and H4) with DNA wrapped around the surface in nearly two left-handed turns, connected by linker DNA associated with one molecule of linker histone (usually H1) to the next subunit. Each repeating unit (core plus linker) packages about 200 bp of DNA.

Further Reading

Fischle, W., Wang, Y., and Allis, C. D. (2003). Histone and chromatin cross-talk. *Curr. Opin. Cell. Biol.* **15**(2), 172–183.

Grewal, S. I., and Elgin, S. C. (2002). Heterochromatin: New possibilities for the inheritance of structure. *Curr. Opin. Genet. Dev.* **12**(2), 178–187.

Luger, K., Mader, A. W., Richmond, R. K., Sargent, D. F., and Richmond, T. J. (1997). Crystal structure of the nucleosome core particle at 2.8Å resolution. *Nature* **389**(6648), 251–260.

Mellone, B. G., and Allshire, R. C. (2003). Stretching it: Putting the CEN(P-A) in centromere. *Curr. Opin. Genet. Dev.* **13**(2), 191–198.

Neidle, S., and Parkinson, G. N. (2003). The structure of telomeric DNA. *Curr. Opin. Struct. Biol.* **13**(3), 275–283.

O'Brien, T. P., Bult, C. J., Cremer, C., Grunze, M., Knowles, B. B., Langowski, J., McNally, J., Pedesson, T., Politz, J. C., Pombo, A., Schmahl, G., Spatz, J. P., and , von Driel, R. (2003). Genome function and nuclear architecture: From gene expression to nanoscience. *Genome Res.* **13**(6A), 1029–1041.

Summer, A. T. (2003). *Chromosomes: Organization and Function*. Blackwell Publishing, Malden, MA.

Swedlow, J. R., and Hirano, T. (2003). The making of the mitotic chromosome: Modern insights into classical questions. *Molecul. Cell.* **11**(3), 557–569.

West, A. G., Gaszner, M., and Felsenfeld, G. (2002). Insulators: Many functions, many mechanisms. *Genes Dev.* **16**(3), 271–288.

Zlatanova, J., and Leuba, S. H. (2003). Chromatin fibers, one-at-a-time. *J. Mol. Biol.* **331**(1), 1–19.

Biography

Sarah C. R. Elgin is a Professor in the Department of Biology at Washington University in St. Louis.

Elena Gracheva is a Research Associate in the Elgin lab. The Elgin lab is interested in the role that chromatin structure plays in gene regulation, considering both effects from packaging large domains and local effects of the nucleosome array. Biochemical, genetic, and cytological studies are conducted using *Drosophila melanogaster* as a model organism. Ongoing projects include investigating the mechanisms of gene silencing associated with heterochromatin formation, and investigating the relationship between heterochromatin and euchromatin. Dr. Gracheva is also involved in investigation of the role of GAGA factor in transcription regulation.

Coenzyme A

M. Daniel Lane
Johns Hopkins University School of Medicine, Baltimore, Maryland, USA

Coenzyme A (CoA) functions as a cofactor for numerous enzyme-catalyzed reactions in animal, plant, and microbial metabolism. The structure of CoA shows that it is composed of the B-vitamin, i.e., pantothenic acid, β-mercaptoethylamine, and an adenine nucleotide with both a 5′-pyrophosphate and a 3′-monophosphate.

Most carboxylic acids, e.g., fatty acids, must be "activated" to enter metabolic pathways by conversion to their corresponding acyl–S–CoA (R–CO–S–CoA) thioesters. The sulfhydryl group (–SH) of the β-mercaptoethylamine component of CoA is the site at which carboxylic acids (R–CO_2H) bond to form acyl–thioester derivatives. Thioesters are the only form in which CoA is known to function in biological systems. Many of the enzyme-catalyzed reactions in which carboxyl groups (–CO_2H) undergo carbon/carbon-, carbon/nitrogen- or carbon/sulfur-bond formation utilize acyl–S–CoA thioesters as the acyl donor substrate.

Background and Discovery

CoA was discovered by Fritz Lipmann and his colleagues in the early 1950s. The coenzyme was first isolated from large quantities of pig liver extract as the factor required for the acetylation of sulfanilamide, the assay system used to track CoA during its purification. The discovery of CoA and the characterization and determination of its structure (Figure 1) led to Lipmann being awarded the 1953 Nobel prize in Physiology or Medicine. Lipmann's findings opened the door for the discovery of the innumerable roles of CoA, most notably the discovery by Feodor Lynen that "active acetate" was acetyl–CoA, a key intermediate in the metabolism of carbon compounds by all organisms. In 1964, Lynen was awarded the 1964 Nobel prize in Physiology or Medicine for his discovery of acetyl–CoA and of the many metabolic systems that CoA functions. We now know that CoA plays a key role in carbohydrate, lipid, and amino acid metabolism.

Enzymatic Functions of CoA and 4′-Phosphopantetheine

Chemical Mechanisms of Action

CoA occurs in cells either as free CoA or in the form its acyl–S–CoA thioester or as 4′-phosphopantetheine (4′-PP), which is part of a multifunctional enzyme. The sulfhydryl (–SH) group of the coenzyme is the functional site that endows it with its unique chemical/enzymatic properties. In all of the reactions in which it participates, CoA serves to "activate" carboxyl groups (R–CO–OH) in the form of an acyl–CoA thioester derivative (R–CO–S–CoA). In this form the acyl group has favorable energetic and mechanistic properties. Energetically, CoA thioesters have high phosphoryl transfer potential (i.e., a high negative free energy change associated with breaking the C–S bond of the thioester) that facilitates driving the acyl transfer reaction in which it participates toward completion. Mechanistically, the chemistry of CoA thioesters facilitates reactions either at the carbonyl carbon (–CH_2–CO–S–CoA) or the adjacent α-carbon atom (–CH_2–CO–S–CoA).

"Activation" of the Carbonyl- and α-Carbon Atoms in Acyl–CoA Thioesters

All enzymatic reactions of CoA thioesters in metabolism involve "activation" either of the carbonyl-carbon or the adjacent α-carbon atom for facile chemical reaction. Mechanistically, the –CO-carbon (i.e., R–CH_2–CO–S–CoA) of the acyl group reacts with a nucleophilic acceptor molecule ('R^-; see Figure 2, Rx′n 1) or the adjacent alpha carbon (i.e., R–CH_2–CO–S–CoA) reacts with an electrophile ('R^+; see Figure 2, Rx'n 2) to produce a new carbon–carbon bond. These reaction types are illustrated below.

CoA as Donor of 4′-Phosphopantetheine for Fatty Acid Synthase

Fatty acid synthase (FAS) is a large multifunctional enzyme that catalyzes all steps in fatty acid synthesis, catalysis being facilitated by a covalently linked 4′-phosphopantetheine (4′-PP) prosthetic group. The 4′-PP group, which is derived from CoA (Figure 1), is enzymatically transferred to the FAS apoenzyme where it becomes covalently linked to the enzyme. The 4′-PP prosthetic group acts as a long sidearm to which intermediates of the pathway are covalently linked. The 4′-PP sidearm allows translocation of the growing

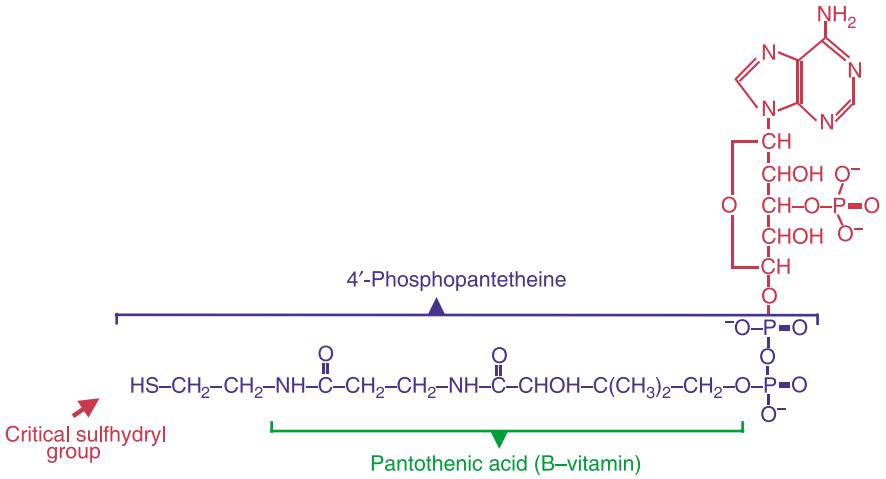

FIGURE 1 Structure of CoA.

fatty acyl chain intermediate from one catalytic site on FAS complex to the next in the cyclic sequence, this leads to formation of a long-chain fatty acid.

Enzymatic Synthesis of Acyl–S–CoA Derivatives from Free Carboxylic Acids and CoA–SH

The enzymatic reactions by which acyl–S–CoA derivative is synthesized from carboxylic acids, such as free fatty acids, occur via a common mechanism (Figure 3).

The reaction illustrated uses fatty acid as example; however, it should be noted that virtually all acyl–CoA's are formed from their cognate carboxylic acids by the same mechanism. The enzymes that catalyze these reactions are referred to as acyl–CoA synthetases. In the initial step (Rx′n 1) the fatty acid attacks the $\tilde{\alpha}$ (innermost) phosphate of ATP releasing pyrophosphate (PP_i) forming an enzyme-bound acyl–AMP intermediate. In the second step (Rx′n 2), CoA–SH attacks the acyl–CO–carbon of the intermediate producing an acyl–S–CoA product and AMP.

Metabolic Roles/Functions

CoA and its derivatives function in a wide variety of metabolic pathways including the tricarboxylic cycle, fatty acid oxidation, ketogenesis, fatty acid biosynthesis, sterol synthesis, complex lipid synthesis, amino acid metabolism, and porphyrin synthesis. (Since most of

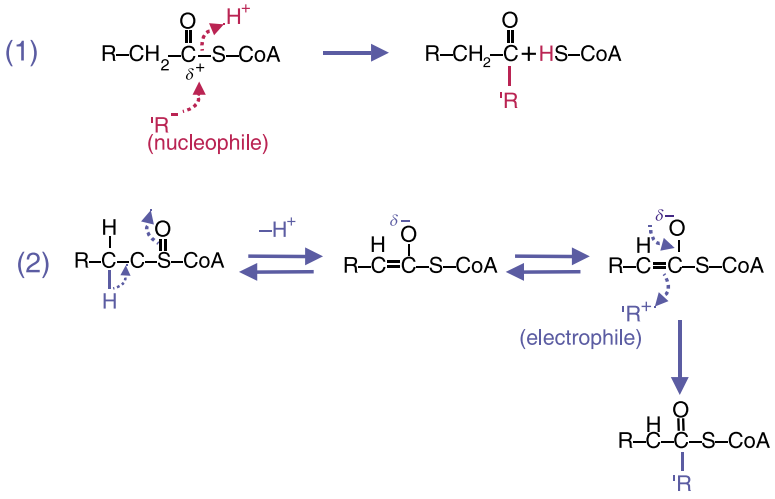

FIGURE 2 Mechanisms of "activation" of the acyl carbonyl- and α-carbon atoms in CoA thioesters.

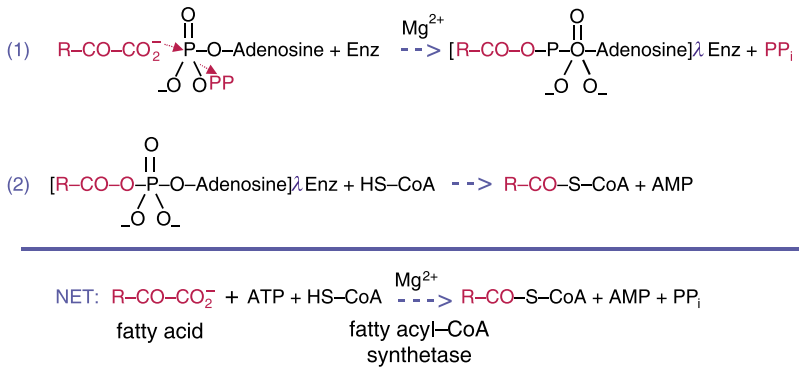

FIGURE 3 Enzymatic synthesis of acyl–S–CoA's.

these are covered elsewhere in this encyclopedia, they are not dealt with in this entry.) As the fatty acid synthase system is unique, in that it makes use of only a fragment of the CoA molecule, 4′-PP, a brief discussion of FAS is warranted.

Fatty Acid Synthase

Fatty acid synthesis in animals is catalyzed by a single large (molecular weight, $\sim 5 \times 10^5$) multifunctional enzyme. All eight steps and thus all eight catalytic centers that carry out fatty acid synthesis occur with the intermediates tethered to the FAS. The intermediates are covalently linked by thioester bonds to the –SH group of the long 4′-PP sidearm which facilitates translocation of intermediates from one catalytic center to the next in sequence until the multiple steps of long-chain fatty acid synthesis are completed. Each round of elongation lengthens the chain by two carbons, a process that is repeated 7 or 8 times for the synthesis of a 16- or 18-carbon containing fatty acids.

The process is initiated by the transfer of an acetyl group to 4′-PP from acetyl–S–CoA. The acetyl group linked to 4′-PP serves as the "primer" onto which the long-chain fatty acid is built. Malonyl units from malonyl–CoA, which serve as the chain-elongating group, condenses with the acetyl-primer concomitant with decarboxylation to produce a 4-carbon intermediate that then undergoes two reductive and "1" dehydration step. Successive malonyl groups are transferred to FAS from malonyl–CoA to provide the basic units for successive steps in the elongation process. The terminal step is catalyzed by a thioesterase releasing the long-chain fatty acid product.

See Also the Following Article

Fatty Acid Synthesis and its Regulation

Glossary

coenzyme A small molecule (molecular weight usually ≤ 1000) that participates chemically in a reaction catalyzed by an enzyme and upon which the reaction depends.

electrophile A compound with an electron-deficient atom that can accept an electron pair from a nucleophilic compound with an electron-rich atom.

nucleophile A compound with an electron-rich atom having an unshared electron pair that can be contributed to an electron-poor atom of an electrophilic compound.

thioester The condensation product of a carboxylic acid and a thiol (–SH) group formed by removal of a water molecule, e.g.,

$$R\text{–}CO_2H + Co\text{–}SH \rightarrow H_2O + R\text{–}CO\text{–}S\text{–}CoA.$$

Further Reading

Berg, J., Tymoczko, J. L., and Stryer, L. (2002). *Biochemistry*, 5th edition, W. H. Freeman and Co., New York.

Lipmann, F. (1953). Development of the acetylation problem: A personal account, Nobel Prize Lecture (in Physiology or Medicine). Available on the Nobel Prize Web Site http://www.nobel.se/ or http://www.nobel.se/medicine/index.html.

Lynen, F. (1964). The pathway from "activated acetic acid" to terpenes and fatty acids. Nobel Prize Lecture (in Physiology or Medicine). Available on the Nobel Prize Web Site http://www.nobel.se/ or http://www.nobel.se/medicine/index.html.

Nelson, D. L., and Cox, M. M. (2005). *Lehninger: Principles of Biochemistry*, 4th edition, W. H. Freeman and Co., New York.

Walsh, C. (1979). *Enzymatic Reaction Mechanisms*. W. H. Freeman and Co., San Francisco.

Biography

M. Daniel Lane is a Distinguished Service Professor in the Department of Biological Chemistry at the Johns Hopkins University School of Medicine. He is a member of the National Academy of Sciences, the American Academy of Arts and Science and has served as President of the American Society of Biochemistry and Molecular Biology. For 19 years he served as Director of the Department of Biological Chemistry at the Johns Hopkins University School of Medicine. His current research interests are on stem cell commitment to the adipocyte lineage, adipocyte differentiation, and the hypothalamic control of food intake, and obesity.

Collagenases

Kenn Holmbeck and Henning Birkedal-Hansen
National Institutes of Health, Bethesda, Maryland, USA

Collagenases are protein capable of cleaving native collagen under physiological conditions *in vivo* and *in vitro*. Here we discuss in brief the history of collagenases, their properties and the definitions assigned to proteins with collagenolytic properties. While collagen cleaving potential is often assessed by simple enzyme substrate incubations it has become increasingly evident that conclusions based on such assay conditions may not necessarily reflect the true nature of enzyme properties. The recent advances in genetic research has demonstrated that some but not all collagen cleaving enzymes functions in that capacity *in vivo*. Conversely, other enzymes previously regarded as unrelated to collagenases have been proven to be important for collagen metabolism.

What Is a Collagenase?

The term "collagenase" was first used by Gross and Lapiere in their 1962 description of an activity released from cultured tissue explants of involuting tadpoles, which dissolved otherwise highly proteinase-resistant, reconstituted collagen fibrils. This was a groundbreaking finding. It was the first demonstration of the existence of an activity operating at neutral pH that was fully capable of dissolving and cleaving native collagen fibrils. It marked the beginning of an exciting period of discovery that led to identification of a large number of distinct matrix metalloproteinases (MMP), almost 6–7 in number with collagen-cleaving capabilities under various *in vitro* conditions (Table I).

Original Definition of Collagenases

The unique resistance of native collagen molecules to proteolysis is a result of the tightly wound, semirigid triple helical structure. However, the resistance is only relative and not absolute. Generally, one of two tests was applied to ascertain whether an enzyme or an activity represented a true collagenase: (1) ability to dissolve reconstituted type I collagen fibrils in the temperature range 35–37°C, and/or (2) ability to cleave type I collagen in solution at neutral pH in the temperature range 15–25°C into two distinct and recognizable 1/4–3/4 fragments (classical collagenase signature cleavage pattern). That the 3/4–1/4 cleavage site is actually utilized *in vivo* was elegantly shown by Robin Poole and co-workers by neo-epitope immunochemistry which convincingly identified collagen molecules in several tissues, which were cleaved at this particular site. Since a number of collagenases cleave this site, the mere detection of this neo-epitope does not necessarily identify any single enzyme responsible for the cleavage. Despite this, the 3/4–1/4 cleavage products are highly useful hallmarks in the analysis and characterization of collagenase activity.

Several lines of evidence support the notion that the collagenase-sensitive cleavage site is subject to local unwinding and therefore constitutes a site of minor resistance. For example, type III collagen has an Arginine-substitution in the susceptible region, and is readily cleaved by trypsin producing a 3/4–1/4 pattern. However, the collagenase-sensitive site in the alpha 1 chain of type I collagen can be mutated in mice without yielding an acute collagen "indigestion" phenotype. The modification leads to a progressive fibrosis, but at a rate indicating that the collagen molecule is cleaved with some efficiency elsewhere. The term "collagenase" based on site specificity may thus be only partially applicable and may in effect obscure the fact that collagen is cleaved at other sites by collagenases, which do not qualify for this designation based on the criteria of generating 3/4–1/4 specific cleavage products.

Revised Definition of "Collagenases"

Based on the observations outlined above, the original definition of a collagenase will therefore have to be revised and broadened to also accommodate other proteinases such as cathepsin K, which clearly is a potent collagen-cleaving enzyme and yet utilizes other cleavage sites in the triple helical region and functions at acidic pH. Ability to cleave native type I collagen in solution within the temperature range 15–25°C at either

TABLE I

Fibrillar Collagenases (Proteinases with Activity Against Fibrillar Collagens)

Enzyme	Other name	Classification	Species
MMP-1	Collagenase-1, interstitial collagenase	Matrix metalloproteinase	Widely expressed except in rodents
McollA		Matrix metalloproteinase	Mice
MMP-2	Gelatinase, type IV collagenase	Matrix metalloproteinase	Widely expressed
MMP-8	Collagenase-2, PMN collagenase	Matrix metalloproteinase	Widely expressed
MMP-13	Collagenase-3, interstitial collagenase	Matrix metalloproteinase	Widely expressed
MMP-14	MT1-MMP	Matrix metalloproteinase	Widely expressed
MMP-18	Collagenase-4	Matrix metalloproteinase	Frog
Cathepsin K		Acidic thiol proteinase	Widely expressed

neutral or acidic pH, or completely dissolve native or reconstituted collagen fibril matrices at 35–37°C still appear to be valid requirements. It is now increasingly being recognized that type I collagen-cleaving ability *in vitro* does not necessarily mean that the enzyme in reality functions as a collagenase *in vivo*. In fact, the assay conditions ordinarily used to assess the collagenolytic activity of putative collagenases may rarely, if ever, entirely mimic the conformation and configuration of the substrate when it is associated with multiple other components of the extracellular matrix and packed to densities rarely achieved in a cell-free system. Conversely, an argument may also be made that enzymes displaying little collagenolytic activity *in vitro* may conceivably be potent collagenases *in vivo*, if by association with other ECM macromolecules, the collagen molecules are made more readily available for cleavage. Standard enzyme kinetic assays measuring substrate conversion are often ill-suited to account for reactions, which take place in a two-dimensional, diffusion-restricted environment such as a cell-membrane or a solid-substrate surface. For collagenolytic enzymes with *trans*-membrane spanning domains, a solution-based assay obviously can change the basic environmental properties under which a molecule ordinarily works, but also molecules commonly recognized as secreted exert their function in close proximity to the peri-cellular (solid phase) environment. Second, the actual enzyme-to-substrate ratio *in vitro* may not adequately mirror that which exists *in vivo*. It may therefore be necessary to revise the definition "collagenase" and assign the term only to enzymes for which there is some evidence, for instance, from naturally occurring mutations or gene ablation studies, that they truly function to cleave collagen *in vivo*.

The Collagenases

Within a few years of the discovery of the tadpole enzyme, similar activities were identified in many vertebrate species including humans. Among these were an enzyme from PMN leukocytes that later turned out to be a genetically distinct collagenase (MMP-8). Gelatinase A/type IV collagenase (MMP-2) was also identified early on and recognized as a probably distinct and separate activity because of its ability to cleave type IV collagen and gelatin. However, it was not recognized until Aimes and Quigley's important study in 1995 that MMP-2 can also be a genuine type I collagen-specific collagenase once the inhibitor TIMP-2, with which it is often complexed, is removed. This finding raises the question whether, and under what conditions, TIMP-2-free proMMP-2 exists *in vivo*? MMP-13 or collagenase-3 is found in both humans and rodents and displays partial homology to the human interstitial collagenase, MMP-1. It was thus originally thought to be the rodent orthologue of MMP-1, but turned out to be a genetically distinct collagenase capable of also dissolving the otherwise highly resistant and slowly cleaved type II collagen. Surprisingly, rodents appear to express MMP-13 in most places where MMP-1 is expressed in humans, thus suggesting that it is a functional equivalent. Yet a closer rodent orthologue of human MMP-1 called Mcol-A has been identified, but so far has been characterized only to some extent. Based on the initial analysis Mcol-A appears to have some collagen-cleaving ability against type I collagen although the specific activity seems fairly low. A collagenase (MMP-18), which was distinct from MMP-1, MMP-13, and MMP-8, was discovered in the frog but no vertebrate orthologue has been identified. The first membrane-type MMP (MT1-MMP or MMP-14) was discovered in 1994 and shortly after, it was shown to have collagen-cleaving activity at least *in vitro*. Later five additional membrane-bound MMPs were identified but it is not yet known whether they possess collagen-cleaving activity. Although most of the collagenases mentioned so far have been matrix metalloproteinases, it is, as previously mentioned, necessary today to also include the thiol cathepsin, cathepsin K. This potent collagen-cleaving enzyme is utilized in the phagocytic pathway of collagen

degradation and in osteoclastic bone resorption, when mineralized type I or type II matrices are dissolved. The various collagenases display somewhat varying substrate preference against type I, II, and III collagens. Type I collagen is most readily cleaved by MMP-8 and MMP-14, while MMP-1 shows preference for type III collagen and MMP-13 for type II collagen.

Recent New Insights

The past decade has dramatically altered our view of the role of classical collagenases in normal growth and development. The advent of gene ablation techniques in combination with various mouse models has enabled detailed exploration of the biologic function of the individual collagenases *in vivo*. Unfortunately, MMP-1 cannot be subjected to this approach because it is not expressed in mice and no human mutations of MMP-1 have been characterized. Although a potent collagenolytic enzyme *in vitro*, the true role of MMP-1 *in vivo* may therefore not be known until a human null-mutation is discovered. No reports have emerged yet with regard to ablation of the weakly collagenolytic, putative murine MMP-1 orthologue, Mcol-A. MMP-2 has been knocked out, but the phenotype is very mild when considering that this enzyme is perhaps the most widely expressed MMP. It was subsequently shown that primary tumor mass and metastatic spread was significantly reduced in MMP-2-deficient animals in two independent tumor models, but it is uncertain whether and/or how these observations relate to collagen degradation. So, at this point there is only limited evidence that MMP-2 indeed serves as a collagenase in mice. Adding confusion to this scenario, however, is the finding by Martignetti and co-workers of the first human MMP-mutation (in MMP-2), which yields a rather spectacular generalized osteolytic bone phenotype. It is dramatically different from that of the mouse but it does have features of a collagen indigestion phenotype. Recently, ablation of the PMN collagenase MMP-8 was reported. Interestingly, MMP-8 deficiency, particularly in male mice, resulted in a dramatic rise in DMBA/TPA-induced skin tumors, diminished inflammatory response, and chemokine processing suggesting that an important protective role, conferred by MMP-8, had been lost. It is so far unresolved whether this effect is a function of the loss of collagenolytic activity by PMNs. An MMP-13-deficient mouse has been generated which shows widening of the growth plate presumably as a result of impairment of cleavage of collagen type II in this area. Moreover, osteoclast differentiation and activity is impaired (S. M. Krane, personal communication) and bone formation is increased. The phenotype is thus consistent with MMP-13 serving as a collagen-cleaving enzyme *in vivo*. MT1-MMP- (MMP-14-) deficient mice display a profound and complex phenotype in which growth, development, and maintenance of multiple collagen-containing matrices (bone, skin, tendon, joints, and ligaments) are severely impaired due to loss of an indispensable and uncompensated collagenolytic activity. Since the MT1-MMP knockout phenotype does not resemble those of either MMP-2 or MMP-13, it is highly unlikely that MT1-MMP functions primarily through activation of these enzymes as has been suggested. Rather, MT1-MMP appears to serve as a highly effective collagenase in its own right *in vivo*. However, it is interesting to note that MT1-MMP displays somewhat weaker collagenolytic activity *in vitro* than, for instance, MMP-1. This finding again points to some level of disconnect between collagenolytic capacity *in vivo* and *in vitro*. In the case of cathepsin K deficiency, the predictions of collagenolytic impairment, however, do hold up *in vivo*. Mouse and human cathepsin K gene mutations give rise to pycnodysostosis in humans and osteopetrosis in the mouse consistent with impairment of osteoclast-mediated type I collagen cleavage. These findings help identify cathepsin K as the acidic collagenase required for removal of type I and type II collagens from mineralized matrices, which can only be dissolved in an acidic environment. It is highly likely that cathepsin K also is responsible for the cleavage of soft tissue collagen fibrils in phago-lysosomes during the often-overlooked phagocytic pathway.

Conclusion

In the aggregate, recent findings have demonstrated that true "collagenases" as defined by their substrate specificity *in vivo* can be found in at least two different classes of proteolytic enzymes (matrix metalloproteinases and cathepsins). Moreover, it is now evident that not all predictions based on enzyme kinetics obtained *in vitro* hold up *in vivo*. Collagenases work in the complex environment of an extracellular matrix. Fortunately, the tools for characterization of enzyme substrate interactions have now entered an exciting new era, which offer multiple genetic approaches to elucidation of these questions. Based on such approaches we have already come to realize that seemingly identical enzymes can perform different roles depending on the species. With this knowledge in mind, the understanding of and search for collagen metabolizing enzymes should continue.

See Also the Following Articles

Collagens • Metalloproteinases, Matrix

Glossary

cathepsins Lysosymal proteinases, mostly thiol-dependent proteinases of the papain family. Present in multiple forms of which cathepsin K seems to be the most potent collagen-cleaving enzyme.

collagen Major structural proteins of the body with type I being the most abundant protein in soft connective tissue and in bone. The major fibrillar collagens (types I, II, and III) provide much of the structural framework for soft connective tissues, cartilage, and bone. They are generally highly resistant to proteolysis.

collagenase Enzyme capable of cleaving native collagen under specified conditions (temperature and pH).

knockout mouse Mouse rendered deficient for a selected gene by targeted inactivation of the encoding locus in embryonic stem cells, subsequent transmission of the trait to the germ line and breeding of the trait to a homozygous state.

matrix metalloproteinases (MMPs) A group of zinc endopeptidases (metzincins) characterized by zinc binding VAAHEXGHXXGXXH amino acid consensus sequence in the catalytic domain and activation by a so-called cysteine switch. This residue is harbored in the latency-conferring prodomain that is proteolytically cleaved upon activation. This group of enzymes does not include the ADAMS, which contains a characteristic disintegrin domain.

Further Reading

Balbin, M., Fueyo, A., Tester, A. M., Pendas, A. M., Pitiot, A. S., Astudillo, A., Overall, C. M., Shapiro, S. D., and Lopez-Otin, C. (2003). Loss of collagenase-2 confers increased skin tumor susceptibility to male mice. *Nat. Genet.* **35**(3), 252–257.

Billinghurst, R. C., Dahlberg, L., Ionescu, M., Reiner, A., Bourne, R., Rorabeck, C., Mitchell, P., Hambor, J., Diekmann, O., Tschesche, H., Chen, J., Van Wart, H., and Poole, A. R. (1997). Enhanced cleavage of type II collagen by collagenases in osteoarthritic articular cartilage. *J. Clin. Invest.* **99**, 1534–1545.

Brinckerhoff, C. E., and Matrisian, L. M. (2002). Matrix metalloproteinases: A tail of a frog that became a prince. *Nat. Rev. Mol. Cell Biol.* **3**, 207–214.

Egeblad, M., and Werb, Z. (2002). New functions for the matrix metalloproteinases in cancer progression. *Nat. Rev. Cancer* **2**, 161–174.

Everts, V., Hou, W. S., Rialland, X., Tigchelaar, W., Saftig, P., Bromme, D., Gelb, B. D., and Beertsen, W. (2003). Cathepsin K deficiency in pycnodysostosis results in accumulation of non-digested phagocytosed collagen in fibroblasts. *Calcif. Tissue Int.* **73**, 380–386.

Garnero, P., Borel, O., Byrjalsen, I., Ferreras, M., Drake, F. H., McQueney, M. S., Foged, N. T., Delmas, P. D., and Delaisse, J. M. (1998). The collagenolytic activity of cathepsin K is unique among mammalian proteinases. *J. Biol. Chem.* **273**(48), 32347–32352.

Hotary, K. B., Allen, E. D., Brooks, P. C., Datta, N. S., Long, M. W., and Weiss, S. J. (2003). Membrane type I matrix metalloproteinase usurps tumor growth control imposed by the three-dimensional extracellular matrix. *Cell* **114**, 33–45.

Krane, S. M., Byrne, M. H., Lemaitre, V., Henriet, P., Jeffrey, J. J., Witter, J. P., Liu, X., Wu, H., Jaenisch, R., and Eeckhout, Y. (1996). Different collagenase gene products have different roles in degradation of type I collagen. *J. Biol. Chem.* **271**(45), 28509–28515.

Liu, X., Wu, H., Byrne, M., Jeffrey, J., Krane, S., and Jaenisch, R. (1995). A targeted mutation at the known collagenase cleavage site in mouse type I collagen impairs tissue remodeling. *J. Cell Biol.* **130**(1), 227–237.

Saftig, P., Hunziker, E., Wehmeyer, O., Jones, S., Boyde, A., Rommerskirch, W., Moritz, J. D., Schu, P., and von Figura, K. (1998). Impaired osteoclastic bone resorption leads to osteopetrosis in cathepsin-K-deficient mice. *Proc. Natl Acad. Sci. USA* **95**, 13453–13458.

Woessner, J., and Nagase, F. H. (eds.) (2000). *Matrix Metalloproteinases and TIMPs*. Oxford University Press, Oxford.

Zucker, S., and Chen, W. (eds.) (2003). *Cell Surface Proteases*. Academic Press, San Diego.

Biography

Henning Birkedal-Hansen is a Scientific Director and Senior Scientist at The National Institute of Dental and Craniofacial Research (NIDCR) at the NIH in Bethesda, Maryland. He also leads the Matrix Metalloproteinase Unit that focuses on the remodeling of collagen fibrils in the extracellular matrix and the biologic function of matrix metalloproteinases and related enzymes. He holds a D.D.S. and a Ph.D. from the Royal Dental College of Copenhagen, Denmark. He served on the faculty of the University of Alabama School of Dentistry in Birmingham, Alabama in various positions from 1979 before becoming Scientific Director at the NIDCR in 1994.

Kenn Holmbeck is a Senior Staff Scientist in the Matrix Metalloproteinases Unit. He holds a Ph.D. from the University of Copenhagen, Denmark, and received postdoctoral training at Children's Hospital Research Foundation, Cincinnati, Ohio and the National Institute of Dental and Craniofacial Research.

Collagens

Darwin J. Prockop
Tulane University Health Sciences Center, New Orleans, Louisiana, USA

Collagens are a large family of proteins widely distributed in nature with a simple, repetitive sequence of amino acids that serves as a defining signature for the proteins. The inherent properties of the signature sequence of amino acids drive spontaneous self-assembly of three similar chains into a distinctive triple-helical structure. The long triple-helical structures found in some collagens drive spontaneous self-assembly of the proteins into large fibrils. The shorter triple helices in other collagens provide rigidity to the proteins to complement the biological activity of other functional domains.

The Signature (Gly-XY-)$_n$ Sequence of Collagens

In the signature amino acid sequence of collagens, every third amino acid is glycine, the amino acid following glycine is usually the five-member ring amino acid proline, and the next amino acid is hydroxyproline. Therefore the signature sequence is usually depicted as (Gly-XY)$_n$ in which the X position is frequently proline and the Y position is frequently hydroxyproline. Under physiological conditions, three chains with the signature (Gly-XY-)$_n$ sequence spontaneously associate into a three-stranded helix that is unique to collagens. The subclass of collagens that form large fibrils consists almost entirely of long (Gly-XY-)$_n$ sequences tightly coiled into triple-helical structures referred to as collagen monomers. The long triple-helical monomers, in turn, spontaneously associate into long, highly ordered fibrils. In some tissues, the long fibrils associate laterally into thick fibers. The two steps in which (Gly-XY-)$_n$ sequences assemble into triple-helical monomers and the triple-helical monomers assemble into fibers resemble the crystallization of small molecules (Figures 1A and 2). Each step is entropy driven by loss of surface water as the larger structure is formed, much as is seen in many crystallization processes. Also, as with crystallizations, each step involves first the slow formation of a small nucleus of a defined structure, and then rapid propagation of the nucleus to form a large structure in which the molecular architecture of the nucleus is extensively replicated. Glycine, the smallest amino acid, must be in every third position in the collagen triple helix because it occupies a very small space where the three chains come together. Additionally, the hydrogens on the α-carbon of glycine allow it to form hydrogen bonds across the three chains. The closed-ring structures of the proline and hydroxyproline residues limit rotation of the polypeptide backbone, thereby providing rigidity to the structure.

Hydroxyproline residues, which are rarely found in other proteins, play a special role in the triple helix. The hydroxyl groups lock the slightly flexible ring of the amino acid into a conformation that further stabilizes the polypeptide backbone. Charged amino acids that occupy the X and Y positions in the repetitive (Gly-XY-)$_n$ sequences point out from the center of the triple helix. The orientation of the charged groups allows them to form salt bridges that bind each triple-helical monomer to surrounding monomers. Most of the monomers in fibrils are staggered one-quarter of their length relative to their nearest neighbors with short gaps between their ends. The gaps are readily seen by staining the surface of the fibrils and examining them by electron microscopy: each fibril has a cross-striated pattern in which the distances between the cross-striations correspond to about one-quarter of the lengths of the monomers. After assembly of the fibrils, the structures are further stabilized by a cross-linking enzyme that generates highly reactive aldehydes by deaminating some of the terminal amino groups on lysine residues that project out from the surface of the monomers. The aldehydes then spontaneously form covalent bonds that link most of the monomers throughout the width and length of the fibril. The result is a highly ordered structure with about the same strength as a steel wire. In essence, the signature (Gly-XY-)$_n$ sequences contain essentially all of the information and driving forces needed to spontaneously generate the highly ordered fibrils and fibers that in some tissues can be several feet long.

The Two Subtypes: The Fibrillar and Non-Fibrillar Collagens

The fibril-forming or fibrillar collagens contain long and uninterrupted (Gly-XY-)$_n$ sequences (Figure 1A). They are among the most abundant proteins in nature,

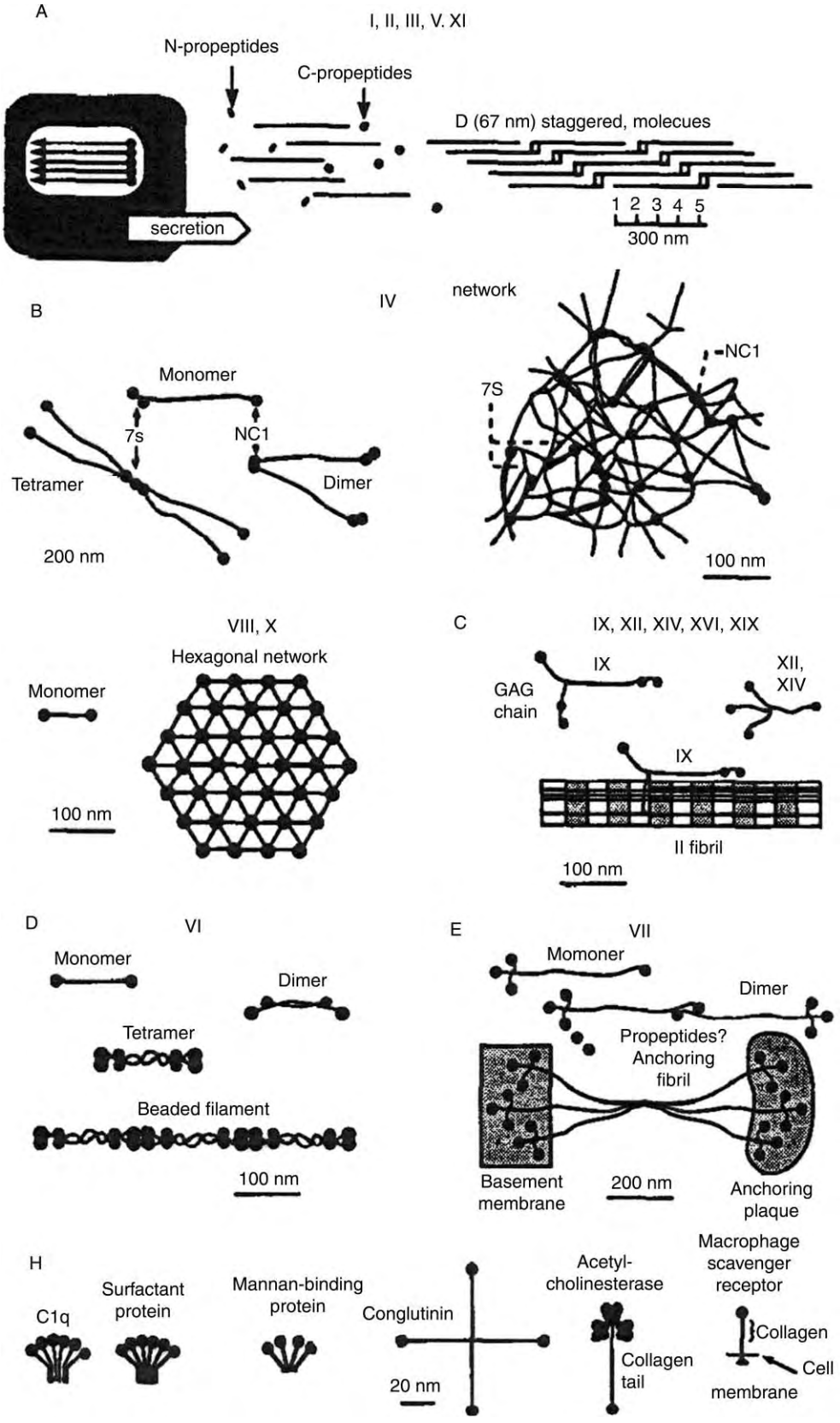

FIGURE 1 Schematic for the structure of various collagens. Reproduced from Prockop, D. J., and Kivirikko, K. I. (1995). Collagens: Molecular biology, diseases, and potentials for therapy. *Annu. Rev. Biochem.* **64**, 403–434.

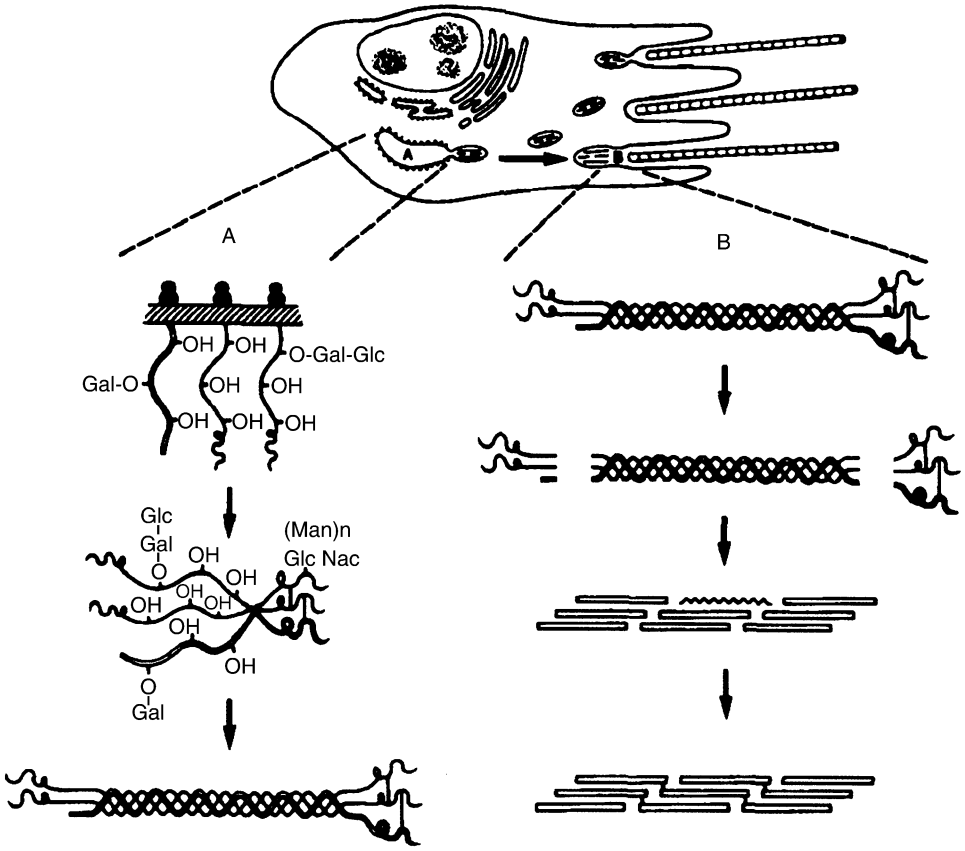

FIGURE 2 Schematic for the biosynthesis of a fibril-forming collagen. (A) Intracellular events that involve posttranslational hydroxylations and glycosylations, association of polypeptide chains, and folding of the triple helix. (B) Extracellular events that involve cleavage of the N- and C-propeptides, self-assembly of collagen into fibrils, and cross-linking of the fibrils. Reproduced from Prockop, D. J., and Kivirikko, K. I. (1995). Collagens: Molecular biology, diseases, and potentials for therapy. *Annu. Rev. Biochem.* **64**, 403–434.

and the most abundant of the fibrillar collagens are referred to as types I, II, and III. They are similar in structure in that each contains three polypeptide chains (α-chains) with approximately 330 -Gly-XY- triplets. They are also similar in that the α-chains spontaneously self-assemble into similar triple-helical monomers and the monomers spontaneously assemble into fibrils. Type I collagen accounts for well over 50% of the dry weight of ligaments, tendons, and demineralized bone. However, the biological properties of the fibrils depend on the still-undefined forces that orient the fibers in tissues. For example, the type I collagen fibrils in ligaments and tendons are present in parallel bundles of thick fibers. In skin, they are randomly oriented in the plane of the skin. In many regions of bone, type I collagen fibrils form highly symmetrical concentric helical arrays around the Haversian canal through which capillaries pass. Type II collagen is very similar to type I collagen in structure, but it is found almost exclusively in cartilage, where it forms very thin fibrils that trap highly charged proteoglycans and water. The result is an arcade-like structure that makes cartilage highly resilient to compression. Type III collagen is also similar to type I collagen in structure and its spontaneous assembly into fibrils. Type III collagen is associated in relatively small amounts with type I collagen in many tissues, but, for reasons that are not apparent, it is particularly abundant in the aorta.

The family of collagen proteins also includes a large number of proteins referred to as nonfibrillar collagens because either they contain only short $(\text{Gly-XY-})_n$ sequences or they contain $(\text{Gly-XY-})_n$ sequences that are interrupted by non-collagen sequences. As a result, the proteins do not assemble into highly ordered fibrils (Figure 1B–1H). One important example of a nonfibrillar collagen is the type IV collagen, which is an abundant constituent of basement membranes (Figure 1B). The protein is a large trimeric monomer with multiple $(\text{Gly-XY-})_n$ sequences that are interrupted by non-collagen sequences; it also contains large globular domains at both ends. The interruptions make the protein flexible, and the globular ends enable the protein to form flexible networks that

bind multiple other proteins. The flexible networks bind epithelial cells and form the barriers that protect the organism from the external environment. Other nonfibrillar collagens are much less abundant and fulfill more specialized functions. Some bind to the surfaces of fibers formed by fibrillar collagens and help either to regulate the assembly process or to provide binding sites for cells or other components of the extracellular matrix. For example, type IX is a short collagen that is flexible because its $(Gly\text{-}XY\text{-})_n$ sequences are interrupted by two non-collagenous sequences (Figure 1C). Type IX collagen binds to both fibrils of type II collagen and proteoglycans to provide one of the connecting links in the arcade-like structure of cartilage. Some nonfibrillar collagens contain very short $(Gly\text{-}XY\text{-})_n$ sequences and triple-helical domains that serve primarily as extension rods for more interactive domains on the ends of the same proteins (Figure 1H).

Collagens and collagen-like proteins are abundant in many multicellular organisms. For example, they are very abundant in diverse invertebrates such as sponges and worms, including the worms found in deep-sea hydrothermal vents. The smallest collagens appear to be minicollagens that contain only 12 to 16 -Gly-XY- repeats, and that are found in the nematocysts with which hydra sting their prey.

The Need to Control the Self-Assembly of $(Gly\text{-}XY\text{-})_n$ Sequences

Viewed with evolution in mind, the special properties of $(Gly\text{-}XY\text{-})_n$ sequences can be seen to have a variety of different purposes. One of the most important of these purposes was to produce tough fibrils to hold together cells and thereby provide a means of developing multicellular organisms. However, it is clear that there had to be controls on the tendency of long polypeptides with repetitive $(Gly\text{-}XY\text{-})_n$ sequences to spontaneously assemble into large fibers. In living systems, the assembly of fibrils cannot be allowed to occur prematurely. If they did, the fibrils would either destroy the cell synthesizing the protein or encase the cell in an impenetrable matrix. Also, the fibrils must be strong but not as rigid as crystals. Their flexibility is critical for most tissues. It is apparently for these reasons that the synthesis of collagens is an elaborate process in which a series of specialized enzymes modifies the polypeptide chains as they are assembled on ribosomes and then pass into the cisternae of the endoplasmic reticulum en route to the Golgi apparatus and secretion from the cell.

Why the Hydroxyproline?

One of the initial intriguing questions about collagens was why they contain large amounts of hydroxyproline, an amino acid very rarely found in other proteins. Early isotope studies demonstrated that after administration of labeled proline to rodents, both labeled proline and hydroxyproline were present in proteins isolated from the animals. After administration of labeled hydroxyproline, however, essentially no labeled hydroxyproline was recovered. Therefore, long before the genetic code was solved, it was apparent that the hydroxyproline in collagen was introduced by an event that did not occur during the initial assembly of the protein but that occurred as a posttranslational event. These observations led to the discovery that the hydroxyproline in collagens was synthesized by prolyl hydroxylase, an enzyme that specifically hydroxylates proline in the Y position in peptides with $(Gly\text{-}XY\text{-})_n$ sequences. The question of why hydroxyproline is introduced in this manner was resolved by demonstrating that if prolyl hydroxylase is inhibited, cells synthesize complete collagen polypeptide chains that cannot fold into a collagen triple helix unless the protein is cooled to about 15 °C below body temperature (Figure 2). The protein folds into a triple helix at body temperature only if about 100 proline residues in each of the 1000-amino-acid-long α-chains of fibrillar collagen are hydroxylated to hydroxyproline. After the protein folds into the triple-helical conformation, prolyl hydroxylase can no longer modify it. In effect, prolyl hydroxylase titers the hydroxyproline content of the proteins so that it folds at body temperature. And, remarkably, the protein is not secreted from cells in significant amounts until it acquires the requisite content of hydroxyproline and folds into a triple helix. This elaborate system is one means of preventing the protein from folding too early in the biosynthetic process. The process by which prolyl hydroxylase gradually titers the hydroxyproline content of collagens serves a second function of ensuring that collagen fibrils are flexible. The monomers are secreted by cells before all the Y position proline residues are fully hydroxylated and before the molecule is a completely rigid rod. Instead, regions of the protein that have low contents of proline and hydroxyproline tend to "breathe" in the sense that they rapidly fold and unfold. Because the monomers are not rigid triple helices, the fibrils they assemble into are not fully crystalline and remain flexible. As might be expected, monomers for fibrillar collagens from organisms with body temperatures ranging from 18° to 40 °C completely unfold at about 4 °C above the body temperatures of the organisms. The fibrillar collagens from organisms with varying body temperatures

have different amino acids found in the X and Y positions that in part explain their different stabilities, but each begins as an unfolded protein that folds as its hydroxyproline content is titered to a critical level by prolyl hydroxylase. After the monomers assemble into fibrils, the lateral interactions of protein make the triple helix stable to about 16 °C above body temperature.

Other Levels of Control

The process of fibril assembly by fibrillar collagens is also controlled at another step. The monomers are first synthesized as larger precursors that are known as procollagens. The procollagens have large non-collagenous domains at both ends that keep the monomers soluble and prevent them from self-assembling until the domains are cleaved by proteinases found outside the cells (Figure 2). Therefore, the proteinases help to regulate the formation of fibrils. In addition, the first fibrils formed begin to accumulate other proteins and components of the extracellular matrix on their surfaces that prevent fusion of the fibrils into large fibers. The rate at which these components are removed provides still another control on the formation of fibrils and fibers.

One Surprise: The Enzymes Involved in Collagen Synthesis Have Other Functions

The biosynthesis of collagen involves processing by a series of separate enzymes that have a number of unusual properties (Figure 2). Because the enzymes carried out processing steps not seen in the synthesis of other proteins, it was initially felt that the enzymes were uniquely dedicated to production of collagen. Subsequently, it became apparent that several of the enzymes had important additional functions. For example, prolyl hydroxylase is unusual among the small number of enzymes that modify proteins in that it requires unfolded peptide substrates. It is also unusual in that it specifically hydroxylates prolyl residues in the Y position of -Gly-X-Pro- sequences. In addition, it is unusual in that the reaction uses iron, molecular oxygen, and ascorbate as well as α-ketoglutarate that is oxidatively decarboxylated to succinate in the reaction. It was surprising, therefore, that cloning of the genes for the two subunits of the enzyme revealed that the β-subunit is identical to protein disulfide isomerase, an enzyme that is required to ensure the correct formation of disulfide bonds during the synthesis of a large number of non-collagen proteins. Perhaps even more surprising was the discovery of three similar but different prolyl hydroxylases that hydroxylate a single proline residue in hypoxia induction factor, a protein that triggers the response of tissues to ischemia. The proline residue in hypoxia induction factor must be hydroxylated for the protein to be degraded by proteosomes. One consequence of this discovery is that inhibitors of prolyl hydroxylase initially designed to limit the excessive deposits of collagen found in scars also increase tissue levels of hypoxia induction factor, thereby enhancing their response to hypoxia. Inhibitors of prolyl hydroxylase therefore appear to provide a new strategy for treatment of diseases such as anemias that are now treated with erythropoietin.

Similar surprises have been encountered with the proteinases that cleave the amino acid extensions on the ends of the procollagen precursors of fibrillar collagens and that keep the proteins from prematurely assembling into collagen fibers. The proteinase that cleaved the large C-terminal globular domains was a large zinc metalloproteinase with an unusual specificity for the similar but different sequences in the cleavage sites for the precursors of types I, II, and III collagens. Therefore, it seemed reasonable to assume that it was a protein with a unique function. Subsequent work demonstrated that the same enzyme was essential for processing a component of basement membranes (laminin-5) and for processing the enzyme (lysyl oxidase) that generates the aldehydes that form the covalent cross-links in fibrils of both collagen and elastin. Even more surprising was the discovery that isoforms of the same enzyme are essential in completely unrelated processes in early embryonic life: they establish a gradient for dorsolateral development by cleaving inhibitors of morphogenic proteins (decapentaplegic/BMP-2/BMP-4).

Evolutionary Origins and Selective Pressures on (Gly-XY-)$_n$ Sequences

The manner in which (Gly-XY-)$_n$ sequences arose and were distributed across biology during evolution cannot be defined any more accurately than many other aspects of evolution. One clue seemed to come from the observation that the genes for the major fibrillar collagens have an unusual structure: most of the codons for the triple helix were found in short exons that were 54 bases long and coded for 18 triplets of (Gly-XY-)$_n$ sequences. Therefore, it appeared that evolutionary pressures had trapped the 54-base exon and replicated it to produce genes for many different collagens. Unfortunately, this attractive hypothesis was not substantiated by data on other collagen genes in which the exons are also relatively short, but the 54-base motif is not a common theme. Independent evidence on the selective pressures on the structure of collagens and the biosynthetic pathway is provided by data on mutations found in patients and a

few animals with genetic diseases. Studies on mutations in fibrillar collagens confirmed that the presence of glycine in (Gly-XY-)$_n$ sequences is critical. Hundreds of mutations that substitute an amino acid with a bulkier side chain for a single glycine distort the triple helix or prevent it from folding. As a result, the mutations produce a large series of diseases of bone, cartilage, blood vessels, and other tissues. Most of the mutations produce severe and rare diseases in children; a few produce variants of common diseases such as osteoporosis or osteoarthritis. The selective pressure for maintaining the signature acid sequences explains why the mutations in collagens differ only slightly from those in organisms that have evolved separately for millions of years. Mutations in the proteinase that cleaves the N-terminal extension on two fibrillar procollagens (types I and II) also produce severe diseases of the skeleton, skin, and other tissues. However, no mutations have been found in either prolyl hydroxylase or the proteinase that cleaves the C-terminal extensions on the procollagen precursors of fibrillar collagens. Such mutations are presumably lethal early in embryonic life.

Summary

The impressive ability of (Gly-XY-)$_n$ sequences to spontaneously undergo self-assembly has been used time and again in biology to provide structures with a variety of important features. However, biological systems need safeguards to control the spontaneous self-assembly of the (Gly-XY-)$_n$ sequences. The principal safeguard is a biosynthetic pathway in which the protein is assembled through a series of complex steps that prevent premature self-assembly and modulate how perfectly the protein crystallizes.

See Also the Following Articles

Amino Acid Metabolism • Collagenases • Metalloproteinases, Matrix

Glossary

collagen fibrils Thin structures, 40 to 500 nm in diameter. Fibrils are assembled laterally into much larger fibers in tissues such as tendons.

collagen monomer A protein containing a collagen triple helix.

collagen triple helix A unique protein structure in which each of three chains with a (Gly-XY-)$_n$ sequence is coiled in a left-handed helix and the three chains are wrapped around each other in a more extended right-handed helix.

procollagens The soluble precursors of fibrillar collagens that contain large, non-collagenous extensions of both ends of the long triple-helical domains.

Further Reading

Boudko, S., Frank, S., Kammerer, R. A., Stetefeld, J., Schulthess, T., Landwehr, R., Lustig, A., Bachinger, H. P., and Engel, J. (2002). Nucleation and propagation of the collagen triple helix in single-chain and trimerized peptides: Transition from third to first order kinetics. *J. Mol. Biol.* **317**, 459–470.

Canty, E. G., and Kadler, K. E. (2002). Collagen fibril biosynthesis in tendon: A review and recent insights. *Comp. Biochem. Physiol. A Mol. Integr. Physiol.* **133**, 979–985.

Engel, J. (1997). Versatile collagens in invertebrates. *Science* **277**, 1785–1786.

Myllyharju, J., and Kivirikko, K. I. (2004). Collagens, modifying enzymes and their mutations in humans, flies and worms. *Trends Genet.* **20**, 43–45.

Prockop, D. J., and Kivirikko, K. I. (1995). Collagens: Molecular biology, diseases, and potentials for therapy. *Annu. Rev. Biochem.* **64**, 403–434.

Pugh, C. W., and Ratcliffe, P. J. (2003). Regulation of angiogenesis by hypoxia: Role of the HIF system. *Nature Med.* **9**, 677–684.

Biography

Darwin J. Prockop is Director of the Center for Gene Therapy at the Tulane University Health Sciences Center. His degrees include an A.B. from Haverford College; an Honors B.A. from Oxford University; an M.D. from the University of Pennsylvania; and a Ph.D. from George Washington University. His former research interests included collagen biosynthesis, structure and function of collagen genes, and genetic mutations that cause bone and cartilage diseases. His current interests are in defining the biological features of adult stem cells and using adult stem cells for therapy of genetic diseases involving collagen and diseases of the central nervous system, lung, and heart.

Cyclic AMP Receptors of *Dictyostelium*

Dale Hereld
The University of Texas Health Science Center, Houston, Texas, USA

Peter N. Devreotes
The Johns Hopkins University School of Medicine, Baltimore, Maryland, USA

When confronted with starvation, the social amoeba *Dictyostelium discoideum* survives by undergoing multicellular development and sporulation. The coordination of these processes is achieved in part through intercellular communication using secreted adenosine 3′,5′-cyclic monophosphate (cAMP) and a family of cell-surface cAMP receptors (cARs). The cARs are examples of G protein-coupled receptors (GPCRs), which enable eukaryotic cells in general to sense and respond to a wide array of environmental and hormonal signals ranging from single photons to large glycoprotein hormones. Due to their involvement in diverse physiological processes, GPCR-targeted drugs are frequently employed in medicine to treat many common conditions including inflammation, hypertension, heart failure, and neurologic and psychiatric disorders. Because GPCRs and the pathways they regulate are conserved in virtually all eukaryotes examined to date, genetically tractable microbes such as *Dictyostelium* have contributed significantly to our understanding of GPCR function and regulation.

Dictyostelium Development and cAMP Signaling

Dictyostelium discoideum is an amoeba found in soil where it feeds on bacteria. In order to survive periods of starvation, 10^4–10^5 amoebae aggregate and execute a 24 h developmental program that yields a fruiting body comprised of a round mass of spores held aloft by a slender stalk (Figure 1A). When nutrients return to the environment, spores germinate to yield amoebae which resume cell division.

Not long after Sutherland and his colleagues discovered cAMP to be an important intracellular second messenger in hormonal signaling, Konijn and his associates demonstrated that cAMP is a potent chemoattractant for *Dictyostelium* and correctly speculated that it was the so-called acrasin secreted by starving amoebae, which mediates their aggregation. Shaffer had proposed that the acrasin would be emitted periodically by cells at aggregation centers and relayed outwardly as waves by surrounding cells. Indeed, exogenous cAMP was shown to elicit the transient activation of adenylyl cyclase and secretion of cAMP. Tomchik and Devreotes later demonstrated the concentric waves of extracellular cAMP waves which arise every ~6 min at aggregation centers and travel radially outward through aggregating populations. Subsequent pharmacologic characterization of these responses established the framework for the identification of the cAMP receptors.

Identification and Properties of cAMP Receptors

The molecular identification of the first cAMP receptor (cAR1) began with its photoaffinity labeling with the cAMP analogue, 8-azido-[^{32}P] cAMP. This approach identified a protein of either 40 or 43 kDa depending on whether or not the cells had been exposed to cAMP, suggesting the existence of a reversible, ligand-induced modification which proved to be phosphorylation. Radiolabeling of cells with [^{32}P] phosphate permitted purification of the 43 kDa phosphorylated form of the receptor. Antibodies directed against purified cAR1 lead to the isolation of a cDNA that encoded a protein of the expected size and hybridized to an mRNA, expressed transiently in early development, consistent with cAMP binding. Formal proof that the isolated cDNA did indeed encode cAR1 came from expression of the cDNA, which resulted in increased cAMP binding, and disruption of the corresponding gene, which obviated cAMP binding and cAR1-mediated responses. The deduced sequence of cAR1 possessed seven putative transmembrane domains (Figure 2) and exhibited weak homology to mammalian G protein-coupled receptors (GPCRs). cAMP stimulation of GTP binding to isolated membranes and GTP hydrolysis was further evidence

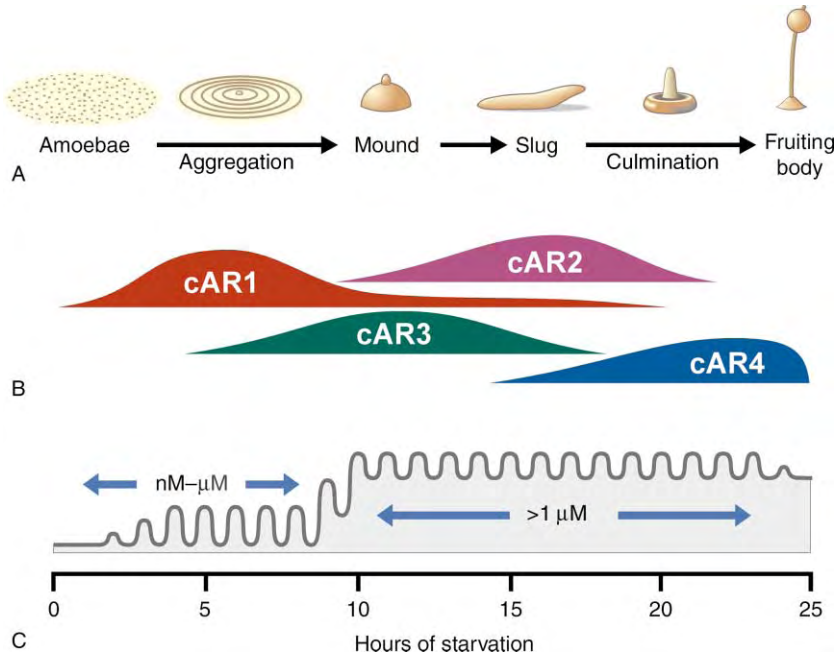

FIGURE 1 Correlation of: (A) developmental morphology, (B) cAR expression, and (C) extracellular cAMP levels. See text for additional details.

that cAR1 is indeed coupled to a G protein. This together with studies of yeast pheromone signaling provided the earliest indications that virtually all eukaryotes have inherited these ancient sensory mechanisms.

Three other highly homologous cAMP receptors, designated cAR2–4, were subsequently identified by hybridization with a cAR1 probe. The cARs are expressed successively during development, peaking in expression at roughly 5 h intervals in the order: cAR1,

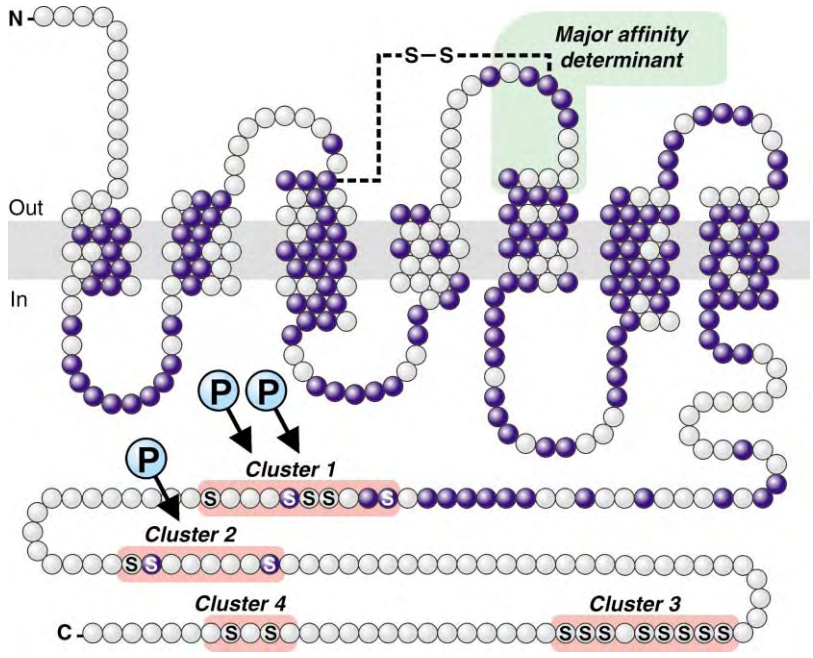

FIGURE 2 Model of cAR1. Dark blue spheres represent amino acids conserved in all four cARs. Densely packed amino acids in the plane of the membrane (gray bar) signify the seven-hydrophobic-transmembrane helices. Nonconserved amino acids (light gray spheres) in the region labeled major affinity determinant are largely responsible for the widely differing cAMP affinities of cAR1 and cAR2 (and possibly other cARs). Clusters of serines in the C-terminal cytoplasmic domain (S), the distribution of ligand-induced phosphorylation (P), and the putative disulfide bridge (––S–S––) are also indicated. cAR2–4 differ in the lengths and sequences of their C-terminal cytoplasmic domains.

cAR3, cAR2, cAR4 (Figure 1B). Disruption of the genes encoding each cAR results in developmental defects consistent with the timing of their expression. cAR1$^-$ cells fail to aggregate. cAR2$^-$ cells arrest shortly after aggregating at the mound stage. cAR3 gene disruption has been variously reported either to have no apparent effect or to interfere with spore cell differentiation late in the mound stage and consequently yield fruiting bodies predominantly comprised of stalk cells. cAR4$^-$ cells develop normally beyond the mound stage but exhibit defects in culmination, resulting in mis-shapen fruiting bodies.

The cARs differ markedly in their affinities for cAMP. The early cARs, cAR1 and cAR3, have high affinities (i.e., low- to mid-nM K_d's), whereas those expressed later in development, cAR2 and cAR4, have low affinities (K_d's > 1 μM). These affinities are appropriate for the extracellular cAMP concentrations that exist at these stages of development (Figure 1C). During aggregation, the cAMP signal oscillates from sub-nM to near-μM concentrations. In contrast, external cAMP oscillates at elevated concentrations exceeding 1 μM in the multicellular stages. Nonconserved residues in the second extracellular loop largely determine whether a cAR has a high or low affinity (Figure 2). By analogy with rhodopsin, this extracellular loop, positioned by disulfide linkage to the extracellular end of the third transmembrane helix, is likely to lie at the entrance to the cAMP binding cleft of cARs and, thereby, influence binding.

Signaling Pathways

cAR1 is perhaps the most versatile GPCR yet to be characterized as it regulates a wide range of downstream effectors and biological responses. Consequently, it serves as a valuable model for understanding diverse modes of GPCR signaling. cAR1 mediates three principal cellular responses during aggregation: (1) propagation of cAMP waves, (2) chemotaxis up the cAMP gradient of each oncoming wave, and (3) regulation of genes required for development. The pathways underlying these responses have been determined to a large extent (Figure 3A). Most striking is the dichotomy between signaling pathways that involve G proteins and those that do not. Comparatively less is known about the pathways governed by cAR2–4 in large measure due to technical challenges posed by multicellularity, although significant progress has been made towards elucidating mechanisms by which these cARs promote cell differentiation in multicellular stages.

G Protein-Dependent Pathways

Dictyostelium possesses at least nine heterotrimeric G proteins composed of distinct α-subunits (designated Gα1–9) and common β- and γ-subunits. Genetic and biochemical evidence indicates that G$\alpha2\beta\gamma$ is the principal G protein to which cAR1 couples. Activation of G$\alpha2\beta\gamma$ by cAR1 liberates the G$\beta\gamma$ dimer and GTP-bound Gα2, which in turn activate various effectors.

The G$\beta\gamma$ dimer is believed to activate the aggregation-stage adenylyl cyclase (ACA) by a mechanism involving activation of phosphoinositide-3-kinase (PI3K), which converts the membrane phospholipid phosphatidylinositol-4,5-bisphosphate (PIP_2) into phosphatidylinositol-3,4,5-trisphosphate (PIP_3). PIP_3, in turn, binds to the PH domain of cytosolic regulator of adenylyl cyclase (CRAC), thus recruiting it to the plasma membrane. How CRAC then activates ACA remains to be determined. The resulting cAMP

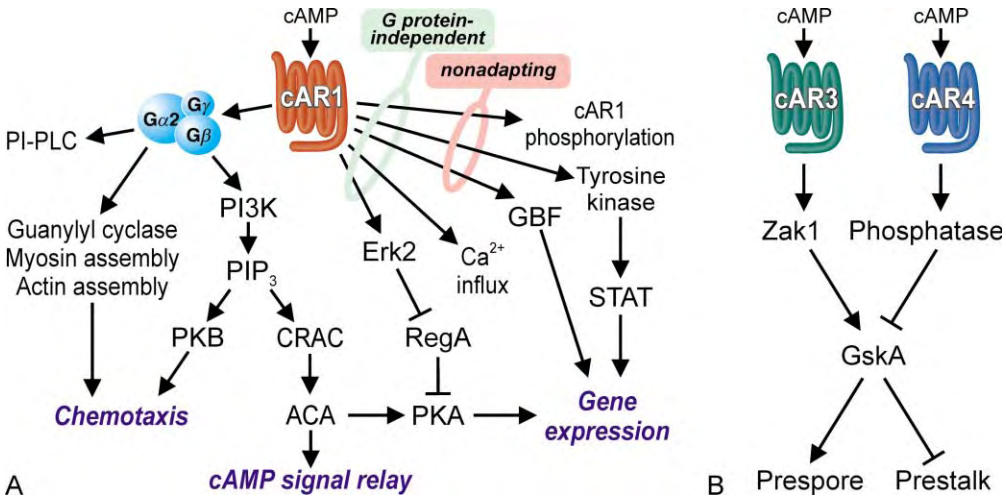

FIGURE 3 cAMP receptor signaling pathways. Pointed (↓) and flat-headed (⊥) arrows indicate activation and inhibition, respectively. (A) cAR1 pathways leading to chemotaxis, cAMP signal relay, and gene regulation. G protein-independent and nonadapting pathways are indicated. In multicellular stages, cAR2–4 might activate some of the pathways shown for cAR1. (B) Role of cARs in the GskA-mediated determination of cell fate. cAR2 (not shown) might promote prestalk cell differentiation at the mound stage in the manner shown for cAR4.

functions intracellularly via protein kinase A (PKA) to modulate gene expression and, in addition, is secreted from the cell in order to relay the cAMP signal to neighboring cells.

G$\beta\gamma$-mediated increases in PIP_3 levels also recruit other PH domain-containing proteins to the plasma membrane including protein kinase B (PKB or Akt), which has been shown to be critical for chemotaxis. In cells undergoing chemotaxis in a shallow cAMP gradient, PKB and other PH domain-containing proteins localize exclusively at the cells' leading edge where they presumably promote actin assembly and pseudopod extension. These mechanistic insights into cAR1-mediated chemotaxis, namely the involvement of PI3K activation and recruitment of PKB to the leading edge, have since been found to also pertain to the chemotaxis of a variety of mammalian cells including neutrophils.

The Gα2 subunit is implicated in the cAR1-dependent activation of guanylyl cyclase (cGMP) which provides another important input to the chemotaxis machinery. The product of cGMP regulates myosin heavy chain kinases and, thereby, promotes the assembly of conventional myosin II in posterior and lateral regions of chemotaxing cells where it can propel the rear of the cell forward upon contraction and suppress lateral pseudopod formation.

G Protein-Independent Pathways

Several cAR-mediated responses appear to be G protein-independent based on their preservation in cells lacking what is believed to be the sole G protein β-subunit gene. These include phosphorylation of cAR1, uptake of Ca^{2+}, and activation of the mitogen-activated protein kinase Erk2, the transcriptional regulators GBF and STAT, and the GSK3 homologue GskA.

cAR1 is phosphorylated on serine residues within its C-terminal cytoplasmic domain. The 18 serines in this domain exist in four clusters (Figure 2). In unstimulated cells, cAR1 is basally phosphorylated within clusters 2 and 3. Upon stimulation with cAMP, cAR1 becomes reversibly hyperphosphorylated due to the addition of approximately two phosphates within cluster 1 and a third phosphate within cluster 2. Cluster 1 phosphorylation causes the 40–43 kDa electrophoretic shift. Other cARs also undergo cAMP-induced phosphorylation commensurate with their affinities.

Erk2 promotes the intracellular accumulation of cAMP by negatively regulating RegA, a cAMP-specific phosphodiesterase. Erk2 is presumably the third of three kinases in a typical MAP kinase cascade. The identity of the upstream kinases as well as the G protein-independent mechanism by which cAR1 activates the cascade remain to be determined.

cAMP triggers the rapid and transient influx of Ca^{2+} ions in aggregation-competent cells. This is mediated largely by cAR1 due to its natural abundance at this stage in development. However, expression of cARs in vegetative cells indicates that the components required for uptake are expressed at this stage and that other cARs can also mediate Ca^{2+} uptake. The magnitude of Ca^{2+} uptake is roughly proportional to receptor level, indicating that cARs are the limiting components for this response.

G-box binding factor (GBF) binds G-rich elements in early postaggregative genes and is required for their induction by cAMP. Gene disruptions suggest that either cAR1 or cAR3 mediate the G protein-independent activation of GBF. In contrast to many aggregation-stage genes whose expression requires periodic cAMP pulses that mimic natural cAMP waves, GBF-mediated gene expression is induced by constant cAMP, indicating that it is not subject to adaptation. Thus, the GBF pathway is appropriately activated upon aggregation when extracellular cAMP rises to levels that persistently occupy cAR1.

STAT proteins have been extensively studied in the context of cytokine signaling in mammalian immune cells. In *Dictyostelium*, exogenous cAMP triggers STATa's phosphorylation on tyrosine, SH2 domain-mediated dimerization, and translocation to the nucleus where it governs prestalk gene expression. cAR1 is required for this response but it can be substituted in this capacity with cAR2, suggesting that multiple cARs might activate STATa during development. The cAR-activated tyrosine kinase involved remains to be identified.

GskA, a homologue of glycogen synthase kinase-3 (GSK3), is an important regulator of cell fate in *Dictyostelium* and cARs play key roles in regulating its activity. GskA activity promotes spore cell differentiation, whereas inactivity results in stalk cell differentiation (Figure 3B). Independent of G proteins, cAR3 activates the nonreceptor tyrosine kinase Zak1 which, in turn, phosphorylates and activates GskA. On the other hand, cAR4 (and perhaps cAR2) activates a phosphotyrosine phosphatase, resulting in the dephosphorylation and inactivation of GskA. The role of G proteins in the latter process, if any, is not known. Therefore, cAR3 signaling promotes spore differentiation and cAR2 and cAR4 favor stalk cell differentiation. Because cAR2 and cAR4 are expressed predominantly in prestalk cells, it is unclear whether these mechanisms determine cell fate or act thereafter in cell-type maintenance.

One known target of cAMP-activated GskA is STATa. GskA phosphorylates multiple serines of STATa, causing it to be exported from the nucleus. This is one mechanism by which cAR3 signaling might oppose prestalk differentiation. As has been described for other developmental systems, GskA may also determine cell fate by phosphorylating β-catenin and thus targeting this transcriptional coactivator for destruction.

Mechanisms of G Protein-Independent Signaling

It remains to be determined how cAMP-occupied cAR1 communicates with and activates these effectors. By analogy with G proteins and also mammalian G protein-coupled receptor kinases (GRKs), the yet to be identified cAR kinase might interact selectively with the ligand-occupied conformation of the receptor's cytoplasmic loops. Other G protein-independent processes such as Ca^{2+} uptake could involve lateral signal transduction within the plane of the membrane by direct interaction of cAR1 with another integral membrane protein, analogous to the interaction of *Halobacterium* sensory rhodopsins (SI and SRII) with their associated histidine kinases (HtrI and HtrII).

Desensitization Mechanisms

In general, receptor-mediated responses are governed by various desensitization mechanisms which attenuate the cell's responsiveness. cAMP triggers the sequential phosphorylation ($t_{1/2} \sim 2$ min) and internalization ($t_{1/2} \sim 15$ min) of cAR1. cAR1 phosphorylation causes a several-fold reduction in the receptor's intrinsic affinity for cAMP, which may extend the range of cAMP concentrations to which the receptor can respond during aggregation. In addition, preliminary results indicate that phosphorylation of cAR1 is a prerequisite for its internalization as in other systems. Prolonged cAMP exposure results in down-regulation of cAR1 levels, the combined effect of diminished cAR1 gene transcription, and cAR1 degradation. Degradation presumably results from delivery of internalized receptors to lysosomes.

On a more rapid timescale, nearly all of the cAR1-mediated responses to abrupt cAMP increases are transient, returning to prestimulus levels in 30 s to several minutes despite constant stimulation. This rapid and reversible attenuation of responses is referred to as adaptation. The few responses that do not adapt include cAR1 phosphorylation and GBF activation. The mechanisms of adaptation are poorly understood and might be distinct for each pathway. cAR1 phosphorylation appears not to be involved as elimination of phosphorylated serine residues in cAR1 by site-directed mutagenesis has little impact on the kinetics of these responses.

Cells adapted to one cAMP concentration can respond to yet higher concentrations (provided the receptor is not saturated). This observation indicates that adaptation is a graded signal that is just sufficient to offset the excitatory signal, the strength of which also reflects receptor occupancy. For the adenylyl cyclase pathway, adaptation can be explained by the transient translocation of PI3K to the plasma membrane and the subsequent degradation of PIP_3 by the phosphatase PTEN. In addition, FRET experiments indicate that the G protein is persistently dissociated in adapted cells. Taken together, these findings suggest that an adaptation pathway emanates from cAR1 and acts upon the adenylyl cyclase excitatory pathway somewhere beyond the G protein, causing PI3K to be released from the membrane. Because PKB activation also depends on PI3K, the same adaptation mechanism is likely to govern chemotaxis.

Gradient Sensing in Chemotaxis

Temporal challenges with fixed cAMP concentrations as described above have been invaluable for deciphering cAR-mediated pathways and revealing the existence of adaptation mechanisms. However, natural cAMP waves also contain spatial information which the cells must rapidly and accurately sense for efficient chemotaxis. Although cAR1 is uniformly distributed in the plasma membrane, shallow cAMP gradients differing by as little as 2% across the length of the cell prompt highly asymmetric localization of various proteins, indicating that the cell senses and amplifies small differences in cAR1 occupancy on this surface. Proteins with PH domains including PKB and CRAC are highly localized to the plasma membrane of cell's leading (or anterior) edge, indicative of elevated PIP_3 levels. This reflects the recruitment of PI3K to the anterior plasma membrane and its subsequent activation. The membrane translocation of PI3K is mediated by its N-terminal domain which presumably binds an entity in the plasma membrane that is generated in response to cAR1 activation. Conversely, PTEN is associated with the posterior plasma membrane via specific interactions with PIP_2. Thus, PTEN is excluded from the anterior membrane where PI3K actively converts PIP_2 to PIP_3 and instead localizes to posterior regions where PIP_2 should be more abundant. Localization of the antagonistic activities of PI3K and PTEN to opposing poles of the cell should result in a steep gradient of PIP_3 and associated PH domain-containing proteins. Precisely how the cell amplifies the directional information of a shallow chemoattractant gradient to achieve extreme gradients of activities within the cell is likely to be critically important for efficient chemotaxis and is under intensive investigation.

See Also the Following Articles

Adenylyl Cyclases • G Protein-Coupled Receptor Kinases and Arrestins • Phosphatidylinositol Bisphosphate and Trisphosphate

Glossary

chemotaxis Directed movement of cells toward (or away from) the source of diffusable chemoattractant (or repellant) molecules.

G protein Heterotrimeric proteins with inactive (GDP-bound) and active (GTP-bound) states which are activated by ligand-occupied receptors and, in turn, activate downstream targets within the cell.

G protein-coupled receptors Cell surface, integral membrane proteins possessing seven membrane-spanning α-helices and usually capable of activating cytosolic G proteins upon binding specific extracellular signaling molecules (also known as seven-transmembrane or serpentine receptors).

signal transduction Molecular events by which the perception of an extracellular signal by a cell is translated into an appropriate cellular response.

Further Reading

Brzostowski, J., and Kimmel, A. (2001). Signaling at zero G: G-protein-independent functions for 7-TM receptors. *Trends Biochem. Sci.* **26**, 291–297.

Chung, C. Y., Funamoto, S., and Firtel, R. A. (2001). Signaling pathways controlling cell polarity and chemotaxis. *Trends Biochem. Sci.* **26**, 557–566.

Iijima, M., Huang, Y. E., and Devreotes, P. (2002). Temporal and spatial regulation of chemotaxis. *Dev. Cell* **3**, 469–478.

Kessin, R. (2001). *Dictyostelium: Evolution, Cell Biology, and the Development of Multicellularity.* Cambridge University Press, Cambridge, UK.

Kim, L., and Kimmel, A. R. (2000). GSK3, a master switch regulating cell-fate specification and tumorigenesis. *Curr. Opin. Genet. Develop.* **10**, 508–514.

Biography

Peter N. Devreotes is a Professor and Chair of the Department of Cell Biology at the Johns Hopkins University School of Medicine in Baltimore, Maryland. His principal research interests include the molecular mechanisms of cell-to-cell signaling, chemoattractant gradient sensing, and chemotaxis. He holds a Ph.D. from Johns Hopkins and obtained postdoctoral training at the University of Chicago.

Dale Hereld, who earned an M.D. and a Ph.D. from Johns Hopkins, was a Damon Runyon-Walter Winchell Fellow under Dr. Devreotes and presently is an Assistant Professor at the University of Texas Health Science Center in Houston, Texas.

Cyclic GMP Phosphodiesterases

Sharron H. Francis and Jackie D. Corbin
Vanderbilt University School of Medicine, Nashville, Tennessee, USA

Cyclic nucleotide (cN) phosphodiesterases (PDEs) are phosphohydrolases that specifically cleave the cyclic phosphodiester bond of 3′,5′-cyclic GMP (cGMP) or 3′,5′-cyclic AMP (cAMP) (Figure 1) to the respective 5′-nucleotides thereby inactivating these signaling molecules. PDEs are largely responsible for lowering the intracellular cN content, and the activities and concentrations of these enzymes are rigorously regulated. Some PDEs are highly specific for either cAMP or cGMP, but others, i.e., dual-specificity PDEs, hydrolyze both. Both types of PDEs contribute importantly to modulation of cGMP-signaling pathways. The competition of cGMP and cAMP for hydrolysis by the dual specificity PDEs can also alter the signaling in the respective pathways. PDEs are integral components in cN signaling pathways (Figure 2) from *Paramecia* through mammals, and in humans, these enzymes are the pharmacological targets for treatment of a number of medical problems including hypertension, male erectile dysfunction, depression, and asthma.

Cyclic GMP and cAMP are prominent second-messenger molecules (Figure 1) and are synthesized by guanylyl cyclases (GC) and adenylyl cyclases (AC), respectively. The balance between the activities of the cyclases and PDEs determines cellular cN levels (see cGMP-signaling pathway, Figure 2). The cyclases specifically synthesize either cAMP or cGMP. The cyclic phosphate ring of cGMP and cAMP is a key feature by which PDEs recognize their substrates, and it is highly resistant to most other phosphohydrolases. Nucleotides lacking this ring do not significantly interact with the catalytic sites of PDEs even at high concentrations. Structural features of the purine (Figure 1) provide the next most critical feature for interaction of the cN with PDEs. For cGMP-specific PDEs, interaction with the oxygen at the C6 position is extremely important.

Distribution of cAMP and cGMP

Cyclic AMP is apparently present in all eukaryotes, but cGMP is less widespread (Figure 1). The yeast genome lacks identifiable sequences for GCs or known cGMP-binding domains. However, *Dictyostelium, Paramecium, Tetrahymena, Trypanosomatids*, and *Plasmodium* contain GCs. The role of cGMP in most of these organisms is not understood, but in *Dictyostelium*, cGMP participates importantly in chemotaxis and osmoregulation. In mammals, cGMP-signaling pathways are prominent in many processes including smooth muscle relaxation, visual transduction, platelet function, neuronal viability, bone growth, apoptosis, water and electrolyte homeostasis, and aldosterone synthesis.

Classification of PDEs

Three evolutionarily distinct classes of PDEs, class I, class II, and class III have been identified; to date, class III contains one PDE that hydrolyzes cAMP and will not be discussed further. Both class I and class II PDEs occur in some species, e.g., *Dictyostelium* and *Saccharomyces*. All known mammalian PDEs and a few PDEs in other species are class I PDEs. In eukaryotes, the cN-binding sites in PDEs are distinguished from those of other known intracellular cN receptors both functionally and evolutionarily; these include cN-binding proteins such as the cAMP- and cGMP-dependent protein kinases (PKA and PKG) which belong to the bacterial catabolite gene activator protein (CAP-related family), the cGMP-binding GAF domains in some PDEs, and some anion transporters.

Class I PDEs

The class I PDE superfamily in mammals contains 11 PDE families that are products of separate genes. Classification is based on the extent of similarity in the DNA sequences. Three are cAMP-specific PDEs (PDEs 4, 7, and 8), three are "cGMP-specific" PDEs (PDEs 5, 6, and 9), and four are dual-specificity PDEs (PDEs 1, 2, 3, 10, and 11) (Figure 3). Among isoforms of the latter group, the relative affinities and turnover rates for cGMP and cAMP can vary significantly as exemplified by PDE1.

Domain Structure of Class I PDEs

Each class I PDE monomer is a chimeric protein that includes a conserved catalytic domain (C domain) of ~270 amino acids that is located more C-terminal to its regulatory domain (R domain); 18 amino acids are

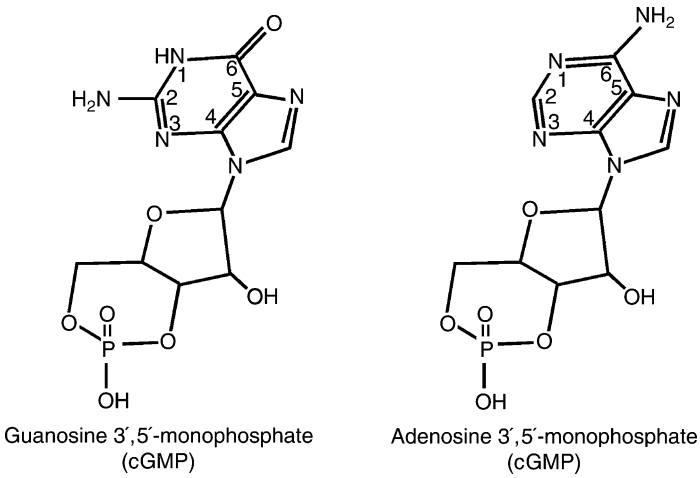

FIGURE 1 Molecular structures of cGMP and cAMP. The structures of cGMP and cAMP differ only at the N-1, C-6, and C-2 positions, but these differences provide for the specific and selective interaction with PDE catalytic sites. The *syn* conformation of both nucleotides is shown.

invariant among mammalian class I PDEs. Among all known class I PEDs, only 14 amino acids are invariant. These most likely provide for critical structural and catalytic features. Diverse regulatory features for each family modulate enzyme functions (Figure 3). The R domains contain varied subdomains including phosphorylation sites, autoinhibitory sequences, subcellular localization signals, dimerization motifs, and GAFs; GAFs are ancient domains of ~120 amino acids that occur in five PDE families. The name is derived from recognition of this motif in a number of diverse proteins (cGMP-binding PDEs, *Anabaena a*denylyl cyclase, and *Escherichia coli F*hla transcription factor). Depending on the PDE in which they are located, GAFs can contribute to for dimerization, interaction with other proteins or with ligands such as cGMP; cAMP interacts weakly with these sites in PDE2, but it does not appear to bind to these sites in other PDEs.

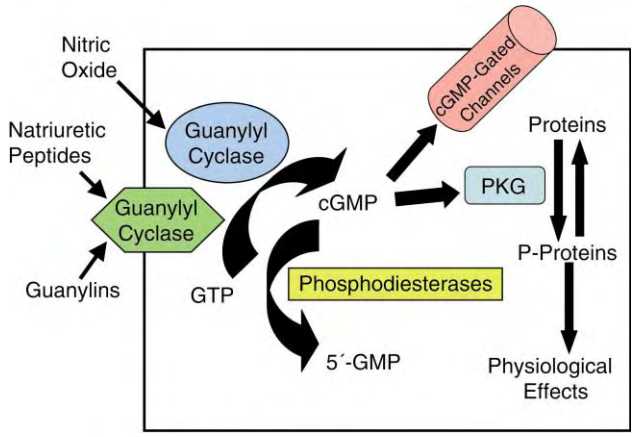

FIGURE 2 Model of cGMP signaling in cells. Intracellular levels of cGMP are determined by the relative activities of guanylyl cyclases and phosphodiesterases. There are two families of guanylyl cyclases; the cytosolic form is activated by nitric oxide and a membrane-bound form is activated by natriuretic peptides and guanylins. Cyclic GMP breakdown is catalyzed by phosphodiesterases that are either cGMP-specific or PDEs that hydrolyzed both cGMP and cAMP, i.e., dual-specificity PDEs. Cyclic GMP interacts with the cGMP-dependent protein kinase (PKG), cGMP-gated cation channels, and cGMP-binding phosphodiesterases to bring about its physiological effects.

C Domains of Class I PDEs

The C domains of class I PDEs contain two prominent functional subdomains; one provides for binding divalent cation(s) and another provides for interaction with the cN purine. Metal and cN apparently bind independently. The subdomains are closely juxtaposed in the tertiary structure in order to effect catalysis. Crystallographic structures of cAMP-specific PDEs (PDE4B and PDE4D), cGMP-specific PDE5, and site-directed mutagenesis of a number of PDEs have identified important amino acids in each subdomain.

Metal Requirements of Class I PDEs

PDEs require divalent cation(s) to support catalysis. Evidence suggests that class I PDEs contain two metals that are bound in close proximity and are critical to the catalytic process. In two cGMP-specific PDEs (PDEs 5 and 6), Zn^{2+} is required for catalysis, and PDE6 contains three Zn^{2+} molecules. Results of site-directed mutagenesis and X-ray crystallographic structures of the catalytic domains of PDEs 4 and 5 indicate that these PDEs contain a tightly bound Zn^{2+} which is coordinated by histidines, aspartic acid, and water molecules. The second metal is coordinated through interactions with an aspartic acid and several water molecules that are in turn linked to histidines and aspartic acid. The metal occupying the second

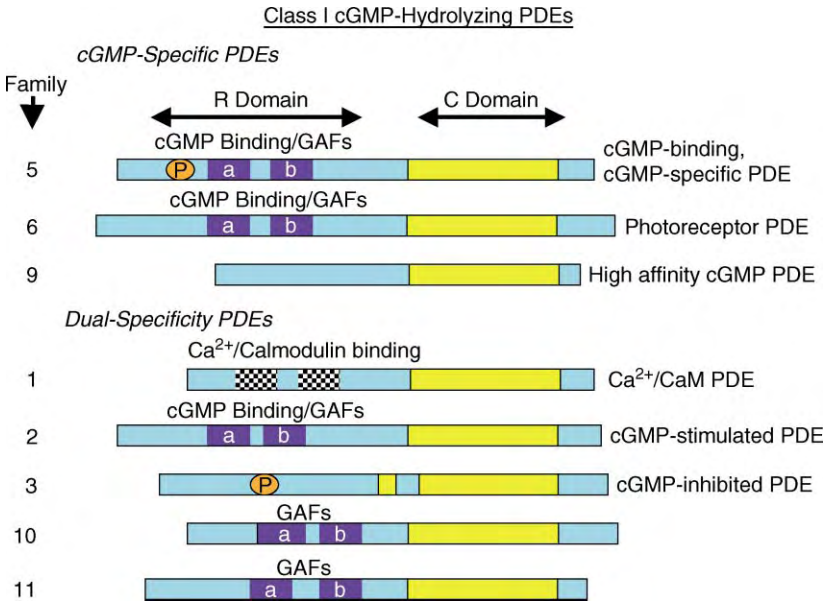

FIGURE 3 Schematic depiction of structural features of mammalian class I cGMP-hydrolyzing PDEs. Arrangements of the regulatory (R) domains and catalytic (C) domains are shown for a monomer, although all known mammalians PDEs exist as dimers. Known sites of phosphorylation (P) are indicated. The cGMP binding/GAFs label denotes allosteric cGMP-binding that is associated with GAF domains in PDEs 2, 5, and 6; all isoforms of these families contain two GAF domains. The role of the GAF domains in PDEs 10 and 11 is not known; isoforms within the PDE11 family contain 1, 2, or no complete GAF domains. The open block in PDE3 is a novel 44 amino acid insert in the catalytic domain of this family. Cross-hatched boxes denote calmodulin-binding domains (1 or 2) in the R domain of PDE1

metal site in PDEs is still unclear and may vary. Both Mg^{2+} and Mn^{2+} have been suggested to be the physiologically relevant cations, but this remains to be definitively demonstrated. Nucleophilic attack by an activated hydroxyl from solvent water that bridges the metals is thought to cleave the phosphodiester bond.

Features that Contribute to cN Specificity

The molecular basis that provides for the affinity and selectivity of PDEs for either cN is poorly understood. Substitution of two amino acids by point mutations shifts the cGMP/cAMP specificity of PDE5 ~100-fold. PDE11, a dual-specificity PDE, and PDE5, a cGMP-specific PDE, are most similar among PDEs. X-ray crystallographic structures of PDEs 4 and 5 suggest that the orientation of the side chain of an invariant glutamine is a critical determinant of specificity for interaction with the purine ring in either cGMP or cAMP.

In solution, cNs are in equilibrium between two conformations, *syn* and *anti*, based on orientation between the purine and ribose moieties. The preferred configuration varies among PDE families, but the *anti* conformer is most commonly preferred. Large substitutions on the ribose 2′-OH or on the N-1 and C-2 positions of the purine are well tolerated by the catalytic sites of both cGMP-specific PDEs 5 and 6 and the dual-specificity PDEs 1 and 2. Some of these analogues are hydrolyzed by the enzymes.

Interaction of Inhibitors with Class I PDEs

Specific structural features in the catalytic sites of cGMP-PDEs provide for interaction with different inhibitors. Some inhibitors compete for access to the catalytic site by mimicking the structure of cGMP. This is true for two specific inhibitors of PDE5, i.e., sildenafil (Viagra) and vardenafil (Levitra); tadalafil (Cialis) also competes with cGMP for the catalytic site, but its structure is not closely patterned on that of cGMP, and it forms different contacts with PDE5 than occur with sildenafil or vardenafil. Studies based on site-directed mutagenesis indicate that sildenafil utilizes many of the amino acids that provide for interaction of cGMP with PDE5. Affinity of PDE5 for these inhibitors is ~1000–10 000 times greater than for cGMP, so additional contacts must be involved.

PDEs 5, 6, and 11 are closely related and share ~50% amino acid sequence homology. Sildenafil inhibits both PDEs 5 and 6, but it has ~4–10 fold lower affinity for isoforms of PDE6 than for PDE5; it is a very weak inhibitor of PDE11. In contrast tadalafil (Cialis) potently inhibits PDE5, is ~40-fold less effective against PDE11, and has little effect on PDE6. PDE1, a dual-specificity PDE, is inhibited by sildenafil with ~100-fold lower potency than that for PDE5. The catalytic sites of

PDEs 1, 5, and 6 have similar preferences for cN analogues, so it is likely that sildenafil exploits shared structural features among these PDEs. In contrast, some other inhibitors selectively inhibit the dual-specificity PDEs 1, 2, and 3 and are ineffective against PDEs 5 and 6. Future development of PDE inhibitors will undoubtedly map the patterns of molecular selectivity to identify compounds that preferentially inhibit particular cGMP PDEs. PDE6 isoforms are novel in that they are specifically inhibited by a small protein, Pγ, that is abundant in photoreceptor cells. Pγ inhibitors appear to be entirely specific for PDE6 isoforms.

Regulation of cGMP-Hydrolyzing Class I PDEs

Cyclic GMP-hydrolyzing PDEs are regulated by both short-term and long-term regulatory mechanisms. These include ligand activation (e.g., Ca^{2+}/calmodulin (PDE1) and cGMP binding to allosteric sites provided by one or more GAF domains (PDEs 2, 5, 6, and perhaps 10 and 11), phosphorylation (PDEs 1, 3, 5, and 11) (Figure 3), and increases in protein levels. In a physiological setting, these provide for sensitive control of PDE activities.

In PDEs 2, 5, and 6, GAFs provide for allosteric cGMP binding, and are evolutionarily distinct from the catalytic sites. Molecular determinants for cGMP interaction with the catalytic site differ markedly from those for cGMP binding to GAF sites. Cyclic GMP is the only ligand that has been shown to bind to GAFs in PDEs; this has been reported only for PDEs 2, 5, and 6. In PDE2, cAMP competes with cGMP binding but with >10-fold lower affinity; it does not measurably compete with cGMP binding in PDEs 5 and 6. In the X-ray crystallographic structure of the PDE2 R domain, cGMP is almost entirely buried within the GAF b site. The tight fit of cGMP agrees well with the fact that few cGMP analogues compete with cGMP at this site. In PDE5, allosteric cGMP binding occurs in the GAF a site.

Characteristics of cGMP-Specific Class I PDEs (PDEs 5, 6, and 9)

PDE5

PDE5 is known as the cGMP-binding, cGMP-specific PDE. There are four isoforms. PDE5 has >100-fold selectivity for cGMP over cAMP at both its catalytic site and allosteric sites; it is a homodimer of ~100 kDa subunits; each R domain contains two GAFs (a and b). GAF*a*, and perhaps GAF*b*, and both provide for allosteric cGMP binding contribute importantly to dimerization. The K_m for cGMP hydrolysis is <1 μM, and the V_{max} is ~5 μmol min^{-1} mg^{-1}. PDE5 is abundant in smooth muscle cells, gastrointestinal epithelial cells, platelets, and certain neuronal cells. It is typically coexpressed with other components of cGMP signaling, including PKGs and GCs. Catalytic activity is stimulated by cGMP binding to the allosteric cGMP-binding sites, by phosphorylation of Ser-102 near the N terminus, and by chemical reduction. Phosphorylation occurs in intact tissues in response to elevation of cGMP and PKG action.

PDE5 is the major cGMP-hydrolyzing PDE in platelets, lung, and the vascular smooth muscle (VSM) of the penile corpus cavernosum (PCC). Sildenafil (Viagra), tadalafil (Cialis), or vardenafil (Levitra) blocks cGMP breakdown by PDE5 leading to increased intracellular cGMP and relaxation of the VSM of blood vessels within and supplying the PCC. The increased blood flow and capacitance of PCC vascular structures facilitate accumulation of blood and improve erectile function. Sildenafil also shows promise in treatment of other diseases involving the vasculature.

PDE6

PDE6 occurs only in mammalian retinal photoreceptor cells. Its activity accounts for the visual response. Rods provide for vision in dim light and contain PDE6$\alpha\beta$, a heterodimer of 100-kDa subunits. Cones provide for vision in bright light and contain PDE6$\alpha'\alpha'$, a homodimer of 100-kDa subunits. In the absence of light, PDE6$\alpha\beta$ and PDE6$\alpha'\alpha'$ are inhibited by specific proteins, Pγs. Activated PDE6 isoforms have high catalytic activity ($V_{max} \sim 300$ μmol min^{-1} mg^{-1}) and $K_m \sim 35$ μM. One or both GAFs in each PDE6 subunit provide for allosteric cGMP binding and/or dimerization.

In the dark, cGMP in photoreceptors is high. This cGMP binds to a cGMP-gated cation channel which then allows for increased conductance of a "dark current." When light strikes the retina, the inhibition of PDE6 by Pγ is relieved, causing a sudden drop in cGMP. At the lower cGMP level cGMP dissociates from the channel; the channel closes, terminating the "dark current." The resulting change in the membrane potential produces the sensation of light. The regulation of PDE6 in cones and rods is specifically adapted to optimally respond to different light intensities, but the overall regulation of the PDE6 isoforms is quite similar.

PDE9

Little is known about the tissue distribution or physiological role of PDE9. It is highly selective for cGMP and has a K_m of 0.1–2 μM for cGMP versus 230 μM for cAMP. It is inhibited by zaprinast ($IC_{50} \sim 35$ μM), but it is insensitive to a wide range of other PDE inhibitors including sildenafil, vinpocetine, IBMX, and dipyridamole.

Characteristics of Class I Dual-Specificity PDEs

A number of mammalian PDEs (PDEs 1, 2, 3, 10, and 11) hydrolyze both cGMP and cAMP. The physiological role of each PDE in hydrolyzing the two nucleotides is likely to be complex. Activities of these PDEs towards either cGMP or cAMP will reflect the respective K_m and V_{max} values for each, but selective action towards one nucleotide can occur simply by mass action. For example, if the cGMP/cAMP content of a tissue selectively changes, increased hydrolysis of one nucleotide (e.g., in response to elevated amounts of that nucleotide) would tend to decrease hydrolysis of the other nucleotide through simple competition for the catalytic site. As a result, the concentration of the second nucleotide would increase.

PDE1

PDE1 is regulated by Ca^{2+}/calmodulin binding (Figure 3). It occurs in many tissues including brain, heart, vascular smooth muscle, and liver. There are three groups of isoforms (PDE1A, IB, and IC) whose relative affinities and turnover rates for cGMP and cAMP vary considerably. In tissues containing primarily one of these isoforms, the relative hydrolytic contribution of PDE1 family to breakdown of cAMP or cGMP will reflect the kinetic features of that particular PDE1. The PDE1 family can provide for responsiveness of cGMP and/or cAMP levels to changes in Ca^{2+} signaling.

PDE2

PDE2 is known as the cGMP-stimulated PDE. It is a homodimer comprised of ~105-kD monomers; there are three isoforms. The V_{max} values for hydrolysis of cAMP and cGMP are similar (150 μmol min^{-1} mg^{-1}), and the K_m values differ ~twofold (15–30 μM for cGMP versus 30–50 μM for cAMP). Cyclic GMP binds to the GAF b in the R domain; this stimulates breakdown of either cAMP or cGMP. PDE2 can therefore potentially lower either or both cNs. PDE2 is abundant in adrenal cortex cells which produce aldosterone in response to cAMP elevation. Elevation of cGMP results in cGMP binding to the PDE2 GAF b, causing increased cAMP hydrolysis and decreased aldosterone production. A similar physiological effect to increase cGMP hydrolysis has not been experimentally demonstrated, but it is likely to occur.

PDE3

PDE3 is abundant in many tissues and occurs as two isoforms (PDE3A and 3B) that are largely membrane bound; both hydrolyze cAMP with a greater V_{max} than cGMP, but the K_m values for the cNs are similar. PDE3B is activated by phosphorylation. Historically, PDE3 was dubbed the "cGMP-inhibited PDE," a misleading descriptor since cGMP "inhibits" cAMP hydrolysis by competing for access to the catalytic site. In platelets, evidence suggests that the antiaggregatory effect of cGMP may occur through a cAMP-signaling pathway due to cGMP competition with cAMP hydrolysis by PDE3. Elevation of cGMP would increase its effectiveness to compete with cAMP for the PDE3 catalytic site, thereby "protecting" cAMP from hydrolysis.

PDEs 10 and 11

Little is known about the physiological functions of these recently characterized PDEs. PDE10 is abundant in neural tissue. It has 26-fold higher affinity for cAMP versus cGMP (K_m values ~0.05 and 13 μM, respectively), but the V_{max} for cGMP is ~5 times that for cAMP. PDE10 R domain contains GAFs, but no ligand has been shown to bind to these GAFs. PDE11 is closely related to PDE5 (50% homology). There are four isoforms whose R domains contain one, two, or partial GAFs, but cN binding has not been demonstrated. PDE11 hydrolyzes cGMP and cAMP at a similar rate, but K_m for cAMP is half that for cGMP (0.5 versus 1 μM, respectively). It is potently inhibited by tadalafil (Cialis) (IC_{50} ~ 80 nM) and by dipyridamole (IC_{50} ~ 0.4–0.9 μM).

Characteristics of Class II PDEs

The few known class II PDEs occur in yeast, bacteria, and *Dictyostelium*. They belong to a family of proteins with a Zn^{2+}-binding hydrolase motif that is thought to mediate hydrolysis of the cN. This family of proteins includes glyoxylases, β-lactamases, and arylsulfatases, but there are no X-ray crystallographic structures. There is no apparent homology with class I PDEs.

Characteristics of Class II PDEs Catalytic Activity

Class II PDEs require divalent cation(s) for catalytic activity. Three of these PDEs hydrolyze cGMP; these include a dual-specificity PDE from *Vibrio fischeri*, and two PDEs from *Dictyostelium* (Figure 4). The *V. fischeri* PDE hydrolyzes cAMP and cGMP with ~20- and 10-fold higher V_{max} values, respectively, than any PDE in either class; one *Dictyostelium* class II PDE is cGMP-specific while the other has dual-specificity.

Regulation of Class II PDEs

Both *Dictyostelium* PDEs described above are activated by cN binding to site(s) in R domains located near the

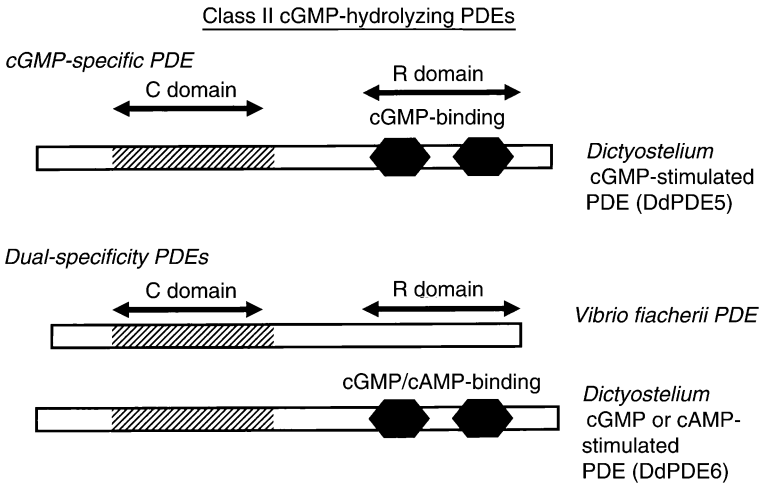

FIGURE 4 Schematic depiction of class II cGMP-hydrolyzing PDEs. Arrangements of functional domains are shown for a monomer. The allosteric cN-binding sites belong to the CAP-related family of cN-binding proteins and are distinct from the allosteric cGMP-binding sites in class I PDEs.

C terminus (Figure 4). In DdPDE5, catalytic activity is stimulated by allosteric cGMP binding, whereas allosteric binding of either nucleotide stimulates catalysis by DdPDE6. This resembles the cGMP effect on catalysis in class I PDEs 2 and 5. However, GAFs are absent in these class II PDEs. Instead, both contain two CAP-related cN-binding domains (Figure 4). Thus, despite little similarity between class I and II PDEs, similar regulatory mechanisms are used, and, remarkably, evolutionarily distinct motifs and arrangements of the motifs in the structures have been employed. In *Dictyostelium*, cellular cGMP is degraded by both of these PDEs as well as by a dual-specificity PDE that is poorly understood.

Concluding Remarks

Cyclic GMP levels are modulated through the action of cGMP-specific PDEs and dual-specificity (cGMP and cAMP) PDEs. Both must be considered when studying physiological changes in intracellular cGMP.

See Also the Following Articles

Cyclic AMP Receptors of *Dictyostelium* • Cyclic Nucleotide Phosphodiesterases • Cyclic Nucleotide-Dependent Protein Kinases • Cyclic Nucleotide-Regulated Cation Channels

Glossary

allosteric binding Binding of ligands to regulatory sites within a protein.

autoinhibition Effect of one region of an enzyme to block the action of the catalytic site of another region of that same enzyme.

CAP-related domains cN-binding domains of ~120 amino acids that provide for cN binding in PKA, PKG, GEFs, and cN-gated cation channels and are evolutionarily related to the bacterial catabolite-gene activator protein.

chimeric proteins Proteins that are composed of multiple subdomains that provide for a specific function of that protein.

dual-specificity Proteins that are not entirely selective among closely related ligands, e.g., cAMP and cGMP.

GAF domains Domains of ~120 amino acids that provide for binding of a variety of ligands and protein–protein interactions in diverse proteins.

phosphohydrolase Enzymes that break a phospho-ester bond.

Further Reading

Bosgraaf, L., Russcher, H., Snippe, H., Bade, S., Wind, J., and Van Haastert, P. J. M. (2002). Identification and characterization of two unusual cGMP-stimulated phoshodiesterases in *Dictyostelium*. *Mol. Biol. Cell.* **13**, 3878–3889.

Chabre, M., and Deterre, P. (1989). Molecular mechanism of visual transduction. *Eur. J. Biochem.* **179**, 255–266.

Corbin, J. D., and Francis, S. H. (1999). Cyclic GMP phosphodiesterase-5: Target of sildenafil. *J. Biol. Chem.* **274**, 13729–13732.

Francis, S. H., Turko, I. V., and Corbin, J. D. (2000). Cyclic nucleotide phosphodiesterases: Relating structure and function. *Prog. Nucleic Acid Res. Mol. Biol.* **65**, 1–52.

Martinez, S. E., Wu, A. Y., Glavas, N. A., Tang, X.-B., Turley, S., Hol, W. G. J., and Beavo, J. A. (2002). The two GAF domains in phosphodiesterase 2A have distinct roles in dimerization and in cGMP binding. *PNAS USA* **99**, 13260–13265.

Shakur, Y., Holst, L. S., Landstrom, T. R., Movsesian, M., Degerman, E., and Manganiello, V. (2001). Regulation and function of the cyclic nucleotide phosphodiesterase (PDE3) gene family. *Prog. Nucleic Acid Res. Mol. Biol.* **66**, 241–277.

Soderling, S. H., and Beavo, J. A. (2000). Regulation of cAMP and cGMP signaling: New phosphodiesterases and new functions. *Curr. Opin. Cell Biol.* **12**, 174–179.

Sung, B.-J., Hwang, K. Y., Jeon, Y. H., Lee, J. I., Heo, Y.-S., Kim, J. H., Moon, J., Yoon, J. M., Hyun, Y.-L., Kim, E., Eum, S. J., Park, S.-Y., Lee, J.-O., Lee, T. G., Ro, S., and Cho, J. M. (2003). Structure of the catalytic domain of human phosphodiesterase 5 with bound drug molecules. *Nature* **425**, 98–102.

Van Haastert, P. J. M., and Kuwayama, H. (1997). cGMP as second messenger during *Dictyostelium* chemotaxis. *FEBS Lett.* **410**, 25–28.

Xu, R. X., Hassell, A. M., Vanderwall, D., Lambert, M. H., Holmes, W. D., Luther, M. A., Rocque, W. J., Milburn, M. V., Zhao, Y., Ke, H., and Nolte, R. T. (2000). Atomic structure of PDE4: Insights into phosphodiesterase mechanism and specificity. *Science* **288**, 1822–1825.

Yarfitz, S., and Hurley, J. B. (1994). Transduction mechanisms of vertebrate and invertebrate photoreceptors. *J. Biol. Chem.* **269**, 14329–14332.

Zhao, A. Z., Yan, C., Sonnenburg, W. K., and Beavo, J. A. (1997). Recent advances in the study of Ca^{2+}/CaM-activated phosphodiesterases. In *Advances in Second Messenger and Phosphoprotein Research: Signal Transduction in Health and Disease*, Vol. 31, pp. 237–251. Lippincott-Raven, Philadelphia.

Biography

Sharron Francis is a Research Professor in the Department of Molecular Physiology and Biophysics at Vanderbilt University School of Medicine. Her interest has been in the mechanism of action of cGMP and cAMP. She has a Ph.D. in Physiology from Vanderbilt University and did postdoctoral training at Washington University in St. Louis, MO and at the National Heart and Lung Institute at the National Institutes of Health in Bethesda, MD. She has made seminal discoveries in the mechanisms and functions of cGMP-dependent protein kinases and cGMP-binding cGMP-specific phosphodiesterase (PDE5).

Jackie Corbin is Professor in the Department of Molecular Physiology and Biophysics at Vanderbilt University School of Medicine. His career interest has been the mechanism of action of cAMP and cGMP. He has a Ph.D. in Physiology from Vanderbilt University and did postdoctoral training at the University of California-Davis. He has made seminal discoveries in the mechanisms and functions of cAMP-dependent protein kinases, cGMP-dependent protein kinases, and cyclic GMP-binding cyclic GMP-specific phosphodiesterase (PDE5).

Cyclic Nucleotide Phosphodiesterases

Vincent C. Manganiello
National Heart, Lung, and Blood Institute, National Institutes of Health, Bethesda, Maryland, USA

Eva Degerman
Lund University, Lund, Sweden

Cyclic nucleotide phosphodiesterases (PDEs) constitute a large, diverse, and complex superfamily of metallohydrolases which cleave the 3′,5′-cyclic phosphate bond of cyclic AMP (cAMP) and cyclic cGMP (cGMP), resulting in production of 5′-AMP and 5′-GMP, respectively. Based on differences in primary structures, PDEs have been divided into two major classes, I and II. Class I PDEs, which contain a conserved catalytic domain (~250–300 amino acids), comprise the majority of known PDEs, including the 11 structurally related, highly regulated, and functionally distinct mammalian gene families (PDEs 1–11). Class I PDEs are also found in the parasites *Trypanosoma brucei* and *cruzi*, and in *Drosophila*, nematodes, yeast, and sponges. Only a few enzymes (no mammalian isoforms) have been classified as class II PDEs, which are structurally unrelated to class I PDEs. The evolutionary relationship between the two PDE classes is also not certain; this brief review will focus on mammalian class I PDEs. By catalyzing hydrolysis of cyclic nucleotides, mammalian PDEs regulate their intracellular concentrations, and, consequently, their signaling pathways and myriad physiological effects, including myocardial contractility, visual transduction, vascular and airway smooth muscle relaxation, immune/inflammatory responses, cell proliferation and apoptosis, memory, and many others. At present, mutations in the PDE6 gene represent the only known association of PDE mutations with human disease, in this instance, with certain subclasses of degenerative retinitis pigmentosa. The mammalian PDE superfamily is a major target for drug discovery in treatment of clinically important diseases, i.e., PDE5 inhibitors (Viagra®) for erectile dysfunction, PDE4 inhibitors for inflammatory disorders, etc.

Molecular Diversity

cAMP and cGMP are important intracellular second messengers that modulate many biological processes. The "classical" mechanism for transduction of cyclic nucleotide signals involves cyclic nucleotide-induced activation of cAMP- and cGMP-dependent protein kinases (PKA and PKG, respectively), with subsequent phosphorylation of critical downstream regulatory effectors. Recently, however, cyclic nucleotide-binding proteins have been recognized as direct mediators of cyclic nucleotide actions, e.g., cyclic nucleotide-gated ion channels, cAMP-activated guanine nucleotide exchange factors (EPACs) which regulate Rap1 GTPases (guanosine triphosphatases), and several PDEs, especially PDEs 2, 5, 6, which contain allosteric, non-catalytic cyclic nucleotide-binding sites.

Molecular genetics has revealed the diversity and complexity of the 11 mammalian PDE gene families (PDEs 1–11). PDE families differ in their primary amino sequences, substrate specificities, sensitivities to endogenous effectors and pharmacological agents, cellular functions, and mechanisms whereby they are regulated. Most PDE families comprise more than one gene; within these families multiple, closely related isoforms are generated from the same gene or different genes via alternative mRNA splicing or utilization of different promoters/transcription initiation sites. More than 20 PDE genes probably encode more than 50 PDE proteins. Some cells are relatively enriched in specific PDEs, e.g., photoreceptor PDE6 is virtually exclusively expressed in the retina. Most cells, however, contain representatives of multiple PDE gene families, and different members of the same family, but in different amounts, proportions and subcellular locations. Redundancy in PDEs, i.e., the presence in the same cell of multiple enymes which essentially perform the same reaction of hydrolyzing cyclic nucleotides, does not merely serve a survival or protective function, but rather allows cells to use distinct subsets of differentially regulated and localized PDEs to specifically and selectively regulate and segregate the generation, amplitude, duration, and compartmentation of cyclic nucleotide signals and actions. It is generally accepted that the cellular capacity to degrade cyclic nucleotides far

exceeds their synthesis, and is a major factor in the very rapid turnover of intracellular cAMP and cGMP. The physiological significance and functional consequences of this rapid turnover, and concomitant heat generation (cyclic nucleotide hydrolysis is accompanied by release of $\sim 7 \text{cal mol}^{-1}$), are not understood. This brief review will discuss some general characteristics of PDEs and then focus on the cellular biology and diverse functions of different PDE isoforms and their potential as therapeutic targets.

Structure/Function Analyses

Catalytic Domain

Mammalian PDEs exhibit a common structural organization, with a conserved catalytic domain ($\sim$250–300 amino acids) in the C-terminal portion of the molecules and divergent regulatory domains and modules in N-terminal portions (Figure 1). The catalytic core, more highly conserved among members of the same gene family than different gene families, contains a signature motif [HD (X_2) H (X_4) N], common to all PDEs, and includes consensus metal-binding domains. In addition to common structural elements responsible for cyclic nucleotide hydrolysis, the catalytic core contains family specific sequences responsible for differences in substrate affinities, catalytic properties, and sensitivities to specific inhibitors (Figure 1). Some PDE families are relatively specific for hydrolysis of cAMP (PDEs 4, 7, 8); others, for cGMP (PDEs 5, 6, 9); and some exhibit mixed specificity for both cAMP and cGMP (PDEs 1, 2, 3, 10, 11). While methylxanthines inhibit almost all PDEs, relatively specific and selective inhibitors, i.e., drugs that target individual PDE families with 10–100-fold greater potency than other PDE families, are available for several families, e.g., PDEs 1, 2, 3, 4, 5, 6. These family specific inhibitors are important for both basic research and clinical applications.

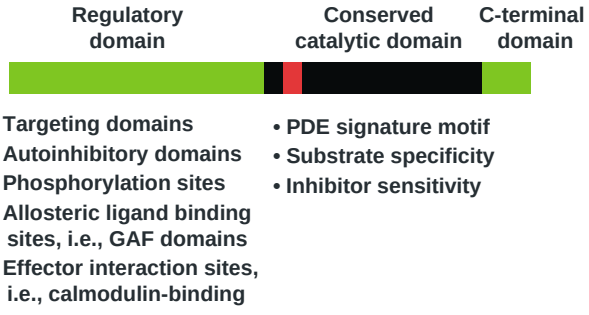

FIGURE 1 Common structural pattern for different PDE gene families.

Regulatory Domain

N-terminal portions of PDE molecules are highly divergent, containing structural determinants and specific amino acid sequences that allow different PDEs to respond selectively to specific regulatory signals (Figure 1). These regulatory regions include autoinhibitory modules (e.g., in PDEs 1, 4, 5), as well as sites and domains that are subject to different types of covalent modification (e.g., sites (in PDEs 1, 3, 4, 5, 10, 11) for phosphorylation by various protein kinases), or that interact with allosteric ligands (e.g., cGMP-binding sites in GAF domains), specific effectors (e.g., Ca^{2+}/calmodulin), protein partners or molecular scaffolds [e.g., AKAPs (anchoring proteins for PKA), B-arrestin], and thereby regulate catalytic activity, protein–protein interactions and/or subcellular compartmentation and localization (Figure 1). Five PDE families (PDEs 2, 5, 6, 10, 11) contain homologous so-called GAF domains, an acronym for proteins (cGMP-binding PDEs, *A*nabena adenylyl cyclase and *f*hlA, an *E. coli* transcriptional regulator) that contain these sequences. Although cGMP binding is not the primary function of GAF domains, in three PDE families (PDEs 2, 5, and 6), GAF domains bind cGMP with high affinity, but with different functional consequences.

PDE Functions

PDEs: Components of Spatially Organized Signaling Networks and Microdomains

PDEs are critical regulators of the generation, amplitude, duration, and termination of intracellular cyclic nucleotide signals. In addition to tight regulation of their concentrations and turnover, intracellular pools of cAMP and cGMP are also temporally, spatially, and functionally compartmentalized. In cardiac myocytes, for example, PGE_1 and catecholamines increase cAMP and activate PKA in different compartments, and cAMP diffusion is spatially restricted and regulated, at least in part, by PDEs. Newer techniques, e.g., use of fluorescence-resonance energy transfer (FRET) and cyclic nucleotide biosensors, also suggest that PDEs play an important role in these spatially-constrained microdomains, i.e., discrete subcellular regions in which cyclic nucleotide gradients are generated, monitored, and regulated, and their signals and effects channeled, transduced, and modulated.

The molecular basis for compartmentalization of cAMP signaling involves anchoring of PKA isoforms at specific intracellular sites via AKAP scaffolding proteins. These proteins organize formation of localized signaling modules/microdomains consisting of kinases, kinase

substrates, phosphatases, PDE4 isoforms, and other proteins. These modules sense intracellular cAMP gradients and effectively compartmentalize activation of substrates and biological responses. In these microdomains, cAMP-induced activation of PKA also results in phosphorylation/activation of PDE4 isoforms associated with AKAPs, resulting in modulation and termination of cAMP signals, and return of PKA to its basal state. For example, in cardiac myocytes, PDE4 isoforms are associated with AKAP complexes thought to modulate effects of cAMP on L-type and ryanodine-sensitive Ca^{2+} channels.

PDE4 isoforms, PKA, and other molecules also interact/associate with β-arrestins, which are scaffolding proteins located in the vicinity of plasma membranes that interact with activated β receptors and are involved in coordination of β receptor signaling and trafficking. This targeting and effective concentrating of PKA and PDE4 in proximity to the activated β receptors not only reduces cAMP generation (via phosphorylation, uncoupling and internalization of β receptors) but also enhances localized degradation of cAMP and desensitizes the complex with respect to further signaling via the β receptor and cAMP.

The subcellular localization of different PDEs, their interactions with molecular scaffolds and interacting partners, and their inclusion in, and contribution to the function of, macromolecular signaling microdomains is becoming a common theme in PDE biology. Anchoring of PDE3B to intracellular membranes via transmembrane hydrophobic helical segments and its interaction with PKB may be important in its activation by insulin. PDE4s also associate, via an N-terminal helical region, with another signaling scaffold protein called RACK1 (receptor for activated protein kinase C 1).

PDEs: Intracellular Effectors

PDEs are not only important determinants in the stringent regulation of intracellular cAMP and cGMP concentrations but they also serve as effectors of cyclic nucleotide actions. Historically, in cells containing multiple PDEs, family specific PDE inhibitors were initially utilized to pharmacologically define roles of specific PDEs in regulating specific signaling pathways and discrete cellular functions. In cultured mammalian oocytes, PDE3 inhibitors, not PDE4 or 5 inhibitors, inhibit meiotic progression and oocyte maturation, implying that PDE3 regulates a cAMP pool that controls maturation. (In fact, female PDE3A KO mice are sterile.) In cultured renal mesangial cells, experiments with PDE3 and PDE4 inhibitors indicated that PDE3 and PDE4 selectively regulated functionally distinct cAMP pools that controlled cell growth, and generation of reactive oxygen species, respectively. These types of studies first suggested a role for PDEs in spatial and/or functional compartmentalization of cyclic nucleotide signals and effects.

In some instances, a specific PDE serves as a critical effector system and regulates a unique cellular function, e.g., in retinal rods and cones, light-induced activation of photoreceptor PDE6 results in hydrolysis of cGMP and initiation of visual signal transduction. Activation of PDE3s by insulin, IGF-1, and leptin is apparently important in their ability to reduce cAMP and thereby regulate lipolysis in adipocytes, glycogenolysis in hepatocytes, insulin secretion from pancreatic β cells, and oocyte maturation. In these instances, PDE3 inhibitors can attenuate or block the effects of insulin, IGF-1 and leptin.

Studies of PDE KO mice do indicate that the ability of specific PDEs to regulate discrete cAMP/cGMP signaling pathways and actions is genetically determined. Female PDE3A KO mice are sterile, most likely due to inhibitory effects of cAMP on meiotic progression and maturation of oocytes, and consequently, their competency for fertilization. PDE3B KO mice, not frankly diabetic, demonstrate signs of disruption in insulin secretion and insulin resistance. Production of TNFα in response to administration of lipopolysaccharide (LPS) in PDE4B KO mice is profoundly ($\sim$90%) inhibited. On the other hand, PDE4D KO mice do not exhibit acetylcholine-induced contraction and hyperreactivity of airway smooth muscle. In PDE4D KO mice, the duration of β-adrenergic-induced anesthesia is reduced by more than 50%, and fertility is decreased due to reduced ovulation.

PDEs: Signal Integrators

With their different intrinsic properties and different responses to regulatory signals, PDEs also integrate multiple inputs, and are a "locus" for crosstalk between different signaling pathways. For example, PDE2, which is allosterically activated by cGMP, is highly concentrated in adrenal zona glomerulosa cells. In these cells, ANF (atrial natriuretic factor) increases cGMP synthesis; cGMP, in turn, activates PDE2, leading to a decrease in cAMP and PKA activity and inhibition of cAMP-stimulated aldosterone production. On the other hand, in other cells, NO activates guanylyl cyclase and increases cGMP, which inhibits PDE3 and increases intracellular cAMP content, resulting, for example, in stimulation of renin secretion from the juxtaglomerular apparatus in the kidney, and inhibition of platelet aggregation.

Newer approaches have suggested that different PDE isoforms may not only coordinate regulation of signals and responses in individual cells, but that differential cellular distribution within tissues may be important in intercellular communication and regulation of tissue

function. Immunohistochemical studies indicate, for example, that PDE1C and PDE2A are expressed in different sets of neurons in the olfactory epithelium, whereas PDE1C and PDE4A are present in different subcellular regions of the same neurons.

PDEs: Homeostatic Regulators

Signaling pathways, in general, also include mechanisms for negative feedback control. PDE3 and PDE4 activities, for example, are acutely up-regulated by cAMP-induced activation of PKA, which results in phosphorylation/activation of PDE3 and PDE4, and enhanced destruction of cAMP. Chronic elevation of cAMP also provides negative feedback, by increasing transcription of PDE3 and PDE4 genes and protein synthesis, resulting in increased enzymatic activities. In some cells, this latter phenomenon is part of mechanisms involved in ligand-induced down-regulation of cellular responses, such as tachyphylaxis or desensitization. Negative feedback control of cGMP hydrolysis by PDE5 is somewhat different, due to the presence of high affinity, non-catalytic, allosteric-binding sites for cGMP in the GAF domains of PDE5. Binding of cGMP to GAF domains results in allosterically-induced conformational changes that increase affinity of the catalytic site for cGMP and also facilitates phosphorylation and activation of PDE5 by PKG. Thus, elevation in intracellular cGMP provides negative feedback control and enhances its own destruction, both via direct cGMP-induced allosteric activation as well as indirect activation due to phosphorylation of PDE5 by PKG.

Family Specific Inhibitors: Clinical Applications

Molecular diversity of PDEs has occasioned the development of family specific PDE inhibitors to replace nonselective PDE inhibitors (theophylline and caffeine) as therapeutic agents for diseases such as asthma. Despite intensive efforts to develop such drugs, only sildenafil (Viagra™), a selective PDE5 inhibitor, has proven to be therapeutically effective in a major disease, i.e. erectile dysfunction, and is showing promise as a treatment modality in pulmonary hypertension. PDE4 enzymes are relatively concentrated in immume/inflammatory cells, and specific PDE4 inhibitors exhibit potent anti-inflammatory actions. Two selective PDE4 inhibitors, cilomilast and rofumilast, are in Phase 3 clinical trials for treatment of chronic obstructive pulmonary disease (COPD) and asthma. PDE3 inhibitors, which enhance myocardial contractility and relaxation of smooth muscle and inhibit platelet aggregation, failed in long-term clinical trials for treatment of chronic heart failure. However, one PDE3 inhibitor, milrinone, is used for acute and short term treatment of adult patients with decompensated and refractory cardiac failure, and another, cilostazol, has FDA approval for treatment for intermittent claudication.

Conclusions

By virtue of their distinct intrinsic characteristics and differential regulation, their intracellular targeting to different subcellular locations and microdomains, and their interactions with cellular structural elements, regulatory partners, and molecular scaffolds such as AKAPs and β arrestin, different PDEs can integrate multiple cellular inputs, and modulate the intracellular diffusion and functional compartmentalization of cyclic nucleotide signals. The combined enormous molecular diversity of receptors and their ligands, adenylyl and guanylyl cyclase systems, PDEs, and cyclic nucleotide-regulated effector systems, coupled with their physical and functional compartmentalization, provides for the complex integration, specificity, and variety of networks and pathways involved in generation, transduction, modulation, and termination of cyclic nucleotide-gated signals and actions. The ability of scaffolding proteins to spatially organize signaling molecules, including protein kinases, phosphatases, kinase substrates, PDEs, and other signaling and effector molecules, effectively allows cells to generate signaling specificity by using small, discrete subsets of proteins which exhibit overlapping or redundant functions. Integration of these myriad combinations establishes the unique cyclic nucleotide networks and phenotypes that characterize individual cells.

See Also the Following Articles

Adenylyl Cyclases • A-Kinase Anchoring Proteins • Cyclic GMP Phosphodiesterases • G Protein-Coupled Receptor Kinases and Arrestins

Glossary

cyclic nucleotide phosphodiesterases (PDEs) Enzymes that catalyze hydrolysis of the 3′-5′-phosphodiester bond of cAMP and/or cGMP.

desensitization Prolonged or repeated exposure of receptors to their ligands leads to reduction or loss of responsiveness, either homologous desensitization with loss of responsiveness only to a specific ligand or heterologous desensitization with loss of responsiveness to multiple ligands.

family specific inhibitors Drugs that inhibit the activity of one PDE gene family with 10–100-fold greater potency than the activities of other PDE gene families.

Further Reading

Beavo, J., and Brunton, L. (2002). Cyclic nucleotide research—still expanding after half a century. *Nat. Rev., Molecul. Cell Biol.* **3**, 710–718.

Conti, M., Richter, W., Mehats, C., Livera, G., Park, J.-Y., and Jin, C. (2003). Cyclic AMP-specific PDE4 phosphodiesterases as critical components of cyclic AMP signaling. *J. Biol. Chem.* **278**, 5493–5496.

Degerman, E., Rahn-Landstrom, T., Stenson-Holst, L., Goranssen, O., Harndahl, L., Ahmad, F., Choi, Y.-H., Masciarelli, S., Lui, H., and Manganiello, V. C (2003). Role for phosphodiesterase 3B in regulation of lipolysis and insulin secretion. In *Diabetes Mellitus: A Fundamental and Clinical Text* (D. LeRoith, S. I. Taylor, and J. M. Olefsky, eds.), 3rd edition. Lippincott-Raven Publishers, Philadelphia, PA, Ch. 24, pp. 373–381.

Francis, S. H., Turko, I. V., and Corbin, J. D. (2001). Cyclic nucleotide phosphodiesterases—relating structure and function. *Prog. Nucleic Acid Res. Mol. Biol.* **65**, 1–52.

Houslay, M. D., and Davis, D. R. (2003). PDE4 cAMP phosphodiesterase: Modular enzymes that orchestrate signaling crosstalk, desensitization and compartmentalization. *Biochem. J.* **370**, 1–18.

Manganiello, V. C., and Degerman, E. (1999). Cyclic nucleotide phosphodiesterases (PDEs): Diverse regulators of cyclic nucleotide signals and inviting molecular targets for novel therapeutic agents. *Thrombosis and Haemostasis* **82**, 407–411.

Mehats, C., Andersen, C., Filopanti, M., Jin, S.-L. C., and Conti, M. (2002). Cyclic nucleotide phosphodiesterases and their role in endocrine cell signaling. *Trends Endocr. Metab.* **13**, 29–35.

Biography

Eva Degerman received her degrees, M.D. in 1991 and Ph.D. in 1988, from Lund University, where she has spent her entire scientific career.

Vincent Manganiello received his degrees, M.D. and Ph.D., from Johns Hopkins University School of Medicine in 1967. After serving as a pediatric intern in the Harriet Lane Service at Johns Hopkins, he came to the National Institutes of Health in 1968, and has pursued his entire scientific career at the National Heart, Lung, and Blood Institute. Drs. Degerman and Manganiello have enjoyed a long-standing collaboration focused on the cyclic nucleotide phosphodiesterase 3 (PDE3) family and its role in metabolic regulation and insulin secretion in adipose tissue, liver and pancreas, important target tissues for actions of insulin, leptin and IGF-1 (insulin-like growth factor-1), and for maintenance of energy homeostasis, as well as for the pathogenesis of type 2 diabetes and obesity.

Cyclic Nucleotide-Dependent Protein Kinases

Sharron H. Francis and Jackie D. Corbin
Vanderbilt University School of Medicine, Nashville, Tennessee, USA

The cyclic nucleotide-dependent protein kinases, cAMP-dependent protein kinase (PKA) and cGMP-dependent protein kinase (PKG), are the major intracellular receptors for adenosine 3′,5′-cyclic monophosphate (cAMP) and guanosine 3′,5′-cyclic monophosphate (cGMP), respectively. Upon elevation of cAMP or cGMP in the cell, these nucleotides can bind to numerous cellular proteins including the cyclic nucleotide-dependent protein kinases. Intracellular levels of cAMP and cGMP are determined by the balance between their synthesis and breakdown. They are synthesized from either ATP or GTP by adenylyl cyclase or guanylyl cyclase, respectively, in response to first messengers in the body (e.g., hormones, neurotransmitters, and various environmental stimuli), and they are broken down by cyclic nucleotide phosphodiesterases (PDEs). The important concept of signaling through second messengers such as cAMP and cGMP is that the hormone, neurotransmitter, or other stimuli can elicit their physiological effects without entering the cell. The protein kinase catalytic activities of cyclic nucleotide-dependent kinases are activated when the cyclic nucleotides bind to their regulatory domains, and the catalytic domains of the kinases can then transfer a phosphate from ATP to many proteins through a process known as phosphorylation. The phosphorylation of these target proteins frequently alters their functions and accounts for most of the known effects of cyclic nucleotides in eukaryotes.

Cyclic Nucleotide-Dependent Protein Kinases as Intracellular Receptors for cAMP and cGMP

The cyclic nucleotide-dependent protein kinases, cAMP-dependent protein kinase (PKA) and cGMP-dependent protein kinase (PKG), are the major intracellular receptors for adenosine 3′,5′-cyclic monophosphate (cAMP) and guanosine 3′,5′-cyclic monophosphate (cGMP), respectively (Figure 1). PKA and PKG are homologous ligand-activated kinases. In the presence of very small amounts of cAMP or cGMP (e.g., concentrations ranging from 10^{-8}–10^{-7} M), these kinases are activated by binding the cyclic nucleotide. The intracellular levels of cAMP and cGMP are determined by the balance between their synthesis and breakdown. They are synthesized from either ATP or GTP by adenylyl cyclase or guanylyl cyclase, respectively, in response to first messengers in the body (e.g., hormones, neurotransmitters, and various environmental stimuli), and they are broken down by cyclic nucleotide phosphodiesterases (PDEs) (Figure 2). The activated PKA or PKG then catalyzes transfer of the γ-phosphate of ATP to selected serine or threonines in many cellular proteins through a process known as phosphorylation. The covalent attachment of phosphate to these proteins converts them into phosphoproteins, a process known as heterophosphorylation because in this case PKA or PKG phosphorylates proteins other than itself. The phosphoproteins frequently have changes in their activities, subcellular localizations, and interactions with other cellular components, including other proteins, DNA, RNA, and lipids. The altered function of these proteins that have been phosphorylated by PKA or PKG mediates the changes induced by many hormones and environmental stimuli, including those in metabolism, gene transcription, neurotransmission, blood pressure, and fluid homeostasis.

Overall Structure of Cyclic Nucleotide-Dependent Protein Kinases

There are several isoforms of PKA and PKG, but all have a similar organization of their functional domains (Figure 3). Both are chimeric proteins comprising a regulatory domain and a catalytic domain, and within each of these there are several subdomains that provide for specific functions. PKA regulatory and catalytic domains are located on separate subunits, the R subunit and C subunit, respectively. In PKG, the regulatory and catalytic domains are on a single polypeptide chain. Both enzymes form dimers through interactions between

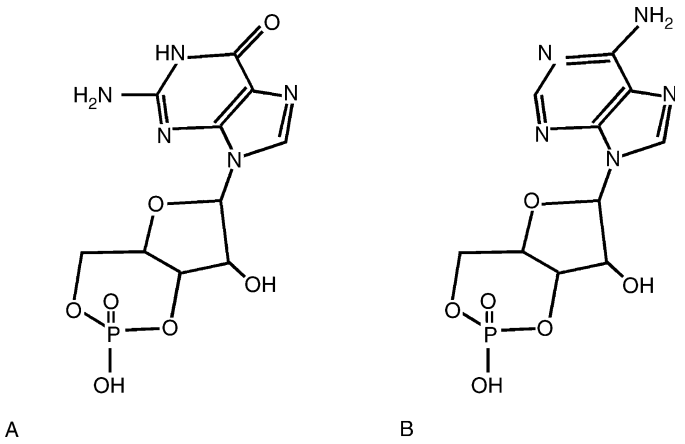

FIGURE 1 Structural models of (A) cGMP and (B) cAMP. cGMP and cAMP differ only in their purine rings. These differences in the purine ring provide for the specificity with which each kinase interacts preferentially with that nucleotide. The cyclic phosphate moiety is required for binding to the cyclic nucleotide-binding sites on PKG and PKA, and the 2′–OH of the ribose provides an important contact in the respective sites. There are two conformations of these nucleotides, *syn* (shown) and *anti*, due to rotation around the bond linking the purine and the ribose. Both PKA and PKG bind the *syn* conformer. Important features of cGMP that contribute to its interaction with PKG include the amino group at C-2 (which interacts with a conserved threonine in sites preferring cGMP), the oxygen at C-6, and a protonated N-1. cAMP has a single substitution on the purine (i.e., an amino group at C-6 and no protonation at N-1).

amino acids near the N terminus within their regulatory domains. However, the salient biochemical features of regulation and catalysis are retained in monomeric forms of PKG and in PKA formed by the combination of a single R subunit and C subunit.

Although dimerization is not necessary for PKA function, it is required for anchoring a portion of the PKA to specific subcellular compartments through a family of proteins known as A kinase anchoring proteins (AKAPs). Anchoring is thought to bring PKA into close proximity with substrates and to thereby facilitate the rapidity and efficiency of cAMP signaling. PKA R

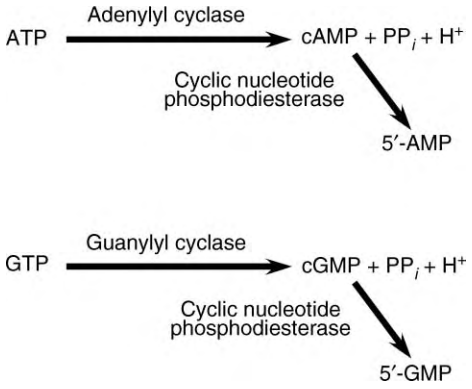

FIGURE 2 The balance between cyclase and phosphodiesterase activities determines cyclic nucleotide levels in the cell. cAMP and cGMP are synthesized from either (A) ATP by adenylyl cyclase or (B) GTP by guanylyl cyclase; when the activities of these cyclases are increased, more cAMP or cGMP is produced. The breakdown of the cyclic nucleotides is catalyzed by cyclic nucleotide phosphodiesterases (PDEs), and the activities of these enzymes lower cAMP and cGMP. The balance between the activities of these two families of enzymes is the major factor in determining the cellular content of cyclic nucleotides.

subunits are aligned in an antiparallel arrangement within the dimer and use hydrophobic interactions, whereas the PKG monomers within the dimer are aligned in a parallel arrangement through interactions of an extended leucine zipper motif.

PKA

PKA is present in the cytosolic and particulate fraction of all mammalian tissues and occurs at concentrations ranging from 0.2 to 2 μM. It is a tetramer comprising two C subunits and two R subunits (R_2C_2) (Figure 3). There are three main genes for mammalian C subunit (Cα, Cβ, Cγ); each is ~36,000 Da. There are two major genes for R subunits (RI and RII) and subtypes within these (RIα, RIβ, RIIα, and RIIβ) are produced by mRNA splicing; each is ~45,000 Da. The nomenclature for PKAs is based on the R subunits; PKAs containing RI subunits are called type I PKA, and those containing RII subunits are called type II PKA. Both types may contain either form of C subunit. Most tissues contain both types of PKA and, in most instances, either type can carry out cAMP-mediated action. Type I PKA is predominantly cytosolic; type II PKA is found in both the cytosol and membrane compartments. The RI and RII content of a particular tissue varies among species.

In the absence of cAMP, an R subunit interacts with a C subunit with high affinity (~0.2 nM) and suppresses its catalytic activity through a process known as autoinhibition. cAMP binding to two cAMP-binding sites on an R subunit causes a conformational change that decreases the affinity of the R subunit for a C subunit by 10,000- to 100,000-fold. An active

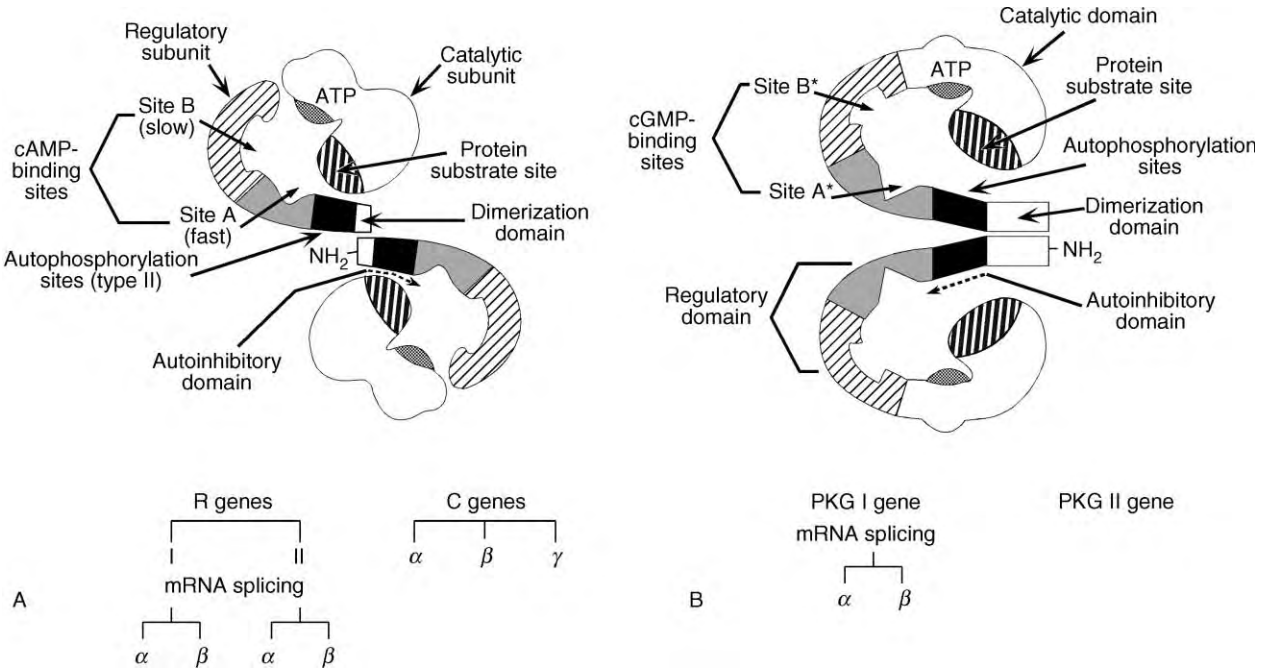

FIGURE 3 Working models of (A) PKAs and (B) PKGs, depicting the overall organization of the functional domains within these enzymes. The major isozymic forms that are products of different genes for each of the kinases are listed below each model. Additional forms of the PKA R subunits and some of the C subunits are produced by alternative mRNA splicing. The alignment of the low-affinity and high-affinity cyclic nucleotide sites within PKA R subunit is the same for all known PKAs. The linear arrangement of the cGMP-binding sites in PKG-II is the same as that found in PKAs. However, in PKG-I, the sites are transposed so that the more N-terminal site is the high-affinity cGMP-binding site and at the more C-terminal position is the low-affinity site.

monomeric C subunit dissociates from the complex and can diffuse throughout the cell, including the nucleus, which excludes R subunits and PKA holoenzymes. The diffusibility of the C subunit is believed to provide for the mechanism by which cAMP elicts its effect in a number of systems. The R subunits remain dimerized and, if anchored to AKAPs, they remain anchored.

X-ray crystallographic structures have been determined for the C subunit and also for the RI and RII subunits, but to date there is no structure for the inactive complex. The C subunit has two lobes that combine to form a catalytic cleft where the phosphate is transferred from ATP to the protein substrate. The smaller, more N-terminal lobe makes most of the contacts with Mg^{2+}/ATP and the larger, more C-terminal lobe makes most of the contacts that precisely position the protein substrate in the catalytic cleft. The binding of Mg^{2+}/ATP and a protein substrate into the catalytic cleft allows a complex set of enzymatic actions to transfer the phosphate from ATP to substrate.

In order to efficiently transfer the phosphate to a peptide or protein, PKA strongly prefers an amino acid sequence of -ArgArgXSer/ThrX- (called a PKA consensus phosphorylation site), and this sequence alone provides in large part for the efficiency with which the C subunit phosphorylates a protein. The amino acids in the positions marked as X affect the affinity of the C-subunit interaction with a substrate and, although arginines (Arg) are highly preferred in this motif, some variation is tolerated.

Each R subunit contains several subdomains. These include an N-terminal dimerization subdomain, a subdomain that includes the autoinhibitory and autophosphorylation regions, and a cyclic nucleotide-binding subdomain that contains two cAMP-binding sites arranged in tandem (Figure 3). In the absence of cAMP, a substrate-like sequence in the R subunit binds tightly to the catalytic site in the C subunit. Although other contacts also contribute to stabilizing the R–C interaction, this substrate-like sequence in the autoinhibitory domain competes with protein substrate binding and provides a major portion of the interactions that hold PKA in a catalytically inactive form in the absence of cAMP. This is known as autoinhibition. The binding of cAMP to both cAMP-binding sites in each R subunit disrupts the R–C subunit interaction.

Most commonly, the PKA tetramer contains a single type of R subunit (either RI or RII). RII subunits contain a sequence in the autoinhibitory domain that mimics a PKA substrate motif, and the serine in this sequence can be autophosphorylated by the C subunit when the subunits are complexed (i.e., in the absence of cAMP). Autophosphorylation of this site in RII increases its affinity for cAMP so that PKA can be activated at lower cAMP concentrations. Type I R subunits contain a pseudosubstrate sequence (-ArgArgXGlyX-), that is, a

substrate-like sequence that lacks a phosphorylatable residue. Therefore, type I PKA R subunits cannot undergo autophosphorylation.

PKA plays a critical role in functions of all mammalian cells. As a result, it is likely that survival requires the presence of the PKA C subunit. A null mutation for C subunit in yeast is lethal. Mice carrying null mutations for either Cα or Cβ are viable, but differ phenotypically; mice lacking either RI or RII subunits are also typically viable and differ phenotypically. These results suggest that these isoforms of the C subunit and R subunit have some selectivity in function.

PKG

The tissue distribution of PKG is more restricted than that of PKA. PKGs play a central role in regulating smooth muscle tone, platelet aggregation, bone growth, and water–salt homeostasis. Cellular concentration of PKG ranges from infinitesimally low to 1 μM. There are two families of PKG (PKG-I and PKG-II) that are the products of separate genes. These families are not co-expressed and appear to have selective functions because the phenotype of PKG-I-null mice differs from that of PKG-II-null animals. PKG-I has two alternative splice variants (PKG-Iα and PKG-Iβ) that vary in the N terminal ~100 amino acids and are typically co-expressed. PKG-I is largely cytosolic, whereas PKG-II is membrane-bound through an N-terminal myristyl group. In some instances, this provides for specific phosphorylation events that do not occur when PKG-II is in its soluble form. The membrane association of PKG-II appears to colocalize PKG-II with the intended substrate. The PKG-I isoforms, PKG-Iα and PKG-Iβ, are largely cytosolic, but they too are specifically localized in some cases. When this occurs, it involves interactions between residues within the conserved leucine zipper motif near the N terminus and another protein, for example, the myosin-binding protein of the myosin phosphoprotein phosphatase. In many cases, the interaction is selective for either PKG-Iα or PKG-Iβ, indicating that the specificity of the interaction involves sequences that are novel to one or the other isoform.

PKG regulatory domains contain several subdomains including an N-terminal dimerization subdomain involving a leucine zipper motif, a subdomain containing both the autoinhibitory and autophosphorylation regions, and a cyclic nucleotide-binding subdomain that contains two cGMP-binding sites arranged in tandem (Figure 3). The role of dimerization is unclear because a monomeric PKG retains the salient features of the dimer.

The autoinhibitory–autophosphorylation subdomain is located just C-terminal to the dimerization domain. This region accounts for autoinhibition of the catalytic site and contains multiple autophosphorylation sites, most of which do not resemble a consensus substrate sequence and are not conserved among PKGs. These sites are autophosphorylated by the catalytic domain within the same PKG monomer; autophosphorylation of PKG-I increases the affinity for cGMP and elevates basal activity. Unlike that for PKA, PKG autophosphorylation increases in the presence of cyclic nucleotide.

The mechanism of autoinhibition of PKGs also differs somewhat from that of PKA. The autoinhibitory domain of all PKGs contains either pseudosubstrate sequences, for example, -LysArgGln*Ala*Ile- in PKG-Iβ, or sequences that only weakly mimic a pseudosubstrate site, for example, -ArgAlaGln*Gly*Ile- in PKG-Iα, where the italicized residue indicates the phosphorylation position in the autoinhibitory PKA sequence. Furthermore, sequences outside the pseudosubstrate sequence contribute more prominently to the autoinhibition of both PKG-I and PKG-II compared to PKA.

PKGs contain two cGMP-binding sites of ~110 amino acids arranged in tandem. A small segment of protein connects the regulatory and catalytic domains of the enzyme. The catalytic domain is thought to resemble that of PKA because the enzymes are homologous. In the absence of cyclic nucleotide, PKG catalytic activity is latent. cGMP binding to the cGMP-binding sites in the regulatory domain causes an elongation of the PKG monomer that relieves the autoinhibition, thereby activating catalytic activity.

Cyclic Nucleotide-Binding Specificity and Affinity

The two homologous cyclic nucleotide-binding sites (~110 amino acids each) in PKA and PKG appear to be the products of an ancient gene duplication that occurred prior to the divergence of these proteins. These sites are evolutionarily related to a bacterial cAMP-binding protein, the catabolite-gene-activating protein (CAP) family of cyclic nucleotide-binding proteins. The cyclic nucleotide-binding sites of cyclic nucleotide-gated channels and cAMP-regulated guanine nucleotide exchange factors (GEFs) are also members of this family. In both PKA and PKG, the two intrasubunit sites differ approximately 10-fold in their affinity for cyclic nucleotide binding and also differ in specificity for cyclic nucleotide analogues. In PKA RI and RII subunits, the more N-terminal site has a lower affinity for cAMP (fast cAMP dissociation) compared to the more C-terminal site (slow cAMP dissociation) (Figure 3). In PKG-II, the cGMP-binding sites are arranged as in PKA, but in PKG-I the higher affinity site is the more N-terminal site. Full activation of either PKA or PKG requires saturation of all the cyclic nucleotide-binding sites.

PKA and PKG have a 50- to 200-fold selectivity for cAMP and cGMP, respectively, and most commonly the

cellular effect of cAMP or cGMP is mediated by the respective kinase. However, in several systems, cAMP or cGMP has been shown to activate the other kinase through a process known as cross-activation. In the X-ray crystallographic structure of the R subunit, cAMP is bound in a deep pocket within each site, and several conserved amino acids (glutamate, arginine, and several glycines) provide direct contact with the cyclic nucleotide or contribute to critical structural features of the site. In sites preferring cGMP, an invariant threonine provides a major portion of the selectivity for cGMP by interacting with the 2′-amino group in the purine (Figure 1). Hydrophobic amino acids in each of the sites contribute importantly to the affinity with which cyclic nucleotide is bound.

Substrate Specificities of PKA and PKG

PKA and PKG-I share many similarities in substrate specificities, and the consensus sequence for phosphorylation by either enzyme is defined as -ArgArgXSer/ThrX-. These kinases can frequently phosphorylate the same proteins, although there are differences. PKG-I phosphorylates numerous proteins in sites that do not conform to this consensus phosphorylation sequence; these sites are not phosphorylated well by PKA. A phenylalanine located C-terminal to the phosphorylation site strongly discriminates against PKA phosphorylation, but not that of PKG, and a basic amino acid adjacent to the phosphorylation site favors PKG-I phosphorylation. The substrate specificity of PKG-II appears to be quite different from those of PKG-I and PKA.

Negative Feedback and Feed-Forward Control of Cyclic Nucleotide Pathways

A two- to fourfold increase in either cAMP or cGMP typically accounts for the physiological responses to these nucleotides. Negative feedback control mechanisms restrict the magnitude or persistence of cyclic nucleotide

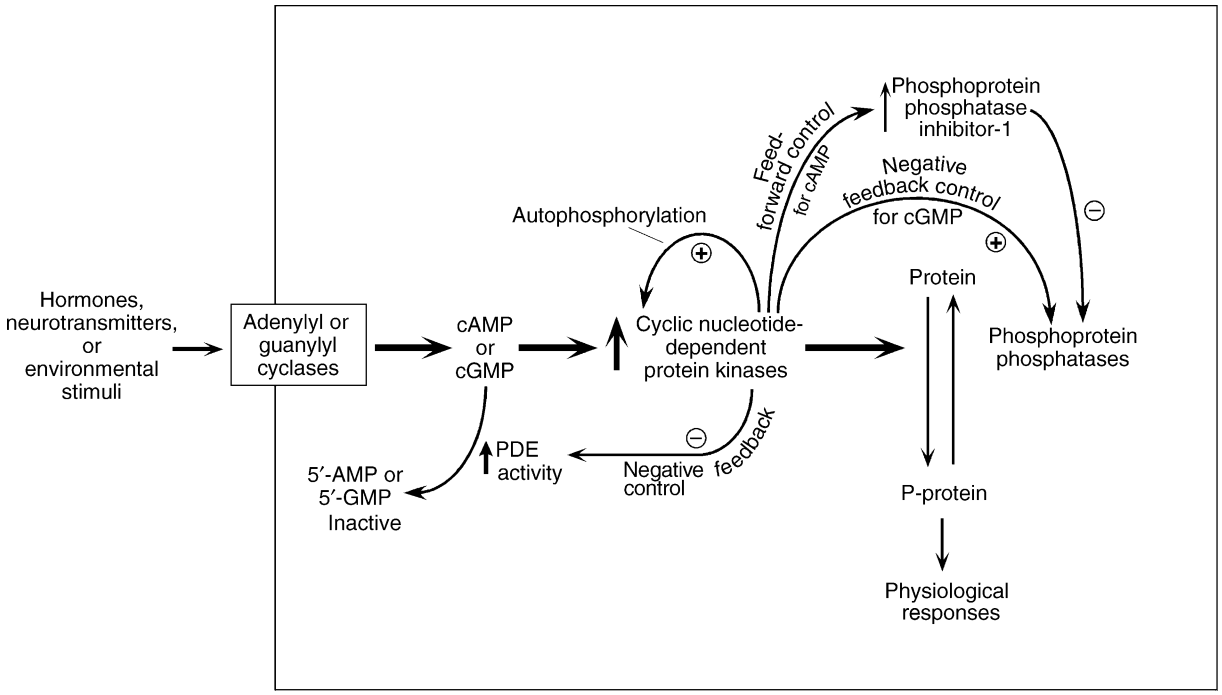

FIGURE 4 Mechanisms involving phosphorylation that contribute to modulation of the cAMP- and cGMP-signaling pathways. Feedback control refers to processes that tend to alter the overall effectiveness of signaling through cyclic nucleotide pathways. Negative feedback control mechanisms decrease the effectiveness of the cyclic nucleotide signal; these include increased activities of cyclic nucleotide phosphodiesterases (PDE activity), which breakdown the cAMP and cGMP, and increased activities of phosphatases that remove phosphates from phosphoproteins that have been phosphorylated by PKG. Feed-forward control (i.e., positive feedback control) mechanisms enhance the effectiveness of the signal. These include autophosphorylation by PKA and PKGI, which increases the affinity of these enzymes for the respective cyclic nucleotides and increases catalytic activity, and increased phosphorylation of the phosphoprotein phosphatase inhibitor-1 by PKA, which inhibits a phosphoprotein phosphatase and blocks its effect of removing phosphate from phosphoproteins involved in the signaling pathway. Circled + and − denote effects that either increase or decrease as the levels of cyclic nucleotides increase or decrease; arrows, ↑ and ↓, denote a change in the catalytic activity of the indicated enzymes that is induced by PKA or PKG phosphorylation or the state of phosphorylation of the phosphoprotein phosphatase inhibitor-1 in response to increased PKA activity.

signaling whereas feed-forward mechanisms potentiate the response to cyclic nucleotide elevation. Both types of mechanisms have been established for the cAMP and cGMP signaling cascades (Figure 4). PKA and PKG can phosphorylate and activate PDEs, which accelerates the breakdown of cyclic nucleotides, thereby favoring inactivation of the kinases. Both cascades also have feed-forward control because the autophosphorylation of type II PKA and PKG-I increases kinase activity and cyclic nucleotide-binding affinity. The cAMP system has an additional feed-forward control because PKA phosphorylates phosphoprotein phosphatase inhibitor-1 to produce a potent inhibition of phosphoprotein phosphatase action, thereby potentiating the effects of PKA phosphorylation.

See Also the Following Articles

Adenylyl Cyclases • A-Kinase Anchoring Proteins • Cyclic GMP Phosphodiesterases • Cyclic Nucleotide Phosphodiesterases

Glossary

autoinhibition The effect of one region of an enzyme blocking the action of the catalytic site of another region of that same enzyme.

autophosphorylation Protein kinase-catalyzed transfer of the γ-phosphate of ATP to a residue within the protein kinase itself.

consensus phosphorylation sequence The amino acid sequence that contains all the determinants that provide for the specific phosphorylation of that sequence by a particular protein kinase.

heterophosphorylation Protein kinase-catalyzed transfer of the γ-phosphate of ATP to another protein substrate.

pseudosubstrate sequence An amino acid sequence that closely resembles the consensus phosphorylation sequence for a protein kinase substrate but lacks the residue that can be phosphorylated.

Further Reading

Cummings, D. E., Brandon, E. P., Planas, J. V., Motamed, K., Idzerda, R. L., and McKnight, G. S. (1996). Genetically lean mice result from target disruption of the RII beta subunit of protein kinase A. *Nature* **382**, 622–626.

Eigenthaler, M., Lohmann, S. M., Walter, U., and Pilz, R. B. (1999). Signal transduction by cGMP-dependent protein kinases and their emerging roles in the regulation of cell adhesion and gene expression. *Rev. Physiol. Biochem. Pharmacol.* **135**, 173–209.

Francis, S. H., and Corbin, J. D. (1999). Cyclic nucleotide-dependent protein kinases: Intracellular receptors for cAMP and cGMP action. *Crit. Rev. Clin. Lab. Sci.* **52**, 275–328.

Johnson, D. A., Akamine, P., Radzio-Andzelm, E., Madhusudan, and Taylor, S. S. (2001). Dynamics of cyclic AMP-dependent protein kinase. *Chem. Rev.* **101**, 2243–2270.

Lincoln, T. M., Dey, N., and Sellak, H. (2001). cGMP-dependent protein kinase signaling mechanisms in smooth muscle: from the regulation of tone to gene expression. *J. Appl. Physiol.* **91**, 1421–1430.

Lohmann, S. M., Vaandrager, A. B., Smolenski, A., Walter, U., and De Jonge, H. R. (1997). Distinct and specific functions of cGMP-dependent protein kinases. *Trends Biochem. Sci.* **22**, 307–312.

Schlossmann, J., Feil, R., and Hofmann, F. (2003). Signaling through NO and cGMP-dependent protein kinases. *Ann. Med.* **35**, 21–27.

Skalhegg, B. S., Huang, Y., Su, T., Idzerda, R. L., McKnight, G. S., and Burton, K. A. (2002). Mutation of the Calpha subunit of PKA leads to growth retardation and sperm dysfunction. *Mol. Endocrinol.* **16**, 630–639.

Smolenski, A., Burkhardt, A. M., Eigenthaler, M., Butt, E., Gambaryan, S., Lohmann, S. M., and Walter, U. (1998). Functional analysis of cGMP-dependent protein kinases I and II as mediators of NO/cGMP effects. *Naunyn Schmiedebergs Arch. Pharmacol.* **358**, 134–139.

Biography

Dr. Jackie D. Corbin is a Professor in the Department of Molecular Physiology and Biophysics at Vanderbilt University School of Medicine. His career interest has been the mechanism of action of cAMP and cGMP. He has a Ph.D. degree in physiology from Vanderbilt University and did postdoctoral training at the University of California, Davis. He has made seminal discoveries in the mechanisms and functions of cAMP-dependent protein kinases, cGMP-dependent protein kinases, and cyclic GMP-binding cyclic GMP-specific phosphodiesterase (PDE5).

Dr. Sharron H. Francis is a Research Professor in the Department of Molecular Physiology and Biophysics at Vanderbilt University School of Medicine. Her research interest has been the biochemical mechanisms by which cGMP-dependent protein kinases and PDE5 effect and modulate the physiological functions of cGMP. She has a Ph.D. degree in physiology from Vanderbilt University and did postdoctoral training at Washington University and at the National Heart and Lung Institute in Bethesda, MD.

Cyclic Nucleotide-Regulated Cation Channels

Martin Biel
Ludwig-Maximilians-Universität München, Munich, Germany

Franz Hofmann
Technischen Universität München, Munich, Germany

Cyclic nucleotides exert their physiological effects by binding to four major classes of cellular receptors: cAMP- and cGMP-dependent protein kinases, cyclic GMP-regulated phosphodiesterases, cAMP-binding guanine nucleotide exchange factors, and cyclic nucleotide-regulated cation channels. Cyclic nucleotide-regulated cation channels are unique among these receptors because their activation is directly coupled to the influx of extracellular cations into the cytoplasm and to the depolarization of the plasma membrane. Two families of channels regulated by cyclic nucleotides have been identified, the cyclic nucleotide-gated (CNG) channels and the hyperpolarization-activated cyclic nucleotide-gated (HCN) channels. The two channel classes differ from each other with regard to their mode of activation. CNG channels are opened by direct binding of cAMP or cGMP. In contrast, HCN channels are principally operated by voltage. These channels open at hyperpolarized membrane potentials and close on depolarization. Apart from their voltage sensitivity, HCN channels are also activated directly by cyclic nucleotides, which act by increasing the channel open probability.

General Features of Cyclic Nucleotide-Regulated Cation Channels

Structurally, both CNG and HCN channels are members of the superfamily of voltage-gated cation channels. Like other subunits encoded by this large gene family CNG and HCN channel subunits assemble to tetrameric complexes. The proposed structure and the phylogenetic relationship of mammalian CNG and HCN channel subunits is shown in Figure 1. The transmembrane channel core consists of six α-helical segments (S1–S6) and an ion-conducting pore loop between the S5 and S6. The amino- and carboxy-termini are localized in the cytosol. CNG and HCN channels contain a positively charged S4 helix carrying three to nine regularly spaced arginine or lysine residues at every third position. In HCN channels, as in most other members of the channel superfamily, the S4 helix functions as "voltage-sensor" conferring voltage-dependent gating. In CNG channels which are not gated by voltage, the specific role of S4 is not known.

CNG and HCN channels reveal different ion selectivities. CNG channels conduct both Ca^{2+} and monovalent cations with permeability ratios P_{Ca}/P_{Na} ranging from about 2 to 25 depending on the respective channel type and the cyclic nucleotide concentration. By providing an entry pathway for Ca^{2+}, CNG channels control a variety of cellular processes that are triggered by this cation. In contrast, HCN channels are not permeable to Ca^{2+}. These channels pass Na^+ and K^+ ion with a relative permeability ratio P_{Na}/P_K of about 0.15–0.25.

In the carboxy-terminus, CNG and HCN channels contain a cyclic nucleotide-binding domain (CNBD) that has significant sequence similarity to the CNBDs of most other types of cyclic nucleotide receptors. In CNG channels, the binding of cyclic nucleotides to the CNBD initiates a sequence of allosteric transitions that lead to the opening of the ion-conducting pore. In HCN channels, the binding of cyclic nucleotides is not required for activation. However, cyclic nucleotides shift the voltage-dependence of channel activation to more positive membrane potentials and thereby facilitate voltage-dependent channel activation. Despite the fact that the CNBDs of HCN and CNG channels show significant sequence homology, the two channel classes reveal different selectivities for cyclic nucleotides. HCN channels display an approximately 10-fold higher affinity for cAMP than for cGMP, whereas CNG channels select cGMP over cAMP.

CNG Channels

CNG channels are expressed in retinal photoreceptors and olfactory neurons and they play a key role in

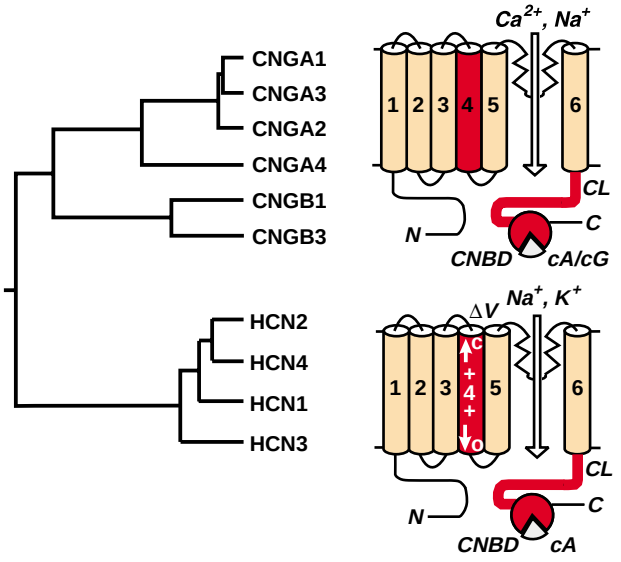

FIGURE 1 Phylogenetic tree and structural model of cyclic nucleotide-regulated cation channels. The CNG channel family comprises six members, which are classified into A subunits (CNGA1–4) and B subunits (CNGB1 and CNGB3). The HCN channel family comprises four members (HCN1–4). CNG and HCN channels share a common transmembrane topology, consisting of six transmembrane segments (1–6), a pore loop, and a cyclic nucleotide-binding domain (CNBD). CNG channels are activated *in vivo* by binding of either cAMP (cA) or cGMP (cG), depending on the channel type. HCN channels activate on membrane hyperpolarization (ΔV) and are enhanced by binding of cAMP. Structures involved in channel gating are shown in red. The positively charged amino acid residues in the S4 segment of HCN channels are indicated by (+). The movement of the S4 leading to channel closure (c) or opening (o) is indicated by arrows. CL denotes the C-linker involved in activation gating of CNG and HCN channels.

visual and olfactory signal transduction. CNG channels are also found at low density in some other cell types and tissues such as brain, testis, and kidney. While the function of CNG channels in sensory neurons has been unequivocally demonstrated, the role of these channels in other cell types remains to be established. Based on phylogenetic relationship, the six CNG channels identified in mammals are divided in two subfamilies, the A subunits (CNGA1-4) and the B subunits (CNGB1 and CNGB3) (Figure 1). CNG channel A subunits (with the exception of CNGA4) can form functional homomeric channels in various heterologous expression systems. In contrast, B subunits do not give rise to functional channels when expressed alone. However, together with CNGA1–3 they confer novel properties (e.g., single-channel flickering, increased sensitivity for cAMP and L-cis diltiazem) that are characteristic of native CNG channels. The physiological role and subunit composition is known for three native CNG channels: the rod photoreceptor channel, the cone photoreceptor channel, and the olfactory channel. The CNG channel of rod photoreceptors is a tetramer composed of three CNGA1 and one long isoform of the CNGB1 subunit (CNGB1a). The cone photoreceptor channel consists of the CNGA3 and the CNGB3 subunit. CNG channels control the membrane potential and the calcium concentration of photoreceptors. In the dark, both channels are maintained in the open state by a high concentration of cGMP. The resulting influx of Na^+ and Ca^{2+} (dark current) depolarizes the photoreceptor and promotes synaptic transmission. Light-induced hydrolysis of cGMP leads to the closure of the CNG channel. As a result, the photoreceptor hyperpolarizes and shuts off synaptic glutamate release. Mutations in CNG channel genes have been linked to retinal diseases. Mutations in the CNGA and CNGB1 subunits have been identified in the genome of patients suffering from retinitis pigmentosa. The functional loss of either the CNGA3 or the CNGB3 subunit causes total color blindness (achromatopsia) and degeneration of cone photoreceptors.

The CNG channel expressed in cilia of olfactory neurons consists of three different subunits: CNGA2, CNGA4, and a short isoform of the CNGB1 subunit (CNGB1b). The channel is activated *in vivo* by cAMP that is synthesized in response to the binding of odorants to their cognate receptors. The olfactory CNG channel is thought to conduct almost exclusively Ca^{2+} under physiological ionic conditions. The resulting increase in cellular Ca^{2+} activates a Ca^{2+}-activated Cl^- channel that further depolarizes the cell membrane. Ca^{2+} is not only a permeating ion of the olfactory CNG channel, it also represents an important modulator of this channel. By forming a complex with calmodulin, which binds to the CNGA2 subunit, Ca^{2+} decreases sensitivity of the CNG channel to cAMP.

The resulting inhibition of channel activity is the principal mechanism underlying odorant adaptation. Recent studies indicate that CNGA4 and the CNGB1b units also contribute to the CaM-dependent feedback inhibition.

HCN Channels

A cation current that is slowly activated by membrane hyperpolarization (termed I_h, I_f, or I_q) is found in a variety of excitable cells including neurons, cardiac pacemaker cells, and photoreceptors. The best understood function of I_h is the control of heart rate and rhythm by acting as "pacemaker current" in the sinoatrial (SA) node. I_h is activated during the membrane hyperpolarization following the termination of an action potential and provides an inward Na^+ current that slowly depolarizes the plasma membrane. Sympathetic stimulation of SA node cells raises cAMP levels and increases I_h by a positive shift of the current activation curve, thus accelerating diastolic depolarization and heart rate. Stimulation of muscarinic receptors slows

down heart rate by the opposite action. In the brain, I_h fulfills diverse functions: it controls the activity of spontaneously spiking neurons (neuronal pacemaking), it is involved in the determination of resting potential, it provides rebound depolarizations in photoreceptors in response to pronounced hyperpolarizations, it is involved in the transduction of sour taste and it is involved in the control of synaptic plasticity.

HCN channels represent the molecular correlate of the I_h current. In mammals, the HCN channel family comprises four members (HCN1–4) that share about 60% sequence identity to each other and about 25% sequence identity to CNG channels. The highest degree of sequence homology between HCN and CNG channels is found in the CNBD. When expressed in heterologous systems, all four HCN channels generate currents displaying the typical features of native I_h: (1) activation by membrane hyperpolarization, (2) permeation of Na^+ and K^+, (3) positive shift of the voltage-dependence of channel activation by direct binding of cAMP, (4) channel blockade by extracellular Cs^+. HCN1–4 mainly differ from each other with regard to their speed of activation and the extent by which they are modulated by cAMP. HCN1 is the fastest channel, followed by HCN2, HCN3, and HCN4. Unlike HCN2 and HCN4 whose activation curves are shifted by about + 15 mV by cAMP, HCN1 is only weakly affected by cAMP (shift of less than +5 mV). Site-directed mutagenesis experiments have provided insight into the complex mechanism underlying dual HCN channel activation by voltage and cAMP. Surprisingly, the voltage-dependent movement of the positively charged S4 helix is fully conserved between HCN channels and depolarization-activated channels such as Shaker K-channels. However, the allosteric coupling between S4 movement and the activation gate is different in the two channel types. In HCN channels, inward movement of S4 leads to the opening of the channel gate, whereas it closes Shaker channels. Major determinants affecting channel activation are the intracellular S4–S5 loop, the S5–P linker, the S1 segment, and the extracellular S1–S2 loop. The CNBD fulfills the role of an auto-inhibitory channel domain. In the absence of cAMP, the cytoplasmic carboxy-terminus inhibits HCN channel gating by interacting with the channel core and thereby shifts the activation curve to more hyperpolarizing voltages. Binding of cAMP to the CNBD relieves this inhibition. Differences in the magnitude of the response to cAMP among the four HCN channel isoforms are largely due to differences in the exent to which the CNBD inhibits basal gating. It remains to be determined if the inhibitory effect of the CNBD is conferred by a direct physical interaction with the channel core domain or by some indirect pathway. There is initial evidence that the so-called C-linker, a peptide of about 80 amino acids that connects the last transmembrane helix (S6) to the CNBD, plays an important role in this process (Figure 1). The C-linker was also shown to play a key role in the gating of CNG channels, suggesting that the functional role of this domain has been conserved during channel evolution.

Genetic deletion experiments in mice have been performed to facilitate the analysis of the physiological and pathophysiological role of individual HCN channel subunits in neuronal and cardiac function. Mice lacking the HCN2-subunit are viable but display a complex neurological–cardiological phenotype including absence epilepsy, ataxia, and sinus arrhythmia. As a likely explanation for this phenotype it was found that the loss of HCN2 induces a pronounced shift of the resting membrane potential and thereby impairs regular cardiac and neuronal rhythmicity. HCN4 represents the predominantly expressed HCN channel isoform in SA node. Deletion of HCN4 results in embryonic lethality after day 9.5 dpc. Electrophysiological studies with HCN4-deficient embryonic heart cells revealed that HCN4 underlies most if not all of the cardiac I_f current at early embryonic stages. Furthermore, HCN4 seems to be required for normal differentiation of the cardiac pacemaker system. Mice lacking the brain-specific HCN1 show a motor deficit, which is likely a result of altered firing rhythms in Purkinje neurons.

See Also the Following Articles

Ligand-Operated Membrane Channels: Calcium (Glutamate) • Ligand-Operated Membrane Channels: GABA • Olfactory Receptors • Photoreceptors

Glossary

channel states Voltage-gated channels have at least three states: a closed, an open, and an inactivated state. Ions conduct through the channel at the open state.

ligand-gated channel In contrast to voltage-gated channels, ligand-gated channels are opened by the occupation of the ligand binding site. HCN channels are gated by the membrane potential and are modulated by the binding of cAMP.

olfaction The processing of smell in the nose and olfactory bulb.

pacemaker Specialized cells that depolarize at a known frequency. The best-known example is the sino-atrial node of the heart.

photoreceptor Part of the rod or cone in the retina that senses light.

Further Reading

Biel, M., Seeliger, M., Pfeifer, A., Kohler, K., Gerstner, A., Ludwig, A., Jaissle, G., Fauser, S., Zrenner, E., and Hofmann, F. (1999). Selective loss of cone function in mice lacking the cyclic nucleotide-gated channel CNG3. *Proc. Natl Acad. Sci. USA* **96**, 7553–7557.

Biel, M., Schneider, A., and Wahl, C. (2002). Cardiac HCN channels: Strucuture, function and modulation. *Trends Cardiovasc. Med.* **12**, 206–213.

Dzeja, C., Hagen, V., Kaupp, U. B., and Frings, S. (1999). Ca^{2+} permeation in cyclic nucleotide-gated channels. *EMBO. J.* **18**, 131–144.

Kaupp, U. B., and Seifert, R. (2002). Cyclic nucleotide-gated ion channels. *Physiol. Rev.* **82**, 769–824.

Ludwig, A., Budde, T., Stieber, J., Moosmang, S., Wahl, C., Holthoff, K., Langebartels, A., Wotjak, C., Munsch, T., Zong, X., Feil, S., Feil, R., Lancel, M., Chien, K. R., Konnerth, A., Pape, H. C., Biel, M., and Hofmann, F. (2003). Absence epilepsy and sinus dysrhythmia in mice lacking the pacemaker channel HCN2. *EMBO J.* **15**, 216–224.

Männikkö, R., Elinder, F., and Larsson, H. P. (2002). Voltage-sensing mechanism is conserved among ion channels gated by opposite voltages. *Nature* **419**, 837–841.

Munger, S. D., Lane, A. P., Zhong, H., Leinders-Zufall, T., Yau, K. Y., Zufall, F., and Reed, R. R. (2001). Central role of the CNGA4 channel subunit in Ca^{2+}-calmodulin-dependent odor adaptation. *Science* **294**, 2172–2175.

Robinson, R. B., and Siegelbaum, S. A. (2003). Hyperpolarization-activated cation currents: From molecules to physiological function. *Ann. Rev. Physiol.* **63**, 453–480.

Wainger, B. J., DeGennaro, M., Santoro, B., Siegelbaum, S. A., and Tibbs, G. R. (2001). Molecular mechanism of cAMP modulation of HCN pacemaker channels. *Nature* **411**, 805–810.

Zhong, H., Molday, L. L., Molday, R. S., and Yau, K. W. (2002). The heteromeric cyclic nucleotide-gated channel adopts a 3A:1B stoichiometry. *Nature* **420**, 193–198.

Biography

Martin Biel is a Professor in Pharmacology and Chair of the Institute of Pharmakologie für Naturwissenschaftler, Science Faculty at the Ludwigs-Maximillian-University München. His research interests are cyclic nucleotide regulated ion channels and CNG and HCN channels. He holds a Ph.D. in Pharmacy. He obtained his Habilitation in Pharmacology at the Medical Faculty of the Technische Universität München.

Franz Hofmann is Professor in Pharmacology and Chair of the Institute for Pharmakologie und Toxikologie, Medical Faculty at the Technische Universität München. His primary research interest is cyclic nucleotide-regulated cellular functions, including cGMP protein kinases and ion channels. He holds an M.D. from the Universität Heidelberg. His group has contributed many seminal papers on the regulation of L-type calcium channels, CNG-channels, pacemaker channels, and the biology of cGMP kinase.

Cysteine Proteases

David J. Buttle
University of Sheffield, Sheffield, UK

John S. Mort
Shriners Hospital for Children, Montréal, Canada

Cysteine proteases represent one of the four main groups of peptide-bond hydrolases. They all use a S^- anion of a cysteine side chain as the nucleophile in peptide-bond hydrolysis. Cysteine proteases are found in all forms of life and mediate a wide variety of physiological and pathological processes, from the bulk digestion of protein, on the one hand, to highly regulated rate-determining and specific peptide-bond cleavages at the opposite extreme. They are implicated in a number of human pathologies, and the development of cysteine protease inhibitors as drugs is a very active field.

Phylogenetic Relationships

The use of the cysteine residue thiolate ion as the nucleophile for peptide-bond cleavage appears to have been derived at least five times during evolution using different structural frameworks, and members of each of these protease families are widely distributed. However, the bulk of these enzymes are members of clans CA and CD as classified in the MEROPS database (a regularly updated and invaluable source of information on proteases) (Figure 1). Clan CA contains the earliest identified cysteine proteases, such as the papaya protease papain, and the mammalian proteases, for example cathepsins B, L, S, and K. These enzymes are generally present in lysosomes or in other membrane-bound compartments where they mediate antigen processing and presentation, or they are secreted from the cell. As a group, clan CA proteases show cleavage selectivity for the residue 2 positions N-terminal to the cleavage site. A related subfamily of papain-like enzymes is the calcium-dependent calpains, which are found in the cytoplasm and mediate various intracellular processes.

The second major group of cysteine proteases, clan CD, has been described much more recently and includes the caspases, legumains, several viral proteases, and separase, which is responsible for the separation of sister chromatids during mitosis. Unlike the papain family, these proteases generally show exquisite specificity for cleavage C-terminal to particular amino acid residues – aspartic acid in the case of caspases, asparagine for legumains, and arginine for separase. The caspases are the mediators of apoptosis.

Mechanism

Proteolytic enzymes are very efficient catalysts that can increase the rate of peptide-bond hydrolysis a billion-fold. In the case of the cysteine proteases, the catalytic mechanism has been most extensively investigated for the clan CA enzymes. Despite their distinct evolutionary origins, it appears that the mechanism of other cysteine proteases is quite similar (an example of convergent evolution). Cleavage of the peptide bond is dependent on a thiolate-imidazolium ion pair provided by the cysteine and histidine residues in the active site (Figure 2). The environment of the active site results in an unusually low pK_a of around 4 for the cysteine thiol group. Nucleophilic attack on the carbonyl group results in the formation of a tetrahedral oxyanion intermediate. This then accepts a proton from the imidazolium group, resulting in the formation of an acyl enzyme intermediate and the release of the C-terminal portion of the substrate. In a second reaction, the acyl enzyme intermediate is deacylated by a water molecule and the remaining portion of the substrate is released.

Control

Activation

As is the case with most proteolytic enzymes, cysteine proteases are synthesized as inactive precursors, allowing them to be delivered to their intended site of action without harming the biosynthetic machinery of the cell. Often these proenzymes are retained in an inactive form until their services are required. Very different strategies have evolved for the activation of the precursors of the different cysteine protease groups. In the case of the

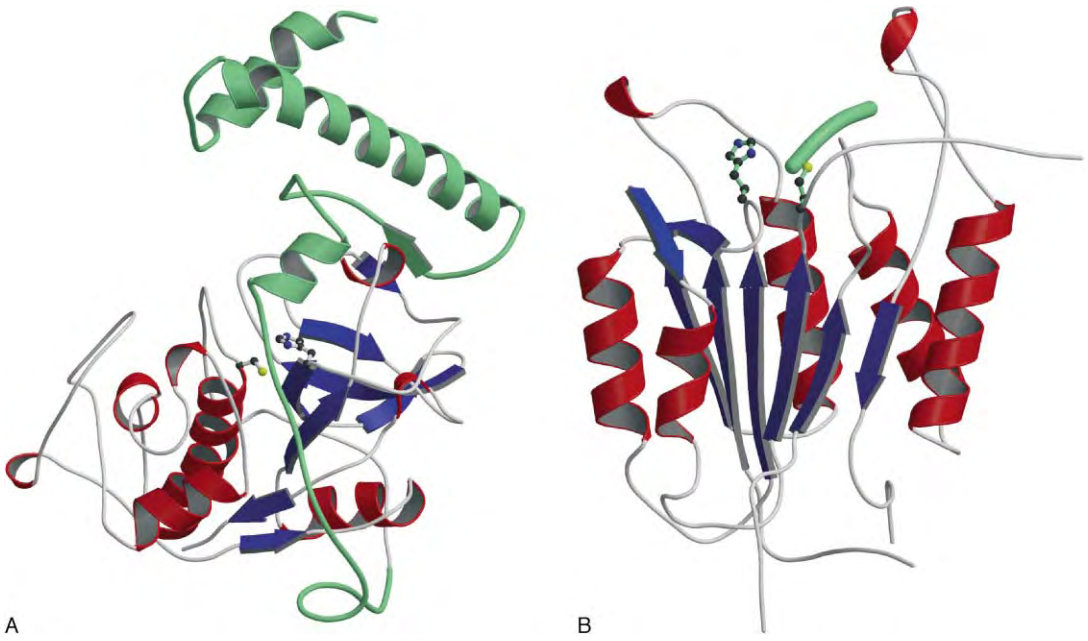

FIGURE 1 Cysteine protease structure. Ribbon diagrams of representative members of the two principal cysteine peptidase clans: (A) cathepsin K (pdb 1by8), a member of the papain family in Clan CA shown as the proenzyme, and (B) caspase-3 (pdb 1cp3), a member of clan CD. The active site cysteine and histidine residues are shown in ball and stick representation. For caspase-3, the position occupied by the substrate is indicated by the green rod. For procathepsin K, the proregion is depicted in green. The extended coil linking the helical region of the propiece passes through the active site in the region normally occupied by the substrate. Processing of the proforms of papain family members requires the proteolytic removal of the proregion without any change to the structure of the protease component. In contrast, major restructuring of the active site occurs during caspase activation and the active form of the enzyme is a dimer of the structure shown.

papain family, an N-terminal propeptide blocks access to the fully functional active site by binding in the reverse orientation to that required for peptide-bond cleavage (Figure 1). Its removal via inter- or intramolecular proteolysis liberates the functional protease. In contrast, the caspases undergo dimerization, which signals a rearrangement of the protein to form the previously incomplete active site.

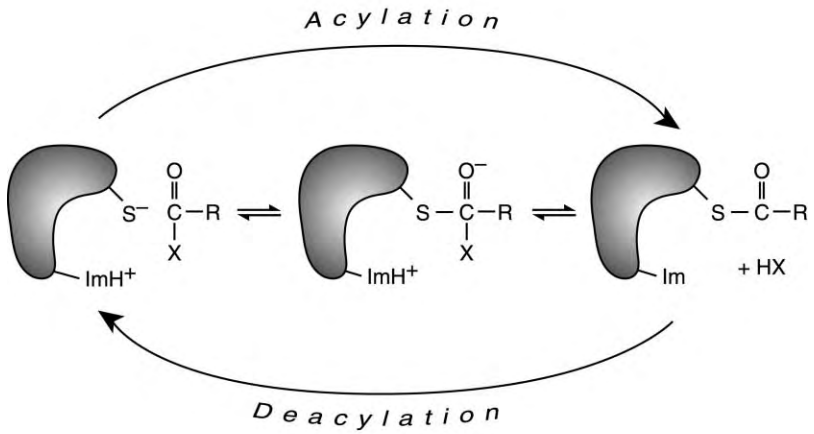

FIGURE 2 Cysteine protease mechanism. Scheme for the reaction mechanism of cysteine protease action. The active-site cysteine and histidine residues are present as a thiolate (S^-)-imidazolium (ImH^+) ion pair. The substrate is represented by the carbonyl group under attack connected to the N-terminal peptide component R and the C-terminal component X. Upon substrate binding, nucleophilic attack by the thiolate ion results in the formation of a tetrahedral oxyanion intermediate. This, following proton donation from ImH^+, breaks down to form an acyl enzyme (thiol ester) intermediate with the release of the C-terminal fragment HX. Adapted from Polgár and Asbóth (1986). The basic difference in catalysis by serine and cysteine proteinases resides in charge stabilization in the transition state. *J. Theor. Biol.* **121**, 323–326.

Inhibitors

A further level of control for unwanted proteolytic activity is provided by the action of a series of cysteine protease inhibitors. Members of the cystatin family are highly effective inhibitors of papain-like enzymes. The N terminus of the cystatin molecule binds in the active site cleft in a substrate-like manner, but the inhibitor evades cleavage by the target protease due to the presence of a glycine residue at what would normally be the site of cleavage. Additional elements in the inhibitor bind to the protease to maneuver the N-terminal substrate region just out of the range of the catalytic residues. A separate family of inhibitors, termed inhibitors of apoptosis proteins (IAPs), is available for the caspases. These proteins bind across the active caspase, obstructing normal substrate access but making limited interactions with the protease. Analogous to the propeptides of the papain family members, IAPs ensure their resistance to proteolysis by binding in the reverse direction to that required for substrate cleavage.

Physiology

Lysosomal Proteolysis

Virtually all eukaryotic cells possess membrane-enclosed organelles known as lysosomes This structure is the site of breakdown of endocytosed or phagocytosed material, and it is also the location for the turnover of certain cytosolic proteins and organelles. In most eukaryotic cells, the lysosome has the highest concentration of cysteine proteases and other hydrolases, which implies that these enzymes are involved in protein degradation for the recycling of amino acids for protein synthesis. This is indeed likely to be the major physiological function of ubiquitously expressed cysteine proteases such as cathepsin L, legumain, cathepsin B, and cathepsin H. Indeed, the last two enzymes, which fragment polypeptides (endopeptidase action) and then attack the fragments at either the C-terminal end, in the case of cathepsin B (carboxypeptidase action), or at the amino terminus, in the case of cathepsin H (aminopeptidase action), are functionally well equipped to fulfill a digestive role.

Antigen-Ii Processing

In the major histocompatibility complex (MHC) class II antigen-presenting cells, such as dendritic cells, macrophages, and B lymphocytes, the lysosomal or endocytic localization of some cysteine proteases has allowed them to participate in antigen presentation to T cells. In this process, the antigen is endocytosed and fragmented into peptides of between 13 and 26 amino acids in length. In order to allow the peptides thus generated to bind to the MHC complexes for presentation at the cell surface, the invariant chain Ii must be cleaved in order to remove it from the peptide-binding groove. Cathepsin S has been known for some time to be highly expressed in antigen-presenting cells and recently the use of selective cathepsin S inhibitors and the generation of cathepsin S-null mice has demonstrated an important, but not solitary, role for this enzyme in Ii processing.

It is likely that a number of endosomal proteases are involved in antigen processing and also that the protease involved is dependent on the nature of the antigen. In some cases at least, legumain appears to play an important role.

Bone Turnover

Bone is continually being broken down and replenished. This is important in calcium homeostasis, in which soluble calcium is provided by the hydrolysis of the mineral fraction of bone. At the same time, the organic component of bone, consisting largely of type I collagen, is also removed. Although a normal physiological process, under some circumstances bone resorption can outstrip synthesis. This can lead to the condition known as osteoporosis or brittle bone disease, which largely affects postmenopausal women. Other situations in which bone resorption is outside normal homeostatic control include bone metastases and some rare genetic diseases. The process of bone resorption is mediated largely by the multinucleated cell type known as an osteoclast. During periods of active resorption, osteoclasts sitting on bone surfaces generate a ruffled membrane, effectively sealing off the area immediately beneath the cell into which proteolytic enzymes and acid are secreted to remove the organic and mineral components, respectively. Both cysteine proteases and matrix metalloproteinases have been implicated in the hydrolysis of the organic component of bone, and it is likely that the relative contributions played by these different enzymes depend on the type of bone, with cysteine proteases playing a dominant role in the resorption of long bone.

The discovery that pycnodysostosis, an autosomal recessive disease leading to short stature and bone fragility, was due to a deficiency in cathepsin K activity, provided the first indication that this cysteine protease played a major role in bone resorption. Laboratory experiments have demonstrated this enzyme's efficiency at cleaving type I collagen, and consequently it has become a major drug target for the treatment of bone-resorbing diseases.

Other cysteine proteases are likely to be involved in bone resorption. For instance, legumain acts as an inhibitor of bone resorption by inhibiting the formation of multinucleated osteoclasts from their mononuclear precursors. The precise mechanism is not known, but it is not linked to the catalytic activity of the enzyme, and

in fact the active component is the C-terminal peptide that is removed upon generation of full catalytic activity.

Thyroglobulin Processing

The distribution of cathepsin K is quite restricted, being found predominantly in the ovary and in the osteoclasts, the bone-degrading cells. The other site where cathepsin K is highly expressed, alongside the more ubiquitously distributed cathepsins B and L, is in the thyroid follicles, which are the site of storage of thyroglobulin, the precursor of the thyroid hormones. It appears from experiments using single- and double-knockout mice that all three of these cysteine proteases are involved in thyroid hormone generation from thyroglobulin. All are found in the lumen of thyroid follicles, where cathepsin L appears to be involved in both the solubilization of cross-linked thyroglobulin and subsequent generation of thyroid hormones. In contrast, cathepsin B may be primarily involved in thyroglobulin solubilization and cathepsin K in thyroid hormone generation.

Apoptosis

The importance of programmed cell death to developmental processes has been recognized for many years. The discovery that the proapoptotic *ced-3* gene of *Caenorhabditis elegans* encodes a protease homologous to the mammalian cysteine protease interleukin-1β-converting enzyme (ICE), together with the demonstration that ICE induces apoptosis in mammals, ignited a great deal of renewed interest in the field, due in large part to the desire of the pharmaceutical industry to control the process. This article is too short to do justice to such a large area of research, which has been the subject of a number of good reviews (see Further Reading). Briefly, the proteases most intricately involved in the process of apoptosis are the caspases (including ICE), all of which have acute specificity for the cleavage of aspartyl bonds and which function in a cascade reaction. Upstream caspases activate downstream caspases, which cleave proteins whose functions are essential to cell survival. One of the initiators of this cascade event is the occupation of cell surface death receptors of the tumor necrosis factor receptor 1 family, which triggers the activation of caspase 8. Alternatively, the formation of a complex with cytochrome c and Apaf-1 in response to DNA damage leads to the activation of caspase 9. Both of these initiating caspases then activate the downstream executioner caspases, such as caspase 3. In cell killing by cytotoxic T cells or NK cells, this pathway is highjacked in the target cell through the ability of the killing cell's serine proteinase, granzyme B, to activate caspases.

It has become increasingly clear that, under some circumstances, cysteine proteases other than caspases are involved in apoptosis. For instance, cathepsin B may be involved in death receptor-mediated apoptosis of tumor cells if downstream caspases are inhibited. This process is expedited by tumor necrosis factor- and caspase 8-induced increases in cytosolic cathepsin B and subsequent release from mitochondria of cytochrome c.

Pathology

Cysteine proteases have been implicated in a wide range of pathologies, including cancer, osteoporosis, and arthritis. Here we concentrate on their involvement in two other pathological situations that may be less fully appreciated.

Allergenic Proteinases

Proteases represent a disproportionately high number of allergens. Examples include the major allergen from the house dust mite (a cysteine protease that is the product of the *Der p*1 gene) and many plant cysteine proteases such as actinidain, bromelain, papain, and glycyl endopeptidase. The normal route for the generation of atopy involves the initiation of a Th2 lymphocyte phenotype and enhanced IgE responses by B cells. Although the mechanisms by which cysteine (and other) proteases favor a switch to a Th2-like response are not completely elucidated, a link with the catalytic activity of these enzymes has been made. The mechanisms may be many and varied and include the cleavage (and activation?) of IgE and IL-2 receptors and disruption of epithelial tight junctions, thus enhancing access by allergens to immune cells. However, a systematic analysis of potential molecular targets for these enzymes has not been undertaken.

Parasitic Proteinases

Many parasites contain cysteine proteases in their phagocytic vacuoles, where they are involved in the digestion of engulfed material to be used in satisfying the nutritional requirements of the organism. As such, these enzymes are potential therapeutic targets. Examples include *Entamoeba histolytica*, a causative agent of amoebic dysentery; trypanosomatids that cause African sleeping sickness and Chagas' disease; schistosomal organisms and the plasmodial parasites that are the causative agents of malaria; and a number of parasitic helminths. In the case of plasmodial parasites, the cysteine proteases are known to be instrumental in the degradation of host hemoglobin, the principal source of amino acids for the parasite, because enzyme inhibition blocks hemoglobin degradation and parasite development. In a mouse model of the human disease, an orally administered inhibitor of the enzyme produced a 40%

cure rate, and a delayed progression of the disease in the remaining animals. New treatments for this and other parasitic diseases that kill millions every year are badly needed, due to increasing resistance to currently available drugs.

See Also the Following Articles

Calpain • Caspases and Cell Death • Cell Death by Apoptosis and Necrosis • Metalloproteases • SUMO Modification

Glossary

endocytosis The taking in by a cell of soluble or membrane-bound material from outside the cell. In the case of eukaryotic cells, endocytosed material passes into the endosome, a membrane-limited organelle that can fuse with lysosomes to allow digestion of the contents.

homeostasis The normal balance of a healthy living organism, in which the status quo is maintained by regulatory mechanisms such as feedback control. In protein turnover, it is the balance between protein synthesis and protein breakdown.

hydrolase An enzyme that breaks peptide, ester, or glycoside bonds by the addition of water. In the case of proteases, water is split, and the resulting oxygen is added to the newly formed carboxyl terminus while the two hydrogens are added to the new amino terminus formed by the breaking of the peptide bond.

protease An enzyme that cleaves proteins or peptides (also called proteinase, peptidase, or proteolytic enzyme).

specificity Susceptibility of an amino acid sequence of a peptide or protein to cleavage by a particular protease. Most proteases possess specificity for the cleavage of particular sequences. For instance, caspases cleave immediately after aspartic acid residues (they cleave aspartyl bonds); most lysosomal cysteine proteases cleave the second peptide bond on the carboxyl side of a hydrophobic residue, the exception being legumain, which cleaves asparaginyl bonds. Specificity is conferred by the structure of the substrate-binding groove on the protease.

Further Reading

Barrett, A. J., Rawlings, N. D., and Woessner, J. F. (eds.) (1998). *Handbook of Proteolytic Enzymes*. Academic Press, London.

Chapman, H. A., Riese, R. J., and Shi, G.-P. (1997). Emerging roles for cysteine proteases in human biology. *Annu. Rev. Physiol.* **59**, 63–88.

Cygler, M., and Mort, J. S. (1997). Proregion structure of members of the papain superfamily: Mode of inhibition of enzymatic activity. *Biochimie* **79**, 645–652.

Delaissé, J.-M., Engsig, M. T., Everts, V., del Carmen Ovejero, M., Ferreras, M., Lund, L., Vu, T. H., Werb, Z., Winding, B., Lochter, A., Karsdal, M. A., Troen, T., Kirkegaard, T., Lenhard, T., Heegaard, A.-M., Neff, L., Baron, R., and Foged, N. T. (2000). Proteinases in bone resorption: Obvious and less obvious roles. *Clin. Chim. Acta* **291**, 223–234.

Elliott, E., and Sloane, B. F. (1996). The cysteine protease cathepsin B in cancer. *Perspect. Drug Discovery Design* **6**, 12–32.

Friedrichs, B., Tepel, C., Reinheckel, T., Deussing, J., von Figura, K., Herzog, V., Peters, C., Saftig, P., and Brix, K. (2003). Thyroid functions of mouse cathepsins B, K, and L. *J. Clin. Invest.* **111**, 1733–1745.

Lang, A., Hörler, D., and Baici, A. (2000). The relative importance of cysteine peptidases in osteoarthritis. *J. Rheumatol.* **27**, 1970–1979.

MEROPS database. Available at: http://merops.sanger.ac.uk.

Polgár, L., and Asbóth, B. (1986). The basic difference in catalysis by serine and cysteine proteinases resides in charge stabilization in the transition state. *J. Theor. Biol.* **121**, 323–326.

Shakib, F., Schulz, O., and Sewell, H. (1998). A mite subversive: Cleavage of CD23 and CD25 by Der p1 enhances allergenicity. *Immunol. Today* **19**, 313–316.

Thornberry, N. A., and Lazebnik, Y. (1998). Caspases: Enemies within. *Science* **281**, 1312–1316.

Biography

David J. Buttle is Reader in Matrix Biology in the Division of Genomic Medicine at the University of Sheffield, U.K. His principal research interests are the turnover of extracellular matrix proteins by proteases and how this relates to various diseases such as arthritis, multiple sclerosis, and cancer. He received a Ph.D. from the Council for National Academic Awards, U.K., before receiving postdoctoral training at the Strangeways Research Laboratory, Cambridge, U.K.

John S. Mort is a Principal Investigator at the Shriners Hospital for Children and an Associate Professor in the Departments of Surgery and Medicine at McGill University in Montreal, Canada. His research program aims to determine the role of specific proteolytic enzymes in connective tissue remodeling during growth and development and in its destruction in arthritis. He received his Ph.D. from McMaster University, Hamilton, Canada, and his postdoctoral training at the University of Western Ontario.

Cytochrome b_6f Complex

Günter A. Hauska and Thomas Schödl
Universität Regensburg, Regensburg, Germany

The cytochrome b_6f-complex connects oxygen evolution by photosystem II, with NADPH production by photosystem I (PSI), in the photosynthetic electron transport (ET) chain of plants, algae, and cyanobacteria. More specifically, it reoxidizes plastoquinol, which has been produced in the membrane by PSII with electrons coming from water, at the expense of plastocyanin or cyt *c*, the electron donors to PSI. It belongs to the family of the cytochrome *bc*-complexes, which function at central position in many eukaryotic and prokaryotic ET chains. They all oxidize quinol in a proton translocating redox reaction, which is best described by the so-called Q-cycle. The resulting transmembrane electrochemical proton gradient drives ATP synthesis in a rotatory mechanism of the H^+-translocating F1Fo-ATP synthases. The scenario holds for respiration and photosynthesis, from higher organisms down to bacteria and archaea.

Quinol oxidation is the rate-limiting step in these ET chains ($\tau \sim$ ms), and therefore a key point for regulation. Plastoquinol oxidation by the cyt b_6f-complex in oxygenic photosynthesis, for example, controls the distribution of light quanta to the two photosystems, via a protein kinase, which by phosphorylation determines the association of chlorophyll antenna proteins with the reaction centers.

Crystal structures of the cytochrome b_6f-complex at atomic resolution have recently been obtained for the prokaryotic cyanobacterium *Mastigogladus laminosus* as well as for the eukaryotic green alga *Chlamydomonas reinhardtii*. They largely resemble the dimeric structures for the cytochrome bc_1-complex from mitochondria, but also reveal some striking differences. In addition to the four redox centers – two hemes *b*, one heme *c*, and a high potential 2Fe2S-cluster per monomeric complex – which are shared with the cyt bc_1-complex, the cyt b_6f-complex per monomer contains one chlorophyll *a*, one carotenoid, and most surprisingly, an extra heme.

Discovery and Isolation

Cytochromes b_6 and f were discovered in leaves by Robin Hill in the middle of last century.

The reduction of cyt f by red light absorbed in PSII and its reoxidation by far-red light absorbed by PSI led to the formulation of the "Z-scheme" of photosynthetic ET in chloroplasts, with the two light reactions acting in series, connected by cyt f.

The first evidence for a complex between these two cytochromes was provided by Nelson and Neumann (Tel-Aviv) in 1972, who recognized that a particle isolated from chloroplasts contained redox centers similar to the cyt bc_1-complex from mitochondria – heme b, heme c, and nonheme iron. A little later Wood and Bendall described a plastoquinol–plastocyanin oxidoreductase activity solubilized from chloroplasts. Both observations were combined by Hurt and Hauska, who succeeded in the isolation of the complex with a well-defined composition in functionally active form from spinach chloroplasts. In addition to plastoquinol–plastocyanin oxidoreductase activity, the isolate catalyzed oxidant-induced reduction of cyt b_6, a signature of the Q-cycle mechanism. Furthermore, during the redox reaction it transcolated protons across the membrane in an electrogenic way, after incorporation into lipid vesicles.

The isolation procedure involved four steps – removal of peripheral proteins, selective solubilization by a mild, nonionic detergent, ammonium sulfate precipitation, and sucrose density gradient centrifugation. These procedures have been modified repeatedly, resulting in improved isolates with turnover numbers up to $500\ s^{-1}$, from spinach as well as from other organisms, but in principle the strategy is followed until today.

Composition and Structure

The cyt b_6f-complex consists of four major polypeptides with two pairs of redox centers which differ by 300–400 mV in the redox potentials under standard conditions. The pair with the higher redox potentials is represented by a heme c (+340 mV) covalently bound to cyt f, and by the 2Fe2S-cluster (+300 mV) of the Rieske FeS–protein. The pair with the lower potentials are the two hemes b on cyt b_6 (−50 and −150 mV). The fourth polypeptide (subunit IV) lacks a redox center. According to a nomenclature for cyanobacteria, cyt f, cyt b_6, the Rieske FeS–protein, and subunit IV are also known as

PetA, PetB, PetC, and PetD, respectively (Pet standing for photosynthetic electron transport), and are coded by the corresponding *pet* genes.

The folding of these subunits in the thylakoid membrane is depicted in Figure 2. They correspond to the central components in the cyt bc_1-complex of mitochondria and bacteria. Cyt c_1 (~33 kDa) resembles cyt *f*, the Rieske FeS–protein (some 20 kDa) occurs in both systems, and the N-terminal part of cyt *b* (~42 kDa) is equivalent to cyt b_6 (24 kDa), while its C-terminal part corresponds to subunit IV (17 kDa).

Several bacterial cyt bc_1-complexes contain just these central components, cyt c_1, cyt *b* and the Rieske FeS–protein, while the eukaryotic bc_1-complexes in mitochondria contain 7–8 "supernumerary" subunits, which do not occur in the cyt b_6f-complex. On the other hand four small hydrophobic polypeptides (3.2–4.2 kDa) have been identified in the cyt b_6f-complex only. These are PetG, PetL, PetM, and PetN, each consisting of little more than a transmembrane helix (Figure 2). In the crystal structure they are found as a transmembrane four-helix bundle, distal to the symmetry axis of the dimer (Figure 3).

Cytochrome *f*

Mature cyt *f* is a 31 kDa protein built from ~290 amino acids. It holds the heme *c* covalently bound to the pentapeptide CxxCH in an elongated, peripheral domain, largely of β-sheet structure. This domain is exposed to the intrathylakoid surface, which becomes positively charged during illumination (p-side, s. Figure 1), and is anchored by a C-terminal transmembrane helix. The fifth ligand to the heme iron is an N-atom of a histidine, while the sixth ligand is exceptional for a *c*-type cytochrome: it is the free α-amino group of the N-terminal tyrosine (Figure 2).

Cytochrome b_6 + Subunit IV

These two subunits are integral membrane proteins, spanning the membrane seven times together. Cyt b_6 (24 kDa, 215 amino acids) contains four hydrophobic helices, the second and fourth holding the two hemes *b* by four H-residues in transmembrane arrangement (Figure 2). These histidines are strictly conserved in all cyt *bc*-complexes. Subunit IV (17 kDa, 160 amino acids) comprises three transmembrane helices. These correspond to helices 5–7 in cyt *b* (42 kDa) from bc_1-complexes, which spans the membrane 8 times. The eighth helix is missing in subunit IV.

In addition to the two hemes *b*, cyt b_6 contains a third heme, which came as a surprise from the crystal structures (Figure 3). It has escaped spectroscopic detection, because it is a low-spin heme. It is of the *c*′-type, being covalently bound by only one of its vinyl groups to C-37 of cyt b_6, which is conserved in all b_6f-complexes. This covalent binding is responsible for the old, but misinterpreted notion that cyt b_6 stains for heme on denaturing SDS-polyacrylamide electrophoresis, in contrast to other cyt's *b*. Noteworthy, this covalently bound heme has been described for the b_6f-type complex of the respiratory, Gram-positive bacterium *Bacillus subtilis* by Yu and LeBrun in 1998 already, without wide recognition, however. It may be involved in ferredoxin–plastoquinone reduction, as an additional entry of electrons into the cyt b_6f-complex.

The hydrophobic region of cyt b_6 and subunit IV furthermore binds a chlorophyll *a* and a carotenoid (Figure 3).

The Rieske FeS–Protein

This protein with a 2Fe2S cluster of +300 mV has been discovered by John S. Rieske in mitochondria in 1964. The unusually high redox potential for a FeS–protein results from "softer" ligation of one Fe to the N-atoms

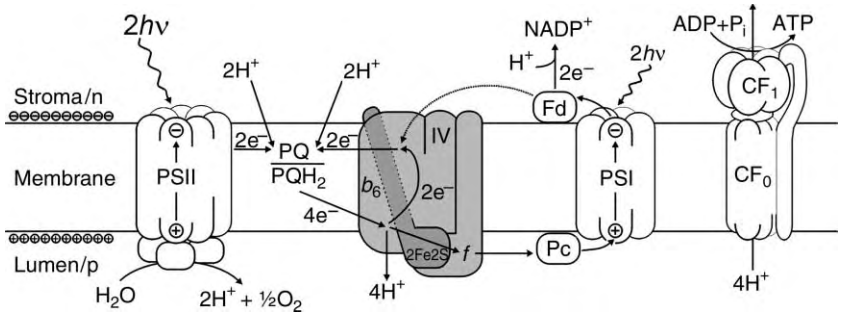

FIGURE 1 The cytochrome b_6f-complex in the chloroplast membrane. The transfer of two electron equivalents from PSII to PSI, and the accompanying proton transfer reactions are shown, indicating the bifurcation of the reduction equivalents from plastoquinol in the Q-cycle of the cyt b_6f-complex. Abbreviations: b_6, cyt b_6; *f*, cyt *f*; 2Fe2S, FeS-cluster of the Rieske protein; IV, subunit IV; PQ, plastoquinone; PC, plastocyanin; Fd, ferredoxin; CF1CFo, H^+-translocating ATP synthase; "p" and "n" denote the positively and negatively charged membrane surfaces; the dotted arrow indicates cyclic electron flow around photosytem I.

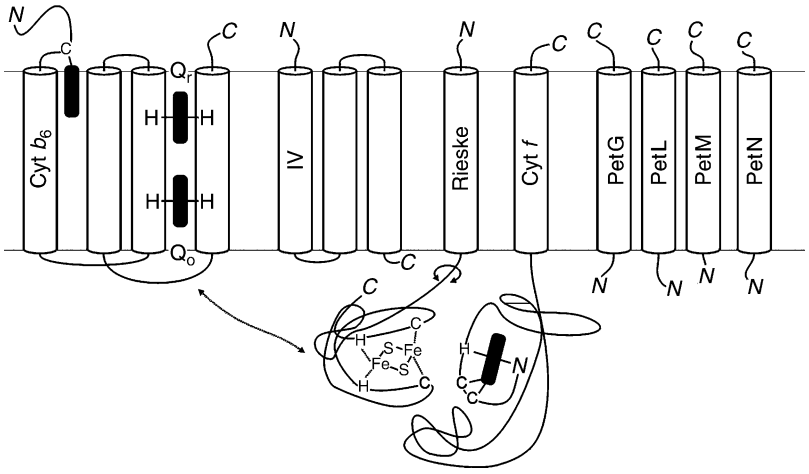

FIGURE 2 Folding of the protein subunits in the cytochrome b_6f-complex across the thylakoid membrane. The solid and dotted double-headed arrows indicate the domain movement of the Rieske FeS–protein by rotation at the "hinge" region. Q_o and Q_r denote the sites of plastoquinol oxidation and plastoquinone reduction, respectively. Italic Ns and Cs stand for N and C termini. Further explanations are given in the text.

of two H-residues, instead of S-atoms of C-residues (Figure 2). The protein of the cyt b_6f-complex consists of 179 amino acids (20 kDa). The two cluster binding peptides are CTHLGC and CPCHGSQY, containing a histidine and two cysteins each. The first cystein in each peptide ligates the other Fe-atom, while the second two cysteins form a stabilizing S–S bond. H-bonds from S and Y in the second peptide stabilize the reduced form of the cluster, additionally increasing the redox potential by some 60 mV per H-bond. Rieske proteins of lower redox potentials occur in menaquinol oxidizing organisms, and carry non-H-bonding residues at these positions.

Like the heme c carrying part of cyt f, the cluster carrying domain of the Rieske FeS–protein is exposed to the p-surface (Figures 1 and 2), and is tied to the membrane by a single transmembrane helix, at the N terminus. Noteworthy, like in the crystal structures of the cyt bc_1-complexes, the Rieske FeS–protein cross-connects the dimer of the cyt b_6f-complex, the

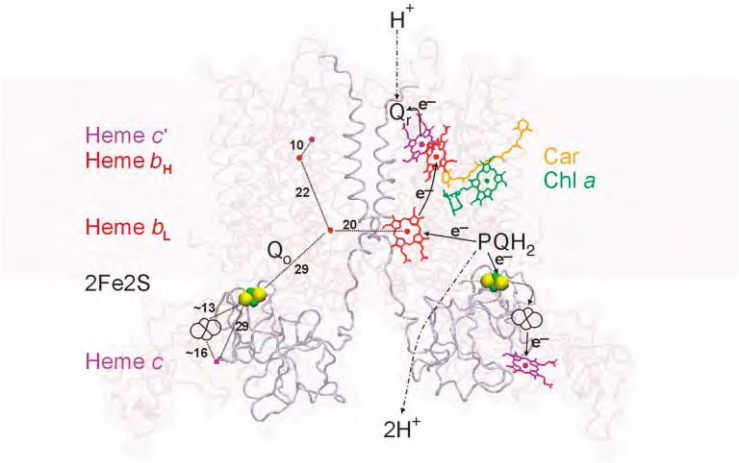

FIGURE 3 Distances, electron and proton transfer in the crystal structure of the dimeric cytochrome b_6f-complex. The figure was constructed from the coordinates for the complex of *Mastigogladus laminosus* submitted to the PDB, accession code 1UM3. The dimeric structure is not totally symmetric, while the one from *Chlamydomonas rheinhardtii* is (PDB accession code 1Q90). Further discrepancies between the two structures are under debate (Daniel Picot, personal communication). In the figure the dimeric structure is depicted in the membrane with its peripheral surface contours and the Cα-backbone in gray. The backbone of the Rieske FeS–protein which cross connects the dimer is emphasized in darker gray. The 2Fe2S cluster is depicted on both halves, the irons in green and the sulfurs in yellow. Its movement to the position closer to the heme c of cyt f is indicated. The positions of the four hemes are shown with the porphyrin rings on the right, and as the central irons on the left. The distances between the metal centers in numbers of Å are given on the left half, while the right includes the electron and proton transfer steps plus the bound molecules of chlorophyll a (Chl a) and carotenoid (Car). Abbreviations: b_H and b_L, high and low potential heme b in cyt b_6; Q_o and Q_r, sites of plastoquinol oxidation and plastoquinone reduction.

FeS-domain being associated with cyt *f* of one-half and the hydrophobic helix with the other (Figure 3). Whether the dimeric structure bears on the function is an unsettled question still. The FeS-domain is linked to the transmembrane helix by a flexible, G-rich "hinge" region, which by rotation allows for the movement of the FeS-domain during the redox cycle. This movement has been documented in oriented samples by polarized EPR, and is indicated by double-headed arrows in Figure 2. The two positions of the FeS-center have been detected in the crystal structure of the mitochondrial cyt bc_1-complex by analyzing preparations with and without the specific inhibitor stigmatellin, which locks the conformation into the form with the FeS-center closer to heme b_L of cyt b_6, at the Qo-site. Only this position of the FeS-center is seen in the structures of cyt b_6f-complex, since the tridecyl derivative of stigmatellin was used to obtain ordered crystals. The second position close to the heme of cyt *f* has been modeled into the cyanobacterial structure, however, and is indicated in Figure 3, which depicts further features of the overall structure. Noteworthy, an electron density close to the heme c' at the Qr-site has been interpreted as bound plastoquinone in the cyanobacterial structure, which has not been identified in the structure for the eukaryotic alga.

Plastoquinol Oxidation – Q-Cycle and Fes-Domain Movement

In 1960, Britton Chance discovered oxidant-induced reduction of cyt *b* during oxygen pulses of anaerobic mitochondria. A decade later Marten Wikström explained this phenomenon as a "pull–push" effect of ubiquinol oxidation in the cyt bc_1-complex, which involves the reactive semiquinone intermediate. Accordingly, Peter Mitchell proposed the Q-cycle mechanism in 1975, which has been reformulated by Antony Crofts, Bernie Trumpower, and others.

The observation of oxidant-induced reduction of cyt b_6 in the isolated cyt b_6f-complex, with pulses of ferricyanide in the presence of excess plastoquinol, was of key importance for acceptance of an operating Q-cycle also in chloroplasts, because the earlier detection in membrane preparations was complicated by reduction of cyt b_6 in cyclic ET around PSI. Quinol oxidation at the Q_o-site is the rate-determining step in ET not only because of second order kinetics, but also because it involves the movement of the 2Fe2S-cluster carrying, peripheral domain in the Rieske protein. The Q-cycle mechanism, as indicated in Figures 1 and 3, comprises the following:

1. Two quinone/quinol interaction sites with different semiquinone stability, and accessible from the aqueous space on opposite membrane surfaces, with two pairs of redox centers at two different redox potential levels.
2. At the Q_o-site the Rieske FeS-center (+300 mV) oxidizes plastoquinol.
3. The resulting instable semiquinone anion is highly reducing (redox potential of semiquinone anion/plastoquinone ~ − 150 mV), and for kinetic reasons does not deliver its electron to the FeS-center but to nearby low-potential heme *b* (− 150 mV) of cyt b_6. This bifurcation is the rate-determining step ($\tau \sim$ ms) of the whole cycle, and causes the oxidant-induced reduction of cyt *b*. It is responsible for the transition from 2e- to 1e-transfer in the electron transport chains of photosynthesis and respiration.
4. Furthermore, this step is linked to the movement of the 2Fe2S-cluster towards the heme *c* of cyt *f* (Figures 2 and 3), close enough for efficient electron transfer. At the same time the oxidized plastoquinone is replaced by plastoquinol from the quinol/quinone pool.
5. The electron from low-potential heme *b* moves across the membrane to the high-potential heme *b* (− 50 mV), and from there to a plastoquinone molecule at the quinone reduction site (Q_r-site), which allows for the electron uptake by stabilizing the resulting semiquinone anion.
6. This semiquinone anion receives a second electron coming from the Q_o-site across the membrane via the two heme *b*, takes up two protons from the n-surface and leaves the site as plastoquinol in exchange for plastoquinone.

An alternative view to the Q-cycle is the "semiquinone cycle," in which the instable semiquinone at the Q_o-site changes into the stable semiquinone at the Q_r-site, either by movement or by conformational dynamics.

In summary, the Q-cycle transports four protons across the membrane per two electrons passing from plastoquinol through the cyt b_6f-complex to plastocyanin. Together with the liberation of two protons in water oxidation inside the thylakoids (p-side), and proton uptake by reduction of CO_2 via $NADP^+$ outside, a total of six protons are translocated across the chloroplast membrane per 2e if the Q-cycle operates (Figure 1). Evidence for a down-regulation to $4H^+/2e$, i.e., a shut down of the Q-cycle at high-energy pressure across the chloroplast membrane has been provided.

One of the two electrons at the bifurcation point reduces cyt b_6, branching off through the membrane. It contributes the "slow phase" to the charge separation across the chloroplast membrane, in addition to the fast phases in the two RCs. These phases are known from the "carotenoid shift," an electrochromic effect on the absorption of carotenoids.

Several inhibitors of electron transport through the cyt b_6f-complex are in use, most of them interfering with quinol oxidation at the Q_o-site. Among them are the antibiotics stigmatellin and myxothiazol, and the quinone analogues DBMIB (2,5-bromo-3-methyl-6-isopropyl-p-benzoquinone) and UHDBT (5-undecyl-6-hydroxy-4,7-dioxobenzothiazole). As mentioned above, the tridecyl derivative of stigmatellin TDS was used to obtain stable crystals. Antimycin A, a Q_r-site inhibitor in cyt bc_1-complexes, and which was valuable in elucidating the Q-cycle mechanism, because it stimulates oxidant-induced reduction of cyt b by blocking its reoxidation with quinone, unfortunately is inefficient in the cyt b_6f-complex. Possibly the additional heme c' at the Q_r-site does not allow the binding of antimycin A. However, MOA-stilbene (β-methoxacrylate-stilbene) acts on the Q_r-site in the cyt b_6f-complex, like antimycin A in the cyt bc_1-complex. Heptyl- or nonyl-4-hydroxyquinoline N-oxides (HQNO and NQNO) block the quinol/quinone interaction at both sites, with a higher affinity for the Q_r-site.

Oxidation of plastoquinol and the coherent movement of the Rieske FeS–protein are rate determining in photosynthetic electron flow, and therefore are linked to regulatory phenomena, like the optimization of the light distribution to the two photosystems via activation of LHCII-kinase (state transitions), but also in light regulation of gene expression.

In the dark and in low light, under aerobic conditions, the chloroplasts are in state 1, with the plastoquinone pool largely oxidized and the outer chlorophyll antenna LHCII associated with PSII for transfer of excitation energy. At high light pressure PSII reduces plastoquinone, and the resulting plastoquinol, via a reduced state of the cyt b_6f-complex, activates a specific kinase which phosphorylates LHCII and causes it to move to PS1. Preferential excitation of PS1 (state 2) reoxidizes plastoquinol leading to deactivation of the LHCII-kinase, deposphorylation of LHCII-P by a phosphatase, and the movement of LHCII back to PSII. This way the distribution of the light quanta between the two photosystems is optimally balanced. LHCII-kinase has been found associated with the cyt b_6f-complex.

Noteworthy, the electron flow through the cyt b_6f-complex *in vivo* can be measured in detail by single turnover laser flash photolysis, or by chlorophyll fluorescence induction (Kautsky-effect) with pulsed light.

Genes, Biogenesis, and Phylogeny

In cyanobacteria, the genes for the major subunits of the cyt b_6f-complex are organized in two transcription units, *petCA* for the Rieske FeS–protein and cyt *f*, and *petBD* for cyt b_6 and subunit IV. The genes for the four small subunits PetG, PetL, PetM, and PetN occur in isolated loci. In eukaryotic plants and algae the genes for the Rieske FeS–protein, *petC*, and for one of the small subunits, *petM*, were moved to the nucleus, while the others remained on the chloroplast genome. In vascular plants *petBD* and *petA* were combined with other genes in transcription units, while in green algae like *Chlamydomonas* these genes have been further rearranged and are transcribed independently.

The nuclear genes *petC* and *petM* acquired N-terminal extensions for signal peptides to recognize the machinery for the uptake of the preproteins into chloroplasts. There they are processed by signal peptidases to the mature proteins during insertion into the thylakoid membrane and assembly with the complex. Since the major part of Rieske FeS–protein faces the intrathylakoid surface (p-side), it has to pass the chloroplast envelope as well as the thylakoid membrane on the path from cytoplasmic ribosomes. Thus it is processed in two steps.

Also cyt *f* faces the p-side and has to pass the membrane. Its plastidal gene *petA*, which is transcribed on stromal ribosomes, also carries an N-terminal extension which targets it across the thylakoid membrane where it is processed. The insertion of cyt *f* and of the Rieske FeS–protein into the complex use different pathways. Cyt *f* follows the secA-route known from bacterial secretion, while the assembly of the Rieske FeS–protein is energized by the proton gradient across the membrane (ΔpH-route). The insertion of the hydrophobic proteins cyt b_6 and subunit IV into the membrane does not require a signal peptide and may follow yet another route. Interestingly cyt *f* controls the stability and assembly of the Rieske FeS–protein and of the other subunits in the cyt b_6f-complex, via a signal in its C terminus which is located on the stromal surface (n-side, see Figure 2). The biosynthesis of 2Fe2S-cluster in the Rieske FeS–protein, and the covalent binding of heme *c* in cyt *f* as well as of the heme c' in cyt b_6 are enzymatic processes governed by several nuclear genes. The insertion of the hemes *b* into cyt b_6 may occur spontaneously.

In many bacteria the genes of the related cyt bc_1-complex, for the Rieske FeS–protein, cyt *b*, and cyt c_1 are joined in the tricistronic *fbc*-operon, while in eukaryotes only the gene for cyt *b* remained in mitochondria, the others were transferred to the nucleus where they were furnished with targeting signal peptides.

The Rieske FeS–protein and cyt *b* in the different cyt *bc*-complexes originate from common ancestors, and since they occur in bacteria as well as in archaea, they appear phylogenetically very old. On the other hand cyt *f* and its *c*-type cyt counterparts have various different ancestors. A "cyt b_6f-complex" without a cyt *f* has been characterized in Gram-positive bacteria, in

respiratory *Bacilli* and in photosynthetic *Heliobacteria*, a notion which is based on the characteristics of the cyt *b*-complement. These are:

1. the splitting into cyt b_6 and subunit IV,
2. 14 instead of 13 amino acid residues between the two histidine ligands of the heme *b* in the fourth transmembrane helix,
3. the loss of the eighth transmembrane helix from subunit IV, and
4. the acquirement of the extra heme c', bound to C-37 of cyt b_6.

Interestingly the cyt *b*-complement from the *bc*-complex from green sulfur bacteria fulfills only the second and third of these criteria, but it is not split, and presumably does not contain the extra heme since C-37 is not conserved. Thus the cyt b_6f-complex has evolved on the path from the common ancestor of green sulfur bacteria (*Chlorobiaceae*) and Gram-positive bacteria (*Firmicutes*), via cyanobacteria to chloroplasts. The addition of a carotenoid and of a chlorophyll *a* molecule should have occurred after the branching of the cyt b_6f-complexes into photosynthetic and respiratory lines.

See Also the Following Articles

Chlorophylls and Carotenoids • Cytochrome bc_1 Complex (Respiratory Chain Complex III) • Cytochrome *c* • Quinones

Glossary

archaea The third domain of life next to eubacteria and eukaryotes, formerly called archaebacteria.

carotenoid shift A bathochromic shift of carotenoid absorption in response to an electric field (Stark effect) across the membranes of photosynthetic organisms.

chlorophyll fluorescence induction The intensity transient of chlorophyll fluorescence in chloroplasts after onset of illumination (Kautsky effect); the initial rise reflects the reduction of plastoquinone by photosystem II, the difference between maximal and actual fluorescence is related to the reoxidation of plastoquinol by the cyt b_6f-complex.

cyclic electron transport Electron transport around photosystem I via plastoquinone and the cyt b_6f-complex which provides extra ATP.

LHCII-kinase An enzyme that phosphorylates LHCII which in that state moves to photosystem I; it is activated by plastoquinol via the reduced state of the cyt b_6f-complex.

light harvesting complex II (LHCII) Also known as chlorophyll *a/b* binding protein (cab-protein), which constitutes the outer antenna of photosystem II.

photosystem The total of pigments assembled around a reaction center.

Q-cycle A mechanism of proton translocating quinol oxidation by cyt *bc*-complexes in respiratory and photosynthetic electron transport, first formulated by Peter Mitchell in 1975.

Q_o-site and Q_r-site The sites for quinol oxidation and quinone reduction in cyt *bc*-complexes are synonymous to Q_p and Q_n, the sites accessible form the positively and negatively charged membrane surface, respectively. Frequently the pair Q_o/Q_i, instead of Q_o/Q_r or Q_p/Q_n is in use, indicating the sites outside and inside the inner mitochondrial and bacterial membrane. Since the sidedness of the thylakoid membrane is turned around the Q_i-denotation is not appropriate for the cyt b_6f-complex.

thylakoid Coined by Wilhelm Menke to denominate the structure of the inner membrane system of the chloroplast which in cross-section appears to be built from stacked "little bags," but their inner space is connected in the third dimension.

Z-scheme Electron transport chain of oxygenic photosynthesis pictured in the redox potential scale, first formulated by Robin Hill and Fay Bendall in 1960.

Further Reading

Allen, J. F. (2002). Plastoquinone redox control of chloroplast protein phosphorylation and distribution of excitation energy between photosystems. *Photosynth. Res.* **73**, 139–148.

Berry, S., and Rumberg, B. (1999). Proton to electron stoichiometries in electron transport of spinach thylakoids. *Biochim. Biophys. Acta* **1410**, 248–261.

Berry, E. A., Guergova-Kuras, M., Huang, L. S., and Crofts, A. R. (2000). Structure and function of cytochrome *bc*-complexes. *Ann. Rev. Biochem.* **69**, 1005–1075.

Brugna, M., Rodgers, S., Schricker, A., Montoya, G., Kazmeier, M., Nitschke, W., and Sinning, I. (2000). A spectroscopic method for observing the domain movement of the Rieske iron–sulfur protein. *Proc. Natl Acad. Sci. USA* **97**, 2069–2074.

Hauska, G. (2003). The isolation of functional cytochrome b_6f complex: From lucky encounter to rewarding experience. *Photosynth. Res.* **120G**, 1–15.

Ke, B. (2001). Photosynthesis – photobiochemistry and photobiophysics. In *Advances in Photosynthesis*, (Govindjee, series ed.) Vol 10/chapter 35, pp. 635–664. Kluwer Academic, Dordrecht, The Netherlands.

Kurisu, G., Zhang, H., Smith, J. L., and Cramer, W. A. (2003). Structure of the cytochrome b_6f-complex of oxygenic photosynthesis: Tuning the cavity. *Science* **302**, 1009–1014.

Schütz, M., Brugna, M., Lebrun, E., Baymann, F., Huber, R., Stetter, K. O., Hauska, G., Toci, R., Lemesle-Meunier, D., Tron, P., Schmidt, C., and Nitschke, W. (2000). Early evolution of cytochrome *bc* complexes. *J. Mol. Biol.* **300**, 663–675.

Stroebel, D., Choquet, Y., Popot, J. L., and Picot, D. (2003). An atypical haem in the cytochrome b_6f-complex. *Nature* **426**, 413–418.

Whitelegge, J. P., Zhang, H., Aguilera, R., Taylor, R. M., and Cramer, W. A. (2002). Full subunit coverage liquid chromatography electrospray ionization mass spectroscopy (LCMS+) of an oligomeric membrane protein: Cytochrome b_6f complex from spinach and the cyanobacterium *Mastigogladus laminosus*. *Mol. Cell. Proteomics* **1**, 816–827.

Wollmann, F.-A., Minai, L., and Nechushtai, R. (1999). The biogenesis and assembly of photosynthetic proteins in the thylakoid membranes. *Biochim. Biophys. Acta* **1411**, 21–85.

Zito, F., Finazzi, G., Delosme, R., Nitschke, W., Picot, D., and Wollman, F. A. (1999). The Qo site of cytochrome b_6f complex controls the activation of the LHCII kinase. *EMBO J.* **18**, 2961–2969.

Biography

Günter Hauska is a Professor of Cell Biology and Plant Physiology at the Institute of Botany, in the Department of Biology at the University of Regensburg, Germany. He obtained his Ph.D. in Chemistry at the

University of Vienna in 1967. Subsequently he served as Postdoctoral Fellow in the Biochemistry Department of the Cornell University, before qualifying as Dozent for Biochemistry at the Ruhr-Universität in Bochum, Germany. His research interest is in energy transduction by membrane protein complexes of electron transport chains, especially in quinol oxidation by cytochrome *bc*-complexes and in photosynthetic reaction centers. In recent years he turned to flavoproteins. He is a member of the German Society for Biochemistry and Molecular Biology.

Thomas Schödl graduated in chemistry at the University of Regensburg and finished his Ph.D. in Biochemistry. He is studying the structure and redox reactions of flavoproteins, in particular of the sulfide quinone reductases from bacteria and eukaryotes.

Cytochrome bc_1 Complex (Respiratory Chain Complex III)

Bernard L. Trumpower
Dartmouth Medical School, Hanover, New Hampshire, USA

The cytochrome bc_1 complex (ubiquinol:cytochrome *c* oxidoreductase complex, E.C. 1.10.2.2) is an energy-transducing, electron transfer enzyme located in the inner mitochondrial membrane of oxygen utilizing eukaryotic cells, where it participates in cell respiration. A functionally similar but structurally simpler version of the bc_1 complex is located in the plasma membrane of many, but not all, bacteria, where it takes part in respiration, denitrification, nitrogen fixation, and cyclic photosynthetic electron transfer, depending on the species. In all of these organisms the bc_1 complex oxidizes a membrane-localized quinol and reduces a water-soluble, *c*-type cytochrome and links this redox reaction to translocation of protons across the membrane in which the bc_1 complex resides. The bc_1 complexes from mitochondria of several species have been crystallized and the mechanism of the enzyme is generally well understood, although some questions remain outstanding.

Function of the bc_1 Complex

The cytochrome bc_1 complex participates in respiration in oxygen utilizing cells and also participates in electron transfer in numerous bacteria that utilize alternative terminal-electron acceptors in addition to oxygen. The functional relationship of the bc_1 complex to other redox enzymes in these linked electron-transfer systems is illustrated in Figure 1. In mitochondria the bc_1 complex is a confluence point for reducing equivalents from the various dehydrogenases and it is essential for mitochondrial respiration, since there is no alternative route to oxidize ubiquinol by molecular oxygen. Bacteria such as *Paracoccus denitrificans* that have a bc_1 complex usually have alternative mechanisms to oxidize ubiquinol or otherwise bypass the bc_1 complex. Consequently, the enzyme is not essential in these organisms. Hydroxyquinone analogues of ubiquinone, such as atovaquone, inhibit the bc_1 complex and are used therapeutically against fungal (e.g., pneumocystis) and parasitic (e.g., malaria) infections, but are ineffective against bacteria in which the enzyme is not essential. In some photosynthetic bacteria, such as *Rhodobacter*, the bc_1 complex is essential for cyclic photosynthetic electron transfer in the absence of a terminal electron acceptor, but is not essential when the cells are growing heterotrophically. In all of these organisms the bc_1 complex is located in the organelle or plasma membrane and converts the energy associated with electron transfer from ubiquinol to cytochrome *c* into an electrochemical proton gradient across the membrane in which the enzyme resides. The resulting protonmotive force is used by the cell for energy-requiring reactions, including ATP synthesis, ion and metabolite transport, and flagellar motion.

Structure, Composition, and Properties of the bc_1 Complex

Protein Subunits

All cytochrome bc_1 complexes contain three protein subunits with redox prosthetic groups, a diheme cytochrome *b* containing a relatively high-potential b_H heme and a lower potential b_L heme, cytochrome c_1, and a Rieske iron–sulfur protein with a 2Fe–2S cluster. In some bacteria, such as *Paracoccus denitrificans* and *Rhodospirillum rubrum*, the bc_1 complex contains only these three subunits. Other bacteria, including the *Rhodobacter*, contain a fourth subunit of unknown function that lacks prosthetic groups. *Rhodobacter* can adapt to grow photosynthetically when this subunit is absent, but the stability of the enzyme is compromised, suggesting at least a structural role.

The cytochrome bc_1 complexes of mitochondria contain as many as seven or eight supernumerary subunits. The enzyme from *Saccharomyces cerevisiae* contains ten subunits, while those from bovine heart and *Schizosaccharomyces pombe* contain 11. The difference between the 10- and 11-subunit enzymes is due to the fact that the 11-subunit enzymes contain one small subunit that is formed when the presequence that targets the Rieske protein to the mitochondria is cleaved from the protein. The cleaved presequence is retained in the

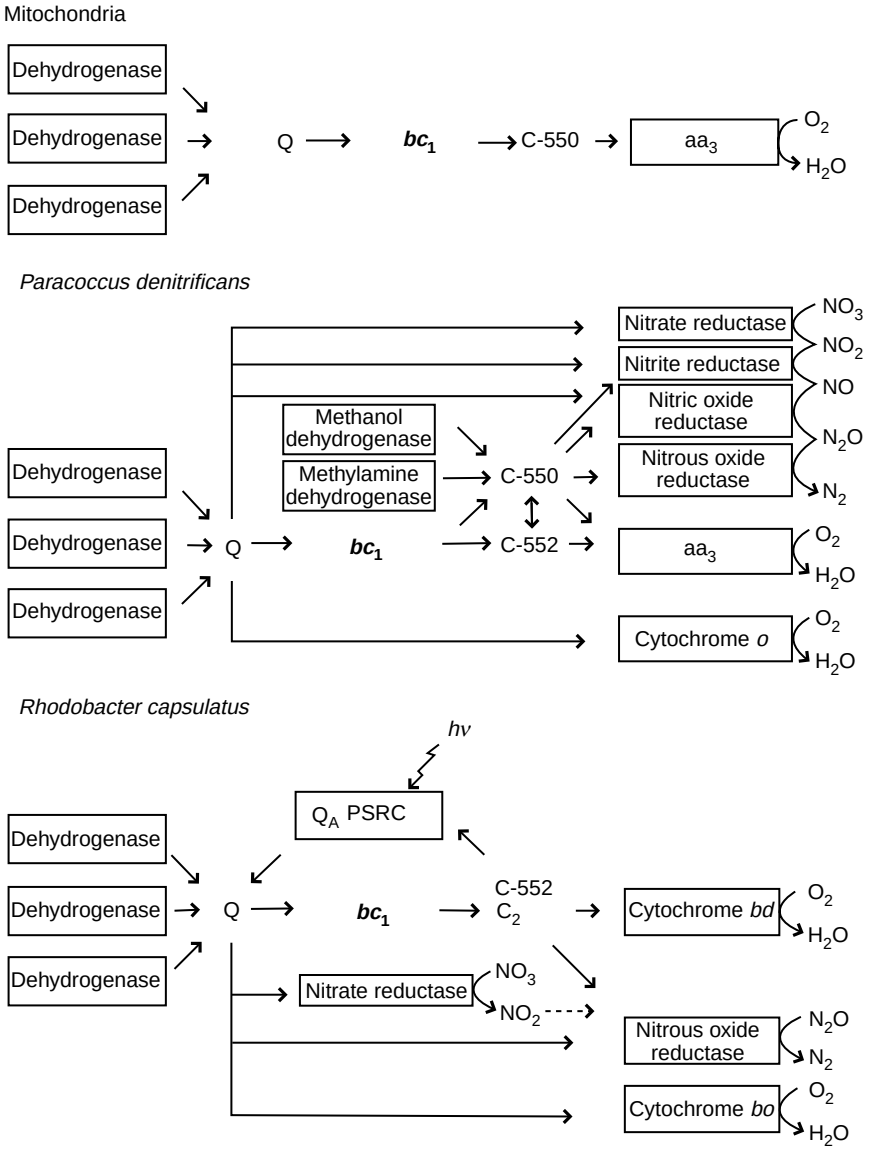

FIGURE 1 Function of the cytochrome bc_1 complex in mitochondria and bacteria. In mitochondria the bc_1 complex oxidizes ubiquinol that is formed by reduction of ubiquinone by various dehydrogenases including glycerol phosphate dehydrogenase, succinate dehydrogenase, NADH dehydrogenase, and ETF dehydrogenase. In bacteria such as *Paracoccus dentrificans*, ubiquinol can be oxidized by various routes that bypass the bc_1 complex, including a terminal oxidase, cytochrome o, which oxidizes ubiquinol directly, without the intervention of cytochrome *c* and cytochrome *c* oxidase. These bacteria can also use alternative terminal electron acceptors, such as nitrate, in which case the bc_1 complex is also not essential for electron transfer from the quinol. In photosynthetic bacteria such as the *Rhodobacter* the bc_1 complex participates in cyclic electron transfer when the bacteria are grown photosynthetically, and is essential under those growth conditions. However, *Rhodobacter* can also grow heterotrophically on a variety of nutrients and can use either oxygen or nitrogen in the form of nitrate and nitrous oxide as terminal electron acceptor. Under these conditions the ubiquinol that is formed by the various dehydrogenases can be oxidized by the bc_1 complex and electrons transferred via the *c* cytochromes to oxygen or nitrous oxide, or electrons from the quinol can bypass the *c*-cytochrome pool and be transferred directly to nitrate, nitrous oxide, or oxygen.

bc_1 complex as an additional subunit. In *Saccharomyces cerevisiae*, the presequence is cleaved from the Rieske protein in two steps and degraded, thus that bc_1 complex contains only 10 subunits.

The functions of the supernumerary subunits in the mitochondrial enzymes are not known. They are not required for the electron transfer and proton translocation activities of the enzyme, since the three-subunit enzyme from *Paracoccus* has the same electron transfer and proton translocation functionality as the mitochondrial enzymes. Possible functions for these nonredox subunits include docking sites for ternary complex formation with the dehydrogenase and oxidase complexes, regulation of half-of-the-sites activity of the

dimeric enzyme, structural stability in the relatively long-lived eukaryotes, and protection against oxygen radicals.

Spectroscopic and Thermodynamic Properties of the bc_1 Complex

The bc_1 complex is visibly red due to the cytochromes. Optical spectra of the yeast enzyme in the visible region of the spectrum are shown in Figure 2. When the enzyme is reduced by dithionite, a difference spectrum of the dithionite reduced versus ferricyanide oxidized enzyme exhibits an absorption maximum at 562 nm due to ferro-cytochrome b and a shoulder at ~553 nm due to ferro-cytochrome c_1. When the enzyme is reduced with ascorbic acid, the reduced versus ferricyanide oxidized difference spectrum consists of only cytochrome c_1, with a maximum at 553 nm (Figure 2B). The extinction coefficient of reduced versus oxidized cytochrome c_1 at 553 nm versus 539 nm is 17.5 $mM^{-1}\,cm^{-1}$, which was obtained from the purified protein. By subtracting the spectrum of c_1 from that of $b+c_1$, it is possible to derive a calculated difference spectrum of the cytochrome b as shown in Figure 2C. The extinction coefficient of reduced versus oxidized cytochrome b at 562 versus 575 nm is 25.6 $mM^{-1}\,cm^{-1}$, which was determined by measuring the fluorescence quenching upon stoichiometric binding of antimycin to the bovine enzyme. This value is an average of the two b hemes. The individual extinction coefficients of the b_H and b_L hemes have not been determined for most bc_1 complexes, but the contribution from the b_H heme at 562 is significantly greater than that from the b_L heme, which has a split absorption maximum with peaks at 564–566 and ~558 nm.

The Rieske iron–sulfur protein is a pale yellow-gold color when isolated from the bc_1 complex in the oxidized form but bleached to colorless when reduced and thus makes no contribution to the optical spectrum of the reduced enzyme. The redox status of the 2Fe–2S cluster is monitored by electron paramagnetic resonance (EPR) spectroscopy since the reduced cluster is paramagnetic. The Rieske cluster exhibits a unique EPR spectrum with peaks at approximately $g_x = 1.76$, $g_y = 1.90$, and $g_z = 2.03$, resulting in $g_{av} = 1.90–1.91$, which is atypical of binuclear iron–sulfur clusters. The unusual EPR spectrum of the Rieske protein is due to bis-histidine coordination of one of the two iron atoms, which was first suggested by spectroscopic studies and confirmed by crystal structures of the enzyme.

The midpoint potentials of the redox centers in the bc_1 complex determine the thermodynamic parameters and in some cases control electron transfer reactions within the enzyme. In *Saccharomyces cerevisiae* the midpoint potentials at pH 7 are as follows: cytochrome c_1, +240 mV; Rieske iron–sulfur cluster, +280 mV; cytochrome b_H, +120 mV; and cytochrome b_L, −30 mV. Although there are species differences in these midpoint potentials it is generally true that the midpoint potential of the Rieske center is ~20–40 mV more positive than that of c_1, and that of the b_L heme is 60–120 mV lower than that of the b_H heme. The midpoint potentials of the b hemes are influenced by the detergents used to purify the enzyme, and may be similarly influenced by bound phospholipids. The midpoint potential at pH 7 of ubiquinone is +90 mV in the membrane, but this value may be altered by preferential binding of either quinone or quinol to reaction sites in the enzyme. These midpoint potentials result in a thermodynamic profile of the bc_1 complex as shown in Figure 3.

Three-Dimensional Structure of the bc_1 Complex

Cytochrome bc_1 complexes from bovine, chicken, and yeast mitochondria have been crystallized and their structures solved to atomic resolution. The yeast enzyme, shown in Figure 4, is the highest resolution structure available at this time. The mitochondrial bc_1

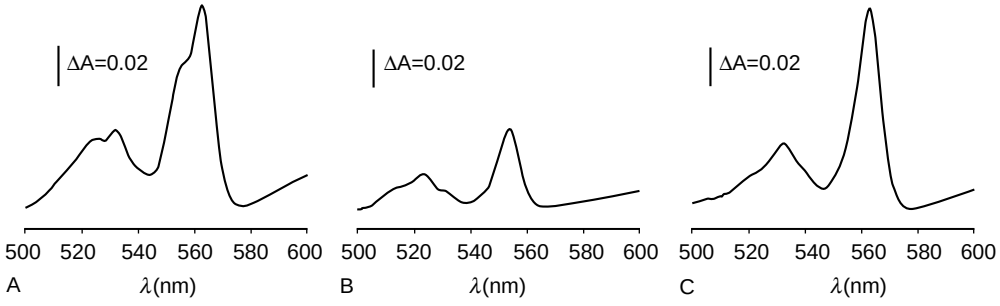

FIGURE 2 Optical spectra of the yeast cytochrome bc_1 complex. Difference spectra of (A) the dithionite reduced versus ferricyanide oxidized enzyme and (B) the ascorbate reduced versus ferricyanide oxidized enzyme. (C) Calculated difference spectrum, obtained by subtracting the spectrum of the ascorbate reduced enzyme from the spectrum of the dithionite reduced enzyme.

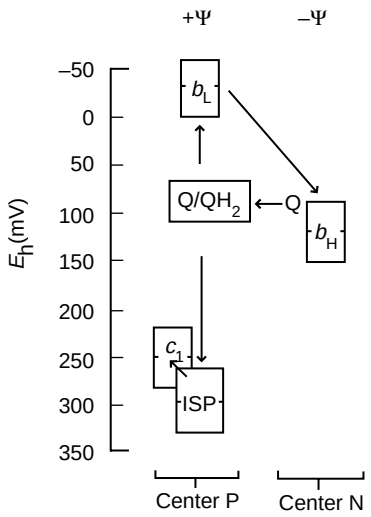

FIGURE 3 Thermodynamic profile of the *Saccharomyces cerevisiae* cytochrome bc_1 complex. The figure illustrates the thermodynamic relationship between the redox components of the cytochrome bc_1 complex. Arrows indicate electron transfer reactions in the enzyme. The redox groups are arranged vertically according to their oxidation–reduction potentials, with the center of the boxes positioned vertically at the midpoint potentials of the redox groups. The open boxes depict the approximate range of potentials spanned by the redox components as their oxidation–reduction status varies in response to changes in rates of electron transfer. The midpoint potentials of the redox components are cytochrome b_L, −30 mV, cytochrome b_H, +120 mV, cytochrome c_1, +240 mV, and Rieske iron–sulfur protein, +280 mV.

complex is a symmetrical, oligomeric dimer, in which the three redox subunits are surrounded by a periphery of nonredox, supernumerary subunits. The dimeric structure of the enzyme was suspected from hydrodynamic measurements and confirmed by the first crystal structure of the bovine enzyme. Although the bacterial enzyme has not yet been crystallized, it will presumably turn out to be a dimeric structure too, but lacking the large number of supernumerary subunits.

One unusual aspect of the dimeric structure is that the iron–sulfur protein spans the dimer. The Rieske protein is anchored in one monomer by a single transmembrane helix, as shown in Figure 4A, while the peripheral domain that contains the 2Fe–2S cluster is located in the other monomer, where it forms part of the ubiquinol oxidation site. Crystal structures of the chicken bc_1 complex in the absence and presence of stigmatellin, an inhibitory ligand, also provided striking evidence that the peripheral domain of the Rieske protein moves back and forth between positions proximal to cytochrome *b* and cytochrome c_1. This suggested that movement of the Rieske protein facilitates electron transfer, which was confirmed by site-directed mutagenesis studies that demonstrated that such movement of the Rieske protein was essential for enzyme activity.

Functionally the enzyme consists of the cytochrome *b* and c_1 subunits from one monomer and the Rieske protein from the other, as shown in Figure 4B. The crystal structures established the location of the sites of ubiquinol oxidation and ubiquinone reduction at topographically separated sites within the enzyme. The structures also confirmed the transmembrane disposition of the *b* hemes, which form a conduit through which electrons are cycled across the membrane in which the enzyme resides. These structural details provided the final confirmatory evidence of the protonmotive Q cycle mechanism of the enzyme.

Mechanism of the Enzyme

The Protonmotive Q Cycle

The bc_1 complex oxidizes ubiquinol and transfers two electrons to two molecules of cytochrome *c*. During this electron transfer reaction two protons are taken up from the mitochondrial matrix or bacterial cytoplasm and four protons are deposited on the other side of the membrane. The mechanism by which the bc_1 complex links the electron transfer and proton translocation reactions is the protonmotive Q cycle, shown in Figure 5. In the Q cycle mechanism proton translocation is the net result of topographically segregated reduction of quinone and reoxidation of quinol on opposite sides of the membrane, with protons being carried across the membrane as hydroxyl hydrogen atoms on the quinol. The sites where quinone is reduced and quinol is oxidized are referred to as center N and center P, respectively, since they are located toward the electronegative and electropositive sides of the membrane. Protons are taken up at center N, carried across the membrane by the quinol, and released at center P.

In the first step of the Q cycle, ubiquinol is oxidized at center P in a reaction that divergently transfers the two electrons from ubiquinol to the Rieske iron–sulfur cluster and the cytochrome b_L heme (reactions 1a–1c in Figure 5). In reaction 2 the reduced Rieske cluster oscillates to within electron transfer distance of cytochrome c_1 and an electron is transferred from the iron–sulfur cluster to the c_1 heme. Two protons are released from center P coincident with ubiquinol oxidation. In reaction 3 an electron is transferred from the b_L to b_H heme, which in turn reduces ubiquinone to ubisemiquinone (reaction 4). Following oxidation of a second ubiquinol at center P and reduction of the *b* cytochromes the b_H heme reduces ubisemiquinone to ubiquinol (reaction 5), accompanied by uptake of two protons at center N.

There is evidence that the mitochondrial bc_1 complex functions by an alternating-sites mechanism, in which binding of ubiquinol in one monomer exerts negative cooperativity on binding of ubiquinol in the other

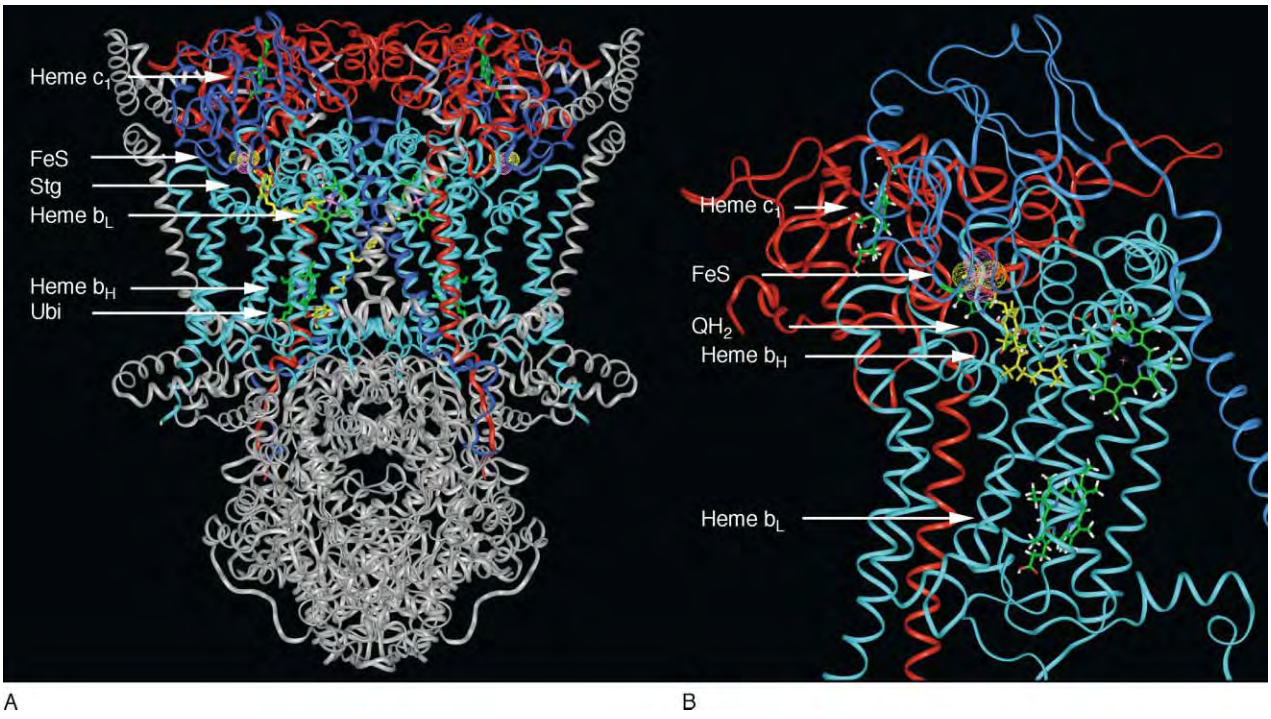

FIGURE 4 Crystal structure of the cytochrome bc_1 complex. The structure in (A) is of the yeast bc_1 complex with stigmatellin bound, resolved to 2.3Å by Hunte and co-workers, and shows all of the subunits of the enzyme dimer, except subunit 10, which is lost during purification. The structure is oriented so that the mitochondrial matrix would be at the bottom and the intermembrane space at the top of the figure. Cytochrome *b* is colored cyan, cytochrome c_1 red, and the Rieske protein blue. The supernumerary subunits are colored gray. The heme groups (heme b_L and heme b_H) are shown as stick structures, colored green. Stigmatellin (Stg) bound at center P in only one monomer is shown as a stick structure, with carbon atoms colored yellow and oxygen atoms red. Ubiquinone (Ubi) bound at center N in only one monomer is also shown as a stick structure, with carbon atoms colored yellow and oxygen atoms red. The iron–sulfur cluster (FeS) is shown with its van der Waals radius, with iron atoms colored purple and sulfur atoms colored yellow. The structure in (B) is of a functional monomer, consisting of cytochrome *b* and cytochrome c_1 from one monomer and the Rieske protein from the other. Ubiquinol (QH_2) containing two isoprenyl groups is hydrogen bonded between His181 of the Rieske protein and Glu272 of cytochrome *b* to form a putative electron-donor complex. An energy-minimized structure of the docked quinol was obtained by replacing stigmatellin in the crystal structure, followed by molecular dynamics and energy minimization calculations. The protein subunits, heme groups, and ubiquinol are colored as in (A).

monomer. If the enzyme can be switched from a form in which ubiquinol oxidation alternates between the two monomers to a form where both monomers are simultaneously active, it would provide a mechanism to regulate the activity of the enzyme, perhaps in response to cellular energy needs. Whether such a regulatory mechanism exists and, if so, how it operates, is not known.

Proton Conduction Pathways

In the Q cycle mechanism, protons are carried across the membrane as hydrogen atoms on the hydroxyl groups of ubiquinol. However, the sites where ubiquinol is oxidized at center P and ubiquinone is reduced at center N are not freely accessible to the bulk aqueous phase at the membrane surface. Consequently, the linkage of proton chemistry to electron transfer requires mechanisms for moving protons to and from the aqueous phase and the hydrophobic sites of quinol and quinone redox reactions.

The crystal structures of the bc_1 complex with bound stigmatellin (Figure 4A) show that the inhibitor is hydrogen bonded between His181 (in the yeast numbering system) of the Rieske protein, which is a ligand to the iron-sulfur cluster, and Glu272 of cytochrome *b*. Since stigmatellin presumably mimics an intermediate in ubiquinol oxidation, this suggests that ubiquinol forms an electron-donor complex involving hydrogen bonds between the quinol hydroxyl groups and these two amino acids, as shown in Figure 4B.

When ubiquinol reduces the Rieske protein, an electron is transferred to the iron–sulfur cluster, while a proton from the quinol hydroxyl group protonates the imidazole nitrogen on His181 of the Rieske protein. The Rieske protein acts as a hydrogen carrier and releases the proton to the aqueous phase when it moves proximal to cytochrome c_1 and is oxidized. The second proton from ubiquinol is transferred to Glu272 and then to a propionate of the cytochrome *b* heme as an electron is transferred to the b_L heme. From the crystal structure of the yeast enzyme it appears that this proton can then

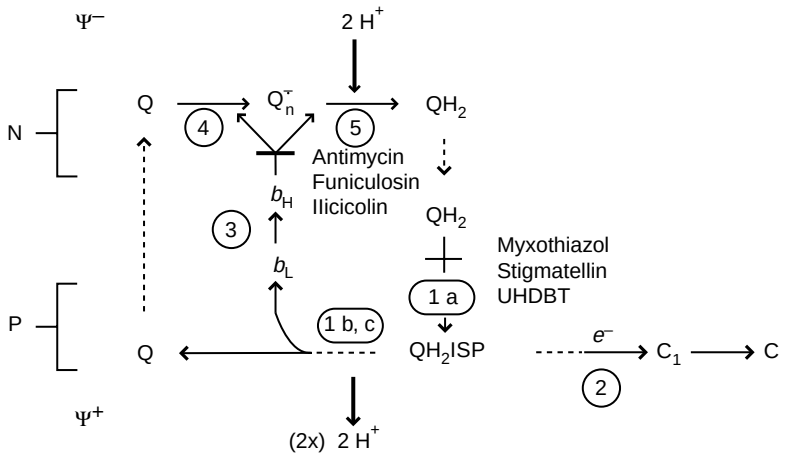

(1a) $QH_2 + ISP \rightleftharpoons QH_2ISP$

(1b) $QH_2\ ISP + b_L \rightleftharpoons QH_2ISP\ b_L$

(1c) $QH_2\ ISP\ b_L \rightleftharpoons Q + ISP^-H^+ + b_L^-H^+$

(2) $ISP^-H^+ + c_1 \rightleftharpoons ISP + c_1^- + H^+$

(3) $b_L^-H^+ + b_H \rightleftharpoons b_L + b_H^- + H^+$

FIGURE 5 Mechanism of electron transfer through the cytochrome bc_1 complex. The scheme shows the pathway of electron transfer from ubiquinol to cytochrome *c* through the redox centers of the cytochrome bc_1 complex. The circled numbers designate electron transfer reactions. Dashed arrows designate movement of ubiquinol (QH_2) or ubiquinone (Q) between center P on the positive side of the membrane and center N on the negative side of membrane, and movement of the iron–sulfur protein between cytochrome *b* and cytochrome c_1. Solid black bars indicate sites of inhibition by antimycin, funiculosin, ilicicolin, myxothiazol, UHDBT, and stigmatellin. In reaction 1, ubiquinol oxidation delivers two electrons divergently to the Rieske iron–sulfur cluster and the b_L heme, two protons are released, and the resulting ubiquinone leaves center P. In reaction 2, the reduced Rieske cluster oscillates to within electron transfer distance of cytochrome c_1, resulting in electron transfer from the iron–sulfur cluster to the c_1 heme. In reaction 3, an electron is transferred from the b_L to b_H heme, which in turn reduces ubiquinone to ubisemiquinone (reaction 4). Following oxidation of a second ubiquinol at center P and reduction of the *b* cytochromes the b_H heme reduces ubisemiquinone to ubiquinol (reaction 5), accompanied by uptake of two protons at center N.

access the aqueous surface from the b_L heme via a conserved arginine (Arg79). In this manner two protons are released from center P with minimal charge separation as the two electrons are divergently transferred from the quinol to the high potential and low-potential electron acceptors (Figure 3).

The crystal structure of the yeast enzyme has also revealed pathways for conduction of two protons into center N. One of these pathways, the (CL)/K pathway, involves a conserved lysine and a bound cardiolipin, which may function as a buffer to concentrate protons at the entrance to the pathway. The second proposed proton conduction pathway at center N is referred to as the E/R pathway and involves a conserved glutamate and a conserved arginine. The high resolution of the yeast crystal structure also reveals that one or two bound water molecules may serve as direct proton donors during quinone reduction. Notably, whereas ubiquinol oxidation at center P proceeds with minimal charge separation, ubiquinone reduction at center N begins with substantial charge separation as electrons and protons enter the reaction site from opposite directions, and the redox reaction is accompanied by charge compensation, which enhances the reaction rate.

Inhibitors

There are numerous inhibitors that act on the cytochrome bc_1 complex and that bind specifically to either the ubiquinol oxidation site at center P or the ubiquinone reduction site at center N. These have proven to be especially useful in establishing the mechanism of the enzyme and for selectively blocking electron transfer reactions at either of the two reaction sites in the enzyme to facilitate kinetic analysis. In addition, some of the inhibitors have antifungal and antiparasitic activity.

Antimycin, funiculosin, and ilicicolin H are produced by micro-organisms as defensive toxins and inhibit the bc_1 complex by binding to center N with near stoichiometric affinity. Under conditions of catalytic turnover, they block reduction of ubiquinone by cytochrome *b* by

binding to the ubiquinone reduction pocket at a site proximal to the b_H heme, causing electrons to accumulate in the *b* hemes. Under presteady-state conditions where the enzyme is reduced by ubiquinol they block reduction of the b_H heme by quinol.

Stigmatellin, also produced by a micro-organism, inhibits the bc_1 complex by binding to the ubiquinol oxidation pocket, simultaneously forming hydrogen bonds to the imidazole nitrogen of His181 on the Rieske protein and a carboxyl oxygen of Glu272 on cytochrome *b*. In this manner the inhibitor locks the Rieske protein in a conformation proximal to cytochrome *b*. Stigmatellin raises the midpoint potential and shifts the EPR spectrum of the iron–sulfur cluster, indicative of its interaction with the Rieske protein.

Hydroxyquinones such as UHDBT, a benzoxythiazole (3-undecyl-2-hydroxy-1,4-benzoxythiazole) and atovaquone, a hydroxynaphthoquinone (2-[trans-4-(4′-chlorophenyl) cyclohexyl]-3-hydroxy-1,4 hydroxynaphthoquinone) also bind to the ubiquinol oxidation pocket and form a hydrogen bond to His181 of the Rieske protein. Like stigmatellin these ligands raise the midpoint potential and change the EPR spectrum of the iron–sulfur cluster. However, the hydroxyquinone inhibitors do not hydrogen bond to Glu272 of cytochrome *b*. Instead, the crystal structure of the yeast bc_1 complex with an analogue of UHDBT bound shows Glu272 rotated toward the heme propionate, which suggested the proton conduction pathway described above.

Methoxyacrylates, such as myxothiazol, also bind to the ubiquinol oxidation pocket but do not interact directly with the Rieske protein. These inhibitors bind proximal to the b_L heme and affect its spectral and thermodynamic properties.

See Also the Following Articles

Heme Proteins • Heme Synthesis • JAK-STAT Signaling Paradigm • Membrane-Associated Energy Transduction in Bacteria and Archaea • Mitochondrial DNA • Respiratory Chain and ATP Synthase • Ubiquitin-Like Proteins

Glossary

protonmotive Q cycle The mechanism of electron transfer by which the cytochrome bc_1 complex transfers electrons from ubiquinol to cytochrome *c* and links the electron transfer to proton translocation. The mechanism is so-named, because the enzyme oxidizes ubiquinol on one side of the membrane and re-reduces ubiquinone on the other side in a cyclic manner, thus bringing about transmembrane movement of protons, carried through the membrane as hydrogen's on the quinol hydroxyl groups.

ubiquinone 2,3-dimethoxyl-5-multiprenyl-6-methyl-1,4-benzoquinone, where the multiprenyl group is an isoprenoid side chain consisting of 6–10 isoprenyl groups, is a lipid-soluble benzoquinone that is reduced to quinol by various dehydrogenases and reoxidized to quinone by the cytochrome bc_1 complex.

Further Reading

Hunte, C., Koepke, J., Lange, C., Roßmanith, T., and Michel, H. (2000). Structure at 2.3 angstrom resolution of the cytochrome bc_1 complex from the yeast *Saccharomyces cerevisiae* co-crystallized with an antibody Fv fragment. *Structure* **8**, 669–684.

Link, T. A. (1999). The structures of Rieske and Rieske-type proteins. *Adv. Inorg. Chem.* **47**, 83–157.

Trumpower, B. L. (1990). The protonmotive Q cycle: Coupling of proton translocation to electron transfer by the cytochrome bc_1 complex. *J. Biol. Chem.* **265**, 11409–11412.

Von Jagow, G., and Link, T. A. (1986). Use of specific inhibitors of the mitochondrial bc_1 complex. *Methods Enzymol.* **126**, 253–271.

Zhang, Z. L., Huang, L. S., Shulmeister, V. M., Chi, Y. I., Kim, K. K., Hung, L. W., Crofts, A. R., Berry, E. A., and Kim, S. H. (1998). Electron transfer by domain movement in cytochrome bc_1. *Nature* **392**, 677–684.

Biography

Bernard L. Trumpower is a Professor of Biochemistry at Dartmouth Medical School. His principal research interest is the function of the cytochrome bc_1 complex. Dr. Trumpower received his Ph.D. from St. Louis University and did his postdoctoral training at Cornell University with Prof. Efraim Racker. Dr. Trumpower has been an established investigator of the American Heart Association and received a Merit Award from the National Institutes of Health. He has authored more than 100 original research articles on the cytochrome bc_1 complex, and in 1984 he was awarded the Humboldt Prize by the Federal Republic of Germany for his contributions to understanding the enzymology of respiratory enzymes.

Cytochrome *c*

Hans Tuppy and Günther Kreil
University of Vienna, Vienna, Austria

Cytochrome *c* is a heme protein that is present in and can easily be isolated from mitochondria of all eukaryotic organisms. The amino acid sequence of the protein moiety was among the first sequences which could be elucidated. This was the starting point for comparative studies about sequence variations found in cytochrome *c* from a wide range of species. A phylogenetic tree constructed on the basis of this information was found to be biologically significant and became exemplary for subsequent studies on molecular evolution. The function of cytochrome *c* in the respiratory chain as an electron carrier is well established. More recently, an additional role of cytochrome *c* was discovered: its release from mitochondria into the cytosol triggers apoptosis – the programmed cell death.

Introduction

Cytochromes are proteins which contain heme as their prosthetic group and whose principal biological function, in the cells of animals, plants, and microorganisms, is electron transport. The foundations of the knowledge of heme proteins and their roles as electron carriers in cell respiration were laid by David Keilin (1887–1963), ~80 years ago. In the cytochromes, the iron which is coordinately linked with four nitrogens within the prosthetic group and with two additional ligands provided by the protein moiety, can alternate between a reduced Fe^{2+} and an oxidized Fe^{3+} state. Different classes of cytochromes (*a*-type, *b*-type, *c*-type) differ in the nature of their heme prosthetic groups. They can be observed and differentiated spectroscopically, on the basis of characteristic absorption bands. The absorption peaks of reduced cytochrome *c* and other *c*-type cytochromes (such as c_1) are at ~550, 520, 416, and 270 nm. The *b*-type and *a*-type cytochromes absorb visible light at higher wavelengths. In eukaryotic cells, cytochromes of types *a*, *b*, and *c* are found predominantly within mitochondria. In the mitochondrial respiratory chain, cytochrome *c* accepts electrons from complex III, which contains cytochromes *b* and c_1 (bc_1), and transmits them to complex IV (cytochrome oxidase), which has two heme prosthetic groups (aa_3). These respiratory complexes, with their respective cytochromes, are firmly integrated in the inner membrane of the mitochondrion. Cytochrome *c*, by contrast, is only loosely bound in the space between the inner and outer mitochondrial membranes and shuttles between bc_1 and aa_3. As shown by Keilin and others, cytochrome *c* can be easily removed experimentally from and reincorporated into isolated mitochondria, their respiratory capacity thereby being impaired and restored, respectively. It has recently been discovered that the release of cytochrome *c* from mitochondria into the cytoplasm is an important step in programmed cell death. This participation in apoptosis of eukaryotic cells is now considered to be another significant function of cytochrome *c*.

Cytochrome *c* and *c*-type cytochromes occur in all eukaryotic organisms. The comparative analysis of the protein structures of cytochromes isolated from a multitude of different species of organisms has made it possible to establish evolutionary relationships between them. The phylogenetic tree based on the slow changes of the structure of cytochrome *c* in the course of evolution is most impressive and biologically relevant.

The *c*-type cytochromes are also present in prokaryotes, where they may function in a respiratory chain or in photosynthesis. Examples are cytochrome c_2 from *Rhodospirillum rubrum* (purple bacteria) and cytochrome c_{551} from *Pseudomonas aeroginosa* (gram-negative bacteria). These are distantly related to mitochondrial cytochromes *c*; however, a more detailed discussion of these diverse hemoproteins is outside the scope of this article.

Attachment of the Heme Prosthetic Group to Cytochrome *c* Apoprotein

The prosthetic group of *c*-type cytochromes, such as cytochrome *c* and c_1 in mitochondria and cytochrome *f* in chloroplasts, unlike that of *a*- and of *b*-type cytochromes, is covalently linked to the polypeptide moiety. The thiol groups of two cysteinyl residues in a Cys-X-Y-Cys-His peptide motif are attached to two vinyl groups of heme through thioether bonds.

This linkage is resistant to heat and hydrolysis, but can be broken with the help of silver or mercury salts. Thus, the polypeptide moiety of cytochrome *c*, or of heme peptides derived from it by proteolytic cleavage, could be obtained. In eukaryotic cells, the apoprotein of cytochrome *c* is encoded by a nuclear gene, translated on cytoplasmic ribosomes and translocated into the intermembrane space of mitochondria, where an enzyme, cytochrome *c* heme lyase, combines it with heme. An *in vitro* synthesis of a microbial *c*-type cytochrome from its apoprotein and reduced heme has recently been achieved.

Amino Acid Sequence Studies

Cytochrome *c* is a small, water-soluble protein that can easily be isolated and purified from cells and tissues of many different eukaryotic organisms. In proteolytic digests of cytochrome *c*, one fragment containing the covalently linked heme group can be separated from all the other ones. Studies on the amino acid sequence of these heme peptides isolated from cytochromes *c* of diverse origin thus became feasible. It turned out that certain sequence elements, like the one mentioned in the introduction were highly conserved from yeast to mammalian cytochromes *c*.

Expanding on this early work, cytochrome *c* from horse heart was one of the first proteins whose complete amino acid sequence could be determined. It consists of a single polypeptide chain of only 104 residues that could be analyzed even with, by modern standards, rather primitive tools available around 1960. The protein contains many (up to 19) lysine residues, whose positive charges can form ionic bonds with constituents of the inner mitochondrial membrane.

With the horse sequence as a reference, cytochrome *c* isolated from diverse species was subsequently analyzed in quick succession. These included other mammals (human, rhesus monkey, pig, dog, rabbit, whale, and kangoroo), birds (chicken, pigeon, king penguin, turtle), reptiles (rattlesnake, alligator), amphibia (bullfrog), fish (tuna, carp, dogfish) and the chordate pacific lamprey. And with unabated pace, additional sequences were determined for cytochromes *c* from flies, moths, yeasts, Neurospora, and a large variety of plants. By now, we know the sequence of this protein from more than 100 eukaryotic species. As a result of these efforts, cytochrome *c* became the first and still is a standard example for studies on the molecular evolution of proteins. Nuclear genes encoding cytochrome *c* have been analyzed from various species. The mammalian gene contains a small intron in the coding sequence and a larger one upstream of the initiation codon.

The recent progress in the sequencing of whole eukaryotic genomes has also yielded information about the number of cytochrome *c* genes in various species. For example, in the human genome, a single gene for cytochrome *c* is present on chromosome 7, along with 49 pseudogenes located on many different chromosomes. These are mostly processed pseudogenes, which were formed by retro-transcription of an mRNA. In rodents, two cytochrome *c* genes are expressed, one of them exclusively in the testis. This latter gene is still present as a pseudogene in the human genome.

Evolutionary Aspects

Cytochrome *c* is a highly conserved protein, which retained many structural characteristics over the eons of evolution of animals and plants. This makes it an ideal tool for amino acid sequence comparisons over a wide range of species (Figure 1). From the sequence differences, a molecular "pedigree" can be constructed based on the original assumption, now corroborated by many examples, that the longer ago the common

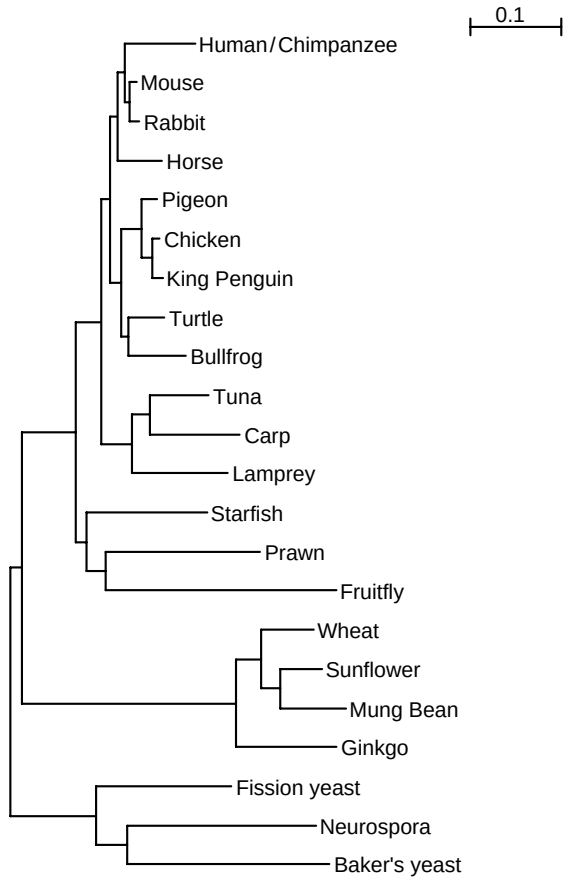

FIGURE 1 Phylogenetic tree constructed from the amino acid sequences of cytochrome *c* using the ClustalW program. The length of the branches corresponds to evolutionary distances (0.1 = 10% amino acid substitutions).

ancestor of two species existed, the more amino acid changes will have accumulated since. As it turned out, the phylogenetic trees constructed on the basis of the sequence of a single protein were surprisingly similar to those derived from comparative anatomy, fossils etc. Moreover, since cytochrome *c* could be extracted from species for which no reliable data were available from other sources, these could now also be included in this analysis.

In this comparison of cytochromes *c* from diverse eukaryotic species, it was found that more than a quarter of the amino acids have been conserved during more than a billion years of evolution. Among these immutable residues are the two cysteines to which the heme is bound via thioether linkages. The central iron of the planar heme is not only bound to four nitrogen atoms of the porphyrin but, in addition, to the side chains of two invariant amino acids of the protein, one being a histidine adjacent to the second cysteine (residue #18 in the vertebrate sequences), the other the sulfur atom of methionine 80, present on opposite sides. Moreover, certain amino acids with hydrophobic side chains, some of which line the crevice where the heme is buried, are also conserved. Surprisingly, it was found that several glycine residues in the sequence were also invariant. Glycine is the smallest amino acid containing only a hydrogen atom where the 19 others have more or less bulky side chains. From the three-dimensional structure, this first puzzling observation could be explained. At these sites, there is simply no space in this tightly folded protein and every other amino acid would presumably prevent proper folding of the polypeptide chain and thus be deleterious. Also, some charged amino acids, mostly lysines, have been conserved. These may be essential for the ionic interaction with two its reaction partners as well as with acidic phospholipids present in the inner mitochondrial membrane.

Three-Dimensional Structure

Using X-ray crystallographic analysis, the three-dimensional structure of tuna cytochrome *c* in its oxidized and reduced forms could be determined. As shown by these studies, the polypeptide chain is tightly wrapped around the heme, which sits in a deep pocket, exposed only on one edge to the solvent. In accordance with the "oil droplet" model of folded proteins, the hydrophobic amino acids are mostly buried inside the protein, some of them surrounding the heme. In the respiratory chain located in the inner membrane of mitochondria, cytochrome *c* shuttles between a reduced ferro-(Fe^{2+}) and ferri-(Fe^{3+}) form. In this redox cycle, the protein changes its conformation, with the reduced form having a more compact structure.

Interactions of Cytochrome *c* in the Respiratory Chain

Cytochrome *c* is loosely bound to the outer surface of the inner mitochondrial membrane. In the respiratory chain, an electron is transferred to cytochrome *c* from cytochrome bc_1. These cytochromes are part of a large, membrane-bound complex, also termed complex III composed of 11 proteins. Subsequently, the electron is delivered to the cytochrome aa_3 of the complex IV, the cytochrome oxidase, which contains 13 proteins. Some of the molecular details of this electron transport has recently also been clarified. In the crystal structure of the yeast cytochrome bc_1 complex with its bound substrate cytochrome *c*, the heme groups of cytochrome c_1 and *c* are in close proximity (see Figure 2). This suggests that the redox process takes place by direct heme-to-heme electron transfer. The same may also be true for the oxidation of cytochrome *c* by cytochrome aa_3.

In both redox reactions, a proton is pumped across the inner membrane. The proton gradient thus formed drives the ATP synthetase motor, which results in the synthesis of ATP.

Cytochrome *c* and Apoptosis

Cells that are damaged or are no longer needed may undergo a form of cell death that is controlled and executed by intracellular programs. One major apoptotic program involves the release of cytochrome *c* from the intermembrane space of mitochondria into the cytosol, together with some other mitochondrial proteins. Once in the cytoplasm, cytochrome *c* combines with an "apoptosis activating factor-1" (Apaf-1) and thus triggers the assembly of a multimeric protein complex, the so-called apoptosome. An inactive proform of a proteolytic enzyme, procaspase-9, is then recruited to the apoptosome and activated. Active caspase-9, in turn, activates other caspases, whose proteolytic actions finally lead to cell death. The crucial role of cytochrome *c* in this process is shown by the fact that microinjection of cytochrome *c* into the cytoplasm suffices to induce apoptosis in several cell lines. In the interaction with Apaf-1, as in the interaction with cytochrome c_1, the exposed heme edge of cytochrome *c* is involved.

When cytochrome *c* molecules are released from the mitochondrion, they have to pass through pores in the outer membrane of the organelle. A group of related proteins, the Bcl-2 family, regulates apoptosis by controlling the permeability of this membrane. Bcl-2 itself and other antiapoptotic proteins are located in the outer mitochondrial membrane and inhibit cytochrome *c* release. Conversely, release of cytochrome *c* is

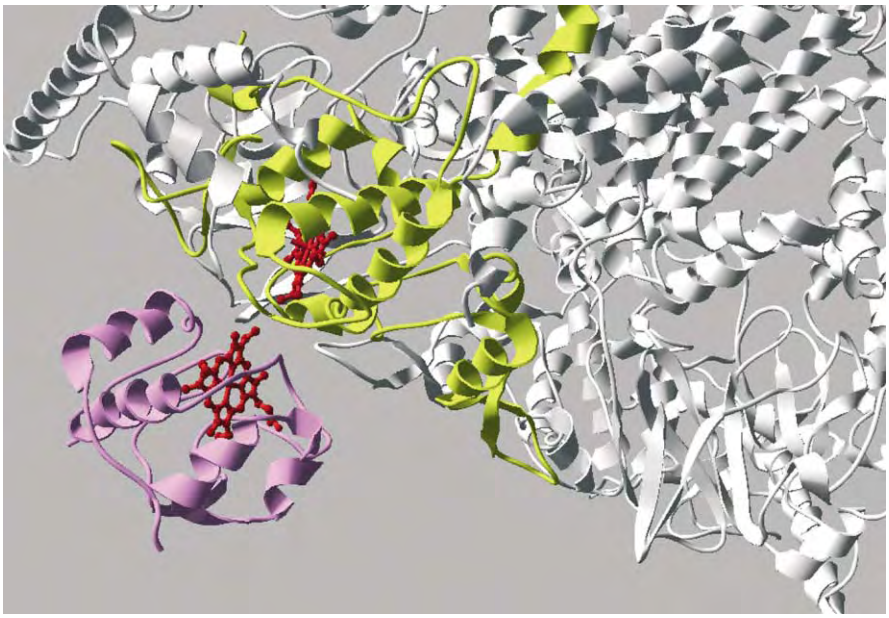

FIGURE 2 Part of the yeast cytochrome bc_1 complex and the bound substrate cytochrome *c* (Protein Data Bank, accession number 1KYO). Cytochrome c_1, yellow; cytochrome *c*, magenta; hemes, red.

triggered by proapoptotic members of the Bcl-2 family, which are induced by a number of stimuli to translocate to the mitochondria. Since one of the functions of apoptosis is to help the multicellular organism get rid of cancer cells, the pro- and antiapoptotic Bcl-2 family members are considered to be oncogenic and antioncogenic proteins, respectively. They control whether cytochrome *c*, besides being a vital mediator of electron transfer in respiration, also gets involved in cell death.

See Also the Following Articles

Cell Death by Apoptosis and Necrosis • Cytochrome Oxidases, Bacterial • Heme Proteins • Heme Synthesis • Purple Bacteria: Electron Acceptors and Donors • Purple Bacteria: Photosynthetic Reaction Centers

Glossary

apoptosis Also called "programmed cell death," a means for the multicellular organism to eliminate cells that are no longer needed or are damaged.

cytochromes Literally "cell pigments," heme proteins chiefly involved in cell respiration and energy supply.

heme An iron porphyrin complex that is attached (as a "prosthetic group") to protein moieties in the red blood pigment hemoglobin, in the cytochromes and in many other heme proteins.

mitochondria Intracellular organelles, the main site of oxidative metabolism which supplies the cell with utilizable energy in the form of ATP. In the course of cellular respiration, elementary oxygen is taken up by mitochondria and reduced to water. The electrons required for reduction are transmitted to oxygen via the respiratory chain, one of the electron transporters being cytochrome *c*.

Further Reading

Dickerson, R. E. (1972). The structure and history of an ancient protein. *Sci. Am.* (April issue), 58–70.

Dickerson, R. E. (1980). Cytochrome c and the evolution of energy metabolism. *Sci. Am.* (March issue), 98–109.

Hengartner, M. O. (2000). The biochemistry of apoptosis. *Nature* **407**, 770–776.

Lange, C., and Hunte, C. (2002). Crystal structure of the yeast cytochrome bc_1 complex with its bound substrate cytochrome *c*. *Proc. Natl. Acad. Sci. USA* **99**, 2800–2805.

Saraste, M. (1999). Oxidative phosphorylation at the *fin de siècle*. *Science* **283**, 1488–1493.

Slater, E. C. (2003). Keilin, cytochromes, and the respiratory chain. *J. Biol. Chem.* **278**, 16455–16461.

Zhang, Z., and Gerstein, M. (2003). The human genome has 49 cytochrome *c* pseudogenes, including a relic of a primordial gene that still functions in mice. *Gene* **312**, 61–72.

Biography

Hans Tuppy is Professor Emeritus and former Chairman of the Institute of Biochemistry at the University of Vienna, Austria. He worked, among other research topics, on the primary structure and species specificity of cytochrome *c*.

Günther Kreil worked in the Institute of Molecular Biology of the Austrian Academy of Sciences in Salzburg. His early work dealt with the amino acid sequence of horse and tuna cytochrome *c*.

Cytochrome Oxidases, Bacterial

Peter Brzezinski and Pia Ädelroth
Stockholm University, Stockholm, Sweden

Bacterial cytochrome *c* oxidases are integral membrane proteins that catalyze the four-electron reduction of dioxygen (O_2) to water and oxidation of different types of water-soluble or membrane-anchored cytochromes *c* (cyt.*c*). The oxygen-reducing site of the enzymes consists of a heme-copper center, which is buried within the protein. Hence, cytochrome *c* oxidases belong to the super-family of heme-copper oxidases, a class of enzymes that also includes the quinol oxidases, which use different types of lipid-soluble quinols (QH_2) instead of cytochrome *c* as their electron donor. The heme-copper oxidases are also often termed *respiratory oxidases* or *terminal oxidases*, terms that refer to the enzymes being the last components of the respiratory chains of aerobic organisms. However, not all terminal oxidases belong to the heme–copper oxidase superfamily. One example is the group of so-called alternative oxidases (e.g., in plants), which do not contain any heme groups.

Chemical Process

In the cytochrome *c* oxidases the protons used for O_2 reduction to water (substrate protons) are taken up from the inner (cytosol) side of the membrane, while cytochrome *c* reacts on the opposite, outer (periplasm) side of the membrane. In the quinol oxidases, the quinol binds from the core of the membrane, and upon oxidation, the protons are released to the periplasm. Thus, the reaction catalyzed by the heme-copper oxidases has a direction not only in time (c.f. any chemical reaction), but also in space, which is referred to as *vectorial chemistry*. The charge distribution across the membrane is such that there are more positive charges on the outer side than on the inner side. Hence, the outer and inner sides are referred to as the positive (*P*) and negative (*N*) sides, respectively:

cytochrome *c* oxidases

$$4\text{cyt.}c_P^{2+} + O_2 + 4H_N^+ \rightarrow 4\text{cyt.}c_P^{3+} + 2H_2O$$

quinol oxidases

$$2QH_2 + O_2 + 4H_N^+ \rightarrow 2Q + 2H_2O + 4H_P^+,$$

where the subscripts *N* and *P* refer to the negative and positive sides, respectively. In both cases outlined above, a net of four positive charges are generated on the *P*-side, while four positive charges are consumed on the *N*-side. Consequently, the chemical reactions catalyzed by heme-copper oxidases are arranged topographically in such a way that they result in a charge separation corresponding to the net transfer of one positive charge from the *N*-side to the *P*-side of the membrane per electron transferred to O_2. In addition, for most heme-copper oxidases characterized to date, part of the free energy released in the catalytic reaction is also used to pump (translocate) protons from the *N*-side to the *P*-side of the membrane, with an average stoichiometry of one proton per electron (see Figure 1 and more detailed discussion below). Hence, on average, two charges are transferred across the inner membrane per electron transferred to oxygen. As suggested by Peter Mitchell and formulated in the Chemiosmotic theory, this transmembrane proton and voltage gradient generated in part by the heme-copper oxidases is used, for example, for synthesis of ATP by the ATP synthase.

Structures

The bacterial heme–copper oxidases consist of several (in many cases four) subunits, located in the (inner) cell membrane of the bacterium. The minimal functional unit of the heme-copper oxidases is the subunit (SU) I–II complex (see also below). The heme–copper oxidase family is defined by the presence in SU I of six conserved histidine residues that coordinate three redox-active metal sites: (1) a six-coordinated heme group which has two axial His ligands and in which the iron ion is in a low-spin state; (2) a five-coordinated heme group with one axial His ligand and in which the iron ion generally is found in the high-spin state; and (3) a copper ion (Cu_B) which is bound by three His ligands. The SU I scaffold, which holds the redox centers, comprises at least 12 transmembrane helices, which span the membrane. The five-coordinated heme is usually denoted with a subscript 3, e.g., heme a_3. In the examples and discussion

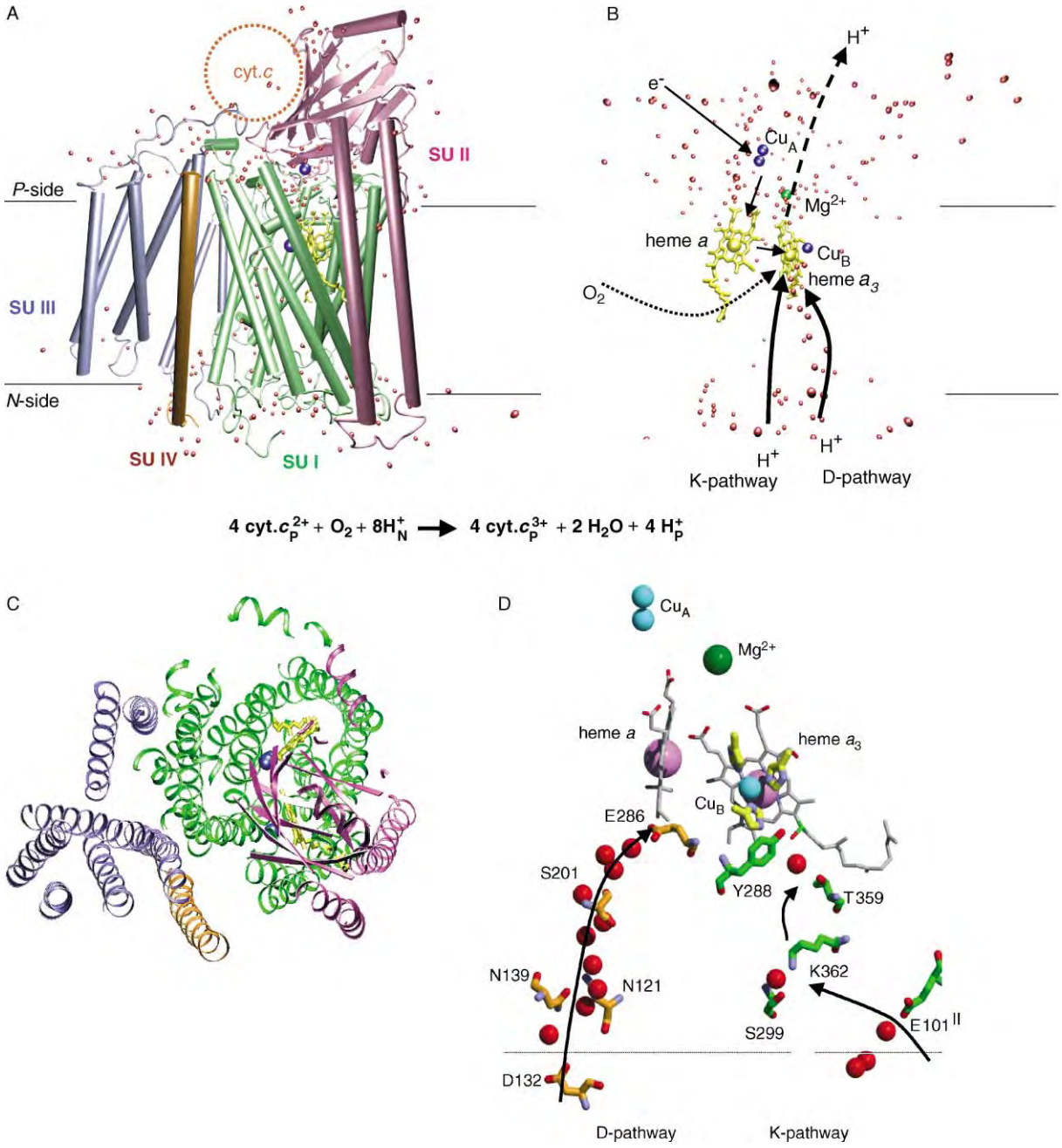

FIGURE 1 (A) The overall structure of the *R. sphaeroides* cytochrome aa_3 (cytochrome *c* oxidase). Subunits I, II, III, and IV are shown in different colors as indicated. The heme groups are shown in yellow, the copper ions in blue, and a redox inactive Mg^{2+} ion in green. Three redox active sites, heme *a*, and the catalytic site consisting of heme a_3 and Cu_B are found in SU I. The Cu_A center is found in SU II. A likely location of the cytochrome *c* binding site is indicated. Water molecules resolved in the structure are shown as red spheres. (B) Only the cofactors are shown together with the water molecules resolved in the structure. Substrate and pumped protons (thick arrows) are taken up from the inner, cytosol side (*N*-side) and the pumped protons (dashed arrow) are released on the outer, periplasm side (*P*-side), as shown. e^- is the electron from cyto *c* (thin arrows). (C) Top view of the enzyme. (D) The redox-active cofactors (and the Mg^{2+} ion) and proton-transfer pathways of cytochrome *c* oxidase. The overall reaction catalyzed by cytochrome c oxidase is described by the reaction formula, where the subscripts *P* and *N* refer to the two sides of the membrane. Subunits I–III of the *R. sphaeroides*, *P. denitrificans*, and the mitochondrial enzymes are highly homologous and their overall structures are very similar.

below, we call the two hemes of the enzyme hemes *a* and a_3, respectively.

Unlike the six-coordinated heme, heme a_3 binds ligands such as O_2, CO, and CN^-. Heme a_3 and Cu_B are collectively called the binuclear center, which is the catalytic site at which O_2 is reduced to water. The heme groups may be of different types, such as heme *a*, *b*, or *o*, where the two hemes in SU I may be of the same or of different types. Heme–copper oxidases are also often given a name that indicates the types of hemes present, e.g., cytochrome aa_3. Many bacteria have several types of oxidases, which are expressed to various degrees

depending on the environmental conditions (e.g., the O_2 concentration). The X-ray structures of heme–copper oxidases that have been determined to date are summarized in Table I.

A common feature of most (but not all) cytochrome *c* oxidases is a copper center (Cu_A) bound in SU II, which is the primary electron acceptor from cytochrome *c*. Hence, the binding site for the water-soluble cytochrome *c* is located near Cu_A (see Figure 1). The Cu_A center is composed of two copper ions coordinated by two –SH groups of two Cys residues (among other ligands), which resembles the [2Fe–2S] centers of iron–sulfur proteins. The Cu_A center can accept and donate one electron switching between the formal charges $[Cu^{1+}–Cu^{1+}]$ and $[Cu^{1.5+}–Cu^{1.5+}]$ in the reduced and oxidized form, respectively. Many cytochrome *c* oxidases that do not have the Cu_A site instead have a cytochrome *c* subunit that protrudes into the inter-membrane space and acts as the primary electron acceptor. In the ubiquinol oxidase from *E. coli*, the ubiquinol binding site was suggested from an analysis of the three-dimensional structure and from experiments using site-directed mutagenesis to be found in the membrane-spanning part of SU I at a cluster of polar residues exposed to the interior of the lipid bilayer.

Subunit III does not contain any redox-active cofactors. Even though the enzyme with SU III removed displays O_2-reduction activity and pumps protons (although with a stoichiometry of less than one proton per electron), this form of the enzyme becomes inactivated after a limited number of reaction cycles. Consequently, SU III is important for the stability of the protein.

Proton-Transfer Pathways

As seen in Figure 1, the O_2-reducing site is located in the membrane-spanning part of the enzyme. Therefore, proton-transfer pathways, leading from the protein surface on the *N*-side to the binuclear center, are needed. Such pathways are typically composed of polar and protonatable amino-acid residues as well as of water molecules forming a hydrogen-bonded chain. The detailed composition of these pathways varies in the bacterial heme–copper oxidases. Two pathways have been identified from an analysis of the three-dimensional structures of heme–copper oxidases determined to date, from a comparison of the amino-acid residue sequences of a large number of other heme–copper oxidases, and from the combined use of site-directed mutagenesis and functional studies. These pathways are found in SU I and are named the D- and K-pathways, after residues Asp(D)132 and Lys(K)-362, respectively. We use the *R. sphaeroides* cytochrome aa_3 amino-acid residue numbering because the structure shown in Figure 1 is from that enzyme. Both pathways start at the inner-side surface and lead to the catalytic site (Figures 1B and 1D). A common feature of a large number of oxidases is a Glu residue in the D-pathway, E(I-286) in the *R. sphaeroides* cytochrome aa_3, located about 25Å from D(I-132) and about 10Å from the binuclear center. In heme–copper oxidases in which the Glu is not conserved, other protonatable residues are found at about the same location in space.

Oxygen Binding and Reduction

Even though the reduction of O_2 to water is a highly exergonic reaction, the O_2 molecule is kinetically stabilized against reduction due to two factors. First, the one-electron reduction of O_2 to form the superoxide radical $O_2^{\cdot-}$ is associated with a positive free energy change, which imposes a thermodynamic barrier in the initial step of the reduction process. Second, in the ground electronic state, O_2 has two unpaired electrons (triplet state), which imposes spin restrictions on many of its reactions. The heme copper oxidases overcome

TABLE I

Structures of Heme–Copper Oxidases from the Protein Data Bank (PDB)* (the Bovine Heart Enzyme is also Included)

Heme–copper oxidase	Source	PDB code	Resolution (Å)	Comment
cytochrome aa_3	*P. denitrificans*	1AR1	2.7	two-subunit enzyme
		1QLE	3.0	four-subunit enzyme
cytochrome bo_3	*E. coli*	1FFT	3.5	
cytochrome ba_3	*T. thermophilus*	1EHK	2.4	
cytochrome aa_3	*R. sphaeroides*	1M56	2.3	wild-type enzyme
		1M57	3.0	EQ(I-286) mutant enzyme
cytochrome aa_3	bovine heart	2OCC	2.3	oxidized state
	mitochondria	1OCR	2.35	reduced state
		1V54	108	oxidized state

*Note. The Protein Data Bank can be found at www.rcsb.org.

these problems by binding O_2 to the heme a_3 iron in the high-spin state and by providing a second electron donor, Cu_B, in the immediate vicinity. The rates at which bacterial oxidases catalyze the O_2 reduction are remarkably rapid with turnover numbers of up to several hundred O_2 molecules per second. The rapid uptake of O_2 may be facilitated by hydrophobic channels leading from the membrane core to the catalytic site, as suggested from analyses of the crystal structures of heme–copper oxidases.

The mechanism of the O_2-reduction has been primarily investigated in detail in cytochromes aa_3 from *R. sphaeroides*, *P. denitrificans*, the closely related mitochondrial enzyme, as well as in cytochrome bo_3 from *E. coli*. The reaction sequence is most likely the same for all oxidases, but the mechanism described below has been identified primarily from studies of these enzymes.

Initially, the electrons are transferred one at a time to the binuclear center. When both heme a_3 and Cu_B are reduced (i.e., $Fe^{2+}_{a_3}$ and Cu^{+}_{B}, state **R** in Figure 2), O_2 binds to heme a_3 (the state is called **A**). After binding of O_2 the O–O bond is cleaved, which results in formation of a ferryl group ($Fe^{4+}_{a_3}{=}O$, see Figure 2), where one electron and a proton are donated by an internal group, presumably a highly conserved Tyr at the catalytic site, which would form a radical. Even though the binuclear center is in a two-electron reduced state, formally four electrons are donated to O_2 in this reaction because two electrons are donated by Fe_{a_3}($Fe^{2+}_{a_3} \rightarrow Fe^{4+}_{a_3}$), one by Cu_B($Cu^{+}_{B} \rightarrow Cu^{2+}_{B}$ and one by the Tyr. For historical reasons, this state is called "peroxy" and denoted **P**.

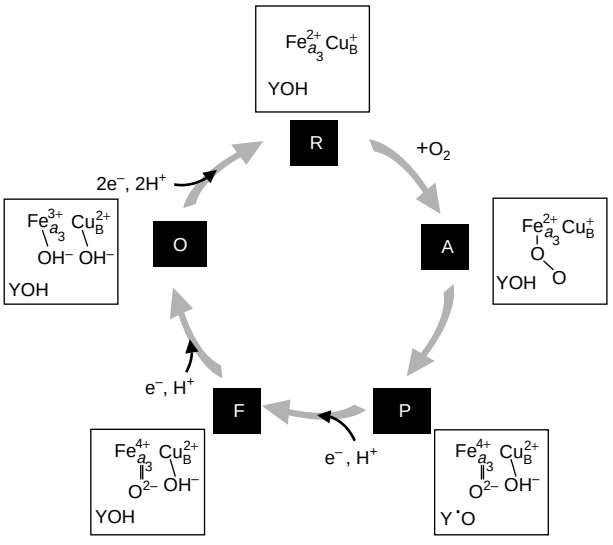

FIGURE 2 The reaction cycle of cytochrome *c* oxidase. State **O** is the oxidized enzyme. The two-electron-reduced catalytic site (state **R**) binds O_2 (forming state **A**). In the first step of O_2 reduction, a ferryl state is formed (**P**), where one electron and one proton are transferred from a Tyr residue at the catalytic site. The transfer of the third electron to the catalytic site is accompanied by proton uptake from the bulk *N*-side solution and the formation of state **F**. In the next step, the fourth electron is transferred to the binuclear center associated with proton uptake from the bulk *N*-side solution.

The transfer of the third electron to the binuclear center is associated with proton uptake from the inside bulk solution. The intermediate that is formed is called "ferryl" and is denoted **F** (Figure 2). It is assumed to have the same chemical structure as **P**, except for the additional electron and proton at the binuclear center, which are presumably transferred to the Tyr radical. The transfer of the next, forth electron to the binuclear center is also associated with proton uptake from the inside bulk solution and results in formation of the oxidized binuclear center, denoted **O**.

Proton Pumping

In 1977, Mårten Wikström showed that in addition to the charge separation associated with the O_2 reduction reaction, cytochrome *c* oxidase also releases protons to the *P*-side of the membrane. In other words, the enzyme is a proton pump, which translocates one proton from the *N*-side to the *P*-side of the membrane per electron transferred to O_2. Consequently, since there is no proton carrier in the enzyme that can bodily move protons across the membrane, there must be a specific mechanism by which the enzyme uses the free energy from reduction of O_2 to translocate protons across the membrane. This function must be reflected in specific structural elements of the molecular machine. The molecular mechanism by which heme–copper oxidases pump protons is not known. The general view is that during the process the enzyme must provide an alternating access of protons to the two sides of the membrane and have this alteration strictly coupled to specific transitions of the catalytic cycle. Such changes in the accessibility for protons to the two sides of the membrane are likely to be achieved by breakage and formation of hydrogen bonds in the proton-transfer pathways, for example, through local rearrangements of amino-acid residue side chains. It has been shown that the **R** → **P** transition is not associated with proton pumping, while the **P** → **F** and **F** → **O** transitions are associated with the translocation of one proton in each step. The definite assignment of other reaction steps in which proton translocation occurs and conditions under which this takes place is at present not definitely settled.

As indicated above, in the initial step of the reaction, the O_2 molecule is formally reduced by four electrons (to form state **P**, Figure 2). An advantage of such a four-electron reduction of O_2 in a single step is that it prevents accumulation of potentially harmful, partly reduced O_2 intermediates. However, since the formation of **P** is not associated with proton translocation, this mechanism

requires that the free energy available from the O_2--reduction reaction is conserved within the enzyme, for example by the formation of high-pK_a internal proton acceptors; and the free energy can be used for proton translocation in the following steps of the reaction.

Some Experimental Techniques Used to Study Heme–Copper Oxidases

Present knowledge about the O_2-reduction mechanism is derived from the use of a large number of experimental techniques. One of these is the "flow-flash" technique, pioneered by Quentin Gibson and Colin Greenwood. The enzyme reduced with 2–4 reduction equivalents and with CO bound to heme a_3 is mixed with an O_2 solution after which the CO ligand is flashed off by means of pulsed illumination, which initiates the reaction of the enzyme with O_2. The application of this technique has made it possible to observe, with microsecond time resolution, the transitions between different states. The progress of the reaction is followed, e.g., by observing absorbance changes of the redox sites, by measuring voltage changes that originate from the movement of charges in enzyme reconstituted in lipid vesicles, or by using time-resolved resonance-Raman spectroscopy to obtain information about the structure of the oxygen intermediates. In addition, Fourier Transform Infrared Difference spectroscopy is used to identify specific residues that undergo changes in their protonation state and/or hydrogen-bonding patterns, and Electron Paramagnetic Resonance spectroscopy is used to explore the electronic configuration and the chemical environment of the redox centers. The use of the techniques discussed above, combined with the use of site-directed mutagenesis, has provided important insights into the catalytic mechanism.

See Also the Following Articles

Cytochrome *c* • Heme Proteins • P-Type Pumps: Copper Pump

Glossary

aerobe Organism that uses oxygen (O_2) as the terminal electron acceptor in respiration.

cytochrome A heme protein serving as an electron carrier.

proton electrochemical gradient Sum of the contributions of the proton concentration difference (pH) and voltage across a membrane (in units of energy, e.g., kJ/mol or eV).

proton pump Integral membrane protein that translocates protons across the membrane without the use of mobile proton carriers (which would bodily carry protons across the membrane, e.g., a quinone).

proton-transfer pathway Typically, an arrangement of protein-bound water molecules and hydrophilic or protonatable amino-acid residues used for the transfer of a proton from a donor to an acceptor (where one of these may be the bulk solution).

redox-active cofactor or redox site Group within a protein (e.g., a metal ion) that can accept and give electrons in its oxidized and reduced states, respectively.

Further Reading

Abramson, J., Riistama, S., Larsson, G., Jasaitis, A., Svensson-Ek, M., Laakkonen, L., Puustinen, A., Iwata, S., and Wikström, M. (2000). The structure of the ubiquinol oxidase from *Escherichia coli* and its ubiquinone binding site. *Nature Str. Biol.* **7**, 910–917.

Brzezinski, P., Larsson, G., and Ädelroth, P. (2003). Functional aspects of heme–copper terminal oxidases. In *Advances in Photosynthesis and Respiration* (D. Zannoni, ed.) Kluwer Academic, Dordrecht/ Norwell, MA.

Ferguson-Miller, S., and Babcock, G. T. (1996). Heme/copper terminal oxidases. *Chem. Rev.* **96**, 2889–2907.

Iwata, S., Ostermeier, C., Ludwig, B., and Michel, H. (1995). Structure at 2.8 Å resolution of cytochrome c oxidase from Paracoccus denitrificans. *Nature* **376**, 660–669.

Soulimane, T., Buse, G., Bourenkov, G. P., Bartunik, H. D., Huber, R., and Than, M. E. (2000). Structure and mechanism of the aberrant ba_3-cytochrome *c* oxidase from *Thermus thermophilus*. *EMBO. J.* **19**, 1766–1776.

Svensson-Ek, M., Abramson, J., Larsson, G., Törnroth, S., Brzezinski, P., and Iwata, S. (2002). The X-ray crystal structures of wild-type and EQ(I-286) mutant cytochrome *c* oxidases from *Rhodobacter sphaeroides*. *J. Mol. Biol.* **321**, 329–339.

Verkhovsky, M. I., Jasaitis, A., Verkhovskaya, M. L., Morgan, J. E., and Wikström, M. (1999). Proton translocation by cytochrome *c* oxidase. *Nature* **400**, 480–483.

Wikström, M. K. F. (1977). Proton pump coupled to cytochrome c oxidase in mitochondria. *Nature* **266**, 271–273.

Yoshikawa, S., Shinzawa-Itoh, K., Nakashima, R., Yaono, R., Yamashita, E., Inoue, N., Yao, M., Fei, M. J., Libeu, C. P., Mizushima, T., Yamaguchi, H., Tomizaki, T., and Tsukihara, T. (1998). Redox-coupled crystal structural changes in bovine heart cytochrome *c* oxidase. *Science* **280**, 1723–1729.

Zaslavsky, D., and Gennis, R. B. (2000). Proton pumping by cytochrome *c* oxidase: Progress, problems and postulates. *Biochim. Biophys. Acta* **1458**, 164–179.

Biography

Peter Brzezinski is Professor of Biochemistry at the Department of Biochemistry and Biophysics at Stockholm University in Stockholm, Sweden. He specializes in the field of bioenergetics, and his principal research interests are mechanisms of electron- and proton-transfer reactions in biological systems, in particular in membrane-bound proteins. He holds a Ph.D. in physics from Chalmers University of Technology in Göteborg, Sweden and received his postdoctoral training at the University of California, San Diego.

Cytochrome P-450

Rita Bernhardt
Saarland University, Saarbrücken, Germany

Cytochromes P-450 are ubiquitously distributed multicatalysts, which were discovered approximately 50 years ago. They possess a high degree of complexity and display a broad field of activity. Although already more than 2500 different P450 forms have been described, new forms are constantly being found, opening up new research fields. They are the key enzymes responsible for the metabolism of many drugs, carcinogens, alkaloids, pesticides, and other important xenobiotics. Moreover, they are involved in a variety of physiological processes such as steroid hormone, eicosanoid, vitamin D, and bile acid biosynthesis. Cytochromes P-450 are hemoproteins that use molecular oxygen to catalyze various reactions. They get the electrons necessary for oxygen activation and substrate hydroxylation from NADH or NADPH, in general via the action of electron-transferring proteins. Most cytochromes P-450 are membrane-bound. Many of them are inducible, but some are constitutively expressed. Defects in some of the cytochromes P-450 lead to pathological effects, such as congenital adrenal hyperplasia and hypertension, and adverse drug effects.

Cytochrome P-450—General Aspects

There are two general classes of enzymes involved in oxygen metabolism: oxidases, transferring electrons from a substrate to oxygen, and oxygenases, transferring oxygen to a substrate after reductive splitting of molecular oxygen. Oxygenases can be divided into dioxygenases and monooxygenases. Monooxygenases (mixed-function oxidases) catalyze the incorporation of a single atom of molecular oxygen into a substrate with the concomitant reduction of the other atom to water. The monooxygenases are divided into two classes, the internal and the external monooxygenases. Internal monooxygenases extract two reducing equivalents from the substrate to reduce one atom of dioxygen to water, whereas external monooxygenases use an external reductant. Cytochromes P-450 are external monooxygenases. Initially the microsomal drug and xenobiotic-metabolizing enzymes were referred to as mixed-function oxidases, but in more recent years the term monooxygenase has become the more accepted one.

Cytochromes P-450 got their name from their character as a hemoprotein and from their unusual spectral properties, displaying a typical absorption maximum of the reduced CO-bound complex at 450 nm (Figure 1)—cytochrome stands for a hemoprotein, P for pigment, and 450 reflects the absorption peak of the CO complex at 450 nm. The ability of reduced P450 to produce an absorption peak at 450 nm upon CO binding is still used for the estimation of P450 content. The red shift of approximately 30 nm observed in cytochromes P-450 means that the distribution of electron density at the heme is significantly perturbed compared to other cytochromes. It has been documented that it is the thiolate sulfur that causes this effect by means of a direct bond to the iron. The Soret band (named after its discoverer) describes the absorption band of hemoproteins at approximately 380–420 nm.

Cytochrome P-450 systems catalyze the following reaction:

$$RH + O_2 + NAD(P)H + H^+ \rightarrow ROH + H_2O + NAD(P)^+$$

They catalyze reactions as diverse as hydroxylation; N-, O-, and S-dealkylation; sulfoxidation; epoxidation; deamination; desulfuration; dehalogenation; peroxidation; and N-oxide reduction. Their substrates include fatty acids, steroids, and prostaglandins, as well as a multitude of foreign compounds such as drugs, anesthetics, organic solvents, ethanol, alkylaryl hydrocarbon products, pesticides, and carcinogens. This diversity of catalyzed reactions and acceptable substrates has attracted researchers from diverse fields to the study of cytochrome P-450 systems (Figure 2). In addition to pharmacologists and toxicologists, endocrinologists, physiologists, microbiologists, organic chemists, plant biologists, and environmental scientists also are working on diverse aspects of P450 function and regulation.

It is obvious that this diversity of substrates and catalyzed reactions cannot be managed by only a few different isoforms. In the human genome alone 57 different P450 genes have been found, and in total more than 3000 different isoforms have been characterized

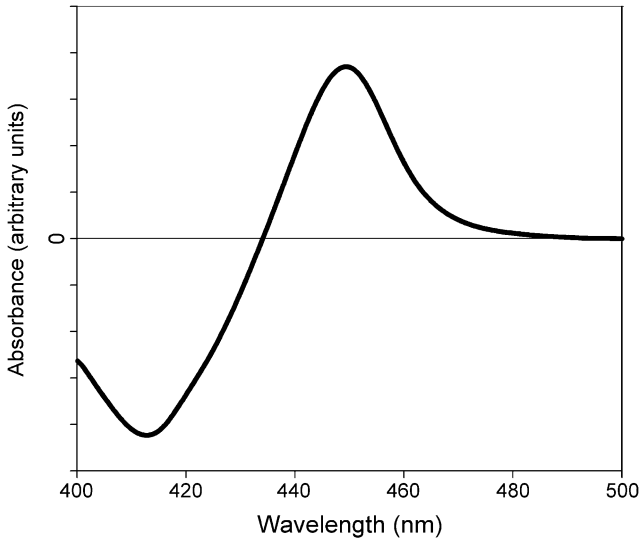

FIGURE 1 CO-difference spectrum of reduced versus oxidized cytochrome P-450 (CYP106A2).

(D. Nelson lists the available P450 sequences identified so far on his website). This superfamily of proteins (and their respective genes) is divided into families, subfamilies, and finally into individual members according to similarities in primary structure. A new nomenclature has been introduced in which CYP and a series of numbers and letters are used to characterize each P450 as a hemoprotein. For example, in CYP1A1, for cytochrome P4501A1 (previously called P450c), the first arabic number defines the gene family, the following letter defines the subfamily, and the second number defines the individual enzyme. Members of the same gene family are defined as usually having $<40\%$ sequence identity to a P450 protein from any other family. Mammalian sequences within the same subfamily are always $>55\%$ identical. The numbers of individual P450 enzymes in different species differ, the highest numbers observed so far being in plants.

Structural Organization of Cytochrome P-450 Systems

As already mentioned, cytochromes P-450 belong to the external monooxygenases. This means that they need an external electron donor to transfer the electrons necessary for oxygen activation and the following substrate hydroxylation. Two main classes of cytochromes P-450 can be defined with respect to their electron-supporting system, although other subclasses also occur: the microsomal type and the mitochondrial/bacterial type (Figure 3).

Microsomal cytochromes P-450 are membrane-bound and accept electrons from a microsomal NADPH–cytochrome P-450 reductase, containing flavin adenine dinucleotide (FAD) and falvin mononucleotide (FMN). All drug- and xenobiotica-metabolizing cytochromes P-450 isolated so far belong to this class. In addition, CYP102 (P450BM-3) isolated from *Bacillus megaterium* was shown to belong to this class. This P450 system consists of a polypeptide chain with two different domains, one containing the hemoprotein and the other containing a flavoprotein with FAD and FMN. Most of the other bacterial cytochromes P-450 belong to

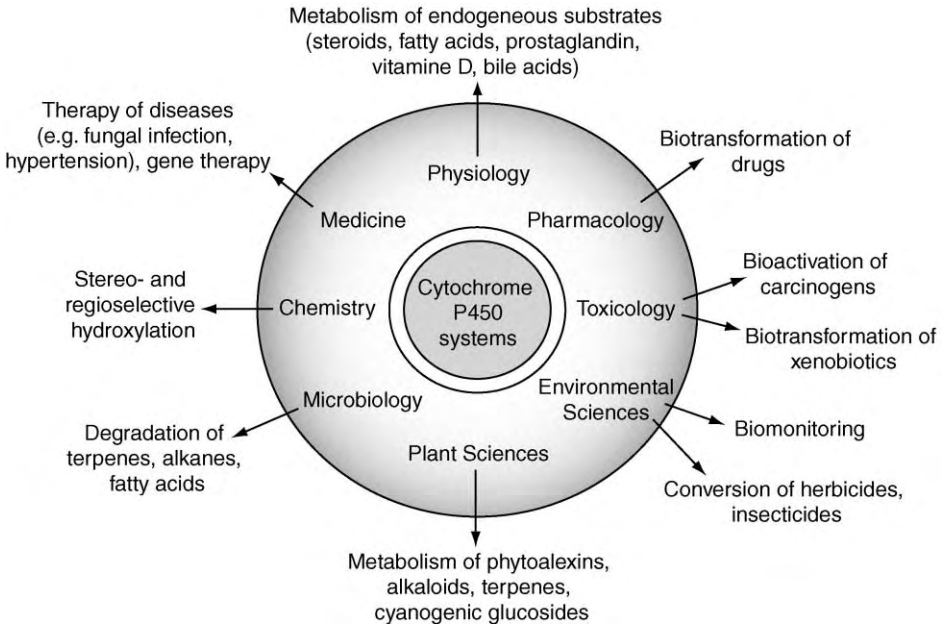

FIGURE 2 Cytochrome P-450 research and application fields.

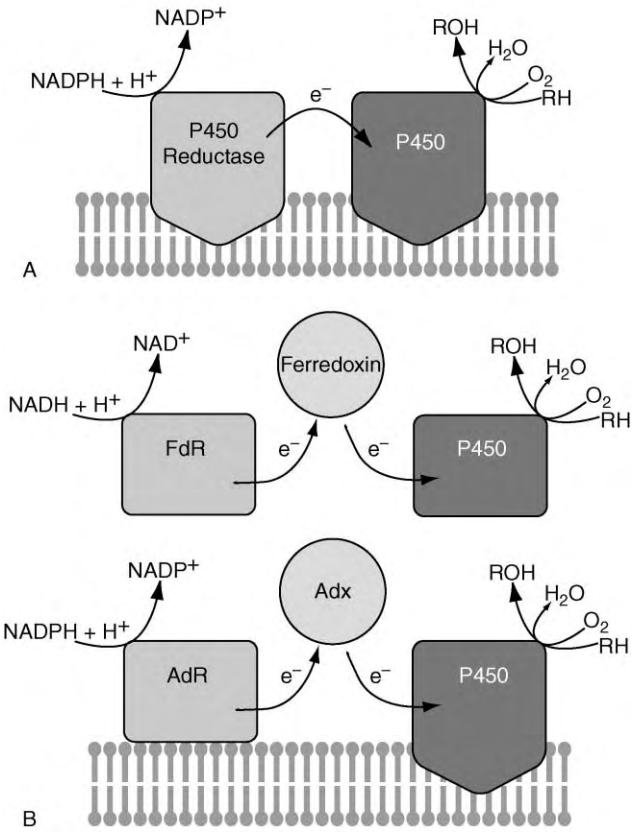

FIGURE 3 Model for the organization of cytochrome P-450 systems. (A) Microsomal type. (B) Mitochondrial/bacterial type.

the second class. They are soluble and obtain the electrons necessary for the reaction mechanism from an NADH-dependent FAD-containing reductase via an iron–sulfur protein of the [2Fe–2S] type.

Mitochondrial cytochromes P450, which are involved e.g., in the side-chain cleavage of cholesterol, the 11β-hydroxylation of deoxycortisol, and the production of aldosterone, also belong to the second class. These cytochromes P-450 are localized in the inner mitochondrial membrane, where the [2Fe–2S] protein, called adrenodoxin in the case of adrenal steroid hydroxylase systems, is a soluble protein of the matrix. The FAD-containing reductase, adrenodoxin reductase, is associated with the inner mitochondrial membrane.

The interaction of the cytochromes P-450 with their corresponding electron donors is a necessary prerequisite of the catalytic cycle. Its specificity guarantees a sufficient reaction rate of catalysis and likewise a discrimination between the different potential donors and acceptors of electrons to protect the system from shunt reactions.

Because many different isoenzymes in liver microsomes have to interact with only one type of reductase, the binding site for reductase is very similar or identical on various cytochromes P450. Salt bridges are responsible for the recognition of reductase by the cytochromes P-450 and for the correct orientation of the proteins to one another. In addition to microsomal reductase, some microsomal cytochromes P-450 are able to accept the second electron from cytochrome b_5. cytochrome b_5 has also been shown to exert a differential stimulatory action, depending on the form of cytochrome P-450 and the substrate metabolized.

In mitochondrial steroid hydroxylases and in the camphor hydroxylating bacterial cytochrome P-450 (CYP101) system, a charge–pair interaction mechanism has been demonstrated by chemical modification, site-directed mutagenesis studies, and structural data of electron-transfer complexes. Like microsomal reductase, the mitochondrial ferredoxin has been shown to deliver electrons to different cytochromes P450. From the available data, a shuttle model is favored, in which the oxidized ferredoxin interacts first with the ferredoxin reductase to undergo reduction, with the formation of a Fe^{3+}–Fe^{2+} iron–sulfur cluster. It dissociates from the reductase and then interacts with the respective cytochrome P450, to which it delivers this electron before going back to the reductase, and transfers the second electron to the cytochrome P450. The mechanism of electron transfer between the components of the different cytochrome P-450 systems, one of the fundamental problems in life sciences, is not well understood.

Reaction Cycle

The generally accepted mechanism of cytochrome P450-dependent substrate conversion is depicted in the overall scheme presented in Figure 4. The first step of the reaction cycle is the formation of the substrate–enzyme complex. Substrate binding induces structural changes in the cytochrome P-450 that may result not only in a

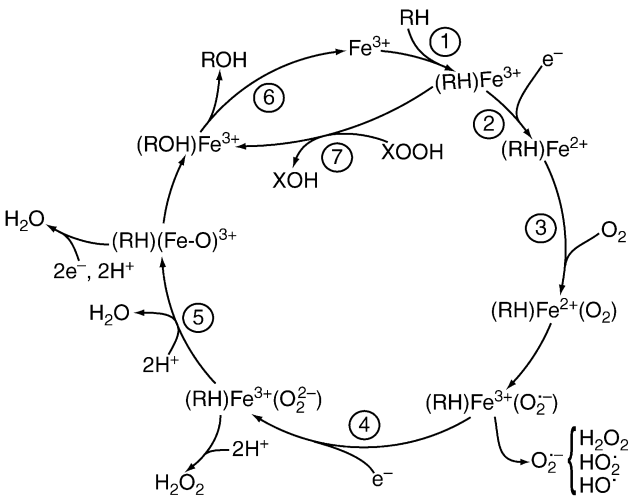

FIGURE 4 Reaction cycle of cytochromes P450.

spin shift, but also in changes of the redox potential and in changed binding affinities between interacting components of the cytochrome P-450 system. The second step of the reaction cycle is the introduction of the first electron, either by NADPH-dependent reductase or via a ferredoxin (see Figure 3). Iron (3+) is reduced to iron (2+). Although in some cytochromes P450 the substrate binding is a prerequisite for electron transfer, this is not a universal requirement. In the third step of the reaction cycle, the hemoprotein reduced by one electron binds the dioxygen molecule. As shown in Figure 4, from this complex a superoxide anion radical can be released. Step 4 of the reaction cycle is the introduction of the second electron. In some instances, another microsomal hemoprotein, cytochrome b_5, can facilitate catalysis by providing the second electron. From the $(RH)Fe^{3+}(O_2^{2-})$ complex, hydrogen peroxide can be split off. The structure of the activated oxygen complex and the precise mechanism of oxygen cleavage are not fully understood yet. Step 5 in the reaction cycle is the removal of the terminal oxygen atom from the dioxygen ligand, that is, the cleavage of the dioxygen bond. Heterolysis of the oxygen–oxygen bond also results in the formation of a putative oxyferryl species. Heterolytic cleavage in P450cam (CYP101), where most of the mechanistic studies have been performed, was shown to be facilitated by hydrogen bonding of the ferric hydroperoxide via a water molecule to a highly conserved threonine residue (Thr252 in CYP101), which is involved in a proton transfer network that promotes oxygen cleavage. The introduction of two electrons and two protons to the putative oxyferryl species may lead to the formation of water. Finally, in step 6 the hydroxylated product dissociates and the cycle can start again. Interestingly, in many but not all cytochromes P450 a shunt reaction can proceed (step 7), in which the substrate can be hydroxylated directly by peroxides such as hydrogen peroxide, cumene hydroperoxide, and *tert*-butyl hydroperoxide without the necessity of an interaction with an electron-donating system. Taken together, cytochromes P-450 do not catalyze just monooxygenase, but also oxidase and peroxidase reactions. Variations of this scheme for the reaction mechanism of cytochromes P-450 occur with different cytochrome P-450 systems such as thromboxane and prostacyclin synthase, nitric oxide reductase (CYP55A1), and others.

Regulation of Cytochrome P-450 Systems

The regulation of enzyme systems is possible at different levels. When considering cytochrome P-450 systems, the complexity of the reaction cycle, the organization within membrane systems for most of the cytochromes P450, and their organ- and tissue-specific expression imply various possible ways for regulatory mechanisms to work. Interaction between these mechanisms then leads to the tuned response of these enzyme systems to endogenous and exogenous signals in terms of acute and long-term reactivities of cytochromes P450.

First it is possible to regulate cytochromes P-450 on the level of the organism. Some of the cytochromes P-450 are expressed in age-, tissue-, and sex-dependent manners. These differences in the expression pattern are governed by sex or other hormones. There are also clearly developmental influences on the expression and function of various cytochrome P-450 systems.

Cellular regulation of cytochromes P-450 is extremely complex and can occur on at least two different levels, enzyme induction and post-translational modification of enzymes. The induction of drug-metabolizing enzymes was noted in the early 1950s. Since then specific inducers for various cytochrome P-450 families and subfamilies have been identified. It can be demonstrated that the inductor functions by enhancing the rate of mRNA synthesis of a special cytochrome P450. In some cases, receptors (the best-studied system currently is the aryl hydrocarbon, Ah, receptor) are involved in mediating the effect of the inducer. Not all cytochromes P450 are, however, inducible; some of them are constitutively expressed.

After the biosynthesis of cytochromes P450, the enzymes might be subject to post-translational modifications to exert a short-term control of activity. One of the most common types of post-translational modifications in eukaryotic organisms is protein phosphorylation, which has been demonstrated for several steroid hydroxylases such as the microsomal CYP7 and the mitochondrial CYP11A1 and also for the drug-metabolizing microsomal CYP2B4.

Because nearly all the cytochromes P-450 are bound to membranes, they can be regulated also at that level. Exclusions are most of the bacterial cytochromes P450, such as CYP101, CYP102, and CYP108, which are soluble. The composition of the membrane (e.g., protein–lipid as well as lipid-mediated protein–protein interactions) exert a functional control on cytochromes P450. Lipids appear to function in at least three ways—they (1) stabilize and induce a functionally active conformation of cytochromes P-450 and the corresponding electron-transfer systems, (2) modulate the electron transfer, and (3) mediate interactions between cytochromes P-450 and the electron-donor systems.

Finally, cytochromes P-450 can be regulated at the molecular level. This includes regulation of the activities by changes of the primary sequence (e.g., by polymorphisms), the spin equilibrium, protein–electron donor interactions, and protein–protein interactions.

Important Functions of Cytochrome P-450 Systems

Cytochromes P-450 and Drug Metabolism

Cytochromes P-450 are able to perform the biotransformation of an enormous variety of substrates. Taking into account all drugs metabolized by enzymes, cytochromes P-450 are responsible for more than two-thirds of these reactions. The most important cytochrome P-450 form for biotransformation in humans is CYP3A4; it is involved in the metabolism of more than one-half of the known drugs and xenobiotics, such as nifedipine, cyclosporin, erythromycin, gestodene, and aflatoxins. This variety of substrates makes CYP3A4 one of the most important enzymes for drug metabolism. The fact that a single cytochrome P-450 is responsible for the metabolism of many different drugs may lead to competition among various drugs for the same enzyme and thus to drug–drug interactions, resulting in higher plasma levels of the less successful (i.e., displaying a lower affinity for the particular cytochrome P450) substrate and even to fatal side effects of the drug treatment.

Another fact complicating drug treatment is the presence of genetic polymorphisms in some of the drug-metabolizing enzymes. It has been shown that 5–10% of Caucasians suffer from a decreased ability to metabolize certain drugs such as debrisoquine and bufuralol (i.e., they are poor metabolizers), due to the presence of nonfunctional alleles of CYP2D6 in these individuals. A smaller portion of patients metabolize the corresponding drugs extremely rapidly (i.e., they are extensive metabolizers), due to having multiple copies of this gene. These pharmacogenetic effects are being studied in many laboratories and will certainly lead to personalized pharmacotherapy.

Physiological Role of Cytochromes P450

In addition to being involved in drug metabolism and xenobiotica degradation, cytochromes P-450 also play a pivotal role in various physiological processes in humans. They are central in the biosynthesis of steroid hormones (sex hormones, glucocorticoids, and mineralocorticoids), vitamin D, fatty acids, bile acids, and eicosanoids. Some severe defects are connected to mutations in cytochrome P-450 genes, such as congenital adrenal hyperplasia, which is mostly due to a steroid 21-hydroxylase (CYP21) deficiency. In addition, human essential hypertension can be caused by the overproduction of aldosterone produced by CYP11B2. More recently, products of cytochrome P-450 reactions such as oxysterols and the endothelium-derived hyperpolarizing factor (EDHF) have been found to play important roles in cellular cholesterol homeostasis, inhibition of cellular proliferation, gene regulation, endothelium-dependent dilation, and enhanced endothelial cell proliferation.

Cytochrome P-450 Diversity

Cytochromes P-450 are found in all kingdoms—eubacteria, archaebacteria, fungi, plants, fish, insects, and vertebrates. More than 250 different forms have been found in the plant *Arabidopsis thaliana*. It was shown that plant cytochromes P450 play a role in the metabolism of a variety of secondary metabolites, in plant–insect interaction, in herbicide metabolism, and in other vital functions. Due to the diversity of catalyzed reactions it can be anticipated that plant cytochromes P450 will offer a broad field for future applications.

See Also the Following Articles

Oxygenases • Vitamin D

Glossary

CYP Nomenclature for the enzymes of the cytochrome P-450 superfamily.

cytochrome P-450 Hemoprotein showing an unusual absorption of the reduced CO complex at 450 nm.

genetic polymorphism Inherited deficiencies of single enzymes such as CYP2D6 and CYP2C19.

glucocorticoids Steroid hormones regulating glucose metabolism, regulating the stress response of the body, and suppressing inflammation.

hormone Chemical messenger secreted into the circulating blood.

mineralocorticoids Steroid hormones regulating the salt and water levels of the body and in this way the blood pressure.

Further Reading

Bernhardt, R. (1996). Cytochrome P450: Structure, function, and generation of reactive oxygen species. *Rev. Physiol. Biochem. Pharmacol.* **127**, 137–221.

Bureik, M., Lisurek, M., and Bernhardt, R. (2002). The human steroid hydroxylases CYP11B1 and CYP11B2. *Biol. Chem.* **383**, 1537–1551.

Guengerich, F. P. (2002). Update information on human P450s. *Drug Metab. Rev.* **34**, 7–15.

Guengerich, F. P., Parikh, A., Yun, C. H., Kim, D., Nakamura, K., Notley, L. M., and Gillam, E. M. (2000). What makes P450s work? Searches for answers with known and new P450s. *Drug Metab. Rev.* **32**, 267–281.

Meyer, U. A. (2000). Pharmacogenetics and adverse drug reactions. *Lancet* **356**, 1667–1671.

Nelson, D. Nelson Lab Homepage. Available at: http://drnelson.utmem.edu/nelsonhomepage.html.

Ruckpaul, K., and Rein, H. (eds.) (1989–1994). *Frontiers in Biotransformation*, Vol. 1–9, Akademie-Verlag, Berlin.

Biography

Rita Bernhardt is a Full Professor at the Saarland University and Head of the Institute of Biochemistry. Her principal research interests are cytochrome P-450 systems. She holds a Ph.D. from Moscow State Lomonossov University and received her postdoctoral training at the Central Institute of Molecular Biology of the Academy of Sciences of the GDR in Berlin–Buch, the University of Illinois at Urbana-Champaign, and the University of Sendai, Japan. She uses a variety of biochemical, biophysical, and engineering techniques to study cytochrome P-450 system functions and improve their catalytic efficiency and stability, with special attention to the structure, function, and regulation of mitochondrial steroid hydroxylase systems.

Cytokines

Andrea L. Wurster and Michael J. Grusby
Harvard School of Public Health, Boston, Massachusetts, USA

Cytokines are a diverse set of small, secreted proteins that help direct many critical aspects of an immune response. Cytokines are rapidly produced in response to foreign antigen exposure and can promote the expansion, activation, recruitment, and differentiation of the responding cell types. However, cytokine expression and signaling must be tightly regulated because dysregulated cytokine responses can lead to pathological conditions such as autoimmunity and asthma.

General Features of Cytokines

Nomenclature

Cytokines have been referred to by a number of labels depending on the cell types that produce them or their functional properties. For example, cytokines that are derived primarily from mononuclear cells such as macrophages have been referred to as monokines while the cytokines produced by activated T lymphocytes are termed lymphokines. Cytokines that specifically regulate the migration of other cells are called chemokines in reference to their chemotactic properties. Historically cytokines were also referred to as interleukins since in a general sense they are being produced by and acting on leukocytes. It is the term interleukin that spawned a universal numerical nomenclature for cataloguing newly identified and characterized cytokines (i.e., IL-4). Sequence comparisons between previously identified cytokines and the recently completed mouse and human genome databases have resulted in a rapid increase in the discovery of new cytokines with the most recently reported being IL-29.

Pleotropism and Redundancy

With so many cytokines now known to exist, an added complexity to their biology is that most cytokines are pleiotropic. This refers to the notion that cytokines do not just act on one particular cell type but can have wide effects on a number of cell types within the immune system as well as on cell types outside of the immune system. A clinically relevant example is the cytokine IL-13. IL-13 is a T cell derived cytokine whose effects on B lymphocytes and monocytes (up-regulation of MHC class II and inhibition of inflammatory cytokine production) have been well described. However, IL-13 has also been shown to be critically involved in the pathogenesis of allergic asthma and is thought to mediate its effects by its actions on epithelial and smooth muscle cells in the lung.

Cytokines are also redundant in nature. This means that many (but not all) biological properties originally described for one cytokine can also be ascribed to others. For instance, when IL-2 was originally discovered it was thought to be the primary T cell growth hormone. Subsequently it has been found that a number of other cytokines can also promote T cell expansion, including IL-4. This redundancy is borne out in genetic knockout experiments of individual cytokines often resulting in mice with subtle defects in their immune responses suggesting that the loss of a particular cytokine can be compensated for by the action of another.

Regulated Expression

The expression of cytokines is also highly regulated. Cytokine gene transcription usually occurs rapidly after an inducing stimulus. The rapid increase in cytokine gene mRNA results in a burst of cytokine protein secretion into the surrounding milieu and can act directly on the cell that produced it or on neighboring cells. For example, T lymphocytes produce large amounts of IL-2 within minutes of encountering antigenic peptides which functions to promote their own expansion. Likewise, when a phagocytic monocyte encounters bacterial lipids it rapidly produces the cytokine TNF resulting in recruitment and activation of additional inflammatory leukocytes. This rapid increase in transcription is usually transient and is extinguished rapidly resulting in a self-limited event. The transitory nature of the cytokine response is imperative since, in the case of TNF, high levels and sustained cytokine production can cause systemic problems such as cachexia and septic shock.

Cytokine expression is not only highly regulated temporally but can also be restricted in a cell type specific manner. For example, CD4+ T helper cells can be divided into two distinct subsets based precisely on

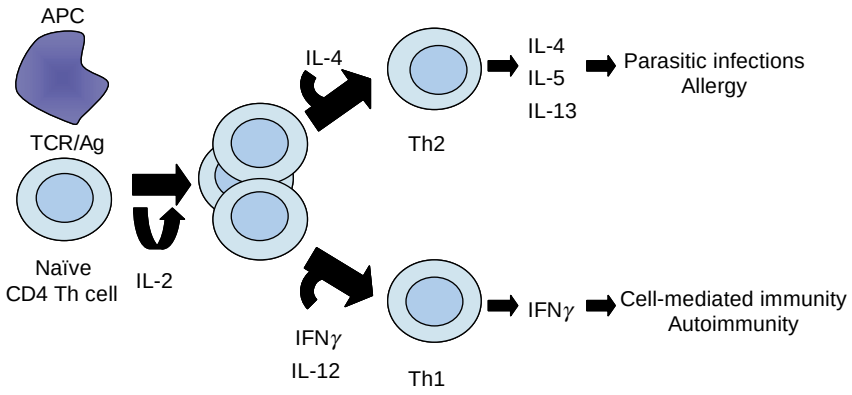

FIGURE 1 T helper cell differentiation. Th cells can differentiate into functionally different subsets depending on the cytokines they are exposed to during antigen activation. Developing Th cells that are exposed to IL-4 differentiate into Th2 cells capable of producing IL-4, IL-5, and IL-13. Th2 cells are important for the clearance of parasitic infections but can also contribute to the pathogenesis of asthma. Th cells that develop in the presence of IFNγ and IL-12 ultimately become IFNγ-producing Th1 cells and play an important role in the clearance of intracellular bacteria but can also contribute to the development of autoimmunity.

their cytokine expression profiles (Figure 1). These individual subsets carry out very different roles in an immune response in part due to the cytokines they produce. T helper type 1(Th1) cells are characterized by the production IFNγ, a cytokine involved in the activation of macrophages to kill phagocytosed microbes. Not surprisingly, Th1 cells are heavily involved in the clearance of intracellular bacteria. Alternatively, T helper type 2 (Th2) cells are characterized by their production of IL-4, IL-5, and IL-13 which directly promote the production of the IgE antibody isotype and stimulate eosinophils. These downstream responses are critical for the clearance of helminthic parasites.

The Role of Cytokines in Immune Responses

It is clear from the discussion above that cytokines can promote a variety of effects on a number of cell types resulting in a wide range of outcomes. Ultimately, the specific expression of and response to cytokines helps orchestrate a tightly regulated immune response.

Cytokines and the Innate Immune Response

Innate immunity is characterized by the initial recognition that a foreign pathogen, such as a virus or bacteria, is in the host. Cytokines play an important role in alerting and activating the immune system to an infection.

Cytokine Response to Bacterial Infection

The cytokine TNF plays an important role in the initial inflammatory response to bacteria especially in the recruitment of leukocytes to the site of infection (Figure 2). When a mononuclear phagocyte, such as a macrophage, encounters gram-negative bacteria it recognizes a product of the cell wall called LPS. LPS binds to a cell surface receptor on the macrophage called CD14 and stimulates the rapid production of TNF. The local presence of TNF serves to recruit other cells, neutrophils and monocytes, to the site of infection. TNF does this by stimulating the expression of adhesion molecules on the surrounding endothelial cells, which capture the leukocytes as they pass by the activated endothelium. TNF also stimulates the production of chemokines from the activated endothelial cells, which further serves to increase recruitment and activation of leukocytes and ultimately results in their transmigration through the vessel wall directly to the infection site. Another cytokine, IL-1, is also produced by macrophages after bacterial exposure and promotes similar inflammatory responses.

Macrophages also respond to bacterial products by producing IL-12 (Figure 2). IL-12 is an important activator of IFNγ production from NK cells and T cells. This IFNγ then feeds back onto the macrophages by enhancing their microbicidal functions to destroy phagocytosed bacteria. IL-12 also directly increases the cytolytic activity of NK cells themselves. Mice made genetically deficient for functional IL-12 have defects in their IFNγ production and NK cell function.

Cytokine Response to Viral Infection

The cytokines IFN-α and IFN-β, also known as type I IFNs, are important mediators of the innate immune

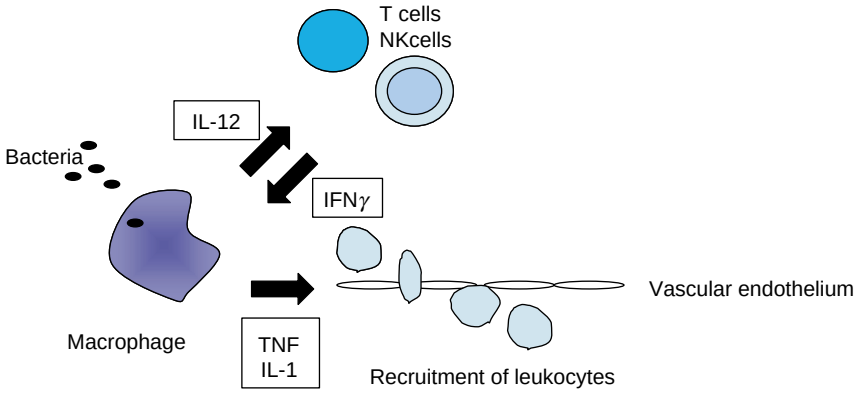

FIGURE 2 Cytokine response to a bacterial infection. Macrophage activation by exposure to bacterial products results in TNF and IL-1 secretion. TNF and IL-1 activate nearby vascular endothelial cells to permit recruitment of leukocytes to the infection site. Activated macrophages also produce IL-12 leading to increased IFNγ production from NK and T cells. IFNγ feeds back on the macrophage to increase the phagocytic potential and microbicidal properties of the macrophage.

response to a viral infection. When a cell is infected with a virus, or exposed to double-stranded RNA molecules that mimic viral replication, production of type I IFNs is dramatically induced. The expression of type I IFNs has a number of consequences in the control of a viral infection. First, exposure to type I IFNs induces the expression of enzymes that directly interfere with viral replication and this helps to protect neighboring cells from becoming infected. Also, type I IFNs act to increase class I MHC expression ultimately resulting in enhanced CTL responses to infected cells. Additionally, type I IFNs directly boost the lytic activity of NK cells.

Cytokines and the Adaptive Immune Response

The adaptive immune response is characterized by the specific activation and expansion of antigen-specific lymphocytes in response to a pathogen as well as immunological memory. Cytokines play a critical role in the proliferation of activated lymphocytes and promoting their differentiation into distinct effector subsets and the induction of memory. Here are just a few examples.

IL-2

As mentioned above, IL-2 has been described chiefly as a T cell growth factor, although it is now recognized that IL-2 plays important roles in several aspects of the adaptive immune response. When a T cell recognizes foreign peptide antigen, IL-2 is produced within minutes and then acts in an autocrine fashion to promote the expansion of that T cell clone. IL-2 also stimulates the proliferation and lytic activity of NK cells. However, IL-2 plays an important role in negatively regulating or terminating an inappropriate T cell response as well. When a cell is repeatedly stimulated with antigen, such as the case with autoantigens, IL-2 exposure renders the cells sensitive to a process called activation induced cell death (AICD) and promotes their elimination. Mice that are deficient for IL-2 or IL-2 receptor subunits develop autoimmunity suggesting an important role for IL-2 in regulating inappropriate T cell responses.

IFNγ

As mentioned, IFNγ plays an important role in activating macrophages during the innate immune response as the downstream target of bacterially stimulated IL-12. However, IFNγ also directly influences the function of antigen-specific lymphocytes during an immune response. For example, IFNγ, along with IL-12, directly promotes the differentiation of CD4+ T cells to become IFNγ-producing Th1 effector cells (Figure 1). As discussed earlier, this T cell subset is critical for the clearance of intracellular bacteria. IFNγ also acts directly on B lymphocytes to promote the production of the specific IgG subclass, IgG2a. This IgG subclass binds to Fcγ receptors on macrophages and promotes phagocytosis of microbes. IFNγ also has indirect effects on T cell function through the up-regulation of MHC molecules on antigen presenting cells, which ultimately increases the opportunity for antigen recognition by the T cell.

IL-4

IL-4 is a cytokine that acts in many ways as an antagonist to the actions of IFNγ described previously. As opposed to the Th1-promoting properties of IFNγ, IL-4 directly promotes the differentiation of CD4+ T cells to become IL-4-producing Th2 cells and inhibits the ability of IFNγ to promote Th1 differentiation (Figure 1). As described, Th2 cells are critical for the clearance of

parasitic infections. IL-4 also promotes the production of the IgE immuno-globulin isotype, which is important for mast cell-mediated immune responses, and inhibits class switching to the IFNγ-stimulated IgG2a. IL-4 has also been shown to inhibit the ability of IFNγ to activate macrophages but promotes MHC class II expression on antigen presenting cells.

Regulatory Cytokines

Most of the features of cytokines described here thus far have involved stimulating the proliferation, differentiation, or microbicidal potential of a responding cell. Recently it has become apparent that certain cytokines have a more regulatory nature. Two of the cytokines that have garnered increased interest recently are TGF-β and IL-10. TGF-β generally inhibits the proliferation and activation of lymphocytes and macrophages. TGF-β also stimulates the production of the immunoglobulin isotype IgA, which plays an important role in mucosal immunity. IL-10 has been described primarily as an inhibitor of macrophage function. Exposure of a macrophage to IL-10 results in decreased IL-12 and TNF production and decreased MHC expression. This decrease in macrophage function then in turn leads to decreased T lymphocyte responses as well. Mice that are deficient for IL-10 develop severe inflammatory bowel disease suggestive of uncontrolled macrophage activation. The expression of these regulatory cytokines have been ascribed to certain T cell subsets (T-regs) thought to be important for specifically suppressing immune responses to autoantigens and preventing the inappropriate activation of bystander lymphocytes.

Cytokines and Immunopathology

As important as cytokines are in orchestrating an immune response, dysregulated cytokine production can have serious and deleterious results. For example, the tissue destruction associated with autoimmune diseases such as type 1 diabetes and rheumatoid arthritis is strongly associated with elevated expression of proinflammatory cytokines such as IFNγ and TNF. Additionally, the airway hyper-responsiveness associated with allergic asthma has been causally linked with the Th2 cytokine IL-13. The notion of a relationship between dysregulated cytokine expression and disease has resulted in clinical applications. In particular, anti-TNF therapies have been effective in treating autoimmune disorders such as rheumatoid arthritis

Cytokine Receptors and Signaling

Cytokines mediate their biological effect through the binding of specific receptors on target cell surfaces. These receptors then convert an external signal (binding of the cytokine to the receptor) to an intracellular biochemical signal, usually resulting in new gene transcription. Cytokine receptors are transmembrane proteins where binding of the cytokine occurs in the extracellular region and interaction with signaling proteins occurs in the cytoplasm.

Cytokine Receptor Classes

Classification of cytokine receptors is based on structural homologies in the cytokine-binding regions. There are five families of cytokine receptors: type I cytokine receptors (IL-2 and IL-4), type II cytokine receptors (type I IFNs and IL-10), Ig superfamily receptors (IL-1), TNF receptors, and serpentine receptors (chemokines).

Cytokine Receptor Expression

Like the highly regulated expression of cytokines described above, expression of the cytokine receptors themselves is also highly regulated and can influence the cellular response to the cytokine. For example, the IL-2 receptor is composed of three polypeptide chains; α, β, and γ. In order for the T cell to maximally respond to IL-2 all three receptor chains must be expressed. When a T cell is specifically activated by antigen, the expression of the α-chain is induced and the cell is capable of expanding to the IL-2 it produces. This provides a link between the antigen specific activation of the T cell and the ability of that cell to subsequently respond to IL-2 ensuring that antigen specific T cells are preferentially and appropriately expanded during an immune response.

JAK/STAT Signaling

The best-defined signaling pathway utilized by type I and type II cytokine receptors involves the activation of Janus kinases (JAKs) and transcription factors called signal transducers and activators of transcription (STATs) (Figure 3). The JAK/STAT signaling pathway provides a direct link between cytokine binding at the cell surface to changes in gene expression at the level of new gene transcription. The general scheme consists of inactive JAK kinases bound specifically to the cytokine receptor cytoplasmic tail. Upon cytokine binding, the receptor chains are brought together and induce the activation of the JAKs through transphosphorylation. The JAKs also phosphorylate specific tyrosine residues on the cytoplasmic portion of the cytokine receptor, serving as a docking site for specific STAT proteins. The STAT proteins are also then phosphorylated, dimerize, and migrate to the nucleus. The dimerized STAT proteins are able to bind to specific DNA sequences in

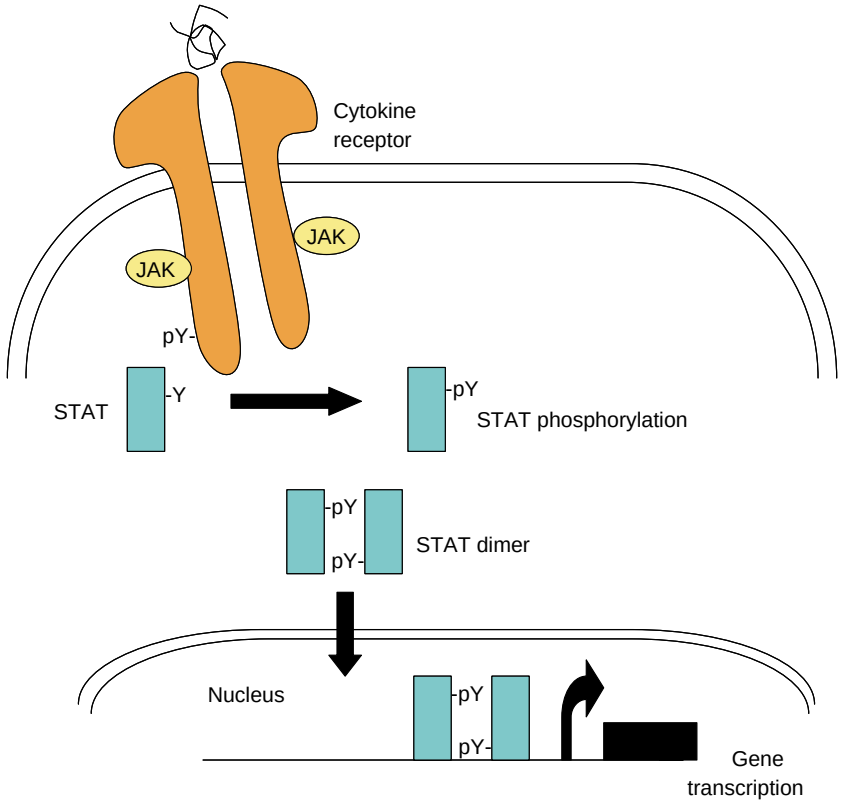

FIGURE 3 JAK/STAT signaling pathway. The activation of the JAKs after cytokine stimulation results in the tyrosine phosphorylation of the cytoplasmic tail of the cytokine receptor and recruitment of the STAT protein. The STAT protein is also tyrosine phosphorylated, forms dimers and migrates to the nucleus to activate the transcription of cytokine responsive genes.

the promoters of cytokine inducible genes and activate the transcription of those genes directly. Different cytokine receptors bind to unique JAK and STAT combinations resulting in specific outcomes to cytokine exposure.

Negative Regulation of Cytokine Signaling

Unopposed cytokine signaling can lead to a number of immune disorders so several regulatory mechanisms are in place to turn off JAK/STAT signaling after cytokine exposure. First, a family of cytoplasmic proteins called suppressor of cytokine signaling (SOCS) can directly interfere with JAK activity or with STAT binding to the cytokine receptor. The expression of the SOCS genes themselves is directly activated by the cytokine-induced STATs, consequently forming a classic negative feedback loop. SOCS1-deficient mice die within a few weeks of birth due to uncontrolled IFNγ responses suggesting a critical role for SOCS proteins in regulating cytokine signaling. JAK and STAT activity can also be negatively regulated by protein tyrosine phosphatases, which return the JAK and STAT proteins to their unphosphorylated, inactive states. STATs are also negatively regulated by their interaction with members of the PIAS protein family. The PIAS proteins in general act to inhibit the ability of STAT proteins to stimulate gene transcription.

See Also the Following Articles

Immunoglobulin (Fc) Receptors • Interferon Receptors • JAK-STAT Signaling Paradigm • Septins and Cytokinesis • T-Cell Antigen Receptor

Glossary

adaptive immunity Immunity mediated by lymphocytes after exposure to foreign pathogen. Characterized by exquisite specificity for antigen and the formation of a memory immune response.

innate immunity The initial and rapid response to invading microbes. The cell types involved include macrophages, NK cells, and neutrophils. The mechanism for response exists before infection and does not result in immunological memory.

JAK/STAT pathway Intracellular signaling pathway induced by triggering of type I and type II cytokine receptors. Involves activation of specific kinases (JAKs), recruitment, and phosphorylation of transcription factors (STATs) and their subsequent

translocation as active dimers to the nucleus to activate gene transcription of cytokine responsive genes.

macrophage A phagocytic cell that plays important roles in both adaptive and innate immune responses. Activated macrophages engulf and kill invading microorganisms, secrete cytokines, and present antigen to T helper cells.

T helper (Th) cell CD4+ T cell subset that mediates cell-mediated responses in the adaptive immune system. Th cells are divided into two distinct subsets (Th1 and Th2) depending on the cytokines they secrete.

Further Reading

Hill, N., and Sarvetnick, N. (2002). Cytokines: Promoters and dampeners of autoimmunity. *Curr. Opin. Immunol.* **14**, 791–797.

Murphy, K., and Reiner, S. (2002). Decision making in the immune system: The lineage decisions of helper T cells. *Nat. Rev. Immunol.* **2**, 933–944.

Renauld, J.-C. (2003). Class II cytokine receptors and their ligands: Key antiviral and inflammatory modulators. *Nat. Rev. Immunol.* **3**, 667–676.

Shuai, K., and Liu, B. (2003). Regulation of JAK–STAT signaling in the immune system. *Nat. Rev. Immunol.* **3**, 900–911.

Biography

Andrea Wurster is an Instructor at the Harvard Medical School. She holds a Ph.D. from the University of California, San Diego. Her research has focused on the role of STAT proteins and cytokines in immune responses.

Michael Grusby is a Professor of Molecular Immunology at the Harvard School of Public Health. He received his Ph.D. from Northwestern University and serves on the editorial boards for the journals *Immunity* and *Journal of Biological Chemistry*. His research has focused on the role STAT proteins and cytokines in immune responses.

Cytokinesis

Masanori Mishima and Michael Glotzer
Research Institute for Molecular Pathology, Vienna, Austria

During cell division the chromosomes are equally segregated to the two poles of the mitotic spindle and the resulting two sets of chromosomes are sequestered into separate cells by a process known as cytokinesis. Cytokinesis must be controlled in both space and time so that the resulting daughter cells each contain a complete copy of the genetic material and other cellular organelles.

Making the Plans: Various Strategies for Coordinating Nuclear and Cytoplasmic Division

Diverse biological constraints dictate that cytokinesis is performed in different ways in various organisms. For example, the presence or absence of a cell wall greatly influences the nature of the cytokinetic process. In plant cells, which have cell walls, the daughter cells are separated by the cell plate, which is formed in the center of the cell by vesicle transport and fusion. In animal cells, the cleavage furrow is generated by constriction of a contractile ring containing actin and myosin II as key components.

A second feature which appears to differ among different cell types is the means by which the division plane is coordinated with nuclear division. For example, in plants and yeast, the division plane is established before mitosis and chromosome segregation is coordinated with this pre-existing spatial determinant. In contrast, in animal cells, the position of the division plane is established by the mitotic spindle in anaphase.

On the other hand, recent data indicate that different modes of cytokinesis rely on common molecular mechanisms. In yeast, cell-wall synthesis had been thought to be the major mechanism of cytokinesis. However, ingression of cell membrane by the constriction of actin ring is now known also to be important. Conversely, in animal cells, although the dominant factor in cell division is constriction of the contractile ring, vesicle trafficking has recently been demonstrated to contribute to this process. A comparison of the molecules required for cytokinesis in various organisms reveals that although some proteins, such as myosin and profilin, are generally required for cytokinesis in all species analyzed thus far, other proteins that are essential in one system are sometimes not even present in other systems (Table I). Thus, the different modes of cytokinesis in various systems may reflect varying degrees of reliance on common basic processes.

Identification and characterization of the molecular machines responsible for cytokinesis has advanced greatly because of the use of genetic analysis in model organisms including yeast, flies, and worms. It is anticipated that the use of RNA-mediated gene silencing (RNAi) will significantly enhance the understanding of cytokinesis in mammalian cells. The proteins involved in cytokinesis conserved among model organisms are summarized in Table I. The mechanism of cytokinesis in animal cells is the primary focus of this article (Figure 1).

Making the Plans: Coordinating Nuclear and Cytoplasmic Division in Animal Cells

In animal cells, the mitotic spindle provides the spatial cue for division. Micromanipulation experiments indicate that microtubules are the critical factor within the spindle; the chromosomes are dispensible. Although it was long thought that microtubules provide a positive signal for cleavage furrow formation, recent evidence suggests that microtubules may generally inhibit cortical contractility and that a local minimum of microtubule density may direct cleavage furrow positioning. However, the underlying molecular mechanism has not been determined.

Since the critical factor required for contractile ring formation is RhoA, a simple, speculative model that could account for cleavage furrow formation is that high microtubule density inhibits RhoA activation and that sites where microtubule density reaches a local minimum induce activation of the small GTPase, RhoA. Like other small GTPases, the activity of RhoA is controlled by guanine nucleotide exchange factors (GEFs) and GTPase activating proteins (GAPs).

TABLE I

Proteins Involved in Cytokinesis Conserved Among Model Organisms

Family	Domains	Mammal	Drosophila	*C. elegans*	*S. pombe*	*S. cerevisiae*	Dictyostelium
Contractile ring							
Myosin II heavy chain	MYSc, CC	Cytoplasmic myosin II	Zipper	NMY-2	Myo2, Myo3/Myp2	MYO1	MHCA
Myosin II light chains	EFh	Essential LC, regulatory LC	Spaghetti squash	MLC-4	Cdc4, Rlc1	Mlc1, Mlc2	Essential LC, regulatory LC
Formin	FH1, FH2, FH3	mDia1, mDia2	Diaphanous, Cappuccino	CYK-1	Cdc12	Bni1, Bnr1	(For A, B, C)
Profilin	PROF	Profilin	Chickadee	PFN-1	Cdc3	Pfy1	Profilin I, II
Rho-kinase	S_TKc, CC, PH	Rho-kinase/ROCK	(Drok)	LET-502	?	?	?
Pebble/ECT2	BRCT, RhoGEF	Ect2	Pebble	LET-21	?	?	?
Cofilin/ADF	ADF	Cofilin/ADF	Twinstar	(UNC-60A, B)	(Cof1/Adf1)	(Cof1)	(Cofilin, cofilin-2)
Central spindle							
PRC1/Ase1	(a Map)	PRC1	(CG11207, CG1655)	(Y34D9A.4)	(CAC21482)	Ase1	?
Centralspindlin kinesin	KISc, CC	MKLP-1/CHO1	Pavarotti	ZEN-4	?	?	?
Centralspindlin RhoGAP	CC, C1, RhoGAP	MgcRacGAP/ HsCYK-4	DRacGAP/acGAP	CYK-4	?	?	?
Mitotic kinase/phosphatase							
AuroraB	S_TKc	AuroraB/ AIM-1/AIRK2	DmAurora B/IAL	AIR-2	(Ark1/Aim1)	(lpl1)	?
INCENP	IN box	INCENP	DmlNCENP	ICP-1	(Pic1)	(Sli15)	?
Survivin	BIR	Survivin	Survivin	BIR-1	(Bir1/Cut17)	(Bir1)	?
Polo kinase	S_TKc, polo box	PLK1	Polo	PLK-1	Plo1	Cdc5	?
Cdc14	Protein phosphatase	hCdc14A, B	(CG7134)	CeCDC-14	Flp1/Clp1	Cdc14	?
Others							
Septin	GTPase	(Nedd5, H5, Diff 6, MSF, etc.)	(Peanut, Sep1, Sep2)	(UNC-59, UNC-61)	Spn1-6	Cdc3, 10, 11, 12	?
IQGAP	CH, IQ, RasGAP	(IQGAP1, 2)	?	(F09C3.1?)	Rng2	Cyk1/lqg1	GAPA, DGAP1
Cdc15	FCH, SH3	(PSTPIP)	?	?	Cdc15, lmp2	Cyk2/Hof1	?

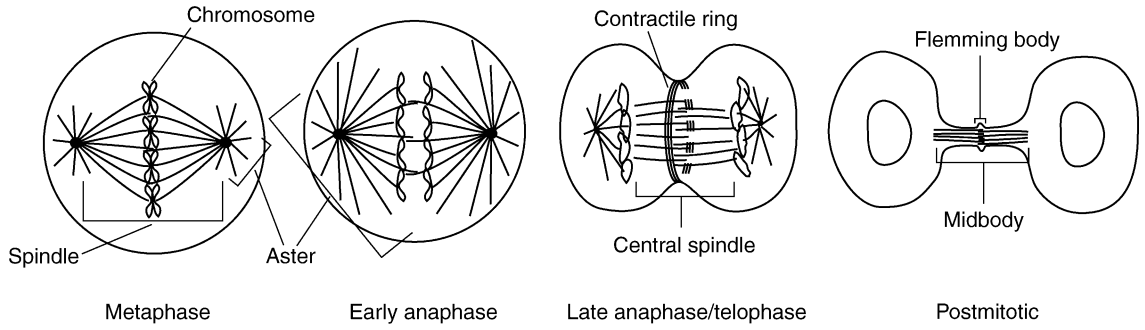

FIGURE 1 The stages of cytokinesis and a guide to the cellular structures involved.

There is strong evidence that a specific GEF regulates cytokinesis. This protein, known as Pebble in flies or ECT2 in mammalian cells, is a multidomain protein whose loss of function parallels that of depletion of RhoA. However, it is not clear if the mitotic spindle generates local activation of RhoA by inducing high GEF activity at regions of low microtubule density. Alternatively RhoA could be activated globally, but other regulatory processes could inhibit the biological function of RhoA where microtubule density is high.

Assembling the Parts 1: Building the Contractile Ring

A number of direct effectors of RhoA have been described and shown to be involved in cytokinesis, including Rho kinase and members of the formin family (Figure 2). Formin family members are auto-inhibitory proteins which are activated by binding of active RhoA. Formins are found concentrated at the contractile ring. They bind to an actin-binding protein, profilin, via a proline-rich sequence. Recently, formin proteins have been shown to have actin-polymerizing activity; this activity is further accelerated by profilin. Thus, formins could contribute to the formation of contractile ring by directing actin polymerization. There is functional evidence for a requirement for formin proteins in cytokinesis in mammals, flies, worms, budding yeast, and fission yeast; so far there is no evidence that formins are required for cytokinesis in plants or *Dictyostelium*.

Like formins, Rho kinase (ROCK) also localizes to the cleavage furrow. One substrate of this kinase is the activation site of the regulatory light chain of myosin II. ROCK also phosphorylates and inactivates the myosin-binding subunit of myosin phosphatase (MBS). Both pathways lead to the activation of myosin-II. In *C. elegans*, mutation of the ROCK orthologue, LET-502, causes defects in cytokinesis. However, these defects can be suppressed by mutation of MBS MEL-11. Thus, ROCK is an important player in cytokinesis, though perhaps it plays an accessory role rather than an essential one.

The contractile ring is a highly dynamic structure. Inhibition of actin polymerization during furrow ingression blocks propagation of the cleavage furrow. Conversely, depolymerization of actin filament in concert with the progression of the constriction is also important for cytokinesis. Indeed, actin depolymerizing factor is required for normal cytokinesis. Moreover, there are indications that inactivation of RhoA is required for completion of cytokinesis, since the CYK-4 RhoGAP is required for completion of cytokinesis.

Assembling the Parts 2: Building the Central Spindle

The central spindle, or spindle midzone, is a barrel-like structure of microtubules formed between the segregating chromosomes during anaphase. The plus ends of nonkinetochore spindle microtubules are bundled to form antiparallel arrays in the spindle midzone. As the cleavage furrow ingresses, these microtubules become compacted. Finally, they form a structure called the midbody with completely constricted contractile ring overlaid by the still continuous cell membrane.

The importance of the central spindle on the promotion and completion (in some systems, initiation) of cytokinesis has been shown by micromanipulation and genetic analysis. For example, depletion or inactivation of *C. elegans* ZEN-4, a kinesin-like molecule that concentrates on the central spindle prevents formation of this structure in early embryos. Contractile ring formation and furrow ingression nevertheless occur. However, the furrow fails to complete and it ultimately regresses. In *Drosophila*, the central spindle seems to be required for early steps in cytokinesis since furrow ingression is not observed in embryos that have mutations in the pavarotti locus (Pav is the orthologue of *zen-4*).

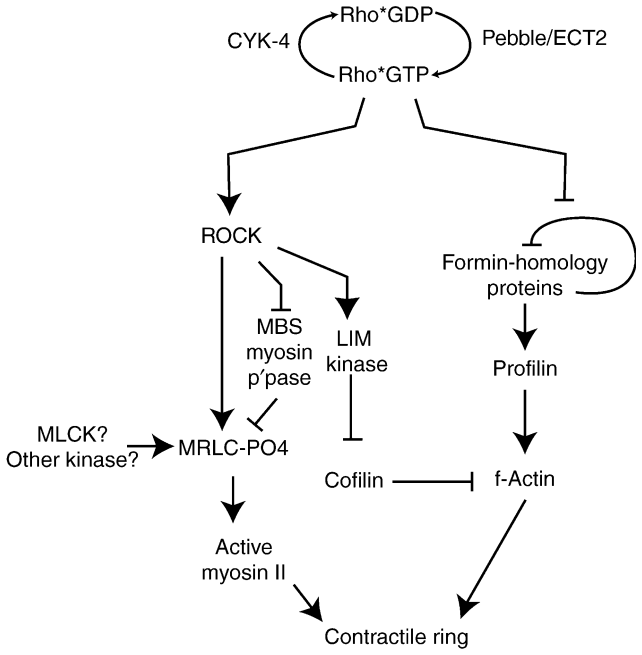

FIGURE 2 The biochemical pathways through which RhoA regulates contractile ring formation.

A RhoGAP, CYK-4, colocalizes with ZEN-4 to the central spindle and midbody. Like ZEN-4, CYK-4 involved the formation of central spindle. CYK-4 forms a stoichiometric complex with ZEN-4 both *in vivo* and *in vitro*. A mutation in the CYK-4 binding domain of ZEN-4 can suppress the embryonic lethality caused by a mutation on the ZEN-4 binding domain of CYK-4, indicating the importance of complex formation for the *in vivo* function of these molecules. This complex is probably directly involved in assembling the central spindle since purified, recombinant CYK-4/ZEN-4 complex has microtubule bundling activity (Figure 3).

Human orthologues of CYK-4 and ZEN-4, HsCYK-4/MgcRacGAP and MKLP-1/CHO1, respectively, also form a similar protein complex. Depletion of HsCYK-4 by RNAi causes cytokinesis defects. Overexpression of MgcRacGAP mutant lacking MKLP-1 binding region or with mutation in the RhoGAP domain inhibits cytokinesis. Overexpression of MKLP-1 with a mutation in the motor domain causes an abnormal central spindle, loss of midbody material, and multinuclear cells. Thus, a protein complex, centralspindlin, containing orthologues of CYK-4 and ZEN-4 has an evolutionary conserved role in the formation and function of central spindle/midbody.

Another molecule, PRC1, is also important for the formation of central spindle. It too has microtubule bundling activity *in vitro*. Antibody injection or depletion by RNAi causes abnormal central spindle and inhibits cytokinesis. In metaphase, PRC1 is phosphorylated by cyclin-dependent kinase 1 (CDK1). This phosphorylation is thought to negatively regulate the protein because a mutant lacking the phosphorylation sites causes abnormal bundling of microtubules in the metaphase spindle. PRC1 contains a conserved central region. Other proteins that have this conserved domain are also implicated in organizing the anaphase spindle, e.g., budding yeast Ase1. In this context it is notable that the centralspindlin complex is not present in yeast. There is no evidence that the anaphase spindle participates in cytokinesis in budding or fission yeast.

Although the mechanism of formation of central spindle has been gradually revealed, the function of the central spindle in cytokinesis remains unclear. There are at least three possibilities.

1. It could be involved in the determination of cleavage site by modulating the distribution of microtubules in the mitotic apparatus during anaphase.
2. It could serve to localize factors that regulate the assembly and/or disassembly of the contractile ring.
3. Like the phragmoplast in plants, it could function to direct vesicle traffic along the ordered microtubule bundles.

These possibilities are not mutually exclusive, although the relative importance might vary among cell types.

Pushing the Envelope: Membrane Fusion

Geometrical considerations require that during cytokinesis, if the total volume of the daughter cells is equivalent to that of the parental cell, the surface area of the cells must increase. Indeed, evidence has accumulated suggesting that vesicle traffic plays an important role in cytokinesis. In *Xenopus*, Zebrafish, and sea urchin embryos, insertion of new cell membrane into cleavage furrow by exocytosis has been observed.

The machinery responsible for this membrane insertion has begun to emerge. Specific syntaxins, rabs, and Golgi proteins have been implicated in cytokinesis and/or cellularization in *Drosophila*, *C. elegans*, and sea urchin embryos. Specific Golgi proteins, such as Lava Lamp, which interacts both with actin and microtubules, are required for cellularization. A lipid kinase, phosphatidylinositol 4-kinase, is required for cytokinesis in spermatocytes (the cell-type specificity may result from genetic redundancy in other cell types).

There are other interesting observations from the point of view of lipid membrane and cytokinesis. Phosphatidylethanolamine (PE) appears on the outer leaflet of cell membrane of cleavage furrow while it is usually enriched in the inner leaflet. A multivalent

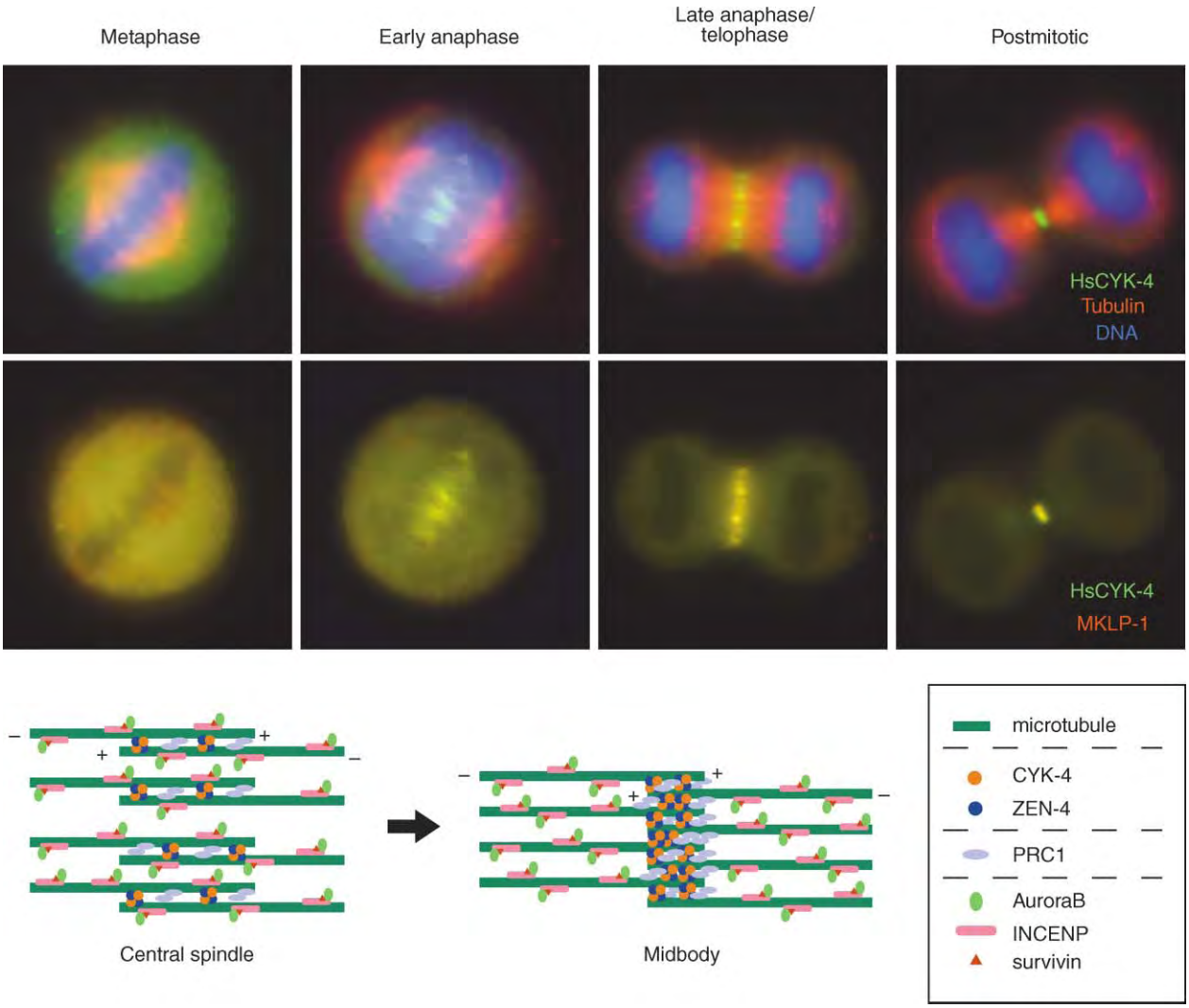

FIGURE 3 The localization of the centralspindlin components MKLP1/HsCYK-4 during the process of cytokinesis. A schematic drawing depicting the assembly of the central spindle.

PE-binding peptide inhibits depolymerization of actin filament at midbody stage, and prevents completion of cytokinesis. Likewise, a sphingolipid, psychosine, causes defect of cytokinesis in some cells.

Getting the Timing Right

In anaphase, activation of anaphase-promoting complex (APC) induces segregation of chromosomes and exit from mitosis by catalyzing the proteolytic destruction of securin and cyclins. Because cytokinesis occurs once per cell cycle and it is coupled to the exit from mitosis, there must be some connection between the cell-cycle engine and cytokinesis. That this is indeed the case is indicated by the fact that a nondegradable mutant of cyclin B prevents assembly of the central spindle and inhibits cytokinesis in mammalian cells, *Drosophila* and sea urchin embryos. This suggests that CDK1/cyclin B negatively regulates cytokinesis. This may be in part due to the regulation of microtubule dynamics. If the spindle is displaced to the vicinity of the cell cortex, furrow ingression can occur in the presence of high levels of CDK1/cyclin B.

CDK1/cyclin B may also regulate central spindle assembly via PRC1, since its function appears to be negatively regulated by CDK1. The RhoGEF, Ect2/Pebble, may also be negatively regulated by CDK1/cyclin B. In addition, cyclic activation of myosin-II in *Drosophila* embryos is indirectly regulated by CDK1 activity.

A conserved signaling cascade called the mitotic exit network (MEN) (budding yeast) or the septation initiation network (SIN) (fission yeast) has been

characterized in detail. At the end of the cascade, a protein phosphatase (Cdc14 in budding yeast and Flp1/Clp1 in fission yeast) is activated. In budding yeast, activation of Cdc14 leads to the activation of APC–Cdh1 through the dephosphorylation of Cdh1. In *S. pombe*, Flp1/Clp1 is involved in the regulation of the timing of septum formation and entry into M-phase. Although their roles are apparently different, antagonism of CDK1 activity could be a common function between Cdc14 and Flp1/Clp1. There are orthologues of Cdc14 in animal cells; however, the conservation of the MEN or SIN cascade is less clear. In mammalian cells, inhibition of Cdc14 causes several mitotic defects including abnormal separation of centrosomes and failure of the completion of cytokinesis. In nematodes, CeCDC-14 localizes to central spindle and its depletion by RNAi causes a similar phenotype to depletion of ZEN-4. Perhaps one conserved role of CeCDC-14 is to relieve the inhibition of cytokinesis by CDK1, though the critical targets may be different in different systems.

Finishing the Job

Daughter cells typically enter G_1 phase connected to each other by the midbody. How they are finally separated (abscission) is not clear, although there is evidence that the midbody and vesicle traffic are involved. Interestingly, it has been observed that the abscission is delayed while the mother centriole, which is loosely connected to the daughter centriole, comes close to the midbody. It has been observed that the timing of abscission correlates with the moment at which the mother centriole moves away from the midbody.

See Also the Following Articles

Mitosis • Rho GTPases and Actin Cytoskeleton Dynamics

Glossary

aster Radial array of microtubules that surrounds each of the spindle poles during mitosis.

central spindle Antiparallel bundle of microtubules that forms in anaphase between the segregating chromosomes.

contractile ring Actomyosin-based structure responsible for constricting the cell cortex.

Flemming body The phase dense structure found in the center of the midbody at late times in cytokinesis.

midbody The thin intercellular bridge connecting the two daughter cells.

Further Reading

Finger, F. P., and White, J. G. (2002). Fusion and fission: Membrane trafficking in animal cytokinesis. *Cell* **108**, 727–730.

Glotzer, M. (2001). Animal cell cytokinesis. *Annu. Rev. Cell Dev. Biol.* **17**, 351–386.

McCollum, D., and Gould, K. L. (2001). Timing is everything: Regulation of mitotic exit and cytokinesis by the MEN and SIN. *Trends Cell Biol.* **11**, 89–95.

Severson, A. F., and Bowerman, B. (2002). Cytokinesis: Closing in on the central spindle. *Dev. Cell* **2**, 4–6.

Straight, A. F., and Field, C. M. (2000). Microtubules, membranes and cytokinesis. *Curr. Biol.* **10**, R760–R770.

Biography

Masanori Mishima is a postdoctoral Fellow at the Research Institute for Molecular Pathology (IMP) in Vienna, Austria. He received his D.Sc. from the University of Tokyo.

Michael Glotzer is a Research Group Leader at the IMP in Vienna, Austria. He received his Ph.D. from the University of California, San Francisco. The Glotzer group studies cytokinesis using *C. elegans* as a principal model system.

Cytokinin

Thomas Schmülling
Free University of Berlin, Berlin, Germany

Cytokinins are plant-specific chemical messengers (hormones) that play a central role in the regulation of the plant cell cycle and numerous developmental processes. Cytokinins were discovered by F. Skoog, C. Miller, and co-workers during the 1950s as factors that promote cell division (cytokinesis). The first cytokinin discovered was an adenine (aminopurine) derivative named kinetin (6-furfuryl-aminopurine), which was isolated as a DNA degradation product. The first common natural cytokinin identified was purified from immature maize kernels and named zeatin. Several other cytokinins with related structures are known today. Cytokinins are present in all plant tissues. They are abundant in the root tip, shoot apex, and immature seeds. Their endogenous concentration is in the low nM range. Typically, several types of cytokinins and their modified forms are present in a given tissue. Cytokinins can act over long distances or in the direct vicinity of the cytokinin producing cells (paracrine signaling). Cytokinins may act also on the cell that produced them (autocrine signaling). Cytokinins are also produced by cyanobacteria, some plant pathogenic bacteria (e.g., *Agrobacterium tumefaciens*, *Pseudomonas savastanoi*, *Rhodococcus fascians*) and the slime-mold *Dictyostelium discoideum*.

Cytokinin Structures

Naturally occuring cytokinins are adenine derivatives with a side chain at the N^6-position (Figure 1). The structure and conformation of the N^6-attached side chain can markedly influence the biological activity of the cytokinin. Depending on the structure of the N^6-substituent, cytokinins are classified as isoprenoid or aromatic cytokinins. The biological activities of both classes are qualitatively similar but they may differ quantitatively in different processes. Isoprenoid cytokinins are the most abundant class. They are either isopentenyl (iP)-type cytokinins, having an isopentenyl N^6-side chain, or zeatin-type cytokinins, having a hydroxylated isopentenyl N^6-side chain. The side chain of a zeatin-type cytokinin occurs in either *cis* or *trans* configuration, depending on which of the two methyl groups is hydroxylated. The *cis* form is usually much less active. Reduction of the double bond in the side chain leads to dihydrozeatin. Aromatic cytokinins have an aromatic benzyl group at N^6. They occur more rarely and much less is known about them. Because of their greater stability, aromatic cytokinins are often used in tissue culture, an example is benzyladenine. In addition, there are the structurally unrelated phenylurea-type cytokinins (e.g., diphenylurea, thidiazuron), a class of synthetic cytokinins. These cytokinins are highly active but do not occur naturally.

Cytokinin Biosynthesis and Metabolism

The rate of *de novo* synthesis, metabolic interconversion, and breakdown are, together with transport processes, relevant to the regulation of cytokinin homeostasis in cells. Cytokinin metabolism includes mainly conversions among cytokinin bases, ribosides, ribotides, side-chain modification, conjugation and conjugate-hydrolyzing reactions, and cytokinin degradation.

Biosynthesis

The initial and rate-limiting step of biosynthesis of isoprenoid-type cytokinins is the transfer of the isopentenyl moiety from dimethylallyl pyrophosphate (DMAPP) to AMP, ADP or ATP. The reaction is catalyzed by DMAPP::AMP/ADP/ATP isopentenyltransferases (IPT). ADP and ATP are the preferred substrates of most of the known plant IPT enzymes, while bacterial enzymes prefer AMP. The reaction leads to the formation of isopentenyl-AMP, -ADP and -ATP, which are the precursor molecules of biologically active cytokinins. The isopentenyl side chain is subsequently hydroxylated to form zeatin-type cytokinins (Figure 1). An alternative pathway, in which an already hydroxylated side chain is directly added to the N^6-position of the adenine moiety, may exist. IPT enzymes are encoded in *Arabidopsis* by a small gene family with seven members (*AtIPT1*, *AtIPT3–AtIPT8*). *AtIPT* genes are expressed in specific tissues of the root and shoot (e.g., vasculature), indicating that cytokinin synthesis

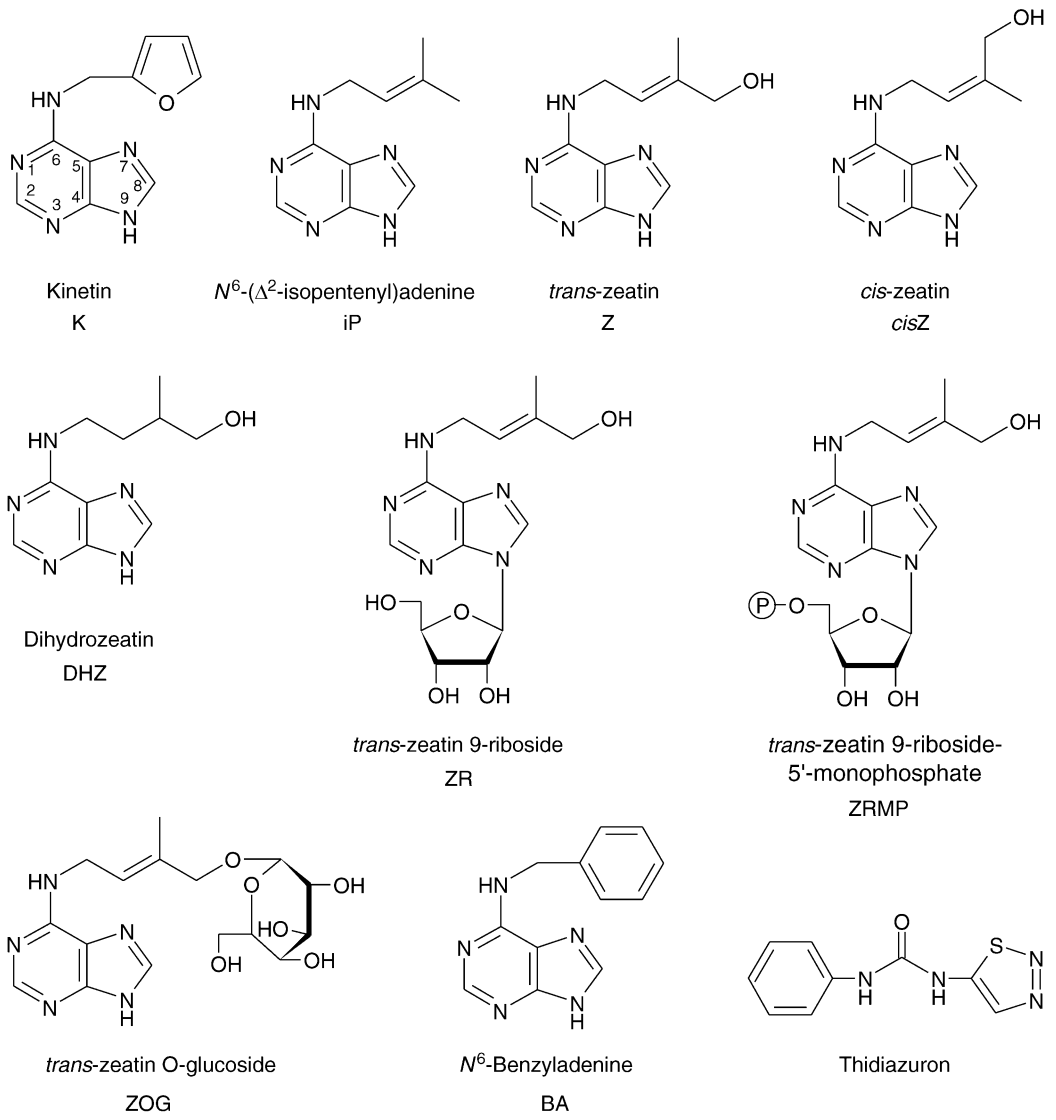

FIGURE 1 Chemical structures of some naturally occurring and synthetic cytokinins. Common names and abbreviations are indicated below the structures. The numbering of purine ring atoms is shown for kinetin.

occurs in all major organs. Another possible source of cytokinins is tRNA, since tRNAs of most organisms contain isopentenylated adenine and other structural derivatives with cytokinin activity. However, it is generally assumed that tRNAs play only a minor role, if any, as a cytokinin source.

Interconversion

A characteristic feature of cytokinin metabolism is the rapid metabolic interconversion of base, ribosides, and ribotides. The biologically most active form of cytokinins is the base. Attachment of ribose or ribose-5′-phosphate to the N^9 atom of the adenine ring leads to the formation of ribosides and ribotides, respectively, which do have lower activities (Figure 1). Interconversion of cytokinins is presumably an important mechanism to regulate the concentration of active compounds. Cytokinin ribosides are probably relevant as a transport form. The interconversions may be catalyzed by the same enzymes that metabolize adenine, adenosine, and AMP. The conversion between the *cis*- and *trans*-isomers of zeatin is catalyzed by the enzyme *cis–trans* zeatin isomerase. Zeatin is converted to dihydrozeatin by a NADPH-dependent zeatin reductase.

Conjugation

Cytokinins can be stably or transiently inactivated by glycosylation of the purine ring or of the side chain. The purine ring can be glycosylated at the N^3-, N^7-, and N^9-positions. In addition, the N^6-side chain group can

form *O*-glycosyl conjugates if it bears a hydroxyl-group. Most often, glucose is the conjugated sugar molecule, more rarely xylose is attached. N^7- and N^9-conjugates are biologically inactive and extremely stable. Thus, they are irreversibly inactivated cytokinins. N^3- and *O*-conjugates are biologically inactive but can be readily hydrolyzed. They are believed to be transient storage forms of cytokinins. Glycosyl conjugation is considered to be important in the regulation of cytokinin activity levels, at least in some tissues and species. Several genes coding for cytokinin glycosyltransferases and glycosidases have been identified. Some conjugates of cytokinins and amino acids (alanine) have been described as well.

Catabolism

Cytokinins are irreversibly degraded in a single enzymatic step by oxidative cleavage of the N^6-side chain. The reaction is catalyzed by cytokinin oxidases/dehydrogenases (CKX), which contain FAD as a cofactor. The reaction products are adenine and an aldehyde. The preferred substrates of CKX are isopentenyladenine, zeatin, and their corresponding ribosides. Ribotides, *O*-glucosides, dihydrozeatin, and aromatic cytokinins are not degraded by CKX. The *Arabidopsis* genome contains seven *AtCKX* genes, which are preferentially expressed in zones of active cell division and growth. The corresponding enzymes are located in the endoplasmatic reticulum, in the apoplast, and in the vacuole.

Cytokinin Transport

Cytokinins are transported from roots to shoots in the xylem, and in the opposite direction in the phloem. Transported cytokinins may have a role in coordinating root and shoot development, for example, by carrying information about nutrient availability. Multiple cellular importers and exporters are required to allow efficient mobilization and targeted translocation of cytokinins, but very little is known about cytokinin transporters. Transport studies indicate that a common H^+-coupled high-affinity purine transport system transports cytokinins.

Cytokinin Signaling

The mechanism of cytokinin signaling is just beginning to emerge. The cytokinin signal is perceived and transduced by a multistep phosphorelay system through a complex form of the two-component system (TCS) pathway. The TCS is common among prokaryotes and lower eukaryotes, among the higher eukaryotes it is unique to plants. In this signaling system, a membrane-located receptor kinase with an extracellular ligand-recognition domain (sensor) dimerizes upon binding a ligand and autophosphorylates a histidine within its cytoplasmic transmitter domain. The phosphoryl group is first transferred to an aspartate residue within the receiver domain at the C terminus of the receptor and from there to a His-containing phosphotransmitter (Hpt), which ultimately phosphorylates and thus activates a response regulator (RR) at a central Asp residue (see Figure 2).

Signal Perception

Cytokinin receptors are histidine kinases consisting of an extracellular sensing domain, a cytoplasmic histidine kinase transmitter and receiver domains. Three cytokinin receptors (CRE1/WOL/AHK4, AHK2, AHK3) have been identified in *Arabidopsis*. They all share a ~270 amino acid long extracellular cyclases/histidine kinases associated sensing extracellular (CHASE) domain, which presumably recognizes cytokinin. This domain might have been acquired by plants through lateral gene transfer from cyanobacteria. Loss-of-function mutants of CRE1/WOL/AHK4 lack the phloem in their primary roots, indicating a role for cytokinins in embryo development.

Signal Transduction

Current knowledge suggests that downstream signaling components of the cytokinin signal-transduction pathway in *Arabidopsis* consist of five Hpt and 22 response regulators of the A- or B-type. Hpts transmit the signal from the receptor, which is presumably localized in the plasma membrane, to B-type RRs, which are in the nucleus. B-type RRs consist of an N-terminal receiver domain and a C-terminal output domain, containing a DNA recognition motif called GARP, which is distantly related to the Myb repeat. The DNA motif optimal for binding is 5′-(A/G)GAT(T/C)-3′. Activated B-type ARRs transcribe primary response genes of cytokinins. Some of the known primary response genes, which are rapidly and specifically up-regulated by cytokinins, code for type A response regulators. Type A RRs resemble type B RRs but lack the C-terminal DNA binding and activation domain. Type A RRs fulfill at least two different functions. On the one hand, they exert a negative feedback regulation of the cytokinin signaling pathway through protein–protein interaction. On the other hand, they mediate the cytokinin-dependent modulation of other pathways, e.g., light signaling. A-Type response regulators can be

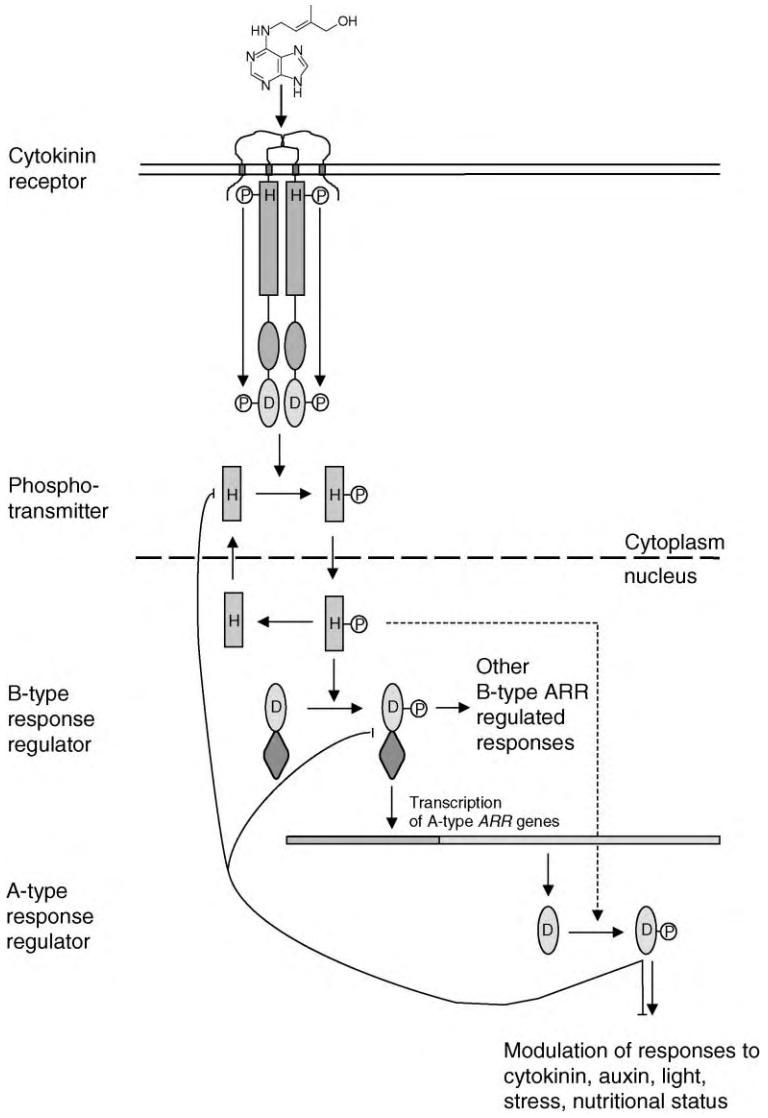

FIGURE 2 A model for cytokinin signal transduction via a His-to-Asp phosphorelay. The structure of CRE1/WOL/AHK4 is shown as an example. Ligand binding induces receptor dimerization and autophosphorylation. Transfer of the phosphoryl group by activated receptors activates histidine phosphotransmitter proteins (Hpts), which transport the signal from the cytoplasm to B-type RRs in the nucleus. B-Type response regulators transcribe target genes, among them A-type *RR* genes. A-Type response regulators may down-regulate the primary cytokinin signal response via a negative feedback loop, modulate downstream activities of cytokinins in a positive or negative fashion, or modulate other signaling pathways through protein–protein interaction. A more complex regulation than shown in the model may exist. D, aspartate residue; H, histidine residue; P, phosphoryl group.

positive or negative regulators, depending on the individual response regulator and the output reaction analyzed.

Cytokinin Functions

Cell Cycle

Cytokinins are required for cell division during embryogenesis in the shoot apical meristem, young leaves, the cambium, and cultured plant cells. In contrast, they have a negative regulatory role in the root meristem. Cytokinin controls the exit of dividing cells from this meristem. Changes in cytokinin levels occur during the cell cycle of cultured cells, the level being highest during the late S and before the M phase. Cytokinins have been functionally linked to all stages of the cell cycle but their mechanism of action has only been partially elucidated. Cytokinin up-regulates expression of the D-type cyclin gene *CycD3*, which is important in regulating the G1/S-transition of the cell cycle. Cytokinin increases the number of replication origins during S-phase and it may also play a role in regulating G2/M transition.

Plant Development and Growth

Cytokinin participates in regulating numerous aspects of plant development throughout the life cycle. These include seed germination, cotyledon expansion, chloroplast differentiation, de-etiolation, differentiation of vascular tissue, apical dominance (shoot branching), root elongation and branching, nutritional signaling, regulation of sink strength, the transition from the vegetative to the reproductive growth phase, flower and fruit development, leaf senescence, and plant–pathogen interactions. A role for the hormone in vascular morphogenesis during embryonic development is firmly established. During post-embryonic development cytokinins are required to maintain meristem activity and leaf development in the plant shoot. Local exogenous cytokinin application to the shoot leads to premature growth of lateral buds, retarded leaf senescence, partial photomorphogenesis in the dark, increased sink strength and an altered vasculature. In contrast to their stimulatory activities in the shoot, cytokinins have a negative regulatory role in the control of root elongation and branching. Additionally, cytokinin regulates important physiological parameters that determine biomass formation and distribution via central genes of primary metabolite pathways, including invertases, hexose transporters, and key genes of phosphate and nitrogen metabolism and signaling (e.g., nitrate reductase). Changes in cytokinin levels are generally positively correlated with levels of mineral nutrients, especially nitrogenous nutrients. Cytokinin levels are decreased by water stress. *In vitro*, the ratio of cytokinin to auxin determines the differentiation of cultured plant tissues to either shoots or roots. A high cytokinin to auxin ratio promotes shoot formation, a low ratio promotes root formation. Owing to their stimulatory effect on plant regeneration, cytokinins are widely used in plant tissue culture.

Pathogenicity

Cytokinins are produced by several plant pathogenic bacteria and play a role in pathogenicity. One such pathogen is *Agrobacterium tumefaciens*, the causative agent of the crown gall disease. During the infection process, *A. tumefaciens* transfers a small stretch of DNA, the T-DNA, to the host plant, where it becomes integrated in the nuclear genome. The T-DNA harbors an *IPT* gene, which is expressed in the host cell and causes cytokinin overproduction. This leads, together with an enhanced auxin content, to tumorous cell proliferation. Other cytokinin-synthesizing pathogens are *Pseudomonas syringae*, which induces gall formation and *Rhodococcus fascians*, which causes fasciation and a growth abnormality called witch's broom disease. The root-nodule forming and nitrogen-fixing plant symbiont *Rhizobium spec.* is also known to produce cytokinin.

Biotechnology

Practical use of cytokinin in agriculture is currently limited. Modulation of the endogenous cytokinin content of plants or interfering with cytokinin signaling has a high potential for biotechnological applications in agriculture. Plants with increased cytokinin content are more branched and senesce later. Moreover, cytokinins alter sink–source relations, a promising approach to improve yield attributes. Plants with reduced cytokinin content develop a larger root system. An improved root system means improved acquisition of minerals and water, factors which are often limiting for plant growth.

See Also the Following Articles

Cytokines • Cytokinesis • Septins and Cytokinesis

Glossary

cell cycle Sequence of events between mitotic divisions, divided into G1, (G standing for gap), S (synthesis phase), G2 and M (mitosis).

cytokinin conjugate Compound formed by the union of a cytokinin and a sugar moiety.

meristem Growing tip of roots and shoots.

senescence Programmed aging leading to organ or plant death.

two-component system Signal transduction system of bacteria, lower eukaryotes and plants; involves autophosphorylation of a histidine kinase that transmits the signal via phosphorelay to response regulator proteins.

Further Reading

Davies, P. J. (1995). *Plant Hormones. Physiology, Biochemistry and Molecular Biology.* Kluwer Academic, Dordrecht.

Heyl, A., and Schmülling, T. (2003). Cytokinin signal perception and transduction. *Curr. Opin. Plant Biol.* **6**, 480–488.

Hoykaas, P. J. J., Hall, M. A., and Libbenga, K. R. (1999). *Biochemistry and Molecular Biology of Plant Hormones*. Elsevier, Amsterdam.

Kakimoto, T. (2003). Biosynthesis of cytokinins. *J. Plant. Res.* **116**, 233–239.

Kakimoto, T. (2003). Perception and signal transduction of cytokinins. *Ann. Rev. Plant Biol.* **54**, 605–627.

Kieber, J. J. (2002). Cytokinins. In *The Arabidopsis Book* (C. Somerville, E. Meyerowitz and M. D. Rockville, eds.) American Society of Plant Biologists, http://www.aspb.org/publications/arabidopsis.

Mok, D. W. S., and Mok, M. C. (1994). *Cytokinins. Chemistry, Activity, and Function*. CRC Press, Boca Raton, FL.

Mok, D. W. S., and Mok, M. C. (2001). Cytokinin metabolism and action. *Annu. Rev. Plant Physiol. Plant Mol. Biol.* **52**, 89–118.

Schmülling, T., Werner, T., Riefler, M., Krupková, E., and Bartrina y Manns, I. (2003). Structure and function of cytokinin oxidase/dehydrogenase genes of maize, rice, Arabidopsis and other species. *J. Plant Res.* **116**, 241–252.

Taiz, L., and Zeiger, E. (2002). *Plant Physiology*. Sinauer, Sunderland, MA.

Biography

Thomas Schmülling is a Professor of Genetics and Chair of Developmental Biology of Plants at the Free University of Berlin. His principal research field is the biology of cytokinins. He studied biology at the University of Cologne, accomplished his doctoral thesis at the Max Planck Institute for Plant Breeding and has been an Assistant Professor at the University of Tübingen. He has made contributions to the understanding of *Agrobacterium rhizogenes* T-DNA genes and cytokinin metabolism and signaling. His laboratory was the first to generate cytokinin-deficient plants by means of genetic engineering.

Desmosomes and Hemidesmosomes

Rachel L. Dusek, Jonathan C. R. Jones and Kathleen J. Green
Northwestern University Feinberg School of Medicine, Chicago, Illinois, USA

Desmosomes and hemidesmosomes are cell junctions important for maintaining adherence within epithelial tissues, a function reflected in the Greek root *desmo*, meaning "bound." Desmosomes facilitate adhesion between adjacent epithelial cells, whereas hemidesmosomes (named for their ultrastructural resemblance to half a desmosome) mediate adhesion between basal cells of epithelial tissues and the substratum. These junctions are functionally alike in their ability to couple the intermediate filament (IF) cytoskeleton to sites of cell–cell or cell–substratum contact at the plasma membrane. However, these organelles differ dramatically in their molecular composition and specialized functions.

The Desmosome

Desmosomes are prominent in tissues that are subjected to mechanical stress. Found most abundantly in epithelial tissues, desmosomes are also present in the myocardium, brain meninges, and follicular dendritic cells of the lymph nodes. These specialized anchoring junctions function to mediate intercellular adhesion and maintain tissue integrity by connecting sites of cell–cell contact to the highly tensile intermediate filament (IF) cytoskeleton.

Desmosome Ultrastructure

Ultrastructurally, the desmosome appears as a symmetrical, highly organized, electron-dense structure that connects neighboring cells (Figure 1A). The plasma membranes of adjacent cells are separated by an ~30-nm space containing an electron-dense midline, composed of the extracellular portion of the transmembrane desmosomal components. Just internal to the plasma membrane is an electron-dense outer plaque containing the intracellular desmosomal components. Interior to this region is a less-dense, IF-rich fibrillar inner plaque.

Structure and Molecular Components of the Desmosome

The basic blueprint of a desmosome comprises molecular components that fall into three main gene families: desmosomal cadherins, armadillo family members, and plakins. Several studies suggest that these molecules are arranged linearly in this order from the cell surface inward and function together to indirectly tether the IF cytoskeleton to the cell membrane. Lateral interactions between these proteins occur as well and enhance the strength of the junction. Nonadhesive functions have also been proposed for several of these molecules. The best characterized desmosomal components (Figure 1B) are discussed in detail here. However, minor components, including pinin and desmocalmin/keratocalmin, have also been described.

Desmosomal Cadherins

Two types of glycosylated, type I transmembrane adhesive cadherin proteins are found in the desmosome, desmogleins (Dsgs), and desmocollins (Dscs). Different genes encode four isoforms of the Dsgs (1–4) and three isoforms of the Dscs (1–3), which are expressed differentially in various cell types and in a differentiation-specific manner in complex stratified epithelia. The Dsc isoforms are further subdivided into two types, a longer "a" form and a shorter "b" form. Like classical cadherins, both Dsgs and Dscs have a highly conserved calcium-binding extracellular domain, membrane-spanning region, and catenin-binding intracellular cadherin segment (ICS) (not present in Dsc b), whereas Dsgs contain additional unique cytoplasmic subdomains of unknown function. Dsgs and Dscs are thought to function primarily in mediating homo- and heterophilic calcium-dependent adhesion across the membranes of adjacent cells. Severe blistering of the skin or lesions on the hands and feet are consequences of genetic, autoimmune, and bacterial diseases that compromise the adhesive function of these molecules (Table I).

Armadillo Family Members

Proteins with homology to the *Drosophila* segment polarity protein armadillo are important structural components of the desmosome, linking the desmosomal cadherins at the plasma membrane with intracellular cytoskeleton components. These proteins contain

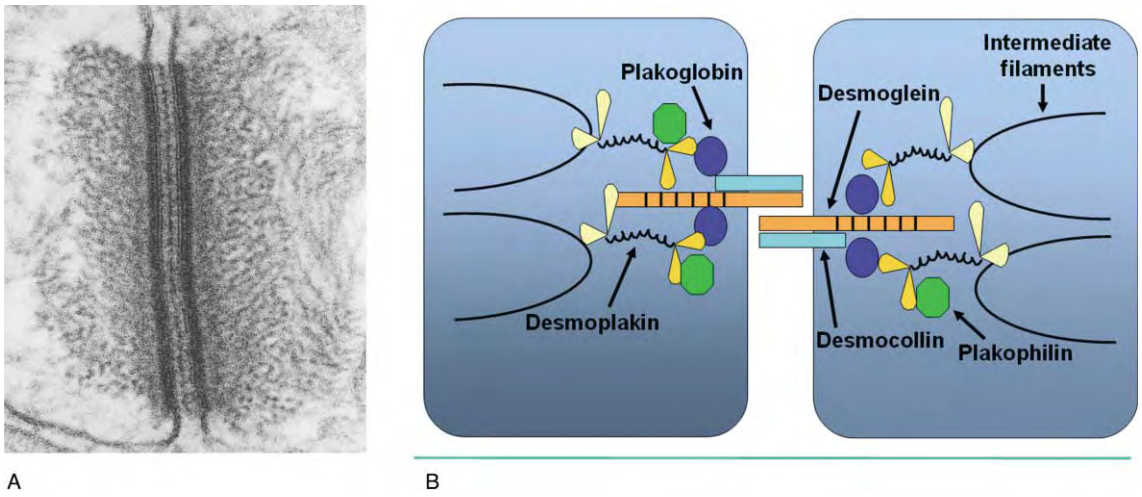

FIGURE 1 Molecular composition and structure of the desmosome. (A) Desmosome ultrastructure is shown in this electron micrograph of bovine tongue epidermis. Reprinted from *Biophysical Chemistry*, Vol. 50, A. P. Kowalczyk, A.P., *et al*., Structure and function of desmosomal transmembrane core and plaque molecules, pp. 97–112, copyright 1994 with permission from Elsevier Science. (B) Desmosomal proteins, their interactions, and their approximate position within the organelle are depicted in this schematic diagram of the desmosome.

a 42-amino-acid repeated motif called the arm repeat, which is thought to mediate protein–protein interactions. Plakoglobin (Pg) is one armadillo protein whose presence in both adherens junctions and desmosomes is selectively regulated. In the desmosome, it binds directly to the cytoplasmic tail of the desmosomal cadherins and to the obligate desmosomal protein, desmoplakin (DP). Pg's adhesive importance is reflected by one genetic disease in which the disruption of its function results in cardiomyopathy, keratoderma, and wooly hair (Table I). In addition to its adhesive role, Pg is also thought to function in a variety of signal transduction pathways.

The plakophilins (PKP1–3) are another group of armadillo family members that contribute to desmosomal adhesion. These proteins have a specific tissue distribution and are differentially expressed in complex stratified epithelia. PKPs are found both in the desmosome and in the nucleus. In the desmosome, PKPs interact cytoplasmically with the desmosomal cadherins, as well as with DP and IFs. The role of PKPs in desmosome assembly and IF attachment is not entirely clear; however, PKP1 is known to enhance the recruitment of DP to the plasma membrane and to facilitate lateral clustering of plaque components. Genetic mutations in both PKP1 alleles negate the protein's function and result in excessive skin fragility (Table I).

Plakins

Although desmosomes consist of various components in different tissues, DP, the most abundant protein in the desmosomal plaque, is an obligate desmosomal constituent. DP is the primary plakin family member found in the desmosome, although other less-abundant plakins include envoplakin, periplakin, and plectin. Structurally, the DP molecule consists of two globular ends connected by a coiled-coil rod whose size is modulated by alternative splicing of the transcript to produce two variants (I and II). The rod domain mediates DP self-dimerization. DP also directly associates with Pg and PKPs through its amino (N) terminus and with IFs through its carboxyl (C) terminus. In addition, direct association of DP with desmosomal cadherin tails has been noted. DP is required for desmosome assembly, linking the IF cytoskeleton to the plasma membrane and anchoring IFs in the plaque. The importance of DP in maintaining epithelial tissue integrity is emphasized by severe keratodermas, sometimes associated with heart defects, affecting patients with genetic diseases in which DP function is compromised by haploinsufficiency, protein truncation, or point mutations (Table I).

Desmosome Assembly and Maintenance

The regulation of the assembly and disassembly of cell–cell junctions is important for normal tissue homeostasis and during junction-remodeling processes such as development or wound healing. One crucial factor controlling desmosome assembly appears to be the prerequisite formation of adherens junctions, perhaps to bring adjacent membranes close together and permit the interaction and clustering of desmosomal molecules. In cultured cells, desmosome assembly occurs in

TABLE I

Human Diseases Associated with Desmosomal Components

Mutated gene/target antigen	Phenotype
Genetic diseases	
Plakoglobin	*Naxos disease*: Autosomal recessive arrythmogenic right ventricular cardiomyopathy (ARVC) combined with striate palmoplantar keratoderma (SPPK) and woolly hair
Plakophilin 1	Autosomal recessive ectodermal dysplasia with a skin fragility syndrome, hair loss, reduced sweating, and nail dystrophy
Desmoglein 1	*Striate palmoplantar keratoderma (SPPK)*: Lesions of the palms and soles exacerbated by mechanical trauma
Desmoglein 4	*Autosomal recessive hypotrichosis* (LAH): Loss of hair on scalp, chest, arms, legs, and face due to hair follicle abnormalities
Desmoplakin (haploinsufficiency)	*Striate palmoplantar keratoderma (SPPK)*: Lesions of the palms and soles exacerbated by mechanical trauma
Desmoplakin (N-terminal missense mutation)	Autosomal dominant arrythmogenic right ventricular cardiomyopathy (ARVD/C)
Desmoplakin (C-terminal missense mutation)	Autosomal dominant arrhythmogenic right ventricular cardiomyopathy (ARVD/C); wooly hair and lesions on the palms of hands and soles of feet
Desmoplakin (C-terminal truncation)	Autosomal recessive left ventricular cardiomyopathy with SPPK and woolly hair
Desmoplakin (compound heterozygosities)	*Palmoplantar keratoderma*: One missense mutation in the N-terminus and one nonsense mutation resulting in a C-terminal deletion; alopecia, hyperkeratosis, acantholysis, and keratin retraction
Autoimmune diseases	
Desmoglein 3	*Pemphigus vulgaris*: Blistering of the oral cavity caused by circulating autoantibodies directed against desmoglein 3; presence of antibodies against both desmoglein 3 and 1 cause the mucocutaneous form with blisters also in the deep epidermis
Desmoglein 1	*Pemphigus foliaceus*: Blistering of the superficial epidermis caused by circulating autoantibodies directed against desmoglein 1
Desmocollin 1, Desmoglein 1, Desmoglein 3	*IgA pemphigus*: Intraepidermal blistering with different forms characterized by circulating autoantibodies against desmocollin 1, desmoglein 1, or desmoglein 3
Plakin family members and desmogleins	*Paraneoplastic pemphigus*: Severe blistering of the skin and mucous membranes caused by circulating autoantibodies against plakin family proteins, desmoglein 1 and desmoglein 3; occurs mainly in patients suffering from malignant lymphomas and thymomas

response to cell–cell contact in a calcium-dependent manner. In low-calcium conditions, newly synthesized desmosomal components are unstable. During assembly, desmosomal cadherins and Pg are delivered together in vesicles to the plasma membrane. Subsequently, DP and IFs are added to the assembling junction. Upon association with the IF cytoskeleton, desmosomal components become stabilized, insoluble, and lose their calcium dependence. The assembly and maintenance of desmosomes is regulated in part by post-translational modification of protein components. Specifically, serine/threonine and tyrosine phosphorylation of several desmosomal components regulates desmosomal assembly and maintenance by modulating the ability of desmosomal proteins to interact with one another.

Desmosome Function

Far from static spot welds, desmosomes are malleable and dynamic structures that respond to extra- and intracellular signals to adapt their functions in cell–cell adhesion, morphogenesis, and signal transduction.

Cell–Cell Adhesive Function

Although desmosomal cadherins were long assumed to function in calcium-dependent cell–cell adhesion, until recently there was a lack of direct evidence demonstrating that ectopically expressed desmosomal proteins promote adhesion in normally nonadherent cells. Evidence now suggests that both Dscs and Dsgs, along with the associated protein Pg, are required for adhesion and that they may interact heterophilically. The existence of autoimmune, genetic, and bacterial diseases that affect the function of desmosomal cadherins and result in compromised epidermal integrity (Table I) support the idea that desmosomes function in intercellular adhesion. Intercellular adhesion may also be disrupted by human diseases that perturb the structure of the desmosomal plaque (Table I). Cell culture models have demonstrated that IF attachment to the desmosome core is a critical aspect in the regulation of desmosome-mediated intercellular adhesion. This is especially important in tissues such as the heart, in which intercellular adhesive defects can have grave consequences.

Morphogenetic Function

Desmosome-mediated intercellular adhesion may be intimately involved in many morphogenetic events. For example, because severe developmental abnormalities lead to embryonic lethality in DP-null mice, desmosomes are thought to play a critical role in maintaining tissue integrity during normal embryogenesis and development. In addition, the importance of desmosomal adhesion in the normal patterning of epithelial cells is demonstrated by the fact that peptide inhibition of desmosomal adhesion can disrupt mammary epithelial cell morphogenesis and positioning.

Signaling Function

Desmosomes may also have a signaling function. A role in outside-in signaling is evidenced by the fact that the ligation of the extracellular domain of Dsg3 by pemphigus vulgaris (PV) antibodies can modulate the intracellular calcium concentration and phospholipid metabolism in keratinocytes. In cultured cells, such ligation results in serine phosphorylation of Dsg3 and its reported dissociation from Pg. Pg-null keratinocytes were used to demonstrate that PV antibody ligation of Dsg3 leads to a Pg-dependent keratin retraction, which may contribute to the epidermal-blistering characteristic of this disease. Intracellular signals can also be propagated by desmosomes. Pg, whether in a desmosomal or nondesmosomal pool, is thought to be the best candidate protein for this process. Although Pg can be found in different junction types, the metabolic stability and cellular localization of Pg are tightly regulated, allowing it to function in cell–cell adhesion, transcriptional activation, proliferation, and programmed cell death.

The Hemidesmosome

Hemidesmosomes are specialized junctions that connect basal epithelial cells to the basement membrane and underlying extracellular matrix. Hemidesmosomes promote the integrity and strength of epithelial tissues by indirectly connecting the intracellular keratin IF cytoskeleton to extracellular matrix proteins.

Hemidesmosome Ultrastructure

The ultrastructure of the hemidesmosome (Figure 2A) includes an electron-dense cytoplasmic triangular plaque, which makes up an inner IF-rich region closest to the cell cytoplasm and a perimembrane plaque containing the cytoplasmic tails of the transmembrane hemidesmosome components. Just adjacent and external to the basal cell membrane is a sub-basal dense plate and thin extracellular anchoring filaments that extend from the plate into the specialized extracellular matrix of the basement membrane.

Structure and Molecular Components of the Hemidesmosome

The major hemidesmosomal components together connect the basal epithelial cell cytoskeleton to the extracellular matrix (Figure 2B). Hemidesmosomal proteins are arranged such that IFs are anchored to the plaque at multiple points, reenforcing the connection to the substratum.

$\alpha 6\beta 4$ Integrin

The $\alpha 6\beta 4$ integrin is the principal factor connecting IFs to the extracellular matrix and, as such, is essential for hemidesmosome formation and the maintenance of epithelial cell attachment to the basement membrane. The $\alpha 6$ integrin can dimerize with $\beta 1$ integrin, but prefers to interact noncovalently with $\beta 4$ integrin. The $\beta 4$ integrin has an unusually long cytoplasmic tail, important for the specialized functions of this molecule. The $\alpha 6\beta 4$ integrin pair is expressed predominantly in epithelial tissues, Schwann cells, and endothelial cells. In complex stratified epithelia, $\alpha 6\beta 4$ integrin is oriented in a polarized fashion on the basal surface of the basal cell layer. The association of the $\alpha 6$ and $\beta 4$ subunits generates a functional transmembrane receptor whose extracellular domain binds to laminin-5, an abundant protein in the extracellular matrix. The interaction of

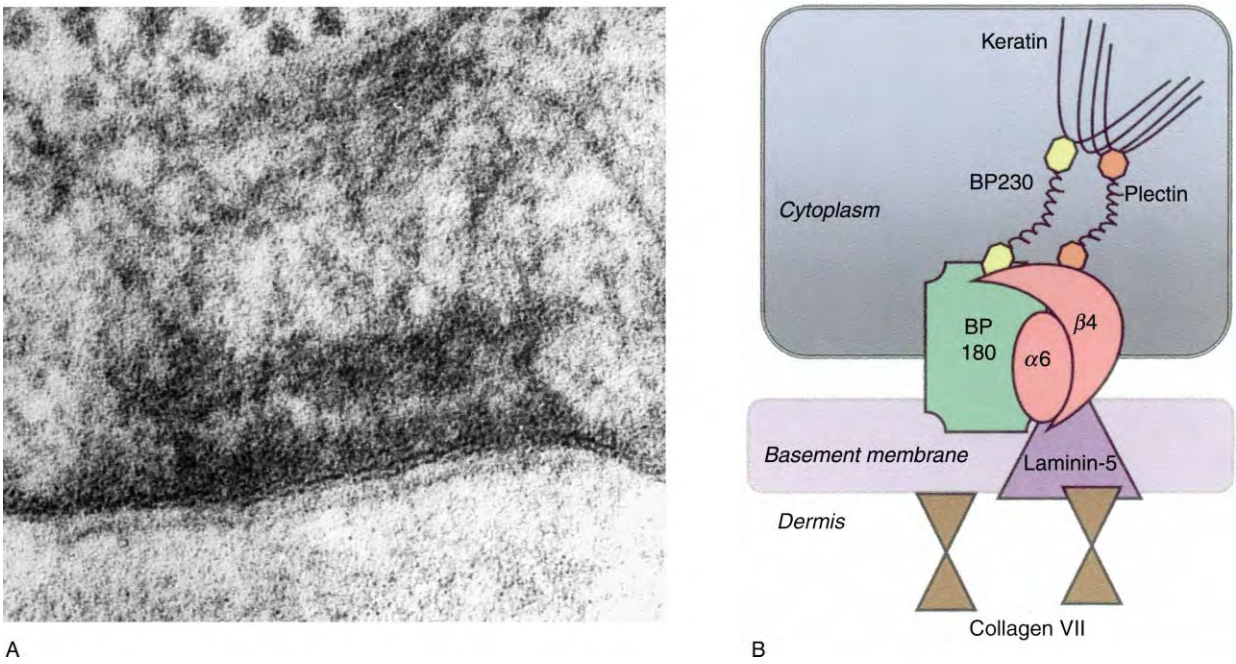

FIGURE 2 Molecular composition and structure of the hemidesmosome. (A) Hemidesmosome ultrastructure is shown in this electron micrograph of bovine tongue epidermis. Reproduced from Is the hemidesmosome a half desmosome? An immunological comparison of mammalian desmosomes and hemidesmosomes, J. C. R. Jones *et al.*, *Cell Motility and the Cytoskeleton*, Vol. 6, pp. 560–569, Copyright (1986). Reprinted by permission of Wiley-Liss, Inc., subsidiary of John Wiley & Sons, Inc. (B) Hemidesmosomal proteins, their interactions, and their approximate position within the organelle are depicted in this schematic diagram of the hemidesmosome.

$\alpha 6\beta 4$ integrin with laminin-5 is thought to be the structural center of the hemidesmosome, as well as the primary channel for the transduction of hemidesmosome-mediated signaling cascades. The $\beta 4$ subunit interacts with another hemidesmosomal protein, plectin, to anchor the IF cytoskeleton to the hemidesmosome core. This interaction is thought to stabilize the association of $\alpha 6\beta 4$ integrin with laminin-5 to enhance adhesion strength.

BP180

Bullous pemphigoid antigen II (BP180) is a 180-kDa type II transmembrane protein component of the hemidesmosome, so named because it is recognized by autoantibodies from the serum of patients with the severe blistering disease bullous pemphigoid (Table II). A member of the collagen family, BP180 is a trimer that contains collagen-like repeats in its C-terminal extracellular domain. These repeats organize into a triple helical coiled-coil arrangement thought to contribute to the structure of anchoring filaments. BP180 interacts with $\beta 4$ integrin in the cytoplasm through its N-terminal domain and binds directly to $\alpha 6$ integrin via its C-terminal extracellular domain, an interaction essential for hemidesmosome formation and stabilization. BP180 is also known to interact with actinin family members and codistributes at sites of cell–cell contact with adherens junction proteins, suggesting a potential role for this molecule in mediating cross-talk between cell–substrate and cell–cell junctions.

BP230

Bullous pemphigoid antigen 230 (BP230) is a 230-kDa cytoplasmic plaque component of the hemidesmosome and a plakin family member. BP230 is known to interact with IFs through its C-terminus. BP230 and BP180 directly interact through their N-terminal domains. BP230 is thought to link the keratin IFs to BP180 and the hemidesmosomal plaque. BP230-null mice have poorly formed hemidesmosomes with few filament attachments.

Plectin

Plectin, a 500-kDa plakin family member, is particularly important for hemidesmosome function in epithelial tissues and as a cytoplasmic cytoskeletal linker in other tissues, but has also been reported in less abundance in desmosomes. Plectin's importance for hemidesmosome stability and tissue integrity is emphasized in patients with genetic mutations in the plectin gene who suffer from severe skin blistering and

TABLE II

Human Diseases Associated with Hemidesmosomal Components

Mutated gene/target antigen	Phenotype
Genetic diseases	
Laminin 5	*Herlitz or Non-Herlitz junctional epidermolysis bullosa (JEB)*: Autosomal recessive severe blistering at the dermal–epidermal junction often coincident with early mortality (Herlitz); less severe form (non-Herlitz) often includes lifelong blistering, loss of hair and nails, and dental abnormalities
β4 Integrin (missense mutation in cytoplasmic tail)	*Non-Herlitz junctional epidermolysis bullosa (JEB)*: Autosomal recessive severe life-long blistering at the dermal–epidermal junction, together with hair, nail, and teeth defects
α6 or β4 Integrin	*Junctional epidermolysis bullosa with pyloric atresia (JEB-PA)*: Mucocutaneous blistering associated with congenital intestinal abnormalities
Collagen VII	*Dystrophic epidermolysis bullosa (DEB)*: The most severe form of epidermolysis bullosa characterized by deep blistering in dermis due to disruption of anchoring fibril stability
BP180	*Non-Herlitz JEB/generalized atrophic benign epidermolysis bullosa (GABEB)*: Autosomal recessive generalized skin blistering, nail dystrophy, enamel hypoplasia, and hair loss
Plectin	*Epidermolysis bullosa with muscular dystrophy (EB-MD)*: Skin blistering noted from birth with late-onset, progressive muscle weakness
Autoimmune diseases	
Laminin-5 and BP180	*Cicatricial pemphigoid*: Chronic subepithelial blistering of mucous membranes and occasionally the skin caused by circulating autoantibodies against laminin-5 or BP180
α6 and β4 Integrin	*Ocular cicatricial pemphigoid*: Subepithelial blistering that mainly affects conjunctiva and other mucous membranes caused by circulating autoantibodies against α6 and β4 integrin
Collagen VII	*Epidermolysis bullosa acquisita*: Minor skin trauma induces severe blistering below the dermal–epidermal junction caused by circulating autoantibodies against collagen VII
BP180 and BP230	*Bullous pemphigoid*: Generalized large subepidermal blisters caused by circulating autoantibodies against BP180 and BP230

muscular dystrophy (Table II). Plectin can interact with itself, with IFs, and with multiple domains of the β4 integrin tail. Plectin has been proposed to cluster $\alpha6\beta4$ molecules at the basal cell surface, a potentially critical step in the formation of hemidesmosomes. In addition, plectin is required for the ligand-independent assembly of hemidesmosomes. However, the primary role for plectin (like BP230) is to link the IF system to the hemidesmosome plaque, stabilizing the junction by connecting the IF cytoskeleton to the hemidesmosome core at multiple points.

CD151

CD151, a member of the tetraspan family, is a potential hemidesmosome component. By immunoelectron microscopy, CD151 appears concentrated at hemidesmosomes in an $\alpha6\beta4$ integrin-dependent manner. Although CD151 associates with $\alpha6\beta4$ integrin and may help stabilize and organize the hemidesmosome, the exact nature of CD151 as a hemidesmosomal component requires further investigation.

Laminin-5

Laminin-5 is a member of the laminin family of large heterotrimeric glycoproteins, which are major constituents of extracellular matrices. Highly expressed in many types of epithelia, laminin-5 is specifically composed of subunits $\alpha3$, $\beta3$, and $\gamma2$, which interact in a noncovalent fashion to form a cross-shaped structure. Laminin-5 is necessary for the firm attachment of basal epithelial cells to the subepithelial basement membrane by linking the hemidesmosome to the underlying tissue. In the hemidesmosome, laminin-5 binds to $\alpha6\beta4$ integrin to mediate cell–substrate attachment. However, laminin-5 is also known to mediate epithelial cell attachment through the nonhemidesmosomal integrin $\alpha3\beta1$. Laminin-5 strongly attaches epithelial cells to the extracellular matrix by interacting with other basement

membrane proteins, including collagen type VII. Laminin-5 can also organize together with BP180 into anchoring filaments thought to extend from the sub-basal dense plate of the hemidesmosome to the deep extracellular matrix. Genetic or autoimmune diseases involving laminin-5 are characterized by complete separation of the epidermis from the dermis (Table II) and further support an important role for laminin-5 in the attachment of basal epithelial cells to the underlying basement membrane.

Hemidesmosome Assembly and Maintenance

The nucleation and assembly of hemidesmosomes is dependent on the $\alpha6\beta4$ integrin pair and its phosphorylation state. The $\beta4$ integrin tail is believed to play important roles in the initiation of hemidesmosome assembly by inducing early clustering of the $\alpha6\beta4$ integrin pair and recruiting BP180, BP230, and plectin to the nucleation site. The $\alpha3\beta1$ integrin pair is also suspected to be an initiator of hemidesmosome assembly, perhaps by preconfiguring the basement membrane into a conformation conducive for stable hemidesmosome formation.

The BP antigens are also thought to be important players in regulating hemidesmosome assembly. Patients with mutations in the BP180 gene have normal $\alpha6\beta4$ integrin and laminin-5 localization but absent or underdeveloped hemidesmosomes. Also, the overexpression of BP230 in cells alters the localization of endogenous BP180, suggesting a role for BP230 in initiating the early interaction of some hemidesmosome proteins prior to junctional incorporation. Laminin-5 also contributes to the regulation and maintenance of hemidesmosomes. Laminin-5 itself is capable of and essential for initiating the formation of hemidesmosome junctions. Hemidesmosome induction, however, is related to the enzymatic cleavage of the $\alpha3$ laminin-5 subunit. The processing of laminin-5 promotes hemidesmosome formation and discourages motility. For adhesion, laminin-5 appears to initially interact with $\alpha3\beta1$ integrin to mediate the attachment of the epithelial cells to the extracellular matrix. Ligation is then transferred to $\alpha6\beta4$ integrin for long-term stable adhesion. The interaction of laminin-5 with $\alpha6\beta4$ integrin induces the formation of the hemidesmosome core.

Hemidesmosome Function

Hemidesmosomes were long thought to be inert adhesive structures with primary importance in maintaining and stabilizing epithelial cell attachment to the underlying basement membrane. However, recent evidence suggests that these structures also exhibit dynamic characteristics that may facilitate tissue-remodeling processes during development and wound healing, as well as permitting rapid responses to biological signals.

Cell–Substrate Adhesive Function

A structural function for hemidesmosomes in initiating and maintaining adhesion between basal epithelial cells and the extracellular matrix is well accepted today, in part because of evidence from autoimmune and genetic human skin diseases that result in epithelial cell-basement membrane separation and severe blister formation (Table II). Other evidence supporting this structural role comes from the noted absence of hemidesmosomes in cells closing wounds and in invasive epithelial tumor cells. Thus, hemidesmosomes appear necessary for stable anchorage of cells to the basement membrane, but may not be required in motile cells.

Morphogenetic Function

The role that hemidesmosomes play in morphogenetic events such as breast epithelial tubule formation indicates the relative dynamic nature of these structures *in vivo*. Indeed, perturbation of the microfilament cytoskeletal architecture in cultured cells results in a redistribution of IF-tethered hemidesmosomes to the cell periphery, highlighting the dynamic nature of the hemidesmosome plaque and its ability to move laterally within the cell membrane.

Transmembrane Signaling Function

Hemidesmosomes are also critical signaling centers competent to transduce both outside-in and inside-out signaling events to regulate such cellular activities as gene expression, cell proliferation, and differentiation. Outside-in signaling during ligation of $\alpha6\beta4$ integrin by laminin-5 is known to regulate cell-cycle progression via the Ras/mitogen-activated protein kinase (MAPK) pathway. Although not fully understood, $\alpha6\beta4$ integrin has also been reported to regulate cell survival. Signal transduction through $\alpha6\beta4$ integrin can modulate cell motility characteristics, particularly through phosphorylation of the $\alpha6\beta4$ integrin pair. Inside-out signaling involving $\alpha6\beta4$ integrin is supported by the dephosphorylation of an 80-kDa membrane-bound protein following the disruption of the $\alpha6\beta4$ integrin–laminin-5 interaction, suggesting that signals inside the cell may contribute to the ligation of $\alpha6\beta4$ integrin by laminin-5.

Conclusion

Despite their ultrastructural and functional similarity as adhesive junctions, desmosomes and hemidesmosomes

are unique structures. Significant progress has been made thus far in the fields of desmosome and hemidesmosome research. The structural organization of these junctions has been examined. Molecular components that make up these junctions have been identified. Protein–protein interactions that contribute to the normal function of these organelles have been characterized. Future studies in these fields will probably focus on further examining the dynamic nature of desmosomes and hemidesmosomes, identifying potential nonadhesive functions for the protein components of these junctional complexes, and investigating junction-mediated signaling cascades and their regulation.

See Also the Following Articles

Cadherin Signaling • Cadherin-Mediated Cell–Cell Adhesion • Integrin Signaling • Intermediate Filament Linker Proteins: Plectin and BPAG1

Glossary

cadherins Single-pass transmembrane proteins that mediate calcium-dependent cell–cell adhesion.

epithelia Sheets of tightly packed cells that cover a body surface or line organs and body cavities.

extracellular matrix An organized network of proteins and polysaccharides that fills the extracellular space of tissues and is produced by the surrounding cells.

integrins Transmembrane linker proteins that are receptors for extracellular matrix proteins and link the extracellular matrix to components of the cytoskeleton.

intermediate filaments (IFs) Cytoskeletal filaments, typically 10 nm in diameter, found in higher eukaryotic cells.

signal transduction The propagation of a chemical or mechanical stimulus to effect a cellular response.

Further Reading

Bannon, L. J., Goldfinger, L. E., Jones, J. C. R., and Green, K. J. (2001). Desmosomes and hemidesmosomes. In *Cell Adhesion*, (M. C. Beckerle, ed.) Vol. 39, pp. 324–368. Oxford University Press, New York.

Borradori, L., and Sonnenberg, A. (1999). Structure and function of hemidesmosomes: More than simple adhesion complexes. *J. Invest. Dermatol.* **112**, 411–418.

Garrod, D. R., Merritt, A. J., and Nie, Z. (2002). Desmosomal cadherins. *Curr. Opin. Cell Biol.* **14**, 537–545.

Getsios, S., Huen, A. C., and Green, K. J. (2004). Working out the strength and flexibility of desmosomes. *Nat. Rev. Mol. Cell Biol.* **5**, 271–281.

Jamora, C., and Fuchs, E. (2002). Intercellular adhesion, signaling, and the cytoskeleton. *Nat. Cell Biol.* **4**, E101–E108.

Jones, J. C. R., Hopkinson, S. B., and Goldfinger, L. E. (1998). Structure and assembly of hemidesmosomes. *Bioessays* **20**, 488–494.

Leung, C. L., Green, K. J., and Liem, R. K. (2002). Plakins: A family of versatile cytolinker proteins. *Trends Cell Biol.* **12**, 37–45.

Nievers, M. G., Schaapveld, R. O., and Sonnenberg, A. (1999). Biology and function of hemidesmosomes. *Matrix Biol.* **18**, 5–17.

Nishiyama, T., Amano, S., Tsunenaga, M., Kadoya, K., Takeda, A., Adachi, E., and Burgeson, R. E. (2000). The importance of laminin-5 in the dermal–epidermal basement membrane. *J. Dermatol. Sci.* **24**(Suppl. 1), s51–S59.

Pulkkinen, L., and Uitto, J. (1999). Mutation analysis and molecular genetics of epidermolysis bullosa. *Matrix Biol.* **18**, 29–42.

Biography

Rachel L. Dusek is a Ph.D. candidate in the Cancer Biology track of the Integrated Graduate Program and is secondarily affiliated with the Departments of Pathology and Dermatology and the R. H. Lurie Comprehensive Cancer Center at Northwestern University Feinberg School of Medicine. Her primary research interest is in the field of cell–cell adhesion, specifically, the potential nonadhesive functions of the desmosome components.

Jonathan C. R. Jones, Ph.D. is a Professor of Cell and Molecular Biology at Northwestern University Feinberg School of Medicine. He is secondarily affiliated with the Pulmonary Division of the Department of Medicine and the Robert H. Lurie Comprehensive Cancer Center of Northwestern University.

Kathleen J. Green, Ph.D. is the Joseph L. Mayberry Professor of Pathology and a Professor of Dermatology at Northwestern University Feinberg School of Medicine and is affiliated with the Robert H. Lurie Comprehensive Cancer Center of Northwestern University.

Detergent Properties

Darrell R. McCaslin
University of Wisconsin, Madison, Wisconsin, USA

A detergent is formed when a hydrophilic group with an affinity for water and a hydrophobic group with an aversion to water are spatially segregated within a molecule's chemical skeleton so as to create a polarity. In aqueous solution, detergents generally exist as a mixture of monomers in equilibrium with a fairly monodisperse population of detergent aggregates known as micelles. In the micelle, the hydrophobic groups are packed together to create a hydrophobic core with the attached hydrophilic groups projecting out from the surface of this core and protecting it from contact with water. As such, detergents have only limited biological functions such as the well-known role in digestion and possibly to some extent in membrane fusion events; however, they play necessary if not essential roles in the isolation, manipulation, and characterization of the constituents of biological membranes.

Chemical Structure of Detergents

The chemical structures of detergents which have been employed in biological studies are quite varied and continues to grow as investigators attempt to develop new entities that will permit the facile isolation of membrane constituents while enhancing their stability once isolated. To reach this goal, various combinations of hydrophobic and hydrophilic groups have been utilized and yield a variety of physical and chemical properties.

Hydrophobic Groups (Tails)

Simple Hydrocarbon Chains

The hydrocarbon chain is the most easily recognized hydrophobic group and when present is often referred to as the molecule's hydrophobic tail (Figure 1). These chains are most often saturated hydrocarbons (Figure 1) and are available in many lengths. The shorter the chain the less well defined the detergent properties tend to be, whereas longer tails become essentially insoluble. Unsaturation and more complex branching structures have been explored as well as chains incorporating phenyl rings. The presence of the ultraviolet light-absorbing phenyl should generally be avoided as it can complicate various spectroscopic techniques.

Ring-Based Hydrocarbons

The naturally occurring bile salts synthesized from cholesterol and utilized in digestive processes are the prototypes for detergents based on ring systems. Figure 1 shows cholic acid, one of the abundant bile salts which is converted to deoxycholate (DOC) by removing the hydroxyl at the arrow. Identifying the spatial segregation of the hydrophilic and hydrophobic groups in these detergents may require careful inspection of their three-dimensional chemical structure. In cholic acid, the carboxyl group is an obvious hydrophilic group, but the effects of the hydroxyl groups located on the rings must also be considered. Viewing the steroid ring nucleus in the molecule as defining a plane, the spatial arrangement of the hydroxyls creates a hydrophilic face on one side and a hydrophobic face on the other side of this plane. The structure of DOC suggests the presence of only a hydrophilic edge along the ring plane, making the whole structure more hydrophobic than cholic acid, which may explain why DOC is generally a more aggressive solubilizer than cholic acid.

Hydrophilic Groups (Headgroups)

Ionic

Positively (e.g., amino) and negatively (e.g., carboxyl) charged groups have been utilized as hydrophilic groups. Single-tailed ionic detergents tend to denature all proteins, with the anionic ones being more aggressive at denaturation than cationic molecules. One of the most familiar examples is the anionic detergent, sodium dodecyl sulfate, $NaDodSO_4$ (Figure 1). It is the denaturing effect of $NaDodSO_4$ on proteins that led to the development of one of the most widely exploited analytical tools of biochemistry, denaturing gel electrophoresis, which permits one to easily assess the number of components present in a sample as well as their approximate molecular weights. Interestingly, it is the monomeric form of the ionic detergent that drives the denaturation process.

The bulk of the lipids which form the basic membrane framework are amphiphiles with two hydrophobic

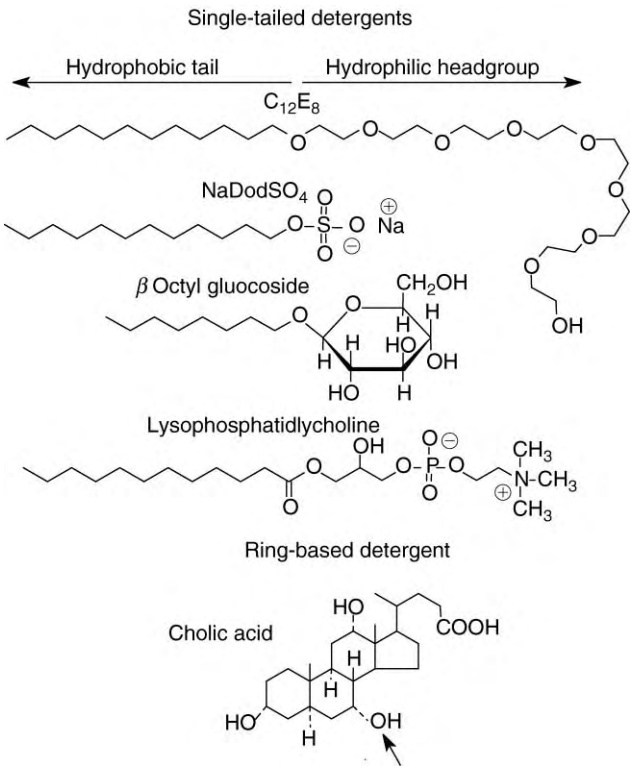

FIGURE 1 Selected chemical structures of detergents. Removal of the hydroxyl near the arrow on cholic acid coverts the molecule to deoxycholic acid.

tails esterified to zwitterionic headgroups (contains both positive and negative charges). While the lipids themselves generally form vesicular structures when dispersed in water, removal of one of the tails creates a detergent such as the lysophosphatidylcholine in Figure 1. Such lysolipids and other zwitterionic detergents (e.g., sulfobetaines) have been used as well as highly dipolar groups (e.g., amine oxide) that lack a formal charge.

Nonionic

Any uncharged group of atoms capable of accepting or donating hydrogen bonds to water can in principle become a nonionic headgroup. The headgroup must be big enough so that the detergent dissolves in solution (as a mixture of monomer and micelles) rather than forming a separate phase. Thus, simple alkyl alcohols tend to phase separate for all but the shortest hydrophobic tails and have no useful detergent properties. Carbohydrate groups are useful headgroups and one of the most frequently encountered is β-octyl glucoside (OG) in Figure 1. Octyl glucoside in the α-anomeric configuration is essentially insoluble, demonstrating how a simple change in chemical structure can dramatically alter detergent properties. More elaborate carbohydrate structures have also been explored.

Commercial applications of detergents have driven the development of a large class of nonionic detergents with polyoxyethylene (POE) headgroups. A chemically homogeneous example is $C_{12}E_8$ (Figure 1), where a 12-C tail (C_{12}) is attached to a polymer with eight repeats of $-CH_2CH_2O-$ (E_8) and terminates with a hydroxyl group. The ether groups of this chain provide sites for hydrogen bonding with water offsetting the hydrophobic nature of the intervening ethylene groups. Most commercially available POE-based detergents have headgroups consisting of a single chain although the length is often heterogeneous; however, highly branched structures have been created by attachment of several POE chains to a central moiety such as sorbitol (e.g., Tweens). The POE chains are subject to peroxidation and breakdown and solutions should only be used when relatively freshly prepared; moreover, when using commercial sources one should be aware that antioxidants are sometimes included.

Connecting Head and Tail

Linkages between the hydrophobic and hydrophilic groups are most often either an ether or ester linkage. The latter can be susceptible to hydrolysis, especially in biological preparations, which in turn could generate an ionic group with denaturing properties.

Detergent Properties

Critical Micelle Concentration (CMC)

The most common concentration-dependent behavior for detergents is illustrated in Figure 2. The monomer concentration increases until the critical micelle concentration (CMC) above which an equilibrium is established between the monomer and an increasing concentration of micelles. The monomer concentration increases very little after reaching the CMC and thus is in effect the highest possible concentration of monomeric detergent. All detergent in excess of the CMC is incorporated into micelles (dashed line in Figure 2). The concentration of micelles increases linearly with total detergent concentration above the CMC, but at a slower rate since a large number of molecules are incorporated into each micelle. Some detergents exhibit more complex behavior, such as secondary association of micelles or even new phases as the total concentration continues to increase.

As illustrated in Figure 2, the CMC is actually a narrow range of concentration over which the formation of micelles becomes dominant. Nonetheless, a single number is usually defined as the CMC and determined by plotting some physical observable whose response differs markedly above and below the CMC against the total

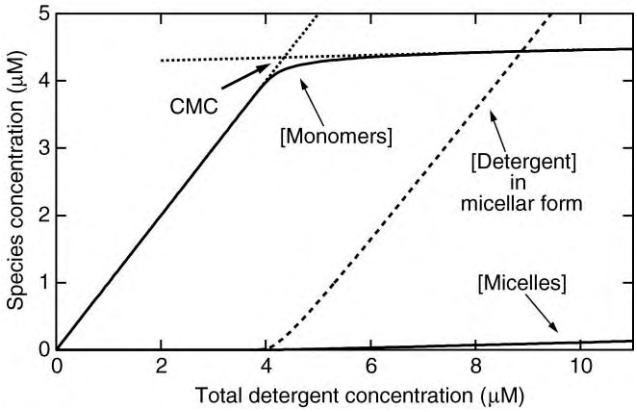

FIGURE 2 Concentration-dependent behavior of a detergent. The calculations are based on the theory of micelle formation developed by Tanford. An aggregation number of 50 was used and the equilibrium constant for micellization was chosen to yield the critical micelle concentration (CMC) indicated.

concentration of detergent. The CMC is then taken as the intersection of lines extrapolated from the nearly linear regions above and below the transition as shown by the dotted lines in Figure 2. Using different observables or concentration ranges for the extrapolation can lead to somewhat different values for the CMC. One of the simplest methods to measure a CMC concentration ranges or for the extrapolation. is by solubilization of heme, which is essentially insoluble below the CMC and increases as the concentration of micelles increases and would be similar to the dashed line in Figure 2.

CMCs range from nanomolar to several millimolar. For single-tailed detergents, the CMC decreases with increasing length of tail and with smaller headgroups. The CMC of nonionics is generally lower than that of ionics with the same length of tail. Ionic headgroups are more susceptible to solution variables than the nonionics. Ionic headgroups that can be titrated are sensitive to pH and may precipitate when the headgroup is in neutral form (both cholic acid and DOC are examples). The CMCs of ionics are also influenced by the type and concentration of counterions present, e.g., using potassium instead of sodium for dodecyl sulfate, results in an insoluble salt. In general, higher salt concentrations will decrease the CMC of an ionic detergent which is a consequence of reducing the headgroup repulsion in the micelle. Even the POE-based nonioncs may be influenced by presence of salts as the ether groups are capable of complexing ions. The solubilization of other components in the micelle (e.g., mixed micelles with lipids) will generally decrease the CMC (i.e., the maximum monomer detergent concentration is decreased). Published values of CMCs are useful guides in experimental design, but should generally be confirmed under the actual experimental conditions.

Aggregation Number

Micelles are formed by self-association of many detergent molecules into a single noncovalent structure. Since the number of molecules in each micelle is somewhat variable, micelle size is characterized by the aggregation number, which is the average number of molecules per micelle and can be determined by standard hydrodynamic methods (e.g., sedimentation equilibrium). The aggregation number is needed to calculate the micelle concentration, which is the total detergent concentration in excess of the CMC divided by the aggregation number.

The CMC transition becomes sharper as the aggregation number increases. The CMC is generally strongly dependent on the size of the hydrophobic moiety, but repulsion between headgroups is the dominant factor for the aggregation number. Thus, nonionics tend to have larger aggregation numbers than ionics of the same tail length. The aggregation number for ionic detergents can be strongly influenced by both the type and concentration of counterions present as well as pH since these factors can dramatically change the electrostatic repulsion between the charged headgroups. Longer hydrophobic tails tend to have larger aggregation numbers. Detergents with high CMCs tend to have more variability in their micelle size distribution. At high concentrations and under certain solution conditions (e.g., elevated temperature) larger structures may be formed which in some cases are new micellar phases and in others simply secondary aggregation of smaller micelles.

Temperature Effects

As a thermodynamic equilibrium, the formation of micelles can be influenced by temperature. At low enough temperatures, solid detergent will exist in equilibrium with monomeric detergent; as the temperature increases, the monomer concentration increases until it reaches the CMC at the critical micelle temperature. Above this temperature, solid detergent will begin to go into solution as micelles. The temperature at which solid, micelles, and monomer at the CMC coexist is called the Kraft point and for most detergents is the same as the critical micelle temperature. An often observed Kraft point, which is near room temperature, is that of sodium dodecyl sulfate and upon cooling one sees precipitation of detergent. A second temperature effect observed at higher temperature, especially with nonionics containing POE, is the cloud point. At this temperature and above the CMC, the solution will turn turbid due to the formation of much larger aggregates. Both the critical micelle temperature and cloud point have been exploited in purification of membrane components.

Micelle Structure

Single-Tailed Detergents

In a micelle, the hydrophobic tails are sequestered into a central core structure with the hydrophilic groups projecting out from the surface of this core into the aqueous surrounding. The tails in the core are not fully extended but are quite flexible, some even lying along the surface of the core rather than within it. The surface of the core should be regarded as having a rippled texture with some tail methylene groups protruding above it. Experimental and theoretical arguments suggest that for most detergent micelles the overall shape is best described as an oblate ellipsoid, although for small aggregation numbers the shape cannot be readily distinguished from spherical. For $C_{12}E_8$ micelles (Figure 1), theoretical calculations constrained by hydrodynamic measurements yield an oblate ellipsoid with dimensions shown in Figure 3. One dimension must be less than the 3.4 nm length of two fully extended 12C chains since the core cannot contain a void. For the same length of tail, the overall dimensions of the micelle will depend on the nature of the headgroup. For POE-based detergents, the headgroup is in a random-coil configuration and consequently occupies a very large region of the space surrounding the core, as illustrated in Figure 3.

Figure 3, while a convenient visualization of micelle structure, cannot convey the highly dynamic processes occurring. Detergent molecules are rapidly exchanged among micelles; whole micelles disappear and reform with slightly different aggregation numbers. The hydrophobic core acts for the most part like a simple liquid hydrocarbon with the tails constantly flexing. POE headgroups occupy a great deal of space around the core and are constantly changing their conformation as well. Finally, it should be obvious that the type and size of headgroup can generate dramatically different chemical environments to which molecules solubilized by detergents are exposed; moreover, the solution composition near a micelle may be quite different from that of the bulk aqueous solution.

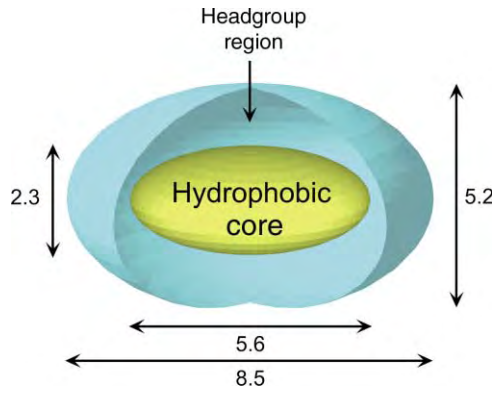

FIGURE 3 Shape of micelles formed by typical single-tailed detergents. The model shown is based on data and calculations for C12E8. The dimensions shown are in nm.

Ring-Based Detergents

Bile salts usually have relatively high CMCs and quite small aggregation numbers (4–10). The small aggregation number does not permit micelles as just described. The micelles are more heterogeneous and are probably best viewed as small assemblies with the hydrophobic surfaces facing each other, presenting their hydrophilic faces to the surrounding solution. The size and shape of these micelles are quite sensitive to the concentration and types of ions, and potentially pH.

Detergents as Tools in Membrane Studies

Membrane Solubilization

Initially when a membrane is exposed to a detergent, monomers partition into the bilayer, so one can imagine that a high CMC might be advantageous (e.g., OG has a very high CMC (>15 mM) and is an efficient solubilizer). As more detergent intercalates into the membrane's bilayer, one reaches a stage where fragmentation occurs, resulting in large mixed micelles containing detergent, lipids, and proteins in various ratios. Continuing to add detergent will eventually disperse the membrane components to the point that any given micelle contains no more than a few lipids, a protein, or the detergent alone. One can apply isolation and enrichment techniques for specific targets to this solubilized mix. The choice of detergent can hinder or help in isolation, e.g., a small aggregation number can facilitate separation of a large protein-containing micelle from those containing only lipid components. It is possible, and perhaps even desirable, to exchange detergents, so that one detergent might be used to speed initial membrane solubilization and another for final isolation of a stable target. It is important to recognize that it is the concentration of micelles that needs to be controlled when one is studying membrane components solubilized by detergents, and generally one should maintain a ratio of several micelles to each solubilized component to avoid the possibility of spurious associations.

Membrane Proteins

A detergent can be found that can reasonably mimic the hydrophobic core of the native membrane. However, the membrane provides a physical constraint to the embedded protein, in that the protein cannot expand

laterally in the plane of the membrane nor can it pull itself through the bilayer; in a detergent solution, such a physical constraint is greatly relaxed and the protein in effect has a much expanded conformational space including conformations where activity will be lost possibly irreversibly. Low CMCs and large aggregation numbers may partially compensate for the loss of the membrane's physical constraints. Moreover, the native environment of the membrane provides a multitude of interactions with a variety of lipid headgroups, tails, and with other proteins and these interactions may differ from one side of the membrane to the other. The roles of these interactions in maintaining an active protein are not well understood and they are radically changed upon solubilization. Studies as a function of micelle concentration should be performed, as there is always a possibility of adventitious interactions, due merely to the fact that too little detergent is present.

Reconstitution of Protein into a Bilayer

Many of the functions of membrane proteins are vectorial in nature, and one must eventually reconstitute the protein into a lipid bilayer where these functions can be probed. Starting with mixed micelles of protein in detergent and lipids in detergent, one must effect a controlled removal of the detergent, permitting the formation of an artificial membrane bearing the protein. This is accomplished largely by trial and error. A high CMC permits the use of dialysis since the monomer should pass through the dialysis membrane. Hydrophobic beads to which the detergent absorbs have also proven effective in reconstitution studies.

Summary

Obviously single-tailed ionic detergents should generally be avoided because of their potential to denature any protein. While zwitterionic headgroups can be identical or at least similar to those of native lipids, to date they have not proven any more useful than others. High CMCs may be appropriate choices for initial solubilization and eventual reconstitution. But long tails and large headgroups (usually accompanied by a low CMC) may enhance stability by restricting the conformational space accessible to the protein in detergent solution. The requirements for efficient solubilization and for the maintenance of activity may to a large extent be antagonistic. The possibility of using one detergent to solubilize and subsequently exchanging into another to enhance stability for isolation and study should always be considered. Finally, there is no perfect detergent for all situations nor are there hard-and-fast rules for choosing a detergent for a specific task. In the end the choice is still largely a matter of trial and error.

See Also the Following Articles

MDR Membrane Proteins • Membrane Transport, General Concepts

Glossary

aggregation number Number of detergent molecules in the average micelle.

CMC (critical micelle concentration) Concentration of detergent in aqueous solution above which micelles begin to form, essentially the maximum concentration of detergent in monomeric form.

detergent A compound having spatially segregated hydrophilic and hydrophobic regions and which, when dissolved in water above the CMC, self-associates to form micelles.

hydrophilic group Structure having an affinity for water with strong favorable noncovalent bonds with water molecules.

hydrophobic group Structure exhibiting an aversion to water and preference for hydrocarbon-type liquids.

micelle Structure formed by the noncovalent and highly cooperative self-association of a detergent molecule so as to form a hydrophobic core from which the hydrophilic groups project into the aqueous surroundings.

Further Reading

Gravito, R. M., and Ferguson-Miller, S. (2001). Detergents as tools in membrane biochemistry. *J. Biol. Chem.* **276**, 32403–32406.

Helenius, A., and Simons, K. (1975). Solubilization of membranes by detergents. *Biochim. Biophys. Acta* **415**, 29–79.

Helenius, A., McCaslin, D. R., Fries, E., and Tanford, C. (1979). Properties of detergents. *Methods Enzymol.* **56**, 734–749.

Tanford, C. (1980). *The Hydrophobic Effect: Formation of Micelles and Biological Membrane.* Wiley, New York.

Tanford, C., and Reynolds, J. A. (1976). Characterization of membrane proteins in detergent solutions. *Biochim. Biophys. Acta* **457**, 133–170.

White, S. H., Ladokhin, A. S., Jayasinghe, S., and Hristova, K. (2001). How membranes shape protein structure. *J. Biol. Chem.* **276**, 32395–32398.

Biography

Dr. Darrell R. McCaslin holds a B.S. with Honors in biochemistry from Oklahoma State University and a Ph.D. in physical biochemistry from Duke University. He has held positions at Duke University Medical Center and Rutgers University in Newark. Presently, he is the Director of Operations for the Biophysical Instrument Facility at the University of Wisconsin in Madison. In addition to overseeing the operations of the facility and training investigators in the use of the instrumentation, he collaborates on a variety of characterization problems.

Diabetes

David W. Cooke
The Johns Hopkins University School of Medicine, Baltimore, Maryland, USA

Diabetes mellitus is among the most common chronic diseases, affecting over 6% of the adult population in Western society, and with a prevalence that is rising dramatically worldwide. However, diabetes mellitus is not a single disease, but rather a number of distinct disorders. They share, in common, deficient action of the hormone insulin. This can be due to an absolute deficiency of insulin production and secretion by the β-cells of the pancreatic Islets of Langerhans. However, in many types o diabetes mellitus there is an impaired cellular response to insulin; this insulin resistance imposes a requirement for increased insulin levels to maintain metabolic control. In this case, diabetes mellitus occurs when there is an inability to secrete sufficient insulin to meet this increased demand. The insulin deficiency, whether absolute or relative, leads to a failure to control carbohydrate and lipid metabolism.

Introduction

The defining feature of diabetes mellitus is an abnormal elevation of the blood glucose level. When the degree of hyperglycemia is mild, there may be no symptoms of diabetes. With greater degrees of hyperglycemia, the concentration of glucose in the blood exceeds the ability of the kidneys to completely reabsorb the glucose delivered to it. The resultant loss of glucose in the urine provides an osmotic force that draws increased water into the excreted urine, causing the patient to experience polyuria (increased urination; this glucosuria gives diabetes mellitus its name, which can be translated from the Greek as "sweet urine" – or more directly as "honey siphon". The osmotic diuresis from glucosuria induces polydipsia (increased drinking) in order to prevent dehydration. When uncontrolled, diabetes mellitus puts patients with these diseases at risk of acute metabolic decompensation, particularly when the insulin deficiency is complete, as in type 1 diabetes mellitus. While this decompensation is life threatening, since the introduction of insulin treatment over 80 years ago these events are generally preventable. It is now the long-term complications that all patients with diabetes mellitus are at risk that has become the most significant burden. Due to these long-term complications, diabetes is a leading cause of blindness and end-stage renal disease. In addition, diabetes is associated with accelerated atherosclerotic vascular disease, leading to a risk of myocardial infarction, stroke, and limb amputation that is increased and occurs at a younger age than in those without diabetes.

Etiology

For each type of diabetes mellitus, the relative contribution of a defect in insulin secretion versus a defect in insulin action will vary. For example, the two most common forms of diabetes are type 1, which is due to an isolated deficiency in insulin, and type 2, which is due to varying degrees of insulin resistance and deficient insulin secretion. In addition, some forms of diabetes have a predominantly genetic etiology, such as the autosomal dominantly inherited maturity-onset diabetes of the young (MODY), whereas in other types both genetic and environmental factors are important, exemplified by type 2 diabetes, where the development of obesity is a significant contributor to the cause of insulin resistance that is central to the pathophysiology of this disease.

Type 1 Diabetes Mellitus

Type 1 diabetes accounts for ~5–10% of all cases of diabetes. It typically has its onset in childhood, although it can occur at any age. Type 1 diabetes is due to the destruction of the insulin-producing β-cells of the pancreas, resulting in an absolute deficiency of insulin. In the vast majority of cases, the destruction is due to a cell-mediated autoimmune attack of the β-cells. This process appears to be precipitated by environmental factors in genetically susceptible individuals. While viral infections, dietary components and specific toxins have been suspected, the true identity of the environmental triggers remains unknown. Similarly, while the immune-recognition genes of the HLA locus account for much of the genetic risk, there are other unidentified genes that also contribute to this risk.

In almost all cases of type 1 diabetes, there is ultimately complete destruction of the pancreatic

β-cells. Because of this, these patients are dependent on treatment with exogenous insulin for their survival, as the absence of such treatment leads to rapid metabolic deterioration into diabetic ketoacidosis and death.

Type 2 Diabetes Mellitus

Over 90% of diabetes is due to type 2 diabetes. The prevalence of this disease increases with age; previously it had been uncommon for children or young adults to be diagnosed with this disease. However, there has been a recent dramatic increase in the prevalence of this disease, and with this, significant numbers of children are now being diagnosed with type 2 diabetes. Although much has been learned about the pathophysiology of type 2 diabetes in the past few decades, there remains much to be learnt about the specific details of its cause. What is known is that two defects are present in patients with type 2 diabetes: insulin resistance and defective insulin secretion. Insulin resistance refers to a decreased effectiveness of insulin in activating signals distal to binding of insulin to the insulin receptor. Insulin resistance itself, except in the most extreme situation, will not lead to diabetes, as normal metabolic control can be maintained by a compensatory increase in insulin secretion. When a second defect results in an inability to respond to the requirement for increased insulin secretion imposed by insulin resistance, type 2 diabetes mellitus occurs.

There is strong familial clustering of type 2 diabetes, and the risk for this disease varies considerably across different ethnic populations. These and other findings indicate that there is a strong genetic component to the development of type 2 diabetes. Multiple genes are most likely to be involved, with each individual with diabetes having altered function of multiple gene products. In addition, the relative contribution of insulin resistance versus defective insulin secretion can vary from patient to patient, so that there is likely a subset of altered genes contributing to the development of type 2 diabetes that differs from one person to the next. The genes involved will include those encoding proteins affecting insulin signaling and insulin secretion, those controlling metabolic pathways, and those contributing to the development of obesity.

Environmental factors play a significant role in determining which genetically predisposed individuals will develop type 2 diabetes. Obesity and low levels of physical activity are strongly associated with insulin resistance, and are the factors to which the rising prevalence of type 2 diabetes in industrialized societies are ascribed. In addition, insulin sensitivity (the inverse of insulin resistance) decreases with age, accounting for much of the increased prevalence of this disease with increasing age.

Insulin Resistance

Both central (hepatic) and peripheral (muscle and adipose) defects contribute to the insulin resistance of type 2 and obesity. (Interestingly, experiments in rodents have indicated that resistance in cells not classically characterized as being insulin-responsive, including the brain and pancreatic β-cells, may contribute to the pathophysiology of obesity and type 2 diabetes.) Hepatic insulin resistance results in increased glucose output from the liver, predominantly due to increased gluconeogenesis. Insulin-resistant muscle and adipose cells have diminished insulin-stimulated glucose uptake, and the muscle cells have a marked decrease in glycogen synthesis. These defects, particularly in the muscle, result in decreased disposal of glucose after a meal. In addition, the decreased metabolism of glucose to glycogen leads to increased glycolysis and production of lactate, which circulates to the liver and provides substrate for increased gluconeogenesis. The increased hepatic glucose production contributes most to fasting hyperglycemia, while the decreased glucose disposal into muscle contributes most to postprandial hyperglycemia.

Although the mechanisms remain incompletely understood, a number of factors have been demonstrated to contribute to the insulin resistance of type 2 diabetes, including free fatty acids and other factors secreted by adipocytes, as well as hyperglycemia itself (Figure 1). Free fatty acids impair insulin sensitivity, both in the liver and in muscle, and increased circulating levels of free fatty acids are found in obese and insulin-resistant subjects, due to increased lipolysis in adipocytes. Importantly, intra-abdominal fat tissue has a higher lipolytic rate compared to subcutaneous adipose tissue, and excess intra-abdominal adiposity has a much higher association with insulin resistance than obesity with a more peripheral (subcutaneous) distribution. Abnormal secretion by the adipocyte of a number of other factors (adipokines) has also been implicated in

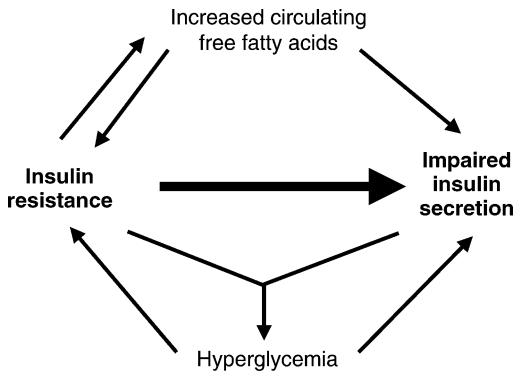

FIGURE 1 Factors contributing to insulin resistance and impaired insulin secretion include the ability for each of them to affect both themselves and each other through direct and indirect mechanisms.

the pathophysiology of insulin resistance, including TNF-α, resistin, adiponectin, and leptin. Hyperglycemia itself causes impaired insulin sensitivity. This may be due to activation of protein kinase C (PKC) by hyperglycemia. Recently, it has also been suggested that hyperglycemia-induced insulin resistance is in some way caused by increased flux of glucose through the glucosamine pathway.

Molecular Mechanisms of Insulin Resistance Insulin is a peptide hormone that binds to a transmembrane-spanning cell surface receptor (Figure 2). The insulin receptor is heterotetrameric in structure, containing two α- and two β-subunits. Insulin binds to the extracellular α-subunit, inducing a conformational change in the transmembrane β-subunit that derepresses intrinsic tyrosine kinase activity contained in the intracellular domain. The activated β-subunit tyrosine kinase activity first trans-phosphorylates the opposite β-subunit of the $\alpha_2\beta_2$ receptor complex. Once autophosphorylated, the insulin receptor is capable of phosphorylating intracellular proteins that propagate the insulin signal within the cell. Proteins of the insulin receptor substrate (IRS) family, the most important of these being IRS-1 and IRS-2, recognize and bind to phosphotyrosine motifs on the activated insulin receptor. Once bound, the IRS proteins are themselves phosphorylated on multiple tyrosine residues by the activated insulin receptor. The IRS proteins do not have intrinsic enzymatic activity, but serve as docking sites to bring other proteins into proximity to the insulin receptor. A signaling cascade is initiated, as proteins recognize and bind to the phosphotyrosine motifs on either the insulin receptor or the IRS proteins. This results in their activation, often through their phosphorylation by the insulin receptor.

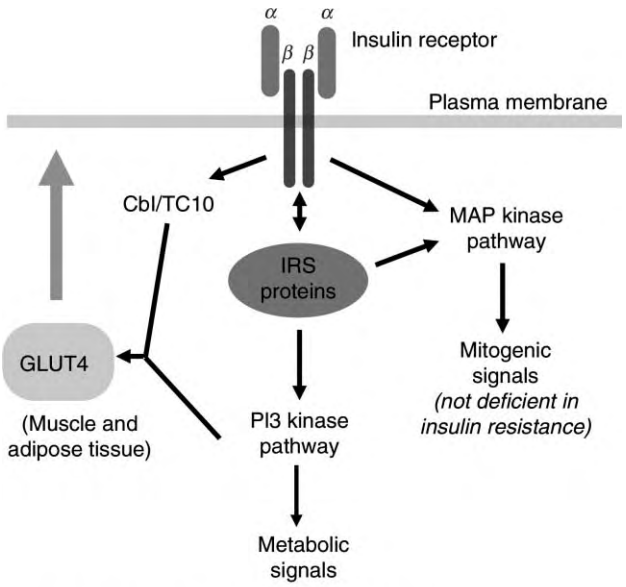

Abnormalities found in insulin resistance:

Insulin receptor:
- decreased number (minor)
- decreased insulin-stimulated tyrosine phosphorylation
- increased serine phosphorylation

IRS proteins:
- decreased protein level
- decreased insulin-stimulated tyrosine phosphorylation
- increased serine phosphorylation
- increased frequency of IRS-1 polymorphisms (some populations)

Decreased insulin-stimulated PI3 kinase associated with IRS proteins

GLUT4:
- decreased expression (adipose tissue)
- decreased insulin-stimulated translocation to the plasma membrane (muscle and adipose)

FIGURE 2 Major signaling pathways of insulin action and abnormalities found in insulin resistance.

The downstream components of the insulin-signaling cascade include protein kinases and phosphatases, and lipid kinases. The two pathways that have been investigated in the most detail are the mitogen-activated protein (MAP) kinase and the phosphatidylinositol-3-OH (PI3) kinase pathways. Although the distinction is not absolute, activation of the MAP kinase pathway is most responsible for the mitogenic actions of insulin, while activation of the PI3 kinase pathway is predominantly involved in the metabolic actions of insulin. This is significant, because activation of the MAP kinase pathway by insulin is not reduced in type 2 diabetes, a result that may be involved in the pathogenesis of the long-term complications of insulin resistance and diabetes. A third pathway involves phosphorylation and activation of the Cbl proto-oncogene by the insulin receptor, which results in activation of the G protein TC10. Many of the pathways that are activated by the insulin receptor are also activated by other means, particularly activation of other growth factor receptors. Specificity of the insulin signal is felt to be due to the integration of the multiple pathways activated, as well as to compartmentalization of the components of the cascade. For example, both the PI3 kinase and Cbl/TC10 pathways appear to be necessary for insulin-stimulated glucose uptake into muscle and adipose cells.

Abnormalities of each of the components of the insulin-signaling cascade, from the insulin receptor at the beginning to the enzymes, transcription factors, and other effector proteins at the end, are potential candidates for contributing to the insulin resistance of type 2 diabetes. Indeed, certain polymorphisms in the IRS-1 gene are found more frequently in individuals with diabetes in some populations (the lack of this association in other populations likely underscores the genetic heterogeneity of this disease). For all the other components, however, mutations or significant alterations in expression have either not been found or have been extremely rare. However, there have been clearly

identified abnormalities in insulin signaling that occur in the insulin resistance of type 2 diabetes (Figure 2). Notably, insulin-stimulated tyrosine phosphorylation of the insulin receptor and IRS proteins is decreased in tissues in insulin-resistant subjects. This is often associated with an increase in phosphorylation on serine residues in these proteins, which may inhibit the protein–protein interactions necessary for proper signaling. Potential mechanisms for this include serine-phosphorylation of the insulin receptor by PKC, and stimulation of serine-phosphorylation of IRS-1 by TNF-α; PKC activity is increased in the presence of hyperglycemia, and adipocytes from obese subjects express increased amounts of TNF-α. The increase in free fatty acids present in obesity and insulin resistance may also lead to increased serine phosphorylation of the insulin receptor and IRS proteins.

In order to enter a cell, glucose requires specialized transporters to be present on the cell surface. GLUT4, the insulin-responsive glucose transporter, is sequestered in intracellular vesicles in the basal state. When muscle or adipose cells are stimulated by insulin, these vesicles translocate and fuse with the plasma membrane, and the increase in transporters at the cell surface results in increased glucose uptake. In the insulin resistance of obesity and type 2 diabetes, there is a decrease in the insulin-stimulated translocation of GLUT4. There may also be a decrease in the intrinsic activity of GLUT4 in insulin-resistant states. Finally, in adipocytes (but not muscle cells) there is significantly decreased expression of GLUT4 that contributes to the diminished insulin-stimulated glucose uptake. Although quantitatively adipose tissue contributes only a small fraction to glucose disposal compared to muscle, evidence from animal models with tissue-specific insulin resistance demonstrates that insulin resistance in one tissue can affect insulin sensitivity in other tissues. Thus, insulin resistance in the adipocyte can cause insulin resistance in liver and muscle, most likely through secreted free fatty acids and adipokines.

Insulin Secretory Defect

Insulin secretion increases to compensate for insulin resistance, so that in obese or otherwise insulin-resistant individuals, fasting and meal-stimulated insulin levels are elevated. When insulin secretion fails to fully compensate for the degree of insulin resistance, glucose levels rise, first to those of mild glucose intolerance (glucose levels above normal but below criteria for a diagnosis of diabetes), and then to those of diabetes. Insulin levels early in this progression are still elevated compared to individuals with normal insulin sensitivity, but are not elevated sufficient to maintain normal glucose control. With time, in most patients, the insulin secretory defect continues to worsen, including loss of β-cells, ultimately requiring exogenous insulin treatment to maintain control of blood glucose levels.

As for insulin resistance, the development of impaired insulin secretion is likely due to both genetic and environmental factors. The persistent stimulus imposed by insulin resistance on the β-cell to oversecrete insulin appears to be a key factor contributing to the loss of β-cell function (Figure 1). This may be due in part to the effect of excessive secretion of islet amyloid polypeptide (IAPP), which is cosecreted with insulin; in the islets in the majority of patients with type 2 diabetes there is the accumulation of amyloid, containing IAPP. Another factor is the elevated free fatty acid level present in insulin resistance, which can contribute to the defective insulin secretion, just as it can contribute to insulin resistance. While short-term exposure to lipids increases insulin secretion, long-term exposure impairs β-cell function, and may be responsible for β-cell death by apoptosis. Similarly, prolonged exposure to increased glucose levels imposes a "glucotoxicity" on the β-cell: if glucose levels are normalized in a patient with diabetes, endogenous insulin secretion will improve. Over time, however, this glucotoxicity may lead to irreversible β-cell damage, perhaps through oxidative injury. Finally, insulin resistance of the β-cell may itself lead to impaired β-cell function, as demonstrated in mice carrying genetic defects of insulin signaling in β-cells.

Other Specific Types

Diabetes of types other than type 1 or type 2 make up a small percentage of the cases of diabetes. For a number of these, however, a single gene defect results in the disease, providing potential insight into what may be the underlying cause of the insulin resistance or insulin secretory defect in type 2 diabetes.

Genetic Defects of β-Cell Function

Insulin Gene Mutations in the insulin gene have been described, but are extremely rare causes of diabetes. In the few families where such mutations have been found, the result is very mildly abnormal glucose control, inherited in an autosomal-dominant manner.

Maturity-Onset Diabetes of the Young Maturity-onset diabetes of the young are a group of diabetes types caused by mutations in single genes. Mutations in six genes have been identified, each of which results in deficient insulin secretion. These mutations result in autosomal dominantly inherited forms of diabetes that have an early onset, usually before the age 25. Because these patients retain some insulin secretion, albeit insufficient to prevent hyperglycemia, these patients are, in general, not ketosis prone, and so are not dependent on insulin treatment for survival. In contrast

to type 2 diabetes, obesity and insulin resistance are not a major feature of MODY; the diabetes in these cases is due to the defective insulin secretion. The severity of the insulin deficiency varies for the different genes involved, and consequently the severity of the untreated diabetes can vary from mild, sometimes unrecognized hyperglycemia with little risk of long-term microvascular diabetic complications, to severe hyperglycemia with a very high risk of microvascular complications.

MODY2 is caused by mutations in the gene for glucokinase, which is expressed in highest levels in the pancreatic β-cell and in the liver. In the β-cell, glucokinase catalyzes the phosphorylation of glucose to generate glucose-6-phosphate, the first step in glucose metabolism. Because glucose metabolism is the stimulus for insulin release, glucokinase functions as the glucose sensor in the β-cell as it is rate limiting for glucose entry into the glycolytic pathway. Thus, glucokinase mutations lead to decreased glucose-stimulated insulin secretion. In the liver, glucokinase affects the storage of glucose as glycogen; this defect may contribute to the hyperglycemia in patients with glucokinase mutations. MODY2 is caused by heterozygous mutations of the glucokinase gene; complete glucokinase deficiency due to homozygous mutations lead to more severe neonatal-onset diabetes.

The other genes that have been identified as having mutations that cause MODY are each transcription factors expressed in the pancreatic β-cell: hepatocyte nuclear factor (HNF)-4α (MODY1); TCF1, which encodes HNF-1α (MODY3); insulin promoter factor-1 (IPF1;MODY4); TCF2, which encodes HNF-1β (MODY5); and neurogenic differentiation 1/β-cell E-box transactivator 2 (NeuroD1/BETA2;MODY6). Each of these genes are expressed in the β-cell and regulate expression of the insulin gene and genes for other factors involved in the regulation of insulin signaling; heterozygous mutations lead to β-cell dysfunction sufficient to cause diabetes. IPF-1 and NeuroD1/BETA2 are also involved in pancreatic development, and homozygous mutations of IPF-1 lead to pancreatic agenesis and congenital diabetes mellitus and pancreatic insufficiency.

Mitochondrial DNA Mutations Mutations in the mitochondrial genome can cause diabetes mellitus, the most common involving the mitochondrial $tRNA^{LEU(UUR)}$. Due to the maternal origin of mitochondria, this type of diabetes is maternally inherited. The pancreatic β-cell is rich in mitochondria and has a high rate of oxidative metabolism; the mitochondrial mutations result in a β-cell defect that causes diabetes through deficient insulin secretion. This form of diabetes is frequently associated with neurosensory deafness.

While inherited mitochondrial genome mutations are rare as a cause of diabetes mellitus, they may provide insight into the worsening insulin secretory defect that occurs in type 2 diabetes. The mitochondrial genome consists only of coding sequences, and its repair mechanisms are poor so that it is highly susceptible to mutation. With age, there is an increase in reactive oxygen species generated in mitochondria, and this may be exacerbated in β-cells with a higher rate of oxidative metabolism due to exposure to elevated glucose levels. With a low expression of enzymes that defend against oxidative damage, β-cells are particularly sensitive to oxidative injury. The inherited mitochondrial genome mutations that cause diabetes demonstrate that these mutations can impair insulin secretion, and it is possible that an accumulation of mitochondrial DNA mutations due to oxidative damage contribute to the β-cell dysfunction of type 2 diabetes.

Genetic Defects in Insulin Action

Insulin Receptor Mutations Insulin resistance can be caused by mutations of the insulin receptor, although these are rare as a cause of diabetes. Most of the subjects identified with insulin resistance and insulin receptor mutations have mutations of both alleles. Some cases of mild insulin resistance have been described in which only one allele carries a mutation, acting as a dominant negative inhibitor of the wild-type allele, due to their combination within the heterotetrameric structure of the receptor. The severity of the phenotype with two mutant insulin receptor alleles can vary from insulin resistance with relatively normal glucose control (type A insulin resistance) to a more severe phenotype evident in infancy (Rabson–Mendenhall syndrome and Leprechaunism, which is usually fatal in infancy).

Secondary Diabetes Mellitus

A number of systemic disorders can cause marked insulin resistance, which can lead to secondary diabetes mellitus (although as for type 2 diabetes and as discussed above, there must be some defect in insulin secretion to prevent complete compensation for the insulin resistance by the β-cell). Excess growth hormone, as in acromegaly, excess glucocorticoid, as in Cushing's disease or exogenous glucocorticoid treatment, or excess catecholamines, as in pheochomacytoma, as well as other diseases such as uremia and hepatic cirrhosis can lead to secondary diabetes primarily through their effect on insulin sensitivity. Similarly, diabetes mellitus will occur if a disorder produces sufficient β-cell damage. Examples of this include pancreatitis, cystic fibrosis, pancreatectomy, and hemochromatosis; in addition, somatostatin-secreting tumors can inhibit insulin secretion sufficient to cause diabetes mellitus.

Rarely, patients with autoimmune disease have been identified where antibodies against the insulin receptor

block signaling, leading to an insulin resistant form of diabetes referred to as type B insulin resistance.

Strikingly, just as the excess adipose tissue in obesity leads to insulin resistance, the deficiency of adipose tissue that is found in lipoatrophy/lipodystrophy also causes insulin resistance, often severe. Mice that are genetically engineered to have a paucity of adipose tissue are also markedly insulin resistant, confirming this association. The cause of insulin resistance in syndromes of adipose deficiency is likely due to intrahepatic and intramuscular accumulation of triglyceride, as well as a loss of normal secreted signals from adipocytes.

Gestational Diabetes

Glucose intolerance that is first identified during pregnancy is referred to as gestational diabetes. The importance of this classification is the significant maternal and fetal morbidity related to diabetes during pregnancy, warranting screening for diabetes mellitus in all pregnant women except those at low risk. In some cases gestational diabetes is merely the identification of glucose intolerance that was previously unrecognized until screening is performed during a pregnancy, or to the temporal development of diabetes (type 1 or type 2) during a pregnancy, perhaps accelerated by the pregnant state, but otherwise predestined to develop. In the majority of cases, however, glucose regulation returns to normal after the pregnancy. Pregnancy is characterized by progressively decreasing insulin sensitivity, due to the insulin antagonizing effects of increases in prolactin, human placental lactogen, estrogens, progesterone, and unbound cortisol levels. In the majority of pregnancies, this insulin resistance is compensated for by increased insulin secretion. However, in the 2–5% of pregnancies that develop gestational diabetes mellitus, there is an inadequate compensation. Thus, gestational diabetes represents the same or similar pathophysiologic abnormality of insulin sensitivity and insulin secretion that occurs in type 2 diabetes, with a portion of the insulin resistance being self-limited due to the pregnant state. However, there is also an underlying defect in insulin sensitivity and insulin secretion, and women who have had gestational diabetes are at a substantially increased risk for the future development of type 2 diabetes.

Metabolic Syndrome and Prediabetes

Insulin resistance often precedes the development of diabetes mellitus by many years. In addition, in some people, β-cell dysfunction does not develop, and insulin resistance exists indefinitely without progressing to diabetes. However, insulin resistance is not without significance of its own. The metabolic syndrome (also referred to as syndrome X) is an association of findings that frequently coexist, and includes insulin resistance, obesity (particularly abdominal/visceral rather than peripheral/subcutaneous), hypertension, and a specific form of dyslipidemia: hypertriglyceridemia and decreased high-density lipoprotein (HDL) cholesterol. These subjects are at risk of developing type 2 diabetes if they do not already have it, but more importantly, even in the absence of progression to diabetes, these individuals are at a markedly elevated risk for atherosclerotic vascular disease. The causality of obesity and insulin resistance in this syndrome is supported by the fact that lipid levels and hypertension may both be improved by decreasing insulin resistance through exercise and weight loss.

The diagnosis of diabetes mellitus is based on blood glucose levels that exceed defined levels, either in the fasting state or after a challenge with an ingested glucose load. The cutoffs are based mostly on levels that predict an increased risk for diabetic microvascular complications. Some individuals with insulin resistance will have glucose levels that do not meet criteria for the diagnosis of diabetes, but are above levels considered normal. Some of these subjects with impaired fasting glucose (IFG) or impaired glucose tolerance (IGT) will have glucose levels that revert to normal, or remain "impaired" over time. However, a large percentage will have progressive β-cell dysfunction (or worsening insulin resistance, or both) that results in progression to type 2 diabetes – ~40% in 5–10 years.

Complications

Acute

Ketoacidosis

Diabetic ketoacidosis (DKA) is the life-threatening acute metabolic decompensation in patients with diabetes mellitus. Because the development of DKA is suppressed by even modest insulin action, DKA is generally only a risk for patients with type 1 diabetes. The pathophysiology of DKA is one of acidosis, hyperosmolarity, and dehydration.

Decompensation towards DKA begins with a fall in insulin action, either due to an absolute decline in the insulin level, or due to antagonism of insulin action by cytokines and stress hormones, including catecholamines, cortisol, glucagons, and growth hormone. As insulin action becomes inadequate, serum glucose levels rise; the loss of insulin suppression of gluconeogenesis and glycogenolysis in the liver results in an increase in hepatic glucose output, and the loss of insulin stimulation of glucose uptake in muscle and adipose tissue results in accumulation of the excess glucose in the blood. The loss of insulin suppression results in unrestrained lipolysis in the adipocyte, releasing free

fatty acids and glycerol. Increased protein breakdown in muscle releases amino acids. These metabolites are taken up by the hepatocytes, where the free fatty acids are metabolized to ketoacids (β-hydroxybutyrate and acetoacetic acid), and the glycerol and amino acids serve as substrates for accelerated gluconeogenesis.

The hyperglycemia and ketoacidosis are initially moderated by the loss of glucose and ketoacids in the urine. However, the glucosuria produces an osmotic diuresis, and the ketoacidosis produce an ileus leading to nausea and vomiting that impairs the ability of the patient to drink to maintain their hydration. As dehydration develops, then worsens, the glomerular filtration rate of the kidney falls, and less glucose and ketoacids can be excreted in the urine, resulting in dramatic accumulation of glucose and ketoacids in the blood. The evolving disease stimulates (further) release of stress hormones that antagonize any remaining insulin action, and further exacerbate the hyperglycemia. The acidosis and the hyperosmolarity caused by the extreme hyperglycemia decrease cerebral function and impair the patient's consciousness, further compromising the patient's ability to drink. Without intervention, death is inevitable.

Nonketotic Hyperosmolar, Coma

Patients with type 2 diabetes are not at much risk of developing DKA. They will generally have sufficient insulin action to restrain lipolysis, limiting free fatty acid delivery to the liver and subsequent ketoacid production. However, decompensation similar to that of DKA, but without the excess ketoacid production, can occur in patients with type 2 diabetes. Nonketotic hyperosmolar coma in patients with type 2 diabetes generally occurs when another illness induces a stress response, and there is an impaired ability to maintain hydration with oral fluids. As in DKA, the increase in stress hormones antagonize insulin action, resulting in increased hepatic glucose production and decreased peripheral glucose utilization. The rising hyperglycemia produces a glucosuria-driven osmotic diuresis. Dehydration is a result of an inability of oral fluid intake to compensate for the osmotic diuresis. As in DKA, the dehydration impairs the renal excretion of glucose, allowing the glucose level to continue to rise. The dehydration and hyperosmolarity impair the patient's consciousness, and oral intake falls further. The final situation is one of marked hyperglycemia, hyperosmolarity, and dehydration. As in DKA, the mortality of nonketotic hyperosmolar coma is high.

Chronic

Patients with diabetes will have bothersome symptoms and are at risk of severe acute metabolic decompensation, even if treatment is successful in avoiding these issues, diabetes can lead to long-term complications that develop over years. These complications can be categorized as microvascular, which are unique to patients with diabetes, and macrovascular, which are complications of atherosclerotic vascular disease that also occur in people without diabetes, but occur with higher frequency in those with diabetes. These complications are felt to be due to a failure of treatment to perfectly normalize insulin and glucose levels, as well as to changes produced by insulin resistance in type 2 diabetes.

Macrovascular Disease

As in individuals without diabetes, atherosclerotic changes in medium- and large-sized arteries that either partly or completely occlude the vessel lumen lead to morbidity and mortality due to impaired blood flow to the heart (angina and myocardial infarction), the brain (stroke), or the periphery (claudication and ischemic damage requiring amputation). These complications occur at a higher frequency and develop at younger ages in patients with diabetes; over half of patients with type 2 diabetes die from cardiovascular disease. It is not fully clear how diabetes contributes to the risk of atherosclerotic vascular disease. The factors that have been implicated include lipid abnormalities, hyperglycemia, and increases in prothrombotic and proinflammatory factors. In addition, the coexistence of other atherosclerotic risk factors, most notably hypertension in obese patients with type 2 diabetes, also plays a role.

In patients with type 2 diabetes, the insulin resistance that is a part of the pathophysiology is associated with a specific pattern of lipid abnormality that increases the atherosclerotic risk: decreased high density lipoprotein (HDL) cholesterol concentration, and elevated triglyceride concentration in the serum. In addition, the inadequate insulin action in poorly controlled diabetes of any type leads to inadequate stimulation of lipoprotein lipase activity and to increased lipolysis and elevated free fatty acids. The free fatty acids that are not oxidized to ketones in the liver are re-esterified to triglycerides and secreted as very low-density lipoproteins (VLDL). Thus, poorly controlled diabetes can lead to atherosclerotic risk by increasing triglyceride and VLDL levels; hypertriglyceridemia can exacerbate the risk by depressing HDL levels. Finally, hyperglycemia may contribute to disordered serum lipids by reducing expression of the heparin sulfate proteoglycan perlecan on hepatocytes, leading to increased levels of the atherogenic cholesterol-enriched apolipoprotein B-containing remnant particles.

Endothelial dysfunction is central to the development of atherosclerosis, with decreased production of the vasodilating molecule nitric oxide and increased production of the prothrombotic factor plasminogen

activator inhibitor-1 (PAI-1) two factors implicated in this dysfunction. In diabetes, hyperglycemia inhibits nitric oxide production and increases production of PAI-1. Hyperglycemia may also contribute to macrovascular disease indirectly through microvascular damage to the nutrient blood vessels supplying the walls of the medium- and large-sized arteries.

Another aspect that is likely to play a role in the development of atherosclerosis in type 2 diabetes relates to the pathway-specific insulin resistance that is present. As noted previously, the insulin resistance of type 2 diabetes has less of an effect on the activation of the intracellular mitogen-activated protein (MAP) kinase pathway than the pathway activating phosphatidylinositol-3-kinase. This may lead to increased activation of the MAP kinase pathway by insulin signaling, which also decreases nitric oxide production and increases PAI-1 production. In addition, as the MAP kinase pathway is a mitogenic pathway, the increased MAP kinase signaling can increase proliferation of the vascular smooth muscle cells, contributing to the atherosclerotic process.

Microvascular Disease

The hyperglycemia of diabetes mellitus leads to damage to the microvascular circulation that results in tissue and organ damage, most notably in the retina, kidneys, and nerves. Due to these microvascular complications, diabetes mellitus is a leading cause of blindness, end-stage renal disease, and neuropathy. Increasing degrees of hyperglycemia are the main risk factor for microvascular complications, with the Diabetes Control and Prevention Trial (for type 1 diabetes) and the United Kingdom Prospective Diabetes Study (for type 2) definitively demonstrating a decreased incidence of microvascular complications with treatments that lower the degree of hyperglycemia. Unfortunately, even the best of current therapies do not completely normalize blood glucose levels. The risk of microvascular complications increases with time, with the earliest evidence uncommon prior to a duration of hyperglycemia of 5 years; note, however, that except for typical type 1 diabetes, hyperglycemia may be present for years before the diagnosis of diabetes is made. Finally, as yet undefined genetic factors also play a role in the risk of microvascular disease.

Microvascular disease begins with abnormal blood flow and increased vascular permeability due to decreased activity of vasodilators, increased activity of vasoconstrictors, and overexpression of permeability factors. Irreversible increases in vascular permeability occur with alterations in the extracellular matrix. Ultimately, there is cell loss, and capillary occlusion from deposition of extravasated plasma proteins and the overproduction of extracellular matrix. Microvascular disease affects the glomerulus in the kidney, with the earliest evidence being leakage of albumin into the urine and progressing to loss of glomerular function. Damage to retinal capillaries causes hypoxic-ischemia, edema, new vessel formation, and hemorrhage. It is the development of new vessels, referred to as proliferative retinopathy, that leads to retinal detachment, vitreous hemorrhage, and loss of sight. Diabetic neuropathy includes degeneration of motor, sensory, and autonomic nerves.

While it is clear that hyperglycemia leads to microvascular disease, the precise mechanism for this has not been completely demonstrated. However, four pathologic processes triggered by hyperglycemia have been identified and proposed as causative mechanisms: increases in the polyol and hexosamine pathways, production of advanced glycation end-products (AGEs), and activation of protein kinase C (PKC). *In vivo* studies with inhibitors, either in animal models or in human subjects, have supported a role for each of these pathways (except the recently implicated hexosamine pathway) in microvascular pathology. The relative contribution of each of these proposed mechanisms likely varies across cell types.

While mechanisms exist for hyperglycemia to directly activate each of the four potential microvascular pathogenic pathways, they may also be activated by the hyperglycemia-induced overproduction of superoxide. The increased metabolism of glucose in the presence of hyperglycemia increases the delivery of electron donors from the tricarboxylic acid (TCA) cycle to mitochondria. This can lead to an increase of the proton gradient across the inner mitochondrial membrane, inhibiting the electron transport chain and increasing superoxide production. Because superoxide inhibits the glycolytic enzyme glyceraldehyde 3-phosphate dehydrogenase (GAPDH), precursors (as noted) can accumulate and be diverted into the polyol pathway (glucose), the hexosamine pathway (fructose-6-phosphate), production of DAG (glyceraldehyde-3-phosphate) which activates PKC isoforms, and production of the reactive dicarbonyl methylglyoxal (glyceraldehyde-3-phosphate) which produces AGEs.

Polyol Pathway Hyperglycemia drives an increased intracellular generation of sorbitol through the NADPH-dependent reduction of glucose by aldose reductase. Increased production of sorbitol could alter cellular functions in a number of ways, including increasing intracellular osmotic stress, decreasing myoinositol and taurine (as compensation for the increase in sorbitol in order to prevent or mitigate an increase in osmolarity), or through an increased NADH/NAD^+ ratio (due to NAD^+-dependent oxidation of sorbitol to fructose). However, the most likely mechanism for cellular dysfunction caused by increased flux through the polyol pathway is due to the consumption of NADPH.

This leads to a lack of NADPH available to regenerate reduced glutathione, limiting the ability of the cell to protect itself against oxidative stress.

Hexosamine Pathway The hexosamine pathway generates UDP-*N*-acetylglucosamine (GlcNAc) from glucose to provide substrate for proteoglycan synthesis and for O-linked glycosylation of certain proteins. The activity or function of many proteins, including transcription factors, can be modified by O-linked glycosylation, often in concert with reciprocal modification by phosphorylation. With hyperglycemia, some of the excess glucose is shunted into the hexosamine pathway. As noted previously, increased flux through this pathway may play a role in insulin resistance. In addition, increased generation of UDP-GlcNAc could alter gene expression and cellular function through excess protein glycosylation, contributing to the pathogenesis of microvascular disease.

Advanced Glycation End-Products Glucose will react with free amino groups on proteins in a nonenzymatic reaction to form glycated proteins. This reaction starts with the formation of a Schiff base (aldamine), which then undergoes an internal Amadori rearrangement. The formation of the Schiff base is rapid and reversible, while the Amadori rearrangement is much slower and results in a more stable ketoamine. This process occurs at a rate proportional to the prevailing glucose level that a given protein is exposed to. The glycation of hemoglobin is used clinically to estimate the average blood sugar in patients with diabetes, as the percent of hemoglobin in the glycated A_{1C} form (HbA_{1C}) is proportional to the average glucose level present over ~3 months prior to testing (roughly the red blood cell life span).

Proteins modified irreversibly through nonenzymatic reaction with glucose or glucose-derived compounds are referred to as advanced glycation end-products (AGEs). Most AGEs are not formed through the reaction of proteins directly with glucose but rather with three reactive dicarbonyl compounds that are produced intracellularly from glucose: glyoxal (an auto-oxidation product of glucose), 3-deoxyglucasone (formed from decomposition of the Amadori product of glucose), and methylglyoxal (from fragmentation of glyceraldehyde-3-phosphate and dihydroxyacetone phosphate generated from glycolysis). The reactive dicarbonyls interact with the amino groups of proteins, and can introduce both intra- and intermolecular cross-links. AGE formation may lead to microvascular damage through alteration of the function of both intracellular and extracellular proteins modified in this way. In particular, the modification of extracellular matrix proteins by this process is likely to contribute to abnormal vascular permeability and elasticity. In addition, however, AGEs formed from plasma proteins bind to and activate specific AGE receptors on endothelial cells, mesangial cells, and macrophages, (one such receptor is RAGE, a member of the immunoglobin superfamily). Activation of AGE receptors induces production of cytokines, growth factors, procoagulatory factors, and reactive oxygen species. Induction of vascular endothelial growth factor (VEGF) by AGE receptor activation most likely contributes to the increased permeability of capillary walls present in diabetes.

Activation of PKC Hyperglycemia increases intracellular diacylglycerol (DAG) levels, which is an activator of many of the PKC isoforms. Hyperglycemia may also activate PKC isoforms indirectly by increasing reactive oxygen species from activation of AGE receptors and from increased activity of the polyol pathway. As discussed above, activation of PKC may play a role in hyperglycemia-induced insulin resistance. Mechanisms through which activation of PKC may be involved in the development of microvascular disease include: inhibiting production of the vasodilator nitric oxide; increasing activity of the vasoconstrictor endothelin-1; increasing expression of VEGF, leading to increased cell permeability; and contributing to the accumulation of extracellular matrix protein by inducing expression of TGF-β1, fibronectin, and type IV collagen.

Diabetes Treatment Medications – Mechanisms of Action

Patients with diabetes of any type can be treated with insulin to overcome the relative or absolute insulin deficiency. For patients with type 1 diabetes, the loss of the ability to produce endogenous insulin because of the loss of pancreatic β-cells makes insulin the only treatment option. Similarly, in many patients with type 2 diabetes, the β-cell dysfunction will progress to a degree that insulin treatment is necessary to maintain glycemic control. However, for many patients with type 2 diabetes, a number of treatments may be effective in lowering the degree of hyperglycemia.

Weight Loss and Exercise

For the majority of patients with type 2 diabetes, obesity is a significant contributor to the insulin resistance that underlies their disease. Therefore, in many cases, if the patient is able to lose weight, insulin sensitivity will improve sufficiently to return metabolic control to normal or near normal. In many cases, only modest weight loss can be effective. A sedentary lifestyle also leads to decreased insulin sensitivity. Therefore, exercise

to improve fitness can also improve insulin sensitivity sufficient to ameliorate the diabetic state, an effect that can occur in the absence of weight loss. AMP-activated kinase (AMPK) functions as an intracellular energy sensor. During exercise, activation of AMPK increases glucose uptake into muscle by stimulating GLUT4 translocation to the plasma membrane in a noninsulin receptor dependent pathway. In addition, the exercise-stimulated activation of AMPK may lead to a prolonged increase in insulin sensitivity by increasing expression of GLUT4, and increasing the insulin sensitivity of the liver.

Insulin Secretagogues

Sulfonylureas and the newer meglitinide analogues lower blood sugar levels by stimulating endogenous insulin secretion. They act by binding to the sulfonylurea receptor (SUR) – one component of the β-cell potassium channel, the other being $Kir_{6.2}$. Binding of these agents to SUR results in closure of the potassium channel, mimicking the effect of a glucose-driven increase in the cellular ATP/ADP ratio, and setting in motion the intracellular signal for exocytosis of insulin. Unfortunately, due to the worsening β-cell dysfunction in most patients with type 2 diabetes, insulin secretagogues often become ineffective over time.

Metformin

Metformin is a biguanide compound that works by increasing insulin sensitivity in diabetic patients. Its main effect is on the liver, to decrease excess hepatic glucose production. The underlying mechanism for metformin's action has not been fully determined. However, it appears to function by activating AMPK. By activating AMPK, the hepatocyte shifts from lipogenesis to fatty-acid oxidation. This reduces hepatic triglyceride content, which has been implicated in the cause of insulin resistance. How metformin activates AMP-kinase is uncertain, but may involve inhibition of the mitochondrial electron transport chain.

Thiazolidinediones

Thiazolidinediones (TZDs) are a second class of insulin-sensitizing drugs. In contrast to metformin, however, their primary action is to increase peripheral insulin sensitivity, increasing glucose uptake into fat and muscle. TZDs are ligands for the peroxisome proliferator-activated receptor-γ (PPAR-γ), which is expressed in high levels only in adipose tissue, although low levels of expression are seen in other tissues, including in muscle, liver, and pancreatic β-cells. PPAR-γ is a transcription factor that alters gene expression in a ligand-dependent manner. The importance of PPAR-γ in the pathophysiology of diabetes is highlighted by the fact that individuals homozygous for a common amino acid polymorphism (Pro12Ala) in the *PPAR*γ gene are more insulin resistant and have an increased risk of diabetes than individuals with one Ala12 allele. The ability of PPAR-γ to improve overall carbohydrate control in spite of the fact that adipocytes are responsible for a relatively minor fraction of insulin-stimulated glucose uptake compared to muscle may be due to direct effects of TZDs on muscle. However, it is most likely that TZDs exert their effect by altering gene expression in adipocytes, which leads to improved insulin action in muscle and liver.

α-Glucosidase Inhibitors

Acarbose and miglitol inhibit the intestinal enzyme α-glucosidase. Given with meals, this delays carbohydrate absorption, leading to a requirement for a lower maximal insulin level to dispose of the absorbed carbohydrate. These drugs do not significantly affect fasting glucose levels, and so are generally ineffective as single agent therapy. However, there is accumulating information demonstrating the importance of controlling postprandial hyperglycemia to minimize long-term diabetic complications.

See Also the Following Articles

Glycogen Metabolism • Insulin- and Glucagon-Secreting Cells of the Pancreas • Insulin Receptor Family • Phosphatidylinositol-3-Phosphate • Protein Kinase C Family

Glossary

β-cell The insulin producing cells in the Islets of Langerhans.

glucose disposal The removal of glucose from the blood, usually in the context of its removal after having been added, as after absorption of a carbohydrate-containing meal.

glucose intolerance The condition where the concentration of glucose in the blood after ingestion of carbohydrate is elevated above normal; may also refer more generally to a condition associated with hyperglycemia.

hyperglycemia An abnormally elevated concentration of glucose in the blood.

kinase An enzyme that modifies a substrate through the addition of a phosphate group.

osmotic diuresis An increase in urine output stimulated by an increase in osmotically active solute in the urine; in diabetes, the solute is glucose.

phosphatase An enzyme that modifies a substrate through the removal of a phosphate group.

prandial Meal associated.

Further Reading

Bell, G. I., and Polonsky, K. S. (2001). Diabetes mellitus and genetically programmed defects in β-cell function. *Nature* **414**, 788–791.

Brownlee, M. (2001). Biochemistry and molecular cell biology of diabetic complications. *Nature* **414**, 813–820.

Cefalu, W. T. (2001). Insulin resistance: cellular and clinical concepts. *Exp. Biol. Med.* **226**, 13–26.

DeFronzo, R. A. (1997). Pathogenesis of type 2 diabetes: metabolic and molecular implications for identifying diabetes genes. *Diabetes Rev.* **5**, 177–269.

Evans, J. L., Goldfine, I. D., Maddux, B. A., and Grodsky, G. M. (2002). Oxidative stress and stess-activated signaling pathways: a unifying hypothesis of type 2 diabetes. *Endo. Rev.* **23**, 599–622.

Kahn, S. E. (2003). The relative contributions of insulin resistance and beta-cell dysfunction to the pathophysioloy of Type 2 diabetes. *Diabetologia* **46**, 3–19.

Maechler, P., and Wollheim, C. B. (2001). Mitochondrial function in normal and diabetic β-cells. *Nature* **414**, 807–812.

Mathis, D., Vence, L., and Benoist, C. (2001). β-Cell death during progression to diabetes. *Nature* **414**, 792–798.

Moller, D. E. (2001). New drug targets for type 2 diabetes and the metabolic sydrome. *Nature* **414**, 821–827.

Saltiel, A. L., and Kahn, C. R. (2001). Insulin signalling and the regulation of glucose and lipid metabolism. *Nature* **414**, 799–806.

Shulman, G. I. (2000). Cellular mechanisms of insulin resistance. *J. Clin. Invest.* **106**, 171–176.

The Expert Committee on the Diagnosis and Classification of Diabetes Mellitus (2003). The Expert Committee on the Diagnosis and Classification of Diabetes Mellitus. *Diabetes Care* **26** (suppl. 1), S5–S20.

Zimmet, P., Alberti, K. G. M. M., and Shaw, J. (2001). Global and societal implications of the diabetes epidemic. *Nature* **414**, 782–787.

BIOGRAPHY

David W. Cooke is an Associate Professor of Pediatrics in the Division of Pediatric Endocrinology at the Johns Hopkins University School of Medicine. His research interest is the molecular basis of insulin resistance, particularly that occurring in the adipocyte. He received S.B. degrees in Mechanical Engineering and Biology from the Massachusetts Institute of Technology and his M.D. from the Duke University School of Medicine. He received his pediatric residency training and his pediatric endocrine fellowship training at the Johns Hopkins Hospital.

Diacylglycerol Kinases and Phosphatidic Acid Phosphatases

Stephen M. Prescott and Matthew K. Topham
Huntsman Cancer Institute, University of Utah, Salt Lake City, Utah, USA

Diacylglycerol (DAG) is an important lipid that initiates specific intracellular signaling events. The majority of signaling DAG is generated by hydrolysis of phosphatidylinositol-4,5-bisphosphate (PIP_2) by the enzyme phospholipase C (PLC). DAG activates protein kinase C (PKC) isoforms, binds to and activates the RasGRP nucleotide exchange factors, and recruits the chimaerins, which are Rac GTPase activating proteins (GAPs), to membrane compartments. Because DAG can modulate a plethora of signaling events, it is crucial that intracellular DAG levels be tightly regulated. Though DAG can be metabolized in various ways, under most circumstances its major route for metabolism is by its phosphorylation (Figure 1), a reaction that is catalyzed by the diacylglycerol kinases (DGKs).

The Diacylglycerol Kinases

Nine mammalian DGK isoforms have been identified (Figure 2). The heterogeneity of the gene family is similar to the PKC and PLC families, suggesting that the DGKs are not simply lipid biosynthetic enzymes, but that they also have signaling roles, since enzymes involved in biosynthetic pathways usually do not have extended families. One or only a few DGK isoforms have been identified in organisms such as *Caenorhabditis elegans*, *Drosophila melanogaster*, and *Arabidopsis thaliana*, and no DGK gene has been identified in yeast. The structural diversity of DGKs in mammals suggests that they may have roles in processes specific to higher vertebrates.

DGK isoforms are categorized based on shared structural motifs. All DGK isoforms have a catalytic domain that is necessary for kinase activity. In most cases, the catalytic domain is a single motif, but DGKs δ and η have bipartite catalytic domains. All DGKs have at least two cysteine-rich regions homologous to the C1A and C1B motifs of PKCs. In theory, these domains may bind DAG, perhaps localizing DGKs to where DAG accumulates. However, no DGK C1 domain has so far been conclusively shown to bind DAG. Structural predictions suggest that most DGK C1 domains may not bind DAG, and most DGKs tested are unable to bind long-lived DAG-like analogues. Houssa and van Blitterswijk noted that in DGKs, the C1 domain closest to the catalytic domain is highly conserved, including an extended motif of 15 amino acids not present in other C1 domains. Conserved residues in this extended motif have been shown to be critical for DAG kinase activity. Together, these data suggest that DGK C1 domains are structurally different from C1 domains in other proteins and that the different C1 domains of a single DGK isoform may have unique functions. Distinct functions of individual C1 domains remain to be definitively demonstrated.

In addition to the C1 and catalytic domains, other regulatory domains are used to group the DGKs into five subfamilies. Type I DGKs have calcium-binding EF hand motifs and have been shown to be more active in the presence of calcium. Type II DGKs have a pleckstrin homology (PH) domain at their amino termini. This domain in DGKδ has been shown to bind weakly and nonselectively to phosphatidylinositols (PIs). DGKδ also has a sterile alpha motif (SAM domain) at its C-terminus that helps localize it to the endoplasmic reticulum (ER). DGKε, a type III enzyme, has an unusual specificity toward acyl chains of DAG, strongly preferring a specific fatty acid – arachidonate – at the *sn*-2 position. This preference suggests that DGKε may be a component of the biochemical pathway that accounts for the enrichment of phosphatidylinositols with arachidonate. Type IV DGKs have a MARCKS phosphorylation domain and, at their C-termini, four ankyrin repeats. The type V enzyme, DGKθ, has three C1 domains and a PH domain.

Regulation of DGK Activity

Activation of the DGKs is complex and unique for each DGK isotype. In most cases, DGKs must translocate to a membrane compartment to access DAG. In addition, their activity can be modified by appropriate cofactors, and several DAG kinases are also regulated by

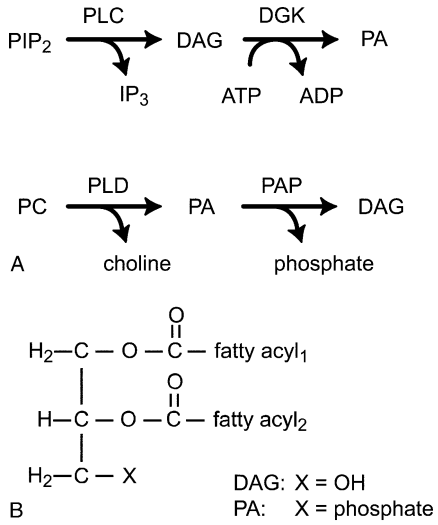

FIGURE 1 (A) Different enzymatic pathways can produce diacylglycerol (DAG) and phosphatidic acid (PA). Phosphatidylinositol-specific PLC enzymes generate DAG that can be phosphorylated by DGKs to produce PA. In another pathway, phospholipase D (PLD) hydrolyzes phosphatidylcholine (PC) – or phosphatidylethanolamine – making PA that can be further hydrolyzed by PAPs to generate DAG. (B) DAG and PA have the same general structure but contain different functional groups attached to the third (*sn*-3) carbon. Depending on their molecular structure, the fatty acyl groups confer different signaling properties to the DAG or PA.

post-translational modifications. Finally, tissue-specific alternative splicing of DGKs β, δ, and ζ, and probably other isotypes, allows additional opportunities for regulation. This complexity permits tissue- or cell-specific regulation of each DGK isotype, depending on the availability of cofactors and the type of stimulus that the cell receives.

DGKα is an example of the contextually dependent differential regulation of DGKs. DGKα translocates to at least two different membrane compartments in T lymphocytes depending upon the agonist used to activate the cells: from the cytosol to a perinuclear region in T cells stimulated with IL-2, and to the plasma membrane upon activation of the T cell antigen receptor. Once at a membrane compartment, the DAG kinase activity of DGKα can be modified by the availability of several cofactors. Calcium is known to bind to EF hand structures and stimulates DGKα activity *in vitro*. Lipids also modify its activity: phosphatidylserine and sphingosine activate DGKα *in vitro* and likely *in vivo* as well. Finally, DGKα can be phosphorylated by several protein kinases including some PKC isoforms and Src kinase, which may enhance its DAG kinase activity.

Like DGKα, other DGK isotypes appear to be sensitively regulated. For example, type II DGKs have a PH domain that may help localize these DGKs, modify their activity, or allow binding to other proteins. The PH domain of the type II DGKδ binds phosphatidylinositols but its DAG kinase activity is not affected by these lipids. In contrast, the activity of DGK types III and IV can be modified by phosphatidylinositols and by phosphatidylserine, sometimes in opposing ways. For example, the type III enzyme, DGKε, is inhibited by, whereas type IV DGKs are activated by, phosphatidylserine. Type IV DGKs are strongly regulated by subcellular translocation. These enzymes have a nuclear localization signal that is regulated by PKC phosphorylation, and there is evidence that the syntrophin family of scaffolding proteins further regulates their subcellular location by anchoring them in the cytoplasm. Finally, DGKθ, a type V DGK, can be regulated through its association with active RhoA, which abolishes its DAG kinase activity and is the only known example of direct regulation of a DGK activity through a protein–protein interaction. Thus, depending on the context of activation, the availability of cofactors, and the activation state of protein kinases, DGKs can be differentially regulated.

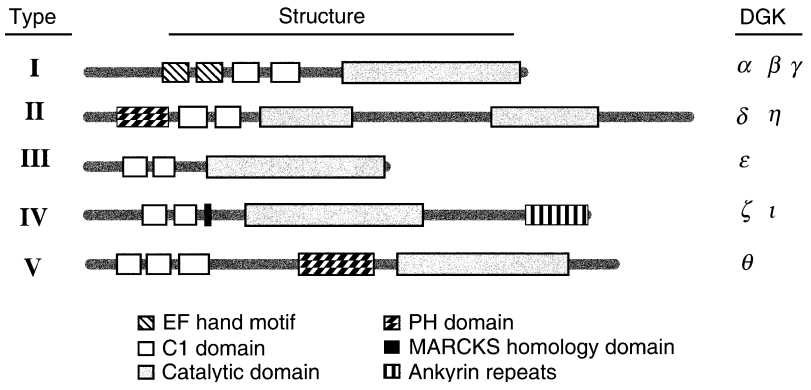

FIGURE 2 The mammalian DGK family. Based on structural motifs, the nine mammalian DGKs are divided into five subtypes. Alternative splicing of some DGK isotypes generates even more structural diversity. Many of the DGKs contain other unique structural domains of unclear significance that are not shown.

Activity of DGKs is Compartmentalized

Evidence suggests that DGK activity is restricted to the area of localized DAG pools generated after activation of receptors. This concept was initially tested in 1994 by Van der Bend *et al.*, who detected DGK activity in cells following receptor activation but could not detect significant DAG kinase activity after treating the cells with exogenous PLC, which caused global, nonspecific DAG generation. Their data suggest that DGKs are active only in spatially restricted compartments following physiologic generation of DAG.

We are only beginning to understand the complexities of spatially restricted DGK function. Several DGKs localize to the cytoskeleton, where they may participate in regulating cytoskeletal dynamics. Investigators have noted that DGK activity associates with a complex of proteins including PI5K, Rac, Rho, Cdc42, and Rho-GDI, all of which regulate cytoskeleton dynamics. Houssa *et al.* showed that RhoA associates with DGKθ – but only when RhoA is in its active form – and that this interaction abolished DGK activity. RhoA appears to bind the catalytic domain of DGKθ, which likely leads to the disruption of DAG kinase activity. DGKζ localizes at the leading edge and cell extensions of glioblastoma cells and can disrupt cell spreading when overexpressed. It and several other DGK isotypes co-immunoprecipitate with Rho family proteins when overexpressed in cells. The physiologic significance of these interactions is not clear, though together, these data suggest that DGKs likely have a role in regulating the cytoskeleton.

In the nucleus, a distinct nuclear phosphatidylinositol cycle is regulated separately from its plasma membrane/cytosolic counterpart. The function of DAG produced in the nucleus has received little attention, but data clearly indicate that in most cases it acts to promote cell growth independently of plasma membrane DAG. For example, some growth factors (e.g., IGF-1) can stimulate a pulse of nuclear DAG without causing a measurable change in extranuclear DAG, and several groups have demonstrated that nuclear DAG fluctuates independently of extranuclear DAG during the cell cycle. Nuclear DAG was shown to peak shortly before S phase, suggesting that it may participate in the G1/S transition. Supporting this conclusion and emphasizing the importance of DAG signaling in the cell cycle, we demonstrated that when a nuclear DGK was overexpressed, cells accumulated at the G0/G1 transition, presumably because the kinase attenuated the nuclear DAG concentration. Within the nucleus, DAG signaling, like its extranuclear counterpart, appears to be compartmentalized. For example, in 1999 D'Stantos *et al.* demonstrated independently fluctuating pools of nuclear diacylglycerol with distinct fatty acid compositions, strongly suggesting the existence of multiple, differentially regulated pools of nuclear DAG.

DGKs are present in nuclei and appear to have prominent and specific roles there. DGKs α, ζ, and ι, translocate to the nucleus, while a fraction of DGKθ is localized there constitutively. Different DGK subtypes are confined to specific, separate compartments within the nucleus, suggesting specificity in their nuclear roles. For example, DGKα associates with the nuclear envelope, while DGKθ and DGKζ are found in discrete regions within the body of the nucleus. Evidence suggests that DGKs likely affect nuclear signaling either by terminating DAG signals or by generating PA. For example, nuclear DGKζ inhibits progression from G1 to S phase of the cell cycle, likely by metabolizing DAG. Conversely, in T lymphocytes, PA generated by nuclear DGKα appears to be necessary for IL-2-mediated progression to S phase of the cell cycle. Thus, DGKα and DGKζ appear to have opposing roles in the nucleus, reflecting the complexity of lipid signaling and DGK activity there.

Coupling of DGKs with Other Signaling Proteins

Recent evidence suggests that in addition to acting locally at sites of DAG pools, DGKs can specifically associate with and regulate signaling proteins that are activated by either DAG or PA. For example, DGKζ associates with and inhibits RasGRP1, a guanine nucleotide-exchange factor for Ras that requires DAG to function. This regulation may be selective: five other DGK isotypes did not significantly inhibit RasGRP1 activity. In *Caenorhabditis elegans*, Nurrish *et al.* found that *dgk-1*, an ortholog of human DGKθ, regulates DAG signaling that is necessary for acetylcholine release. Combined, these data demonstrate that DGK activity is not only targeted at sites of DAG production, but is also specifically directed toward a subset of DAG-activated proteins.

PA as a Signal

The DGK reaction is of special interest because it removes one signaling molecule, DAG, while generating another, phosphatidic acid (PA). PA can stimulate DNA synthesis and is potentially mitogenic. It modulates the activity of several enzymes, including phosphatidylinositol 5-kinases (PI5Ks), PAK1, Ras-GAP, and PKCζ, and it has a prominent role in vesicle trafficking. At the plasma membrane, PA also helps recruit Raf to the Ras signaling complex. Although phospholipase D (PLD)

generates the bulk of signaling PA (Figure 1), DGKs likely also contribute to its intracellular concentration.

The PA species generated by DGK and PLD reactions are distinct from each other by virtue of their initial substrates. Phosphatidylcholine, which is largely composed of saturated and mono-unsaturated fatty acids is the predominant substrate of PLD, while PA produced by DGKs is derived from DAG that is enriched in polyunsaturated fatty acids – particularly arachidonate. There is good evidence that each PA species – saturated and unsaturated – can differentially activate targets. For example, saturated PA species induce MAPK activation to a greater extent than unsaturated PAs; Flores and colleagues presented evidence that the PA produced by DGKα was necessary for stimulated T lymphocytes to progress to S phase of the cell cycle. Thus, DGKs can influence signaling events either by metabolizing DAG or by generating PA.

PA Conversion to DAG by PA Phosphatase

Just as PA can be generated by more than one enzymatic pathway, DAG is also the product of several enzymatic reactions. The PLC reaction is generally thought to be the major route to generate signaling DAG, but some lipid phosphate phosphatases (LPPs) can also produce DAG by dephosphorylating phosphatidic acid (Figure 1). Most LPPs are integral membrane proteins thought to act on extracellular lipids, but some of them are clearly intracellular proteins. Type I LPPs specifically dephosphorylate phosphatidic acid and are also known as PA phosphatases (PAPs). Though their cDNAs have not been cloned and the proteins have not been purified to homogeneity, PAPs are known to be cytosolic proteins that can translocate to membrane compartments. Historically, PAP activity is thought to be coupled with PLD activity to generate DAG. But very little published work supports that this DAG can initiate signaling. Due to the identity of its precursor, DAG generated by PAP activity is composed of predominantly saturated fatty acids, and like PA, the signaling properties of DAG depend on these fatty acid components. Evidence suggests that DAG composed of saturated fatty acids – like that produced by PAP activity – has weak signaling properties compared to unsaturated DAG. Thus, PAPs are not thought to initiate DAG signaling. Instead, PAPs may terminate PA signals that were initiated by phospholipase D. It is possible that PAP activity could couple with DGK activity to regenerate unsaturated DAG that could initiate signaling, but no one has demonstrated that this cycle exists. Thus, PAPs theoretically could contribute to DAG signaling but evidence is lacking that they do so; it is generally agreed that PAP activity is coupled with PLDs and not DGKs.

Conclusions

As evidence accumulates, it is apparent that the structural diversity of DGK isoforms mirrors the range of functions and sites of action of these enzymes. Further studies of the regulation of lipid signaling should reveal additional roles for DGKs and more precise information about their regulation. Phosphatidic acid phosphatases, in contrast, appear to be a less diverse family of enzymes that are coupled to PLD activity.

See Also the Following Articles

Phosphatidylinositol Bisphosphate and Trisphosphate • Phospholipase C

Glossary

diacylglycerol A lipid composed of a glycerol backbone with fatty acids attached by ester bonds to its first (*sn-1*) and second (*sn-2*) carbons.

fatty acid Monobasic acids containing long hydrocarbon chains that can be either saturated (no double bonds) or unsaturated (one or more double bonds).

phosphatidic acid Diacylglycerol with a phosphate group attached to the third (*sn-3*) carbon of the glycerol backbone.

phosphatidylinositol Phosphatidic acid with an inositol group attached to the phosphate.

phospholipid The major structural lipids of most cellular membranes. They contain one or more phosphate groups and, if derived from glycerol, are known as phosphoglycerides.

Further Reading

Hodgkin, M. N., Pettitt, T. R., Martin, A., Michell, R. H., Pemberton, A. J., and Wakelam, M. J. O. (1998). Diacylglycerols and phosphatidates: Which molecular species are intracellular messengers? *Trends Biochem. Sci.* **23**, 200–204.

Nurrish, S., Segalat, L., and Kaplan, J. M. (1999). Serotonin inhibition of synaptic transmission: Gα_o decreases the abundance of UNC-13 at release sites. *Neuron* **24**, 231–242.

Sanjuan, M. A., Jones, D. R., Izquierdo, M., and Merida, I. (2001). Role of diacylglycerol kinase α in the attenuation of receptor signaling. *J. Cell Biol.* **153**, 207–219.

Sciorra, V. A., and Morris, A. J. (2002). Roles for lipid phosphate phosphatases in regulation of cellular signaling. *Biochim. Biophys. Acta* **1582**, 45–51.

Topham, M. K., and Prescott, S. M. (2001). Diacylglycerol kinase ζ regulates Ras activation by a novel mechanism. *J. Cell. Biol.* **152**, 1135–1143.

Topham, M. K., and Prescott, S. M. (2002). Diacylglycerol kinases: Regulation and signaling roles. *Thromb. Haemostasis* **88**, 912–918.

van Blitterswijk, W. J., and Houssa, B. (2000). Properties and functions of diacylglycerol kinases. *Cell. Signalling* **12**, 595–605.

Van der Bend, R. L., de Widt, J., Hilkmann, H., and van Blitterswijk, W. J. (1994). Diacylglycerol kinase in receptor-stimulated cells converts its substrate in a topologically restricted manner. *J. Biol. Chem.* **269**, 4098–4102.

Biography

Stephen M. Prescott is the Executive Director of the Huntsman Cancer Institute at the University of Utah in Salt Lake City. His research explores the enzymes that generate lipid signals for growth and differentiation, and the role that they play in cancer. Another major area of interest is how inflammation is regulated.

Matthew K. Topham is an Assistant Professor of Internal Medicine at the University of Utah and an Investigator at the Huntsman Cancer Institute. He studies lipid signaling in cancer and is particularly interested in the diacylglycerol kinases and cyclooxygenases.

Disulfide Bond Formation

Hiram F. Gilbert
Baylor College of Medicine, Houston, Texas, USA

Disulfide bond formation is a posttranslational protein modification that introduces a covalent cross-link between the sulfhydryl groups of specific cysteine residues. Biologically, disulfide bonds are most often used to increase the conformational stability of extracellular proteins, but disulfides may also serve catalytic or regulatory roles through their effects on protein structure. Disulfide bonds are formed as the protein folds into its correct biological structure. Elaborate quality control systems in the bacterial periplasm and eukaryotic endoplasmic reticulum assure that correct disulfides are formed as the proper conformation is achieved.

Chemistry of Disulfide Formation as a Posttranslational Modification

Disulfide Formation

Extracellular and secreted proteins often contain many disulfides, with pairs of cysteines linked to each other in a specific configuration in the folded protein (Figure 1). Biochemically, disulfide formation is an oxidation (the loss of electrons). Not all of the cysteines in a protein form disulfides. Disulfides form only when the structure of the protein places two cysteines in the proper spatial location and when an oxidizing agent is available. The chemical reaction is reversible, and high concentrations of a reductant can reverse or prevent disulfide formation.

Disulfide Rearrangements

Through a chemical process called thiol-disulfide exchange, one disulfide may serve as an oxidizing agent to form a disulfide between two different cysteines (Figure 2). If this leads to connecting the cysteines in a different configuration, it is termed disulfide isomerization.

Oxidative Protein Folding

Since many disulfides will be buried in the core of the protein and link cysteines that are not adjacent in sequence, disulfide formation and rearrangements often occur as the protein attains a three-dimensional structure (protein folding). The coupling of disulfide formation and protein folding is termed "oxidative protein folding."

Structure is Linked to Disulfide Formation

In the 1960s, Anfinsen and his colleagues used the reversible nature of disulfide formation to demonstrate that the primary sequence of a protein contains sufficient information to define the final, biologically active structure of a protein. Disulfide bonds stabilize protein structure by organizing and destabilizing the denatured protein relative to the native structure. Usually, both the disulfides and noncovalent interactions (hydrophobic interaction, hydrogen bonds, etc.) are needed to specify the structure of ribonuclease A (RNase). Reducing the disulfides or using urea to disrupt the noncovalent structure causes a loss in biological activity. After removing the urea and including an oxidizing agent to reform the disulfides, the protein spontaneously refolds, forming the correct disulfides and a biologically active structure. However, if disulfide formation is permitted without removing the urea, random disulfides form (scrambled RNase) and there is no regain of biological activity. If disulfide formation is inhibited (by including a reducing agent), the native structure does not form when the urea is removed. Disulfide bonds are essential for forming the native structure but when the noncovalent structure is disrupted by denaturants disulfides are usually not sufficient to specify the tertiary structure.

Disulfide Bond Formation during Protein Folding

Even with two disulfides, there are numerous ways to connect the cysteines (Figure 3), and the problem increases greatly as the number of disulfides to be formed increases. Early in protein folding, disulfide formation tends to be error-prone. Two types of

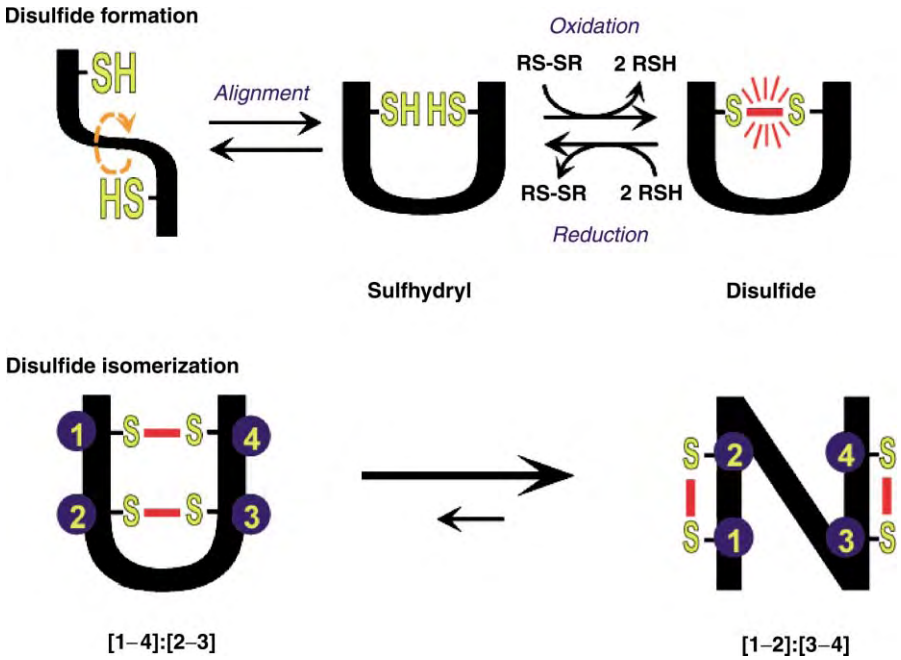

FIGURE 1 Disulfide formation and isomerization. An alignment step is needed to bring two sulfhydryl groups from cysteine residues into close proximity. Disulfide formation represents an oxidation where the electrons from disulfide formation must be transferred to an oxidizing agent. Disulfide isomerization does not formally require a change in the oxidation state of the protein; however, a thiol group is needed to initiate and propagate the change in disulfide connectivity.

error have been found: disulfides may be formed between the wrong pairs of cysteines or the correct cysteines may be paired but in a temporal order that interferes with the assembly of the rest of the structure. In both cases, the incorrect disulfides are replaced with correct ones through disulfide isomerization. In the cases examined so far, many incorrect disulfides accumulate early in oxidative folding. These are slowly replaced by correct disulfides through isomerization which requires the breaking and reforming of disulfide bonds.

Catalysis of Disulfide Formation

Soon after discovering that native proteins can be regenerated from reduced, denatured ones, Anfinsen realized that *in vitro* oxidative folding was often too

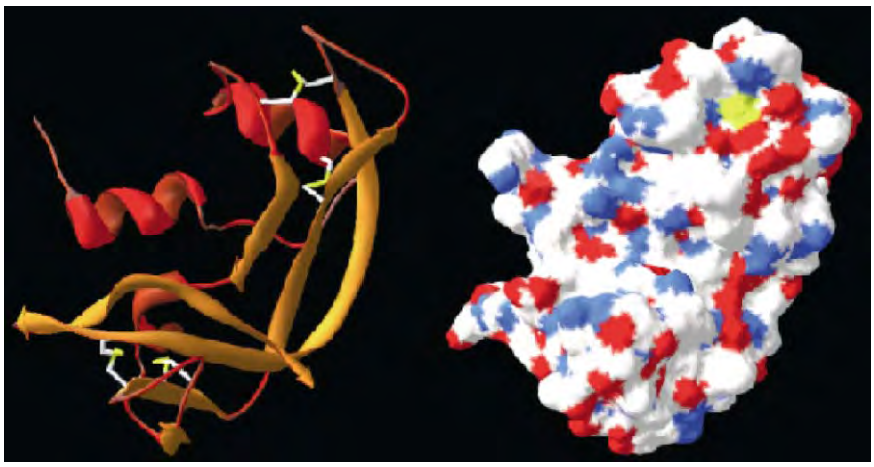

FIGURE 2 Structure of disulfide bonds. (Left) Disulfide bonds cross-link cysteines in various parts of the protein structure. (Right) Some disulfides (yellow) are exposed to solution in the tertiary structure of the protein but others are buried in the core of the protein and not exposed to solution.

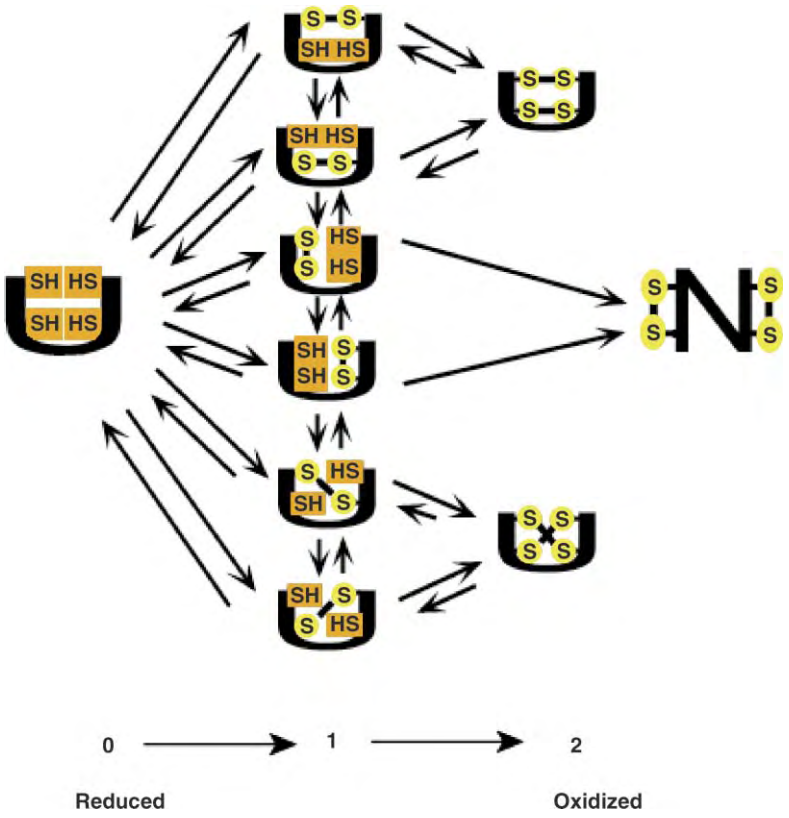

FIGURE 3 Generalized mechanism of oxidative protein folding. The initial stages of oxidative folding are error-prone and often lead to the connection of cysteines that are not connected in the native structure. Different proteins will generate a different population of misoxidized species which are converted to the native structure (N) by disulfide bond isomerization.

slow (hours to days) to be biologically relevant. The resulting search for a biological catalyst for oxidative folding led to the discovery of the first catalyst of protein folding, protein disulfide isomerase (PDI).

Protein Disulfide Isomerase

PDI accelerates the regain of native structure by catalyzing the formation of disulfide bonds and by providing a way to correct mistakes in connecting cysteines. PDI is an enzyme that has both oxidase (disulfide formation) and isomerase (disulfide rearrangement) activities. PDI accelerates thiol/disulfide exchange reactions (Figure 1) with proteins and small-molecule substrates. The final outcome of the reaction will depend on the redox conditions. The catalytic sites are contained in two thioredoxin homology domains located at each end of the PDI molecule. These active sites, both with the sequence CGHC, have the correct redox potential to effectively catalyze oxidation, reduction, and exchange reactions under the redox conditions of the endoplasmic reticulum. PDI interacts with its protein substrates but in a way that does not direct which cysteines are connected in the substrate. The mechanism involves several rounds of making and breaking disulfide bonds until the final structure becomes resistant to further isomerization of its disulfides.

The Thioredoxin Family

Many of the thiol–disulfide exchange reactions of the cell are mediated by members of the thioredoxin family. This large family of proteins is characterized by an active site sequence of CXXC and an α–β secondary structure. The structure greatly affects the redox potential for reducing the active site disulfide. Thioredoxin, the patriarch of the family, is an excellent reducing agent involved in the biosynthesis of deoxyribonucleotides for DNA synthesis and in helping maintain reduced proteins in the cellular cytoplasm. DsbA, a periplasmic oxidase in bacteria is an excellent oxidizing agent that inserts disulfides into secreted proteins. The ease of forming the CXXC disulfide varies by a factor of over 10^5, corresponding to a redox potential difference of more than 0.15 V.

Disulfide Formation in the Cell

Disulfide bond formation state is influenced by the thiol/disulfide redox environment of the cellular compartment where the protein is located. Most disulfides are found in secreted or extracellular proteins where the environment is oxidizing. Generally, the cytoplasm of most cells, bacterial and eukaryotic, is very reducing, due to the high concentration of glutathione (GSH, a tripeptide, γ-glutamylcysteinylglycine) and the low concentration of glutathione disulfide.

Extracellular Proteins

Proteins destined for the extracellular environment acquire disulfides after they are secreted from the cytoplasm during translation. In bacteria, an elaborate system of periplasmic and membrane-bound proteins, comprising the Dsb system, provides the periplasm with oxidizing equivalents to enable disulfide formation and reducing equivalents and catalytic isomerases to correct errors during protein folding (Figure 4). DsbB couples the bacterial electron transport system to disulfide formation, providing a source of oxidizing agent which are delivered directly to folding proteins by DsbA. Reducing equivalents to enable disulfide isomerization are provided by thioredoxin in the cytosol and transferred across the inner bacterial membrane by DsbD to DsbC, the periplasmic isomerase.

A similar system operates in eukaryotic cells, although all the elements of the system have not been found. Extracellular proteins are synthesized on the rough endoplasmic reticulum and translocated into the lumen (inside) during translation. The lumen of the endoplasmic reticulum is a more oxidizing intracellular compartment than the cytoplasm. Oxidizing equivalents are transferred from Ero1 to PDI and then to the folding proteins. The ultimate source of the oxidizing agent is not yet known. Reducing agents of the endoplasmic reticulum enable PDI and other catalysts to correct any errors in pairing cysteines by reducing the incorrect disulfide bond. Reducing agents are provided by glutathione, presumably by importing GSH from the cytoplasm. The endoplasmic reticulum has an elaborate quality control mechanism, which prevents misfolded proteins from exiting the endoplasmic reticulum or directs them to degradation pathways. The error-correction activity of PDI plays a critical role in this system. Depending on the details of the folding mechanism dictated by the primary sequence, different extracellular proteins may use different components of the complex folding and quality control apparatus of the endoplasmic reticulum to gain their correct three-dimensional structure, including the disulfide bonds that stabilize the structures.

Disulfide Formation as a Regulatory Mechanism

Because disulfide bond formation is reversible, disulfide bonds can also regulate biological activity through their ability to stabilize specific protein structures. For example, the bacterial transcription factor, OxyR, senses the redox environment of the aerobic bacterial cell

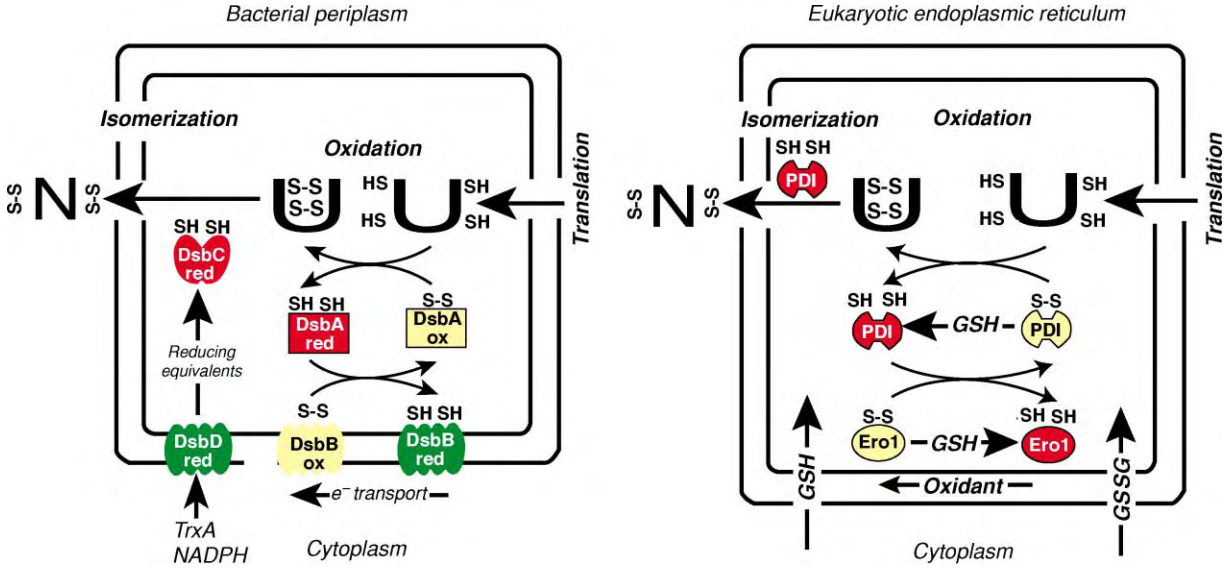

FIGURE 4 Disulfide bond formation in bacterial and eukaryotic cells. In both cells, the major pathways for disulfide formation are located in specialized cellular compartments where the redox state of the environment is maintained in a more oxidized state than the cytosol.

through reversible disulfide bond formation linked to the cellular redox state and oxygen metabolism. Reduced OxyR is inactive as a transcription factor and upon oxidation and disulfide formation, the transcription factor can regulate the transcription of genes involved in the protection of the cell against oxidative stress and reactive oxygen species. Similar mechanisms operate in eukaryotic cells.

See Also the Following Articles

Glycoprotein Folding and Processing Reactions • Protein Folding and Assembly

Glossary

bacterial periplasm A specialized compartment in between the inner and outer membrane of bacteria. Disulfide formation occurs in this compartment.

disulfide bond A covalent bond between two sulfhydryl groups. In proteins, this bond covalently connects the sulfur atoms of two cysteine residues.

endoplasmic reticulum A specialized compartment of eukaryotic cells in which extracellular proteins are processed for secretion or inclusion in other cellular compartments.

glutathione (GSH) A tripeptide, γ-glutamylcysteinylglycine found at high concentrations in cells. It is the major thiol compound in most cells involved in redox reactions and the protection of cells against reactive oxygen species and toxic compounds.

oxidation Disulfide bond formation (formally, the loss of electrons) oxidation.

oxidative folding The coupling of disulfide formation to the folding of a protein into its correct three-dimensional structure. Disulfides stabilize protein structure and *vice versa*.

protein folding The process by which an unfolded protein gains its three-dimensional structure.

reduction Formally, the gain of electrons. Disulfide bonds are reduced to two thiols.

thiol A sulfhydryl (–SH) group.

Further Reading

Collet, J.-F., and Bardwell, J. C. A. (2002). Oxidative protein folding in bacteria. *Mol. Microbiol.* **44**, 1–8.

Creighton, T. E. (1984). Disulfide bond formation in proteins. *Method Enzymol.* **107**, 305–329.

Frand, A. R., Cuzzo, J. W., and Kaiser, C. A. (2000). Pathways for protein disulphide bond formation. *Trends Cell Biol.* **10**, 203–210.

Gilbert, H. F. (1998). Protein disulfide isomerase. *Method Enzymol.* **290**, 26–50.

Gitler, C., and Danon, A. (eds.) (2003). *Cellular Implications of Redox Signaling*. Imperial College Press, London.

Goldberger, R. F., Epstein, C. J., and Anfinsen, C. B. (1963). Acceleration of reactivation of reduced bovine pancreatic ribonuclease by a microsomal system from rat liver. *J. Biol. Chem.* **238**, 628–635.

Helenius, A. (2001). Quality control in the secretory assembly line. *Philos. Trans. R. Soc. Lond. B Biol. Sci.* **356**, 147–150.

Ritz, D., and Beckwith, J. (2001). Roles of thiol-redox pathways in bacteria. *Annu. Rev. Microbiol.* **55**, 21–48.

Scheraga, H. A., Konishi, Y., and Ooi, T. (1984). Multiple pathways for regenerating ribonuclease A. *Adv. Biophys.* **18**, 21–41.

Weissman, J. S., and Kim, P. S. (1991). Reexamination of the folding of BPTI: predominance of native intermediates. *Science* **253**, 1386–1390.

Biography

Hiram F. Gilbert is a Professor of Biochemistry and Molecular Biology and Associate Dean of the Graduate School of Biomedical Sciences at Baylor College of Medicine in Houston, Texas. His principal research interests are in the catalysis of disulfide bond formation in the eukaryotic endoplasmic reticulum and the cellular function of disulfides. He holds a Ph.D. in Organic Chemistry from the University of Wisconsin, Madison and received his postdoctoral training at Brandeis University.

DNA Base Excision Repair

Hilde Nilsen and Tomas Lindahl
Cancer Research UK, London Research Institute, London, UK

DNA decomposes spontaneously as a result of chemical modifications inflicted by water and reactive by-products of normal aerobic metabolism. This spontaneous DNA base damage has both mutagenic and cytotoxic consequences. The quantitatively most important classes of such endogenous DNA damage are (1) loss of the purine bases guanine (G) and adenine (A) due to hydrolysis of the *N*-glycosyl bond between the DNA base and the backbone, leaving an abasic (AP) site in the DNA; (2) hydrolytic deamination of cytosine (C) and 5-methylcytosine (5-mC) to generate U:G and T:G base pairs, respectively; (3) formation of base oxidation products by reactive oxygen species, the most studied being 8-hydroxyguanine (8-oxoG) and ring-saturated pyrimidines, such as thymine glycol (Tg); (4) methylation of bases by nuclear methyl donors at reactive nitrogen or oxygen groups, one important product being the cytotoxic residue 3-methyladenine (3-mA); and (5) oxidation of nucleotide precursors resulting in the incorporation of damaged bases into DNA during semiconservative replication, such as the misincorporation of 8-oxodGMP to form 8-oxoG:A base pairs. DNA base excision repair (BER) is the main repair pathway for these lesions, both in the nucleus and in the mitochondria.

Core Base Excision Repair Factors

DNA base excision repair (BER) involves one damage-specific step to identify and release the damaged or, in some cases, mispaired base and a subsequent set of general steps that result in the reinsertion of one or a few nucleotides. There are three major modes of the DNA BER pathway that can be executed by a set of core factors (Figure 1). The choice of pathway is influenced by the initiating DNA glycosylase and the nature of the 3′ and 5′ residues generated during the repair process.

DNA Base Excision

The damaged base is recognized by one of several DNA glycosylases (Table I), which initiate repair by hydrolyzing the *N*-glycosyl bond linking the base and the DNA backbone, leaving an AP site in the DNA. Notwithstanding limited sequence homologies, structural studies of the three-dimensional protein folds have revealed that DNA glycosylases can be divided into two main families. The mammalian members of the smaller family are UNG, TDG, and SMUG1. Members of the larger family are characterized as having a common structural motif and include the OGG1, MYH, NTH, and MBD4 enzymes. In addition, DNA glycosylases are classified as being either monofunctional or bifunctional, with the latter having an associated DNA lyase activity for chain cleavage at AP sites. Several DNA glycosylases can excise the same substrates, but the substrate specificities differ due to architectural diversity of the substrate-binding pockets of the enzymes. Furthermore, variations in biochemical properties, subcellular localization, and regulation suggest that their functions are not entirely overlapping.

Uracil-DNA Glycosylases

Human cells have at least four enzymes that can remove uracil from DNA (UNG, SMUG1, TDG, and MBD4). The UNG and SMUG1 enzymes are unusual in that they can remove uracil from single-stranded DNA as well as from double-stranded DNA. UNG is highly specific for uracil, with a very high turnover number, whereas SMUG1 has broader substrate specificity with lower turnover number. UNG accumulates at sites of active DNA replication in S-phase nuclei via interaction with PCNA and is the main enzyme responsible for post-replicative removal of uracil resulting from dUMP misincorporation. UNG may also be important for the removal of deaminated cytosine residues in single-stranded regions of DNA, in front of the replication fork, or in highly transcribed genes, but the relative contributions of UNG and SMUG1 in the repair of deaminated cytosine residues in general is not clear. In contrast, both TDG and MBD4 require double-stranded DNA as substrates and remove U or T resulting from the deamination of cytosine or 5-methylcytosine (5-mC). MBD4 contains a 5-mCpG binding domain in addition to the DNA glycosylase domain and is probably restricted to repair in a TpG or UpG context, whereas TDG has broader substrate specificity. These are enzymes with very low turnover numbers as a result of strong binding to AP sites.

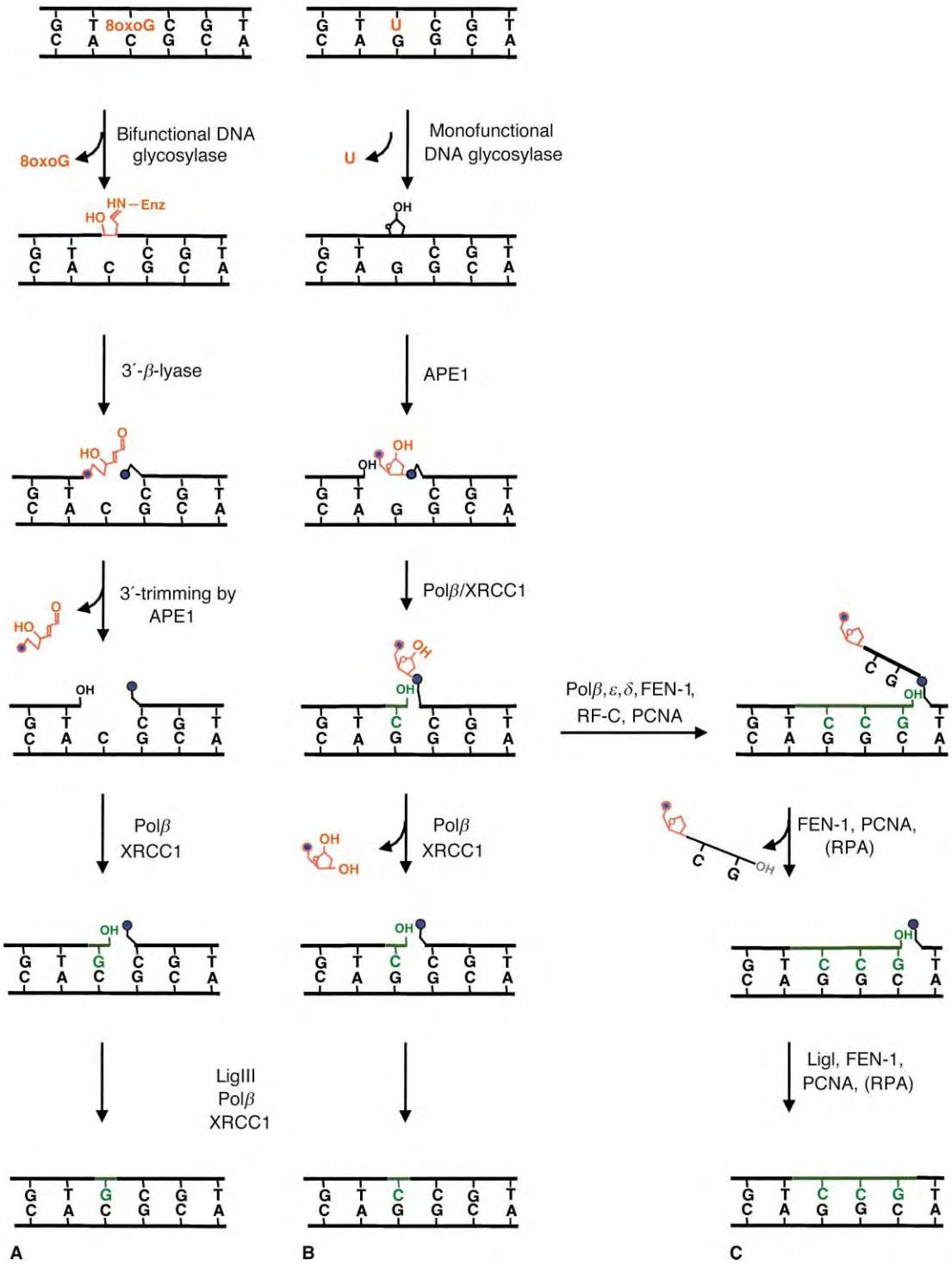

FIGURE 1 DNA base excision repair pathways. (A) One nucleotide gap repair initiated by a bifunctional DNA glycosylase. (B) Short-patch repair is the major mode of repair initiated by a monofunctional DNA glycosylase. (C) Long-patch repair is used when short-patch repair is blocked. Reactive groups in each step are shown in red, phosphate groups are indicated as blue circles, and green blocks represent newly synthesized DNA. Adapted from Krokan, H. E., Nilsen, H., Skorpen, F., Otterlei, M., and Slupphaug, G. (2000) Base excision repair of DNA in mammalian cells. *FEBS Lett.* **476**, 73–77 and Klungland, A., Hoss, M., Gunz, D., Constantinou, A., Clarkson, S. G., Doetsch, P. W., Bolton, P. H., Wood, R. D., and Lindahl, T. (1999) Base excision repair of oxidative DNA damage activated by XPG protein. *Mol. Cell* **3**, 33–42.

TABLE I

Human DNA Glycosylases and their Major Substrates

Enzyme name	Lyase activity	Cellular localization[a]	Major substrates[b]
UNG	No	N/M	U in single- or double-stranded DNA
SMUG1	No	N	U in single- or double-stranded DNA
TDG	No	N	U, T or ethenoC opposite G
MBD4	No	N	U or T opposite G in U/TpG context
MPG	No	N	3-mA
MYH	No	N/M	A opposite 8-oxoG
OGG1	Yes	N/M	8-oxoG opposite C
NTH1	Yes	N/M	Ring-saturated or fragmented pyrimidines
NEIL1	Yes	N	Tg
NEIL2	Yes	N	Oxidation products of C or U
NEIL3	Yes	N	Fragmented or oxidized pyrimidines

[a] The enzyme or specific isoforms of it are sorted to nuclei (N) or mitochondria (M).
[b] Only major substrates are shown. A comprehensive list of substrates for each DNA glycosylase can be found in Wood *et al.* (2001) and a regularly updated version can be found at that article's supplementary Web site.

Methylpurine DNA Glycosylase

Methylpurine DNA glycosylase (MPG, also called 3-alkyladenine DNA glycosylase, AAG) is a monofunctional DNA glycosylase that structurally forms a class of its own. The major substrate for MPG is 3-methyladenine (3-mA) in double-stranded DNA, but the enzyme has an unusually wide substrate binding pocket that can accommodate a wide range of modified purine bases. Interestingly, MPG has a weak, but significant activity toward normal purine bases, illustrating the importance of tight regulation of individual BER enzymes.

DNA Glycosylases for Removal of Oxidized Bases

The repair of oxidized DNA bases is predominantly initiated by bifunctional DNA glycosylases that use an amino group of the enzyme rather than a water molecule as a nucleophile to cleave the *N*-glycosyl bond. Enzyme-catalyzed resolution of the resulting Schiff-base intermediate, referred to as the AP-lyase activity, leads to the incision of the DNA backbone 3′ to the AP site. Several DNA glycosylases specific for oxidized DNA bases have been identified (Table I). Similar to the uracil-DNA glycosylases, they have different but overlapping substrate specificity. Oxidized purines are primarily removed by OGG1, whereas oxidized and fragmented pyrimidines are removed by the NTH1 and NEIL enzymes.

Despite having structural homology to the bifunctional DNA glycosylases, MYH acts as a monofunctional DNA glycosylase when removing unmodified adenine base-paired with 8-hydroxyguanine (8-oxoG). MYH colocalizes, via interaction with PCNA, with replication foci in the S-phase nuclei, where it removes adenine misincorporated opposite 8-oxoG during semi-conservative replication.

Base-Flipping and Release

Despite the lack of sequence homology, DNA glycosylases show structural similarities, which allow base recognition and catalysis to proceed by related mechanisms. Pinching of the DNA backbone followed by intercalation of amino acid side chains into the DNA provides the basis for substrate recognition and catalysis. Consequently, the damaged nucleotide is flipped out of the helix and the scissile bond is exposed upon the stabilization of the base in the substrate-binding pocket. DNA glycosylases then release the damaged base after cleavage of the *N*-glycosyl bond.

Backbone Incision

Following excision of the damaged base, BER can proceed through several routes. Subsequent to base excision by a monofunctional DNA glycosylase, the DNA backbone is incised 5′ of the AP site by AP-endonuclease 1 (APE1), creating a 3′OH group and a 5′-dRP moiety (Figure 1B). Upon resolution of the Schiff-base intermediate formed by a bifunctional DNA glycosylase, the DNA backbone is cleaved 3′ to the damage to give a 5′-phosphate and a blocked, 3′ α, β unsaturated aldehyde or a 3′-phosphate by elimination reactions. Although the NEIL enzyme domains deviate from the OGG1/NTH1 superfamily, they are believed to act by similar mechanisms. The blocked 3′ residue must

be removed to generate a 3′-OH group that is a substrate for DNA polymerases. This is achieved by the 3′ phosphodiesterase activity of APE1, leaving a one nucleotide gap in DNA (Figure 1A).

Base Insertion

DNA polymerase β (Polβ) is the main DNA polymerase involved in BER and comprises a polymerase domain and a dRP-lyase domain. The 3′-OH group is a substrate for the polymerase function of Polβ. Polβ is distributive and will only synthesize a few nucleotides before disengaging. If the 5′-dRP moiety is a substrate for the dRP-lyase activity of Polβ, then one or two nucleotides will be inserted in concert with the removal of the dRP moiety and BER will proceed through the short-patch pathway (Figure 1B). If, however, the dRP moiety is modified, making it a poor substrate for the dRP-lyase activity of Polβ, this polymerase may still incorporate one nucleotide, but BER will then be funneled into the long-patch pathway, which uses DNA replication factors to synthesize a longer repair patch (Figure 1C). In this case, DNA polymerase δ/ε performs strand-displacement synthesis, supported by replication factor C (RF-C) and proliferating cell nuclear antigen (PCNA), and the modified dRP moiety is removed as part of an oligonucleotide released upon Flap endonuclease 1 (FEN1) incision. Finally, because a 1-nucleotide gap in DNA is a poor substrate for the strand-displacement activity of Polβ, a single nucleotide will be inserted when repair is initiated by a bifunctional DNA glycosylase (Figure 1A). Oxidative base lesions frequently occur in clusters, and this pathway might have evolved to prevent the collision between closely spaced repair tracts on different strands, which otherwise could generate double-strand breaks.

Polβ lacks the editing 3′-exonuclease function characteristic of replicative DNA polymerases. Consequently, the accuracy of DNA synthesis by Polβ is relatively low. In the case of BER, the proofreading required is probably performed by a cryptic 3′-exonuclease activity of the APE1 enzyme.

Nick Rejoining

Both DNA ligase III (LigIII) and DNA ligase I participate in BER. Polβ interacts directly with X-ray cross complementing factor 1 (XRCC1). XRCC1 also interacts with LigIII, and this interaction stabilizes LigIII. Polβ, XRCC1, and LigIII form a trimeric complex on substrate DNA, and LigIII is the main nick rejoining activity for short-patch and 1-nucleotide gap repair. DNA ligase I predominantly seals nicks after long-patch repair via direct protein–protein interaction with PCNA.

Pathway Orchestration

One characteristic of the BER pathway is the highly orchestrated manner with which proteins interact sequentially on the DNA substrate, as opposed to the assembly of large preformed nuclear complexes. The DNA glycosylases all remain bound at AP sites, albeit to varying degrees, but are efficiently displaced by APE1. Polβ is in turn recruited through interaction with APE1, and the trimeric complex of DNA Polβ-XRCC1-LigIII ensures that the repair intermediates are protected. There is a progressive bending of the DNA backbone during the repair pathway, starting from a 30° kink when the DNA glycosylase is bound to the substrate, progressing to 45° (APE1-bound), and then becoming almost a 90° bend when the trimeric Polβ-XRCC1-LigIII is bound. Progressive bending and pairwise protein–protein interactions probably aid substrate recognition and give directionality to the pathway without exposure of cytotoxic repair intermediates, such as AP sites and dRP moieties, thus preventing aberrant processing of intermediates and premature activation of cell cycle checkpoints in response to DNA damage.

Base Excision Repair in Chromatin

The organization of DNA into chromatin in eukaryotic cells restricts access for several DNA binding proteins to their substrates and introduces steric constraints that might hamper catalytic reactions on the nucleosome surface. Although BER proceeds more slowly in chromatin than in free DNA, the core BER proteins are apparently able to access DNA on the surface of a nucleosome. Chromatin remodeling might therefore not be a prerequisite for repair of DNA in nucleosomes, but it would presumably facilitate repair in chromatin. Furthermore, mammalian cells might circumvent a need for rapid DNA repair in condensed chromatin by coupling BER to other DNA transactions where the chromatin structure is relaxed. This would ensure efficient repair when speed is of importance, for example, in the cases of UNG and MYH, by targeting the enzymes to sites of active replication.

Base Excision Repair in Mitochondria

Being close to the centers for oxidative metabolism in the cell, mitochondrial DNA is particularly exposed to reactive oxygen species. Several alternatively spliced forms of DNA glycosylases have been identified, and some isoforms are specifically sorted to mitochondria (denoted M in Table I). APE1 is transported to mitochondria and the mitochondrial DNA polymerase

γ has dRP-lyase activity. mtDNA ligase is a processed form of DNA LigIII. Thus, the mitochondria have all the activities required for BER, and BER might be the most important mode of DNA repair in this organelle.

The Cancer Connection

Bacterial and yeast mutants deficient in DNA glycosylases often exhibit elevated spontaneous mutation frequencies. Despite an observed accumulation of DNA base damage in gene-targeted knockout mice, they generally show weaker phenotypes in this regard, presumably because of the high degree of functional overlap among different DNA glycosylases (Table I) and the existence of several efficient and specialized DNA polymerases for translesion synthesis. There are at least four mammalian DNA glycosylases that can remove uracil from DNA and, although Ung-deficient mice accumulate uracil in the genome, they show only a modest increase (less than 50%) in the mutation frequency of a transcriptionally inactive transgene. Nevertheless, the Ung-deficient mice are susceptible to the spontaneous development of B-cell lymphomas. No spontaneous tumor development has been observed in other DNA glycosylase deficient mice, but Mbd4-deficiency accelerates tumor development in a tumor-prone mouse strain. However, human polymorphisms have been identified in most BER genes, and mutations in MYH have been linked convincingly to a higher susceptibility to colorectal cancer.

Base Excision Repair Branching Out

Interestingly, attempts to generate gene-targeted knockout mice for genes downstream of the DNA glycosylases result in embryonic lethality. Similarly, genetic studies with budding yeast have shown that mutants unable to repair AP sites in DNA are not viable. This could be a result of the accumulation of cytotoxic repair intermediates, AP sites or dRP moieties in particular, or a consequence of the involvement of these proteins in other cellular pathways. BER factors associated with the long-patch pathway exert their main function during DNA replication, but other BER factors may also be employed in DNA transactions in addition to classical BER, for example, the involvement of Polβ in meiosis. Mammalian APE1 has an N-terminal domain that allows it to function as a redox factor; this domain is required for redox activation of various spontaneously oxidized transcription factors, such as AP1. Recently, the Ung uracil-DNA glycosylase was shown to be central in the diversification of immunoglobulin genes, a finding that opens up new and exciting prospects for research into the biological significance of DNA BER.

See Also the Following Articles

Chromatin: Physical Organization • DNA Glycosylases: Mechanisms • DNA Polymerase β, Eukaryotic • DNA Polymerases: Kinetics and Mechanisms • Mitochondrial DNA • Nuclear Organization, Chromatin Structure, and Gene Silencing • Nucleotide Excision Repair and Human Disease • Nucleotide Excision Repair, Bacterial: The UvrABCD System • Nucleotide Excision Repair: Biology • Nucleotide Excision Repair in Eukaryotes

Glossary

cytotoxic DNA base A DNA base that blocks the progression of replication forks or transcription.

hydrolysis A chemical reaction involving a water elimination reaction; a reaction in which a molecule decomposes to two molecules, one smaller than the other.

mutagenic DNA base A DNA base that introduces changes in the coding sequence of DNA.

Schiff base A covalent compound formed by a condensation reaction between an aromatic amine in the enzyme and an aldehyde or ketone of the deoxyribose group of DNA.

Further Reading

Bogenhagen, D. F., Pinz, K. G., and Perez-Jannotti, R. M. (2001). Enzymology of mitochondrial base excision repair. *Prog. Nucleic Acid Res. Mol. Biol.* **68**, 257–271.

Friedberg, E. C., and Meira, L. B. (2000). Database of mouse strains carrying targeted mutations in genes affecting cellular responses to DNA damage: Version 4. *Mutat. Res.* **459**, 243–274.

Friedberg, E. C., Walker, G. C., and Siede, W. (1995). *DNA Repair and Mutagenesis*. ASM Press, Washington D.C.

Hosfield, D. J., Daniels, D. S., Mol, C. D., Putnam, C. D., Parikh, S. S., and Tainer, J. A. (2001). DNA damage recognition and repair pathway coordination revealed by the structural biochemistry of DNA repair enzymes. *Prog. Nucleic Acid Res. Mol. Biol.* **68**, 315–347.

Klungland, A., Hoss, M., Gunz, D., Constantinou, A., Clarkson, S. G., Doetsch, P. W., Bolton, P. H., Wood, R. D., and Lindahl, T. (1999) Base excision repair of oxidative DNA damage activated by XPG protein. *Mol. Cell* **3**, 33–42.

Krokan, H. E., Nilsen, H., Skorpen, F., Otterlei, M., and Slupphaug, G. (2000) Base excision repair of DNA in mammalian cells. *FEBS Lett.* **476**, 73–77.

Lindahl, T. (2001). Past, present and future aspects of base excision repair. *Prog. Nucleic Acid Res. Mol. Biol.* **68**, 17–30.

Rada, C., Williams, G. T., Nilsen, H., Barnes, D. E., Lindahl, T., and Neuberger, M. S. (2002). Immunoglobulin isotype switching is inhibited and somatic hypermutation perturbed in Ung-deficient mice. *Curr. Biol.* **12**, 1748–1755.

Wood, R. D., Mitchell, M., Sgourous, J., and Lindahl, T. (2001). Human DNA repair genes. *Science* **291**, 1284–1289.

Wood, R. D., Mitchell, M., Sgourous, J., and Lindahl, T. Human DNA repair genes supplement. Available at: http://www.cgal.icnet.uk/DNA_Repair_Genes.html.

Biography

Dr. Hilde Nilsen is a postdoctoral research fellow at the Cancer Research U.K., London Research Institute. Her research interests are cellular responses to spontaneous DNA damage. She received her Ph.D. from the Norwegian University of Science and Technology in Norway. She has been awarded fellowships from EMBO and the EU Marie Curie program.

Dr. Tomas Lindahl is Director of Research at the Clare Hall Laboratories of the Cancer Research U.K., London Research Institute. His research interests are in DNA repair of spontaneous DNA damage and genome instability. He has an M.D. from the Karolinska Institute, Stockholm. He is a member of EMBO, a fellow of the Royal Society, and a member of the Swedish and Norwegian Academies of Science, and he has published extensively over a period of 30 years.

DNA Damage: Alkylation

Anton B. Guliaev and B. Singer
Lawrence Berkeley National Laboratory, Berkeley, California, USA

Alkylation is the reaction of electrophilic chemical compounds or alkylating agents with the nucleophilic centers in organic macromolecules. Alkylating agents include a large variety of chemicals, some of which are potent mutagens or carcinogens. It is well known that DNA is a key structure that determines development and reproduction of the leaving organisms ranging from simple cells to humans. The sequence and structure of individual nucleotides in DNA are essential for the high degree of fidelity required for generating a "blueprint" during the process of the storing and passing of genetic information from one organism to another. However, DNA is subject to alteration in structure and/or sequence of individual bases. These changes can result in errors during the steps of the DNA replication, recombination, and repair, thus leading to the modification of the molecular structure of genetic material. Most of these modifications can be successfully removed by the DNA repair machinery. However, a significant amount of DNA remains unrepaired, which can lead to mutagenesis.

The common source of the modifications in DNA, particularly the alteration in the nucleotide structure, can be found in the instability of specific chemical bonds of nucleotides under different physiological conditions, such as temperature or pH. Moreover, the DNA structure readily reacts with multiple chemical compounds and physical agents found in the environment. These mutagens and carcinogens can be produced by a variety of chemical reactions, metabolism of other living forms, and they also can be manmade. Modifications of the DNA molecular structure can be characterized as DNA damage. DNA damage is unavoidable and can be divided into two categories: (1) spontaneous, such as formation of mismatches, deamination of bases, loss of base, oxidative damage; (2) environmental, such as ionizing radiation, UV radiation, and chemical agents, including ubiquitous alkylating agents. DNA alkylation, which is a part of the DNA damage, is the reaction of the alkylating agents with the nucleophilic centers, such as oxygen or nitrogen in the DNA base or backbone. The result of the reaction is the formation of the modified DNA bases called *adducts* or formation of the phosphotriesters in the case of the interaction of the agent with the oxygen in the DNA phosphodiester backbone. The adduct together with the opposite base is usually called a *lesion*.

Alkylating Agents and Mechanism of the Reaction with DNA

The first chemical evidence of alkylation damage to DNA was reported in 1962 by the observation of 7-methylguanine as an *in vivo* product of dimethylnitrosamine administered to rats. Since that time, the list of alkylation agents and sites of alkylation has significantly increased, so that now we know that almost all nitrogens and oxygens of nucleotides in DNA can be modified. Alkylating agents include a large number of molecules, which can efficiently react with DNA causing structural modification of the base and phosphate group in DNA. The most common agents are alkyl sulfates, alkyl sulfonates, alkyl halides, dialkyl nitrosamine, alkyl nitrosoureas, acyl nitrosamides, mustards, diazo compounds, lactones, epoxides, etc. (Figure 1). These agents can be divided into two major groups: monofunctional and bifunctional. The monofunctional agents have only one reactive group that is involved in covalent interaction with the single center on DNA. The bifunctional agents have two reactive groups and have the ability to react with two centers on DNA. If the two centers are on the opposite strands of the DNA, the reaction of a bifunctional agent, such as sulfur or nitrogen mustards, can produce an interstrand cross-link. Many of the alkylating agents have a mutagenic effect and are known or suspected carcinogens. The reaction specificity of these compounds is different with different bases. Diazoalkanes react readily with guanosine and thymidine, but only under extreme conditions with adenosine and cytosine. In contrast, alkyl sulfates, alkyl sulfonates, mustards, epoxides, and nitroso compounds alkylate bases in the following order: $G > A > C \gg T$. The rate of ethylation is much slower than that of methylation for all classes of alkylating agents except alkyl iodides, which readily alkylate G, A and C.

The main chemical mechanism of DNA alkylation is a S_N2 and S_N1 type reaction in which the electrophile (alkylating agent) reacts with the electron-rich regions of the base residues and phosphodiester

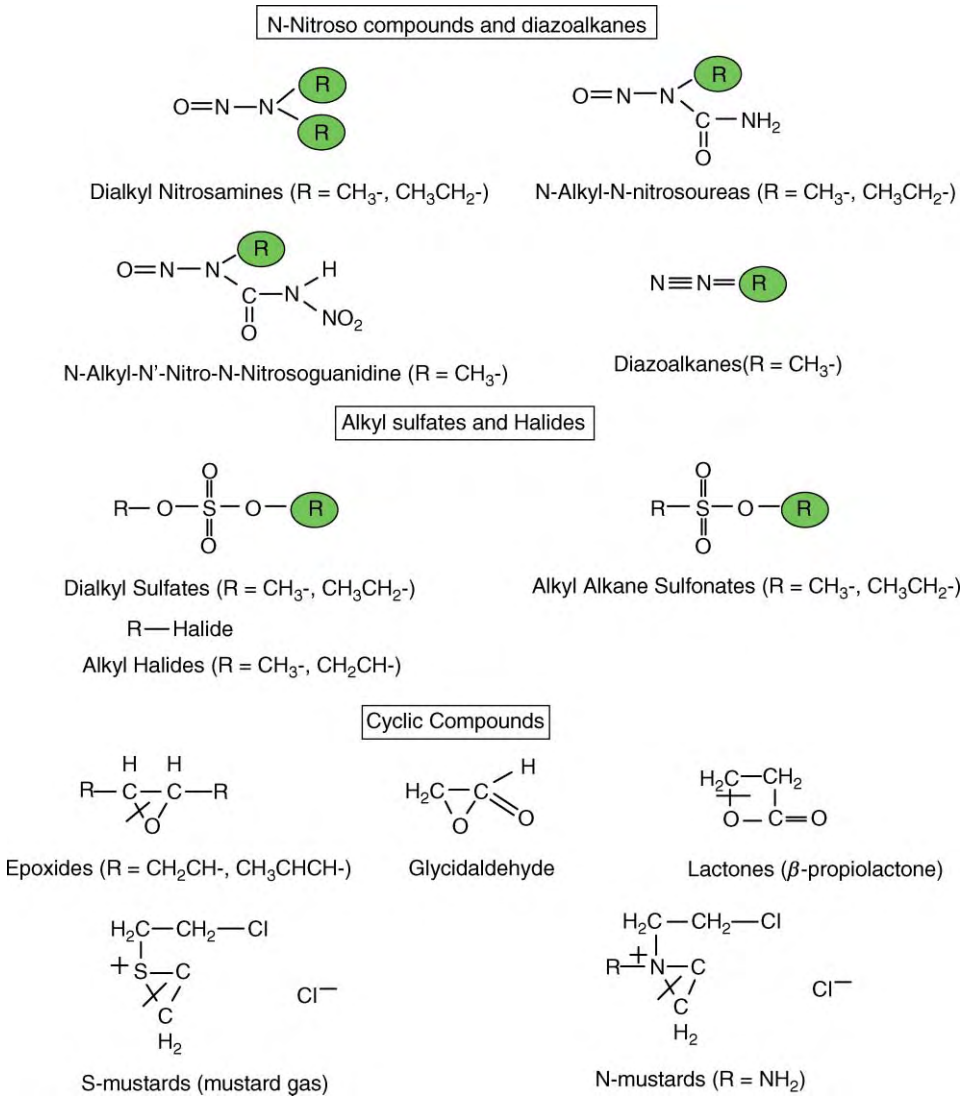

FIGURE 1 Structural formulas of alkylating agents. The alkyl groups are indicated by R. Circled R shows which group of the molecule is being transferred. The opening of the ring for the cyclic compounds is indicated by the line, and the whole molecule acts as a substituent.

backbone. Figure 2 shows possible sites of alkylation on the DNA bases and the relative reactivity of these sites as measured by the presence of the alkylated base after the reaction with carcinogenic alkylating agents. The ring nitrogens, being more nucleophilic than the oxygens, are known to be more reactive with the alkylating agents. Thus, the N7 of guanine and N3 of adenine are the most reactive. The DNA phosphodiester backbone can also undergo an alkylation reaction through interaction of the agent with the oxygen, which results in the formation of phosphotriesters (Figure 2). However, not all alkylating agents react directly with the DNA bases. Some of them, such as dialkylnitrosamines or vinyl chloride (group of R-halides), must be metabolically activated.

Effect of DNA Conformation on the Alkylation

There are at least two significant differences between alkylation of nucleosides and polynucleotides. One is the presence of the phosphate in the phosphodiester bonds, which can form phosphotriesters, and the other is the effect of secondary structure on the availability of reactive sites. In general, the major sites of alkylation of single-stranded synthetic polynucleotides are the same as those for nucleosides, but the extent of reaction is different. The neighboring base or the overall charge of the nucleotide can affect the nucleophilic potential of the DNA base. For example, if the guanine residue is flanked by another guanine, the negative electrostatic

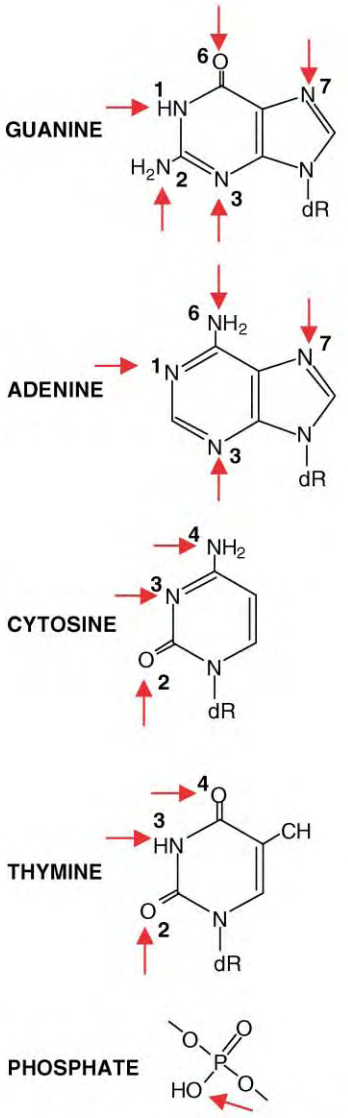

Adduct \ Carcinogenic alkylating agent	Percentage of total alkylation: DMN MNU SDMH	DEN ENU	MM S
N^3-Alkylguanine	0.6	1.5	0.7
O^6-Alkylguanine	3–6	8	0.3
N^7-Alkylguanine	69	12	8.3
N^1-Alkyladenine	0.8	0.1	1.2
N^2-Alkyladenine	4	4	11
N^7-Alkyladenine	1.5	0.6	1.9
O^2-Alkylcytosine	0.1	2	
N^3-Alkylcytosine	0.5	0.3	
O^2-Alkylthymine	0.1	7	
N^3-Alkylthymine	0.3	0.4	
O^4-Alkylthymine	0.1	2.5	
Triester	12	58	1

DMN – Dimethylnitrosamine
MNU – Methylnitrosourea
SDMN – 1,2-Dimethylhydrazine
DEN – Diethylnitrosamine
ENU – Ethylnitrosourea
MMS – Methyl methanesulfonate

FIGURE 2 Structural formulas of the DNA bases with the possible sites of the modification by alkylating agents indicated by red arrows. dR indicates sugar. The table on the right shows the percentage of total alkylation after reaction with the carcinogenic alkylating agent. The data presented in the table are available only for the subset of the sites shown.

potential of the N7 position of guanine is enhanced, thus providing a better environment for the electrophilic attack of the alkylating agent. However, the increase of the negative charge of the alkylating moiety diminishes the nucleophilic potential of the base. Steric effects also play an important role in the reaction between the alkylating agents and the nucleophilic sites in DNA. For the normal right-handed (B-form) helix conformation, the access to sites in DNA differs between the major and minor groove. For the guanine residue in the B-form DNA the O6 and N7 atoms are in the major groove, which can be easily accessed by the alkylating agent. In contrast, the relatively reactive N3 of the adenine lies in the minor groove, which is less accessible due to the steric implications of the B-form DNA.

Methods of Identification of Alkyl Derivatives of Nucleic Acids

The initial identification and characterization of the alkylation products can be made using UV absorption

spectroscopy. The nature of the alkyl group introduced to the base does not affect the λ_{max} or λ_{min} significantly. However, the position of the base modification results in the spectral changes that make it possible to distinguish among derivatives. In addition to spectra maxima and minima of the cationic and anionic forms, the shape of the spectra changes significantly depending on the base modification. The characteristic shoulders and alteration in the curve profile can be assigned to a particular adduct. Additional identification can be performed using other methods such as mass spectrometry, nucleic magnetic resonance, and infrared spectroscopy. The detailed description of these methods and their use for identification of alkyl derivatives can be found in the Further Reading.

Cytotoxic and Mutagenic Effects of Alkylation: Methylation

Mutation can be described as a change of one base to another, leading to a change in coding information. The change in the base structure, which is lethal to the cell, can be characterized as a cytotoxic.

Direct alkylation of DNA, particularly methylation, acting through the covalent modification of the base, has the ability to generate miscoding base derivatives and lesions that block replication. The major adducts generated in double-stranded DNA by methylating agents such as methyl methanesulfonate (MMS), dimethylsulfate (DMS) and methyl iodide (MeI)

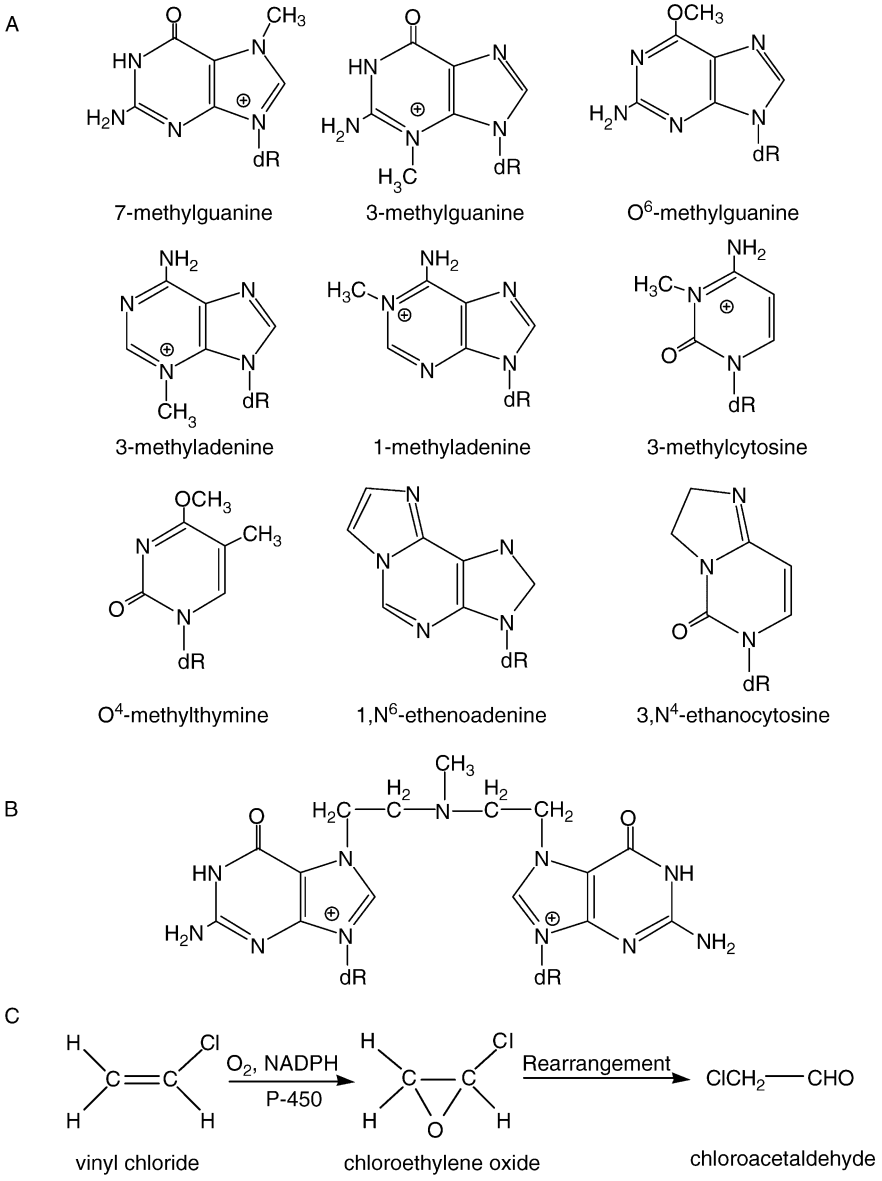

FIGURE 3 (A) Selective structures of the DNA adducts formed by the alkylation reaction. (B) Intrastrand cross-link product of the reaction of nitrogen mustard with N-7 of guanine. (C) Mechanism of the metabolism of vinyl chloride.

are: 7-methylguanine (7-meG), 3-methyladenine (3-meA), 3-methylguanine (3-meG), and O^6-methylguanine (O^6-meG) (Figure 3A). In single stranded DNA, these methylating agents form 1-methyladenine (1-meA) and 3-methylcytosine (3-meC) (Figure 3A). The formation of these adducts in the single-stranded, but not in double-stranded DNA is due to the fact that these modification sites are involved in base-pairing and are therefore protected from alkylation. Adducts 3-meA, 3-meG and 3-meC have the ability to block DNA replication, thus having cytotoxic effects. In contrast, O^6-meG and O^4-methylthymine (O^4-meC) are miscoding base derivatives that mispair during replication thus leading to possible mutations. Environmental mutagens such as 1,2-dimethylhydrazine, diazoquinones, and tert-butylhydroperoxide generate methyl radicals that readily react with the guanine residue to form 8-methylguanine, which also has a high miscoding potential. However, the most common methylation product in DNA, 7-meG, is not mutagenic and basepairs normally in polynucleotides. Most of the adducts produced by methylation can be efficiently removed by a variety of DNA glycosylases through the base excision repair mechanism (BER). This process involves cleavage of a base–sugar bond in order to release the modified base and generate an apurinic/apyrimidinic site that is repaired by endonucleases. This is followed by the action of the DNA polymerase that incorporates the correct base. In contrast, O6-methylguanine is corrected by the direct transfer of the methyl group to a cysteine residue of the methyltransferase repair enzyme. Intrastrand cross-links (Figure 3B), generated by bifunctional alkylating agents, such as nitrogen mustard, represent an important class of DNA damage, since they prevent DNA strand separation, which is crucial to the processes of replication and transcription. The cell has the ability to repair this damage through the mechanism of nucleotide excision repair (NER), which uses multiple enzymes.

The nitroso compounds and hydrocarbons, which are well-known environmental carcinogens, react through a number of metabolic intermediates. However, the most effective direct alkylating agents, such as alkyl sulfates (Figure 1), in turn, are poor carcinogens. In contrast, the metabolically activated alkylating agents are very efficient carcinogens. One of the widely used common chemicals, which is carcinogenic in man and experimental animals, is vinyl chloride (Figure 3C). The industrial use of vinyl chloride is estimated to be about 4×10^9 kg/year in the United States. The exposure to vinyl chloride is generally by inhalation and results in angiosarcoma of the liver or other tumors in the brain, lung, and hematolymphopoietic system in humans. Vinyl chloride is readily metabolized into chloroethylene (CEO) oxide, which rapidly changes to chloroacetaldehyde (CAA) (Figure 3C). Both CEO and CAA are highly mutagenic and carcinogenic and react with the DNA bases to form etheno derivatives (e.g., 1,N^6-ethenoadenine and 3,N^4-ethanocytosine (Figure 3A)). These adducts have a high miscoding potential and also an ability to block DNA replication.

See Also the Following Articles

DNA Base Excision Repair • Nucleotide Excision Repair, Bacterial: The UvrABCD System • Nucleotide Excision Repair in Eukaryotes

Glossary

adduct Structurally modified DNA nucleotide.

alkylating agent Chemical compound that has the ability to react with the DNA through the reaction of alkylation.

DNA Deoxyribonucleic acid.

nucleoside Compound that consists of a purine or pyrimidine base linked to a pentose.

nucleotide Compound that consists of a nitrogeneous base, a sugar, and one or more phosphate groups.

Further Reading

Lindahl, T., and Sedgwick, B. (1988). Regulation and expression of the adaptive response to alkylating agents. *Ann. Rev. Biochem.* **57**, 133–157.

Sedgwick, B., and Lindahl, T. (2002). Recent progress on the ada response for inducible repair of DNA alkylation damage. *Oncogene* **21**, 8886–8894.

Singer, B. (1975). The chemical effects of nucleic acid alkylation and their relation to mutagenesis and carcinogenesis. *Prog. Nucleic Acid Res. Mol. Biol.* **15**, 219–284.

Singer, B., and Grunberger, D. (1983). *Molecular Biology of Mutagens and Carcinogens*. Plenum Press, New York.

Biography

B. Singer is a Research Professor Emeritus at the Virus Laboratory and Department of Molecular Biology at the University of California, Berkeley; she is currently Senior Scientist at Lawrence Berkeley National Laboratory. She has coauthored the text, "Molecular Biology of Mutagens and Carcinogens," as well as numerous papers on chemistry, molecular biology, and virology. In 1957, together with her husband, H. Fraenkel-Conrat, they discovered that all the genetic information for tobacco mosaic virus was coded by RNA alone. Her current research interests are in the chemical reactions of environmental carcinogens.

Anton B. Guliaev is a Physicist Scientist at Lawrence Berkeley National Laboratory, Berkeley, California.

DNA Glycosylases: Mechanisms

Daniel J. Krosky and James T. Stivers
The Johns Hopkins University School of Medicine, Baltimore, Maryland, USA

The highly accurate replication of an organism's DNA is necessary for it to maintain genetic stability over many generations. Thus, cells need to aggressively repair DNA damage in order to prevent mutations and to eliminate toxic base modifications that can interfere with DNA replication. To this end, cells have evolved several DNA repair pathways geared toward processing different types of DNA lesions. One of these systems, the base excision repair (BER) pathway, recognizes and removes chemically modified DNA bases and replaces them with the correct nucleotides. The first step in BER is catalyzed by a family of functionally related enzymes known as DNA glycosylases that hydrolytically cleave the glycosidic bond between the damaged base and its deoxyribose sugar.

The Biological Function of DNA Glycosylases

DNA bases can be damaged by a variety of mechanisms that include alkylation, deamination, oxidation, and ultraviolet light, each of which produces a different base alteration. Repair of each of these diverse lesions begins with the action of a unique DNA glycosylase (to date, eight have been identified in humans) that is specific for the particular damaged base. This hydrolysis reaction results in a common intermediate, an abasic site, which can be processed by either short- or long-patch repair. In short-patch repair, only the damaged nucleotide is replaced, whereas in long-patch repair, the damaged base and three or four additional nucleotides are excised and replaced.

Types of DNA Glycosylases

Substrate Range and Specificity

The DNA glycosylases have evolved varying degrees of substrate specificity. For example, uracil–DNA glycosylase (UDG) will efficiently cleave uracil that has been misincorporated into DNA, but not thymine, which only differs from uracil by one methyl group. Other DNA glycosylases not only possess high specificity for the cleaved base, but also for the context in which it appears. Examples of these include the bacterial mismatch-specific UDG (MUG), which excises uracil paired with guanine but not with adenine, and the mammalian 8-oxoguanine glycosylase (OGG), which only cleaves the oxidized base 8-oxoguanine when it is opposite cytosine.

In contrast, other DNA glycosylases cleave a relatively wide spectrum of chemically related damaged bases. For instance, *Escherichia coli* 3-methyladenine glycosylase II (AlkA) catalyzes the hydrolysis of a wide range of cationic *N*-alkylated purines, such as 3-methyladenine and 7-methylguanine. In addition, AlkA can cleave undamaged purine bases, although with much lower efficiency than *N*-alkylated purines. Other broad-specificity glycosylases include mammalian methylpurine glycosylase (MPG), which has a substrate range similar to AlkA, and endonuclease III (Endo III), which processes a variety of oxidized pyrimidines (e.g., thymine glycol and 5-hydroxycytosine).

In addition to simply excising damaged DNA bases resulting in an abasic site, a subset of bifunctional DNA glycosylases can subsequently catalyze an elimination reaction in which the 3′-phosphate of the abasic site is expelled. Members of this bifunctional DNA glycosylase family include OGG, Endo III, and pyrimidine dimer DNA glycosylase (PDG). Other enzymes in the base excision repair (BER) pathway then process the resulting repair intermediate, mostly via the short-patch pathway.

Structural Superfamilies of DNA Glycosylases

Even though DNA glycosylases catalyze similar reactions, these enzymes share minimal primary sequence homology with one another. However, X-ray crystallography and nuclear magnetic resonance (NMR) analyses have revealed that many of these proteins share a common fold and have allowed the classification of these proteins into several structural superfamilies. One of these structural superfamilies is defined by the helix-hairpin-helix (HhH) motif, which is found in many non-sequence-specific DNA-binding proteins. This α-helical fold allows these enzymes to make

nonspecific contacts with the DNA phosphodiester backbone, thus permitting sequence-independent excision of their cognate lesions. Other DNA glycosylases, such as UDG, have evolved alternate structural motifs that also result in nonspecific DNA binding and fufill the same function as the HhH domain.

Functional Commonalities of DNA Glycosylases

Base Flipping

Despite differences in substrate specificity, structure, and primary sequence, all DNA glycosylases are functionally related in their ability to extrude DNA bases from the double helix and to catalyze the hydrolysis of the glycosidic bond between the cognate base and the deoxyribose. Extruding a base from duplex DNA, or base flipping, is the process by which an enzyme facilitates the rotation of the DNA phosphodiester backbone such that a base flips from within the double helix to an extrahelical position located within the binding pocket of the enzyme (Figure 1). The most common mode of base flipping occurs when the enzyme flips the damaged base from the DNA double helix. However, some DNA glycosylases use different base-flipping strategies. PDG, which is responsible for cleaving the glycosidic bond of thymine photodimers, flips the adenine that is opposite the target base. *E. coli* MutY, which removes adenine misincorporated opposite to the oxidized base 8-oxoguanine, appears to flip both bases from the duplex.

There are several elements common to the base-flipping mechanisms of DNA glycosylases. First, the enzyme makes extensive nonspecific contacts with the phosphodiester backbone of the DNA (Figure 1). In addition to allowing sequence-independent binding of the DNA glycosylase to DNA, these protein–DNA interactions provide a stable architecture from which the enzyme can distort the DNA. All structural studies of DNA glycosylases bound to DNA have revealed that the DNA is significantly bent at the site of enzyme binding, albeit to differing degrees with different enzymes (Figure 1). Although the exact role of DNA bending is unclear, it may help certain glycosylases locate lesions in DNA. In addition, computational studies have suggested that DNA bending may play an important role in lowering the activation barrier for base flipping, thus providing an explanation for why DNA bending is such a ubiquitous feature of these interactions (Figure 1). Finally, all DNA glycosylases insert a bulky amino acid side chain, such as leucine or phenylalanine, inside the DNA double helix (Figure 1). This group serves as a structural wedge to both push the base out and to act as a barrier to prevent the base from slipping back into the double helix.

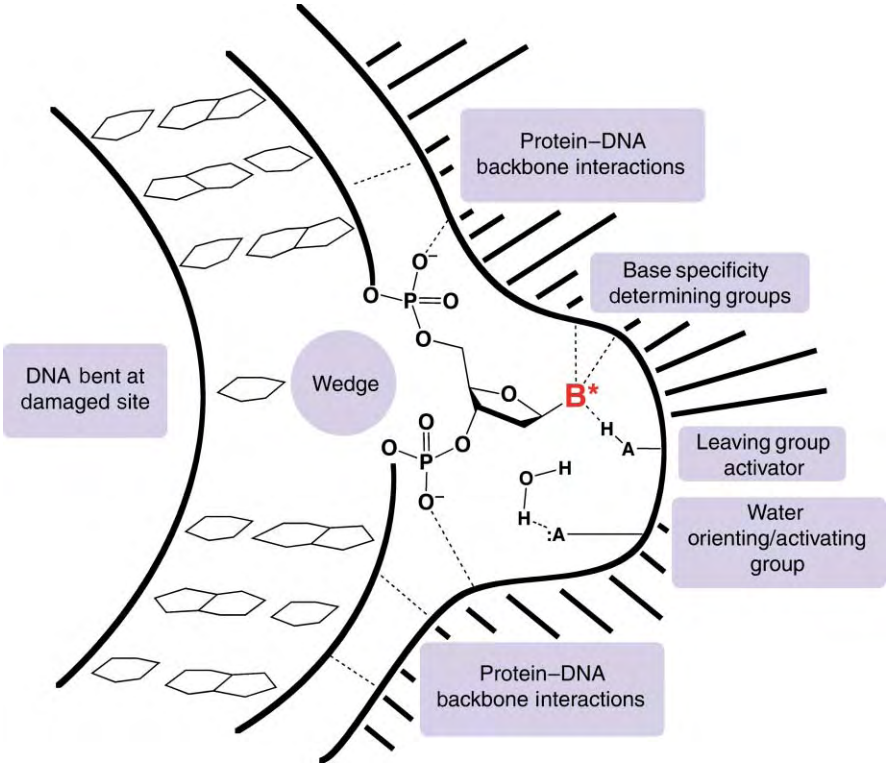

FIGURE 1 Schematic representation of base flipping and other common interactions of DNA glycosylases with DNA. B*, damaged base; (---), hydrogen bond.

Base flipping plays an important role in facilitating base recognition and glycosidic bond cleavage. Extrusion of the base juxtaposes its unique functional groups with complementary groups in the enzyme active site. These specific interactions promote the recognition of the damaged base and largely exclude binding of undamaged bases. Differences in the amino acid residues of the base binding pocket among DNA glycosylases, in part, account for differences in their substrate specificity and catalytic mechanisms (see later discussion). Base flipping also exposes the anomeric carbon (the deoxyribose carbon that is attached to the base) to attack by water in the enzyme active site. Thus, base flipping enables DNA glycosylases to couple damaged base recognition to enzyme catalysis.

Catalytic Strategies for Glycosidic Bond Hydrolysis

At neutral pH and ambient temperature, the glycosidic bond of a deoxynucleotide is a very stable linkage toward hydrolysis ($t_{1/2} = 109$ years for thymidine; $t_{1/2} = 3.9$ years for deoxyadenosine). The stability of this bond stems in part from the poor leaving-group ability of the electron-rich nucleobase, the poor nucleophilicity of water, and the poor electrophilicity of the anomeric carbon. DNA glycosylases have evolved remarkably similar strategies to overcome these chemical problems and remove these lesions rapidly enough to preserve the integrity of the genomic information.

Making the Cognate Nucleobase a Better Leaving Group

Most neutral deoxynucleotide bases are poor leaving groups because they cannot effectively stabilize the developing negative charge that forms on the base during the reaction. Some DNA glycosylases stabilize this negative charge by donating specific hydrogen bonds from active-site residues to acceptors on the base (Figure 1). This type of catalysis has been most clearly shown for UDG, in which an unusually strong hydrogen bond from a histidine residue in the enzyme active site stabilizes the uracil anion leaving group. In other cases, leaving group departure may be facilitated by the full transfer of a proton from an active site donor to a proton-accepting atom on the nucleobase, as has been suggested for MutY.

N-alkylated purines (i.e., 3-methyladenine and 7-methylguanine) are unique in that they are positively charged and electron-deficient; therefore, they are excellent leaving groups in the absence of any enzymatic activation. Accordingly, DNA glycosylases use different types of catalytic interventions to affect the hydrolysis of these labile bases. For example, the cationic base binding site of AlkA lacks the constellation of highly specific hydrogen-bonding groups that line the active sites of DNA glycosylases that recognize neutral damaged bases. Instead, its active site is rich in aromatic amino acids, such as tryptophan and tyrosine, that allow AlkA to bind purine bases of varying shape and account for the promiscuous activity of this enzyme. The unique chemical character of the AlkA active site may facilitate damaged-base recognition by forming favorable stacking interactions between the cationic *N*-alkylpurine and the aromatic side chains. Alternatively, positioning the cationic damaged base in a hydrophobic active site may serve to lower the activation barrier by electrostatic destabilization of the charged ground state. These key questions are still under active investigation.

The Nature of the Transition State

The rupture of the glycosidic bond in DNA can proceed through two limiting routes (Figure 2). In the first route (Figure 2A), the attack of water is coincident with departure of the leaving base, resulting in a concerted transition state. In a concerted reaction, the anomeric carbon is relatively electron rich, and little negative charge has built up on the leaving nucleobase. In the second route (Figure 2B), the bond between the anomeric carbon and the nucleobase is completely broken before the new bond with water forms, and the reaction proceeds via a stepwise mechanism with a discrete intermediate. Thus, in a stepwise reaction, the anomeric carbon is electron poor and has a significant positive charge, and the bonding electrons have migrated fully onto the leaving-group nucleobase.

Although comprehensive mechanistic studies for most DNA glycosylases have not been performed, it appears that these enzymes may catalyze their reactions using mechanisms in which the glycosidic bond is mostly broken and the new bond between water and the deoxyribose is only partially formed. In support of these electronic features, custom oligonucleotides containing a positively charged deoxyribose analogue that mimics the electron-deficient anomeric carbon at the transition state are potent inhibitors of several DNA glycosylases, including UDG and AlkA (Figure 2C). Such inhibitors of DNA glycosylases may someday find use in increasing the efficacy of anticancer agents that modify the bases of DNA by disabling the repair pathways that reverse the effects of these chemotherapeutics.

One way in which DNA glycosylases stabilize stepwise reactions is by surrounding the positively charged deoxyribose with negatively charged groups. For example, UDG engulfs the cationic deoxyribose intermediate with a negatively charged aspartate residue, DNA phosphodiester groups, and the uracil anion leaving group.

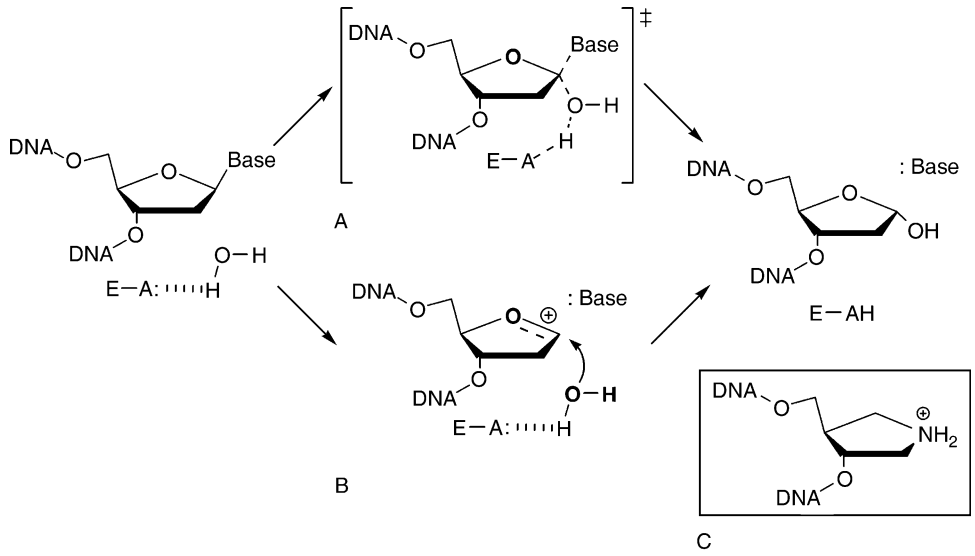

FIGURE 2 Two limiting reaction pathways for DNA glycosylases. (A) Concerted pathway; (B) stepwise pathway; (C) DNA glycosylase inhibitor based on the cationic deoxyribose intermediate of the stepwise reaction.

Helping Water Attack the Anomeric Carbon

Most DNA glycosylases possess a polar amino acid near the anomeric carbon of the target deoxyribose that can accept a hydrogen bond or proton from the attacking water (i.e., aspartate, glutamate, or asparagine) (Figure 1). Depending on the mechanism, this group may simply orient the water close to the anomeric carbon or, alternatively, may actively facilitate its attack by deprotonation. In concerted reactions, when there is significant bond formation between the attacking water and the anomeric carbon in the transition state, the activation barrier is lessened by partial or full deprotonation of the water. For stepwise reactions, the water needs only to be oriented close to the positively charged anomeric carbon because such species are highly reactive even with poor nucleophiles such as water (Figure 2B).

See Also the Following Article

DNA Base Excision Repair

Glossary

abasic site A deoxyribose residue in DNA that lacks a base.

base flipping The process by which an enzyme extrudes a base from within the DNA double helix into an extrahelical position inside the active site of the enzyme.

DNA glycosylase A family of functionally related enzymes that catalyze the hydrolytic cleavage of a damaged base from DNA.

glycosidic bond The bond connecting the anomeric carbon of the deoxyribose to the nitrogen on the purine or pyrimidine base.

transition state The highest potential energy species in the overall transformation of reactants to products. The difference in energy between the reactants and the transition state (the activation barrier) determines the rate of reaction.

Further Reading

Hollis, T., Ichikawa, Y., and Ellenberger, T. (2000). DNA bending and a flip-out mechanism for base excision by the helix-hairpin-helix DNA glycoyslase, *Escherichia coli* AlkA. *EMBO J.* **19**, 758–766.

Jiang, Y. L., Drohat, A. C., Ichikawa, Y., and Stivers, J. T. (2002). Probing the limits of electrostatic catalysis by uracil DNA glycosylase using transition state mimicry and mutagenesis. *J. Biol. Chem.* **277**, 15385–15392.

Pearl, L. H. (2000). Structure and function in the uracil–DNA glycosylase superfamily. *Mutat. Res.* **460**, 165–181.

Stivers, J. T., and Drohat, A. C. (2001). Uracil DNA glycosylase: Insights from a master catalyst. *Arch. Biochem. Biophys.* **396**, 1–9.

Stivers, J. T., and Jiang, Y. L. (2003). A mechanistic perspective on the chemistry of DNA repair glycosylases. *Chem. Rev.* **103**, 2729–2759.

Biography

Daniel J. Krosky is currently a graduate student at the Johns Hopkins University School of Medicine, studying the energetics of base flipping by uracil DNA glycosylase. Prior to attending Johns Hopkins University, he was a Senior Research Associate at AstraZeneca R&D, Boston, developing novel antibacterial agents.

James T. Stivers is an Associate Professor in the Department of Pharmacology and Molecular Sciences at Johns Hopkins Medical School. His research focuses on understanding the nature of enzyme catalysis and inhibition for a number of enzymes involved in DNA repair and recombination. He obtained his Ph.D. in biochemistry from Johns Hopkins University in 1992. He received postdoctoral training in heteronuclear NMR and enzymology in the laboratory of Professor Albert Mildvan at Johns Hopkins Medical School.

DNA Helicases: Dimeric Enzyme Action

Timothy M. Lohman
Washington University School of Medicine, St. Louis, Missouri, USA

DNA helicases are a class of motor proteins that function to generate the transient single-stranded DNA required as intermediates in DNA and RNA metabolism. These enzymes couple the energy obtained from the binding and hydrolysis of nucleoside 5′-triphosphates (NTP) to perform the work of DNA duplex unwinding (strand separation) and translocation of the helicase along the linear DNA filament. Helicases function in a variety of processes including DNA replication, DNA repair, recombination, and bacterial conjugation, and are components of eukaryotic transcription complexes. Mutations in enzymes with helicase activity result in a variety of human genetic diseases. This article focuses on the *Escherichia coli* Rep and UvrD helicases, both members of the SF1 helicase superfamily.

Function

The *Escherichia coli* Rep helicase is involved in replication, most likely playing a role in replication restart. Rep was first identified as being required for replication of bacteriophage ϕX174. Rep in complex with the phage ϕX174 gene A protein is highly processive, being able to unwind the entire genome ($>$6000 bp). However, in the absence of this accessory protein, Rep unwinds DNA with significantly lower processivity. *E. coli* UvrD, also known as helicase II, is involved in nucleotide excision repair and methyl-directed mismatch repair of DNA, as well as in plasmid replication. In the absence of accessory proteins, the unwinding processivity of UvrD is also relatively low. However, UvrD must be able to unwind at least 1000 bp processively during methyl-directed mismatch repair. Therefore, the processivity of each of these helicases can be increased through interactions with accessory proteins.

Most DNA helicases show a preference for unwinding duplex DNA possessing a ss-DNA flanking region or "tail" *in vitro*, and generally display a defined "polarity of unwinding" with respect to the backbone polarity of the ss-DNA tail that flanks the duplex DNA. Helicases that initiate unwinding more efficiently on DNA substrates with a 3′-ss-DNA tail are referred to as "3′–5′ helicases," whereas those that prefer DNA substrates possessing a 5′-ss DNA tail are referred to as "5′–3′ helicases." The *E. coli* Rep, UvrD and *B. stearothermophilus* PcrA helicases are 3′–5′ helicases, whereas the phage T4 Dda protein is a 5′–3′ helicase. These results suggest that a 3′–5′ helicase translocates in that direction along ss-DNA and this appears to be the case. At high-protein concentrations, *E. coli* UvrD can also initiate DNA unwinding at a nick *in vitro*, which is the biologically important site for initiation of unwinding in its roles in methyl-directed mismatch repair and excision repair.

Helicases are allosteric enzymes, many of which function as oligomeric assemblies. The class of hexameric DNA helicases exemplifies such oligomerization. The general importance of oligomerization for the function of SF1 helicases is less clear and is the subject of current study. Although there is evidence that a monomer of the phage T4 Dda helicase, an SF1 helicase, displays limited helicase activity *in vitro*, monomers of *E. coli* Rep and UvrD do not display helicase activity *in vitro*, but must dimerize in order to unwind DNA *in vitro*. The role of this dimerization may be to activate the enzyme and to provide the functional enzyme with multiple DNA-binding sites that are important for increasing the processivity of DNA unwinding.

Structural Features of SF1 DNA Helicases

Primary Structures

Helicases have been classified into families and superfamilies (SF1, SF2, SF3, F4, and F5) based on conserved amino acid sequence patterns. The SF1 superfamily (containing *E. coli* Rep and UvrD) is defined by seven conserved regions of primary structure, referred to as "helicase motifs." The only regions of sequence similarity that are shared uniformly among all of the helicase families are motifs I and II, which correspond to the

"Walker A" and "B" boxes that form part of the nucleoside-5′-triphosphate-binding site. The presence of these two motifs is necessary but not sufficient for a protein to have helicase activity. The remaining conserved regions of the SF1 helicases are involved in binding of nucleoside-5′-triphosphate and/or DNA.

Crystal Structures of SF1 Helicases

Crystal structures have been solved for three SF1 DNA helicases, *B. stearothermophilus* PcrA, *E. coli* Rep, and *E. coli* UvrD. The apo form of PcrA as well as PcrA in complex with ADP, was solved at 2.5 and 2.9Å resolution, respectively. Structures of *E. coli* Rep bound to ss-DNA ($dT(pT)_{15}$) and Rep bound to ss-DNA and ADP were solved at 3.0 and 3.2Å, respectively. Structures of PcrA in complex with a 3′-ss-ds DNA junction, both in the presence and absence of the nonhydrolyzable ATP analogue, AMPPNP, were solved at 3.3 and 2.9Å, respectively.

The Rep (673 amino acids), PcrA (675 amino acids), and UvrD (720 amino acids) proteins are structurally homologous; a structure of the Rep-ss-DNA-ADP ternary complex is shown schematically in Figure 1. These SF1 proteins consist of two domains (1 and 2), separated by a cleft; domains 1 and 2 are further composed of subdomains 1A, 2A, 1B, and 2B (Figures 1 and 2). Subdomains 1A and 2A are composed of central

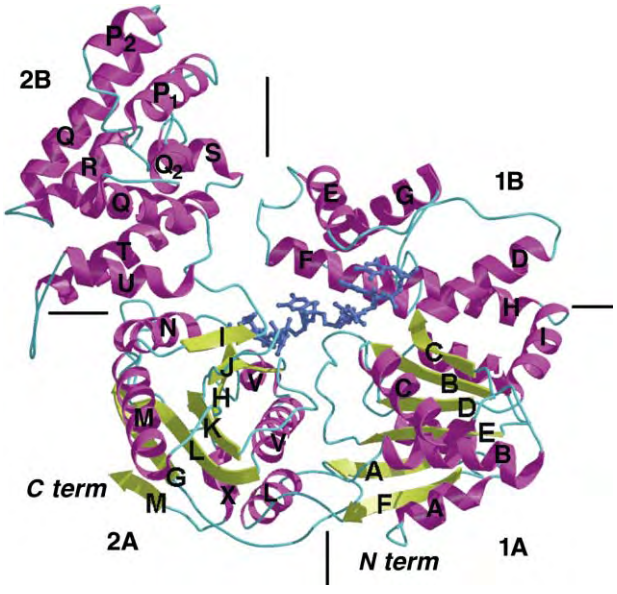

FIGURE 1 Structure of the *E. coli* Rep monomer bound to a single-stranded DNA (6 nucleotides shown in blue). Subdomains 1A, 1B, 2A, and 2B are indicated. The 3′ end of the ss-DNA resides near domain 1. Reprinted from Korolev, S., Hsieh, J., Gauss, G. H., Lohman, T. M., and Waksman, G. (1997). Major domain swiveling revealed by the crystal structures of complexes of *E. coli* Rep helicase bound to single-stranded DNA and ADP. *Cell* **90**, 635–647.

β-sheets flanked by α-helical regions and are homologous to each other as well as to the nucleoside-5′-triphosphate-binding domain of the *E. coli* RecA protein. Subdomains 1A and 2A both contain large insertions which form the α-helical 1B and 2B domains.

The crystal structures of *E. coli* Rep and *B. stearothermophilus* PcrA in conjunction with mutagenesis studies on several helicases indicate that amino acid residues in the seven conserved SF1 "helicase motifs," I–VI and IA are involved in either nucleotide and/or DNA binding. As shown in Figure 2, motifs I, IA, II, and III are contained within domain 1A, motifs V and VI are contained within domain 2A, whereas domain IV is found at the cleft formed between domains 1A and 2A. In general, ADP interacts with residues in motifs I and IV, whereas ATP interacts with residues within or near all of the motifs, with the apparent exception of motif IA.

Rep binds ss-DNA with a defined orientation with respect to the polarity of the sugar-phosphate backbone. In the crystal structures, the 3′–5′ direction runs from domain 1 to domain 2 across the cleft between the two domains, with the 3′ end of the ss-DNA located in a groove formed between subdomains 1A and 1B.

Several of the "helicase motifs" appear to be involved in the transmission of information between the ATP and ss-DNA-binding sites within a Rep monomer. Motif V residues are also likely to be involved in both ss-DNA binding as well as ATP binding through interactions with the γ-phosphate. Motif VI interacts directly with the γ-phosphate of ATP, as well as with motif IV. The above summary considers only interactions that occur within a single monomer or subunit. However, since oligomerization of both Rep and UvrD is functionally important for helicase activity *in vitro*, important allosteric interactions also occur between subunits of a Rep dimer.

"Open" and "Closed" Conformations

The asymmetric unit of the Rep-ssDNA crystal structure shows two molecules of Rep bound to a single molecule of $dT(pT)_{15}$. The conformations of the two Rep monomers are strikingly different with respect to the orientation of the 2B subdomain relative to the other three subdomains. These two conformations, referred to as "closed" and "open," respectively, differ by a ~130° rotation of the 2B subdomain about a hinge region connecting it to the 2A subdomain. It has been speculated that the 2B subdomain might be part of the interface between subunits within the Rep dimer, while others have suggested that the 2B subdomain forms part of the duplex DNA-binding site in the closed form of the PcrA monomer and plays a role in

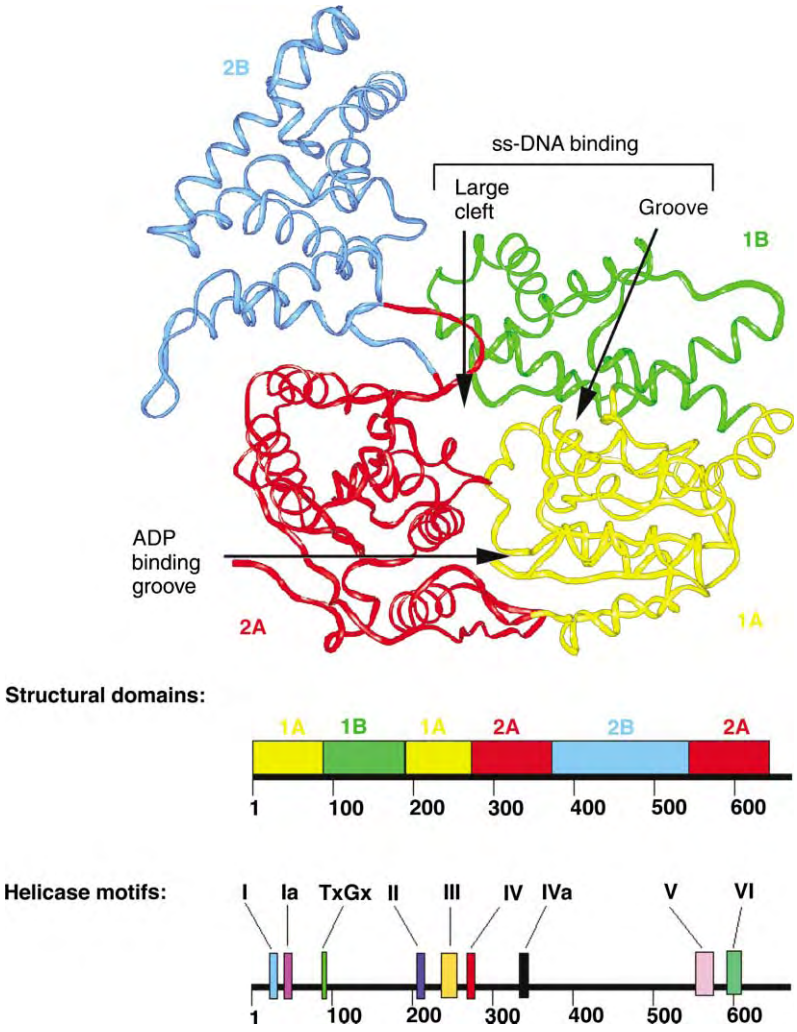

FIGURE 2 The domain structure of *E. coli* Rep monomer. The positions of the subdomains and the helicase motifs within the primary structure of Rep are also shown. The color scheme for the individual motifs corresponds to that shown in Figure 1. Modified from Korolev, S., Hsieh, J., Gauss, G. H., Lohman, T. M., and Waksman, G. (1997). Major domain swiveling revealed by the crystal structures of complexes of *E. coli* Rep helicase bound to single-stranded DNA and ADP. *Cell* **90**, 635–647.

duplex DNA stabilization. The essential nature of the 2B subdomain in Rep was tested by making a *rep* gene construct in which the coding region for the entire 2B domain was deleted and replaced by three glycines. The resulting RepΔ2B protein retains helicase activity *in vitro* and can also support ϕX174 phage replication *in vivo*, thus ruling out models invoking an essential role for the 2B domain in the helicase activity of Rep. In fact, a monomer of the RepΔ2B protein displays limited helicase activity *in vitro* in stark contrast to a wild-type Rep monomer which displays no helicase activity *in vitro*. This indicates that individual Rep monomers do possess all that is needed to unwind duplex DNA. However, the 2B subdomain appears to be inhibiting helicase activity of the monomer, and thus may have a regulatory function. This inhibition is relieved upon formation of a Rep or UvrD dimer.

Single-Stranded DNA Translocation by Monomers of SF1 Helicases

Recent studies have demonstrated that monomers of *B. stearothermophilus* PcrA can indeed translocate with biased directionality (3′–5′) along ss-DNA in an ATP-dependent reaction. In fact, monomers of *E. coli* Rep and UvrD, which are structural homologues of PcrA, also have been shown to be able to translocate along ss-DNA with biased (3′–5′) directionality. However, since monomers of Rep and UvrD are unable to unwind duplex DNA *in vitro*, it is clear that ss-DNA translocation alone is insufficient for DNA helicase activity for these helicases, and that dimerization is required.

DNA Unwinding by *E. coli* Rep and UvrD Helicases

Rep and UvrD Monomers are Unable to Unwind Duplex DNA and Protein Oligomerization is Required for Helicase Activity *in vitro*

Single-turnover DNA-unwinding studies indicate that Rep monomers are unable to unwind DNA *in vitro* and that Rep oligomerization is required for initiation of DNA helicase activity *in vitro*. Single-molecule fluorescence techniques have shown that a monomer of Rep uses ATP hydrolysis to translocate toward the ss/dsDNA junction, but then displays futile ATP-dependent conformational fluctuations, followed by dissociation of the monomer. DNA unwinding is initiated only if a functional oligomeric helicase is formed. Significantly, partial dissociation of the oligomeric helicase during unwinding leaves an inactive Rep monomer, resulting in a stalled complex. This stalled complex can be resolved in two ways. Dissociation of the remaining bound monomer leads to rewinding of the DNA duplex; however, re-initiation of unwinding can occur upon re-formation of the functional helicase by binding of additional Rep protein. These results show that a Rep monomer is unable to sustain DNA unwinding after the active Rep oligomeric complex disassembles. This also suggests that the low unwinding processivity observed for Rep DNA unwinding *in vitro* may be due to the relative instability of the functional dimer.

Initiation of DNA unwinding *in vitro* also requires a dimeric UvrD complex in which one subunit is bound to the ss/ds-DNA junction, while the second subunit is bound to the 3′ ss-DNA tail. Since the assay used in these UvrD studies relies on complete unwinding of an 18 base pair duplex, these results cannot exclude the possibility that monomers might unwind a short stretch of DNA duplex; however, processive unwinding of an 18 bp duplex requires UvrD oligomerization. Therefore, simple unidirectional translocation of a UvrD or Rep monomer along ss-DNA is not sufficient for helicase activity, and thus do not support "passive" models of DNA unwinding which assume that a translocating enzyme can unwind a duplex by simply taking advantage of the thermal fluctuations at the ss–ds DNA junction that result in transient fraying of the duplex end.

Kinetic Estimate of the DNA Unwinding "Step-Size" for *E. coli* UvrD Helicase

A kinetic approach indicates that UvrD unwinds 4–5 bp in each step (called the kinetic step size). This indicates that a rate-limiting step is repeated during the unwinding cycle and the unwinding "step-size" of 4–5 bp represents the number of base pairs unwound between two successive rate-limiting steps. It is not yet known how this kinetic step-size is related to a mechanical step size. Similar experiments performed with *E. coli* RecBCD helicase yield a step size of 3.9 ± 1.3 bp. A value of ~ 6 bp per step has also been estimated for the vaccinia NPH-II helicase. The similarities among these step sizes suggest mechanistic similarities, although this remains to be determined.

Mechanisms for DNA Unwinding and Translocation by SF1 Helicases

Whereas it seems likely that SF1 helicases may share some features of their unwinding mechanisms, it is still too early to conclude whether a single mechanism applies to all SF1 helicases. In fact, there are clear differences among some of the SF1 helicases studied to date. Although *E. coli* Rep and UvrD must oligomerize to function as helicases *in vitro*, a monomer of the phage T4 Dda helicase possesses limited unwinding activity *in vitro*. It is therefore possible that some SF1 helicases function as monomers to unwind short stretches of duplex nucleic acids, while oligomerization may be necessary to activate some SF1 helicases or to enhance their processivity. Of course, interaction of a helicase with an accessory protein may also modify the need for the helicase to oligomerize by providing a second DNA-binding site.

Most proposed mechanisms for DNA unwinding and helicase translocation assume the functional helicase to possess at least two DNA-binding sites. Differences in current models for DNA unwinding center on three aspects: (1) whether translocation of the helicase along ss-DNA is sufficient for helicase activity or whether the helicase also interacts directly with the duplex DNA; (2) whether the two DNA-binding sites are contained within a single polypeptide; and (3) whether the same DNA-binding site remains as the lead site (inch-worm model) or whether multiple sites alternate as the lead subunit ("rolling" or "hand-over-hand" models).

Active Versus Passive Mechanisms of DNA Unwinding

One operational distinction among DNA unwinding models is whether the helicase participates directly in destabilizing the duplex DNA (active mechanism), or whether the helicase interacts solely with the ss-DNA and waits for transient fluctuations in the duplex to form a ss-DNA region (end fraying) onto which the helicase can then translocate (passive mechanism).

"Active" mechanisms would generally involve direct binding of the helicase to the duplex DNA (or the duplex–ss DNA junction), in addition to the ss-DNA, although a "torsional" mechanism is possible in which binding of the helicase to both single strands might unwind the duplex without direct duplex interactions.

Tests of a "passive" mechanism of unwinding have been made for *E. coli* Rep and UvrD helicases using non-natural DNA substrates in which a region of the ss-DNA adjacent to the duplex was reversed in its backbone polarity or replaced by polyethylene glycol. The segments of polyethylene glycol or reversed polarity ss–DNA would prevent a helicase from translocating up to the ss–ds DNA junction, thus a helicase operating by a "passive" mechanism would not be expected to unwind such DNA substrates. However, Rep and UvrD can unwind such DNA molecules, ruling out a passive mechanism for these helicases.

Dimeric, Subunit Switching Models

Active, "Rolling" or "Hand-Over-Hand" Models for a Dimeric Helicase

An "active, rolling" mechanism (Figure 3A) has been proposed for how a Rep dimer might unwind DNA and translocate along the DNA filament. In this model, the individual subunits alternate as the lead subunit, which binds to duplex DNA, followed by unwinding. However, all of the evidence upon which this model was based is also consistent with a "dimeric inch-worm" model shown schematically in Figure 3B.

Dimeric Inch-Worm Models

The only difference between the "rolling" and "dimeric, inch-worm" models is that the same subunit remains as the lead subunit in the "dimeric inch-worm" model. In fact, recent evidence with both Rep and UvrD favors a "dimeric, inch-worm" model rather than a "rolling" or "hand-over-hand" model. Based on the fact that monomers of Rep and UvrD are able to translocate along ss-DNA with biased (3′–5′) directionality, it seems most likely that in a "dimeric inch-worm" model, the trailing subunit of the dimer might maintain continuous contact with the 3′ ss-DNA, possibly providing the motor component of the helicase, whereas the leading subunit would interact with the ss–ds DNA junction. However, such details are still speculative and need to be tested.

Monomeric Inch-Worm Models

It has been proposed that that a PcrA monomer unwinds DNA by an inch-worm mechanism. Support for the monomeric inch-worm model proposed for PcrA comes from the fact that PcrA monomers are able to translocate along ss-DNA with biased (3′–5′) directionality. However, both Rep and UvrD monomers also possess this ability, yet cannot unwind DNA *in vitro*.

Summary

It is now clear that monomers of SF1 helicases are able to translocate along ss-DNA with biased directionality in an ATP-dependent reaction. These monomers must use some sort of inch-worm mechanism for this translocation. However, monomers of *E. coli* Rep and UvrD are not able to initiate DNA unwinding *in vitro*, despite the fact that these monomers can translocate along ss-DNA with directional bias. Therefore, the ability to translocate with unidirectional bias along ss-DNA is not sufficient for a protein to have helicase activity. In fact, to date, only the phage T4 Dda and a deletion mutant of *E. coli* Rep (RepΔ2B) have been shown to unwind DNA *in vitro* as monomers, and these do so with low processivity. The 2B subdomain of Rep is not required for its helicase activity *in vitro*; in fact, this domain inhibits the ability of a Rep monomer to unwind

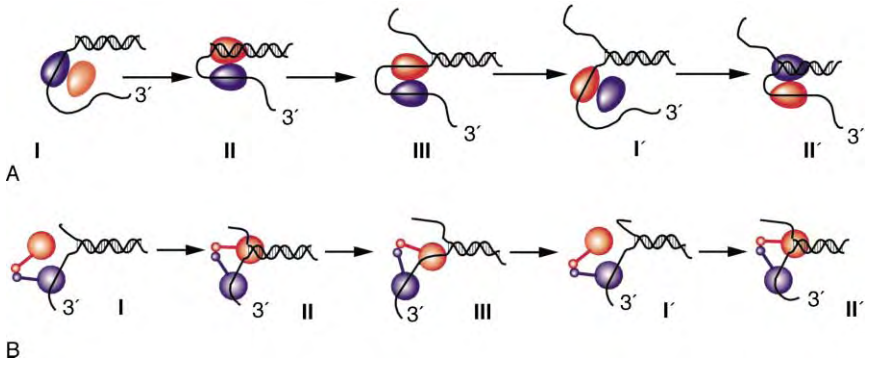

FIGURE 3 Models for DNA unwinding and translocation by a dimeric helicase. (A) Active, "rolling" or "hand-over-hand" model, and (B) dimeric "inch-worm" model.

DNA *in vitro*. Both *E. coli* Rep and UvrD are required to dimerize in order to initiate DNA unwinding *in vitro*, thus the inhibition of helicase activity by the 2B subdomain of Rep appears to be relieved through Rep oligomerization.

See Also the Following Articles

DNA Helicases: Hexameric Enzyme Action • DNA Mismatch Repair in Bacteria • DNA Replication Fork, Bacterial • DNA Replication: Initiation in Bacteria • DNA Topoisomerases: Type III–RecQ Helicase Systems • recQ DNA Helicase Family in Genetic Stability

Glossary

helicase An enzyme that utilizes nucleoside 5′-triphosphates to separate the two strands of the DNA double helix in order to form the single-stranded DNA intermediates that are required for DNA metabolism (i.e., replication, recombination, and repair).

kinetic step size The average number of base pairs unwound between successive, repeated rate-limiting steps in the DNA unwinding cycle.

processivity A measure of the average number of base pairs that can be unwound by a helicase before it dissociates from the DNA.

Further Reading

Ellis, N. A. (1997). DNA helicases in inherited human disorders. *Curr. Opin. Genet. Dev.* **7**, 354–363.

Geider, K., and Hoffmann-Berling, H. (1981). Proteins controlling the helical structure of DNA. *Annu. Rev. Biochem.* **50**, 233–260.

Kornberg, A., and Baker, T. A. (1992). *DNA Replication*. W.H. Freeman, New York.

Korolev, S., Hsieh, J., Gauss, G. H., Lohman, T. M., and Waksman, G. (1997). Major domain swiveling revealed by the crystal structures of complexes of *E. coli* Rep helicase bound to single-stranded DNA and ADP. *Cell* **90**, 635–647.

Lohman, T. M., and Bjornson, K. P. (1996). Mechanisms of helicase-catalyzed DNA unwinding. *Annu. Rev. Biochem.* **65**, 169–214.

Matson, S. W., and Kaiser-Rogers, K. A. (1990). DNA helicases. *Annu. Rev. Biochem.* **59**, 289–329.

Matson, S. W., Bean, D. W., and George, J. W. (1994). DNA helicases: Enzymes with essential roles in all aspects of DNA metabolism. *Bioessays* **16**, 13–22.

Modrich, P. (1987). DNA mismatch correction. *Annu. Rev. Biochem.* **56**, 435–466.

Modrich, P. (1994). Mismatch repair, genetic stability, and cancer. *Science* **266**, 1959–1960.

Patel, S. S., and Picha, K. M. (2000). Structure and function of hexameric helicases. *Annu. Rev. Biochem.* **69**, 651–697.

Soultanas, P., and Wigley, D. B. (2001). Unwinding the gordian knot of helicase action. *TIBS* **26**, 47–54.

Biography

Timothy M. Lohman is the Marvin A. Brennecke Professor of Biological Chemistry and a member of the Department of Biochemistry and Molecular Biophysics at Washington University School of Medicine, St. Louis, MO. His principal research interests are in the study of energetics and kinetic mechanisms of protein–DNA interactions, focusing on helicases and SSB proteins. He holds a Ph.D. in Physical Chemistry from the University of Wisconsin, Madison and did postdoctoral research at the University of California, San Diego and the University of Oregon.

DNA Helicases: Hexameric Enzyme Action

Smita S. Patel
Robert Wood Johnson Medical School, Piscataway, New Jersey, USA

Helicases are molecular motor proteins that use the energy of nucleoside triphosphate (NTP) hydrolysis to unidirectionally translocate along nucleic acid while separating the double-strand (ds) DNA strands, removing secondary structures in RNA, and displacing proteins bound to nucleic acids. Helicases are integral parts of the cellular machinery involved in DNA and RNA metabolic processes. Thus, it is not surprising that helicases and helicase-related proteins constitute more than 2% of the eukaryotic genome. Mutations in human genes coding for helicases result in several diseases that result in cancer and premature aging. Helicases also play a key role in viral life cycles such as viral genome replication and genome packaging/unpackaging. Viral helicases are therefore attractive targets for antiviral therapy. The topic of helicase structure, function, and mechanisms has been widely discussed in the literature. Oligomeric state divides helicases into two groups: ring (hexameric) helicases and all other. In this article, we start by discussing general mechanisms of translocation and strand separation of nucleic acid by helicases, which is followed by a discussion of the mechanisms of ring helicases.

Nucleic Acid Strand Separation Activity of Helicases

A long stretch of ds DNA or RNA is unwound by the helicase in a step-wise manner as shown in Figure 1. In each step, the helicase translocates and separates the duplex strands.

Most helicases require a stretch of single-stranded (ss) nucleic acid of a specific polarity adjacent to the duplex region to initiate strand separation. Helicases that require a 3′ ss tail to initiate strand separation are assumed to translocate in the 3′ to 5′ direction, and *vice versa*. Some helicases including hexameric ring helicases like T7 phage gp4 helicase, T4 phage gp41 helicase, and bacterial DnaB helicase require both 5′ and 3′ non-complementary tails to initiate strand separation, in which case it is difficult to determine the directionality of translocation using this assay.

Nucleic acid strand separation is commonly measured using short duplexes that contain a labeled strand of nucleic acid. Helicase is mixed with the substrate and MgNTP is added to initiate the reaction. This is a discontinuous assay, and after various reaction times, sodium dodecylsulfate (SDS) and ethylenediaminetetraacetic acid (EDTA) are added to stop the reaction. It is assumed that partially separated strands reanneal and only the completely separated strands are observed as products by native polyacrylamide gel electrophoresis. Alternatively, strand separation is measured in real time by using fluorescently labeled nucleic acids. This can be measured in ensemble reactions by the stopped flow method by monitoring fluorescence change or loss of fluorescence resonance energy transfer (FRET) as the strands are separated or by using FRET in single molecule experiments.

Multiple enzymatic activities are required for the helicase function, including NTPase, translocation, and strand separation. All helicases hydrolyze NTP, commonly ATP, both in the absence and in the presence of nucleic acid. The NTPase activity in the absence of nucleic acid is low and is stimulated many fold in the presence of nucleic acid. The stimulated NTPase activity is coupled to strand separation and unidirectional translocation of the helicase along nucleic acid. It is believed that as the helicase cycles through different NTP ligation states, the reactions of NTP binding, hydrolysis and product release induce conformational changes in the helicase's nucleic acid binding site. These conformational changes alter the affinity of the helicase for the substrate and/or to perform a power stroke to somehow drive unidirectional translocation and strand separation.

The helicase activity can be broadly divided into two reactions: unidirectional translocation and strand separation, both of which are fueled by the NTPase activity of the helicase. Several studies indicate that helicases translocate unidirectionally along ss DNA and that unidirectional translocation does not require the presence of the ss/ds DNA junction. Thus, it is likely that unidirectional translocation along nucleic acid is

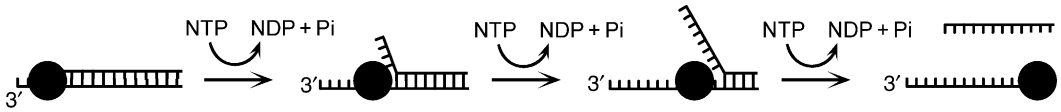

FIGURE 1 Helicase separating the strands of nucleic acid in the 3′–5′direction. The helicase (black circle) initiates strand separation by binding to the 3′-tail, translocating along a strand of the ss/ds nucleic acid substrate, and separating the strands of the substrate as it hydrolyzes NTP to NDP and phosphate (Pi).

the basic activity of helicases that also facilitates the strand separation process. A number of mechanisms of strand separation and NTPase-coupled translocation have been proposed from studies of different helicases. Some of the differences in the proposed mechanisms result from the different biochemical properties of the helicases, such as the protein oligomeric state, the interactions with ss versus ds substrates, and the effect of the nucleotide ligation state of the helicase on its substrate binding properties. Thus, it might appear that there are several ways to separate the strands of nucleic acid; although, it is likely that as detailed studies are carried out, a general mechanism of translocation and strand separation by helicases will emerge.

Mechanisms of Unidirectional Translocation

Stepping Model

It is commonly believed that translocation requires at least two nucleic acid binding sites that independently bind and release nucleic acid as the helicase goes through the NTPase cycle. Such stepping models have been discussed widely and proposed for helicases such as PcrA, Rep, and UvrD. The two nucleic acid binding sites move with respect to each other in response to the conformational changes induced by NTP binding, hydrolysis, and product release at the NTP binding site of the helicase. In an oligomeric helicase, the NTPase activity of each subunit controls the conformation of the nucleic acid binding site; thus, coordinated NTPase activity leads to coordinated binding and release of the helicase from nucleic acid. Several helicases including PcrA, HCV helicase, and T4 DdaA are active as monomers. A monomeric helicase with one nucleic binding site cannot use the stepping mechanism described above. The monomer of PcrA has been proposed to contain two DNA binding sites that coordinate DNA binding and release. In this case, the two DNA binding sites on a monomer are controlled by one nucleotide binding site.

Brownian Motor Model

An alternative model of translocation integrates Brownian motion into a molecular motor. Such a Brownian motor mechanism has been proposed for motors such as kinesin, myosin, and ion pumps. A Brownian motor uses thermal fluctuations from its surroundings and the NTPase reaction to achieve unidirectional movement. Brownian motor model can be applied to monomeric helicases with one nucleic acid binding site, although it predicts limited processivity of translocation and strand separation. The helicase holds on to the ss nucleic acid only via one binding site, and therefore it is more likely to dissociate during the weak binding sliding phase. A dimeric helicase with two and a hexameric helicase with six nucleic acid binding sites can use a Brownian motor mechanism and translocate with a greater efficiency. This is especially true if the helicase subunits coordinate their NTPase cycles and take turns binding and hydrolyzing NTP. In fact, a coordinated dimer or hexamer should appear as if it is stepping, because its subunits are taking turn moving forward.

Figure 2 shows a mechanism in which we suppose that in the absence of NTP the helicase is tightly bound to the nucleic acid and hence is in its lowest energy state unable to move along the substrate. When NTP binds to the helicase, it causes a conformational change in its nucleic acid binding site, resulting in a weakening of the nucleic acid binding affinity. In this weak binding state, the helicase's binding free energy is constant along the nucleic acid length (Figure 2, dotted line), which allows the helicase to slide along randomly in either direction influenced by thermal fluctuations, this is Brownian motion (Figure 2, position 4). It is important that the random movement of the helicase lasts only for a short time, and this is achieved by rapid NTP hydrolysis. After NTP hydrolysis, the tight rebinding to the nucleic acid is associated with a forward movement of the helicase along the direction of translocation. The forward movement of the helicase occurs along a decreasing energy slope and can be considered a power stroke. The forward movement does not require specific interactions with the ss/ds junction; hence, it can provide unidirectional movement along ss nucleic acid. If Brownian motion moves the helicase backward, a forward power stroke while rebinding to the nucleic acid will bring the helicase back to the same position it started, without net movement (position 3). The helicase molecules that diffuse in the forward direction (position 5) will end up one step forward from their original position upon tight

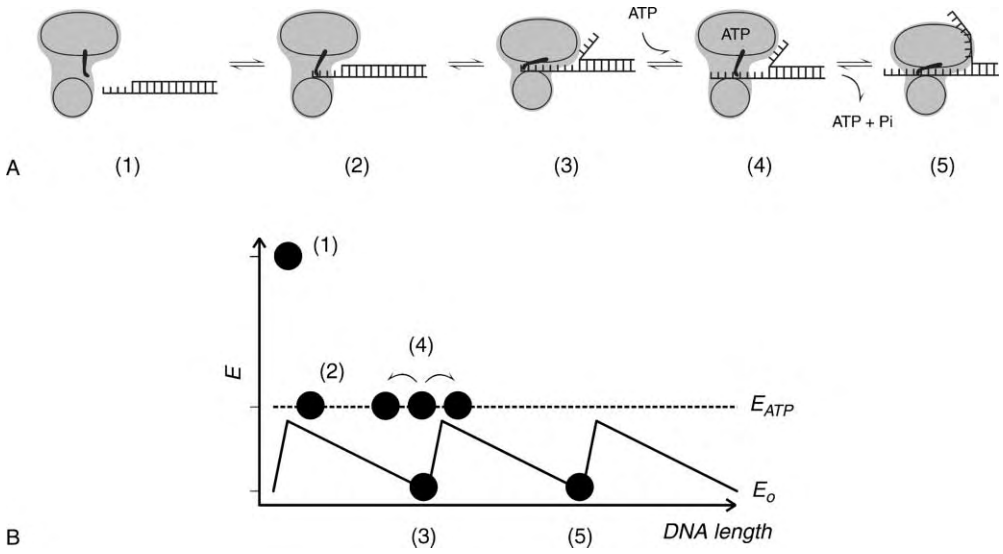

FIGURE 2 Translocation of the helicase by a Brownian motor mechanism. (A) Transition of the helicase from a weakly nucleic-acid-bound state (helicase-ss nucleic acid-ATP state, (2)) to a tightly nucleic acid-bound state (helicase-ss nucleic acid state, (3)) is coupled to unidirectional movement. (B) Helicase binding free energy (E) along the length of ss nucleic acid. The helicase–nucleic acid complex has an asymmetric saw tooth profile along the length of ss nucleic acid, E_o (solid line) in the nucleotide-free state and a flat energy profile in the ATP-bound state, E_{ATP} (dotted line). The helicase position on ss nucleic acid is represented by gray circles: (1) free helicase; (2) helicase bound to ss nucleic acid weakly; (3) helicase bound to ss nucleic acid tightly; (4) helicase bound weakly to ss nucleic acid that can diffuse in either direction; (5) rebinding of the helicase from position (4) results in a net forward movement.

rebinding to the nucleic acid. A helicase can move forward even against a moderate external force (such as strand separation) as long as a significant fraction of the helicase can diffuse forward to position 5. Repeated binding and release of the helicase catalyzed by NTPase cycles results in a net unidirectional translocation of the helicase. This mechanism may be considered a combination of power stroke and Brownian ratchet.

The efficiency of a motor is defined as the fraction of productive steps per round of NTP hydrolysis. Several factors affect the efficiency of a Brownian motor. The greater the asymmetry of the saw tooth energy profile, the greater the efficiency of the motor. The steeper energy profile will increase the fraction of helicase molecules that reach position 5. The efficiency is also highly dependent on the rate of NTP hydrolysis, which determines the lifetime of the weakly bound state (Figure 2, position 4). If NTP hydrolysis is too fast, the lifetime of the weakly bound state will be too short and most molecules will end up in the same position they started with no net directed motion. If NTP hydrolysis is too slow, the molecules will have time to spread broadly in both directions with no net directed motion.

Mechanisms of Nucleic Acid Strand Separation

Separating the strands of a duplex nucleic acid involves breaking the hydrogen bonds that hold the base pair (bp) together. At physiological temperature, nucleic acid bps open and close spontaneously. The rates of spontaneous bp opening as measured by imino proton exchange range from 30 s^{-1} for internal bp to 1000 s^{-1} for bp at the ss/ds junction. Individual bps open at a fast rate but the equilibrium for this reaction is toward bp formation. Therefore, bp closing is fast and it poses a kinetic barrier against the movement of helicase at the ss/ds nucleic acid junction.

At physiological temperatures, nucleic acid strand separation is a thermodynamically unfavorable process. In order to make the process thermodynamically favorable, the helicase must stabilize the transition state and/or stabilize the open bps. This can be accomplished either actively or passively. In an active mechanism, the helicase increases the rate of bp opening. If the helicase separates the nucleic acid strands by the passive mechanism, by definition, it does not change the rate of bp opening. A helicase can increase the rate of strand separation by lowering the transition state energy by binding to an intermediate such as a distorted duplex region or the ss/ds nucleic acid junction. Interaction of the helicase with ds nucleic acid has been viewed as an indication of an active mechanism of strand separation. Another way to actively disrupt bps is by unidirectional translocation or by a wedge mechanism. In this mechanism, the helicase translocates unidirectionally along ss nucleic acid and along its way it is able to capture base-pairs generated by thermal fluctuation. Helicases have been shown to move unidirectionally

along ss nucleic acid. Helicases have also been shown to displace proteins on their path and break the streptavidin–biotin linkage at the end of ssDNA without specifically interacting with them. Unidirectional translocation could be the driving force for strand separation and a basic property of helicases, making helicases similar to motor proteins that move on filaments.

Step-Size of the Helicase

The physical step-size of a helicase is the number of bases it travels in a single cycle during unidirectional translocation; its measurement provides critical insights into the mechanism of translocation. Methods for measuring the physical step-size of a helicase directly have been reported, and there is a need to develop methods to quantitatively measure the stepping motion of the helicase. Kinetic step-size of a helicase can be measured by globally fitting the single turnover kinetics of strand separation of duplexes of various lengths. This method assumes that all species have identical stepping properties. In cases where multiple populations with different stepping rates exist, the kinetics will exaggerate the estimation of step-size. In the case of a helicase whose ATPase cycles are tightly coupled to movement, the step-size can also be obtained by measuring the coupling ratio, which is the number of bases the helicase can travel per NTP hydrolyzed.

Hexameric Helicases

Hexameric ring helicases are found in all organisms including bacteriophage, viruses, bacteria, and eukaryotes. These helicases are often integral parts of protein complexes that catalyze nucleic acid replication, recombination, and transcription (Figure 3).

Ring Structure

In most helicases, six identical polypeptides assemble into a hexameric ring. Eukaryotic minichromosome maintenance (MCM) helicases on the other hand assemble into a heterohexamer of Mcm2–7 proteins with a unique arrangement of the six subunits. The three-dimensional structure of ring helicases from various organisms has been characterized extensively by electron microscopy and image analysis. These studies show that the ring structure is conserved from bacteriophage to viruses and from prokaryotes to eukaryotes as shown in Figure 4. The six subunits are arranged in a toroidal shape. On an average, the outer diameter of the ring is approximately 12 nm and the diameter of the central channel is approximately

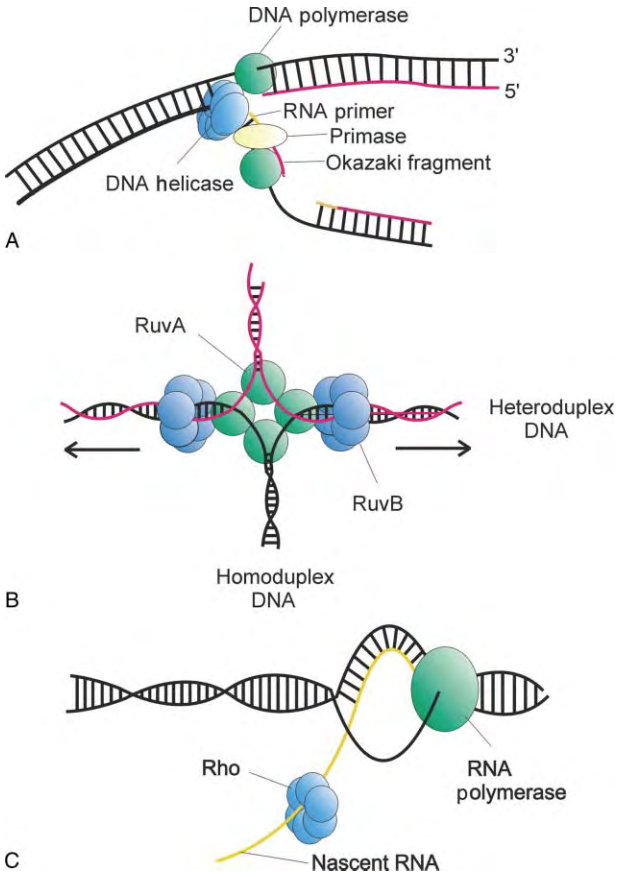

FIGURE 3 Functions of ring helicases in (A) DNA replication, (B) recombination, and (C) transcription.

2 nm. The central channel is therefore wide enough to accommodate duplex DNA or RNA.

Crystal structures of ring helicases including RepA, RuvB, Rho, and fragments of T7 gp4 and SV40 Large T antigen provide atomic details of the subunit interface and the NTP binding site (Figure 5A). The crystallized RepA helicase ring in the absence of NTP has a sixfold symmetry, Rho ring was open, and the T7 gp4 ring with four NTPs bound has a twofold symmetry. The structure of the N-terminal fragment of archaea MCM protein reveals a double hexamer arrangement. The major subunit–subunit contact in RepA and T7 gp4 is between an N-terminal loop (in RepA) or the linker region between the helicase and primase domains (in T7 gp4) contacting helices between H1a and H2 of a neighboring subunit.

The structure of ring helicases shows that most of the helicase-conserved motifs including H1, H1a, H2, and H3 appear at the subunit interface, where they participate in NTP binding (Figure 5). Thus, NTP bound at the interface interacts with residues from adjacent subunits. A critical arginine (Arg 522 in T7 gp4) is found in hexameric helicases that come from a neighboring subunit and is within hydrogen bonding distance of the

Helicase	Mol. Wt.	Direction	Activities	Function	EM
E. coli DnaB	52,390	5' to 3'	NTPase Helicase	DNA Replication	
E. coli Bacteriophage T7 gp4	62,655	5' to 3'	Primase NTPase Helicase	DNA Replication	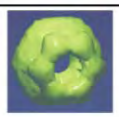
E. coli Bacteriophage T4 gp41	53,601	5' to 3'	NTPase Helicase	DNA Replication	
Plasmid Encoded RSF1010 RepA	29,909	5' to 3'	NTPase Helicase	DNA Replication	
Simian virus large T antigen	81,907	3' to 5'	NTPase Origin Binding Helicase	DNA Replication	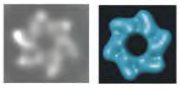
Bovine papillomavirus E1	68,246	3' to 5'	NTPase Origin Binding Helicase	DNA Replication	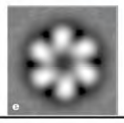
B. subtilis Phage SPP1 gene 40	46,746	5' to 3'	NTPase Helicase	DNA Replication	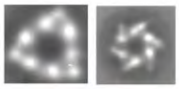
E. coli RuvB	37,174	5' to 3'	NTPase Branch Migration Helicase	DNA Recombination	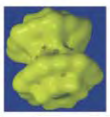
E. coli Rho	47,004	5' to 3'	NTPase Helicase	Transcription Termination	
Human Bloom's syndrome helicase	159,000	3' to 5'	NTPase Helicase	Unknown	

FIGURE 4 Structures of ring helicases. Electron microscopy images of several ring helicases are shown.

gamma phosphate of NTP bound at the interface, as shown in Figure 5B. This residue is important for catalyzing NTP hydrolysis and is implicated in transducing conformational changes between subunits of the hexamer.

Nucleic Acid Binding in the Central Channel

Detailed structural information is not available for the helicase nucleic acid binding site. Electron microscopy studies of ring helicases and biochemical studies indicate that nucleic acid binds in the central channel. Since the nucleic acid is confined within the central channel, its dissociation would require subunit–subunit disruption. This mode of nucleic acid binding is believed to confer processivity in translocation and strand separation activities of the hexameric helicases.

Processivity is the measure of the number of bases translocated or bp unwound before the helicase dissociates from the nucleic acid. Processivity, *P*, can be obtained from the measured stepping rate and the dissociation rate of the helicase. High processivity of translocation distinguishes the ring helicases from helicases such as *E. coli* UvrD, PcrA, and hepatitis C virus (HCV) helicases that do not assemble into rings.

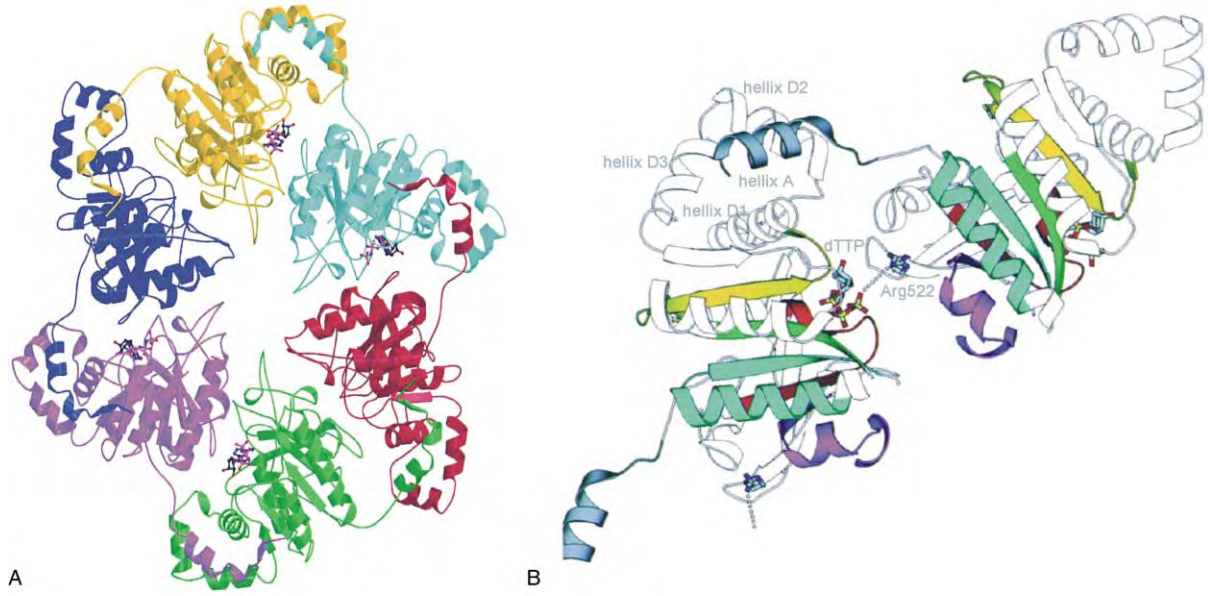

FIGURE 5 Crystal structure of the helicase domain of T7 gp4 protein. (A) Model of a closed ring shaped hexamer with four adenosine 5′-(β,γ-imido)triphosphates (ADPNP) bound at the subunit interfaces. (B) Arginine 522 (arginine-finger) contacting the nucleotide at the subunit interface.

Exceptions include RecBCD that may not encircle the DNA but shows a high processivity. The average processivity of ssDNA translocation by T7 gp4 hexamer on the other hand is $P = 0.99997$, a number close to one, which indicates that the probability of T7 helicase dissociating from ssDNA during translocation is very small. The processivity of T7 gp4 is only moderate because it is translocating and separating the strands of ds DNA, indicating that the association of T7 gp4 helicase with T7 DNA polymerase is necessary to achieve the high processivity observed during DNA replication. High processivity has been observed also for T4 gp41 and *E. coli* DnaB helicase in the replication complex.

How does the ring helicase bind nucleic acid in the central channel? The individual subunits can assemble around the nucleic acid, or the ring can open to accommodate the nucleic acid. Most helicases appear to use the ring-opening mechanism and they require a loader to efficiently bind nucleic acid. The loader is either part of the helicase or a separate protein or set of proteins that interact with the helicase. The primase site of T7 gp4 faces the outer surface of the ring and is proposed to play a role in loading the DNA into the central channel. Similarly, RNA wraps around the N-terminal domain of *E. coli* Rho protein, which plays a role in loading the RNA into the central channel. SV40 large T antigen and papilloma virus E1 contains origin binding domains that assist in DNA loading. In other ring helicases, accessory proteins are required to load the nucleic acid efficiently into the central channel. *E. coli* DnaB requires DnaC, T4 gp41 requires gp59, and MCM 2–7 helicase complex requires Cdc6 in addition to the single-stranded DNA binding proteins and origin recognition complex proteins to load at the replication origins.

Mechanism and Role of NTP Hydrolysis

The role of NTPase activity in ring helicases is similar to that of other helicases, in that NTP acts as a molecular switch. For example, T7 gp4 binds ssDNA in the presence of deoxythymidine (β, γ, methylene)triphosphate (dTMP-PCP), a nonhydrolyzable analog of dTTP with a K_d around 10 nM, and dTTP hydrolysis and Pi release leads to weakening of the interactions with ssDNA. Thus, dTTP binding and Pi release promote DNA binding and release events.

A negative cooperativity in nucleotide binding is observed in most hexameric helicases. A hexamer may bind only three nucleotides or show three high affinity and three low affinity nucleotide binding sites. T7 gp4 binds 3–4 nucleotides tightly in the presence or absence of Mg(II) ion. *E. coli* DnaB and Rho proteins have three high affinity and three low affinity nucleotide binding sites.

All six subunit interfaces of the hexamer can potentially bind and hydrolyze NTP. However, it has been proposed in T7 gp4 *E. coli* Rho as well as in MCM proteins that three subunits may have a regulatory role similar to that of the F_1-ATPase protein. Several possible mechanisms of NTP hydrolysis by ring helicases have

been discussed. The most appealing mechanism is sequential NTP hydrolysis by three or six of the hexameric subunits. Such a mechanism of NTP hydrolysis at three sites has been proposed based on pre-steady-state kinetic experiments in Rho protein with RNA and in T7 gp4 protein in the absence of ssDNA.

Translocation along Single-Stranded and Double-Stranded Nucleic Acid

Hexameric helicases such as T7 gp4 and T4 gp41 have been shown to translocate unidirectionally along ssDNA. T4 gp41 was able to displace streptavidin complexed to biotin placed at the 3′-end but not the 5′-end, suggesting that it translocates in the 5′–3′ direction. Similarly, utilization of primase sites on ssDNA was used to show that T7 gp4 translocates in the 5′–3′ direction. The DNA-dependent NTPase rate of these helicases also shows a dependence on ssDNA length that can be interpreted as unidirectional translocation along DNA. The translocation rate on ssDNA was measured for T7 gp4 as 130 base/s (at 18°C), and while translocating, gp4 hydrolyzes dTTP at a rate of 50 s^{-1}. This indicates that the energy from hydrolysis of one dTTP on average leads to translocation of the helicase along three bases of ssDNA. T7 gp4 helicase therefore translocates with a minimal step-size of three bases along ssDNA. RuvB helicase binds and translocates on dsDNA, catalyzing Holliday junction migration. Recently, *E. coli* DnaB and T7 gp4 helicases have been shown to migrate on dsDNA, but the rate of translocation has not been determined.

Translocation along nucleic acid by hexameric helicases appears to require functional subunits. Mutant poisoning experiments show that substitution of one or two of the hexamer subunits with a mutant inhibits the helicase and nucleic acid-dependent NTPase activity. Pre-steady-state NTPase kinetic experiments have indicated that the subunits of the ring act in a cooperative manner. The crystal structure of T7 gp4 fragment reveals that three adjacent subunits are in different conformational state (Figure 5A). Based on the structure, it was proposed that the hexamer subunits interact sequentially with the DNA during translocation. The stepping mechanism consisting of sequential NTP hydrolysis by the hexameric subunits coupled to sequential binding and release of nucleic acid is an attractive mechanism, but it requires more experimental evidence. An alternative mechanism of translocation to that discussed above is the Brownian motor mechanism that cannot be ruled out for hexameric helicases.

Binding and Strand Separation at the Fork Junction

Ring helicases encircle either the ss nucleic acid or the ds nucleic acid at the fork junction, as shown in Figure 3. Helicases involved in DNA replication are believed to encircle one of the ssDNA strands at the fork junction and to exclude the complementary strand from the central channel, as shown in Figure 3A. This mode of DNA binding minimizes immediate reannealing of the DNA strands after they are separated. The RuvB–RuvA complex involved in recombination (shown in Figure 3B) encircles dsDNA to drive Holliday junction movement. Recently, it was shown that when *E. coli* DnaB helicase and T7 gp4 helicase are presented with a substrate that contains only the 5′ ss DNA tail adjacent to the duplex they encircle and translocate along ds DNA and also drive movement of the Holliday junction. Transcription termination factor Rho is believed to translocate along RNA (shown in Figure 3C) to disrupt the transcription complex.

The kinetics of strand separation by helicase alone can be measured as described earlier using a small ds nucleic acid oligomer and by monitoring the release of ss nucleic acid. It was found with T7 gp4 that the rate of translocation along ssDNA is faster than the rate of ds DNA strand separation. Thus, T7 gp4 separates the ds DNA strands with a rate of about 15 bp/s. This rate depends on the concentration of NTP and temperature. Under the same experimental conditions, the rate of translocation along ssDNA is more than six times faster. Thus, dsDNA presents a barrier to the movement of helicase along DNA. The strand separation rate of helicases involved in replication also increases in the presence of the DNA polymerase. The replicative complex consisting of T7 gp4 helicase, gp2.5 protein, and T7 DNA polymerase catalyzes DNA replication at a rate greater than 200 bp/s at 30°C.

Conclusion

A large number of helicases and helicase-like proteins have been identified by genome sequencing efforts. These proteins play essential roles in almost all nucleic acid metabolism processes, and many are known to be associated with human diseases such as cancer and premature aging. Interestingly, many viruses code for their own helicases, which make them unique targets for antiviral therapy. Understanding the structure and mechanisms of helicases is an important means to find the link between the complex human diseases and helicases and to aid in the drug discovery process. From the viewpoint of understanding how helicases work, there is still a lack of a general mechanism that would

explain nucleic acid strand separation and other functions performed by helicases at the molecular level. Despite all the differences in the properties and structures of helicases, it is possible that they function by similar mechanisms. It is likely that unidirectional translocation is a basic activity of all helicases responsible for nucleic acid strand separation and all other functions of helicases. This makes helicases similar to general motor proteins that translocate on lattices, and their mechanism of operation may apply to helicases as well. New methodologies such as analysis of single helicase molecules will allow direct observation of the helicase reaction, and more detailed information from these experiments will provide physical parameters that will reveal how helicases work.

See Also the Following Articles

DNA Helicases: Dimeric Enzyme Action • DNA Polymerases: Kinetics and Mechanism • DNA Secondary Structure • recQ DNA Helicase Family in Genetic Stability

Glossary

Holliday junction A four-stranded DNA structure that is an intermediate in DNA recombination.

transition state The highest energy species in a chemical reaction pathway.

Further Reading

Astumian, R. D. (2001). Making molecules into motors. *Sci. Am.* **285**, 56–64.

Egelman, E. H., Yu, X., Wild, R., Hingorani, M. M., and Patel, S. S. (1995). Bacteriophage T7 helicase/primase proteins form rings around single-stranded DNA that suggest a general structure for hexameric helicases. *Proc. Natl Acad. Sci. USA* **92**, 3869–3873.

Hall, M. C., and Matson, S. W. (1999). Helicase motifs: The engine that powers DNA unwinding. *Mol. Microbiol.* **34**, 867–877.

Hingorani, M. M., Washington, M. T., Moore, K. C., and Patel, S. S. (1997). The dTTPase mechanism of T7 DNA helicase resembles the binding change mechanism of the F1-ATPase. *Proc. Natl Acad. Sci. USA* **94**, 5012–5017.

Kim, D. E., Narayan, M., and Patel, S. S. (2002). T7 DNA helicase: A molecular motor that processively and unidirectionally translocates along single-stranded DNA. *J. Mol. Biol.* **321**, 807–819.

Levin, M. K., and Patel, S. S. (2003). Helicases as molecular motors. In *Molecular Motors* (M. Schliwa, ed.) pp. 179–198. Wiley-VCH Verlag GmbH, Weinheim, Germany.

Lohman, T. M., and Bjornson, K. P. (1996). Mechanisms of helicase-catalyzed DNA unwinding. *Annu. Rev. Biochem.* **65**, 169–214.

Patel, S. S., and Picha, K. M. (2000). Structure and function of hexameric helicases. *Annu. Rev. Biochem.* **69**, 651–697.

Singleton, M. R., Sawaya, M. R., Ellenberger, T., and Wigley, D. B. (2000). Crystal structure of T7 gene 4 ring helicase indicates a mechanism for sequential hydrolysis of nucleotides. *Cell* **101**, 589–600.

Soultanas, P., and Wigley, D. B. (2001). Unwinding the 'Gordian knot' of helicase action. *Trends Biochem. Sci.* **26**, 47–54.

von Hippel, P. H., and Delagoutte, E. (2001). A general model for nucleic acid helicases and their "coupling" within macromolecular machines. *Cell* **104**, 177–190.

Biography

Smita Patel is a Professor in the Department of Biochemistry at the University of Medicine and Dentistry of New Jersey–Robert Wood Johnson Medical School in Piscataway, New Jersey. Research in her laboratory is focused on understanding the mechanisms of enzymes involved in DNA replication and transcription. She holds a Ph.D. from Tufts University and received postdoctoral training at Pennsylvania State University. Her laboratory is continuing to elucidate the mechanisms of DNA and RNA helicases from phage T7 and hepatitis C virus. In addition, she is interested in understanding the mechanism of transcription and its regulation and has elucidated the kinetic pathway of transcription initiation of a DNA-dependent RNA polymerase and the mechanism of open complex formation using transient state kinetic approaches.

DNA Ligases: Mechanism and Functions

Alan E. Tomkinson and John B. Leppard
University of Texas Health Science Center at San Antonio, Institute of Biotechnology, San Antonio, Texas, USA

DNA ligases are involved in DNA replication, genetic recombination, and DNA repair. These enzymes belong to a larger superfamily of nucleotidyl transferases that also includes RNA ligases and mRNA capping enzymes. Specifically, DNA ligases catalyze phosphodiester bond formation at breaks in the phosphate backbone of duplex DNA. The DNA ligase family can be subdivided into two groups based on cofactor specificity. Prokaryotic enzymes use either nicotinamide adenine dinucleotide (NAD) or adenosine triphosphate (ATP) as a cofactor, whereas viral, archael, and eukaryotic DNA ligases use ATP almost exclusively. DNA ligases share a common core catalytic domain, but the regions flanking the core domain are widely divergent. These unique regions mediate the specific participation of DNA ligases in different DNA transactions.

Reaction Mechanism

DNA ligase activity was first identified in 1967 in five different laboratories. In the years that followed, the Lehman laboratory was primarily responsible for elucidating the three-step reaction catalyzed by the NAD-dependent *Escherichia coli* DNA ligase and the ATP-dependent DNA ligase encoded by bacteriophage T4 that is described in this article.

Adenylation

In the first step, DNA ligase reacts with either nicotinamide adenine dinucleotide (NAD) or ATP to form a covalent enzyme—adenosine monophosphate (-AMP) intermediate (Figure 1). The AMP group is linked via a phosphoramidate bond to a conserved lysine residue that defines the active site of the core catalytic domain (Figure 2A). Formation of the enzyme–AMP intermediate induces a conformational change that is required for the recognition of a nicked DNA substrate in the next step.

AMP–DNA Intermediate

The second step in the reaction involves the transfer of the AMP group to the 5′-phosphate terminus at the nick in duplex DNA (Figure 1). The previous step leaves the enzyme in an open conformation that exposes the DNA binding site. Specific amino acid residues in the enzyme coordinate the AMP group such that an oxygen atom of the 5′-phosphate in the DNA substrate can attack the phosphoryl group of AMP, generating a DNA–AMP intermediate.

Phosphodiester Bond Formation

The third and final step of ligation is catalyzed by the nonadenylated form of DNA ligase. In this reaction, esterification of the 5′-phosphoryl group to the 3′-hydroxyl group completes phosphodiester bond formation with the concomitant release of AMP (Figure 1).

Structure

Gene cloning and, more recently, genome sequencing has led to a rapid growth in the number of DNA ligase genes identified. Alignment of DNA ligase amino acid sequences indicates that these enzymes share a conserved catalytic domain (Figure 2A). Furthermore, a comparison with the catalytic domains of mRNA capping enzymes revealed the presence of six conserved motifs (I, III, IIIa, IV, V, VI) that are characteristic of nucleotidyl transferases. In recent years, our understanding of how the DNA ligase catalytic domain catalyzes DNA joining has been advanced by a combination of approaches that include the use of site-directed mutagenesis to elucidate the role of individual amino acids within the catalytic domain and the determination of the three-dimensional structure of several DNA ligases by X-ray crystallography.

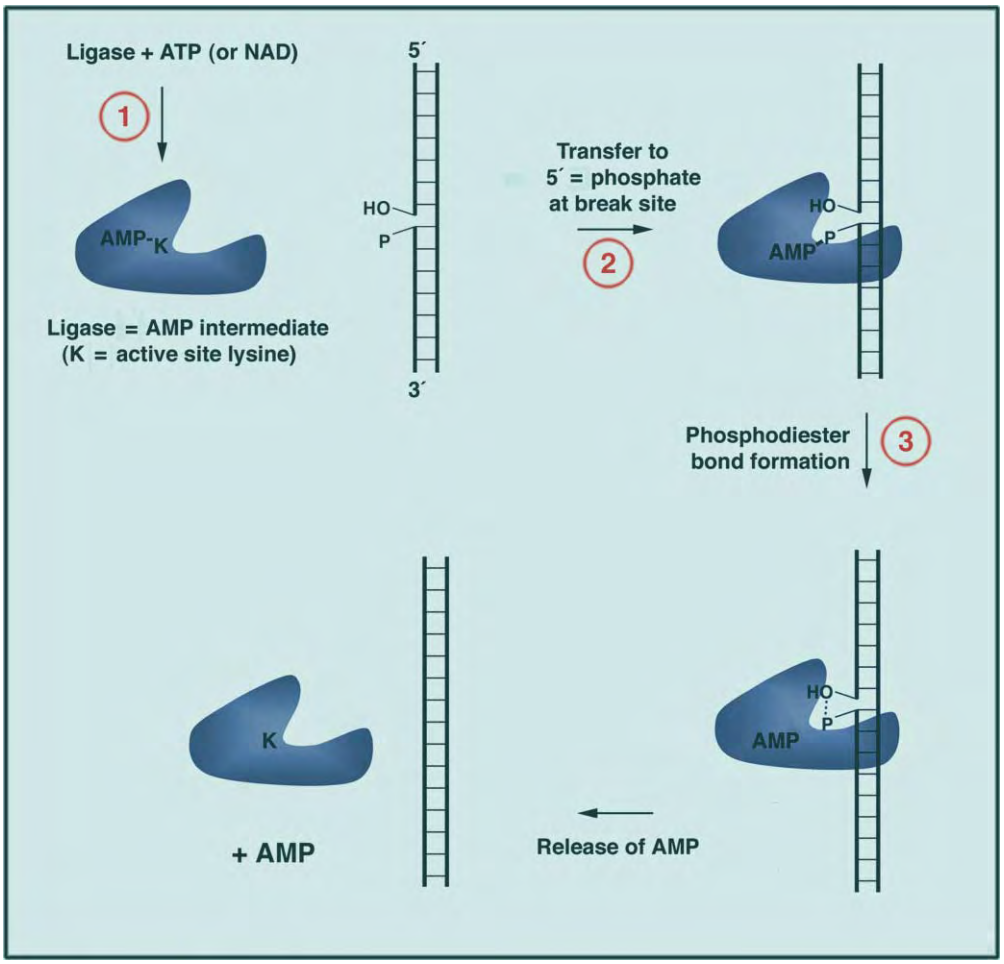

FIGURE 1 Mechanism of phosphodiester bond formation by DNA ligase. Step 1, DNA ligase interacts with ATP or NAD, forming a covalent enzyme–AMP intermediate. Step 2, after nick recognition, the AMP group is transferred to the 5′-phosphate terminus, forming a high-energy phosphate bond. Step 3, DNA ligase catalyzes phosphodiester bond formation, releasing AMP.

Crystal Structures

X-ray crystallographic studies of both NAD- and ATP-dependent DNA ligases have provided important insights into the three-dimensional structure of these enzymes. In 1996, the Wigley laboratory solved the first crystal structure of an ATP-dependent DNA ligase, the bacteriophage T7 DNA ligase, in a complex with ATP. More recently, the structure of the enzyme–AMP intermediate formed by the *Chlorella* virus DNA ligase was determined by the Shuman laboratory. A comparison of these structures revealed a conformational change in the DNA ligase catalytic domain that allows binding to nicked DNA. The structures of the ATP-dependent DNA ligases together with those of NAD-dependent enzymes such as *Thermus filiformis* DNA ligase (Figure 2B) and other members of the nucleotidyl transferase superfamily represent snapshots of this family of enzymes at different stages of the catalytic cycle. Thus, they provide a framework for understanding the dynamic conformational changes that occur when nucleotidyl transferases interact with their nucleotide cofactor and polynucleotide substrate.

Domains Constituting the Core Catalytic Domain

There are two subdomains known as the adenylation domain and the oligomer-binding (OB) fold (Figure 2A) within the DNA ligase catalytic domain. The larger adenylation domain is the minimum region required for formation of an enzyme–AMP intermediate, whereas the OB fold allows the enzyme to bind to DNA and coordinates the ligation event. Residues from motifs I through V line a cleft formed between the two subdomains to generate a positively charged nucleotide-binding pocket. The active-site lysine residue, which is contained within motif I, sits at the bottom of the cleft close to where the adenylation domain and the OB fold are linked. In the nonadenylated form, the enzyme is in an open conformation with the DNA-binding surface of

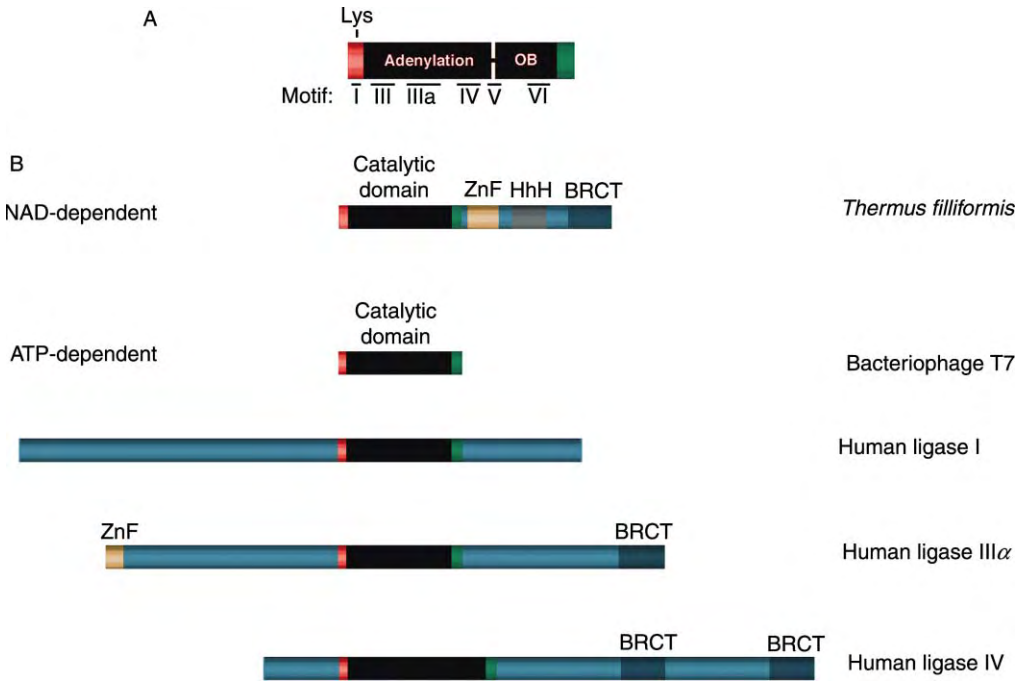

FIGURE 2 (A) Schematic representation of the core catalytic domain shared by all DNA ligases. (B) Comparison of a prokaryotic NAD-dependent DNA ligase (*Thermus filiformis*) and ATP-dependent DNA ligases from virus (bacteriophage T7) and humans (DNA ligases I, IIIα, and IV). BRCT, BRCA1 C-terminus domain; HhH, helix–hairpin–helix domain; Znf, zinc-finger motif.

the OB fold rotated away from the active site, thus preventing nonproductive DNA binding. Upon adenylation, the enzyme undergoes a conformational change such that the DNA binding surface of the OB fold faces in toward the cleft, making the active site accessible.

Other Common Domains of NAD-Dependent DNA Ligases

NAD-dependent DNA ligases are relatively uniform in size (~70 kDa). In addition to the adenylation domain and OB fold, they contain several other common motifs (Figure 2B) that are thought to mediate protein–DNA and protein–protein interactions. The zinc-finger (ZnF) and helix–hairpin–helix (HhH) motifs confer DNA binding activity. The BRCT domain, which was first identified in the breast cancer susceptibility gene 1, is probably involved in protein–protein interactions that recruit the enzyme to its site of action.

Sequences Flanking the Core Catalytic Domain of ATP-Dependent DNA Ligases

Unlike NAD-dependent ligases, ATP-dependent DNA ligases are heterogeneous in size (40–125 kDa) (Figure 2B). The amino acid residues that flank the catalytic domain of ATP-dependent DNA ligases contain a wide variety of sequences that mediate specific protein–protein interactions and protein–DNA interactions (Figure 2B). Intriguingly, recent sequencing studies have identified open reading frames in bacterial genomes whose sequences suggest that ATP-dependent DNA ligase activity may reside in the same polypeptide as nuclease and primase activities.

Biological Functions

The notion that cells may contain more than one species of DNA ligase was based on initial studies in the Lindahl laboratory describing the properties of various species of DNA ligase in mammalian cell extracts. These biochemical studies led to the cloning of three mammalian genes, *LIG1*, *LIG3*, and *LIG4*, that encode DNA ligases (Table I). More recent genome sequencing has led to the identification of additional DNA ligase genes in organisms such as *S. cerevisiae* and *E. coli* that were thought to have only a single DNA ligase gene. Because DNA joining is required to complete DNA replication, DNA repair, and genetic recombination, it appears likely that the multiple species of DNA ligase have evolved to participate in specific DNA transactions. Insights into the biological functions of the various DNA ligases have been obtained by examining the phenotype of DNA ligase-deficient cells and by identifying protein partners of the DNA ligases (Table I).

TABLE I

Mammalian DNA Ligases[a]

Gene	Gene product	Interacting protein	Function
LIG1	DNA ligase I	PCNA, Polβ	DNA replication, BER, NER, recombination
LIG3	DNA ligase IIIα (nuclear)	XRCC1	Single-strand break repair, BER
	DNA ligase IIIα (mitochondrial)	?	Single-strand break repair, BER?
	DNA ligase IIIβ	?	Postmeiotic repair?, meiotic recombination?
LIG4	DNA ligase IV	XRCC4	NHEJ, V(D)J recombination

[a] BER, base excision repair; NER, nucleotide excision repair; NHEJ, nonhomologous end-joining; PCNA, proliferating cell nuclear antigen; XRCC1, XRCC4, X-ray cross complementing factor 1 and factor 4.

DNA Replication

The ability to make a copy of their genetic information is essential for all organisms. During DNA replication, DNA joining events are required to link together DNA intermediates known as Okazaki fragments that are generated by discontinuous DNA synthesis on the lagging strand at the replication fork. As expected, inactivation of genes encoding replication proteins, including the replicative DNA ligase, results in cell lethality. Because DNA replication involves the coordinated actions of many different proteins, it seems reasonable to assume that the DNA ligase involved in DNA replication will interact with one or more of the other replication proteins. In mammalian cells, proliferating cell nuclear antigen (PCNA), a homotrimeric ring-shaped clamp protein that was identified as an accessory factor of the replicative DNA polymerase, specifically interacts with the N-terminal region of DNA ligase I. This interaction is critical for the recruitment of DNA ligase I to the sites of DNA replication and for the efficient joining of Okazaki fragments. A similar protein–protein interaction occurs in *E. coli* between the NAD-dependent DNA ligase and β-clamp, the functional homologue of PCNA, indicating that the interaction between the replicative DNA ligase and the clamp protein is conserved in prokaryotic and eukaryotic DNA replication.

DNA Excision Repair

Exposure to endogenous DNA-damaging agents such as reactive oxygen species and exogenous DNA-damaging agents such as ultraviolet light results in damage to the nitrogenous bases of DNA. In addition, the DNA replication machinery makes errors that result in mispaired or unpaired nucleotides. Damaged and mispaired nucleotides are removed from the genome by excision repair pathways that share three common steps: (1) excision of the damaged or mispaired DNA, (2) gap-filling DNA synthesis using the undamaged strand as template, and (3) DNA ligation to complete the repair.

The pathways for the repair of damaged bases can be divided into two types based on whether the damage is removed as a nitrogenous base, base excision repair (BER), or as a nucleotide, nucleotide excision repair (NER). In mammalian cells, there are two subpathways of BER, long patch and short patch, that appear to involve two different DNA ligases. Short-patch BER events are mostly completed by DNA ligase IIIα in a complex with its partner protein X-ray cross complementing factor 1 (XRCC1), whereas long-patch BER is completed by DNA ligase I. NER events are probably completed by DNA ligase I.

In DNA mismatch repair, specific protein factors recognize the mispaired or unpaired nucleotides and direct the excision proteins to the newly synthesized strand. After the removal of a section of newly synthesized DNA containing the mispaired or unpaired nucleotides, the resultant single-strand gap is filled in by a DNA polymerase and repair is completed by a DNA ligase, presumably DNA ligase I.

Genetic Recombination and Recombinational Repair

Genetic recombination is the major process by which diversity is generated in living organisms. In mammals, exchanges between homologous chromosomes that occur during meiosis contribute to the generation of genetically diverse gametes. It is assumed that DNA ligase I, the replicative DNA ligase, also completes the meiotic recombination events. However, in vertebrates, there is a germ-cell-specific isoform of DNA ligase III, DNA ligase IIIβ, that may also participate in the completion of meiotic recombination. Alternatively, DNA ligase IIIβ may function in DNA transactions in haploid gametes.

Recombination pathways are also critical for the maintenance of genome stability in somatic cells, in particular for the repair of DNA double-strand breaks. This lesion presents a difficult challenge because both strands of the DNA duplex are broken. Recombinational repair pathways can be divided into two types

based on whether they are dependent on DNA sequence homology or not. It is generally assumed that homology-dependent recombinational repair pathways, in particular those involving sister chromatids, are completed by DNA ligase I. In the non-homology-directed repair pathways, the ends of broken DNA molecules are simply brought together by DNA end-bridging factors, processed, and then ligated. Surprisingly, this inaccurate repair pathway, which can result in a wide spectrum of genetic alterations ranging from small deletions to chromosomal translocations, makes a major contribution to the repair of DNA double-strand breaks in mammalian cells. Genetic and biochemical studies have shown that this so-called nonhomologous end-joining (NHEJ) is dependent on DNA ligase IV and its partner protein XRCC4. The same DNA ligase IV/XRCC4 complex is also required for the completion of *** V(D)J recombination, a site-specific recombination mechanism that is required for the rearrangement of immunoglobulin genes to develop a diverse repertoire of antibodies and T-cell receptors.

Mitochondrial DNA Metabolism

The DNA transactions just described occur in the nucleus. However, the eukaryotic organelles, mitochondria and chloroplasts, contain their own genetic information that must be replicated and repaired. Studies in the Campbell laboratory have shown that nuclear and mitochondrial forms of DNA ligase III are generated by translation initiation at different sites within the same open reading frame encoded by DNA ligase IIIα mRNA. Although the yeast *S. cerevisiae* lacks a homologue of the *LIG3* gene, it uses the same mechanism to generate mitochondrial and nuclear forms of the Cdc9 DNA ligase.

Concluding Remarks

Although the basic reaction mechanism catalyzed by DNA ligases was elucidated over 30 years ago, the recent determination of the three-dimensional structure of both NAD- and ATP-dependent DNA ligases has provided exciting new molecular insights into this reaction mechanism. However, structures of DNA ligases interacting with their DNA substrate are needed for a better understanding of the final two steps of the ligation reaction. Because DNA strand breaks are a common intermediate in many different DNA transactions, the study of DNA ligases by genetic and biochemical approaches will continue to provide information about the molecular mechanisms of DNA replication, DNA repair, and genetic recombination. Finally, mutations in DNA ligase genes have been associated with human diseases, highlighting the importance of these enzymes.

See Also the Following Articles

DNA Base Excision Repair • DNA Ligases: Structures • DNA Mismatch Repair in Bacteria • DNA Mismatch Repair in Mammals • DNA Replication: Eukaryotic Origins and the Origin Recognition Complex • DNA Replication: Initiation in Bacteria • DNA Replication, Mitochondrial • Recombination-Dependent DNA Replication

Glossary

adenylation The reaction in which DNA ligase interacts with ATP or NAD to form a covalent enzyme–adenylate complex.

motif An amino acid sequence found to be conserved in various proteins.

phosphodiester bond Bond that links deoxynucleotides in DNA, forming the sugar phosphate backbone of the DNA polymer.

phosphoramidate bond The covalent bond formed between a phosphoryl group and an amino group. For DNA ligases, the phosphoryl group of AMP is linked to the amino group of the active-site lysine.

Further Reading

Doherty, A. J., and Suh, S. W. (2000). Structural and mechanistic conservation in DNA ligase. *Mutat. Res.* **28**, 4051–4058.

Lehman, I. R. (1974). DNA ligase: Structure, mechanism and function. *Science* **186**, 790–797.

Lindahl, T., and Barnes, D. E. (1992). Mammalian DNA ligases. *Annu. Rev. Biochem.* **61**, 251–281.

Shuman, S. (1996). Closing the gap on DNA ligase. *Structure* **4**, 653–658.

Timmons, D. J., Singleton, M. R., and Wigley, D. B. *Mutat. Res.* **460**, 301–318.

Tomkinson, A. E., and Mackey, Z. B. (1998). Structure and function of mammalian DNA ligases. *Mutat. Res.* **407**, 1–9.

Biography

Alan Tomkinson is a Professor in the Department of Molecular Medicine at The University of Texas Health Science Center at San Antonio. His research focuses on the function of eukaryotic DNA ligases in DNA replication, DNA repair, and genetic recombination. He holds a Ph.D. from the University of Newcastle upon Tyne, UK, and received postdoctoral training at the University of California, Berkeley, and the Imperial Cancer Research Fund, UK.

DNA Ligases: Structures

C. Kiong Ho
State University of New York, Buffalo, New York, USA

Mark Odell
University of Westminster, London, UK

Dimitar B. Nikolov
Memorial Sloan-Kettering Cancer Center, New York, USA

DNA ligases are enzymes that catalyze the formation of phosphodiester bonds at the site of DNA nicks or breaks. They are responsible for maintaining the continuity of DNA, which is of paramount importance for the survival of all organisms. While many different safeguards exist to repair DNA damage and to accurately replicate or recombine DNA, they all share a common, final procedure, the ligation of DNA. The fundamental nature of this process explains why the DNA ligase family of enzymes is represented in all cellular organisms and in a number of DNA virus genomes. High-resolution crystal structures of DNA ligases and important reaction intermediates illuminate the mechanism of covalent catalysis and provide a framework for understanding the results of preceding investigations of ligase biochemistry.

Introduction

The copying and maintenance of the genetic material takes place through the processes of DNA replication, repair, and recombination. In all cases, the final step in these fundamental cellular processes is the sealing of the DNA strands to maintain their fidelity. DNA ligases catalyze the formation of phosphodiester bonds at the site of DNA nicks or breaks via three sequential nucleotidyl transfer steps. In the first step, the enzyme reacts with a high-energy cofactor (ATP or NAD^+) to form a covalent ligase-AMP intermediate with a release of pyrophosphate or nicotinamide mononucleotide. In the second step, the ligase-AMP binds a DNA nick and the AMP moiety is transferred from the enzyme to the 5′ phosphate terminated DNA molecule. The resulting stable DNA adenylate has an inverted 5′–5′ pyrophosphate bridge structure, AppDNA. In the final step, the ligase catalyzes the nucleophillic attack by the 3′ hydroxyl group present on the juxtaposed nucleotide of the discontinuous strand, resulting in closure of the gap between the two polynucleotides and release of AMP.

The ATP-dependent ligases and the GTP-dependent capping enzymes are defining members of the superfamily of the covalent nucleotidyltransferases. The first two steps of DNA ligation are analogous to the steps of GTP-dependent mRNA capping that result in guanylate RNA (GpppRNA). The lysine residue located within a conserved Lys-X-Asp-Gly-X-Arg element (named motif I) is the site of covalent linkage of AMP to the ligase and of GMP to the capping enzyme. In addition to this sequence, the members of this enzyme superfamily share five other conserved regions, referred to as motifs III, IIIa, IV, V, and VI. The numbering corresponds to the position within the primary sequence, with motif I being the most proximal to the protein amino terminus, and motif VI to the carboxy terminus. Mutational analysis of the residues within these motifs has documented their essential role in the catalytic activity of both ligases and capping enzymes.

The multi-step, nucleotidyltransferase reactions are catalyzed by single enzymes, which suggests that these proteins undergo dynamic conformational changes to accommodate the distinct substrates utilized at each step. Crystal structures of a number of ATP- and NAD^+-dependent ligases, as well as the related mRNA capping enzymes, at intermediate steps along the reaction coordinate have provided insights into the catalytic mechanism of the enzymes.

Overall Structure of DNA Ligases

DNA ligases are grouped into two families according to their high-energy cofactor requirements for either ATP or NAD. Those utilizing ATP are more widely distributed and are present in eubacteria, bacteriophages, archaebacteria, eukaryotes, and eukaryotic viruses. They vary in size between the 268 amino acid enzyme of *Haemophilus influenzae* and the larger cellular ligases of vertebrates, which are 912 and 844 amino

acids, respectively, for the human DNA ligase I and IV enzymes. The first reported three-dimensional structure of an ATP-dependent DNA ligase was that of the bacteriophage T7 enzyme, followed by the structure of the eukaryotic DNA ligase from the *Paramecium Bursari Chlorella Virus*, the smallest known (298 residues) eukaryotic ATP-dependent ligase. In addition, the structures of the GTP-dependent mRNA capping enzymes from *Chlorella* virus and *Candida albicans* were also determined. These studies reveal a common molecular architecture of the ligases and capping enzymes, with a large amino-terminal domain (domain 1) and a smaller carboxy-terminal domain (domain 2) separated by a deep cleft. The amino-terminal domain 1 of the *Chlorella* virus ligase consists of two twisted antiparallel β-sheets packing against six α-helices. This domain contains the nucleotide-binding site, which is generated by the spatial approximation of five of the six conserved nucleotidytransferase motifs (I, III, IIIa, IV, and V), and is located between the two β-sheets. The carboxy-terminal domain 2 contains an antiparallel β-sheet and a α-helix and folds into an OB-fold, commonly found in nucleic acid-binding proteins. The sixth nucleotidyltransferase motif (motif VI), which is required for covalent enzyme-nucleotide monophosphate (enzyme-NMP) formation, is located within domain 2 in both the ATP-dependent ligases and the mRNA capping enzymes. The conserved spatial arrangement of critical residues and functional groups in the two enzyme classes suggests a common ancestral protein from which the two enzymatic lineages have descended.

Analysis of the structures presented in Figure 2 demonstrates that the *Chlorella* ligase represents the core catalytic element found in all nucleotidyltransferase enzymes. The sequence alignment of known DNA ligases reveals that in addition to this more conserved core element, most members of this enzyme family contain a variety of amino- and carboxy-terminal sequence motifs and domains, which are likely to mediate interactions with other proteins that participate in DNA replication and repair (illustrated in Figure 1). Mammals encode for four distinct DNA ligases (I, IIIα, IIIβ, and IV). Ligase I contains a proliferating cell nuclear antigen (PCNA) binding motif, which likely functions to coordinate protein-protein interactions at the DNA replication fork. The DNA ligase III gene encodes for two isoforms, IIIα and IIIβ, which are produced by alternative splicing and are found in the nucleus and the mitochondria, respectively. Both ligase III isoforms harbor a putative zinc-finger motif, which could facilitate the DNA-enzyme interactions. In addition, the larger ligase IIIα isoform contains a carboxy-terminal BRCT domain that interacts with XRCC1, a multi-domain protein implicated in base excision-repair. Ligase IV possesses two BRCT domains, and the region between them was shown to bind the repair factor XRCC4 that functions in V(D)J recombination and nonhomologous end joining.

The NAD-dependent DNA ligases are found exclusively in eubacteria, and have a relatively conserved length and sequence. The crystal structures of the NAD-dependent ligase from the thermophilic bacterium *Thermus filiformi* and of the adenylation domain of the *Bacillus stearothermophilus* ligase have been determined. The *T. filiformi* structure documents that the protein contains four discrete domains. Domains 1 and 2 are analogous both in structure and function to

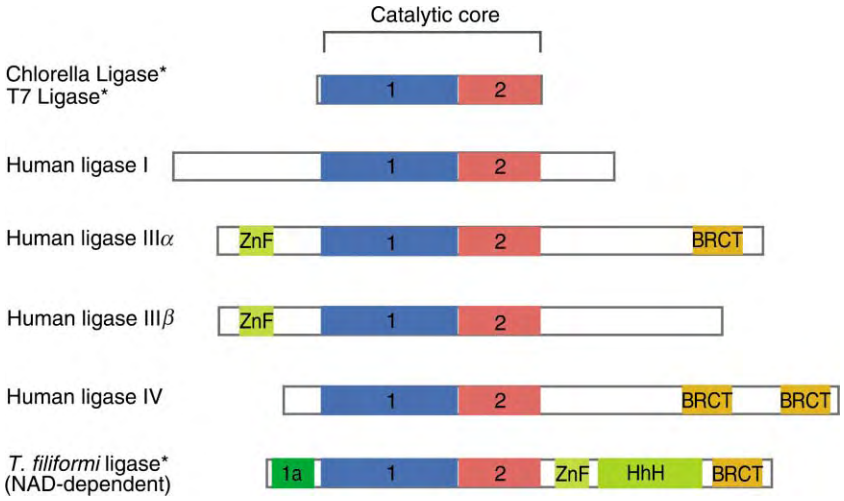

FIGURE 1 Schematic representation of the domain architecture of known DNA ligases. The domains are color-coded. The asterisk indicates that the high-resolution structure is known. The catalytic core consists of two subdomains: 1 (adenylation), blue; and 2 (oligonucleotide-binding or OB), red. In addition to the catalytic core, some DNA ligases contain other domains and/or motifs, such as zinc fingers (ZnF), helix–hairpin–helix (HhH), and BRCT. Many NAD-dependent DNA ligases also have a small amino-terminal helical subdomain (1a).

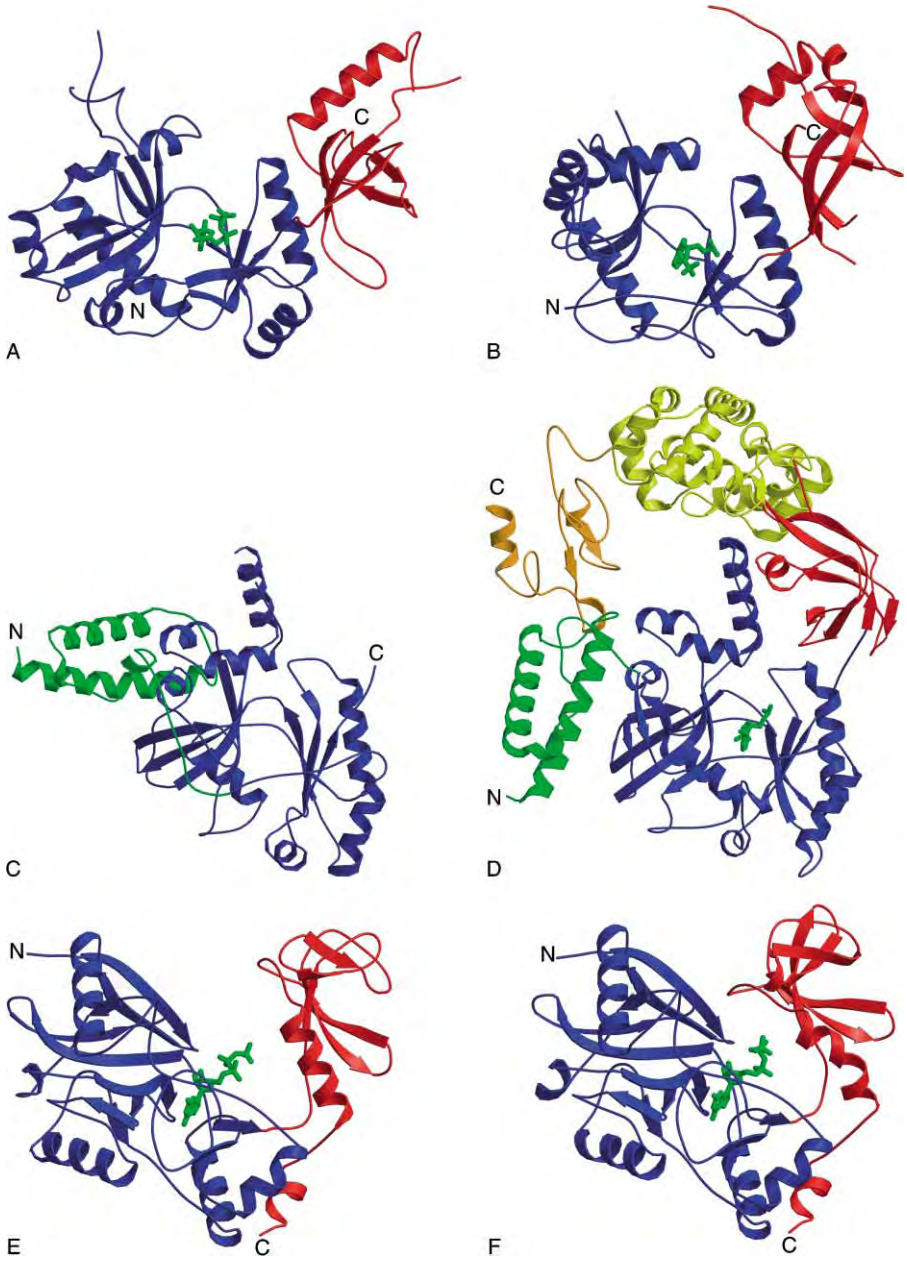

FIGURE 2 Structures of DNA ligases and the related capping enzymes. The structural domains are color-coded as in Figure 1. The protein amino and carboxy termini are indicated. Bound nucleotides in the active sites are in green. (A) The ATP-dependent DNA ligase of bacteriophage T7, PDB-ID: 1AOI. (B) The ATP-dependent *Chlorella* virus DNA ligase, PDB-ID: 1FVI. (C) The adenylation domain (domain 1) of NAD-dependent DNA ligase from *B. stearothermophilus*, PDB-ID: 1BO4. (D) The NAD-dependent DNA ligase from *T. filiformis*, PDB-ID: 1DGS, 1DGT. (E) *Chlorella* virus capping enzyme open conformation. (F) *Chlorella* virus capping enzyme closed conformation, PDB-ID: 1CKM, 1CKN.

the two catalytic domains of the ATP-dependent enzymes (Figures 1 and 2). Within this region, the five amino-terminal nucleotidyltransferase motifs adopt nearly identical spatial organization to their ATP-dependent counterparts. Domain 1 of the NAD-dependent DNA ligases contains an additional amino-terminal α-helical subdomain 1a, which may participate in the recognition and binding of the second nicotinamide mononucleotide moiety of NAD^+. Interestingly, domain 2 of the NAD-dependent DNA ligases lacks the motif VI sequence, but still adopts an OB-fold similar to that of the T7 and *Chlorella* ligases. Domain 3 is unique for the NAD-dependent DNA ligase subfamily, and is predicted to be involved in nonsequence-specific DNA binding. It contains a four-cysteine zinc finger and four helix-hairpin-helix (HhH) motifs, which fold around each other to form a compact three-dimensional structure. The carboxy-terminal domain 4 has a BRCT motif similar to those present in mammalian ligases III and IV.

The Nucleotide-Binding Pocket

The structure of the T7 DNA ligase with bound ATP (Figure 2A) reflects the state of the enzyme prior to the first chemical step of nucleotidyl transfer. The ATP is located in a hydrophobic pocket of the active site with the adenosine base adopting a *syn* conformation relative to the sugar (Figure 3A). The active site lysine (Lys-34) in motif I is positioned close to the α-phosphate of the ATP molecule, marking the future site of the covalent AMP-enzyme adduct. Arg-39 in motif I is hydrogen-bonded to the 3′ oxygen of the ribose sugar. Motif III contains two acidic residues, Asp-91 and Glu-93. Asp-91 forms a salt bridge with Arg-39 in motif I, while Glu-93 is hydrogen-bonded to the ribose oxygen at the 2′ position. Two positively charged residues in motif V, Lys-232 and Lys-238, are positioned close to the γ- and β-phosphate groups and stabilize the negative charges on the ATP molecule. The aromatic residue Try-149 in motif IIIa stacks against the purine ring of ATP, positioning the adenine base in an optimal orientation for catalysis. The key residues involved in nucleotide binding are conserved both in the ATP- and in the NAD-dependent DNA ligases (as well as in the capping enzymes) and perform similar catalytic functions as visualized in the corresponding *Chlorella* ligase-AMP and *T. filiformi* ligase-AMP structures, suggesting that the reaction mechanism is conserved throughout evolution.

The *Chlorella* ligase–AMP structure reveals that the adenosine-binding pocket is remodeled upon covalent ligase-adenylate complex formation. In contrast to the *syn* conformation of the ATP adenosine bound in the active site of the T7 ligase, the adenosine nucleoside present in the *Chlorella* ligase–AMP complex is in the *anti* conformation (Figure 4A). As a consequence, the contacts between the enzyme and the ribose oxygen are altered during enzyme-adenylate complex formation. The arginine in motif I forms a hydrogen bond to the ribose 2′ oxygen, rather than the 3′ oxygen, while the glutamate side chain in motif III no longer contacts the ribose sugar, leaving the 3′ oxygen without any direct contacts with the protein. The observation that both the *C. albicans* capping enzyme-GMP and NAD-dependent *T filiformi* ligase-AMP (Figure 3B) intermediates adopt an *anti* conformation suggests that the change in conformation from *syn* to *anti* during enzyme-NMP formation is a general feature of the nucleotidyltransferase superfamily. The wider implication of this structural rearrangement is that the ribose 3′ oxygen is free to directly coordinate the 5′ nucleotide phosphate group of the nucleic acid substrate.

Mechanism of Nucleotidyl Transfer

The first direct evidence for conformational change during the covalent enzyme–NMP complex formation was evinced by crystal structures of two distinct conformations of the *Chlorella* virus mRNA capping enzyme bound to GTP. The two states are referred to as "open" and "closed" capping enzyme-GTP complexes (Figures 2E and 2F). The open conformation corresponds to the enzyme making an initial or transient contact with GTP. The closed complex structure represents the conformation in which the enzyme is stably bound to GTP, and is committed to the nucleotidyl transfer reaction. The two structural forms differ in the relative position of domain 2 with respect to the GTP-binding pocket: in the open complex, the cleft between the domains is wider and as a result the residues within motif VI are unable to make direct contact with GTP. In the closed complex structure, the positively charged amino acids in motif VI make direct contact with the β- and γ-phosphates of GTP, suggesting that these conserved residues function to facilitate the release of pyrophosphate after the formation of the lysyl–NMP

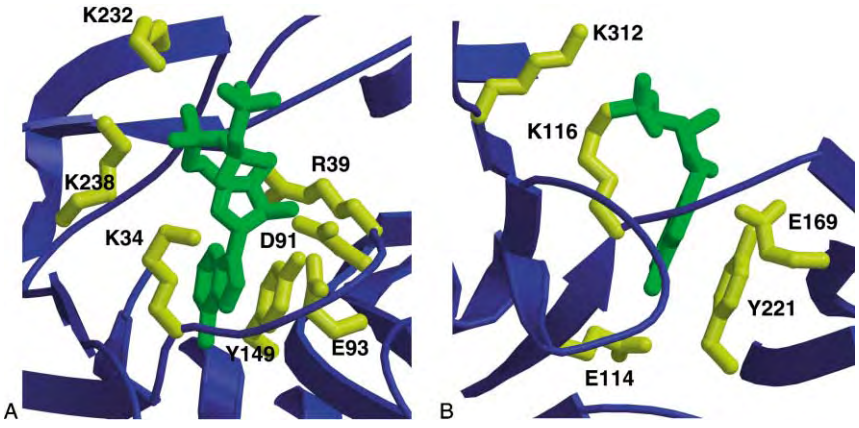

FIGURE 3 The nucleotide-binding pocket of DNA ligases. The ligase adenylation domain (domain 1) is in blue; the side chains of important residues (discussed in the text) are in yellow; and the bound nucleotide is in green. (A) ATP bound in the active site of the bacteriophage T7 DNA ligase. (B) AMP covalently bound to the active-site lysine of the NAD-dependent *T. filiformis* DNA ligase.

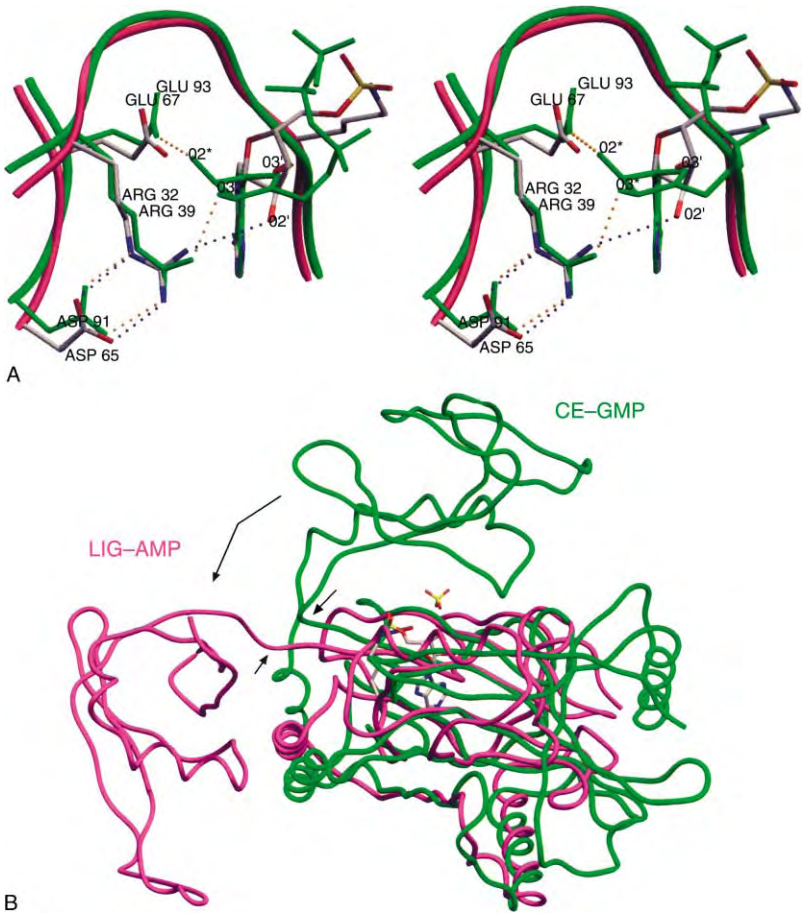

FIGURE 4 Conformational changes in DNA ligases during catalysis. (A) Remodeling of the adenosine-binding pocket after ligase–adenylate formation. Stereoview of the nucleotide-binding pocket of *Chlorella* ligase (purple, with side chains in CPK) highlighting interactions of motif I and III side chains with the ribose sugar of the lysyl-adenylate adduct. The superimposed equivalent structural elements of the T7 ligase–ATP complex are in green. Hydrogen bonds are denoted by dashed lines. (B) Comparison of the *Chlorella* virus ligase (purple) and capping enzyme (green) structures. The structures are superimposed with reference to the nucleotide-binding pocket of domain 1. The lysyl–AMP adduct and the sulfate in the ligase are shown. The guanylate and a sulfate are similarly positioned in the capping enzyme structure. The figure highlights the large movement of domain 2 from the closed state (capping enzyme) to the wide-open conformation (ligase) that exposes a DNA-binding surface. The principal flexion points within the inter-domain linkers (in motif V) are indicated by the short arrows. Reproduced with permission from Odell, M., Sriskanda, V., Shuman, S., and Nikolov, D. B. (2000). Crystal structure of eukaryotic DNA ligase–adenylate illuminates the mechanism of nick sensing and strand joining. *Mol. Cell.* **6**, 1183–1193 with permission from Elsevier.

covalent complex. The requirement of the equivalent motif VI residues in the ATP-dependent ligases for enzyme activity strongly suggests that they undergo a similar conformational change during the first step of the reaction.

While the structure of a ligase bound to DNA has yet to be determined, the ligase-AMP structures of the *Chlorella* virus DNA ligase provide valuable insight into the mechanism of nicked duplex DNA recognition. Occupation of the adenylate binding site is known to be crucial to nick recognition, and in this "DNA-binding-competent" state, domain 2 of the *Chlorella* ligase-AMP complex is pivoted away from domain 1 via a bending in the flexible inter-domain linker region (Figure 4B). The cleft between domains 1 and 2 is substantially wider than in the open complex form of the capping enzyme-GTP complex, and this ligase-adenylate structure is therefore referred to as the "wide-open" complex. The "wide-open" conformation is proposed to expose the DNA-binding surface on domain 1 allowing the 5′ phosphate of the nicked DNA substrate to make direct contact with the adenylation site on the enzyme. Analysis of the surface properties of the *Chlorella* ligase further suggests that the ligase–AMP is ready to bind DNA. In this conformation the electrostatically positive surface of domain 1 favors interaction with the negatively charged phosphodiester backbone of DNA. The relatively flat surface of the ligase molecule (Figure 4B) could allow direct interactions with one face of the DNA double helix. The remodeling of the active site leaves the 3′ oxygen of the ribose sugar free to participate directly in the coordination of

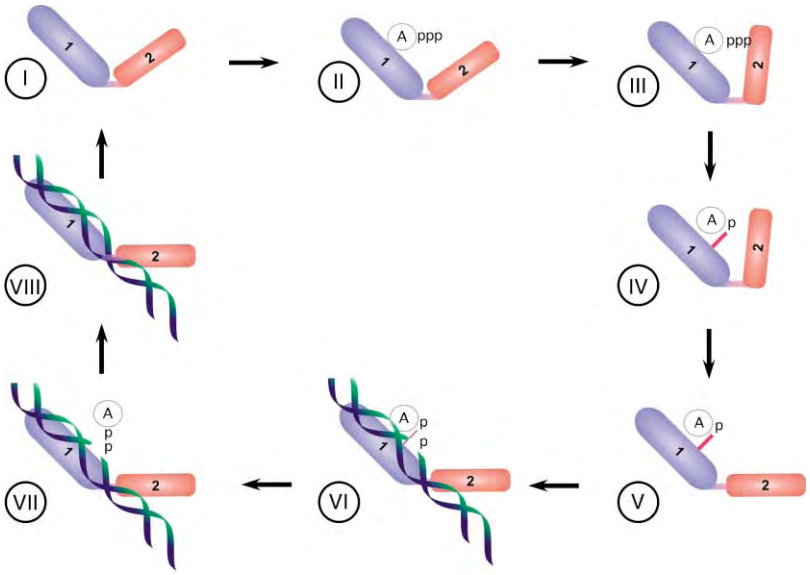

FIGURE 5 Schematic model of ATP-dependent DNA ligation showing the individual catalytic steps and the corresponding conformational changes in the enzyme. Only the catalytic core (domains 1 and 2) of the DNA ligase is shown. See text for details.

the 5′ phosphate of the DNA substrate. This indicates that only catalytically licensed forms of DNA ligases will be able to stably interact with a nicked DNA substrate. The structural data also suggest that domain 2 might not directly participate in the subsequent catalytic events that result in the adenylation of DNA (step 2) and in phosphodiester bond formation (step 3).

A model of ATP-dependent ligation consistent with the known ligase and capping enzyme structures is shown in Figure 5. Specifically, the structural data support a common mechanism of catalysis by nucleotidyltransferases that is carried out through a series of conformational changes induced by substrate binding. In the first step, the energy cofactor, ATP, binds to the open form of enzyme (state I on Figure 5). The binding of this substrate and/or of a divalent cation promotes domain closure, bringing the positively charged residues of the OB-fold into direct contact with the pyrophosphate leaving group (II and III). As a result of the structural rearrangement, the active site lysine is positioned to make an in-line attack on the α-phosphate of the ATP (III). The following formation of the ligase-AMP complex is accompanied by release of pyrophosphate (IV). The ligase undergoes a transition from a "closed" (IV) to a "wide-open" complex (V). This transition is an example of ping-pong kinetics where the active site is initially modified by the first substrate (ATP) to permit recognition of the second substrate (DNA). While structures of DNA ligases in complex with DNA are not yet reported, it is hypothesized that the wide-open complex would allow the nicked duplex DNA to be recognized and bound by the positively charged surface on the nucleotidyltransferse domain 1 (VI) and stabilized by bonding of the 5′ phosphate of DNA by the 3′ oxygen of the NMP sugar moiety, facilitating the transfer of AMP to the 5′-phosphate terminated DNA strand (VII). Once the DNA-adenylate is formed, the enzyme remains bound to the activated nick and catalyzes its sealing via an attack of the 3′ OH on the 5′ adenylated DNA, producing a phosphodiester linkage with the concomitant release of AMP (VIII). It should be emphasized that this model is consistent with ligation of a single nick in an otherwise duplex DNA molecule. The ligation of double-stranded DNA breaks is catalyzed by the mammalian DNA ligase IV, and requires additional proteins to stabilize the free DNA ends. The functional catalytic complex in this case may contain two molecules of DNA ligase, each sealing a single DNA strand.

See Also the Following Articles

ATP Synthesis in Plant Mitochondria: Substrates, Inhibitors, Uncouplers • DNA Ligases: Mechanism and Functions

Glossary

ATP Adenosine triphosphate. An adenosine-containing nucleotide that harbors high-energy phosphate bonds and is used to transport energy to cells for biochemical processes through its hydrolysis.

covalent nucleotidyltransferase Enzyme that reacts with nucleotides and transfers the nucleoside moiety to an acceptor molecule

through the formation of a covalent nucleoside monophosphate (NMP)-enzyme intermediate.

mRNA cap Structure found at 5′ end of the eukaryotic mRNAs, consists of 7-methylguanosine linked to the end of the transcript via a 5′–5′ triphosphate bridge (m7GpppN). The cap structure enhances mRNA stability, splicing of pre-mRNAs, and initiation of protein synthesis.

NAD Nicotinamide adenine dinucleotide (oxidized form). A coenzyme present in all cells that assists enzymes by accepting electrons during metabolic reactions. Acts as an energy donor in bacteria by virtue of a high-energy P–P bond.

Further Reading

Cherepanov, A. V., and de Vries, S. (2002). Dynamic mechanism of nick recognition by DNA ligase. *Eur. J. Biochem.* **269**, 5993–5999.

Doherty, A. J., and Suh, S. W. (2000). Structural and mechanistic conservation in DNA ligases. *Nucleic Acids Res.* **28**, 4051–4058.

Hakansson, K., Doherty, A. J., Shuman, S., and Wigley, D. B. (1997). X-ray crystallography reveals a large conformational change during guanyl transfer by mRNA capping enzymes. *Cell* **89**, 545–553.

Lee, J. Y., Chang, C., Song, H. K., Moon, J., Yang, J. K., Kim, H. K., Kwon, S. T., and Suh, S. W. (2000). Crystal structure of NAD(+)-dependent DNA ligase: Modular architecture and functional implications. *EMBO J.* **19**, 1119–1129.

Odell, M., Sriskanda, V., Shuman, S., and Nikolov, D. B. (2000). Crystal structure of eukaryotic DNA ligase–adenylate illuminates the mechanism of nick sensing and strand joining. *Mol. Cell.* **6**, 1183–1193.

Shuman, S. (1996). Closing the gap on DNA ligase. *Structure* **4**, 653–656.

Subramanya, H. S., Doherty, A. J., Ashford, S. R., and Wigley, D. B. (1996). Crystal structure of an ATP-dependent DNA ligase from bacteriophage T7. *Cell* **85**, 607–615.

Timson, D. J., Singleton, M. R., and Wigley, D. B. (2000). DNA ligases in the repair and replication of DNA. *Mutat. Res.* **460**, 301–318.

Tomkinson, A. E., and Mackey, Z. B. (1998). Structure and function of mammalian DNA ligases. *Mutat. Res.* **407**, 1–9.

Biography

C. Kiong Ho is an Assistant Professor in the Department of Biological Sciences at the State University of New York, Buffalo. His laboratory is taking a molecular and biochemical approach to study mRNA processing events (mRNA capping and RNA editing) in parasitic protozoa.

Mark Odell studied DNA ligase enzymology for his doctorate at the University of Oxford, then subsequently in the USA at the Sloan-Kettering Institute with Professor Stewart Shuman. He now runs a research group at the University of Westminster, London, using structure and biochemistry to understand how proteins function.

Dimitar B. Nikolov is an Associate Member of the Memorial Sloan-Kettering Cancer Center and an Associate Professor at the Weill Medical College of Cornell University in New York City. He holds a Ph.D. degree from The Rockefeller University. His laboratory uses X-ray crystallography combined with other biophysical methods to study the structure, function, and mechanism of action of proteins.

DNA Methyltransferases, Bacterial

Albert Jeltsch
International University Bremen, Bremen, Germany

Richard I. Gumport
University of Illinois, Urbana, Illinois, USA

DNA methylation has a number of important roles in bacteria including the control of gene expression, DNA replication, and the cell cycle. In addition, it is involved in mismatch repair and protection of bacteria from foreign DNA in restriction modification systems. DNA methyltransferases (MTases) are the enzymes that methylate DNA. They deposit methyl groups on DNA at the N6-position of adenine, or the N4- or C5-positions of cytosine in a sequence-specific reaction using S-adenosyl-L-methionine (AdoMet) as the methyl group donor. Their reaction mechanism includes rotating the target base completely out of the DNA helix in a biphasic process, where fast flipping of the base out of the double helix is followed by a slower binding of the flipped base into a hydrophobic pocket of the enzyme. DNA MTases comprise two structural domains: the larger domain contains the cofactor-binding site and the binding pocket for the flipped base and the smaller domain is responsible for most of the sequence-specific contacts of the enzyme to the target site. The structures of large domains from all known DNA MTases are similar, whereas the small domains are more heterogeneous in sequence and structure. DNA MTases are an attractive model system to study how proteins recognize specific sequences of DNA and how the specificity of DNA recognition changes during molecular evolution. In addition, they illustrate how the biochemical properties of the enzymes are related to their biological functions. In this article, we shall describe the biological roles of DNA methylation in prokaryotes, discuss the chemistry of the enzymatic methylation reaction performed by the DNA methyltransferases (the focus of the review), and finally discuss aspects of the enzymology of this fascinating family of enzymes that reveal how these molecular machines perform their complicated biochemical tasks.

Introduction

After their discovery during the 1940s, methylated nucleobases have been found in the DNA of most species. DNA methyltransferases (MTases) produce three types of methylated bases, C5-methylcytosine, N4-methylcytosine, and N6-methyladenine (Figure 1). Based on the identity of the acceptor atom for the methyl group, C-MTases forming C5-methylcytosine can be distinguished from N-MTases forming N6-methyladenine and N4-methylcytosine. Whereas C5-methylcytosine occurs in higher eukaryotes and prokaryotes, the N-modified bases (N4-methylcytosine and N6-methyladenine) are present only in prokaryotes and some lower eukaryotes. Usually, DNA MTases are DNA sequence specific. In higher eukaryotes, cytosine methylation occurs mainly at CG sequences, and in plants also at CNG sequences. Such DNA methylation leads to chromatin condensation and silencing of gene expression. In prokaryotes, DNA methylation is involved in the control of gene expression, but it has a multitude of additional roles including control of initiation of DNA replication, correction of errors in DNA replication, and modulation of the destruction of DNA by restriction endonucleases.

Biological Function of DNA Methylation in Prokaryotes

Molecular Recognition of the Presence of the Methyl Groups on the DNA

DNA methylation adds an extra layer of information, viz., epigenetic information, to the genome that extends the intrinsic genetic information encoded in the unmodified sequence composed of the four usual Watson–Crick base pairs. In this sense, it can be compared to the different written diacritic marks in the French language, which are not required to read a word but rather define how the words are pronounced. Thus, diacritic signs do not carry essential information for the meaning of text, but impart important information beyond that level. Likewise, DNA methylation adds information that influences the stability, regulation, and expression of the encoded genetic information.

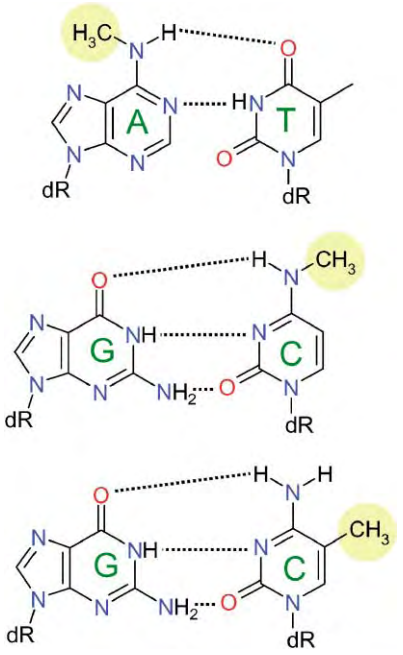

FIGURE 1 Structures of 6-methyladenine and of 5- and 4-methylcytosine in the context of an AT and GC base pairs. In all cases, the methyl group is located in the major group of the DNA and it does not interfere with the Watson–Crick base pairing.

Methylation of the DNA at the cytosine-C5, N4, and adenine-N6 positions does not interfere with Watson–Crick base pairing (Figure 1). It represents a minimal change of the molecular structure of the DNA. However, the methyl groups are positioned in the major groove of the DNA, a region where many proteins recognize the sequence of the DNA by formation of specific contacts to the edges of the base pairs. Such recognition can be severely disturbed by the presence of a single methyl group in the major groove as illustrated by the complexes of restriction endonucleases with specific DNA. These enzymes form a very tight interface with their target DNA, stabilized, in part, by several base-specific interactions. Methylation of the target DNA base sequence prevents close approximation of the enzyme and the DNA through steric hindrance, thereby effectively preventing DNA cleavage by the restriction enzyme. Thus, the introduction of a single methyl group onto a DNA base can have a profound effect on the biological functions of the modified sequence.

The Molecular Logic of DNA Methylation

The effect of DNA MTase action is to give DNA a methylation pattern that will affect its biological function. In prokaryotes, we can discern several levels of biological responses to methylation.

Sequence Context of DNA Methylation

Most prokaryotic DNA MTases are parts of restriction/modification (RM) systems, which are widely distributed in the bacterial and archeal kingdoms. These systems comprise two enzymes, a restriction endonuclease that specifically recognizes and cleaves DNA usually within or near short, often palindromic sequences. The cellular DNA is protected from cleavage by the MTase, because it modifies the DNA within the same sequence and prevents endonuclease action. Since different RM systems have different recognition sequences, the methylation pattern basically imprints a bar code on the DNA that allows the bacterium to distinguish between its own and foreign DNA. Since DNA from bacteriophages is often not modified at the sites of the resident RM systems, these systems efficiently protect against bacteriophage infection. In addition, they serve to control the uptake and incorporation of foreign DNA from any source into the bacterial chromosome. Because RM systems distinguish between self and nonself DNA and protect bacteria from phage infection, they can be compared, in biological function, to the immune system of higher eukaryotes. Like the immune system, RM systems are also involved in a molecular arms race between the invader and the host, and bacteriophages have evolved many antirestriction systems, such as multispecific MTases that modify the phage genome at many sites, and thereby provide a broad protection against the endonucleases of different RM systems.

Regulation by Hemimethylation

Coordination of DNA Replication and Cell Division In addition to the MTases that are part of RM systems, solitary MTases also occur. These enzymes are not accompanied by a restriction enzyme and are exemplified by the *Escherichia coli* dam or *Caulobacter cresentus* CcrM MTases. Both modify adenine residues; their palindromic recognition sequences are GATC and GANTC, respectively. Therefore, both strands of the DNA usually carry a methyl group, and the duplex sites are fully methylated (5′-G^{m}ATC-3′/3′-CT^{m}AG-5′ in the case of dam). Since only unmodified nucleotides are incorporated during DNA replication, the newly synthesized strand of the DNA lacks methyl groups. Therefore, replication transforms the DNA methylation status from a fully methylated into a hemimethylated state. In *E. coli*, the dam sites in most parts of the genome are remodified rapidly after replication. In contrast, the SeqA protein tightly binds to the origin of replication and protects it from being remethylated for several minutes. During this time, the origin cannot initiate a new round of DNA replication thereby coupling DNA replication and cell division. Thus, in

this system the hemimethylated status of the dam sites determines whether DNA replication will occur again.

Postreplicative Mismatch Repair As described, DNA replication generates hemimethylated dam sites in *E. coli*. Such strand-specific methylation distinguishes the parental and daughter DNA strands; the residual methylation always marks the parental strands. Strand-specific asymmetric methylation is the basis for a directed repair of replication errors by the *E. coli* Mut HLS system. Mismatched base pairs resulting from erroneous nucleotide incorporation by the DNA polymerase are recognized by the MutS protein or homologues in a mechanism that is conserved from *E. coli* to man. In *E. coli*, MutH, a partner in a complex with MutS and MutL, specifically cleaves the DNA at hemimethylated GATC sites in the unmodified, newly synthesized daughter strand. This allows differentiating the erroneous new strand from the original stand and directs the repair process to the proper strand. Therefore, strand discrimination and postreplicative mismatch repair in *E. coli* and other dam-positive bacteria is connected to dam methylation. Loss of the dam methylation generates a hypermutational phenotype that contributes to pathogenicity of *Neisseria meningitides*. Other mechanisms of strand discrimination, which do not depend on DNA methylation, are operative in higher eukaryotes and bacteria not having dam methylation.

Cell-Cycle Control *Caulobacter cresentus* is an α-proteobacterium with a well-controlled cell cycle that is coordinated to a phase transition between mobile swarmer cells and stalk cells. Its genome changes from the fully methylated to the hemimethylated state during DNA replication. The CcrM Mtase in *Caulobacter cresentus* is among the proteins whose expression is regulated during the cell cycle such that it is present only during a short time near the end of S phase. The CcrM MTase is a master regulator gene, because the change between the hemimethylated and fully methylated state itself regulates a variety of other proteins, including the CtrA global regulator.

Regulation of Gene Expression by Methylation Pattern

Examples of gene regulation by the dam MTase in *E. coli* were detected several years ago, when it was shown that the pap operon in uropathogenic *E. coli* strains is regulated by differential methylation. Analyses of the *E. coli* genome showed that there are stably undermethylated sets of GATC sites whose position can vary with environmental conditions. Most likely, these sites are blocked by other proteins tightly bound to the DNA such that the dam enzyme cannot gain access. Recent whole-genome expression profiles have revealed a much higher number of genes whose expression is regulated by dam methylation. Regulation of gene expression by dam methylation contributes to phase variations of *E. coli* and other γ-proteobacteria. This is the most likely reason that dam-negative strains of *Salmonella thyphimurium* are not pathogenic and can serve as live vaccines.

Chemistry of DNA Methylation

DNA MTases use S-adenosyl-L-methionine (AdoMet) as the donor of an activated methyl group. The activated methylsulfonium of AdoMet can be attacked by a nucleophile to effect the methylation (Figure 2). However, methylation of either the exocyclic amino groups of adenine and cytosine or the C5-position of cytosine is a difficult chemical task, because these positions are not intrinsically nucleophilic. For instance, chemical alkylation of adenine and cytosine occurs at positions 3 of cytosine and 1 or 7 of adenine rather than the atoms modified by the MTases. To overcome this intrinsic lack of reactivity, the two families of DNA MTases, N-MTases and C-MTases, have evolved highly sophisticated reaction mechanisms. Both mechanisms have in common the necessity for close contact between the

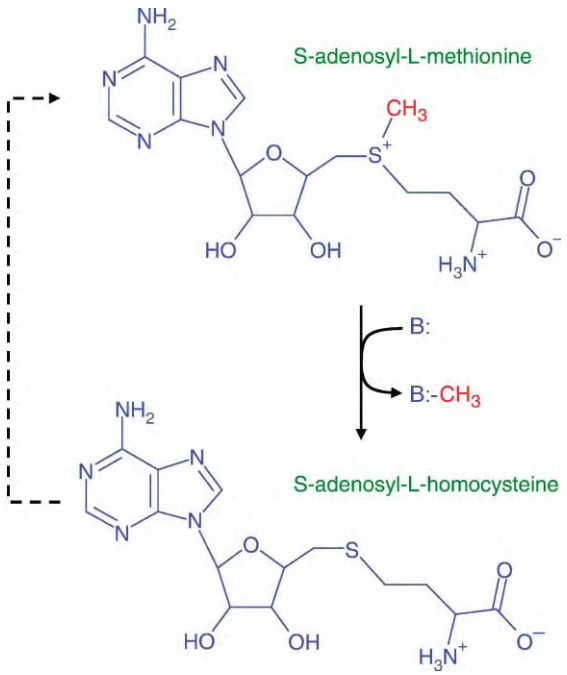

FIGURE 2 The structure of AdoMet, the cofactor of the methylation reactions catalyzed by DNA MTases. In the methylation reaction AdoMet is converted into S-adenosyl-L-homocysteine (AdoHcy). AdoMet can be regenerated from AdoHcy in a multistep pathway depending on tetrahydrofolate and Coenzyme-B12 that employs serine, which itself can be derived from 3-phosphoglycerate or glycine as the ultimate donor of a C1-group.

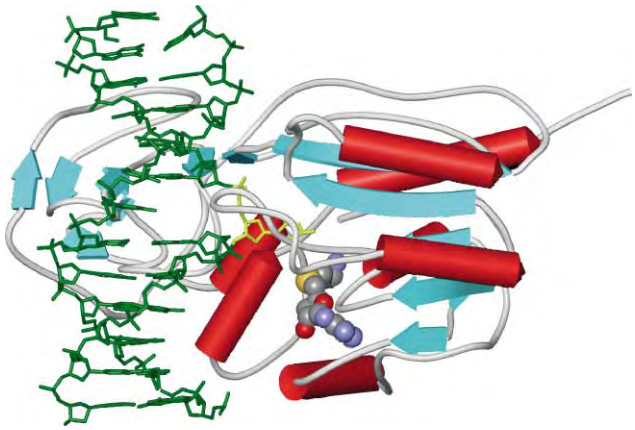

FIGURE 3 Structure of M.HhaI (gray, blue, and red) showing the target base (yellow) flipped out of the DNA helix (black). The bound cofactor AdoMet (purple) is displayed in its space-filling form.

enzyme active site and the target base. Such proximity is not possible while the base is located within the DNA double helix. In seminal studies, X. Cheng, S. Klimasauskas, R. Roberts, and co-workers demonstrated that the cytosine-C5 Mtase HhaI completely flips its target base out of the DNA double helix during catalysis – an unprecedented, dramatic conformational change in the DNA (Figure 3). Later, similar mechanisms were observed with another cytosine-C5 MTase (HaeIII) and more recently with an adenine-N6 MTase (TaqI).

Reaction Mechanism of Cytosine-C5 MTases

Methylation of the C5-position of cytosine follows a two-step reaction mechanism (Figure 4) that resembles a Michael addition and is analogous to the mechanism used by thymidylate synthase to convert dUMP to dTMP. In the first step, a cysteine residue in the active site of the DNA MTase performs a nucleophilic attack on the C6-position of the cytosine that is flipped out of the DNA and bound in a hydrophobic pocket of the enzyme. Thereby, a transient carbanion is generated, which is stabilized by a protonated glutamic acid residue that hydrogen-bonds to the flipped base and protonates the N3 atom of the base. Since the carbanion has a high negative charge density at position 5, the activated base can attack the methyl group of the cofactor yielding a stable intermediate comprising a covalently linked complex of the methylated DNA and the MTase. The catalytic cysteine and glutamic acid residues are located in two highly conserved amino acid motifs found in cytosine-C5 MTases, the PCQ motif and the ENV motif also called motif IV and motif VI. The second step of the reaction resolves the covalent intermediate. It is initiated by deprotonation of C5 catalyzed by an unknown proton acceptor; deprotonation leads to the elimination of the cysteine residues and re-establishment of aromaticity.

This mechanism is supported by several lines of evidence. The covalent complex has been detected in crystal structures and in biochemical studies, the catalytic cysteine and glutamic acid residues are highly conserved in all cytosine-C5 MTases, and mutational analyses have supported their importance. Moreover, MTases effect the methylation reaction by positioning of the substrate and the cofactor in the active site and by tight binding to the transition state of the reaction.

Reaction Mechanism of N-MTases

Chemically, methylation of either adenine and cytosine residues at their exocyclic amino group is similar, because in each case the substrate amino group is part of an electron-poor, heterocyclic, aromatic system. The reaction is difficult, because the free electron pairs formally present at the amino groups are delocalized into the aromatic system and not readily available for nucleophilic attack on the AdoMet. The catalytic center of the MTases that acts on exocyclic amino groups (N-MTase) is formed by a (D/N/S)PP(Y/F) motif. The reaction mechanism of the N-MTases (Figure 5) is illuminated by the structure of the TaqI adenine-N6 MTase. The carboxyamide group of the active site asparagine and the backbone carbonyl group of the second proline residue of the active site tetrapeptide contact the amino group of the flipped adenine target. Since the hydrogen acceptor groups are presented in a tetrahedral geometry,

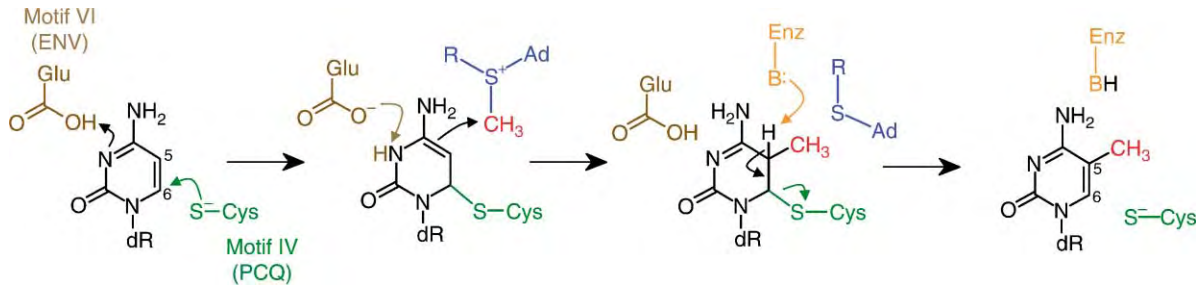

FIGURE 4 Schematic drawing of the catalytic mechanisms of C-methylation. The conserved motifs ENV and PCQ are indicated.

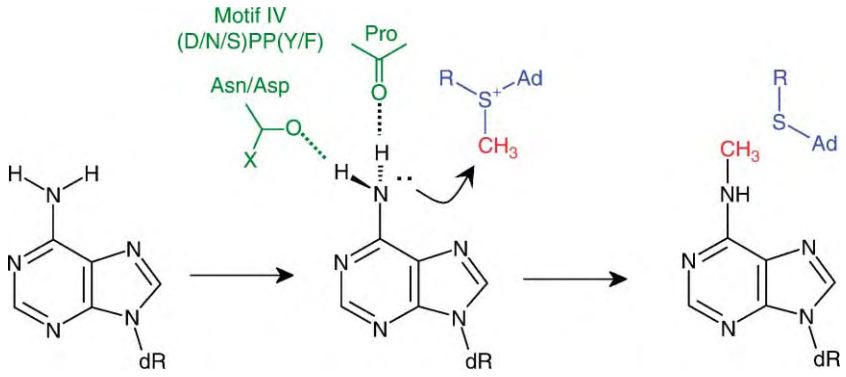

FIGURE 5 The catalytic mechanism of N-methylation. The conserved catalytic motif (D/N/S)PP(YF) is indicated.

formation of the hydrogen bonds induces a change in hybridization of the amino group from sp^2 to sp^3. This localizes the free electron pair and makes it available for the nucleophilic attack on the methyl group of the AdoMet. This mechanism is consistent with results from site-directed mutagenesis studies with many different DNA N-MTases, which demonstrate the importance of the active site (D/N/S)PP(Y/F) motifs. In addition, positioning of the base and the cofactor appear to be critical elements for catalysis by N-MTases.

It is interesting that the recognition of the flipped target base by the MTase is not necessarily precise; adenine-N6 MTases modify cytosine residues at position N4 and cytosine-N4 MTases modify adenine residues at position N6. Although these reactions occur with reduced efficiencies, they prove that the catalytic mechanisms of adenine-N6 and cytosine-N4 MTases are similar. Surprisingly, it has been shown recently that HemK enzymes, which are conserved from bacteria to human and strongly resemble adenine-N6 MTases in all their characteristic primary sequence motifs, are Glutamine-N5 methyltransferases. This unexpected finding demonstrates that the (D/N/S)PP(Y/F) tetrapeptide is a versatile active-site motif that supports methylation of various amino groups that are conjugated to an electron poor π-conjugation system, viz., the purine ring in adenine-N6 methylation, the pyrimidine ring in cytosine-N4 methylation, or a carbonyl group of glutamine-N5 methylation. It will be interesting to see whether (D/ N/S)PP(Y/ F)-containing enzymes have even more substrates, for instance if they can support methylation of arginine.

Mechanism of Base Flipping

Base flipping is a prerequisite for the catalytic mechanism of all DNA MTases; all structures of DNA MTases in complex with DNA solved so far show base flipping (Figure 3). In addition, numerous biochemical studies with different MTases demonstrate base flipping in solution. Three lines of biochemical evidence support a base flipping mechanism: (1) DNA MTases often bind substrates that contain a base mismatch at the target site more tightly than a normal substrate, because base flipping requires disruption of the base pairing between the target base and its partner base. (2) 2-Aminopurine, a base analogue that is fluorescent in solution but is highly quenched in the DNA by base stacking to its neighbor bases can be incorporated in the DNA as target base. Base flipping destroys the stacking interactions and sometimes leads to a strong and specific increase of fluorescence that is correlated with the flipping process. (3) The target base of DNA MTases shows a high propensity to react with the protein during cross-linking experiments. This result suggests that the base is flipped out of the helix and thereby available for much closer contact with the protein than it could if it remained inside the DNA helix. However, one should bear in mind that none of these assays is sufficient to prove or disprove unequivocally base flipping.

Our understanding of base flipping is limited by the high efficiency of the process, because so far no structural information is available for the specific DNA MTase complex prior to base flipping. The equilibrium favoring the flipped-base state is related to structural relaxations of the protein–DNA complex that prevent back-rotation and reinsertion of the flipped base into the DNA helix. Interestingly, these structural changes are different in all three complexes of DNA MTase with specific DNA available so far. In the case of M.HhaI, the DNA retains an almost perfect B-DNA-like conformation and the enzyme inserts a glutamine residue from the small domain into the cavity, left by the flipped base. In the case of the M.HaeIII enzyme (another cytosine-C5 MTase), the orphan G pairs with a C on the 3′ side of the target base. The partner of this C is orphaned and the large cleft in the DNA is filled with solvent. In the case of the TaqI enzyme (an adenine-N6 MTase) the orphan T moves towards the center of the DNA helix. Thereby, in part, it occupies the space left by the flipped A, and in this way optimizes its base stacking interactions.

Base flipping is at least a two-step process. The base is first extruded from the DNA and then tightly contacted by the enzyme in a binding pocket in the catalytic domain allowing base recognition and catalysis to occur. Whereas the first step of the flipping process is very fast (milliseconds), the second is much slower (seconds). It is not clear how flipping of the target base is initiated; it could simply be spontaneous DNA breathing where thermal energy occasionally leads to the flipping of the base. The function of the enzyme would be to catch the flipped base and prevent its back-rotation until after methylation had occurred. Alternatively, contacts of the enzyme with the phosphodiester groups of the backbone of the DNA might impose torsional stress on the DNA that would induce the flipping. It is clear that the interactions of the enzyme with the target base itself are not required for base flipping, at least in the case of the HhaI MTase, because with this enzyme a rotation of the deoxyribose analogous to base flipping is also observed using substrates carrying an abasic site at the target position. Finally, we do not know whether base flipping is correlated with DNA recognition. In principle, two alternative reaction schemes are possible. The enzyme could scan the DNA, recognize its target base in the unflipped state, and then induce flipping only at the specific site. Alternatively, flipping could occur anywhere and the enzyme recognized the target site only after flipping. Then it would lock the flipped base only if the correct sequence is bound.

Molecular Enzymology of DNA MTases

In this section, we shall briefly describe some features of DNA MTases, which explain how these fascinating enzymes are able to perform their complicated function.

Structures of DNA MTases

Structures of six DNA MTases are presently available: M.HhaI, M.HaeIII, M.TaqI; M.PvuII, DpnM, M.MboII, and M.RsrI. Whereas for M.HhaI, M.HaeIII, and M.TaqI ternary complexes between cofactor, DNA and enzyme are solved, all other structures are binary complexes between the Mtase and different forms of the cofactor. The single present exception is the structure of a catalytically compromised mutant of M.RsrI, L72P, that lacks bound ligand. All DNA MTases analyzed so far comprise two domains, one large and one small.

Structure and Function of the Large Domain

The large domain consists of a central mixed β-sheet, flanked by α-helices. The overall structure consists of two subdomains, which both form a hydrophobic pocket, the cofactor-binding site, and the binding site for the flipped target base. The AdoMet-binding site is composed of a subset of the conserved amino acid motifs that are found in most AdoMet-interacting enzymes, with conserved motif I ((D/E/S)XFXGXG) contributing important contacts to the AdoMet. Surprisingly, C-MTases and N-MTases show a striking similarity in the structure of their catalytic domains, with important catalytic residues (motif IV: PCQ in the case of cytosine-C5 MTases and (D/N/S)PP(Y/F) in the case of N-MTases) occupying equivalent positions in the three-dimensional structures of both MTase families. This finding was surprising, given the apparent differences in the catalytic mechanisms of both types of enzymes. It suggests an evolutionary relationship of both classes of MTases. In this context, it is interesting to note that three families of N-MTases exist that are related by circular permutations of the catalytic domain, but all known cytosine-C5 MTases belong to just one form that corresponds to the γ-family of N-MTases. Given the fact that N-MTases are structurally much more diverse and that they have a wider range of substrates (adenine, cytosine, and also amino acids), one might speculate that the C-MTases could be derived from the N-MTases, taking advantage of their established AdoMet-binding site and ability to flip the target base.

Structure and Function of the Small Domain

The second, smaller, domain of DNA MTases is much more heterogenous in size and structure. It contains most of the residues that mediate sequence-specific recognition of the DNA. Therefore, the variability of the target sequence is reflected by the loss of sequence conservation of the small DNA MTase domains. Upon specific DNA binding, base flipping is initiated or stabilized and conformational changes of the enzyme are induced. For example, in the case of M.HhaI, the loop comprising the catalytic motif IV of the enzyme undergoes a massive conformational change and approaches the DNA. Moreover, the small domain itself also moves towards the DNA. These changes are induced by the formation of base-specific contacts in a highly cooperative process that mediates the sequence specificity of DNA recognition. Thereby, the activation of the catalytic center is coupled to DNA recognition – a mechanism that is generally used by enzymes that interact with DNA in a sequence-specific manner.

Mechanism of DNA Recognition

DNA recognition by MTases arises from sequence-specific contacts of the enzymes in the major and minor grooves of the DNA as well as to its phophodiester backbone. The small domain of the MTases contacts the

DNA from the major groove side, and the body of the large domain interacts with the minor groove. For example, M.HhaI contacts the edges of the bases of the recognition sequence with 14 hydrogen bonds. In addition, in M.HhaI and M.HaeIII, residues following the active-site motif IV are involved in DNA recognition and form base-contacts with the target sequence. A contribution of loops of the catalytic domain in sequence recognition was confirmed by biochemical experiments with M.SinI and M.EcoRII, which are both C-MTases, as well as with the adenine-N-MTase M.EcoRV.

Depending on the particular enzyme, specific-complex formation sometimes, but not always, leads to strong bending of the DNA. Unfortunately, structural information is available only for enzymes that do not induce bending of the DNA. It is interesting to note that the specificities of different DNA MTase can vary dramatically. Some MTases display a very high specificity that is comparable to that of restriction enzymes whereas others interact with the DNA in a more relaxed manner, such that sites differing from the consensus target site are modified at reasonable rates. Relaxed target specificity may arise because RM systems are steadily evolving and are regularly changing or modifying their recognition sites. Most likely, MTases with relaxed specificity have been caught in the act of molecular evolution and have not yet optimized selectivity for their new target site. The EcoRV MTase provides revealing details of this process. GATATC is the target site of this enzyme, and according to multiple sequence alignments, it is most closely related to dam MTases whose target site is GATC. Interaction with the same sequence expanded by two base pairs at the 3′ end suggests that EcoRV could have been derived from a GATC methylating enzyme. In support of this model, EcoRV also modifies GATC sites. The contacts of the EcoRV and dam enzymes to the GAT-part of their recognition sites are conserved in both enzyme families. The contacts to the ATC-part of the recognition site by EcoRV supplements the contacts to the conserved core GAT sequence. Interestingly, the contacts between M.EcoRV and the conserved core occur earlier in complex formation than those to the supplemental sites suggesting a pathway by which evolution could change the specificity of protein–DNA interaction.

Mechanism of Target Site Location and Processivity of DNA Methylation

Ordinarily, DNA MTases methylate DNA only at specific sites. Localization of these specific sites in the sea of non-specific sites is a challenging process. Like most other proteins or enzymes that interact with DNA in a sequence-specific manner, DNA MTases make use of facilitated diffusion to accelerate the search for target sites. In this mechanism, the enzyme first binds to the DNA at a nonspecific site in a very fast reaction that often is close to the theoretical limit for a bimolecular association process. Then, the enzyme follows the DNA in a one-dimensional random movement.

One interesting facet in the target-acquisition mechanism of the DNA MTases is the manner in which several target sites are modified when they reside on the same DNA molecule. Enzymes can react with substrates containing several target sites in two principal ways: processively or distributively. In a processive reaction, after one turnover, the enzyme remains bound to the same substrate molecule, moves to the next target site and modifies it. Therefore, in a completely processive reaction, a DNA molecule is modified at all its target sites before the enzyme dissociates. In contrast, in a distributive reaction the enzyme releases the DNA after turnover at each site. As a consequence of these two mechanisms, the distribution of substrates, methylation intermediates, and products are completely different: methylation intermediates are not generated in a processive multiple-turnover reaction, whereas intermediates are necessarily formed in a distributive reaction. Recently, experiments with different MTases demonstrate that the solitary M.SssI, the CcrM MTase, and *E. coli* dam methylate DNA in a highly processive reaction. In contrast, the RM enzymes M.HhaI, M.HpaI, EcoRI, and EcoRV react distributively. This difference is particularly striking in the case of the EcoRV–*E. coli* dam pair, because they share high sequence similarity and show overlapping specificity.

Most likely, processive and distributive mechanisms are correlated with the biological roles played by the enzymes. One function of RM systems is to protect cells from bacteriophage infections, by cleavage of the phage DNA catalyzed by the restriction enzyme. The role of the MTase is to prevent cleavage of the host genome by methylation. However, the MTase must not modify the incoming DNA too rapidly or the phage DNA would be protected. The distributive reaction mechanism of the RM MTases would slow the complete methylation of any one molecule leaving it more vulnerable to restriction enzyme, because cleavage of one or a few sites is sufficient for inactivation of the phage. In agreement with this model, all RM MTases examined to date show a distributive reaction. However, mechanisms other than distributive ones such as compartmentation or tight control of the expression levels of both types of enzymes could also ensure proper RM MTase function. For the solitary MTases, no such evolutionary pressure against processive methylation exists, because rapid methylation of the chromosomal DNA after replication is desirable. For instance, prolonged hemimethylation of the newly replicated DNA, by delay of methylation

completion, would confuse the dam mismatch-repair system. Dam repair depends on the damage residing in the unmethylated strand, which holds true only for polymerase mistakes and not for other lesions in the DNA that might have occurred after replication.

The difference in processivity between EcoRV and *E. coli* dam is due to a pronounced difference in the order of DNA and AdoMet binding. Whereas EcoRV first binds to the cofactor and then to the DNA, *E. coli* dam prefers the opposite order of binding. Microscopic reversibility dictates that the order of DNA and cofactor release must reflect the order of binding. Thus, EcoRV first releases the DNA and then the cofactor. This mechanism precludes EcoRV from modifying DNA in a processive fashion, because it cannot exchange the product AdoHcy with AdoMet while bound to the DNA. What prevents an exchange of the cofactor in the ternary complex of M.EcoRV is presently unknown, but one could easily imagine that slight conformational changes of a few amino acid residues could open or block a channel that would permit cofactor exchange. Strikingly, subtle changes of the structure of the enzyme can be responsible for fundamental differences in the mechanism and thereby effect the adaptation of the enzymes to their biological functions.

See Also the Following Articles

DNA Methyltransferases: Eubacterial GATC • DNA Mismatch Repair in Bacteria • DNA Replication: Initiation in Bacteria • DNA Restriction and Modification: Type I Enzymes • DNA Restriction and Modification: Type II Enzymes • DNA Restriction and Modification: Type III Enzymes

Glossary

base flipping The process by which a base in the DNA is rotated so that it is no longer inside the DNA double helix, and is available for binding to an enzyme.

epigenetic information Genetic information arising from modifications of the bases in DNA.

hemimethylation Condition in which only one strand of the DNA double helix is methylated at a given site.

nucleobase One of the heterocyclic structures, adenine, cytosine, guanine, or thymine, that is attached to the phosphodiester-linked deoxyribose backbone of DNA.

nucleophile An atom or molecule group that is electron rich and reacts readily with a positively charged atom.

Further Reading

Cheng, X. (1995). Structure and function of DNA methyltransferases. *Annu. Rev. Biophys. Biomol. Struct.* **24**, 293–318.

Cheng, X. (1995). DNA modification by methyltransferases. *Curr. Opin. Struct. Biol.* **5**, 4–10.

Cheng, X., and Blumenthal, R. M. (1999). *S-Adenosylmethionine-Dependent Methyltransferases: Structures and Functions*. World Scientific, Singapore.

Cheng, X., and Roberts, R. J. (2001). AdoMet-dependent methylation, DNA methyltransferases and base-flipping. *Nucl. Acids Res.* **29**, 3784–3795.

Jeltsch, A. (2002). Beyond Watson and Crick: DNA methylation and molecular enzymology of DNA methyltransferases. *Chem. Bio. Chem.* **3**, 274–293.

Klimasauskas, X., Kumar, S., Roberts, R. J., and Cheng, X. (1994). HhaI methyltransferase flips its target base out of the DNA helix. *Cell* **76**, 357–369.

Low, D. A., Weyand, N. J., and Mahan, M. J. (2001). Roles of DNA adenine methylation in regulating bacterial gene expression and virulence. *Infect Immun.* **69**, 7197–7204.

Reisenauer, A., Kahng, L. S., McCollum, S., and Shapiro, L. (1999). Bacterial DNA methylation: A cell cycle regulator? *J. Bacteriol.* **181**, 5135–5139.

Roberts, R. J., and Cheng, X. (1998). Base flipping. *Annu. Rev. Biochem.* **67**, 181–198.

Biography

Albert Jeltsch is a Professor of Biochemistry at the School of Engineering and Science of the International University Bremen, Germany. He received his diploma from the University of Hannover, Germany and his doctoral degree from the Hannover Medical School, Germany. His research interests are DNA methylation and the molecular enzymology of DNA enzymes.

Richard I. Gumport is a Professor in the Department of Biochemistry and College of Medicine at the University of Illinois at Urbana-Champaign. He received his bachelor and doctoral degrees from the University of Chicago. His research interests are nucleic acid enzymology with an emphasis on protein–DNA interactions.

DNA Methyltransferases, Structural Themes

Sanjay Kumar
New England Biolabs, Beverly, Massachusetts, USA

DNA methyltransferases (MTases) are enzymes that catalyze the transfer of a methyl group from a donor molecule to DNA. On the basis of their chemistry, MTases can be grouped into two general categories: C5-MTases and N-MTases (Figure 1). The C5-MTases methylate the 5-carbon of the cytosine ring forming 5-methylcytosine. The N-MTases, which can be subclassed as N4- and N6-MTases, transfer a methyl group to an exocyclic nitrogen to form N_4-methylcytosine or N_6-methyladenine, respectively. The donor molecule in all known cases is the ubiquitous, small cofactor S-adenosyl-L-methionine (AdoMet or SAM). In the process of methylation, MTases employ a unique method called *base flipping* to access the target base. These enzymes are also highly selective DNA binding proteins and will only methylate their target bases within the context of a specifically recognized DNA sequence. MTases are widely distributed and have been isolated from or identified in the genomes of a wide variety of higher eukaryotes, lower eukaryotes, bacteria, and bacteriophage.

Function

The existence of DNA methylation (and hence MTases) has been known since 1948, even before the structure of DNA was discovered. Although much has been learned, the functional role of MTases in the molecular biology of the cell is still being uncovered today. DNA methylation is not essential for survival in all organisms, as both prokaryotes and eukaryotes that lack detectable methylation are known to exist. This is especially true in simpler organisms. However, as genome size increases (with some exceptions, of course), methylation takes on an increasingly important regulatory role, and defects in methylation are often strongly deleterious in plant and vertebrate embryonic development. The role of DNA methylation in human diseases is just beginning to be understood.

MTases impart epigenetic information to an organism's genome in the form of methylated bases. The primary purpose of this information is to modulate the interaction between DNA and the proteins that bind to it, whether directly by interacting with the proteins or indirectly by altering DNA structure. In general, methylation interferes with the binding of proteins to DNA; however, proteins whose DNA-binding is enhanced by methylation also exist. The effects of methylation on DNA structure are subtler. Methylation influences a variety of properties such as the stability of the double helix, DNA curvature, and the formation of DNA triple helices and left-handed Z-form DNA.

DNA methylation is closely tied to DNA replication. When a replication fork moves through a region of methylated DNA, the replicated DNA will be hemi-methylated with methyl groups *only* on the parental template strands. Soon afterward, the hemi-methylated DNA is recognized by MTases and becomes fully methylated once again. This transient undermethylated state can be used in a variety of ways: to monitor the replication state of DNA, to differentiate between the parental strand (methylated) and the newly synthesized strand (unmethylated), and to couple cellular functions to the cell cycle.

While MTases can aid in the correction of replication errors immediately after replication (called postreplicative mismatch repair) by using methylation to mark the strand carrying the original information, C5-MTases also contribute to the mutability of genomes. Cytosine spontaneously deaminates by hydrolysis at a very low rate, converting itself to uracil. Uracil is obviously foreign to DNA and the cell easily repairs the mutation. When 5-methylcytosine is deaminated it becomes thymine, giving rise to C → T transition mutations that are difficult for the cell to correct because T is a normal constituent of DNA. In addition, C5-MTases, in the presence of low concentrations of AdoMet, accelerate the rate of deamination. Sites of cytosine methylation are therefore mutagenic hotspots, and the genomes of higher eukaryotes such as vertebrates show significant depletion in the dinucleotide CG (the target sequence for vertebrate MTases).

Prokaryotes

Prokaryotes have both C5-MTases and N-MTases (Figure 1). A significant characteristic of prokaryotic

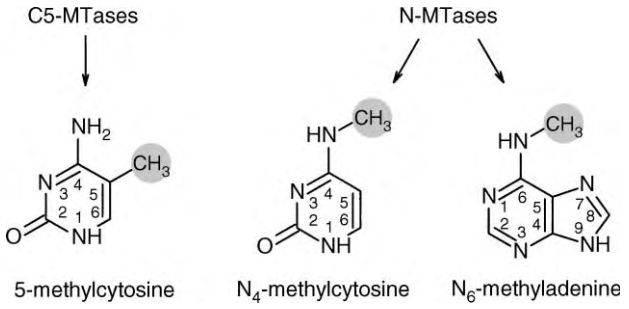

FIGURE 1 Products of DNA methylation by MTases. A shaded gray circle highlights the added methyl group.

DNA methylation is its promiscuity: prokaryotic MTases will methylate all available target sites, and do not discriminate between hemi-methylated and unmethylated targets. DNA binding proteins may, however, delay this methylation at some sites by temporarily sequestering the target sequences. MTases in prokaryotes are involved in two major groups of functions: (1) restriction–modification (RM) systems that serve as immune defenses against phage infection and (2) regulation of cellular processes.

RM Systems

In RM systems, MTases are paired with restriction endonucleases (RE). RE are enzymes that recognize target sequences in DNA with very high sequence specificity and then cleave the DNA. DNA methylation of the target sequence inhibits binding and cleavage by the RE. In an RM system, the MTase and RE have identical or overlapping target sequence specificity. The bacterium's DNA is protected from RE cleavage by prior methylation at the recognition site. Incoming foreign DNA (classically phage DNA), which does not display the same pattern of methylation as the host, is quickly fragmented by the host's REs. In this way, the bacterium uses MTases to effectively discriminate between self and foreign DNA.

Regulation of Cellular Processes

Our knowledge of the regulation of prokaryotic cellular processes by methylation is almost entirely focused on the action of one MTase: the Dam MTase, a solitary N-MTase (not part of an RM system) that recognizes the sequence GATC and methylates the adenine residue. The primary signal used for regulation is the transient undermethylation of Dam sites after replication. Dam MTase is involved in postreplicative mismatch repair, as well as controlling aspects of the initiation of chromosomal and plasmid DNA replication, transposition of transposable elements, and gene expression.

Eukaryotes

DNA methylation in eukaryotes is exclusively in the form of 5-methylcytosine and is confined to the dinucleotide CG (or CNG in plants, where N is any nucleotide), and C5-MTases are the only type of MTases found in eukaryotes. While little or no methylation is detected in unicellular, insect or invertebrate cells, both plant and vertebrate DNA are significantly methylated. Approximately 3–8% of the cytosine residues in vertebrates and 4–40% in plants are methylated. Unlike the prokaryotes, where the distribution of methylated bases mirrors the distribution of target sequences, only 60–80% of eukaryotic CG sites have methyl groups attached; however, for any given site, the cytosines in both strands of the DNA are methylated.

Pattern of Methylation

While eukaryotic DNA methylation is incomplete, it is not random. The pattern of methylation can be tissue specific and maintainable across cell generations. This implies the existence of at least two types of MTase functions: a *de novo* function to establish methylation patterns and a maintenance function to faithfully copy those patterns following DNA replication. The maintenance methylase function, exemplified by mammalian DNMT1, preferentially targets the hemi-methylated sequences that are present after DNA replication, a preference not shared by bacterial MTases. The CG dinucleotide distribution is also nonrandom. In mammals, while CG is generally depleted, it occurs at its expected frequency in blocks of sequence called CpG islands. CpG islands are often located near sites that regulate the transcription of genes. While they contain only 15% of the genome's CG sites, over half the target CG sequences in CpG islands are unmethylated. In contrast, 80% of the remaining CG sites in the genome are methylated.

Transcriptional Silencing

The effects of DNA cytosine-5 methylation in eukaryotes are complex and a thorough discussion is beyond the scope of this entry. However, there is strong evidence for its involvement in partitioning the genome into transcriptionally active and inactive functional compartments, where DNA methylation is generally correlated with silencing of gene expression. Methylation appears to accomplish this silencing by recruiting transcriptional repressors to the methylation sites, as well as histone deacetylases. The latter are involved in remodeling the chromatin structure that packages eukaryotic DNA into

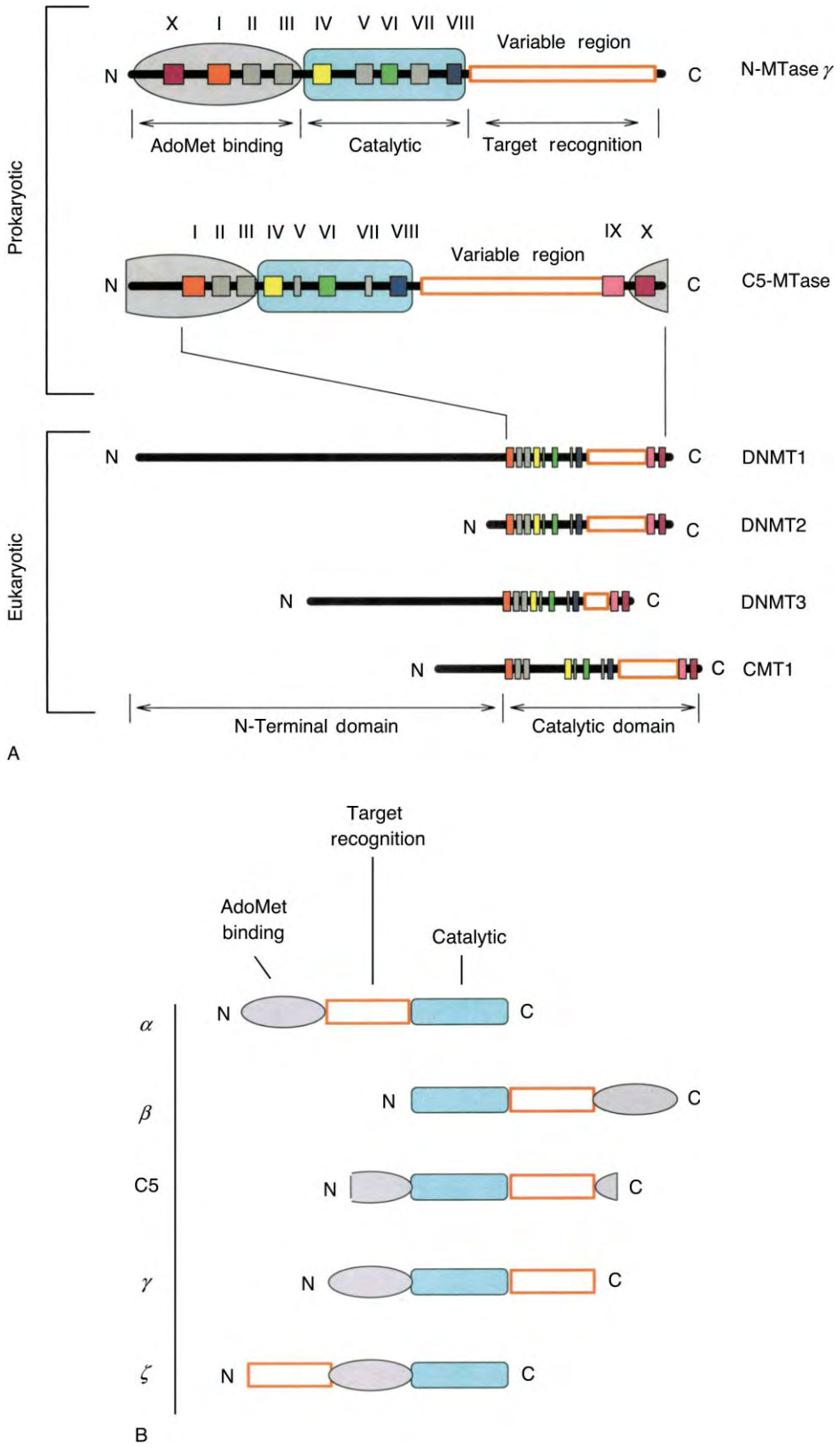

FIGURE 2 Schematic of MTase motifs and domains. (A) Sequence motifs and modules: Motifs are numbered I through X (Roman numerals). Conserved motifs are consistently represented by the same color square in all figures (not to scale). The MTase structure is divided into three modules: AdoMet Binding (gray oval), Catalytic (cyan rectangle), and Target Recognition (thin brown rectangle). The Target Recognition module and the variable region overlap completely. The N-MTase schematic is specific for the γ class of N-MTases. In C5-MTases, the components of the AdoMet Binding module are split and portions reside on the N and C termini of the sequence. The eukaryotic enzyme families (DNMT1, 2, 3,

a transcriptionally silent state. Methylation induced transcriptional silencing is believed to play a role in such processes as embryonic development, genomic imprinting, X-chromosome inactivation, and silencing of transposons and other mobile repetitive elements.

Primary Sequence Organization

Modular Arrangement

MTases are built from three basic modules that perform the primary functions required of these enzymes: DNA recognition, AdoMet binding and catalysis of methylation (Figure 2A). With few exceptions, they are monomeric proteins that range in size from approximately 300–500 amino acids in prokaryotes to over 1500 amino acids in eukaryotes. The amino acid sequence of MTases is divided into two distinct regions. The first region contains many sequence motifs that are conserved between groups of MTases. The core enzymatic functionality, consisting of the AdoMet binding and catalytic domains, is located in this region. The other region, termed the "variable region" (because its size and sequence varies greatly between otherwise related MTases), is almost completely devoid of such motifs (Figure 2A). The variable region contains the target recognition domain (TRD) and forms the third basic module. Theoretically, six permutations of the linear order of these three modules are possible (Figure 2B). To date, examples of four of the six have been identified.

Conserved Sequence Motifs

The signatures of their sequence motifs can often identify different classes of MTases. C5-MTases share a set of up to 10 motifs (labeled I–X in Figure 2A), six of which are strongly conserved. Each motif spans a total of 8–20 amino acids and usually contains two or three highly conserved positions. The linear order of these motifs is also conserved in virtually every member of the C5-MTase family, and the variable region is always located between motifs VIII and IX. The 10 motifs are also found in eukaryotic MTases, but they are confined to the roughly 500 amino acid long C-terminal catalytic domain of these larger enzymes. The eukaryotic MTases often possess an additional very large N-terminal domain that modulates their biological function.

Nine motifs can be located within N-MTases at positions that spatially overlap their C5-MTase counterparts on protein structures (Figure 2A); however, the level of similarity at the primary sequence level between corresponding C5 and N-MTase motifs is very low. Even corresponding motifs in different groups of N-MTases can show substantial differences. Only two of the sequence motifs, motif I and motif IV, can be identified without the aid of protein structure information. The N-MTases can be grouped into subclasses on the basis of motif order, but these groupings do not distinguish between N_4-cytosine and N_6-adenine MTases. The variable region is inserted in different, but conserved, positions relative to the motifs in each group.

Tertiary Structure

Reflecting the modularity seen in the primary sequences, MTases fold into structures with two domains: the core methylation machinery is localized in one large domain and the sequence recognition functions are concentrated in a second usually smaller domain. DNA binds in the cleft between the two domains, which are connected by a stalk or hinge (Figures 3 and 4).

Large Domain

The large domain is dominated by a structural motif termed the AdoMet-dependent methyltransferase fold that is conserved across a wide variety of AdoMet-dependent methyltransferases. The AdoMet fold spans both the AdoMet binding module and the catalytic module (Figure 3). It is composed of a core seven-stranded β sheet with strand order 6↓, 7↑, 5↓, 4↓, 1↓, 2↓, 3↓ (the arrows indicate relative strand direction), though strand 3 is sometimes not well formed. A characteristic feature is the insertion of strand 7 between strands 6 and 5 and antiparallel to the other six strands. The topological switch point (where the strand order changes) between strands 4 and 1 is situated in the active site. The switch point roughly divides the AdoMet fold into two parts, with strands 1 to 3 forming the core of the AdoMet binding module and strands 4 to 7 forming parts of the catalytic module including the substrate binding pocket. The two sections of the AdoMet fold β-sheet are each flanked by α helices to form β-α-β-α sandwiches. The core structure of the large domain is structurally quite similar to the Rossman fold of proteins that bind NAD or NADP.

Small Domain

The small domain corresponds to the "variable region" in primary sequence alignments of MTases.

and CMT1) all share the same motif arrangement as the prokaryotic C5-MTases, but the region of similarity is entirely confined to the C-terminal catalytic domain of these larger enzymes. (B) The modular arrangement of known MTases: The α, β, γ, and ζ classes are exclusively N-MTases. The C5 class (C5-MTases) and the (N-MTases are essentially the same class. The arrangements of domains in the β, C5, γ, and ζ classes are circular permutations of each other.

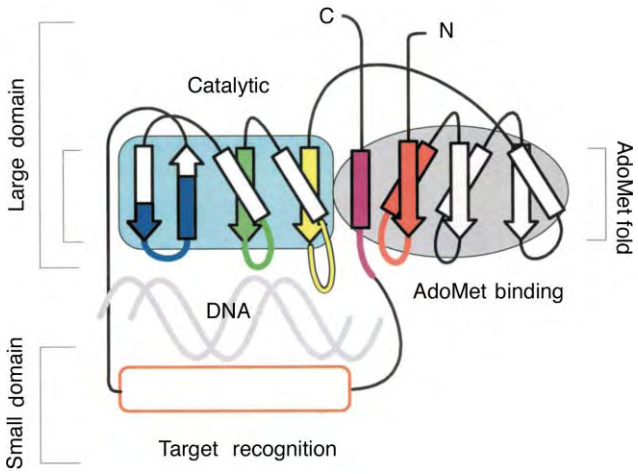

FIGURE 3 Structure of MTases: An idealized representation of the structure of a C5-MTase is shown. β strands are represented by arrows, α helices by rectangles, and loops by curved lines. Gray wavy double lines indicate DNA. Colored regions represent the locations of sequence motifs (Figure 2A). Other symbols and colors represent the same as those described in Figure 2. β strands are numbered 6, 7, 5, 4, 1, 2, and 3, from left to right as shown.

Not surprisingly, this domain is varied in size and structural arrangement. The small domain contacts the major groove face of the target DNA. In C5-MTases, the residues that specify the choice of target sequence and the base to be methylated generally reside on the small domain. In N-MTases, the contacts are more distributed between the two DNA grooves and the two domains of the enzyme.

Mechanism

Chemistry

The methylation reaction catalyzed by MTases requires only the DNA substrate and AdoMet. The products of the reaction are the various methylated bases and S-adenosyl-L-homocysteine (AdoHcy or SAH). The methylated bases are relatively stable, and the reverse reaction (demethylation) is not known to be mediated by MTases.

AdoMet

AdoMet is the most commonly used methyl donor in cellular biochemistry and the second most common

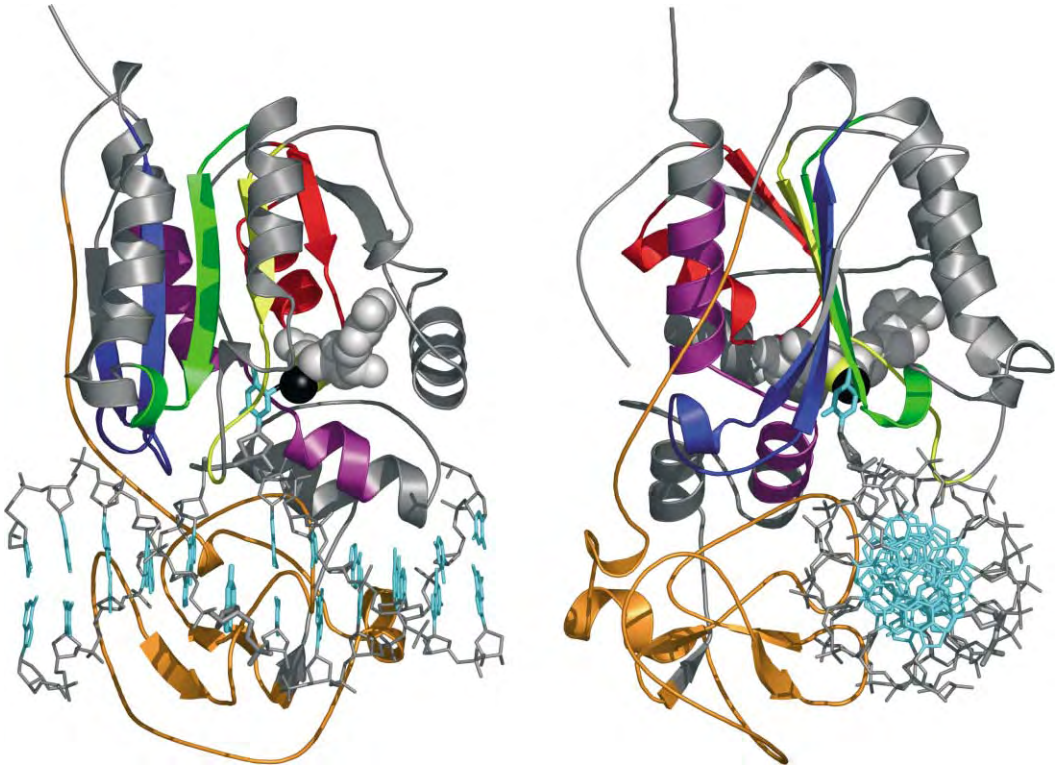

FIGURE 4 Crystallographic Structure of a C5-MTase: A three-dimensional cartoon representation of the structure of the C5-MTase M.HhaI. β strands are represented by arrows, α helices by helical flat coils, and loops by thin, curved lines. Protein is gray. The variable region is shown in brown. Other colors represent the same as those in Figures 2 and 3. DNA is seen in the lower part of the structure, with a gray sugar-phosphate backbone and cyan bases. The target base near the center of the structure is flipped out. The small gray molecule represented by space-filling spheres is AdoMet. The carbon to be transferred is colored black. The two views are related by a 90° rotation around the vertical axis of the structure.

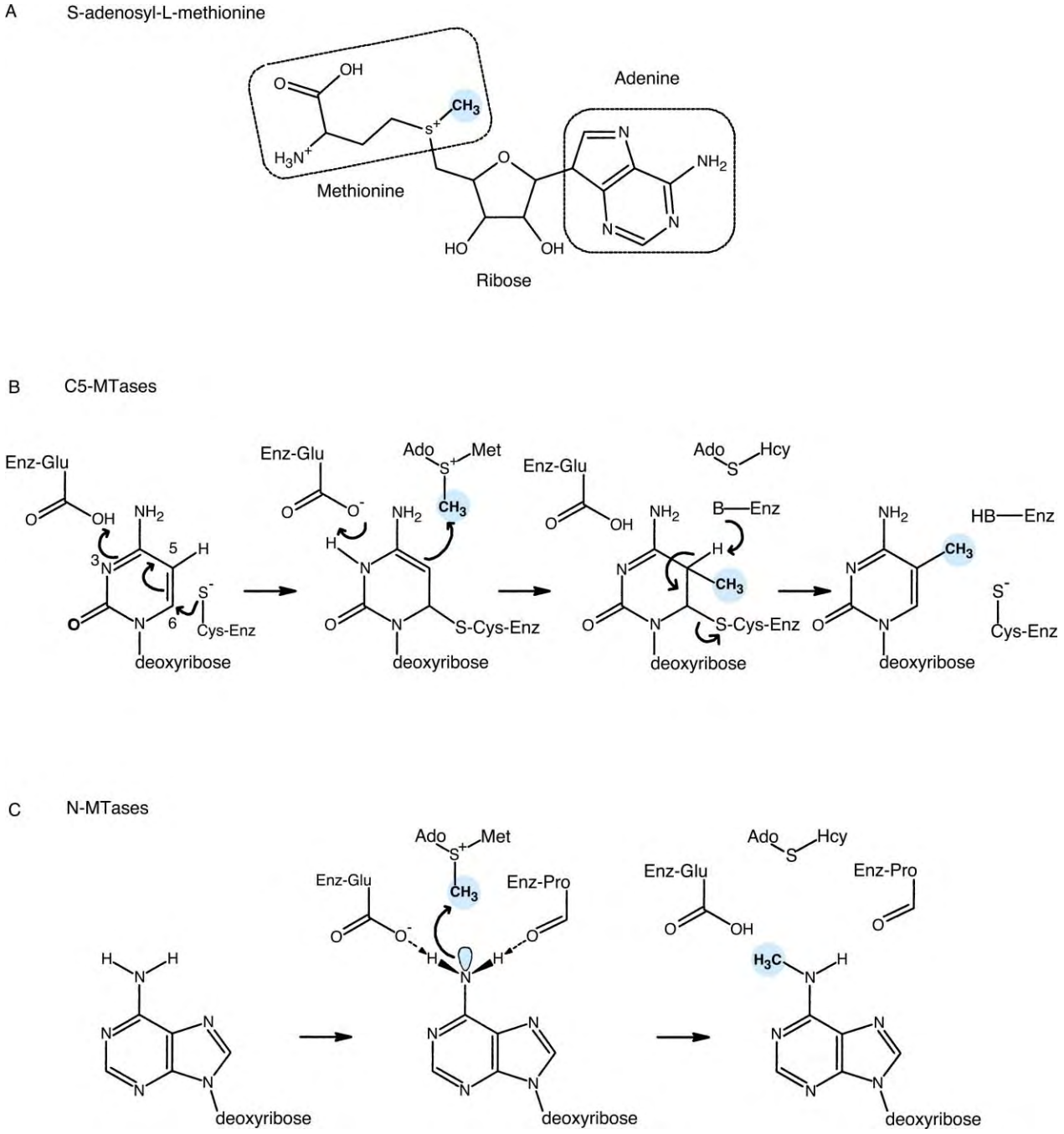

FIGURE 5 Reaction mechanisms of MTases: In each panel, a shaded gray circle indicates the transferred methyl group. The enzyme is represented by the symbol Enz. The symbol B refers to a generic basic residue. In (B) and (C), AdoMet is represented by the symbol Ado-S-Met and AdoHcy by Ado-S-Hcy. (A) The structure of S-adenosyl-L-methionine (AdoMet or SAM). (B) C5-MTase reaction mechanism. The mechanism is described in the text. Though not obvious from the diagram, the mechanism requires that the sulfhydryl group of Cys-Enz and the methyl group of AdoMet must approach perpendicular to and on opposite faces of the target cytosine. (C) N-MTase reaction mechanism based on the M.Taq I MTase. In the central structure, the coordinating hydrogen bonds (shown by dashed lines) are situated in a tetrahedral arrangement relative to the nitrogen and change the hybridization state of the nitrogen from sp^2 to sp^3. This localizes and repositions the free lone pair electrons, shown as a shaded orbital above the nitrogen, for nucleophylic attack on the methyl group.

cofactor after ATP (Figure 5A). The transferable methyl group resides on a charged sulfur atom, making it very reactive to nucleophiles such as polarized N, S, O, and activated carbons or carbanions. Interestingly, the synthesis reaction for AdoMet is the only one known to require hydrolysis of all three phosphates of ATP to drive the reaction. Transfer of the methyl group converts AdoMet to AdoHcy.

C5-MTases

C5-MTases transfer a methyl group to the 5-carbon of the cytosine base (Figure 5B). The 5-carbon of cytosine is not normally reactive enough to attack the methyl group on AdoMet to effect transfer. C5-MTases catalyze this unfavorable reaction in the following way, with a key feature of this process being the formation of a transient covalent complex between the enzyme and the DNA. First, a cysteine thiol on the enzyme serves as a nucleophile that attacks the 6-carbon of the pyrimidine ring, forming a covalent DNA-protein intermediate. This is aided by the protonation of N3 on the ring by the enzyme. The sulfhydryl is provided by the Cys in the highly conserved PC dipeptide (motif IV) found in all C5-MTases. A Glu in the highly conserved ENV tripeptide (motif VI) carries out the protonation. An Arg residue from motif VIII assists the process. This addition activates the 5-carbon and allows it to attack the AdoMet methyl group. Following transfer, AdoHcy is released. The proton left at the 5-position is abstracted by a nearby basic residue leading to resolution of the DNA-protein complex by β-elimination.

N-MTases

N_4-cytosine and N_6-adenine N-MTases methylate an exocyclic nitrogen atom (Figure 5C). Their mechanisms are believed to be similar, but they are not as clearly understood as for the C5-MTases. Methylation occurs by direct transfer from AdoMet and does not involve a covalent DNA-protein intermediate. Each of the first two residues of conserved motif IV (N/S/DPPY/F) donates a hydrogen bond to the target exocyclic nitrogen. This activates the exocyclic N for subsequent nucleophylic attack on the AdoMet methyl group. Following transfer, AdoHcy is released.

AdoMet and DNA Binding

Association of the Reactants

Methylation reactions proceed via a complex between the MTase, DNA, and AdoMet. The order of association of these components varies among MTases (sometimes being random) and no general rule applies to all MTases. The binding to DNA occurs in two discrete steps. The initial nonspecific DNA binding is accompanied by scanning linear diffusion, in which the MTase slides along the DNA in search of a specific recognition site. In the second step, the MTase binds tightly to a specific recognition sequence. When specific binding is observed, it is often associated with a substantial conformational change in the DNA and/or the MTase.

Sequence-Specific DNA Recognition

Sequence-specific recognition of DNA is achieved through multiple contacts between the MTase and the target DNA, both direct and water-mediated. The target base itself does not seem to be part of the recognition sequence as DNA sequences with missing, modified, or alternate target bases are still recognized by the appropriate MTase. In fact, several MTases show preferential affinity for DNA substrates containing base mismatches at the target base position. The vast majority of MTases recognizes palindromic sequences and thus methylates both strands of a target sequence.

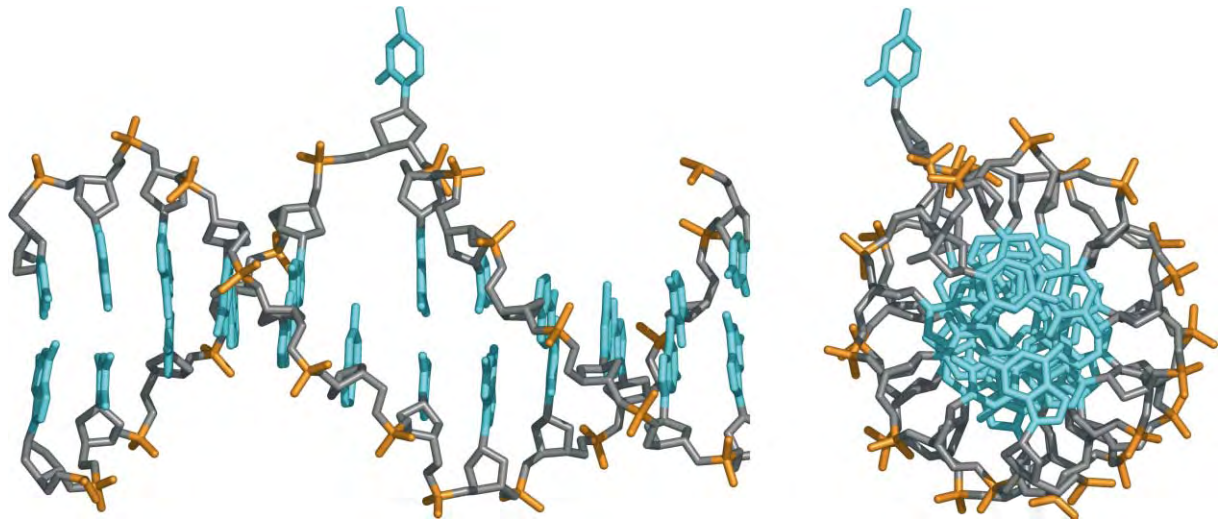

FIGURE 6 DNA base flipping: The DNA (shown from the side and end-on) is in the same orientation as in the structure shown in Figure 4. The backbone is gray with orange phosphates and the bases are cyan. With the exception of the flipped cytosine, the structure is classical B-Form DNA.

Base Flipping

The target base for MTases is normally buried in the DNA helix stack, a location that is incompatible with the stereochemical requirements of the reacting groups on the cofactor and the enzyme. The MTases overcome this spatial hurdle in a surprising and elegant manner: without seriously distorting the remainder of the DNA helix or breaking any bonds, they rotate the target base and its sugar phosphate backbone 180° out of the helix stack and into a pocket in the active site (Figures 4 and 6). This process has been termed "base flipping." The precise mechanism of base flipping is unknown. However, the identity of the target base or even its presence appears irrelevant to the mechanism, as mismatched, modified, methylated, or even missing bases at the target site still display base-flipping, or flipping of the remaining sugar-phosphate backbone at the target position. Subsequent to its discovery in MTases, base flipping was shown to be utilized by other proteins that need access to bases buried within DNA, including DNA glycosylases and AP endonucleases.

See Also the Following Articles

Chromatin Remodeling • Chromatin: Physical Organization • DNA Methyltransferases, Bacterial • DNA Methyltransferases: Eubacterial GATC • Nuclear Organization, Chromatin Structure, and Gene Silencing • Transcriptional Silencing

Glossary

beta sheet A flat, side-by-side arrangement of polypeptide chains linked together by hydrogen bonds. Each chain is in a zigzag conformation called a beta strand. Beta strands that run in the same direction (from amino terminal to carboxyl terminal) are termed parallel, while those that run in opposite directions are termed antiparallel.

chromatin DNA packaged around small protein cores. Roughly 200 base pairs of DNA are wound twice around an octamer of proteins called histones to form a nucleosome. Nucleosomes are the basic repeating structure of chromatin in eukaryotes.

CpG island A short region of DNA (one kilobase or less in length) that contains clusters of CG dinucleotides (the p in CpG refers to the intervening phosphodiester) at a frequency that is expected from the base composition of the DNA. CpG islands are often located in proximity to the transcriptional control regions of genes. They are normally undermethylated.

hemi-methylated Referring to a double-stranded DNA segment containing a recognition sequence for a MTase in which only one strand of the target sequence is methylated.

palindromic sequence A DNA sequence in which the sequence and its complement are identical when each is read in the standard 5′ to 3′ direction. CG, GATC, and GAATTC are examples of palindromic sequences.

Further Reading

Alberts, B., Lewis, M., Raff, M., Johnson, A., and Roberts, K. (2002). *Molecular Biology of the Cell*. Taylor & Francis, New York.

Cheng, X., and Blumenthal, M. (eds.) (1999). *S-Adenosylmethionine-Dependent Methyltransferases: Structures and Functions*. World Scientific, New Jersey.

Cheng, X., and Roberts, R. J. (2001). AdoMet-dependent methylation, DNA methyltransferases and base flipping. *Nucl. Acids Res.* **29**, 3784–3795.

Jeltsch, A. (2002). Beyond Watson and Crick: DNA methylation and molecular enzymology of DNA methyltransferases. *Chem. Bio. Chem.* **3**, 275–293.

Jones, P. A., and Takai, D. (2001). The role of DNA methylation in mammalian epigenetics. *Science* **293**, 1068–1070.

Jost, J. P., and Saluz, H. P. (eds.) (1993). *DNA Methylation: Molecular Biology and Biological Significance*. Birkhäuser Verlag, Basel.

Kumar, S., Cheng, X., Klimasauskas, S., Mi, S., Posfai, J., Roberts, R. J., and Wilson, G. G. (1994). The DNA (cytosine-5) methyltransferases. *Nucl. Acids Res.* **22**, 1–10.

Robertson, K., and Wolffe, A. P. (2000). DNA methylation in health and disease. *Nat. Rev. Genet.* **1**, 11–19.

Biography

Sanjay Kumar is a Staff Scientist at New England Biolabs in Beverly, Massachusetts. His research interests include DNA methyltransferases, DNA and chromatin structure, and the development of bioinformatic tools. He holds a Ph.D. in biomedical sciences from Wright State University in Dayton, Ohio. He received his postdoctoral training with Dr. Richard Roberts at Cold Spring Harbor Lab in Cold Spring Harbor, New York. Dr. Kumar and his associates authored the first paper to detail the crystallographic structure of a DNA methyltransferase, and later they made the first discovery of base flipping in DNA.

DNA Methyltransferases: Eubacterial GATC

Martin G. Marinus
University of Massachusetts Medical School, Worcester, Massachusetts, USA

Eubacterial GATC methyltransferases transfer methyl groups from S-adenosyl-L-methionine to the N-6 position of the adenine ring. Only adenines in the tetranucleotide sequence GATC in double-stranded DNA are methylated. Unlike other methyltransferases that function to protect DNA from restriction endonucleases, the eubacterial GATC methyltransferases have other biological functions that are described in this article. In general, the cell uses DNA methylation primarily to control the rate at which these functions exert their effects. Most of our knowledge about eubacterial GATC methyltransferases has come from studies using the Dam methyltransferase of *Escherichia coli* as a model system and this article will focus primarily on it.

Properties of Dam Methyltransferase

The Dam methyltransferase is encoded by the *dam* (*D*NA *a*denine *m*ethyltransferase) gene of *Escherichia coli*, which has a complex mechanism of gene regulation involving multiple promoters and terminators. The major promoter for transcription of the gene is regulated by growth rate of the cells; that is, the faster the growth rate the greater the level of initiation of transcription.

During chromosome replication, the replication fork is followed by a region of hemimethylated DNA which comprises new unmethylated DNA and the complementary methylated template strand. After ~1 min, on average, the newly synthesized DNA is methylated so that both strands are fully methylated. This delay in methylation is due to the concentration of the Dam methyltransferase; it is present at ~130 molecules per cell. Increasing the cellular concentration of the enzyme decreases proportionately the amount of hemimethylated DNA.

The enzyme is a single polypeptide chain of 278 amino acids with a molecular weight of 32 kDa and exists in solution as a monomer. The enzyme has a turnover number of 19 methyl transfers per min and an apparent K_m of 3.6 nM for DNA and double-stranded DNA is a better methyl acceptor than denatured DNA and there is one methyl transfer per site per binding event even if the substrate DNA is fully unmethylated. The protein may have two SAM binding sites: a catalytic site and one which increases specific binding to DNA perhaps as a result of an allosteric change. The methyltransferase is thought to bind the template and slide processively along the DNA, methylating about 50 sites before dissociating.

Properties and Uses of *∂am* Mutant Strains

The commonly used *dam* mutant strains do not have detectable residual methyltransferase activity nor detectable methylation at GATC sequences. *Dam* mutants are most often used to "launder" DNA molecules that have sites that are resistant to digestion with specific restriction endonucleases. These include: AlwI, BcgI, BclI, BsaBI, BspDI, BspEI, BspHI, ClaI, HphI, NruI, TaqI, and XbaI. Resistance occurs because these enzymes have recognition sequences that overlap with the GATC tetranucleotide and almost all of these are methylated in wildtype *E. coli*. After transfer through the *dam* mutant strain, there is no methylation at GATCs and DNA molecules are now sensitive to digestion with the restriction endonucleases listed above.

Dam mutants have also been useful to define the biological roles of methyl groups on adenine in DNA. The mutant strain shows a large number of phenotypic differences compared to wild type suggesting multiple functions. All the known mutant phenotypes in *E. coli* can be explained by the involvement of GATC methylation in mismatch repair, regulation of gene expression, and initiation of chromosome replication.

Dam-Directed Mismatch Repair

During chromosome replication, errors are made at low frequency by the replicative polymerase to form base

mismatches in newly synthesized DNA. Such errors need to be removed because they are potentially mutagenic. *E. coli* and most other organisms, including humans, have a highly conserved repair system that removes such mismatches in newly synthesized DNA. The Dam- (or methyl-) directed mismatch repair system in *E. coli* uses only hemimethylated DNA as a substrate thereby restricting its activity to the region of the chromosome immediately trailing the replication fork. The repair system is outlined in Figure 1. Briefly, base mismatches in hemimethylated DNA are recognized by the MutS protein followed by formation of a ternary complex with two additional proteins, MutL and MutH. MutH is an endonuclease active on hemimethylated GATC sites but only when complexed with the other Mut proteins on DNA. Following DNA incision, the UvrD helicase unwinds DNA in either the 5′ to 3′ direction or the reverse. The directionality is dependent on the location of the mismatch relative to the nearest GATC sequence. The unwound nicked DNA strand is digested by one or more exonucleases followed by resynthesis using the replicative polymerase. DNA ligation of the nick at the end of replication completes the process of repair and the hemimethylated DNA is eventually methylated.

Three lines of genetic evidence indicate the importance of DNA methylation in the process. First, overproduction of Dam methyltransferase inhibits the repair process by reducing the amount of hemimethylated DNA. Under these conditions mismatches are not repaired and lead to an increase in mutation frequency. Second, in a *dam* mutant the repair system is active but cannot discriminate the template strand from the daughter strand.

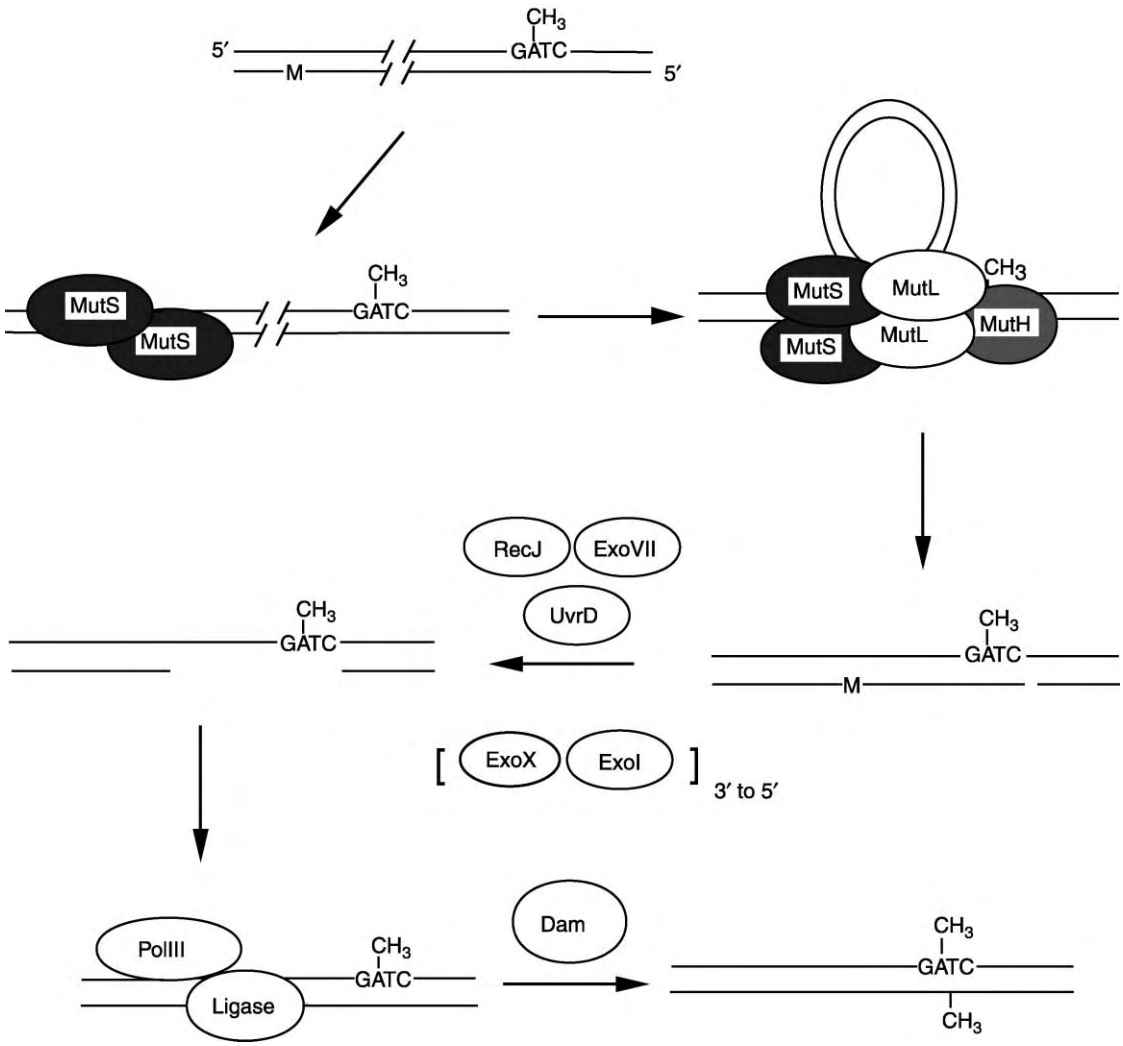

FIGURE 1 DNA mismatch repair. A base mismatch (M) in the newly synthesized unmethylated DNA strand is some distance from the nearest GATC sequence. MutS protein binds the mismatch and a complex with MutL and MutH is formed leading to cleavage of the unmethylated strand. The UvrD helicase unwinds the unmethylated strand which is digested by an exonuclease. Excision can occur in either the 3′ to 5′ direction (ExoI, ExoX) or the reverse (RecJ, ExoVII) depending on the orientation of the mismatch relative to the GATC sequence. DNA polymerase III holoenzyme synthesizes a new strand and the resultant nick is ligated by DNA ligase. The GATC sequence is eventually methylated by Dam methyltransferase.

Consequently, the repair system removes mutations from the newly synthesized strand but also introduces mutations into the parental strand yielding an increased mutation frequency. Third, DNA duplexes containing a mismatch can be constructed with no methylation, methylation on both strands, or on only one of the two strands. When introduced into cells the fully methylated DNA is not repaired, hemimethylated DNA is repaired using the methylated strand as template and the unmethylated duplex is repaired using either strand as template.

In a *dam* mutant, mismatch repair produces detectable nicks or gaps in DNA but it is not known if the nicks or gaps occur exclusively behind the replication fork as a result of replication errors or in any part of the chromosome as a result of mismatches formed spontaneously. The nicks or gaps are converted to double-strand breaks either by a replication fork encountering an unrepaired gap or by activated MutH cleavage on complementary strands at the same GATC sequence or by a combination of these (Figure 2). It is not yet known which of these mechanisms (or both) generates double-strand breaks *in vivo* but *in vitro* evidence supports the MutH cleavage model.

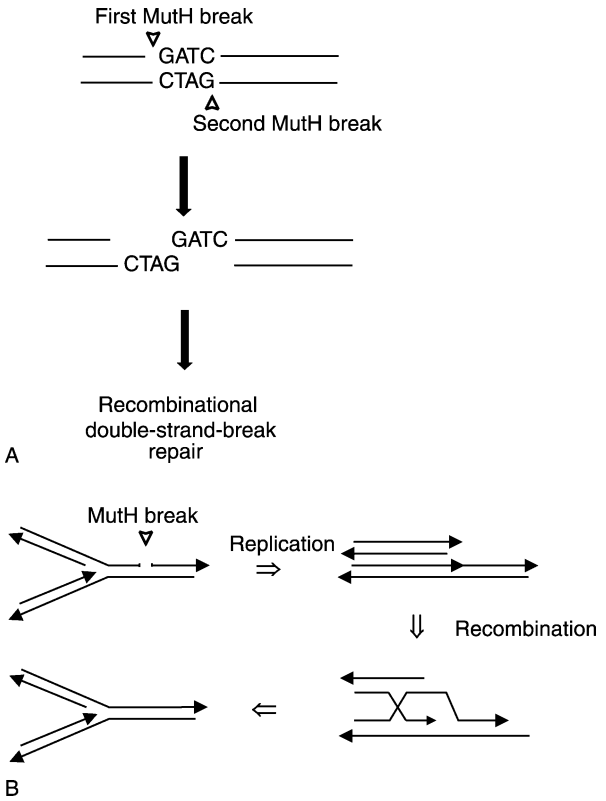

FIGURE 2 Generation of double-strand DNA breaks. (A) Mismatch repair endonuclease MutH introduces nicks on either side of a GATC sequence to produce a double-strand break. (B) Mismatch repair introduces a nick ahead of a replication fork producing a double-strand break when the fork encounters it. Recombination is required to restore the fork.

Mismatch repair in *dam* mutants is also the basis for the phenomenon of drug tolerance. The mutants are more sensitive than wild type to certain anticancer agents such as cisplatin, and methylating agents like streptozotocin. Inactivation of mismatch repair, however, renders the cell tolerant to these agents. In other words, mismatch repair sensitizes *dam* cells to the effects of these deleterious agents. This is of interest because mammalian cells in culture respond in exactly the same way; that is, they are sensitive to these agents but become tolerant upon loss of mismatch repair capacity. The molecular basis for this phenomenon has yet to be defined.

Initiation of Chromosome Replication

In *E. coli*, chromosome replication is initiated only once per cell cycle and Dam methylation is involved in this process. Chromosome replication is initiated at *oriC*, a region which has a 10 times higher than expected density of GATC sequences, by the initiation protein DnaA. The promoter region of the *dnaA* gene must be methylated for maximal expression and methylated origins are more efficiently initiated than unmethylated ones. The neighboring hemimethylated *oriC* and *dnaA* gene region is bound specifically and with high affinity by the SeqA protein which prevents methylation by Dam methyltransferase and renders the origin inert to further initiation (the eclipse period). By a process that is not understood, SeqA is released from *oriC* later in the cell cycle and methylation ensues followed by another initiation event.

Fast-growing wild type cells contain multiple origins and these initiate synchronously. The eclipse period is dependent on the level of Dam methyltransferase and can be lengthened or shortened by decreasing or increasing the enzyme level respectively. *In vivo*, *dam* and *seqA* mutants have an asynchronous initiation pattern and the eclipse period is shortened or absent. The *seqA* mutant, as expected, performs extra initiations each cell cycle but the *dam* mutant does not. This indicates that in *dam* mutants there must be an alternative mechanism preventing excessive initiation.

Altered Gene Expression

The state of GATC methylation can affect protein–DNA interaction and if this tetranucleotide sequence occurs in promoter or regulatory DNA regions, gene expression can be altered. As discussed, the *dnaA* gene is maximally transcribed only if the promoter region is fully methylated. This is consistent with its role in the initiation of chromosome replication. Another example is the

promoter for the *tsp* (transposase) gene of the mobile genetic element, *Tn*10, which controls the rate of transposition. This promoter is active only when it is hemimethylated thereby ensuring that transposition is coupled with chromosome duplication and occurs only once per cell cycle. A further example is the *pap* (pyelonephritis-associated pilus) operon in pathogenic *E. coli*, where Dam and the transcriptional activator Lrp compete for binding to specific symmetrically unmethylated GATC sequences. Depending on which protein is bound, *pap* expression is either off or on.

There are few other genes where the rationale of coupling methylation to gene expression is so clear-cut. High-density oligonucleotide array analysis of mRNA from *dam* mutants indicates that expression of many genes is altered. In several instances this is due to competition between Dam methyltransferase and transcriptional activators such as Fnr and Cap competing for the GATC sites that overlap their recognition sequences. For other genes such as *sulA* (involved in control of cell division) and *glnS* (glutamyl-tRNA synthetase), which have GATCs in their promoter regions, expression is increased when they are unmethylated. The biological rationale for this is unclear especially since in a wild type background these promoter regions would never be unmethylated. There are also many examples where GATCs in the promoter region have no effect on initiation of transcription. At present, there are no rules to predict if a GATC sequence in the promoter will increase, decrease, or have no effect on the frequency of transcription initiation.

As discussed, *dam* mutant DNA is subjected to DNA breakage *in vivo*. This results in the induction of a stress response termed SOS in which transcription of about 50 genes is increased. The gene products include those that repair DNA damage, recombination, and control cell division. In *dam* mutants, this response is constitutively expressed because three recombination proteins (RecA, RuvA, and RuvB), which are part of the response, are required for cell viability.

Role of Dam Methylation in Bacterial Pathogenesis

Altered levels of Dam methyltransferase can modulate the virulence of certain bacterial pathogens including *Salmonella*, *Yersinia*, and *Vibrio* in animal models and in *Erwinia*, a plant pathogen. The best-studied system is the *Salmonella*-mouse model. *Dam* mutant *Salmonella* are 10 000 times less capable of killing mice than wild type but a low level of tissue infectivity occurs. Mice that have been infected with the avirulent *dam* mutant become much more resistant to killing by wild-type *Salmonella* suggestive of a vaccine effect. The molecular basis for the role of Dam methylation in bacterial pathogenesis has yet to be elucidated but mismatch repair-deficient *Salmonella* are fully virulent. As there is a large group of virulence genes in *E. coli* and *Salmonella* whose expression is altered in *dam* mutants, it is likely that the basis for the avirulent phenotype of *dam* mutants is due to gene expression at inappropriate times allowing the animal hosts to mount an effective challenge to bacterial invasion.

A contrast to the *Salmonella* example is provided by *Neisseria* that can cause meningitis. These bacteria have a *dam* gene but it is not involved in pathogenesis. Rather, it is defects in the mismatch repair system (*mutS* and *mutL* gene inactivation) that allows for frameshift mutations to occur in DNA sequences controlling expression of certain virulence genes. There is no general rule about the effect of Dam methylation on virulence; it has to be investigated for each organism.

Role of Dam Methylation in Other Bacteria and Their Viruses

At present, little is known about the role of Dam methylation in other bacteria. Inactivation of the *dam* gene in *Yersinia* and *Vibrio*, however, is a lethal event, although the reason is not known. In contrast, inactivation of the *dam* gene in *Neisseria meningitidis* is not lethal, does not lead to a mutator phenotype and inactivation of recombination does not lead to lethality. This suggests a fundamentally different role for Dam methyltransferase in this species compared to the *E. coli* paradigm.

The bacterial virus P1 has its own *dam* gene that is related to that of its *E. coli* host and is essential for its life cycle. Dam methylation is required at the stage where the viral DNA is packaged into the heads. This is accomplished by filling the head with genomic DNA and then cleaving it at specific sequences, termed *pac* sites. These *pac* sites are flanked by multiple GATC sequences which must be methylated in order for cleavage to occur. In other *E. coli* bacterial viruses, however, such as T2 and T4, deletion of the *dam* gene has no discernable effect on their life cycle. Again, no generalizations can be made regarding the essentiality of the *dam* gene for viability.

See Also the Following Articles

DNA Methyltransferases, Structural Themes • DNA Mismatch Repair in Bacteria • Exonucleases, Bacterial

Glossary

DNA methyltransferase Enzyme that transfers a methyl group to a base in DNA.

epigenetic Pertaining to phenotypic, but not genotypic, change.

exonuclease Enzyme that digests DNA strand from an end.

hemimethylated Describing DNA in which one strand contains methylated residues but the complementary strand does not.

promoter Sequence at which RNA polymerase initiates transcription.

Further Reading

Casadesus, J., and Torreblanca, J. (1996). Methylation-related epigenetic signals in bacterial DNA. In *Epigenetic Mechanisms of Gene Regulation* (V. E. A. Russo, R. A. Martienssen and A. D. Riggs, eds.) pp. 141–153. Cold Spring Harbor Laboratory, Cold Spring Harbor, New York.

Cheng, X., and Roberts, R. J. (2001). Ado-Met-dependent methylation, DNA methyltransferases and base flipping. *Nucleic Acids Res.* **29**, 3784–3795.

Low, D. A., Weyand, N. J., and Mahan, M. J. (2001). Roles of DNA adenine methylation in regulating bacterial gene expression and virulence. *Infect. Immun.* **69**, 7197–7204.

Marinus, M. G. (1996). Methylation of DNA. In *Escherichia coli and Salmonella: Cellular and Molecular Biology* (F. C. Neidhardt, R. Curtiss, J. L. Ingraham, E. C. C. Lin, K. B. Low, B. Magasanik, W. S. Reznikoff, M. Riley, M. Schaechter and H. E. Umbarger, eds.) 2nd edition, pp. 782–791. American Society for Microbiology, Washington, DC.

Biography

Dr. Martin G. Marinus is a Professor in the Department of Biochemistry and Molecular Pharmacology at the University of Massachusetts Medical School in Worcester. His principal research interest is the molecular biological processes that involve DNA adenine methylation in *Escherichia coli*. He holds a Ph.D. from the University of Otago, New Zealand, and received his postdoctoral training at Yale University.

DNA Mismatch Repair and Homologous Recombination

Ivan Matic and Miroslav Radman
INSERM U571, Faculté de Médecine Necker-Enfants Malades, Université Paris V, Paris, France

Mismatches are mispaired or unpaired bases in the double-strand DNA molecule. Mismatches are generated as a consequence of errors during DNA replication or during homologous recombination involving nonidentical sequences. Specific mismatches can be formed by DNA damage. Enzymes that recognize and process mismatches have been identified in prokaryotes and eukaryotes. Different mismatch repair systems (MRS) are distinguished on the basis of their mismatch specificity and the size of excision tract that varies from single nucleotide to over a kilobase. The long-patch, also called the general, MRS (because it recognizes a variety of mismatches) is highly conserved during evolution. This repair system controls the fidelity of chromosomal replication by eliminating DNA biosynthetic errors and participates in the processing of some DNA lesions in transcription-coupled repair and in meiotic and mitotic recombination processes. The control of homologous recombination is particularly important because this fundamental biological process is essential for the maintenance of chromosomal integrity, generation of genetic diversity, proper segregation of meiotic chromosomes, and the speciation. Specific mismatches created by chemical modification of DNA bases (e.g., G:T mismatch due to deamination of 5-methyl-C to T or 8-oxo-G:A mismatch due to oxidation of G) are repaired by specialized short-patch MRS. When such mismatches occur in the course of recombination, their localized repair in heteroduplex DNA creates mosaic sequences, i.e., an apparent hyper-recombination effect.

Generalized Mismatch Repair Systems

Escherichia coli Methyl-Directed Mismatch Repair Pathway

The best characterized generalized MRS is *Escherichia coli* methyl-directed MRS. It has been completely reconstituted *in vitro* and involves three dedicated proteins: MutS, MutL, and MutH. Other proteins that participate in the processing of mismatches are shared with other repair pathways. MutS protein recognizes and binds to mismatches, MutL associates with MutS-mismatch complex and activates MutH, which incises the newly synthesized strand at a nearby unmethylated 5′-GATC-3′ site. GATC sites are hemimethylated because methylation of adenine by Dam methylase lags behind replication by several minutes. Thus, MutH directs the mismatch repair process to the newly synthesized strand. Neither MutH nor nonmethylated GATC are required if a single strand break is present in the substrate DNA. The helicase II (MutU) unwinds the DNA allowing degradation of the displaced single-strand DNA, assuring the irreversibility of this repair process. The involvement of different exonucleases in this repair pathway depends on orientation of the nick relative to the mismatch. The repair process is finalized by DNA polymerase III and DNA ligase activity.

MutS protein recognizes seven of eight possible base pair mismatches, C-C mismatches (the least frequent replication error) being refractory. In addition, MutS protein binds up to four unpaired bases allowing for repair of frameshift errors. MutS does not recognize mismatches in a sequence-specific manner, although sequence context does influence the efficiency of repair. MutS protein binds to mismatches as a homodimer and has affinities for various mismatches that reflect the efficiency of *in vivo* repair. MutS proteins possess an intrinsic ATPase activity, which is essential for mismatch repair. The inactivation of *mutS*, or any other of *mut* genes coding for general MRS, show identical strong mutator phenotypes with 10^2- to 10^3-fold increased rates of transition (G:C → A:T and A:T → G:C) and frameshift mutations, as compared to mismatch repair proficient bacteria.

Generalized Mismatch Repair in Eukaryotes

The knowledge about *E. coli* general MRS greatly facilitated identification and comprehension of homologous MR systems in other organisms. However, there are significant differences between these repair systems.

In most organisms, DNA strand recognition is not governed by DNA methylation. Dam methylase, coupled with the presence of *mutH* gene, has been identified in only a limited number of bacterial species. The mechanism of strand discrimination in other prokaryotes and eukaryotes is not yet elucidated.

Core functions of MRS, MutS, and MutL proteins are conserved in prokaryotes and eukaryotes. However, unlike its prokaryotic homologs, these proteins function as heteromers. The most extensively characterized eukaryotic generalized MRS is that of *Saccharomyces cerevisae*. In this organism, six MutS homologues (Msh1-6) have been identified. Msh1 functions in mitochondria, while others act in the nucleus. Heterodimers of the MutS homologs cooperate with heterodimers of MutL homologs to process different mismatches. Msh2–Msh6 (MutSα) complex preferentially targets base pair mismatches and insertions/deletions of one or two nucleotides. Msh2–Msh3 (MutSβ) binds 1–10 nucleotides large insertion/deletions loops.

Four MutL homologs (Mlh1-3 and Pms1) were identified in *S. cerevisae*. These proteins also form heterodimers. The majority of mismatch-repair activity is carried out by Mlh2-Pms1 heterodimer interacting with either MutSα or MutSβ complex. Mlh1 forms complexes with either Pms1, Mlh2, or Mlh3, each having distinct roles in the repair of mutational intermediates. As in prokaryotes, additional factors participate in *S. cerevisae* mismatch repair: proliferating cell nuclear antigen (PCNA; processivity factor for replication machinery) Exo1 ($5' \rightarrow 3'$ exonuclease), and the DNA polymerases δ and β.

In other eukaryotic organisms, invertebrates, vertebrates, and plants, multiple MutS and MutL homologs have also been identified. Different species contain different sets of homologs, without an obvious correlation to their position in the evolutionary tree. The eukaryotic mismatch-repair deficient mutants show mutator phenotypes similar to prokaryotic ones, i.e., increased rate of transition and frameshift mutations.

Mismatch Repair System and Homologous Recombination

Anti-Recombination Activity in *Escherichia coli*

Homologous recombination can be defined as interaction between two DNA sequences sharing extensive nucleotide sequence identity, present on a single or two different DNA molecules, that results in generation of mixed sequences derived from two parental ones. The homologous recombination process occurs in four basic steps: initiation, homologous pairing and DNA exchange, DNA heteroduplex extension, and resolution. The recombination process is initiated by combined action of a variety of nucleases and helicases that generate single-strand DNA. Single-strand DNA is substrate for proteins that catalyze homologous pairing and DNA exchange. The best studied homologous pairing and DNA exchange protein is *Escherichia coli* RecA.

RecA protein binds to single-strand DNA, or double-strand DNA containing single-strand DNA gaps, and forms a nucleoprotein complex containing one RecA protein monomer for every three nucleotides. RecA-single-strand DNA filaments engage search for homologous target DNA sequences. Scanning DNA for homologous sites is very fast and highly accurate even when they are very rare in the genome. *In vitro* data show that one helical turn of a RecA nucleoprotein filament containing approximately six RecA monomers and 15 bases of single-strand DNA is the functional unit sufficient to carry out the homology search. *In vivo* data show that RecA-catalyzed pairing is effective providing that the length of shared uninterrupted identity is at least 26 nucleotides.

After homologous pairing is achieved, the resultant joint molecules exchange homologous strands and establish heteroduplex DNA, where each parental DNA contributes one complementary strand. Heteroduplex DNA is extended by a unidirectional branch migration step. At this step of recombination, RecA protein tolerates DNA lesions, large heterologies, and up to 30% nucleotide sequence divergence between recombining molecules. However, pairing of nonidentical DNA sequences produces mismatched heteroduplex molecules, a substrate for MRS (Figure 1). *In vitro* experiments demonstrated that MutS and MutL proteins block RecA catalyzed strand-exchange and elongation of heteroduplex. *In vivo* MRS is capable of impeding recombination even between sequences with very low divergence. For example, transductional recombination between two serovars (Typhimurium and Typhi) of *S. enterica*, whose genomes differ only 1–2% at DNA sequence level, increases 10^2- to 10^3-fold in MRS deficient genetic background.

The antirecombination activity of the MRS is a consequence of blocking the RecA-catalyzed heteroduplex elongation but also of reducing the length of sequence identity needed for RecA-mediated homologous pairing and DNA exchange. The increased concentration of RecA protein does not prevent mismatch-repair antirecombination activity, whereas the overproduction of MutS and MutL proteins severely reduces recombination frequency between diverged DNAs (Figure 2).

Unlike the identical effect of MRS mutants on spontaneous mutagenesis, the inactivation of different MRS genes has distinct and characteristic effect on the recombination between diverged sequences. Very strong

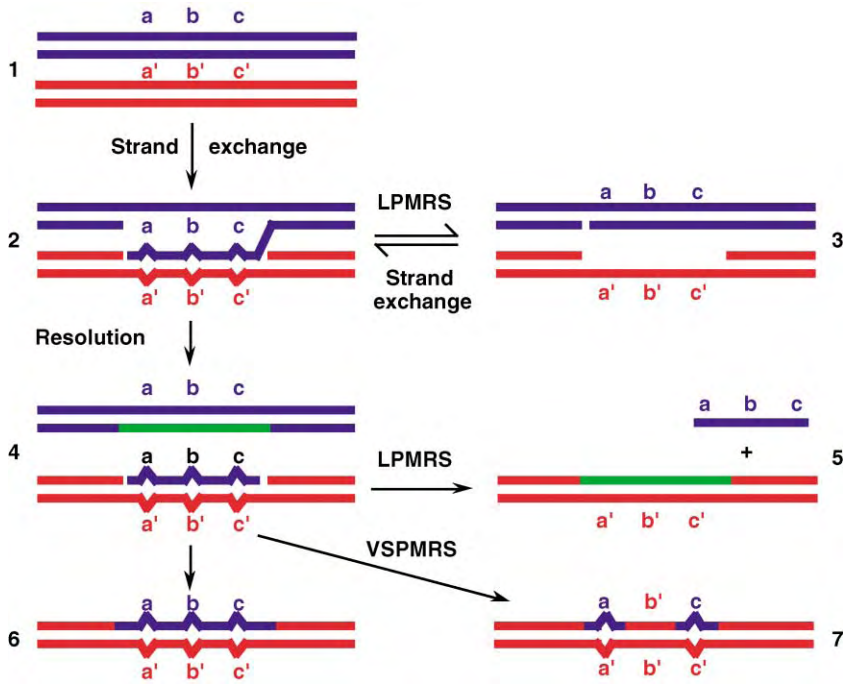

FIGURE 1 Anti-recombination by long patch mismatch repair system (LPMRS) and hyper-recombination by very short patch mismatch repair system (VSPMRS). a/a′, b/b′, and c/c′ represent single nucleotide polymorphisms between two recombining DNA molecules (blue and red) (1). For simplicity, only one kind of strand exchange (asymmetric strand exchange) is shown; a:a′, b:b′ and c:c′ are mismatched bases in the heteroduplex intermediate (2). LPMRS can destroy mismatched heteroduplex before (3) of after (4 and 5) resolution of recombination intermediates. Heteroduplexes that escape LPMRS, and which are sealed by ligase (6), will be separated by subsequent replication producing one recombinant and one parental DNA molecule. If some of the mismatches (e.g., b:b′) in this heteroduplex molecule are substrate for VSPMRS, its activity will generate a complex recombinant on the repaired strand (7). Green lines represent tracts of DNA repair synthesis.

hyper-recombination effect is observed upon inactivation of *mutS* and *mutL* genes (Figure 2), while the effect of inactivation of *mutU* and *mutH* genes is relatively weak. The presence of single strand ends in recombination intermediates (Figure 1) can explain the weak effect of *mutH* gene inactivation. The helicase II can probably be replaced by other enzymes that are involved in recombination, e.g., RecG.

Anti-Recombination Activity in *Saccharomyces cerevisae*

The anti-recombination activity of the eukaryotic MRS has been best characterized in *S. cerevisiae*, where it can inhibit recombination between diverged sequences both in mitosis and in meiosis. Even a single mismatch is sufficient for MRS to inhibit recombination, while additional mismatches have a cumulative negative effect on recombination efficiency. When DNA sequence divergence reaches several percent, the probability of a heteroduplex recombination intermediate to escape detection by the MRS is so low that the additional mismatches fail to increase anti-recombination activity. The MutSα or MutSβ complexes recognize the same types of mismatches in recombination intermediates as in replication intermediates. Although *msh2* and *mlh1* or *pms1* mutants have identical mutator phenotypes, *msh2* mutants exhibit higher recombination rates between diverged DNAs than do *pms1* or *mlh1* mutants. This indicates that Msh binding to mismatch may by itself inhibit the recombination process.

In *S. cerevisiae*, MRS processing of recombination intermediates results in gene conversion or complete destruction of recombination intermediates. Gene conversion is a genetic phenomenon in which information on one chromosome is replaced with information from the homologous chromosome, which remains unchanged (nonreciprocal recombination). In *S. cerevisae*, where it is possible to analyze all four products derived from a single meiosis, a non-Mendelian 3:1 segregation pattern of allelic sequences is diagnostic of a gene conversion event. In the absence of a functional MRS, mismatches in heteroduplex recombination intermediates are not repaired and the mismatch-containing DNA strands segregate at the first mitotic division following meiosis (postmeiotic segregation or PMS). The frequency of PMS reflects the repair efficiency for the particular mismatch. In *msh2*, *pms1*, *mlh1*, and to a lesser extent *msh3* and *msh6* mutants, meiotic gene

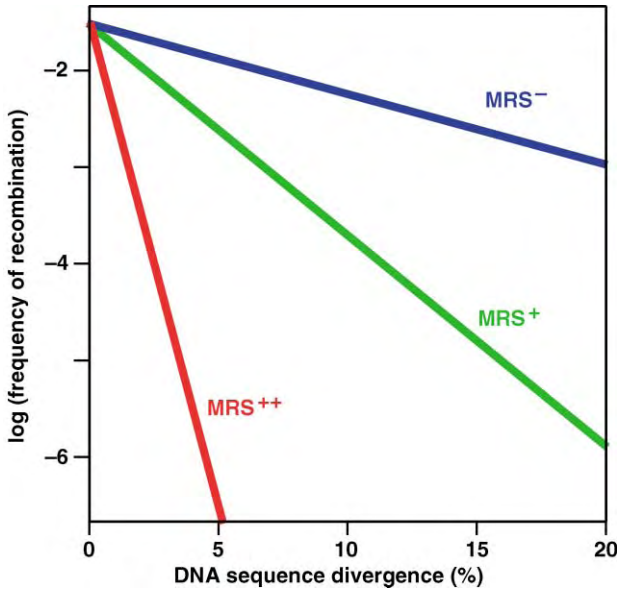

FIGURE 2 The relationship between DNA sequence divergence, homologous recombination, and mismatch repair system (MRS). Conjugational crosses between enterobacterial strains and species show that linear increase of sequence divergence between recombining genomes results in the exponential decrease in recombination frequency. This relationship shows that an increase in DNA divergence increases the difficulty for RecA protein to find the sites for initiation of homologous pairing and strand exchange. The MRS activity reduces the apparent length of these sites and blocking the maturation of RecA-catalyzed recombination intermediates. Consequently, the inactivation of MRS decreases the slope of correlation between recombination and DNA divergence, i.e., increasing the frequency of recombination between diverged sequences. In contrast, the overproduction of the key MRS proteins (MutS and MutL) increases the slope (MRS^{++}), i.e., creates new genetic barriers.

conversion events are reduced while PMS events are elevated. Since the repair patch is shorter than the meiotic heteroduplex DNA, the repair process does not necessarily interfere with the formation of crossing overs. Although the same mismatch-repair machinery detects mismatches in both recombination and replication intermediates, some accessory proteins are probably unique to each type of repair. For example, PCNA appears to play a role in correcting DNA replication errors but has not been implicated in the correction of heteroduplex recombination intermediates.

MRS inhibits crossing-over between diverged chromosomes in interspecific hybrids during meiosis, and therefore it is also important for establishing and maintaining interspecific genetic barriers. In addition, the mismatch-triggered anti-recombination activity of eukaryotic MRS proteins inhibits ectopic interactions between diverged, repetitive DNA sequences during both mitosis and meiosis, and therefore it maintains genome stability by preventing genome rearrangements. Interestingly, mitotic recombination in yeast is more sensitive (in a mismatch repair-dependent manner) to low levels of sequence divergence than is meiotic recombination, which may help reinforce the strong bias for sister chromatid versus interhomolog interactions during mitosis.

Two *S. cerevisiae* MutS homologs Msh4 and Msh5 have completely lost the ability to participate in a standard mismatch repair reaction but have acquired novel, meiosis-specific roles. The loss of either MSH4 or MSH5 is associated with an approximately 50% reduction in meiotic crossing-over, in increased levels of homolog nondisjunction, and decreased viability of meiotic products. The Msh4 and Msh5 genes are in the same epistasis group and, like the other MutS homologs, physically interact to form heterodimers. As gene conversion levels are normal in *msh4* or *msh5* mutants, the Msh4-Msh5 complex is assumed to act late in recombination. Genetic data indicate that the Msh4–Msh5 heterodimer interacts specifically with the Mlh1-Mlh3 complex to promote meiotic crossing-over. Both *mlh1* and *mlh3* mutants exhibit a reduction in meiotic crossover events, and epistasis analysis indicates that Mlh1 and Msh4 act in the same crossover pathway.

DNA Sequence Divergence, Mismatch Repair, Loss of Heterozygosity, and Cancer

Carcinomas evolve by accumulation of several somatic mutations, of which some are recessive (e.g., in tumor suppressor genes). Such mutations are expressed only when homozygous, i.e., when both alleles in diploid cells are inactivated by mutation. The transition from the heterozygous (m/+) to homozygous (m/m) or hemizygous (m/o) state usually occurs due to a chromosomal rearrangement leading to the loss of the functional gene copy (Figure 3). Such rearrangement can be due to (i) the loss of the (+) allele (e.g., a small or large deletion, or the loss of the entire chromosome), or (ii) a homologous recombination event, such as gene conversion of the allele to (m/m) or a mitotic crossover anywhere between the centromere and the allele (Figure 3). All these events, with the exception of gene conversion, lead to the loss of heterozygosity (LOH) initially present because of the maternal/paternal sequence divergence (about 0.1% of nucleotides in human population).

Two lines of experiments suggest that the functionally largely neutral sequence polymorphism between the two parental lines effectively suppresses the mitotic recombination mechanism for LOH:

(a) Gene targeting in mouse embryonic stem cells is highly sensitive to the natural sequence polymorphism of the parental strains. That suppression of mitotic

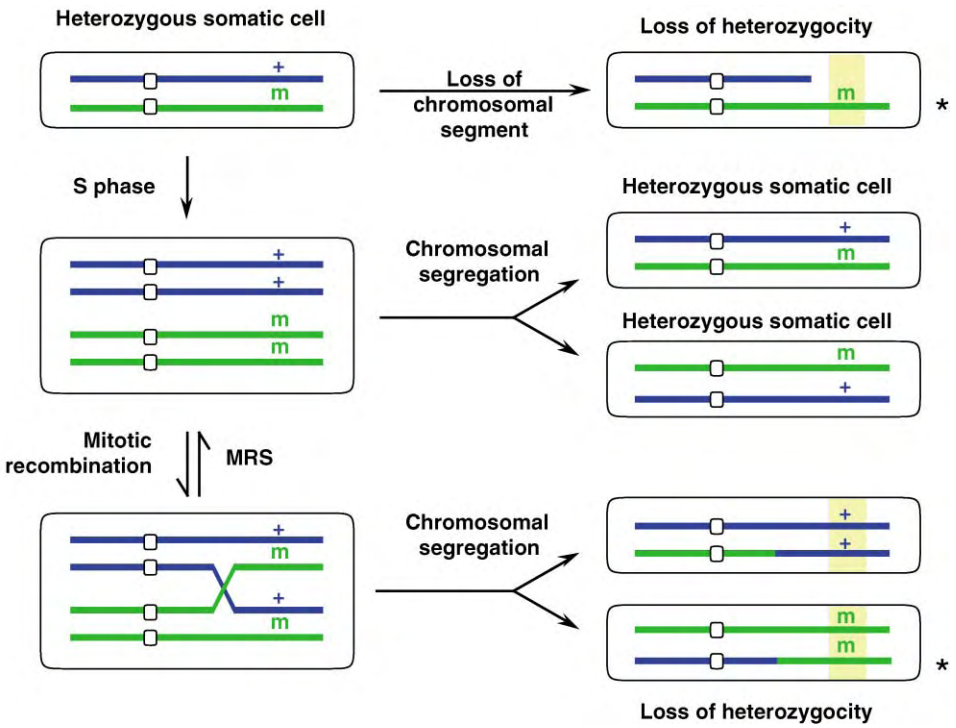

FIGURE 3 DNA sequence divergence, mismatch repair, and loss of heterozygosity. Only one pair of homologous chromosomes is shown. The chromosome colors (blue and green) indicate the sequence polymorphism between the maternal and paternal line (0.1% in human population). The symbol (m) stands for a specific recessive mutation. Only cells (*) having lost the wild type (+) allele express the (m) mutation. Such cells show loss of heterozygocity (LOH; yellow). In human tumors, most LOH occurs by chromosomal rearrangements (top right). However, in inbred mice, with little or no sequence divergence between homologs, most LOH occurs by mitotic recombination. The recombination-suppressing effect of sequence polymorphism is relieved in MRS deficient mouse cells (see Figure 1). Because LOH is an obligate step in the expression of recessive mutations in tumor suppressor genes, sequence polymorphism protects against cancer due to MRS activity.

recombination can be relieved by the defect in mismatch repair, i.e., it appears that the mammalian mismatch repair acts to prevent mitotic recombination between nonidentical sequences.

(b) The expression of a recessive heterozygous (m/+) mutation in inbred, globally highly homozygous mice, occurs at elevated frequency *via* mitotic recombination, i.e., LOH from the crossover point to the end of the chromosome including the recessive mutation (Figure 3). In hybrids between different strains, the LOH frequency is much lower than in inbred strains. The decrease in LOH is accounted by the loss of mitotic recombination due to the activity of the MRS.

Thus, it appears that – like in bacteria and yeast – the editing (suppression) of homologous recombination by the MRS, based on the sequence divergence between the recombining sequences, functions also in mammalian cells. Such genetic barriers based on the genomic sequence polymorphism are expected to: (i) delay the process of carcinogenesis by delaying the expression of relevant recessive somatic and inherited mutations, and (ii) enhance sympatric speciation by creating genetic isolation on the germ line level.

Evolutionary Role of the Control of Homologous Recombination by Mismatch Repair

Evolutionary conservation of key MRS functions illustrates the importance of this genetic system in the preservation of genomic integrity in prokaryotes and eukaryotes. In bacteria, the loss of MRS activity can provide transient selective advantage when adaptation is limited by the supply of mutations. However, the restoration of MRS proficiency is prerequisite for evolutionary success because upon adaptation, the load of deleterious mutations is no longer counterbalanced by the generation of beneficial mutations resulting in fitness reduction. In eukaryotes, the increased genomic instability resulting from MRS deficiency is apparently never advantageous. For example, in mammals, the loss of MRS activity is associated with male or female sterility and tumorigenesis.

Increased frequency of chromosomal rearrangements is a particularly deleterious phenotype of MRS deficiency in prokaryotes and eukaryotes. For example,

the inactivation of MRS increases 10-fold the frequency of chromosomal duplications resulting from recombination between *E. coli rhsA* and *rhsB* loci (0.9% divergent) and about 10^3-fold gene conversion between *Salmonella enterica tufA* and *tufB* genes (about 1% divergent). The MRS-mediated recombination surveillance is particularly important for eukaryotes because their genomes contain a multitude of repetitive DNA sequences. MRS in *S. cerevisiae* prevents intra- and inter-chromosomal crossovers and gene conversions resulting from recombination between nonidentical DNA sequences.

By controlling homologous recombination, MRS controls also the process of speciation. In bacteria, MRS controls conjugational, transductional, and transformational recombination between strains and species, thus reducing gene flow between diverged populations. Similarly, by controlling crossing-over and chromosome segregation in meiosis, MRS prevents hybridization between diverged organisms resulting in reproductive isolation of closely related species.

See Also the Following Articles

DNA Ligases: Mechanism and Functions • DNA Ligases: Structures • DNA Mismatch Repair and the DNA Damage Response • DNA Mismatch Repair Defects and Cancer • DNA Mismatch Repair: *E. coli* Vsr and Eukaryotic G–T Systems • DNA Mismatch Repair in Bacteria • DNA Mismatch Repair in Mammals • DNA Polymerase III, Bacterial • Mitosis • Recombination: Heteroduplex and Mismatch Repair *in vitro*

Glossary

homologous recombination Interaction between two DNA sequences sharing extensive nucleotide sequence identity, present on a single or two different DNA molecules, that results in generation of mixed sequences derived from two parental ones. Such recombination events can be nonreciprocal (gene conversion or "patch" recombinants) or reciprocal (crossover or "splice" recombinants).

meiosis (from Greek, *meion*, smaller) Two successive nuclear and cellular divisions resulting in the reduction of the chromosome number from diploid to haploid. The products of meiosis are haploid gametes. Because chromosome segregation in meiosis requires physical attachment of homologous chromosomes (chiasmata), each chromosome in the gamete is recombinant.

mismatch Mispaired or unpaired bases in the double-strand DNA molecule.

mitosis (from Greek, *mitos*, thread) Nuclear and cellular division of a eukaryotic somatic cell resulting in the generation of two daughter cells having the same number of chromosomes as the parent cell.

mutation (from Latin *mutare*, to change) Any heritable modification of genetic material.

Further Reading

Borts, R. H., Chambers, S. R., and Abdullah, M. F. (2000). The many faces of mismatch repair in meiosis. *Mutat. Res.* **451**, 129–150.

Chang, D. K., Metzgar, D., Wills, C., and Boland, C. R. (2001). Microsatellites in the eukaryotic DNA mismatch repair genes as modulators of evolutionary mutation rate. *Genome Res.* **11**(7), 1145–1146.

Datta, A., Hendrix, M., Lipsitch, M., and Jinks-Robertson, S. (1997). Dual roles for DNA sequence identity and the mismatch repair system in the regulation of mitotic crossing-over in yeast. *Proc. Natl Acad. Sci. USA* **94**, 9757–9762.

de Wind, N., Dekker, M., Berns, A., Radman, M., and te Riele, H. (1995). Inactivation of the mouse Msh2 gene results in mismatch repair deficiency, methylation tolerance, hyperrecombination, and predisposition to cancer. *Cell* **82**, 321–330.

Friedberg, E. C., Walker, G. C., and Siede, W. (1995). *DNA Repair and Mutagenesis*. ASM Press, Washington, D.C.

Harfe, B. D., and Jinks-Robertson, S. (2000). Mismatch repair proteins and mitotic genome stability. *Mutat. Res.* **451**, 151–167.

Hunter, N., Chambers, S. R., Louis, E. J., and Borts, R. H. (1996). The mismatch repair system contributes to meiotic sterility in an interspecific yeast hybrid. *EMBO J.* **15**, 1726–1733.

Jones, M., Wagner, R., and Radman, M. (1987). Mismatch repair and recombination in *E. coli*. *Cell* **50**, 621–626.

Matic, I., Taddei, F., and Radman, M. (1996). Genetic barriers among bacteria. *Trends Microbiol.* **4**, 69–73.

Modrich, P., and Lahue, R. (1996). Mismatch repair in replication fidelity, genetic recombination and cancer biology. *Annu. Rev. Biochem.* **65**, 101–133.

Rayssiguier, C., Thaler, D. S., and Radman, M. (1989). The barrier to recombination between *Escherichia coli* and *Salmonella typhimurium* is disrupted in mismatch-repair mutants. *Nature* **342**, 396–401.

Shao, C., Yin, M., Deng, L., Liskay, R. M., Stambrook, P. J., Doetschman, T. C., and Tischfield, J. A. (2002). Loss of heterozygosity and point mutation at Aprt locus in T cells and fibroblasts of Pms2-/- mice. *Oncogene* **21**, 2840–2845.

Vulic, M., Dionisio, F., Taddei, F., and Radman, M. (1997). Molecular keys to speciation: DNA polymorphism and the control of genetic exchange in enterobacteria. *Proc. Natl Acad. Sci. USA*. **94**, 9763–9767.

Biography

Miroslav Radman is Professor of cell biology at the Medical School Necker of the University Paris 5. He is also the Director of the research Unit No. 571 of INSERM entitled "Evolutionary and Medical Molecular Genetics." He is a member of the EMBO, Academia Europea, French Academy of Science and Croatian Academy of Sciences and Arts. He is a pioneer in the study of DNA repair and mutagenesis, in particular of mutagenic SOS repair and the antimutagenic mismatch repair.

Ivan Matic is an Associate Research Professor of the French National Center for Scientific Research (CNRS). He directs the research group "Evolution of Enterobacteria" in the INSERM Unit No. 571 at the Medical School Necker, University Paris 5. He studies the mechanisms of mutation and recombination in bacteria, as well as their role in adaptive evolution of bacteria.

DNA Mismatch Repair and the DNA Damage Response

Guo-Min Li and Steven R. Presnell
University of Kentucky Medical Center, Lexington, Kentucky, USA

DNA mismatches are base-pairing errors that deviate from the Watson-Crick rules that stipulate that A pairs with T and G with C. In addition, small insertion/deletion structures, in which one DNA strand contains a small number of unpaired nucleotides, are also considered mismatches. Mismatched base pairs occur as errors during the normal course of DNA replication and recombination, and they are mutagenic if left uncorrected. DNA mismatch repair (MMR) is a cellular process that rectifies mismatches to yield correct Watson-Crick base pairs. MMR is an important genome maintenance system because defects in the system cause genomewide instability and have been implicated in the development of certain types of human cancer. In the past, the ability of the MMR system to correct DNA heteroduplexes has been considered the primary mechanism by which it contributes to genomic stability. However, more recent studies indicate that the MMR system also contributes to genomic stability by mediating protective cellular responses to DNA damage.

Mismatch Repair Proteins and Their Role in Mismatch Correction

The eukaryotic MMR pathway is similar to the *Escherichia coli* MutHLS pathway with respect to features of mechanism and involvement of several homologous activities. In fact, many of the eukaryotic MMR components were initially identified by their sequence homology to the *E. coli* MMR proteins (see Table I). The eukaryotic MMR proteins are known to include the MutS homologues (MutSα, MutSβ), the MutL homologues (MutLα, MutLβ, MutLγ), exonuclease I (ExoI), replication protein A (RPA, a eukaryotic, SSB (single strand DNA-binding protein)), and DNA polymerase δ. Although eukaryotic homologues of the bacterial MutH and helicase II have not yet been identified, studies in human nuclear extracts have demonstrated that the human MMR reaction possesses a mechanism similar to that of *E. coli*; that is, the repair is targeted to the newly synthesized strand and can occur bidirectionally. The eukaryotic system appears, however, to be more complex than the *E. coli* pathway. For example, whereas only a single form of MutS or MutL in *E. coli* has been documented, at least two MutS homologues and three MutL homologues have been identified in eukaryotic cells, each of which is a heterodimer. For example, MutSα consists of the polypeptides MSH2 and MSH6, and MutLα comprises MLH1 and PMS2 (see Table I). These MutS and MutL heterodimers, although redundant, play special roles in MMR subpathways. In human cells, MutSα and MutLα are the most abundant species among the MutS and MutL heterodimers, respectively.

Mismatch Repair Function is Required for Drug Cytotoxicity

Although MMR is well known for its role in correcting biosynthetic errors, other important roles for MMR proteins are being recognized; one of these is the mediation of programmed cell death (or apoptosis) in cells with heavily damaged DNA. This apoptotic function of the MMR system was realized from both basic and clinical studies on how chemical or physical DNA damaging agents induce tumor cells to undergo cell death.

Treatment of cells with chemical DNA-damaging agents, such as the alkylating agents, *N*-methyl-*N*′-nitro-*N*-nitrosoguanidine (MNNG), temozolomide, or procarbazine, leads to increased amounts of cell death. For this reason, these cytotoxic agents are often used in chemotherapy to destroy rapidly growing tumor cells. There is great interest in the cancer research community in understanding the mechanism by which these agents cause cell death. Interestingly, it has been found almost universally that, whereas cells that are proficient in MMR are sensitive to these agents, cells that are deficient in MMR are more resistant to killing by these agents. This was first observed with *E. coli* in the 1980s when *E. coli* MMR mutants (*mutS*$^-$ or *mutL*$^-$) were found to be more resistant to killing by

TABLE I

MMR Components and Their Function[a]

E. coli	Human	Function
MutS	MutSα (MSH2-MSH6)[b] MutSβ (MSH2-MSH3)	DNA mismatch/damage sensor
MutL	MutLα (MLH1-PMS2)[b] MutLβ (MLH1-PMS1) MutLγ (MLH1-MLH3)	Molecular chaperon and/or DNA damage signal transducer?
MutH	?	Strand discriminator
Helicase II	?	Unwinding DNA helix
ExoI, ExoVII, ExoX, RecJ	ExoI, ?	Removing mispaired base
Pol III holoenzyme	Pol δ, PCNA	Repair DNA synthesis
SSB	RPA	Protecting template DNA from degradation
DNA ligase	?	Nick ligation

[a] ExoI, exonuclease I; PCNA, proliferating cell nuclear antigen; Pol δ, polymerase δ; RPA, replication protein A; ?, not yet identified.
[b] Major components in cells.

MNNG than were wild-type bacterium. In addition, resistance to cytoxic agents such as cisplatin (a cross-linking agent) and MNNG has also been observed in human cells that are defective in MutSα or MutLα. An interesting example is afforded by the development of the lymphoblastoid cell line MT1. This cell line was derived from the TK6 cell line by selection with a high dose of MNNG. MT1 cells are 500-fold more resistant to killing by this agent than the parental cells and exhibit an elevated spontaneous mutation rate. The MT1 cell line was subsequently found to be defective in *MSH6*, the gene that encodes a subunit of MutSα that is necessary for MMR. Conversely, many human tumor cells that are defective in MMR have been found to be relatively resistant to alkylating agents. For example, the *MLH1*-defective colorectal tumor cell line HCT116 is resistant to killing by MNNG, and the MNNG resistance is lost by these cells when they have received a wild-type copy of the *MLH1* gene by chromosome transfer. Therefore, the cytotoxicity of DNA damaging agents is dependent on a functional MMR system.

Mismatch Repair Proteins Promote DNA Damage-Induced Cell Cycle Arrest and Apoptosis

Normal cells are known to undergo growth arrest at cell-cycle checkpoints when exposed to DNA-damaging agents. This response allows cells to respond to DNA damage either by repairing the damage or by committing programmed cell death (apoptosis). Interestingly, cells defective in MMR fail to arrest at crucial checkpoints after exposure to DNA-damaging agents. For example, MMR-proficient cells undergo growth arrest at the G2 phase of the cell cycle after treatment with alkylating agents, but MMR-deficient cells do not. The G2 phase arrest in MMR-proficient cells has been found to be associated with apoptosis. As illustrated in Figure 1, when wild-type TK6 cells and MutSα-deficient MT1 cells were treated with MNNG, apoptotic cell death was observed in TK6 cells (see the pattern of DNA

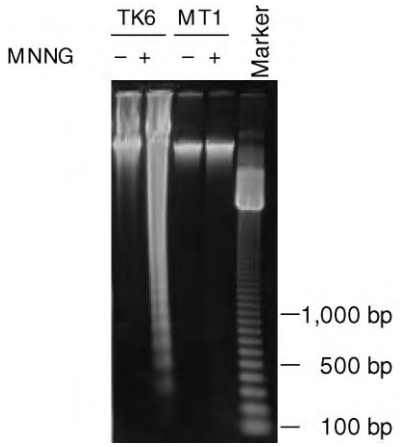

FIGURE 1 MNNG induces apoptosis in MMR-proficient cells. MMR-proficient TK6 and MMR-deficient MT1 cells were treated with MNNG for 1 h and then cultured in fresh medium for 24 h before harvesting. Genomic DNAs isolated from MNNG-treated (+) and untreated cells (−) were electrophoresed in a 2% agarose gel and detected by UV-illumination in the presence of ethidium bromide. Notice that DNA fragmentation is observed in MNNG-treated TK6 cells, but not in MNNG-treated MT1 cells. This DNA fragmentation pattern is diagnostic of apoptosis, or programmed cell death.

fragmentation, a classical characteristic of apoptosis), but not in MT1 cells. Similarly, MutLα is also required for alkylating agent-induced apoptosis. This MMR-dependent apoptotic response can be also induced by other DNA-damaging agents, including cisplatin, certain environmental carcinogens, and ionizing radiation. In addition to cell lines, DNA-damage-induced MMR-dependent apoptosis also occurs in classic laboratory animals such as the mouse and the soil nematode *Caenorhabditis elegans*.

How is the MMR pathway involved in the apoptotic response? Although the details are far from clear, MMR initiation factors may play a crucial role in this response by recognizing DNA damage. For example, it has been established that the *E. coli* mismatch recognition protein MutS and its eukaryotic homologues recognize DNA bases damaged or modified by a variety of agents. These agents include MNNG, cisplatin, chemical carcinogens, oxidative free radicals, and ultraviolet (UV) light. These damaged DNA bases, or DNA adducts, possess structures different from regular bases, thereby causing conformational changes in the DNA duplex. For example, whereas the 8-hydroxyguanine adduct generated by ionizing radiation is approximately the same size as guanine, the guanine adduct of benzo[a]pyrene dihydrodiol epoxide, an environmental chemical carcinogen, is twice as large as guanine. However, a common feature shared by these DNA adducts, as well as DNA base–base mismatches, is that they more or less distort the structure of the DNA helix. This distortion may constitute the basis of their recognition by MutS and its eukaryotic homologues.

Mismatch Repair Proteins Interact with Apoptotic Transducer in Response to DNA Damage

Apoptosis is normally mediated by the transcription factor p53 and its cousin, p73. Recent studies have indicated that both proteins are also implicated in MMR-dependent apoptosis. Upon treating cells with DNA damaging agents (e.g., MNNG), increased expression of p53 has been noted in MMR proficient cells, but not in cells defective in either MutSα or MutLα. The increased level of p53 is due to its phosphorylation by a protein kinase, whose activation is dependent on a functional MMR system. In addition to p53, cells also use p73 for MMR-dependent apoptotic response. Recent studies have shown that phosphorylation and stabilization of p73 occur in an MMR-dependent manner during cellular response to cisplatin-induced DNA damage. The phosphorylation of p73 is carried out by the c-Abl protein kinase and the stabilization of p73 requires the interaction of the protein with the MutL homologue protein, PMS2. These observations indicate that MMR-dependent apoptosis in response to DNA damage involves a signaling cascade.

Mismatch Repair-Mediated Apoptosis Eliminates Damaged Cells from Tumorigenesis

The molecular events involved in the MMR-dependent apoptotic response have not yet been established. However, based on what is already known, the apoptotic signaling is probably initiated by binding of MMR proteins to DNA adducts. This event stimulates the interactions between MMR proteins and an apoptotic transducer, p53 or p73. Two possible mechanisms for this signaling process are depicted in Figure 2. One model proposes that repetitive attempts by MMR to remove a DNA adduct in the template DNA strand cause cell death. DNA adducts in the template strand can pair with appropriate bases or lead to mispairs during DNA replication. MutSα, along with MutLα, recognizes these unusual base pairs as mismatches and provokes a strand-specific MMR reaction. However, because MMR is always targeted to the newly synthesized strand, adducts in the template strand cannot be removed and thus unusual base pairs reform upon DNA resynthesis during repair. As a result, the repair cycle can be perpetually reinitiated. Such a futile repair cycle may signal cells to switch on apoptotic machinery. Alternatively, the death signal could come from the binding of MutSα/MutLα to DNA adducts in the replication fork, the unwound DNA helix, or both and may be unrelated to the repair process. These protein–DNA adduct complexes may block DNA transactions such as replication, transcription, and repair and could be recognized as a signal for cell-cycle arrest and death. In both models, the action on DNA adducts by MMR proteins activates protein kinases to phosphorylate apoptotic transducers such as p73 and p53 that have just established their physical interactions with MMR proteins upon the MMR processing of DNA adducts. The phosphorylation of p73/p53 activates apoptotic machinery and takes the cell down the road to eventual death.

The MMR pathway is well known for its function of promoting genomic stability. The newly identified apoptotic function of MMR, however, may be as important as its replication-fidelity function for maintaining genomic stability. Normally, base excision repair and nucleotide excision repair pathways are responsible for the repair of DNA damage induced by

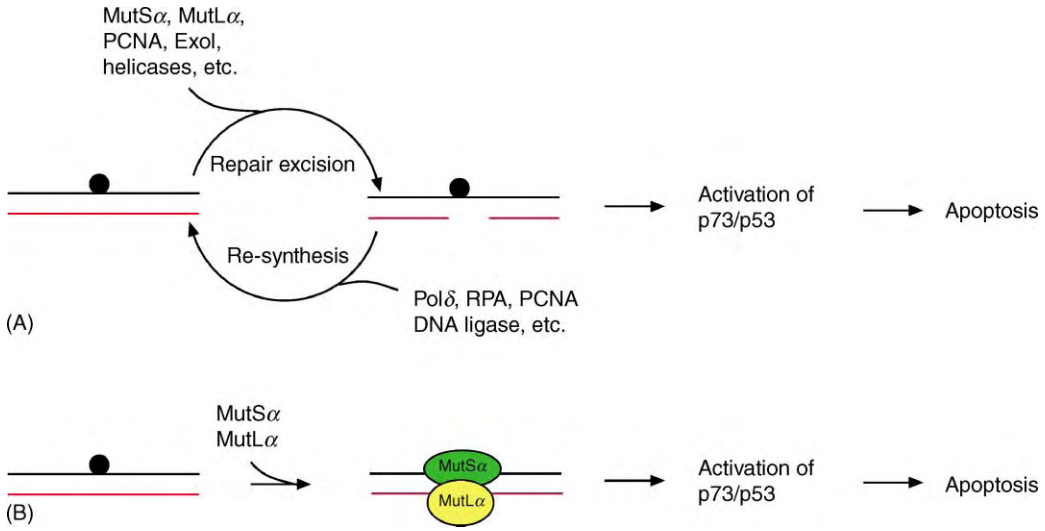

FIGURE 2 Proposed models of how MMR mediates apoptosis in response to DNA damage. (A) The futile repair cycle model. The adducted base (solid circle) could pair with an appropriate base or lead to a mispair during DNA replication. This abnormal structure can be recognized by MutSα (MSH2–MSH6) and provoke a strand-specific MMR reaction. However, because MMR can be only targeted to the newly synthesized strand (red line), the offending adduct in the template strand (black line) cannot be removed and will initiate a new cycle of MMR upon repair resynthesis. Such a futile repair cycle stimulates an interaction between MMR proteins and apoptotic transducers, including ATM/ATR, c-Abl, and p73/p53. These interactions may activate the apoptotic machinery. (B) The blockage model. The binding of MutSα/MutLα to a DNA adduct in the replication fork, the unwound DNA helix, or both could block DNA transactions such as replication, transcription, and repair. The blockage promotes MMR proteins to interact with apoptotic transducers to switch on apoptotic machinery. ExoI, exonuclease I; PCNA, proliferating cell nuclear antigen; Pol δ, polymerase δ; RPA, replication protein A.

physical and chemical agents. However, when excision repair pathways are not available or there is too much damage to be repaired, genomic DNA is in danger of accumulating a large number of mutations, a process that is tumorigenic. Eliminating these damaged cells from the body would be beneficial. It is the MMR system that initiates the elimination of these pre-tumorigenic cells by promoting apoptosis. The inability of the MMR system to commit genetically damaged cells to apoptosis may contribute to a molecular basis for cancer development.

See Also the Following Articles

Cell Death by Apoptosis and Necrosis • DNA Mismatch Repair Defects and Cancer • DNA Mismatch Repair: *E. coli* Vsr and Eukaryotic G–T Systems

Glossary

apoptosis An active cell death process that requires RNA and protein synthesis to specifically digest cellular DNA into nucleosomal fragments; also known as programmed cell death.

cytotoxicity The degree to which an agent possesses a specific destructive action on certain cells or the possession of such action; often used when referring to the action of antineoplastic drugs that selectively kill dividing cells.

DNA mismatch Non-G:C or -A:T DNA base pairs or small insertion/deletion (unpaired) nucleotides in duplex DNA; also called a heteroduplex.

DNA mismatch repair A DNA repair pathway that specifically coverts mismatched DNA bases (heteroduplexes) into normal G:C or A:T base pairs (homoduplexes).

tumorigenesis The process that generates tumors.

Further Reading

Aquilina, G., and Bignami, M. (2001). Mismatch repair in correction of replication errors and processing of DNA damage. *J. Cell Physiol.* **187**, 145–154.

Bellacosa, A. (2001). Functional interactions and signaling properties of mammalian DNA mismatch repair proteins. *Cell Death Differ.* **8**, 1076–1092.

Karran, P., and Bignami, M. (1994). DNA damage tolerance, mismatch repair and genome instability. *Bioessays* **16**, 833–839.

Li, G. M. (1999). The role of mismatch repair in DNA damage-induced apoptosis. *Oncol. Res.* **11**, 393–400.

Modrich, P. (1997). Strand-specific mismatch repair in mammalian cells. *J. Biol. Chem.* **272**, 24727–24730.

Biography

Guo-Min Li is an Associate Professor in the Department of Pathology at the University of Kentucky. His principal research interests are in mammalian DNA mismatch repair and its role in DNA damage response. He holds a Ph.D. from Wayne State University and received his postdoctoral training at Duke University His laboratory was among the first to demonstrate that the recognition and the processing of DNA adducts by mismatch repair proteins trigger apoptosis.

Steven R. Presnell is a Research Associate in Dr. Li's laboratory. He holds a Ph.D. from the Georgia Institute of Technology and received his postdoctoral training at the University of North Carolina, Chapel Hill.

DNA Mismatch Repair Defects and Cancer

Richard D. Kolodner
Ludwig Institute for Cancer Research, University of California, San Diego School of Medicine, La Jolla, California, USA

A major source of mutagenic mispaired bases is misincorporation errors that occur during DNA replication. If such errors are not repaired prior to the next round of DNA replication, they result in mutations. These misincorporation errors are normally corrected by DNA mismatch repair (MMR). MMR recognizes the resulting mispaired base in DNA and excises the misincorporated base from the newly synthesized DNA strand, which is then resynthesized. This process significantly increases the fidelity of DNA replication. Because of the critical role of MMR in suppressing DNA replication errors, MMR defects cause an increased rate of accumulating mutations. Such mutations can activate oncogenes or inactivate tumor suppressor genes and contribute to the process of carcinogenesis.

Introduction

It has been demonstrated that increased mutation rates resulting from DNA replication errors (Figure 1) can play a role in the development of cancer by the discovery that (1) hereditary nonpolyposis colorectal carcinoma (HNPCC) can be caused by inherited mutations in some genes encoding mismatch repair (MMR) proteins, (2) somatically acquired MMR defects underlie some sporadic cancers, and (3) mice containing mutations in MMR genes or mutations that decrease the fidelity of the replicative DNA polymerases result in increased cancer susceptibility. This entry briefly reviews our understanding of MMR.

Proteins Involved in Mismatch Repair

MutS Homologue Proteins Involved in Mismatch Repair

A model has been proposed for eukaryotic MMR in which mispaired bases in DNA are recognized by heterodimeric complexes of proteins that are homologues of the bacterial MutS protein (Figure 2). MutS is the bacterial MMR protein that recognizes mispaired bases in DNA (Mut is an abbreviation for Mutator, because mutations in the *mutS* gene cause high mutation rates or a mutator phenotype). Three different MutS homologues, called MSH proteins, function in MMR. These three different MSH proteins (MSH2, MSH3, and MSH6) form two different heterodimeric complexes, the MSH2–MSH6 (MutSalpha) and MSH2–MSH3 (MutSbeta) complexes (see Figure 2). Extensive genetic studies indicate that the MSH2–MSH6 (MutSalpha) complex is the major mismatch recognition complex that functions in repair of base:base mispairs and a broad spectrum of insertion/deletion mispairs. The MSH2–MSH3 (MutSbeta) complex appears to be able to substitute for the MSH2–MSH6 (MutSalpha) complex in the repair of many insertion/deletion mispairs and may be primarily responsible for the repair of larger insertion/deletion mispairs.

The MSH2–MSH6 (MutSalpha) and MSH2–MSH3 (MutSbeta) complexes have been purified and extensively studied. Consistent with genetic studies, MSH2–MSH6 (MutSalpha) is able to support the repair of both base:base mispairs and insertion/deletion mispairs in *in vitro* MMR reactions, whereas MSH2–MSH3 (MutSbeta) is only able to support the repair of insertion/deletion mispairs. The MSH2–MSH6 (MutSalpha) and MSH2–MSH3 (MutSbeta) complexes have also been shown to preferentially bind to mispaired bases in DNA. Upon mispair recognition they appear to form a ring around the DNA that can then move along the DNA and function in MMR. The MSH2–MSH6 (MutSalpha) complex binds to both base:base mispairs and insertion/deletion mispairs, whereas the MSH2–MSH3 (MutSbeta) complex appears to bind only insertion/deletion mispairs. There is some indication that the *Saccharomyces cerevisiae* and mouse MSH2–MSH3 (MutSbeta) complex may have a relatively greater ability to function in the repair of single base insertion/deletion mispairs than the human MSH2–MSH3 (MutSbeta) complex.

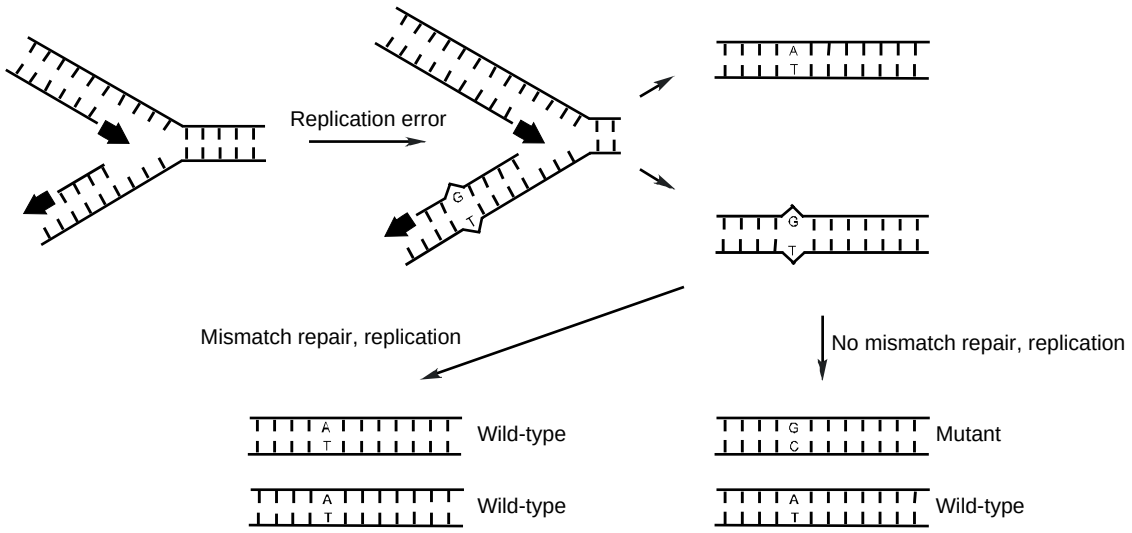

FIGURE 1 The origin of mutations as a result of errors during DNA replication. A DNA molecule in the process of being copied by DNA polymerases (large arrows) is illustrated at the upper left. Such structures are often called replication forks. After an error occurs in which a G is misincorporated opposite a T, as illustrated at the upper center, replication completes and yields one correctly paired DNA and one mispaired DNA as illustrated at the upper right. If the mispaired DNA is then replicated before it is repaired, a mutant and a wild-type DNA result as illustrated at the lower right. If mismatch repair occurs prior to DNA replication, then two wild-type DNAs result as illustrated at the lower left.

One of the key properties of the MSH protein complexes [MSH2–MSH6 (MutSalpha) and MSH2–MSH3 (MutSbeta)] is that they are partially redundant. This is relevant to the observation that defects in MMR can cause cancer (discussed later). Because MSH2 is the only protein present in both complexes, defects in the MSH2 gene completely inactivate MMR (see Figure 2). As a consequence, MSH2 defects result in increased rates of accumulation of both base substitution and frameshift mutations. Interestingly, short mononucleotide repeat sequences are often found within genes, and frameshift errors that occur by the copying of such sequences during replication are the most frequent misincorporation errors made by DNA polymerases. Thus, in MSH2-defective cells, frameshift mutations in mononucleotide repeats often occur more frequently than base substitution mutations. MSH6 and MSH3 gene defects inactivate only the MSH2–MSH6

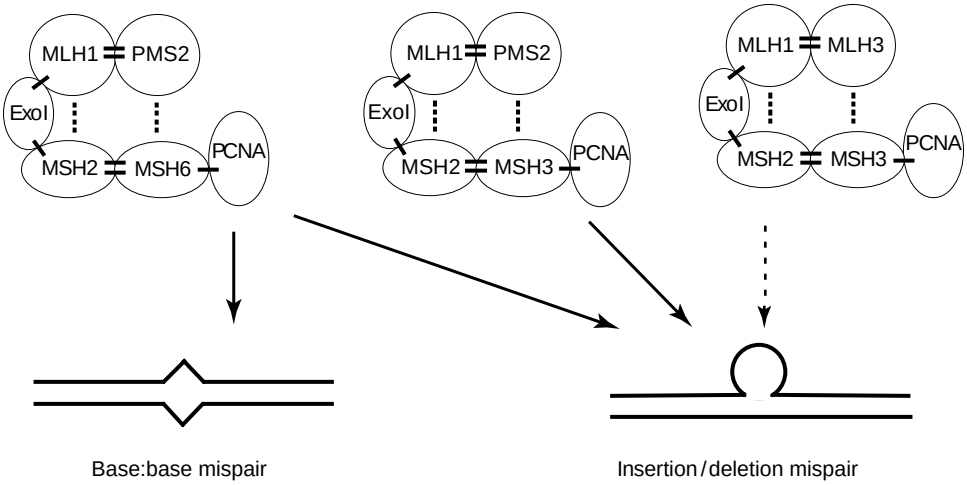

FIGURE 2 Illustration of the protein complexes that function in mismatch repair. The circles and ovals represent the MSH2, MSH3, MSH6, MLH1, MLH3, PMS2, exonuclease I, and PCNA proteins, as indicated. The double solid connecting lines indicate known stable protein–protein interactions, the single solid connecting lines indicate known, less stable protein–protein interactions, and the dashed connecting lines indicate interactions between protein assemblies in which the exact protein contacts are not yet known. Below these illustrated protein complexes are the mispaired based containing DNAs they interact with during mismatch repair. The solid connecting arrows indicate the major repair reactions, and the dashed connecting arrow indicates a minor repair pathway.

(MutSalpha) and MSH2–MSH3 (MutSbeta) complexes, respectively. Because of the partially overlapping mispair recognition specificity of each complex, defects in MSH6 cause only large increases in the rate of base substitution mutations, like that seen in MSH2 mutants, and cause small increases in the rate of frameshift mutations relative to that seen in MSH2 mutants. Defects in MSH3 have very little effect on mutation rates except for frameshift mutations in repeating sequences where the repeat unit length is 2 bases and larger. Dinucleotide and larger repeats are found less frequently in sequences encoding genes than short mononucleotide repeats, indicating that MSH3 defects should have little effect on the accumulation of mutations within the majority of genes.

MutL Homologue Proteins Involved in Mismatch Repair

MutL is a bacterial protein that is required for MMR; it is known to interact with MutS and then activate other proteins that function in MMR. There are three MutL homologues, called MLH proteins: MLH1, PMS2 (called PMS1 in *S. cerevisiae*), and MLH3, for which there is good evidence for a function in MMR in eukaryotes. These proteins form two different heterodimeric complexes, MLH1–PMS2 (MutLalpha) and MLH1–MLH3 (see Figure 2). Biochemical experiments have shown that the MLH1–PMS2 (MutLalpha) complex forms a higher order complex with both MSH2–MSH6 (MutSalpha) and MSH2–MSH3 (MutSbeta) when these MSH complexes interact with DNA. Presumably the MLH complex then acts to activate other components of MMR; however, little is yet known about this process. Neither is much yet known about the biochemical properties of the MLH1–MLH3 complex. A fourth MutL-related protein, human PMS1 (called MLH2 in *S. cerevisiae*), which appears to be able to form a complex with MLH1, was initially suggested to function in MMR. Genetic and biochemical studies performed to date, however, have failed to provide evidence that this protein plays an important role in MMR.

Genetic studies have shown that the MLH1–PMS2 (MutLalpha) complex is the major MutL-related complex that functions in MMR. The MLH1–MLH3 complex appears to play only a minor role in MMR. Like the situation with the two different MSH complexes discussed previously, the observation that two different MutL-related protein complexes function in MMR indicates that defects in each of the three MutL-related genes may cause different MMR defects. Because MLH1 is the only protein present in both MutL-related complexes, only defects in the MLH1 gene completely inactivate MMR (see Figure 2). However, since the MLH1–PMS2 (MutLalpha) complex is the major complex that functions in MMR, defects in the PMS2 gene cause almost as strong a defect in MMR as do defects in the MLH1 gene. In contrast, because the MLH1–MLH3 complex plays a minor role in MMR, defects in the MLH3 gene cause only a partial defect in MMR, resulting in a small but significant increase in the rate of accumulating frameshift mutations in mutant cells. Defects in human PMS1 or its *S. cerevisiae* homologue MLH2 cause little if any significant increase in mutation rate.

Other Proteins Implicated in Mismatch Repair

One of the important problems in the study of eukaryotic MMR is the identification of the other proteins required for MMR. Some progress has been made in this area, but unfortunately, little is known about how MMR initiates and how the newly synthesized DNA strand is recognized, nor has eukaryotic MMR been reconstituted from purified proteins.

DNA polymerase delta is required for the DNA synthesis step of MMR; similarly, there is also a requirement for its accessory factors proliferating cell nuclear antigen (PCNA), replication protein A (RPA/RFA), and replication factor C (RFC). PCNA has also been suggested to be involved in MMR at an early step prior to the resynthesis step. PCNA interacts with the MSH2–MSH6 (MutSalpha) and MSH2–MSH3 (MutSbeta) complexes through a specific motif located in the MSH6 and MSH3 subunits. This has led to the suggestions that PCNA may be required for the activity of the MSH2–MSH6 (MutSalpha) and MSH2–MSH3 (MutSbeta) complexes or that PCNA may target these MMR proteins to regions of newly replicated DNA. In considering the possibility that defects in genes encoding DNA polymerase delta, PCNA, RPA, and RFC might play a role in cancer susceptibility (see following discussion), it is important to note that each of these genes is an essential gene that would preclude mutations that cause complete loss-of-function defects.

In bacteria, at least four exonucleases have been shown to be able to function in the degradation step of MMR; each can substitute for all of the others. This redundancy of exonucleases appears to occur in eukaryotic MMR. Exonuclease 1 is a 5′ to 3′ double-strand DNA-specific exonuclease encoded by the EXO1 gene that is thought to be one of a number of redundant exonucleases that function in eukaryotic MMR. Exonuclease 1 physically interacts with both MSH2 and MLH1, and genetic studies have suggested that exonuclease 1 may in some way help to assemble higher order protein complexes that function in MMR. Biochemical studies have shown that exonuclease 1

can function in the excision step of MMR *in vitro* and plays a role in excision in both 5′ to 3′and 3′ to 5′ directions. Consistent with the view that exonuclease 1 is only one of many exonucleases that function in MMR, mutations in the EXO1 gene cause only partial MMR defects. Other exonucleases that have been suggested to function in MMR are the endo/exonuclease FEN1/RAD27 and the 3′ to 5′ editing exonuclease functions of DNA polymerases delta and epsilon. However, whether these latter three exonucleases play a direct role in MMR has been difficult to determine because these exonucleases all function in other critical aspects of DNA synthesis.

Defects in Mismatch Repair Cause Increased Cancer Susceptibility

HNPCC is a common inherited cancer susceptibility syndrome that in its most striking examples is characterized by a dominant mode of transmission, high penetrance, significantly earlier age of onset than sporadic cancers, multiple primary tumors, and a high proportion of colorectal as well as many other types of cancer, including endometrial, genitourinary, extracolonic GI cancers, ovarian, brain, and sebaceous skin tumors. A number of clinical criteria for the identification of HNPCC have been used, ranging from the highly stringent Amsterdam criteria (see Table I) that identify kindreds based on clustering of colorectal cancer and an early age of onset, to less restrictive criteria that allow inclusion of individuals with a less well documented family history of cancer and families with colorectal cancer and HNPCC-associated cancers as well as early onset colorectal cancer cases without a documented family history of cancer. DNA from HNPCC tumors often shows a high frequency of frameshift mutations in microsatellite sequences, a phenotype called microsatellite instability (MSI). MSI is an important diagnostic tool for identifying cases of HNPCC that are due to MMR defects. Tumors showing a high proportion of unstable microsatellite sequences are often designated MSI-High (MSI-H).

A high proportion of HNPCC cases defined by the Amsterdam criteria show tumor MSI, whereas a lower proportion of HNPCC cases defined by other clinical criteria show tumor MSI. Recent genetic studies suggest that almost all HNPCC cases showing tumor MSI can be accounted for by inherited defects in the MSH2 gene or the MLH1 gene. These two genes encode the common subunits of the MutS-related and MutL-related family of heterodimeric complexes, respectively, that function in MMR. The types of inherited mutations observed in these two genes include frameshift and nonsense mutations (protein-truncating mutations), missense mutations (protein sequence changes), and deletion mutations; deletion mutations appear to be more prevalent in MSH2 than MLH1, and missense mutations appear to be more prevalent in MLH1 than MSH2. There are no simple, routine molecular diagnostic methods for diagnosing mutations that cause HNPCC. However, in combination with an appropriate family history of cancer, complete MSH2 and MLH1 gene sequencing and deletion analysis along with testing of HNPCC tumors for MSI using a standard set of microsatellite markers and analysis of tumors for loss of MSH2 or MLH1 protein expression using immunohistochemistry (sometimes called IHC analysis) have proven to be useful in detecting MMR defects in suspected HNPCC families. Through the application of these methods, most HNPCC cases that have MSI-H tumors have been linked to a mutation in MSH2 or MLH1. In addition, in some cases in which inherited mutations have not been found, altered expression of MSH2 or MLH1 has been identified, indicating the presence of some type of MSH2 or MLH1 defect. It should be noted that the less restrictive clinical criteria for HNPCC (see Table I) identify many more patients suspected of having HNPCC compared to the Amsterdam criteria, but a smaller proportion of these patients ultimately prove to have inherited MMR defects.

Many other genes encoding proteins implicated in MMR have been considered as potential HNPCC genes. Of these, the most studied is MSH6. Defects in the MSH6 gene cause a partial loss of MMR due to the partial redundancy between MSH6 and MSH3. MSH6 mutations result in a large increase in the rate of accumulation of base substitution mutations but only modest increases in the rate of accumulation of single base frameshift mutations. Different studies have reported that perhaps up to 3% of HNPCC families can be accounted for by germline MSH6 defects, with these kindreds having a higher proportion of endometrial cancer than MSH2- or MLH1-detective HNPCC families. In contrast, approximately 8% of familial, non-HNPCC colorectal cancer cases were found to have germline MSH6 defects; similarly, germline MSH6 defects have been found in endometrial cancer cases associated with a weak family history of cancer. Such familial cancer cases constitute a much larger number of total cancer cases than HNPCC, indicating that germline defects in MSH6 could be almost as prevalent in the population as germline MSH2 and MLH1 defects. Compared to MSH2- or MLH1-defective HNPCC kindreds, MSH6-defective kindreds had a less striking family history and later age of onset of cancer, a result that parallels the results obtained in studies of MSH2-, MSH6-, and MLH1-defective mice. While more work on MSH6 is needed, it

TABLE I

Clinical Criteria for HNPCC[a]

Name	Criteria
Amsterdam[b]	Three relatives with CRC, one of which must be a first-degree relative of the other two; CRC involving at least two generations of the family; one or more CRC cases diagnosed before age 50.
Modified Amsterdam[c]	1. Small pedigrees, which cannot be further extended, can be considered as HNPCC if they contain CRCs in first-degree relatives; CRC must involve at least two generations and one or more CRC cases must be diagnosed before age 55. 2. In pedigrees where CRC is found in two first-degree relatives, a third relative with an unusually early-onset cancer or endometrial cancer is sufficient.
Young age of onset	A CRC case diagnosed at less than 40 years of age, without a family history fulfilling Amsterdam or modified Amsterdam criteria.
HNPCC variant	A family history of cancer suggestive of HNPCC, but not fulfilling Amsterdam, modified Amsterdam, or young age of onset criteria.
Bethesda[c]	1. Individuals in families that fulfill Amsterdam criteria. 2. Individuals with two HNPCC-related cancers, including synchronous and metachronous CRCs or associated extracolonic cancers. 3. Individuals with CRC who have a first-degree relative with CRC and/or a HNPCC-related extracolonic cancer and/or colorectal adenoma; one of the cancers diagnosed before age 45 and the adenoma diagnosed before age 40. 4. Individuals with CRC or endometrial cancer diagnosed before age 45. 5. Individual with right-sided CRC with an undifferentiated pattern (solid/cribform) on histopathology diagnosed before age 45. 6. Individuals with signet-ring-cell-type CRC diagnosed before age 45. 7. Individuals with adenomas diagnosed before age 40.

Adapted from Syngal S., Fox, E. A., Li, C., Dovidio, M., Eng, C., Kolodner, R. D., and Garber J. E., (1999). Interpretation of genetic test results for hereditary nonpolyposis colorectal cancer: implications for clinical predisposition testing. *J. Am. Med. Assoc.* **282**, 247–253.

[a] HNPCC, hereditary nonpolyposis colorectal carcinoma; CRC, colorectal cancer.

[b] All criteria must be met.

[c] Meeting all features under a single numbered criteria is sufficient.

appears that germline MSH6 defects cause an attenuated form of HNPCC.

A number of other MMR genes have been considered as possible HNPCC genes, including the MSH3 gene encoding a MutS homologue, the MutL homologue genes PMS1 (MLH2 in *S. cerevisiae*), PMS2 (PMS1 in *S. cerevisiae*) and MLH3, and the exonuclease encoding gene EXO1. However, defects in these genes have not been found to make a major contribution to HNPCC. This observation is consistent with many studies, indicating that defects in these genes do not cause complete loss of MMR because they encode partially redundant functions. It is also possible that these genes do not play roles in other MMR-related functions such as DNA damage-induced cell cycle arrest and apoptosis. Germline mutations in PMS2 appear to be only a rare cause of HNPCC, and most germline PMS2 mutations have been found to be associated with Turcot syndrome. In some sense this is surprising, because mutations in PMS2 cause strong MMR defects; however, PMS2-defective mice, while cancer prone, have a much different tumor spectrum compared to MSH2-, MSH6-, or MLH1-defective mice. Following the initial report of a germline PMS1 mutation, no other mutations have been reported, and recently the original PMS1 mutant family was shown to contain a MSH2 mutation. Mutations in MLH3 are also likely to be rare in HNPCC. Most studies have not identified germline MLH3 mutations in HNPCC cases, whereas the one study that did report potential mutations only identified missense variants that could be rare polymorphisms. Similarly, after an initial report of EXO1 mutations in HNPCC cases, a follow-up study showed that most of the initially reported variants, including a splice site mutation, were actually polymorphisms. This is consistent with the observation that EXO1 mutant mice show increased but much later onset

cancer susceptibility than MSH2 or MLH1 mutant mice. No germline defects in the MSH3 have been reported to date, although somatic mutations in MSH3 have been found as modifiers of germline MSH6 mutations consistent with studies of mutant yeast and mice. It is conceivable that defects in these genes could cause cancer susceptibility, although extrapolating from studies in model systems suggests such cancer susceptibility might be of later onset and weaker family history than HNPCC.

A variable proportion of sporadic cancers of many types has been observed to show tumor MSI indicative of a MMR defect. For example, in the case of sporadic colorectal cancer, the reported proportion of MSH-H tumors (note that MSI-H indicates a MMR defect) is around 18%. Most tumors showing MSI have been shown to lose expression of either MSH2 or MLH1, although the majority of cases show the loss of MLH1 expression. Most cases showing loss of MLH1 expression are due to somatic silencing of both copies of the MLH1 gene associated with hypermethylation of the MLH1 promoter. A small number of sporadic cases have been attributed to somatic mutations in MMR genes. These results indicate that there are both inherited and sporadic forms of MMR defective cancers, although the etiology of the two different types of cases is quite different.

How do MMR defects actually cause the development of cancer? Loss of MMR results in increased rates of accumulating mutations. This would be expected to increase the rate of accumulation of mutations that inactivate tumor suppressor genes and activate proto-oncogenes and consequently increase the rate of tumorigenesis. Considerable data exist that support this view. In addition, MMR-defective cells have checkpoint defects and are resistant to killing by DNA-damaging agents, suggesting that MMR defects also cause a defect in apoptosis that may also contribute to tumorigenesis. Because of this resistance to killing by DNA-damaging agents, MMR-defective tumors may also not be as responsive to some chemotherapeutic agents as non-MMR defective tumors.

Summary

MMR requires two different heterodimeric complexes of MutS-related proteins, MSH2–MSH3 and MSH2–MSH6, that recognize mispaired bases in DNA. Two different heterodimeric complexes of MutL-related proteins, MLH1–PMS2 (*S. cerevisiae* PMS1) and MLH1–MLH3, also function in MMR and appear to interact with other MMR proteins, including the MSH complexes and replication factors. Additional proteins, including DNA polymerase delta, RPA, PCNA, RFC, and exonuclease 1, have been implicated in MMR. Loss of function of three of these genes, MSH2, MSH6, and MLH1, has been shown to be the cause of both hereditary cancer susceptibility syndromes and sporadic cancers, whereas mutations in other MMR genes have not yet been shown to be associated with a significant number of hereditary or sporadic cancer cases.

See Also the Following Articles

DNA Mismatch Repair and Homologous Recombination • DNA Mismatch Repair and the DNA Damage Response • DNA Mismatch Repair: *E. coli* Vsr and Eukaryotic G–T Systems • DNA Mismatch Repair in Mammals • DNA Polymerase δ, Eukaryotic

Glossary

base substitution mutation The class of mutations that result when an incorrect base is paired with the correct base that is present in the DNA.

DNA polymerase The class of enzymes that synthesize DNA using one DNA strand as a template to direct DNA synthesis.

DNA replication The process by which cells make an exact copy of their DNA.

exonuclease The class of enzymes that degrade DNA molecules starting from the ends of DNA or breaks in DNA strands.

first-degree relative A parent, sibling, or child of the individual in question.

frameshift mutation Type of mutation that results from either insertion or deletion of one or a small number of extra bases in DNA.

germline mutation Mutation that is transmitted through the germline (e.g., inherited mutation).

heterodimer Complex composed of two different proteins.

immunohistochemistry (IHC) Use of antibodies to stain tissue slices to detect the presence of the antigen (protein or other molecule to which the antibody binds).

microsatellite instability (MSI) The accumulation of frameshift mutations within the simple repeat sequences found ubiquitously in most eukaryotic chromosomal DNA.

mispaired base An incorrectly paired base in DNA, e.g., an A paired with a C instead of a T, or an extra base inserted into DNA so that it is not paired with any base.

mutation Change in the normal sequence of a DNA molecule.

MutL Bacterial MutL protein or gene. MutL is a protein that interacts with the MutS protein during bacterial MMR.

MutS Bacterial MutS protein or gene. Mut is an abbreviation for mutator, because inactivation of a mutator gene results in increased rates of accumulating mutations. MutS is the protein that recognizes mispaired bases in DNA during bacterial MMR.

oncogene Gene whose increased or altered activity promotes the development of tumors. Oncogenes often accumulate activating mutations or are amplified during tumor development.

penetrance The percent chance that a mutation carrier will develop the disease in the individual's lifetime.

proliferating cell nuclear antigen (PCNA) A protein that forms a ring around DNA and functions to keep proteins such as DNA polymerases attached to the DNA.

redundancy Two genes or proteins are redundant when they can substitute for each other.

replication protein A (RPA)/replication factor A (RFA) Protein complex that binds to single-strand DNA, allowing it to be a better template for DNA polymerases.

replication factor C (RFC) Protein complex required to load PCNA onto DNA.

somatic mutation Mutation that occurs in a somatic cell. Such mutations are not inherited.

tumor suppressor gene Gene whose product prevents the development of a tumor. Tumor suppressor genes accumulate inactivating mutations during tumor development.

Further Reading

Fishel, R. (2001). The selection of mismatch repair defects in hereditary nonpolyposis colorectal cancer: Revising the mutator hypothesis. *Cancer Res.* **61**, 7369–7374.

Harfe, B. D., and Jinks-Robertson, S. (2000). DNA mismatch repair and genetic instability. *Annu. Rev. Genet.* **34**, 359–399.

Kolodner, R. D., and Marsischky, G. T. (1999). Eukaryotic DNA mismatch repair. *Curr. Opin. Genet. Dev.* **9**, 89–96.

Li, G.-M. (1999). The role of mismatch repair in DNA damage-induced apotosis. *Oncol. Res.* **11**, 393–400.

Loeb, L. A. (2001). A mutator phenotype in cancer. *Cancer Res.* **61**, 3230–3239.

Modrich, P., and Lahue, R. (1996). Mismatch repair in replication fidelity, genetic recombination, and cancer biology. *Annu. Rev. Biochem.* **65**, 101–133.

Nakagawa, T., Datta, A., and Kolodner, R. D. (1999). Multiple functions of MutS- and MutL-related heterocomplexes. *Proc. Natl. Acad. Sci. USA* **95**, 14186–14188.

Peltomake, P. (2003). Role of DNA mismatch repair in the pathogenesis of human cancer. *J. Clin. Oncol.* **21**, 1174–1179.

Sixma, T. K. (2001). DNA mismatch repair: MutS structure bound to mismatches. *Curr. Opin. Struct. Biol.* **11**, 47–52.

Wei, K., Kucherlapati, R., and Edelmann, W. (2002). Mouse models for human DNA mismatch-repair gene defects. *Trends Mol. Med.* **8**, 346–353.

Biography

Richard D. Kolodner is Head of the Laboratory of Cancer Genetics at the Ludwig Institute, San Diego, and Professor, Department of Medicine and Department of Cellular and Molecular Medicine at the University of California at San Diego, School of Medicine. He is an Associate Editor of *Cell* and serves on the editorial board of *Cellular and Molecular Biology*, the *Journal of Biological Chemistry*, and *DNA Repair*. He has published more than 200 papers on DNA repair and recombination and received numerous awards for this work.

DNA Mismatch Repair in Bacteria

A-Lien Lu
University of Maryland, Baltimore, Maryland, USA

There are two major DNA mismatch repair (MMR) systems in bacteria to correct DNA biosynthetic errors. Long-patch repair systems involve a long-patch excision and resynthesis (up to 1000 nt) and are specific to a particular DNA strand. Short-patch repair systems have a repair tract shorter than 15 nt and are dictated by the nature of the mismatches. MMR enhances the fidelity of DNA replication and genetic recombination, and it participates in the cellular response to certain types of DNA damage. The inactivation of DNA repair systems can lead to genomewide instability and a predisposition to cancers in mammals. The importance of MMR in mutation avoidance is widely documented. Mutations in long-patch MMR genes result in a mutator phenotype with a spontaneous mutation frequency elevated approximately 100-fold. The mutation spectrum reveals that transitions and short nucleotide insertions/deletions predominant. MMR-defective strains are also hypersensitive to base-substitution mutagenesis and resistant to some types of alkylating agents. MMR also has an antirecombination function in limiting recombination between divergent sequences and preventing gross chromosomal rearrangement. MMR proteins have been shown to function in preventing interspecies recombination between *Escherichia coli* and *Salmonella typhimurium*.

Escherichia coli Long-Patch Mismatch Repair is Dependent of *dam* Methylation

For mismatch repair (MMR) to correct replication error, a strand-discrimination system must target the repair to the daughter DNA strand that contains the incorrect nucleotides. *E. coli* MMR is dependent on *dam* (DNA adenine methylation) methylation and is biased to unmethylated DNA strands. The *dam* methylase modifies the adenine at the 6-NH_2 group in GATC sequences. Wagner and Meselson proposed in 1976 that transient undermethylation of GATC sites in newly synthesized DNA provides the basis to direct the MMR to the daughter strands, an idea that has been confirmed both *in vivo* and *in vitro*. Because methylation is a postsynthetic process, methylation on the parental strands and transient unmethylation on the newly synthesized strands provide the signal to direct the repair to the daughter strands. MMR can be directed by hemimethylated sites located either 5′ or 3′ to the mismatch at a separation distance of up to 1 kb.

Specificity of Mismatch Repair

Methyl-dependent MMR has a broad specificity. Of the eight possible base-base mismatches, only C–C is refractory to the repair. Heteroduplexes containing short insertion/deletion loops (IDL) derived from DNA polymerase slippage can also be repaired. IDL with three unpaired nucleotides are efficiently repaired, but IDL with four to seven unpaired nucleotides are poorly repaired. The efficiency of MMR is influenced by the sequence flanking the mismatch. The MMR system has also been shown to be involved in repair of oxidative DNA damage. The major oxidative lesion, 7,8-dihydro-8-oxo-guanine (8-oxoG), can mispair with adenine during DNA replication. *E. coli* MMR can also act on A-8-oxoG mismatches that result from replication errors.

Mechanism of *E. coli* Long-Patch Mismatch Repair

An *in vitro* assay developed by Lu *et al.* has provided the basis for purifying and characterizing the *E. coli* MutH, MutL, and MutS proteins. Biochemical studies from P. Modrich's laboratory show that *E. coli* MMR involves 11 protein activities: MutS, MutL, MutH, UvrD (DNA helicase II), four single-strand specific exonucleases, a single-strand DNA binding protein (SSB), DNA polymerase III (Pol III) holoenzyme, and DNA ligase (Table I). Whereas MutH, MutL, and MutS proteins are specific for MMR, the other activities are involved in other DNA metabolic pathways, including replication and recombination. The mechanism of *E. coli* long-patch MMR is depicted in Figure 1.

TABLE I

Functions of *E. coli* Mismatch Repair Enzymes

Enzyme	Function
MutS	DNA mismatch/damage recognition
MutL	Molecular matchmarker; Enhances mismatch recognition; stimulates MutH and UvrD activities
MutH	Strand discrimination; cleaves at unmethylated DNA strands
UvrD	DNA helicase II; unwinding DNA
ExoI, ExoX	3′ to 5′ exonuclease; removes nucleotides
ExoVII, RecJ	5′ to 3′ exonuclease; removes nucleotides
DNA Pol III holoenzyme	DNA resynthesis of the long-patch mismatch repair pathway
β Sliding clamp	A subunit of DNA Pol III holoenzyme; interacts with MutS
SSB	Protecting DNA from degradation and re-anneal
DNA ligase	Nick ligation
MutY	DNA glycosylase; excises A from A/G, A/8-oxoG, A/C and G-8-oxoG mismatches and removes G from G/8-oxoG mismatches
Vsr	Endonuclease; removes T from T-G mismatch
DNA polymerase I	Repair synthesis of short-patch mismatch repair pathways

Initiation of Mismatch Repair

MMR requires specifically MutH, MutL, and MutS proteins in the initiation steps. MutS recognizes base–base mismatches and short insertion/deletion loops. MutL serves to couple mismatch recognition by MutS to activate several downstream activities, such as MutH and DNA helicase II. MutH endonuclease cleaves at the 5′ of G of an unmethylated GATC sequence. In a similar manner, MutS and MutL activate the excision process.

MutS

MutS is a homodimer of a 95-kDa polypeptide that recognizes all base-base mismatches except C–C mismatch and small insertion/deletion loops up to five unpaired nucleotides. The discrimination of a mismatch-containing heteroduplex from a homoduplex by MutS protein is not great; there is only 10- to 20-fold preference. It has been suggested that mismatch recognition by MutS may be enhanced by MutL or by the association with replication proteins. MutS has ATPase activity, which is essential for the MMR function. ATP binding reduces the MutS affinity for heteroduplex DNA. Although several models have been proposed, the role of ATPase of MutS is still under investigation. The translocation and sliding clamp models suggest that MutS moves away from the mismatch site to activate MMR. The translocation model suggests that ATP hydrolysis provides the energy and enables MutS to move like a motor protein. This model is supported by a α-loop-like DNA structure visualized under electron microscopy. The sliding clamp model or molecular switch model suggests that ATP-bound MutS slides along DNA without ATP hydrolysis. There is a conformation change from ADP-bound MutS to ATP-bound MutS. The third model suggests that the ATPase activity of MutS plays a proofreading role in MMR. The structure of MutS-DNA-ADP suggests that MutS has to bind both ATP and the mismatched DNA simultaneously to activate the repair process. Thus, the model suggests that MutS remains bound to the mismatch site and recruits MutL and MutH to initiate MMR.

The structure of *E. coli* MutS complexed with a G–T mismatch and *Thermus aquaticus* MutS with a + 1T IDL have been solved recently by the W. Yang and T. Sixma groups. Although different types of mismatches were used, both MutS structures are very similar. These structures show that a truncated form of MutS is a homodimer like an oval disk with two channels, one of which forms by domains I and IV and binds to the DNA. The bound DNA is kinked by 60° at the mismatch and the minor groove is widened and contacted extensively by MutS. Interestingly, MutS forms an asymmetric dimer with only one monomer making direct contact with the mismatched base. MutS contacts the mismatched bases through a highly conserved N-terminal motif Phe-X-Glu. The Phe residue in this conserved motif is inserted into the double helix and stacks with the mismatched thymine. The ATP binding site at the C terminus (domain V) of the protein is composed of residues from both subunits and is located far from the DNA-binding site. Domains II and III connect the mismatch-binding and ATPase domains. In the absence of DNA, domains I and IV are disordered in the crystal structure. DNA binding also alters the conformation of the ATPase domain.

MutL

MutL is a dimer of a 68-kDa polypeptide that operates as a molecular matchmaker in MMR to assemble a functional repair complex. In the presence of ATP, MutL binds to the MutS-heteroduplex complex and activates MutH and UvrD helicase activities. The divergent C-terminal domain of MutL is responsible for the dimer formation. The conserved N-terminal domain has weak ATPase activity that is stimulated by DNA. Structural and biochemical studies indicate that ATP binding and hydrolysis modulate the conformation, oligomeric state of MutL, and interactions of MutL with MutS, MutH, and UvrD helicase. Upon ATP

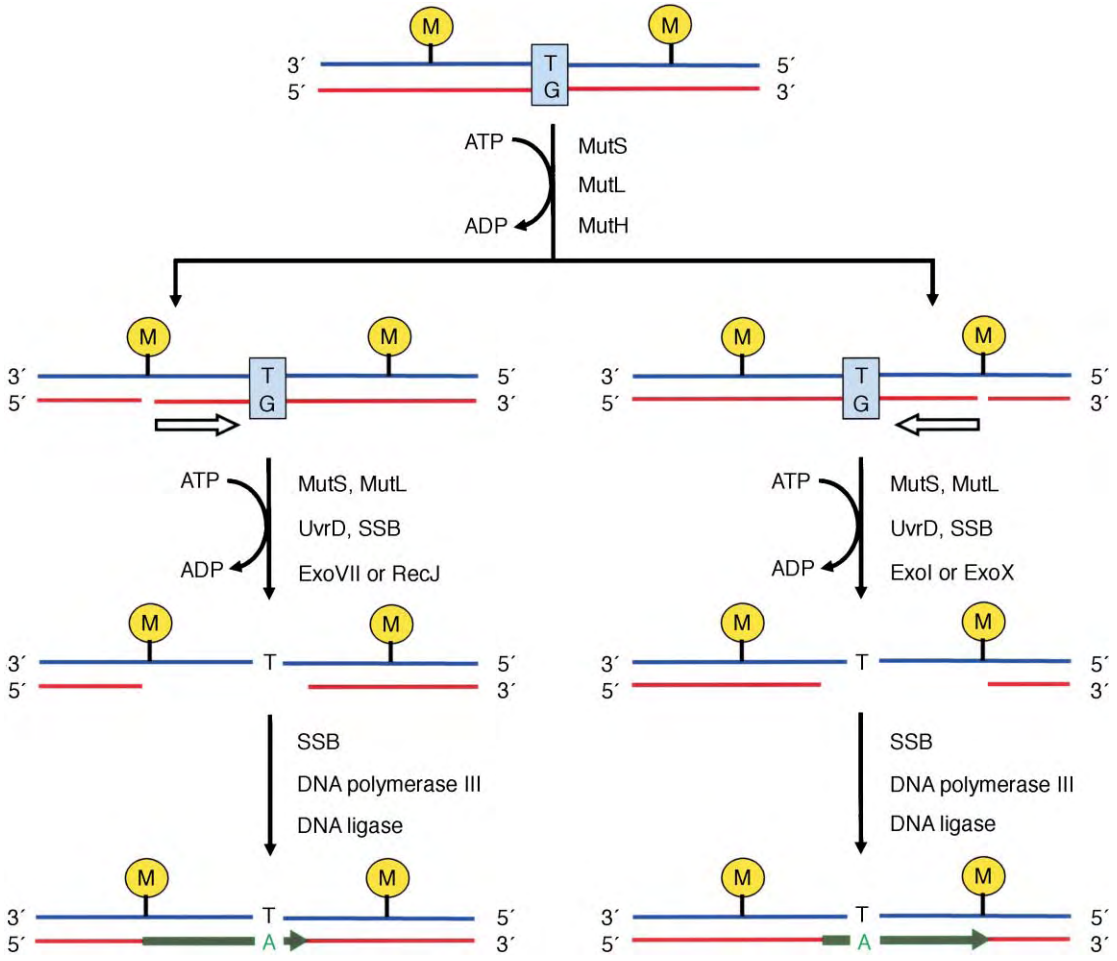

FIGURE 1 The long-patch methyl-dependent mismatch repair system of *E. coli*. Mismatches (G–T, as shown) are recognized by dimeric MutS protein. After binding of MutL and MutH, the unmethylated strand in red is nicked by MutH at the hemimethylated GATC sites (M in yellow circle represents for methyl groups). ATP hydrolysis by MutS and MutL triggers the downstream repair process. DNA unwinding by UvrD (DNA helicase II) in the presence of ATP from the nick site toward the mismatch reveals a single-stranded DNA region that is protected by SSB. Depending on the position of the nick relative to the mismatch, ExoVII or RecJ with 5′ to 3′ exonuclease activity and ExoI or ExoX with 3′ to 5′ exonuclease activity degrade the nicked strand from the nick site up to and slightly past the mismatch. The resulting single-stranded gap undergoes repair resynthesis by the DNA polymerase III holoenzyme and the nick is finally sealed by DNA ligase. Open arrows represent the direction of exonuclease degradation and thick green arrows show the direction of repair resynthesis.

binding, the N-terminal domain undergoes conformation changes and dimerizes, although the native protein exists as a dimer in solution.

MutH

The 25-kDa monomer MutH belongs to a family of type II restriction enzyme. MutH activity is activated by MutS and MutL in the presence of ATP and a mismatch-containing DNA. MutH cleaves at the 5′ side of the G of the GATC sequence on unmethylated strand located on either the 5′ or 3′ side of the mismatch. Tyr212 of MutH is important in sensing the methylation status of DNA. The structure of MutH is like a clamp with a cleft and two arms. DNA may be bound in the cleft.

Excision and Repair Synthesis of Mismatch Repair

The strand break created by MutH at a GATC site of the unmethylated strand serves as the starting point for the excision of the mispaired base. UvrD (DNA helicase II) physically interacts with MutL and its unwinding activity is dramatically stimulated by MutL. MutL facilitates the loading of helicase II on the appropriate strand to unwind DNA in the proper direction and allows repeated loading of additional helicase II molecules to continue the unwinding reaction. DNA helicase II unwinds the DNA from the nick toward the mismatch and reveals a single-stranded DNA region that is protected by SSB.

The excision of the displaced strand is then initiated from the nick by exonucleases and is dependent on MutS, MutL, and UvrD helicase. Depending on the position of the nick relative to the mismatch, ExoVII or RecJ with 5′ to 3′ exonuclease activity and ExoI or ExoX with 3′ to 5′ exonuclease activity degrade that portion of the nicked strand displaced by the helicase up to and slightly past the mismatch. The resulting single-stranded gap is repaired by the DNA polymerase III holoenzyme, and the nick is finally sealed by DNA ligase. MMR may be coupled with DNA replication via physical interaction between MutS and the β-clamp of DNA polymerase III holoenzyme.

MutY Repair Pathway

In addition to the long-patch methyl-dependent MMR, two short-patch repair pathways have been characterized in *E. coli*. Only the MutY repair pathway is described here and the very short patch (VSP) pathway initiated by Vsr endonuclease is covered elsewhere in this encyclopedia.

Oxidative damage is a major source of mutation load in living organisms. 8-OxoG is one of the most stable products of oxidative DNA damage and has the most deleterious effects because it can mispair with adenine. In *E. coli*, MutT, MutS, MutM, and MutY are involved in defending against the mutagenic effects of 8-oxoG lesions (Figure 2). The MutT protein eliminates 8-oxo-dGTP from the nucleotide pool with its pyrophosphohydrolase activity, whereas the MutM glycosylase (Fpg protein) removes both mutagenic 8-oxoG adducts and ring-opened purine lesions. MutS and MutY increase replication fidelity by removing the adenines misincorporated opposite 8-oxoG or G during DNA replication. The *E. coli* MutY protein specifically removes mispaired adenines from A–G, A-8-oxoG, and A-C mismatches and removes guanines from G-8-oxoG mismatches. A-8-oxoG mismatches are particularly important biological substrates for MutY. The mutY mutants have approximately 50-fold higher mutation frequencies of G–C to T–A transversions than wild-type cells.

MutY is a 39-kDa DNA glycosylase that removes a free base from DNA to initiate a base excision repair (BER) process. The MutY BER pathway involves DNA polymerase I and DNA ligase and may involve apurinic–apyrimidinic (AP) endonuclease (EndoIV or ExoIII). Both AP endonucleases enhance the product release with A–G but not A–8-oxoG substrates. Although MutY can form a covalent Schiff base intermediate with its DNA substrates, it is controversial whether MutY has AP lyase (β-elimination) activity in addition to the DNA glycosylase activity. It has been suggested that coupling to DNA replication ensures that MutY BER is targeted to the daughter DNA strands but not the parental strands.

MutY glycosylase contains a [4Fe–4S] iron–sulfur cluster and it belongs to a conserved helix–hairpin–helix (HhH) family that includes several DNA glycosylases.

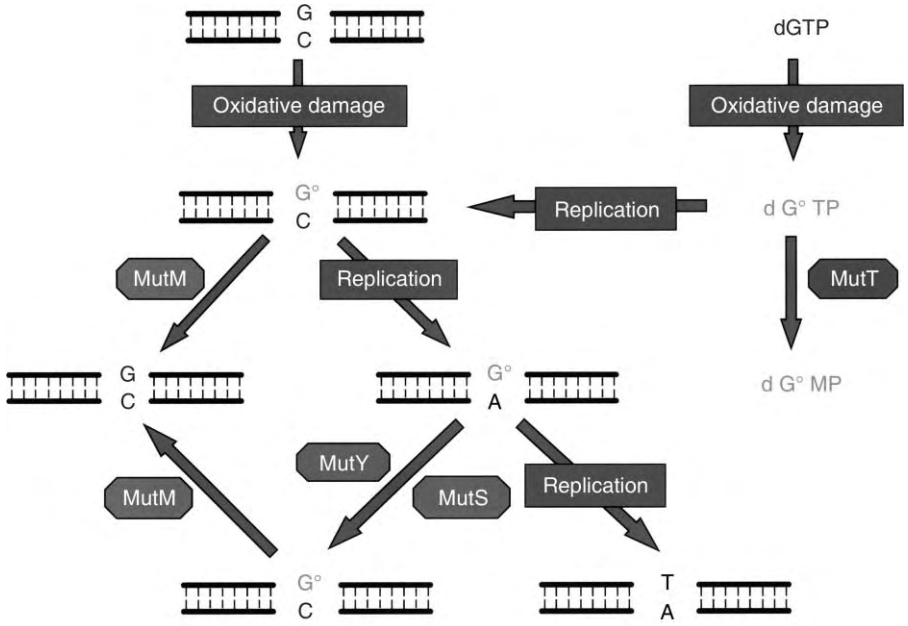

FIGURE 2 8-OxoG repair in *E. coli*. The MutT protein hydrolyzes 8-oxo-dGTP (dG°TP) to 8-oxo-dGMP (dG°MP) and pyrophosphate. The MutM glycosylase (Fpg protein) removes mutagenic 8-oxoG (G°) adducts while they are paired with cytosines. When C–8-oxoG is not repaired by MutM, adenines are frequently incorporated to the 8-oxoG bases during DNA replication. MutS and MutY increase replication fidelity by removing the adenines misincorporated opposite 8-oxoG.

The X-ray crystal structure of the catalytic domain of D138N-MutY with bound adenine shows that adenine is buried in the active site of the catalytic domain, suggesting that the mismatched adenine must flip out of the DNA helix for glycosylase action. The iron–sulfur cluster loop is important in substrate recognition and MutY stability, and the HhH motif is involved in binding to the phosphate backbone. The structure of MutY from *Bacillus stearothermophilus* in complex with A-8-oxoG-containing DNA was recently determined. Similar to several DNA glycosylases, MutY distorts the bound DNA and flips out the mismatched adenine out of the helix but the mismatched GO remains intrahelical. The C-terminal domain of MutY has been shown to play an important role in the recognition of GO lesions. The C-terminal domain of MutY has no homology to other members of the HhH superfamily, but shares some sequence and structural similarities to MutT.

See Also the Following Articles

DNA Base Excision Repair • DNA Helicases: Dimeric Enzyme Action • DNA Ligases: Mechanism and Functions • DNA Ligases: Structures • DNA Mismatch Repair and Homologous Recombination • DNA Mismatch Repair: *E. coli* Vsr and Eukaryotic G–T Systems • DNA Polymerase III, Bacterial • Recombination: Heteroduplex and Mismatch Repair *in vitro*

Glossary

base excision repair (BER) A DNA repair pathway that is initiated by a DNA glycosylase to remove relatively small lesions. Some glycosylases are highly specific to certain lesions or mismatches.

***dam* methylation** The methylation of the adenine at the 6-NH2 group in GATC sequences by *dam* methylase. Methylation on the parental strands and transient unmethylation on the newly synthesized strands provide a signal to direct the mismatch repair to the daughter strands.

mismatch repair (MMR) Process in which the long-patch MMR removes replicative errors that are missed by DNA polymerase's proofreading activity. MMR also functions during genetic recombination and corrects certain types of DNA damage.

mutator phenotype A phenotype that is associated with elevated genomewide spontaneous mutation frequencies and is usually caused by mutations at the DNA repair genes.

replication fidelity The extremely low error rate of DNA replication, which is achieved by the accuracy of DNA replication and mismatch repair.

Further Reading

Friedberg, E. C., Walker, G. C., and Siede, W. (1995). *DNA Repair and Mutagenesis*. ASM Press, Washington, D.C.

Hsieh, P. (2001). Molecular mechanisms of DNA mismatch repair. *Mutat. Res.* **486**, 71–87.

Lindahl, T., and Wood, R. D. (1999). Quality control by DNA repair. *Science* **286**, 1897–1905.

Lu, A.-L., Li, X., Gu, Y., Wright, P. M., and Chang, D.-Y. (2001). Repair of oxidative DNA damage. *Cell Biochem. Biophys.* **35**, 141–170.

Modrich, P. (1991). Mechanisms and biological effects of mismatch repair. *Annu. Rev. Genet.* **25**, 229–253.

Modrich, P., and Lahue, R. (1996). Mismatch repair in replication fidelity, genetic recombination, and cancer biology. *Annu. Rev. Biochem.* **65**, 101–133.

Yang, W. (2000). Structure and function of mismatch repair proteins. *Mutat. Res.* **460**, 245–256.

Biography

A-Lien Lu is a Professor in the Department of Biochemistry and Molecular Biology at the University of Maryland, Baltimore. Her principal research interest is in DNA repair, including long-patch MMR and short-patch MutY repair. She holds a Ph.D. from the University of North Carolina at Chapel Hill and received her postdoctoral training at Duke University. As a postdoctoral fellow, she developed an *in vitro* MMR assay that has been used to purify and characterize MMR proteins, and her laboratory was the first to discover the *E. coli dam*-independent MutY pathway.

DNA Mismatch Repair in Mammals

James T. Drummond
Indiana University, Bloomington, Indiana, USA

When DNA polymerases copy an organism's genomic DNA, errors that escape the replication complex appear as mismatches. Virtually every mispairing may be recognized and corrected by a set of activities known collectively as the mismatch repair (MMR) pathway. When this pathway is disabled in humans, either via mutation or epigenetic silencing, the mutation rate rises approximately 100- to 1000-fold. There is a generally predictable outcome when dividing cells become mutators; deleterious changes within critical genes that regulate cell growth or suppress tumors result in a clonal expansion that fuels a cycle of further mutation and selection for phenotypes that spur growth or avoid death. Such a sequence describes tumors in hereditary cancer syndromes such as Muir–Torre and hereditary nonpolyposis colorectal cancer (HNPCC), and it frequently can explain sporadic tumor initiation in many tissue types.

Historical Perspective and Overview

Our understanding of the contributions of the DNA MMR pathway to the long-term well being of humans has exploded over the past decade. Substantial literature describing repair processes in model organisms such as bacteria and yeast has provided an indispensable road map for identifying mammalian homologs involved in tumor initiation and progression, beginning with the identification of human *MSH2* (*MutS Homolog 2*) in 1993. It quickly became apparent that the two primary genetic loci defective in HNPCC families corresponded to human *MSH2* and *MLH1* (*MutL homolog 1*), homologs of proteins essential for repairing mismatches in most complex organisms. The cast of participants rapidly evolved with revelations that MSH2 and MLH1 were isolated as heterodimeric species with distinct MutS and MutL homologs, each with different but often overlapping mechanistic contributions. In contrast to DNA repair pathways that remove site-specific lesions, repair of mismatches depends on identifying both the mismatch and a remote site that allows discrimination between parent and daughter strand. Large tracts of DNA may therefore be excised and resynthesized during a repair event. The replication machinery that restores the excised DNA sequence also participates in genomic replication, adding these proteins to the list of participants. Many of the proteins essential for DNA replication were found to have distinct roles in mismatch correction, most prominently PCNA (identified as a proliferating cell nuclear antigen). Despite the many advances, neither the full cast of players nor the specific mechanism for mismatch correction is fully characterized.

Mechanistic Contributions of the Key Participants in Mammalian MMR

MutS and Some of Its Homologs Recognize Mismatches

During a search for genetic defects that conferred a *Mut*ator phenotype in *E. coli*, inactivation of the *MutS* gene resulted in roughly a 1000-fold increase in the mutation rate. The MutS protein proved to be a mismatch-binding homodimer composed of 90 kD monomers with an inherent weak ATPase activity that plays an essential but incompletely defined role in mismatch correction. In mammals, the corresponding protein activities are more complex (Figure 1). The MSH2 protein forms tight complexes with either MSH6 or MSH3 (not shown); defects in *MSH2* apparently eliminate all nuclear MMR activity and increase the mutation rate from 100- to 1000-fold. Partnered with MSH6, MSH2 forms a heterodimer called MutSα that can recognize base–base and many small insertion-deletion mismatches. The MSH2/MSH3 heterodimer (MutSα) is present in substantially lower amounts in tumor cells, and it recognizes primarily insertion–deletion mutations in which two or more unpaired nucleotides are present in either strand. These two mismatch-binding heterodimers provide partially overlapping mismatch recognition capabilities, and defects in either *MSH6* or *MSH3* are less severe mutators than *MSH2*. Each individual defect confers a mutation

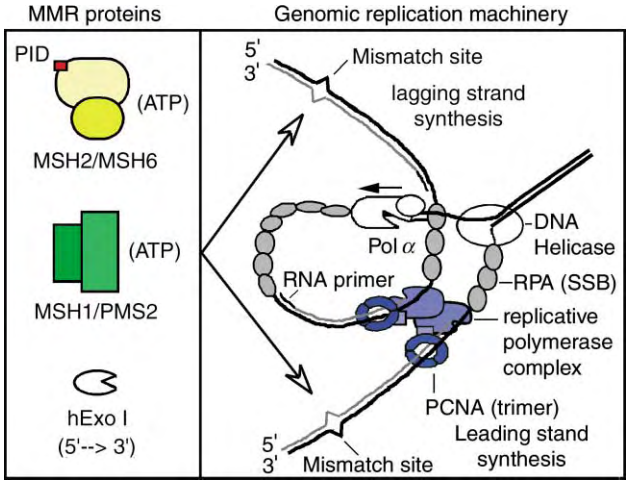

FIGURE 1 MMR activities cooperate with the DNA replication apparatus. The box on the left shows the proteins specific to mismatch correction. DNA replication is illustrated on the right as a process where leading and lagging strand synthesis is coordinated. Mismatches, identified as inverted triangles, are corrected such that the daughter strand (light gray) is targeted specifically for excision and removal. Resynthesis restores the parental strand information (darker strand). Several key proteins in replication, such as PCNA, RPA (a single-stranded binding protein complex), and polymerase delta, are also required for mismatch correction.

spectrum consistent with the selective failure to recognize different classes of mutations.

While the MSH6 and MSH3 proteins form heterodimers with MSH2 that are involved in recognizing mismatches, other MutS homologs have distinct roles in DNA metabolism. The mammalian MSH4 and MSH5 proteins also heterodimerize, yielding a complex that participates in meiotic recombination. While the precise mechanistic contribution of this complex is not known, it does not appear to recognize DNA mismatches in an error avoidance pathway. One further MutS homolog identified in yeast that might be expected in human cells, MSH1, has not surfaced. This mitochondrial protein is known to recognize DNA mismatches and stabilize the yeast mitochondrial genome by an undefined mechanism.

MutL and its Homologs are Essential to MMR

In prokaryotes such as *E. coli*, loss-of-function mutations in *Mut* L confer up to a 1000-fold increase in the mutation rate, much like defects in the *MutS* homologs. In parallel with MutS homologs, mammalian MutL homologs form heterodimers in which the MLH1 protein is central to complexes active in nuclear mismatch correction (Figure 1). MLH1 forms the primary heterodimer with PMS2 (PMS1 in yeast), which is also a *Mut* L homolog.

The mechanistic contribution of the MutL homolog heterodimers to repair, let alone other processes, is one of the least well-understood aspects of MMR. Some clues to MutL function are available from studies using yeast or *E. coli* proteins, but very little is known of their mammalian counterparts. Some MutL homologs are known to bind and utilize ATP, which is essential for mismatch correction. The nucleotide-binding motif is most similar to those of the growing category of AAA^+ proteins, which carry out diverse roles but often utilize ATP to drive dissociation of protein–protein or protein–DNA complexes. The purified human MutSα and MutLα heterodimers, as well as homologs from model organisms, have been shown to interact on longer DNA templates in the presence of ATP. This has led to models that suggest migration of a complex of both heterodimers along the DNA helix as part of the repair mechanism.

PCNA and the Replication Apparatus

When MutSα recognizes mismatches and triggers a strand-specific excision event, hundreds to thousands of nucleotides may be removed. A processive, PCNA-dependent polymerase is required to fill in the gap, which in human cells has been identified as polymerase delta. In Figure 1, the replicative polymerase complex shown synthesizing the daughter strand contains polymerase delta, and the MMR and replication functions are likely to be closely linked. A central player shared by both processes is the PCNA molecule, which forms a trimeric sliding clamp for replication and plays a complex in mismatch correction. It is essential for the MMR reaction prior to strand excision, and it interacts with MSH2 and MSH6 via a small, conserved domain through which many other repair proteins also bind PCNA (labeled PID for *P*CNA *I*nteracting *D*omain in Figure 1). Consistent with the biochemical and genetic evidence for this interaction, the key MMR proteins can be identified within replication foci *in situ*. Precisely how MMR is coupled to replication, or how the processes are coordinated, remains poorly understood.

Orchestration of Mismatch Correction in Mammals

The mechanism through which a DNA mismatch is repaired remains an intensely investigated field of research. Based on a wealth of genetic and biochemical data generated in model organisms, we have a clear idea of several participants and mechanistic intermediates along the pathway. How repair events are coordinated,

and the precise role of each of the players, remains unknown or a matter of dispute. Therefore, a series of intermediates in the process in which the proteins involved or the DNA structure is known, but for which the understanding of the mechanism remains incomplete, will be presented (Figure 2).

How Does Mismatch Binding Trigger Repair?

To be corrected, a mismatched site needs to be distinguished from correctly paired DNA. While no crystal structure is available for any eukaryotic heterodimer, prokaryotic MutS homodimers (from *E. coli* and *Thermus aquaticus*) have been crystallized complexed with either base–base or base–insertion mismatches. These structures reveal that mismatch recognition depends on the ability of MutS to kink the DNA helix sharply at the mismatch site by approximately 60°. The bend is partially enforced by the insertion of a phenylalanine side chain that stacks within the helix at the mismatch site. The MutS protein contains a domain that is poorly structured in the absence of DNA, and binding to the mismatch site orders the protein fold and sandwiches the DNA between the two halves of the homodimer. It has also been shown that eukaryotic MutS heterodimers are also capable of bending DNA upon mismatch binding.

As described above, MutSα in mammals is an ATPase, and it is clear that ATP triggers a conformational change that modifies DNA binding at the mismatch site. Precisely how that occurs, or which other protein activities might be involved *in vivo* (such as PCNA or MutLα), remains to be established. The three competing models that address this question each have clear experimental support or mechanistic plausibility, yet none provide a satisfactory overall answer.

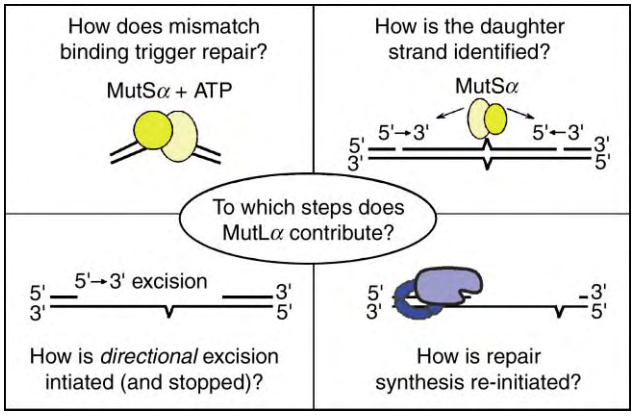

FIGURE 2 Five prominent unanswered questions about human MMR. Note that the MMR pathway is bidirectional, and that the nick shown to the right of MutSα in the upper right box could also have been accessed to trigger a 3′ to 5′ excision event toward the mismatch.

Mechanisms that suggest ATP-dependent DNA looping provide an elegant solution for how bidirectional scanning for a repair-directing signal may occur. Mechanisms that suggest diffusion-controlled migration along the DNA helix are plausible and well supported, but they require multiple copies of MutSα *in vivo* to drive bidirectional scanning. Neither of these models provides a memory for the mismatch site, since the protein that originally binds the mismatch leaves the site and travels hundreds of base pairs away. A third model suggests that MutSα might stay associated with the mismatch site and communicate through space with a marker for the daughter strand, such as with PCNA within the replication complex (see Figure 1). This allows for an anchor at the mismatch site, but it fails to provide an explanation for how directional excision is initiated.

How Is the Daughter Strand Identified?

Once a mismatch has been identified, the mandate of the MMR pathway is to target the newly synthesized DNA strand for excision and resynthesis. In a small group of prokaryotes that includes *E. coli*, the methylation status at GATC sequences reveals the daughter strand. The transient lack of methylation allows the MutH protein, stimulated by MutS and MutL at a nearby mismatch, to nick the daughter strand. However, such a methylation-based strategy apparently does not operate in mammalian cells. Instead, the most plausible mechanism to date suggests that mismatch correction is coupled with replication. By definition, the replication machinery generates the daughter strand, yielding a strand discrimination mechanism if the DNA end where synthesis occurs may be accessed.

How is Directional Excision Initiated and Controlled?

One of the hallmarks of MMR in all organisms is a bidirectional capability. In other words, the information used to distinguish DNA strands may be either "upstream" or "downstream" with respect to the mismatch (Figure 2). This capability demands that any mechanism to explain mismatch correction must account for identifying nearby signals in both directions along the DNA helix simultaneously. Once a strand signal is identified, several further constraints are introduced. The system must identify the relative orientation between the mismatch site and the point of excision, then correctly initiate an excision event that moves toward and through the mismatch site. This requires competence for degrading the intervening DNA by correctly accessing an exonuclease with either a

5′ → 3′ or a 3′ → 5′ strand polarity. It has been shown that the human Exonuclease I (Exo I) is essential for repair with either strand polarity, but only a 5′ → 3′ excision capability has been demonstrated. Note that for clarity, only a 5′ to 3′ excision reaction is illustrated in Figure 2.

How is Repair Synthesis Reinitiated?

Once DNA excision with either polarity is initiated, the replicative polymerase machinery must bring closure to it. It is clear that excision proceeds to relatively random sites approximately 150 nucleotides beyond the mismatch, with a wide variance and a few favored stopping points. Given that the single-strand excision event could span a few hundred to over a thousand base pairs, the MMR pathway must have a mechanism to ensure that excision proceeds until the mismatch site is removed. Once excision gives way to resynthesis, a new logistical problem is now apparent – if excision proceeds 5′ → 3′, the gap-filling polymerase (delta) has access to the DNA priming end from which the excision was initiated. In principle, resynthesis could track the excision process, leaving little or no gapped DNA as an intermediate. In the case of 3′ → 5′ excision, the entire excision event must be completed before the priming strand may be revealed to the polymerase. A long DNA gap is a required intermediate in this case. The repair process is formally concluded by the action of a DNA ligase that seals the nick that remains after resynthesis.

In summary, the MMR machinery is a complex assembly of proteins that can recognize DNA mismatches and restore the original DNA sequence. Failure of this pathway results in an increased mutational load and relaxed oversight of recombination events, wherein mismatches are also generated when the participating DNA strands are not identical. Such events are associated with tumorigenesis, revealing the crucial role of the MMR pathway in maintaining the genome of complex organisms under normal circumstances.

See Also the Following Articles

DNA Mismatch Repair and Homologous Recombination • DNA Mismatch Repair Defects and Cancer • DNA Polymerase δ, Eukaryotic

Glossary

exonuclease Enzyme that hydrolyzes nucleic acid polymers, usually to nucleotide monophosphates or short oligonucleotides, in a reaction initiated from a single- or double-stranded terminus.

mismatch Any pairing of DNA bases not described by the classical Watson–Crick G–C or A–T pairing, including addition or deletion of up to ~12 nucleotides in one DNA strand.

mutation Alternations in DNA sequence that result from processes such as unrepaired replication errors or DNA damage, which may or may not result in detectable phenotypic changes.

PCNA Proliferating cell nuclear antigen, a trimeric protein that forms a ring that can be pried open and loaded on double-stranded DNA to act as a platform for processive DNA synthesis or DNA repair activities.

Further Reading

Bellacosa, A. (2001). Functional interactions and signaling properties of mammalian DNA mismatch repair proteins. *Cell Death Different.* **8**(11), 1076–1092.

Hsieh, P. (2001). Molecular mechanisms of DNA mismatch repair. *Mutat. Res.* **486**(2), 71–87.

Lynch, H. T., and de la Chapelle, A. (2003). Hereditary colorectal cancer. *N. Engl. J. Med.* **348**(10), 919–932.

Modrich, P. (1991). Mechanisms and biological effects of mismatch repair. *Annu. Rev. Genet.* **25**, 229–253.

Wei, K., Kucherlapati, R., and Edelmann, W. (2002). Mouse models for human DNA mismatch repair defects. *Trends Mol. Med.* **8**(7), 346–353.

Biography

James T. Drummond is an Associate Professor of Biology at Indiana University in Bloomington, Indiana. He earned his doctoral degree in Biological Chemistry from the University of Michigan Medical School; he received his postdoctoral training at Duke University. His research interest in DNA metabolism is focused on two major goals: defining the mechanism through which human DNA mismatch repair pathway distinguishes the parent from the daughter strand, and how the pathway responds to lesions.

DNA Mismatch Repair: *E. coli* Vsr and Eukaryotic G–T Systems

Margaret Lieb
Keck School of Medicine, University of Southern California, Los Angeles, California, USA

5-Methylcytosine (5meC) is found at specific sites in the DNA of *Escherichia coli* and related bacteria, and also in eukaryotes, where it functions in the regulation of gene expression. Hydrolytic deamination of 5meC produces thymine (T) (Figure 1), which is mispaired with guanine (G) in the sister DNA strand. In *E. coli*, the very-short patch (VSP) repair system replaces the mismatched T with cytosine (C), thus preventing the occurrence of a C:G to T:A mutation during the next replication of the DNA (Figure 2). In the absence of VSP repair, spontaneous mutation at the sites of 5meC increases manyfold. VSP repair requires the specific endonuclease Vsr and also a DNA polymerase, pol I, and DNA ligase. MutS and MutL, proteins that are essential for the correction of mispairs arising during DNA replication, are required for efficient VSP repair. In mammals, 5meC occurs in CpG sequences. At least two different enzymes appear to preferentially excise T in a T:G mispair that arises in this context.

VSP Repair in *E. coli*

Structure and Regulation of *vsr*

A small gene, *vsr*, coding for only 156 amino acids is present in *E. coli* and related enteric bacteria. It is located adjacent to *dcm*, whose product adds a methyl group to the second cytosine in a 5′ CC (A or T) GG sequence (Figure 2). The first seven codons of *vsr* overlap the 3′ end of *dcm* and both genes are transcribed from a single promoter. While their gene transcripts are present on the same mRNA, Dcm and Vsr proteins are expressed independently. In actively growing cultures, little Vsr is present in the bacteria, and mutation hot spots are found at the sites of 5meC. In nondividing bacteria, the concentration of Vsr increases significantly and, although deamination of 5meC continues at a rate that is time and temperature dependent, mutations do not accumulate at 5meC. Since the bacteria are expected to divide infrequently under natural conditions, VSP repair is an efficient mechanism to prevent mutation at 5meC.

Biochemistry of Vsr

Vsr endonuclease is a monomeric protein whose overall structure and active site have similarities to type II restriction endonucleases. Vsr binds to DNA containing a T:G mispair resulting from the deamination of 5meC (Figure 2). It also binds, with lower affinity, to related sequences lacking the 5′C or the 3′G of the cognate sequence. Binding requires a divalent cation; however, magnesium but not calcium promotes subsequent Vsr activity. Crystallographic studies have shown that Vsr spreads apart the DNA strands at the mispair site by inserting amino acid side chains, causing the DNA to bend. *In vitro*, absence of 5meC from the strand opposite the mispaired T reduces both the rate of DNA binding and the efficiency of enzyme action. This effect has not been observed *in vivo*, where additional factors influence VSP repair.

Biochemical studies show that Vsr nicks DNA 5′ to the mismatched T. When large amounts of Vsr are present, the endonuclease activity does not require an additional protein. However, in replicating bacteria, VSP repair activity is enhanced significantly by MutS and MutL. Since the absence of either protein, or of both, has the same effect, it is likely that these products act cooperatively, as they are known to cooperate in mismatch correction of replication errors (MMR). MutS binds to T:G mispairs in any sequence context and recruits MutL resulting in a MutL–MutS complex that interacts with an endonuclease called MutH. Dominant negative mutations in MutS that block MMR also prevent VSP repair. Although the biochemistry has not been demonstrated *in vitro*, it is likely that MutS helps to attract Vsr to T:G mispairs, perhaps because Vsr can bind to MutL *in vitro*. If Vsr is brought to a T:G that is in the DNA sequence that it recognizes, it may cause MutS and MutL to disassociate from the mispair, allowing Vsr to replace MutS.

In addition to Vsr, VSP repair requires pol I, which has an intrinsic 5′–3′ exonuclease activity that digests away a small number of nucleotides starting at the nick immediately upstream of T. It simultaneously

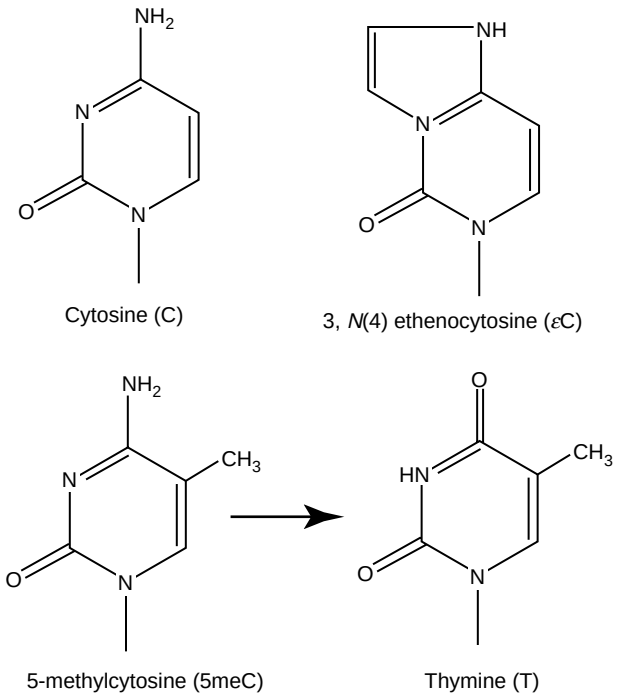

FIGURE 1 Chemical structures of cytosine and cytosine derivatives. 3,N(4) ethenocytosine is a mutagen produced in DNA by endogenous products of lipid peroxidation and by industrial pollutants such as vinyl chloride.

resynthesizes DNA in the 5′–3′ direction. Since pol I is an error-free polymerase, it inserts a C in place of the T that it has removed from the mismatch. The actual number of bases removed is known to be less than 10, and is perhaps as few as 1 or 2. This is why this repair is referred to as very-short patch. The repair is completed by DNA ligase, an enzyme that seals single-strand nicks in double-stranded DNA.

Mutagenesis by Vsr

Overproduction of Vsr increases the frequency of mutation at many sites in *E. coli*, mimicking the effect of mutations in *mutS* or *mutL*. Mutagenesis by Vsr can be attributed to its competition for a component of the MMR system. MutL has been shown to interact physically with Vsr *in vitro* and additional MutL reduces the mutagenic effect of excess Vsr. Thus, it is likely that the concentration of Vsr is maintained at a low level in dividing bacteria to prevent its titration of MutL. Vsr would also have a mutagenic effect if it corrected to C:G a T:G mispair in which the G was a replication error in a newly synthesized strand. It should be noted that MutS has a higher affinity for T:G than for any other mispair. Therefore, it is not surprising that excess MutS reduces VSP repair by competing with Vsr for binding at T:G mispairs that result from deamination of 5meC.

VSP Repair and Marker Effects

Before the advent of DNA sequencing, the relative location of different mutation sites on microbial chromosomes was determined by crossing different mutants and observing the frequency of wild-type recombinants. The frequency of recombination generally decreases with the distance between mutation sites on the parental genomes. Certain mutations (or markers) appear to recombine with other mutations in their vicinity more frequently than expected. This "marker effect," which has also been referred to as "high negative interference," is often the result of VSP repair of a C to T mutation that occurred at a 5meC.

Methyl-CpG Binding Domain 4 (MBD4) Protein in Eukaryotes

Structure and Biochemistry of MBD4

The gene for MBD4 was identified in a search of the human sequence database for a methyl-CpG-binding domain. Mbd4 genes in both the human and mouse code for a 580 amino acid protein with a methyl-CpG-binding domain near the amino-terminal end, and a carboxy-terminal glycosylase domain. The glycosylase region of the protein is related to bacterial glycosylases such as MutY. The enzyme has no lyase activity, so that the removal of the mismatched base

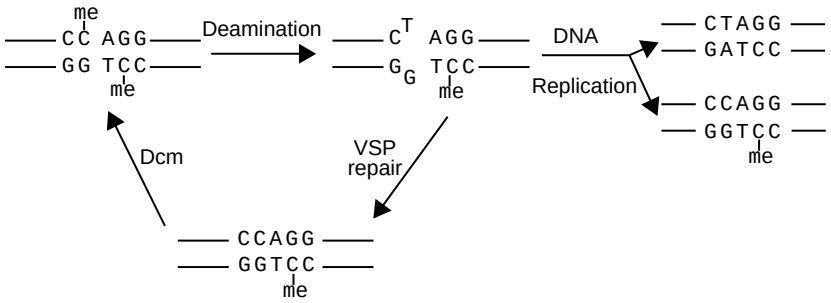

FIGURE 2 The life cycle of a dcm site in *E. coli*.

leaves an abasic site. The sugar-phosphate backbone of DNA can subsequently be cleaved by the human AP endonuclease HAP1 but other endonucleases may also perform this function. There is evidence suggesting that processing of the abasic site also involves interaction with MLH1, a homologue of bacterial MutL.

Specificity

Investigations with human MBD4 have shown that only T:G and U:G mispairs are good substrates for the enzyme. The human MBD4 enzyme binds preferentially to T:G mismatches in the meCpG/TpG context. However, removal of the mismatched base was observed when U:G and T:G mismatches were in a nonmethylated substrate. T:G mismatches in other contexts are processed at a greatly reduced rate. The fact that U is removed from a mispair with G more rapidly than T suggests that removal of T resulting from deamination of meC may not be the primary function of MBD4.

Cancer Prevention

In the cells of the intestinal mucosa of mice containing inactive *Mbd4* genes there was a two- to threefold increase in C to T mutations in CpG sequences. In combination with mutations in the adenomatosis polyposis (Apc) genes, MBD4 inactivation increased the number of tumors and tumor progression. A 3.3-fold increase of C to T mutations at 5meC was also observed in the liver and spleen of mice lacking MBD4. Therefore, it is clear that MBD4 is a significant factor in the prevention of mutations leading to cancer.

Thymine-DNA Glycosylase (TDG)

Structure and Biochemistry of TDG

TDG is an enzyme with homologues found in the cells of humans and other animals, and also in *E. coli*. It has no apparent amino acid similarity to MBD4.The enzyme is characterized by low abundance and slow action. TDG can remove from DNA the bases T or U that arise by deamination of 5meC or C, and are thus mispaired with G. Removal of the base from the DNA backbone results in an abasic site to which the TDG remains bound. Studies of human TDG *in vitro* have indicated that an apurinic exonuclease (HAP1) helps TDG turnover and cleaves the abasic sugar phosphate. Repair of the resulting nick in the DNA strand requires both a DNA polymerase and DNA ligase.

Specificity

TDG was first isolated in a search for a Vsr-like activity in extracts of human cells. The enzyme has a higher affinity for U:G mispairs than for T:G, and also significant affinity for 3,N(4) ethenocytosine (Figure 1) paired with G. TDG has a strong preference for mispairs arising in the CpG context. However, there is as yet no direct evidence that it has an important role in preventing mutation resulting from deamination of 5meC.

See Also the Following Articles

DNA Mismatch Repair Defects and Cancer • DNA Mismatch Repair in Bacteria • DNA Restriction and Modification: Type II Enzymes • Recombination: Heteroduplex and Mismatch Repair *in vitro*

Glossary

AP endonuclease An enzyme that makes incisions in DNA on the 5′ side of either apurinic or apyrimidinic sites.

deamination Hydrolytic replacement of an amino group ($-NH_2$) from a chemical compound with a hydroxyl group.

dominant negative mutation A mutation that results in a protein that is inactive and, in addition, competes with an active form of the same protein.

glycosylase (glycosidase) A hydrolytic enzyme that cleaves the bond between a sugar molecule and a nucleic acid base such as thymine.

monomeric enzyme An enzyme composed of a single polypeptide.

type II restriction endonuclease An enzyme that cuts both DNA strands at defined positions close to or within a specific base sequence.

Further Reading

Bellacosa, A. (2001). Role of MED1(MBD4) gene in DNA repair and human cancer. *J. Cell Physiol.* **178**, 137–144.

Bhagwat, A. S., and Lieb, M. (2002). Cooperation and competition in mismatch repair: Very short patch repair and methyl-directed mismatch repair in *Escherichia coli*. *Mol. Microbiol.* **44**, 1421–1428.

Hardeland, U., Bentel, M., Lettieri, T., Jiricny, J., and Schar, P. (2003). The versatile thymine DNA glycosylase: A comparative characterization of the human, Drosophila and fission yeast orthologs. *Nucleic Acids Res.* **312**, 261–271.

Lieb, M., and Bhagwat, A. S. (1996). Very short patch repair: Reducing the cost of cytosine methylation. *Mol. Microbiol.* **20**, 467–473.

Miller, C. B., Guy, J., Sansom, O. J., Selfridge, J., MacDougall, E., Hendrich, B., Keightley, P. D., Bishop, S. M., Clarke, A. R., and Bird, B. (2002). Enhanced CpG mutability and tumorigenesis in MBD4-deficient mice. *Science* **297**, 403–405.

Wu, P., Qiu, C., Sohail, A., Zhang, X., Bhagwat, A. S., and Cheng, X. (2003). Mismatch repair in methylated DNA. *J. Biol. Chem.* **278**, 5285–5291.

Biography

Margaret Lieb is Professor Emerita in the Department of Molecular Microbiology and Immunology at the Keck School of Medicine in Los Angeles. She holds degrees from Smith College, Indiana University and Columbia University, and pursued postdoctoral studies at Caltech and the Pasteur Institute. Her research on bacteriophage lambda genetics has focused on the lambda repressor. VSP repair was discovered in a study of recombination between mutations in the repressor gene.

DNA Oxidation

Arthur P. Grollman
State University of New York, Stony Brook, New York, USA

Dmitry O. Zharkov
Novosibirsk Institute of Chemical Biology and Fundamental Medicine, Russia

Oxygen-releasing photosynthesis and aerobic respiration have provided the basic machinery of life for almost three billion years and have driven the evolution of complex life forms. Molecular oxygen is a powerful oxidizing agent whose metabolic products can cause serious damage to proteins and DNA. As the integrity of genomic DNA is critical to cell survival, a variety of intracellular systems have evolved to repair oxidative DNA damage.

Oxidants and Antioxidants

The reduction of oxygen to water consists of several sequential steps involving the reactive oxygen species (ROS) superoxide anion radical, hydrogen peroxide, and hydroxyl radical. Thus,

$$O_2 \rightarrow {}^{\cdot}O_2^- \rightarrow H_2O_2 \rightarrow HO^{\cdot} \rightarrow H_2O$$

Additionally, molecular oxygen in the $^1\Delta_g$ excitation state ("singlet oxygen") is included in the category of reactive oxygen species. In cells, ROS react with many molecules, with their average lifetime and distance of diffusion from the point of generation being inversely proportional to their reactivity. Free radicals, such as ${}^{\cdot}O_2^-$ and $HO^{\cdot}$, trigger chain reactions of oxidation, allowing unpaired electrons to propagate over longer distances. Polyunsaturated fatty-acid side chains are especially prone to reactions with free radicals; the resulting peroxyl radicals propagate by a chain reaction. Given the ubiquitous presence of lipid bilayers in cells, lipid peroxidation also plays an important role in the toxicity associated with ROS.

The primary source of ROS in eukaryotes is the mitochondrial respiratory chain. Approximately 0.1% of cellular oxygen is converted to superoxide, primarily through auto-oxidation of the semiquinone forms of ubiquinone and flavin mononucleotides, which occurs during the NADH dehydrogenase electron transfer process. In mitochondria, superoxide anions generate hydrogen peroxide and hydroxyl radicals. In plants, photosystem I is also a major producer of ROS. Other cellular redox systems also are capable of producing ROS. For example, nonmitochondrial endogenous sources of ROS include reactions catalyzed by cytochrome P450, NADPH:cytochrome P450 reductase, and xanthine oxidase. Recently, immunoglobulins were identified as a major ROS source in mammals.

The major environmental source of ROS is ionizing radiation. Radiolysis of water releases hydroxyl radicals and other reactive entities, such as solvated electrons and ${}^{\cdot}H$ and ${}^{\cdot}O^-$ radicals. Other sources of ROS include microwave radiation, ultrasound, photosensitizing dyes (methylene blue, rose bengal), transition metal ions, ozone, and a variety of salts (e.g., $KBrO_3$), as well as certain drugs and chemicals.

Hydroxyl radicals and singlet oxygen are the most reactive forms of ROS and, consequently, the most damaging to biomolecules. Hydroxyl radicals are generated from superoxide and H_2O_2 by Fenton chemistry when Fe^{2+} or other low-valency transition metal ions are present; such ions bind to DNA and these reactions play an important role in DNA damage:

$$H_2O_2 + Fe^{2+} \rightarrow HO^{\cdot} + OH^- + Fe^{3+}$$
$${}^{\cdot}O_2^- + Fe^{3+} \rightarrow O_2 + Fe^{2+}$$

In living organisms, various mechanisms have evolved to minimize the effects of oxidative damage, including deactivation of ROS by superoxide dismutases, catalases, and peroxidases. Superoxide dismutases (SODs) are ubiquitous metal-dependent enzymes that contain Cu and Zn, Mn, or Fe metal ions. All forms of SOD catalyze the dismutation of superoxide radicals into hydrogen peroxide and oxygen:

$$2\,{}^{\cdot}O_2^- + 2H^+ \rightarrow H_2O_2 + O_2$$

In the next stage of oxygen reduction, hydrogen peroxide is converted to water and oxygen by catalase:

$$2H_2O_2 \rightarrow 2H_2O + O_2$$

or peroxidase:

$$R_1SH + R_2SH + H_2O_2 \rightarrow R_1SSR_2 + 2H_2O$$

Almost any low-molecular-weight substance that contains a reducing moiety can react with ROS. Such nonenzymatic radical scavengers are present in significant quantities in cells or concentrated at ROS target sites. These scavengers include lipophilic substances (α-tocopherol, β-carotene) and hydrophilic molecules (ascorbic acid, uric acid, glucose, and glutathione) that prevent transition metals from producing hydroxyl radicals, thereby performing an antioxidant function. The low concentrations of free Fe^{2+} in living cells is a consequence of the presence of proteins in the cell that bind and sequester iron (ferritin, transferrin) or oxidize it (ceruloplasmin).

DNA Damage

DNA is an important target of oxidative damage. Both the sugar-phosphodiester backbone and the bases are subject to attack by ROS, producing single- and double-strand breaks, intra- and interstrand cross-links, abasic (AP) sites, cyclonucleotides, and a variety of modified bases. ROS also damage DNA by lipid peroxidation. All DNA bases are subject to direct oxidation; the principal lesions detected in cellular DNA are shown in Figure 1.

The most prevalent oxidized base in DNA, 8-oxoguanine (8-oxoG), is formed by oxidation of guanine at C8. Like all purine nucleotides substituted at C8, 8-oxo-2′-deoxyguanosine (8-oxodG) adopts the *syn* rather than *anti* conformation unless additional restraints, such as Watson–Crick pairing, are present. In the *anti* conformation, 8-oxodG forms a Watson–Crick pair with dC, whereas in the *syn* conformation, it forms a Hoogsteen pair with dA.

Biological Effects

Cytotoxicity and Mutagenesis

The major cytotoxic effects of ROS represent responses to DNA double-strand breaks and lesions that block DNA replication. Certain oxidized bases are mutagenic, e.g., 8-oxoG accommodates a miscoding base (A) during DNA synthesis. The proofreading activity of DNA polymerases fails to remove this base when it is incorporated opposite 8-oxodG. Thus, mutations at 8-oxoG are predominantly G → T transversions. Interestingly, DNA polymerases differ significantly with respect to nucleotide insertion opposite 8-oxoG. Thus, replicative polymerases (DNA polymerase α, DNA polymerase δ, DNA polymerase III) preferentially insert dAMP opposite the damaged base, while polymerases involved in DNA repair (DNA polymerase β, DNA polymerase I) mainly incorporate dCMP opposite the lesion. Deoxynucleotide triphosphates are also subject to damage by ROS, promoting base misincorporation, which may lead to mutational events.

Carcinogenesis

Oxidative stress is an important factor in tumor initiation and promotion. Its relative impact can be appreciated by noting that the amount of oxidized bases in DNA is significantly higher than the amount of DNA adducts formed by environmental mutagens. It is clear that somatic mutations play a central role in carcinogenesis and oxidative DNA damage has been implicated as an initiating event in this process. The role of ROS in tumor development also may be attributed, in part, to

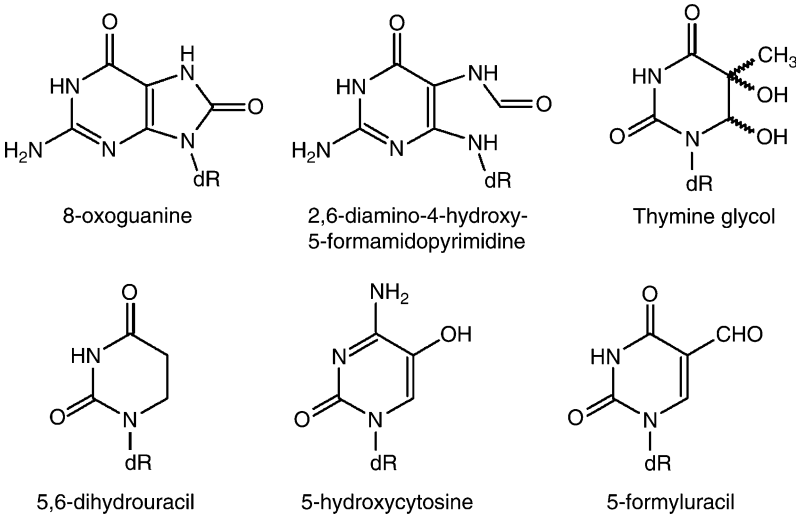

FIGURE 1 Examples of major oxidative lesions in DNA.

their mitogenic properties and their ability to damage cellular proteins and membranes.

8-oxoG and thymine glycol are frequently used as biomarkers for oxidative DNA damage. Interestingly, tumor tissue sometimes contains increased amounts of oxidized bases. As most solid tumors are anoxic and generally display *lower* levels of general oxidative damage, this increase in DNA damage appears to be a cause rather than a consequence of neoplastic transformation. For tumor development to occur, a series of mutations are generally required to inactivate tumor suppressor genes and/or alter the status of protooncogenes. The presence of G → T transversions, characteristic of 8-oxoG, suggests that oxidative damage may have been involved in these instances. This signature base-substitution mutation is found in mutated p53 and *ras* genes in many human cancers and experimental systems.

Aging

In 1956, D. Harman proposed a free-radical theory of aging. Oxidative DNA damage increases with age and the correlations between aging and DNA oxidation are reflected in increasing levels of 8-oxoG and thymine glycol. The relationship between an organism's life span and its ability to repair oxidatively damaged DNA has also been reported. Although the frequency of mutations increases with age, there are no documented cases of somatic mutations in the nuclear genome that are directly involved in causing age-related changes or age-related diseases (such as hypertension or Alzheimer's disease). There are, however, known, well-established mutations that are associated with certain spontaneous, nonhereditary cancers. Mitochondrial DNA (mtDNA), rather than nuclear DNA, has been proposed as a principal site of age-related damage accumulation. In fact, direct estimates of oxidative damage in mtDNA usually are higher than those in nuclear DNA. A specific, age-related deletion in the mtDNA of postmitotic cells, as well as multiple rearrangements, has been documented.

Repair of Oxidative DNA Damage

General

DNA damage occurs to a significant degree despite the ubiquitous presence of ROS scavengers. However, several cellular mechanisms are available to effect repair: direct reversal, base excision repair (BER), nucleotide excision (NER), methyl-directed mismatch repair, and recombination repair. Double-strand breaks are generally repaired by recombination repair; interstrand cross-links by a combination of NER and recombination repair; and intrastrand cross-links and cyclonucleotides by NER. Most oxidative damage is dealt with by BER. Here, damaged bases are excised by specific DNA glycosylases, creating an apurinic/apyrimidinic (AP) site. If the glycosylase has AP lyase activity, it can immediately cleave 3′ to the AP site; otherwise, a separate AP endonuclease cleaves 5′ to this position. Deoxyribose phosphate lyase (dRPase) removes the sugar residue, creating a substrate for a DNA polymerase. After this polymerase fills the resulting gap, a DNA ligase restores the double-stranded DNA.

Despite the wide variety of oxidatively damaged bases found in DNA, only a few glycosylases are involved in their repair. These enzymes necessarily exhibit broad substrate specificity, with some acting primarily on oxidized pyrimidines and others on oxidized purines. In *Escherichia coli*, oxidative damage to pyrimidines is repaired by endonucleases III and VIII (Nth and Nei); structurally related enzymes (NTH and NEIL) perform similar functions in eukaryotes. About 20 types of oxidized bases are excised by these DNA glycosylases. Depending on the type of chemistry performed by DNA glycosylases, modified AP sites are generated and processed by AP endonucleases to generate a suitable end for the DNA polymerase.

GO System

8-oxoG presents special problems for DNA repair. Since either dAMP or dCMP can be incorporated opposite 8-oxodG, the repair system for this lesion must convert both 8-oxodG:dC and 8-oxodG:dA mispairs into a dG:dC pair. At least two cycles of BER are required to repair 8-oxodG:dA. First, adenine, the normal base, is excised, a process followed by insertion of dCMP opposite the lesion. The resulting 8-oxodG:dC mispair is then repaired by excision of 8-oxoG and subsequent insertion of dGMP.

In *E. coli*, a system of three enzymes – Fpg (MutM), MutT, and MutY (GO system) – counters the deleterious effects of 8-oxoG (Figure 2). MutT protein, a nucleoside triphosphate hydrolase, cleanses the cellular nucleotide pool of 8-oxodGTP. Fpg is an 8-oxoguanine-DNA glycosylase/AP lyase that excises 8-oxoG from 8-oxodG:dC but not from 8-oxodG:dA. MutY protein is an adenine glycosylase specific for dA:8-oxodG and dA:dG pairs. If 8-oxoG DNA arises by spontaneous oxidation of guanine or by incorporation of 8-oxodGMP opposite dC, it is excised by Fpg. However, if dA:8-oxodG is present because of incorporation of 8-oxodGMP opposite dA, it becomes a substrate for MutY. DNA polymerase I, the principal repair polymerase in *E. coli*, preferentially inserts dCMP opposite 8-oxodG. If dAMP is again inserted, the cycle of MutY repair may repeat. If dCMP is inserted during postreplication repair, the 8-oxodG:dA mispair is converted

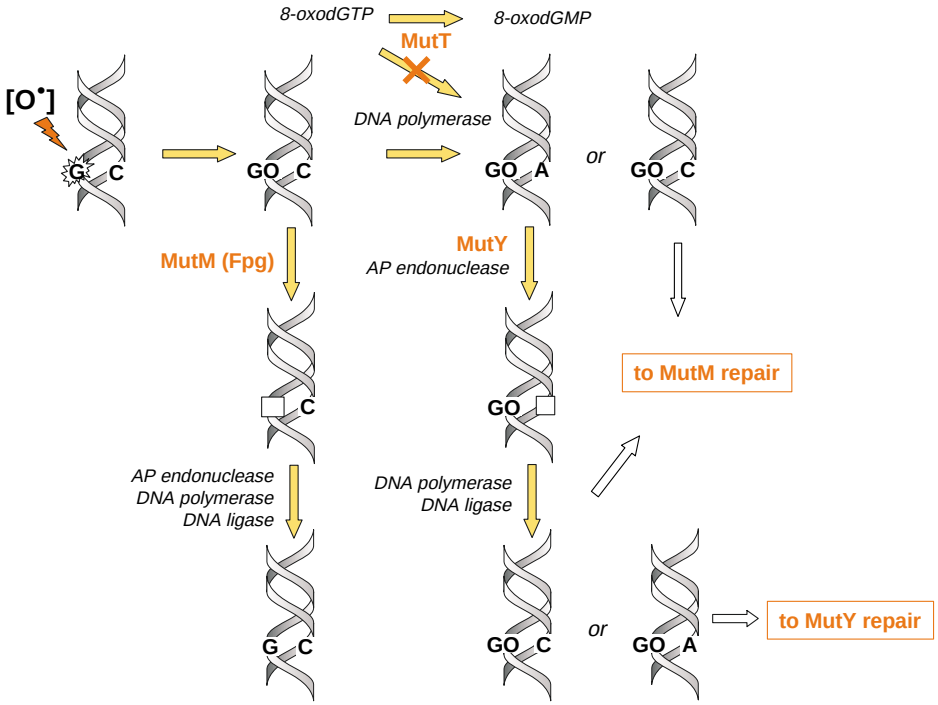

FIGURE 2 GO system in bacteria.

to 8-oxodG:dC, a substrate for Fpg. This GO system also operates in most eukaryotes.

See Also the Following Articles

DNA Glycosylases: Mechanisms • DNA Mismatch Repair and the DNA Damage Response • Superoxide Dismutase

Glossary

DNA damage Any change in the bases (A, C, G, and T) or phosphodiester backbone structure that comprise canonical DNA.

DNA repair Any process, usually enzymatic, which participates in purging DNA of damaged elements and returns it to its canonical form.

reactive oxygen species A molecule that contains an oxygen atom with a highly reactive configuration of electrons.

Further Reading

Aruoma, O. I., and Halliwell, B. (eds.) (1998). *DNA and Free Radicals: Techniques, Mechanisms, and Applications*. OICA International, London.

Friedberg, E. C., Walker, G. C., and Siede, W. (1995). *DNA Repair and Mutagenesis*. ASM Press, Washington, DC.

Grollman, A. P., and Moriya, M. (1993). Mutagenesis by 8-oxoguanine: an enemy within. *Trends Genet.* **9**, 246–249.

Halliwell, B., and Gutteridge, J. (1999). *Free Radicals in Biology and Medicine*. Oxford University Press, Oxford.

Moldave, K., Mitra, S., and McCullough, A. (eds.) (2001). *Base Excision Repair (Progress in Nucleic Acid Research and Molecular Biology)*, *Vol 68*. Academic Press, London.

Stivers, J. T., and Jiang, Y. L. (2003). A mechanistic perspective on the chemistry of DNA repair glycosylases. *Chem. Rev.* **103**, 2729–2760.

von Sonntag, C. (1987). *The Chemical Basis of Radiation Biology*. Taylor and Francis, London.

Biography

Arthur P. Grollman is Distinguished Professor of Pharmacological Sciences and Glick Professor of Experimental Medicine at the State University of New York at Stony Brook, where he heads the Laboratory of Chemical Biology. The Laboratory's research focuses on mechanisms of DNA damage, mutagenesis and DNA repair.

Dmitry O. Zharkov is a senior research scientist at the Novosibirsk Institute of Chemical Biology and Fundamental Medicine, Russia. His principal research interests are in the field of DNA repair and protein–nucleic acid interactions. He obtained a Ph.D. from the State University of New York at Stony Brook, where he later investigated the structure and mechanism of action of DNA glycosylases.

DNA Photolyase

Carrie L. Partch and Aziz Sancar
University of North Carolina School of Medicine, Chapel Hill, North Carolina, USA

Ultraviolet irradiation from sunlight damages DNA, and the growth of cells containing DNA lesions can lead to mutations, cell death, and cancer. Photolyase repairs UV-induced pyrimidine dimers by splitting the DNA photoproducts into individual pyrimidine bases through a process of photo-induced cyclic electron transfer using near-UV/blue light as an energy source. The reversal of the effect of far-UV (200–300 nm) by near-UV/visible light (300–500 nm), known as photoreactivation, is the most direct mechanism for repair of DNA photoproducts. Phylogenetically, the closest homolog of photolyase is a UV/blue light photo-receptor named cryptochrome, which regulates growth and development in plants and the circadian clock in animals and plants.

Classification

All members of the photolyase/cryptochrome family share a common evolutionary origin, high sequence homology, and identical chromophore/cofactors. Despite these similarities, their activities are directed toward unique substrates; photolyases repair either cyclobutane pyrimidine dimers or (6-4) photoproducts, induced in DNA by ultraviolet light. Cryptochromes do not have any repair activity; instead, they function as photoreceptors to regulate development in plants and synchronize circadian rhythms with the solar cycle in animals. Circadian rhythms are the daily oscillation of physiological processes designed to coordinate organismal activity with the solar cycle. Photoreactivation and circadian phototransduction may conceivably have had a common evolutionary origin. In the distant past, when more UV light reached the surface of the Earth, a primitive organism may have used the same protein to repair UV-induced DNA lesions and regulate daily behavior in order to minimize exposure to the harmful effects of sunlight.

Species Distribution

The two members of the photolyase/cryptochrome family are found in many members of the three kingdoms of life. Cyclobutane photolyases are by far the most predominant across species. The two most abundant photoproducts formed by absorption of far-UV light (200–300 nm) by DNA are *cis,syn*-cyclobutane pyrimidine dimers (CPD) and pyrimidine–pyrimidone (6-4) photoproducts (Figure 1). UV induces cyclobutane pyrimidine dimers in DNA 10 times more frequently than (6-4) photoproducts. Many species that contain a cyclobutane photolyase lack a (6-4) photolyase, but those with a (6-4) photolyase always contain a cyclobutane photolyase, highlighting the importance of the cyclobutane photolyase for survival. Despite the relatively widespread distribution of photolyases in the three kingdoms, many microorganisms such as *Bacillus subtilis* and *Schizosaccharomyces pombe* do not have any photolyase. In contrast, *Escherichia coli* and *Saccharomyces cerevisiae* have cyclobutane photolyase and *Drosophila* has cyclobutane photolyase, (6-4) photolyase and cryptochrome. Of special interest, placental mammals such as mice and humans have two cryptochromes but do not possess either photolyase. UV photoproducts in these organisms are removed exclusively by the nucleotide excision repair pathway. Cryptochromes are expressed in plants, most animals, and some bacteria, frequently with more than one isoform in a species.

Photolyase

Primary Structure and Chromophores

Photolyases are 50- to 55-kDa monomeric proteins with two chromophore/cofactors. Sequence identity among the 50 or so known photolyases ranges from 15 to 70% with maximal sequence conservation in the catalytic FAD-binding domain. All photolyase/cryptochrome family proteins contain two noncovalently bound chromophores: a primary chromophore, FAD (flavin adenonucleotide), required for specificity in binding damaged DNA and catalysis, and a second, or "antenna" chromophore. The second chromophore is a folate (or rarely, a deazaflavin) and increases the rate of catalysis in

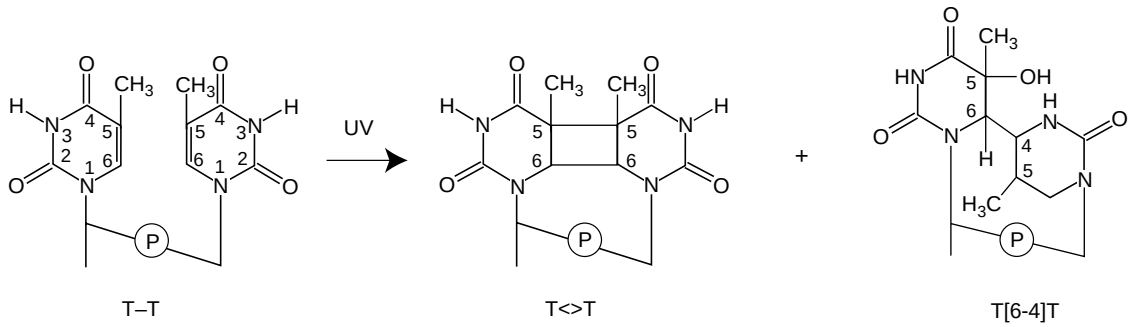

FIGURE 1 Structure of UV-induced DNA photoproducts. The two major DNA photoproducts induced by far-UV irradiation are pyrimidine cyclobutane dimers (80–90% of lesions) and pyrimidine–pyrimidone (6-4) photoproducts (10–20% of lesions). The same type of photoproduct may form between any adjacent pyrimidines, including T–T, T–C, C–T, and C–C sites, except that (6-4) photoproducts do not form at C–T sites.

limiting light by absorbing light and transferring the energy to the FAD catalytic cofactor. Native photolyase contains FAD in the two-electron reduced and deprotonated form ($FADH^-$). This is the only active form of the cofactor. During purification the flavin is often converted to the catalytically inactive neutral radical ($FADH^\circ$) form, but it can be converted back to the $FADH^-$ either chemically or photochemically.

Tertiary Structure

Crystal structures have been solved for several members of the photolyase family and despite their low sequence homology (~25% identity), the structures are remarkably similar. Photolyases exhibit a rather compact structure composed of two distinct domains: an N-terminal α/β domain (residues 1–131, *E. coli* photolyase numbering) and a C-terminal α-helical domain (residues 204–471), connected to one another by a long loop (residues 132–203) (Figure 2). The FAD cofactor is buried deep within the α-helical domain, held tightly in place by contact with 14 highly conserved amino acids. The antenna chromophore is bound loosely in a cleft between the two domains. An electrostatic representation of the surface of photolyase illustrates the presence of a large, shallow, positively charged groove that comprises the DNA-binding interface. A cavity in the middle of the groove allows the damaged nucleotide bases to fit in close proximity to the FAD during catalysis (Figure 2).

Reaction Mechanism

The cyclobutane photolyase has been extensively studied and a detailed model for its reaction mechanism had been made. The enzyme binds pyrimidine dimers

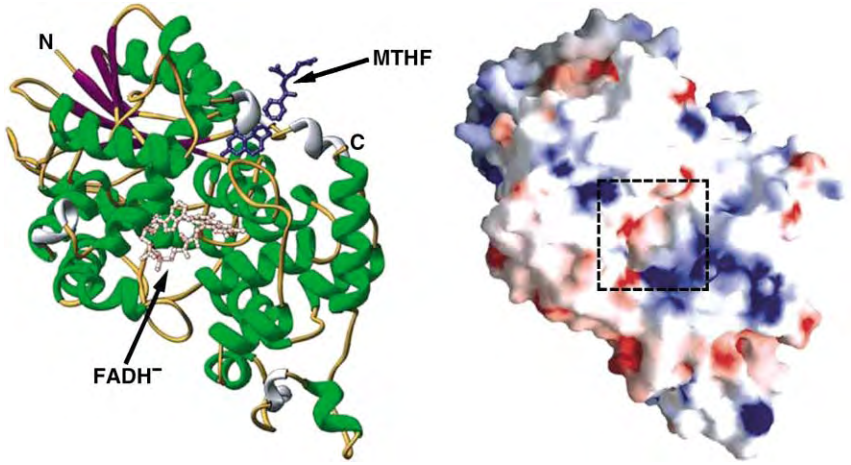

FIGURE 2 The structure of *E. coli* photolyase. The ribbon diagram representation (left) of the crystal structure of *E. coli* photolyase obtained at 2.3Å shows the placement of the two chromophores and the distinct N-terminal α/β domain and C-terminal α-helical domain. An electrostatic representation (right) of the surface illustrates the positive DNA-binding groove (shown in blue) that runs diagonally down the length of the protein and the dimer binding cavity (indicated by the dashed square).

independently of light, specifically attracted to the distorted DNA helix (bent approximately 30°) created by the DNA lesion. The dimer is flipped out of the double helix of the DNA into the active site cavity of photolyase, positioned in close proximity to the flavin (Figure 3A). Catalysis is initiated by light. A photon of near-UV/blue light (300–500 nm) is absorbed by the antenna chromophore and the excitation energy is transferred to the flavin ($FADH^-$) by fluorescence resonance energy transfer. The excited singlet state flavin $^1(FADH^-)^*$ then transfers an electron to the dimer, splitting the cyclobutane ring to form two pyrimidines. Concomitantly, an electron from the pyrimidine radical is transferred back to the neutral radical flavin ($FADH^\circ$) formed during catalysis to regenerate the active form of flavin ($FADH^-$) without a net redox change in the chromophore or substrate (Figure 3B). The repair of photoproducts by CPD photolyases occurs with a high quantum yield (photolesion repaired per absorbed photon) of 0.7–0.98.

The (6-4) photolyase has not been studied to the same extent as the cyclobutane photolyase, but it is believed to function in a similar manner with one significant difference. Upon binding the damaged DNA, the enzyme first thermally converts the (6-4) photoproduct to a four-membered ring intermediate closely resembling a cyclobutane dimer. The photo-induced electron transfer mechanism is presumed to be the same as for the classical cyclobutane photolyase, although there is no direct evidence for this mechanism and the quantum yield of repair is significantly lower for (6-4) photolyases, in the range of 0.05–0.10.

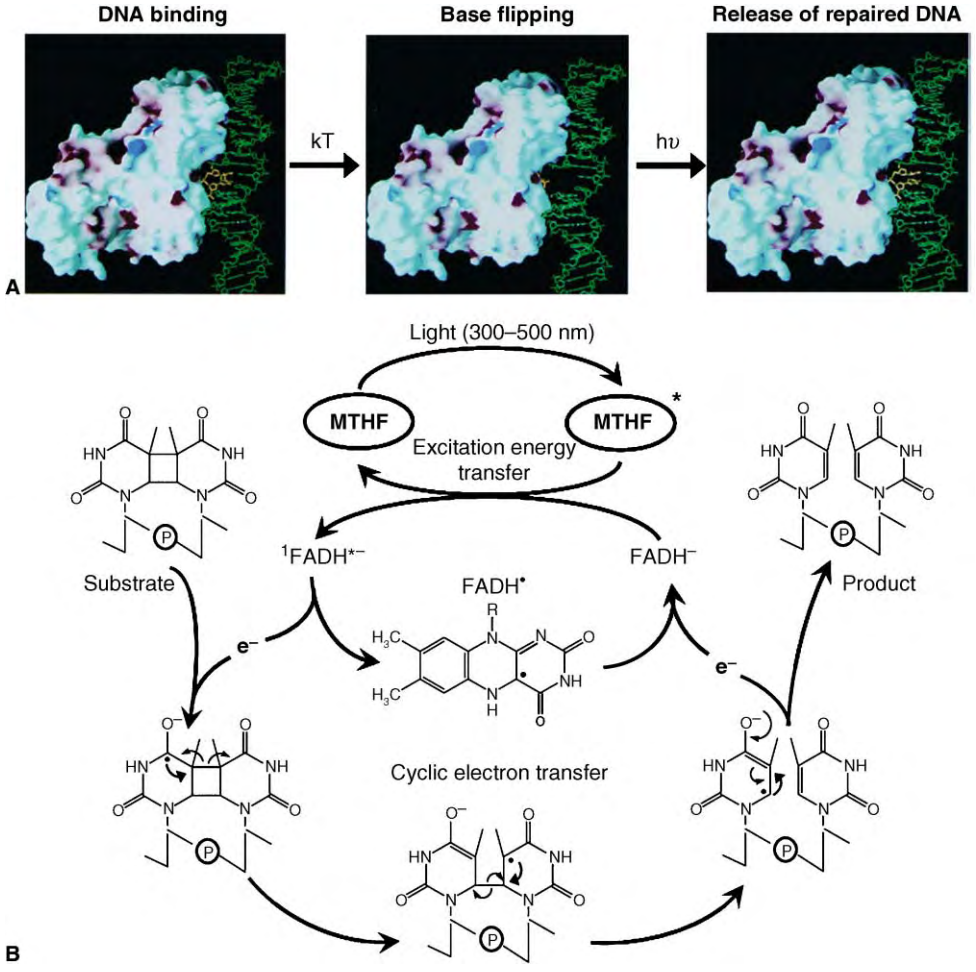

FIGURE 3 Reaction mechanism of photoreactivation by *E. coli* photolyase. (A) General outline of the repair reaction. Photolyase binds to the damaged DNA (shown in yellow), flips the dimer into its active site cavity thermally (kT) for repair, and, following photorepair ($h\nu$), ejects the repaired DNA bases into the DNA helix. (B) Photochemical steps of dimer splitting. After absorption of a photon by the folate, energy is transferred to the flavin, which donates an electron to break the cyclobutane ring. An electron is transferred back from the product to the flavin, restoring the flavin to its ground state with no net change in redox status in either the substrate or cofactor.

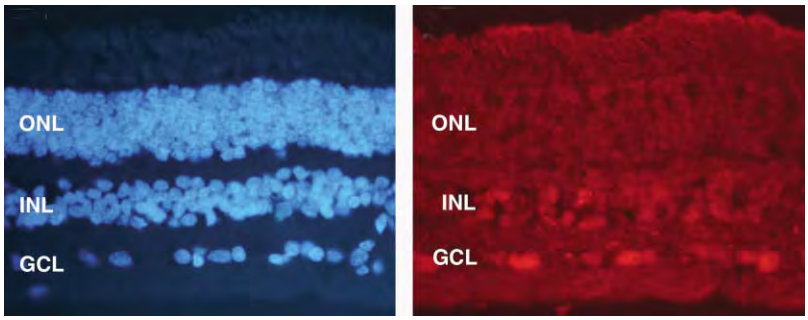

FIGURE 4 Cryptochrome expression in the human retina. Human cryptochrome 2 (Cry2) is expressed in the inner retina. DAPI staining of nuclei (left, shown in blue) and Cry2 immunofluorescence (right, shown in red) are shown. Note the exclusive expression of Cry2 in the inner retina (INL and GCL). ONL, outer nuclear layer; INL, inner nuclear layer; GCL, ganglion cell layer.

Dark Repair Function

Even in the absence of photoreactivating light, photolyase plays an advantageous role in the cell by stimulating the repair of damaged DNA. This "dark function" is due to the stimulation of the nucleotide excision repair pathway by photolyase. As a general rule, the more a lesion distorts the DNA structure, the more efficiently it is recognized and removed by the excision nuclease system. Cyclobutane pyrimidine dimers cause only modest distortions of the DNA helix compared to (6-4) photoproducts and are repaired at a much lower rate in the absence of photolyase. Photolyase, presumably by binding the damage and flipping the dimer out of the helix, increases distortion of the DNA and accelerates the rate-limiting damage recognition step of the excision repair complex. In addition, photolyase recognizes DNA lesions caused by other chemical agents such as cisplatin, stimulating excision of the DNA adduct and increasing cellular survival without photoreactivation.

Cryptochromes

Structure

The basic architecture of cryptochrome is remarkably similar to photolyase. However, cryptochromes are structurally distinguished from photolyases by the presence of extended C-terminal domains ranging from 40 to 250 amino acids in length. These domains are thought to be important to the unique function of cryptochromes in circadian rhythms and growth control.

Function

In nearly all organisms, the daily oscillation of physiological and behavioral processes such as sleep, body temperature, and metabolic rate are regulated by a transcription-based endogenous clock called the circadian (circa = about, dies = day) clock. These oscillations are kept in harmony with the solar cycle by photoreceptors that adjust the phase of the endogenous clock to coordinate rest or activity with the appropriate light cycle. Cryptochromes have two roles in maintaining circadian rhythms: photoreception and light-independent control of the endogenous clock. In mammals, circadian phototransduction is mediated solely through the eye and is not dependent on the outer retina containing the visual photoreceptors. Human cryptochromes are highly expressed in the inner retina (Figure 4). Elimination of cryptochromes by genetic means seriously compromises circadian phototransduction in mice and *Drosophila*, indicating that cryptochromes are the primary circadian photoreceptors. However, in the absence of cryptochromes there is some residual circadian photoreception, indicating that functional redundancy exists between cryptochromes and opsins in circadian phototransduction.

Reaction Mechanism

The mechanism of photoreception/phototransduction by cryptochromes is not known at this time. However, catalytic residues from photolyase are conserved in cryptochromes and the unique C-terminal domains interact with effector proteins in a light-dependent manner in several organisms. It has been hypothesized that an intra- or intermolecular electron transfer mechanism may regulate accessibility of the C-terminal domain to effector proteins in response to light, thereby providing a regulated mechanism of signal transduction. The light-independent function of cryptochromes is to downregulate the expression of several clock genes by acting as a negative transcription factor.

See Also the Following Articles

Nucleotide Excision Repair, Bacterial: The UvrABCD System • Nucleotide Excision Repair in Eukaryotes

Glossary

cryptochrome Flavoprotein photoreceptor with homology to DNA photolyase that regulates the circadian clock.

DNA adduct Complex formed when a chemical is covalently bound to a DNA base.

photolyase Flavoprotein photoreceptor that uses UV/blue light to repair UV-induced photoproducts in DNA.

pyrimidine dimer Covalent linkage formed between two adjacent pyrimidine bases when DNA is exposed to far-UV light (200–300 nm).

Further Reading

Carell, T., Burgdorf, L. T., Kundu, L. M., and Cichon, M. (2001). The mechanism of action of DNA photolyases. *Curr. Opin. Chem. Biol.* **5**, 491–498.

Sancar, A. (2000). Cryptochrome: The second photoactive pigment in the eye and its role in circadian photoreception. *Ann. Rev. Biochem.* **69**, 31–67.

Sancar, A. (2003). Structure and function of DNA photolyase and cryptochrome blue light photoreceptors. *Chem. Rev.* **103**, 2203–2237.

Sancar, A., Thompson, C., Thresher, R. J., Araujo, F., Mo, J., Ozgur, S., Vagas, E., Dawut, L., and Selby, C. P. (2000). Photolyase/cryptochrome family blue-light photoreceptors use light energy to repair DNA or set the circadian clock. *Cold Spring Harb. Symp. Quant. Biol.* **65**, 157–171.

Sancar, G. B. (2000). Enzymatic photoreactivation: 50 years and counting. *Mut. Res. Fund. Molec. Mech. Mutagen.* **451**, 25–37.

Biography

Carrie Partch is a graduate student in the laboratory of Dr. Aziz Sancar at the University of North Carolina School of Medicine, Chapel Hill. She received her B.S. in 1997 from the University of Washington. She is investigating vertebrate cryptochrome function for her graduate work.

Aziz Sancar is a Distinguished Professor of Biochemistry and Biophysics at the University of North Carolina School of Medicine, Chapel Hill. He holds an M.D. from Istanbul University School of Medicine and a Ph.D. in molecular biology from the University of Texas at Dallas. He carried out his postdoctoral work at Yale University. He works on mechanisms of DNA repair and DNA damage checkpoints, as well as DNA photolyase/cryptochrome and circadian photoreception.

DNA Polymerase α, Eukaryotic

Teresa S.-F. Wang
Stanford University School of Medicine, Stanford, California, USA

DNA polymerase α (polα) is a replicative DNA polymerase in eukaryotic cells essential for initiation of chromosome replication. Polα exists in cells as a four-subunit enzyme complex often referred as polα-primase complex. The enzyme complex uniquely contains a RNA polymerase activity called primase activity that synthesizes a short RNA primer to sever as primer for the DNA polymerase activity of polα to extend for DNA synthesis. This unique nature of polα-primase complex to perform *de novo* synthesis bequeaths it a critical role not only in initiation of chromosome replication but also in repair, recombination, checkpoint activation, telomere maintenance, and mutation avoidance. Thus, polα-primase plays a critical role in maintenance of genomic stability of cells.

Protein Structure and Subunit Components

DNA polα consists of four subunits: a catalytic subunit of 165–180 kDa that contains the polymerase activity, a subunit of 70 kDa that has no detectable enzymatic activity but is essential for the initiation of replication both *in vivo* and *in vitro*, and two subunits with approximate molecular masses of 48 and 59 kDa that together contain the DNA primase activity. The ability of the primase subunits to synthesize a short RNA primer *de novo* renders polα unique among other eukaryotic replicative DNA polymerases. The subunit composition of polα from different organisms is conserved; their nomenclatures are listed (Table 1).

Although the predicted molecular mass of the polα catalytic subunit calculated from the mammalian cDNA or yeast gene sequence is 165 kDa, the polypeptide often appears as a 180 kDa protein due to posttranslational modifications, including glycosylation and cell-cycle-dependent phosphorylation. A degraded form with a molecular mass of 160 kDa is also frequently seen. The B-subunit (p70) of human polα as well as the budding yeast Pol12p protein are also phosphorylated in a cell cycle-dependent manner, whereas primase subunits from either human or yeast are not phosphorylated.

The human polα catalytic subunit is localized on the short (p) arm of X chromosome at Xp21.3–22.1 (not on the q-arm as erroneously indicated in other review articles). The budding yeast *POL1* is localized on chromosome XIV and the fission yeast *polα^+* is localized on chromosome 1.

Enzymatic Properties and Catalytic Mechanisms

Optimal Conditions for DNA Polymerase Activity and Mechanisms of DNA Polymerase Action

Optimal assay conditions for DNA polymerase α activity include a pH of 8.0, a DNA primer-template with a gap size of 60–150 nucleotides, four deoxynucleotide triphosphates (dNTPs), and Mg^{2+} as the metal ion activator. Polα is sensitive to inhibitors such as aphidicolin and N-ethylmaleimide, and is highly sensitive to butylphenyl-dGTP and butylphenyl-dATP. In contrast to polβ and polγ, but similar to polδ and polε, polα is not sensitive to dideoxynucleotide triphosphates (ddNTPs).

Under the optimal assay conditions, polα polymerizes DNA with moderate processivity and medium levels of fidelity, interacting first with template and then with primer. The minimum effective length of primer is eight nucleotides; the terminal three to five nucleotides of primer must be complementary to the template. Polα can interact with a primer terminating in either 3′-H or 3′-OH, but not in 3′-PO_4. Following the interaction with template and primer, polα recruits specific dNTPs as dictated by template nucleotide sequence. Hence, polα interacts with its substrates in an ordered sequential mechanism.

DNA Primase Activity and Mechanisms of Primer Synthesis

De novo initiation of primer synthesis requires the formation of a dinucleotide with a purine ribonucleotide triphosphate at the 5′ end by both primase subunits. Once the initial dinucleotide is formed, the catalytic

TABLE 1

Nomenclatures of Polα Subunits in Different Organisms

	Mammalian cells	Budding yeast (*Saccharomyces cerevisiae*)		Fission yeast (*Schizosaccharomyces pombe*)	
	Protein	Protein	Gene	Protein	Gene
Polymerase					
Catalytic subunit	p180–p165	Pollp	*POL1*	Polα	*polα*$^+$
B-subunit	p70	Poll2p	*POL12*	Spb70	*spb70*$^+$
Primase					
Catalytic subunit	p49	Pri1p	*PRI1*	Spp1	*spp1*$^+$
Coupling subunit	p58	Pri2p	*PRI2*	Spp2	*spp2*$^+$

subunit of primase, p49, is sufficient to extend the ribo-primer. The formation of the initial dinucleotide suggests that the primase complex contains two proximate separate ribonucleotide triphosphate (rNTP)-binding sites. One site specifically binds the purine ribonucleotide triphosphate, while the other site offers the 3′-OH group of the ribonucleotide triphosphate to the second incoming ribonucleotide, located in the RNA polymerase domain of the heterodimeric primase protein complex. Although p49 is the catalytic subunit of primase, the p58 subunit is absolutely required for the p49 subunit to bind the purine ribonucleotide triphosphate to form the initial dinucleotide, and both the rate of extension of the ribo-primer and the binding affinity (K_m) of p49 for ribonucleotides (rNTPs) are influenced by the presence of p58 subunit. Immunoprecipitation analyses of the two primase subunits in cell extracts from both human cells and fission yeast cells indicate that the human p58 and fission yeast Spp2 physically couple the polymerase catalytic subunit p180 with the primase catalytic subunit, p49.

Structure and Function of the Polymerase Catalytic Subunit

DNA polymerases are classified into A, B, C, X, and Y families, based on the similarities of their primary sequences to the three *E. coli* DNA polymerases I, II, and III, and to DNA polymerases from various organisms and DNA viruses. The primary sequences of polα from mammalian cells, budding yeast, and fission yeast cells contain six motifs that are highly conserved among many other prokaryotic, eukaryotic, and viral DNA polymerases. These conserved motifs are designated regions I–VI according to their extent of conservation; region I is the most conserved and region VI is the least conserved. Polymerases containing these six motifs are members of the B-family, or polα-family, of polymerases. Structural analysis of a polα-family member from bacteriophage RB69 (gp43) has revealed that the protein is shaped like a disk with a hole in the center that contains the active site. Similar to the Klenow fragment of *E. coli* Pol1, it also has a "right hand"-like structure composed of palm, finger and thumb domains. A 2.6 Å structural analysis of the ternary complex of RB69 polymerase in the presence of dTTP and duplex DNA primer-template revealed potential functions for many residues that have been confirmed by mutagenesis studies.

Residues Responsible for Interactions with the Metal Ion-dNTP Complex

Analyses of the ternary complex of RB69 polymerase revealed two highly conserved motifs responsible for metal ion-dNTP binding in the polα-family (B-family) polymerases: -YGDTDS- and -DFNSLYPSII-, corresponding to regions I and II, also termed motifs C and A, respectively. These two motifs form a three-stranded anti-parallel β-sheet. The aspartate residue in region II (motif A) and the second aspartate residue in region I (motif C), together with the dTTP tail, coordinate two divalent metal ions for catalysis. Mutagenesis of these residues followed by steady-state kinetic analyses has confirmed that the second aspartate residue in region I (motif C) chelates the metal ion activator-nucleotide complex and is critical for catalysis. Structure analysis also indicates that the phenyl ring of Tyr (-Y-) in region II (motif A) stacks with the ribose ring of the incoming dNTP. This interaction is confirmed by mutagenesis studies in other polα-family polymerases. Furthermore, three positively charged residues in the finger domain: Arg (-R-) and a Lys (-K-) in region VI, interact with the γ-phosphate of dNTP and a Lys (-K-) in region III forms a hydrogen bond with the bridging oxygen between α- and β-phosphates of the dNTP. Comparison of the structures of apo RB69 polymerase and its ternary

complex indicates that binding of the incoming dNTP induces a 60° rotation of the finger domain allowing the three highly positive residues, Arg and Lys in region VI and Lys in region III, to move closer to the active site.

Residues Responsible for Interactions with the Primer-Template DNA

Structural analyses of RB69 polymerase in complex with B-form duplex DNA have revealed that DNA primer-template binds in a groove between the palm domain and the thumb. Because residues involved in these interactions are not conserved among the polα-family (B-family) polymerases, the interactions most likely occur via hydrogen bonding between phosphates of the primer-template strand with the side chains of non-specific aggregates of residues. The polymerase protein or side chains directly form hydrogen bonds linking the primer-strand's phosphates, while a number of charged residues appear to interact with the template. The conserved motif of Lys-Lys-Arg-Tyr- (-KKRY-), unique to the polα-family polymerases, is involved in stabilizing the B-form DNA. The Tyr (-Y-) residue in this motif forms a hydrogen bond with the phosphodiester at the 3′-terminus of the primer, while the Lys (-K-) and Arg (-R-) interact with template phosphate to bring the primer and template strand backbones near one another.

Biological Role in the Cell

Initiation of Chromosome Replication

DNA polα primase has been regarded as the principal DNA polymerase involved in the initiation of chromosomal DNA synthesis. Reconstituted replication of an SV40 origin-containing plasmid by purified replication factors confirms that the polα-primase complex is essential to initiate both the leading and lagging strand DNA synthesis in a coordinated manner. Initiation of cell-free SV40 DNA replication requires the physical interaction of the SV40 viral large T-antigen in the pre-initiation complex with the amino terminal region residues 195–313 of the catalytic subunit of human pol α. After the synthesis of the initiation DNA primer (iDNA) by polα-primase complex, polα-primase complex is replaced by the more processive polδ, which extends the iDNA primer and completes elongation synthesis with the help of replication factor C (RFC) and proliferating cell antigen (PCNA). The human papillomavirus type 11 (HPV-11) origin recognition and initiator protein E1 also interacts with both the polα catalytic subunit (p180) and the B-subunit (p70) and the interactions are critical for the initiation of HPV-11 DNA replication. In addition, species-specific replication of polyomavirus (Py) DNA *in vitro* is dependent on the mouse primase catalytic subunit p48.

Finally, yeast cells harboring a conditional mutation in polα or primase exhibit an initiation defective phenotype when grown under restrictive conditions. Thus, biochemical studies of viral replication and yeast genetic analyses all indicate that the polα-primase complex is the principal cellular DNA polymerase for the initiation of chromosome replication.

DNA Repair and Recombination

Mutations in budding yeast (*S. cerevisiae*) polα (*POL1*) or primase (*PRI2*) compromise completion of double strand break (DSB)-induced gene conversion at the *MAT* locus. Mutation of a glycine residue (Gly^{493}) to glutamate (Glu) in an evolutionarily conserved amino terminal region of budding yeast *POL1* induces a hyper-recombination (*hpr*) phenotype; mutation of this same Gly^{493} residue to arginine (Arg) induces a high mutation rate, plasmid loss, and chromosome loss in budding yeast cells. Finally, mutation in budding yeast *POL12* (B-subunit of yeast) enhances the levels of ribosomal-DNA Holliday junction formation during S phase.

In fission yeast, developmentally programmed cell-type switching requires a strand-specific imprinting event at the mating type locus (*mat1*). This process requires the gene product of $swi7^{+}$, which encodes polα. A mutation in fission yeast *polα* can induce a defect in mating, indicating that polα is essential for mating type switching. Together, these findings indicate that polα is required for DNA repair and recombination processes in both mitotic and meiotic cells.

Mutation Avoidance

Mutations in replication genes can often induce a mutator phenotype characterized by point mutations, single base frameshifts, and deletion or duplication of sequences flanked by short homologous repeats. Mutations in budding yeast polα (*pol1*) have been shown to induce dinucleotide repeat instability, deletion mutations, gross chromosomal alterations, and high frequencies of plasmid and chromosome loss. Among all of the replication mutators analyzed, mutations in the polα catalytic subunit (*pol1* or *polα*) in either budding or fission yeast induce a higher mutation rate in cells than do mutations in primase, polδ, polδ-subunits, and DNA ligase, indicating that polα plays an important role in mutation avoidance and genomic stability of cells.

Checkpoint Activation

Checkpoints are surveillance mechanisms that monitor genomic integrity to signal the cell cycle machinery

monitor genomic integrity, the cell cycle machinery to delay mitosis to allow time for recovery and repair of replication perturbation or DNA damage. Genetic analyses and physiological studies of budding and fission yeasts have shown that checkpoint pathways are directly linked to DNA metabolism. Importantly, the establishment of a DNA replication fork is required for activation of checkpoint response. Since polα and primase are essential for replication fork establishment, their functions are required for checkpoint activation to delay the mitotic entry until completion of DNA replication.

Genetic analyses of the budding yeast *pri1* mutant have suggested that the catalytic subunit of DNA primase (Pri1p) is linked to checkpoint response. In addition, genetic and biochemical studies of fission yeast primase (Spp1 and Spp2) have shown that Spp2 plays an essential role in maintaining the physical stability of polα-primase complex in cells, which has critical impact on the intra-S phase checkpoint kinase Cds1 (the homologue of budding yeast Rad53p and mammalian tumor suppressor Chk2). Fission yeast genetic data also indicate that the initiator DNA (iDNA) synthesized by polα-catalytic activity activates the checkpoint responsible for delaying premature mitotic entry during replication. Biochemical studies of *Xenopus* extracts, however, have shown that synthesis of RNA primer by primase is sufficient to activate the checkpoint.

Initiation defects caused by mutations in polα-primase can induce replication stalling and checkpoint activation. Checkpoint activation caused by mutation in a fission yeast polα has been shown to promote tolerance through induction of mutagenic synthesis by error-prone translesional DNA polymerases κ and ζ. Furthermore, replication perturbation caused by mutations in the fission yeast polα catalytic subunit activates the checkpoint kinase Cds1, which prevents mutagenesis and stabilizes the replication fork. Thus, polα-primase complex plays a direct as well as indirect role in checkpoint processes.

Telomerase Stability and Telomere Length Maintenance

Eukaryotic chromosome ends are capped by telomeres consisting of simple tandem arrays of short G-rich repeats. Because DNA polymerases synthesize DNA in 5′–3′ polarity, the telomeric G-rich strand is synthesized by the leading strand replication machinery and the C-rich strand is synthesized by the lagging strand replication machinery. Removal of the terminal RNA primer leaves a gap of 8–12 nucleotides at the 5′-end of the newly synthesized lagging strand that cannot be synthesized by conventional DNA replication, resulting in a so-called "end replication problem". A special telomere synthesis polymerase, telomerase, containing an integral RNA molecule with a small template domain can add telomeric repeats onto the 3′-end of the telomeric G-strand to resolve the end replication dilemma.

Studies of budding yeast have shown the polα-catalytic subunit physically interacts with the telomere binding protein Cdc13. Mutations in the budding yeast or fission yeast polα catalytic subunit, as well as the fission yeast primase subunits Spp1 and Spp2, result in abnormal telomeric length extension. Moreover, the fission yeast polα catalytic subunit physically associates with the telomerase catalytic subunit (Trt1). A mutation in fission yeast polα that causes abnormal telomere lengthening also compromises both the polα-telomerase association and telomerase protein stability. Ectopic expression of wild type fission yeast polα in this *polα* mutant can restore cellular telomerase protein to normal level and returns the telomere length to near wild type. Hence, the polα-primase complex co-exists with telomerase in the telomeric complex and is important for maintaining both telomere length equilibrium and telomerase protein stability.

See Also the Following Articles

DNA Polymerase I, Bacterial • DNA Polymerase II, Bacterial • DNA Polymerase III, Bacterial • DNA Polymerases: Kinetics and Mechanism • DNA Polymerase β, Eukaryotic • DNA Polymerase δ, Eukaryotic • DNA Polymerase ε, Eukaryotic • DNA Replication: Eukaryotic Origins and the Origin Recognition Complex • DNA Replication Fork, Eukaryotic • Translesion DNA Polymerases, Eukaryotic • umuC,D Lesion Bypass DNA Polymerase V • XPV DNA Polymerase and Ultraviolet Damage Bypass

Glossary

checkpoints Signal transduction surveillance pathways that coordinate cell cycle transitions with the detection of unfinished DNA replication or damaged DNA to activate tolerance or repair processes to overcome the lesion or to induce apoptosis.

fidelity of DNA polymerase The error-free nature of a DNA polymerase in template-dictated incorporation of nucleotides.

klenow fragment A proteolytic fragment of *E. coli* Pol1 containing only the polymerase and the 3′–5′ proofreading exonuclease domains.

mutator A gene mutation of which causes the cells to have additional new mutations.

processivity of DNA polymerase The uninterrupted repetitive DNA polymerase interaction with its DNA primer-template without dissociation.

Further Reading

Bhaumik, D., and Wang, T. S.-F. (1998). Mutational effect of fission yeast polα on cell cycle event. *Molecul. Biol. Cell* **9**, 2107–2123.

Copeland, W. C., and Wang, T. S.-F. (1993). Enzymatic characterization of the individual mammalian primase subunits reveals a biphasic mechanism for initiation of DNA replication. *J. Biolog. Chem.* **268**, 26179–26189.

Dahlén, M., Sunnerhagen, P., and Wang, T. S.-F. (2003). Replication proteins influence the maintenance of telomere length and telomerase protein stability. *Molecul. Cell. Biol.* **23**, 3031–3042.

Franklin, M. C., Wang, J., and Steitz, T. A. (2001). Structure of the replicating complex of a polα family DNA polymerase. *Cell* **105**, 657–667.

Griffiths, D. J. F., Liu, V. F., Nurse, P., and Wang, T. S.-F. (2001). Role of fission yeast primase catalytic subunit in the replication checkpoint. *Molecul. Biol. Cell* **12**, 115–128.

Gutierrez, P. J. A., and Wang, T. S.-F. (2003). Genomic instability induced by mutations in *Saccharomyces cerevisiae POL1*. *Genetics* **165**, 65–81.

Kai, M., and Wang, T. S.-F. (2003). Checkpoint activation regulates mutagenic translesion synthesis. *Genes Develop.* **17**, 64–76.

Liu, V. F., Bhaumik, D., and Wang, T. S.-F. (1999). Mutator phenotype induced by aberrant replication. *Molecul. Cell. Biol.* **19**, 1126–1135.

Tan, S., and Wang, T. S.-F. (2000). Analysis of fission yeast primase defines the checkpoint responses to aberrant S phase initiation. *Molecul. Cell. Biol.* **20**, 7853–7866.

Wang, J., Sattar, A. K. M. A., Wang, C. C., Karam, J. D., Konigsberg, W. H., and Steitz, T. A. (1997). Crystal structure of polα family replication DNA polymerase from bacteriophage RB69. *Cell* **89**, 1087–1099.

Biography

Dr. Teresa S.-F. Wang is a professor in the Department of Pathology at the Stanford University School of Medicine in Stanford, California. Her principal research interests are in enzymatic mechanisms of DNA polymerases and biological responses to mutations of DNA polymerases. She holds a Ph.D. from the University of Texas at Austin, Texas, and received her postdoctoral training at Stanford University.

DNA Polymerase β, Eukaryotic

William A. Beard and Samuel H. Wilson
National Institute of Environmental Health Sciences, Research Triangle Park, North Carolina, USA

DNA polymerase β (pol β) plays a crucial role in the base excision repair pathway that cleanses the genome of apurinic/apyrimidinic (AP) sites. AP sites arise in DNA from spontaneous base loss (depurination) and DNA damage-specific glycosylases that hydrolyze the *N*-glycosidic bond between the deoxyribose and damaged base. Pol β contributes two enzymatic activities, DNA synthesis and lyase, during the repair of AP sites. AP sites represent a potentially dangerous lesion to a cell since they can be mutagenic or cytotoxic.

Introduction

Endogenous and environmental agents continually threaten cellular DNA. These threats can result in physical damage (e.g., DNA strand breaks or base loss) or modification (e.g., alkylation and cross-links). Since these genetic insults lead to an altered DNA structure that can result in deleterious outcomes, cells have evolved DNA repair mechanisms to correct these abnormalities. The base excision repair (BER) pathway is responsible for removing simple base lesions and AP sites in DNA. The repair of an AP site minimally requires four coordinated enzymatic activities: strand incision by AP endonuclease, removal of the resulting deoxyribose phosphate (dRP) backbone of the AP site by a pol β-associated lyase, single-nucleotide DNA synthesis by pol β, and ligation of the DNA nick by DNA ligase. These steps are illustrated in Figure 1.

Pol β is the smallest eukaryotic cellular DNA polymerase (335 residues; 39 kDa) and it lacks a $3' \rightarrow 5'$ proofreading exonuclease activity that enhances the accuracies of replicative DNA polymerases (e.g., DNA polymerase ε and δ). Based on primary sequence alignments, pol β belongs to the X-family of DNA polymerases that also includes pol λ and pol μ.

Biological Role

Based upon the high level of sequence conservation of pol β among mammalian species, it seemed highly likely that pol β is conducting a role that is essential for animal survival. This is consistent with the embryonic lethality of pol β null mice. Pol β preferentially fills short DNA gaps (<6 nucleotides). Because of this attribute, it had generally been assumed that pol β is involved in short-gap DNA repair synthesis. In addition, early studies implicated pol β in gap-filling DNA synthesis during mammalian BER of alkylation damage and the repair of UV DNA damage, and inhibitor studies also implicated pol β in other types of DNA repair, such as the repair of oxidative DNA damage. Although these attributes and studies implicated pol β in BER and in other types of short gap-filling DNA repair, pol β's role in BER was confirmed when mouse cells lacking pol β were found to be hypersensitive to DNA-damaging agents believed to be repaired by the BER pathway.

In addition to the "simple" single-nucleotide BER pathway illustrated in Figure 1, alternate BER pathways are needed to remove modified dRP-moieties that cannot be excised by the pol β lyase activity. In this situation, pol β strand displacement DNA synthesis creates a DNA flap of about four nucleotides with a 5′-modifed dRP group that can be subsequently removed by flap endonuclease-1 (FEN-1), thereby creating a nick that will be sealed by DNA ligase. This alternate pathway is referred to as "long-patch" BER.

Pol β Domain Organization

Controlled proteolytic or chemical cleavage of pol β first demonstrated that it is folded into discrete domains. Subsequently, the X-ray crystal structure of the ternary substrate complex with DNA and an incoming nucleoside triphosphate (dNTP) defined the location of these domains in relation to the tertiary structure of the polymerase. Pol β is organized into two domains: an 8 kDa amino-terminal lyase domain and a 31 kDa carboxyl-terminal polymerase domain (Figure 2).

The structures of DNA polymerases derived from other polymerase families indicate that they also have a modular domain organization. The polymerase domain is typically composed of three functionally distinct subdomains. The catalytic subdomain coordinates two divalent metal cations that promote DNA synthesis. The other two subdomains are spatially situated on opposite

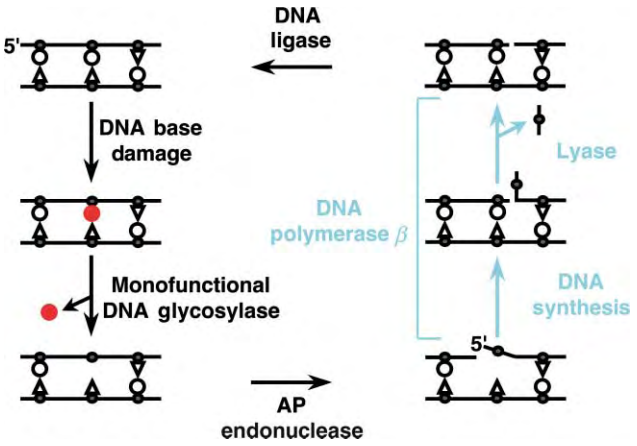

FIGURE 1 Single-nucleotide BER. AP sites are lesions in DNA that originate from spontaneous or enzymatic (glycosylase) removal of a damaged base (red). These sites are removed from DNA by four coordinated enzymatic activities, two of which are contributed by pol β (blue).

sides of the catalytic subdomain. DNA polymerases outside the X-family of polymerases share structural homology within their catalytic subdomains. This has perpetuated a nomenclature based on an architectural analogy to a right hand where the subdomains are referred to as palm, thumb, and fingers. However, the catalytic subdomain of X-family members is not structurally homologous to other DNA polymerases. Application of the "hand analogy" to the polymerase subdomains of pol β is ambiguous. To highlight the intrinsic function of the polymerase subdomains of pol β, a functionally based nomenclature has been proposed. Accordingly, the pol β polymerase domain is composed of the C- (*C*atalytic), D- (*D*uplex DNA binding), and N-subdomains (*N*ascent base pair binding) (Figures 2 and 3). These correspond to the palm, thumb, and fingers subdomains of the right-handed DNA polymerases.

Lyase Domain

The amino-terminal lyase domain (residues 1–90) has an associated lyase, metal-independent, activity that removes the 5′-dRP moiety generated during single-nucleotide BER (Figure 1). This activity plays a pivotal role in BER in that it represents the slowest step in the overall process, and if the lyase reaction is inhibited (e.g., modified dRP-moiety), alternate BER pathways will be initiated. The lyase reaction proceeds by β-elimination through a Schiff base intermediate. A stable covalently bound intermediate can be formed between the dRP-containing DNA substrate and the enzyme by $NaBH_4$ trapping. Lys72 is preferentially modified by primary amine reactive agents in both full-length pol β and the isolated lyase domain. Site-directed mutagenesis of Lys72 diminishes dRP lyase activity nearly 2 orders of magnitude indicating that this residue is the likely nucleophile that forms the Schiff base intermediate. The lyase domain is highly basic (net charge = +10), and the positively charged surface potential predicts that it would interact with the DNA backbone.

In addition to providing a crucial enzymatic activity for single-nucleotide BER, the lyase domain possesses a 5′-phosphate binding site that facilitates targeting of pol β into the 5′-position in a DNA gap. Importantly, pol β binds tightly to the 5′-phosphate only when there is DNA adjacent to the 5′-phosphate. This can be double-stranded or single-stranded DNA since a 3′-primer terminus is not required for optimum binding. Accordingly, pol β is expected to bind to the 5′-phosphate in a DNA gap of any size. The observation that pol β can processively (i.e., insert several nucleotides before dissociating from the DNA substrate) fill short gaps

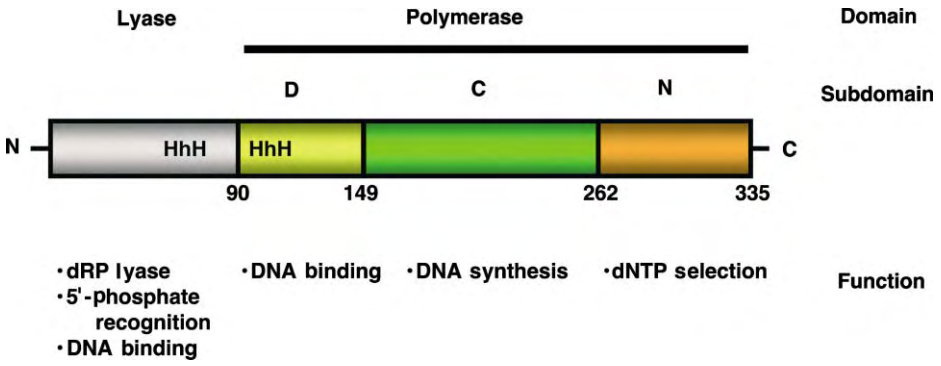

FIGURE 2 Domain and subdomain organization of pol β. Pol β is composed of a polymerase (colored) and an amino-terminal lyase domain (gray). The polymerase domain is composed of three subdomains: D- (yellow), C- (green), and N- (orange) subdomains. These correspond to the thumb, palm, and fingers subdomains of DNA polymerases that utilize an architectural analogy to a right hand, respectively. The lyase domain and the D-subdomain each have a HhH motif that interacts with the DNA backbone of the incised DNA strand downstream and upstream of the gap, respectively.

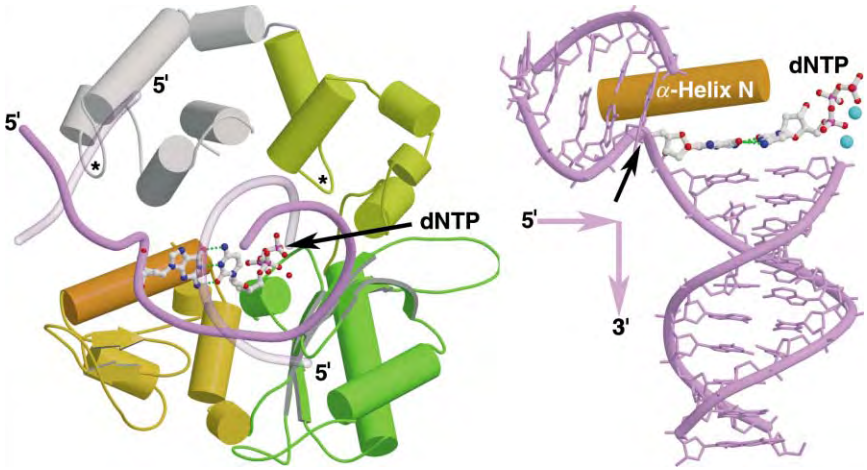

FIGURE 3 Structure of the pol β-substrate complex. Left panel: The domains and subdomains are colored as in Figure 2 and the 5′-ends of the DNA strands forming a one-nucleotide gap are indicated. The trajectory of the template strand (purple) is altered dramatically as it enters the polymerase active site. The complementary DNA strands (primer and downstream oligonucleotides) are semitransparent. Except for the nascent base pair (templating and incoming nucleotides), the sugars/bases of the duplex DNA are not illustrated for clarity. An α-helix of the N-subdomain (dark orange) contributes one face of the binding pocket for the nascent base pair. The hairpins, of the HhH motifs, are highlighted with an asterisk. Right panel: The perspective is from the major groove edge of the nascent base pair and only α-helix N of pol β is shown for clarity. The 5′ → 3′ trajectory of the template strand is indicated and the radical bend in the 5′-phosphodiester bond of the templating base is highlighted (black arrow). The active site metals that coordinate the incoming dNTP and assist catalysis are illustrated as light blue spheres.

(<6 nucleotides) suggests that the lyase domain tethers the polymerase domain to the downstream position in gapped DNA. When the primer terminus (i.e., 3′-OH) is within six nucleotides of the 5′-phosphate on the downstream DNA strand, the polymerase domain will be "within reach" of the primer terminus thereby facilitating processive DNA synthesis.

The lyase domain is composed of five α-helices (Figure 3). Structural characterization of this domain has identified a structural motif that binds monovalent metals and interacts with the DNA backbone. The helix–hairpin–helix (HhH) motif (residues 55–79) has also been identified in other DNA repair proteins as well as many proteins that bind either single- or double-stranded DNA in a nonsequence-specific manner. The crystal structure of pol β bound to a one-nucleotide gap DNA substrate indicates that the lyase domain and the N-subdomain of the polymerase domain interact (Figure 3). The interaction of the lyase domain and the N-subdomain results in a donut-like structure. The interactions between these subdomains are altered upon binding substrates resulting in a tighter complex.

Polymerase Domain

D-Subdomain

As noted above, the polymerase domain is composed of three functionally distinct subdomains. The lyase domain is connected to the D-subdomain (residues 91–149) with a protease-hypersensitive hinge region. The D-subdomain interacts with the DNA sugar-phosphate backbone of the duplex DNA upstream of the polymerase active site. In addition to the HhH motif found in the lyase domain, a second HhH motif (residues 92–118) is also found in the D-subdomain. This HhH motif interacts with the primer strand phosphate backbone through a monovalent metal ion. Thus, the two HhH motifs in pol β are observed to make DNA backbone interactions with each end of the incised DNA strand. In the crystal structure of pol β bound with an incoming nucleotide and a one-nucleotide DNA gap, the DNA is bent ~90° (Figure 3). The DNA template does not travel through the hole in the donut-like structure. The sharp bend occurs at the 5′-phosphodiester bond of the templating base and is also observed in a product complex where pol β is bound to nicked DNA. The 3′-hydroxyl and 5′-phosphate groups on the nicked DNA strand, which need to be ligated in the final step of BER, are observed to be over 27Å apart. For pol β, the function of the HhH motifs is that a sequence nonspecific phosphate-backbone binding motif that stabilizes the pronounced bend observed in the pol β-gapped DNA structure. The 90° bend also exposes the terminal base pairs of each DNA duplex that is situated in the gap. His34 of the lyase domain interacts with the first base pair of the downstream duplex, whereas the N-subdomain contributes interactions with the nascent base pair (see below). The dramatic bend of the template strand as it enters the polymerase active site is a general feature observed in crystal structures of substrate complexes of all DNA polymerases.

C-Subdomain

The C-subdomain (residues 150–262) of pol β includes three acidic residues that coordinate two essential magnesium ions. One magnesium coordinates nonbridging oxygens on the three phosphates of the incoming nucleotide (nucleotide-binding metal), whereas the other coordinates oxygens on the α-phosphate of the incoming dNTP and the DNA primer terminus (catalytic metal). These metals are believed to play critical and conserved roles in catalysis (nucleotidyl transfer) in all DNA polymerases. Although the C-subdomains of X-family members are not homologous to those of other polymerase families, crystal structures of substrate complexes of DNA polymerases from other families indicate that the reactive groups (i.e., metals, incoming nucleotide, and DNA) have a similar three-dimensional arrangement. Likewise, all DNA polymerases also follow an ordered binding of substrates where DNA binds first. The polymerase then selects a nucleoside triphosphate from a pool of structurally similar molecules to preserve Watson–Crick base pairing rules. The ability to choose between "right and wrong" is highly dependent on the identity of the polymerase. Pol β has a moderate ability to select the correct (i.e., right) nucleotide and capacity for DNA synthesis. Since it does not have an intrinsic proofreading activity, it has the potential to be highly mutagenic. The fidelity of pol β is too low (1 error per ~2000 nucleotides synthesized) for pol β DNA synthesis errors to be tolerated during DNA repair. It is generally believed that the proofreading activity of AP endonuclease, or some other extrinsic $3' \rightarrow 5'$-exonuclease, may proofread base substitution errors generated by pol β.

N-Subdomain

The N-subdomain (residues 263–335) contributes important interactions to the binding pocket of the nascent base pair (templating and incoming nucleotides). Comparison of DNA polymerase structures bound to DNA with those that include an incoming complementary dNTP reveals that the N-subdomain repositions itself to "sandwich" the nascent base pair between the growing DNA terminus and the polymerase. In the absence of an incoming nucleotide, the N-subdomain is "open," but forms a "closed" complex upon binding a correct nucleotide. Thus, the dNTP-binding pocket is formed by the template base, DNA duplex terminus, and enzyme. For pol β, subdomain interactions with the nascent base pair are contributed primarily through α-helix N (Figure 3). These include stacking interactions with Lys280 and Asp276 with the templating and incoming nucleotide bases, respectively. Additionally, Asn279 and Arg283 contribute DNA minor groove interactions. Alanine substitution for Arg283 results in a dramatic decrease in fidelity. Since Arg283 plays a critical role in the formation of the closed complex, the low-fidelity mutant (i.e., R283A) is believed to be in an open conformation thereby losing the ability to promote efficient DNA synthesis when a correct nucleotide binds. Thus, the ability to choose the correct nucleotide has been lost. As noted above, the trajectory of the duplex DNA into the polymerase active site requires that the templating strand bend by 90° (Figure 3). This bend in the template strand serves at least two functions: (1) it provides access for the N-subdomain to check whether geometrical constraints imposed by correct Watson–Crick hydrogen bonding occurs; (2) it discourages the next templating base from entering the polymerase active site prematurely which could result in the incorrect template base coding for nucleotide insertion (deletion mutagenesis).

Pol β–BER–Protein Interactions

In addition to its catalytic function, pol β also interacts with several proteins known to be involved in BER. These interactions may facilitate the coordination of the necessary enzymatic steps required in alternate BER pathways. In this context, the observations that pol β interacts with other DNA repair proteins such as AP endonuclease, DNA ligase I, X-ray cross-complementing factor-1 (XRCC1), poly(ADP-ribose) polymerase-1 (PARP-1), and proliferating cell nuclear antigen (PCNA), among others, suggest complex regulatory mechanisms that are not fully understood. Thus, pol β interacts with the enzymes involved in the steps immediately upstream and downstream of its own steps in single-nucleotide BER. Importantly, formation of binary or ternary protein complexes, rather than a "super" BER complex, has the advantage of flexibility that can accommodate alternate pathways. The influence of these protein–protein interactions on catalytic function and processing of BER intermediates remains to be determined.

See Also the Following Articles

DNA Polymerase α, Eukaryotic • DNA Polymerase δ, Eukaryotic • DNA Polymerase ε, Eukaryotic • DNA Polymerases: Kinetics and Mechanism • Translesion DNA Polymerases, Eukaryotic• XPV DNA Polymerase and Ultraviolet Damage Bypass

Glossary

AP site DNA lesion resulting from the loss of a base (i.e., abasic site). These sites can be mutagenic since they have lost their coding potential, or cytotoxic since they are quickly incised resulting in DNA strand breaks.

DNA polymerase β A small eukaryotic DNA polymerase involved in short gapped DNA repair synthesis. In addition to its polymerase activity, this polymerase contributes an accessory lyase activity required to remove the backbone of an AP site (i.e., deoxyribose) during BER.

HhH The helix–hairpin–helix structural motif binds single- or double-stranded DNA in a nonsequence-specific manner and has been identified in a number of DNA repair proteins. Two such motifs in pol β are observed to make DNA backbone interactions with the incised DNA strand downstream and upstream of the gap suggesting that they stabilize the pronounced DNA bend observed when gapped DNA binds to pol β.

lyase In the context of single-nucleotide BER, this reaction results in the removal of the 5′-deoxyribose phosphate backbone after incision of an AP site by an endonuclease. The reaction proceeds by β-elimination through a Schiff base intermediate. The ε-NH_2 group of a lysine side chain (Lys72 of pol β) serves as a nucleophile, resulting in transient covalent attachment of the enzyme to its substrate. This Schiff base intermediate can be trapped by sodium borohydride, resulting in conversion to an irreversibly linked lyase–DNA complex.

N-subdomain One of three subdomains found in all DNA polymerases. This subdomain forms one face of the nascent base pair (templating and incoming nucleotide bases) binding pocket and it is involved in selecting the correct dNTP. It is also referred to as the fingers or thumb subdomain in the polymerase nomenclature that utilizes the analogy to a right or left hand, respectively.

Further Reading

Beard, W. A., and Wilson, S. H. (1995). Purification and domain-mapping of mammalian DNA polymerase β. *Methods Enzymol.* **262**, 98–107.

Beard, W. A., and Wilson, S. H. (2000). Structural design of a eukaryotic DNA repair polymerase: DNA polymerase β. *Mutat. Res.* **460**, 231–244.

Beard, W. A., and Wilson, S. H. (2003). Structural insights into the origins of DNA polymerase fidelity. *Structure* **11**, 489–496.

Beard, W. A., Shock, D. D., Vande Berg, B. J., and Wilson, S. H. (2002). Efficiency of correct nucleotide insertion governs DNA polymerase fidelity. *J. Biol. Chem.* **277**, 47393–47398.

Horton, J. K., Joyce-Gray, D. F., Pachkowski, B. F., Swenberg, J. A., and Wilson, S. H. (2003). Hypersensitivity of DNA polymerase β null mouse fibroblasts reflects accumulation of cytotoxic repair intermediates from site-specific alkyl DNA lesions. *DNA Repair (Amst.)* **2**, 27–48.

Lindahl, T., and Wood, R. D. (1999). Quality control by DNA repair. *Science* **286**, 1897–1905.

Sawaya, M. R., Prasad, P., Wilson, S. H., Kraut, J., and Pelletier, H. (1997). Crystal structures of human DNA polymerase β complexed with gapped and nicked DNA: Evidence for an induced fit mechanism. *Biochemistry* **36**, 11205–11215.

Sobol, R. W., Horton, J. K., Kühn, R., Gu, H., Singhal, R. K., Prasad, R., Rajewsky, K., and Wilson, S. H. (1996). Requirement of mammalian DNA polymerase β in base excision repair. *Nature* **379**, 183–186.

Wilson, S. H., and Kunkel, T. A. (2000). Passing the baton in base excision repair. *Nat. Struct. Biol.* **7**, 176–178.

Biography

Samuel H. Wilson is Head of the DNA Repair and Nucleic Acid Enzymology Section in the Laboratory of Structural Biology at NIEHS/NIH in Research Triangle Park, NC. Prior to this, Dr. Wilson was the founding Director of the Sealy Center for Molecular Science at the University of Texas Medical Branch-Galveston.

William A. Beard holds a Ph.D. from Purdue University and did postdoctoral training at St. Jude Children's Research Hospital, Memphis. He joined Dr. Wilson's group in 1990 and is currently a Staff Scientist in the Laboratory of Structural Biology at NIEHS/NIH.

Their common research interests are to understand basic mechanisms of biological catalysis and substrate recognition through a combination of site-directed mutagenesis, kinetic analysis, molecular modeling and structure determination. They have effectively applied these approaches to derive a molecular and biological description of DNA polymerase β function.

DNA Polymerase δ, Eukaryotic

Antero G. So and Kathleen M. Downey
University of Miami, Miami, Florida, USA

DNA polymerase δ (pol δ) is an essential DNA polymerase that is required for DNA replication and participates in several DNA repair pathways. It is a proofreading DNA polymerase; that is, it is capable not only of catalyzing template-directed nucleotide incorporation, but also of editing errors of incorporation by virtue of a 3′ to 5′ exonuclease activity. Pol δ is highly conserved and has been identified in multiple eukaryotic species from yeast to humans.

Structure

Pol δ comprises a core enzyme and one or more loosely associated subunits.

The Core Enzyme

The pol δ core enzyme is a heterodimer comprising a catalytic subunit of approximately 125 kDa and a small subunit of approximately 50 kDa. The catalytic subunit contains the active sites for both the DNA polymerase and 3′ to 5′ exonuclease activities, as well as a putative nuclear localization signal. The small subunit is not associated with any catalytic activity, but it is required for the interaction of the core enzyme with more loosely associated subunits and accessory proteins.

Cloning and sequencing of the cDNAs for the catalytic and small subunits of pol δ from various species demonstrated that pol δ is the most highly conserved among the eukaryotic DNA polymerases, with sequence identity of 94% between both subunits of the human and bovine enzymes and 44% identity between the subunits of the human and budding yeast enzymes. The human gene for the catalytic subunit of pol δ has been mapped to chromosome 19q13.3 and that for the small subunit has been located on chromosome 7.

Pol δ belongs to the class B, or α-like, DNA polymerases, which are found in both prokaryotes and eukaryotes. The class B polymerases include pol α, pol δ, pol ε, the herpes virus family of DNA polymerases, and the T4 and RB69 bacteriophage DNA polymerases. These enzymes contain six highly conserved domains and, in addition, pol δ also contains three highly conserved regions (ExoI, ExoII, and ExoIII), which are responsible for the 3′ to 5′ proofreading exonuclease activity and are found in all exonuclease-containing DNA polymerases.

Pol δ is very sensitive to inhibition by aphidicolin, N-ethylmaleimide, and carbonylphosphonate; moderately sensitive to butylphenyl-dGTP and butylphenyl-dATP; and resistant to dideoxynucleotides.

Other Subunits

The third subunit of pol δ is a polypeptide of 42–66 kDa that has been found in both mammalian and yeast enzyme preparations. It interacts with both the small subunit of the enzyme and the processivity factor for pol δ, the proliferating cell nuclear antigen (PCNA). The fourth subunit of pol δ, which has been identified only in fission yeast and mammalian cells thus far, is a polypeptide of approximately 12 kDa, whose function has not yet been elucidated.

Several other proteins have been identified as interacting specifically with the small subunit of pol δ. In addition to the third subunit, these proteins include the Werner's syndrome protein (WRN) and pol δ interacting protein 1 (PDIP1). All of these proteins have been shown to physically and functionally interact with the small subunit of pol δ as well as with its processivity factor PCNA.

Processivity Factor

Core pol δ is essentially a distributive DNA polymerase that is capable of synthesizing only short stretches of DNA (10–20 nt) before dissociating from the template. However, when bound to its processivity factor PCNA, pol δ becomes a highly processive enzyme, capable of synthesizing stretches of DNA containing up to 5×10^4 nucleotides before being released from the template. PCNA is a homotrimer that has a subunit size of approximately 29 kDa and forms a ring with an internal diameter capable of accommodating double-stranded DNA. PCNA, which has been called a sliding clamp, is

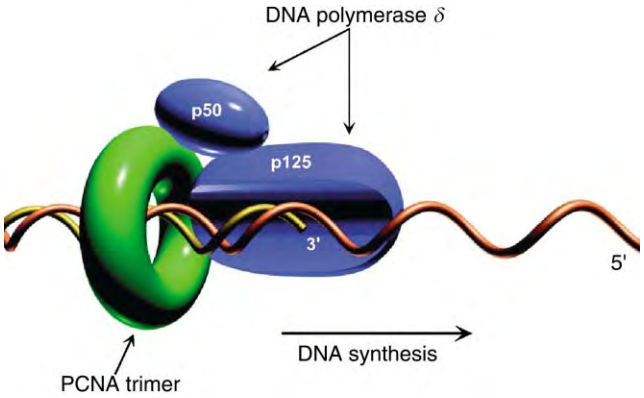

FIGURE 1 Schematic model of the pol δ-PCNA–DNA complex during DNA replication. Reprinted from Mozzherin, D. J., Tan, C.-K., Downey, K. M., and Fisher, P. A. (1999) Architecture of the active DNA polymerase d–proliferating cell nuclear antigen–template primer complex. *J. Biol. Chem.* **274**, 19862–19867 with permission from the American Society for Biochemistry and Molecular Biology.

loaded onto DNA by a clamp loader, replication factor C (RFC), in a reaction that requires ATP hydrolysis. PCNA binds to pol δ and, by virtue of being topologically linked to the DNA template primer, causes pol δ to become highly processive (see Figure 1).

Functional studies with recombinant p125 from human, mouse, and fission yeast have shown that DNA synthesis catalyzed by p125 alone is not stimulated by PCNA, whereas the activity and processivity of the recombinant human p125/p50 heterodimer is fully stimulated by PCNA to the same extent as the native two-subunit enzyme isolated from calf thymus tissue, suggesting that p50 is required for the functional interaction of PCNA with pol δ.

Functions of Pol δ

DNA Replication

There is strong evidence from studies in both higher and lower eukaryotes that pol δ plays an essential role in DNA replication. The development of an *in vitro* simian virus 40 (SV40) DNA replication system led to the identification of both pol δ and PCNA as mammalian replication proteins. Furthermore, studies in both fission and budding yeast have shown that the catalytic and small subunits of pol δ are the products of essential genes, and the phenotypes of mutants that are temperature-sensitive in these genes are consistent with a role for pol δ in replication. However, the precise role of pol δ at the replication fork is still unclear. Although it is clear that pol δ is capable of catalyzing the synthesis of the leading strand as well as elongation of the lagging-strand Okazaki fragments, after priming of these strands by the action of pol α-primase, whether either of these functions is exclusively attributable to pol δ *in vivo* and whether pol ε can carry out these functions have not yet been resolved.

DNA Repair

Although there are highly specialized DNA polymerases that are involved in the repair of specific lesions in DNA, the replicative polymerases pol δ and pol ε appear to carry out the bulk of DNA synthesis involved in filling in the gaps generated during the repair of DNA damaged by ultraviolet (UV) irradiation or the chemical alteration of bases (i.e., nucleotide excision repair and base excision repair). Genetic studies in yeast and biochemical studies in mammalian cells have also demonstrated a role for pol δ in postreplication mismatch repair.

See Also the Following Articles

DNA Mismatch Repair in Mammals • DNA Polymerase α, Eukaryotic • DNA Polymerase β, Eukaryotic • DNA Polymerase ε, Eukaryotic • DNA Replication: Eukaryotic Origins and the Origin Recognition Complex • Translesion DNA Polymerases, Eukaryotic

Glossary

base excision repair A repair characterized by excision of nucleic acid base residues in free form.

nuclear localization signal The amino acid sequence responsible for proteins being actively and selectively imported into the nucleus.

nucleotide excision repair A repair in which damaged nucleotides are removed as part of DNA fragments.

processivity The extent of nucleotide incorporation per DNA polymerase binding event.

proofreading The correction of mispaired nucleotides at the end of a growing DNA chain during replication.

Further Reading

Burgers, P. M. J. (1998). Eukaryotic DNA polymerases in DNA replication and DNA repair. *Chromosoma* **107**, 218–227.

DePamphilis, M. L. (1996). *DNA Replication in Eukaryotic Cells*. Cold Spring Harbor Laboratory Press, New York.

Hubscher, U. (1997). DNA polymerase δ, an essential enzyme for DNA transactions. *Biol. Chem.* **378**, 345–362.

Kornberg, A., and Baker, T. (1992). *DNA Replication*. W. H. Freeman and Company, New York.

Waga, S., and Stillman, B. (1998). The DNA replication fork in eukaryotic cells. *Annu. Rev. Biochem.* **67**, 721–751.

Biography

Antero G. So is a Professor in the Departments of Medicine and of Biochemistry and Molecular Biology at the University of Miami. His principal interest is in the field of mammalian DNA replication, with major emphasis on mammalian DNA polymerases. He holds an M.D. from the University of Santo Tomas and a Ph.D. from the University of Washington; he did his postdoctoral training at Case Western University and the University of Geneva.

Kathleen M. Downey is a Professor in the Departments of Medicine and of Biochemistry at the University of Miami. Her principal interest is in mammalian DNA replication and repair. She holds a Ph.D. from the University of Washington in Seattle, Washington and received her postdoctoral training at the Swiss Federal Institute of Technology in Zurich, Switzerland.

DNA Polymerase ε, Eukaryotic

Yasuo Kawasaki and Akio Sugino
Osaka University, Suita, Osaka, Japan

DNA polymerase ε is one of the least understood cellular DNA polymerases. Recent studies have revealed that it plays a central role in chromosomal DNA replication. DNA polymerase ε activity was reported in the extract from rabbit bone marrow cells in 1985. Although DNA polymerase ε was purified from calf thymus and human cells in the late 1980s, it was described initially as a "large form" of DNA polymerase δ or PCNA-independent DNA polymerase δ whose activity is not affected by proliferating cell nuclear antigen (PCNA). This DNA polymerase is a high-molecular-weight, aphidicolin-sensitive enzyme that copurifies with a tightly associated 3′–5′ exonuclease. In addition, it is highly processive in the absence of polymerase-loading factor, PCNA. In budding yeast *Saccharomyces cerevisiae*, DNA polymerase activity called DNA polymerase II was already known in the 1970s. The complete enzyme complex was purified in 1990 and it turned out to be the yeast homologue of DNA polymerase ε. It was in 1990 that the nomenclature of "DNA polymerase ε" was established. Since then, molecular structure and biological function have been extensively studied especially in budding yeast.

Molecular Structure

DNA polymerase ε (Pol ε) is purified from yeast as a four-subunit holoenzyme. It consists of four subunits, Pol2p, Dpb2p, Dpb3p, and Dpb4p in budding yeast and p261, p59, p12, and p17 in human. The genes encoding all four subunits of yeast and human enzyme have been cloned and sequenced. The genes for the largest and the second largest subunit, *POL2* and *DPB2* respectively, were shown to be essential for budding yeast cell growth, while *DPB3* and *DPB4* are not essential.

Catalytic Subunit

The largest subunit of budding yeast Pol ε is encoded by *POL2* gene and the molecular mass is 256 kDa. Its human counterpart, encoded by *POLE*, is 261 kDa. Homologues in other eukaryotes were also found including that in fission yeast *Schizosaccharomyces pombe*, encoded by *cdc20*$^+$ gene. The catalytic domain has the consensus amino acid sequences common to B family DNA polymerases (Figure 1). Eukaryotic DNA polymerases α, δ, ε, and ζ, *Escherichia coli* DNA polymerase II, and several viral DNA polymerases (T4 phage, HSV, and EBV) belong to B family. Unlike the other catalytic subunits of eukaryotic B family DNA polymerases, Pol2p has a long stretch at carboxyl-terminal half that is not related to the catalytic activity (Figure 1). There are two putative zinc-finger motifs at the carboxyl terminus, which is required for complex formation with the other three subunits. Overlapping partly with the catalytic domain, it has 3′–5′ exonuclease activity, which is responsible for editing during DNA biosynthesis. These molecular structures are conserved in all eukaryotes.

Other Subunits

The second largest subunit of Pol ε is encoded by the budding yeast *DPB2* gene, which is essential for viability, and by *POLE2* in humans. The molecular mass is 80 kDa in yeast and 59 kDa in humans, and they share 26% amino acid sequence identity. The function of this subunit is not known yet.

Budding yeast 34 kDa subunit of Pol ε is encoded by *DPB3* gene and the 29 kDa subunit is encoded by *DPB4* gene. These genes are not essential for growth since deletion mutants are viable. However, the DNA polymerase activity from either *DPB3* or *DPB4* deletion strain is less than that from wild-type cells, presumably because the complex formation is unstable. p17 and p12 correspond to the human homologues of Dpb4p and Dpb3p. They interact physically with p261 and p59, although a four-subunit human holoenzyme has not yet been isolated. These two subunits have a so-called histone-fold motif that is found in many transcription factors and is utilized for interaction with DNA. However, the significance of these motifs with respect to biological function of Pol ε is not yet known.

Biochemical Character

The biochemical properties of Pol ε are very similar to those of DNA polymerase δ; its activity is sensitive to aphidicolin, resistant to deoxyribonucleotide analogue

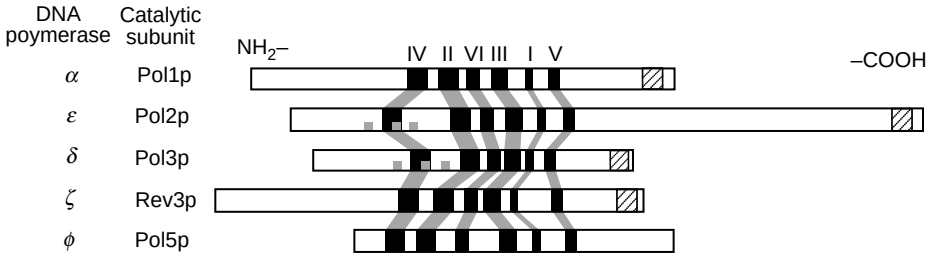

FIGURE 1 Eukaryotic B family DNA polymerases. DNA polymerases that possess B family catalytic domain are aligned. Closed boxes (I–V) represent the subdomains conserved among B family DNA polymerases. Gray boxes represent the exonuclease domains. Shaded boxes represent cysteine-rich domain which can form Zinc-fingers.

ddTTP, and characterized by high fidelity. Pol ε is distinguished from DNA polymerase δ by its high processivity in the absence of the cofactors PCNA, RFC, and RPA. However, under some conditions, it complexes with and is stimulated by PCNA, although the physiological significance of this interaction is unknown. During purification of Pol ε from yeast or mammalian cells, a small form of Pol2p ("145-kDa form" in yeast) has been identified in addition to the holoenzyme (Figure 2). Purified 145-kDa form, which lacks the carboxyl-terminal half, does not associate with the other three subunits. Both 145-kDa form and holoenzyme are highly processive and have an intrinsic proofreading $3'-5'$ exonuclease activity.

Role in DNA Replication

Role at Replication Fork

The SV40 DNA replication system, which serves as a model for eukaryotic DNA replication, has been successfully reconstituted *in vitro* with SV40 large T-antigen and mammalian proteins. Analysis of this system, which includes DNA polymerases α and δ, led to the conclusion that DNA polymerase α and δ are sufficient for synthesis of both leading and lagging strands in eukaryotes. These studies showed that DNA polymerase α, which is associated with primase activity, is required for initiation of new DNA chains. Only DNA polymerase δ was required to replicate both leading and lagging strands, leaving a replication role for Pol ε in doubt. However, several lines of evidence indicate the presence of Pol ε at the eukaryotic replication fork. Evidence for a physical interaction came from cross-linking experiments, which showed that Pol2p is located at or near the replication fork. Furthermore, the mutation rate is increased about tenfold in a yeast strain carrying a *pol2* mutation that inactivates the Pol ε proofreading capability (mutation in $3'-5'$ exonuclease domain) suggesting that this enzyme contributes to the synthesis of newly replicated DNA. A yeast double mutant lacking proofreading

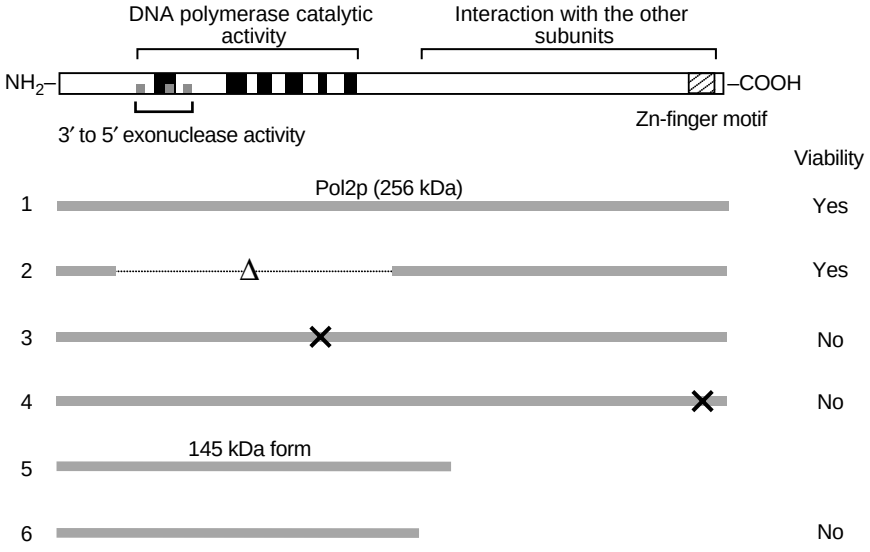

FIGURE 2 Domain structure of the yeast Pol2p subunit. Closed, gray, and shaded boxed are as described in Figure 1. Mutated or truncated versions of Pol2p are schematically shown and the viability of yeast cells which express each mutant Pol2p are indicated. 1, full-length Pol2p; 2, complete deletion of catalytic domain; 3, missence mutation in domain I; 4, missence mutation in zinc-finger motif; 5, endogenous 145 kDa form; 6, deletion of carboxyl terminus.

capability of both Pol2p and Pol3p cannot survive, presumably because the mutations accumulate to a lethal level. In addition, it has also been shown that loss of the exonuclease activity in either Pol2p or Pol3p alters the mutation spectra in a strand-specific manner. It has also been shown that DNA replication activity was drastically lost in *Xenopus* egg extracts when Pol ε was removed immunologically from the egg extract. Several conditionally lethal mutants of *POL2* have been isolated and characterized in budding yeast. Chromosomal DNA synthesis in these mutant cells ceases under the restrictive condition, indicating that Pol ε is required for normal chromosomal DNA replication. Consistent with this conclusion, the terminal morphology of mutant cells is the same as those of other DNA replication mutants in budding yeast, namely a dumbbell shape with a single nucleus localized between mother and daughter cells. Furthermore, a temperature-sensitive mutant of the *DPB2* gene also results in temperature-sensitive chromosomal DNA replication. Pol ε also exhibits the highest processivity among replicative DNA polymerases, suggesting that Pol ε synthesizes the leading strand, while the lagging strand is synthesized by DNA polymerase α and δ in a discontinuous manner.

Distinct Roles and Domain Structure

Yeast cells carrying a point mutation in the conserved catalytic domain of Pol2p are not viable. By contrast yeast mutant cells that have an internal deletion of *POL2*, resulting in loss of the DNA polymerase catalytic domain and the 3′–5′ exonuclease domain, can survive (Figure 2). However, this strain is temperature sensitive for cell growth, exhibits slow growth phenotype even at permissive temperature, and the elongation of DNA strands in the mutant cells is slow. This apparent discrepancy can be explained by considering the discrete functional domains of Pol ε. Although Pol ε may normally be present at the replication fork, in the complete absence of the catalytic domain, another DNA polymerase, presumably DNA polymerase δ, can substitute. On the other hand, the carboxyl terminus that is dispensable for the processive DNA synthesis *in vitro* is essential for growth (Figure 2). The *in vivo* requirement of carboxyl terminus may involve function in the initiation of DNA replication via interaction with the other subunits.

Role in DNA Repair

Apart from DNA replication, Pol ε participates in DNA repair and recombination. It was first suggested in human cells that Pol ε, is involved in DNA repair processes initiated by UV-damage. Human DNA polymerase ε and/or δ are required in the repair DNA synthesis step of nucleotide excision repair *in vitro*. It was also shown that the recombinational repair pathway, which repairs double strand breaks, requires both DNA polymerase δ and ε. *In vitro* studies have shown that crude extracts of temperature-sensitive *pol2* mutant cells have reduced activity in nucleotide excision repair and base excision repair. However, the suggestion that Pol ε functions in DNA repair has been questioned based on the observation that several mutant *pol2* alleles that have temperature-sensitive Pol ε activity *in vitro* do not show any significant sensitivity to DNA-damaging reagents. Since most of the evidence that Pol ε participates in DNA repair and recombination derives from *in vitro* experiments, further studies are required to confirm that this is also the case *in vivo*.

Role in Checkpoint Control

In order to prevent premature mitosis before the whole genome is completely duplicated, the S phase checkpoint is activated when S phase progression is inhibited, for example, by DNA damage. This process involves a protein phosphorylation signal cascade, slowing down of DNA synthesis, and induced transcription of certain genes. Several mutations that cannot induce checkpoint-dependent transcription after DNA damage have been isolated and characterized in budding yeast. One of these mutations is located in the carboxyl-terminal region of the *POL2* gene, suggesting that Pol ε may act as a DNA-damage "sensor" that triggers expression of checkpoint and repair genes. Additional evidence for this view is provided by the observation that Pol ε binds to a factor which participates in S phase checkpoint control under certain conditions.

See Also the Following Articles

Cell Cycle: DNA Damage Checkpoints • Cell Cycle: Mitotic Checkpoint • DNA Mismatch Repair in Mammals • DNA Polymerase α, Eukaryotic • DNA Polymerase β, Eukaryotic • DNA Polymerase δ, Eukaryotic • DNA Polymerases: Kinetics and Mechanism • DNA Replication Fork, Eukaryotic • Translesion DNA Polymerases, Eukaryotic • Zinc Fingers

Glossary

B family DNA polymerase DNA polymerases in bacteria, archaea, and eukarya are classified into six groups (A, B, C, D, X, and Y) based on their amino acid sequences.

exonuclease activity An activity which digests single-stranded DNA from an end. The direction of exonuclease activity is specific: 5′–3′ or 3′–5′.

replication fork During DNA replication, the template strands of the duplex DNA separate to form a replication fork. Leading strand is continuously synthesized and lagging strand is synthesized discontinuously.

zinc-finger motif Amino acid sequences that bind zinc, composed with two repeats of two closely spaced cysteine or histidine. It mediates protein–protein interaction or protein–DNA interaction.

Further Reading

Kawasaki, Y., and Sugino, A. (2001). Yeast replicative DNA polymerases and their role at the replication fork. *Molecul. Cells* **12**, 277–285.

Newlon, C. S. (1996). DNA replication in yeast. In *DNA Replication in Eukaryotic Cells* (M. L. DePamphilis, ed.) pp. 873–914. Cold Spring Harbor Laboratory Press, Cold Spring Harbor.

Wang, T. S.-F. (1996). Cellular DNA polymerases. In *DNA Replication in Eukaryotic Cells* (M. L. DePamphilis, ed.) pp. 461–493. Cold Spring Harbor Laboratory Press, Cold Spring Harbor.

Biography

Yasuo Kawasaki is an Assistant Professor of the Graduate School of Frontier Biosciences at Osaka University in Osaka, Japan. His principal research interests are in the regulation of S phase and the mechanism of chromosomal DNA replication in eukaryotes. He holds a Ph.D. from Kyoto University and received his postdoctoral training at Cornell University. He is actively studying the regulation and mechanism of chromosomal DNA replication in budding yeast *Saccharomyces cerevisiae*.

Akio Sugino is a Professor of the Graduate School of Frontier Biosciences at Osaka University in Osaka, Japan. His principal research interests are in the regulation of S phase and characterization of DNA polymerases in eukaryotes. He holds a Ph.D. from Nagoya University. He started his research career with Professor Reiji Okazaki and participated in the works for finding the discontinuous DNA replication of the lagging strand synthesis.

DNA Polymerase I, Bacterial

Catherine M. Joyce
Yale University, New Haven, Connecticut, USA

DNA polymerase I is the most abundant DNA polymerase in eubacteria. Although it lacks the speed and processivity of the more complex polymerases which replicate the bacterial chromosome, it is ideally suited for the synthesis of short stretches of DNA in excision repair and in the removal of RNA primers during lagging strand replication. DNA polymerase I (pol I) of *Escherichia coli*, the first DNA polymerase to be discovered and studied, has long served as the prototype for this class of enzymes. Other homologues that have been extensively studied are the thermostable DNA polymerase I from *Thermus aquaticus* (*Taq* DNA pol) and the DNA polymerase of bacteriophage T7.

Overview of Structure

Pol I enzymes are multifunctional and follow the pattern seen throughout the polymerase superfamily: a modular structure with a common polymerase domain (described below) and auxiliary enzyme activities located on separate protein domains. All bacterial pol Is have an N-terminal domain with 5′ nuclease activity; this activity is responsible for the removal of DNA ahead of the growing primer strand. Attachment of the 5′ nuclease domain to the rest of the polymerase is protease sensitive; in *E. coli* pol I mild protease digestion was originally used to remove the 5′ nuclease (35 kDa) from the remainder of the molecule (called Klenow fragment, 68 kDa); nowadays this is accomplished by recombinant DNA manipulations. The linkage between the 5′ nuclease and Klenow fragment is almost certainly flexible, as shown by the observation that the 5′ nuclease does not occupy the same position relative to the rest of the molecule in different crystal forms of *Taq* DNA pol. The pol I homologues found in bacteriophage genomes resemble the Klenow fragment portion of the bacterial pol Is, in that they lack the 5′ nuclease portion of the sequence. In some cases, such as bacteriophage T7, the 5′ nuclease is encoded as a separate gene product.

The Klenow fragment portion of pol I also contains two domains. In about half of the bacterial pol Is, the N terminal of the two domains contains a 3′–5′ exonuclease (3′ exo) activity which serves as a proofreader to eliminate polymerase errors. If the polymerase were to insert an incorrect nucleotide, resulting in a terminal mispair, the 3′–5′ nuclease would remove the incorrect primer-terminal nucleotide and provide a second opportunity for correct insertion. The bacterial pol I enzymes that lack 3′–5′ exonuclease activity (from species including *Thermus*, *Bacillus*, and *Rickettsiae*) nevertheless contain the domain, though key active site side chains are absent. Aside from the thermophiles, where fraying of double-stranded DNA termini at high temperatures might encourage excessive nuclease degradation, it is unclear why certain bacterial pol I enzymes have proofreading activity and others do not.

Polymerase

Domain Structure and Relation to Other Polymerases

When the structure of Klenow fragment (the first polymerase to be studied crystallographically) was reported in 1985, the polymerase domain structure was described as resembling a half-open right hand, with subdomains called “fingers,” “palm,” and “thumb” forming a cleft. Currently, structures are available for more than 30 polymerases, encompassing all four biochemical categories of polymerase (DNA or RNA dependent, with DNA or RNA as product), and it is clear that the domain structure originally observed in Klenow fragment is a common theme (Figure 1). The palm subdomain is the most highly conserved across polymerase families; it contains a conserved structural motif (the “polymerase fold”) consisting of a three-stranded antiparallel β-sheet supported by two α-helices. This serves as the scaffold for important active site residues, in particular a pair of carboxylate ligands to the two divalent metal ions that catalyze the phosphoryl transfer reaction. The fingers and thumb subdomains are structurally much more divergent, but carry out analogous functions in all polymerases – the fingers providing important active site residues, particularly those involved in nucleotide binding, and the thumb binding the primer-template duplex.

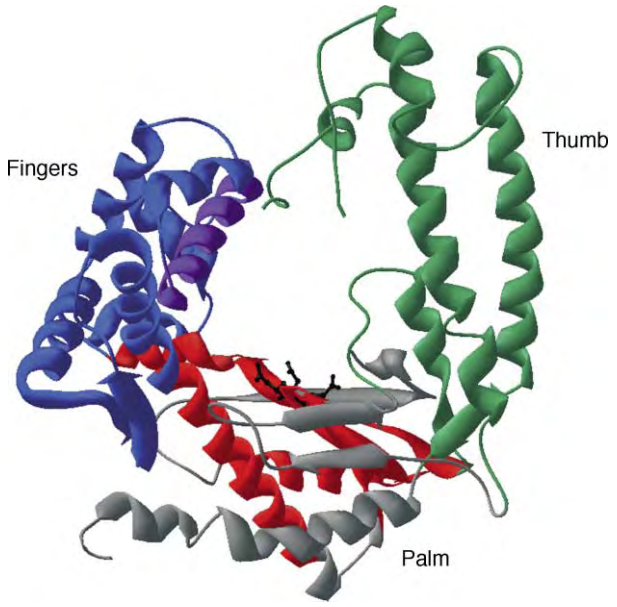

FIGURE 1 Three-dimensional structure of the polymerase domain of *E. coli* DNA polymerase I (from the work of T. A. Steitz and colleagues). The thumb and fingers subdomains are colored green and blue, respectively, with the O-helix on the fingers subdomain in purple. The palm subdomain is gray, except for the "polymerase fold," a conserved structural motif found in the majority of nucleic acid polymerases, which is shown in red. Three conserved carboxylate side chains, two of which are ligands to the catalytic metal ions, mark the location of the polymerase active site.

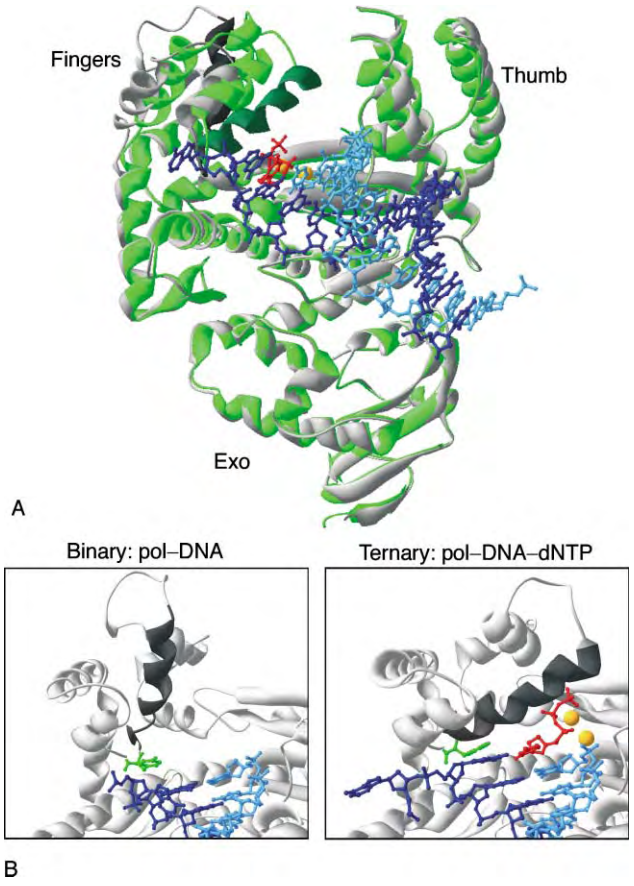

FIGURE 2 (A) Superposition of binary (pol–DNA) and ternary (pol–DNA–dNTP) complexes of Klentaq, the Klenow fragment portion of *Taq* DNA pol (from the work of G. Waksman and colleagues). The DNA template (dark blue) and primer (cyan), incoming nucleotide (red) and active-site metal ions (gold) are shown in their positions in the ternary complex. The protein backbone in the binary complex is gray, and in the ternary complex green. The two protein structures are essentially superimposable except within the fingers subdomain, where the largest movement involves the O-helix (shown in darker shades of gray and green, respectively). The domain marked "Exo" corresponds to the 3′–5′ exonuclease domain in Klenow fragment, though it has no enzymatic activity in Klentaq. (B) Detailed comparison of the active site regions in the two complexes. In each case the protein is shown in gray, with the O-helix in a darker shade. Coloring of the DNA, nucleotide, and metal ions is the same as in the top panel. The structures are oriented so that the palm subdomain and the DNA are in similar positions in both panels, emphasizing the movement of the O-helix. The side chain of the conserved Tyr at the C-terminus of the O-helix (Tyr671 in Klentaq, Tyr 766 in Klenow fragment) is shown in green. This side chain is stacked with the template side of the terminal base pair in the binary complex; in the ternary complex it has moved out of the way to allow the next template base to enter the active site (note that this template base is folded back over the template strand in the binary complex). For clarity, the top of the thumb subdomain is omitted in all the structures illustrated in this figure.

Substrate Binding

The binding of substrates at the polymerase active site has been revealed in cocrystals of several pol I homologues. The template-primer duplex (corresponding to the product of DNA synthesis) is bound in a shallow cleft between the thumb and 3′ exo domains, with the largely α-helical thumb providing important binding contacts to the phosphate backbone. In a polymerase–DNA binary complex, the primer terminal base pair abuts the side of the polymerase cleft formed by the fingers subdomain. This wall, which defines one side of the active site, is formed primarily by a long α-helix (the O-helix, shown in purple in Figure 1) which runs the length of the fingers subdomain and has a group of important and highly conserved side chains on the surface pointing into the cleft. At the C terminus of the O-helix is an invariant Tyr side chain which is stacked against the template side of the terminal base pair.

When the dNTP complementary to the templating position is added so as to form a polymerase–DNA–dNTP ternary complex, cocrystal structures indicate that the polymerase must have undergone a conformational change (Figure 2). The novel conformation seen in ternary complex structures differs from the apoenzyme and binary complex structures by a substantial movement of the fingers subdomain so as to close the polymerase cleft. In conjunction with the transition from the open (binary complex) to closed (ternary complex) conformation, the Tyr side chain at the C-terminus of the O-helix moves further down into

the active site, away from its stacked position with the terminal base pair. This allows the templating base to stack with its 3′ neighbor at the duplex terminus, and to base pair with the incoming dNTP in a snug binding pocket formed by side chains of the O-helix and nearby residues on one side and the primer-terminal base pair on the other side. Analogous conformational transitions have been inferred from crystal structures of a diverse variety of polymerases, suggesting that the formation of a closed ternary complex may be a common feature of the polymerase reaction pathway.

DNA Polymerase Reaction Mechanism

Extensive work by Benkovic and co-workers has defined the polymerase reaction pathway of Klenow fragment. There is an obligatory order of substrate binding – DNA before dNTP – as would be expected, given that templating information is required for nucleotide selection. As mentioned above, the chemical step of dNTP addition is catalyzed by two divalent metal ions coordinated at the active site (Figure 3). One metal ion facilitates deprotonation of the primer 3′-OH, making it a better nucleophile, while the other stabilizes the pyrophosphate leaving group. Both metals also stabilize the developing negative charge on the α-phosphate in the transition state. This two-metal-catalyzed reaction mechanism is beautifully illustrated in the ternary complex cocrystal structures, and is widespread in phosphoryl transfer reactions, including the 3′–5′ exonuclease reaction (discussed below). The work of Benkovic and co-workers indicates that the phosphoryl transfer step of Klenow fragment is rapid, but is preceded and followed by slow noncovalent steps. These steps must correspond to some kind of conformational transition and it is tempting to equate the step preceding phosphoryl transfer with formation of the closed complex inferred from the crystal structures. However, it is important to realize that there is currently no experimental evidence in support of this idea.

DNA Polymerase Reaction Specificity

Base Pairing

DNA polymerases function with extraordinary specificity, selecting the complementary dNTP and rejecting incorrect choices in the majority of cases. Klenow fragment makes approximately one error for every 10^5 nucleotides synthesized, about 1000-fold more accurate than would be predicted solely from the energetics of base pairing. Three major mechanisms have been proposed to account for the way in which the polymerase enhances the accuracy of DNA synthesis.

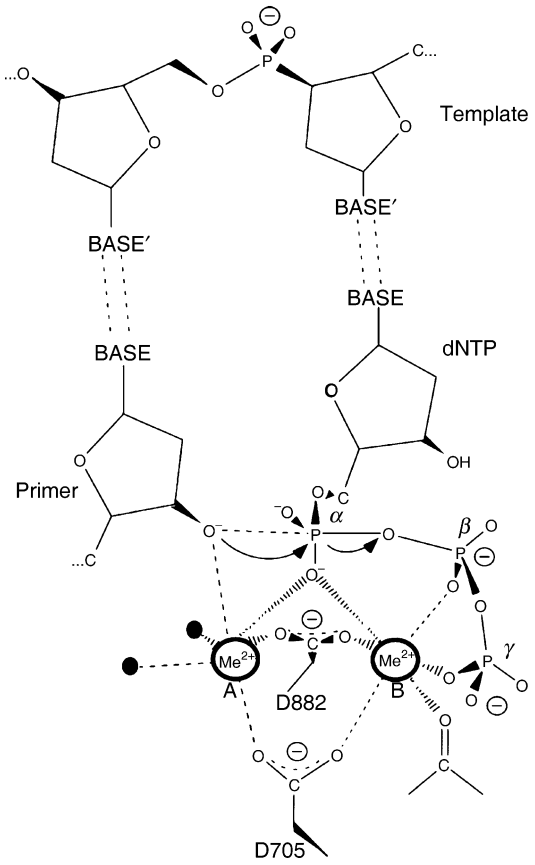

FIGURE 3 Mechanism of phosphoryl transfer, resulting in nucleotide addition, at the polymerase active site. Catalysis is mediated by two divalent metal ions, coordinated, in Klenow fragment, by Asp705 and Asp882. Metal ion A activates the primer 3′-OH for nucleophilic attack on the α-phosphate of the dNTP. Metal ion B stabilizes the negative charge that develops on the pyrophosphate leaving group. Both metal ions also assist the reaction by stabilizing the negative charge on the α-phosphate in the pentacovalent transition state. Adapted from Brautigam and Steitz (1998).

The first is exclusion of water from the active site which should amplify the energetic differences between correct and incorrect base pairings. The second is geometric selection in the binding pocket for the nascent base pair such that there is good steric complementarity to the rather symmetrical shape of a Watson–Crick base pair, but exclusion of mispairs. This model is consistent with the very snug fit seen in the binding pocket of polymerase ternary complex structures. Moreover, several polymerases, including Klenow fragment, have been shown to incorporate template-primer pairings that mimic the shape of a Watson–Crick base pair but lack any hydrogen bonds. These first two specificity mechanisms are proposed to operate at the level of nucleotide addition, and should weaken the binding or slow the incorporation of an incorrectly paired incoming nucleotide. The third selection method would operate after nucleotide addition and relies on hydrogen-bonding interactions between the polymerase and

the minor groove at or close to the primer terminus. The hydrogen-bond acceptors on N3 of purines and O2 of pyrimidines occupy similar positions in all Watson–Crick base pairs but are mispositioned in incorrect pairings, thus providing a mechanism for scanning the minor groove to ensure that template information has been correctly read. A mispair located at the primer terminus will fail to make the minor groove interactions that are seen for correct base pairs in polymerase cocrystal structures, and this, together with other geometric abnormalities, results in a much slower rate of addition of the next nucleotide. Slower polymerase addition to a mispaired primer terminus reduces the likelihood of a mispair becoming fixed as a mutation by continued synthesis, and also increases the time window during which the error may be proofread, or the mispaired DNA may dissociate.

As might be expected from the different geometries of various mispairs, a polymerase such as Klenow fragment does not make all errors at the same frequency, so that insertion of dGTP opposite a template T is relatively facile, whereas insertion of dCTP opposite C is rare. Klenow fragment mutator mutants change not only the frequency of errors but also the specificity, and may provide a valuable window into the recognition processes that take place at the polymerase active site.

Sugar Specificity

Bacterial pol Is also have stringent specificity for the sugar of the incoming nucleotide. A DNA polymerase must reject ribonucleotides, despite their higher concentration *in vivo*, and this is achieved by an invariant Glu residue positioned so as to obstruct any substituent on the C2′ position of the sugar. Mutation of this Glu to the smaller Ala in Klenow fragment results in a polymerase that can add a ribonucleotide almost as easily as a deoxyribonucleotide. However, the mutant enzyme does not function as a true RNA polymerase because it cannot efficiently add multiple ribonucleotides, most probably because the duplex binding site cannot accommodate a DNA–RNA product.

Pol I enzymes fall into two classes regarding their handling of nucleotide analogues which lack the sugar 3′ hydroxyl (dideoxy nucleotides) and therefore function as chain terminators. The majority, exemplified by Klenow fragment, discriminate very strongly against dideoxy nucleotides. The ternary complex cocrystal structures show a hydrogen bond between the 3′ hydroxyl and the β-phosphate of the incoming nucleotide; presumably, the loss of this interaction compromises the alignment of reactive groups in the transition state, resulting in a slower reaction rate. A minority of pol Is, exemplified by T7 DNA pol, discriminate only slightly against dideoxy nucleotides. In these polymerases, a conserved aromatic side chain that forms part of the nucleotide binding pocket is present as Tyr, instead of the more usual Phe, and the Tyr hydroxyl provides the missing interaction with the β-phosphate. The ability to manipulate chain terminator specificity via a single active-site point mutation has proven invaluable in DNA sequencing and related biotechnology applications.

3′–5′ Exonuclease

The 3′–5′ exonuclease, present in about half of pol Is, carries out its editing function by means of hydrolysis of the terminal nucleotide of the DNA primer strand. The hydrolysis reaction is a phosphoryl transfer, analogous to that described above for the polymerase reaction, catalyzed by a pair of metal ions liganded by a cluster of conserved carboxylate side chains. The other important component of the 3′ exo site is a binding site for single-stranded DNA. In model studies, the exonuclease can be studied using single-stranded DNA as the substrate, though the natural substrate *in vivo* is a duplex DNA whose primer terminus is frayed so as to present three or four bases of single-stranded DNA for binding at the 3′ exo site. The requirement for fraying in order to bind at the 3′ exo active site provides the specificity for editing, because a mismatched primer terminus is more easily melted and is therefore a better substrate for the 3′ exo than a correctly paired DNA. Indeed, studies have shown that, whereas a correctly paired DNA duplex is bound predominantly at the polymerase site of Klenow fragment, a single terminal mismatch results in $\approx$50:50 partitioning between polymerase and 3′ exo sites. The preference of the 3′ exo for a mispaired substrate is amplified by the slowing of the polymerase reaction caused by a mispaired primer terminus (discussed above), so that a mispair is likely to be targeted for proofreading, while a correct primer terminus will serve as a substrate for continued addition.

The contribution of proofreading to polymerase fidelity is quite variable in the pol Is. As already noted, some pol Is do not proofread at all. In others, such as *E. coli* pol I, the contribution of proofreading is relatively modest, about tenfold. Others, such as the polymerases from bacteriophages T5 and T7, have more active exonucleases. Additionally, depending on the strength of the polymerase–DNA interaction, the DNA may stay associated with the polymerase during the transfer from polymerase to editing site, as in T5 and T7, or it may reach the proofreading site via dissociation from the polymerase site and binding to the exonuclease site of another enzyme molecule. Because the selectivity of editing is determined by the structure of the DNA substrate (paired or mispaired) and does not require presentation of the primer terminus in a particular way, the intermolecular transit from polymerase to

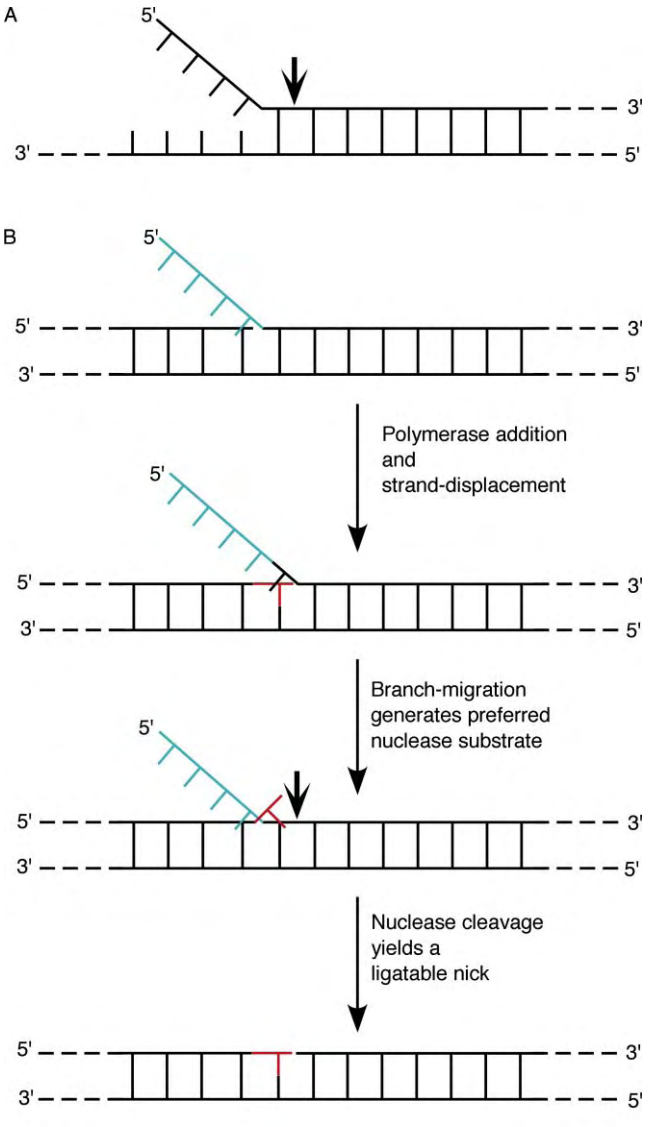

FIGURE 4 (A) Site of cleavage by the 5′ nuclease on a model substrate containing noncomplementary 5′ and 3′ extensions. The nuclease cuts between the first two paired bases. (B) The polymerase and 5′ nuclease activities collaborate in processing a DNA molecule with a 5′ single-stranded tail so as to produce a nicked product that can be sealed by DNA ligase. Cleavage of the first structure, between the first two paired bases adjacent to the 5′ tail, would yield a single-base gap. Nucleotide addition by the polymerase (in red), together with the preference of the 5′ nuclease for a melted base at the 3′ end of the adjacent primer strand, favors the formation of a ligatable product.

exonuclease site would not be expected to compromise the editing process.

5′ Nuclease

The 5′ nuclease of the bacterial pol I enzymes was described as the "5′–3′ exonuclease" in the earlier literature. However, it is now recognized that this activity is not a true exonuclease, but is a structure-specific nuclease that recognizes the junction between duplex DNA and a single-stranded 5′ end, and cuts between the first two paired bases (Figure 4A). On a nicked DNA molecule, polymerase-catalyzed synthesis causes strand displacement and generates the substrate for the 5′ nuclease, so that together the polymerase and 5′ nuclease cause "nick translation," the movement of a nick along a duplex DNA molecule. DNA binding experiments show that the polymerase and 5′ nuclease compete for binding to a DNA substrate, and this implies a mechanism in which the DNA is passed from one active site to the other, and rules out mechanisms in which both reactions take place within a single bound species. The preferred substrate for the 5′ nuclease has, in addition to the unpaired 5′ strand, an unpaired base at the 3′ end of the primer strand abutting the ss–ds junction. This substrate could be formed by rearrangement of the product of polymerase extension and, when cleaved by the 5′ nuclease, will leave a junction ready for ligation (see Figure 4B). The observed specificity of the 5′ nuclease fits well with the *in vivo* functions of the bacterial pol I enzymes in DNA repair and in the removal of primers from Okazaki fragments on the lagging strand. In both cases, the desired endpoint of pol I action is a nick that can be sealed by DNA ligase.

Several 5′ nuclease structures have been solved in the absence of substrates, but our structural understanding of the 5′ nuclease is less good than for the polymerase or 3′–5′ exonuclease because of the absence of cocrystal structures. The location of the 5′ nuclease active site has been inferred from the position of conserved sequence motifs. These contain a large number of conserved carboxylate residues, inviting speculation that, like the polymerase and 3′–5′ exonuclease activities, the 5′ nuclease may carry out phosphoryl transfer using bound divalent metal ions. The bacterial 5′ nucleases and their archaeal homologues have a protein loop or arch in their structures, and it has been hypothesized that the single-stranded 5′ end of the DNA substrate is threaded through the protein.

See Also the Following Articles

DNA Polymerase II, Bacterial • DNA Polymerase III, Bacterial • DNA Polymerases: Kinetics and Mechanism • Exonucleases, Bacterial • umuC,D Lesion Bypass DNA Polymerase V

Glossary

apo-enzyme Enzyme in the absence of bound substrates.
mispair Two opposed bases in DNA that do not conform to the Watson–Crick rules of complementarity, i.e., not A–T or G–C.
primer In duplex DNA, the strand that presents a 3′ end for extension by a DNA polymerase.

template In duplex DNA, the strand that is paired with the primer, and therefore provides the information for copying by DNA polymerase.

Further Reading

Benkovic, S. J., and Cameron, C. E. (1995). Kinetic analysis of nucleotide incorporation and misincorporation by Klenow fragment of *Escherichia coli* DNA polymerase I. *Methods Enzymol.* **262**, 257–269.

Brautigam, C. A., and Steitz, T. A. (1998). Structural and functional insights provided by crystal structures of DNA polymerases and their substrate complexes. *Curr. Opin. Struct. Biol.* **8**, 54–63.

Ceska, T. A., and Sayers, J. R. (1998). Structure-specific DNA cleavage by 5′ nucleases. *Trends Biochem. Sci.* **23**, 331–336.

Joyce, C. M. (1997). Choosing the right sugar: How polymerases select a nucleotide substrate. *Proc. Natl Acad. Sci. USA* **94**, 1619–1622.

Kunkel, T. A., and Bebenek, K. (2000). DNA replication fidelity. *Annu. Rev. Biochem.* **69**, 497–529.

Li, Y., Korolev, S., and Waksman, G. (1998). Crystal structures of open and closed forms of binary and ternary complexes of the large fragment of *Thermus aquaticus* DNA polymerase I. Structural basis for nucleotide incorporation. *EMBO J.* **17**, 7514–7525.

Biography

Catherine M. Joyce is a Senior Research Scientist in the Department of Molecular Biophysics and Biochemistry at Yale University. Her research is directed toward a structural interpretation of DNA polymerase reaction mechanisms.

DNA Polymerase II, Bacterial

Judith L. Campbell
California Institute of Technology, Pasadena, California, USA

DNA must be synthesized during cellular reproduction to produce an identical copy of the chromosome, a process known as DNA replication. In addition, DNA synthesis is needed during the process of DNA repair. After DNA damage is removed from one strand, the complementary strand can serve as a template for correct resynthesis of an intact chain. DNA is synthesized from deoxynucleoside triphosphate building blocks through the action of enzymes called DNA polymerases. All cells contain several DNA polymerases, each of which is specialized either for DNA replication or for different repair pathways. *Escherichia coli* contains five DNA polymerases. DNA polymerase III is essential for DNA replication, while the remaining DNA polymerases are for DNA repair. The specific DNA polymerase being recruited to sites of DNA damage depends on a number of factors. DNA polymerase II, so-called because it was the second DNA polymerase described in *E. coli*, is specialized for DNA repair that occurs when moving replication forks encounter damaged DNA templates.

DNA Polymerase II: Structure and Biochemical Functions

DNA polymerase II (pol II) is a single polypeptide of 783 amino acids with a predicted mass of 89.9 kDa, and is encoded by the *polB* (a.k.a. *dinA*) gene. DNA pol II is the founding member of the B family of DNA polymerase structures, and contains the five motifs characteristic of this family, including both DNA polymerase and exonuclease domains. (DNA pol I belongs to family A, DNA pol III to family C, and DNA poly IV and V to family Y.) Members of the family B polymerases are found throughout the Archaea; and, interestingly, the three replicative DNA polymerases of eukaryotic cells, as well as additional repair DNA polymerases, belong to family B. This suggests the evolutionary importance of pol II.

DNA pol II is a monomeric enzyme but interacts with accessory subunits of the pol III replicase, the γ–δ clamp loading complex and the β clamp. The clamp tethers the DNA polymerase to the terminus of the growing DNA chain. These subunits confer high processivity on both enzymes, a property consistent with a role in synthesizing long stretches of DNA, either during repair or replication. In fact, all five bacterial polymerases interact with the β-clamp. This interaction is competitive, suggesting that all polymerases use the same interface on the β-clamp. This observation suggests a mechanism by which the polymerases may be transiently interchanged with the replicase to copy sites in the template that pose blocks to pol III, such as modification of the bases, bound proteins, or sequences that are inherently inhibitory to polymerase translocation because of their structure. This polymerase switching phenomenon is important for the coordination of DNA replication and DNA repair, and thus for the maintenance of DNA synthesis fidelity.

In addition to being capable of highly processive DNA synthesis, DNA pol II is highly accurate, with *in vitro* error rate as low as one in a million. Mutations in the $3'$–$5'$ proofreading exonuclease domain of the pol II protein result in a 13–240-fold increase in the error rate, depending on the type of error being edited. *In vivo*, defects resulting in a 1000-fold reduction in the proofreading exonuclease activity of pol II cause no increase in mutation frequency in cells containing normal DNA pol III. When an antimutator allele of DNA pol III was present in the cells, however, the pol II proofreading mutant experienced a significant increase in chromosomal base substitution and frameshift mutation frequencies in dividing cells. This suggests that, while pol III is the normal replicase, pol II can replace pol III at the replication fork under some circumstances. In non-dividing cells, pol II exonuclease-defective mutants and mutants completely lacking pol II due to deletion of the *polB* gene have a mutator activity for adaptive mutation. (Adaptive mutations in *E. coli* are episomal mutations arising in stationary phase, nongrowing cells, and the highly conserved pol IV is thought to introduce the mutations during synthesis initiated at the conjugal origin or by DNA repair and recombination.) Thus, an additional role of the pol II exonuclease activity may be to control the level of adaptive mutation by pol IV.

Biological Function: Replication Restart

Given that pol II is a high-fidelity polymerase and that it is highly processive in the presence of the β-clamp, pol II has properties characteristic of replicative DNA polymerases, i.e., ability to synthesize long stretches of DNA at high rates and with high fidelity. However, deletion of pol II from the cell is not deleterious to growth of *E. coli* cells, suggesting that the polymerase is present in order to carry out repair of damaged DNA. This appears to be the case, since the levels of pol II are induced sevenfold by treatment of cells with UV light, which causes lesions in the DNA. In fact, pol II is one of ~40 genes that comprises of the SOS regulon. SOS is a global response to DNA damage that induces ~40 genes, ~30 of which, like *polB*, are induced specifically by inactivating a repressor known as LexA. The level of pol II rises from ~50 molecules in normally replicating cells to ~350 after derepression. Two additional DNA polymerases (pol V and pol IV), both of which have low fidelity, are also induced after cells are treated with DNA-damaging agents.

Although the level of pol II increases in cells after DNA damage, *polB* mutants are not sensitive to DNA-damaging agents such as UV. This is because pol V can carry out repair in the absence of pol II. This conclusion derives from the observations that pol V mutants are UV sensitive and mutants lacking both pol V and pol II are even more so. The mechanism of repair catalyzed by the two polymerases is quite different, however. After treatment with UV, DNA replication is transiently inhibited. Within ~10–15 min, DNA replication resumes, eventually returning to the normal rate. Pol II is induced 30 s after treatment with UV and is required for this replication restart, also known as replisome reactivation. During replisome reactivation, efficient repair mechanisms remove most of the DNA damage. Repair carried out in the presence of pol II is error free and does not give rise to increased mutation. The steps in error-free replication restart involving pol II are shown in Figure 1. When the replisome encounters damage in the template that blocks the progress of pol III, there is a rearrangement of the replication fork. The replication of the two complementary strands, which is usually concurrent, is uncoupled. Synthesis on the damaged template strand is blocked but synthesis on the undamaged strand can continue, resulting in faithful copying of the undamaged strand beyond the site of the lesion. Next, the nascent DNA chains unwind from the parental templates in a process of rotary diffusion called branch migration, and then reassociate with each other by virtue of their complementarity. The longer nascent strand then serves as a template for the shorter, previously blocked strand, which can now be extended past the site of the lesion using the undamaged, and therefore instructional, bases from the newly synthesized complementary strand. This synthesis is thought to occur by substituting pol II for pol III, perhaps via the β-clamp, as already suggested. This part of the reaction is sometimes called template switching. In order to recreate the rapidly moving replication fork, the process is then reversed. The nascent strands unwind and switch back to the parental template, restoring the replication fork at a position downstream of the lesion. As a result of these isomerizations, the lesion is effectively bypassed by the normal replication fork and moved into the fully duplex region upstream of the fork, where it can be recognized and dealt with by the various repair systems in the cell. To complete the process of replication restart, both kinetic and genetic evidence support the notion that after restoration of the replication fork, there is a switch back to

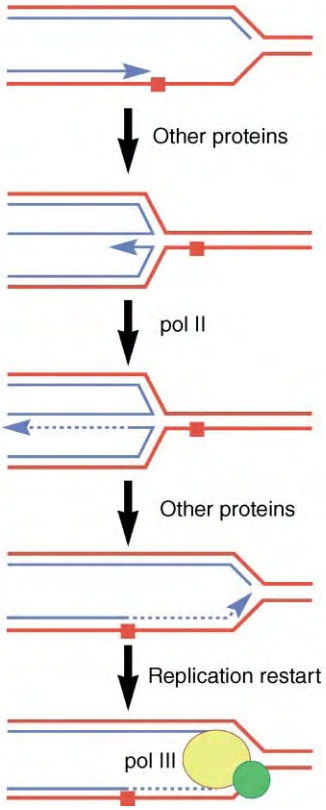

FIGURE 1 A hypothetical scheme for replication restart using bacterial DNA polymerase II. The red lines represent template DNA, and the blue lines newly synthesized DNA. The arrow represents the end of the chain where the polymerase switch occurs. The dotted line represents a lesion in the DNA that cannot be copied by pol III. Pol III replicase, depicted as the yellow and green ovals, is shown after reassociation with the fork at the bottom of the figure. The various steps are described in the text in detail. (Modified from Rangarajan, S., Woodgate, R., and Goodman, M. F., (2002). Replication restart in UV-irradiated *Escherichia coli* involving pols II, III, V, PriA, RecA, and RecFOR proteins. *Mol. Microbiol.* **43**, 617–628, with permission of Blackwell Publishing Ltd.)

the pol III replicase in order to complete normal replication. Thus, pol II carries out only transient synthesis. Several proteins in addition to pol II, as indicated in Figure 1, genetically implicated in replication restart after UV irradiation, are likely to aid in the uncoupling, branch migration, and recruitment of pol II described in the model. Since the reaction has not been reconstituted from purified proteins, however, the molecular mechanism remains to some extent conjectural. One enigma with respect to the role of pol II in replication restart is the finding that levels of pol II are substantial even in cells lacking DNA damage. This has led to speculation that pol II might be involved in error-free replication restart in the presence of endogenous blocks to replication, such as oxidative damage due to normal metabolism, deamination of cytosine, or protein blocks.

In the absence of pol II, DNA replication is still inhibited immediately following DNA damage, but replication restart is delayed for ~50 min after UV irradiation. Biochemical studies suggest that pol V directly substitutes for pol III at the growing fork, and that pol V then inserts a base directly across from the lesion. This process is called translesion synthesis (TLS). After insertion, there is a switch back to pol III for continued replication. TLS is not only fundamentally different in mechanism from pol II catalyzed replisome reactivation, it also has a very different outcome for the surviving cells. Pol V has more relaxed base recognition properties than pol II or pol III, and can efficiently incorporate bases opposite certain lesions and abasic sites, thus giving rise to mutations primarily targeted to the lesions. Thus, repair in the absence of pol II is mutagenic and is therefore known as error-prone repair. Even in the presence of pol II, mutation frequency is induced 100-fold by UV irradiation of *E. coli* cells. It is reasonable that the pol II pathway temporally precedes TLS, since pol II-dependent replication restart does not increase the mutational load. Apparently, however, TLS is a fail-safe pathway which is employed because the organism prefers high survival rates, even with increased mutation load, pending return to an environment supporting more robust growth.

While the polymerase chosen for repair of damage that blocks replication forks depends on availability of polymerase (pol II must be induced), the repair pathway chosen also depends on the type of damage. In the case of N-2 acetylaminofluorene (AAF) guanine adducts, pol II acts as an error-prone TLS polymerase and generates frameshift mutations, while pol V carries out error-free translesion synthesis.

In summary, pol II can, under some conditions, replace pol III in chromosomal replication, but its primary role is in error-free replication restart in response to DNA damage.

See Also the Following Articles

DNA Polymerase I, Bacterial • DNA Polymerase III, Bacterial • DNA Replication Fork, Bacterial

Glossary

adaptive mutation Mutations that arise presumably during DNA repair in cells that are not otherwise undergoing DNA replication. In bacteria, such mutations have been shown to occur on episomes. This process is probably important in evolution.

episome An extrachromosomal DNA molecule, residing in a cell, that cannot replicate on its own but needs the proteins encoded by the cellular chromosome.

processivity With respect to DNA polymerases, the ability to copy long stretches of template without dissociating from the template.

repressor A protein that shuts down production of RNA from specific genes (i.e., turns them off). Repressors can be removed or inactivated by inducers.

Further Reading

Campbell, J. L., Soll, L., and Richardson, C. C. (1972). Isolation and partial characterization of a mutant of *Escherichia coli* deficient in DNA polymerase II. *Proc. Natl Acad. Sci. USA* **69**, 2090–2094.

Cox, M. M., Goodman, M. F., Kreuzer, K. N., Sherratt, D. J., Sandler, S. J., and Marians, K. J. (2000). The importance of repairing stalled replication forks. *Nature* **404**, 37–41.

Goodman, M. F. (2002). Error-prone repair DNA polymerases in prokaryotes and eukaryotes. *Annu. Rev. Biochem.* **71**, 17–50.

Hirota, Y., Gefter, M., and Mindich, L. (1972). A mutant of *Escherichia coli* defective in DNA polymerase II activity. *Proc. Natl Acad. Sci. USA* **69**, 3238–3242.

Knippers, R. (1970). DNA polymerase II. *Nature* **228**, 1050–1053.

Moses, R. E., and Richardson, C. C. (1970). A new DNA polymerase activity of *Escherichia coli*. II: Properties of the enzyme purified from wild-type *E. coli* and DNA-ts mutants. *Biochem. Biophys. Res. Commun.* **41**, 1565–1571.

Pham, P., Rangarajan, S., Woodgate, R., and Goodman, M. F. (2001). Roles of DNA polymerases V and II in SOS-induced error-prone and error-free repair in *Escherichia coli*. *Proc. Natl Acad. Sci. USA* **98**, 8350–8354.

Rangarajan, S., Woodgate, R., and Goodman, M. F. (1999). A phenotype for enigmatic DNA polymerase II: A pivotal role for pol II in replication restart in UV-irradiated *Escherichia coli*. *Proc. Natl Acad. Sci.USA* **96**, 9224–9229.

Rangarajan, S., Woodgate, R., and Goodman, M. F. (2002). Replication restart in UV-irradiated *Escherichia coli* involving pols II, III, V, PriA, RecA, and RecFOR proteins. *Mol. Microbiol.* **43**, 617–628.

Biography

Dr. Judith Campbell is a Professor of Biology and Chemistry at the California Institute of Technology. In the 1970s her laboratory made contributions to the studies of the regulation of DNA replication of episomes in bacteria. Currently her laboratory studies include DNA replication and control of the cell cycle in the yeast *Saccharomyces cerevisiae*, with emphasis on DNA polymerases and DNA helicases.

DNA Polymerase III, Bacterial

Hisaji Maki
Nara Institute of Science and Technology, Ikoma, Japan

DNA polymerase III holoenzyme (pol III HE) is an enzyme that catalyzes elongation of DNA chains during bacterial chromosomal DNA replication. Bacterial cells contain several distinct DNA polymerases. In *Escherichia coli*, five DNA polymerases have been found and designated as DNA polymerase I to V in the order of their discovery. The main function of the third polymerase, pol III, is duplication of the chromosomal DNA, while other DNA polymerases are involved mostly in DNA repair and translesion DNA synthesis. Together with a DNA helicase and a primase, pol III HE participates in the replicative apparatus that acts at the replication fork. Unlike other bacterial DNA polymerases, pol III HE is a multisubunit complex, in which twin catalytic subassemblies, called the pol III core, are embedded with several other auxiliary subunits. Cooperative and coordinated action of these subunits enables pol III HE to function as the chromosomal replicase, concurrently synthesizing the leading and lagging strands of DNA. DNA synthesis by pol III HE is also characterized by a rapid chain-elongation reaction, high processivity, and high fidelity, all of which are essential for chromosomal DNA replication.

Replicative Apparatus in Bacterial Cells

In bacterial cells, the circular chromosome contains a unique origin, and DNA replication proceeds bidirectionally from the origin to the terminus. Replication of the whole bacterial genome (4700 kb for *E. coli*) is continuous from the origin to the terminus, and is accompanied by movement of the replicating point, called the replication fork. Both parental DNA strands are concurrently replicated at the fork. Since DNA polymerase can extend a DNA chain only in the $5' \rightarrow 3'$ direction, replication at a fork is semi-discontinuous: DNA synthesis is continuous on one strand (the leading strand) and discontinuous on the other (the lagging strand). Short pieces of DNA, called Okazaki fragments, are repeatedly synthesized on the lagging strand template. These Okazaki fragments are a few thousand nucleotides long in bacterial cells.

DNA replication is a complex process, involving numerous enzymes at the replication fork. In *E. coli*, more than 20 different proteins participate in DNA replication. Among these proteins, DnaB, DnaG, and pol III HE are the three basic components acting at the replication fork, forming a multiprotein complex called the "replisome" (Figure 1). The DnaB protein is a major replicative DNA helicase which moves along the lagging strand in the $5' \rightarrow 3'$ direction and opens up the duplex DNA at the tip of the replication fork to expose a pair of single-stranded DNA templates. The DnaG protein is a primase which synthesizes a short RNA to prime DNA chain elongation catalyzed by pol III HE.

The highly organized and remarkably efficient process needed for replicating chromosomal DNA is achieved by physical and functional interactions among these three components. Pol III HE associates with DnaB protein and pushes the helicase forward as it proceeds along the leading strand. Thus, the velocity of replication fork movement is determined mainly by the rate of chain elongation by pol III HE, $\sim$1000 bp s^{-1}. DnaB interacts with DnaG and activates cyclically the primase activity as the helicase moves along the lagging strand, resulting in timely initiation of Okazaki fragment synthesis. Finally, the proper recruitment of pol III HE to the replisome requires an RNA primer formed within the origin and, thus, depends upon the function of DnaG.

In bacterial cells, pol III HE and the other components of the replisome localize to discrete positions, predominantly at or near the midcell throughout the cell cycle. It is thought that the DNA is threaded through the centrally positioned replisome during duplication, and then extruded from the replisome after duplication.

Subunits and Subassembly of Pol III Holoenzyme

The machine-like action of pol III HE at the replication fork, far more complex than what is necessary for mere DNA polymerization, is based on its subunit structure. Ten different polypeptides form an isolable 17-subunit pol III HE complex in *E. coli*. The whole assembly is very stable while participating in the replisome at

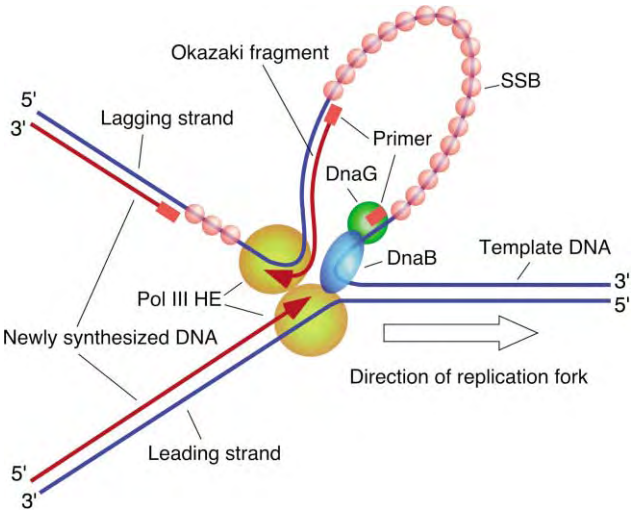

FIGURE 1 The replication fork and three basic components of the replicative apparatus in bacteria.

the replication fork. However, during the course of purification, pol III HE readily disassembles into free subunits and various subassemblies, analyses of which have greatly helped to clarify the biochemical function of each subunit and the architecture of the holoenzyme (Figure 2). Smaller numbers of subunits assemble to form the holoenzyme in *Bacillus subtilis* and other bacterial species, although the basic architecture is conserved in most bacteria.

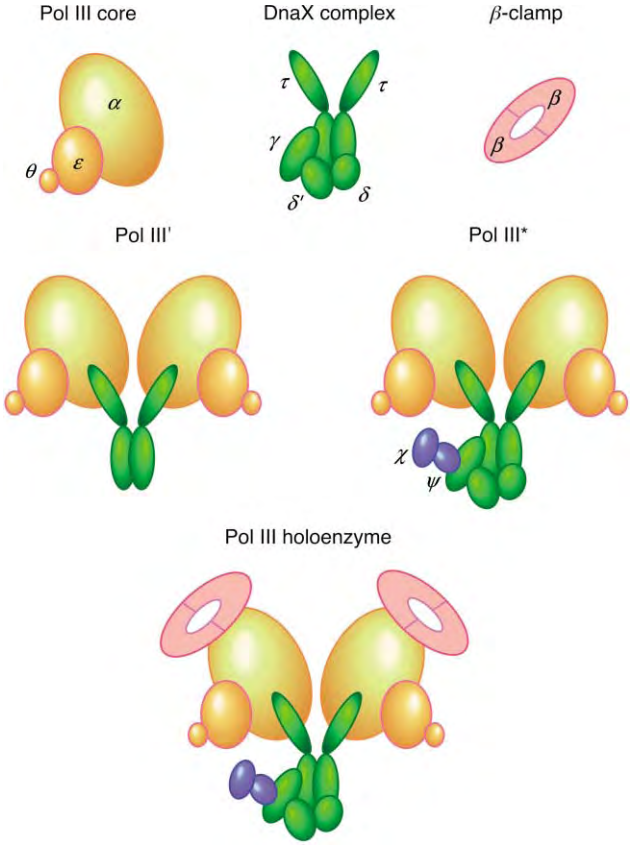

FIGURE 2 A schematic view of the architecture of DNA polymerase III holoenzyme.

Pol III Core

The α-subunit, the largest polypeptide among the holoenzyme subunits, possesses DNA polymerase activity and forms a catalytic core subassembly, called the pol III core, with one molecule each of the ε and θ subunits. The α-subunit shares an amino-acid-sequence motif with bacterial DNA polymerases I and II, and with eukaryotic DNA polymerases α, δ, ε, and ζ, which consists of six segments each containing 5–10 residues. This polymerase motif corresponds to catalytically important structural determinants for the active center of DNA polymerases. Based on small differences in the sequences of this motif, the DNA polymerases are divided into three classes: type A (pol I), type B (pol II and catalytic subunits of the eukaryotic polymerases), and type C (α-subunit of pol III). In contrast to the type A and type B polymerases, the α-subunit lacks the $3' \rightarrow 5'$ exonuclease activity required for the proofreading function, which removes nucleotides that have been incorrectly inserted by the polymerase. In the pol III core, the ε-subunit acts as the editing exonuclease and ensures highly accurate DNA synthesis by the polymerase. Cells that are defective in ε-subunit function show a strong mutator phenotype, with remarkably elevated frequencies of spontaneous mutation.

Although the pol III core has high catalytic efficiencies for DNA synthesis and proofreading, it cannot extend more than 10 nucleotide residues at once. This relatively low processivity of DNA synthesis by the pol III core is due to a low affinity of the core subassembly for template-primer DNA. Other subunits, especially the β-subunit, greatly enhance and regulate the processivity of the core.

τ-Subunit and Pol III′

The τ-subunit is the second largest subunit, and forms a stable homodimer complex when it is free in solution. An important function of the τ-subunit is to make the pol III core into a dimer. The C-terminal domain of the τ-subunit interacts with the α-subunit, and the dimeric nature of the τ-subunit itself facilitates dimerization of the pol III core. The resulting subassembly, called pol III′, consists of two pol III cores and two τ-subunits. The τ-subunit improves the low processivity displayed by the pol III core, resulting in a moderately increased processivity for pol III′.

Besides dimerization of the pol III core, the τ-subunit plays multiple roles at the replication fork. In the HE complex, the τ-dimer bridges between dimeric polymerases and other auxiliary subunits. In addition, as

a scaffold of the replisome, the τ-dimer connects pol III HE and the DnaB helicase at the replication fork.

β-Subunit and Pol III*

Among the holoenzyme subunits, the β-subunit most easily dissociates from the holoenzyme complex. Phosphocellulose or cation-exchange column chromatography effectively separates the holoenzyme into the β-subunit and pol III*, a subassembly that retains all the subunits except β. However, the association of the β-subunit with pol III* is very stable when they form a ternary complex with template-primer DNA.

The β-subunit is a crescent-shaped polypeptide, and forms a homodimer with a doughnut-like structure which encircles double-stranded DNA and slides along the DNA. The β-dimer binds to the α-subunit, even in the absence of other HE-subunits, and it tethers the α-subunit to template DNA during DNA synthesis. The sliding-clamp nature of the β-subunit and the α–β interaction are the basis of the ability of pol III HE to perform highly processive DNA synthesis. The β-subunit also interacts with the δ-subunit in an ATP-dependent manner when β is functioning in the HE complex. Albeit much more weakly than its interaction with the α-subunit, the β-dimer can associate with other proteins including all the other *E. coli* DNA polymerases, a mismatch repair protein (MutS), DNA ligase, and a replication initiator protein (DnaA). Involvement of the β-subunit in many aspects of DNA transactions other than DNA replication has been suggested.

Pol III*, the largest subassembly of pol III HE, consists of two pol III cores, two molecules of τ-subunit, and one molecule each of the $\gamma, \delta, \delta', \chi$, and ψ subunits. The architecture of pol III* is semi-symmetrical. As in pol III′, the τ-dimer connects two pol III cores in a symmetrical configuration. On the other hand, the other five auxiliary subunits impose an asymmetry on the dimeric polymerases. Among these auxiliary subunits, γ, δ, and δ' form a pentameric circular complex (the DnaX complex) with the τ-dimer, while the χ and ψ subunits form another complex that bridges the DnaX-complex and SSB (single-stranded DNA-binding protein).

DnaX Complex

The biochemical function of the DnaX complex is to load the β-clamp on DNA. The δ-subunit directly interacts with the β-subunit and opens the β-ring. Other subunits assist and regulate the action of the δ-subunit. The τ- and γ-subunits are encoded by the *dnaX* gene and, thus, are called DnaX proteins. τ is the full-length translation product, while γ is a truncated protein that arises by translational frameshifting. Hence, the N-terminal portion of τ is identical to that of the γ-subunit. Furthermore, all the subunits of the DnaX complex are structurally related to the AAA^+ ATPase family, although only τ and γ show ATPase activity.

ATP-binding and hydrolysis of ATP are crucial events for the clamp-loading action of the DnaX complex. In the absence of ATP, the five-subunit circular complex is in a tightly closed configuration, and inert for loading the β-subunit. In particular, the δ'-subunit blocks the δ-subunit's interaction with the β-subunit. When all three DnaX proteins in the complex bind ATP, the DnaX complex attains a more relaxed form in which the δ-subunit readily gains access to the β-subunit. Upon association with the δ-subunit, the β-ring is opened and mounted on primer-template DNA. Contact between the β–DnaX-complex and DNA activates hydrolysis of ATP bound to the DnaX-complex, which leads to dissociation of β from the δ-subunit, leaving the closed β-ring on the primer-template DNA.

Pol III HE in Other Bacteria

Genes encoding the subunits of pol III HE have been identified in the genomes of many species of eubacteria. Among these genes, those encoding the $\alpha, \beta, \tau, \delta$, and δ'-subunits are well conserved, while those for other subunits seem to be significantly divergent or lost. In many bacterial species, the *dnaX* gene does not show an obvious frameshifting signal sequence and, therefore, likely produces only the τ-subunit as a single DnaX protein. A group of bacterial species (gram-positive, G + C low) including *B. subtilis*, *Staphylococcus aureus*, and *Streptococcus pyogenes* possess two distinct type-C DNA polymerases, both of which are required for chromosomal replication. Despite the apparent diversity among different species, analyses of pol III HE in bacterial species that are evolutionarily distant from *E. coli* have demonstrated that the basic architecture and biochemical functions of pol III HE are common throughout the eubacteria.

Concurrent DNA Synthesis of Leading and Lagging Strands

In vitro reconstitution of the replisome with purified pol III*, β-subunit, DnaB helicase, DnaG primase, and SSB has indicated that a single pol III HE particle can simultaneously synthesize both leading and lagging strands at a replication fork. Pol III HE is a functionally and structurally asymmetric complex with twin polymerases, one of which participates in leading-strand synthesis and the other in lagging-strand synthesis. The leading-strand polymerase remains continuously

clamped to DNA, but the lagging-strand polymerase is repeatedly clamped and unclamped from DNA, to cycle from one Okazaki fragment to the next. Since the lagging-strand polymerase is held at the replication fork via the τ-subunit bridge and the leading-strand polymerase, retargeting of the lagging-strand polymerase to the next primer is so efficient and rapid that the overall rate of lagging strand synthesis matches the rate of leading strand synthesis (Figure 3).

Pol III HE is initially loaded on the chromosome DNA after the first RNA primer is synthesized within or near the replication origin. One polymerase clamped on the initial RNA primer becomes the leading polymerase, and the other polymerase in the same HE complex serves

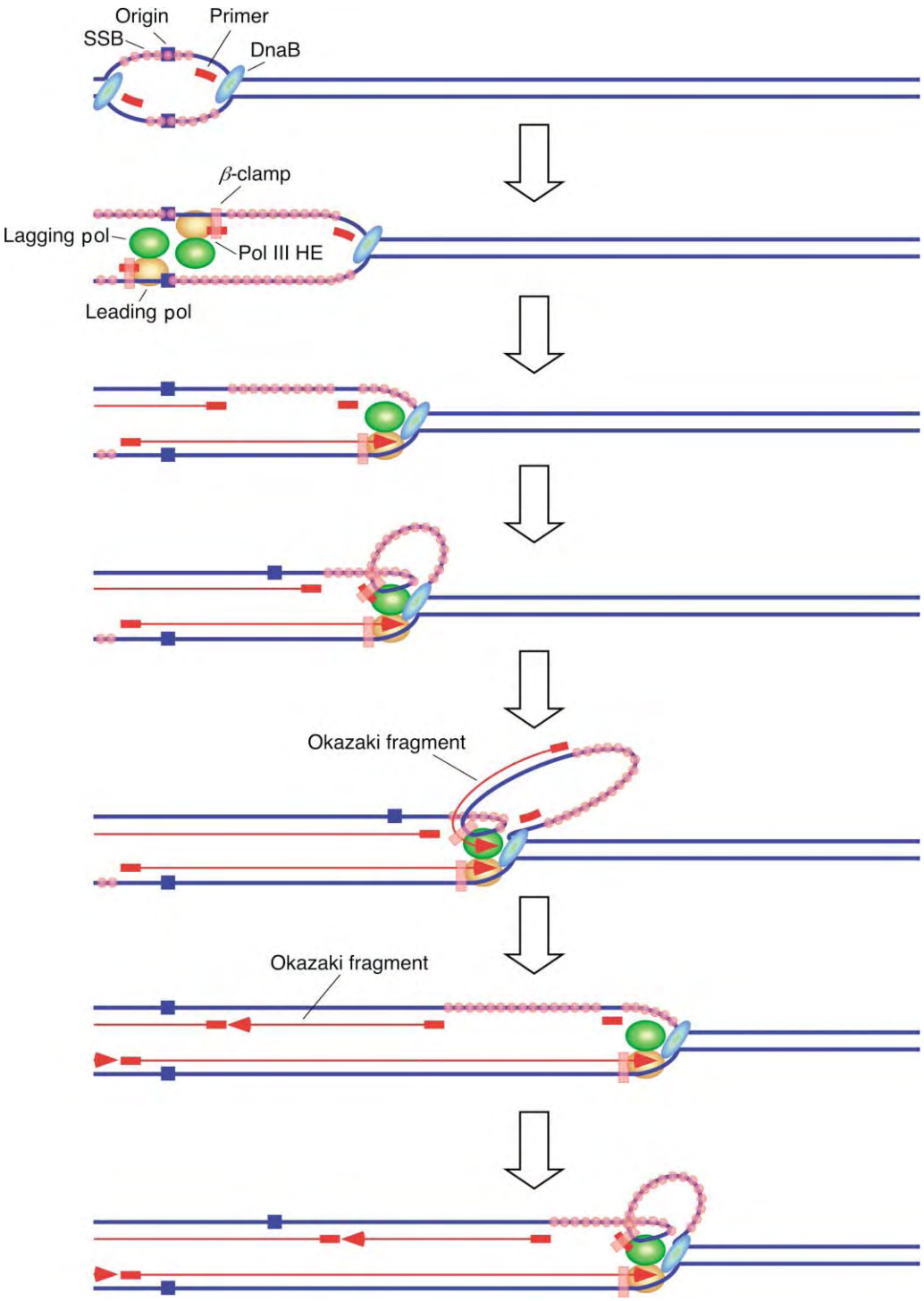

FIGURE 3 Concurrent DNA synthesis of leading and lagging strands by the bacterial replisome.

as the lagging polymerase. An asymmetric arrangement of the DnaX complex in pol III HE is the basis for the functional asymmetry of the replicative polymerase. It has been hypothesized that the position of the DnaX complex is biased to the lagging polymerase, which limits its clamp-loading activity exclusively to the lagging strand.

Other Biological Functions

Almost all plasmids, and the majority of bacteriophages, use pol III HE for their DNA replication. Pol III HE is involved in several kinds of DNA transactions that require synthesis of relatively long segments of DNA. These include long-patch nucleotide excision repair, *mutS*-dependent mismatch repair, homologous recombination, and replicative translocation of transposons.

See Also the Following Articles

DNA Helicases: Dimeric Enzyme Action • DNA Helicases: Hexameric Enzyme Action • DNA Mismatch Repair and the DNA Damage Response • DNA Mismatch Repair in Bacteria • DNA Polymerase I, Bacterial • DNA Polymerase II, Bacterial • DNA Topoisomerases: Type III–RecQ Helicase Systems • recQ DNA Helicase Family in Genetic Stability

Glossary

AAA$^+$ ATPase family An extension of the AAA (for ATPases associated with a variety of cellular activity) family, originally defined to include proteins with a common ~200 residue ATPase core.

mismatch repair A class of DNA repair that corrects mispairs and small bulge structures in DNA, which are caused mainly by replication errors.

mutator A phenotype showing an increased rate of spontaneous mutation, which is caused by a mutation within one of the genes for maintenance of replicational fidelity or repair of spontaneous damage to DNA and substrate nucleotides.

nucleotide excision repair A class of DNA repair by which a segment of DNA containing lesions is excised and replaced with resynthesized DNA.

translesion DNA synthesis A cellular process involving specialized DNA polymerases that counteract the replication-blocking damage to DNA.

Further Reading

Kelman, Z., and O'Donnell, M. (1995). DNA polymerase III holoenzyme: Structure and function of a chromosomal replicating machine. *Annu. Rev. Biochem.* **64**, 171–200.

Kornberg, A., and Baker, T. (1992). *DNA Replication,* 2nd edition. Freeman, New York.

Marians, K. J. (1992). Prokaryotic DNA replication. *Annu. Rev. Biochem.* **61**, 673–719.

McHenry, C. S. (1988). DNA polymerase III holoenzyme of *Escherichia coli*. *Annu. Rev. Biochem.* **57**, 519–550.

Biography

Dr. Hisaji Maki is a Professor in the Department of Molecular Biology at the Nara Institute of Science and Technology in Ikoma, Japan. His principal research interests are in maintenance of genetic information, spontaneous mutagenesis, and chromosome aberration. He holds a Ph.D. from Kyushu University and received his postdoctoral training in Professor Arthur Kornberg's laboratory at Stanford University. He has isolated and analyzed several mutator genes in *E. coli*, including *dnaE* and *dnaQ* which encode the α- and ε-subunits of pol III holoenzyme, respectively.

DNA Polymerases: Kinetics and Mechanism

Kenneth A. Johnson
University of Texas, Austin, Texas, USA

Polymerases can replicate DNA with extraordinary speed and fidelity, copying a template strand at a rate of 300 base pairs per second and making a mistake only one time out of a million. When the polymerase does make a mistake, it stalls by slowing the incorporation of the next correct base pair on top of the mismatch, giving time for a proofreading exonuclease to remove the mismatched base. Selective removal of mismatched bases by the proofreading exonuclease contributes an additional factor of ~1000, resulting in a net fidelity of approximately one error in a billion bases copied. Not all polymerases achieve such high fidelity, however. Rather, each polymerase has evolved a fidelity that balances the biological needs for stability and adaptability. Although the fidelity varies greatly among the polymerases that have been examined in detail, the pathway by which a correct base pair is selected remains invariant. This article briefly summarizes our understanding of the kinetic, structural, and thermodynamic bases governing the fidelity of DNA replication.

Elementary Steps in Polymerization

The free energy difference between a correct and incorrect base pair is quite small (1–2 kcal/mole), which leads to a selectivity factor of only 5–30 in favoring the correct base pair over a mismatch. Therefore, the polymerase does not simply stitch together base pairs that form in solution; rather, the fidelity of DNA replication is largely a function of the kinetics of the reactions, involving nucleotide binding, recognition, and incorporation. The polymerase uses not only the base pair free energy but also the base pair geometry in selecting the correct base pair. The new base pair is buried at the active site of the polymerase, shielding it from water molecules, which enhances the free energy difference between correct and incorrect base pairs and facilitates rapid catalysis.

DNA polymerases achieve their extraordinary fidelity by using a two-step nucleotide-binding sequence to select the proper nucleotide for incorporation, as shown in Figure 1.

The deoxynucleoside triphosphate (dNTP) initially binds in a rapid equilibrium reaction to an "open" state of the enzyme to form the "ground state" complex (E·DNA·dNTP). A correct base pair enables a change in enzyme structure (at rate k_2) to a "closed" form in which the active catalytic residues are brought in to the proper orientation necessary for catalysis of the chemical reaction (at rate k_3). This two-step nucleotide-binding sequence is important for two reasons. First, the binding of the nucleotide to the open enzyme form allows a rapid selection of the correct base pair from the four competing nucleotides in solution, using base pair free energy to favor the correct base. Second, the conformational change in the enzyme to the closed form provides additional selectivity dependent upon the proper base pair geometry, and it leads to a close alignment of protein residues around the reactants, shielding them from solvent and bringing about rapid catalysis. A mismatched base pair is discriminated against at each step in the sequence. An incorrect base binds weaker in the ground state, inhibits the rate of the conformational change, and may lead to a misalignment of the reactive groups necessary for catalysis, leading to a much slower rate of incorporation.

Selectivity Contributions of Each Step

Fidelity varies greatly for different DNA polymerases. The DNA polymerase responsible for replicating the viral genome of HIV (human immunodeficiency virus), known as reverse transcriptase (RT) because it copies RNA templates as well as DNA, has a much lower fidelity, making one mistake in only 10,000 base pairs. This higher error rate is essential for the survival of HIV by affording a fast mutation frequency that gives the virus the ability to evade the immune system and all modern drugs, by constantly changing and evolving resistance via the process of natural selection.

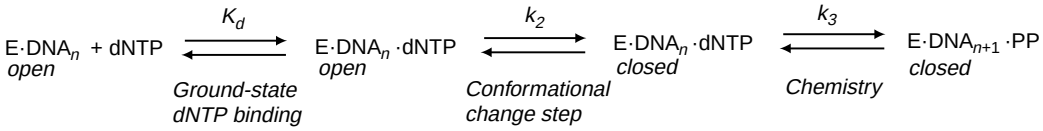

FIGURE 1 Pathway of nucleotide binding and incorporation.

In contrast, the human DNA polymerase responsible for replicating the mitochondrial genome has an intermediate fidelity, making one error in 300,000; with proofreading, the error frequency is increased to one error in 1.5 million.

Table I shows the net selectivity observed in each step of the reaction for several polymerases. It is interesting to note that each of the polymerases shows a nearly constant selectivity of approximately 200–300 for the ground state nucleotide binding, whereas the selectivity afforded by the conformational change step (and ensuing chemistry step) contributes a widely varying selectivity. For a high-fidelity enzyme such as T7 DNA polymerase, the selectivity in the second step is 5000, leading to a net fidelity of 1.5 million. In contrast, the HIV RT shows a selectivity factor of only 50 in the conformational change step, leading to an average overall fidelity of only 13,000. Effectively, HIV RT makes at least one error each time it replicates the 9 kb viral genome, allowing the virus to rapidly evolve to evade the host immune system and any single antiviral drug. Its low fidelity is due to the small contribution of the conformational change and/or chemistry toward the net fidelity. Moreover, because HIV RT lacks a proofreading exonuclease, once a mismatch is incorporated it is not readily removed.

Measurement of the Kinetics of Incorporation

Measurement of the kinetics of DNA polymerization is complicated by the processivity of the enzyme, defined by the tendency of the polymerase to remain bound to the DNA template/primer and to continue multiple rounds of polymerization (Table II). The processivity is calculated by the rate of polymerization divided by the rate of dissociation of the E·DNA complex and is equal to the average number of bases incorporated before the complex dissociates. Although polymerization can be quite fast (50–300 s^{-1}), the rate of dissociation is slow (typically 0.02–0.2 s^{-1}). Therefore, in the measurement of the kinetics of incorporation of a single nucleotide in the steady state with an excess of DNA and limiting enzyme, the rate that is measured is due solely to the dissociation reaction and provides no information pertaining to the nucleotide incorporation reaction, unless incorporation is slower than DNA dissociation. Therefore, steady-state rate measurements are virtually meaningless. To circumvent these difficulties, the kinetics of incorporation are measured by examining the rate of extension using single-turnover kinetic methods. A stoichiometric E·DNA complex is rapidly mixed with the correct dNTP and Mg^{2+} and then quenched by mixing with EDTA to chelate metal ions needed for catalysis. The time course of extension of the DNA by one base pair is then quantified after resolution on a DNA sequencing gel.

To resolve the time dependence of extension, the reaction must be examined on the time scale of a single turnover, which usually is in the range of milliseconds. Definitive experiments require a rapid mixing device to achieve rapid mixing of small volumes. Compared to experiments using steady-state kinetic methods, single-turnover kinetic experiments may be slightly more difficult to perform, but they can be interpreted directly and often unambiguously. The nucleotide concentration dependence of the rate of the incorporation in the single-turnover reaction defines the maximum rate of incorporation, k_{pol}, which may be limited by k_2, k_3, or a combination of the two steps (Figure 1) and the ground state nucleotide dissociation constant, K_d. Because the nucleotide binding is a rapid equilibrium reaction and k_{pol} is the single, rate-limiting step in polymerization, the ratio of k_{pol}/K_d is equal to k_{cat}/K_m, the specificity constant for the reaction. Thus, this one experiment defines the key kinetic parameter governing nucleotide selectivity and resolves it into the two steps contributing to fidelity, the ground state nucleotide dissociation constant and the rate of incorporation, k_{pol}. Most importantly, these methods provide a measurement of

TABLE I

Fidelity Contributions of Ground State Binding and Polymerization[a]

Polymerase	$K_{d,inc}/K_{d,cor}$	$k_{pol,cor}/k_{pol,inc}$	Overall fidelity
T7 DNA polymerase	300	5,000	1,500,000
Pol γ DNA polymerase	200	1,500	300,000
Klenow	170	2,300	210,100
Pol β	290	610	19,700
HIV RT	260	50	13,000

[a] The average contribution of ground state binding ($K_{d,inc}/K_{d,cor}$) and the maximum rate of polymerization ($k_{pol,cor}/k_{pol,inc}$) to the net fidelity are shown for various polymerases, where *inc* represents an incorrect while *cor* represents a correct nucleotide, respectively.

TABLE II

Kinetics of Polymerization

Polymerase	K_d (nM)	k_{pol} (s^{-1})	k_{pol}/K_d ($\mu M^{-1}s^{-1}$)	k_{off} (s^{-1})	Processivity	$K_{d,DNA}$ (nM)
T7 DNA polymerase	18	300	15	0.2	1500	18
Pol γ DNA polymerase	0.8	40	50	0.02	2250	10
Klenow	5	50	5	0.2	250	5
Pol β	10	10	1	0.3	30	50
HIV RT	4	30	8	0.2	150	5

the equilibrium constant for the binding of the substrate to the enzyme in a complex that is poised for catalysis.

Structural Determinants of Fidelity

The structure of T7 DNA polymerase in the closed complex is shown in Figure 2. The E·DNA·dNTP closed complex was formed with the correct dNTP and a dideoxy-terminated DNA primer/template to prevent the chemical reaction from occurring. It shows the tight arrangement of the protein around the DNA and the dNTP poised for the chemical reaction to proceed. The DNA lies largely on the surface of the protein, making contacts through the phosphodiester backbone. As the DNA approaches the active site, the structure changes from standard B-DNA to an A-form DNA with a more open minor groove that allows contacts with several residues that are thought to be important for sensing mismatches in the incoming base pair as well in the primer/template. Also important to note is that the next residue in the template strand is rotated out from the active site at 90°, and protein residues stack with both the templating base and the incoming dNTP. These contacts are all thought to be important in enforcing the proper base pair geometry.

Comparison of the T7 DNA polymerase closed complex with the structures of other polymerases in

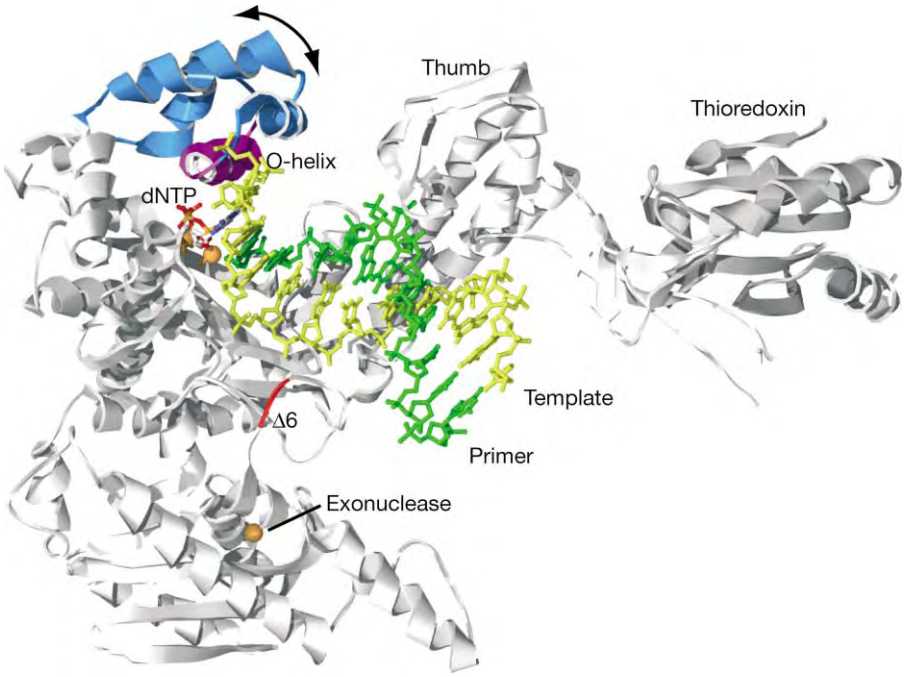

FIGURE 2 Structure of T7 DNA polymerase. The structure shows the "closed" complex resulting from the rotation (arrow) of the recognition domain (blue) to bring the O-helix (magenta) into contact with the incoming dNTP (CPK colors). The template strand is shown in yellow, the primer strand in green, and the thioredoxin accessory protein in gray. The two metal ions at the polymerase active site and the single metal ion at the exonuclease site are shown in gold. The location of the six-residue deletion (Δ6) to create the exo-mutant is shown in red. Drawn from Protein Data Bank structure file 1T7P.

the E·DNA state reveals that there is a large conformational change in a nucleotide recognition domain involving a 45° rotation to bring key residues into contact with the dNTP at the active site. Included among these residues are positively charged lysine and arginine, amino acids that bind to the β- and γ-phosphates to facilitate catalysis, and a tyrosine that stacks with the dNTP to help align the reaction center. This conformational change step provides the most significant contribution to nucleotide selectivity by sensing the proper base pair geometry and leading to fast catalysis of the chemical reaction.

Chemistry of Catalysis

A close-up view of the reaction center is shown in Figure 3. Two tetrahedrally coordinated Mg^{2+} ions are ligated by conserved acidic residues at the active site (D475 and D654), orient the reactants, and facilitate catalysis. Metal A activates the 3′ OH and is ligated to the non-bridging oxygen of the α-phosphate of the incoming dNTP, while metal B is ligated to non-bridging oxygens of α-, β-, and γ-phosphates and stabilizes the pyrophosphate leaving group as the reaction proceeds.

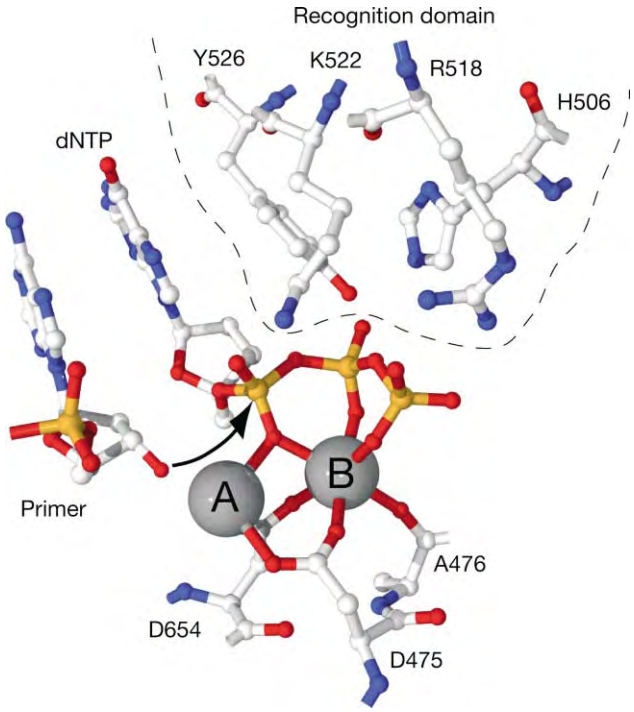

FIGURE 3 Two-metal ion mechanism. A close-up view of the active site shows the 3′ OH of the terminal base in position to react with the incoming dNTP, bound to the two metal ions. Residues from the recognition domain contact the incoming dNTP to facilitate catalysis. Drawn from Protein Data Bank structure file 1T7P.

This two-metal ion mechanism appears to be common for all polymerases.

Catalysis is also critically dependent upon contacts made involving residues from the recognition domain. Positively charged residues K522, H506, and R518 contact the α-, β-, and γ-phosphates, respectively; and Y526 stacks against the incoming dNTP. These contacts are formed following the conformational change and facilitate catalysis by binding and orienting the dNTP for reaction and stabilizing the development of negative charge on the pyrophosphate. Thus, the structure provides a rationale for the importance of the conformational change in nucleotide selectivity and incorporation efficiency.

Selectivity of the Proofreading Exonuclease

The polymerase contains a proofreading function to efficiently remove mismatches after they are formed. This is accomplished by the polymerase recognizing it has made an error by stalling in its attempt to insert the next correct base on top of the mismatch to give time for the primer strand to flip over into the exonuclease site to have the 3′-terminal base excised. Although the exonuclease active site is 25 Å away from the polymerase site (see Figure 2), the DNA primer strand is able to flip back and forth between the two sites.

The selectivity of the exonuclease is governed by kinetic partitioning between the polymerase and exonuclease active sites, with the decision to excise being made at the polymerase site. As summarized in Figure 4, during successive correct nucleotide incorporation reactions, the polymerase continues down the DNA template, inserting bases at a rate of $300\ s^{-1}$. Occasionally, the DNA will dissociate from the polymerase or flip into the exonuclease site at a rate of $0.2\ s^{-1}$. Therefore, the cost of having a proofreading exonuclease site next to the polymerase active site is $0.2/(300 + 0.2) = 0.07\%$ of the correct nucleotides removed after correct incorporation. However, after the polymerase inserts a mismatched dNTP (occurring at an infrequent rate of $0.002\ s^{-1}$), the rate of incorporation of the next correct base on top of the mismatch is reduced to $0.012\ s^{-1}$, while the rate at which the primer flips over into the exonuclease site is increased to $2.3\ s^{-1}$. The probability of removing the mismatch increases to $2.3/(2.3 + 0.012) = 99.5\%$. Thus, the kinetic partitioning defining the relative probability of reaction at the polymerase and exonuclease sites is inverted when the polymerase encounters a mismatch in the primer/template.

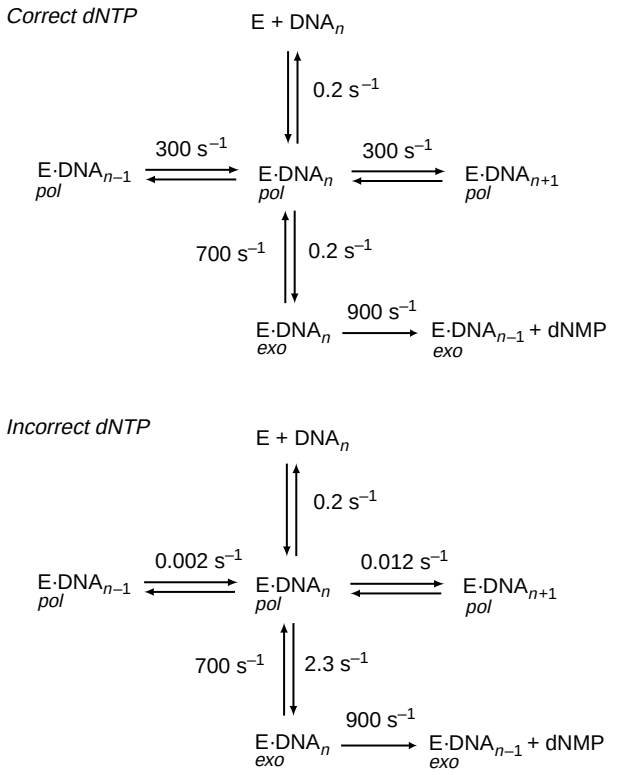

FIGURE 4 Kinetic partitioning for exonuclease proofreading. The changes in the rates of polymerization and exonuclease removal for correct and incorrect base pairs are summarized. Correct base pairs are incorporated sequentially at a rate of 300 s^{-1}, while occasionally the DNA will dissociate (0.2 s^{-1}) or slide into the exonuclease site (0.2 s^{-1}). Mismatches are incorporated at a slow rate (0.002 s^{-1}) and extension to incorporate the next correct base is also slow (0.012 s^{-1}), but the rate of sliding into the exonuclease site is increased to 2.3 s^{-1}. This change in kinetic partitioning leads to selective removal of mismatches based upon testing for proper base pairing at the polymerase site.

The dynamics of the reaction provides a perfect solution to the problem of designing a proofreading function. A single-stranded primer in the exonuclease site is needed to excise the 3′-terminal base, but the DNA must be in duplex form in order to know whether the base pair is correct. According to the kinetics, the DNA spends most of the time at the polymerase site and makes only brief excursions to the exonuclease site, by melting out a single-stranded segment of the primer strand sufficient to reach the exonuclease site 25Å away. The decision as to whether to remove a base pair is made solely at the polymerase site, based upon the ability of the enzyme to sense a mismatch in the primer template and inhibit the rate of forward reaction, thereby changing the probability of excision versus extension.

It is interesting to note that the binding of the next correct base pair is not significantly impaired with a mismatch in the primer/template; rather, the rate of the conformational change and/or the chemical reaction is reduced by the presence of a mismatch. This again is in keeping with the postulate that one purpose of the conformational change step is to test for mismatches. The proofreading selectivity demonstrates that the polymerase is capable of sensing a mismatch not only in the incoming base pair but also at the adjacent position in the primer/template, and this ability is used to increase the selectivity at each step.

Summary

DNA polymerases are remarkable machines central to the replication of all life forms on earth. The fidelity of different DNA polymerases varies widely in order to meet the requirements of the biology in balancing the conflicting needs for stability and adaptability. All polymerases studied in sufficient detail show a similar two-step binding mechanism to select the correct base pair using both the base pair free energy and base pair geometry.

See Also the Following Articles

DNA Polymerase α, Eukaryotic • DNA Polymerase β, Eukaryotic • DNA Polymerase δ, Eukaryotic • DNA Polymerase ε, Eukaryotic • DNA Polymerase I, Bacterial • DNA Polymerase II, Bacterial • DNA Polymerase III, Bacterial • Exonucleases, Bacterial • Reverse Transcriptase and Retroviral Replication • Translesion DNA Polymerases, Eukaryotic • umuC,D Lesion Bypass DNA Polymerase V

Glossary

discrimination The ratio of the specificity constant for a correct base pair divided by that for a particular mismatch.

fidelity The reciprocal of the error frequency; for example, an error frequency of 0.000002 is expressed as a fidelity of one error in 500,000.

proofreading exonuclease An exonuclease that removes a single base from the 3′ end of the primer strand.

selectivity The fidelity contribution of individual constants; for example, the selectivity in the ground state binding is equal to the ratio of the K_d for the incorrect dNTP divided by the K_d for the correct dNTP binding.

specificity constant The apparent second-order rate constant for nucleotide binding and incorporation, defined by the steady-state kinetic parameters, k_{cat}/K_m, but more accurately measured using pre-steady-state kinetic methods to define k_{pol}/K_d, where k_{pol} is the maximum rate of incorporation and K_d is the apparent ground state nucleotide dissociation constant.

Further Reading

Doublie, S., Tabor, S., Long, A. M., Richardson, C. C., and Ellenberger, T. (1998). Crystal structure of a bacteriophage T7 DNA replication complex at 2.2 A resolution. *Nature* **391**, 251–258.

Johnson, K. A. (1993). Conformational coupling in DNA polymerization. *Ann. Rev. Biochem.* **62**, 685–713.

Johnson, A. A., and Johnson, K. A. (2001). Fidelity of nucleotide incorporation by human mitochondrial DNA polymerase. *J. Biol. Chem.* **276**, 38090–38096.

Johnson, A. A., Ray, A. S., Hanes, J., Suo, Z., Colacino, J. M., Anderson, K. S., and Johnson, K. A. (2001). Toxicity of antiviral nucleoside analogs and the human mitochondrial DNA polymerase. *J. Biol. Chem.* **276**, 40847–40857.

Lee, H., Hanes, J., and Johnson, K. A. (2003). Toxicity of nucleoside analogs used to treat AIDS and the selectivity of the mitochondrial DNA polymerase. *Biochemistry* **42**, 14711–14719.

Spence, R. A., Kati, W. M., Anderson, K. S., and Johnson, K. A. (1995). Mechanism of inhibition of HIV-1 reverse transcriptase by nonnucleoside inhibitors. *Science* **267**, 988–993.

Biography

Kenneth A. Johnson is the Roger J. Williams Centennial Professor of Biochemistry at the University of Texas at Austin. His research focus is on the mechanistic and kinetic basis for DNA polymerase selectivity, especially as it pertains to the effectiveness and toxicity of drugs used to combat viral infections, especially HIV and HCV. He holds a Ph.D. from the University of Wisconsin and received postdoctoral training at the University of Chicago. He is President and CEO of KinTek Corporation, a company he founded to manufacture instruments that he designed to examine enzyme reaction kinetics on the millisecond time scale.

DNA Replication Fork, Bacterial

Nancy G. Nossal
National Institutes of Health, Bethesda, Maryland, USA

The complete duplex DNA chromosome of bacteria is replicated before each cell division. In *E. coli* the length of the single circular chromosome is 4.6×10^6 base pairs, and it can be copied in 40 min in rich media. Replication of bacterial DNA is thus rapid and is also extremely accurate. The error frequency during *E. coli* replication is estimated to be about 10^{-7}, before additional correction by the mismatch-repair system. The timing of replication must be coordinated with the cell division cycle, and the synthesis of the two strands of the DNA duplex must be coordinated with each other. Replication in *E. coli* is initiated when the dnaA protein binds to a specific DNA sequence, the *oriC* origin, beginning a series of reactions in which the DNA duplex is opened to allow the binding of the other replication proteins. Replication from the origin is bidirectional, so that two replication forks moving in opposite directions are established. DNA synthesis at each fork is accomplished by a complex of many proteins, called the replisome. It includes the leading- and lagging-strand DNA polymerases, and their associated polymerase clamps and clamp loader, collectively known as the polymerase holoenzyme, which synthesize the new DNA on each strand. The replisome also contains a primosome with a primase to make short RNA chains to initiate new DNA fragments, a helicase to unwind the parental duplex, and a helicase loading protein.

The Two Strands of the DNA Duplex are Copied by Different Mechanisms

The two strands of a DNA duplex have opposite polarity, one goes 5′–3′ and the other 3′–5′ (Figure 1). All known DNA polymerases add new nucleotides only to the 3′ end of the chain. The parent strand that runs 3′–5′ is called the leading-strand template and serves as a template for the continuous synthesis of the new leading strand, which grows in the 5′–3′ direction. The lagging-strand template runs 5′–3′, so that the polymerase copying this strand moves away from the fork. However, microscopic studies have shown that the most recently replicated DNA on each strand is located close to the fork. On the lagging strand this is accomplished by a discontinuous mechanism of replication in which the polymerase makes short fragments that begin near the fork and extend for 1000–3000 bases (Figure 1). These fragments, which are often called Okazaki fragments in honor of their discoverer, are subsequently joined to each other by DNA ligase. Since DNA polymerases cannot begin new chains, each fragment is started by a short RNA chain (primer) that is made by a specialized RNA polymerase called a primase. To allow synthesis on the leading and lagging strands to be coordinated, Bruce Alberts proposed that the lagging strand folds into a loop, bringing the two polymerases together (Figure 2). This has been called a trombone replication model, because the expansion of the loop as each fragment is synthesized resembles a trombone slide.

Proteins Required for DNA Replication

Much of our current understanding of bacterial replication comes from the characterization of the replication system of *E. coli*, and the simpler but mechanistically similar systems of the *E. coli* bacteriophage T7 and T4. The classes of proteins needed at the fork are shown in Figure 2, and the specific proteins in these three replication systems are shown in Table I.

DNA Polymerase Holoenzymes

The distinguishing feature of a replicative DNA polymerase is that it is highly processive, which means that it can incorporate thousands of nucleotides each time it binds to the template. *E. coli* polymerase III and T4 polymerase remain bound because they are connected to circular-clamp proteins that surround the duplex and move with the polymerase. These clamp proteins are in turn loaded on the DNA by multisubunit complexes of proteins called clamp loaders. *E. coli* Pol III holoenzyme can be isolated as a complex containing a leading and a lagging DNA polymerase core, two clamps, and a single multi-subunit clamp loader. The clamp loader (γ-complex) is physically attached to each polymerase by the C-terminal domain of the one of two τ-subunits in

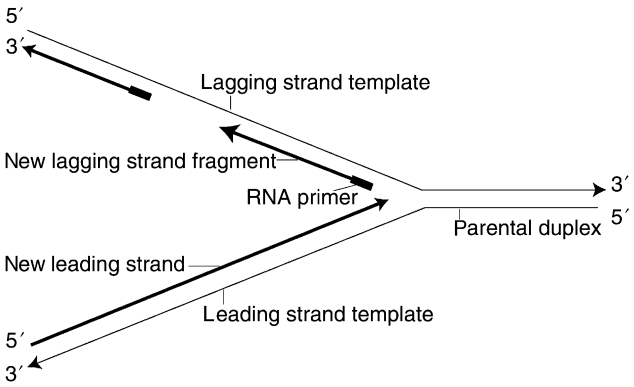

FIGURE 1 Synthesis of the leading- and lagging-strands at a DNA replication fork. Because the two strands in a DNA duplex are antiparallel (run in opposite directions), and strands grow by addition of nucleotides to the 3′ end, the lagging strand is made by the synthesis of short fragments that are then joined together. Light lines: parental DNA template; heavy lines: new DNA.

the complex, and travels with the polymerases. The T4 proteins are less tightly connected, and are isolated as separate proteins. There is evidence that the two T4 polymerases at the fork do interact with each other at least transitorily. T7 DNA polymerase is isolated as a complex with *E. coli* thioredoxin, which increases the processivity of the polymerase.

Primosomes

In the bacterial replication systems there is a close physical and functional relationship between the primase that makes the very short RNA chains (4–12 b) initiating each lagging-strand fragment and the helicase that unwinds the duplex ahead of the leading-strand polymerase. The length and sequences of the primers are different in each of these systems. The bacterial replicative helicases are hexamers that surround the lagging-strand template strand, and move 5′–3′ on that strand to unwind the duplex by a reaction that requires hydrolysis of nucleotide triphosphates. The loading of the *E. coli* dnaB helicase is promoted by dnaC protein, which is thought to open the preformed helicase hexamer to allow ssDNA to bind inside. The T4 59 helicase loading protein binds to the replication fork, and facilitates the assembly of the 41 helicase subunits into a hexamer surrounding the lagging-strand template. The T7 helicase and primase activities are both catalyzed by the gene 4 protein, a hexamer with adjoining rings of the primase and helicase domains of the protein.

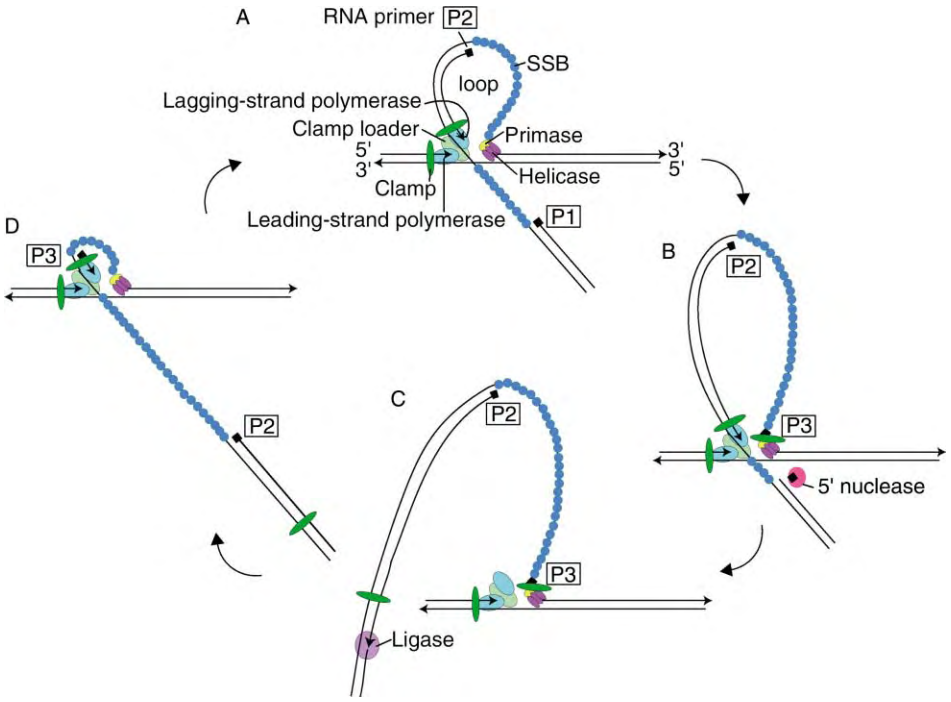

FIGURE 2 Cycle of the reactions on the lagging strand of a bacterial DNA replication fork. The functions of the proteins are described in the text. In this model, the lagging strand has been folded to bring the leading- and lagging-strand polymerases together. (A) Extension of a lagging-strand fragment that began with primer P2 in the early elongation stage. (B) Late elongation-synthesis of a new primer (P3) for the next fragment, and hydrolysis of the primer (P1) from the previous fragment, occur as the nascent fragment is extended. (C) Fragment termination-polymerase is released after it completes the fragment. The clamp is frequently left behind. The nick between fragments is sealed by DNA ligase. (D) Polymerase is transferred to the new primer (P3) to begin elongation of the next fragment. This figure shows the reactions that must be completed in each cycle, but the order of some of the reactions, such as ligation of the adjacent fragments relative to polymerase transfer, has not been established.

TABLE I

Proteins in the *E. coli* and Bacteriophage T4 and T7 DNA Replication Systems

Replication system	*E. coli*	Phage T4	Phage T7
Polymerase holoenzyme	Pol III holoenzyme		
Polymerase	Polymerase core (α, ε, θ)	T4 DNA polymerase (gp43)[a]	T7 DNA polymerase (T7 gp5 + *E. coli* thioredoxin)
Clamp	β (dimer)	gp45 (trimer)	
Clamp loader	γ-complex (γ, τ, τ, δ, δ')	gp44/62 complex	
Primosome			
Primase	dna G	gp61 primase	gp 4[b] (hexamer)
Helicase	dna B (hexamer)	gp41 helicase (hexamer)	gp 4[b] (hexamer)
Helicase loader	dna C (hexamer)	gp59 helicase loader	
ssDNA-binding protein	SSB	gp 32	gp 2.5
5′ nuclease	DNA pol I 5′ nuclease	T4 RNaseH	T7 exo6
DNA ligase	*E. coli* DNA ligase	T4 DNA ligase	T7 DNA ligase

[a] gp stands for gene product. The gene name is 43.
[b] T7 gp4 hexamer catalyzes both primase and helicase reactions.

Kinetic studies of the T7 primase–helicase show that DNA binds first to the primase site on the outside of the ring, before the ring opens to allow the DNA to reach the helicase active site in the center.

Single-Stranded DNA-Binding Proteins

The single-stranded DNA (ssDNA) regions of the lagging strand are covered by tight single-stranded DNA-binding proteins called SSB = s. In addition to protecting the ssDNA from nucleases, SSB proteins bind specifically to several other replication proteins, including polymerases, primases, and in the T4 system, the helicase loading protein, and modulate their activities.

5′–3′ Nucleases and DNA Ligases

The RNA primers on lagging-strand fragments must be removed before the fragments can be joined by DNA ligase. The enzymes responsible for removing the primers are 5′–3′ nucleases that are capable of degrading both RNA:DNA and DNA:DNA duplexes. Thus, they can remove the RNA primers and a short stretch of adjoining DNA from the discontinuous fragments.

DNA Replication Cycle

Leading-Strand Synthesis

The leading strand at the replication fork is synthesized continuously (Figure 2), beginning with an RNA primer that is made, in different systems, by either an RNA polymerase or a primase. Once the leading-strand polymerase and helicase are loaded, this polymerase can in principle remain bound to complete synthesis of the chromosome. The rate of synthesis by the polymerase, and duplex unwinding by the helicase, are much greater when these proteins work together at a replication fork, than when these reactions occur separately. The τ-subunit of the *E. coli* clamp loader connects the polymerase holoenzyme with the helicase. Although synthesis on the leading strand is extremely processive, recent evidence shows that bacterial replication forks frequently stall before completing the chromosome and need to be reassembled.

Lagging-Strand Synthesis

Because the lagging strand is made by joining short fragments, there is a cycle of reactions needed to initiate, elongate, and seal these fragments (Figure 2A–D). These reactions must be coordinated with each other, as well as with the reactions on the leading strand. The lagging-strand cycles are completed in only a few seconds because the fragments are 1000–3000 bases, and replication is proceeding at 400–1000 bases/second.

Early Elongation Stage

In the beginning of the elongation stage of this cycle, the clamped lagging strand polymerase is synthesizing a fragment that began with the primer labeled P2 (Figure 2A). At the same time, the helicase surrounding the lagging-strand template at the fork is unwinding the duplex ahead of the leading-strand polymerase.

SSB proteins coat the ssDNA between the helicase and the nascent elongating fragment, and the ssDNA between the lagging-strand polymerase and the previous fragment. Although the protein-covered ssDNA in Figure 2 is shown as a linear array for simplicity, there is evidence discussed below that it is actually in a more compact structure.

Late Elongation and Primer Synthesis

Each lagging-strand cycle can be completed rapidly because reactions required to prime the next fragment, elongate the present fragment, and remove primers from the previous fragment can occur simultaneously. In the latter part of the elongation stage (Figure 2B) as synthesis of the nascent fragment continues, primase, associated with the helicase at the fork, makes the RNA primer (P3) that will be used to start the next fragment. In the *E. coli* and T4 systems a clamp is loaded on the new primer by the clamp loader. The *E. coli* clamp loader is bound to the two polymerases at the fork, as well as to the helicase, while the clamp is recruited from solution. Dilution experiments suggest that both the T4 clamp and clamp loader must be provided from solution at the beginning of each cycle. At the same time, the $5'-3'$ nuclease is removing the RNA primer (P1) and a small amount of adjacent DNA from the previous fragment. This is the DNA that was first added to the primer, and its removal may increase the accuracy of replication. In the T4 system the SSB (T4 32 protein) between the polymerase and the nuclease increases the rate of these two reactions, and controls the extent of DNA removed along with the RNA primer.

Fragment Termination

When the lagging-strand polymerase completes the nascent fragment (Figure 2C), creating a nick, polymerase is released, but the clamp is frequently left behind on the DNA. In *E. coli*, the C-terminal domain of the τ-subunit of the clamp loader acts as an unloader, releasing the lagging-strand polymerase core from the β-clamp. The T4 proteins are less tightly bound, and there is no evidence that the clamp loader is needed to disengage the clamp and polymerase. If the polymerase fails to be released at the nick, it can continue strand-displacement synthesis, forming a flap from the $5'$ end of the downstream fragment. However, all of the prokaryotic $5'$ nucleases with a role in primer removal have flap endonuclease activities, which can remove these displaced strands. The nicks that are formed between adjacent fragments are sealed by DNA ligase.

Transfer of Polymerase to the New Primer

The *E. coli* lagging-strand polymerase released from the completed fragment remains attached to the clamp loader at the fork, and can be transferred directly to the clamped new primer (P3) to begin synthesis of the next fragment (Figure 2D). Under some conditions, the addition of primase acts as a signal that causes the lagging-strand polymerase to be released prematurely, before the previous fragment is finished. This leaves a gap between fragments that must ultimately be repaired by loading another polymerase. Structural and functional studies of the T7 primase-helicase show that the DNA-binding domain of the primase binds the new primer and transfers it to the lagging-strand polymerase.

Coordination of Leading and Lagging-Strand Synthesis

The *E. coli* leading and lagging-strand polymerases are connected because they are each joined to the same clamp-loading complex. The two polymerases at the T4 and T7 replication fork are not joined through a clamp loader. However, on synthetic templates in which dGTP can only be incorporated into the leading

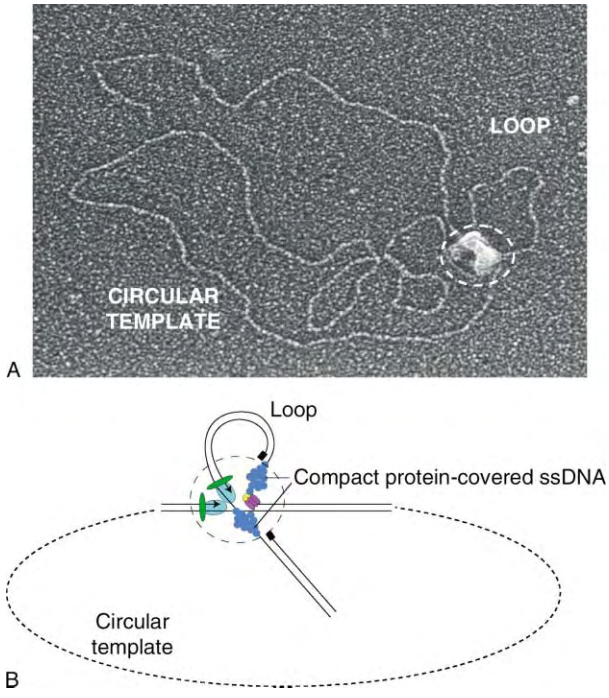

FIGURE 3 The single-stranded DNA on the lagging template is in a compact structure. (A) Electron micrograph of a replication fork with bacteriophage T4 proteins. The loop at the fork is all duplex DNA. The dense complex at the fork contains the replication proteins, as well as protein-covered ssDNA that has been folded into a compact structure. (Adapted from Chastain *et al.* (2003) *J. Biol. Chem.* **278**, 21276). (B) Model of a fork with compact ssDNA. Compare this model with that in Figure 2A.

strand and dCTP into the lagging strand, leading-strand synthesis stopped when a chain terminator was added to block lagging-strand synthesis, indicating a close interaction between the polymerases on the two strands. In addition, dilution experiments suggest that these phage polymerases can recycle from one lagging-strand fragment to the next.

The ssDNA on the Lagging Strand is in a Compact Structure

Electron microscopic analysis of DNA being replicated by the phage T7 or T4 proteins has confirmed that there is a loop at the replication fork, as predicted by the trombone replication model. While the model envisioned that the loops would be composed of the new duplex lagging-strand fragment and the ssDNA behind it (Figure 2A), the observed loops were entirely double stranded (Figure 3). The dense complex at the fork contains the replication proteins, as well as the protein-covered ssDNA folded into a compact structure. The path of the DNA and the proteins in this structure remain to be determined. The compact nature of the lagging-strand template may limit access of the primase and clamp loader, and thus be a factor in controlling when new lagging-strand fragments are initiated.

Replication Factories

Studies of the location of *B. subtilis* DNA polymerase first showed that replisome proteins are concentrated into discrete regions of living cells that have been called replication factories. It is likely that the reactions at a replication fork take place as DNA template is pulled through a stationary replisome, rather than having the replisome proteins move along the DNA.

See Also the Following Articles

DNA Helicases: Hexameric Enzyme Action • DNA Polymerase III, Bacterial • DNA Replication: Initiation in Bacteria • Processivity Clamps in DNA Replication: Clamp Loading • Sliding Clamps in DNA Replication: *E. coli* β-Clamp and PCNA Structure

Glossary

DNA helicase An enzyme that unwinds the two strands of a DNA duplex.

DNA ligase An enzyme that covalently joins two DNA strands together.

DNA polymerase An enzyme that synthesizes DNA by incorporating nucleotides at the 3′ end of the new strand that are complementary to the nucleotides on the strand serving as the template.

lagging strand The strand at the replication fork that is synthesized discontinuously by making shorter fragments that are sealed together by DNA ligase.

leading strand The strand at the replication fork that is synthesized continuously as one long strand.

primase An enzyme that synthesizes the short RNA primers that are used to begin the discontinuous fragments on the lagging strand of a replication fork.

Further Reading

Ahnert, P., Picha, K. M., and Patel, S. S. (2000). A ring-opening mechanism for DNA binding in the central channel of the T7 helicase-primase protein. *Embo. J.* **19**, 3418–3427.

Alberts, B. (2003). DNA replication and recombination. *Nature* **421**, 431–435.

Chastain, P., Makhov, A. M., Nossal, N. G., and Griffith, J. D. (2003). Architecture of the replication complex and DNA loops at the fork generated by the bacteriophage T4 proteins. *J. Biol. Chem.* **278**, 21276–21285.

Davey, M. J., Jeruzalmi, D., Kuriyan, J., and O'Donnell, M. (2002). Motors and switches: AAA+ machines within the replisome. *Nat. Rev. Mol. Cell Biol.* **3**, 826–835.

Kato, M., Ito, T., Wagner, G., Richardson, C. C., and Ellenberger, T. (2003). Modular architecture of the bacteriophage T7 primase couples RNA primer synthesis to DNA synthesis. *Mol. Cell* **11**, 1349–1360.

Kornberg, A., and Baker, T. (1992). *DNA Replication*, 2nd edition. W. H. Freeman, San Francisco.

Lemon, K. P., and Grossman, A. D. (1998). Localization of bacterial DNA polymerase: Evidence for a factory model of replication. *Science* **282**, 1516–1519.

Leu, F. P., Georgescu, R., and O'Donnell, M. (2003). Mechanism of the *E. coli* tau processivity switch during lagging-strand synthesis. *Mol. Cell* **11**, 315–327.

Biography

Dr. Nancy Nossal is Head of the Laboratory of Molecular and Cellular Biology in the National Institute of Diabetes and Digestive and Kidney Diseases at the National Institutes of Health. Her research interests are in understanding the molecular mechanisms of DNA replication, and she has worked extensively with the phage T4 replication system. She holds a Ph.D. in biological chemistry from the University of Michigan and was a postdoctoral fellow at the National Institutes of Health.

DNA Replication Fork, Eukaryotic

Lori M. Kelman
Montgomery College, Germantown, Maryland, USA

Jerard Hurwitz
Memorial Sloan-Kettering Cancer Center, New York, USA

Zvi Kelman
University of Maryland Biotechnology Institute, Rockville, Maryland, USA

During the S phase of the cell cycle, DNA replication duplicates chromosomes into two identical copies, which segregate to daughter cells during mitosis. In DNA replication, a double-stranded molecule of DNA is copied into two daughter molecules. DNA replication occurs at replication forks – structures consisting of DNA and replication proteins that allow the two strands of DNA to be copied accurately and completely.

Introduction

All organisms must replicate their chromosomal DNA in order to propagate their genetic information. During the S phase of the cell cycle, DNA replication duplicates chromosomes into two identical copies that segregate to daughter cells during mitosis. Chromosomal DNA replication begins at regions of the chromosomes called origins of replication and can be divided into three phases: initiation, elongation, and termination. In the initiation stage, an origin recognition protein (ORP) binds the origin of replication and recruits additional initiation factors to the origin. Next the helicase is recruited to the DNA to form the initial replication bubble. The single-stranded DNA (ssDNA) exposed behind the helicase is coated with ssDNA-binding protein (SSB). The polymerase and the rest of the replication machinery are associated with the SSB/origin complex to form the two replication forks and to initiate bidirectional DNA synthesis (the elongation phase). During termination, replication forks collide and are resolved, and the resulting daughter DNA molecules are completed and separated. A number of proteins and complexes that participate in replication fork progression are described below.

Due to the antiparallel nature of DNA and the unidirectionality of the polymerase, one strand of the chromosome is synthesized continuously (the leading strand) while the other is copied discontinuously (the lagging strand) as a series of Okazaki fragments (Figure 1). It is believed that at the replication fork, the two polymerases responsible for replicating the leading and lagging strand are associated (either directly or indirectly via other molecules) (Figure 1). Thus, the replication of the two strands is coupled.

Minichromosome Maintenance (MCM) Complex

MCM is a family of six proteins (Mcm2–7, molecular masses of 101, 91, 97, 82, 93, and 81 kDa, respectively) with highly conserved amino acid sequences between the six different polypeptides. All MCM proteins are essential for cell viability and have been identified in all eukarya. In addition to forming a heterohexamer, *in vivo* and *in vitro* studies have revealed the presence of several additional MCM complexes composed of different combinations of the MCM proteins. Biochemical studies with the various complexes in yeast and mammals have shown that a dimeric complex of the Mcm4,6,7 heterotrimer contained $3'–5'$ DNA helicase activity, ssDNA binding, and DNA-dependent ATPase activities, while its interactions with either Mcm2 or Mcm3,5 inhibited the helicase activity. However, all six proteins were shown to be essential for replication fork movement. Based on genetic and biochemical studies, the MCM complex is presumed to be the helicase responsible for the separation of duplex DNA during chromosomal replication.

Replication Protein A (RPA)

RPA (also called replication factor A, RFA) is the eukaryotic single-stranded DNA-binding protein. It is a heterotrimeric complex of proteins with molecular

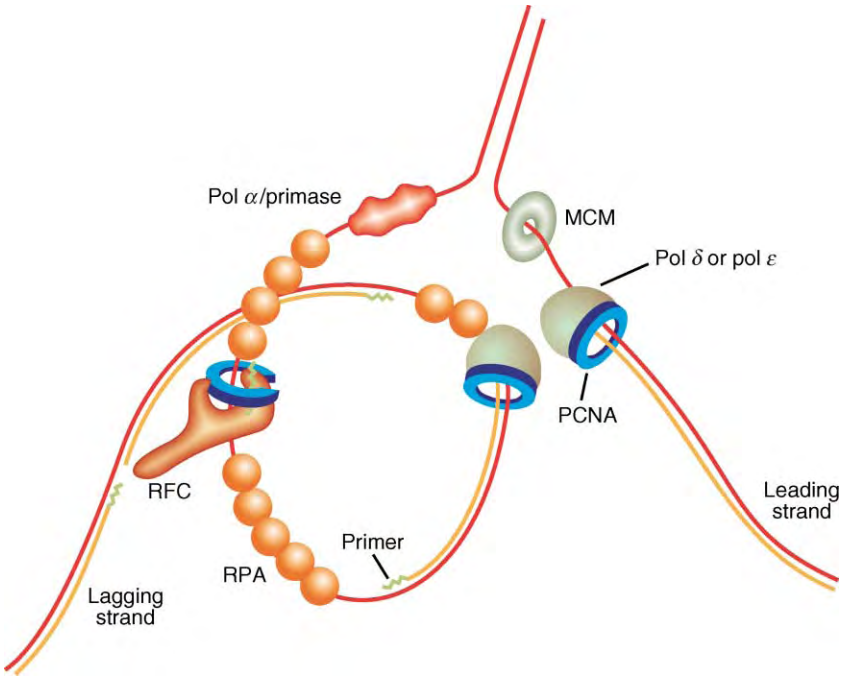

FIGURE 1 A schematic representation of the proteins at the eukaryotic replication fork. Although it is not shown in the figure, it is thought that all proteins shown interact with each other.

masses of 14, 32, and 70 kDa; these essential proteins have been found in all eukarya studied. SSBs are essential components of all replication systems. The protein coats the ssDNA exposed behind the helicase, thus protecting it from attack by nucleases and chemical modification. In addition, RPA stimulates the activity of DNA polymerases by removing secondary structures that interfere with polymerase movement, creating a uniform substrate for polymerase activity. RPA was shown to play an instrumental role in the coordination of DNA synthesis on the lagging strand and to interact with a large number of cellular factors needed for DNA metabolism.

DNA Polymerase α/Primase (Pol α/Primase) Complex

DNA polymerases are incapable of initiating DNA synthesis *de novo* and require DNA primases, which synthesize short RNA primers on template DNA that are subsequently extended by the polymerase. In eukarya, DNA primase is part of a four-subunit complex, the Pol α/primase complex, containing subunits with molecular masses of 180, 68, 58, and 48 kDa. Two of the subunits, p48 and p58, are required for primase activity, with p48 serving as the catalytic unit. Primase synthesizes short RNA primers (8–12 nucleotides (nt)) which are then elongated by Pol α to ~30 nt, forming pre-Okazaki fragments. These RNA–DNA hybrid molecules are recognized by the polymerase accessory complex, replication factor C (RFC) to initiate processive DNA synthesis by the replicative polymerase. On the lagging strand Pol α/primase activity is required at the initiation of each Okazaki fragment.

Polymerase Accessory Proteins

The processivity of DNA polymerases is quite low. This means that only a few nucleotides are incorporated into the newly synthesized DNA before the polymerase dissociates from the substrate. Processivity is conferred by a ring-shaped protein, referred to as the DNA polymerase sliding clamp (also called DNA polymerase processivity factor) that encircles DNA and acts to tether the polymerase catalytic unit to the primed template for processive DNA synthesis. The eukaryotic sliding clamp is proliferating cell nuclear antigen (PCNA). However, PCNA cannot assemble itself around the DNA, but must be loaded onto DNA by a protein complex, known as the clamp loader (also called polymerase accessory complex), which in eukarya is RFC. RFC recognizes the 3′ end of the single strand/duplex (primer–template) junction of the pre-Okazaki fragment and utilizes ATP hydrolysis to assemble PCNA around the primer. PCNA encircles the primer DNA and then binds the polymerase catalytic

unit, allowing rapid and processive DNA synthesis. Upon completion of an Okazaki fragment, the polymerase dissociates, leaving the clamp assembled around the duplex DNA.

Proliferating Cell Nuclear Antigen (PCNA)

PCNA, the eukaryotic sliding clamp, is a ring-shaped homotrimer of a 29 kDa protein. Upon its assembly around the primer of the pre-Okazaki fragment by RFC, PCNA associates with Pol δ or Pol ε to initiate processive DNA synthesis. *In vitro* studies demonstrated that upon assembly around duplex DNA, PCNA could slide freely and bidirectionally along the duplex. Although PCNA has no enzymatic activity, it plays a major role in chromosomal DNA replication. Besides its role as a processivity factor for Pol δ and Pol ε, PCNA was shown to play a regulatory role during chromosomal replication. A number of proteins that inhibit DNA synthesis were shown to operate via interaction with PCNA, preventing its association with the polymerase. Upon completion of an Okazaki fragment, PCNA disengages from the polymerase and is left on the duplex DNA. The PCNA molecules left on replicated DNA play diverse roles in postreplication DNA metabolic processes.

Replication Factor C (RFC)

RFC, the eukaryotic clamp loader, is a five-subunit complex of 140, 40, 38, 37, and 36 kDa proteins (for Rfc1–5, respectively). All five subunits are essential for cell viability. The amino acid sequences of each subunit reveal significant homology in seven regions (boxes II–VIII). The large subunit (Rfc1) contains an additional box (box I) within its N-terminal region. RFC recognizes the 3′ end of the pre-Okazaki fragment and utilizes ATP hydrolysis to assemble PCNA around the duplex DNA. It was shown that the interactions between RFC and RPA play a role in the switch that removes Pol α/primase from the DNA, allowing the loading of PCNA. In addition to its role as a clamp loader, *in vitro* studies suggest that RFC also functions as a clamp unloader, i.e., removing free PCNA from DNA.

Polymerase δ (Pol δ) and Polymerase ε (Pol ε)

Both Pol δ and Pol ε are essential polymerases required for chromosomal replication. However, their precise function at the replication fork remains unclear. Although Pol δ is found in all eukarya, its polypeptide composition is different in different organisms. To date, Pol δ isolated from either mammals or *Schizosaccharomyces pombe* is a heterotetramer of 125, 66, 50, and 12 kDa protein (only the human molecular masses are given) while the *Saccharomyces cerevisiae*, Pol δ, is a heterotrimer. *In vitro* studies with these enzymes indicate that all Pol δ complexes are monomers. Following the assembly of PCNA at the primer, Pol δ associates with the clamp to initiate rapid and processive DNA synthesis.

Pol ε is a four-subunit complex of proteins with molecular masses of 261, 59, 17, and 12 kDa (for the mammalian complex). As is the case with Pol δ, Pol ε is a monomeric polymerase. Like Pol δ, the PCNA clamp is required for the Pol ε-catalyzed DNA synthesis in the presence of physiological salt concentrations. However, at low ionic strength Pol ε alone can elongate primed DNA chains, in contrast to Pol δ.

Reconstitution of the simian virus 40 (SV40) DNA replication system with mammalian enzymes demonstrated that only Pol δ was required for replication of both leading and lagging strands and did not require Pol ε. Both *in vivo* experiments in yeast and *in vitro* experiments with the *Xenopus* cell free replication system indicate that Pol ε and Pol δ are required for replication. Genetic experiments in yeast showed that Pol ε is located at the replication fork. Furthermore, mutational rate studies in *S. cerevisiae* suggest that the proofreading functions of Pol δ and Pol ε act on different DNA strands. However, the precise location of each polymerase (i.e., lagging or leading strand) could not be deduced. These results suggest that each polymerase acts on a specific strand during replication. However, conflicting results in yeasts indicate that cells deleted of the catalytic domain of the large subunit of Pol ε (at the N terminus) are viable, provided that the C terminus of this subunit is expressed. The C terminus was shown to play an important role in the regulation of DNA replication. Interestingly, point mutations in the conserved catalytic site of Pol ε result in loss of viability. Thus, although Pol ε is normally present at the replication fork, in the absence of the catalytic portion of its large subunit, it is likely that Pol δ can substitute for its function. Further studies are needed to determine the cellular functions of Pol δ and Pol ε.

Topoisomerases

During replication, DNA is supercoiled in front of and behind the polymerase. Positive supercoils are produced in front of the replication fork, while negative supercoils result behind it. Topoisomerases prevent excessive supercoiling and regulate the level of supercoiling within the DNA molecule. These enzymes are essential for replication fork progression.

Topoisomerases introduce transient breaks in the phosphodiester backbone of the DNA, which allow supercoils to be added or removed.

Conclusion

The replication of eukaryotic chromosomes is a very complex and highly coordinated process involving dozens of proteins. Although most of the proteins assembled at the replication forks have been identified and isolated, the precise biochemical properties and roles of some of these proteins remain to be elucidated.

See Also the Following Articles

DNA Polymerase α, Eukaryotic • DNA Polymerase β, Eukaryotic • DNA Polymerase δ, Eukaryotic • DNA Polymerase ε, Eukaryotic • DNA Polymerases: Kinetics and Mechanism • DNA Replication: Eukaryotic Origins and the Origin Recognition Complex • DNA Topoisomerases: Type I • DNA Topoisomerases: Type II • DNA Topoisomerases: Type III–RecQ Helicase Systems • Translesion DNA Polymerases, Eukaryotic

Glossary

bidirectional DNA replication DNA synthesis that originates at a bidirectional origin results in the formation of two replication complexes leading to two replication forks that move in opposite directions.

DNA polymerase Enzyme that utilizes a primed DNA template to catalyze the synthesis of DNA.

helicase Enzymes that use the energy derived from hydrolysis of nucleoside triphosphates to sever the hydrogen bonds that hold each strand of duplex DNA together.

primase Enzyme that synthesizes small RNA chains *de novo* on ssDNA resulting in RNA–DNA hybrids which are used to prime DNA synthesis.

Further Reading

Baker, T. A., and Bell, S. P. (1998). Polymerases and the replisome: Machines within machines. *Cell* **92**, 295–305.

Bambara, R. A., Murante, R. S., and Henricksen, L. A. (1997). Enzymes and reactions at the eukaryotic DNA replication fork. *J. Biol. Chem.* **272**, 4647–4650.

DePamphilis, M. L. (ed.) (1996). *DNA Replication in Eukaryotic Cells*. Cold Spring Harbor Laboratory Press, New York.

Hübscher, U., and Seo, Y. S. (2001). Replication of the lagging strand: A concert of at least 23 polypeptides. *Mol. Cells* **12**, 149–157.

MacNeill, S. A., and Burgers, P. M. J. (2000). Chromosomal DNA replication in yeast: Enzymes and mechanisms. In *Frontiers in Molecular Biology: The Yeast Nucleus* (P. Fontes and J. Beggs, eds.) pp. 19–57. IRL Press, Oxford.

O'Donnell, M., Jeruzalmi, D., and Kuriyan, J. (2001). Clamp loader structure predicts the architecture of DNA polymerase III holoenzyme and RFC. *Curr. Biol.* **11**, R935–R946.

Tye, B. K. (1999). MCM proteins in DNA repelication. *Ann. Rev. Biochem.* **68**, 649–686.

Vivona, J. B., and Kelman, Z. (2003). The diverse spectrum of sliding clamp interacting proteins. *FEBS Lett.* **546**, 167–172.

Waga, S., and Stillman, B. (1998). The DNA replication fork in eukaryotic cells. *Annu. Rev. Biochem.* **67**, 721–751.

Biography

Lori M. Kelman is a Professor of biotechnology at Montgomery College, Germantown, MD. She received an A.B. in biochemistry from Mount Holyoke College, a M.S. in biology from St. John's University, a MBA in Management from Iona College, and a Ph.D. in molecular biology from Cornell University. She is Editor of *BIOS*, a quarterly journal of biology.

Zvi Kelman is an Assistant Professor at the Center for Advanced Research in Biotechnology, one of the University of Maryland Biotechnology Institutes. His work is focused on DNA replication. He received his Ph.D. in Molecular Biology from the Cornell University School of Medicine.

Jerard Hurwitz, whose research is focused on DNA replication, is a Member of the Molecular Biology Program at Memorial Sloan-Kettering Cancer Center. He received his Ph.D. in Biochemistry from Western Reserve University and has held faculty positions at Washington University, St. Louis, New York University School of Medicine and Albert Einstein College of Medicine.

DNA Replication, Mitochondrial

David A. Clayton
Howard Hughes Medical Institute, Chevy Chase, Maryland, USA

Nearly all eukaryotic cells contain organelles called mitochondria that contain enzymes which utilize oxygen and nutrient molecules, such as sugars, to produce most of the ATP that in turn provides energy to support cellular molecular activities. The mitochondria, in addition to being the principal sites of energy production, contain their own genomes, mitochondrial DNA (mtDNA), which are different structurally and functionally from the much larger nuclear genome. DNA replication is the process by which new DNA is synthesized by copying the strands of pre-existing DNA. Replication of mtDNA occurs by a distinctive mechanism independent of the replication of DNA in the cell nucleus. Proper synthesis and maintenance of mtDNA and the mitochondrion as a whole requires the coordinated participation of both nuclear and mtDNA gene products.

Mitochondrial Constituents and their Functions

Mitochondria comprise several hundred macromolecules, including mtDNA, mitochondrial RNA (mtRNA), and proteins.

mtDNA

Although certain cells can exist without mtDNA under special nutrient and growth conditions, where oxidative phosphorylation activity is not essential, in all other cases, mtDNA is needed. This is due to the fact that mtDNA encodes some of the proteins necessary for mitochondrial function in energy production. The sizes of mitochondrial genomes are quite broad. Vertebrate mtDNAs are typically 16–18 Kb in size, with yeast mtDNA being several times larger. Plant mtDNAs can be 30-fold larger than vertebrate mtDNA. In addition, the number and identity of mtDNA genes is not constant across all mtDNAs. Human (and vertebrate) mtDNAs contain 37 genes, of which 13 are for proteins involved in bioenergetics. Although larger mtDNAs can contain more genes, the coding information is not directly linear with genome size.

RNA

The RNA inside the mitochondrion is almost exclusively that which is encoded by mtDNA. For mammals, this generally includes two rRNAs and 22 tRNAs. These 24 RNAs are thought to be necessary and sufficient to support fully the mitochondrial translation machinery, responsible for decoding the 13 mammalian mRNAs for mtDNA-encoded proteins.

Other RNAs, encoded by nuclear genes, include additional tRNAs, in cases where mtDNA contains an insufficient number of its own tRNA genes. In addition, certain RNA-processing activities, consisting of enzymes with nucleus-encoded RNA components, have been implicated as participants in processing mtRNA sequences. These include an RNase P for processing tRNA precursors and an RNase that cleaves mtRNA sequences at the origin of leading-strand DNA replication. This latter activity is thought to provide 3′-primer RNA ends for elongation by mtDNA polymerase.

Protein

The protein components of mitochondria are of several classes. Although mitochondria play key roles in apoptosis, calcium regulation, iron metabolism, and the synthesis of amino acids, sterols, and heme, the principal function of the organelle is energy production. It is, therefore, not surprising that all of the mtDNA-encoded proteins participate in the formation of one or another of the several bioenergetic complexes that support the chain of reactions leading to ATP production. Although the vast majority of mitochondrial proteins are encoded by nuclear genes, those encoded by mtDNA are essential and there are no nuclear genes present that can substitute for a loss of mtDNA.

The several hundred nucleus-encoded proteins that comprise the bulk of mitochondrial proteins fall roughly into two classes. One class is devoted to the task of energy production and mitochondrial function, including maintenance and expression of mtDNA. The second population consists of structural elements that provide the infrastructure that maintains basic mitochondrial morphology, mobility, and organelle physiology.

Most mitochondrial proteins, being nuclear-gene products, are produced by translation on cellular ribosomes and then targeted to mitochondria by their sequence (the most common feature directing the process is a signal sequence at one end of the protein, the amino terminus). Physical importation of the protein involves specific portions of the mitochondrion's inner and outer membranes that form ports for entry of these proteins. Initially, a general internalizing import mechanism applies to most proteins regardless of their final destination within the mitochondria. This is followed by other mechanisms leading to sorting of protein according to function.

Replication of the Mitochondrial Genome

Replication of mtDNA occurs within the confines of the mitochondrial-organelle network, which is usually organized dispersively throughout the cell's cytoplasm. As such, it represents a separately managed genome, physically and functionally distinct from nuclear DNA replication. The cellular copy number of mtDNA varies according to cell type. For example, mature lymphocytes have a few hundred mitochondrial genomes, whereas mammalian oocytes contain tens of thousands. Unlike nuclear DNA replication, which is subject to cell cycle control, it appears that mtDNA is able to initiate and complete a round of replication in dividing cells at any time.

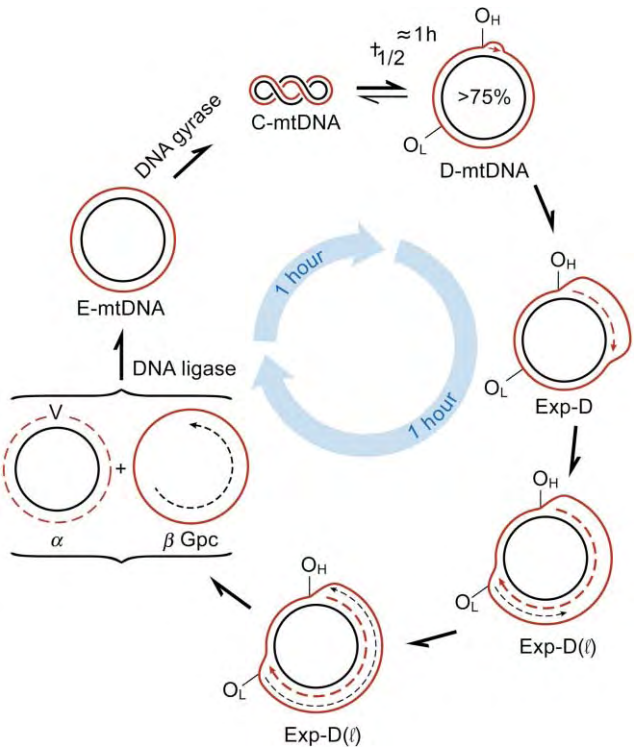

FIGURE 1 Diagram of mtDNA replicative intermediates. In the strand-displacement model closed-circular mtDNA (C-mtDNA) is in equilibrium with D-loop mtDNA (D-mtDNA). Productive replication is defined by elongation of the leading strand (red), which progresses around the genome (dashed red; Exp-D) until exposure of the major lagging-strand origin, which sponsors initiation of synthesis in the counterclockwise direction. End products are the new α- and β-circles, which are finished to closed circles (E-mtDNA). Superhelical turns are introduced (C-mtDNA) and finally a new D loop is synthesized. There is a rapid conversion back-and-forth between D-mtDNA and C-mtDNA.

Mammalian mtDNA

The historic replication model posits that leading-strand replication of mammalian mtDNA begins at closely spaced, defined sites located downstream from a major transcription promoter and proceeds unidirectionally with displacement of the parental leading strand until approximately two-thirds of the closed circular mtDNA has been copied (Figure 1). As a consequence, the replication fork passes a major origin for lagging-strand synthesis, leaving it in single-stranded form. Displacement as a single strand is thought to allow the characteristic secondary structure of this origin to occur, thereby permitting initiation of lagging-strand synthesis. A natural consequence of the separate and distinct locations of the two origins is that the two segregated progeny mtDNA circles are of two types: one a duplex circle with a newly synthesized leading strand and the other a gapped circle with a partial newly synthesized lagging strand. In each case, the final steps of synthesis and closure result in the mature closed circular mtDNA products.

Convincing biochemical isolation and characterization of mammalian mtDNA began in the 1960s. The key technical breakthrough was the use of dye-salt buoyant density centrifugation to isolate even relatively rare closed-circular DNAs in highly purified form. This technique was exploited to perform mtDNA analyses by sophisticated analytical centrifugation techniques, by electron microscopy, and eventually by gel electrophoresis. It is fortuitous that mammalian mtDNA molecules are small enough to be easily manipulated and analyzed by a variety of techniques.

Unique to mammalian mtDNA and a few viral DNA genomes is a bias in the content of guanosine plus thymine in one strand of the double helix compared to the other strand. A consequence of this situation is that the two strands of mammalian mtDNA can be physically separated to an extent that allows their individual identification. Therefore, one can isotopically label mtDNA and directly assay the extent of mtDNA synthesis that has occurred in each strand.

Perhaps the most signature feature of mammalian mtDNA is the displacement-loop (D loop). The D-loop nomenclature follows from the fact that closed-circular

mtDNA contains a region of varying size, depending on the species, in which leading-strand DNA synthesis has initiated and elongated to a size between 0.5–1 Kb. Molecules exhibiting progressive growth of this nascent leading strand, approaching full genomic size, were identified and argued as support for the proposed model for replication.

Lagging-strand synthesis is revealed by the appearance of duplex DNA within the context of the ever-increasing displaced parental-single strand. A preferred initiation site is located about two-thirds of the genomic distance away from the D-loop origin of leading-strand synthesis. Recent studies have suggested that other sites can serve as points of lagging-strand DNA replication initiation and thereby provide a broader range of duplex replicative intermediates.

Future Studies

In contrast to studies on mtDNA, the mitochondrial system has been challenging with respect to identifying, purifying, and characterizing the critical proteins and other factors that sponsor mtDNA replication. A principal reason for this is that although low-abundance mammalian mtDNA can be successfully purified to a high state because of its closed circular physical form, in general, the mitochondrial proteins involved in mitochondrial nucleic acid syntheses tend to be similar to their much more abundant nuclear counterparts. With the current availability of mammalian genomic sequences, and cloning and expression technologies, it should be possible to make more advances in this area. A partial listing of known and predicted activities include mtDNA and mtRNA polymerases, transcription factors, single-strand DNA binding protein, specialized RNase activities, helicases, and topoisomerases.

It is now clear that mitochondrial function and the integrity of normal mtDNA are important for normal physiology in mammals. There are numerous reports of human disease in particular that have mtDNA mutations, and even loss of mtDNA, as the underlying basis for what is usually manifested as neuromuscular disorder phenotypes.With this understanding, it will be important to learn the nature and rate of mtDNA turnover in different cells and tissues. Unlike nuclear DNA, which is not replicating in nondividing cells, mtDNA continues in its need to replicate due to continuous turnover and renewal of the mitochondrial organellar population. Thus, at least the opportunity to accumulate mutations in mtDNA during an individual's lifetime can be appreciated. Knowledge of the global pattern of mtDNA-turnover rates could prove valuable in predicting risk factors for human mitochondrial disease.

There are now a number of studies that are identifying the key activities that regulate the fission and fusion of individual organelles. This will likely involve further consideration of how the mitochondrial network travels along microfilaments and is positioned within the cellular cytoplasm. In turn, it will be important to learn more about the precise location of mtDNA-replication sites to determine if replication is site-specific or can occur generally.

Yeast and Others

Historically, the yeast system has been the most widely used to study almost all aspects of mitochondrial biogenesis. It has provided a wealth of information on bioenergetics, organelle assembly, protein import, and other areas of mitochondrial biology, including the details of mtDNA gene expression.

However, studies of mtDNA replication in yeast have been challenging due, in part, to the plasticity of the genome and the very aggressive rate of recombination of yeast mtDNA in cells. Thus the isolation and analysis of productive replicative intermediates have proved much more difficult than for mammalian systems with their small genomes and almost complete absence of recombination, including the nucleases usually associated with breakage and rejoining of DNA strands. Nevertheless, there are a few intriguing similarities between yeast and mammalian mtDNAs with regard to potential yeast mtDNA origins resembling origin sequences in D loops. It will be interesting to learn whether origins of replication have been conserved over this period of evolution, or whether other roles for these sequences, such as attachment to membranes to facilitate segregation of mtDNA molecules after replication, are the driving force for these similarities. In this regard, recent studies have suggested that mtDNA can be isolated in close association with specific proteins, which may be key to understanding genomic placement in the organelle.

See Also the Following Articles

Mitochondrial DNA • Mitochondrial Genes and Their Expression: Yeast • Mitochondrial Genome Evolution • Nuclear Genes in Mitochondrial Function and Biogenesis

Glossary

closed-circular DNA DNA in which the double helix forms a continuous circular structure with no ends nor any interruptions in either strand.

DNA replication The process by which a given DNA molecule duplicates itself. This process occurs in different ways depending on the form of DNA and the enzymes and factors supporting replication.

mitochondria The organelles in cells primarily responsible for energy production.

mtDNA The genome of mitochondria; every species has a characteristic mtDNA sequence.

origin A DNA sequence region in which new DNA synthesis begins.

promoter A DNA sequence recognized by enzymes and factors that copy genes into RNA molecules. Like an origin, a promoter marks the beginning of a nucleic acid synthesis event.

transcription The overall process by which DNA sequence is copied into RNA sequence. This is the first major step in gene expression.

Further Reading

Attardi, G. (1986). The elucidation of the human mitochondrial genome: A historical perspective. *Bioessays* **5**(1), 34–39.

Clayton, D. A. (1982). Replication of animal mitochondrial DNA. *Cell* **28**, 693–705.

Larsson, N.-G., and Clayton, D. A. (1995). Molecular genetic aspects of human mitochondrial disorders. *Annu. Rev. Gen.* **29**, 151–178.

Scheffler, I. E. (1999). *Mitochondria*. Wiley-Liss, New York.

Shadel, G. S., and Clayton, D. A. (1997). Mitochondrial DNA maintenance in vertebrates. *Annu. Rev. Biochem.* **66**, 409–435.

Biography

David A. Clayton is Vice President and Chief Scientific Officer of the Howard Hughes Medical Institute. Responsible for the institute's Science Department, he led the early phase of planning for the Janelia Farm Research Campus. He received his Ph.D. from the California Institute of Technology, and is a biochemist and geneticist whose research focuses on understanding the nature and role of mitochondrial DNA in cells. He is also a Professor at Stanford University and a member of the Institute of Medicine of the National Academy of Sciences.

DNA Replication: Eukaryotic Origins and the Origin Recognition Complex

Melvin L. DePamphilis
National Institute of Child Health and Human Development, National Institutes of Health, Bethesda, Maryland, USA

Cong-jun Li
Animal and Natural Resources Institute, US Department of Agriculture, Beltsville, Maryland, USA

Eukaryotic DNA replication is a highly conserved process that begins with the assembly of an origin recognition complex (ORC) composed of six different subunits (Orc1 to Orc6) at DNA replication origins distributed throughout the genome. Thus, it is the interaction between ORC and DNA that determines where DNA replication begins in the genomes of eukaryotic cells. Moreover, regulation of ORC activity is the premier step in determining when replication will occur. Pre-replication complexes (pre-RCs) are assembled at ORC/chromatin sites during the G1 phase of the cell division cycle. Pre-RCs consist of six ORC proteins, Cdc6, Cdt1, and six Mcm proteins. The role of Cdc6 is to identify ORC/chromatin sites; the role of Cdt1 is to load Mcm(2–7) hexamers onto these sites. The role of Mcm(2–7) hexamers is to unwind the DNA into two single-stranded DNA templates. DNA synthesis (S phase) is triggered by the addition of Mcm10 followed by the action of three protein kinases: Cdc7/Dbf4, Cdk2/cyclin E, and Cdk2/cyclin A. These events allow Cdc45 to escort DNA polymerase-α:DNA primase to the pre-RC and initiate RNA-primed DNA synthesis at or close to the ORC-binding site.

DNA Replication Origins

The Generic DNA Replication Origin

All DNA replication origins require two core components: (1) one or more binding sites for an origin recognition protein or protein complex, and (2) an easily unwound sequence called the DNA-unwinding element (DUE). A DUE is not sequence specific, but consists of a nucleotide composition with a low melting temperature. DNA unwinding begins within the DUE, and then DNA synthesis begins on each of the resulting single-stranded DNA templates. Additional "auxiliary" components may include one or more transcription factor binding sites that facilitate either binding of origin recognition proteins or DNA unwinding, but that are not required for origin activity. Auxiliary components are commonly found in viral replication origins. In cellular genomes, the sites where DNA replication begins, particularly in multicellular organisms, are determined by epigenetic as well as genetic parameters. This allows metazoans the flexibility to change their pattern of replication origins to accommodate changes in the length of S phase and in the pattern of gene expression that can occur during animal development. Thus, evolution has retained the same basic mechanism for DNA replication throughout the eukaryotic kingdom without sacrificing the flexibility needed in gene expression and genomic changes needed to create complex, multicellular organisms.

Eukaryotic replication origins initiate DNA replication in both directions, resulting in a transition from discontinuous to continuous DNA synthesis on each template strand (origins of bidirectional replication (OBR)) (Figure 1). This transition occurs because the two complementary DNA strands are antiparallel ($5' \rightarrow 3' : 3' \leftarrow 5'$), and all DNA polymerases travel along their template in only one direction ($5' \rightarrow 3'$). Therefore, DNA synthesis can occur continuously on one template of a replication fork in the same direction as DNA unwinding (this process is termed leading strand synthesis), but it must occur discontinuously on the complementary template, in the direction opposite to DNA unwinding, through the repeated initiation of short nascent DNA fragments called Okazaki fragments (lagging strand synthesis). Okazaki fragments are initiated by the enzyme DNA polymerase-α:DNA primase, extended by DNA polymerase-α:PCNA, and eventually ligated to the $5'$ end of the long growing daughter strand by DNA ligase I. The two leading strand initiation events that mark the OBR are separated by only one or two nucleotides.

Eukaryotic replication origins depend on DNA sequence information, although the requirements are less stringent than viral replication origins. Cellular

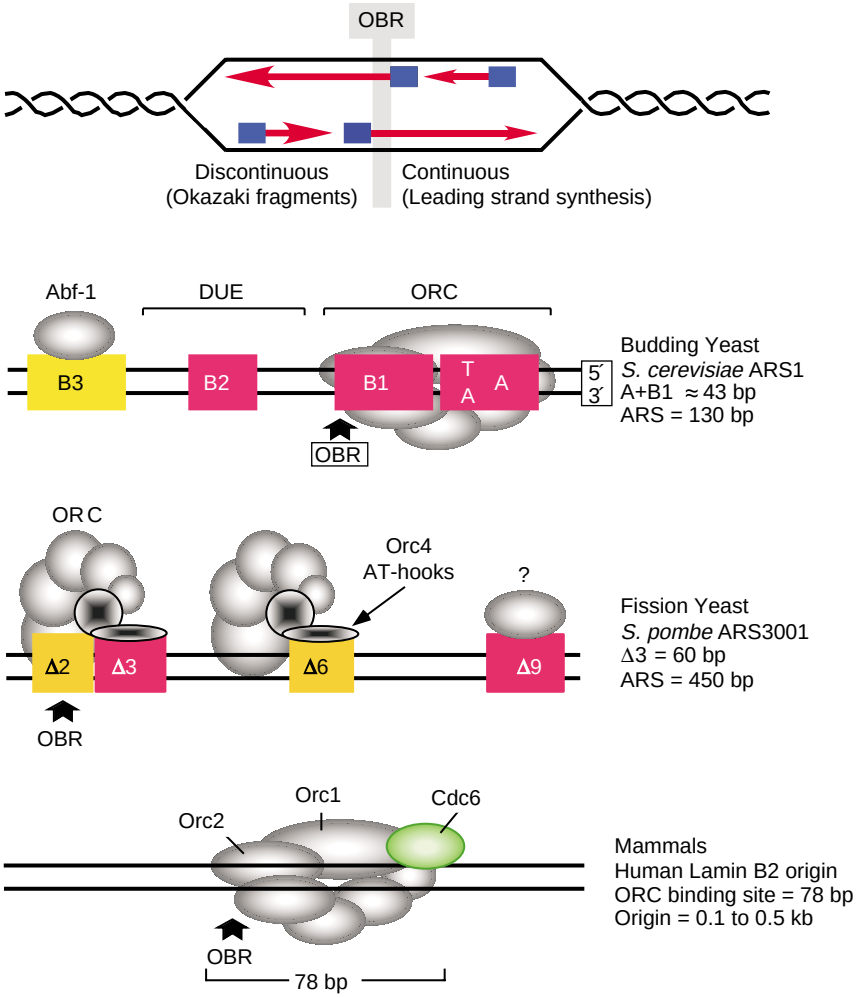

FIGURE 1 Replication origins. Some sequence elements are required for origin activity (red) while others facilitate origin activity (yellow). The *S. cerevisiae* ARS1 origin consists of a binding site (elements A + B1) for the six subunit origin recognition complex (ORC), and a large DNA-unwinding element (DUE) that contains a genetically defined B2 element. It also contains a binding site for transcription factor Abf-1. The origin of bidirectional replication (OBR) is the site where leading strand synthesis begins on each template. The *S. pombe* ARS3001 origin consists of four genetically defined elements. Δ3 and Δ6 bind SpORC. Δ2 contains the OBR. Δ9 is required for origin activity, but its function is unknown. The human lamin B2 origin has been mapped to a ~0.6 kb site at the 3′-end of the lamin B2 gene. No genetically defined elements (replicators) have been reported, but other mammalian replicators occupy <1 kb. The OBR and DNA contact points for Orc1, Orc2, and Cdc6 have been identified.

replication origins contain a "replicator" sequence that imparts origin activity when translocated to other chromosomal sites; this can be inactivated by sequence alterations. The genomes of viruses, yeast, and protozoa also contain an autonomously replicating sequence (ARS) that allows extrachromosomal DNA (e.g., plasmids) to replicate when provided with the cognate origin recognition proteins and essential replication proteins. All ARSs exhibit replicator activity, but all replicators do not exhibit ARS activity. Such differences presumably reflect the effects of sequence context and chromatin structure on origin activity.

The most well characterized replication origins are found in the genomes of animal viruses and yeast cells. Genomes such as simian virus 40 (SV40), polyomavirus, and papillomavirus contain a single species-specific sequence of approximately 60 bp that is the binding site for the single origin recognition protein encoded by the virus. For example, SV40 encodes T-antigen, which in the presence of ATP binds specifically to the SV40 replication origin where it assembles into two hexamers with the DNA passing through their centers. The two hexamers unwind DNA in opposite directions, one hexamer for each newly formed replication fork. T-antigen hexamers assembled in the absence of DNA cannot unwind the origin. Thus, viral replication origins not only determine where replication begins, but also are required for assembly of an active helicase to initiate DNA unwinding, a prerequisite to DNA synthesis.

Yeast origins are similar to animal virus origins in that they both exhibit ARS activity. However, yeast origins differ from viral origins in four ways: (1) Viral origins initiate replication many times per cell division cycle, whereas yeast origins (like all eukaryotic origins) are activated once and only once per cell cycle. (2) Viral origins exhibit a rigid modular anatomy in which the sequence elements require a specific spacing and orientation with respect to one another, whereas yeast origins exhibit a flexible modular anatomy in which the same functional modules from different origins are interchangeable, even though they are not similar in sequence. (3) Viral origins function independently of their DNA context, whereas both the activity and the timing of the activation of yeast origins are strongly influenced by neighboring sequences. (4) Finally, viral origins are sequence-specific binding sites for a unique virally encoded origin recognition protein, whereas yeast origins exhibit little sequence specificity and bind a complex of six different proteins (ORC). ORC, in turn, recruits a helicase [Mcm(2–7)] to the replication origin.

The Budding Yeast Paradigm

Replication begins at specific DNA sites in *Saccharomyces cerevisiae* consisting of 100 to 150 bp. The core component consists of an ScORC binding site (~30 bp) that includes two genetically identifiable elements, A and B1, as well as a DUE that usually contains the genetically identifiable B2 element (Figure 1). (Note that species is indicated by prefixes such as Sc, Sp, Xl, Dm, and Hs for *Saccharomyces cerevisiae*, *Schizosaccharomyces pombe*, *Xenopus laevis*, *Drosophila melanogaster*, and *Homo sapiens*, respectively.) Element A contains an asymmetric A:T-rich ARS consensus sequence that is required for origin activity. B1 facilitates A in binding ScORC. B2 appears to be a weak ScORC binding site that facilitates pre-RC assembly. Some origins also contain an auxiliary component, element B3 (~22 bp), that binds transcription factor Abf-1. The OBR is marked by two start sites for leading strand DNA synthesis at specific nucleotides separated by only 1 bp. The OBR resides between the ScORC binding site and the DUE. Despite the fact that only ~15% of the sequences in *S. cerevisiae* origins are shared (parts of elements A and B1), they exhibit a flexible modular anatomy in which homologous elements from different origins are interchangeable. Yeast origins vary considerably in the frequency at which they are activated during cell proliferation and in the temporal order they are activated during S phase. Sensitivity to their DNA (chromatin?) context most likely accounts for the facts that not all ARS elements function as replication origins in yeast chromosomes and that some origins can bind ORC but still cannot initiate replication.

The Fission Yeast Paradigm

S. pombe replication origins (0.5 to 1 kb) are five to ten times larger than those in *S. cerevisiae*. *S. pombe* replication origins contain ARSs that function *in vivo* as replication origins, but *S. pombe* ARSs are not interchangeable with those in *S. cerevisiae*. Furthermore, they lack a genetically required consensus sequence. *S. pombe* replication origins contain two or more regions that are required for full ARS activity. These regions consist of asymmetric A:T-rich sequences with A residues clustered on one strand and T residues on the other. Some exhibit either orientation or distance dependence, and some bind SpORC, assemble a pre-RC, and initiate bidirectional DNA replication, while others with a similar AT content do not. Thus, despite the absence of a required consensus sequence, *S. pombe* origins still exhibit sequence specificity in their design.

For example, ARS3001 (Figure 1) consists of four genetically required sites contained within ~570 bp; Δ2 and Δ6 are weakly required while Δ3 and Δ9 are strongly required. SpORC binds strongly to the Δ3 site, weakly to the Δ6 site, and not at all to the remaining sequences. Pre-RC assembly appears to occur primarily at the Δ3 + Δ2 region, and an OBR has been mapped to the Δ2 site. Thus, the Δ3 + Δ2 region (~100 bp) is equivalent to a simple *S. cerevisiae* origin. Δ6 appears similar to the B2 element in *S. cerevisiae* origins in that it is a weak SpORC binding site that facilitates origin activity. Remarkably, the Δ9 region, which is required for origin activity to the same extent as the Δ3 region, neither binds ORC nor functions as a centromere, although it does bind an as yet unidentified protein throughout the cell cycle. Therefore, Δ9 may be a novel origin component. This and other examples suggest that *S. pombe* replication origins contain at least two SpORC binding sites, consisting of asymmetric A:T-rich sequences, that act synergistically to facilitate assembly of a single pre-RC at an adjacent site.

Metazoan Replication Origins

Replication origins in multicellular animals such as flies, frogs, and mammals differ in two critical ways from those found in animal viruses and in yeast. First, metazoan replication origins exhibit replicator activity more readily than they do ARS activity, suggesting that metazoan replication origins function better in large chromosomes than in small extrachromosomal elements. Second, metazoan ORCs do not require binding to specific DNA sequences in order to initiate assembly of a pre-RC. For example, early embryos undergoing rapid cell cleavage (e.g., frogs, flies, sea urchin, fish) initiate DNA replication with no obvious requirement for any specific DNA sequences,

and DmORC or HsORC can replace XlORC in frog egg extracts with the same result.

Nevertheless, in the differentiated cells of flies, frogs, and mammals, OBRs have been mapped repeatedly to specific genomic loci. The nature of these loci, however, is not clear. Studies employing 2D gel fractionation of total genomic DNA to detect replication bubbles or to map the polarity of replication forks generally conclude that initiation events are distributed uniformly over intergenic regions as large as 55 kb (initiation zones), whereas methods that map either the relative distribution or the relative abundance of nascent DNA strands along the genome invariably conclude that initiation events originate within specific loci of ~1 kb or smaller, similar in size to fission yeast origins. Moreover, these specific loci contain replicators that can be inactivated by internal deletions, but they lack an identifiable, genetically required consensus sequence, such as the ARS consensus sequence found in budding yeast replicators. They also contain an OBR that is comparable to those found in yeast, and at least one ORC-binding site (e.g., lamin B2) (Figure 1). In addition, origin activity can be regulated from sequences such as locus control regions that are many kilobases distal to the OBR but affect the accessibility of initiation sites to replication proteins. Thus, replication origins in mammals appear more similar to those in fission yeast than to those in budding yeast.

How might such disparate data be reconciled? The answer is that metazoan genomes contain many potential initiation sites for DNA replication, but during animal development some of these sites are selectively activated whereas others are suppressed. This is evident from the simple fact that site-specific initiation is developmentally acquired. Initiation sites are uniformly distributed throughout the genome in embryos undergoing rapid cell cleavages prior to the onset of zygotic gene expression, with no apparent preference for specific sequences. After this stage, initiation events become restricted to specific sites. Therefore, epigenetic as well as genetic parameters determine where initiation will occur.

Epigenetic Parameters

Epigenetic parameters that can affect origin activity include nucleotide pool levels, transcription factor binding sites, concentration of replication proteins, transcription, chromosome structure, nuclear organization, and DNA methylation. For example, under normal culture conditions, one particular 128 kb locus in the hamster cell genome initiates predominately at a single primary (high-frequency) origin. However, reducing dNTP pools distributes initiation events equally among six different origins within this locus (the primary origin plus five secondary or low frequency origins). This implies that synchronization of cells at their G1/S boundary by reducing nucleotide pools would favor the appearance of initiation zones, a caveat that may account for some of the data in the literature. It also implies that the frequency of initiation sites in mammals is similar to the frequency in yeast and in frog eggs (1/20 to 1/30 kb).

Similarly, transcription factors binding close to ORC-binding sites can facilitate origin activity. Because they are expressed in specific cells and at specific times during development, transcription factors could impart both developmental and DNA site specificity to origins. High ratios of ORC to DNA should favor initiation at low- as well as high-affinity DNA binding sites, whereas low ratios would favor initiation at high-affinity sites only. Since the concentration of ORC in the eggs of the frog, *Xenopus laevis*, is about 10^5 greater than in frog somatic cells, this could account for the transition from "random" to site-specific initiation events that is observed during frog development. In addition, the onset of zygotic gene expression will repress initiation events in the transcribed regions, because RNA synthesis through replication origins represses their activity. Similarly, changes in chromosome structure will make some genomic sites more accessible to ORC while making others less accessible. Changes in nuclear organization may also contribute to origin specification, because site-specific initiation of DNA replication has been observed only with intact cells or with intact (impermeable) nuclei incubated in cell extracts. Finally, DNA methylation is associated with repressed chromatin, and changes in DNA methylation patterns have been correlated with changes in initiation site activity.

Primary and secondary origins clearly exist in yeast, where some origins are activated once each cell division cycle while others are not, and in bacteriophage such as T7, where deletion of the primary origin simply shifts replication to a secondary origin. Most mammalian origins contain AT-rich sequences of the type commonly found at matrix attachment regions and in the replication origins of fission yeast and flies. In fact, ORCs from *S. pombe*, *Xenopus* eggs, and human cells all target asymmetric A:T-rich sequences. Perhaps their affinity for a particular site depends on epigenetic factors.

The Origin Recognition Complex

Eukaryotic ORCs are functionally, if not structurally, conserved among yeast, frogs, flies, and mammals. They all bind to DNA with nanomolar affinity, and they all bind preferentially to asymmetric A:T-rich sequences. ORC subunits 1, 4, and 5 bind ATP. The ATP-binding site in Orc1 is required for ORC

activity, and ORC exhibits ATPase activity. Only two of the six ORC subunits contain multiple consensus sites for phosphorylation by cyclin-dependent protein kinases, suggesting that these subunits are targets for regulation. These are Orc1 and Orc2 in the metazoa and Orc2 and Orc6 in yeast. Nevertheless, there are notable differences.

The ability of ORC to bind specific DNA sequences appears to be species dependent. Site-specific DNA binding by *S. cerevisiae* ORC requires subunits 1 to 5 and ATP; once ScORC is bound to origin DNA, it remains there throughout the cell division cycle. ScORC covers ~80 to 90 bp, and origin binding is facilitated by Cdc6. ScORC bound to dsDNA origins exists in an extended conformation, whereas ScORC bound to ssDNA forms a bent conformation. In addition, ScORC ATPase activity is stimulated by ssDNA but inhibited by dsDNA. Thus, it appears that *S. cerevisiae* double-stranded origin DNA, ATP, and Cdc6 stabilize bound ScORC in a conformation that allows pre-RC assembly, whereas ssDNA, ATP hydrolysis, and the loss of Cdc6 converts ScORC into a form that may release the Mcm(2–7) helicase to continue unwinding DNA at replication forks.

Like *S. cerevisiae*, all six *S. pombe* ORC subunits remain tightly bound to chromatin throughout the cell cycle. In contrast to *S. cerevisiae*, however, site-specific DNA binding by *S. pombe* ORC requires only the SpOrc4 subunit; neither the presence nor the absence of ATP and the other five subunits affects SpOrc4 binding to DNA *in vitro*. The SpOrc4 subunit is unique among eukaryotes in that its N-terminal half contains nine AT-hook motifs that specifically bind the minor groove of AT-rich DNA. The C-terminal half of SpOrc4 is 35% identical and 63% similar to the human and *Xenopus* Orc4 proteins. SpOrc4 has a general affinity for all AT-rich DNA, but it has a higher affinity for specific asymmetric A:T-rich sequences found within *S. pombe* replication origins. In fact, chromatin immunoprecipitation assays reveal that SpORC is bound to *S. pombe* origins and not to other AT-rich sequences in the regions between origins. Thus, while each AT-hook motif binds tightly to [AAA(T/A)], site specificity likely results from the arrangement of all nine motifs acting in concert.

Whereas the six ORC subunits in yeast and frogs form a stable complex *in vitro*, human ORC consists of a stable ORC[2–5] subcomplex to which Orc1 and Orc6 are only weakly bound. Both frog and human ORC binds preferentially to asymmetric A:T-rich sequences *in vitro* or during DNA replication in frog egg extracts, and the sequences selected by these metazoan ORCs are the same as those targeted by SpOrc4. Nevertheless, HsORC is localized at specific DNA replication origins *in vivo*.

Regulating ORC Activity: The ORC Cycle

One universal feature of eukaryotic DNA replication is that the genome is replicated once and only once each time a cell divides. This is accomplished in two ways. First, pre-RCs that are assembled during the M to G1 phase transition are inactivated during S phase, and second, new pre-RCs cannot be assembled until G1 phase. This is accomplished by blocking pre-RC assembly and activation at multiple steps such as the Cdc6, Cdt1, Mcm(2–7), and Cdk2 functions. However, the premier step in determining both where and when DNA replication begins is the assembly of functional ORC/chromatin sites, and this step appears to be regulated by inactivating ORC during the G1 to S phase transition and then preventing re-establishment of ORC activity until mitosis is completed and, in the metazoa, a nuclear membrane is reassembled.

In contrast to mammals and frogs, all six ORC subunits in yeast remain tightly bound to chromatin throughout their cell division cycles. Nevertheless, yeast ORC subunits undergo cell cycle-dependent phosphorylation that contributes to preventing reinitiation of DNA replication before cell division is finished. Orc2 and Orc6 are phosphorylated by Cdk1(Cdc28)/cyclin B during the S to M transition, and then dephosphorylated during early G1 phase when pre-RC assembly occurs. In *S. pombe*, Cdk1(Cdc2)/cyclin B associates with replication origins during S phase and remains there during G2 and early M phases. This association is ORC dependent and prevents reinitiation of DNA replication before mitosis has been completed (Figure 2).

In frog eggs, all six ORC subunits remain stably bound to one another throughout the cell division cycle, but their affinity for chromatin is cell cycle dependent. When sperm chromatin replicates in a *Xenopus* egg extract, the affinity of XlORC for chromatin becomes salt-labile following pre-RC assembly and then appears to be released during G2/M phase as a result of hyperphosphorylation by Cdk1/cyclin A. However, when somatic cell chromatin replicates under the same conditions, XlORC binds to the chromatin, initiates pre-RC assembly, and is then released upon completion of pre-RC assembly. Thus, the affinity of XlORC for chromatin depends on at least three factors: pre-RC assembly, chromatin structure, and the action of Cdk1/cyclin A (Figure 2).

In mammalian cells, ORC subunits two to five remain bound to chromatin throughout the cell division cycle, but the affinity of the largest subunit, Orc1, for chromatin is selectively reduced during S phase and then restored during the M to G1 phase transition (Figure 3). During G1 phase, Orc1, Orc2, Cdc6, and Mcm3 proteins can be cross-linked to replication origins (e.g., lamin B2

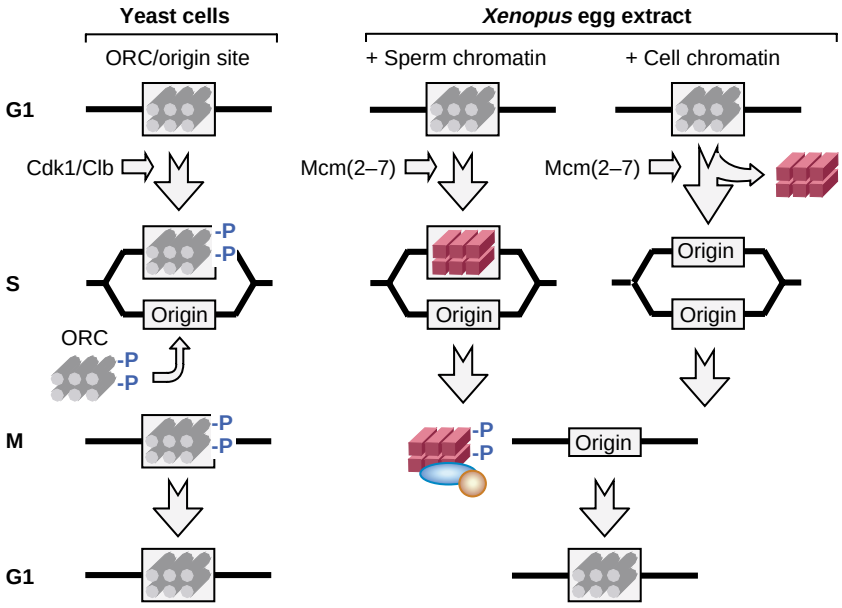

FIGURE 2 Three manifestations of the ORC cycle in eukaryotes. Yeast cells: ORC (six gray cylinders) remains bound to replication origins throughout the cell cycle, but ORC is phosphorylated (-P) during the S to M periods; this phosphorylation inhibits its ability to assemble a pre-RC. *Xenopus* egg extract: ORC binds to sperm chromatin, but the stability of ORC/chromatin sites is reduced (red boxes) following pre-RC assembly. ORC is phosphorylated by Cdk1/cyclin A (yellow ball) during G2/M and released from chromatin. If somatic cell chromatin is incubated in the extract instead of sperm chromatin, then ORC is released from chromatin following pre-RC assembly.

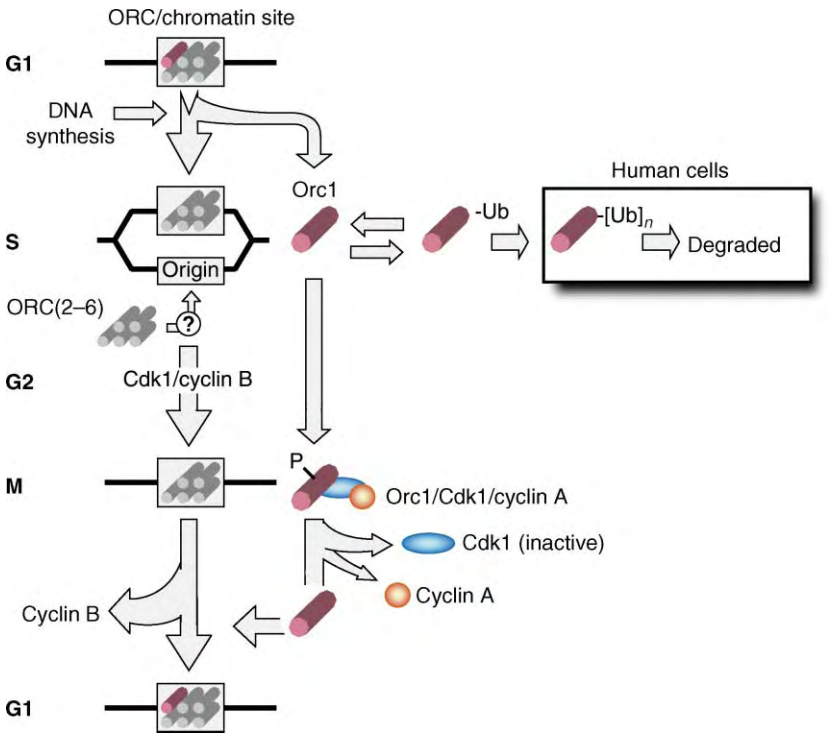

FIGURE 3 The ORC cycle in mammalian cells. ORC subunits 2 to 6 (grey cylinders) remain bound to chromatin throughout the cell cycle, but the Orc1 subunit (red cylinder) is selectively destabilized and released from chromatin when DNA synthesis begins (S phase). Orc1 is then mono-ubiquitinated (Ub) and in some cases polyubiquitinated ($[Ub]_n$) and degraded. Orc1 in mitotic cells is hyperphosphorylated by its association with Cdk1/cyclin A. When this enzyme is inhibited during the M to G1 transition, the phosphorylated state of Orc1 is reduced and it binds to chromatin.

origin; Figure 1), but during S phase, only the Orc2 protein can be cross-linked, consistent with release of Orc1 and disassembly of a pre-RC and with the fact that mammalian metaphase chromatin lacks functional ORCs. Rebinding of Orc1 to chromatin follows the same time course as degradation of cyclin B, suggesting that exiting mitosis triggers Orc1 binding to chromatin. Furthermore, Orc1 binding to chromatin precedes the appearance of functional pre-RCs at specific origins of bidirectional replication, suggesting that assembly of functional ORC/chromatin sites is the rate-limiting step in the assembly of pre-RCs at specific genomic sites.

What prevents Orc1 from rebinding to chromatin? In human cells, most of the Orc1 is selectively released, polyubiquitinated, and degraded during S phase. However, in hamster cells, the Orc1 is released but it is mono-ubiquitinated and not degraded *in vivo*. Moreover, during the S to M transition in hamster cells, mono-ubiquitinated Orc1 is replaced by Orc1, and the Orc1 in G2/M phase cells is hyperphosphorylated by its association with Cdk1/cyclin A (Figure 3). Inhibition of protein kinase activity in M phase cells allows dephosphorylation of Orc1 and rapid reassociation of Orc1 with chromatin. The association of Orc1 with chromatin appears to be the rate-limiting step in assembly of functional pre-RCs during the M to G1 phase transition. Thus, there is a universal control point in eukaryotic cell division cycles: the same cyclin-dependent protein kinase that regulates the onset of mitosis (Cdk1) also prevents premature assembly of functional ORC/chromatin sites until mitosis is complete and a nuclear membrane is present.

See Also the Following Articles

Cell Cycle: Control of Entry and Progression Through S Phase • Chromatin: Physical Organization • Chromatin Remodeling • DNA Replication Fork, Eukaryotic • Nuclear Organization, Chromatin Structure, and Gene Silencing

Glossary

autonomously replicating sequence (ARS) A DNA sequence that imparts origin activity to extrachromosomal elements in the presence of appropriate replication proteins, and whose activity is sensitive to genetic alterations.

Cdc Cell division cycle protein. A large number of Cdc genes have been identified in eukaryotes that affect various stages in cell division. Cdc6 is the name used in the budding yeast, *Saccharomyces cerevisiae*; Cdc18 is the name used in the fission yeast, *Schizosaccharomyces pombe*. The nomenclature for budding yeast proteins is generally applied to other organisms.

Cdk Cyclin-dependent protein kinase. This phosphorylates specific amino acids in proteins, but only when associated with a cyclin protein.

Cdt1 A protein encoded by Cdc10-dependent transcript 1 in *S. pombe*. Cdt1 is the same as RLF-B in *Xenopus laevis*.

DNA replication origin The DNA site where replication begins; also called an origin of bidirectional replication.

Mcm Minichromosome maintenance proteins. These were identified as genes required to maintain plasmids in *S. cerevisiae*. At least seven of these proteins are involved in DNA replication.

origin recognition complex (ORC) Six different proteins that bind to DNA replication origins and thereby initiate assembly of a pre-replication complex.

pre-replication complex (pre-RC) Fourteen different proteins consisting of ORC, Cdc6, Cdt1, and Mcm(2–7) that form a complex with chromatin during G1 phase of the cell cycle and that become the site where DNA replication begins during S phase.

replicator A DNA sequence that imparts origin activity when translocated to other chromosomal regions, and whose activity is sensitive to genetic alterations.

Further Reading

Abdurashidova, G., Danailov, M. B., Ochem, A., Triolo, G., Djeliova, V., Radulescu, S., Vindigni, A., Riva, S., and Falaschi, A. (2003). Localization of proteins bound to a replication origin of human DNA along the cell cycle. *EMBO J.* **22**, 4294–4303.

Anglana, M., Apiou, F., Bensimon, A., and Debatisse, M. (2003). Dynamics of DNA replication in Mammalian somatic cells. Nucleotide pool modulates origin choice and inter-origin spacing. *Cell* **114**, 385–394.

Bell, S. P. (2002). The origin recognition complex: From simple origins to complex functions. *Genes Dev.* **16**, 659–672.

Bell, S. P., and Dutta, A. (2002). DNA replication in eukaryotic cells. *Annu. Rev. Biochem.* **71**, 333–374.

Bogan, J. A., Natale, D. A., and DePamphilis, M. L. (2000). Initiation of eukaryotic DNA replication: Conservative or liberal? *J. Cell. Physiol.* **184**, 139–150.

DePamphilis, M. L. (1999). Replication origins in metazoan chromosomes: Fact or fiction? *Bioessays* **21**, 5–16.

DePamphilis, M. L. (2003). The 'ORC cycle': A novel pathway for regulating eukaryotic DNA replication. *Gene* **310**, 1–15.

Kong, D., Coleman, T. R., and DePamphilis, M. L. (2003). *Xenopus* origin recognition complex (ORC) initiates DNA replication preferentially at sequences targeted by *Schizosaccharomyces pombe* ORC. *EMBO J.* **22**, 3441–3450.

Li, C-J., Vassilev, A., and DePamphilis, M. L. (2004). A role for Cdk1(Cdc2)/Cyclin A in preventing the mammalian Origin Recognition Complex's largest subunit (Orc1) from binding to chromatin during mitosis. *Mol. Cell. Biol.*, in press.

Prioleau, M. N., Gendron, M. C., and Hyrien, O. (2003). Replication of the chicken beta-globin locus: Early-firing origins at the 5′ HS4 insulator and the rho- and betaA-globin genes show opposite epigenetic modifications. *Mol. Cell. Biol.* **23**, 3536–3549.

Takahashi, T., Ohara, E., Nishitani, H., and Masukata, H. (2003). Multiple ORC-binding sites are required for efficient MCM loading and origin firing in fission yeast. *EMBO J.* **22**, 964–974.

Vashee, S., Cvetic, C., Lu, W., Simancek, P., Kelly, T. J., and Walter, J. C. (2003). Sequence-independent DNA binding and replication initiation by the human origin recognition complex. *Genes Dev.* **17**, 1894–1908.

Biography

Melvin L. DePamphilis began his career in the field of DNA replication as a postdoctoral fellow with Paul Berg at Stanford University Medical School, and continued in this field as a Professor at Harvard Medical School, an Adjunct Professor at Columbia Medical School, a member of the Roche Institute of Molecular Biology, and most recently a Section Chief at the National Institutes of Health. He has published over 150 papers, reviews, and books on the subject of DNA

replication, chromatin structure, and gene expression in a variety of experimental systems.

Cong-jun Li began his career in the field of DNA replication as a graduate student with the late Earl F. Baril at the Worcester Foundation for Experimental Biology and continued in this field as a postdoctoral fellow with Paul T. Englund at the Johns Hopkins School of Medicine and then with Melvin L. DePamphilis at the National Institutes of Health. He has published over 20 papers and reviews on DNA replication and related subjects. Currently he is a Principal Investigator at the Animal and Natural Resources Institute, a division of the U.S. Department of Agriculture.

DNA Replication: Initiation in Bacteria

Jon M. Kaguni
Michigan State University, East Lansing, Michigan, USA

The study of *Escherichia coli* as a model organism has led to significant advancements in understanding the molecular mechanisms of DNA replication. This bacterium carries a circular duplex genome of 4.7×10^6 bp, and DNA replication initiates from a single replication origin, *oriC*. This locus is the site at which the duplex DNA opens to become single stranded. The replication fork machinery then assembles at this site, and moves bidirectionally as it copies the parental DNA to terminate chromosomal DNA replication in a region 180° opposite *oriC*. The daughter chromosomes are then segregated to progeny cells at cell division.

The *E. coli* Replication Origin, *oriC*

Escherichia coli oriC was identified genetically, then more precisely mapped by molecular DNA methods. Its isolation was based on its ability to confer autonomous replication to a plasmid formed by joining *oriC* to a DNA fragment that conferred drug resistance and lacked a replication origin. Subsequently, *oriC* was studied extensively by mutational analysis which, together with biochemical studies, showed that it carries five similar 9 bp motifs called DnaA boxes that are bound by DnaA protein, the initiator of bacterial chromosomal replication (see Figure 1). Each of the DnaA boxes (R1–R5) and their orientation relative to one another is critical for the function of *oriC* as the replication origin. For example, insertions are not tolerated in the region between the AT-rich region and R1, R5, and R1 or R5 and R2, indicating that the spacing between respective sequence elements in the left half of *oriC* must be rigorously preserved. In the right half, the spacing can be varied as long as the helical phasing of DnaA boxes is maintained. Collectively, these results suggest that the geometry of DnaA protein monomers relative to the DnaA boxes is critical for the initiation process.

oriC also contains binding sites for factor for inversion stimulation (FIS) and integration host factor (IHF). Mutation of these sites inactivates *oriC*, confirming their functional importance. IHF acts directly in initiation by stimulating DnaA-dependent opening of an AT-rich region of *oriC*, perhaps by bending the DNA to bring DnaA bound to DnaA boxes near the AT-rich region to support opening (Figure 1). Alternatively, IHF may act by binding to the unwound single-stranded DNA to stabilize it. IHF also contributes to the proper timing of initiation. Whereas wild type strains growing exponentially initiate new rounds of DNA replication synchronously, a null mutant of *himA*, encoding one of the subunits of the IHF heterodimer, is defective in this timing.

Similarly, *fis* mutants are asynchronous in initiation, and maintain *oriC* plasmids poorly at temperatures ≥ 37°C. Furthermore, deletion of DnaA box R4 at the chromosomal *oriC* locus, but not when *oriC* is carried in a plasmid, can only be tolerated when the *fis* gene is functional. Whereas these observations suggest a positive role for FIS, it is not required *in vitro* for *oriC* plasmid replication. Instead, FIS is inhibitory by sequestering the negative superhelicity that is essential for *oriC* plasmid replication.

IciA protein binds to 13-mer sequence motifs in the AT-rich region of *oriC* to prevent DnaA-dependent unwinding of this region. Because *iciA* null mutants are viable and do not show an asynchrony phenotype, the physiological importance of IciA as a regulator of initiation is uncertain.

Finally, *oriC* has eleven copies of the sequence GATC which is recognized by DNA adenine methyltransferase (Dam). This enzyme acts in mismatch repair in the discrimination of the parental DNA from the unmethylated progeny DNA strand after a cycle of DNA replication. The GATC sites in *oriC* remain hemimethylated for about one-third of the cell cycle whereas most other sites are methylated much more rapidly. Hemimethylated *oriC* associates with proteins in the inner membrane, including SeqA and SeqB to prevent premature reinitiation.

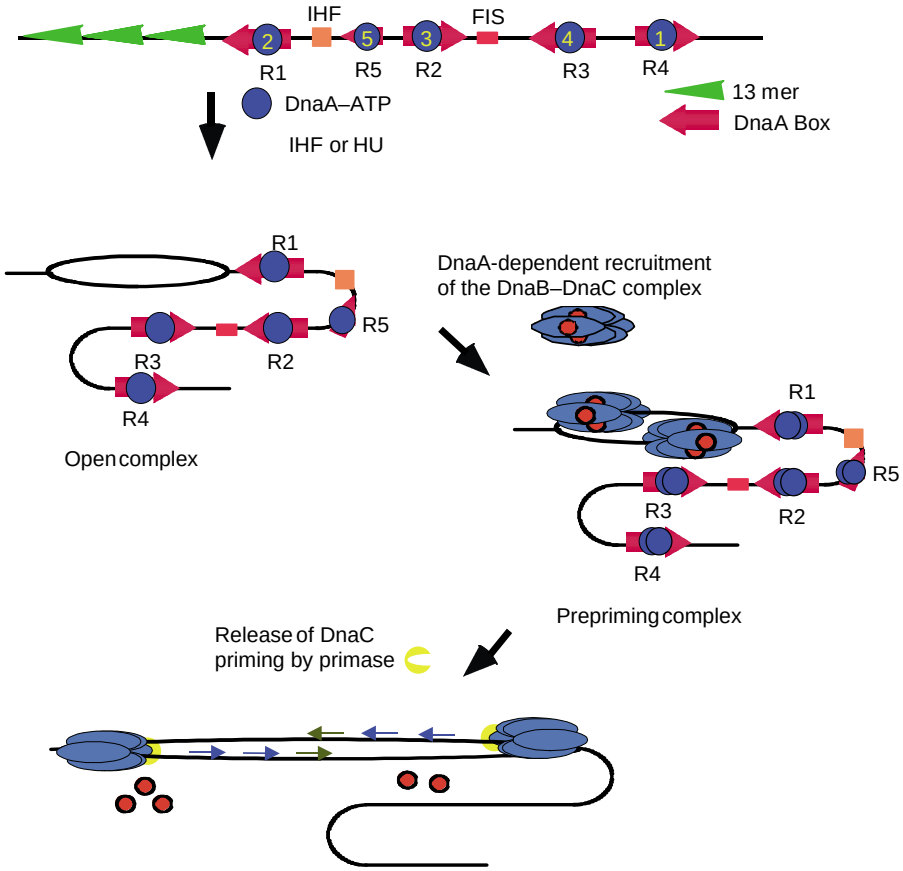

FIGURE 1 Mechanism of initiation of DNA replication from the *E. coli* replication origin, *oriC*. Sequence elements in *oriC* include the DnaA boxes (red arrows), 13-mer motifs (green triangles) in the AT-rich region near the left border, and binding sites for IHF and FIS. In the first step, DnaA protein binds to respective DnaA boxes sequentially, as indicated by the superimposed numbers. Complexed to ATP, DnaA then opens an AT-rich region that contains 13-mer sequences near the left *oriC* boundary to form the open complex. Entry of hexameric DnaB (blue ellipse) from the DnaB–DnaC complex follows to assemble the prepriming complex. In the import of DnaB to *oriC*, DnaB initially binds to *oriC*-bound DnaA protein. The hydrolysis of ATP bound by DnaC (red circle) in the DnaB–DnaC complex releases DnaC. Bound to each parental DNA template, DnaB then moves in the 5′–3′direction and interacts periodically with primase, which synthesizes RNA primers necessary for both leading and lagging strand synthesis. These primers are then extended by DNA polymerase III holoenzyme during semiconservative DNA replication.

Mechanism of Initiation at *oriC*

The molecular mechanism describing initiation of DNA replication from *oriC* is based primarily on the study of plasmids carrying this sequence. Such plasmids are useful model systems because its DNA replication resembles that which occurs at the chromosomal *oriC* locus. First, *oriC* plasmids replicate in synchrony with the bacterial chromosome. Second, they are duplicated with bidirectional fork movement. Third, *oriC* plasmids require the same gene products needed for copying the bacterial genome. Purified enzyme systems have been developed that sustain DNA replication on a plasmid carrying the *oriC* sequence. This has led to the biochemical analysis of the replication process, including the function of DnaA protein, the replication initiator.

DnaA Protein and the DnaA Box

DnaA protein performs a number of essential functions in initiation, including recognition of each DnaA box sequence in *oriC*. DNA binding assays first showed that DnaA specifically recognizes *oriC* as well as to other DNAs carrying the DnaA box sequence. DNase I foot-printing revealed that DnaA protected the DnaA box in addition to flanking sequences. In *oriC*, DnaA binds to the five boxes with different affinities, apparently as a monomer to each site. Whereas DnaA box R3 is the weakest site, DnaA must be bound to it and to the other DnaA boxes to promote initiation *in vitro*. This finding corroborates *in vivo* foot-printing studies showing that DnaA bound to R1, R2, and R4 throughout the cell cycle, but that it bound to DnaA box R3 only at the time of initiation.

Unwinding of the AT-Rich Region

DnaA is a nucleotide binding protein with a preference for ATP. In a complex with ATP and bound to *oriC*, DnaA induces unwinding of an AT-rich region near the left border of *oriC*. Whereas DnaA alone can induce this topological alteration, IHF stimulates this reaction, perhaps by binding to the IHF site in *oriC*. HU, a small basic protein that binds with higher affinity to nicked, gapped or cruciform DNA than to duplex DNA or RNA can replace IHF, and may stabilize the region of single-stranded DNA opened by DnaA. If so, IHF may similarly act to stabilize the single-stranded DNA as it is similar to HU in amino acid sequence.

DnaA is a weak ATPase, but ATP hydrolysis is not required for unwinding because a nonhydrolyzable ATP analogue is as effective as ATP in supporting strand opening of *oriC* and initiation. As DnaA bound to ADP is far less active in both unwinding and initiation, a nucleoside triphosphate or its analogue is required. A discrepancy is that the binding affinity (K_d) for ATP of 0.03 μM is much greater than the 1–5 mM ATP that is optimal for the unwinding reaction. It is likely that the complex of DnaA bound to *oriC* is reduced in its affinity for ATP.

Helicase Recruitment

Following the unwinding of *oriC*, DnaA then directs the binding of two DnaB helicase molecules to *oriC* to assemble the prepriming complex. The function of DnaB as a helicase is to unwind the parental duplex DNA so that it can be copied by the replication fork machinery. Helicase recruitment involves a physical interaction between DnaA and DnaB in the DnaB–DnaC complex. The interaction of DnaA with DnaB is interesting to consider in the context of the orientation of DnaA boxes in *oriC* and in plasmid replicons that require DnaA, DnaB, and DnaC protein for DNA replication. In these plasmids that replicate unidirectionally, the DnaA boxes can be viewed to "point" in the direction of replication fork movement. In *oriC*, four of the boxes are arranged as two sets of repeats that point in both directions, corresponding to the bidirectional mode of replication fork movement. An attractive model is that DnaA orients the binding of DnaB at *oriC* so that it is pointed in the proper direction for replication fork movement.

If DnaA orients the binding of DnaB to *oriC*, inverting the DnaA boxes should affect the directionality of replication fork movement. However, inverting DnaA boxes R1, R2, and R4 individually abolished *oriC* function, probably because this perturbs the architecture of the nucleoprotein complex. Recall that the spatial arrangement of the DnaA boxes relative to each other is critical for *oriC* function.

Hexameric DnaB of identical subunits is a ring-shaped molecule with a central cavity. One of the two strands of duplex DNA passes through the central cavity of DnaB as it unwinds DNA. For its assembly into the prepriming complex, DnaC transiently bound to the unwound region of *oriC* via its cryptic single-stranded DNA-binding activity may assist at this step in loading DnaB onto the DNA. ATP hydrolysis is then required to liberate DnaC from DnaB, a necessary step for DnaB to act as a helicase else the helicase activity of DnaB is suppressed.

Events after Prepriming Complex Formation

Upon the delivery of DnaB to *oriC*, DnaB is first bound to the unwound region of *oriC*. DnaB then unwinds the parental duplex, driven by ATP hydrolysis. Primase transiently interacts with the translocating DnaB to synthesize primers that are extended by DNA polymerase III holoenzyme. Single-strand DNA-binding protein binds to the single-stranded DNA formed by DnaB helicase activity. DNA gyrase and topoisomerase IV relieve the positive superhelicity created ahead of the replication fork. To process the Okazaki fragments formed on the lagging strand template, DNA polymerase I removes the RNA primers by nick translation, and DNA ligase seals the resulting discontinuities to make the progeny DNA fully duplex.

Functional Domains of DnaA Protein

The alignment of many *dnaA* homologues led to the proposal that DnaA is composed of four structural domains (see Figure 2). A small region of moderate sequence conservation near the N terminus is followed by a region of variable length that is species-dependent and not conserved. The C-terminal two-thirds of DnaA protein is highly conserved in this broad range of species. Most notable is the absolute conservation of the P-loop motif or Walker A box (residues 172–179 in *E. coli* DnaA) involved in nucleotide binding. The region of DnaA carrying this portion forms a Rossmann fold by the EMBL PHD method of secondary structure prediction.

In addition to these in silico observations, characterization of a large collection of *dnaA* alleles led to the identification of functionally distinct domains that correspond well with the domain structure derived from sequence homology, and from the crystal structure of the C-terminal two-thirds of *Aquifex aeolicus* DnaA. As a brief summary, domain I functions in self-oligomerization and in retention of DnaB in the

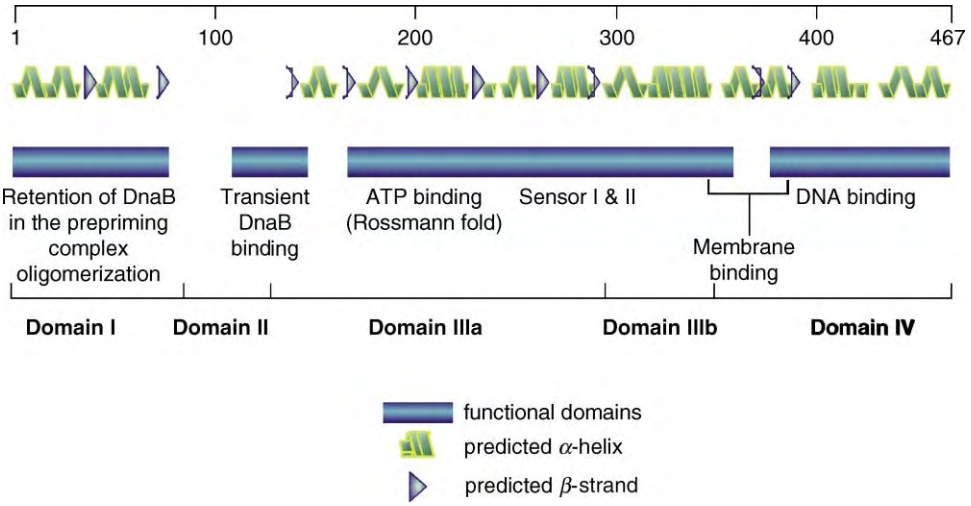

FIGURE 2 Functional domains of DnaA protein. The top line represents the primary sequence of DnaA protein of 467 amino acids. The predicted secondary structure is below, with α-helices in yellow and β-strands in purple. DnaA is a member of the AAA^+ family of proteins (ATPases associated with a variety of cellular activities) which have Walker A and B motifs involved in nucleotide binding and hydrolysis, and the sensor 1 and sensor 2 motifs that may function to sense nucleotide binding and hydrolysis. The Walker A motif is also known as the P-loop. The colored diagram near the bottom represents functional domains of DnaA in comparison to the domain structure of DnaA predicted by amino acid sequence alignment, and confirmed by analysis of the crystal structure of *A. aeolicus* DnaA protein.

prepriming complex. Domain II varies in length and sequence among bacteria and apparently functions as a flexible linker because an in-frame deletion of amino acids 87–104 of *E. coli* DnaA does not affect replication activity. A region overlapping domain II and III interacts with DnaB, and is involved in loading of the helicase at *oriC*. Domain III contains the Walker A and B boxes, and the sensor I and II motifs shared among AAA^+ proteins that typically bind ATP to regulate protein function. ATP binding induces a conformational change of DnaA, and mutant proteins bearing amino acid substitutions in or adjacent to the Walker A box are defective in ATP-binding activity. Domain IV carries a helix-turn-helix motif that recognizes nucleotides in the major groove of the DnaA box sequence via amino acids in the DnaA signature sequence. Near the N-terminal border of domain IV, a region involved in phospholipid binding has been described.

Regulation of DNA Replication in *E. coli*

DNA replication is regulated at the step of initiation at *oriC*. For example, *E. coli* cultures can have generation times that vary over a tenfold range from 20 to 200 min. In cultures growing faster than 60 min, the time needed to duplicate the genome is relatively constant at about 40 min. For a culture with a 20 min generation time, new initiations occur before the replicating chromosome is completed. In cells growing more slowly, the time needed to duplicate the chromosome is interspersed by a period when no DNA replication occurs. Under these conditions, replication forks move at constant speed due to the concerted actions of DnaB helicase and DNA polymerase III holoenzyme. Thus, DNA replication is controlled by modulating the frequency of initiation, occurring more often in rapidly growing cells compared to more slowly growing *E. coli*.

Because DNA replication in *E. coli* and all other free-living organisms is a periodic event in the cell cycle, factors act to regulate DNA replication either prior to or after initiation to prevent DNA synthesis from occurring at the wrong time. Several concepts have emerged from physiological studies in bacteria. One is initiation mass, the ratio of cell mass per replication origin. This ratio is a constant value, and DnaA protein contributes to setting this ratio. Other cellular factors that govern how this ratio is kept constant have not been identified. Thus our understanding of this process is rudimentary. A second concept is initiation synchrony. In rapidly growing cultures, individual cells initiate additional rounds of DNA replication synchronously, as measured by flow cytometry under conditions in which cell division and new initiations are blocked, but ongoing DNA replication proceeds to completion, so that cells carry 2^n chromosomes where $n \geq 0$ and is an integer. In contrast, asynchronous DNA replication results in odd numbers of chromosomes (1^n) as observed in mutants carrying *dnaA*(Ts) alleles defective in ATP binding, suggesting that ATP binding by DnaA

is necessary for proper regulation of initiation. Other mutations in *fis*, *himA*, *seqA*, *dam*, *hupA*, and *hda* also result in an asynchrony phenotype because the respective mutations perturb the initiation process by direct or indirect effects.

DnaA Protein and the Regulation of Chromosomal Replication

Among the genes required for *E. coli* DNA replication, the *dnaA* locus is unique in that conditionally defective mutations specifically affect initiation of DNA replication. By comparison, mutations in the *dnaB* and *dnaC* genes result in either an elongation- or initiation-defective phenotype, consistent with biochemical studies which show their dual roles in initiation at *oriC* and during elongation. All other replication genes display an elongation-defective phenotype because the respective proteins function in progression of the replication fork.

Several observations indicate that DnaA protein acts as a regulatory factor in the initiation process. First, DnaA protein appears to be limiting for initiation because its overproduction increases the frequency of initiation. In one study, the *dnaA*$^+$ gene (plasmid borne) was expressed from a regulated promoter in a *dnaA*(Ts) strain at nonpermissive temperature, causing initiation to be dependent on the level of induced expression. At an intermediate level of expression (13%), the synchrony of replication was comparable to the wild type control. Apparently, cyclic variation of DnaA protein is not required for initiation synchrony despite experiments showing that expression of the *dnaA* gene is autoregulated, to maintain a relatively constant cellular level of DnaA. Recent evidence implicates the *datA* locus in regulating initiation by controlling the availability of DnaA. A second line of evidence is the hyperactive initiation promoted by a mutant *dnaA* allele named *dnaAcos*. Recent experiments show that the replication activity of DnaA$^+$ protein is normally regulated to prevent unscheduled initiations whereas DnaAcos fails to respond to negative regulation. Third, some *dnaA* mutations at permissive temperature display an increased initiation mass. As the mutant proteins have reduced initiation activity *in vitro*, the lower frequency of initiation *in vivo* may lead to an increased initiation mass by promoting initiation later in the cell cycle. Together, these results suggest that DnaA protein activity controls initiation in the cell cycle.

The *datA* Locus

Interestingly, a 1 kbp chromosomal segment called *datA* is one of eight sites in the *E. coli* genome that are bound by DnaA with high affinity. The *datA* locus carries five DnaA boxes to which several hundred DnaA monomers can bind. Strains lacking this chromosomal segment exhibit both asynchronous initiations as well as an increased frequency of initiation. The *datA* site is unique among the eight strong binding sites for DnaA in that its deletion and not others leads to aberrant initiation. Apparently, when the level of DnaA is elevated that would otherwise lead to increased initiations, the extra DnaA can bind to the *datA* locus, thus modulating the initiation process.

SeqA at *oriC*

E. coli DNA replication occurs only once per cell cycle. Several proteins have been identified that bind to newly duplicated origins to block premature initiations. Specific binding to the newly replicated origins is by virtue of hemimethylated GATC sequences, as exists when the progeny DNA strand annealed to the methylated parental DNA has not yet been modified by DNA adenine methylase (the *dam* gene product). One protein is SeqA, which binds to the left half of *oriC* with tenfold greater affinity when this DNA is hemimethylated compared to when it is fully methylated. Footprinting experiments showed that SeqA specifically recognizes the hemimethylated GATC sequence in each 13-mer motif of *oriC* (Figure 1). These observations support a model in which SeqA blocks reinitiation by inhibiting the unwinding of the 13-mer region of *oriC*. In addition, SeqA seems to limit the binding of DnaA to *oriC*.

In *E. coli* with a generation time of 30 min, methylation of *oriC* after its duplication is delayed for ~13 min (~one-third of the cell cycle). In *seqA* mutants, methylation occurs after 5 min, so the 8 min difference is apparently because SeqA protein complexed to hemimethylated *oriC* impedes methylation. However, the 5 min delay indicates the participation of other factors. One of these is SeqB, a membrane-associated protein which appears to act in concert with SeqA. SeqB in a membrane fraction stimulates the binding of SeqA to hemimethylated *oriC* by at least 30-fold in DNA binding assays.

Interaction of DnaA with Hda and the β-Subunit of DNA Polymerase III Holoenzyme

DnaA complexed to ATP is more active than the DnaA–ADP complex in initiation and unwinding of *oriC*, leading to the notion that the nucleotide bound state of DnaA controls initiation. Although DnaA alone can slowly hydrolyze ATP, hydrolysis is stimulated by

incubation with a recently discovered protein named Hda (for homologous to DnaA, specifically domain III), duplex or single-stranded DNA, and the β-subunit of DNA polymerase III holoenzyme. The β-subunit confers processive DNA synthesis to DNA polymerase III holoenzyme by tethering the enzyme to DNA during DNA synthesis. Because any duplex or single-stranded DNA suffices, ATP hydrolysis is not necessarily coupled to DNA replication. However, under appropriate *in vitro* conditions, the ATP bound to DnaA can by hydrolyzed by incubation with the β-subunit and Hda in coordination with DNA replication.

Hda protein is similar at the amino acid level to domain III of DnaA, and carries AAA^+ sequence motifs. Initially, the *hda* gene was described to be essential for viability. More recent experiments showed that viability, growth rate, initiation frequency, and replication synchrony were unaffected when a drug resistance gene interrupted the *hda* coding region. However, deletion of *hda* coding sequences caused asynchronous initiation. A model has been proposed that the interaction of DnaA with Hda and the β-subunit of DNA polymerase III holoenzyme, in coordination with DNA replication, stimulate the hydrolysis of ATP bound to DnaA to modulate the frequency of initiation. If so, the capacity for initiation after one round of initiation should diminish, reflecting the inactivation of DnaA function by ATP hydrolysis. However in the absence of sequestration, the initiation activity of DnaA was not diminished but was elevated instead. This suggests that the hydrolysis of ATP bound to DnaA does not control initiation frequency.

Summary and Perspectives

Studies of the process of initiation from *oriC* has led to a molecular understanding of the events that lead to assembly of the replication fork machinery. Determination of the biochemical mechanisms that control this process will reveal how DNA replication occurs only once per cell cycle.

See Also the Following Articles

Cell Cycle: Control of Entry and Progression Through S Phase • DNA Polymerase III, Bacterial • DNA Replication Fork, Bacterial

Glossary

DnaA box A 9 bp DNA sequence motif recognized by DnaA protein.

DnaA protein The initiator of DNA replication, recognizing the chromosomal replication origin by binding to DnaA box sequences.

DnaB protein The replicative helicase that functions to unwind the parental duplex. Composed of six identical subunits, the single-stranded DNA passes through the central cavity of this ring-shaped protein when it unwinds double-stranded DNA.

DNA polymerase III holoenzyme The replicative DNA polymerase.

DNA replication The process of duplication of DNA.

oriC The *Escherichia coli* chromosomal replication origin where DNA replication is initiated by recognition of DnaA box sequences.

primase The enzyme that forms primers needed for DNA replication by DNA polymerase III holoenzyme.

Further Reading

Baker, T. A., and Bell, S. P. (1998). Polymerases and the replisome: Machines within machines. *Cell* **92**, 295–305.

Donachie, W. D., and Blakely, G. W. (2003). Coupling the initiation of chromosome replication to cell size in *Escherichia coli*.

Kornberg, A., and Baker, T. A. (1992). *DNA Replication*, 2nd edition. W.H. Freeman, New York.

Neidhardt, F. C., Ingraham, J. L., and Schaechter, M. (1990). *Physiology of the Bacterial Cell: A Molecular Approach*. Sinauer Associates, Sunderland, MA.

Nelson, D. L., and Cox, M. M. (2000). *Lehninger Principles of Biochemistry*, 3rd edition. Worth Publishers, New York.

Biography

Jon M. Kaguni is a Professor in the Department of Biochemistry and Molecular Biology at Michigan State University. His principal research interests are on the mechanisms of DNA replication and its regulation. He holds a Ph.D. from the University of California, Los Angeles and received his postdoctoral training at the Stanford University School of Medicine. He developed the enzymatic system to study DNA replication from the *Escherichia coli* replication origin, and has studied the process of initiation of DNA replication throughout his professional career.

DNA Restriction and Modification: Type I Enzymes

David T. F. Dryden
University of Edinburgh, Edinburgh, UK

The original genetic studies of type I DNA restriction and modification (R/M) enzymes were published in 1953 by Bertani and Weigle, the same year that Watson and Crick presented their structural model of B-form DNA. Bertani and Weigle showed that some strains of *Escherichia coli* could reduce (restrict) the ability of bacteriophage to propagate through the bacterial population. Arber and colleagues later showed that surviving phage acquired a modification specific to the host bacterial strain, a modification which was lost upon subsequent passage through different hosts. The biological results were eventually linked to an enzyme-specific modification of DNA by type I R/M enzymes. These enzymes were designated *Type I* because they were the first restriction enzymes to be purified and characterized biochemically by Meselson and Yuan. The type II restriction enzymes prepared some years later had the very desirable property of cutting DNA into defined pieces, and they became the backbone of the genetic engineering revolution. In contrast, the type I enzymes, which cut DNA into unpredictable pieces, have provided important molecular models for complex biological mechanisms.

Biochemical Function

Type I restriction enzymes are large complexes with multiple enzymatic functions, and they possess the ability to switch between these functions depending upon the chemical nature of specific nucleotides within a target DNA sequence. A demonstrated function of type I enzymes in their natural hosts, eubacteria and archaea, is to protect the host from infection by foreign DNA from bacteriophage. This is achieved by two processes; modification of the host DNA by methylation at the N6 position of adenine nucleotides within the recognition sequence targeted by the enzyme and destruction of invading DNA, which typically lacks the appropriate modification of the target sequence. For a host specifying a type I restriction enzyme, typically far fewer than one in one thousand phage successfully infect the host. Therefore, they are a very effective defence system despite the considerable resources devoted by the host cell to their synthesis. This protective function is termed *restriction* and results in the destruction of the phage DNA once it has entered the host cell. Methylation of host DNA occurs during each round of DNA replication. The newly synthesized DNA strand lacks the appropriate methylation; the type I restriction enzyme recognizes this DNA as hemimethylated and adds the methyl group to the adenine in the target sequence in the newly synthesized strand. In this way, the type I restriction enzyme recognizes three different states of methylation of its target sequence, unmodified, hemimethylated, and fully modified, and performs a different reaction on each form of DNA, Figure 1. *In vitro*, the efficiency or accuracy of the switching between activities varies depending upon the particular type I restriction enzyme. For example, EcoKI, the type I restriction enzyme in *E. coli* K12 and EcoR124I, a plasmid encoded type I R/M system, are very precise—methylating only hemimethylated targets and cutting only unmodified ones. In contrast, EcoAI from *E. coli* 15T$^-$ methylates unmodified targets as effectively as hemimethylated targets, and, as a result, this activity competes with the restriction of unmodified DNA. These three enzymes are the best characterized examples of the type I restriction enzymes.

Genes and Protein Structure

It has been shown that three genes are required to specify a type I system, *hsdS*, *hsdM*, and *hsdR*, where *hsd* refers to host specificity for DNA and *S*, *M*, and *R* stand for specificity, modification, and restriction, respectively. Typically, the *hsdR* gene is expressed from its own promoter and the *hsdM* and *hsdS* genes are expressed from a single promoter upstream of *hsdM*. *hsdR* is typically close to *hsdM/hsdS*, although some genome sequences suggest that this is not always the case. Genome rearrangements also occur around the *hsd* locus and this is used to induce some interesting switching of the expression and target sequence specificity of alternative type I R/M systems within a cell. Most studies

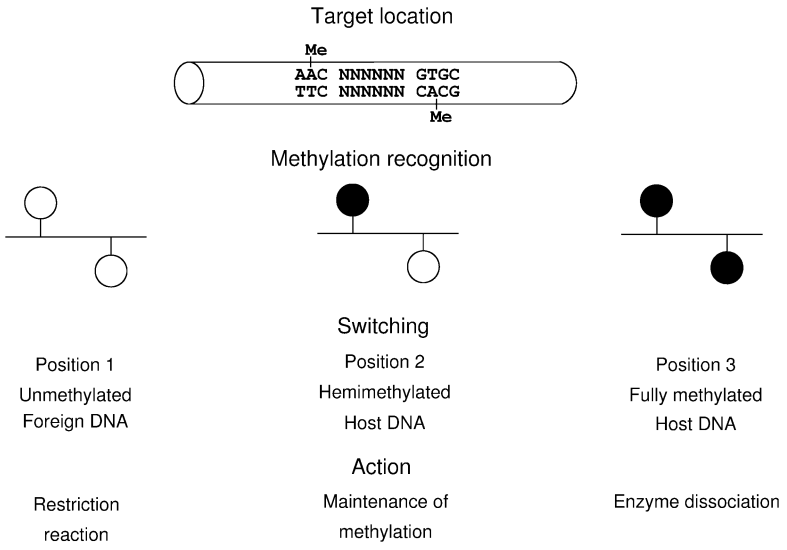

FIGURE 1 The operations performed by a typical type I restriction enzyme are illustrated using the EcoKI enzyme binding to its DNA target sequence AACNNNNNNGTGC and determining the methylation status of the target. The sequence of operations is target location, methylation recognition, switching between different activities, and performance of the selected action.

have concentrated upon the type I systems of *E. coli* and *Salmonella enterica*, and it has been found in these hosts that type I R/M systems can be divided into at least four families based upon the following criteria: DNA hybridization, antibody cross reactivity, and genetic complementation of the *hsd* genes from different systems. These families are known as types IA, IB, IC, and ID. Structural and bioinformatics studies of the Hsd subunits have been used to understand the basis of these families. Within a family, amino acid sequence identity of the three expressed polypeptides is very high except for two regions of HsdS involved in DNA target recognition. Amino acid sequence identity between polypeptides from different families is much lower and is usually confined to regions of HsdS involved in DNA target recognition if the R/M systems being compared share at least part of the same DNA target sequence specificity, and to short motifs involved in catalysis.

The Sequence Specificity Subunit

HsdS, often referred to as the S subunit, is responsible for recognizing the characteristic bipartite, asymmetric DNA target sequence of type I restriction enzymes, for example, the target for EcoKI is 5′-AACNNNNNNGTGC-3′, where N is any base. S subunits have a mass of approximately 50000 and comprise five regions of primary structure (polypeptide sequence), Figure 2. There are sequences (conserved regions) at the N terminus, the central part of the polypeptide, and at the C terminus that are highly conserved within a family of type I restriction enzymes and show some identity between families. Separating these three conserved regions are two longer sequences that display very limited sequence identity between different S subunits unless the different S subunits recognize the same DNA target sequence or one part of the same target sequence. These polypeptide sequences (variable regions) are associated with recognition of DNA target sequence and each region recognizes one part of the bipartite target sequence of the enzyme. These two variable regions each fold into a tertiary structure domain referred to as a target recognition domain (TRD). A weak sequence identity exists between the TRDs of S subunits and the TRD of methyltransferases from type II R/M systems. This identity covers a region involved in DNA sequence

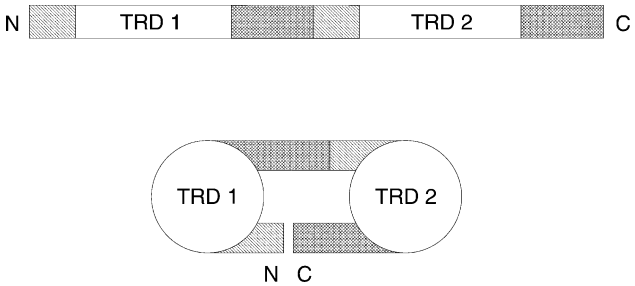

FIGURE 2 Diagrams of a typical S subunit of a type I restriction enzyme. The upper diagram shows the subunit as a linear representation from the N terminus to the C terminus. Regions of sequence conservation between different S subunits are shown hatched. Regions within the subunit with sequence conservation have the same sort of hatching. The conserved regions flank the target recognition domains responsible for DNA sequence recognition. Each TRD recognizes one part of the bipartite target sequence. The lower diagram depicts the folded arrangement of these regions making apparent the approximate twofold rotational symmetry axis of the S subunits.

recognition, and extensive mutagenesis of a TRD from HsdS of EcoKI corroborated this similarity between TRDs from type I and type II R/M systems. The conserved polypeptide regions flanking the TRDs are structural components required to position the TRDs against the DNA target and to act as a scaffold for the binding of the M and R subunits. Some *hsdS* genes have been manipulated to exchange TRDs from different type I R/M systems. The resulting chimeric HsdS recognize new target DNA sequences. In addition, sequence similarity between conserved regions within an S subunit suggested an approximate twofold degree of symmetry in the subunit. A polypeptide comprising one TRD and part of the conserved regions formed a dimeric protein recognizing a twofold symmetrical DNA target. Within a family, the length of the central conserved region influences the number of nonspecific bases found in the DNA target sequence. Naturally occurring variation in the structure of *hsdS* genes has led to the evolution of new target specificities.

The Modification Subunit

Two M subunits bind to HsdS to form a core trimeric enzyme with the properties of sequence specificity, detection of DNA methylation (whether hemimethylated or unmethylated), binding of methylation cofactor S-adenosyl-methionine (SAM), and methyltransferase activity. These M subunits are approximately 60000 molecular mass. The central one-third of the polypeptide sequence contains a series of amino acid motifs that are found in SAM-dependent methyltransferases and are involved in binding of the cofactor, binding of the adenine base specified for methylation, and catalytic transfer of the methyl group from SAM to the N6 position of the adenine base. This region of the M subunit has been successfully modeled upon the catalytic domain of the methyltransferases of type II R/M systems. Mutations in the motifs found in this catalytic domain have deleterious effects on activity. Methylation by type I restriction enzymes almost certainly occurs via the same nucleotide flipping mechanism used by methyltransferases of type II R/M systems in which the base targeted for modification is displaced from the DNA double helix into a catalytic pocket in the SAM-binding catalytic domain. The N terminal part of the M subunit of EcoKI appears to play a role in recognition of the methylation status of the DNA target sequence and mutations reduce the preference of EcoKI for methylating only hemimethylated DNA. The C terminal region of M subunits appears to play a role in interacting with the S subunit to form the core assembly. The polypeptide sequence of M subunits are almost identical within the same type I family but identity between families is mostly confined to the motifs in the catalytic domain.

The Restriction Subunit

The complete type I restriction enzyme is formed by adding two R subunits to the core trimer to form a complex with subunit stoichiometry $R_2M_2S_1$ and a mass of around 440000, an enormous multifunctional molecular machine. As for HsdM, the R subunits show high sequence identity for members in the same family but lower identity, confined to a series of amino acid motifs, for comparisons between families. The complete restriction enzyme is still capable of methylating the DNA target sequence if it is hemimethylated and, if it is a type I system of low preference such as EcoAI, of methylating unmodified targets as well. However, unmethylated DNA target sequences primarily trigger the restriction reaction. The R subunits contain three main regions. An N terminal domain contains an amino acid motif found in DNA endonucleases particularly endonucleases from type II R/M systems. Mutagenesis experiments reveal that this domain is responsible for DNA cleavage by type I restriction enzymes. The central portion of the subunit contains a further set of amino acid motifs characteristic of the so-called DEAD-box helicases, enzymes which translocate or move DNA. These motifs form a multidomain structure that binds and hydrolyzes ATP and couples this hydrolysis to the movement of DNA relative to the enzyme (DNA translocation). Mutation abolishes the ability to hydrolyze ATP and translocate DNA. In the absence of translocation, the enzyme cannot cut DNA and restriction activity is lost even though the endonuclease domain is unaltered. The C terminal region of HsdR appears to be required for interaction with the core trimer.

Assembly and Control of the Type I Restriction Enzyme

The assembly of the complete type I restriction enzyme is a complex affair and many type I R/M systems can form proteins with different subunit stoichiometries. The main partially assembled form of type I restriction enzymes is a trimer M_2S_1, which forms a fully functional modification methyltransferase recognizing the same DNA target as the complete enzyme. Other partially assembled forms and even individual subunits can be isolated and can display some limited activities such as sequence specificity, cofactor binding, and, for the $R_1M_2S_1$ form of EcoR124I, DNA methylation and ATP hydrolysis-driven DNA translocation. Intracellular concentrations of the Hsd subunits may vary with host conditions and it has been suggested that concentration-dependent assembly may play a role in the establishment of type I R/M systems in new hosts. It has also been shown that when the host cell acquires unmodified target sequences after suffering DNA

damage, the restriction activity of type IA and IB R/M systems is controlled by proteolytic digestion of hsdR. This control process prevents the type I restriction enzyme from attacking the unmodified target sequences in the damaged host chromosome.

The Restriction Reaction

DNA Binding and Recognition of Unmodified DNA

The type I restriction enzymes display a strong preference, in the presence of their cofactors, for binding to their DNA target sequence rather than to other DNA sequences. Although sequence specificity resides within HsdS, the presence of HsdM appears to be essential for strong binding to DNA. Once bound, the HsdM plus SAM detect the presence of adenine methylation on each strand of the DNA target using the base flipping mechanism. If the adenine is already methylated, then it will not be able to fit properly into the catalytic site as the methyl group will clash with the methyl group of SAM. This steric hindrance appears to change the conformation of the enzyme to allow the methylation reaction to proceed upon hemimethylated DNA or to dissociate from fully modified DNA. However, if both adenines are unmethylated, they can be accommodated within the HsdM along with SAM. The absence of steric hindrance for both target adenines appears to be the trigger for the highly complicated restriction reaction.

Upon recognition of an unmodified target site, the restriction enzyme becomes strongly attached to the DNA target site and does not appear to dissociate from the DNA after carrying out the restriction reaction. Strictly speaking, this lack of enzymatic turnover in the complete process means that type I restriction enzymes are not "enzymes." If the DNA molecule contains more than one target site, the type I restriction enzymes bound at each site can stick to each other to form a large complex. This additional DNA-dependent dimerization of the enzyme arises from diffusional motion of the DNA molecule bringing the bound enzymes into contact and does not depend upon enzyme activity. The functional role, if any, of this dimerization is not known, as it is not necessary for restriction.

ATP Hydrolysis

Unmodified DNA target sequences trigger the hydrolysis of large amounts of ATP. The ATPase activity continues throughout the DNA translocation and cleavage process and even continues after DNA cleavage. The purpose of this continuing ATP hydrolysis observed *in vitro* is not known but may represent continuing DNA translocation on the cleaved DNA substrate.

DNA Translocation

The enzyme remains bound to the target sequence and commences pulling DNA on either side of the target sequence toward itself. Because it is still attached at the target sequence, loops of DNA appear to be extruded from the enzyme, Figure 3. This process requires ATP hydrolysis and generates extensive supercoiling in the DNA. The reeling in of DNA occurs at approximately 100 to 400 base pairs per second and has been shown to occur over huge distances up to approximately 50000 base pairs. Stalling of the movement appears to occur when the translocating enzyme collides with a blockage on the DNA. This blockage can be another translocating type I restriction enzyme if there are two or more target sequences on a particular DNA molecule, stalling on a circular DNA molecule containing only one target sequence or collision with a complex DNA structure such as a fixed Holliday junction.

Cleavage of DNA

Translocation blockage appears to be the signal for cutting of the DNA strands at the stalling location. Cutting does not occur at the original target sequence. As translocation rates of individual type I restriction enzymes on a DNA molecule may vary depending upon

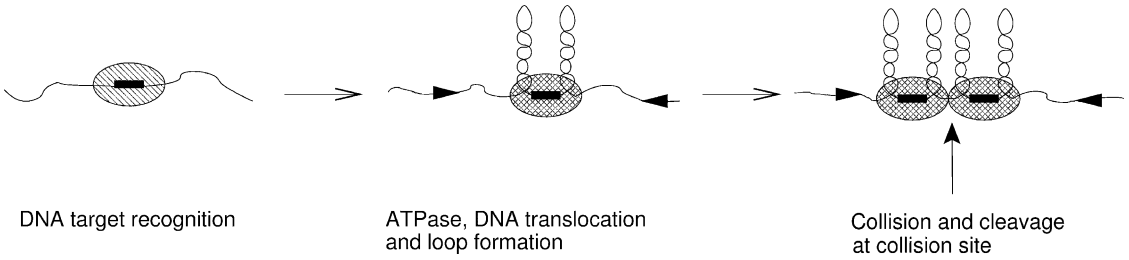

FIGURE 3 The sequence of events occurring after the type I restriction enzyme (oval) has bound and recognized an unmodified DNA target sequence (black box) on a DNA molecule (thin line). ATP hydrolysis drives the translocation of DNA, reeling the DNA in toward the enzyme with, as a consequence, the extrusion of loops of DNA. Eventually, translocation is blocked by, in this example, collision with a second translocating type I restriction enzyme, whereupon cleavage occurs at the collision point. After cleavage *in vitro*, the enzymes remain bound to their target sequence.

the particular enzyme species and upon the sequence being translocated, individual enzymes will stall or collide with each other at different locations on the DNA. Therefore, in a solution containing many DNA molecules, translocation blockage and DNA cleavage occur at a range of locations. For a DNA molecule containing two or more target sequences for the same type I restriction enzyme, cleavage occurs approximately half way between the original DNA target sequences. For a DNA molecule containing target sequences for different type I restriction enzymes, the approximate location of cleavage depends on the relative translocation speeds of the different enzymes. DNA cleavage by type I restriction enzymes does not produce DNA fragments of defined length and sequence but rather a broad range of fragment lengths. Circular DNA molecules containing one target sequence are also cleaved at an undefined distance from the target sequence. The presence of a nick in a DNA molecule appears to bias the cleavage event to be close to the nick.

Antirestriction

Despite their complexity, type I restriction enzymes are very effective barriers against bacteriophage propagation. Bacteriophage have developed a range of countermeasures to overcome this barrier. These antirestriction strategies include selection against presence of target sequences, modification of DNA bases, coinjection of bacteriophage proteins to inhibit restriction enzymes, hydrolysis of the SAM cofactor, and the use of genes encoding specialized proteins that act as competitive inhibitors of DNA binding by type I restriction enzymes. This last strategy is employed by bacteriophage T7, which produces gene 0.3 protein, also known as Ocr (overcome classical restriction), immediately upon infection of *E. coli*. This protein binds very strongly to all characterized type I restriction enzymes, irrespective of their DNA target sequences, and prevents the enzyme from binding to DNA. The structure of Ocr shows that negatively charged aspartate and glutamate side chains are arranged on the protein surface to perfectly match the three-dimensional positioning of the phosphate groups on DNA. Ocr appears to fit perfectly into the DNA-binding site of type I restriction enzymes and acts as a DNA mimic.

See Also the Following Articles

DNA Restriction and Modification: Type II Enzymes • DNA Restriction and Modification: Type III Enzymes

Glossary

hsd Host specificity of DNA. In a host expressing a type I R/M system, DNA containing the specificity target sequence becomes modified or restricted depending upon the methylation status of the target sequence.

modification The process accompanying restriction by which host DNA is maintained in a state of sequence-specific methylation. Most restriction enzymes cannot cleave DNA that has been modified by the methyltransferase partner. Type I restriction enzymes combine both restriction endonuclease and methyltransferase in one protein complex.

restriction The process of hindering the propagation of bacteriophage through a bacterial culture. This process requires cleavage of the bacteriophage DNA by DNA-sequence-specific endonucleases commonly referred to as restriction enzymes.

translocation Usually, the processive motion of an enzyme along DNA. However, for type I restriction enzymes which remain bound to their initial target sequence, refers to the pulling in of DNA toward the enzyme.

Further Reading

Bertani, G., and Weigle, J. J. (1953). Host controlled variation in bacterial viruses. *J. Bacteriol.* **65**, 113–121.

Bickle, T. A., and Kruger, D. H. (1993). Biology of DNA Restriction. *Microbiol. Rev.* **57**, 434–450.

Burckhardt, J., Weisemann, J., Hamilton, D. L., and Yuan, R. (1981). Complexes formed between the restriction endonuclease EcoK and heteroduplex DNA. *J. Mol. Biol.* **153**, 425–440.

Davies, G. P., Martin, I., Sturrock, S. S., Cronshaw, A., Murray, N. E., and Dryden, D. T. F. (1999). On the structure and operation of type I DNA restriction enzymes. *J. Mol. Biol.* **290**, 565–579.

Davies, G. P., Kemp, P., Molineux, I. J., and Murray, N. E. (1999). The DNA translocation and ATPase activities of restriction-deficient mutants of EcoKI. *J. Mol. Biol.* **292**, 787–796.

Meselson, M., and Yuan, R. (1968). DNA restriction enzyme from *E. coli*. *Nature* **217**, 1110–1114.

Murray, N. E. (2000). Type I restriction systems: Sophisticated molecular machines (a legacy of Bertani and Weigle). *Microbiol. Mol. Biol. Rev.* **64**, 412–434.

Studier, F. W., and Bandyopadhyay, P. K. (1988). Model for how type I restriction enzymes select cleavage sites in DNA. *Proc. Natl. Acad. Sci. U.S.A.* **85**, 4677–4681.

Walkinshaw, M. D., Taylor, P., Sturrock, S. S., Atanasiu, C., Berge, T., Henderson, R. M., Edwardson, J. M., and Dryden, D. T. F. (2002). Structure of Ocr from bacteriophage T7, a protein that mimics B-form DNA. *Mol. Cell.* **9**, 187–194.

Biography

David Dryden is a lecturer in physical chemistry at Edinburgh University, Scotland. He earned a degree in chemical physics and a Ph.D. in chemistry from Glasgow University. He gained postdoctoral experience with Roger Pain at Newcastle University. In 1989, he joined Noreen Murray at Edinburgh University to study type I DNA restriction enzymes. He started research on antirestriction proteins after being awarded a University Research Fellowship by the Royal Society in 1994. In 2002, he published, with Malcolm Walkinshaw (Edinburgh University), the first atomic structure of an antirestriction protein.

DNA Restriction and Modification: Type II Enzymes

Darren M. Gowers and Stephen E. Halford
University of Bristol, Bristol, UK

Type II restriction–modification (RM) enzymes are two separate proteins that act in concert to destroy foreign DNA as it enters a bacterial cell, while protecting the host DNA. Destruction of the foreign DNA is accomplished by a sequence-dependent restriction endonuclease, while a modification methyltransferase protects identical sequences in the host DNA. Restriction–modification systems are present in virtually all bacterial genera and show a huge range of DNA specificities. A complete listing can be found at REBASE (rebase.neb.com).

History

The ability of bacteria to defend themselves from viral infection was first reported by Luria and Bertani in 1952, who noted that some strains of *Escherichia coli* could restrict the growth of bacteriophage λ. This was accounted for a decade later by W. Arber, who proposed the existence of restriction–modification (RM) enzymes; the restriction enzymes were envisaged to cleave DNA in response to a particular sequence of bases, but only if the sites had not been protected by prior modification.

A landmark was reached in 1970, when H. O. Smith identified a novel restriction enzyme that cleaved DNA at a specific sequence. In collaboration with D. Nathans, he showed that this enzyme could be used to dissect DNA into discrete fragments. By 1978, when Arber, Nathans, and Smith shared the Nobel Prize in Medicine, nearly 50 restriction enzymes had been discovered. Today, that number stands near 3700. The early availability of restriction enzymes as off-the-shelf reagents heralded the age of recombinant DNA technology.

Classification

At least three distinct categories of RM systems have been identified from their subunit compositions and their modes of action: types I, II, and III. This article focuses on the type II systems. In brief, most type II systems consist of two proteins: a restriction endonuclease that, in the presence of Mg^{2+}, cleaves DNA at a particular sequence, its recognition site; and a modification methyltransferase that blocks restriction activity by transferring a methyl group from S-adenosyl methionine (AdoMet) to a particular base in the recognition site. Only the nucleases from type II systems cleave DNA at specific positions and it is these, unlike the type I and the type III enzymes, which have the myriad applications in recombinant DNA technology.

The enzymes within the type II category display a variety of reaction mechanisms and subunit compositions. Many have been allotted to various subtypes, for example, the type IIS, IIB, IIE, and IIF enzymes.

Discovery of New Restriction–Modification Systems

The value of type II restriction enzymes for DNA manipulations has driven extensive searches for more enzymes of this sort. A common means of identifying new restriction enzymes has been to screen bacterial lysates for endonucleases that cleave DNA into discrete fragments. Phage or adenoviral DNA are often used as test substrates. The recognition sites are then determined by sequencing methods. About one-half of the bacterial strains tested in this way are found to have a RM system, in some cases two or three such systems. But if the enzyme fails to cleave the test DNA for some reason, it will not be detected by this procedure.

New RM systems have also been identified by analyzing the genome sequences of bacteria. Such analyses show that almost all bacteria possess multiple candidates for RM genes, in some cases over 10 such candidates. Subsequent studies showed that a high proportion of the candidate genes were active RM systems, although some did not encode an active endonuclease.

Organization of Genes

Modification and Restriction Genes

The type II systems generally feature two separate genes: one for the restriction enzyme and one for the modification enzyme. In all such systems examined to date, the gene for the endonuclease is adjacent to that for the methyltransferase, although the order of the genes varies between systems. In some cases, they are in head-to-tail orientation and in others head-to-head or tail-to-tail.

Modification genes from different type II systems are often homologous to one another. In many cases, the methyltransferase genes encode 10 highly conserved blocks of amino acid sequence which are involved directly in catalysis and S-adenosyl methionine and AdoMet binding. Another block of protein sequence, which is not conserved, is involved in DNA recognition.

The restriction genes in the type II systems are never homologous to the modification gene from the same system, despite coding for proteins recognizing the same DNA sequence. Moreover, the restriction enzymes from different type II systems have dissimilar amino acid sequences, apart from enzymes with the same recognition site. The only well-conserved feature is the motif Pro-Asp-X_{10-20}-(Asp/Glu)-X-Lys (where X is any amino acid), which is often found at the active site. The aspartate and glutamate residues form part of the binding site for Mg^{2+}.

There are, however, many type II systems that deviate from the standard pattern of one modification gene and one restriction gene. For instance, some systems employ two modification enzymes, one for each strand of the DNA. Others have two restriction genes to encode an enzyme comprising two different subunits. In further cases, one gene encodes a single polypeptide with both modification and restriction activities.

Regulating Restriction–Modification Expression

Whenever a bacteria gains a new RM system, expression of the RM genes has to be stringently coordinated. The methyltransferase must be produced first, to protect all the recognition sites in the chromosome, before significant amounts of the endonuclease are made. To do this, some type II RM systems, such as PvuII and BamHI, contain a gene upstream of the restriction gene that codes for a protein that regulates gene expression in this manner.

The Type II Restriction Endonucleases

Recognition Sequences

The recognition sequences for the majority of the type II restriction enzymes possess three attributes (Table I). First, the sites are usually 4–8 bp long. Second, the sites are palindromic: they read the same in 5′–3′ directions on both strands. Third, the sites are fully specified, in that every position in the sequence is occupied by a particular base. These enzymes cleave DNA at their recognition sites much more rapidly than any other sequence.

For some other enzymes, the recognition sequence is degenerate, in that certain positions can be occupied by alternative bases. For example, the recognition sequence for Cfr10I (Table I) has either G or A at its 5′-end and either C or T at its 3′-end. Similarly, the central base pair in the target site for EcoRII can be either an A:T or a T:A. For some systems, the recognition sequence is discontinuous, for example, SfiI (Table I). Such sites contain two blocks of specified sequence interrupted by a section of unspecified sequence but defined length that varies from just 1 bp (e.g., HinfI at GANTC) to 9 bp (e.g., XcmI at CCA$(N)_9$TGG). In most cases, the specified base pairs in the degenerate and in the discontinuous sites are still symmetrical palindromes.

Some recognition sites are truly asymmetric. For example, the 5′–3′ sequence in the top strand of the recognition site for BbvCI is not the same as the bottom strand (Table I). Many enzymes that recognize asymmetric sequences cleave the DNA some distance away from the site, at fixed positions on one side of the site. These are called the type IIS enzymes. One example is FokI at GGATG(9/13); it cleaves 9 bases downstream from its site on the top strand and 13 bases away on the bottom strand (Table I). However, some cut just one strand, for example, N.BstNBI (Table I). Conversely, some enzymes that recognize asymmetric sequences cleave both upstream *and* downstream of the recognition site, for example, BcgI (Table I). They cut four phosphodiester bonds in their reactions to liberate a small DNA fragment, 32 bp in the case of BcgI, which contains the intact recognition site. Such enzymes belong to the type IIB category.

The 3700 known enzymes have only 230 different recognition sequences, so enzymes from different species often have the same recognition site. Those that cut at exactly the same position are called isoschizomers; for example, HhaI and CfoI both cut GCG↓C. Those that cut at different positions within the same sequence are called neoschizomers; HinP1I, which cuts G↓CGC, is thus a neoschizomer of HhaI.

TABLE I

Recognition Sites for Type II Restriction Endonucleases

Site	Enzyme	Genus	Recognition site
Palindromic			
4 bp			
5′ overhangs	Sau3AI	*Staphylococcus aureus*	5′ ↓ G-A-T-C 3′ 3′ C-T-A-G ↑ 5′
Blunt ends	AluI	*Arthrobacter luteus*	A-G ↓ C-T T-C ↑ G-A
3′ overhangs	HhaI	*Haemophilus haemolyticus*	G-C-G ↓ C C ↑ G-C-G
6 bp			
5′ overhangs	EcoRI	*Escherichia coli*	G ↓ A-A-T-T-C C-T-T-A-A ↑ G
Blunt ends	EcoRV	*Escherichia coli*	G-A-T ↓ A-T-C C-T-A ↑ T-A-G
3′ overhangs	PvuI	*Proteus vulgaris*	C-G-A-T ↓ C-G G-C ↑ T-A-G-C
8 bp			
5′ overhangs	NotI	*Nocardia otitidis*	G-C ↓ G-G-C-C-G-C C-G-C-C-G-G ↑ C-G
Blunt ends	PmeI	*Pseudomonas mendocina*	G-T-T-T ↓ A-A-A-C C-A-A-A ↑ T-T-T-G
3′ overhangs	SgfI	*Streptomyces griseoruber*	G-C-G-A-T ↓ C-G-C C-G-C ↑ T-A-G-C-G
Degenerate			
	Cfr10I	*Citrobacter freundii*	(G/A) ↓ C-C-G-G-(C/T) (C/T)-G-G-C-C ↑ (G/A)
	EcoRII	*Escherichia coli*	↓ C-C-(A/T)-G-G G-G-(T/A)-C-C ↑
Discontinuous			
	SfiI	*Streptomyces fimbriatus*	G-G-C-C-N_4 ↓ N-G-G-C-C C-C-G-G-N ↑ N_4-C-C-G-G
Asymmetric			
Cleaves within site	BbvCI	*Bacillus brevis*	C-C ↓ T-C-A-G-C G-G-A-G-T ↑ C-G
Cleaves outside site	FokI	*Flavobacterium okeanokoites*	G-G-A-T-G-N_9 ↓ N-N-N-N C-C-T-A-C-N_9-N-N-N-N ↑
Cleaves one strand	N.BstNBI	*Bacillus stearothermophilus*	G-A-G-T-C-N-N-N-N ↓ N C-T-C-A-G-N-N-N-N-N
Cleaves both sides	BcgI	*Bacillus coagulans*	↓ N_{10}-C-G-A-N_6-T-G-C-N_{12} ↓ ↑ N_{12}-G-C-T-N_6-A-C-G-N_{10} ↑

Protein Structures

The enzymes that recognize palindromic DNA sequences are generally dimers of identical subunits. They interact with their recognition sequences symmetrically so that all the contacts between one subunit of the protein and one half of the recognition site are duplicated by the second subunit with the other half of the DNA. One active site in the dimer is positioned against the scissile phosphodiester bond in one strand of the DNA and likewise the second active site on the other strand.

The structures of several type II endonucleases, and their complexes with DNA, have been determined by X-ray crystallography. As with most other proteins that act at specific DNA sequences, restriction enzymes recognize their target sequences primarily by multiple hydrogen bonds to the bases in the major groove of the DNA. However, the restriction enzymes do not usually employ the elements of protein structure that are common amongst DNA-binding proteins, such as the helix–turn–helix or the zinc-finger. Instead, their DNA-recognition

elements encompass a wide variety of nonstandard structures, including loops, sheets, and helices. These also differ considerably from one enzyme to the next. In some cases, such as EcoRV, contacts to the specific sequence also depend on deformations to DNA structure.

Despite the differences in their structural elements for DNA recognition, and indeed in the overall dissimilarity in their amino acid sequences, some type II restriction enzymes have similar tertiary structures, for example, EcoRI and BamHI or EcoRV and PvuII. Similar structures have since been found in many other proteins that act on DNA, including enzymes involved in replication, recombination, repair, and transposition.

Cleavage of Specific DNA Sequences

Enzymes such as EcoRI or EcoRV find their recognition sites in long DNA molecules by first binding to the DNA anywhere along the chain and then translocating to the recognition site. The transfer seems to occur primarily by multiple rounds of dissociation and reassociation events with the same chain. However, one-dimensional diffusion along the chain may also play a role, particularly over short distances of DNA. Once at the recognition site, each active site in the dimeric enzyme catalyzes the hydrolysis of its target phosphodiester bond in independent reactions. Both reactions are usually complete within the lifetime of the DNA–protein complex, so the initial product released from the enzyme is the DNA cut in both strands. However, if the complex dissociates before both strands are cut, for example, in reactions at high ionic strength, DNA cleaved in one strand is liberated.

With very few exceptions, the type II endonucleases require Mg^{2+} for their reactions. Some other metal ions, such as Mn^{2+} or Co^{2+}, give low levels of activity but others, such as Ca^{2+}, give no activity at all. The Mg^{2+} ions play direct roles in the catalytic reaction, but the precise roles vary from enzyme to enzyme. Some, such as EcoRI and BglII, seem to have one metal ion at each active site, whereas EcoRV, BamHI, and many others use two ions.

The hydrolysis of phosphodiester bonds by type II endonucleases yields termini with 5′-phosphate and 3′-hydroxyl groups. Some enzymes introduce staggered breaks into the DNA, leaving fragments of double-stranded DNA with single-strand extensions at either their 5′-ends (e.g., EcoRI in Table I) or their 3′end (e.g., PvuI in Table I). Others cut both strands at equivalent positions, producing blunt-ended fragments (e.g., EcoRV in Table I).

Interactions with Nonspecific DNA

The type II restriction enzymes are extremely specific for their cognate sequences. They cleave their recognition sites over a million times more rapidly than DNA sequences that differ from the recognition site by just 1 bp. Surprisingly, this specificity in catalysis need not be accompanied by an equivalent specificity in DNA binding. In the absence of Mg^{2+} ions, many restriction enzymes bind to all DNA sequences with equal affinities. Their extraordinary specificities for DNA cleavage arise instead from the catalytic reaction, with only the cognate DNA giving rise to a catalytically competent enzyme–Mg^{2+}–DNA complex. For example, the complex of EcoRV with nonspecific DNA has a low affinity for Mg^{2+}, whereas its complex with specific DNA has a high affinity for Mg^{2+}, so only the specific DNA is cleaved.

Certain reaction conditions can, however, enhance the activities of these enzymes at alternative sites. This is termed star activity. The star sites are generally sequences that differ from the recognition site by 1 bp; sequences differing in two or more positions are normally resistant even under star conditions. The conditions that cause star activity include high pH, low ionic strength, the addition of organic solvents, and the replacement of Mg^{2+} with Mn^{2+}.

Subsets of Type II Restriction Enzymes

In recent years, many type II enzymes have been found to have distinctive properties and have been classified into subsets. Most of these enzymes have to interact with two copies of their recognition site before cleaving DNA. The restriction enzymes that need two sites are in effect double-checking the DNA to ensure that they cleave DNA only at the correct sequence.

Type IIS

Type IIS enzymes recognize asymmetric sequences and cleave the DNA short distances downstream of the recognition site, typically 1–20 bp away. FokI (Table I) is the archetype of the type IIS enzymes. It is a monomeric protein containing two domains connected by a flexible linker: a DNA recognition domain that makes all of the contacts to the recognition site and a catalytic domain that has an active site capable of cleaving one DNA strand. To cut both strands, two monomers of FokI have to aggregate to a dimer via their catalytic domains to create a unit with two active sites. The dimer is formed most readily when both monomers are bound to separate FokI sites in the same DNA molecule. FokI is thus more active on molecules with two sites than on DNA with one site. This is a common feature of the type IIS enzymes. Most of them cleave DNA with two target sites more rapidly than DNA with one site even though they are not all monomers. Instead,

some are dimers, such as BfiI at ACTGGG(5/4), and others are tetramers, such as BspMI at ACCTGC(4/8).

Type IIE

Another subset of type II enzymes is the type IIE group, typified by EcoRII and NaeI, which consists of dimers of identical subunits. In these enzymes, the interface between the subunits has two binding clefts for the recognition sequence rather than the single cleft in enzymes such as EcoRV and BamHI. One cleft has the catalytic functions for DNA cleavage, but these are inactive unless the other cleft has bound another copy of the recognition site. Interactions spanning two DNA sites occur more readily with sites in *cis* on the same molecule of DNA than with sites in *trans* on different molecules. The type IIE enzymes thus cleave DNA with two recognition sites faster than DNA with one site, but only one of the two sites is cut per turnover.

Type IIF

SfiI, Cfr10I, NgoMIV, and several other restriction enzymes show further differences from the orthodox pattern, and this group is now known as the type IIF enzymes. They are tetramers of identical subunits, two of which interact with one copy of a palindromic recognition sequence while the other two interact with a second copy. To cleave DNA, both binding sites must be filled with cognate DNA. Hence, like the type IIE enzymes, the type IIF enzymes also interact with two copies of the target sequence, but, in contrast to the IIE systems, the IIF enzymes cut both sites in both strands. They thus cleave four phosphodiester bonds per turnover to convert a DNA with two sites into the product cut at both sites. They display optimal activity with sites in *cis* – the concurrent binding of the enzyme to sites in the same molecule of DNA traps the intervening DNA in a loop. Nevertheless, they can also act, albeit less efficiently, with sites in *trans* by bridging separate molecules.

Type IIB

By cutting both strands of the DNA on both sides of their recognition sites, the type IIB enzymes such as BcgI (Table I) cut four phosphodiester bonds at *each* recognition site. Moreover, like many other restriction enzymes, the IIB enzymes are more active against DNA with two recognition sites than DNA with a single site. They thus have the potential to cleave eight phosphodiester bonds per turnover. The IIB enzymes also differ from the orthodox enzymes in subunit composition. For instance, BcgI contains two different subunits: one carries both the endonuclease and methyltransferase activities and the other recognizes the cognate DNA. Other type IIB enzymes contain a single subunit with endonuclease, methyltransferase, and DNA recognition functions. Moreover, some require AdoMet for not only the methyltransferase but also the endonuclease activity.

The Type II Modification Methyltransferases

Purpose of Methylation

The methyltransferases of type II RM systems are altogether different from the partner endonucleases; their only commonality is recognition of the same DNA sequence. The purpose of the modification enzyme is to protect recognition sites in the host DNA from the restriction enzyme. They achieve this by transferring a methyl group from AdoMet to a particular base in the recognition sequence. Some methylate the carbon at position 5 (C5) of the cytosine ring, some the exocyclic amino group at position 4 in cytosine, and some the exocyclic amino group at position 6 in adenine. Each turnover of a modification enzyme methylates the recognition sequence in one strand. This is sufficient to block the activity of the restriction endonuclease. Hence, following semiconservative replication of fully methylated DNA, the hemimethylated daughter strands are protected. The unmethylated strand must then be modified by the methyltransferase before the next round of replication.

The Methyltransferase Enzymes

The methyltransferases from type II RM systems are monomeric proteins. The same enzyme methylates both strands of palindromic sites, but two methyltransferases are needed at asymmetric sites: one for the top strand and another for the bottom strand, although both activities are sometimes present in one polypeptide. The crystal structures of these enzymes have revealed two domains, one on either side of a DNA-binding cleft. One domain contains the DNA-recognition functions, which are unique to each methyltransferase, and the other the binding site for AdoMet and the catalytic residues for the transfer reaction.

The crystal structure of the HhaI methyltransferase bound to its recognition sequence revealed a novel perturbation of the DNA. Remarkably, the target cytidine had been swiveled completely out of its stacked conformation in the DNA helix and into the active site of the enzyme, deep in the catalytic domain. Other DNA-processing enzymes also use this mechanism, for example, the uracil DNA glycosidases in DNA repair. Base flipping may be a ubiquitous device used by enzymes that require access to the nucleotide bases in DNA that are otherwise buried in the double helix.

All methyltransferases use AdoMet as the methyl donor. With the cytosine C5 methyltransferases, the

carbon must first be activated. This is achieved by forming a covalent bond between the adjacent C6 position on the cytosine and the thiol group of a cysteine in the active site of the protein. The subsequent transfer of the methyl group to C5 expels the cysteine from C6, thus breaking the covalent link between protein and DNA. With the cytosine N4 and the adenine N6 methyltransferases, the exocyclic amino group may function directly as a nucleophile to attack the transferable methyl group of AdoMet.

Restriction Enzymes in the Laboratory

Various factors have contributed to the adoption of type II restriction enzymes as essential research tools. The foremost is their specificity in cleaving DNA at fixed positions at particular sequences, that is, their abilities to recognize simple DNA sequences within any DNA molecule and to cleave the DNA at those sites without cleaving other sites to any detectable extent. Consequently, a restriction digest yields a discrete set of defined fragments determined by the positions of the recognition sites in the DNA molecule. Moreover, the resultant fragments of duplex DNA may, depending on the restriction enzyme being used (Table I), possess single-strand extensions that are mutually complementary. Such fragments can be then ligated to other DNA molecules with the same single-strand extensions.

The applications of restriction enzymes have led to the emergence of several companies for whom restriction enzymes are the primary product line. The availability of these enzymes permitted far-reaching technical advances, such as the construction of recombinant DNA molecules, restriction mapping, DNA sequencing, and the use of restriction-fragment-length polymorphisms (RFLPs) as genetic markers for genealogical analysis and gene isolation.

One feature of type II nucleases that concerns users is their star activity (noted previously). Under altered conditions, the barriers that prevent the enzymes from cleaving DNA at noncognate sites are less severe than those under optimal conditions. There is no general remedy for this, other than avoiding the conditions that cause it: low ionic strength, high pH, organic solvents, and Mn^{2+}. A further concern is the fact that many restriction enzymes cleave DNA only after interacting with two recognition sites. Such enzymes have low activities against DNA molecules with one target site, but they can be activated against single-site substrates by adding oligonucleotide duplexes that have the recognition sequence.

See Also the Following Articles

DNA Restriction and Modification: Type I Enzymes • DNA Restriction and Modification: Type III Enzymes

Glossary

S-adenosylmethionine (AdoMet) The cofactor for methyltransferases.

palindromic DNA A DNA in which the 5′–3′ sequence of one strand is the same as that of the complementary strand.

recognition site A sequence of nucleotide bases recognized by a restriction enzyme.

restriction digest The cleavage of DNA molecules into defined fragments by the action of a (type II) restriction enzyme.

restriction mapping Placing the series of DNA fragments from a restriction digest into the order in which they occur along the DNA.

restriction–modification (RM) The bipartite bacterial defense system. Unmethylated phage DNA is hydrolyzed at specific sites by a *R*estriction enzyme; host DNA containing the same sequences is guarded from destruction by methylation from a *M*odification methyltransferase.

Further Reading

Cheng, X., and Roberts, R. J. (2001). AdoMet-dependent methylation, DNA methyltransferases and base flipping. *Nucleic Acids Res.* **29**, 3784–3795.

Halford, S. E. (2001). Hopping, jumping and looping by restriction enzymes. *Biochem. Soc. Trans.* **29**, 363–373.

Pingoud, A., and Jeltsch, A. (2001). Structure and function of type-II restriction endonucleases. *Nucleic Acids Res.* **29**, 3705–3727.

REBASE. Available at: http://rebase.neb.com/rebase.

Roberts, R. J., and Macelis, D. (2001). REBASE-restriction enzymes and methylases. *Nucleic Acids Res.*, **29**, 268–269.

Roberts, R. J., Belfort, M., Bestor, T., Bhagwat, A. S., Bickle, T. A., Bitinaite, J., Blumenthal, R. M., Degtyarev, S. K., Dryden, D. T. F., Dybvig, K., Firman, K., Gromova, E. S., Gumport, R. I., Halford, S. E., Hattman, S., Heitman, J., Hornby, D. P., Janulaitis, A., Jeltsch, A., Josephsen, J., Kiss, A., Klaenhammer, T. R., Kobayashi, I., Kong, H., Kruger, D. H., Lacks, S., Marinus, M. G., Miyahara, M., Morgan, R. D., Murray, N. E., Nagaraja, V., Piekarowicz, A., Pingoud, A., Raleigh, E., Rao, D. N., Reich, N., Repin, V. E., Selker, E. U., Shaw, P-C., Stein, D. C., Stoddard, B. L., Szybalski, W., Trautner, T. A., Van Etten, J. L., Vitor, J. M. B., Wilson, G. G., and Xu, S-Y. (2003). A nomenclature for restriction enzymes, DNA methyltransferases, homing endonucleases and their genes. *Nucleic Acids Res.*, in press.

Biography

Darren Gowers is a postdoctoral researcher at Bristol University. His interests include the mechanisms of restriction enzymes that interact with two DNA sites, and the mechanisms by which sequence-specific DNA-binding proteins locate their target sequences. He gained his Ph.D. degree in 1998 from Southampton University.

Stephen Halford has led a research group at the University of Bristol since 1976, examining several different sorts of enzyme reactions on DNA, primarily the type II restriction endonucleases. He received his Ph.D. from Bristol University in 1970. In 2000, he was awarded the Novartis Medal of the Biochemical Society.

DNA Restriction and Modification: Type III Enzymes

Desirazu N. Rao and S. Srivani
Indian Institute of Science, Bangalore, India

Type III restriction–modification (RM) enzymes are multifunctional proteins that exhibit both restriction and modification activities. Five members in this class of enzymes have been characterized to some extent: *Eco*PI from prophage P1, *Eco*P15I from the prophage P1-related plasmid p15B in *Escherichia coli*, *Hin*fIII from *Haemophilus influenzae*, *Sty*LTI from *Salmonella typhimurium*, and *Lla*FI from *Lactococcus lactis*. These enzymes are composed of two subunits, products of the *res* and *mod* genes, and require ATP, S-adenosyl-L-methionine (AdoMet) and Mg^{2+} for restriction. The Mod subunit alone functions as a methyltransferase in the presence of AdoMet, whereas restriction activity requires the cooperation of both the Res and Mod subunits. Type III restriction enzymes characteristically recognize DNA sequences that lack symmetry and cleave DNA 25–27 base pairs downstream of the sequence. Two inversely oriented (→←) unmethylated sites are the substrates for cleavage by type III restriction enzymes. It has been shown that ATP hydrolysis is required for DNA cleavage by the type III enzymes. In contrast, methylation proceeds regardless of the number and orientation of recognition sequences.

*Eco*PI and *Eco*P15I

*Eco*PI and *Eco*P15I restriction enzymes (R.*Eco*PI and R.*Eco*P15I) recognize the sequences 5′-AGACC-3′ and 5′-CAGCAG-3′, respectively. The *res* gene product is a 106-kDa protein, while the product of the *mod* gene is a 75-kDa protein. Analytical ultracentrifugation and gel quantification of *Eco*PI and *Eco*P15I restriction enzymes revealed a common Res_2Mod_2 subunit stoichiometry. The *Eco*PI and *Eco*P15I systems are closely related, in which complementation as well as recombination between the structural genes are possible. Electron microscopic analysis of heteroduplexes between the *Eco*P1 and *Eco*P15 genes reveals that the *res* genes of the two systems are largely homologous. The *mod* genes are a mosaic of homologous and nonhomologous regions, the latter being responsible for sequence specificity of these enzymes.

Substrate Requirements

Cleavage of DNA by *Eco*P15I restriction enzyme (and the type III restriction enzymes in general) can be explained by a tracking–collision model (Figure 1). The model states that one *Eco*P15I molecule bound to a recognition site produces a DNA loop of increasing size as it tracks along the DNA until it collides with another *Eco*P15 molecule bound to another site tracking in the opposite direction. Translocation thus positions the two inversely oriented enzyme–site complexes appropriately for cleavage to occur. However, cleavage occurs at only one of the two possible cleavage positions and is a random event.

DNA translocation requires a driving force (ATP hydrolysis). It has been shown that the ATPase activity of *Eco*P15I and *Eco*PI is uniquely recognition site-specific. The collision complex is considered to be the endonucleolytically active form of the enzyme. Both cleavage products contain the original recognition sites, allowing the enzyme to remain bound and continue tracking. A DNA substrate possessing one *Eco*PI and one *Eco*P15I site in a head-to-head configuration was cleaved only in the presence of both enzymes, clearly demonstrating that these two different type III enzymes can functionally cooperate in DNA cleavage. Results from such cooperation assays using mutant enzymes suggest that double-strand breaks result from top strand cleavage by a Res subunit proximal to the site of cleavage, while bottom strand cleavage is catalyzed by a Res subunit supplied in trans by the distal endonuclease in the collision complex. DNA translocation appears not to be required for cleavage initiation, as two adjacent head-to-head or tail-to-tail oriented sites are efficiently cleaved. Post cleavage, the enzyme remains bound to the DNA. An exonuclease is required to act on these molecules releasing the enzyme for subsequent rounds of catalysis. Thus, efficiency of enzyme increases with decreased affinity for cleaved DNA.

One of the fundamental differences between type I and type III enzymes is that cleavage occurs at the point where the two DNA-translocating restriction enzyme complexes collide. While the cleavage by type III R–M

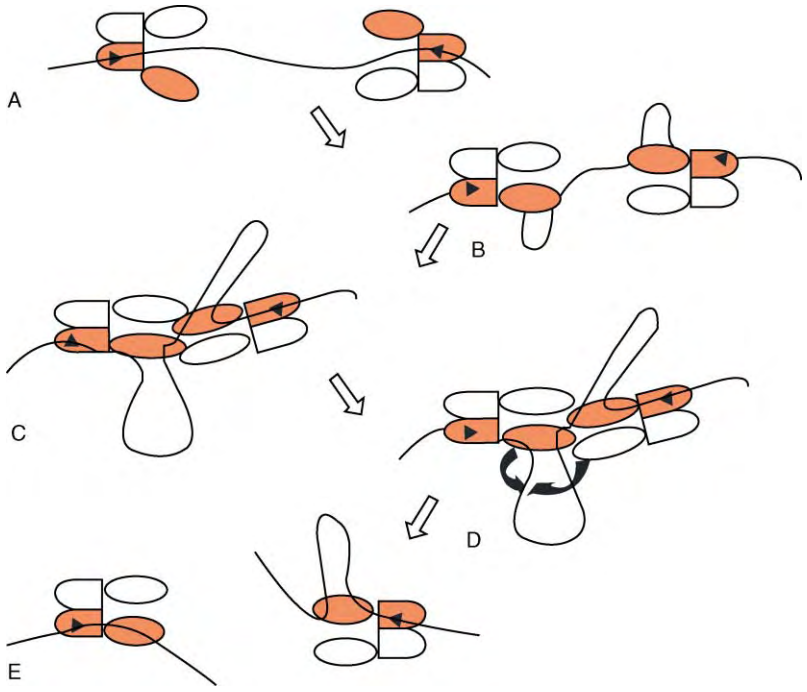

FIGURE 1 Schematic diagram showing the model proposed for DNA cleavage by type III RM enzymes (and represent Mod subunit; and represent Res subunit). (**A**) Enzyme binds two inversely oriented recognition sequences. (**B**) ATP-dependent DNA-translocation commences resulting in looping of DNA. (**C**) Collision of the two complexes results in conformational changes in Res subunit. (**D**) DNA cleavage: top strand is cut by the proximally attached Res subunit and bottom strand is cut by the distally attached Res subunit. (**E**) Cleaved DNA with the RM enzyme attached.

enzymes occurs 25–27 base pairs from the recognition sites, type I enzymes cleave 1000–7000 base pairs away from their recognition sites. Type III enzymes cleave at the recognition site proximal end of the tracking loop as illustrated in Figure 1. An unspecific molecular barrier such as a bound Lac-repressor, which would halt DNA translocation, is not adequate to evoke DNA cleavage by the type III enzyme, *Eco*P15I. Despite differences in structure and mode of action, type I and type III enzymes appear closely related mechanistically.

Cofactor Requirements

Both *Eco*P15I and *Eco*PI restriction enzymes possess sequence-specific ATPase activity. Nonhydrolyzable analogs of ATP, such as AMP-PNP or ATP-γS, cannot replace ATP in the reaction. DNA restriction by *Eco*PI restriction enzyme requires exogenous addition of AdoMet, while the closely related *Eco*P15I enzyme has bound AdoMet and therefore, does not require the addition of this cofactor for DNA cleavage. Reconstitution experiments, which involve mixing of the isolated subunits of R.*Eco*P15I result in an apoenzyme form, which is restriction proficient only in the presence of AdoMet. However, mixing the Res subunit with Mod subunit deficient in AdoMet binding does not result in a functional restriction enzyme, suggesting that AdoMet binding causes a conformational change, which is necessary for DNA cleavage.

Organization of Genes and Regulation of Restriction Activity

Several observations implied that the *mod–res* operon was transcribed as a single unit. Sequence analysis of the genes showed a two base pair gap between the end of *mod* and the beginning of *res* gene. This led to the conclusion that translation of the *res* gene was due to ribosomal shuffling from the terminator to the initiator codon, an initiation factor independent event.

A tight control of the potentially lethal activity of the restriction enzyme must be ensured for efficient establishment of type III restriction–modification (RM) system in a cell. Two independent post-transcriptional regulatory mechanisms control the expression of restriction activity: (a) The modification activity is expressed immediately after the RM genes enter the cell, whereas the expression of restriction activity is delayed until the complete protection of cellular DNA is achieved by methylation. The expression of the modification subunit regulates the amount of restriction subunit present in the cell, suggesting that the correct folding of Res into active and stable configuration is promoted by its interaction with the Mod subunit. (b) *In vivo* restriction activity is modulated by a decrease in the efficiency of translation and by varying ribosomal accuracy conditions.

Domainal Organization in Restriction Subunit

Multiple sequence alignment of all known and putative Res subunits suggests a modular structure (Figure 2). The ATPase and helicase domains are present in the N-terminal region of Res subunit. The C-terminus contains the P-D…(D/E)-X-K motif that is commonly present in the catalytic center of type II restriction endonucleases. Amino acid sequence comparison of the restriction subunit of *Eco*PI and several putative Res subunits revealed the so-called DEAD box motif that is present in the helicase superfamily II. The members of the DEAD family have seven conserved motifs (motifs I, IA, II–VI). The first of the seven motifs of the DEAD family of helicases resembles the Walker A domain. Mutational analysis of motif I resulted in a loss of DNA cleavage and ATP hydrolysis, while that of motif II significantly decreased ATP hydrolysis but had no effect on DNA cleavage. These motifs must, therefore, clearly play a role in ATP hydrolysis. Mutations in motif VI abolished both activities while mutations in the putative endonuclease active site of Res P1 and Res P15 abolished DNA cleavage, but not ATP hydrolysis.

*Eco*PI and *Eco*P15I restriction enzymes are also modification methylases, more efficient than their methylase counterparts. Studies with *Eco*P15I enzyme revealed that the cofactor requirements for methylation by the modification methylase were different from those for the restriction enzyme. Mg^{2+} is an absolute requirement for the modification methylase, while the restriction enzyme could methylate DNA in the absence of Mg^{2+}. Another contrasting feature is that while ATP stimulates methylation activity of the restriction enzyme, the activity of the modification methylase is not altered. It is thought that stimulation of methylation activity of *Eco*P15I restriction enzyme could be due to DNA tracking which transforms modification from a distributive to a processive reaction.

Hinf III

Hinf III and *Hine*I restriction enzymes recognize the sequence 5′-CGAAT-3′. *Hinf* III enzyme exists as a large complex of two subunits with a molecular size greater than 200 kDa. Two forms of the enzyme, one with AdoMet bound and the other without the cofactor bound are known to occur. Both forms of the enzyme cleave DNA, only in the presence of ATP and Mg^{2+}, which is stimulated by AdoMet.

A search of the whole genome sequence of *H. influenzae* strain Rd identified tetra nucleotide repeats in a gene, with low homology to *Eco*PI *mod* gene. The adjacent downstream gene in the *H. influenzae* genome has low homology to the *res* gene of the type III family. This homology and organization is a strong indication that these genes indeed encode a type III restriction system. It is, therefore, likely that *Hinf* III purified from *H. influenzae* Rf strain is encoded by the *mod* and *res* genes described above. The number of repeats within the *mod* gene influences the rate of phase variation and expression of the *mod* gene. Similarly, a pentanucleotide repeat in the *mod* gene of *Pasteurella haemolytica* may modulate expression of a resident type III system.

Other Type III RM Systems

With the sequencing of a number of genomes, a number of putative RM systems have been discovered. A few RM systems have been characterized but not in extensive detail such as those mentioned earlier.

The *res* and *mod* genes for *Sty*LTI system have been cloned and sequenced. The sequence 5′-CAGAG-3′ was found to be the canonical recognition sequence and methylation was limited to the second adenine in this sequence. Based on the derived amino acid sequence, the *Sty*LT system shows a high degree of homology with the other type III systems. *Lla*FI is the first type III RM system to be characterized from a Gram-positive bacterium, *Lactococcus lactis*. *Lla*FI has cofactor

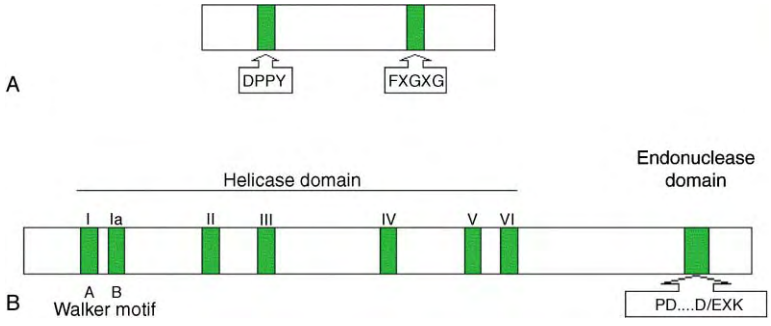

FIGURE 2 Modular structure of type III restriction enzyme. (**A**) Mod subunit showing the location of conserved amino acid sequence regions; catalytic motif, DPPY (motif IV) and AdoMet binding motif, FXGXG (motif I). (**B**) Res subunit showing the location of conserved sequences, helicase motif, and putative endonuclease motif.

requirements that are characteristic of type III enzymes. ATP and Mg^{2+} are required while AdoMet stimulates DNA cleavage. An open reading frame (ORF) from an 8 kb fragment from *Bacillus cereus* ATCC 10987 showed 29.3% identity with the *Eco*PI *res* gene product and 67.6% identity with the deduced amino acid sequence of *Sty*LTI system. Based on these observations, a type III system has been suggested to exist in *B. cereus*. The complete genome sequence of the gastric pathogen *Helicobacter pylori* has revealed four type III RM systems identified on the basis of gene order and similarity to endonucleases and methyltransferases.

DNA Methyltransferases

One unique feature of methylation by *Eco*PI and other type III RM systems is that only one strand of the asymmetric recognition sequence is methylated. Thus, unmodified DNA is the only substrate for the reaction. *Eco*P15I DNA methyltransferase (*Eco*P15I MTase) adds a methyl group to the second adenine in the recognition sequence 5′-CAGCAG-3′ in the presence of AdoMet and Mg^{2+}. *Eco*P15I MTase occurs as a dimer in solution. The kinetic mechanism for *Eco*P15I MTase has been elucidated and the order of substrates binding is random. *Eco*P15I MTase binds about threefold more tightly to DNA containing its recognition sequence 5′-CAGCAG-3′ than to nonspecific sequences in the absence or presence of cofactors. In the presence of ATP, the discrimination between specific and nonspecific sequences increases significantly, suggesting a role for ATP in DNA recognition by these enzymes. *Eco*P15I DNA MTase makes contacts in the major groove of its substrate DNA. The first guanine of the recognition sequence does not show any altered reactivity toward dimethyl sulfate, but the second guanine was modified 3.5-fold better in the presence of the enzyme. This hypermethylation of guanine next to the target adenine could be due to a conformational change in the DNA as a result of protein binding. This probably indicates that the protein flips out the target adenine residue. Both potassium permanganate footprinting and fluorescence spectroscopic measurements support a base flipping mechanism for *Eco*P15I DNA MTase. *Eco*P15I MTase and *Eco*PI MTase, like other N^6-MTases, contain two highly conserved sequences, FxGxG (motif I) and DPPY (motif IV) postulated to form the AdoMet binding site and catalytic site, respectively. Mutations in motif I completely destroy AdoMet binding but leave target DNA recognition unaltered. Mutations in motif IV result in loss of enzyme activity but enhance crosslinking of AdoMet and DNA, implying that DNA and AdoMet binding sites are close to motif IV.

*Eco*PI DNA methyltransferase methylates the second adenine in the recognition sequence 5′-AGACC-3′. Replacement of tyrosine in the conserved DPPY motif with tryptophan results in a mutant enzyme that binds AdoMet almost as well as the wild-type but is catalytically inactive. However, DNA binding is at least threefold stronger than that of the wild-type enzyme.

Clear plaque mutants of phage P1 were isolated to those defective in DNA modification and map to the nonhomologous region of the *mod* gene of P1. These mutant methylases (*c*2 mutants) have either very little or no AdoMet binding and therefore have very weak or no methylating activity. However, the mutant proteins bind specifically to DNA containing *Eco*P1 recognition sequences.

See Also the Following Articles

DNA Methyltransferases, Bacterial • DNA Restriction and Modification: Type I Enzymes • DNA Restriction and Modification: Type II Enzymes

Glossary

base flipping Process in which a base in the normal B-DNA is swung out of the helix into an extrahelical position.

DNA translocation Movement of DNA through a region of protein, an energy-dependent process.

methylation Modification of target base within the recognition sequence by the transfer of a methyl group from AdoMet.

restriction DNA cleavage by a restriction enzyme within or outside the recognition site.

Further Reading

Aude, A., Bourniquel, A., and Bickle, T. A. (2002). Complex restriction enzymes: NTP-driven molecular motors. *Biochimie* **84**, 1047–1059.

Dryden, D. T. F., Murray, N. E., and Rao, D. N. (2001). Nucleoside triphosphate-dependent restriction enzymes. *Nucleic Acids Res.* **29**, 3728–3741.

Krüger, D. H., Küpper, D., Meisel, A., Reüter, M., and Schroeder, C. (1995). The significance of distance and orientation of restriction endonuclease recognition sites in viral DNA genomes. *FEMS Microbiol. Rev.* **17**, 177–184.

Rao, D. N., Saha, S., and Krishnamurthy, V. (2000). ATP-dependent restriction enzymes. *Prog. Nucl. Acid Res. Mol. Biol.* **64**, 1–63.

Biography

Desirazu N. Rao is a Professor in the Department of Biochemistry at the Indian Institute of Science, Bangalore, India. His principal research interests are in the area of DNA–protein interactions using restriction–modification enzymes and DNA mismatch repair proteins as model systems. He holds a Ph.D. from the Indian Institute of Science and received his postdoctoral training at the National Institutes of Health, Bethesda, Maryland; Biozentrum, University of Basel, Switzerland; and the University of Cambridge, United Kingdom.

S. Srivani is a Ph.D. student in the Biochemistry Department, Indian Institute of Science.

DNA Secondary Structure

Albino Bacolla and Robert D. Wells
Institute of Biosciences & Technology, Houston, Texas, USA

The term secondary structure refers to all DNA conformations (non-*B*-DNA) other than the antiparallel right-handed double helix (*B*-DNA). The conventional and commonly accepted structure of the majority of DNA in a cell is that of *B*-DNA, as first proposed by Watson and Crick in 1953. However, experimental data have shown for almost 50 years that nucleic acids exist in a variety of other conformations, including left-handed duplexes and three- and four-stranded helices, with parallel and antiparallel strand orientations. In addition, recent nuclear magnetic resonance (NMR) studies have revealed the assembly of nucleic acids into pentameric and hexameric architectures. These non-*B* conformations are favored by specific sequence motifs at certain chromosomal loci and by defined topological or environmental conditions, such as negative supercoil density or cations.

B-DNA

In 1980, the crystal structure of a helix turn of DNA was reported, which confirmed the Watson and Crick model. Since then, analyses of many sequences agree that the structure of DNA (*B*-DNA) is a right-handed double helix rotating about a central axis of symmetry and forming a major and a minor groove (Figure 1A). The Watson and Crick base-pairing scheme between a purine and pyrimidine base (adenine (A) with thymine (T) and cytosine (C) with guanine (G)) was confirmed. Deviations from these pairings (mismatches) perturb the helix structure and are readily corrected by the cellular DNA repair enzymes.

Z-DNA

The first crystal structure of a DNA minihelix, reported in 1979, revealed a left-handed double helix. It was called *Z*-DNA because of the zigzag shape of the phosphate and sugar backbone.

Structure

Z-DNA is formed by alternating purine–pyrimidine (RY·RY) sequences (where R indicates a purine, A or G, and Y indicates a pyrimidine, C or T; the dot designates the complementary strands), such as the repeating $(CG{\cdot}CG)_n$ and $(CA{\cdot}TG)_n$ motifs (Table I). Structurally, the *Z*-DNA helix is slimmer and more elongated than *B*-DNA, and it lacks a major groove (Figure 1B). *Z*-DNA represents a high-energy state for DNA; *in vivo*, most energy required for the *B* to *Z* transition is supplied by negative supercoiling, a topological state found in chromosomal DNA.

Biology

Alternating (RY·RY) tracts are common in eukaryota, and *Z*-DNA formation has been found mostly in transcribed regions of the genome. In the current model, high negative supercoiling generated behind RNA polymerase complexes during transcription drives the (RY·RY) tracts into a left-handed conformation. The alternative structure, in turn, regulates gene expression. For example, the rat nucleolin promoter contains a $[(CA)_{10}(CG)_8]$ motif that represses promoter activity upon adopting a left-handed conformation. Allelic variants differing in the number of dinucleotide repeats show a quantitative effect on the rate of gene transcription that correlates with the stability of *Z*-DNA. Sera from patients with the autoimmune systemic disease *Lupus erythematosus* contain antibodies against *Z*-DNA. Two eukaryotic proteins, both γ-interferon-inducible, bind and stabilize *Z*-DNA structure: ADAR1, an RNA-editing enzyme, and DLM-1, a protein that is up-regulated in tumor stromal cells.

Triplex DNA

The association of synthetic nucleic acids into three-stranded structures (three-stranded DNA or H-DNA) was reported in 1957 and was confirmed in 1968 with naturally occurring sequences.

Structure

In a three-stranded nucleic acid, consecutive purine bases in a *B*-DNA duplex engage a third base through additional hydrogen bonds, referred to as Hoogsteen hydrogen bonds. These bonds differ from the Watson

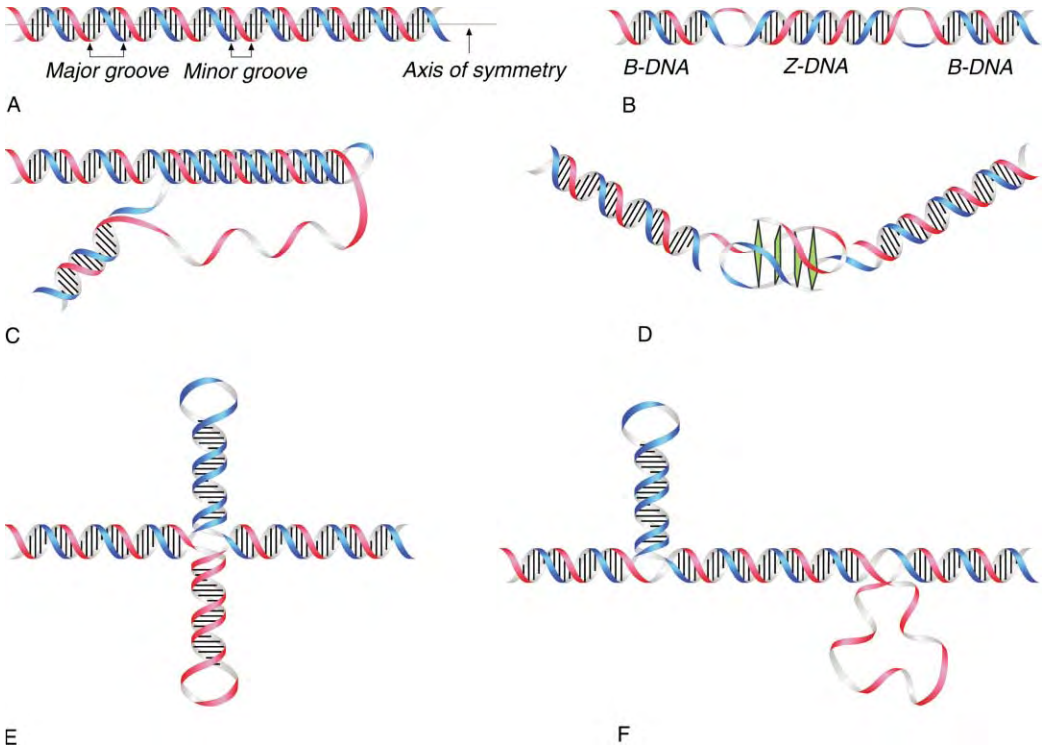

FIGURE 1 DNA secondary structures. (A) *B*-DNA, a canonical antiparallel right-handed double helix with major and minor grooves. (B) *Z*-DNA, a left-handed double helix. The ribbons show the transition between right-handed and left-handed sections. (C) Triplex DNA; ribbon shows a third strand wrapping in the major groove and the complementary strand unpaired. (D) Tetraplex DNA; the model shows an intermolecular tetraplex containing antiparallel strands from two duplex molecules. (E) Cruciforms; the model shows a four-way junction and single-stranded loops. (F) Slipped DNA; the ribbons illustrate two conformationally different slipped structures, a base-paired hairpin and an unpaired loop. Reprinted from R. D. Wells and S. T. Warren, *Genetic Instabilities and Hereditary Neurological Diseases*, p. 563, Copyright 1998, with permission from Elsevier.

and Crick model and were described by Hoogsteen in 1963 when an A·T base pair was first reported. The formation of a triplex requires DNA to contain only purines in one strand and pyrimidines in the complementary strand (R·Y) in a mirror repeat orientation (Table I). In an intramolecular triplex, one-half of the purine-rich (or pyrimidine-rich) strand dissociates and folds back to engage the remaining Watson and Crick paired purine-rich strand in the major groove (Figure 1C). Alternatively, in an intermolecular triplex, a purine (or pyrimidine) strand from one DNA tract engages in Hoogsteen bonds with a duplex from a different DNA tract. Specific bonds form between A and A, G and G, A and T, and G and protonated C.

Biology

R·Y tracts are common in eukaryotic genomes. In humans, sequences with thousands of such asymmetric base pairs exist, such as in the intron 21 of the

TABLE I

DNA Secondary Structures, Sequence, Sequence Features, and Biology

Secondary structure	Sequence requirements	Examples	Biology
Left-handed DNA (*Z*-DNA)	$(RY{\cdot}RY)_n$	$(CG{\cdot}CG)_{40}$ $[(CA)_{10}(CG)_8{\cdot}(CG)_8(TG)_{10}]$	Gene expression
Triplex DNA (H-DNA)	$(R{\cdot}Y)_n$ (mirror repeats)	$(GAA{\cdot}TTC)_{18}$ $(GA{\cdot}TC)_n$	Gene expression, chromatin organization, genetic instability
Tetraplex DNA (G4-DNA)	Repeating G-tracts	$(TTAGGG)_4$ $[(TGGGGAGGG)_2TGGGGAAGG]$	Telomere capping, gene expression
Cruciforms	Inverted repeats	GTCCAGTATACTGGAC	Replication origins, genetic instability
Slipped DNA (hairpins)	Direct repeats	$(CTG{\cdot}CAG)_{180}$	Gene expression, genetic instability

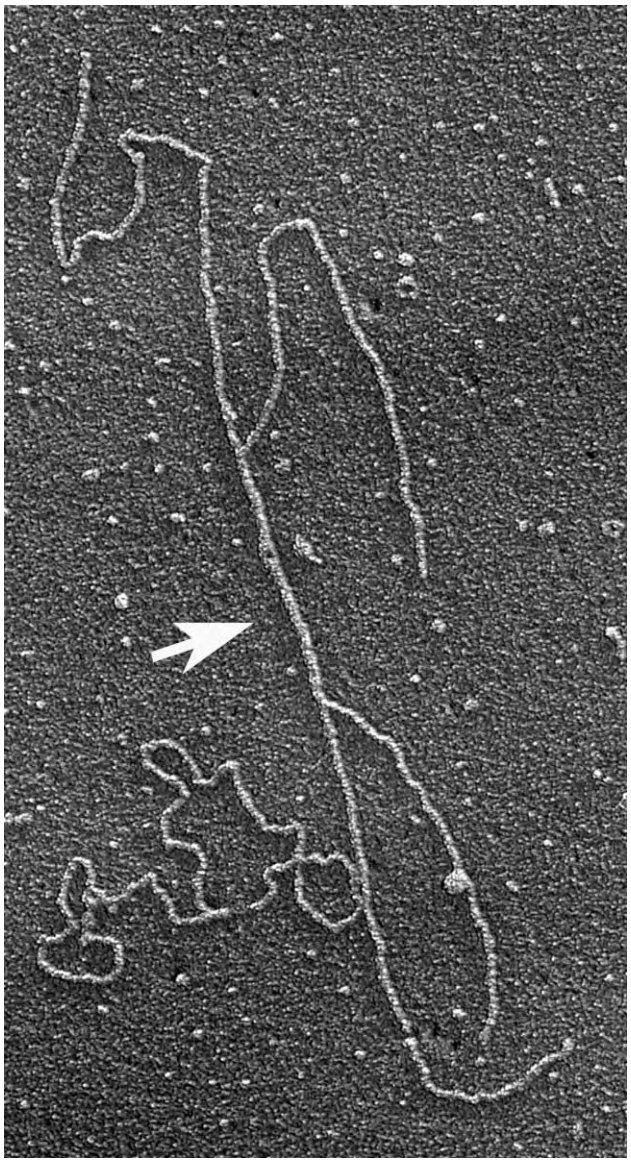

FIGURE 2 Electron micrograph of sticky DNA. Two linear DNA molecules interact (arrow) and are held together by a pair of long GAA·TTC tracts from a Friedreich's ataxia patient. Courtesy of Dr. Jack Griffith of the University of North Carolina, Chapel Hill, NC.

polycystic kidney disease gene 1. Triplex structures have been shown to inhibit transcription and replication, but increase recombination rates and promote genome instability. Sticky DNA (Figure 2) is a long triplex between two tracts of $(GAA{\cdot}TTC)_n$ (where $n = 59-270$) that are distantly located in a circular DNA. Friedreich's ataxia (FRDA), the most common hereditary ataxia, is caused by the expansion of the GAA·TTC tract in intron 1 of the frataxin gene, which subsequently inhibits its transcription. Sticky DNA is likely to be involved in the etiology of this neurological disease. In mammalian nuclei, actively transcribed chromatin is organized in specific domains, and centromeres are involved in such organization. Visualization of triplexes in nuclei revealed a colocalization of such structures from centromeres and other loci, supporting a model in which triplexes are implicated in the organization of chromatin domains.

Pharmacology

The delivery of synthetic triplex-forming oligonucleotides (TFOs) that adopt Hoogsteen pairs with complementary purine-rich genomic targets has been shown to form triplexes in nuclei. This strategy has been explored as a therapeutic tool to inhibit gene expression. For example, a TFO targeting an R·Y tract in the third intron of the *ICAM-1* gene, whose up-regulation is associated with inflammatory diseases, inhibited protein synthesis in human keratinocytes in cell culture and is considered a therapeutic agent in the treatment of psoriasis.

Tetraplex DNA

The ability of G residues to assemble in tetrameric arrangements (quadruplex DNA, four-stranded DNA, or G4 DNA) was noted in 1962. In 1988, tetraplex DNA was reported in biological systems.

Structure

Tetraplex DNA (also called G4 DNA because of the G quartets) forms when DNA sequences are composed of four repeating motifs that contain G residues (Figure 1D, Table I). Gs from each motif stack on one another and the four stacks form the sides of a cube. In each stack, four Gs hydrogen-bond and constitute a tetrad. NMR and X-ray crystallography studies showed that, in fact, all four nucleotides can form heterotetrads (or homotetrads), and therefore tetraplex DNA is likely to be observed with a greater variety of sequences *in vivo*.

Biology

Tetraplex DNA is involved in the maintenance of telomere ends and in the control of gene expression.

Maintenance of Telomere Ends

The DNA sequence at the ends of eukaryotic linear chromosomes, the telomeres, is a repetitive sequence that contains tetraplex-forming Gs. It is postulated that such capping protects the chromosome ends from being degraded and mediates chromosome condensation. Several proteins assist in the formation of tetraplex DNA; others disassemble the structure.

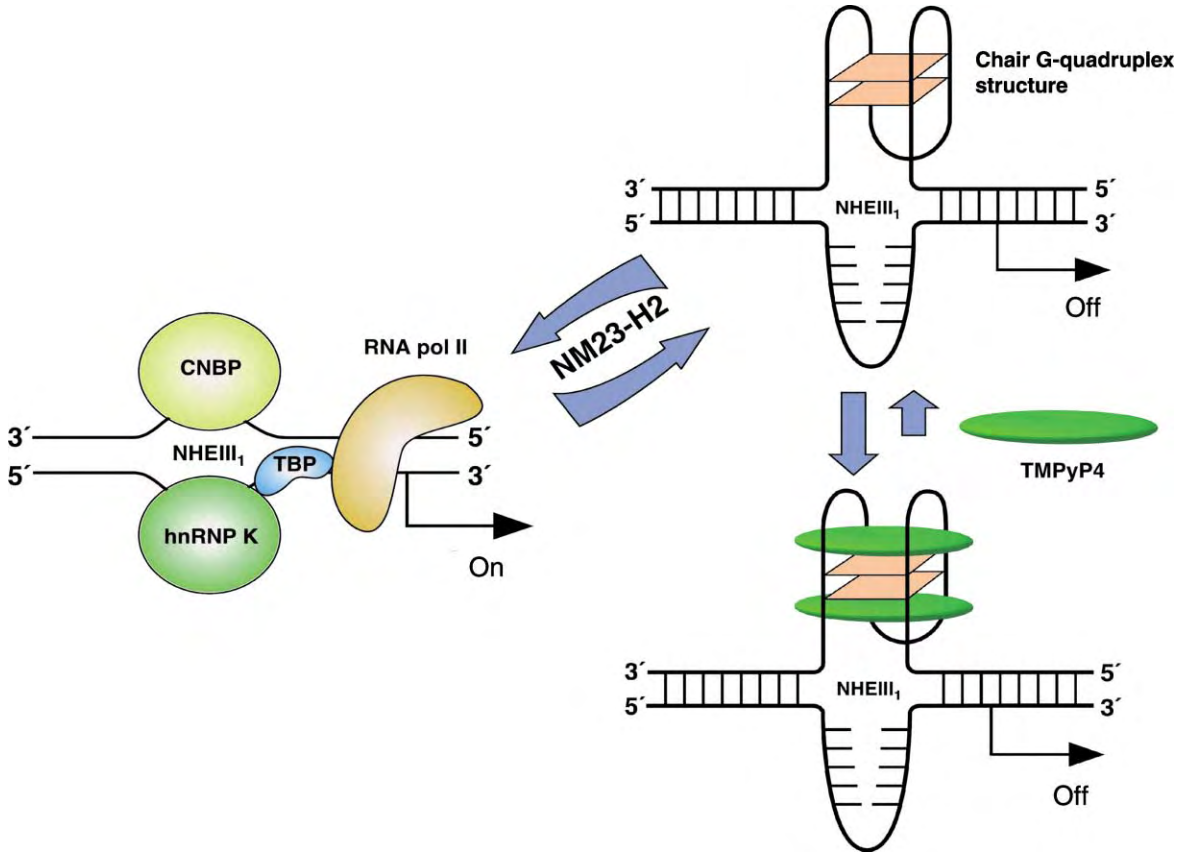

FIGURE 3 Inhibition of transcription by tetraplex DNA, a model for the inhibition of transcription at the *c-MYC* promoter. Left, the transcriptional complex assembles at the promoter and supports initiation of transcription by an RNA polymerase II complex. Top right, the cellular factor NM23-H2 promotes the transition from duplex to tetraplex, preventing assembly of transcription factors. Bottom right, TMPyP4 binds to, and stabilizes, the tetraplex structure driving the equilibrium toward stable transcriptional repression. TMPyP4, 5,10,15,20-tetra(*N*-methyl-4-pyridyl)porphine, a porphyrin derivative, and pyrelene derivatives such as *N*,*N*′(-bis[2-(1-piperidino)-ethyl]-3,4,9,10-perylenetetracarboxylic diimide (PIPER) are explored as therapeutic agents because their tetraplex binding activity inhibits telomerase, which is up-regulated in 80–90% of malignant tumors. Nuclear hypersensitive element III_1 ($NHEIII_1$) is a 27-bp promoter sequence cleaved when probed with single-stranded-specific nucleases or other chemicals. This sequence is shown in Table I. Reprinted from Siddiqui-Jain, A., Grand, C. L., Bears, D. J., and Hurley, L. H. (2002). Direct evidence for a G-quadruplex in a promoter region and its targeting with a small molecule to repress a c-*MYC* transcription. *Proc. Natl Acad. Sci. USA* **99**, 11593–11598. Copyright 2002, with permission of National Academy of Sciences, U.S.A.

Control of Gene Expression

Human sequences in the immunoglobulin switch region and in the promoters of other genes, including the oncogenes *c-MYC*, *c-MYB*, *c-FOS*, and *c-ABL*, contain repeating Gs that have been shown to form G-quartets. Experiments in cell cultures indicate that the promoter region of *c-MYC* is under the regulatory control of a secondary DNA structure, including a tetraplex. Specifically, its formation decreases transcriptional activity by interfering with the assembly of an RNA–polymerase complex (Figure 3).

Cruciforms and Slipped Structures

Cruciforms and slipped structures are formed by repetitive DNA sequences, but do not require a specific base composition.

Cruciforms

In inverted repeats, a DNA sequence is followed by its complementary sequence read in the opposite orientation (Table I). Thus, each strand may form a fully paired duplex, giving rise to a cruciform (Figure 1E). Inverted repeats are common at replication origins and at chromosomal locations associated with genomic instability.

Origins of Replication

Bacteria may carry extra-chromosomal DNA elements called plasmids. pT181 belongs to a class of plasmids whose replication requires nicking on one strand; under optimal conditions, negative supercoiling drives the formation of a cruciform that positions the nicking site on a single-stranded loop, allowing

nicking and the replisome to assemble and carry out replication. Studies have indicated a dynamic distribution of cruciforms in mammalian nuclei, their number being maximal at the G_1/S phase boundary, when DNA synthesis takes place. The concentration of a family of proteins (called 14-3-3) with cruciform-binding activities is also maximal in this period. Experiments on monkey *ors8* and *ors12* replication origins support the involvement of such proteins and DNA secondary structures in the initiation of DNA replication.

Genetic Instability

The recurrent human translocation t(11;22) involves the fusion of chromosomes 11 and 22. The site of translocation contains several hundred base pairs of AT-rich sequences on both chromosomes that may form large cruciforms. Breaking points were observed at the center of an inverted repeat sequence on both chromosomes, supporting the formation of a cruciform structure as the cause of translocation (Figure 4).

Slipped DNA

Repeating motifs of identical sequence composition (direct repeats) may base-pair in an out-of-register manner and thus form looped-out (slipped) structures (Figure 1F). Di-, tri-, tetra-, and pentanucleotide repeats are common in prokaryotes and eukaryotes and are often present in regulatory regions. Their copy number varies within a population, and this variation modulates gene expression (Table I). The simple sequence contingency loci are repeating tracts (microsatellites) in pathogens, such as *Haemophilus influenza* and *Neisseria meningitis*, that are involved in phase variation, a high-frequency gain or loss of the expression of virulence associated with changes in the number of repeats. Slippage of the complementary strands during replication is the accepted mechanism involved in such length changes. The involvement of slipped structures in the genetic instabilities of triplet repeat sequences has probably been studied most extensively. At least 14 hereditary neurological diseases, including myotonic dystrophy, fragile X syndrome, and FRDA, are caused by the massive expansion of CTG·CAG, CGG·CCG, and GAA·TTC, respectively. The capacity of one of the complementary strands in each duplex to preferentially adopt a quasi-stable slipped structure during replication–repair–recombination, thus causing primer realignment, is the mechanism. Also, the first two repeating sequences are flexible and writhed, contributing to their genetic instability.

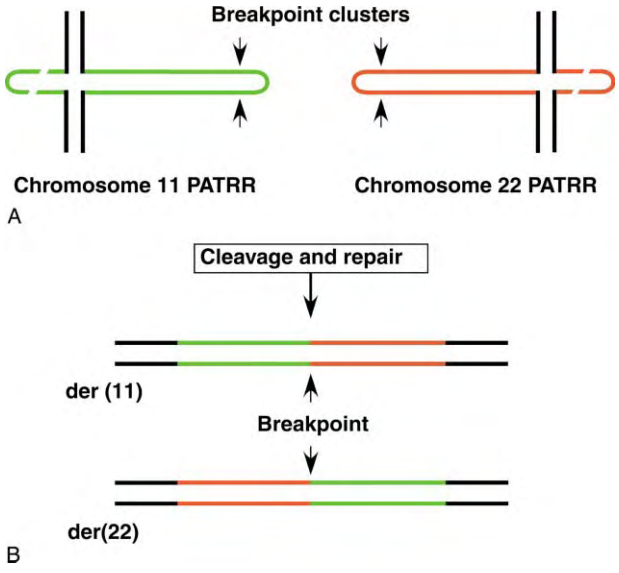

FIGURE 4 Human t(11;22) translocation. (A) Chromosomes 11 and 22 contain A/T-rich inverted repeats (PATRR) that form cruciform structures cleaved by nucleases. (B) Cleavage sites are repaired by joining chromosome 11 with 22, which yields the translocations der(11) and der(22). Adapted from Kurahashi, H., and Emanuel, B. S. (2001). Long AT-rich palindromes and the constitutional t(11;22) breakpoint. *Hum. Mol. Genet.* **10**, 2605–2617, by permission of Oxford University Press.

See Also the Following Articles

DNA Supercoiling • Friedreich's Ataxia

Glossary

base pairs Bases associated by hydrogen bonds and hydrophobic forces.

DNA secondary structure A DNA conformation (non-*B*-DNA) different from the antiparallel right-handed double helix, *B*-DNA.

supercoiling The folding and wrapping of a constrained DNA duplex onto itself.

Further Reading

Brown, B. A., II, and Rich, A. (2001). The left-handed double helical nucleic acids. *Acta Biochim. Pol.* **48**, 295–312.

Casey, B. P., and Glazer, P. M. (2001). Gene targeting via triple-helix formation. *Prog. Nucleic Acid Res. Mol. Biol.* **67**, 163–192.

Kurahashi, H., and Emanuel, B. S. (2001). Long AT-rich palindromes and the constitutional t(11;22) breakpoint. *Hum. Mol. Genet.* **10**, 2605–2617.

Shafer, R. H., and Smirnov, I. (2001). Biological aspects of DNA/RNA quadruplexes. *Biopolymers* **56**, 209–227.

Siddiqui-Jain, A., Grand, C. L., Bears, D. J., and Hurley, L. H. (2002). Direct evidence for a G-quadruplex in a promoter region and its targeting with a small molecule to repress a c-*MYC* transcription. *Proc. Natl Acad. Sci. USA* **99**, 11593–11598.

Sinden, R. R. (1994). *DNA Structure and Function.* Academic Press, San Diego, CA.

Soyfer, V. N., and Potaman, V. N. (1996). *Triple-Helical Nucleic Acids.* Springer-Verlag, New York.

Wells, R. D., and Warren, S. T. (1998). *Genetic Instabilities and Hereditary Neurological Diseases*. Academic Press, San Diego, CA.

Biography

Robert D. Wells is Director of the Center for Genome Research at the Institute of Biosciences and Technology in Houston, TX, and a Professor in the Department of Biochemistry and Biophysics at Texas A&M University. His principal research interest is in alternative DNA structures and their roles in medicine and biology. He holds a Ph.D. from the University of Pittsburgh and received his postdoctoral training at the University of Wisconsin. He has served as the President of the American Society for Biochemistry and Molecular Biology and the Federation of American Societies for Experimental Biology.

Albino Bacolla is a Senior Research Associate at the Institute of Biosciences and Technology in Houston, TX. His research interest is in the biological role of secondary DNA structure and topology. He holds a Ph.D. in Biology from the University of Turin, Italy.

DNA Sequence Recognition by Proteins

Arabela A. Grigorescu and John M. Rosenberg
University of Pittsburgh, Pittsburgh, Pennsylvania, USA

Recognition of specific DNA sequences by proteins refers to the ability of proteins to distinguish and preferentially bind particular DNA sequences in the genome. DNA sequence recognition is vital to cellular processes such as regulation of gene expression, site-specific recombination, DNA replication, and DNA repair; accordingly, in all living organisms, there are many different families of DNA binding proteins. The primary mechanism for this recognition is the formation of a tight complex between the target DNA sequence and a specific protein that has evolved to recognize it. The shapes of the protein and the DNA match each other precisely across the protein–DNA interface. That match is chemically complementary: opposite charges are situated across the interface from each other, as are hydrogen bond donors and acceptors. How they get there is the basis of sequence-specific recognition.

What Features of DNA Sequences are Recognized by Proteins?

The Watson-Crick model of the DNA double helix is a uniform structure with a negatively charged phosphate backbone at the exterior and a core of stacked base pairs forming a column up the center. What unique features of a DNA sequence can be recognized by a protein?

Functional Groups on DNA

The four constituent bases of DNA, adenine (A), thymine (T), guanine (G), and cytosine (C) have unique chemical groups available at their edges to interact with atoms of the protein. These chemical groups – termed functional groups of the DNA bases – are lying on the floors of the two DNA grooves (the concave surfaces of the double helix formed by the edges of the DNA deoxynucleosides (Figure 1)). Because of the asymmetric attachment of the DNA base pairs to the furanose rings, the two grooves of the double-helical DNA molecule have different dimensions. The narrower groove is referred to as the minor groove while the wider groove is referred to as the major groove.

Complementary Interactions with the Functional Groups

As initially pointed out by A. Rich and co-workers, the A-T and G-C base pairs display unique patterns of hydrogen bond donors and acceptors in the DNA grooves (Figure 1B). Also, the methyl group on the C5 position of the thymine base can interact favorably with CH_2 and CH_3 groups on amino acid side chains of the protein. The shape of a particular base pair can be recognized by proteins through series of adjacent van der Waals contacts.

Thus, recognition interactions require precise juxtaposition of complementary chemical groups on the protein and on the DNA (chemical complementarity). This complementarity is the basis of recognition, because once a particular protein has achieved the positioning of its functional groups such that they are complementary to those presented by one base sequence, they would not match the functional groups presented by a different sequence.

Water-mediated interactions are also common at protein–DNA interfaces. Polar atoms from amino acid side chains such as Asn, Gln, Thr, and Ser, as well as the amino and carboxyl groups of the protein's main chain, often trap water molecules between the protein and the DNA. The water molecules bridge the protein and the DNA, forming hydrogen bonds to both. Because of the functional groups often involved, these bridging interactions can form simple extensions of the complementarity described above.

Reading Heads

In order to "read" even a short sequence of DNA, the protein must group appropriate amino acid side chains in close proximity. Indeed, some short sequences are recognized by the single structural element of the protein (sometimes referred to as a reading head) that is brought in close proximity to the functional groups of the DNA bases. These structural elements, often called

motifs, provide a scaffold for functional groups that do the reading.

Reading heads can be α-helices, β-sheets, or loops. In some cases, they pre-exist as rigid secondary structural elements in the unbound protein, but in others they represent flexible protein regions that adopt a regular structure in response to DNA binding (many proteins couple local folding with site-specific DNA binding – an idea originally proposed by T. Record based on thermodynamic premises).

In the example shown in Figure 2A, the reading head is an α-helix inserted into the DNA major groove. In the example shown, the α-helix positions four protein side chains for recognition of a total of three base pairs of the DNA. The dimensions of the protein α-helix and of the DNA major groove are ideal for this mode of interaction.

Although not as common as α-helices, two stranded β-sheets have also been observed to serve as reading heads. In the example shown in Figure 2B, the convex side of a curved, two-stranded β-sheet runs parallel to the surface of the major groove; six amino acid residues (three in each β-strand) make direct readout interactions with a total of six consecutive DNA base pairs.

Indirect Readout

Despite the existence of several such simple and attractive examples, in general, direct readout by a rigid fit of α-helices and/or β-sheets to the DNA major groove is not the predominant mechanism employed by proteins for DNA recognition. Only a limited number of sequence-specific DNA-binding proteins exclusively use direct readout, and very often direct readout alone cannot explain the energetic preference of a protein for a particular DNA site. A second, more subtle mechanism for sequence discrimination originates in the distortability of the DNA helix, as shown by structural analysis of a large number of protein–DNA complexes. They reveal that DNA is characterized by remarkable flexibility. In a complex with a protein, the DNA often adopts a conformation that departs significantly from a regular double helix. Several examples given in Figure 3 show that DNA can be, for example, bent, kinked, elongated, and wrapped around a protein. Many lines of experimental evidence suggest that the energetic cost of distorting the DNA into a particular conformation is sequence dependent, and this dependence is exploited by proteins for sequence recognition.

As the DNA is distorted, its chemical groups change their spatial positions. Because the energy required to achieve that distortion is sequence dependent, the resulting spatial positioning of the functional groups reflects the sequence. This is true even for functional groups that do not change with base sequence, such as backbone phosphate groups. Thus, the energy liberated by contacts between a protein and a distorted DNA molecule depend subtly on the distortability of the base sequence. This mechanism of sequence recognition is referred to as indirect readout.

Most site-specific DNA-binding proteins combine the direct and indirect readout mechanisms in order to maximize the information content of DNA sequences. This combination also diversifies the available structural strategies for DNA binding. For example, certain distortions of the DNA helix can alter the dimensions of the DNA grooves such that they can accommodate α-helices, β-sheets, or loops in various orientations. In some cases, dramatic bending of the DNA molecule can completely open up the major or minor groove. In the specific complex of the TATA-binding protein (TBP) and DNA (Figure 3E), the protein is bound on the minor groove side of the DNA, but the DNA is bent by approximately 80° toward the major groove. This distortion alters the minor groove such that it becomes a wide concave surface that is complementary to the curved surface of the TBP protein. In the specific protein–DNA complex of the prokaryotic integration host factor (IHF) (Figure 3F), the DNA molecule is wrapped around the protein. This is possible because the protein induces a bend of approximately 160° in the DNA, and three distinct regions of the DNA molecule are directly contacted and held in place by the IHF protein.

Structural Motifs in Protein–DNA Recognition

As exemplified in Figure 3, the structural strategies for DNA recognition and binding are remarkably diverse among various classes of DNA-binding proteins. Similar binding strategies and common design principles, however, appear to exist between members of a given protein family; several structural motifs for DNA recognition have been identified in families such as bacterial repressors, eukaryotic transcription factors and other gene regulatory proteins, and particular classes of DNA enzymes.

The Helix-Turn-Helix Motif

Historically, the helix-turn-helix (HTH) motif was one of the first DNA-binding motifs to be identified and analyzed. DNA recognition by the HTH motif has been reviewed by S. Harrison and A. Aggarwall and more recently by C. Garvie and C. Wolberger.

Common to many prokaryotic gene regulatory proteins and also found in eukaryotic homeodomain proteins, the HTH motif consists of two α-helices connected by a turn (Figure 3A). One of the α-helices (termed the recognition helix) inserts into the major

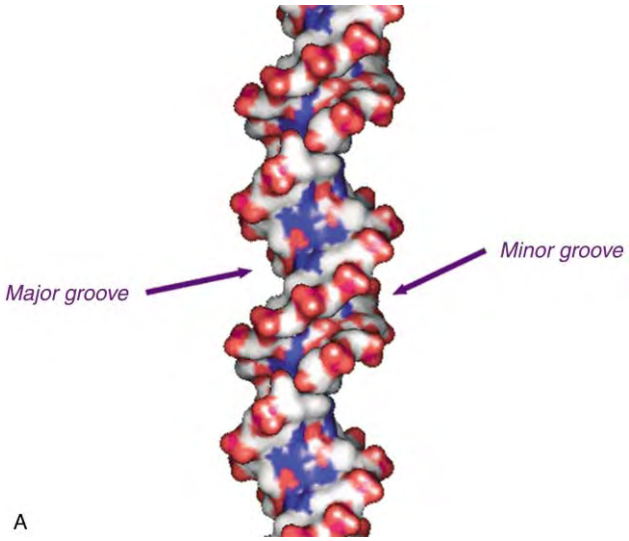
Major groove
Minor groove
A

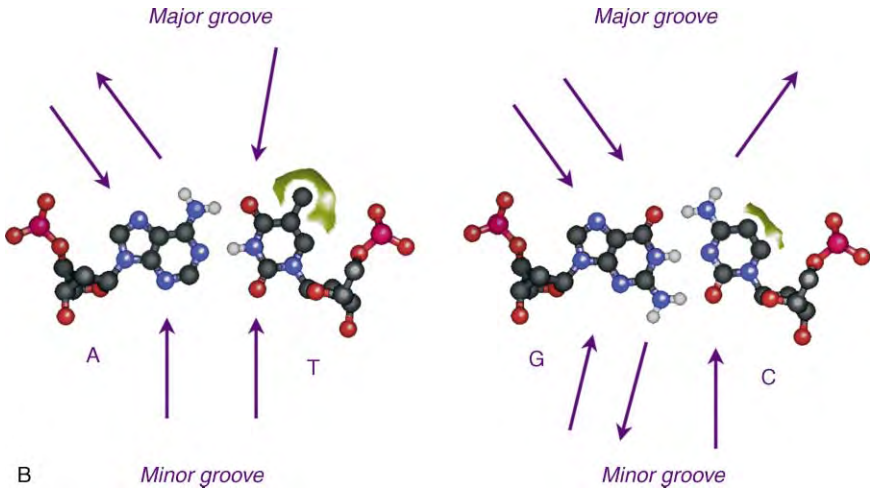
Major groove
Major groove
A
T
G
C
B
Minor groove
Minor groove

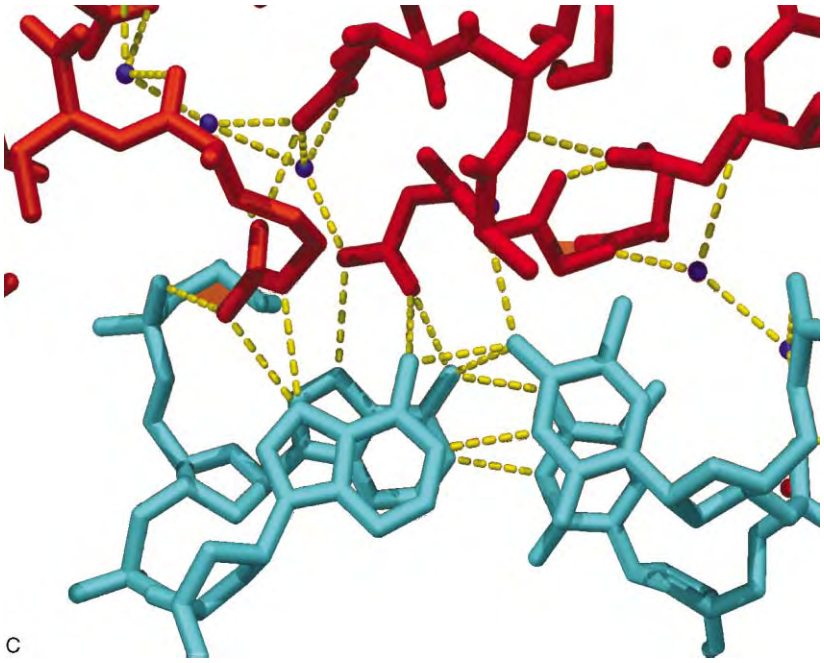
C

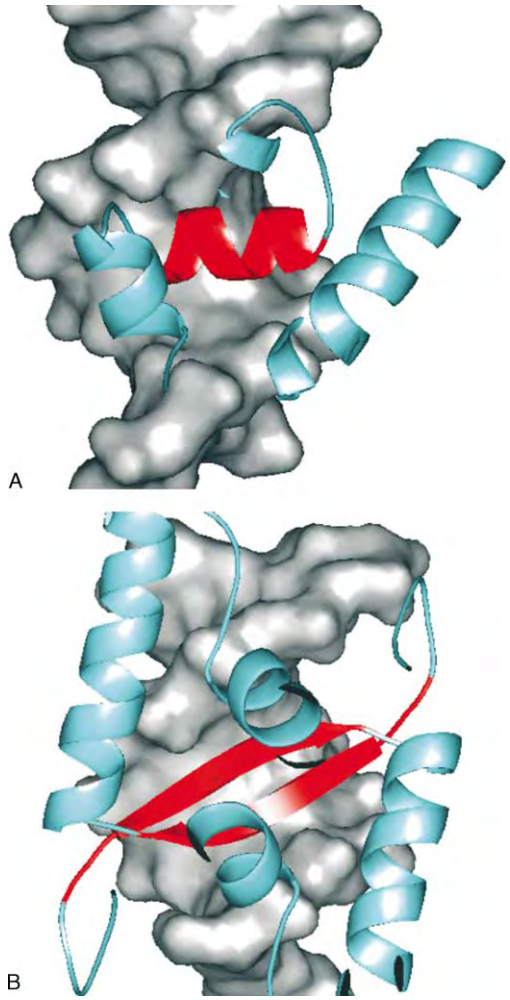

FIGURE 2 Reading heads in the DNA major groove. The DNA molecular surface is shown in gray. The proteins are shown with a cartoon representation, emphasizing their secondary structure. The amino acid side chains are omitted for clarity. Only regions of the protein that are close to the DNA are visible in the figure. In the examples shown, the DNA reading heads (highlighted in red) are (A) an α-helix in λ repressor, (B) a two-stranded β-sheet in MetJ repressor.

groove, making direct or water-mediated contacts with the DNA bases. The other α-helix acts primarily to spatially stabilize the motif through hydrophobic interactions in the interior of the two-helix elbow but, in some cases, also contributes to the binding specificity by interacting with the DNA phosphate backbone. Most of the proteins that use this motif for DNA recognition are homodimers; by using two symmetrical HTH motifs, recognition of longer DNA sequences as well as modulated affinity for a series of closely related DNA sequences can be achieved.

Although highly conserved in its internal structure, the HTH motif is highly variable in its precise placement within the major groove of DNA, i.e., the geometry of the DNA–HTH interaction is not as highly conserved. This apparent paradox has been resolved by noting that the HTH motif forms a highly stable bulge on the surface of a protein, a structural requirement for an effective reading head. Thus, although primarily found in DNA-recognition roles, HTH motifs have been found in other situations where there is a structural requirement for a small bulge.

The Zinc Finger Motif

The zinc finger DNA-binding motif is common to many transcription factors in the human genome. The first zinc finger domains were identified in the structure of *Xenopus* transcription factor IIIA in 1985. This motif consists of a relatively short α-helix and a two-stranded antiparallel β-sheet (Figure 3C). The fold is stabilized by a core of residues (most commonly two cysteines and two hystidines) coordinating a Zn^{2+} ion. Typically, the N-terminal part of the α-helix is inserted in the major groove, contacting 3 to 4 DNA bases. Many gene regulatory proteins in eukaryotes contain several copies of this motif connected by linkers; variations in the number and sequence of the zinc finger motifs and the length and flexibility of the linker regions allow transcription factors and other similar proteins to recognize long and complex DNA target sites using a relatively simple structural motif. Here, too, the zinc finger forms a bulge found most often, but not exclusively, as a DNA recognition element.

The Leucine Zipper Motif

The basic leucine zipper (bZIP) binding motif is another structural motif employed by eukaryotic gene regulatory proteins for DNA recognition. It consists of two long, approximately parallel α-helices wrapped partially around each other to form a type of structure called a coiled coil. The contacts between the α-helices are stabilized by hydrophobic interactions made by a series of leucine residues. The N termini of the α-helices are the DNA reading heads that insert into the major groove (Figure 3B). They are unstructured in the absence of DNA; thus, the basic leucine zipper motif couples local

FIGURE 1 (A) The molecular surface of B-DNA; the major groove and minor groove are indicated. (B) The A-T and G-C DNA base pairs. The coloring scheme for the atoms is carbon, black; oxygen, red; nitrogen, blue; hydrogen, white. The arrows illustrate the hydrogen-bonding potential of the functional groups and point from the hydrogen bond donor toward the hydrogen bond acceptor. The methyl group of the thymine and C-H groups of cytosine can be contacted by the protein through van der Waals interactions. (C) View of a typical protein–DNA recognition interface. The hydrogen bonds between the protein and the DNA are indicated by dashed lines.

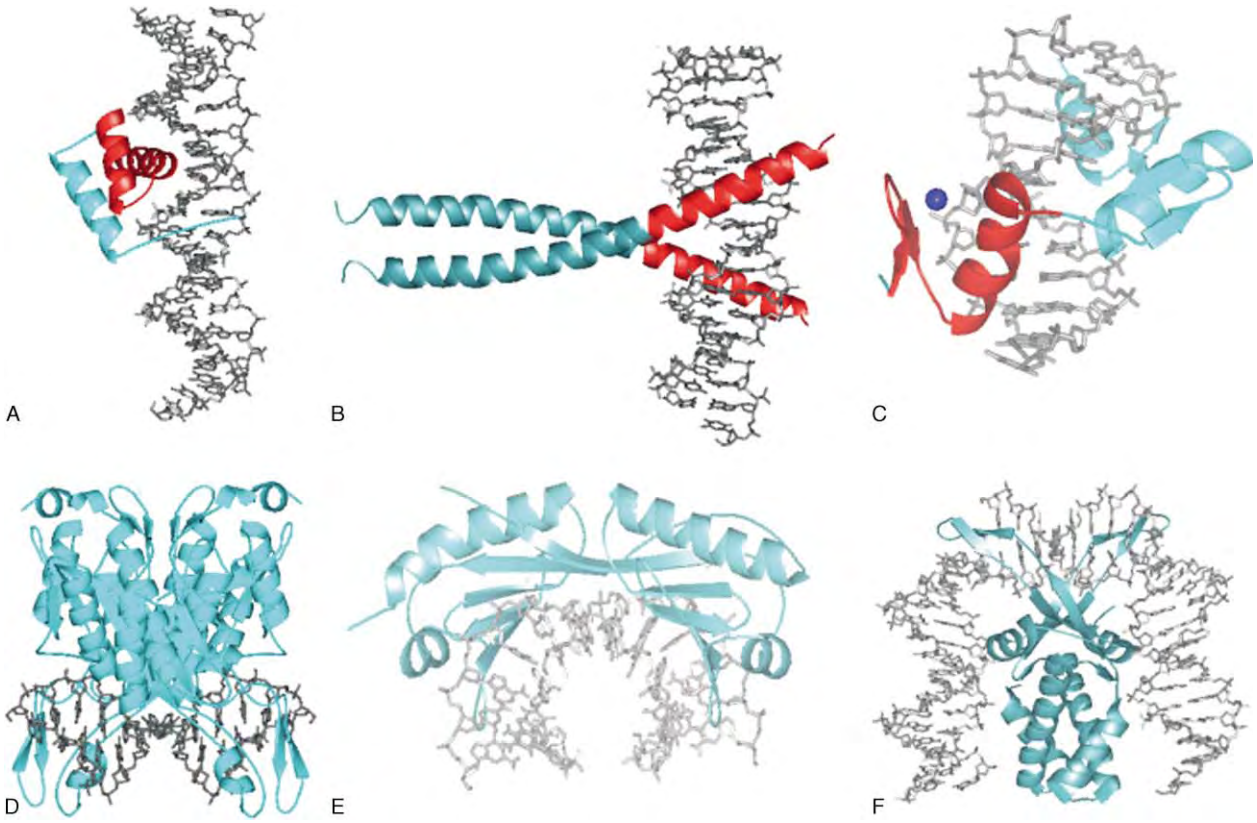

FIGURE 3 Diverse structural strategies for DNA binding and recognition are employed by proteins. Top: examples of structural motifs (highlighted in red) for DNA recognition: (A) helix-turn-helix (HTH) in prokaryotic λ repressor, (B) leucine zipper (bZIP) in yeast transcriptional activator GCN4, (C) zinc finger in mouse transcription factor ZIF268. Bottom: examples of protein–DNA complexes with significant DNA distortion: (D) bacterial type II endonuclease *Eco*RI, (E) yeast TATA-binding protein (TBP), (F) prokaryotic integration host factor (IHF).

folding with DNA recognition. T. Hakoshima and co-workers have reviewed the structural basis of DNA recognition by bZIP transcription factors.

Diverse Structural Strategies are Employed by Proteins for DNA Recognition

In general, structural DNA-binding motifs such as helix-turn-helix, zinc fingers, and leucine zipper are used by proteins as DNA-binding modules. In some proteins, they facilitate multiple independent intermolecular contacts and allow modulated affinity for a series of related sites. Proteins with stringent sequence specificity, such as restriction enzymes, use a more integrated recognition mode. Several structural elements of the protein are involved in DNA recognition over a large structural area, but these interactions are not independent. Extensive networks of hydrogen bonds and other favorable interactions form cooperatively at the molecular interface upon site-specific binding; such networks contribute to the specificity and stability of these complexes. These networks often extend to enzymatic active sites, e.g., the cleavage sites of restriction enzymes, thereby integrating recognition and cleavage.

One of the few common trends among the various families of DNA-binding proteins is that most proteins bind to DNA as homodimers, heterodimers, or pseudo-dimers. This strategy has several purposes: first, it is a relatively simple way to bring two or more DNA reading heads in proximity at the interface and to create a larger interface from a globular protein and a helical DNA molecule. Second, additional specificity can be achieved by coupling DNA recognition interactions with quaternary structure interactions within the dimer. Third, the symmetry or the asymmetry of these dimers is often required for the specific function of the protein. For example, type II bacterial restriction endonucleases that recognize short palindromic DNA sites make double-strand breaks in DNA by positioning the two scissile bonds in the two symmetric catalytic sites of the homodimeric enzyme. Proteins that are required to bind DNA in a precise orientation are often

pseudodimers or heterodimers; such examples include eukaryotic TATA-binding protein and prokaryotic integration host factors, respectively.

Conclusion

As the number of structurally characterized protein–DNA complexes continues to expand, it is becoming evident that evolution has engineered a diversity of DNA-binding proteins and DNA recognition modes. By correlating the structural analysis with energetic and functional characterization of DNA-binding proteins, it is becoming increasingly clear that DNA recognition is tightly coupled with the protein function. Conservation of DNA-binding motifs and design principles within protein families reflects the fact that the structural strategies and energetic principles for DNA recognition have been shaped by evolution such that proteins can achieve simultaneously both the desired level of sequence specificity and optimal functionality in their complexes with DNA.

See Also the Following Articles

DNA Base Excision Repair • DNA Replication: Eukaryotic Origins and the Origin Recognition Complex • DNA Replication: Initiation in Bacteria • DNA Replication, Mitochondrial • Recombination-Dependent DNA Replication • Transcription-Coupled DNA Repair, Overview • Zinc Fingers

Glossary

direct readout Recognition of the identity of the functional groups of the DNA bases by a protein through specific interactions (hydrogen bonds, hydrophobic, van der Waals contacts, etc).

DNA distortion in a protein–DNA complex A significant departure of the DNA conformation within the complex from that of the free DNA (with the same sequence) in solution (under physiological conditions).

DNA reading head A structural element or motif of the protein that makes specific contacts with functional groups of the DNA bases when it is brought in close proximity to those bases; typically contains several amino acid residues that are involved in the recognition interaction.

indirect readout Recognition of the sequence-dependent conformational features of the DNA, including the energetic cost of distorting the DNA into a particular conformation.

sequence specificity in DNA binding The preference of a given protein for binding DNA of a particular sequence over binding DNA independently of its sequence (nonspecific binding); typically expressed via the differential free energy of binding.

Further Reading

Fujii, Y., Shimizu, T., Toda, T., Yanagida, M., and Hakoshima, T. (2000). Structural basis for the diversity of DNA recognition by bZIP transcription factors. *Nat. Struct. Biol.* **7**, 889–893.

Garvie, C. W., and Wolberger, C. (2001). Recognition of specific DNA sequences. *Mol. Cell* **8**, 937–946.

Harrison, S. C., and Aggarwal, A. K. (1990). DNA recognition by proteins with the helix-turn helix motif. *Annu. Rev. Biochem.* **59**, 933–969.

Miller, J., McLachlan, A. D., and Klug, A. (1985). Repetitive zinc-binding domains in the protein transcription factor IIIA from Xenopus oocytes. *EMBO J.* **4**, 1609–1614.

Pabo, C. O., and Nekludova, L. (2000). Geometric analysis and comparison of protein–DNA interfaces: Why is there no simple code for recognition? *J. Mol. Biol.* **301**, 597–624.

Rosenberg, J. M. (1991). Structure and function of restriction endonucleases. *Curr. Opin. Sruct. Biol.* **1**, 104–113.

Seeman, N. A., Rosenberg, J. M., and Rich, A. (1976). Sequence specific recognition of double helical nucleic acids by proteins. *Proc. Natl. Acad. Sci. USA* **73**, 804–808.

Steitz, T. A. (1990). Structural studies of protein-nucleic acid interaction: The sources of sequence-specific binding. *Quart. Rev. Biophys.* **23**, 205–280.

Tateno, M., Yamasaki, K., Amano, N., Kakinuma, J., Koike, H., Allen, M. D., and Suzuki, M. (1997). DNA recognition by beta-sheets. *Biopolymers* **44**, 335–359.

Wodak, S. J., and Janin, J. (2002). Structural basis of macromolecular recognition. *Adv. Prot. Chem.* **61**, 9–73.

Wolberger, C. (1993). Transcription factor structure and DNA binding. *Curr. Opin. Struct. Biol.* **3**, 3–10.

Biography

John M. Rosenberg is a member of the Department of Biological Science at the University of Pittsburgh. He holds a Ph.D. from the Massachusetts Institute of Technology. His major research interest is in the structural basis of sequence-specific DNA–protein interactions.

Arabela A. Grigorescu is a research associate in the Department of Biological Sciences at the University of Pittsburgh. She holds a Ph.D. from the University of Pittsburgh.

DNA Supercoiling

Tao-shih Hsieh
Duke University Medical Center, Durham, North Carolina, USA

DNA supercoiling describes a higher-order DNA structure. The double-helical structure of DNA entails the interwinding of two complementary strands around one another and around a common helical axis. The writhing of this helical axis in space defines the DNA superhelical structure (DNA tertiary structure). For a circular DNA or a linear DNA with its ends anchored to create a loop, there is a tight topological coupling between the DNA superhelical structure and the double-helical structure (DNA secondary structure). Hence, DNA superhelicity can influence the DNA winding/unwinding, thereby affecting the biological functions of DNA. In nature, there exists a ubiquitous class of enzymes, DNA topoisomerases, that can mediate the topological transformation in DNA molecules.

Background

The beauty and elegance of the double-helical structure of DNA, as first proposed by Watson and Crick in 1953, also imparts critical functions of DNA. However, the unwinding of the DNA double helix during the process of replication, transcription, and recombination creates intriguing topological problems. The potential topological problem intrinsic to a circular, double-stranded DNA molecule was first noted by Cairns in 1963. In his autoradiographic analysis of chromosome replication in the bacterium *Escherichia coli*, Cairns pointed out that the bihelical DNA structure of a circular molecule poses a topological constraint on the strand separation necessary in the process of DNA replication. Vinograd and his associates about the same time demonstrated that an animal virus, polyomavirus, also has a circular genome. Furthermore, the helical axis itself winds and turns in space, thus producing a superhelix. Since then, circular genomes have been discovered in many organisms, including most bacteria, bacterial plasmids, and organelles such as mitochondria and chloroplasts. For example, Figure 1 shows an electron micrograph of a small bacterial plasmid DNA. The DNA superhelicity results in a duplex making crossovers (intersections) with itself. For most circular DNAs isolated from natural sources, the number of superhelical turns is directly proportional to the length of DNA. There are approximately six to eight superhelical turns per 1 kb DNA. We discuss the quantitative details in later sections.

The biological significance of DNA superhelicity was first realized when Vinograd and his co-workers discovered that there is a tight coupling between the DNA secondary structure and superhelical structure. Therefore, DNA superhelicity can influence the unwinding and rewinding of DNA duplex, and vice versa. Because such a coupling is direct, it allows one a rare opportunity in molecular biology to design experiments to gain insight into the structure of DNA and to probe the mechanism of the enzymes that affect DNA structure. The theoretical consideration of the coupling between DNA secondary and tertiary structures, based on mathematical topology, was later extended in the treatises by Fuller, White, and Crick. It should be pointed out that such a topological coupling also applies to linear DNA with anchored sites to create the loop structure that is found in the chromosomes of essentially all cells.

Nature has evolved unique enzymes to solve the topological problems that arise during the process of unwinding/rewinding DNA helix. The first such enzyme, topoisomerase I from the bacterium *E. coli*, discovered by Wang in 1970, can remove negative supercoils efficiently. Many new families of topoisomerases have since been discovered, and these enzymes are present in all organisms and have essential biological functions.

Quantitative Relationship between Twist and Supercoil

For a circular DNA without any nicks, in which both DNA strands are covalently continuous, the sum of DNA twists (*Tw*) and writhes of the DNA helical axis (*Wr*), a measure of DNA superhelical structure, is invariant. Because the algebraic sum of these two numbers is equal to the number of times that one of the DNA strands winds around its complementary strand in space, it defines the topological linkage between DNA strands, termed the linking number (*Lk*).

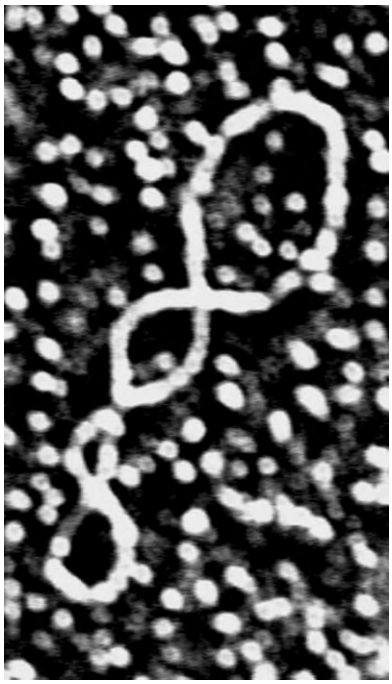

FIGURE 1 An electron micrograph of a bacterial plasmid DNA. The DNA has about 3 superhelical turns, as evidenced by the number of crossovers made by the DNA duplex.

We therefore have the following equation:

$$Tw + Wr = Lk$$

where Lk is a constant for a covalently closed circular DNA. Tw is related to the DNA secondary structure, the bihelical winding of two DNA strands, and it can be calculated if one knows the size of the DNA and the average helical pitch in this DNA. For example, in a 1-kb B-form DNA with a helical pitch of 10.5 bp/turn, $Tw = 95$. Wr is a measure of the superhelical structure of DNA. It relates to the number of times that the helical axis crosses itself in space. The higher the Wr, the more supertwisted the DNA. Lk is a topological quantity and defines the total linkage between the two complementary strands. Whereas Tw and Wr can be any real number, Lk is always an integer. This is because, for a closed circular DNA, strands have to wind around one another an integral number of turns to avoid nicks or gaps.

Handedness and the Sign of *Tw* and *Wr*

An important feature for all three parameters is that each has a sign, positive or negative, depending on the handedness of the double helix and superhelix. Because most of the DNA duplexes are right-handed, we define right-handed as positive and left-handed as negative. We can define whether the crossover of two curves in space is left-handed or right-handed if an axis is clearly marked. For example, Figure 2 shows two curves, denoted as two arrows in space, one making a left-handed cross and the other a right-handed one. The axis is shown as a thin vertical line going through the crossover. The significance of the definition of the axis can be visualized in this figure as well. If one chose instead a horizontal line as the axis, then the assignment of handedness is reversed. Figure 2B would then be left-handed and Figure 2A would be right-handed. For the duplex DNA structure, the axis definition is rather intuitive and straightforward. The helical axis is the axis around which the two strands are wrapped with respect to one another. For the DNA superhelix, it is necessary to define an axis in a manner that is consistent with what we defined for secondary structure. An example is shown in Figure 3. A figure-eight superhelix is the simplest possible DNA supercoil. If one lays down the figure-eight superhelix horizontally, then the axis is the vertical line going through the crossover. With this definition of axis, the superhelix shown in Figure 3A has a left-handed crossover, and thus it has a negative superhelical turn ($Wr = -1$). Figure 3B has a positive superhelical turn ($Wr = +1$).

Because it is not practical to measure the absolute value of Wr or Lk, they are usually determined experimentally with respect to a reference state, DNA in a relaxed state. The linking number and writhe for the relaxed state are denoted with a subscript zero.

Because $Wr_0 = 0$, the measure of DNA supercoils, Wr, is equal to the writhe difference with respect to the reference state:

$$Wr = \Delta Wr = Wr - Wr_0$$

Assuming that Tw for the supercoiled and relaxed DNA is about the same ($Tw = Tw_0$), then it follows that:

$$\Delta Wr = \Delta Lk$$

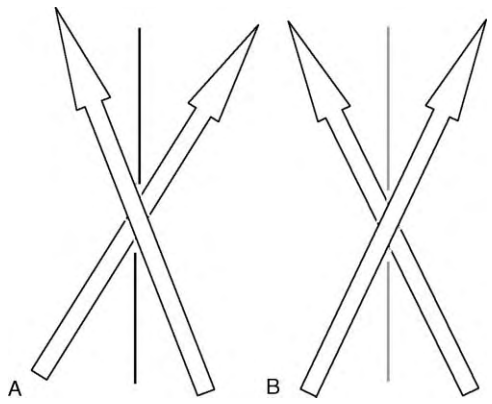

FIGURE 2 Diagrams of (A) a left-handed crossover and (b) a right-handed one. The arrows shown here simply serve to illustrate the point that the two perpendicular axes, one vertical and one horizontal, are not equivalent. The vertical line has been chosen arbitrarily as the axis for determining handedness.

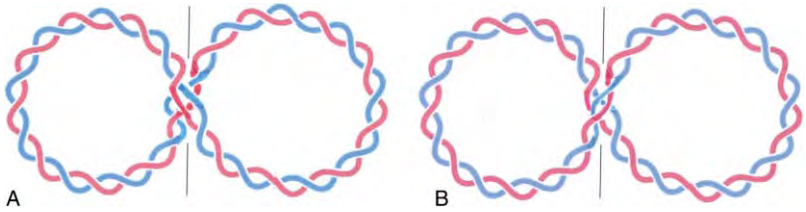

FIGURE 3 Diagram of a DNA with (A) a left-handed supercoil and (B) with a right-handed supercoil. Notice the two complementary strands (in red and blue) are wound in a right-handed helix. The axis for determining the handedness of the superhelical turn is shown as a vertical line going through the DNA crossover.

Because *Lk* is a topological invariant, it does not change for a given DNA in different environments. It is thus a more useful parameter for tracking the structure of DNA. ΔLk is thus frequently used to mark the superhelicity of DNA. If ΔLk is negative, DNA is underwound; the absolute value of ΔLk in this case gives a measure of negative supercoils or linking deficiency. If ΔLk is positive, then the DNA is overwound; its absolute value relates to the number of positive superhelical turns. DNA superhelicity can also be expressed as a fraction with respect to the linking number in a relaxed DNA. This is usually referred to as superhelical density, σ.

$$\sigma = \Delta Lk/Lk_0 = \Delta Lk/Tw_0$$

because $Lk_0 = Tw_0$, when $Wr_0 = 0$.

Most of the circular DNAs isolated from natural sources are negatively supercoiled. An interesting exception is the DNA in hyperthermic bacteria, which is positively supercoiled. For the numerous negatively supercoiled DNAs studied so far, the superhelicity mostly falls within a narrow range, with σ between -0.06 and -0.08.

Biological Effects of Supercoiling and Enzymes That Can Change DNA Supercoiling

To access the genetic information embedded within the double helix, most of the biological processes associated with critical functions of DNA involve unwinding or rewinding of the twin DNA strands. With a covalently closed circular DNA for which *Lk* stays constant, any change in *Tw* will be compensated by a change in *Wr* that is equal in magnitude but opposite in sign:

$$\Delta Tw = -\Delta Wr$$

This quantitative coupling between the DNA secondary structure and superhelical structure suggests that supercoiling can profoundly influence DNA structure and function. DNA with supercoils, either positive or negative, is thermodynamically less stable than its relaxed counterpart. For a negatively supercoiled DNA, any reactions associated with a reduction in the negative superhelical turns ($\Delta Wr > 0$) are energetically favored. These reactions will also be coupled with the unwinding of the DNA duplex because $\Delta Tw < 0$ if $\Delta Wr > 0$. Therefore negative DNA supercoiling facilitates the unwinding of DNA. In many instances, it has been demonstrated that replication, transcription, and recombination, all of which require the unwinding of DNA, are promoted by negative supercoiling. In an interesting corollary, DNA with positive supercoils will favor winding and disfavor unwinding of duplex structure (i.e., $\Delta Tw > 0$ if $\Delta Wr < 0$). It has been hypothesized that positive supercoiling found in some of the hyperthermophiles serves to stabilize the DNA double-helical structure in the extreme temperatures at which these organisms find home.

Nature has harnessed the use of DNA supercoiling for regulating the biological functions of DNA; it has also developed tools to modulate supercoiling. A ubiquitous class of enzymes, DNA topoisomerases, evolved to carry out the topological transformation in DNA. In order to break the hold of the topological constraint on closed circular DNA, these enzymes can make transient and reversible DNA breaks. There are two important features in these topoisomerase-mediated breaks in comparison with those made by nucleases. One is that a specific tyrosyl residue in the enzyme is joined covalently to the phosphate at the breakage site through a phosphodiester bond. Because this enzyme–DNA bridging bond is made at the expense of the neighboring DNA backbone bond, there is no significant energy change associated with the process of strand scission, thus assuring that the cleavage/religation is readily reversible. The enzyme-mediated DNA breakage is also accompanied by strand passage through the break or a rotation of the strand with the transient break around the intact strand. Both processes result in a change of DNA supercoiling or other topological transformation in DNA. Indeed, genetic experiments have demonstrated essential functions of these enzymes in the cell. These results also

underscore the importance of supercoiling in the biological functions of DNA.

See Also the Following Articles

DNA Secondary Structure • DNA Topoisomerases: Type I • DNA Topoisomerases: Type II

Glossary

DNA twist The number of times that two complementary strands wind around one another in the double-helical structure.

kilobase (kb) One thousand base pairs.

linking number The number of times that DNA strands wind around one another in space. For a closed circular DNA, it is an integer and a topological invariant.

supercoil The winding of the DNA helical axis in space.

topoisomerase An enzyme that can change supercoiling or other aspects in the topological structure without altering any covalent structure in DNA.

Further Reading

Cozzarelli, N. R., and Wang, J. C. (eds.) (1990). *DNA Topology and Its Biological Effects*. Cold Spring Harbor Laboratory Press, New York.

Wang, J. C. (1980). Superhelical DNA. *Trends Biochem. Sci.* **5**, 219–221.

Wang, J. C. (1994). Appendix I: An introduction to DNA supercoiling and DNA topoisomerase-catalyzed linking number changes of supercoiled DNA. In *Advances in Pharmacology Vol. 29B, DNA Topoisomerases: Biochemistry and Molecular Biology* (L. Liu, ed.) pp. 257–270. Academic Press, San Diego, CA.

Biography

Tao-shih Hsieh is a Professor in the Department of Biochemistry at Duke University Medical Center, Durham, NC. His general research area is in the structure and function of eukaryotic chromosomes. He received a Ph.D. from the University of California at Berkeley and did his postdoctoral fellowship at the Stanford University Medical Center. His research has contributed to the discovery of new DNA topoisomerases and the unraveling of their biological functions.

DNA Topoisomerases: Type I

James J. Champoux
University of Washington, Seattle, Washington, USA

The large size of DNA molecules and the double-helical nature of DNA create unique topological problems during replication, transcription, recombination, and chromatin remodeling that are solved by a family of enzymes called DNA topoisomerases. Members of the type II subfamily of DNA topoisomerases alter the supercoiling of DNA and disentangle chromosomes by introducing temporary double-strand breaks into the DNA. Type I DNA topoisomerases, the subject of this review, manage DNA topology in the cell by transiently cleaving only one of the two DNA strands.

Reactions Catalyzed by Type I DNA Topoisomerases

To introduce a temporary single-strand break into duplex DNA, type I DNA topoisomerases must catalyze the cleavage and subsequent religation of a DNA strand. Since these two reactions occur without an external energy source such as ATP, cleavage cannot result from simple hydrolysis of a phosphodiester bond in the DNA. Instead, a covalent enzyme–DNA intermediate is generated that makes the religation step energetically feasible. The formation of the covalent intermediate involves nucleophilic attack by the O-4 atom of the active site tyrosine in the enzyme on a phosphodiester bond in the DNA to produce a phosphodiester bond between the tyrosine and the DNA and leave a free DNA hydroxyl end. DNA religation and release of the enzyme is the reverse reaction with the oxygen of the free DNA hydroxyl acting as the nucleophile. The type I enzymes display a loose preference for certain nucleotides in the vicinity of a cleavage site, and therefore a cleavage site typically occurs every 5–20 base pairs along the DNA.

Type I topoisomerases act on closed circular DNAs to change the number of times one strand winds around the other, a parameter referred to as the linking number of the DNA. Changes in the linking number are reflected in a reduction or an increase in the supercoiling of a plasmid DNA, a property that is most often measured by gel electrophoresis. In addition to altering the supercoiling of a plasmid DNA, many type I topoisomerases are capable of catalyzing a number of other transactions involving both single- and double-stranded DNAs. Most of these enzymes can catenate (interlock), decatenate, knot, and unknot single-stranded DNA circles. The same series of reactions can be carried out with duplex circular DNAs providing at least one of the circular molecules possesses a nick or gap. In some cases, the enzymes can facilitate the interwinding required for the renaturation of two complementary single-stranded circular DNAs, a reaction that could be important during homologous recombination. Interestingly, topoisomerase V, which has only been described in the hyperthermophilic archaeon *Methanopyrus kandleri*, possesses, in addition to the usual topoisomerase activity, an apurinic/apyrimidinic site-processing activity that would appear to implicate the enzyme in DNA repair. Finally, with certain unusual DNA substrates, a block to religation leads to permanent suicide cleavage and the enzyme remains covalently linked to the DNA.

Classification, Nomenclature and General Properties

Type I topoisomerases are classified into two structurally and mechanistically distinct subfamilies based on which DNA end becomes covalently attached to the enzyme during the cleavage reaction: type IA enzymes attach via a tyrosine phosphodiester linkage to the 5′ end of the DNA, whereas type IB enzymes attach to the 3′ end of the DNA. Table I lists the known type I DNA topoisomerases in the two subfamilies with their common names and origins. The common names have generally been assigned in the order of discovery using odd Roman numerals (even Roman numerals are similarly used for type II DNA topoisomerases). Type I enzymes with unusual properties or origins have been given unique names (reverse gyrase, poxviral topoisomerase, and mitochondrial topoisomerase). The recently described IB enzymes in some eubacteria are currently referred to as bacterial topoisomerases IB.

The three categories of type IA enzymes listed in Table I can be distinguished on the basis of the types of

TABLE I

Type I DNA Topoisomerases

Subfamily	Common name	Source	Structure
IA	Topoisomerase I	All eubacteria and some archaebacteria	Monomer
IA	Topoisomerase III	Some eubacteria and most eukaryotes	Monomer
IA	Reverse gyrase	All hyperthermophilic eubacteria and archaea	Monomer
IA	Reverse gyrase	Archaeon *Methanopyrus kandleri*	Heterodimer
IB	Topoisomerase I	Nucleus of all eukaryotes	Monomer
IB	Mitochondrial topoisomerase	Mitochondria of higher eukaryotes	Monomer
IB	Poxviral topoisomerase	All members of poxviridae family	Monomer
IB	Topoisomerase V	Archaeon *Methanopyrus kandleri*	Monomer
IB	Topoisomerase IB	Some eubacteria (see Table II)	Monomer
IB	Topoisomerase I	Trypanosomatids *Trypanosoma brucei* and *Leishmania donovani*	Heterodimer

reactions they catalyze. Topoisomerases I relax negative but not positive supercoils in plasmid DNAs; but since relaxation does not go to completion, some residual negative supercoils remain in the product. Topoisomerases III require hypernegatively supercoiled plasmid DNA as a substrate and again relaxation is incomplete. Interestingly, topoisomerases III are much more proficient than the topoisomerases I in DNA catenation and decatenation (see below). Reverse gyrases, which are only found in hyperthermophilic eubacteria and archaebacteria, introduce positive supercoils into plasmid DNAs at the expense of ATP hydrolysis. All of the type IA enzymes require Mg^{2+} and are monomeric with the exception of the reverse gyrase from the archaeon *Methanopyrus kandleri* which is a heterodimer.

The type IB DNA topoisomerases are capable of relaxing both positive and negative supercoils in a reaction that does not require ATP or divalent cations. The reactions go to completion to produce a completely relaxed set of plasmid DNA topoisomers. With the exception of the recently discovered heterodimeric topoisomerases I from trypanosomatids, all of the type IB enzymes are monomeric.

Type IA DNA Topoisomerases

Protein Domains

All type IA topoisomerases (Table I) share a highly conserved "cleavage/strand passage" domain that contains the active site tyrosine. This domain is also responsible for promoting the structural change in the DNA during the interval between the cleavage and religation reactions that results in a linking number change (see below) (Figure 1, red boxes). As indicated in Figure 1, all type IA enzymes contain a poorly conserved

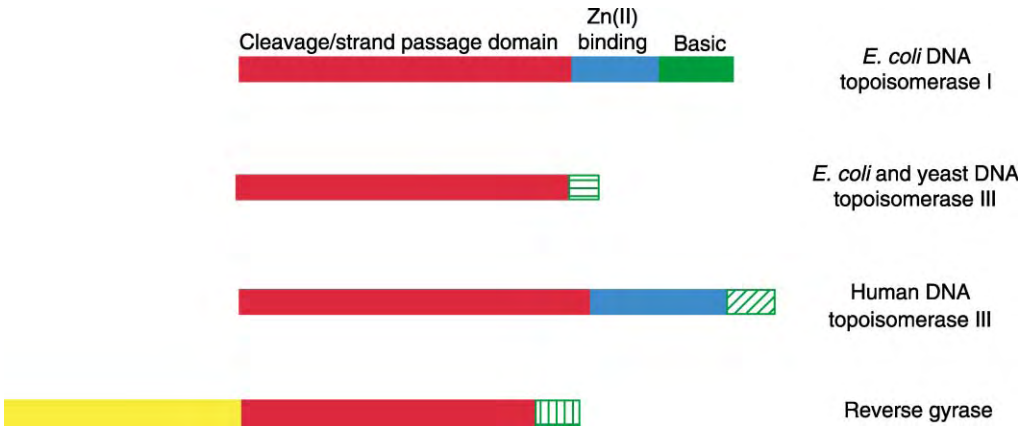

FIGURE 1 Domain structure and sequence relationships between type IA DNA topoisomerases. The domain structure of representative type IA topoisomerases is denoted by colored boxes. The names of the domains for the prototypic *E. coli* DNA topoisomerase I are given along the top. The cleavage/strand passage domains shared by all the IA enzymes are shown in red. Green is used to denote the basic C-terminal domains, but the different types of fill for these boxes indicate that these domains are poorly conserved. Some type IA enzymes contain a Zn(II) binding domain shown in blue. The helicase-like domain of reverse gyrase is shown in yellow.

basic C-terminal domain (solid or hatched green boxes) and some contain a Zn(II) binding domain as well (blue boxes). These latter two features appear to be important for the interaction of the enzyme with DNA. Finally, reverse gyrases contain an N-terminal domain, which resembles the ATPase domains of helicases (yellow box), and is connected to two domains that are structurally very similar to the cleavage/strand passage and basic domains of the typical type IA topoisomerases.

Crystal Structure of the Conserved Cleavage/Strand Passage Domain

The crystal structure of the cleavage/strand passage domain of *E. coli* DNA topoisomerase I shown in Figure 2 provides key insights concerning the substrate preference of the enzyme and the mechanism of DNA relaxation. Notably, the cleavage/strand passage domains of all type IA topoisomerases bear a strong resemblance to the *E. coli* structure. The hallmark of the crystal structure is a toroidal shape in which the diameter of the hole in the center of the torus is sufficient to accommodate either single- or double-stranded DNA.

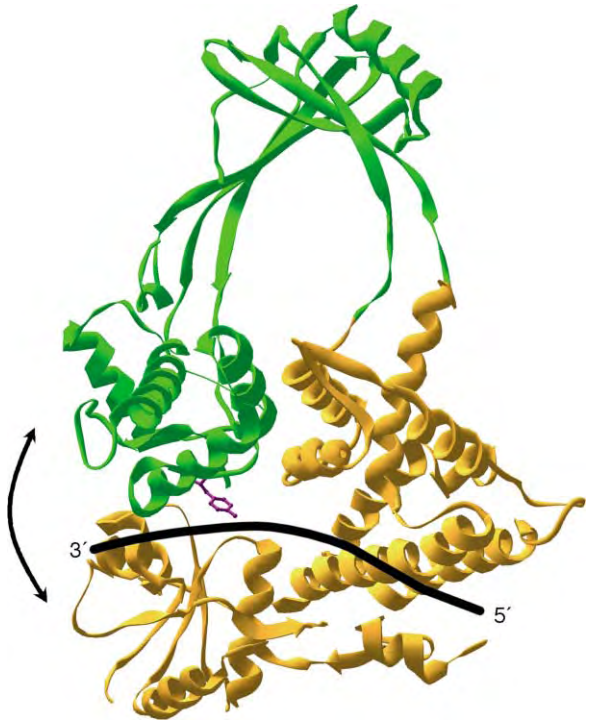

FIGURE 2 A ribbon diagram showing the crystal structure of the cleavage/strand passage domain of *E. coli* DNA topoisomerase I (pdb entry 1ecl) drawn with Swiss-Pdb Viewer software (Glaxo Wellcome Experimental Research). The approximate path of the bound single-stranded substrate DNA is indicated by the solid black line, and the active site tyrosine is shown in magenta. The two regions of the protein that move relative to each other (double-headed arrow) to open and close the torus during the strand passage reaction and to release the DNA are shown in green and orange.

The requirement for a negatively supercoiled substrate and the inability to completely relax negative supercoils is best explained by supposing that these enzymes will only bind an otherwise duplex DNA substrate if it contains a single-stranded region resulting from local unwinding of the helix. A plasmid DNA that is highly negatively supercoiled is energetically disposed toward helix unwinding, which explains why such a DNA is a good substrate for the enzyme. However, relaxation ceases when the negative supercoiling falls to a level below which there is insufficient energy to promote the required opening of the helix. As shown in Figure 2, a single strand of DNA (solid black line) binds to a narrow groove on the cleavage/strand passage domain of the enzyme in close proximity to the active site tyrosine (magenta).

Enzyme-Bridging Mechanism for Strand Passage

To change the linking number of a closed circular DNA during relaxation, one strand of DNA must pass through a break in the other strand. Knotting, catenation, and decatenation of either single or double-stranded DNAs similarly require such a strand passage event. The strand passage reaction for type IA topoisomerases occurs by what is referred to as an enzyme-bridging mechanism. Once the scissile DNA strand is cleaved, both DNA ends remain tightly associated with the enzyme; the 5′ end is bound covalently to the active site tyrosine and the 3′ end is bound noncovalently to the enzyme. To orchestrate strand passage, the enzyme undergoes a conformational change in which the top half of the protein containing the 5′ end of the cleaved strand (Figure 2, shown in green) lifts upward to generate a gate in the DNA through which another strand of DNA is passed. After strand passage, the broken strand is religated and the enzyme opens up a second time to release the strand that had been passed into the hole of the torus. A correlate of this model is that the linking number can only be changed in steps of one and this prediction has been verified biochemically.

This same scheme can explain how the enzyme can catenate or decatenate a DNA containing a nick or gap. However, it is unclear whether the DNA that passes through the temporary gate in the cleaved strand is captured in the hole of the torus before strand cleavage and is then passed out of the hole after cleavage or vice versa as described above.

Reverse Gyrase Mechanism

Despite the presence of a helicase-like ATPase domain in the N-terminal region of reverse gyrases, these enzymes

lack helicase activity when assayed under conditions that would require processive translocation along the DNA. Instead, the binding of the N-terminal domain to DNA is believed to simply unwind a region of the helix. Subsequently, in a reaction dependent on ATP, one of the two strands is cleaved and the other strand is passed through the resultant gate by the cleavage/strand passage domain present in the C-terminal half of the molecule. The key to positive supercoiling is that the strand passage event that occurs in the presence of ATP is directional such that the linking number of the DNA is increased and therefore the DNA ends up positively supercoiled. The structural basis for the unidirectional nature of the strand passage event remains unknown.

Type IB DNA Topoisomerases

Domain Structure and Sequence Conservation

Type IB DNA topoisomerases are present in the nucleus of all eukaryotic cells and the mitochondria of higher eukaryotes, as well as in at least one archaeon and some eubacteria (Table I). The typical eukaryotic type IB enzyme possesses the four domains shown in Figure 3. A highly charged and poorly conserved N-terminal domain (red box) is followed by the core domain (blue box), which binds DNA and contains most of the catalytic residues. The active site tyrosine is found in the C-terminal domain (yellow box) that is connected to the remainder of the protein by a poorly conserved linker region (orange box).

All of the other type IB enzymes share at least partial sequence and structural homology with the catalytically important core domain as can be seen from the color scheme in Figure 3 (blue boxes). Where present, the sequence of the mitochondrial enzyme is very similar to the nuclear enzyme with the exception of the N-terminal region (green box), which contains the organelle targeting signals. The eubacterial IB enzyme and the vaccinia topoisomerase are very similar to each other, but they lack most of the core domain as well as the conserved C-terminal domain that is characteristic of the other IB enzymes; instead, they share unique N-terminal and C-terminal regions (white and magenta boxes). The topoisomerase I found in the trypanosomatids is a heterodimer with one subunit containing the catalytic core (blue box) and the other subunit containing a region homologous to the C-terminal domain of the prototypic eukaryotic sequence (yellow box).

Crystal Structure of Human Topoisomerase I

Two views of the crystal structure of human topoisomerase I (missing the N-terminal domain) with a bound 22 base pair duplex oligonucleotide are shown in Figure 4. The protein is a bi-lobed structure that clamps completely around the DNA with the active site tyrosine (shown in black in Figure 4A) juxtaposed to the scissile phosphate. The linker region comprises the coiled-coil structure that protrudes conspicuously from the bottom portion of the enzyme and has an unknown function (Figure 4A). To release the DNA, the top half of the protein (shown in blue) must shift upward relative to the bottom half as indicated in Figure 4B by the double-headed arrow. Likewise, DNA binding requires that the protein clamp be in an open conformation. The region of

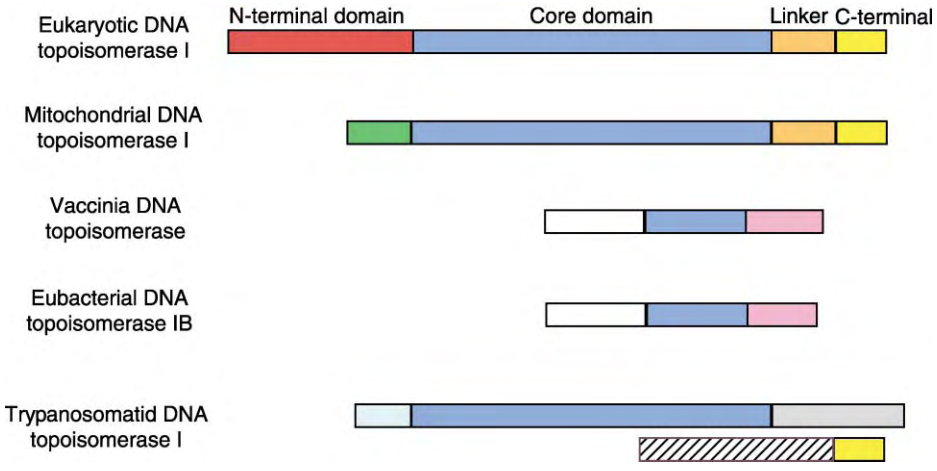

FIGURE 3 Domain structure and sequence relationships between type IB topoisomerases. The domain structure of the type IB topoisomerases from the indicated sources are denoted by colored boxes with similar domains aligned vertically. The names of the domains for the eukaryotic type IB topoisomerases are shown along the top. Regions that are similar in amino acid sequence share the same color; distinct sequences are assigned different colors. The two subunits of the heterodimeric topoisomerase I from trypanosomatids are shown with these same color conventions.

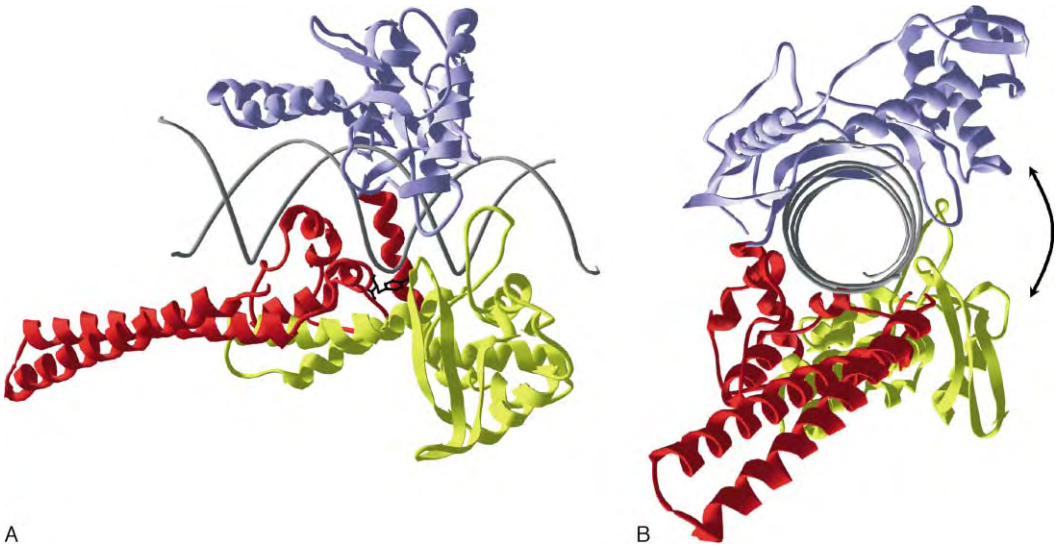

FIGURE 4 The ribbon diagrams show two views of the crystal structure of human topoisomerase I clamped around a 22 base pair duplex DNA, shown in gray (pdb entry 1a36). The top lobe of the enzyme is shown in blue and the bottom lobe is shown in red and yellow. The poxviral topoisomerase and the eubacterial topoisomerases IB are structurally very similar to the region of the bottom lobe, shown in yellow. The coiled-coil linker region in bottom lobe (in red) is most easily seen in the side view shown in (A). The active site tyrosine (in black) is shown in (A). Panel (B) shows a view of the structure looking down the axis of the DNA. The double-headed arrow in (B) indicates the nature of the conformational change that is required to open and close the clamp during binding and release of the DNA.

the human topoisomerase I structure shared by the poxviral and eubacterial IB enzymes corresponds to the portion of the core domain depicted in yellow in Figure 4. Tyrosine recombinases such as the bacteriophage λ and HP1 integrases, and cre recombinase are also structurally very similar to approximately this same region.

Catalysis

The co-crystal structure of human topoisomerase I with bound DNA reveals which amino acid residues in the protein are directly involved in catalysis. It is worth noting that the nucleophilic tyrosine O-4 does not appear to be activated for cleavage by general base catalysis, although a lysine residue acts as a general acid to protonate the leaving 5′ oxygen. The pentavalent transition state is stabilized by hydrogen-bonding interactions between three basic amino acid side chains and the scissile phosphate oxygens. An interaction between a lysine residue and the base of the nucleotide where cleavage occurs is also important for catalysis. Religation is likely to proceed by a pathway that is essentially the reverse of cleavage.

Rotational Mechanism for Strand Passage

Examination of the crystal structure of human topoisomerase I (Figure 4A) suggests that the strand passage reaction required to change the linking number of the DNA during DNA relaxation occurs by a rotational mechanism rather than by the enzyme-bridging mechanism described above for the type IA enzymes. However, there appears to be insufficient space within the confines of the enzyme to accommodate unrestricted rotation of the DNA. This feature of the structure suggests that the enzyme probably undergoes a conformational change after cleavage to open up the space downstream of the cleavage site to allow rotation. Unlike the enzyme-bridging model, a rotational mechanism places no *a priori* limit on the number of rotational events that can occur for each cycle of cleavage and religation. Indeed, in the case of vaccinia topoisomerase, five rotations of the DNA occur on the average between each cleavage and religation reaction.

Cellular Roles

Although much is yet to be learned about how the various topoisomerases collaborate to manage DNA topology in the cell, a partial picture has emerged based on work in bacteria and simple eukaryotes. Although the type II topoisomerases are not the subject of this review, the activities of these enzymes are briefly considered in the sections to follow for the sake of completeness. The type II enzymes are important for any cellular process that requires the passage of a region of duplex DNA through a double-strand break in the same or a different DNA molecule. The allocation of functions to

the known topoisomerases in setting the global levels of supercoiling, in transcription and in DNA replication, are discussed below.

Types of Supercoiling in Eukaryotic Versus Prokaryotic Cells

Two different situations lead to the supercoiling of DNA *in vivo*. First, DNA will assume a supercoiled configuration through an interaction with certain proteins or other cellular components. Alternatively, a closed domain of DNA (e.g., a closed circular DNA) will spontaneously supercoil if the linking number is not the same as the helical winding (referred to as twist) of the DNA helix. This latter type of supercoil is often referred to as torsionally strained supercoils. The chromosomal DNA of eukaryotes is wrapped into a protein-constrained solenoidal superhelix in nucleosomes and, except for the transient occurrence of torsionally strained supercoils associated with replication and transcription, is maintained in a relaxed state by DNA topoisomerases. However, in prokaryotes it appears that although some supercoils are constrained by virtue of an interaction with proteins as in eukaryotes, there exists, in addition, a fixed steady-state level of torsionally strained supercoiling generated by gyrases (see below).

Generation of Supercoiling Stress in Prokaryotes

Mesophilic Bacteria

The DNA in all mesophilic eubacteria and archaebacteria contains torsionally strained negative supercoils that are introduced by the type II enzyme called DNA gyrase. It appears that this steady-state level of negative superhelicity is required to facilitate helix opening during the initiation of DNA replication and transcription. To prevent the introduction of excess negative supercoils by the gyrase, these bacteria also contain one or two type IA DNA topoisomerases (topoisomerases I or III or both) to counteract the effects of DNA gyrase. The inability of the type IA enzymes to remove negative supercoils below a critical threshold level prevents these enzymes from negating the effects of DNA gyrase and is crucial for fine-tuning the negative supercoiling levels in these organisms. Some eubacteria also contain a type IB enzyme (Table II), which could also balance the effects of DNA gyrase; but the apparent ability of these enzymes to completely relax the DNA suggests that their activity would have to be regulated in some way. The exact role played by the bacterial topoisomerase IB and why this enzyme is only present in a subset of the mesophilic eubacteria remains unknown.

TABLE II

Occurrence of DNA Topoisomerase IB in Eubacteria

Known species possessing type IB topoisomerase	Examples of species lacking type IB topoisomerase
Mycobacterium avium	
Mycobacterium smegmatis	*Streptomyces coelicolor*
Cytophaga hutchinsonii	*Chlamydia trachomatis*
Agrobacterium tumefaciens	*Bacillus anthracis*
Bradyrhizobium japonicum	*Bacillus subtilis*
Mesorhizobium loti	*Clostridium tetani*
Sinorhizobium meliloti	*Mycoplasma pneumoniae*
Rhodobacter sphaeroides	*Listeria monocytogenes*
Novosphingobium aromaticivorans	*Staphylococcus aureus*
Bordetella parapertussis	*Streptococcus pneumoniae*
Burkholderia fungorum	*Streptococcus pyogenes*
Xanthomonas axonopodis	*Caulobacter crescentus*
Xanthomonas campestris	*Rickettsia conorii*
Pseudomonas aeruginosa	*Neisseria meningitidis*
Pseudomonas fluorescens	*Helicobacter pylori*
Pseudomonas putida	*Escherichia coli*
Pseudomonas syringae	*Yersinia pestis*
Deinococcus radiodurans	*Vibrio cholerae*
	Xylella fastidiosa
	Haemophilus influenzae
	Salmonella typhimurium
	Borrelia burgdorferi
	Treponema pallidum

Hyperthermophilic Bacteria

All hyperthermophilic eubacteria and archaebacteria possess a reverse gyrase that actively maintains positive supercoils in the chromosomal DNA. It appears this positive supercoiling is necessary to stabilize the DNA helix against denaturation at the high growth temperatures of these organisms. The mechanism for preventing excess positive supercoiling is not known, but it is likely that a type II enzyme that can relax positive supercoils (DNA gyrase or the archaeal topoisomerase VI) counteracts the effects of reverse gyrase to set the final steady-state level of positive supercoiling.

Transcription

During transcription, the movement of RNA polymerase along a DNA that is rotationally fixed transiently generates positive supercoils in front of the translocating polymerase and negative supercoils behind the polymerase (Figure 5A). The type IA enzymes present in all organisms relax the negative supercoils that accompany transcription, but the mechanism for the removal of the positive supercoils depends on the organism.

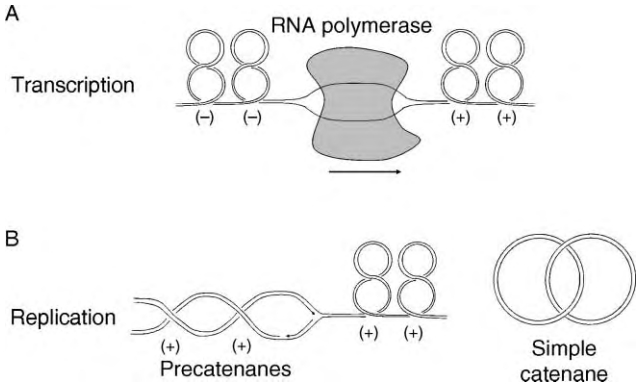

FIGURE 5 Topological transformations of DNA during transcription and replication. (A) The generation of positive supercoils (+) in front of and negative supercoils (−) behind a translocating RNA polymerase during transcription are depicted. (B) Replication fork movement in a closed domain results in an overwinding of the DNA ahead of the replication fork and the interwinding of the two daughter helices to form precatenanes behind the replication fork, as shown in (B). Any precatenanes remaining at the end of replication for a circular replicon will result in the catenation of the two daughter circular molecules. A simple catenane with a single interlink is also shown.

In prokaryotes, positive supercoils are relaxed by a type II enzyme such as DNA gyrase or in the archaea by topoisomerase VI, and in the case of select eubacteria (see Table II) probably by a combination of a type II enzyme and the type IB topoisomerase.

In eukaryotes, it is likely that the type IB DNA topoisomerase I relaxes the supercoils of both signs associated with transcription. Based on the known complete genome sequences, most eukaryotes, but not fungi or *Caenorhabditis elegans*, contain two distinct genes for type IB enzymes, one for the nuclear enzyme and a second for an enzyme that is imported into the mitochondrion to presumably function in transcription. In those eukaryotic organisms with only a single type IB enzyme, topoisomerase I likely plays a dual role, acting in both the nucleus and the mitochondrion.

DNA Replication

As the two DNA strands are separated during DNA replication, the DNA helix in front of the replication fork becomes at least transiently overwound or positively supercoiled (Figure 5B). This overwinding of the helix has been shown to be at least partially transmitted to the region behind the replication fork to cause an interwinding of the two daughter helices. These interwindings are referred to as precatenanes (Figure 5B), since in a circular replicon, if any remain at the end of replication, the two daughter circular molecules will be catenated. Resolution of the overwound structure of a replicating chromosome can be accomplished by relaxing positive supercoils in front of the fork, or by decatenating (or unlinking) the precatenanes behind the moving fork, or both.

As in transcription, positive supercoils can be removed in prokaryotes by a type II topoisomerase such as the DNA gyrase, the archaeal topoisomerase VI, or, for those eubacteria that have it, topoisomerase IB. Precatenanes can be resolved by a type II topoisomerase, most notably topoisomerase IV in eubacteria or topoisomerase VI in archaea. As long as gaps exist during discontinuous DNA synthesis, precatenanes can also be unlinked in some eubacteria either by topoisomerase IB (Table II) or by the potent type IA decatenating enzyme, topoisomerase III. Segregation of true catenanes lacking nicks or gaps in either of the two strands can only be accomplished by a type II enzyme.

In eukaryotes, the type IB topoisomerase relaxes the positive supercoils ahead of the replication fork and during synthesis can probably decatenate the precatenanes by acting at gaps in the DNA. However, most of the precatenanes and terminally interlinked or catenated structures are likely resolved by a type II topoisomerase. In mitochondria, replication-associated positive supercoils are relaxed by a type IB topoisomerase as described above for transcription. A mitochondrial type II topoisomerase and a type IA enzyme (topoisomerase III) are likely involved in unlinking precatenanes and catenated circular DNAs that occur during mitochondrial DNA replication.

See Also the Following Articles

DNA Supercoiling • DNA Topoisomerases: Type II

Glossary

catenane Two interlocked circular DNA molecules in which the two duplexes are wound around each other one or more times.

catenate The process whereby two circular DNAs are interlocked to form a catenane. The unlocking of catenated DNAs is referred to as decatenation.

closed circular DNA Circular DNA in which both strands are intact.

DNA gyrase DNA topoisomerase that couples the hydrolysis of ATP to the introduction of negative supercoils into a closed circular DNA.

DNA supercoiling The coiling of the axis of a DNA molecule in three-dimensional space. Supercoiling may result from an interaction of the DNA with protein or from an inequality between the number of helical turns dictated by the structure of the DNA helix under a particular set of conditions (the twist of the DNA) and the linking number of the DNA.

linking number Topological property of a closed circular DNA that is a measure of the fixed interwinding of the two DNA strands.

precatenanes The interwinding of the two daughter duplexes behind a replication fork.

reverse gyrase DNA topoisomerase that couples the hydrolysis of ATP to the introduction of positive supercoils into a closed circular DNA.

scissile strand The strand of DNA that is cleaved by a type I topoisomerase.

topoisomerase Enzyme that changes the linking number of a closed circular DNA by temporarily breaking one (type I) or both (type II) of the strands of the DNA.

topoisomers Variants of a closed circular DNA that have different linking numbers.

torsionally strained supercoils Supercoils that result from an inequality between the number of helical turns dictated by the structure of the DNA helix under a particular set of conditions and the linking number of the DNA.

Further Reading

Alexandrov, A. I., Cozzarelli, N. R., Holmes, V. F., Khodursky, A. B., Peter, B. J., Postow, L., Rybenkov, V., and Vologodskii, A. V. (1999). Mechanisms of separation of the complementary strands of DNA during replication. *Genetica* **106**, 131–140.

Champoux, J. J. (2001). DNA topoisomerases: Structure, function, and mechanism. *Annu. Rev. Biochem.* **70**, 369–413.

Wang, J. C. (1996). DNA topoisomerases. *Annu. Rev. Biochem.* **65**, 635–692.

Wang, J. C. (2002). Cellular roles of DNA topoisomerases: A molecular perspective. *Nat. Rev. Mol. Cell. Biol.* **3**, 430–440.

Biography

James J. Champoux is a Professor in the Department of Microbiology in the School of Medicine at the University of Washington. His research focuses on topoisomerases and reverse transcription. He holds a Ph.D. from Stanford University and carried out his postdoctoral work at the Salk Institute in San Diego, California. He discovered the eukaryotic type IB topoisomerase and was the first to show that the reaction proceeds through an enzyme–DNA covalent intermediate. He has been instrumental in elucidating the roles of the RNase H activity of reverse transcriptase in retroviral replication.

DNA Topoisomerases: Type II

Renier Vélez-Cruz and Neil Osheroff
Vanderbilt University School of Medicine, Nashville, Tennessee, USA

Although the genetic information of an organism is encoded by the linear array of DNA bases that make up its genome, the three-dimensional properties of the double helix dramatically affect how this information is expressed and passed from generation to generation. Some of the most important three-dimensional relationships in the genetic material are topological in nature, including DNA under- and overwinding, knotting, and tangling. The enzymes that modulate the topological properties of DNA are termed DNA topoisomerases. There are two classes of topoisomerases, type I and type II, which are defined by their reaction mechanisms. Type I topoisomerases alter DNA topology by creating a transient single-stranded break in the genetic material and facilitating controlled rotation of the double helix about (or strand passage through) the nick. Type II topoisomerases act by passing an intact double helix through a transient double-stranded break that they generate in a separate DNA segment. As a consequence of their reaction mechanisms, both classes of enzymes can regulate DNA under- and overwinding. However, because type II topoisomerases cut both strands of the double helix, they also are able to resolve knots and tangles in the genetic material. Type II topoisomerases are essential to all species. Beyond their critical physiological functions, these enzymes are the targets for some of the most important anticancer and antibacterial drugs in clinical use.

DNA Topology

The topological properties of DNA are defined as those that cannot be altered without breaking one or both strands of the double helix. Because DNA comprises two interwound nucleic acid strands and the genomes of all known organisms are very long or circular (or both), two distinct topological issues arise as a result of the genetic material. Proliferating cells must be able to cope with both of these in order to survive.

The first issue is related to the torsional stress on the double helix. The DNA from all species of eukaryotes and eubacteria is globally underwound ~5–10%. DNA under torsional stress is termed supercoiled (underwound molecules are negatively supercoiled and overwound molecules are positively supercoiled) because underwound or overwound DNA writhes about itself to form superhelical twists. Negative supercoiling puts energy into the genetic material and makes it easier to separate the two strands of the double helix for replication and transcription. Thus, DNA underwinding dramatically increases the rates of these two fundamental processes. In contrast, the movement of DNA tracking systems (such as replication forks and transcription complexes) through the double helix locally overwinds the DNA ahead of their actions. Because overwinding makes it much harder to pull apart the double helix, it blocks many essential cellular processes.

The second issue is related to the extreme length of genomic DNA. Nucleic acid knots (intramolecular) and tangles (intermolecular) are formed routinely during a variety of ongoing cellular processes including DNA recombination and replication. Both knots and tangles must be resolved in order for daughter chromosomes to segregate properly during meiosis and mitosis.

DNA Topoisomerases

Cells contain ubiquitous enzymes known as DNA topoisomerases that maintain the appropriate level of DNA supercoiling and remove knots and tangles from the genetic material. These enzymes modulate the topological structure of the genetic material by creating transient breaks in the backbone of DNA. There are two classes of topoisomerases that can be distinguished by the number of DNA strands that they cleave during their catalytic cycles. Type I enzymes create transient single-stranded DNA breaks, whereas type II enzymes create transient double-stranded breaks. To maintain genomic integrity during their DNA cleavage events, topoisomerases form covalent linkages between active-site tyrosyl residues and the newly generated DNA termini. These covalent protein-cleaved DNA complexes, known as cleavage complexes, are the hallmarks of all topoisomerases irrespective of enzyme classification. Because type I topoisomerases create single-stranded breaks in the genetic material, they can regulate DNA supercoiling. However, because type II topoisomerases generate double-stranded breaks in the DNA backbone, they can

resolve knots and tangles in addition to removing torsional stress from the genetic material.

Type II topoisomerases are essential to all eukaryotic and prokaryotic organisms. They are highly conserved among species, and the eukaryotic enzymes appear to be direct descendents of ancestral bacterial proteins.

Eukaryotic Type II Topoisomerases

The eukaryotic type II enzyme is called topoisomerase II. It was discovered in 1980 and is a member of the type IIA homology subfamily. Topoisomerase II can remove positive and negative superhelical twists from the double helix and can resolve DNA knots and tangles.

Enzyme Mechanism

Topoisomerase II interconverts different topological forms of DNA by the double-stranded DNA passage reaction depicted in Figure 1, which shows the products of each individual step. Briefly, it is proposed that topoisomerase II (1) binds two DNA segments, (2) creates a double-stranded break in one of the segments, (3) translocates the other DNA segment through the cleaved double helix, (4) rejoins (i.e., ligates) the cleaved DNA, (5) releases the translocated segment through a gate in the protein, and (6) closes the protein gate and regains the ability to start a new round of catalysis. The scissile bonds on the two strands of the double helix that are cut by topoisomerase II are staggered. Thus, the enzyme generates cleaved DNA molecules that contain four-base single-stranded ends at their 5′-termini. During its cleavage event, topoisomerase II covalently attaches to these newly generated 5′-termini.

Topoisomerase II requires two cofactors in order to carry out its catalytic double-stranded DNA passage reaction. First, it needs a divalent cation for all steps beyond enzyme-DNA binding (Figure 1, complex 1). Magnesium(II) appears to be the divalent cation that the enzyme uses *in vivo*. Second, topoisomerase II uses the energy of adenosine triphosphate (ATP) to drive the overall DNA strand passage reaction. Although ATP is not required for either DNA cleavage or ligation, the binding of this nucleoside triphosphate triggers DNA translocation (which converts complex 2 to complex 3)

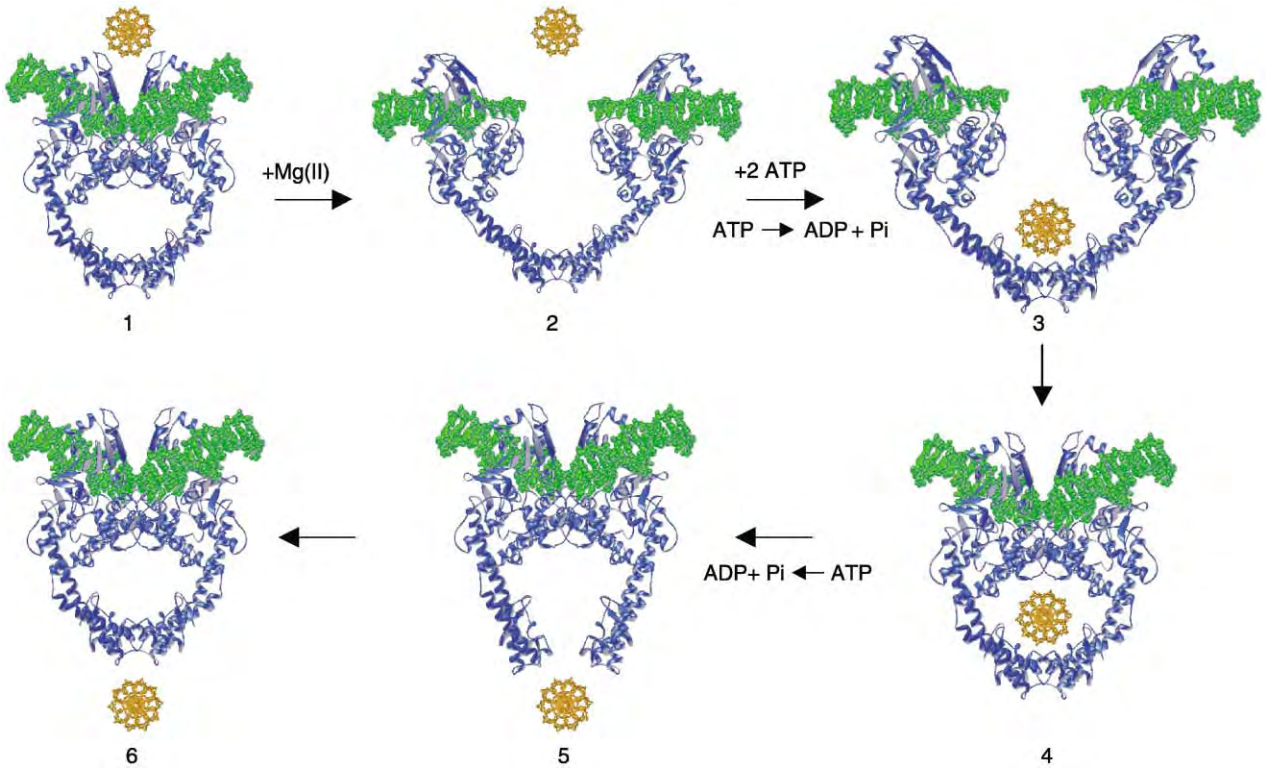

FIGURE 1 Catalytic cycle of type IIA topoisomerases. The complete double-stranded DNA passage reaction is shown as a series of discrete steps (the products of each step are shown). (1) Enzyme–DNA binding, (2) DNA cleavage (formation of cleavage complex), (3) double-stranded DNA passage, (4) DNA ligation, (5) gate opening and release of the translocated DNA helix, and (6) enzyme recycling. The protein (shown in blue) is based on the crystallographic structure of the catalytic core of yeast topoisomerase II. Modeled DNA helices are shown in green (horizontal) and orange (coming out of the plane of the paper). Structures are courtesy of Dr. James M. Berger, University of California, Berkeley.

and its hydrolysis to adenosine diphosphate (ADP) and inorganic phosphate (Pi) is necessary for enzyme recycling (which converts complex 5 to complex 6). Normally, topoisomerase II binds two molecules of ATP. Although hydrolysis of the cofactor is not a prerequisite for the strand passage event, it appears that this step proceeds more rapidly if it is preceded by hydrolysis of one of the bound ATP molecules.

Enzyme Domain Structures and Isoforms

Eukaryotic type II topoisomerases are homodimeric enzymes with protomer molecular masses ranging from ~160 to 180 kDa (depending on the species). On the basis of amino-acid-sequence comparisons with the bacterial type II enzyme, DNA gyrase, each enzyme monomer can be divided into three distinct domains (Figure 2). The N-terminal domain of the enzyme is homologous to the B-subunit of DNA gyrase (GyrB) and contains consensus sequences for ATP binding. The central domain is homologous to the A-subunit of DNA gyrase (GyrA) and contains the active-site tyrosyl residue that forms the covalent bond with DNA during scission. The C-terminal domain is not highly conserved and appears to have no corresponding region of homology with DNA gyrase. This variable region of the eukaryotic enzyme contains nuclear localization sequences as well as amino acid residues that are phosphorylated *in vivo*.

Although some eukaryotic species such as yeast and *Drosophila* appear to have only a single type II topoisomerase (i.e., topoisomerase II), vertebrates contain two closely related isoforms, topoisomerase IIα and β. These two isoforms share extensive amino acid sequence identity (~70%), but are encoded by separate genes (located at chromosomal bands 17q21–22 and 3p24 in humans, respectively) and can be distinguished by their protomer molecular masses (~170 and ~180 kDa, respectively).

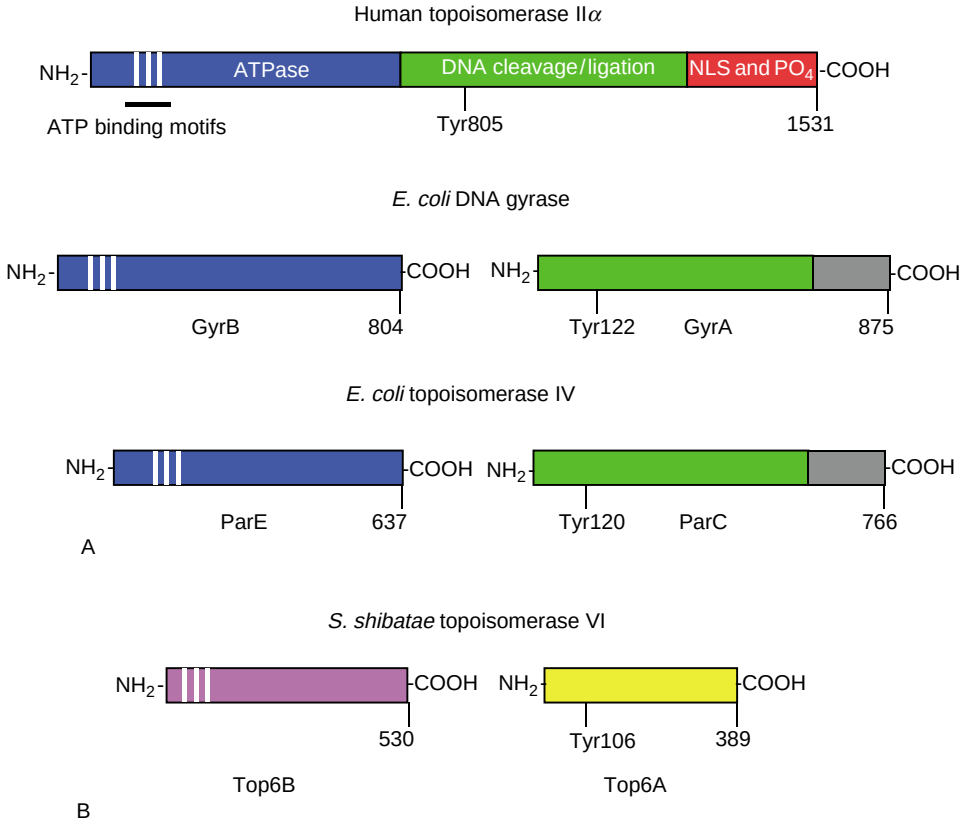

FIGURE 2 Domain structures of type II topoisomerases. (A) The domain structures of three type IIA topoisomerases: human topoisomerase IIα and bacterial (*Escherichia coli*) DNA gyrase and topoisomerase IV. Regions of homology among the enzymes are indicated by colors. The N-terminal (i.e., GyrB) homology domains contain the regions responsible for ATP binding and hydrolysis. The vertical white stripes represent the three conserved motifs of the Bergerat fold that define the ATP-binding domain. The central (i.e., GyrA) homology domains contain the active site tyrosyl residue (Tyr805 in human topoisomerase IIα) that forms the covalent bond with DNA during scission. For human topoisomerase IIα, the variable C-terminal domain contains nuclear localization sequences (NLS) and phosphorylation sites (PO_4). (B) The Top6A and Top6B subunits of the archaeal type IIB topoisomerase, *Sulfolobus shibatae* topoisomerase VI, shown for comparison.

Physiological Functions

Topoisomerase II plays a number of essential roles in eukaryotic cells and participates in virtually every major process that involves the genetic material. It unlinks daughter chromosomes that are tangled following replication and resolves DNA knots that are formed during recombination. It also helps to remove the positive DNA supercoils that are generated ahead of replication forks and transcription complexes. Topoisomerase II is required for proper chromosome condensation, cohesion, and segregation and appears to play roles in centromere function and chromatin remodeling. Finally, the type II enzyme is important for the maintenance of proper chromosome organization and structure, and it is the major nonhistone protein of the mitotic chromosome scaffold and the interphase nuclear matrix.

It is not obvious why vertebrate species possess two distinct topoisomerase II isoforms. Enzymological differences between topoisomerase IIα and β are subtle and the relationships between these isoforms are not well defined. Although either enzyme can complement yeast strains lacking topoisomerase II activity, topoisomerase IIα is essential for proliferating mammalian cells and its loss cannot be compensated by the β isoform. Topoisomerase IIβ appears to be dispensable at the cellular level, but is required for proper neural development in mice.

The specific cellular functions of topoisomerase IIα and β probably reflect their physiological regulation more than their enzymological characteristics. Topoisomerase IIα is regulated over both cell and growth cycles. Enzyme levels increase throughout the S-phase of the cell cycle and peak at the G_2-M boundary. Furthermore, this isoform is found almost exclusively in rapidly proliferating tissues. In contrast, the concentration of topoisomerase IIβ is independent of the cell cycle and this isoform is found in most cell types regardless of proliferation status. Taken together, these characteristics suggest that topoisomerase IIα is the isoform responsible for events associated with DNA replication and chromosome segregation, whereas topoisomerase IIβ is the isoform that probably functions in ongoing nuclear processes.

Prokaryotic Type II Topoisomerases

Eubacteria contain two distinct type II topoisomerases, DNA gyrase and topoisomerase IV. Both are members of the type IIA subfamily. In addition to these two enzymes, many archaeal species contain a third type II enzyme, topoisomerase VI. This last enzyme is a member of the type IIB subfamily.

DNA Gyrase

DNA gyrase was discovered in 1976. It was the first type II topoisomerase to be described and is the only one to retain its historical name (in the modern nomenclature, type II topoisomerases are denoted by even numbers). In contrast to the eukaryotic type II enzymes, DNA gyrase is comprised of two distinct subunits, GyrA and GyrB (molecular mass $\approx$96 kDa and 88 kDa, respectively) and is arranged as an A_2B_2 tetramer. GyrA contains the active site tyrosine used in DNA cleavage and ligation, and GyrB contains the binding site for ATP (Figure 2A).

In contrast to all other type II topoisomerases, DNA gyrase is the only enzyme that is capable of actively underwinding (i.e., negatively supercoiling) the double helix. It accomplishes this feat by wrapping DNA around itself in a right-handed fashion and carrying out its strand-passage reaction in a unidirectional manner.

The negative supercoiling activity of DNA gyrase far exceeds the ability of the enzyme to remove either knots or tangles from the genetic material. Consequently, the major physiological roles of DNA gyrase stem directly from its ability to underwind the double helix. DNA gyrase plays a critical role in opening DNA replication origins and removing positive supercoils that accumulate in front of replication forks and transcription complexes. In addition, this enzyme works in conjunction with the ω protein (a type I topoisomerase that removes negative supercoils from the double helix) to maintain the global balance of DNA supercoiling in bacterial cells.

Topoisomerase IV

Topoisomerase IV is an A_2B_2 tetramer that is comprised of two distinct subunits, ParC (molecular mass $\approx$88 kDa), and ParE (molecular mass $\approx$70 kDa), which are homologous to the A- and B-subunits of DNA gyrase (Figure 2B). (In gram-positive bacterial species, the subunits of topoisomerase IV are designated GrlA and GrlB, respectively.) It was known for several years that the ParC and ParE proteins were necessary for proper chromosome segregation in bacteria. However, it was not discovered until 1990 that these two subunits together constituted a type II topoisomerase.

The catalytic properties of topoisomerase IV can be distinguished from those of DNA gyrase in two important ways. First, although topoisomerase IV can remove positive and negative superhelical twists from DNA, it cannot actively underwind the double helix. Second, the ability of topoisomerase IV to resolve DNA knots and tangles is dramatically better than that of DNA gyrase. Because of these differences, the physiological roles of topoisomerase IV are distinct from those of DNA gyrase. The primary cellular functions of topoisomerase IV are to unlink daughter chromosomes following DNA replication and to resolve DNA knots

that are formed during recombination. Recently, it was found that topoisomerase IV removes positive supercoils from DNA more efficiently than it removes negative supercoils. This has led to speculation that the enzyme also may act ahead of DNA tracking systems to alleviate overwinding of the double helix. However, the precise role of topoisomerase IV in this process has yet to be defined.

Archaeal Topoisomerase VI

In 1997, a novel type II topoisomerase, topoisomerase VI, was discovered in hyperthermophilic archaeal species. This enzyme was designated as the first member of the topoisomerase IIB subfamily due to its lack of homology to previously identified type II enzymes.

Topoisomerase VI has two subunits, Top6A and Top6B (molecular masses ≈47 and 60 kDa, respectively), and is arranged as an A_2B_2 tetramer. Both subunits are considerably smaller than those of bacterial DNA gyrase or topoisomerase IV (Figure 2B). Although short regions of Top6B surrounding the ATP-binding domain are homologous to portions of GyrB, and Top6A contains an active-site tyrosine that is required for DNA cleavage, the primary structure of topoisomerase VI displays little similarity to the type IIA enzymes.

Archaeal topoisomerase VI appears to alter DNA topology by using a double-stranded DNA passage reaction like that described for other type II topoisomerases. During this reaction, it generates DNA breaks with 5′ overhangs that are covalently attached to its active-site tyrosyl residues. Topoisomerase VI relaxes positively and negatively supercoiled DNA, but cannot actively underwind the double helix. In addition, it can unlink (i.e., untangle) interwound double-stranded DNA circles.

The catalytic properties of topoisomerase VI differ from those of the type IIA enzymes in two significant aspects. First, topoisomerase VI requires ATP binding in order to cleave its DNA substrate. Second, in marked contrast to the type IIA enzymes (which produce four-base staggered ends during scission), topoisomerase VI-mediated DNA cleavage generates DNA termini that contain only two-base overhangs. Although the physiological functions of topoisomerase VI have yet to be determined, the enzyme is believed to play a role in unlinking daughter chromosomes following replication in archaeal cells.

With the exception of plants, no Top6B homologue has been identified in eukaryotic species. However, a Top6A homologue, Spo11, has been found in eukaryotes ranging from yeast to humans. Spo11 generates the double-stranded DNA breaks that initiate meiotic recombination. Like its topoisomerase relatives, Spo11 forms a covalent bond between an active-site tyrosyl residue and the 5′-DNA termini generated by its scission reaction. At the present time there is no evidence that Spo11 has topoisomerase (i.e., DNA strand passage) activity.

Type II Topoisomerases as Therapeutic Targets

In addition to their varied and critical physiological functions, the type IIA topoisomerases are targets for some of the most active anticancer and antibacterial drugs in clinical use. In contrast to most enzyme-targeted drugs, these agents do not act by robbing cells of an essential enzyme activity. Rather, drugs that target type II topoisomerases kill cells by dramatically increasing the concentration of covalent enzyme-cleaved DNA complexes (i.e., cleavage complexes) that are requisite intermediates formed during the double-stranded DNA passage reaction. Normally, cleavage complexes are present at low steady-state levels and are tolerated by cells. However, conditions that significantly increase either their concentration or lifetime trigger numerous mutagenic events.

The potential lethality of cleavage complexes rises dramatically when DNA tracking enzymes such as polymerases or helicases attempt to traverse the covalently bound topoisomerase roadblock in the genetic material. Such an action disrupts cleavage complexes and converts transient enzyme-mediated DNA breaks to permanent DNA breaks. These permanent breaks in the genome trigger the generation of chromosomal insertions, deletions, translocations, and other aberrations, and, when present in sufficient numbers, they initiate a series of events that culminates in cell death. Because the drugs that target type II topoisomerases convert these essential enzymes to potent cellular toxins that fragment the genome, they are referred to as topoisomerase poisons to distinguish them from drugs that act as catalytic inhibitors.

Anticancer Drugs

At the present time, six topoisomerase II-targeted anticancer agents (Figure 3A) are approved for use in the United States. Drugs such as etoposide and doxorubicin are front-line therapy for breast and lung cancers, as well as for a variety of leukemias, lymphomas, and germ-line malignancies. Approximately one-half of all cancer chemotherapy regimens contain drugs targeted to topoisomerase II. Moreover, every form of cancer that can be cured by systemic chemotherapy is treated with these agents.

Due to the high concentration of topoisomerase IIα in rapidly proliferating cells, this isoform probably is the major important target of anticancer therapy. However, circumstantial evidence suggests that the β-isoform also contributes to drug efficacy.

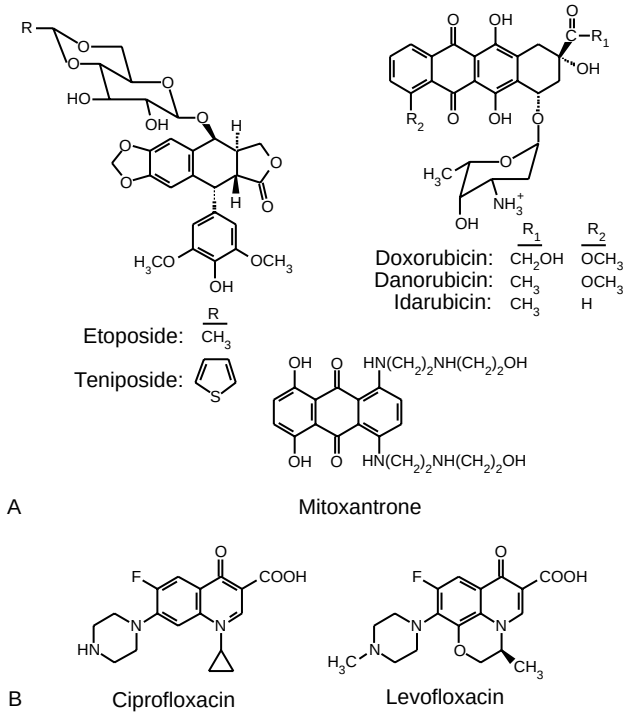

FIGURE 3 Structures of selected (A) anticancer drugs targeted to topoisomerase II and (B) antibacterial drugs targeted to DNA gyrase and topoisomerase IV.

Antibacterial Drugs

DNA gyrase and topoisomerase IV are the targets for quinolone-based antibacterial agents (Figure 3B). Quinolones are the most active and broad-spectrum antibacterial drugs currently available. Drugs such as ciprofloxacin are prescribed routinely for a wide variety of gram-negative bacterial infections, including gastrointestinal tract, respiratory tract, and bone and joint infections. Ciprofloxacin also is used to treat a number of sexually transmitted diseases as well as infection with anthrax. Newly developed quinolones, such as levofloxacin, display significant efficacy against gram-positive bacterial infections.

DNA gyrase is the primary cytotoxic target of quinolones in gram-negative bacteria. However, topoisomerase IV appears to be the more important target for many of these drugs in gram-positive species.

See Also the Following Articles

DNA Supercoiling • DNA Topoisomerases: Type I

Glossary

adenosine triphosphate (ATP) A cofactor that supplies energy for many enzymatic processes.

cell cycle The process by which a cell grows, replicates its genome, and divides. The cell cycle is divided in four distinct phases: G_1, a growth phase; S, the phase in which the cell duplicates (i.e., synthesizes) its genetic material; G_2, a second growth phase in which the cell prepares to divide; and M, the phase in which the cell divides (i.e., mitosis).

DNA recombination The process by which the cell reorganizes its genetic material in order to repair certain forms of DNA damage (including double-stranded DNA breaks) or promote genetic diversity.

DNA replication The process by which the cell duplicates (i.e., synthesizes) its genetic material.

DNA supercoiling The underwinding (i.e., negative supercoiling) or overwinding (i.e., positive supercoiling) of the genetic material.

topoisomerase poison A drug that increases levels of topoisomerase-cleaved DNA complexes.

topology A field of mathematics that deals with relationships that are not altered by elastic deformation.

transcription The process by which the cell expresses its genetic material; the generation of messenger RNAs from a DNA template.

Further Reading

Anderson, V. E., and Osheroff, N. (2001). Type II topoisomerases as targets for quinolone antibacterials: Turning Dr. Jekyll into Mr. Hyde. *Curr. Pharm. Des.* **7**, 337–353.

Champoux, J. J. (2001). DNA topoisomerases: Structure, function, and mechanism. *Annu. Rev. Biochem.* **70**, 369–413.

Fortune, J. M., and Osheroff, N. (2000). Topoisomerase II as a target for anticancer drugs: When enzymes stop being nice. *Prog. Nucl. Acid Res. Mol. Biol.* **64**, 221–253.

Gadelle, D., Filee, J., Buhler, C., and Forterre, P. (2003). Phylogenomics of type II DNA topoisomerases. *BioEssays* **25**, 232–242.

Heddle, J. G., Barnard, F. M., Wentzell, L. M., and Maxwell, A. (2000). The interaction of drugs with DNA gyrase: A model for the molecular basis of quinolone action. *Nucleosides Nucleotides Nucleic Acids* **19**, 1249–1264.

Li, T. K., and Liu, L. F. (2001). Tumor cell death induced by topoisomerase-targeting drugs. *Annu. Rev. Pharmacol. Toxicol.* **41**, 53–77.

Osheroff, N (ed.) (1998). DNA topoisomerases. *Biochim. Biophys. Acta* **1400**.

Wang, J. C. (2002). Cellular roles of DNA topoisomerases: A molecular perspective. *Nat. Rev. Mol. Cell. Biol.* **3**, 430–440.

Biography

Renier Vélez-Cruz is completing his doctoral studies in the Department of Biochemistry, Vanderbilt University School of Medicine.

Neil Osheroff is a Professor in the Departments of Biochemistry and Medicine at the Vanderbilt University School of Medicine and holds the John G. Coniglio Chair in Biochemistry. His principal research interests are the fields of DNA topoisomerases, topoisomerase-targeted drugs, and DNA repair. He holds a Ph.D. in Biochemistry and Molecular Biology from Northwestern University and received his postdoctoral training in the Department of Biochemistry at the Stanford University School of Medicine. He has authored more than 170 articles and has contributed significantly to our understanding of the mechanism of action of type II topoisomerases and topoisomerase II poisons.

DNA Topoisomerases: Type III–RecQ Helicase Systems

Rodney Rothstein and Erika Shor
Columbia University College of Physicians and Surgeons, New York, USA

DNA helicases and topoisomerases belong to the category of proteins that physically manipulate and alter the structure of DNA molecules. DNA helicases are enzymes that separate the strands of double-stranded (ds) DNA molecules, thus catalyzing DNA unwinding. Topoisomerases transiently create breaks in a DNA strand(s), pass other strands through the broken strand(s), and reseal the breaks. Topoisomerase activity can change levels of DNA supercoiling or result in catenation (interlinking) or decatenation (unlinking) of two DNA molecules. Both DNA helicases and topoisomerases are key players in various DNA transactions, such as replication, transcription, and recombination. Different classes and families of helicases and topoisomerases have been identified based on their protein sequence conservation, substrate preference, directionality on DNA, and other properties. DNA helicases of the RecQ family have garnered much interest lately because of the involvement of three human RecQ helicase family members in genetic disorders characterized by genomic instability and cancer predisposition. RecQ helicases are evolutionarily conserved proteins found in organisms ranging from bacteria to humans. Interestingly, an association between RecQ-type helicases and type III topoisomerases has been observed throughout the evolutionary tree, suggesting that these two proteins act in concert to promote genomic stability.

Structure and Molecular Mechanisms

Topoisomerase III

Topoisomerase III belongs to the type IA topoisomerases (also known as type I-5′). This subfamily of topoisomerases acts on DNA that is negatively supercoiled (underwound) and/or contains single-stranded (ss) regions. The topoisomerase, which functions as a monomer, makes a break in a ssDNA region via a transesterification reaction between an active site tyrosine of the enzyme and a DNA phosphate group (Figure 1). A transient covalent linkage between the tyrosine and the 5′-phosphoryl group of the DNA is thus formed. After passage of other DNA strand(s) through the break, the reverse transesterification reaction leads to the rejoining of the DNA backbone. Topoisomerase III activity can result in relaxation/removal of negative supercoiling from DNA, (de)catenation and knotting of ss circular DNA molecules, and (de)catenation of ds DNA molecules that contain ss regions. Topoisomerase III does not require energy in the form of nucleoside triphosphates, such as ATP. Hence, the directionality of the topoisomerase III-driven reactions is toward the DNA conformation with the lowest free energy.

RecQ Helicases

The RecQ family of DNA helicases is defined by homology to the bacterial RecQ protein. Like other helicases, these proteins contain seven signature helicase motifs, including sequences that contain Walker A (required for ATP binding and hydrolysis) and B boxes. In addition to the core helicase motifs, all RecQ helicases share additional regions of homology not shared by other families of helicases.

The functional unit of a helicase is generally composed of a dimer or a hexamer that forms a ring around its substrate DNA. However, examples of monomeric helicases are also known. Whereas several early studies have indicated that RecQ-like helicases form hexamers, two recent studies suggest that DNA helicase activities *in vitro* of both *E. coli* RecQ and human BLM proteins are associated with a monomeric form of the protein. Thus, the composition of a functional unit of RecQ-like helicases is still being explored.

All RecQ-type helicases examined to date display $3' \rightarrow 5'$ directionality on DNA with respect to the strand to which the protein is bound (Figure 2A). *In vitro* substrate preference studies have indicated that these helicases can act on a variety of DNA structures, possibly reflecting the diversity of their *in vivo* activities. Among the structures that RecQ helicases can unwind are branched molecules, four-way dsDNA junctions, G-quartets, and D-loops (Figure 2B). ATP and Mg^{2++} are necessary cofactors for RecQ-driven reactions.

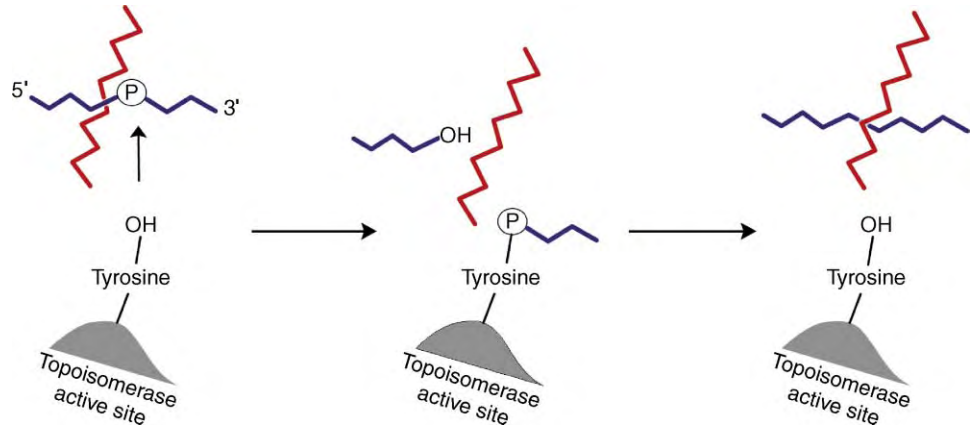

FIGURE 1 The mechanism of strand passage by a type IA topoisomerase. The topoisomerase makes a break in the blue strand by catalyzing a trans-esterification reaction between the tyrosine at the topoisomerase active site and a 5′ phosphate group of the DNA. Only the reacting phosphate is depicted as a P for clarity. The intact red strand is passed through the break, and a reverse trans-esterification reaction reseals the blue strand.

The RecQ Helicase–Topoisomerase III Connection

Physical Association

Two widely used model organisms, budding and fission yeast, each has one RecQ-like helicase and one topo III. In both organisms, the two proteins have been shown to physically interact with each other and/or to associate in cellular extracts. In human cells, the RecQ homolog BLM physically interacts with an isoform of topoisomerase III, Top3α, via the N-terminus of BLM. Mutation or deletion of BLM in human cells has several detrimental consequences on genome stability, including a marked increase in recombination between sister chromatids. Interestingly, cells expressing BLM protein that lacks its N-terminus and fails to interact with Top3α (but retains DNA unwinding activity) show increased levels of sister chromatid exchange, similar to cells that lack the entire BLM protein. This demonstrates that, in order to perform its role in suppressing recombination between sister chromatids, BLM needs to interact with Top3α *in vivo*, which supports other evidence that the two act as a complex with key roles in maintenance of genome stability.

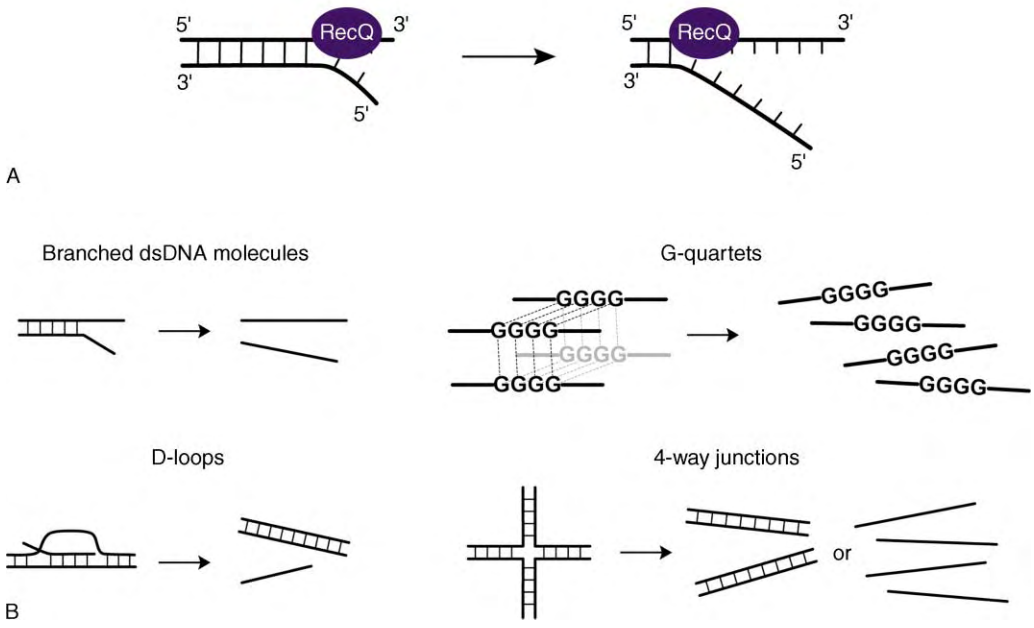

FIGURE 2 (A) RecQ helicases unwind DNA in the 3′ to 5′ direction with respect to the strand to which the helicase is bound. (B) Several of the known *in vitro* substrates of RecQ helicases before and after incubation with the protein.

Genetic Interactions in Yeast

As mentioned above, the genomes of both budding and fission yeast encode a single topoisomerase III gene. In both organisms, loss or mutation of the topo III protein is detrimental, resulting in slow growth or lethality. Concomitant loss of RecQ helicase function in mutants lacking topo III largely restores normal growth and viability. These genetic observations have led to the following model of RecQ–Topoisomerase III interaction *in vivo*. It is proposed that in wild-type cells, the activity of the RecQ helicase creates a DNA structure that is normally acted on and resolved by topo III. When topo III is inactivated, this structure is not processed properly and causes slow growth or lethality. In mutants lacking the RecQ helicase, this structure is not created, eliminating the need for a functional topo III. While this model is supported by genetic evidence, experimental data confirming the existence of such a DNA structure are lacking to date.

Combined Mode of Action

The genetic and physical interactions between RecQ-like helicases and type III topoisomerases in several organisms have prompted investigation and speculation regarding their combined mode of action. One possibility first put forth upon the discovery of the budding yeast RecQ homolog Sgs1 and its genetic and physical association with the budding yeast topo III was that the two proteins form a complex that functions like a eukaryotic reverse gyrase. A reverse gyrase is an enzyme found in several species of *Archaea*. A hallmark feature of the reverse gyrase protein is the presence of a type I topoisomerase-like domain and a helicase domain as part of the same polypeptide. *In vitro*, the enzyme introduces positive supercoiling into dsDNA molecules. This is thought to happen in the following manner. The helicase domain of reverse gyrase unwinds a region of dsDNA, creating local negative supercoiling on one side of the enzyme and local positive superoiling on the other. The topoisomerase domain relaxes the negative supercoiling, resulting in a net overall increase in positive supercoiling in the dsDNA molecule. However, despite the attractiveness of the hypothesis that the RecQ–topoIII complex resembles reverse gyrase, the few *in vitro* studies done on RecQ and topo III have not reported increased positive supercoiling as a result of the combined action of the two enzymes.

Another hypothesis regarding the role of the RecQ–topoIII complex suggests a role in catenation or decatenation of ds DNA molecules. This idea is supported by a study that examined the consequences of concerted action of bacterial RecQ and topo III in an *in vitro* system. It was shown that both bacterial and yeast topo III proteins are specifically stimulated by the bacterial RecQ helicase to fully catenate or decatenate (depending on the conditions of the reaction) covalently closed circular dsDNA molecules. *In vivo*, a decatenation activity may be used to separate such interlinked dsDNA substrates as sister chromatids following DNA replication or homologous chromosomes following mitotic or meiotic recombination. Their complete decatenation is essential for subsequent faithful chromosomal segregation, which in turn ensures accurate transfer of genetic material into daughter cells. On the other hand, a catenating activity may be used *in vivo* to suppress recombination, as DNA sequences that are highly catenated undergo fewer recombination events.

Cellular Roles of the RecQ–TopoIII Complex in DNA Metabolism

The Recombination Connection

Inactivation of a RecQ-type helicase or topoisomerase III generally causes a variety of detrimental consequences on the genomic integrity of an organism. One consequence that is shared by all organisms examined to date is an increase in genetic recombination. As mentioned above, hyper-recombination between sister chromatids is a hallmark of human cells expressing mutant versions of BLM protein. In budding yeast, inactivation of the RecQ homolog Sgs1 or of the topo III homolog Top3 leads to an increase in several kinds of recombination, such as recombination between tandemly repeated DNA sequences. In *E. coli*, inactivation of the *recQ* gene leads to an increase in illegitimate recombination (i.e., recombination between nonhomologous DNA sequences). These observations have suggested that RecQ helicases generally control or suppress recombination. This idea is supported by a series of genetic experiments with budding yeast and mirrored by observations in fission yeast. In these organisms, concomitant mutation of the RecQ family member and of another helicase, Srs2, causes extreme slow growth and frequent lethality. However, these defects are fully rescued by mutation of any of several proteins that perform homologous recombination. This indicates that in the absence of a functional homologous recombination pathway, deletion of the two helicases is no longer detrimental to the cell. This can be explained by proposing that in the absence of the two helicases, incorrectly regulated or uncontrolled recombination is responsible for the poor growth and increased lethality. Physical interactions between RecQ helicases and proteins that function in recombination add further support to the connection between the RecQ family and recombination. In both yeast and humans, a RecQ

family member was shown to physically interact with Rad51, a protein that performs key steps in homologous recombination, such as the invasion of a DNA duplex by a homologous single strand and subsequent branch migration. Also, biochemical activities of several RecQ helicases are consistent with a direct role in suppressing recombination. Human BLM and yeast Sgs1 proteins efficiently unwind or branch-migrate four way DNA junctions *in vitro* (Figure 2B). Interestingly, four-way junctions closely resemble the structure of an intermediate in genetic recombination, a Holliday junction. Another human RecQ homolog, WRN, unwinds D-loops, DNA intermediates formed by the first step of homologous recombination—the strand invasion of a duplex by a ssDNA molecule (Figure 2B). Thus, RecQ helicases may control recombination *in vivo* by disrupting recombination intermediates.

The Replication Connection

Several lines of evidence indicate that RecQ-like helicases and topo III function during DNA replication. Analyses of mRNA and protein levels of the budding yeast RecQ and topo III homologs have shown that expression of these genes fluctuates throughout the cell cycle, peaking during and right after the period of active DNA replication. Also, yeast mutants lacking the RecQ helicase or topo III are sensitive to chemicals that arrest DNA replication by depleting cellular pools of deoxynucleotide triphosphates (dNTP's)—the building blocks necessary to assemble new DNA molecules. For instance, wild-type fission yeast cells are able to resume normal replication after transient exposure to one such chemical, hydroxyurea, whereas mutants that lack the RecQ helicase fail to make the recovery. These observations indicate that the function of RecQ family proteins is especially important for cellular survival if DNA replication is stalled.

Whereas chemicals such as hydroxyurea can arrest the progress of DNA replication throughout the entire genome, occasional pausing in the progression of individual replication forks is thought to occur spontaneously in a high proportion of cells. Accordingly, proteins that are necessary for proper handling and eventual restart of these paused forks are required throughout DNA replication even in cells unchallenged by exogenous agents. Consistent with a role for RecQ helicases during normal cell cycle, analysis of human cells expressing mutant versions of BLM or WRN proteins has shown that these cells exhibit delayed replication progression and accumulate abnormal replication intermediates.

There are several non-mutually exclusive possibilities for the roles of RecQ family members during DNA replication. These proteins could physically manipulate or maintain replication fork structure. The importance of RecQ helicases for normal progression of DNA replication combined with their previously discussed roles in controlling recombination have led to the idea that these proteins function specifically to suppress recombination initiated at stalled replication forks. Also, RecQ helicases may be involved in replicating "difficult" regions of the genome, such as telomeres. Telomeric DNA is very GC-rich and may form alternative conformations, such as G-quartets (Figure 2B). Several RecQ homologs can unwind G-quartet DNA *in vitro*, and yeast RecQ homolog Sgs1 has been implicated in telomere maintenance *in vivo*. Alternatively, these proteins could detect fork stalling and signal to other molecules, resulting in recruitment of factors necessary for resumption of fork movement. Indeed, recent evidence suggests that some RecQ family members may be involved in DNA damage surveillance and signaling mechanisms called checkpoints. In particular, the budding yeast RecQ homolog Sgs1 has been shown to participate in such signaling mechanisms specific to DNA damage occurring during DNA replication.

RecQ Helicases and Human Disease

The human genome encodes five proteins that belong to the RecQ class of helicases. Mutations in three of these proteins, BLM, WRN, and RECQ4, cause genetic disorders: Bloom, Werner, and (at least a subset of) Rothmund–Thomson syndromes, respectively. Among other symptoms, Bloom syndrome patients exhibit short stature, immunodeficiency, impaired fertility, and a predisposition to a variety of cancers. At the cellular level, the syndrome is characterized by genomic instability, including hyper-recombination between sister-chromatids and homologous chromosomes. Werner and Rothmund-Thomson syndrome patients exhibit symptoms of premature aging, as well as a predisposition to certain types of cancer. Both syndromes are also characterized by increased genomic instability at the cellular level. Cells cultured from Werner syndrome patients exhibit an increase in illegitimate recombination, resulting in chromosomal deletions and translocations. Less is known about the cellular characteristics of the Rothmund–Thomson syndrome, but these cells also display increased chromosomal abnormalities.

Whereas no genetic disorder is known to result from mutation of a human topo III homolog, mouse knock-out strains have provided important information about the role of these proteins in higher eukaryotes. Deletion of the *TOP3α* gene, encoding one of the two isoforms of topo III in mice and humans, results in embryonic lethality, indicating that this protein has essential functions during development. Deletion of the other topo III isoform, *TOP3β*, does not result in lethality, but

causes a decrease in lifespan, reduced fertility, and increased incidence of aneuploidy. Thus, topo III-like proteins, similar to RecQ helicases, play important roles in mammalian development, aging, and chromosomal integrity.

See Also the Following Articles

DNA Helicases: Dimeric Enzyme Action • DNA Helicases: Hexameric Enzyme Action • DNA Replication Fork, Eukaryotic • DNA Supercoiling • Glutamate Receptors, Ionotropic

Glossary

DNA recombination Exchange or transfer of genetic material between two DNA molecules, such as two chromosomes in the cell.

DNA replication The process of faithful copying of genetic information in a cellular genome prior to cell division. This is accomplished by separating the strands of duplex chromosomal DNA and synthesizing new DNA strands that are complementary to the parental strands.

replication fork Y-shaped DNA structure formed during DNA synthesis when the parental DNA strands are separated to provide a template for DNA replication.

sister chromatids The identical copies of a single chromosome produced after DNA replication.

supercoiling The topological state achieved by twisting a duplex DNA molecule around its axis.

telomere Region of DNA at the end of a linear chromosome.

Further Reading

Champoux, J. J. (2001). DNA topoisomerases: Structure, function, and mechanism. *Annu. Rev. Biochem.* **70**, 369–413.

Lohman, T. M., and Bjornson, K. P. (1996). Mechanisms of helicase-catalyzed DNA unwinding. *Annu. Rev. Biochem.* **65**, 169–214.

Lombard, D. B. (2001). *Biochemistry and Genetics of RecQ-Helicases*. Kluwer Academic, Boston.

Oakley, T. J., and Hickson, I. D. (2002). Defending genome integrity during S-phase: Putative roles for RecQ helicases and topoisomerase III. *DNA Repair* **1**, 175–207.

van Brabant, A. J., Stan, R., and Ellis, N. A. (2000). DNA helicases, genomic instability, and human genetic disease. *Annu. Rev. Genomics Hum. Genet.* **1**, 409–459.

Wang, J. C. (2002). Cellular roles of DNA topoisomerases: A molecular prospective. *Nature Rev.* **3**, 430–440.

Biography

Rodney Rothstein is a Professor of Genetics and Development at Columbia University College of Physicians and Surgeons in New York. His principal research interests are in the mechanisms of DNA recombination and the cellular response to DNA damage. He holds a Ph.D. from The University of Chicago and received postdoctoral training at the University of Rochester and Cornell University. He developed one-step gene disruption in yeast and is one of the authors of the double-strand break repair model. His laboratory discovered the first eukaryotic topoisomerase III gene family member and the first eukaryotic RecQ homolog, Sgs1.

Erika Shor, a senior graduate student in the Rothstein laboratory, studies the budding yeast RecQ and topoisomerase III family members.

Dopamine Receptors

Kim A. Neve
VA Medical Center, Portland, Oregon, USA

Dopamine receptors are rhodopsin-like seven transmembrane receptors (also called G protein-coupled receptors) that mediate the central and peripheral actions of dopamine. Dopamine receptors are most abundant in pituitary and brain, particularly in the basal forebrain, and are also found in the retina and peripheral organs such as the kidney. Stimulation of dopamine receptors modulates excretion of sodium by the kidney, and both cell division and hormone synthesis and secretion in the pituitary. Brain dopamine receptors regulate movement and locomotion, motivation, and working memory. Five subtypes of mammalian dopamine receptors have been identified that are divided into D1-like (D1, D5) or D2-like (D2, D3, D4) groups. The D1-like receptors couple primarily to the $G_{\alpha s}$ family of G proteins ($G_{\alpha s}$ and $G_{\alpha olf}$), whereas the D2-like receptors couple primarily to the $G_{\alpha i/o}$ family. Drugs that block D2 receptors are useful for the treatment of schizophrenia and other psychoses, while drugs that stimulate D1-like or D2-like receptors alleviate the motor symptoms that result from degeneration of dopamine-containing neurons in Parkinson's disease.

Introduction

Nobel prize-winning work by Arvid Carlsson and colleagues in 1958 first demonstrated that dopamine is a neurotransmitter, rather than being only an intermediate step in the synthesis of norepinephrine (noradrenaline), and a neurotransmitter that plays an important role in regulating motor behavior. The first pharmacological evidence for the existence of specialized receptors for dopamine was obtained five years later, but it was not until 1972 that the identification of dopamine-stimulated adenylate cyclase, the enzyme that converts ATP into the "second messenger" cyclic AMP, made possible the biochemical characterization of a dopamine receptor. Later that decade, further pharmacological and biochemical chacterization of dopamine receptors, including their division into D1 and D2 subtypes, was made possible by the development of radioisotopically labeled ligands, or radioligands, that bind to dopamine receptors with high affinity and selectivity. What might be considered the modern era of dopamine receptor research began with the determination of the DNA sequence and predicted protein sequence of the D2 dopamine receptor and the subsequent identification of additional dopamine receptor subtypes.

Dopamine Receptor Subtypes

Virtually all neurotransmitters and hormones activate multiple receptor subtypes—distinct classes of receptors that share relatively high affinity for a single neurotransmitter but that differ in structure, affinity for drugs, signaling, and distribution. It is common for the distribution of receptor subtypes to overlap, so that one organ or brain region may have multiple receptor subtypes for any neurotransmitter or hormone that is present.

D1-Like and D2-Like Receptor Subfamilies

Prior to the molecular cloning of dopamine receptors, they were divided into D1 and D2 subtypes on the basis of several criteria. D1 and D2 receptors have distinct pharmacological profiles; in particular, D2 receptors have high affinity for benzamide and butyrophenone antagonists such as sulpiride and spiperone, respectively, while D1 receptors have high affinity for benzazepine antagonists such as SCH23390. D1 receptors stimulate adenylate cyclase and cyclic AMP accumulation, while D2 receptors inhibit the enzyme. Finally, the D1 and D2 receptors are physically distinct. For example, there are tissues such as the anterior and intermediate pituitary gland that have an abundance of D2 receptors but no D1 receptors. Furthermore, it is possible to cause selective damage to cell bodies in the substantia nigra or in the neostriatum of the rat brain, using lesions that spare axons and axon terminals, and with these lesions to cause a preferential reduction in the abundance of D2 receptors (substantia nigra) or D1 receptors (neostriatum), thus demonstrating the differential localization of the subtypes on cell bodies and axon terminals in these brain regions. The molecular cloning of additional subtypes of dopamine receptors revealed the existence of

two receptor subfamilies, in each of which the subtypes share D1-like or D2-like characteristics.

Molecular Cloning of Dopamine Receptor Subtypes

Following the cloning of DNA encoding receptors determined to be identical to the pharmacologically characterized D1 and D2 receptors, several additional subtypes were identified in 1990–91. DNA sequence information was a new tool for classification of receptors, in that receptors belonging to the same subfamily are more similar in DNA and protein sequence. Thus, there are many amino acids that are common in D1 and D5 receptors (Figure 1A), but fewer that are shared among all the dopamine receptor subtypes (Figure 1B). D1 and D5 receptors are both D1-like receptors, whereas D2, D3, and D4 receptors belong to the D2-like receptor subfamily in terms of sequence identity and affinity for drugs.

Structural Characteristics of Dopamine Receptors

Most hormone and neurotransmitter receptors are integral membrane proteins that span the cell membrane at least once, so that one portion of the receptor lies outside the cell and another portion lies inside. Dopamine receptors all belong to the superfamily of proteins called 7-transmembrane receptors, because they traverse the membrane seven times, serpentine receptors because of the manner in which the wind back and forth across the membrane, or G protein-coupled receptors because most of the effects of neurotransmitter binding to the receptors are mediated by activation of G proteins. The superfamily of 7-transmembrane receptors includes receptors for light, odors, and calcium, in addition to most neurotransmitters. Although all dopamine receptors have seven membrane-spanning regions with four intracellular domains (loops 1–3 and the carboxy terminus) and four extracellular domains (the amino terminal extension and extracellular loops 1–3), the D1-like receptors have relatively short third intracellular loops and relatively long carboxy termini compared to the D2-like receptors (Figure 1).

As illustrated in Figure 1, the presence of specific amino acid residues at certain locations across receptor subtypes, or amino acid sequence homology, is highest within the membrane-spanning regions of 7-transmembrane receptors. This is primarily because maintaining the three-dimensional structure of a receptor so that it is relatively quiescent until activated by the binding of a neurotransmitter such as dopamine requires precise packing of the membrane-spanning alpha-helices and a network of interhelical bonds that constrain the movement of the helices. Random mutations in these regions would be often deleterious and selected against because of the relatively high likelihood of disrupting helix packing or interhelical bonds. Within a family of receptors for one neurotransmitter or for several structurally related neurotransmitters such as the catecholamines dopamine and norepinephrine (noradrenaline), sequence homology also reflects the conservation of amino acids that bind the neurotransmitter; for small molecule neurotransmitters such as dopamine, these amino acids are typically in the membrane-spanning helices, which form a water-accessible binding pocket within the membrane lipid bilayer.

Dopamine Receptor Subtype-Selective Drugs

D1 and D2 receptor-selective drugs have been very useful for differentiating between the behavioral and biochemical effects of D1-like or D2-like receptor stimulation. There are numerous commercially available potent and selective D2-like receptor agonists such as quinpirole and 7-OH DPAT, and antagonists such as spiperone and nemonapride (YM-09151-2). Although there are fewer D1-like receptor-selective drugs, the selective benzazepine antagonist SCH23390 and agonists such as SKF38393 and 6-chloro-APB (SKF82958) have been used to demonstrate that blockade or stimulation of D1-like receptors has significant behavioral consequences.

There is great interest in developing drugs that differentiate between D1 and D5 receptors or among the D2-like receptors, both as research tools and because of the possibility that selective blockade or stimulation of only one subtype will be a more effective treatment for a disease that is currently treated by blockade or stimulation of the D1-like or D2-like subfamily (Table I). It is still not possible to differentiate pharmacologically between D1 and D5 receptors, two subtypes with very similar sequence in the membrane-spanning helices (Figure 1A). On the other hand, the use of antagonists that are highly selective for only one of the three subtypes of the D2-like receptor subfamily, particularly for the D4 receptor, has demonstrated that dopamine binding to D3 or D4 receptors in rats has behavioral effects that are very different from D2 receptor-stimulated locomotor activation.

Dopamine Receptor Signaling

Most of the effects of dopamine receptors on cellular function are mediated by activation of heterotrimeric

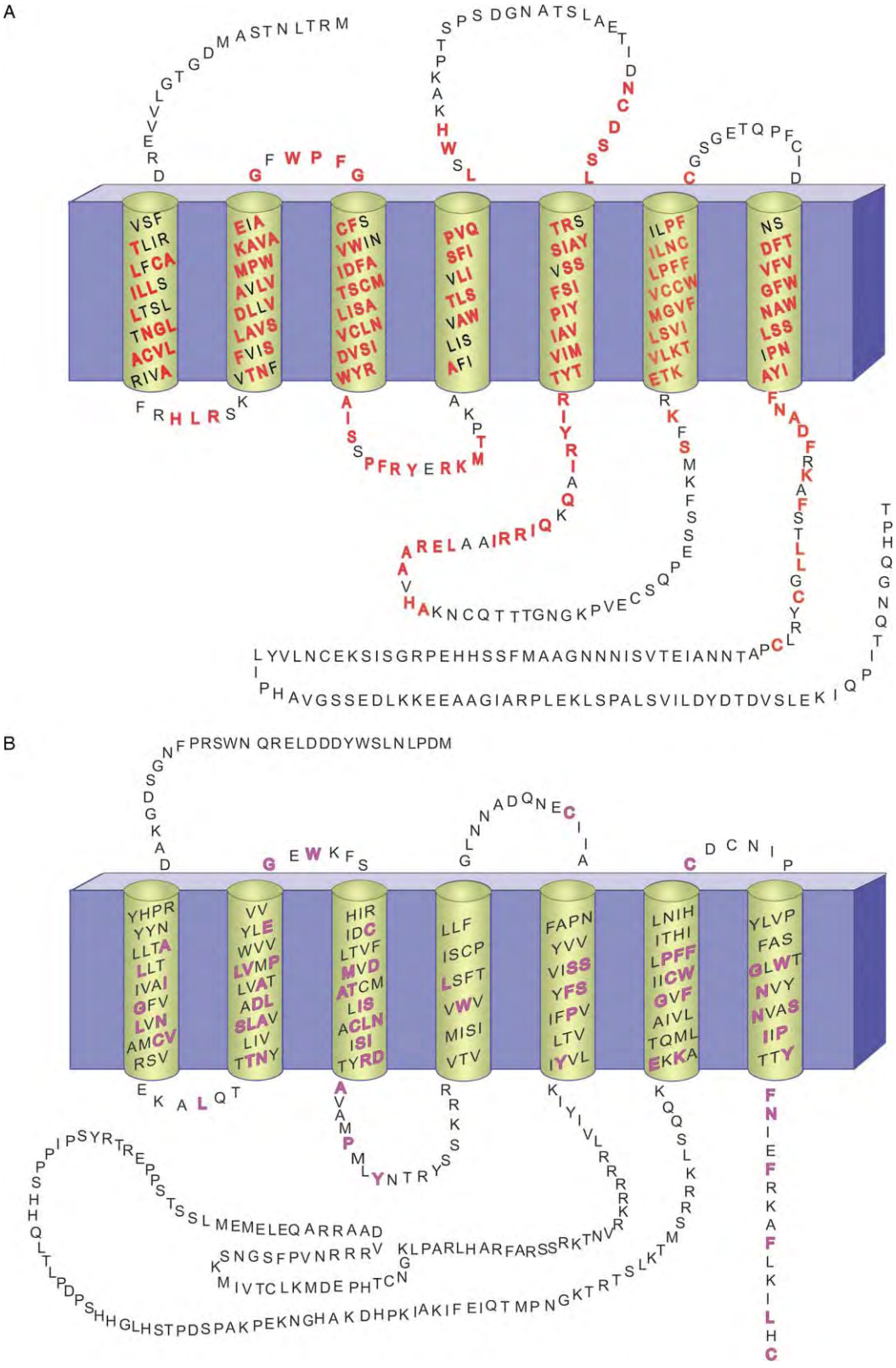

FIGURE 1 Predicted amino acid sequence and membrane-spanning segments of the D1 (A) and D2 (B) dopamine receptor subtypes. The figure is oriented so that the extracellular regions of each receptor are above the shaded transmembrane helices and the intracellular regions are below. Amino acids colored red (A) are shared between D1 and D5 receptors, whereas amino acids colored purple (B) are shared among all of the dopamine receptor subtype.

TABLE I

Features of Human Dopamine Receptor Subtypes

Type of feature	Dopamine receptor subtype				
	D1	**D5**	**D2**	**D3**	**D4**
Length (amino acids)	446	477	443[a]	400	387[b]
Introns in coding region	No	No	Yes	Yes	Yes
G protein coupling	$G\alpha_s/G\alpha_{olf}$	$G\alpha_s$	$G\alpha_{i/o}$	$G\alpha_{i/o}$	$G\alpha_{i/o}$
Agonists	SKF38393	SKF38393	Quinpirole	Quinpirole	Quinpirole
	6-Cl-APB	6-Cl-APB	7-OH-DPAT	7-OH-DPAT	7-OH-DPAT
				PD128907	PD168077
Antagonists	SCH23390	SCH23390	L-741,626	GR 103691	L-741,742
				U99194	L-745,870
Radioligands	[^{3}H]SCH23390	[^{3}H]SCH23390	[^{3}H]spiperone	[^{3}H]spiperone	[^{3}H]spiperone
	[^{125}I]SCH23982	[^{125}I]SCH23982	[^{3}H]YM-09151-2	[^{3}H]YM-09151-2	[^{3}H]YM-09151-2
				[^{3}H]7-OH-DPAT	
Localization[c]	Caudate-putamen, cerebral cortex, substantia nigra, parathyroid gland	Hippocampus, cerebral cortex	Caudate-putamen, substantia nigra, intermediate and anterior pituitary gland	Nucleus accumbens, olfactory tubercle	Cerebral cortex, hypothalamus, olfactory bulb
Splice variants	None	None	$D2_L/D2_S$	D3nf[d]	None
Allelic variants[e]	None	Leu88 → Phe	Val96 → Ala	Ser9 → Gly	Gly11 → Arg
		Ala269 → Val	Pro310 → Ser		12 bp repeat in exon 1
		Pro330 → Gln	Ser311 → Cys		21 bp deletion in exon 1
		Cys-335 → stop			13 bp deletion in exon 1
		Asn351 → Asp			Val194 → Gly
		Ser453 → Cys			48 bp repeat in exon 3

[a] Length of $D2_L$; $D2_S$ is 414 amino acids long.

[b] Length of the variant with two repeats (D4.2) although actual length depends on the number of repeat units, which varies from 2 to 10.

[c] Selected tissues and brain regions with relatively high expression of the subtype are listed.

[d] D3nf is a frame-shifted variant with D3 receptor sequence only through the fifth membrane-spanning helix. Although shorter truncated splice variants of D3 mRNA also exist, D3nf is the only one for which expression of the protein has been demonstrated.

[e] Only variants that alter the protein sequence are listed.

GTP-binding proteins called G proteins. Binding of dopamine to amino acids within the membrane-spanning helices of a dopamine receptor disrupts the interhelical bonds that hold the receptor in an inactive state. The resulting movement of one or more of the helices exposes amino acids on the cytoplasmic face of the membranes that bind to and activate G proteins. D1-like and D2-like receptor have very different signaling properties as a result of differential selection of G protein subtypes.

G Protein Coupling

Heterotrimeric G proteins are composed of α-, β-, and γ-subunits, and are generally named according to the subtype of G_α subunit. D1-like receptors that have been stimulated by dopamine or other D1 receptor agonists activate two G proteins that stimulate adenylate cyclase, $G_{\alpha s}$ and the closely related G protein $G_{\alpha olf}$ (Table I). (The latter G protein was first identified as mediating olfactory responses to receptors for odorants.) D2-like receptors activate the $G_{\alpha i}$ subtypes, named after their ability to inhibit adenylate cyclase, and the closely related G protein $G_{\alpha o}$. That these G proteins are substrates for ADP-ribosylation by cholera toxin, which persistently activates $G_{\alpha s}$, or pertussis toxin, which inactivates $G_{\alpha i/o}$, has contributed importantly to determining their role in dopamine receptor signaling.

Signaling Pathways

As suggested by their activation of G proteins that stimulate adenylate cyclase, most effects of D1-like receptor stimulation are mediated by increased levels of cyclic AMP and cyclic AMP-dependent protein phosphorylation. D1 receptor-stimulated protein phosphorylation alters the activity of other protein kinases, receptors, protein phosphatases, ion channels, and transcription factors. D2-like receptors inhibit the activity of adenylate cyclase via $G_{\alpha i}$. D2-like receptors also modulate many other signaling pathways, most of them as a result of the liberation of G protein $\beta\gamma$-subunits that occurs when 7-transmembrane receptors activate $G_{\alpha i/o}$ proteins. $G_{\beta\gamma}$-regulated pathways that are regulated by stimulation of D2-like receptors include several forms of adenylate cyclase, ion channels, phospholipase C, and mitogen-activated protein (MAP) kinases. Although the basic mechanism of activation of heterotrimeric G proteins by receptors is probably the same for all receptor-G protein combinations, for reasons that have not been determined, activation of other types of G proteins such as $G_{\alpha s}$ does not produce the same $G_{\beta\gamma}$-mediated signaling that is observed after receptor-mediated activation of $G_{\alpha i/o}$.

Distribution of Dopamine Receptors

The D1 and D2 dopamine receptors are overall the most abundant dopamine receptor subtypes. The D1 receptor is expressed most highly in brain, with lower expression in periperheral tissues such as the parathyroid gland, renal, mesenteric, and coronary vascular beds, and the kidney. Within the brain, the D1 receptor is most abundant in the caudate-putamen and other basal forebrain nuclei such as the nucleus accumbens, and is also found in the cerebral cortex and the substantia nigra *pars reticulata*. The D5 receptor is expressed at much lower levels in the same basal forebrain nuclei, the cerebral cortex, and hippocampus. The D2 receptor is expressed most highly in the intermediate pituitary gland, with abundant expression also observed in the anterior pituitary and in a number of brain regions including the caudate-putamen and other nuclei of the basal ganglia, the substantia nigra *pars compacta*, and the cerebral cortex. The D4 receptor is expressed in most of the same forebrain regions as the D2 receptor and in the cerebral cortex, albeit at a lower level. Whereas the D2 receptor is most abundant in dorsal areas of the striatum, the D3 receptor is also expressed in the basal forebrain but is more abundant in the ventral nuclei (nucleus accumbens, olfactory tubercle).

Dopamine Receptor Variants

Although there are only five mammalian dopamine receptor genes that give rise to D1–5 receptors, four of the genes produce multiple receptor variants (Table I). For example, the D2 receptor has two variants that result from alternative splicing of the RNA that is transcribed from the *DRD2* gene. The long form of the D2 receptor, $D2_L$, contains a 29-amino-acid insert encoded by an exon that is spliced out of the short form, $D2_S$. Recent evidence suggests that $D2_S$ and $D2_L$ might serve very different functions as autoreceptors that regulate dopamine release and as postsynaptic receptors that mediate the actions of dopamine on non-dopaminergic neurons, respectively. In contrast to splice variants that are derived from a single gene sequence and that are present in everybody, there are also dopamine receptor variants transcribed from distinct gene sequences, so that each individual expresses only one or two of the two or more existing variants. For example, there are at least 27 allelic variants of the human D4 receptor that have from 2 to 10 copies of an imperfectly repeated 48 nucleotide (16 amino acid) sequence in the third intracellular loop of the receptor. There is considerable interest in the possibility that these allelic variants also vary in functional characteristics.

Therapeutic Uses for Dopamine Receptor Agonists and Antagonists

By far the most common therapeutic purpose for drugs that act on dopamine receptors is the use of D2 receptor antagonists for the treatment of schizophrenia and other psychoses. D2-like receptor antagonists are also used for the treatment of nausea and vomiting, for delerium or dementia of unknown cause, and for symptomatic treatment of hyperactive movement disorders such as Tourette's syndrome and Huntington's disease. Dopamine receptor agonists alleviate the symptoms of Parkinson's disease, and are often used in combination with the dopamine precursor L-DOPA. The D2-like receptor agonist bromocriptine is used to treat hyperprolactinemia because of the inhibitory effect of anterior pituitary D2 receptors on prolactin secretion. When hyperprolactinemia results from a prolactin-secreting tumor, treatment with bromocriptine also decreases the size of the tumor. Dopamine or D1 agonists such as fenoldopam cause D1 receptor-mediated vasodilation, thus increasing glomerular filtration, renal blood flow, and sodium excretion, and are used to manage types of shock associated with loss of cardiac output and compromised renal function.

See Also the Following Articles

G_i Family of Heterotrimeric G Proteins • G_q Family • G_s Family of Heterotrimeric G Proteins • G_{12}/G_{13} Family • Neurotransmitter Transporters

Glossary

affinity Term for how tightly a drug binds to a receptor, expressed as the concentration of drug that occupies half of the available receptors. High affinity means that a drug will bind at very low concentrations.

agonist A drug that binds to and activates a receptor. Dopamine is the endogenous agonist for dopamine receptors.

antagonist A drug that binds to a receptor without activating it, and thus prevents the binding of an agonist.

receptor A protein, usually associated with the cell membrane, that binds a neurotransmitter or hormone and initiates a biological response.

second messenger A chemical signal elicited by an activated receptor that transmits information within a cell. The extracellular neurotransmitter is the first messenger, and whereas some receptors transduce information about the neurotransmitter concentration into an electrical response, other receptors convert that information into altered abundance of an intracellular second messenger such as cyclic AMP.

Further Reading

Bunzow, J. R. (1988). Cloning and expression of a rat D2 dopamine receptor cDNA. *Nature* **336**, 783–787.

Emilien, G., Maloteaux, J. M., Geurts, M., Hoogenberg, K., and Cragg, S. (1999). Dopamine receptors – physiological understanding to therapeutic intervention potential. *Pharmacol. Ther.* **84**, 133–156.

Jose, P. A., Eisner, G. M., and Felder, R. A. (1998). Renal dopamine receptors in health and hypertension. *Pharmacol. Ther.* **80**, 149–182.

Meador-Woodruff, J. A., Damask, S. P., Wang, J., Haroutunian, V., Davis, K. L., and Watson, S. J. (1996). Dopamine receptor mRNA expression in human striatum and neocortex. *Neuropsychopharmacology* **15**, 17–29.

Neve, K. A., and Neve, R. L. (eds.) (1997). *The Dopamine Receptors*. Humana Press, Totowa, NJ.

Sealfon, S. C., and Olanow, C. W. (2000). Dopamine receptors: From structure to behavior. *Trends Neurosci.* **23**, S34–S40.

Sidhu, A., Laruelle, M., and Vernier, P. (eds.) (2003). *Dopamine Receptors and Transporters: Function, Imaging, and Clinical Implication*. Marcel Dekker, New York.

Vallone, D., Picetti, R., and Borrelli, E. (2000). Structure and function of dopamine receptors. *Neurosci. Biobehav. Rev.* **24**, 125–132.

Biography

Kim A. Neve is a Senior Research Career Scientist at the Portland Veterans Affairs Medical Center and a Professor in the Department of Behavioral Neuroscience at Oregon Health & Science University in Portland, Oregon. He holds a Ph.D. from the University of California, Irvine and received his postdoctoral training at the University of Pennsylvania. His principal research interest concerns the structure and function of dopamine receptors, and he has worked extensively on determining how the responsiveness of the receptors is regulated by dopamine.

Dynactin

Trina A. Schroer
The Johns Hopkins University, Baltimore, Maryland, USA

Dynactin is a multi-subunit protein complex that links many components of cells to microtubules and microtubule-based motors. In addition to serving as an adapter that tethers and/or allows movement of cellular structures, dynactin also enhances the activity of some motors by increasing their processivity.

Overview of Dynactin Composition and Structure

Dynactin contains a total of 24 individual polypeptide subunits that are encoded by 11 different genes (Figure 1). The locations and nearest neighbors of most dynactin subunits have been identified using antibody labeling and biochemical analysis (Figure 2). Most of dynactin's mass is contained in a rod-like structure that is an octameric polymer of the actin-related protein, Arp1. The subunits p62, Arp11, p27, and p25 are organized into a disk-shaped complex that sits at one end of this polymer. The actin-capping protein (CapZ) α/β heterodimer is present at the other end of the Arp1 polymer. Dynactin also contains a single monomer of conventional cytoplasmic β-actin, the precise location of which has not been rigorously defined. The entire rod-like domain is thought to mediate interactions of dynactin with a wide variety of cellular structures.

The other prominent structural domain of dynactin is a flexible shoulder and arm complex that projects away from the Arp1 rod. This complex contains the largest dynactin subunit, $p150^{Glued}$, dynamitin (p50), and p24 in a stoichiometric ratio of 2:4:2. The projecting domain is where dynactin binds motors and microtubules.

Dynactin structure has been imaged in the electron microscope (EM) by a variety of methods, including negative-staining EM and scanning transmission EM. The most detailed information has been derived from platinum replicas of rotary shadowed, quick-frozen, deep-etched molecules. The dynactin structure obtained in this manner is the basis of the cartoon shown in Figure 2. Till the time of preparation of this entry, no high resolution structural information about dynactin as a whole or any of its individual subunits (aside from actin and CapZ) was available.

Dynactin Functions

Functions Associated with Dynein-Based Motility

Dynactin was first discovered as a large (20S) protein complex that copurified with the minus end-directed motor, cytoplasmic dynein. Dynactin was found to stimulate dynein's ability to translocate membrane vesicles *in vitro*. The name dynactin derives from its *dyn*ein-*act*ivating activity.

Adapter Function

An important function of dynactin is to serve as an "adapter" that allows cytoplasmic dynein to bind a variety of cargoes. This adapter function relies on dynactin's distinct dynein and cargo-binding domains. Dynein is the predominant minus end-directed motor activity in most cells and therefore virtually any subcellular structure or macromolecular complex that moves toward the cell center is translocated by dynein, usually in conjunction with dynactin. Dynein cargoes include membranous organelles such as the Golgi complex, the ER–Golgi intermediate compartment (ERGIC), endosomes, lysosomes, and mitochondria. Dynein can also move lipid droplets, aggresomes, viral capsids, and centrosome components toward the cell center.

Dynactin also contributes to the binding of dynein to large cellular structures such as centrosomes, mitotic spindle poles, chromosomes, the nucleus, and the plasma membrane. Dynein associates with centrosomes beginning in S-phase and remains at spindle poles during mitosis. Centrosomal dynactin is required for dynein binding. The persistent action of dynein at spindle poles is required for the retention and organization of microtubules. Dynactin is also required for proper binding of dynein to chromosome kinetochores, which is important for capture of spindle microtubules in prometaphase. Dynein may also power the lateral sliding of chromosomes along microtubules and contribute to attachment to microtubules that must undergo

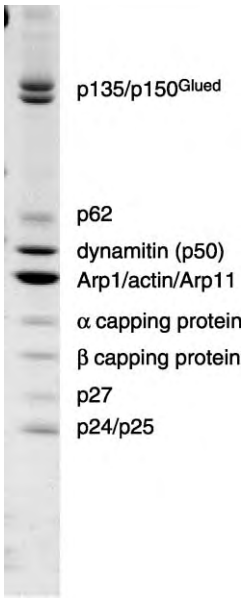

FIGURE 1 Dynactin composition. Dynactin's 11 distinct polypeptide subunits are shown on this Coomassie blue-stained, SDS polyacrylamide gel.

disassembly at their plus ends during prometaphase and anaphase. Just prior to mitosis, dynactin and dynein are recruited to the outer nuclear membrane. Dynein-driven movement of the nuclear envelope along microtubules pulls the entire centrosomal microtubule array toward the nucleus. This causes centrosomes to become closely associated with the nuclear surface and contributes to nuclear envelope rupture.

Dynein binds to the cell cortex via dynactin. As in the case of dynein bound to the nuclear envelope, the force exerted by cortical dynein "reels in" microtubules, pulling with them any structures to which they might be attached. This process can reorient the entire microtubule array and contributes to the long-range movements of nuclei that occur during mitosis and cellular morphogenesis.

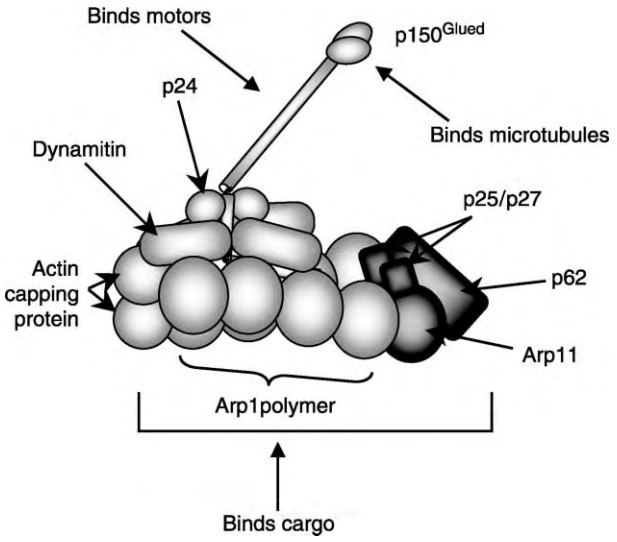

FIGURE 2 Subunit organization in dynactin. The three different binding domains are indicated. The precise location of conventional actin is unknown.

Processivity Enhancement

In the absence of dynactin, cytoplasmic dynein's two motor domains are able to travel only a very short distance along the microtubule lattice. Dynactin's $p150^{Glued}$ subunit provides a second set of microtubule binding sites that holds dynein in the vicinity of the microtubule. This low affinity binding allows dynein to move over longer distances, making it a more processive motor.

Interactions with other Motors

Dynactin may bind motors of the kinesin family to target them to cargoes and enhance processivity. Evidence exists suggesting that $p150^{Glued}$ binds Eg5/BimC, a plus end-directed motor that is localized at spindle poles where it contributes to microtubule organization. Membranous organelles that undergo dynamic bidirectional movements, such as late endosomes and pigment granules, must also be able to bind multiple motors. Dynactin on the surface of such membranes may be able to recruit both dynein and the heterotrimeric, plus end-directed motor, kinesin II (KIF3), thereby allowing bidirectional translocation.

Dynein-Independent Functions

Dynactin can support non-motile interactions of microtubules with cellular components in a manner that is independent of motor binding. This cross-linking function depends on dynactin's distinct microtubule and cargo-binding domains. Dynactin associates with microtubules at their plus ends, their minus ends, and along their length. At plus ends, dynactin may help control the rate of microtubule growth and shrinkage, perhaps by recruiting or working with other plus end-binding factors. Dynactin is also seen at sites where microtubule minus ends converge, such as centrosomes, at times when dynein is not. Centrosomal dynactin is required for microtubule anchoring at this site. Dynactin may interact with microtubule minus ends directly, or it might recruit other minus end-binding factors. Subunits of dynactin's cargo-binding domain are able to associate with a wide array of intracellular molecules and macromolecular complexes that are still being identified. This may allow dynactin to bind cellular components to microtubules transiently. This would prevent them from diffusing freely in cytosol and could cause them to be retained at particular sites within the cell, for example, in the cytoplasm rather than the nucleus.

Structure and Function of Individual Dynactin Subunits

Structure

Dynactin subunits can be grouped into four structural families: (1) proteins whose structures resemble actin (actin itself, plus the actin-related proteins Arp1 and Arp11) or actin-binding proteins (CapZ), (2) α-helical, elongated proteins (p150^{Glued}, dynamitin and p24), (3) β-helix proteins (p25 and p27), and (4) Cys/His RING/LIM domain proteins (p62).

Actin-Related or Actin-Binding Proteins

Dynactin contains three proteins of the actin superfamily: β-(cytoplasmic) actin, Arp1, and Arp11. Arp1 is quite similar (~65% identical) to conventional actin and is the only Arp that has been shown to assemble into filaments in vitro and hydrolyze ATP. Arp11 is less similar to actin but can copolymerize with actin and bind Arp1 *in vitro*. Sequence comparisons suggest that Arp11 is most divergent at its pointed end face. Arp11 has been localized to the pointed end of the Arp1 filament where it may bind Arp1 directly. The CapZ species found in dynactin contains the β_2 isoform only. Among the dynactin subunits, these five dynactin polypeptides are the most highly conserved between species.

α-Helical Proteins

The polypeptides p150^{Glued}, dynamitin and p24 are the least highly conserved of all the dynactin subunits, suggesting that their overall structures may play a more important role in dynactin function than their specific sequences. p150^{Glued} forms a parallel homodimer that is stabilized by two long coiled coils, one ~300 amino acids long and the other ~125 amino acids long (Figure 3). The 200 amino acid N-terminal domains comprise the globular heads found at the tip of the projecting arm. Only the N-terminal ~400 amino acids are exposed in the projecting arm, leaving the C-terminal two-thirds to associate with other dynactin subunits in the elastic shoulder that is associated with the Arp1 filament. The structural features of the central region and C terminus of p150^{Glued} have not yet been defined. The p150^{Glued} mRNA is spliced at multiple sites that are still being characterized. This may yield p150^{Glued} protein isoforms that exhibit differential binding to microtubules and other dynactin subunits.

Isolated dynamitin is an elongated tetramer, but it folds into a more compact structure when associated with other dynactin subunits. Dynamitin and p24 (2:1 stoichiometric ratio) associate stably with each other to form a complex that plays a critical role in dynactin integrity. Free dynamitin is able to displace endogenous dynamitin, p24 and p150 from the Arp1 filament. The location of dynamitin within the dynactin molecule has not been rigorously determined, but its known neighbors and general structural properties suggest that it is a major structural component of the shoulder.

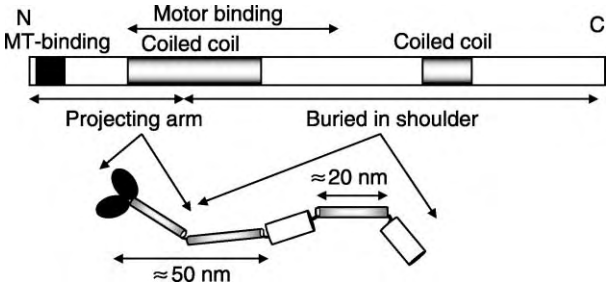

FIGURE 3 Two representations of the domain organization of p150^{Glued}. Top: A schematic of the primary sequence with predicted structural features and sites of known interactions indicated. Bottom: A cartoon illustrating the N-terminal globular heads and location and approximate lengths of the two coiled-coil domains. The structural features of the open boxed regions have not been determined.

β-Helix Proteins: p25 and p27

Dynactin contains one copy each of p27, p25, Arp11, and p62, which are closely associated in with each other. p27 and p25 are evolutionarily related and contain a polypeptide repeat motif that is characteristic of β-helical proteins. β-helix proteins are common in proteins from plants and pathogenic organisms, but rarer in animal cells. Most β-helices are elongated and possess an extended binding face or groove. The β-helices in p25 and p27 are predicted to be short, but the two proteins may associate with each other end-to-end to provide a longer-binding face. The unusually alkaline pI of the p25/p27 dimer suggests this part of dynactin may associate with acidic binding partners.

RING/LIM Domain Protein: p62

Very little is known about p62 structure, but it has been shown to associate with actin, Arp11, and Arp1. p62 contains a Cys/His-rich motif of the RING/LIM type that may chelate a metal ion and contribute to interactions with other dynactin subunits and/or other proteins. p62 contains a single consensus site for phosphorylation by cell cycle kinases (Cdks) that may govern its cell cycle-dependent binding to nuclei.

Binding Activities

Dynactin can interact with a wide variety of different cellular components. Its binding partners fall into three

classes: (1) microtubules, (2) motors, and (3) motile cargoes or non-motile subcellular docking sites. Each type of interaction is supported by a different part of the dynactin molecule (Figure 2).

Microtubule Binding

Microtubule binding is mediated by a CAP-Gly (i.e., cytoskeleton-associated protein that is glycine-rich) motif found in the N-terminal "head" domain of each $p150^{Glued}$ subunit (Figure 3). CAP-Gly motifs have been found in other microtubule binding proteins such as CLIP-170, Bik1 and the tubulin-folding cofactors, Factor B and E. The affinity of microtubule binding is regulated by phosphorylation, possibly at multiple sites. The ability of dynactin to bind microtubules with a range of affinities may allow it to work as either a processivity factor or a tethering molecule.

Motor Binding

$p150^{Glued}$ also contributes to motor binding. Its best-characterized binding partner is cytoplasmic dynein, but $p150^{Glued}$ has also been reported to interact with the kinesin family motors, Eg5 and kinesin II. Motors bind to the central portion of $p150^{Glued}$ (amino acids ~200–800; Figure 3). It is not known whether this element contains a single-motor-binding site or whether distinct sites bind different motors. In addition to $p150^{Glued}$, nearby dynactin subunits such as dynamitin and p24 may contribute to binding to cytoplasmic dynein and other motors.

Binding to other Cellular Components

Membranes Dynactin localizes to many cellular membranes, including the Golgi complex, ERGIC, endocytic pathway components, the nuclear envelope and the plasma membrane. All these interactions are thought to involve dynactin's Arp1 filament domain. Arp1 can associate with the actin-binding region of at least one spectrin isoform, which might provide a general mechanism for binding to the Golgi complex, nuclear envelope, and plasma membrane. Nuclear envelope binding also utilizes p62 and Arp11.

Other Cytoplasmic Structures The association of dynactin with lipid droplets, intracellular pathogens and cytoplasmic signaling complexes also appears to involve the Arp1 filament domain. The mechanisms for binding to most of these structures have not yet been defined. Cytoplasmic signaling complexes appear to bind dynactin via p27 and p25. These subunits are loosely associated with dynactin and may provide a mechanism for promoting transient and/or regulated interactions with a variety of cellular components.

Chromosomes Dynactin is bound to chromosome kinetochores during mitosis. As in the case of other structures that bind dynactin, kinetochore binding probably involves multiple dynactin subunits. One known contributor to this interaction is dynamitin, which binds the kinetochore component, ZW10, directly.

See Also the Following Articles

Actin-Related Proteins • Centrosomes and Microtubule Nucleation • Dynein • Microtubule-Associated Proteins

Glossary

centrosome A complex organelle located at the center of many cells that is the major site of microtubule nucleation and in some cells, focusing of minus ends.

dynein A massive, multisubunit mechanoenzyme that powers movement toward the minus ends of microtubules.

microtubule A 25 nm diameter hollow cytoskeletal polymer comprising 11–15 parallel protofilament strands of α/β tubulin heterodimers.

motor An ATPase that performs mechanical work as part of its ATP hydrolytic cycle.

processivity The ability of an enzyme to catalyze a reaction on multiple, successive subunits of a polymeric substrate.

Further Reading

Allan, V. (2000). Dynactin (Quick guide). *Curr. Biol.* **10**, R432.

Holleran, E. A., Karki, S., and Holzbaur, E. L. (1998). The role of the dynactin complex in intracellular motility. *Int. Rev. Cytol.* **182**, 69–109.

Schafer, D. A., and Schroer, T. A. (1999). Actin-related proteins. *Annu. Rev. Cell Dev. Biol.* **15**, 341–363.

Vale, R. D. (2003). The molecular motor toolbox for intracellular transport. *Cell* **112**, 467–480.

Biography

Dr. Trina A. Schroer is a Professor in the Department of Biology at The Johns Hopkins University in Baltimore, Maryland. Her principal research interests are cytoarchitecture and subcellular motility, with a particular focus on the functions of the microtubule cytoskeleton and microtubule-based motors. She holds a Ph.D. from the University of California, San Francisco and received postdoctoral training at the Washington University School of Medicine. Dr. Schroer discovered dynactin as a postdoctoral fellow and has made significant contributions toward determining its composition, structure, and functions.

Dynein

K. Kevin Pfister
University of Virginia School of Medicine, Charlottesville, Virginia, USA

Dyneins are motor proteins that move along microtubules toward their minus ends. They are members of the AAA family of ATPases. Dyneins were first identified by Gibbons as the ATPases that are responsible for the propulsive flagella bending and he named them after the unit of force, the dyne. Many members of the dynein family have been found in organisms from yeast to humans. All dyneins are large protein complexes composed of one or more ~530 kDa polypeptides, known as heavy chains, and various accessory subunits from 10 to 150 kDa.

Characteristics of Dynein Complexes

Dyneins are found in many eukaryotes, including, fungi, worms, insects, and vertebrates, but analysis of *Arabidopsis* genome indicates that they are not found in plants. Dyneins are classified as either cytoplasmic or flagellar, and the flagellar dyneins are further divided into the outer arm and inner arm dyneins. Cytoplasmic dynein moves membranous organelles, kinetochores, and viruses along microtubules and assists in the assembly and function of the mitotic spindle. Cytoplasmic dynein is also responsible for retrograde axonal transport. The flagellar dyneins, also called axonemal dyneins, are the arms that project from the doublet axonemal microtubules of flagella and cilia. The flagellar dyneins generate the sliding force between outer doublet microtubules that is converted by other axonemal structures into the bending of cilia and flagella. The outer arms specify the flagellar beat frequency and the inner arms specify flagellar waveform. There is also a dynein responsible for the transport of protein complexes from the tip of cilia and flagella to their base that occurs between the axonemal microtubules and the flagellar membrane, known as intraflagellar transport.

Fungi, *Drosophila,*and mammals have provided the major sources and systems for the study of cytoplasmic dynein. The alga *Chlamydomonas*, which has two flagella, has been a useful model system for the study of flagellar dyneins. As many as ten different dynein complexes are found in animals and most of these are components of the flagella. Molecular genetic analyses indicate that genomes contain more than ten flagellar dynein heavy chain genes, one cytoplasmic dynein heavy chain gene, and the intraflagellar transport dynein heavy chain, which is most related to the cytoplasmic dynein heavy chain. Dynein complexes are composed of one, two, or three heavy chains, and each complex has various smaller accessory subunits (Tables I and II). Cytoplasmic dynein has two identical heavy chains. Flagellar outer arm dyneins have two or three different heavy chains depending on the species. Each flagella has many different inner arm dyneins. Inner arm dynein 1 has two different heavy chains, and there are at least six different inner arm dyneins each with one unique heavy chain.

The different dynein complexes hydrolyze MgATP at different rates, for example, the microtubule stimulated ATPase activity of cow brain cytoplasmic dynein is 0.3 μmol min^{-1} mg^{-1} and the activity of flagellar outer arm dynein is 2.0 μmol min^{-1} mg^{-1}. Different dynein complexes also move along microtubules at different rates. An *in vitro* motility assay is used to quantify the velocity of dynein-based movement by using computer-enhanced video microscopy. Dynein is attached to a glass coverslip and when microtubules are added the dynein motor domains bind the microtubules. In the presence of MgATP, the dynein moves microtubules across the coverslip with the microtubule-plus ends leading. Cytoplasmic dynein from bovine brain moves microtubules at the rate of ~1 μs^{-1} while sea urchin outer arm dynein moves microtubules at the rate of 3.5 μs^{-1}.

The Dynein Heavy Chain

The central component of the dynein complex is the heavy chain, an ~530 kDa polypeptide of that contains the ATP-binding and hydrolysis site and a microtubule-binding domain. Often the heavy chain alone is referred to as a dynein. The heavy chain is an AAA ATPase. The C-terminal two-thirds of the heavy chain, ~350 kDa, is necessary for ATP-dependent microtubule binding. This domain contains six sequential AAA domains, with

TABLE I

Composition of Cytoplasmic Dynein Complexes

	Cytoplasmic dynein	Intraflagellar transport dynein
Heavy chain	HC1a	HC1b
Number of heavy chains	2	nd (1?)
Intermediate chain[a]	IC74-1 IC74-2	n
Light intermediate chain[a]	LIC1 LIC2	LIC3
Light chain[b]	Tctex1 family Roadblock family LC8 family	n

n, none identified; nd, not determined.

[a] It is not known if the intermediate chains associate in the dynein complex as homodimers or heterodimers. The light intermediate chains associate in the dynein complex only as homoligomers.

[b] Each light chain family has at least 2 members.

~350 amino acid microtubule-binding region inserted between AAA domains 4 and 5. Consensus nucleotide-binding sites known as P loops are components of AAA domains 1 through 4, while AAA domains 5 and 6 lack consensus P loop motifs. The first P loop, P1, is the site of ATP binding and hydrolysis which generates force. In the presence of vanadate and inorganic phosphate, the heavy chains are cleaved by photolysis with ultraviolet light into two fragments at P1. The role of the other P loops is unknown although at least one of them binds nucleotide.

Structural analysis of the heavy chain indicates that the C-terminal motor portion forms a large globular domain known as the head (Figure 1). The head is made up of six or seven lobes arranged in a ring surrounding a central cavity. The individual AAA domains make six of the lobes. The microtubule binding region, two anti-parallel coiled coils separated by a globular region, projects from the head as a stalk. The N-terminal portion of the heavy chain extends from the head as a thin flexible stem across the head from the microtubule binding stalk. Two or three dynein heavy chains are often connected by their stems to form a common base. Most of the other subunits of the dynein complexes bind to the N terminus of the heavy chain at the base and they contribute to the motor protein's cargo-binding domain.

Cytoplasmic Dynein

The mammalian cytoplasmic dynein (Figure 1 and Table I) has a native molecular weight of 1.5×10^3 kDa. It is a homodimer of two identical heavy chains associated with two ~74 kDa intermediate chains, two to four ~55 kDa light intermediate chains (LIC) and three pairs of light chains, the Tctex1, roadblock, and LC8 families. The heavy chain of this dynein is encoded by a single gene, but two genes have been identified for the mammalian intermediate and light intermediate chains and for each of the three light chain families. Intermediate chain and light intermediate chain isoforms are also generated by mRNA alternative

TABLE II

Composition of Chlamydomonas Flagellar Dynein Complexes

	Outer arm	Inner arm 1	Inner arm (a, c, d)	Inner arm (b, e, g)
Heavy chains	α, β, and γ	Iα and Iβ	a, c, or d	b, e, or g
Number of heavy chains	3	2	1	1
Intermediate chain	IC1 IC2	IC140 IC138 IC110	None	None
Light intermediate chain	None	None	None	None
Light chain	LC1/leucine rich LC2/tctex2 LC3/Thioredoxin LC4/Ca + 2 binding LC5/Thioredoxin LC6/LC8 homolog LC7/roadblock homolog LC8	p22 (nk) Tctex1 LC8	Actin p28	Actin Centrin Novel actin Related protein

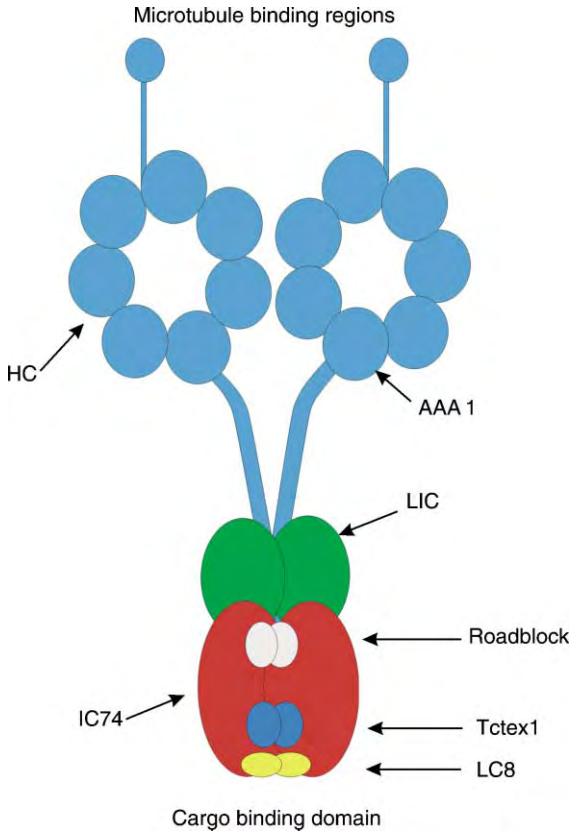

FIGURE 1 Model for the structure of cytoplasmic dynein. The two heavy chains, in light blue, have heads with six to seven lobes. A microtubule binding stalk projects from each head, and the N-terminal stem binds the light intermediate chains (LIC) and the intermediate chains (IC74). The three light chains bind the intermediate chain. The smaller subunits define the cargo-binding domain.

splicing. The heavy chain dimerization domain is a large portion of its N terminus. Also in this region are the overlapping binding sites for the light intermediate chains and the intermediate chains.

The intermediate chains play an important scaffold role in the structure of the cytoplasmic dynein complex. In addition to binding the heavy chains, the intermediate chain binds the three light chain families. It also binds other proteins including the p150 subunit of dynactin, a protein that links dynein to its cargo. The intermediate chain has seven WD domains at its C terminus, which are necessary for binding to the heavy chain. The intermediate chain N terminus is a region predicted to form a coiled coil followed by the alternative splicing regions. The binding site for the dynactin subunit, p150 contains the N-terminal coiled coil region and the next ~60 amino acids. The Tctex1 and LC8 light chains bind the intermediate chain N terminus near to the alternative splicing region, while the Roadblock light chain binds near the first of the WD domains.

Cytoplasmic dyneins have many functions in cells, including transporting many organelles. They are important for maintaining Golgi position near the centrosome, for endosome movement, and for nuclear migration. During mitosis, they assist in the assembly of spindle poles, are used by kinetochore to move along microtubules, and generate pulling forces from the cell cortex to separate the spindle poles. In axons, cytoplasmic dynein is essential for retrograde membrane-bounded organelle transport in fast transport and for the movement of microtubules and neurofilaments. Several viruses including Adenovirus, Herpes, and HIV also utilize cytoplasmic dynein to move along microtubules during the infection process. The cytoplasmic dynein cargo-binding domain is made up of the intermediate chains, light intermediate chains, and the three light chain families. The best-characterized protein responsible for linking dynein to cargo is the dynactin complex, it is important for dynein binding to kinetochores and most membrane-bounded organelles. Dynactin also increases the processivity of cytoplasmic dynein, the distance dynein travels along a microtubule before detaching. Cytoplasmic dynein binds liposomes, artificial lipid membranes, so it may bind directly to some membranes. Cytoplasmic dynein also transports individual proteins, which bind directly to the intermediate chains, light intermediate chains, or the light chains.

The cytoplasmic dynein heavy chain, light intermediate chain, and intermediate chain subunits are phosphorylated *in vivo*. Light intermediate chain phosphorylation is correlated with cell-cycle regulation of dynein binding to membrane-bounded organelles. Intermediate chain phosphorylation regulates dynein binding to the p150 subunit of dynactin.

In yeast deletion mutations of dynein subunits are not lethal, but mitosis is disrupted. Deletion of the cytoplasmic dynein heavy chain is lethal in multicellular organisms such as mouse and *Drosophila*. Non-lethal mutations of cytoplasmic dynein heavy and light chains lead to axonal pathfinding defects and other pleotrophic developmental defects in *Drosophila*, and mutations in the mouse heavy chain result in age-dependent progressive degeneration of motor neurons. Cytoplasmic dynein also binds to and is modulated by the lissencephaly disease protein, Lis1. Lissencephaly is characterized by defects in the organization of the cortical regions of the mammalian brain.

Flagellar Dyneins

Dyneins are the motor proteins that drive the bending of cilia and flagella. The flagellar dyneins are attached to the outer doublet microtubules of axonemes and generate the sliding force between neighboring outer doublet microtubules that is the basis for the propulsive bending of flagella that move cells through fluids.

The base of a flagellar dynein binds to one of the axonemal outer doublet microtubules, the A microtubule. The dynein head binds to the B microtubule of the neighboring outer doublet in an ATP-sensitive manner and utilizes the hydrolysis of ATP to push the B microtubule toward the tip of the axoneme. The arms are arranged in two rows along the microtubules, the outer and inner arms, and the dyneins in each row are different and have different functions. The outer arms specify the flagellar beat frequency and the inner arms specify waveform. While *Chlamydomonas* has fourteen flagellar dynein heavy chain genes, eight different flagellar dynein complexes have been purified from their flagella to date. There is one outer arm dynein complex and at least seven different inner arm complexes (Table II).

Outer Arm Dynein

The *Chlamydomonas* outer arm dynein is a heterotrimer of three different heavy chains, however in some species, such as sea urchin, the outer arm is a heterodimer. The outer arm dynein also has two different intermediate chains, and eight light chains. Outer arm dynein binds to the microtubule through the outer arm docking complex. The outer arm dynein light chains are well characterized. LC1 is a member of a leucine-rich repeat family, and unlike the other light chains, it binds to the motor domain of the gamma heavy chain, not to its N terminus. LC3 and LC5, are thioredoxin homologues. LC4 is involved in the regulation of dynein by Ca^{+2}. LC6 and LC8 are members of the LC8 family. There is also a roadblock light chain, LC7, and LC2 is Tctex2. Although they bind to different cargo, the intermediate chain and light chain subunits, which make up the cargo-binding domains of cytoplasmic dynein and outer arm dynein are closely related. The C termini of the intermediate chains, the region, which interacts with the heavy chains, are conserved between outer arm and cytoplasmic dynein complexes. However, the N termini of outer arm and cytoplasmic dynein are different and are thought to allow the binding to the different cargo. Both cytoplasmic dynein and outer arm dynein have light chains that are members of the Tctex family. The two complexes also have roadblock light chains and share identical LC8 light chains. LC8 is also a component of the two-headed inner arm dynein, and is thus associated with all dynein complexes that have more than one heavy chain.

Inner Arm Dynein

The inner arm dyneins are very heterogeneous (Table II). Inner arm dynein 1 has two different heavy chains, three different intermediate chains, and three light chains, including Tctex1 and LC8, both of which are also components of cytoplasmic dynein. The other six inner arm dyneins are organized into two groups. Each of the six dyneins has a single unique heavy chain and the heavy chains associate with two different sets of light chains. Three inner arm dynein heavy chains associate with actin and p28. The other three heavy chains associate with actin, an actin-related protein, and centrin. The functional significance the association of actin with these dyneins is unknown.

To convert from dynein-driven microtubule sliding to flagellar bending, the flagellar dyneins must be regulated. During flagellar bending, only a subset of the flagellar dyneins function at a time. The phosphorylation state of the inner arm dynein intermediate chain IC138 modulates this regulation. Genetic analysis has also identified several proteins that make up a dynein-regulatory complex, though the mechanism of the complex remains unknown.

Intraflagellar Transport Dynein

The intraflagellar transport dynein is encoded by a single unique heavy chain. To date a unique light intermediate chain is the only identified accessory subunit which binds to this heavy chain. This dynein moves protein complexes from the flagellar tip to the base in the space between the outer double microtubules and the flagellar membrane. It is most closely related to the cytoplasmic dynein heavy chain.

See Also the Following Articles

Actin Assembly/Disassembly • Actin-Capping and -Severing Proteins • Dynactin • Mitosis

Glossary

AAA ATPase Super family of ATPases associated with various cellular activities found in all kingdoms of living organisms.

axoneme Cytoskeletal structure of the cilia and flagella composed of nine outer doublet microtubules with dynein arms and radial spokes, and two central microtubules with central pair projections.

head Globular C-terminal portion of the dynein heavy chain containing six AAA domains and the microtubule-binding stalk. It is the smallest portion of the heavy chain that has ATP-dependent microtubule binding.

microtubule A cytoskeletal polymer of tubulin dimers in ~13 protofilaments arranged as a hollow tube with two distinct ends, the plus and minus ends.

stem N-terminal of the dynein heavy chain, binds most other subunits of the dynein complex and can participate in dimerization with one or more other heavy chains.

Further Reading

DiBella, L. B., and King, S. M. (2001). Dynein motors of the chlamydomonas flagellum. *Intl. Rev. Cytol.* **210**, 227–268.

Gibbons, I. R. (1988). Dynein ATPases as microtubule motors. *J. Biol. Chem.* **263**, 15837–15840.

Porter, M. E., and Sale, W. S. (2000). The 9 + 2 axoneme anchors multiple inner arm dyneins and a network of kinases and phosphatases that control motility. *J. Cell Biol.* **27**, F37–F42.

Vale, R. D. (2003). The molecular motor toolbox for intracellular transport. *Cell* **112**, 467–480.

Vallee, R. B., Shpetner, H. S., and Paschal, B. M. (1989). The role of dynein in retrograde axonal transport. *Trends Neurosci.* **12**, 66–70.

Biography

K. Kevin Pfister is an Associate Professor of Cell Biology at the University of Virginia School of Medicine. His current major research interest is the function of cytoplasmic dynein in axonal transport. His lab characterized the cytoplasmic dynein intermediate chains, and with Dr. S. King identified the cytoplasmic dynein light chains. He earned a Ph.D. from Princeton University and served as a postdoctoral fellow at the University of Texas Southwestern Medical Center.

Editors-in-Chief

William J. Lennarz

State University of New York at Stony Brook, Stony Brook, New York, USA

Section: Lipids, Carbohydrates, Membranes and Membrane Proteins

WILLIAM J. LENNARZ received his B.S. in Chemistry from Pennsylvania State University and a Ph.D. in Organic Chemistry from the University of Illinois. Subsequently he carried out postdoctoral work at Harvard with Konrad Bloch on fatty acid biosynthesis. In 1962 he was appointed Assistant Professor at Johns Hopkins in the Department of Physiological Chemistry. After promotion to Associate Professor in 1967, and full Professor in 1971, he remained at Hopkins until 1983. At that time, he was appointed Robert A. Welch Professor and Chair of the Department of Biochemistry and Molecular Biology at the University of Texas Cancer Center, M.D. Anderson Hospital. In 1989 he became a Leading Professor and Chair of the Department of Biochemistry and Cell Biology at SUNY at Stony Brook. In 1990 he founded and became Director of the Institute for Cell and Developmental Biology at Stony Brook.

Dr. Lennarz has served on many national and international committees. He has served as President of the Biochemistry Chairman's Organization, President of the American Society for Biochemistry and Molecular Biology and President of the Society for Glycobiology. He was a member of the Executive Committee of the International Union of Biochemistry and Molecular Biology for almost a decade.

He has presented special lectures at the University of Notre Dame, the NIH, the University of West Virginia, Johns Hopkins University, Florida State University, the University of California at San Diego, the University of Arkansas, Indiana University and the Medical College of Virginia.

He is a member of the National Academy of Sciences. The focus of his early work was on lipids and bacterial cell surfaces. More recent efforts have been in the structure, biosynthesis and function of cell surface glycoproteins. The biosynthesis studies initially were carried out in liver and oviduct, but these efforts now are focused in yeast. The functional studies have concentrated on the role of cell surface glycoproteins in fertilization and early development in the sea urchin and, more recently, the frog. For over 30 years Dr. Lennarz' research has been supported by federal sources, primarily the National Institutes of Health. Recently he was appointed Distinguished Professor and Chair of his department.

M. Daniel Lane

The Johns Hopkins University, School of Medicine, Baltimore, Maryland, USA

Section: Metabolism, Vitamins and Hormones

M. DANIEL LANE received B.S. and M.S. degrees in 1951 and 1953 from Iowa State University and a Ph.D. in 1956 from the University of Illinois. He was a Senior Postdoctoral Fellow with Professor Feodor Lynen at the Max-Planck Institute Fur Zellchemie in Munich. Following faculty positions at Virginia Polytechnic Institute and New York University School of Medicine, he joined the faculty at the Johns Hopkins University School of Medicine in 1969 and served as DeLamar Professor and Director of the Department of Biological Chemistry from 1978 to 1997. He is presently Distinguished Service Professor at Johns Hopkins. In 2002 he received an honorary degree, Doctor of Humane Letters, from Iowa State University.

Dr. Lane was elected to membership in the National Academy of Sciences (in 1987) and was elected as a Fellow of the American Academy of Arts and Sciences (in 1982) and of the American Society of Nutritional Sciences (in 1996). He received the Mead Johnson Award from the American Society for Nutritional Sciences in 1966 for his research on biotin-dependent enzymes and in 1981, the William C. Rose Award from the American Society for Biochemistry and Molecular Biology for his work on the insulin receptor. In 1990–1991 Lane served as President of the American Society of Biochemistry and Molecular Biology. He has presented many named lectureships (including the

Feodor Lynen Lecture in Germany in 1999) and served on numerous editorial boards including the Journal of Biological Chemistry and the Annual Reviews of Biochemistry. Currently he is Associate Editor for Biochemical and Biophysical Research Communications.

Dr. Lane has published 280 research papers in major scientific journals. His early work focused on various enzymatic CO_2 fixation reactions, notably the mechanisms by which the B-vitamin, biotin, functions in enzymes to catalyze carboxylation. Dr. Lane's work on the regulation of acetyl-CoA carboxylase, the key regulatory enzyme of fatty acid synthesis, led him to his present interests which are to understand the basic mechanisms of lipogenesis, adipogenesis and the consequence of aberrations in these processes, most notably obesity. Research currently underway in his laboratory focuses on: (1) the genes that signal stem cell "commitment" to the adipocyte lineage and subsequent differentiation into adipocytes, and (2) the mechanisms by which the region of the brain, known as the hypothalamus, monitors and controls the drive to eat.

Associate Editors

Ernesto Carafoli

Università degli Studi di Padova, Padova, Italy
Section: Bioenergetics

ERNESTO CARAFOLI earned his M.D. degree at the University of Modena in Italy in 1957. After postdoctoral studies in the Laboratory of Albert L. Lehninger at Johns Hopkins University in the mid 1960s he returned to his home institution in Italy where he worked until 1973, when he was appointed Professor of Biochemistry at the Swiss Federal Institute of Technology (ETH) in Zurich. He returned to Italy in 1998 as a Professor of Biochemistry at the University of Padova, where he now also directs the newly founded Venetian Institute of Molecular Medicine (VIMM).

Dr. Carafoli became interested in calcium as a signaling agent during his post-doctoral days at Johns Hopkins. When he arrived there his main interests were in mitochondrial bioenergetics and it was thus natural for him to expand them to the newly discovered area of mitochondrial calcium transport. He was involved in most of the early discoveries in the field, and he continued to work on mitochondria and calcium after his return to Italy and until he moved to the ETH. There his interests still remained focused on calcium, but the emphasis shifted to the proteins that transport it across membranes and to those that process its signal. His favorite object of study became the calcium pumps, especially that of the plasma membrane, an enzyme which is essential to the regulation of calcium homeostasis and thus to the well being of cells. His contributions on the enzyme, especially after he purified it in 1979, have helped establishing most of its properties and have clarified important problems of mechanism, regulation and structure.

Dr. Carafoli has authored or co-authored about 450 peer-reviewed articles and reviews, and has edited or co-edited about 20 books. He has served on the Editorial or Advisory Boards of several periodicals and has organized about 30 International Workshops and Symposia. He has been featured as a plenary or honorary lecturer at numerous events ranging from specialized Workshops to International Symposia and Congresses. Dr. Carafoli's honors and awards include several international prizes and medals, memberships in several Academies, and three honorary degrees.

Don W. Cleveland

University of California, San Diego, La Jolla, CA, USA
Section: Cell Architecture and Function

DON W. CLEVELAND has been a longstanding contributor to the elucidation of regulation of assembly of mitotic spindles and chromosome movement and how errors in these contribute to the chromosome loss characteristic of human tumors. He discovered the tubulin gene families encoding the major subunits of microtubules and the first mammalian example of control of gene expression through regulated RNA instability. He identified components required for microtubule nucleation and anchoring during spindle assembly. He identified the first human centromeric protein (CENP-B). He then discovered CENP-E, the centromere-associated, microtubule-motor that he showed to be essential for chromosome attachment and for activation and silencing of the mitotic checkpoint, the cell cycle control mechanism that prevents errors of chromosome segregation in mitosis.

Dr. Cleveland has also been a leading force in dissecting the disease mechanism for major human neurodegenerative disorders. He initially purified and characterized tau, the microtubule-associated protein that assembles aberrantly in human dementias including Alzheimer's disease and Pick's disease. He established that the extreme asymmetry of neurons acquired during development is achieved with a deformable array of interlinked neurofilaments, microtubules and actin. He showed that disorganization of neurofilament arrays caused selective death of motor neurons in mice and humans. He also demonstrated that neuronal death could also arise by a toxicity of mutant superoxide dismutase unrelated to its normal activity, thereby uncovering the mechanism underlying the major genetic form of amyotrophic lateral sclerosis. He showed that this toxicity could be

sharply ameliorated by lowering the content of neurofilaments.

Dr. Cleveland is currently Head, Laboratory for Cell Biology in the Ludwig Institute for Cancer Research and Professor of Medicine, Neurosciences and Cellular and Molecular Medicine at the University of California at San Diego. He is also the Editor of the Journal of Cell Biology and Current Opinion in Cell Biology.

Jack E. Dixon

University of California, San Diego School of Medicine,
La Jolla, CA, USA
Section: Protein/Enzyme Structure, Function, and Degradation

JACK E. DIXON earned his Ph.D. in Chemistry at the University of California, Santa Barbara in 1971 and did his postdoctoral training in Biochemistry at the University of California, San Diego.

Dr. Dixon is a pioneer and leader in the structure and function of the protein tyrosine phosphatases (PTPases). He demonstrated that the unique catalytic mechanism of the PTPases proceeds via a novel cysteine-phosphate intermediate. He discovered the first dual-specificity phosphatase, which led to the identification of the cell cycle protein, $p80^{cdc25}$, as a phosphatase. He also showed that the bacteria responsible for the plague or "black death" harbor the most active PTPase ever described. He and his colleagues went on to demonstrate that this PTPase gene product is essential for the pathogenesis of the bacteria. Dr. Dixon and his colleagues determined X-ray structures for both tyrosine and dual specificity phosphatases. Dr. Dixon also found that sequences outside of the PTPase catalytic domain could function to direct the subcellular localization of the PTPases and to restrict their substrate specificity. This is now a widely acknowledged regulatory paradigm for the PTPases. Recently, his laboratory demonstrated that the tumor suppressor gene, PTEN, which shares sequence identity with the PTPases, catalyzes the dephosphorylation of a lipid second messenger, phosphatidylinositol 3,4,5-trisphosphate (PIP3). This represents the first example of a PTPase dephosphorylating a lipid second messenger. PIP3 activates the protein kinase, AKT, which plays a critical role in controlling the balance between apoptosis and cell survival. The loss of the PTEN gene elevates PIP3 levels leading to constitutive activation by AKT and oncogenesis. Recently, Dr. Dixon in collaboration with Nikola Pavletich determined the X-ray structure of PTEN. Their structure–function studies explain the PIP3 substrate specificity of PTEN and also provide a rationale for many of the mutations seen in human cancers. Earlier in his career, Dr. Dixon adopted the tools of molecular biology as they became available in the 1970s, and his laboratory was among the first to use synthetic oligonucleotides to isolate and extensively characterize cDNAs encoding peptide hormones.

Dr. Dixon is Professor of Pharmacology, Cellular and Molecular Medicine and Chemistry and Biochemistry and Dean of Scientific Affairs at the University of California, San Diego. He is a member of the National Academy of Sciences, the Institute of Medicine and the American Academy of Arts and Sciences. Dr. Dixon was the recipient of the 2003 William C. Rose Award from the American Society for Biochemistry and Molecular Biology.

John H. Exton

Howard Hughes Medical Institute, Vanderbilt University School of Medicine, Nashvillie, TN, USA
Section: Signaling

JOHN H. EXTON was born and educated in New Zealand where he received his medical training and a Ph.D. in Biochemistry from the University of Otago in 1963. He did postdoctoral work at Vanderbilt University under Charles R. Park and Earl W. Sutherland, and became an Investigator of the Howard Hughes Medical Institute in 1968 and Professor of Physiology in 1970. He is presently Professor of Molecular Physiology and Biophysics, Professor of Pharmacology and a Hughes Investigator at Vanderbilt.

Dr. Exton's research initially focused on the changes in carbohydrate metabolism in liver during diabetes and treatment with various hormones using the perfused rat liver as the experimental system. His work concentrated on gluconeogenesis and identified the enzymatic reactions that were under control by insulin, epinephrine (adrenaline), glucagon and glucocorticoids, and demonstrated the importance of cyclic AMP in the regulation of these reactions. The role played by the supply of substrates, especially of alanine, was also shown.

Dr. Exton then turned his attention to the action of epinephrine (adrenaline) and demonstrated that many of its actions were not mediated by cyclic AMP but by calcium ions. This led to study of the breakdown of inositol phospholipids by phospholipase C that underlay the increase in calcium. Later this resulted in the discovery of G_q, a novel G protein that activated phospholipase C. Further studies demonstrated that agonists caused the breakdown of another phospholipid (phosphatidylcholine) by another phospholipase (phospholipase D). Current work is focused on the physiological role of phospholipase D.

Dr. Exton has authored over 350 scientific articles and is presently an Associate Editor of the Journal of Biological Chemistry. He has served on many scientific review groups and as a reviewer for many journals. He has won numerous awards, most notably the Lilly

Award of the American Diabetes Association, Fellow of the American Association for the Advancement of Science and election to membership in the National Academy of Sciences.

Paul Modrich

Duke University Medical Center, Durham, NC, USA
Section: Molecular Biology

PAUL MODRICH is an Investigator of the Howard Hughes Medical Institute and James B. Duke Professor of Biochemistry at Duke University Medical Center. He received his undergraduate degree from M.I.T. and his Ph.D. in Biochemistry from Stanford University. His current research addresses the mechanisms of DNA repair. He has served on the editorial boards of the Journal of Biological Chemistry, Biochemistry, Proceedings of the National Academy of Sciences, and DNA Repair. His honors include election to National Academy of Sciences and the Institute of Medicine, the Pfizer Award in Enzyme Chemistry, the General Motors Mott Prize in Cancer Research, and the Pasarow Foundation Award in Cancer Research.

Preface

Biological Chemistry is defined as the chemistry of the compounds and processes that constitute living organisms. The ultimate goal, of course, is to understand and define biology at a mechanistic level. This was aptly stated in an historical treatise on the founding of the *Journal of Biological Chemistry*, where John Edsall quoted a statement in a letter from J. L. Loeb (in Berkeley), "The future of biology lies with those who attack its problems from a chemical point of view." What was an emerging field in 1900 with its origins in physiology, nutrition and chemistry has broadened and expanded to include numerous other fields including mechanistic enzymology, molecular biology, structural biology, cell biology, genomics, proteomics, bioinformatics, metabolomics and others, that were not defined as discrete fields at that time.

Modern biochemistry (biological chemistry) began with the accidental discovery by Eduard Buchner in 1897 that a cell-free yeast extract could carry out fermentation of glucose to alcohol and CO_2 *in the absence of intact cells*. He named the dissolved substance responsible for this process zymase, the substance(s) we now refer to as enzymes. Importantly, Buchner recognized the significance of his discovery. This ended the dogma of the time, perpetuated by Pasteur, the concept of *vitalism*; i.e., that fermentation (and presumably other complex biological phenomena) required the action of intact cells. Thus, serendipity and a prepared mind ushered in a new era of discovery. Now it became possible to dissect complex physiological processes and to study them with preparations free of the constraints of intact cells. Once a metabolic pathway/process was established, it became possible to purify the enzymes, cofactors and substrates involved, to reconstitute the process with purified components and to characterize the components chemically. What followed was an information explosion in the field of biochemistry and progression through a series of trends, each "in vogue" in its time. The identification of the dietary essentials, the hunt for the vitamins/cofactors, the hormones, identification of metabolic pathways and the enzymes involved, oxidative phosphorylation, protein synthesis, molecular biology—each developed as a primary focus.

The need to associate chemistry with function came early and was evident in the naming of departments and journals. Over time names changed from Agricultural Chemistry to Physiological Chemistry to Biochemistry to Biological Chemistry. An example is the Department of Biochemistry at the University of Wisconsin, which began in 1883 as the Department of Agricultural Chemistry.

Where are we headed? We have reached the point where the borders of these areas have become blurred. What constitutes cell biology, molecular biology/genetics, developmental biology, physiology, immunology—ultimately reduces to chemistry. To understand these processes we must know what the molecules are and understand how they interact, i.e. the basic chemistry. That is what this encyclopedia is about.

The breadth of content of this encyclopedia aims to cover major topics of modern biochemistry, each authored by an expert in the area. We feel that the coverage is broad and we have been inclusive in choice of topics. The encyclopedia is a reference work encompassing four volumes containing over 500 articles with more than 750 authors or coauthors. Each article/topic covers an important area of the field which reflects the point of view of the authors. Together the articles cover virtually every aspect of biology for which we have "mechanistic" information. For those who wish to probe more deeply into a topic, references to further readings are included at the end of each article. The editorial board that made decisions on coverage consists of seven members, each an expert representing a major area in the field of biochemistry. A dedicated effort was made to provide coverage that is as complete as possible. The content is presented at a level that we hope will be interpretable to interested individuals with some background in chemistry and biology. It is intended for such individuals rather than specialists with extensive scientific backgrounds in specific areas. It is aimed at the generalist as opposed to the specialist.

Finally, we would like to single out Gail Rice and Dr. Noelle Gracy for their enormous contribution in putting this encyclopedia together. They, in fact, were a driving force that brought this major work to completion.

Notes on the Subject Index

Abbreviations used in subentries without explanation:

CoA	coenzyme A
DAG	diacylglycerol
ELISA	enzyme-linked immunosorbent assay
ERK	extracellular-signal regulated kinase
GlcNAC	N-Acetylglucosamine
HPLC	high-pressure liquid chromatography
IP_3	inositol 1,4,5-triphosphate
MAP	mitogen-activated protein
MMP	matrix metalloproteinase
mtDNA	mitochondrial DNA
NADPH	nicotinamide-adenine dinucleotide phosphate
PFK-2/ FBPase-2	6-phosphofructo-2-kinase/fructose-2,6-bisphosphatase
PI3K	phosphatidylinositol 3-kinase
PIP_2	phosphatidylinositol 4,5-bisphosphate
PIP_3	phosphatidylinositol-3,4,5-triphosphate
PPAR	peroxisome proliferator-activated receptor
RPLC	reversed-phase high-performance liquid chromatography

Volume 1

ABC Transporters, Pages 1-5, Andre Goffeau, Benoit De Hertogh and Philippe V. Baret

Abscisic Acid (ABA), Pages 6-11, Ramanjulu Sunkar and Jian-Kang Zhu

Actin Assembly/Disassembly, Pages 12-18, Henry N. Higgs

Actin-Capping and -Severing Proteins, Pages 19-26, Sankar Maiti and James R. Bamburg

Actin-Related Proteins, Pages 27-33, R. Dyche Mullins

Adenosine Receptors, Pages 34-39, Lauren J. Murphree and Joel Linden

Adenylyl Cyclases, Pages 40-45, Ronald Taussig

Adrenergic Receptors, Pages 46-50, David B. Bylund

Affinity Chromatography, Pages 51-56, Pedro Cuatrecasas and Meir Wilchek

Affinity Tags for Protein Purification, Pages 57-63, Joseph J. Falke and John A. Corbin

A-Kinase Anchoring Proteins, Pages 64-67, Lorene K. Langeberg and John D. Scott

Allosteric Regulation, Pages 68-73, Barry S. Cooperman

Alternative Splicing: Regulation of Fibroblast Growth Factor Receptor (FGFR), Pages 74-77, Mariano A. Garcia-Blanco

Alternative Splicing: Regulation of Sex Determination in Drosophila melanogaster, Pages 78-84, Jill K. M. Penn, Patricia Graham and Paul Schedl

Amine Oxidases, Pages 85-89, Giovanni Floris and Alessandro Finazzi Agro

Amino Acid Metabolism, Pages 90-95, Luc Cynober

Aminopeptidases, Pages 96-98, Ralph A. Bradshaw

Amyloid, Pages 99-104, Ronald Wetzel

Anaplerosis, Pages 105-110, Raymond R. Russell, III and Heinrich Taegtmeyer

Angiotensin Receptors, Pages 111-115, Tadashi Inagami

ara Operon, Pages 116-119, Robert F. Schleif

ARF Family, Pages 120-122, Gustavo Pacheco-Rodriguez, Joel Moss and Martha Vaughan

Aspartic Proteases, Pages 123-127, Ben M. Dunn

ATP Synthesis in Plant Mitochondria: Substrates, Inhibitors, Uncouplers, Pages 128-132, Kathleen L. Soole and R. Ian Menz

ATP Synthesis: Mitochondrial Cyanide-Resistant Terminal Oxidases, Pages 133-137, James N. Siedow

Autophagy in Fungi and Mammals, Pages 138-143, Daniel J. Klionsky and Ju Guan

B12-Containing Enzymes, Pages 145-151, Vahe Bandarian and Rowena G. Matthews

Bax and Bcl2 Cell Death Enhancers and Inhibitors, Pages 152-154, David L. Vaux

B-Cell Antigen Receptor, Pages 155-158, Thomas M. Yankee and Edward A. Clark

Bile Salts and their Metabolism, Pages 159-163, Ulrich Beuers and Thomas Pusl

Biliary Cirrhosis, Primary, Pages 164-169, Marshall M. Kaplan

Bioenergetics: General Definition of Principles, Pages 170-173, David G. Nicholls

Biotin, Pages 174-178, Steven W. Polyak and Anne Chapman-Smith

Biotinylation of Proteins, Pages 179-181, Ronald A. Kohanski

Bradykinin Receptors, Pages 182-185, Ronald M. Burch

Branched-Chain -Ketoacids, Pages 186-191, David T. Chuang

Brassinosteroids, Pages 192-197, Steven D. Clouse

Cadherin Signaling, Pages 199-204, David B. Sacks and Jonathan M. G. Higgins

Cadherin-Mediated Cell-Cell Adhesion, Pages 205-211, Frauke Drees and W. James Nelson

Calcitonin Gene-Related Peptide and Adrenomedullin Receptors, Pages 212-216, Debbie L. Hay, Alex C. Conner and David R. Poyner

Calcitonin Receptor, Pages 217-220, Samia I. Girgis, Niloufar Moradi-Bidhendi, Lucia Mancini and Iain MacIntyre

Calcium Buffering Proteins: Calbindin, Pages 221-225, Willi Hunziker and Igor Bendik

Calcium Buffering Proteins: ER Luminal Proteins, Pages 226-230, Jody Groenendyk and Marek Michalak

Calcium Oscillations, Pages 231-234, Marisa Brini

Calcium Sensing Receptor, Pages 235-240, Jacob Tfelt-Hansen and Edward M. Brown

Calcium Signaling: Calmodulin-Dependent Phosphatase, Pages 241-245, Claude Klee, Hao Ren and Shipeng Li

Calcium Signaling: Cell Cycle, Pages 246-249, Luigia Santella

Calcium Signaling: Motility (Actomyosin-Troponin System), Pages 250-255, Takeyuki Wakabayashi and Setsuro Ebashi

Calcium Signaling: NO Synthase, Pages 256-260, Zhi-Qiang Wang and Dennis J. Stuehr

Calcium Transport in Mitochondria, Pages 261-266, Rosario Rizzuto and Marisa Brini

Calcium Waves, Pages 267-269, Lionel F. Jaffe

Calcium, Biological Fitness of, Pages 270-273, Robert J. P. Williams

Calcium/Calmodulin-Dependent Protein Kinase II, Pages 274-280, Andy Hudmon and Howard Schulman

Calcium/Calmodulin-Dependent Protein Kinases, Pages 281-286, J. Robison and Roger J. Colbran

Calcium-Binding Proteins: Cytosolic (Annexins, Gelsolins, C2-Domain Proteins) , Pages 287-293, Joachim Krebs

Calcium-Modulated Proteins (EF-Hand), Pages 294-299, Robert H. Kretsinger

Calpain, Pages 300-306, Hiroyuki Sorimachi and Yasuko Ono

Carbohydrate Chains: Enzymatic and Chemical Synthesis, Pages 307-313, Thomas J. Tolbert and Chi-Huey Wong

Carnitine and -Oxidation, Pages 314-318, Janos Kerner and Charles L. Hoppel

Caspases and Cell Death, Pages 319-327, Don W. Nicholson, Pierluigi Nicotera and Gerry Melino

Cell Cycle Controls in G1 and G0, Pages 328-331, WengeShi and Steven F. Dowdy

Cell Cycle: Control of Entry and Progression Through S Phase, Pages 332-337, Susan L. Forsburg

Cell Cycle: DNA Damage Checkpoints, Pages 338-344, Jean Y. J. Wang

Cell Cycle: Mitotic Checkpoint, Pages 345-351, Tim J. Yen

Cell Death by Apoptosis and Necrosis, Pages 352-355, Pierluigi Nicotera

Cell Migration, Pages 356-361, J. Victor Small and Emmanuel Vignal

Cell-Matrix Interactions, Pages 362-366, Janet A. Askari and Martin J. Humphries

Centromeres, Pages 367-371, Beth A. Sullivan

Centrosomes and Microtubule Nucleation, Pages 372-376, Reiko Nakajima, Ming-Ying Tsai and Yixian Zheng

c-fes Proto-Oncogene, Pages 377-382, Thomas E. Smithgall and Robert I. Glazer

Chaperones for Metalloproteins, Pages 383-386, Valeria C. Culotta and Edward Luk

Chaperones, Molecular, Pages 387-392, Sue Wickner and Joel R. Hoskins

Chaperonins, Pages 393-398, Arthur L. Horwich, Wayne A. Fenton and George W. Farr

Chemiluminescence and Bioluminescence, Pages 399-404, Thomas O. Baldwin

Chemiosmotic Theory, Pages 405-412, Keith D. Garlid

Chemokine Receptors, Pages 413-418, Ann Richmond and Guo-Huang Fan

Chemolithotrophy, Pages 419-424, Alan B. Hooper

Chemotactic Peptide/Complement Receptors, Pages 425-429, Eric R. Prossnitz and Larry A. Sklar

Chlorophylls and Carotenoids, Pages 430-437, Hugo Scheer

Chloroplast Redox Poise and Signaling, Pages 438-445, John F. Allen

Chloroplasts, Pages 446-450, Nicoletta Rascio

Cholesterol Synthesis, Pages 451-455, Peter A. Edwards

Chromatin Remodeling, Pages 456-463, Eric Kallin and Yi Zhang

Chromatin: Physical Organization, Pages 464-468, Christopher L. Woodcock

Chromosome Organization and Structure, Overview, Pages 469-474, Elena Gracheva and Sarah C. R. Elgin

Coenzyme A, Pages 475-477, M. Daniel Lane

Collagenases, Pages 478-481, Kenn Holmbeck and Henning Birkedal-Hansen

Collagens, Pages 482-487, Darwin J. Prockop

Cyclic AMP Receptors of Dictyostelium, Pages 488-493, Dale Hereld and Peter N. Devreotes

Cyclic GMP Phosphodiesterases, Pages 494-500, Sharron H. Francis and Jackie D. Corbin

Cyclic Nucleotide Phosphodiesterases, Pages 501-505, Vincent C. Manganiello and Eva Degerman

Cyclic Nucleotide-Dependent Protein Kinases, Pages 506-511, Sharron H. Francis and Jackie D. Corbin

Cyclic Nucleotide-Regulated Cation Channels, Pages 512-515, Martin Biel and Franz Hofmann

Cysteine Proteases, Pages 516-520, David J. Buttle and John S. Mort

Cytochrome b6f Complex, Pages 521-527, Gunter A. Hauska and Thomas Schodl

Cytochrome bc1 Complex (Respiratory Chain Complex III), Pages 528-534, Bernard L. Trumpower

Cytochrome c, Pages 535-538, Hans Tuppy and Gunther Kreil

Cytochrome Oxidases, Bacterial, Pages 539-543, Peter Brzezinski and Pia Adelroth

Cytochrome P-450, Pages 544-549, Rita Bernhardt

Cytokines, Pages 550-555, Andrea L. Wurster and Michael J. Grusby

Cytokinesis, Pages 556-561, Masanori Mishima and Michael Glotzer

Cytokinin, Pages 562-567, Thomas Schmulling

Desmosomes and Hemidesmosomes, Pages 569-576, Rachel L. Dusek, Jonathan C. R. Jones and Kathleen J. Green

Detergent Properties, Pages 577-581, Darrell R. McCaslin

Diabetes, Pages 582-592, David W. Cooke

Diacylglycerol Kinases and Phosphatidic Acid Phosphatases, Pages 593-597, Stephen M. Prescott and Matthew K. Topham

Disulfide Bond Formation, Pages 598-602, Hiram F. Gilbert

DNA Base Excision Repair, Pages 603-608, Hilde Nilsen and Tomas Lindahl

DNA Damage: Alkylation, Pages 609-613, Anton B. Guliaev and B. Singer

DNA Glycosylases: Mechanisms, Pages 614-617, Daniel J. Krosky and James T. Stivers

DNA Helicases: Dimeric Enzyme Action, Pages 618-623, Timothy M. Lohman

DNA Helicases: HexamericEnzyme Action, Pages 624-631, Smita S. Patel

DNA Ligases: Mechanism and Functions, Pages 632-636, Alan E. Tomkinson and John B. Leppard

DNA Ligases: Structures, Pages 637-643, C. Kiong Ho, Mark Odell and Dimitar B. Nikolov

DNA Methyltransferases, Bacterial, Pages 644-651, Albert Jeltsch and Richard I. Gumport

DNA Methyltransferases, Structural Themes, Pages 652-659, Sanjay Kumar

DNA Methyltransferases: Eubacterial GATC, Pages 660-664, Martin G. Marinus

DNA Mismatch Repair and Homologous Recombination, Pages 665-670, Ivan Matic and Miroslav Radman

DNA Mismatch Repair and the DNA Damage Response, Pages 671-674, Guo-Min Li and Steven R. Presnell

DNA Mismatch Repair Defects and Cancer, Pages 675-681, Richard D. Kolodner

DNA Mismatch Repair in Bacteria, Pages 682-686, A-Lien Lu

DNA Mismatch Repair in Mammals, Pages 687-690, James T. Drummond

DNA Mismatch Repair: E. coli Vsr and Eukaryotic G-T Systems, Pages 691-693, Margaret Lieb

DNA Oxidation, Pages 694-697, Arthur P. Grollman and Dmitry O. Zharkov

DNA Photolyase, Pages 698-702, Carrie L. Partch and Aziz Sancar

DNA Polymerase, Eukaryotic α, Pages 703-707, Teresa S. -F. Wang

DNA Polymerase, Eukaryotic β, Pages 708-712, William A. Beard and Samuel H. Wilson

DNA Polymerase, Eukaryotic δ, Pages 713-715, Antero G. So and Kathleen M. Downey

DNA Polymerase, Eukaryotic ε, Pages 716-719, Yasuo Kawasaki and Akio Sugino

DNA Polymerase I, Bacterial, Pages 720-725, Catherine M. Joyce

DNA Polymerase II, Bacterial, Pages 726-728, Judith L. Campbell

DNA Polymerase III, Bacterial, Pages 729-733, Hisaji Maki

DNA Polymerases: Kinetics and Mechanism, Pages 734-739, Kenneth A. Johnson

DNA Replication Fork, Bacterial, Pages 740-744, Nancy G. Nossal

DNA Replication Fork, Eukaryotic, Pages 745-748, Lori M. Kelman, Jerard Hurwitz and Zvi Kelman

DNA Replication, Mitochondrial, Pages 749-752, David A. Clayton

DNA Replication: Eukaryotic Origins and the Origin Recognition Complex, Pages 753-760, Melvin L. DePamphilis and Cong-jun Li

DNA Replication: Initiation in Bacteria, Pages 761-766, Jon M. Kaguni

DNA Restriction and Modification: Type I Enzymes, Pages 767-771, David T. F. Dryden

DNA Restriction and Modification: Type II Enzymes, Pages 772-777, Darren M. Gowers and Stephen E. Halford

DNA Restriction and Modification: Type III Enzymes, Pages 778-781, Desirazu N. Rao and S. Srivani

DNA Secondary Structure, Pages 782-787, Albino Bacolla and Robert D. Wells

DNA Sequence Recognition by Proteins, Pages 788-793, Arabela A. Grigorescu and John M. Rosenberg

DNA Supercoiling, Pages 794-797, Tao-shih Hsieh

DNA Topoisomerases: Type I, Pages 798-805, James J. Champoux

DNA Topoisomerases: Type II, Pages 806-811, Renier Velez-Cruz and Neil Osheroff

DNA Topoisomerases: Type III-RecQ Helicase Systems, Pages 812-816, Rodney Rothstein and Erika Shor

Dopamine Receptors, Pages 817-822, Kim A. Neve

Dynactin, Pages 823-826, Trina A. Schroer

Dynein, Pages 827-831, K. Kevin Pfister

Volume 2

EF-G and EF-Tu Structures and Translation Elongation in Bacteria, Pages 1-5, Poul Nissen and Jens Nyborg

Eicosanoid Receptors, Pages 6-9, Richard M. Breyer and Matthew D. Breyer

Elastin, Pages 10-12, Judith Ann Foster

Endocannabinoids, Pages 13-15, Daniele Piomelli

Endocytosis, Pages 16-19, Julie G. Donaldson

Endoplasmic Reticulum-Associated Protein Degradation, Pages 20-23, Maurizio Molinari

Energy Transduction in Anaerobic Prokaryotes, Pages 24-30, Gottfried Unden

Enzyme Inhibitors, Pages 31-37, Vern L. Schramm

Enzyme Kinetics, Pages 38-44, Irwin H. Segel

Enzyme Reaction Mechanisms: Stereochemistry, Pages 45-50, Ming-Daw Tsai, Li Zhao and Brandon J. Lamarche

Epidermal Growth Factor Receptor Family, Pages 51-55, Denis Tvorogov and Graham Carpenter

ER/SR Calcium Pump: Function, Pages 56-60, Giuseppe Inesi

ER/SR Calcium Pump: Structure, Pages 61-65, Chikashi Toyoshima and Yuji Sugita

Exonucleases, Bacterial, Pages 66-72, Susan T. Lovett

F1-F0 ATP Synthase, Pages 73-79, Donata Branca

FAK Family, Pages 80-84, Steven K. Hanks

Fat Mobilization: Perilipin and Hormone-Sensitive Lipase, Pages 85-89, Constantine Londos and Alan R. Kimmel

Fatty Acid Oxidation, Pages 90-94, Horst Schulz

Fatty Acid Receptors, Pages 95-98, Christer Owman and Bjorn Olde

Fatty Acid Synthesis and its Regulation, Pages 99-103, Steven D. Clarke and Manabu T. Nakamura

Ferredoxin, Pages 104-106, Giuliana Zanetti and Vittorio Pandini

Ferredoxin-NADP+ Reductase, Pages 107-111, Giuliana Zanetti and Alessandro Aliverti

Fibroblast Growth Factor Receptors and Cancer-Associated Perturbations, Pages 112-117, Marko Kornmann and Murray Korc

Flavins, Pages 118-122, Barrie Entsch and David P. Ballou

Flippases, Pages 123-127, Charles J. Waechter

Focal Adhesions, Pages 128-133, Eli Zamir and Benjamin Geiger

Free Radicals, Sources and Targets of: Mitochondria, Pages 134-142, Alberto Boveris and Enrique Cadenas

Friedreich's Ataxia, Pages 143-145, Paul E. Hart and Anthony H. V. Schapira

G Protein Signaling Regulators, Pages 147-151, John H. Exton

G Protein-Coupled Receptor Kinases and Arrestins, Pages 152-157, Jeffrey L. Benovic

G12/G13 Family, Pages 158-161, Stefan Offermanns

GABAA Receptor, Pages 162-166, Richard W. Olsen and Gregory W. Sawyer

GABAB Receptor, Pages 167-170, S. J. Enna

Galectins, Pages 171-174, R. Colin Hughes

Genome-Wide Analysis of Gene Expression, Pages 175-180, Karine G. Le Roch and Elizabeth A. Winzeler

Gi Family of Heterotrimeric G Proteins, Pages 181-185, Maurine E. Linder

Giant Mitochondria (Megamitochondria), Pages 186-188, Bernard Tandler and Charles L. Hoppel

GlcNAc Biosynthesis and Function, O-Linked, Pages 189-192, Kaoru Sakabe and Gerald W. Hart

Glucagon Family of Peptides and their Receptors, Pages 193-196, Laurie L. Baggio and Daniel J. Drucker

Gluconeogenesis, Pages 197-203, Richard W. Hanson and Oliver E. Owen

Glucose/Sugar Transport in Bacteria, Pages 204-207, Lan Guan and H. Ronald Kaback

Glucose/Sugar Transport in Mammals, Pages 208-212, Silvia Mora and Jeffrey Pessin

Glutamate Receptors, Ionotropic, Pages 213-219, Derek B. Scott and Michael D. Ehlers

Glutamate Receptors, Metabotropic, Pages 220-223, P. Jeffrey Conn

Glutathione Peroxidases, Pages 224-228, Fulvio Ursini and Matilde Maiorino

Glycation, Pages 229-236, Suzanne R. Thorpe and John W. Baynes

Glycine Receptors, Pages 237-243, Bodo Laube and Heinrich Betz

Glycogen Metabolism, Pages 244-248, Peter J. Roach

Glycogen Storage Diseases, Pages 249-254, George H. Sack, Jr.

Glycogen Synthase Kinase-3, Pages 255-260, James R. Woodgett

Glycolipid-Dependent Adhesion Processes, Pages 261-265, Senitiroh Hakomori

Glycolysis, Overview, Pages 266-271, Robert A. Harris

Glycoprotein Folding and Processing Reactions, Pages 272-276, Armando J. Parodi

Glycoprotein-Mediated Cell Interactions, O-Linked, Pages 277-282, Robert S. Haltiwanger

Glycoproteins, N-Linked, Pages 283-292, Mark A. Lehrman

Glycoproteins, Plant, Pages 293-296, Carolyn J. Schultz

Glycosylation in Cystic Fibrosis, Pages 297-301, Andrew D. Rhim, Thomas F. Scanlin and Mary Catherine Glick

Glycosylation, Congenital Disorders of, Pages 302-307, Hudson H. Freeze

Glycosylphosphatidylinositol (GPI) Anchors, Pages 308-311, Anant K. Menon

Golgi Complex, Pages 312-315, Mark Stamnes

Gq Family, Pages 316-320, Wanling Yang and John D. Hildebrandt

Green Bacteria: Secondary Electron Donor (Cytochromes), Pages 321-324, Hirozo Oh-oka and Robert E. Blankenship

Green Bacteria: The Light-Harvesting Chlorosome, Pages 325-330, John M. Olson

Green Sulfur Bacteria: Reaction Center and Electron Transport, Pages 331-336, Gunter A. Hauska and Thomas Schodl

Gs Family of Heterotrimeric G Proteins, Pages 337-341, Susanne M. Mumby

Heat/Stress Responses, Pages 343-347, Davis T. W. Ng

Hematopoietin Receptors, Pages 348-353, Barbara A. Miller and Joseph Y. Cheung

Heme Proteins, Pages 354-361, Johannes Everse

Heme Synthesis, Pages 362-366, Gloria C. Ferreira

Hepatocyte Growth Factor/Scatter Factor Receptor, Pages 367-371, Selma Pennacchietti and Paolo M. Comoglio

Hexokinases/Glucokinases, Pages 372-377, Emile Van Schaftingen

Histamine Receptors, Pages 378-383, Stephen J. Hill and Jillian G. Baker

HIV Protease, Pages 384-387, Ben M. Dunn

HIV-1 Reverse Transcriptase Structure, Pages 388-392, Kalyan Das, Stefan G. Sarafianos, Eddy Arnold and Stephen H. Hughes

Homologous Recombination in Meiosis, Pages 393-397, Nancy M. Hollingsworth

HPLC Separation of Peptides, Pages 398-403, James D. Pearson

Imaging Methods, Pages 405-410, Gyorgy Szabadkai and Rosario Rizzuto

Immunoglobulin (Fc) Receptors, Pages 411-416, Mark Hogarth

Inorganic Biochemistry, Pages 417-420, Robert J. P. Williams

Inositol Lipid 3-Phosphatases, Pages 421-426, Gregory S. Taylor and Jack E. Dixon

Inositol Phosphate Kinases and Phosphatases, Pages 427-429, Stephen B. Shears

Insulin- and Glucagon-Secreting Cells of the Pancreas, Pages 430-435, Franz M. Matschinsky

Insulin Receptor Family, Pages 436-440, Paul F. Pilch and Jongsoon Lee

Integrin Signaling, Pages 441-445, Lawrence E. Goldfinger and Mark H. Ginsberg

Interferon Receptors, Pages 446-451, Christopher P. Elco and Ganes C. Sen

Intermediate Filament Linker Proteins: Plectin and BPAG1, Pages 452-457, Peter Fuchs and Gerhard Wiche

Intermediate Filaments, Pages 458-464, Kelsie M. Bernot and Pierre A. Coulombe

Intracellular Calcium Channels: cADPR-Modulated (Ryanodine Receptors), Pages 465-468, Antony Galione

Intracellular Calcium Channels: NAADP+-Modulated, Pages 469-472, Armando A. Genazzani and Marcella Debidda

Ion Channel Protein Superfamily, Pages 473-477, William A. Catterall

IP3 Receptors, Pages 478-481, Colin W. TaylorEdward Morris and Paula da Fonseca

Iron-Sulfur Proteins, Pages 482-489, Helmut Beinert

JAK-STAT Signaling Paradigm, Pages 491-496, Edward Cha and Christian Schindler

Keratins and the Skin, Pages 497-504, Pierre A. Coulombe and Kelsie M. Bernot

Ketogenesis, Pages 505-507, Janos Kerner and Charles L. Hoppel

Kinesin Superfamily Proteins, Pages 508-516, Nobutaka Hirokawa and Reiko Takemura

Kinesins as Microtubule Disassembly Enzymes, Pages 517-521, Susan L. Kline-Smith and Arshad Desai

Kinetic Isotope Effects, Pages 522-527, Justine P. Roth and Judith P. Klinman

lac Operon, Pages 529-534, Liskin Swint-Kruse and Kathleen S. Matthews

Lectins, Pages 535-540, Nathan Sharon and Halina Lis

Leptin, Pages 541-545, Thomas W. Gettys

LexA Regulatory System, Pages 546-550, Veronica G. Godoy, Penny J. Beuning and Graham C. Walker

Ligand-Operated Membrane Channels: Calcium (Glutamate), Pages 551-561, Elias K. Michaelis

Ligand-Operated Membrane Channels: GABA, Pages 562-566, F. Minier and Erwin Sigel

Light-Harvesting Complex (LHC) I and II: Pigments and Proteins, Pages 567-570, Stefan Jansson

Lipases, Pages 571-575, Howard L. Brockman

Lipid Bilayer Structure, Pages 576-579, Erwin London

Lipid Modification of Proteins: Targeting to Membranes, Pages 580-583, Marilyn D. Resh

Lipid Rafts, Pages 584-587, Deborah A. Brown

Lipoproteins, HDL/LDL, Pages 588-593, Fayanne E. Thorngate and David L. Williams

Low Barrier Hydrogen Bonds, Pages 594-598, Perry A. Frey

Luft's Disease, Pages 599-601, Salvatore DiMauro

Lysophospholipid Receptors, Pages 602-604, Gabor J. Tigyi

MDR Membrane Proteins, Pages 605-609, Nathan C. Rockwell

Meiosis, Pages 610-616, Neil Hunter

Melanocortin System, Pages 617-620, Roger D. Cone

Membrane Fusion, Pages 621-626, Joshua Zimmerberg and Leonid V. Chernomordik

Membrane Transport, General Concepts, Pages 627-630, Stanley G. Schultz

Membrane Transporters:Na+/Ca2+ Exchangers, Pages 631-636, Jonathan Lytton

Membrane-Associated Energy Transduction in Bacteria and Archaea, Pages 637-645, Gunter Schafer

Metabolite Channeling: Creatine Kinase Microcompartments, Pages 646-651, Uwe Schlattner and Theo Wallimann

Metalloproteases, Pages 652-656, David S. Auld

Metalloproteinases, Matrix, Pages 657-665, Hideaki Nagase and Gillian Murphy

Metaphase Chromosome, Pages 666-671, Sharron Vass and Margarete M. S. Heck

Methyl-CpG-Binding Proteins, Pages 672-675, David G. Skalnik

Microtubule-Associated Proteins, Pages 676-682, Nobutaka Hirokawa and Reiko Takemura

Mitochondrial Auto-Antibodies, Pages 683-688, Harold Baum

Mitochondrial Channels, Pages 689-692, M. Catia Sorgato and Alessandro Bertoli

Mitochondrial DNA, Pages 693-696, Gottfried Schatz

Mitochondrial Genes and their Expression: Yeast, Pages 697-702, Piotr P. Slonimski and Giovanna Carignani

Mitochondrial Genome, Evolution, Pages 703-708, B. Franz Lang, Dennis V. Lavrov and Gertraud Burger

Mitochondrial Genome, Overview, Pages 709-715, Douglas C. Wallace

Mitochondrial Inheritance, Pages 716-719, Eric A. Shoubridge

Mitochondrial Membranes, Structural Organization, Pages 720-724, Carmen A. Mannella

Mitochondrial Metabolite Transporter Family, Pages 725-732, Ferdinando Palmieri and Martin Klingenberg

Mitochondrial Outer Membrane and the VDAC Channel, Pages 733-736, Marco Colombini

Mitogen-Activated Protein Kinase Family, Pages 737-742, Hidemi Teramoto and J. Silvio Gutkind

Mitosis, Pages 743-747, Patricia Wadsworth and Nasser M. Rusan

mRNA Polyadenylation in Eukaryotes, Pages 748-752, Mary Edmonds

mRNA Processing and Degradation in Bacteria, Pages 753-757, Deborah A. Steege

Mucin Family of Glycoproteins, Pages 758-764, Juan Perez-Vilar and Robert L. Hill

Mucins in Embryo Implantation, Pages 765-769, Daniel D. Carson

Multiple Sequence Alignment and Phylogenetic Trees, Pages 770-774, Russell F. Doolittle

Muscarinic Acetylcholine Receptors, Pages 775-777, Neil M. Nathanson

Myosin Motors, Pages 778-781, Roy E. Larson

Volume 3

Natriuretic Peptides and their Receptors, Pages 1-5, Lincoln R. Potter

N-End Rule, Pages 6-10, Alexander Varshavsky

Neoglycoproteins, Pages 11-15, Y. C. Lee and Reiko T. Lee

Neuronal Calcium Signal, Pages 16-20, Hilmar Bading

Neuronal Intermediate Filaments, Pages 21-25, Ronald K. H. Liem

Neuropeptide Y Receptors, Pages 26-31, Eric M. Parker

Neurotensin Receptors, Pages 32-36, William Rostene, Patrick Kitabgi and Didier Pelaprat

Neurotransmitter Transporters, Pages 37-40, Aurelio Galli, Randy D. Blakely and Louis J. DeFelice

Neurotrophin Receptor Signaling, Pages 41-45, Jennifer J. Gentry and Bruce D. Carter

Nicotinamide Nucleotide Transhydrogenase, Pages 50-56, Jan Rydstrom

Nicotinic Acetylcholine Receptors, Pages 57-61, Nivalda O. Rodrigues-Pinguet and Henry A. Lester

Nitric Oxide Signaling, Pages 62-65, Michael A. Marletta

N-Linked Glycan Processing Glucosidases and Mannosidases, Pages 46-49, Linda O. Tremblay and Annette Herscovics

Non-Homologous End Joining, Pages 66-70, Penny A. Jeggo

Nonhomologous Recombination: Bacterial Transposons, Pages 71-79, Bao Ton Hoang and Michael G. Chandler

Nonhomologous Recombination: Retrotransposons, Pages 80-86, Siew Loon Ooi and Jef D. Boeke

Nuclear Compartmentalization, Pages 87-91, Kelly P. Smith and Jeanne B. Lawrence

Nuclear Envelope and Lamins, Pages 92-95, Bryce M. Paschal

Nuclear Factor kappaB, Pages 96-99, Thomas D. Gilmore

Nuclear Genes in Mitochondrial Function and Biogenesis, Pages 100-104, Alexander Tzagoloff and Carol L. Dieckmann

Nuclear Organization, Chromatin Structure, and Gene Silencing , Pages 105-108, Lori L. Wallrath, John R. Danzer, Oya Yazgan and Pamela K. Geyer

Nuclear Pores and Nuclear Import/Export, Pages 109-114, Anita H. Corbett

Nucleoid Organization of Bacterial Chromosomes, Pages 115-118, Charles J. Dorman

Nucleolus, Overview, Pages 119-122, Thoru Pederson

Nucleotide Excision Repair and Human Disease, Pages 123-129, James E. Cleaver

Nucleotide Excision Repair in Eukaryotes, Pages 130-133, Laura A. Lindsey-Boltz and Aziz Sancar

Nucleotide Excision Repair, Bacterial: The UvrABCD System, Pages 134-142, Bennett Van Houten and Lawrence Grossman

Nucleotide Excision Repair: Biology, Pages 143-147, Errol C. Friedberg

Olfactory Receptors, Pages 149-154, Sigrun I. Korsching

Oligosaccharide Analysis by Mass Spectrometry, Pages 155-160, Andrew J. Hanneman and Vernon N. Reinhold

Oligosaccharide Chains: Free, N-Linked, O-Linked, Pages 161-164, Tadashi Suzuki

Oncocytes, Pages 165-166, Bernard Tandler and Charles L. Hoppel

Opioid Receptors, Pages 167-171, P. Y. Law and Horace H. Loh

Ornithine Cycle, Pages 172-177, Malcolm Watford

Oxygenases, Pages 178-182, Osamu Hayaishi

P2X Purinergic Receptors, Pages 183-187, Annmarie Surprenant

P2Y Purinergic Receptors, Pages 188-191, George R. Dubyak

p53 Protein, Pages 192-195, Jamie Hearnes and Jennifer Pietenpol

p70 S6 Kinase/mTOR, Pages 196-200, Christopher G. Proud

Parathyroid Hormone/Parathyroid Hormone-Related Protein Receptor, Pages 201-207, Thomas J. Gardella

PCR (Polymerase Chain Reaction), Pages 208-210, Michael J. Brownstein

Pentose Phosphate (Hexose Mono Phosphate) Pathway, Pages 211-215, Bernard R. Landau

Pentose Phosphate Pathway, History of, Pages 216-225, John F. Williams

Peptide Amidation, Pages 226-230, Mark J. Niciu, Richard E. Mains and Betty A. Eipper

Periplasmic Electron Transport Systems in Bacteria, Pages 231-238, David J. Richardson, Gary Sawers and Rob J. M. Van Spanning

Peroxisome Proliferator-Activated Receptors, Pages 239-245, Mary C. Sugden, Edward A. Sugden and Mark J. Holness

Peroxisomes, Pages 246-250, Suresh Subramani

Phage Display for Protein Binding, Pages 251-255, Henry B. Lowman

Pheromone Receptors (Yeast), Pages 256-261, James B. Konopka and Jeremy W. Thorner

PHO Regulon, Pages 262-265, Bengt L. Persson

Phosphatidylinositol Bisphosphate and Trisphosphate, Pages 266-271, Alex Toker

Phosphatidylinositol-3-Phosphate, Pages 272-276, Joseph V. Virbasius and Michael P. Czech

Phosphofructokinase-2/Fructose Bisphosphatase-2, Pages 277-280, Daniel M. Raben

Phosphoinositide 3-Kinase, Pages 281-286, Khatereh Ahmadi and Michael Waterfield

Phosphoinositide 4- and 5-Kinases and Phosphatases, Pages 287-291, Shawn F. Bairstow, Matthew W. Bunce and Richard A. Anderson

Phosphoinositide-Dependent Protein Kinases, Pages 292-296, Nick R. Leslie and C. Peter Downes

Phospholipase A2, Pages 297-300, Timothy R. Smith and Edward A. Dennis

Phospholipase C, Pages 301-305, Fujio Sekiya, Yeun Ju Kim and Sue Goo Rhee

Phospholipase D, Pages 306-313, Mary M. LaLonde and Michael A. Frohman

Phospholipid Metabolism in Mammals, Pages 314-320, Claudia Kent

Phospholipid Synthesis in Yeast, Pages 321-325, Gil-Soo Han and George M. Carman

Photoreceptors, Pages 326-329, King-Wai Yau

Photosynthesis, Pages 330-335, Richard C. Leegood

Photosynthetic Carbon Dioxide Fixation, Pages 336-341, Matthew J. Paul

Photosystem I, Structure and Function, Pages 342-347, Petra Fromme

Photosystem I: FX, FA, and FB Iron-Sulfur Clusters, Pages 348-356, Mikhail L. Antonkine and John H. Golbeck

Photosystem II Light Harvesting System: Dynamic Behavior, Pages 357-362, Peter Horton and Alexander Ruban

Photosystem II: Assembly and Turnover of the D1 Protein, Pages 363-366, Eira Kanervo and Eva-Mari Aro

Photosystem II: Protein Components, Pages 367-374, James Barber

Photosystem II: Water Oxidation, Overview, Pages 375-380, Fabrice Rappaport and Pierre Joliot

Plant Signaling: Peptides, Pages 381-384, Clarence A. Ryan and Gregory Pearce

Plasma-Membrane Calcium Pump: Structure and Function, Pages 385-389, Emanuel E. Strehler

Plastocyanin, Pages 390-393, Elizabeth L. Gross

Platelet-Activating Factor Receptor, Pages 394-398, Katherine M. Howard and Merle S. Olson

Platelet-Derived Growth Factor Receptor Family, Pages 399-406, Marina Kovalenko and Andrius Kazlauskas

Polysialic Acid inMolecular Medicine, Pages 407-414, Frederic A. Troy, II

Porphyrin Metabolism, Pages 415-419, Mark Shepherd and Harry A. Dailey

Pre-tRNA and Pre-rRNA Processing in Bacteria, Pages 420-424, Sidney R. Kushner

Pre-tRNA and Pre-rRNA Processing in Eukaryotes, Pages 425-431, Hendrik A. Raue

Prions and Epigenetic Inheritance, Pages 432-436, Reed B. Wickner

Prions, Overview, Pages 437-440, Cedric Govaerts and Fred E. Cohen

Processivity Clamps in DNA Replication: Clamp Loading, Pages 441-446, Megan J. Davey and Mike O'Donnell

Propionyl CoA-Succinyl CoA Pathway, Pages 447-451, Wayne A. Fenton

Prostaglandins and Leukotrienes, Pages 452-456, William L. Smith and Robert C. Murphy

Proteases in Blood Clotting, Pages 457-463, John D. Kulman and Earl W. Davie

Proteasomes, Overview, Pages 464-468, Martin Rechsteiner

26S Proteasome, Structure and Function, Pages 469-473, Peter Zwickl and Wolfgang Baumeister

Protein Carboxyl Esterification, Pages 474-477, Shilpa G. Lalchandani and Jeffry B. Stock

Protein Data Resources, Pages 478-483, Philip E. Bourne

Protein Degradation, Pages 484-492, Tomo ari and Alfred L. Goldberg

Protein Folding and Assembly, Pages 493-499, David P. Goldenberg

Protein Glycosylation Inhibitors, Pages 500-503, Alan D. Elbein

Protein Glycosylation, Overview, Pages 504-509, Natasha E. Zachara and Gerald W. Hart

Protein Import into Mitochondria, Pages 510-515, Johannes M. Herrmann and Walter Neupert

Protein Kinase B, Pages 516-522, Bettina A. Dummler and Brian A. Hemmings

Protein Kinase C Family, Pages 523-526, Alexandra C. Newton

Protein N-Myristoylation, Pages 527-531, Erica Dutil Sonnenburg and Jeffrey I. Gordon

Protein Palmitoylation, Pages 532-535, Robert J. Deschenes

Protein Tyrosine Phosphatases, Pages 536-542, David J. Pagliarini, Fred L. Robinson and Jack E. Dixon

Proteinase-Activated Receptors, Pages 543-548, Kristina K. Hansen and Morley D. Hollenberg

Proteoglycans, Pages 549-555, Sara K. Olson and Jeffrey D. Esko

Pteridines, Pages 556-560, S. Colette Daubner and Paul F. Fitzpatrick

P-Type Pumps: Copper Pump, Pages 561-564, Ilia Voskoboinik and James Camakaris

P-Type Pumps: H+/K+ Pump, Pages 565-570, Jai Moo Shin and George Sachs

P-Type Pumps: Na+/K+ Pump, Pages 571-576, Peter L. Jorgensen

P-Type Pumps: Plasma-Membrane H+ Pump, Pages 577-581, A. Brett Mason and Carolyn W. Slayman

Purple Bacteria: Electron Acceptors and Donors, Pages 582-585, Evaldas Katilius and Neal W. Woodbury

Purple Bacteria: Photosynthetic Reaction Centers, Pages 586-594, C. Roy D. Lancaster

Pyridoxal Phosphate, Pages 595-599, David E. Metzler

Pyrimidine Biosynthesis, Pages 600-605, Monika Loffler and Elke Zameitat

Pyruvate Carboxylation, Transamination, and Gluconeogenesis, Pages 606-610, Sarawut Jitrapakdee and John C. Wallace

Pyruvate Dehydrogenase, Pages 611-615, Sam A. Johnson and James G. McCormack

Pyruvate Kinase, Pages 616-619, Kosaku Uyeda

Quinones, Pages 621-627, Giorgio Lenaz and Maria Luisa Genova

Rab Family, Pages 629-634, Mary W. McCaffrey and Andrew J. Lindsay

Ran GTPase, Pages 635-639, Mary Shannon Moore

Ras Family, Pages 640-644, Lawrence A. Quilliam

Recombination: Heteroduplexand Mismatch Repair in vitro, Pages 645-648, Leroy Worth

Recombination: Strand Transferases, Pages 649-653, Floyd R. Bryant

Recombination-Dependent DNA Replication, Pages 654-659, Kenneth N. Kreuzer

recQ DNA Helicase Family in Genetic Stability, Pages 660-664, Mary A. Risinger and Joanna Groden

Regulated Intramembrane Proteolysis (Rip), Pages 665-670, Jin Ye, Michael S. Brown and Joseph L. Goldstein

Respiratory Chain and ATP Synthase, Pages 671-675, David G. Whitehouse and Anthony L. Moore

Respiratory Chain Complex I, Pages 676-680, Ulrich Brandt

Respiratory Chain Complex II and Succinate: Quinone Oxidoreductases, Pages 681-687, C. Roy D. Lancaster

Respiratory Chain Complex IV, Pages 688-694, Hartmut Michel

Respiratory Processes in Anoxygenic and Oxygenic Phototrophs, Pages 695-699, Roberto Borghese and Davide Zannoni

Retinoblastoma Protein (pRB), Pages 700-703, Nicholas Dyson and Maxim Frolov

Retinoic Acid Receptors, Pages 704-707, Martin Petkovich

Reverse Transcriptase and Retroviral Replication, Pages 708-713, Laura Tarrago-Litvak, Marie-Line Andreola and Simon Litvak

Rho GTPases and Actin Cytoskeleton Dynamics, Pages 714-718, Priam Villalonga and Anne J. Ridley

Ribosome Assembly, Pages 719-724, John L. Woolford

Ribosome Structure, Pages 725-732, Brian T. Wimberly

Ribozyme Mechanisms, Pages 733-737, John Hsieh and Carol A. Fierke

Ribozyme Structural Elements: Group I Introns, Pages 738-742, Barbara L. Golden

Ribozyme Structural Elements: Hairpin Ribozyme, Pages 743-746, Adrian R. Ferre-D'Amare

Ribozymes and Evolution, Pages 747-752, Niles Lehman

RNA Editing, Pages 753-758, Charles E. Samuel

RNA Polymerase I and RNA Polymerase III in Eukaryotes, Pages 759-762, Robert J. White

RNA Polymerase II and Basal Transcription Factors in Eukaryotes, Pages 763-765, Joan Weliky Conaway and Ronald C. Conaway

RNA Polymerase II Elongation Control in Eukaryotes, Pages 766-769, David H. Price

RNA Polymerase II Structure in Eukaryotes, Pages 770-774, Patrick Cramer

RNA Polymerase Reaction in Bacteria, Pages 775-780, Arkady A. Mustaev and Alexander D. Goldfarb

RNA Polymerase Structure, Bacterial, Pages 781-784, Michael Anikin, Dmitri Temiakov and William T. McAllister

Volume 4

Secondary Structure in Protein Analysis, Pages 1-6, George D. Rose

Secretases, Pages 7-10, Robert L. Heinrikson

Secretory Pathway, Pages 11-16, Karen J. Colley

Selenoprotein Synthesis, Pages 17-21, August Bock

Septins and Cytokinesis, Pages 22-26, Makoto Kinoshita and Christine M. Field

Serine/Threonine Phosphatases, Pages 27-32, Thomas S. Ingebritsen

Serotonin Receptor Signaling, Pages 33-37, Paul J. Gresch and Elaine Sanders-Bush

Siglecs, Pages 38-40, Ajit Varki

Sigma Factors, Pages 41-44, John D. Helmann

Sliding Clamps in DNA Replication: E. coli -Clamp and PCNA Structure, Pages 45-47, Eric R. Goedken and John Kuriyan

Small GTPases, Pages 48-54, Adam Shutes and Channing J. Der

Somatostatin Receptors, Pages 55-60, Agnes Schonbrunn

Spastic Paraplegia, Pages 61-66, Elena Irene Rugarli and Andrea Ballabio

Spectrophotometric Assays, Pages 67-75, Britton Chance

Sphingolipid Biosynthesis, Pages 76-81, Martina Leipelt and Alfred H. Merrill

Sphingolipid Catabolism, Pages 82-87, Akira Abe and James A. Shayman

Spliceosome, Pages 88-92, Timothy W. Nilsen

Src Family of Protein Tyrosine Kinases, Pages 93-98, Jonathan A. Cooper

Starvation, Pages 99-110, Oliver E. Owen and Richard W. Hanson

Steroid/Thyroid Hormone Receptors, Pages 111-116, Ramesh Narayanan and Nancy L. Weigel

Store-Operated Membrane Channels: Calcium, Pages 117-122, Indu S. Ambudkar

Substrate Binding, Catalysis, and Product Release , Pages 123-126, W. Wallace Cleland

Sugar Nucleotide Transporters, Pages 127-129, Carlos B. Hirschberg

SUMO Modification, Pages 130-134, Frauke Melchior and Andrea Pichler

Superoxide Dismutase, Pages 135-138, Irwin Fridovich

Syk Family of Protein Tyrosine Kinases, Pages 139-145, Andrew C. Chan

T7 RNA Polymerase, Pages 147-151, Rui Sousa

Tachykinin/Substance P Receptors, Pages 152-157, Mark D. Richardson and Madan M. Kwatra

Taste Receptors, Pages 158-161, John D. Boughter, Jr. and Steven D. Munger

T-Cell Antigen Receptor, Pages 162-168, Andrea L. Szymczak and Dario A. A. Vignali

Tec/Btk Family Tyrosine Kinases, Pages 169-173, Shuling Guo and Owen N. Witte

Telomeres: Maintenance and Replication, Pages 174-179, Alessandro Bianchi and David Shore

Thyroid-Stimulating Hormone/Luteinizing Hormone/Follicle-Stimulating Hormone Receptors, Pages 180-186, Deborah L. Segaloff, Dario Mizrachi and Mario Ascoli

Tight Junctions, Pages 187-189, Shoichiro Tsukita

Title, Pages, Authors

Toll-Like Receptors, Pages 190-194, Himanshu Kumar, Kiyoshi Takeda and Shizuo Akira

Transcription Termination, Pages 195-199, Thomas J. Santangelo and Jeffrey W. Roberts

Transcriptional Silencing, Pages 200-203, Ann Sutton and Rolf Sternglanz

Transcription-Coupled DNA Repair, Overview, Pages 204-208, Isabel Mellon

Transforming Growth Factor-β Receptor Superfamily, Pages 209-213, Mark de Caestecker

Translation Elongation in Bacteria, Pages 214-223, Oliver Vesper and Knud H. Nierhaus

Translation Elongation in Eukaryotes, Pages 224-229, William C. Merrick and Anton A. Komar

Translation Initiation in Bacteria: Factors and Mechanisms, Pages 230-236, Cynthia L. Pon and Claudio O. Gualerzi

Translation Initiation in Eukaryotes: Factors and Mechanisms, Pages 237-241, Tatyana V. Pestova and Christopher U. T. Hellen

Translation Termination and Ribosome Recycling, Pages 242-246, Nadja Koloteva-Levin and Mick F. Tuite

Translesion DNA Polymerases, Eukaryotic, Pages 247-250, Alexandra Vaisman and Roger Woodgate

Trehalose Metabolism, Pages 251-255, Alan D. Elbein

Tricarboxylic Acid Cycle, Pages 256-262, Richard L. Veech

tRNA Synthetases, Pages 263-266, Karla L. Ewalt and Paul Schimmel

trp Operon and Attenuation, Pages 267-271, Paul Gollnick

Tubulin and its Isoforms, Pages 272-276, Eva Nogales

Tumor Necrosis Factor Receptors, Pages 277-283, Karen G. Potter and Carl F. Ware

Two-Dimensional Gel Electrophoresis, Pages 284-289, Gerhard Schmid, Denis Hochstrasser and Jean-Charles Sanchez

Two-Hybrid Protein-Protein Interactions, Pages 290-293, Ilya Serebriiskii and Erica A. Golemis

Tyrosine Sulfation, Pages 294-297, Denis Corbeil and Wieland B. Huttner

Ubiquitin System, Pages 299-303, Aaron Ciechanover and Michael H. Glickman

Ubiquitin-Like Proteins, Pages 304-307, Edward T. H. Yeh

UmuC, D Lesion Bypass DNA Polymerase V, Pages 308-312, Zvi Livneh

Uncoupling Proteins, Pages 313-318, Daniel Ricquier and Frederic Bouillaud

Unfolded Protein Responses, Pages 319-325, David Ron

Urea Cycle, Inborn Defects of, Pages 326-330, Marsha K. Fearing and Vivian E. Shih

Vacuoles, Pages 331-336, Christopher J. Stefan and Scott D. Emr

Vascular Endothelial Growth Factor Receptors, Pages 337-342, Kenneth A. Thomas

Vasopressin/Oxytocin Receptor Family, Pages 343-348, Michael J. Brownstein

V-ATPases, Pages 349-353, Michael Forgac

Vitamin A (Retinoids), Pages 354-359, Joseph L. Napoli

Vitamin B12 and B12-Proteins, Pages 360-366, Bernhard Krautler

Vitamin C, Pages 367-371, Robert B. Rucker and Francene Steinberg

Vitamin D, Pages 372-377, Hector F. DeLuca and Margaret Clagett-Dame

Vitamin D Receptor, Pages 378-383, Diane R. Dowd and Paul N. MacDonald

Vitamin E, Pages 384-388, Ute C. Obermuller-Jevic and Lester Packer

Vitamin K: Biochemistry, Metabolism, and Nutritional Aspects, Pages 389-393, J. W. Suttie

Vitamin K: Blood Coagulation and Use in Therapy, Pages 394-398, Matthew D. Stone and Gary L. Nelsestuen

Voltage-Dependent K+ Channels, Pages 399-404, Ramon Latorre and Francisco J. Morera

Voltage-Sensitive Ca2+ Channels, Pages 405-408, Harald Reuter

Voltage-Sensitive Na+ Channels, Pages 409-415, William J. Brammar

Von Hippel-Lindau (VHL) Protein, Pages 416-418, Ronald C. Conaway and Joan Weliky Conaway

XPV DNA Polymerase and Ultraviolet Damage Bypass, Pages 419-421, Alan R. Lehmann

X-Ray Determination of 3-D Structure in Proteins, Pages 422-428, Martha L. Ludwig

Yeast GAL1-GAL10 System, Pages 429-433, Dennis Lohr and Ralph Bash

Zinc Fingers, Pages 435-439, Mark Isalan

Lipids, Carbohydrates, Membranes and Membrane Proteins

Carbohydrate Chains: Enzymatic and Chemical Synthesis; Vol.1 - Pages 307-313, Thomas J. Tolbert and Chi-Huey Wong

Cell–Matrix Interactions; Vol.1 - Pages 362-366, Janet A. Askari and Martin J. Humphries

Detergent Properties; Vol.1 - Pages 577-581, Darrell R. McCaslin

Endocytosis; Vol.2 - Pages 16-19, Julie G. Donaldson

Flippases; Vol.2 - Pages 123-127, Charles J. Waechter

Galectins; Vol.2 - Pages 171-174, R. Colin Hughes

GlcNAc Biosynthesis and Function, O-Linked; Vol.2 - Pages 189-192, Kaoru Sakabe and Gerald W. Hart

Glycation; Vol.2 - Pages 229-236, Suzanne R. Thorpe and John W. Baynes

Glycolipid-Dependent Adhesion Processes; Vol.2 - Pages 261-265, Senitiroh Hakomori

Glycoprotein Folding and Processing Reactions; Vol.2 - Pages 272-276, Armando J. Parodi

Glycoprotein-Mediated Cell Interactions, O-Linked; Vol.2 - Pages 277-282, Robert S. Haltiwanger

Glycoproteins, N-Linked; Vol.2 - Pages 283-292, Mark A. Lehrman

Glycoproteins, Plant; Vol.2 - Pages 293-296, Carolyn J. Schultz

Glycosylation in Cystic Fibrosis; Vol.2 - Pages 297-301, Andrew D. Rhim, Thomas F. Scanlin and Mary Catherine Glick

Glycosylation, Congenital Disorders of; Vol.2 - Pages 302-307, Hudson H. Freeze

Glycosylphosphatidylinositol (GPI) Anchors; Vol.2 - Pages 308-311, Anant K. Menon

Ion Channel Protein Superfamily; Vol.2 - Pages 473-477, William A. Catterall

Lectins; Vol.2 - Pages 535-540, Nathan Sharon and Halina Lis

Lipases; Vol.2 - Pages 571-575, Howard L. Brockman

Lipid Bilayer Structure; Vol.2 - Pages 576-579, Erwin London

Lipid Rafts; Vol.2 - Pages 584-587, Deborah A. Brown

Lipoproteins, HDL/LDL; Vol.2 - Pages 588-593, Fayanne E. Thorngate and David L. Williams

MDR Membrane Proteins; Vol.2 - Pages 605-609, Nathan C. Rockwell

Membrane Fusion; Vol.2 - Pages 621-626, Joshua Zimmerberg and Leonid V. Chernomordik

Mucin Family of Glycoproteins; Vol.2 - Pages 758-764, Juan Perez-Vilar and Robert L. Hill

Mucins in Embryo Implantation; Vol.2 - Pages 765-769, Daniel D. Carson

Neoglycoproteins; Vol.3 - Pages 11-15, Y. C. Lee and Reiko T. Lee

N-Linked Glycan Processing Glucosidases and Mannosidases; Vol.3 - Pages 46-49, Linda O. Tremblay and Annette Herscovics

Oligosaccharide Chains: Free, N-Linked, O-Linked; Vol.3 - Pages 161-164, Tadashi Suzuki

Phospholipid Metabolism in Mammals; Vol.3 - Pages 314-320, Claudia Kent

Phospholipid Synthesis in Yeast; Vol.3 - Pages 321-325, Gil-Soo Han and George M. Carman

Prostaglandins and Leukotrienes; Vol.3 - Pages 452-456, William L. Smith and Robert C. Murphy

Protein Glycosylation Inhibitors; Vol.3 - Pages 500-503, Alan D. Elbein

Proteoglycans; Vol.3 - Pages 549-555, Sara K. Olson and Jeffrey D. Esko

Secretory Pathway; Vol.4 - Pages 11-16, Karen J. Colley

Siglecs; Vol.4 - Pages 38-40, Ajit Varki

Sphingolipid Biosynthesis; Vol.4 - Pages 76-81, Martina Leipelt and Alfred H. Merrill, Jr.

Sphingolipid Catabolism; Vol.4 - Pages 82-87, Akira Abe and James A. Shayman

Sugar Nucleotide Transporters; Vol.4 - Pages 127-129, Carlos B. Hirschberg

Trehalose Metabolism; Vol.4 - Pages 251-255, Alan D. Elbein

Metabolism, Vitamins and Hormones

Amino Acid Metabolism; Vol.1 - Pages 90-95, Luc Cynober

Anaplerosis; Vol.1 - Pages 105-110, Raymond R. Russell, III and Heinrich Taegtmeyer

Bile Salts and their Metabolism; Vol.1 - Pages 159-163, Ulrich Beuers and Thomas Pusl

Biliary Cirrhosis, Primary; Vol.1 - Pages 164-169, Marshall M. Kaplan

Branched-Chain -Ketoacids; Vol.1 - Pages 186-191, David T. Chuang

Carnitine and -Oxidation; Vol.1 - Pages 314-318, Janos Kerner and Charles L. Hoppel

Cholesterol Synthesis; Vol.1 - Pages 451-455, Peter A. Edwards

Diabetes; Vol.1 - Pages 582-592, David W. Cooke

Fat Mobilization: Perilipin and Hormone-Sensitive Lipase; Vol.2 - Pages 85-89, Constantine Londos and Alan R. Kimmel

Fatty Acid Oxidation; Vol.2 - Pages 90-94, Horst Schulz

Fatty Acid Synthesis and its Regulation; Vol.2 - Pages 99-103, Steven D. Clarke and Manabu T. Nakamura

Gluconeogenesis; Vol.2 - Pages 197-203, Richard W. Hanson and Oliver E. Owen

Glucose/Sugar Transport in Bacteria; Vol.2 - Pages 204-207, Lan Guan and H. Ronald Kaback

Glucose/Sugar Transport in Mammals; Vol.2 - Pages 208-212, Silvia Mora and Jeffrey Pessin

Glycogen Metabolism; Vol.2 - Pages 244-248, Peter J. Roach

Glycogen Storage Diseases; Vol.2 - Pages 249-254, George H. Sack, Jr.

Glycolysis, Overview; Vol.2 - Pages 266-271, Robert A. Harris

Hexokinases/Glucokinases; Vol.2 - Pages 372-377, Emile Van Schaftingen

Insulin- and Glucagon-Secreting Cells of the Pancreas; Vol.2 - Pages 430-435, Franz M. Matschinsky

Ketogenesis; Vol.2 - Pages 505-507, Janos Kerner and Charles L. Hoppel

Ornithine Cycle; Vol.3 - Pages 172-177, Malcolm Watford

Pentose Phosphate (Hexose Mono Phosphate) Pathway; Vol.3 - Pages 211-215, Bernard R. Landau

Pentose Phosphate Pathway, History of; Vol.3 - Pages 216-225, John F. Williams

Phosphofructokinase-2/Fructose Bisphosphatase-2; Vol.3 - Pages 277-280, Daniel M. Raben

Photosynthesis; Vol.3 - Pages 330-335, Richard C. Leegood

Photosynthetic Carbon Dioxide Fixation; Vol.3 - Pages 336-341, Matthew J. Paul

Porphyrin Metabolism; Vol.3 - Pages 415-419, Mark Shepherd and Harry A. Dailey

Propionyl CoA–Succinyl CoA Pathway; Vol.3 - Pages 447-451, Wayne A. Fenton

Pyruvate Carboxylation, Transamination, and Gluconeogenesis; Vol.3 - Pages 606-610, Sarawut Jitrapakdee and John C. Wallace

Pyruvate Dehydrogenase; Vol.3 - Pages 611-615, Sam A. Johnson and James G. McCormack

Pyruvate Kinase; Vol.3 - Pages 616-619, Kosaku Uyeda

Starvation; Vol.4 - Pages 99-110, Oliver E. Owen and Richard W. Hanson

Tricarboxylic Acid Cycle; Vol.4 - Pages 256-262, Richard L. Veech

Urea Cycle, Inborn Defects of; Vol.4 - Pages 326-330, Marsha K. Fearing and Vivian E. Shih

Vitamin A (Retinoids); Vol.4 - Pages 354-359, Joseph L. Napoli

Vitamin B12 and B12-Proteins; Vol.4 - Pages 360-366, Bernhard Krautler

Vitamin C; Vol.4 - Pages 367-371, Robert B. Rucker and Francene Steinberg

Vitamin D; Vol.4 - Pages 372-377, Hector F. DeLuca and Margaret Clagett-Dame

Vitamin E; Vol.4 - Pages 384-388, Ute C. Obermuller-Jevic and Lester Packer

Vitamin K: Biochemistry, Metabolism, and Nutritional Aspects; Vol.4 - Pages 389-393, J. W. Suttie

Vitamin K: Blood Coagulation and Use in Therapy; Vol.4 - Pages 394-398, Matthew D. Stone and Gary L. Nelsestuen

Cell Architecture and Function

Actin Assembly/Disassembly; Vol.1 - Pages 12-18, Henry N. Higgs

Actin-Capping and -Severing Proteins; Vol.1 - Pages 19-26, Sankar Maiti and James R. Bamburg

Actin-Related Proteins; Vol.1 - Pages 27-33, R. Dyche Mullins

Autophagy in Fungi and Mammals; Vol.1 - Pages 138-143, Daniel J. Klionsky and Ju Guan

Bax and Bcl2 Cell Death Enhancers and Inhibitors; Vol.1 - Pages 152-154, David L. Vaux

Cadherin-Mediated Cell–Cell Adhesion; Vol.1 - Pages 205-211, Frauke Drees and W. James Nelson

Caspases and Cell Death; Vol.1 - Pages 319-327, Don W. Nicholson, Pierluigi Nicotera and Gerry Melino

Cell Cycle Controls in G1 and G0; Vol.1 - Pages 328-331, WengeShi and Steven F. Dowdy

Cell Cycle: Control of Entry and Progression Through S Phase; Vol.1 - Pages 332-337, Susan L. Forsburg

Cell Cycle: DNA Damage Checkpoints; Vol.1 - Pages 338-344, Jean Y. J. Wang

Cell Cycle: Mitotic Checkpoint; Vol.1 - Pages 345-351, Tim J. Yen

Cell Migration; Vol.1 - Pages 356-361, J. Victor Small and Emmanuel Vignal

Centromeres; Vol.1 - Pages 367-371, Beth A. Sullivan

Centrosomes and Microtubule Nucleation; Vol.1 - Pages 372-376, Reiko Nakajima, Ming-Ying Tsai and Yixian Zheng

Chaperones for Metalloproteins; Vol.1 - Pages 383-386, Valeria C. Culotta and Edward Luk

Chaperones, Molecular; Vol.1 - Pages 387-392, Sue Wickner and Joel R. Hoskins

Chaperonins; Vol.1 - Pages 393-398, Arthur L. Horwich, Wayne A. Fenton and George W. Farr

Chromosome Organization and Structure, Overview; Vol.1 - Pages 469-474, Elena Gracheva and Sarah C. R. Elgin

Cytokinesis; Vol.1 - Pages 556-561, Masanori Mishima and Michael Glotzer

Desmosomes and Hemidesmosomes; Vol.1 - Pages 569-576, Rachel L. Dusek, Jonathan C. R. Jones and Kathleen J. Green

Dynactin; Vol.1 - Pages 823-826, Trina A. Schroer

Dynein; Vol.1 - Pages 827-831, K. Kevin Pfister

Endoplasmic Reticulum-Associated Protein Degradation; Vol.2 - Pages 20-23, Maurizio Molinari

Focal Adhesions; Vol.2 - Pages 128-133, Eli Zamir and Benjamin Geiger

Golgi Complex; Vol.2 - Pages 312-315, Mark Stamnes

Heat/Stress Responses; Vol.2 - Pages 343-347, Davis T. W. Ng

Inositol Lipid 3-Phosphatases; Vol.2 - Pages 421-426, Gregory S. Taylor and Jack E. Dixon

Intermediate Filament Linker Proteins: Plectin and BPAG1; Vol.2 - Pages 452-457, Peter Fuchs and Gerhard Wiche

Intermediate Filaments; Vol.2 - Pages 458-464, Kelsie M. Bernot and Pierre A. Coulombe

Keratins and the Skin; Vol.2 - Pages 497-504, Pierre A. Coulombe and Kelsie M. Bernot

Kinesin Superfamily Proteins; Vol.2 - Pages 508-516, Nobutaka Hirokawa and Reiko Takemura

Kinesins as Microtubule Disassembly Enzymes; Vol.2 - Pages 517-521, Susan L. Kline-Smith and Arshad Desai

Meiosis; Vol.2 - Pages 610-616, Neil Hunter

Metalloproteinases, Matrix; Vol.2 - Pages 657-665, Hideaki Nagase and Gillian Murphy

Microtubule-Associated Proteins; Vol.2 - Pages 676-682, Nobutaka Hirokawa and Reiko Takemura

Mitosis; Vol.2 - Pages 743-747, Patricia Wadsworth and Nasser M. Rusan

Myosin Motors; Vol.2 - Pages 778-781, Roy E. Larson

N-End Rule; Vol.3 - Pages 6-10, Alexander Varshavsky

Neuronal Intermediate Filaments; Vol.3 - Pages 21-25, Ronald K. H. Liem

Nuclear Compartmentalization; Vol.3 - Pages 87-91, Kelly P. Smith and Jeanne B. Lawrence

Nuclear Envelope and Lamins; Vol.3 - Pages 92-95, Bryce M. Paschal

Nuclear Pores and Nuclear Import/Export; Vol.3 - Pages 109-114, Anita H. Corbett

Peroxisomes; Vol.3 - Pages 246-250, Suresh Subramani

26S Proteasome, Structure and Function; Vol.3 - Pages 469-473, Peter Zwickl and Wolfgang Baumeister

Protein Glycosylation, Overview; Vol.3 - Pages 504-509, Natasha E. Zachara and Gerald W. Hart

Rho GTPases and Actin Cytoskeleton Dynamics; Vol.3 - Pages 714-718, Priam Villalonga and Anne J. Ridley

Septins and Cytokinesis; Vol.4 - Pages 22-26, Makoto Kinoshita and Christine M. Field

SUMO Modification; Vol.4 - Pages 130-134, Frauke Melchior and Andrea Pichler

Tight Junctions; Vol.4 - Pages 187-189, Shoichiro Tsukita

Transcriptional Silencing; Vol.4 - Pages 200-203, Ann Sutton and Rolf Sternglanz

Tubulin and its Isoforms; Vol.4 - Pages 272-276, Eva Nogales

Unfolded Protein Responses; Vol.4 - Pages 319-325, David Ron

Vacuoles; Vol.4 - Pages 331-336, Christopher J. Stefan and Scott D. Emr

Protein/Enzyme Structure Function and Degradation

Allosteric Regulation; Vol.1 - Pages 68-73, Barry S. Cooperman

Aminopeptidases; Vol.1 - Pages 96-98, Ralph A. Bradshaw

Amyloid; Vol.1 - Pages 99-104, Ronald Wetzel

Aspartic Proteases; Vol.1 - Pages 123-127, Ben M. Dunn

B12-Containing Enzymes; Vol.1 - Pages 145-151, Vahe Bandarian and Rowena G. Matthews

Biotin; Vol.1 - Pages 174-178, Steven W. Polyak and Anne Chapman-Smith

Biotinylation of Proteins; Vol.1 - Pages 179-181, Ronald A. Kohanski

Calpain; Vol.1 - Pages 300-306, Hiroyuki Sorimachi and Yasuko Ono

Chemiluminescence and Bioluminescence; Vol.1 - Pages 399-404, Thomas O. Baldwin

Coenzyme A; Vol.1 - Pages 475-477, M. Daniel Lane

Collagenases; Vol.1 - Pages 478-481, Kenn Holmbeck and Henning Birkedal-Hansen

Collagens; Vol.1 - Pages 482-487, Darwin J. Prockop

Cysteine Proteases; Vol.1 - Pages 516-520, David J. Buttle and John S. Mort

Disulfide Bond Formation; Vol.1 - Pages 598-602, Hiram F. Gilbert

Elastin; Vol.2 - Pages 10-12, Judith Ann Foster

Enzyme Inhibitors; Vol.2 - Pages 31-37, Vern L. Schramm

Enzyme Kinetics; Vol.2 - Pages 38-44, Irwin H. Segel

Enzyme Reaction Mechanisms: Stereochemistry; Vol.2 - Pages 45-50, Ming-Daw Tsai, Li Zhao and Brandon J. Lamarche

Flavins; Vol.2 - Pages 118-122, Barrie Entsch and David P. Ballou

Heme Proteins; Vol.2 - Pages 354-361, Johannes Everse

HIV Protease; Vol.2 - Pages 384-387, Ben M. Dunn

Kinetic Isotope Effects; Vol.2 - Pages 522-527, Justine P. Roth and Judith P. Klinman

Lipid Modification of Proteins: Targeting to Membranes; Vol.2 - Pages 580-583, Marilyn D. Resh

Low Barrier Hydrogen Bonds; Vol.2 - Pages 594-598, Perry A. Frey

Metalloproteases; Vol.2 - Pages 652-656, David S. Auld

Peptide Amidation; Vol.3 - Pages 226-230, Mark J. Niciu, Richard E. Mains and Betty A. Eipper

Phage Display for Protein Binding; Vol.3 - Pages 251-255, Henry B. Lowman

Prions, Overview; Vol.3 - Pages 437-440, Cedric Govaerts and Fred E. Cohen

Proteases in Blood Clotting; Vol.3 - Pages 457-463, John D. Kulman and Earl W. Davie

Proteasomes, Overview; Vol.3 - Pages 464-468, Martin Rechsteiner

Protein Carboxyl Esterification; Vol.3 - Pages 474-477, Shilpa G. Lalchandani and Jeffry B. Stock

Protein Degradation; Vol.3 - Pages 484-492, Tomo ari and Alfred L. Goldberg

Protein Folding and Assembly; Vol.3 - Pages 493-499, David P. Goldenberg

Protein N-Myristoylation; Vol.3 - Pages 527-531, Erica Dutil Sonnenburg and Jeffrey I. Gordon

Protein Palmitoylation; Vol.3 - Pages 532-535, Robert J. Deschenes

Pteridines; Vol.3 - Pages 556-560, S. Colette Daubner and Paul F. Fitzpatrick

Pyridoxal Phosphate; Vol.3 - Pages 595-599, David E. Metzler

Regulated Intramembrane Proteolysis (Rip); Vol.3 - Pages 665-670, Jin Ye, Michael S. Brown and Joseph L. Goldstein

Secretases; Vol.4 - Pages 7-10, Robert L. Heinrikson

Selenoprotein Synthesis; Vol.4 - Pages 17-21, August Bock

Substrate Binding, Catalysis, and Product Release; Vol.4 - Pages 123-126, W. Wallace Cleland

Two-Hybrid Protein–Protein Interactions; Vol.4 - Pages 290-293, Ilya Serebriiskii and Erica A. Golemis

Tyrosine Sulfation; Vol.4 - Pages 294-297, Denis Corbeil and Wieland B. Huttner

Ubiquitin System; Vol.4 - Pages 299-303, Aaron Ciechanover and Michael H. Glickman

Ubiquitin-Like Proteins; Vol.4 - Pages 304-307, Edward T. H. Yeh

Zinc Fingers; Vol.4 - Pages 435-439, Mark Isalan

Bioenergetics

ABC Transporters; Vol.1 - Pages 1-5, Andre Goffeau, Benoit De Hertogh and Philippe V. Baret

Amine Oxidases; Vol.1 - Pages 85-89, Giovanni Floris and Alessandro Finazzi Agro

ATP Synthesis in Plant Mitochondria: Substrates, Inhibitors, Uncouplers; Vol.1 - Pages 128-132, Kathleen L. Soole and R. Ian Menz

ATP Synthesis: Mitochondrial Cyanide-Resistant Terminal Oxidases; Vol.1 - Pages 133-137, James N. Siedow

Bioenergetics: General Definition of Principles; Vol.1 - Pages 170-173, David G. Nicholls

Calcium Buffering Proteins: Calbindin; Vol.1 - Pages 221-225, Willi Hunziker and Igor Bendik

Calcium Buffering Proteins: ER Luminal Proteins; Vol.1 - Pages 226-230, Jody Groenendyk and Marek Michalak

Calcium Oscillations; Vol.1 - Pages 231-234, Marisa Brini

Calcium Sensing Receptor; Vol.1 - Pages 235-240, Jacob Tfelt-Hansen and Edward M. Brown

Calcium Signaling: Calmodulin-Dependent Phosphatase; Vol.1 - Pages 241-245, Claude Klee, Hao Ren and Shipeng Li

Calcium Signaling: Cell Cycle; Vol.1 - Pages 246-249, Luigia Santella

Calcium Signaling: Motility (Actomyosin–Troponin System); Vol.1 - Pages 250-255, Takeyuki Wakabayashi and Setsuro Ebashi

Calcium Signaling: NO Synthase; Vol.1 - Pages 256-260, Zhi-Qiang Wang and Dennis J. Stuehr

Calcium Transport in Mitochondria; Vol.1 - Pages 261-266, Rosario Rizzuto and Marisa Brini

Calcium Waves; Vol.1 - Pages 267-269, Lionel F. Jaffe

Calcium, Biological Fitness of; Vol.1 - Pages 270-273, Robert J. P. Williams

Calcium/Calmodulin-Dependent Protein Kinase II; Vol.1 - Pages 274-280, Andy Hudmon and Howard Schulman

Calcium-Binding Proteins: Cytosolic (Annexins, Gelsolins, C2-Domain Proteins); Vol.1 - Pages 287-293, Joachim Krebs

Calcium-Modulated Proteins (EF-Hand); Vol.1 - Pages 294-299, Robert H. Kretsinger

Cell Death by Apoptosis and Necrosis; Vol.1 - Pages 352-355, Pierluigi Nicotera

Chemiosmotic Theory; Vol.1 - Pages 405-412, Keith D. Garlid

Chemolithotrophy; Vol.1 - Pages 419-424, Alan B. Hooper

Chlorophylls and Carotenoids; Vol.1 - Pages 430-437, Hugo Scheer

Chloroplast Redox Poise and Signaling; Vol.1 - Pages 438-445, John F. Allen

Chloroplasts; Vol.1 - Pages 446-450, Nicoletta Rascio

Cytochrome b6f Complex; Vol.1 - Pages 521-527, Gunter A. Hauska and Thomas Schodl

Cytochrome bc1 Complex (Respiratory Chain Complex III); Vol.1 - Pages 528-534, Bernard L. Trumpower

Cytochrome c; Vol.1 - Pages 535-538, Hans Tuppy and Gunther Kreil

Cytochrome Oxidases, Bacterial; Vol.1 - Pages 539-543, Peter Brzezinski and Pia Adelroth

Cytochrome P-450; Vol.1 - Pages 544-549, Rita Bernhardt

Energy Transduction in Anaerobic Prokaryotes; Vol.2 - Pages 24-30, Gottfried Unden

ER/SR Calcium Pump: Function; Vol.2 - Pages 56-60, Giuseppe Inesi

ER/SR Calcium Pump: Structure; Vol.2 - Pages 61-65, Chikashi Toyoshima and Yuji Sugita

F1–F0 ATP Synthase; Vol.2 - Pages 73-79, Donata Branca

Ferredoxin; Vol.2 - Pages 104-106, Giuliana Zanetti and Vittorio Pandini

Ferredoxin-NADP+ Reductase; Vol.2 - Pages 107-111, Giuliana Zanetti and Alessandro Aliverti

Free Radicals, Sources and Targets of: Mitochondria; Vol.2 - Pages 134-142, Alberto Boveris and Enrique Cadenas

Friedreich's Ataxia; Vol.2 - Pages 143-145, Paul E. Hart and Anthony H. V. Schapira

Giant Mitochondria (Megamitochondria); Vol.2 - Pages 186-188, Bernard Tandler and Charles L. Hoppel

Glutathione Peroxidases; Vol.2 - Pages 224-228, Fulvio Ursini and Matilde Maiorino

Green Bacteria: Secondary Electron Donor (Cytochromes); Vol.2 - Pages 321-324, Hirozo Oh-oka and Robert E. Blankenship

Green Bacteria: The Light-Harvesting Chlorosome; Vol.2 - Pages 325-330, John M. Olson

Green Sulfur Bacteria: Reaction Center and Electron Transport; Vol.2 - Pages 331-336, Gunter A. Hauska and Thomas Schodl

Heme Synthesis; Vol.2 - Pages 362-366, Gloria C. Ferreira

Intracellular Calcium Channels: cADPR-Modulated (Ryanodine Receptors); Vol.2 - Pages 465-468, Antony Galione

Intracellular Calcium Channels: NAADP+-Modulated; Vol.2 - Pages 469-472, Armando A. Genazzani and Marcella Debidda

IP3 Receptors; Vol.2 - Pages 478-481, Colin W. TaylorEdward Morris and Paula da Fonseca

Iron–Sulfur Proteins; Vol.2 - Pages 482-489, Helmut Beinert, Jacques Meyer and Roland Lill

Ligand-Operated Membrane Channels: Calcium (Glutamate); Vol.2 - Pages 551-561, Elias K. Michaelis

Ligand-Operated Membrane Channels: GABA; Vol.2 - Pages 562-566, F. Minier and Erwin Sigel

Light-Harvesting Complex (LHC) I and II: Pigments and Proteins; Vol.2 - Pages 567-570, Stefan Jansson

Luft's Disease; Vol.2 - Pages 599-601, Salvatore DiMauro

Membrane Transport, General Concepts; Vol.2 - Pages 627-630, Stanley G. Schultz

Membrane Transporters:Na+/Ca2+ Exchangers; Vol.2 - Pages 631-636, Jonathan Lytton

Membrane-Associated Energy Transduction in Bacteria and Archaea; Vol.2 - Pages 637-645, Gunter Schafer

Metabolite Channeling: Creatine Kinase Microcompartments; Vol.2 - Pages 646-651, Uwe Schlattner and Theo Wallimann

Mitochondrial Auto-Antibodies; Vol.2 - Pages 683-688, Harold Baum

Mitochondrial Channels; Vol.2 - Pages 689-692, M. Catia Sorgato and Alessandro Bertoli

Mitochondrial DNA; Vol.2 - Pages 693-696, Gottfried Schatz

Mitochondrial Genes and their Expression: Yeast; Vol.2 - Pages 697-702, Piotr P. Slonimski and Giovanna Carignani

Mitochondrial Genome, Evolution; Vol.2 - Pages 703-708, B. Franz Lang, Dennis V. Lavrov and Gertraud Burger

Mitochondrial Genome, Overview; Vol.2 - Pages 709-715, Douglas C. Wallace

Mitochondrial Inheritance; Vol.2 - Pages 716-719, Eric A. Shoubridge

Mitochondrial Membranes, Structural Organization; Vol.2 - Pages 720-724, Carmen A. Mannella

Mitochondrial Metabolite Transporter Family; Vol.2 - Pages 725-732, Ferdinando Palmieri and Martin Klingenberg

Mitochondrial Outer Membrane and the VDAC Channel; Vol.2 - Pages 733-736, Marco Colombini

Neuronal Calcium Signal; Vol.3 - Pages 16-20, Hilmar Bading

Nicotinamide Nucleotide Transhydrogenase; Vol.3 - Pages 50-56, Jan Rydstrom

Nuclear Genes in Mitochondrial Function and Biogenesis; Vol.3 - Pages 100-104, Alexander Tzagoloff and Carol L. Dieckmann

Oncocytes; Vol.3 - Pages 165-166, Bernard Tandler and Charles L. Hoppel

Oxygenases; Vol.3 - Pages 178-182, Osamu Hayaishi

Periplasmic Electron Transport Systems in Bacteria; Vol.3 - Pages 231-238, David J. Richardson, Gary Sawers and Rob J. M. Van Spanning

Phosphatidylinositol-3-Phosphate; Vol.3 - Pages 272-276, Joseph V. Virbasius and Michael P. Czech

Photosystem I, Structure and Function; Vol.3 - Pages 342-347, Petra Fromme

Photosystem I: FX, FA, and FB Iron–Sulfur Clusters; Vol.3 - Pages 348-356, Mikhail L. Antonkine and John H. Golbeck

Photosystem II Light Harvesting System: Dynamic Behavior; Vol.3 - Pages 357-362, Peter Horton and Alexander Ruban

Photosystem II: Assembly and Turnover of the D1 Protein; Vol.3 - Pages 363-366, Eira Kanervo and Eva-Mari Aro

Photosystem II: Protein Components; Vol.3 - Pages 367-374, James Barber

Photosystem II: Water Oxidation, Overview; Vol.3 - Pages 375-380, Fabrice Rappaport and Pierre Joliot

Plasma-Membrane Calcium Pump: Structure and Function; Vol.3 - Pages 385-389, Emanuel E. Strehler

Plastocyanin; Vol.3 - Pages 390-393, Elizabeth L. Gross

Protein Import into Mitochondria; Vol.3 - Pages 510-515, Johannes M. Herrmann and Walter Neupert

P-Type Pumps: Copper Pump; Vol.3 - Pages 561-564, Ilia Voskoboinik and James Camakaris

P-Type Pumps: H+/K+ Pump; Vol.3 - Pages 565-570, Jai Moo Shin and George Sachs

P-Type Pumps: Na+/K+ Pump; Vol.3 - Pages 571-576, Peter L. Jorgensen

P-Type Pumps: Plasma-Membrane H+ Pump; Vol.3 - Pages 577-581, A. Brett Mason and Carolyn W. Slayman

Purple Bacteria: Electron Acceptors and Donors; Vol.3 - Pages 582-585, Evaldas Katilius and Neal W. Woodbury

Purple Bacteria: Photosynthetic Reaction Centers; Vol.3 - Pages 586-594, C. Roy D. Lancaster

Pyrimidine Biosynthesis; Vol.3 - Pages 600-605, Monika Loffler and Elke Zameitat

Quinones; Vol.3 - Pages 621-627, Giorgio Lenaz and Maria Luisa Genova

Respiratory Chain and ATP Synthase; Vol.3 - Pages 671-675, David G. Whitehouse and Anthony L. Moore

Respiratory Chain Complex I; Vol.3 - Pages 676-680, Ulrich Brandt

Respiratory Chain Complex II and Succinate: Quinone Oxidoreductases; Vol.3 - Pages 681-687, C. Roy D. Lancaster

Respiratory Chain Complex IV; Vol.3 - Pages 688-694, Hartmut Michel

Respiratory Processes in Anoxygenic and Oxygenic Phototrophs; Vol.3 - Pages 695-699, Roberto Borghese and Davide Zannoni

Spastic Paraplegia; Vol.4 - Pages 61-66, Elena Irene Rugarli and Andrea Ballabio

Store-Operated Membrane Channels: Calcium; Vol.4 - Pages 117-122, Indu S. Ambudkar

Superoxide Dismutase; Vol.4 - Pages 135-138, Irwin Fridovich

Uncoupling Proteins; Vol.4 - Pages 313-318, Daniel Ricquier and Frederic Bouillaud

V-ATPases; Vol.4 - Pages 349-353, Michael Forgac

Voltage-Dependent K+ Channels; Vol.4 - Pages 399-404, Ramon Latorre and Francisco J. Morera

Voltage-Sensitive Ca2+ Channels; Vol.4 - Pages 405-408, Harald Reuter

Voltage-Sensitive Na+ Channels; Vol.4 - Pages 409-415, William J. Brammar

Molecular Biology

Alternative Splicing: Regulation of Fibroblast Growth Factor Receptor (FGFR); Vol.1 - Pages 74-77, Mariano A. Garcia-Blanco

Alternative Splicing: Regulation of Sex Determination in Drosophila melanogaster; Vol.1 - Pages 78-84, Jill K. M. Penn, Patricia Graham and Paul Schedl

ara Operon; Vol.1 - Pages 116-119, Robert F. Schleif

Chromatin Remodeling; Vol.1 - Pages 456-463, Eric Kallin and Yi Zhang

Chromatin: Physical Organization; Vol.1 - Pages 464-468, Christopher L. Woodcock

DNA Base Excision Repair; Vol.1 - Pages 603-608, Hilde Nilsen and Tomas Lindahl

DNA Damage: Alkylation; Vol.1 - Pages 609-613, Anton B. Guliaev and B. Singer

DNA Glycosylases: Mechanisms; Vol.1 - Pages 614-617, Daniel J. Krosky and James T. Stivers

DNA Helicases: Dimeric Enzyme Action; Vol.1 - Pages 618-623, Timothy M. Lohman

DNA Helicases: HexamericEnzyme Action; Vol.1 - Pages 624-631, Smita S. Patel

DNA Ligases: Mechanism and Functions; Vol.1 - Pages 632-636, Alan E. Tomkinson and John B. Leppard

DNA Ligases: Structures; Vol.1 - Pages 637-643, C. Kiong Ho, Mark Odell and Dimitar B. Nikolov

DNA Methyltransferases, Bacterial; Vol.1 - Pages 644-651, Albert Jeltsch and Richard I. Gumport

DNA Methyltransferases, Structural Themes; Vol.1 - Pages 652-659, Sanjay Kumar

DNA Methyltransferases: Eubacterial GATC; Vol.1 - Pages 660-664, Martin G. Marinus

DNA Mismatch Repair and Homologous Recombination; Vol.1 - Pages 665-670, Ivan Matic and Miroslav Radman

DNA Mismatch Repair and the DNA Damage Response; Vol.1 - Pages 671-674, Guo-Min Li and Steven R. Presnell

DNA Mismatch Repair Defects and Cancer; Vol.1 - Pages 675-681, Richard D. Kolodner

DNA Mismatch Repair in Bacteria; Vol.1 - Pages 682-686, A-Lien Lu

DNA Mismatch Repair in Mammals; Vol.1 - Pages 687-690, James T. Drummond

DNA Mismatch Repair: E. coli Vsr and Eukaryotic G–T Systems; Vol.1 - Pages 691-693, Margaret Lieb

DNA Oxidation; Vol.1 - Pages 694-697, Arthur P. Grollman and Dmitry O. Zharkov

DNA Photolyase; Vol.1 - Pages 698-702, Carrie L. Partch and Aziz Sancar

DNA Polymerase α, Eukaryotic; Vol.1 - Pages 703-707, Teresa S. -F. Wang

DNA Polymerase β, Eukaryotic; Vol.1 - Pages 708-712, William A. Beard and Samuel H. Wilson

DNA Polymerase δ, Eukaryotic; Vol.1 - Pages 713-715, Antero G. So and Kathleen M. Downey

DNA Polymerase ε, Eukaryotic; Vol.1 - Pages 716-719, Yasuo Kawasaki and Akio Sugino

DNA Polymerase I, Bacterial; Vol.1 - Pages 720-725, Catherine M. Joyce

DNA Polymerase II, Bacterial; Vol.1 - Pages 726-728, Judith L. Campbell

DNA Polymerase III, Bacterial; Vol.1 - Pages 729-733, Hisaji Maki

DNA Polymerases: Kinetics and Mechanism; Vol.1 - Pages 734-739, Kenneth A. Johnson

DNA Replication Fork, Bacterial; Vol.1 - Pages 740-744, Nancy G. Nossal

DNA Replication Fork, Eukaryotic; Vol.1 - Pages 745-748, Lori M. Kelman, Jerard Hurwitz and Zvi Kelman

DNA Replication, Mitochondrial; Vol.1 - Pages 749-752, David A. Clayton

DNA Replication: Eukaryotic Origins and the Origin Recognition Complex; Vol.1 - Pages 753-760, Melvin L. DePamphilis and Cong-jun Li

DNA Replication: Initiation in Bacteria; Vol.1 - Pages 761-766, Jon M. Kaguni

DNA Restriction and Modification: Type I Enzymes; Vol.1 - Pages 767-771, David T. F. Dryden

DNA Restriction and Modification: Type II Enzymes; Vol.1 - Pages 772-777, Darren M. Gowers and Stephen E. Halford

DNA Restriction and Modification: Type III Enzymes; Vol.1 - Pages 778-781, Desirazu N. Rao and S. Srivani

DNA Secondary Structure; Vol.1 - Pages 782-787, Albino Bacolla and Robert D. Wells

DNA Sequence Recognition by Proteins; Vol.1 - Pages 788-793, Arabela A. Grigorescu and John M. Rosenberg

DNA Supercoiling; Vol.1 - Pages 794-797, Tao-shih Hsieh

DNA Topoisomerases: Type I; Vol.1 - Pages 798-805, James J. Champoux

DNA Topoisomerases: Type II; Vol.1 - Pages 806-811, Renier Velez-Cruz and Neil Osheroff

DNA Topoisomerases: Type III–RecQ Helicase Systems; Vol.1 - Pages 812-816, Rodney Rothstein and Erika Shor

EF-G and EF-Tu Structures and Translation Elongation in Bacteria; Vol.2 - Pages 1-5, Poul Nissen and Jens Nyborg

Exonucleases, Bacterial; Vol.2 - Pages 66-72, Susan T. Lovett

HIV-1 Reverse Transcriptase Structure; Vol.2 - Pages 388-392, Kalyan Das, Stefan G. Sarafianos, Eddy Arnold and Stephen H. Hughes

Homologous Recombination in Meiosis; Vol.2 - Pages 393-397, Nancy M. Hollingsworth

lac Operon; Vol.2 - Pages 529-534, Liskin Swint-Kruse and Kathleen S. Matthews

LexA Regulatory System; Vol.2 - Pages 546-550, Veronica G. Godoy, Penny J. Beuning and Graham C. Walker

Metaphase Chromosome; Vol.2 - Pages 666-671, Sharron Vass and Margarete M. S. Heck

Methyl-CpG-Binding Proteins; Vol.2 - Pages 672-675, David G. Skalnik

mRNA Polyadenylation in Eukaryotes; Vol.2 - Pages 748-752, Mary Edmonds

mRNA Processing and Degradation in Bacteria; Vol.2 - Pages 753-757, Deborah A. Steege

Non-Homologous End Joining; Vol.3 - Pages 66-70, Penny A. Jeggo

Nonhomologous Recombination: Bacterial Transposons; Vol.3 - Pages 71-79, Bao Ton Hoang and Michael G. Chandler

Nonhomologous Recombination: Retrotransposons; Vol.3 - Pages 80-86, Siew Loon Ooi and Jef D. Boeke

Nuclear Organization, Chromatin Structure, and Gene Silencing; Vol.3 - Pages 105-108, Lori L. Wallrath, John R. Danzer, Oya Yazgan and Pamela K. Geyer

Nucleoid Organization of Bacterial Chromosomes; Vol.3 - Pages 115-118, Charles J. Dorman

Nucleolus, Overview; Vol.3 - Pages 119-122, Thoru Pederson

Nucleotide Excision Repair and Human Disease; Vol.3 - Pages 123-129, James E. Cleaver

Nucleotide Excision Repair in Eukaryotes; Vol.3 - Pages 130-133, Laura A. Lindsey-Boltz and Aziz Sancar

Nucleotide Excision Repair, Bacterial: The UvrABCD System; Vol.3 - Pages 134-142, Bennett Van Houten and Lawrence Grossman

Nucleotide Excision Repair: Biology; Vol.3 - Pages 143-147, Errol C. Friedberg

PHO Regulon; Vol.3 - Pages 262-265, Bengt L. Persson

Pre-tRNA and Pre-rRNA Processing in Bacteria; Vol.3 - Pages 420-424, Sidney R. Kushner

Pre-tRNA and Pre-rRNA Processing in Eukaryotes; Vol.3 - Pages 425-431, Hendrik A. Raue

Prions and Epigenetic Inheritance; Vol.3 - Pages 432-436, Reed B. Wickner

Processivity Clamps in DNA Replication: Clamp Loading; Vol.3 - Pages 441-446, Megan J. Davey and Mike O'Donnell

Recombination: Heteroduplexand Mismatch Repair in vitro; Vol.3 - Pages 645-648, Leroy Worth, Jr.

Recombination: Strand Transferases; Vol.3 - Pages 649-653, Floyd R. Bryant

Recombination-Dependent DNA Replication; Vol.3 - Pages 654-659, Kenneth N. Kreuzer

recQ DNA Helicase Family in Genetic Stability; Vol.3 - Pages 660-664, Mary A. Risinger and Joanna Groden

Reverse Transcriptase and Retroviral Replication; Vol.3 - Pages 708-713, Laura Tarrago-Litvak, Marie-Line Andreola and Simon Litvak

Ribosome Assembly; Vol.3 - Pages 719-724, John L. Woolford

Ribosome Structure; Vol.3 - Pages 725-732, Brian T. Wimberly

Ribozyme Mechanisms; Vol.3 - Pages 733-737, John Hsieh and Carol A. Fierke

Ribozyme Structural Elements: Group I Introns; Vol.3 - Pages 738-742, Barbara L. Golden

Ribozyme Structural Elements: Hairpin Ribozyme; Vol.3 - Pages 743-746, Adrian R. Ferre-D'Amare

Ribozymes and Evolution; Vol.3 - Pages 747-752, Niles Lehman

RNA Editing; Vol.3 - Pages 753-758, Charles E. Samuel

RNA Polymerase I and RNA Polymerase III in Eukaryotes; Vol.3 - Pages 759-762, Robert J. White

RNA Polymerase II and Basal Transcription Factors in Eukaryotes; Vol.3 - Pages 763-765, Joan Weliky Conaway and Ronald C. Conaway

RNA Polymerase II Elongation Control in Eukaryotes; Vol.3 - Pages 766-769, David H. Price

RNA Polymerase II Structure in Eukaryotes; Vol.3 - Pages 770-774, Patrick Cramer

RNA Polymerase Reaction in Bacteria; Vol.3 - Pages 775-780, Arkady A. Mustaev and Alexander D. Goldfarb

RNA Polymerase Structure, Bacterial; Vol.3 - Pages 781-784, Michael Anikin, Dmitri Temiakov and William T. McAllister

Sigma Factors; Vol.4 - Pages 41-44, John D. Helmann

Sliding Clamps in DNA Replication: E. coli -Clamp and PCNA Structure; Vol.4 - Pages 45-47, Eric R. Goedken and John Kuriyan

Spliceosome; Vol.4 - Pages 88-92, Timothy W. Nilsen

T7 RNA Polymerase; Vol.4 - Pages 147-151, Rui Sousa

Telomeres: Maintenance and Replication; Vol.4 - Pages 174-179, Alessandro Bianchi and David Shore

Transcription Termination; Vol.4 - Pages 195-199, Thomas J. Santangelo and Jeffrey W. Roberts

Transcription-Coupled DNA Repair, Overview; Vol.4 - Pages 204-208, Isabel Mellon

Translation Elongation in Bacteria; Vol.4 - Pages 214-223, Oliver Vesper and Knud H. Nierhaus

Translation Elongation in Eukaryotes; Vol.4 - Pages 224-229, William C. Merrick and Anton A. Komar

Translation Initiation in Bacteria: Factors and Mechanisms; Vol.4 - Pages 230-236, Cynthia L. Pon and Claudio O. Gualerzi

Translation Initiation in Eukaryotes: Factors and Mechanisms; Vol.4 - Pages 237-241, Tatyana V. Pestova and Christopher U. T. Hellen

Translation Termination and Ribosome Recycling; Vol.4 - Pages 242-246, Nadja Koloteva-Levin and Mick F. Tuite

Translesion DNA Polymerases, Eukaryotic; Vol.4 - Pages 247-250, Alexandra Vaisman and Roger Woodgate

tRNA Synthetases; Vol.4 - Pages 263-266, Karla L. Ewalt and Paul Schimmel

trp Operon and Attenuation; Vol.4 - Pages 267-271, Paul Gollnick

UmuC, D Lesion Bypass DNA Polymerase V; Vol.4 - Pages 308-312, Zvi Livneh

XPV DNA Polymerase and Ultraviolet Damage Bypass; Vol.4 - Pages 419-421, Alan R. Lehmann

Yeast GAL1–GAL10 System; Vol.4 - Pages 429-433, Dennis Lohr and Ralph Bash

Signaling

Abscisic Acid (ABA); Vol.1 - Pages 6-11, Ramanjulu Sunkar and Jian-Kang Zhu

Adenosine Receptors; Vol.1 - Pages 34-39, Lauren J. Murphree and Joel Linden

Adenylyl Cyclases; Vol.1 - Pages 40-45, Ronald Taussig

Adrenergic Receptors; Vol.1 - Pages 46-50, David B. Bylund

A-Kinase Anchoring Proteins; Vol.1 - Pages 64-67, Lorene K. Langeberg and John D. Scott

Angiotensin Receptors; Vol.1 - Pages 111-115, Tadashi Inagami

ARF Family; Vol.1 - Pages 120-122, Gustavo Pacheco-Rodriguez, Joel Moss and Martha Vaughan

B-Cell Antigen Receptor; Vol.1 - Pages 155-158, Thomas M. Yankee and Edward A. Clark

Bradykinin Receptors; Vol.1 - Pages 182-185, Ronald M. Burch

Brassinosteroids; Vol.1 - Pages 192-197, Steven D. Clouse

Cadherin Signaling; Vol.1 - Pages 199-204, David B. Sacks and Jonathan M. G. Higgins

Calcitonin Gene-Related Peptide and Adrenomedullin Receptors; Vol.1 - Pages 212-216, Debbie L. Hay, Alex C. Conner and David R. Poyner

Calcitonin Receptor; Vol.1 - Pages 217-220, Samia I. Girgis, Niloufar Moradi-Bidhendi, Lucia Mancini and Iain MacIntyre

Calcium/Calmodulin-Dependent Protein Kinases; Vol.1 - Pages 281-286, J. Robison and Roger J. Colbran

c-fes Proto-Oncogene; Vol.1 - Pages 377-382, Thomas E. Smithgall and Robert I. Glazer

Chemokine Receptors; Vol.1 - Pages 413-418, Ann Richmond and Guo-Huang Fan

Chemotactic Peptide/Complement Receptors; Vol.1 - Pages 425-429, Eric R. Prossnitz and Larry A. Sklar

Cyclic AMP Receptors of Dictyostelium; Vol.1 - Pages 488-493, Dale Hereld and Peter N. Devreotes

Cyclic GMP Phosphodiesterases; Vol.1 - Pages 494-500, Sharron H. Francis and Jackie D. Corbin

Cyclic Nucleotide Phosphodiesterases; Vol.1 - Pages 501-505, Vincent C. Manganiello and Eva Degerman

Cyclic Nucleotide-Dependent Protein Kinases; Vol.1 - Pages 506-511, Sharron H. Francis and Jackie D. Corbin

Cyclic Nucleotide-Regulated Cation Channels; Vol.1 - Pages 512-515, Martin Biel and Franz Hofmann

Cytokines; Vol.1 - Pages 550-555, Andrea L. Wurster and Michael J. Grusby

Cytokinin; Vol.1 - Pages 562-567, Thomas Schmulling

Diacylglycerol Kinases and Phosphatidic Acid Phosphatases; Vol.1 - Pages 593-597, Stephen M. Prescott and Matthew K. Topham

Dopamine Receptors; Vol.1 - Pages 817-822, Kim A. Neve

Eicosanoid Receptors; Vol.2 - Pages 6-9, Richard M. Breyer and Matthew D. Breyer

Endocannabinoids; Vol.2 - Pages 13-15, Daniele Piomelli

Epidermal Growth Factor Receptor Family; Vol.2 - Pages 51-55, Denis Tvorogov and Graham Carpenter

FAK Family; Vol.2 - Pages 80-84, Steven K. Hanks

Fatty Acid Receptors; Vol.2 - Pages 95-98, Christer Owman and Bjorn Olde

Fibroblast Growth Factor Receptors and Cancer-Associated Perturbations; Vol.2 - Pages 112-117, Marko Kornmann and Murray Korc

G Protein Signaling Regulators; Vol.2 - Pages 147-151, John H. Exton

G Protein-Coupled Receptor Kinases and Arrestins; Vol.2 - Pages 152-157, Jeffrey L. Benovic

G12/G13 Family; Vol.2 - Pages 158-161, Stefan Offermanns

GABAA Receptor; Vol.2 - Pages 162-166, Richard W. Olsen and Gregory W. Sawyer

GABAB Receptor; Vol.2 - Pages 167-170, S. J. Enna

Gi Family of Heterotrimeric G Proteins; Vol.2 - Pages 181-185, Maurine E. Linder

Glucagon Family of Peptides and their Receptors; Vol.2 - Pages 193-196, Laurie L. Baggio and Daniel J. Drucker

Glutamate Receptors, Ionotropic; Vol.2 - Pages 213-219, Derek B. Scott and Michael D. Ehlers

Glutamate Receptors, Metabotropic; Vol.2 - Pages 220-223, P. Jeffrey Conn

Glycine Receptors; Vol.2 - Pages 237-243, Bodo Laube and Heinrich Betz

Glycogen Synthase Kinase-3; Vol.2 - Pages 255-260, James R. Woodgett

Gq Family; Vol.2 - Pages 316-320, Wanling Yang and John D. Hildebrandt

Gs Family of Heterotrimeric G Proteins; Vol.2 - Pages 337-341, Susanne M. Mumby

Hematopoietin Receptors; Vol.2 - Pages 348-353, Barbara A. Miller and Joseph Y. Cheung

Hepatocyte Growth Factor/Scatter Factor Receptor; Vol.2 - Pages 367-371, Selma Pennacchietti and Paolo M. Comoglio

Histamine Receptors; Vol.2 - Pages 378-383, Stephen J. Hill and Jillian G. Baker

Immunoglobulin (Fc) Receptors; Vol.2 - Pages 411-416, Mark Hogarth

Inositol Phosphate Kinases and Phosphatases; Vol.2 - Pages 427-429, Stephen B. Shears

Insulin Receptor Family; Vol.2 - Pages 436-440, Paul F. Pilch and Jongsoon Lee

Integrin Signaling; Vol.2 - Pages 441-445, Lawrence E. Goldfinger and Mark H. Ginsberg

Interferon Receptors; Vol.2 - Pages 446-451, Christopher P. Elco and Ganes C. Sen

JAK-STAT Signaling Paradigm; Vol.2 - Pages 491-496, Edward Cha and Christian Schindler

Leptin; Vol.2 - Pages 541-545, Thomas W. Gettys

Lysophospholipid Receptors; Vol.2 - Pages 602-604, Gabor J. Tigyi

Melanocortin System; Vol.2 - Pages 617-620, Roger D. Cone

Mitogen-Activated Protein Kinase Family; Vol.2 - Pages 737-742, Hidemi Teramoto and J. Silvio Gutkind

Muscarinic Acetylcholine Receptors; Vol.2 - Pages 775-777, Neil M. Nathanson

Natriuretic Peptides and their Receptors; Vol.3 - Pages 1-5, Lincoln R. Potter

Neuropeptide Y Receptors; Vol.3 - Pages 26-31, Eric M. Parker

Neurotensin Receptors; Vol.3 - Pages 32-36, William Rostene, Patrick Kitabgi and Didier Pelaprat

Neurotransmitter Transporters; Vol.3 - Pages 37-40, Aurelio Galli, Randy D. Blakely and Louis J. DeFelice

Neurotrophin Receptor Signaling; Vol.3 - Pages 41-45, Jennifer J. Gentry and Bruce D. Carter

Nicotinic Acetylcholine Receptors; Vol.3 - Pages 57-61, Nivalda O. Rodrigues-Pinguet and Henry A. Lester

Nitric Oxide Signaling; Vol.3 - Pages 62-65, Michael A. Marletta

Nuclear Factor kappaB; Vol.3 - Pages 96-99, Thomas D. Gilmore

Olfactory Receptors; Vol.3 - Pages 149-154, Sigrun I. Korsching

Opioid Receptors; Vol.3 - Pages 167-171, P. Y. Law and Horace H. Loh

P2X Purinergic Receptors; Vol.3 - Pages 183-187, Annmarie Surprenant

P2Y Purinergic Receptors; Vol.3 - Pages 188-191, George R. Dubyak

p53 Protein; Vol.3 - Pages 192-195, Jamie Hearnes and Jennifer Pietenpol

p70 S6 Kinase/mTOR; Vol.3 - Pages 196-200, Christopher G. Proud

Parathyroid Hormone/Parathyroid Hormone-Related Protein Receptor; Vol.3 - Pages 201-207, Thomas J. Gardella

Peroxisome Proliferator-Activated Receptors; Vol.3 - Pages 239-245, Mary C. Sugden, Edward A. Sugden and Mark J. Holness

Pheromone Receptors (Yeast); Vol.3 - Pages 256-261, James B. Konopka and Jeremy W. Thorner

Phosphatidylinositol Bisphosphate and Trisphosphate; Vol.3 - Pages 266-271, Alex Toker

Phosphoinositide 3-Kinase; Vol.3 - Pages 281-286, Khatereh Ahmadi and Michael Waterfield

Phosphoinositide 4- and 5-Kinases and Phosphatases; Vol.3 - Pages 287-291, Shawn F. Bairstow, Matthew W. Bunce and Richard A. Anderson

Phosphoinositide-Dependent Protein Kinases; Vol.3 - Pages 292-296, Nick R. Leslie and C. Peter Downes

Phospholipase A2; Vol.3 - Pages 297-300, Timothy R. Smith and Edward A. Dennis

Phospholipase C; Vol.3 - Pages 301-305, Fujio Sekiya, Yeun Ju Kim and Sue Goo Rhee

Phospholipase D; Vol.3 - Pages 306-313, Mary M. LaLonde and Michael A. Frohman

Photoreceptors; Vol.3 - Pages 326-329, King-Wai Yau

Plant Signaling: Peptides; Vol.3 - Pages 381-384, Clarence A. Ryan and Gregory Pearce

Platelet-Activating Factor Receptor; Vol.3 - Pages 394-398, Katherine M. Howard and Merle S. Olson

Platelet-Derived Growth Factor Receptor Family; Vol.3 - Pages 399-406, Marina Kovalenko and Andrius Kazlauskas

Protein Kinase B; Vol.3 - Pages 516-522, Bettina A. Dummler and Brian A. Hemmings

Protein Kinase C Family; Vol.3 - Pages 523-526, Alexandra C. Newton

Protein Tyrosine Phosphatases; Vol.3 - Pages 536-542, David J. Pagliarini, Fred L. Robinson and Jack E. Dixon

Proteinase-Activated Receptors; Vol.3 - Pages 543-548, Kristina K. Hansen and Morley D. Hollenberg

Rab Family; Vol.3 - Pages 629-634, Mary W. McCaffrey and Andrew J. Lindsay

Ran GTPase; Vol.3 - Pages 635-639, Mary Shannon Moore

Ras Family; Vol.3 - Pages 640-644, Lawrence A. Quilliam

Retinoblastoma Protein (pRB); Vol.3 - Pages 700-703, Nicholas Dyson and Maxim Frolov

Retinoic Acid Receptors; Vol.3 - Pages 704-707, Martin Petkovich

Serine/Threonine Phosphatases; Vol.4 - Pages 27-32, Thomas S. Ingebritsen

Serotonin Receptor Signaling; Vol.4 - Pages 33-37, Paul J. Gresch and Elaine Sanders-Bush

Small GTPases; Vol.4 - Pages 48-54, Adam Shutes and Channing J. Der

Somatostatin Receptors; Vol.4 - Pages 55-60, Agnes Schonbrunn

Src Family of Protein Tyrosine Kinases; Vol.4 - Pages 93-98, Jonathan A. Cooper

Steroid/Thyroid Hormone Receptors; Vol.4 - Pages 111-116, Ramesh Narayanan and Nancy L. Weigel

Syk Family of Protein Tyrosine Kinases; Vol.4 - Pages 139-145, Andrew C. Chan

Tachykinin/Substance P Receptors; Vol.4 - Pages 152-157, Mark D. Richardson and Madan M. Kwatra

Taste Receptors; Vol.4 - Pages 158-161, John D. Boughter, Jr. and Steven D. Munger

T-Cell Antigen Receptor; Vol.4 - Pages 162-168, Andrea L. Szymczak and Dario A. A. Vignali

Tec/Btk Family Tyrosine Kinases; Vol.4 - Pages 169-173, Shuling Guo and Owen N. Witte

Thyroid-Stimulating Hormone/Luteinizing Hormone/Follicle-Stimulating Hormone Receptors; Vol.4 - Pages 180-186, Deborah L. Segaloff, Dario Mizrachi and Mario Ascoli

Toll-Like Receptors; Vol.4 - Pages 190-194, Himanshu Kumar, Kiyoshi Takeda and Shizuo Akira

Transforming Growth Factor-β Receptor Superfamily; Vol.4 - Pages 209-213, Mark de Caestecker

Tumor Necrosis Factor Receptors; Vol.4 - Pages 277-283, Karen G. Potter and Carl F. Ware

Vascular Endothelial Growth Factor Receptors; Vol.4 - Pages 337-342, Kenneth A. Thomas

Vasopressin/Oxytocin Receptor Family; Vol.4 - Pages 343-348, Michael J. Brownstein

Vitamin D Receptor; Vol.4 - Pages 378-383, Diane R. Dowd and Paul N. MacDonald

Von Hippel-Lindau (VHL) Protein; Vol.4 - Pages 416-418, Ronald C. Conaway and Joan Weliky Conaway

Techniques and Methodology

Affinity Chromatography; Vol.1 - Pages 51-56, Pedro Cuatrecasas and Meir Wilchek

Affinity Tags for Protein Purification; Vol.1 - Pages 57-63, Joseph J. Falke and John A. Corbin

Genome-Wide Analysis of Gene Expression; Vol.2 - Pages 175-180, Karine G. Le Roch and Elizabeth A. Winzeler

HPLC Separation of Peptides; Vol.2 - Pages 398-403, James D. Pearson

Imaging Methods; Vol.2 - Pages 405-410, Gyorgy Szabadkai and Rosario Rizzuto

Inorganic Biochemistry; Vol.2 - Pages 417-420, Robert J. P. Williams

Multiple Sequence Alignment and Phylogenetic Trees; Vol.2 - Pages 770-774, Russell F. Doolittle

Oligosaccharide Analysis by Mass Spectrometry; Vol.3 - Pages 155-160, Andrew J. Hanneman and Vernon N. Reinhold

PCR (Polymerase Chain Reaction); Vol.3 - Pages 208-210, Michael J. Brownstein

Polysialic Acid inMolecular Medicine; Vol.3 - Pages 407-414, Frederic A. Troy, II

Protein Data Resources; Vol.3 - Pages 478-483, Philip E. Bourne

Secondary Structure in Protein Analysis; Vol.4 - Pages 1-6, George D. Rose

Spectrophotometric Assays; Vol.4 - Pages 67-75, Britton Chance

Two-Dimensional Gel Electrophoresis; Vol.4 - Pages 284-289, Gerhard Schmid, Denis Hochstrasser and Jean-Charles Sanchez

X-Ray Determination of 3-D Structure in Proteins; Vol.4 - Pages 422-428, Martha L. Ludwig

ENCYCLOPEDIA OF
Biological Chemistry

Editors
William J. Lennarz
M. Daniel Lane

EF-G and EF-Tu Structures and Translation Elongation in Bacteria

Poul Nissen and Jens Nyborg
University of Aarhus, Aarhus, Denmark

The elongation cycle is the productive phase of protein biosynthesis. The genetic message in mRNA is a working transcript of a gene on DNA and it is translated one triplet codon at a time during this phase. Thereby, a specific amino acid sequence is synthesized and the final product represents a functional protein of the living cell. The translation is performed on the ribosome, which is a large complex of ribosomal RNA and ribosomal proteins. The ribosome is organized into two subunits, the large 50S subunit and the small 30S subunit. tRNA molecules provide amino acids for the protein biosynthesis and they are activated by the attachment to tRNA by an aminoacyl bond. During the elongation phase the ribosome is assisted by three elongation factors: (1) elongation factor Tu (EF-Tu), which brings to the ribosome amino-acylated tRNAs (aa-tRNAs) for decoding at the 30S subunit, (2) elongation factor G (EF-G), which assists the ribosome in translocating mRNA and tRNAs, and (3) elongation factor Ts (EF-Ts), which reactivates EF-Tu by exchanging its cofactor GDP for GTP. EF-Tu and EF-G are both G proteins that are active when GTP is bound as cofactor and inactive when GDP is bound. There is no nucleotide exchange factor for EF-G. The elongation phase and both EF-Tu and EF-G are surprisingly well preserved during evolution, for all living organisms. The proteins corresponding to EF-Ts are more complex in eukaryotes.

Elongation

The process by which the growing polypeptide on the ribosome is elongated by one amino acid according to the codon on mRNA involves the activities of the three elongation factors: EF-Tu, EF-Ts, and EF-G. EF-Tu in its active complex with GTP interacts with any aa-tRNA and prevents the spontaneous hydrolysis of the ester bond between the amino acid carboxyl acid moiety and the terminal 3′-ribose hydroxyls of the tRNA. EF-Tu in this so-called ternary complex interacts with the ribosome in its decoding activity where the correct match between the codon positioned in the decoding center of the 30S subunit and the anti-codon on tRNA is achieved. A signal is sent through as yet unknown routes to the 50S subunit, which reacts by inducing hydrolysis of GTP on EF-Tu at the GTPase center of the ribosome. EF-Tu in its GDP form undergoes a large conformational change and is released from the ternary complex and from the ribosome. The universal 3′-CCA end of tRNA is then free to swing into the peptidyl transferase center of the 50S subunit, where the formation of a new peptide bond between the growing polypeptide and the incoming amino acid is performed with the help of catalytic residues of the ribosomal RNA. The released EF-Tu:GDP is reactivated to EF-Tu:GTP with the help of the nucleotide exchange factor EF-Ts.

After peptidyl transfer the nascent polypeptide chain is attached to the incoming tRNA, with its anticodon still at the A site of the 30S subunit. It must be shifted to the P site together with the mRNA by exactly one codon. This is performed by EF-G in the translocation stage of elongation, where EF-G pushes the tRNA and the attached codon of the mRNA from the A site into the P site of the 30S subunit. After this the GTP of EF-G is hydrolyzed to GDP at the GTPase center of the ribosome, and EF-G:GDP is released. The high level of GTP in the cell and the relatively low affinity of GDP for EF-G is enough to ensure that EF-G reactivates into EF-G:GTP spontaneously, without the aid of a nucleotide exchange factor.

The ribosome has now completed one elongation cycle, and is left with a tRNA with its attached polypeptide in the P site of both the 50S and 30S subunits, and with the previous tRNA pushed into the E (exit) site. The ribosome exposes the next codon in the A site of the 30S subunit and is ready to receive the next cognate tRNA in its complex with EF-Tu:GTP.

Elongation Factor EF-Tu

EF-Tu has been the focus of structural studies for several decades. The name stems from early characterization of this factor as “translation factor unstable”. The biochemically most stable form is the biologically inactive EF-Tu:GDP, and was therefore the first form to be

structurally investigated. It was shown that EF-Tu consists of ~400 amino acids containing three domains (Figure 1). Domain 1 is a typical nucleotide binding domain with a central β-sheet surrounded by α-helices on both sides. This domain also contains all the consensus sequences now recognized as typical for a GTP-binding protein (G protein). Of these, there is a P-loop GXXXXGK(S/T) and a DXXG sequence motif also found in many ATP-binding proteins, where they are called Walker A and B motifs, respectively. Furthermore, there is a NKXD sequence motif involved in specific recognition of the G base of GTP, and a threonine residue in the so-called switch I region, which is now known to be involved in Mg^{2+} binding, and in the large conformational change of EF-Tu. A similar domain is found in all known G proteins, like the small GTPases (ras P21 or ran) and in the α-subunit of the heterotrimeric G proteins involved in cellular responses to external signals. The domain is therefore often referred to as the G domain. The remaining two domains, domain 2 and domain 3, of EF-Tu are both β-barrel structures and are in all known conformations of EF-Tu kept together as a single structural unit.

The biologically active form, EF-Tu:GTP, has been structurally determined with a nonhydrolyzable GDPNP nucleotide, where the O atom between the β- and γ-phosphate of GTP has been altered to the electronically similar NH group (Figure 1). The presence of the extra γ-phosphate in EF-Tu:GDPNP, when comparing to EF-Tu:GDP, has a dramatic effect on the overall conformation of the EF-Tu molecule. First of all, the γ-phosphate attracts the DXXG sequence motif, such that the peptide bond between the G residue and its preceding P residue is rotated by ~150°, and such that the NH group of this peptide bond makes a hydrogen bond with the γ-phosphate group. Like all G proteins, EF-Tu has switch regions of the G-domain that have significantly different structures in the GDP and GTP forms. The DXPGH motif of EF-Tu is at the beginning of its switch region II. This region in both the GDP and the GTP form includes an α-helix. However, between the two forms the helix is shifted by 4 residues along the sequence, and the position of its axis is therefore rotated by ~45°. As this helix is a major part of the interface towards domain 3 this change results in an overall rotation of the G-domain relative to domains 2 and 3 by ~90°. From biochemical studies, the histidine residue of the DXPGH motif of EF-Tu is known to be involved in the intrinsic GTPase activity of EF-Tu, and is presumably involved in stabilization of the transition state of GTP hydrolysis on the ribosome. Secondly, the presence of the γ-phosphate, and the shift in position of the proline residue of the DXPGH motif alters the conformation of the switch I region of EF-Tu such that its

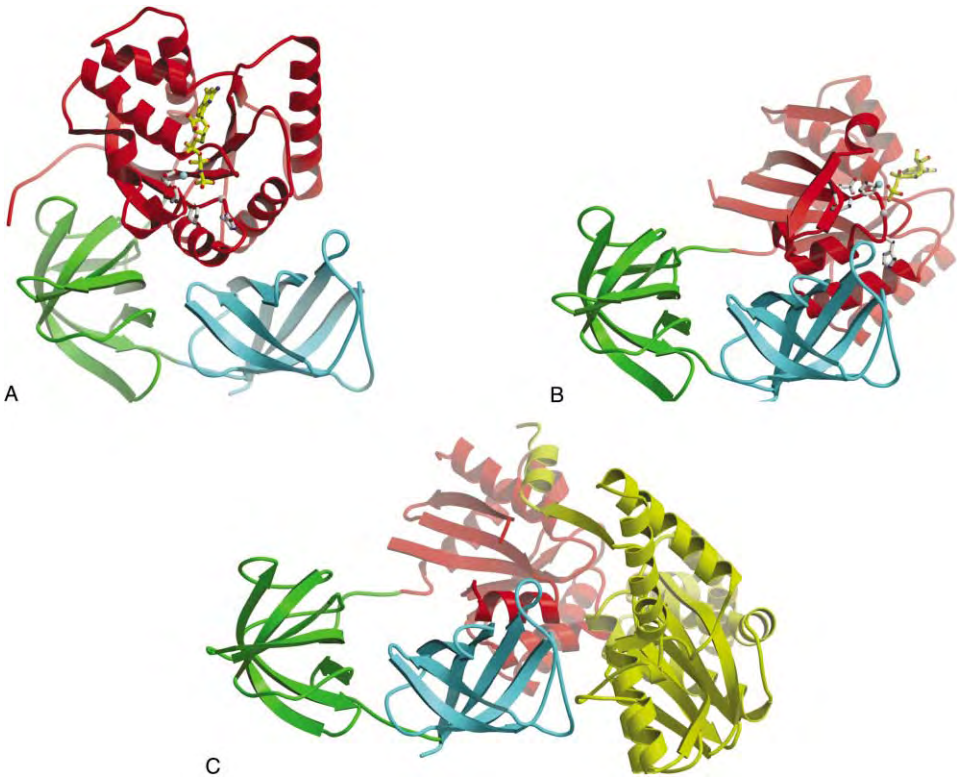

FIGURE 1 Structures of various forms of EF-Tu complexes: (A) EF-Tu:GDP, (B) EF-Tu:GTP, and (C) EF-Tu:EF-Ts. Domains of EF-Tu are colored: domain 1, red with nucleotides in yellow ball-and-stick where present; domain 2, green; domain 3, blue. EF-Ts is in yellow.

T residue becomes a ligand to the Mg^{2+} ion of the GTP form, and part of its secondary structure interchanges between a β-hairpin in the GDP form and an α-helix in the GTP form.

The structure of the complex between EF-Tu and its nucleotide exchange factor EF-Ts is also known. EF-Ts interacts with the G-domain of EF-Tu at the loops responsible for the nucleotide binding, and in many ways it alters the GDP binding pocket. Furthermore, EF-Ts interacts with the tip of domain 3 of EF-Tu in such a way that the G-domain and domain 3 are separated from each other. This separation represents an intermediate in the large conformational change of EF-Tu, and is also part of the catalysis of nucleotide exchange.

Elongation Factor EF-G

The structure of EF-G is known in its GDP-bound and in its nucleotide-free form (Figure 2). EF-G is much larger than EF-Tu and contains ~690 residues organized in five domains. The first domain of EF-G is the G-domain that has many similarities with the G-domain of EF-Tu in structure and in amino acid sequence. Apart from that, it contains an insert of ~90 residues (the G′-domain). The switch I region of EF-G in the GDP form is disordered. Domain 2 of EF-G is also similar to that of EF-Tu although it has a β-hairpin in the cleft between the G-domain and domain 2. The arrangement of the two domains in EF-G:GDP is like that of EF-Tu:GTP. Domains 3–5 have folds containing a small β-sheet with helices on one side only. This fold is very similar to that of some ribosomal proteins. Domain 4 contains an unusual left-handed $\beta-\alpha-\beta$ folding motif. Furthermore, this domain is more elongated and sticks out from the rest of the protein. It is known that the very tip of this domain is functionally important in translocation, as a histidine residue in the eukaryotic factor is modified into the unusual diftamide, and that ADP-ribosylation of this residue by difteria toxin blocks its function on the ribosome.

Despite numerous attempts by several research groups, it has not been possible to determine the structure of the biologically active EF-G:GTP. Studies by cryo-electron microscopy indicate that significant conformational changes occur when EF-G is bound on the ribosome.

The Ternary Complex of EF-Tu

Two structures have been determined of the ternary complex of EF-Tu (Figure 2). The first one was a complex between yeast Phe-tRNA and bacterial EF-Tu:GDPNP, while the second one was of bacterial Cys-tRNA and bacterial EF-Tu:GDPNP. The two are very similar and point to the fact that tRNAs are very similar in all organisms and that therefore the ternary complex is most likely to have the same general structures in all kingdoms of life. The large conformational change of EF-Tu from the GDP to the GTP form creates

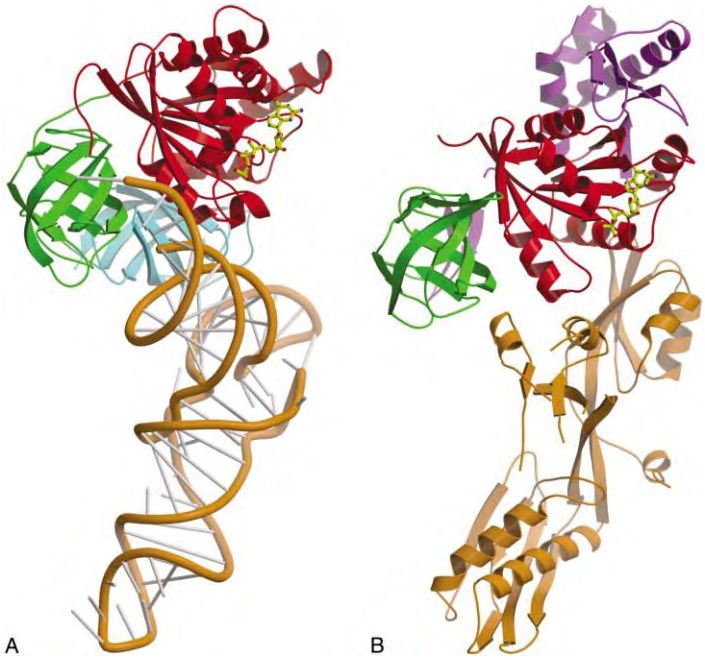

FIGURE 2 Structures of (A) the ternary complex of EF-Tu, and (B) EF-G:GDP. EF-Tu is colored as in Figure 1. The tRNA is in orange, domains 1 and 2 of EF-G are colored as for EF-Tu with an insert in domain 1 in magenta. Domains 3, 4, and 5 of EF-G are in orange.

a preformed binding surface for the tRNA. The structures of both tRNA and EF-Tu:GDPNP in the ternary complex are thus very similar to the structures of the free components. The universally conserved 3′-CCA end of tRNA is bound to a cleft between the G-domain and domain 2 of EF-Tu. This cleft as mentioned above is filled with a β-hairpin in EF-G. The terminal A base is recognized in a deep pocket on the surface of domain 2, while a pocket between the G-domain and domain 2 holds the amino acid attached to tRNA. The aminoacyl bond of the amino acid is recognized by main chain groups of EF-Tu in such a way that the amino group must be deprotonated in the complex. Other contacts involve general features of the tRNA structure.

The Structural Similarity of EF-G and the Ternary Complex

When the structure of the first ternary complex of EF-Tu was determined it was observed that its shape was very similar and points to that of the previously known EF-G:GDP (Figure 2). Domains 3, 4, and 5 of EF-G are thus a structural mimic of the tRNA of the ternary complex. The elongated domain 4 of EF-G directly mimics the anti-codon stem-and-loop of tRNA. There has been much speculation why this should be, and whether this would be a general phenomenon for parts of proteins known to interact with the A site of the ribosome. This does not seem to be the case according to recent results, and the simplest explanation of the mimicry is that the ternary complex has to interact with the ribosome after EF-G:GDP left the ribosome. Possibly, EF-G reshapes the ribosome into a form that is ready to interact with a ternary complex.

Action of Elongation Factors on the Ribosome

Electron microscopy of ribosomal particles in flash-frozen vitreous ice (cryo-EM) has revealed information on how elongation factors interact with the ribosome. The results obtained make use of the fact that some antibiotics interact specifically with the elongation factors on the ribosome. The antibiotic fusidic acid is thus known to interact with EF-G, while the antibiotic kirromycin interacts with the ternary complex of EF-Tu. Both antibiotics block the release of the target proteins on the ribosome after GTP hydrolysis has been induced. The antibiotics are believed to prevent conformational changes in the elongation factors that are needed for their release from the ribosome. The cryo-EM reconstructions of both EF-G and of the ternary complex on the ribosome reveal that they indeed occupy very similar positions and are found to have very similar shapes. The G-domain is seen to be very close to features of the 50S subunit that are very close to the GTPase-activating center of the ribosome. Domain 2 interacts with the 30S subunit such that the G-domain and domain 2 together fill the gap between ribosomal subunits.

The tip of domain 4 of EF-G and the tip of the anti-codon stem-and-loop of tRNA both reach into the decoding center of the 30S subunit. Thus, the similarity in the structures of EF-G:GDP and of the ternary complex of EF-Tu is reflected in their similar interaction with the ribosome.

Antibiotic Action on EF-Tu

A few families of antibiotics are known to interact directly with the function of EF-Tu. These families seem

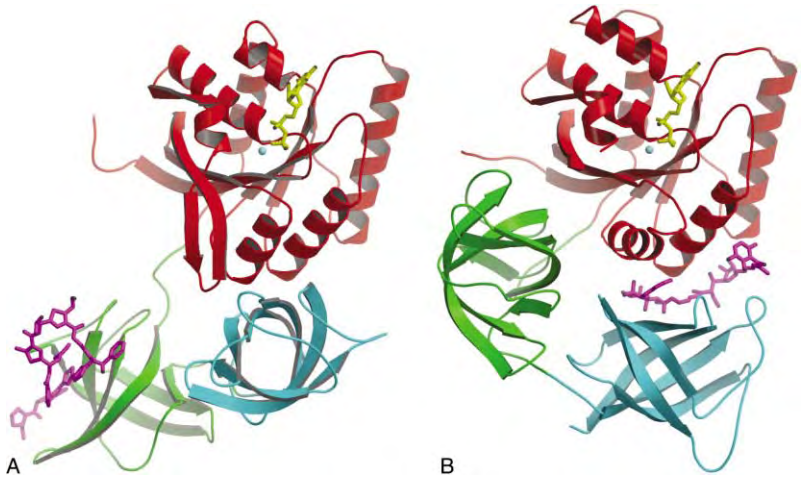

FIGURE 3 Structures of complexes of EF-Tu and antibiotics: (A) GE2770A bound to EF-Tu:GDP, and (B) aurodox bound to EF-Tu:GDP. Antibiotics are shown in magenta.

to fall into two functional groups. One group (examples are GE2270A and pulvomycin) prevents the formation of the ternary complex, while another group (examples kirromycin and enacyloxin IIa) prevents the release of EF-Tu from the ribosome. A structural complex of GE2270A with EF-Tu:GDP has been determined, and reveals that the antibiotic partly occupies the pocket on domain 2, which in the ternary complex accommodates the terminal A base. Furthermore, GE2270A stabilizes EF-Tu in the GDP-bound conformation and prevents the formation of the GTP-bound conformation. This structure thus explains how this group of antibiotics prevents the formation of a ternary complex of EF-Tu.

A structure of EF-Tu:GDP in complex with aurodox (a methylated version of kirromycin) shows the antibiotic in a cleft between the G-domain and domain 3, keeping the two together in a GTP-like form of EF-Tu although the nucleotide bound is GDP. This will explain how kirromycin blocks the release of EF-Tu from tRNA and from the ribosome upon GTP hydrolysis.

These results (Figure 3) may indicate that the conformations trapped by antibiotics are biologically relevant forms, which effectively can be blocked by inhibitors aimed at stopping protein biosynthesis in bacteria.

See Also the Following Articles

G_i Family of Heterotrimeric G Proteins • G_q Family • G_s Family of Heterotrimeric G Proteins • G_{12}/G_{13} Family • Translation Elongation in Bacteria

Glossary

anti-codon A triplet of bases on tRNA that by Watson–Crick base pairing can decode a codon.

codon A triplet of bases on mRNA that codes for one amino acid.

EF-G Translation factor controlled by GTP.

EF-Ts Translation factor (stable).

EF-Tu Translation factor (unstable).

G protein Protein whose action is controlled by GTP and GDP. The protein is active in its GTP-bound form, while hydrolysis of GTP into GDP inactivates the protein.

GDP Guanosine di-phosphate.

GTP Guanosine tri-phosphate.

mRNA Messenger ribonucleic acid containing the triplet codons, each specifying one amino acid.

ribosome Cellular particle that synthesizes proteins with the amino acid sequence given by the sequence of triplet codons of mRNA.

tRNA Transfer ribonucleic acid that carries on its 3′ CCA end an amino acid corresponding to its anti-codon.

Further Reading

Kjeldgaard, M., Nyborg, J., and Clark, B. F. C. (1996). The GTP-binding motif—variations on a theme. *FASEB J.* **10**, 1347–1368.

Krab, I. M., and Parmeggiani, A. (1998). EF-Tu, a GTPase odyssey. *Biochim. Biophys. Acta* **1443**, 1–22.

Merrick, W. C., and Nyborg, J. (2000). The protein biosynthesis elongation cycle. In *Translational Control of Gene Expression* (N. Sonenberg, J. W. B. Hershey and M. B. Mathews, eds.) CSHL Press, New York.

Nissen, P., Kjeldgaard, M., and Nyborg, J. (2000). Macromolecular mimicry. *EMBO J.* **19**, 489–495.

Nyborg, J., Nissen, P., Kjeldgaard, M., Thirup, S., Polekhina, G., Clark, B. F. C., and Reshetnikova, L. (1996). Structure of the ternary complex of EF-Tu: Macromolecular mimicry in translation. *TIBS* **21**, 81–82.

Ramakrishnan, V. (2002). Ribosome structure and the mechanism of translation. *Cell* **108**, 557–572.

Valle, M., Zavia lov, A., Li, W., Stagg, S. M., Sengupta J., Nielsen, R. C., Nissen, P., Harvey, S. C., Ewemberg, M., and Frank, J. (2004). Incorporation of aminoacyl tRNA into the ribosome as seen by cryo-electron microscopy. *Nat. Struct. Biol.* **10**, 899–906.

Biography

Poul Nissen is an Associate Professor at the University of Aarhus, Denmark. His major scientific interest has been the structural investigation of the ternary complex of EF-Tu and of the large 50S ribosomal subunit and the transition state of its peptidyl transferase center. He received his Ph.D. in protein crystallography at the University of Aarhus, and spent his postdoctoral period at Yale University. He is now working on the yeast ribosome and membrane transport proteins. He is an EMBO Young Investigator and a Danish Research Council Ole Rømer Stipendiate.

Jens Nyborg is an Associate Professor at the University of Aarhus, Denmark. His major scientific interests have been the structural investigations of translation factors and of components of the innate immune system. He received his Ph.D. in crystallography on inorganic chemical compounds and spent his postdoctoral period at the Medical Research Councils Laboratory of Molecular Biology in Cambridge, UK. He is a member of the Royal Danish Academy of Sciences and Letters and EMBO.

Eicosanoid Receptors

Richard M. Breyer and Matthew D. Breyer
Vanderbilt University, Nashville, Tennessee, USA

Eicosanoids are the oxygenated metabolites of the 20-carbon polyunsaturated fatty acid arachidonic acid. These compounds are locally acting autacoids and are rapidly metabolized with a half-life of minutes to seconds. Once formed, eicosanoids exert their physiologic effects via interaction with specific receptors. The best characterized of these receptors belong to the superfamily of G protein-coupled receptors, although some eicosanoids are thought to interact with nuclear hormone receptors as well.

Eicosanoid Biosynthesis Pathways

The 5,8,11,14-eicosatrienoic acid, a 20-carbon polyunsaturated fatty acid with the trivial name arachidonic acid, is esterified in the lipid bilayer of cell membranes. Upon its enzymatic release by the action of phospholipase, free arachidonate is rapidly metabolized. Oxygenated metabolites of arachidonic acid are collectively known as the eicosanoids. These compounds are formed by the action of three distinct enzymatic pathways.

The Lipoxygenase (LO) Pathway

This pathway leads to the formation of the monoxygenated compounds such as hydroperoxytetraenoic acids (HPETEs), hydroxytetraenoic acids (HETEs), and trihydoxylated metabolites known as lipoxins via three principal enzymes: 5-LO, 12-LO, and 15-LO. The 5-HPETEs are substrates for the leukotriene synthases that lead to the formation of a series of key inflammatory mediators, the leukotrienes, including the unstable intermediate LTA_4, which is converted to the potent mediator LTB_4 and the cysteinyl leukotrienes LTC_4, LTD_4, and LTE_4. Sequential oxidation of arachidonic acid by the action of both 12-LO and 5-LO or 12-LO and 15-LO leads to the formation of the lipoxins LXA_4 and LXB_4. The lipoxins are structurally related to the leukotrienes, but appear to act through a distinct set of receptors and have very different actions *in vivo*. Finally, the 5-LO metabolite HPETE can be further metabolized to the 5-oxo ETE(5-oxo-6E,8Z,11Z,14Z-eicosatetraenoic acid), for which a unique receptor has recently been cloned.

The Cyclooxygenase (COX) Pathway

Cyclooxygenase metabolism leads to the production of the five principal prostanoids via two distinct isozymes, COX-1 and COX-2. Four of the principal prostaglandins, PGE_2, PGD_2, $PGF_{2\alpha}$, and PGI_2 are analogues of the 20-carbon unnatural fatty acid prostanoic acid, which is distinguished by its five carbon "prostane" ring group comprised of carbons five through eight. The fifth prostanoid, thromboxane, has an inserted ether oxygen and thus has a six-member ring structure and is an analogue of the unnatural fatty acid thrombanoic acid.

The Epoxygenase Pathway

Oxidation of arachidonic acid by the cytochrome P450 pathway leads to the formation of epoxytrienoic acids (EETs). Although physiologic effects have been attributed to these compounds no specific EET receptors have been identified to date.

Eicosanoid Action

As a class, eicosanoids mediate a wide array of physiologic effects including pain, inflammation, and modulation of smooth muscle tone. Many of these effects are receptor-mediated by cell surface G protein-coupled receptors (GPCRs). There is recent evidence that some PG metabolites can activate nuclear hormone receptors of the peroxisome-proliferation-activated receptor family (PPARs). In addition to the enzymatic products of arachidonic acid metabolism, prostanoid-like products resulting from nonenzymatic oxidation have also been described and designated isoprostanes. These products are structurally related to the COX-derived prostanoids, but are the product of non-enzymatically free radical oxidation. Isoprostanes are markers of oxidative stress and evidence suggests that these metabolites can also evoke receptor-mediated physiologic effects.

Receptors of Lipoxygenase Metabolites

The action of lipoxygenase metabolites of arachidonic acid is mediated by a distinct family of GPCRs. Six GPCRs have been identified that bind lipoxygenase metabolites of arachidonic acid: four leukotriene receptors designated BLT_1, BLT_2, $CysLT_1$, and $CysLT_2$ have been described, a lipoxin receptor designated ALX, and the receptor for 5-oxo ETE.

Leukotriene Receptors

The leukotriene receptors fall into two groups of structurally related GPCRs: the chemoattractant-like BLT receptors and the CysLT receptors, which are related to the family of nucleotide-binding receptors. Of the four cloned leukotriene receptors, BLT_1 and BLT_2 receptors have highest affinity for the leukotriene LTB_4 with BLT_1 binding LTB_4 with much higher affinity as compared to BLT_2. The BLT receptors are predominantly expressed in the peripheral blood including leukocytes, granulocytes, macrophages, and eosinophils. The $CysLT_1$ and $CysLT_2$ receptors in contrast each bind the cysteinyl leukotrienes LTC_4 and LTD_4 with high affinity. CysLT receptors are expressed in peripheral blood leukocytes, spleen, and lung as well in a number of other tissues at lower levels. The $CysLT_1$ receptor has been implicated as an important mediator in asthma, and antagonists of this receptor such as monteleukast have been used clinically in the treatment of asthma.

Lipoxin Receptors

The lipoxin A_4 receptor (ALX), is a member of the GPCR family of chemoattractant receptors, as are the BLT receptors discussed above. This receptor was identified as an orphan receptor cDNA sharing significant homology with the fMLP chemoattractant receptor and was designated FMLP-like receptor 1 (FPLR1). Subsequent identification of this receptor as a mediator of LXA_4 action resulted in its designation as the ALX receptor. Activation of this receptor mediates the anti-inflammatory actions of lipoxin LXA_4. Northern blot analysis of ALXR mRNA in mouse tissues demonstrates that the receptor is most highly expressed in neutrophils, lung, and spleen with lower levels detected in the liver and heart. Some actions of lipoxins cannot be accounted for by the ALXR, and the existence of other lipoxin receptors has been postulated, but existence of other lipoxin receptor cDNAs has not been confirmed.

The 5-Oxo-ETE Receptor

The orphan GPCR TG1019 and closely related R527 have been identified as receptors for 5-oxo-ETE. These receptors have no official designation at this time. These receptors have been shown to be highly expressed in the kidney and may mediate the observed hemodynamic effects of 5-oxo-ETE described in this tissue.

Prostaglandin (PG) Receptors

The local action of PGs depends in part, on activation of a family of specific GPCRs, designated EP for E-prostanoid receptors, FP, DP, IP, and TP receptors respectively, for the other prostanoids. The EP receptors are unique in that four receptors, designated EP1 through EP4, have been described for PGE_2 each encoded by a distinct gene. A second class of Prostaglandin D receptor designated chemoattractant receptor-homologous molecule expressed on Th2 cells (CRTH2) has been identified, which has no sequence homology to the remaining PG receptors. This receptor has been unofficially designated "DP2." Each of the other PGs has a single receptor, and taken together there are nine PG GPCRs, each encoded by distinct genes. Alternative mRNA splice variants have been cloned for the EP1, EP3, TP, and FP receptors. In each case, these splice variants generate receptor sequence diversity in the intracellular C-terminal tail of the receptor protein (Figure 1). Functionally, these splice variants appear to modulate the specificity of G protein coupling, as well as regulation of receptor desensitization by encoding alternate phosphorylation sites. Pharmacologically, the PG receptors are distinguished by their ligand-binding selectivity as well as the signal transduction pathway they activate. In general, PG receptors may have significant affinity for more than one prostanoid ligand. Moreover, multiple PG receptors are frequently coexpressed in a single cell type or tissue. COX activation and resulting PG production may lead to complex effects in the target tissue by activation of multiple PG receptor subtypes. Thus, a given PG ligand may elicit multiple, and at times apparently opposing, functional effects on a given target tissue. For example, prostaglandin receptors were initially characterized by their actions on smooth muscle, where they may lead to either smooth muscle contraction or relaxation. The vasodilator effects of PGE_2 have long been recognized in both arterial and venous beds. Smooth muscle relaxation by PGE_2 is, however, not uniformly observed, and PGE_2 is a potent constrictor in other smooth muscle beds, including trachea, gastric fundus, and ileum. Importantly, some structural analogues of PGE_2 are capable of reproducing the dilator effects of PGE_2, but are inactive on tissues where it is a constrictor. Conversely, analogues that reproduce the constrictor effects of PGE_2 may fail to affect tissues where PGE_2 is a dilator. The EP receptor mRNAs exhibit differential

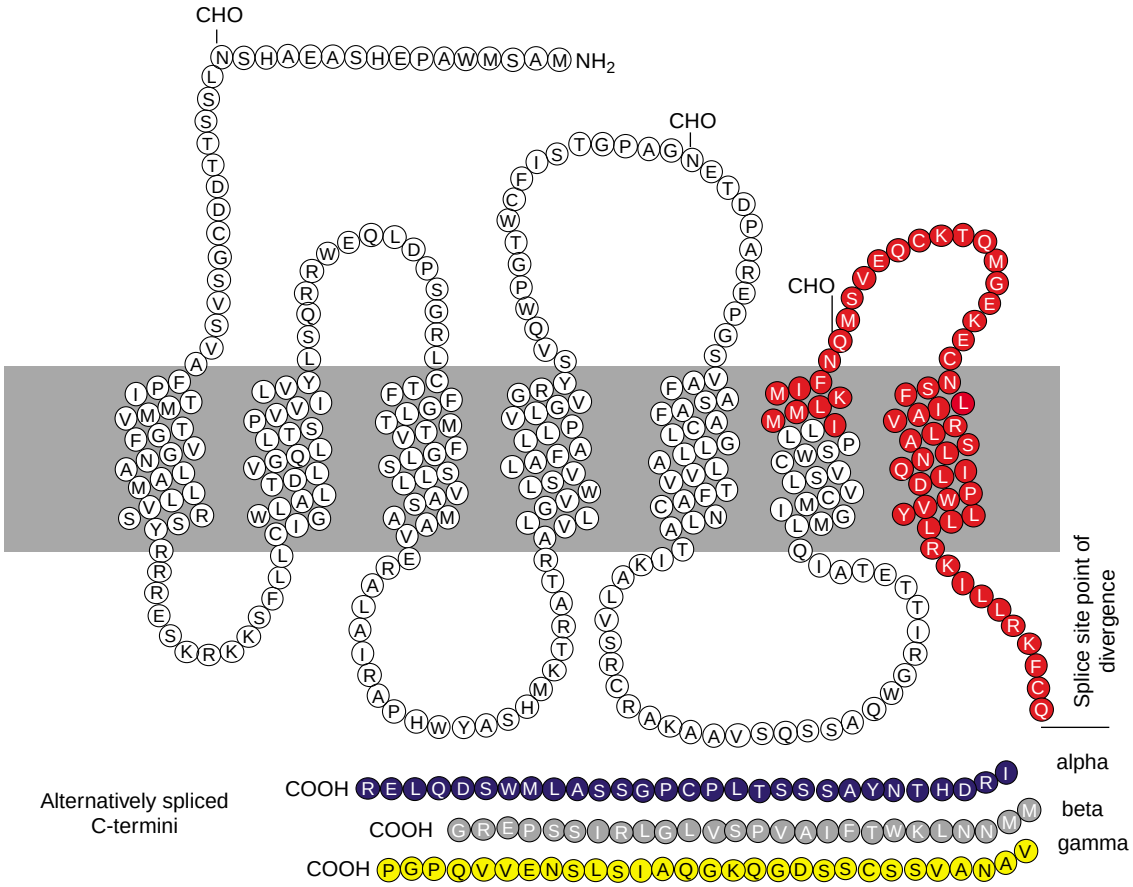

FIGURE 1 EP_3 receptor sequence of three mouse EP_3-receptor splice variants differing only in their intracellular carboxyl termini. The predicted amino acid sequences of each splice variant is represented by the one-letter amino acid code. Exons are color-coded. The common region is comprised of two exons (in white and red circles) which are spliced to three possible C-terminal tails. The carboxyl variable tails are designated alpha (blue), beta (gray), and gamma (yellow), each encoded by distinct exons.

expression in a number of tissues with distinct functional consequences of activating each receptor subtype. Functional antagonism among PGs can also be observed in platelet aggregation, where TXA_2 activation of the TP receptor causes platelet aggregation. Conversely, prostacyclin activates platelet IP receptors which opposes this platelet aggregation. Thus, the balance of PGs synthesized as well as the complement of PG receptors expressed determines the net effect of COX metabolism on platelet function.

PPARs

In addition to the GPCR-mediated effects there is evidence that prostaglandin metabolites are capable of activating some nuclear transcription factors. This action is exemplified by the cyclopentenone prostaglandins of the J-series, e.g., 15-deoxy -Δ12,14-PGJ_2 (15d-PGJ_2) which are derived from PGD_2. 15d-PGJ_2 activates a nuclear hormone receptor designated peroxisome proliferation activated receptor gamma (PPARgamma). There is also evidence that prostacyclin (PGI_2) also activates another member of this family designated PPARdelta. It is unclear whether the PGs represent true endogenous ligands of these receptors, as their affinity is generally in the micromolar range, which is two to three orders of magnitude lower than the nanomolar affinities observed for PGs at the GPCRs; nonetheless, these concentrations could be achieved in the intracellular environment.

See Also the Following Articles

DNA Polymerase δ, Eukaryotic • Peroxisome Proliferator-Activated Receptors • Processivity Clamps in DNA Replication: Clamp Loading • Prostaglandins and Leukotrienes

Glossary

autacoid A class of physiologically active substances that act upon the cell that elaborated this compound or on adjacent cells.

cyclooxygenase (COX) Enzymes that catalyze the oxidation of arachidonic acid. Also known as PGH synthase. COX catalyzes two sequential reactions, a *bis* oygenase, or cycloxygenase, reaction leading to the formation of PGG_2 and a subsequent peroxidase activity at the C15 position leading to the conversion of PGG_2 to PGH_2.

eicosanoid Any of the collections of oxygenated metabolites of the 20-carbon fatty acid, 5,8,11,14-eicosatetranoic acid (arachidonic acid) that are the products of cyclooxygenase, cytochrome P450, lipoxygenase, and nonenzymatic pathways.

GPCRs G protein-coupled receptors. A class of integral membrane protein cell-surface receptors that change conformation upon binding cognate agonists. This conformational change causes the dissociation of heterotrimeric G proteins leading to the initiation of the signal transduction cascade.

leukotriene Monoxygenated metabolites of arachidonic acid formed by the action of the lipoxygenases.

nonsteroidal anti-inflammatory drugs (NSAIDs) A class of drugs that effect their action by inhibiting the activity of cyclooxygenase. They have potent analgesic, antipyretic, and anti-inflammatory properties.

prostanoids Oxygenated metabolites of the 20-carbon essential fatty acid arachidonic acid. They are analogues of the 20-carbon unnatural fatty acids, prostanoic, and thrombanoic acid, produced by the action of cyclooxygenase.

Further Reading

Breyer, R. M., Bagdassarian, C. K., Myers, S. A., and Breyer, M. D. (2001). Prostanoid receptors: subtypes and signaling. *Annu. Rev. Pharmacol. Toxicol.* **41**, 661–690.

Brink, C., Dahlen, S. E., Drazen, J., Evans, J. F., Hay, D. W., Nicosia, S., Serhan, C. N., Shimizu, T., and Yokomizo, T. (2003). International union of pharmacology XXXVII. Nomenclature for leukotriene and lipoxin receptors. *Pharmacol. Rev.* **55**, 195–227.

Forman, B. M., Tontonoz, P., Chen, J., Brun, R. P., Spiegelman, B. M., and Evans, R. M. (1995). 15-Deoxy-delta 12, 14-prostaglandin J2 is a ligand for the adipocyte determination factor PPAR gamma. *Cell* **83**, 803–812.

Hosoi, T., Koguchi, Y., Sugikawa, E., Chikada, A., Ogawa, K., Tsuda, N., Sato, N., Tsunoda, S., Taniguchi, T., and Ohnuk, T. (2002). Identification of a novel eicosanoid receptor coupled to Gi/o. *J. Biol. Chem.* **277**, 31459–31465.

Jones, C. E., Holden, S., Tenaillon, L., Bhatia, U., Seuwen, K., Trantes, P., Turner, J., Kettle, R., Bouhelal, R., Charlton, S., Nirmala, N. R., Jarai, G., and Finun, P. (2003). Expression and characterization of a 5-oxo-6E,8Z,11Z,14Z-eicosatetraenoic acid receptor highly expressed on human eosinophils and neutrophils. *Mol. Pharmacol.* **63**, 471–477.

Morrow, J. D., and Roberts, L. J. (2001). Lipid-derived autacoids. In *Goodman & Gilman's the Pharmacological Basis of Therapeutics* (J. G. Hardman, L. E. Limbird and A. G. Gilman, eds.) 2nd edition. McGraw-Hill, New York.

Biography

Richard M. Breyer is an Associate Professor of Medicine (Nephrology) and Pharmacology at Vanderbilt University. His principal research interests are in prostaglandin receptor structure, function, and pharmacology. He holds a Ph.D. in biochemistry from the Massachusetts Institute of Technology, and received his postdoctoral training at the Pasteur Institute in Paris, France.

Matthew D. Breyer is a VA Merit Awardee and Professor of Medicine (Nephrology) and Molecular Physiology and Biophysics at Vanderbilt University. His principal research interests are in eicosanoid regulation of renal physiology. He holds an M.D. from Harvard University, and received his postdoctoral fellowship training at the University of Texas, Southwestern Medical Center in Dallas, Texas.

Elastin

Judith Ann Foster
Boston University School of Medicine, Boston, Massachusetts, USA

Elastin is a protein that exists as fibers in the extracellular spaces of many connective tissues. Elastin derives its name from its ability to act as an elastic band, i.e., to stretch and recoil with transient force. It is located throughout many tissues and organs of higher vertebrates and plays an important functional role in maintaining pressures associated with liquid and air flow in the cardiovascular and pulmonary systems. Elastogenic cells synthesize and secrete a soluble monomeric form of elastin into the extracellular space. The enzyme, lysyl oxidase, initiates cross-linking of the soluble monomers into insoluble fibers. Extracellular elastin associates closely with other proteins in the matrix including microfibrillar proteins and collagens. Once laid down in the matrix, the insoluble protein is very stable and resistant to degradation. Because of its critical role in the normal development and function of vital organs, impairment of elastin synthesis or proteolytic degradation of the insoluble fibers results in major clinical pathologies.

Composition and Primary Sequence

Elastin, as any protein, possesses a unique amino acid composition and a unique sequence of those amino acid residues along the polypeptide chain.

Amino Acid Composition

The soluble form of elastin, sometimes referred to as tropoelastin, contains a preponderance of uncharged and nonpolar amino acids. The polypeptide chain contains appropriately 850 amino acids and a molecular mass of 65–72 kDa. The actual size varies somewhat among different species. Glycine (33%), alanine (18%), proline (13%), valine (17%), and leucine (5%) residues represent 86% of the total amino acids. Prolyl hydroxylase converts 1–2% of the proline residues to hydroxyproline but it is unclear as to the significance of this cotranslational modification. There are ~36–38 lysine residues per molecule so the overall charge of monomer is basic with an isoelectric point over pH 10. Once lysyl oxidase deaminates the epsilon amino group of most lysine residues in the protein, the resulting semialdehydes undergo a series of aldol condensations and Schiff bases to form the desmosine cross-links. At this stage, the protein is irreversibly insoluble and any success in extracting soluble fragments requires cleavage of peptide bonds.

Amino Acid Sequence

Unlike the classical triple repeat of collagen wherein glycine residues occupy every third position of the triplet, elastin does not contain a uniform repeating structure. Instead, elastin contains two broad sequence motifs that accommodate much subdivision. Most lysine residues segregate together with alanine residues to create pairs of lysines separated by two or three alanine residues. These sequences exist within stretches of uncharged, nonpolar amino acid residues such as glycine, valine, and proline. The latter amino acid residues occur together with other nonpolar, hydrophobic, and polar residues, form tri, tetra, penta, and hexa repeats with not a single consistent motif. The carboxy terminal sequence is unique and highly conserved among different species. It contains the only cysteine residues within the molecule.

Isolation of Elastin

Insoluble Elastin

An early operational definition of elastin was that it represented the protein remaining after one extracted all other connective tissue proteins. Consequently, the insolubility of elastin serves as the basis for all isolation methods. Isolation procedures involve very harsh treatments such as autoclaving, extraction with hot alkali or strong denaturants, and exposure to cyanogen bromide or collagenases. Amino acid analysis of the material remaining insoluble after these treatments confirms the presence and homogeneity of the elastin.

Soluble Elastin

In vivo the conversion of soluble to insoluble elastin occurs rapidly making the isolation of soluble elastin very difficult. In order to isolate quantitative amounts of soluble elastin from a tissue, one must block the

conversion of the soluble to the insoluble form. Inhibition of the cross-linking enzyme, i.e., lysyl oxidase, is the most effective approach for isolating intact elastin monomers. Since lysyl oxidase is a copper-dependent enzyme that is specific for lysine residues it can be inhibited by removing copper or adding a noncompetitive inhibitor. In practice, this involves rendering an animal copper deficient by dietary restriction or by adding β-aminopropionitrile, a lathyrogen, to the diet of young animals. The procedure for isolating soluble elastin is based primarily on its unique solubility in organic solvents.

The Elastin Gene

Gene Structure

The single copy, elastin gene spans ~35–40 kb of DNA but only 7% of the sequences represent exons that are transcribed into the mRNA. The huge amount of intron sequences in the gene (19:1, intron to exon) makes this one of the most disperse genes reported. The short exon sequences (less than 190 bp) encode separate cassettes for the nonpolar and lysine/alanine residues of the protein. Many of the intron sequences encode elastin-like sequences.

Gene Promoter

The elastin gene promoter contains features of a constitutively expressed (housekeeping) gene. It lacks a classic TATA box, is very GC rich (67%), has two CAAT boxes and possesses multiple transcription start sites. There are also several Sp1 sites as well as a cryptic GC box and several consensus AP2 sequences within the proximal promoter. In addition, consensus sequences for glucocorticoid, TPA-inducible, and CRE response elements reside in the distal promoter regions.

Elastin Gene Expression

Elastin mRNAs

Transcription of the elastin gene results in multiple mRNAs. The multiple forms all possess a size in the 24S range arising from alternate splicing of several different exons. All of the transcripts contain ~3.5 kb that includes a large untranslated 3′ region of ~1.0 kb in addition to the polyA tail.

Elastin Protein Isoforms

Translation of multiple mRNA results in different isoforms of soluble elastin that reflect insertion of different exons sequences. Although there is variance in the presence of isoforms dependent on cell type and age, the function of the different variations of soluble elastin is still not clear. There is speculation that different isoforms play a major role in the early phase of elastic fiber assembly by providing interactive sites for specific binding to other components of the extracellular matrix.

Regulation of Elastin Gene Expression

The expression of elastin is high in developing tissues and through early growth to maturity. In the adult animal, elastin synthesis is very low and its reinitiation occurs only in normal injury/repair situations or in some pathological conditions. Many studies have focused on understanding how elastin expression is regulated in development and disease conditions. The results show that expression is regulated at both the transcriptional and posttranscriptional levels.

Transcriptional Regulation

Many studies have shown that elastin expression in developing pulmonary and cardiovascular tissues is controlled primarily at the transcriptional level. These results have been confirmed in transgenic animals carrying the transgene with a reporter driven by the elastin promoter and by *in vitro* tissue transfections of the same reporter gene. In addition, primary cultures of elastogenic cells demonstrate that elastin transcription plays a major role in the action of elastin modulators such as basic fibroblast growth factor and insulin-like growth factor. Putative *cis*-acting elements in the 5′ flanking region of the gene have been broadly defined through transient transfections of various cell types with a series of deletion reporter constructs. Of the *cis*-acting elements identified within the elastin promoter, few have been functionally shown to convey an increase in elastin transcription. In fact, the majority were found to be repressors. These latter observations suggest that a possible route to increase elastogenesis is to block the repressor complex from binding via the disruption of the receptor and/or ligand binding, as well as blocking the resultant signal pathway.

Posttranscriptional Regulation

Studies on the expression of elastin in cultures of elastogenic cells challenged with biologically significant factors show that elastin mRNA stability is important in regulating expression especially in the adult animal.

See Also the Following Articles

Amino Acid Metabolism • Collagens

Glossary

cyanogen bromide A chemical reagent used to cleave peptide bonds adjacent to methionine residues.

desmosine A pyridinium ring alkylated in four positions; serves as a cross-link derived from four lysine residues.

lathyrism A disease caused by ingestion of seeds of *Lathyrus odoratus*, a sweet pea. The active agent is β-aminopropionitrile which inhibits lysyl oxidase.

polyA tail A string of adenine nucleotides added to the 3′ end of most eukaryotic mRNAs.

promoter A DNA sequence that binds RNA polymerase resulting in transcription initiation.

svedberg unit (S) A unit used for the sedimentation coefficient; equivalent to 10–13 s.

Further Reading

Franzblau, C., and Lent, R. W. (1968). Studies on the chemistry of elastin. In *Structure, function, and evolution of proteins* Vol 21, Brookhaven Symposia in Biology, pp. 358–377.

Gallop, P. M., and Paz, M. A. (1975). Posttranslational protein modifications, with special attention to collagen and elastin. *Physiol. Rev.* **55**, 418–487.

Gray, W. R., Sandberg, L. B., and Foster, J. A. (1973). Molecular model for elastin structure and function. *Nature* **246**, 461–466.

Indik, Z., Yeh, H., Ornstein-Goldstein, N., Kucich, U., Abrams, W., Rosenbloom, J. C., and Rosenbloom, J. (1989). Structure of the elastin gene and alternative splicing of elastin mRNA: Implications for human disease. *Am. J. Med. Genet.* **34**, 81–90.

Lansing, *et al.* (1952). *Anat. Rec.* **114**,550–575.

Partridge and Davis (1955). *J. Biochem.* **61**, 21–30.

Perrin, S., and Foster, J. A. (1997). Developmental regulation of elastin gene expression. *Crit. Rev. Eukaryot. Gene Expr.* **7**, 1–10.

Sandberg, L. B., Weissman, N., and Smith, D. W. (1969). The purification and partial characterization of a soluble elastin-like protein from copper-deficient porcine aorta. *Biochemistry* **8**, 2940–2945.

Biography

Dr. Judith Ann Foster is currently a Professor of Biochemistry at Boston University School of Medicine. She has held faculty positions at the Utah University School of Medicine, the University of Georgia and served as the Chairperson of the Biology Department at Syracuse University. She has been studying elastin for the last 30 years. She began her work on characterizing soluble elastin and the regions of cross-link formation and progressed to examining the biosynthesis and expression of elastin in lung and aortic cells. Dr. Foster has spent the last decade studying the regulation of elastin gene transcription.

Endocannabinoids

Daniele Piomelli
University of California, Irvine, California, USA

The endocannabinoids are a family of biologically active lipids that bind to and activate cannabinoid receptors, the G protein-coupled receptors targeted by Δ^9-tetrahydrocannabinol in marijuana. The term encompasses several derivatives of arachidonic acid, which are generated on demand by neurons and other cells in response to physiological or pathological stimuli. The two best-characterized endocannabinoids are anandamide (arachidonoylethanolamide) and 2-arachidonoylglycerol (2-AG). Others are noladin ether (2-arachidonoyl glyceryl ether) and virodhamine (O-arachidonoyl ethanolamine).

Synthesis

Anandamide

Anandamide is produced from the hydrolysis of an N-acylated species of phosphatidylethanolamine (PE), called N-arachidonoyl-PE. This reaction is initiated by activating neurotransmitter receptors and/or by elevating intracellular levels of Ca^{2+} ions and is probably catalyzed by phospholipase D. The anandamide precursor, N-arachidonoyl-PE, is present at low levels in nonstimulated cells, but its formation can be stimulated by Ca^{2+} and occurs simultaneously with that of anandamide. N-arachidonoyl-PE synthesis is catalyzed by membrane-bound N-acyltransferase, which has been partially purified. (See Figures 1 and 2.)

2-Arachidonoylglycerol

In brain neurons, 2-AG formation is probably initiated by the activation of phospholipase C, which cleaves membrane phospholipids (e.g., phosphatidylinositol-4,5-bisphosphate) at the proximal phosphate ester bond, producing 1,2-diacylglycerol. This intermediate is broken down by diacylglycerol lipase to yield 2-AG and free fatty acid. Another pathway of 2-AG release might involve the hydrolytic cleavage of a phospholipid at the *sn*-1 position of the glycerol backbone, catalyzed by phospholipase A_1. This reaction yields a *sn*-2 lysophospholipid, which can be further hydrolyzed to produce 2-AG (Figure 3). Finally, 2-AG might be formed by hormone-sensitive lipase acting on triacylglycerols or by lipid phosphatases acting on lysophosphatidic acid. However, as these enzymes preferentially target lipids enriched in saturated or monounsaturated fatty acids, they are unlikely to play a role in the synthesis of a polyunsaturated species such as 2-AG.

Physiological Regulation of Endocannabinoid Synthesis

Anandamide

Anandamide synthesis is initiated by intracellular Ca^{2+} rises and/or by activation of G protein-coupled receptors. For example, activation of vanilloid receptors elevates intracellular Ca^{2+} levels and stimulates anandamide synthesis in rat sensory neurons in culture. In addition, activation of dopamine D_2-receptors enhances anandamide release in the brain striatum of the rat *in vivo*. The molecular steps involved in these effects have not yet been clarified.

2-Arachidonoylglycerol

2-AG formation is also linked to intracellular Ca^{2+} rises. For example, in freshly dissected slices of rat hippocampus, electrical stimulation of the Schaffer collaterals (a glutamatergic fiber tract that projects from CA3 to CA1 neurons) produces a fourfold increase in 2-AG levels, which is prevented by the Na^+ channel blocker tetrodotoxin or by removing Ca^{2+} from the medium. It is notable that anandamide levels are not changed by the stimulation, suggesting that the syntheses of 2-AG and anandamide can be independently regulated. This idea is supported by the fact that activation of D_2 receptors, a potent stimulus for anandamide release in the rat striatum, has no effect on striatal 2-AG levels.

Deactivation

In the brain and other tissues, anandamide and 2-AG are rapidly eliminated through a two-step process consisting of uptake into cells and enzymatic hydrolysis.

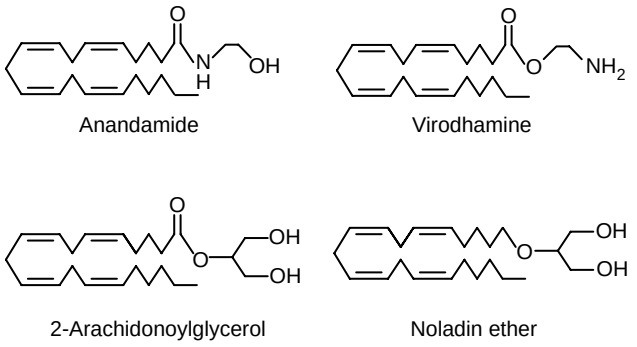

FIGURE 1 Chemical structures of the endocannabinoids anandamide (arachidonoylethanolamide), 2-arachidonoylglycerol (2-AG), noladin ether, and virodhamine.

The two endocannabinoids share a functionally similar transport mechanism, but they follow distinct routes of intracellular degradation.

Transport into Cells

The transport of anandamide and 2-AG into neurons and astrocytes is structurally specific, displays classical saturation kinetics, and is selectively inhibited by compounds such as N-(4-hydroxyphenyl)-arachidonamide (AM404). The putative transporter involved has not yet been identified, but transport has been shown to be Na^+-independent, which is suggestive of a facilitated diffusion mechanism.

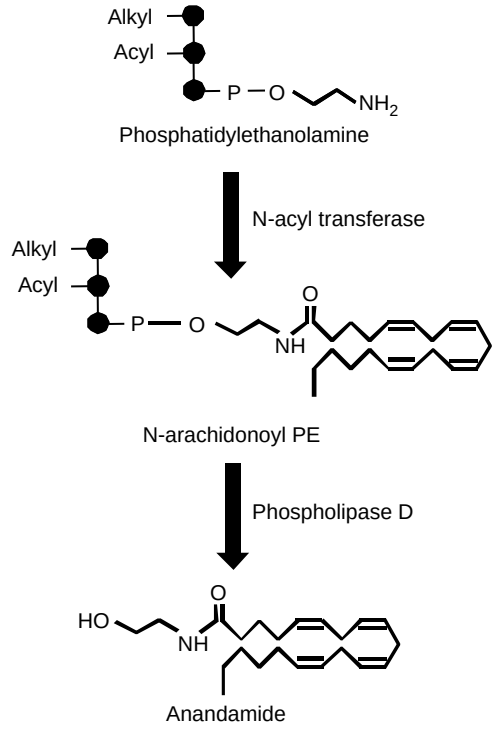

FIGURE 2 Anandamide biosynthesis. PE, phosphatidylethanolamine.

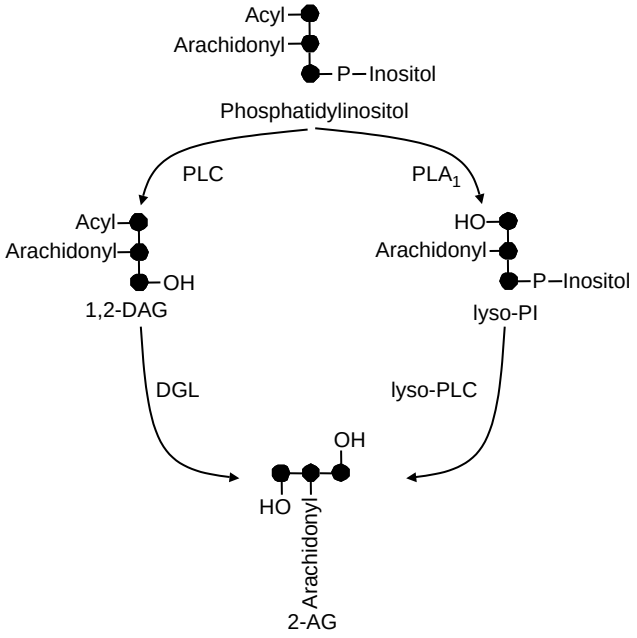

FIGURE 3 2-AG biosynthesis. 1,2,-DAG, 1,2- diacylglycerol; DGL, diacylglycerol lipase; PL, phospholipase.

Intracellular Hydrolysis

Inside cells, anandamide is metabolized by fatty acid amide hydrolase (FAAH), a membrane-bound intracellular serine hydrolase that also cleaves oleoylethanolamide, an endogenous satiety factor, and other lipid amides. Hydrolysis of 2-AG is catalyzed instead by monoglyceride lipase (MGL), a cytosolic serine hydrolase that converts 2- and 1-monoglycerides into fatty acid and glycerol. The contribution of other lipases to 2-AG degradation cannot be excluded at present.

Cannabinoid Receptors

The endocannabinoids regulate the function of multiple organs and tissues of the body. These regulatory effects are primarily mediated by two G protein-coupled receptors: CB_1 and CB_2. CB_1 is highly expressed in the central nervous system, but is also present at lower levels in a variety of peripheral tissues. By contrast, CB_2 is mostly found in immune cells such as lymphocytes. Both subtypes are linked to G_i/G_o proteins and can initiate signaling events typical of these transducing proteins, which include inhibition of adenylyl cyclase activity, opening of K^+ channels, closing of Ca^{2+} channels, and stimulation of protein kinase activities. Nevertheless, CB_1 and CB_2 are structurally different (they have only 44% sequence homology), which has allowed the development of subtype-selective ligands such as the CB_1 antagonist SR141716A (rimonabant) and the CB_2 antagonist SR144528. There is evidence for the

existence of at least two additional cannabinoid-sensitive sites in the brain and vasculature, which remain however uncharacterized.

Functions

In broad terms, the endocannabinoids are considered paracrine mediators, substances that act on cells near their sites of synthesis without entering the bloodstream. For example, they are formed by circulating leukocytes and platelets during hypotensive shock and induce the vascular relaxation that accompanies this phenomenon by activating CB_1 receptors on the surface of smooth muscle cells. Similar paracrine actions occur in the brain, where the endocannabinoids mediate a localized signaling mechanism through which neurons modify the strength of incoming inputs. The endocannabinoids are generated by neuronal depolarization and travel backward across the synapse to regulate the release of neurotransmitters from neighboring axon terminals, a process called retrograde signaling.

See Also the Following Articles

Adenylyl Cyclases • G Protein-Coupled Receptor Kinases and Arrestins • Neurotransmitter Transporters • Phospholipase C

Glossary

arachidonic acid Common name for eicosatetraenoic acid (eicosatetraenoic acid, $20{:}4\Delta^{5,8,11,14}$), an essential fatty acid that serves as metabolic precursor for eicosanoids and endocannabinoids.

axon terminal Specialized structure of a neuron that secretes neurotransmitters.

G proteins Heterotrimeric proteins with GTPase activity that link the occupation of certain cell surface receptors to cellular responses.

neurotransmitter Substance secreted by a neuron at a synapse.

phospholipase A group of enzymes that catalyze the hydrolysis of phospholipids at their glycerol ester (PLA) of phosphodiester (PLC, PLD) bonds.

protein kinase Enzyme that transfers a phosphate group from ATP to a protein.

stereospecific numbering (sn) A convention on how to designate the stereochemistry of glycerol-based lipids. When the glycerol moiety is drawn with the secondary hydroxyl to the left, the carbons are numbered 1,2,3 from top to bottom.

striatum A subcortical brain structure involved in the control of movement, habit learning, and the rewarding properties of drugs of abuse.

synapse Specialized junction between the ending of the presynaptic neuron and the dendrite, cell body, or axon of a postsynaptic neuron.

vanilloid receptor A receptor channel permeable to monovalent cations and activated by heat, acid, and capsaicin, the active ingredient of chili peppers.

Further Reading

Devane, W. A., Hanus, L., Breuer, A., Pertwee, R. G., Stevenson, L. A., Griffin, G., Gibson, D., Mandelbaum, A., Etingers, A. and Mechoulam, R. (1992). Isolation and structure of a brain constituent that binds to the cannabinoid receptor. *Science* **258**, 1946–1949.

Di Marzo, V., Fontana, A., Cadas, H., Schinelli, S., Cimino, G., Schwartz, J. C. and Piomelli, D. (1994). Formation and inactivation of endogenous cannabinoid anandamide in central neurons. *Nature* **372**, 686–691.

Piomelli, D. (2003). The molecular logic of brain endocannabinoid signaling. *Nat. Neurosci. Rev.* **4**, 873–884.

Wagner, J. A., Varga, K. and Kunos, G. (1998). Cardiovascular actions of cannabinoids and their generation during shock. *J. Mol. Med.* **76**, 824–836.

Biography

Daniele Piomelli is a Professor in the Department of Pharmacology at the University of California, Irvine. His principal research interest is in the field of lipid signaling, including the endocannabinoids. He holds a doctorate in pharmacy from the University of Naples (Italy) and a Ph.D. in pharmacology from Columbia University, New York. He served as postdoctoral fellow at the Rockefeller University, New York, and worked at the INSERM, Paris, and at the Neurosciences Institute in La Jolla, California. He is a member of the American College of Neuropsychopharmacology.

Endocytosis

Julie G. Donaldson
National Heart, Lung, and Blood Institute, National Institutes of Health, Bethesda, Maryland, USA

Endocytosis is a process carried out by all eukaryotic cells that involves the invagination of the cell surface membrane and constricted closure to form a vesicle that enters the cell interior. Included in the internalized vesicle are extracellular fluid and plasma membrane proteins and lipids. Endocytosis enables the cell to take up extracellular nutrients, remove activated receptors from the cell surface, and turnover cell surface proteins and lipids. Endocytosis is also used for the removal of extracellular debris such as dead cells and bacteria, and as a cellular port of entry for infectious bacteria and viruses. Endocytosis can be broadly divided into pinocytosis (cell drinking) and phagocytosis (cell eating) (Figure 1). There are several types of pinocytosis. The best-characterized type is that involving endocytosis of vesicles coated on the cytoplasmic surface with a protein called clathrin. Phagocytosis involves ingestion of particles by extension and wrapping of plasma membrane around the particle, bringing it into the cell. After internalization, the endocytosed material meets different fates: degradation, recycling back to the cell surface, or routing to other destinations within the cell.

Clathrin-Mediated Endocytosis

Endocytosis that is associated with clathrin coating enables certain plasma membrane proteins to be concentrated and efficiently internalized (Figure 1A). The transferrin receptor and low-density lipoprotein (LDL) receptor are cell surface proteins that are internalized by this mechanism, carrying iron-loaded transferrin protein and cholesterol-bearing LDL particles bound to these receptors into the cell. The clathrin coat that assembles on these structures forms a distinctive basket-like structure that can be visualized by electron microscopy. The polymerization of the clathrin coat is believed to facilitate changes in membrane curvature, deformation of the surface membrane, and formation of the vesicle. Once the vesicle has separated from the cell surface (fission), the clathrin coat is rapidly shed and then reutilized for additional endocytic events. Clathrin-coated pits cover 2% of the plasma membrane and since they are believed to have a lifetime of ~1 min, ~2% of the cell surface membrane is internalized each minute in the average cell. Clathrin-mediated endocytosis accounts for the bulk of pinocytosis in most cells. Clathrin assembly onto membrane requires the prior binding of a set of cytosolic adaptor proteins onto the plasma membrane.

Adaptor Proteins

The clathrin adaptor protein 2 complex (AP2) is composed of four different cytosolic proteins that bind to specific lipids and proteins at the plasma membrane and to clathrin, thus initiating clathrin assembly at distinct sites along the cell surface. There are three additional AP complex proteins in cells that associate with other cellular membranes such as the Golgi complex where they also facilitate clathrin assembly. One of the subunits of AP2 specifically binds to tyrosine-based, amino acid sorting signals in the cytoplasmic regions of plasma membrane proteins. The transferrin receptor contains such a tyrosine signal that sorts transferrin receptor into forming clathrin-coated PM vesicles enabling the transferrin receptor to be efficiently and rapidly internalized into cells. The ability to concentrate specific surface cargo proteins into clathrin-coated pits is the hallmark of clathrin-mediated endocytosis (Figure 2). There are other amino acid sorting signals that allow for rapid internalization via clathrin endocytosis including paired leucine and/or isoleucine residues. Plasma membrane proteins that contain these sorting sequences are continually brought into cells by clathrin-mediated endocytosis. Some hormone receptors such as the β2-adrenergic receptor lack these sorting sequences and do not appreciably enter clathrin-coated vesicles in the absence of hormonal stimulation. However, when the receptor is activated by a hormone, a special adaptor protein called β-arrestin binds to the receptor, allowing the receptor–arrestin complex to associate with AP2 and be rapidly internalized by the clathrin-dependent pathway.

Dynamin

The final step in endocytosis is membrane fission that allows the vesicle to detach from the cell surface. A GTP-binding protein called dynamin facilitates this process

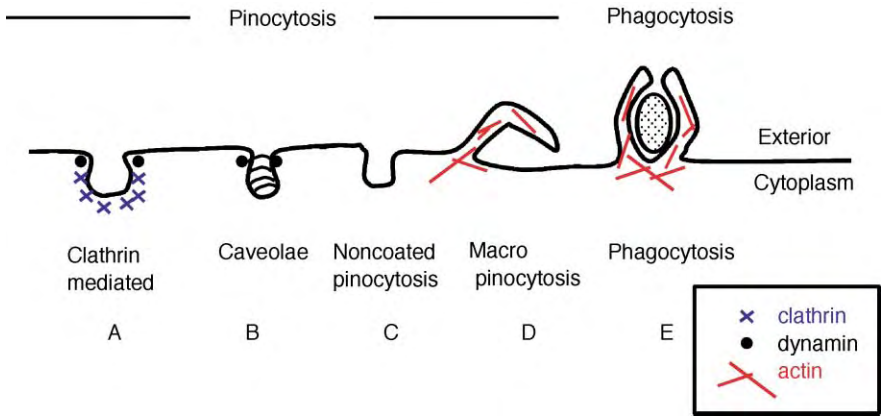

FIGURE 1 Types of endocytosis. Features of the various types of endocytosis (pinocytosis and phagocytosis) are shown. (A) Clathrin-mediated pinocytosis is associated with a cytosolic coat of clathrin (X) and uses dynamin (black spots) for vesicle fission. (B) Caveolae are flask-shaped structures coated with caveolin that also use dynamin for vesicle fission. (C) Non-coated pinocytosis involves invagination of membrane that does not have a recognizable protein coat. (D) Macropinocytosis is associated with cell surface actin-dependent protrusions and forms by fusion of the protruding membrane back onto the cell surface. (E) Phagocytosis is a process that is stimulated by an extracellular particle that induces actin-dependent cell extensions to envelope the particle.

by assembling into ring-like structures and constricting at the necks forming clathrin-coated vesicles. Mutations in dynamin, originally described for *Drosophila melanogaster* mutants, freeze clathrin-forming vesicles at the constricted state and the vesicles are not released. All clathrin-mediated and some other types of endocytosis are dependent upon the function of dynamin. Dynamin also associates with other factors that may facilitate the fission process. Rearrangements in membrane lipids and changes in lipid composition also contribute to the changes in membrane curvature required for vesicle budding and vesicle fission.

Clathrin-Independent Endocytosis

Several other types of pinocytosis have been identified that are not associated with clathrin coats. We know less about the mechanisms of these processes and how they are regulated. Plasma membrane proteins that lack the

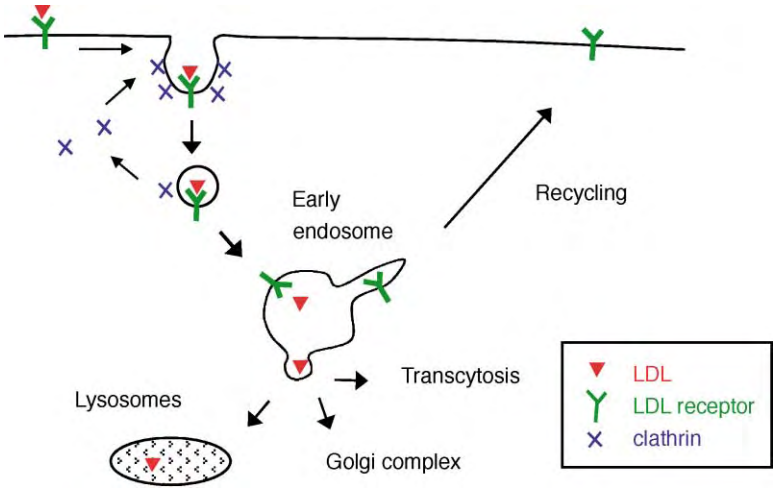

FIGURE 2 Itinerary of internalized cell surface receptors and vesicle contents. Shown here is the pathway followed by internalized LDL bound to the LDL receptor. Cell surface–LDL receptor binds to LDL and is sorted into forming clathrin-coated vesicles at the plasma membrane. After vesicle fission, the clathrin coat is rapidly released from the vesicle so it can assemble again onto the plasma membrane. The vesicle membrane then fuses with the early endosome, a membrane compartment that serves as a sorting station for membrane proteins and lipids. The low pH of the early endosome causes release of LDL from its receptor. The LDL particle and other molecules present in the fluid portion of the early endosome can then be routed to lysosomes for degradation. The LDL receptor enters regions of the early endosome that break off and carry these receptors and membrane back to the plasma membrane. Some membrane proteins leave the early endosome and are transported to other regions of the plasma membrane (transcytosis) or to the Golgi complex.

cytoplasmic amino acid sequences specifying association with AP2 and clathrin, can be endocytosed into cells by these processes.

Caveolae

Some proteins associate with cholesterol and glycosphingolipid-enriched regions of the plasma membrane referred to as membrane raft domains. In many cells, especially in endothelial cells that line blood vessels, these raft domains are present in flask-shaped invaginations of the plasma membrane. These flask-shaped invaginations are called caveolae (caves), and the cytoplasmic coat protein associated with these structures that give them their distinctive shape is called caveolin (Figure 1B). Caveolar endocytosis is dependent upon dynamin and is used as an endocytic mechanism for the transport of materials across endothelial cells. Interestingly, simian virus 40 stimulates caveolar endocytosis and enters many types of cells through this mechanism. Finally, there are cells that lack caveolin and hence caveolae and yet endocytose proteins that associate with membrane raft domains.

Noncoated Endocytosis and Macropinocytosis

Plasma membrane proteins and lipids are also observed in invaginations budding from the membrane that lack any identifiable protein coat (Figures 1C and 1D). This process may or may not require dynamin function depending upon the cell type. Although this process may account for a smaller fraction of cell-surface endocytosis than clathrin-mediated endocytosis, it can be greatly stimulated when cells get activated and form membrane ruffles and protrusive structures. In this case, the membrane ruffle can fuse with the plasma membrane forming a large, macropinosome that internalizes a large amount of surrounding fluid. Dendritic cells of the immune system are very active in macropinocytosis as a means of sampling foreign material in the extracellular fluid. Macropinosome formation is actin dependent. Some bacteria, notably *Salmonella typhi*, stimulate host cells to form membrane ruffles and macropinosomes, and then use these structures as a port of entry into the cells.

Phagocytosis

In lower eukaryotes, such as protozoa, this process of particle ingestion is used for nutrient uptake. However, in mammals phagocytosis is observed in specialized cell types, namely, macrophages and neutrophils that ingest bacteria and dead cells and degrade them. When a macrophage encounters a bacterium that has been coated with antibodies generated by the immune system, cell surface receptors that recognize the Fc portion of the antibodies get activated. This stimulates changes in the macrophage actin cytoskeleton and leads to the extension of membrane around the bacteria, and final closure of the structure through membrane fusion (Figure 1E). Macrophages are also active in phagocytosing senescent-red blood cells and other cells that have undergone programmed cell death. It is believed that macrophages can detect alterations on the cell surface of the senescent cell, such as appearance of a phospholipid on the outer surface that is normally present only on the cytoplasmic side of the plasma membrane. After phagocytosis, the resulting phagosome usually fuses with lysosomes and membrane-bound organelles that contain hydrolytic enzymes that degrade the bacteria. However, some bacteria such as *Mycobacterium tuberculosis*, can actively prevent the fusion of the phagosome with lysosomal membranes, and hence escape degradation.

Fate of Internalized Membrane and Content

After endocytosis, the endocytic vesicle usually fuses with a membrane-bound structure called the early endosome (Figure 2). The early endosome accepts newly endocytosed material and serves as a sorting station that directs incoming proteins and lipids to their final destination. The early endosomal membrane contains a special membrane lipid, phosphatidylinositol 3-phosphate that recruits cytosolic proteins onto these membranes and facilitates the fusion of incoming vesicles with the early endosome. The interior, lumenal environment of the early endosome is moderately acidic (pH 6.5–6.0). The low pH facilitates the sorting process, releasing bound proteins from their receptors and sorting membrane proteins and lipids into different domains. A good example of how low pH serves this function is the itinerary of the transferrin receptor that carries iron-saturated transferrin into the cell. The acidic environment of the early endosome causes the release of iron from transferrin. The iron is then transferred across the membrane into the cytosol, while the transferrin bound to the transferrin receptor is recycled back to the cell surface via membrane carriers that are released from the early endosome. Another example of this sorting of incoming material is the fate of internalized LDL particles bound to the LDL receptor (shown in Figure 2). LDL is released from the receptor in the early endosome and is transferred with other lumenal material to late endosomes and lysosomes. There the LDL is degraded, causing cholesterol

release inside the cell. Meanwhile, the LDL receptor returns to the cell surface to carry out additional rounds of endocytosis. For the transferrin and LDL receptors, endocytosis is a mechanism for delivery of iron and LDL into the cell. By contrast, for signaling receptors, such as those activated by hormones and growth factors, endocytosis is generally used to halt the signaling process by removal of the receptor from the cell surface. An exception to this is the recent observation that the epidermal growth factor (EGF) receptor may require endocytosis for some signaling functions.

Endocytosed membrane proteins can be transported to different locations in the cell (Figure 2). Some membrane proteins are sorted into vesicles that fuse to another region of the plasma membrane, a process called transcytosis. Mucosal immunoglobulins such as IgA are transcytosed across intestinal epithelia via IgA receptors that ferry IgA from the basal (serosal) side to the apical (mucosal) surface of the epithelia. Other proteins leave the early endosome in vesicles that fuse with membranes adjacent to the *trans* side of the Golgi complex.

Regardless of how a membrane is brought into the cell, it must be balanced by addition of membrane back to the plasma membrane. This is accomplished by endosomal-membrane recycling and also through the contribution of newly synthesized membranes from the secretory pathway. The cell has to regulate and coordinate the flux of membrane into and out of the cell to maintain cell surface area and for proper localization of important cell surface receptors.

See Also the Following Articles

Epidermal Growth Factor Receptor Family • Glycoprotein Folding and Processing Reactions • Lipoproteins, HDL/LDL

Glossary

caveolae Flask-shaped invaginations from the plasma membrane that are enriched in cholesterol and glycosphingolipids and are coated with the protein caveolin.

clathrin Cytosolic protein that polymerizes into basket-like coat complex on membranes, facilitating deformation of the plasma membrane to form a vesicle.

dynamin GTP-binding protein that assembles at the necks of forming vesicles and facilitates the fission of membranes to release the vesicle.

phagocytosis Endocytic process involving particle ingestion through extension of cell-surface membranes around particle (typically >250 nm in diameter) and membrane fusion to form phagosome.

pinocytosis Endocytic process involving invaginations of the plasma membrane to generate small (~ 100 nm in diameter) intracellular vesicles.

Further Reading

Alberts, B., Johnson, A., Lewis, J., Raff, M., Roberts, K., and Walter, P. (2002). *Molecular Biology of the Cell*, 4th edition, Garland Science, New York.

Conner, S. D., and Schmid, S. L. (2003). Regulated portals of entry into the cell. *Nature* **422**, 37–44.

Lodish, H., Berk, A., and Zipursky, L. (1999). *Molecular Cell Biology*, 4th edition, W.H. Freeman, New York.

Marsh, M. (ed.) (2001). *Endocytosis*. Oxford University Press, New York.

Slepnev, V. I., and DeCamilli, P. (2000). Accessory factors in clathrin-dependent synaptic vesicle endocytosis. *Nat. Rev. Neurosci.* **1**, 161–172.

Sorkin, A., and von Zastrow, M. (2002). Signal transduction and endocytosis: Close encounters of many kinds. *Nat. Rev. Mol. Cell Biol.* **3**, 600–614.

Biography

Julie G. Donaldson is a Senior Investigator in the Laboratory of Cell Biology in the National Heart, Lung, and Blood Institute at the National Institutes of Health in Bethesda, Maryland. Her research interests are in understanding the mechanisms and regulation of endosomal and secretory membrane traffic in the cell. She holds a Ph.D. from the University of Maryland and was a Postdoctoral Fellow in the National Institute of Child Health and Human Development prior to her current position.

Endoplasmic Reticulum-Associated Protein Degradation

Maurizio Molinari
Institute for Research in Biomedicine, Bellinzona, Switzerland

For proper functioning, a protein has to fold into a characteristic three-dimensional structure and may have to form a multimeric complex. The endoplasmic reticulum (ER) provides an environment optimized for the folding and assembly of proteins that will then be secreted (hormones, antibodies, pancreatic enzymes, etc.), or displayed at the plasma membrane (receptors, channels, etc.), or that reside in intracellular compartments such as the lysosomes and the Golgi. Only native proteins leave the ER to be transported along the secretory pathway to their final destination. A quality control system is in place to prevent forward transport of polypeptides for which folding and assembly have failed. To prevent their accumulation in the lumen of the ER, a series of events regulated by luminal and cytosolic components, and collectively named ER-associated protein degradation (ERAD) ensures that terminally misfolded polypeptides are transferred into the cytosol to be degraded by the 26S proteasome. This article summarizes recent advances in understanding how malfolded glycoproteins are cleared from the ER lumen of mammalian cells.

Protein Synthesis and Folding in the ER

In mammalian cells, secreted proteins are expressed by ribosomes attached at the cytosolic face of the endoplasmic reticulum (ER) at an average synthesis rate of three to five amino acids per second. Nascent chains are translocated into the ER lumen and most of them become N-glycosylated upon addition of pre-assembled, branched oligosaccharides (N-glycans) at asparagines in Asn–Xaa–Ser/Thr sequons. The highly hydrophilic N-glycans preserve the solubility of yet unstructured chains likely to expose hydrophobic, aggregation-prone patches. Moreover, they are the ligands of calnexin and calreticulin, two lectin chaperones that make nascent chains accessible to ERp57. ERp57 is an oxidoreductase that catalyzes the formation of disulfide bonds, a rate-limiting step of the folding process peculiar for proteins expressed in the ER. As thoroughly reviewed by Armando Parodi and Ari Helenius, calnexin, calreticulin and ERp57, together with the sugar-processing enzymes glucosidase I and II and UDP-glucose:glycoprotein glucosyltransferase (GT) compose the calnexin/calreticulin cycle, a chaperone network that assists folding and quality control of glycoproteins.

The kinetics and the efficiency of the folding process are highly variable and depend on the substrate protein considered, and on the cell type where folding occurs. Somewhat surprisingly, the folding of heterologous proteins may be faster and significantly more efficient compared to the maturation of cell-self proteins. So it may take only ten minutes for a viral glycoprotein (e.g., influenza virus hemagglutinin) to complete the folding and oligomerization processes and to leave the ER with an efficiency approaching 100%. On the other hand, it may take several hours before ~20% of the cystic fibrosis channel (CFTR) expressed in the ER lumen becomes native and leaves the compartment. About 80% of the wild-type CFTR is produced just to be degraded, a fate probably shared with a significant fraction of any cellular protein. In some cases, degradation may actually start even before the synthesis of a given polypeptide has been completed. This has no consequences for cell viability and ER-associated protein degradation (ERAD) actually plays an important regulatory role, as shown by Randy Hampton for the HMG-CoA reductase, a rate-limiting enzyme for production of sterols and a variety of essential isoprenoids, whose intracellular level is controlled, at least partially, by regulated degradation.

Folding efficiency may drop substantially, and can be the cause of impaired cell, organ, and/or organism viability when genetic mutations occur that change or delete amino acids in polypeptides (e.g., deletion of phenylalanine at position 508 of the CFTR). If the mutated protein cannot fold properly, it will not fulfill the quality control standard for ER exit and will eventually become a substrate of the ERAD machinery.

Diseases Related to Failure of Protein Folding and Quality Control in the ER

An increasing number of strongly debilitating human diseases has been ascribed to defective protein folding and quality control. Together with cystic fibrosis, one could mention the hereditary lung emphysema and liver failure caused by alpha1-antitrypsin deficiency, diabetes mellitus caused by retention and degradation from the ER of mutant insulin receptors, familial hypercholesterolemia (low-density lipoprotein receptor), osteogenesis imperfecta (type I procollagen), retinitis pigmentosa, and several neurodegenerative diseases. In these so-called "conformational diseases," mutated proteins that do not acquire their native structure are diverted to ERAD. If their disposal is not efficient, they accumulate intra- or extracellularly triggering severe damages to cells and tissues. In some cases, such as the hereditary lung emphysema caused by alpha1-antitrypsin deficiency (alpha1-antitrypsin is the principal blood-borne inhibitor of the destructive neutrophil elastase in the lungs), the lack-of-function phenotype observed at the level of patient's lungs is accompanied by a gain-of-toxic-function phenotype at the level of the patient's liver because the mutated protein accumulates in the ER of hepatocytes.

Degradation of Aberrant Proteins Expressed in the ER: The Mannose Timer

But how are polypeptides recognized as being "non-native," retained in the ER, and targeted for ERAD? The mechanisms, better known for glycoproteins and named GERAD for glycoprotein ERAD by Rick Sifers, are summarized in the following paragraphs.

The quality control machinery of the ER checks the structure and not the function of newly synthesized proteins. Therefore, function-competent proteins can be retained in the ER and destroyed because they are structurally imperfect, as exemplified by the case of the ΔPhe508 CFTR.

The modification of N-glycans can determine the fate of newly synthesized glycoproteins. Glycans are added as preassembled units composed of two N-acetyl-glucosamine, nine mannose, and three glucose residues. Two glucoses are removed in a matter of seconds after addition of the N-glycan to nascent chains. In the minutes following the synthesis of a glycoprotein, the number of glucoses on N-glycans can vary from zero to one in response to the counteracting enzymatic activities of glucosidase II and GT. These modifications control cycles of dissociation from/association with the lectin chaperones, calnexin and calreticulin (as described in Armando Parodi's review). How long newly synthesized proteins are retained in the calnexin/calreticulin cycle depends on their rate of folding. N-glycans of native glycoproteins are inaccessible to GT; they are therefore not re-glucosylated so that mature proteins exit the folding cycle, leave the ER, and are transported along the secretory pathway.

In this model, proteins unable to fold properly persist in the calnexin/calreticulin cycle. To prevent accumulation of aberrant polypeptides in the ER, the terminally misfolded polypeptides have to be released from the calnexin/calreticulin cycle and targeted for degradation. After several unsuccessful folding attempts, N-glycans become substrates of ER-resident mannosidases. Therefore, long retention in the ER as signaled by a reduced number of mannose residues on N-glycans is a clear symptom of a problematic folding. It has originally been proposed by Helenius in 1994 that a timer based on mannose cleavage exists in the ER that decides when it is time to stop folding attempts and to divert unlucky polypeptides for degradation. The timer function that mannosidase activities play during ER quality control is supported by findings which show that cleavage of mannoses from the N-glycans has to take place for GERAD to proceed (as first shown by Green and then elucidated by Sifers, mannosidase inhibitors interfere potently and specifically with GERAD). It is conceivable that GERAD candidates are subjected to folding attempts and remain shielded from the degradation machinery while in the calnexin/calreticulin cycle. Accordingly, the degradation of glycoproteins is usually preceded by a lag phase whose length is determined by the retention of the GERAD candidates in association with the ER lectins.

Distinct ER Chaperone Networks are Involved in the GERAD Process

Involvement of at least two distinct chaperone networks (the calnexin/calreticulin cycle and the BiP/PDI system) has been shown (by the groups of Rick Sifers and Maurizio Molinari) to regulate degradation of GERAD candidates in mammalian cells. Interestingly, misfolded glycoproteins remain in the calnexin/calreticulin cycle when degradation is blocked by mannosidase inhibitors; they are released from the lectin chaperones to remain trapped in the BiP/PDI system, in the lumen of the ER when the proteasome activity is specifically shut down. These data show that the two chaperone networks work sequentially and offer the appealing view that GERAD

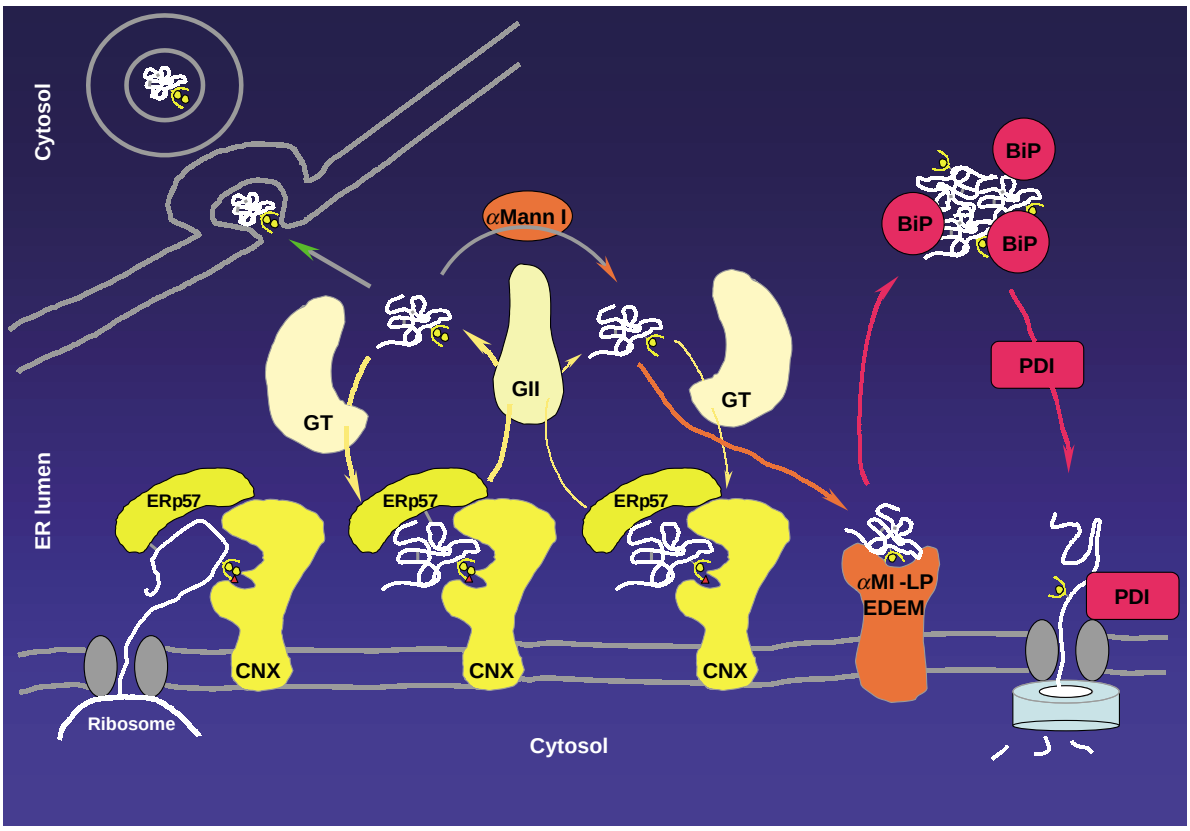

FIGURE 1 The GERAD mechanism can be divided into four steps. First, the GERAD candidate is subjected to folding attempts in the calnexin cycle. Second, the folding-incompetent protein is extracted from the calnexin cycle by the concerted activity of a mannose-trimming enzyme (the ER α-mannosidase I) and a mannose-binding lectin (EDEM). Third, the aberrantly folded polypeptide has to be unfolded (e.g., the wrong disulfide bonds formed during the folding attempts have to be reduced) in order to (fourth) allow dislocation of the GERAD candidate across the ER membrane to be degraded by the proteasome.

candidates are first subjected to folding attempts in the calnexin/calreticulin cycle (lag between synthesis and degradation onset) to be then transferred into the BiP/PDI system that would regulate unfolding and dislocation of the aberrant polypeptide into the cytosol for proteasome-mediated degradation (Figure 1).

A Role for a Mannose-Binding Lectin in GERAD

Mechanistically, the sequential cleavage of mannoses affects the retention of the aberrant protein in the calnexin/calreticulin cycle by decreasing the capacity of glucosidase II and GT to further re- and de-glucosylate the sugar moiety associated with a misfolded chain. Moreover, at least one mannose-binding lectin (EDEM for ER degradation enhancing alpha mannosidase-like protein) is present in the ER lumen and is involved in recognition of aberrant proteins carrying N-glycans with a reduced number of mannose residues, and in deviating them from the folding into the GERAD machinery. The role of EDEM as an acceptor of misfolded glycoproteins released from the calnexin/calreticulin cycle has been recently elucidated by the groups of Kazuhiro Nagata and Maurizio Molinari. It has actually been shown that the intracellular level of EDEM regulates kinetics of the GERAD process by determining the permanence of misfolded proteins in the calnexin cycle. Importantly, as shown by Kazutoshi Mori, the level of EDEM is adapted to the cargo load of the ER, so as to ensure, at any time, optimal disposal of wastes produced during secretory protein synthesis and to prevent processes, which may ultimately lead to cell death through intracellular accumulation of malfolded proteins. Whether EDEM represents the last acceptor of ERAD candidates before their dislocation into the cytosol for proteasome-mediated degradation, or if EDEM regulates the transfer of GERAD candidates from the folding into the unfolding cycles driven by the ER lectins and by the BiP/PDI system, respectively, remains an open question.

See Also the Following Articles

Chaperones, Molecular • Glycoprotein Folding and Processing Reactions • *N*-Linked Glycan Processing

Glucosidases and Mannosidases • Protein Degradation • Protein Folding and Assembly • 26S Proteasome, Structure and Function • Proteoglycans

Glossary

calnexin and calreticulin Calnexin is a nonglycosylated, type I protein of the ER membrane with 573 amino acids. Most of them are in the lumen of the ER and comprise a glucose-binding site for transient association with folding substrates and a P-domain for noncovalent association with the co-chaperone ERp57; 89 residues are cytosolic and contain a RKPRRE ER-retention sequence. Calreticulin is the soluble homologue of calnexin; it has 400 amino acids with a KDEL ER-retrieval sequence.

EDEM *E*R *d*egradation *e*nhancing α-*m*annosidase-like protein is a type II glycoprotein of the ER membrane that shares sequence homology with ER mannosidases. It has, however, no enzymatic activity possibly because it lacks two cysteines conserved in all active mannosidases. The intracellular level of EDEM is increased in response to accumulation in the lumen of the ER of misfolded proteins.

ERAD ER-associated protein degradation (also GERAD for glycoproteins), the processes leading to recognition of misfolded proteins present in the ER lumen and their dislocation into the cytosolic compartment for proteasome-mediated destruction.

quality control The capacity of cells to distinguish and retain in the ER lumen to be eventually targeted for degradation, proteins that have structural defects.

Further Reading

Cabral, C. M., Liu, Y., and Sifers, R. N. (2001). Dissecting glycoprotein quality control in the secretory pathway. *Trends Biochem. Sci.* **26**, 619–624.

Cabral, C., Liu, Y., Moremen, K. W., and Sifers, R. N. (2002). Organizational diversity among distinct glycoprotein ER-associated degradation programs. *Molecul. Biol. Cell* **13**, 2651–2663.

Ellgaard, L., Molinari, M., and Helenius, A. (1999). Setting the standards: Quality control in the secretory pathway. *Science* **286**, 1882–1888.

Hampton, R. Y. (2002). ER-associated degradation in protein quality control and cellular regulation. *Curr. Opin. Cell Biol.* **14**, 476–482.

Helenius, A. (1994). How N-linked oligosaccharides affect glycoprotein folding in the endoplasmic reticulum. *Molecul. Biol. Cell* **5**, 253–265.

Hosokawa, N., Wada, I., Hasegawa, K., Yorihuzi, T., Tremblay, L. O., Herscovics, A., and Nagata, K. (2001). A novel ER {alpha}-mannosidase-like protein accelerates ER-associated degradation. *EMBO Rep.* **2**, 415–422.

Molinari, M., Galli, C., Piccaluga, V., Pieren, M., and Paganetti, P. (2002). Sequential assistance of molecular chaperones and transient formation of covalent complexes during protein degradation from the ER. *J. Cell Biol.* **158**, 247–257.

Molinari, M., Calanca, V., Galli, C., Lucca, P., and Paganetti, P. (2003). Role of EDEM in the release of misfolded glycoproteins from the calnexin cycle. *Science* **299**, 1397–1400.

Oda, Y., Hosokawa, N., Wada, I., and Nagata, K. (2003). EDEM as an acceptor of terminally misfolded glycoproteins released from calnexin. *Science* **299**, 1394–1397.

Parodi, A. J. (2000). Protein glucosylation and its role in protein folding. *Annu. Rev. Biochem.* **69**, 69–93.

Parodi, A. J. (2000). Role of N-oligosaccharide endoplasmic reticulum processing reactions in glycoprotein folding and degradation. *Biochem. J.* **348**, 1–13.

Yoshida, H., Matsui, T., Hosokawa, N., Kaufman, R. J., Nagata, K., and Mori, K. (2003). A time-dependent phase shift in the mammalian unfolded protein response. *Dev. Cell* **4**, 265–271.

Biography

Maurizio Molinari obtained a Ph.D. from the ETH in Zurich, Switzerland, under the guidance of Ernesto Carafoli in 1995. He then performed two postdoctoral training periods in the group of Cesare Montecucco (University of Padua, Italy), and in the group of Ari Helenius (ETH, Zurich). Since October 2000 he has been Group Leader at the Institute for Research in Biomedicine in Bellinzona, Switzerland. His research interests are in the characterization of the mechanisms of folding and degradation of proteins expressed in the endoplasmic reticulum of mammalian cells.

Energy Transduction in Anaerobic Prokaryotes

Gottfried Unden
Johannes-Gutenburg-Universität Mainz, Mainz, Germany

Many prokaryotes (bacteria and archaea) are able to grow in the absence of molecular O_2. In the absence of O_2 metabolic energy can be gained by the catabolic reactions of fermentation, anaerobic respiration, anoxygenic photosynthesis, decarboxylation of dicarboxylic acids, or electrogenic transport of substrate and product molecules. Many of the reactions are unique for prokaryotes. Anaerobic metabolism is essential for many biotopes which are permanently or occasionally anoxic. The bacteria responsible for anaerobic metabolism and mineralization are either strictly anaerobic and restricted to anaerobic biotopes, or facultatively anaerobic, using either aerobic or anaerobic metabolism depending on the O_2 supply. The facultative bacteria switch between aerobic and anaerobic metabolism by using molecular O_2 sensors, which control the expression of aerobic or anaerobic metabolic systems mostly at the transcriptional level.

ADP Phosphorylation Driven by Chemical Coupling or by the Membrane Potential

Synthesis of ATP by fermentation relies on substrate level phosphorylation, whereas the other reactions for anaerobic energy conservation use a membrane potential as the coupling device between energy-supplying and energy-consuming reactions, in particular ADP phosphorylation (Figure 1). Phosphorylation of ADP for generation of ATP requires a free energy ($\Delta G_0'$) of $\sim +50\ \mathrm{kJ\ mol^{-1}}$ under cellular conditions. This amount of free energy has to be supplied in fermentation by one chemical reaction and direct coupling. In the metabolic systems using the membrane or proton potential (Δp) as the coupling device (Figure 1), the energy-supplying reaction on the other hand has to supply only $12-17\ \mathrm{kJ\ mol^{-1}}$ per reaction which is the amount required for translocating 1 H^+ (or Na^+) across the membrane. Three or four H^+ are then used to drive ADP phosphorylation. Therefore, storing the free energy in a membrane potential is favorable for anaerobic catabolic processes which often provide only small amounts of free energy.

The overview will demonstrate, by examples, the functioning of anaerobic metabolism of prokaryotes, in particular fermentation and reactions using a membrane potential for coupling between energy-supplying and energy-consuming reactions.

Fermentation

Typical habitats for fermentation are sediments in freshwater, sewage fermenters, or the digestive tract of vertebrates and insects. Fermentation means growth in the absence of external electron acceptors or light. ADP is phosphorylated under these conditions by substrate level phosphorylation, or direct chemical coupling, without involvement of membranes or membrane potential. Most common substrates for fermentative metabolism are sugars and amino acids. The substrates are first degraded in an oxidative part of metabolism yielding pyruvate or related compounds plus NAD(P)H. For oxidation of the sugars, most bacteria use the glycolytic (Embden–Meyerhof–Parnas, EMP) pathway to pyruvate (glucose + $2NAD^+$ + 2ADP + 2 $P_i \rightarrow$ 2pyruvate + 2NADH + $2H^+$ + 2ATP). Some bacteria use the phosphoketolase (modified pentose-phosphate) pathway (glucose + $3NAD(P)^+$ + ADP + P_i + HSCoA → pyruvate + acetyl-CoA + 3NADH + $3H^+$ + 1ATP) for pyruvate formation, whereas the Entner–Doudoroff (or 2-keto-3-deoxy-6-P-gluconate, KDPG) pathway (glucose + $2NAD(P)^+$ + ADP + $P_i \rightarrow$ 2pyruvate + 2NAD(P)H + $2H^+$ + 1ATP) is found only rarely in anaerobic bacteria.

In simple fermentations pyruvate is used as the electron acceptor for reoxidation of the NAD(P)H formed in sugar oxidation, yielding lactate or ethanol as the fermentation products. In more complicated fermentation reactions (mixed acid fermentation, butyrate fermentation, and others), pyruvate is further oxidized yielding acetate and additional ATP. In these

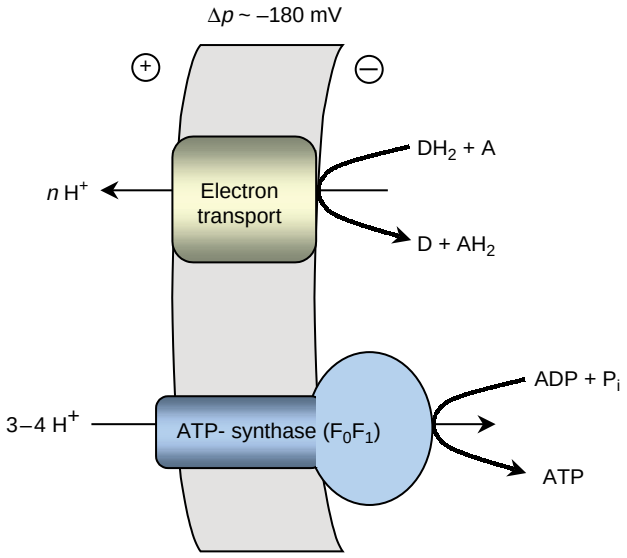

FIGURE 1 Generation of a proton potential (Δp) by translocation of protons across a cytoplasmic membrane by anaerobic respiration and coupling to ADP phosphorylation by ATP synthase. DH_2, electron donor; A, electron acceptor.

pathways butyrate or ethanol (plus acetate) can be obtained as fermentation products among others.

Typical fermentation products derived from sugars and amino acids are carboxylic acids (formate, acetate, propionate, butyrate, and lactate), alcohols (ethanol, 2-propanol, *n*-butanol, and 2,3-butandiol), but also polyols (glycerol, erythritol, and mannitol), CO_2, and H_2 (Table I). The well-known fermentation reactions of this type are homo- and heterofermentative lactic acid, propionic acid, butyric acid, mixed acid, or ethanolic fermentations which are named according to the major or characteristic products (Table I). The ATP yields of the fermentation reactions are generally in the range of 1–3 ATP mol^{-1} of hexose (compared to up to 38 ATP mol^{-1} glucose in aerobic metabolism).

The most important primary or energy-conserving reactions in fermentation are the oxidation of aldehyde to carbonates (thioester formation by glyceroaldehyde-3-phosphate dehydrogenase), the oxidative decarboxylation of α-ketoacids (thioester formation by pyruvate-ferredoxin oxidoreductase), and phosphoroklastic cleavage of ketuloses (acetyl-phosphate formation by phosphoketolase) which are all located in the oxidative part of fermentative metabolism. Reductive desamination of amino acids (acetyl-phosphate formation by glycine reductase) is an example for an energy-conserving reaction in the reductive branch of Stickland fermentation. The energy-rich products obtained from these reactions are then used finally for the phosphorylation of ADP yielding ATP.

Organic matter (polysaccharides, proteins, fats, and monomers derived thereof) can be mineralized in the absence of electron acceptors to methane and CO_2 by interaction of fermenting and methanogenic prokaryotes. The primary fermenters degrade sugars and amino acids to propionate, butyrate, succinate, lactate, acetate, alcohols, CO_2, H_2, and NH_3. H_2, CO_2, and acetate are converted by homoacetogenic and methanogenic prokaryotes to methane and CO_2. Alcohols and fatty acids (short chain fatty acids such as propionate, up to C_{18}), on the other hand, are degraded by secondary fermenters to methane and CO_2. The secondary fermenters are synthrophic bacteria which convert alcohols, fatty acids, and aromatic compounds such as benzoate to H_2, CO_2, and acetate. Secondary fermentation is an endergonic process under standard conditions (e.g., butyrate + $2H_2O \rightarrow$ 2acetate + $H^+ + 2H_2$; $\Delta G_0' = +48.2$ kJ mol^{-1} butyrate) and becomes only exergonic in the presence of syntrophic prokaryotes which consume H_2 to keep it at very low levels. By this the reaction becomes exergonic under environmental conditions ($\Delta G_{env} = -18$ kJ mol^{-1} butyrate) enabling growth of the bacteria. Acetate, H_2, and CO_2 are metabolized by methonogenic archaea and the homoacetogenic bacteria finally to methane and CO_2. In this way fatty acids, alcohols, and aromatic compounds are mineralized yielding CO_2 and methane as the final products.

TABLE I

Fermentation Products of Sugars (Primary Fermentations)

Fermentation (pathway for sugar degradation)	Products per mol glucose (ATP yield per glucose)	Bacterium or microorganism
Lactic acid, homof ermentative (EMP)	2 lactate (+2ATP)	*Lactobacillus lactis*
Lactic acid, heterof ermentative (PK)	1 lactate + 1 ethanol + $1CO_2$ (+1ATP)	*Leuconostoc*
Propionic acid (EMP)	2 propionate (+2–3ATP)	*Propionibacterium*
Butyric acid (EMP)	1 butyrate + $2CO_2$ + $2H_2$ (+3ATP)	*Clostridium butyricum*
Mix acid (EMP)	1 acetate + 1 ethanol + 2 formate (+3ATP)	*Escherichia coli*
Ethanolic (ED)	2 ethanol + $2CO_2$ (+1ATP)	*Zymomonas mobilis*
Ethanolic (EMP)	2 ethanol + $2CO_2$ (+2ATP)	*Saccharomyces cerevisiae* (yeast)

EMP, Embden–Meyerhof–Parnas pathway (glycolysis); PK, phosphoketolase pathway; ED, Entner–Doudoroff pathway.

Fermentation reactions are used on a large scale for preparation of food and beverages. The fermentation reactions and products improve food (nutritional) quality, taste, and durability. For this purpose mainly primary fermentation reactions such as ethanol (beverages), lactic acid (dairy products, vegetables, sour dough), propionic acid fermentation (cheese), and others are used. Solvent production (ethanol, propanol, butanol, and acetone) by Clostridia also depend on type I fermentations. Biotechnological processes for microbiological production of amino acids, citrate, and others, on the other hand, rely on an overflow metabolism of central pathway and anabolic reactions.

Electron Transport Phosphorylation in Anaerobic Respiration

Anaerobic respiration is able to generate an electrochemical proton potential ($\Delta p \sim -0.18$ V) over the membrane which is driven by the oxidation of an electron donor by an (mostly externally added) electron acceptor. The free energy of the redox reaction is converted to and conserved in a proton potential (Figure 1). The proton potential then drives phosphorylation of ADP and formation of ATP by ATP synthase. The Δp generating respiratory chain and the Δp consuming ATP synthase are thus coupled only by the Δp. The free energy of the redox reaction of the respiratory chain under standard conditions and pH 7 is directly related to the difference in the redox potentials of the electron donors and acceptors ($\Delta E_0'$), the Faraday constant ($F = 96.5 \times 10^3$ J mol^{-1} V^{-1}) and the number of participating electrons (n):

$$\Delta G_0' = -nF\Delta E_0'$$

Figure 2 gives a selection of important electron donors and acceptors used by prokaryotes in anaerobic respiration and the corresponding midpoint potentials. The $\Delta E_0'$ value sets the maximal (theoretical) amount of electrons (H^+/e ratio) which can be translocated across the membrane for the given Δp value (-0.18 V):

$$(H^+/e)_{max} = \Delta E_0'/\Delta p$$

The actual H^+/e ratio generally is lower than the calculated value due to lower coupling efficiency, and since some electron transport enzymes lack coupling mechanisms for H^+ translocation. From the above equations it follows that the minimal amount of free energy required for translocation of 1 H^+ across membranes ($\Delta p = -180$ mV) amounts to -17.4 kJ mol^{-1}. Thus free energy as low as $\Delta G_0' = -17$ kJ mol^{-1} can be conserved in a membrane potential by anaerobic respiration (or other Δp generating reactions) compared to $\Delta G_0'$ value of ~ -50 kJ mol^{-1} required in substrate level phosphorylation. Therefore storage of free energy in a membrane potential allows use of energy-supplying reaction with low $\Delta G_0'$ values, since 3–4 translocated H^+ or Na^+ ions are equivalent to phosphorylation of one ADP. This coupling mechanism is of particular significance for reactions of anaerobic metabolism which are only weakly exergonic.

In anaerobic respiration a large number of different electron acceptors can be used, including S^0, CO_2, sulfate, fumarate, nitrate, tetrachlorethen, and Fe^{3+} (Figure 2). The free energy, and thus the ATP yields, are distinctly lower than in aerobic respiration due to the more negative redox potentials (and thus $\Delta E_0'$ values) of the electron acceptors. Most of the anaerobic respiratory systems are composed of two enzymes, a dehydrogenase and a terminal reductase. The enzymes are linked by diffusible low molecular redox mediators (quinones). In anaerobic respiration menaquinone (MK, a lipophilic naphtoquinone derivative with $E_0' = -80$ mV) replaces ubiquinone (Q, a lipophilic benzoquinone derivative with $E_0' = +110$ mV) from aerobic respiratory chains. Figure 3 gives a schematic presentation on the topology and arrangement of enzymes in fumarate and nitrate respiration with formate as the electron donor. The biochemistry and energetics of the enzymes have been studied in detail, and the structures of the enzymes have been solved by X-ray cristallography. Each of the enzymes is anchored in the membrane with a hydrophobic anchor protein, which contains the active site for the lipophilic quinone. The second active site for the hydrophilic substrates formate, fumarate, or nitrate, is located in the cytoplasmic or periplasmic protrusions of the enzymes.

In formate:fumarate reductase respiration the enzymes catalyze the following reactions:

Formate dehydrogenase :

$$\text{Formate} + \text{MK} + 2H^+_{in} \rightarrow CO_2 + \text{MKH}_2 + 2H^+_{ex}$$

Fumarate reductase :

$$\text{Fumarate} + \text{MKH}_2 + 2H^+_{in} \rightarrow \text{succinate} + \text{MK} + 2H^+_{in}$$

Formate : fumarate reduction :

$$\text{Formate} + \text{fumarate} + 2H^+_{in} \rightarrow \text{Succinate} + CO_2 + 2H^+_{ex}$$

The overall reaction of formate : fumarate respiration results in the release of $2H^+$ at the periplasmic, and consumption of $2H^+$ at the cytoplasmic side of the membrane resulting in a H^+/2e ratio of 2, which is due to the action of formate dehydrogenase. The enzyme has the

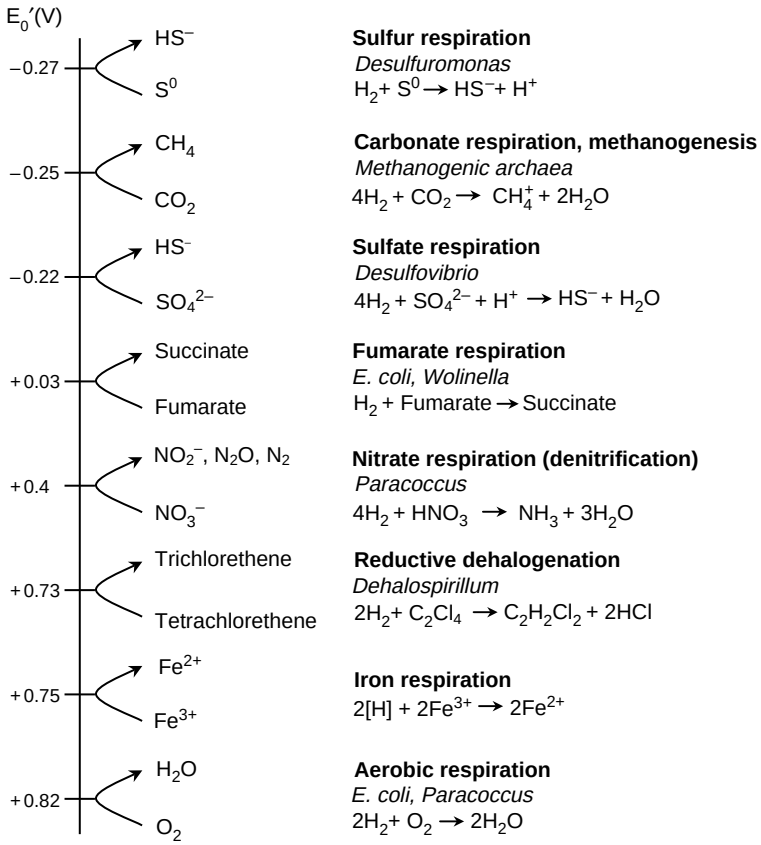

FIGURE 2 Important electron acceptors of anaerobic respiration by prokaryotes. The scheme gives the redox potentials of the redox pairs, the type of respiration, the metabolic balance using H_2 as the electron donor and examples for prokaryotes catalyzing the reaction. The free energy of the reaction can be calculated from $\Delta G_0' = -nF\Delta E_0'$, and is for example for fumarate respiration (H_2 + fumarate → succinate) $\Delta G_0' = -87$ kJ mol^{-1}.

active sites for formate oxidation and menaquinone reduction on opposite sides of the membrane, and translocates $2e^-$ from the formate to the quinone site, resulting in an overall translocation of two charges across the membrane (without actual translocation of H^+) and generation of Δp. Many anaerobic respiratory enzymes generate Δp in the same way. This mechanism of Δp generation has to be distinguished from proton-pumping redox enzymes, such as cytochrome *c* oxidase, which transfer protons across the membrane in a reaction, which is driven by a redox reaction (proton pump).

In fumarate reductase the protons are released (menaquinol site) and consumed (fumarate site) finally on the same (cytoplasmic) side of the membrane. The reaction therefore is not electrogenic and does not contribute to the formation of Δp, and fumarate reductase functions only as an electron sink. The overall $H^+/2e^-$ ratio of formate fumarate reduction is 2 (2 from formate dehydrogenase, 0 from fumarate reductase). These findings are in agreement with the energetics of the overall formate fumarate reduction, and of the partial reactions. The big difference in the redox potentials of the electron donor formate and of the electron acceptor menaquinone of formate:menaquinone reductase ($\Delta E_0' = -340$ mV) allows generation of a proton potential (max. H^+/e^- ratio ≤ 1.9). For fumarate reductase $\Delta E_0'$ is much lower ($\Delta E_0' = -110$ mV) which is not sufficient for generation of a proton potential in agreement with the scheme of Figure 3. In the same way other terminal reductases such as nitrite reductase from *Wolinella succinogenes* function as electron acceptors without contributing directly to Δp production.

Formate–nitrate respiration is catalyzed by an electron transport chain consisting of formate dehydrogenase and nitrate reductase:

Formate dehydrogenase:

$$\text{Formate} + \text{MK} + 2\text{H}^+_{\text{in}} \rightarrow \text{CO}_2 + \text{MKH}_2 + 2\text{H}^+_{\text{ex}}$$

Nitrate reductase:

$$\text{Nitrate} + \text{MKH}_2 + 2\text{H}^+_{\text{in}} \rightarrow \text{Nitrite} + \text{MK} + \text{H}_2\text{O} + 2\text{H}^+_{\text{ex}}$$

Formate:nitrate reduction:

$$\text{Formate} + \text{nitrate} + 4\text{H}^+_{\text{in}} \rightarrow \text{nitrite} + \text{CO}_2 + 4\text{H}^+_{\text{ex}}$$

For quinol:nitrate reduction with nitrate ($E_0' = +430$ mV) as the electron acceptor, $\Delta E_0'$ amounts to -510 mV with

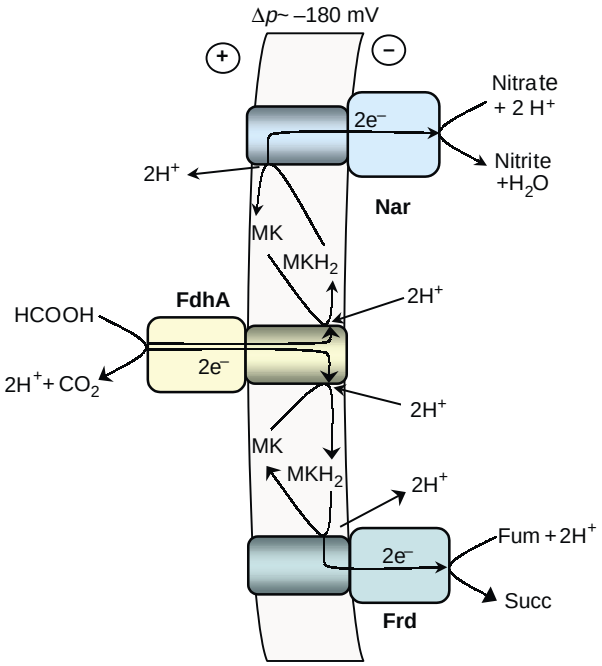

FIGURE 3 Formate–fumarate and formate–nitrate respiration. The figure shows topology and reactions of formate dehydrogenase (formate:quinol reductase), fumarate reductase (quinol:fumarate reductase) and nitrate reductase (quinol:nitrate reductase). Note the topology of the active sites for formate, fumarate, nitrate, and the quinones, the release and consumption of H^+ at the active sites, and transmembrane transfer of electrons in formate dehydrogenase and nitrate reductase. Frd, fumarate reductase; Nar, Nitrate reductase; Fdh, formate dehydrogenase. Examples of this type of fumarate respiration are found in *E. coli* and *Wolinella* of the nitrate respiration in *E. coli*.

menaquinol, or to -350 mV with ubiquinol as the electron donor, which allows conservation of the redox energy in a proton potential (Figure 3). Accordingly, the enzyme functions as a redox half-loop very similar to (but mirror-inverted) formate dehydrogenase, resulting in the translocation of two positive charges across the membrane (inside to outside).

A similar organization is found for many anaerobic respiratory chains, which are composed of one respiratory dehydrogenase and terminal reductase each, and which are linked by the quinones. In this way a large number of different respiratory dehydrogenases and terminal reductases can be linked to each other in branched respiratory chains.

Decarboxylation of Dicarboxylic Acids

Some anaerobic bacteria grow at the expense of decarboxylation of dicarboxylic acids such as oxaloacetate or succinate. The free energy of this reaction amounts to ~ -20 kJ mol^{-1} and is used for translocation of one Na^+ across the membrane by a membraneous decarboxylase as the energy-conserving reaction. The sodium motive force generated in this way can be used to drive secondary substrate transport, flagella, motility, or for phosphorylation of ADP if the bacteria contain an Na^+ potential-driven ATP synthase. The Na^+-dependent ATP synthase is very similar in function and composition to H^+-translocating F_1F_0-ATP synthase. In this way 3–4 decarboxylation reactions are required for phosphorylation of one ADP. *Propionigenium modestum* grows by conversion of succinate to propionate, including decarboxylation of methylmalony-CoA by a membraneous decarboxylase (Figure 4). Succinate is converted to methylmalonyl-CoA which is then decarboxylated in a reaction coupled to Na^+ translocation. The enzyme in addition consumes one H^+ from the periplasmic side of the membrane for the formation of propionyl-CoA + CO_2. Thus, the free energy of decarboxylation is used for generating an electrochemical Na^+ potential. The decarboxylation represents an intramolecular redox reaction producing an oxidized (CO_2) and a reduced (propionate) product. The reaction, however, does not comprise electron transport and depends only on the membraneous decarboxylase for generation

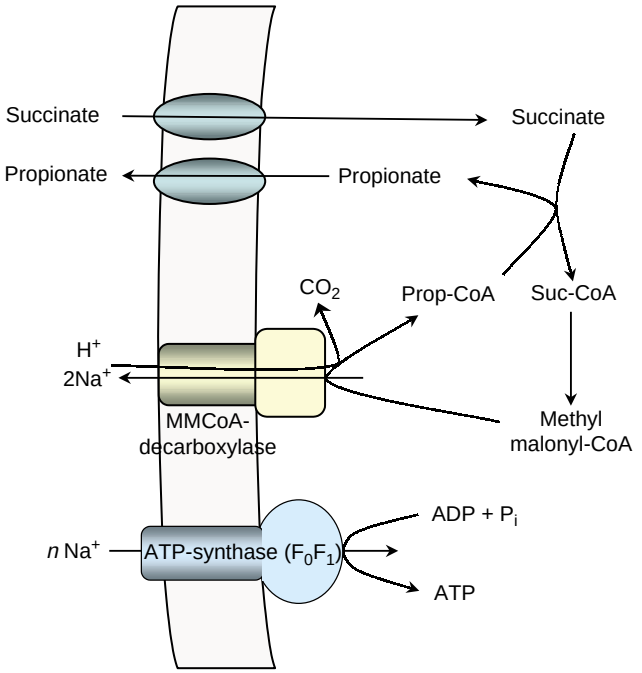

FIGURE 4 Anaerobic growth on succinate by *P. modestum* (succinate + $H_2O \rightarrow$ propionate + CO_2; $\Delta G_0' = -21$ kJ mol^{-1}) and generation of an Na^+ potential by decarboxylation. The membraneous methylmalony-CoA decarboxylase couples decarboxylation to translocation of $2Na^+$ ions over the membrane. H^+ for the decaroxylation reaction is derived from the outside.

of the electrochemical potential. In *Klebsiella*, an enterobacterium closely related to *Escherichia coli*, a membraneous Na^+ translocating decarboxylase of this type (oxaloacetate decarboxylase) is part of citrate fermentation and decarboxylates oxaloacetate yielding pyruvate which can be further converted to acetate + formate. In citrate fermentation ATP is formed in addition by substrate level phosphorylation, or a H^+ potential is generated in respiratory pathways. Therefore, the ATP synthase of *Klebsiella* is H^+ dependent, and the Na^+ potential is used mainly for secondary substrate transport.

Generation of a H^+-Potential by Transport of Charged Substrate and Product Molecules

Some bacteria use the (electrogenic) transport of substrate and product molecules for the generation of a proton potential. *Oxalobacter formigenes* and lactic acid bacteria like *Lactococcus lactis* or *Oenococcus oeni* are able to generate a proton potential by decarboxylation of the dicarboxylic acids oxalate or malate. The decarboxylation is catalyzed by cytoplasmic enzymes, and the free energy of the reaction is not directly stored in a membrane potential as in the membraneous decarboxylases. In *Oxalobacter* oxalate^{2-} is taken up by an electrogenic antiport with formate, the end product of the pathway (Figure 5). Decarboxylation of activated oxalate (oxalyl-CoA) produces CO_2 and consumes one H^+. The antiport of the dianionic oxalate against the monoanionic formate generates an electrical gradient (outside positive), and consumption of $1H^+$ by the decarboxylation generates a ΔpH (alkaline inside). The resulting proton potential is then used to drive ADP phosphorylation by a H^+-ATP synthase.

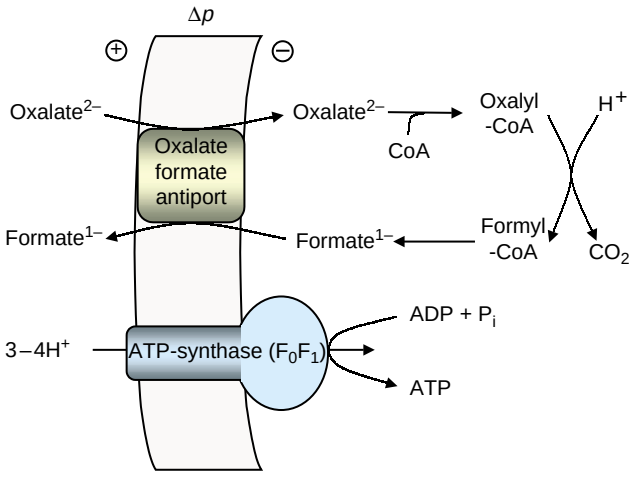

FIGURE 5 Anaerobic growth on oxalate by *Oxalobacter formigenes* (oxalate → formate + CO_2; $\Delta G_0' = -27$ kJ mol^{-1}) and generation of a H^+ potential by electrogenic oxalate^{2-}/formate^{1-} antiport and decarboxylation of oxalate by a cytoplasmic (H^+ consuming) decarboxylase.

Decarboxylation of malate by lactic acid bacteria (malolactic fermentation: malate^{2-} + H^+ → lactate$^-$ + CO_2) uses a similar mechanism of energy conservation. In *Lactococcus lactis* malate^{2-} is taken up and converted by a cytoplasmic decarboxylase to lactate$^-$ + CO_2, consuming H^+ as a cosubstrate. Malate^{2-} and lactate$^-$ are transported by an electrogenic antiporter generating an electrical potential (outside positive), and H^+ consumption in the cytoplasm during decarboxylation generates a ΔpH value (inside alkaline). The proton potential can be used for driving ADP synthesis by a membraneous ATP synthase.

Anoxygenic Photosynthetic Prokaryotes

Anoxygenic photosynthetic bacteria use only one photosystem for converting light energy into an electrochemical proton potential which is then used for driving ADP phosphorylation. Anoxygenic photosynthetic bacteria are found in three different phylogenetic groups which contain different photosynthetic systems: the purple bacteria, the green phototrophic bacteria with the subgroups of green sulfur bacteria (Chlorobiaceae) and *Chloroflexus*, and the gram-positive Heliobacteria. The three groups show differences in the type of photosynthetic reaction center, photosynthetic electron transfer and the electron donors used, pigments, and the pathway for CO_2 fixation. In anoxygenic photosynthesis, light is used to raise electrons to a more electronegative redox potential and to feed the electrons into a cyclic electron transport to generate a proton potential. The cyclic electron transport systems contain only one reaction center in contrast to oxygenic photosynthesis in cyanobacteria, green algae, or plants. The archaeon *Halobacterium salinarum*, on the other hand, contains a proton pump which is directly driven by light to translocate protons over the membrane without involvement of a photosynthetic electron transport. In contrast to the photosynthetic bacteria using chlorophyll containing proteins for photosynthesis and energy conversion, *Halobacterium* contains bacteriorhodopsin with retinal as a chromophor for light absorption and conversion to an electrochemical proton potential.

See Also the Following Articles

Chemiosmotic Theory • Energy Transduction in Anaerobic Prokaryotes • Pentose Phosphate (Hexose Mono Phosphate) Pathway • Pentose Phosphate Pathway, History of • Photosynthesis • Propionyl CoA–Succinyl CoA Pathway • Respiratory Chain and ATP Synthase

Glossary

ATP synthase (F_0F_1-ATPase) Enzyme in mitochondria and bacteria for the phosphorylation of ADP which is driven by the proton potential over the membrane.

chemiosmotic hypothesis Mechanisms for the coupling of the endergonic ATP synthesis by ATP synthase to the exergonic electron transport via a proton potential over the membrane.

prokaryotes Microorganisms, mostly unicellular, in which the chromosome is organized in a nucleoid (rather than a nucleus) which is not separated from the cytoplasm by a membrane. Bacteria and Archaea, two of the three major domains of living organisms, are prokaryotes.

Further Reading

Lengeler, J. W., Drews, G., and Schlegel, H. G. (1999). *Biology of the Prokaryotes.* Thieme, Stuttgart and Blackwell Science, Oxford.

Madigan, M. T., Martinko, J. M., and Parker, J. (2000). *Brock Biology of Microorganisms*, 9th edition, Prentice-Hall, Upper Saddle River, NJ.

Mitchell, P. (1961). Coupling of phosphorylation to electron and hydrogen transfer by a chemi-osmotic type of mechanism. *Naturwissenschaften* **191**, 144–148.

Unden, G., and Bongaerts, J. (1997). Alternative respiratory pathways of *Escherichia coli*: Energetics and transcriptional regulation in response to electron acceptors. *Biochim. Biophys. Acta* **1320**, 217–234.

Biography

Dr. Gottfried Unden is a professor for microbiology at the department for Microbiology and Wine Research at the Johannes Gutenberg-University, Mainz, Germany. His principal research interest is in facultatively anaerobic bacterial metabolism, function of bacterial sensors for environmental stimuli, and bacterial fermentation reactions in wine.

Enzyme Inhibitors

Vern L. Schramm
Albert Einstein College of Medicine, Yeshiva University, Bronx, New York, USA

Enzymes catalyze the chemical reactions necessary for life. They typically increase chemical reaction rates by factors of 10^{10}–10^{15}. The first step to initiate catalysis is binding the reactant molecules into the catalytic sites to form the Michaelis complex. In most enzymes, a conformational change occurs to enclose the reactants tightly in the enzyme and to make contacts between reactants and the enzyme that will achieve the transition state and subsequently form products. The enzyme then relaxes to open the catalytic site and release products. Enzyme inhibitors prevent enzymes from their catalytic function by interfering with any step in this catalytic cycle. Four common types of enzyme inhibitors are given as follows:

1. catalytic site inhibitors that compete with the substrate for formation of the Michaelis complex, traditionally called competitive inhibitors;

2. inhibitors that alter formation of the Michaelis complex and full expression of catalytic potential are called noncompetitive inhibitors;

3. covalent inhibitors that form a Michaelis complex followed by a chemical reaction with the enzyme to form a stable and inactive complex, often called mechanism-based inhibitors or "suicide inhibitors"; and

4. transition-state analogue inhibitors that resemble the unstable reactant complex at the transition state of the reaction.

Reversible Catalytic-Site Inhibitors

Reactant and Product Analogues

Molecules with shape and charge similar to the substrate or products may bind to the catalytic site similar to the normal reactants. When they are bound, substrate cannot bind and the enzyme is prevented from catalyzing the reaction. The relative affinity of these competing molecules for the catalytic site and their abundance relative to substrate will determine if they prevent substrate binding (Figures 1 and 2). Thus, if reactants and inhibitors bind with equal affinity, at equal concentrations, the enzyme catalytic site will be equally occupied with reactants and inhibitor resulting in 50% inhibition. This relationship is described in quantitative terms by the competition between an inhibitor (I) and a reactant (A) for a simple enzyme with one reactant by the equation: $v = (k_{cat})(A)/(K_m + A(1 + I/K_i))$, where v is the enzymatic reaction rate, k_{cat} is the maximum catalytic rate of the enzyme, K_m is related to the binding affinity between enzyme and substrate, defined as the concentration of substrate to achieve 50% of k_{cat} in the absence of inhibitor, and K_i is the dissociation constant for the enzyme–inhibitor complex, defined by the equation: $K_i = (E)(I)/(EI)$, and A and I are reactant and inhibitor concentrations. Diagrams of substrate and product inhibition illustrate the mutually exclusive or "competitive" inhibition relative to the catalytic site (Figure 2). Complete graphical and mathematical analyses of enzyme inhibition cases are available.

Bisubstrate Mimics

Many enzymatic reactions combine two different molecules at the catalytic site to transfer a chemical group between them. An example is the enzyme adenylate kinase that transfers the terminal phosphoryl group of ATP to AMP to generate two molecules of ADP (Figure 3). The catalytic site must accommodate ATP and AMP at the same time in preparation for group transfer. The bisubstrate mimic for the adenylate kinase reaction is chemically similar to ATP combined with AMP to make a bisubstrate molecule called AP_5A (Figure 3). Such molecules compete for both substrate sites, since they prevent either substrate from binding by competition for the same sites. Bisubstrate mimics can bind tightly to the enzyme since connected molecules bind with affinity equal to the product of the affinity of the individual molecules. For example, if individual dissociation constants (K_i values) for ATP and AMP are both 10^{-4} M, the dissociation constant for the bisubstrate mimic would be expected to be related to the product of these constants or $10^{-4} \times 10^{-4}$ M $= 10^{-8}$ M.

Transition-State Analogues

A special class of competitive inhibitors resembles the reactant molecule at the very point where it

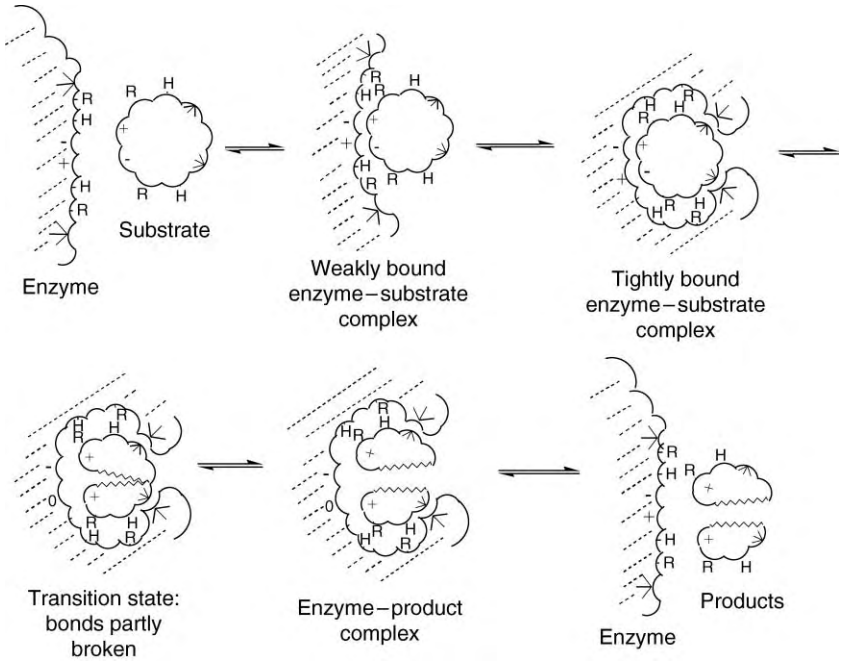

FIGURE 1 A schematic for the steps in enzyme-catalyzed reactions. In the first step diffusion causes collision between the substrate and an open catalytic site. The weakly bound enzyme–substrate complex causes the protein to close to form the tightly bound enzyme–substrate complex. Hydrogen bonds (H–R), ionic bonds (+ −), and hydrophobic interactions (><) in this closed complex at the transition state are shown. Following bond changes, the enzyme–product complex relaxes to release product and regenerate the original form of the enzyme to repeat the cycle.

crosses the chemical energy equivalence point of bond breaking/bond making called the transition state. These inhibitor molecules must be chemically stable, but have close similarity to the unstable transition state. Based on the theory of transition-state stabilization for enzyme-catalyzed reactions, the perfectly designed transition-state analogue is capable of binding to the enzyme by the factor: K_i for transition state inhibitor $= K_m$/catalytic rate enhancement. Since enzymatic catalytic rate enhancements are typically 10^{10}–10^{15}, perfectly designed transition-state inhibitors can bind 10^{10}–10^{15} times better than substrate. These incredibly large affinities have been rarely achieved. It is impossible to match the nonequilibrium bond lengths and partial charges present at the precise moment of the transition state with chemically stable molecules. However, incorporation of even modest similarities between the actual transition-state and transition-state analogues can achieve binding affinities 10^5–10^7 times that of reactants, and this improvement is adequate to achieve inhibition of the targeted enzymes in biological systems.

Enzymatic Transition States

This point of the chemical reaction is often the most energetic point in the reaction cycle, and therefore the rarest and the most difficult to detect. The exact shape and charge of the substrate molecule at the moment of the transition state is of great interest, since chemically stable molecules that resemble the substrate molecule at the transition state bind extremely tightly to the enzyme, as discussed above. This concept was proposed early in the history of biochemistry by Linus Pauling, and was formalized several decades later by Richard Wolfenden. An example of the substrate, enzyme-stabilized transition state and a transition analogue for purine nucleosidase phosphorylase is shown (Figure 4). These inhibitors commonly bind to the catalytic sites of enzymes millions of times more tightly than the substrates. Many of the antibiotics isolated in nature have been found to be transition-state analogues. Recently, molecules designed to be transition-state analogues are being tested in medical applications such as anticancer agents. Transition-state inhibitors compete at the catalytic site and cause the enzyme to fold into its tightly binding mode and keep it closed for long times, preventing catalysis (see Figure 1).

Design of Transition-State Analogues

Both the shape and charge of reactant molecules change as they reach the transition state (see Figure 1). The structure of the transition state can be experimentally measured by using kinetic isotope effects, combined with computational chemistry to locate the enzymatic

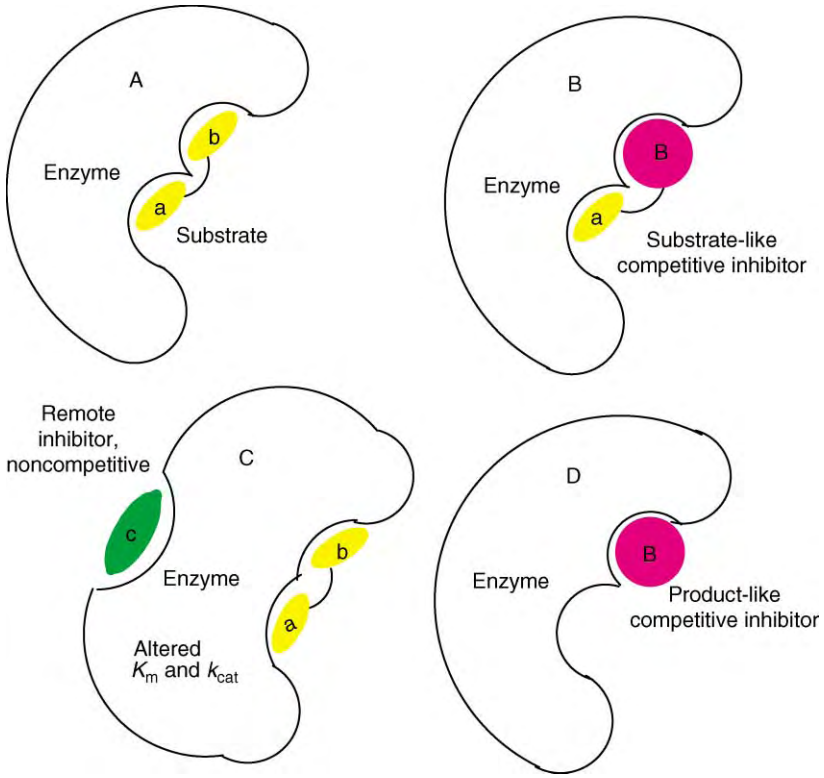

FIGURE 2 Enzyme A is a normal Michaelis complex with substrate a–b at the catalytic site (yellow). The bond to be broken by the enzyme connects a and b. The substrate-like competitive inhibitor (pink, enzyme B) has a difference in the B part of the bound molecule and is not a substrate but competes directly for a–b at the catalytic site. Since this is a competition, large amounts of a–b will displace a–B. A noncompetitive inhibitor binds to influence catalysis but does not directly compete for the catalytic site. There are many variants of noncompetitive inhibition and binding at a remote site to change features of the catalytic site is one example (green in enzyme C). Competitive inhibitors can also be product-like as shown in enzyme D (pink).

transition state. The electron distribution at the van der Waals surface of a molecule is called its molecular electrostatic potential surface. This can be described for substrate and transition states for enzyme reactions provided the transition-state structure is known, and can also be established for proposed inhibitor molecules. Electrostatic matches to the transition state make powerful inhibitors by capturing some of the transition-state energy usually applied to catalysis (Figure 4).

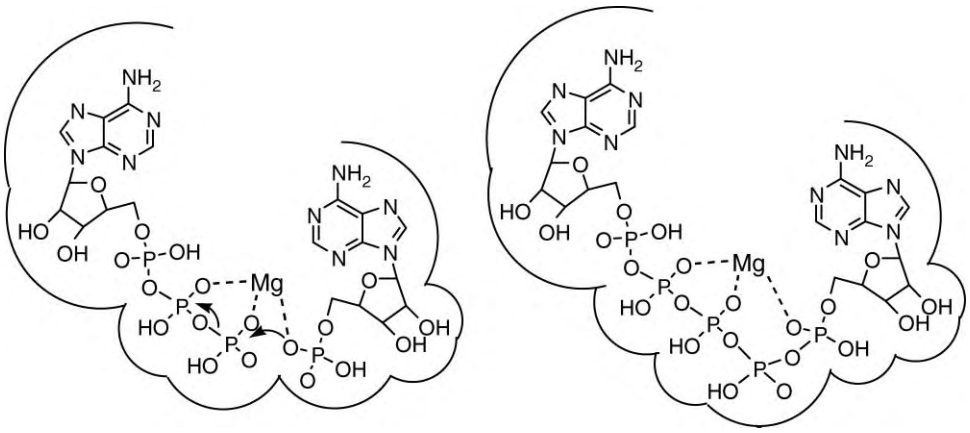

FIGURE 3 The Michaelis complex for adenylate kinase (ATP + AMP → 2ADP) is shown on the left with the arrows indicating electron flow for the phosphoryl group transfer. The inhibited complex with adenosyl–pentaphosphate–adenosine (A–P5–A) is on the right. The bisubstrate inhibitor competes for both ATP- and AMP-binding sites. Ionic charges are omitted for clarity and the ribosyl groups are all β-D-ribose in stereochemistry.

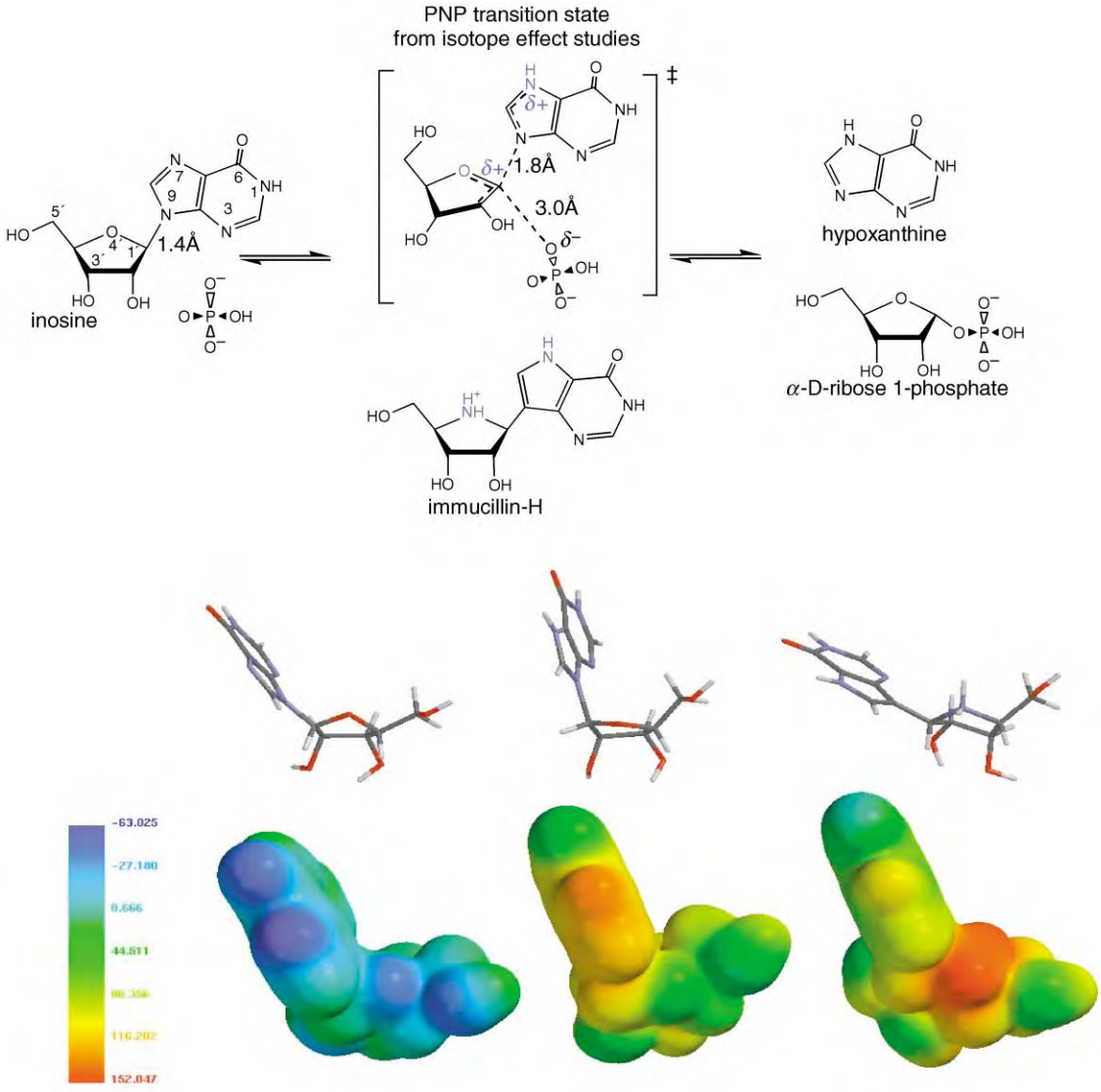

FIGURE 4 The reaction catalyzed by bovine purine nucleoside phosphorylase (PNP), transition-state structure, and a transition-state analogue inhibitor (immucillin-H). Novel features of the transition state are protonation at N7 and the partial positive charge on the ribosyl group. Both are represented in the inhibitor, shown in blue. Immucillin-H binds approximately 1 million times more tightly to PNP than does the substrate inosine. Shown below are the electronic van der Waals surfaces of inosine (left), transition state (middle), and Immucillin-H (right). Note the electrostatic similarity between transition state and Immucillin-H. Reproduced with permission of Elsevier Ltd., from Vern, L. Schramn. Development of transition state analogues of purine nucleoside phosphorylase as anti-T-cell agents. (2002) *Biochem. Biophys. Acta* **1587**, 107–117.

Natural Product Transition-State Analogues

Many antibiotics isolated from natural sources are transition-state inhibitors. One example is an antibiotic formed in the culture medium of *Streptomyces antibioticus* that is apparently made as an agent of microbial warfare between species of soil organisms. R-Coformycin binds to the catalytic sites of adenine nucleoside and nucleotide deaminases millions of times tighter than the reactant molecules. The transition-state structure for deaminase enzymes has been solved and the similarity of transition-state analogue and transition state is greater than either to the substrate (Figure 5).

Noncatalytic Site Inhibitors

Noncatalytic site inhibitors include all inhibitors binding at sites other than the catalytic site. These inhibitor molecules can cause several different types of enzymatic inhibition, both competitive inhibition and noncompetitive inhibition. The reason for this diversity arises by inhibitor binding distant to the catalytic site but, in so doing, changing the enzyme conformation to prevent proper function of the enzyme either in binding its substrate or in formation of the products.

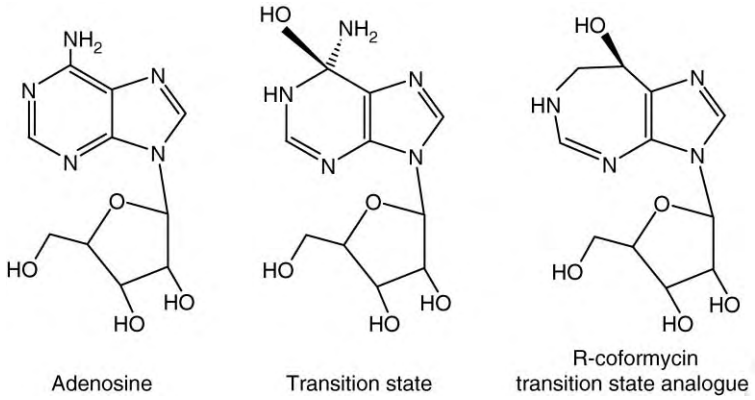

FIGURE 5 Reactant (adenosine), transition state, and transition-state analogue inhibitor for adenosine deaminase. R-Coformycin is a natural product transition state analogue inhibitor that binds 10 million times tighter to adenosine deaminase than does adenosine.

Prevent Catalytic-Site Binding

An inhibitor may bind remote from the catalytic site to change the protein conformation to cause mutual exclusion between reactant binding at the catalytic site and inhibitor binding at the remote site. For this interaction, kinetic analysis of the type shown above will be kinetically indistinguishable from competitive inhibition. The surfaces of proteins contain highly irregular and charged surfaces that interact with specific molecules. Current practice of testing libraries of diverse chemical compounds against a specific enzyme to find any type of interaction that can cause inhibition often discovers this class of inhibitor.

Prevent Subunit Formation

Most enzymes have multiple protein subunits that must interact to provide a functional catalytic unit. An example is the ribonucleotide diphosphate reductase required to form deoxynucleotides for the biological production of DNA. During cellular protein synthesis of these enzymes, the protein subunits are formed separately and must then combine to make the functional catalyst. In the cell, these subunits are thought to separate and recombine many times, providing an opportunity to insert an inhibitory molecule in the protein interface between subunits. Selection of such molecules from chemical libraries or designing them from known protein–protein interfaces prevents formation of the active enzyme molecule in the cell. Inhibitors of this type have been designed for ribonucleotide diphosphate reductase and show promise in this new area of specific inhibitor design.

Prevent Conformational Change for Catalysis

A related inhibitor type is one binding remote from the catalytic site to prevent an enzymatic conformational change that is required for catalysis. Most enzymes require protein motion to close the catalytic site prior to formation of the transition state. These loop or domain motions involve physical motion of segments of the proteins, often over relatively large distances. A consequence of the motion is to position amino acid residues in the catalytic site where they are required for catalysis. An inhibitor that binds outside the catalytic site and prevents this protein motion required for catalysis will provide complete loss of enzyme function without blocking access of reactants to the catalytic site. As knowledge of the protein surfaces becomes more complete, it will be increasingly possible to design molecules that act in these novel inhibitory roles.

Mechanism-Based Inhibitors

Mechanism-based enzymatic inhibitors are designed to be stable molecules that resemble the substrate. They bind at the catalytic site of the target enzyme and are converted by the enzyme to a chemically reactive form that covalently reacts with the catalytic site of the enzyme. This covalent intermediate of enzyme inhibitor differs from normal catalytic intermediates by its chemical stability and long lifetime. Trapping the enzyme in a stable covalent complex blocks the catalytic site from normal interaction and provides long-term inhibition of the enzyme. Mechanism-based inhibitors are in broad use in biology, and our example of this chemical inhibitor logic is in the pathway of polyamines (Figure 6).

Polyamine Synthesis

The polycationic polyamines are essential counterions for DNA replication in dividing cells. The first step in

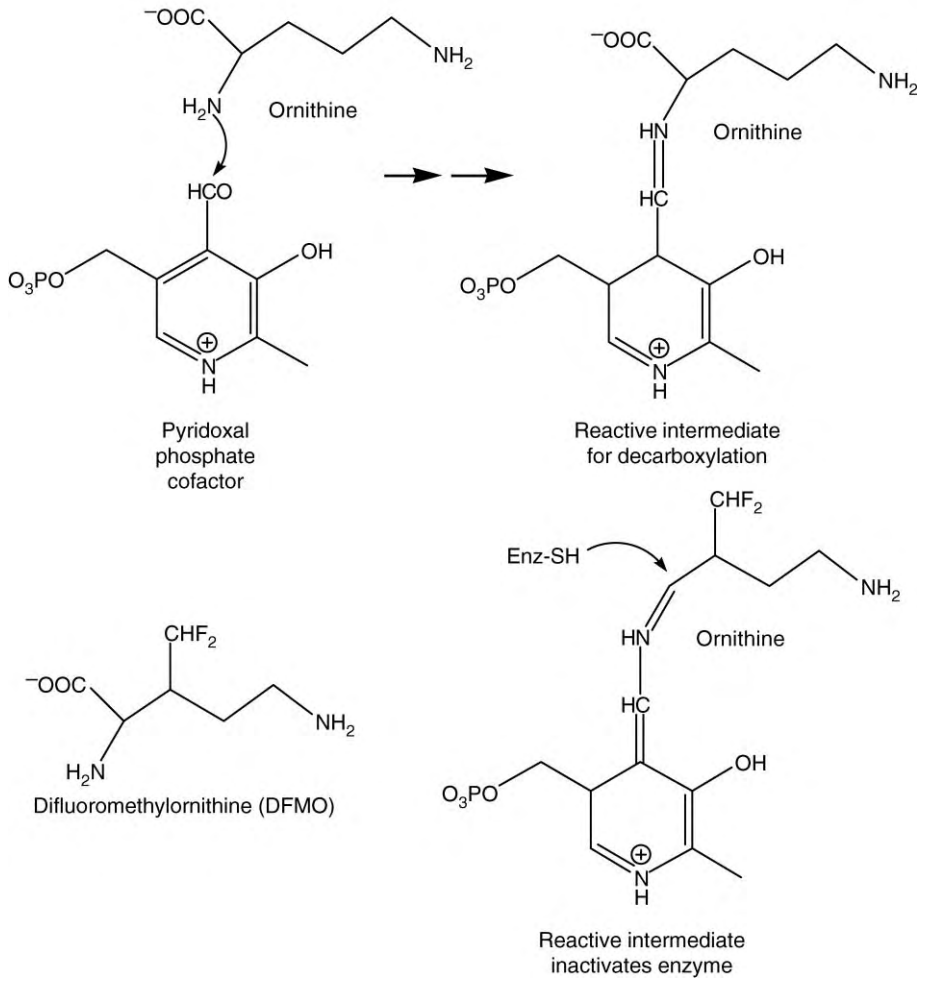

FIGURE 6 Covalent suicide inhibition of ornithine decarboxylase by DFMO. In the normal reaction, the enzymatic cofactor, pyridoxal phosphate, forms a Schiff base favoring decarboxylation of ornithine. With DMFO, the same steps occur but decarboxylation generates a reactive difluoro-conjugated imine. A nearby cysteine nucleophile reacts to form a stable, inactive enzyme.

polyamine synthesis is catalyzed by ornithine decarboxylase which uses a transient covalent intermediate to the enzymatic cofactor pyridoxal phosphate. Difloromethylornithine (DFMO) is decarboxylated in similar fashion to orinithine, but the reaction creates a highly reactive intermediate that reacts with a nearby group on the enzyme to form a stable covalent intermediate, resulting in an inactive ornithine decarboxylase. It therefore stops polyamine biosynthesis. It has been used as an anticancer agent and an antibiotic against *Trypanosoma* species that cause sleeping sickness. Specificity is provided by the binding of DFMO only to the target enzyme and long biological action is provided by the stable covalent interaction with the enzyme. These are features of most mechanism-based enzyme inhibitors. Care is needed that chemical reactivity causing enzymatic inactivation is revealed only to the target enzyme.

Other Mechanism-Based Inhibitors

Many of the common antimetabolites are mechanism-based inhibitors. Thus, certain insecticides form covalent interactions with the catalytic site of enzymes involved in insect neurotransmission. Deprenyl is a drug used to treat Parkinson's disease and mental depression by increasing brain dopamine levels. It functions by suicide inhibition at the catalytic site of monamine oxidase, the enzyme that degrades dopamine.

Conclusion

The intricate steps in enzymatic action can be disrupted in numerous ways, each causing inhibition of catalytic steps. Enzymes have evolved to function in the presence of the complex mixture of normal cellular components, but inhibitors can be designed to specifically target a

single enzyme of the thousands that function in coordination in a normal cell.

See Also the Following Articles

Enzyme Kinetics • Enzyme Reaction Mechanisms: Stereochemistry • Substrate Binding, Catalysis, and Product Release

Glossary

biological efficency The ability of an enzyme inhibitor to achieve significant inhibition at the physiological conditions of substrates and cofactors.

catalytic site A cavity on the enzymatic surface that binds substrates and causes them to be converted to product by increasing the probability that they will achieve the transition state.

inhibitor design Selection or synthesis of stable molecules intended to disrupt catalytic function of a specific enzyme.

mechanism-based inhibitor A molecule resembling a substrate that is chemically activated by the action of the enzyme to form a stable covalent link with the enzyme – also known as suicide substrates or suicide inhibitors.

substrate analogue A molecule with shape and charge features similar to a substrate of the enzyme that binds at the catalytic site and prevents substrate binding.

transition-state analogue A chemically stable molecule with shape and electrostatic features that mimic those of the transition state and that inhibit at the catalytic site by converting energy of catalysis to energy of binding.

Further Reading

Abeles, R. H., and Alston, T. A. (1990). Enzyme inhibition by fluoro compounds. *J. Biol. Chem.* **265**, 16705–16708.

Cleland, W. W. (1970). Steady state enzyme kinetics. In *The Enzymes*, 3rd edition, Vol. 2, (P. S. Boyer, ed.) Academic Press, New York pp. 1–65.

Northrop, D. B. (1999). Rethinking fundamentals of enzyme action. *Adv. Enzymol. Relat. Areas Mol. Biol.* **73**, 25–55.

Schramm, V. L. (1998). Enzymatic transition states and transition state analog design. *Ann. Rev. Biochem.* **67**, 693–720.

Schramm, V. L. (2003). Enzymatic transition state poise and transition state analogues. *Acc. Chem. Res.* **36**, 588–596.

Wolfenden, R. (1976). Transition state analog inhibitors and enzyme catalysis. *Ann. Rev. Biophys. Bioeng.* **5**, 271–306.

Biography

Vern Schramm received his Ph.D. at the Australian National University, John Curtain School of Medical Research in 1968. In the Department of Biochemistry at the Temple University School of Medicine (1971), he began to apply isotope effects to the study of enzymatic transition states. At the Albert Einstein College of Medicine in 1987, he began a systematic program of solving enzymatic transition states by kinetic isotope effects. Enzymatic transition-state information is then applied to the design of transition-state analogue inhibitors. The inhibitors are applied to biomedical problems.

Enzyme Kinetics

Irwin H. Segel
University of California, Davis, California, USA

Enzymes are protein catalysts that accelerate the rates at which reactions approach equilibrium. *Enzyme kinetics* is the branch of biochemistry that deals with a quantitative description of this process, mainly, how experimental variables affect reaction rates. The variables that are studied include the concentrations of the enzyme, substrates (reactants), products, inhibitors, activators, the pH, temperature, and ionic strength. A complete kinetic analysis (together with complementary studies of equilibrium ligand binding, isotope exchange, covalent modification of amino acid side chains, etc.) can disclose most of the functional characteristics of a particular enzyme. These include (1) the specificities and affinities of the ligand subsites, (2) the order in which substrates bind and products leave, (3) the enzyme species that are intermediates in the overall reaction, (4) the magnitudes of component rate constants, (5) the possible identities of active-site residues, (6) the mode of action of an inhibitory drug, and (7) how the enzyme might be regulated *in vivo*. Enzyme kinetics combined with related approaches can show how the functional properties of a mutant or "engineered" enzyme compare to those of its wild-type parent. Many of the equations of enzyme kinetics are also applicable to other saturable biological processes, e.g., membrane transport and receptor–ligand interactions.

Unireactant Enzymes and the Michaelis–Menten Equation

By the mid- to late 1800s, most of the laws governing the effect of reactant concentrations on the rates of chemical reactions were known. But enzyme-dependent reactions did not always follow these simple rate laws. In 1902, Victor Henri proposed the first useful equation for an enzyme-dependent reaction. Henri's equation took into account the known properties of enzymes, including that (1) an enzyme was highly specific for a particular substrate (or class of substrates), (2) substrates often protected an enzyme from inactivation by heat, and (3) a plot of initial velocity versus substrate concentration was hyperbolic. (These properties all pointed to the participation of an enzyme–substrate complex.) Subsequent workers, including Michaelis and Menten (1913), Van Slyke and Cullen (1914), and Briggs and Haldane (1925) confirmed and/or extended Henri's equation, which is derived below.

The Rapid Equilibrium Assumption

The following assumptions and procedures led Henri and others to the relationship between substrate concentration and reaction rate, which is now known as the Michaelis–Menten equation:

1. The overall reaction occurs in two steps, as shown below:

$$\mathrm{E} + \mathrm{S} \underset{k_{-1}}{\overset{k_1}{\rightleftharpoons}} \mathrm{ES} \xrightarrow{k_2} \mathrm{E} + \mathrm{P}. \qquad (1)$$

This sequence recognizes that the enzyme is not consumed in the reaction, but rather, is a recycling catalyst. The first step is the rapid equilibration of the free enzyme, E, and the free substrate, S, to form an ES complex. This is followed by the unidirectional, rate-limiting decomposition of ES to E + P. The rapid equilibrium between E, S, and ES is maintained throughout the course of the reaction. (This condition requires that $k_{-1} >> k_2$.) The equilibrium is described by the dissociation constant, K_s of the ES complex:

$$K_s = [E][S]/[ES] = k_{-1}/k_1. \qquad (2)$$

Equation (2) allows the concentration of the ES complex to be expressed in terms of the concentration of free E, free S, and K_s:

$$[ES] = [S][E]/K_s. \qquad (3)$$

2. At any time, the total enzyme, $[E]_t$ is present as either free E or as the ES complex. Thus, the mass balance (conservation) equation is

$$[E]_t = [E] + [ES]. \qquad (4)$$

The total substrate is also distributed between the free and complexed species:

$$[S]_t = [S] + [ES]. \qquad (5)$$

However, for most enzyme-dependent reactions that are studied *in vitro*, the enzyme is present at a very low (catalytic) level (i.e., $[E]_t << [S]_t$), so that the

maximum $[ES]$ that can form will be much smaller than the $[S]_t$ added. Consequently, it can be assumed that the free S concentration is essentially identical to the total added S (i.e., $[S] \approx [S]_t$). This assumption is not valid for many enzymes inside the cells, where $[E]_t$ may be in the same range as $[S]_t$.

3. The instantaneous or "initial" rate, $\mathrm{d}[P]/\mathrm{d}t$ or $-\mathrm{d}[S]/\mathrm{d}t$ (usually indicated as "v" for "velocity"), is proportional to the concentration of the ES complex:

$$v = k_2[ES]. \tag{6}$$

4. It is assumed that the accumulating product has no effect on the reaction. That is, the P concentration remains close to zero throughout the course of the reaction, or P has no affinity for the enzyme.

5. The final velocity equation is obtained by dividing eqn. (6) by eqn. (4) and substituting for $[ES]$ from eqn. (3):

$$\frac{v}{[E]_t} = \frac{k_2[ES]}{[E] + [ES]} \quad \text{or} \quad v = \frac{k_2[E]_t \dfrac{[S][E]}{K_S}}{[E] + \dfrac{[S][E]}{K_S}} \tag{7}$$

$k_2[E]_t$ is defined as V_{max} because when all the enzyme is in the ES form, the observed velocity will be maximal. This substitution and canceling $[E]$ in eqn. (7) yields the final Michaelis–Menten equation:

$$v = \frac{V_{max} \dfrac{[S]}{K_s}}{1 + \dfrac{[S]}{K_s}} = \frac{V_{max}[S]}{K_s + [S]}. \tag{8}$$

The Steady-State Assumption

By the 1920s, researchers realized that the rapid equilibrium assumption was too restrictive and would not be valid for enzymes where the ES complex proceeds on to E + P much faster than it dissociates back to E + S. In such cases, E, S, and ES would not attain equilibrium. In 1925, Briggs and Haldane offered a more general method for deriving velocity equations that did not require a rapid equilibrium assumption. Their *steady-state* approach recognized that under most assay conditions, $[E]$ and $[ES]$ would attain certain levels very quickly after mixing E and S, but that the concentrations of these enzyme species would change very little thereafter. In other words, for the duration of the assay, the rate at which ES is formed (from E + S) remains identical to the rate at which it decomposes (back to E + S, plus forward to E + P). Similarly, the rate at which E is produced from ES equals the rate at which E is used to form ES. Scheme (1) is still applicable, but now rate constants for individual steps must be taken into account. Applying the steady-state assumption we can write

$$\mathrm{d}[ES]/\mathrm{d}t = 0 \quad \text{or} \quad k_1[E][S] = (k_{-1} + k_2)[ES] \tag{9}$$

and

$$\mathrm{d}[E]/\mathrm{d}t = 0 \quad \text{or} \quad (k_{-1} + k_2)[ES] = k_1[E][S]. \tag{10}$$

Solving either equation for $[ES]$ yields

$$[ES] = k_1[E][S]/(k_{-1} + k_2) \quad \text{or} \quad [ES] = [S][E]/K_m \tag{11}$$

where in the latter expression, the three rate constants are combined into a single kinetic constant, K_m, as shown below:

$$K_m = (k_{-1} + k_2)/k_1. \tag{12}$$

The initial velocity, v, at any $[S]$ still equals $k_2[ES]$. So, proceeding as described earlier, but substituting for $[ES]$ from eqn. (11), we obtain

$$v = \frac{V_{max}[S]}{K_m + [S]}. \tag{13}$$

Thus, the velocity equation is the same as that derived for rapid equilibrium conditions, except that the constant in the denominator (now called a Michaelis constant) is more complex than a simple dissociation constant. The Briggs–Haldane approach is more general than the rapid-equilibrium approach because it makes no assumptions about the relative magnitudes of the various rate constants. If $k_2 \ll k_{-1}$, K_m reduces to k_{-1}/k_1, which is equivalent to the simpler K_s.

Equation (13) is valid throughout the experimental [S] range provided that the rate of P formation is measured before [S] changes appreciably. (In practice, substrate use should be restricted to less than 5% (or at most 10%) of $[S]_t$.) When $[S] \ll K_m$, eqn. (13) reduces to $v = V_{max}[S]/K_m = k[S]$, i.e., the reaction is *first order* with respect to $[S]$ with a rate constant equivalent to V_{max}/K_m. When $[S] >> K_m$, v is essentially constant at V_{max} and independent of $[S]$. (The reaction is *zero order* with respect to $[S]$.)

A More Realistic Unireactant Reaction Sequence

Equation (1) contains the minimum number of steps that must be considered in the description of a uni–uni (one substrate, one product) reaction. A more realistic scheme takes into account the conversion of enzyme-bound S to enzyme-bound P (before P is released) and the reversibility of each step as shown below:

$$\mathrm{E} + \mathrm{S} \underset{k_{-1}}{\overset{k_1}{\rightleftharpoons}} \mathrm{ES} \underset{k_{-2}}{\overset{k_2}{\rightleftharpoons}} \mathrm{EP} \underset{k_{-3}}{\overset{k_3}{\rightleftharpoons}} \mathrm{P} + \mathrm{E}. \tag{14}$$

A steady-state treatment of the above reaction sequence once again yields the familiar Michaelis–Menten equation when $[P] = 0$, except that now

$$K_m = \frac{k_{-1}k_3 + k_{-1}k_{-2} + k_2k_3}{k_1(k_2 + k_{-2} + k_3)} \tag{15}$$

and

$$V_{max} = \frac{k_2k_3[E]_t}{k_2 + k_{-2} + k_3}. \tag{16}$$

So, in the absence of other information, the rate constant compositions of the two kinetic constants, K_m and V_{max}, are not usually known. But regardless of its makeup, K_m is a valuable characteristic because it is equivalent to the substrate concentration that yields half-maximal velocity. V_{max} is not a true constant because it depends on the enzyme concentration. However, $V_{max}/[E]_t$, expressed as moles of S converted to P per second per mole of enzyme active site (which reduces to per second, or s^{-1}) is the *catalytic rate constant* (or *turnover number*) of the enzyme, k_{cat}. The ratio k_{cat}/K_m has been used to compare the action of an enzyme on a series of related substrates. The higher the value of this *specificity constant*, the better the substrate. If an enzyme is evolutionarily perfected so that the catalytic and product release rate constants are very much larger than any of the reverse first-order rate constants, the ratio k_{cat}/K_m reduces to k_1, the second-order rate constant for the interaction of E and S to form ES. In aqueous solution, this constant has a maximum, diffusion-limited value of $\sim 10^9\ M^{-1}\ s^{-1}$. Many enzymes have k_{cat}/K_m values that approach this maximum.

Reversible Reactions

In the presence of both the substrate and product, the net steady-state velocity is given by the difference between the forward and reverse rates of any step, e.g.,

$$v = k_2[ES] - k_{-2}[EP] \tag{17}$$

or

$$\frac{v}{[E]_t} = \frac{k_2[ES] - k_{-2}[EP]}{[E] + [ES] + [EP]}. \tag{18}$$

After substituting for $[ES]$ and $[EP]$ and grouping rate constants into kinetic constants, the equation is

$$v = \frac{V_{max,f}\dfrac{[S]}{K_{mS}} - V_{max,r}\dfrac{[P]}{K_{mP}}}{1 + \dfrac{[S]}{K_{mS}} + \dfrac{[P]}{K_{mP}}} \tag{19}$$

where $V_{max,f}$ and $V_{max,r}$ are the forward and reverse maximal velocities, respectively; K_{mS} and K_{mP} are the Michaelis constants of S and P, respectively. Equation (19) can also be written as

$$v = \frac{V_{max,f}[S]}{K_{mS}\left(1 + \dfrac{[P]}{K_{mP}}\right) + [S]} - \frac{V_{max,r}[P]}{K_{mP}\left(1 + \dfrac{[S]}{K_{mS}}\right) + [P]} \tag{20}$$

which shows that in this unireactant process, P acts as a competitive inhibitor of the forward reaction and S acts as a competitive inhibitor of the reverse reaction. (In reactions catalyzed by multireactant enzymes, individual products might be competitive, uncompetitive, or noncompetitive with respect to different substrates.)

The Velocity Curve and its Linear Forms

Figure 1 shows the typical hyperbolic dependence of the velocity of an enzyme-catalyzed reaction on the substrate concentration. The kinetic constants, K_m and V_{max}, can be obtained by fitting the v versus $[S]$ data directly to the Michaelis–Menten equation using an appropriate computer application. Alternatively, K_m and V_{max} can be obtained by plotting the data in a linear form such as $1/v$

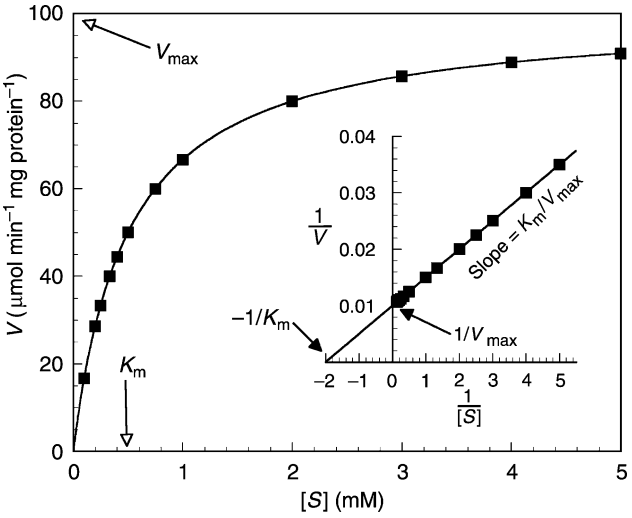

FIGURE 1 Theoretical plot of initial velocity versus substrate concentration in the absence of the product for an enzyme with a K_m of 0.5 mM and a V_{max} of 100 μmol min^{-1} mg^{-1} protein. The $[S]$ at which v is 50% of V_{max} (i.e., $[S]_{0.5}$) is equivalent to K_m. The curvature of the plot is the same for all enzymes obeying Henri–Michaelis–Menten kinetics, regardless of the absolute values of the kinetic constants. For example, the ratio of substrate concentration that yields 90% of V_{max} ($[S]_{0.9}$) to that yielding 10% of V_{max} ($[S]_{0.1}$) is always 81. Similarly, the $[S]_{0.75}/[S]_{0.5}$ ratio is always 3. Note that V_{max} is difficult to determine visually. But a computer-assisted fit to $v = Vmax^*[S]/(Km + [S])$ will return both V_{max} and K_m. (Inset) Double-reciprocal plot of the data. A wide range of substrate concentrations is needed to construct both the primary plot and the double-reciprocal plot because $[S]$ values that are evenly spaced on one plot do not space evenly on the other.

versus $1/[S]$ (usually called the Lineweaver–Burk or double-reciprocal plot), $v/[S]$ versus v (usually called the Scatchard plot), v versus $v/[S]$, or $[S]/v$ versus $[S]$. The most popular of these is the double-reciprocal plot, which is based on the linear transformation of the Michaelis–Menten equation shown below.

$$\frac{1}{v} = \frac{K_m}{V_{max}}\frac{1}{[S]} + \frac{1}{V_{max}}. \quad (21)$$

A major advantage of a linear plot is that data obtained at several different fixed concentrations of a second ligand (e.g., a cosubstrate, product, inhibitor, or activator) can be displayed simultaneously and the resulting slope and intercept characteristics used to diagnose the kinetic mechanism or the mode of inhibition or activation.

Multireactant Enzymes

Common Mechanisms

Most enzymes catalyze reactions between two or more substrates to yield two or more products. The substrates bind to the enzyme either in a random manner or in a compulsory order. Similarly, product release is random in some cases, and ordered in others. Mechanisms in which catalysis occurs only after two (or more) substrates are brought together on the enzyme are called "sequential." Some enzymes catalyze the formation and release of a product before all the substrates have bound. For example, an enzyme might capture a substrate, A, and retain part of that molecule (sometimes as a covalent adduct with the enzyme) releasing the rest of the molecule as product P. Only then does substrate B bind and combine with the part of A that was left on the enzyme to form product Q, which then leaves. This type of substituted enzyme or "ping-pong" mechanism is common for transaminases; the amino group of substrate A is left temporarily on the enzyme. A reaction catalyzed by a terreactant (three-substrate) enzyme might proceed by a combination of sequential and ping-pong steps. The order of addition of substrates and release of products is called the *kinetic mechanism*. Four bireactant examples are shown in Figure 2.

Velocity Equations for Some Bireactant Mechanisms

In some cases, different kinetic mechanisms are described by different velocity equations. (See standard enzyme kinetics texts for the procedures used to derive these equations.) Consequently, it is sometimes possible to distinguish between mechanisms from the characteristics of the double-reciprocal plots. For example, the velocity equation for an ordered bireactant mechanism under steady-state conditions in the absence of products is

$$v = \frac{V_{max}[A][B]}{K_{ia}K_{mB} + K_{mB}[A] + K_{mA}[B] + [A][B]} \quad (22)$$

where K_{mA} and K_{mB} are the Michaelis constants of the two substrates and K_{ia} is the simple dissociation constant of the EA complex. (Velocity equations for multireactant mechanisms often contain both types of constants.) When $[A]$ is varied at different fixed concentrations of B, the velocity dependence can be written in the form of the Michaelis–Menten equation:

$$v = \frac{V_{max}[A]}{K_{mA}\left(1 + \frac{K_{ia}K_{mB}}{K_{mA}[B]}\right) + [A]\left(1 + \frac{K_{mB}}{[B]}\right)}. \quad (23)$$

Or, in double reciprocal form:

$$\frac{1}{v} = \frac{K_{mA}}{V_{max}}\left(1 + \frac{K_{ia}K_{mB}}{K_{mA}[B]}\right)\frac{1}{[A]} + \frac{1}{V_{max}}\left(1 + \frac{K_{mB}}{[B]}\right). \quad (24)$$

When $[B]$ is varied at different fixed concentrations of A, the equations are

$$v = \frac{V_{max}[B]}{K_{mB}\left(1 + \frac{K_{ia}}{[A]}\right) + [B]\left(1 + \frac{K_{mA}}{[A]}\right)} \quad (25)$$

and

$$\frac{1}{v} = \frac{K_{mB}}{V_{max}}\left(1 + \frac{K_{ia}}{[A]}\right)\frac{1}{[B]} + \frac{1}{V_{max}}\left(1 + \frac{K_{mA}}{[A]}\right). \quad (26)$$

At a fixed concentration of one substrate, e.g., A, the velocity dependence on the concentration of substrate B can also be described by a simplified form of eqn. (25):

$$v = \frac{V_{max,app}[B]}{K_{mB,app} + [B]} \quad (27)$$

where the *apparent constants* are related to the true or limiting constants as shown below.

$$V_{max,app} = \frac{V_{max}}{\left(1 + \frac{K_{mA}}{[A]}\right)} \quad \text{and} \quad K_{mB,app} = \frac{\left(1 + \frac{K_{ia}}{[A]}\right)}{\left(1 + \frac{K_{mA}}{[A]}\right)}. \quad (28)$$

In other words, the experimentally determined "K_m" and "V_{max}" depend on the concentration of the co-substrate and will not equal the limiting values unless that concentration is infinitely high ("saturating"). In practice, the limiting kinetic constants are obtained from appropriate replots of the slopes and $1/v$-axis intercepts

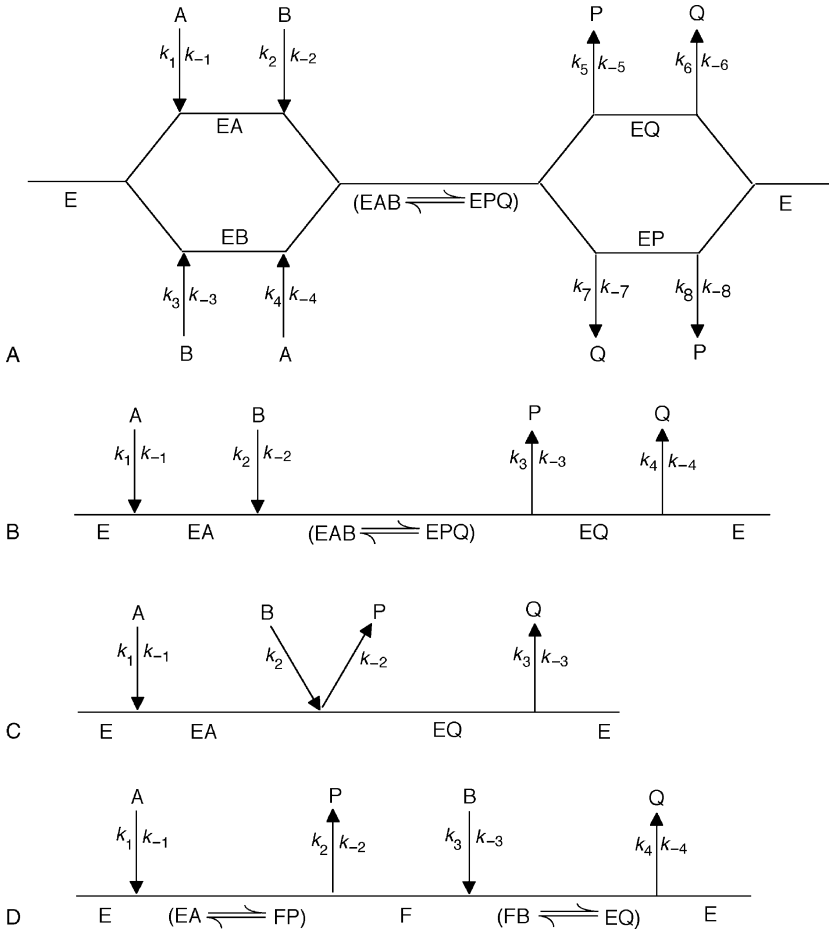

FIGURE 2 Four common kinetic mechanisms for bireactant enzymes shown in the Cleland shorthand notation. Substrates are indicated above a horizontal line as A, B, C, etc., in the order in which they add to the enzyme. Products are indicated as P, Q, R, etc., in the order in which they dissociate from the enzyme. Arrows are shown pointing in a single direction, but all the reactions are reversible. Rate constants for each reversible reaction are shown alongside of the arrows. For computer-based derivations of the velocity equation, it is usually more convenient to indicate all rate constants with positive subscripts (odd numbers for the forward steps; even numbers for the reverse direction). The various enzyme species present in the mechanism are placed below the horizontal line (in sequence of their formation). Species that are interconverted by a unimolecular step are usually grouped together within parentheses. (A) Random mechanism, (B) ordered mechanism, and (C) Theorell–Chance mechanism. The last is a limiting case of an ordered mechanism in which the EAB + EPQ central complex does not account for a significant fraction of the total enzyme in the steady state. (D) Ping-pong mechanism where stable enzyme form F may be a covalent adduct of E with the part of substrate A left behind.

of the double-reciprocal plots. (The former is a replot of $K_{m,app}/V_{max,app}$; the latter is a replot of $1/V_{max,app}$.) For example, the replots for the family of $1/v$ versus $1/[B]$ plots at different fixed $[A]$ are described by the following linear equations:

$$\text{int} = \frac{K_{mA}}{V_{max}}\frac{1}{[A]} + \frac{1}{V_{max}} \tag{29}$$

$$\text{slope} = \frac{K_{mB}K_{ia}}{V_{max}}\frac{1}{[A]} + \frac{K_{mB}}{V_{max}}. \tag{30}$$

V_{max}, K_{mA}, K_{mB}, and K_{ia} can be determined from the intercepts of the replots.

The equations for the substituted enzyme (ping-pong) bireactant mechanism in the absence of products is

$$v = \frac{V_{max}[A][B]}{K_{mB}[A] + K_{mA}[B] + [A][B]}. \tag{31}$$

When $[A]$ is varied at different $[B]$, the Michaelis–Menten and double reciprocal equations are

$$v = \frac{V_{max}[A]}{K_{mA} + \left(1 + \dfrac{K_{mB}}{[B]}\right)} \tag{32}$$

and

$$\frac{1}{v} = \frac{K_{mA}}{V_{max}}\frac{1}{[A]} + \frac{1}{V_{max}}\left(1 + \frac{K_{mB}}{[B]}\right). \qquad (33)$$

The equations for varied $[B]$ at different $[A]$ are symmetrical to those shown for varied $[A]$. Figure 3 shows the families of $1/v$ versus $1/[A]$ plots for an ordered and a ping-pong mechanism. In both mechanisms different fixed $[B]$ values affect the vertical-axis intercepts. In the ordered mechanism, changing $[B]$ also affects the slopes of the $1/v$ versus $1/[A]$ plots. But in the ping-pong mechanism, changing the fixed $[B]$ has no effect on the slopes. (Note that eqns. (24) and (33) predict these effects.) The absence of a slope effect is often sufficient to identify the ping-pong mechanism. But the presence of both slope and intercept effects (as shown in Figure 3A) is not sufficient to diagnose the mechanism as ordered because in the absence of products, a steady-state ordered, a Theorell–Chance, and a rapid-equilibrium random mechanism all have the same velocity equation. Consequently, the double-reciprocal plot patterns of the three different mechanisms are the same. Additional measurements are needed to distinguish between these mechanisms. Product inhibition studies can be informative. For example, in a steady-state ordered mechanism, one of the products (P, the first to dissociate from the enzyme) is noncompetitive with respect to both substrates, but in a Theorell–Chance and random mechanism, each product is competitive with at least one substrate. Dead-end inhibition studies may also be useful. For example,

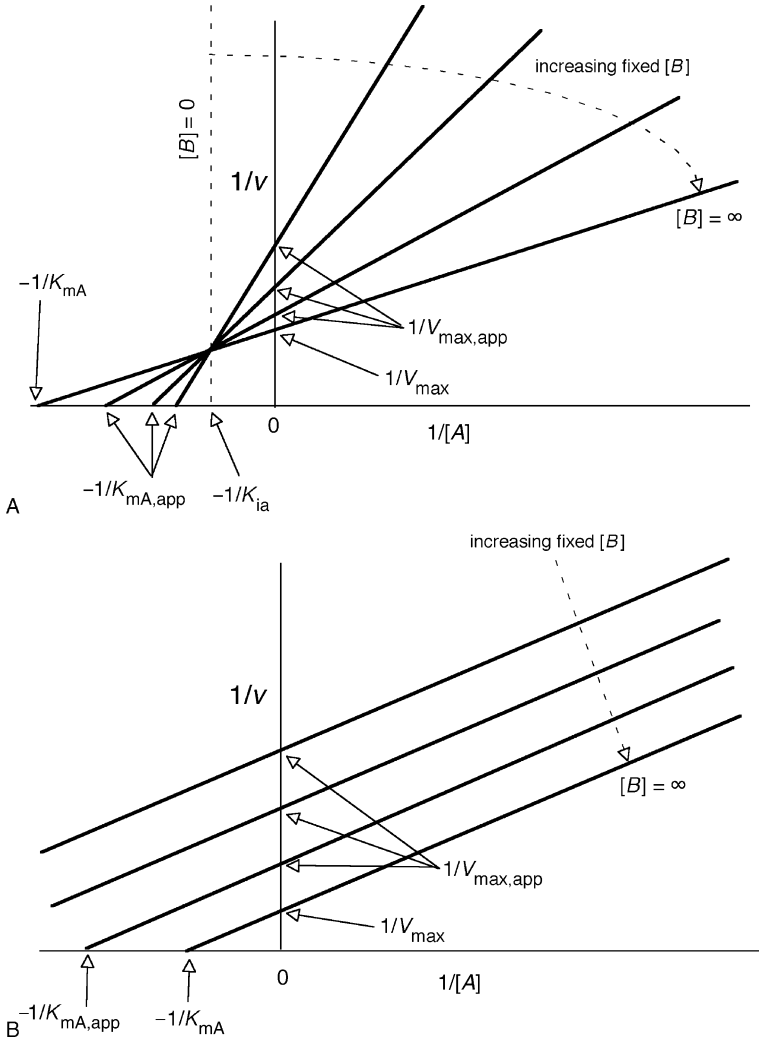

FIGURE 3 Double-reciprocal plots of $1/v$ versus $1/[A]$ at different fixed concentrations of B. A is called the varied substrate; B is called the changing fixed substrate. (A) A sequential mechanism. The plots could be for a steady-state ordered, Theorell–Chance, or a rapid-equilibrium random mechanism. (B) Ping-pong mechanism. For the above mechanisms, the plots of $1/v$ versus $1/[B]$ at different fixed $[A]$ have the same appearance as for varied $1/[A]$. The limiting kinetic constants, K_{mA}, K_{mB}, K_{ia}, V_{max}, etc., are obtained by replotting the slopes and/or $1/v$-axis intercepts of the double-reciprocal plots against the reciprocal of the changing fixed substrate concentration.

a nonreactive analogue that is competitive with B will be uncompetitive with A in the ordered and Theorell–Chance mechanisms, but noncompetitive with A in the random mechanism. (This assumes that the inhibitor forms an EAI complex in the Theorell–Chance mechanism and mimics substrate B completely in the random mechanism by binding to both E and EA.)

Cleland's Slope and Intercept Rules

W. W. Cleland has presented a series of rules for predicting the effect of changing the fixed concentration of a co-substrate or product on the slopes and vertical-axis intercepts of $1/v$ versus 1/[varied substrate] plots. The slope and intercept effects are predicted separately and then combined to deduce the appearance of the double-reciprocal plot family. Conversely, the slope and intercept patterns can help to diagnose the kinetic mechanism. The rules are as follows.

Intercept Effect

A changing fixed substrate or product will cause an intercept effect if it and the varied substrate combine with different enzyme forms. Exceptions: an intercept effect will not be seen for a changing fixed ligand that adds to the enzyme before the varied substrate under rapid-equilibrium conditions, or in a Theorell–Chance "hit-and-run" sequence between a substrate and the immediately released product (B and P in Figure 2C).

Slope Effect

A changing fixed substrate or product will cause a slope effect if it and the varied substrate combine with the same enzyme form, or with different forms that are "reversibly connected" in the upstream or downstream direction. Two enzyme forms will not be reversibly connected if either (1) a product release step occurs between them and that product is at zero concentration in the assay solution, or (2) a substrate addition step occurs between the two enzyme forms and that substrate is present at a saturating concentration. Both the upstream and downstream directions must be blocked to eliminate reversibility.

A product will have no effect on slopes or intercepts if the steady-state level of the enzyme form with which it combines is zero because of saturation with a competitive substrate.

Similar rules predict the slope and intercept effects produced by dead-end inhibitors.

See Also the Following Articles

Allosteric Regulation • Enzyme Inhibitors

Glossary

catalytic rate constant (k_{cat}) Moles of substrate converted to product per second per mole of enzyme active site; also called active-site turnover number.

kinetic mechanism The order in which substrates add and products are released in an enzyme-catalyzed reaction.

maximal velocity (V_{max}) Maximum reaction rate (v observed at saturating substrate concentrations) for a given concentration of enzyme: $V_{max} = k_{cat}[E]_t$.

Michaelis constant (K_m) Kinetic constant equivalent to the concentration of the varied substrate that yields half-maximal velocity when all other substrates are saturating.

rapid equilibrium Condition where the ligands and enzyme species present are at chemical equilibrium.

steady state Condition where the rate of formation of an intermediate is equal to the rate of its utilization.

Further Reading

Cleland, W. W. (1963). The kinetics of enzyme-catalyzed reactions with two or more substrates or products. *Biochim. Biophys. Acta* **67**, 104–137, 173–187, 188–196.

Cornish-Bowden, A. (1995). *Fundementals of Enzyme Kinetics*. Portland Press, London.

Fromm, H. J. (1975). *Initial Rate Enzyme Kinetics*. Springer, Berlin.

Gutfreund, H. (1995). *Kinetics for the Life Sciences*. Cambridge University Press, Cambridge.

Kuby, S. A. (1991). *A Study of Enzymes, Vol 1: Enzyme Catalysis, Kinetics, and Substrate Binding*. CRC Press, Boca Raton, FL.

Purich, D. L., and Allison, R. D. (2000). *Handbook of Biochemical Kinetics*. Academic Press, San Diego, CA.

Segel, I. H. (1976). *Biochemical Calculations*. 2nd edition, Ch. 4, Wiley, New York.

Segel, I. H. (1993). *Enzyme Kinetics: Behavior and Analysis of Rapid Equilibrium and Steady State Enzyme Systems*. Wiley Classics Library, Wiley-Interscience, New York.

Biography

Irwin H. Segel is a Professor in the Section of Molecular and Cellular Biology at the University of California, Davis. His major research interests are in the structure–function relationships of the inorganic sulfate activating enzymes, ATP sulfurylase and APS kinase. He received his Ph.D. from the University of Wisconsin and did postdoctoral research at the Centre National de la Recherche Scientifique in Marseille. He is a Fellow of the American Association for the Advancement of Science.

Enzyme Reaction Mechanisms: Stereochemistry

Ming-Daw Tsai, Li Zhao and Brandon J. Lamarche
The Ohio State University, Columbus, Ohio, USA

Stereochemistry **is the facet of chemistry concerned with the three-dimensional properties of molecules. The history of stereochemistry began in 1815 when Jean-Baptiste Biot discovered that some molecules are capable of rotating the plane of polarized light. Louis Pasteur suggested in 1850 that this phenomenon could be attributed to the stereochemical properties of molecules. In the subsequent 150 years it has come to be understood that stereochemistry is all-important in biology, where a molecule's structure and function are inextricably related. Though synthetic chemists are increasingly adept at controlling the stereochemistry of chemical reactions, enzymes – nature's catalysts – remain the paradigm for stereochemical control. Stereochemical analysis of enzymatic reactions can therefore yield information about the mechanism of enzyme action. That is the focus of this entry.**

Explanation of Stereochemical Terms

Figure 1 uses chemical structures to illustrate key stereochemical terms. *Stereomers* (or stereo isomers) are molecules that have the same molecular formula and the same order of attachment of atoms, but they differ in the way their atoms are oriented in space. Any molecule that cannot be superimposed on its mirror image is said to be *chiral*. Though chirality can result from a number of molecular properties, it is usually due to the presence of one or more carbon or phosphorus atoms, called chiral centers, which are surrounded by four unique substituents. Chiral molecules are classified as either *enantiomers* (stereoisomers that are mirror images of each other) or *diastereomers* (stereoisomers that are not mirror images of each other).

Configuration specifies how substituents are oriented around a chiral center and is determined by the *R*–*S* notation system, where *R* and *S* refer to the Latin terms *rectus* (right) and *sinister* (left). To assign *R*/*S* configuration, a priority rating is given to each substituent at a chiral center using the following rules: Priority is first assigned on the basis of atomic number with highest priority given to the atom with the highest atomic number. When identical atoms are directly attached to the chiral center, the next atoms on the substituent are compared, until a difference is noted. Once priority has been established, the molecule is oriented so that the lowest priority substituent is pointing away from the viewer. The direction of rotation observed when moving from the highest to lowest priority will now be either clockwise or counterclockwise and the configuration is designated *R* or *S*, respectively.

An atom that is attached to two unique substituents and two identical substituents is said to be prochiral. The two identical groups at a prochiral center can be designated as pro-*R* and pro-*S* following a prochirality rule. As shown in Figure 1C, the pro-*R* hydrogen (H_R) is the one that leads to R configuration if it is given a higher priority than the other hydrogen atom. When a chiral center or prochiral center is phosphorus instead of carbon, a subscript p is added (i.e., R_P, S_P, pro-R_P, pro-S_P).

Stereoselectivity, Stereospecificity, and Stereochemical Course of Enzymatic Reactions

If exposed to a racemic mixture of substrates, most enzymes utilize one enantiomer or diastereomer preferentially. In reactions where chemistry is occurring at a prochiral center, an enzyme is also likely to act on just one of the two available enantiotopic or diastereotopic groups. The enzyme is said to be *stereoselective* in both cases.

Enzymatic reactions are almost always *stereospecific*, which means that they convert one stereoisomer of substrate to one stereoisomer of product. For substitution reactions, *stereochemical course* refers to the change (or lack thereof) in configuration at the reaction center in a stereospecific reaction. While *retention* means the new group occupies the same position as the

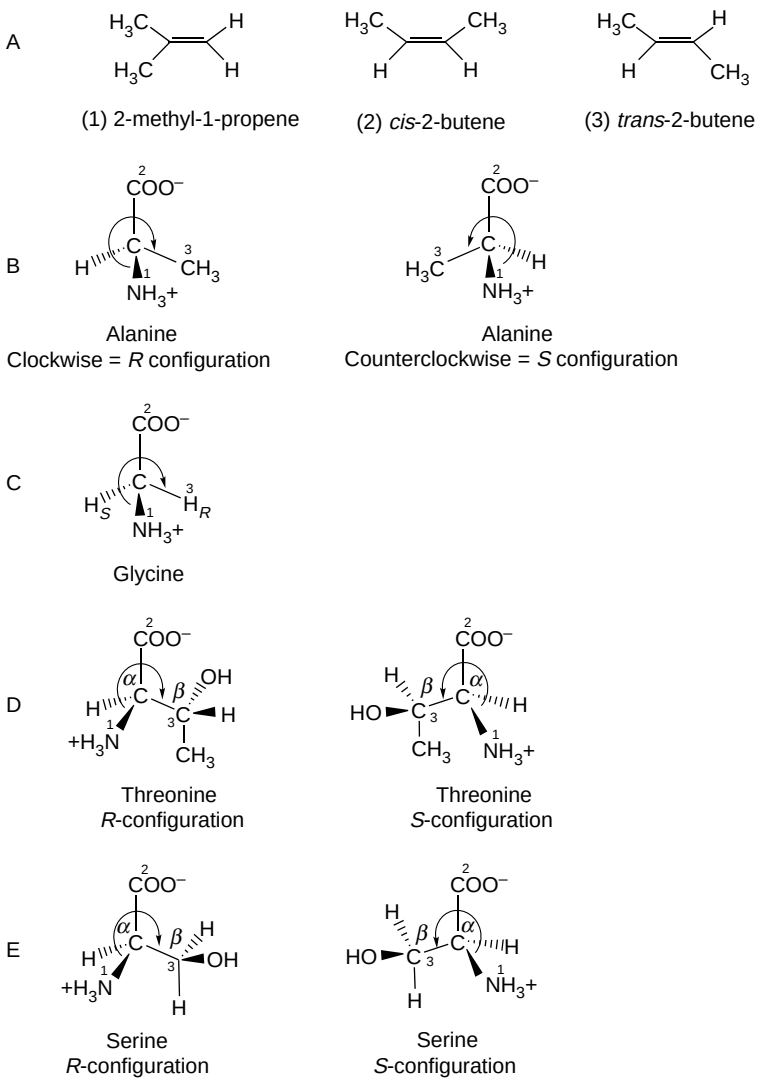

FIGURE 1 Demonstration of stereochemical terms using structures. (A) Though molecules 1, 2, and 3 have the same molecular formula, only 2 and 3 are stereoisomers. Molecule 1 has a different pattern of bonding (i.e., a different linkage of atoms) and is therefore a structural isomer of molecules 2 and 3. (B) Alanine stereoisomers are *enantiomers* since they are mirror images of each other. Note that the different configuration of substituents about the central carbon makes it impossible to superimpose the two isomers. (C) Glycine is *achiral* and therefore does not have stereoisomers. However, the central carbon is a prochiral center since it can be converted to a chiral center by replacing one of the two hydrogens with a different group. The two hydrogens are said to be *enantiotopic* since the separate replacement of each hydrogen results in a pair of enantiomers. (D) The two stereoisomers of threonine shown are diastereomers, i.e., stereo isomers that are not complete mirror images of each other. Note that this pair of molecules results by altering the configuration at C_α while leaving the configuration at the C_β unmodified. (E) Serine contains a chiral center at C_α and a prochiral center at C_β. Unlike glycine, the two hydrogen atoms at the prochiral center of serine are *diastereotopic* groups since the separate replacement of each hydrogen results in a pair of diastereomers.

displaced group, *inversion* means it occupies the opposite position. If the reaction is non-stereospecific, it leads to racemization, with both isomers being formed at a ratio close to 1:1. Note that an *R*-substrate does not necessarily give an *S*-product in an inversion reaction, since the priority of the substituents at the reaction center can be altered on going from substrate to product. Also note that there is a steric course (inversion or retention) even when the displacement occurs at a prochiral center or a pro-prochiral center (a methyl group or phosphoryl group). The three hydrogen atoms of a methyl group and the three oxygen atoms of a phosphoryl group are homotopic and cannot be differentiated from one another by an enzyme. In these cases, there is no issue of stereoselectivity, only steric cause. Experimentally, pro-prochiral centers can be made chiral via isotope substitution, which in turn allows elucidation of the steric course of the reaction as illustrated in Figures 2B and 2C.

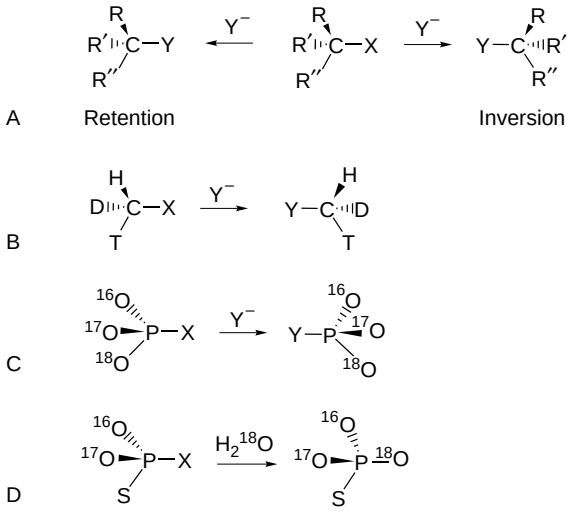

FIGURE 2 Illustration of possible steric courses of enzymatic reactions and application of isotope substitutions to elucidate the steric course. Steric courses shown in B, C, and D are inversion, inversion, and retention, respectively.

In addition to the use of oxygen isotopes, an oxygen atom at a prochiral or pro-prochiral center can also be replaced by a sulfur atom. These phosphorothioate analogs have found broad applications in the study of diverse biological systems. The stereochemical course of phosphatases, which convert a phosphomonoester to inorganic phosphate, have been deciphered in this manner, as illustrated in Figure 2D.

Key steps in conducting stereochemical experiments are the synthesis of isomers of chiral substrates and/or substrate analogs and the analysis of a compound's stereochemical configuration before and after being processed by an enzyme. Since different substrate analogs are required for each enzyme studied, and since isotopes are frequently used, these studies are particularly challenging.

Pioneering Study: Alcohol Dehydrogenase (ADH)

Yeast alcohol dehydrogenase (ADH) catalyzes the reversible transfer of a hydrogen atom between a molecule of ethanol and a molecule of the coenzyme nicotinamide-adenine dinucleotide (NAD^+). By use of deuterated ethanol or coenzyme, ADH was shown to abstract the pro-*R* hydrogen of ethanol and adding it to the *re* face of NAD^+, as illustrated in Figure 3.

Analysis of Steric Course to Probe an Enzymatic Reaction Pathway

In nonenzymatic reactions, a bimolecular S_N2 reaction leads to inversion of configuration of the chiral carbon, while a unimolecular S_N1 reaction generates a planar carbonium ion that reacts randomly at each face to generate a racemic product. In enzymatic reactions, however, the steric course is usually an inversion for both types of mechanisms, since the carbonium ion is not free to rotate within the active site. Thus, an inversion of steric course can be used to conclude that the reaction involves an odd number of displacements (most likely single displacement), whereas retention can be used to conclude that the reaction involves an even number of displacements (most likely two displacements involving an E–S intermediate).

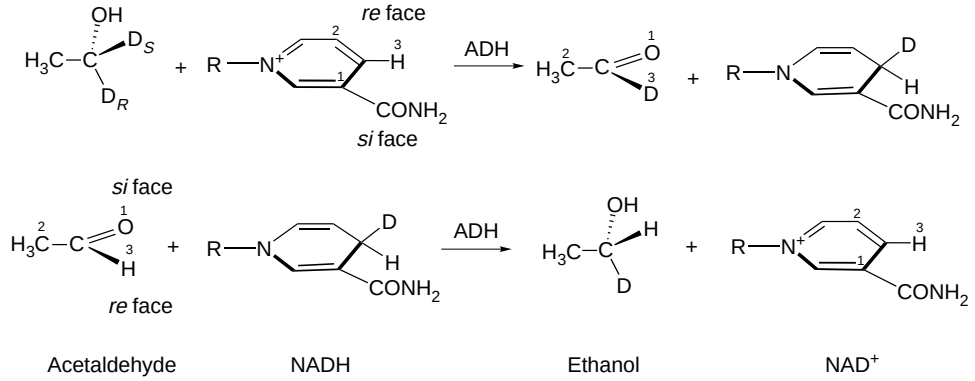

FIGURE 3 Stereochemistry involved in the reaction catalyzed by yeast alcohol dehydrogenase (ADH). In the forward reaction, the pro-*R* hydrogen of ethanol is transferred to the *re* face of NAD^+ to give NADH and acetaldehyde. In the reverse reaction, the pro-*R* hydrogen of NADH is transferred to the *re* face of acetaldehyde. The numbers 1, 2, and 3 designate the priorities of the substituents at the sp^2 carbon. The *re* and *si* faces of NADH are diastereotopic faces (since "R" includes stereocenters) whereas those of acetaldehyde are enantiotopic faces.

Phosphoryl transfer reactions are described by different terminology, where dissociative and associative mechanisms generally correspond to S_N1 and S_N2, respectively. The associative mechanism can be executed via in-line or adjacent mechanisms. In the adjacent mechanism, the nucleophile enters on the same side as the leaving group, generating a pentavalent intermediate with trigonal bipyramidal geometry. However, for the reaction to proceed, both the nucleophile and the leaving group must occupy apical positions. Therefore, pseudorotation – rearrangement of substituents about the reaction center such that the leaving group shifts from an equatorial to an axial position – must occur before the leaving group can be expelled. Except when the adjacent mechanism appears likely, the steric course of the reaction is also used to obtain information about the number of phosphoryl transfers.

Information about an enzyme's steric course is very useful for elucidating the reaction pathway as illustrated by the following example: mammalian phosphatidylinositol-specific lipase C (mPI-PLC) catalyzes the simultaneous formation of 1,2-cyclic phosphate (IcP) and inositol phosphate (IP) from phosphatidylinositol (DPPI). Two reaction schemes, sequential and parallel, can account for this behavior (Figure 4). Examination of the steric course of the mPI-PLC catalyzed reaction, where inversion of configuration at the phosphate center of IcP and retention of configuration at the phosphate center of IP were found, led to the conclusion that the reaction pathway is sequential.

Stereoselectivity Can Probe Metal–Nucleotide or Enzyme–Substrate Interactions at the Transition State

Enzymes catalyze reactions by stabilizing the transition state. Knowledge of enzyme substrate interactions at the transition state is therefore requisite for understanding the mechanism of enzyme action. Though structures of enzyme–substrate complexes are useful, they can only provide information about ground state interactions. Since enzymatic stereoselectivity is a consequence of steric and electronic constraints within the enzyme active site at the transition state, stereochemical studies can provide information about catalytic interactions that is often unattainable via structural work alone.

Since there are numerous points of contact between an enzyme and its substrate throughout a reaction pathway, stereoselectivity alone is often not sufficient for providing information about a particular enzyme–substrate interaction. However, this difficulty is circumvented by employing substrate analogs in conjunction with stereochemical analysis. For example, most enzymes that utilize ATP prefer one isomer of ATPαS or ATPβS over the other. Such R_P/S_P (or S_P/R_P) stereoselectivity can be caused by phosphate–metal-ion interactions, phosphate–enzyme interactions, or both types of interactions. A reversal (or a dramatic change) of stereoselectivity in the presence of an

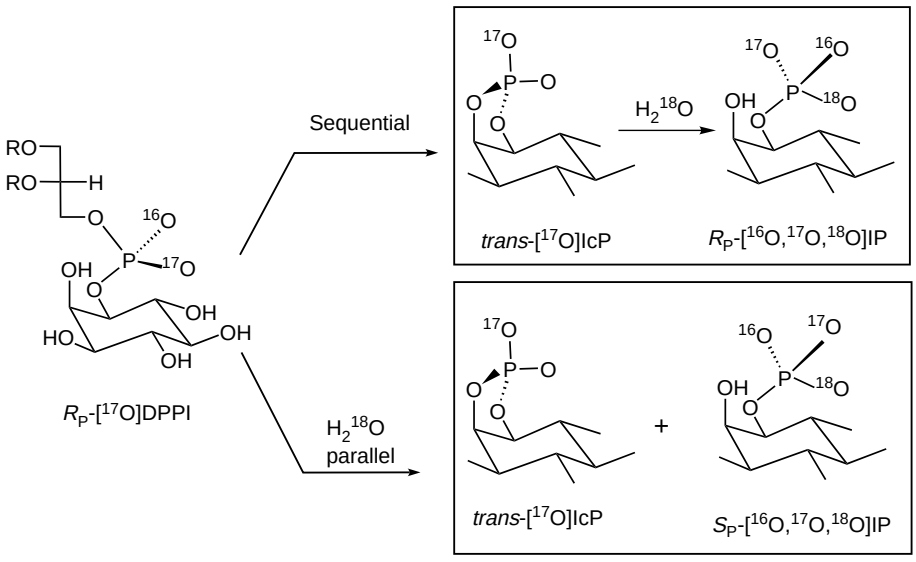

FIGURE 4 Proposed sequential and parallel mechanisms for the formation of IcP and IP catalyzed by mPI-PLC. In the sequential mechanism, intramolecular attack by the axial ring hydroxyl forms the cyclic intermediate (IcP), which is then broken down by hydrolysis ($H_2^{18}O$) to give R_P-[^{16}O, ^{17}O, ^{18}O] IP. In the parallel mechanism, intramolecular attack by the axial ring hydroxyl and direct water ($H_2^{18}O$) attack gives S_P-[^{16}O, ^{17}O, ^{18}O] IP, respectively.

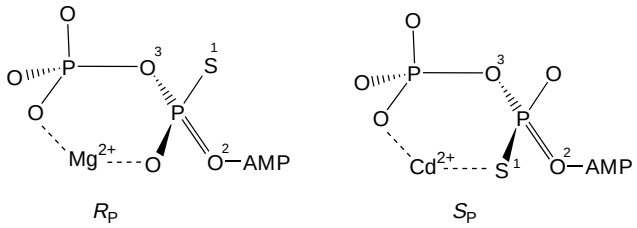

FIGURE 5 Metal–nucleotide interactions showing that substitution of Mg^{2+} by Cd^{2+} leads to a change in the stereoselectivity of AK from R_P-ATPβS to S_P-ATPβS.

"unnatural" metal ion or upon mutating an active site residue provides strong evidence that the metal ion or mutated residue interacts with that particular phosphate moiety. Studies of adenylate kinase (AK) described below further illustrate this point.

AK catalyzes the reversible phosphoryl transfer reactions: $Mg^{2+} \cdot ATP + AMP \leftrightarrow Mg^{2+} \cdot ADP + ADP$. Of the R_P and S_P isomers of ATPβS shown in Figure 5, AK prefers the S_P isomer by a factor of 9 in the presence of Mg^{2+}. However, this stereoselectivity is reversed (R_P isomer is preferred by a factor of 10) when Mg^{2+} is substituted by Cd^{2+}. Since Cd^{2+} preferentially coordinates sulfur over oxygen, which is opposite to the ligand preference of Mg^{2+}, the switch of stereospecificity upon Cd^{2+} substitution is strong evidence for direct coordination of the metal ion by the pro-*S* oxygen of the

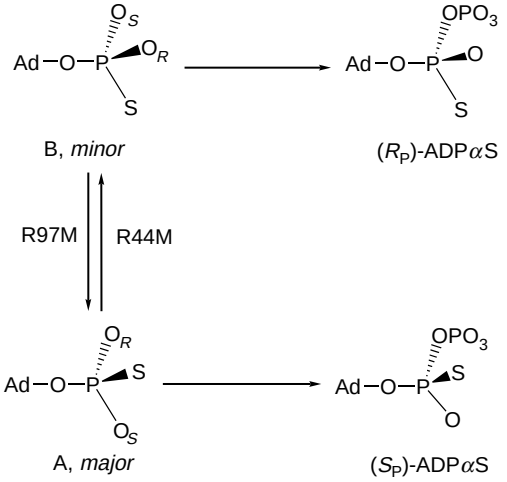

FIGURE 6 Enhancement and reversal of adenylate kinase stereoselectivity by site-directed mutagenesis (Ad, adenosine). In the reaction catalyzed by WT protein, phosphate is preferentially attached to the pro-*R* oxygen of AMPS. The R97M and R44M mutations enhance and reverse this stereoselctivity, respectively. This provides strong evidence that R97 and R44 interact with the phosphate moiety of AMP at the transition state. A and B represent two "conformers" of AMPS when bound to the active site of the enzyme.

β-phosphate of ATP. Additional mechanistic information for AK was derived using active site mutants. Wild type AK catalyzes the stereoselective conversion of AMPS to S_P-ADPαS. Such stereoselectivity could be achieved by restricting orientation of the P–S and P–O bonds at the active site as shown in Figure 6. Experimental results demonstrated that the stereoselectivity of this reaction is further enhanced by the R97M mutant, but is completely reversed in the reaction catalyzed by the R44M mutant. These results indicate that the conformational equilibrium of the AMPS substrate in the active site is perturbed in both mutants, suggesting that the Arg97 and Arg44 residues interact with the phosphate moiety of AMPS.

See Also the Following Articles

Carbohydrate Chains: Enzymatic and Chemical Synthesis • Enzyme Inhibitors • Substrate Binding, Catalysis, and Product Release

Glossary

enzyme-catalyzed reaction Usually stereospecific; many of them are also stereoselective. The stereochemical property of an enzymatic reaction is useful in elucidating its reaction mechanism.

stereoselectivity The ability of an enzyme to choose from two or more possible stereoisomers as a preferred substrate, to choose from two enantiotopic groups or from two diastereotopic groups, or to produce one stereoisomer as a preferred product when more than one stereoisomeric products are possible.

stereospecificity The ability of an enzyme to convert a particular stereoisomeric substrate to a specific stereoisomeric product. For a substitution reaction, the stereochemical course of a stereospecific reaction can be retention or inversion.

Further Reading

Bruzik, K. S., and Tsai, M.-D. (1991). Phospholipase stereospecificity at phosphorus. *Methods Enzymol.* **197**, 258–269.

Fersht, A. (1998). *Structure and Mechanism in Protein Science: A Guide to Enzyme Catalysis and Protein Folding*. Freeman, New York.

Floss, H. G., and Tsai, M.-D. (1979). Chiral methyl groups. *Adv. Enzymol.* **50**, 243–302.

Knowles, J. R. (1980). Enzyme-catalyzed phosphoryl transfer reactions. *Ann. Rev. Biochem.* **49**, 877–919.

Tomasselli, A. G., and Noda, L. H. (1983). Baker's yeast adenylate kinase. Evidence of conformational change from intrinsic fluorescence and difference spectra. Determination of the structure of enzyme-bound metal-nucleotide by use of phosphorothioate analogues of ATP. *Eur. J. Biochem.* **132**, 109–115.

Tsai, M.-D. (1982). Use of $^{31}P(^{18}O)$, $^{31}P(^{17}O)$, and ^{17}O NMR methods to study enzyme mechanisms involving phosphorus. *Methods Enzymol.* **87**, 235–279.

Tsai, M.-D., Jiang, R. T., Dahnke, T., and Shi, Z. (1995). Manipulating phosphorus stereospecificity of adenylate kinase by site-directed mutagenesis. *Methods Enzymol.* **249**, 425–443.

Biography

Ming-Daw Tsai is a Professor in the Departments of Chemistry and Biochemistry at The Ohio State University. Dr. Tsai's overall research interest lies at the interface between chemistry and biology, in particular, the structure–function relationship of enzymes and proteins. He holds a Ph.D. in Medicinal Chemistry from Purdue University.

Li Zhao holds a Ph.D. in Chemistry from The Ohio State University. Her research focus has been the catalytic mechanism of Phosphatidylinositol-specific lipase C.

Brandon J. Lamarche earned a B.Sc. in Chemistry from Westmont College. In 1999 he started doctoral work in the Department of Chemistry at The Ohio State University. His research interests involve the enzymology of DNA repair.

Epidermal Growth Factor Receptor Family

Denis Tvorogov and Graham Carpenter
Vanderbilt University School of Medicine, Nashville, Tennessee, USA

The physiological state of a single cell in a multicellular organism is generally determined by different extracellular signals presented to the cell. Many of these extracellular signals transduce their cellular response by recognizing and activating a receptor with intrinsic tyrosine kinase activity. Among these is the epidermal growth factor receptor family, also known as the ErbB family of receptors.

Receptors and Ligands

The ErbB family is comprised of four receptor tyrosine kinases: ErbB-1 (also known as an epidermal growth factor [EGF] receptor), ErbB-2, ErbB-3, and ErbB-4. These receptors are thought to mediate signal for cell proliferation, differentiation, migration, or apoptosis. Deregulated expression or mutational activation of ErbB receptors, especially ErbB-1 and ErbB-2, has been found in numerous types of human cancer.

Eleven different EGF-like growth factors, which directly activate ErbB receptors, have been identified: EGF, transforming growth factor alpha (TGF-α), amphiregulin, heparin-binding-EGF (HB-EGF), epiregulin, betacellulin, epigen, and the neuregulins (NRG-1, NRG-2, NRG-3, NRG-4) also known as heregulins. ErbB receptors are subgrouped by their ligand-binding properties. ErbB-1 recognizes EGF, TGF-α, amphiregulin, HB-EGF, epiregulin, epigen, and betacellulin. ErbB-3 binds NRG-1 and NRG-2. ErbB-4 binds NRG-1–4, betacellulin, epiregulin, and HB-EGF (Figure 1). As yet no ligand has been identified for ErbB-2, but significant data suggest that ErbB-2 serves as a coreceptor for all other ErbBs. The binding of a ligand with an ErbB receptor induces the formation of homodimers and heterodimers, particularly with ErbB-2. Dimerization is a mechanism to provoke receptor autophosphorylation and thereby stimulate the intrinsic tyrosine kinase activity of the receptors.

The Structure of ErbB Receptors

The domain structure of the ErbB receptors consists of an extracellular ligand-binding domain, a single transmembrane (TM) domain, and an intracellular region (Figure 1). The extracellular domains of all ErbB receptors are highly glycosylated and are subdivided into four subdomains, termed I, II, III, and IV. Domains II and IV are cysteine-rich regions, and are highly conserved among the ErbBs. Domains I and III cooperate to form a growth factor-binding site as demonstrated by the crystal structure of the extracellular region of the ErbB-1 receptor with EGF and TGF-α. These data further indicate that growth factor binding induces conformational changes in subdomain II, which leads to dimerization through a direct receptor:receptor interaction.

The TM domain of each ErbB receptor contains 20–25 amino acid residues forming five loops of α-helical structure, and probably plays a passive role in signal transduction. This conclusion is based on experiments with ErbB-1 receptors containing a mutated TM region. Different forms of the ErbB-1 receptor with extended or shortened TM regions were able to bind EGF and dimerize. Alterations generated within the TM domain did not prevent receptor autophosphorylation.

The intracellular domain of ErbB receptors contains a tyrosine kinase domain and autophosphorylation sites (Figure 1). The tyrosine kinase domain is highly conserved among all four ErbB receptors; however, the ErbB-3 has a defective tyrosine kinase domain due to several residue changes. ErbB-3, therefore, must dimerize with a kinase competent receptor (ErbB-2 is preferred) to form a signaling competent complex.

Binding of ligand to an ErbB receptor provokes autophosphorylation of multiple tyrosine residues within the carboxy-terminal domain. Together with adjacent residues each phosphotyrosine residue serves as a receptor docking site for proteins involved in

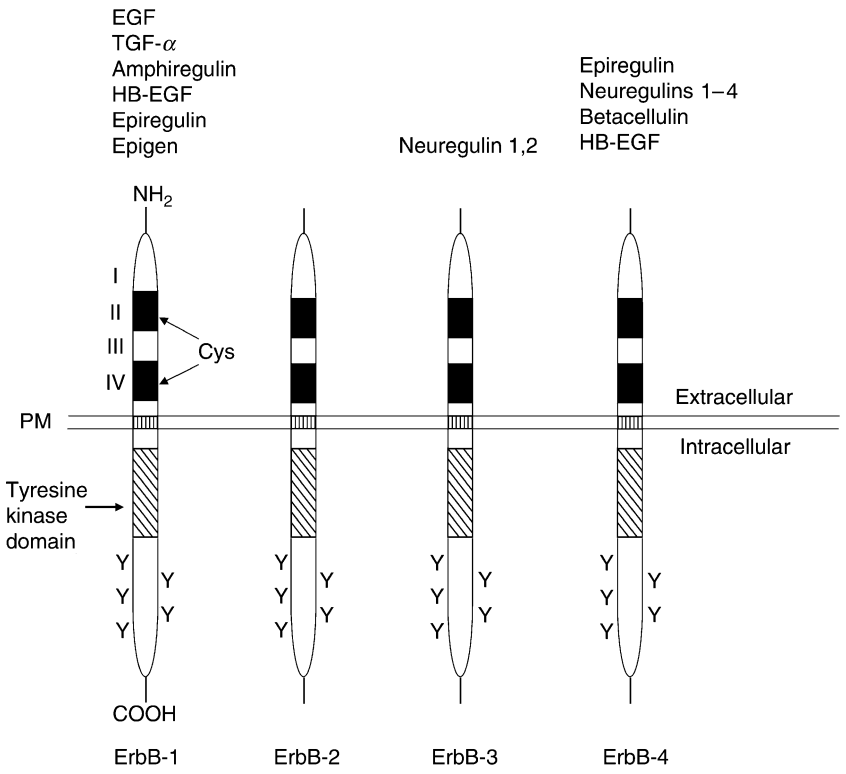

FIGURE 1 Structure of ErbB receptors. Each receptor contains an extracellular region bearing with cysteine-rich domains (Cys, filled), a single TM domain (vertical hatched), and a cytoplasmic region consisting of a tyrosine kinase domain (diagonal hatched) and tyrosine residues (Y) on the C-terminal domain which can be phosphorylated by the tyrosine kinase domain. The ErbB-3 receptor has a deficient tyrosine kinase domain (diagonal hatched with a cross). The ligands which bind to these receptors are listed above each receptor.

downstream signaling events (Figure 2). The association between tyrosine phosphorylated sequences and each signaling protein is facilitated by the presence of either an Src homology 2 (SH2) or a phosphotyrosine binding (PTB) domain in the signaling protein. The specificity of the interaction of any given ErbB receptor with an SH2 or PTB domain-containing protein is determined by the exact amino acid sequences surrounding the phosphorylated tyrosine residue, as well as sequences within each SH2 or PTB domain. Generally, receptor docking of these proteins is a prerequisite for tyrosine phosphorylation of these signaling proteins by the receptor and the activation of signal transduction pathways that cooperate to produce cellular responses.

ErbB-1	ErbB-2	ErbB-3	ErbB-4
Shc	Shc	Shc	Shc
Cb1			
Grb2	Grb2		
PLCγ1			
Shp1			
		p85	p85
		Grb7	
STAT	STAT	STAT	STAT

FIGURE 2 Subsets of signaling proteins activated by each ErbB receptor.

ErbB Receptor Substrates

ErbB receptors are involved in the initiation of a variety of cell responses, such as proliferation, differentiation, or cell locomotion, which require changes in gene expression, intracellular Ca^{2+} level, protein and lipid phosphorylation, and other intracellular conditions. Therefore, every activated ErbB receptor interacts with a battery of proteins involved in different signal intracellular pathways. Different ErbB receptors associate with overlapping subsets of intracellular proteins to activate subsets of the same downstream signaling pathways (Figure 2). The list of signaling partners for each ErbB receptor is not entirely determined and most data have been obtained from experiments with the ErbB-1 (or EGF) receptor. Proteins that interact with activated ErbB receptors can be categorized according to

their signaling properties: enzymes participating in phosphatidylinositol metabolism, such as phospholipase Cγ1 and the regulatory subunit of phosphatidylinositol 3-kinase; protein kinases, such as Src; phosphatases, such as Shp1 and Shp2; adaptor proteins, such as Cbl, Shc, Grb2, Nck; and transcription factors, such as STATs. As shown in Figure 2. the signaling pathways activated by the four ErbB receptors frequently overlap. How signaling pathways are actually integrated to provoke a cellular response, such as proliferation, is unknown.

Receptor-Mediated Endocytosis

A second consequence of ligand binding to ErbB receptors is an initiation of rapid receptor-mediated endocytosis (Figure 3). During this process ligand–receptor complexes cluster in cell-surface clathrin-coated pits, which subsequently become intracellular clathrin-coated endosomes. The clathrin coat is then removed to produce early endosomes and this compartment matures to form multivesicular bodies. There are two fates for internalized receptor. First, receptors may undergo recycling, from early endosomes or from multivesicular bodies, to the plasma membrane. Multivesicular bodies become late endosomes and then primary lysosomes where receptor and ligand degradation occurs. Hence, a receptor may be degraded or recycled following the endocytic pathway. Under most circumstances the degradation route is kinetically favored.

Interestingly, only ErbB-1 receptors have been shown to be rapidly internalized following ligand binding. Other ErbB receptors are endocytosis impaired or demonstrate only a very slow endocytotic rate. Experiments with chimeric receptors containing the ErbB-1 extracellular domain and different ErbB-2, ErbB-3, ErbB-4 cytoplasmic regions show extremely low rates of internalization. These data suggest that the structure of the ErbB cytoplasmic domains determines whether or not a given ErbB receptor will be rapidly internalized by clathrin-coated pits. It also has been shown that ErbB-1 tyrosine kinase activity is necessary for ligand-dependent receptor trafficking into clathrin-coated pits and subsequent internalization.

There are two different points of view regarding the significance of endocytosis for growth factor receptor signal transduction. One view is that endocytosis serves as a desensitization mechanism by removing the receptors from the plasma membrane and degrading the activated receptors in the lysosome. Indeed, introduction of a truncated form of EGF receptor that retains kinase activity is internalization defective and leads to enhanced mitogenic responses and cellular transformation after treatment with EGF. A second viewpoint is that positive signaling occurs during endocytosis. It has been shown that EGF receptors in endosomes retain bound EGF, are authophosphorylated, and are able to activate some intracellular signaling pathways. This suggests that receptor-mediated endocytosis may serve as a mechanism for spatial redistribution of activated EGF receptors and transduction of signals.

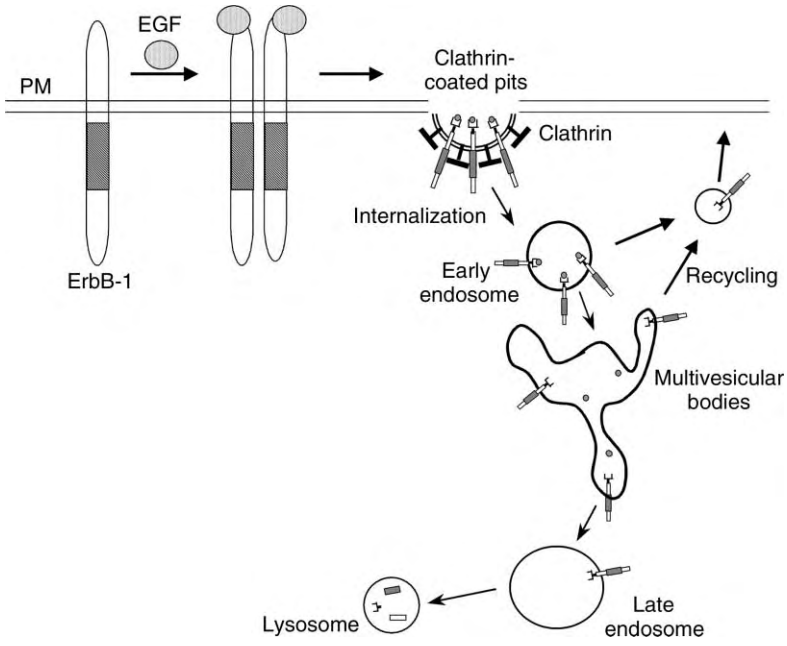

FIGURE 3 Schematic representation of ErbB-1 receptor trafficking following EGF binding.

Targeting ErbB Receptors in Cancer Therapy

During the past several years it has become clear that deregulated signaling from ErbB receptors is involved in cancer development. Among the ErbB receptors, the overexpression or abnormal activation of ErbB-1 or ErbB-2 is most often observed in epithelial carcinomas and glioblastomas. There are three possible mechanisms by which an ErbB pathway may be hyperactivated: ligand overproduction, receptor overexpression, or mutation to produce activated receptors in the absence of a growth factor. Expression of ErbB-1 or its ligand has been reported in over 80% of head and neck squamous cell carcinomas, while its overexpression occurs in breast carcinomas and its mutational activation occurs in glioblastomas. Overexpression of the ErbB-2 receptor is common in breast cancer, ~25% of invasive ductal breast cancers have overexpressed ErbB-2 due to gene amplification. The level of ErbB-2 overexpression correlates with tumor size and its spread to lymph nodes. Breast cancers with ErbB-2 overexpression have a poorer prognosis and are more resistant to chemotherapy. Among all ErbB ligands, the role of TGF-α in human cancer is most characterized. Co-overexpression of TGF-α and ErbB-1 has been found in several types of carcinomas, and overproduction of TGF-α in lung and colon tumors coexpressing ErbB-1 correlates with poor prognosis.

In general, there are two different but related approaches to inhibit Erb-B-mediated signaling in human tumors and both are now in clinical trials. These include monoclonal antibodies and tyrosine kinase selective inhibitors. Several ErbB-1-specific antibodies against the extracellular region of receptor have been developed. The mechanism of inhibiting the activity of the receptor involves antibody binding to the receptor and masking the ligand-binding site. This prevents ligand-binding and receptor activation. Additionally the antibody may enhance receptor internalization and degradation. It is also possible that the antibody marks cells that express an increased level of ErbB-1 and targets them for destruction by the immune system. A humanized antibody to ErbB-2 termed Herceptin has been validated for clinical use and represents one of the first successes of biotechnology in clinical settings. Herceptin slows the proliferation rate of breast cancer cells overexpressing ErbB-2, by increasing the percentage of the cell population in G0/G1 or quiescent states of the cell cycle.

Low-molecular-weight inhibitors are another strategy used *in vivo* to suppress hyperactivated ErbB signaling in human tumors. These compounds competitively inhibit ATP binding at the tyrosine kinase active site and thereby block proliferation. One of these compounds, Iressa, has been cleared for clinical use.

Conservation of ErbB Receptor Signaling during Evolution

ErbB signaling is present not only in mammalians, but also in less-developed organisms such as the nematode *Caenorhabditis elegans* and the fruitfly *Drosophila melanogaster.* The nematode has one EGF-like ligand (Lin-3) and one ErbB-like receptor (Let23). These components are required for correct development in the nematode. In the fruitfly the ErbB signaling network consists of four EGF-like ligands (Vein, Gurken, Spitz, and Argos) and one EGF-like receptor (*Drosophila* EGF receptor – DER). Argos is a unique ligand as it acts negatively to inhibit receptor signaling. In *Drosophila*, ErbB signaling is also required for several developmental pathways. Interestingly, many of the signaling elements found downstream of the mammalian EGF receptor are highly conserved in the nematode and fruitfly. Hence, this growth factor signaling system has been highly conserved throughout millions of years of evolution.

See Also the Following Articles

Phosphatidylinositol Bisphosphate and Trisphosphate • Phospholipase C • Src Family of Protein Tyrosine Kinases • Syk Family of Protein Tyrosine Kinases • Tec/Btk Family Tyrosine Kinases

Glossary

autophosphorylation The process by which a receptor phosphorylates itself. This can be cisphosphorylation or, with context of a dimmer, transphosphorylation.

dimerization The tight association of two proteins, such as receptor tyrosine kinase.

growth factor A small protein which binds to a cell-surface receptor and induces proliferation, differentiation, or other cellular responses dependent on cell type.

receptor A cell-surface molecule that binds a cognate growth factor with high specificity and high affinity and which mediates a biologic response to the growth factor.

tyrosine kinase An enzyme that uses ATP as a phosphate donor to catalyze the formation of phosphotyrosine residues on substrate proteins.

Further Reading

Carpenter, G. (2000). The EGF receptor: A nexus for trafficking and signaling. *Bioessays* **22**, 697–707.

Cho, H. S., and Leahy, D. J. (2002). Structure of the extracellular region of HER3 reveals an interdomain tether. *Science* **297**, 1330–1333.

Garrett, T. P., McKern, N. M., Lou, M., Elleman, T. C., Adams, T. E., Lovrecz, G. O., Zhu, H. J., Walker, F., Frenkel, M. J., Hoyne, P. A., Jorissen, R. N., Nice, E. C., Burgess, A. W., and Ward, C. W. (2002). Crystal structure of a truncated epidermal growth factor receptor extracellular domain bound to transforming growth factor alpha. *Cell* **110**, 763–773.

Ogiso, H., Ishitani, R., Nureki, O., Fukai, S., Yamanaka, M., Kim, J. H., Saito, K., Sakamoto, A., Inoue, M., Shirouzu, M., and Yokoyama, S. (2002). Crystal structure of the complex of human epidermal growth factor and receptor extracellular domains. *Cell* **110**, 775–787.

Olayioye, M. A., Neve, R. M., Lane, H. A., and Hynes, N. E. (2000). The ErbB signaling network: Receptor heterodimerization in development and cancer. *EMBO J.* **19**, 3159–3167.

Sorkin, A., and Von Zastrow, M. (2002). Signal transduction and endocytosis: Close encounters of many kinds. *Nat. Rev. Mol. Cell Biol.* **3**, 600–614.

Sweeney, C., and Carraway, K. L. III., (2000). Ligand discrimination by ErbB receptors: Differential signaling through differential phosphorylation site usage. *Oncogene* **19**, 5568–5573.

BIOGRAPHY

Denis Tvorogov is a Postdoctoral Fellow in the laboratory of Graham Carpenter at Vanderbilt University School of Medicine. He received his Ph.D. from the Institute of Cytology, St. Petersburg, Russia in 2002.

Graham Carpenter's Ph.D. was awarded from the University of Tennessee in 1974. He is a Professor of Biochemistry at Vanderbilt University School of Medicine, where he is also Ingram Professor of Cancer Research.

ER/SR Calcium Pump: Function

Giuseppe Inesi
University of Maryland School of Medicine, Baltimore, Maryland, USA

The sacro-endoplasmic reticulum Ca^{2+} ATPase (SERCA) utilizes ATP for active transport of cytosolic Ca^{2+} into membrane bound intracellular compartments. Intracellular storing of Ca^{2+} by SERCA is an integral part of signaling mechanisms for a large number of cellular functions. The catalytic and transport cycle of SERCA includes formation of a phosphorylated enzyme intermediate and protein conformational changes, leading to vectorial translocation of Ca^{2+} across the membrane.

ATP Use for Ca^{2+} Transport

The sarcoendoplasmic reticulum calcium ATPase (SERCA) is the Ca^{2+} pump of intracellular membranes. The pump plays a prominent role in numerous cytosolic signaling mechanisms that require the sequestration of intracellular Ca^{2+}. The SERCA pump was first noted in a microsomal fraction of rabbit skeletal muscle homogenates, which was found to prevent activation of glycerinated muscle fibers or isolated contractile models upon the addition of ATP. The microsomes were then identified with vesicular fragments of sarcoplasmic reticulum (SR), and the relaxing effect was attributed to sequestration of Ca^{2+} from the medium through active transport by a membrane-bound ATPase. cDNA cloning identified three gene products (SERCA 1, SERCA2, and SERCA3) with two to three splice variants for each primary transcript. The related isoforms display specific tissue distribution, functional roles, and regulatory mechanisms.

The SR vesicles obtained from skeletal muscle contain a high quantity of Ca^{2+} ATPase (SERCA1A isoform), which accounts for approximately 50% of the total protein and which is densely spaced within the plane of the membrane (Figure 1). These vesicles provide a very useful experimental system inasmuch as they allow parallel measurements of ATPase activity and Ca^{2+} transport, as well as control of the ionic environment in compartments delimited by the native membrane. For this reason, they have been used extensively in biochemical and structural studies to clarify the mechanism of ATP use for Ca^{2+} transport.

Steady-State Behavior

Active transport of Ca^{2+} into the lumen of SR vesicles occurs with a stoichiometric ratio of two Ca^{2+} per hydrolyzed ATP under optimal steady-state conditions. Acetyl phosphate or *p*-nitrophenyl phosphate can be used as substrate by the enzyme instead of ATP, although with lesser kinetic competence. The maximal levels of ATP-dependent Ca^{2+} uptake by the vesicles is increased by Ca^{2+} binding to a native acidic protein, calsequestrin, in the lumen of the vesicles. It can also be increased by complexation with anions such as oxalate or phosphate in the lumen of the vesicles.

Independent of the substrate, the ATPase has a strict requirement for Ca^{2+} activation. In fact the enzyme is activated by medium containing free Ca^{2+} within the micromolar range and is inhibited by lumenal free Ca^{2+} in the millimolar range. This indicates that ATP is used to change the affinity and orientation of the Ca^{2+}-binding sites, resulting in a three-orders-of-magnitude Ca^{2+} gradient across the membrane. Furthermore, in reconstituted ATPase preparations that are deprived of pathways for passive leakage, it was shown that Ca^{2+} transport is accompanied by H^+ countertransport at a 1:1 ratio and that the pump is electrogenic.

Considering these functional features, the free energy required for active transport of Ca^{2+} into the vesicles can be defined, at first approximation, as:

$$\Delta G = RT \ln\left(\left[Ca^{2+}_{in}\right]/\left[Ca^{2+}_{out}\right]\right) + zF\Delta V$$

where $[Ca^{2+}_{in}]$ and $[Ca^{2+}_{out}]$ refer to the Ca^{2+} concentration in the lumen of the vesicles and in the outer medium, z is the electrical charge of the transported species, R and F are the gas and Faraday constants, respectively, and ΔV is the transmembrane electrical gradient. The free-energy requirement, estimated in this manner, provides a satisfactory match of the experimentally observed gradients with the chemical potential of ATP.

The Partial Reactions of the Catalytic and Transport Cycles

The Ca^{2+} ATPase catalytic cycle includes a phosphorylated intermediate formed by covalent transfer of the

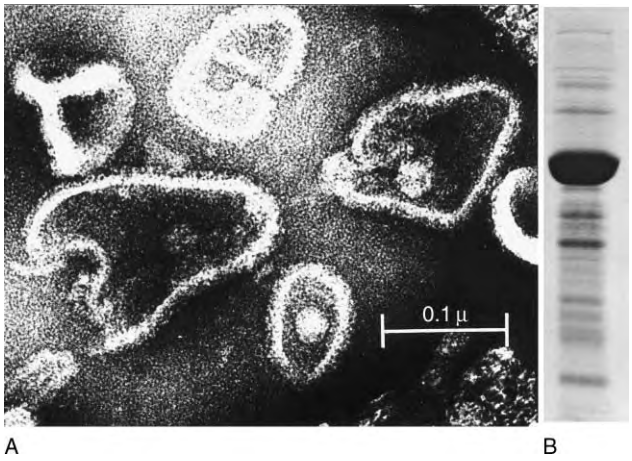

FIGURE 1 Structural characterization of SR vesicles. (A) Negatively stained SR vesicles, obtained from rabbit skeletal muscle, are visualized by electron microcopy. The densely spaced granules on the surface of the membrane correspond to Ca^{2+} ATPase molecules. (B) Electrophoretic analysis demonstrating that the Ca^{2+} ATPase separates as a prominent band that accounts for the major portion of the membrane protein. Adapted from Scales, D. and Inesi, G. (1976). Assembly of ATPase protein in sarcoplasmic reticulum membranes. *Biophys. J.* **16**, 735–751, with permission from the Biophysical Society.

ATP terminal phosphate to an aspartyl residue (Asp351) at the catalytic site. Phosphoryl transfer requires activation by the same Ca^{2+} concentration as ATP hydrolysis, indicating that enzyme activation by Ca^{2+} must occur early in the catalytic cycle. In fact, cooperative binding of two Ca^{2+} per ATPase in the absence of ATP, with an apparent K_d in the micromolar Ca^{2+} range, was demonstrated by direct equilibrium measurements (Figure 2A).

The sequence of partial reactions making up the catalytic cycle was unveiled by transient-state experiments showing that addition of ATP to SR vesicles preincubated with micromolar Ca^{2+} is followed by the rapid formation of phosphorylated intermediate and vectorial displacement of two bound Ca^{2+} per ATPase. These initial events are then followed by hydrolytic cleavage of inorganic phosphate (Pi) after a time lag (Figure 2B). On the other hand, the ATPase cycle is highly reversible, as demonstrated by ATP synthesis coupled to the Ca^{2+} efflux from loaded vesicles. The partial reactions of the reverse cycle were further clarified by the finding that, in the absence of bound Ca^{2+}, the enzyme can be phosphorylated with Pi to yield ADP-insensitive phosphoenzyme (E-P). This phosphoenzyme can then be made ADP-sensitive by the addition of millimolar Ca^{2+}, whereupon it reacts with ADP to form ATP.

These functional findings have been attributed to a mechanism based on the interconversion of two enzyme states. One state (E_1), stabilized by Ca^{2+} binding, has the Ca^{2+} sites in high affinity and cytosolic orientation.

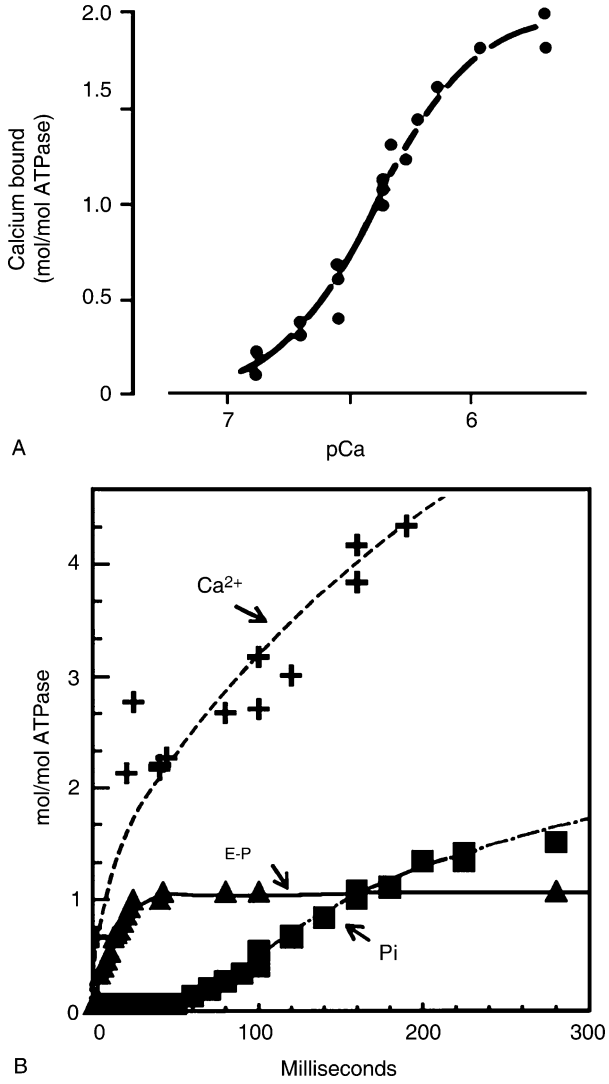

FIGURE 2 Functional characterization of SR vesicles. (A) Calcium binding at equilibrium in the absence of ATP, demonstrating cooperative binding of two Ca^{2+} per ATPase. From Inesi G., Kurzmack M., Coan C., and Lewis D. (1980). Cooperative calcium binding and ATPase activation in sarcoplasmic reticulum vesicles. *J. Biol. Chem.* 255, 3025–3031 with permission from The American Society for Biochemistry & Molecular Biology. (B) Rapid enzyme phosphorylation and inward displacement of the two bound Ca^{2+} upon addition of ATP. Hydrolytic cleavage of inorganic phosphate (Pi) occurs after a lag period. E-P, phosphoenzyme. From Inesi, G., Watanabe, T., Coan, C., and Murphy, A. (1978). The mechanism of sarcoplasmic reticulum ATPase. *Ann. N.Y. Acad. Sci.* **402**, 515–534 with permission.

The alternate state (E_2), stabilized by enzyme phosphorylation, has the Ca^{2+} sites in low affinity and lumenal orientation. A more explicit view of the coupling mechanistic can be obtained by considering a minimal number of partial reactions and their equilibrium constants, as follows:

$$H_2E + 2Ca^{2+}_{out} \equiv E{\cdot}Ca_2 + 2H^+_{out} \qquad (10^{12}\ M^{-2}) \quad (1)$$

$$E{\cdot}Ca^{2+} + ATP \equiv ATP{\cdot}E{\cdot}Ca_2 \qquad (10^{5}\ M^{-1}) \quad (2)$$

$$ATP{\cdot}E{\cdot}Ca_2 \equiv ADP{\cdot}E{\cdot}P{\cdot}Ca_2 \quad (1.0) \qquad (3)$$

$$ADP{\cdot}E{\cdot}P{\cdot}Ca_2 \equiv E - P{\cdot}Ca_2 + ADP \quad (10^{-4}\,M) \qquad (4)$$

$$E - P{\cdot}Ca_2 + 2H^+_{in} \equiv H_2E{-}P + 2Ca^{2+}_{in} \quad (10^{-6}\,M^2) \qquad (5)$$

$$H_2E{-}P \equiv H_2E{\cdot}Pi \quad (1) \qquad (6)$$

$$H_2E{\cdot}Pi \equiv H_2E + Pi \quad (10^{-2}\,M) \qquad (7)$$

where the equilibrium constants (listed after each reaction) relate to conditions allowing constant temperature (25 °C) and pH (7.0).

In the reaction sequence given, the initial high-affinity binding (reaction 1) of two Ca^{2+} activates the enzyme, permitting the use of ATP and the formation of a phosphorylated intermediate (reactions 2–4). In turn, enzyme phosphorylation destabilizes and changes the vectorial orientation of the bound Ca^{2+}, thereby increasing the probability of its dissociation into the lumen of the vesicles (reaction 5). Note that the equilibrium constant for the enzyme phosphorylation by ATP is nearly 1, indicating that the free energy of ATP is conserved by the enzyme and used to change the Ca^{2+}-binding characteristics. Finally, the phosphoenzyme undergoes hydrolytic cleavage and releases Pi (reactions 6 and 7) before entering another cycle. The reaction sequence shows clearly that the direct mechanistic device for translocation of bound Ca^{2+} is enzyme phosphorylation rather than hydrolytic cleavage of Pi.

The Coupling Mechanism

Free-Energy Use

Because the catalytic and transport cycles are likely to include conformational transitions, it should be noted that such transitions are coupled intrinsically with the chemical reactions subjected to experimental measurement and that their influence is reflected by the equilibrium constants just listed. In fact, the standard free energies ($-RT \ln K$) of the partial reactions add up to the standard free energy of ATP hydrolysis (γ-phosphate), as expected. Most interestingly, the standard free-energy diagram for the partial reactions reveals that the chemical potential of ATP does not manifest itself in the phosphoryl transfer or hydrolytic cleavage reactions (K_4 and K_6 near 1) but rather in the drastic reduction of the enzyme affinity for Ca^{2+} (compare K_1 to $1/K_5$). We can, then, write that, under standard conditions:

$$\Delta G = nRT \ln\left(K_a^{\text{CaE-P}}/K_a^{\text{CaE}}\right) \qquad (8)$$

per n calcium ions (2 in our case) transported per cycle, and where the equilibrium constant (listed after the reaction) relates to conditions allowing constant temperature (25 °C and pH 7.0). $K_a^{\text{CaE-P}}/K_a^{\text{CaE}}$ are the association constants of the enzyme for Ca^{2+} in the ground state and following activation by ATP. With reference to the reaction scheme given previously, the two relevant constants are K_1 and $1/K_5$. Note that, as written in the scheme and in the forward direction of the cycle, the equilibrium constant for reaction 1 is Ka, while it is Kd for reaction S.

It is then apparent that the basic coupling mechanism of catalysis and transport consists of the mutual destabilization of Ca^{2+} and phosphorylation sites. Analysis of the amino acid sequence, electron microscopy of ordered ATPase arrays, and diffraction patterns obtained from three-dimensional crystals have shown that the SERCA enzyme is a 100-kDa protein, folded into a membrane-bound region, an extramembranous (cytosolic) region, and a short stalk between them. The membrane-bound region includes 10 helical segments (M1, …, M10) and the calcium-binding domain. On the other hand, the extramembranous region, or headpiece, comprises the nucleotide-binding (N) domain and a phosphorylation (P) domain, in addition to a smaller actuator (A) domain. It is clear that the Ca^{2+}-binding domain and the catalytic domain are separated by a large distance (~ 50Å). Therefore, the interconversion of cation-binding and phosphorylation potentials requires a long-range intramolecular linkage, rendered possible by protein conformational changes. It is, then, useful to relate the binding and covalent reactions to conformational changes that may occur through the catalytic and transport cycles.

Ca^{2+} Binding and Catalytic Activation

Binding of two calcium ions per ATPase molecule is an absolute requirement for enzyme activation. The cooperative character of binding is consistent with a sequential binding mechanism to two interdependent sites (I and II). Spectroscopic studies provided early suggestions of Ca^{2+}-induced conformational effects, accounting for binding cooperativity and enzyme activation. A detailed characterization of the large conformational changes produced by Ca^{2+} binding was recently obtained by high-resolution diffraction studies.

The functional role of the Ca^{2+}-induced conformation change lies in its absolute requirement for enzyme activation, rendered possible by the long-range intramolecular linkage. The requirement for Ca^{2+} involves both ATP use for phosphoenzyme formation in the forward direction of the cycle and the formation of ATP upon addition of ADP to

phosphoenzyme formed with Pi in the reverse direction of the cycle. Activation is not obtained by Ca^{2+} occupancy of the first binding site only but requires the occupancy of the second site, which may then be considered a Ca^{2+} trigger point for enzyme activation. Ca^{2+}-binding affects directly the M4, M5, and M6 transmembrane helices and is then transmitted to the extramembranous region, resulting in the large displacement of the headpiece domains and catalytic activation. Single mutations of several residues in the segments connecting the Ca^{2+}-binding region with the phosphorylation domain, such as M4, M5, and the M6–M7 loop, interfere with the phosphorylation reactions.

Nucleotide Binding and Substrate-Induced Conformational Fit

Nucleotide protection of the ATPase from digestion with proteinase and the mutational analysis of this phenomenon suggest that ATP binding produces a conformational change that includes repositioning of the A domain, concomitant with approximation of the N and P domains to match the molecular geometry of ATP. This substrate effect appears similar to the approximation of nucleotide binding (fingers) and catalytic (palm) domains that occurs in DNA polymerases. Although ATP is likely to form an initial complex with Mg^{2+} due to the cation-binding property of the nucleotide, ATP and Mg^{2+} reach the catalytic site through a random mechanism. Accordingly, the initial nucleotide binding at the substrate site does not include Mg^{2+}, even though the subsequent phosphoryl transfer and hydrolytic reactions require Mg^{2+}. The stabilization provided by Mg^{2+} to the transition state, relative to that of the enzyme–substrate complex, is of definite kinetic advantage.

Phosphoryl Transfer and Hydrolytic Cleavage

The Ca^{2+} ATPase mechanism includes a covalent intermediate, general acid–base catalysis and metal ion assistance. The covalent intermediate is formed through an attack on the electrophilic ATP terminal phosphate by a nucleophilic carboxylate group (D531) within the catalytic site. The phosphoenzyme intermediate reacts, then, with water to yield Pi.

It is useful to consider the Ca^{2+} ATPase catalytic mechanism in the light of the phosphorylserine phosphatase (PSPase), due to a remarkable structural and functional analogy and the high definition available for the PSPase catalytic intermediates. Based on this analogy, and on ATPase mutational analysis, it appears that the terminal phosphate of ATP comes in close proximity to Asp351, stabilized by neighboring residues such as K352, T353, G626, K684, and N706. Mg^{2+} is then coordinated by D703, T353, D351, and phosphate oxygen, participating in the transition state and in all subsequent steps. Furthermore, T353 is likely to serve as a general acid for proton donation to the leaving ADP. The same residue then acts as a general base, extracting a proton from nucleophilic water for hydrolytic cleavage of the phosphoenzyme.

Interconversion of Phosphorylation and Ca^{2+}-Binding Potentials

The specific step related to interconversion of phosphorylation and Ca^{2+}- binding potentials is often referred to as the $E_1P{\cdot}Ca_2 \rightleftharpoons E_2P{\cdot}Ca_2$, to indicate the transition of an intermediate of high phosphorylation potential and high Ca^{2+} affinity to an intermediate of low phosphorylation potential and low Ca^{2+} affinity. The functional and structural information described so far indicates that small conformational changes occurring in concomitance with ATP use at the catalytic site (phosphorylation trigger point) are amplified and transmitted to the Ca^{2+}-binding domain through a long-range relay mechanism. The inversion of phosphoryl oxygen atoms during the transition state of the phosphorylation reaction and the displacement of residues interacting with these oxygen atoms may be the triggering perturbation. This is then followed by large motions of the headpiece domains, which are transmitted to the Ca^{2+}-binding domain in the membrane-bound region. Accordingly, the ability of headpiece domains to chemically cross-link changes drastically as they are displaced by intermediate reactions of the catalytic cycle.

In conclusion, the transduction mechanism relies on a long-range linkage of transmembrane helices and cytosolic domains, whereby large-scale and mutually exclusive motions are triggered by Ca^{2+} binding at one end and ATP use at the other. This is rendered possible by the ability of the protein to use free energy derived from binding and phosphorylation reactions. The cycle proceeds forward to Ca^{2+} release or in reverse to ATP synthesis, depending on the concentrations of ligands, substrate, and products.

Physiological Regulation and Experimental Inhibitors

The SERCA2 isoform of cardiac muscle is subject to physiological regulation by phospholamban (PLB), a 22-kDa pentameric protein undergoing reversible association and dissociation. The PLB monomer

interacts with the ATPase at the level of both the membrane-bound and extramembranous regions of the enzyme. In the presence of PLB, the ATPase activation curve is displaced to a higher Ca^{2+} concentration range. The velocity at nonsaturating Ca^{2+} concentrations is thereby reduced, although the maximal velocity at saturating Ca^{2+} concentrations remains unchanged. This inhibition is reversed when PLB undergoes phosphorylation catalyzed by cAMP and calmodulin-dependent kinases. The phosphorylation-dependent relief of inhibition by PLB is related to the physiological mechanism whereby adrenergic stimuli increase Ca^{2+} storing by SR and improve the contractile performance of the heart muscle *in vivo*. Another small protein, sarcolipin, appears to regulate the Ca^{2+} ATPase in skeletal muscle.

Thapsigargin (TG), a plant-derived sesquiterpene lactone, is a very potent and specific SERCA inhibitor. Although TG is not likely to be a physiologic inhibitor, it is nevertheless an extremely useful experimental tool. TG interferes with all partial reactions of the catalytic cycle and induces stabilization of ordered ATPase arrays, suggesting a general effect on the enzyme. Mutational and structural studies indicate that the TG-binding site resides in a cavity delimited by the M3, M5, and M7 helices near the cytosolic surface of the membrane. It is likely that the presence of TG in this cavity confers structural stabilization to the enzyme, thereby preventing conformational responses to Ca^{2+} binding and phosphorylation reaction, as required for the progression of the catalytic cycle.

See Also the Following Articles

Calcium/Calmodulin-Dependent Protein Kinase II • Calcium/Calmodulin-Dependent Protein Kinases • Calcium-Binding Proteins: Cytosolic (Annexins, Gelsolins, C_2-Domain Proteins) • ER/SR Calcium Pump: Structure

Glossary

long-range linkage A conformational mechanism whereby phosphorylation and Ca^{2+}-binding domains are functionally coupled through a large intramolecular distance, within the ATPase molecule.

partial reactions The sequential steps of the SERCA catalytic and transport cycles, including Ca^{2+} and ATP binding to the enzyme, formation of phosphoenzyme intermediate, translocation of bound Ca^{2+} against a concentration gradient, and hydrolytic cleavage of phosphate.

sarcoendoplasmic reticulum Ca^{2+} ATPase (SERCA) The membrane-bound ATPase involved in Ca^{2+} transport and refilling of intracellular Ca^{2+} stores.

trigger points The phosphorylation domain and Ca^{2+}-binding site II where phosphorylation and occupancy by a Ca^{2+} trigger the long-range linkage for interconversion of phosphorylation and Ca^{2+}-binding potentials.

Further Reading

Andersen, J. P. (1995). Dissection of the functional domains of the sarcoplasmic reticulum Ca^{2+} ATPase by site-directed mutagenesis. *Biosci. Rep.* **15**, 243–261.

East, J. M. (2000). Sarco(endo)plasmic reticulum Ca^{2+} pumps: Our advances in understanding of structure/function and biology. *Mol. Membr. Biol.* **17**, 189–200.

Green, N. M., and Stokes, D. L. (2003). Structure and function of the calcium pump. *Annu. Rev. Biophys. Biomol. Struct.* **32**, 445–468.

Inesi, G., Watanabe, T., Coan, C., Murphy, A. (1978). The mechanism of sarcoplasmic reticulum ATPase. *Ann. N.Y. Acad. Sci.* **402**, 515–534.

Inesi, G., Kurzmack, M., Coan, C., and Lewis, D. (1980). Cooperative calcium binding and ATPase activation in sarcoplasmic reticulum vesicles. *J. Biol. Chem.* **255**, 3025–3031.

Maclennan, D. H., Rice, W. J., and Green, N. M. (1997). The mechanism of Ca^{2+} transport by sarco(endo)plasmic reticulum ATPase. *J. Biol. Chem.* **272**, 28815–28818.

Moller, J. V., Juul, B., and le Maire, M. (1996). Structural organization, ion transport and energy transduction of P-type ATPases. *Biochim. Biophys. Acta* **1286**, 1–51.

Scales, D., and Inesi, G. (1976). Assembly of ATPase protein in sarcoplasmic reticulum membranes. *Biophys. J.* **16**, 735–751.

Toyoshima, C., Nomura, H., and Sagita, Y. (2003). Structural basis for ion pumping by Ca^{2+}-ATPase of sarcoplasmic reticulum. *FEBS Lett.* **555**, 106–110.

Biography

Giuseppe Inesi is a Professor in and Chair of the Department of Biochemistry at the University of Maryland, School of Medicine, Baltimore. His research interest is the mechanism of Ca^{2+} transport by Ca^{2+} ATPase, including kinetic and equilibrium characterizations, protein biochemistry, and mutational analysis. He received an M.D. at the University of Modena, and a Ph.D. at the University of Bologra (Italy). He participated in the initial recognition of Ca^{2+} ATPase and has made major contributions to its characterization.

ER/SR Calcium Pump: Structure

Chikashi Toyoshima and Yuji Sugita
University of Tokyo, Tokyo, Japan

The structures of the Ca^{2+}-ATPase of skeletal muscle sarcoplasmic reticulum (Sarco(Endo)plasmic Reticulum Calcium ATPase 1, SERCA 1) have been determined to 2.4Å resolution for the Ca^{2+}-bound form ($E1Ca^{2+}$, PDB entry code: 1SU4) and to 3.1Å for the unbound (but thapsigargin(TG) bound) form (E2(TG), PDB entry code: 1IWO). Detailed comparison of these two structures reveals that very large rearrangements of the transmembrane helices take place accompanying Ca^{2+} dissociation and binding and that they are mechanically linked with equally large movements of the cytoplasmic domains. Such domain movements are thermal in nature and used efficiently for rearranging various domains to alter the functional properties (e.g., affinity for Ca^{2+}) of the ion pump.

Overall Description of the Structure

Ca^{2+}-ATPase is a tall molecule, ~150Å high and 80Å thick, and comprises a large cytoplasmic headpiece, transmembrane domain made of ten (M1–M10) α-helices, and small lumenal domain (Figure 1). The cytoplasmic headpiece consists of three domains, designated as A (actuator), N (nucleotide binding), and P (phosphorylation) domains. They are widely split in the presence of Ca^{2+} but gather to form a compact headpiece in the absence of Ca^{2+}. The A-domain is connected to M1–M3 helices, and the P-domain to M4 and M5 helices. The N-domain is a long insertion between two parts of the P-domain. The M5 helix runs from the lumenal surface to an end of the P-domain and works as the "spine" of the molecule. On the lumenal side, there are only short loops connecting transmembrane helices, except for the loop of ~40 residues connecting the M7 and M8 helices. The distance between the Ca^{2+}-binding sites and the phosphorylation site is larger than 50Å. For the phosphoryl transfer from ATP to Asp351 to take place, the N-domain has to approach the P-domain even closer than that observed in the E2(TG) form.

The orientations and positions of atomic models with respect to the lipid bilayer are determined from crystallographic constraints and illustrated in Figure 1, in which the models are positioned in the bilayer of dioleoylphosphatidylcholine generated by molecular dynamics calculation. The orientations were found to be the same as in the original crystals. The coordinates of the aligned models can be downloaded from the author's web site (http://www.iam.u-tokyo.ac.jp/StrBiol/models).

Organization of the Transmembrane Domain

Transmembrane Helices

As expected from the amino acid sequence, SERCA1 has ten (M1–M10) transmembrane α-helices, two of which (M4 and M6) are partly unwound for efficient coordination of Ca^{2+}. M6 and M7 are far apart and are connected by a long cytosolic loop that runs along the bottom of the P-domain. The amino acid sequence is well conserved for M4–M6 but not for M8 even within the members of closely related P-type ATPases, such as Na^+K^+- and H^+K^+-ATPases. M7–M10 helices are in fact lacking in bacterial-type I P-type ATPases, and are apparently specialized for each subfamily. Nevertheless, M5 and M7 are packed very tightly at Gly770 (M5) and Gly841 (M7) and Gly845 (M7), forming a pivot for the bending of M5. The M7–M10 helices appear to work as a membrane anchor.

Details of the Ca^{2+}-Binding Sites

It is well established that SR Ca^{2+}-ATPase has two high-affinity transmembrane Ca^{2+}-binding sites and the binding is cooperative. X-ray crystallography of the rabbit SERCA1a in 10 mM Ca^{2+} identified two binding sites in the transmembrane but none outside the membrane.

Figure 2 illustrates the structure of the Ca^{2+}-binding sites. The two Ca^{2+}-binding sites (I and II) are located side by side near the cytoplasmic surface of the lipid bilayer, with the site II ~3Å closer to the surface (Figure 1). Site I, the binding site for the first Ca^{2+},

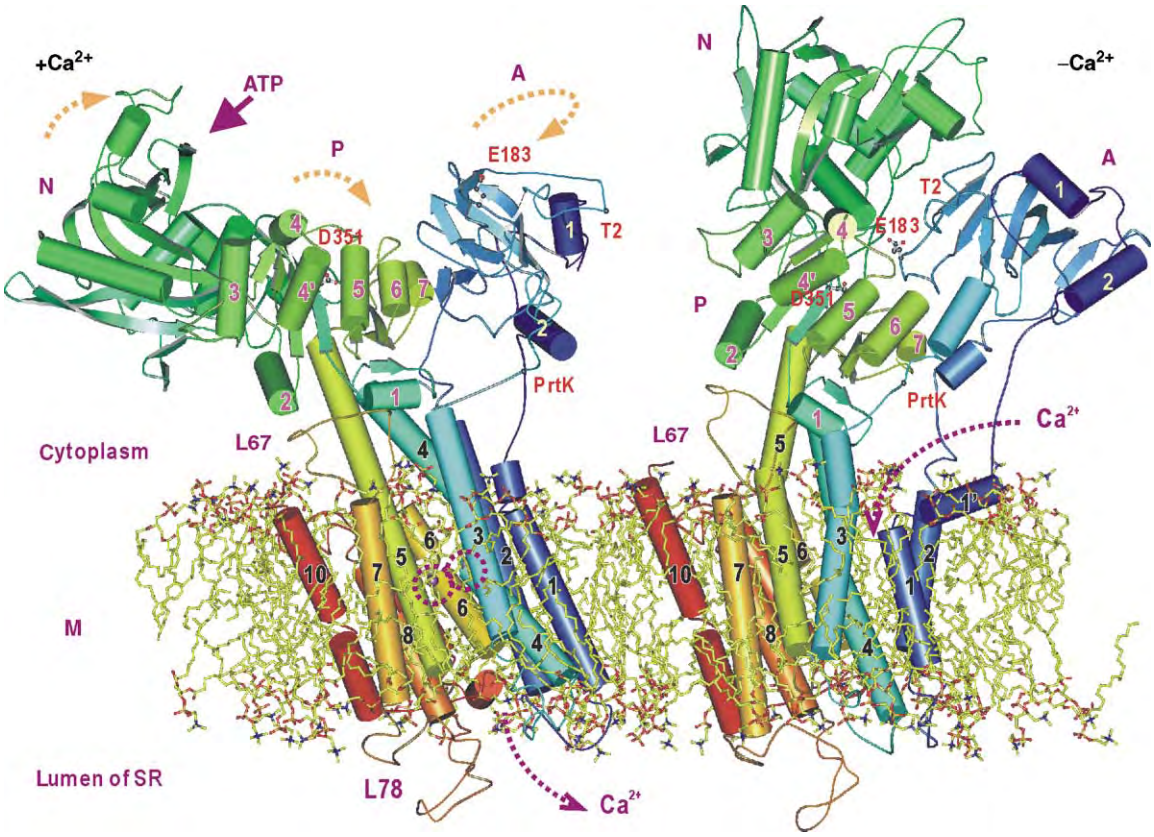

FIGURE 1 Ca^{2+}-bound and unbound forms of Ca^{2+}-ATPase in the lipid bilayer. The bilayer is generated by molecular dynamics simulation of dioleoylphosphatidylcholine. M3 and M5 helices in the unbound form are approximated with two and three cylinders, respectively. The color changes gradually from the N-terminus (blue) to the C-terminus (red). The arrows indicate the directions of movements accompanying the dissociation of Ca^{2+}. Two bound $Ca^{2+}$are shown as purple spheres (circled). T2 trypsin digestion site and a proteinase K digestion site (PrtK) are also marked.

is located at the center of the transmembrane domain in a space surrounded by M5, M6, and M8 helices. Ca^{2+} is coordinated by side chain oxygen of Glu771 (M5), Thr799, Asp 800 (M6), and Glu908 (M8) and two water molecules. M8 is located rather distally and the contribution of Glu908 is not essential in that Gln can substitute Glu908 to a large extent. Any substitutions to other residues totally abolish the binding of Ca^{2+}.

Site II is nearly "on" the M4 helix with the contribution of Asp800 (M6) and Asn768 (M5). The M4 helix is partly unwound (between Ile307 and Gly310). This part provides three main chain oxygen atoms to the coordination of Ca^{2+}. Glu309 provides two oxygen atoms and caps the bound Ca^{2+}. This arrangement of oxygen atoms is reminiscent of the EF-hand motif.

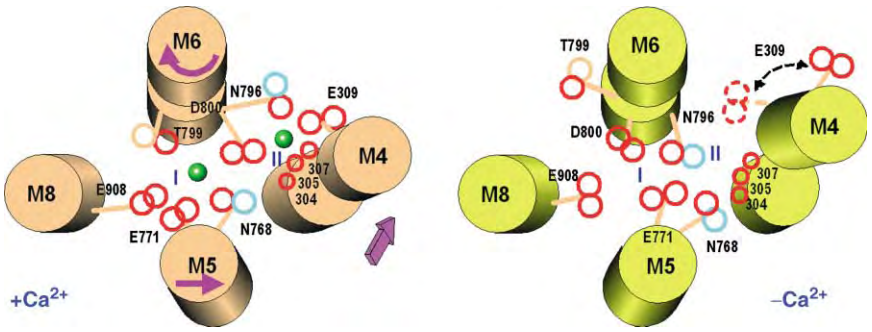

FIGURE 2 Schematic diagram of the Ca^{2+}-binding sites and the movements accompanying the dissociation of Ca^{2+}. The arrows indicate the movements of the helices in the transition from $E1Ca^{2+} \rightarrow E2(TG)$. Red circles, oxygen atoms (carbonyl oxygen atoms appear smaller); cyan circles, nitrogen; orange circles, carbon.

Thus, both site I and site II have seven coordination but have different characteristics. Asp800, on the unwound part of M6, is the only residue that contributes to both sites. Even double mutations of Glu309 and Asn768 leave 50% Ca^{2+} binding, indicating that site II is the binding site for the second Ca^{2+}.

Organization of the Cytoplasmic Domain

Structure of the P-Domain

The P-domain contains the residue of phosphorylation, Asp351. There are three critical aspartate (627, 703, 707) residues clustered around the phosphorylation site, in addition to an absolutely conserved Lys residue (Lys684). These key residues are very well conserved throughout the haloacid dehalogenase (HAD) superfamily, but also shared by bacterial two-component response regulator proteins, such as CheY and Fix J, which have folding patterns different from that of HAD. The P-domain has a Rossmann fold, commonly found in nucleotide-binding proteins, consisting of a parallel β-sheet (seven strands in Ca^{2+}-ATPase) and associated short α-helices. The catalytic residue (i.e., Asp351 in Ca^{2+}-ATPase) is always at the C-terminal end of the first β-strand, which is connected to a long insertion, the N-domain. Thus, the P-domain is formed by two regions far apart in the amino-acid sequence. This is why the P-type ATPase was thought to be an orphan in evolution for a long time. This system requires Mg^{2+} for phosphorylation. Mg^{2+} is coordinated by carboxyls of Asp351, Asp703, carbonyl of Thr353 and two water molecules. It is not known whether this Mg^{2+} is the same as that bound to ATP. Lys684 is particularly important for the binding of γ-phosphate of ATP.

Structure of the N-Domain

N-domain is the largest of the three cytoplasmic domains, containing residues Asn359–Asp601 (Figure 1), and connected to the P-domain with two strands. These strands bear a β-sheet like hydrogen-bonding pattern, presumably to allow large domain movements with a precise orientation. In particular, consecutive prolines (Pro602–603) appear to serve as a guide that determines the orientation of the movement. The N-domain contains the binding site for the adenosine moiety of ATP. Phe487 makes an aromatic–adenine ring interaction, which is a common feature in many ATP binding sites. Lys515, a critical residue, is located at one end of the binding cavity. This residue can be labeled specifically with FITC at alkaline pH and has been used for many spectroscopic studies. The binding of the adenine ring appears predominantly hydrophobic.

Structure of the A-Domain

A-domain is the smallest of the three cytoplasmic domains and consists of the N-terminal ~50 residues that form two short α-helices and ~110 residues between the M2 and M3 helices (Figure 1), which form a deformed jelly role structure. The A-domain contains a sequence motif ^{183}TGE, one of the signature sequences of the P-type ATPase. This sequence represents a loop that comes very close to the phosphorylation site Asp351, in the E2 and E2P states. Because this domain is directly connected to the M1–M3 helices and more indirectly to the M4–M6 helices, this domain is thought to act as the "actuator" of the gates that regulate the binding and release of Ca^{2+} ions.

Structural Changes Accompanying the Dissociation of Ca^{2+}

Rearrangement of the Transmembrane Helices

As illustrated in Figure 2, Ca^{2+}-ATPase undergoes large structural changes upon the dissociation of Ca^{2+}. Three cytoplasmic domains change their orientations and gather to form a compact headpiece. The P-domain inclines 30° with respect to the membrane and N-domain inclines 60° relative to the P-domain, whereas the A-domain rotates ~110° horizontally. The structure of each domain, however, is hardly altered. In contrast, some of the transmembrane helices are bent or curved (M1, M3, and M5) or partially unwound (M2); M1–M6 helices undergo drastic rearrangements that involve shifts normal to the membrane (M1–M4). Thus, the structural changes are very large and global; they are mechanically linked and coordinated by the P-domain.

M3–M5 helices are directly linked to the P-domain by hydrogen bonds (Figure 3). M3 is connected to the P1 helix at the bottom of the P-domain through a critical hydrogen bond involving Glu340. The top part of M5 is integrated as a part of the Rossmann fold (Figure 3) and moves together with the P-domain as a single entity. M4 and M5 are "clamped" by forming a short antiparallel β-sheet. M6 is also connected, though less directly, to the P-domain through L67 (Figure 1), which is, in turn, linked to M5 through a critical hydrogen bond. If the P-domain inclines, for instance, due to the bending of M5, all these helices (M3–M6) will incline and generate movements that have components normal

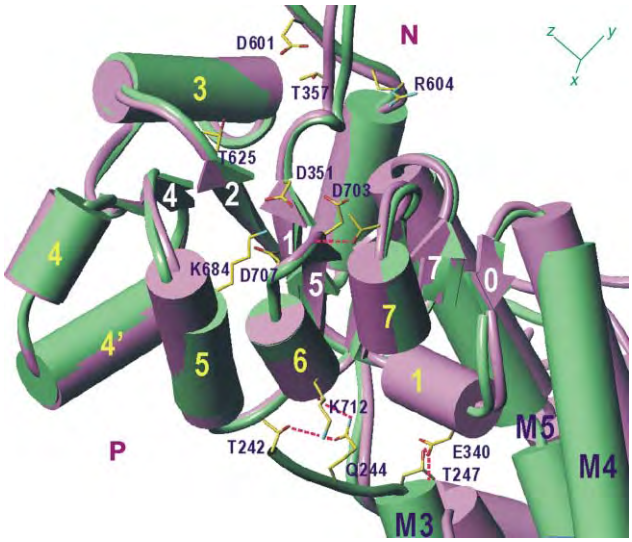

FIGURE 3 Organization of the P-domain and the linkage with the transmembrane helices. Superimposition of the E1Ca^{2+}(violet) and E2(TG) (light green) forms fitted with the P domain. The residues (in atom color) represent those in E2(TG).

to the membrane (Figure 4). Their amounts depend on the distances from the pivoting point, located around Gly770 at the middle of the membrane (double circle in Figure 4). The lower part below Gly770 hardly moves.

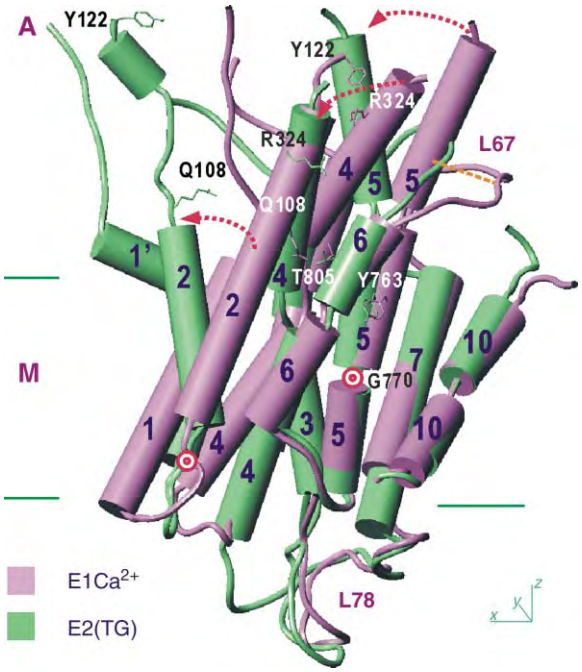

FIGURE 4 Rearrangement of transmembrane helices on the dissociation of Ca^{2+}. The models for E1Ca^{2+}(violet) and E2(TG) (light green) are superimposed. The M5 helix lies along the plane of the paper. M8 and M9 are removed. Double circles show pivot positions for M2 and M5. Arrows indicate the directions of movements during the change from E1Ca^{2+}to E2(TG). Orange broken line shows a critical hydrogen bond between the L67 loop and M5 helix.

The shift is therefore small for M6 and large for M3 and M4; whole M3 and M4 helices move downwards upon dissociation of Ca^{2+}, whereas M6 undergoes rather local changes around Asn796–Asp800.

Ca^{2+}-Binding Sites in the E2(TG) State

The most important movements of the transmembrane helices directly relevant to the dissociation of Ca^{2+} are: (1) a shift of M4 towards the lumenal (extracellular) side by one turn of an α-helix (5.5Å), (2) bending of the upper part of M5 (above Gly770) towards M4, and (3) nearly 90° rotation of the unwound part of M6. As a result, profound reorganization of the binding residues takes place and the number of coordinating oxygen atoms decreases (Figure 2). For site I, this is due to the movement of Asn768 toward M4 caused by the bending of M5; for site II, replacement of Asp800 by Asn796 (i.e., rotation of M6) is critical.

Role of the Large Conformational Movements

Homology modeling of the cation binding sites of Na$^+$K$^+$-ATPase suggests that a large downward movement of M4 (and M3) is needed for counter-transport. With the arrangements of residues observed with E2(TG) structure, it is straightforward to make two high-affinity K$^+$-binding sites, provided that Asn796 is replaced by Asp following Na$^+$K$^+$-ATPase sequence: the other coordinating residues are common to both ATPases. The key feature in the model is that the Asp (Asn796) is coordinated to both K$^+$, similar to Asp800 in coordination of 2Ca^{2+}. Because Asn796 is located one turn below where Asp800 is, M4 must move downwards to provide carbonyl groups for coordination of K$^+$. These rearrangements ensure that release of one type of cation coordinates with the binding of the other and allow the binding of ions of different radii with high affinity.

In summary, ion pumps use thermal movements of various domains very efficiently. Most of the movements described here can be related to the bending of the M5 helix. Because M5 participates in Ca^{2+} coordination and moves together with the P-domain, it is understandable that the phosphorylation (binding of phosphate and Mg^{2+}) at the phosphorylation site and the binding of Ca^{2+} to the transmembrane binding sites will alter the properties of the other. This appears to be the mechanism of long-distance (>50Å) intramolecular communication. Animations showing the conformation changes accompanying Ca^{2+}-dissociation are available (http://www.iam.u-tokyo.ac.jp/StrBiol/animations).

See Also the Following Articles

Calcium, Biological Fitness of • Calcium-Binding Proteins, Cytosolic (Annexins, Gelsolins, C_2-Domain Proteins) • ER/SR Calcium Pump: Function

Glossary

EF-hand motif Most common calcium-binding motif that has a helix–loop–helix motif with a seven-coordinate geometry.

HAD superfamily A large family found by Aravind *et al.* in 1998 including P-type ion transporting ATPases, haloacid dehalogenase (HAD) and phosphoserine phosphatase, structurally the best studied member.

Rossmann fold A supersecondary structure, consisting of a pair of $\beta\alpha\beta$ structures arranged so that at least four β-strands form a single parallel β-sheet flanked by two layers of α-helices.

Further Reading

Aravind, L., Galperin, M. Y., and Kunin, E. V. (1998). The catalytic domain of the P-type ATPase has the haloacid dehalogenase fold. *Trends Biochem. Sci.* **23**, 127–129.

Møller, J. V., Juul, B., and le Maire, M. (1996). Structural organization, ion transport, and energy transduction of P-type ATPases. *Biochim. Biophys. Acta* **1286**, 1–51.

Ogawa, H., and Toyoshima, C. (2002). Homology modeling of the cation binding sites of Na^+K^+-ATPase. *Proc. Natl Acad. Sci. USA* **25**, 15977–15982.

Toyoshima, C., and Inesi, G. (2004). Structural basis of ion pumping by Ca^{2+}-ATPase of the sarcoplasmic reticulum. *Ann. Rev. Biochem.* **73**, 269–292.

Toyoshima, C., and Nomura, H. (2002). Structural changes in the calcium pump accompanying the dissociation of calcium. *Nature* **418**, 605–611.

Toyoshima, C., Nakasako, M., Nomura, H., and Ogawa, H. (2000). Crystal structure of the calcium pump of sarcoplasmic reticulum at 2.6 A resolution. *Nature* **405**, 647–655.

Biography

Chikashi Toyoshima is a Professor in the Institute of Molecular and Cellular Biosciences at the University of Tokyo. His principal research interest is structural understanding of ion transport.

Yuji Sugita is a Lecturer in the Institute of Molecular and Cellular Biosciences at the University of Tokyo. His principal research interests are in the development of new molecular simulation methodologies and in their application to the biological phenomena.

Exonucleases, Bacterial

Susan T. Lovett
Brandeis University, Waltham, Massachusetts, USA

Exonucleases are enzymes that catalyze hydrolysis of DNA or RNA from a free end. Exonucleolytic digestion of nucleic acids may be required for processing and for turnover of these macromolecules. In addition, RNA exonucleases contribute to the maturation of stable RNA molecules. The action of DNA exonucleases permits diverse processes such as mutation avoidance, repair, and genetic recombination.

Introduction

Nucleases are defined as enzymes that hydrolyze the phosphodiester bond of nucleic acids. Borrowing the system developed for proteases, nucleases have been classified whether they cleave internally in the DNA or RNA molecule (endonucleases) or from an end in a stepwise fashion producing mononucleotide products (exonucleases). This distinction is complicated by the fact that several enzymes require entry at a free DNA or RNA end but cleave internally (often referred to as endo/exonucleases). An example is the RecBCD recombination nuclease that unwinds DNA from an end and cleaves it as it travels, producing oligonucleotide products. Some exonuclease activities are found within proteins with other distinct catalytic activities, such as the 3′ DNA exonuclease activities associated with DNA polymerases.

The systematic purification and characterization of more than 20 exonuclease activities from *Escherichia coli* extracts have provided much of our knowledge about this group of enzymes (Tables I and II). Most *E. coli* exonucleases on DNA and RNA were identified and named arbitrarily (DNA exonucleases Exo I–X and RNase II) or by reference to their substrate specificity (RNase H, R, D, T oligoribonuclease, etc.). A few nucleases were identified first and named by their genetic function (such as RecJ exonuclease required for genetic recombination). The biological role of most *E. coli* exonucleases has now been confirmed by genetic experiments, although many exonucleases have redundant genetic function and genetic phenotypes are not manifested until multiple members are inactivated. Such overlapping functions are not surprising, given the great number of these enzymes in *E. coli* (at present count 15 DNA, 9 RNA exonucleases.) Orthologues of many of the *E. coli* exonucleases can be found in diverse bacterial genera and often in archaea and eukaryotes. *E. coli* appears to be especially rich in exonucleases, in contrast to other bacteria that have only a few exonucleases, as predicted by sequence similarity. However, since most exonuclease families were defined first by purification and characterization of representatives from *E. coli*, this may represent an ascertainment bias and there may be additional, presently unknown exonuclease families in other bacterial species but not in *E. coli*.

Biochemical Properties of Exonucleases

Mechanism

All DNA and RNA exonucleases, with the exception of DNase Exo VII, require a divalent-cation cofactor, commonly Mg^{2+} or Mn^{2+}, to accomplish hydrolysis of the phosphodiester bond. The crystal structures of many exonucleases have now been solved and reveal coordination of one or more divalent cations by aspartate, glutamate, or histidine residues. Such residues are found as evolutionarily conserved amino acid motifs within related exonucleases. A role for the metal ions was suggested by the structure published by Beese and Steitz for the 3′–5′ exonuclease of *E. coli* polymerase I, which contains two metal atoms, a single-strand DNA (ss DNA) substrate and deoxynucleoside monophosphate. They proposed that one metal activates a water molecule for the nucleophile in an SN2-type reaction; the other closely positioned metal is poised to stabilize the pentacovalent intermediate in the reaction and the leaving oxyanion. The universality of this two-metal-ion scheme is not clear: some exonuclease structures, such as that of the 5′ nuclease FEN-1, contain two more widely separated metal ions and other structures, such as DNA exonucleases Exo III and RecJ, reveal only one metal cation.

Two RNases, acting from a 3′ end, polynucleotide phosphorylase (PNPase) and RNase PH, are not, strictly

TABLE I

DNA Exonucleases of *E. coli*[a]

Enyzme	Gene(s)	Preferred substrate	Polarity	Other features	Biological role in DNA metabolism
Exo I	*xonA* (= *sbcB*)	ssDNA	3′–5′	Processive	Recombination, damage repair, mutation avoidance, MMR
Exo III	*xth*	dsDNA	3′–5′	Acts at nicks and ends, abasic endonuclease	Base excision repair
Exo IV	?[b]	Oligonucleotides	?	May be identical to oligoribonuclease[b]	?
Exo VII	*xseA*, *xseB*	ssDNA	3′–5′ 5′–3′	Heterodimer, processive, Oligonucleotide products, metal cofactor-independent	Damage repair, mutation avoidance, MMR
Exo VIII	*recE*	dsDNA	5′–3′	Processive, encoded by cryptic Rac prophage	Recombination, damage repair
Exo IX	*xni*	dsDNA	3′–5′	In 5′ nuclease/FEN-1 family[c]	?
Exo X	*exoX*	ssDNA, dsDNA	3′–5′	Distributive	Mutation avoidance, MMR
DNA pol I 5′ exo	*polA*	ssDNA	5′–3′	Flap endonuclease	Replication (Okazaki fragment maturation)
DNA pol I 3′ exo	*polA*	ssDNA	3′–5′		Proofreading
DNA pol II 3′ exo	*polB*	ssDNA	3′–5′		Proofreading
DNA pol III 3′ exo	*dnaQ* (= *mutD*)	ssDNA	3′–5′	ε Subunit	Proofreading
RecBCD	*recB*, *recC*, *recD*	dsDNA, ssDNA	3′–5′ 5′–3′	Exo V, highly processive, ATP-dependent, oligonucleotide products, helicase activity	Recombination, DSB repair
RecJ	*recJ*	ssDNA	5′–3′	Processive	Recombination, damage repair, MMR
RNase T	*rnt*	ssDNA	3′–5′	Activity on DNA > RNA, homodimer, distributive	Repair?[d]
SbcCD	*sbcC*, *sbcD*	dsDNA	3′–5′ 5′–3′	ATP-dependent, processive	Repair

[a] Abbreviations: pol, polymerase; Exo, exonuclease, dsDNA, double-strand DNA; ssDNA single-strand DNA; MMR, mismatch repair; DSB, double-strand break.
[b] Eukaryotic oligoribonuclease has activity on oligodeoxynucleotides and *E.coli* oligoribonuclease may be identical to exonuclease IV.
[c] Although the polarity of Exo IX-mediated digestion is reported to be 3′–5′, it is a member of the 5′ flap endonuclease family by amino acid sequence similarity.
[d] RNase T can act as a high-copy suppressor of some DNA repair defects of RecJ$^-$ ExoI$^-$ ExoVII$^-$ strains, has potent DNase activity and so could play a redundant function in DNA metabolism.

TABLE II

RNA Exonucleases[a] of *E. coli*

Enzyme	Gene	Preferred substrate[b]	Biological role in RNA metabolism
RNase II	*rnb*	Unstructured RNA	mRNA degradation, stable RNA maturation
RNase R	*rnr*	rRNA, homopolymers	?
RNase D	*rnd*	Denatured tRNAs	Defective tRNA degradation, stable RNA maturation
RNase H	*rnhA*	RNA/DNA hybrid	Repair
RNase T	*rnt*	tRNA[c]	tRNA end turnover, stable RNA maturation
Oligoribonuclease	*orn*	Oligoribonucleotides[d]	mRNA degradation
Polynucleotide phosphorylase (PNPase)	*pnp*	Unstructured RNAs	mRNA degradation, stable RNA maturation
RNase PH	*rph*	tRNA precursors	Stable RNA maturation
RNase BN	*rbn*	tRNA with aberrant 3′ ends, tRNA precursors	Stable RNA maturation defective tRNA degradation

[a] Although PNPase and RNase PH are phosphorylases not nucleases, they act to digest RNA in a polar fashion from a 3′ end.
[b] All *E. coli* exoribonucleases act 3′–5′.
[c] RNase T also possesses a potent exonuclease activity on single-strand DNA in a 3′–5′ fashion.
[d] May be identical to DNA exonuclease IV.

speaking, "nucleases," because they are not hydrolases but phosphorylases, using inorganic phosphate to attack the phosphodiester bond and releasing nucleoside diphosphate reaction products. These are, however, of related biological function and are included here and in many reviews of exoribonucleases.

Specificity

Many exonucleases have strict specificity for the sugar moiety in nucleic acids and therefore cleave only RNA or DNA. (RNase H is specific for RNA within a DNA hybrid.) Other nucleases, however, may cleave both RNA and DNA, e.g., RNase T of *E. coli*. It is difficult to tell from amino acid sequence information alone whether any given exonuclease will have a preference for DNA or RNA. Exonuclease superfamilies include both RNase and DNase members. Steric considerations may exclude RNA as a substrate for DNA-specific exonucleases; 2′-OH specific interactions may specify RNA as a preferred substrate.

Almost all exonucleases have a strict polarity of digestion, initiating attack from either the 3′- or 5′-end of a nucleic acid molecule. This polarity reflects the exonuclease's particular architecture of the amino acids and bound metal atoms that interact with the nucleic acid. Exceptions to strict polarity include those "exo/endonucleases" that cleave internally within DNA, producing oligonucleotide products, but require an end for entry, such as Exo VII, SbcCD, and RecBCD. The latter two DNA exonucleases are ATP dependent and may require ATP for associated helicase activity to move the enzyme along its DNA substrate. Some exonucleases are specific for the phosphorylation status of the end, indicating a specific interaction with the nucleic acid terminus. For example, many 3′–5′ exonucleases such as *E. coli* exonuclease I cannot attack a nucleic acid with 3′-phosphate; similarly, lambda bacteriophage exonuclease requires a 5′-phosphate in a double-strand DNA (dsDNA) end and will not initiate cleavage on a 5′-OH-containing DNA molecule. Many DNA exonucleases are specific for double-strand (Exo III, Exo VIII) or single-strand (RecJ, Exo I, Exo VII) DNA. Likewise, certain RNases may prefer unstructured RNA regions. The ssDNA-specific exonucleases accomplish their specificity sterically: they either possess a pore or have a deep cleft in which ssDNA but not dsDNA can reach the catalytic center of the enzyme. Oligoribonuclease has a size specificity and prefers short oligonucletide substrates less than five nucleotides in length but the molecular basis for this specificity is not understood.

Processivity

Exonucleases are classified "processive" if they catalyze multiple cleavage events upon a single binding to their nucleic acid substrates. In contrast, "distributive" must rebind substrate after each cleavage. The biochemical property of processivity has important biological consequence and allows exonucleases to rapidly digest appropriate substrates. Several processive nucleases (bacteriophage lambda exonuclease, *E. coli* Exo I) have toroidal or clamp-like structures that allow the enzyme to encircle its substrate, a simple way of

achieving processivity. Processivity can also be achieved by multiple binding interactions of the exonuclease to its substrate, as has been proposed for RNase II.

Structural Families

Comparison of exonuclease sequences from bacteria shows that the primary amino acid sequence of these proteins has diverged rather quickly. Nevertheless, conserved motifs emerge and several extensive sequence families can be recognized and are briefly discussed below. Members of these exonuclease families can often be found in all three domains of life: archaea, eubacteria and eukaryotes. In exonucleases for which there is structural information, these conserved motif residues coordinate metal cofactor or interact with substrate. These structural families can include members with diverse substrate specificities, including both exonucleases and endonucleases, and even phosphatases, RNases and DNases, processive and distributive enzymes, and a few are discussed briefly.

DEDD/DNAQ

An extensive group of 3′–5′ exonucleases is defined by three motifs carrying conserved aspartate and glutamate residues (Figure 1); hence, the alternate designation "DEDD" for this family of nucleases found in eukaryotes as well as prokaryotes. This family includes exonucleases with specificity for DNA (the proofreading exonucleases of DNA polymerases, *E. coli* exonucleases I and X), RNA (RNase D, oligoribonuclease), and those with dual specificity (RNase T). Both distributive and processive exonucleases are members of this family. *E. coli* possesses eight enzymes in this family (alignment shown in Figure 1). Structural information is available for several members of this superfamily including the proofreading exonuclease domain of DNA polymerases I and III of bacteria, and *E. coli* exonuclease I. The fold of these enzymes resembles RNase H1. Most structures include two metal atoms at the active site.

DHH/RecJ

The founding member of this family, RecJ, is a 5′–3′ ssDNA exonuclease involved in genetic recombination and DNA repair. The RecJ family encompasses a large family of proteins found in archaea and bacteria, very few of which have been characterized at the biochemical level. This family is defined by seven conserved motifs, primarily acidic residues, or histidines; the family is sometimes termed "DHH" after the amino acid sequence within one of these motifs. The RecJ family is particularly expanded in the archaea; for example, *Archaeoglobus fulgidus* possesses seven members of this family. There are eukaryotic members, but the yeast DHH protein is a phosphatase (polyphosphatase PPX1), not a nuclease. Therefore, the RecJ family is, more broadly, a phosphoesterase rather than a nuclease family.

XthA

E. coli exonuclease III is a 3′–5′ DNA exonuclease active on dsDNA; it also possesses 3′ phosphatase activity and endonuclease activity at abasic (apurinic/apyrimidinic) sites. Exo III is an important protein for base excision repair, as is its eukaryotic counterpart Ape1. Structurally, Exo III resembles eukaryotic DNase I, with a single metal at its active site and a large group of phosphatases, primarily involved in eukaryotic cell signaling processes.

FEN-1/5′ Nucleases

The founding member of this group is FEN-1 "flap-endonuclease" from eukaryotes and archaea; the eubacterial counterpart, both structurally and functionally, is the 5′ exonuclease domain of DNA polymerase I. Both proteins possess 5′–3′ exonuclease activity and endonuclease activity on ssDNA "flaps" adjacent to region of duplex DNA. These 5′-nucleases play an important role in processing of Okazaki fragments during lagging strand DNA synthesis. Structural information of archaeal FEN-1, DNA polymerase I, and the related RNase H activity from bacteriophage T4 shows two metals coordinated by glutamate and aspartate

```
ExoI        11 LFHDYETFGTHPALDRPAQFAA 66 LGYNNVRFDDEVTRN 64 SNAHDAMADVYAT
ExoX         2 RIIDTETCGLQGGIVEIASVDV 52 YVAHNASFDRRVLPE 39 LHHHRALYDCYIT
OligoRNase  31 IWIDLEMTGLDPERDRIIEIAT 73 ICGNSIGQDRRFLFK  6 AYFHYRYLDVSTL
RNase T     19 VVIDVETAGFNAKTDALLEIAA 75 MVAHNANFDHSFMMA 37 CQTAGMDFDSTQA
RNase D     24 IALDTEFVRTRTYYPQLGLIQL 30 KFLHAGSEDLEVFLN 55 RQCEYAAADVWYL
PolI       123 FAFDTETDSLDNISANLVGLSF 42 KVGQNLKYDRGILAN 62 EAGRYAAEDADVT
PolII      353 VWVEGDMHNGTIVNARLKPHPD 75 IGWNVVQFDLRMLQK 91 ALATYNLKDCELV
DnaQ         8 IVLDTETTGMNQIGAHYEGHKI 62 LVIHNAAFDIGFMDY 49 RTLHGALLDAQIL
```

FIGURE 1 *E. coli*'s DnaQ superfamily members. Shown are aligned amino acid sequences of exonuclease I, exonuclease X, oligoribonuclease, RNase D, RNase T, and the 3′-exonucleases of DNA polymerases I, II, and III. Conserved acid residues are shown in bold and comprise metal coordination residues for those proteins with determined three-dimensional structure. Numbers refer to amino acid residues not shown.

residues. This family also includes eukaryotic Exo 1, a 5′-exonuclease implicated in eukaryotic mismatch repair, and *E. coli* exonuclease IX of unknown biological function.

Mre11/SbcD

Eukaryotic and archaeal Mre11 is the catalytic subunit of an ATP-dependent exonuclease with associated endonuclease activity. Mre11 shares sequence homology with bacterial SbcD protein. The nuclease activity specified by these subunits requires assembly of an active complex with one or two other additional proteins. One of these additional subunits possesses a coiled-coil structure: Rad50 in eukaryotes and archaea, SbcC in bacteria. Structural data are available for archaeal Mre11, showing two Mn^{2+} atoms, and Rad50. The Mre11 fold resembles metal-dependent phosphatases with the conserved phosphoesterase motifs (histidines, aspartates, and asparagines) making interactions with substrate or metal cofactors. Mre11 and SbcD exonucleases play a role in DNA repair and genomic surveillance.

Biological Roles of RNA Exonucleases

Turnover

mRNA half-lives in bacteria are short and degradation of mRNA is essential for viability. After initial endonucleolytic cleavage, degradation of mRNA in *E. coli* is accomplished by the combined action of RNase II and PNPase to produce short oligomers that are then digested by oligoribonuclease. These bacterial enzymes attack RNA in a 3′–5′ direction. Loss of either RNase II (a true exoribonuclease) or PNPase (a phosphorylase) can be tolerated by *E. coli*; however, inactivation of both enzymes or of oligoribonuclease is lethal to the cell. Aberrant or misfolded stable RNAs may also be subject to turnover by exoribonuclease action.

Processing

Proper maturation of stable RNAs requires the action of exoribonucleases. In *E. coli* several exoribonucleases act redundantly in processing of tRNA or rRNA. Maturation of stable RNAs seems to be most dependent on RNase T and RNase PH; the double mutant accumulates tRNA precursors and although viable, grows more slowly. Upon loss of five activities, RNase II, D, BN, T, and PH, *E. coli* becomes inviable; any single one of these enzymes can suffice to support viability, indicating significant functional overlap.

Biological Roles of DNA Exonucleases

Replication Fidelity

Exonucleases are integral to two major mechanisms that insure the fidelity of DNA replication: polymerase proofreading and mismatch repair. 3′–5′ exonuclease activity is a component of many bacterial DNA polymerases at a site or within a subunit distinct from the polymerase activity. Unpaired 3′-residues are more likely to be degraded by the exonuclease than to support polymer extension; this proofreading reaction contributes substantially to the accuracy of replication. Complete absence of 3′–5′ exonuclease activity of *E. coli* replicative polymerase, the DnaQ or ε-subunit of DNA polymerase III, causes cellular inviability due to the catastrophic accumulation of replication errors.

Misincorporations that escape polymerase proofreading can be recognized and excised by the mismatch repair pathway, which is initiated by the MutHLS proteins of *E. coli*. The excision tract, up to thousands of bases in length, can be directed either 3′ or 5′ to the mismatch and is catalyzed by the redundant action of four exonucleases, RecJ, Exo I, Exo VII, or Exo X, aided by the UvrD helicase of *E. coli*. Loss of mismatch repair elevates the frequency of spontaneous mutational events several orders of magnitude.

Scavenging of ssDNA by the 3′–5′ DNA exonucleases (*E. coli* Exo I, Exo VII, and Exo X) aborts a wide range of mutational events believed to be caused by nascent strand displacement and mispairing, including frameshifts, deletions, and quasipalindrome-associated mutational hotspots. These enzymes act redundantly in this process, which can be considered a type of "proofreading in trans."

Maturation of Okazaki fragments during DNA replication in *E. coli* is catalyzed by the 5′-exonuclease domain of polymerase I, functionally and structurally homologous to the FEN-1/Rad27 nuclease of eukaryotes and archaea. In addition to a nonspecific 5′-exonuclease activity, these enzymes specifically cleave the junction between ss and dsDNA, an activity often termed "flap" endonuclease activity. In some bacteria such as *Streptococcus pneumoniae*, loss of the 5′ nuclease domain of DNA polymerase I is lethal. *E. coli* mutants are viable and may, therefore, use a backup mechanism of Okazaki fragment maturation. The absence of the 5′-nuclease domain of polymerase I in *E. coli* elevates spontaneous mutation rates, as was first described for the related Rad27 of yeast; this elevated class of mutations consists largely of short sequence duplications. In a similar fashion, these 5′-nucleases also suppress expansion of tandem repeat arrays.

The SbcCD nuclease appears to play a role in genome surveillance and repair. Through its endonuclease activity, SbcCD breaks the chromosome at large inverted DNA repeats that form secondary structures, which can impede DNA replication. Such breakage and subsequent exonucleolytic processing may selectively remove such structures from the genome. The SbcCD nuclease may also mediate certain modes of double-strand break repair, independent of DNA secondary structures.

Recombination and DNA Repair

Exonucleases play an essential role in homologous recombination. Strand exchange is initiated by ssDNA, which binds the strand transfer protein RecA and initiates the homology-search process. Nicks or double-strand breaks in DNA are converted by exonucleases to recombinogenic ssDNA gaps or tails, respectively, by the degradation of one strand of the DNA duplex. During recombinational double-strand break repair in *E. coli*, the RecBCD nuclease provides this function by its combined ATP-dependent helicase and nuclease activities. RecBCD's nuclease activity is modulated by octameric "Chi" DNA sequences that act *in vivo* as hot spots of recombination by a molecular mechanism yet to be deciphered. In pathways of recombination independent of RecBCD, exonuclease function for recombination can be provided by the RecJ $5'-3'$ ssDNA exonuclease, acting in conjunction with a DNA helicase, such as RecQ. After recombinational joint molecules are formed by synapsis, degradation of one strand ("post-synaptic" DNA degradation) can extend and stabilize the heteroduplex intermediate by removing a competitor strand for pairing. It may be for this reason that in *E. coli* either RecJ ($5'-3'$) and Exo I ($3'-5'$) are required for efficient recombination, even when the presynaptic degradation is presumably occurring via the RecBCD nuclease. After exchange is complete, exonucleases may also participate in the trimming of unpaired ends to form mature recombinant molecules.

Conclusions

Exonucleases comprise a large set of structurally and biochemically characterized enzymes with diverse properties. Systematic characterization of exonucleases from the bacterium *E. coli* has provided much of our knowledge of this class of enzymes. Certain families of related exonucleases are found widely throughout bacteria, archaea, and eukaryotes, indicating the early evolution of nucleases and their important role in all cells. However, primary amino acid sequence cannot predict many elements of substrate specificity (such as DNase or RNase), other enzymatic properties such as processivity or biological function. A single *E. coli* cell contains more than 20 different exonuclease activities. Exonucleases often act redundantly in biological functions of RNA processing and degradation, mutation avoidance, and in DNA repair and recombination. Therefore, several biological functions of exonucleases probably remain unknown and are the focus of current work in the field.

See Also the Following Articles

DNA Polymerase I, Bacterial • Recombination: Heteroduplex and Mismatch Repair *in vitro* • Transcription-Coupled DNA Repair, Overview

Glossary

base excision repair A repair mechanism that removes damaged nucleotide bases from duplex DNA. The resulting abasic site is then incised by abasic endonucleases and repaired by exonucleases, polymerase and ligase.

genetic recombination A process by which homologous segments of DNA molecules are exchanged. Recombination serves as a relatively error-free mechanism for repair of chromosomal single-strand gaps or double-strand breaks.

heteroduplex A DNA duplex region formed by the pairing of two strands from different DNA molecules. Heteroduplex joint formation is the first step of homologous genetic recombination.

mismatch repair A conserved repair mechanism by which many replication errors ("mismatches") are detected and excised from duplex DNA.

okazaki fragments Short, discontinuous pieces of DNA, primed by RNA and synthesized during lagging strand DNA replication.

proofreading The $3'-5'$ exonucleolytic removal of polymerase incorporation errors in newly synthesized DNA.

Further Reading

Beese, L. S., and Steitz, T. A. (1991). Structural basis for the $3'-5'$ exonucleases activity of *Escherichia coli* DNA polymerase: I. A two metal ion mechanism. *EMBO J.* **10**, 25–33.

Ceska, T. A., and Sayers, J. R. (1998). Structure-specific cleavage by $5'$ nucleases. *Trends Biochem. Sci.* **23**, 331–336.

D'Alessio, G., and Riordan, J. F. (eds.) (1997). *Ribonucleases – Structures and Functions*. Academic Press, San Diego, CA.

Deutscher, M. P., and Li, Z. (2001). Exoribonucleases and their multiple roles in RNA metabolism. *Prog. Nucleic Acids Res.* **66**, 67–105.

Kunkel, T. A., and Bebenek, K. (2000). DNA replication fidelity. *Annu. Rev. Biochem.* **69**, 497–529.

Linn, S. M., and Roberts, R. J. (eds.) (1993). *Nucleases*, 2nd Edition. Cold Spring Harbor Laboratory Press, Cold Spring Harbor, NY.

Nishino, T., and Morikawa, K. (2002). Structure and function of nucleases in DNA repair: Shape, grip and blade of the DNA scissors. *Oncogene* **21**, 9022–9032.

Shevelev, I. V., and Hübscher, U. (2002). The $3'-5'$ exonucleases. *Nat. Rev. Molecul. Cell Biol.* **3**, 1–12.

Zuo, Y., and Deutscher, M. P. (2001). Exoribonuclease superfamilies: Structural analysis and phylogenetic distribution. *Nucleic Acids Res.* **29**, 1017–1026.

Biography

Susan T. Lovett is a Professor in the Department of Biology and Rosenstiel Basic Medical Sciences Research Center at Brandeis University in Waltham, Massachusetts. Among her research interests are the DNA exonucleases that mediate genetic recombination, repair, and mutation avoidance. She and her colleagues discovered and characterized the RecJ exonuclease and Exonuclease X from *E. coli*. She received her Ph.D. in Molecular Biology from the University of California at Berkeley and trained as a postdoctoral fellow at Lawrence Berkeley Laboratory in Berkeley, California and the Harvard Medical School in Boston, Massachusetts.

F1–F0 ATP Synthase

Donata Branca
University of Padova, Padova, Italy

F1–F0 ATP synthases (also called F1–F0 or F-ATPases) are large protein complexes, weighing 550–650 kDa, located in the inner mitochondrial membrane, in the chloroplast thylakoid membrane and in the bacterial plasma membrane. They are the major ATP suppliers of most cells, synthesizing ATP in the terminal phase of oxidative phosphorylation or photophosphorylation. The synthesis of ATP from ADP and inorganic phosphate (Pi) is driven by protons (H^+) moving through the complex down the transmembrane H^+ gradient built by the respiratory or photosynthetic electron-transfer chains (or by light-driven H^+ pumps in some bacteria). The ATP synthases may also operate in the opposite direction, as H^+-pumping ATPases; this reversal, which may be accomplished by any ATP synthase *in vitro*, is physiologic in anaerobic bacteria, allowing them to build a transmembrane H^+ gradient (e.g., as required for the movement of flagella or for the uptake of nutrients). Thus, the ATP synthases reversibly convert the energy stored in the proton gradient into the chemical energy of ATP. The ATP synthases of all organisms are believed to have evolved from a common protobacterial ancestor. In fact they have a high degree of sequence homology within structurally and functionally important regions, display similar architectures, and operate with the same basic mechanism. Moreover, in eukaryotes, they are partially encoded by mitochondrial or chloroplast DNA.

Structure of the ATP Synthase Complex

ATP synthases are traditionally described as bipartite complexes, composed of two structurally and functionally distinct multisubunit portions (Figure 1A): a membrane-embedded F0, which translocates protons, and a membrane-peripheral F1 comprising a globular head, which synthesizes ATP, and a central stalk, which interacts with F0. A second, peripheral stalk, contributed by F1 and F0 subunits, also connects the outer regions of F1 and F0. F1 may be reversibly dissociated from F0 *in vitro*, with the isolated F1 still active, but only capable of hydrolyzing ATP (hence the ATPase designation), and the membrane-associated F0 retaining the ability to translocate protons down a concentration gradient. The isolated F1, and the F1-depleted membranes containing F0 are invaluable tools to investigate the structure and the enzymology of the synthases, even if lacking the coupling mechanism which allows the H^+-driven ATP synthesis by the intact complex. As to the operation of the complex, there is wide agreement that H^+ translocation through F0 triggers the rotation of the central stalk, which in turn promotes the synthesis of ATP by F1.

Structural, biochemical, and molecular biological studies have contributed to the knowledge of the architecture of the ATP synthases. The landmark achievement has been the high-resolution structure of the mitochondrial F1: the X-ray crystallographic studies on bovine heart F1 by Walker and co-workers (Figure 2A) have established the essential features of the mammalian complex. X-ray crystallographic work by Amzel, Pedersen and co-workers (Figure 2B) has contributed significant results on the rat liver F1 enzyme. Much less is known on F0, due to its membrane-intrinsic nature; the structural analysis of this portion of the synthase is so far limited to its isolated subunits or subcomplexes.

Subunit Composition

In the simplest ATP synthase, that of bacteria (Figures 1A and B), F1 contains five different subunits with a stoichiometry $\alpha_3,\beta_3,\gamma_1,\delta_1,\varepsilon$. F0 is composed of three kinds of subunits with a stoichiometry a_1,b_2,c_{10-14}. This core structure is substantially conserved in all ATPases, but for the presence of two homologous b and b′ subunits in chloroplast F0, of a single copy of the b subunit in mitochondrial F0 and of several additional subunits, whose roles are still poorly defined, in the stalk and in the membrane sector of the mitochondrial complex(Figure 1C). Finally, an inhibitor peptide (IF_1), unique to mitochondria, may reversibly associate to the synthase.

At present, the subunit nomenclature for the ATP synthases from different sources is confusing, partly due to historical reasons; as an example, the bacterial ε-subunit corresponds to the mitochondrial δ, and the bacterial δ-subunit to the mitochondrial oligomycin sensitivity conferring protein (OSCP), while the

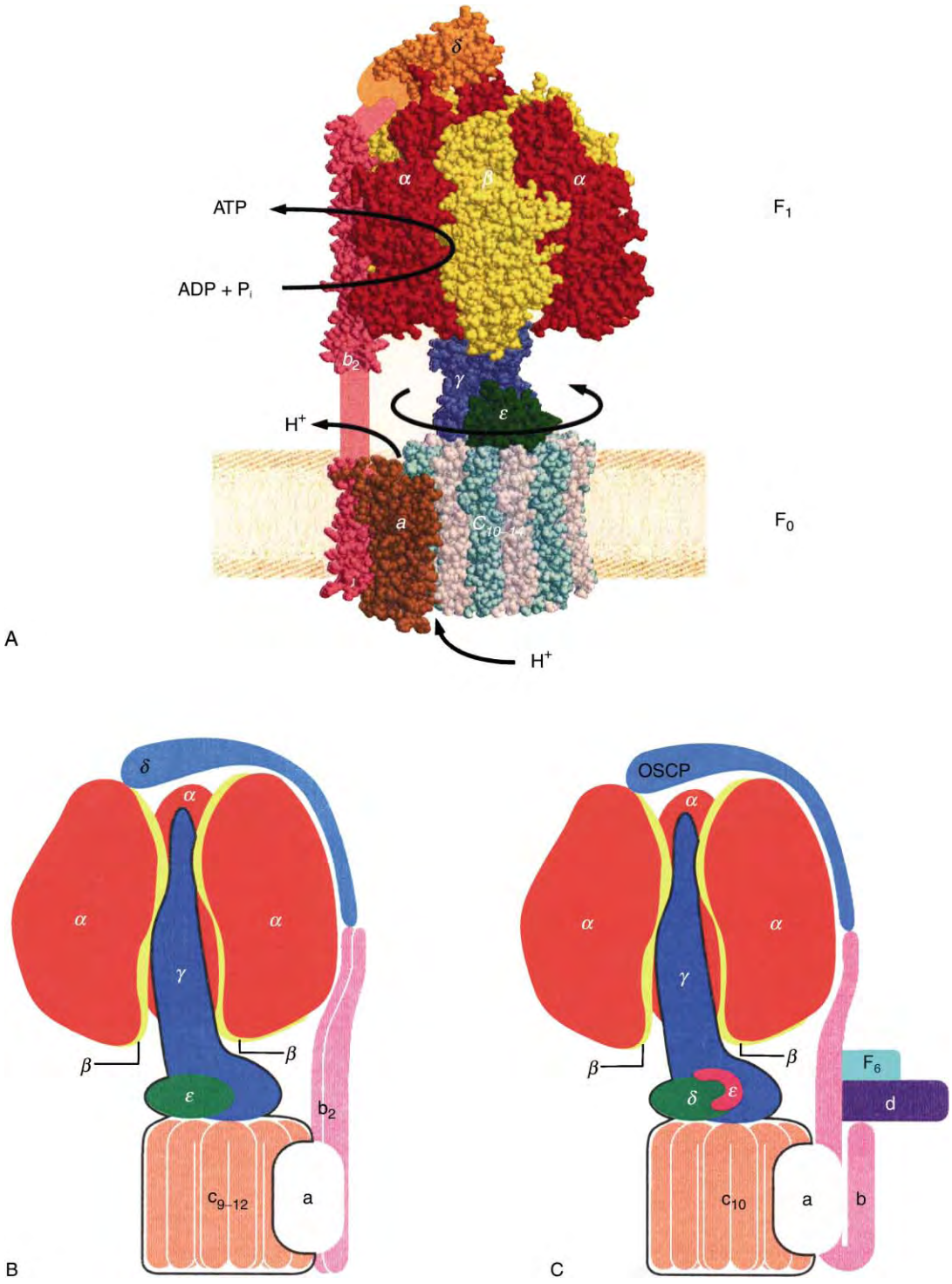

FIGURE 1 Structure of the F1F0 ATP synthase. (A) Space filling model of the F1–F0 complex of *E. coli*. The uniformly coloured parts correspond to domains whose high-resolution structure is lacking. (Reproduced from Weber, J., and Senior, A. E. (2003). ATP synthesis driven by proton transport in F_1F_0-ATP synthase. *FEBS Lett.* **545**, 152–160, with permission.) (B and C) Schematic model of the ATP synthase from bacteria (B) and mitochondria (C). One of the three β subunits has been omitted to reveal the g subunit within the $\alpha_3\beta_3$ hexamer. In (C), some minor subunits (e, f, g, A6L) are not shown. (Reproduced from Stock, D., Gibbons, C., Arechaga, I., Leslie, A. G. W., and Walker, J. E. (2000). The rotary mechanism of ATP synthase. *Curr. Opin. Struct. Biol.* **10**, 672–679, with permission from Elsevier.)

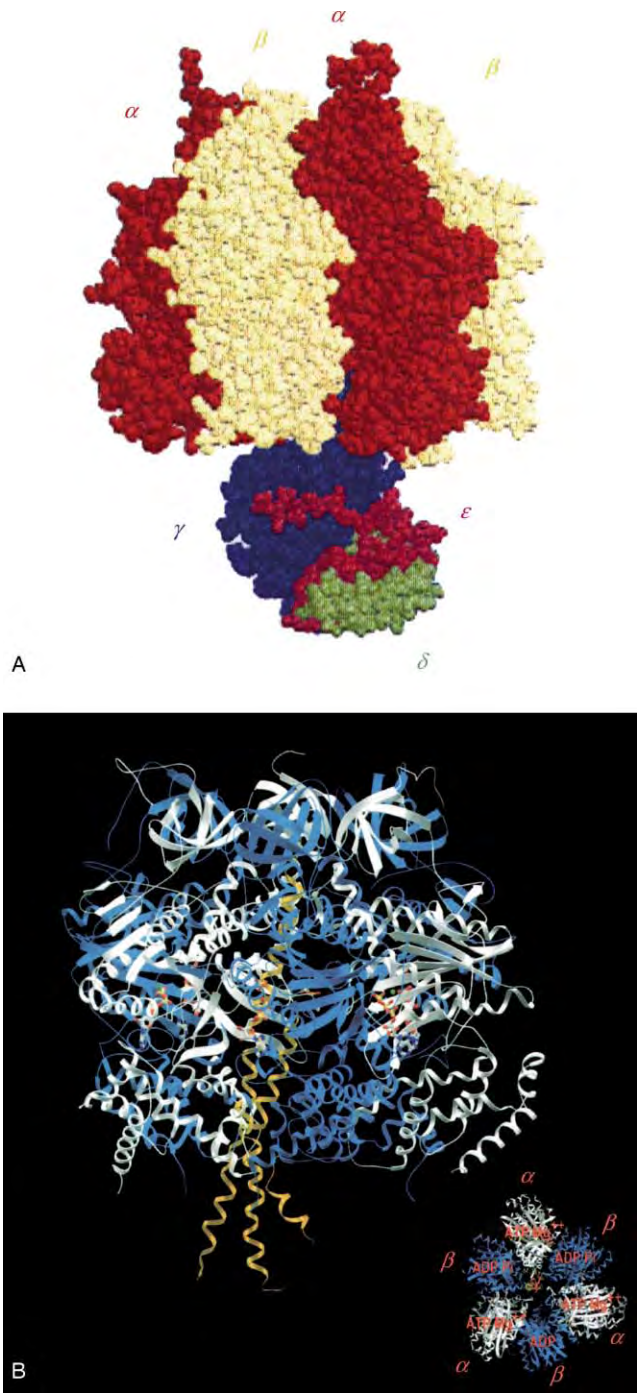

FIGURE 2 Structure of F1. (A) Side view of bovine F1 crystallized in the presence of the synthase inhibitor dicyclohexylcarbodiimide (DCCD). Reproduced from Gibbons, C., Montgomery, M. G., Leslie, A. G. W., and Walker, J. E. (2000). The structure of the central stalk in bovine F1-ATPase at 2.4Å resolution. *Nature Struct. Biol.* 7, 1055–1061. (B) Side view (large) and top view (small) of the $\alpha_3\beta_3\gamma$ complex of rat liver F1 crystallized in the presence of ATP and Pi. The α subunits are in white, the β subunits are in blue, and the γ subunit (part of which is lacking, since it was disordered in the crystal) is in yellow; the nucleotides bound to all β/α and α/β interfaces are shown. Reproduced from Bianchet, M. A., Pedersen, P. L., and Amzel, L. M. (2000). Notes on the mechanism of ATP synthesis. *J. Bioenerg. Biomembr.* **32**, 517–521 with permission of Kluwer Academic/Plenum Publishers.

mitochondrial ε-subunit has no bacterial counterpart (Figures 1B and C).

F1

The three α- and the three β-subunits of F1 are arranged alternately in an hexagonal ring of 90–100Å diameter, forming the bulk of the globular head of F1 (Figure 2A). The α- and β-subunits of F1 are homologous and share similar folds, comprising an N-terminal β-barrel domain, a central domain which includes the nucleotide-binding site, and a C-terminal bundle of α-helices. The γ-subunit has an elongated shape: a long C-terminal and a shorter N-terminal α-helix wrap in an antiparallel, asymmetric coiled-coil, and the central section of the chain folds in a globular domain. The terminal portion of the coiled coil inserts into the large central cavity of the $\alpha_3\beta_3$ hexamer (Figure 2A), making minimal contacts with its interior surface and reaching its top. The remainder of the γ-subunit protrudes to form a 47Å stalk, which contacts F0 at the membrane surface by means of a foot-shaped structure (Figures 1 and 2B), resulting from the interaction of its globular domain with the ε-subunit (or the δ- and ε-subunits in mitochondria). The bacterial δ-subunit (or the equivalent mitochondrial OSCP) is located externally on the upper half of the $\alpha_3\beta_3$ assembly, interacting with the N-terminal domains of at least one α-subunit (Figure 1).

F0

In F0 (Figure 1) the a subunit (the only main subunit still lacking a high resolution structure) is thought to be folded into five-transmembrane α-helices, the b-subunit comprises an α-helical hydrophilic and a potentially α-helical transmembrane domain, and the c-subunit folds in a hairpin-like structure, with two transmembrane α-helices linked by a short polar loop. Several c-subunits pack to form an oligomeric membrane-spanning ring, probably filled by membrane lipids. The number of monomers in the ring is generally thought to vary between species, and stoichiometries of 9–14 c-subunits have been proposed for the synthases of different sources. In bacteria, the packing of the c-subunits is suggested to vary even within a single species, as a result of modifications in the membrane lipid composition induced by different growing conditions. Irrespective of its stoichiometry, the c-ring spans the membrane, interacting with the foot of the F1 stalk by means of the polar loops of the c-subunits, while its external surface contacts the highly hydrophobic a subunit and the transmembrane domains of the b-subunit dimer (in bacteria and chloroplasts). The hydrophilic α-helices of the b-subunits project from

the membrane reaching the δ-subunit of F1. The b-subunit of mitochondrial F0, although monomeric, is thought to have an analogous organization and to contact the OSCP subunit of F1. The interaction between the F0 b and the F1 δ (or OSCP) subunits results in the second, peripheral stalk connecting the catalytic head to the membrane-intrinsic footpiece of the ATP synthase complex.

ATP Synthesis by F1

Catalytic Process

The catalytic cycle leading to the production of ATP involves three main steps: binding of Mg–ADP and P_i to the enzyme (both ADP and ATP are complexed with Mg^{2+}, as in all known reactions of these nucleotides), formation of the γ-phosphoanhydridic bond by removal of a water molecule, and release of Mg–ATP to the aqueous phase. Reversal of these steps leads to the hydrolysis of ATP, which is often studied as it requires simpler experimental systems (e.g., the isolated F1, or the complete F1–F0 complex in the absence of a proton gradient) than the synthesis. ATP is synthesized (or hydrolyzed) at three catalytic sites located on the β-subunits at the interface with an α-subunit (Figure 3). The α-subunits also contain nucleotide-binding sites which, although homologous to those of the β-subunits, are catalytically inactive (Figure 2A). Most of the amino acids involved in catalysis belong to the β-chain, but the adjacent α-chain also contributes essential residues, so that the enzyme functionally consists of three αβ catalytic pairs. As in many ATP-utilizing proteins, each nucleotide-binding site contains a P-loop, i.e., a conserved sequence motif – Gly-X-X-X-X-Gly-Lys-Thr/Ser – which participates in the binding of the phosphate groups. Other amino acids involved in the synthesis/hydrolysis of ATP have been identified by mutational and structural data; among them, the side chain of a glutamic acid, which has no equivalent in the inactive sites of the α-chains, appears essential for the formation/hydrolysis of the anhydridic bond of ATP.

Analysis of ATP synthesis has unexpectedly shown that the γ-phosphoanhydridic bond of ATP readily forms within the complex, owing to the much higher affinity of the catalytic sites for ATP than for ADP and Pi. However, the newly formed ATP remains tightly bound to the enzyme unless protons are flowing through F0 down a transmembrane gradient. This observation has provided evidence that the translocated protons are not directly involved in catalysis, suggesting instead that the H^+ flow is the exergonic process driving the major energy-requiring step of ATP synthesis, i.e., the decrease of the enzyme affinity for ATP.

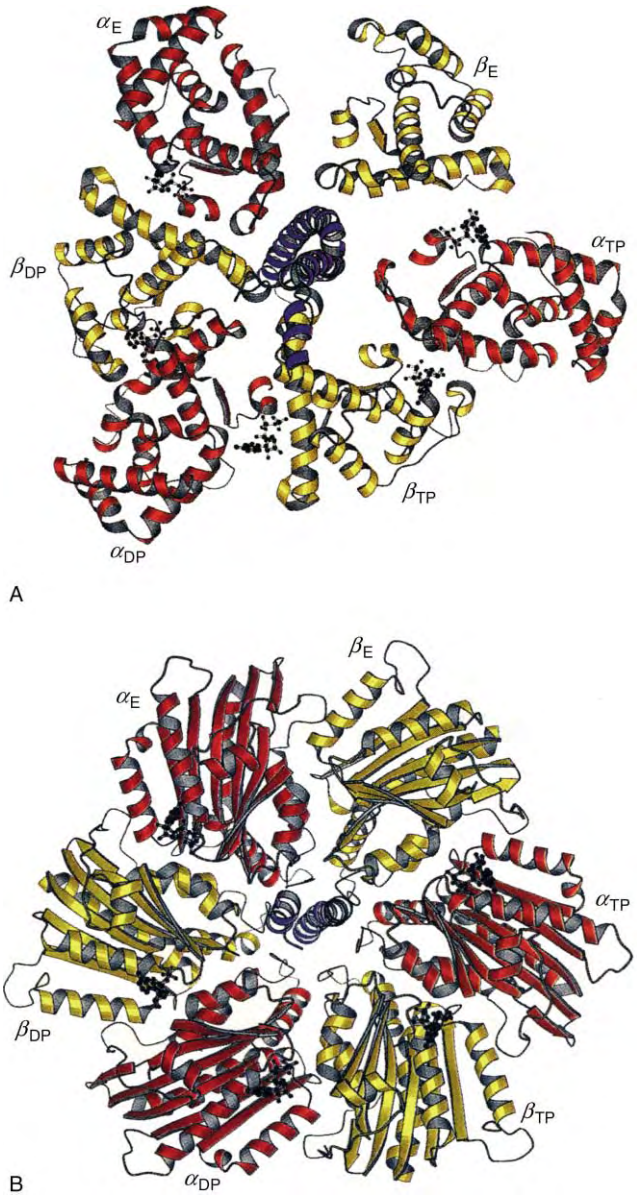

FIGURE 3 Asymmetric features of bovine F1. F1 was crystallized in the presence of AMP–PNP and ADP. The α-subunits are in red, the β-subunits are in yellow, and the γ-subunit (part of which is lacking, since it was disordered in the crystal) is in blue. All the α-subunits and the β_{TP}-subunit have AMP–PNP bound; β_{DP} has ADP and β_E has no nucleotide. (Reproduced from Abrahams, J. P., Leslie, A. G. W., Lutter, R., and Walker, J. E. (1994). Structure at 2.8Å resolution of F1-ATPase from bovine heart mitochondria. *Nature* **370**, 621–628, with permission.) (A) The γ-subunit coiled-coil and the C-terminal domains of the α- and β-subunits (viewed from the membrane side). (B) The γ-subunit coiled-coil and the nucleotide-binding domains of the α- and γ-subunits (viewed from the membrane side).

Binding Change Model

A further peculiar aspect of F1 revealed by the enzymological data is cooperative catalysis: the three β-subunit cannot operate independently, as revealed by the complete loss of enzymatic activity of the synthase

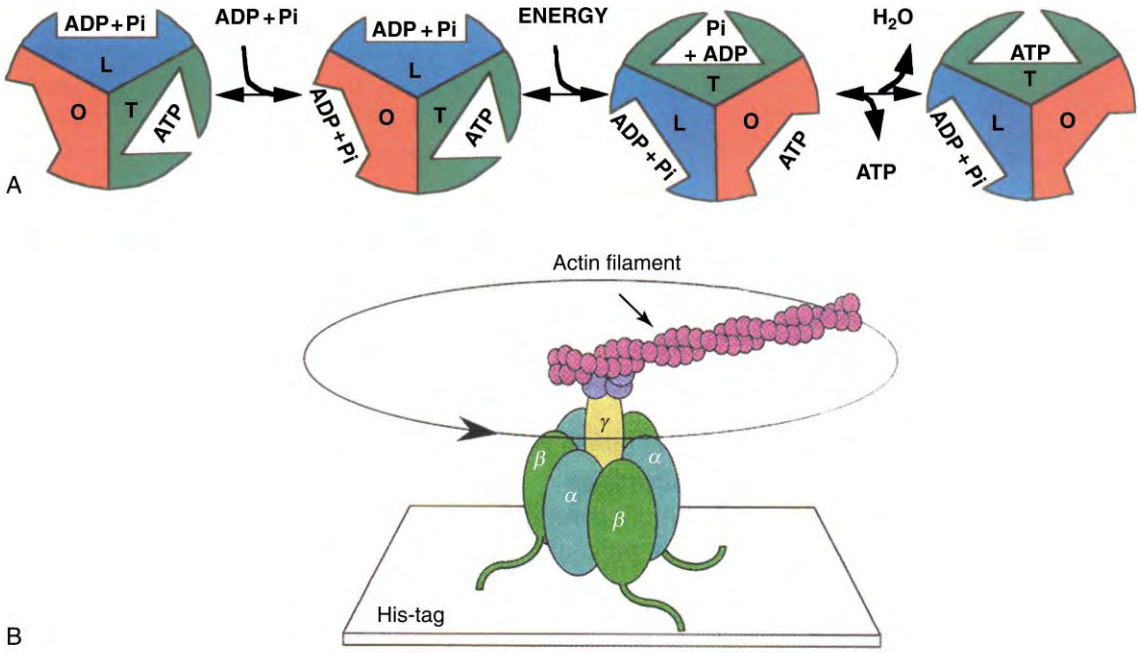

FIGURE 4 The binding change model of ATP synthesis and the rotation of the γ-subunit(A) Each circle represents a different conformation of $\alpha_3\beta_3$, the three sectors corresponding to the three $\alpha\beta$ pairs. Green sectors represent the "tight" (T) conformation, blue sectors represent the "loose" (L) conformation, and red sectors represent the "open" (O) conformation. (Reproduced from Bianchet, M.A., Pederson, P. L., and Amzel, L. M. (2000). Notes on the mechanism of ATP synthesis. *J. Bioenerg. Biomembr.* **32**, 517–521, with permission of Kluwer Academic/Plenum Publishers.) (B) The $\alpha_3\beta_3\gamma$ complex was immobilized on a microscope slide coated with Ni^{2+}-nitrilotriacetic acid, by means of polyhistidine tags (that bind strongly to nickel ions) attached to the N termini of the β-subunits. A fluorescently labelled actin filament (length 2 μm) was attached to the γ-subunit, and the rotation of the γ-subunit was observed directly during the hydrolysis of ATP by epifluorescence microscopy. (Reproduced from Junge, W., Lill, H., and Engelbrecht, S. (1997) ATP synthase: an electrochemical transducer with rotatory mechanics. *Trends Biochem. Sci.* **22**, 420–423, with permission from Elsevier.)

upon inhibition of a single catalytic site of F1, implying that site-to-site interactions are essential to complete the catalytic cycle. According to the widely accepted binding change model (Figure 4A), proposed by Boyer in 1973 to explain the unusual catalytic features of the F1–F0 ATPase, as the synthesis of ATP proceeds each β-subunit sequentially adopts three conformations, corresponding to different binding affinities of the catalytic site for ATP, ADP, and Pi: the loose (L) conformation binds ADP and P_i with low affinity, the tight (T) conformation allows ATP to be synthesized by binding it with very high affinity, and the open (O) conformation releases the newly formed ATP to the medium. At any time the three β-subunits within F1 have different conformations and distinct steps of the enzymatic reaction take place at each catalytic site: when one β-subunit changes from the L to the T conformation, forming ATP from ADP and P_i, another β-subunit converts from the T to the O state, releasing ATP, and the third one shifts from the O to the L conformation, binding ADP and P_i. Thus, ATP is released by a catalytic site only upon binding of the substrates to another site, and the synthesis of ATP is the result of the concerted operation of the three $\alpha\beta$ pairs of F1.

The functional asymmetry predicted by the binding change mechanism has been substantiated by structural information. In fact, in the first F1 crystal described by Walker (Figure 3) the β-subunits have distinct tridimensional structures, arising principally from domain shifts, and the catalytic sites contain different nucleotides: one binds the ATP analogue AMP–PNP, one ADP, while the third one has no ligand. However, two main problems concerning the catalytic cycle are still debated: (1) the actual number of the catalytic sites of F1 involved in the synthesis of ATP and (2) the number of the distinct conformations cyclically adopted by each β-subunit.

Rotational Catalysis

The tridimensional structure of F1 has also revealed that the γ-subunit contributes to the asymmetry of F1 (Figure 3): its coiled-coil displays different interactions with each $\alpha\beta$-subunit pair, correlating with the conformational differences among the catalytic sites. These structural features support the rotary mechanism of ATP synthesis, as predicted by Boyer to account for the binding change model. According to this mechanism the asymmetric γ-subunit triggers the conformational transitions required to synthesize ATP by rotating relative to the $\alpha_3\beta_3$ ring, therefore interacting differently with each $\alpha\beta$ pair at any instant. The contact sites between the γ-subunit and each $\alpha\beta$ pair which are specifically

responsible for the conformational transitions envisaged by the binding change model remain controversial; however, an inventive experiment designed in 1997 by the groups of Yoshida and Kinosita has visually documented the rotation of the γ-subunit during ATP hydrolysis (Figure 4B). A single recombinant $\alpha_3\beta_3\gamma$ bacterial complex was anchored to a microscope slide, so that the γ-subunit projected upwards. An actin filament, much bigger than the enzyme and bearing a fluorescent tag, was linked to the γ-subunit, at a distance from the ring, to provide a long adjunct that could be observed under a fluorescent microscope. When Mg–ATP was added to this ATPase preparation, the actin filament began to rotate unidirectionally proving that the hydrolysis, and presumably the synthesis, of ATP entailed the physical rotation of the γ-subunit. At very low concentrations of ATP the rotary motion apparently splits into 120° steps, each evidently corresponding to the hydrolysis of one molecule of ATP. The efficiency of the conversion of the chemical energy from ATP hydrolysis into the mechanical energy of rotation was estimated to approximate 90%, consistent with the fully reversible operation of F1. The same biophysical approach has subsequently demonstrated that the whole central stalk assembly (i.e., the bacterial γ- and ε-subunits) revolves during the catalytic process.

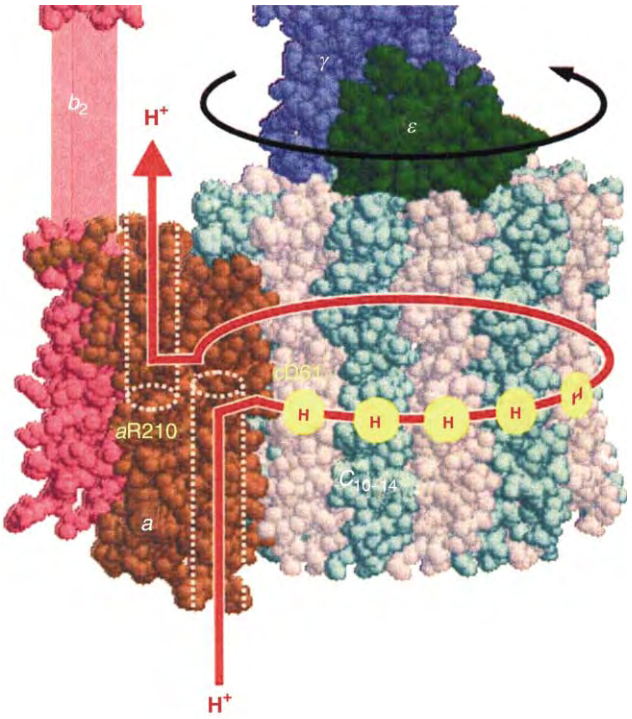

FIGURE 5 Structure of the ATP synthase showing a proposed proton transport path. aR210 and cD61 indicate the a-subunit arginine and the c-subunit aspartate required for the transmembrane movement of H^+; the dotted lines represent the putative half-channels for H^+. (Reproduced from Weber, J., and Senior, A. E. (2003). ATP synthesis driven by proton transport in F_1F_0-ATP synthase. *FEBS Lett.* **545**, 152–160 with permission of Federation of the European Biochemical Societies.)

Proton Translocation by F0

To mechanically connect the synthesis of ATP by F1 to the translocation of protons by F0, the rotation of the central stalk must be driven by protons moving through F0. However, the abovementioned lack of a high resolution structure of the intact F0 has so far hampered the efforts to define its fine molecular mechanism.

Amino acids essential for the transmembrane movement of protons have been identified both in the a-subunit and in the c-subunit, but not in the b-subunit, implying that the H^+ path is formed by a- and c-subunits. In particular, two interacting amino acids, predicted to be near the middle of the hydrophobic core of the membrane, are apparently crucial to H^+ transport: an aspartate (or glutamate) in the c-subunit, and an arginine in the a-subunit (Figure 5). The acidic residue reacts specifically with the synthase inhibitor dicyclohexylcarbodiimide (DCCD), and the translocation of protons through F0 is completely blocked by the binding of DCCD to just one of the several c-subunits, meaning that the c-subunits in the ring operate cooperatively.

In 1986, these experimental findings have led Cox and co-workers to propose that the c-ring rotates against the a-subunit so that, as each c-subunit moves past the a-subunit, a proton moves across F0. Recently, cross-linking studies have established that H^+ translocation does cause the c-ring to revolve, and that the central stalk is forced to rotate synchronously with the ring due to the connections between its foot-shaped portion and the c-subunits. In addition, extension of the procedure of Yoshida and Kinosita to the F1–F0 complex has confirmed the rotation of the c-ring.

The generally accepted model for the operation of F0 (Figure 5) envisages two disaligned half-channels (mainly located in the a-subunit) extending from the opposite surfaces of the membrane to the depth of the essential aspartate/arginine pair. To cross the membrane, a proton moves through one half-channel and binds to the negatively charged aspartate of one c-subunit, relieving the electrostatic interaction with the positively charged arginine. The uncharged c-subunit can thus come into contact with the hydrophobic core of the membrane, and the c-ring may rotate, therefore allowing the aspartate of the contiguous c-subunit to align to the half-channel and to bind another H^+. Protons are discharged to the opposite side of the membrane by means of the other half-channel following the rotation of the ring. Consistent with the actual operation of F0 and of the intact F1–F0 complex, the translocation of protons by this mechanism is passive and bidirectional,

unless a proton gradient across the membrane imposes a single direction of rotation.

Peripheral Stalk

The peripheral stalk is the least defined portion of the ATP synthase, consisting of b- and δ- (or OSCP) subunits, whose high resolution structures are still partially unknown. It is believed to act as a stator, i.e., to keep the catalytic head and the proton channel in the right relative orientation by preventing the a-subunit and the $\alpha_3\beta_3$ ring from rotating with the c-ring–γ–ε assembly (often referred to as the rotor of the complex).

See Also the Following Articles

Membrane-Associated Energy Transduction in Bacteria and Archaea • P-Type Pumps: H^+/K^+ Pump • P-Type Pumps: Plasma Membrane H^+ Pump

Glossary

electron transfer chain A functional assembly of membrane-associated redox compounds which transfers electrons down a redox potential difference. It uses the energy thus made available to pump protons across the membrane, thereby generating a transmembrane proton gradient

F1–F0 Abbreviation of "coupling *f*actor *1*" and "*f*actor conferring sensitivity to *o*ligomycin": the proteins originally identified in mitochondria by E. Racker and co-workers as necessary for the synthesis of ATP, but not for the activity of the respiratory chain.

(ion) channel A transmembrane pathway that allows a passive flow of ions down a concentration or an electrical gradient. It may shift from an open to a closed state.

oligomycin An antibiotic that blocks both the synthesis and the hydrolysis of ATP in mitochondria. It does not block the hydrolysis of ATP by purified F1 preparations.

Further Reading

Abrahams, J. P., Leslie, A. G. W., Lutter, R., and Walker, J. E. (1994). Structure at 2.8Å resolution of F_1-ATPase from bovine heart mitochondria. *Nature* **370**, 621–628.

Boyer, P. D. (1997). The ATP synthase – A splendid molecular machine. *Annu. Rev. Biochem.* **66**, 717–749.

Capaldi, R. A., and Aggeler, R. (2002). Mechanism of the F_1F_0-type ATP synthase, a biological rotary motor. *Trends Biochem. Sci.* **27**, 154–160.

Junge, W., Pänke, O., Cherepanov, D. A., Gumbiowski, K., Müller, M., and Engelbrecht, S. (2001). Inter-subunit rotation and elastic power transmission in F_1F_0-ATPase. *FEBS Lett.* **504**, 152–160.

Nicholls, D. G., and Ferguson, S. J. (2002). *Bioenergetics*. Academic Press, London.

Noji, H., Yasuda, R., Yoshida, M., and Kinosita Jr., K. (1997). Direct observation of the rotation of F_1-ATPase. *Nature* **386**, 299–302; http://www.res.titech.ac.jp/seibutu/main_html.

Pedersen, P. L., Ko, Y. H., and Hong, S. (2000). ATP synthases in the year 2000: Defining the different levels of mechanism and getting a grip on each. *J. Bioenerg. Biomembr.* **32**, 423–432.

Richter, M. L., Hein, R., and Huchzermeyer, B. (2000). Important subunit interactions in the chloroplast ATP synthase. *Biochim. Biophys. Acta* **1458**, 326–342.

Sambongi, Y., Ueda, I., Wada, Y., and Futai, M. (2000). A biological molecular motor, proton-translocating ATP synthase: Multidisciplinary approach for a unique membrane enzyme. *J. Bioenerg. Biomembr.* **32**, 441–448.

Stock, D., Gibbons, C., Arechaga, I., Leslie, A. G. W., and Walker, J. E. (2000). The rotary mechanism of ATP synthase. *Curr. Opin. Struct. Biol.* **10**, 672–679.

Weber, J., and Senior, A. E. (2003). ATP synthesis driven by proton transport in F_1F_0-ATP synthase. *FEBS Lett.* **545**, 152–160.

Yoshida, M., Muneyuki, E., and Hisabori, T. (2001). ATP synthase – A marvellous rotary engine of the cell. *Nat. Rev. Mol. Cell Biol.* **2**, 669–677.

Biography

Donata Branca is a Research Associate in the Department of Biological Chemistry at the University of Padova and the Venetian Institute of Molecular Medicine. In the past, she has worked on the relationship between H^+ translocation and ATP synthesis in mitochondria. Her present interest is the role of calcium in intracellular proteolysis.

FAK Family

Steven K. Hanks
Vanderbilt University School of Medicine, Nashville, Tennessee, USA

The focal adhesion kinase (FAK) family is a small family of nonreceptor tyrosine kinases that function in adhesion-mediated signaling. The family contains just two vertebrate members: FAK and *p*roline-rich *t*yrosine *k*inase 2 (PYK2). Also included are homologues from invertebrate metazoans: DFak56 from *Drosophila* and KIN-31 from *C. elegans*. The FAK family is defined by the presence of three major conserved domains: central tyrosine kinase catalytic domain, amino-terminal FERM domain (related to domains found in the red blood cell band 4.1 protein, *e*zrin, *r*adixin, and *m*oesin), and carboxyl-terminal *f*ocal *a*dhesion *t*argeting (FAT) domain.

FAK

Focal adhesion kinase (FAK) (Figure 1) was the first member of the family to be described and has been most extensively studied, primarily in cultured fibroblasts. Its name derives from its prominent localization to cellular focal adhesions (Figure 2). Focal adhesions are sites where cell surface integrins cluster and make strong adhesive contact with components of the extracellular matrix (ECM) such as fibronectin, vitronectin, and collagen. Focal adhesion localization was the first indication that FAK could be involved in regulating aspects of cell behavior resulting from integrin-mediated adhesion. The FAT domain is necessary and sufficient for focal adhesion localization.

FAK Expression and Role in Development

FAK is widely expressed throughout embryogenesis and appears to function in many developmental processes. A role for FAK in gastrulation is suggested by observations, made in early embryos from *Xenopus* and chicken, of prominent FAK expression in the involuting mesoderm. FAK-deficient mouse embryos fail to develop past late stages of gastrulation, and exhibit dramatically retarded development of the antero-posterior axis, suggestive of defects in mesodermal migration. Studies using late-stage embryos from mouse, *Xenopus*, and zebrafish indicate high FAK expression associated with several developing systems including the central nervous system, somites, arterial walls, myotendinous junctions, and germ cells. FAK is ubiquitously expressed in adult tissues, with high levels found in brain, lung, and testis. In neuronal cells FAK is enriched in growth cones. Neuronal FAK is expressed from alternatively spliced transcripts resulting in short insertions in the region between the FERM and kinase domains.

FAK Activation and Signaling Mechanism

Like most tyrosine kinases, FAK is in its active signaling state when phosphorylated on tyrosine residues. FAK tyrosine phosphorylation results from integrin-mediated cell adhesion to the ECM and is maintained by Rho-mediated contraction of the actin cytoskeleton. The initial step in FAK activation is phosphorylation of Tyr-397, which occurs through intermolecular autophosphorylation. Neuronal-specific isoforms of FAK have a higher intrinsic capacity to autophosphorylate. A critical aspect of FAK signaling is the recruitment of Src-family kinases, which bind via their SH2 domains to the phosphorylated Tyr-397 site. This leads to Src-mediated phosphorylation of five other FAK tyrosine residues: 407, 576, 577, 861, and 925 (Figure 1). Tyrosines 576 and 577 reside in the kinase domain "activation loop," and evidence indicates that phosphorylation of these sites elevates catalytic activity. Phosphorylated Tyr-925 can bind the SH2 domain of the adaptor protein Grb2, suggesting a mechanism for integrin stimulation of "extracellular-signal regulated kinase" (ERK) via a FAK > Grb2/SOS > Ras pathway. The signaling functions of the Tyr-407 and Tyr-861 sites are unknown.

Src-family kinases recruited to the Tyr-397 site also phosphorylate two FAK-associated proteins: "Crk-associated substrate" (CAS) and paxillin. CAS, via its SH3 domain, interacts with either of two proline-rich motifs (PR1 and PR2) that reside in the region linking the kinase and FAT domain. Paxillin interacts with the FAT domain. For both CAS and paxillin, the major tyrosine phosphorylation sites are in Tyr-X-X-Pro (YxxP) motifs. Fifteen YxxP motifs constitute the major region of CAS tyrosine phosphorylation (known as the "substrate domain") while two YxxP motifs are

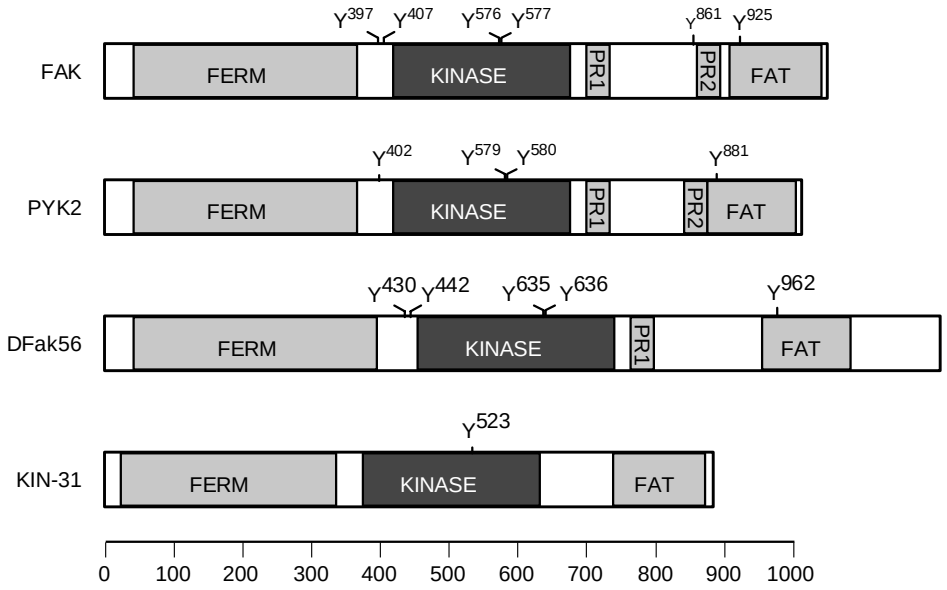

FIGURE 1 Members of the FAK family. FAK and PYK2 are vertebrate family members, DFak56 is from *Drosophila*, and KIN-31 is from *C. elegans*. Shown in the linear structures are major conserved domains, protein interaction motifs, and sites of tyrosine phosphorylation (see text for details). The scale bar represents number of amino acid residues.

the major paxillin sites. Phosphorylation of YxxP sites promotes downstream signaling events through recruitment of additional SH2-containing effector molecules. The c-Crk adaptor molecule binds to YxxP sites of both CAS and paxillin and appears to be a major downstream effector in signaling from the FAK/Src complex.

In addition to Src family kinases, the phosphorylated Tyr-397 site mediates interactions with SH2 domains of other signaling proteins including phosphatidylinositol 3-kinase (PI3K), the γ1 isoform of phospholipase C (PLC-γ1), Shc, Grb7, and Nck-2. Thus FAK likely promotes assembly of several distinct signaling complexes within a larger integrin-associated protein network.

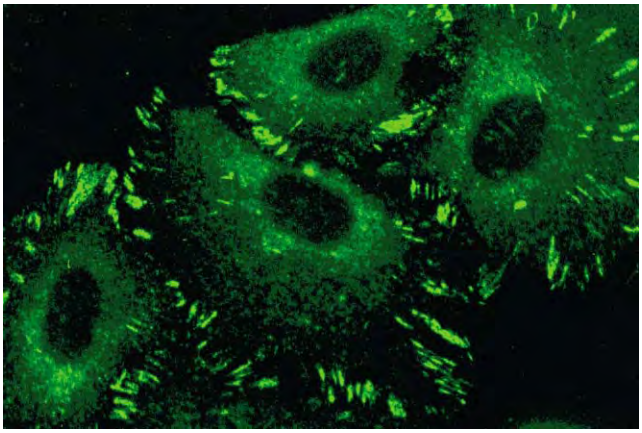

FIGURE 2 Localization of FAK in focal adhesions. Primary cultures of mouse keratinocytes were plated on fibronectin and stained using an antibody against FAK. The highly immunoreactive structures observed at the cell peripheries are focal adhesions.

Cellular Responses to FAK Signaling

Much evidence indicates that FAK functions to enhance the rate of cell motility. For example, fibroblasts derived from *FAK* −/− mouse embryos exhibit poor motility compared to cells from normal embryos, and the motility defect can be rescued by re-expressing wild-type FAK. Mutant FAK variants, either lacking the Tyr-397 site or deficient in catalytic activity, are unable to efficiently promote the motility response, indicating that FAK signaling is involved. A likely mechanism by which FAK promotes cell motility is by directing the extension of leading-edge lamellipodia. This occurs, in part, through activation of the small GTPase Rac, which can result from the recruitment of c-Crk to phosphorylated CAS and paxillin. One of the c-Crk SH3 domains interacts with the protein DOCK180 that promotes Rac GDP–GTP exchange. Interactions of the FAK Tyr-397 site with PI3K and Grb7 have also been implicated in the motility response.

In addition to regulating motility, FAK also functions as a positive regulator of cell growth by triggering both survival and proliferative signals. FAK-mediated signaling (requiring the Tyr-397 site) confers resistance to apoptosis resulting from various stimuli including loss of anchorage to the ECM (anoikis), oxidative stress, UV irradiation, and exposure to anti-cancer drugs. FAK survival signals can result from multiple downstream events including CAS/Crk complex formation and PI3K-mediated activation of Akt. FAK may also help

drive progression through G1 phase of the cell cycle through its ability to activate ERK kinases and promote transcriptional activation of the gene encoding cyclin D1.

PYK2

PYK2 is also known as CAK-β (cellular adhesion kinase β), RAFTK (related adhesion focal tyrosine kinase), and CADTK (calcium-dependent tyrosine kinase). The FAT and kinase domains of PYK2 each exhibit ~60% amino acid identity with the homologous domains of FAK, while the FERM domain is slightly less conserved (Table I). Both PR motifs in the kinase-FAT linking region are present in PYK2 (and capable of mediating interactions with CAS) but otherwise this region is poorly conserved, as is the short region amino-terminal to the FERM domain. Four tyrosine residues corresponding to sites of FAK phosphorylation are functionally conserved (Figure 1): phosphorylated Tyr-402 mediates interactions with Src-family kinases, phosphorylated activation loop tyrosines 579 and 580 stimulate PYK2 catalytic activity, and phosphorylated Tyr-881 binds Grb2.

PYK2 Expression and Roles in Development

PYK2 is expressed at high levels in the central nervous system and cells of hematopoietic origin, but is also detected in a variety of other cell types including fibroblasts, osteoclasts, epithelial cells, and smooth muscle cells. PYK2 levels increase dramatically in the forebrain around birth. A splice variant encoding a 42 amino acid insert between the two PR regions is predominantly expressed in neuronal cells. PYK2-deficient mice develop normally, but lack marginal zone B cells and have suppressed immunoglubulin production.

TABLE I

Conservation of FAK Family Domains[a]

	PYK2	DFak56	KIN-31
FERM	47	26	19
Kinase	58	63	47
PR linker	25	19	7
FAT	61	43	18

[a] Percent amino acid identities are shown compared to human FAK. Human PYK2 was used for the comparison. "PR linker" refers to the region containing proline-rich motifs that lies between the kinase and FAT domains.

PYK2 Activation and Signaling Mechanism

Like FAK, PYK2 activation can result from integrin stimulation. For example, PYK2 undergoes tyrosine phosphorylation following plating of megakaryocytes onto fibronectin and upon antibody stimulation of B cell integrins. In fibroblasts, PYK2 is detected in focal adhesions, consistent with the high conservation of the FAT domain. It is notable, however, that the FAT domain of PYK2 targets to focal adhesions inefficiently compared to that of FAK. PYK2 activation in response to integrin-mediated adhesion has been observed in *FAK −/−* fibroblasts. But re-expression of FAK in these cells effectively suppresses the PYK2 response, probably by displacing PYK2 from the adhesion sites. These observations suggest that PYK2 may not play as widespread a role in integrin signaling as does its sister molecule, FAK.

In contrast to FAK, PYK2 can be activated by extracellular signals that elevate levels of intracellular calcium and stimulate calcium-dependent isoforms of protein kinase C. These include agonists for G protein-coupled receptors, voltage-gated calcium channels, and the nicotinic acetylcholine receptor. Since protein kinase C is a protein-serine/threonine kinase it must stimulate PYK2 tyrosine phosphorylation through an indirect means, but the exact mechanism is unknown.

The downstream signaling events resulting from PYK2 activation are generally similar to those of FAK, involving autophosphorylation, recruitment of Src family kinases, and Src-mediated phosphorylation of other sites on PYK2 as well as PYK2-associated CAS and paxillin (Figure 3). The interaction of Grb2 with the PYK2 Tyr-881 site suggests a possible link between G protein-coupled receptors and ERK activation.

Cellular Responses to PYK2 Signaling

Unlike FAK, PYK2 overexpression does not efficiently promote fibroblast motility and results in apoptosis, rather than cell survival. Nevertheless, a critical role for PYK2 in the motility and migration of macrophages and B cells has been demonstrated using cells derived from PYK2-deficient mice. Defects in lymphocyte motility could explain the absence of marginal zone B cells in these animals. Through its ability to be activated by both integrin- and calcium/PKC-dependent mechanisms, PYK2 can function in numerous and diverse signaling pathways regulating a wide variety of cellular activities. In neuronal cells, for example, PYK2 has been implicated as a positive regulator of neurite outgrowth and NMDA channel activity. Other consequences of PYK2 signaling include inhibition of voltage-gated potassium channels leading to membrane depolarization of vascular smooth muscle cells, translocation of the

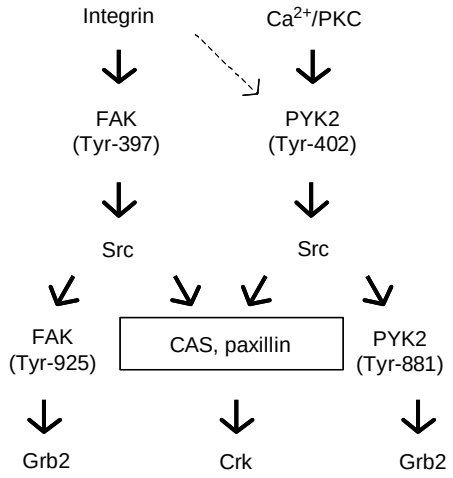

FIGURE 3 Signaling by FAK and PYK2. Both FAK and PYK2 can be activated by integrin-mediated adhesion, while PYK2 is uniquely activated through a calcium/PKC-dependent mechanism. A critical element of FAK and PYK2 signaling involves the recruitment of Src family kinases to sites of autophosphorylation. The associated Src family kinases then phosphorylate a conserved FAK/PYK2 tyrosine site to promote Grb2 binding, and also phosphorylate FAK/PYK2-associated proteins CAS and paxillin to promote binding of Crk. The adaptor molecules Grb2 and Crk interact with guanine-nucleotide exchange factors for small G proteins, including Ras and Rac, to promote downstream signals.

GLUT4 glucose transporter to the plasma membrane of adipocytes, stimulation of Na-HCO^{3-} cotransporter activity in renal epithelial cells, and angiogenesis of vascular endothelial cells.

Invertebrate Members of the FAK Family

Drosophila and *C. elegans* genomes each contain a single member of the FAK family: DFak56 in *Drosophila* and KIN-31 in *C. elegans*. FAK and PYK2 are more closely related to one another than they are to either DFak56 or KIN-31, indicating that the two vertebrate family members arose through a gene duplication event that occurred sometime after evolutionary separation from the invertebrates.

Drosophila DFak56 shows strong overall conservation with the two vertebrate family members, but is slightly more similar to FAK than to PYK2. The kinase domain of DFak56 is most highly conserved in comparison to FAK, followed in order by the FAT domain, the FERM domain, and the kinase-FAT linker region (Table I). Within the kinase-FAT linker, DFak56 contains a proline-rich motif corresponding to the PR1 site, but lacks the PR2 site. Of the six sites of FAK tyrosine phosphorylation, DFak56 lacks only the site corresponding to FAK Tyr-861. But DFak56 Tyr-962, which corresponds to the Grb2 binding sites in FAK and PYK2, lacks the asparagine residue at the +2 position necessary for Grb2 SH2 binding. A unique structural feature of DFak56 is an extended carboxyl-terminal region of unknown function. Like the vertebrate members of the FAK family, DFak56 exhibits autophosphorylation activity and undergoes tyrosine phosphorylation in response to integrin-mediated adhesion. DFak56 is broadly expressed during embyrogenesis, with strongest expression in the developing gut and central nervous system. The role of DFak56 in *Drosophila* development has yet to be defined through loss of function studies. However, overexpression of DFak56 in the wing imaginal disk leads to wing blistering, a phenotype associated with weakened integrin linkage to the actin cytoskeleton.

C. elegans KIN-31 is a predicted protein product of gene C30F8.4 that has yet to be characterized biochemically. Compared to other members of the FAK family, KIN-31 contains a well-conserved and apparently functional kinase domain, while both the FAT and FERM domains are rather poorly conserved (Table I). Interestingly, KIN-31 lacks key motifs associated with FAK family signaling including a tyrosine corresponding to the autophosphorylation site and proline-rich motifs in the kinase-FAT linker region. Thus the functional role of KIN-31 could be quite distinct from the other FAK family members. KIN-31 is expressed in all larval stages and is prominent in bodywall muscle cells. Surprisingly, there is no obvious phenotype associated with a deletion of the gene encoding KIN-31.

See Also the Following Articles

Focal Adhesions • Integrin Signaling • Src Family of Protein Tyrosine Kinases

Glossary

activation loop A region within protein kinase catalytic domains that is often phosphorylated to promote catalytic activity.

integrins A large family of cell surface adhesion receptors, composed of α- and β-subunits, that link the extracellular matrix to the actin cytoskeleton and transmit biochemical signals across the plasma membrane.

SH2 "Src-homology 2," a domain that mediates protein–protein interactions by binding to sites of tyrosine phosphorylation.

SH3 "Src-homology 3," a domain that mediates protein–protein interactions by binding to proline-rich motifs with a core sequence of Pro-X-X-Pro.

tyrosine kinase A kinase that phosphorylates protein substrates on tyrosine residues.

Further Reading

Avraham, H., Park, S. Y., Schinkmann, K., and Avraham, S. (2000). RAFTK/Pyk2-mediated cellular signalling. *Cell Signal.* **12**, 123–133.

Girault, J.-A., Costa, A., Derkinderen, P., Studler, J.-M., and Toutant, M. (1999). FAK and PYK2/CAKβ in the nervous system: A link between neuronal activity, plasticity and survival? *Trends Neurosci.* **22**, 257–263.

Hanks, S. K., Shin, N.-Y., Ryzhova, L., and Brabek, J. (2003). Focal adhesion kinase signaling activities and their implications in the control of cell survival and motility. *Front Biosci.* **8**, d982–d996.

Hauck, C. R., Hsia, D. A., and Schlaepfer, D. D. (2002). The focal adhesion kinase—A regulator of cell migration and invasion. *IUBMB Life* **53**, 115–119.

Parsons, J. T., Martin, K. H., Slack, J. K., Taylor, J. M., and Weed, S. A. (2000). Focal adhesion kinase: A regulator of focal adhesion dynamics and cell movement. *Oncogene* **19**, 5606–5613.

Schaller, M. D. (2001). Biochemical signals and biological responses elicited by the focal adhesion kinase. *Biochim. Biophys. Acta* **1540**, 1–21.

Biography

Steven K. Hanks is a Professor in the Department of Cell and Developmental Biology at Vanderbilt University School of Medicine. His principal research interest is the role of tyrosine phosphorylation in integrin signaling. He holds a Ph.D. from the University of Texas Health Science Center at Houston Graduate School of Biomedical Sciences and received postdoctoral training at the Salk Institute. He pioneered homology-based approaches to identify novel protein kinases, which led to the recognition of CDK4 and FAK. He developed an approach to classify eukaryotic protein kinases based on catalytic domain phylogeny.

Fat Mobilization: Perilipin and Hormone-Sensitive Lipase

Constantine Londos and Alan R. Kimmel
National Institutes of Health, Bethesda, Maryland, USA

Nature's solution for packaging energy reserves in organisms ranging from plants to mammals is to sequester energy-rich fatty acids, in the form of triacylglycerols (TAG) or cholesteryl esters, within intracellular neutral lipid storage droplets. The great survival value for this type of packaging is attributed to the high density of energy in fatty acids and the relatively low amount of water necessary for their storage. If man were to carry the energy equivalent of fat as carbohydrate, the additional required water would render man immobile. Typically, intracellular lipid droplets are coated with specific targeting classes of proteins, but enzymes involved in lipid metabolism may also be found in tight association.

Plant Lipid Droplets

The oleosins of plant seeds and tapeta were the first to be identified, and remain the most extensively studied, lipid droplet coat proteins. The oleosins are thought to protect the lipid depositions during dessication.

Animal Lipid Droplets

The first animal lipid droplet protein to be identified was perilipin of mammalian adipocytes. While perilipin has no obvious sequence relationship to the oleosins, it is related to several other animal proteins that also target lipid droplets. One of these, the adipose differentiation-related protein (ADRP), also termed adipophilin, was first identified as a gene that is highly expressed very early during adipocyte differentiation; subsequently, ADRP was found to be expressed ubiquitously and to coat the lipid droplets of all cells, excepting mature adipocytes. A third related protein, TIP47, was identified initially by a screen for proteins that interact with the mannose 6-phosphate/IGF2 receptor and was later also found to associate with lipid droplets. Based upon the sequence similarities among perilipin, ADRP, and TIP-47, the grouping has been described as the PAT protein family. S3-12 is an even more distantly related mammalian protein that is found on adipocyte plasma membranes and also on their intracellular lipid droplets. Several genes that encode PAT proteins in *Drosophila melanogaster* and *Dictyostelium discoideum* have also been identified. These genes are related to the mammalian counterparts not only in their protein-coding sequences, but also in their overall genomic structural organizations, indicating that they derive from a gene family of ancient origin. Further, the *Drosophila* and *Dictyostelium* PAT proteins localize to lipid droplets in fusion with green fluorescent protein (GFP) when expressed heterologously in the mammalian CHO fibroblasts. It is suggested that the PAT proteins share a specific and novel structural motif that determines their unique intracellular lipid droplet targeting ability. Moreover, each member of this protein family is likely to have an essential role in lipid metabolism.

Perilipin

The most extensively studied PAT protein is perilipin. There is a single gene for perilipin in mouse (and in human) that encodes multiple mRNA and protein species, resulting from differential splicing. The mRNAs encode identical amino termini but utilize distinct stop codons and display tissue-specific variants. Perilipin expression is highest in adipose tissue, with lesser amounts in steroidogenic tissue and only trace amounts elsewhere. Although cells contain a wide variety of lipid docking sites, the perilipins localize exclusively to the phospholipid monolayer that covers the underlying neutral lipid deposits of the droplet core (Figure 1). The perilipins are found on or within this phospholipid monolayer that forms the boundary between the aqueous cytosol and the hydrophobic lipid core of the droplet. Perilipin A (Peri A) is the largest and most abundant form. It has six consensus protein kinase A (PKA) sites that are phosphorylated upon elevation of cAMP during the lipolytic stimulation of adipocytes. Since lipolysis in

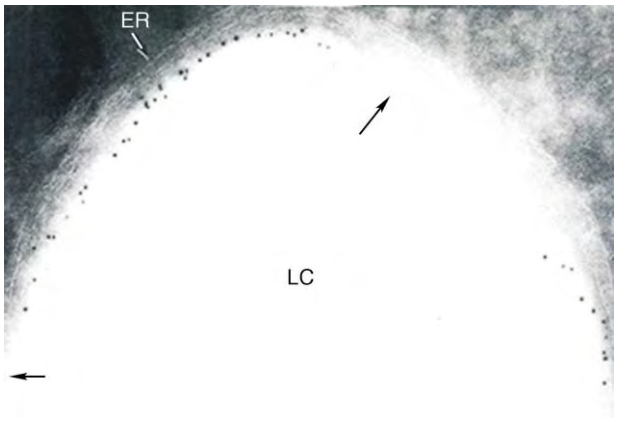

FIGURE 1 Immunogold labeling of perilipin at the surface of adipocyte lipid droplet. Electron micrograph of section through a lipid droplet immunostained with antiperilipin Ab. Note that the gold particles occur at the surface of the lipid droplet core (LC). (Reprinted from Blanchette-Mackie, E. J., Duyer, N. K. Barber, T. Coxay, R. A. Takeda, T. Rondinono, C. M. Theodorakis, J. L., Greenberg, A. S., and Londos, C. (1995). Perilipin is located on the surface layer of intracellular lipid droplets in adipocytes. *J. Lipid Res.* **36**, 1216–1226.)

adipocytes is driven by a cAMP-mediated process, and given perilipin's subcellular localization and tissue specificity, it was predicted that it would play a central role in the regulation of adipocyte lipolysis. Functional analyses has confirmed this speculation.

Perilipin Function

Depending on its PKA-dependent phosphorylation state, Peri A exhibits two opposing functional properties. Nonphosphorylated Peri A serves to shield the triacylglycerols (TAG) within the droplets from lipases. By contrast, when phosphorylated by PKA, the protein facilitates TAG hydrolysis. The importance of the protective function of perilipin is best illustrated by the *peri*-null mouse that exhibits a ~70% decrease in adipose tissue weight without a change in gross animal weight or in caloric intake. This loss in adipose tissue is attributed to the constitutively high rate of basal lipolysis in the adipocytes lacking perilipin. Thus, perilipin is essential for animals to package and retain their energy reserve supply. These *peri*-null animals also revealed the critical role for perilipin in regulated lipolysis; in the absence of perilipin, adipocytes fail to respond maximally to lipolytic stimuli. Thus, in *peri*-null adipocytes as compared to wild type, quiescent cells have an elevated basal lipolytic rate, while PKA-activated cells have an attenuated lipolysis. These dual functions have been recreated and the mechanism confirmed by expressing wild type and mutant forms of Peri A in fibroblastic cells which lack endogenous perilipin protein. Perilipin, thus, protects lipids from hydrolysis in unstimulated cells, whereas PKA-phosphorylated perilipin is required for regulated lipid hydrolysis.

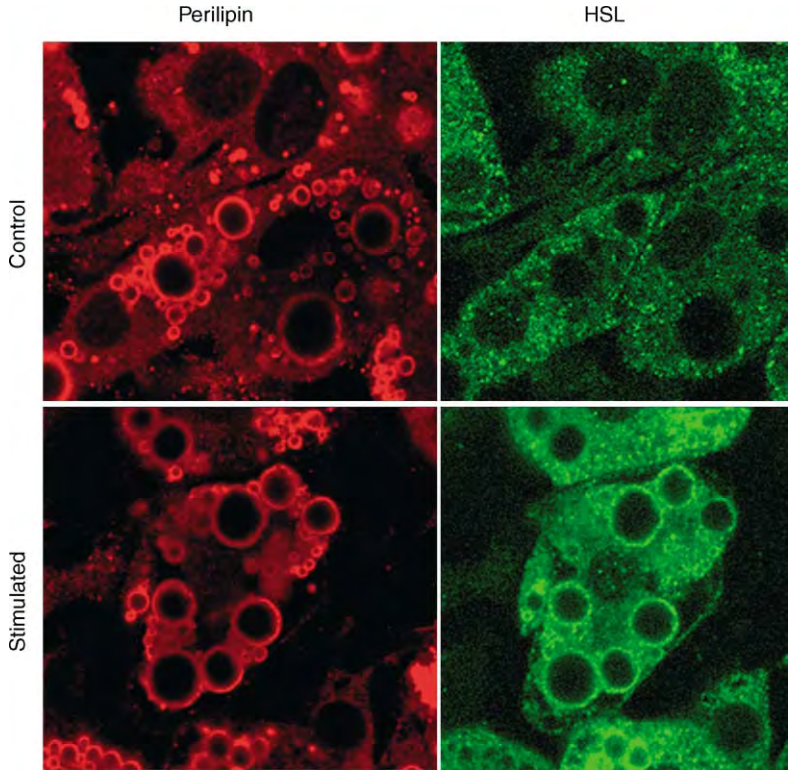

FIGURE 2 Migration of HSL from cytosol to lipid droplet surface upon stimulation. Red staining is perilipin at the lipid droplet surface. Green staining is HSL. Lower panels are resting adipocytes; upper panels show isoproterenol-stimulated cells. (Image courtesy of Dr. Carole Sztalryd, NIH.)

Adipocyte Lipolysis Catalyzed by Hormone-Sensitive Lipase

For many years, the prevailing model for adipocyte lipolysis was that hormone-sensitive lipase (HSL) was the rate-limiting enzyme and that the lipolytic rate *in vivo* was regulated exclusively by the PKA-dependent activation of HSL. This mechanism was questioned because phosphorylation of HSL *in vitro* elicits no more than a doubling of activity, whereas activation of cellular PKA increases lipolysis *in vivo* by 50- to 100-fold. The simple doubling of enzymatic activity was inadequate to explain the large increase in cellular lipolytic activity. Also, while HSL is easily identified in the cytosol of homogenates from quiescent adipocytes, the enzyme is absent from the aqueous fraction of homogenates from stimulated cells. HSL in stimulated cells was found subsequently to be associated with the cellular fraction containing the lipid storage. These data were confirmed by immunocytochemistry (Figure 2). It was not a great leap to conclude that PKA activation led to the translocation of HSL from the cytosol to the surface of the lipid storage droplet; subsequent experiments confirmed this hypothesis. An important breakthrough in understanding this mechanism came from studies with cells from the *peri*-null animals. Again, adipocytes from these animals exhibit elevated basal lipolysis, but are refractory to stimulation upon elevation of cAMP. The latter defect is downstream of the β-adrenergic receptor/G-protein/adenylyl cyclase complex that generates cAMP at the plasma membrane. Further exploration revealed that in the absence of perilipin, HSL cannot translocate from the cytosol to the lipid droplet surface in response to PKA activation. This finding established HSL translocation, and not activation per se, as the key reaction that elicits stimulated lipolysis in adipocytes and revealed the central role of perilipin in regulated lipid hydrolysis. Moreover, the HSL translocation reaction was reconstructed in nonadipocyte, CHO fibroblasts. HSL can be induced to translocate to the lipid droplet from the cytosol when coexpressed with wild-type perilipin. Translocation is not observed in the absence of perilipin or the presence of phosphorylation-defective variants of perilipin. Further, PKA-dependent phosphorylation of HSL itself was required to facilitate the translocation process.

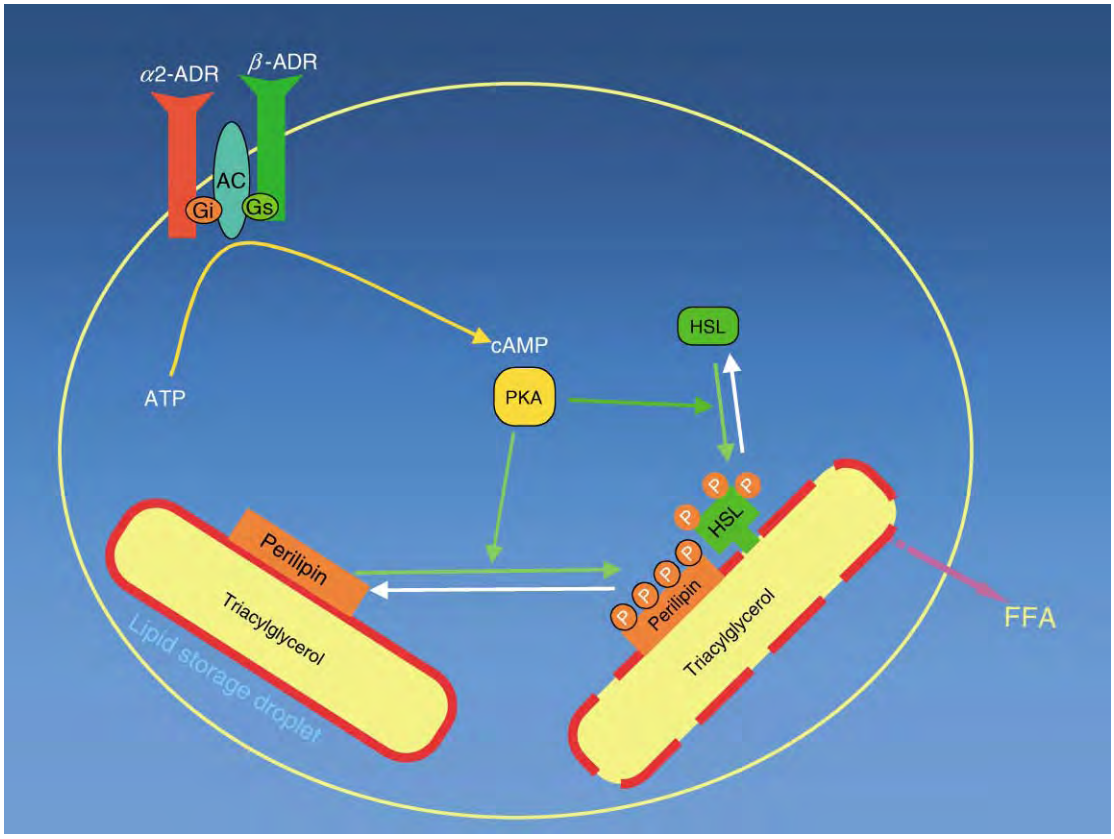

FIGURE 3 Model of the lipolytic reaction in adipocytes. Lipolytic stimulants activate adenylyl cyclase to increase cAMP which, in turn, activates protein kinase A which polyphosphorylates both hormone-sensitive lipase (HSL) and perilipin A. HSL then translocates from the cytosol to the lipid droplet surface. Phosphorylation of perilipin modifies the lipid droplet surface to accommodate the HSL.

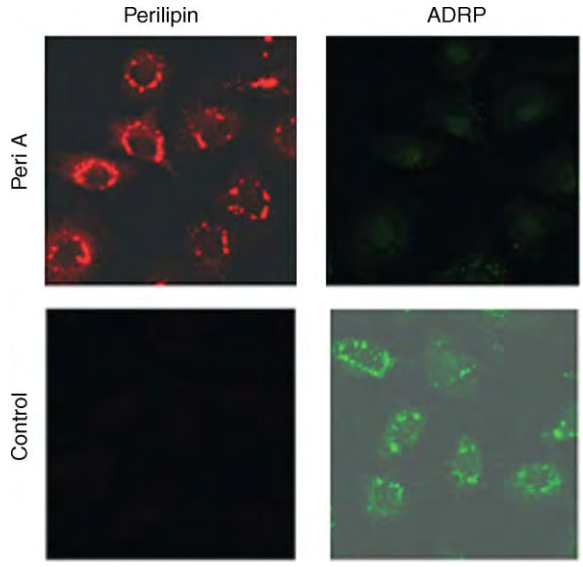

FIGURE 4 Displacement of ADRP by perilipin. Lipid droplets in lipid-loaded CHO fibroblasts stain for ADRP, but upon expression of perilipin A, the ADRP disappears and perilipin staining is seen around the lipid droplets.

Lipolysis Model

The current model for PKA-mediated lipolysis is depicted in Figure 3. In quiescent cells, cAMP levels are low, PKA is minimally active, and Peri A is unphosphorylated. Under these conditions, Peri A serves as a functional barrier for HSL access to the TAGs in the inner core of the intracellular neutral lipid droplets. Upon hormonal stimulation, cAMP levels rise, leading to the activation of PKA and the phosphorylation of both Peri A and HSL. Phosphorylation of Peri A at its three most N-terminal PKA sites readies the droplet surface to "accept" HSL. Phosphorylation of HSL at one of its two C-terminal PKA sites promotes the translocation of HSL from the cytosol to the lipid droplet surface. While it may be tempting to speculate that phospho-Peri A serves as the site for HSL docking at the droplet surface, it is difficult to believe this is the case. Potentially, unphosphorylated Peri A acts to sterically restrict access of all lipases to the surface of intracellular lipid droplets. It is, thus, not surprising that Peri A will inhibit lipolysis when expressed in cells that only possess PKA-insensitive lipases. However, phosphorylation of Peri A by PKA will stimulate lipolytic rates in these cells in excess of those observed in control cells that lack Peri A. Thus, it is suggested that Peri A phosphorylation alters the droplet surface to favor binding of all lipases, whether or not they are subject to PKA regulation. Perilipin may serve a space-making function. Phosphorylation of HSL separately facilitates binding to this "prepared" surface, effecting a synergism between Peri A and HSL during stimulation that raises the lipolytic rate 50- to 100-fold above basal levels and that is not observed with nonregulatable lipases.

It has been suggested that members of the PAT family of proteins play central roles in the regulation of lipid metabolism and energy homeostasis in organisms as diverged as *Dictyostelium* and mammals. This has been proven unequivocally for Perilipin and is strongly implied for ADRP. Recent data in *Drosophila* now extend these observations. *Drosophila* lacking one of their two PAT proteins exhibit a lean phenotype, while overexpression of the same protein leads to an increase in TAG stores, phenotypes that largely parallel those observed for perilipin (Figure 4).

See Also the Following Articles

Diacylglycerol Kinases and Phosphatidic Acid Phosphatases • Fatty Acid Oxidation • Fatty Acid Receptors • Fatty Acid Synthesis and its Regulation • Lipases • Lipid Bilayer Structure • Lipid Modification of Proteins: Targeting to Membranes • Lipid Rafts • Lipoproteins, HDL/LDL

Glossary

adipocyte The cell that stores most animal energy reserves as triacylglycerols (TAGs). Commonly known as the fat cell.

ADRP/adipophilin A protein that occurs ubiquitously and coats lipid droplets, especially in lung lipofibroblasts and secreted milk lipid globules.

hormone-sensitive lipase (HSL) The adipocyte enzyme responsible for catalyzing the rate-limiting step in TAG hydrolysis.

PAT family A family of genes that encode perilipins, ADRP/adipophilin/TIP-47 and related genes.

perilipin A protein that coats lipid droplets, primarily in adipocytes.

Further Reading

Blanchette-Mackie, E. J., Duyer, N. K., Barber, T., Coxay, R. A., Takeda, T., Rondinono, C. M., Theodorakis, J. L., Greenberg, A. S., and Londos, C. (1995). Perilipin is located on the surface layer of intracellular lipid droplets in adipocytes. *J. Lipid Res.* **36**, 1216–1226.

Brasaemle, D. L., Barber, T., Wolins, N. E., Serrero, G., Blanchette-Mackie, E. J., and Londos, C. (1997). Adipose differentiation-related protein is an ubiquitously expressed lipid storage droplet-associated protein. *J. Lipid Res.* **38**, 2249.

Gronke, S., Beller, M., Fellert, S., Ramakrishnan, H., Jackle, H., and Kuhnlein, R. P. (2003). Control of fat storage by a Drosophila PAT domain protein. *Curr. Biol.* **13**, 603.

Heid, H. W., Schnolzer, M., and Keenan, T. W. (1996). Adipocyte differentiation-related protein is secreted into milk as a constituent of milk lipid globule membrane. *Biochem. J.* **320**, 1025.

Londos, C., Brasaemle, D. L., Schultz, C. J., Segrest, J. P., and Kimmel, A. R. (1999). Perilipins, ADRP and other proteins that associate with intracellular neutral lipid droplets in animal cells. *Semin. Cell Dev. Biol.* **10**, 51.

Lu, X., Gruia-Gray, J., Copeland, N. G., Gilbert, D. J., Jenkins, N. A., Londos, C., and Kimmel, A. R. (2001). The murine perilipin gene: The lipid droplet-associated perilipins derive from tissue-specific, mRNA splice variants and define a gene family of ancient origin. *Mamm. Genome* **12**, 741.

Miura, S., Gan, J. W., Brzostowski, J., Parisi, M. J., Schultz, C. J., Londos, C., Oliver, B., and Kimmel, A. R. (2002). Functional conservation for lipid storage droplet association among perilipin, ADRP, and TIP47 (PAT)-related proteins in mammals, drosophila, and dictyostelium. *J. Biol. Chem.* **277**, 32253.

Murphy, D. J. (2001). The biogenesis and functions of lipid bodies in animals, plants and microorganisms. *Prog. Lipid Res.* **40**, 325–438.

Schultz, C. J., Torres, E., Londos, C., and Torday, J. S. (2002). Role of adipocyte differentiation-related protein in surfactant phospholipid synthesis by type II cells. *Am. J. Physiol. Lung Cell Mol. Physiol.* **283**, L288.

Sztalryd, C., Xu, G., Dorward, H., Contreras, J. A., Tansey, J. T., Kimmel, A. R., and Londos, C. (2002). Perilipin A is essential for the translocation of hormone-sensitive lipase during lipolytic activation of adipocytes. *J. Cell Biol.* **161**, 1103.

Tansey, J. T., Sztalryd, C., Gruia-Gray, J., Roush, D. L., Zee, J. V., Gavrilova, O., Reitman, M. L., Deng, C. X., Li, C., Kimmel, A. R., and Londos, C. (2001). Perilipin ablation results in a lean mouse with aberrant adipocyte lipolysis, enhanced leptin production, and resistance to diet-induced obesity. *Proc. Natl. Acad. Sci. USA* **98**, 6494.

Tansey, J. T., Hunl, A. M., Vogt, R., Davis, K. E., Jones, J. M., Fraser, K. A., Braesamle, D. L., Kimmel, A. R., and Londos, C. (2003). Functional studies on native and mutated forms of perilipins: A role in protein kinase A-activated lipolysis of triacylglycerols. *J. Biol. Chem*, **278**, 8401–8406.

Biography

Constantine Londos received D.D.S. from Ohio State University and Ph.D. from the University of Louisville School of Medicine. He worked with Dr. Martin Rodbell from 1971 through 1985, where he contributed to the G protein research for which Rodbell was awarded the Nobel prize in medicine or physiology in 1994. He currently heads the Membrane Regulation Section of Laboratory of Cellular and Developmental Biology, NIDDK, National Institutes of Health.

Alan Kimmel received Ph.D. from the University of Rochester and currently heads the Molecular Mechanisms of Development Section of LCDB, NIDDK, NIH, with a primary focus on developmental regulation of *Dictyostelium discsoideum*.

Fatty Acid Oxidation

Horst Schulz
City College and Graduate School of the City University of New York, New York, USA

Fatty acid oxidation is the process by which fatty acids are degraded in living organisms. The initial event is the activation of fatty acids by esterification with coenzyme A (CoA). The degradation of the resultant fatty acyl coenzyme A (acyl-CoA) thioesters proceeds by a cyclic process named β-oxidation. Passage through one cycle of β-oxidation produces fatty acids that are shortened by two carbon atoms and yields acetate in the form of acetyl coenzyme A (acetyl-CoA). Repetitive cycling through β-oxidation results in the complete degradation of fatty acids.

Cellular Uptake and Activation of Fatty Acids

The uptake of fatty acids by animal cells seems to be a facilitated process even though fatty acids can diffuse unassisted across biological membranes. A number of proteins of the cellular membrane are thought to be involved in this process. However, their specific functions in fatty acid uptake have not been elucidated. Once fatty acids have crossed the cellular membrane, they either diffuse or are transported to mitochondria, peroxisomes, and the endoplasmic reticulum where they are activated by esterification with coenzyme A (CoA). The transfer of fatty acids from the cellular membrane to sites of their activation may be facilitated by fatty-acid-binding proteins (FABPs), a group of low-molecular-weight (14–15 kDa) proteins that are present in the cytosol of various animal tissues. The function of FABP as an intracellular carrier of fatty acids has not been proven nor other suggested roles of this protein in the uptake and storage of fatty acids have been established.

The cellular uptake of fatty acids is tightly coupled to their intracellular esterification with CoA. Acyl-CoA synthetases catalyze the ATP-dependent esterification of fatty acids and CoA to produce fatty acyl-CoA, AMP, and pyrophosphate. Long-chain specific acyl-CoA synthetases are associated with the outer mitochondrial membrane and the membranes of the endoplasmic reticulum and peroxisomes. Acyl-CoA synthetases with a preference for medium-chain fatty acids are mostly located in the matrix of mitochondria while short-chain specific acyl-CoA synthetases are found in the mitochondrial matrix and/or in the cytosol depending on the organ of the animal.

Fatty Acid Oxidation in Mitochondria

In animal cells, fatty acids are degraded both in mitochondria and peroxisomes, whereas in lower eukaryotes fatty acid oxidation is generally confined to peroxisomes. Acetyl-CoA formed by mitochondrial fatty acid oxidation is further oxidized to release energy that drives the formation of ATP by oxidative phosphorylation. In liver, acetyl-CoA is also utilized for the synthesis of ketone bodies.

Mitochondrial Uptake of Fatty Acids

Fatty acids are activated by their conversion to fatty acyl-CoA thioesters at the outer mitochondrial membrane while their degradation by β-oxidation takes place in the mitochondrial matrix. Because acyl-CoAs cannot efficiently cross the inner mitochondrial membrane, an uptake system exists that shuttles fatty acyl residues across the inner membrane. As illustrated in Figure 1, the acyl residue of fatty acyl-CoA is transferred from CoA to carnitine at the outer mitochondrial membrane catalyzed by carnitine palmitoyltransferase I (CPT I). The resultant fatty acylcarnitine can cross the inner mitochondrial membrane in exchange for carnitine. This exchange is catalyzed by carnitine:acylcarnitine translocase (T). Once fatty acylcarnitine is in the mitochondrial matrix, it is converted back to fatty acyl-CoA by carnitine palmitoyltransferase II (CPT II), which is associated with the inner mitochondrial membrane. Medium-chain and short-chain fatty acids are not activated in the cytosol but directly enter the mitochondrial matrix where they are converted to their acyl-CoAs by medium-chain and short-chain acyl-CoA synthetases, respectively.

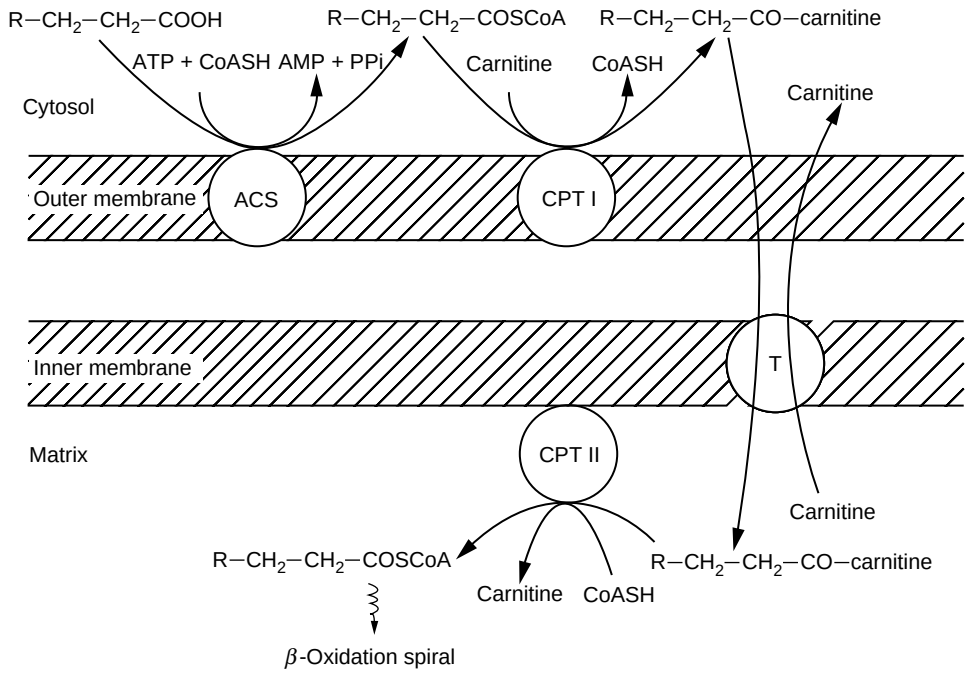

FIGURE 1 Carnitine-dependent transfer of fatty acyl groups across the inner mitochondrial membrane. ACS, acyl-CoA synthetase; CPT I and CPT II, carnitine palmitoyltransferase I and II, respectively; T, carnitine:acylcarnitine translocase.

β-Oxidation in Mitochondria

Fatty acyl-CoAs in the mitochondrial matrix are substrates of β-oxidation. This cyclic process consists of four reactions that shorten the acyl chain of fatty acyl-CoA by two carbon atoms at a time and produce acetyl-CoA. As shown in Figure 2, reaction 1a, β-oxidation begins with the removal of two hydrogens from carbon atoms 2 (α-carbon) and 3 (β-carbon) of acyl-CoA to form the corresponding 2-*trans*-enoyl-CoA. The hydrogens are initially accepted by the flavine adenine dinucleotide (FAD) cofactor of acyl-CoA dehydrogenase, the enzyme that catalyzes this reaction, then are transferred to the FAD of a soluble matrix enzyme named electron transferring flavoprotein and finally are fed into the mitochondrial electron transport chain, which supplies the energy for ATP formation by oxidative phosphorylation. In the second β-oxidation reaction, water is added across the double bond of 2-*trans*-enoyl-CoA by enoyl-CoA hydratase to yield L-3-hydroxyacyl-CoA (see Figure 2, reaction 2). The third reaction is the NAD^+-dependent dehydrogenation of L-3-hydroxyacyl-CoA catalyzed by L-3-hydroxyacyl-CoA dehydrogenase (see Figure 2, reaction 3). The product of this reaction, 3-ketoacyl-CoA, is the substrate of the fourth and last reaction of β-oxidation catalyzed by 3-ketoacyl-CoA thiolase, which cleaves the compound in the presence of CoA between carbons 2 and 3 to yield an acyl-CoA shortened by two carbon atoms and acetyl-CoA (see Figure 2, reaction 4). Repetitive cycles of β-oxidation result in the complete degradation of fatty acids to acetyl-CoA and also propionyl-CoA, if fatty acids with an odd-numbered number of carbon atoms are involved.

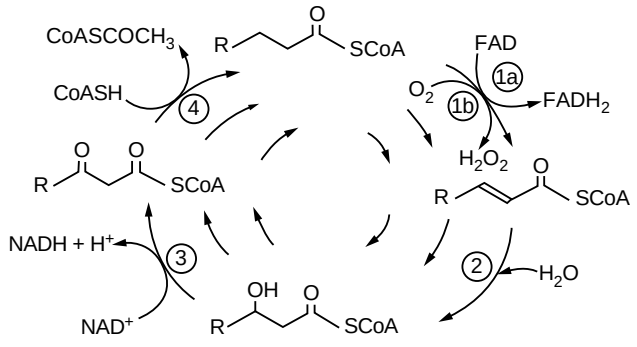

FIGURE 2 β-Oxidation of fatty acyl-CoA. Reactions 1a, 1b, 2, 3, and 4 are catalyzed by acyl-CoA dehydrogenase, acyl-CoA oxidase, enoyl-CoA hydratase, 3-hydroxyacyl-CoA dehydrogenase, and 3-ketoacyl-CoA thiolase, respectively. Abbreviations: FAD, oxidized form of flavine adenine dinucleotide; $FADH_2$, reduced form of flavine adenine dinucleotide.

Two or more enzymes with different acyl chain length specificities participate in each of the four reactions. Four acyl-CoA dehydrogenases are required for the β-oxidation of fatty acids. Their names, very long-chain acyl-CoA dehydrogenase, long-chain acyl-CoA dehydrogenase, medium-chain acyl-CoA dehydrogenase, and short-chain acyl-CoA dehydrogenase reflect their preferences for substrates of different acyl chain lengths.

Together they efficiently dehydrogenate all acyl-CoAs that are formed during the β-oxidation of most dietary fatty acids. Two enzymes, one with a preference for short-chain and medium-chain substrates and another most active with long-chain substrates, cooperate in each of the three other reactions to metabolize a range of β-oxidation intermediates of different acyl chain lengths.

β-Oxidation of Unsaturated Fatty Acids

Unsaturated and polyunsaturated fatty acids also are degraded by β-oxidation. However, additional reactions are required to metabolize pre-existing double bonds that would otherwise interfere with the complete β-oxidation of unsaturated fatty acids. All double bonds found in unsaturated fatty acids can be classified as either odd- or even-numbered double bonds. Both classes are present in linoleic acid, which contains an odd-numbered double bond at position 9 and an even-numbered double bond at position 12 (see Figure 3).

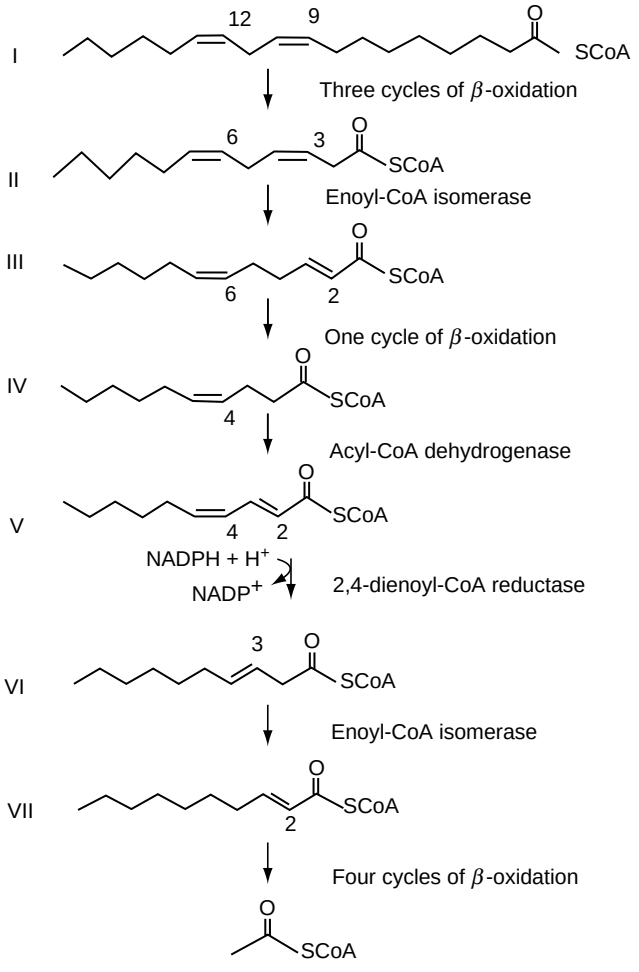

FIGURE 3 Pathway for the β-oxidation of linoleoyl-CoA.

The degradation of linoleic acid therefore illustrates the β-oxidation of all unsaturated fatty acids. As outlined in Figure 3, linoleoyl-CoA (I; all Roman numerals refer to compounds shown in Figure 3), after passing three times through the β-oxidation cycle, yields 3-*cis*,6-*cis*-dodecadienoyl-CoA (II). This metabolite cannot enter another cycle of β-oxidation due to interference by the double bond at position 3. However, an additional (auxiliary) enzyme, Δ^3,Δ^2-enoyl-CoA isomerase (enoyl-CoA isomerase), converts 3-*cis*,6-*cis*-dodecadienoyl-CoA (II) to 2-*trans*,6-*cis*-dodecadienoyl-CoA (III) that can complete its pass through one cycle of β-oxidation to yield 4-*cis*-decenoyl-CoA (IV). 4-*cis*-Decenoyl-CoA is dehydrogenated by acyl-CoA dehydrogenase to 2-*trans*,4-*cis*-decadienoyl-CoA (V), which is not a substrate of β-oxidation but which is reduced by NADPH in the presence of 2,4-dienoyl-CoA reductase, the second auxiliary enzyme, to 3-*trans*-decenoyl-CoA (VI). The latter compound is converted by enoyl-CoA isomerase to 2-*trans*-decenoyl-CoA (VII) that can be completely degraded by β-oxidation. A third auxiliary enzyme, $\Delta^{3,5}$,$\Delta^{2,4}$-dienoyl-CoA isomerase (dienoyl-CoA isomerase), catalyzes the isomerization of 3,5-dienoyl-CoA to 2,4-dienoyl-CoA. This reaction facilitates the complete β-oxidation of 3,5-dienoyl-CoAs that are minor metabolites of unsaturated fatty acids with odd-numbered double bonds.

Regulation of Mitochondrial Fatty Acid Oxidation

The rate of fatty acid oxidation changes in response to the nutritional and hormonal state of the animal. The rate of fatty acid oxidation is high during fasting but low in the fed animal. One cause for this change is the higher concentration of unesterified (free) fatty acids in the circulation of the fasting animal as compared to the concentration in the fed animal. An increased concentration of free fatty acids results in higher rates of cellular uptake and oxidation of fatty acids. In liver, which has high capacities for both synthesizing and oxidizing fatty acids, a reciprocal relationship exists between these two processes. After feeding, when carbohydrates are converted to triacylglycerols, the rate of fatty acid synthesis is high because acetyl-CoA carboxylase is active. This enzyme catalyzes the carboxylation of acetyl-CoA to malonyl-CoA, the first committed intermediate in fatty acid synthesis. Malonyl-CoA binds to and effectively inhibits CPT I that initiates the uptake of fatty acids by mitochondria. Thus, when fatty acids are rapidly synthesized, the cytosolic concentration of malonyl-CoA is high and the mitochondrial uptake and oxidation of fatty acids are inhibited. This situation is reversed during fasting when lower blood glucose levels cause the plasma

concentration of the hormone glucagon to increase and that of insulin to decrease. Glucagon promotes the phosphorylation and inactivation of acetyl-CoA carboxylase with the result that the cytosolic concentration of malonyl-CoA declines. The lower concentration of malonyl-CoA causes fatty acid synthesis to decrease and fatty acid oxidation to increase. The same regulatory mechanism may be effective in tissues like heart and skeletal muscle that oxidize fatty acids but do not synthesize them. Although malonyl-CoA is generated in these tissues by acetyl-CoA carboxylase, it seems to be metabolized by decarboxylation catalyzed by malonyl-CoA decarboxylase.

Fatty Acid Oxidation in Peroxisomes

Peroxisomes of animal cells contain a β-oxidation system that partially degrades fatty acids in contrast to mitochondria that break down fatty acids completely. The enzymes of peroxisomal and mitochondrial β-oxidation are not the same. Different genes encode most of the peroxisomal and mitochondrial enzymes. Substrates of peroxisomal β-oxidation are the CoA derivatives of fatty acids and carboxylic acids that are poorly or not at all taken up by mitochondria as, for example very long-chain fatty acids, methyl-branched carboxylic acids like pristanic acid, prostaglandins, dicarboxylic acids, xenobiotic compounds like phenyl fatty acids, and hydroxylated cholestanoic acids that are precursors of cholic acid. However, peroxisomes of lower eukaryotes catalyze the complete β-oxidation of fatty acids, whereas mitochondria in the same organisms generally are devoid of a functional β-oxidation system.

The uptake and activation of fatty acids by peroxisomes remain poorly understood. While some fatty acids like very long-chain fatty acids may be activated by conversion to CoA esters in the peroxisomal matrix after directly entering animal peroxisomes, other fatty acids or carboxylic acids seem to be activated outside of peroxisomes. The uptake of fatty acyl-CoAs by peroxisomes is suspected to take place but has not been demonstrated. Carnitine does not seem to be required for this uptake.

The four reactions of β-oxidation in peroxisomes are similar to the corresponding mitochondrial reactions (see Figure 2). An exception is the first reaction, in which fatty acyl-CoA is dehydrogenated to 2-*trans*-enoyl-CoA by acyl-CoA oxidase while oxygen is reduced to H_2O_2 (see Figure 2, reaction 1b). The latter product is converted to H_2O and O_2 by catalase that is present in peroxisomes. At least two acyl-CoA oxidases exist in animal peroxisomes; one named palmitoyl-CoA oxidase is active with long-chain and medium-chain, but not short-chain acyl-CoAs that have straight acyl chains while the second acyl-CoA oxidase also acts on branched-chain acyl-CoAs. Since the acyl-CoA oxidase activity of lower eukaryotes extends over the whole spectrum of acyl-CoAs of various chain lengths, peroxisomes in these organisms, in contrast to those in animals, can degrade fatty acids completely. The second and third reactions of peroxisomal β-oxidation are catalyzed by enoyl-CoA hydratase and 3-hydroxyacyl-CoA dehydrogenase, respectively, that are associated with a same polypeptide. Two such multifuntional enzymes, MFE 1 and MFE 2, are present in animal peroxisomes. They differ from each other in that the 3-hydroxyacyl-CoA intermediate formed and acted upon by MFE 1 has the L configuration, whereas the intermediate of MFE 2 is the D isomer. Peroxisomes of yeast and fungi only contain the type 2 multifunctional enzymes. Two types of 3-ketoacyl-CoA thiolases are present in rat peroxisomes. One of these thiolases, referred to as SCP_x-thiolase, is unusual because it is part of a bifunctional protein that additionally contains a lipid-binding segment named sterol carrier protein (SCP). Studies with β-oxidation mutants have led to the conclusion that the partial β-oxidation of straight-chain fatty acyl-CoAs, like very long-chain fatty acyl-CoAs, in animal peroxisomes requires palmitoyl-CoA oxidase, MFE 2, and 3-ketoacyl-CoA thiolase, whereas the partial degradation of branched-chain acyl-CoAs, like pristanoyl-CoA, involves branched-chain acyl-CoA oxidase, MFE 2, and SCP_x-thiolase. Unsaturated and polyunsaturated fatty acids also are partially degraded in peroxisomes. The necessary additional enzymes, enoyl-CoA isomerase, 2,4-dienoyl-CoA reductase, and even dienoyl-CoA isomerase, are present in this organelle. The products of peroxisomal β-oxidation are chain-shortened acyl-CoAs, NADH, and acetyl-CoA. Additionally propionyl-CoA is formed when methyl-branched-chain substrates are degraded. Acyl-CoAs may be converted to the corresponding acylcarnitines before they exit from peroxisomes. The necessary carnitine acyltransferases active with medium-chain and short-chain acyl-CoAs have been identified in peroxisomes. However, little is known about transporters that facilitate the efflux of products from peroxisomes.

α-Oxidation and ω-Oxidation

α-Oxidation is the process that results in the oxidative removal of the first carbon atom, the carboxyl group, of a fatty acid or carboxylic acid to yield CO_2 and a fatty acid or carboxylic acid shortened by one carbon atom. In animals, this process occurs in peroxisomes where, for example phytanic acid, which is derived from phytol of chlorophyll and which cannot be degraded by β-oxidation, is chain-shortened by one carbon atom to

pristanic acid that can be degraded by β-oxidation. ω-Oxidation is the process by which fatty acids are oxidized at their terminal (ω) or penultimate (ω-1) carbon atom to form dicarboxylic acids. This process occurs at the endoplasmic reticulum and requires molecular oxygen. When β-oxidation of fatty acids is impaired, more fatty acids are converted to dicarboxylic acids by ω-oxidation.

See Also the Following Articles

Anaplerosis • Carnitine and β-Oxidation • Cholesterol Synthesis • Fatty Acid Synthesis and its Regulation • Gluconeogenesis • Insulin- and Glucagon-Secreting Cells of the Pancreas • Ketogenesis • Lipases • Lipid Modification of Proteins: Targeting to Membranes • Lipoproteins, HDL/LDL • Peroxisomes • Protein Palmitoylation

Glossary

activation of fatty acids The conversion of fatty acids to thioesters with coenzyme A.

β-oxidation Degradation of fatty acyl coenzyme A thioesters by the sequential removal of two carbon atoms at a time in the form of acetyl coenzyme A.

peroxisome Subcellular organelle that is enclosed by a single membrane.

unsaturated fatty acids Fatty acids that contain one or more double bonds.

Further Reading

Eaton, S. (2002). Control of mitochondrial β-oxidation flux. *Prog. Lipid Res.* **41**, 197–239.

Kunau, W.-H., Dommes, V., and Schulz, H. (1995). Beta oxidation of fatty acids in mitochondria, peroxisomes, and bacteria. *Prog. Lipid Res.* **34**, 267–341.

McGarry, J. D. (2001). Travels with carnitine palmitoyltransferase: I. From liver to germ cell with stops in between. *Biochem. Soc. Trans.* **29**, 241–245.

Ruderman, N. B., Saha, A. K., Vavas, D., and Witters, L. A. (1999). Malonyl-CoA, fuel sensing, and insulin resistance. *Am. J. Physiol.* **276**, E1–E18.

Schulz, H., and Kunau, W.-H. (1987). Beta-oxidation of unsaturated fatty acids: A revised pathway. *Trends Biochem. Sci.* **12**, 403–406.

Van Veldhoven, P. P., Casteels, M., Mannaerts, G. P., and Baes, M. (2001). Further insight into peroxisomal lipid breakdown via α- and β-oxidation. *Biochem. Soc. Trans.* **29**, 292–298.

Wanders, R. J. A., Vreken, P., Ferdinandusse, S., Jansen, G. A., Waterham, H. R., van Roermund, C. W. T., and van Grunsven, E. G. (2001). Peroxisomal fatty acid α- and β-oxidation in humans: Enzymology, peroxisomal metabolite transporters, and peroxisomal diseases. *Biochem. Soc. Trans.* **29**, 250–267.

Watkins, P. A. (1997). Fatty acid activation. *Prog. Lipid Res.* **36**, 55–83.

Biography

Horst Schulz is a Professor in the Department of Chemistry at City College of the City University of New York. His main research interest is the β-oxidation of saturated and unsaturated fatty acids with an emphasis on fatty acid oxidation in mitochondria. He received a Ph.D. from the Technische Universität Berlin in Germany and carried out research as a postdoctoral fellow at Cornell University Medical College and Duke University Medical Center.

Fatty Acid Receptors

Christer Owman and Björn Olde
Lund University, Lund, Sweden

Lipids provide energy to the organism and contribute to various cellular components, including organelles and plasma membranes. A particular class of lipids are unesterified and are usually known as free fatty acids. Although dietary fatty acids have a major role as nutrients in various types of metabolic functions, some of them also exert more specialized functions as signaling molecules when they act as messengers between cells and within tissues.

It became evident in the early 1990s that such functions were mediated via a family of transcription factors called peroxisomal proliferator-activated receptors (PPARs). This class of nuclear receptors plays a central role in regulating the storage and degradation of dietary lipids. However, not all biological effects of free fatty acids can be explained by nuclear receptor signaling, but rather show the characteristics of a cell surface receptor involvement. Indeed, a decade after the discovery of the PPARs, a group of free-fatty acid-activated receptors (FFARs), expressed on the cell surface, could be identified. They all belong to the superfamily of G protein-coupled receptors (GPCRs), which is the most widely distributed class of receptors on eukaryotic cells.

The two classes of fatty acid-activated receptors appear to have an overlapping, but not identical, function. It should now be possible to unfold many hitherto unexplained observations on the actions of free fatty acids in both normal and pathophysiological situations.

The PPAR Family of Receptors

The PPARs (Figure 1) constitute a family of three nuclear receptor isoforms named PPARα, PPARδ (sometimes called PPARβ), and PPARγ. They function as transcription factors in response to specific ligands and thereby control gene expression by binding to various response elements within gene promoters. The receptors always bind as heterodimers together with the so-called retinoid X receptor. Like the PPARs, the retinoid X receptor exists in three isoforms which are all activated by the naturally occurring 9-*cis* retinoic acid. After binding of the ligand to the receptor dimers, these interact with cofactors, resulting in increased rate of transcription initiation. All three receptor subtypes are localized in different chromosomes. The PPAR receptors have a physiological role as regulators in the metabolism of dietary lipids. Free fatty acids with long carbon chains, and particularly polyunsaturated fatty acids, constitute the major natural ligands for PPARs. The nuclear receptor family also includes receptors for steroid, thyroid, and retinoid hormones.

PPARα

The receptor PPARα is expressed in many metabolically active tissues, including heart, skeletal muscle, kidney, liver, as well as brown fat. In addition, it has a vascular localization, both in endothelium and smooth muscle cells, and is also present in monocytes (Figure 1). Accordingly, PPARα has been found to effectively improve cardiovascular risk factors, and it also enhances cardiovascular performance. It exerts a critical function in the regulation of the cellular uptake, activation, and β-oxidation of fatty acids; the receptor directly up-regulates enzymes in the peroxisomal β-oxidation pathway. PPARα was also suggested to be involved in immunmodulatory functions when it was found that leukotriene B_4 could specifically activate the receptor.

PPARδ

This receptor subtype (Figure 1) was first cloned as PPARβ in frog, but the generally agreed name for the receptor is now PPARδ. It has a ubiquitous localization in the body (often at lower expression levels than PPARα and γ), with a particularly high expression in brain, adipose tissue, and in skin. It is likely that PPARδ is involved in lipid homeostasis since, like the other two isoforms, it is activated by fatty acids and fatty acid metabolites. The ligand-binding profile is intermediate between PPARα and PPARγ. PPARδ has been suggested to be involved in the differentiation of cells within the central nervous system, and it may also have a role in myelinization and lipid metabolism in brain. The receptor has been reported to have importance for wound healing as well as in female fertility.

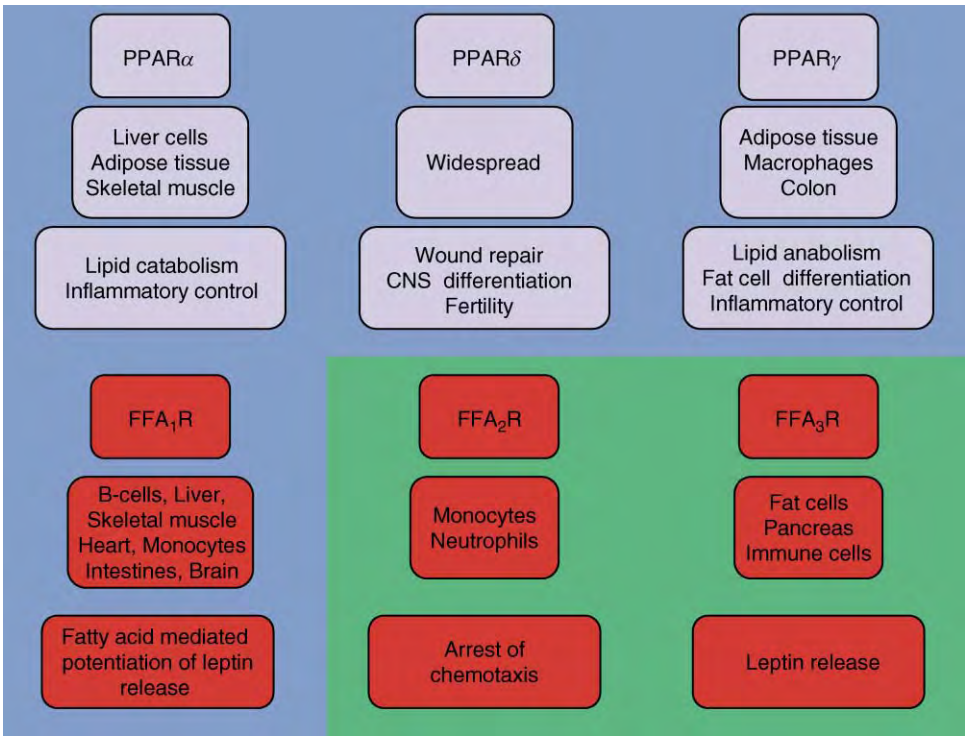

FIGURE 1 Panel summarizing the expression patterns (upper boxes) and the functional characteristics (lower boxes) of the two fatty acid receptor families, the PPARs and the FFARs. The blue background shading indicates the four receptors that are activated by medium- to long-chain free fatty acids, whereas the green background points out the two receptors that are activated by short-chain free fatty acids.

PPARγ

PPARγ is the most extensively studied of the three receptor subtypes. It shows, in contrast to the two other receptors, a considerable degree of conservation – some 95% identity at the protein level – among the various species from which is has been cloned. Three receptor isoforms, numbered 1–3, have been reported to arise from different promoter utilization. While PPARγ1 is expressed in a wide range of tissues, PPARγ2 is found predominantly in adipose tissue, whereas PPARγ3 is expressed only in adipose tissue, macrophages, and colon epithelium (Figure 1). PPARγ is a critical transcription factor in the regulation of adipocyte differentiation, and it also exerts an important function in insulin sensitization, atherosclerosis, and cancer. Activation of the receptor induces differentiation of cells into adipocytes, and it promotes the transcription of numerous important lipogenic proteins. It appears that PPARα and γ exert opposite but complementary functions in fat energy homeostasis; the former having a catabolic function whereas the latter is involved in lipid anabolism and energy storage.

It is evident from the above descriptions that the PPAR receptor family should play important roles in various types of life-style diseases. Actually, much of the focus on PPARγ is related to fatty acids being risk factors in type 2 diabetes, and to the fact that modern anti-diabetic substances of the thiazolidinedione class may use this receptor as a target, although other pathways for thiazolidinedione actions seem to exist. The compounds, also known as glitazones, exert their beneficial effect by enhancing the sensitivity of target tissues to insulin and by reducing the plasma levels of fatty acids, glucose, and insulin.

The FFAR Family of Receptors

In contrast to the nuclear PPAR receptors, the FFAR family consists of receptors that are localized to the plasma membrane of cells. Here, the receptor protein anchors as a serpentine with seven membrane-spanning helical segments, a typical feature of the superfamily of GPCRs. Based on this general structure they are also known as 7TM (for transmembrane) or heptahelix receptors. The three separate genes encoding the receptors of this family are present in a cluster on chromosome 19. As illustrated in Figure 1, the PPARs are activated only by free fatty acids having a carbon chain length above twelve, while the ligand spectrum for the FFARs include chain lengths down to one (formiate). The receptors are well conserved both in mammals and fish.

FFA_1R

This receptor was originally presented as an orphan receptor (i.e., without known ligand/function) with the provisional designation GPR40. Its identity and function was reported independently by three groups early in the year 2003. The encoded human receptor protein consists of 300 amino acid residues. FFA_1R is characteristically activated by medium-length (down to 10 carbons) to long-chain free fatty acids. Besides the effect of the natural ligands, a very intriguing observation was that also the anti-diabetic thiazolidinedione compound, rosiglitazone, activated the receptor.

According to the current understanding this novel receptor is primarily expressed in the insulin-producing pancreatic islets. It has also been reported to be present in liver, skeletal muscle, heart, intestines, monocytes, as well as in brain. FFA_1R has been tied to the so-called fatty acid potentiation of glucose-stimulated insulin secretion (GSIS) by pancreatic β-cells. In fact, fatty acids, like linoleic acid and γ-linoleic acid, have been shown to stimulate insulin release in mouse insulinoma cells through FFA_1R.

The identification of FFA_1R, having a ligand spectrum that is overlapping that of PPARγ (Figure 1), offers a new type of nutrient sensor in lipid homeostasis. It may provide a basis for understanding hitherto unexplained mechanisms involved in insulin release as well as in thiazolidinedione functions related to various therapeutic areas.

FFA_2R

The second FFAR, FFA_2R (previously known as GPR43), has the same general structure as FFA_1R and consists of 330 amino acid residues. In contrast to the latter, it is activated by short-chain (C1–C6) fatty acids, acetate (C2) being the most effective. It has a different expression pattern (Figure 1) in that it is found mainly in polymorphonuclear leukocytes, predominantly in monocytes and neutrophils.

Activation of FFA_2R expressed on immune cells causes pertussis toxin sensitive calcium mobilization and also leads to arrest of cellular chemotaxis. It is likely that this response is part of an immunmodulatory mechanism within the alimentary tract whereby short-chain fatty acids, known to be produced by the enteric bacteria, control the invasion of immune cells.

FFA_3R

The receptor, FFA_3R, was previously known as GPR41 and is structurally more closely related to FFA_2R than to FFA_1R. It forms a seven membrane-spanning protein comprising 346 amino acid residues. (A fourth annotated receptor, designated GPR42, has 98% deduced amino acid homology with GPR41; the corresponding gene is probably a pseudogene.) As depicted in Figure 1, the fatty acid ligand spectrum for FFA_3R is similar to that of FFA_2R, although butyrate (C4) and pentanoate (C5) are the most potent agonists for FFA_3R. The elicited response (as in the case of FFA_2R) is clearly pertussis toxin-sensitive. FFA_3R is predominantly expressed in adipose tissue, although expression has been reported also in pancreas and immune cells, as well as in placenta. FFA_3R has recently been shown to control leptin production in adipocytes.

See Also the Following Articles

Adenylyl Cyclases • Fatty Acid Receptors • Fatty Acid Synthesis and its Regulation • Peroxisome Proliferator-Activated Receptors • Peroxisomes

Glossary

G protein Abbreviated term for "GTP (guanosine triphosphate)-binding regulatory protein," which, upon membrane receptor activation, serves as an intermediary protein between the receptor and a cell membrane-bound enzyme or ion channnel.

peroxisome Membrane-surrounded cell organelle where, e.g., hydrogen peroxide is generated and degraded.

promoter Specific DNA sequence containing the start site for RNA synthesis.

pseudogene Nonfunctional gene closely related to functional genes.

transcription factor Controls gene transcription and is one of several sequence-specific DNA-binding regulatory proteins.

Further Reading

Berger, J., and Moller, D. E. (2002). The mechanisms of action of PPARs. *Ann. Rev. Med.* **53**, 409–435.

Brown, A. J., Goldsworthy, S. M., Barnes, A. A., Eilert, M. M., Tcheang, L., Daniels, D., Muir, A. I., Wigglesworth, M. J., Kinghorn, I., Fraser, N. J., Pike, N. B., Strum, J. C., Steplewski, K. M., Murdock, P. R., Holder, J. C., Marshall, F. H., Szekeres, P. G., Wilson, S., Ignar, D. M., Foord, S. M., Wise, A., and Dowell, S. J. (2003). The orphan G protein-coupled receptors GPR41 and GPR43 are activated by propionate and other short chain carboxylic acids. *J. Biol. Chem.* **278**, 11312–11319.

Nilsson, N. E., Kotarsky, K., Owman, C., and Olde, B. (2003). Identification of a free fatty acid receptor, FFA_2R, expressed on leukocytes and activated by short-chain fatty acids. *Biochem. Biophys. Res. Commun.* **303**, 1047–1052.

Poitout, V. (2003). The ins and outs of fatty acids on the pancreatic β cells. *Trends Endocrinol. Metab.* **14**, 201–203.

Rutter, G. A. (2003). Insulin secretion: Fatty acid signalling via serpentine receptors. *Curr. Biol.* **13**, R403–R405.

Sawzdargo, M., George, S. R., Nguyen, T., Shijie, X., Kolakowski, L. F. Jr., and O'Dowd, B. F. (1997). A cluster of four novel human G protein-coupled receptor genes occurring in close proximity to CD22 gene on chromosome 19q13.1. *Biochem. Biophys. Res. Commun.* **239**, 543–547.

Wahli, W. (2002). Peroxisome proliferator-activated receptors (PPARs): From metabolic control to epidermal wound healing. *Swiss Med. Wkly* **132**, 83–91.

Willson, T. M., Brown, P. J., Sternbach, D. D., and Henke, B. R. (2000). The PPARs: From orphan receptors to drug discovery. *J. Med. Chem.* **43**, 527–550.

Xiong, Y., Miyamoto, N., Shibata, K., Valasek, M. A., Motoike, T., Kedzierski, R. M., and Yanagisawa, M. (2004). Short-chain fatty acids stimulate leptin production in adipocytes through the G protein-coupled receptor GPR41. *Proc. Natl Acad. Sci. USA* **101**, 1045–1050.

Biography

Christer Owman is M.D. and Ph.D. (Lund University, Sweden) and Professor and Chair of the Division of Molecular Neurobiology, Department of Physiological Sciences, Wallenberg Neuroscience Center at the same University. He has published extensive work on autonomic neuro-receptor mechanisms. His present research interest is in molecular aspects of GPCRs, and he has discovered several previously unknown GPCRs. He is scientific founder of the small biotech company, HeptaHelix AB. He has served two terms as Dean of the Medical Faculty, Lund University.

Björn Olde is a Ph.D. from Lund University and is an associate professor there. He spent most of an extensive postdoctoral period with Dr. Craig Venter. His principal interest is in basic research and drug development focusing on GPCRs. He has developed uniquely sensitive cell-based reporter systems successfully applied to "deorphanize" several hitherto unknown GPCRs, followed by their further functional characterization.

Fatty Acid Synthesis and its Regulation

Steven D. Clarke
McNeil Nutritionals, New Brunswick, New Jersey, USA

Manabu T. Nakamura
University of Illinois at Urbana-Champaign, Illinois, USA

Fatty acid synthesis involves the *de novo* assembly of acetate into saturated fatty acids as well as the desaturation and elongation of the dietary essential fatty acids linoleic acid (C18:2$_{n-6}$) and α-linolenic acid (C18:3$_{n-3}$) to highly unsaturated 20- and 22-carbon fatty acids essential to reproduction, cell differentiation, inflammation, and cognition. Short-chain fatty acids are derived largely from bacterial fermentation such as that which occurs in the gut or rumen. Medium-chain fatty acids are characteristic of milk fat and are absorbed from the intestine directly into the portal blood, and subsequently metabolized largely by the liver. Fatty acids containing 14 or more carbons are absorbed from the intestine and transported to the periphery as chylomicrons. Very long chain fatty acids are largely found in neural tissue and used for myelin formation. Net fatty acid synthesis by humans is relatively small, but the *de novo* fatty acid biosynthetic pathway is essential for the production of malonyl-CoA, a metabolite inhibitor of carnitine palmitoyltransferase. Consequently, substrate flux through the *de novo* lipogenic pathway plays a key role in determining if a fatty acid is partitioned to fatty acid oxidation or triglyceride assimilation.

De novo Fatty Acid Biosynthesis of Saturated Fatty Acids

Saturated fatty acids are categorized as short (C2–C6), medium (C8–C12), long (C14–C18), and very long (C20–C24) fatty acids. Short-chain fatty acids are derived largely from bacterial fermentation such as that which occurs in the gut or rumen. Medium-chain fatty acids are characteristic of milk fat and are absorbed from the intestine directly into the portal blood, and subsequently metabolized largely by the liver. Fatty acids containing 14 or more carbons are absorbed from the intestine and transported to the periphery as chylomicrons. Very long chain fatty acids are largely found in neural tissue and used for myelin formation. The liver and adipose tissue of humans are the primary sites of conversion of excess carbohydrate to fatty acids, but fatty acid synthesis is more than just for conserving excess glucose as fat. Fatty acid synthesis is essential for cell membrane production, lung surfactant function, milk fat production, brain myelination, and fat storage. Consequently, nearly all tissues have the capacity to synthesize fatty acids.

De novo fatty acid biosynthesis in humans occurs in cytosol. Two enzymes, acetyl CoA carboxylase and fatty acid synthase, are required for this process. The first and rate-limiting step is the conversion of acetyl CoA to malonyl CoA by acetyl CoA carboxylase:

$$\begin{aligned} &CH_3CO-S-CoA + HCO_3^- + ATP \\ &\quad \rightarrow {}^-OOC-CH_2CO-S-CoA + H_2O + ADP + Pi \end{aligned}$$

Fatty acid synthase catalyzes all of the subsequent steps for the synthesis of long-chain saturated fatty acids. Fatty acid synthase is made of a single peptide chain that possesses seven distinct catalytic domains. Fatty acid synthase first adds two carbons to acetyl CoA using malonyl CoA. NADPH is used as a reducing power in this reaction:

$$\begin{aligned} &CH_3CO-S-CoA + {}^-OOC-CH_2CO-S-CoA \\ &\quad + Enzyme-SH + 2NADPH + 2H^+ \\ &\quad\quad \rightarrow CH_3CH_2CH_2CO-S-Enzyme + 2CoA-SH \\ &\quad\quad\quad + HCO_3^- + 2NADP^+ \end{aligned}$$

Fatty acid synthase repeats this acyl chain elongation two carbons at a time using malonyl CoA as a substrate:

$$\begin{aligned} &CH_3CH_2CH_2CO-S-Enzyme \\ &\quad + {}^-OOC-CH_2CO-S-CoA + 2NADPH + 2H^+ \\ &\quad\quad \rightarrow CH_3(CH_2)_3CH_2CO-S-Enzyme \\ &\quad\quad\quad + CoA-SH + HCO_3^- + 2NADP^+ \end{aligned}$$

When the carbon chain reaches 16, the thioesterase domain of fatty acid synthase releases free palmitate,

completing fatty acid biosynthesis.

$$CH_3(CH_2)_{14}CO-S-Enzyme + H_2O \rightarrow CH_3(CH_2)_{14}COO^- + H^+ + HS-Enzyme$$

Regulation of Pyruvate Entry into Mitochondria

Malonyl-CoA is the substrate used by fatty acid synthase to assemble the acetate units into fatty acids. Malonyl-CoA is produced from pyruvate through a series of reactions. The first step involves the mitochondrial formation of acetyl-CoA by pyruvate dehydrogenase's decarboxylation of pyruvate. This is followed by the intramitochondrial synthesis of citrate from acetyl-CoA and oxaloacetate. Citrate is transported from the mitochondria to the cytosol where it is cleaved by citrate lyase to cytosolic acetyl-CoA and oxaloacetate. The acetyl-CoA is available for carboxylation to malonyl-CoA by the biotin-containing enzyme acetyl-CoA carboxylase. The liver and adipose tissue of humans are the primary sites of conversion of excess carbohydrate to fatty acids. The source of hepatic or adipose pyruvate for fatty acid biosynthesis may be derived from the metabolism of glucose via the glycolytic pathway with the liver or adipocyte itself, or it may be provided to the liver and/or adipose tissues as lactate or alanine that is produced by glucose metabolism in peripheral tissues such as the small intestine and muscle. Entry of pyruvate into the tricarboxylic acid pathway of the mitochondria is determined by the activity of pyruvate dehydrogenase. The concentration of pyruvate dehydrogenase does not widely fluctuate, but its catalytic activity is suppressed by phosphorylation and enhanced by dephosphorylation of the enzyme. Insulin and glucose stimulate dephosphorylation, whereas glucagon and fatty acids enhance the phosphorylation. Thus, pyruvate entry into the mitochondria is highly dependent upon the macronutrient composition of the diet, and the ratio of insulin to glucagon.

Regulation of Malonyl-CoA Synthesis

The synthesis of malonyl-CoA is catalyzed by the biotin-containing enzyme acetyl-CoA carboxylase. Acetyl-CoA carboxylase exists as two isoforms: a liver or type I, and muscle or type II. Like pyruvate dehydrogenase, the catalytic activity, and hence the production of malonyl-CoA, of both acetyl-CoA carboxylase isoforms is regulated by phosphorylation and dephosphorylation of the protein. Acetyl-CoA carboxylase I and II are substrates for AMP kinase and cyclic AMP kinase. AMP kinase activity is enhanced by leptin and adiponectin, two hormones that stimulate fatty acid oxidation and inhibit fatty acid biosynthesis. The dephosphorylation of acetyl-CoA carboxylase is carried out by phosphatase 1 and 2, and phosphatase activity appears to be stimulated under conditions where glucose flux through glycolysis is high. Muscle acetyl-CoA carboxylase is not adaptive, but hepatic acetyl-CoA carboxylase, like other lipogenic enzymes, increases and decreases its concentration depending upon nutritional conditions, dietary composition, and hormonal milieu. For example, the hepatic abundance of acetyl-CoA carboxylase is low during fasting and diabetes, but is greatly induced by refeeding glucose or administering insulin.

Malonyl-CoA and Fatty Acid Metabolism

Malonyl-CoA is not only the substrate for fatty acid synthase, but it is a key determinant for the entry of fatty acids into the mitochondria, and appears to play a pivotal signaling role in appetite regulation. Malonyl-CoA is an inhibitor of carnitine palmitoyltransferase. Thus, high levels of malonyl-CoA suppress fatty acid entry into the mitochondria and this in turn leads to increased flux of fatty acids to triglycerides. On the other hand, conditions that lead to low cellular concentrations of malonyl-CoA favor fatty acid oxidation because the inhibition of carnitine palmitoyltransferase is released. Consequently, even though net fatty acid synthesis by humans may be relatively small, the fatty acid biosynthetic pathway plays an instrumental role in determining whether a fatty acid is stored as triglyceride or undergoes oxidation. Since excessive cellular triglyceride production and accumulation is causatively linked to the development of insulin resistance and type 2 diabetes, factors regulating the fatty acid biosynthetic pathway will exert a direct influence on the development of diabetes.

Nutritional Regulation of Lipogenic Gene Expression

Hepatic and adipose fatty acid biosynthesis is increased by the ingestion of a high-carbohydrate diet and decreased by the consumption of a high-fat diet. Dietary regulation of lipogenesis is not simply a product of nutritional manipulation of hormonal balance. Rather, nutrients exert a specific influence on the expression of glycolytic and lipogenic proteins. Nutrients exercise their influence by modulating gene transcription, mRNA processing, mRNA decay, and by stimulating posttranslational protein modifications.

Carbohydrate Induction of Lipogenic Gene Transcription

Since the early 1990s, a collection of transcription factors that are specifically targeted by glucose and fatty acids have been identified. Dietary carbohydrate induces lipogenic gene transcription in two ways. First, glucose increases the nuclear concentration of the potent lipogenic transcription factor, SREBP-1. SREBPs are a family of transcription factors that were first isolated as a result of their properties for binding to the sterol regulatory element of genes encoding proteins of sterol metabolism. SREBP-2 is a regulator of genes encoding proteins of cholesterol metabolism. SREBP-1 exists in two forms, 1a and 1c. SREBP-1a is the dominant form in cell lines and is a regulator of genes encoding proteins involved in fatty acid biosynthesis as well as cholesterolgenesis. SREBP-1c constitutes 90% of the SREBP-1 found *in vivo* and is a determinant of lipogenic gene transcription. SREBP-1 is synthesized as a 125 kDa precursor protein that is anchored in the endoplasmic reticulum membrane. Proteolytic release of the 68 kDa mature SREBP-1 occurs in the Golgi system, and movement of SREBP-1 from the endoplasmic reticulum to the Golgi requires the trafficking protein SREBP cleavage-activating protein. Once released, mature SREBP-1 translocates to the nucleus and binds to the classic sterol response element and/or to a palindrome CATG sequence. Glucose increases the abundance of precursor SREBP-1 by inducing SREBP-1 gene transcription. In addition, glucose elevates the nuclear concentration of SREBP-1 by stimulating the proteolytic release of mature SREBP-1 from its membrane-anchored precursor. A second effect of glucose is to stimulate the DNA binding activity of select transcription factors involved with the transcription of lipogenic genes, notably a unique carbohydrate response factor (CHORF). Glucose exerts its effect by elevating the cellular concentration of the pentose shunt metabolite xylulose-5-phosphate. Xylulose-5-phosphate is a positive metabolite effecter of phosphatase 2A, and increased phosphatase activity leads to the dephosphorylation of CHORF and a subsequent increase in its DNA binding to a specific carbohydrate response element (CHORE) in select glycolytic (e.g., pyruvate kinase) and lipogenic (e.g., fatty acid synthase) genes. The consequence is an increase in gene transcription followed by a rise in the abundance of glycolytic and lipogenic enzymes.

Suppression of Lipogenic Gene Expression by omega-6 and -3 Fatty Acids

Glucose stimulation of lipogenesis is a nice example of a feedforward regulatory mechanism that functions to enhance glucose storage as fatty acids. Interestingly the saturated fatty acid products of the *de novo* fatty acid synthetic pathway do not feedback and suppress glycolytic and lipogenic gene expression or activity. Only omega-6 and -3 fatty acids (e.g., linoleic ($C18:2_{n-6}$) and α-linolenic ($C18:3_{n-3}$)) interfere with glycolytic and lipogenic gene expression (Figure 1). Highly unsaturated 20- and 22-carbon omega-6 and -3 fatty acids (HUFAs) inhibit glycolytic and lipogenic gene transcription through two different types of DNA regulatory response regions (HUFA-RR). One type overlaps with the insulin response element (HUFA-RR/IRE), while the second region colocalizes with the carbohydrate response element (HUFA-RR/CHORE).

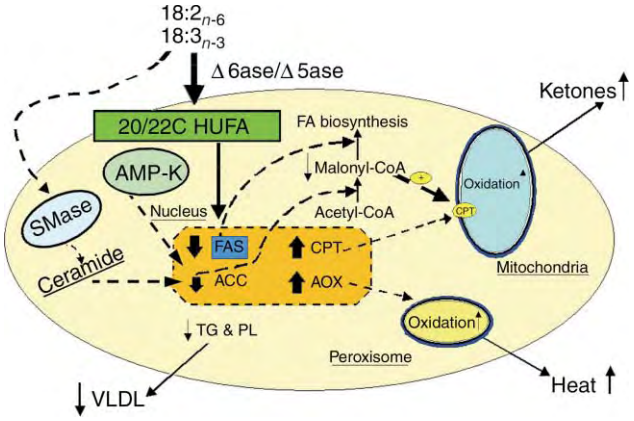

FIGURE 1 Regulation of hepatic gene expression and lipid metabolism by highly unsaturated fatty acids. Δ6ase, Δ-6 desaturase; Δ5ase, Δ-5 desaturase; HUFA, highly unsaturated fatty acids; AMP-K, AMP-kinase; SMase, sphingomyelinase; TG, triglyceride; PL, phospholipid; FA, fatty acids; FAS, fatty acid synthase; ACC, acetyl-CoA carboxylase; CPT, carnitine palmitoyltransferase; AOX, acyl-CoA oxidase; VLDL, very low density lipoproteins.

Colocalization of the HUFA-Response Region with the Insulin Response Element

The HUFA-RR/IRE contains recognition sequences for SREBP-1c, NF-Y, Sp1, and USF. HUFAs inhibit the activity of promoters containing the HUFA-RR/IRE by decreasing SREBP-1c and NF-Y interactions with their respective recognition sequences. HUFAs lower the concentration of SREBP-1 precursor protein as well as inhibit the proteolytic release and nuclear localization of mature SREBP-1. The HUFA-dependent inhibition of the proteolytic release of mature SREBP-1 and -2 may involve a stimulation of sphingomyelin hydrolysis and subsequent ceramide signaling. In addition to inhibiting the proteolytic release of SREBP-1, HUFAs reduce the cellular content of precursor SREBP-1 protein by reducing the cellular abundance of SREBP-1 mRNA. HUFAs decrease the hepatic abundance of SREBP-1 mRNA, and consequently the

hepatic content of precursor SREBP-1 protein, by accelerating SREBP-1 mRNA decay and by suppressing SREBP-1 gene transcription. The mechanisms by which HUFAs accelerate SREBP-1 mRNA decay remain unclear, but the mechanisms by which HUFAs suppress SREBP-1 gene transcription are beginning to emerge. The SREBP-1 gene contains two response elements for the lipogenic transcription factor LXR. Oxysterol ligand activation of LXR induces the transcription of SREBP-1. HUFAs reportedly displace oxysterol from LXR and in this way antagonize the transactivation activity of LXR. In addition, HUFAs may stimulate the "trapping" of LXR as a PPARα/LXR heterodimer. Thus, when the ratio of HUFA to oxysterol is low LXR/RXR heterodimers favor lipogenic gene expression, but when the ratio of HUFA to oxysterol is high, the PPARα/LXR and PPARα/RXR heterodimer mixtures are poised towards a gene profile that favors fatty acid oxidation over fatty acid synthesis. Although SREBP-1 metabolism is highly responsive to HUFA, it is only one of several transcription factors targeted by HUFA. In fact, $>50\%$ of the HUFA control of fatty acid synthase gene transcription can be attributed to the NF-Y site at $-99/-93$. NF-Y is an abundant heterotrimeric nuclear protein that interacts with histone acetyl transferases, and consequently plays a role in modifying histone structure. HUFAs do not reduce the nuclear abundance of NF-Y but rather suppress NF-Y transactivation activity by decreasing its DNA binding activity.

A Cho-Response Element within a Hufa-Response Region

The HUFA-RR of certain lipogenic genes, notably fatty acid synthase, contains DNA-binding sites for several transcription factors (e.g., carbohydrate response factor, HNF-4) whose DNA-binding activity is governed by the amount and type of fat in the diet. One factor that binds to this region and has received significant attention has been the carbohydrate response factor that uniquely interacts with the CHORE. The DNA binding activity of carbohydrate response factor is dependent upon its state of phosphorylation. Fatty acid activation of AMP-kinase leads to increased phosphorylation of the carbohydrate response factor and consequently decreased DNA binding and trans-activation activity. How HUFAs selectively activate AMP-kinase remains to be determined, but HUFA inhibition of lipogenesis and HUFA stimulation of fatty acid oxidation are consistent with the established role that AMP-kinase plays in the partitioning of fatty acids between triglyceride storage and fatty acid oxidation.

Unsaturated Fatty Acid Synthesis

Oleic and Palmitoleic Acid Synthesis

Palmitate (C16:0) and stearate (C18:0) are rapidly desaturated to mono-unsaturated palmitoleic (C16:1) and oleic (C18:1) acids by the stearoyl-CoA desaturase (also known as Δ-9 desaturase) system (Figure 2). Stearoyl-CoA desaturase exists in multiple isoforms that are derived from separate genes. The dominant form within a cell depends upon the origin of the cell. Stearoyl-CoA desaturase inserts a double bond between carbons 9 and 10. This desaturation reaction requires three different components: the desaturase itself, cytochrome b5, and cytochrome b5 reductase. Oleic acid synthesis is required for a variety of reasons. In particular it appears to be required for the hepatic secretion of very low-density lipoproteins.

Arachidonic and Docosahexenoic Acid Synthesis

While oleic acid clearly plays an important role in overall energy metabolism, it cannot fulfill the biological requirements for growth, reproduction, cell signaling, and cell differentiation. These requirements can only be fulfilled by long chain fatty acids from the omega-6 and omega-3 fatty acid family, i.e. linoleic ($C18:2_{n-6}$)

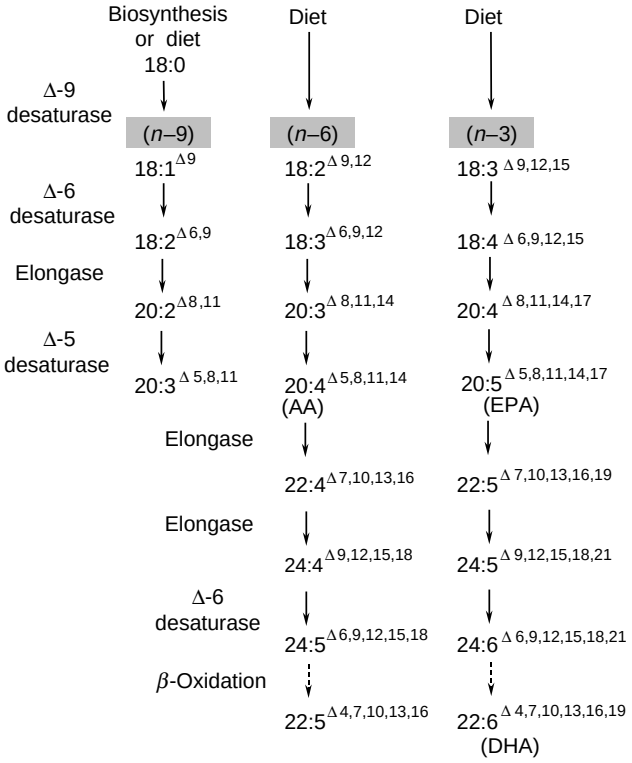

FIGURE 2 Synthesis of highly unsaturated fatty acids.

and α-linolenic (C18:3$_{n-3}$), respectively (Figure 2). Linoleate and α-linolenate undergo desaturation and elongation to 20- and 22-carbon highly unsaturated fatty acids. Prostaglandins and leukotrienes produced from arachidonic acid (C20:4$_{n-6}$) are required for blood clotting, cardiac function, reproduction, inflammatory response, and cell differentiation. Docosahexaenoic acid (C22:6$_{n-3}$) is required for cognition and brain development. Formation of bio-active 20- and 22-carbon highly unsaturated omega-6 and -3 fatty acids requires that the dietary essential fatty acids, linoleate and α-linolenate undergo two steps of desaturation that are catalyzed by the Δ-6 desaturase and Δ-5 desaturase. Both desaturases are expressed in all tissues. The human desaturase genes are members of a gene cluster on chromosome 11 that includes a third desaturase of unknown function, and a non-coding RNA gene that encodes an anti-sense transcript for Δ-5 desaturase. Nearly all human tissues express the products of the Δ-6 desaturase gene cluster. Unlike the stearoyl-CoA desaturase, the Δ-6 and Δ-5 desaturases contain a cytochrome b5 domain within the desaturase peptide. The rate of production of 20- and 22-carbon highly unsaturated fatty acids is dependent upon the tissue content of the two desaturases, and this in turn in determined by nutritional and hormonal factors that are similar to those that regulate the expression of lipogenic genes. The one notable difference between lipogenic and desaturase genes is that while HUFAs suppress both gene families, activators of peroxisome proliferator activator receptor-α induce desaturase genes but they suppress lipogenic genes. The increase in desaturase expression may be in response to a greater need for unsaturated fatty acids for the production of phospholipids, particularly in the liver for the secretion of very low density lipoproteins.

See Also the Following Articles

Cholesterol Synthesis • Fatty Acid Oxidation • Fatty Acid Receptors • Lipoproteins, HDL/LDL • Pyruvate Carboxylation, Transamination, and Gluconeogenesis • Pyruvate Dehydrogenase • Pyruvate Kinase

Glossary

carbohydrate response element (**ChoRE**) A DNA sequence that binds a unique carbohydrate response protein whose DNA-binding and transactivation activities are up-regulated by glucose ingestion.

HUFA Highly unsaturated omega-6 and -3 fatty acids that uniquely regulate gene expression, cell differentiation, and are required for cognition and neural function.

liver-X receptor (**LXR**) A nuclear transcription factor that is activated by the binding of oxysterols and stimulates the transcription of lipogenic genes.

sterol regulatory element binding protein-1 (**SREBP-1**) Protein required for the transcription of genes encoding proteins of fatty acid biosynthesis.

Further Reading

Berger, J., and Moller, D. E. (2002). The mechanisms of action of PPARs. *Annu. Rev. Med.* **53**, 409–435.

Clarke, S. D., Gasperikova, D., Nelson, C., DeMar, J., Lapillonne, A., and Heird, W. C. (2002). Fatty acid regulation of gene expression: A genomic explanation for the benefits of the Mediterranean diet. *Ann. N. Y. Acad. Sci.* **967**, 283–298.

Horton, J. D., Goldstein, J. L., and Brown, M. S. (2002). SREBPs: Activators of the complete program of cholesterol and fatty acid synthesis in the liver. *J. Clin. Invest.* **109**, 1125–1131.

Loewen, C. J. R., and Levine, T. P. (2002). Cholesterol homeostasis: Not until the SCAP lady INSIGs. *Curr. Biol.* **12**, R779–R781.

Puigserver, P., and Spiegelman, B. M. (2003). Peroxisome proliferator-activated receptor-gamma coactivator 1 alpha (PGC-1 alpha): Transcriptional coactivator and metabolic regulator. *Endocr. Rev.* **24**, 78–90.

Vessby, B., Gustafsson, I. B., Tengblad, S., Boberg, M., and Andersson (2002). Desaturation and elongation of Fatty acids and insulin action. *Ann. N. Y. Acad. Sci.* **967**, 183–195.

Biography

Steven D. Clarke is a Director of Science Research at McNeil Nutritionals. Dr. Clarke's research for over 25 years has addressed the nutrient control of the lipid metabolism with particular interest in nutrient–gene interactions. His research has resulted in over 100 publications, and he was among the first to recognize the unique role that polyunsaturated fatty acids play as nutrient sensors for the regulation of fatty acid synthesis and oxidation.

Manabu T. Nakamura received a Ph.D. from the University of California at Davis and is an Assistant Professor of Nutrition at the University of Illinois at Urbana-Champaign. Dr. Nakamura's research focuses on the mechanism by which animals adapt to a wide variety of diets. In particular, he has been working on the regulation of highly unsaturated fatty acid synthesis in mammals.

Ferredoxin

Giuliana Zanetti and Vittorio Pandini
Università degli Studi di Milano, Milan, Italy

Under the name ferredoxin (Fd) are comprised ubiquitous, small proteins containing one or two iron-sulfur clusters. These prosthetic groups contain iron and sulfur atoms, organized in three different types of centers: 2Fe–2S, 4Fe–4S, and 3Fe–4S. The presence of the cluster(s) confers to the protein the property of absorbing light in the visible region. Fd solutions are thus reddish brown in the oxidized state and fade upon reduction. Despite the type and number of clusters bound, Fds generally function in oxidoreduction reactions. Many Fds are involved as electron carrier of low redox potential in electron transport chains of fundamental metabolic processes like photosynthesis, nitrogen fixation, and assimilation of hydrogen, nitrogen, and sulfur. The first report of a nonheme iron protein in the bacterium *Clostridium pasteurianum* appeared in 1962, and was immediately followed by the discovery of a Fd in spinach chloroplast. By now, the family of Fds is greatly increased. Bacteria generally harbor many Fds, which differ in amino acid sequence, FeS cluster type, redox potential, and function. Eukaryotic organisms instead contain just one or two Fds of the 2Fe–2S type, except for plants in which several isoforms coexist. Here we will focus on this type of Fds with special emphasis on ferredoxin I of chloroplast.

2Fe Ferredoxins

The 2Fe ferredoxins (Fds) are hydrophilic, acidic proteins of 11–15 kDa which harbor a single 2Fe–2S cluster coordinated by four cysteine residues. They function as single-electron shuttle in fundamental metabolic processes. The family can be subdivided in two major classes, the mitochondrial-type and the plant-type Fds, based on the cysteine spacing in the iron–sulfur binding motif, the three-dimensional structure, and function. A third class of bacterial 2Fe–Fds has recently been recognized on the basis of sequence and spectroscopic properties.

Plant-Type 2Fe Fds

More than a hundred sequences of 2Fe Fds have been deposited in sequence databases. The polypeptide chain is 93–98 residues long, yielding a protein of molecular mass ~11 kDa. The archetype of this class is the chloroplast ferredoxin I (FdI), which in addition to its main role in the photosynthetic electron transfer to Fd–$NADP^+$ reductase (FNR), provides electrons to a large number of Fd-dependent enzymes involved in assimilatory and regulatory pathways (Figure 1).

Molecular Structure

The characteristic spacing of the cysteinyl residues in the iron-sulfur cluster binding motif for this class is $C–X_4–C–X_2–C$, which provides three of the four thiolate ligands to the two iron atoms, with the fourth ligand 29 residues downstream in the primary structure. Several Fds have been structurally characterized either by X-ray crystallography or NMR spectroscopy. They show a folding motif, dubbed β-grasp, which is similar to that of ubiquitin. It is constituted by a four-stranded antiparallel β-sheet and an α-helix lying perpendicularly to the sheet. A representation of the structure of recombinant spinach FdI is depicted in Figure 2 to show the secondary structure elements. The central core (β-grasp) holds the loop which harbors the Cys motif for binding the iron-sulfur cluster. In addition, two short β-strands, a second α-helix and a short C-terminal helical turn are present. The binuclear iron cluster is located near the surface of the protein with Fe1 atom more exposed to solvent. Upon protein reduction, Fe1 has been shown to become reduced. The surface of the Fd molecule shows an asymmetry in distribution of the many acidic residues, which cluster in two distinct areas around the FeS prosthetic group. This feature common to all plant-type Fds has been shown to be important for interaction with protein partners.

Physiological Function

The nuclear encoded FdI is imported in the chloroplast as an apoprotein, where it acquires the prosthetic group. FdI biosynthesis is under the control of light. As depicted in Figure 1, FdI forms transient electron transfer complexes with several different proteins. First it is reduced through electron transfer from the 4Fe–4S

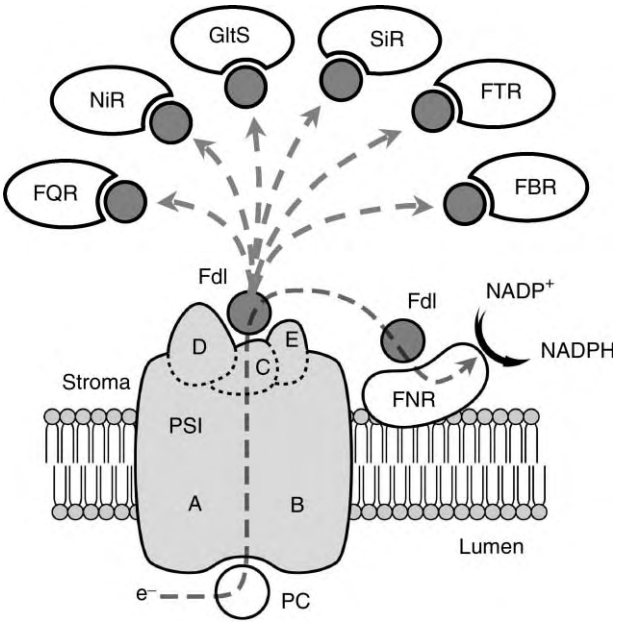

FIGURE 1 Schematic representation of the photosynthetic chain indicating the electron transfer pathways from photosystem I (PSI) to several metabolic processes of chloroplast by FdI servicing. FNR, Fd-$NADP^+$ reductase (carbon assimilation); FBR, Fd-bilin reductase (phytochromobilin synthesis); FTR, Fd-thioredoxin reductase (regulation of Calvin cycle enzymes); SiR, sulfite reductase (sulfur assimilation); GltS, glutamate synthase (amino acid synthesis); NiR, nitrite reductase (nitrogen assimilation); FQR, hypothetical Fd-quinone reductase (cyclic electron flow). PC, plastocyanin. A, B, C, D, and E indicate the PsaA, PsaB, PsaC, PsaD, and PsaE subunits of PSI, respectively.

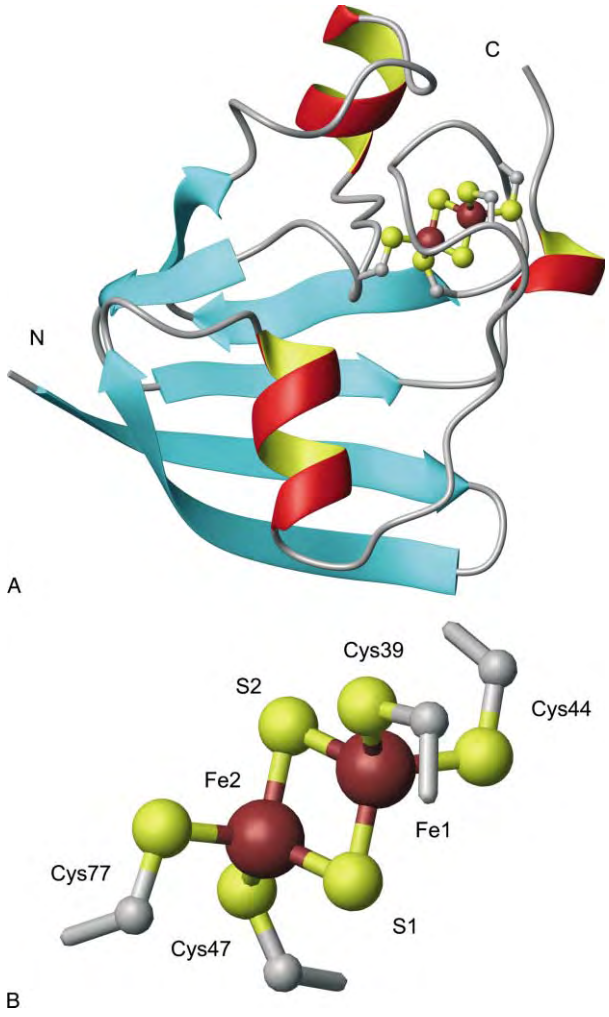

FIGURE 2 Ribbon representation of the three-dimensional structure of spinach FdI showing secondary structure elements. (A) N and C define the N terminus and C terminus, respectively. (B) Detail of the iron–sulfur cluster showing the side chains of the cysteines (residues 39, 44, 47, and 77) and the two sulfide sulfur atoms which coordinate the two iron atoms. The figure was made with Molmol.

centers (F_A and F_B) of the subunit PsaC of photosystem I, by docking both to the PsaD and the PsaE subunits at the stromal side of the thylakoid membrane. Then, the reduced protein donates its electron to either one of the various enzymes known to be Fd dependent. NADPH production through FNR is the main role of FdI. Several studies employing a number of different techniques have attempted to define the binding region of FdI for its various redox partners. The three-dimensional structure of the Fd-FNR complexes both from *Anabaena* spp. and maize leaves have recently been obtained. Overall, the picture which comes out is that FdI acts a mobile electron shuttle between photosystem I and the enzyme partners, utilizing for the interaction the same acidic surface area surrounding the iron-sulfur cluster. The binding sites do not need to be exactly the same but may be just overlapping.

Fd isoforms are present in plastids of nongreen plant tissues and most recently, such type of Fd has been found in the organelle called apicoplast of protozoan parasites Apicomplexa (*Plasmodium* spp., *Toxoplasma gondii*, etc.). These Fds, which have a more positive redox potential than the photosynthetic ones are reduced by FNR isoforms at the expenses of NADPH and act as reductant of Fd-dependent pathways in these organelles.

Mitochondrial-Type 2Fe Fds

Mammalian adrenodoxin (Adx) is the prototype of this class, other well-known members are putidaredoxin of *Pseudomonas putida*, yeast Fd, and *Escherichia coli* Fd. The first two Fds have the role of providing electrons to cytochrome P450-catalyzed hydroxylation reactions, the latter two have been more recently implicated in iron-sulfur cluster biogenesis. They are 105–128 residues long, thus are up to 4 kDa larger than plant Fds. The typical Fe-S binding sequence is $C–X_5–C–X_2–C$, which provides three of the four thiolate ligands to the iron atoms, with the fourth ligand 35–37 residues downstream in the sequence. The three-dimensional structures of these Fds show high similarity to those of the plant Fds in the fold of the core involving

the N-terminal moiety (i.e., the β-grasp), but they have an additional C-terminal lobe, called interaction domain, which has been shown to be involved in binding both the redox partners, Adx reductase and cytochrome P450. As in the case of FdI, the binding sites may be separate but overlapping.

Thioredoxin-Type 2Fe Ferredoxins

Thioredoxin-like Fds were first identified in *Azotobacter vinelandii* and *C. pasteurianum*. They seem to be present only in bacteria. The polypeptide chain length is that usually reported for 2Fe Fds, i.e., 100–120 residues, but these Fds, being dimer, have a larger molecular mass. The cysteine motif for binding the iron-sulfur cluster is rather unique: $C-X_{10-12}-C-X_{29-34}-C-X_3-Cys$ and the crystal structure of *Aquifex aeolicus* Fd revealed a fold unusual for Fds and quite similar to that of thioredoxin. The function of these Fds is not yet known, although there are some indications for their involvement in nitrogen fixation.

Ferredoxins Containing 4Fe and 3Fe Iron–Sulfur Clusters

This class comprises 3Fe, 4Fe, 7Fe, and 8Fe Fds, which are small, bacterial proteins containing one or two FeS clusters of the cubane type. The iron and sulfide atoms alternate on the corners of a distorted cube. In the case of the 3Fe cluster, one corner is devoid of the fourth iron atom. The two types of clusters are in some cases interconvertible. The cysteine motif for the coordination of these iron–sulfur centers is $C-X_2-C-X_2-C$ with the middle cysteine replaced by aspartic acid or any residue in the case of 3Fe clusters, in a polypeptide chain of 60–100 residues. These Fds generally function as electron carrier in several metabolic pathways including pyruvate metabolism, nitrogen fixation, sulfate reduction, hydrogen production, and cytochrome P450 hydroxylations.

See Also the Following Articles

Ferredoxin-NADP$^+$ Reductase • Iron–Sulfur Proteins • Photosynthesis

Glossary

iron–sulfur cluster A prosthetic group containing iron and sulfur atoms liganded by protein cysteine residues.

isoform Any of multiple forms of a protein differing in primary structure but having similar function.

photosynthesis A process that converts the light energy in the chemical energy of NADPH and ATP.

thioredoxin A small protein containing an oxidoreducible disulfide.

Further Reading

Beinert, H., Holm, R. H., and Münck, E. (1997). Iron–sulfur clusters: Nature's modular, multipurpose structures. *Science* **277**, 653–659.

Grinberg, A. V., Hannemann, F., Schiffler, B., Müller, J., Heinemann, U., and Bernhardt, R. (2000). Adrenodoxin: Structure, stability, and electron transfer properties. *Proteins* **40**, 590–612.

Knaff, D. B. (1996). Ferredoxin and ferredoxin-dependent enzymes. In *Oxygenic Photosynthesis: The Light Reactions* (D. R. Ortand and C. F. Yocum, eds.) Vol 4, pp. 333–361. Kluwer, Dordrecht.

Meyer, J. (2001). Ferredoxin of the third kind. *FEBS Lett.* **509**, 1–5.

Tagawa, K., and Arnon, D. I. (1962). *Nature* **195**, 537–543.

Zanetti, G., Binda, C., and Aliverti, A. (2001). The [2Fe–2S] ferredoxins. In *Handbook of Metalloproteins* (A. Messerschmidt, R. Huber, T. Poulos and K. Wieghardt, eds.) Vol 1, pp. 532–542. Wiley, Chichester.

Biography

Giuliana Zanetti is full Professor of Biochemistry in the Department of General Physiology and Biochemistry at the Università degli Studi di Milano, Italy. Her principal research interests are in the field of flavo/iron–sulfur proteins advanced enzymology. She holds a Libera Docenza in plant physiology and underwent postdoctoral training at the University of Michigan. She contributed to the mechanism of action of the photosynthetic Fd-NADP$^+$ reductase, and of several other reductases.

Vittorio Pandini is a Research Scientist in the Dept of Scienze Biomolecolari e Biotecnologie at the Università degli Studi di Milano, Italy. He holds a Ph.D. from the Università di Milano. His current interests are in the ferredoxin redox system of apicomplexan parasites.

Ferredoxin-NADP$^+$ Reductase

Giuliana Zanetti and Alessandro Aliverti
Università degli Studi di Milano, Milan, Italy

The photosynthetic ferredoxin-NADP$^+$ reductase (FNR) is the prototype of a functional group of flavoenzymes that catalyze the exchange of reducing equivalents between NADP(H) and ferredoxins. In photosynthesis, FNR provides NADPH by pairing electrons supplied by photosystem I through ferredoxin. It is a monomeric protein comprising two domains, one for FAD binding and a Rossmann fold for NADP binding. Interactions with either substrates have been elucidated by biochemical studies and by solving the three-dimensional structures of their complexes with the enzyme. The other members of the group catalyze the reduction of ferredoxin at the expense of NADPH, and vary in physiological function, structure and localization.

Introduction

Ferredoxin-NADP$^+$ reductase (FNR) is the common name of members of a broad group of flavoenzymes (classified as EC 1.18.1.2) sharing the ability to catalyze the transfer of reducing equivalents between NADP(H) and ferredoxins (Fds). The best-known example is the photosynthetic FNR, the terminal component of the photosynthetic electron transport chain, both in eukaryotic and prokaryotic phototrophic organisms. In addition to this photosynthetic oxidoreductase, isoforms exist in non-photosynthetic cells. The subdivision between photosynthetic and non-photosynthetic FNRs is functional, and is based on the physiological direction of the catalyzed reaction, i.e., towards NADP$^+$ reduction in the case of photosynthetic FNR, and towards Fd reduction for heterotrophic FNRs (Figure 1). Besides such functional classification, a structural/phylogenetic one is possible, which distinguishes between plant-type and glutathione reductase-type FNRs. While all photosyntetic FNRs are plant-type, non-photosynthetic reductases are distributed between both structural classes.

Furthermore, the plant-type FNR is the prototype of a large superfamily of homologous enzymes, which display a great variety of catalytic functions. All members of this family possess the two-domain FNR unit and additional domains that modify and extend their functional properties.

Photosynthetic FNR

FNR was first discovered in 1956 by Avron and Jagendorf, who isolated it from pea chloroplasts as a NADPH-dependent diaphorase (i.e., a flavin-containing enzyme that catalyzes the transfer of reducing equivalents from NADPH to various electron acceptors). This chloroplast oxidoreductase was later shown by Shin and Arnon to mediate the transfer of electrons from ferredoxin to NADP$^+$.

Molecular Structure

Photosynthetic FNRs are monomeric proteins of about 35 kDa molecular mass, containing one molecule of non-covalently but tightly bound flavin adenine dinucleotide (FAD) as prosthetic group. FNRs from different eukaryotic sources show a high sequence similarity (~80% identity), which is spread over the entire polypeptide chain of ~300 amino acid residues. Cyanobacterial FNR possesses an additional N-terminal sequence of ~10 kDa involved in binding to phycobilisomes, light-harvesting structures of the thylakoid membrane of cyanobacteria. The three-dimensional (3D) structures of photosynthetic FNRs have been determined at high resolution (up to 1.7Å) by X-ray crystallography for the proteins from spinach, pea, paprika, and maize leaves, as well as from the cyanobacterium *Anabaena* spp. The enzyme molecule consists of two structural domains, each of ~150 residues (Figure 2). The N-terminal domain, comprising a six-stranded antiparallel β-barrel, a small β-sheet and an α-helix, provides most of the residues involved in FAD binding and is thus also known as the FAD-binding domain. The C-terminal domain, topologically similar to the supersecondary structure named Rossmann fold, binds NADP(H) and is thus indicated as the NADP-binding domain. However, both dinucleotides interact also with residues belonging to the other domain. Indeed, FAD- and NADP(H)-binding sites are located within a deep cavity at the interface of the two domains. The isoalloxazine ring of FAD, as in many flavoproteins, is sandwiched between the side-chains of two aromatic residues. In particular, the C-terminal tyrosine residue

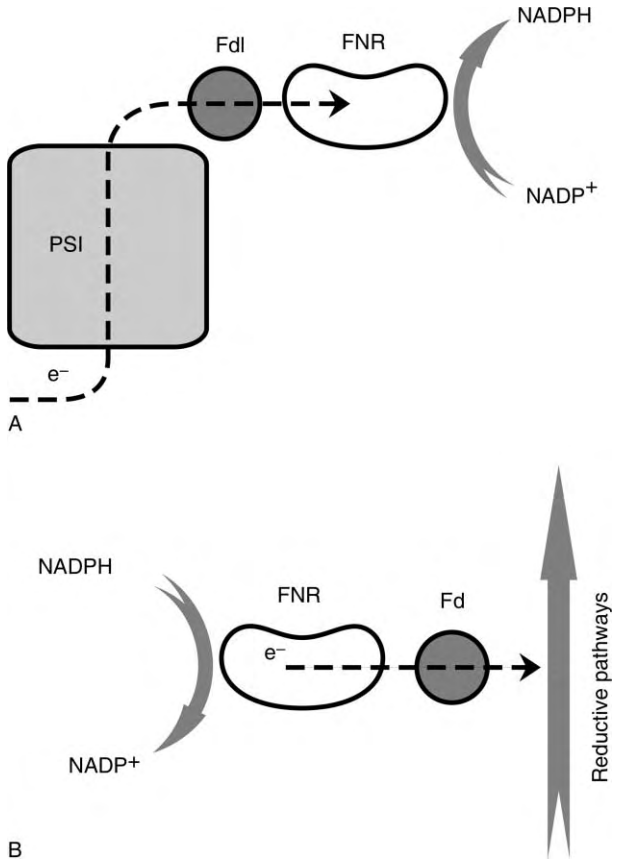

FIGURE 1 Comparison of the physiological reactions catalyzed by photosynthetic and non-photosynthetic FNR isoforms. (A) Scheme of the reaction catalyzed by FNR in chloroplasts. PSI, photosystem I; FdI, photosynthetic isoform of Fd. (B) Scheme of the reaction catalyzed by non-photosynthetic FNR isoforms. Fd indicates any non-photosynthetic Fd isoform, including adrenodoxin. The dashed line indicates the electron transfer path.

makes an aromatic stacking interaction with the *re*-face of the isoalloxazine ring.

Subcellular Localization and Physiological Role

FNR is present in the chloroplasts of algae and higher plants. It is an extrinsic membrane protein localized on the side facing the stroma of the thylakoid membrane. FNR is the catalyst of the last step in the light-driven electron transport. FNR is thus directly responsible for producing the NADPH required in the Calvin cycle for carbohydrate biosynthesis. Reducing power is in turn provided to FNR by Fd, which acts as an electron shuttle by diffusing in the stroma between photosystem I and FNR and being reduced by the former and oxidized by the latter.

Catalytic Mechanism

FNR catalyzes the reversible transfer of reducing equivalents between the obligatory one-electron carrier ferredoxin (Fd) to the obligatory two-electron carrier NADP(H), according to the following balanced chemical equation:

$$2\mathrm{Fd}(\mathrm{Fe}^{2+}) + \mathrm{NADP}^{+} + \mathrm{H}^{+} \Leftrightarrow 2\mathrm{Fd}(\mathrm{Fe}^{3+}) + \mathrm{NADPH}. \quad (1)$$

The ability of FNR to pair single electrons in order to transfer them as a couple to a two-electron acceptor is a feature of the dehydrogenase-electron transferases class of flavoproteins to which FNR belongs, and is mediated by the FAD prosthetic group. FAD can exist in three redox states: oxidized, one-electron reduced (semiquinone form), and two-electron reduced (dihydroquinone form). During turnover, enzyme-bound FAD cycles among the three redox states described above, according to the reaction scheme shown in Figure 3. Two reduced Fd molecules sequentially transfer one electron at the time to FAD, before FNR can complete the catalytic cycle transferring a couple of electrons to $NADP^+$. Electron transfer is strictly coupled to proton (H^+) transfer, at least in steps 2 and 4. FAD protonation in step 2 is required to yield the neutral semiquinone form observed during turnover. In step 4, two electrons are transferred simultaneously with one H^+ in the form of a hydride ion (H^-). Catalysis proceeds according to a sequential ordered mechanism, through the formation of ternary complexes of FNR with both substrates. The redox potential of the FAD/$FADH^-$ couple in FNR is −360 mV, a value intermediate between that of FdI (−400 mV) and that of the $NADP^+$/NADPH couple (−320 mV).

Interaction with NADP(H)

FNR is a remarkably specific enzyme, showing a strong preference for $NADP^+$ over NAD^+. Substrate discrimination is due to a number of interactions that FNR establishes with the 2′-phosphate group of NADP(H). NADP(H) interactions with FNR have been described in terms of a bipartite binding mode, where the adenylate moiety of the dinucleotide binds independently of the nicotinamide one. Binding of the adenylate moiety occurs with high affinity and is the leading event in substrate recognition. In order to allow hydride transfer to occur between the reduced isoalloxazine ring and the nicotinamide, FNR has to undergo an induced-fit process where the nicotinamide ring of $NADP^+$ displaces the phenol ring of the C-terminal tyrosine residue from its stacking interaction with *re*-face of the isoalloxazine (Figure 2). A detailed picture of the enzyme–NADP(H) interaction has been obtained by producing an engineered FNR, where the C-terminal tyrosine was changed to a non-aromatic residue. This greatly stabilized the interaction between the flavin and the nicotinamide ring. Thus, X-ray crystallography of the NADP(H) complex with the mutant FNR revealed the hydride-transfer competent binding mode of the substrate (Figure 2).

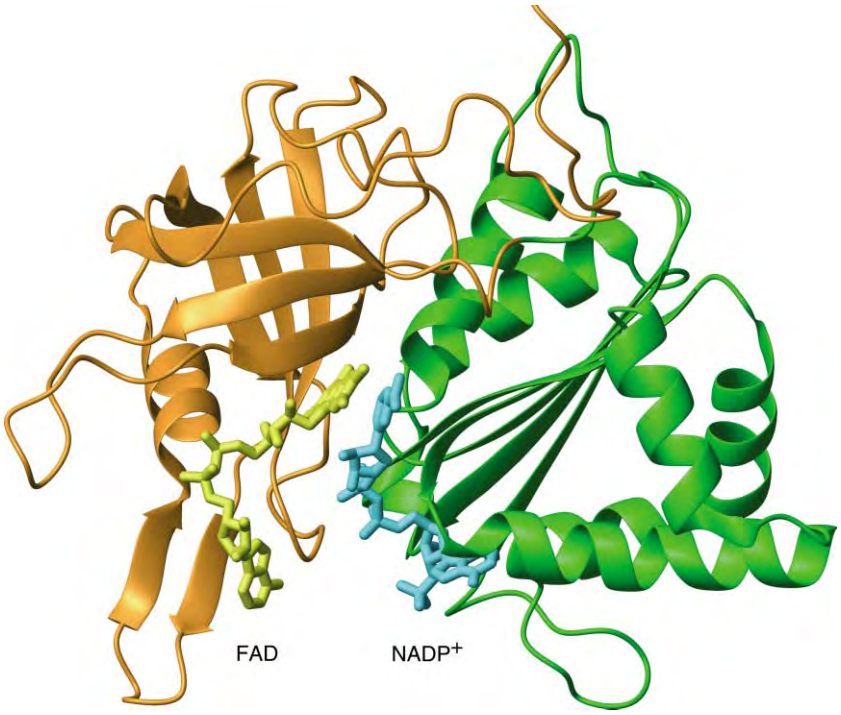

FIGURE 2 Ribbon model of the 3D structure of the pea photosynthetic FNR mutant with a serine replacing the C-terminal tyrosine residue. The FAD-binding and the NADP-binding domains are depicted in orange and green, respectively. The wireframes of bound FAD and NADP$^+$are shown in yellow and cyan, respectively. The figure was made with Molmol.

Interaction with Fd

Crystals of the complexes between FNR and Fd, both in the oxidized state, have been obtained for the eukaryotic (maize leaf) and the prokaryotic (*Anabaena* spp.) protein couples. X-ray structures are similar (Figure 4). Fd binds to a large concave region of FNR, which is contributed by both structural domains of the reductase, with the FAD-binding domain providing most of the interactions. Complex formation places the redox active prosthetic group at a distance (6.0–7.4Å) compatible with high-rate electron transfer. Protein–protein complex formation is thought to be initially driven by the mutual orientation of the dipole moments of the two molecules as they approach. After initial docking, minor adjustments are expected to occur to reach a conformation optimal for intermolecular electron-transfer, with the formation of a network of intermolecular weak bonds (salt bridges, hydrogen bonds, van der Waals, and hydrophobic interactions). Charge–charge interactions, which play a major role in the stabilization of the Fd–FNR complex, are formed between basic groups provided by FNR and acidic groups of Fd.

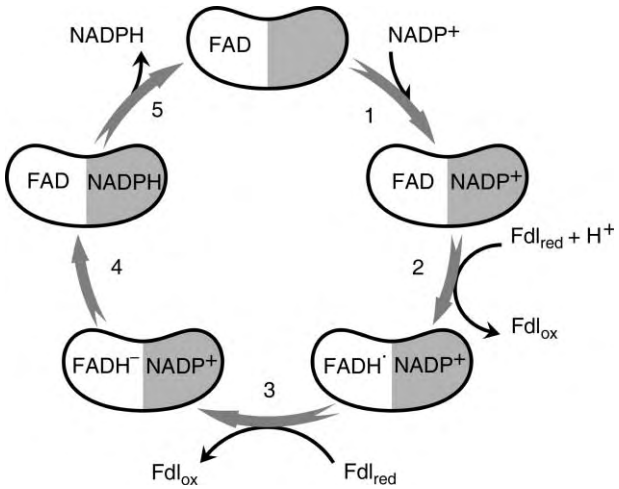

FIGURE 3 Simplified scheme of the mechanism of the reaction catalyzed by the photosynthetic FNR isoform. FdI indicates the photosynthetic Fd isoform present in chloroplasts. FdIox and FdIred indicate oxidized and reduced forms of FdI, respectively. FADH$^{\cdot}$ and FADH$^-$ indicate the neutral semiquinone and the hydroquinone anion of FAD, respectively.

Non-Photosynthetic Plant-Type FNRs

Root FNR

Non-photosynthetic plastids of higher plants contain an isoform of FNR, also known as root FNR. Root and leaf isoforms of FNR are clearly homologous, showing a sequence identity of ~48%, which corresponds to highly similar 3D structures. Isoform-specific

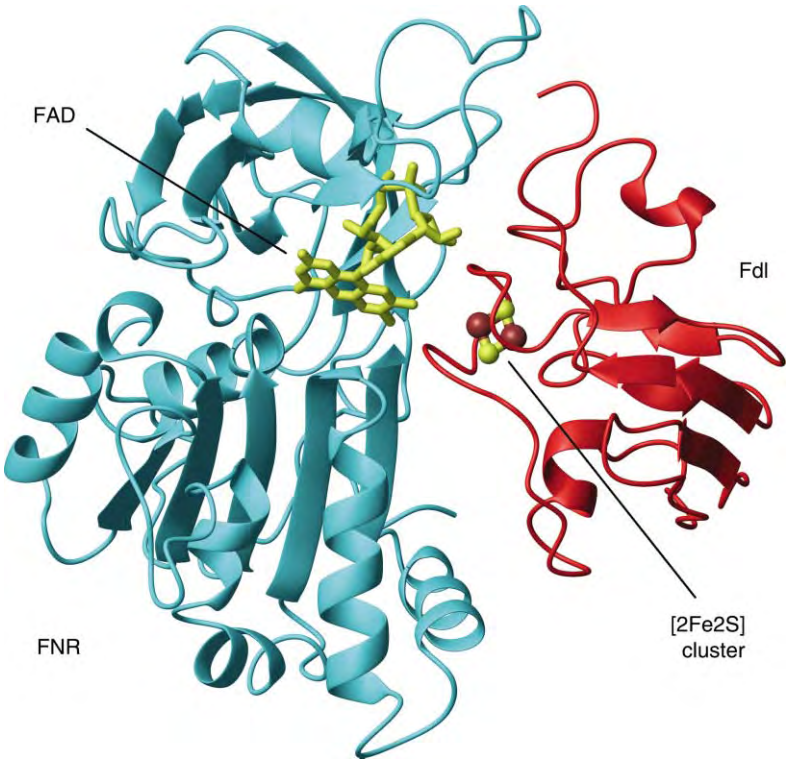

FIGURE 4 Ribbon model of the binary complex between maize photosynthetic FNR and FdI. FNR is depicted in cyan, while FdI is in red. The wireframe of FAD is shown in yellow. The iron–sulfur cluster is represented as a ball and stick model, with the iron atoms in brown and the sulfur atoms in yellow. The figure was made with Molmol.

differences are limited to the structure of surface loops of the molecules, the presence of a conserved disulfide bridge in the FAD-binding domain of the root isoform, a higher redox potential for the bound FAD of the root isoform, and different affinities for the Fd isoforms. Many of these structural and functional differences are instrumental for the diverse physiological role played by the two FNR isoforms. Indeed, the role of root FNR is opposite to that of the leaf isoform, i.e., transfer of reducing equivalents from NADPH to a root-specific Fd isoform to yield reduced Fd for several Fd-dependent pathways.

Bacterial and Apicomplexan FNR

FNRs belonging to the FNR structural family are present in some prokaryotic organisms such as *Escherichia coli* and *Azotobacter vinelandii*. A plant-type FNR has been recently identified in different species belonging to the *Apicomplexa*, a phylum of obligatory eukaryotic unicellular parasites, including the causative agents of malaria, toxoplasmosis, and coccidiosis. In the apicomplexan cell, the FNR is localized, together with a plant-type Fd, in a peculiar organelle, the apicoplast. Apicomplexan FNR is thus expected to play a metabolic function similar to that of root FNR, i.e., production of reduced Fd to be used in reductive biosynthetic pathways. Due to the increasing importance attributed to the apicoplast metabolism in parasite pathogenicity, apicomplexan FNR is an attractive target for novel antiparasitic drugs.

Heterotrophic Glutathione Reductase-Type FNRs

In addition to plant-type FNRs, various FNRs exist that – while being structurally and phylogenetically distinct from the former – show essentially the same catalytic activity, thus representing a noteworthy example of convergent evolution. Such FNRs show a significant sequence identity. The 3D structures of two of them (bovine adrenodoxin reductase and *Mycobacterium tuberculosis* FprA) have been determined and shown to be similar to that of glutathione reductase (GR). FNRs of the GR-like class thus have both domains based on the Rossmann fold motif for binding the nucleotides (FAD and NADPH). The prototype of such enzymes is adrenodoxin reductase (AdR), found in vertebrate mitochondria, where it transfers electrons from NADPH to an Fd known as adrenodoxin (Adx). AdR and Adx form an electron supply system for the cytochrome P450-catalyzed hydroxylation reactions to

produce steroid hormones, vitamin D metabolites, and bile acids. An AdR-homologous protein (Arh1) has been recently found in *Saccharomyces cerevisiae*. By now AdR and Adx have been shown to be ubiquitous in mitochondria of eukaryotes, where they play a role in the biogenesis of iron–sulfur clusters. More recently, an AdR-like enzyme (FprA) has been identified in *Mycobacterium tuberculosis*, showing that they are not restricted to eukaryotes. FprA is thought to have a critical role in the complex lipid metabolism of this pathogen as a source of reducing power for the unusually large numbers (~20) of cytochromes P450 present in this organism. This observation could eventually lead to novel pharmacological treatment for tuberculosis.

See Also the Following Articles

Ferredoxin • Photosynthesis • Photosystem I: F_X, F_A, and F_B Iron–Sulfur Clusters • Protein Folding and Assembly

Glossary

domain An independently folded structural region of a protein molecule.

flavoprotein A protein that contains a flavin nucleotide (FAD or FMN) as prosthetic group.

photosynthesis A process that converts the light energy into chemical energy of NADPH and ATP.

prosthetic group A tightly bound cofactor that contributes to the biological activity of a protein.

Rossmann fold A protein structural motif for nucleotide binding.

Further Reading

Arakaki, A. K., Ceccarelli, E. A., and Carrillo, N. (1997). Plant-type ferredoxin-NADP$^+$ reductase: A basal structural framework and a multiplicity of functions. *FASEB J.* **11**, 133–139.

Deng, Z., Aliverti, A., Zanetti, G., Arakaki, A. K., Ottado, J., Orellano, E. G., Calcaterra, N. B., Ceccarelli, E. A., Carrillo, N., and Karplus, P. A. (1999). A productive NADP$^+$ binding mode of ferredoxin-NADP$^+$ reductase revealed by protein engineering and crystallographic studies. *Nat. Struct. Biol.* **6**, 847–853.

Hurley, J. K., Morales, R., Martínez-Júlvez, M., Brodie, T. B., Medina, M., Gómez-Moreno, C., and Tollin, G. (2002). Structure–function relationships in Anabaena ferredoxin/ferredoxin: NADP$^+$ reductase electron transfer: insights from site-directed mutagenesis, transient absorption spectroscopy and X-ray crystallography. *Biochim. Biophys. Acta* **1554**, 5–21.

Karplus, P. A., Daniels, M. J., and Herriott, J. R. (1991). Atomic structure of ferredoxin-NADP$^+$ reductase: Prototype for a structurally novel flavoenzyme family. *Science* **251**, 60–66.

Zanetti, G., and Aliverti, A. (1991). Ferredoxin-NADP$^+$ oxidoreductase. In *Chemistry and Biochemistry of Flavoenzymes II* (F. Müller, ed.) pp. 305–315. CRC Press, Boca Raton, FL.

Biography

Giuliana Zanetti is a Professor of Biochemistry in Scienze Biomolecolari e Biotechnologie at the Università degli Studi di Milano, Italy. Her principal research interests are in the field of flavo/iron–sulfur proteins advanced enzymology. She holds a Libera Docenza in Plant Physiology and underwent a two-year postdoctoral training at the University of Michigan. She contributed to clarifying the mechanism of action of the photoysnthetic ferredoxin-NADP$^+$ reductase, and of several other reductases.

Alessandro Aliverti is an Assistant Professor of Biochemistry in Scienze Biomolecolari e Biotechnologie at the Università degli Studi di Milano, Italy. He holds a Ph.D. from the University of Milan. His current research is on the enzymology of ferredoxin reductases from both plants and pathogens.

Fibroblast Growth Factor Receptors and Cancer-Associated Perturbations

Marko Kornmann
University of Ulm, Ulm, Germany

Murray Korc
Dartmouth Medical School, Lebanon, New Hampshire, USA

Fibroblast growth factors (FGFs) constitute a family of homologous heparin-binding polypeptides that presently consists of at least 23 members. FGFs play important roles in many biological functions, including development, pattern formation, cellular differentiation, metabolic regulation, tissue repair, angiogenesis, and mitogenesis. FGFs act by binding to a family of specific, high-affinity FGF receptors (FGFRs) that possess a discontinuous intracellular kinase domain. Perturbations in FGF–FGFR expression, localization, and signaling have been implicated in several pathological processes, including malignant transformation and tumor spread and metastasis.

Fibroblast Growth Factors

Genes

To date, 23 *Fgf* genes have been identified in vertebrates. Although human *Fgf15* and mouse *Fgf19* have not been described, human *Fgf19* is most closely related to mouse *Fgf15*, and both genes are closely linked to the *Fgf3* and *Fgf4* genes, raising the possibility that human *Fgf19* may be identical to mouse *Fgf15*. According to their evolutionary relationship, the 22 *Fgfs* in humans can be classified into several subgroups (Figure 1). Members of each subgroup may also share similar biochemical and developmental properties. For example, members of the *Fgf8* subgroup display similar receptor-binding properties and overlapping yet distinct expression patterns during development, underscoring both their commonality and uniqueness.

Proteins

Among vertebrates, fibroblast growth factors (FGFs) share 13–71% of their amino acid sequence homology. Most notably, there is an internal core region consisting of six identical and 28 highly conserved amino acids, which include the ten amino acid residues interacting with the high-affinity FGF receptors (FGFRs) within ~120 amino acid region. In FGF-1 and FGF-2 this areas consists of 12 antiparallel β-strands forming a structure exhibiting a threefold internal symmetry called a β-trefoil.

FGF4–8, 10, 17–19, 21, 23 possess classical N-terminal leader sequences that may allow for rapid and efficient secretion. This sequence is also present in FGF3 and 22. However, neither of these FGFs is efficiently secreted. By contrast, FGF-1, 2, 9, and 11–14, 16, and 20 lack a leader sequence for secretion. Nonetheless, FGF9, 16, and 20 have a hydrophobic region in the core domain allowing for secretion. Moreover, FGF1 and FGF2 may be released by an exocytotic mechanism, while FGF11–14 are thought to remain intracellularly. Posttranslational glycosylation, alternative splicing, and initiation of synthesis from N-terminal CUG sequences can result in several different molecular weight forms in the case of several FGFs.

Physiologic Actions

FGFs regulate diverse processes during development and exert a broad variety of functions in the adult organisms including growth, survival, apoptosis, motility, and differentiation.

Fibroblast Growth Factor Receptors

Genes

FGFRs are transmembrane proteins that are encoded by five distinct *Fgfr* genes. The extracellular portion of these receptors is usually composed of three immunoglobulin (Ig)-like domains (I–III), including a stretch of acidic residues (acidic box) between domain I and II, which is unique for the FGFRs. The hydrophobic

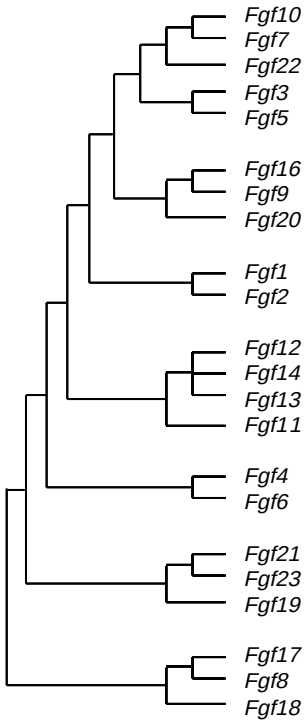

FIGURE 1 Evolutionary relationships within the human FGF family. (Adapted from Ornitz, D. M., and Itoh, N. (2001). Protein family review: Fibroblast growth factors. *Genome Biol.* **2**, 30051–300512, with permission.)

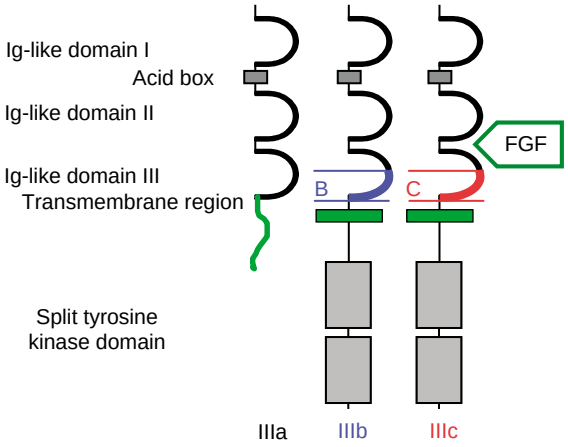

FIGURE 2 Schematic diagram of structural features of FGF receptors. FGFRs are usually composed of three extracellular immunoglobulin (Ig)-like domains (I–III) including a stretch of acidic residues (acidic box) unique for FGFRs, a hydrophobic transmembrane region followed by a juxtamembrane and a split tyrosine kinase catalytic domain. The IIIa isoform is devoid of any signaling capacity. In case of the IIIc isoform, the second half of the Ig-like domain III (solid) corresponds to the exon 7 sequence of the *FGFR1* gene and in case of IIIb, the second half of the Ig domain III (open) corresponds to the exon 6 sequence of the *Fgfr1* gene.

transmembrane region is followed by a juxtamembrane domain and a split tyrosine kinase catalytic domain (Figure 2). In contrast to FGFR1–4, FGFR5 contains a transmembrane domain, but no intracellular kinase domain. A special feature of the FGFR family is the existence of several receptor isoforms for FGFR1, 2, 3, and 4 that are generated by alternative mRNA splicing and result in different ligand-binding specificities.

Proteins

FGF signaling is generally mediated by a dual-receptor system, consisting of the high-affinity FGFRs and of low-affinity heparan sulfate proteoglycan receptors that are most often devoid of signaling capabilities but enhance ligand presentation to the receptors. The function of FGFR5, which is also devoid of intracellular signaling capacity, is presently unknown, but it may provide a binding site for FGFs. FGF binding results in receptor oligomerization, activation of the cytoplasmic tyrosine kinase domains and receptor autophosphorylation. Intracellular signaling is then mediated through the tyrosine phosphorylation of key substrates, and the activation of downstream pathways such as the mitogen-activated protein kinases (MAPK), extracellular signal regulated kinase-1 (ERK-1), and ERK-2. In general, activation of these pathways occurs following phosphorylation of FGF receptor substrate-2 (FRS-2) (Figure 3). However, the same signaling cascades can also be activated under certain circumstances through FRS-2 independent mechanisms (Figure 3).

The existence of at least 23 FGF ligands, 5 FGFRs, and multiple FGF isoforms and FGFR splice variants can potentially result in a large combinatorial set of interactions. This further increases the complexity, diversity, and functional specificity of FGFs. Most notably, alternative splicing of the second half of the Ig-like domain III results in three receptor variants, termed IIIa, IIIb, and IIIc (Figure 2). Due to the fact that FGF binding occurs between the Ig-like domains II and III, these splice variants are important for defining ligand binding. Thus, the IIIa splice variant yields a secreted receptor that is devoid of any signaling capacity. The expression of the IIIb variant is believed to be restricted to epithelial cell types, whereas the expression of the IIIc variant, especially in the case of FGFR2 and FGFR3, is believed to be restricted to mesenchymal cell types.

Physiologic Actions

The expression of FGFRs seems to be fundamental for many processes including limb, craniofacial, and lung development, hepatogenesis, osteogenesis, and inner ear formation. Mutations of *Fgfr1–3* genes have been linked to syndromes characterized by specific craniofacial and limb malformations. For example, mutations of *Fgfr2* were found in patients with Apert syndrome and mutations of *Fgfr3* in patients with achondroplasia.

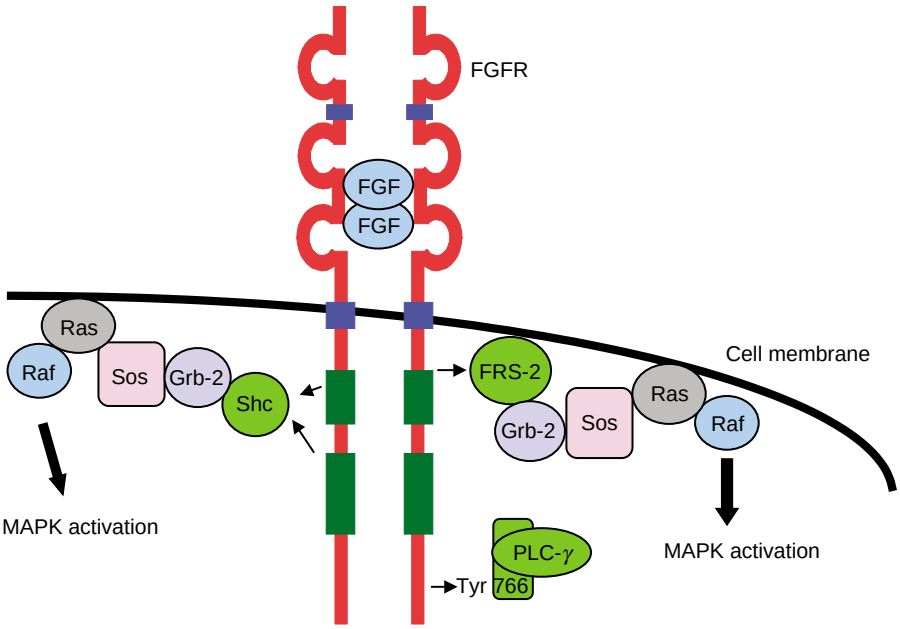

FIGURE 3 Schematic diagram of FGF signaling. FGF binding between Ig domain II and III results in receptor oligomerization, activation of the split cytoplasmic tyrosine kinase domains (rectangles) and receptor autophosphorylation. This is followed by binding, phosphorylation, and activation of fibroblast growth factor receptor substrate 2 (FRS2) or phospholipase C-γ (PLC-γ), which binds to tyrosine residue 766. Activation of the downstream mitogen-activated protein kinases (MAPK), extracellular signal regulated kinase-1 (ERK-1), and ERK-2 generally occurs via FRS2, but may also be mediated by an FRS2 independent pathway through the signaling molecules Shc, Grb-2, SOS, ras, and raf.

FGF Actions in Cancer

Many studies demonstrate that alterations of the expression of FGFs and FGFRs play an important role in the development and progression of various malignant diseases.

FGF2

FGF2 exerts mitogenic effects on various endothelial, mesothelial, and epithelial cell types. It is overexpressed in a great portion of human tumor cell lines and various human malignancies. High levels of FGF2 in the serum of patients or in tumor specimens have been correlated with advanced tumor stage and poor prognosis in several gastrointestinal and other cancers, including thyroid, lung, and renal cell cancer. However, FGF2 expression may be associated with favorable prognosis in ovarian and breast cancer.

FGF1

FGF1 is also a potent mitogenic factor for many normal and malignant cells and is also expressed in a variety of cultured cell lines and tissues. Although FGF1 is present in many malignancies and can display similar biological activities as FGF2, FGF1 expression has not been clearly demonstrated to correlate with clinico-pathological parameters in human cancers.

FGF3

The *Fgf3* gene was initially identified as murine mammary tumor virus integration site oncogene homologue (*int2*) implicated in mouse mammary tumors. *Fgf3* is localized on chromosome 11q13, a locus frequently amplified in malignant diseases. Amplification of *Fgf3* was associated with poor prognosis in breast cancer and biological aggressiveness in ovarian and esophageal cancer. The overexpression of FGF3 in normal mouse mammary cells resulted in the development of orthotopically implanted tumors in nude mice, underscoring the important role of FGF3 in mammary tumorigenesis.

FGF-4

Fgf4, also called "human stomach cancer transforming factor-1" (*hst-1*), was discovered when DNA from stomach tissues was shown to induce the malignant transformation of fibroblasts. The same oncogene was isolated by transfection of Kaposi sarcoma DNA and is therefore also called "kaposi sarcoma *Fgf*" (*kFgf*). *Fgf4* is also located on chromosome 11q13 together with *Fgf3*. Amplification of *Fgf4* correlates with increased risk of systemic recurrence after resection of esophageal

cancer and with nodal involvement in head and neck cancers. Moreover, FGF4 overexpression increases the metastasic potential of breast cancer cells in association with altered expression of matrix metallo-proteinases.

FGF5

Fgf5 was also initially identified as a transforming proto-oncogene. In addition to being expressed in fibroblasts, FGF5 is expressed in breast cancer and several cancers of the gastrointestinal and urinary tract. Exogenous FGF5 exerts proliferative effects on cultured pancreatic cancer cells which express FGFR1 IIIc suggesting that FGF5 may act as paracrine and autocrine factor in pancreatic cancer.

FGF6

FGF6 or human stomach transforming factor-2 also displays transforming potential and was found in prostate cancer in conjunction with FGFR4. Exogenous FGF6 enhances the proliferation of primary prostatic epithelial and stromal cells and prostate cancer cell lines suggesting that FGF6 may act as paracrine and autocrine factor in prostate cancer.

FGF7

FGF7 is an important mitogen for a variety of epithelial and cancer cells, including liver, pancreas, gastrointestinal tract, lung, and breast. Inhibition of FGF7 signaling results in reduced mobility and invasion of breast and gastric cancer cells. FGF7 is overexpressed in many cancers, but is expressed at lower levels in squamous cell carcinomas of the head and neck and endometrial cancers by comparison with the corresponding normal tissue. In many cases, FGF7 is not expressed in the cancer cells, but in the adjoining cellular elements within these pathological tissues. Moreover, serum FGF7 levels are lower in patients with prostate cancer in comparison to patients with benign prostatic hyperplasia. Together, these observations suggest that FGF7 may differentially modulate tumor growth depending on its site of expression and on the expression and localization of the FGF receptors in these tissues.

FGF8

FGF8 or androgen-induced growth factor was isolated from SC-3 androgen-stimulated mouse mammary carcinoma cells and found to be overexpressed in breast cancer. *Fgf8* has been proposed to enhance murine mammary tumorigenesis in cooperation with the *Wnt-1* proto-oncogene. It was found that the four known human FGF8 isoforms (a, b, e, and f) display different proliferating and transforming potencies, the FGF8b isoform being the most potent. Constitutive expression of FGF8b resulted in enhanced invasion, angiogenic capacity, and tumor growth of breast cancer cells, underscoring its potential role in this malignancy.

FGF9-23

Expression of FGF9 or glia-activating factor, FGF10, and FGF19 was detected in various cancer tissues and these FGFs are also able to act as mitogens. FGF19 transgenic mice that overexpress FGF19 in skeletal muscle, exhibits elevated hepatic α-fetoprotein levels at 2 months of age and develop hepatocellular carcinomas by 10 months of age.

FGFR Actions in Cancer

In order to exert their activities, FGFs are dependent on the presence of high-affinity FGFRs. Changes in isoform expression of various FGFRs appear to be important for the enhancement of tumorigenesis and transformation.

FGFR1

FGFR1 is expressed in a wide variety of cell types and tissues including many malignancies. Amplification of the *Fgfr1* locus on chromosome 8p12 was associated with nodal involvement in breast cancer and poor prognosis of patients with bladder cancer. An atypical stem-cell myeloproliferative disorder evolving toward acute myelogenous leukemia is characterized by a 8p12–11 breakpoint and at (8;13) translocation, resulting in an aberrant formation of a tyrosine kinase with the catalytic domain of FGFR1 and constitutive kinase activity. This translocation was also found in breast cancer. Expression of *Fgfr1* in transgenic mice suggests that FGFR1 plays an important role in mammary gland tumorigenesis. Deletions of 8p12 have been reported for choriocarcinoma and frequent disturbances including amplification or deletions have been reported in prostate cancer. FGFR1 expression can also be induced by overexpression of cyclin D1 in fibroblasts via the pRb/E2F pathway. Cyclin D1 is known to be overexpressed in many malignancies and correlates with poor prognosis in several malignancies. Recent evidence also suggests that N-cadherin expression can enhance tumorigenesis via FGFR1. FGFR1 ligand-induced internalization was reduced by N-cadherin mediated by the first two Ig-like domains and resulted in increased FGFR1 stability and sustained activation of mitogen-activated protein kinase.

A potent ligand of FGFR1, FGF2, has been shown to be an important prognostic factor for many malignancies. Nevertheless, high FGFR1 expression was only associated with poor differentiation in prostate cancer,

advanced stage in head and neck squamous cell carcinoma, and nonsmall-cell lung cancer. In addition, recent evidence suggests that alterations in the expression of certain splice variants may be responsible for malignant transformation. Thus, expression of FGFR1 IIIc in normal ductal pancreatic epithelial cells resulted in the establishment of an autocrine loop and cellular transformation with increased proliferation and *in vivo* tumor formation. Expression of FGFR1 IIIc in the cancer cells, which are of epithelial origin, has been linked to the pathogenesis of pancreatic and prostate cancers. Additionally, altered expression of FGFR1 splice variants have been reported in breast cancer. Specifically, the 2-Ig like isoform (also called FGFR1β) is up-regulated in pancreatic, prostate, and breast cancers, and in astrocytomas and glioblastomas in comparison to the 3-Ig form (FGFR1α).

Inhibition of FGFR1 signaling using dominant-negative or soluble forms of the receptor resulted in significant growth inhibition in pancreatic, breast, prostate, and several other cancer cell lines. Using vaccination with *Xenopus* FGFR1 in a murine tumor model resulted in the production of FGFR1-specific autoantibodies and effective antitumor activity and suppression of angiogenesis.

FGFR2

FGFR2 is also found in a wide variety of cell types and tissues and was first identified as an amplified gene from a human gastric cancer cell line. Amplification of *Fgfr2* on chromosome 10q26 was also observed in breast and oral squamous cell carcinomas. One important isoform, keratinocyte growth factor (KGFR), is devoid of the Ig-like domain I and the acidic box and contains sequences encoding the IIIb variant. Overexpression of KGFR occurs in gastric and pancreatic cancers, and is associated with poor differentiation in prostate cancer, whereas KGFR expression is lower in endometrial cancer in comparison to the normal endometrium.

An essential feature of *Fgfr2* is its proposed strictly tissue-specific expression using exon IIIb in epithelial cells and IIIc in mesenchymal cells. Exon switching from IIIb to IIIc in conjunction with the presence of stromal cell-derived FGF7 was accompanied with malignant progression in a prostate cancer model, down-regulation of IIIb with malignant progression of the prostate, and dedifferentiation of normal oral keratinocytes into a malignant phenotype. This exon switch from FGFR2 IIIb to FGFR2 IIIc can be induced by the presence of FGF1 and 2 in keratinocytes, fibroblasts, and bladder carcinoma cells. Re-expression of KGFR by transfection in human salivary gland adenocarcinoma cells which lost KGFR expression in the process of malignant transformation, resulted in growth inhibition, induction of differentiation, and apoptosis. *Fgfr2* mutations linked to craniosynostosis syndromes and resulting in constitutive receptor activation with transforming potential were also detected in gastric cancers, suggesting that gain-of-function mutations of *Fgfr2* can also play a role in tumorigenesis.

FGFR3

Mutations of *Fgfr3* were identified in a great portion of bladder carcinomas and at low frequency in cervical, urothelial cell, and colorectal carcinomas. Many of these mutations occurred at highly conserved sequences in the Ig-like domain III, highlighting the functional importance of this domain. Mutations were not detected in stomach, rectum, prostate, ovarian, breast, brain, or renal tumors or cell lines. Interestingly, the presence of FGFR3 mutations in bladder and urothelial cell carcinoma was associated with better clinical outcome.

Nuclear accumulation of FGFR3 has been reported in breast cancer samples. This is probably related to a splice variant in which exons 7 and 8 are deleted resulting in the translation of a soluble intracellular FGFR3 missing the transmembrane domain, but with an intact kinase domain. Using other splice variants that are devoid of the acidic box, it could be shown that inhibitory functions of FGFR3 can be abolished. Other variants with altered ligand-binding specificities were described in osteosarcoma and squamous carcinoma cell lines. Thus, depending on the mutations and the receptor splice variant expressed, FGFR3 can display transforming potential, supporting the possible role of FGFR3 in the pathogenesis of some malignancies.

FGFR4

G to A conversions resulting in a substitution of glycine by arginine at position 388 in the transmembrane domain of the *Fgfr4* gene have been described. Expression of this receptor in mammary tumor cells increased cell mobility and the presence of this allele was associated with lymph node metastases and more advanced disease in colon cancer and reduced disease-free survival in breast cancer. Amplification of *Fgfr4* on 5q35.1-qter has been reported in some breast and ovarian cancers, leukemias, and lymphomas. FGFR4 overexpression was also reported in endocrine tumors of the digestive system, several gastrointestinal and urinary tract cancers as well as breast and lung cancers. FGFR4 expression has also been correlated with a lower differentiation state and tends to be associated with shorter patient survival in astrocytomas. Furthermore, a truncated form of FGFR4 lacking the first two Ig-like domains was identified in human pituitary tumors. Because the N terminus of this truncated receptor lacks a signal peptide, it is not inserted into

the plasma membrane and resides in the cytoplasm. The truncated receptor is constitutively phosphorylated and exhibits transforming potential in fibroblasts. Its expression in transgenic mice results in formation of pituitary tumors suggesting that this isoform may play a role in the development of pituitary tumors.

Experiments using dominant-negative FGFR4 also suggest that FGFR4 may be involved in matrix adhesion and therefore tumor dissemination. Expression of FGFR4 induced membrane ruffling, a sign of transformation of breast cells, in the presence of FGF1 or 2. Furthermore, the differentiation of teratocarcinoma cells was associated with loss of FGFR4 expression.

Nothing is presently known about involvement of FGFR5 in any malignancies.

Summary

In addition to their role in many biological processes during development and in the adult, FGFs and FGFRs are involved in the pathobiology of many malignancies. One important reason for this seems to be the altered expression of FGFs and FGFRs and their isoforms resulting in the aberrant activation of autocrine and paracrine signaling loops that eventually promote tumorigenesis. Other changes include the expression of abnormal FGFs or FGFRs with constitutive activation of FGFR tyrosine kinase signaling. Thus, the functional analysis of the role of FGF–FGFR alterations in specific cancer entities may lead to novel and highly specific treatment strategies.

See Also the Following Articles

Alternative Splicing: Regulation of Fibroblast Growth Factor Receptor (FGFR) • Immunoglobulin (Fc) Receptors • Phospholipase C

Glossary

malignant transformation Process of exhibiting qualities of malignancies including uncontrolled growth, anchorage-independent cell growth, and *in vivo* tumor formation.

mRNA splice variant An isoform of a protein resulting from the processing of different exons of a gene.

Further Reading

Burgess, W. H., and Winkles, J. A. (1996). The fibroblast growth factor family: Multifunctional regulators of cell proliferation. In *Cell Proliferation in Cancer, Regulatory Mechanisms of Neoplastic Cell Growth* (L. Pusztai, C. E. Lewis and E. Yap, eds.) pp. 154–217. Oxford University Press, New York.

Ford-Perriss, M., Abud, H., and Murphy, M. (2001). Fibroblast growth factors in the developing central nervous system. *Clin. Exp. Pharmacol. Physiol.* **28**, 493–503.

Johnson, D. E., and Williams, L. T. (1993). Structural and functional diversity in the FGF receptor multigene family. *Adv. Cancer Res.* **60**, 1–41.

Klint, P., and Claesson-Welsh, L. (1999). Signal transduction by fibroblast growth factor receptors. *Front. Biosci.* **4**, D165–D177.

Lax, I., Wong, A., Lamothe, B., Lee, A., Frost, A., Hawes, J., and Schlessinger, J. (2002). The docking protein FRS2alpha controls a MAP kinase-mediated negative feedback mechanism for signaling by FGF receptors. *Molecul. Cell* **10**, 709–719.

Ornitz, D. M., and Itoh, N. (2001). Protein family review: Fibroblast growth factors. *Genome Biol.* **2**, 30051–300512.

Biography

Marko Kornmann is an Assistant Professor of Surgery in the Department of Visceral and Transplantation Surgery at the University of Ulm in Germany. His principal research interests are in molecular and biological alterations of growth factor pathways in gastrointestinal malignancies. He holds an M.D. and Ph.D. from the University of Ulm and received his postdoctoral training at the University of California, Irvine.

Murray Korc is the Joseph M. Huber Professor and Chairman in the Department of Medicine at Dartmouth-Hitchcock Medical Center and Professor of Pharmacology and Toxicology at Dartmouth Medical School in Hanover, New Hampshire. His principal research interests are in the elucidation of the molecular alterations that occur in pancreatic cancer.

Flavins

Barrie Entsch and David P. Ballou
University of Michigan, Ann Arbor, Michigan, USA

The word flavin in biochemistry comes from the Latin word meaning yellow. The root word flavin was used in the early twentieth century to refer to yellow compounds extracted from tissue samples. Richard Kuhn is credited with the preparation of pure riboflavin (which he called lactoflavin – from milk) and its structural determination. Kuhn received the Nobel prize for this and other work in 1938. Today, the term flavin is reserved for a group of compounds that contain the fused three-ring structure called isoalloxazine which is responsible for the yellow color.

The most important flavins in nature are riboflavin, flavin mononucleotide (FMN), and flavin adenine dinucleotide (FAD) as shown in Figure 1. Riboflavin is often known as vitamin B2 (one of the soluble vitamins), which is an essential requirement in the diet of mammals and many other organisms. Riboflavin is manufactured by most microorganisms and plants. There is now a great deal of information on the process of biosynthesis. Organisms that require riboflavin as a vitamin use specific enzymes and ATP to convert the compound into both FMN and FAD. These nucleotides are used as cofactors (or prosthetic groups) in the structure and function of many proteins. The relationship with proteins is so important that we normally think of flavins in the context of protein structures. Thus, we refer constantly to flavoproteins as proteins with a flavin cofactor. This article describes the fundamentally important functions of these compounds in a wide variety of chemical processes in nature.

Chemistry

The chemistry of flavins has been studied extensively. Riboflavin is a stable compound with a variety of interesting properties. FMN and FAD are much more important in cells, but are less stable in solution because of the presence of phosphate ester and anhydride bonds. Riboflavin is responsible for the important biological chemistry of all flavins. Only the reactions most relevant to life are mentioned below. One reason that flavoproteins have been so extensively analyzed is that they can be studied by examining the properties of their cofactor that is nearly always involved in the core function of each protein. Another reason is the variety of chemical properties that have been exploited for important biological functions of considerable diversity.

Redox Properties

Oxidized flavins (called flavoquinones) can be reduced by two electrons and protons, and the redox potential for reduction is ~ -0.2 V at pH 7 (Figure 2). Reduced flavins (flavohydroquinones) are thus moderate reducing agents and can occur as either a neutral or an anionic form. Part of the versatility of flavins comes from their ability to be reduced in one-electron steps because flavins are capable of forming stable free radicals (flavosemiquinones in Figure 2). A neutral and an anioic free radical can be formed by flavins and both occur in nature. Proteins modify these redox properties by the interactions formed with the flavin cofactor to establish a wide variety of biological processes. Flavins can pass electrons to transition metal ions. Many proteins make use of this property to link stable reducing compounds (e.g., NADH) to reactive metal ions and one-electron processes in electron transport chains. Flavins are almost always involved as the transforming molecule.

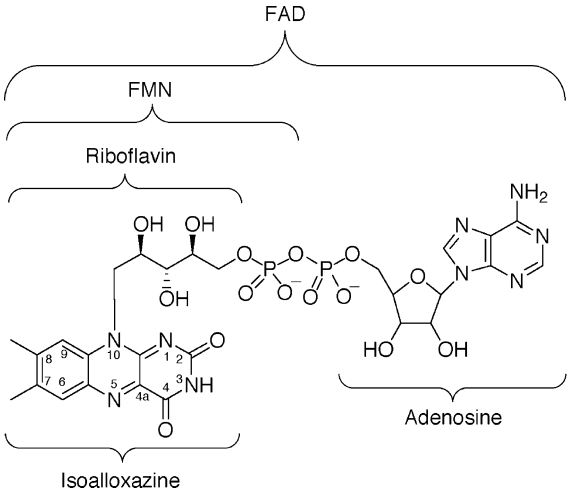

FIGURE 1 The structures of flavins discussed in this article. The numbering system shown for the isoalloxazine ring is used in the text.

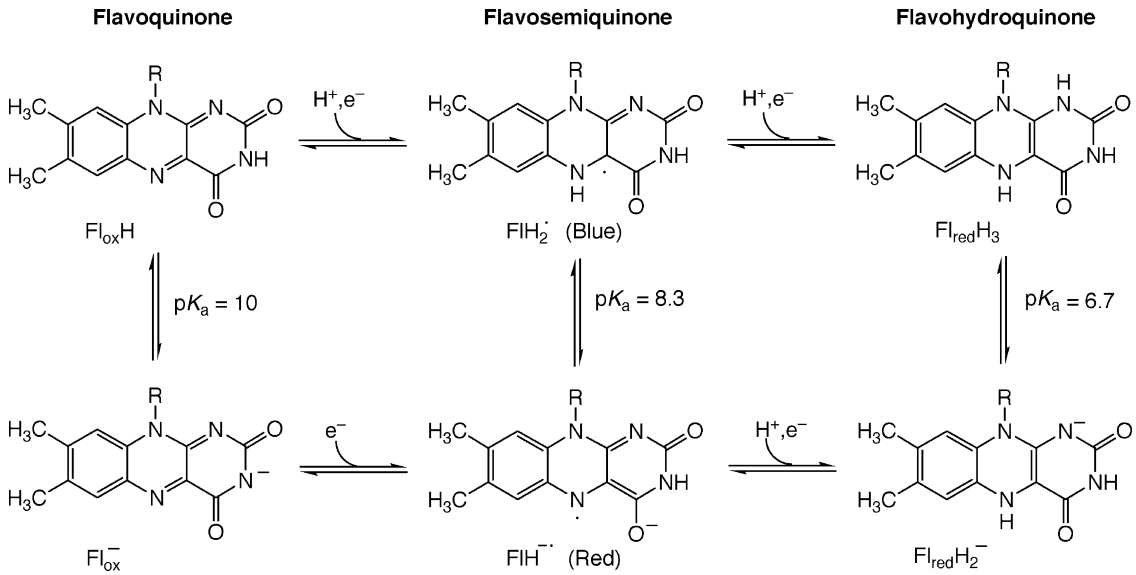

FIGURE 2 The redox states of the isoalloxazine ring that are observed in natural systems.

Oxygen and Other Derivatives

Flavins, unlike most organic molecules, react with oxygen. This reactivity is a product of the redox properties mentioned above. Oxygen is unreactive without the formation of free-radical intermediates. Reduced flavins provide the capacity for one-electron reductions and have the additional ability of forming reactive covalent adducts with oxygen and other molecules. Bruice and colleagues have shown that the reactions between reduced flavins and oxygen involve covalent adducts and free-radical intermediates. Many proteins take advantage of the oxygen adducts (Figure 3) to help carry out chemical reactions. A wide variety of biological processes depend upon the specific interactions between particular proteins and these flavin adducts. A small number of proteins form stable covalent bonds to the flavin through the 8-position (Figure 1).

Spectroscopic Properties

Oxidized flavins (the stable form) are normally yellow due to a major electronic transition observed at ~450 nm (Figure 4). Full reduction of flavins (two equivalents) gives a structure that has a low absorbance beyond 400 nm, and thus looks almost colorless (pale yellow) by comparison to oxidized flavins. Free-radical flavins (flavosemiquinones) have complex spectra with spectacular colors – either red or blue (Figure 4), depending on the state of protonation. Flavins also form charge-transfer complexes with a variety of other compounds. These complexes have a range of different visible spectra with a corresponding variety of colors. Various proteins can stabilize one or more of these chemical species, so that flavoproteins can

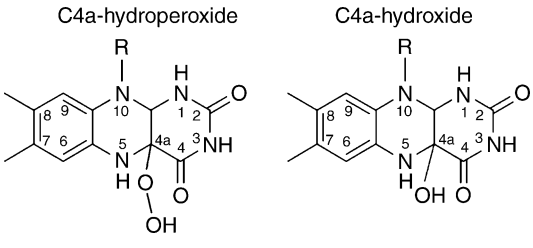

FIGURE 3 The structure of transient oxygen derivatives of the isoalloxazine ring that are important in protein function. Note that thiol groups can form a similar structure to the C4a-hydroxide. The biological function of the sulfur derivative is discussed in this article.

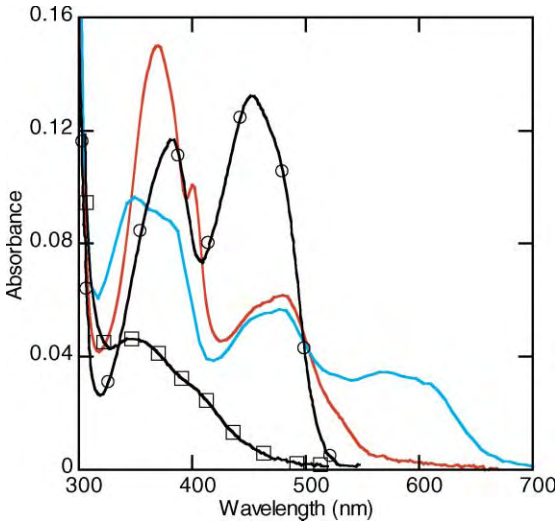

FIGURE 4 Absorption spectra of the redox states of FAD in glucose oxidase. A solution of 9.5 μM oxidized enzyme (solid line/open circles) was photoreduced in anaerobic conditions at pH 9.2 to form the red, anionic semiquinone. The solution was shifted to pH 5.0 with citric acid to form the blue semiquinone, and then reduced with glucose to form the hydroquinone (solid line/open squares).

have many colors, as well as change color during catalytic function.

Flavins have important luminescent spectral properties. Many flavins are fluorescent, and the fluorescence properties are strongly influenced by association with proteins and by the oxidation state or formation of derivatives. These properties can be studied in biological systems because the flavin can be excited by light (between 350 and 480 nm) and the emitted light is a broad band with a peak near 530 nm. This property provides a sensitive assay of flavins down to $\sim 10^{-9}$ M. The fluorescent properties of flavoproteins often provide information not available from absorbance properties. Flavins can even be trapped in excited states and this has been exploited in living systems. Nature has also utilized the enhanced reactivity of the excited states of flavins that last long enough to be chemically useful.

Types of Flavoproteins

To try to display the diversity and utility of flavin function in living systems, we adapt below the classification system for flavoproteins developed by Massey.

Pyridine Nucleotide Oxidoreductases

There is a diverse group of proteins that connects the stable reducing currency of cells (NADH/NADPH) with other redox processes required for cellular function. For example, glutathione reductase is one of a group of related disulfide reductases that contain both FAD and a pair of reactive cysteine residues in the active site. The function of this enzyme is to help maintain a reducing environment within cells by keeping glutathione reduced. Glutathione then carries out many important functions such as reducing disulfides in proteins and removing hydrogen peroxide from cells (catalyzed by glutathione peroxidase). Through the flavin buried in the protein, the enzyme can use the reducing power of NADPH to reduce the disulfide of glutathione, because the flavin reacts rapidly with thiols by the formation of a transient covalent adduct (Figure 3). Another example is ferredoxin reductase, the enzyme principally associated with photosynthesis that enables reactive, strongly reducing proteins such as ferredoxin to provide stable reducing equivalents in the cell as NADPH. Through the FAD in the active site, the enzyme can accept single reducing electrons from ferredoxin (electrons collected from the reactive free-radical photochemical process) that can then be safely stored as NADPH.

Dehydrogenase/Electron Transferase

There are a limited number of enzymes that use flavins to link oxidation of a stable metabolite to electron transport chains for energy conservation in cells. For example, succinate dehydrogenase is a component of the "citric acid cycle" in mitochondria and it links directly into the respiratory complexes through an iron/sulfur cluster complex. The FAD in this enzyme is covalently linked to the protein where it accepts a pair of electrons from the oxidation of succinate and then transfers single reducing electrons into the respiratory complex II. The acyl-CoA dehydrogenases in animals have a similar fundamental role in obtaining energy from the oxidation of fats. These enzymes contain FAD and the latter accepts electrons from a fatty acyl-CoA to initiate oxidation of a fatty acid. In this case, the electrons are transferred to the respiratory chain in mitochondria through another soluble flavoprotein called the electron transferring flavoprotein. In plants, the process of fatty acyl-CoA oxidation occurs in glyoxisomes (rather than mitochondria) by the use of similar enzymes that are oxidases. That is, after being reduced by the fatty acyl-CoA, the enzyme flavin reacts with oxygen to dispose of the reducing electrons. The difference between these enzymes in animals and plants is a subtle change in the protein interactions with the FAD that changes the course of the reaction.

Electron Transfer Proteins

There is a small group of proteins that act to provide single reactive reducing electrons for a variety of biological reactions. Most of these proteins contain iron/sulfur complexes, but a few are flavoproteins that use the ability of flavins to form stable free radicals. For example, flavodoxins are widespread in microorganisms and have been extensively studied. The protein in flavodoxins makes a specific interaction with the isoalloxazine ring that stabilizes the blue neutral radical (Figures 2 and 4), and makes further reduction difficult. Thus, when reduced, flavodoxins are strong one-electron reducing agents. Electron transferring flavoprotein referred to earlier is a different member of this family of proteins.

Oxygenases

Flavins are widely employed in cells to unlock the reactivity of the oxygen molecule. Oxygenases not only react with oxygen, but they also incorporate oxygen into metabolites. There are many types of flavoprotein oxygenases that tame oxygen for useful purposes. For example, *p*-hydroxbenzoate hydroxylase adds one atom of oxygen to an aromatic ring so that it

can eventually be used for carbon and energy supply for a microorganism. Oxygenated aromatic rings are then converted to aliphatic compounds by subsequent metabolic steps. *p*-hydroxybenzoate hydroxylase contains FAD in the structure and has been studied extensively to understand this type of reaction. In catalysis, the reduction of FAD by NADPH is tightly controlled in a remarkable process. The enzyme senses the presence of the substrate *p*-hydroxybenzoate in the active site and responds by swinging the isoalloxazine ring to the surface of the protein where it contacts the NADPH. This process makes use of the flexibility of the ribityl side chain of FAD. Then, after reduction, the isoalloxazine swings back into the interior of the protein where it not only reduces oxygen, but also forms a transient covalent adduct (Figure 3, hydroperoxide) in the controlled environment of the enzyme. The peroxide provides the reactive oxygen to oxygenate the substrate. Cyclohexanone monooxygenase provides a different example where the FAD, after reduction by NADPH, reacts with oxygen to form a peroxide anion that reacts rapidly with the carbonyl group of cyclohexanone. Another variation is found in lactate monooxygenase. Here, the enzyme flavin (FMN) is reduced by the substrate lactate to form pyruvate that is held by the enzyme and oxygenated by the peroxide formed from the reaction between reduced FMN and oxygen.

Oxidases

Flavoproteins can also use oxygen as a sink for removing unwanted reducing electrons. This process was briefly referred to above in relation to fatty acyl-CoA oxidase in plants. Another important example is glycolate oxidase in plants. During photosynthesis, glycolate is formed as an unwanted byproduct and must be removed. Glycolate oxidase uses FMN to oxidize glycolate to glyoxalate, which is then aminated to glycine, a normal metabolite. This process occurs in peroxisomes where oxygen is used to react with reduced FMN to remove the reducing electrons from glycolate, rather than through an electron transport chain. The oxygen is reduced to hydrogen peroxide (similar to the oxygenases), but the peroxide is released from the enzyme and must be removed from the cell by other enzymes such as catalase to prevent dangerous side reactions. Other examples of this use of oxygen by flavoproteins are D-aminoacid oxidase in kidneys and glucose oxidase in fungi. It is the absence of a flavoprotein oxidase function (gulonolactone oxidase) that explains why humans require vitamin C in their diets, when most animals can make this molecule. In humans, the gene for this enzyme has mutated and no longer codes for a functional protein.

Photochemistry

Flavoproteins show some really novel functions when the properties of their excited states are utilized in cells. A classic example is bacterial luciferase, which is an enzyme that produces lime-green light from chemical energy. The light-producing process is an outgrowth of the reactions of the oxygenases. NADH is used to reduce FMN by one enzyme and then the reduced FMN binds to luciferase where it reacts with oxygen to form the flavin C-4a-hydroperoxide (Figure 3). The novel reaction occurs when the hydroperoxide oxidizes a fatty aldehyde to form the corresponding fatty acid. In this reaction the protein traps the FMN in an excited state of the flavin C-4a-hydroxide (Figure 3), which can decay with the release of a photon. Many marine animals in the deep oceans form symbiotic relationships with the bacteria that make luciferase. The animal can then form light-emitting organs essential for communication, hunting, or defense.

Just as remarkable as luciferase is DNA photolyase, which is found in all cells. An essential part of cellular survival is the maintenance of the integrity of genetic information in the face of damage by environmental factors. One source of damage is UV light, which can cause cross-linking of bases in the DNA helix. It is the task of DNA photolyase to repair the damage often by using the same source of light that caused the damage. This enzyme contains both an FAD and an accessory pigment. The flavin functions in the protein in the reduced state, where it is converted to a powerful reducing agent when excited by energy from light. The excited reduced state is powerful enough to break down the unwanted covalent bonds in damaged DNA and thus repair the integrity of the genetic information. Electrons used for this purpose are then recovered to reform the reduced FAD.

Another developing story about flavoprotein photochemistry involves flavins as blue-light photoreceptors. For example, phototropins are photoreceptors for some plant responses to light. These proteins contain FMN that forms a transient and reversible covalent bond to an active site cysteine upon illumination. This complex is thought to form through a free-radical mechanism of excited state flavin chemistry.

Medical Significance

It is extremely rare for riboflavin deficiency to occur in humans because of its widespread occurrence in food. However, some flavoproteins are important in medical practice. A few examples are mentioned below.

A common medication for gout (caused by excess uric acid) is allopurinol. This drug inhibits xanthine oxidase, a complex flavoprotein involved in formation of the uric

acid that causes gout. Uric acid is the end product of the natural breakdown of purines in the body.

Another complex flavoprotein, monoamine oxidase is a target for modulation by drug therapy, particularly for depression, because this enzyme degrades some of the potent natural neurotransmitters involved in mental disorders.

The flavoprotein, methylenetetrahydrofolate reductase is involved in the formation of the amino acid methionine. About 12% of the human population has a form of the enzyme that leads to elevated homocysteine in the blood, a major risk factor in cardiovascular disease.

Some medications for stomach ulcers work because they are substrates for the bacterial flavoprotein, nitroreductase produced by the ulcer-causing *Helicobacter pylori*. The reduced products formed from the drug by the enzyme kill the bacterial cells.

See Also the Following Articles

Fatty Acid Synthesis and its Regulation • Peroxisomes • Tricarboxylic Acid Cycle

Glossary

fatty acyl-CoA Derivatives of fatty acids (CoA thioesters) formed in cells to initiate oxidation of the fatty acid.

glyoxisome/peroxisome Common membrane-enclosed compartments in plant and animal cells.

hydroperoxide A derivative of hydrogen peroxide where one of the H atoms is replaced by a chemical group.

isoalloxazine Fused three-ring structure that forms the core chemical function of flavins (Figure 1).

redox Shorthand for reduction and oxidation processes.

Further Reading

Flavins and Flavoproteins. A series of books that report the Proceedings of the International Symposia on Flavins and Flavoproteins are published every three years. Since 1990 this series has been published by Walter de Gruyter and Rudolf Weber, Berlin.

Massey, V. (1994). Activation of molecular oxygen by flavins and flavoproteins. *J. Biol. Chem.* **269**, 22459–22462.

Massey, V., and Ghisla, S. (1974). Role of charge-transfer interactions in flavoprotein catalysis. *Annu. N.Y. Acad. Sci.* **227**, 446–465.

Müller, F. (ed.) (1991). *Chemistry and Biochemistry of Flavoenzymes*, Vols. I–III, CRC Press, Boca Raton.

Palfey, B. A., and Massey, V. (1998). Flavin-dependent enzymes. In *Comprehensive Biological Catalysis: Vol. III Radical Reactions and Oxidation/Reduction* (M. Sinnott, ed.) pp. 83–154. Academic Press, London.

Biography

Dr. Barrie Entsch retired from the position of Associate Professor of Biochemistry at the University of New England, Australia in 2002. He now works as a Research Fellow in Biological Chemistry at the University of Michigan, Ann Arbor. He has collaborated on mechanistic studies of flavoproteins with David Ballou and Vincent Massey for more than 30 years. He was awarded several Australian Research Council Grants for research with flavoproteins, particularly oxygenases.

David Ballou has been a Professor on the faculty of the Department of Biological Chemistry at the University of Michigan since 1972. His work has mainly been mechanistic and structural studies on a wide variety of redox enzymes. These include flavoproteins, cytochrome P450, cobalamin-containing enzymes, non-heme iron oxygenases, and copper enzymes. He has specialized in the development of rapid kinetic and spectroscopic methods for studying these systems.

Flippases

Charles J. Waechter
University of Kentucky College of Medicine, Lexington, Kentucky, USA

Membrane proteins referred to as flippases play a vital role in membrane biology by overcoming the biophysical barrier imposed by the greasy, hydrophobic core of the bilayer common to biological membranes, and facilitating the transbilayer movement of the hydrophilic headgroups of phospholipids and glycolipids. This article summarizes the transbilayer events involved in biosynthetic processes and establishing phospholipid asymmetry and speculates on the mechanism(s) that could overcome the thermodynamically unfavorable spontaneous flip-flopping of the various polar lipids. More detailed reviews of some aspects of the flip-flopping of phospholipids and dolichol-linked saccharide intermediates can be found in the references cited at the end of this article.

Introduction

During the bioassembly of N-linked oligosaccharides, C- and O-linked mannosyl units in proteins, glycosylphosphatidylinositol (GPI) anchors, glycosphingolipids, and newly formed phospholipid bilayers in eukaryotic cells, charged hydrophilic headgroups must diffuse transversely through the hydrophobic core of the endoplasmic reticulum (ER) and an early Golgi compartment. Similarly, in prokaryotes phospholipids and undecaprenyl pyrophosphate-linked glycosyl building blocks must be translocated from the inner leaflet to the outer monolayer during the expansion of the cytoplasmic membrane and the biosynthesis of cell-wall components. Biochemical and biophysical model systems indicate that the unassisted transbilayer movement of polar lipids with charged headgroups is highly unfavorable thermodynamically and much too slow to allow cells to synthesize the essential glycoconjugates in a physiologically requisite time frame. Thus, it has been proposed that the "flip-flopping" of the amphipathic precursors/intermediates is mediated by a class of membrane proteins referred to as flippases. The term "flippase" was originally suggested by Mark Bretscher during the 1970s.

The transbilayer movement of lipids with the generalized structure of a polar lipid (A) and of mannosylphosphoryldolichol (Man-P-Dol) (B) mediated by a flippase is illustrated in Figure 1. Table I summarizes several examples of polar lipids whose transverse diffusion is believed to be facilitated by flippases in prokaryotic and eukaryotic cells. Despite the critical function of flippases in membrane biology, there are still very large gaps in the information about their structures, the genes encoding this vital class of proteins and the mechanism(s) by which they shield and permit the passage of the polar moieties through the hydrophobic core of the ER and other cellular membranes.

Expansion of the ER Bilayer during Membrane Biogenesis

It is well established that the major site of phospholipid biosynthesis *de novo* in eukaryotes is on the cytoplasmic leaflet of the ER membrane. Clearly, to have uniform expansion of the bilayer during active membrane biogenesis, ~50% of the newly formed phospholipids must be translocated to the lumenal monolayer. The landmark study of Kornberg and McConnell proved that the unassisted movement of spin-labeled phosphatidylcholine (PC) molecules between the two leaflets of pure lipid vesicles did not occur fast enough to maintain bilayer expansion at physiological rates. Further emphasizing the essential role of flippases, the classic experiments of James Rothman and Eugene Kennedy demonstrated that movement of phosphatidylethanolamine molecules, newly synthesized on the cytoplasmic leaflet of a *B. megaterium* cell, to the extracellular monolayer was remarkably faster than the rate of spontaneous diffusion in artificial lipid bilayers. Primarily due to severe technical difficulties inherent in studying the phospholipid flippase(s), there is still very little known about the structure and mechanism of this eminently important class of membrane proteins. Bishop and Bell proposed the novel idea of following the transport of a water-soluble analogue (diC_4PC) of PC by sealed microsomal vesicles to implicate one or more ER proteins in the transbilayer movement of the major membrane phospholipid. The PC flippase is

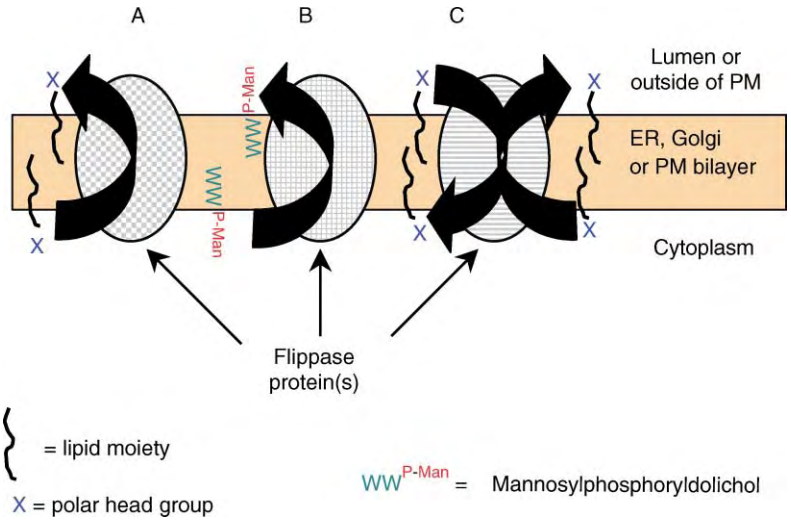

FIGURE 1 Illustration of the flippase-mediated transbilayer movement of a membrane lipid with the generalized structure of a polar lipid (A) or mannosylphosphoryldolichol (B) from the cytoplasmic leaflet to the lumenal monolayer in the ER or Golgi. The ATP-dependent flip-flopping of a phospholipid from the outer surface of the PM (C, left) or the bidirectional, ATP-independent movement of a polar lipid mediated by scramblases is depicted in model (C). Although the translocation in examples in A and B are illustrated as being unidirectional, these processes appear to be bidirectional.

depicted in Figure 1A. The basic principle of this experimental approach is to design a water-soluble form of the polar lipid in which the hydrophobic groups are reduced in size to increase their solubility in aqueous solutions while retaining the essential structural features recognized by the proteins mediating their translocation. Although this experimental approach and alternate methods have been utilized by other researchers more recently to make progress toward these goals, the PC and other phospholipid flippases in biogenic membranes remain to be identified, isolated, and cloned. Presumably, neutral lipids such as cholesterol, coenzyme Q, and neutral glycerides diffuse transversely in cellular membranes by a protein-unassisted process since they lack charged, hydrophilic groups.

Aminophospholipid Flippases/ Translocases, Floppases, Scramblases, and Phospholipid Asymmetry

In most, if not all, cellular membranes phospholipids are distributed asymmetrically between the two leaflets, a property that is critical to membrane function. Thus, in addition to the flippases crucial to uniform expansion of the bilayer in the ER during membrane biogenesis, another set of flippases is required to maintain the proper distribution of phospholipids between the two leaflets of membranes in the various cellular compartments. The combined action of aminophospholipid flippases, two types of outwardly driven floppases (multidrug resistance, MDR, P-glycoprotein, other

TABLE I

Summary of Specific Flip-Flopping Events in Prokaryotic and Eukaryotic Cells

Polar lipid	Membrane site	Transbilayer movement from
Aminophospholipids (PS/PE)	Plasma membrane	Outer leaflet to inner monolayer
PC and other glycerophospholipids, GlcN-Pl, Man-P-Dol, Glc-P-Dol and $Man_5GlcNAc_2$-P-P-Dol	ER	Cytoplasmic to lumenal leaflet
Glucosylceramide	Early Golgi	Cytoplasmic to lumenal leaflet
Glycerophospholipids, and undecaprenyl-P(P)-linked cell-wall intermediates	Bacterial cytoplasmic membrane	Cytoplasmic leaflet to exterior monolayer (or outer membrane)

members of the MDR family and members of the multidrug resistance-associated protein, MRP, subfamily) and possibly the ATP-independent, bidirectional scramblases (Figure 1C) are believed to play a role in the asymmetric distribution of PC and other membrane phospholipids between the two leaflets of the plasma membrane (PM) and other cellular membranes. The best characterized of the candidate flippases is the ATP/Mg^{2+}-dependent aminophospholipid flippase. The properties of this type of flippase have been studied extensively, and progress has been made in purifying the protein component(s). It has been found in the PM of erythrocytes and other mammalian cells, synaptosomes, chromaffin granules, and secretory vesicles. This flippase appears to play a direct role in maintaining the enrichment of PS and PE in the inner leaflet of the PM by moving the two aminophospholipids from the outer to the inner leaflet of the plasma membrane against a concentration gradient at the expense of ATP. In Figure 1C (left) the lipid moiety would be diacylglycerol and the polar headgroup (X) would be either phosphorylserine or phosphorylethanolamine. The loss of this activity due to diminishing ATP pools or the loss of the protein(s) allows PE/PS to diffuse back to the outer monolayer where the surface alteration is recognized by the immune system as an early signal in apoptosis.

However, inhibition of the flippase or loss of ATP is insufficient to cause a rapid loss of plasma membrane PS asymmetry. Rapid PS externalization requires the additional activation of a (Ca^{2+}-dependent) scramblase. The bidirectional, ATP-independent scramblase (Figure 1C) plays an important role in platelet activation, blood clotting, and apoptosis.

There is good evidence that floppases (Figure 1A) mediate the ATP-dependent translocation of cholesterol, PC, and sphingolipids from the cytoplasmic to the external leaflet of the plasma membrane. More details of the latter two classes of "flippases" can be found in the excellent review by Dr. D. Daleke cited at the end of this article.

Protein N-Glycosylation

N-linked oligosaccharide chains are initially synthesized as the dolichyl pyrophosphate (Dol-P-P) linked precursor oligosaccharide by a two-stage process in the ER. In the first stage, three lipid intermediates, mannosylphosphoryldolichol (Man-P-Dol), glucosylphosphoryldolichol (Glc-P-Dol), and a heptasaccharide intermediate ($Man_5GlcNAc_2$-P-P-Dol) are synthesized in the ER by enzymes with active sites facing the cytoplasm. In the next stage these three glycolipid intermediates diffuse transversely to the lumenal monolayer where four more mannosyl units are added to $Man_5GlcNAc_2$-P-P-Dol with Man-P-Dol (Figure 1B) functioning as the mannosyl donor. Finally, three glucosyl units are donated by Glc-P-Dol, completing the synthesis of the oligosaccharyl donor, $Glc_3Man_9GlcNAc_2$-P-P-Dol. Based on evidence obtained from biophysical and enzymological topological studies, it is very likely that the transverse diffusion of the three intermediates requires ER proteins functioning as flippases to maintain lipid intermediate biosynthesis and protein N-glycosylation at physiologically relevant rates. Evidence has been obtained for the presence of ER proteins that mediate the transbilayer movement of short-chain, water-soluble analogues of Man-P-Dol and Glc-P-Dol by sealed vesicles from rat liver and brain by a variation of the experimental approach pioneered by Bishop and Bell. Preliminary studies using this transport technique indicate that the flippases are bidirectional and ATP independent. It is plausible that this class of flippase acts by facilitated diffusion, and the transbilayer movement of the lipid intermediates is driven by mass action as they are consumed during $Glc_3Man_9GlcNAc_2$-P-P-Dol synthesis on the lumenal surface. Hopefully, the *in vitro* assays will provide a means to isolating the ER proteins involved in this flip-flopping process. More recently, genetic and biochemical studies have implicated the *Rft1* protein in the transbilayer movement of $Man_5GlcNAc_2$-P-P-Dol in the yeast, *S. cerevisiae*. The structure of the yeast protein may provide clues to the identity of the gene encoding the corresponding protein in mammalian cells. The identification of the flippase proteins involved in the "dolichol pathway" and the corresponding genes should ultimately be relevant to the diagnosis of related genetic defects in patients with as yet uncharacterized forms of congenital disorders of glycosylation.

Relationship of a Man-P-Dol Flippase to the Biosynthesis of Other Mannose-Containing Glycoconjugates

Protein O- and C-Mannosylation

In yeast and mammalian cells, many proteins are modified by the addition of mannosyl units from Man-P-Dol to either serine/threonine in O-mannosidic linkage or to the indole ring of tryptophan residues in a C-mannosidic linkage. Since Man-P-Dol is believed to be formed only on the cytosolic face of the ER (Figure 1B), and these modifications appear to occur on the lumenal side of the ER, a Man-P-Dol flippase is essential for O- and C-mannosylation of proteins, as well as completing the synthesis of $Glc_3Man_9GlcNAc_2$-P-P-Dol and to maintain normal rates of protein N-glycosylation.

GPI Anchors

One class of proteins that is associated with membranes, despite not having any transmembrane domains, is attached by an amide linkage to GPI anchors. The biosynthesis of the GPI anchors theoretically requires at least two ER flippases. The best current evidence indicates that the early intermediate, GlcN-PI, is formed on the cytoplasmic face of the ER, and is subsequently translocated to the lumenal monolayer where the GPI anchor is completed and the appropriate polypeptides are covalently attached to the ethanolamine moiety by a transpeptidation reaction. The completion of the anchor on the lumenal surface also requires Man-P-Dol as a mannosyl donor, and the transverse diffusion of the mannolipid intermediate requires a flippase that is discussed above.

Glucosylceramide

The enzyme that synthesizes glucosylceramide (Glc-Cer) from UDP-glucose and ceramide in an early Golgi compartment has an active site that is oriented toward the cytoplasm. Since more complex cerebrosides and gangliosides are elaborated on the interior of the Golgi compartments, it is necessary for the Glc-Cer formed on the cytosolic side to be translocated to the lumenal leaflet where the glucosyl unit can be elongated by lumenally oriented glycosyltransferases. Thus, in this flippase-mediated event the lipid moiety would be ceramide and the polar headgroup would be a β-linked glucosyl group as illustrated in Figure 1A. The biosynthesis of the complex glycosphingolipids also requires a set of Golgi proteins to mediate the transbilayer movement of the sugar nucleotides required for ganglioside synthesis. Since there is experimental evidence that some fraction of the Glc-Cer formed on the cytoplasmic leaflet of an early Golgi compartment can be translocated directly to the inner surface of the PM, there may also be a PM flippase that mediates the movement of Glc-Cer to the outer leaflet.

Bacterial Cell Walls

In gram-positive and gram-negative bacteria, some of the building blocks for the assembly of peptidoglycan, lipopolysaccharide, and several other cell-wall complex glycoconjugates are synthesized on the inner face of the cytoplasmic membrane while attached to undecaprenyl pyrophosphate (Und-P-P). There is solid genetic evidence for the presence of membrane proteins that mediate the transbilayer movement of the bacterial lipid intermediates so the assembly of the cell-wall components can be completed on the exterior face of the cytoplasmic membrane, or in the case of gram-negative bacteria, on the outer membrane. The *Wzx* family has been proposed to encode proteins involved in the translocation of Undec-P-P linked intermediates in bacteria. There is recent evidence that the *wzxE* gene encodes a protein involved in the transbilayer movement of a trisaccharide lipid intermediate in the biosynthesis of the enterobacterial common antigen in *E. coli*. Although there is very limited information about their structures at this time, it is quite possible that the prokaryotic flippases resemble their eukaryotic counterparts. The intriguing question of why the polyisoprenoid glycosyl carrier lipids became longer (C55 for prokaryotes to C75–95 for eukaryotes) and acquired the saturated α-isoprene unit in dolichols during evolution remains to be explained.

See Also the Following Articles

Glycosylphosphatidylinositol (GPI) Anchors • Lipid Bilayer Structure • Protein Glycosylation, Overview

Glossary

dolichyl monophosphate An eukaryotic glycosyl carrier lipid containing 15–20 isoprene units in which the α-isoprene unit is saturated.

flippase A general term for a class of membrane proteins proposed to facilitate the transbilayer movement of the polar headgroup of a phospholipid, glycosphingolipid, or a polyisoprenyl-P(-P) linked glycosyl intermediate.

scramblase Bidirectional, ATP-independent transporters that randomly redistribute polar lipids formed *de novo* in the endoplasmic reticulum. This class also facilitates the nonspecific, bidirectional movement of phospholipids in the plasma membrane.

transverse diffusion The "flip-flopping" or transbilayer movement of a polar membrane lipid from one leaflet to the opposite monolayer of a cellular membrane.

undecaprenyl phosphate A fully unsaturated bacterial glycosyl carrier lipid containing eleven isoprene units.

Further Reading

Bishop, W. R., and Bell, R. M. (1985). Assembly of the endoplasmic reticulum phospholipid bilayer: The phosphatidylcholine transporter. *Cell* **42**, 51–60.

Bratton, D. L., Fadok, V. A., Richter, D. A., Kailey, J. M., Guthrie, and Henson, P. M. (1997). Appearance of phosphatidylserine on apoptotic cells requires calcium-mediated nonspecific flip-flop and is enhanced by loss of the aminophospholipid translocase. *J. Biol. Chem.* **272**, 26159–26165.

Daleke, D. L. (2003). Regulation of transbilayer plasma membrane phospholipid asymmetry. *J. Lipid Res.* **44**, 233–242.

Dolis, D., Moreau, C., Zachowski, A., and Devaux, P. F. (1997). Aminophospholipid translocase and proteins involved in transmembrane phospholipid traffic. *Biophys. Chem.* **68**, 221–231.

Helenius, J., Ng, D. T. W., Marolda, C. L., Walter, P., Valvano, M., and Aebi, M. (2002). Translocation of lipid-linked oligosaccharides

across the ER membrane requires Rft1 protein. *Nature* **415**, 447–450.

Kornberg, R. D., and McConnell, H. M. (1971). Inside-outside transitions of phospholipids in vesicle membranes. *Biochemistry* **10**, 1111–1120.

Menon, A. (1995). Flippases. *TICB* **5**, 355–360.

McCloskey, M. A., and Troy, F. A. (1980). Paramagnetic isoprenoid carrier lipids: 2. Dispersion and dynamics in lipid membranes. *Biochemistry* **19**, 2061–2066.

Rick, P. D., Barr, K., Sankaran, K., Kajimura, J., Rush, J. S., and Waechter, C. J. (2003). Evidence that the *wzxE* gene of *E. coli* K-12 encodes a protein involved in the transbilayer movement of a trisaccharide-lipid intermediate in the assembly of enterobacterial common antigen. *J. Biol. Chem.* **278**, 16534–16542.

Rothman, J. E., and Kennedy, E. P. (1977). Rapid transmembrane movement of newly synthesized phospholipids during membrane assembly. *PNAS* **74**, 1821–1825.

Schenk, B., Fernandez, F., and Waechter, C. J. (2001). The ins(ide) and outs(ide) of dolichyl phosphate biosynthesis and recycling in the endoplasmic reticulum. *Glycobiology* **11**, 61R–70R.

Sprong, M., van der Sluijs, P., and van Meer, G. (2001). How proteins move lipids and lipids move proteins. *Nat. Rev. Mol. Biol.* **2**, 504–513.

Biography

Charles Waechter received a Ph.D. in biochemistry in 1971 studying the regulation of membrane phospholipid biosynthesis in *S. cerevisiae* with Robert L. Lester (University of Kentucky College of Medicine). His major research interest, in the biosynthesis and function of lipid intermediates in protein N-glycosylation in mammalian cells, began as a postdoctoral fellow with Dr. William Lennarz (The Johns Hopkins University School of Medicine) during 1971–74. He is currently professor of Molecular and Cellular Biochemistry at the University of Kentucky College of Medicine, and has served on the editorial board of *The Journal of Biological Chemistry and Glycobiology*, in the Neurological Sciences Study Section at NIH, and in the Tumor Biochemistry Study Section of the ACS.

Focal Adhesions

Eli Zamir and Benjamin Geiger
The Weizmann Institute of Science, Rehovot, Israel

Focal adhesions (also known as focal contacts) are integrin-dependent adhesions in which the cell membrane is attached at its external surface to the extracellular matrix (ECM) and at its internal aspect to the actin cytoskeleton. These transmembrane interactions are mediated via a complex network of cytoplasmic proteins, forming a submembrane plaque. Additional ECM–integrin–actin-mediated adhesion sites, termed focal complexes, fibrillar adhesions, 3D-matrix adhesions, and podosomes, are related to focal adhesions, although the details of their molecular structures and functions differ. In addition to playing central roles in cell migration and morphogenesis, focal adhesions and related structures convey adhesion-triggered signals across the cell membrane, regulating cell proliferation, differentiation, and death.

Cell Adhesion

In multicellular organisms, cells adhere to their neighbors either directly or via a complex meshwork of fibers, known as the extracellular matrix (ECM). This adhesion is not a passive attachment but rather a complex process mediating specific, and dynamically regulated, cell interactions as well as crucial signaling cross-talks between the cell and its environment. Indeed, cell adhesion plays a fundamental role in embryogenesis and organogenesis as well as in cellular processes such as cytoskeletal organization, cell motility, and regulation of cell cycle and differentiation.

Moreover, cell adhesion is not a single molecularly uniform event but rather a highly diversified process at the cellular, molecular, and functional levels. For example, cell-to-cell adhesion occurs at tight junctions, gap junctions, chemical synapses, adherens junctions, desmosomes, and various carbohydrate-mediated contacts. Cell–ECM adhesions can involve a large variety of ECM proteins and glycosaminoglycans and their respective receptors, and they occur at specialized cellular sites such as intermediate-filament-associated hemidesmosomes and the widely occurring actin-associated contacts of the focal-adhesion type, which is addressed here.

Focal Adhesions—A Historical Perspective

Specialized adhesions between cultured fibroblasts and the underlying substrate were revealed over 30 years ago by interference–reflection microscopy and electron microscopy. These studies showed that the attached cells contain many specialized and defined regions (commonly measuring 0.25–2 by 2–10 μm) along the ventral plasma membrane, which are in a very tight contact (10- to 15-nm gap) with the substrate. Moreover, these sites, which were termed focal contacts or focal adhesions, appeared to be associated with the termini of actin microfilaments. These early studies revealed that focal adhesions are responsible for tight ECM contacts in which the extracellular substrate and the actin cytoskeleton are physically linked.

Following the early structural studies, the molecular composition of focal adhesions was addressed by immunofluorescence and immunoelectron microscopy, yielding a long list of diverse proteins, starting with α-actinin and vinculin. Biochemical examination of these proteins suggested that they are capable of establishing a complex network of protein–protein interactions with both cytoskeletal and signaling partners and implicated focal adhesions in both mechanical and signaling processes. Studies carried out with different cell types, in culture and *in vivo*, exposed to a variety of conditions established that focal adhesions are not the only sites mediating ECM–integrin–actin binding, and added to this group focal complexes, fibrillar adhesions, 3D-matrix adhesions, and podosomes (Figure 1).

The Molecular Organization of Focal Adhesions

Focal-adhesion components were identified, primarily by immunofluorescence, in studies conducted in many laboratories for the last two decades. More than 50 distinct proteins were reported to localize, stably or transiently, in focal adhesions and related cell–matrix

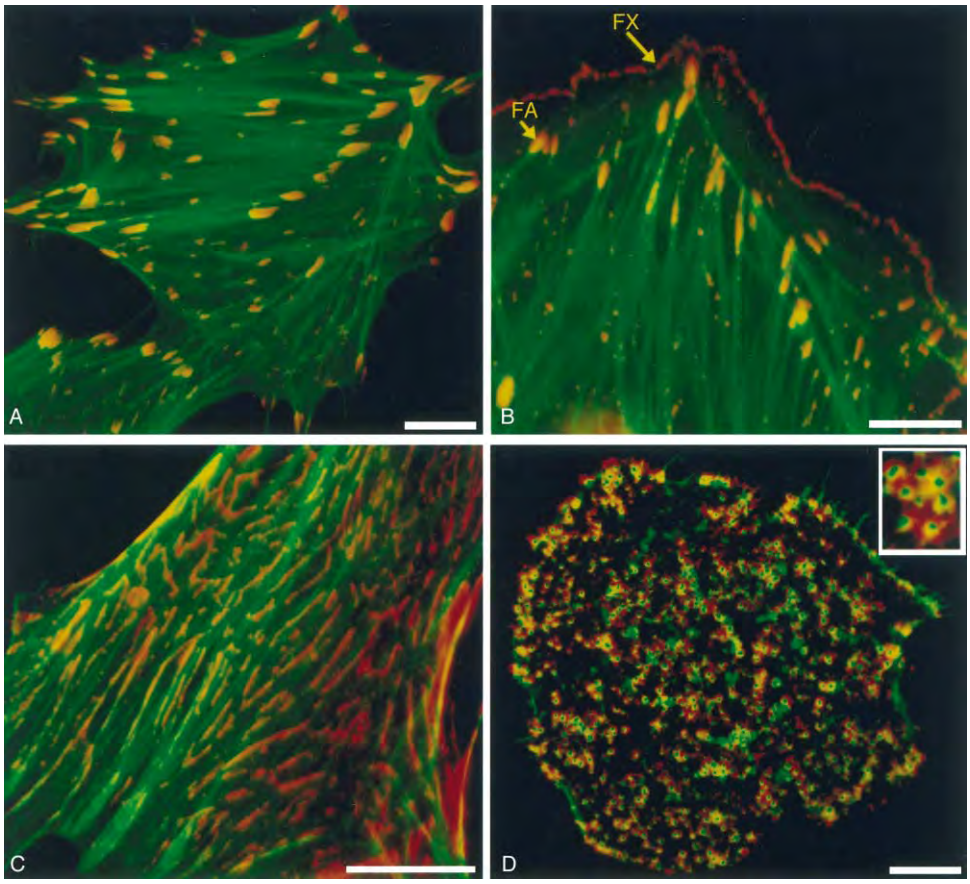

FIGURE 1 Focal adhesions and related adhesion sites. (A) Stationary human fibroblasts, stained for actin (green) and vinculin (red), having typical ovular focal adhesions located at the ends of actin stress fibers. (B) Migrating endothelial cells (porcine aortic endothelial cells, PAEC) stained for actin (green) and phosphotyrosine (red), displaying both focal adhesions (FA) and focal complexes (FX). Focal complexes have a circular morphology and are located at the edge of the lamellipodium where actin is organized as a dense network of highly branched fibers. (C) Human fibroblasts stained for actin (green) and for the fibronectin receptor $\alpha_5\beta_1$ integrin (red), which is enriched in fibrillar adhesions. (D) A mouse osteoclast, stained for actin (green) and paxillin (red), showing typical podosomes—doughnut-shaped adhesions with an actin core. The insert shows a cluster of podosomes at a higher magnification. Scale = 10 μm.

contacts. These molecules are largely segregated into three major structural domains, including the transmembrane domain, the cytoskeleton domain, and the interconnecting submembrane plaque (Figure 2).

The Receptors and their ECM Ligands

The membrane domains of ECM adhesions contain-specific integrins, which are heterodimers of α- and β-subunits that bind the ECM via a large extracellular domain. Integrins span the membrane and contain a cytoplasmic region through which they interact with plaque proteins. The most common integrins found in focal adhesions and related ECM adhesions are the fibronectin receptor, $\alpha_5\beta_1$, and the vitronectin receptor, $\alpha_V\beta_3$.

Additional, somewhat less characterized, membrane-bound components of focal adhesions include potentially adhesive molecules such as syndecan-4 and the hyaluronan-binding protein layilin, as well as the tyrosine phosphatase LAR and the glycoprotein SHPS-1, a substrate of the tyrosine phosphatase SHP-2 (Figure 2). The role of these membrane molecules is still not known.

The Cytoskeletal Domain

Focal adhesions are associated with the termini of actin bundles termed stress fibers. The polarity of the attached actin filaments is apparently uniform, with their barbed ends pointing to the membrane. That area of the actin cable is particularly enriched with actin-associated proteins such as the actin-bundling protein α-actinin. Actin is also associated with the other forms of integrin-mediated adhesion, although not in a form of stress fibers (Figure 1).

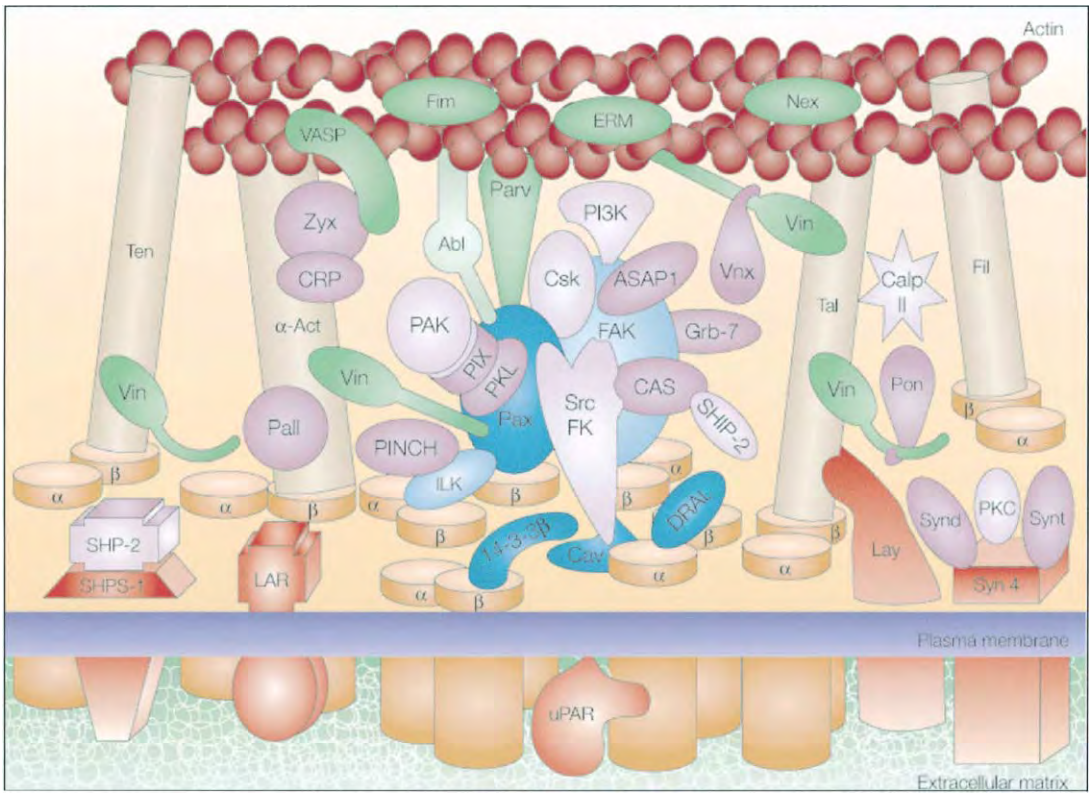

FIGURE 2 A scheme depicting the complexity of the main molecular domains of cell–matrix adhesions. The main adhesion receptors are heterodimeric (α and β) integrins. Additional membrane-associated molecules enriched with these adhesions include syndecan-4 (Syn4); layilin (Lay); the phosphatase LAR; SHPS-1, the substrate of the cytoplasmic phosphatase SHP-2; and the urokinase receptor (uPAR). Proteins that interact with both integrin and actin, and that function as the structural scaffolds of focal adhesions, include α-actinin (α-Act), talin (Tal), tensin (Ten), and filamin (Fil). Integrin-associated molecules include focal adhesion kinase (FAK), paxillin (Pax), integrin-linked kinase (ILK), DRAL, 14-3-3β, and caveolin (Cav). Actin-associated proteins include VASP, fimbrin (Fim), ezrin-radixin-moesin proteins (ERM), Abl kinase, nexillin (Nex), parvin/actopaxin (Parv), and vinculin (Vin). Other proteins, many of which may serve as adapter proteins, include zyxin (Zyx), CRP, palladin (Pall), PINCH, PKL, PIX, vinexin (Vnx), ponsin (Pon), Grb-7, ASAP1, syntenin (Synt), and syndesmos (Synd). Among these are several enzymes, such as SHP-2, SHIP-2, PAK, PI-3 kinase (PI3K), Src-family kinases (Src FK), Csk, the protease calpain II (Calp II), and PKC. Reprinted by permission from Geiger, B., Bershalsky, A., Pankov, R., and Yamada, K. M. (2001). Extracellular matrix-cytoskeleton crosstalk. *Nat. Rev. Mol. Cell Biol.* **2**, 793-805. Copyright 2001, Macmillan Magazines, Ltd.

The Submembrane Plaque

The submembrane plaque is a multiprotein complex that interconnects actin to the membrane in focal adhesions and related adhesions. Some of the plaque components contain binding domains for both actin and integrin, including talin, α-actinin, tensin, and filamin, and may function as direct integrin-actin linkers (Figure 2). Additional integrin-associated molecules do not bind directly to actin and may link the cytoskeleton to the membrane indirectly, via other plaque components. Some of them, such as focal adhesion kinase (FAK), the LIM-domain protein DRAL, integrin-linked kinase (ILK), and 14-3-3β, are signaling molecules (Figure 2).

Yet another group of focal-adhesion-associated proteins includes actin-binding proteins that were not shown to interact directly with integrins, including vinculin, VASP/Ena, and ezrin–radixin–moesin (ERM) proteins (Figure 2). Vinculin plays a pivotal role as a central linker interacting with many plaque proteins (e.g., talin, α-actinin, VASP/Ena, ponsin, and vinexin), acidic phospholipids, and actin. Finally, a very large group of proteins consists of adapter proteins, which apparently interact with actin-bound and integrin-bound components and link them to one another.

The components of cell–matrix adhesions have an unusual wide range of intrinsic activities. Beyond their protein–protein binding specificities, many of these proteins are enzymes, such as tyrosine kinases (e.g., members of the Src family and FAK), serine/threonine kinases (e.g., ILK, PKC, and PAK), tyrosine phosphatases (e.g., SHP-2 and LAR-PTP), inositol 5′-phosphatase (SHIP-2), modulators and adapters of small GTPases (e.g., ASAP1, DOCK180, PIX and GRAF),

and other enzymes such as PI 3-kinase and the protease calpain II (Figure 2). It should be pointed out that the true molecular complexity of focal adhesions is probably greater than depicted in Figure 2 because many of these components represent products of multigene families and may undergo posttranslational modification and proteolytic cleavage.

A striking characteristic of many focal-adhesion components is that they are multidomain proteins that can interact with several distinct partner molecules. For example, vinculin, FAK, Src family kinases, and paxillin can each bind to more than 10 different partners. Thus, the theoretical number of different combinations of molecular interactions that might be involved in linking integrins to actin is enormous.

Diversity of Cell–Matrix Adhesion Sites

Adhesions with the ECM are formed by essentially all adherent cells, in culture and *in vivo*. Yet their morphology, size, molecular composition, and subcellular distribution can be quite heterogeneous. These adhesions share, however, two common features: they are mediated by integrins and they interact with the actin cytoskeleton. Focal adhesions, the best-characterized form, are flat elongated structures, several square microns in area and are usually located near the periphery of cells, associated with bundles of actin microfilaments (Figures 1A and 3). The development

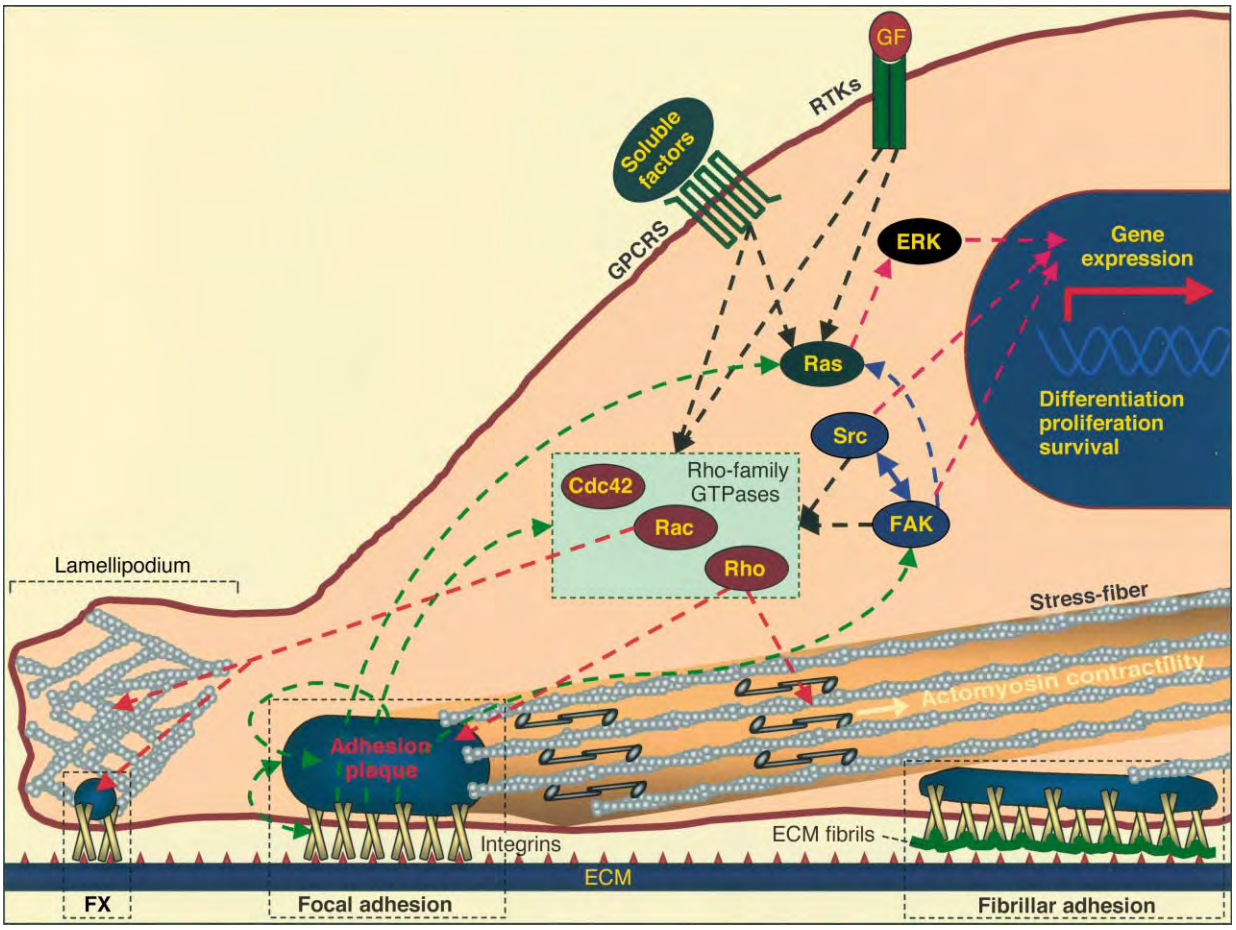

FIGURE 3 A simplified scheme highlighting the major pathways of focal adhesion mediated signaling. Rho family GTPases, including Rho, Rac and Cdc42, are regulated by integrins, growth factors (GFs), receptor tyrosine kinases (RTKs) and G protein coupled receptors (GPCRs). Cdc42 induces the formation of filopodia (not shown) and activates Rac. Rac induces the formation of a meshed network of branched actin filaments, extension of lamellipodia, and formation of focal complexes (FX). Rho induces actomyosin contractility and organizes actin in contractile bundles called stress fibers. Rho activation drives the development of focal adhesions from focal complexes. Rho-induced contractility is also essential for the development of fibrillar adhesions and their translocation toward the cell center. In adhesion sites, integrins activate locally the tyrosine kinases FAK and Src, which then regulate the enzymatic activities and interactions of many other focal-adhesion components. Integrins also affect gene expression, mainly through the activation of the Ras-ERK pathway, and thereby regulate differentiation, proliferation, and survival.

of focal adhesions is stimulated by the small GTPase Rho and requires actomyosin contractility. Characteristic focal-adhesion plaque proteins include vinculin, talin, paxillin, and tyrosine-phosphorylated proteins. Focal adhesions are particularly prominent in cultured cells growing on solid surfaces, yet structures with similar molecular properties are also found *in vivo*.

Another group of matrix adhesions is the focal complexes, which are small, dot-like adhesions present mainly close to the edges of the lamellipodium (Figures 1B and 3). These sites can be associated with cell migration or serve as precursors of focal adhesions. Their formation is induced by the Rho family GTPase Rac.

In the more central locations of many cell types, there are the fibrillar adhesions (also referred to as ECM contacts), which are elongated or dot-like structures associated with ECM fibrils (Figures 1C and 3). The typical components of fibrillar adhesions are extracellular fibronectin fibrils, the fibronectin receptor $\alpha_5\beta_1$ integrin, and the cytoplasmic protein tensin. Fibrillar adhesions emerge from focal adhesions in an actomyosin-dependent fashion.

Another form of ECM adhesions is the podosomes, which are small ($\sim 0.5\ \mu m$ diameter) cylindrical structures containing typical focal-adhesion proteins such as vinculin and paxillin (Figure 1D). Podosomes are found in a variety of malignant cells and in some normal cells such as macrophages and osteoclasts. Characteristic and indispensable proteins of podosomes are gelsolin and dynamin, which localize to tubular invaginations of the plasma membrane typical for these structures. Finally, another type of adhesion is the 3D-matrix adhesions, formed with three-dimensional ECM, which differ from focal adhesions in their overall morphology, fine molecular composition, and function.

Signaling

Focal adhesions and related structures are involved in adhesion-mediated signaling processes affecting various cellular processes such as proliferation, differentiation, anchorage-dependent survival, spreading, and migration. The main signaling paths include the stimulation of local tyrosine phosphorylation driven by FAK and Src, activation of small GTPases of the Rho and Ras family, and the extracellular signal-regulated kinase (ERK) pathway (Figure 3). It is proposed that tethering of FAK to clustered integrins leads to its autophosphorylation, recruitment of Src, and phosphorylation of their downstream targets. The presence of a variety of kinases and their substrates in the submembrane plaque suggests that additional signaling processes are activated by matrix adhesion, yet definitive information about these signaling processes is still scarce.

Focal adhesions themselves are regulated by several signaling systems. In addition to Rho and Rac, excessive Src-mediated phosphorylation and stimulation of appropriate cells by growth factors (e.g., EGF or neuregulin), phosphatases, and proteases have a profound effect on the organization of cell–matrix adhesions.

Focal Adhesions and Mechanosensitivity

Mechanical forces play a key role in the development and fate of focal adhesions and focal complexes. The transition from focal complex to focal adhesion and the growth of focal adhesions require local tension and are dramatically suppressed following treatment with inhibitors of Rho kinase or myosin light-chain kinase (Figure 4). Focal complexes do not appear to depend on actomyosin contractility and even become abundant upon inhibition of cellular contractility. Similarly, the

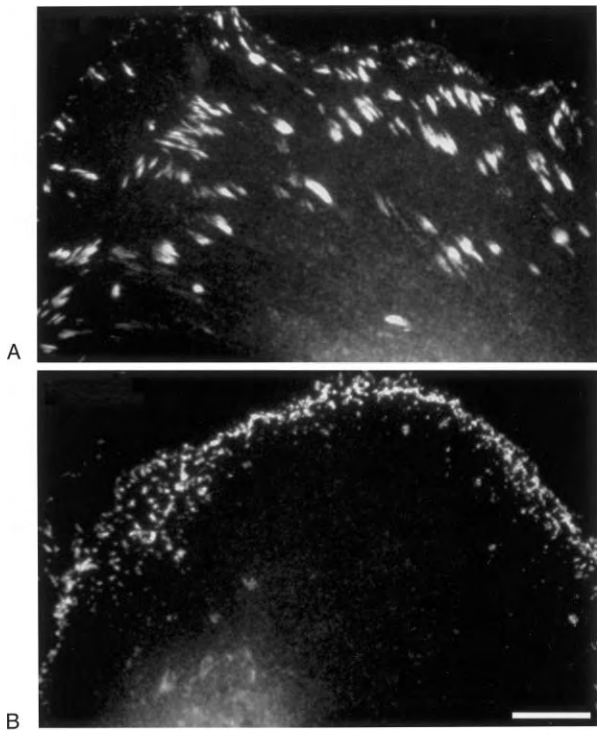

FIGURE 4 The key role of actomyosin contractility in the organization of adhesion site. Rat embryonic fibroblasts (REF52), stably expressing β_3-integrin-GFP, were either (A) untreated (control) or (B) treated with the Rho-kinase inhibitor Y-27632 prior to fixation. Inhibition of actomyosin contractility by Y-27632 causes disassembly of focal adhesions and accumulations of focal complexes. Scale = 10 μm.

maintenance of fibrillar adhesions is not affected by the inhibition of contractility, yet their emergence from peripheral focal adhesions requires actomyosin-driven tension.

See Also the Following Articles

Actin Assembly/Disassembly • Actin-Capping and -Severing Proteins • Actin-Related Proteins • Cell–Matrix Interactions • Integrin Signaling • Rho GTPases and Actin Cytoskeleton Dynamics • Src Family of Protein Tyrosine Kinases

Glossary

fibrillar adhesions Elongated or dot-like adhesions that are associated with fibronectin fibrils, mostly along the central areas of the cell.

focal adhesions Flat elongated adhesions associated with prominent actin bundles (stress fibers); also known as focal contacts. They are usually located near the periphery of the cell.

focal complexes Small dot-like adhesions located mainly at the edge of lamellipodium. They are induced by Rac, are associated with cell migration, and can develop into focal adhesions.

podosomes Small cylindrical adhesions found in osteoclasts, macrophages, and various malignant cells.

Rac A Rho family GTPase that stimulates the extension of the lamellipodium and formation of focal complexes.

Rho A Rho family GTPase that stimulates stress-fiber and focal-adhesion formation.

Further Reading

Alberts, B., Johnson, A., Lewis, J., Raff, M., Roberts, K., and Walter, P. (2002). *Molecular Biology of the Cell*. Garland Publishing, New York.

Beckerle, M. C. (2001). *Frontiers in Molecular Biology, Vol 39. Cell Adhesion*. Oxford University Press, New York.

Geiger, B., Bershadsky, A., Pankov, R., and Yamada, K. M. (2001). Extracellular matrix-cytoskeleton crosstalk. *Nat. Rev. Mol. Cell Biol.* **2**, 793–805.

Kreis, T., and Vale, R. (eds.) (1999). *Guidebook to the Extracellular Matrix, Anchor, and Adhesion Proteins*. Oxford University Press, New York.

Zamir, E., and Geiger, B. (2001). Molecular complexity and dynamics of cell–matrix adhesions. *J. Cell Sci.* **114**, 3583–3590.

Biography

Benjamin Geiger is the Head of the Department of Molecular Cell Biology, The Weizmann Institute of Science, Israel, and the incumbent of the E. Neter Chair in Cell and Tumor Biology. His research interests are the molecular basis for cell adhesion. He received a B.Sc. from Tel Aviv University, an M.Sc. from Hebrew University, Israel and a Ph.D. and Professorship from The Weizmann Institute of Science, Israel.

Eli Zamir is a Postdoctoral Fellow in the Department of Molecular Cell Biology, The Weizmann Institute of Science, Israel. His research interests are in the structural and functional diversity of cell–matrix adhesions, and in resolving the structure and function of multi-component interaction networks in cells. He received a B.Sc. from Tel Aviv University, Israel and an M.Sc. and a Ph.D. from The Weizmann Institute of Science, Israel.

Free Radicals, Sources and Targets of: Mitochondria

Alberto Boveris
University of Buenos Aires, Buenos Aires, Argentina

Enrique Cadenas
University of Southern California, Los Angeles, California, USA

Mitochondria constitute an active source of free radicals, continuously producing $O_2^{\cdot-}$ (superoxide radical) and $^{\cdot}NO$ (nitric oxide), by auto-oxidation of ubisemiquinone ($UQH^{\cdot}$) and by the enzymatic action of mitochondrial nitric oxide synthase (mtNOS), respectively. These two primary products generate a series of derived and reactive oxidizing species, as H_2O_2 and alkyl and peroxyl radicals. $^{\cdot}NO$ inhibits cytochrome oxidase, competitively with O_2, and ubiquinol–cytochrome c reductase activities. Peroxynitrite ($ONOO^-$), the product of the reaction of $^{\cdot}NO$ with $O_2^{\cdot-}$, inhibits NADH-dehydrogenase. The $[O_2]/[^{\cdot}NO]$ ratio in the tissues is consistent with a respiratory inhibition of 16–26%. The intramitochondrial production of free radicals is involved in a series of oxidative stress situations, in the syndrome of mitochondrial dysfunction, in mitochondrion-dependent apoptosis, in aging and in neurodegenerative diseases. At the same time, $^{\cdot}NO$ and H_2O_2 seem to constitute a pleitrophic signal indicating high mitochondrial energy charge.

Introduction

More than two centuries after Lavoisier's description of animal respiration as a biological oxidation, there is still a fresh and active interest in the mechanisms and the regulation of the processes that link the oxidation of food components to energy production in mammals and in the recognition that the modulation of energy production and expenditure underlies the whole process of life and death of a cell. At the foundation of biochemistry, in the 1920s, there was a controversy on how the hydrogen atoms of organic molecules would end in the H_2O molecule: there were two views – hydrogen activation and oxygen activation, championed by Wieland and Warburg, respectively. The first view involved H_2O_2 as an important intermediate and the second one supported the idea of H_2O as the direct product of O_2 reduction. The monumental contribution of Warburg, identifying cytochrome oxidase as the enzyme catalyzing the overwhelming part of O_2 uptake in biological systems, eclipsed the dispute. However, the concept of the partial reduction of O_2 in biological systems emerged again in 1946 with Michaelis' ideas of univalent electron transfer between biological molecules when he described hydroperoxyl radical ($HO_2^{\cdot}$, the protonated base of superoxide free radical: $O_2^{\cdot-}$), hydrogen peroxide (H_2O_2), hydroxyl radical ($HO^{\cdot}$), and water (H_2O) as the four steps of the univalent reduction of the O_2 molecule. These concepts were strengthened when Gerschman postulated in 1954 that oxygen-free radicals were the common biochemical mechanisms of oxygen and radiation toxicity. At that time, $HO^{\cdot}$ and $HO_2^{\cdot}$ were known as toxic species in radiation chemistry and biology, but by no means it was admitted that these highly reactive free radicals could be produced in physiological conditions. Gerschman exposed small mammals to hyperbaric O_2 to increase the tissue levels of oxygen-free radicals and found synergism between radiation and hyperbaric O_2 in decreasing the survival time of exposed mice.

The transcendental and landmark discovery of superoxide dismutase (SOD) by McCord and Fridovich in 1969 introduced a new dynamism to the understanding of free radical reactions in biological systems. The existence of the enzyme, first described in erythrocytes and later in bacteria and in mammalian organs, implied that its substrate, $O_2^{\cdot-}$, was a normal biological metabolite. In a few years, a dogma advanced by Fridovich evolved: $O_2^{\cdot-}$ and H_2O_2 interact in biological systems and produce the highly toxic $HO^{\cdot}$, which is the chemical species responsible for biological damage. The elegant classification of bacteria as aerobes (protected by superoxide dismutase and catalase), aerotolerant anaerobes (protected by superoxide dismutase but not by catalase), and anaerobes (without protection by superoxide dismutase and catalase) paved the way to the extension of the concept to mammalian biology, oxygen toxicity, and human pathology.

In parallel, mitochondria were recognized by Boveris and Chance in 1972–73 as an active source of H_2O_2 that diffuses to the cytosol. The concept collided with the idea of H_2O_2 produced and utilized in the intraperoxisomal space and avoided as a cellular metabolite. Shortly after, Boveris and Cadenas described $O_2^{\cdot-}$ as the stoichiometric precursor of mitochondrial H_2O_2 and suggested ubisemiquinone ($UQH^{\cdot}$) as the main source of $O_2^{\cdot-}$ upon auto-oxidation. Mitochondria were recognized as the more generalized and quantitatively main source of $O_2^{\cdot-}$ in mammalian organs by 1980. Other sources of $O_2^{\cdot-}$, such as polymorphonuclear leukocytes, xanthine oxidase, and liver endoplasmic reticulum, were also identified as active $O_2^{\cdot-}$ sources that proved to be decisive in specific conditions.

The existence of the family of superoxide dismutases with one of them, Mn-SOD, specific for the mitochondrial matrix, and the mitochondrial production of $O_2^{\cdot-}$ in all aerobic cells were the two ideas that gave the strongest support for the participation of oxygen-free radicals in mammalian and human physiology, pathology, and aging.

The mechanistic concept that was currently accepted for the deleterious action of oxygen-free radicals in biological systems, called the Fenton/Haber–Weiss pathway, involved a primeval and dual role for $O_2^{\cdot-}$, as precursor of H_2O_2 and as reductant of cellular Fe^{3+}, and a second reaction between H_2O_2 and Fe^{2+}, involving the homolytic scission of the peroxide bond and the generation of the highly toxic $HO^{\cdot}$.

The discovery of the generation of nitric oxide ($^{\cdot}NO$) in mammals as a signaling molecule, with roles as intercellular messenger in the cardiovascular system, as neurotransmitter, and as component of the signaling and cytotoxic mechanisms of the immunological system along with the identification of $^{\cdot}NO$ as a free radical, produced a revolution in the concepts of free radical metabolism and signaling in mammalian organs. The linear Fenton/Haber–Weiss pathway evolved to a Y-shaped scheme of the pathways of free radical reactions in mammalian organs (Figure 1).

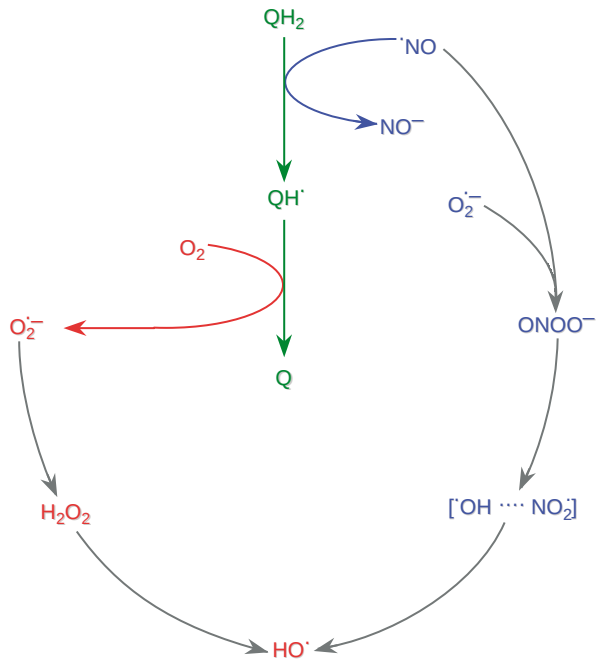

FIGURE 1 The biochemical free radical chain reactions encompassed by the redox transitions of oxygen, nitric oxide, and ubiquinone. The redox transitions of ubiquinone, oxygen, and nitric oxide are shown in green, red, and blue, respectively. $O_2^{\cdot-}$, superoxide anion, H_2O_2, hydrogen peroxide; $HO^{\cdot}$, hydroxyl radical; $^{\cdot}NO$, nitric oxide; $ONOO^-$, peroxynitrite; UQH_2, ubiquinol; $UQH^{\cdot}$, ubisemiquinone; UQ, ubiquinone.

The Mitochondrial Production of $O_2^{\cdot-}$ and H_2O_2

Mitochondria were recognized as subcellular organelles by application of supravital stainings by the end of 19th century, and as the powerhouses of cells, sites of the biochemical process of oxidative phosphorylation in the 1950s, after the availability of electron microscopy and the modern methods of cell fractionation. Mitochondrial isolation permitted the identification of the inner mitochondrial membrane as the site in which the mitochondrial complexes I–V were constitutive proteins and as the coupling membrane for the transduction of the redox chemical energy of NADH oxidation into ATP high-energy phosphate bond. By 1955, Chance and Williams produced a complete description of the redox states of the components of the mitochondrial respiratory chain, and defined the operational concepts of mitochondrial metabolic states and respiratory control. The latter concept elegantly describes the state 4 to state 3 transition in which ADP regulates the rate of mitochondrial electron transfer and respiration. State 4, with availability of respiratory substrate but not of ADP, was described as "controlled or resting respiration," whereas state 3, with ample respiratory substrate and ADP availability, was defined as the "active respiration," i.e., the maximal physiological rate of ATP production and O_2 consumption. By determination of the rates of mitochondrial O_2 uptake in both state 4 and state 3, and of the O_2 uptake of tissue slices and perfused organs, it was estimated that mammalian tissue mitochondria under physiological conditions are mostly (60–70%) in state 4, whereas the rest (30–40%) are in state 3, thus meaning that in a physiological setting there is a 30–40% utilization of the ATP-producing capacity.

Isolated mitochondria were identified as sources of H_2O_2, in a process modulated by the mitochondrial state 4/state 3 transition; the rate of H_2O_2 generation in state 4 is about 4–6 times higher than that in state 3.

This fact indicates that a component of the respiratory chain, markedly changing its redox steady state level in the state 4/state 3 transition is the H_2O_2 generator. The rates of H_2O_2 production of mitochondria isolated from mammalian organs are in the range of 0.3–0.8 nmol $H_2O_2 min^{-1} mg^{-1}$ protein for state 4 and 0.05–0.15 nmol $H_2O_2 min^{-1} mg^{-1}$ protein for state 3. In the case of rat heart and liver, mitochondrial H_2O_2 production accounts for ~0.5% of the physiological O_2 uptake.

The mechanistic option for O_2 reduction, between either one 2-electrons step to yield H_2O_2 or two 1-electron steps to yield $O_2^{\cdot-}$ as intermediate, was solved by the fact that submitochondrial particles show a 2 to 1 ratio of $O_2^{\cdot-}$ and H_2O_2 productions, thus establishing $O_2^{\cdot-}$ as the stoichiometric precursor of mitochondrial H_2O_2. The main part of mitochondrial $O_2^{\cdot-}$, ~70%, is vectorially released to the mitochondrial matrix, where it encounters specific intramitochondrial Mn-SOD. Steady state concentrations of 0.08–0.2 nM $O_2^{\cdot-}$ and 5–50 nM H_2O_2 are estimated for the mitochondrial matrix, with a content of 3–10 μM Mn-SOD. The release of $O_2^{\cdot-}$ to the mitochondrial intermembrane space, accounting for ~30% of the mitochondrial $O_2^{\cdot-}$ production, was recognized, being probably in functional relationship to the Cu,Zn-SOD of this compartment. $O_2^{\cdot-}$, from the intermembrane space is released into the cytosol through a voltage-dependent anion channel. Hence, mitochondria may be considered as effective sources of cytosolic $O_2^{\cdot-}$ and this species may contribute to the redox regulation of cell signaling.

Two main $O_2^{\cdot-}$ generating reactions have been described for the mitochondrial respiratory chain. In both cases the intermediate semiquinone form of redox pairs components of the respiratory chain, ubiquinol/ubiquinone, and the $FMNH_2$/FMN component of NADH dehydrogenase, i.e., $UQH^{\cdot}$ and $FMNH^{\cdot}$, respectively, are collisionally and nonenzymatically auto-oxidized by molecular O_2 to yield $O_2^{\cdot-}$. In the case of $UQH^{\cdot}$ auto-oxidation, the chemical process is called the Boveris–Cadenas reaction (reaction [1]) with a second-order reaction constant of $8 \times 10^3\ M^{-1}\ s^{-1}$; it is considered the main mitochondrial $O_2^{\cdot-}$-producing reaction and a biological pacemaker of the aging process.

$$UQH^{\cdot} + O_2 \rightarrow UQ + H^+ + O_2^{\cdot-} \qquad [1]$$

Figure 2 illustrates the mitochondrial reactions that produce $O_2^{\cdot-}$ as well as their vectorial release to the cytosol and to the intermembrane space. Auto-oxidation of other components of the mitochondrial respiratory chain is thermodynamically feasible, but these reactions are not kinetically important on quantitative basis.

The spontaneous surface chemiluminescence of *in situ* organs supported the idea of mitochondria as the main physiological source of oxidizing free radicals. The assay is based in the production of the chemiluminescent species singlet oxygen ($^1O_2$), a downstream by-product of the free radical recombination reactions in biological systems (Figure 1). Liver and brain chemiluminescence increased under hyperbaric O_2 and in ischemia reperfusion following a dependence on mitochondrial $O_2^{\cdot-}$ generation in these conditions.

The Mitochondrial Production of $^{\cdot}NO$

At the beginning of the 1990s, the extraordinary research activity on biological $^{\cdot}NO$ production,

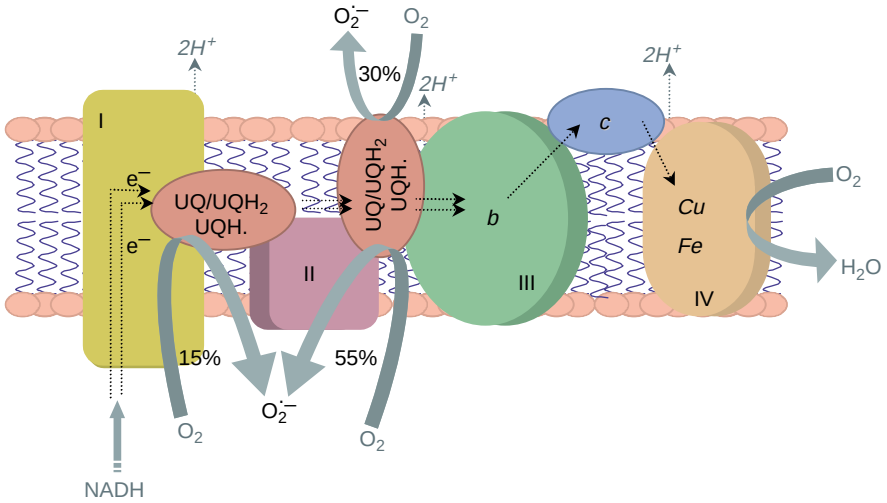

FIGURE 2 Sites of superoxide anion production in the mitochondrial respiratory chain. UQH_2: ubiquinol; UQ: ubiquinone; and $UQH^{\cdot}$: ubisemiquinone. The percentages close to superoxide anion ($O_2^{\cdot-}$) indicate the relative contribution of each reaction to the total mitochondrial $O_2^{\cdot-}$ production.

identified three different nitric oxide synthases (NOS): neuronal NOS (nNOS or NOS-I), inducible or macrophage NOS (iNOS or NOS-II), and endothelial NOS (eNOS or NOS-III). Immunocytochemical assays with antibodies against eNOS gave evidence of a nitric oxide synthase (NOS) located in mitochondria, which was named mtNOS and advanced as a regulator of mitochondrial and cellular respiration. The determination of mtNOS enzymatic activity was elusive for a few years, until two independent groups located in Zurich and Los Angeles/Buenos Aires, succeeded in showing $^{\cdot}NO$ production by rat liver mitochondria and mitochondrial fragments. The original observations in liver mitochondria were later extended to mitochondria from brain, heart, thymus, kidney, and diaphragm, thus dissipating the skepticism on mtNOS activity stemming from a contamination produced during cell fractionation. Mitochondrial $^{\cdot}NO$ production is carried out by mtNOS, a classic NOS, that requires NADPH (K_M = 12–20 μM), arginine (K_M = 5–50 μM), O_2 (K_M = 35–70 μM), and Ca^{2+} for enzyme activity. Calmodulin, tetrahydrobiopterine, and thiols increase the enzymatic activity. The intramitochondrial concentrations of NADPH, arginine, O_2, and Ca^{2+} are in excess or in the range needed for enzymatic activity. The methodology currently used to measure mtNOS activity determines NO production rates of 0.30–1.20 nmol $^{\cdot}NO\ min^{-1}\ mg^{-1}$ protein in mitochondria and submitochondrial preparations.

Recently, in a pivotal contribution, Giulivi and coworkers sequenced the 1429 amino acids of rat liver mtNOS and found it identical to nNOS splice variant αmirystoylated and phosphorylated in posttranslational processes. Transcripts corresponding to nNOSα were found in liver, brain, heart, kidney, skeletal muscle, lung, testis, and spleen. Hence, it is clear that mtNOS is a constitutive protein of the inner mitochondrial membrane with its substrates present in the mitochondrial matrix. Interestingly, a whole series of physiological situations were reported to regulate the level and activity of mtNOS that were up-regulated during brain development, by cold exposure, and by acute hypoxia, and down-regulated by thyroxin and angiotensin II. Treatments with enalapril, the converting-enzyme inhibitor, increased mtNOS activity. Pharmacological administration of haloperidol and chlorpromazine decreased brain mtNOS activity.

Intramitochondrial steady-state concentrations of $^{\cdot}NO$ are calculated as 20·50 nM and a release of 29 nM $^{\cdot}NO$ was electrochemicaly measured after supplementation of a single mitochondrion with Ca^{2+}. In the tissues under physiological conditions with a steady-state oxygenation of 20 μM O_2, the $[O_2]/[^{\cdot}NO]$ ratio is 500–1000, which competitively inhibit cytochrome oxidase by 16–26%. $^{\cdot}NO$ and $O_2^{\cdot-}$ metabolism in the mitochondrial matrix are linked by the very fast reaction between $^{\cdot}NO$ and $O_2^{\cdot-}$ to produce $ONOO^-$. This oxidative utilization of $^{\cdot}NO$ is the main (60–70%) pathway of $^{\cdot}NO$ metabolism, but at the same time it is only a minor part (15%) of intramitochondrial $O_2^{\cdot-}$ utilization. The reductive utilization of $^{\cdot}NO$ by ubiquinol and cytochrome oxidase provides a minor (20%) pathway of $^{\cdot}NO$ catabolism. The cellular conditions in which $^{\cdot}NO$ diffuses from mitochondria to cytosol, as well as the conditions in which $^{\cdot}NO$ diffuses from cytosol to mitochondria are unsolved questions for the complex process of intracellular signaling. Figure 3 shows a view of the integrated metabolism of $O_2^{\cdot-}$ and $^{\cdot}NO$ in mitochondria.

The effects of $^{\cdot}NO$ on mitochondrial electron transfer were reported in 1994 by two British research groups as the inhibition of brain and muscle cytochrome oxidase (complex IV) activity by low $^{\cdot}NO$ concentrations within a reversible and O_2-competitive biochemical process. The observation was rapidly confirmed by other groups using $^{\cdot}NO$ donors and pure $^{\cdot}NO$ in liver, heart, and brown fat mitochondria. $^{\cdot}NO$ levels of 0.1–0.3 μM decreased cytochrome oxidase activity and mitochondrial respiration to one half. The inhibition is reversible by dilution, hemoglobin supplementation, or exposure to $O_2^{\cdot-}$. The O_2-competitive inhibition of cytochrome oxidase renders the inhibition more important at low O_2 concentrations; ratios of $^{\cdot}NO/O_2$ affinities of 150–500 were reported for enzymatically active cytochrome oxidase. A second sensitive point in the mitochondrial respiratory chain is at the ubiquinol–cytochrome *c* reductase segment (complex III); half inhibition of electron transfer between cytochromes *b* and *c* occurs at 0.2–0.4 μM $^{\cdot}NO$, enhancing the production of $O_2^{\cdot-}$ and H_2O_2 in submitochondrial particles and in mitochondria. A third sensitive point is located at NADH-dehydrogenase (complex I), in this case, $ONOO^-$ appears as the effective inhibitory agent.

Figure 4 illustrates the direct and indirect effects of $^{\cdot}NO$, in the latter case through $ONOO^-$ formation, on the mitochondrial respiratory chain. The reversible effects of $^{\cdot}NO$ on cytochrome oxidase and ubiquinol-cytochrome *c* reductase are two sides of the regulation of mitochondrial respiration by $^{\cdot}NO$. On the one hand, the inhibition of cytochrome oxidase and, on the other, the supply of $O_2^{\cdot-}$ to remove the respiratory inhibition, as it may become a physiological need with high steady-state concentrations of $^{\cdot}NO$, as it is the case in ischemiareperfusion and in inflammation. The irreversible effects of $ONOO^-$ on complexes I and III are related to situations in which sustained high levels of $ONOO^-$ lead to mitochondrial dysfunction and apoptosis.

Concerning the important question of whether or not mtNOS enzymatic activity regulates mitochondrial functions under physiological conditions, several reports described the modulation of mitochondrial O_2 uptake and H_2O_2 production by the activity of mtNOS in

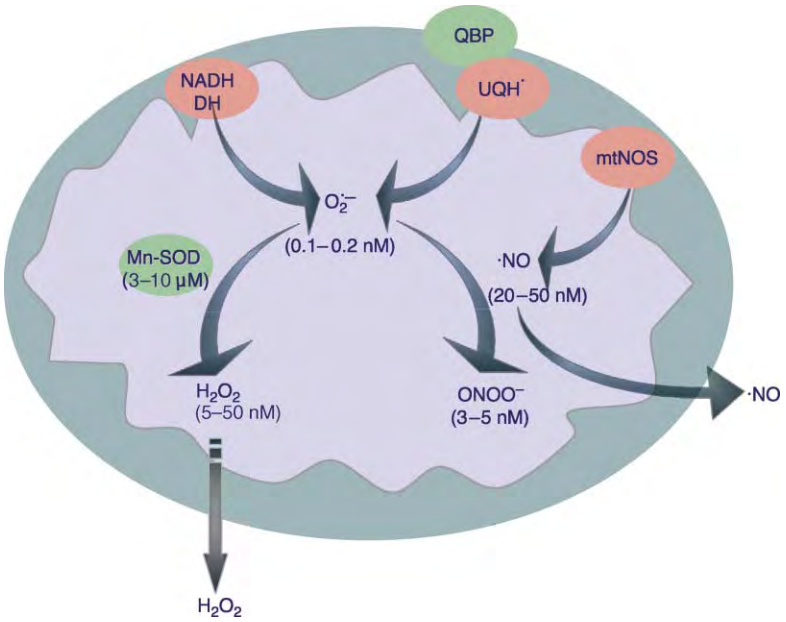

FIGURE 3 Metabolism of superoxide radicals and nitric oxide in the mitochondrial matrix. The numbers below the symbols indicate physiological steady-state concentrations for mammalian organs. The arrows reaching outside the mitochondrion indicate diffusion of H_2O_2 and ·NO to the cytosol. QBP: ubiquinone binding protein; NADH DH, NADH dehydrogenase; mtNOS, mitochondrial nitric oxide synthase; Mn-SOD, Mn-superoxide dismutase.

isolated mitochondria. The current view is that mtNOS does regulate mitochondrial respiration; hence, mtNOS, cytochrome oxidase, and F_1-ATPase are the three regulatory proteins of cellular O_2 uptake and energy production. The biochemical activity of mtNOS (expressed as nmol ·NO min^{-1} mg^{-1} protein) is usually measured as the difference in ·NO production between the assay performed in the presence of arginine and in the presence of a competitive inhibitor of NOS, such as NMMA or NNA. The *regulatory activity* of mtNOS is best expressed by the difference in the rates of O_2 uptake or H_2O_2 production between the system supplemented with arginine, the highest mtNOS activity, and the system in the presence of the NOS inhibitor, the lowest

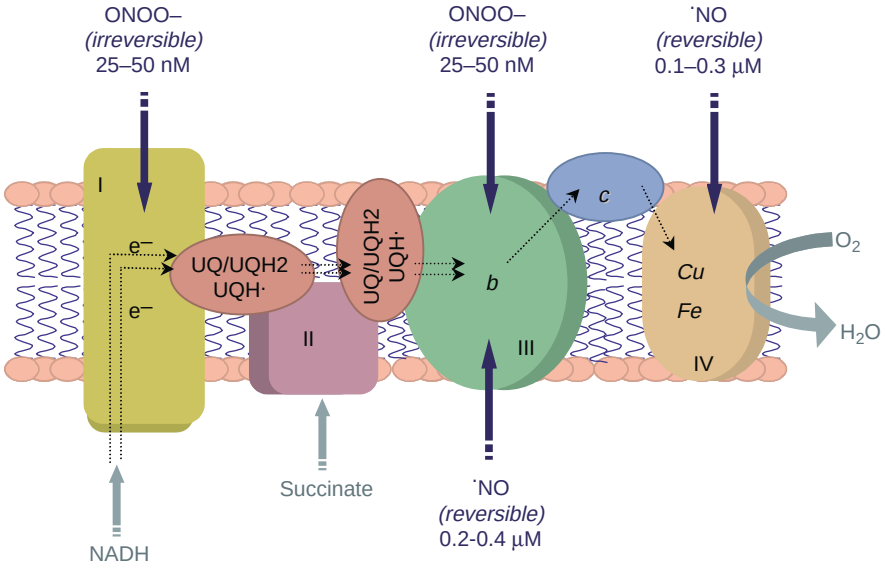

FIGURE 4 Sites of action of nitric oxide and peroxynitrite in the mitochondrial respiratory chain. Reversible and irreversible indicate the type of inhibition and are understood as regulatory or toxic processes, respectively. The indicated steady-state concentrations were determined or estimated to reduce enzymatic activity to one half, at a concentration of 100–150 μM O_2.

mtNOS activity. The *regulatory capacity* of ·NO, estimated as the ratio of the rates of *regulated* O_2 *uptake*/·NO production or of *regulated* H_2O_2 *production*/·NO production is ~70 for O_2 uptake and ~0.4 in H_2O_2 production. The activity of mtNOS in isolated mitochondria markedly increased the $[O_2]_{0.5}$ of mitochondrial O_2 uptake from 1.1 μM O_2 in the case of inactive mtNOS, to 2.2 μM O_2 in the case of an active mtNOS. However, it is not clear to what extent these effects, observed with isolated mitochondria, occur under physiological conditions in myoglobin-containing tissues and in blood-perfused organs, due to the high affinity of the two mentioned hemoproteins for ·NO.

The Physiological Role of the Mitochondrial Production of $O_2^{\cdot-}$, H_2O_2, and ·NO

The early recognition that $O_2^{\cdot-}$ and H_2O_2 are both able to initiate reactions harmful to cell and tissues is now complemented by the concept that both $O_2^{\cdot-}$ and H_2O_2 are carefully regulated metabolites capable of signaling the regulatory devices of the biochemical and genetic systems of the cell. ·NO was initially recognized as an intercellular messenger and later as an intracellular regulator. At present, the three chemical species are considered to participate in integrated processes of intracellular regulation and in intercellular signaling, communication, and cytotoxicity. The redox regulation of gene expression and intercellular communication is just starting to be understood as a vital mechanism in health and disease.

The fine regulation by H_2O_2 of cell function was advanced by Antunes and Cadenas in 2001 when they showed that in Jurkat T-cells, steady-state concentrations below 0.7 μM H_2O_2 place cells in a proliferative state, whereas at 1.0–3.0 μM, H_2O_2 cells develop programmed cell death, and at levels higher than 3.0 μM H_2O_2 cells undergo necrosis. H_2O_2 and ·NO share the chemical properties of being uncharged and the biological property of being highly diffusible through biological membranes, at variance with $O_2^{\cdot-}$ and $ONOO^-$ that are charged and non-diffusible molcules. Consequently, the first two species are suitable for cellular and intercellular signaling, and the two latter for signaling and cytotoxicity in confined spaces.

There is evidence that H_2O_2 and ·NO are able to modulate mitogen-activated protein kinases (MAPKs), the widespread integral components of intracellular phosphorylation and dephosphorylation signaling cascades involved in cell survival, proliferation, differentiation, and death. The interactions are complex and seem to involve intracellular glutathione and $ONOO^-$. Both, H_2O_2 and ·NO diffusing from mitochondria to the cytosol are considered to constitute a pleiotropic signal involved in the regulation of a series of cellular processes, among them JNK signaling…NO diffusing from mitochondria may also modulate (inactivate) JNK1 via S-nitrosylation. The concept of narrow ranges of intracellular messenger molecules for different or opposite biological actions, as observed for H_2O_2 levels in the proliferation/apoptosis transition, is now applied to effector systems with two regulators, H_2O_2 and ·NO, with the consequence of four different responses for the combination of the two binary conditions of low and high level of the two signals (Figure 5).

It has been understood for the last 30 years that excess generation of $O_2^{\cdot-}$ and H_2O_2 leads to oxidative stress and harmful biological situations. ·NO has been added to these two species in the last decade. The classical concept of oxidative stress, as brought forward by Sies implies an imbalance between oxidants and antioxidants, in favor of the former. The situation is understood as reversible, especially by supplementation with antioxidants, and also as leading, sooner or later, to biological dysfunction. The concept is applicable to subcellular organelles, cells, organs, systems, or whole organisms. From a biochemical perspective, oxidative stress is determined by an increased steady-state level of at least one of the oxidant species ($O_2^{\cdot-}$, H_2O_2, ·NO, $ONOO^-$, $HO^{\cdot}$, $ROO^{\cdot}$, and $^1O_2$) that leads to increased levels of the other oxidizing species downstream of the

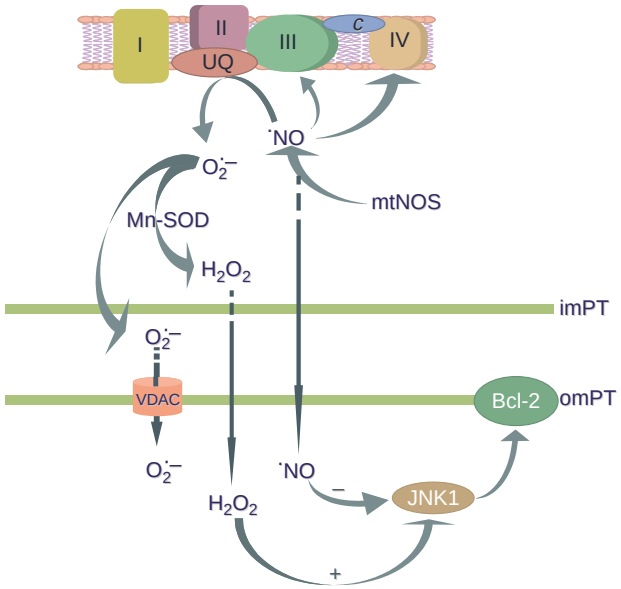

FIGURE 5 Mitochondrial production of oxygen- and nitrogen-centered radicals and cell signaling. The scheme shows the sites of action of nitric oxide (·NO) on the respiratory chain, the ensuing production of $O_2^{\cdot-}$ and H_2O_2, the release of these reactive species from the mitochondrion (controlled by VDAC in the case of $O_2^{\cdot-}$), and their effect on JNK signaling.

free radical pathways (Figure 1) and to biochemical damage.

Oxidative Stress and Dysfunctional Mitochondria: Mitochondria as Targets of Free Radicals

In the last few years, the concept of dysfunctional mitochondria was associated with mitochondrial features under oxidative stress, biological damage, and pathological conditions. Mitochondria are considered dysfunctional by comparison of their functions and properties with normal control mitochondria. The classic mitochondrial properties, that reflect their energy-producing physiological function, i.e., the state 3 rate of O_2 uptake, the respiratory control, the membrane potential, and the ADP:O ratio, are the parameters that, when decreased, support the contention of dysfunctional mitochondria. In addition, dysfunctional mitochondria frequently show increased rates of $O_2^{\cdot-}$ and H_2O_2 production.

Mitochondrial dysfunction is a mitochondrial syndrome that has been observed in ischemia/reperfusion, endotoxic and septic shock, a series of pathological situations, and aging. The syndrome is characterized by decreases in the rates of state 3 respiration and ATP synthesis, in mitochondrial membrane potential, and in respiratory control ratio, and by increases in the rate of state 4 respiration, and mitochondrial size and fragility. The reported decreases in the rates of state 3 respiration and of mitochondrial electron transfer are in the range of 30–40%; it seems that more damaged mitochondria are not compatible with living cells. There are three main chemical species involved in the molecular mechanism of this syndrome; the triad is constituted by $O_2^{\cdot-}$, $^{\cdot}NO$, and peroxynitrite ($ONOO^-$). The first chemical species is the free radical $O_2^{\cdot-}$, that is continuously produced in the auto-oxidation of $UQH^{\cdot}$ and $FMNH^{\cdot}$, intermediates of the respiratory chain function, and mainly dismutates to H_2O_2. The second free radical is $^{\cdot}NO$, that is continuously produced by mtNOS as regulator of respiration and mainly converted to $ONOO^-$. The latter, the third member of the triad, is produced by collision of $O_2^{\cdot-}$ and $^{\cdot}NO$ in the fastest reaction known in biological systems ($k = 1.9 \times 10^{10}\ M^{-1}\ s^{-1}$), except for the neutralization reaction of H^+ and HO^- ($k = 14 \times 10^{10}\ M^{-1}\ s^{-1}$). Peroxynitrite is a powerful oxidant, that when produced in excess, as in ischemia/reperfusion and inflammation, produces tyrosine nitration of intramitochondrial proteins. Intramitochondrial levels of 3–5 nM $ONOO^-$ have been estimated for physiological conditions, and levels above 20−30 nM are considered cytotoxic. The whole syndrome of dysfunctional mitochondria appears mainly driven by excess $^{\cdot}NO$ and $ONOO^-$.

Selective inhibition of NADH-dehydrogenase (complex I) activity in submitochondrial particles by $ONOO^-$ has been reported. Complex I dysfunction was also reported in animal models and in human neurodegenerative diseases. This selective mitochondrial defect is understood as secondary to a sustained oxidative stress and was reported in aged humans and in patients with neurodegenerative disorders, among them Parkinson's and Alzheimer's diseases. The near-target generation of $O_2^{\cdot-}$ by NADH-dehydrogenase and of $ONOO^-$ after molecular collision of $O_2^{\cdot-}$ with matrical $^{\cdot}NO$, is considered determinant in the selective impairment of complex I in neurodegenerative diseases.

The continuous mitochondrial production of free radicals and oxidizing species makes mitochondria the quantitatively most important source of these harmful species in the cell, and, at the same time, the sensitivity of mitochondrial functions to increased levels of the oxidizing free radicals and related chemical species renders mitochondria the most sensitive cellular target for the deleterious action of free radicals. The rapid mitochondrial turnover ($t_{1/2}$ of about 7 and 28 days in liver and brain, respectively) seems to reflect this double role of mitochondria as source and target of biologically harmful free radicals.

Mitochondrion-Dependent Apoptosis

The role of mitochondria in apoptosis is now well-established; a specific mitochondrion-dependent pathway of cell death is differentiated from the death-receptor-mediated apoptosis. Mitochondrion-dependent apoptosis entails oxidative stress and is modulated by MAPK signaling through JNK activation associated with Bcl-2 down-regulation, cytochrome *c* release, and the downstream activation of caspases. A very early activation of mtNOS has been reported in thymocyte-induced apoptosis. Thapsigargin supplementation of isolated thymocytes sequentially increases cytosolic Ca^{2+} and the activities of mtNOS and of the NOS of endoplasmic reticulum. A crosstalk between mitochondria and endoplasmic reticulum, in which Ca^{2+} and $^{\cdot}NO$ are the signals, is established in the initial phase of thymocyte apoptosis followed by the well-established mitochondrial changes that are characteristic of mitochondrion-mediated apoptosis: fall in mitochondrial membrane potential, mitochondrial dysfunction, opening of the membrane transition pores (MTP), and cytochrome *c* release.

The central role of mitochondria in the cell death program is exerted during the first and reversible phase of early apoptosis through the release of H_2O_2 and $^{\cdot}NO$ to either activate or inhibit cytosolic JNK, respectively, which attached to mitochondria catalyzes phosphorylation of Bcl-2 and Bcl-x_L and other not yet identified mitochondrial proteins. JNK-mediated phosphorylations initiate the steps to the second and irreversible phase of apoptosis by opening the inner membrane transition pore and by releasing $Ca^{2+}$and $O_2^{\cdot -}$ to the intermembrane space, followed by the opening of the outer membrane transition pore and release of cytochrome *c* to the cytosol. The next steps in the execution of the cell death program, such as apoptosome assembly and caspase activation, are independent of mitochondrial intervention.

The Mitochondrial Hypothesis of Aging

In the last few years, a strong current of opinion has linked the processes of mitochondrial oxyradical production, continuous oxygen toxicity, aging, and lifespan, in "the mitochondrial hypothesis of aging" following the idea of mitochondria as the biological clock. The free radical theory of aging was proposed by Harman in 1956 and considered that aging was caused by the cumulative and random effects of free radicals; an increased median lifespan in rats and mice supplemented in their food with organic antioxidants was observed. The continuous mitochondrial production of $O_2^{\cdot -}$ and $^{\cdot}NO$ as primary free radicals, with a whole series of derived reactive species, such as H_2O_2, $ONOO^-$, $HO^{\cdot}$, $ROO^{\cdot}$, and $^1O_2$, supports the notion of mitochondria as pacemakers of organ aging. As mentioned above, increased intramitochondrial steady-state concentrations of reactive oxygen and nitrogen species have been associated to the appearance of dysfunctional mitochondria in situations of acute oxidative stress, such as ischemia/reperfusion, and endotoxic or septic shocks. The persistence of a chronic oxidative stress situation is considered an effective aging factor. It is worth noting that increased levels of oxidative stress markers, such as 8-hydroxydeoxyguanosine, protein carbonyls, hydroperoxides, and TBARS, have been reported upon aging. Dysfunctional mitochondria, with decreases in the state 3 respiration, membrane potential, and respiratory control, and with increased size have been reported upon aging. Interestingly, some of the altered parameters were partially or totally normalized by treatment with antioxidants.

It is noteworthy that some mitochondrial macromolecules appear selectively damaged upon aging. In this way, mitochondria are the pacemaker of aging, both as the main continuous source and as the main target of oxidizing free radicals. Ames and co-workers pioneered the field with the observation of increased mtDNA damage, expressed as the level of 8-hydroxy-deoxyguanosine in tissues and in urine and in old animals as compared with young ones. Other mitochondrial macromolecules, such as mtRNA and the regulatory factor Bcl-2, have been reported damaged upon aging. Some mitochondrial enzymatic activities as NADH-dehydrogenase, cytochrome oxidase, adenine nucleotide translocase, and carnitine-acyl transferase are selectively decreased upon aging. There is a hypothesis linking these observations that considers that damaged mtDNA and mtRNA will produce, through mitochondrial protein synthesis, faulty polypeptides that would contribute along with protein carbonyls, hydroperoxides, and TBARS, to sub-optimal enzyme function and the appearance of dysfunctional mitochondria. The latter would signal for lysosomal digestion and for apoptosis. The decrease in energy availability and in tissue-active cells, as consequence of the decreased amount of mitochondria and of the enhanced apoptosis, would lead to the reduction in tissue function that is characteristic of tissue aging.

See Also the Following Articles

Cell Death by Apoptosis and Necrosis • Cytochrome *c* • Mitogen-Activated Protein Kinase Family • Nitric Oxide Signaling • Superoxide Dismutase

Glossary

apoptosis The active process by which cells execute a series of processes leading to cell death in a way that is not harmful for the tissue and the organism. It is opposite to inflammation and necrosis, a process in which toxic products reach the neighbor cells.

free radicals Molecules, better understood as chemical species, having an unpaired electron in their external orbitals. The feature makes the chemical species unstable and highly reactive with low specificity. However, some biologically produced free radicals, such as superoxide radicals ($O_2^{\cdot -}$) and nitric oxide ($^{\cdot}NO$), are relatively stable and quite selective in their reactions. Other biologically produced radicals, such as hydroxyl, alkyl and peroxyl ($HO^{\cdot}$, $R^{\cdot}$, $ROO^{\cdot}$) radicals, are highly reactive and unspecific. The point near the chemical symbols indicates the unpaired electron.

hydrogen peroxide The product of the bivalent reduction of the oxygen molecule (HOOH; H_2O_2); it is not a free radical, but originates $HO^{\cdot}$ radical upon interaction with Fe^{2+}.

mitochondrial electron transfer chain A series of biological and organic molecules embedded in the inner mitochondrial membrane that have chemical groups able to undergo reversible cycles of reduction/oxidation. The function of the mitochondrial respiratory chain channels the reducing equivalents from food components to the oxygen molecules and constitute the biochemical basis of respiration.

Further Reading

Beckman, K. B., and Ames, B. N. (1998). The free radical theory of aging matures. *Physiol. Rev.* **78**, 547–581.

Boveris, A., and Cadenas, E. (1982). Production of superoxide radicals and hydrogen peroxide in mitochondria. In *Superoxide Dismutase* (L. W. Oberley, ed.) Vol II, pp. 15–30. CRC Press, Boca Raton, Florida.

Boveris, A., and Cadenas, E. (2000). Mitochondrial production of hydrogen peroxide, regulation by nitric oxide and the role of ubisemiquinone. *IUBMB Life* **50**, 1–6.

Boveris, A., Cadenas, E., Reiter, R., Filipkowski, M., Nakase, Y., and Chance, B. (1980). Organ chemiluminescence: Non-invasive assay for oxidative radical reactions. *Proc. Natl. Acad. Sci. USA* **77**, 347–351.

Chance, B., Sies, H., and Boveris, A. (1979). Hydroperoxide metabolism in mammalian organs. *Physiol. Rev.* **59**, 527–605.

Elfering, S. L., Sarkela, T. M., and Giulivi, C. (2002). Biochemistry of mitochondrial nitric oxide synthase. *J. Biol. Chem.* **277**, 38079–38086.

Fridovich, I. (1976). Oxygen radicals, hydrogen peroxide and oxygen toxicity. In *Free Radicals in Biology* (W. A. Pryor, ed.) Vol 1, pp. 239–277. Academic Press, New York.

Gerschman, R., Gilbert, D., Nye, S. W., Dwyer, P., and Fenn, W. O. (1954). Oxygen poisoning and X-irradiation: A mechanism in common. *Science* **119**, 623–626.

Greenamyre, J. T., Sherer, T. B., Betarbet, R., and Panov, A. V. (2001). Complex I and Parkinson's disease. *IUBMB Life* **52**, 135–141.

Ignarro, L. J. (2000). Introduction and overview. In *Nitric Oxide: Biology and Pathobiology* (L. J. Ignarro, ed.) pp. 3–19. Academic Press, New York.

Kroemer, G., Dallaporta, B., and Resche-Rigon, M. (1998). The mitochondrial death/life regulators in apoptosis and necrosis. *Annu. Rev. Physiol.* **60**, 619–642.

Biography

Alberto Boveris is a Professor of Physical Biochemistry at the University of Buenos Aires (Argentina). He has B.S. degrees in pharmacy and biochemistry and a Ph.D. from the same university. During 1975–79, Boveris and Cadenas described the mitochondrial production of superoxide radical and hydrogen peroxide. His current research interests are aging mechanisms, organ chemiluminescence, and mitochondrial nitric oxide synthase.

Enrique Cadenas is a Full Professor and Chairman of Molecular Pharmacology and Toxicology at the School of Pharmacy of the University of Southern California. He holds an M.D. and a Ph.D. from the University of Buenos Aires (Argentina) and an honorary Ph.D. from the University of Linköping (Sweden). His fields of investigation include quinone redox reactions and mitochondrial metabolism and signaling.

Friedreich's Ataxia

Paul E. Hart and Anthony H. V. Schapira
University College London, London, UK

Friedreich's ataxia (FRDA) is an autosomal-recessive disorder that causes ataxia, sensory loss, cardiomyopathy, skeletal abnormalities, and in a proportion of patients diabetes and optic atrophy. It is the commonest inherited ataxia with an estimated prevalence of 1:29 000. Carrier prevalence is between 1:60 and 1:90. The responsible gene and its gene product, frataxin, have both been identified. Ongoing investigations into the function of frataxin, and the pathophysiology of FRDA are opening up new avenues for therapeutic intervention in this devastating neurodegenerative disorder.

Historical Perspective

In a series of five papers published between 1863 and 1877, Nicholaus Friedreich reported nine members of three families who had onset in puberty of ataxia, dysarthria, sensory loss, muscle weakness, scoliosis, foot deformity, and cardiac symptoms. Areflexia was only described in the final two reports, but was later adopted as one of the clinical diagnostic criteria. Over a century later the elucidation of the molecular mechanism of Friedreich's ataxia (FRDA), and the availability of genetic testing for diagnosis, allowed greater clarity regarding the phenotypic spectrum of this disorder.

Clinical Features

Disease onset ranges from 1.5 to 51 years in reported series. Loss of ambulation has been reported to occur at a mean of 15.5 $\pm$ 7.4 years after disease onset but ranges between 3 and 44 years. Death is most commonly as a consequence of cardiomyopathy and is at a mean age of 37.5 $\pm$ 14.4 years. Retrospective analysis of disease progression has reported a mean time to wheelchair confinement of 11 years. Atypical presentations include onset over the age of 25 years (late-onset Friedreich's ataxia (LOFA)), the preservation of lower limb reflexes (Friedreich's ataxia with retained reflexes (FARR)), and presentation as a pure spastic paraparesis, spastic ataxia (Acadian FRDA), pure sensory ataxia, or chorea.

Pathology

Pathological studies of FRDA report changes maximal in dorsal root ganglia, dorsal columns, corticospinal tracts, and heart. Macroscopically the spinal cord is atrophic with the posterior and lateral columns particularly affected. Changes within the nervous system are thought to be the consequence of a dying back process from the periphery affecting the longest and largest myelinated fibres that show changes of an axonopathy. Demyelination is seen in the dorsal columns. The cerebellar cortex shows only mild neuronal loss, but the dentate nucleus, and Clarke's column in the cord show marked changes. The cerebellar and occipital cortex, show reduced phospholipid levels in the absence of neuronal loss.

Genetics

In 1988 the FRDA gene was mapped to chromosome 9. The gene was linked to 9q13-21.1 in 1990 and cloned in 1996. Ninety-eight percent of cases are now known to be the result of a homozygous GAA triplet repeat expansions in intron 1 of the FRDA gene. This is a unique trinucleotide repeat (TNR) disorder in that its inheritance is autosomal recessive, its location is intronic, and it involves a GAA trinucleotide as opposed to CAG repeat as found in the majority of TNR disorders. The repeat length in normal individuals is 6-34, but is expanded in patients and carriers to between 67 and 1700. Repeat lengths are unstable. Paternal transmission is associated with a reduction in repeat length, an effect that increases with increasing paternal age. Maternal transmission can cause an increase or decrease in repeat length, and expansions are greater with increasing maternal age. The remaining 2% of patients are compound heterozygotes harboring an expanded repeat on one allele and a point mutation on the other. Twenty-three different point mutations are described to date and include missense, frameshift, splice site, initiation codon, and nonsense mutations. The former are found only in the C-terminal suggesting that functional domains reside in this part of the protein.

The location of these mutations in highly or poorly conserved amino acids correlates with the severity of the phenotype and the presence of atypical features. No cases resulting from homozygous point mutations have been described, although the population incidence of such individuals has been calculated to be $1{:}100 \times 10^6$. Clinically typical FRDA may occur in individuals in the absence of linkage to chromosome 9 suggesting that a second locus may exist.

Phenotype–Genotype Correlations

Clinical parameters correlate with the repeat length size. The size of GAA1 (the larger repeat allele) accounts for between 33% and 73% of the variation in the age of onset in various studies. GAA2 (the smaller allele) accounts for less than 20% of this variability. Indeed, GAA1 correlated better than GAA2 for several disease parameters and disease complications, including cardiomyopathy, in all studies except one. By contrast, the development of diabetes mellitus in FRDA correlated in only one study.

Further variation may result from other factors. The GAA repeat length may vary in a tissue-specific pattern due to mitotic instability, and peripheral blood samples may be a poor indicator of repeat lengths in pathologically affected tissues. GAA1 has been shown to differ in different brain regions and in various tissues. *Cis*-acting factors may also influence the phenotype. Potential mechanisms would include effects upon the stability of the trihelix structure by sequence alterations within or flanking the GAA expansion. Other genetic or environmental factors may also exert an influence on the phenotype. This is illustrated by the finding that the age of onset in sibs correlates strongly regardless of the degree of difference between their repeat lengths.

Gene and Gene Product

The FRDA gene contains seven exons within 80 kb of nuclear DNA. Transcription most commonly generates a 1.3 kb product translated into a 210 amino acid protein named frataxin. Alternative splicing generates a 171 amino acid protein of uncertain significance. Frataxin and mRNA levels are maximal in tissues of high mitochondrial content (heart, pancreas, liver, and skeletal muscle), although not all of these exhibit obvious clinical involvement in FRDA. Within the CNS, mRNA levels are highest in the cord, low in the cerebellum, and very low in the cerebral cortex. Frataxin appears to play a role in development; its homozygous knockout is lethal at an early embryological stage. Frataxin mRNA levels are high in fetal spinal cord, dorsal root ganglion, heart, liver, skeletal muscle, and skin. Lymphocytes from patients with homozygous expansions contain low levels of frataxin and these levels, and that of the mRNA, are inversely related to the size of the smaller repeat. The block is thought to occur at the level of transcript elongation, and the mechanism for this is believed to be through the formation of unusual DNA structures, such as DNA triplexes, by the GAA/TTC repeats. Several point mutations appear to alter the secondary structure of the protein and thus influence mitochondrial uptake or cleavage.

The function of frataxin is incompletely understood. The amino acid sequence shows no strong homology to any proteins of known function. It has, however, been shown to contain an N-terminal mitochondrial targeting sequence in its first 55 amino acids. The predicted mitochondrial location was confirmed when tagged expressed frataxin was shown to colocalize with mitochondrial markers in HeLa and COS cells. An inner membrane and a matrix location within the mitochondrion have both been proposed. X-ray crystallography studies reveal similarities to ferritin, a site for protein–protein interaction, and the ability to bind one molecule of iron. Point mutations in the protein core cause more severe phenotypes than those within the ferritin-like anionic patch, or flat external protein interaction surface.

A number of animal and cell models of FRDA, including transgenic mice, have provided insights into the pathogenesis of FRDA. Increased susceptibility to oxidative stress, increase in cellular and mitochondrial iron content, defects of the iron–sulfur center containing complexes of the mitochondrial respiratory chain, and reduced mitochondrial DNA levels have all been reported. Some of these changes have also been reported in human tissue. A role for frataxin in mitochondrial iron–sulfur (Fe–S) center synthesis has been proposed. The exact relationship between these biochemical perturbations remains incompletely understood.

Therapeutic Intervention

Based on the improved understanding of the pathogenesis of FRDA, a number of novel therapeutic strategies have been evaluated. Iron chelation restores mitochondrial iron levels and prevents MRC dysfunction in yeast models, but their *in vivo* use has been problematic. Antioxidants, including idebenone, coenzyme Q_{10}, vitamin E, N-acetyl cysteine, and selenium, have also been used. In some studies idebenone has resulted in a decrease in cardiac hypertrophy and decreases in surrogate markers of oxidative damage to DNA. Other studies have failed to show a benefit. Combined therapy with coenzyme Q_{10} and vitamin E has shown improvement in magnetic resonance spectroscopy and echocardiographic parameters.

Future therapeutic trials in FRDA may make use of antioxidants or other agents coupled to the triphenylphsphonium cation, which facilitates mitochondrial targeting of the agent. Potentials for gene therapy are also being explored, and may utilize drugs that interfere with the "sticky DNA" structures that are thought to be the cause of the transcription blockade that occurs in FRDA.

See Also the Following Articles

Diabetes • Mitochondrial DNA

Glossary

antioxidant Any substance that delays or prevents the process of oxidation.

ataxia Incoordination of voluntary muscle action.

mitochondria A cytoplasmic organelle, consisting of an outer membrane and an inner folded membrane, and containing its own DNA.

mitochondrial DNA A circular DNA molecule of 16.5 kb contained within the mitochondrion, and inherited maternally.

mitochondrial respiratory chain A series of enzyme complexes located on the mitochondrial inner membrane responsible for generating a proton gradient, which is itself required for the conversion of ADP to ATP by complex V (ATP synthase) of this chain.

trinucleotide repeat A three-nucleotide sequence, present in normal individuals as a set number of repeats, but which causes disease when a threshold number of repeats is exceeded.

Further Reading

Campuzano, V., Montermini, L., Molto, M. D., Pianese, L., Cossee, M., Cavalcanti, F., Monros, E., Rodius, F., Duclos, F., Monticelli, A., *et al.* (1996). Friedreich's ataxia: Autosomal recessive disease caused by an intronic GAA triplet repeat expansion. *Science* **271**(5254), 1423–1427.

Campuzano, V., Montermini, L., Lutz, Y., Cova, L., Hindelang, C., Jiralerspong, S., Trottier, Y., Kish, S. J., Faucheux, B., Trouillas, P., Authier, F. J., Durr, A., Mandel, J. L., Vescovi, A., Pandolfo, M., and Koenig, M. (1997). Frataxin is reduced in Friedreich ataxia patients and is associated with mitochondrial membranes. *Hum. Mol. Genet.* **6**(11), 1771–1780.

Delatycki, M. B., Williamson, R., and Forrest, S. M. (2000). Friedreich ataxia: An overview (Review). *J. Med. Genet.* **37**(1), 1–8.

Durr, A., Cossee, M., Agid, Y., Campuzano, V., Mignard, C., Penet, C., Mandel, J. L., Brice, A., and Koenig, M. (1996). Clinical and genetic abnormalities in patients with Friedreich's ataxia. *N. Engl. J. Med.* **335**(16), 1169–1175.

Harding, A. E. (1981). Friedreich's ataxia: A clinical and genetic study of 90 families with an analysis of early diagnostic criteria and intrafamilial clustering of clinical features. *Brain* **104**(3), 589–620.

Lodi, R., Hart, P. E., Rajagopalan, B., Taylor, D. J., Crilley, J. G., Bradley, J. L., Blamire, A. M., Manners, D., Styles, P., Schapira, A. H., and Cooper, J. M. (2001). Antioxidant treatment improves *in vivo* cardiac and skeletal muscle bioenergetics in patients with Friedreich's ataxia. *Ann. Neurol.* **49**(5), 590–596.

Lodi, R., Rajagopalan, B., Bradley, J. L., Taylor, D. J., Crilley, J. G., Hart, P. E., Blamire, A. M., Manners, D., Styles, P., Schapira, A. H., and Cooper, J. M. (2002). Mitochondrial dysfunction in Friedreich's ataxia: From pathogenesis to treatment perspectives (Review). *Free Radic. Res.* **36**(4), 461–466.

Muhlenhoff, U., Richhardt, N., Ristow, M., Kispal, G., and Lill, R. (2002). The yeast frataxin homolog Yfh1p plays a specific role in the maturation of cellular Fe/S proteins. *Hum. Mol. Genet.* **11**(17), 2025–2036.

Rustin, P., Rotig, A., Munnich, A., and Sidi, D. (2002). Heart hypertrophy and function are improved by idebenone in Friedreich's ataxia. *Free Radic. Res.* **36**(4), 467–469.

Wilson, R. B., and Roof, D. M. (1997). Respiratory deficiency due to loss of mitochondrial DNA in yeast lacking the frataxin homologue. *Nat. Genet.* **16**(4), 352–357.

Biography

Paul Hart is a Wellcome Research Training Fellow and Neurologist at the Department of Clinical Neurosciences, Royal Free Campus, University College London. His Ph.D. and primary research interests are on the interactions between nuclear and mitochondrial DNA, and the role of mitochondrial dysfunction in neurodegeneration.

A. H. V Schapira is Chairman, University Department of Clinical Neurosciences at the Royal Free and University College Medical School, and Professor of Neurology at the Institute of Neurology, Queen Square, London. His primary research interests are into the aetiology and pathogenesis of neurodegenerative diseases including Parkinson's disease, Huntington's disease, and Friedreich's Ataxia.

G Protein Signaling Regulators

John H. Exton
Vanderbilt University, Nashville, Tennessee, USA

Regulators of G protein signaling are important controllers of the system by which many agonists (hormones and neurotransmitters) transmit their signals across the cell membrane to influence intracellular processes. This system involves heterotrimeric G proteins, which are activated when the agonists bind to their specific receptors, and effectors (enzymes and ion channels), which are the targets of the G proteins. Activation of the G proteins by the receptors involves the release of GDP from their α-subunits and the subsequent binding of GTP, and the dissociation of the $\beta\gamma$-subunits from the G proteins. The GTP-bound α-subunits and the free $\beta\gamma$-subunits then act on their target effectors. Turning off the system requires the hydrolysis of GTP to GDP by the intrinsic GTPase of the α-subunits and this is a relatively slow process. Regulators of G protein signaling accelerate the GTPase activity thereby terminating the stimulation of effectors and allowing the G protein to revert to its GPD-liganded heterotrimeric state where it can activate again by agonist binding to receptor.

Discovery of Regulators of G Protein Signaling

Regulators of G protein signaling (RGSs) were discovered as negative regulators of G protein signaling in *S. cerevisiae* and *C. elegans*. In *S. cerevisiae*, a mutation termed *sst2* caused the yeast to become supersensitive to mating pheromone. However, at the time the *SST2* gene was identified, knowledge of signaling pathways was rudimentary and the connection to G proteins could not be made. Later it became clear that signaling in yeast was similar to that in mammals, i.e., the topology of pheromone receptors was similar to that of G protein-coupled receptors and the yeast G_α subunit shared considerable identity with mammalian $G_{i\alpha}$. Later, genetic evidence indicated a direct interaction between SST2 and G_α, and studies of mutations in G_α and SST2 led to the conclusion that SST2 acted as a GTPase-activating protein (GAP) for G_α.

Genetic analysis of *C. elegans* revealed a gene (*egl-10*) that encoded a protein that was similar in its C-terminal region to SST2. Similar to what was found in *S. cerevisiae*, the function of EGL-10 (to increase the frequency of egg laying via serotonergic motor neurons) depended on the presence of a G_α protein (GOA-1) that was homologous to mammalian $G_{o\alpha}$.

Multiple homologues of SST2 and EGL-10 have been identified in higher eukaryotes, utilizing yeast two-hybrid screens, database searches for related sequences, polymerase chain reaction, and rescue of the SST2-deficient phenotype in yeast. A large family of RGS proteins (more than 30 members) that show activity to different G proteins has now been identified in mammals (Table I). They differ significantly in size, but all have a diagnostic RGS core domain and exhibit GAP activity towards heterotrimeric G proteins.

Structure of RGS Proteins

RGS proteins have a conserved RGS domain of ~130 amino acids (Figure 1). This domain is capable of binding G_α subunits and stimulating GTP hydrolysis. In addition, certain RGSs have other domains in their N- and C-terminal regions. These may be PDZ, PTB, GGL, PH, DH, PX, and DEP domains, transmembrane spans, cysteine strings, and domains that bind the adenomatous polyposis coli protein (APC), GSK3, β-catenin, PKA, GRK, and G$\beta\gamma$ (Figure 1, see legend for definitions). The presence of these domains illustrates that RGSs have more functions than GAP activity and are targeted to membranes by multiple mechanisms.

The RGS domain has been defined by X-ray crystallography as a complex between RGS4 and $G_{\alpha i}1$, and by NMR analysis of a fragment of GAIP. The domain is globular and mostly helical in structure, based on a four-helix bundle and a second domain composed of the N- and C-terminal helices. Many of the most conserved residues face into the helical bundles, and others are involved in G_α binding. Three interhelix loops make contact with the three switch regions of G_α (those regions that show the greatest conformational changes when GDP is replaced by GTP), but there is no contact with bound GTP.

TABLE I

Mammalian RGS Proteins

Protein	Gα interactions	Tissue distribution
hRGS1	$G\alpha_i$ family, $G\alpha_q$	Activated B cells
hRGS2	$G\alpha_q > G\alpha_{i1}$	Biquitous
hRGS3	$G\alpha_i$ family, $G\alpha_q$	Ubiquitous
rRGS4	$G\alpha_i$ family, $G\alpha_q$	Brain
mRGS5	$G\alpha_i$ family	Heart, lung, brain, muscle
hRGS6	$G\alpha_o$	Brain
hRGS7	$G\alpha_i$ family, $G\alpha_q$	Brain, retina
rRGS8	$G\alpha_i$ family	Brain
hRGS9	$G\alpha_i$ family, $G_t\alpha$	Brain, retina
hRGS10	$G\alpha_i$ family	Brain
hRGS11	$G\alpha_o$	Brain, retina, pancreas
rRGS12	$G\alpha_i$ family, $G\alpha_{12}$, $G\alpha_{13}$	Brain, lung, liver, heart, spleen
hRGS13	N.D.	N.D.
rRGS14	$G\alpha_i$ family, $G\alpha_{12}$, $G\alpha_{13}$	Brain, lung, spleen
hRGS15	$G\alpha_{12}$, $G\alpha_{13}$	N.D.
mRGS16	$G\alpha_i$ family, $G\alpha_q$	Retinal, pituitary, liver
hRGS-GAIP	$G\alpha_i$ family, $G\alpha_q$	Heart, lung, liver
bRET-RGS1	$G\alpha_t$	Retina
hRGSZ1	$G\alpha_z$	Brain
hRGSZ2	$G\alpha_z$	N.D.
h115RhoGEF	$G\alpha_{13}$, $G\alpha_{12}$	Ubiquitous
mLscRhoGEF	N.D.	N.D.
hRhoGEF	N.D.	N.D.
mD-AKAP2	N.D.	Ubiquitous
rAxin	N.D.	Ubiquitous
mConductin	N.D.	Brain, lung, liver
bGRK2	$G\alpha_q$	Brain

N.D., no data.

Mechanisms of RGS Proteins

RGS proteins interact with active (GTP-bound) G_α-subunits and accelerate the hydrolysis of GTP. In the absence of RGSs and certain effectors, the rate of hydrolysis of GTP by G_α-subunits is very slow and inappropriate for rapid on/off signaling. RGSs can increase the rate of GTP hydrolysis by up to 2000-fold. RGSs act by altering the conformation of the G_α–GTP complex thus causing G_α to be a more efficient GTPase. The transition state intermediate involved in the hydrolysis of GTP can be mimicked by the complex G_α–GDP–$A1F_4$, and this has helped elucidate the mechanism of action of RGSs through crystallographic and other studies. As noted above, RGS proteins have a broad interface with G_α-subunits that includes the three switch regions. In the case of RGS4, the major change exerted on $G_{\alpha i}1$ is decreased mobility of switch II, and it has been suggested that switch II is stabilized in a catalytically active conformation. Because of the conservation of key residues in the contact site of the RGS domain, this mechanism is probably general. Other residues that have been shown by mutation to affect the GAP activity of the RGSs are probably involved in stabilizing the catalytic conformation of the G_α-subunit or altering the affinity of RGS for G_α. Although the usual mode of action of RGSs is to interact with G_α-subunits, some of them can also interact directly with effectors. For example, RGS2 can inhibit type V adenylyl cyclase.

From their structure, RGS proteins are predicted to be soluble. However, their mechanism requires that they act at the plasma membrane. The generation of GTP-liganded G_α-subunits in response to receptor activation would be expected to recruit RGSs to the membrane. However, transmembrane segments, lipid modifications, e.g., palmitoylation, and domains that interact with membrane lipids may also be involved, and there is evidence that some RGSs can be recruited selectively to the plasma membrane by receptors.

Selectivity of RGS Action

In view of the large number of RGSs, some selectivity in their interactions with G_α-subunits would be expected (Table I). Since certain receptors can couple to more than one G protein, the selective modulation of one G_α by an RGS protein can change the output from such receptors. However, selectivity has been hard to define *in vitro* and may involve restrictive patterns of cellular expression of the RGS and G_α proteins. *In vitro* analysis of RGS selectivity has involved single-turnover GAP assays, studies of competition with substrate and coimmunoprecipitation and coadsorption assays. For example, GAIP displays activity towards G_i and G_q class α-subunits, but the closely related RGSZ1 and RGSZ2 are selective for $G_{\alpha z}$ and display low activity towards $G_{\alpha q}$. RGS6 and RGS11 are selective for $G_{\alpha o}$ compared with other $G_{\alpha i}$ class subunits, and RGS2 prefers $G_{\alpha q}$. Surprisingly, only one RGS (sorting nexin 13) has been reported to act on $G_{\alpha s}$.

In a cellular setting, the selectivity of RGSs for certain G_α-subunits is less readily defined than *in vitro* since the readouts are quite distal from the interactions. RGS2 displays selectivity for $G_{\alpha q}$, in accordance with *in vitro* studies. RGS16 inhibits the activation of p38 MAP kinase by PAF more effectively than the activation of ERK2, whereas RGS1 has the opposite effects. In dorsal root ganglion cells, α_2-adrenergic activation of $G_{\alpha i}$ and $G_{\alpha o}$ was enhanced by antibodies against RGS4 and GAIP, whereas antibodies to other RGSs had no effect. Microinjection of the RGS proteins confirmed these results.

Concerning the receptor selectivity of RGS proteins, there have been few studies. In pancreatic acinar cells,

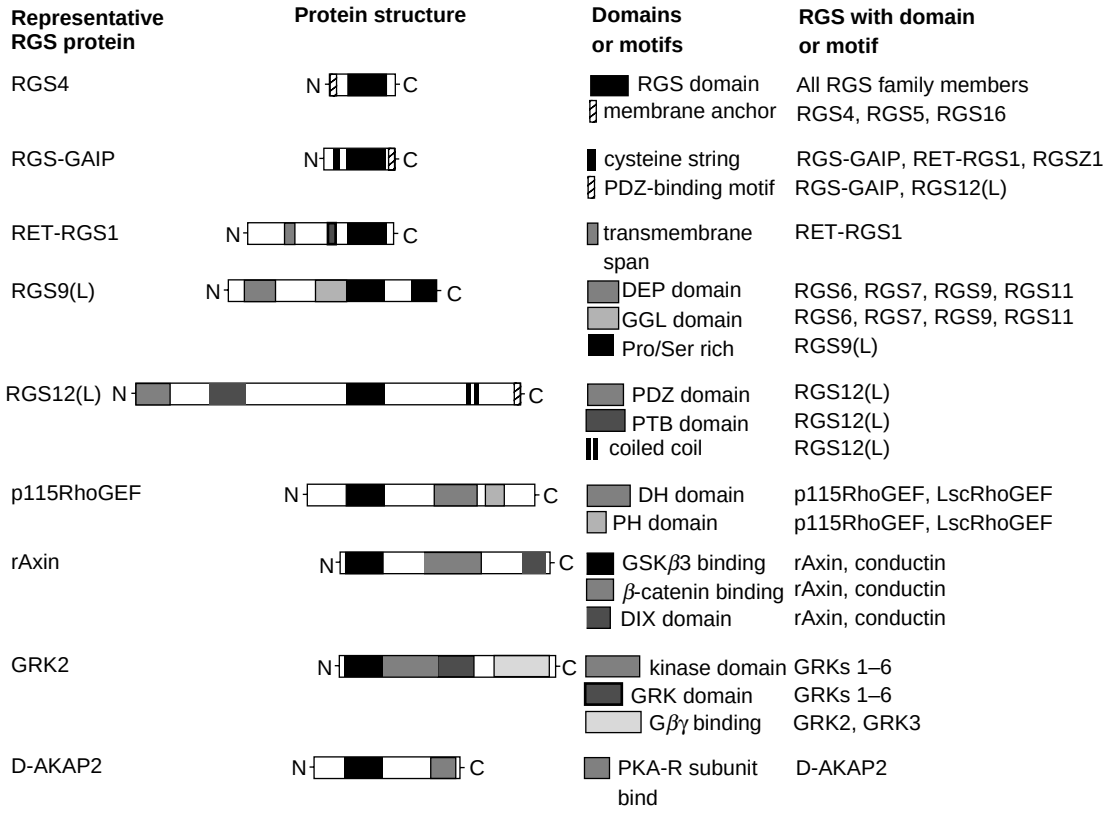

FIGURE 1 Structural organization and motifs in RGS proteins. (Modified from Hepler, J. R. (1999) Emerging roles for RGS proteins in cell signalling. *Trends Physiol. Sci.* **20**, 376–382.) PDZ (PSD-95, disk-large and zo-1), DEP (disheveled, egl-10 and pleckstrin), GGL (Gγ subunit-like), PTB (phosphotyrosine binding), DH (Dbl homology), PH (pleckstrin homology), GSKβ3 (glycogen synthase kinase β3-binding), DIX (disheveled homology), GRK (G protein-coupled receptor kinase), PKA-R (regulatory subunit of cAMP-dependent protein kinase).

RGS4 blocked G_q-mediated PLC activation initiated by M_3 muscarinic, cholecystokinin, and bombesin receptors. However, it was more potent against the muscarinic receptors. RGS1 and RGS16 were also more selective against M_3 muscarinic receptors. Surprisingly RGS2, which has activity towards $G_{\alpha q}$, did not show the same selectivity. The molecular basis for this receptor selectivity is presently unknown.

Significance of RGS Action

The primary action of RGSs is to induce rapid signal termination upon removal or inactivation of agonists in G protein-coupled receptor systems. The "knockout" of RSG9 prolongs photon responses because $G_{\alpha t}$ remains active. In addition this approach has been used to show that RGS3 and RGS5 selectively suppress MAP kinase activation by M_3 muscarinic and AT_{1A}-angiotensin receptors, respectively, in vascular smooth muscle. On the other hand, transgenic mice overexpressing RGS4 in ventricular tissue develop less ventricular hypertrophy in response to pressure overload, apparently because of reduced $G_{\alpha q}$ action. It should also be noted that RGSs can inhibit effectors by mechanisms not involving their GAP activity. This may be because the RGSs compete with the effectors for binding the G_α-subunits or because the RGSs inhibit the effectors directly.

Although signal termination is an important component of RGS action, this is not the whole story. There are interesting kinetic aspects to RGS action which arise from the cycle of activation/deactivation that G protein-coupled receptor systems undergo. For example, the activating receptors can only interact with the GDP-liganded form of G_α. Thus RGS activity can promote the association of G_α with the receptor through the generation of G_α–GDP, and permit G protein activation to continue.

Through their actions, RGS proteins modulate a variety of hormone- and neurotransmitter-stimulated responses in cells. These include the activity of adenylyl cyclase, the mitogen-activated protein kinase (MAP kinase) family, phospholipase C (with attendant changes in inositol trisphosphate and Ca^{2+} ions), G protein-gated inward rectifying K^+ (GIRK) channels, and cGMP phosphodiesterase in the retina (with altered phototransduction). Studies of the GIRK channels have revealed that RGS proteins can alter the timing,

amplitude and duration of the K^+ currents. An interesting group of RGSs is the RhoGEFs. These are guanine-nucleotide-exchange factors for the small G protein Rho. The first of these was discovered in *Drosophila*, where genetic analysis indicated that a RhoGEF (DRhoGEF2) acted downstream of the concertina gene, which is the *Drosophila* homologue of $G_{\alpha 12}$. Several laboratories then showed that $G_{\alpha 12}$ acted directly on three mammalian homologues of DRhoGEF2 (p115 RhoGEF, PDZ-RhoGEF, and LARG). In particular, the N-terminal region of p115 was observed to be similar to the conserved region of RGSs, and p115 was found to associate with $G_{\alpha 12}$ and $G_{\alpha 13}$ through its RGS domain. Even more interesting were the findings that $G_{\alpha 13}$ could stimulate the GEF activity of p115 towards Rho, and that the RGS domain of p115 displayed GAP activity towards $G_{\alpha 12}$ and $G_{\alpha 13}$. There is now much evidence that p115 and related RhoGEFs mediate the activation of Rho induced by agonists whose receptors are coupled to G_{13}. RGS16 inhibits $G_{\alpha 13}$-mediated activation of Rho by binding directly to $G_{\alpha 13}$ and disrupting its interaction with p115. The binding does not involve the RGS domain of RGS16.

Although they do not contain the RGS domain, many effectors of G proteins act as GAPs towards G_α-subunits. Examples are phospholipase C, which acts on $G_{\alpha q}$, and the γ-subunit of cGMP phosphodiesterase, which acts on transducin. In the case of transducin, RGS proteins and the phosphodiesterase act synergistically to inactivate the G protein.

Regulation of RGS Proteins

RGS proteins can be regulated by various mechanisms. One is by transcriptional regulation of their cellular levels. Other mechanisms include covalent modification, cellular relocalization, and interaction with regulatory proteins and lipids. The yeast RGS SST2 can be regulated at the transcriptional level by mating factor. Almost all RGSs are expressed in brain, although they are restricted to certain regions. They can be regulated by neurotransmitters through changes in their mRNA levels. In other tissues, there is transcriptional regulation involving growth factors and other peptides.

Regulation of RGSs also occurs at the post-transcriptional level. For example, phosphorylation can alter their degradation through ubiquitin-dependent proteolysis or by affecting a PEST sequence(s). For example, TNFα can protect RGS7 from proteolysis through phosphorylation of a Ser/Thr sequence near the GGL and RGS domains. RGS activity can also be modified by phosphorylation of its G_α targets. Phosphorylation of $G_{\alpha z}$ by protein kinase C inhibits the GAP activity of RGS5. Another modification is reversible palmitoylation of either the RGS or its substrate G_α. The effects on the RGS may be positive or negative, depending on the assay used, but palmitoylation of G_α-subunits usually results in inhibition of the GAP activity of the RGS.

RGS proteins can bind to a variety of cellular proteins (Figure 1). As noted in the section on structure, they contain many different protein-binding motifs. They can also bind lipids, e.g., PIP_3, Ca^{2+}-calmodulin, and the APC protein. RGS12 is the only RGS that contains a PDZ domain and thus can interact with proteins that contain a PDZ-binding motif, e.g., IL-8. AKAP2 binds the regulatory subunit of cAMP-dependent protein kinase (PKA). RGS6, RGS7, RGS9, and RGS11 contain a DEP domain and this is involved in membrane localization. Axin and conductin, which are scaffolding proteins, block signaling by Wnt proteins, which are involved in development. The RGS domains of these proteins bind the APC protein, whereas other domains bind β-catenin and GSK3.

Important interacting partners of the RGSs are the $\beta\gamma$-subunits of G proteins ($G_{\beta\gamma}$). These bind to G_α cooperatively with respect to GDP and suppress receptor-independent activation of G proteins. They also anchor G_α to the plasma membrane and regulate many effector proteins, e.g., adenylyl cyclase, phospholipase C, ion channels, and lipid kinases. With respect to RGS proteins, $G_{\beta\gamma}$ inhibits the GAP activity of many of these proteins. It appears that $G_{\beta\gamma}$ interacts with both the RGS and its target G_α-subunits. Several RGSs contain a GGL domain that is similar in sequence to $G_{\beta\gamma}$. It has also been shown that RGS11 binds Gβ5, and that the binding involves the GGL domain. Binding of $G_{\beta 5}$ to other RGSs has been demonstrated *in vivo*. In addition, RGSs can inhibit the effects of $G_{\beta\gamma}$-subunits on effectors by virtue of the generation of G_α·GDP which recombines with $G_{\beta\gamma}$ to reform inactive heterotrimeric G proteins. In the case of RGS3, there is another mechanism, namely its binding to $G_{\beta 1\gamma 2}$-subunits to inhibit signaling to effectors. This effect involves two regions of RGS3 separate from the RGS domain.

RGS Proteins as Drug Targets

Because the importance of G protein-coupled receptors in regulating a large variety of physiological processes, the RGSs represent very attractive targets for therapeutic intervention. Alterations in their expression indicate that they regulate cardiac function, immune responses, neuronal function, behavior, vision, and embryonic development. There is also evidence that they may be involved in the diseases of retinitis pigmentosa, schizophrenia, Parkinson's disease, chronic heart failure, drug addiction, and prostate cancer. Drugs could be targeted to RGSs in several ways, and could act as agonists or inhibitors. The first approach is to target the RGS/G_α

interface, which involves certain amino acids that are essential for the contact. The second is through modulation of the proteins and lipids that act as allosteric modifiers of RGS action. This also includes covalent modifications. The third is modification of the membrane attachment of the RGSs since it is essential for them to be recruited to the plasma membrane in order to exert their effects. In all cases, determination of the amino acid residues involved in RGS selectivity and in their interactions with allosteric regulators will be essential for the development of drugs of sufficient specificity to be therapeutically useful.

See Also the Following Articles

Adenylyl Cyclases • G_{12}/G_{13} Family • G_i Family of Heterotrimeric G Proteins • G_q Family • G_s Family of Heterotrimeric G Proteins • Mitogen-Activated Protein Kinase Family • Phospholipase C

Glossary

GAP A GTPase-activating protein that acts on monomeric and heterotrimeric G proteins to inactivate them. GAPs for heterotrimeric G proteins are RGSs and certain effectors.

G protein A signal-transducing protein that binds GTP (active form) or GDP (inactive form). Occurs in monomeric and heterotrimeric forms. Heterotrimeric G proteins are comprised of α-, β-, and γ-subunits. The α-subunit binds the guanine nucleotides and interacts with effector enzymes or ion channels. Heterotrimeric G proteins are activated by receptors with seven-transmembrane-spanning domains termed G protein-coupled receptors.

phosphorylation The modification of proteins by protein kinases and lipids by lipid kinases involving the addition of phosphate groups. This results in changes in the activity of the proteins or in the generation of new lipids with different functions.

receptor A membrane protein that binds and is activated by hormones, neurotransmitters, growth hormones, and cytokines.

Further Reading

Berman, D. M., and Gilman, A. G. (1998). Mammalian RGS proteins: Barbarians at the gate. *J. Biol. Chem.* **273**, 1269–1272.

Dohlman, H. G., and Thorner, J. (1997). RGS proteins and signaling by heterotrimeric G proteins. *J. Biol. Chem.* **272**, 3871–3874.

Fukuhara, S., Chikumi, H., and Gutkind, J. S. (2001). RGS-containing RhoGEFs: The missing link between transforming G proteins and Rho? *Oncogene* **20**, 1661–1668.

Hepler, J. R. (1999). Emerging roles for RGS proteins in cell signalling. *Trends Physiol. Sci.* **20**, 376–382.

Hollinger, S., and Hepler, J. R. (2002). Cellular regulation of RGS proteins: Modulation and integrators of G protein signaling. *Pharmacol. Rev.* **54**, 527–559.

Ross, E. M., and Wilkie, T. M. (2000). GTPase-activating proteins for heterotrimeric G proteins: Regulators of G protein signaling (RGS) and RGS-like proteins. *Annu. Rev. Biochem.* **69**, 795–827.

Biography

John Exton is a Professor of Molecular Physiology and Biophysics, Professor of Pharmacology and Investigator of the Howard Hughes Medical Institute at Vanderbilt University. His principal research interests relate to signal transduction involving G proteins and phospholipases. He received an M.D. and Ph.D. from the University of Otago, New Zealand, and was a postdoctoral fellow under Charles R. Park and Earl W. Sutherland at Vanderbilt. He is a member of the National Academy of Sciences.

G Protein-Coupled Receptor Kinases and Arrestins

Jeffrey L. Benovic
Thomas Jefferson University, Philadelphia, Pennsylvania, USA

Many transmembrane signaling systems consist of specific G protein-coupled receptors (GPCRs), which transduce the binding of a diverse array of extracellular stimuli into intracellular signaling events. GPCRs function to regulate many biological processes including neurotransmission, sensory perception, cardiovascular function, chemotaxis, embryogenesis, cell growth and development, differentiation, and apoptosis. To ensure that extracellular signals are translated into intracellular signals of appropriate magnitude and specificity, most signaling cascades are tightly regulated. GPCRs are subject to three principal modes of regulation: (1) desensitization, in which a receptor becomes refractory to continued stimuli; (2) endocytosis, whereby receptors are removed from the cell surface; and (3) down-regulation, where total cellular receptor levels are decreased. GPCR desensitization is primarily mediated by second-messenger-dependent kinases, such as protein kinase A (PKA) and protein kinase C (PKC), and by G protein-coupled receptor kinases (GRKs). GRKs specifically phosphorylate activated GPCRs and initiate the recruitment of arrestins, which mediate receptor desensitization, endocytosis, and down-regulation.

The GRK Family of Proteins

GRKs are found in metazoans and, in mammals, the seven GRKs can be divided into three subfamilies based on overall structural organization and homology: GRK1 (also termed rhodopsin kinase) and GRK7; GRK2 (βARK1), and GRK3 (βARK2); and GRK4, GRK5, and GRK6. GRKs are serine/threonine kinases with a tripartite modular structure. A central ~330 amino acid catalytic domain, most related to those of other AGC kinases such as protein kinase A, protein kinase C, and PDK1, is flanked by an ~180 residue N-terminal region that contains a regulator of G protein signaling homology (RH) domain, and an ~80–180 amino acid C-terminal lipid-binding domain that varies in structure (Figure 1) .

Specificity of GRK Interaction with GPCRs

GRKs specifically phosphorylate agonist-occupied GPCRs. While no clear consensus sequence for GRK-mediated phosphorylation has been identified, specific sites for GRK-mediated phosphorylation have been mapped to either the carboxyl terminal tail or the third intracellular loop of a number of GPCRs. Experiments with synthetic peptide substrates have revealed a preference of GRK1 and GRK2 family members for serines/threonines flanked by acidic residues, whereas GRK4 family members appear to prefer serines/threonines flanked by basic residues. Overall, the specificity of receptor phosphorylation by GRKs appears to be determined by a combination of binding determinants between the receptor and GRK.

Important insight has also been provided by manipulation of GRK expression in intact cell systems. Co-expression studies have revealed that a wide variety of GPCRs can serve as GRK substrates. Several strategies that reduce endogenous GRK levels/function in cells, including inhibitory antibodies, antisense DNA and dominant negative GRKs have also been used to assess specificity. For example, incubation of inhibitory GRK-specific monoclonal antibodies with various permeabilized cell types suggests the preferential regulation of both β_2- and α_2-adrenergic receptors (β_2AR and α_2AR) by the GRK2 subfamily. Similarly, the use of GRK-specific antisense constructs in various cell types reveals subtype-specific regulation of H2 histamine receptors (by GRK2), PACAP type 1 and CRF1 receptors (by GRK3), D1 dopamine and metabotropic glutamate type 1 receptors (by GRK4), thyrotropin receptors (by GRK5), and CGRP receptors (by GRK6).

Insight into GRK specificity/function has also been gained from *in vivo* strategies. Transgenic mice with cardiac-specific overexpression of GRK2 or a carboxyl-terminal GRK2 mini-gene, which serves as a GRK2 inhibitor, demonstrate *in vivo* effects on cardiac function.

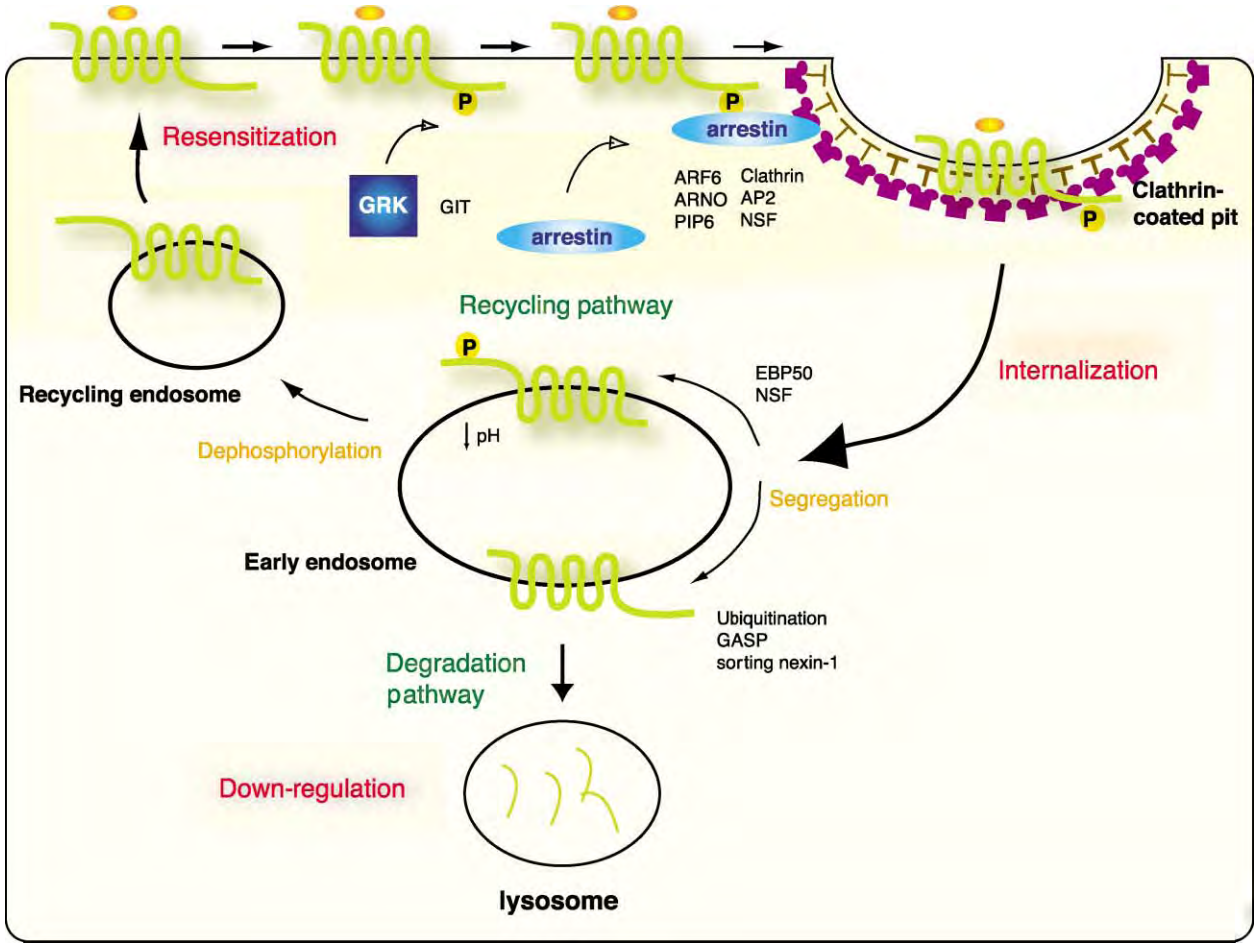

FIGURE 1 Schematic representation of G protein-coupled receptor (GPCR) trafficking. Agonist-activated receptors are phosphorylated by a GRK leading to the recruitment of arrestins. Arrestins serve as adaptor proteins by virtue of their ability to link receptors to components of the transport machinery such as clathrin, AP-2, and phosphoinositides leading to internalization. Additional interactions with GRKs and arrestins appear to play a role in this process. Once in endosomes, recycling receptors (recycling pathway) are readily segregated from receptors destined for lysosomes (degradation pathway). Although poorly understood, the sorting decision may be regulated by specific and distinct protein interactions or modification by ubiquitin. Receptors that enter the recycling pathway enter recycling endosomes and traffic back to the cell surface resulting in resensitization. Receptors that enter the degradation pathway traffic to lysosomes where they are proteolyzed, leading to a loss in the total cellular complement of the receptor, a process known as down-regulation.

Specifically, while GRK2 overexpression leads to increased uncoupling of the βAR from adenylyl cyclase and an associated decrease in left ventricular contractility, mice overexpressing the GRK2 inhibitor demonstrate increased left ventricular contractility even in the absence of β-agonist. Cardiac-specific overexpression of GRK5 in transgenic mice has a similar effect on βAR-mediated signaling and contractility, while the angiotensin II-mediated contractile response is attenuated only in the GRK2-overexpressing mice. Further demonstration of specificity is suggested in transgenic mice with myocardial overexpression of GRK3, where no effect on βAR response is observed. Moreover, studies involving cardiac overexpression of individual GRKs in mice revealed that GRK3 > GRK5 > GRK2 at desensitizing α_{1B}-adrenergic receptor signaling in the heart.

Functional knockouts of GRKs have provided unique insight into potential physiological roles of these proteins. Disruption of the GRK2 gene in mice by homologous recombination results in embryonic lethality as a consequence of hypoplasia of the ventricular myocardium, suggesting a role for GRK2 in cardiac development. In contrast, disruption of the mouse GRK3 gene results in normal development and physiology, although specific defects in desensitization of odorant-induced cAMP responses in olfactory epithelium and cholinergic response of airway smooth muscle are observed. A GRK5 knockout results in muscarinic supersensitivity and impaired receptor desensitization, while disruption of the GRK6 gene results in altered SDF-promoted chemotaxis of lymphocytes, supersensitivity to the locomoter-stimulating

effects of cocaine and amfetamine, and enhanced coupling of postsynaptic D2-like dopamine receptors. These findings suggest that GRKs are involved not only in regulating signaling, but may also have critical roles in regulating growth and development.

Regulation of GRK Function

A critical component in generating specificity is the molecular mechanism responsible for regulating the activity and cellular localization of GRKs. Recent studies have provided increased detail for known regulatory mechanisms as well as revealing previously unrecognized forms of regulation. For example, phosphorylation appears to play an important role in regulating GRK activity. GRK2 phosphorylation by ERK1/2 inhibits GRK2 activity while phosphorylation by PKA, Src, and PKC results in increased activity. In contrast, GRK5 activity is attenuated by PKC phosphorylation, but stimulated by autophosphorylation. GRK function is also regulated by interaction with a large number of additional proteins including G protein α- and $\beta\gamma$-subunits, clathrin, the GRK-interacting protein GIT1, caveolin-1, phosphoinositide 3-kinase-α and γ, cytoskeletal proteins such as tubulin and actin, and various calcium-binding proteins.

Phospholipids also play an important role in regulating GRK function since G$\beta\gamma$-mediated activation of GRK2 is dependent on negatively charged phospholipids including PIP_2. Interestingly, while GRK4 subfamily members do not bind G$\beta\gamma$-subunits, these kinases share an N-terminal PIP_2-binding domain that may facilitate receptor phosphorylation. These kinases also have the ability to associate with phospholipids via a C-terminal domain that is either palmitoylated (GRK4 and 6) or can directly bind phospholipids (GRK5). Thus, the immediate phospholipid environment may have a general and critical role in modulating GRK function. Taken together, multiple mechanisms including GPCR, G protein, and phospholipid binding play an important role in regulating GRK activity and function.

Structural Basis of GRK Function

The X-ray crystal structure of GRK2 complexed with G$\beta\gamma$ provides significant insight into GRK function. GRK2 is composed of three primary domains, an N-terminal RH domain, a central kinase catalytic domain, and a C-terminal PH domain. Interestingly, the crystal structure reveals that the RH, kinase, and PH domains form an equilateral triangle that is $\sim$80Å on a side. The RH domain consists of two discontinuous regions and contacts both the kinase and PH domains. The kinase domain is most similar to that of PKA and PDK1 and appears to be in an inactive conformation in the crystal structure. Interestingly, the structure of the RH and kinase domain core appears to have similarities to the inactive structure of Src with one region of the RH domain (the α10 helix) potentially functioning to regulate GRK activation. The C-terminal PH domain of GRK2 mediates phospholipid and G$\beta\gamma$ binding. Docking analysis of the GRK2/G$\beta\gamma$ complex with a GPCR and Gαq suggests that all three proteins should be able to bind to GRK2 simultaneously. This would represent an effective way of turning off signaling by phosphorylating receptor and sequestering Gαq and G$\beta\gamma$, thereby preventing interaction with effector molecules.

Role of GRKs in Disease

While various *in vitro* and *in vivo* manipulations of GRKs have provided significant insight into their function, various experimental approaches have led to a growing appreciation of the physiological and pathophysiological roles of GRKs in human disease. Several studies have demonstrated increased expression of GRKs associated with congestive heart failure (CHF), hypertension, and myocardial ischemia. In experimentally induced models of CHF, both GRK2 and GRK5 expression and activity was enhanced 2–3 fold in the left ventricular myocardium early in CHF progression. While it is not clear whether this increase in GRK levels is causal or a byproduct of elevated hormones secondary to disease, it is interesting that myocardial ischemia, which is associated with a large local release of noradrenaline, also produces a rapid increase in GRK2 mRNA levels. Since cardiac-specific overexpression of either GRK2 or GRK5 in transgenic mice produces decreases in cardiac function, the myocardial GRK overexpression that occurs during CHF could potentially contribute to pathology through increased βAR desensitization.

Several studies have also shown that GRK expression is selectively regulated as a function of the hypertensive state. In a comparison of normotensive and mildly hypertensive subjects, GRK2 protein expression in lymphocytes was positively correlated with blood pressure and negatively correlated with β_2AR-mediated adenylyl cyclase activity. These results suggest that GRK2 expression may underlie reduced β_2AR responsiveness characteristic of the hypertensive state. Another form of hypertension (human essential hypertension) involves impairment in dopamine-promoted urinary sodium excretion. Defective D1 dopamine receptor/G protein coupling in the kidney proximal tubule is the cause of the impaired renal dopaminergic action in this form of hypertension. Recent studies suggest that single nucleotide polymorphisms of GRK4 increase GRK activity and cause D1 receptor/G protein uncoupling in the renal proximal tubule. Moreover, expression of polymorphic GRK4 in transgenic mice produces

hypertension. Taken together, these findings suggest that GRKs play a role in vascular and renal control and may represent novel therapeutic targets for the treatment of human hypertension.

The visual transduction system provides another example of the critical role of GRKs in pathophysiology. Various methods of genetic analysis have revealed inherited mutations in GRK1 associated with a visual degenerative disease known as stationary night blindness or Oguchi's disease. Genetic analysis of several Oguchi patients demonstrated a lack of functional *grk1* alleles. A more detailed analysis of this disruption uncovered a profound abnormality in recovery of rod photoreceptors after light activation. These discoveries clearly demonstrate the sensitivity of phototransduction to GRK1 dysfunction and suggest potential future targets for gene therapy.

The Arrestin Family of Proteins

Arrestin (also termed S-antigen, visual arrestin, or arrestin-1) was initially identified in the visual system as a 48-kDa protein that redistributed from the cytoplasm to the disk membrane following light activation of bovine rod cell outer segments. Arrestin-1 is a 404 amino acid protein and binds to the light-receptor rhodopsin in a light- and phosphorylation-dependent manner resulting in suppression of G protein signaling. Gene targeting has demonstrated a clear physiological role for arrestin-1 in quenching phototransduction in mice. In addition, mutations in human arrestin-1 have been identified in Oguchi's disease.

Evidence for the involvement of arrestins in the regulation of additional GPCRs was initially suggested by the finding that purified arrestin-1 could impair β_2AR/G protein coupling in a phosphorylation-dependent manner. Subsequent studies identified a 418 amino acid arrestin-1 homologue (termed β-arrestin-1 or arrestin-2) that could effectively uncouple phosphorylated β_2AR from G protein. Arrestin-2 is widely expressed and has been broadly implicated in regulating GPCR desensitization. Subsequent studies identified two additional members of the arrestin family, arrestin-3 (also termed β-arrestin-2) and arrestin-4 (also termed cone arrestin). The four mammalian arrestins are divided into two major classes, visual and nonvisual, based on their localization and function. The nonvisual arrestins, arrestin-2 and arrestin-3, are broadly distributed and function in multiple processes including GPCR desensitization, endocytosis, recycling, down-regulation, and signaling. The visual arrestins, arrestin-1 in rod cells and arrestin-4 in cone cells are highly localized and play a primary role in quenching phototransduction.

Molecular Nature of Arrestin Interaction with GPCRs

An important feature of arrestin interaction with GPCRs is the ability of arrestins to recognize both the activation- and phosphorylation-state of the receptor. The observation that arrestins discriminate between agonist-activated and nonactivated GPCRs suggests that arrestins contain domains that specifically contact regions of the receptor exposed following receptor activation. Initial localization of such domains was provided by the observation that truncated arrestin-1 partially retained the ability to bind with light-activated rhodopsin. It was further demonstrated that at least three regions within the N-terminal half of arrestin-1 were involved in recognizing light-activated rhodopsin.

The importance of receptor phosphorylation in arrestin binding has also been explored in significant detail. The phosphorylation-recognition domain within arrestin-1 (residues 163–179) has been extensively characterized. These studies revealed two relatively independent changes that occur in arrestin on receptor binding: (1) increased binding affinity of the phosphorylation-recognition region of arrestin for the phosphorylated C terminus of rhodopsin, and (2) mobilization of additional receptor binding sites. These experiments also revealed that charge inversion of Arg-175 generates an "activated" form of arrestin that demonstrates phosphorylation-independent receptor binding. These studies and others provide the basis for a model of GPCR/arrestin interaction that is initiated by the activation- and phosphorylation-dependent binding of arrestin to receptor, culminating in a conformational change in arrestin that promotes additional interactions with the receptor.

Role of Arrestins in GPCR Endocytosis

Radioligand binding and immunocytochemical techniques have demonstrated that many GPCRs undergo endocytosis and multiple studies have implicated an important role for GRKs and arrestins in this process. Initial efforts revealed that GRK2 and nonvisual arrestins could enhance agonist-dependent endocytosis of the β_2AR. Additional analysis revealed that arrestins promoted endocytosis of agonist-activated GPCRs via an ability to interact with clathrin, the major protein component of the clathrin-based endocytic machinery. Predictably, arrestin mutants impaired in clathrin binding are largely defective in promoting β_2AR endocytosis. Consistent with these findings, minigenes expressing the C-terminal clathrin-binding domains of arrestin-2 or -3 are constitutively localized to clathrin-coated pits and function as dominant negative inhibitors of GPCR endocytosis. Additional studies have implicated a role

for nonvisual arrestin interaction with the β-subunit of the adaptor protein AP-2 in GPCR endocytosis and there also appears to be a critical role for arrestin interaction with PIP_2 in this process. In fact, a mutant arrestin-3 that is defective in phosphoinositide binding can still interact with the agonist-activated receptor but does not localize to clathrin-coated pits. Thus, nonvisual arrestin interaction with clathrin, AP-2, and PIP_2 contribute to arrestin-promoted endocytosis of GPCRs.

Role of Arrestins as Scaffolds in Cell Signaling

Several studies suggest that arrestins also have roles beyond regulating GPCR desensitization and trafficking. The finding that arrestin-2 binds directly to c-Src provided initial insight into this possibility. This interaction appears to be mediated via a proline-rich region in arrestin-2 interacting with the SH3 domain in Src, although the catalytic domain of Src may also contribute to binding. Since arrestin-2–Src interaction may be regulated by arrestin phosphorylation, the current model proposes that arrestin-2 binding to receptor promotes arrestin dephosphorylation enabling c-Src to bind and be recruited to clathrin-coated pits as part of a receptor–arrestin–Src complex. This localization may regulate Src-mediated phosphorylation of components (e.g., dynamin) that may, in turn, contribute to the regulation of GPCR trafficking and/or signaling.

Additional studies have suggested a role for arrestins as MAP kinase scaffolds. Several studies have focused on the potential involvement of arrestin-2 in GPCR-mediated activation of ERK1/2 and have demonstrated formation of complexes that contain receptor, arrestin-2, ERK1/2, and either raf-1 or Src. Studies have also demonstrated that arrestin-3 can directly bind to JNK3 and ASK1, a JNK kinase kinase, suggesting a role for arrestin-3 as a MAP kinase scaffold. Interestingly, stimulation of the AT_{1A} angiotensin receptor resulted in JNK3 activation and triggered the colocalization of arrestin-3 and active JNK3 to intracellular vesicles. Thus, arrestins may serve as scaffolds to mediate GPCR activation of various MAP kinase complexes.

The Structural Basis for Arrestin Function

Initial structural insight on arrestins was provided by the X-ray crystal structure of arrestin-1 while more recently the crystal structure of arrestin-2 has been solved. In general, arrestins have an elongated shape and are almost exclusively made up of β-sheets and connecting loops with the exception of one short α-helix. Each arrestin molecule is composed of two major domains termed the N domain and C domain that are held together by a set of buried salt bridges termed the polar core. The N and C domains are connected by a short hinge and are thought to move relative to each other in the process of arrestin's transition into an active conformation. The arrestin polar core is comprised of charged residues from the N-terminus, N domain, C domain, and C-terminus, thus bringing different parts of the molecule together to maintain a basal conformation. The residues involved in formation of the polar core are highly conserved, suggesting that this structural element is conserved in all arrestins and critical for function. Because the buried side chains of the polar core achieve neutrality by an elaborate network of electrostatic interactions, it has been suggested that disturbance of the polar core by introduction of a phosphate group from the receptor promotes structural changes that result in an active conformation of the protein. Disruption of polar core interactions can be simulated by charge inversion of an arginine (Arg-175, 169, and 170 in arrestin-1, -2, and -3, respectively) that lies in the center of the polar core. Mutation of this arginine results in an arrestin that binds equally well to phosphorylated and non-phosphorylated GPCRs suggesting that this residue plays a key role in recognition of phosphorylated receptor and in maintaining the basal conformation of arrestin. Taken together, these studies suggest that activation of arrestin results in significant structural changes that play an important role in mediating the various protein interactions and cellular functions of arrestin.

See Also the Following Articles

Adenylyl Cyclases • Brassinosteroids • Endocytosis • Histamine Receptors • Protein Kinase C Family

Glossary

desensitization A loss in responsiveness of a signaling system often due to an agonist-promoted decrease in coupling between receptor and G protein.

down-regulation A decrease in the total cellular level of a receptor typically due to prolonged incubation with agonist.

endocytosis The process of cellular uptake of a protein that often occurs through clathrin-coated pits for G protein-coupled receptors (GPCRs).

phosphorylation The transfer of phosphate from ATP to a serine, threonine, or tyrosine on a protein.

Further Reading

Benovic, J. L., DeBlasi, A., Stone, W. C., Caron, M. G., and Lefkowitz, R. J. (1989). Primary structure of the beta-adrenergic receptor kinase delineates a potential multigene family of receptor specific kinases. *Science* **246**, 235–240.

Ferguson, S. S. (2001). Evolving concepts in G protein-coupled receptor endocytosis: The role in receptor desensitization and signaling. *Pharmacol. Rev.* **53**, 1–24.

Krupnick, J. G., and Benovic, J. L. (1998). The role of receptor kinases and arrestins in G protein-coupled receptor regulation. *Annu. Rev. Pharmacol. Toxicol.* **38**, 289–319.

Lodowski, D. T., Pitcher, J. A., Capel, W. D., Lefkowitz, R. J., and Tesmer, J. J. (2003). Keeping G proteins at bay: A complex between G protein-coupled receptor kinase 2 and G$\beta\gamma$. *Science* **300**, 1256–1262.

Marchese, A., Chen, C., Kim, Y.-M., and Benovic, J. L. (2003). The ins and outs of G protein-coupled receptor trafficking. *Trends Biochem. Sci.* **28**, 369–376.

Perry, S. J., and Lefkowitz, R. J. (2002). Arresting developments in heptahelical receptor signaling and regulation. *Trends Cell Biol.* **12**, 130–138.

Biography

Jeffrey L. Benovic is Professor and Vice Chair in the Department of Microbiology and Immunology at Thomas Jefferson University in Philadelphia. His principal research interests are on the regulation of GPCR signaling with particular emphasis on the role of GRKs and arrestins in this process. He holds a Ph.D. in biochemistry from Duke University, where he also received his postdoctoral training. He has authored over 200 articles on GPCR signaling and regulation.

G_{12}/G_{13} Family

Stefan Offermanns
University of Heidelberg, Heidelberg, Germany

The ubiquitously expressed mammalian G proteins, G_{12} and G_{13}, constitute one of the four families of heterotrimeric G proteins (G_s, $G_{i/o}$, $G_{q/11}$, and $G_{12/13}$). Heterotrimeric G proteins, which consist of α-, β-, and γ-subunits, are defined by their α-subunit and act as molecular switches, which transmit signals from heptahelical G-protein-coupled receptors (GPCRs) at the plasma membrane to intracellular effectors. Orthologues of the mammalian G_{12} and G_{13} α-subunits, $G\alpha_{12}$ and $G\alpha_{13}$, have also been found in other multicellular organisms like *Drosophila melanogaster* and *Caenorhabditis elegans*. G_{12}/G_{13} regulate cytoskeletal rearrangements and cell growth in part via the small GTPase Rho.

General Properties and Modifications

The α-subunits of G_{12} and G_{13}, $G\alpha_{12}$ and $G\alpha_{13}$, have been identified by Mel Simon's group using a PCR cloning approach. $G\alpha_{12}$ and $G\alpha_{13}$ share 67% sequence identity and have a length of 377–380 amino acids. Biochemical analysis of purified $G\alpha_{12}$ and $G\alpha_{13}$ has revealed a relatively low rate of GTP hydrolysis, as well as a relatively slow guanine nucleotide exchange rate. Their expression levels in most cells appear to be lower than those of other G protein α-subunits. Both, $G\alpha_{12}$ and $G\alpha_{13}$, undergo palmitoylation, a reversible post-translational modification, which occurs at cysteine residues close to their N termini. Palmitoylation localizes G_{12} and G_{13} to the inner side of the plasma membrane and is required for proper signaling via G_{12}/G_{13}. *In vitro* experiments have shown that purified $G\alpha_{12}$ is a substrate for protein kinase C, whereas $G\alpha_{13}$ can be phosphorylated by protein kinase A. The physiological significance of these phosphorylations is unclear.

Receptor-Mediated Activation of G_{12} and G_{13}

It has been difficult to provide direct evidence for the coupling of a defined receptor to G_{12}/G_{13}. However, for a variety of GPCRs coupling to G_{12}/G_{13} could be demonstrated using different methods including the immunoprecipitation of receptor-activated G proteins, as well as genetic approaches. These studies revealed that some lipid mediators such as lysophospholipids or thromboxane A_2, various peptides such as endothelin, angotensin II, or substance P as well as the protease thrombin act on receptors, which are able to couple to G_{12}/G_{13} (Table I). G_{12} and G_{13} appear to be activated by GPCRs, which also couple to G_q/G_{11} and in some cases to G_i/G_o. However, not all G_q/G_{11}-coupled receptors are also able to activate G_{12}/G_{13}.

Cellular Functions of G_{12}/G_{13}

Most information on the cellular functions regulated via G_{12}/G_{13} came from indirect experiments employing constitutively active mutants of $G\alpha_{12}/G\alpha_{13}$ which lack the intrinsic GTPase activity due to an exchange of a glutamine residue (Q231 and Q226 in human $G\alpha_{12}$ and $G\alpha_{13}$, respectively) to a leucine residue. Several laboratories could show that transfection of these mutants into different cell types leads to cellular transformation. Interestingly, human $G\alpha_{12}$ was first cloned in a screen for transforming oncogenes from a Ewing Sarcoma cDNA library. However, it is still unknown whether $G\alpha_{12}$ or $G\alpha_{13}$ are involved in the pathogenesis of any neoplastic disease. In subsequent studies, the expression of constitutively active mutants of $G\alpha_{12}/G\alpha_{13}$ was shown to induce a variety of signaling pathways leading to the activation of various downstream effectors including phospholipase A_2, Na^+/H^+ exchanger or c-Jun N-terminal kinase.

Another important cellular function of G_{12}/G_{13} is their ability to regulate the formation of actomyosin-based structures and to modulate their contractility by increasing the activity of the small GTPase RhoA. The RhoA-mediated formation of actin stress fibers in fibroblasts activated by various G-protein-coupled receptor agonists is one of the best described cellular paradigms for G_{12}/G_{13}-mediated Rho activation and subsequent rearrangement of the actin cytoskeleton. This phenomenon involves a Rho-induced bundling of

TABLE I

GPCRs Shown to Couple to G_{12}/G_{13}

Receptor	Endogenous ligand(s)	G-protein subclass(es)
AT_1	Angiotensin II	$G_{12/13}$, $G_{q/11}$, $G_{i/o}$
B_2	Bradykinin	$G_{12/13}$, $G_{q/11}$
ET_A	Endothelin-1, -2	$G_{q/11}$, $G_{12/13}$, G_s
ET_B	Endothelin-1, -2, -3	$G_{12/13???}$
GAL2	GALP, Galanin	$G_{i/o}$, $G_{q/11}$, $G_{12/13}$
5-HT_{2C}	Serotonin	$G_{12/13}$, $G_{q/11}$
LPA_1 (Edg2) LPA_2 (Edg4)	Lysophosphatidic acid	G_i, $G_{q/11}$, $G_{12/13}$
LPC_1 (G2A)	Lysophosphatidylcholine	$G_{12/13}$, $G_{q/11}$,
NK_1	Substance P	$G_{12/13}$, $G_{q/11}$
PAR-1 PAR-3/4	Thrombin and others	$G_{12/13}$, $G_{q/11}$, G_i
$S1P_2$ (Edg5) $S1P_3$ (Edg3)	Spingosine-1-phosphate	$G_{12/13}$, G_i, $G_{q/11}$ $G_{12/13}$, G_i, $G_{q/11}$
TP	Thromboxane A_2	$G_{q/11}$, $G_{12/13}$
TSH	Thyrotropin	$G_{12/13}$, G_s, $G_{q/11}$, G_i
V_{1A}	Vasopressin	$G_{12/13}$, $G_{q/11}$

Summarized are findings from various laboratories which are based on the immunoprecipitation of receptor activated $G\alpha_{12}/G\alpha_{13}$ using photoaffinity labeling or a GDP/[^{35}S]GTPγS exchange assay as well as on genetic evidence from $G\alpha_{12}/G\alpha_{13}$ deficient cells. Please note that this list is far from being complete.

actin filaments into stress fibers and the clustering of integrins and associated proteins into focal adhesion complexes. The ability of $G\alpha_{12}/G\alpha_{13}$ to induce actin stress fiber formation in fibroblasts was first described by the group of Gary Johnson. Regulation of actin-based structures via a G_{12}/G_{13}-mediated and Rho-dependent pathway has also been shown to occur in many other eukaryotic cells. For instance, in neuronal cells, activation of Rho through lysophosphatitic acid or thrombin receptors leads to the formation of contractile actomyosin filaments eventually leading to the induction of neurite retraction, cell rounding, or axonal growth cone collapse. In vascular smooth muscle cells, the G_{12}/G_{13}-Rho-mediated pathway has been shown to contribute to the vasoconstrictor-induced actomyosin-based cell contraction, and the same pathway appears to be involved in the platelet shape change response.

Proteins Directly Interacting with $G\alpha_{12}/G\alpha_{13}$

Until recently, it was not clear how G_{12} and G_{13} regulate the function of RhoA. In general, the activation of Rho by exchange of GDP for GTP is catalyzed by guanine nucleotide exchange factors (GEFs), which in turn are regulated by various, mostly ill-defined mechanisms in the cell. First indications that a RhoGEF protein is regulated by G_{12}/G_{13} came from studies on early gastrulation events in *Drosophila*. Genetic analysis indicated that DRhoGEF2, a *Drosophila* RhoGEF protein, functions downstream of the *Drosophila* $G\alpha_{12}/G\alpha_{13}$ orthologue, the *concertina* gene product. Subsequently, three mammalian RhoGEF proteins (p115RhoGEF, PDZ-RhoGEF, and LARG) were described which are able to interact with activated $G\alpha_{12}/G\alpha_{13}$. This family of RhoGEF proteins is characterized by the presence of a "regulator of G protein signaling" (RGS)-domain, which mediates the interaction with the α-subunits of G_{12}/G_{13}. While the RhoGEF activity of PDZ-RhoGEF and LARG appears to be activated by both, $G\alpha_{12}$ and $G\alpha_{13}$, p115 RhoGEF activity is stimulated only by $G\alpha_{13}$. In addition, the RGS domains of these RhoGEF proteins accelerate the intrinsic GTP hydrolysis activity of $G\alpha_{12}/G\alpha_{13}$ *in vitro* and, thus, function as "GTPase-activating proteins" (GAPs). While it is now well established that RhoGEF proteins which contain an RGS-domain interact with $G\alpha_{12}/G\alpha_{13}$, the precise mode of this interaction is still not completely clear. In addition, several groups have found evidence for an involvement of tyrosine kinases in the regulation of Rho via G_{12}/G_{13}. In any case, regulation of RhoGEF proteins by $G\alpha_{12}/G\alpha_{13}$ provided the missing link between G_{12}/G_{13} and their ability to activate the small GTPase RhoA, which then mediates the effects of G_{12}/G_{13} on the cytoskeleton and may also be involved in the transforming activity of these G proteins (Figure 1).

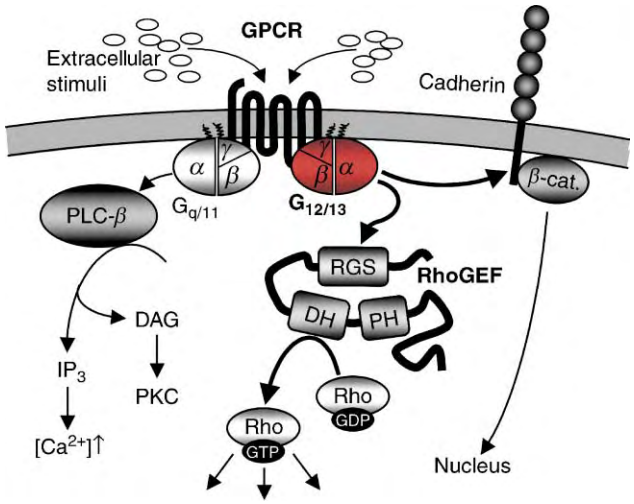

FIGURE 1 Some of the signaling processes mediated by G_{12}/G_{13}. G-protein-coupled receptors (GPCRs) which couple to G_{12}/G_{13} also activate G_q/G_{11}. RhoGEF, guanine nucleotide exchange factor for Rho proteins; PLC-β, phospholipase C β; β-cat., β-catenin; DAG, diacylglycerol; IP_3, inositol-1,4,5-trisphosphate; PKC, protein kinase C; RGS, "regulator-of-G-protein-signaling" domain; DH, "dbl-homology" domain; PH, "pleckstrin-homology" domain; see text for details.

Recently, an interesting link between G_{12}/G_{13} and cadherin-mediated signaling was described by the group of Pat Casey. Active $G\alpha_{12}$ and $G\alpha_{13}$ interact with the cytoplasmic domain of some type I and type II class cadherins, such as E-cadherin, N-cadherin, or cadherin-14, causing the release of β-catenin from cadherins (Figure 1). This down-regulates cadherin-mediated cell activation, and the release of β-catenin from cadherins may be a mechanism, by which $G\alpha_{12}/G\alpha_{13}$ induces cellular transformation.

Various other proteins including Bruton's tyrosine kinase, the Ras GTPase-activating protein Gap1m, radixin, heat shock protein 90, or protein phosphatase type 5 have been shown to interact with $G\alpha_{12}$ and/or $G\alpha_{13}$. However, the biological significance of these interactions are not yet clear.

In vivo Functions of G_{12}/G_{13}

The fact that G_{12}/G_{13} appear to be the major mediators of the activation of RhoA via GPCRs suggests that they are involved in multiple biological processes including morphogenetic processes, regulation of cell shape, or regulation of cell movements. Strong evidence for *in vivo* functions of G_{12}/G_{13} came so far mainly from the analysis of phenotypical changes of null-mutants of these G protein α-subunits in mice, flies, and worms. Experiments in *Drosophila* have provided genetic evidence for a physiological role of the G_{12}/G_{13}/RhoGEF-mediated pathway leading to Rho activation. By gene inactivation and epistasis experiments it could be shown that a signaling pathway, consisting of the G_{12}/G_{13} orthologue *concertina*, the *Drosophila* RhoGEF protein DRhoGEF2, as well as of Rho is involved in the actin/myosin-mediated cellular shape change, which results in the ventral furrow formation of the *Drosophila* embryo. Interestingly, loss of DRhoGEF2 results in a more severe phenotype than observed in *concertina* mutant embryos, suggesting that the *concertina* gene product conveys only part of the upstream regulation of DRhoGEF2.

While mice lacking the $G\alpha_{12}$ gene (*gna12*) are phenotypically normal, deletion of the $G\alpha_{13}$ gene (*gna13*) results in embryonic lethality at embryonic day 9.5 due to a defect in angiogenesis. Chemokinetic effects of thrombin were completely abrogated in fibroblasts lacking $G\alpha_{13}$, indicating that $G\alpha_{13}$ is required for full migratory responses of cells to certain stimuli. The defects observed in $G\alpha_{13}$-deficient embryos and cells occurred in the presence of $G\alpha_{12}$, and loss of $G\alpha_{12}$ did not result in any obvious defects. However, $G\alpha_{12}$-deficient mice, which carry only one intact $G\alpha_{13}$ allele also die *in utero*, and $G\alpha_{12}/G\alpha_{13}$ double deficient mice die even earlier than $G\alpha_{13}$ single deficient animals. This genetic evidence indicates that $G\alpha_{13}$ and its closest relative, $G\alpha_{12}$, fulfill at least partially nonoverlapping cellular and biological functions, which are required for proper mammalian development. Mouse lines carrying conditional mutants of the $G\alpha_{12}/G\alpha_{13}$ genes might allow one to analyze some of the functions of these proteins in the adult mammalian organism.

See Also the Following Articles

Cadherin Signaling • Cytokines • G Protein-Coupled Receptor Kinases and Arrestins • Phospholipase A_2 • P-Type Pumps: Na^+/K^+ Pump • Rho GTPases and Actin Cytoskeleton Dynamics • Small GTPases

Glossary

actin stress fiber Bundles of actin microfilaments which are found on the ventral side of cells cultured on artificial surfaces. They contain myosin and α-actinin as well as a variety of other structural and regulatory proteins which allow them to contract and to exert tension. The ends of stress fibers terminate at specific sites at the plasma membrane (focal adhesions) which are involved in cell adhesion. Activation of RhoA has been shown to induce actin stress fiber formation.

angiogenesis Growth of new blood vessels by sprouting from existing ones.

cadherins Calcium-dependent adhesion proteins, characterized by the presence of cadherin repeats, which are present in the extracellular part of the protein. Cadherins mediate Ca^{2+}-dependent homophilic adhesion. Cadherins are divided into two subfamilies, the classic cadherins and the protocadherins. Classic cadherins are subdivided into four subfamilies, the type I classic

cadherins, the type II classic cadherins, the desmosomal cadherins, and the so-called "other classic cadherins."

guanine nucleotide exchange factor (GEF) Guanine nucleotide exchange factors (GEFs) are proteins which catalyze the release of nucleotide bound to small GTPases like RhoA. In most cases, GEFs bind to the GDP bound GTPase, causing dissociation of the GDP. GTP, which is present at higher concentrations in the cell than GDP, then binds to the GTPase, and the GEF is released.

RhoA Small GTP-binding protein (small GTPase). Being one of the best studied members of the Rho-family of small GTPases, it has been shown to play an important role in the regulation of the actin cytoskeleton.

Further Reading

Buhl, A. M., Johnson, N. L., Dhanasekaran, N., and Johnson, G. L. (1995). $G\alpha_{12}$ and $G\alpha_{13}$ stimulate Rho-dependent stress fiber formation and focal adhesion assembly. *J. Biol. Chem.* **270**, 24631–24634.

Fukuhara, S., Chikumi, H., and Gutkind, J. S. (2001). RGS-containing RhoGEFs: The missing link between transforming G proteins and Rho? *Oncogene* **26**, 1661–1668.

Gutkind, J. S. (1998). Cell growth control by G protein-coupled receptors: From signal transduction to signal integration. *Oncogene* **17**, 1331–1342.

Kozasa, T., Jiang, X., Hart, M. J., Sternweis, P. M., Singer, W. D., Gilman, A. G., Bollag, G., and Sternweis, P. C. (1998). p115 RhoGEF, a GTPase activating protein for $G\alpha_{12}$ and $G\alpha_{13}$. *Science* **280**, 2109–2111.

Meigs, T. E., Fields, T. A., McKee, D. D., and Casey, P. J. (2001). Interaction of $G\alpha_{12}$ and $G\alpha_{13}$ with the cytoplasmic domain of cadherin provides a mechanism for beta-catenin release. *Proc. Natl. Acad. Sci. USA* **98**, 519–524.

Offermanns, S., Mancino, V., Revel, J.-P., and Simon, M. I. (1997). Vascular system defects and impaired cell chemokinesis as a result of $G\alpha_{13}$ deficiency. *Science* **275**, 533–536.

Parks, S., and Wieschaus, E. (1991). The Drosophila gastrulation gene concertina encodes a $G\alpha$-like protein. *Cell* **64**, 447–458.

Sah, V. P., Seasholtz, T. M., Sagi, S. A., and Brown, J. H. (2000). The role of Rho in G protein-coupled receptor signal transduction. *Annu. Rev. Pharmacol. Toxicol.* **40**, 459–489.

Singer, W. D., Miller, R. T., and Sternweis, P. C. (1994). Purification and characterization of the α-subunit of G_{13}. *J. Biol. Chem.* **269**, 19796–19802.

Strathmann, M. P., and Simon, M. I. (1991). $G\alpha_{12}$ and $G\alpha_{13}$ subunits define a fourth class of G protein α-subunits. *Proc. Natl. Acad. Sci. USA* **88**, 5582–5586.

Biography

Stefan Offermanns is a Professor of pharmacology and Head of the Department of Pharmacology at the University of Heidelberg, Germany. He received an M.D. from the Free University Berlin and was a postdoctoral fellow at the California Institute of Technology. His principal research interests are the cellular and biological roles of signalling pathways involving heterotrimeric G-proteins and small GTPase of the Rho family.

$GABA_A$ Receptor

Richard W. Olsen
University of California, Los Angeles, California, USA

Gregory W. Sawyer
Oklahoma State University, Tulsa, Oklahoma, USA

γ-Aminobutyric acid (GABA) is the neurotransmitter at most inhibitory synapses in the central nervous system. This amino acid is synthesized in one step from L-glutamate by the enzyme glutamic acid decarboxylase (GAD). GAD is present only in GABAergic neurons, comprising up to 30% of those in the nervous system of all organisms, and is a marker for GABA synapses. Dysfunction of GABA, including GAD, is implicated in a variety of neuropsychiatric disorders, including epilepsy, anxiety, depression, and drug dependence.

Fast inhibitory synaptic transmission is mediated primarily by the GABA-type A receptor ($GABA_A$ receptor (GABAR)), a ligand-gated chloride ion channel. Some slow inhibition is mediated by GABA at the GABA-type B ($GABA_B$) receptor, a G protein-coupled receptor. GABAR are members of a neurotransmitter receptor superfamily that includes the nicotinic acetylcholine receptors, glycine receptors, and serotonin $5HT_3$ receptors. The nicotinic acetylcholine receptors and the GABAR are families of heteropentameric isoforms, or receptor subtypes. These have different age-dependent and brain regional localization, circuit participation, and, thus, involvement in different functions and behaviors. Despite the lack of X-ray crystallographic data on the structure of GABAR, considerable information about functional domains within the protein is evolving. GABAR are the targets of important drugs, including general anesthetics and agents, such as the benzodiazepines used to treat epileptic seizures, anxiety, and sleep disorders. Benzodiazepines are synthetic compounds with important clinical utility (neuroactive drugs). The benzodiazepine "receptor," or site that mediates their pharmacological effects, is a portion of the GABAR protein itself; indeed, the binding site appears to be a modified version of the binding site for GABA.

Molecular Structure

Heteropentamers

The members of the superfamily share a pseudo-symmetric, pentameric membrane-spanning structure, with all subunits contributing equally to the ion channel (Figure 1). Each member of the superfamily is made from a family of homologous subunits of 45–67 kDa, with a conserved topology. These subunits each possess a long extracellular N terminus, which in some cases carries the neurotransmitter-binding site, four membrane-spanning domains, including the ion channel wall in M2, and a large variable sequence intracellular loop between M3 and M4. Although the structure of these complicated oligomeric receptor-channel membrane proteins has so far not been solved by crystallographic methods, some structural information has been obtained for other kinds of membrane receptors, ion channels, and, particularly, the extracellular domain of the nicotinic acetylcholine receptor, found to be exactly homologous to a snail acetylcholine-binding protein.

A Family of Isoforms

The heteropentameric GABAR protein is most often made from α, β, and γ subunits. The most common combination contains two copies of one α-subunit, two copies of one β-subunit, and one copy of $\gamma 2$, arranged as in Figure 2. The isoform most abundantly expressed in the CNS contains $\alpha 1\beta 2\gamma 2$. Those containing $\alpha 2$ or $\alpha 3$ are less abundant, and $\alpha 4$, $\alpha 5$, and $\alpha 6$-containing GABAR are even less abundant, with very restricted regional expression. Each α has a preferential β-partner ($\beta 1$, $\beta 2$, $\beta 3$, or θ, similar to avian $\beta 4$), although some α can combine with different β-subunits in different regions. Some GABAR isoforms appear to contain two different α-subunits, but these are relatively nonabundant. Additional rare isoforms have subunits substituted for $\gamma 2$. For example, the $\alpha 4$ and $\alpha 6$ subunits can combine with $\gamma 2$ or with δ in cerebellar and dentate gyrus granule cells and thalamic relay cells. Rarely, $\gamma 1$, $\gamma 2$, or ε (related to avian $\gamma 4$) can substitute for $\gamma 2$ in pentamers containing certain $\alpha\beta$ combinations.

Anatomical Localization and Functional Heterogeneity

Each GABAR subunit shows a specific anatomic and cellular localization as determined by assay of mRNA

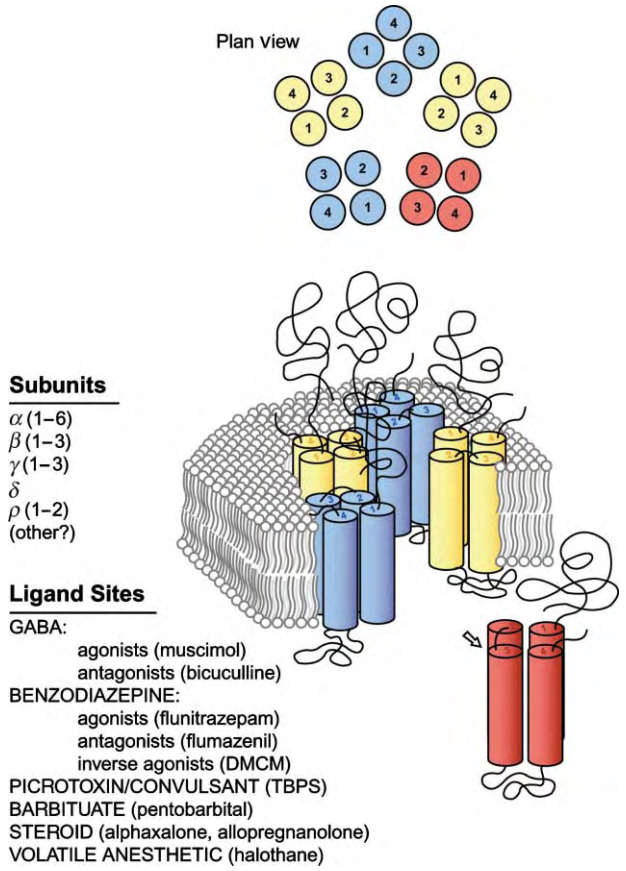

FIGURE 1 Schematic of GABA$_A$ Receptors. The protein is shown as a pseudo-symmetric membrane-spanning ion channel protein made of five homologous subunits, each of which has four membrane-spanning regions as shown in the pull-out subunit. The view from outside the cell (plan view) shows the arrangement around the central core, the chloride ion channel. Also indicated are the subunit families that can be utilized in composing each receptor, and the ligand-binding sites present on the receptor.

and polypeptides, indicating tissue-specific gene expression. Subunit–subunit associations and heteropentamer localization have been revealed by colocalization, copurification, or coimmunoprecipitation studies. Furthermore, there is specific localization to subcellular sites on the plasma membrane, such as synaptic versus nonsynaptic regions, cell bodies versus axons and dendrites, including positioning at postsynaptic locations apposed to specific cellular inputs. For example, the abundant isoform $\alpha1\beta2\gamma2$ is found primarily on inhibitory interneurons, thus inhibiting inhibition and producing a net excitatory circuit. Alternatively, many isoforms containing $\beta3$ are partnered with $\alpha2$, $\alpha3$, and $\alpha5$ subunits and localized on cells that use neurotransmitters other than GABA. These include principal excitatory cells, in which case GABAR inhibit a local circuit. The $\alpha1$ subunit appears to occur at any and all subcellular locations within a given cell, while the $\alpha2$ is limited to axo-axonal synapses in some cells. Thus the nature of the α-subunit, or perhaps specific partnering, may play a role in localization. In addition, heterogeneity has been demonstrated in the developmental profile of individual subunits in brain regions and cells.

The heterogeneity in subunit composition for the GABAR isoforms provides an explanation for pharmacological subtypes based primarily on ligand affinities, and secondarily on other factors such as sensitivity to regulatory systems. GABAR in certain brain regions, with certain subunit compositions, vary in their sensitivity to modulatory drugs like general anesthetics, including barbiturates, and benzodiazepines, as well as the biologically endogenous modulators, the neurosteroids. The neurosteroids are hormone metabolites that have rapid and direct effects on neurons, such as modulation of GABAR. Metabolites of the female sex hormone progesterone (allopregnanolone), corticosteroids (tetrahydrocorticosterone), and possibly androgens, enhance GABAR currents and appear to reach effective concentrations during certain physiological and pathological conditions. This field of research is just in its infancy.

Insights Gained from Transgenic Mice

Interestingly, the specific anatomical location and circuitry of GABAR subtypes dictates the specificity of functions and involvement in specific behaviors. Thus, transgenic and gene-targeted mice have demonstrated a role for certain subunits in particular functions and abnormalities, as well as pharmacology. For example, a mouse knockout for the $\gamma2$ subunit reveals a role for this subunit in proper synaptic localization and clustering of GABAR, and a role in anxiety, stress, and fear conditioning. Knockout of the $\beta3$ subunit produces a severe phenotype with epilepsy, motor incoordination, hyperactivity, and cognitive defects. These observations suggest that decreased levels of $\beta3$ subunit expression may contribute to Angelman syndrome, a human genetic disease with similar phenotype. Knockout of the common $\alpha1$ and $\beta2$ subunits have surprisingly little phenotype, perhaps due to compensatory increases in other subunits. Knockout of the $\alpha6$ subunit reveals its obligatory partnership with the δ subunit in the cerebellum, since no δ peptide is expressed in surface receptors. Knockout or knockdown of the $\alpha5$ subunit yields an animal with improved spatial memory acquisition, implicating $\alpha5$-containing GABAR in the CA1 region in mechanisms that are inhibitory for learning. Genetic knockins of point mutations for drug-binding sites have revealed subunit and subtype functions such as the differential importance of the $\alpha1$-subunit and its sites of expression in sedative/hypnotic functions, the $\alpha2$-subunit in anxiety, and the $\beta3$-subunit but not $\beta2$-subunit in the action of the intravenous anesthetic etomidate. Aberrant plasticity of GABAR in

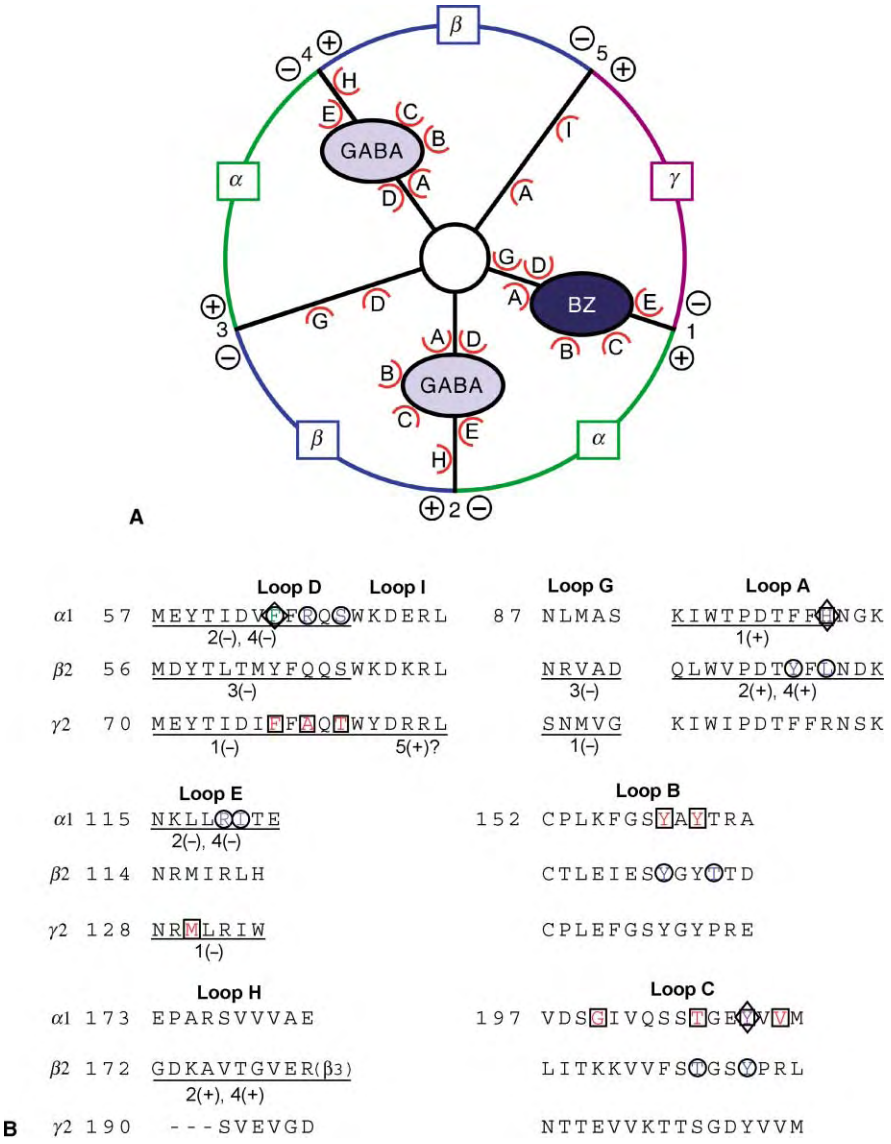

FIGURE 2 Donut model of GABA$_A$ receptor heteropentamer showing ligand-binding and subunit interaction domains. (A) The 5 subunits (-β–γ–α–β–α-) and 5 subunit interfaces (1–5) are shown, indicating the two different subunit interfaces for each subunit ((−) and (+)), the ligand-binding pockets for GABA and benzodiazepines (BZ), and the various peptide loops (A–I) involved in ligand-binding or subunit interfaces. The pore in the center represents the chloride channel. (B) The sequences represent the loops A–I within the N-terminal extracellular domain of the α1, β2, and γ2 subunits (numbering corresponds to mature subunits from rat). Circles: GABA site; squares: BZ site; diamonds (α1): photoaffinity label sites identified by sequencing: F64 (Muscimol); H101 (Flunitrazepam); Y209 (Ro15-4513). Underlines: subunit interaction loops, indicated under the line.

which a subunit switch occurs, such as α1 to α4, appear to contribute to drug withdrawal and seizure susceptibility. A summary of current (incomplete) knowledge of subtype localization and function is given in Table I.

Subcellular Localization, Associated Proteins, and Synaptic Plasticity

The localization of GABAR likewise involves events other than gene expression. These include intracellular trafficking, surface membrane insertion, synaptic clustering, removal of GABAR from synapses, and recycling or degradation. For example, the nature of the β-subunit seems to determine the subcellular location of GABAR. Regulation of these activities allows some plasticity of subunit composition of adult brain.

Several associated proteins have been identified in GABAR cell biology. These include especially gephyrin, originally isolated as a glycine receptor-associated synaptic clustering protein, that also appears to colocalize at synapses with some isoforms of GABAR. Likewise, GABARAP, a microtubule-associated protein, is involved

TABLE I

Summary of Native GABA$_A$ Receptor Subtypes

Subunit composition	Location	Function	Comments
$\alpha1\beta2\gamma2$	Widespread, esp. GABA neurons	Sedation, anticonvulsant	Adult, BZ1 pharmacology reduced in drug tolerance?
$\alpha2\beta3\gamma2$	Forebrain spinal cord	Anxiety, muscle relaxant	Axon hillock in some cells embryonic and adult
$\alpha2\beta1\gamma1$	Glia		
$\alpha3\beta3\gamma2$	Cortex	Anticonvulsant	Embryonic and adult
$\alpha4\beta2\gamma2$	Thalamus Dentate gyrus		Insensitive to agonist BZ elevated in drug withdrawal?
$\alpha4\beta2\delta$	Thalamus Dentate gyrus	Tonic inhibition	Extrasynaptic, BZ-insensitive, adult
$\alpha5\beta3\gamma2$	Hippocampus CA1 sensory ganglia	Tonic inhibition	Extrasynaptic, BZ-sensitive
$\alpha6\beta2\gamma2$	Cerebellar granule cells		Insensitive to agonist BZ
$\alpha6\beta2\delta$	Cerebellar granule cells	Tonic inhibition	Extrasynaptic, BZ-insensitive, adult
$\gamma3$, θ, ε	Little information		

in intracellular membrane vesicle trafficking and targeting of GABAR. GABARAP binds to the intracellular loop of the γ subunits but not others. Since the $\gamma2$ subunit is needed to direct GABAR to synapses, this interaction, as well as those with other proteins, may contribute to the process. Some aspects of channel function, allosteric modulation, and cell biology are regulated by post-translational mechanisms including protein phosphorylation. Many such topics are still controversial.

Functional Domains

Assembly

Rules determining which pentamers are produced are built in to the sequences of the subunits, primarily in the extracellular N-terminal domains. These residues involved in subunit partnering, assembly, and stoichiometry have been identified by subunit sequence scanning, site-directed chimeras and mutagenesis. They involve homologous positions in different subunits and are located at regions of subunit interfaces (Figure 2). Thus, approximately two dozen isoforms are significantly present in the nervous system, out of the literally thousands of possible permutations of heteropentamers.

Ligand-Binding Sites

Although the presence of a γ-subunit (generally $\gamma2$) in the pentamer is required for benzodiazepine (BZ) sensitivity, the nature of the α subunit determines the BZ site selectivity. The δ subunit is selectively associated with the $\alpha6$ subunit in cerebellar granule cells and with the $\alpha4$ subunit elsewhere. Although isoforms containing $\alpha4/6$ and $\gamma2$ can bind BZ inverse agonists, $\alpha4/6$-γ isoforms are totally BZ-insensitive, and they are excluded from synapses. The δ-containing isoforms are involved in producing tonic inhibition involving spillover of synaptic transmitter or other long-lasting pools of extrasynaptic GABA. These tonic currents are therefore affected by the activity of GABA transporters in nerve endings, postsynaptic cell bodies, and surrounding glia. The extrasynaptic δ-receptors appear to have higher affinity for GABA than synaptic receptors, slower desensitization, and they are the main targets of endogenous neurosteroid modulation.

Inspection of sequences for the BZ-sensitive and insensitive α-subunits suggested amino acid residues critical for BZ binding. The contribution of these residues was subsequently verified by site-directed mutagenesis and functional analysis by recombinant expression in heterologous cells. Additional information on ligand-binding site residues was obtained by microsequencing of peptides covalently attached by radioactive photaffinity labeled BZ ligand. Figure 2 summarizes results from the two approaches, indicating the residues participating in the BZ-binding site, one per pentamer; this is localized at the interface of α- and γ-subunits.

Similar approaches have identified residues involved in the agonist (GABA)-binding sites (two per pentamer), which are localized at the interface between α- and β-subunits. In fact, the residues in the β subunit that participate in the GABA-binding pocket are part of the BZ-binding pocket in the α subunit. This suggests that the binding site for BZ, a synthetic drug, is an evolutionary development of an agonist site. In addition, it is clear that the same residues in homologous sequences of other members of the receptor super-family are involved in the neurotransmitter-binding pocket, involving 5–6 small loops in the extracellular domain (Figure 2).

Ion Channel/Sites for Action of Allosteric Blockers and Enhancers

As in other members of the superfamily, the second transmembrane domain M2 has been shown to form the ion channel in GABAR. Residues in this domain affect

ion selectivity, gating, conductance, kinetics, and desensitization of the channel. This area is also involved in the action of picrotoxin and cage convulsants that functionally block the channel, as well as certain allosteric modulators like general anesthetics that enhance GABA or activate the channel. Residues have been identified within the mouth of the ion channel in M2, as well as on the back side of the M2 helix, that are required for general anesthetic modulation of GABAR. Other residues at the extracellular ends of M3 and M1 have been implicated and appear to be spatially situated near the position of the identified M2 residues, suggesting the possibility of an anesthetic-binding pocket, although this area may be involved only in allosteric coupling.

See Also the Following Articles

Allosteric Regulation • GABA$_B$ Receptor • Ion Channel Protein Superfamily

Glossary

allosteric Literally, "at another site": proteins have domains, or sites, that carry out their functions, termed "active" sites, such as the binding site on a receptor for the neurotransmitter ligand. Other ligands bind at different, or allosteric sites, to modulate the activity of the protein.

ligand-gated ion channel receptor Some receptors are coupled to effector systems in the cells, possibly a cascade of events, while other receptors are themselves ion channels, regulated by binding of the neurotransmitter ligand.

neurosteroid Steroids that are found endogenously in the nervous system and have some function there. Neuroactive steroids have some action in the nervous system but may originate there or have exogenous sources, elsewhere in the body, or be administered as drugs.

receptor protein Proteins that recognize the signal molecule, the neurotransmitter, bind it, and trigger a response.

transgenic mouse An animal that has been genetically engineered to express a foreign gene (a "trans" gene) or a mutated version of its own gene (knockout or knockin).

Further Reading

Jones-Davis, M., and Macdonald, R. L. (2003). GABA$_A$ receptor function and pharmacology in epilepsy and status epilepticus. *Curr. Opin. Pharmacol.* **3**, 12–18.

Martin, D. L., and Olsen, R. W. (eds.) (2000). *GABA in the Nervous System: The View at 50 Years*. Lippincott, Williams and Wilkins, Philadelphia.

McKernan, R. M., and Whiting, P. J. (1996). Which GABA$_A$ receptor subtypes really occur in the brain? *Trends Neurosci.* **19**, 139–143.

Möhler, H., Fritschy, J. M., and Rudolph, U. (2002). A new benzodiazepine pharmacology. *J. Pharmacol. Exp. Ther.* **300**, 2–8.

Moss, S. J., and Smart, T. G. (2001). Constructing inhibitory synapses. *Nat. Rev. Neurosci.* **2**, 240–250.

Olsen, R. W., and Macdonald, R. L. (2002). GABA$_A$ receptor complex: Structure and function. In *Glutamate and GABA Receptors and Transporters: Structure, Function, and Pharmacology* (J. Ejeberg, A. Schousboe and P. Krogsgaard-Larsen, eds.) pp. 202–235. Routledge, London.

Sieghart, W., and Sperk, G. (2002). Subunit composition, distribution and function of GABA$_A$ receptor subtypes. *Curr. Top. Med. Chem.* **2**, 795–816.

Sigel, E. (2002). Mapping of the benzodiazepine recognition site on GABA$_A$ receptors. *Curr. Top. Med. Chem.* **2**, 833–840.

Biography

Richard W. Olsen is a Professor of Neuroscience, Pharmacology, and Anesthesiology at the University of California, Los Angeles, School of Medicine. His principal research interest is in the structure and function of GABA$_A$ receptors. He received his Ph.D. in Biochemistry from the University of California, Berkeley, and did postdoctoral research at the Pasteur Institute in Paris, France.

Gregory W. Sawyer is a Professor in the Department of Pharmacology and Physiology at Oklahoma State University, Center for Health Sciences in Tulsa. His primary research interests are in the cell biology and structure/function of G protein-coupled receptors. He obtained his Ph.D. from the University of California, Irvine and received his postdoctoral training at the University of California, Los Angeles.

$GABA_B$ Receptor

S. J. Enna
University of Kansas Medical Center, Kansas City, Kansas, USA

γ-Aminobutyric acid (GABA) is a major inhibitory neurotransmitter in the central nervous system (CNS). The responses to GABA are mediated by two classes of receptors, $GABA_A$ and $GABA_B$. While the former is a pentameric, ionotropic chloride ion channel, the $GABA_B$ site is a heterodimeric, Group 3 G-protein coupled receptor. Structurally, the $GABA_B$ receptor consists of two 7 transmembrane spanning subunits, $GABA_{B(1)}$ and $GABA_{B(2)}$. Whereas the orthosteric-binding site for the neurotransmitter is located on the $GABA_{B(1)}$ subunit, G protein coupling is associated with the $GABA_{B(2)}$ component. The functional and pharmacological characteristics of $GABA_B$ receptors have been defined using potent and selective agonists and antagonists. Studies with both wild type and expressed $GABA_B$ receptors indicate that a $GABA_{B(1)}$/$GABA_{B(2)}$ dimerization is obligatory for receptor function. The discovery of positive allosteric modulators may pave the way for the development of $GABA_B$-receptor subtype-selective drugs. Such compounds, along with competitive agonists and antagonists, may be of value in treating a host of neurological and psychiatric conditions including spasticity, epilepsy, depression, cognitive impairments, and pain.

$GABA_B$-Receptor Structure and Function

The $GABA_B$ receptor was first identified in 1981. Studies revealed that (R,S)-β-aminomethyl-β-(4-chlorophenyl)-propanoic acid (baclofen), a drug used to treat spasticity, and GABA inhibit depolarization-induced neurotransmitter release and compete for a specific binding site in brain tissue. Since neither the functional response to baclofen nor its binding are inhibited by bicuculline, a competitive $GABA_A$-receptor antagonist, it was proposed that baclofen interacts with a different class of receptors, which were designated $GABA_B$ sites. Subsequent work demonstrated further that $GABA_A$ and $GABA_B$ receptors are distinct entities. Thus, although baclofen, like $GABA_A$-receptor agonists, hyperpolarizes neurons, the baclofen-sensitive receptors are coupled to G proteins, unlike the ionotropic $GABA_A$ site. Activation of the $GABA_B$ receptor decreases Ca^{2+} and increases K^+ membrane conductance, whereas the $GABA_A$ receptor regulates chloride ion flux. Although baclofen inhibits forskolin-stimulated adenylyl cyclase activity in brain tissue, it enhances cAMP production in brain slices if they are exposed simultaneously to agents, such as β-adrenoceptor agonists, that activate receptors coupled to G_s. Thus, depending on the conditions, $GABA_B$-receptor stimulation either enhances or inhibits cAMP accumulation, suggesting an effector system associated with both G_i and G_o proteins. Furthermore, $GABA_B$ receptor stimulation induces nuclear accumulation of the transcription factors ATF4 and ATFx, suggesting genomic consequences to activation of this site.

Definitive proof that the $GABA_B$ receptor is molecularly distinct from the $GABA_A$ site came from expression cloning experiments. These studies revealed that the $GABA_B$ receptor is a heterodimer composed of two 7-transmembrane-spanning proteins (Figure 1). The first protein to be identified was designated $GABA_{B(1)}$, and the second $GABA_{B(2)}$. These subunits, which have 54% amino acid similarity and 35% sequence homology, are characterized by a large extracellular N-terminal domain. Heterodimerization, which is essential for receptor trafficking to the membrane as well as receptor function, occurs predominately through association of the intracellular α-helical portions of the C termini (Figure 1). The orthosteric-binding site for GABA is located within a conserved Venus flytrap region of the $GABA_{B(1)}$, but not $GABA_{B(2)}$, subunit N-terminal domain, whereas the affiliated G proteins are coupled to the $GABA_{B(2)}$ component (Figure 1). The $GABA_B$ site is a group 3 receptor, a category that includes vomeronasal organ, metabotropic glutamate, and calcium-sensing receptors. Indeed, calcium is absolutely required for agonist binding to the $GABA_B$ site. While several splice variants have been identified for the $GABA_{B(1)}$-receptor subunit, not all are capable of forming functional receptors when coupled to $GABA_{B(2)}$. The most extensively studied $GABA_B$-receptor subunit combinations are $GABA_{B(1a)}$/$GABA_{B(2)}$ and $GABA_{B(1b)}$/$GABA_{B(2)}$. A variety of studies, including those with $GABA_B$ subunit deletion mutant mice, have demonstrated that heterodimerization of these two distinct gene products is absolutely essential for a functional receptor, with homodimers being biologically inert.

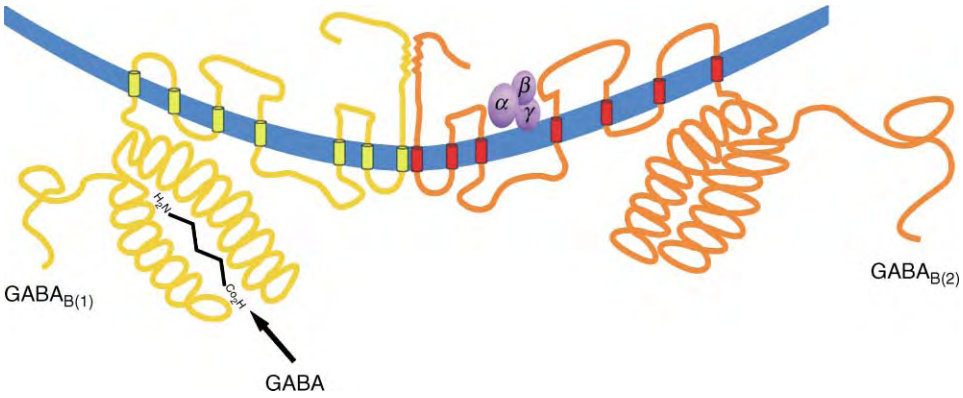

FIGURE 1 Structure and function of the GABA$_B$ receptor. Attachment of GABA to the receptor recognition site located on the GABA$_{B(1)}$ component causes dissociation of the α- and $\beta\gamma$-subunits from the G protein affiliated with the GABA$_{B(2)}$ component of the receptor dimer. The liberated G-protein subunits influence cellular activity by regulating Ca^{2+} and K^+ flux, adenylyl cyclase activity, and transcription factors. (Modified from Enna, S. (2001). A GABA$_B$ mystery: The search for pharmacologically distinct GABA$_B$ receptors. *Mol. Interventions* **1**, 208–218.)

GABA$_B$ receptors are located pre- and postsynaptically throughout the central nervous system (CNS) and in some peripheral organs, although the physiological significance of the latter remains to be determined. Given the obligatory nature of heterodimerization for GABA$_B$-receptor function, it is somewhat surprising that the distribution of GABA$_{B(1)}$ and GABA$_{B(2)}$ expression differs among brain regions, and that drug- or physiologically induced changes in subunit expression varies between the two. This suggests a differential regulation of these genes, pointing to the possibility that the protein products may serve functions other than formation of GABA$_B$ receptors. For example, it has been reported that GABA$_B$-receptor subunits can directly associate with other proteins, in particular transcription factors such as CREB2.

The restricted number of GABA$_B$-receptor subunits, the 1:1 stoichiometry of the system, and the conserved nature of the GABA$_{B(1)}$-neurotransmitter recognition site, limits the possibilities for pharmacologically distinct GABA$_B$ receptors. Although there is indirect evidence that certain GABA$_B$ receptors may be more responsive to some agents than to others, there is no direct proof of molecularly or pharmacologically distinct sites. While it has been suggested that GABA$_{B(1a)}$/GABA$_{B(2)}$ may be pharmacologically different from the GABA$_{B(1b)}$/GABA$_{B(2)}$, this has not been substantiated. Since the neurotransmitter recognition site on the GABA$_{B(1)}$ splice variants are identical, any difference in their responsiveness to a ligand would most likely be due to an allosteric modification mediated by attachment of the agonist or antagonist to some portion of the receptor complex separate from the recognition site. The lack of evidence supporting pharmacologically distinct GABA$_B$-receptor subtypes has limited the clinical development of GABA$_B$-receptor agonists and antagonists since dose-limiting side effects accompany a generalized modification of GABA$_B$ receptor function.

GABA$_B$-Receptor Agonists and Allosteric Modulators

Baclofen is the prototypical GABA$_B$-receptor agonist (Figure 2). In ligand-binding assays with rat brain membranes its affinity for the receptor is approximately 40 nM, with its EC_{50} values in functional assays being in the low μM range. Baclofen has been employed for years as a treatment for spasticity associated with multiple sclerosis and spinal cord injuries, for nocturnal myoclonus, and for trigeminal neuralgia. It is the only GABA$_B$-receptor agent approved for clinical use.

A series of phosphinic acid analogues of GABA has yielded a number of potent and selective GABA$_B$-receptor agonists, including CGP 44532 and CGP 27492, that

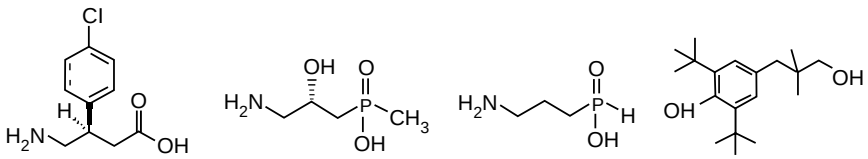

FIGURE 2 Chemical structures of some GABA$_B$-receptor agonists and a positive allosteric modulator.

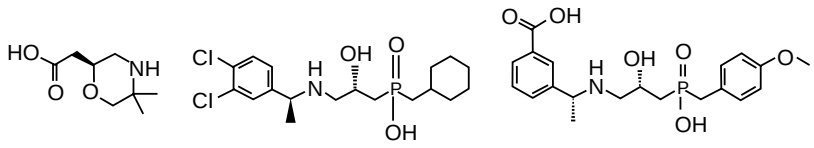

FIGURE 3 Chemical structures of some GABA$_B$-receptor antagonists.

have been used for experimental purposes (Figure 2). Other compounds in this series include CGP 44533, the less active (R)-(+) enantiomer of CGP 34938, of which CGP 44532 is the more active (S)-(−) enantiomer, and SKF 97541, also known as CGP 35024. Rat brain membrane GABA$_B$-receptor binding affinities for CGP 44532 and CGP 27492 are ~45 nM and 6.0 nM, respectively, with the corresponding values for CGP 44533 and SKF 97541 being 150 nM and 1.0 nM, respectively. Both tritiated baclofen and tritiated CGP 27492 are available as radioligands for labeling GABA$_B$ receptors.

In vivo studies indicate that GABA$_B$ agonists display sedative, muscle relaxant, and antinociceptive properties. They also impair memory performance, reduce the craving for cocaine, and are anticonvulsants. Tolerance develops to some of these responses upon repeated administration of agonist, and sedation precludes their use in many situations.

Another approach to activating GABA$_B$ receptors is with selective allosteric modulators, as exemplified by CGP 7930 (Figure 2). Modulators differ from conventional agonists in that they do not directly interact at the GABA$_B$-receptor recognition site, but rather attach to some other portion of the receptor complex causing an allosteric modification in the neurotransmitter-binding site, or enhancing the efficiency of the receptor coupling with the effector system. Allosteric modulators, such as CGP 7930 and GS 39738, increase both receptor affinity and the maximal response to the neurotransmitter. Certain arylalkylamines, some L-amino acids and selected dipeptides have been proposed as GABA$_B$-receptor allosteric modulators, although these claims have been disputed. Nonetheless, because allosteric modulators indirectly influence receptor sensitivity by acting at a site distinct from that utilized by the neurotransmitter, such agents may be capable of distinguishing subtypes of GABA$_B$ receptors, making it possible to more selectively modify this system for therapeutic gain.

GABA$_B$-Receptor Antagonists

The absence of selective receptor antagonists initially hindered the pharmacological characterization of the GABA$_B$ site. The first antagonists developed for this purpose were phaclofen, a phosphonic acid analogue of GABA, and saclofen, a sulfonic acid analogue. While both are highly selective as GABA$_B$-receptor antagonists, their affinities for this site are quite low, being greater than 100 μM. Subsequently, a series of selective, high-affinity, and in some cases, systemically active phosphinic acid derivatives were developed as GABA$_B$-receptor antagonists. Included in this group are CGP 54626 and CGP 62349 (Figure 3). Both of these compounds display K_d values at the GABA$_B$-binding site of 1s nM or less, and both have been radiolabeled for use as ligands for studying the localization, molecular properties, and pharmacological selectivity of this receptor. Other notable phosphinic acid GABA$_B$-receptor antagonists are CGP 36742, CGP 35348, CGP 55845, CGP 46381, and CGP 51176.

Morpholine derivatives have also been found to display GABA$_B$-receptor antagonist properties. This is exemplified by SCH 50911, a systemically active agent with a K_i of ~300 nM at the GABA$_B$ receptor (Figure 3).

While no GABA$_B$-receptor antagonists have been approved for clinical use, laboratory animal studies suggest they may be effective in treating absence epilepsy, cognitive impairments, and affective illness. One of the phosphinic acid analogues, CGP 51176, is currently undergoing clinical trails as a possible antidepressant.

Glossary

allosterism A change induced in the properties and function of a receptor by attachment of a ligand to a site other than that utilized by the endogenous substrate.

heterodimer A complex consisting of two different proteins.

ligand A drug, hormone, or neurotransmitter that attaches to a receptor.

recognition site That portion of a receptor to which the neurotransmitter or hormone attaches.

Further Reading

Bowery, N., Bettler, B., Froestl, W., Gallagher, J., Marshall, F., Raiteri, M., Bonner, T., and Enna, S. (2002). Mammalian γ-aminobutyric acid B receptors: Structure and function. *Pharmacol. Rev.* **54**, 247–264.

Bowery, N., and Enna, S. (2000). γ-Aminobutyric acid$_B$ receptors: First of the functional metabotropic heterodimers. *J. Pharmacol. Exptl. Ther.* **292**, 2–7.

Bythin, D., Kuo, S., Shue, H., and McPhail, A. (1996). Substituted morpholine-2S-acetic acid derivatives: SCH 50911 and related compounds. *Bioorg. Med. Chem. Lett.* **6**, 1529–1534.

Enna, S. (2001). A GABA$_B$ mystery: The search for pharmacologically distinct GABA$_B$ receptors. *Mol. Interventions* **1**, 208–218.

Froestl, W., Mickel, S., Hall, R., von Sprecher, G., Strub, D., Baumann, P., Brugger, F., Gentsch, C., Jaekel, J., Olpe, H., Rihs, G., Vassout, A., Waldmeier, P., and Bittiger, H. (1995a). Phosphinic acid analogues of GABA. 1. New potent and selective GABA agonists. *J. Med. Chem.* **38**, 3297–3312.

Froestl, W., Mickel, S., von Sprecher, G., Diel, P., Hall, R., Maier, L., Strub, D., Mellilo, V., Baumann, P., Bernasconi, R., Gentsch, C., Hauser, K., Jaekel, J., Karlsson, G., Klebs, K., Maitre, L., Marescaux, C., Pozza, M., Schmutz, M., Steinman, M., van Reizen, H., Vassout, A., Mondadori, C., Olpe, H., Waldmeier, P., and Bittiger, H. (1995b). Phosphinic acid analogues of GABA. 2. Selective, orally active GABA$_B$ antagonists. *J. Med. Chem.* **38**, 3313–3331.

Hill, D., and Bowery, N. (1981). ^{3}H-Baclofen and ^{3}H-GABA bind to bicuculline-insensitive GABA$_B$ sites in rat brain. *Nature* **290**, 149–152.

Kaupmann, K., Malitschek, B., Schuler, V., Heid, J., Froestl, W., Beck, P., Mosbacher, J., Bischoff, S., Kulik, A., Shigemoto, R., Karschin, A., and Bettler, B. (1998). GABA$_B$-receptor subtypes assemble into functional heteromeric complexes. *Nature* **396**, 683–687.

Kerr, D., and Ong, J. (2003). Potentiation of metabotropic GABA$_B$ receptors by L-amino acids and dipeptides in rat neocortex. *Eur. J. Pharmacol.* **468**, 103–108.

Sands, S., McCarson, K., and Enna, S. (2003). Differential regulation of GABA$_B$ receptor subunit expression and function. *J. Pharmacol. Exptl. Ther.* **305**, 191–196.

Urwyler, S., Pozza, M., Lingenhoehl, K., Mosbacher, J., Lampert, C., Froestl, W., Koller, M., and Kaupmann, K. (2003). N, N′-Dicyclopentyl-2-methylsulfanyl-5-nitor-pyrimidine-4,6-diamine (GS39783) and structurally related compounds: Novel allosteric enhancers of γ-aminobutyric acid$_B$ receptor function. *J. Pharmacol. Exptl. Ther.* **307**, 322–330.

BIOGRAPHY

S. J. Enna is a Professor of Pharmacology and former Chair of the Department of Pharmacology, Toxicology, and Therapeutics at the University of Kansas Medical Center in Kansas City, Kansas. He is past-president of the American Society for Pharmacology and Experimental Therapeutics and has served as editor of the *Journal of Pharmacology and Experimental Therapeutics, Biochemical Pharmacology*, and *Pharmacology and Therapeutics*. His research interests include neuropsychiatric disorders, neurotransmitter receptors, and GABA.

Galectins

R. Colin Hughes
Medical Research Council, London, UK

Galectins, a family of proteins that bind to galactose residues of glycoproteins and glycolipids, represent a special group of a large number of carbohydrate-binding proteins known as lectins. Galectins are found in tissues of organisms ranging from lower inverterbrates to mammals, and participate in many essential biological processes. Different members play roles in growth regulation, cell adhesion, and migration and are in some cases associated with the neoplastic transformation of cells and metastasis. Galectins are also involved in cell signaling and the regulation of immune responses, and recently have become the focus of intensive research in many areas of cell and developmental biology, immunology, and pathology.

Galectin Structure

The galectin family at present consists of 14 identified members (Figure 1). Several galectins are small proteins of 14–16 kDa with a single carbohydrate recognition domain (CRD) of ~130 amino acid residues (galectin-1, 2, 5, 7, 10, 11, 13, and 14). Many of these form noncovalent homodimers, and hence are functionally bivalent molecules. Others are constitutively bivalent molecules of 30–35 kDa containing two CRDs joined by a short link sequence as in galectin-4, 6, 8, 9, and 12. Galectin-3 is unique in that it contains an N-terminal extension that is very much larger than those seen in other galectins. Under normal conditions galectin-3 is monomeric, probably due to the masking by the N-terminal tail of a site on the CRD known to be the subunit interaction site of dimeric galectins. The N-terminal domain of galectin-3 is similar to sequences found in other proteins that promote self-aggregation. Galectin-3 also readily forms multimers at high concentrations or when bound to ligand-coated surfaces, mainly through interactions between the N-terminal extensions. Galectin-5 is also a monomer normally, but has weak agglutinating activity indicative of at least bivalent interactions.

The valency of galectins is functionally important. First, the binding of single CRDs even to a preferred carbohydrate is often relatively weak. Assembly of CRDs can lead to cooperative binding between multiple CRDs and ligand, with greatly increased avidity. Second, multivalent galectins are capable of cross-linking receptor glycoproteins at cell surfaces or in the extracellular matrix, and have the potential to form clusters or lattices of receptors, for example, at cell surfaces. There is a close correlation between the ability of lectins to cluster cell-surface ligands and their effects in initiating cellular signals, e.g., a mitogenic stimulus. Third, multivalency is essential for the proposed roles of some galectins in linking cell surface receptors such as integrins to extracellular matrix components, leading to cell–substratum adhesion. In addition to their relatively low avidity of binding to carbohydrates, monovalent galectins cannot participate in cross-linking of glycoproteins, and indeed may function to competitively inhibit such cross-linking activity, for example, to block signal transduction or to weaken cell adhesions.

Binding Specificity

Carbohydrate Structures

Many galectins bind, albeit with low affinity, to the monosaccharide galactose (hence the name GALectin) or simple galactosides such as the disaccharides lactose and lactosamine (respectively a galactose residue joined in a β1,4 linkage to glucose or N-acetylglucosamine). Crystal structures of complexes between galectin CRDs and lactose show in each case six conserved hydrophilic residues essential for galactose binding. However, high-affinity binding requires additional features and longer carbohydrate chains. These requirements for high-affinity binding to larger oligosaccharides vary considerably between the various galectins. In agreement with these differences, there is significant sequence variation among the various galectin CRDs in their extended binding sites adjacent to the primary binding site for galactose. In the case of the constitutively bivalent galectins containing two CRDs, each CRD may have different preferences for carbohydrate ligands, indicating that these galectins may bind to and cross-link different glycoproteins.

Several galectins bind with high affinity to polylactosamines, oligosaccharide chains made up of repeating units of lactosamine residues. These chains can be

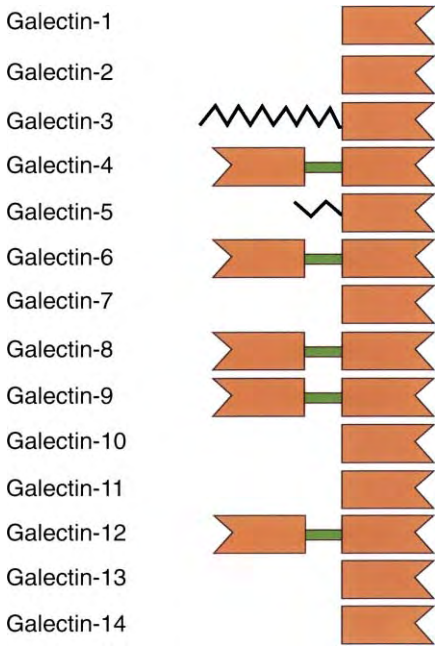

FIGURE 1 Schematic of the overall structures of galectins. The proteins are shown as linear diagrams of single polypeptide chains with N- and C-termini at the left- and right-hand side, respectively. The CRDs are in red, and the short sequences linking the N- and C-terminal CRDs of galectin-4,6,8, and 9 are in green. The extra-long N-terminal domain of galectin-3, and the slightly elongated N-terminal domain of galectin-5, are in yellow.

expressed on the N- or O-glycans of glycoproteins, and their expression is controlled by specific N-acetylglucosaminyl transferases (GlcNAcT). Two GlcNAcTs are particularly important in the initiation of polylactosamine synthesis and hence production of high-affinity galectin ligands. The GlcNAcT V enzyme allows elongation of N-linked polylactosamines. It is crucial for production of specific cell surface galectin-3 receptors on certain thymus-derived lymphocytes (T-cells), and activation of these cells. Another GlcNAcT enzyme starts polylactosamine chain extension on O-glycans. Its expression is crucial for the production of other specific receptors required for binding of galectin-1 to T-cells, and elimination of these cells by apoptosis.

Glycoprotein Receptors

The significant differences in carbohydrate-binding specificities between different CRDs are functionally important since it implies that different galectins may bind preferentially to unique glycoprotein receptors that bear glycans carrying the preferred saccharide sequences. Galectin-1 and -3 both bind to the lysosomal associated membrane proteins (LAMPs), and to some isoforms of the extracellular matrix components fibronectin, laminin, and tenascin. These receptors all contain high amounts of N- and/or O-linked polylactosamine chains. Similarly, both galectins bind the T-cell receptor (TCR) complex and regulate lymphocyte activation, possibly by effects on TCR clustering at the lymphocyte surface. On the other hand, galectin-3 specifically recognizes Mac2-binding protein, a cell-adhesive protein present in the extracellular matrix and a secreted tumor-associated antigen. Similarly, galectin-1 specifically recognizes the lymphocyte surface antigens CD7 and CD45. Activated cells exposed to galectin-1 undergo apoptosis, mediated by binding and clustering of cell-surface CD7/CD45 complexes by the lectin.

Galectin Distribution

Species

In addition to the galectins present in mammalian species, galectins are found in birds, fish, and amphibians, in invertebrates such as worms and insects and even in protists such as sponges. In the human and *Caenorhabditis elegans* genomes, ~17–20 galectin-like genes are identifiable. This is likely to be a minimal estimate, since several galectins can undergo alternative splicing to produce separate transcripts from a single gene. However, not all of these have been isolated as yet and shown directly to be active as galactose-binding lectins: the latter point also includes some of those proteins listed in Figure 1.

Tissues

The known galectins have distinct patterns of expression during development and in the mature organism. Galectin-1 and -3 have a rather broad distribution, the former in tissues of mesodermal origin and the latter being mainly in epithelial cells, tumor cells, as well as macrophages and other inflammatory cells. Other galectins are more restricted, e.g., galectin-2, -4, and -6 in the gastrointestinal tract, galectin-5 in erythrocytes, and galectin-7 in skin and tumors of epidermal origin. A particular tissue may express more than one galectin, e.g., galectin-1, -3, -8, and -9 in the kidney. In the kidney, galectin-3 expression is strongly regulated during development, whereas the expression of other galectins is more constant. Galectin expression is also often regulated physiologically Thus, galectin-1 and -3 expression is strongly increased upon activation of T-cells, and macrophages or Schwann cells, respectively. Upstream elements in several galectin genes are identified that account for transcriptional activation by glucocorticoids, phorbol esters, retinoic acid, and other factors. Galectin gene sequences have also been found that account for the tissue-specific expression of galectins, e.g., binding sites for transcription factors

implicated in up-regulation of galectin-3 and -11 in activated macrophages and differentiating eye lens epithelia, respectively.

Cells

Galectins are characteristic cytoplasmic proteins in that they lack signal sequences for transfer into endoplasmic reticulum (ER)/Golgi compartments, are acetylated at the N-terminus but are not glycosylated even though some contain concensus sites for N-glycosylation within the ER. However, following synthesis there is selective intracellular trafficking of some galectins (galectin-1, -3, -7, -10, -11, and -12) to the nucleus. Nuclear localization, at least for galectin-3, is correlated with cell proliferation, and redistribution of galectins is often observed in actively dividing cancer cells relative to their normal counterparts. In addition, many galectins are secreted from cells by unknown mechanisms distinct from conventional transfer through the ER/Golgi pathway. In polarized cells, which have physically segregated surface domains with distinct functions, galectins may be secreted preferentially from a particular surface domain. This complex distribution of galectins inside and outside cells is consistent with these proteins having different functions intra- and extracellularly (Figure 2).

Multiple Roles

Nuclear Functions

Galectin-1 and -3 are present in the cell nucleus in association with ribonucleoprotein complexes involved in RNA splicing. Removal of the galectins from such complexes by treatment with inhibitory sugars, such as lactose, results in loss of splicing activity. Conversely addition of either galectin to the depleted nuclear extracts restores activity, showing directly that these galectins are splicing factors. The galectins appear to be critically involved in assembly of higher-order complexes of nucleoproteins leading to functional splicing particles.

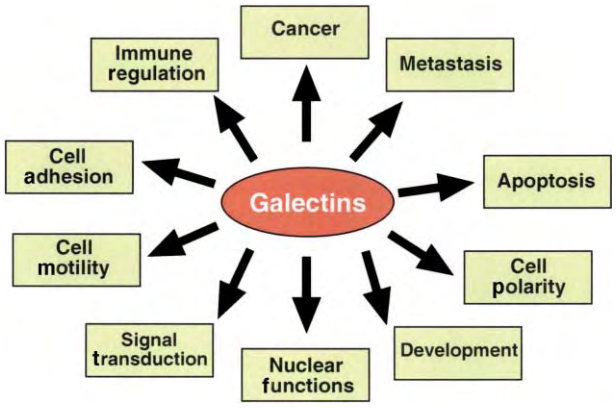

FIGURE 2 Galectins participate in a wide range of biological functions, including regulation of cell proliferation and death, modulation of cell adhesion, and motility in normal and cancer cells, cell signaling, and immuno-regulation. The particular effect of a galectin in any one situation depends on its valency of binding and ability to cross-link receptors, the appropriate glycosylation of specific receptors, cell activation state, developmental and tissue-type expression, and subcellular localization.

Cell Growth and Apoptosis

In complex organisms, homeostasis requires a balance between cell growth and cell death. A galectin may either promote or suppress the form of programmed cell death known as apoptosis. Galectin-1, 7, 9, and 12 promote, while galectin-3 inhibits, this process. Galectin-3 and -12 also regulate the cell cycle. Hence, the growth and survival of some cell types and tissues may be controlled by the relative levels of expression of multiple galectins.

Cell Adhesion and Motility

Galectins bind to many key molecules involved in cell adhesion. These include various subunits of the integrins, as well as extracellular matrix glycoproteins such as laminin and fibronectin, which interact in cell adhesion to substratum. Others bind to members of the cadherin family of cell adhesion molecules, active in cell–cell adhesion. Typically, galectins may act to enhance or antagonize cell adhesion, as mentioned above. These effects on the strength of cell adhesions also influence the ability of cells to dissociate and migrate, for example, during gastrulation, or in wound healing. Enhanced adhesion is likely due to direct binding of a galectin to the glycans of molecules on adjacent cells or within the extracellular matrix. Additionally, galectins may act synergistically to strengthen adhesive interactions, for example, between integrins and their matrix counter-receptors. Pro-adhesive or anti-adhesive effects of galectins, especially galectin-1 and -3, are important in many processes during fetal development. The anti-adhesive effects of galectin-1 influence the motility of myoblasts during muscle differentiation, and the projection of axons during establishment of neural networks, e.g., in the olfactory bulb. Conversely, galectin-3 promotes adhesion of various metastatic tumor cells and inflammatory cells to extracellular matrices, and limits growth and differentiation of epithelial structures during kidney development.

Cancer and Metastasis

Galectin gene expression is, in many cases, up-regulated by growth factors and oncogenes, and down-regulated

by tumor suppressors. Thus, galectin-3 is found in a wide variety of malignances. In most cases, increased expression renders tumor cells more invasive and is associated with a negative prognosis. Probably, the galectins increase the invasive potential of the tumors by modulating the interactions with the endothelium and by assisting the formation of homotypic cell aggregates, important for homing of metastatic tumors to secondary tissue sites.

Immune Response and Regulation

Galectins are important regulators of immune cell homeostasis, as well as immune responses. Some galectins, e.g., galectin-3, act to enhance immune responsiveness and the inflammatory cascade. Others, such as galectin-1, play key roles in shutting off immune cell functions, for example, by triggering their apoptosis as discussed before for T-cells. These diverse effects are propagated by interactions of particular galectins with specific receptor glycoproteins. Specific interactions can lead to regulation of immune cell survival and signaling, their growth and chemotaxis, and the secretion of various cytokines influencing the differentiation of particular immune cell types. Recent evidence also shows the roles of galectins in infection by important human pathogens. Consequently, galectins are attractive therapeutic targets in autoimmune, inflammatory, allergic as well as neoplastic and infective diseases.

See Also the Following Articles

Caspases and Cell Death • Cell Death by Apoptosis and Necrosis • Glycoproteins, N-linked • Lectins • *N*-Linked Glycan Processing Glucosidases and Mannosidases • Glycoprotein-Mediated Cell Interactions, O-Linked • Proteoglycans

Glossary

apoptosis A form of programmed cell death observed in animal tissues during embryogenesis, and in the mature organism in regulation of tissue homeostasis. A family of cytoplasmic proteases, caspases, are key effector molecules of apoptosis.

glycan A chain of sugar residues added covalently to proteins. A given protein may have several attached glycans, the composition and sequence of which may vary with developmental stage and tissue type. Glycans are classified as N-glycans containing an N-acetylglucosamine to asparagine linkage, or as O-glycans containing an N-acetylgalactosamine to serine/threonine linkage.

immune homeostasis The maintenance of steady-state levels of functionally distinct leukocyte populations in the adult immunologically competent organism.

lectins Lectins (from the Latin *legere*, to select) are specific carbohydrate-binding proteins that are ubiquitous, being found in animals, plants, and microorganisms. Lectins can be grouped in distinct families on the basis of homologies in amino-acid sequence and three-dimensional structure, and carbohydrate-binding specificity.

splicing The process by which pre-RNA is modified by intron removal and exon ligation during production of fully mature RNA transcripts.

Further Reading

Cooper, D. N. W., and Barondes, S. H. (1999). God must love galectins: He made so many of them! *Glycobiology* **9**, 979–984.

Hernandez, J. D., and Baum, L. G. (2002). Ah, sweet mystery of death! Galectins and the control of cell fate. *Glycobiology* **12**, 127R–136R.

Hughes, R. C. (2001). Galectins as modulators of cell adhesion. *Biochemie* **83**, 667–676.

Kasai, K.-I., and Hirabayashi, J. (1996). Galectins: A family of animal lectins that decipher glycocodes. *J. Biochem.* **119**, 1–8.

Liu, F.-T., Patterson, R. J., and Wang, J. L. (2002). Intracellular functions of galectins. *Biochim. Biophys. Acta* **1572**, 263–273.

Rabinovich, G. A., Baum, L. G., Tinari, N., Paganelli, R., Natoli, C., Liu, F.-T., and Iacobelli, S. (2002). Galectins and their ligands: Amplifiers, silencers or tuners of the inflammatory response. *Trends Immunol.* **23**, 313–320.

Rini, J. M., and Lobsanov, Y. D. (1999). New animal lectin structures. *Curr. Opin. Struct. Biol.* **9**, 578–584.

Biography

R. Colin Hughes has been a UK Medical Research Council scientist at the National Institute for Medical Research in Mill Hill, London, since 1970. His main research interests have been in the structure and biosynthesis of the complex carbohydrates attached to proteins, and more recently in the functional significance of their recognition by antibodies and lectins. He holds a Ph.D. from the University of London and received postdoctoral training at the University of Washington and the Massachusetts General Hospital.

Genome-Wide Analysis of Gene Expression

Karine G. Le Roch and Elizabeth A. Winzeler
Scripps Research Institute, La Jolla, California, USA

Genome-wide expression experiments, like genetics, can reveal new genes involved in a process, or can allow two or more biological states to be distinguished from one another. Both serial and parallel approaches can be used to collect genome-wide expression data. In both cases RNA (target) from conditions of interest is isolated. For serial methods, the RNA is converted to cDNA and the relative number of cDNA molecules per condition is counted. For parallel methods the RNA is labeled directly either with a biochemical marker (such as biotin), a radioisotope, or with fluorescence; or is converted to cDNA and then labeled. This target is then incubated with a microarray in buffered solution. The labeled RNA molecules then seek out their complementary sequences on the array. The amount of RNA that has hybridized at each location on the array is determined. By comparing the patterns that are obtained for two different conditions, it is possible to monitor how gene expression changes.

Uses for Genome-Wide Expression Datasets

Using Gene Expression Data for Discovery

The primary use for whole genome expression analysis is in the identification of novel genes involved in a particular molecular process. Such genes may encode novel drug targets, may be used as molecular reporters, or may provide a better description of the biological process under study. RNA is collected from the condition of interest and from a control condition. If genes that are known to be involved in a process are included on the microarray, the researcher can find genes with similar expression patterns by cluster analysis. Alternatively, genes can be identified that show a large induction in the condition of interest relative to the reference condition. Because a block in a metabolic pathway may result in a transcriptional upregulation of the genes in the pathway, new members of the pathway may be discovered using this approach.

Using Gene Expression Data for Classification

Genome-wide analysis of gene expression can be used to distinguish two different biological states such as acute myoblastic leukemia and acute lymphoblastic leukemia, which are relatively difficult to distinguish from one another using conventional cytological approaches. Here RNA is isolated from two distinct populations and RNA from each individual is labeled and hybridized to a cDNA or oligonucleotide array containing probes to the genome from which the RNA was derived. Then software is used to identify genetic markers that can be used to classify the two populations. By subsequently analyzing only the expression patterns of genes that distinguish two patient populations, physicians may be able to predict a patient's disease classification and optimize treatment.

Serial Methods for Global Analysis of Gene Expression

Serial analysis of gene expression (SAGE) is a technique for collecting genome-wide expression data in which short sequence tags (7–9 bases in length) are isolated from near the 3′ end of transcripts using biochemical methods (Figure 1). The short tags (usually 10,000–20,000 per condition) are concatenated and then sequenced. Finally each SAGE tag is mapped back to the gene from which it originated by using full-genome sequence data. By counting the number of SAGE tags for a gene for several different conditions, one can obtain an estimate of how the gene's expression is changing. This technique which does not depend on constructing a microarray, can be initiated with full genome sequence information, and is very quantitative, especially for highly expressed genes.

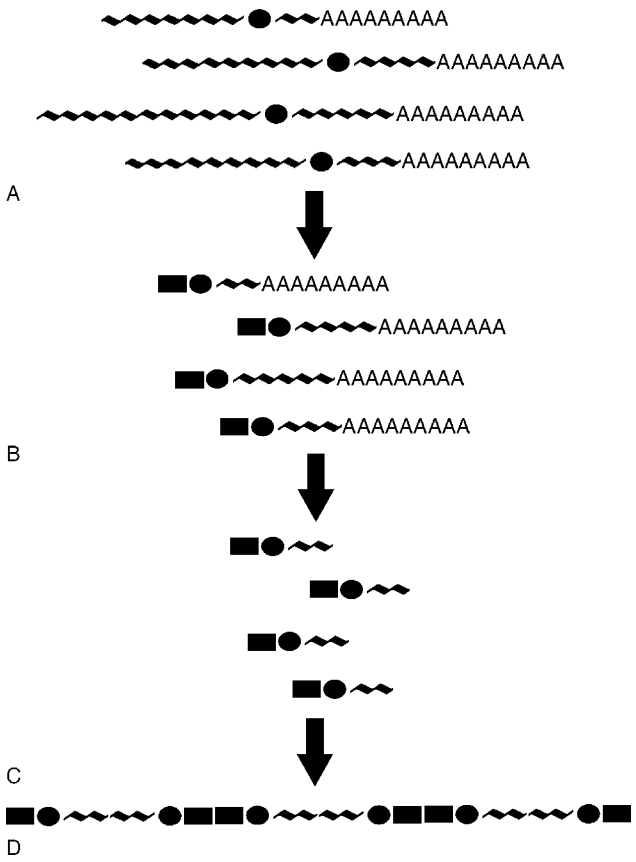

FIGURE 1 Serial analysis of gene expression. RNA from the condition of interest is first converted to double-stranded cDNA using reverse transcriptase and DNA polymerase enzymes (A). The double-stranded cDNA is then cleaved with a restriction enzyme that cuts every few hundred bases in the genome of interest (usually NlaIII, whose site is here represented by solid circles). A short piece of DNA is then ligated at the cut site of the first restriction enzyme (B), generating a recognition site for a type II restriction enzyme (usually BsmFI, whose recognition site is shown as a solid rectangle) which cuts a defined distance from its recognition site, creating a 15 bp SAGE tag. After restriction with the type Ii enzyme (C), the tags are then biochemically linked to one another and finally sequenced (D). The number of SAGE tags mapping to a gene is then tabulated to determine the gene's expression level.

The technique is relatively expensive and is much more time consuming than microarray analysis. Other serial methods include sequencing libraries of expressed sequence tags (ESTs).

Analysis of Gene Expression Using Microarrays

Microarrays Created by Robotic Deposition or Ink-Jetting

Printed microarrays, which are used to measure gene expression in parallel, can be readily constructed in most laboratory settings using a robotic microarraying device that is able to dispense small quantities of solution at precise locations on a solid support. Genes or DNA fragments of interest such as members of complete or partial cDNA libraries (or ESTs) are selected and amplified by the polymerase chain reaction. The probes are then cleaned before being printed using a pin-based robotic arrayer or an inkjet microdispensing liquid-handling system on the selected matrix in a two-dimensional array format (Figure 2B). Alternatively, oligonucleotides can be designed that probe genes of interest. Because of its low inherent fluorescence, glass is the most common substrate when the target is to be fluorescently labeled. The glass slides are typically coated with poly-lysine or aminosilanes, which improve the hydrophobicity and limit the spread of the spotted DNA on the slide.

Microarrays Synthesized *in situ* by Photolithography

An alternative technique for creating microarrays was first implemented by Affymetrix (Santa Clara, CA). In this method light-directed oligonucleotide chemistry is combined with photolithography for solid-phase *in situ* synthesis of DNA probes from the gene of interest (Figures 2A and 3). The advantage of photolitography is that arrays with extremely high information content can be manufactured. Up to 1,000,000 oligonucleotides can be specifically selected from sequencing databases and synthesized in a highly specific manner on a small 1.28×1.28 cm array. Because such arrays are designed *in silico* and there is no need to handle intermediate such as clones, PCR product, or cDNA libraries, the risk of mislabeling is reduced. Furthermore, it is easier to control the amount of product that it is deposited at each location on the array. Because of the combinatorial synthesis and high density, a typical array may contain 16 or more individual oligonucleotide probes per gene. Such redundancy is used in the data analysis to gain confidence.

Microarray Target Preparation and Hybridization

Creating labeled target for hybridization to microarrays can be accomplished in a variety of ways (Figure 2C). Arrays constructed from nylon membranes typically use target that is labeled with radioactive isotopes, while glass arrays use fluorescence. For most methods mRNA is first converted to cDNA using a polydT-primed reverse transcriptase reaction. Because it can be difficult to be sure that the same quantity of probe is placed at the each position in

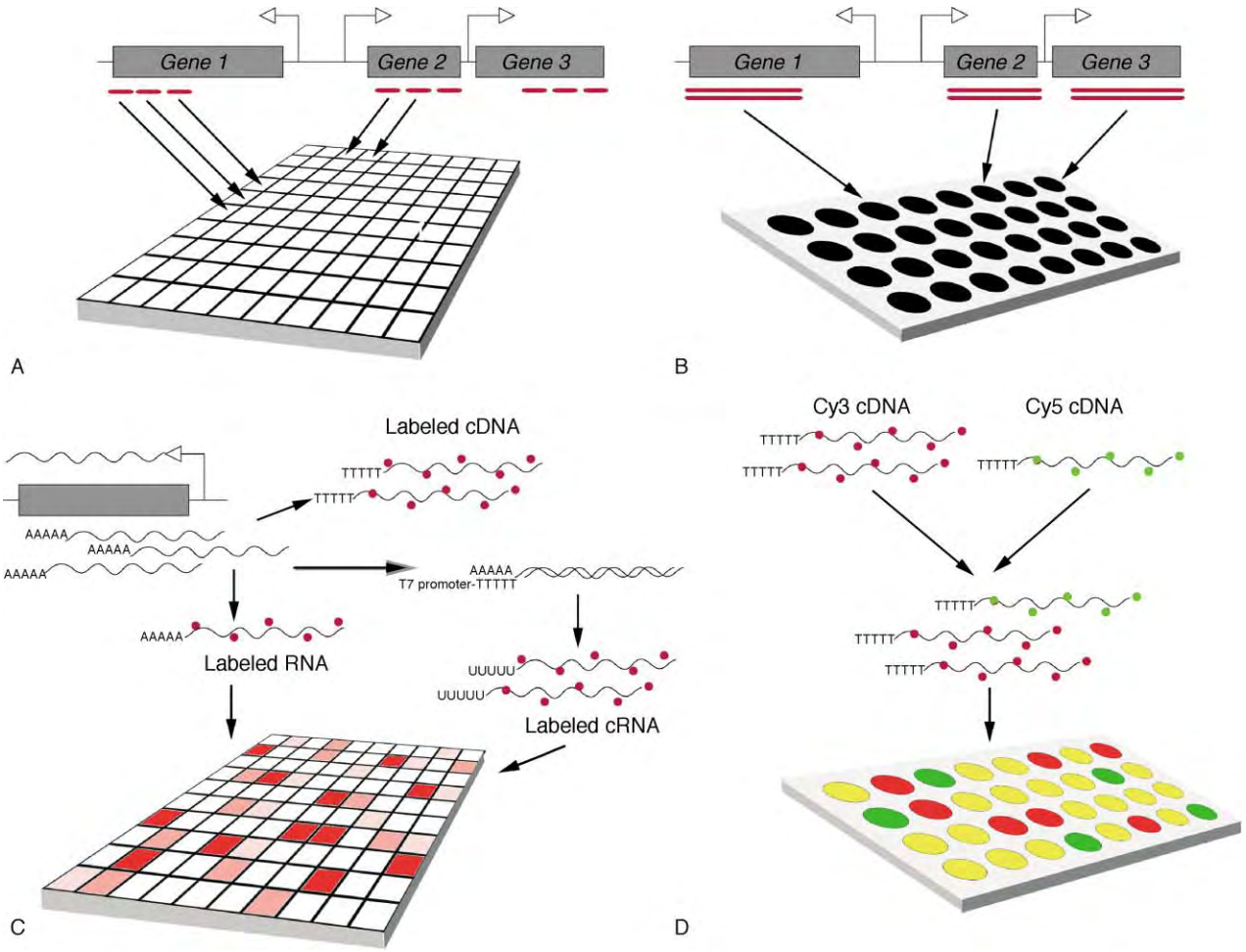

FIGURE 2 Comparison of most commonly used microarray methods. Nucleic acid microarrays are generally produced in one of two ways: by *in situ* synthesis (A) or by robotic deposition of nucleic acids (PCR products, plasmids or oligonucleotides) onto a glass slide (B). Typically for oligonucleotide arrays produced *in situ* (A), multiple probes per gene are placed on the array, while in the case of robotic deposition, a single, longer (up to 1,000 bp) double-stranded DNA probe is used for each gene. Different methods can be used for preparing labeled material for measurements of gene expression (C) including direct labeling of RNA, incorporation of labeled nucleotides into cDNA during or after reverse transcription of polyadenylated RNA; or construction of cDNA that carries a T7 promoter at its 5′ end. In the last case, the double-stranded cDNA serves as template for a reverse transcription reaction in which labeled nucleotides are incorporated into cRNA. Commonly used labels include the fluorophores fluorescein, Cy3 (or Cy5), or nonfluorescent biotin, which is subsequently labeled by staining with a fluorescent streptavidin conjugate. Two-color hybridization strategies are often used with spotted microarrays (D).

a microarray created by robotic deposition, most researchers favor a hybridization scheme in which two different fluorophores are incorporated during the cDNA synthesis reaction for RNA targets from the test and reference conditions (Figure 2D). The two labeled targets are mixed in the appropriate hybridization buffer mix and hybridized. Laser excitation of the incorporated targets yields an emission with characteristic spectra. The fluorescent intensity of each element on the array is measured using a scanning confocal laser microscope.

For targets that are to be hybridized to photolithographic arrays, a phage T7 promoter is attached to the end of double-stranded cDNA and used to drive an *in vitro* transcription (IVT) reaction during which biotin or other labels are incorporated. The IVT reaction results in a linear amplification of the original mRNA population of up to 100-fold. In contrast to the two-color method described above, target from each biological condition is hybridized separately to its own array.

Microarray Data Analysis Methods

Detection of mRNA Levels

Typically only SAGE methods or oligonucleotide arrays that use multiple probes per gene can be used to determine the approximate number of transcripts for genes that are present in a given sample.

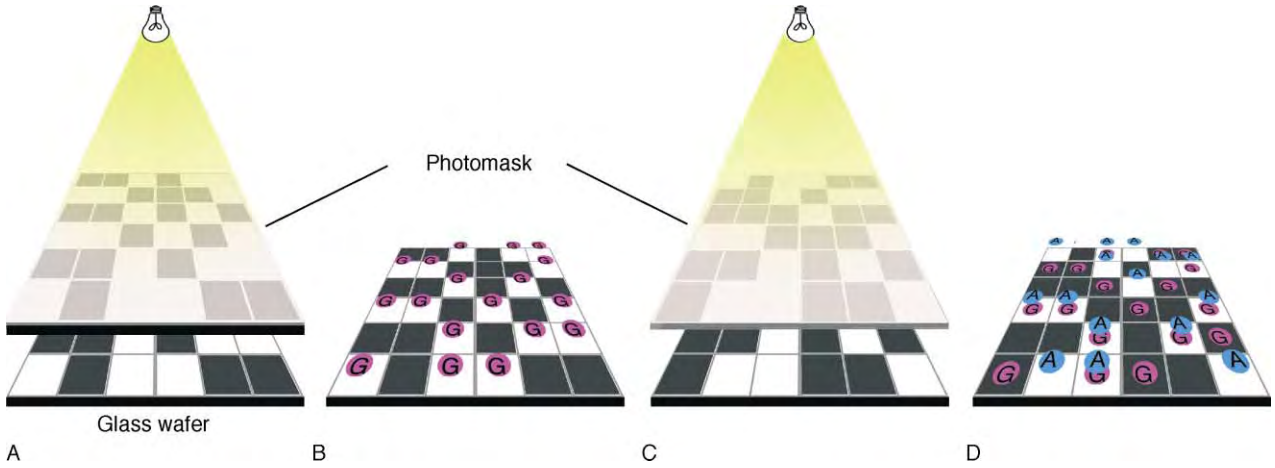

FIGURE 3 Photolithographic synthesis of oligonucleotide arrays. Here quartz wafers are placed in a bath of silane, which reacts with the hydroxyl group of the quartz to form a matrix of covalently linked molecules. Light is directed through a series of photomasks placed over the coated wafer that determine which regions will be activated by light and are thus capable of receiving a nucleotide in each step (A). The wafers are then bathed in the appropriate nucleotide (ACG or T) containing a photoprotective group (B). The photoprotective group is removed at the next step (C) before the next nucleotide is added (D). Using this method any 25 mer can be synthesized in no more than 100 such steps.

For oligonucleotide arrays with multiple probes per gene, an estimate of transcript levels can be obtained by averaging the background-subtracted intensity values from usually 16 or more individual probes to a given gene. Values from multiple probes need to be considered because different oligonucleotide probes have different hybridization properties. Such an approach can be used to distinguish genes that are highly expressed from ones which are poorly expressed.

Computation of Gene Expression Ratios

Microarrays that contain only a single probe per gene can generally just be used to calculate how a gene's expression changes when two conditions are compared. Monochrome images from each condition output by the scanner are read by software that locates each element within the grid and converts the images to pseudo-color and merges them. The ratio of the dye signals for each probe on the array is used to determine the relative proportion of a transcript in the two different conditions (Figure 2D).

Analysis of Genome-Wide Expression Datasets

Cluster Analysis

Gene expression experiments typically generate tens of thousands of data points. It has been shown that genes with similar biological roles will often have similar patterns of expression. Clustering as a method of analysis can be used to organize data and to group genes according to their similarity in gene expression patterns so that genes involved in similar processes can be identified (Figure 4). Pairwise average-linkage cluster analysis is the most widely used. This method creates hierarchical clusters in which relationships between genes are represented by trees whose branch lengths reflect the degree of similarity between genes.

Ontology Analysis

This method can be used to determine the biological pathway that is active in one condition relative to another pathway that is activated when an organism is treated with a chemical compound. Here a group of genes that is up-regulated in one condition relative to another condition is determined. It is assumed that many of the genes in this group will be uncharacterized, but the function of others will be well understood and can be accessed by examining catalogues that group genes by function (e.g., nucleic acid metabolism or maintenance of the cytoskeleton). By comparing the size and membership of the group of up-regulated genes to the size and membership of different functional groups, it is possible to calculate statistics describing whether or not the amount of overlap would be expected by chance. Thus, one might find that the probability that a group of genes that is induced by a drug shows significant overlap with a group of genes that have a role in sulfur metabolism, suggesting that the drug may disrupt sulfur metabolism.

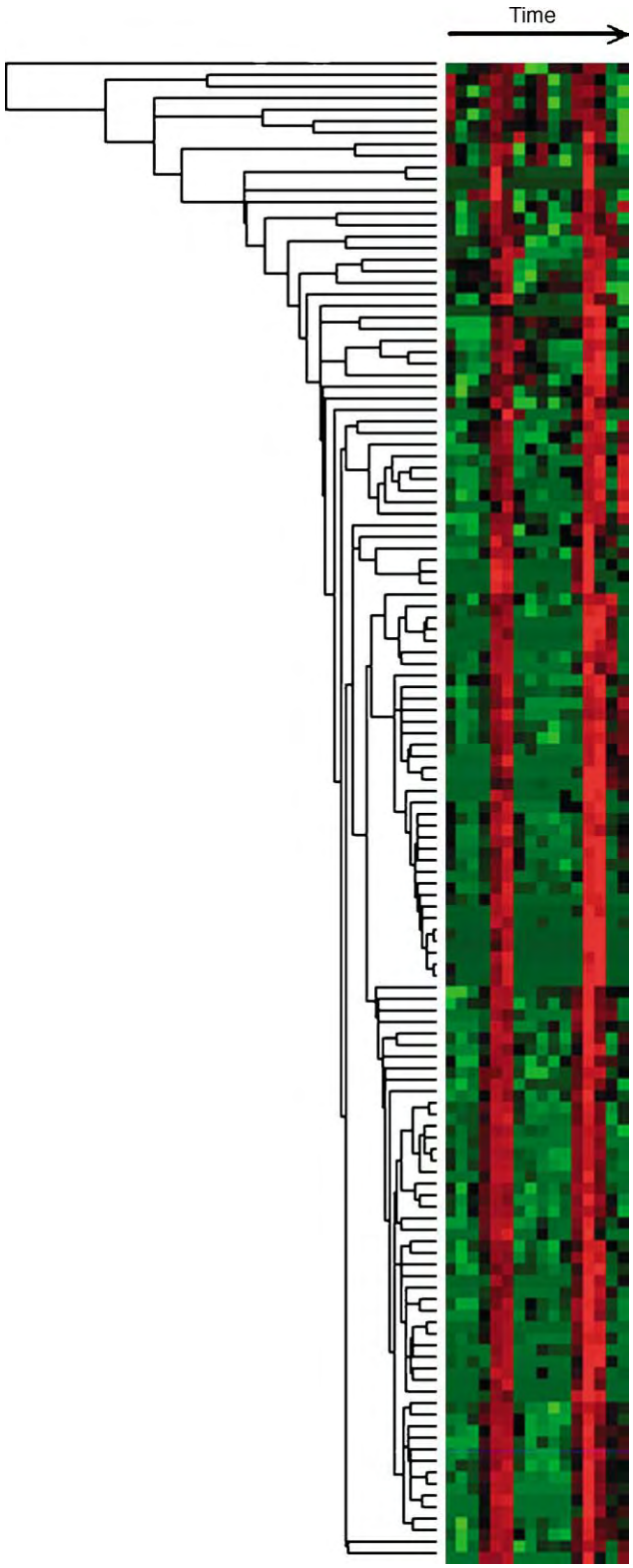

FIGURE 4 Clustergram showing gene expression patterns in the malaria parasite's lifecycle. Each gene is represented by a single row of colored boxes and each time point is represented by a single column. The hue (red or green) indicates the relative expression relative to a reference condition.

See Also the Following Articles

Mitochondrial Genes and their Expression: Yeast • Mitochondrial Genome, Evolution • Mitochondrial Genome, Overview • Nuclear Genes in Mitochondrial Function and Biogenesis • Protein Data Resources

Glossary

cDNA DNA that has been created from RNA using reverse transcription.

cluster analysis The process of grouping genes or other array elements based on their similarity of behavior over many different conditions. Both hierarchical (tree-based) or nonhierarchical methods (k-means, self-organizing maps) can be used to accomplish the same organizational goal.

EST library A library created by cloning the 3′ end of individual cDNA molecules into a vector.

microarray A device typically used for monitoring gene expression for a large number of genes. They consist of an ordered array of different elements (usually nucleic acids complementary to the genes of interest) that are printed or synthesized *in situ* on a solid surface (usually a glass slide).

probe The individual elements on a microarray consisting of long oligonucleotides, short oligonucleotides (25mers), fragments of genomic DNA, or cDNAs.

RNA The molecular messages produced when genes are transcribed.

serial analysis of gene expression (SAGE) A method used in the genome-wide monitoring of gene expression in which short sequence tags from different cDNAs are isolated, sequenced, and counted.

target Uncharacterized RNA that is labeled and hybridized to the microarray.

Further Reading

Chee, M., Yang, R., Hubbell, E., Berno, A., Huang, X. C., Stern, D., Winkler, J., Lockhardt, D. J., Morris, M. S., Fodor, S. P. (1996). Accessing genetic information with high-density DNA arrays. *Science* **274**(5287), 610–614.

DeRisi, J. L., Iyer, V. R., and Brown, P. O. (1997). Exploring the metabolic and genetic control of gene expression on a genomic scale. *Science* **278**(5338), 680–686.

Golub, T. R., Slonim, D. K., Tamayo, P., Huard, C., Gaasenbeek, M., Mesirov, J. P., Coller, H., Loh, M. L., Downing, J. R., Caligiuri, M. A., Bloomfield, C. D., Lander, E. S. (1999). Molecular classification of cancer: Class discovery and class prediction by gene expression monitoring. *Science* **286**(5439), 531–537.

Hughes, J. D., Estep, P. W., Tavazoie, S., Church, G. M. (2000). Computational identification of *cis*- regulatory elements associated with groups of functionally related genes in *Saccharomyces cerevisiae*.. *J. Mol. Biol.* **296**(5), 1205–1214.

Pease, A. C., Solas, D., Sullivan, E. J., Cronin, M. T., Holmes, C. P., Fodor, S. P. (1994). Light-generated oligonucleotide arrays for rapid DNA sequence analysis. *Proc. Natl. Acad. Sci. USA* **91**(11), 5022–5026.

Schena, M., Shalon, D., Davis, R. W., Brown, P. O. (1995). Quantitative monitoring of gene expression patterns with a complementary DNA microarray. *Science* **270**(5235), 467–470.

Velculescu, V. E., Zhang, L., Vogelstein, B., Kinzler, K. W. (1995). Serial analysis of gene expression. *Science* **270**(5235), 484–487.

Biography

Elizabeth Winzeler is a Professor at the Scripps Research Institute and the Head of Cellular Biology Research at the Genomics Institute of the Novartis Research Foundation. She trained in the laboratory of Dr. Ron Davis at Stanford University during the time that many of the important developments in global gene expression monitoring were unfolding and were being developed in this laboratory. She has used many of these methods described here in her search for new drugs for malaria and has developed other full-genome methods using the yeast, *Saccharomyces cerevisiae* as a model system.

Karine Le Roch is a postdoctoral fellow in Dr. Winzeler's laboratory at the Scripps Research Institute.

G_i Family of Heterotrimeric G Proteins

Maurine E. Linder
Washington University School of Medicine, St. Louis, Missouri, USA

Hormones, neurotransmitters, and sensory inputs elicit responses by binding to cell surface receptors. Heterotrimeric G proteins are poised at the inner face of the plasma membrane to respond to the activated receptors and relay signals by changing the activity of intracellular effector molecules. A detailed discussion of the shared properties of heterotrimeric G proteins can be found in the entry on the G_s family. This entry focuses on the G_i family, which regulates a broad array of physiological processes. These include vision, taste, heart rate, neural activity, cell migration, survival, and proliferation.

Overview of the G_i Family

G_i was discovered in the early 1980s as the G protein that mediates hormonal inhibition of cAMP production. Its discovery followed that of G_s, the G protein that stimulates cAMP production and G_t, the G protein that regulates cGMP levels in the retina (see below). Characterization of G_s, G_i, and G_t revealed a structurally homologous family of guanine nucleotide-binding proteins. Over time, many additional G proteins were identified biochemically or through cloning of cDNAs. By the mid-1990s, it was appreciated that 16 distinct genes encode G-protein α-subunits in mammalian genomes. The α-subunits could be grouped into families based on sequence similarity and were assigned to four families: G_s, G_i, G_q, and G_{12}. The G_s, G_q, and G_{12} families are covered in separate articles.

The G_i family is the most functionally diverse of the G-protein families. It can be subdivided into five groups: G_i, G_o, G_t, G_g, and G_z, according to the identity of the α-subunit. The evolutionary relationship among the G_i family α-subunits is shown in Figure 1. G_α subunits associate with $G_{\beta\gamma}$ dimers composed of combinations of the 5 G_β and 12 G_γ subunits. Although not all combinations are possible, a large number of heterotrimers can be generated within this family. Like all heterotrimeric G proteins, G_i family members undergo a cycle of nucleotide exchange and hydrolysis when activated by receptors (Figure 2). Binding of GTP to G_α induces dissociation from $G_{\beta\gamma}$ and both G_α–GTP and $G_{\beta\gamma}$ can interact with effector molecules and regulate their activity. Although in principle all G-protein families can signal through $G_{\beta\gamma}$ subunits, this mode of signaling is most prevalent with signaling pathways regulated by G_i, G_o, and G_z.

G-protein pathways are deactivated when G_α hydrolyzes GTP to GDP. In the GDP-bound form, G_α binds efficiently to $G_{\beta\gamma}$ and restores the heterotrimer to its inactive state. The length of time that G_α is in its GTP-bound state determines the duration of the signal. Regulators of G-protein signaling (RGS) bind to G_α and accelerate the rate of GTP hydrolysis by acting as GTPase activating proteins (GAPs). Thus, RGS proteins are important regulators of the timing of G-protein responses. Members of the G_i family are targets for RGS proteins.

Signaling through $G_{\beta\gamma}$

Many receptors coupled to G_i and G_o exert their effects through signals propagated to downstream effectors by $G_{\beta\gamma}$ subunits. Similar to G_α subunits, $G_{\beta\gamma}$ subunits regulate the activity of enzymes involved in the generation of second messengers. These are adenylyl cyclase, phospholipase Cβ, and phosphatidylinositol 3-kinase. $G_{\beta\gamma}$ exhibits type-specific regulation of adenylyl cyclase, inhibiting some isotypes, but activating others synergistically with $G_{s\alpha}$. $G_{\beta\gamma}$ activates certain isoforms of phospholipase Cβ, an enzyme that converts phosphatidylinositol into diacylglycerol and inositol trisphosphate. The second messenger inositol trisphosphate induces the release of calcium from intracellular stores, whereas diacylglycerol recruits protein kinase C to the plasma membrane. Phosphatidylinositol 3-kinase (PI3K) is also activated by $G_{\beta\gamma}$ subunits. The generation of phosphatidylinositol 3,4,5-trisphosphate (PIP_3), the product of PI3K, mediates important cellular responses. Production of PIP_3 in white blood cells is an essential step in inducing the cells to migrate to sites of cell injury. PI3K activation by $G_{\beta\gamma}$ is also associated with signaling pathways that regulate cell survival.

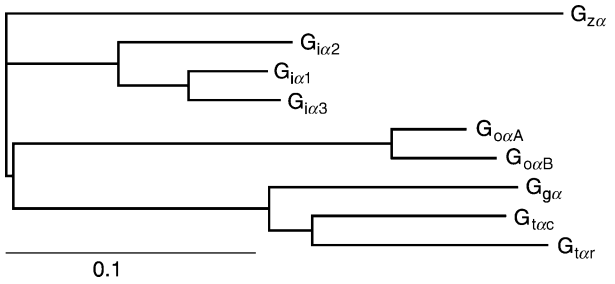

FIGURE 1 Sequence comparison of $G_{i\alpha}$ family members. A nearest-neighbor dendrogram of $G_{i\alpha}$ family sequences. The scale bar represents a measure of evolutionary distances between the sequences analyzed.

In addition to regulating second messengers, $G_{\beta\gamma}$ subunits modulate the activity of numerous ion channels. The best characterized are potassium channels in the heart which slow heart rate when activated. $G_{\beta\gamma}$ subunits bind directly to the channel and cause it to open (Figure 2).

The effectors described above are regulated through direct binding of the $G_{\beta\gamma}$ subunits. $G_{\beta\gamma}$ is also an important regulator of MAP kinase pathways. The direct target of $G_{\beta\gamma}$ in these pathways has not been identified.

G_i

G_i, the founding member of the family, is named for its ability to inhibit the enzyme adenylyl cyclase. There are three forms of $G_{i\alpha}$, designated $G_{i\alpha1}$, $G_{i\alpha2}$, and $G_{i\alpha3}$, each encoded by a separate gene. The three isoforms share many functions and will be considered together here. Heterotrimeric G_i couples to many different receptors, including those for catecholamines, neurotransmitters, and chemokines. Many of the effects associated with activation of G_i by receptors are mediated by $G_{\beta\gamma}$ subunits as discussed above. The best characterized effector for $G_{i\alpha}$ is adenylyl cyclase. $G_{i\alpha}$ binds to this

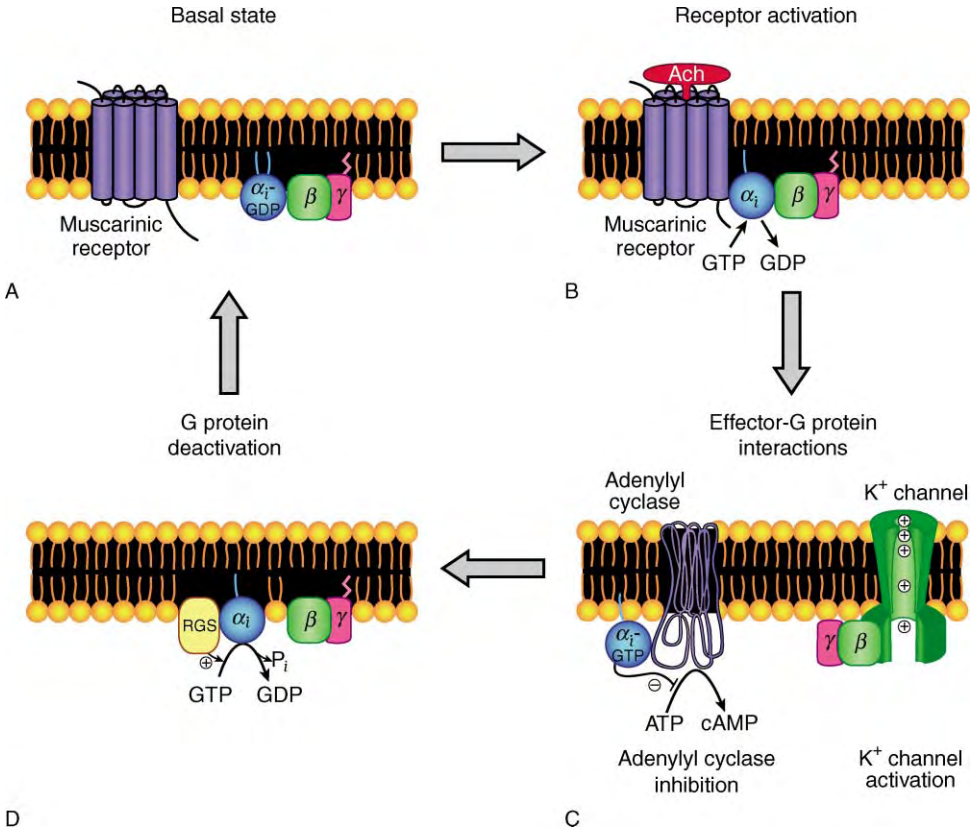

FIGURE 2 G_i signaling in the heart. In heart cells, the neurotransmitter acetylcholine elicits a slowing of heart rate by activating a G_i-coupled signaling pathway. (A) In the basal state, $G_{i\alpha}$ is in the GDP-bound state and associated with $G_{\beta\gamma}$. The receptor is unoccupied and effectors (not shown) are inactive. (B) The neurotransmitter acetylcholine is released at the terminal of the vagus nerve that innervates the heart. Binding of acetylcholine activates the receptor, which in turn stimulates the release of GDP from $G_{i\alpha}$. GTP is present intracellularly at high concentration and quickly diffuses into the guanine nucleotide-binding pocket on $G_{i\alpha}$. GTP binding induces a conformational change in $G_{i\alpha}$, causing it to dissociate from $G_{\beta\gamma}$. (C) $G_{i\alpha}$–GTP interacts with adenylyl cyclase in the plasma membrane and inhibits its activity. $G_{\beta\gamma}$ subunits bind to the K^+ channel, causing it to open. The cell membrane becomes hyperpolarized, slowing action potential frequency and heart rate. (D) $G_{i\alpha}$ hydrolyzes its GTP to GDP to deactivate the pathway. The rate of GTP hydrolysis is accelerated by $G_{i\alpha}$ interaction with an RGS protein. Once in its GDP-bound state, $G_{i\alpha}$ reassociates with $G_{\beta\gamma}$ and the system is returned to the basal state.

enzyme and inhibits its activity, thereby reducing intracellular levels of the second messenger cAMP (Figure 2). $G_{i\alpha}$ (and $G_{o\alpha}$) can propagate signals to protein kinases (e.g., the MAP kinase pathway or c-Src), but the direct target of $G_{i\alpha}$ in these pathways is unknown.

$G_{i\alpha}$'s are ubiquitously expressed and most cell types contain more than one form. Eliminating the gene for $G_{i\alpha1}$ or $G_{i\alpha3}$ in mice does not have any obvious effects on the organism's ability to develop or to reproduce. Mice lacking a functional gene for $G_{i\alpha2}$ appear to develop normally, but exhibit growth retardation, inflammatory bowel disease, and are prone to developing adenocarcinomas, demonstrating that $G_{i\alpha2}$ is essential for normal function of the intestine. The relatively mild phenotypes associated with inactivation of the individual $G_{i\alpha}$ genes probably reflect an ability of one $G_{i\alpha}$ subtype to compensate for the function of another.

G_o

$G_{o\alpha}$ is a close relative of the $G_{i\alpha}$'s, with 70% sequence identity to $G_{i\alpha1}$ (Table I). Two forms of $G_{o\alpha}$ ($G_{o\alpha A}$ and $G_{o\alpha B}$) are generated by alternative splicing of mRNA. G_o is very abundant in the nervous system where it represents 0.5% of total membrane protein. It is also expressed in neuroendocrine tissues and at low levels in the heart. In general, receptors coupled to G_o bind neurotransmitters that mediate inhibitory, rather than excitatory, responses in the central nervous system. The best-studied effectors regulated by G_o are voltage-gated calcium channels, which are inhibited by $G_{\beta\gamma}$ subunits released upon receptor activation of G_o. Direct effectors of $G_{o\alpha}$ are not as well characterized. Inactivation of the $G_{o\alpha}$ gene in mice results in central nervous system dysfunction and abnormal regulation of calcium channels in the nervous system and heart.

G_z

$G_{z\alpha}$ is the most distantly related member of the $G_{i\alpha}$ family based on sequence comparison (Figure 1). Its expression pattern is more restricted than $G_{i\alpha}$, with abundant expression in brain, neuroendocrine tissues, and platelets. G_z has several properties that distinguish it from the other members of the G_i family. It is the only family member that is not a substrate for ADP-ribosylation by pertussis toxin (see below). $G_{z\alpha}$ also has an intrinsic rate of GTP hydrolysis that is much slower than G_i or G_o. Thus, G_z pathways may be slow to turn off unless regulated by RGS proteins. $G_{z\alpha}$ interacts with several RGS family members that show marked specificity for $G_{z\alpha}$ over other G-protein α-subunits. The complement of receptors that G_z responds to overlaps extensively with those that couple to $G_{i\alpha}$ and $G_{o\alpha}$. Given its abundant expression in brain, G_z is coupled to many neurotransmitters and can regulate ion channels, adenylyl cyclase, and MAP kinase pathways similar to G_i and G_o. $G_{z\alpha}$–GTP binds directly to Rap1GAP, a GTPase-activating protein for the monomeric GTPase Rap1, an interaction that may modulate neuronal differentiation.

The gene for $G_{z\alpha}$ has been knocked out in mice. The $G_{z\alpha}$-deficient mice develop normally and are fertile. However, they exhibit altered responses to psychoactive drugs and a mild impairment in platelet function. These phenotypes are consistent with the restricted distribution of $G_{z\alpha}$ in neural tissues and platelets.

G_t (Transducin)

G_t is the G protein that mediates the visual signal transduction cascade. It is also known as transducin.

TABLE I

$G_{i\alpha}$ Family Members

Protein	Gene name	% Amino acid identity[a]	PTX substrate[b]	Fatty acylation[c]	Major tissue distribution
$G_{i\alpha1}$	GNAI-1	100	Yes	Myr, Palm	Nearly ubiquitous
$Gi_{\alpha2}$	GNAI-2	87	Yes	Myr, Palm	Ubiquitous
$G_{i\alpha3}$	GNAI-3	93	Yes	Myr, Palm	Nearly ubiquitous
$G_{o\alpha A}$	GNAO	70	Yes	Myr, Palm	Brain neuroendocrine, heart
$G_{o\alpha B}$	GNAO	69	Yes	Myr, Palm	Brain, neuroendocrine, heart
$G_{t\alpha r}$	GNAT-1	67	Yes	Myr	Retinal rods
$G_{t\alpha}$	GNAT-2	69	Yes	Myr	Retinal cones
$G_{g\alpha}$	GNAG	68	Yes	Myr	Taste buds
$G_{z\alpha}$	GNAZ	66	No	Myr, Palm	Brain, adrenal, platelets

[a] Amino acid sequence (human) comparison with $G_{i\alpha1}$.
[b] PTX, pertussis toxin, see text.
[c] Myr, amide-linked myristate; Palm, thioester-linked palmitate; see text.

There are two closely related forms of $G_{t\alpha}$ that are encoded by separate genes. $G_{t\alpha r}$ is expressed in retinal rods, whereas $G_{t\alpha c}$ is found in cone cells. $G_{t\alpha r}$ and $G_{t\alpha c}$ both associate with specific $G_{\beta\gamma}$ complexes: $G_{t\alpha r}$ with $G_{\beta 1\gamma 1}$ and $G_{t\alpha c}$ with $G_{\beta 1\gamma 14}$. The receptor in the visual signal transduction cascade is rhodopsin, which harbors a covalently attached 11-*cis*-retinal. When a photon of light is absorbed by the retinal, it undergoes a *cis–trans* isomerization that induces a conformational change in rhodopsin. The activated receptor then promotes nucleotide exchange and subunit dissociation of G_t. $G_{t\alpha}$–GTP propagates the signal by stimulating cGMP phosphodiesterase (PDE), an enzyme that hydrolyzes cGMP. PDE consists of two catalytic subunits and two inhibitory subunits (called PDE_γ). $G_{t\alpha}$ binds PDE_γ and relieves the inhibitory constraint on the catalytic subunits. Reduction of cellular levels of cGMP causes closure of cGMP-gated ion channels in the plasma membrane. This reduces the influx of Na^+ and Ca^{2+}, increasing the negative charge inside the cell, and causing the cell to become hyperpolarized. The net effect is a change in the signals that photoreceptors send to the brain. Mice lacking a functional $G_{t\alpha r}$ gene demonstrate defective light responses and develop a mild retinal degeneration with age.

An important mechanism for deactivating the phototransduction process is the hydrolysis of GTP by $G_{t\alpha}$. The intrinsic rate of GTP hydrolysis measured for $G_{t\alpha}$ *in vitro* is too slow to mediate the physiological response. *In vivo*, the GTPase rate of $G_{t\alpha}$ is accelerated by the GAP activity of a protein complex of the retinal RGS protein RGS9 and its binding partner $G_{\beta 5L}$. RGS9 has a G_γ-like domain that mediates its association with $G_{\beta 5L}$. The effector molecule PDE_γ also promotes GAP activity by increasing the affinity of $G_{t\alpha}$ for the RGS9–$G_{\beta 5L}$ complex. Thus, timely inactivation of G_t is achieved through cooperation between RGS9–$G_{\beta 5L}$ and PDE_γ.

G_g (Gustducin)

G_g is a signal transducer for bitter and sweet taste signaling pathways. Its expression is restricted primarily to taste buds. $G_{g\alpha}$ is closely related to $G_{t\alpha r}$ and $G_{t\alpha c}$ (Figure 1). G_g couples receptors for bitter and sweet tastants to specific taste cell phosphodiesterases. Transducins and gustducin therefore share a common family of effectors. In mice deficient for $G_{g\alpha}$, the animals show impaired responses to bitter and sweet agents, but are normal in their responses to sour and salty tastants. Thus, animals use a different signal transduction pathway to experience sour and salty taste.

Post-translational Modifications

Members of the G_i family are subject to a number of post-translational modifications (Table I). All family members except $G_{z\alpha}$ are modified with ADP–ribose at a cysteine residue near the C terminus by a bacterial toxin from *Bordatella pertussis*. The C terminus of G_α is an important site of interaction with G-protein-coupled receptors. Modification of G_α with the bulky ADP–ribose group interferes with receptor–G-protein coupling. Therefore, cells treated with pertussis toxin cannot respond to ligands that bind to G_i-coupled receptors. Pertussis toxin has been a useful experimental tool to define cellular responses that are mediated by members of the G_i family.

All G-protein α-subunits are modified with fatty acids at or near the amino terminus. Fatty acylation provides a hydrophobic anchor that mediates binding to the plasma membrane. Members of the G_i family (but not G_s, G_{12}, or G_q families) are N-myristoylated. Myristic acid is added through an amide linkage to a glycine residue exposed after removal of the initiator methionine. This is the only modification found on $G_{t\alpha}$ and $G_{g\alpha}$. However, $G_{i\alpha}$, $G_{o\alpha}$, and $G_{z\alpha}$ undergo a second type of fatty acylation, S-palmitoylation, which occurs at a cysteine residue adjacent to the N-myristoylated glycine. Whereas N-myristoylation is a stable modification, S-palmitoylation is reversible and can be regulated.

Heterotrimeric G proteins are generally not regulated by protein phosphorylation and dephosphorylation, in contrast to many signaling proteins. $G_{z\alpha}$ is an exception. It is phosphorylated by protein kinase C and p21-activated kinase 1. Phosphorylation of $G_{z\alpha}$ reduces its ability to bind $G_{\beta\gamma}$, and interact with RGS proteins, thereby prolonging $G_{z\alpha}$ activation.

See Also the Following Articles

Adenylyl Cyclases • Cyclic GMP Phosphodiesterases • G_{12}/G_{13} Family • G Protein Signaling Regulators • G_q Family • G_s Family of Heterotrimeric G Proteins

Glossary

chemokine Small, secreted protein that guides the migration of white blood cells.

effector A protein whose activity is changed in response to a stimulus.

hormone A circulating peptide or chemical that acts on target organs at a distance from its site of synthesis.

neurotransmitter A chemical messenger released by a nerve cell at a synapse.

second messenger A small molecule synthesized intracellularly in response to an extracellular stimulus that propagates the signal by binding to an effector and modulating its activity.

Further Reading

Arshavsky, V. Y., Lamb, T. D., and Pugh, E. N. (2002). G proteins and phototransduction. *Annu. Rev. Physiol.* **64**, 153–187.

Clapham, D. E., and Neer, E. J. (1997). G protein $\beta\gamma$ subunits. *Annu. Rev. Pharmacol. Toxicol.* **37**, 167–203.

Gilman, A. G. (1995). Nobel lecture. G proteins and regulation of adenylyl cyclase. *Biosci. Rep.* **15**, 65–97.

Ho, M. K.-C., and Wong, Y. H. (2001). G_z signaling: emerging divergence from G_i signaling. *Oncogene* **20**, 1615–1625.

Margolskee, R. F. (2002). Molecular mechanisms of bitter and sweet taste transduction. *J. Biol. Chem.* **277**, 1–4.

Neves, S. R., Ram, P. T., and Iyengar, R. (2002). G protein pathways. *Science* **296**, 1636–1639.

Offermans, S. (2001). *In vivo* functions of heterotrimeric G proteins: studies in G_α-deficient mice. *Oncogene* **20**, 1635–1642.

Biography

Maurine Linder is an Associate Professor of Cell Biology and Physiology at Washington University School of Medicine in St. Louis. Her principal research interests are in the organization and regulation of signal transduction pathways in cell membranes. She holds a Ph.D. in molecular and cell biology from the University of Texas at Dallas and received her postdoctoral training in the Department of Pharmacology at UT Southwestern Medical Center in Dallas.

Giant Mitochondria (Megamitochondria)

Bernard Tandler and Charles L. Hoppel
Veterans Affairs Medical Center, Cleveland, Ohio, USA

Mitochondria are extremely sensitive indicators of the health of their host cells. Even slight perturbations in cellular metabolism can evoke morphological alterations in these organelles. One way in which mitochondria respond to metabolic disturbances is by increasing in size, often to a point where they outstrip the cell nucleus in diameter. Such outsize organelles are also referred to as megamitochondria, a term that appears to have found increasing favor. Hepatic megamitochondria can measure ~14 μm, giving them a volume >1,400 mm^3, compared to the volume of ~0.5 mm^3 exhibited by typical liver mitochondria. Enlarged mitochondria can be induced by various nutritional and pharmacological manipulations. They occur naturally in certain human disease states and in a few cell types in exotic organisms; e.g., the larger of the paired mitochondria in the spermatozoan tail of the hemipteran *Gerris* has a volume of ~10,000 mm^3.

Megamitochondrial Structure

Under some conditions, the megamitochondria are virtual simulacra of their normal size counterparts; i.e., on a unit mitochondrial area basis they display the same number and arrangement of cristae as do normal mitochondria (Figure 1), although in some cases they may contain within their matrix a small stack of closely packed, short cristae. In other conditions, the megamitochondria have very short cristae that protrude inward from the boundary membrane in a manner not unlike a picket fence. In still others, the cristae are very rare, with the megamitochondria consisting of a morphologically conventional outer membrane and a smooth inner boundary membrane that is almost devoid of cristae. In all types of megamitochondria, the inner compartment contains moderately dense, homogeneous material. In some cases of human thyroid tumors, the matrix compartment contains a jumble of dense ribbons of undefinable length. In certain types of giant mitochondria, an expanded crista contains a bundle of helical filaments. Filaments of this type occurring in normal hepatic mitochondria consist of three distinct, but otherwise uncharacterized, proteins.

Formation of Megamitochondria

The manner in which megamitochondria arise is somewhat controversial. In riboflavin deficiency (the first experimental protocol to evoke the production of giant hepatic mitochondria), this size increase results from two distinct processes, growth and organelle fusion. The earliest step in fusion is signaled by the touching of adjacent mitochondria (under normal conditions, hepatic mitochondria repel one another because of their identical surface charge). One of the paired organelles forms a protrusion that fits into an appropriately shaped invagination in its partner. A myelin figure, which may be indicative of membrane flux, forms at the point of deepest penetration. Eventually, the surface membranes become melded, with the result of a single mitochondrion of enhanced size. That mitochondria are capable of fusing even under physiological conditions is shown by the formation of mitochondrial nebenkerns in insect spermatids, where numerous small mitochondria combine to form two extremely large mitochondria that ultimately twine about the elongating axoneme. Repetition of the fusion process in hepatocytes eventually results in significantly enlarged mitochondria. But the fractional volume of the hepatocytes occupied by the megamitochondria is considerably larger than that of mitochondria in control hepatocytes. In addition to fusion, there clearly has been growth of the mitochondria. It would appear that these two processes constitute an invariant mechanism for formation of giant mitochondria. Therefore, mitochondria that evince a minor increase in size probably as a result of growth or swelling alone should not be categorized as megamitochondria; it is recommended that only those organelles that achieve a diameter greater than 4 μm be designated as giant mitochondria or as megamitochondria.

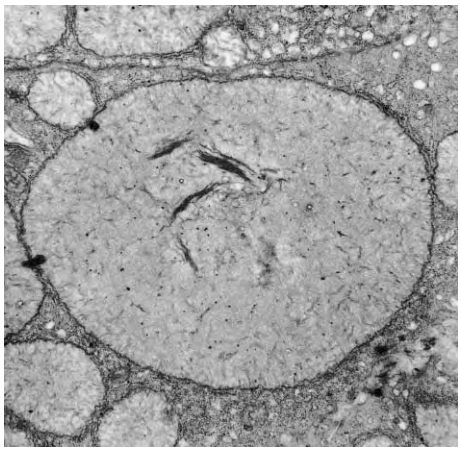

FIGURE 1 Transmission electron micrograph of a hepatic megamitochondrion induced in a mouse by riboflavin deficiency. Note the typical distribution of cristae and the presence of dense matrix granules. The diameter of this organelle is approximately six times as large as that of normal hepatic mitochondria. At the left, the large mitochondrion is linked to two smaller organelles by means of small myelin figures, indicating that it is still in the process of enlargement. Original magnification, ×9,000.

Biochemistry

Little is known of the functional capabilities of megamitochondria. A number of laboratories have reported on biochemical studies carried out on alleged megamitochondria, but inspection of the accompanying electron micrographs of the tested mitochondrial fractions invariably reveals that these organelles are of normal size. When all fractions obtained from livers known to contain megamitochondria are examined, the giant mitochondria are found to have co-sedimented with the nuclei, which they match in size and density, rather than in the mitochondrial fraction. So virtually all published accounts of megamitochondrial function are actually based on normal-sized mitochondria. In such normal-sized mitochondria, oxidative metabolism is significantly decreased even before giant mitochondria appear. In those tissues in which only sporadic megamitochondria are elicited, the normal size mitochondria showed no change. Only when giant mitochondria can be obtained in pure yield will questions concerning mitochondrial DNA content, enzyme content, membrane composition, and oxidative capacity be addressed.

Involvement in Apoptosis

The logistics involved in the experimental evocation of megamitochondria in intact animals are formidable. Recently, it has been proven possible to produce enlarged mitochondria (although such organelles have been referred to as megamitochondria, they rarely exceed 2 μm in diameter) in tissue culture cells by administration of hydrazine to these cells; this compound is normally toxic, but if the cells are protected by prior administration of inducers of cytochrome P450, they survive the hydrazine and produce large mitochondria that can be monitored by confocal laser microscopy. Based on such preparations, it has been suggested that megamitochondria represent a way station on the road to apoptosis induced by free radicals. Although this concept may be true in specific cases, there is no evidence that there is in every case a direct association between megamitochondria formation and apoptosis. There are ample examples of apoptotic cells that clearly are devoid of megamitochondria; conversely, many of the tissues that contain megamitochondria show no evidence of apoptotic decline.

Restoration to Normal Size

It is well established that normal mitochondria replicate by division, but the morphological pathway by which this process is accomplished was unclear. The megamitochondrial model has been used successfully to settle this point. Based on restoration to normal size of experimentally induced megamitochondria, there

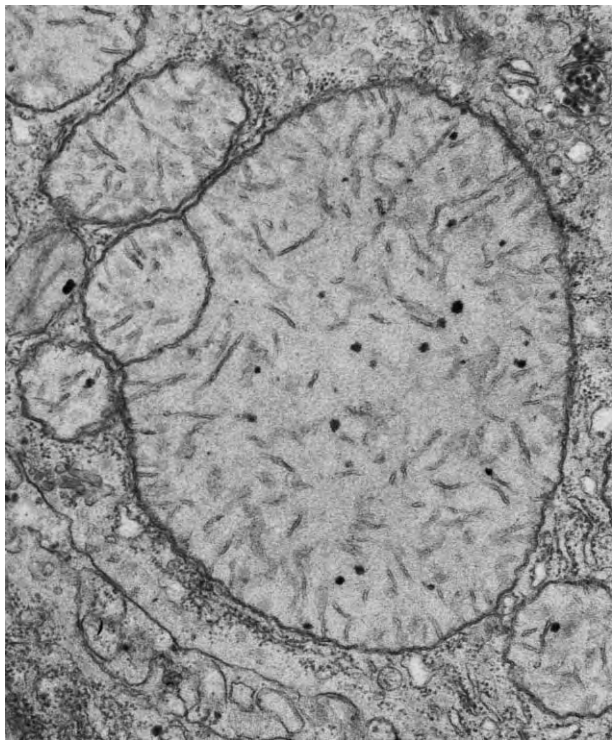

FIGURE 2 Transmission electron micrograph of a dividing hepatic megamitochondrion during recovery from ariboflavinosis. A small bud is subtended by a membranous partition; ingrowth of the outer membrane ultimately leads to the separation of the bud, which is equal in size to a typical mitochondrion, from the enlarged organelle. Repetition of this process results in mitochondrial normalization in terms of size. Original magnification, ×34,000.

appear to be two distinct pathways in mitochondrial division; during recovery, only one of the two mechanisms is called upon, depending on the agent that evoked the megamitochondria in the first place. The first mechanism involves the formation of a membranous partition, probably of boundary membrane origin, that spans the organelle, frequently at the base of a bud (Figure 2). This is followed by ingrowth of the outer membrane into the partition. Like a closing iris diaphragm, the outer membrane eventually completes its incursion, and two daughter mitochondria result. Repetition of this process ultimately leads to the disappearance of megamitochondria and to the appearance of organelles of normal size. The second pathway involves a simple elongation and attenuation of the equator of the megamitochondrion until membranes from opposite sides of the organelle touch and fuse. In effect, the giant mitochondrion has been pulled apart. The progeny of such division repeatedly undergo the same process to finally restore the mitochondria to their accustomed dimensions. What controls the selection of a particular pathway for mitochondrial division is completely unknown.

See Also the Following Articles

Cell Death by Apoptosis and Necrosis • Flavins • Hepatocyte Growth Factor/Scatter Factor Receptor • Vitamin B_{12} and B_{12}-Proteins

Glossary

ariboflavinosis A deficiency of riboflavin in the diet.

crista (pl. cristae) Any of numerous infoldings of the inner mitochondrial membrane in eukaryotic cells.

nebenkern A globular structure in a spermatid that results from interlocking and fusion of the mitochondria during spermatogenesis.

Further Reading

Hoppel, C. L., and Tandler, B. (1993). Megamitochondria. *Meth. Toxicol.* **2**, 191–206.

Karbowski, M., Kurono, C., Wozniak, M., Ostrowski, M., Teranishi, M., Nishizawa, Y., Usukura, J., Soji, T., and Wakabayashi, T. (1999). Free radical-induced megamitochondria formation and apoptosis. *Free Radical Biol. Med.* **26**, 396–409.

Tandler, B., and Hoppel, C. L. (1973). Division of giant mitochondria during recovery from cuprizone intoxication. *J. Cell Biol.* **56**, 266–272.

Tandler, B., and Hoppel, C. L. (1986). Studies on giant mitochondria. *Ann. N.Y. Acad. Sci.* **488**, 65–81.

Tandler, B., Erlandson, R. A., and Wynder, E. L. (1968). Riboflavin and mouse hepatic cell structure and function. I. Ultrastructural alterations in simple deficiency. *Am. J. Pathol.* **52**, 69–95.

Tandler, B., Erlandson, R. A., Smith, A. L., and Wynder, E. L. (1969). Riboflavin and mouse hepatic cell structure and function. II. Division of mitochondria during recovery from simple deficiency. *J. Cell Biol.* **41**, 477–493.

Tandler, B., Dunlap, M., Hoppel, C. L., and Hassan, M. (2002). Giant mitochondria in a cardiomyopathic heart. *Ultrastruct. Pathol.* **26**, 1–7.

Biography

Bernard Tandler was a long-time Professor of Oral Biology and of Anatomy at the Case Western Reserve University Schools of Dentistry and Medicine, Cleveland, where he currently is a Visiting Professor of Oral Diagnosis, as well as a Consultant at the VA Medical Center in Cleveland. He also served as Visiting Professor of Anatomy at Kyushu Dental College and of Biological Sciences at Texas Tech University. His major research interests concern the biogenesis, structure, and physiology of giant mitochondria, as well as the structure, function, and evolution of mammalian salivary glands and of secretory cells in general.

GlcNAc Biosynthesis and Function, O-Linked

Kaoru Sakabe and Gerald W. Hart
The Johns Hopkins University School of Medicine, Baltimore, Maryland, USA

O-GlcNAc is a dynamic posttranslational modification of proteins in which a single β-N-acetylglucosamine (O-GlcNAc) is added enzymatically to Ser or Thr residues through a glycosidic linkage. Much like phosphorylation, the emerging evidence shows a regulatory role for O-GlcNAc on proteins. In addition, misregulation of this posttranslational modification has been linked to diseases such as type 2 diabetes, Alzheimer's disease, and cancer.

Background

The modification of nuclear and cytoplasmic proteins on Ser and Thr residues by the addition of a single sugar moiety β-N-acetylglucosamine (O-GlcNAc) through an O-glycosidic linkage was originally described in 1984. The dogma at that time limited covalent modification of proteins by carbohydrates to occur solely in the extracellular space and within the ER, Golgi, and other subcellular organelles. Since then, O-GlcNAc has been found in all multicellular plants and animals. It is generally not elongated to more complex structures like other types of glycosylation.

The addition of O-GlcNAc to proteins, termed O-GlcNAcylation, is analogous to phosphorylation in its use as a signaling intermediate and regulatory mechanism. Indeed, global changes of O-GlcNAc have been observed during different stages of cell cycle, as well as upon mitogen stimulation. Similarly to O-Phosphate, O-GlcNAc is abundant, occurs posttranslationally and is dynamic. In fact, all proteins known to be O-GlcNAcylated are also modified with O-Phosphate. Often the sites of glycosylation are near or the same as phosphorylation sites, leading to the complex interplay on the protein by both modifications. In several cases in which the protein is glycosylated, the site can no longer be phosphorylated even if it is a few amino acids away, presumably due to steric hindrance. The converse is also true (refer to Figure 1).

The enzymes catalyzing the addition and removal of O-GlcNAc have been cloned and characterized. UDP-GlcNAc:polypeptide transferase or O-GlcNAc transferase (OGT) catalyzes the transfer of the N-acetylglucosamine from uridine diphosphate N-acetylglucosamine (UDP-GlcNAc) to the hydroxyl group of specific Thr and Ser residues. β-D-N-acetylglucosaminidase or O-GlcNAcase, on the other hand, hydrolyzes the sugar moiety from the protein.

Many proteins have been identified as O-GlcNAc-modified proteins, with many more yet to come. The proteins identified so far include RNA polymerase II and transcription factors, tumor suppressors and oncogenes, chromatin and nuclear pore proteins, RNA processing proteins, protein translation regulatory proteins, cytoskeletal proteins, and cytosolic enzymes.

Biosynthesis of UDP-GlcNAc

The activated sugar donor, UDP-GlcNAc, is an example of a molecule exquisitely controlled by multiple different pathways of cellular metabolism including nucleotide, glucose, amino acid, and fatty acid metabolism. In addition, the sugar nucleotide is sensitive to the overall energy status of the cell. The relative levels of each component determine the availability of UDP-GlcNAc for modifying different proteins; therefore, this sugar donor serves an important function by sensing the nutrient status of the cell.

UDP-GlcNAc is synthesized via the hexosamine biosynthetic pathway. Approximately 2–5% of the glucose taken up by the cell is shunted through this pathway to generate amino sugars and activated amino sugars. The rate-limiting enzyme glutamine-fructose-6-phosphate-transaminase, or GFAT, controls how much glucose is diverted into UDP-GlcNAc. The amount of UDP-GlcNAc available correlates well with the O-GlcNAc levels within the cell (Figure 2).

O-GlcNAc Transferase (OGT)

OGT is evolutionarily conserved from *Caenorhabditis elegans* to *Homo sapiens*, diverging little from organism to organism, indicating the importance of this enzyme in

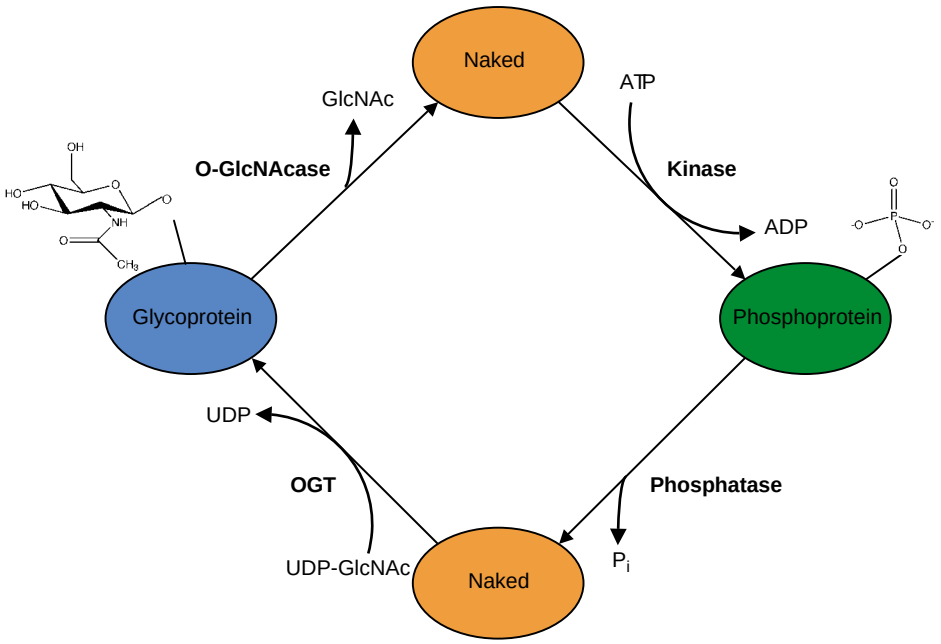

FIGURE 1 Interrelationship between O-GlcNAc and O-phosphate.

metazoans. In addition, ablation of this gene is lethal down to the single cell level. Therefore, evolution seems to have kept tight control on this enzyme, not allowing it to diverge greatly, signifying the importance of its function. In plants, OGT regulates growth via the gibberellin acid hormonal system.

The native enzyme in most tissues is comprised of three identical polypeptides. Each polypeptide consists of two domains: a tetratricopeptide repeat (TPR) domain and the catalytic domain. The TPR domain contains 9–13 tandem repeats of 34 amino acids, depending on species. These domains have been characterized as protein–protein interaction domains and are important for trimerization of the subunits as well as for substrate interaction. For example, OGT interacts with a repressor complex, mSin3a, through its TPR domain to inhibit transcription.

No consensus sequence has yet been identified for OGT; however, it seems that a Pro residue within one to three amino acids of the modification site occurs frequently. In addition, O-GlcNAc sites are usually found in regions rich in Ser and Thr residues.

O-GlcNAcase

The enzyme that catalyzes the hydrolysis of the O-GlcNAc moiety, O-GlcNAcase, is a monomer of 130 kDa. A 75 kDa alternate splice variant has also been described which lacks the catalytic C-terminal end of the enzyme. Both forms are expressed ubiquitously.

Not much is known about O-GlcNAcase; however, when purified, O-GlcNAcase is found within a high-molecular-weight complex suggesting that it associates with other proteins for regulation and specificity. Additionally, O-GlcNAcase is a substrate for proteolytic cleavage by one of the executioner caspases, caspase-3. Cleavage by this aspartyl protease has no effect on *in vitro* O-GlcNAcase activity.

Function

Different studies have ascribed varied roles of O-GlcNAc on certain proteins. These functions include involvement in nuclear transport, regulation of protein–protein interactions, regulation of protein degradation, and regulation of protein activity.

The proteins constituting the nuclear pore are enriched with O-GlcNAc. In fact, the nucleus contains the greatest concentration of O-GlcNAcylated proteins and many proteins that are O-GlcNAcylated are known to exist both in the cytoplasm and in the nucleus. It has been suggested that O-GlcNAc may be an alternative nuclear localization sequence or cytosolic retention sequence; however, this hypothesis has yet to be confirmed.

Early observations of O-GlcNAcylated proteins demonstrated an involvement of the modification in forming multimeric complexes, suggesting that O-GlcNAc may be important for regulating protein–protein interactions. These proteins include cytoskeletal proteins such as cytokeratins, neurofilaments, microtubule associated proteins, tau, crystallin, and synapsin.

The half-life of a protein dictates the temporal effect that it exerts on the cell. PEST sequences, Pro, Glu, Ser, and Thr enriched regions, are efficient in targeting proteins to the proteasome. Glycosylation has been

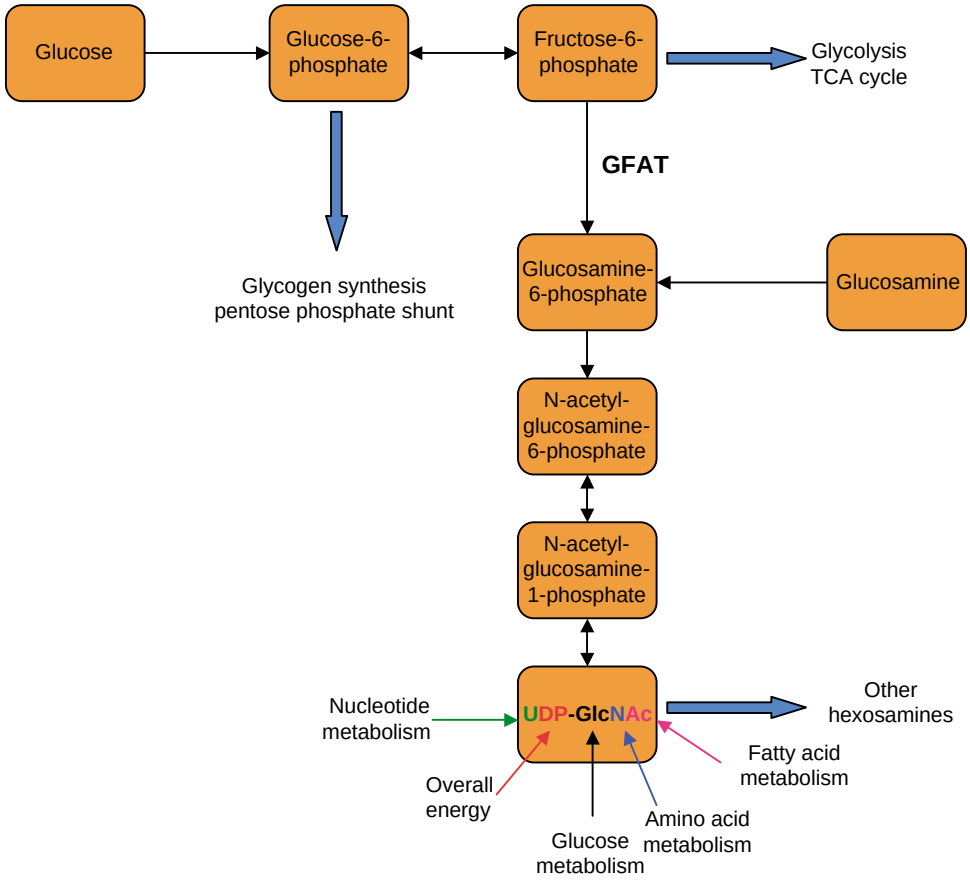

FIGURE 2 Hexosamine biosynthetic pathway.

shown to protect the translation activator p67, the transcription factor Sp1, and the nuclear hormone receptor estrogen receptor-β from degradation.

Physiological Importance

Misregulation of O-GlcNAc has been implicated in numerous disease pathologies such as type 2 diabetes, Alzheimer's disease, and cancer. Hyperglycemia and insulin resistance are hallmarks of type 2 diabetes. Since generation of UDP-GlcNAc is sensitive to the amount of glucose and glucosamine available, hyperglycemic conditions are believed to increase UDP-GlcNAc levels within the cell and thus increase the amount of O-GlcNAcylated proteins. Exogenously increasing O-GlcNAc levels have been shown to cause insulin resistance; therefore, OGT appears to play a key role in the pathology of type 2 diabetes.

A major component of neurofibrillary tangles associated with Alzheimer's disease is the microtubule-associated protein tau. In the diseased state, tau becomes hyperphosphorylated. It is known that under normal conditions, tau is modified with O-GlcNAc; it is hypothesized that by decreasing the amount of this modification on tau, it becomes hyperphosphorylated and forms the aggregates associated with Alzheimer's disease.

Finally, a decrease in O-GlcNAc has been seen in cancerous tissue. In fact, increased O-GlcNAcase activity and decreased O-GlcNAc levels correlated with tumor grade, indicating a protective role for this modification. In fact, Thr 58 of c-myc, an oncoprotein, is the major O-GlcNAc site on this oncogene protein and is also a hotspot for mutation in Burkitt's lymphoma.

In summary, O-GlcNAc is an abundant and dynamic posttranslational modification in all metazoans. It has a complex interplay with phosphorylation and in turn plays a key role in regulating cell signaling, transcription, and cytoskeletal functions.

See Also the Following Articles

Diabetes • Oligosaccharide Chains: Free, *N*-Linked, *O*-Linked • Glycosylation, Congenital Disorders of • RNA Polymerase I and RNA Polymerase III in Eukaryotes • RNA Polymerase II and Basal Transcription Factors in Eukaryotes • RNA Polymerase II Elongation Control in Eukaryotes • RNA Polymerase II Structure in Eukaryotes

Glossary

hexosamine biosynthetic pathway The pathway by which the activated sugar donor, UDP-GlcNAc, for O-glycosylation is generated.

O-GlcNAcase or β-D-N-acetylglucosaminidase The enzyme that hydrolyzes O-GlcNAc from the target protein.

O-GlcNAc transferase or UDP-GlcNAc:polypeptide transferase (OGT) The enzyme that catalyzes the transfer of O-GlcNAc from UDP-GlcNAc to its target substrate.

O-GlcNAcylation or O-glycosylation The modification of Ser or Thr residues with a single sugar moiety N-acetylglucosamine or O-GlcNAc. This modification occurs in the nucleus or cytoplasm and is analogous to O-phosphorylation.

Further Reading

Fang, B., and Miller, M. W. (2001). Use of galactosyltransferase to assess the biological function of O-linked *N*-acetyl-D-glucosamine: A potential role for O-GlcNAc during cell division. *Exp. Cell Res.* **263**, 243–253.

Iyer, S. P., and Hart, G. W. (2003). Dynamic nuclear and cytoplasmic glycosylation: Enzymes of O-GlcNAc cycling. *Biochemistry* **42**, 2493–2499.

Kearse, K. P., and Hart, G. W. (1991). Lymphocyte activation induces rapid changes in nuclear and cytoplasmic glycoproteins. *Proc. Natl Acad. Sci. USA* **88**, 1701–1705.

McClain, D. A., and Crook, E. D. (1996). Hexosamines and insulin resistance. *Diabetes* **45**, 1003–1009.

Miller, M. W., Caracciolo, M. R., Berlin, W. K., and Hanover, J. A. (1999). Phosphorylation and glycosylation of nucleoporins. *Arch. Biochem. Biophys.* **367**, 51–60.

Torres, C.-R., and Hart, G. W. (1984). Topography and polypeptide distribution of terminal N-acetylglucosamine residues on the surfaces of intact lymphocytes. *J. Biol. Chem.* **259**, 3308–3317.

Wells, L., Vosseller, K., and Hart, G. W. (2001). Glycosylation of nucleocytoplasmic proteins: Signal transduction and O-GlcNAc. *Science* **291**, 2376–2378.

Yang, X., Zhang, F., and Kudlow, J. E. (2002). Recruitment of O-GlcNAc transferase to promoters by corepressor mSin3A: Coupling protein O-GlcNAcylation to transcriptional repression. *Cell* **110**, 69–80.

Biography

Kaoru Sakabe is a graduate student in the Program of Biochemistry, Cellular, and Molecular Biology at the Johns Hopkins University School of Medicine. She graduated with a B.S. in Biochemistry from the University of North Carolina Chapel Hill before completing a fellowship at the National Institutes of Health.

Gerald W. Hart is Director and DeLamar Professor of Biological Chemistry at the Johns Hopkins University School of Medicine. He received his Ph.D. in developmental biology at Kansas State University in 1977 and did his postdoctoral work with William J. Lennarz at Johns Hopkins before joining the faculty in the Department of Biological Chemistry (1979). He was the founding editor-in-chief of *Glycobiology.*

Glucagon Family of Peptides and their Receptors

Laurie L. Baggio and Daniel J. Drucker
University of Toronto, Toronto, Canada

Glucagon and the glucagon-like peptides are produced in the gut, pancreas, and brain, and exert multiple biological actions converging on energy homeostasis via activation of distinct G protein-coupled receptors. Glucagon, liberated from the islet A cells, promotes glucose homeostasis via control of glucose production and glycogenolysis. GLP-1 and GLP-2 are secreted from gut endocrine cells and regulate energy disposal and the functional integrity of the gastrointestinal epithelium. The actions of these peptides and related analogues are relevant to the treatment of disordered energy homeostasis as exemplified by diabetes, obesity, and intestinal insufficiency.

In mammals, the proglucagon gene is expressed as a single messenger RNA (mRNA) transcript in the α-cells of the endocrine pancreas, the enteroendocrine L-cells of the small and large intestine, and in brainstem neurons within the central nervous system (CNS). Pancreatic proglucagon gene expression is up-regulated in the fasting state and by hypoglycemia and inhibited by insulin. In the intestine, proglucagon gene expression is stimulated by the presence of nutrients and by a gut-endocrine axis which in rodents, includes the peptide hormones gastrin-releasing peptide and gastric-inhibitory polypeptide. In contrast, very little is known about the factors responsible for regulating proglucagon gene expression in the CNS. Proglucagon mRNA transcripts are translated into a single 160 amino acid precursor in the pancreas, intestine, and brain that undergoes prohormone convertase (PC) enzyme-mediated tissue-specific posttranslational processing to generate structurally related yet distinct proglucagon-derived peptides (PGDPs); These PGDPs in turn activate specific seven-transmembrane G protein-coupled receptors and play important roles in modifying nutrient intake, absorption and assimilation.

Pancreatic PGDPs

In pancreatic α-cells, the action of PC-2 liberates glucagon, a hormone that is important for regulating carbohydrate metabolism, as well as the major proglucagon fragment (MPGF), a larger peptide with no known biological function (Figure 1).

Glucagon

Glucagon is a 29 amino acid hormone whose effects converge on hepatic glucose output and oppose those of insulin. Thus, glucagon elevates blood glucose levels primarily by stimulating glucose output via enhancement of glycogenolysis and promotion of gluconeogenesis in the liver.

Secretion

Glucagon secretion from pancreatic α-cells into the bloodstream is stimulated chiefly by hypoglycemia and inhibited by hyperglycemia, insulin, or somatostatin. GLP-1 can also inhibit glucagon secretion either directly, through interaction with GLP-1 receptors on pancreatic α-cells, or indirectly, through its ability to stimulate insulin and somatostatin release.

Physiological Actions

Glucagon increases hepatic glucose production in both animals and humans and plays a key role in maintaining blood glucose levels in the physiological range during periods of prolonged fasting or between meals. When blood glucose levels fall, glucagon is released into the circulation and binds to specific glucagon receptors on hepatocyte membranes. The binding of glucagon to its receptor leads to the activation of adenylyl cyclase, elevation of intracellular cAMP, and activation of protein kinase A (PKA). Activation of this glucagon receptor-signaling pathway in the liver ultimately leads to stimulation of glycogenolysis and gluconeogenesis and inhibition of glycogen synthesis and glycolysis. Glucagon typically functions as a counter regulatory hormone of insulin and can elevate blood glucose levels in response to insulin-induced hypoglycemia. However, in the diabetic state where insulin secretion may be deficient or the A cell may be less

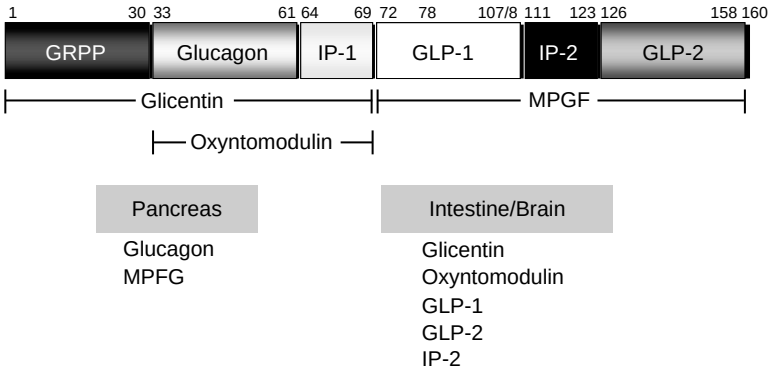

FIGURE 1 Structure of the mammalian proglucagon precursor protein and products of tissue-specific posttranslational processing in the pancreas, intestine, and brain. The numbers indicate amino acid positions in proglucagon. GRPP, glicentin-related pancreatic polypeptide; IP-1 and IP-2, intervening peptide 1 and 2; GLP-1 and GLP-2, glucagon-like peptide-1 and -2; MPGF, major proglucagon fragment.

insulin-responsive, glucagon levels are often elevated, and the resultant hyperglucagonemia is believed to play a role in the disordered glucose homeostasis characteristic of type 2 diabetes.

The glucagon receptor is also expressed in pancreatic islets, adipose tissue, heart, and kidney, and glucagon exerts a number of effects in these tissues including: enhancement of glucose-stimulated insulin secretion from pancreatic β-cells, stimulation of lipolysis in adipose tissue, elevation of heart rate and blood pressure, and regulation of renal function. Glucagon receptors are also detectable in brain and injection of glucagon into the CNS has a potent inhibitory effect of food intake in rats. Glucagon may also play a role in regulating meal size as studies in rodents and humans demonstrate that glucagon administration during a meal can reduce meal size. Lower levels of glucagon receptor mRNA are present in the stomach and intestine, and the administration of supraphysiological doses of glucagon pharmacologically inhibits gastrointestinal motility in humans. The glucagon receptor is also present in several other tissues, however, the physiological action of glucagon in these tissues is not clearly established.

Metabolism and Clearance

In both humans and animals, the kidney is the major organ responsible for glucagon metabolism and clearance, although some studies suggest the liver may also contribute significantly to glucagon degradation. Although the ubiquitous protease dipeptidyl peptidase IV (DPP IV) can also degrade glucagon, recent studies assessing (1) arteriovenous glucagon concentrations across the vascular beds of different organs and (2) inhibition of DPP IV activity *in vivo*, demonstrated that glucagon metabolism occurs primarily in the kidney and that DPP IV has no significant effect on glucagon degradation *in vivo*.

PGDPs in the Intestine and Brain

In the L-cells of the intestine, proglucagon is processed by PC1/3 to glicentin, oxyntomodulin (OXM), glucagon-like peptides-1 and -2 (GLP-1 and GLP-2), and a peptide of unknown function designated intervening peptide-2 (IP-2; Figure 1). Although the specific PC enzymes responsible for posttranslational processing of proglucagon in the CNS are not known, the brain displays a similar profile of PGDPs to that of the intestine (Figure 1).

Secretion

Intestinal PGDPs are co-released from enteroendocrine L-cells in a one-to-one molar ratio in response to an appropriate stimulus, primarily nutrients, as well as neural and hormonal agents. Nutrient ingestion, particularly carbohydrates and fats, is the primary stimulator of PGDP secretion. Nutrients produce a biphasic increase in levels of circulating PGDPs. An early (within 10–15 min) phase is likely mediated by neural and hormonal factors (including acetylcholine, muscarinic agonists, gastrin-releasing peptide, gastric inhibitory peptide, and calcitonin gene-related peptide), and a later (30–60 min) phase is mediated by direct contact of nutrients with open type L-cells. Conversely, insulin and somatotstatin-28, as well as the neuropeptide galanin, inhibit the secretion of intestinal PGDPs.

Physiological Actions

Glicentin

Glicentin is a 69 amino acid peptide whose essential physiological importance remains poorly defined. In rats, glicentin has been reported to stimulate insulin secretion, inhibit gastric acid secretion and intestinal

motility, and stimulate intestinal growth. However, since these effects are similar to those described for other PGDPs and, as a glicentin-specific receptor has not yet been identified, it is unclear whether glicentin mediates these pharmacological effects via a unique glicentin receptor or through activation of receptors for other PGDPs.

Oxyntomodulin (OXM)

OXM is a 37 amino acid peptide that inhibits gastric emptying and gastric acid secretion in both rodents and humans. OXM also stimulates intestinal glucose uptake and reduces pancreatic enzyme secretion in rats. More recent studies in rodents and humans indicate that OXM can also reduce food intake and promote satiety. However, a specific unique receptor for OXM has not yet been identified. Furthermore OXM is able to bind to and activate receptors for GLP-1 and glucagon, hence the receptor(s) responsible for mediating the biological effects of OXM are not clearly defined.

GLP-1

The GLP-1 receptor (GLP-1R) is widely expressed in multiple tissues including the endocrine pancreas, the gastrointestinal tract, lung, kidney, and many regions of the CNS, including those known to regulate energy homeostasis. GLP-1 circulates as a 30 or 31 amino acid peptide that exhibits numerous biological effects in both animals and humans which converge on the lowering of blood glucose in the postprandial state. These include potentiation of glucose-stimulated insulin secretion, enhancement of insulin gene transcription and biosynthesis, and inhibition of glucagon secretion, gastric emptying, and food intake. GLP-1 may also enhance glucose disposal through effects on liver, muscle, and adipose tissues. More recently, cell culture experiments and studies with rodents demonstrated that GLP-1 stimulates islet cell differentiation, proliferation and neogenesis, increases β-cell mass, and inhibits β-cell apoptosis. As the glucose lowering actions of GLP-1 are retained in subjects with type 2 diabetes, GLP-1R agonists are being evaluated as therapeutic agents for the treatment of diabetes.

Several actions of GLP-1 are not directly related to acute lowering of blood glucose, and include stimulation of somatostatin secretion and inhibition of pentagastrin- and meal-induced gastric acid secretion. GLP-1 receptors are also found on the heart and GLP-1 administration in rodents is associated with elevations in heart rate and blood pressure. GLP-1 also elicits several effects in the CNS that include activation of aversive pathways, prevention of apoptosis, neuroprotection, and modulation of learning and memory.

GLP-2

Studies in rodents revealed that the major biological role for GLP-2, a 33 amino acid peptide, is that of an intestinotrophic factor, an effect mediated through regulation of both proliferative and anti-apoptotic mechanisms in intestinal crypt and villus cells. GLP-2 also inhibits gastric emptying and gastric acid secretion and stimulates intestinal hexose transport by increasing the expression and activity of intestinal glucose transporters. GLP-2 administration enhanced epithelial integrity and reduced permeability in the intestinal mucosa of rodents with experimental gut injury. More recently, intracerebroventricular injection of GLP-2 into the rodent CNS was shown to transiently reduce food intake.

Metabolism and Clearance

All PGDPs are cleared primarily through the kidney, via mechanisms that include glomerular filtration and tubular catabolism. The half-life of GLP-1 is $\sim$90 s, due to its rapid inactivation by DPP IV, which is present on the surface of circulating lymphocytes and on vascular endothelial cells in the small intestine, in close proximity to the sites of PGDP release from gut endocrine cells. In addition, the neutral endopeptidase (NEP-24.11) has an endoproteolytic effect on GLP-1 *in vitro*, and may play a role in GLP-1 metabolism. GLP-2 is also inactivated by DPP IV, although it has a considerably longer half-life (5–7 min) relative to GLP-1. Glicentin and OXM are also potential substrates for DPP IV activity, however, the physiological relevance, if any, of DPP IV for the biological activity of glicentin and OXM has not been determined.

PGDP Receptors

Thus far, individual receptors for glicentin or OXM have not been identified and experimental evidence indicates that these peptides likely mediate their physiological actions via known PGDP receptors. Glucagon, GLP-1, and GLP-2 exert their biological effects through unique specific receptors that belong to the seven transmembrane-spanning, heterotrimeric G protein-coupled family of receptors.

The human and rat glucagon receptor (GluR) cDNAs encode proteins that are 82% identical and 485 and 477 amino acids in length, respectively. The human GluR gene has been mapped to chromosome 17, band q25. Glucagon receptors are widely expressed in multiple mammalian tissues including liver, heart, kidney, spleen, ovary, pancreatic islets, thymus, stomach, adrenals, intestine, thyroid, skeletal muscle, adipose tissue, lung, and brain. Studies examining the regulation of GluR

mRNA expression in rat islet and primary liver cultures indicate that glucagon, dexamethasone, and agents that increase cAMP levels inhibit, whereas somatostatin increases, GluR expression. The promoter region of the GluR gene contains a glucose regulatory element and levels of liver GluR mRNA increase in response to high glucose concentrations. GluR activation leads to stimulation of adenylyl cyclase, elevations in intracellular cAMP levels, and activation of PKA. Glucagon can also activate phospholipase C and increase intracellular levels of inositol triphosphates and Ca^{2+}. Structure–function studies of the glucagon receptor indicate that sequences in the N-terminal extra cellular domain, in particular aspartic acid residue 64, as well as the first extra cellular loop and the third and fourth transmembrane domains are essential for ligand binding. Intracellular loops two and three are important for GluR signaling.

The human *GLP-1R* (GLP-1R) gene encodes a 463 amino acid protein and has been mapped to chromosome 6, band p21.1. The rat *GLP-1R* also consists of 463 amino acids and is 90% identical to the human receptor. The GLP-1R is expressed in pancreatic islet α-, β-, and δ-cells, lung, heart, kidney, gastrointestinal tract, CNS, and the pituitary. GLP-1R mRNA levels are down-regulated in response to GLP-1, activation of protein kinase C (PKC), and high concentrations of glucose or dexamethasone in cell lines *in vitro*. The GLP-1R engages multiple G proteins and activate several intracellular signal transduction pathways including the cAMP/PKA and phospholipase C/PKC pathways. GLP-1R activation also leads to increased intracellular Ca^{2+} levels and activation of phosphatidylinositol 3-kinase and mitogen-activated protein kinase signaling pathways. The N-terminal extra cellular domain of the GLP-1R is essential for GLP-1 binding, whereas the third intracellular loop is required for coupling of the receptor to G proteins.

Human and rat GLP-2 receptor (GLP-2R) cDNAs, originally isolated from hypothalamic and intestinal cDNA libraries, encode proteins of 553 and 550 amino acids, respectively. The human GLP-2R gene has been localized to chromosome 17, band p13.3. The GLP-2R is expressed in the stomach, intestine, lung, subsets of enteric neurons, and the CNS; the factors that regulate GLP-2R gene expression remain unknown. Studies using heterologous cells transfected stably with rat or human GLP-2R cDNAs demonstrate that the receptor is coupled to induction of adenylyl cyclase activity, cAMP production and activation of PKA. The anti-apoptotic effects of GLP-2R activation are mediated by both PKA-dependent and -independent signaling pathways. In contrast to the glucagon and GLP-1 receptors, specific GLP-2R regions important for ligand binding and G protein coupling have not yet been identified.

See Also the Following Articles

Adenylyl Cyclases • A-Kinase Anchoring Proteins • Calcitonin Gene-Related Peptide and Adrenomedullin Receptors • Diabetes • Insulin- and Glucagon-Secreting Cells of the Pancreas • Phospholipase C • Protein Kinase C Family

Glossary

DPP-IV A serine protease that specifically cleaves dipeptides from the amino terminus of peptides or small proteins that contain an alanine or proline residue in amino acid position 2.

enteroendocrine cells Hormone-producing cells of the gastrointestinal tract.

G protein-coupled receptors A family of receptors that consists of seven-transmembrane-spanning domains and that utilizes GTP-binding proteins (G proteins) to transmit signals from the surface to the interior of the cell.

prohormone convertase Endoproteolytic enzymes that cleave C-terminal to paired basic amino acid residues. PGDPs are flanked by pairs of basic amino acids, the recognition sites for prohormone convertase cleavage.

Further Reading

Drucker, D. J. (2002). Biological actions and therapeutic potential of the glucagon-like peptides. *Gastroenterology* **122**, 531–544.

Drucker, D. J. (2003). Enhancing incretin action for the treatment of type 2 diabetes. *Diabetes Care* **26**(10), 2929–2940.

Jiang, G., and Zhang, B. B. (2003). Glucagon and regulation of glucose metabolism. *Am. J. Physiol. Endocrinol. Metab.* **284**, E671–E678.

Kieffer, T. J., and Habener, J. F. (1999). The glucagon-like peptides. *Endocr. Rev.* **20**, 876–913.

Mayo, K. E., Miller, L. J., Bataille, D., Dalle, S., Goke, B., Thorens, B., and Drucker, D. J. (2003). International union of pharmacology. XXXV. The glucagon receptor family. *Pharmocol. Rev.* **55**, 167–194.

Biography

Laurie Baggio is a Research Associate Scientist in the Banting and Best Diabetes Centre.

Daniel Drucker is Director, Banting and Best Diabetes Centre, University of Toronto.

Gluconeogenesis

Richard W. Hanson and Oliver E. Owen
Case Western Reserve University School of Medicine, Cleveland, Ohio, USA

Gluconeogenesis is the major route for the synthesis of glucose in all mammals. This pathway is present in the liver and kidney cortex and is active during starvation and after a meal high in protein and fat, but low in carbohydrate. The major substrates for gluconeogenesis are lactate, pyruvate, 18 of the 20 amino acids (leucine and lysine are not gluconeogenic), propionate and glycerol. During periods of prolonged starvation, the concentration of ketone bodies in the blood can rise from undetectable levels (after a meal containing carbohydrate) to as high as 5 mM after a week of starvation. A fraction of these ketone bodies are excreted in the urine. To buffer the acidity of the tubular urine, the kidney cortex generates ammonia from the glutamine produced by muscle. The carbon skeleton of glutamine (α-ketoglutarate) enters the citric acid cycle and is converted to glucose. Thus the kidney can become a major source of blood glucose during prolonged starvation. Insulin represses transcription of many of the genes involved in hepatic gluconeogenesis, so that during diabetes gluconeogenesis is markedly induced. This results in elevated rates of hepatic glucose output.

History

Claude Bernard first noted the synthesis of glucose in his famous description of glucose turnover during fasting. However, it is the work of Carl and Gerty Cori that established gluconeogenesis as critical for the synthesis of glucose from lactate as part of what is now known as the Cori Cycle. Gluconeogenesis is not a reversal of glycolysis, although the two pathways share a number of enzymes. A major advance in the understanding of the specific reactions in the pathway of glucose synthesis occurred when Merton Utter and his colleagues discovered two of the major enzymes of the pathway, phosphoenolpyruvate carboxykinase and pyruvate carboxylase. In the 1960s and 1970s, the research of Hans Krebs, Charles Park and John Exton, John Williamson and Henry Lardy, among others, set out the metabolic parameters of the pathway as it known today. Finally, the elevated rate of synthesis and release of glucose by the liver and kidney cortex during diabetes mellitus is a major factor in the pathogenesis of this disease.

Overview of Gluconeogenesis

Gluconeogenesis is defined as the *de novo* synthesis of glucose from nonhexose precursors. Gluconeogenesis does not include the conversion of fructose or galactose to glucose in the liver or the generation of glucose from glycogen via glycogenolysis. The pathway of gluconeogenesis (Figure 1) occurs mainly in the liver and kidney cortex and to a lesser extent in the small intestine. The major substrates for gluconeogenesis are lactate, pyruvate, propionate, glycerol, and 18 of the 20 amino acids (the exceptions are leucine and lysine). Glucose cannot be synthesized from fatty acids, since they are converted by β-oxidation to acetyl CoA, which subsequently enters the citric acid cycle and is oxidized to CO_2. The three-carbon fatty acid, propionate is an exception since it is carboxylated, converted to succinyl-CoA and enters the citric acid cycle as a four-carbon intermediate, not as acetyl CoA. One exception is acetone, which is converted to propanediol, a minor gluconeogenic precursor. Also, the last three carbon atoms of the odd-chain fatty acids generate proprionyl CoA during β-oxidation and are thus partly gluconeogenic. There are 14 enzymes involved in the conversion of lactate to glucose; three of these enzymes are classified as gluconeogenic (phosphoenolpyruvate carboxykinase, fructose-1,6-bisphosphatase, and glucose-6-phosphatase) and one is anaplerotic (pyruvate carboxylase), since it is important in both gluconeogenesis and lipogenesis. The remainder of the pathway is simply a reversal of the enzymes of glycolysis, which is responsible for the breakdown of glucose. Gluconeogenic enzymes are present in the cytosol, mitochondria, and endoplasmic reticulum of the tissues in which this pathway is present. Net gluconeogenesis occurs during starvation and after a meal high in fat and protein but no carbohydrate.

The Enzymes of Gluconeogenesis

The unique properties of gluconeogenesis are attributable to the three gluconeogenic and one anaplerotic enzyme in the pathway. The following will describe each of these enzymes and review their regulatory properties.

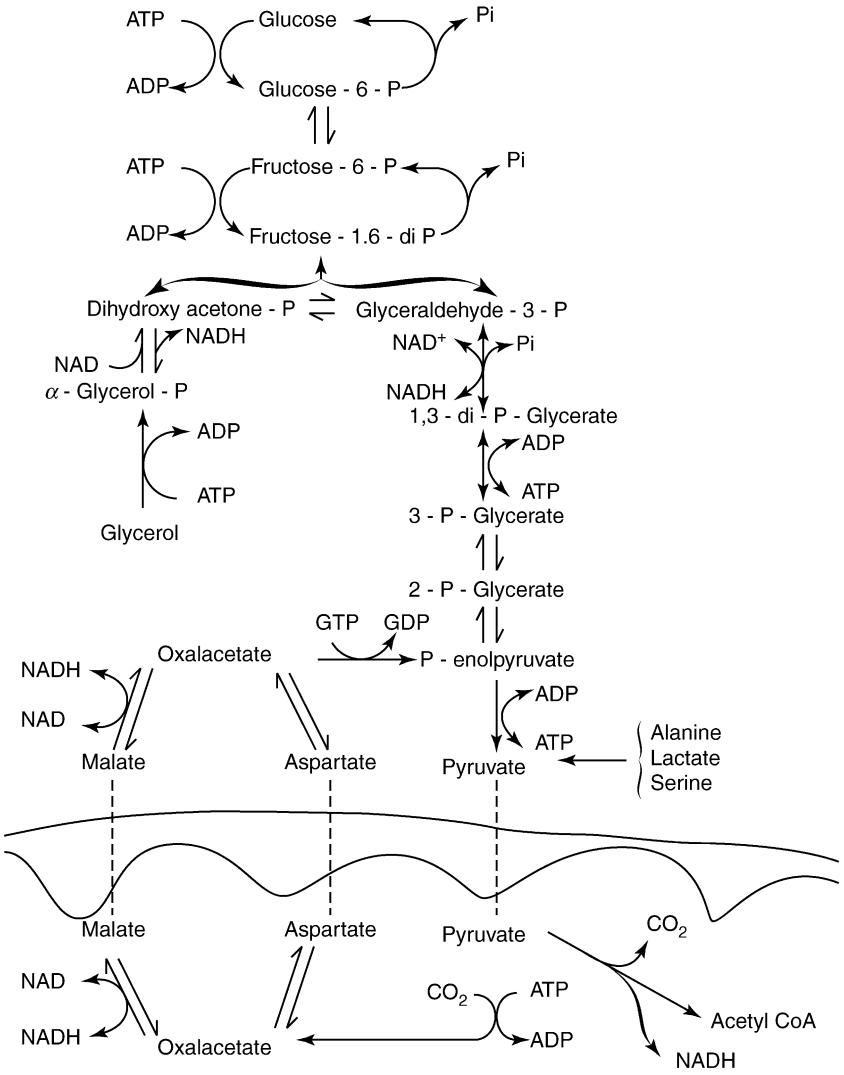

FIGURE 1 The pathway of hepatic gluconeogenesis. The figure demonstrates the reactions involved in gluconeogenesis in the liver starting with alanine, lactate or serine as precursors. The movement of aspartate and malate from the mitochondria is also indicated to demonstrate the redox state balance that occurs between the mitochondria and the cytosol during gluconeogenesis.

Pyruvate Carboxylase (PC)

PC is found in the mitochondria, catalyzes the following reaction:

$$\text{Pyruvate} + CO_2 + \text{ATP} \rightarrow \text{Oxalacetate} + \text{ADP} + \text{Pi}$$

Pyruvate carboxylase is a multisubunit enzyme that has acetyl CoA as a positive allosteric regulator. The enzyme is critical for both gluconeogenesis and fatty acid synthesis, since it replenishes the citric acid cycle intermediates (malate or citrate) that leave the mitochondria as part of biosynthetic processes. Since it is essentially irreversible under biological conditions, PC does not generate pyruvate from oxalacetate. Pyruvate carboxylase is generally considered an anaplerotic (to refill) enzyme since it functions to replace the oxalacetate that is reduced to malate and used in the synthesis of glucose. Since the citric acid cycle is important in both gluconeogenesis and lipogenesis, PC plays a role in both pathways.

Phosphoenolpyruvate Carboxykinase (PEPCK)

PEPCK catalyzes the following reaction:

$$\text{Oxalacetate} + \text{GTP} \rightarrow \text{Phosphoenolpyruvate} + \text{GDP} + CO_2$$

It is found in both the mitochondria (PEPCK-M) and the cytosol (PEPCK-C). Two different nuclear genes encode these two isoforms of PEPCK. Expression of the gene PEPCK-C is inducible by diet and hormones, while PEPCK-M is constitutive. Species vary in the amount

of the two isoforms expressed in gluconeogenic tissues. Rodent species such as the rat and mouse have 90% PEPCK-C in their liver and kidney cortex while birds have 100% PEPCK-M. Humans and most other mammalian species studied to date have ~50% of both isoforms. The exact metabolic significance of having two isoforms of PEPCK is not entirely clear but it has been proposed that PEPCK-M allows the direct synthesis of PEP in the mitochondria thus bypassing the need to transport reducing equivalents out of the mitochondria. This point will be discussed in more detail in the latter section of this article. PEPCK is generally considered to be the pace-setting enzyme in gluconeogenesis, but it has no known allosteric regulators. The enzyme has a relatively short half-life of 6 h and alterations in the rate of gene transcription are rapid. For example, the rate of PEPCK-C gene transcription in the liver is increased tenfold in 30 min after the administration of cAMP to animals. Insulin administration causes an equally rapid decrease in the transcription of the gene. It has thus been suggested that the level of enzyme protein in the liver is a critical determinant in the overall activity of the enzyme. Transcription of the gene for PEPCK-C has been studied in considerable detail and many of the transcription factors that regulate the tissue-specific expression of the gene have been identified. A detailed discussion of this area is beyond the scope of this article but the reader is directed to several reviews on the subject listed in the Further Reading.

Fructose-1,6-Bisphosphatase (FBPase)

FBPase is found in the cytosol. In mammalian liver, the enzyme is a homotetramer with a subunit molecular weight of 38–41 kDa, depending on the species. FBPase catalyzes the following reaction:

$$\text{Fructose-1, 6-bisphosphate} \rightarrow \text{Fructose-6-Phosphate} + \text{Pi}$$

The enzyme is regulated allosterically by a number of small molecules including AMP and fructose-2,6-phosphate, which are negative regulators, and ATP that is a positive regulator. The enzyme is also covalently modified by phosphorylation by protein kinase A, which decreases its activity.

Glucose-6-Phosphatase (G6Pase)

G6Pase is present in the endoplasmic reticulum of the liver, kidney cortex, and small intestine. The role of this enzyme in the synthesis of glucose was first suggested by the Coris' cycle in 1938 and finally demonstrated by Marjorie Swanson in the United States and Christian deDuve and colleagues in Belgium in the early 1950s. For a detailed review of the early work with this important enzyme, the reader is directed to a review by Nordlie referenced at the end of this article. The activity of G6Pase can be induced by starvation, cAMP, and glucocorticoids. Somewhat paradoxically, glucose at high concentrations will also stimulate transcription of the gene for this enzyme.

Physiological Control of Gluconeogenesis

Dietary Status Determines the Extent of Gluconeogenesis

There are two normal metabolic situations during which gluconeogenesis occurs in mammals. In addition, gluconeogenesis increases during diabetes, resulting in an increased rate of glucose output by the liver. The first physiological situation involves the gluconeogenesis, characteristic of starvation, and the second, the gluconeogenesis that occurs after a meal that contains minimal carbohydrate. During starvation, the source of carbon for gluconeogenesis is body protein, largely from the muscle and lactate and pyruvate from glycolysis and glycerol from lipolysis. The muscle undergoes proteolysis, largely due to the fall in insulin. Proteolysis in muscle results in the generation of 20 amino acids. However, reactions in the muscle convert these amino acids mainly to alanine and glutamine, which are leased for subsequent metabolism. Both alanine and glutamine can be converted to glucose in the liver but in starvation it is the kidney cortex that utilizes glutamine. The kidney synthesizes glucose from the carbon skeleton of glutamine and uses the ammonia derived from this process to maintain the acid–base balance of the tubular urine. Later in this article, the metabolic role of renal gluconeogenesis will be discussed in detail. The gluconeogenesis that occurs after a meal containing protein and fat, but no carbohydrate, involves the 18 gluconeogenic amino acids found in dietary protein (degradation of the amino acids leucine and lysine contributes no carbon for glucose synthesis). The carbon skeletons of most of the amino acids enter the citric acid cycle, proceed forward to malate and are subsequently converted to glucose via the gluconeogenesis as described in detail below.

The Role of Fatty Acid Oxidation in the Control of Gluconeogenesis

Gluconeogenesis occurs during fasting but the amount of glucose supplied by this process is far less than can be generated by glycogenolysis during the immediate post-absorptive period. Blood glucose homeostasis is possible only because other substrates (fatty acids, ketone bodies) are used as fuels by peripheral tissues, thus sparing the use

of glucose. In general, the rate of gluconeogenesis is increased in the liver during starvation due to a fall in the concentration of insulin and a rise in glucagon; glucocorticoids play a permissive role in stimulating this process. This change in hormone status results in profound alterations in the metabolism of both skeletal muscle and adipose tissue. There is an increased rate of lipolysis in the adipose tissue and a net protein breakdown (proteolysis) in muscle. This results in an elevated rate of delivery to the liver of fatty acids from adipose tissue and primarily alanine from muscle. Fatty acid oxidation by hepatic mitochondria raises the concentration of acetyl CoA and shifts the redox state of that organelle toward reduction; there is a concomitant increase in ATP synthesis. In the rat, for example, the hepatic NAD/NADH ratio shifts from 700 to 550 after 48 h of starvation. The net effect of this increase in fatty acid oxidation is a stimulation of gluconeogenesis and an inhibition of glycolysis. This stimulatory effect is exerted at several levels. First, the rise in NADH and ATP inhibits multiple steps in the tricarboxylic acid cycle (TCA cycle), including citrate synthase, isocitrate dehydrogenase, and α-ketoglutarate dehydrogenase complex. Most importantly, the increased concentrations of ATP, NADH, and acetyl CoA that occur in the liver during fasting inhibit flux through the pyruvate dehydrogenase complex. The importance of the latter step will be stressed subsequently.

Pathway of Gluconeogenesis

During starvation, alanine is transported from the muscle to the liver, where it is converted to pyruvate. As mentioned above, during fasting the pyruvate dehydrogenase complex is inhibited by the products of fatty acid oxidation. At the same time, acetyl CoA activates PC, thus converting pyruvate to oxalacetate, which is then reduced to malate by the mitochondrial isoform of NAD malate dehydrogenase. Malate leaves the mitochondria and is oxidized to oxalacetate via the cytosolic isoform of NAD malate dehydrogenase; the oxalacetate is decarboxylated to PEP by PEPCK-C and the PEP is further metabolized via a reversal of glycolysis to fructose-1,6-bisphosphate. This intermediate is then converted to fructose-6-phosphate by the gluconeogenic enzyme, FBPase. Finally, G6Pase, which is present in the endoplasmic reticulum, generates free glucose from glucose-6-phosphate; GLUT 2 transports the glucose from the liver to the blood.

Redox Balance for Gluconeogenesis

It is important to note that gluconeogenesis requires two molecules of NADH for every molecule of glucose that is synthesized. The NADH is required to reverse the glyceraldehyde-3-phoshate dehydrogenase reaction. The source of this NADH varies according to the substrate used for gluconeogenesis. When oxidized compounds such as pyruvate and alanine are used for glucose synthesis, the pathway involves malate transport from the mitochondria, essentially generating reducing equivalents in the cytosol for gluconeogenesis, as described above. There is a slight variation in this pathway of glucose synthesis when the starting substrate in lactate. In this case, the conversion of lactate to pyruvate in the cytosol generates NADH, which obviates the necessity of transporting malate from the cytosol to produce NADH. There are two possible routes for the movement of intermediates from the mitochondria that is not linked to the transport of reducing equivalents. The first involves the transamination of mitochondrial oxalacetate to aspartate via aspartate aminotransferase. The aspartate is transported to the cytosol and converted to oxalacetate by the cytosolic isoform of aspartate aminotransferase (Figure 1). The second variation in metabolite transfer involves the generation of oxalacetate in the mitochondria via PC, followed by the synthesis of PEP directly in the mitochondria via PEPCK-M. PEPCK-C is readily transported from the mitochondria on the tricarboxylate carrier in the inner mitochondria membrane. This role of PEPCK-M in avian metabolism supports the physiological role of the two isoforms of PEPCK. In birds, the liver uses only lactate for gluconeogenesis, and the avian liver contains only PEPCK-M. Gluconeogenesis from amino acids occurs in the kidney.

Regulation of Gluconeogenesis

Gluconeogenesis is regulated at four fundamental levels, discussed below.

Substrate Delivery to the Liver and Kidney

The rate of delivery of substrates such as lactate, which is derived from glycolysis in skeletal muscle (Cori cycle) or glycolysis in erythrocytes, glycerol from the breakdown of triglycerides in adipose tissue and amino acids from proteolysis in skeletal muscle and other protein rich tissues, greatly influences the level of hepatic gluconeogenesis. Thus, the control of the release and delivery of precursors from peripheral tissues is an important controlling factor in the rate of gluconeogenesis in the liver and kidney cortex. For example, insulin controls the rate of gluconeogenesis, in part, by regulating the delivery of substrates from muscle and adipose tissue to the liver.

Mass Action Regulation of Enzymes

As an example of this type of regulation, the activity of glyceraldehyde-3-P dehydrogenase (in the direction of gluconeogenesis) is stimulated by a rise in NADH in cytosol (the NAD/NADH ratio). The activity of G6Pase is increased by a rise in the concentration of G6Pase and PEPCK activity is stimulated by a rise in the concentration of oxalacetate.

Allosteric Activation of Key Enzymes

As an example of this type of regulation of gluconeogenesis, acetyl-CoA allosterically activates PC, while FBPase is activated by ATP and inhibited by AMP and fructose-2,-6,bisphosphate. In addition, during gluconeogenesis, pyruvate kinase must be inhibited in order to prevent the conversion of PEP back to pyruvate ("futile cycling") by liver-type pyruvate kinase (PK-L). A rise in the concentration of alanine or ATP and a decrease in the level of fructose-1,6-bisphosphate that occurs in the liver during fasting, results in the allosteric inhibition of the activity of this enzyme (Figure 2).

Covalent Modification

Phosphorylation of gluconeogenic enzymes by a cAMP-dependent protein kinase (PKA) regulates the rate of key steps in gluconeogenesis. PK-L (not the muscle isozyme, PK-M) is inhibited by cAMP-induced phosphorylation via PKA. This, together with the allosteric regulation mentioned above, prevents the conversion of PEP to pyruvate in the liver and thus limits possible "futile cycling" of carbon and resulting energy loss. The PKA regulation of hepatic gluconeogenesis is controlled in part by changes in the concentration of fructose-2,6-bisphosphate. As mentioned above, this compound allosterically regulates two critical enzymes, phosphofructokinase, the rate-controlling enzyme in glycolysis, and FBPase the key gluconeogenic enzyme. Fructose-2,6-bisphosphate is both synthesized and degraded by a single, "bifunctional" enzyme 6-phosphofructo-2-kinase/fructose-2,6-bisphosphatase, which can act as a kinase (it synthesizes fructose-2,6-bisphosphate using ATP as a source of phosphate) or a phosphatase (it converts fructose-2,6-bisphosphate to fructose-6-phospahte plus inorganic phosphate. Phosphorylation of this enzyme by PKA, induces the phosphatase function of the enzyme. This results in a decrease in the concentration of fructose-2,6-bisphosphate, thereby inhibiting the activity of phosphofructokinase (the rate-limiting enzyme in glycolysis), which requires fructose-2,6-bisphosphate as an allosteric activator) and simulating the activity of FBPase, for which fructose-2,6-bisphosphate is an inhibitor (Figure 2). Thus the covalent modification of the bifunctional enzyme has a reciprocal effect on the gluconeogenesis (stimulation) and glycolysis (inhibition).

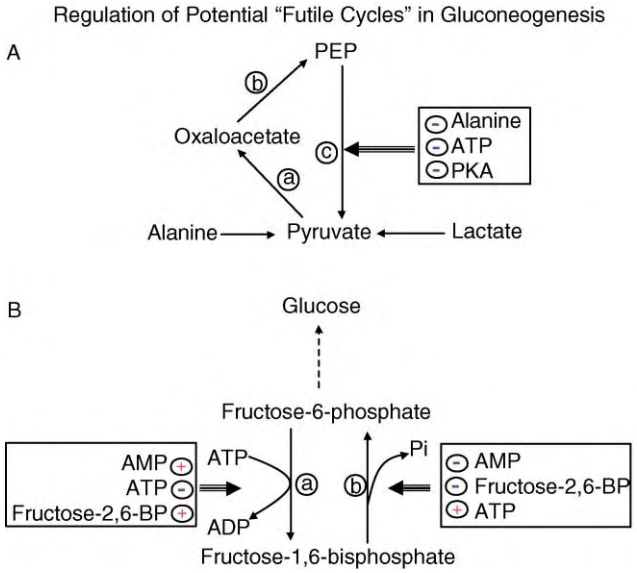

FIGURE 2 Regulation of potential "futile cycles" during gluconeogenesis. (A) The control of the oxalacetate/PEP/pyruvate futile cycle. The enzymes shown in this panel are (a) pyruvate carboxylase, (b) PEP carboxykinase, and (c) liver-type pyruvate kinase. This cycle is regulated by inhibition of liver-type pyruvate kinase by allosteric regulation by alanine and ATP and by phosphorylation of the enzyme by PKA. In addition, the decreased glycolytic flux that occurs during periods of gluconeogenesis (starvation) reduces the concentration of fructose-6-phosphate, a positive allosteric regulator of liver-type pyruvate kinase. (B) The control of the fructose-1,6-bisphosphate/fructose-6-phosphate futile cycle. The enzymes shown in this panel are (a) phosphofructokinase and (b) fructose-1,6-bisphosphatase (FBPase). Phosphofructokinase is activated by AMP, and fructose-2,6-bisphosphate and inhibited by ATP, while fructose-1,6-bisphosphatase is regulated in the opposite manner by the same intermediates. The result is a coordinated control of carbon flux via glycolysis and gluconeogenesis in the liver.

Alteration in Gene Expression

The expression of several of the genes in the gluconeogenic pathway is modified by starvation, diabetes, or by diets high in carbohydrate. Transcription of the genes coding for PEPCK-C, FBPase, and G6Pase are increased by fasting and during diabetes while transcription of the genes for several of the glycolytic enzymes, such as PK-L, phosphofructokinase, and glucokinase is decreased. Alterations in the rate of gene transcription change the levels of mRNA for a specific enzyme, resulting in a change in the rate of synthesis for the enzyme. An increase or decrease in enzyme content usually occurs over a period of several hours and is mediated by hormones such as glucagon (acting via cAMP), insulin, and glucocorticoids that stimulate the transcription of the genes for these enzymes. Metabolites such as glucose and fatty

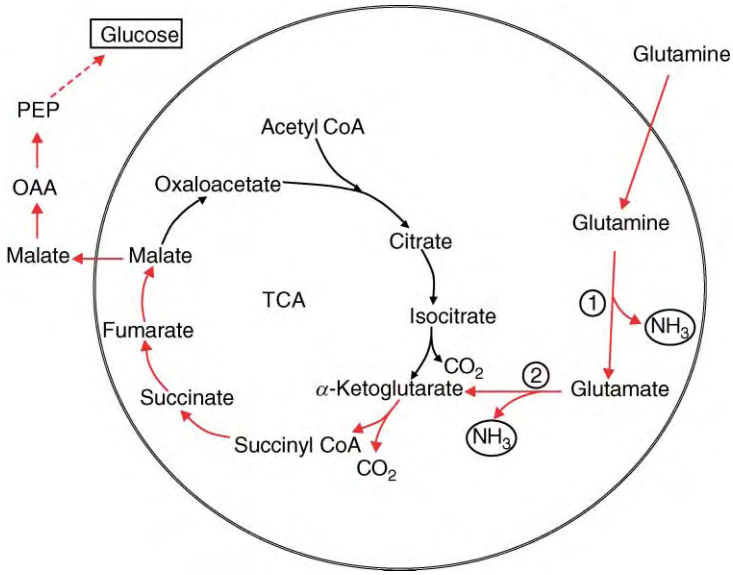

FIGURE 3 Gluconeogenesis from glutamine in the kidney. Glutamine from the muscle is metabolized by the kidney cortex to generate ammonia (circled) that is used to titrate the acidity of the tubular urine. This involves two enzymatic reactions, both of which are in the renal mitochondria, (1) glutaminase, and (2) glutamate dehydrogenate. The α-ketoglutarate that is produced by the removal of the two amino groups of glutamine enters the citric acid cycle, is oxidized to malate and then proceeds to glucose via gluconeogenesis. The large circle in the figure represents the renal mitochondria.

acids also exert control of the expression of specific genes involved in their metabolism.

Renal Gluconeogenesis

The synthesis of glucose in the kidney cortex is directly related to the loss of ketone bodies in the urine. During periods of fasting, the kidney excretes large amounts of ketone bodies (weak acids), but produces urine that is near neutrality. The relative acidity of the tubular urine is maintained at about pH 6.0 by the generation of ammonia from the metabolism of glutamine that has been mobilized from the muscle during starvation. Glutamine is converted to glutamate by "glutaminase" and glutamate to α-ketoglutarate by "glutamate dehydrogenase;" this generates 2 molecules of ammonia that are released into the urine to maintain the neutrality of the urine. The α-ketoglutarate is then converted to glucose. Thus, ammoniagenesis in the kidney is linked to gluconeogenesis (Figure 3). Interestingly, acidosis induces transcription of the gene for PEPCK-C, increasing its concentration in the kidney cortex. This elevation in the activity of PEPCK-C is critical for the increased rates of gluconeogenesis noted during acidosis.

Final Words

Glucose oxidation is essential for human metabolism and thus gluconeogenesis is a critical element in the maintenance of glucose homeostasis in all mammals. In humans, this process is continuous and augmented after the depletion of liver glycogen. Gluconeogenesis is the sole source of glucose during starvation. Since gluconeogenesis from amino acids results in a depletion of lean body mass, a number of metabolic accommodations occur to minimize the use of glucose by tissues such as the brain and skeletal muscle (fuel sparing). The details of these processes appear elsewhere in this encyclopedia. It is impossible to reference all of the research responsible for a detailed understanding of the pathway of gluconeogenesis and its regulation. A select number of more general articles that reflect the field are included in the Further Reading section.

See Also the Following Articles

Carnitine and β-Oxidation • Diabetes • Diacylglycerol Kinases and Phosphatidic Acid Phosphatases • Fatty Acid Oxidation • Glucose/Sugar Transport in Bacteria • Glucose/Sugar Transport in Mammals • Pyruvate Carboxylation, Transamination, and Gluconeogenesis • Pyruvate Dehydrogenase • Pyruvate Kinase • Regulated Intramembrane Proteolysis (Rip) • Starvation

Glossary

anaplerotic reactions Enzymatic reactions that produce citric acid cycle anions to replace those that leave the cycle for the synthesis of compounds such as glucose and fatty acids.

Cori cycle Process in which the lactate generated in the red blood cells and muscle is converted to glucose in the liver and cycled back to these tissues for reconversion to lactate.

gluconeogenesis The *de novo* synthesis of glucose from nonhexose precursors.

ketone bodies Water-soluble fuels produced by the liver from the acetyl CoA that is generated from the β-oxidation of fatty acids.

lipolysis The degradation of triglyceride to free fatty acids and glycerol; occurs primarily in the white adipose tissue.

β-oxidation The oxidation of fatty acids to acetyl CoA in the mitochondria.

proteolysis The breakdown of proteins to their component amino acids.

Further Reading

Granner, D. K., and O'Brien, R. M. (1992). Molecular physiology and genetics of NIDDM. *Diabetes Care* **15**, 369.

Hanson, R. W., and Patel, Y. M. (1994). P-enolpyruvate carboxykinase: The gene and the enzyme. In *Advances in Enzymology* (A. Meister, ed.) Vol 69, Wiley, New York.

Nordlie, R. C., Foster, J. D., and Lange, A. J. (1999). Regulation of glucose production by the liver. *Annu. Rev. Nutr.* **19**, 379.

Owen, O. E., Felig, P., Morgan, A. P., Wahren, J., and Cahill, G. F. Jr. (1969). Liver and kidney metabolism during prolonged starvation. *J. Clin. Invest.* **48**, 584.

Pilkis, S. J., and Claus, T. H. (1991). Hepatic gluconeogenesis/glycolysis: Regulation and structure/function relationships of substrate cycle enzymes. *Ann. Rev. Nutr.* **11**, 465.

Pilkis, S. J., Claus, T. H., Kurland, I. J., and Lange, A. J. (1995). 6-Phosphofructo-2-kinase/fructose-2,6-bisphosphatase: A metabolic signaling enzyme. *Annu. Rev. Biochem.* **64**, 799.

Soling, H.-D., and Kleineke, J. (1976). Species dependent regulation of gluconeogenesis in higher animals. In *Gluconeogenesis, Its Regulation in Mammalian Species* (R. W. Hanson and M. A. Mehlman, eds.) Wiley, New York.

Watford, M., Hod, Y., Chiao, Y.-B., Utter, M. F., and Hanson, R. W. (1981). The unique role of the kidney in gluconeogenesis in the chicken: The significance of a cytosolic form of PEPCK. *J. Biol. Chem.* **256**, 10023.

Utter, M. F., and Kolenbrander, H. M. (1972). Formation of oxalacetate by CO_2 fixation on P-enolpyruvate. In *The Enzymes* (P. D. Boyer, ed.) Vol VI, 117pp. Academic Press, New York.

Biography

Richard W. Hanson is Professor of Biochemistry at Case Western Reserve University School of Medicine in Cleveland, Ohio. For many years, he has been an Associate Editor of the *Journal of Biological Chemistry*, and he was the President of the American Society of Biochemistry and Molecular Biology. His research interests include the dietary and hormonal control of gene transcription and the regulation of gluconeogenesis and glyceroneogenesis in mammals.

Oliver E. Owen was previously Professor of Medicine and coprincipal Investigator and Program Director, General Clinical Research Center, Temple University School of Medicine and Hospital, and formerly Professor and Chair of Medicine, Southern Illinois University School of Medicine.

Glucose/Sugar Transport in Bacteria

Lan Guan and H. Ronald Kaback
University of California, Los Angeles, California, USA

Sugar transport in bacteria involves highly specific membrane proteins that catalyze translocation and accumulation of various sugars from the outside environment across the cytoplasmic membrane and into the cell where they are metabolized. As with other membrane proteins that catalyze transport of metabolites other than sugars, these proteins are called transporters or permeases. When the translocation of sugar takes place against a concentration gradient (from a low concentration outside of the cell to higher concentrations inside), the transport process requires energy, and is called active transport. In bacteria, there are three types of systems involved in sugar transport, and each one utilizes distinct energy sources.

The Phosphoenolpyruvate: Sugar Phosphotransferase System (PTS)

Classification

According to the Transport Commission (TC) classification, the PTS represents a distinct family found only in certain bacteria. It is a bacterial sugar transport system which also plays an essential role in the phenomena of catabolite repression and inducer exclusion, particularly in *Escherichia coli* (*E. coli*) and *Salmonella typhimurium*.

Functional Properties

The PTS is a multicomponent system and catalyzes vectorial phosphorylation of various sugars. Thus, in *E. coli*, for example, glucose and other sugars are translocated across the membrane by PTS-catalyzed phosphorylation (Figure 1) (i.e., glucose appears in the cytoplasm as glucose-6-phosphate). Therefore, translocation across the membrane and the first step in metabolism are one and the same. Many sugars are transported by PTS systems (glucose, mannitol, fructose, mannose, galactitol, sorbitol, xylitol, and N-acetylglucosamine), and specificity for each sugar is provided by the membrane-embedded component of the system. In *E. coli*, only monosaccharides and their derivatives are substrates for PTS systems, but in other bacteria, disaccharides are also utilized by this system.

The PTS is also involved in the regulation of uptake and metabolism of many other sugars, as discussed in this entry, as well as bacterial chemotaxis toward these sugars, which is not covered here.

Assembly and Phosphoryl Transfer Reaction

The PTS includes three essential enzymes, termed Enzyme I (EI), Enzyme II (EII), and *H*istidine *Pr*otein (HPr) (Figure 1). EI is a soluble protein kinase encoded by *ptsI* gene that catalyzes the phosphorylation of HPr from phospho*enol*pyruvate (PEP). HPr, encoded by the *ptsH* gene, is a small monomeric protein that is phosphorylated on a histidine residue at position 15. Both proteins are involved only in phosphoryl transfer reactions and are not sugar specific. PEP autophosphorylates EI on His189, and the phosphoryl group is sequentially transferred to HPr. EII consists of three functional domains – IIA, IIB, and IIC. The organization of these domains is dependent on the specific sugar transported. In the case of glucose transport in *E. coli* (Figure 1), IIA^{Glc}, encoded by the *crr* gene, exists as a separate polypeptide, which enables it to have multiple functions. IIA^{Glc} receives a phosphoryl group at His90 from HPr and transfers the phosphoryl group to Cys421 of IIB^{Glc} which is a part of the membrane protein complex $IIBC^{Glc}$ (Figure 1). IIB^{Glc} directly donates the phosphoryl group to sugar to catalyze translocation through the membrane. IIC^{Glc} consists of multiple transmembrane helices and is likely responsible for allowing access of the sugar to IIB^{Glc} for phosphorylation and release on the inner surface of the membrane (i.e., vectorial phosphorylation). With some PTS systems in *E. coli*, the three domains are contained within a single polypeptide (e.g., mannitol) or domains IIA and IIB are in a single polypeptide, but domain C consists of two polypeptides (e.g., mannose).

Preferential Utilization of Carbohydrate

In *E. coli*, there is a preferential growth on glucose via the PTS in the presence of several sugars (diauxie). This phenomenon involves regulatory functions of the PTS with respect to transcription of a wide variety of

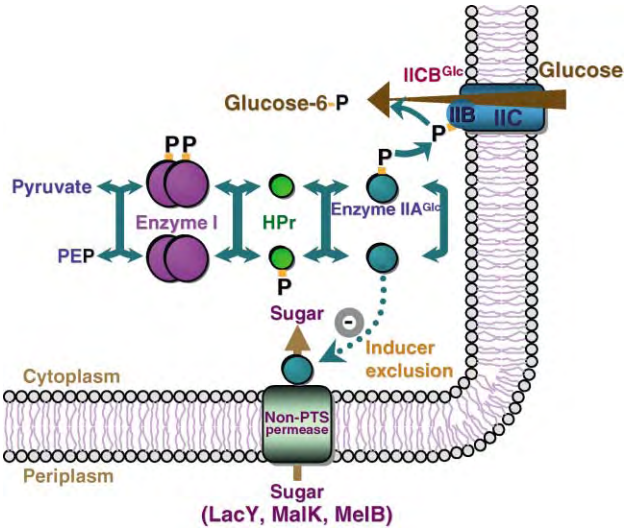

FIGURE 1 The glucose PTS system in *E. coli*. Shown is the sequence of phosphoryl transfer reaction through PEP → EI → HPr → EIIA → EIIB domain → glucose during vectorial phosphorylation across the membrane through EIIC domain. Glucose enters the cells as glucose-6-phosphate. Dephosphorylated IIA^{Glc} is able to bind to non-PTS permeases to inhibit transport of non-PTS sugars.

inducible proteins that are dependent upon cyclic-AMP (cAMP; catabolite repression), as well as regulation of the activity of endogenous levels of inducible permeases (inducer exclusion). Both regulatory activities are properties of $EIIA^{Glc}$. In the presence of glucose, the steady-state level of phosphorylated enzyme IIA^{Glc} is diminished leading to decreased adenylate cyclase activity, low intracellular levels of cAMP, and low levels of the catabolite receptor protein (CRP)-cAMP complex. Therefore, when glucose is present, transcription cannot be activated for most inducible PTS systems and non-PTS sugar permeases.

Another way to ensure preferential utilization of glucose is by inducer exclusion (Figure 1). In the presence of glucose, not only is the expression level of inducible transport systems dramatically reduced due to decreased transcription, but the activity of the non-PTS sugar permeases expressed at a basal level is inhibited by binding of unphosphorylated IIA^{Glc}. These proteins include lactose permease (LacY), melibiose permease (MelB), and MalK (a component of the maltose transport system). For example, with LacY, binding of IIA^{Glc} blocks entry of lactose and subsequent formation of allolactose, the inducer of the lactose operon.

Electrochemical Ion-Gradient-Driven Symporters

Classification

Electrochemical ion-gradient-driven symporters belong to a large and diverse superfamily, the *m*ajor *f*acilitator *s*uperfamily (MFS), members of which are found ubiquitously in all living organisms. Among the superfamilies, the sugar porter family (e.g., galactose permease (GalP) and arabinose permease (AraE)) and the oligosaccharide/proton symporter family (e.g., LacY and sucrose permease (CscB)) are two large groups involved in the bacterial sugar transport. In addition, the glycoside-pentoside-hexuronide:cation symporter family (e.g., melibiose permease (MelB)) is also responsible for transport of disaccharides.

Structural Features

Electrochemical ion-gradient-driven symporters are composed of a single polypeptide with 12 membrane-spanning helices, and for those studied intensively, a single polypeptide is able to catalyze translocation and accumulation. The X-ray structure of LacY from *E. coli* (Figure 2) provides a structural model for this family. The N-terminal six-helix and C-terminal six-helix bundles are highly symmetrical, and many of the helices are irregular. The helices are arranged so that they form a hydrophilic cavity open to the cytoplasm and closed to the periplasm, representing the inward-facing conformation. Bound sugar is located at the twofold axis of symmetry and approximately equidistant from both sides of the membrane.

Functional Properties

The sugar permeases in the MFS catalyze the transport of the mono- and disaccharides as well as their

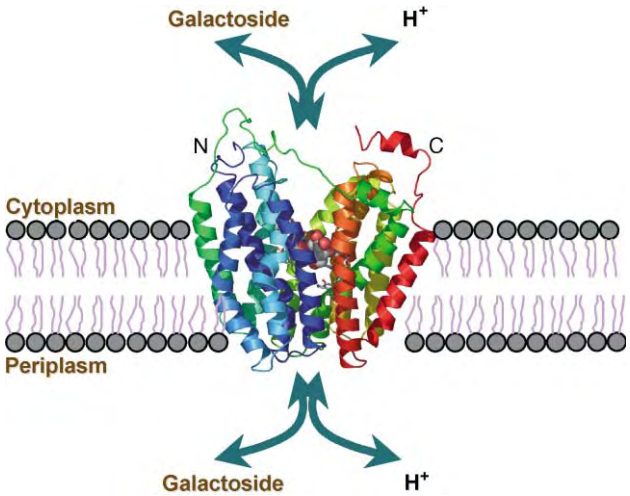

FIGURE 2 Overall structure of LacY in *E. coli*. The figure is based on the X-ray structure of the C154G mutant with a bound sugar. Ribbon representation of LacY viewed parallel to the membrane with a sugar bound in middle of the membrane at the approximate twofold axis of symmetry. As shown the protein catalyzes the stoichiometric translocation of sugar and H^+ in either direction across the membrane.

derivatives. They do not utilize ATP, but are driven by the free energy released from the energetically downhill movement of a cation (H^+ or Na^+) in response to an electrochemical ion gradient to accumulate sugar against concentration gradient. Unlike the case with the PTS, with ion-gradient-driven transport, sugar enters the cell in an unchanged form. Mechanistically and thermodynamically, it is noteworthy that MFS sugar permeases catalyze sugar/ion symport in both directions across the membrane (influx and efflux), unlike the other transport systems described.

Representatives

LacY

LacY is encoded by the *lacY* gene in the *lac* operon and consists of 417 amino acid residues. LacY is solely responsible for all the translocation reactions catalyzed by the β-galactoside system in *E. coli*. LacY is a particular well-studied representative of the oligosaccharide/proton symport family of the MFS. Like many other MFS transporters, LacY utilizes free energy released from the downhill translocation of H^+ in response to an electrochemical H^+ gradient ($\Delta\bar{\mu}_{H^+}$, interior negative and/or alkaline) to drive the stoichiometric accumulation of a galactopyranoside against a concentration gradient. In the absence of electrochemical proton gradient, LacY catalyzes the converse reaction, utilizing free energy released from downhill translocation of sugar to drive uphill stoichiometric accumulation of H^+. LacY is selective for disaccharides containing a D-galactopyranosyl ring, as well as D-galactose, but has no affinity for D-glucopyranosides or D-glucose.

By regulation of both transcription of *lacY*, as well as LacY activity by IIA^{Glc} of the PTS, *E. coli* grown in the presence of a mixture of glucose and lactose will utilize the lactose only when the glucose in the medium is completely exhausted, leading to diauxic or biphasic growth.

MelB

MelB, encoded by the *melB* gene, consists of 473 amino acid residues and is a well-studied member of the glycoside-pentoside-hexuronide:cation symporter family. A topological model indicates that the molecule contains 12-transmembrane domains with the N and C termini facing the cytoplasm, like LacY. MelB catalyzes the accumulation of galactopyranosides in *E. coli* by utilizing the free energy from the energetically downhill inward movement of Na^+, Li^+, or H^+ to drive the stoichiometric accumulation of sugar, and the symported ion is dependent on the nature of the sugar that is transported. Generally, it is believed that the α-galactosides melibiose, raffinose, and *p*-nitrophenyl-α-galactoside are transported with either H^+ or Na^+, while the β-galactosides lactose, methyl-1-β-D-galactopyranoside, or *p*-nitrophenyl-β-galactoside are symported with Na^+ but not with H^+.

Binding Protein-Dependent ATP-Binding Cassette (ABC) Transport System

Classification

Although ABC transporters are broadly distributed in archaea, prokaryotes, and eukarotes, ABC transport systems that require binding proteins for function are found only in archaea and prokaryotes. All members share the common feature that turnover involves the utilization of energy released from the hydrolysis of ATP to translocate solute across the membrane.

Structural Architecture

The binding protein-dependent ABC transporters have a common global organization with two integral membrane proteins, each of which has multiple-transmembrane helices, and two cytoplasmic proteins, each of which has one ATP-binding cassette (Figure 3). Both the integral membrane protein and the cytoplasmic ATP-binding protein may be present as homodimers or heterodimers. Both ATP-binding cassettes are required for transport activity. The X-ray structure of the vitamin B_{12} transporter $BtuFC_2D_2$ from *E. coli* provides a

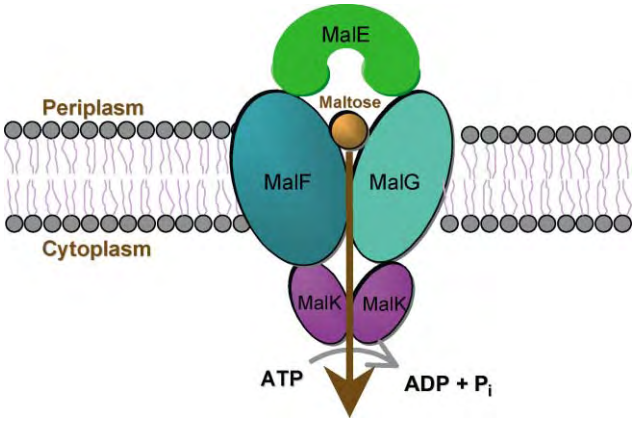

FIGURE 3 Model of MalEFGK2 complex of *E. coli*. The periplasmic binding protein MalE tightly binds to the membrane proteins MelF/MelG, delivering maltose and stimulating ATPase activity of the cytoplasmic protein MalK. The energy released from the hydrolysis of ATP drives the translocation of maltose across the membrane. The sugar enters the cells in an unchanged form.

structural example of a binding protein-dependent ABC transport complex. The two membrane-spanning subunits (BtuC) group around the translocation pathway, and the two ATP-binding cassettes (BtuD) are in close contact. In gram-negative bacteria, this family possesses periplasmic substrate-binding proteins and in gram-positive bacteria, there are membrane-bound, substrate-binding lipoproteins. Although these binding proteins have diverse specificity, the X-ray structures indicate a similar bilobate architecture composed of two symmetrical lobes surrounding the binding site.

Functional Properties

The binding protein selectively binds the substrate with high affinity and delivers it to the cognate permease. Interaction of the sugar-bound periplasmic binding protein with the membrane permease stimulates the ATPase activity of the cytoplasmic ATP-binding domains and initiates the transport process. The sugar enters the cell in an unchanged form. This system has the capacity to accumulate sugars to extremely high levels, and translocation is unidirectional.

Maltodextrin/Maltose Transport

Maltodextrin/maltose transport $MalEFGK_2$ (Figure 3), encoded by the maltose operon of *E. coli*, is the most extensively studied representative of the binding protein-dependent sugar transporters. MalE binds maltodextrin/maltose with high affinity and is the main determinant of substrate specificity. MalE releases the sugar into the MalF/MalG complex, two membrane proteins with multiple transmembrane helices through which the sugar enters into the cytoplasm of the bacterium. There are two copies of MalK, and each has a highly conserved ATP-binding cassette which is responsible for ATPase activity and a C-terminal regulatory domain for $EIIA^{Glc}$ regulation.

See Also the Following Articles

ABC Transporters • Carbohydrate Chains: Enzymatic and Chemical Synthesis • Oligosaccharide Chains: Free, *N*-Linked, *O*-Linked

Glossary

ATP-binding cassette The catalytic domain of the protein that binds ATP.

electrochemical ion gradient The electrochemical potential difference of an ion on either side of a membrane.

symporter A transporter that catalyzes the concomitant translocation of an ion and the substrate across the membrane in the same direction.

Further Reading

Abramson, J., Smirnova, I., Kasho, V., Verner, G., Kaback, H. R., and Iwata, S. (2003). Structure and mechanism of the lactose permease of *Escherichia coli*. *Science* **301**, 310–315.

Cordat, E., Mus-Veteau, I., and Leblanc, G. (1998). Structural studies of the melibiose permease of *Escherichia coli* by fluorescence resonance energy transfer: II. Identification of the tryptophan residues acting as energy donors. *J. Biol. Chem.* **273**, 33198–33202.

Duan, X., Hall, J. A., Nikaido, H., and Quiocho, F. A. (2001). Crystal structures of the maltodextrin/maltose-binding protein complexed with reduced oligosaccharides: Flexibility of tertiary structure and ligand binding. *J. Mol. Biol.* **306**, 1115–1126.

Fetsch, E. E., and Davidson, A. L. (2003). Maltose transport through the inner membrane of *E. coli*. *Front Biosci.* **8**, d652–d660.

Kaback, H. R. (1968). The role of the phospho*enol*pyruvate-phosphotransferase system in the transport of sugars by isolated membrane preparations of *Escherichia coli*. *J. Biol. Chem.* **243**, 3711–3724.

Kaback, H. R., Sahin-Tóth, M., and Weinglass, A. B. (2001). The kamikaze approach to membrane transport. *Nat. Rev. Mol. Cell Biol.* **2**, 610–622.

Locher, K. P., Lee, A. T., and Rees, D. C. (2002). The *E. coli* BtuCD structure: A framework for ABC transporter architecture and mechanism. *Science* **296**, 1091–1098.

Postma, P. W., Lengeler, J. W., and Jacobson, G. R. (1996). In *Escherichia coli and Salmonella typhimurium: Cellular and Molecular Biology* (F. C. Neidhardt, ed.) pp. 1149–1174. Am. Soc. Microbiol., Washington, DC.

Saier, Jr M. H. (2000). Families of transmembrane sugar transport proteins. *Mol. Microbiol.* **35**, 699–710.

Biography

Lan Guan, M.D., Ph.D., is a Research Associate of the Howard Hughes Medical Institute at the David Geffen School of Medicine at UCLA.

H. Ronald Kaback, M.D., is an investigator at the Howard Hughes Medical Institute, Professor in the Departments of Physiology and Microbiology, Immunology, and Molecular Genetics, and a Member of the Molecular Biology Institute at UCLA. Recently, the laboratory collaborated with So Iwata's laboratory at Imperial College, London to solve the X-ray structure of LacY. He is a member of the National Academy of Sciences and a Fellow of the American Academy of Arts and Sciences.

Glucose/Sugar Transport in Mammals

Silvia Mora and Jeffrey Pessin
State University of New York, Stony Brook, New York, USA

Glucose is the primary energy source for mammalian cells and its oxidation provides ATP under both anaerobic and aerobic conditions. Moreover, its storage as glycogen in the liver provides a ready source of glucose during states of fasting through the catabolism of glycogen and the release of glucose back into the circulation. Glycogen storage also represents the primary source of energy for muscle. In adipocytes, glucose can be converted to triglycerides, a more energetically compact fuel store that can be better metabolized to fatty acids and glycerol. Apart from being a major source of metabolic energy, glucose is also a source of structural moieties for other macromolecules including glycoproteins, proteoglycans, glycolipids, and nucleic acids. However, glucose is a highly polar molecule that is impermeable across cell membrane and therefore two specific families of mammalian glucose transporters, the sodium-dependent glucose transporters (SGLT) and the facilitative glucose transporters (GLUT), have evolved.

Sodium-Dependent Glucose Transporters

The Na^+/glucose cotransporters are responsible for the absorption of glucose against its concentration gradient by utilizing the energy generated by the electrochemical Na^+ gradient (Figure 1A). These transporters are primarily located in the brush border (apical) membranes of intestinal and kidney epithelial cells and are responsible for the absorption of glucose from the lumen of the small intestine and proximal tubule of the kidney. In the intestines, this transporter functions in the absorption of dietary glucose from the lumen and is then transported across the basolateral membrane into the circulation by the facilitative glucose transporters. Similarly, in the kidneys glucose is filtered into the lumen of the proximal tubule and is reabsorbed by the Na^+/glucose cotransporters such that under normal physiological conditions, urine is completely depleted of glucose. However, in states of insulin resistance and diabetes, the concentration of lumenal glucose may reach such high levels that it exceeds the capacity of the Na^+/glucose cotransporters to fully reabsorb the filtered glucose.

There are three different isoforms of sodium/glucose cotransporters named SGLT1, SGLT2, and SGLT3. Amino acid sequence alignments show that SGLT3 and SGLT2 have identities of 70% and 59% to SGLT1, respectively. The secondary structure model predicted for SGLT1 contains 14 transmembrane α-helices (TMH) with both the hydrophobic NH_2 terminus and the COOH terminus of TMH 14 facing the extracellular solution (Figure 2A). All SGLTs probably use the consensus N-linked glycosylation site (*N*248) between TMH 6 and 7. The predicted molecular weight of these transporters is 73 kDa with the proteins having 659–672 amino acids. The major differences in function between SGLT1 and SGLT2/SGLT3 resides in the selectivity for sugar transport. SGLT1 accepts the natural sugars D-glucose and D-galactose with comparable affinities and a variety of synthetic sugars such as 3-*O*-methyl-D-glucose. SGLT2 and SGLT3 are much more restrictive in that they prefer D-glucose to D-galactose or 3-*O*-methyl-D-glucose. The affinity of SGLT1 for D-glucose is tenfold higher than that of SGLT2 or SGLT3.

Facilitative Glucose Transporters

The facilitative glucose transporters comprise a relatively large family of structurally related proteins that are encoded by distinct genes and are expressed in an overlapping yet tissue-specific manner (Table I). All the facilitative glucose transporters are predicted to have 12 membrane-spanning domains and allow for the stereospecific transport of glucose through the lipid bilayer. The transport of glucose is energy-independent and is solely driven by the relative glucose concentration across the plasma membrane (Figure 1B). Since under most conditions, the cytoplasmic glucose is rapidly phosphorylated by hexokinase or glucokinase, the relative levels of intracellular glucose are compared to the extracellular concentration resulting in net inward flux of glucose. However, in some instances glucose can be

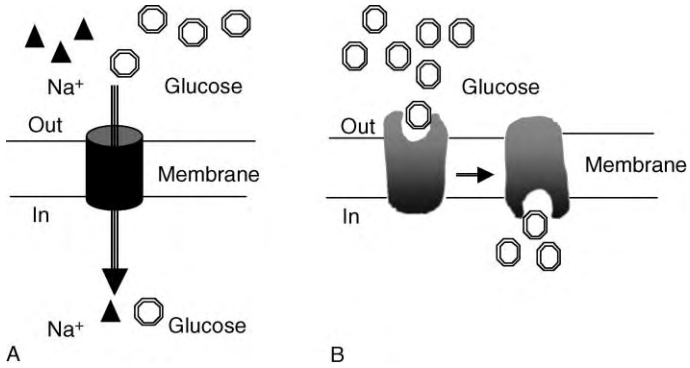

FIGURE 1 Distinct glucose transport mechanisms in mammalian cells: (A) sodium-glucose cotransport and (B) facilitative diffusion.

secreted into the circulation under normal physiological conditions. For example, in hepatocytes facilitative glucose transporters participate in the uptake of glucose from the portal circulation following a meal and in the release of glucose generated by glycogenolysis or glucogenesis in the postabsorptive state and during fasting.

Currently, there are 12 identified facilitative glucose transporters in mammalian cells, with GLUT1, GLUT2, GLUT3, GLUT4, GLUT8, and GLUT9 established as functional facilitative glucose transporters. GLUT5 is primarily a fructose transporter and the other isoforms have only been identified based upon amino acid sequence homology. Each of these transporters have distinct but overlapping tissue distributions, which underscores their specific physiologic function. For example, GLUT1 is generally expressed and is thought to be responsible for the basal uptake of glucose. GLUT2 is predominantly expressed in the liver and pancreatic β-cells where it functions as part of a sensor-mediating hepatic glucose output during states of fasting and insulin secretion in the postprandial absorption state. In contrast, neurons primarily express the relatively high-affinity GLUT3 isoform necessary to maintain high rates of glucose metabolism for energy production. GLUT8 appears to provide important function during early embryogenesis, whereas GLUT4 is exclusively expressed in insulin responsive tissues, adipose, and striated muscle. These latter tissues provide the key functional elements responsible for the insulin stimulation of glucose uptake and are key targets for dysregulation in states of insulin resistance and diabetes. The latest GLUT member identified, GLUT14, is present in the testis and seems to have evolved from a gene duplication of GLUT3.

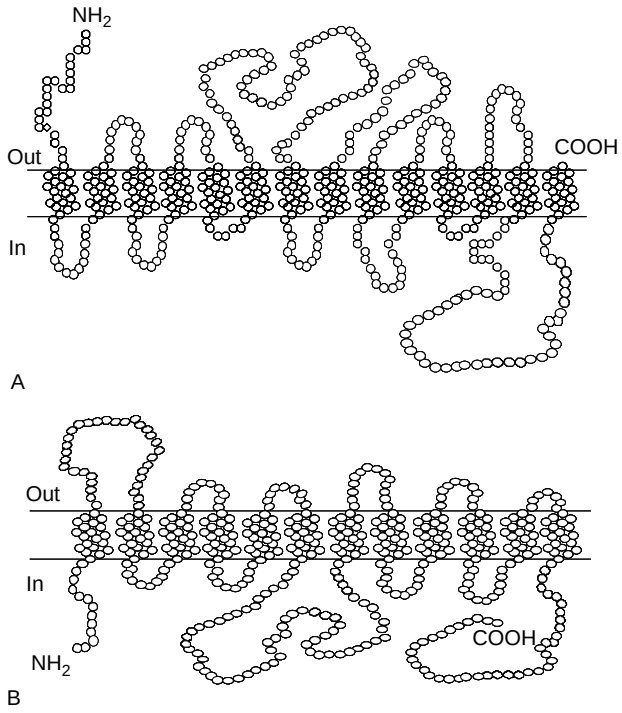

FIGURE 2 Predicted structure of glucose transporters: (A) SGLT-1 and (B) GLUT-1.

GLUT1

GLUT1 was originally identified as the erythrocyte-type facilitative glucose transporter and was the first isoform to be purified and eventually cloned. The amino acid sequence of GLUT1 is highly conserved among different species (i.e., 98% identity between human and rat). Computer analysis of the primary sequence of GLUT1 has revealed that GLUT1 is a hydrophobic protein, with ~50% located within the lipid bilayer. Several lines of evidence have supported a structural model for GLUT1 that consists of 12-membrane-spanning α-helical segments and an intracellular located NH_2 and COOH termini. According to this model a large intracellular segment of 33 amino acids connects transmembrane domains M1 and M2, and an extremely hydrophilic intracellular segment of 65 amino acids joins M6 and M7. Short regions of 7–14 amino

TABLE I

Mammalian Facilitative Sugar Transporters

Isoform	Tissue distribution	Function
GLUT-1	Brain, endothelial cells, placenta, erythrocyte, mammalian gland	Basal transport, transport in fetal tissues
GLUT-2	Liver, small intestine, pancreatic cells, kidney	Basolateral transport in epithelial cells, glucose release form liver
GLUT-3	Neurones Placenta	Basal transport
GLUT-4	Muscle, heart, white and brown adipose tissue	Insulin-stimulated glucose transport
GLUT-5	Small intestine, kidney, testis and sperm	Fructose transporter
GLUT-6	Spleen, leukocytes, brain	Unknown
GLUT-7	Unknown	Unknown
GLUT-8	Testis, blastocyst, brain	Unknown
GLUT-9	Liver, kidney	Unknown
GLUT-10	Liver, pancreas	Unknown
GLUT-11	Heart, muscle	Unknown
GLUT-12	Heart, prostate	Unknown
GLUT-13	Unknown	Unknown
GLUT-14	Testis	Unknown

acids connect the remaining membrane-spanning regions. There are two potential N-linked glycosylation sites in GLUT1 at Asn-45 and Asn-411, but only the former site in the large extracellular loop has been shown to be glycosylated (Figure 2B). Although other models have been proposed, structural analysis of GLUT1 topography has confirmed the originally proposed 12-transmembrane-spanning model. The other members of the glucose transporter family are similar in size (between 492 and 524 amino acids) and all are predicted to maintain the 12-transmembrane-spanning structure, although the sites of glycosylation and length of the different intracellular and extracellular loops appear to vary (Table I).

GLUT1 is highly expressed in placenta, brain, epithelial cells of the mammary gland, transformed cells, and fetal tissues. Because of its ubiquitous expression it has been proposed that GLUT1 might be responsible, at least in part, for basal glucose uptake. Kinetic studies in erythrocytes have demonstrated that GLUT1 has a K_m of ~2 mM for D-glucose, whereas the K_m is greater than 3 M for L-glucose. In addition, it has been postulated that GLUT1 functions in either a dimeric or tetrameric oligomeric state. This appears to account for the various kinetic properties of glucose transport and, in addition to expression levels and localization, provides another level of control of transporter function.

GLUT2

The low-affinity GLUT2 facilitative glucose transporter functions in the β-cells of the pancreas to transport glucose in direct proportion to the circulating glucose concentration. This transporter functions in concert with glucokinase such that small increases in glucose influx can signal changes in the ATP/ADP ratio, resulting in a highly sensitive mechanism regulating insulin secretion. The central importance of GLUT2 in the regulation of pancreatic insulin secretion was established with the identification of a patient expressing a defective GLUT2 mutation. This transporter also functions in the liver to allow for shuttling of increased glucose load into glycogen. GLUT2 also appears to play a significant role in the reabsorption of filtered glucose in the kidney and in the basolateral transport of glucose from the digestive tract epithelium into the circulation.

GLUT3

GLUT3 was originally isolated from a fetal skeletal muscle library but is not significantly expressed in adult muscle. This isoform is primarily expressed in the brain (astrocytes), but it has also been detected in placenta endothelial cells and in human skeletal muscle. Recently, it has also been detected in human condrocytes. The localization of this transporter is in the plasma membrane.

GLUT4

In 1989, five research groups independently cloned the insulin-responsive glucose transporter isoform GLUT4. This isoform is predominantly expressed in striated muscle (skeletal and cardiac) and adipose tissue (white and brown), the major tissues that display insulin-stimulated glucose uptake. Sequence analysis of GLUT4 suggests that its secondary structure and orientation in the plasma membrane is similar to GLUT1 with an overall 65% amino acid identity.

In contrast to the other glucose transporters under basal conditions GLUT4 is predominantly localized intracellularly. The primary mechanism responsible for the increase in glucose uptake in insulin-sensitive tissues upon insulin treatment is the recruitment or translocation of glucose transporters from these intracellular storage sites to the plasma membrane. Although the molecular mechanisms that regulate GLUT4 translocation are poorly understood, the trafficking of the GLUT4 protein has several similarities with the trafficking, docking, and fusion of synaptic vesicles in neurons responsible for neurotransmitter release.

The long-term expression of the GLUT4 gene is also controlled during development and during various hormonal, nutritional, and metabolic states. For example, fetal tissues contain very little GLUT4 and expression of this transporter increases after birth. In addition, during states of insulin deficiency such as fasting and following destruction of the insulin secreting β-cells by streptozotocin (STZ)-induced diabetes, GLUT4 expression levels are severely reduced in adipose, heart, and skeletal muscle. Similarly, obesity, high-fat feeding, and muscle denervation also result in a decrease in GLUT4 expression and subsequent insulin resistance. In contrast, GLUT4 is up-regulated, by exercise training, thyroid hormone treatment, and insulin therapy, treatments that increase insulin sensitivity.

GLUT5

The GLUT5 fructose transporter is highly conserved among species with a 69–88% amino acid identity between mice, human, rat, and rabbit. In mice, expression is highest in small intestine, kidney, and testis. In humans, it is also present in skeletal muscle. Studies in rats and rabbits have shown that the expression of this transporter is highest in the upper part of the small intestine (duodenum and proximal jejunum). Expression of GLUT5 in the intestine is highly regulated, showing circadian rhythm, dependence on dietary fat and carbohydrate content, and insulin levels.

GLUT6

The GLUT6 gene encodes a cDNA which exhibits significant sequence similarity with the other members of the glucose transporter family, particularly GLUT8. GLUT6 protein has been detected in spleen, peripheral leucocytes, and brain. When heterologously expressed in 3T3L1 adipocyte cells this transporter is localized intracellularly, but unlike GLUT4 does not translocate to the plasma membrane in response to insulin.

GLUT7

GLUT7 is an uncharacterized protein. The pattern of expression of this gene and the transport substrate specificity of the protein are currently unknown. However, the genomic sequence of GLUT7 is 59% similar to that of GLUT5.

GLUT8

GLUT8, previously known as GLUTX1, is a newly characterized glucose transporter isoform that is expressed at high levels in the testis and brain and at lower levels in several other tissues. In the brain GLUT8 is expressed in the neuronal cell bodies of excitatory and inhibitory neurons in the rat hippocampus. It was found in hippocampal and dentate gyrus neurons as well as in amygdala and primary olfactory cortex. In these neurons, its location was close to the plasma membrane of cell bodies and sometimes in proximal dendrites. High GLUT8 levels were detected in the hypothalamus, supraoptic nucleus, median eminence, and the posterior pituitary. In the testis, it is found in differentiating spermatocytes of type 1 stage and in the acrosomal region it is found in mature spermatozoa.

GLUT9–14

Other than sequence analysis and tissue distribution of mRNA expression, little information is available about the function and properties of GLUT9–14. GLUT9 has a high-sequence similarity to the fructose transporter GLUT5 and is mainly expressed in kidney and liver. GLUT10 is primarily expressed in human heart, lung, brain, liver, skeletal muscle, pancreas, placenta, and kidney. GLUT11 gene has two splice variants and is most abundant in skeletal muscle and heart. GLUT12 is expressed in heart, prostate and has also been detected in breast cancer cells and in epithelial cells of rat mammary gland during pregnancy and lactation. The tissue distribution of GLUT13 is unknown and GLUT14 is expressed in the testis.

See Also the Following Articles

Gluconeogenesis • Glycogen Metabolism • Insulin- and Glucagon-Secreting Cells of the Pancreas • Membrane Transport, General Concepts • Sugar Nucleotide Transporters

Glossary

insulin resistance A state in which the same concentration of insulin elicits a decreased biological response compared to normal conditions.

isoform A protein with similar amino acid sequence and same function.

splice variant Different mRNA sequences that originate from the same gene.

Further Reading

Holloszy, J. (2001). A forty-year memoir of research on the regulation of glucose transport into muscle. *Am. J. Physiolo. Endocrinol. Metab.* **284**, E453–E467.

Joost, H., and Thorens, B. (2001). The extended GLUT family of sugar/polyol transport facilitators: Nomenclature sequence characteristics and potential function of its novel members. *Mol. Memb. Biol.* **18**, 247–256.

Koistinen, H., and Zierath, J. (2003). Regulation of glucose transport in human skeletal muscle. *Ann. Med.* **34**, 410–418.

Watson, R., and Pessin, J. (2001). Subcellular compartmentalization and trafficking of the insulin-responsive glucose transporter, GLUT4. *Exp. Cell Res.* **15**, 75–83.

Wright, E. (2001). Renal sodium-glucose cotransporters. *Am. J. Renal. Physiol.* **280**, F10–F18.

Biography

Jeffrey E. Pessin is a Professor in and Chair of the Department of Pharmacological Sciences at the State University of New York in Stony Brook. His research interests include the molecular mechanisms of insulin action, intracellular signaling, and the regulation of glucose transport in muscle and adipose tissue.

Silvia Mora is an Assistant Professor in the Division of Biology, Kansas State University. Her interests are focused on the intracellular trafficking of GLUT4 and the regulated secretion of adipokines.

Glutamate Receptors, Ionotropic

Derek B. Scott and Michael D. Ehlers
Duke University Medical Center, Durham, North Carolina, USA

Ionotropic glutamate receptors (iGluRs) are ion channels that respond to the amino acid neurotransmitter L-glutamate—the major excitatory neurotransmitter in the mammalian nervous system. Localized to excitatory synapses, iGluRs mediate a net influx of positively charged ions into the postsynaptic cell when activated by glutamate that is released from presynaptic terminals. The net influx of positive ions through iGluRs raises the membrane potential of the postsynaptic cell, thus increasing neuronal excitability and making it more likely that an action potential will be initiated. The combination of ligand activation and channel gating in the same protein complex enables iGluRs to directly convert chemical presynaptic signals to electrical responses in the postsynaptic neuron. In addition to mediating synaptic transmission, iGluRs play important roles in synapse formation during brain development, in synaptic plasticity during learning and memory, and in many neurological diseases. Thus, much focus has been given to understanding the biophysical properties—the structure, pharmacology, and physiology—of these glutamate-gated channels.

Ionotropic Glutamate Receptor Subtypes

Ionotropic glutamate receptors (iGluRs) are a family of receptors comprised of three related ion channel types: α-amino-3-hydroxy-methyl-4-isoxazole (AMPA) receptors, kainate receptors, and *N*-methyl-D-aspartate (NMDA) receptors. These three iGluR subtypes are named after specific agonists that selectively activate each channel type, namely AMPA, kainate, or NMDA. A fourth iGluR subtype, termed delta, is an "orphan" subtype as it does not form functional ion channels and has unknown cellular functions. Although these glutamate-gated channels have distinct physiological and pharmacological properties, they share structural similarities (Figure 1).

Ionotropic Glutamate Receptor Structure

Current evidence indicates that iGluRs are tetramers formed by the assembly of four integral membrane protein subunits (Figure 1A). These subunits, unique to each iGluR subtype, were initially isolated using expression cloning techniques and share similar structural and topological properties. There are 18 known mammalian iGluR subunits that together make a gene family (Table I). A typical iGluR subunit consists of an extracellular amino-terminal domain (NTD), a ligand-binding domain (S1–S2), four membrane domains including three transmembrane segments (M1, M3, and M4) and one re-entrant pore loop (M2), and an intracellular carboxyl-terminal domain (Figure 1B).

Extracellular and Ligand-Binding Domains

The large extracellular domains of iGluRs share sequence and structural homology with bacterial amino-acid-binding proteins. The NTD at the distal amino terminus participates in subunit assembly, whereas the S1–S2 domains together form a cleft where ligands, including L-glutamate, bind and activate the opening of the channel (Figure 1B). Crystal structures of iGluR S1–S2 domain bound to ligands have revealed that the relative movements of the S1 and S2 segments are critical parameters during iGluR activation. At rest, the ligand-binding cleft is in an open conformation, while ~20° cleft closure occurs following ligand binding that results in full channel activation.

Pore Structure

In addition to an S1–S2 ligand-binding site, each subunit within the tetrameric complex also contributes a polypeptide sequence (the M2 pore-loop) that lines the channel pore (Figures 1B and 1C). The channel pore segments share common structural signatures across the family of iGluRs that are similar to and have been found to be evolutionarily conserved in K^+ channels. This has allowed researchers to model the structure of the iGluR M2 pore-loop domain using the crystal structure of the P-loop pore domain of K^+ channels. The M2 pore-loop domain of iGluRs is believed to be composed of two parts, a short α-helix and a random-coil domain

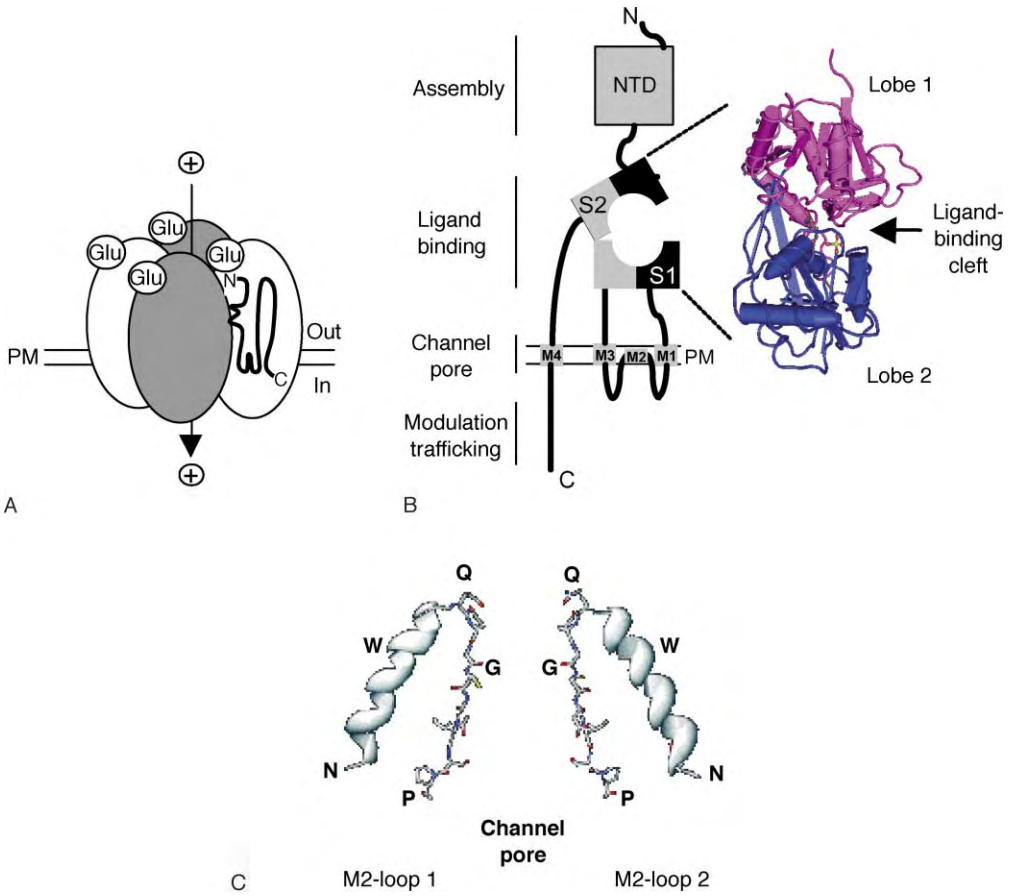

FIGURE 1 Structural features of iGluRs. (A) All iGluRs are heterotetramers formed by the regulated assembly of transmembrane subunits. Upon glutamate binding, a conformational change opens the channel pore leading to a net influx of positive ions into the postsynaptic neuron. PM designates the plasma membrane, Glu designates glutamate. (B) iGluR subunits have a modular domain organization including (1) a large extracellular amino-terminal domain (NTD), (2) a two-segment extracellular ligand-binding domain (S1–S2), (3) a membrane domain consisting of three transmembrane segments (M1, M3, and M4) and a re-entrant loop whose residues form the channel pore (M2), and (4) an intracellular C-terminal domain. The crystal structure of the S1–S2 ligand-binding domain is shown in an enlarged form as a ribbon diagram. Ligands such as L-glutamate bind to the ligand-binding cleft between the two lobes (lobe 1 and lobe 2) that are formed by the S1 and S2 domains. Domains are not drawn to scale. S1–S2 structure courtesy of E. Gouaux and can be viewed at the Molecular Modeling Database, NCBI, National Library of Medicine. MMDB# 21762 or PDB# 1MM6. (Reproduced from Armstrong, N., Sun, Y., Chen, G. Q., and Gouaux, E. (1998). Structure of a glutamate-receptor ligand-binding core complex with kainate. *Nature* **395**, 913–917, with permission.) (C) The proposed structure of the iGluR channel pore. The structure of the M2 pore-loop domain of iGluRs was modeled using the crystal structure of the highly homologous P-loop region in K^+ channels. A side view of the modeled iGluR channel pore composed of two M2 pore-loop domains is shown. The M2 pore-loop domain is ~23 amino acids long and begins as an ascending α-helix (N) that quickly becomes a random coil structure. A tryptophan residue (W) within the ascending α-helix, a glycine (G) residue within the channel pore and a proline (P) residue at the end of the M2 pore-loop together constitute the WGP signature that represents the minimal structural conservation between iGluR and K^+channel pore loops. The last residues within the α-helical region of the M2 pore-loop domain (Q) achieve ion selectivity. (Reproduced from Kuner, T., Seeburg, P. H., and Guy, H. R. (2003). A common architecture for K^+ channels and ionotropic glutamate receptors? *Trends Neurosci.* **26**, 27–32, with permission from Elsevier.)

(Figure 1C). Ion selectivity is determined by residues located immediately after the α-helical portion of M2. Constriction of the pore is achieved by several residues that span the end of the α-helical portion and beginning of the random coil domain of M2.

Intracellular Domain

Much less structural information is available on the carboxyl-terminal domains of iGluRs, which vary greatly in size and sequence between the different iGluR subunits. This intracellular domain is subject to protein phosphorylation and participates in numerous protein interactions that regulate iGluR channel activity and intracellular trafficking.

Ionotropic Glutamate Receptor Subunits and Molecular Diversity

Although all iGluRs are activated by L-glutamate and share structural similarities, each channel type has

TABLE I

Molecular Diversity of Ionotropic Glutamate Receptor Subunits

Receptor	Subunits	Assemblies	Molecular diversity/alternative isoforms
AMPA	GluR1 GluR2 GluR3 GluR4	• Homomeric assemblies between all subunits observed • GluR2 heteromers predominate *in vivo*	GluR1–4: flip/flop: 38 aa sequence near M4 GluR2 and GluR4: splicing yields 2 different intracellular C termini (short and long) GluR2: RNA edited in pore domain (Q/R) GluR2–4: RNA edited in S2 domain (R/G)
Kainate	GluR5 GluR6 GluR7 KA1 KA2	• Homomeric GluR5–7 observed • KA1–2 do not form homomeric channels	GluR5: splicing yields 4 different intracellular C termini GluR5 and GluR6: RNA edited in pore domain (Q/R) GluR6: RNA edited in M1 domain at 2 sites GluR6: splicing yields 2 different intracellular C termini GluR7: splicing yields 2 different intracellular C termini
NMDA	NR1 NR2A NR2B NR2C NR2D NR3A NR3B	Strict heteromer: NR1/NR2 heteromers most abundant, also NR1/NR2/NR3 NR1/NR3	NR1: alternative splicing of 5 aa near N terminus NR1: splicing yields 4 different intracellular C termini NR1: total of eight different splice variants
Orphan receptors	δ1 δ2	Unknown	Unknown A spontaneous mutation in δ2 forms functional channels in *lurcher* mice

Abbreviations: aa, amino acid; Q/R, glutamine/arginine; R/G, arginine/glycine.

unique pharmacological and physiological properties. The varied functional properties of iGluRs arise from the molecular diversity of the protein subunits that assemble to form AMPA receptors, kainate receptors, or NMDA receptors (Table I).

AMPA Receptors

AMPA receptors are composed of four subunits (GluR1–4) that are encoded by four different genes (Table I). Animals with targeted disruptions of AMPA receptor subunit genes are severely impaired in basal excitatory synaptic transmission, are unable to induce activity-dependent changes in synaptic transmission, and have memory defects in spatial learning tasks. All AMPA receptor subunits are capable of homotetrameric assembly to form functional channels. However, heterotetrameric combinations containing GluR2 subunits predominate *in vivo*.

Tetrameric combinations of GluR1–4 give rise to AMPA receptors with distinct properties and regulation. Additional molecular diversity within AMPA receptor subunits is achieved by mRNA splicing and RNA editing. Alternate mRNA splicing of exon 14 and 15 includes or excludes a 38-amino-acid segment termed the "flip/flop site" near the beginning of M4 in the S2 segment that regulates channel properties (Table I). This splicing event is developmentally regulated as flip-containing subunits predominate in very young animals, while flip- and flop-containing subunits are expressed at the same level in adults. Alternative mRNA splicing at the C terminus of GluR2 or GluR4 subunits gives rise to splice forms that possess either short or long intracellular domains. These different intracellular domains regulate intracellular trafficking and targeting of GluR2- or GluR4-containing AMPA receptors to synaptic sites. In addition, RNA editing of the mRNA encoding GluR2 subunits results in replacement of a

glutamine (Q) residue with an arginine (R) residue within the M2 pore-loop domain (termed the Q/R site). The editing of GluR2 subunits is very significant since AMPA receptors containing unedited GluR2 subunits are Ca^{2+} permeable, while those containing normal edited versions cannot flux Ca^{2+} ions. The regulated influx of Ca^{2+} into postsynaptic neurons triggers synaptic plasticity and other long-lasting changes in synaptic efficacy, and if excessive can lead to neurotoxic effects including cell death. Quite strikingly, animals that completely fail to edit GluR2 subunits are nonviable, while others that can only edit half of their complement of GluR2 develop seizures. As these observations suggest, the majority of GluR2 subunits *in vivo* are edited at the Q/R site. RNA editing also occurs at other sites within AMPA receptor subunits (Table I), causing more subtle changes in channel physiology.

Kainate Receptors

Unlike AMPA receptors and NMDA receptors, kainate receptors are located at both presynaptic and postsynaptic sides of the synapse, where they modulate presynaptic neurotransmitter release as well as synaptic transmission. Kainate receptors are composed of five subunits (GluR5–7, KA1–2), each encoded by a separate gene (Table I). Various homomeric and heteromeric combinations of kainate receptor subunits give rise to functional receptors with very different properties. For example, GluR5–7 homomeric receptors (low-affinity subunits) have a tenfold lower affinity to L-glutamate than KA1–2-containing receptors (high-affinity subunits). KA1–2 subunits do not form homomeric receptors and must assemble with GluR5–7 subunits to form functional channels.

Much like the AMPA receptor GluR2 subunits, mRNAs encoding GluR5 and GluR6 undergo RNA editing at the Q/R site (Table I). In addition, GluR6 subunits undergo RNA editing at two other sites within the M1 segment that also influence Ca^{2+} permeability. Unedited GluR5 and GluR6 are more abundant during embryonic development, while edited subunits predominate in adults. Alternative splicing of intracellular C-terminal domains yields multiple GluR5 (A–D), GluR6 (A–B), and GluR7 (A–B) subunits; however, the functional significance of these splicing events is still unknown.

NMDA Receptors

NMDA receptor subunits fall into three separate groups—NR1, NR2, and NR3. NR1 subunits are encoded by a single gene; NR2 subunits are encoded by four genes (NR2A–D); and NR3 subunits are encoded by two genes (NR3A–B) (Table I). NR1 and NR2B subunits are essential, as animals containing targeted disruptions in the genes encoding either subunit die from respiratory and feeding deficits soon after birth. In contrast, animals with NR2A-, 2C-, 2D-, or NR3-targeted disruptions are viable, but display deficiencies in synaptic plasticity and neuronal development. Unlike AMPA and kainate receptors, NMDA receptors are strict heteromers that require the assembly of NR1 subunits with either NR2 or NR3 subunits to form functional channels. NR1 is expressed in almost all neurons in the brain and spinal cord, while the expression of NR2 and NR3 subunits is spatially restricted and developmentally regulated.

Alternative splicing generates eight different NR1 splice variants that differ in the presence or absence of a small five-amino-acid segment near the N terminus (N1), a 21 amino-acid sequence in the middle portion of the carboxyl terminus (C1), and two alternate ending sequences at the very distal carboxyl terminus (C2 and C2′) (Table I). Splicing at the N1 site regulates channel sensitivity to allosteric modulators (e.g., polyamines and Zn^{2+}). Splicing at the C1 and C2/C2′ sites generates receptors with unique trafficking signals that regulate the speed and efficiency of synaptic delivery of NMDA receptor complexes.

Orphan (δ) Receptors

Two orphan receptors (δ1–2) share considerable sequence homology with other iGluRs, but fail to form functional glutamate-gated channels when expressed alone or in combination with other iGluR subunits. However, spontaneous mutations of δ2—*hotfoot* and *lurcher* mutant mice—cause ataxia and impaired synaptic plasticity by transforming quiescent δ2-containing receptors into functional channels.

Ionotropic Glutamate Receptor Pharmacology and Physiology

An important step in studying the physiological properties of iGluRs *in vivo* has been the development of unique agonists and antagonists that specifically activate or inhibit distinct types of iGluRs. A limited list of the most commonly used pharmacological agents used to activate or inhibit iGluRs is presented in Table II. Each type of iGluR has distinct channel properties—including ligand affinity, ionic permeability, channel conductance, and gating kinetics—that are determined by subunit composition. Table III includes some of the physiological characteristics of AMPA receptor, kainate receptor, and NMDA receptor synaptic responses and single channel properties, illustrating the diverse properties of the different iGluRs.

TABLE II

Ionotropic Glutamate Receptor Pharmacology

Receptor	Agonists	Activation of channels (EC_{50})	Antagonists and mode of action
AMPA	• Glutamate • AMPA • Kainate[a]	• L-glutamate (450–600 μM) • AMPA (3–5 μM) • Kainate (50–60 μM)	CNQX and NBQX: competitive inhibitors GYKI53655: noncompetitive inhibitor
Kainate	• Glutamate • Kainate	• L-glutamate (500–6000 μM) • Kainate (6–33 μM) • AMPA (2000 μM)	CNQX: competitive inhibitor LY382884: GluR5-specific inhibitor
NMDA	• Glutamate • Glycine[b] • NMDA	• L-glutamate (0.4–1.8 μM) • Glycine (0.1–2.1 μM) • Depolarization of membrane to release Mg^{2+} block	Mg^{2+}: channel pore blocker at resting potential AP5: competitive inhibitor MK801: channel pore blocker

EC_{50} is the concentration of agonist that evokes a half-maximal activation. These values were determined for peak responses of recombinant receptors in heterologous cells.

[a] Nondesensitizing agonist for AMPA receptors.

[b] Coagonist.

AMPA Receptor Physiology

Activated AMPA receptors carry most of the ionic current into postsynaptic neurons following presynaptic glutamate release, and therefore mediate most of the fast excitatory neurotransmission in the brain. GluR2-containing AMPA receptors are permeable to Na^+ and K^+ ions, while AMPA receptors lacking GluR2 also flux Ca^{2+} ions. AMPA receptor currents have rapid kinetics (Table III); channels open rapidly with a very high probability ($P_o = 0.4–1.0$), deactivate rapidly (dissociation of ligand from agonist binding site), desensitize rapidly (closing of channel in the presence of agonist), and recover fully from desensitization in about 100 ms. Once gated, individual AMPA channels have several conductance states ranging from 4 to 24 pS, depending upon the exact subunit composition of the AMPA receptor complex studied. GluR2-containing channels possess a linear current–voltage (*I/V*) relationship over a wide range of membrane potentials. On the other hand, channels lacking GluR2 do not have a linear *I/V* relationship, but rather are inwardly rectified (preferentially pass current at negative membrane potentials). Determining the *I/V* relationship of AMPA receptor currents is thus a common technique to reveal subunit composition *in vivo*.

Kainate Receptor Physiology

Kainate receptor-mediated currents are similar to those of AMPA receptors (Table III), but do not contribute nearly as much to excitatory neurotransmission. Like AMPA receptors, kainate receptors have fast activation

TABLE III

General Characteristics of Ionotropic Glutamate Receptor Physiology

Receptor	Ions in[a]	Ions out[b]	Activation kinetics (τ)[b] (ms)	Open times (ms)	Deactivation (ms)	Desensitization (ms)	Single channel conductance (pS)
AMPA	Na^+	K^+	Very fast 0.2–0.4	0.14–3.3	0.6–1.1	0.8–8.1	Multiple states 4–24
Kainate	Na^+	K^+	Very fast 0.2–0.4	0.3–2.1	2.5	1.4–9	Multiple states 0.2–25
NMDA	Na^+ Ca^{2+}	K^+	Slow 10–50	0.06–8	33–4400	650–750	Multiple states 17–75

Ranges are presented because there are different values for different subunit compositions. For measurements of specific subunit combinations see Dingledine, R., Borges, K., Bowie, D., and Traynelis, S. F. (1999). The glutamate receptor ion channels. *Pharmacol. Rev.* **51**, 7–61.

ms = milliseconds; pS = picosiemens.

[a] Assuming a resting membrane potential of −70 mV.

[b] Kinetic and channel conductance measurements are reported following a brief application of glutamate (AMPA and kainite receptors) or glutamate plus glycine (for NMDA receptors).

kinetics with high probabilities ($P_o = 0.5–1.0$), similar open times, deactivation and desensitization kinetics, and are permeable primarily to Na^+ and K^+ (Table III). However, kainate receptors recover slowly following glutamate-induced desensitization (20-fold slower than AMPA receptors; ~2000 ms), and some kainate receptors (GluR5 homomers) have very small single-channel conductances (as low as 0.2 pS). As with AMPA receptors, a range of single channel conductances has been measured depending on the exact subunit composition of the kainate receptor complex studied.

NMDA Receptor Physiology

NMDA receptors possess a number of properties unique among the iGluRs. They are highly permeable to Ca^{2+} ions, have much slower activation kinetics, and remain open much longer than either AMPA or kainate receptors (Table III). Although glutamate binding is sufficient to open AMPA or kainate receptors, three separate events must occur for NMDA receptor activation—the binding of glutamate, the binding of the coagonist glycine, and a large enough membrane depolarization to remove Mg^{2+} ions that at resting membrane potentials enter and block the channel pore (Table II). This dual requirement for ligand binding and membrane depolarization allows NMDA receptors to act as "coincidence detectors" of simultaneous presynaptic and postsynaptic activity—presynaptic activity represented by glutamate present in the synaptic cleft and postsynaptic activity reflected by membrane depolarization. Since both AMPA and NMDA receptors colocalize at excitatory synapses, AMPA receptor activation is often critical for activation of synaptic NMDA receptors. Concurrent or repetitive glutamate release in conjunction with AMPA receptor activation can depolarize the postsynaptic cell to a level at which the Mg^{2+} block of NMDA receptors is lifted, thereby allowing Ca^{2+} influx through NMDA receptors into the postsynaptic cell.

Tight regulation of NMDA receptor activation is essential for brain function. Under normal physiological conditions, Ca^{2+} influx through NMDA channels triggers intracellular pathways that alter synaptic efficacy. Such synaptic plasticity modifies neural circuits during learning and memory. Excess Ca^{2+} influx through NMDA receptors causes neurotoxic effects (termed excitotoxicity) that contribute to neuron loss in stroke, epilepsy, and neurodegenerative diseases. Like AMPA and kainate receptors, different subunit combinations lead to differences in channel properties. Specifically, NR2B-containing channels are open much longer than NR2A-containing channels, resulting in a prolonged influx of Ca^{2+} ions. The more recently identified NR3 subunits are believed to attenuate NMDA receptor responses by decreasing single-channel conductance and lower Ca^{2+} permeability.

Summary

iGluRs are the major excitatory neurotransmitter receptor in the mammalian central nervous system. They comprise a diverse family of ligand-gated ion channels that flux cations across the plasma membrane in response to glutamate binding. All iGluRs share similar structural features including oligomeric assembly from four subunits. Three major subtypes of iGluR are expressed in the brain—AMPA receptors, kainate receptors, and NMDA receptors—each with separate sets of subunits, unique pharmacologies, and distinct channel properties. Functionally, iGluRs conduct synaptic transmission and play a central role in synaptic plasticity, neural development, and neurologic disease.

See Also the Following Articles

Glutamate Receptors, Metabotropic • Ligand-Operated Membrane Channels: Calcium (Glutamate)

Glossary

agonists/antagonists Pharmacological agents that activate/inhibit receptor activation.

alternative splicing The generation of multiple mRNAs from a single gene by the combination of different sets of exons during mRNA processing.

coincidence detection Concurrent postsynaptic membrane depolarization (that removes Mg^{2+} block of NMDA receptors) and presynaptic glutamate release (that binds to and gates NMDA receptors) that is required for full NMDA receptor activation.

excitotoxicity Neuronal cell death due to an inappropriate or extremely strong activation of iGluRs.

synaptic plasticity Long-lasting changes in synaptic responses following repeated stimulation of excitatory synapses that lead to either stronger excitatory postsynaptic currents (long-term potentiation) or weaker excitatory postsynaptic currents (long-term depression) often by modulating the number or properties of postsynaptic AMPA receptors.

Further Reading

Aidley, D. J., and Stanfield, P. R. (1996). *Ion Channels Molecules in Motion.* Cambridge University Press, United Kingdom.

Armstrong, N., Sun, Y., Chen, G. Q., and Gouaux, E. (1998). Structure of a glutamate-receptor ligand-binding core complex with kainate. *Nature* **395**, 913–917.

Dingledine, R., Borges, K., Bowie, D., and Traynelis, S. F. (1999). The glutamate receptor ion channels. *Pharmacol. Rev.* **51**, 7–61.

Hammond, C. (2001). *Cellular and Molecular Neurobiology.* 2nd edition, Academic Press, London.

Hille, B. (2001). *Ionic Channels and Excitable Membranes*, 3rd edition, Sinauer Associates, Sunderland, MA.

Johnston, D., and Wu, S. M. (1997). *Foundations of Cellular Neurophysiology*. The MIT Press, London.

Kuner, T., Seeburg, P. H., and Guy, H. R. (2003). A common architecture for K^+ channels and ionotropic glutamate receptors? *Trends Neurosci.* **26**, 27–32.

Madden, D. R. (2002). The structure and function of glutamate receptor ion channels. *Nat. Rev. Neurosci.* **3**, 91–101.

Biography

Michael D. Ehlers is Assistant Professor of Neurobiology at Duke University. His research focuses on the interface between neuronal cell biology and the plasticity of neural circuits, with emphasis on protein trafficking mechanisms in dendrites. He holds an M.D. and a Ph.D. from the Johns Hopkins University School of Medicine, where he also conducted postdoctoral research. He is the recipient of numerous awards in neuroscience and is a scholar of the Ruth K. Broad Foundation.

Glutamate Receptors, Metabotropic

P. Jeffrey Conn
Vanderbilt University Medical Center, Nashville, Tennessee, USA

In addition to eliciting fast excitatory synaptic responses, the neurotransmitter glutamate can modulate neuronal excitability, synaptic transmission, and other cell functions by activation of a family of G protein-coupled receptors termed metabotropic glutamate (mGlu) receptors. Because of the ubiquitous distribution of glutamatergic synapses and the broad range of functions of the mGlu receptors, members of this receptor family participate in a broad range of functions of the central nervous system.

Fast Synaptic Transmission and Neuromodulation in the Central Nervous System

The majority of connections that make up a neural network in the mammalian central nervous system are synaptic connections in which a neurotransmitter released from the presynaptic neuron activates postsynaptic receptors that are neurotransmitter-gated ion channels. Opening of these ion channels, results in either excitation or inhibition of a receptive neuron, a process known as fast excitatory and inhibitory synaptic transmission. Normal function of the central nervous system requires a delicate balance between excitatory and inhibitory transmission. In mammalian brain, two major neurotransmitters are responsible for most fast inhibitory and excitatory synaptic responses. Gamma-aminobutyric acid (GABA) is the principal inhibitory neurotransmitter whereas the amino acid glutamate is the primary excitatory neurotransmitter. Transmission through a neuronal circuit can be fine-tuned or regulated by activation of another class of receptor that couples to activation of second messenger systems and various biochemical processes through GTP-binding proteins. This form of synaptic transmission is often referred to as slow synaptic transmission or neuromodulation to differentiate it from fast excitatory and inhibitory transmission.

Fast Excitatory and Neuromodulatory Actions of Glutamate

As the primary fast excitatory neurotransmitter, glutamate plays an important role in virtually all major functions of the CNS. Traditionally, the actions of glutamate were thought to be mediated exclusively by activation of glutamate-gated cation channels termed ionotropic-glutamate receptors (iGluRs). Fine tuning or modulation of transmission through glutamatergic circuits was thought to require neuromodulators from extrinsic afferents such as dopamine, acetylcholine, serotonin, and norepinephrine that activate GTP-binding protein (G protein)-linked receptors (GPCRs). However, in the mid-1980s, evidence for the existence of glutamate receptors directly coupled to second-messenger systems through G proteins began to appear with the discovery of glutamate receptors coupled to activation of phosphoinositide hydrolysis. Since that time, it has become clear that glutamate activates a large family of receptors, termed metabotropic glutamate (mGlu) receptors, which signal by coupling to GTP-binding proteins.

The discovery of mGlu receptors dramatically altered the traditional view of glutamatergic neurotransmission since activation of mGlu receptors can modulate activity in glutamatergic circuits in a manner previously associated only with neuromodulators from nonglutamatergic afferents. However, unlike receptors for monoamines and other neuromodulators, the mGlu receptors provide a mechanism by which glutamate can modulate or fine tune activity at the same synapses at which it elicits fast synaptic responses. Because of the ubiquitous distribution of glutamatergic synapses, mGlu receptors participate in a wide variety of functions of the CNS.

Eight mGlu Receptor Subtypes

Eight mGlu receptor subtypes have been identified and placed into three major groups based on structural, functional, and pharmacological properties. A major breakthrough in the understanding of mGlu receptors occurred in 1991 when groups led by Shigetada Nakanishi at Kyoto University in Japan and by Eileen Mulvihill and F.S. Hagen at ZymoGenetics, Inc., in Seattle, Washington independently cloned the first gene encoding an mGlu receptor. The predicted topology of this receptor, based on its deduced amino acid sequence, suggests that this receptor is similar to β-adrenergic receptors and other G protein-coupled receptors in that it contains seven predicted transmembrane-spanning domains. However, the primary structure of this receptor revealed no sequence homology with other G protein-coupled receptors, suggesting that it was a member of a new receptor gene family. Moreover, the mGlu receptor is distinct from members of the β-adrenergic receptor family in that it contains a large extracellular N-terminal domain and a large intracellular carboxy terminal tail. Structure–function studies performed since the initial cloning suggest that the extracellular N-terminal domain of mGlu receptors is made up of two globular domains with a hinge region. This forms a clam shell-shaped structure with the glutamate binding site between the two globular domains (see Figure 1). Evidence suggests that when glutamate binds, the globular domains close into a stable conformation with glutamate inside.

After cloning of the first mGlu receptor, a search for related cDNA resulted in the isolation of seven other genes encoding different mGlu receptor subtypes. These receptors are named mGlu1 through mGlu8. Also, several alternatively spliced forms or structural variants have been isolated for many of the cloned mGlu receptors. These include splice variants for mGlu1 (mGlu1a–1d), mGlu4 (mGlu4a and 4b), mGlu5 (mGlu5a and b), mGlu7 (mGlu7a and b) and mGlu8 (mGlu8a and b). Thus, it is now clear that there is tremendous diversity within the mGlu receptor family.

The cloned mGlu receptors have been classified into three major groups based on sequence homology, pharmacological properties, and coupling to different second-messenger pathways. Group I includes mGlu1 and mGlu5, group II, mGlu2 and mGlu3, and group III, all the others. mGlu receptors of the same group show ~70% sequence identity whereas between groups this percentage falls to ~45% (Figure 2) Group I mGlu receptors preferentially couple to activation of the $G_{q/11}$ G proteins and activate phosphoinositide hydrolysis as a major signaling mechanism. In contrast, group II and group III mGlu receptors preferentially couple to $G_{i/o}$ and inhibition of adenylyl cyclase. Members of each group have a unique pharmacological profile and can be selectively activated by specific agonists that have no effects on members of the other groups of mGlu receptors. Also, in recent years, progress has been made in developing drugs that differentiate between members of a single group. These drugs are having a major impact on the understanding of the physiological roles and pharmacological properties of the different mGlu receptor subtypes.

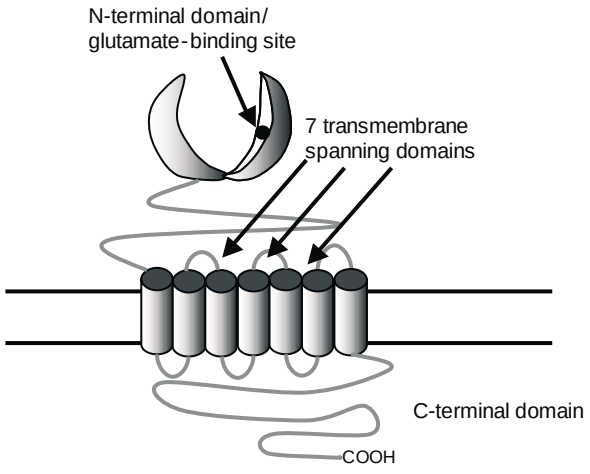

FIGURE 1 Schematic representation of an mGlu receptor. The mGlu receptors contain a large extracellular N-terminal domain, seven-transmembrane-spanning regions and an intracellular carboxy terminal domain. Glutamate binds in the large extracellular domain.

mGlu Receptors Play Diverse Roles in Regulating Neuronal Excitability and Synaptic Transmission

Anatomical studies using probes that specifically interact with individual mGlu receptor subtypes, coupled with electrophysiological studies have revealed that each of the individual mGlu receptor subtypes is differentially localized in different brain regions where they play a number of important physiological roles. While the specific mGlu receptor subtype involved in mediating a given effect varies in different brain regions, some generalizations can be made regarding the major roles of different groups of mGlu receptors. Elucidation of these roles of mGlu receptors suggests that specific agonists and antagonists of specific mGlu receptor subtypes could subtly alter transmission in glutamatergic circuits in a way that would provide a therapeutic benefit without eliciting the side effects commonly associated with drugs that interact with members of the ionotropic glutamate receptor family.

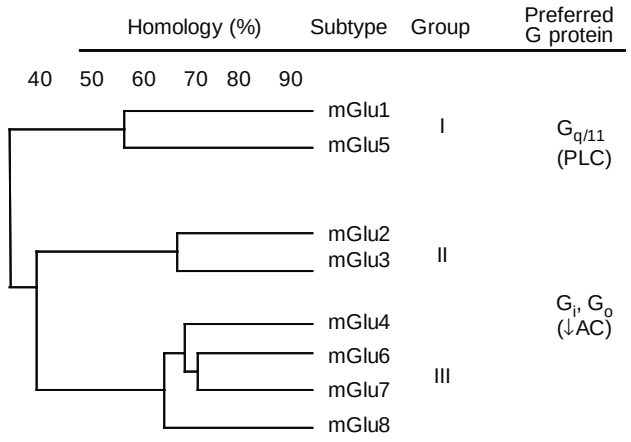

FIGURE 2 Dendrogram and classification of the members of the mGlu receptor family. The mGlu receptors are divided into three major groups, based on sequence homology, pharmacological profile, and second-messenger coupling.

One of the most common physiological functions of mGlu receptors, which is seen throughout the CNS, is as autoreceptors present at presynaptic terminals at glutamatergic synapses. Activation of these presynaptic receptors by glutamate released from the presynaptic neuron results in a reduction of glutamate release at that synapse. It is likely that this provides a negative feedback mechanism for tightly controlling transmission at glutamatergic synapses. This presynaptic function of mGlu receptors is usually subserved by a group II mGlu receptor or by one of the group III mGlu receptors (typically mGlu receptor 4, 7, or 8). While multiple mGlu receptor subtypes can serve this role, the specific mGlu receptor subtype(s) involved varies from synapse to synapse. mGlu receptors also exist postsynaptically where they play an important role in regulating cell excitability. The most common postsynaptic effect of mGlu receptor activation is induction of an increase in neuronal excitability. Again, the specific mGlu receptor subtype involved varies from synapse to synapse but typically involves one of the group I mGlu receptors (mGlu1 or mGlu5). In some cells, activation of postsynaptic mGlu receptors can lead to hyperpolarization and a reduction in neuronal excitability. This has been observed for both group I and group II mGlu receptors. Finally, a commonly observed effect of mGlu receptor activation is regulation of transmission at inhibitory GABAergic synapses. Thus, mGlu receptors are often localized at presynaptic GABAergic terminals where they regulate GABA release. In addition to these effects on neuronal function, mGlu receptors can also exist on glial cells. While mGlu receptors can have a number of effects on glial function, Ferdinando Nicoletti and co-workers have reported a series of studies revealing that one important effect of mGlu receptors in glia is induction of release of neuroprotective factors that reduce excitotoxicity and protect neurons from damage. The most prominent mGlu receptors in glia are mGlu3 and mGlu5.

Therapeutic Potential of mGlu Receptor Ligands

In recent years, major efforts have been made to develop new therapeutic agents for disorders of the central nervous system by targeting glutamatergic synapses in the circuits impacted by a particular disease. A potential advantage of developing new therapeutic agents that specifically target mGlu receptors is that it provides a rational approach for subtle fine-tuning of activity at synapses that have been identified as playing an important role in a given disorder. Because of the wide diversity, heterogeneous distribution, and diverse physiological roles of mGlu receptor subtypes, the opportunity exists for developing therapeutic agents that selectively interact with mGlu receptors involved in only one or a limited number of CNS functions. Such drugs could have a dramatic impact on development of novel treatment strategies for a variety of psychiatric and neurological disorders. Because of this, a great deal of effort has been focused on developing small molecules that selectively activate or inhibit specific mGlu receptor subtypes. One of the most important and earliest breakthroughs in developing drugs that target the mGlu receptors was development of highly selective agonists for the group II mGlu receptors by Jim Monn, Darryle Schoepp, and their coworkers at Eli Lilly. The first of these mGlu receptor agonists is now in clinical trials and preliminary proof of concept studies have been presented that suggest that this compound may have clinical efficacy for treatment of generalized anxiety disorder and panic attack. This represents a major breakthrough in the mGlu receptor field. A number of other compounds that selectively block or activate mGlu receptors have been developed by several drug companies and are now in preclinical stages of development.

See Also the Following Articles

$GABA_B$ Receptor • Glutamate Receptors, Ionotropic • Ligand-Operated Membrane Channels: Calcium (Glutamate) • Ligand-Operated Membrane Channels: GABA

Glossary

GABA An amino acid that serves as the primary inhibitory neurotransmitter in the central nervous system.

glutamate An amino acid that serves metabolic functions and as a component of proteins and polypeptides in all cells. In addition,

glutamate serves as a major excitatory neurotransmitter in the central nervous system.

G protein Membrane associated protein that interacts with a particular class of cell-surface receptor and participates in receptor-induced activation of intracellular enzymes, ion channels, and other signaling molecules. Also known as GTP-binding protein.

Further Reading

Alagarsamy, S., Sorensen, S. D., and Conn, P. J. (2001). Coordinate regulation of metabotropic glutamate receptors. *Curr. Opin. Neurobiol.* **11**, 357–362.

Conn, P. J., and Pin, J. P. (1997). Pharmacology and functions of metabotropic glutamate receptors. *Annu. Rev. Pharmacol. Toxicol.* **37**, 205–237.

Coutinho, V., and Knopfel, T. (2002). Metabotropic glutamate receptors: Electrical and chemical signaling properties. *Neuroscientist* **8**, 551–561.

Dingledine, R., Barges, K., Bowie, D., and Traynelis, S. F. (1999). The glutamate receptor ion channels. *Pharmacol. Rev.* **51**, 7–61.

Fagni, L., Chavis, P., Ango, F., and Bockaert, J. (2000). Complex interactions between mGluRs, intracellular Ca^{2+} stores and ion channels in neurons. *Trends Neurosci.* **23**, 2380–2388.

Pin, J. P., and Acher, F. (2002). The metabotropic glutamate receptors: Structure, activation mechanism and pharmacology. *Curr. Drug Target CNS Neurol. Disord.* **1**, 297–317.

Schoepp, D. D. (2001). Unveiling the functions of presynaptic metabotropic glutamate receptors in the central nervous system. *J. Pharmacol. Exp. Ther.* **299**, 12–20.

Schoepp, D. D., Jane, D. E., and Monn, J. A. (1999). Pharmacological agents acting at subtypes of metabotropic glutamate receptors. *Neuropharmacology* **38**, 1431–1476.

Biography

P. Jeffrey Conn is a Professor in the Department of Pharmacology and Director of the Program in Translational Pharmacology at Vanderbilt University Medical Center in Nashville, Tennessee. Prior to his current position, he was Head of the Department of Neuroscience at Merck and Company and Professor of Pharmacology at Emory University. He holds a Ph.D. in Pharmacology from Vanderbilt University and received his postdoctoral training at Yale University. Dr. Conn has played a major role in determining the functional roles of metabotropic glutamate receptors and in development of small molecules that interact with members of this receptor family.

Glutathione Peroxidases

Fulvio Ursini and Matilde Maiorino
University of Padova, Padova, Italy

Glutathione peroxidases (GPxs) form a superfamily of oxidoreductases distributed in all living domains. They may contain cysteine or selenocysteine as part of the catalytic site. The cysteine homologues prevail in prokaryotes, yeasts, and land plants, while selenocysteine-containing enzymes have been considered peculiar of mammals. This view has been expanded since selenium peroxidases have been recently identified in two distinct poxviruses: the platyhelminth *Schistosoma mansoni* and the green alga *Chlamidomonas rheinhardtii*.

Mammalian Se-GPxs are four different gene products, namely cGPx (or GPx-1), GI-GPx (or GPx-2), pGPx (or GPX-3), and PHGPx (or GPx-4), in humans mapping to chromosome 3, 14, 5, and 19, respectively. The typical reaction of GPxs is the reduction of a hydroperoxide coupled to the oxidation of two thiols. The most characteristic substrates are hydrogen peroxides (H_2O_2) and glutathione (GSH), which undergo a two-electron redox transition to water and glutathione disulfide (GSSG), respectively. Since reduction of hydroperoxides prevents the formation of reactive oxygen species (ROS), which have a strong pro-oxidant character, an antioxidant role has been classically ascribed to GPxs. The cysteine-containing homologues have an order of magnitude lower efficiency in catalyzing a peroxidatic cycle than that of the corresponding selenoperoxidases, therefore posing the question of their actual function as efficient hydroperoxide detoxifying enzymes.

History

The first glutathione peroxidase ("classical" or "cytosolic" GPx, cGPx) was discovered in 1957 by Mills as an enzymatic activity that protects hemoglobin in red blood cells from oxidative denaturation. At the time, the notion that an enzyme catalyzing the reduction of hydrogen peroxide at the expense of GSH could be physiologically relevant was not immediately accepted, since heme peroxidases (including catalase) were considered much more efficient. The work by Choen and Hochstein in 1963 disclosed the real physiological value of this enzyme, showing that H_2O_2 does not denature hemoglobin until red blood cells, that contain catalase, are fully depleted of GSH. Kinetic analysis and subcellular localization of enzymes, eventually clarified the issue, showing the glutathione peroxidase is the most efficient hydroperoxide removing system in almost every cell.

In 1972 the groups of Rotruck in Wisconsin and Flohé in Germany provided evidence that cGPx contains one mole of selenium per mole of homotetrameric enzyme. The selenium moiety was later identified as a selenocysteine. This discovery led to the formulation of the dogma of the antioxidant effect of selenium. This view is now considered quite limited owing the discovery of both, other selenoenzymes and functions of GPxs, different from antioxidant protection.

The second GPx, "phospholipid hydroperoxide glutathione peroxidase" (PHGPx), was first described as a monomeric enzyme, distinct from cGPx in 1982. Subsequently, the list of the members of the GPxs family grew with the discovery of the tetrameric "plasma" pGPx in 1987 and of the gene of the "gastro-intestinal" GI-GPx in 1993.

Enzymology and Kinetics

cGPx, GI-GPx, and pGPx are homotetrameric proteins and rather similar to one another (overall homology $>80\%$). PHGPx is monomeric and presents an overall homology $< 35\%$ when compared to the monomer of tetrameric enzymes. The X-ray structure has been elucidated only for cGPx, and the conformation of the other GPxs has been obtained by molecular modeling based on the cGPx structure.

A relevant feature of the superfamily of GPxs is the catalytic triad, which is highly conserved in all members, including the cysteine homologues. This is made by loops rather distant in primary structure, contains one selenocysteine, one tryptophan, and one glutamine residue, and has been functionally proved by site directed mutagenesis. The catalytic triad of Gpx1 and PHGPx is reported in Figure 1. The tryptophan and the glutamine residue are assumed to "activate" by hydrogen bonding the dissociated selenol. However, it could also be possible that the residues "activate" the hydroperoxide, thus facilitating the nucleophilic

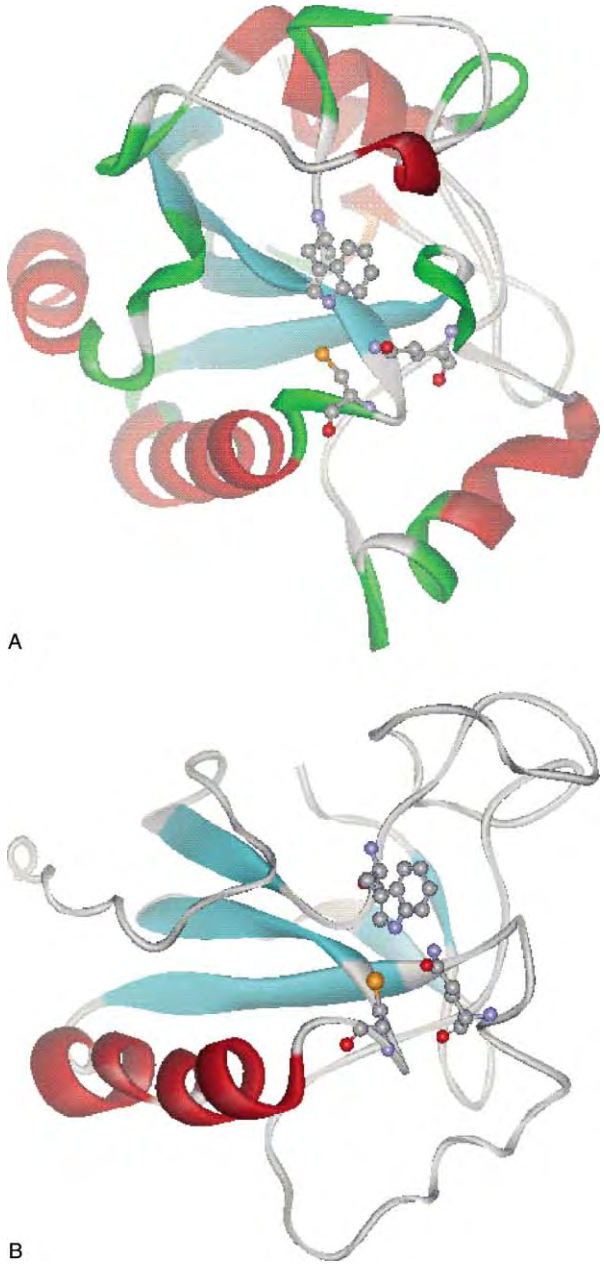

FIGURE 1 Structure of catalytic site of glutathione peroxidases, showing catalytic selenocysteine, tryptophan and glutamine. The structure of Gpx1 (A) has been constructed from crystallographic data. The structure of PHGPx (B) has been calculated by homology modeling and energy minimization.

displacement leading to oxidation of selenol, the first step of the catalytic cycle.

Kinetic analysis of the peroxidase reaction has been carried out on cGPx and PHGPx. During the catalytic cycle, the selenol at the active site is oxidized by the hydroperoxide. The product is assumed a selenenic acid derivative (Se-OH), although, due to the extreme reactivity of the group, a chemical evidence for the nature of the first oxidized species is so far missing. This intermediate reacts with a suitable thiol (usually GSH) to produce a mixed selenadisulfide (Se-SG), the nature of which has been positively determined by mass spectrometry. The selenadisulfide is then reduced by another thiol (usually GSH) to produce the leaving disulfide (usually GSSG) and the native, reduced, form of the enzyme.

This reaction mechanism is described by ping-pong kinetics typical of an enzyme substitution mechanism, following the simplified Dalziel equation:

$$\frac{[E_0]}{V} = \frac{\phi_1}{[\mathrm{ROOH}]} + \frac{\phi_2}{[\mathrm{GSH}]}$$

where ϕ_1 is the reciprocal of the rate constant for the reduction of the hydroperoxide and ϕ_2 the empirical coefficient accounting for the sum of the two steps of GSH oxidation.

The corollary of this kinetic mechanism, where reactions at the active site are much faster than the enzyme substrate complex formation, is that V_{max} and K_m remain undefined, and apparent kinetic constants for one substrate are dependent on the concentration of the other substrate.

The specificity for the oxidizing substrate is maximal in cGPx that reduces only hydrogen peroxide and some small organic hydroperoxides, and minimal in PHGPx that reduces large lipophilic substrates such as hydroperoxide derivatives of phospholipids and cholesterol esters as well. Intermediate specificity, although closer to that of cGPx, has been observed for pGPx. No kinetic data are available for GI-GPx, which has never been isolated as a protein, although specificity similar to that of cGPx can be assumed from structure homology. The different specificity for oxidizing substrate is accounted for by the active site that in tetrameric enzymes is located in the valley among subunits while in PHGPx is at the center of an exposed lipophilic depression.

In addition, the specificity for the donor substrate is maximal for cGPx and minimal for PHGPx. This has been attributed to the mutation/deletion of four Arginine residues surrounding the active site and alleged to be involved in binding of GSH. According to this observation, the specificity of GPxs toward GSH should decline in the following order: cGPx > GI-GPx > pGPx > PHGPx. Therefore the family of GPxs appears diversified in function so that the classification as *glutathione* peroxidases may be too restrictive. For PHGPx, although the interaction with GSH is energetically favored by the formation of hydrogen bonding with lysines in the proximity of the active site, the specificity for this substrate is low and this turned out definitely relevant for the recently disclosed role of the protein in spermatogenesis.

Biosynthesis of Selenoperoxidases

Selenocysteine is a rare but widely distributed amino acid in the living kingdom, and selenoproteins containing this amino acid as a part of the active site have been described in prokarya, archaea, and eukarya. In mammals, besides GPxs, at least 16 other selenocysteine-containing proteins have been described.

The elucidation of selenocysteine biosynthesis and its cotranslational incorporation into proteins occurred in the last two decades by elegant studies carried out independently by Böck, Berry, Stadtman, and co-workers. These studies followed the discovery of an in-frame TGA codon in the cDNA of *gpx-1* by Chambers and co-workers. The process represents a special case in protein biosynthesis, being peculiar in several respects and exhibiting several common features among the different organisms.

1. Among all the organisms of the living kingdom, selenocysteine biosynthesis occurs from serine, while this amino acid is bound to the $tRNA^{Sec}$ (the *SelC* gene product). This is structurally different from the canonical tRNA for serine. The conversion of serine into selenocysteine requires SelA (the selenocysteine synthase) and selenophosphate. The latter is produced from ATP and selenide by the specific synthetase SelD, a selenoprotein itself.

2. The use of an in-frame TGA for selenocysteine insertion is also peculiar and common to all the organisms. This triplet was formerly known just as "stop codon" in the nuclear genome. Therefore, a complex decoding mechanism has evolved to read TGA as selenocysteine insertion instead of protein termination.

3. Decoding requires a hairpin structure called selenocysteine inserting sequence (SECIS) and proteins that recognize the SECIS acting as elongation factors. SECIS location differs among the different organisms, being located immediately downstream the stop codon in prokarya or in the 3′ UTR in archaea and eukarya. In prokarya, one protein acts both as SECIS binding protein and elongation factor (the *SelB* gene product), while in archea and eukarya two distinct proteins are involved in this process. In eukarya (mammals), these are the specialized elongation factors mSelB/EFsec and SBP-2, which bind both the SECIS elements and mSelB/EF.

In condition of limited selenium supply, eukaryotic selenoproteins are differentially expressed, a phenomenon referred to as "selenoprotein hierarchy." The mRNA of cGPx, and the level of expressed protein, decreases under conditions of low availability of selenium, while GI-GPx and PHGPx results remarkably stable. Although the underlying mechanism is far from being clear, the affinity of SBP2 for the different SECIS seems to play a key role, but phenomena such as tissue levels of SB2, tissue specific accumulation of selenium, and tissue specific transcription and mRNA stability might also contribute. The priority of the synthesis of GI-GPx and PHGPx over cGPx under limited conditions of selenium supply indirectly suggests a more relevant biological function. Moreover, in a selenium status where other peroxidases are saturated, cGPx keeps increasing, an evidence that led to speculations about a "selenium deposit" role for cGPx.

Biological Functions

The common catalytic mechanism suggests a similar function for GPxs, although in different cell compartments and with different specificity toward peroxidic and reducing substrate. On the other hand, inverse genetics experiments showed an unambiguous antioxidant function only for cGPx.

cGPX

cGPx is a widely distributed, intracellular protein. The cGPx (−/−) mouse develops and grows normally, unless challenged by an oxidative stress induced by redox-cycling compounds or activation of an oxidative burst of macrophages. These challenges mimic the pathological condition of the inadequate antioxidant protection seen in favism and related diseases. Moreover, in (−/−) mouse, a nonvirulent strain of Coxsackie's virus mutates into a virulent form. Thus, silencing cGPx appears as a perfect model of the Kashan disease (a syndrome due to severe selenium deficiency) where, due to the oxidizing intracellular environment produced, a nonvirulent virus becomes virulent, apparently in relation to higher mutation rate. The pathophysiological feature of cGPx knockout is independent of selenium status, suggesting that other selenoperoxidases are unable to substitute for the antioxidant function of cGPx.

pGPX

pGPx is an extracellular protein secreted by organs such as kidney or ciliar body. It has been suggested to reduce lipid hydroperoxides in circulating lipoproteins, thus playing a role in protecting against the oxidation claimed to be involved in atherogenesis. Against this hypothesis argues the evidence that reducing equivalents (either from GSH or thioredoxin) are extremely limited in plasma and that the enzyme is not active on cholesterol ester hydroperoxides, a major lipid oxidation product in LDL. A possible, although purely speculative, role could be seen in the regulation of the flux of oxidant produced by phagocytes and thus in the control of inflammatory response.

Indeed, no information from inverse genetics exists for pGPx.

GI-GPx

A reasonable function of GI-GPx is suggested by the localization in the digestive tract. Since traces of lipid hydroperoxides, within food or produced during gastric digestion, can be detected in postprandial plasma, the peroxidase could work in minimizing the absorption of harmful lipid hydroperoxides. However, this appealing hypothesis has been neither fully confirmed nor excluded so far.

The GI-GPx (−/−) mouse has a normal phenotype, while the double knockout (GI-GPx and cGPx) shows major alterations of the intestinal mucosa. These data and peculiar localization allow speculation on a possible function of GI-GPx acting synergically with cGPx in regulating proliferation, differentiation, and apoptosis in cells of intestinal villi.

PHGPx

PHGPx has been discovered as a ubiquitous, intracellular antioxidant enzyme. By reducing all types of lipid hydroperoxide in membranes, PHGPx prevents lipid peroxidation initiated *in vitro* by homolytic or heterolytic decomposition of these compounds. This reaction is synergic with the reduction by vitamin E of lipid hydroperoxy radicals propagating lipid peroxidation. Thus, a complete and fully efficient antioxidant system is accomplished by a one-electron reduction of hydroperoxy radicals (chain-breaking reaction, accomplished by vitamin E) followed by a two-electron reduction of lipid hydroperoxides (peroxidolytic reaction, accomplished by PHGPx). This mechanism accounts for by the synergism in antioxidant protection between vitamin E and selenium, evidenced by nutritional studies.

More recently, a major role in spermatogenesis has been documented. PHGPx appears involved in both the formation of the keratinous material embedding the mitochondria of the spermatozoon, a structure called mitochondrial capsule, and in chromatin condensation. PHGPx is orders of magnitude more abundant in male germ cells with respect to other somatic cells, where different mRNAs are translated into proteins specifically addressed to the mitochondria or to the nucleus by organelle-specific sequences. Distinct transcripts are generated by alternative transcription of the gene. Furthermore, the expression of the individual PHGPx transcripts appears stage specific during spermatogenesis, mitochondria and cytosolic PHGPx peaking in round spermatids, and nuclear PHGPx in later stages of spermatogenesis, together with protamine expression. In the mitochondrial capsule, PHGPx is found as catalytically inactive protein cross-linked with other proteins, including PHGPx itself. The presence of inactive PHGPx as a major component of the mitochondrial capsule suggests a moonlighting from an active peroxidase to a structural element during sperm maturation. Several evidences indicate that this function switch is primed by GSH depletion and the capability of PHGPx to use alternative thiol substrates, including PHGPx itself. Mass spectrometry data showed that, the oxidized selenium moiety of PHGPx reacts with a specific surface cysteine of another PHGPx molecule. This accounts for the first elements of the cross-linked matrix. A similar mechanism thus leads to the copolymerization of other still undefined proteins, eventually leading to the formation of the capsule. By a similar mechanism, nuclear PHGPx results involved in chromatin condensation, when protamine thiols are used as donor substrate for the peroxidatic reaction.

A definitely relevant physiological role for PHGPx has been suggested by inverse genetics, since *gpx-4* revealed to be a vital gene. Furthermore, as a confirmation of a major role in spermatogenesis, PHGPx chimeric mice show mosaic testicular atrophy and abnormal sperm morphology.

The reason why PHGPx (−/−) mice are not vital cannot be reconciled with either the specific function in spermatogenesis or the other proposed functions, such as inhibiting lipoxygenases, stifling the nuclear factor κB, or controlling apoptosis, and implies additional and undisclosed functions of this gene product.

Future Perspectives

Mammalian cells contain four different selenium-dependent GPxs plus other cysteine-containing homologues. Only selenium-containing homologues are efficient peroxidases in principle, but an antioxidant function (related to reduction of hydroperoxides) has been unambiguously demonstrated by reverse genetics only for cGPx. Indeed, the major role of PHGPx in spermatogenesis appears the oxidation of protein thiols. Thus, the catalysis operated by the selenocysteine residue in PHGPx can be interpreted in considering the capability of the enzyme to address the oxidation potential of hydroperoxides toward specific protein thiols. The mechanisms of redox regulation of enzymes or nuclear factors are attracting more and more efforts by scientists, and it seems reasonable to suggest that specific redox transitions occurring in cells must undergo a kinetic more than a thermodynamic control. On this light, it is predictable that forthcoming studies will revisit the catalysis operated by the selenol moiety of some GPxs shifting from the antioxidant defense area to the control of redox-mediated processes.

See Also the Following Article

Selenoprotein Synthesis

Glossary

antioxidant A molecule or an enzymatic system that prevents or slows down a free radical oxidative chain reaction, by either preventing the formation of initiating radicals or reducing the concentration of propagating radicals.

glutathione A tripeptide (γ-glutamyl-cysteinyl-glycine) widely distributed, involved in antioxidant protection and regulation of the redox status of the cell.

kashan disease A cardiomyopathy described in a selenodeficient area of China.

mitochondrial capsule (of spermatozoa) A keratinous-like structure containing large amounts of disulfides, present in the mid-piece of spermatozoa and embedding mitochondria, fibers, and centriole.

peroxidase An oxidoreductase catalyzing the reduction of a hydroperoxide to the corresponding alcohol and water by using the reducing potential of a specific substrate.

peroxidation Free-radical-driven oxidative degradation of fatty acids (mainly polyunsaturated) producing lipid hydroperoxides and their degradation products.

selenium A nutritionally essential oligoelement inserted in specific proteins as a selenocysteine that undergoes redox transitions.

thioredoxin A pleiotropic, low-molecular-weight protein containing a redox sensitive thiol/disulfide couple.

Further Reading

Atkins, J. F., and Gesteland, R. F. (2000). The twenty-first amino acid. *Nature* **407**, 463–465.

Brigelius-Flohé, R. (1999). Tissue-specific functions of individual glutathione peroxidases. *Free Radic. Biol. Med.* **27**, 951–965.

Flohé, L., and Brigelius-Flohé, R. (2001). Selenoproteins of the glutathione system. In *Selenium; its Molecular Biology and Role in Human Health* (D. L. Hatfield, ed.) pp. 157–178. Kluwer Academic, Norwell Massachusetts (USA).

Low, S. C., and Berry, M. J. (1996). Knowing when not to stop: selenocysteine incorporation in eukaryotes. *Trends Biochem. Sci.* **21**, 203–208.

Maiorino, M., Aumann, K.-D., Brigelius-Flohé, R., Doria, D., van Den Heuvel, J., McCarthy, J., Roveri, A., Ursini, F., and Flohé, L. (1995). Probing the presumed catalytic triad of selenium-containing peroxidases by mutational analysis of phospholipid hydroperoxide glutathione peroxidase (PHGPx). *Biolog. Chem. Hoppe-Seyler* **376**, 651–660.

Stadtman, T. C. (1996). Selenocysteine. *Annu. Rev. Biochem.* **65**, 83–100.

Ursini, F., Maiorino, M., Brigelius-Flohé, R., Aumann, K. D., Roveri, A., Schomburg, D., and Flohé, L. (1996). Diversity of glutathione peroxidases. *Methods in Enzymol.* **252**, 38–53.

Ursini, F., Heim, S., Kiess, M., Maiorino, M., Roveri, A., Wissing, J., and Flohé, L. (1999). Dual function of the selenoprotein PHGPx during sperm maturation. *Science* **285**, 1393–1396.

Biography

Fulvio Ursini holds an M.D. degree from the University of Padova and serves as full Professor of Biochemistry at the same University. His main research fields are: (1) biochemistry of selenium-dependent peroxidases; (2) mechanism of antioxidant effect of natural compounds and role of antioxidants on cellular functions; (3) lipid peroxidation and its impact on molecular mechanism of disease; and (4) mechanism of protein thiol oxidation during cell differentiation.

Matilde Maiorino is Associate Professor of Biochemistry at the School of Medicine of the University of Padova. She contributed to the discovery of PHGPx and to its functional characterization. In 1997 she was awarded the Klaus Schwarz Commemorative Medal for her research in trace elements. Her current interest is focused on molecular biology of Se-peroxidases and on the impact of selenium on male fertility.

Glycation

Suzanne R. Thorpe and John W. Baynes
University of South Carolina, Columbia, South Carolina, USA

Glycation is a term describing the adduction of a carbohydrate to another biomolecule, such as a protein or lipid. Glycation may occur either enzymatically or nonenzymatically. The common term for enzymatic glycation is glycosylation, e.g., formation of a glycosidic bond using a sugar nucleotide donor during synthesis of glycoproteins. The terms nonenzymatic glycation, nonenzymatic glycosylation, or glycation (without a modifier) are commonly used in reference to direct chemical reactions of reducing sugars with proteins, illustrated by the reaction of glucose with lysine residues in protein to form a ketoamine (Amadori) adduct (Figure 1). Glucation, fructation, ribation, etc., are used in reference to glycation by specific sugars.

Although glycation is a reversible reaction, it is considered a first step in the Maillard or browning reaction, which leads to irreversible chemical modification, browning, generation of fluorescence, and cross-linking of proteins during cooking, and in the body during aging and in disease. The irreversible adducts and cross-links in protein are known as advanced glycation end products (AGEs). Most AGEs are formed by a combination of glycation and oxidation reactions and are termed glycoxidation products. AGEs accumulate with age in long-lived extracellular proteins, such as collagen, and are also formed from glycolytic intermediates on shorter-lived intracellular proteins. Increased rates of formation of AGEs in tissue proteins during hyperglycemia and oxidative stress or inflammation are implicated in the pathophysiology of aging, and diabetes and other chronic diseases.

Glycation of Proteins in Blood

Glycated Hemoglobin

Interest in the Maillard reaction in biochemistry began with the identification of HbA_{Ic}, an anodic variant of adult hemoglobin (Hb), discovered during screening of diabetic patients. HbA_{Ic} contains glucose bound to the amino-terminal valine residues of the Hb β-chains. The glucose–valine adduct was characterized as an aminoketose or ketoamine (fructosevaline), formed by nonenzymatic reaction of glucose with protein (Figure 1). The high reactivity of the β-chain valine residues of Hb results from catalysis of the Amadori rearrangement by phosphate or 2,3-bisphosphoglycerate bound near these valine residues in the allosteric site regulating the oxygen affinity of Hb. The α-chain valines, which have similar exposure to solvent and the same low pK_a, but are not in the allosteric site, are only ~10% as glycated as the β-chain valines. HbA_{II} also has 66 lysine residues, but there are only about twice as many fructoselysine (FL) as fructosevaline residues in the protein. The more reactive lysines are adjacent to basic or acidic amino acid in the primary or three-dimensional structure of the protein, which either affect the nucleophilicity of the lysine amino group or catalyze the Amadori rearrangement. The primary sites of glycation of ribonuclease by glucose *in vitro* are at lysine residues in the active site. Glycation of some, but not all of these residues is catalyzed by phosphate and other anionic buffers that bind in the basic, RNA-binding region of the enzyme. Thus, glycation, although not as specific as enzymatic glycosylation of protein, is not a random modification of protein, but is affected by the pK_a of the amino acid, amino acid sequence, protein conformation, and ligand binding.

Clinical Significance of Glycated Hb

Assays of glycated Hb (GlcHb) are a powerful tool for the clinical management of diabetes. Glycation is a slow reaction. The rate of formation of HbA_{Ic} is ~0.1% of HbA_{II} per day at normal blood glucose concentration (5 mM), and is first order in glucose concentration. Since the red cell is long-lived (life span ~120 days) and is freely permeable to glucose, the mean extent of glycation of Hb varies with mean blood glucose concentration. The average percent glycation of Hb, ranges from 4 to 6% HbA_{Ic} in a control population, to 16% or higher in poorly controlled diabetic patients. Based on clinical studies, assays of percent HbA_{Ic} integrate the mean blood glucose concentration during the previous 4–6 weeks. These assays complement acute blood glucose measurements for assessment of long-term glycemic control in diabetes.

Assays for HbA_{Ic} use an anion exchange procedure that depends on the shift in pK_a of the protein, which occurs on glycation of the valine residues. Alternatively,

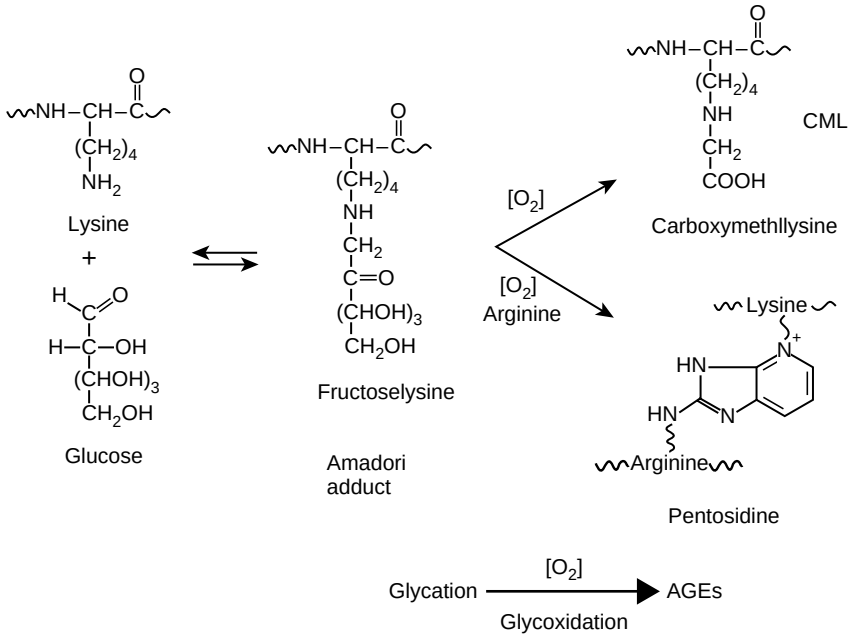

FIGURE 1 Pathway for glycation of protein. Glucose reacts reversibly with amino groups in protein, e.g., lysine, forming a Schiff base (not shown), which rearranges to the Amadori compound (ketoamine), fructoselysine. Oxidation of the Amadori compound is one route to formation of advanced glycation or glycoxidation end products, such as CML and pentosidine.

total GlcHb may be measured by an affinity chromatography assay that depends on interaction of Amadori adducts on the surface of the protein with phenylboronate resins; this assay measures primarily the glycation of lysine residues. While assays of HbA_{Ic} and GlcHb actually measure different aspects of GlcHb, the two assays yield similar quantitative results and correlate strongly with one another. Both the ion-exchange and affinity chromatography assays are available as mini-column kits and HPLC methods. Electrophoretic, nephelometric (immuno-turbidimetric), and ELISA assays are also used, but less commonly, for measurement of glycation of Hb and assessment of long-term glycemic control.

Glycation of Extracellular and Plasma Proteins

Glucose is ubiquitous in body fluids, and therefore all tissue proteins are subject to glycation. The steady-state extent of glycation of a protein depends on the inherent reactivity of the protein with glucose under physiological conditions, the protein's biological half-life or lifespan, and the ambient glucose concentration. The fractional glycation of lysine in lens proteins is ~40% that of skin collagen in humans, reflecting the lower glucose concentration in the lens, compared to extracellular fluids. Collagen accounts for about one-third of total body protein mass and is accessible by biopsy. Like glycation of Hb, the extent of glycation of skin collagen may be used as an index of very long-term hyperglycemia or glycative stress. In addition to Hb, other intracellular proteins are also subject to glycation, e.g., superoxide dismutase in the lens, alcohol dehydrogenase in the liver, and the actomyosin complex in muscle.

Assays for glycated plasma proteins, which have relatively short half-lives compared to hemoglobin or collagen, provide an index of intermediate-term blood glucose concentration, during the previous 7–10 days. In addition to ELISA and phenylboronate affinity chromatography assays for glycated albumin, total Amadori adducts on plasma proteins can be measured by the fructosamine assay. This assay measures the reduction of a tetrazolium dye by the Amadori compound on plasma proteins. The Amadori adduct has much stronger reducing activity than glucose at pH 10, so that the reducing activity of Amadori adducts on glycated plasma proteins can be measured without significant interference by blood glucose.

Glycation of Other Amino Acids and Biomolecules

Glucose appears to react only with primary amino groups on protein. However, Amadori compounds undergo facile rearrangement and oxidation reactions. They may rearrange nonoxidatively to form deoxyglucosones, regenerating free lysine, or undergo autoxidative decomposition to form glucosone. These dicarbonyl compounds react with the side chains of lysine, arginine, cysteine, histidine, and probably tryptophan residues, expanding the range of glycative damage to protein. Amadori adducts to phosphatidylethanolamine and

phosphatidylserine have also been measured in tissues. DNA undergoes glycation *in vitro*, although glycated DNA has not been identified *in vivo*, perhaps because of the involvement of the amino groups of nucleic acids in intrahelical hydrogen bonds and the shielding provided by histones and other nuclear proteins.

Reactivity of Glucose

The rate of reaction of a sugar with protein depends on the fraction of the sugar in the open-chain, aldehyde conformation. Glucose, among all sugars, exists to the greatest extent in the cyclic, hemiacetal conformation. It is therefore the least reactive in glycating proteins, in comparison to other hexoses, pentoses, ketoses, or phosphorylated metabolic intermediates. Another unique feature of glucose is that, although it is a reducing sugar and is readily oxidized, it is the least active among all sugars in oxidation or autoxidation (oxidation by molecular oxygen) reactions—again, because it exists largely in a hemiacetal rather than aldehyde conformation. In the Fehling and Benedict assays for reducing sugars, oxidation is promoted by strongly basic conditions that catalyze the enolization and isomerization of glucose. Its low reactivity with protein and its resistance to autoxidation was probably important in the evolutionary selection of glucose as blood sugar in mammals. Despite its chemical inertness, however, glucose does react with proteins at a measurable rate. Glycation occurs and advanced glycation end products (AGEs) accumulate on tissue proteins with age.

Advanced Glycation and Glycoxidation Reactions

Advanced Glycation

Food scientists learned early in the twenty-first century that glycation was one of the early steps in the Maillard or browning reaction of proteins during cooking, part of the process of caramelization that enhances the color, taste, aroma, and texture of cooked foods. The Maillard reaction also contributes to the loss in nutritional value of cooked foods, because of the chemical modification of the essential amino acids, lysine and arginine. When biomedical scientists discovered that hemoglobin was glycated *in vivo*, it was reasonable to speculate that advanced stages of the Maillard reaction should also proceed *in vivo*–the human body could be viewed, at one level, as a low-temperature oven (98.6°F) with a long cooking cycle (~80 years). The Maillard reaction was seen as a possible source of the brown color and fluorescence that develops with age in long-lived proteins, such as crystallins and collagens, and as a contributing factor in both the normal aging of tissue proteins and the acceleration of age-like pathology by hyperglycemia in diabetes.

More than 20 AGEs have now been detected in tissue proteins (Figure 2), including amines, amides, pyrroles, imidazolones, imidazolium salts, and several bicyclic heteroaromatic compounds. The first two AGEs to be identified *in vivo* were N^{ε}-(carboxymethyl)lysine (CML) and pentosidine. Because of their stability during acid hydrolysis of proteins, these compounds are still the most frequently measured AGEs. CML, which is quantitatively the most abundant AGE, is measured by GC/MS or ELISA. Although present at much lower concentration, pentosidine is highly fluorescent and is measured by HPLC with fluorescence detection. Other AGEs are measured less frequently because they are either present at lower concentrations in tissues or are labile to acid or base hydrolysis and must be measured following enzymatic digestion of proteins. The known AGEs are only trace components of proteins *in vivo*. Even in skin collagen and lens proteins of elderly diabetic patients, CML and CEL (Figure 2) typically account for modification of less than 1% of the lysine residues in the protein. However, these biomarkers are thought to represent only a fraction of the total chemical modification of amino acids and cross-linking of proteins *in vivo*.

Glycoxidation

Although oxygen is not required for glycation, formation of CML and pentosidine from FL requires oxidation of the Amadori compound: cleavage between C-2 and C-3 of the carbohydrate to form the lysine adduct CML; and loss of one carbon from glucose during the formation of pentosidine. The development of brown color and fluorescence and formation of AGEs during incubation of proteins with glucose *in vitro* are also accelerated by oxygen. The oxidation reactions are more rapid in phosphate and carbonate buffers, compared to organic buffers, because of the presence of trace amounts of redox-active, metal ions, such as iron and copper in inorganic buffers, which catalyze oxidation and glycoxidation reactions.

The term, glycoxidation, was coined in recognition of the importance of both glycation and oxidation in the formation of AGEs. Oxidation reactions often have high-negative free energies, and, especially in oxidative cleavage reactions, oxygen can be viewed as the fixative of irreversible damage to protein during the Maillard reaction. However, some AGEs, such as pyrraline and the cross-lines, may be formed from glucose under nonoxidative conditions. Likely precursors to these compounds include the dicarbonyl sugars 1- and 3-deoxygluosone, which are formed from Amadori compounds under nonoxidative conditions.

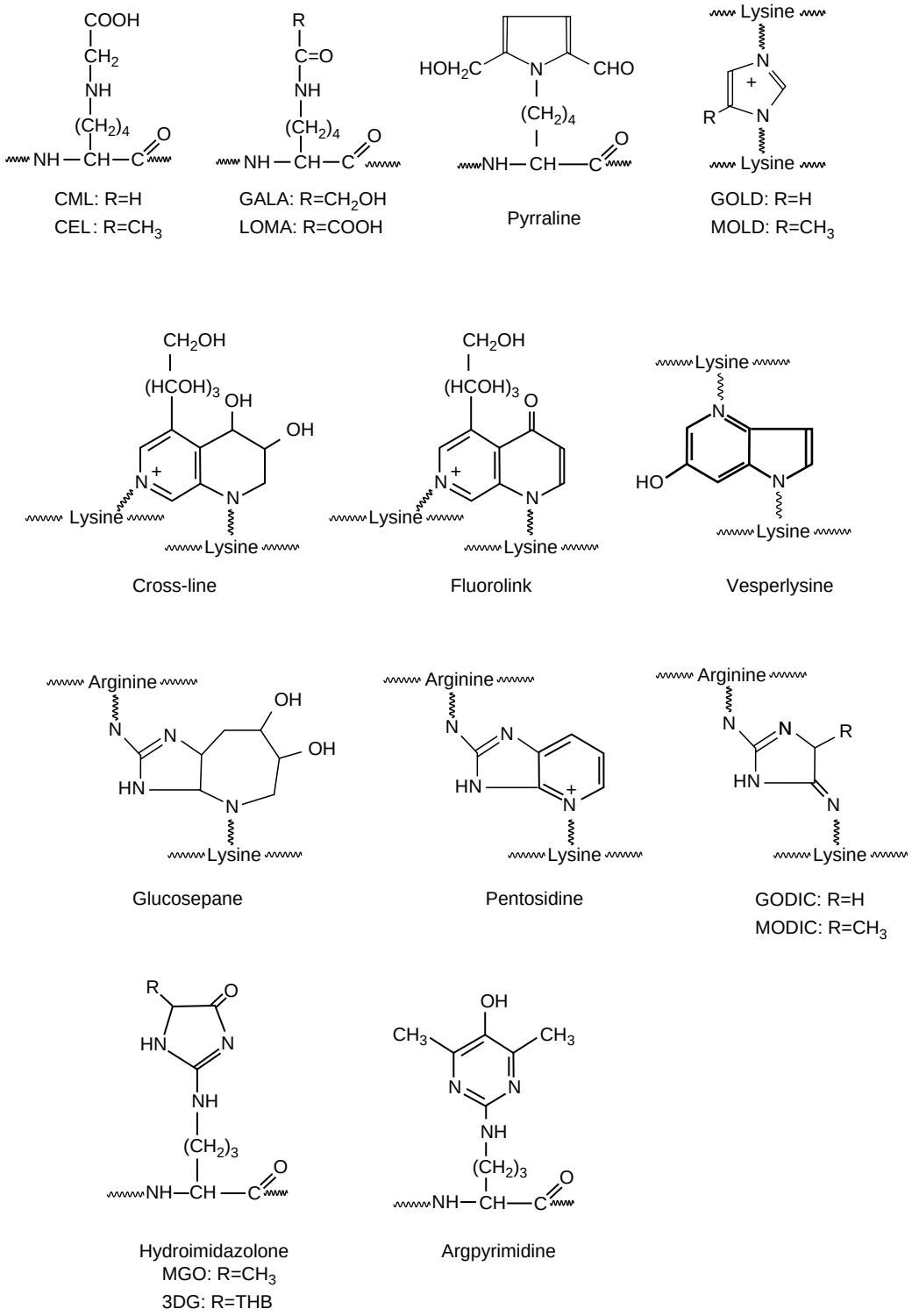

FIGURE 2 Structure of AGEs that have been detected in tissue proteins by chemical and/or immunological methods. Top: Nonfluorescent lysine adducts and cross-links, including amides, amines and imidazolium salts. Second row: Fluorescent lysine-lysine cross-links. Third row: Fluorescent arginine-lysine cross-links. Bottom: Arginine derivatives. CML, N^{ε}-(carboxymethyl)lysine; CEL, N^{ε}-(carboxyethyl)lysine; GALA, glycolic acid lysine monoamide; LOMA, lysine oxalic acid monoamide; GOLD and MOLD, GO and MGO lysine dimer (imidazolium salts); and GODIC and MODIC, GO and MGO dihydroimidazolylidene cross-links.

Alternative Pathways to AGEs and Glycoxidation Products

In the early 1980s, the Amadori adduct was considered an obligate intermediate in the formation of AGEs (Figure 1). However, it is now clear that there are multiple precursors and pathways to formation of the same AGE (Figure 3). CML, for example, may be formed from glyoxal or glycolaldehyde which are produced on autoxidation of many carbohydrates, or by autoxidation of Schiff base intermediates and Amadori adducts, or from ascorbate and dehydroascorbate and phosphorylated intermediates in glycolysis. To complicate the issue further, glycolaldehyde, formed on oxidation of serine by myeloperoxidase, and glyoxal formed during lipid peroxidation reactions, may also contribute to the formation of CML. Thus, the measurement of CML provides little information regarding its origin. Lipid-derived adducts to protein, such as malondialdehyde and hydroxynonenal adducts to protein, are known as advanced lipoxidation end-products (ALEs), so that CML and GOLD, and the homologous compounds, CEL and MOLD, are now considered AGE/ALEs, reflecting the fact that they may be derived from a variety of carbohydrate and non-carbohydrate precursors *in vivo*. Some AGEs, such as pentosidine and cross-lines, which contain 5–6 carbon rings or side-chains (Figure 2), are clearly derived from carbohydrates, but may be formed from a variety of carbohydrate precursors, including reducing sugars, sugar phosphates, and ascorbate.

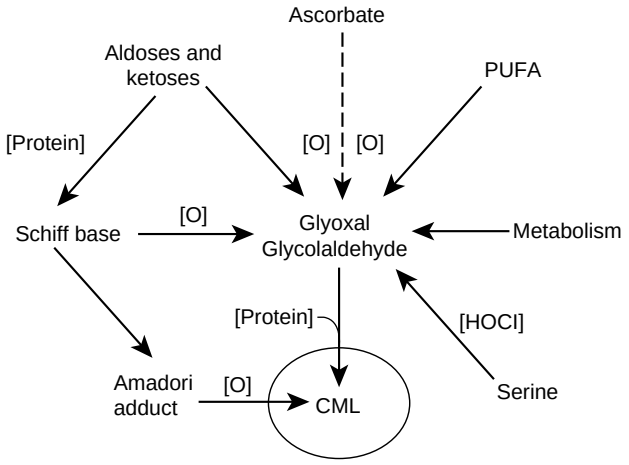

FIGURE 3 Alternative sources of the AGE/ALEs. CML may be formed from reducing sugars, either directly by oxidative cleavage of Schiff base or Amadori adducts on protein, or indirectly through glyoxal or glycolaldehyde formed on oxidation of glucose or glucose adducts to protein. CML may also be formed from ascorbate, through glyoxal, glycolaldehyde, or tetroses formed on oxidative degradation of dehydroascorbate. Glyoxal or glycolaldehyde are also formed during peroxidation of polyunsaturated fatty acids, or during myeloperoxidase-mediated degradation of amino acids.

Recognition and Turnover of AGE-Proteins

Nearly a dozen AGE-binding proteins have also been identified to date. The best characterized among the AGE receptors are RAGE (receptor for AGE), which is widely distributed among endothelial and parenchymal cells, and the macrophage scavenger receptors (MSRs). An unusual feature of these receptors is their range of ligand binding. In addition to binding of heterogeneously modified AGE-proteins, RAGE also recognizes the peptide amphoterin, which is involved in neuronal development, and the Aβ-amyloid peptide found in Alzheimer's plaque. MSRs were originally described as receptors for acetyl-LDL, later for their role in macrophage uptake of oxidized lipoproteins, then for their role in the recognition of AGE-proteins. The rapid uptake of injected AGE proteins (and oxidized LDL) in liver is consistent with a role for MSRs and the reticuloendothelial system in the removal of AGE-proteins from the circulation. A number of other candidate AGE receptor proteins have also been identified, based on interaction with AGE-proteins, but the determinants or motifs recognized by these receptors are, in most cases, unknown. Scavenger receptors recognize both AGE-proteins and oxidized lipoproteins, suggesting that common products are formed on chemical modification of proteins by both carbohydrates and lipids. CML has been proposed as a ligand for RAGE.

Binding of AGE-proteins to AGE-receptors appears to induce oxidative stress to cells, possibly because of the activity of AGEs, a source of reactive oxygen, in much the same way that binding and uptake of oxidized lipoproteins causes oxidative stress to cells bearing MSR. Thus, there is some risk to the cell involved in recognition and catabolism of AGEs, and chronic increases in AGE-induced oxidative stress have been invoked as a source of damage to endothelial cells and development of vascular and renal disease in diabetes. Under normal conditions, oxidative stress and protein turnover induced by AGE-proteins may have a role in the remodeling and rejuvenation of tissues, however this process may become pathogenic in chronic disease.

The Maillard Reaction in Aging and Disease

Aging

The age-dependent browning of tissue proteins is most apparent in the lens, which becomes visibly yellow with age. This change in color is accompanied by insolubilization, aggregation, and precipitation of lens crystallins, which may proceed to formation of cataracts.

Collagens and other long-lived proteins in the body undergo similar changes with age. The increased cross-linking of collagen contributes to the decrease in elasticity and resiliency of the extracellular matrix with age. By interfering with turnover of matrix components by metalloproteinases, browning reactions may also contribute to the age-dependent thickening of basement membranes in the microvasculature of the kidney, retina, and other tissues, affecting the permeability and transport properties of the matrix. The accumulation of AGEs in long-lived proteins (Figure 4) is accompanied by an age-dependent increase in protein fluorescence and by a parallel increase in other chemical modifications of proteins, including products of both nonoxidative (e.g., aspartate racemization, spontaneous deamidation) and oxidative damage (*o*-tyrosine, nitrotyrosine, dityrosine, and methionine sulfoxide). Research on the Maillard hypothesis today is focused on increasing evidence that AGEs have effector functions, i.e., they activate or participate in physiological responses to stress, including inflammation, hyperglycemia, and hyperlipidemia, and oxidative stress. Although proteins serve as the register or accumulator of Maillard reaction damage *in vivo*, glycoxidative and oxidative modifications of DNA are certain to have significant effects on the integrity of the genome during aging.

Diabetes

The glycation, AGE, or Maillard hypothesis identifies glucose as the culprit in diabetes, and proposes that diabetic complications result from accelerated Maillard reaction damage to tissue protein. Consistent with the hypothesis, both the extent of glycation of protein and the rate of accumulation of AGEs are accelerated by hyperglycemia in diabetes (Figure 4). The damage, like hyperglycemia, is systemic, and age-adjusted levels of AGEs in skin collagen are also correlated with the

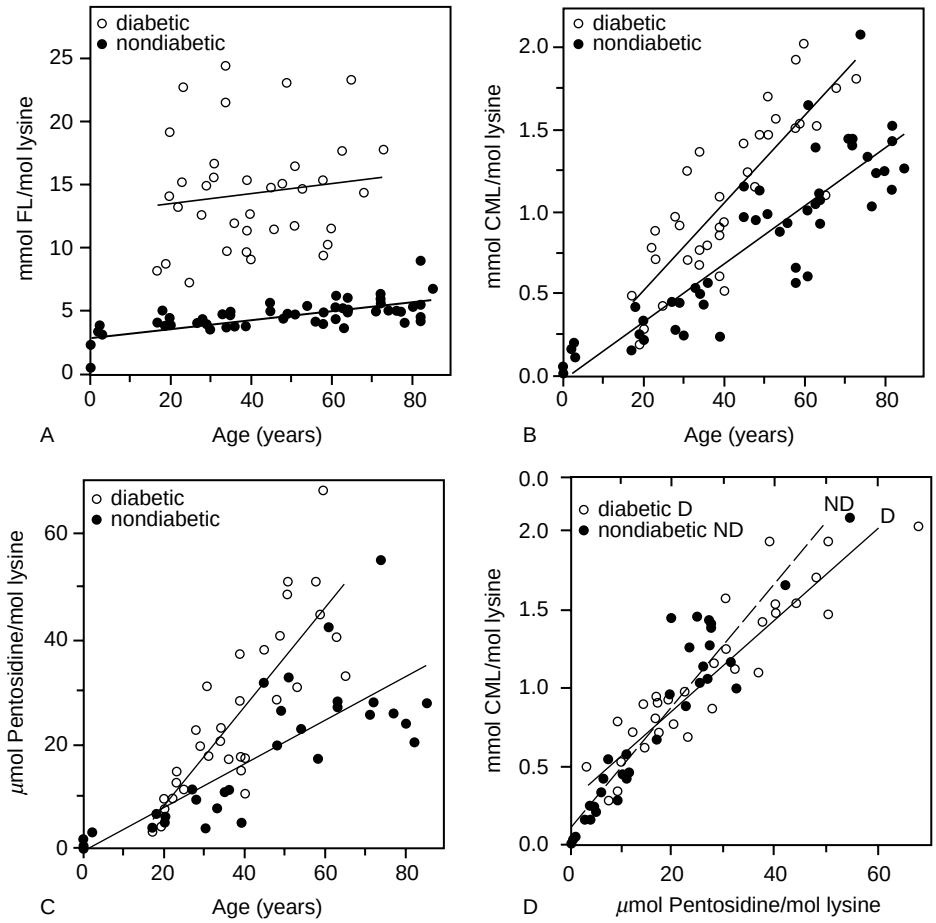

FIGURE 4 Influence of age and diabetes on glycation and glycoxidation of skin collagen. (A) Glycation of protein is reversible and relatively constant with age. Glycation of collagen increases with mean blood glucose concentration and correlates with GlcHb in diabetic patients. (B) and (C) The concentrations of the AGE/ALE, CML, and of the AGE, pentosidine, increase with age in the nondiabetic population and at an increased rate in diabetic patients. (D) Despite differences in origin and mechanism of formation and significant differences in their concentrations, the levels of CML and pentosidine in skin collagen correlate more closely with one another than with age in either control or diabetic populations. (Reproduced from Dyer, D. G., Dunn, J. A., Thorpe, S. R., Bailie, K. E., Lyons, T. J., McCance, D. R., and Baynes, J. W. (1993). Accumulation of Maillard reaction products in skin collagen in diabetes and aging. *J. Clin. Invest.* **91**, 2463–2469, with permission.)

severity of renal, retinal, and vascular complications of diabetes. The Maillard hypothesis is a chemical rather than metabolic theory on the origin of diabetic complications; it explains the development of similar complications in both type 1 (juvenile-onset, insulin-dependent) and type 2 (adult-onset, noninsulin-dependent) diabetes, despite the differences in etiology of these diseases (insulin deficiency versus insulin resistance). It also explains the development of complications in kidney, nerve, retina, and vasculature, since endothelial and parenchymal cells in these tissues are mostly independent of insulin for glucose transport. In these tissues, intracellular glucose tracks extracellular glucose concentration. These tissues are also rich in long-lived extracellular proteins, such as collagens, elastin, and myelin. In addition to the gradual accumulation of AGEs on extracellular proteins, AGEs are also formed on intracellular proteins in these tissues, probably from glycolytic intermediates, such as the triose phosphates. Research on intracellular glycation and AGE formation is still at an early stage, but is essential for a comprehensive understanding of the role of the Maillard reaction in the pathogenesis of diabetic complications.

AGE Inhibitors

Perhaps the most convincing evidence for the AGE hypothesis is the demonstrated efficacy of AGE-inhibitors in retarding the development of a wide range of complications in animal models of diabetes. Both aminoguanidine (AG) and pyridoxamine (PM) are potent inhibitors of formation of AGEs by autoxidation of sugars and Schiff base adducts to proteins, while PM, described as an Amadorin, also inhibits formation of AGEs from Amadori compounds. AG and PM inhibit the formation of AGEs and cross-linking of collagen *in vivo*, and also limit the increase in immunohistochemically detectable AGEs in tissues in diabetes. Other activities of these inhibitors may contribute to their efficacy *in vivo*, since they inhibit amine oxidases, including some isoforms of nitric oxide synthase, have weak chelating activity, and also have antihypertensive and hypolipidemic effect *in vivo*.

Other Diseases

AGEs and ALEs are increased in tissues in a wide range of age-related, chronic diseases, including diabetes, atherosclerosis, dialysis-related amyloidosis, arthritis, and neurodegenerative diseases. The increase in glycoxidative and lipoxidative damage reflects, in part, uncontrolled chemistry occurring, either locally or systemically, in biological systems as a result of tissue damage, decreased antioxidant defenses and increased decompartmentalization of metal ions. Although the AGE/ALEs are not the primary source of pathology in these diseases, they are macrophage chemoattractants and proinflammatory molecules, acting as both intermediaries in pathogenic processes and biomarkers of resultant tissue damage. AGE/ALE inhibitors may eventually prove useful for limiting damage or complications from a wide range of chronic, age-related diseases. Their effects on health and longevity are being explored in studies in animal models.

See Also the Following Articles

Collagens • Diabetes • Glycogen Storage Diseases • Insulin- and Glucagon-Secreting Cells of the Pancreas

Glossary

advanced glycation end-product (AGE) Irreversible end-product of nonenzymatic reaction of carbohydrates with protein; includes fluorescent and nonfluorescent adducts and cross-links in protein.

advanced lipoxidation end-product (ALE) Stable end-product of chemical modification of protein by reactive carbonyl intermediates formed during lipid peroxidation reactions.

Amadori adduct or **compound** First stable product of glycation of protein; a ketoamine.

glycation Enzymatic or nonenzymatic adduction of a carbohydrate to a biomolecule.

glycoxidation product AGE formed by a combination of glycation and oxidation chemistry.

Further Reading

Baynes, J. W., and Thorpe, S. R. (2000). Glycoxidation and lipoxidation in atherogenesis. *Free Radic. Biol. Med.* **28**, 1708–1716.

Bucciarelli, L. G., Wendt, T., Rong, L., Lalla, E., Hofmann, M. A., Goova, M. T., Taguchi, A., Yan, S. F., Yan, S. D., Stern, D. M., and Schmidt, A. M. (2002). RAGE is a multiligand receptor of the immunoglobulin superfamily: Implications for homeostasis and chronic disease. *Cell Mol. Life Sci.* **59**, 1117–1128.

Dyer, D. G., Dunn, J. A., Thorpe, S. R., Bailie, K. E., Lyons, T. J., McCance, D. R., and Baynes, J. W. (1993). Accumulation of Maillard reaction products in skin collagen in diabetes and aging. *J. Clin. Invest.* **91**, 2463–2469.

Miyata, T., Devuyst, O., Kurokawa, K., and van Ypersele de Strihou, C. (2002). Toward better dialysis compatibility: Advances in the biochemistry and pathophysiology of the peritoneal membranes. *Kidney Int.* **61**, 375–386.

Schleicher, E. D., Bierhaus, A., Haringm, H. U., Nawroth, P. P., and Lehmann, R. (2001). Chemistry and pathobiology of advanced glycation end products. *Contrib. Nephrol.* **131**, 1–9.

Stitt, A. W., Jenkins, A. J., and Cooper, M. E. (2002). Advanced glycation end products and diabetic complications. *Expert Opin. Invest. Drugs* **11**, 1205–1223.

Thorpe, S. R., and Baynes, J. W. (2003). Maillard reaction products in tissue proteins: New products and new perspectives. *Amino Acids* **25**, 275–281.

Ulrich, P., and Cerami, A. (2001). Protein glycation, diabetes, and aging. *Recent Prog. Horm. Res.* **56**, 1–21.

Vlassara, H. (2001). The AGE-receptor in the pathogenesis of diabetic complications. *Diabetes Metab. Res. Rev.* **17**, 436–443.

Vlassara, H., and Palace, M. R. (2002). Diabetes and advanced glycation endproducts. *J. Intern. Med.* **251**, 87–101.

Biography

Suzanne Thorpe and John Baynes are a husband-and-wife team who have worked together for over 25 years in teaching and research at the University of South Carolina. They study chemical modifications of proteins by carbohydrates, lipids, and oxidation reactions, focusing on the role of nonenzymatic chemistry in regulatory biology and in the pathogenesis of aging and age-related, chronic diseases.

Glycine Receptors

Bodo Laube and Heinrich Betz
Max-Planck Institute for Brain Research, Frankfurt, Germany

Glycinergic inhibition of neuronal excitability in spinal cord and brain stem is mediated via inhibitory glycine receptors (GlyRs). These receptors are composed of two types of homologous membrane-spanning subunits (α and β) and belong to the pentameric nicotinic acetylcholine receptor superfamily of ligand-gated ion channels. Binding of presynaptically released glycine to postsynaptically enriched GlyRs prevents membrane depolarization of nerve cells by opening receptor-intrinsic chloride channels and is specifically antagonized by the convulsant alkaloid strychnine. Mutations in *GlyR* genes give rise to neuromotor and startle disorders in humans and animals and underline the important roles of GlyRs in motor coordination and sensory processing.

Distribution of Glycine in the Brain

Although glycine is the simplest of all amino acids, it has diverse functions within the central nervous system (CNS). It serves as an inhibitory neurotransmitter at the GlyR and as a coagonist essential for the activation of excitatory *N*-methyl-D-aspartate receptors, in addition to being involved in the metabolism of proteins and nucleotides in all cells. The regional levels of glycine in the CNS mainly reflect its role in inhibitory neurotransmission, being highest in the medulla oblongata, pons, and spinal cord, and lowest in the cerebral hemispheres and the cerebellum.

Physiological Role and Functional Properties of Glycine Neurotransmission

Principal Properties of Glycinergic Inhibition

Excitation of glycinergic neurons in the CNS causes Ca^{2+} triggered release of presynaptic glycine into the synaptic cleft and results in the activation of postsynaptic GlyRs, which mediate an increase in the chloride conductance of the postsynaptic plasma membrane (Figure 1). These glycinergic synaptic currents have a complex time course with a fast rising phase and an exponential deactivation, which reflect the synchronous activation of GlyR channels by glycine released during exocytosis and the subsequent closure of individual channels, respectively. After receptor unbinding, glycine is removed from the synaptic cleft by rapid reuptake into presynaptic nerve terminals or surrounding glial processes to allow termination of the transmission process (Figure 1).

Roles in Spinal Control of Motor Activity and Sensory Processing

Inhibition at central synapses is mediated by both glycine and γ-aminobutyric acid (GABA). Whereas GABA is primarily used in higher brain regions, glycinergic synapses are particularly abundant in spinal cord and brain stem, i.e., structures involved in the control of motor rhythm generation, the coordination of spinal reflex responses and the processing of sensory signals. Ia glycinergic interneurons in spinal cord mediate reciprocal inhibition in stretch reflex circuits, allowing relaxation of the antagonist muscle, and thus contribute to the coordination of opposing muscles. Renshaw interneurons regulate motoneuron excitability by producing a recurrent inhibition via a negative feedback system. In sensory processing, glycine modulates neuronal circuits in the auditory system and in the retina and suppresses nociceptive signals in the spinal cord.

Synaptic Versus Extrasynaptic Inhibition

Although neurotransmission between nerve cells is mainly mediated by synaptic contacts, GlyRs are also found outside synapses in noninnervated plasma membrane regions (Figure 1). These extrasynaptic receptors are thought to be persistently activated by low concentrations of extracellular agonists and/or glycine spillover from active glycinergic synapses and have been implicated in the tonic inhibition of neurons and the development of the neocortex.

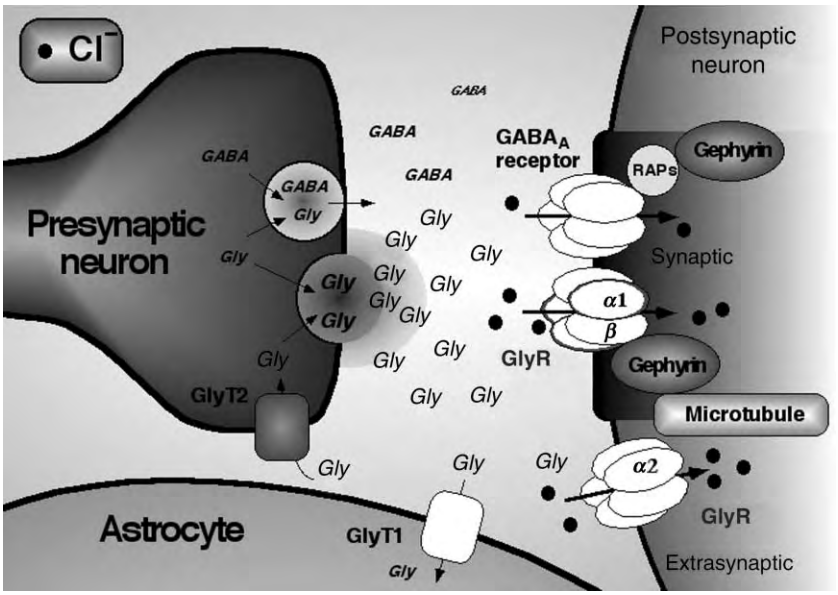

FIGURE 1 The glycinergic synapse. Excitation of the glycinergic terminal of interneurons causes Ca^{2+}-triggered fusion of glycine (and GABA) containing synaptic vesicles with the presynaptic plasma membrane, thus initiating glycine (and GABA) release into the synaptic cleft. This results in the activation of postsynaptic GlyRs which, by opening of the receptor integral anion channel in response to agonist binding, results in an increase in chloride conductance. Upon receptor unbinding, glycine is removed by specific glycine transporters located in the presynaptic (GlyT2) and the glial (GlyT1) plasma membranes. The synaptically localized GlyR interacts via its β-subunit with the submembraneous scaffold protein gephyrin, which binds to cytoskeletal components (tubulin) and receptor-associated proteins (RAPs), and thereby targets and anchors the GlyR (and $GABA_A$Rs) to postsynaptic specializations. Extrasynaptic GlyRs might play an important role in the tonic inhibition of neurons, due to persistent activation by low extracellular glycine concentrations or glycine spillover from adjacent glycinergic synapses.

Long-Term Plasticity of Glycinergic Synapses

Activity-dependent long-term changes in synaptic efficacy are important for many higher brain functions. Different forms of plasticity have been described for glycinergic synapses. For example, auditory stimulation triggers a form of long-term potentiation of glycinergic synapses that shares similarities with the long-term potentiation seen upon tetanic stimulation of excitatory connections. Consequently, increases in postsynaptic Ca^{2+} concentrations after high-frequency presynaptic activity are likely to affect the insertion and/or retrieval of GlyRs, and to thus modify inhibitory synaptic currents.

Switch from Excitatory to Inhibitory GlyR Function During Development

While glycine is a major inhibitory neurotransmitter in the adult CNS, activation of GlyRs does not always lead to membrane hyperpolarization and neuronal inhibition. During prenatal development of the brain, glycine acts as an excitatory transmitter that induces a depolarising chloride-dependent response, due to a more positive chloride equilibrium potential of embryonic neurons mediated by actively regulated chloride transport. This excitatory GlyR function seems to be important for synapse formation, since glycine-triggered rises in intracellular Ca^{2+} are crucial for the correct formation of glycinergic postsynaptic membrane specializations.

Mixed GABA and Glycinergic Synapses

The inhibitory neurotransmitters glycine and GABA are often colocalized in terminals of premotor inhibitory interneurons in the spinal cord. Furthermore, the protein gephyrin, which links GlyRs to the cytoskeleton, can promote clustering of major $GABA_A$ receptor subtypes at the same postsynaptic site. Since the relative strengths of the glycinergic and GABAergic components of "mixed" inhibitory synaptic transmission can change during development, this might reflect a complex interaction of these two inhibitory neurotransmitters at central synapses (Figure 1).

Structure and Diversity of GlyR Channels

Purification and Isolation of the GlyR

The GlyR was the first neurotransmitter receptor protein that was isolated from the mammalian CNS by affinity purification, using adsorption of the detergent-solubilized receptor on aminostrychnine-agarose followed by elution with the agonist glycine. The resulting preparation contained the pentameric GlyR composed of α- and β-subunits and the associated anchoring protein gephyrin.

Glycine Receptor Isoforms

Cloning of GlyR subunit cDNAs revealed that the GlyR belongs to the same superfamily of group I ligand-gated ion channels (LGICs) as the nicotinic acetylcholine receptor (nAChR), the GABA type A and C receptors ($GABA_{A/C}R$), the serotonin type 3 receptor ($5\text{-}HT_3R$) and the glutamate gated-chloride channel receptor (GluClR). The GlyR α- and β-subunits share significant sequence homology with each other ($>40\%$) and, to a lesser extent, with other proteins of the nAChR family. Homology is particularly high within the four transmembrane domains and a cysteine loop located within the N-terminal extracellular region. Four different genes encoding GlyR α-subunits ($\alpha 1\text{–}4$) have been identified in vertebrates with an overall sequence identity of $>80\%$. Alternative splicing in the extracellular N-terminal region and in the intracellular loop between transmembrane domains 3 and 4 generates further diversity. So far, only a single GlyR β-subunit gene has been found.

Spatial and Developmental Expression of GlyR Subunits in the Brain

In situ hybridization studies revealed that $\alpha 1$-GlyR subunit mRNA is mainly found in spinal cord, brain stem, and the colliculi, whereas GlyR $\alpha 2$-transcripts are found in the hippocampus, cerebral cortex, and thalamus (Figure 2). Low levels of $\alpha 3$-mRNA are detected in spinal cord, cerebellum, and olfactory bulb. The β-subunit gene is expressed throughout the entire CNS. GlyR $\alpha 1$- and $\alpha 2$-gene expression is subject to developmental regulation; $\alpha 1$-transcripts increase, and $\alpha 2$-mRNA decreases, after birth. This change in mRNA expression is reflected in an altered GlyR subunit composition and a faster decay time of inhibitory glycinergic postsynaptic currents. The neonatal form primarily composed of $\alpha 2$-homo-oligomers exhibits long channel open times, while the adult isoform is a $\alpha 1\beta$-hetero-oligomer characterized by fast channel kinetics.

Heterologous Expression of the GlyR

After heterologous expression, all GlyR α-subunits form functional homo-oligomeric channels with properties resembling those of native GlyRs. Single expression of the β-subunit does not result in either glycine-activated currents or [^{3}H]strychnine binding. Coexpression of α- and β-subunits generates hetero-oligomeric GlyRs that differ from homo-oligomeric α-GlyRs by their insensitivity to the channel blocker picrotoxinin and a reduced main state conductance.

Structural Features of the GlyR

Cross-linking and heterologous expression experiments have shown that the adult spinal GlyR is a pentameric complex composed of multiple copies of the ligand-binding $\alpha 1$- and β-subunits, which have molecular masses of 48 and 58 kDa, respectively. All subunits share a large and highly conserved N-terminal extracellular domain, four putative transmembrane domains (M1–M4), and a short extracellular C-terminus (Figure 2). Hydropathy analysis suggests that all four transmembrane segments are α-helices.

Molecular Model of the Ligand-Binding Region

The significant extent of sequence homology within the group I ligand-gated ion channel superfamily indicates that its members share a common structural organization. Composite ligand-binding sites, conserved throughout this receptor family, are located at the extracellular interface between subunits and involve contact residues that belong to distinct loops of two adjacent subunits. Homology modeling of the $\alpha 1$-subunit of the GlyR based on the crystal structure of the homologous soluble acetylcholine-binding protein from the snail *Lymnea stagnalis* (Brookhaven PDB entry 1I9B) has provided intriguing clues about the subunit architecture and the ligand-binding sites of these receptors.

Ion Channel Function

The second transmembrane domain M2 forms the ion channel of the GlyR. It is highly anion selective, with a

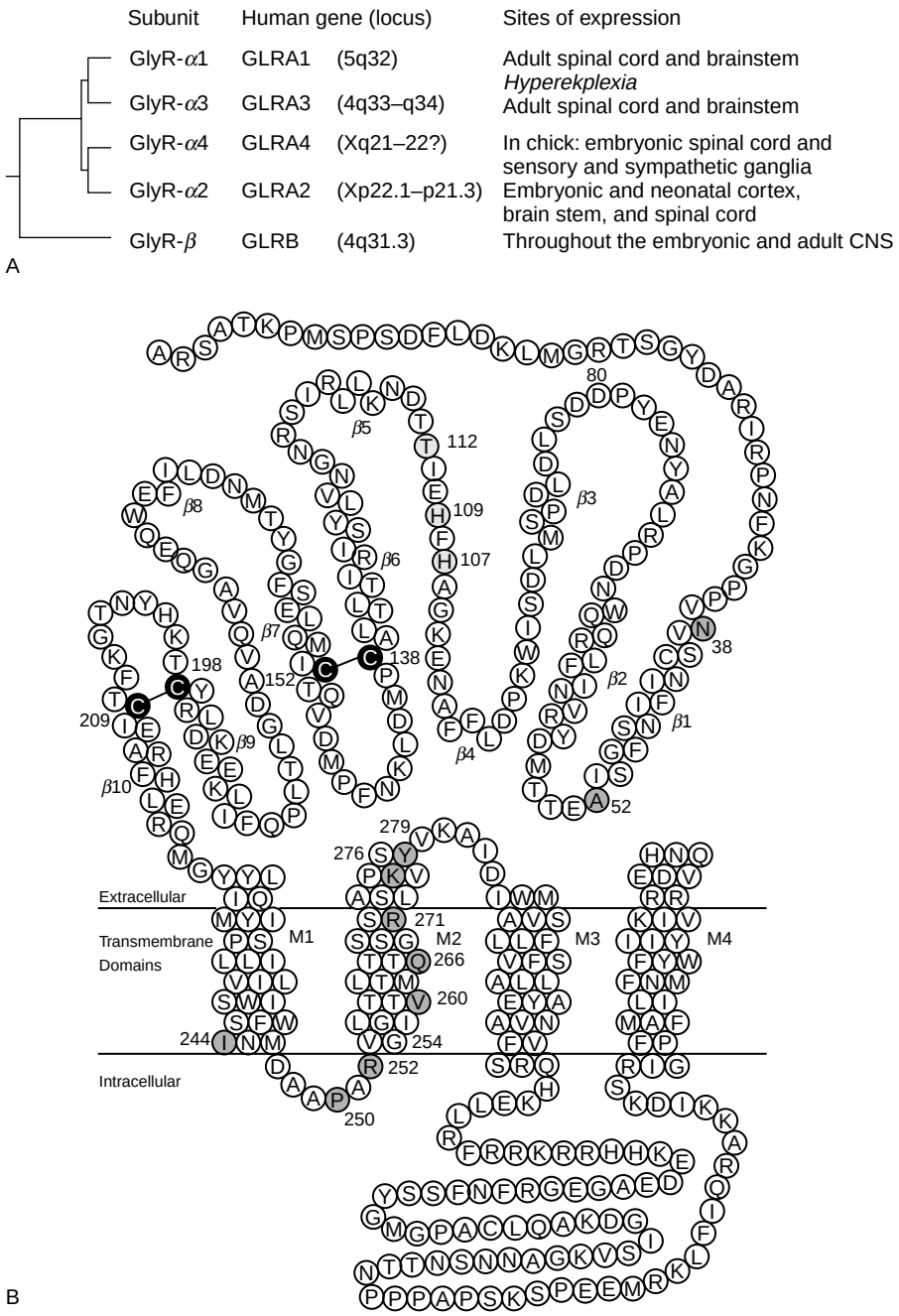

FIGURE 2 Phylogenetic relationships between and transmembrane topology of vertebrate GlyR subunits. (A) Evolutionary relationships between GlyR subunits. In addition to individual subunits, the chromosomal localizations of the human genes and their major sites of expression are indicated. (B) Transmembrane topology of the human GlyR-α1-subunit, with amino acid residues mutated in human hyperekplexia (gray residues) being indicated. Conserved cysteine residues forming disulfide bridges are shown in black. Residue N38 constitutes the sole N-glycosylation site. Mutation A52S is found in the *spasmodic* mouse. G254 in M2 of the α1-subunit determines the main conductance and sensitivity to the channel blocker CTB. Residue D80 is an important determinant of Zn^{2+} potentiation, whereas residues H107, H109, and T112 are essential for Zn^{2+} inhibition. Secondary structure predictions for the extracellular and transmembrane domains are indicated by amino acid residues being arranged in β-sheet (β1–β10), or α-helical (M1–M4), structures, respectively.

halide selectivity sequence of $I^- > Br^- > Cl^-$, and is significantly permeable to bicarbonate. A characteristic of GlyRs is that they do not exhibit a single conductance state but instead display a range of conductance states, with residue Gly 254 within the second transmembrane domain constituting a major determinant of ion flux (Figure 2). Hetero-oligomeric α1/β-GlyRs show lower subconductance state levels than α1-homomeric receptors, and in this respect resemble the adult native receptors.

The Cytoplasmic Loop of the β-Subunit is Crucial for Postsynaptic Receptor Clustering

A protein of 93 kDa, named gephyrin, copurifies with the GlyR and is enriched on the cytoplasmic face of the postsynaptic membrane. A short amino acid motif within the cytoplasmic loop, linking the third and fourth transmembrane domains of the GlyR β-subunit, forms the binding site for gephyrin. Thus, synaptically localized GlyR is bound via its β-subunit to the submembraneous scaffold protein, gephyrin, which interacts with cytoskeletal components and receptor-associated proteins, and thereby targets and anchors the GlyR to postsynaptic membrane specializations (Figure 1).

Pharmacological Properties of the GlyR

The Classical Antagonist Strychnine

The alkaloid strychnine constitutes a unique tool in the investigation of the GlyR. In electrophysiological studies, it is the most reliable antagonist to distinguish glycinergic from GABAergic inhibition. Biochemists use glycine-displaceable [^{3}H]strychnine binding to quantify the GlyR in radioligand-binding assays. The physiological symptoms of strychnine poisoning emphasize the importance of glycinergic inhibition in the control of both motor behavior and sensory processing. Due to its high toxicity, which causes convulsions and, at higher doses, death, strychnine is of low therapeutical value but serves as a rat poison.

Agonistic Amino Acids

In addition to glycine, the endogenous amino-acids β-alanine and taurine display inhibitory activity when applied to neurons. Taurine released nonsynaptically from immature cortical neurons has been found to influence cortical development by activating extrasynaptic GlyRs. The role of β-alanine is less clear. Despite being synthesized endogenously, evidence for an *in vivo* transmitter function of this amino acid is lacking. Both β-alanine and taurine are partial agonists, which can elicit only submaximal currents.

Antagonism by Channel Block

The alkaloid picrotoxinin acts as a use-dependent but voltage-independent open-channel blocker of the GlyR and can be used to discriminate homo- from hetero-oligomeric receptors. Hetero-oligomeric GlyRs composed of α- and β-subunits are relatively resistant to block by picrotoxinin, whereas homo-oligomeric GlyRs containing only α-subunits are sensitive to low micromolar alkaloid concentrations. The bulky organic anion cyanotriphenylborate (CTB) blocks GlyR channels in a use-dependent fashion, with the exception of homomeric α2-GlyRs.

Allosteric Modulation of the GlyR

Only a few agents are known to potentiate GlyR function. Therapeutically, potentiation of glycinergic inhibition in the mammalian CNS has substantial promise for both normalizing pathological states and for lowering sensory and motor activity under different conditions including narcosis.

Anesthetics and Alcohol

Since decades, anesthetics and alcohols are known to potentiate GlyR responses. Anesthetic concentrations of propofol and volatile halogenated hydrocarbons such as halothane, enflurane, isoflurane, methoxyflurane, and sevoflurane enhance the effects of low concentrations of glycine at the GlyR. The potencies of n-alcohols increase with chain length of their alkyl groups, up to a cut-off value of twelve carbon atoms. Using site-directed mutagenesis, residues within the transmembrane domains have been shown to be important for the potentiating effect of anesthetics and alcohol.

Zinc

The divalent cation Zn^{2+} exhibits biphasic effects on both native and recombinantly expressed GlyRs. Low concentrations of Zn^{2+} (0.1–10 μM) potentiate submaximal glycine-induced currents about threefold, while higher concentrations cause inhibition. Since Zn^{2+} is present within presynaptic secretory vesicles and is coreleased with the neurotransmitter upon stimulation, this modulation might be of considerable physiological significance. Mutational studies indicate that the Zn^{2+}-binding sites for potentiation and inhibition are located at subunit interfaces, as are the agonist-binding sites.

Neurosteroids

Steroids markedly affect glycinergic transmission; however, their actions are variable and show a strong dependence on subunit composition. This has been interpreted as evidence for heterogenous binding sites of neurosteroids existing on the GlyR. *In vivo*, steroid

effects on GlyR activity may be particularly important at the time of birth and during adolescence.

Posttranslational Modifications

GlyR subunits contain consensus sequences for glycosylation (Figure 2), phosphorylation (protein kinases A and C, Ca^{2+}-dependent kinases), and ubiquitination. Although a regulation of GlyR channel activity by phosphorylation was observed in different preparations, consistent with a potential role of protein kinases in the modulation of synaptic efficacy, the functional significance of GlyR phosphorylation is far from being clear. Also, ubiquitin-mediated internalization and degradation of the GlyR have been suggested to constitute important mechanisms for regulating receptor numbers in the neuronal plasma membrane.

Disorders of Glycinergic Neurotransmission

Mutations in GlyR subunits causing an impairment of glycinergic transmission result in neurological malfunction and hereditary neuromotor disease.

Human Disorders

The first disorder associated with a mutation in a neurotransmitter receptor was found by positional cloning. Hyperekplexia (startle disease, Kok disease) is characterized by muscle rigidity of nervous system origin, particularly in neonates, and by an exaggerated startle response to unexpected auditory or tactile stimuli. The underlying genetic defect was mapped to chromosome 5q by genetic linkage using DNA markers defining the GlyR-α1 gene, *GLRA1*, as the prime candidate. Substitutions of the charged residue Arg 271 by uncharged amino acids (Leu or Gln) were identified in four families with autosomal dominant hyperekplexia. These substitutions result in a reduction of agonist sensitivity and glycine-activated current. Recombinant expression of the mutant GlyRs revealed that the reduced glycine current is due to a decrease in single-channel conductance levels. Recessive forms of hyperekplexia have subsequently been identified in other families, which carry other missense or null mutations in the *GLRA1* locus (Figure 2). However, in only 40–50% of the human patients displaying hyperekplexia-like symptoms *GLRA1* mutations have been found, suggesting that genes other than *GLRA1* could be involved in hyperekplexia.

Animal Mutants

The syntenies between human chromosome 5q and mouse chromosome 11 led to the discovery that recessive mutations in mouse *GLRA1* underlie two mouse neurological mutants, *spasmodic* and *oscillator*. *Spasmodic* displays a phenotype similar to human hyperekplexia and is caused by missense mutation of Ala 52 to Ser (Figure 2). *Oscillator* has a more severe phenotype, including progressive tremor and muscle spasms, leading to death by 3 weeks of age. Lethality is caused by a frameshift-producing deletion predicted to eliminate the large cytoplasmic loop and the fourth transmembrane domain. Homozygous *spastic* mice develop at ~2 weeks postnatally a hyperekplexic phenotype that is associated with a marked reduction in the density of GlyRs in brain stem and spinal cord. The disorder results from the insertion of a LINE-1 element into an intronic region of the gene encoding the β-subunit of the GlyR (GLRB), thereby causing delayed and aberrant splicing of the β-subunit mRNA. A disease resembling the human and murine startle diseases is found in Poll-Hereford cattle and Peruvian Paso horses. These animals display strong myoclonus resulting from reduced or absent GlyR expression in the spinal cord. In the Poll-Hereford cattle, a missense mutation at Thr24 of the *GlyR-α1* gene has been shown to cause a translational stop, and thus a complete α1-subunit deficiency in homozygous animals.

See Also the Following Articles

Amino Acid Metabolism • $GABA_B$ Receptor • Ligand-Operated Membrane Channels: GABA • Protein Kinase C Family • Ubiquitin System

Glossary

gephyrin From the Greek word for bridge. Protein that anchors the GlyR to the subsynaptic cytoskeleton.

LGICs Family of receptor proteins composed of homologous subunits, whose intrinsic ion channel opens after binding of neurotransmitter.

startle disease Human hereditary disorder characterized by an exaggerated startle reaction in response to unexpected stimuli.

strychnine A plant alkaloid derived from the Indian tree *Strychnos nux vomica*. A potent convulsant antagonizing glycinergic inhibition.

Further Reading

Becker, C. M. (1992). Convulsants acting at the inhibitory glycine receptor. In *Handbook of Experimental Pharmacology* (H. Herken and F. Hucho, eds.) pp. 539–575. Springer, Berlin, Heidelberg.

Kneussel, M., and Betz, H. (2000). Clustering of inhibitory neurotransmitter receptors at developing postsynaptic sites: The membrane activation model. *Trends Neurosci.* **23**, 429–435.

Kuhse, J., Betz, H., and Kirsch, J. (1995). The inhibitory glycine receptor: Architecture, synaptic localization and molecular pathology of a postsynaptic ion channel complex. *Curr. Opin. Neurobiol.* **5**, 318–323.

Laube, B., and Betz, H. (1999). Purification and heterologous expression of inhibitory glycine receptors. *Meth. Enzymol.* **294**, 260–273.

Laube, B., Maksay, G., Schemm, R., and Betz, H. (2002). Modulation of glycine receptor function: A novel approach for therapeutic intervention at inhibitory synapses? *TiPS* **23**, 519–527.

Rajendra, L., Lynch, J. W., and Schofield, P. (1997). The glycine receptor. *Pharmacol. Ther.* **73**, 121–146.

Schofield, P. (2002). The role of glycine and glycine receptors in myoclonus and startle syndromes. *Adv. Neurol.* **89**, 263–274.

Biography

Bodo Laube studied biology in Frankfurt, where he received his Diploma of Zoology (1991), Ph.D. (1995) and *venia legendi* (2003) from the Johann Wolfgang Goethe Universität. Since 1997, he is a Staff Scientist in the Neurochemistry Department of the MPI for Brain Research in Frankfurt.

Heinrich Betz studied biochemistry and medicine in Tübingen and Munich and obtained his M.D. from the University of Tübingen. After working in Freiburg, Paris, and Munich, he was a Professor of Molecular Neurobiology and Neuropharmacology at the University of Heidelberg. He is currently the Head of the Neurochemistry Department at the MPI for Brain Research in Frankfurt.

Glycogen Metabolism

Peter J. Roach
Indiana University School of Medicine, Indianapolis, Indiana, USA

Glycogen, a polymer of the sugar glucose, functions as a reserve of energy and structural building blocks in organisms from bacteria to humans. It is synthesized when nutrients are available for utilization in times of need. In mammals, the two largest deposits of glycogen are in skeletal muscle and liver; muscle glycogen is utilized locally to help fuel muscular activity, whereas liver glycogen is broken down to glucose that is delivered into the bloodstream. After a meal, elevated blood glucose causes the hormone insulin to be released from the pancreas and to stimulate conversion of ingested glucose into glycogen in muscle, liver, and other tissues. Upon fasting, such as overnight, the pancreatic hormone glucagon signals the breakdown of liver glycogen to stabilize blood glucose levels, essential for brain and blood cell function. The hormone epinephrine stimulates glycogen breakdown in liver and muscle to cope with stressful situations.

Glycogen Structure

Many nutrients contain either glucose or compounds that are easily converted to glucose, so that it is an important nutritional currency for many organisms. Glycogen is a glucose polymer meaning that individual glucose units are joined together by repeated chemical linkages to form large molecules containing thousands of glucose residues (Figure 1). Two types of linkages are present in glycogen causing a branched polymeric structure. These same two linkages are present in plant starches which serve a similar function as glycogen. When needed, the glucose units can be recovered by breaking down the glycogen. A possible explanation for the storage of glucose as glycogen rather than glucose monomers is the lower osmotic activity of the polymer.

Glycogen Metabolism

Glycogen exists as a particle in which the carbohydrate core is associated with several of the proteins needed to make it and to degrade it. The glycogen molecule expands or contracts due to growth or breakdown of the outer branches of the molecule (Figure 1).

Synthesis

Glycogen in cells is either synthesized directly from glucose transported into the cells by transporter proteins or from other cellular metabolites that are converted to the activated sugar precursor, UDP-glucose in animals, and ADP-glucose in bacteria (or for starch biosynthesis in plants). Three enzymes are needed to synthesize glycogen: an initiator protein called glycogenin that attaches glycogen residues to itself; the enzyme glycogen synthase responsible for incorporating most of the glucose moieties of glycogen from UDP-glucose; and a special enzyme, branching enzyme, to introduce the branchpoints (Figure 2).

Degradation

Controlled degradation of glycogen requires two enymes (Figure 2). Glycogen phosphorylase releases a glucose unit from the polymer as a metabolite, named glucose-1-P, that can be used by the cell. Since phosphorylase stalls at the branch points, a second specialized enzyme, the debranching enzyme, is needed to degrade past them. In muscle, the process stops at another metabolite of glucose, called glucose-6-phosphate, which is used in the muscle cell to provide energy or building blocks. In liver the glucose-6-phosphate can be converted, by an enzyme called glucose-6-phosphatase, to free glucose that is exported to the bloodstream. There is a second pathway to degrade glycogen. In most cell types, there is a house-cleaning process whereby a portion of the cellular content is continuously being delivered to an organelle, called a lysozome or vacuole, to recycle the building blocks of the macromolecules, like amino acids from proteins and glucose from glycogen. A specialized enzyme, called an α-glucosidase, is present in the lysosome to break glycogen down to glucose.

Glycogen Function and Control

Metabolic Role

Whether in bacteria or mammals, glycogen serves as a reservoir of energy and/or building blocks that can be

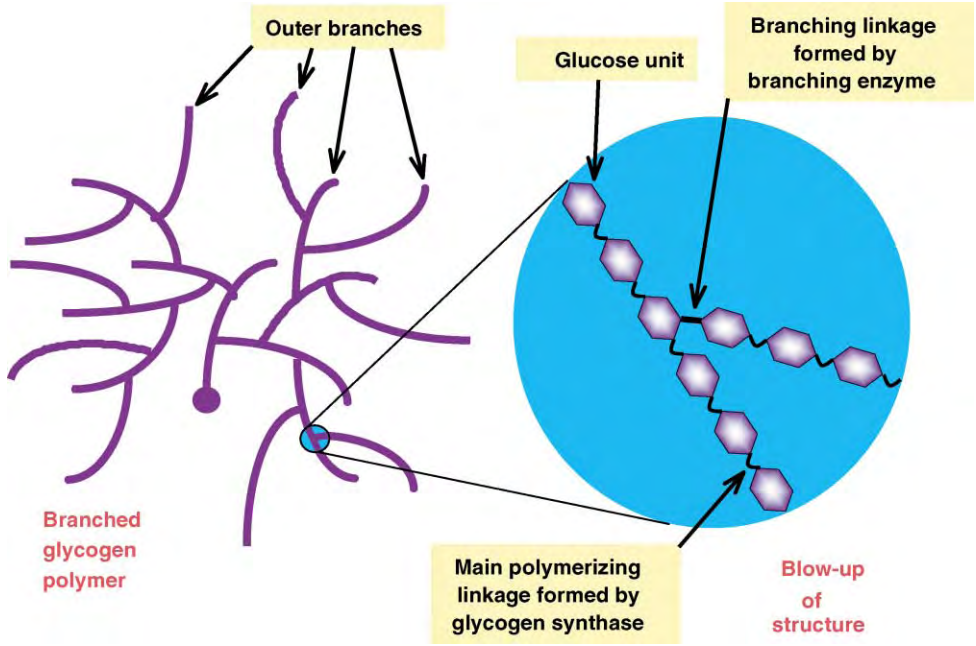

FIGURE 1 Glycogen is a polymer of glucose units.

called upon in times of need. In microorganisms, glycogen is generally made in response to impending nutritional deprivation, as judged by sensing the composition of the environment, and stored for use later during starvation. In mammals, the nutritional cues that govern glycogen metabolism in tissues are indirect and are borne by the blood levels of glucose itself and several important regulatory hormones. After a meal, nutrients enter the gut and lead to increased blood glucose which triggers the pancreas to release the hormone insulin, a signal of the fed condition. Insulin-sensitive tissues, liver, fat, and especially skeletal muscle, respond by increasing transport of glucose into the cells (Figure 3A). Insulin also causes activation of the enzyme

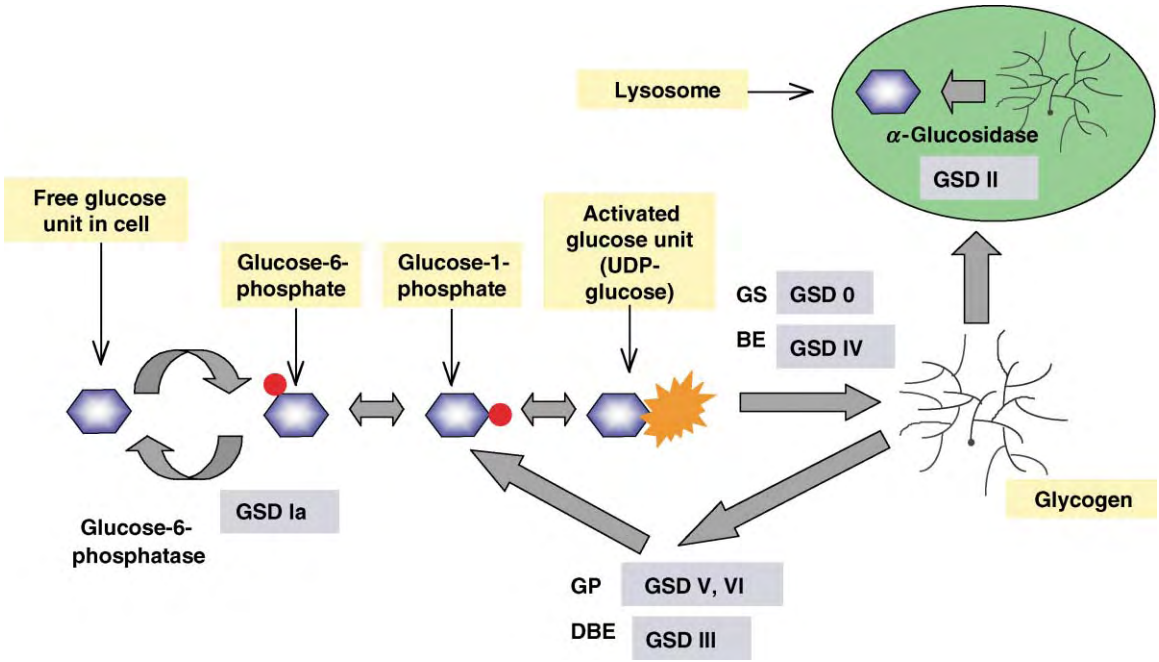

FIGURE 2 The pathways of glycogen production and degradation. GSD, glycogen storage disease; GS, glycogen synthase; BE, branching enzyme; GP, glycogen phosphorylation; DBE, debranching enzyme.

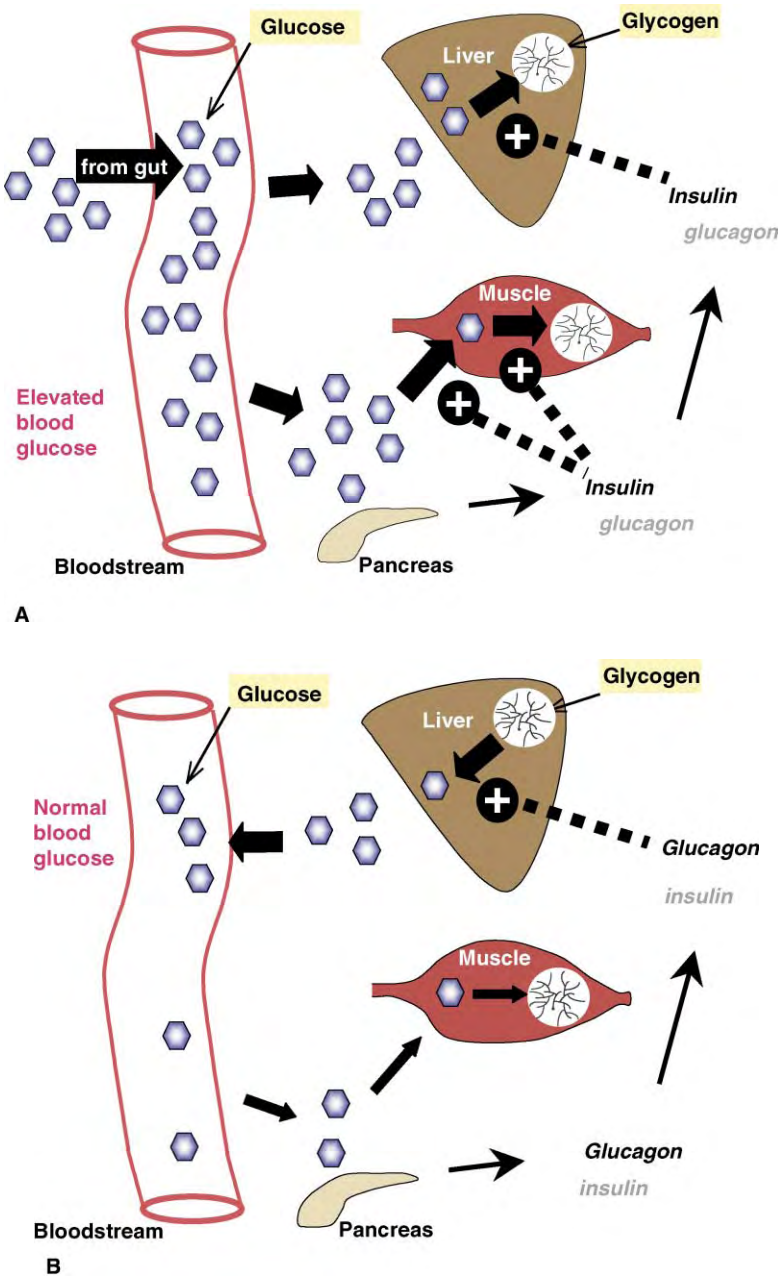

FIGURE 3 The interconversion of glucose and glycogen in the fed (A) and fasted (B) states.

glycogen synthase enhancing the conversion of glucose to glycogen. This is part of the process of blood glucose homeostasis whereby the body seeks to maintain the blood glucose level within safe limits. As the time after the last meal increases, the blood glucose level normalizes, the pancreas delivers less insulin and begins to secrete the hormone glucagon, which signals the unfed state (Figure 3B). The primary target is the liver which responds by breaking down glycogen to produce glucose that can be delivered to the bloodstream – another contribution to blood glucose homeostasis.

Role in Muscle or Exercise

Unlike the liver, muscle cannot breakdown glycogen all the way to free glucose for export to the bloodstream. Muscle glycogen is instead broken down to metabolites that can be converted to energy to fuel muscular contraction. The stimulus for the breakdown of muscle glycogen is the same as for contraction, and nerve signals telling the muscle to contract concurrently activate glycogen phosphorylase, which breaks down glycogen. Most muscles do not rely entirely on glycogen, and other fuels, such as fat, can also be utilized. Increased muscular

TABLE I

Selected Glycogen Storage Diseases (GSD)

GSD type	Name	Enzyme affected	Affected organ(s)	Glycogen	Description
0		Glycogen synthase	Liver	Reduced amount	Hypoglycemia
Ia	Von Gierke's disease	Glucose-6-phosphatase	Liver	Normal structure, increased amount	Massive liver enlargement, multiple metabolic problems, treatment improving
II	Pompe's disease	Lysosomal α-glucosidase	All	Increased glycogen in lysosomes	Usually death before age 2
III	Cori's disease	Debranching enzyme	Muscle, liver	Short outer branches, increased amount	Similar to type I, but less severe
IV	Andersen's disease	Branching enzyme	Liver	Long outer branches, normal amount	Usually death from liver failure before age 2
V	McArdle's disease	Muscle glycogen phosphorylase	Muscle	Normal structure, moderate increase in amount	Impaired exercise capability
VI	Hers' disease	Liver glycogen phosphorylase	Liver	Increased amount	Similar to type I but less severe

activity is often associated with increased levels of the stress hormone, epinephrine (also called adrenaline). In response to anxiety, which in evolution might have involved fleeing an aggressor, the adrenal gland produces epinephrine which activates phosphorylase in muscle and liver, providing enhanced muscle performance and increased fuel to the bloodstream respectively. Muscular activity also sensitizes the tissue to insulin and activates glycogen synthase, so that it is ready to reform glycogen once contraction ceases.

Glycogen and Disease

Glycogen Storage Diseases

A number of genetic diseases are known in which genes encoding the enzymes involved in glycogen metabolism are mutated (Table I and Figure 2). These diseases range in severity from relatively mild to early death. Their frequency is for the most part relatively low. Most of these diseases are associated with overaccumulation of glycogen or the formation of abnormally branched glycogen. One disease called glycogen storage disease 0, is associated with mutations that impair liver glycogen synthesis, and patients are prone to low blood glucose (hypoglycemia).

Diabetes Mellitus

Diabetes occurs when blood glucose homeostasis fails and blood glucose levels are elevated. High blood glucose (hyperglycemia) leads to many complications including heart, kidney, nerve, and eye disease. This disease is extremely common and growing in epidemic fashion as enrichments in diets around the world are coupled with diminished physical activity and obesity. The more prevalent form, type 2 diabetes, has a genetic component, likely linked to multiple genes, and an environmental component, lack of exercise and unhealthy diet. Type 2 diabetes is associated with an impaired ability to store glucose as glycogen but whether there is a causal relationship with defective glycogen metabolism is still not certain.

See Also the Following Articles

Diabetes • Glycogen Storage Diseases • Insulin- and Glucagon-Secreting Cells of the Pancreas

Glossary

enzyme A protein that catalyzes or accelerates chemical reactions, such as those involved in metabolism, to interconvert compounds in cells.

hormone A compound in the blood released from specialized organs, called endocrine glands, that acts as a messenger within the body to regulate the function of individual target tissues.

metabolism The process by which molecules are interconverted within cells among different related chemical forms, called metabolites.

pancreas An organ with multiple functions related to the utilization of foods. The endocrine pancreas responds to the nutrient levels in the blood to release the hormones insulin and glucagon.

Further Reading

Chen, Y.-T. (2001). Glycogen storage diseases. In *The Metabolic and Molecular Bases of Inherited Disease* (C. R. Scrives, W. S. Sly, B. Childs *et al*. eds.) 8th edition, Vol 1, pp. 1521–1551. McGraw-Hill, New York.

Harris, R. A. (2002). Carbohydrate metabolism I: Major metabolic pathways and their control. In *Textbook of Biochemistry with Clinical Correlations* (T. M. Devlin, ed.) 5th edition, pp. 597–664. Wiley-Liss, New York.

Harris, R. A., and Crabb, D. W. (2002). Metabolic interrelationships. In *Textbook of Biochemistry with Clinical Correlations* (T. M. Devlin, ed.) 5th edition, pp. 861–902. Wiley-Liss, New York.

Preiss, J., and Walsh, D. A. (1981). The comparative biochemistry of glycogen and starch. In *Biology of Carbohydrates* (V. Ginsburg and P. Robbins, eds.) Vol 1. Wiley, New York.

Roach, P. J., Skurat, A. V., and Harris, R. A. (2001). Regulation of glycogen metabolism. In *Handbook of Physiology Section 7, The Endocrine Pancreas and Regulation of Metabolism* (L. S. Jefferson and A. D. Cherrington, eds.) Vol. 2, pp. 609–647. Amer Physiological Society, MD.

Biography

Peter J. Roach, graduate of Glasgow University, is Chancellor's Professor at Indiana University School of Medicine in the Department of Biochemistry and Molecular Biology. His research addresses biological regulation at the molecular level and has focused on the control of glycogen synthesis in mammals and yeast. His principal contributions have been in defining the phosphorylation and control of glycogen synthase, including the concept of heirarchal phosphorylation, and the characterization of the self-glucosylating initiator of glycogen synthesis, glycogenin.

Glycogen Storage Diseases

George H. Sack, Jr.
The Johns Hopkins University, Baltimore, Maryland, USA

Glycogen storage diseases (GSDs) comprise a group of inherited disorders caused by dysfunction of the synthesis or degradation of glycogen. Manifestations of GSDs are largely related to their direct effects on liver and/or muscle metabolism. The medical consequences of GSDs directly relate to glycogen's central role in glucose homeostasis. Analysis of this group of disorders has identified most of the enzymes directly related to glycogen metabolism. Recognition of the presence and consequences of GSD is the basis for rational treatment of individuals with these rare conditions.

Glycogen Structure

As shown in Figure 1, glycogen is composed of a large number of glucose polymers with (α1–4) linkages that are branched with (α1–6) linkages every 4–10 units. The resulting particles, called β-particles, can become large and contain 6×10^5 individual glucose monomers and these can be grouped into even larger particles called α-particles. The β-particles are organized around a central protein called glycogenin upon which the initial glucose polymerization is based. There is also a thin bounding membrane that appears to contain most of the enzymes of glycogen metabolism. Glycogen is found mainly in liver and muscle.

Glycogen Function

Glycogen is a source of glucose for both muscle and liver. As such it serves as a short-term buffer for glucose homeostasis (liver) and a source of immediate glucose for energy (muscle). The synthesis and degradation of glycogen are closely regulated. Consistent with its function in homeostasis, these processes are controlled by different enzyme systems and hormones. Synthesis is not the reverse of degradation and most of the enzymes catalyze reactions strongly in favor of their products (i.e., they are not at equilibrium). Several of the enzymes are regulated by covalent modification.

Glycogen Metabolism

Figure 2 presents a summary of the pathways involved in glycogen metabolism. Note that several are unique to either liver or muscle. Considerable metabolic control is also exerted on these enzymes as shown.

Glycogen Synthesis

The first committed step in glycogen synthesis is the formation of UDP glucose by UDP glucose pyrophosphorylase. The glycogen polymer begins with the attachment of glucose to the protein glycogenin. UDP glucose is the substrate for polymerization via (α1–4) linkages catalyzed by glycogen synthase. The branching enzyme is bifunctional, cleaving the linear chain and creating a branch via an (α1–6) linkage. This leads to a reduced length of the final polymer and the production of more termini—leading to a more compact particle and providing a substrate suitable for very rapid degradation.

Glycogen Degradation

Most individual glucose residues are removed from the glycogen polymer by phosphorolysis. Different phosphorylase enzymes catalyze this reaction in muscle and liver. These proteins are genetically unique—synthesized from different loci. Muscle phosphorylase has been studied in particularly great detail. It functions as a dimer and contains sites for both covalent and allosteric modifications. Phosphorylase must itself be phosphorylated to be active, a reaction catalyzed by phosphorylase kinase (which itself is dependent on modification by a cAMP-dependent kinase and calcium).

Because of the branched nature of mature glycogen, either muscle or liver phosphorylase by itself can only partially degrade the polymer. Phosphorylase cannot cleave beyond four glucose residues from the branch point. Glycogen subjected to treatment with phosphorylase alone is converted into limit dextran—itself a still very large molecule. The action of the debranching enzyme eliminates the barrier to phosphorolysis by transferring the three distal glucose residues from the

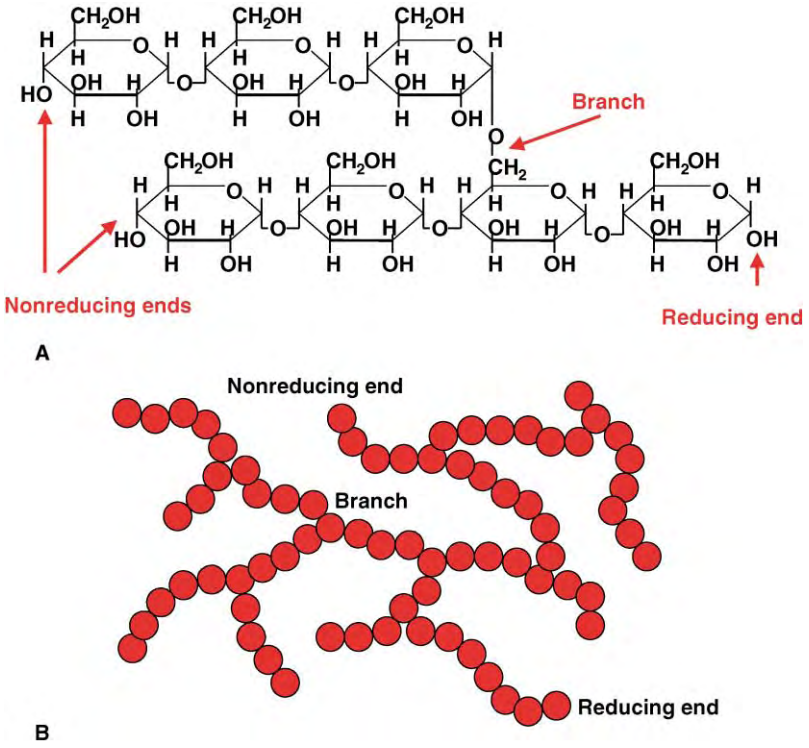

FIGURE 1 (A) Details of glycogen polymer showing linear (α1–4) and branch (α1–6) linkages. (B) Example of glycogen at lower resolution showing branches and reducing and nonreducing ends.

side chain to the nonreducing terminus of the parent chain. This leaves a single glucose remaining from the side chain attached by an α1–6 linkage. The debranching enzyme also hydrolyzes this remaining side-chain residue, freeing a single glucose molecule and leaving a continuous chain connected by α1–4 linkages, a substrate suitable for phosphorylase.

The products of glycogen degradation are thus predominantly glucose-1-phosphate and a small amount of free glucose from hydrolysis of the single remnant glucose of the side chain. The reversible phosphoglucomutase converts glucose-1-phosphate to glucose-6-phosphate. Because glucokinase is irreversible, the glucose-6-phosphate enters the endoplasmic reticulum (ER) by its own transporter. Within the liver ER, the glucose-6-phosphate is hydrolyzed and another specialized transporter transfers the free glucose outside the cell. The phosphate is also removed by its own transporter. Glucose-6-phosphatase is largely confined to the liver and thus the degradation of glycogen in muscle is not a source of blood glucose.

Control of Glycogen Metabolism

Because of the irreversibility of many of the enzymes involved and consideration of the details of Figure 2, the synthesis and degradation of glycogen do not use the same pathways. Furthermore, the enzymes mediating both sets of reactions are under tight control. This control often is mediated by addition and removal of phosphate to and from the proteins as shown. Several critical control points are given as follows:

1. The phosphorylated form of glycogen synthase (noted as "b" in the figure) is activated by removal of the phosphate to the "a" form by the active form of phosphoprotein phosphatase. The latter is produced by phosphorylation using ATP, stimulated by insulin.
2. Phosphorylase is active in its phosphorylated form, produced by the active form of phosphorylase kinase and ATP.
3. Phosphorylase kinase itself is activated by phosphorylation by cAMP-dependent protein kinase A.
4. The active, phosphorylated forms of both phosphorylase kinase and phosphorylase are inactivated through removal of the activating phosphate by the active form of phosphoprotein phosphatase as shown.

Thus, modification of existing enzymes regulates glycogen metabolism. This exquisitely sensitive system is subject to hormonal control. For example, a rise in insulin (the "fed" state with high blood glucose levels) activates phosphoprotein phosphatase (by phosphorylation). This enzyme then activates glycogen synthase and *in*activates phosphorylase and phosphorylase

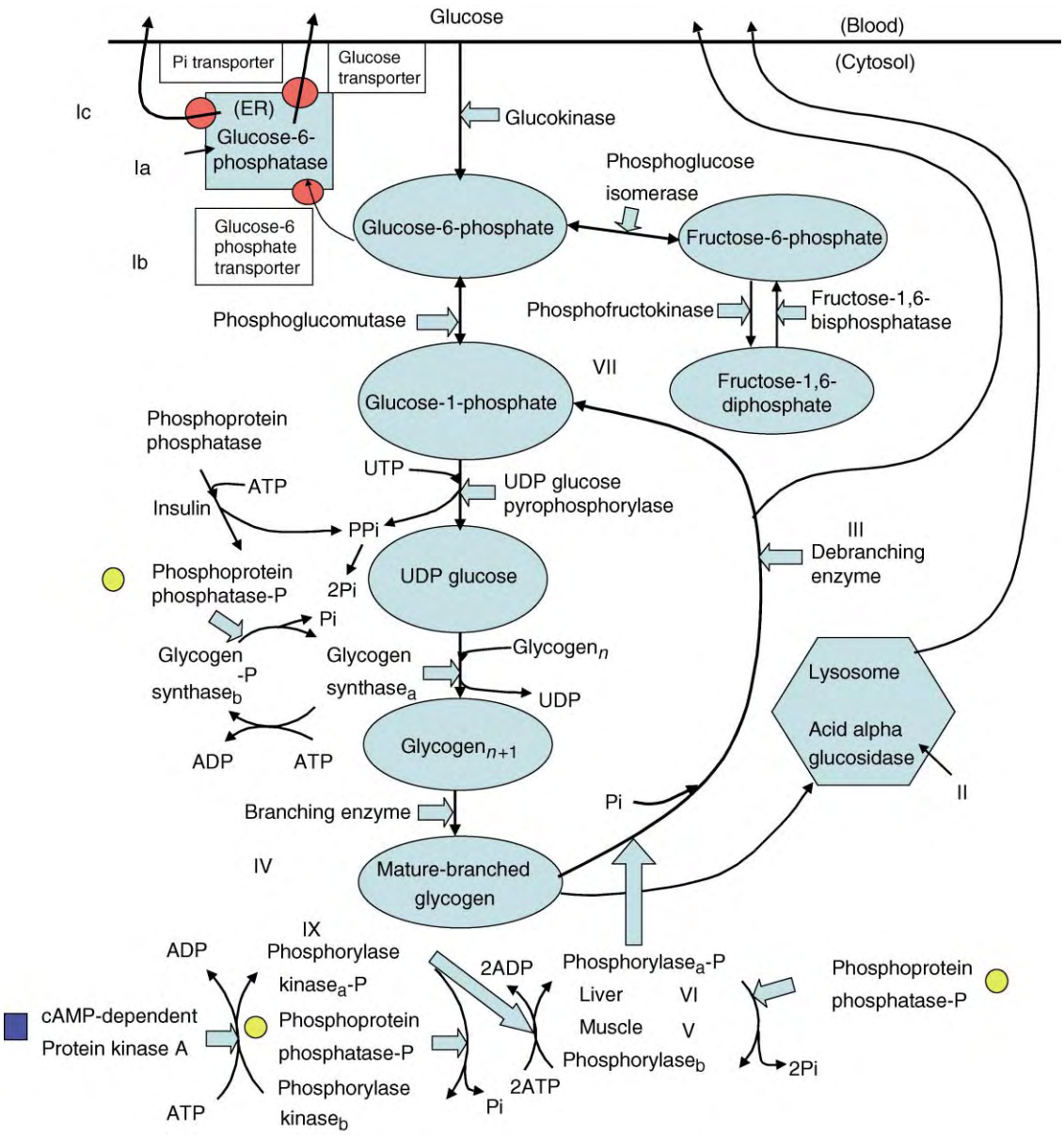

FIGURE 2 Metabolic pathways directly involved in the synthesis and degradation of glycogen. Note that blood glucose (top) is both the source of substrates for glycogen synthesis as well as the product of glycogen degradation. Compounds in ovals are biochemical intermediates. The rectangle represents the ER and the hexagonal structure represents a lysosome. Small closed circles show three sites for participation by the phosphorylated form of phosphoprotein phosphatase, formed by insulin stimulation. The small, closed square shows the site of stimulation by glucagon and epinephrine (adrenaline) through cAMP-dependent protein kinase A. The sites of enzyme defects in GSDs are indicated by the bold roman numerals.

kinase. The result is synthesis and accumulation of glycogen.

By contrast, in the "fasting" state (low blood glucose levels), insulin levels are low, inactivating phosphoprotein phosphatase. Other hormones—glucagon and epinephrine (adrenaline)—activate cAMP-dependent protein kinase A which phosphorylates (thereby activating) phosphorylase kinase. The latter, in turn, activates phosphorylase itself by phosphorylation leading to glycogen degradation.

This complex but sensitive system provides a critical buffer for blood glucose under common, relatively short-term, conditions.

Defects in Glycogen Metabolism and their Consequences

The remarkably sensitive metabolic system represented by glycogen is central to normal physiology and is an

essential defense against wide fluctuations in blood glucose levels. Because of this, defects in the pathway are often manifested by failure of glucose homeostasis with the frequent development of symptomatically low blood glucose levels (hypoglycemia). Furthermore, the shear mass of the glycogen polymer can cause organ enlargement and, ultimately, dysfunction when its degradation is inadequate. The central position of blood-borne glucose in the energy metabolism of many organs (especially the brain) has meant that careful management of glucose levels is often a prime emphasis of care for affected individuals. The disorders we consider are shown in Figure 2 and Table I. It is of historic interest that the definition and biochemical characterization of many of the enzymes of this system were based on detailed study of affected individuals. Although the general features of individual types are presented, it is important to remember that the genetic changes underlying the disorders both within and among clinical categories are not uniform. Much clinical heterogeneity likely reflects the fact that different mutations are often responsible for the failure or dysfunction of a given enzyme in different kindreds. This latter fact also complicates diagnostic studies that rely on mutation analysis alone.

Type I(a,b,c)

Originally described in 1929, individuals with one of this group of disorders have early difficulties with low blood glucose levels (hypoglycemia). In the neonatal period this can lead to seizures. Slightly later, enlargement of the liver is detected. The first biochemical study of the liver of affected individuals showed defective activity of glucose-6-phosphatase. Subsequent study of a larger number of individuals with similar manifestations led to dissection of more details of the pathway. The largest fraction of individuals shows defects in the gene and protein for glucose-6-phosphatase and this type is now known as Ia. Subsequently, it was determined that the active site of glucose-6-phosphatase lies within the ER and the glucose-6-phosphate translocase was suspected (and later shown) to be defective in another subgroup of individuals—this type is now known as Ib. Finally, a smaller group of patients has shown defects in the transport of phosphate out of the ER—these are known as type Ic.

The care of individuals affected with these three types is similar and is initially based on prevention of hypoglycemia by frequent feedings, often with the use of a slowly hydrolyzable glucose polymer (e.g., cornstarch). Liver transplantation has also been used. The long-term complications of this group of disorders are still being determined, but their prognosis is considerably improved with adequate control of blood glucose levels.

Type II

This type of GSD is unique because it involves dysfunction of an intralysosomal enzyme—α-1, 4-glucosidase (also called acid maltase). The characteristic feature of this group of individuals is the accumulation of glycogen within lysosomes. Historically, type II GSD was the first of the so-called "lysosomal storage diseases" to be defined. It is important to recall that glycogen storage and the enzymes for its synthesis and degradation are found in the cytoplasm. It has been proposed that lysosomes take up cytoplasmic glycogen and hydrolyze it within their unique low- pH environment.

Intralysosomal accumulation of glycogen in type II individuals is more notable in muscle than in liver and,

TABLE I

The Glycogen Storage Diseases

Designation	Enzyme	Eponym	OMIM#	Locus
Ia	Glucose-6 phosphatase	vonGierke	232220	17q21
Ib	Glucose-6 phosphate translocase		602671	11q23
Ic	Phosphate transporter		232240	11q23
II	Lysosomal (α-1,4-glucosidase)	Pompe	232300	17q25.2–q25.3
III	Debranching enzyme	Cord/Forbes	232400	1q21
IV	Branching enzyme	Andersen	232500	3p12
V	Muscle phosphorylase	McArdle	232600	11q13
VI	Liver phosphorylase	Hers	232700	14q21–q22
VII	Phosphofructokinase	Tarui	232800	12q13.3
IX[a]	Phosphorylase kinase		306000	Xp22.2–p22.1

[a] As noted in the text, the numerical designation(s) for defects in phosphorylase kinase have been confused, because the active enzyme comprises four subunits derived from genes at different loci. Only one of these is one the X-chromosome and that is shown in this table.

thus, many of the manifestations are related to muscle dysfunction. The disease often presents as a "myopathy" with symptoms and signs of muscle abnormalities. Muscle biopsy usually shows the characteristic glycogen accumulation within vacuoles. The severity and rate of progression of the disorder vary widely from individuals with severe disease presenting in infancy to those with a more gradual adult onset. In general, these clinical differences reflect different mutations in the same gene, but a direct correlation is not always possible. Blood glucose levels are not usually affected. Treatment is not available.

Type III

Absence or dysfunction of the debranching enzyme leads to the accumulation of glycogen with abnormal structure as noted above. This "limit dextran" represents the product of phosphorolysis up to the limits imposed by the branches. Such products are bulky with short outer branches.

Affected individuals resemble those with type I GSD as infants—they have hypoglycemia and liver enlargement. In general, the manifestations become less severe with age and individuals can survive to adulthood. Because both liver and muscle forms of the enzyme exist, rare individuals can show selective organ involvement.

Treatment is generally the same as for individuals with type I GSD, although the requirements are generally less stringent. Liver transplantation has also been used but does not affect problems in muscles.

Type IV

Consistent with the structure and synthesis of mature glycogen, defective formation of branches leads to very long polymers and bulky particles. The structure of the resulting molecules resembles amylopectin and the manifestations are related to their accumulation in the liver with attendant dysfunction of the metabolic activity and, particularly, derangement of liver architecture known as cirrhosis. Complications of cirrhosis ensue in many individuals leading to liver failure and death. Because the polymers are degradable, low blood glucose complications are not generally found. A rare variety appears to largely involve muscle. Liver transplantation has been successful in selected individuals.

Type V

Types V and VI represent the consequences of organ-specific dysfunction of phosphorylase, the primary enzyme for glycogen degradation. Type V, the muscle-specific form, is recognized by intolerance to significant muscle activity. In most individuals, quiet activities are managed well and no symptoms develop but rapid exercise can cause severe, acute muscle pain and the loss of muscle tissue integrity. Muscle cramps after exercise are common and may progress to the destruction of muscle—rhabdomyolysis. Usually, symptoms develop in adolescence or young adulthood. Because muscle glycogen is the source of energy for acute contraction, the manifestations of type V GSD are often related to the intensity of the exercise. The phosphorylase found in muscle is unique to muscle and thus its mutations do not directly affect other tissues. The most effective treatment is avoidance of intense exercise; this often can lead to a relatively good course.

Type VI

The mutations in this disorder are the hepatic counterpart of those in type V GSD. In general, the manifestations are milder than for individuals with type I(a,b,c), but poor blood glucose control and liver enlargement due to glycogen storage are seen. Muscle problems are not encountered (cf. type V). The prognosis is usually good if control of blood glucose levels can be maintained; often this can be accomplished through diet alone.

Type VII

Dysfunction of the muscle form of phosphofructokinase leads to individuals with manifestations similar to those with GSD type V—exercise-related muscle pain and fatigue. The likely pathophysiology involves elevation of the level of glucose-6-phosphate in muscle cells leading to increased glycogen synthesis. Giving glucose to affected individuals leads to lower levels of fatty acids which normally would serve as an important energy source for muscle during contraction. Thus, while administering glucose can be helpful for muscle cells in type V GSD, it can aggravate the consequence of the mutation in type VII. There is no specific treatment for this form of GSD. Avoidance of strenuous exercise (similar to the advice for individuals with type V GSD) generally is effective.

Type IX

This is a complex category, now grouped by effects on a single function. It comprises several different disorders, reflecting the fact that four individual protein subunits make up the functional phosphorylase kinase; one of these is on the X-chromosome. Although all types are rare, the X-linked form is the most frequently recognized (and is the only X-linked form of GSD).

Individuals with the X-linked form usually show moderate liver enlargement and liver function abnormalities early in life; growth often is delayed. Problems due to low blood sugar levels are not common.

In general, the manifestations become less prominent with age. Treatment is not generally required once the diagnosis has been recognized.

Because of the diversity of subunits contributing to the functional mature enzyme complex, several rare types of dysfunction have also been recognized that may be limited to the skeletal muscle or the heart. Individuals with these forms, also, generally do not require specific treatment.

Summary

Although they are rare, as a group, the GSDs have led to the understanding of many aspects of glycogen metabolism. Affected individuals develop difficulties based on the site of their underlying defect. The care of affected individuals is directed to controlling blood glucose levels and minimizing organ damage that can result from inadequate glucose mobilization and/or glycogen accumulation. Liver transplantation is a treatment option for selected patients.

See Also the Following Articles

Glycogen Metabolism • Glycogen Synthase Kinase 3 • Insulin- and Glucagon-Secreting Cells of the Pancreas • Insulin Receptor Family

Glossary

glycogen A complex, branched polymer of glucose that serves as a site of short-term glucose storage as well as a source of blood glucose during fasting.

hypoglycemia The clinical condition of low blood glucose levels with physiologic consequences including seizures caused by brain dysfunction.

myopathy Disease of muscle, in this context reflecting inadequate glucose (and, hence, energy) supply or mobilization from glycogen stores.

phosphorolysis The use of phosphate to remove successive glucose residues from the reducing end of the glycogen polymer.

Further Reading

Chen, Y.-T. (1999). Glycogen storage diseases. In *Metabolic and Molecular Basis of Inherited Disease* (C. R. Scriver, A. L. Beaudet, W. S. Sly and D. Valle, eds.) 8th edition, Ch. 71, Vol I, pp. 1521–1551. McGraw-Hill, New York.

Chou, J. Y., and Mansfield, B. C. (1999). Molecular genetics of type I glycogen storage disease. *Trends Endocr. Metab.* **10**, 104–113.

Cori, G., and Cori, C. (1952). Glucose-6-phosphatase of the liver in glycogen storage disease. *J. Biol. Chem.* **199**, 661–667.

Hirschhorn, R., and Reuser, A. J. J. (1999). Glucogen storage disease type II: Acid α-glucosidase (acid maltase) deficiency. In *Metabolic and Molecular Basis of Inherited Disease*. (C. R. Scriver, A. L. Beaudet, W. S. Sly and D. Valle, eds.) 8th edition, Ch. 135, Vol III, pp. 3389–3420. McGraw-Hill, New York.

Kazemi-Esfarjani, P., Skomorowska, E., Jensen, T. D., Haller, R. G., and Vissing, J. (2002). A nonischemic forearm exercise test for McArdle disease. *Ann. Neurol.* **52**, 153–159.

National Library of Medicine (2003). OMIM – Online Mendelian Inheritance in Man. http://www.ncbi.nlm.nih.gov/omim.

Biography

George Sack is an Associate Professor of Medicine, Pediatrics, and Biological Chemistry at the Johns Hopkins University School of Medicine. His principal research interests are in amyloid proteins and their diseases and inherited metabolic disorders affecting adults. He holds an M.D. and a Ph.D. (Molecular Biology) from Johns Hopkins where he also completed a residency in Internal Medicine and a fellowship in Medical Genetics. He is the author of the textbook "Medical Genetics" (McGraw-Hill, 1999) and a founding fellow of the American College of Medical Genetics.

Glycogen Synthase Kinase-3

James R. Woodgett
Ontario Cancer Institute, Toronto, Ontario, Canada

Glycogen synthase kinase-3 (GSK-3) is a widely expressed, multifunctional serine/threonine protein kinase that plays a role in a wide variety of regulatory processes and is implicated in diabetes, cancer, neurodegenerative diseases, and inflammation. Unlike the majority of protein kinases, this enzyme is active in resting cells and is regulated by signal-dependent inactivation. GSK-3 is a critical component of several signal transduction pathways including those that respond to Wnt and Hedgehog and receptor-tyrosine kinase pathways. GSK-3 modulates proteins involved in metabolism, transcriptional regulation, the cytoskeleton and the cell cycle and due to its role in pathophysiologically relevant conditions, is a potential therapeutic target.

GSK-3 Genes and Proteins

Mammalian genomes harbor two genes that encode for three isoforms of glycogen synthase kinase-3 (GSK-3) (Figure 1). The GSK-3α gene is located on human chromosome 19q13.2 and codes for a 51 kDa protein. The GSK-3β gene is located on human chromosome 3q13.33 and expresses a 47 kDa protein that is $>95\%$ identical to GSK-3α in the kinase catalytic domain. Through differential splicing, the GSK-3β gene also encodes a variant termed β' in which a 39 bp exon is included, adding 13 amino acids within the catalytic core. Both genes are widely expressed in all mammalian tissues and the crystal structure of GSK-3β has been solved.

GSK-3 is an ancient and conserved protein, with clear homologues in all eukaryotes. Much of the functional knowledge of the enzyme has been derived from analysis in genetically tractable organisms such as fruit flies, slime mold, and yeast.

Regulation of GSK-3

Protein kinases are typically subject to intricate modes of regulation – in most cases their activity is not induced unless a specific signal is received by a cell. GSK-3 displays the rare behavior of being fully active in the absence of cellular stimulation. Thus, in resting cells, the protein phosphorylates its catalog of substrate proteins and upon stimulation by growth factors, hormones, and other agents, GSK-3 activity is repressed, relieving phosphorylation of its targets. In general, the substrate proteins of GSK-3 are inhibited by phosphorylation. Hence, GSK-3 acts like a brake to suppress the activity of its targets (see Figure 2). This strategy allows cells to quickly respond to stimuli by activating a litany of pre-existing proteins through deactivation of just one enzyme.

There are two modes by which GSK-3 activity is regulated. Both GSK-3α and β are inhibited by phosphorylation of a serine residue located within the N-terminal regulatory domain (serine 21 in the α-isoform and serine 9 in β).

Several protein kinases phosphorylate these regulatory residues including protein kinase B(PKB)/Akt, cyclic AMP-dependent protein kinase, and several protein kinase C isoforms. As a consequence, a wide variety of stimuli result in GSK-3 inactivation including receptor-tyrosine kinases, such as the insulin receptor, that activate phosphatidylinositol 3′ kinase (which activates PKB) and agonists of G protein-coupled receptors that result in elevated cyclic AMP (Figure 2).

GSK-3 activity is also inhibited by the Wnt signaling pathway by a completely distinct and insulated mechanism (Figure 3). Wnt-mediated inhibition of GSK-3 specifically targets a select fraction of GSK-3 molecules that are associated with the Axin/adenomatous polyposis Coli (APC) complex. In resting cells, this high-molecular mass protein system acts as an efficient machine to degrade cytoplasmic β-catenin, an oncoprotein associated with colon cancer and other neoplasms. In the absence of a Wnt signal, β-catenin binds to a scaffolding protein termed Axin. Axin also sequesters a portion of GSK-3 molecules within the cell. Although GSK-3 cannot phosphorylate soluble β-catenin, when both molecules are cobound to Axin GSK-3 efficiently targets three serine residues within the amino-terminal domain of β-catenin. These phosphorylated residues form a recognition motif for E3 ligases that add a ubiquitin molecule to β-catenin which signals its rapid destruction by the 26S proteosome. In the presence

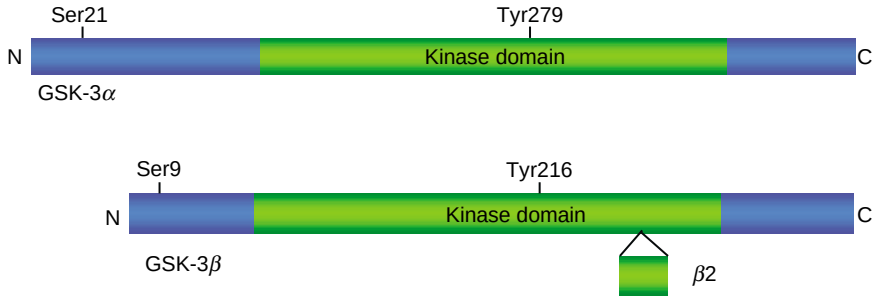

FIGURE 1 Domain structure of the two human GSK-3 genes. The regulatory phosphorylation sites are indicated.

of Wnt (a large family of secreted glycoproteins), a signaling cascade is initiated through engagement of the Frizzled class of receptors, leading to modification of an adaptor molecule termed Dishevelled that results in inhibition of phosphorylation of β-catenin by GSK-3. As a consequence β-catenin accumulates within the cytoplasm, binds to the TCF family of DNA-binding proteins, translocates to the nucleus, and modulates expression of genes such as *cyclin D* and c-*myc*. Mutations in APC or the phosphorylation domain of β-catenin result in elevated levels of the protein within cells and loss of growth control. Indeed, mutations in one of these two molecules are found in the majority of colon cancers.

Although two distinct pathways converge to inhibit the same signaling molecule, GSK-3, the cellular consequences of inactivation are specific to the signal. This, inactivation of GSK-3 via N-terminal phosphorylation of serine 21/9 does not cause stabilization of β-catenin. Nor does Wnt signaling impact metabolic targets that are regulated by insulin or growth factors. The mechanism underlying the specificity determinants remains unclear but is likely related to sequestration of a subset of GSK-3 molecules in the APC/Axin complex, effectively shielding this subset from external regulation.

GSK-3 is also phosphorylated on a tyrosine residue within the P-loop of the catalytic center. Although

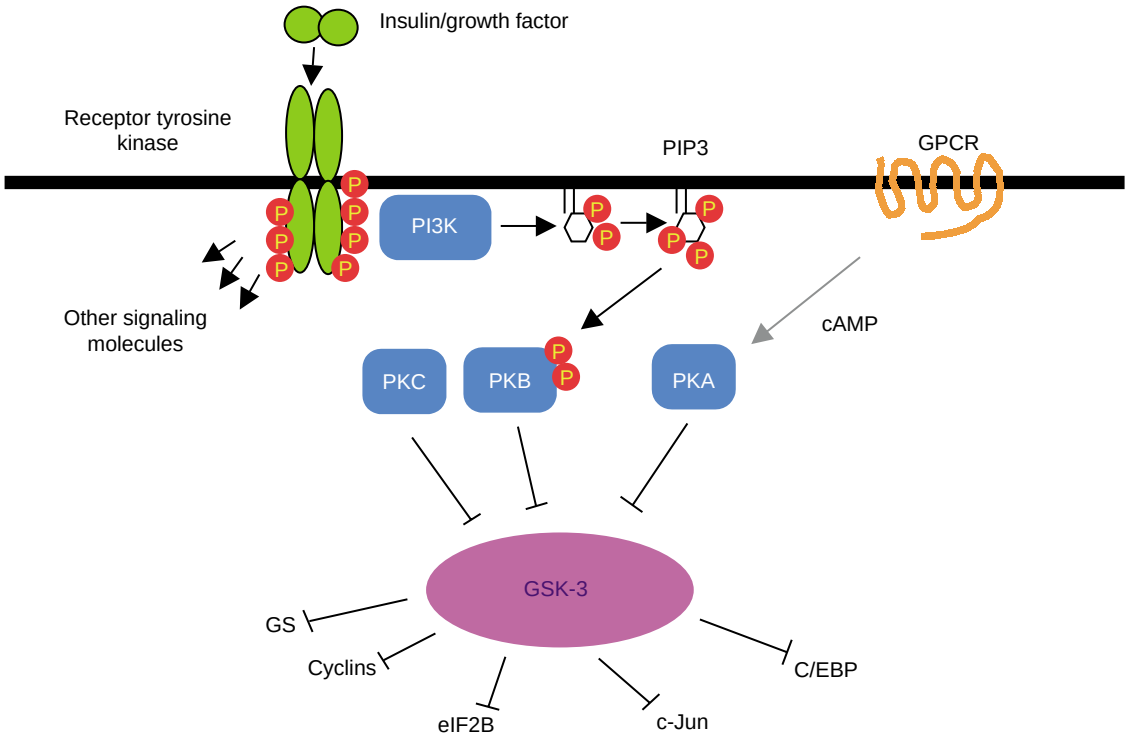

FIGURE 2 Simplified map of the regulation of GSK-3 by growth factors and mitogens. Several GSK-3 target proteins are indicated to represent the different classes of molecules regulated by GSK-3.

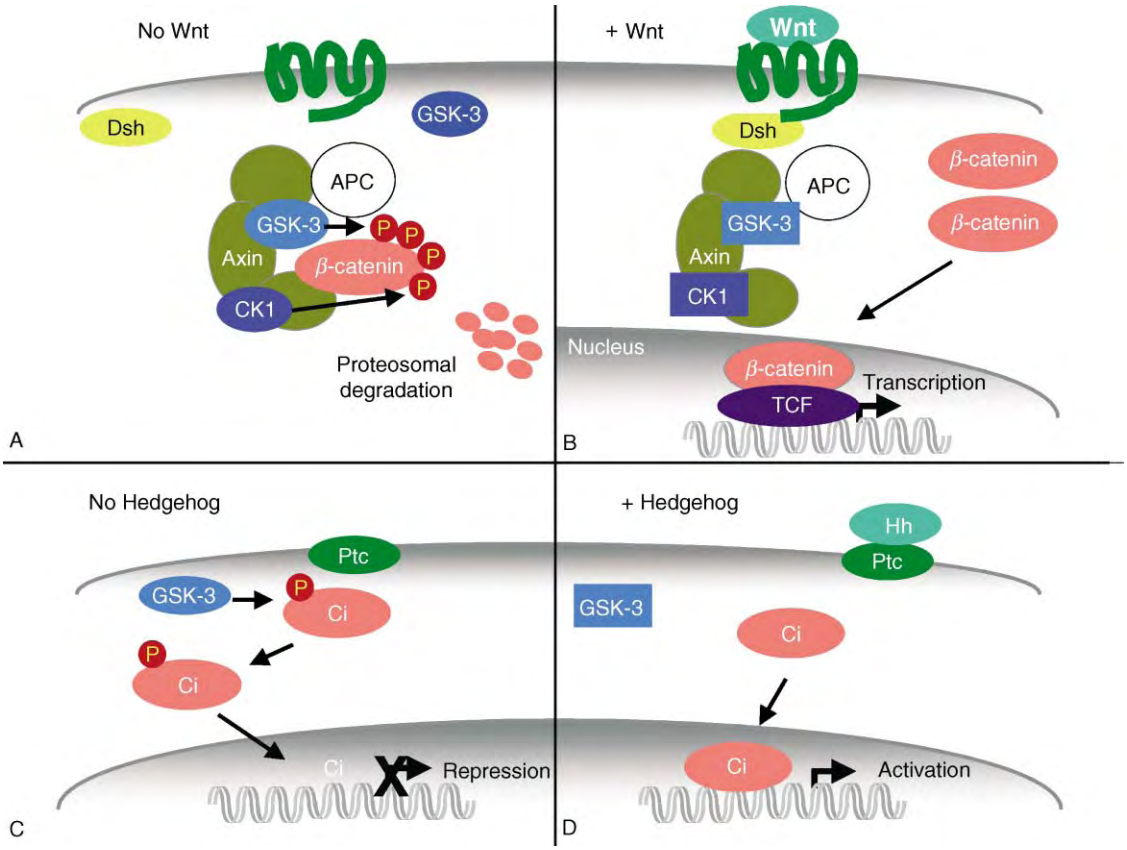

FIGURE 3 Regulation of GSK-3 by the Wnt and Hedgehog signaling proteins. The resting and stimulated states of these pathways are indicated for comparison.

phosphorylation of this site is required for full activity, the level of phosphorylation does not appear to be regulated (unlike, for example, the analogous tyrosine residues in MAP kinases). A protein-tyrosine kinase has been identified (Zak1) that targets the tyrosine in slime mold. However, in mammals, the residue is likely modified by autophosphorylation.

A Primer on GSK-3 Substrates

Many (but not all) of the proteins that are phosphorylated by GSK-3 require prior phosphorylation by a distinct protein kinase (Table I). The primary substrate recognition sequence of GSK-3 is Ser/Thr-X-X-X-Ser/Thr-phosphate where X is any amino acid but with a preference for prolines. In theory, this prerequisite for prior phosphorylation provides an additional regulatory step but in practice, many of the primed phosphorylation sites are unregulated and fully phosphorylated. Instead, the priming mechanism appears to allow a distinct form of regulatory control at the level of GSK-3 itself. The crystal structure of GSK-3β revealed the presence of several positively charged residues including a critical arginine (Arg 96) within the substrate-binding domain in a location that would permit interaction with the priming phosphorylated amino acid in the incoming substrate. In other words, the primed phospho-amino acid is an important contributor to substrate binding. However, when GSK-3 is phosphorylated within its N-terminal domain (serine 21 or 9 in GSK-3α or β respectively), this phosphorylated serine competes for the primed phosphorylation site docking motif and when bound occludes the active site. Hence, the protein kinase activity is effectively inhibited.

Substrates that require priming include glycogen synthase, CREB, inhibitor-2, cyclin E, Tau, and β-catenin. The inclusion of β-catenin in this list introduces a caveat since phosphorylation of this target is not affected by N-terminal phosphorylation of GSK-3. Since β-catenin is only phosphorylated by GSK-3 when both molecules are bound to Axin, it is possible that Axin shields GSK-3 from the inhibitory effect of a phosphorylated N-terminal domain (since β-catenin stabilization is insensitive to signals that promote N-terminal domain phosphorylation of GSK-3. Enzymes that catalyze priming of GSK-3

TABLE I

GSK-3 Substrates. GSK-3 Targets are Grouped Along with the Sequences of Known Phosphorylation Sites

GSK-3 substrate	Phosphorylation site
Wnt pathway related	
Axin	**S**AND**S**EQQ**SS**DAD**T**LSL**TS**LTD**S**
β-Catenin	D**S**GIH**S**GAT**T**TAPS LSGKGNPEEED
Cyclin D1	EEVDLAC**T**PTDVR
Cyclin E	ASPLPSGLL**T**PPQSGKK
Transcription factors	
c-Jun	**T**PPL**S**PIDME**S**QER
JunD	**S**PPL**S**PIDME**T**QER
CREB	KRREIL**S**RRPS YR
NF-ATc	PYA**S**PQT**S**PWQ**S**PCV**S**P
	LG**S**PQH**S**PST**S**P
	PY**S**PHH**S**PTP**S**PHG**S**PRV
C/EBPα	**T**PPP**T**PVP**S**P
Heat shock factor-1	EEPP**S**PPQS P
c-Myc	DIWKKFELLP**T**PPL**S**PSRRSG
L-myc	DIWKKFELVP**S**PPT**S**PPWGL
Metabolism	
ATP-citrate lyase	LLNASGSTS**T**PAP**S**RTAS FSESR
Glycogen synthase	RPA**S**VPP**S**PSL**S**RHS**S**PHQS EDEE
eIF-2B translation factor	DSEELD**S**RAGS PQLDDIKVF
G subunit of phosphatase 1	GF**S**PQP**S**RRGSSESSE
Inhibitor-2	DEPS**T**PYHSMIGDDDDAYS D
RII subunit of cAMP-dependent protein kinase	LREAR**S**RA**S**TPPAAPPS
Neuronal/structural	
Tau	TPPK**S**PSAAK VVSGDT**S**PR
Presenilin 1	NAES**T**ERE**S**QDTVAEN
Kinesin light chain	LSD**S**RTL***S***SS**S**MDL**S**RRS***S***LVG

The residues phosphorylated by GSK-3 are in bold type (if known) whereas residues that act as priming sites are underlined.

substrates include casein kinases 1 and 2 and cyclic-AMP-dependent protein kinase.

Physiological Functions of GSK-3

GSK-3 has been implicated in a wide variety of cellular processes and pathologies. The first genetic analysis of the protein kinase occurred in the fruitfly where mutants of the *Drosophila melanogaster* GSK-3 gene, termed Zeste-White3 or Shaggy, were found to display a phenotype similar to continuous signaling of the Wingless pathway, the fly counterpart of the mammalian Wnt signaling system. As described, this pathway plays an important role in controlling the activity of the β-catenin oncogene that is mutationally activated in several cancers. Since GSK-3 negatively regulates this onco-protein (in addition to other onco-proteins such as the c-Jun and c-Myc transcription factors and cyclin D, a CDK activator), it is a candidate tumor suppressor gene. However, mutations in GSK-3 have not been found in human cancers. The most likely reason is that the two mammalian isoforms of GSK-3 are encoded by distinct genes and many (but not all) of their functions are redundant. Thus, both alleles of both genes would have to be inactivated to effect complete disruption of function – an unlikely event given that loss of the first would confer no selective advantage. A second possibility is that mutational inactivation of GSK-3 is incompatible with basic cellular properties that are requisite for tumor growth such as proliferation.

A developmental pathway that often works in concert with the Wnt pathway is the Hedgehog pathway. Hedgehog, like Wnt, is a secreted factor but instead of targeting β-catenin, Hedgehog signaling prevents the cleavage of a protein termed Gli in mammals and Cubitus interruptus (Ci) in flies (Figure 3). In resting cells, Ci is processed into two fragments, one of which acts as a transcriptional repressor. This cleavage requires phosphorylation of Ci by GSK-3. Upon binding of Hedgehog to its receptor (Patched) cleavage is inhibited. The pathway thus has several parallels to Wnt signaling, although it is unclear whether GSK-3 is directly regulated by Hedgehog signaling or is, instead, a passive player that maintains low amounts of the uncleaved Ci protein under resting conditions.

Neurological Diseases

Dysregulation of GSK-3 has been implicated in neurological diseases such as Alzheimer's disease and bipolar disorder. This protein kinase is one of several that targets sites of phosphorylation of the microtubule-associated protein Tau that are hyperphosphorylated in insoluble structures termed neurofibrilliary tangles. These deposits are found in the brains of patients with Alzheimer's disease and are associated with neuronal death. Transgenic mice expressing a mutant of GSK-3β that cannot be inhibited by N-terminal phosphorylation demonstrate higher than normal Tau phosphorylation. A further connection to this debilitating disease was recently uncovered by the finding that inhibition of GSK-3 reduced the generation of Aβ peptide from the amyloid precursor protein. This peptide is the product of the γ-secretase protease complex that is responsible to overproduction of Aβ that aggregates to form the primary constituent of amyloid plaques. These deposits are early markers of the disease. Activation of GSK-3 in neuronal cells has also been correlated with induction of apoptosis such that

death induced by serum deprivation can be suppressed by GSK-3 inhibition. Finally, GSK-3 is inhibited by lithium ions at concentrations that are therapeutically effective for the treatment of bipolar disorder. Inhibitors of GSK-3 therefore have potential therapeutic value in the control of at least two neurological disorders.

Knockout Mice

Mice lacking GSK-3β die during embryogenesis from liver failure. The defect was traced to aberrant induction of the NF-κB transcription factor by TNF-α in the liver that leads to hepatocyte cell death. TNF-α typically induces both a proapoptotic and an NF-κB-mediated survival signal within cells. However, in the cells lacking GSK-3β, induction of survival genes by NF-κB was found to be defective, leading to dominance of the proapoptotic signal and the demise of the hepatocytes. The mechanism by which GSK-3β influences NF-κB is unclear, although there is evidence of both positive and negative regulation. Chemical inhibition of GSK-3 also leads to sensitization of cells to TNF-α. Of note, although the embryonic lethality of the mice lacking GSK-3β can be rescued by either injection of anti-TNF-α antibodies or by breeding with mice that lack the 55 kDa receptor for TNF-α, the mice still die shortly after birth indicating additional critical roles for the protein kinase during development.

Metabolism and Diabetes

While the initial identification of GSK-3 was rooted in the study of glycogen metabolism, study of this kinase has largely focused on its roles in other processes, perhaps as a result of genetic analysis. However, GSK-3 is the predominant regulator of glycogen synthase inhibition. This role has been resurrected by studies assessing the effects of GSK-3 inhibitors on glucose uptake and metabolism in response to insulin. Insulin acts to activate phosphatidylinositol 3′ kinase and PKB leading to phosphorylation and inactivation of GSK-3 (Figure 2). Inhibitors of this protein kinase may therefore be predicted to act as insulin sensitizers. Such drugs are highly sought in the treatment of type 2 diabetes, a growing health problem as populations increase their degree of obesity and age. Small molecule inhibitors of GSK-3 have been shown to act as effective insulin sensitizers in several animal models of diabetes, reducing circulating blood glucose and enhancing glycogen deposition. In addition to negatively regulating glycogen synthase, GSK-3 also phosphorylates and inhibits other proteins important to insulin's mechanism of action including IRS1, ATP-citrate lyase, and eIF2B. Thus, GSK-3 inhibition promotes anabolic processes such as fatty acid and protein synthesis.

One potential spoiler to the use of GSK-3 inhibitors as insulin sensitizers is the concern that chronic inhibition of this protein kinase may lead to inappropriate accumulation of β-catenin, a potent oncogene. However, cells appear to have a built-in fail-safe mechanism that normally prevents unscheduled induction of β-catenin. For example, loss of 50% of total GSK-3 activity results in virtually no increase in noncadherin-associated β-catenin. Inhibition of at least 75% of GSK-3 activity is required for substantial stabilization in the absence of a specific signal (one of the Wnts). The reason for this is at least partially related to the relative levels of the Wnt signaling components compared to GSK-3. Axin is present at significantly lower concentrations than GSK-3($\alpha + \beta$). Hence, only when total GSK-3 levels decrease below that of Axin will processing of β-catenin be affected in the absence of a Wnt signal. Since most therapeutics are used at concentrations that dampen rather than eradicate activity, there exists likely a therapeutic window that allows tempering of aberrant GSK-3 activity without impacting stabilization of β-catenin. However, this Damacles Sword will dangle over the use of GSK-3 inhibitors until at least preclinical trials demonstrate no increase in tumor incidence upon chronic administration of the drugs. Given rapid progress in the development of potent and specific inhibitors of GSK-3, an answer to this question is not far away.

See Also the Following Articles

Diabetes • Glycogen Metabolism • Glycogen Storage Diseases • Secretases

Glossary

adenomatous polyposis coli (APC) A large protein that is frequently mutated in colorectal cancer that is a component of the β-catenin destruction complex.

glycogen synthase (GS) The rate-limiting enzyme of glycogen deposition that is inhibited by phosphorylation.

nuclear factor of κB (NF-κB) An important transcription that binds specific sequences in DNA and plays roles in regulating inflammatory responses and in deciding whether a cell will live or die following stress.

protein kinase An enzyme that catalyzes the transfer of phosphate from adenosine triphosphate (ATP) to the serine, threonine, or tyrosine residues.

Wnt An evolutionarily conserved family of extracellular proteins that regulate developmental processes by binding to a specific receptor (Frizzled) and initiating a cascade of events within cells that includes the accumulation of β-catenin.

Further Reading

Dajani, R., Fraser, E., Roe, S. M., Young, N., Good, V., Dale, T. C., and Pearl, L. H. (2001). Crystal structure of glycogen synthase kinase 3

beta: Structural basis for phosphate-primed substrate specificity and autoinhibition. *Cell* **105**, 721–732.

Doble, B. W., and Woodgett, J. R. (2003). GSK-3: Tricks of the trade for a multi-tasking kinase. *J. Cell Sci.* **116**, 1175–1186.

Eldar-Finkelman, H., and Ilouz, R. (2003). Challenges and opportunities with glycogen synthase kinase-3 inhibitors for insulin resistance and Type 2 diabetes treatment. *Expert Opin. Invest. Drugs* **12**, 1511–1519.

Gurvich, N., and Klein, P. S. (2002). Lithium and valproic acid: Parallels and contrasts in diverse signaling contexts. *Pharmacol. Ther.* **96**, 45–66.

Jope, R. S. (2003). Lithium and GSK-3: One inhibitor, two inhibitory actions, multiple outcomes. *Trends Pharmacol. Sci.* **24**, 441–443.

Nusse, R. (2003). Wnts and Hedgehogs: Lipid-modified proteins and similarities in signaling mechanisms at the cell surface. *Development* **130**, 5297–5305.

Biography

Jim Woodgett is a Senior Scientist at the Ontario Cancer Institute and Amgen Professor of Cancer Biology at the University of Toronto. His research interests focus on the dysregulation of signaling pathways in human cancer. His research group is studying the molecular biology of the phosphatidylinositol 3′ kinase and Wnt systems using transgenic mice, cell biology, genetic and functional genomic approaches. He has enjoyed working on the biology of GSK-3 for over 20 years and still marvels at the diversity of functions of the enzyme.

Glycolipid-Dependent Adhesion Processes

Senitiroh Hakomori
University of Washington, Seattle, Washington, USA

The majority of glycolipids in mammalian cells are glycosphingolipids (GSLs), with the exception of sulfated galactosyl diglyceride (seminolipid) present in testis, seminal fluid, and a very small quantity in brain. Therefore, this article is limited to cell adhesion caused by GSLs. Although >500 GSLs are known, only ~10 species of GSLs have been studied and found to mediate cell-to-cell adhesion. Change of signal transduction and cell phenotype take place in most cases of GSL-dependent cell adhesion. The known examples may constitute only a small proportion of the existing cases, since this area of research is still in the early stage of development. There may be a number of cell adhesion systems mediated by GSLs that are not yet known. Glycolipid-dependent cell adhesion requires a specific assembly in which a cluster of GSLs is present as a functional center. Because GSL-dependent adhesion takes place through clustered GSLs in microdomain, we will first explain GSL assembly in membrane, then report cases of cell adhesion mediated through such microdomains.

GSL Assembly in Membrane as GSL-Enriched Microdomain

Cluster Formation by GSL-to-GSL *Cis* Interaction

Ceramide, the lipid moiety of glycosphingolipids (GSLs), has aminoacyl (N-acyl) residue and hydroxyl group that act as hydrogen bond donors, whereas glycerides and glycerophospholipids have only O-acyl group that act as hydrogen bond acceptor. In addition, GSLs have a number of hydroxyl groups and N-acyl residues at the sugar moiety, that may provide a much stronger hydrogen bond donor (Figure 1A). At the plane of lipid bilayer, the presence of sphingolipids and GSLs therefore provides higher and stronger *cis* interaction, i.e., GSL-to-GSL side-by-side interaction. Glycerides and glycerophospholipids in the same lipid bilayer plane, although they constitute the major lipid components, show much weaker *cis* interaction. By a similar mechanism, glycoproteins show strong *cis* interaction, possibly through their hydrogen bonds, to form clusters separable from GSL clusters. Thus, GSLs and glycoproteins are clustered to form independent patches or islands separated from the sea of glycerophospholipids on the cell surface, as shown in Figure 1B. Sphingomyelin interacts with cholesterol but is separated from glycerophospholipids in gel state, as evidenced by ESR and IR spectroscopy. GSL clusters occur in the absence of cholesterol.

Association of Clustered GSLs with Lipophilic Signal Transducers and Proteolipids: Assembly of "Glycosynapse"

Clustered GSLs in cell membranes can be separated as insoluble low-density membrane by homogenization in high-salt, or in lysis buffer containing neutral detergent, followed by density-gradient ultracentrifugation. The GSL-enriched buoyant fraction contains >95% of GSLs originally present in cells, but <1% of total cellular protein. The proteins found in this fraction, from many cell types, are cSrc, other Src family kinases, and small G proteins (Ras, RhoA, RAC), which contain long-chain aliphatic acyl groups and are closely associated with GSLs. In addition, the fraction has proteolipid proteins and tetraspanins, which are also closely associated with GSLs and signal transducers. Molecular assembly of these components in microdomain forms a functional unit in membrane essential for cell adhesion with concurrent signal transduction; the unit is collectively termed "glycosynapse."

Cell Adhesion Through Clustered GSLs

Two types of GSL-dependent cell adhesion processes can be considered.

1. GSL cluster is recognized by or bound to complementary GSL cluster expressed on counterpart cell surface glycosynapse, i.e., GSL-to-GSL *trans* interaction.

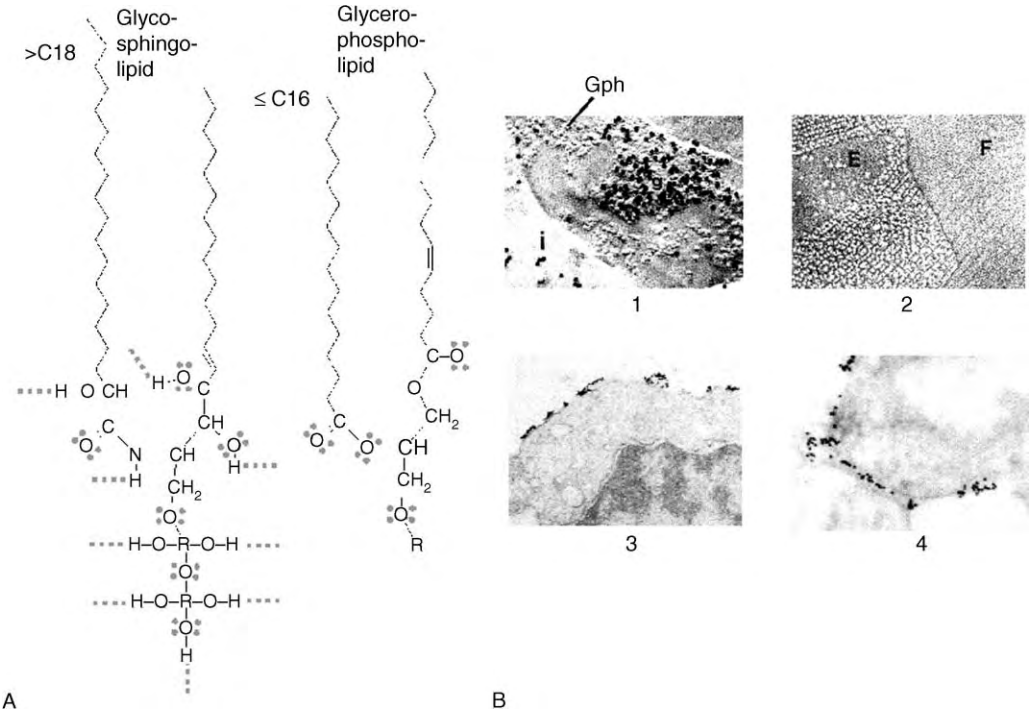

FIGURE 1 Clustering of glycosphingolipids and glycoproteins on membrane due to *cis* interaction. (A) Contrasting properties of GSLs and glycerophospholipids in ability for hydrogen bond formation. GSLs are both hydrogen bond donors and acceptors (indicated respectively by ····H—O and Ö═C), whereas glycerophospholipids only accept hydrogen bond, due to absence of hydroxyl group (OH). (B) Clustering is visualized by scanning electron microscopy following freeze-fracture technique: glycophorin (Gph) clustering, and globoside (Gb4) clustering on erythrocyte membrane (in 1), GM1 clustering on dipalmitoyl phosphatidylcholine liposome surface (in 2). Cell surface GSL clustering is also observed by transmission electron microscopy using specific antibody-gold sol conjugates: GM3 clustering on T-lymphocyte surface (in 3), polysialoganglioside clustering in neuronal cells (in 4).

Such interaction takes place through specific complementary structures. The binding between carbohydrate moieties of GSLs is catalyzed, in many cases, by Ca^{2+}. There is a steadily increasing number of examples of such complementary GSL pairs, providing the basis of GSL-dependent adhesion. A model of such interaction involving single molecules of Gb4 and nLc_4, as a basis of cell adhesion, is shown in Figures 2A–2C. In reality, however, GSLs are not present as single molecules, but are clustered on membrane. Cell adhesion occurs through such GSL clusters in association with signal transducers (glycosynapse), to activate or inhibit signaling. A model is shown in Figure 3.

2. GSL cluster, particularly ganglioside cluster, is bound to ganglioside-binding lectin (siglec) such as siglec-4 or -7. Alternatively, GSL having βGal residue (e.g., GM1) is recognized by galectin, or GSL having SLe^x or SLe^a residue is recognized by E-selectin.

Processes 1 and 2 are shown schematically in Figure 4. In either process, structure of GSLs is the target of cell adhesion, recognized by complementary GSL (Figure 4A) or by specific binding protein (Figure 4B), which triggers activation or inhibition of signal transducers.

Types of Cell Adhesion Mediated by GSL-to-GSL Interaction

Mouse Melanoma B16 Cell Adhesion to Mouse Endothelial Cells Through GM3-to-LacCer or GM3-to-Gg3Cer Interaction

B16 cells are characterized by predominance of GM3 ganglioside. Their adhesion to mouse or human endothelial cells (ECs) is based on interaction of GM3 (on melanoma cells) with LacCer or Gg3Cer (on ECs). LacCer is present on essentially all types of ECs, whereas Gg3Cer has more restricted distribution on lung microvascular ECs, where metastasis may occur preferentially. The degree of this "GM3-dependent adhesion" is closely correlated with metastatic and invasive potential of B16 cells, based on the following observations: (1) *in vitro* GM3-dependent adhesion was inhibited by liposomes containing GM3, LacCer, or Gg3Cer; (2) *in vivo* metastatic potential of B16 cells in terms of lung colonization was inhibited by administration of GM3- or Gg3Cer-liposomes; (3) enhancement of B16 cell motility and invasiveness following

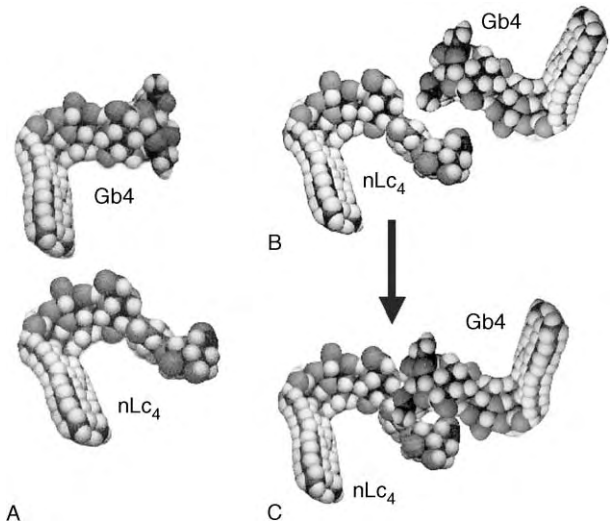

FIGURE 2 *trans* interaction of GSLs as a basis of glycolipid-dependent cell adhesion. (A) Minimum-energy conformational model of Gb4 and nLc_4. Note that axis of carbohydrate is perpendicular to that of sphingosine and fatty acid (ceramide). (B) Gb4 on the surface of one cell and nLc_4 on surface of counterpart cell have complementary surface profile. (C) Gb4 and nLc_4 adhere to each other, by carbohydrate-to-carbohydrate interaction, as a basis for cell adhesion.

GM3-dependent adhesion was indicated by activation of cSrc, RhoA, and FAK at glycosynapse. GM3-to-Gg3Cer and -LacCer interactions were well studied recently by surface plasmon resonance spectroscopy.

F9 Cell Autoaggregation Through Le^x-to-Le^x Interaction

Mouse embryonal carcinoma F9 cells show strong autoaggregation, simulating morula-stage preimplantation embryo. Both F9 cell autoaggregation and compaction of morula are inhibited by a trivalent Le^x-lysyllysine conjugate. The molecular mechanism of Le^x-dependent autoaggregation was found to be Le^x-to-Le^x interaction in the presence of Ca^{2+}. The process was recently well elucidated by molecular force microscopy and by surface plasmon resonance spectroscopy.

Human Embryonal Carcinoma Autoaggregation Through Gb4-to-nLc_4 or Gb4-to-Gb5 Interaction

Gb4, Gb5, and nLc_4 are highly expressed, in addition to Le^x, in mouse preimplantation embryo. Expression of Gb5 is much higher than that of Le^x in human embryonal carcinoma and in primate preimplantation embryo, although the expression status of these GSLs and carbohydrate antigens in human embryo has not been studied for ethical reasons. Autoaggregation of human embryonal carcinoma, which may mimic the compaction process of human embryo, is mediated by Gb4-to-nLc_4 or Gb4-to-Gb5 interaction (Gb4-dependent adhesion). These GSLs are closely associated with cSrc, RhoA, and Ras in glycosynapse, and may induce differentiation following Gb4-dependent adhesion.

Rainbow Trout Sperm Binding to Egg Mediated by (KDN)GM3 Interaction with Gg3-Like Epitope

A novel deaminated analogue of sialic acid, 2-keto-3-deoxy-D-*glycero*-D-*galacto*-nononic acid (KDN), is found in fish egg and sperm. The head of rainbow trout

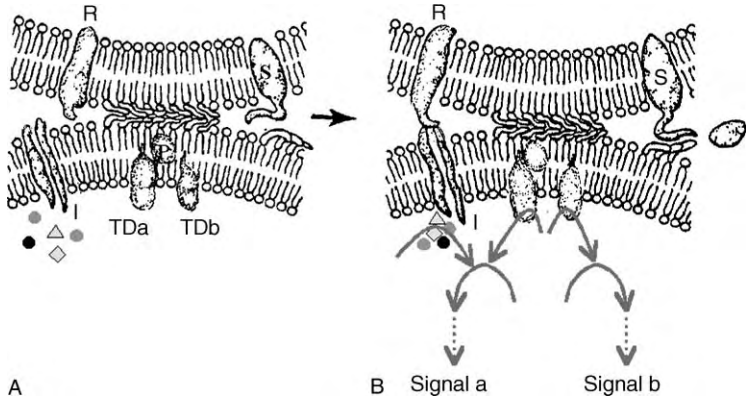

FIGURE 3 Model of GSL-based glycosynapse, and GSL-dependent adhesion through carbohydrate-to-carbohydrate interaction. (A) Clustered GSLs on the surface membrane of one cell are bound to cluster of another type of GSL on surface membrane of counterpart cell, through *trans* interaction of GSLs as in Figure 2. (B) Such adhesion induces change (activation or inhibition) of signal transducers (TDa, TDb) to send signals (a, b). In some cases, this process is synergistic with another adhesion system, such as integrin receptor (I) and its binding counterpart (R, e.g., ICAM1), or other type of carbohydrate-dependent receptor (S, e.g., CD44).

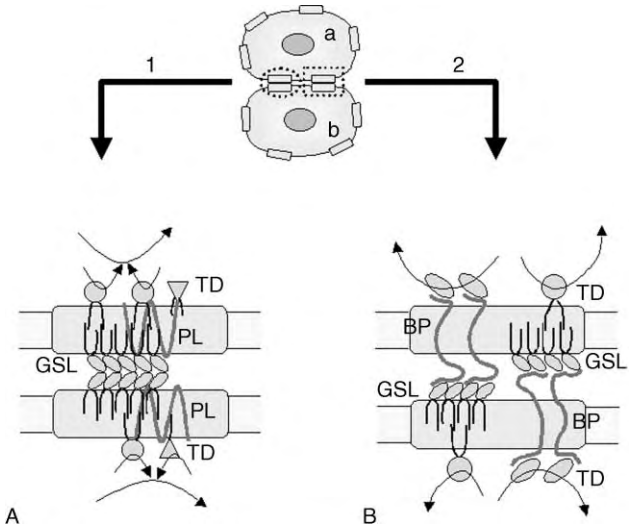

FIGURE 4 Two types of GSL clusters in glycosynapse function in GSL-dependent adhesion. Adhesion of cell a to cell b occurs via adhesion processes 1 and 2. (A) Process 1 is based on GSL clusters associated directly with signal transducers (TD), and stabilized by proteolipids (PL). Adhesion proceeds through interfacing of the two glycosynapses, and carbohydrate-to-carbohydrate interaction, and concurrent activation or inhibition of signal transducers. (B) Process 2 is based on GSL clusters and their binding protein (BP). Through interfacing of the two glycosynapses, GSLs are bound to BP, whereby TD is activated or inhibited.

sperm has a high content of (KDN)GM3, as indicated by reactivity with specific anti-(KDN)GM3 mAb kdn3G, and binds strongly to plates coated with Gg3, but not other GSLs. This binding is inhibited by kdn3G and by anti-Gg3 mAb 2D4. Vitelline envelope membrane isolated from rainbow trout egg has a glycoconjugate containing Gg3-like epitope, defined by antibody 2D4. Immunoelectron microscopy revealed that the Gg3-like epitope is highly expressed in exposed second layer of vitelline envelope surrounding the micropyle, a narrow channel through which a sperm enters the egg cell. Thus, interaction of (KDN)GM3 at sperm head with Gg3-like epitope surrounding the micropyle is a crucial event in the process of rainbow trout fertilization.

Types of Cell Adhesion Mediated by Interaction of GSL with GSL-Binding Protein

Neuronal Axon Binding to Myelin Through Interaction of Ganglioside with Siglec-4

Neuronal cell membranes are characterized by the presence of ganglio-series gangliosides. Gangliosides expressed at neuronal cell axons interact with myelinating glial cells through myelin-associated glycoprotein (MAG), which was known previously as sialic acid-binding protein siglec4. GD1a and GT1b, which have sialyl $\alpha 2 \rightarrow 3$Gal terminal residue, are specific functional ligands of MAG that inhibit nerve regeneration and neurite formation. Inhibition of ganglioside synthesis by P4, or blocking of ganglioside interaction with MAG by anti-ganglioside IgG antibodies, reversed the MAG-dependent inhibitory effect on neurite formation.

Aggregation of Renal Cell Carcinoma TOS1 Cells with Peripheral Blood Mononuclear Cells Through Interaction of Disialoganglioside with Siglec-7

Renal cell carcinoma (RCC) has high metastatic potential to lung, and the degree of metastatic potential is correlated with RCC expression of disialogangliosides, which are ligands of sialic acid-binding protein siglec-7, the major siglec expressed in peripheral blood mononuclear cells (PBMC). These disialogangliosides expressed in RCC were identified as disialyl-Lc_4 (defined by mAb FH9), GalNAc-disialyl-Lc_4 (defined by mAb RM2), disialyl-Gb5 (defined by mAb 5F3), and GD3 (defined by mAb R24). RCC cell line TOS1 is characterized by expression of disialyl-Lc_4, GalNAc-disialyl-Lc_4, and GD3, and interacts with siglec-7 on the surface of PBMC, causing aggregation of TOS1 cells with PBMC. Large aggregates of this type may result in microembolisms that initiate metastasis, particularly in lung.

Adhesion of Neutrophils or Myelogenous Leukemia HL60 Cells to E-Selectin Through Fucosyl-poly-LacNAc Ganglioside (Myeloglycan)

Sialyl-Le^x (SLe^x) has been regarded as the major ligand of human neutrophils, or myelocytic, or monocytic leukemia cell lines (e.g., HL60, U937) that interact with E-selectin expressed on ECs. Extensive studies on human neutrophils and HL60 cells indicated that SLe^x epitope is absent from GSLs and gangliosides of these cells. Instead, E-selectin-binding epitopes were identified as poly-LacNAc with multiple $\alpha 1 \rightarrow 3$ fucosylation and terminal $\alpha 2 \rightarrow 3$ sialylation:

$$\text{NeuAc}\alpha 3\text{Gal}\beta 4\,\text{GlcNAc}\beta 3\,[\text{Gal}\beta 4\text{GlcNAc}\beta 3\text{Gal}\beta 4\,\underset{\text{Fuc}\alpha}{\overset{3}{\text{GlcNAc}}}\,]_n\beta 3\,\text{Gal}\beta\text{GlcCer} \qquad n \geq 1$$

These GSLs display strong E-selectin-dependent adhesion, particularly under dynamic flow conditions, and are collectively termed "myeloglycan."

Human Neuroblastoma Adhesion through GM1-to-Galectin-1 Interaction

Human neuroblastoma expresses ganglio-series gangliosides and galectin-1. Neuroblastoma cell contact activates endogenous sialidase, which causes conversion of GD1a, GD1b, GT1b, etc. to GM1, and consequent accumulation of GM1. GM1 is one of the ganglio-series gangliosides having terminal βGal residue that is recognized by galectin-1; therefore, GM1 at the neuroblastoma cell surface promotes cell-to-cell adhesion. Galectin-mediated cell adhesion has been proposed, but the target carbohydrate was identified as glycoprotein, and little attention has been paid to GSLs.

See Also the Following Articles

Glycolysis, Overview • Lipid Modification of Proteins: Targeting to Membranes • Lysophospholipid Receptors • Sphingolipid Biosynthesis • Sphingolipid Catabolism

Glossary

glycosphingolipid Carbohydrate glycosidically bound to primary hydroxyl group of N-fatty acyl sphingosine.

glycosynapse The assembly of glycosphingolipids and other glycoconjugates in membrane, associated with cytoplasmic signal transducers having long-chain acyl group, and with hydrophobic transmembrane proteins. The assembly performs carbohydrate-dependent cell adhesion with concurrent signaling.

GSL structures Gb4, GalNAcβ3Galα4Galβ4Glcβ1Cer; Gb5, Galβ3GalNAcβ3Galα4Galβ4Glcβ1Cer; Gg3, GalNAcβ4Galβ4Glcβ1Cer; GM3, NeuAcα3Galβ4GlcCer; LacCer, Galβ4Glcβ1Cer; LacNAc, Galβ4GlcNAc$\beta \rightarrow$ R; Lc_4, Galβ3GlcNAcβ3Galβ4GlcCer; Le^x, Galβ4[Fucα3]GlcNAcβ3Gal$\beta \rightarrow$ R; nLc_4, Galβ4GlcNAcβ3Galβ4Glcβ1Cer.

Further Reading

Hakomori, S. (2000). Traveling for the glycosphingolipid path. *Glycoconj. J.* **17**, 627–647.

Hakomori, S. (2002). The glycosynapse. *Proc. Natl. Acad. Sci. USA* **99**(1), 225–232.

Hakomori, S., and Handa, K. (2002). Glycosphingolipid-dependent cross-talk between glycosynapses interfacing tumor cells with their host cells: Essential basis to define tumor malignancy. *FEBS Lett.* **531**(1), 88–92.

Handa, K., Stroud, M. R., and Hakomori, S. (1997). Sialosyl-fucosyl poly-LacNAc without the sialosyl-Le^x epitope as the physiological myeloid cell ligand in E-selectin-dependent adhesion: Studies under static and dynamic flow conditions. *Biochemistry* **36**, 12412–12420.

Ito, A., Handa, K., Withers, D. A., Satoh, M., and Hakomori, S. (2001). Binding specificity of siglec7 to disialogangliosides of renal cell carcinoma: Possible role of disialogangliosides in tumor progression. *FEBS Lett.* **504**(1–2), 82–86.

Kopitz, J., von Reitzenstein, C., Burchert, M., Cantz, M., and Gabius, H. J. (1998). Galectin-1 is a major receptor for ganglioside GM1, a product of the growth-controlling activity of a cell surface ganglioside sialidase, on human neuroblastoma cells in culture. *J. Biol. Chem.* **273**, 11205–11211.

Rojo, J., Morales, J. C., and Penades, S. (2002). Carbohydrate–carbohydrate interactions in biological and model systems. *Topics Curr. Chem.* **218**, 45–92.

Vyas, A. A., Patel, H. V., Fromholt, S. E., Heffer-Lauc, M., Vyas, K. A., Dang, J., Schachner, M., and Schnaar, R. L. (2002). Gangliosides are functional nerve cell ligands for myelin-associated glycoprotein (MAG), an inhibitor of nerve regeneration. *Proc. Natl. Acad. Sci. USA* **99**(12), 8412–8417.

Biography

Dr. Senitiroh Hakomori is Professor of Pathobiology and Microbiology, University of Washington, and Head, Division of Biomembrane Research, Pacific Northwest Research Institute, Seattle, Washington. His major work has been focused on structure, function, and organization of glycosphingolipids. He was also involved in discovery of fibronectin, and systematic analysis of blood group ABH including cloning and structure of their genes. He has received many national and international awards, and was elected to the National Academy of Sciences in 2000.

Glycolysis, Overview

Robert A. Harris
Indiana University School of Medicine, Indianapolis, Indiana, USA

Glycolysis is a linear metabolic pathway of enzyme-catalyzed reactions that convert glucose to two molecules of pyruvate in the presence of oxygen or to two molecules of lactate in the absence of oxygen. Anaerobic glycolysis is likely the first pathway that evolved in nature to produce ATP and it remains the only pathway for ATP production in some cells. In most cells, however, glycolysis serves to convert glucose to pyruvate rather than lactate, with pyruvate subsequently being oxidized to carbon dioxide and water by mitochondrial enzymes. Since oxygen is necessary for complete pyruvate oxidation, glycolysis is the only option cells have for the production of ATP in the absence of oxygen. Glycolysis is frequently elevated in malignant tumors and may favor survival and proliferation of cancer cells. Overproduction of lactic acid by glycolysis leads to lactic acidosis, a life-threatening condition.

Role of Glycolysis

ATP Production

In the absence of either oxygen or mitochondria, glycolysis operates as a self-contained pathway with lactate as its end product (Figure 1A). Energy released by exergonic reactions is captured with the formation of two molecules of ATP from two molecules of ADP and inorganic phosphate (Pi):

$$\text{Glucose} + 2\text{ADP} + 2\text{Pi} \rightarrow 2\text{Lactate} + 2\text{ATP}$$

Production of ATP by this overall sum equation for the pathway is the most important function of glycolysis. Some cells depend entirely upon the ATP produced by glycolysis. For example, mature red blood cells obtain all of their ATP in this manner because they lack mitochondria, the oxygen-consuming organelles responsible for production of practically all of the ATP in most cells. Uninterrupted production of ATP is required for proper function and survival of all cells. The simplest of all cells in the body, red blood cells still require the continuous operation of the glycolytic pathway to produce ATP to power their Na^+, K^+-ATPase and a number of processes.

Preparatory Pathway for Glucose Oxidation

The function of glycolysis changes when oxygen is available and mitochondria are present. When oxygen and mitochondria are both present, glucose is completely oxidized to carbon dioxide and water (Figure 1B) by the sum reaction:

$$\text{Glucose} + 6\text{O}_2 + 32\text{ADP} + 32\text{Pi} \rightarrow 6\text{CO}_2 + 6\text{H}_2\text{O} + 32\text{ATP}$$

Glycolysis sets the stage for the complete oxidation of glucose, a process that produces 16 times more ATP per glucose molecule than anaerobic glycolysis. In the absence of either oxygen or mitochondria, glycolysis yields two molecules of pyruvate that must be reduced to lactate for glycolysis to proceed (Figure 1A). When oxygen is present, pyruvate is taken up by mitochondria and the entire molecule is oxidized to carbon dioxide and water by the sequential actions of the pyruvate dehydrogenase complex, citric acid cycle, and the electron transport chain (Figure 1B).

Because mitochondria are present in most cells and there is continuous supply of oxygen from the blood, virtually every tissue of the body uses glycolysis as a preparatory pathway, which provides them with much greater amounts of ATP from each glucose than anaerobic glycolysis. The human brain, for example, completely oxidizes about 120 g of glucose each day, all via pyruvate molecules produced from glucose by glycolysis. Lactate is present in the brain, but the amount is small and none is released into the blood because the brain is well oxygenated and mitochondria are abundant.

Three Stages of the Glycolytic Pathway

Conversion of glucose to lactate occurs in three stages in the cell cytoplasm (Figure 2).

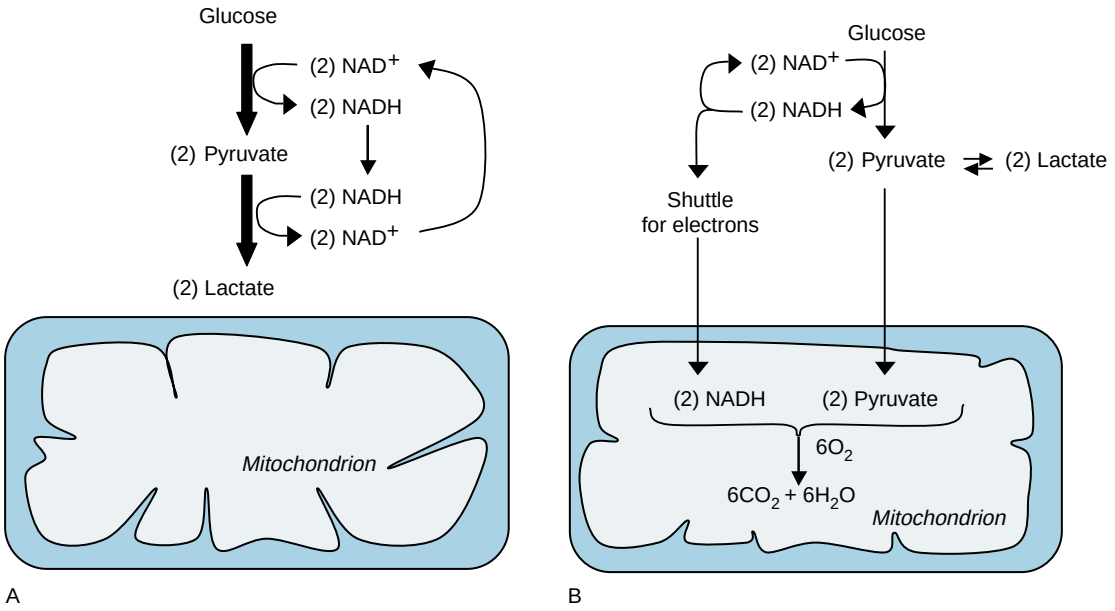

FIGURE 1 Overviews of glycolysis. (A) Lactate is the product of glycolysis in the absence of oxygen. (B) Glycolysis serves as a preparatory pathway for the complete oxidation of glucose in the presence of oxygen.

Priming Stage

The first three reactions of the pathway prime the glucose molecule for use by subsequent enzymes. ATP molecules are invested in the reactions catalyzed by hexokinase and 6-phosphofructo-1-kinase. Phosphorylation traps glucose inside the cell and sets the stage for subsequent cleavage of the glucose into two 3-carbon fragments. The priming stage sums up to be simply:

$$\text{Glucose} + 2\text{ATP} \rightarrow \text{Fructose 1,6-bisphosphate} + 2\text{ADP}$$

Splitting Stage

Fructose 1,6-biphosphate undergoes cleavage by aldolase between carbons 3 and 4 in the first step of the splitting stage. Dihydroxyacetone phosphate and glyceraldehyde 3-phosphate, known collectively as triose phosphates, are produced by an aldol cleavage of fructose 1,6-bisphosphate. Interconversion of the triose phosphates by an isomerase completes the splitting stage, which sums up to be:

$$\text{Fructose 1,6-bisphosphate} \rightarrow 2\text{Glyceraldehyde 3-phosphate}$$

Energy-Trapping Stage

Six enzymes are required to capture the energy made available in this stage. All of the ATP produced by glycolysis is generated in this stage by the reactions catalyzed by 3-phosphoglycerate kinase and pyruvate kinase. Since two glyceraldehyde 3-phosphate molecules are converted to two lactate molecules, a total of 4 ATPs are produced in this stage, which sums up to be:

$$2\text{Glyceraldehyde 3-phosphate} + 4\text{ADP} + 2\text{Pi} \rightarrow 2\text{Lactate}^- + 4\text{ATP}$$

The sum of the three stages yields the overall equation for anaerobic glycolysis in which one molecule of glucose is converted to two molecules of lactate with the production of two molecules of ATP:

$$\text{Glucose} + 2\text{ADP} + 2\text{Pi} \rightarrow 2\text{Lactate}^- + 2\text{ATP}$$

Anaerobic Glycolysis is a Type of Fermentation

Fermentations are pathways that (1) produce ATP, (2) do not involve oxygen, (3) involve an intermediate that becomes oxidized, and (4) involve an intermediate that becomes reduced. That ATP is produced and oxygen is not required can be seen from the overall equation for glycolysis:

$$\text{Glucose} + 2\text{ADP} + 2\text{Pi} \rightarrow 2\text{Lactate}^- + 2\text{ATP}$$

Whether an intermediate becomes oxidized and another reduced is not shown. However, during the first reaction of the energy trapping stage of glycolysis (Figure 2), the aldehyde group ($-$CHO) of glyceraldehyde 3-phosphate is oxidized to a carboxylic acid ($-CO_2^-$) and then phosphorylated to give a mixed anhydride of a carboxylic acid and phosphoric acid

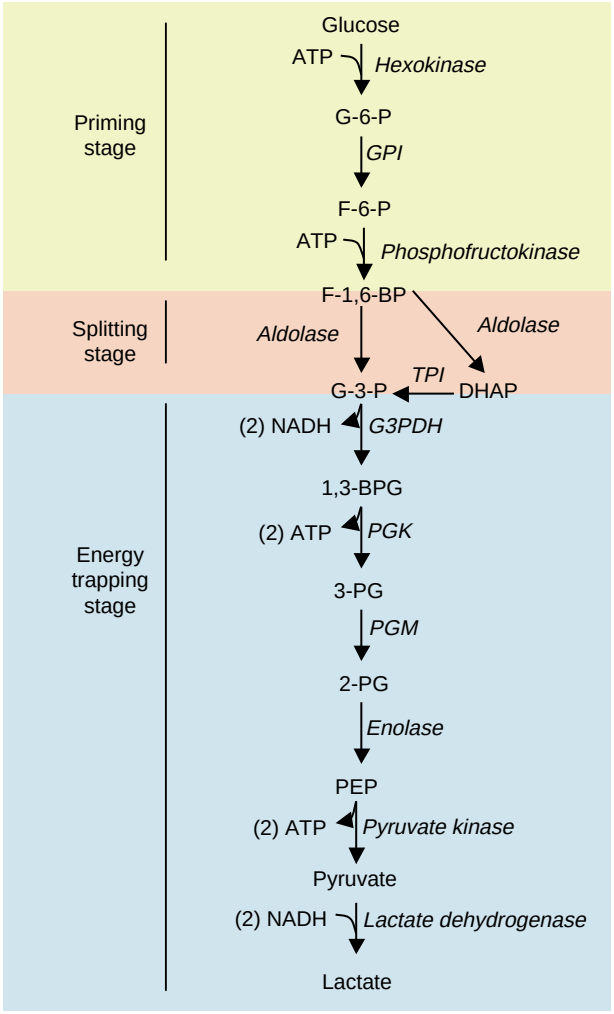

FIGURE 2 The three stages of the glycolytic pathway: Priming, splitting, and energy trapping. Abbreviations for glycolytic intermediates: G-6-P, glucose 6-phosphate; F-6-P, fructose 6-phosphate; F-1,6-BP, fructose 1,6-bisphosphate; G-3-P, glyceraldehyde 3-phosphate; DHAP, dihydroxyacetone phosphate; 1,3-BPG, 1,3-bisphosphoglycerate; 3-PG, 3-phosphoglycerate; 2-PG, 2-phosphoglycerate; PEP, phosphoenolpyruvate. Abbreviations for glycolytic enzyme names: GPI, glucose phosphate isomerase; TPI, triose phosphate isomerase; G3PDH, glyceraldehyde-3-phosphate dehydrogenase; PGK, phosphoglycerate kinase; PGM, phosphoglycerate mutase.

(1,3-biphosphoglycerate):

$$R-CHO + Pi + H_2O \rightarrow R-CO_2P + 2e^- + 2H^+$$

$$NAD^+ + 2e^- + 2H^+ \rightarrow NADH + H^+$$

$$\text{Sum}: \; R-CHO + NAD^+ + H_2O + Pi \rightarrow R-CO_2P + NADH + H^+$$

In the last reaction of the energy trapping stage of glycolysis (Figure 2), the α-keto group of pyruvate is reduced to give the α-hydroxyl group of lactate:

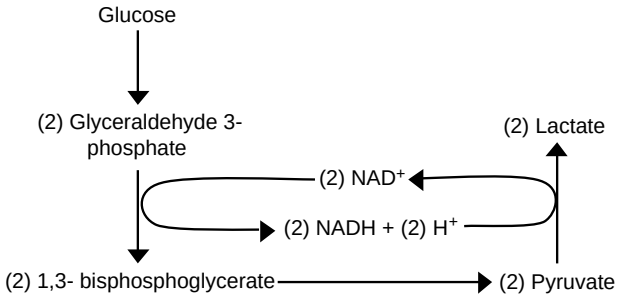

FIGURE 3 NAD^+ serves as a bridge molecule to couple the oxidation of glyceraldehyde 3-phosphate to the reduction of pyruvate during anaerobic glycolysis.

$$NADH + H^+ \rightarrow NAD^+ + 2e^- + 2H^+$$

$$CH_3-CO-CO_2^- + 2e^- + 2H^+ \rightarrow CH_3-CHOH-CO_2^-$$

$$\text{Sum}: \; CH_3-CO-CO_2^- + NADH + H^+ \rightarrow CH_3-CHOH-CO_2^- + NAD^+$$

NAD^+ serves as a bridge compound for these reactions (Figure 3), accepting two electrons and one H^+ to become NADH during the oxidation of the aldehyde group of glyceraldehyde 3-phosphate and subsequently donating two electrons and one H^+ when it returns to being NAD^+ during the reduction of the α-keto group of pyruvate. The result is a perfect balance between the production of NADH in an oxidation step and its utilization in a reduction step. Anaerobic glycolysis is therefore a type of fermentation.

Control of Glycolysis

The rate at which ATP is hydrolyzed back to ADP and Pi by energy requiring reactions is a major determinant of flux through the glycolytic pathway. In other words, ATP turnover caused by energy required to perform the work being done by a cell greatly affects the rate of glycolysis. The presence or absence of oxygen also has a profound effect upon the rate of glycolysis.

ATP Turnover

Two molecules of ATP are produced for each molecule of glucose utilized by glycolysis. Less obvious, but important for an understanding of what controls the rate of glycolysis, "two molecules of ATP must be hydrolyzed to ADP and Pi for each glucose utilized." This is because the amount of ADP present in cells is quite small relative to the large amount of glucose that has to be utilized to meet the energy needs of cells. Glycolysis can therefore

not proceed without hydrolyzing ATP to make ADP available for energy conserving steps. Hydrolysis of ATP to ADP plus Pi is usually rate limiting for the process of glycolysis. Thus, an increase in ATP turnover caused by an increase in the amount of work being done by a cell has a profound effect upon the rate of glycolysis. For example, strenuous exercise induces a marked increase in glycolysis because of ATP hydrolysis by the contractile machinery of muscle.

Oxygen

A remarkable "decrease" in glycolysis occurs when cells that lack oxygen are transferred into an environment in which oxygen is abundantly available. Carbon dioxide production starts immediately but cells use much less glucose and accumulate little or no lactate. This illustrates the Pasteur effect, which refers back to Louis Pasteur's observation ~150 years ago that oxygen inhibits the fermentation of glucose by yeast. The Pasteur effect reflects the marked difference in cellular capacity for ATP production in the presence and absence of oxygen. Relative to anaerobic glycolysis, 16 times more ATP is produced when glucose is completely oxidized to carbon dioxide and water by the combined actions of glycolytic and mitochondrial enzymes. The rate of glycolysis decreases greatly in the presence of oxygen because the ATP needed to meet the energy needs of a cell can be supplied by the catabolism of much less glucose.

Lactate is not produced when oxygen is available to cells. Less glucose has to be used to meet the need for ATP, which automatically means less pyruvate is produced and available for reduction to lactate by NADH. The pyruvate that is produced by glycolysis is also rapidly oxidized by the mitochondria, leaving less available for reduction to lactate by NADH. And finally, less NADH is available for the reduction of pyruvate to lactate because shuttle mechanisms operate in the presence of oxygen to transport the electrons of NADH into mitochondria by the net equation:

$$\mathrm{NADH_{cytosol} + H^{+}_{Cytosol} + NAD^{+}_{Mitosol} \rightarrow NAD^{+}_{Cytosol} + NADH_{Mitosol} + H^{+}_{Mitosol}}$$

NADH generated in the mitochondria is oxidized by the electron transport chain, which provides energy for the synthesis of ATP by oxidative phosphorylation according to net equation:

$$\mathrm{NADH + H + \tfrac{1}{2}O_2 + 2\tfrac{1}{2}ADP + 2\tfrac{1}{2}Pi \rightarrow NAD^{+} + 2\tfrac{1}{2}ATP + H_2O}$$

Removal of oxygen from the environment of cells utilizing glucose has the opposite effect. Glycolysis is greatly stimulated as evidenced by increased glucose utilization and lactate production. Anaerobic glycolysis

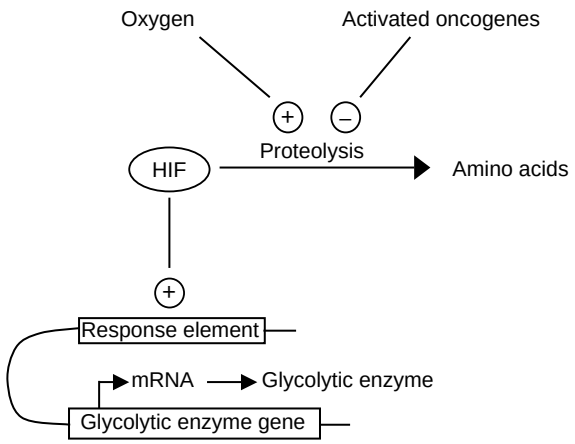

FIGURE 4 Oxygen controls glycolytic enzyme expression by controlling the amount of HIF (hypoxia inducible factor), a transcription factor that regulates transcription of genes that encode glycolytic enzymes.

can sometimes meet the need of cells for ATP. Sometimes it is inadequate, in spite of an increase in its rate. Cells can and do die when ATP is not generated fast enough to keep them viable, which is what happens in the heart during a heart attack or in the brain as a consequence of a stroke. Cells that survive in an oxygen-poor environment are usually able to elevate their capacity for glycolysis by increasing the amounts of the glycolytic enzymes present. This in turn increases the activities of the glycolytic enzymes and therefore the capacity for ATP synthesis by glycolysis. Lack of oxygen signals an increase in the transcription of the genes that encode the glycolytic enzymes. This occurs because lack of oxygen (hypoxia) causes an increase in the amount of a protein called hypoxia *i*nducible *f*actor (HIF) (Figure 4). HIF is a transcription factor that promotes transcription when it binds to a specific sequence of nucleotides in promoter region of genes encoding glycolytic enzymes. Oxygen stimulates proteolytic degradation of HIF (Figure 4), which keeps the amount of HIF very low in cells, which in turn keeps the amounts of the glycolytic enzymes also low. Hypoxia maximizes the amount of HIF, which greatly increases expression of the glycolytic enzymes and therefore cellular capacity for glycolysis.

Cancer

Malignant tumors make good use of glycolysis as a source of ATP. Rates of glycolysis are often faster in malignant tumors than normal tissues. Radiologists and oncologists take advantage of this phenomenon in the diagnosis of cancer by PET imaging. Radioactive glucose derivatives accumulate in cancer cells because of their greater glycolytic capacity. Surprisingly, tumor cells often metabolize glucose to lactate even in the

"presence" of oxygen. This is unusual and stands in contrast to normal cells that only metabolize glucose to lactate in the "absence" of oxygen, as discussed previously. The conversion of glucose to lactate in the presence of oxygen is called aerobic glycolysis, to distinguish it from anaerobic glycolysis which refers to the conversion of glucose to lactate in the absence of oxygen. The high rate of aerobic glycolysis exhibited by some cancer cells is called the Warburg effect, in recognition of Otto Warburg's discovery ~80 years ago that tumor cells produce lactate in the presence of oxygen. Based on this observation Warburg championed the idea that aerobic glycolysis is the cause of cancer. Now, however, it is appreciated that up-regulation of the enzymatic capacity of glycolysis occurs frequently in cancer cells because of a higher concentration of HIF, the transcription factor responsible for regulation of the transcription of genes encoding glycolytic enzymes (Figure 4). HIF is highly expressed in many tumor cells even in the presence of oxygen, most likely as a consequence of mutations that have occurred in genes that either prevent (tumor suppressors) or promote (oncogenes) the development of cancer. Since tumors sometimes outgrow their blood supply and cancer cells frequently migrate into areas of the body where the oxygen concentration is low, an exceptionally high capacity for ATP production that does not require oxygen may provide cancer cells with a metabolic advantage for survival and growth.

Lactic Acidosis

Regardless of whether anaerobic or aerobic, glycolysis produces acid if lactate is the end product of the pathway. The acid produced by glycolysis lowers the pH both inside cells where lactate is produced as well as outside where protons can diffuse. Since the pH range in which cells can function is quite narrow (pH 7.0–7.6), uncontrolled glycolysis can lead to cell death. This is the Achilles' heel of glycolysis. Indeed, in the final analysis it is overproduction of acid and lowering of the pH by glycolysis that kills most organisms, including humans. In an effort to emphasize the production of ATP by glycolysis, unbalanced reactions were used in the description of glycolysis. The production of protons by glycolysis was ignored. However, cells incubated under anaerobic conditions produce large amounts of acid by anaerobic glycolysis. Likewise, forcing an area of the heart to obtain all of its energy from glycolysis by occluding a coronary artery causes rapid production of large amounts of acid, which lowers the pH, activates nerve endings, and registers as pain. That the conversion of glucose to lactate produces acid is apparent when we write the "balanced" overall equation for glycolysis in the following manner:

$$\text{Glucose} \rightarrow 2\,\text{Lactate}^- + 2\text{H}^+$$

Since the empirical formula for glucose is $C_6H_{12}O_6$, and there are 6 carbons, 12 hydrogens, and 6 oxygens in the products, this equation is balanced for mass and charge. Thus, two protons are produced for every glucose molecule converted to lactate molecules by glycolysis. Since glycolysis produces 2 ATPs per glucose, the equation seems incomplete, and in one sense it is incomplete. Expanding the equation to include ADP, Pi, and ATP in their predominant ionization states at physiological pH yields:

$$\text{Glucose} + 2\text{ADP}^{3-} + 2\text{Pi}^{2-} \rightarrow 2\,\text{Lactate}^- + 2\text{ATP}^{4-} + 2\text{H}_2\text{O}$$

If this is accepted as the appropriate equation for glycolysis, balanced as it is for mass and charge, the pathway does not produce acid and therefore should have no effect on cellular pH. However, anaerobic glycolysis can clearly be shown to produce acid experimentally, and the reason it does so is again because the pool size of ATP is small compared to the amount of glucose that is converted to lactate to meet the energy needs of a cell. For every glucose molecule converted to lactate, two ATP molecules have to be hydrolyzed according to the equation:

$$2\text{ATP}^{4-} + 2\text{H}_2\text{O} \rightarrow 2\text{ADP}^{3-} + 2\text{Pi}^{2-} + 2\text{H}^+ + \text{"work"}$$

Work in this equation refers to any of the many energy-requiring processes that can only occur as a consequence of ATP hydrolysis, such as muscle contraction, Na^+, K^+-ATPase activity, etc. Summing up the last two equations brings us back to the overall balanced equation that shows acid production by glyolysis:

$$\text{Glucose} \rightarrow 2\,\text{Lactate}^- + 2\text{H}^+$$

Anaerobic glycolysis therefore produces acid. Conditions in humans that greatly increase anaerobic glycolysis because of a shortage of oxygen and the resulting Pasteur effect, such as failure of the respiratory system or the blood circulatory system, often cause the production of more acid than can be handled by the buffering systems of the body. The consequence is lactic acidosis, a life-threatening condition that can be dealt with most effectively by supplying oxygen, which will block the Pasteur effect and inhibit the production of lactic acid.

See Also the Following Articles

N-Linked Glycan Processing Glucosidases and Mannosidases • Pyruvate Dehydrogenase • Pyruvate Kinase

Glossary

cancer Unlike normal tissue or a benign tumor, cancer cells exhibit the property of invasion of other organs of the body.

hypoxia Condition in which the oxygen content of a tissue is so low that it limits electron transport activity by mitochondria.

Na^+, K^+-ATPase Enzyme complex present in the plasma membrane of all cells that utilizes the energy provided by ATP hydrolysis to drive the transport of Na^+ out and K^+ into cells.

oxidation–reduction reactions Reaction in which one compound gets oxidized (loses electrons) and another compound gets reduced (gains electrons).

PET imaging A technique for creating an image of a tissue that relies upon the use of positron emission tomography (PET) to measure a signal produced by a short-lived radionuclide such as ^{18}F-fluorodeoxyglucose.

Further Reading

Berg, J. M., Tymoczko, J. L., and Stryer, L. (1995). Glycolysis. In *Biochemistry*, 5th edition, pp. 425–449. W. H. Freeman, New York.

Gibson, D. M., and Harris, R. A. (2002). *Metabolic Regulation in Mammals*. Taylor and Frances, London.

Harris, R. A. (2002). Carbohydrate metabolism I: Major metabolic pathways and their control. In *Textbook of Biochemistry with Clinical Correlations* (T. M. Devlin, ed.) 5th edition, pp. 597–664. Wiley-Liss, New York.

Harris, R. A., and Crabb, D. W. (2002). Metabolic interrelationships. In *Textbook of Biochemistry with Clinical Correlations* (T. M. Devlin, ed.) 5th edition, pp. 861–902. Wiley-Liss, New York.

Semenza, G. L. (2002). Signal transduction to hypoxia-inducible factor 1. *Biochem. Pharm.* **64**, 993–998.

Stubbs, M., Bashford, C. L., and Griffiths, J. R. (2003). Understanding the tumor metabolic phenotype in the genomic era. *Curr. Mol. Med.* **3**, 485–505.

Biography

Robert A. Harris, a graduate of Purdue University, is Distinguished Professor, Showalter Professor, and Chairman of Biochemistry and Molecular Biology at the Indiana University School of Medicine. Postdoctoral training was completed in the laboratories of David Green (Wisconsin) and Sir Hans Krebs (Oxford). Dr. Harris teaches metabolism and directs the medical biochemistry course for first year medical students. His research contributions include the identification and characterization of several mitochondrial enzymes involved in pyruvate and the branched-chain amino acids metabolism.

Glycoprotein Folding and Processing Reactions

Armando J. Parodi
Fundacion Instituto Leloir, Buenos Aires, Argentina

The term glycoprotein folding and processing reactions refers to the mechanisms by which cells ensure that only properly folded glycoproteins follow the secretory pathway. The concept of quality control of protein folding first appeared in the late 1970s and early 1980s when it was noticed that not in all cases insertion of proteins or glycoproteins in the endoplasmic reticulum (ER) leads to their expected final destination, either intracellular (for instance, the lysosomes) or secretion. Several experimental results showed that cells displayed mechanisms that ensured that only proteins in their native conformations could be produced by the secretory pathway. Those mechanisms received the collective denomination of "quality control." By far the best-studied quality control mechanism is that occurring in the ER but more recent studies revealed that it also takes place at the Golgi apparatus. The scope of this article will be limited to the quality control occurring on glycoproteins in the ER.

Protein Folding in the Endoplasmic Reticulum

The endoplasmic reticulum (ER) quality control system is adapted to handling virtually any condition that results in a protein conformation other than the native state. Accordingly, multiple scenarios of quality control arise from the many ways in which proteins can fail to achieve their native conformation. All kinds of polypeptides inserted into the ER are subject to quality control, including soluble and membrane proteins (type I, II, and multispan). It applies to proteins regardless of their quaternary structure and whether they are glycosylated or contain intra- or intermolecular bonds. Proteins can fail the quality control due to multiple factors, such as truncations or mutations that interfere with proper folding, as well as orphan subunits of hetero-oligomeric complexes or homo-oligomers that cannot reach their proper structure. The lack of ligand binding or post-translational modifications (signal sequence cleavage, disulfide bond formation, *N*-glycosylation or glycosylphosphatidylinositol (GPI) anchor addition) can prevent proteins from folding correctly. Moreover, normal proteins that do not have any of the mentioned defects can also be targets of the quality control system, as protein folding is an extremely hazardous process whose efficiency heavily depends not only on particular environmental conditions but also on the amino acid primary sequence. In fact, almost never do all normal protein molecules manage to reach their proper native structure; there is always a variable fraction of newly synthesized proteins that do not fold efficiently.

A number of abundant ER resident proteins that participate in retention of non-native conformers have been identified as chaperones and folding-assisting proteins. Protein disulfide isomerase (PDI), one of the first facilitators of protein folding described, is an abundant ER chaperone. PDI and other members of the thioredoxin family participate in disulfide bond formation as well as retention and degradation of targets of the quality control system. Of particular interest is one member of this family (ERp57) that specifically associates with two ER resident lectins and contributes to proper glycoprotein folding. Another abundant ER protein, binding protein (BiP) that was originally identified as an ER retention factor for immunoglobulin heavy chains, participates in assisting protein folding through cycles of ATP hydrolysis that regulate substrate binding and release.

N-Glycan Processing Reactions in the Endoplasmic Reticulum

Glycosylation of asparagine residues (*N*-glycosylation) in the mammalian cell ER presents two basic differences with respect to glycosylation of Ser/Thr units (*O*-glycosylation) in either the cystosol or the Golgi apparatus: (1) in the former case a glycan containing 14 monosaccharide units in most cell types is transferred "*en bloc*" to the polypeptide chain whereas in *O*-glycosylation either a variable number of

monosaccharide units are sequentially transferred (Golgi *O*-glycosylation) or a single of such units is added (cytosolic *O*-glycosylation) and (2) *N*-glycosylation occurs on not yet properly folded polypeptide moieties, whereas in all cases *O*-glycosylation is a post-folding event. After being transferred to nascent chains in the ER, *N*-glycans are processed all along the secretory pathway. Whereas processing in the ER is basically similar in all eukaryotic cells for all *N*-glycans, Golgi processing reactions present a broad variation not only among different cell types but also different *N*-glycans belonging to the same or different glycoproteins may be differently processed within the same cell, thus yielding mature glycoproteins bearing glycan moieties with widely different structures. This diversity presents certain logic as the roles of protein-linked glycans in mature glycoproteins are mainly related to recognition phenomena. On the contrary, glycan processing in the ER is basically similar in all cells because the role of those reactions directly relates to a process common to all glycoproteins, namely the acquisition of their proper tertiary structures.

Addition of *N*-glycans has several effects on protein folding, at least two of which may be observed not only *in vivo* but also in folding assays performed in test tubes with pure glycoproteins: (1) *N*-glycans provide bulky, highly hydrophilic groups that help to maintain glycoproteins in solution during the folding process and (2) the presence of glycans modulates protein conformation by forcing amino acids close to the linking Asn unit to be in the proximity of the water-glycoprotein interphase. This article will not deal with those effects but with *in vivo* folding facilitation and ER retention of improperly folded structures mediated by the interaction of a specific glycan structure (monoglucosylated glycans) with ER lectins as calnexin (CNX) and calreticulin (CRT).

The saccharide transferred in most wild-type cells from a lipid (dolichol) derivative to polypeptide chains as they enter the ER lumen has the composition $Glc_3Man_9GlcNAc_2$ and the structure depicted in Figure 1. This is a well-conserved structure in nature as the same glycan is transferred in wild-type mammalian, plant, and fungal cells. There are some exceptions to this common pattern in certain protozoa, in which truncated *N*-glycans are transferred. The consensus glycosylation sequence (Asn–X–Ser/Thr, where X may be any amino acid except for Pro) is not necessarily glycosylated. Apparently, *N*-glycosylation, which occurs when the involved Asn unit is about 10–12 amino acids far from the inner ER membrane surface, is hindered if the polypeptide chain rapidly adopts a secondary structure. Cell-free assays showed that the oligosaccharyltransferase transfers the triglucosylated glycan about 20–25-fold faster than $Man_9GlcNAc_2$. This property, as well as the strict distance between the receptor amino acid and the ER inner surface required for glycan transfer, determine a severe underglycosylation of glycoproteins synthesized by cell mutants unable to glucosylate the lipid-linked glycan. Folding is severely impaired in many (but not all) underglycosylated glycoproteins.

The external Glc unit (residue *n*, Figure 1) is immediately removed from the protein-linked glycan by glucosidase I (GI), a membrane bound α-(1,2)-glucosidase (see mammalian cell ER processing of *N*-glycans in Figure 2). Further deglucosylation mediated by glucosidase II (GII), an α-(1,3)-glucosidase, may remove the remaining Glc units (residues *l* and *m*, Figure 1). GII is a soluble heterodimer composed of catalytically active and inactive subunits. The latter, but not the former, contains an ER retrieval sequence at its C terminus. Depending on the species, one or two Man units may be removed in the ER. Mammalian mannosidases I and II excise Man units *i* and *k*, respectively (Figure 1). A single ER α-mannosidase occurs in *Saccharomyces cerevisiae* that yields the same product as mammalian α-mannosidase I.

An additional *N*-glycan processing reaction occurring in the ER lumen is the transient glucosylation of

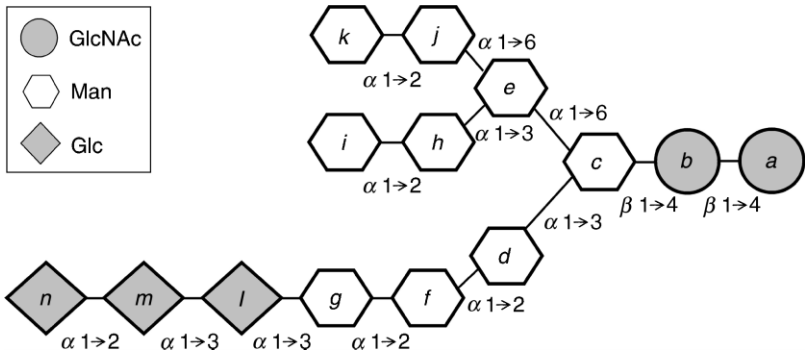

FIGURE 1 Glycan structures. Lettering (*a*–*n*) follows the order of addition of monosaccharides in the synthesis of $Glc_3Man_9GlcNAc_2$-P-P-dolichol. GI removes residue *n* and GII residues *l* and *m*. GT adds residue *l* to residue *g*. The $Man_8GlcNAc_2$ isomer formed by mammalian cell or *S. cerevisiae* ER α-mannosidase I lacks residues *i*, and *l*–*n* and that formed by mammalian cell ER α-mannosidase II is devoid of residues *k* and *l*–*n*.

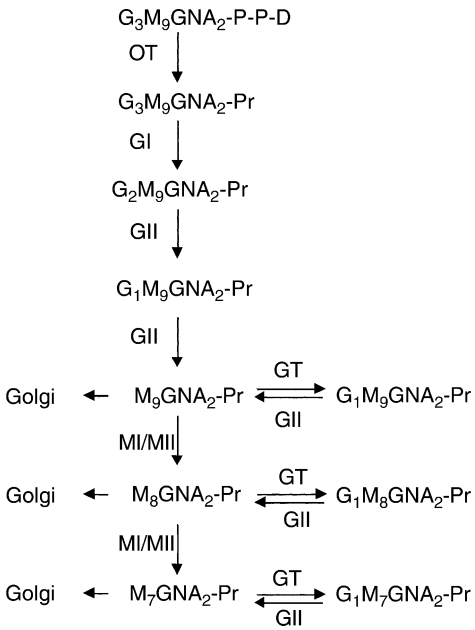

FIGURE 2 Glycan processing in the ER. G, M, GNA, D, and Pr stand for Glc, Man, GlcNAc, dolichol, and protein, respectively. OT, GI, GII, GT, MI, and MII stand for oligosaccharyltransferase, glucosidase I, glucosidase II, UDP-Glc:glycoprotein glucosyltransferase, mannosidase I, and mannosidase II, respectively.

glycoproteins: glucose-free glycans may be reglucosylated by the UDP-Glc:glycoprotein glucosyltransferase (GT) yielding $Glc_1Man_9GlcNAc_2$, $Glc_1Man_8GlcNAc_2$ and $Glc_1Man_7GlcNAc_2$ as reaction products. The structure of the first one is identical with that produced by partial deglucosylation of $Glc_3Man_9GlcNAc_2$ (Figure 1) and GII is also responsible for the *in vivo* deglucosylation of the monoglucosylated compounds formed by GT. This enzyme is present not only in mammalian but also in plant, fungal, and protozoan cells. *S. cerevisiae* is the only cell known so far to lack GT.

The Golgi apparatus of species belonging to the chordate phylum display an endomannosidase activity that degrades monoglycosylated *N*-glycans yielding Glc_1Man (plus $Man_{6\text{-}8}GlcNAc_2$, depending on the substrate used). This enzyme has been described to occur also in the mammalian cell ER-Golgi intermediate compartment. It may be speculated that the role of this enzyme is to ensure a complete removal of Glc units, as their presence would hinder formation of complex-type glycans in the Golgi apparatus.

The UDP-Glc:glycoprotein Glucosyltransferase

The transient addition of a terminal glucose residue to protein-linked glycans was discovered while studying *N*-glycan processing in trypanosomatid cells pulse-chased with [^{14}C]Glc. These *in vivo* observations were then extended to other eukaryotes, and it was soon established that transient reglucosylation of completely deglucosylated, protein-bound high-mannose-type glycans was a general glycoprotein processing reaction. Since glucose is not normally found on mature glycoproteins, transient reglucosylation was intriguing and the function of such apparent futile cycle of glucose addition and removal was not understood at the time. The reglucosylation of endogenous glycoproteins observed *in vivo* was reproduced in cell-free systems and the activity was localized by subcellular fractionation to the ER, where as mentioned above, deglucosylated glycoproteins that are subject to reglucosylation are formed by the action of GI and GII. As an *in vitro* assay for exogenous glycoprotein reglucosylation was developed, it was noticed that the substrate glycoprotein had to be denatured in order to be an acceptor in the reglucosylation reaction. This observation raised the radical notion that glycoproteins had to be devoid of a native conformation to be recognized as substrates by GT. Based on this unique property, it was suggested that the enzyme (and monoglucosylated glycans) could be somehow involved in the so-called "quality control" of glycoprotein folding in the ER.

The involvement of protein recognition in glycosylation reactions was not without precedent. While most glycosyltransferases display specificity at the carbohydrate level (sugar acceptor, sugar donor, and linkage formed), some glycosyltransferases also recognize the protein to which the substrate glycan is bound to. The UDP-N-acetylglucosamine:lysosomal enzyme N-acetylglucosamine phosphotransferase selectively initiates the formation of the Man 6-P epitope in lysosomal glycoproteins. Also, the UDP-GalNAc:glycoprotein hormone N-acetylgalactosaminyltransferase, selectively adds a GalNAc residue to secreted hormones. The substrates that reacted with GT *in vitro* did not appear to share any apparent common feature, except for their non-native conformation, as opposed to the other two glycosyltransferases, which maintain their rather narrow selectivity towards their respective glycoprotein substrates (lysosomal enzymes or glycoprotein hormones) when assayed *in vitro*. The requirement for non-native conformations implied that a wide range of substrates could be reglucosylated *in vivo*, since a large number of glycoproteins could potentially be recognized as substrates during their folding in the ER. Indeed, it is now accepted that all glycoproteins, independently from their final destination or of their soluble or membrane-bound status, behave as GT substrates during their folding process.

Purification of the enzyme from rat liver or *Schizosaccharomyces pombe* showed that activity resided in a single polypeptide of 170 kDa, significantly larger than

most glycosyltransferases. While most, if not all, glycosyltransferases and glycosidases in the secretory pathway are type II membrane proteins, GT and its counteracting enzyme GII are so far the only soluble carbohydrate-processing enzymes described in the secretory pathway. The purified GT has a neutral pH optimum, requires millimolar Ca^{2+} concentrations for activity, and uses UDP-Glc as substrate donor.

The ER membrane contains an integral protein responsible for the specific transport of UDP-Glc from its site of synthesis (the cytosol) into the lumen of the ER, where the sugar nucleotide serves as substrate for glycoprotein reglucosylation. Further, two GDPase/UDPases have been described recently in the mammalian cell ER lumen. Their role is probably to allow transport of UDP-Glc into the lumen by the known antiport mechanism, by which entrance of sugar nucleotides into the ER or Golgi lumen is coupled to exit of the corresponding nucleoside monophosphates.

The most significant finding in the isolation of GT was that the purified enzyme maintained its selectivity for denatured substrates. While it may still cooperate with other factors to recognize non-native conformations *in vivo*, the finding that pure GT exclusively reglucosylates non-native glycoproteins strongly suggests that the conformational sensing is performed primarily by the GT itself. No cofactors were found so far to modify the activity of isolated GT *in vitro*, and expression of GT cDNA is sufficient for glycoprotein reglucosylation in cells devoid of such activity (*S. cerevisiae*). It is now accepted that GT recognizes hydrophobic amino acid patches exposed in molten globule-like folding intermediates, that is, in polypeptides in which there is enough primary sequence information to allow adoption of a collapsed conformation. Moreover, *N*-glycans have to be relatively close to protein structural perturbations to be glucosylated.

The Quality Control Mechanism of Glycoprotein Folding

The information mentioned above supports the mechanism depicted in Figure 3 for the quality control mechanism of glycoprotein folding occurring in the ER. According to it, monoglucosylated glycoproteins generated either by partial deglucosylation of the transferred glycan or by GT-mediated glucosylation interact with CNX/CRT. This interaction is followed by a shuttle between glucosylated (CNX/CRT-bound) and

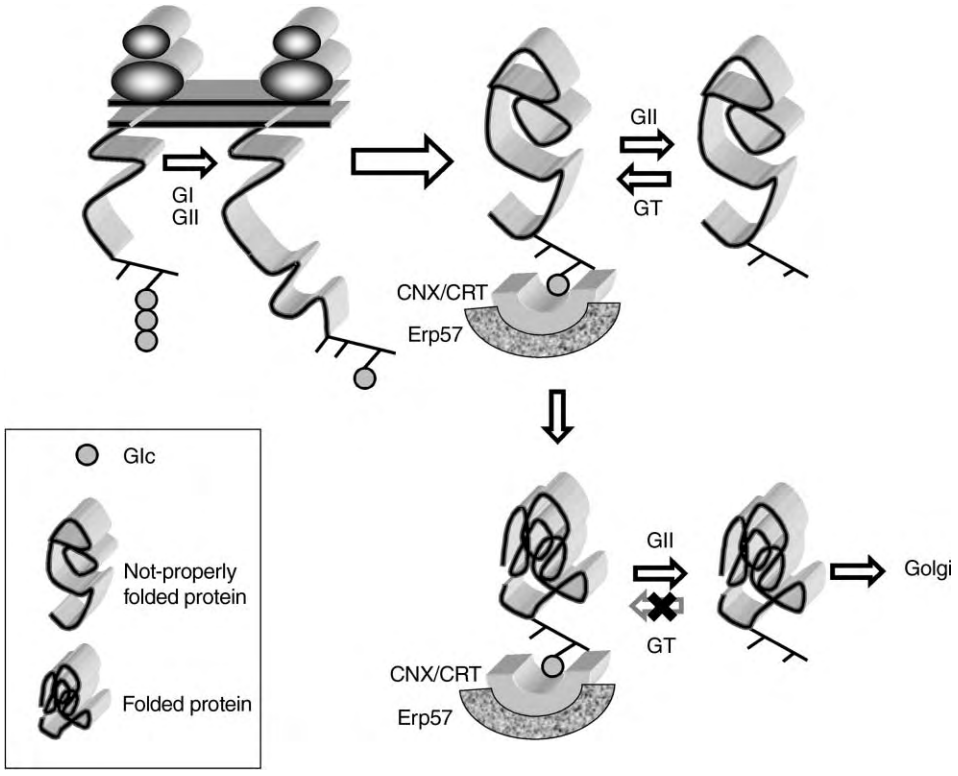

FIGURE 3 Model proposed for the quality control of glycoprotein folding. Protein linked $Glc_3Man_9GlcNAc_2$ is partially deglucosylated to the monoglucosylated derivative by GI and GII, and this structure is recognized by CNX/CRT. $Man_9GlcNAc_2$ is glucosylated by GT if complete deglucosylation occurs before lectin binding. The glycoprotein is liberated from the CNX/CRT anchor by GII and reglucosylated by GT only if not properly folded. On adoption of the native structure, the glycoprotein is released from CNX/CRT by GII and not reglucosylated by GT.

deglucosylated (CNX/CRT-free) forms catalyzed by the opposing activities of GT and GII. After acquiring their proper tertiary structure, glycoproteins are deglucosylated by GII but not reglucosylated by GT and no longer bind to CNX/CRT. Permanently misfolded molecules continue to interact with the lectins, which are not sensing the conformation of their glycoprotein ligands. This task, all over the quality control process, is reserved to the reglucosylating enzyme, and cycles of binding and release to the lectins are mediated by independently acting enzymes (GT and GII) that covalently modify glycans. The CNX/CRT–glycoprotein interaction not only prevents secretion of folding intermediates and irreparably misfolded molecules, but also enhances folding efficiency as it prevents protein aggregation, premature oligomerization, and promotes formation of the correct disulfide bonds by the CNX/CRT–ERp57 complex. It is worth mentioning that GT and BiP apparently recognize different folding conformers. The latter specifically binds heptapeptides with bulky hydrophobic amino acids in alternating positions exposed in early, extended conformations. As predicted by the different recognition patterns, sequential BiP-CNX/CRT interaction has been described for the *in vivo* folding of several glycoproteins. Folding facilitation mediated by CNX/CRT–glycoprotein interaction is not essential for the eukaryotic cell viability. Hindering monoglucosylated *N*-glycan formation by either disrupting GI-, GII-, or GT-encoding genes or by the addition cell permeable inhibitors of the first two enzymes leads to the up-regulation of other chaperones and folding assisting proteins that compensate the absence of lectin–glycoprotein interaction (unfolded protein response). Finally, it should be mentioned that irremediably misfolded glycoproteins are retained in the ER and eventually transported through a complex and not yet fully understood process to the cytosol to be degraded in the proteasomes.

See Also the Following Articles

Glycoproteins, N-linked • Glycoprotein-Mediated Cell Interactions, O-Linked

Glossary

calnexin A membrane-bound endoplasmic reticulum-resident lectin that binds monoglucosylated *N*-glycans.

calreticulin The soluble homologue of calnexin.

quality control Mechanisms by which cells ensure that only properly folded proteins are produced by the secretory pathway.

UDP-Glc:glycoprotein glucosyltransferase A soluble, endoplasmic reticulum-resident enzyme that exclusively glucosylates glycoproteins displaying non-native conformations.

Further Reading

Elgaard, L., and Helenius, A. (2003). Quality control in the endoplasmic reticulum. *Nat. Rev. Mol. Cell Biol.* **4**, 181–191.

Ellgaard, L., Molinari, M., and Helenius, A. (1999). Setting the standards: Quality control in the secretory pathway. *Science* **286**, 1882–1888.

Hammond, C., and Helenius, A. (1997). Quality control in the secretory pathway. *Curr. Opin. Cell Biol.* **7**, 523–529.

Helenius, A. (1994). How *N*-linked glycans affect glycoprotein folding in the endoplasmic reticulum. *Mol. Biol. Cell* **5**, 253–265.

Helenius, A., and Aebi, M. (2000). Intracellular functions of *N*-linked glycans. *Science* **291**, 2364–2369.

Parodi, A. J. (2000a). Protein glucosylation and its role in protein folding. *Annu. Rev. Biochem.* **69**, 69–95.

Parodi, A. J. (2000b). The role of oligosaccharide ER processing reactions in glycoprotein folding and degradation. *Biochem. J.* **348**, 1–13.

Trombetta, E. S., and Helenius, A. (1998). Lectins as chaperones in glycoprotein folding. *Curr. Opin. Struct. Biol.* **8**, 587–592.

Trombetta, E. S., and Parodi, A. J. (2002). *N*-glycan processing and glycoprotein folding. *Adv. Prot. Chem.* **59**, 303–344.

Trombetta, E. S., and Parodi, A. J. (2003). Quality control and protein folding in the secretory pathway. *Annu. Rev. Cell Dev. Biol.* **19**, 649–676.

Biography

Armando Parodi is a Professor of Biochemistry at the School of Sciences of the University of Buenos Aires, and a Foreign Associate of the National Academy of Sciences (USA). He obtained an M.Sc. (organic chemistry) and a Ph.D. (biochemistry) from the School of Sciences of the University of Buenos Aires. Except for two postdoctoral training periods abroad, Dr. Parodi has spent most of his scientific career at the Instituto de Investigaciones Bioquimicas Fundacion Campomar (now Fundacion Instituto Leloir).

Glycoprotein-Mediated Cell Interactions, O-Linked

Robert S. Haltiwanger
State University of New York, Stony Brook, New York, USA

Glycoproteins can be divided into two large classes of molecules based on the atom linking the carbohydrate to the protein. N-linked glycoprotein refers to the subset where carbohydrates are linked to protein through the amide nitrogen of an asparagine residue and are discussed in other entries in this volume. O-linked glycoprotein refers to glycoproteins where the carbohydrate is linked to the protein through an oxygen atom. The fact that cell surfaces are coated with numerous glycoproteins bearing thousands of different, structurally complex carbohydrate structures caused researchers over 30 years ago to propose that these carbohydrates would play roles in communication between cells and their environment. Since then, numerous examples demonstrating that such communication exists have been uncovered. In the past few years, several specific examples showing functional roles for cell-surface oligosaccharides have been poignantly provided through the study of unusual forms of O-linked oligosaccharides. In particular, roles for these carbohydrates in both regulation of signal transduction events and in cell-surface binding events have been demonstrated. These examples have provided firm evidence that the predictions of 30 years ago were true and are now serving as paradigms for the functional relevance of many different forms of glycosylation.

Classes of O-Glycans

O-linked carbohydrate modifications are defined as any carbohydrate covalently linked to protein through a hydroxyl group, most commonly the hydroxyl of a serine or threonine residue. The classes of O-linked carbohydrate modifications are defined by the sugar directly linked to the hydroxyl group. In mammalian systems, at least six classes of O-glycans exist: O-GalNAc (N-acetylgalactosamine), O-GlcNAc (N-acetylglucosamine), O-xylose, O-fucose, O-glucose, and O-mannose. With the exception of O-GlcNAc, all of these modifications are found on proteins in extracellular spaces. O-GlcNAc is uniquely found on nuclear and cytoplasmic proteins. The O-GalNAc and O-xylose modifications constitute the largest and most structurally heterogeneous classes of O-linked modifications. The O-GalNAc modifications are usually referred to as "mucin-type" O-glycosylation since they are prevalent on mucins, and the O-xylose modifications are the glycosaminoglycans, the carbohydrate portion of proteoglycans. Two other O-linked modifications found on the hydroxyls of amino acids other than serine or threonine also exist in mammals: O-galactose on hydroxylysine of collagen and O-glucose on tyrosine of glycogenin.

O-Fucose on Epidermal Growth Factor-Like Repeats

O-fucose modifications were initially identified on a number of serum glycoproteins involved in blood clot formation or dissolution including urinary-type plasminogen activator (uPA), tissue-type plasminogen activator, and factors VII, IX, and XII. Analysis of the sites of fucosylation on these proteins revealed that the fucose was attached to a serine or threonine in a consensus sequence within a protein module known as an epidermal growth factor (EGF)-like repeat. EGF-like repeats are small protein modules of ~40 amino acids found in dozens of cell-surface and secreted proteins (Figure 1). They are defined by the presence of six conserved cysteine residues that form three disulfide bonds. The O-fucose modification occurs between the second and third conserved cysteine of the EGF-like repeat at the sequence $C^2XXGG(S/T)C^3$, where X can be any amino acid and *S/T* is the modified amino acid. More recent work has shown that this consensus site is too narrow and can be broadened to include EGF-like repeats containing $C^2X_{4-5}(S/T)C^3$. Nonetheless, the $C^2XXGG\ (S/T)C^3$ sequence has been extremely useful for identifying other proteins that bear O-fucose such as Notch and Cripto.

The O-fucose is added to EGF-like repeats by protein O-fucosyltransferase I (O-FucT-1, Figure 2A). It will only transfer fucose to serine or threonine in a consensus sequence within a properly folded EGF-like

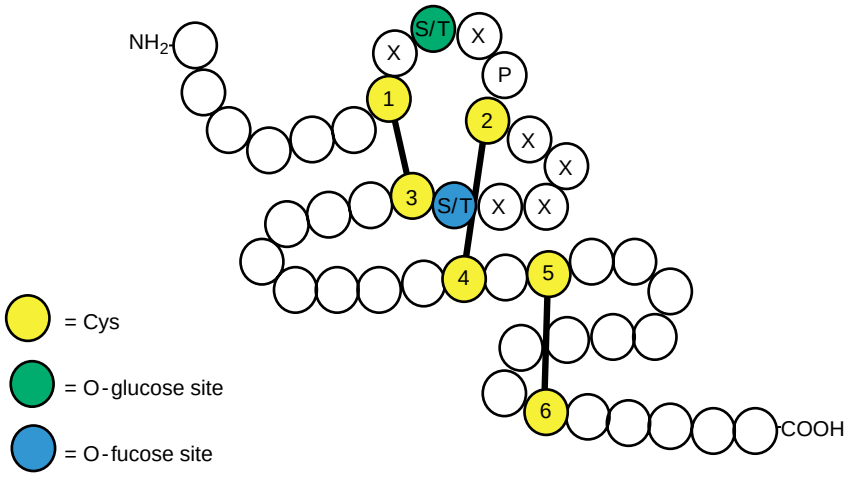

FIGURE 1 O-fucose and O-glucose modifications occur within epidermal growth factor (EGF)-like repeats. A schematic representation of an EGF-like repeat is shown. Each circle represents an amino acid. Cysteines are shown in yellow, the O-glucose modification site is shown in green, and the O-fucose modification site is shown in blue. Amino acids important for defining the glycosylation sites are indicated. Disulfide linkages are represented by lines.

repeat, suggesting that the three-dimensional structure of the EGF-like repeat is necessary for recognition of the site. The gene for O-FucT-1 is highly conserved in metazoans, and mutations in the gene result in embryonic lethality in mice and fruit flies. The O-fucose can be elongated with a β1,3-GlcNAc by a fucose-β1,3-GlcNAc transferase called Fringe (Figure 2A). The GlcNAc can be further elongated with a galactose and sialic acid to form a mature tetrasaccharide. Elongation of the O-fucose monosaccharide is dependent on both the protein being modified and the tissue-dependent expression of the Fringe proteins. Fringe will modify O-fucose on some EGF repeats but not others, suggesting it recognizes not just the O-fucose, but also the surrounding protein structure.

O-Glucose on EGF Repeats

O-glucose modifications were also initially described on EGF-like repeats of serum glycoproteins such as factors VII and IX. Analysis of the sites of glycosylation revealed that the O-glucose modifies serine residues between the first and second conserved cysteine of the EGF-like repeat at the sequence: C^1XSXPC^2 (Figure 1). Other proteins that bear O-glucose modifications have been identified by searching databases using this sequence, including the Notch receptor. O-glucose is added to EGF-like repeats by a protein O-glucosyltransferase, and the O-glucose can be further elongated with xyloses (Figure 2B). Although enzymatic activities capable of adding O-glucose to EGF-like repeats and addition of the xyloses have been detected, the genes encoding these enzymes have not yet been identified.

O-Fucose on TSRs

O-fucose modifications have also been identified in a separate sequence context, that of thrombospondin type 1 repeats (TSRs). TSRs are a protein module found in numerous cell surface and secreted molecules of ~60 amino acids (Figure 3). TSRs are identified by the presence of several conserved residues, including six conserved cysteines that form internal disulfide bonds. The O-fucose modification on TSRs was first identified on human thrombospondin 1, and based on comparison of sequences surrounding the site of glycosylation on several TSRs, a consensus sequence for modification has been proposed: $WX_5C^1X_{2-3}(S/T)C^2X_2G$. Modification of TSRs with O-fucose in other proteins, such as properdin and F-spondin, has been accurately predicted using this sequence. The O-fucose is added to the TSR by protein O-fucosyltransferase 2 (O-FucT-2), a distinct gene product from O-FucT-1 with non-overlapping specificity (Figure 2C). The O-fucose can be elongated with a β1,3-glucose by the action of an O-fucose-β1,3-glucosyltransferase.

O-Mannose

O-mannose modifications of proteins were originally described in yeast, but more recently have been shown to occur on mammalian proteins as well. The first description of O-mannose glycans in mammals has been on brain proteoglycans. Recently, O-mannose glycans were detected on a specific protein, α-dystroglycan.

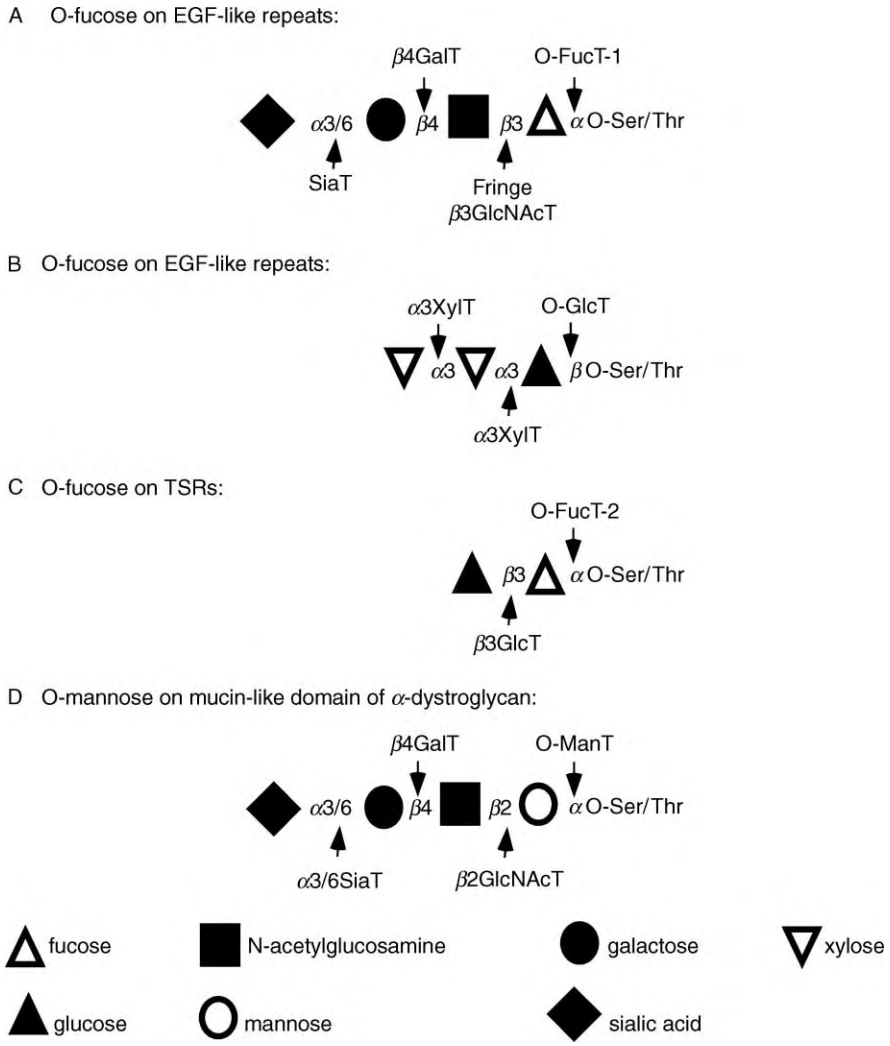

FIGURE 2 Structures of O-linked carbohydrate modifications. For each modification, the potential structures are shown. Each monosaccharide is represented by the symbols defined at the bottom. The enzyme responsible for addition of each sugar is indicated with an arrow. O-FucT-1: protein O-fucosyltransferase-1; O-GlcT: protein O-glucosyltransferase; O-ManT: protein O-mannosyltransferase. All of the other enzymes are described by the linkage they form (e.g., β3GlcNAcT is a β1,3-N-acetylglucosaminyltransferase, forming a β1,3GlcNAc linkage).

Numerous O-mannose chains are attached to α-dystroglycan in a "mucin-like" domain. This is a region of the protein rich in serine, threonine, and proline where many of the serines and threonines appear to be modified. The mannose is added to the mucin-like domain by a protein O-mannosyltransferase. Seven different genes encoding protein O-mannosyltransferases have been identified with yeast, and at least two homologues exist in higher eukaryotes. Although none of these homologues has been shown to have *in vitro* protein O-mannosyltransferase activity, they are believed to be responsible for addition of O-mannose to protein in mammals. The O-mannose can be elongated with a β1,2-GlcNAc by an O-mannose-β1,2-GlcNAc transferase, and the GlcNAc can be further elongated to a mature tetrasaccharide by the addition of galactose and sialic acid (Figure 2D).

Functions of O-Glycans

Determining the function of protein glycosylation has remained a problem for many years, partly because so many different proteins bear carbohydrate modifications. Carbohydrate modifications differ in function, depending on the protein they modify. Nonetheless, recent work has revealed specific functions for some of the O-linked modifications. The fact that these modifications are found on a smaller subset of proteins than more common types of glycosylation (e.g., N-glycosylation, mucin-type O-glycosylation, glycosaminoglycans) has made evaluation of their functions somewhat more straightforward. Still, the principles learned from studying these modifications should be applicable to our understanding of other forms of glycosylation.

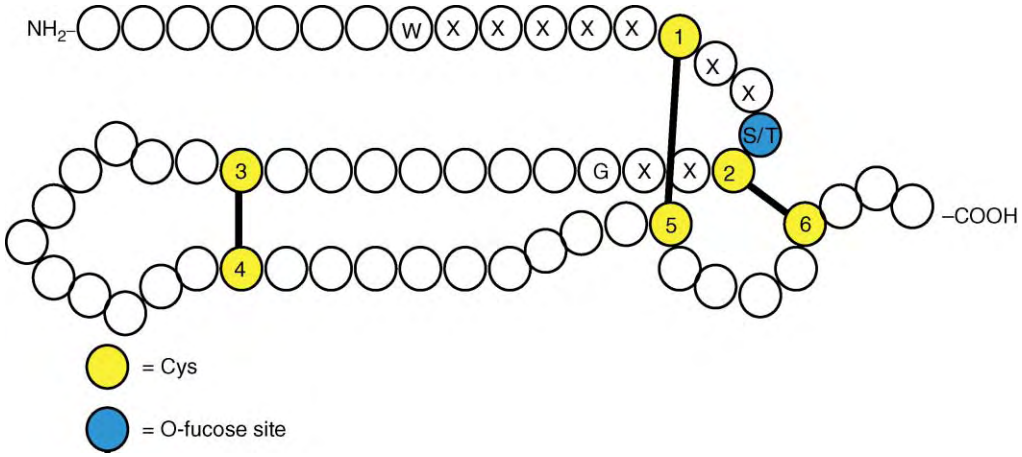

FIGURE 3 O-fucose modifications occur on thrombospondin type 1 repeats (TSRs). A schematic representation of a TSR is shown. Each circle represents an amino acid. Cysteines are shown in yellow, and the O-fucose site is shown in blue. Amino acids important for defining the glycosylation sites are indicated. Disulfide linkages are represented by lines.

The Role of O-Fucose in Regulating Signal Transduction

The Effects of O-Fucose in uPA–uPA Receptor Signaling

A role for the O-fucose modification in modulation of signal transduction was first proposed for the activation of the uPA receptor. As mentioned, the EGF-like repeat of uPA was one of the first proteins to be demonstrated to bear an O-fucose modification. The uPA receptor is a mitogenic receptor, and it becomes activated upon binding to the EGF-like repeat of uPA. Interestingly, removal of O-fucose from the EGF-like repeat abrogates uPA receptor activation, although it has little or no effect on binding. Thus, the O-fucose appears to be essential for activation of the uPA receptor, and alterations in the level of O-fucose on uPA could potentially serve as a mechanism for modulating this activation.

The Effects of O-Fucose in Notch Signaling

The concept that O-fucose modifications can regulate signal transduction events is strengthened by work on the Notch receptor. Notch is a cell surface signaling receptor that plays many essential roles in the development of metazoans. Defects in the Notch signaling pathway lead to a number of human diseases, including several types of cancer, CADASIL (an inherited disease that results in recurrent strokes and early death), and a group of developmental disorders termed Alagille syndrome. Recent work has also implicated Notch in the pathogenesis of multiple sclerosis. Notch becomes activated upon binding to its ligands (members of the Delta family or the Serrate/Jagged family of proteins). Interestingly, the ligands are also cell surface, transmembrane proteins. Thus, Notch becomes activated when an adjacent cell expresses ligand. Ligand binding causes the activation of proteases, releasing the cytoplasmic domain of Notch into the cytoplasm. The cytoplasmic domain then moves into the nucleus, where it associates with other proteins to regulate the transcription of a number of genes.

The extracellular domain of the Notch receptor is composed largely of EGF-like repeats (36 consecutive EGF-like repeats in mammalian Notch1), many of which are modified with O-fucose. The O-fucose modifications are essential for Notch function. Abrogation of O-FucT-1 activity in *Drosophila* (by RNA interference) or in mice (by gene knockout) results in Notch phenotypes (i.e., the same phenotype observed when mutations are made in the Notch gene itself). These results imply that if O-fucose is not added to Notch, it does not function. Since most Notch phenotypes arise early in development, these defects result in embryonic lethality.

In addition to being essential for Notch function, the O-fucose modification on Notch serves a regulatory role. The O-fucose on the EGF-like repeats of Notch can exist in either the monosaccharide or the tetrasaccharide form, depending on whether Fringe is expressed in the same cell. Fringe is a known modifier of Notch function, potentiating the signal received from Delta-like ligands, but inhibiting the signal received from Serrate/Jagged-like ligands. Although the details of how this modulation occurs are not known, these results indicate that the activation of Notch can be regulated by altering the structure of the O-fucose glycans on Notch. These results provide one of the clearest examples known of how a signal transduction pathway can be regulated by alterations in the glycosylation of the receptor.

The Effects of O-Fucose on the Nodal/Cripto Signaling Pathway

In addition to its role in the Notch and uPA receptors signaling pathways, recent work has suggested a role for O-fucose in the Nodal/Cripto pathway. Nodal is a member of the transforming growth factor β (TGFβ) superfamily that plays a key role in establishing polarity early in vertebrate embryogenesis. Mutations in Nodal cause defects in left–right asymmetry and mesoderm formation. Nodal is a secreted protein that binds to and activates members of the type I/type II activin receptor family. Interestingly, Nodal only activates these receptors in the presence of a coreceptor. The coreceptors include the proteins Cripto and Criptic, both of which contain an EGF-like repeat that is modified with O-fucose. Without the O-fucose, neither Cripto nor Criptic will support Nodal-dependent activation of the receptors, demonstrating that the O-fucose modification is essential for Cripto/Criptic-dependent Nodal signaling. Alterations in the levels of O-fucose on Cripto and Criptic could be a mechanism for modulating Nodal signaling. Surprisingly, the mouse knockouts of O-FucT-1 do not show severe Nodal phenotypes, even though Nodal actually functions at an earlier stage of development than Notch. This result suggests either that a different enzyme is responsible for addition of O-fucose to Cripto and Criptic or that the role of O-fucose in Nodal function is more complicated than previously believed and requires further investigation.

The Role of O-Mannose in α-Dystroglycan Function

The recent demonstration of O-mannose on α-dystroglycan has led to the discovery of an essential role for these glycans in the musculoskeletal system. α-Dystroglycan forms a portion of an essential link between the cytoskeleton and the extracellular matrix in the sarcolemma. Specifically, α-dystroglycan binds to β-dystroglycan, a transmembrane protein that in turn interacts with cytoskeletal components. In addition, α-dystroglycan binds to laminin, an extracellular matrix component. Interestingly, the interaction with laminin appears to be mediated through the O-mannose oligosaccharides on α-dystroglycan, and alteration in the O-mannose tetrasaccharide appears to disrupt this interaction. Defects in any of the components in the link between the cytoskeleton and laminin in the muscle are known to cause various muscular dystrophies. For instance, defects in the enzyme that adds a GlcNAc to the O-mannose on α-dystroglycan, preventing formation of the mature tetrasaccharide, result in a form of congenital muscular dystrophy: muscle-eye-brain disease. These results demonstrate that the O-mannose saccharides of α-dystroglycan play an essential role in the function of the dystroglycan–laminin interaction.

Potential Roles for O-Glucose on EGF-Like Repeats and O-Fucose on TSRs

Although specific functions for the O-glucose modifications on EGF-like repeats and O-fucose on TSRs are not known, some functions have been proposed based on the proteins they modify. For instance, many of the EGF-like repeats in the Notch receptor contain evolutionarily conserved O-glucose modification sites. The large number of predicted O-glucose sites, the presence of sites in EGF-like repeats with known functions (e.g., ligand-binding regions), and the fact that many of the sites are evolutionarily conserved argues for a significant biological role for the O-glucose modifications in Notch function. Similarly, the O-fucose modification sites on TSRs are evolutionarily conserved and are predicted to fall within a sequence involved in interactions between cell surface receptors and proteins such as thrombospondin-1. It will be very interesting to examine whether the presence or absence of the O-fucose modification at these sites on TSRs will modulate interactions between thrombospondin-1 and cells, much like the role of O-fucose on the EGF-like repeats of uPA and Cripto.

See Also the Following Articles

Epidermal Growth Factor Receptor Family • Glycoprotein Folding and Processing Reactions • *N*-Linked Glycan Processing Glucosidases and Mannosidases • GlcNAc Biosynthesis and Function, O-Linked • Polysialic Acid in Molecular Medicine

Glossary

cripto/criptic Coreceptors for Nodal that are modified with O-fucose.

α-dystroglycan An essential component of the link between the cytoskeleton and the extracellular matrix in sarcolemma.

fringe A β1,3-N-acetylglucosaminyltransferase that modifies O-fucose residues on Notch (see Figure 2A). Alteration of the O-fucose structures results in modulation of Notch activity.

nodal A member of the TGFβ superfamily that plays an essential role in establishing polarity in vertebrate embryos.

notch A genetic locus originally identified in *Drosophila* that encodes a large cell surface receptor essential for many stages of development. The Notch receptor is modified with both O-fucose and O-glucose.

O-linked carbohydrates Carbohydrate covalently linked to a protein through a hydroxyl group, usually of serine or threonine.

Further Reading

Gonzalez de Peredo, A., Klein, D., Macek, B., Hess, D., Peter-Katalinic, J., and Hofsteenge, J. (2002). C-mannosylation and O-fucosylation of thrombospondin type 1 repeats. *Mol. Cell Proteomics* **1**, 11–18.

Haltiwanger, R. S. (2002). Regulation of signal transduction pathways in development by glycosylation. *Curr. Opin. Struct. Biol.* **12**, 593–598.

Haltiwanger, R. S., and Stanley, P. (2002). Modulation of receptor signaling by glycosylation: Fringe is an O-Fucose-β1,3-N-acetylglucosaminyltransferase. *Biochem. Biophys. Acta* **1573**, 328–335.

Harris, R. J., and Spellman, M. W. (1993). O-linked fucose and other post-translational modifications unique to EGF modules. *Glycobiology* **3**, 219–224.

Michele, D. E., and Campbell, K. P. (2003). Dystrophin–glycoprotein complex: Post-translational processing and dystroglycan function. *J. Biol. Chem.* **278**, 15457–15460.

Biography

Robert S. Haltiwanger is a Professor in the Department of Biochemistry and Cell Biology at the State University of New York at Stony Brook. His research interests are in the role of glycosylation in the regulation of signal transduction events. He obtained a Ph.D. from Duke University in the laboratory of Dr. Robert L. Hill and performed his postdoctoral work at the Johns Hopkins University School of Medicine in the laboratory of Dr. Gerald W. Hart.

Glycoproteins, N-Linked

Mark A. Lehrman
University of Texas Southwestern Medical Center, Dallas, Texas, USA

Proteins that are either secreted from eukaryotic cells or expressed on their surfaces are usually modified with structures called asparagine-linked, or N-linked, oligosaccharides. These are short sugar polymers or glycans attached to the nitrogen atoms of asparaginyl residues. The resulting glycan–protein conjugates are termed N-linked glycoproteins. There are many different kinds of N-linked oligosaccharides with roles in a wide array of biological functions, and a basic knowledge of the pathways responsible for their synthesis is necessary to understand these functions. This article will cover the key concepts behind the synthesis, structures, analysis, functions, and diseases of N-linked glycoproteins, and will illustrate concepts with well-established examples from the literature.

Biosynthesis and Structures of N-Linked Oligosaccharides

Synthesis of a Dolichol Pyrophosphate-Linked Oligosaccharide

N-linked glycosylation begins not with a polypeptide substrate, but rather with the polyisoprenoid lipid dolichol phosphate (Dol-P; also referred to as dolichyl phosphate by many workers). Dolichols are the longest lipids in humans, most commonly consisting of 95 carbons (19 isoprenyl units). Originating from the terminal phosphate of Dol-P, a 14-sugar oligosaccharide unit with a pyrophosphate linkage is assembled in a stepwise manner (Figure 1). The initial seven sugar additions of this pathway utilize enzymes and substrates present on the cytoplasmic leaflet of the endoplasmic reticulum (ER) membrane. First, a residue of GlcNAc-1-P is transferred from UDP-GlcNAc to Dol-P with release of UMP. The enzyme catalyzing this reaction, GlcNAc-1-P-transferase, is selectively inhibited by tunicamycin (TN). The resulting GlcNAc-P-P-Dol is sequentially modified with an additional residue of GlcNAc from UDP-GlcNAc and five residues of mannose from GDP-mannose. The product, $Man_5GlcNAc_2$-P-P-Dol, then flips to the lumenal leaflet of the ER membrane. The subsequent extension of this molecule to $Glc_3Man_9GlcNAc_2$-P-P-Dol, the completed dolichol-linked oligosaccharide (Figure 1, violet), requires a second function of Dol-P. On the cytoplasmic leaflet, Dol-P is modified with single residues of either mannose (from GDP-mannose) or glucose (from UDP-glucose). The resulting mannose-P-Dol (MPD) and glucose-P-Dol (GPD) then flip to the lumenal leaflet where they serve as enzymatic donors for the final seven sugar residues of $Glc_3Man_9GlcNAc_2$-P-P-Dol. The specific arrangement of sugars in $Glc_3Man_9GlcNAc_2$-P-P-Dol, including linkages and anomeric conformations, is highly conserved among eukaryotes and is essential for the functions of the oligosaccharide.

Genetic defects in the synthesis of dolichol-P-P-linked oligosaccharides are responsible for the type-I congenital disorders of glycosylation (CDG). To date, eleven distinct genetic disorders (CDG types Ia–Ik) have been reported, all but type Ia since 1998. The type-I CDGs affect specific sugar transferases as well as enzymes and factors involved in the synthesis of their donor substrates (Figure 1). Given the diversity of functions of N-linked glycans, it is not surprising that type-I CDG patients suffer from abnormalities of many organ systems. In contrast, the type-II CDGs affect remodeling of the oligosaccharide once transfer to newly synthesized protein has occurred, and may be caused by defects in processing glycosidases, glycosyltransferases, and nucleotide-sugar transporters.

Transfer of the Preformed Oligosaccharide Unit to Newly Synthesized Protein

The lumenally oriented oligosaccharide unit of $Glc_3Man_9GlcNAc_2$-P-P-Dol is transferred to newly synthesized polypeptides that are also within the lumen of the ER, with release of Dol-P-P (Figure 1). The reaction is catalyzed by the multi-subunit enzyme oligosaccharyltransferase (OT). OT transfers oligosaccharide to sterically accessible asparaginyl residues in the tripeptide context asparagine-X-serine or threonine, where X can be any residue except proline. Transfer generally occurs cotranslationally; that is, once the polypeptide has emerged inside the lumenal space but before its synthesis by the ribosome is completed.

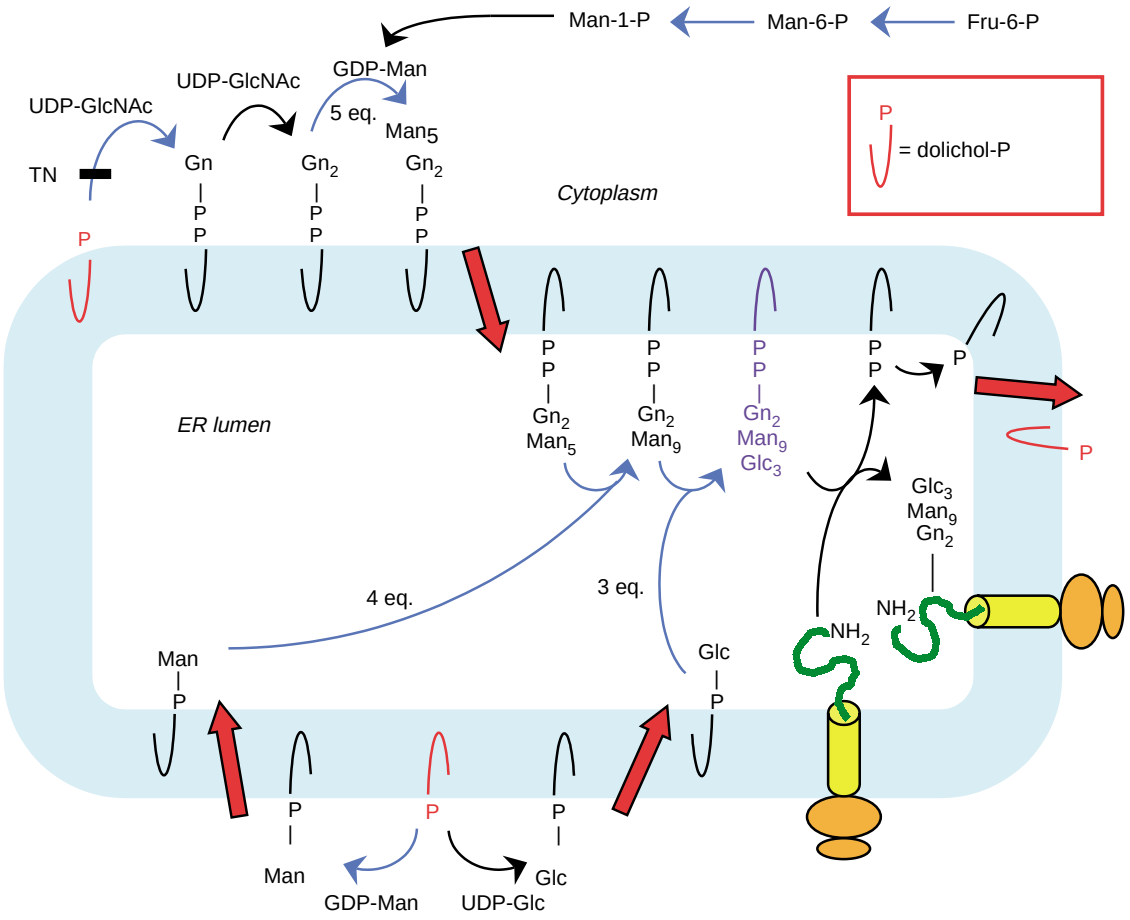

FIGURE 1 Biosynthesis of the lipid-linked oligosaccharide $Glc_3Man_9GlcNAc_2$-PP-Dol in the endoplasmic reticulum. A molecule of Dol-P (upper left-hand corner) is converted into a dolichol pyrophosphate-linked 7-sugar saccharide ($Man_5GlcNAc_2$-PP-Dol) at the cytoplasmic face of the ER membrane. It is then extended in the lumen to the 14-sugar $Glc_3Man_9GlcNAc_2$-PP-Dol (violet; the detailed structure of the glycan is identical to that shown in Figure 2, structure A). The glycan unit is transferred to polypeptides synthesized by membrane-associated ribosomes (orange) as the polypeptides (green) emerge from the translocation pore (yellow). The resulting Dol-PP is converted to Dol-P and recycled to replenish the cytoplasmically-oriented pool of Dol-P (red) used for synthesis of GlcNAc-PP-Dol, Man-P-Dol, and Glc-P-Dol. The latter two molecules are synthesized cytoplasmically and translocated to the lumenal face. Dol-P resulting from their consumption is not shown. Blue arrows indicate steps known to be defective in Type I Congenital Disorders Of Glycosylation. Bold red arrows represent flipping reactions. The site of action of tunicamycin (TN) is shown.

The resulting molecule of Dol-P-P is believed to be recycled back to Dol-P and returned to the cytoplasmic face to participate in additional synthesis of $Glc_3Man_9GlcNAc_2$-P-P-Dol, MPD, and GPD.

Glycosidase Digestion in the ER Lumen

Within minutes after transfer to protein, glycosidic digestion of the N-linked $Glc_3Man_9GlcNAc_2$ (Figure 2, structure A) unit begins by the action of a family of ER-resident glycosidases. In a sequential manner, the terminal glucose residue is removed by ER glucosidase I, the remaining two glucose residues are removed by ER glucosidase II, and a single mannose is removed by ER mannosidase I. The resulting $Man_8GlcNAc_2$ oligosaccharide is depicted in Figure 2 (structure B). As discussed below, the intermediates $Glc_1Man_9GlcNAc_2$, $Man_9GlcNAc_2$, and $Man_8GlcNAc_2$ are particularly significant for folding and processing of glycoproteins. Cell-permeant inhibitors are available that block both of the ER glucosidases (castanospermine (CSN) and deoxynojirimycin (DN)), or ER mannosidase I (kifunensine (KF) and deoxymannojirimycin (DMN)). All of the N-linked oligosaccharide intermediates normally found within the ER are termed *high-mannose-type* to reflect the high proportion of mannosyl residues. Glycoproteins exported to the Golgi apparatus typically have glycans with eight mannosyl residues and no glucosyl residues, but in the event that a glycoprotein is exported before glucosidase digestion is completed, a Golgi endomannosidase exists that can remove any attached glucosyl residues plus the underlying mannosyl residue as a single unit (Figure 3).

Remodeling by Golgi Apparatus Glycosidases and Glycosyltransferases

The steps reviewed to this point are similar for all eukaryotes. However, within the Golgi apparatus N-linked oligosaccharides are remodeled with extensive variations in structure. These variations occur between different species, different organ systems of an individual species, different cell types of an organ system, different glycoproteins of a particular cell, and even among different sub-populations (glycoforms) of a given glycoprotein. Many features of remodeling of N-glycans by the Golgi apparatus are covered in other articles.

The remainder of this article will be limited to remodeling in mammalian cells. It is useful to recall that the mammalian Golgi apparatus can be divided structurally and functionally into three components, known as the *cis*, *medial*, and *trans* Golgi compartments, and is associated with the *trans*-Golgi network (TGN). The key enzymes involved in glycan remodeling are usually found in specific Golgi compartments or the TGN, and their physical locations in these secretory pathway organelles reflect both their order of action on secreted glycoproteins and their distinct substrate specificities (Figure 2). Enzymes involved in specialized remodeling (Figures 3 and 4) are also optimally located for access to the correct oligosaccharide intermediate.

An elegant example of the orchestration of enzyme location and specificity comes from reactions that occur in the *cis* and *medial* Golgi compartments (Figure 2). Recall that $Man_8GlcNAc_2$ is the typical oligosaccharide intermediate on glycoproteins leaving the ER (structure B). Golgi mannosidase I, a resident of the *cis*-Golgi compartment, digests this oligosaccharide to form $Man_5GlcNAc_2$ (structure C; a different isomer than $Man_5GlcNAc_2$ formed as a dolichol-PP-linked intermediate). Upon arrival at the *medial*-Golgi compartment, the $Man_5GlcNAc_2$ is modified by the first in a series of Golgi-associated glycosyltransferases, GlcNAc transferase I. Like all Golgi-associated glycosyltransferases, this enzyme uses a nucleotide-sugar donor. GlcNAc transferase I transfers a residue of N-acetylglucosamine (GlcNAc) from UDP-GlcNAc, forming a β1,2 linkage with a specific mannosyl residue to yield $GlcNAc_1Man_5GlcNAc_2$ (structure D). GlcNAc transferase I is unable to recognize $Man_8GlcNAc_2$, and therefore the prior action of Golgi mannosidase I is essential. After addition of the GlcNAc residue, in most cases the $GlcNAc_1Man_5GlcNAc_2$ oligosaccharide is digested by another *medial*-Golgi enzyme, Golgi mannosidase II (which is inhibited by swainsonine (SW)), to generate $GlcNAc_1Man_3GlcNAc_2$ (structure E). Golgi mannosidase II is unable to recognize $Man_5GlcNAc_2$, and therefore requires the prior action of GlcNAc transferase I. Thus, it is clear that the subcellular locations of these enzymes must reflect their substrate specificities. Consequently, each enzyme is membrane associated and contains appropriate sorting/retention signals.

It is important to note that not all N-linked glycans are digested by Golgi mannosidases, and thus pass through the secretory pathway without further processing. This can be due to steric inaccessibility of the oligosaccharide or, as discussed later in the entry, specialized competing reactions that supercede the typical processing reactions.

Digestion of $GlcNAc_1Man_5GlcNAc_2$ by Golgi mannosidase II uncovers a key mannosyl residue (structure E), allowing it to be modified by the addition of a residue of GlcNAc by GlcNAc transferase II (Figure 2). The resulting $GlcNAc_2Man_3GlcNAc_2$ oligosaccharide (structure F) has two exposed GlcNAc residues, and extension of these by additional transferases associated with the Golgi complex results in *complex-type* N-linked glycans such as structures G and H. As indicated earlier, the exact structures of *complex-type* glycans depend heavily on the organism, tissue, cell type, and protein, and are governed by which glycosyltransferases are expressed. These transferases differ with regard to the sugar residue transferred (galactose, GlcNAc, fucose, GalNAc, sialic acid), the anomeric conformation of the new linkage (α or β), the acceptor saccharide, and the hydroxyl on the acceptor that participates in formation of the glycosidic linkage. As expected from the topological locations of the glycoprotein substrates, these transferases have catalytic sites facing the lumenal spaces of Golgi compartments. The donor requirements of these transferases are met by specific transporters that import nucleotide sugars from the cytoplasm. These transporters also export the nucleotide mono- or di-phosphate byproducts back to the cytoplasm. For a small fraction of oligosaccharides that fail to be digested by Golgi mannosidase II, the single exposed GlcNAc is available for extension to form *hybrid-type* N-linked glycans. These are so-named because they retain elements of both *high mannose-type* and *complex-type* oligosaccharides.

A key variable among *complex-type* oligosaccharides is the number of branches, or antennae, that are formed. Each branch is initiated by a residue of GlcNAc attached to one of mannosyl residues in the $Man_3GlcNAc_2$ "core." *Complex-type* structures with two to five branches have been reported, termed bi-antennary (Figure 2, structure G), tri-antennary, tetra-antennary (structure H), and penta-antennary. In most cases sialic acid is the final sugar attached to N-linked glycans, introducing negative charges onto each branch of the *complex-type* oligosaccharide. However, negative charges can also result from sulfation. It is with these

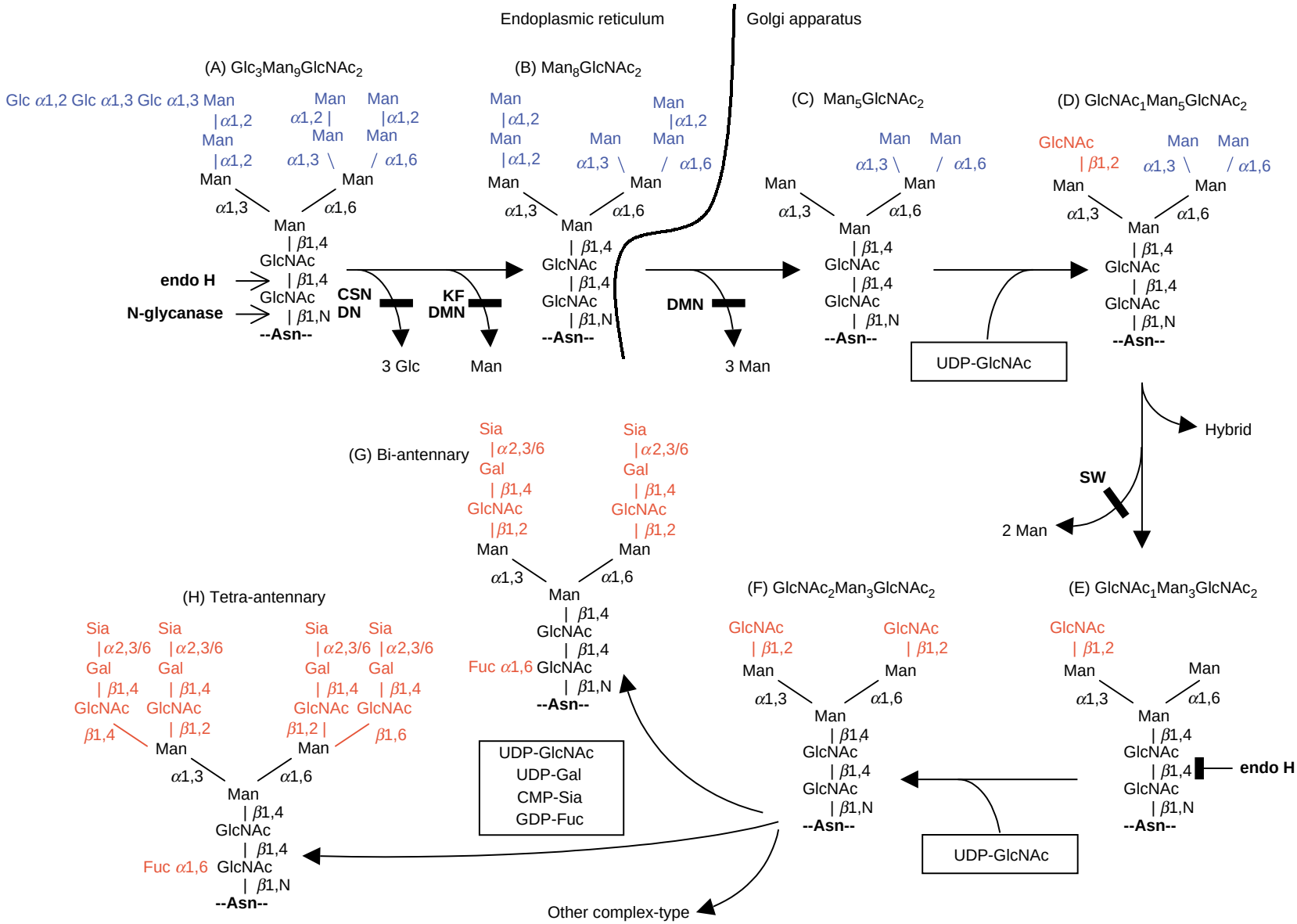
Endoplasmic reticulum
Golgi apparatus
(A) Glc3Man9GlcNAc2
(B) Man8GlcNAc2
(C) Man5GlcNAc2
(D) GlcNAc1Man5GlcNAc2
endo H
N-glycanase
CSN
DN
KF
DMN
DMN
3 Glc
Man
3 Man
UDP-GlcNAc
Hybrid
SW
2 Man
(G) Bi-antennary
(H) Tetra-antennary
(F) GlcNAc2Man3GlcNAc2
(E) GlcNAc1Man3GlcNAc2
UDP-GlcNAc
UDP-Gal
CMP-Sia
GDP-Fuc
UDP-GlcNAc
endo H
Other complex-type

final modifications that the glycoprotein is secreted or retained at the cell surface.

Methods for Analysis of N-Linked Glycoprotein Structure and Function

Binding to Plant Lectins

Plant lectins with a diverse range of specificities for the exposed monosaccharide, anomeric linkage, and other features of the oligosaccharide unit are commercially available. These can be used in many different ways: for example, as immobilized adsorbents attached to column matrices, as histochemical reagents when tagged with a reporter such as horseradish peroxidase, or to isolate sub-populations of cells when conjugated with fluorescent probes for flow sorting. Perhaps the best-known plant lectin is concanavalin A, which is selective for oligosaccharides with exposed α-mannosyl or α-glucosyl residues. Concanavalin A binds tightly to *high mannose-type* and *hybrid-type* oligosaccharides, and weakly to bi-antennary *complex-type* oligosaccharides, but not to *complex-type* oligosaccharides with three or more branches.

Radiolabeling of Oligosaccharides

Incorporation of an isotopic label is a simple and highly sensitive way to permit study of the oligosaccharides themselves. In principle, to label the oligosaccharide unit in intact cells a radiolabeled metabolic precursor of any of the sugar residues can be used, but in practice the choice of precursor is limited by the specific radioactivity, intracellular pool dilution, and competing metabolic fates of precursors. [2-^{3}H]mannose is frequently used because it can label all classes of N-linked oligosaccharides with high specific activity, and labeling is selective for glycoconjugates because diversion of the mannose to glycolysis by phosphomannose isomerase results in loss of the tritium from the sugar ring. *In vitro*, oligosaccharides are typically radiolabeled by incubation with an appropriate glycosytransferase and a nucleotide sugar with an isotopically labeled sugar residue, or by selective oxidation of hydroxyls to aldehydes followed by reduction with [^{3}H]$NaBH_4$.

Digestion with Purified Endo- and Exo-Glycosidases

A useful selection of glycosidases that can be used to characterize N-linked glycans is now commercially available. Endoglycosidases cleave the bonds of unexposed sugar residues; two widely used ones are endoglycosidase H and peptide:N-glycosidase F (also known as N-glycanase) as indicated by Figure 2. N-glycanase cleaves the asparaginyl–GlcNAc bond of almost all N-linked glycans, generating a free oligosaccharide with conversion of the asparaginyl residue to aspartic acid. Endoglycosidase H cleaves the β-linkage between the two GlcNAc residues. The asparaginyl–GlcNAc bond remains intact, and an oligosaccharide released by endoglycosidase H will have one fewer GlcNAc residue than the same oligosaccharide released by N-glycanase. Importantly, endoglycosidase H only cleaves *high mannose-type* and *hybrid-type* oligosaccharides that have not been digested by Golgi mannosidase II (Figure 2).

Exoglycosidases cleave the linkages of exposed sugar residues. Specific glycosidases are available that can remove essentially every sugar found in N-glycans, and are often used sequentially as one glycosidase exposes the substrate of another. For example, the presence of sialic acid residues on an N-glycan can be determined with enzymes called sialidases or neuraminidases. As for other families of glycosidases, these can be obtained with broad or narrow specificities for the type of glycosidic linkage. After removal of sialic acid, the

FIGURE 2 Remodeling of mammalian N-linked glycans in the endoplasmic reticulum, Golgi apparatus, and *trans* Golgi network. Sugars in *black* form the invariant core that is retained after remodeling of N-linked glycans is completed; those in blue are removed by processing glycosidases; and those in red are added by Golgi-associated glycosyltransferases. The anomeric conformation of each glycosidic linkage is denoted α or β, with the linking group of the donor sugar preceding the comma and the linking group of the acceptor following the comma (GlcNAc, N-acetyl-D-glucosamine; Gal, D-galactose; Sia, sialic acid; Fuc, L-fucose). Processing of structure A ($Glc_3Man_9GlcNAc_2$) begins by digestion with ER glucosidases I and II. Structures B through F are each formed by specific enzymes: B, ER mannosidase I; C, Golgi mannosidase I; D, GlcNAc transferase I; E, Golgi mannosidase II; F, GlcNAc transferase II. Structures A and B are associated with the ER; structure C is associated with the *cis* Golgi apparatus; structures D–F are associated with the medial Golgi apparatus; and structures G and H are associated with the *trans* Golgi apparatus and the *trans* Golgi network. Note that structure D can be converted to a hybrid-type glycan or, via structure E, a complex-type glycan such as those shown here (G and H). Sialic acid is commonly found in both α2,3 and α2,6 linkages on complex-type structures. The sites of cleavage by N-glycanase and endoglycosidase H (endo H) are indicated on structure A. Structure E and its products are resistant to endo H. Sites of action of the inhibitors castanospermine (CSN), deoxynojirimycin (DN), kifunensine (KF), deoxymannojirimycin (DMN), and swainsonine (SW) are shown.

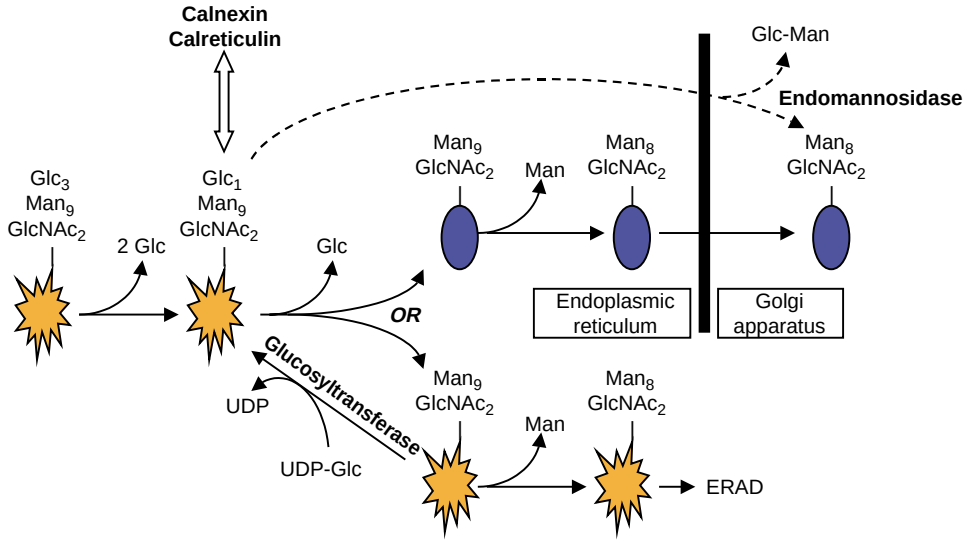

FIGURE 3 The roles of calnexin, calreticulin, unfolded glycoprotein glucosyltransferase, and endomannosidase in the formation and function of glucosylated N-linked oligosaccharides. A newly synthesized glycoprotein with a $Glc_3Man_9GlcNAc_2$ glycan is shown in its unfolded state (orange). Removal of two glucose units forms a monoglucosylated glycan which can interact with the lectin sites of the chaperones calnexin and calreticulin. Subsequent dissociation from the lectin site allows the 3rd glucose residue to be removed by glucosidase II. At this point, if the glycoprotein is properly folded (blue) an additional mannose unit will be removed and the glycoprotein will be exported to the Golgi apparatus. However, if the glycoprotein remains misfolded, its Man_9Gn_2 glycan can be recognized by the unfolded glycoprotein glucosyltransferase to regenerate the monoglucosylated glycan and allow additional interaction with calnexin or calreticulin. The cycle of glucose removal and re-addition can be repeated many times for glycoproteins that are unable to fold. Eventually, on such misfolded glycoproteins a single mannose unit is removed from the Man_9Gn_2 glycan, and the glycoprotein is destroyed by a process termed ER-associated degradation (ERAD). If a glycoprotein folds properly, but exits the ER before glucose removal is completed, a Golgi-associated endomannosidase exists presumably to remove a disaccharide containing the remaining glucose unit and its underlying mannose unit (dashed arrows). Two distinct $Man_8GlcNAc_2$ isomers are formed by ER mannosidase I and Golgi endomannosidase, but each can be remodeled by Golgi-associated enzymes to form complex-type structures.

nature of the underlying sugar can be deduced with other exoglycosidases.

Inhibitors of Glycan Assembly and Processing

TN, a specific inhibitor of initiation of synthesis of dolichol-P-P-linked oligosaccharides, and CSN, DN, KF, DMN, and SW, inhibitors of N-glycan processing, can be valuable tools for determining the presence or class of an N-glycan, as well as for assessment of N-glycan function. These inhibitors are effective with intact cells and purified enzymes. Their sites of action are shown in Figures 1 and 2.

Introduction of Mutations in Genes Encoding Glycosidases and Glycosytransferases

A very powerful approach for assessment of N-glycan function and structure is the use of cell lines and rodent strains in which one or more glycosidases or glycosyltransferases have been inactivated by a spontaneous mutation, a chemically induced mutation, or a targeted gene disruption. The extensive collection of N-glycosylation mutations in Chinese hamster ovary cells has proved valuable in elucidating key steps in both the biosynthetic pathway discussed earlier in the article and the secretory pathway, in addition to testing the functions of specific intermediates and production of useful glycoproteins with defined N-glycans. Many of these cell lines were isolated by their resistance to toxicity of specific plant lectins. For example, cells of the *Lec*1 complementation group lack GlcNAc transferase I activity. These have been used to establish the order of reactions discussed previously, to produce N-linked glycoproteins with $Man_5GlcNAc_2$ glycans instead of *complex-type* glycans, and to establish *in vitro* conditions for transfer of glycoprotein cargo between Golgi-derived vesicles.

Chemical and Physical Analysis of N-Glycans

The combined uses of glycosylation inhibitors, genetic mutations, and glycosidases can reveal a great deal of information about the number and types of N-linked glycans attached to a protein and their functions. Detailed structural information requires removal of the oligosaccharide unit from the polypeptide, followed by

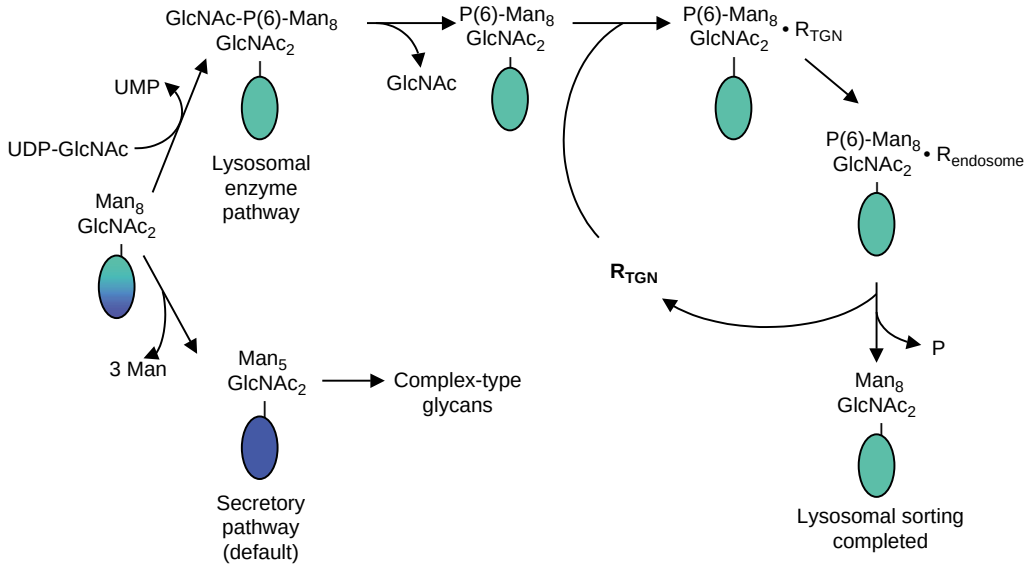

FIGURE 4 Formation of the mannose-6-phosphate sorting signal for lysosomal enzymes. Glycoproteins enter the *cis* Golgi compartment with Man_8Gn_2 glycans (Figure 2, structure B). The majority of glycoproteins (blue) are processed normally and enter the secretory pathway by default. However, a specific UDP-GlcNAc:lysosomal enzyme GlcNAc-1-P transferase recognizes protein determinants that are common to lysosomal enzymes (green), and modifies the 6-hydroxyls of mannosyl residues of the Man_8Gn_2 glycan with GlcNAc-1-P. An uncovering enzyme then removes the GlcNAc unit, leaving a mannosyl unit with a 6-phosphate modification. In the *trans* Golgi network (TGN), enzymes with mannose-6-P units are then bound by mannose-6-P receptors (R), which escort the enzymes to endosomes. The acidic pH of the endosome allows the enzyme-receptor complex to dissociate. The receptors recycle to the TGN, and normal endocytic flow transports the released enzymes to lysosomes where the phosphate modification is removed. Thus, mature lysosomal enzymes have no trace of the mannose-6-P sorting signal. In certain disorders, addition of the GlcNAc-1-P unit is defective, resulting in generation of a complex-type glycan and secretion of enzymes rather than delivery to lysosomes.

chemical and physical analysis. Conventional liquid chromatography, high-pressure liquid chromatography, and gel electrophoresis have been used extensively for both purification of oligosaccharides and determination of structural features. These are effective for separation of oligosaccharides by size, by charge, or by differences in column adsorption due to the particular arrangements of functional groups in the molecule. Several strategies are available to determine the monosaccharide compositions of purified oligosaccharides, including gas chromatography and liquid chromatography. The actual arrangements of the sugar residues, including linkage assignments, are achieved through a combination of glycosidase digestion, gas chromatography, mass spectrometry, and/or nuclear magnetic resonance spectroscopy.

N-Linked Oligosaccharides as Experimental Aids

Purification of N-Linked Glycoproteins

The presence of an N-linked glycan gives biological chemists a simple and effective way to enrich a glycoprotein of interest, by the use of lectin-affinity chromatography. A knowledge of the sub-cellular location of the glycoprotein allows the likely identity of the glycan class to be surmised, and an appropriate immobilized lectin to be chosen. A column prepared with such an immobilized lectin can then be used to isolate glycoproteins bearing the appropriate N-glycan from remaining cellular components. These glycoproteins can then be gently eluted from the adsorbent by the addition of the correct competing saccharide. For example, chromatography with immobilized concanavalin A will strongly retain glycoproteins with *high mannose-type* or *hybrid-type* glycans, which can be recovered by elution with a solution of α-methylmannoside. A similar approach can be used to prepare an enriched fraction of proteins that have traversed the Golgi apparatus, and therefore bear *complex-type* glycans, by chromatography with immobilized wheat germ agglutinin and elution with the competitor disaccharide chitobiose.

Radiolabeling and Tagging of N-Linked Glycoproteins

The methods described earlier for radiolabeling of N-glycans to facilitate glycan analysis are also useful for incorporating a radiolabel for other experimental purposes, without modification of the peptide backbone.

A classic example is the sequential treatment of ceruloplasmin with neuraminidase and galactose oxidase, followed by reduction of the 6-aldehyde with [^{3}H]$NaBH_4$ to generate an exposed tritium-labeled β-galactosyl residue. The resulting labeled asialoceruloplasmin is found to be rapidly cleared from the circulation by the liver. This result allows the identification of a novel β-galactoside selective "asialoglycoprotein receptor" in the liver. It has become an important model for receptor-mediated endocytosis studies.

Trafficking Through the Secretory Pathway

As discussed earlier, N-linked glycan structures are modified as glycoproteins pass through the various compartments of the mammalian secretory pathway (Figure 2). This feature makes N-linked glycans extremely useful for monitoring the subcellular location of a glycoprotein of interest. The presence of a glycoprotein in almost any compartment along the secretory pathway can be determined by information gained from binding to plant lectins, reactivity with glycosidases, and/or labeling with sugar precursors. The most common use of these techniques takes advantage of the sensitivity of *high mannose-type* glycans to endoglycosidase H, and the resistance to this enzyme that occurs after digestion with Golgi mannosidase II. Thus, the acquisition of endoglycosidase H sensitivity by a newly synthesized protein signifies that it is in fact a glycoprotein, and that a portion or all of its sequence is present in the ER lumenal space. The subsequent loss of endoglycosidase H sensitivity reflects the arrival of the protein at the *medial* compartment of the Golgi apparatus (for most glycoproteins, 30–60 min after synthesis).

Functions of Selected N-Linked Glycans and their Specific Cognate Lectins

Since the 1990s, there has been an explosion of discoveries of specific functions for protein-linked glycans, both asparagine-linked and serine/threonine-linked. Some functions of N-linked glycans are covered in detail in other articles. A central concept revealed by these studies is that glycan function usually requires recognition by a specific cognate lectin. In this section, two functions that highlight reactions covered in earlier sections are selected for discussion. These two examples illustrate how certain glycosyltransferases may recognize features of the polypeptide in addition to the glycan, and thus restrict modification to only special sub-classes of glycoproteins. They also show how certain key modifications are transient, and are not found on the mature glycoproteins.

Monoglucosylated Oligosaccharides in ER Quality Control

As discussed earlier, removal of two glucosyl residues from the $Glc_3Man_9GlcNAc_2$ N-linked oligosaccharide by the CSN-sensitive glucosidases I and II results in a monoglucosylated processing intermediate, $Glc_1Man_9GlcNAc_2$. This intermediate is recognized by calnexin and calreticulin, resident ER chaperones with lectin activities specific for monoglucosylated oligosaccharides (Figure 3). Interactions with one of these lectin-chaperones can be crucial for folding and processing of nascent N-linked glycoproteins. Calnexin and calreticulin have essentially negligible recognition of $Glc_3Man_9GlcNAc_2$ (as well as oligosaccharides with zero or two glucose residues). Thus, treatment of cells with CSN blocks glycan-dependent interactions of chaperones with misfolded nascent N-linked glycoproteins because it prevents formation of $Glc_1Man_9GlcNAc_2$ N-linked oligosaccharides. Calnexin and calreticulin bind to $Glc_1Man_9GlcNAc_2$ reversibly, and once dissociated from the lectin site of calnexin or calreticulin, the $Glc_1Man_9GlcNAc_2$ glycan can be digested to $Man_9GlcNAc_2$ by glucosidase II according to the scheme discussed earlier. After release of the glycan from the lectin site, calnexin and calreticulin appear to mediate further folding of their glycoprotein substrates due to lectin-independent chaperone activities.

In addition to processing of $Glc_3Man_9GlcNAc_2$, $Glc_1Man_9GlcNAc_2$ can be formed by reglucosylation of N-linked $Man_9GlcNAc_2$. This is achieved by a remarkable enzyme, the UDP-glucose:unfolded glycoprotein glucosyltransferase (Figure 3). The glucosyltransferase has two functional domains. A "catalytic" domain mediates the transfer of glucose from UDP-glucose to $Man_9GlcNAc_2$, forming the same $Glc_1Man_9GlcNAc_2$ structure as achieved by processing of $Glc_2Man_9GlcNAc_2$. A second "recognition" domain is able to identify physical features characteristic of misfolded proteins, presumably exposed hydrophobic surfaces. The binding of a $Man_9GlcNAc_2$-bearing misfolded glycoprotein to the recognition domain allows reglucosylation by the catalytic domain. The regenerated $Glc_1Man_9GlcNAc_2$ glycan then gives the misfolded glycoprotein another opportunity to interact with calnexin/calreticulin and be folded properly. The repeated actions of the lectin-chaperones calnexin and calreticulin, of glucosidase II, and of the ER glucosyltransferase account for the observation

that certain glycoproteins with mutations that affect folding may retain the $Glc_1Man_9GlcNAc_2$ glycan for extended periods. Properly folded glycoproteins can be exported to the Golgi apparatus, while glycoproteins unable to achieve a properly folded conformation are destroyed by a process termed ER-associated degradation (ERAD) (Figure 3).

High-Mannose Oligosaccharides Bearing Mannose-6-Phosphate Residues as Sorting Signals for Lysosomal Hydrolases

The processing of $Man_8GlcNAc_2$ to $Man_5GlcNAc_2$ by the *medial* Golgi enzyme mannosidase I was discussed earlier. However, hydrolases destined for the lumenal space of the lysosome undergo a very different fate (Figure 4). On these proteins the 6-hydroxyl groups of mannosyl residues are phosphorylated, producing high-mannose oligosaccharides containing mannose-6-phosphate. The mannose-6-phosphate then serves as a specific trafficking signal and allows the hydrolase to be deposited in the lysosome.

The mannose-6-phosphate recognition marker is created in two steps. First, GlcNAc-1-P is transferred to the 6-hydroxyl of a mannosyl residue of $Man_8GlcNAc_2$ by a specialized transferase, the UDP-GlcNAc:lysosomal enzyme GlcNAc-1-P transferase. Like the UDP-glucose:unfolded glycoprotein glucosyltransferase, this enzyme has two functional domains. The catalytic domain mediates transfer of GlcNAc-1-P to *high mannose-type* glycans. The recognition domain binds to lysosomal hydrolases due to a special arrangement of amino acid side chains found only on these enzymes. Thus, the GlcNAc-1-P transferase is effective only with lysosomal hydrolases bearing *high mannose-type* glycans. The GlcNAc-1-P transferase is found in the *cis*-Golgi compartment, and thus its reaction with $Man_8GlcNAc_2$ glycans can take place before digestion with Golgi mannosidase I. The product is the substrate for another enzyme, known as the "uncovering enzyme," which removes the GlcNAc residue and exposes the phosphate. Unlike the GlcNAc-1-P transferase, the uncovering enzyme has a catalytic domain but no known polypeptide recognition domain. The resulting mannose-6-phosphate labeled hydrolase continues its movement along the secretory pathway, but undergoes no additional modifications of its glycan.

In the *trans*-Golgi network, receptors for glycans with mannose-6-phosphate bind the hydrolases and escort them to endosomes. Usually, at least two mannose-6-phosphates must be generated per hydrolase for effective receptor binding. The acidic pH of the endosome causes release of the hydrolase from the receptor, which then recycles back to the *trans*-Golgi network for additional rounds of sorting. The hydrolase is then deposited in the lysosome by normal vesicular traffic, and phosphatases remove the phosphate modification. Thus, mature lysosomal hydrolases bear *high mannose-type* glycans without phosphate. Elucidation of this unique process has been aided by the discovery that it is disrupted in patients with I-cell disease and pseudo-Hurler polydystrophy. In these patients, heritable mutations cause loss of UDP-GlcNAc:lysosomal enzyme GlcNAc-1-P transferase activity. As a result, the mannose-6-phosphate sorting signal is not formed and lysosomal enzymes are secreted instead of being deposited in lysosomes. This accounts for the storage of pathological waste products in the lysosomes of I-cell and pseudo-Hurler patients.

See Also the Following Articles

Glycosylation, Congenital Disorders of • *N*-Linked Glycan Processing Glucosidases and Mannosidases • Glycoproteins, Plant • Secretory Pathway • Siglecs • Sugar Nucleotide Transporters

Glossary

asparagine-linked glycan An oligosaccharide covalently attached to the nitrogen atom of an asparaginyl residue of a protein or peptide.

dolichol A polyisoprenoid lipid composed of five-carbon isoprene units and terminating with a hydroxyl that can be modified with groups such as phosphate, sugar phosphate, or oligosaccharyl pyrophosphate. The "business-end" (α) isoprene unit is reduced, while the remaining isoprene units in dolichol retain double bonds.

glycosidase An enzyme that can release a monosaccharide or oligosaccharide by cleavage of a glycosidic linkage.

glycosyltransferase An enzyme that transfers a sugar residue from a donor substrate to a saccharide, protein, or lipid acceptor.

lectin A protein with a binding site that is specific for sugars.

Further Reading

Beeley, J. G. (1985). *Glycoprotein and Proteoglycan Techniques*. Elsevier, New York.

Lehrman, M. A. (2001). Oligosaccharide-based information in endoplasmic reticulum quality control and other biological systems. *J. Biolog. Chem.* **276**, 8623–8626.

Lennarz, W. J., and Hart, G. (eds.) (1994). *Methods in Enzymology*, Vol. 230, Academic Press, New York.

Varki, A., Cummings, R., Esko, J., Freeze, H., Hart, G., and Marth, J. (eds.) (1999). *Essentials of Glycobiology*. Cold Spring Harbor Laboratory Press, Cold Spring Harbor.

Voet, D., and Voet, J. G. (1995). *Biochemistry*, 2nd edition, Wiley, New York.

Biography

Mark A. Lehrman received his B.S. in biochemistry from the State University of New York at Stony Brook in 1977, and his Ph.D. in biochemistry from Duke University Medical Center in 1982. He is currently Professor of Pharmacology at the University of Texas Southwestern Medical Center at Dallas. His areas of research involve the structures, biosynthesis, functions, and disorders of mammalian glycoconjugates. He has served on the editorial board of the *Journal of Biological Chemistry* and of *Glycobiology*, and was a member of the Pathobiochemistry Study Section (Center for Scientific Review, National Institutes of Health).

Glycoproteins, Plant

Carolyn J. Schultz
University of Adelaide, Glen Osmond, SA, Australia

A glycoprotein is a compound containing carbohydrate (or glycan) covalently linked to protein (International Union of Pure and Applied Chemistry). Plants contain a spectrum of glycoproteins, such as the heavily glycosylated arabinogalactan-proteins (AGPs) which can contain more than 90% carbohydrate, to the minimally glycosylated proline-rich proteins containing only 1–2% carbohydrate. This article highlights the different types of glycoproteins in plants, how they are made, and the approaches being used to determine their function(s). The focus will be on glycoproteins containing *O*-linked glycans such as the AGPs and extensins, because these are unique to plants and are abundant components of the plant cell wall.

Types of Glycosylation

The classification of glycans as *N*-linked or *O*-linked reflects the type of covalent linkages between the amino acid residue in the core protein, and the first sugar of the glycan chain.

N-Linked Glycans

N-linked glycans are attached to core proteins through an amide nitrogen (N) on the side chain of selected asparagine (Asn) residues. They are attached to some, but not all, Asn residues in the motif Asn-Xaa-(Ser/Thr), where Xaa can be any amino acid except proline (Pro). Although the motif for the attachment of *N*-linked glycans is conserved in eukaryotes, the structure of the *N*-linked glycans differs in different organisms.

Attachment of an *N*-linked glycan is a multistep process. The first step is the addition of a 14-sugar preformed precursor oligosaccharide. This oligosaccharide contains *N*-acetylglucosamine (GlcNAc), mannose (Man), and glucose (Glc) and is the same in most eukaryotes (Figure 1A). This oligosaccharide is subsequently modified by glycosidases that remove selected sugars and by glycosyltransferases that selectively add sugars to specific positions.

The modifications can be temporally and spatially regulated, and are different in different organisms. An example of a "complex" type *N*-linked glycan found in plants is shown in Figure 1B. The $Man_3GlcNAc_2$ core (boxed) is found in all eukaryotic *N*-linked glycans; however, the terminal α-1,3-linked fucose and β-1,2 linked xylose residues attached to the $Man_3GlcNAc_2$ core are specific to plants. These plant specific sugars on *N*-linked glycan are believed to contribute to the response suffered by people who are allergic to pollen and certain plant foods.

N-linked glycosylation is a common motif occurring on many plant proteins. *N*-linked glycans assist protein folding and are important for ensuring that only correctly folded proteins pass through the secretory system.

O-Linked Glycans

O-linked glycans are attached to the core protein through the oxygen (O) moiety of selected serine (Ser), threonine (Thr), and hydroxyproline (Hyp) residues. Hyp is a posttranslational modification of proline that is commonly glycosylated in plants. Although Hyp is found in animal proteins (e.g., collagen), glycosylation of Hyp does not occur.

Glycosylation of Hyp exists in two different forms that depend on the arrangement of Hyp residues in the core protein. The first type of *O*-linked glycans attached to Hyp are short Ara chains (one to four) and are typically found on extensins (Figure 1B). In contrast, the arabinogalactan–proteins (AGPs) contain large arabinogalactan (AG) polysaccharides attached to Hyp residues (Figure 1C). *O*-linked glycosylation of Thr is rare in plants, although it is common in animals. Glycosylation of Ser in plants is also relatively rare and usually consists of the addition of a single galactosyl residue.

In general, glycoproteins containing *O*-linked glycans are destined for the cell surface and are found in the cell-wall/extracellular matrix (ECM), or in vesicles either in transit to/from the cell surface. The addition of carbohydrate to proteins provides unique structural properties and informational complexity to the cell. The remainder of this article will focus on the *O*-linked glycosylation of Hyp residues.

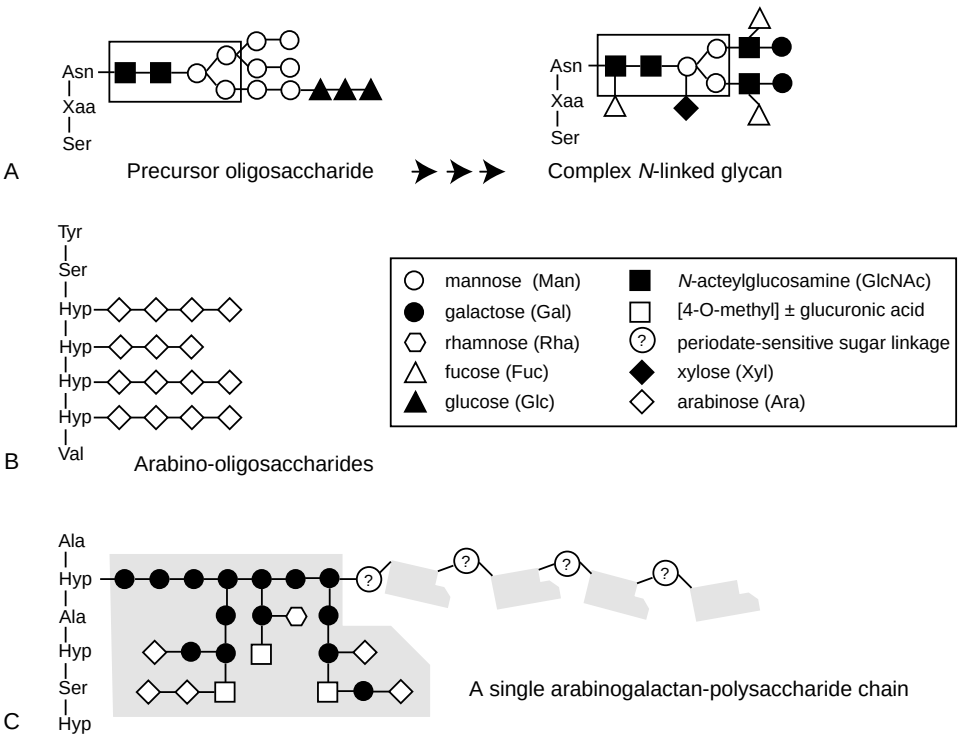

FIGURE 1 (A) The first step in *N*-linked glycosylation is the addition of a 14-sugar preformed precursor oligosaccharide. This is subsequently modified by a series of glucanases and glycosyltransferases to produce a variety of *N*-linked glycans. An example of a complex-type *N*-linked glycan from plants is shown. The five core sugars (boxed) are conserved in plants, insects, and mammals. (B) An example of the *O*-linked glycosylation that occurs on extensins. Attached to the contiguous (uninterrupted) Hyp residues are one to four (1 → 2)α-L-Ara*f* residues. (C) An example of the *O*-linked glycosylation found on AGPs. Attached to the predominantly noncontiguous Hyp residues are repeats of (1 → 3)β-D-linked Gal*p* oligosaccharides with a degree of polymerization of about seven (large shaded region), separated by a periodate sensitive linkage. The branching from the (1 → 3)β-D-linked Gal*p* oligosaccharide backbone (as seen in the large shaded region) can occur from any Gal in the backbone. There may be as many as ten repeats (only five are shown here). For simplicity, only a single Hyp residue has a polysaccharide chain attached. Reprinted from Gaspar, Y. M., Johnson, K. L., McKenna, J. A., Bacic, A., and Schultz, C. J. (2001). The complex structures of arabinogalactan-proteins and the journey towards a function. *Plant Mol. Biol.* **47**, 161–176.

Synthesis of *O*-Linked Glycans

Hydroxylation of Proline

For proteins to be glycosylated they must enter the secretory system via the endoplasmic reticulum (ER) and subsequently the Golgi apparatus. Targeting is achieved by an *N*-terminal signal sequence of ~20 amino acids in length and this signal is subsequently cleaved. In plants, the hydroxylation of Pro occurs in the ER as it does for animals.

Glycosyl Transferases

O-linked glycosylation is poorly understood in plants. It is believed to occur sequentially with the addition of single sugars by a multitude of glycosyltransferases, starting in the ER and then further elaborated in the Golgi apparatus. The recent sequencing of several plant genomes has identified hundreds of plant glycosyl transferases (http://afmb.cnrs-mrs.fr/CAZY/). The lack of knowledge of these enzymes and the abundant heterogeneity of the *O*-linked glycans in plants means that it will be many years before we have a good understanding of the structure and synthesis of these glycans in plants.

Arrangement of Hyp Residues Dictates the Type of Glycans

Our understanding about the arrangement of glycans on the Hyp-rich glycoproteins is more advanced than our understanding of the individual glycan structures. In 1994, Marcia Kieliszewski and Derek Lamport developed the Hyp contiguity hypothesis. This hypothesis suggests that contiguous (uninterrupted) Hyp residues are glycosylated with arabino-oligosaccharides (Figure 1B) and noncontiguous Hyp residues are glycosylated with arabinogalactan (AG) polysaccharides (Figure 1C). Experimental support for this hypothesis continues to grow and recent work by Kieliszewski and colleagues shows that *O*-linked oligosaccharides and AG polysaccharides can be found in the same

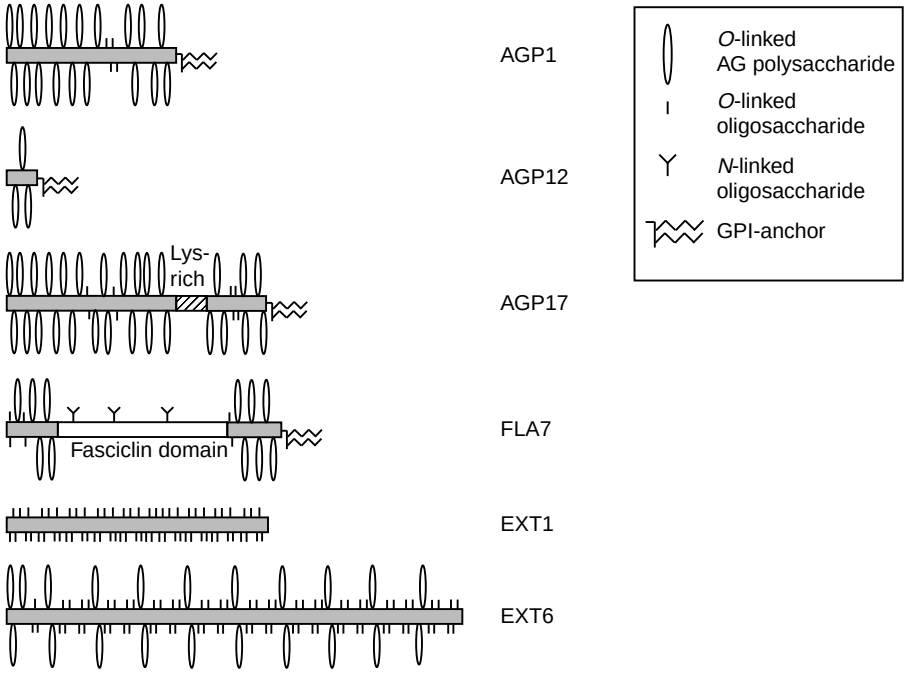

FIGURE 2 Schematic representation of the major classes of glycoproteins from *Arabidopsis thaliana*. The models are based on AGP1 (At5g64310), AGP12 (At3g13520), AGP17 (At2g23130), FLA7 (At2g04780), EXT1 (At1g76930), and EXT6 (At2g24980), as downloaded from http://www.tigr.org/tdb/e2k1/ath1/LocusNameSearch.shtml. For the AGPs and FLA7, all of the predicted Hyp glycosylation sites are shown. For the longer extensin protein backbones, the relative placement of the predicted arabino-oligosaccharides and the AG polysaccharides is shown, but the number of glycan chains is not accurate. Not drawn to scale.

molecules, e.g., LeAGP1 from tomato and gum arabic from *Acacia senegal*.

The Hyp contiguity hypothesis is useful for predicting O-linked glycosylation, although the precise rules governing the minimum length of clustered noncontiguous Hyp residues is not yet established. This is useful for modern biology where genes are generally characterized before the corresponding protein. Figure 2 shows the predicted arrangement of glycosylation of the major classes of Hyp-rich glycoproteins in *Arabidopsis thaliana*.

Hyp-Rich Glycoproteins Belong to Multigene Families

It is ~10 years since the first extensin and AGP core protein genes were cloned from plants. The completion of the sequencing of the first plant genome, from *A. thaliana*, has provided a better understanding of the size and complexity of the hydroxyproline-rich glycoprotein gene families. For example, the AGP gene family consists of ~50 different genes, in four distinct subclasses and there are at least 20 different extensin genes. A major challenge for the future is determining the function of each family member.

Approaches for Determining the Function of Plant Glycoproteins

Structural Studies

The two best-studied classes of plant glycoproteins, the extensins and AGPs, have different structures and it is widely accepted that they have different functions. Extensins are an integral part of the insoluble plant cell wall. The addition of arabino-oligosaccharides to the extensin core proteins induces an extended polyproline-II helical structure giving extensins a rod-like property. The Ser-Hyp_{3-4} regions of extensins are interspersed with amino acid residues (e.g., Tyr and Lys) that are important for cross-linking.

In contrast, AGPs are highly soluble components of the ECM. Rather than forming rods, they are believed to be almost spherical. In addition to polysaccharides, many AGPs also possess a lipid modification at their C terminus, in the form of a glycosylphosphatidylinositol (GPI) anchor. The finding that AGPs are GPI-anchored helped explain their frequent association with the plasma membrane and provided additional clues to how they might be involved in signaling.

GPI-anchors confer many different properties to animal proteins. These include (1) regulated release from cell surfaces, (2) inclusion in lipid rafts where they

may be important components of signaling cascades, and (3) polarized targeting of proteins to specific cell surfaces. Although none of these features have been confirmed for AGPs, there is recent evidence suggesting that a GPI-anchored plant protein, COBRA, is polarized in specific cells of the root.

Immunohistochemistry

Much of the original interest in AGPs came from their abundance in female reproductive tissues. The two most commonly used tools for detecting AGPs are monoclonal antibodies that recognize carbohydrate epitopes, and the artificial carbohydrate antigen, β-glucosyl Yariv reagent (β-glcY). A variety of experiments using these tools suggest that AGPs are important for cell expansion and somatic embryogenesis. However, because these tools interact with carbohydrate epitopes present on multiple AGPs, they have limited use in determining the function of individual AGPs.

Genetic Approaches

Genetic approaches offer the best hope for finding the function(s) of individual plant glycoproteins. Identification of insertion (knockout) mutants in specific genes by sequencing the DNA flanking the site of DNA insertions is well advanced in *A. thaliana*. Current research efforts around the world aim to identify insertion mutants for every gene by 2010. By studying the phenotype of knockout mutants for genes involved in the synthesis and assembly of plant glycoproteins, it should be possible to determine the function of individual family members.

Future Studies

Once we know the function of individual glycoproteins, we can begin to answer the key question of whether the function of each glycoprotein resides in the protein core or in the microheterogeneity of the glycan epitopes, or in both. It is now widely recognized that carbohydrate epitopes on mammalian, *Drosophila*, and protozoan parasite glycoproteins are key determinants of biological specificity/function. The carbohydrate component of plant glycoproteins is expected to be equally important.

See Also the Following Articles

Oligosaccharide Chains: Free, *N*-Linked, *O*-Linked • Glycosylphosphatidylinositol (GPI) Anchors • *N*-Linked Glycan Processing Glucosidases and Mannosidases • Glycoprotein-Mediated Cell Interactions, O-Linked • Protein Glycosylation, Overview

Glossary

arabinogalactan protein (AGP) A heavily glycosylated cell surface glycoprotein composed of large branched polysaccharide chains (containing predominantly arabinosyl and galactosyl residues) attached to hydroxyproline residues.

extensin A moderately glycosylated cell surface glycoprotein containing short linear arabinosyl chains attached to hydroxyproline residues and which may also contain single galactosyl residues attached to Ser residues.

glycoprotein A compound containing carbohydrate (or glycan) covalently linked to protein (International Union of Pure and Applied Chemistry). The carbohydrate may be in the form of a monosaccharide, disaccharide(s), oligosaccharides, and polysaccharides.

glycosylphosphatidylinositol (GPI) anchor A lipid modification added to the C terminus of selected proteins that anchors them in the outer layer of the lipid bilayer of the plasma membrane.

Further Reading

Buchanan, B. B., Gruissem, W., and Jones, R. L. (eds.) (2000). *Biochemistry and Molecular Biology of Plants*. American Society of Plant Physiologists, Rockville.

Fincher, G. B., and Stone, B. A. (1983). Arabinogalactan-proteins: structure, biosynthesis and function. *Ann. Rev. Plant Physiol.* **34**, 47–70.

Gaspar, Y. M., Johnson, K. L., McKenna, J. A., Bacic, A., and Schultz, C. J. (2001). The complex structures of arabinogalactan-proteins and the journey towards a function. *Plant Mol. Biol.* **47**, 161–176.

Haltiwanger, R. S. (2002). Regulation of signal transduction pathways in development by glycosylation. *Curr. Opin. Struct. Biol.* **12**, 593–598.

Johnson, K. J., Jones, B. J., Schultz, C. J., and Bacic, A. (2003). Non-enzymic cell wall (glyco)proteins. In *The Plant Cell Wall* (J. Rose, ed.) Blackwell Publishing Ltd, Oxford.

Lerouge, P., Cabanes-Macheteau, M., Rayon, C., Fischette-Lainé, A.-C., Gomord, V., and Faye, L. (1998). *N*-glycoprotein biosynthesis in plants: recent developments and future trends. *Plant Mol. Biol.* **38**, 31–48.

Schindelman, G., Morikami, A., Jung, J., Baskin, T. I., Carpita, N. C., Derbyshire, P., McCann, M. C., and Benfey, P. N. (2001). COBRA encodes a putative GPI-anchored protein, which is polarly localized and necessary for oriented cell expansion in *Arabidopsis*. *Genes Dev.* **115**, 1115–1127.

Schultz, C. J., Rumsewicz, M. P., Johnson, K. L., Jones, B. J., Gasar, Y. M., and Bacic, A. (2002). Using genomic resources to guide research directions. The arabinogalactan protein gene family as a test case. *Plant Physiol.* **129**, 1448–1463.

Wilson, I. B. H. (2002). Glycosylation of proteins in plants and invertebrates. *Curr. Opin. Struct. Biol.* **12**, 569–577.

Zhao, Z. D., Tan, L., Showalter, A. M., Lamport, D. T., and Kieliszewski, M. J. (2002). Tomato LeAGP-1 arabinogalactan-protein purified from transgenic tobacco corroborates the Hyp contiguity hypothesis. *Plant J.* **31**, 431–444.

Biography

Carolyn Schultz is a Lecturer in the School of Agriculture and Wine at the University of Adelaide's Waite Agricultural Research Institute. Her primary research interests are in understanding the role of AGPs in plant growth and development. She holds a Ph.D. from New York University and did her postdoctoral work at the University of Melbourne. She has been instrumental in defining the classes of hydroxyproline-rich glycoproteins in plants and her most recent paper won *Plant Physiology*'s best paper award for 2002.

Glycosylation in Cystic Fibrosis

Andrew D. Rhim, Thomas F. Scanlin and Mary Catherine Glick
Children's Hospital of Philadelphia and University of Pennsylvania School of Medicine, Philadelphia, Pennsylvania, USA

Cystic fibrosis (CF) is a common, ultimately fatal, genetic disease. The complex pathophysiology of CF included chronic lung disease and malnutrition. The gene that is responsible for CF was identified in 1989. Its gene product is named the cystic fibrosis transmembrane conductance regulator (CFTR). The mechanisms for many manifestations of this disease, such as chronic airway infection and inflammation, have yet to be elucidated. The glycosylation of surface membrane components has been shown to be altered in CF. This article will discuss these findings and provide an insight into how the complete understanding of the altered regulation of glycosylation in CF may eventually provide new approaches to therapy.

Cystic Fibrosis

Cystic fibrosis (CF) is the most common inherited disease in Caucasians today, affecting ~30 000 people in the US. CF is a complex multi-system disease, with initial manifestations of this disease occurring as early as the prenatal period. CF patients frequently display a unique combination of medical problems affecting multiple organ systems which can be manifested by chronic lung infection, meconium ileus, lung inflammation in the neonatal period, pancreatic insufficiency leading to malabsorption of nutrients, infertility, and excessive loss of salt in sweat. Almost invariably, the lungs are most severely affected by this disease. Patients with CF are usually colonized with either *Staphylococcus aureus* or *Haemophilus influenzae* in early childhood followed by *Pseudomonas aeruginosa*. Chronic infection by these and other types of bacteria not found in normal lungs and the hyperstimulation of the immune response of the patient eventually leads to destruction and scarring of formerly functional airways. Over time, lung function of the CF patient deteriorates to the point of failure.

In 1989, the gene responsible for CF was identified by positional cloning. Since then, more than 1000 CF gene mutations have been identified. This gene normally codes for a glycoprotein which functions as a cAMP-regulated chloride channel at the apical surfaces of epithelial cells and is known as the cystic fibrosis transmembrane conductance regulator (CFTR). Patients with CF, an autosomal-recessive disease, have two mutations in their CFTR alleles.

While there have been numerous studies on the relationship of CFTR to the pathogenesis of CF, it is still not clear how the mere absence of a normal copy of CFTR (and hence altered chloride conductance) could lead to the complex and diverse pathology of CF, and, in particular, the associated lung disease. Therefore, investigators have turned to post-translational modifications to provide further understanding of this disease.

It has been shown that the process of glycosylation, the systematic addition of carbohydrates to proteins and lipids, is altered in the tissues of patients with CF, particularly in the airways. Glycosylation is an important factor in a number of biological processes, including bacterial adhesion and the initiation of the inflammatory response. Hence, altered glycosylation of CF cells may play an important role in the pathophysiology of CF.

Glycosylation

Glycosylation refers to the systematic addition of one or more carbohydrates to proteins or lipids. This process requires specific glycosyltransferases, usually located in the smooth endoplasmic reticulum and the Golgi apparatus. Glycosylation is an important cellular function that often confers additional specific biological function to glycosylated products. For example, certain carbohydrate moieties can serve as ligands for bacterial binding, whereas others allow for recruitment of neutrophils in the inflammatory response. Additionally, it has been shown in a number of biological systems that the alteration of normally glycosylated carbohydrates of cellular components can lead to the acquisition of significantly different properties which are important in health and disease.

It is thought that CF also involves a modification in normal glycosylation processes. Two of the most prominent characteristics of the CF airway disease are chronic infection with bacterial pathogens, especially

P. aeruginosa, and a robust but ineffective inflammatory response. While it is unclear how the absence of normal CFTR chloride channels could lead to these observations, an alteration in glycosylation may be the common denominator. As will be discussed later, bacteria such as *P. aeruginosa* require the presence of specific carbohydrates on the surfaces of host for proper binding and function.

Terminal Glycosylation of CF Cells

CF Glycosylation Phenotype

It has been shown by ~50 different studies that material obtained from patients with CF display a specific glycosylation phenotype. This phenotype of increased fucose and decreased sialic acid in the terminal positions of membrane glycoconjugates has been confirmed by many different methods and in multiple cell types. This section will focus on the glycosylation of cell surface components.

Glycosylation of CF Fibroblasts

Early work on CF glycosylation focused on skin fibroblasts as these cells were readily accessible, relatively easy to maintain in culture, and not subjected to the same chronic infections as airway cells. Secreted and membrane glycoproteins from fibroblasts have significantly more fucosyl residues compared to normal controls by biochemical analyses. In addition, the ratio of fucose to sialic acid of membrane glycoproteins is significantly greater in fractions from CF fibroblasts compared to non-CF controls. Perhaps the most striking findings were obtained by 500 MHz ^{1}H-NMR spectroscopic analyses of secreted and membrane-bound glycoproteins from fibroblasts. Interpretation of the data from these analyses has led to the proposed structure of the oligosaccharide chains derived from CF fibroblast glycoconjugates shown in Figure 1.

Glycosylation of CF Airway Epithelial Cells

As the site of the most lethal pathology in CF, studies have focused on the airway, and, in particular, the airway epithelium. Similar to results obtained from fibroblast studies, increased fucosyl residues linked α1,3 or 4 to *N*-acetylglucosamine (Fucα1,3/4GlcNAc) were found in CF compared to non-CF fractions of the airway cells. Also, significantly less terminal sialic acid residues were found on CF membrane glycoproteins compared to non-CF membrane glycoproteins. Hence, the increased ratio of Fucα1,3/4GlcNAc to sialic acid in CF compared to non-CF airway cells mirrored that seen in fibroblasts.

In airway epithelial cells, the glycosylation phenotype of increased Fucα1,3/4GlcNAc and decreased sialic acid is modulated by the degree of wild-type CFTR expression (Figure 2). In other words, when normal copies of the CF gene are successfully transferred into CF airway epithelial cells so that these cells express normal copies of CFTR, the amount of sialic acid and Fucα1,3/4GlcNAc found on membrane glycoproteins changed to levels seen in non-CF cells. Conversely, if mutated copies of the CF gene are transferred into non-CF airway epithelial cells, the amount of sialic acid would decrease. The dependence on CFTR was seen in primary and corresponding immortalized cells (Table I). Therefore, in airway epithelial cells, the presence of CFTR affects glycosylation.

It has also been shown that not all fucose moieties are increased in CF airway cells. Specifically, the amount of fucose in α1,2 linkage to galactose is decreased in CF airway cells compared to non-CF airways. The Fucα1,3/4GlcNAc-to-Fucα1,2Gal ratio reflects the Fucα1,3/4GlcNAc-to-sialic acid ratio in airway cells. Moreover, the amount of Fucα1,2Gal is increased once wtCFTR cDNA is transferred into and expressed in CF airway epithelial cells. On the other hand, the mRNA expression for the corresponding fucosyltransferases does not correlate with the chemical structures found on the surface membranes of CF and non-CF airway

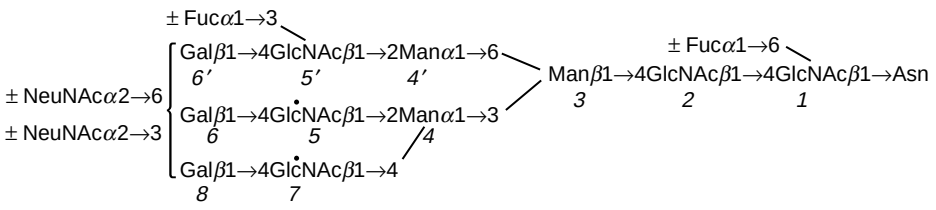

FIGURE 1 Oligosaccharide structure obtained by ^{1}H-NMR spectroscopy of glycopeptides isolated from membrane glycoprotiens of CF fibroblasts represents the CF glycosylation phenotype. α1,3 fucosyl residues can also occur on GlcNAc 5 or 7. ± denotes the decrease in sialic acid on one or more branches. Reproduced from Rhim, A. D., Stoykova, L., Glick, M. C., and Scanlin, T. F. (2001). Terminal glycosylation in cystic fibrosis (CF): A review emphasizing the airway epithelial cell. *Glycoconjugate J.* **18**, 649–660, with permission of Nature.

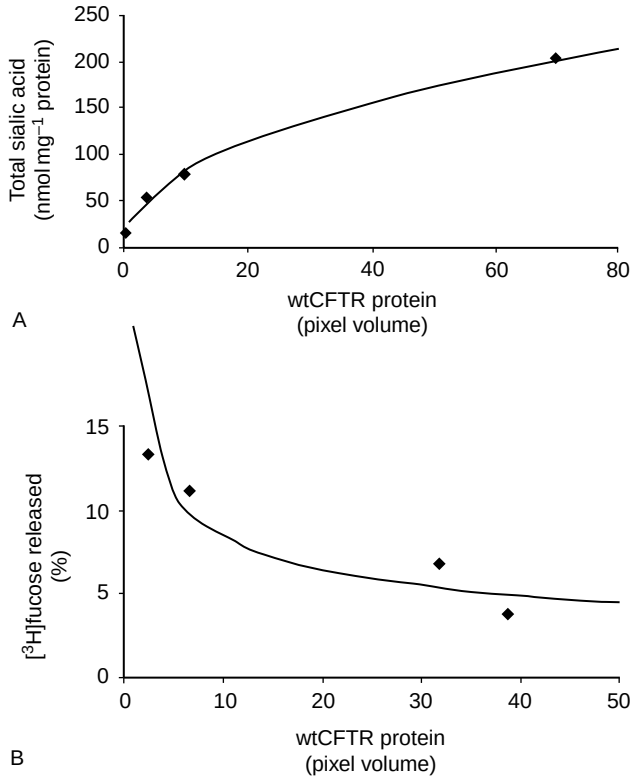

FIGURE 2 The dependence on the expression of wtCFTR of sialic acid and Fucα1,3/4GlcNAc content of peripheral glycopeptides of airway epithelial cells. Line represents the exponential equation generated characterizing this relationship based on data. (A) The sialic acid content of CF cells is increased with the expression of wtCFTR whereas (B) Fucα1,3GlcNAc is decreased. Sialic acid content was determined by the thiobarbituric acid assay and fucose by α1,3/4 fucosidase. Reproduced from Rhim, A. D., Stoykova, L., Glick, M. C., and Scanlin, T. F. (2001). Terminal glycosylation in cystic fibrosis (CF): A review emphasizing the airway epithelial cell. *Glycoconjugate J.* **18**, 649–660, with permission of Nature.

epithelial cells. This has led to the proposal that the compartmentalization of the glycosyltransferases in the Golgi apparatus is affected by CFTR resulting in modified glycosylation products.

Glycosylation of CF Airway Mucins

Respiratory mucus serves as a defense against the entry of foreign particles (bacteria and viruses included) by forming a protective layer over the epithelial surfaces of the human airway. Mucus is secreted both constitutively and in response to inflammatory cytokines by a relatively small number of specialized glandular cells that are intrinsically different from other epithelial cells. Mucins are the main constituents of respiratory mucus. Mucins are a family of high-molecular-weight

TABLE I

Sialic Acid and Fucose Content in Membranes of Immortalized or Primary Airway Epithelial Cells

Airway cells	Sialic acid (nmol mg^{-1} protein)	Fucose (% released)
BEAS-2B	7.64 ± 4.01^a	3.28 ± 0.03^b
CF/T43	2.34 ± 0.32^a	27.45 ± 0.35^b
Non-CF (primary)	37.45 ± 1.45^c	2.75 ± 0.35^d
CF (primary)	16.42 ± 2.00^c	18.45 ± 0.42^d

Reproduced from Rhim, A. D., Kothari, V. A., Park, P. J., Mulberg, A. E., Glick, M. C., and Scanlin, T. F. (2000). Terminal glycosylation of cystic fibrosis airway epithelial cells. *Glycoconjugate J.* **17**, 385–391, with permission of Nature.

[a] $p < 0.021$.
[b] $p < 0.013$.
[c] $p < 0.00064$.
[d] $p < 0.0009$, by Student's *t*-test.

proteins that are highly glycosylated (50–80% of molecular weight). As opposed to *N*-linked carbohydrate residues on most glycoproteins, mucins are by definition *O*-glycosylated at either a threonine or serine. Therefore, the types of glycosylation seen in mucin glycoconjugates are inherently different from most other membrane-bound glycoproteins, particularly when compared to membrane glycoconjugates of nonmucus-secreting airway epithelial cells which are the vast majority of cells lining the airways.

Mucins obtained from CF patients have significantly more sialic acid and fucose than those obtained from non-CF controls. In particular, the specific carbohydrate epitope, Neu5Ac2,3Galβ1,4[Fucα1,3]GlcNAcβ, was found to be increased in mucins from CF patients. However, since the expression of this motif is increased in the presence of cytokines, as in chronic bronchitis, some of the differential glycosylation of CF mucins may be a result of the state of chronic respiratory infection that CF patients endure.

Interestingly enough, the same glycosyltransferases that are involved in the CF glycosylation phenotype seen in CF airway cell membranes are also implicated in the alteration of mucin carbohydrate composition in patients with chronic lung infections. However, it should be emphasized that the mechanisms behind both observations are different – the glycosylation of CF airway cell membranes is dependent upon the presence or absence of wtCFTR whereas mucin glycosylation is apparently not affected by the presence or absence of CFTR. While confirmatory studies on the subject are necessary, the alteration in glycosylation of CF mucins is a phenomenon that may not be entirely specific to the disease of CF, but rather an observation which is influenced by chronic airway infection.

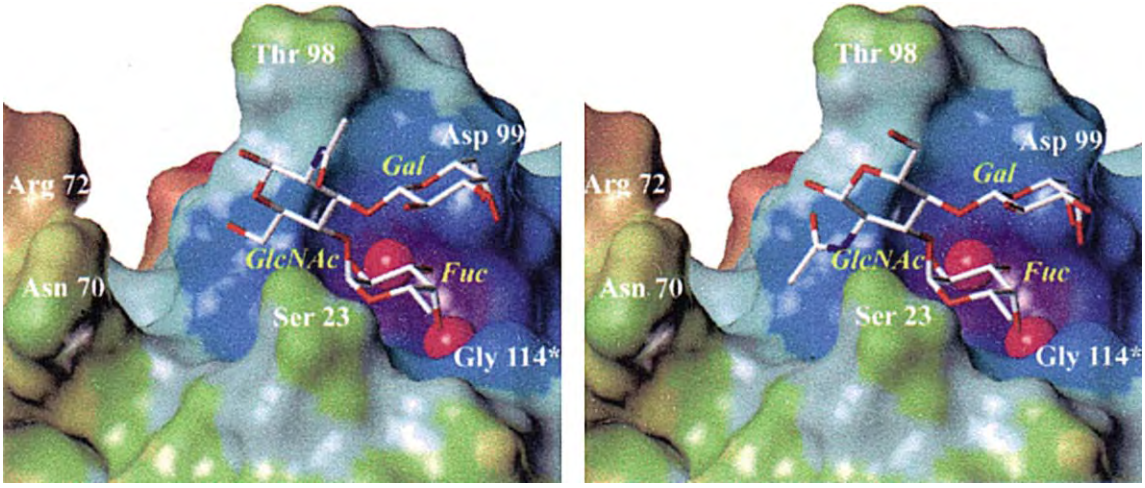

FIGURE 3 Molecular model based on crystallography experiments of PA-IIL, a lectin found on pili of *P. aeruginosa*. Two fucosylated oligosaccharides similar to those detected on the membranes of CF airway cells are shown to be optimally docked in the binding site of this protein. (Left) Galβ1,3[Fucα1,4]GlcNAcβ has a better fit than (Right) Galβ1,4[Fucα1,3]GlcNAcβ, where the position of GlcNAc interferes slightly. Both feature a terminal fucosyl residue linked to *N*-acetylglucosamine. The surface of the protein model has been color coded according to the electrostatic potential (from violet for negative to orange for positive). Reproduced from Mitchell, E., Houles, C., Sudakevitz, D., Wimmerova, M., Gautier, C., Perez, S., Wu, A. M., Gilboa-Garber, N., and Imberty, A. (2002). Structural basis for oligosaccharide-mediated adhesion of *Pseudomonas aeruginosa* in the lungs of cystic fibrosis patients. *Nat. Struct. Biol.* **9**, 918–921.

Functional Implications of Altered Glycosylation

As the major virulent bacterium infecting cystic fibrosis airways, *P. aeruginosa* almost exclusively infects CF patients in the immunocompetent pediatric population. Hence, the CF airway is intrinsically predisposed to colonization by *P. aeruginosa*. A recent crystallography study provided the structural basis for increased adhesion by *P. aeruginosa* in CF patients. The focus of their study was PA-IIL, a lectin on the pili of *P. aeruginosa* that binds to specific carbohydrates and is involved in colonization. It was shown that PA-IIL contains an anionic "dock" which allows optimal binding of fucosylated carbohydrate structures (Figure 3). Therefore, it is thought that the mechanism of increased and efficient *P. aeruginosa* adherence is due to the increased constitutive expression of terminal α1,3/4 fucose-containing carbohydrate motifs on CF airway epithelial cell membranes. In addition, as the negatively charged sialic acid occupies the terminal end of oligosaccharide branches, a decrease in sialic acid residues, as observed in CF airway membranes, could lead to the removal of a potential inhibitor of *P. aeruginosa* binding to fucose-containing moieties.

See Also the Following Articles

Glycosylation, Congenital Disorders of • Mucin Family of Glycoproteins • *N*-Linked Glycan Processing Glucosidases and Mannosidases • Protein Glycosylation, Overview

Glossary

cystic fibrosis (CF) A common autosomal-recessive genetic disease where no copies of wild-type cystic fibrosis transmembrane conductance regulator protein (CFTR) are expressed. This disease varies in severity but is characterized by chronic lung infection, eventual failure of pulmonary function, pancreatic insufficiency, and infertility.

fucose A monosaccharide which can be found on glycoconjugates in α1,3 or α1,4 linkage to branched *N*-acetylglucosamine (Fucα1,3/4GlcNAc).

glycosylation The biological process whereby carbohydrates are enzymatically linked to proteins and lipids by specific glycosyltransferases in a discrete, organized fashion to create glycoconjugates.

mucin A large glycoprotein composed of glycans *O*-linked to serine or threonine.

sialic acid A family of negatively charged nine-carbon monosaccharide frequently found on the terminal end of glycoconjugates.

Further Reading

Lamblin, G., Degroote, S., Perini, J.-M., Delmotte, P., Scharfman, A., Davril, M., Lo-Guidice, J.-M., Houdret, N., Dumur, V., Klein, A., and Roussel, P. (2001). Human airway mucin glycosylation: A combinatory of carbohydrate determinants which vary in cystic fibrosis. *Glycoconjugate J.* **18**, 661–684.

Mitchell, E., Houles, C., Sudakevitz, D., Wimmerova, M., Gautier, C., Perez, S., Wu, A. M., Gilboa-Garber, N., and Imberty, A. (2002). Structural basis for oligosaccharide-mediated adhesion of *Pseudomonas aeruginosa* in the lungs of cystic fibrosis patients. *Nat. Struct. Biol.* **9**, 918–921.

Rhim, A. D., Kothari, V. A., Park, P. J., Mulberg, A. E., Glick, M. C., and Scanlin, T. F. (2000). Terminal glycosylation of cystic fibrosis airway epithelial cells. *Glycoconjugate J.* **17**, 385–391.

Rhim, A. D., Stoykova, L., Glick, M. C., and Scanlin, T. F. (2001). Terminal glycosylation in cystic fibrosis (CF): A review emphasizing the airway epithelial cell. *Glycoconjugate J.* **18**, 649–660.

Robinson, C., and Scanlin, T. F. (1997). Cystic fibrosis. In *Pulmonary Diseases and Disorders* (A. P. Fishman, ed.) pp. 1273–1294. McGraw-Hill, New York.

Scanlin, T. F., and Glick, M. C. (1999). Terminal glycosylation in cystic fibrosis. *Biochim. Biophys. Acta* **145**, 241–253.

Varki, A., Cummings, R., Esko, J., Freeze, H., Hart, G., and Marth, J. (eds.) (1999). *Essentials of Glycobiology.* Cold Spring Harbor Laboratory Press, Cold Spring Harbor, New York.

Biography

Mary Catherine Glick received a Ph.D. from the University of Pennsylvania and soon thereafter began her studies of surface membranes from mammalian cells and the glycoconjugates thereof. She became a Professor of Pediatric Research at the University of Pennsylvania. She studies the glycoconjugates of CF airway cells with Dr. Thomas F. Scanlin.

Thomas Scanlin received his M.D. from the University of Pennsylvania. He is Director of the Cystic Fibrosis Center and is a Professor of Pediatrics at the University of Pennsylvania. Both are at the Children's Hospital of Philadelphia.

Andrew D. Rhim is a candidate for the M.D. degree from the University of Pennsylvania. He is studying in the laboratory of Drs. Glick and Scanlin as an NIH Medical Student Research Program Fellow, where he continues the research he began as an undergraduate.

Glycosylation, Congenital Disorders of

Hudson H. Freeze
The Burnham Institute, La Jolla, California, USA

All cells are covered with a dense forest of glycosylated molecules that consist of glycoproteins and glycolipids. These frostings often dictate and monitor the stability of newly synthesized proteins and glycolipids within the cell. On the surface, they help cells communicate with their neighbors to assess the state of the local neighborhood. Hundreds of enzymes are used in making the sugar chains and adding them to thousands of proteins. Inherited mutations in some of the biosynthetic enzymes cause human diseases that affect the function of many organs during embryonic development, childhood, and even as adults. This article will cover these inherited protein glycosylation diseases and show where glycobiologists studying sugar chain biosynthesis and function team up with physicians to define and understand the basis of these diseases.

Setting the Stage

About 1–2% of the human genome encodes proteins that synthesize or recognize sugar chains. Hundreds of different sugar chains decorate the surface of eukaryotic cells. The immense variety of sugar chains stems from variability in length (number of monosaccharides), kinds of linkage (alpha versus beta), spatial orientation (linkage) of the sugar, branching patterns (two or more sugars attached to another sugar), and modifications by nonsugar elements (e.g., phosphate or sulfate). Adding each of these sugars or modifications requires one or more separate enzymes. Sometimes coordinated groups of enzymes work in a specific order to add some sugars, or cleave others from the maturing chain. Cells express different complements of sugar biosynthetic enzymes (glycosyl transferases and glycosidases) and glycosylation of a single protein can vary in different cells. Moreover, the same sugar chain can have different functions depending on the protein it is on and the cell expressing it. Loss of glycosylation capacity can have serious effects in some cells and much milder effects in others. This complexity means that the function of sugar chains has to be investigated case by case, protein by protein.

The linkage joining the sugar chain to the protein defines the type of glycosylation, as shown in Table 1. Most of the glycosylation disorders have been identified in the N-linked oligosaccharide biosynthetic pathway since 1995. In 2002, incomplete glycosylation of α-dystroglycan with O-mannose based sugar chains was found to be the cause of rare forms of muscular dystrophy. Defects in the biosynthesis of chondroitin and heparin sulfate chains also cause diseases that affect growth of bone and connective tissues. The failure to add phosphate or sulfate to sugar chains also causes glycosylation-based disorders. No specific human diseases in the O-GalNAc (mucin) pathway are yet known.

Congenital Disorders of Glycosylation

Biosynthetic Overview

All N-linked chains are derived from a common dolichyl pyrophosphate (Dol-PP)-linked 14-sugar oligosaccharide (lipid linked oligosaccharide (LLO)). It is composed of 3 glucose (Glc), 9 mannose (Man) and 2 N-acetylglucosamine (GlcNAc) residues, forming a $Glc_3Man_9GlcNAc_2$ chain which is transferred *en bloc* from the lipid carrier to proteins. Addition of each sugar unit occurs in a preferred order and requires at least 13 glycosyltransferases. The completed oligosaccharide chain is then transferred to the nascent polypeptide chain by the oligosaccharyl transferase complex located in the endoplasmic reticulum (ER) membrane. After the transfer, the sugar chain is processed. Specific glycosidases trim the $Glc_3Man_9GlcNAc_2$ chain, removing all Glc and some Man in the ER. As the proteins move to the Golgi, additional Man is often carved away and the chain is extended once again by addition of 2–4 branches composed of GlcNAc, galactose (Gal) and sialic acid (Sia) to form complex-type sugar chains (Figure 1). Literally hundreds of different sugar chain structures can be made by variations of this pathway.

TABLE I

Major Types of Glycan-Protein Linkages

Glycan type	Linkage	Typical proteins	Location
N-linked	GlcNAc-β-Asn	Cell surface receptors secreted proteins	All cells, blood, sub-cellular compartments (e.g., lysosomes)
O-linked	GalNAc-α-Ser/Thr	Secreted and cell surface mucins	Cell surface, gastrointestinal, and reproductive tracts
O-linked	Xyl-α-Ser	Chondroitin/dermatan sulfate	Extracellular matrix, cartilage
O-linked	Man-β-Ser/Thr	Heparan sulfate/heparin α-dystroglycan	Muscle, nerve cells

Scope of the Disorders

Congenital Disorders of Glycosylation (CDG) result from defects in the assembly, transfer, and processing of N-linked oligosaccharides. For convenience, the CDGs are divided into groups I and II. Defective genes are lettered in chronological order of their discovery. The first group includes defects in the assembly of the LLO and its transfer to proteins, which probably requires about 40 nonredundant genes. Defects in nine of these 40 genes have been shown to cause CDG. These include defects in the mobilization and interconversion of monosaccharide precursors or defective glycosyltransferases used to link these sugar units. The second group involves processing of the sugar chains, requiring a minimum of 20 genes. Some of them encode enzymes that may catalyze the same or similar sugar transfer reactions. Defects in four of the genes from this group cause CDG and involve mutations in glycosidases, glycosyl transferases, and Golgi-associated sugar nucleotide transporters that carry these donors from their origin in the cytosol to the Golgi lumen where they are added to their acceptor oligosaccharides. It is likely that serious mutations in any of these genes will cause CDG.

Although there are currently ~300–400 cases of all types of CDG worldwide, it is probably only a few percent of the total patients. It is safe to say that the entire group of CDGs is severely underdiagnosed, and that we are now only seeing the "tip of the iceberg."

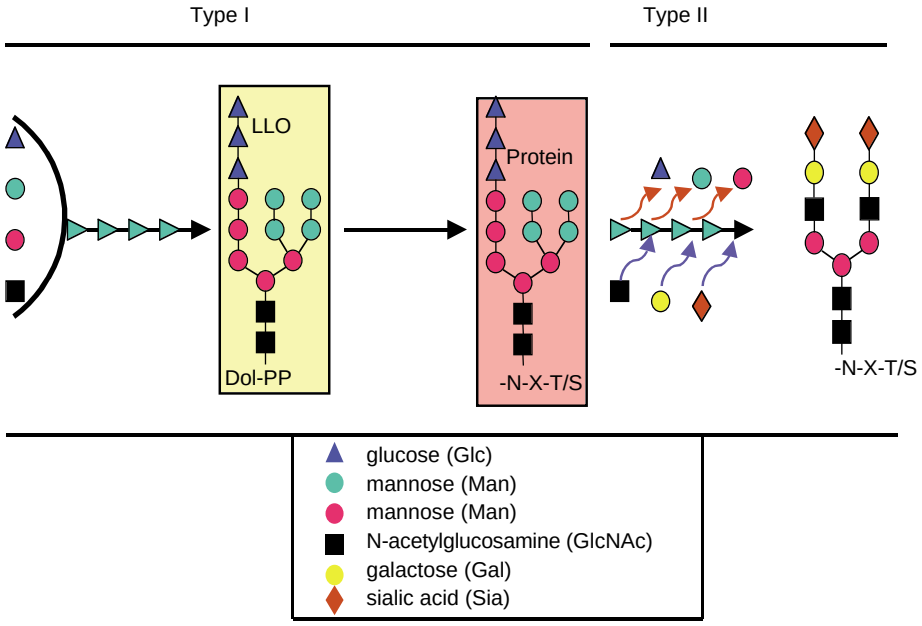

FIGURE 1 Defining Types of Congenital Disorders of Glyosylation (CDG). CDG types are based on finding mutations in genes whose products are involved in glycosylation. Type I CDGs are defined by mutations in steps leading to the assembly and transfer of the lipid linked oligosaccharide chain (LLO) from the carrier lipid to potential N-glycosylation sites (N-X-T/S) on newly synthesized proteins in the ER. At the extreme left, the various monosaccharides (see symbol key below) are first activated, and then they are incorporated one-by-one into a growing chain assembled on the carrier lipid, Dol-PP. The complete sugar chain is then transferred to protein in a single step. Approximately 40 genes are needed to carry out the first stage. Type II CDG defects are defined as those that involve the sequential, highly ordered removal and, addition of individual sugars on protein-bound N-linked sugar chains. More than 20 additional genes are needed to synthesize a sugar chain typical of mammalian plasma glycoprotein, shown on the extreme right side. To date only 16 types of CDG have been identified. It is likely that many more will be found.

Laboratory Diagnosis of CDG

CDG patients are often misdiagnosed early on because their symptoms resemble other generic disorders. CDG-Ia patients are sometimes mistaken for having inherited mitochondrial disorders or cerebral palsy. This is understandable since glycobiology is not part of a typical medical education or training program and most practicing physicians have a limited awareness of glycosylation. Fortunately, most CDG patients can be diagnosed by a simple blood test to analyze the glycosylation status of transferrin (Tf). Abnormal Tf is detected by isoelectric focusing, or by electrospray ionization-mass spectrometry. Many other proteins are misglycosylated, but Tf appears to be especially sensitive to limitations in the amount of LLO precursor. These biochemical analyses provide clues to the defect, but they cannot pinpoint the defective gene, since many defects produce the same altered pattern.

Biochemical Overview

All of the CDGs are autosomal recessive disorders and they result from an insufficient amount of precursor molecules or from deficient glycosyltransferases or sugar processing glycosidases. For a complete listing see Table 2. By far the most common type, CDG-Ia (OMIM 212066), is caused by mutations in the gene encoding phosphomannomutase (Man-6-P → Man-1-P). Mutations reduce the amount of GDP-Man, resulting in insufficient LLO. This leaves some of the normal glycosylation sites on many proteins unoccupied, which can lead to their misfolding and degradation. Sometimes the misfolded proteins accumulate in the ER, activating cell apoptosis. CDG-Ib (OMIM 602579) results from mutations in the *MPI* gene encoding phosphomannose isomerase (PMI) (fructose-6-P → Man-6-P), just one metabolic step away from phosphomannomutase. The clinical pictures of CDG-Ib and CDG-Ia patients are quite different. CDG-Ic (OMIM 603147) is caused by mutations in *ALG6*, which encodes an α-1,3-glucosyltransferase used to add the first Glc to the immature LLO precursor. Chains lacking glucose are transferred to proteins less efficiently than full-sized ones. Group II CDGs are defined as those that affect the processing of the protein-bound sugar chains. Only a few patients have been identified with these disorders, and most, but not all of them can be diagnosed by analysis of Tf.

Clinical Features of CDG

The most common clinical features in various types of CDG are shown in Table 2. There is considerable clinical heterogeneity even within a specific type of CDG. Psychomotor retardation ranging from mild to severe and hypotonia are consistent features in all patients except Type-Ib. Other neurological findings include ataxia (Ia and Ic), seizures, and stroke-like episodes. Cerebellar hypoplasia (Ia, Ic), delayed myelination (Ie, IIa, IIb), microcephaly, and atrophy of the cerebrum (Ia, Ic, Id, Ie) are seen. Sometimes the cognitive deficiency can be mild. Nearly all patients have feeding problems and fail to thrive. Strabismus, abnormal fat distribution, and retracted nipples are common, especially in the CDG-Ia group.

Mortality in CDG-Ia children is about 20% during the first few years, but they stabilize after childhood. Substantial survival means that many adult CDG patients remain undiagnosed.

CDG-Ib, caused by deficiency in MPI, is substantially different from all the others in that mental development and the nervous system are normal. The reason for this is unknown. These patients have serious gastrointestinal problems, protein-losing enteropathy (loss of proteins through the intestine), low plasma albumin, coagulopathy (fast clotting), and hyopoglycemia. A substantial number of patients died before they received a diagnosis, which is unfortunate, since this type of CDG can be treated effectively.

Therapy for CDG

The effective therapy for CDG-Ib is oral mannose. Mannose bypasses the fructose-6-P → Man-6-P block to replenish the depleted GDP-Man pools. A mannose transporter delivers mannose to the cells and hexokinase converts it into Man-6-P. Mannose therapy reverses the hypoglycemia and coagulopathy within a few weeks, and within 1–2 months plasma protein levels become normal and protein-losing enteropathy disappears. Some patients have been treated for over 6 years without side effects. Growth during childhood is metabolically demanding and mannose supplements are most important then. It is encouraging that none of the adult patients with proven CDG-Ib is currently taking mannose, suggesting that it will not be a lifelong requirement. It is important to point out that there is no evidence that healthy people require mannose supplements. Vendors of complex nutraceutical mannose fail to point out that the natural plant polysaccharides they sell are nondigestible. Fucose supplements have also been used to treat patients with CDG-IIc who have a defective GDP-Fucose transporter. Fucose enters the cell and apparently increases the GDP-Fucose pool driving it into the Golgi through the transporter. Within a day, fucose treatment corrects the patients' elevated circulating neutrophil by generating a selectin ligand needed for neutrophil rolling on the endothelium prior to their transmigration into the tissues. Infections cease and health improves. Unfortunately, fucose does not improve or reverse the mental retardation.

TABLE II

Inherited Glycosylation Disorders

Disorders	Enzymatic or protein defect	Gene	OMIM	Frequent clinical features
CDG type				
Ia	Phosphomannomutase Man-6-P → Man-1-P	*PMM2*	212065 601785	Variable psychomotor retardation, hypotonia, seizures, coagulopathy, feeding problems, liver fibrosis.
Ic	α-1,3-glucosyltransferase	*ALG6*	603147 604566	
Id	α-1,3-mannosyltransferase	*ALG3*	601110	
Ie	Dolichol-P-Man synthase	*DPM1*	603503	
If	Dolichol-P sugar utilization protein	*MPDU1*	604041	
Ig	α-1,2-mannosyltransferase	*ALG12*		
Ih	α-1,3-glucosyltransferase	*ALG8*		
Ii	GlcNAc-1-P transferase	*GNT*		
IIa	N-acetylglucosaminyltransferase II	*MGAT2*	212066 602616	
IIb	α-1,2-glucosidase	*GCS1*	601336	
IId	β-1,4-galactosyltransferase	*B4GALTI*	607091	
IIc	GDP-fucose transporter	*FUCTI*	266265	Severe psychomotor retardation, hypotonia, elevated peripheral neutrophils.
Ib	Phosphomannose isomerase (PMI) Fru-6-P ⇄ Man-6-P	*MPI*	602579 154550	Normal development, hypoglycemia, coagulopathy, diarrhea protein-losing enteropathy, vomiting, liver fibrosis.
Muscular dystrophy				
Muscle–eye–brain disease (MEB)	O-mannosyl glycan synthesis	*POMGnT1*	253280	Severe muscle weakness, mental retardation, epilepsy, neuronal migration disorder, ocular abnormalities.
Fukuyama-type congenital muscular dystrophy (FCMD)	Putative glycosyltransferase	Fukutin	253800	Severe proximal and axial weakness, mental retardation, epilepsy neuronal migration disorder.
Walker–Warburg syndrome	Putative O-mannosyltransferase	*POMT1*	268870	Severe muscle weakness, death in infancy, absent psychomotor development, neuronal migration disorder, ocular abnormalities.
Inclusion body myopathy	UDP-GlcNAc epimerase/kinase	*GNE*	600737	Adult onset myopathy that spares quadriceps.
Limb–girdle muscular dystrophy IC	Putative glycosyltransferase	Fukutin-related protein (FKRP)	607155 606612	Variable proximal and axial muscle weakness, cardiomyopathy.
Other types				
1-cell disease	GlcNAc-1-P transferase	*GNPTA*	252500	Severe developmental abnormalities.
Multiple hereditary exostoses	Heparan sulfate co-polymerase	*EXT1, EXT2*	133701	Bony outgrowths.
Macular corneal dystrophy	GlcNAc-6-sulfotransferase	*CHST6*	605294	Progressive corneal opacity.
Ehlers–Danlos syndrome progeroid form	Xylosylprotein β-1,4-galactosyltransferase	*B4GALT7*	130070 604327	Hypotonia, delayed development, connective tissue abnormalities, loose skin.
Diastrophic dysplasia achondrogenesis	Anion (sulfate) transporter	*DTDST*	606718 600972	Scoliosis, club foot, premature calcification.

[a]OMIM: Online Mendelian Inheritance in man (http://www.ncbi.nlm.nih.gov/).

Congenital Muscular Dystrophies: The Most Recently Discovered Glycosylation Deficiencies

α-Dystroglycan is a peripheral membrane component of the dystrophin–glycoprotein complex (DGC) found in muscle, nerve, heart, and brain. This protein binds to merosin in extracellular matrix bridging it to the cytoskeleton molecules that include dystrophin and actin. Mutations in dystrophin cause Duchenne and Becker muscular dystrophies, while assorted mutations in merosin and sarcoglycans cause other inherited muscular dystrophies. Total systemic loss of α-dystroglycan is embryonic lethal. In addition, this protein is the major carrier of O-mannose-based sugar chains. In α-dystroglycan, these sugar chains cluster together in a small "mucin-like" domain of where they mediate many of the critical stabilizing interactions with the other matrix molecules such as merosin, neurexin, and agrin, depending on which cells express α-dystroglycan. Several kinds of muscular dystrophies including muscle–eye–brain (MEB) disease, Fukuyama-type congenital muscular dystrophy (FCMD), Walker–Warburg syndrome, and limb–girdle muscular dystrophy, involve mutations in the genes needed for the biosynthesis of these chains (Table 2). These mutations also appear to affect neuronal migration in the developing brain, thus accounting for the combined effects on muscle and brain development. Studying the glycosylation of α-dystroglycan will be important to understand how these pathologies develop. However, α-dystroglycan is not the only protein that carries these sugar chains. In fact, one out of four O-linked chains in the brain are O-mannose based.

One form of adult onset muscular dystrophy, hereditary inclusion body myopathy Type II, is due to mutations in an enzyme involved in the biosynthesis of CMP-sialic acid, the universal activated donor for addition of sialic acid. The mutations appear to have a minor affect on the activity of the enzyme (UDP-GlcNAc epimerase-kinase) which is lethal when totally deleted. Preliminary studies in fibroblasts and muscle cells from the patients show that addition of sialic acid is reduced and that supplying sialic acid or N-acetylmannosamine (the product of the impaired enzyme) can correct the glycosylation. This suggests that patients might benefit from supplements of these sugars.

Defects in Proteoglycan Biosynthesis Cause Disease

Incomplete or impaired synthesis of glycosaminoglycan (GAG) chains also cause inherited disorders. The bony outgrowths found in patients with multiple hereditary exostoses (MHE) result from mutations in the co-polymerase that assembles alternating units of glucuronic acid and GlcNAc in heparan sulfate. Elhers–Danlos syndrome, which causes a form of progeria is caused by mutations a galactosyltransferase used for assembly of the tetrasaccharide core linkage common to heparin, heparan sulfate, chondroitin, and dermatan sulfate. Macular corneal dystrophy that leads to corneal opacity is caused by loss of a specific sulfotransferase that modifies a special type of keratan sulfate found in the cornea. Sulfate is such an important component for making extracellular matrices that cells have a cell surface transporter that delivers sulfate to the cytoplasm. Mutations in the transporter cause multiple cartilage and bone malformations and in the most severe forms prenatal lethality results from respiratory insufficiency.

Glycosylation Disorders: The Next Generation

The very complexity of sugar chain assembly practically guarantees that more glycosylation disorders will be discovered. Finding defects in the N-linked pathway has been relatively easy because many of the steps involve only a single enzyme, many of which have strict substrate requirements. In addition, Tf provides an unusually robust assay for defective N-glycosylation. Except for α-dystroglycan, the other pathways lack a similar diagnostic champion. New disorders that compromise glycosylation will probably be discovered in the synthesis of O-GalNAc-linked sugar chains, glycosaminoglycans, and in the assembly, organization, or recycling of proteins in the Golgi apparatus. These causes may be more difficult to identify because many of these pathways are composed of redundant, sometimes, overlapping enzymes with tissue specific distributions.

Understanding the role of sugar chains in building cell-surface signaling complexes and finding how to boost sugar donors in cells may help to understand and treat these pathologies. Interactions among basic scientists focused on glycobiology and glycosylation-savvy clinicians will be the key to further discoveries.

See Also the Following Articles

Glycosylation in Cystic Fibrosis • *N*-Linked Glycan Processing Glucosidases and Mannosidases • Protein Glycosylation, Overview • Proteoglycans

Glossary

congenital disorders of glycosylation Inherited disorders of protein glycosylation involving the synthesis and transfer of the Dol-PP-oligosaccharide precursor sugar chain to protein or the subsequent processing of these N-linked oligosaccharides. The term

can also apply to the addition of other types of sugar chains to proteins.

α-dystroglycan An extrcellular DGC component which is one of the major proteins known to contain O-mannose-based oligosaccaharides. Mutations in genes that encode proteins needed for this type of glycosylation cause several types of muscular dystropy.

dystrophin–glycoprotein complex (DGC) A large protein complex found in muscle, nerve, heart, and brain. It is composed of extracellular, transmembrane and intracellular proteins. Mutations in different proteins of this complex cause different types of muscular dystrophy.

glycosaminoglycan (GAG) A large complex sugar chain composed of alternating amino-sugar and uronic acid units. The disaccharides uronic acid disaccharide unite.

glycosylation The process of adding single (monosaccharides) or multiple sugars to proteins or lipids.

glycosyltransferase An enzyme that transfers a sugar from an activated nucleotide donor to an acceptor protein, carbohydrate, or lipid.

lipid linked oligosaccharide (LLO) Structure that is the precursor for N-linked glycans; composed of a sugar chain linked to dolichol through a pyrophosphate linkage.

multiple hereditary exostosis (MHE) A dominant inherited disorder caused by mutations in two genes (*EXT1* and *EXT2*) that encode a polymerase needed for the synthesis of heparan sulfate. Mutations cause painful recurrent outgrowths of bone and must be surgically removed.

oligosaccharyl transferase complex A protein complex found in the endoplasmic reticulum where it recognizes the LLO sugar chain and attaches it to the newly synthesized proteins having the N-X-Thr/Ser consensus sequence for N-glycosylation.

transferrin (Tf) An iron-carrying plasma glycoprotein that is especially susceptible incomplete N-glycosylation caused by an insufficient amount of LLO or one that is inefficiently transferred to proteins.

Further Reading

Freeze, H. H. (2001). Update and perspectives on congenital disorders of glycosylation. *Glycobiology* **11**, 29R–143R.

Jaeken, J., and Matthijs, G. (2001). Congenital disorders of glycosylation. *Annu. Rev. Genomics Hum. Genet.* **2**, 129–151.

Martin, P. T., and Freeze, H. H. (2003). Glycobiology of neuromuscular disorders. *Glycobiology* **13**, 67R–75R.

Muntoni, F., Brockington, M., Black, D. J., Torelli, S., and Brown, S. C. (2002). Defective glycosylation in muscular dystrophy. *Lancet* **360**, 1419–1421.

Biography

Hudson H. Freeze is Professor and Director of the Glycobiology and Carbohydrate Chemistry Program at The Burnham Institute in La Jolla, California, and specializes in congenital disorders of glycosylation. He received his Ph.D. in biology in 1976 from the University of California, San Diego and later joined the UCSD Department of Medicine faculty where he is an adjunct professor.

Glycosylphosphatidylinositol (GPI) Anchors

Anant K. Menon
University of Wisconsin-Madison, Madison, Wisconsin, USA

Glycosylphosphatidylinositol (GPI)-anchored proteins are a class of lipid-anchored membrane proteins that is ubiquitously expressed at the surface of eukaryotic cells. GPI proteins differ from traditional membrane proteins in that they rely on a complex glycolipid, GPI, rather than a hydrophobic transmembrane sequence for their association with membranes. GPI anchors are found on a variety of functionally diverse proteins (as well as glycoconjugates) including cell surface receptors (folate receptor, CD14), cell adhesion molecules (neural cell adhesion molecule (NCAM) isoforms, carcinoembryonic antigen variants), cell surface hydrolases (5′-nucleotidase, acetylcholinesterase), complement regulatory proteins (decay accelerating factor), and protozoal surface molecules (*Trypanosoma brucei* variant surface glycoprotein, *Leishmania* lipophosphoglycan). Along with serving to attach proteins to the cell surface, GPI-anchored proteins appear to be markers and major constituents of "detergent-resistant" lipid rafts, the sphingolipid- and sterol-rich domains in membranes that are postulated to play an important role in the activation of signaling cascades.

GPI Structure

The structure of a GPI-anchored protein is displayed in Figure 1. The carboxy terminus of the protein is linked via an ethanolamine residue to GPI, a complex glycolipid. The core GPI structure consists of ethanolamine phosphate linked via a series of three mannose residues and a single glucosamine residue to the phospholipid phosphatidylinositol (PI).

GPI Biosynthesis

Outline of the Biosynthetic Pathway

The GPI structure is assembled via a biosynthetically and topologically complex metabolic pathway composed of at least ten steps and requiring the participation of at least 20 distinct gene products. GPI biosynthesis occurs in the endoplasmic reticulum (ER), but may be spatially segregated in a subdomain of the ER that is associated with mitochondria. In basic terms, synthesis occurs in the ER and involves the sequential addition of monosaccharides to PI yielding the core GPI structure that is then added to proteins. Many of the genes encoding enzymes involved in synthesis have been identified. Figure 2 illustrates the sequence of reactions involved in the assembly of a GPI protein anchor precursor in mammalian cells; variations of this general sequence are found in all organisms studied thus far.

GPI biosynthesis is initiated on the cytoplasmic face of the ER via the addition of *N*-acetylglucosamine (GlcNAc) from UDP-GlcNAc to PI yielding GlcNAc-PI (Figure 2, step 1). The enzyme which mediates this first step is an unusual complex consisting of six membrane proteins in mammalian cells. GlcNAc-PI is subsequently de-*N*-acetylated to generate GlcN-PI (Figure 2, step 2). The third step in biosynthesis is the acylation of the inositol residue of GlcN-PI at the 2-position (Figure 2, step 3). The acylation step is required prior to the addition of three mannose residues to GlcN-(acyl)PI (Figure 2, step 5), and modification of the mannose residues with phosphoethanolamine (EtNP) side chains (Figure 2, step 6). In contrast to the first two steps of synthesis that occur on the cytoplasmic leaflet of the ER, the mannosylation reactions are thought to occur lumenally based on the predicted membrane topology of the mannosyl transferases. This indicates that the substrate (GlcN-PI or GlcN-(acyl)PI) must be flipped across the ER membrane bilayer (Figure 2, step 4). Both mannose and EtNP residues are contributed by lipids. Dolichol-P-mannose serves as the mannose donor for all three mannosylation steps and EtNP residues are added from the phospholipid phosphatidylethanolamine (PE). The terminal EtNP residue is critical since it is this residue that is involved in the linkage of GPI to the carboxy terminus of proteins destined to be GPI-anchored (Figure 2, step 7). Fully assembled GPI structures, or the GPI moiety in GPI-anchored proteins, are frequently subject to lipid re-modeling reactions in

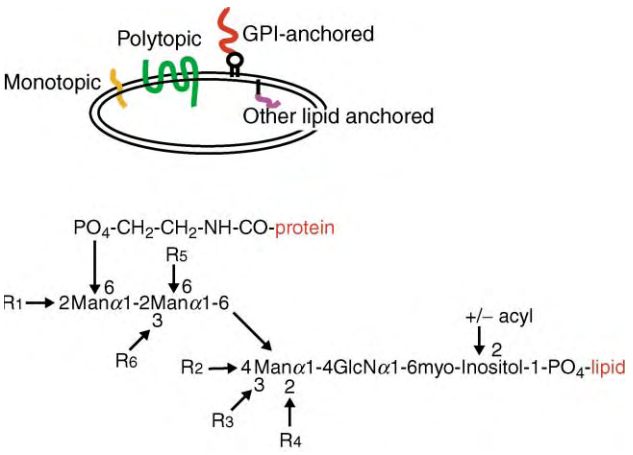

FIGURE 1 The top schematic illustrates different membrane and membrane-associated proteins in the cell surface membrane of a eukaryotic cell (internal membranes of the cell are not shown). Proteins containing hydrophobic stretches of amino acids may span the membrane once (monotopic membrane proteins) or several times (polytopic). GPI-anchored proteins are firmly associated with the cell surface membrane, but confined to the outer leaflet of the membrane bilayer since the anchor cannot span the membrane. Other lipid-anchored proteins (such as N-myristoylated, palmitoylated, and prenylated proteins) are attached to the cytoplasmic leaflet of the cell surface membrane. GPIs attached to protein have the conserved structure shown in the lower part of the figure. Variations of the structure include substituents on each of the mannose residues (phosphoethanolamine groups, monosaccharides, etc.; indicated R1–R6), differences in the lipid moiety (diacylglycerol, alkylacylglycerol, ceramide, etc.), and the presence of a fatty acyl chain attached to the 2-position of the *myo*-inositol ring. Redrawn from Ferguson, M. A. J., Brimacombe, J. S., Brown, J. R., Crossman, A., Dix, A., Field, R. A., Guther, M. L., Milne, K. G., Sharma, D. K., and Smith, T. K. (1999). The GPI biosynthetic pathway as a therapeutic target for African sleeping sickness. *Biochim. Biophys. Acta* **1455**, 327–340.

which fatty acids or the entire lipid moiety is replaced with different fatty acids or lipids.

GPI Attachment to Proteins

Newly synthesized proteins are attached to pre-existing GPIs in the lumenal leaflet of the ER by a GPI:protein transamidase complex. Proteins to be GPI-anchored contain an N-terminal signal sequence that targets them to the ER and a C-terminal signal sequence that directs GPI-anchoring. The N-terminal signal sequence is cleaved by signal peptidase during or after translocation of the nascent polypeptide into the ER lumen. The C-terminal GPI signal sequence is then cleaved and replaced with a GPI anchor through the action of GPI transamidase.

The C-terminal GPI-signal peptide, which is cleaved at what is referred to as the ω site, is necessary and sufficient for designating that a protein becomes GPI-anchored. The GPI transamidase complex responsible for attaching the protein to the GPI-anchor consists of at least five subunits. The enzyme recognizes a protein containing a GPI-anchoring signal sequence, cleaves the signal sequence and attaches the new carboxy terminus to the terminal EtNP of a pre-existing GPI.

GPI-Anchoring in Mammals, Parasitic Protozoa, and Yeast

GPI-deficient mammalian cells are viable in tissue culture, but a GPI defect has clear consequences for multicellular organisms. Transgenic mouse embryos lacking the ability to initiate GPI biosynthesis (defective in PIG-A) do not develop beyond the ninth day of gestation. The inability of certain blood cells to express GPI-anchored proteins results in the rare human disease, paroxysmal nocturnal hemoglobinuria (PNH), characterized by intravascular hemolysis, thrombosis, and bone marrow failure. The disease is caused by a somatic mutation of the X-linked PIG-A gene (encoding the catalytic component of the enzyme responsible for the first step in GPI biosynthesis) in hematopoietic stem cells. Cells defective in PIG-A are either unable to synthesize GPIs or exhibit a significant decrease in the synthesis of GPIs and thus decreased expression of GPI-anchored proteins. Red blood cells no longer expressing GPI-anchored complement regulatory proteins (e.g., CD55 and CD59) become susceptible to complement-mediated lysis, resulting in the release of heme and hemoglobin into the blood, filtering by the kidney, and excretion in the urine. Interestingly, while the GPI-deficient phenotype of hematopoietic stem cells makes the cells more sensitive to complement-mediated lysis, the defective PNH clone still persists. This implies that there must be other factors which select for clonal expansion and maintenance of GPI-deficient blood cells. One proposal is that PNH patients possess autoreactive T cells that target GPI on the surface of hematopoietic stem cells, thus PNH cells would evade damage because they lack surface GPI molecules.

GPI anchoring is the most prominent mode of attachment for cell surface proteins and glycans in parasitic protozoa. Pathogenic protozoa, including species of the genera *Trypanosoma*, *Leishmania*, and *Plasmodium*, display abundant GPI-anchored cell surface macromolecules that play crucial roles in parasite infectivity and survival. An example is the GPI-anchored variant surface glycoprotein (VSG) of bloodstream forms of *Trypanosoma brucei*, the causative agent of African sleeping sickness.

GPIs serve a unique function in yeast (*S. cerevisiae*). In addition to anchoring secretory proteins to the cell surface, GPIs play an additional role in yeast cell wall biosynthesis. The yeast cell wall consists of a fibrous lattice of mannoproteins, β1,3-glucan, β1,6-glucan, and chitin. During cell wall biosynthesis GPI-anchored

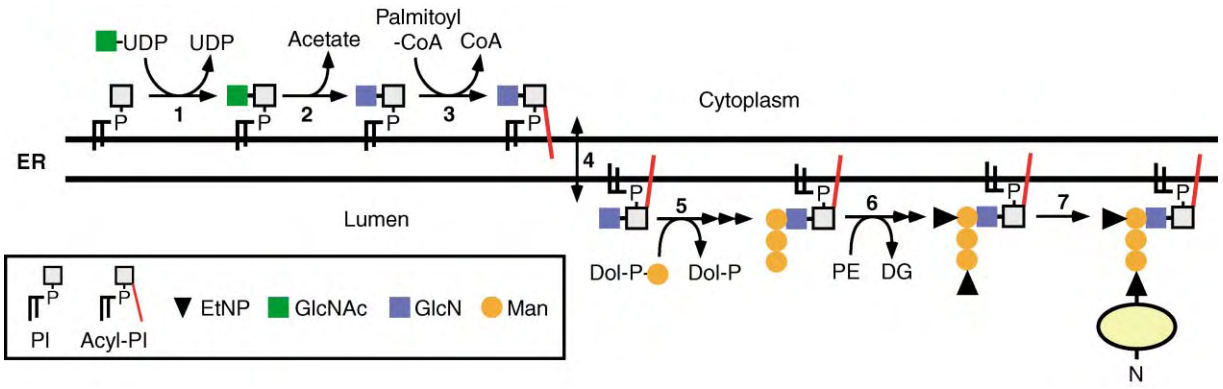

FIGURE 2 GPI biosynthesis in the ER. The pathway is a simplified version of the biosynthetic process in mammalian cells. The pathway is similar in broad terms in all other eukaryotic organisms. Biosynthesis is initiated on the cytoplasmic face of the ER by the transfer of GlcNAc from UDP-GlcNAc to PI (step 1). GlcNAc-PI is de-*N*-acetylated (step 2), then acylated on the inositol residue (step 3) to yield GlcN-acyl PI. This lipid is flipped across the ER membrane (step 4), triply mannosylated (step 5) (dolichol-phosphate-mannose (Dol-P-Man) contributes each of the mannose residues) and capped with a phosphoethanolamine residue (step 6) (donated by the phospholipid phosphatidylethanolamine (PE)). Other phosphoethanolamine residues may also be added, some prior to the completion of mannosylation. The mature GPI structure is then attached to ER-translocated proteins bearing a C-terminal, GPI-directing signal sequence, to yield a GPI-anchored protein (step 7).

mannoproteins are transported through the secretory pathway to the cell surface. After arrival at the plasma membrane a transglycosylation reaction (catalyzed by an unknown enzyme) results in cleavage of the GPI moiety between GlcN and the first mannose residue and formation of a glycosidic linkage between the manno-protein-GPI-remnant and β1,6 glucan. Mutations in GPI biosynthesis are lethal in yeast and decreased levels of GPI biosynthesis cause growth defects and aberrant cell wall biogenesis. However, not all GPI-anchored proteins become cross-linked to β1,6 glucan; the amino acids within four or five residues upstream of the ω-site determine whether the protein becomes incorporated into the cell wall or remains anchored to the plasma membrane. A unique characteristic of yeast GPIs is the addition of a fourth mannose residue to the core GPI structure (via an α1–2 linkage to the third mannose). Most GPI-anchored proteins in yeast also undergo lipid remodeling replacing the glycerolipid backbone with ceramide. The remodeling occurs after the attachment of protein to the GPI and can occur in both the ER and the Golgi.

Functions of GPIs

GPIs function as membrane anchors for secretory proteins and are believed to provide targeting signals that influence the intracellular trafficking of these proteins. Recent results indicate that GPI-proteins are packaged into unique transport vesicles, distinct from those carrying other secretory proteins, for export from the ER. GPI-anchored proteins have been shown to coalesce with sphingolipids and cholesterol into detergent-insoluble membrane domains, or lipid rafts. Association of molecules in rafts at the plasma membrane, including GPI-anchored proteins (in the exoplasmic leaflet) and acylated signaling molecules (in the cytoplasmic leaflet), is postulated to play an important role in the activation of signaling cascades. In some polarized epithelial cells, GPI-anchored proteins and many glycosphingolipids are sorted in the *trans* Golgi network and specifically targeted to the apical membrane. Once at the plasma membrane GPI-anchored proteins can undergo endocytosis and recycling back to the cell surface. However, uptake of GPI-anchored proteins is ~5 times slower than that of receptor-mediated endocytosis and recycling to the plasma membrane is ~3 times slower than that of recycling receptors. The current view is that GPI-anchoring of proteins directs their segregation into lipid rafts and affects their sorting in both the exocytic and endocytic pathways.

A GPI-anchor may also allow a protein to be selectively released from the cell surface upon hydrolysis by a GPI-specific phospholipase (e.g., PI-PLC or GPI-PLD). This has been shown to occur for certain GPI-anchored proteins in mammalian cell culture. One example is GPI-anchored membrane dipeptidase which is released from the adipocyte cell surface by a phospholipase C in response to insulin. Interestingly, other GPI-anchored proteins are not released indicating a level of regulation in insulin-stimulated hydrolysis of GPI-anchored proteins. GPI-anchored molecules have also been to shown to transfer between cells and stably insert in the external leaflet of the acceptor cell's plasma membrane. The biological significance of this is unclear, however the ability of GPI-anchored proteins to transfer between cells has implications for the expression of foreign proteins on the cell surface.

Acknowledgments

Sections of this article are reproduced and/or adapted with permission from an article by Baumann and Menon that provides a summary of all types of lipid anchored proteins. Baumann, N.A., and Menon, A.K. (2002) Lipid Modifications of Proteins. *In* "Biochemistry of Lipids, Lipoproteins and Membranes", (D.E. Vance, and J. Vance, eds.), Ch. 2, pp 37–54. Elsevier, Amsterdam, The Netherlands.

See Also the Following Articles

Protein N-Myristoylation • Protein Palmitoylation

Glossary

endoplasmic reticulum Intracellular meshwork of membranes in eukaryotic cells; the ER is endowed with the ability to synthesize lipids and is a departure point for the transport of proteins to the cell surface and extracellular space.

glycoconjugate Macromolecule containing sugars.

glycolipid Lipid molecule to which sugars are covalently attached.

lipid modified proteins Proteins, including GPI-anchored proteins, to which lipids (fatty acids, isoprenoids, or GPI) are covalently attached.

phospholipid Amphipathic molecule with a hydrophobic tail consisting typically of two fatty acids linked to glycerol, and a hydrophilic head also attached to a glycerol backbone.

Further Reading

Eisenhaber, B., Bork, P., and Eisenhaber, F. (2001). Post-translational GPI lipid anchor modification of proteins in kingdoms of life: Analysis of protein sequence data from complete genomes. *Prot. Eng.* **14**, 17–25.

Ferguson, M. A. J. (2000). Glycosylphosphatidylinositol biosynthesis validated as a drug target for African sleeping sickness. *Proc. Natl Acad. Sci. USA* **97**, 10673–10675.

Ferguson, M. A. J., Brimacombe, J. S., Brown, J. R., Crossman, A., Dix, A., Field, R. A., Guther, M. L., Milne, K. G., Sharma, D. K., and Smith, T. K. (1999). The GPI biosynthetic pathway as a therapeutic target for African sleeping sickness. *Biochim. Biophys. Acta* **1455**, 327–340.

Karadimitris, A., and Luzatto, L. (2001). The cellular pathogenesis of paroxysmal nocturnal hemoglobinuria. *Leukemia* **15**, 1148–1152.

Kinoshita, T., and Inoue, N. (2000). Dissecting and manipulating the pathway for glycosylphosphatidylinositol-anchor biosynthesis. *Cur. Opin. Chem. Biol.* **4**, 632–638.

Lipke, P. N., and Ovalle, R. (1998). Cell wall architecture in yeast: New structure and new challenges. *J. Bacteriol.* **180**, 3735–3740.

Low, M. G., Ferguson, M. A. J., Futerman, A. H., and Silman, I. (1986). Covalently attached phosphatidylinositol as a hydrophobic anchor for membrane proteins. *Trends Biochem. Sci.* **11**, 212–215.

McConville, M. J., and Menon, A. K. (2000). Recent developments in the cell biology and biochemistry of glycosylphosphatidylinositol lipids. *Mol. Membr. Biol.* **17**, 1–16.

Simons, K., and Toomre, D. (2000). Lipid rafts and signal transduction. *Nat. Rev (Molecular Cell Biology)* **1**, 31–39.

Tiede, A., Bastisch, I., Schubert, J., Orlean, P., and Schmidt, R. E. (1999). Biosynthesis of glycosylphosphatidylinositols in mammals and unicellular microbes. *Biol. Chem.* **380**, 503–523.

Udenfriend, S., and Kodukula, K. (1995). How glycosyl-phosphatidylinositol-anchored proteins are made. *Annu. Rev. Biochem.* **64**, 563–591.

Biography

Anant K. Menon is a Professor of Biochemistry at the University of Wisconsin-Madison. His research interests lie in the area of membrane biogenesis, particularly the synthesis and intracellular trafficking of simple and complex lipids, and the transport of lipids and peptides across biomembranes. Dr. Menon obtained his Ph.D. at Cornell University and pursued postdoctoral work on the biosynthesis of GPI anchors in the Laboratory of Molecular Parasitology at the Rockefeller University. He was an Assistant Professor at The Rockefeller University for three years before moving to the University of Wisconsin-Madison. His work at The Rockefeller (in collaboration with George Cross, Mark Field, Satyajit Mayor, Ralph Schwarz, and Jolanta Vidugiriene) was instrumental in establishing the pathway shown in Figure 2.

Golgi Complex

Mark Stamnes
University of Iowa, Iowa City, Iowa, USA

The Golgi complex or Golgi apparatus is an organelle of eukaryotic cells involved in the processing and transport of proteins. The Golgi complex is one of a group of cellular organelles including the endoplasmic reticulum, endosomes, and lysosomes that compose the secretory pathway. Proteins are transported through the organelles of the secretory pathway en route to the plasma membrane for secretion into the extracellular space or insertion into the membrane. This pathway also transports and sorts the resident proteins of many cellular organelles. Secreted proteins such as hormones enter the secretory pathway by translocation into the endoplasmic reticulum. They are then concentrated and transported via vesicle intermediates to the Golgi complex. At the Golgi complex, proteins can undergo processing events such as proteolytic cleavage and the removal or addition of sugar moieties. Proteins are finally sorted into various classes of post-Golgi vesicles for transport to the proper location in the cell. Hence, the Golgi complex plays a central role in the function of the secretory pathway and is the subject of intense investigation by cell biologists. While important aspects of Golgi function remain to be fully characterized, previous studies have revealed many interesting features of its morphology and its role in the transport and processing of proteins.

Morphology of the Golgi Complex

The Golgi complex is often found as a set of 3-5 stacked saccules or cisternae (Figure 1A). The cisternae are organized with a polarity such that there is a *cis*-cisterna where proteins arriving from the endoplasmic reticulum enter and a *trans*-cisterna where proteins exit the Golgi complex. Proteins pass through the medial cisternae that are present between the *cis*- and *trans*-cisternae. The *cis* and *trans*faces of the Golgi apparatus are often reticulated and thus referred to as the *cis*-Golgi network and the *trans*-Golgi network.

The stacked Golgi complexes are frequently localized together at a single site adjacent to the cell nucleus (Figure 1B). This site is near the centrosome, a cellular structure involved in the assembly and organization of microtubules, which are one of the key components of the cell cytoskeleton. In mammalian cells, the juxtanuclear localization of the Golgi complex involves the translocation of pre-Golgi vesicles along microtubules using a molecular motor protein called dynein. The Golgi stacks are often organized into interconnected ribbon-like structures. Although there is some variability in the morphology and organization of the Golgi complex among eukaryotic cells, in all cases, the Golgi is a critical site for processing and sorting of proteins that are transiting the secretory pathway.

Protein Processing in the Golgi Complex

Protein Glycosylation

Many proteins, especially those localized to the cell surface, are covalently attached to complex sugar moieties called oligosaccharides to form glycoproteins. One of the best-characterized functions for the Golgi apparatus is in the addition and modification of oligosaccharides on glycoproteins. Many proteins are modified at specific asparagine amino-acid residues in the endoplasmic reticulum in a process called N-linked glycosylation, which is carried out by the enzyme oligosaccharyl transferase. In the Golgi complex, additional oligosaccharide chains can be attached to certain serine or threonine amino-acid residues via the enzyme peptidyl N-acetylgalactosamine-transferase. This process is referred to as O-linked glycosylation. Both N-linked and O-linked oligosaccharides are further modified in the Golgi complex through both the removal and addition of specific sugars. The processing of N-linked oligosaccharides by the Golgi complex is understood in some detail. In the Golgi complex, mannose is trimmed from N-linked oligosaccharides through the action of mannosidase II. This is followed by the addition of N-acetylglucosamine, galactose, and sialic acid by sugar-specific transferases. The enzymes that catalyze the various processing steps are spatially organized throughout the Golgi stacks in the order in which they function. For example, N-acetylglucosamine transferase is mostly enriched in the *cis*-Golgi cisterna,

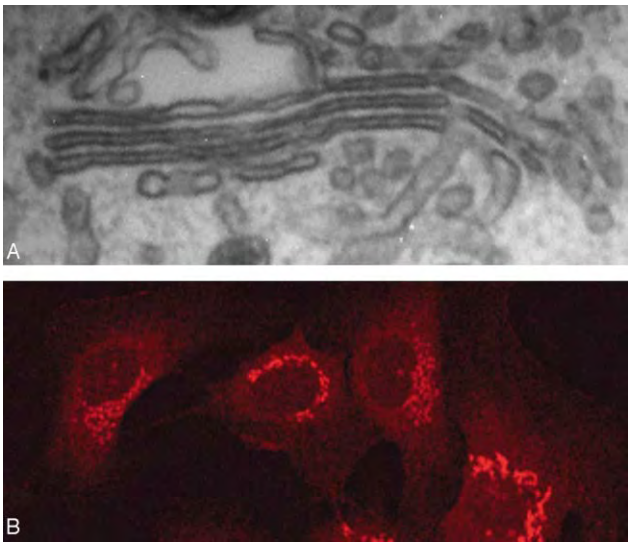

FIGURE 1 The morphology and localization of Golgi complexes. (A) Shown is a transmission electron micrograph of a Golgi complex from a rat kidney cell. Note that it is composed of three stacked cisternae: *cis*, medial, and *trans*. Transport vesicles are apparent near the Golgi complex as circular profiles. (B) Shown is a fluorescence micrograph of normal rat kidney cells that are decorated with an antibody against the Golgi enzyme, mannosidase II. Note that the labeled Golgi stacks (red) are concentrated in a region next to the cell nucleus.

while sialic acid transferase is found predominantly in the *trans*-cisterna. The role of protein glycosylation is still not fully understood, but one described function includes protein sorting.

Proteolytic Processing

Some proteins must be cleaved within the secretory pathway before they are functional. Examples of such proteins include various proteases, hormones, and transcription factors.

Prohormone Processing

Many peptide hormones are first synthesized as part of a larger inactive polypeptide, which is then cleaved by enzymes called endoproteases into a smaller active form. For example the metabolic hormone, insulin, folds first as a long polypeptide, which is then cleaved at two sites releasing an inactive fragment, the C-peptide, to form the fully active insulin molecule. Many of these proteolytic processing steps occur in the trans-Golgi network and in post-Golgi secretory vesicles. The endoproteases that carry out this processing are generally referred to as prohormone convertases. One *trans*-Golgi-network-localized endoprotease, furin, has been extensively characterized and is involved in processing a wide variety of receptors and hormones.

Proteolytic Regulation of Transcription Factors

Regulation of a Transcription Factor Involved in Cholesterol Metabolism In some cases, Golgi-localized endoproteases are used for the activation of proteins that function as part of regulatory signaling pathways. A very interesting example of this type of regulation is the proteolytic activation of sterol-response-element-binding protein (SREBP). SREBP is a transcription factor that activates genes that are involved in cholesterol uptake and biosynthesis. It resides as an integral membrane protein on the endoplasmic reticulum when cellular cholesterol levels are elevated. However, when cholesterol levels in the cell are low, SREBP is transported out of the endoplasmic reticulum to the Golgi complex where it is cleaved by two endoproteases. One of these enzymes is unique since it cleaves the transmembrane domain of SREBP within the plane of the membrane. The result of this proteolysis in the Golgi complex is the release of an active transcription factor from the membrane, which is then translocated into the nucleus to activate genes involved in sterol metabolism.

A Golgi-Localized Endoprotease is Involved in Alzheimer's Disease The toxic peptide β-amyloid accumulates in plaques found within the brain of individuals with Alzheimer's disease. β-amyloid is generated through inappropriate proteolytic cleavage of amyloid precursor protein. A Golgi-localized endoprotease called presenilin is important for normal processing of amyloid precursor protein. Presenilin is similar to the Golgi-localized endoprotease that activates SREBP since it cleaves the amyloid precursor protein within the membrane.

The examples of endoprotease function described here are illustrative of the wide variety of proteins and cellular processes that utilize proteolytic processing at the Golgi complex.

Mechanisms of Protein Transport at the Golgi Complex

Vesicular Transport at the Golgi Complex

One important mechanism for moving proteins and phospholipids to, from, and within the Golgi complex is via transport vesicles. These small, spherical, membrane-limited structures are formed on organelles through the assembly of a protein coat. The coat deforms the membrane into a vesicle and plays a role in selecting the appropriate cargo proteins. Once formed, the vesicles are translocated to the target organelle where they fuse with the membrane and

deliver their contents. Several types of transport vesicles, each with a distinct protein coat, function at the Golgi complex. Two well-studied examples are clathrin-coated vesicles that mediate transport of proteins leaving the trans-Golgi network, and COPI vesicles that mediate transport among the cisternae and backwards transport out of the Golgi complex.

Cisternal Progression

A second mechanism for moving proteins through the Golgi complex is cisternal progression. Here, the *cis*-cisternae are transformed into medial cisternae, and medial cisternae are transformed into *trans*-cisternae. New *cis*-cisternae are created by vesicles arriving from the endoplasmic reticulum. The *trans*-cisternae are expended by the formation of transport vesicles involved in post-Golgi trafficking. Progressive changes in the repertoire enzymes within the cisternae occur through vesicle-mediated protein transport and sorting of the resident Golgi proteins. During cisternal progression, forward moving cargo proteins are carried along with the cisternae as they progress from the *cis* to medial to *trans* positions.

Protein Sorting at the Golgi Complex

Proteins must be properly sorted and targeted as they traverse and exit the Golgi complex. At the *trans*-Golgi network, proteins are destined for several different locations. Many proteins are sent to the cell surface for insertion into the plasma membrane or for release into the extracellular space. Other proteins must be targeted to intracellular organelles such as late endosomes or lysosomes. In addition to the sorting of forward moving proteins, some proteins are retrieved or recycled back to earlier compartments. For example, proteins that function within the Golgi complex are recognized and retained at or retrieved to the proper cisterna. Two sorting mechanisms that have been characterized at the Golgi complex are receptor-mediated packaging into transport vesicles and protein aggregation.

Receptor-Mediated Sorting into Transport Vesicles

A key aspect of protein sorting throughout the secretory pathway is the selective packaging of cargo proteins into transport vesicles. This involves either direct or indirect (receptor-mediated) interactions with the vesicle-coat proteins. Thus, a vesicle targeted for a specific organelle in the cell can select cargo proteins that are destined for the same location. Discussed next are two receptor proteins that function in cargo selection during protein transport from the Golgi complex, namely the mannose-6-phosphate receptor and the KDEL receptor.

The Mannose-6-Phosphate Receptor

The mannose-6-phosphate receptor sorts proteins into clathrin-coated vesicles that are leaving the trans-Golgi network and are destined for organelles called lysosomes involved in breaking down cellular waste products. Mannose-6-phosphate is an N-linked oligosaccharide generated by enzymes present in the cis-Golgi cisterna. It is formed specifically on proteins destined for the lysosome. The mannose-6-phosphate receptor spans the Golgi membrane and binds to coat proteins on the cytosolic side of the membrane and to the mannose-6-phosphate-containing protein on the luminal side of the membrane. Thus, mannose-6-phosphate-containing proteins are sorted and concentrated into the correct clathrin-coated vesicles for transport to the lysosome.

The KDEL Receptor

Many resident proteins of the endoplasmic reticulum are retrieved from the Golgi complex if they escape. The KDEL receptor functions in this retrieval process by sorting proteins that belong in the endoplasmic reticulum into COPI vesicles for backwards transport. KDEL refers to the single-letter code for the amino acid residues lysine, aspartic acid, glutamic acid, leucine, which are present on many endoplasmic reticulum-resident proteins. Similar to the mannose-6-phosphate receptor, the KDEL receptor binds to COPI-coat proteins on the cytosolic side of the membrane and to KDEL-containing protein on the luminal side. This allows for sorting and retrieval of endoplasmic reticulum-localized proteins via COPI vesicles.

Protein Aggregation as a Sorting Mechanism

Another way that proteins are sorted in the Golgi complex is through aggregation. Some resident Golgi proteins, such as the enzyme mannosidase II, form aggregates with themselves and other Golgi-resident proteins. Golgi proteins may be retained at the proper cisternae through the exclusion of the large aggregates from transport vesicles. By contrast, some proteins – for example, insulin and many other hormones – may cluster within the *trans*-Golgi network to facilitate their concentration and packaging into vesicles. Aggregation continues in the secretory vesicles before its delivery to the plasma membrane and release into the extracellular space.

In higher eukaryotes, thousands of proteins must be properly transported, processed, and sorted through the Golgi complex. Some of the properties of this organelle that have been revealed by cell biologists and briefly outlined in this article are beginning to explain how this remarkable feat might be achieved.

See Also the Following Articles

Amyloid • Cholesterol Synthesis • Dynein • Oligosaccharide Chains: Free, *N*-Linked, *O*-Linked • *N*-Linked Glycan Processing Glucosidases and Mannosidases • Protein Glycosylation, Overview • Secretory Pathway

Glossary

cisternae Flattened membrane-limited structures that stack together to form the Golgi complex.

endoprotease An enzyme that cleaves a protein into two or more fragments.

glycoprotein A protein that is attached to complex sugar molecules called oligosaccharides.

secretory vesicles Specialized transport vesicles that transport proteins from the trans-Golgi network to the plasma membrane. These vesicles can sometimes be regulated to allow release of proteins such as hormones from cells only under certain conditions.

transport vesicle A small spherical structure that mediates protein transport between organelles. It is formed by the assembly of a protein coat.

Further Reading

Berger, E. G., and Roth, J. (eds.) (1997). *The Golgi Apparatus*. Birkhauser, Boston.

Hong, W. (1996). *Protein Trafficking along the Exocytic Pathway*. Landes Bioscience, Georgetown, TX.

Short, B., and Barr, F. (2000). The Golgi apparatus. *Curr. Biol.* **10**, R583–R585.

Shorter, J., and Warren, G. (2002). Golgi architecture and inheritance. *Annu. Rev. Cell Dev. Biol.* **18**, 379–420.

Thomas, G. (2002). Furin at the cutting edge: From protein traffic to embryogenesis and disease. *Nat. Rev. Mol. Cell Biol.* **3**, 753–766.

Varki, A. (1998). Factors controlling the glycosylation potential of the Golgi apparatus. *Trends Cell Biol.* **8**, 34–40.

Biography

Mark Stamnes is an Associate Professor in the Department of Physiology and Biophysics of the Roy J. and Lucille A. Carver College of Medicine at the University of Iowa. His research interest is in the mechanisms of protein transport and sorting in the secretory pathway. He holds a Ph.D. from the University of California, San Diego and has completed his postdoctoral studies at the Memorial Sloan-Kettering Cancer Center in New York. He is a member of the American Society for Cell Biology.

G_q Family

Wanling Yang and John D. Hildebrandt
Medical University of South Carolina, Charleston, South Carolina, USA

Guanine-nucleotide-binding proteins (G proteins) are heterotrimeric proteins composed of α-, β-, and γ-subunits. Activated by G protein-coupled receptors (GPCRs) in the plasma membrane, G proteins play pivotal roles in signal transduction from hormones, neurotransmitters, and drugs to cellular responses. So far a total of 16 α-, 5 β-, and 12 γ-subunits have been described in mammals. Based on functional and structural similarities, G proteins are grouped into four families named by the α-subunits they contain: G_s, G_i/G_o, G_q, and G_{12}/G_{13}. Activation of members of the G_q family of G proteins directly activates phospholipase Cβ (PLCβ) isozymes to produce the second messengers inositol 1, 4, 5-trisphosphate (IP_3) and diacylglycerol (DAG). Unlike G_s or G_i/G_o families, the G_q family proteins are insensitive to cholera toxin and pertussis toxin.

G_q Family of G Proteins

Phosphatidylinositol metabolites are primary intracellular regulators of eukaryotic cells. Studies of hormone and neurotransmitter regulation of phosphatidylinositol turnover implicated the frequent involvement of a specific class of G proteins. The subsequent purification of pertussis toxin-insensitive G_α subunits led to the demonstration of guanine nucleotide regulation of phospholipase Cβ isoforms through G_q. The G_q family includes $G_{\alpha q}$, $G_{\alpha 11}$, $G_{\alpha 14}$, and $G_{\alpha 15}$ (previously referred to in some species as $G_{\alpha 16}$), which are expressed from individual genes with different expression patterns. $G_{\alpha q}$ and $G_{\alpha 11}$ are the most similar (89% identical amino acids), whereas $G_{\alpha 15}$ shares only about 56% identities with other family members (Figure 1). Nevertheless, the genes encoding these proteins may have arisen from a pair of gene duplications since $G_{\alpha q}$ and $G_{\alpha 14}$ are within 70 kb of each other on human chromosome 9 or mouse chromosome 19, and $G_{\alpha 11}$ and $G_{\alpha 15}$ are within 7 kb of each other on human and mouse chromosomes 19 and 10, respectively. All four genes have similar structures and contain seven coding exons. Proteins likely related to the G_q family are found in the genome of many species throughout the animal kingdom, but their relationship to G_α subunits in other kingdoms is unclear.

G_q is Activated by Hormones, Neurotransmitters, and Drugs through Multiple GPCRs

The G_q family of G proteins is responsible for cellular responses to a plethora of hormones, neurotransmitters, and drugs, and is involved in the corresponding physiological, pathophysiological, and pharmacological processes (Table I). In the CNS, M_1, M_3, and M_5 muscarinic receptors, group I metabotropic glutamate receptors ($mGluR_1$ and $mGluR_5$), and serotonin 5-HT_2 receptors, all couple to G_q family of G proteins and thus activate the PLCβ signal transduction pathway. Activation of this pathway in the CNS is involved in synaptic transmission and modulation, neuronal development, and long-term depression (LTD) and long-term potentiation (LTP). In the cardiovascular system, α_1 adrenergic receptors, endothelin receptors, angiotensin receptors, and prostaglandin F receptors modulate cardiovascular function through activation of G_q and are especially involved in cardiac hypertrophy and congestive heart failure, a compensation process induced by hemodynamic stress and myocardial injury and subsequent decompensation after sustained stimulation. Thromboxane A_2 receptors, thrombin receptors, and purinergic receptors induce platelet aggregation and granule secretion through activation of the G_q/PLCβ pathway. The G_q family of G proteins is also involved in hormone secretion, inflammation, and allergy through the activation of many other receptors including those for TRH, GnRH, leukotrienes, bradykinin, and histamine.

PLCβ Activation and Calcium Mobilization are Downstream Responses to G_q Activation

Phospholipases are membrane-associated proteins involved in the biosynthesis and degradation of membrane lipids. They include phospholipase (PL) A_1, A_2, C,

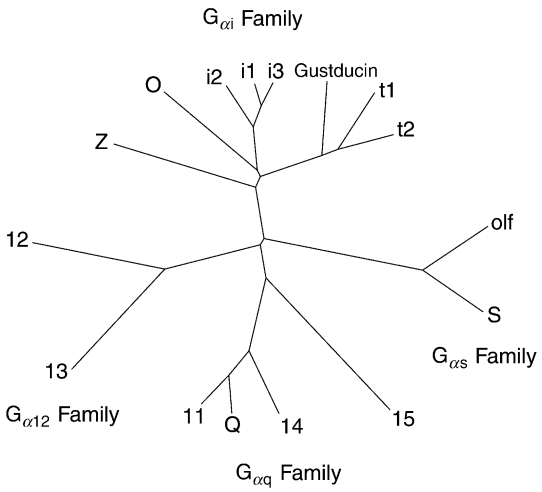

α_q Homologues	
Human α_q	100%
Mouse α_q	100%
Rat α_q	98%
Xenopus	96%
Turkey α_q	90%
Human α_{11}	89%
Drosophila	84%
Lobster	83%
C. elegans	82%
Snail	81%
Human α_{14}	80%
Squid	77%
Sponge	62%
Human α_{15}	57%
Aspergillus	50%
Penicillium	49%
Human α_i	49%

FIGURE 1 Homology of $G_{\alpha q}$ to other human G_α proteins and to related proteins in other species. The phylogenetic tree diagram was generated by TreeView from human G protein α-subunit protein sequences aligned with ClustalX. The length of the bars connecting different G_α proteins is proportional to the similarity of their aligned sequences. The α_q homologues listed are based upon percent identical amino acids in the aligned sequences.

TABLE I

Receptors that Couple to the G_q Family of G Proteins and their Ligands and Physiological Functions

Ligands	Receptors	Function
Acetylcholine carbachol	M_1, M_3, M_5 muscarinic	Memory and cognition, smooth muscle contraction, and salivary secretion
Adenine nucleotides	P_2Y purinergic	Vasodilation
Angiotensin II, Losartan	AT_{1a}, AT_{1b}	Modulation of cardiovascular activities
Bradykinin	B_2 bradykinin	Hyperalgesia, smooth muscle contraction
C_{5a} anaphylatoxin	C_{5a}	Chemoattraction
Cholecystokinin (CCK)	CCK_a and CCK_b	Gastrointestinal activities
Endothelins	ET_a and ET_b	Regulation of cardiovascular activities
Glutamate	$mGluR_1$ and $mGluR_5$	Modulation of neuronal activities
Gonadotrophin-releasing hormone (GnRH)	GnRH	Synthesis and release of FSH and LH
Histamines	H_1	Inflammation and allergy
5-hydroxytryptamine, α-methyl-5-HT	5-HT_{2a}, 5-HT_{2b} and 5-HT_{2c}	Modulation of neuronal activities of the brain
Neurotensin	Neurotensin	Modulation of gastrointestinal and brain activities
Norepinephrine (noradrenaline), epinephrine (adrenaline), phenylephrine, prazosin	α_{1a}, α_{1b}, α_{1c}, α_{1d} adrenergic	Modulation of cardiovascular activities
Platelet activating factor	PAF	Platelet activation and aggregation
Prostaglandin $F_{2\alpha}$	Prostaglandin F (FP)	Bronchoconstriction and luteolysis
Thromboxane A_2	TXA_2 (TP)	Smooth muscle contraction and platelet aggregation
Tachykinins	NK_1, NK_2, NK_3	Smooth muscle contraction, transmission of sensory information
Thrombin	Thrombin	Platelet aggregation
Thyrotrophin-relasing hormone (TRH)	TRH	Synthesis and release of thyroid-stimulating hormone
Vasopressin	V_{1a}, V_{1b}	Smooth muscle contraction, platelet activation, glycogenolysis, and ACTH release
Leukotrienes	$CysLT_1$, $CysLT_2$	Bronchoconstriction and vasodilation

and D (PLA_1, PLA_2, PLC, and PLD). PLC contains three subclasses on the basis of size and amino acid sequences: PLCβ, PLCγ, and PLCδ. PLCβ isotypes (β1–4) are activated by GPCRs via G_q family and/or $\beta\gamma$-subunits primarily from activation of the G_i/G_o family. Activated α-subunits of the G_q family stimulate all four isoforms of PLCβ with the potency rank order of $\beta1 \geq \beta3 \geq \beta4 \gg \beta2$ (Figure 2). PLCβ hydrolyzes the membrane phospholipid phosphatidylinositol 4,5-bisphosphate (PIP_2) and generates two signal molecules: diacylglycerol (DAG) and inositol 1,4,5-trisphosphate (IP_3). While DAG remains membrane-associated, IP_3 is released into cytosol and binds to IP_3 receptors, which are ligand-gated Ca^{2+} channels, in the endoplasmic reticulum or sarcoplasmic reticulum (cardiac muscle cells). Binding of IP_3 induces calcium release from intracellular stores and causes a rise in cytosolic free calcium concentration. One result of the increase in calcium concentration is its binding to calmodulin. Calcium–calmodulin complexes bind to other proteins and change their functional activities. Isozymes of protein kinase C (PKC) translocate from cytosol to plasma membrane and bind to DAG in the presence of calcium. Activated PKC phosphorylates other proteins and alters their functional state. PKC is known to have a wide variety of effects including receptor desensitization, activation of gene transcription, immune regulation, and regulation of cell growth.

The regulation of gene expression by cell surface receptors often involves the stimulation of signaling pathways including one or more members of the mitogen-activated protein kinases (MAPKs). The MAPKs are a family of evolutionarily conserved serine/threonine kinases that transmit externally derived signals regulating cell growth, division, differentiation, and apoptosis. MAPKs are activated in response to stimulation of GPCRs that couple to the G_q family of G proteins such as α_{1b} adrenergic receptors or M_1 muscarinic cholinergic receptors. This process involves PLCβ, intracellular Ca^{2+}, and PKC. PKC activation leads to MAPK activation through both Ras-dependent and Ras-independent mechanisms. PKCα can apparently activate Raf-1 by direct phosphorylation. In many cases, however, $G_{q/11}$ activation causes MAPKs activation that is unaffected by PKC inhibition.

G_q in Cardiovascular Disease, Platelet Aggregation, and Cerebellum Development

The study of the functions of the G_q family of proteins has been greatly facilitated by the use of various animal models that overexpress the wild-type $G_{\alpha q}$ protein or that express a constitutively active form (gain of function mutations). Also useful have been animal models deficient in the protein, or that overexpress an inhibitor (loss of function mutations). Some well-characterized functions of the G_q proteins include roles in the development of cerebellum and motor coordination, platelet aggregation, heart development and cardiac adaptation, and development of heart failure.

$G_{\alpha q}$ is essential for the signaling processes used by different platelet activators. It has been reported that a defect in human platelet G_q function leads to impaired

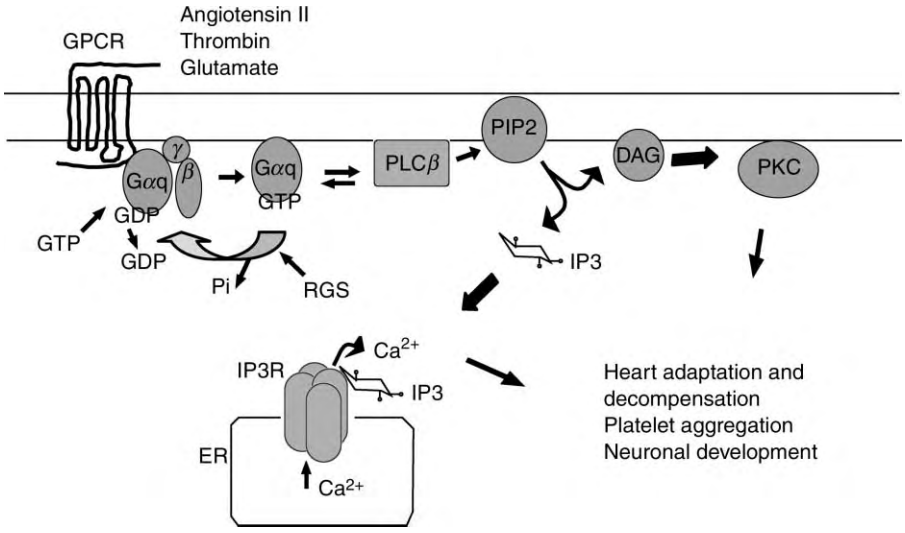

FIGURE 2 The G_q signal transduction pathway. Activation of many GPCRs leads to activation of G_q. $G_{\alpha q}$ activates PLCβ that subsequently cleaves PIP_2 to generate DAG and IP_3. IP_3 binds to the IP_3 receptor (IP_3R) on the endoplasmic reticulum (ER) and induces release of calcium. DAG remains membrane bound and activates PKC. Both calcium and PKC are important signaling molecules that are involved in many cellular functions including cell growth and differentiation. PLCβ and RGS proteins can work as GAPs to facilitate the termination of G_q signaling by enhancing its GTPase activity.

platelet aggregation, secretion, and calcium mobilization, in response to a number of agonists. Platelets from $G_{\alpha q}$-deficient mice are unresponsive to a variety of physiologic platelet activators. As a result, these mice have increased bleeding times, which is an *in vivo* measure of platelet function.

Mice with a null mutation in the $G_{\alpha q}$ gene suffer from ataxia with typical signs of motor coordination defects. In the cerebellum of newborn rodents, each Purkinje cell (PC) is innervated by multiple climbing fibers (CFs). Massive elimination of supernumerary CF–PC synapses occurs during the first three postnatal weeks, and by about postnatal day 20, most PCs are innervated by a single CF. In $G_{\alpha q}$-deficient mice, ~40% of adult PCs remain innervated by multiple CF because of a defect in regression of supernumerary CFs. PLCβ_4, which shows predominant expression in cerebellar PCs, and $mGluR_1$ may be involved in this function of $G_{\alpha q}$ since in $mGluR_1$- or PLCβ_4-deficient mice, a similar phenotype was observed. LTD of the PF–PC synapse in mice lacking $G_{\alpha q}$ was also deficient. Cerebellar LTD is a form of synaptic plasticity believed to be related to motor learning.

The G_q family of G proteins has been implicated in signaling pathways regulating cardiac growth under physiological and pathological conditions. The ability of cardiomyocytes to undergo hypertrophic growth is an important adaptive response to a wide range of conditions that require the heart to work more effectively. Norepinephrine (noradrenaline) (NE) and other hormones or regulators such as endothelin, prostaglandin F2α, and angiotensin II induce cardiomyocyte growth through activation of G_q-coupled receptors. A relatively modest degree of wild-type $G\alpha_q$ overexpression in transgenic mice produced many of the features of compensated left ventricular hypertrophy. Conversely, expression of a $G_{\alpha q}$ inhibitor peptide that prevents receptor coupling to $G_{\alpha q}$ in mouse myocardium, or RGS4, which binds to and activates the GTPase activity of $G\alpha_q$, significantly attenuated hypertrophy induced by pressure overload. The ability of cardiomyocytes to function at high capacity under increased workload usually cannot be sustained and ventricular failure develops after prolonged stimulation. One event associated with this transition to heart failure is the apoptotic death of cardiomyocytes. It has been shown that sustained or excessive activation of the G_q signaling pathway results in apoptotic loss of cardiomyocytes. Expression of a constitutively activated mutant of $G_{\alpha q}$, which further increased G_q signaling, produces initial hypertrophy, which rapidly progresses to apoptotic cardiomyocyte death. Conversely, inhibition of specific components of the pathway prevents or ameliorates heart failure. Experimental and clinical evidence supports the benefit of reduced G_q-coupled receptor signaling in modifying the progression of left ventricular remodeling and heart failure.

Modulation of G_q Functions

The G_q family of G proteins undergoes palmitoylation at N-terminal cysteine residues. Mutation of cysteines 9 and 10 in $G_{\alpha q}$ to serine profoundly alters the behavior of the subunit. Mutant $G_{\alpha q}$ cannot couple a coexpressed receptor to stimulation of PLCβ. Cysteine substitution also prevented a constitutively active form of $G_{\alpha q}$ from stimulating PLC directly. However, a substitution of a single cysteine in $G_{\alpha q}$ did not alter its activity.

Long-term activation of GPCRs coupled to G_q induces down-regulation of the $G_{\alpha q}$ subunit. For example, prolonged exposure of αT3-1 pituitary cells to a gonadotrophin-releasing hormone receptor agonist results in marked down-regulation of $G_{\alpha q}$ and $G_{\alpha 11}$. Chinese hamster ovary cells stably transfected with human M_3 muscarinic acetylcholine receptors show a 40–50% reduction in $G_{\alpha q}$ and $G_{\alpha 11}$ when stimulated with the cholinergic agonist carbachol. Usually, levels of mRNA encoding $G_{\alpha q}$ and $G_{\alpha 11}$were not greatly altered, suggesting a change in protein degradation.

The intrinsic GTPase activity of G_α-subunits acts as a timer to limit the duration of G protein activation. PLCβ works as a GAP (GTPase-activating protein) to increase the intrinsic GTPase activity of $G_{\alpha q}$. The ability of PLCβ to act as a GAP for $G_{\alpha q}$ provides negative feedback, limiting PLC activity. In addition, a family of proteins known as the regulators of G protein-signaling (RGS) proteins has been identified as GAPs for G_α-subunits. RGS4 and GAIP are known to act as GAPs for the G_q family. Furthermore, these RGS proteins block activation of PLCβ by $G_{\alpha q}$, which apparently results from occlusion of the effector-binding site on $G_{\alpha q}$. The presence of RGS proteins with GAP activity is also thought to increase the selectivity of GPCRs that couple to G_q by filtering out low-efficacy responses.

G_q Family Members are Functionally Complementary to Each Other

Mammals express four G_q class α-subunits of which two, $G_{\alpha q}$ and $G_{\alpha 11}$, are widely expressed and are primarily responsible for coupling receptors to PLCβ. In contrast, expression of $G_{\alpha 14}$ and $G_{\alpha 15}$ is restricted to certain tissues. $G_{\alpha 14}$ is predominantly expressed in spleen, lung, kidney, and testis, whereas $G_{\alpha 15}$ is primarily restricted to hematopoietic lineages. In most tissues, $G_{\alpha q}$ and $G_{\alpha 11}$ are functionally complementary to each other. Receptors activating G_q family members in mammalian systems do not discriminate between $G_{\alpha q}$ and $G_{\alpha 11}$. Similarly, there appears to be little difference between the abilities of these G proteins in regulating PLCβ functions. Functional

redundancy of G_q family proteins is also demonstrated by knocking-out individual genes that code for the proteins of this family. Only $G_{\alpha q}$-deficient mice revealed obvious phenotypic defects, including cerebellar ataxia and deficiencies in primary hemostasis due to a defect in platelet activation. The observed phenotypes correlated with preferential or exclusive expression of $G_{\alpha q}$ in the affected cell types of the cerebellum and platelets. Despite the specific expression patterns of $G_{\alpha 14}$ and $G_{\alpha 15}$, which may indicate tissue-specific functions for these proteins, no obvious phenotypic changes were observed in mice carrying inactivating mutations of the $G_{\alpha 14}$ and $G_{\alpha 15}$ genes. $G_{\alpha 11}$-deficient mice were also viable and fertile with no apparent behavioral or morphologic defects. Their functions may be dispensable or compensated for by other members of the $G_{\alpha q}$ family, although subtle phenotypes from loss of their functions may be difficult to detect with current methodology.

A gene dosage effect between $G_{\alpha q}$ and $G_{\alpha 11}$ was observed after breeding $G_{\alpha q}$-deficient mice with $G_{\alpha 11}$-deficient mice. Embryos lacking both genes died in uterus with heart malformations. Mice inheriting a single copy of either gene died within hours of birth with craniofacial and/or cardiac defects. Apparently, two active alleles of these genes are required for life after birth. Analyses of intercross offspring inheriting different combinations of these two mutations indicated that $G_{\alpha q}$ and $G_{\alpha 11}$ have overlapping functions in embryonic cardiomyocyte proliferation and craniofacial development.

See Also the Following Articles

G Protein Signaling Regulators • G_{12}/G_{13} Family • G_i Family of Heterotrimeric G Proteins • G_s Family of Heterotrimeric G Proteins • IP_3 Receptors • Phospholipase C • Protein Kinase C Family • Protein Palmitoylation

Glossary

ataxia An inability to coordinate muscle activity during voluntary movement. It is often caused by disorders of the cerebellum.

cardiac hypertrophy Enlargement of cardiomyocytes and thickening of the walls of the heart in response to hemodynamic stress and myocardial injury.

primary hemostasis The formation of a primary platelet plug and involving platelets, the blood vessel wall and von Willebrand factor. The process includes contraction of injured vessel, platelet adhesion, activation, aggregation, and secretion. Platelet secretion triggers the coagulation process and proceeds in a positive feedback loop to further stop bleeding.

Further Reading

Adams, J. W., and Brown, J. H. (2001). G proteins in growth and apoptosis: Lessons from the heart. *Oncogene* **20**, 1626–1634.

Alliance for Cell Signaling/Nature, The Signaling Gateway, http://www.signaling-gateway.org/

Cockcroft, S., and Gomperts, B. D. (1985). Role of guanine nucleotide binding protein in the activation of polyphosphoinositide phosphodiesterase. *Nature* **314**, 534–536.

Exton, J. (1996). Regulation of phosphoinositide phospholipases by hormones, neurotransmitters, and other agonists linked to G proteins. *Annu. Rev. Pharmacol. Toxicol.* **36**, 481–509.

Hermans, E., and Challiss, R. A. J. (2001). Structural, signaling and regulatory properties of the group I metabotropic glutamate receptors: Prototypic family C G protein-coupled receptors. *Biochem. J.* **359**, 465–484.

Iyengar, R., and Hildebrandt, J. D. (eds.) (2002). *G Protein Pathways, Part B, G Proteins and their Regulators, Methods in Enzymology*, Vol 344. Academic Press, New York.

Litosch, I., and Wallis, C., and Fain, J. N. (1985). 5-Hydroxytryptamine stimulates inositol phosphate production in a cell-free system from blowfly salivary glands. Evidence for a role of GTP in coupling receptor activation to phosphoinositide breakdown. *J. Biol. Chem.* **260**, 5464–5471.

Offermanns, S. (2001). In vivo functions of heterotrimeric G proteins: Studies in Gα-deficient mice. *Oncogene* **20**, 1635–1642.

Pang, I. H., and Sternweis, P. C. (1990). Purification of unique alpha subunits of GTP-binding regulatory proteins (G Proteins) by affinity chromatography with immobilized beta gamma subunits. *J. Biol. Chem.*, **265**, 18707–18712.

Simon, M. I., Strathmann, M. P., and Gautam, N. (1991). Diversity of G proteins in signal transduction. *Science* **252**, 802–808.

Smrcka, A.V., Hepler J. R., Brown K. O., and Sternweis, P. C. (1991). Regulation of polyphosphoinositide-specific phospholipase c activity by purified G_q. *Science* **251**, 804–807.

Sternweis, P.C., and Smrcka, A.V. (1993). G proteins in signal transduction: The regulation of phospholipase C. *Ciba Found. Symp.* **176**, 96–111.

Strathmann, M., Wilkie, T. M., and Simon M. I. (1989). Diversity of the G-protein family: sequences from five additional alpha subunits in the mouse. *Proc. Natl Acad. Sci. USA* **86**, 7407–7409.

Taylor, S. J., Smith, J. A., and Exton, J. H. (1990). Purification from bovine liver membranes of a guanine nucleotide-dependant activator of phosphoinositide-specific phospholipase C. Immunologic identification as a novel G-protein alpha subunit. *J. Biol. Chem.* **265**, 17150–17156.

Taylor, S. J., Chae, H. Z., Rhee, S. G., and Exton, J. H. (1991). Activation of the 1 isozyme of phospholipase C by subunits of the G_q class of G proteins. *Nature* **350**, 516–518.

Uhing, R. J., Popic, V., and Exton, J. H. (1986). Hormone-stimulated polyphosphoinositide breakdown in rat liver plasma membranes. Roles of quanine nucleotides and calcium. *J. Biol. Chem.* **261**, 2140–2146.

Biography

John D. Hildebrandt is a Professor in the Department of Molecular and Cell Pharmacology at the Medical University of South Carolina. He received his Ph.D. from the University of Iowa and did postdoctoral training in the Department of Physiology at the University of Pittsburgh and in the Department of Cell Biology at Baylor College of Medicine. His main research interest is G protein structure and function. He has made numerous contributions to the identification of G protein subunits and isoforms, and the relationship between the generation of G protein subunit diversity and G protein-dependent signaling mechanisms.

Wanling Yang is a postdoctoral Fellow in the Medical University of South Carolina. He holds a Ph.D. in Pharmacology and Bioinformatics from the University of Minnesota. He has studied the structure and function of opiate receptors and is currently working on the structure and function of the G protein subunit genes.

Green Bacteria: Secondary Electron Donor (Cytochromes)

Hirozo Oh-oka
Osaka University, Osaka, Japan

Robert E. Blankenship
Arizona State University, Tempe, Arizona, USA

Green photosynthetic bacteria are a class of photosynthetic organisms that carry out light-driven electron transfer that leads to long-term energy storage. A reaction center, pigment–protein complex, mediates the electron transfer process. Cytochromes, proteins that contain Fe-containing heme prosthetic groups, are an essential part of the photosynthetic electron transfer system. The green photosynthetic bacteria contain a rich variety of different cytochromes. Various cytochromes act as either soluble or membrane-bound electron carriers and are involved in substrate oxidation processes, as well as proton translocation across the membrane.

Cytochromes in Green Bacteria

There are two phyla of green photosynthetic bacteria, green sulfur bacteria and green nonsulfur bacteria; the latter group is now more correctly called filamentous anoxygenic phototrophic bacteria. Both groups of organisms contain cytochromes, although the patterns and types of cytochromes in the two phyla are very different.

Green sulfur bacteria (chlorobiaceae) are strictly anaerobic, photosynthetic organisms whose reaction center (RC) complex shares common structural and functional features with the photosystem (PS) I RC complex of plants and cyanobacteria or the heliobacterial RC complex. This type-1 (also called Fe–S-type) RC complex consists of five subunits, including a homodimeric core RC (with two identical subunits with molecular mass of 65 kDa), Fenna Matthews Olson (FMO) antenna protein (41 kDa), Fe–S protein that includes the early electron acceptors F_A and F_B (31 kDa), cytochrome c_z (22 kDa) and 18 kDa protein, respectively. Cytochrome c_z serves as a secondary electron donor to the primary electron donor P840. The green sulfur bacteria utilize sulfur compounds as a source of reducing power and therefore also contain additional electron transfer components, primarily soluble cytochromes *c*, which are involved in the metabolic pathway of sulfur oxidation (Figure 1).

Filamentous anoxygenic phototrophic (FAP) bacteria are not closely related organisms to the green sulfur bacteria, with the exception of the primary shared characteristic, the chlorosome antenna complex. Many of these organisms are facultatively aerobic photosynthetic bacteria that are often found in microbial mat environments with cyanobacteria. The only member of this group that has been well studied is *Chloroflexus aurantiacus*, which is found in hot spring environments all over the world. FAP bacteria contain a type-2 (also called quinone-type) RC complex that includes bacteriopheophytins and quinones as early electron acceptors. The type-2 RC is similar to that found in purple photosynthetic bacteria and photosystem II of oxygenic photosynthetic organisms. The FAP RC consists of a heterodimeric complex of two proteins, L and M, plus a tightly bound tetraheme *c*-type cytochrome, *c*-554. Cyt *c*-554 is a membrane-associated cytochrome of molecular mass 48 kDa, which serves as a secondary electron donor to the primary electron donor P870. FAP bacteria have not been reported to contain any soluble *c*-type cytochromes. They also do not appear to contain a membrane-bound cytochrome bc_1 complex.

Types of *c*-Type Cytochromes in Green Sulfur Bacteria

Green sulfur bacteria contain a number of *c*-type cytochromes. These include soluble cytochromes *c*-555, *c*-553, and *c*-551, the membrane-bound cytochrome c_z, and the membrane-bound cytochrome bc_1 complex. The first three were isolated from *Chlorobium limicola* f. *thiosulfatophilum*, and extensively studied biochemically by Yamanaka's group in the 1970s and have been extensively characterized. The others are less

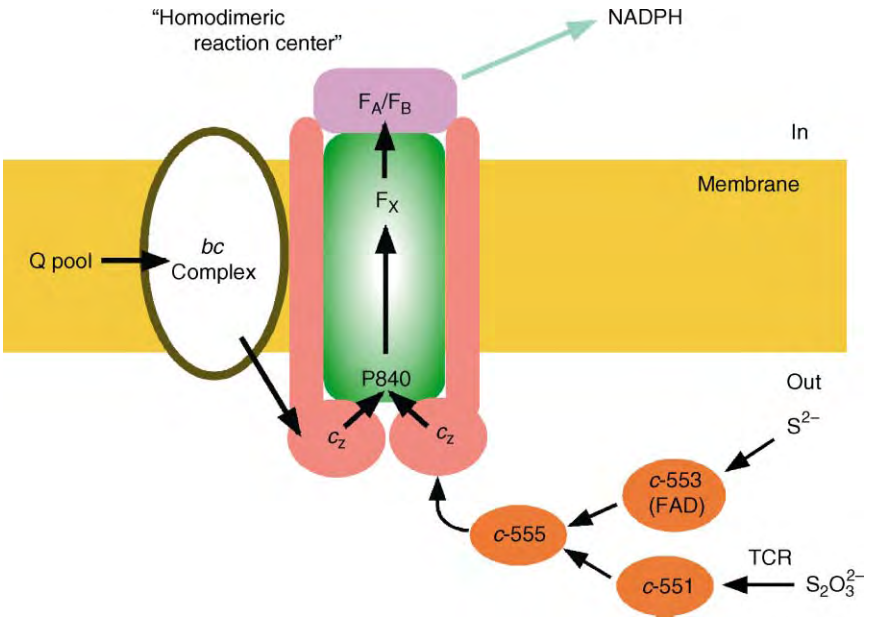

FIGURE 1 Schematic structural model for the reaction center and associated cytochromes involved in electron transport in photosynthetic green sulfur bacteria. Details of the various cytochromes can be found in the text.

well characterized. The cytochromes together make up essential components of the photosynthetic electron transport chain. The pattern described here is similar in most species of green sulfur bacteria.

Cytochrome c_z (PscC)

This cytochrome c_z (PscC) is a monoheme type with a molecular mass of 23 kDa and is tightly bound to the RC complex with putative amino-terminal helices that span the membrane three times. Two molecules of cytochrome c_z are present in one RC complex. Each of them donates an electron to the P840 in a reaction mode with high viscosity dependence. The carboxyl-terminal heme-containing hydrophilic moiety seems to fluctuate on the RC surface and search for an appropriate site for the reaction to proceed. The cytochrome c_z was designated in order to characterize its functional similarity to the membrane-bound cytochrome c_y in *Rhodobacter capsulatus* and mediates the electron transfer between quinol oxidoreductase and P840 RC complex. Although there had been a controversial point concerning the exact α-peak wavelength of the relevant cytochrome *c* that donates an electron directly to P840, its value was found to vary from 553 nm in membranes to 552–551 nm in a solubilized RC complex in the case of *Chl. tepidum*.

Cytochrome *c*-555

This water-soluble cytochrome *c*-555 has a molecular mass of 10 kDa and gives a characteristic asymmetric α-absorption peak, similar to that of algal water-soluble cytochrome c_6 that serves as an electron donor to PSI RC. The cytochrome *c*-555 appears to donate an electron to the membrane-bound cytochrome c_z. Note that the cytochrome in the case of *Chl. tepidum*, to which a locus accession number is CT0075, shows the α-absorption peak at 554 nm.

Cytochrome *c*-553 (Fcc/SoxEF1)

This cytochrome *c*-553 (Fcc/SoxEF1) is a flavo-cytochrome *c* that consists of an 11-kDa cytochrome *c* (FccA/SoxE) plus a 47-kDa flavoprotein (FccB-2/SoxF1) subunits and serves as a sulfide–cytochrome *c* reductase. The flavoprotein subunit contains FAD that is covalently bound to a cysteine residue through a thioether linkage. The electron transfer proceeds as follows: $S^{2-} \rightarrow$ cytochrome *c*-553 (FAD $\rightarrow$ heme *c*-553) $\rightarrow$ cytochrome *c*-555 $\rightarrow$ cytochrome c_z.

Cytochrome *c*-551 (SoxA)

This cytochrome *c*-551 (SoxA) is a dimer of 30-kDa cytochrome *c* and serves as an electron acceptor from a thiosulfate-cytochrome *c* reductase (TCR). Since the pathway is exclusively involved in the oxidation of thiosulfate ($S_2O_3^{2-}$) as a source of reducing power, there is no cytochrome *c*-551 in those green sulfur bacteria that cannot utilize thiosulfate as a reductant. The reduction of cytochrome *c*-555 by a TCR can be accelerated dramatically by the addition of a small amount of cytochrome *c*-551. Furthermore, the reduction of cytochrome *c*-551, itself, can also be accelerated by the

addition of a small amount of cytochrome *c*-555. Cytochrome *c*-555 seems to function as an effector for a TCR.

Cytochrome bc_1 Complex

The cytochrome bc_1 complex is a multisubunit membrane-bound quinone-cytochrome *c* oxidoreductase found in many bacteria and in mitochrondria, where it is also called complex III. It consists of a *b*-type cytochrome, a *c*-type cytochrome, cyt c_1, a Rieske Fe–S protein, and in some cases additional subunits. It oxidizes reduced quinone (quinol) and transfers the electrons to soluble *c*-type cytochromes, at the same time pumping protons across the membrane and creating a protonmotive force that is used to make ATP. The cytochrome bc_1 complex from green sulfur bacteria is not as well characterized as those from other organisms. An unusual aspect of it is that it uses menaquinone, which is lower in redox potential than ubiquinone, which is used in the better-characterized complexes.

Other Cytochromes in Green Sulfur Bacteria

The genome project of *Chl. tepidum* has revealed seven more *c*-type cytochromes (CT0073, CT0188, CT1016, CT1704, CT1734, CT2026, CT2242) whose molecular weights are ~13–17 kDa. *CT1016* has recently been reported to correspond to a *soxX* gene, which is located in the thiosulfate-utilizing genes cluster, although its role is not known at present. Furthermore, one of the residual proteins may be the counterpart of cytochrome c_1 which has not been identified biochemically as yet but is supposed to be present from spectroscopic data.

Cytochromes in Filamentous Anoxygenic Phototrophic Bacteria

The pattern of cytochromes in FAP bacteria is strikingly different from that found in green sulfur bacteria. The only cytochrome that has been characterized in detail is the reaction center associated cytochrome *c*-554.

Cytochrome *c*-554

Cytochrome *c*-554 is a membrane-bound tetraheme cytochrome in which all four of its heme groups have α-band maxima ~554 nm. This cytochrome is the secondary electron donor to the reaction center and bears considerable similarity to the tetraheme cytochrome that is found in many purple photosynthetic bacteria, the best characterized is the tetraheme cytochrome from *Rhodopseudomonas viridis* (recently renamed *Blastochloris viridis)*. The four heme groups in *c*-554 have redox potentials of 0 to +300 mV (versus NHE).

Other Cytochromes in Filamentous Anoxygenic Phototrophic Bacteria

The genomes of FAP bacteria contain other open reading frames that appear to code for *c*-type cytochromes, although none have been characterized. Apparently, there is no cytochrome bc_1 complex present, as indicated both by genetic and biochemical analysis.

See Also the Following Articles

Cytochrome bc_1 Complex (Respiratory Chain Complex III) • Cytochrome *c* • Green Bacteria: The Light-Harvesting Chlorosome • Green Sulfur Bacteria: Reaction Center and Electron Transport • Heme Proteins • Iron–Sulfur Proteins

Glossary

c-type cytochrome A class of cytochromes in which the heme cofactor is covalently attached to the protein via thioether linkages to cysteine amino acid residues.

cytochrome A heme-containing protein that serves as an electron transfer cofactor in biological systems.

Fe-S protein An iron–sulfur protein which holds a [2Fe-2S], [3Fe-4S], or [4Fe-4S]-type cluster and functions as an electron transfer cofactor in biological systems.

flavoprotein A FAD (flavin adenine dinucleotide)-containing protein that serves as an electron transfer cofactor in biological systems.

P840 A special pair of bacteriochlorophyll *a* in green sulfur bacterial RC, which serves as the primary electron donor.

P870 A special pair of bacteriochlorophyll *a* in green nonsulfur bacterial RC, which serves as the primary electron donor.

reaction center (RC) A pigment–protein complex that converts light energy into chemical energy in photosynthetic organisms.

Further Reading

Blankenship, R. E., Madigan, M. T., and Bauer, C. E. (eds.) (1995). *Anoxygenic Photosynthetic Bacteria*. Kluwer Academic, Dordrecht, The Netherlands.

Chen, Z. W., Koh, M., Van Driessche, G., Van Beeumen, J. J., Bartsch, R. G., Meyer, T. E., Cusanovich, M. A., and Mathews, F. S. (1994). The structure of flavocytochrome *c* sulfide dehydrogenase from a purple phototrophic bacterium. *Science* **266**, 430–432.

Dracheva, S., Williams, J. C., Van Driessche, G., Van Beeumen, J. J., and Blankenship, R. E. (1991). The primary structure of cytochrome *c*-554 from the green photosynthetic bacterium *Chloroflexus aurantiacus*. *Biochem.* **30**, 11451–11458.

Eisen, J. A., Nelson, K. E., Paulsen, I. T., Heidelberg, J. F., Wu, M., Dodson, R. J., Deboy, R., Gwinn, M. L., Nelson, W. C., Haft, D. H., Hickey, E. K., Peterson, J. D., Durkin, A. S., Kolonay, J. L., Yang, F., Holt, I., Umayam, L. A., Mason, T., Brenner, M.,

Shea, T. P., Parksey, D., Nierman, W. C., Feldblyum, T. V., Hansen, C. L., Craven, M. B., Radune, D., Vamathevan, J., Khouri, H., White, O., Gruber, T. M., Ketchum, K. A., Venter, J. C., Tettelin, H., Bryant, D. A., and Fraser, C. M. (2002). The complete genome sequence of *Chlorobium tepidum* TLS, a photosynthetic, anaerobic, green-sulfur bacterium. *Proc. Nat'l. Acad. Sci. USA* **99**, 9509–9514.

Hauska, G., Schoedl, T., Remigy, H., and Tsiotis, G. (2001). The reaction center of green sulfur bacteria. *Biochim. Biophys. Acta* **1507**, 260–277.

Oh-oka, H., Iwaki, M., and Itoh, S. (1997). Viscosity dependence of the electron transfer rate from bound cytochrome *c* to P840 in the photosynthetic reaction center of the green sulfur bacterium *Chlorobium tepidum*. *Biochem.* **36**, 9267–9272.

Oh-oka, H., Iwaki, M., and Itoh, S. (1998). Membrane-bound cytochrome c_z couples quinol oxidoreductase to the P840 reaction center complex in isolated membranes of the green sulfur bacterium *Chlorobium tepidum*. *Biochem.* **37**, 12293–12300.

Okkels, J. S., Kjaer, B., Hansson, Ö., Svendsen, I., Møller, B. L., and Scheller, H. V. (1992). A membrane-bound monoheme cytochrome-c_{551} of a novel type is the immediate electron donor to P840 of the *Chlorobium vibrioforme* photosynthetic reaction center complex. *J. Biol. Chem.* **267**, 21139–21145.

Sakurai, H., Kusumoto, N., and Inoue, K. (1996). Function of the reaction center of green sulfur bacteria. *Photochem. Photobiol.* **64**, 5–13.

Yanyushin, M. (2002). Fractionation of cytochromes of phototrophically grown *Chloroflexus aurantiacus*. Is there a cytochrome *bc* complex among them? *FEBS Lett.* **512**, 125–128.

BIOGRAPHY

Hirozo Oh-oka is an Associate Professor of the Department of Biology, the Graduate School of Science at Osaka University in Japan. His research interests are in the area of photosynthetic electron transport systems. He has a Ph.D. from Osaka University.

Robert E. Blankenship is Professor and Chair of the Department of Chemistry and Biochemistry at Arizona State University. His research interests are in the area of photosynthetic energy and electron transfer processes. He has a Ph.D. from the University of California, Berkeley. Dr. Blankenship has been the Editor-in-Chief of the scientific research journal *Photosynthesis Research* and has served as the President of the International Society of Photosynthesis Research.

Green Bacteria: The Light-Harvesting Chlorosome

John M. Olson
University of Massachusetts, Amherst, Massachusetts, USA

Chlorosomes are the main light-harvesting structure of green filamentous bacteria and green sulfur bacteria and are filled with aggregated bacteriochlorophyll (BChl) *c*, *d*, or *e*. BChl *a* is associated with a small protein in the envelope of the chlorosome, whereas the other BChls are organized in rod-like structures located in the interior of the chlorosome and containing little or no protein. Chlorosomes are appressed to the cytoplasmic side of the cytoplasmic membrane and the main path of excitation energy transfer can be written as BChl *c*, *d*, or *e* (chlorosome) → BChl *a* (chlorosome) → BChl *a* (FMO or membrane proteins) → BChl *a* (reaction center).

Chlorosomes are the characteristic light-harvesting complexes of green filamentous bacteria (green non-sulfur bacteria, Chloroflexaceae) and green sulfur bacteria (Chlorobiaceae). Chlorosomes are filled with bacteriochlorophyll (BChl) *c*, *d*, or *e* molecules in a highly aggregated state and are appressed to the cytoplasmic side of the cytoplasmic membrane. BChl *c*, *d*, and *e* form a family of chlorophylls (chlorosome chlorophyll) that contain a hydroxyethyl group at position 3 as shown in Figure 1. The main esterifying alcohol is farnesol in green sulfur bacteria and stearol in filamentous bacteria, which contain only BChl *c*. In some green sulfur bacteria there are at least four chemically distinct homologues of BChl *c* that differ in the degree of alkylation on the chlorin ring at positions 8 and 12 (see Figure 1 and Table I). In addition to chlorosome chlorophyll all chlorosomes contain a small amount of BChl *a*, the same chlorophyll found in proteobacteria (purple bacteria). BChl *a* is associated with a small protein in the envelope of the chlorosome, whereas chlorosome chlorophyll is located in the interior and is organized in rod-like structures containing little or no protein.

Phylogeny

From a phylogenetic viewpoint green filamentous bacteria and green sulfur bacteria are two distinct groups based on 16S rRNA, reaction center (RC) type, and physiology. Green filamentous bacteria contain a quinone-type RC similar to that found in proteobacteria and also similar to the RC of photosystem II in cyanobacteria and plant chloroplasts. Green sulfur bacteria contain an iron–sulfur-type RC similar to those found in heliobacteria and in photosystem I of cyanobacteria and chloroplasts. The filamentous bacteria live either as facultative photoautotrophs or as respiring chemoheterotrophs. They are found mostly in hot springs, often in mixed populations with cyanobacteria. The sulfur bacteria are obligate photoautotrophs and strict anaerobes that grow in dim light in sulfide-rich environments such as effluents of sulfur springs and the lower layers of stratified lakes and in marine habitats. In one extreme case, green sulfur bacteria have been found at a depth of 80 m in the Black Sea.

Structural Features

Size and Internal Structure

Chlorosomes are mostly made up of chlorophyll, but lipid, protein, carotenoid, and quinone are also present. Typically the chlorosomes from *filamentous* bacteria (designated F-chlorosomes) are ~100 nm long, 20–40 nm wide and 10–20 nm high. Chlorosomes from *sulfur* bacteria (designated S-chlorosomes) are considerably larger with lengths 70–260 nm and widths 30–100 nm. All chlorosomes consist of a core and a 2–3 nm envelope as shown in Figure 2. The core consists of rod elements made up of aggregated chlorosome chlorophyll, while the envelope is a monolayer of mostly galactolipid and some protein. Each chlorosome may contain 10–30 rod elements. The rod elements of S-chlorosomes are 10 nm in diameter, whereas those of F-chlorosomes are only 5.2–6 nm. The envelopes of both F- and S-chlorosomes contain BChl *a* associated with a specific protein, CsmA. The molar ratio of chlorosome chlorophyll to BChl *a* in S-chlorosomes is ~90/1, whereas in F-chlorosomes it is ~25/1.

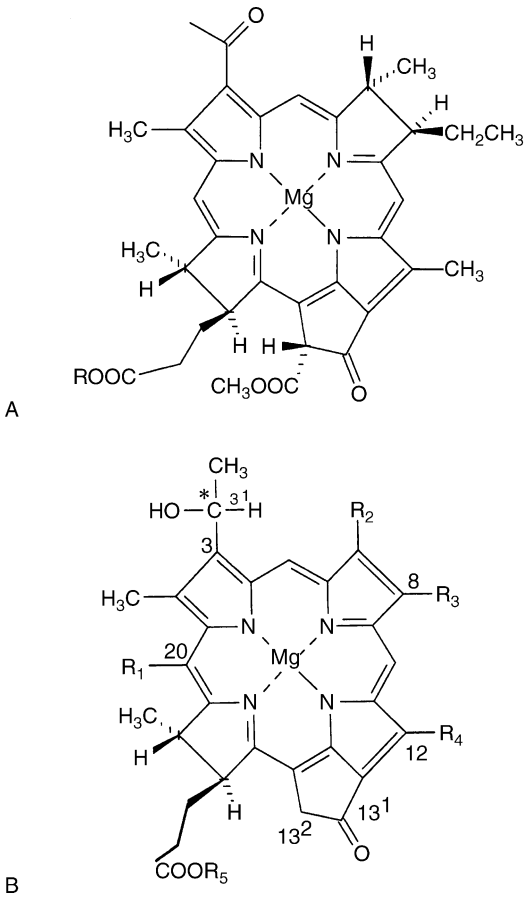

FIGURE 1 Structures of (A) BChl *a* and (B) the chlorosome chlorophylls (BChl *c*, *d*, and *e*). For BChl *a* R = phytyl. See Table I for details about the chlorosome chlorophylls.

Proteins

In highly purified S-chlorosomes the mass ratio of protein to chlorophyll is very low—only 0.5 compared to 6.3 for the Fenna–Matthews–Olson (FMO) BChl a protein found in green sulfur bacteria. The proteins of chlorosomes are localized in the envelope. In F-chlorosomes these proteins are called CsmA, CsmM, and CsmN. In S-chlorosomes they are called CsmA, CsmB, CsmC, CsmD, and CsmE. The major component in both kinds of chlorosomes is CsmA with a molecular mass of 5.7 kDa in F-chlorosomes and 6.3 kDa in S-chlorosomes. This protein binds BChl *a* in both kinds of chlorosomes, and the BChl *a*–CsmA complexes are thought to be concentrated in a "baseplate" that is in contact with BChl *a* proteins associated with the cytoplasmic membrane. Some chlorosome proteins may be responsible for maintaining the native shape.

TABLE I

Ring Substituents Found on Chlorosome Chlorophylls (see Figure 1)

Chlorophyll	R_1	R_2	R_3	R_4	R_5
BChl *c* (F-chlorosomes)	Methyl	Methyl	Ethyl	Methyl	Stearyl (mostly)
BChl *c* (S-chlorosomes)	Methyl	Methyl	Ethyl *n*-Propyl Isobutyl	Methyl Ethyl	Farnesyl (mostly)
BChl *d* (S-chlorosomes)	H	Methyl	Ethyl *n*-Propyl Isobutyl	Methyl Ethyl	Farnesyl (mostly)
BChl *e* (S-chlorosomes)	Methyl	Formyl	Ethyl *n*-Propyl Isobutyl	Ethyl	Farnesyl (mostly)

Carotenoids

All chlorosomes contain carotenoids which function as light-harvesting pigments and triplet-state quenchers.

Spectral Properties

In Figure 3 the absorbance and fluorescence emission spectra of F-chlorosomes indicate the presence of a large amount of BChl *c*, a small amount of BChl *a*, and energy transfer from BChl *c* to BChl *a*. The absorbance and fluorescence peaks at 740 and 750 nm respectively belong to BChl *c*, while the peaks at 795 and 801 nm belong to BChl *a*. The circular dichroism (CD) spectrum (not shown) demonstrates a strong excitonic interaction among the BChl *c* molecules. All these properties of BChl *c* in both F- and S-chlorosomes are completely different from those of monomeric BChl *c* dissolved in polar solvents. Monomeric BChl *c* has absorption and fluorescence peaks at ~660 and 665 nm, and a CD spectrum with a very small negative peak at 660 nm. Pure BChl *c* forms aggregates in dried films or when dissolved in non-polar solvents such as hexane and carbon tetrachloride. The spectral properties of these aggregates are similar to those of chlorosomes and suggest that in chlorosomes BChl *c* exists in an aggregated state. The absence of proteins from the aggregates *in vitro* supports the idea that BChl *c* does not require protein to form aggregates in the chlorosome.

Models of Chlorophyll Organization

Although it is not yet possible to present a definitive structure for the chlorophyll aggregates in the chlorosome, several characteristics have been established:

1. The aggregates of chlorosome chlorophyll (BChl *c*, *d*, or *e*) are the result of chlorophyll–chlorophyll interactions. The molecules are close together and oriented so as to give a strong excitonic interaction.

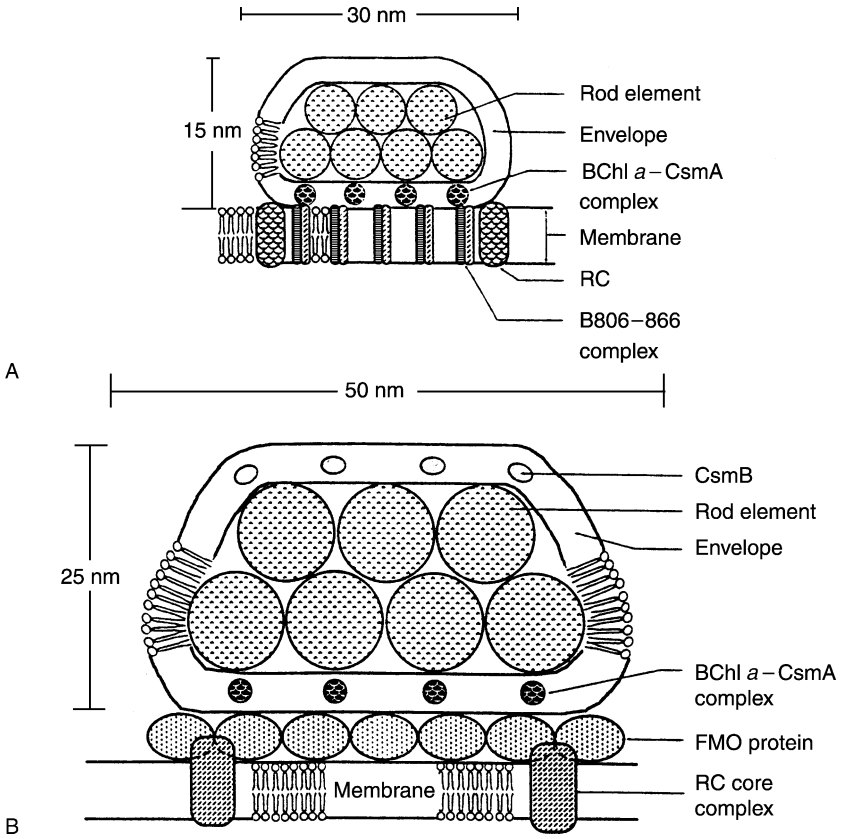

FIGURE 2 Cross-sectional views of antenna system models for (A) green filamentous bacteria and (B) green sulfur bacteria. Relatively small chlorosomes are shown in both cases. Adapted from Olson, J. M. (1998). Chlorophyll organization and function in green photosynthetic bacteria. *Photochem. Photobiol.* **67**, 61–75 with permission from the American Society for Photobiology.

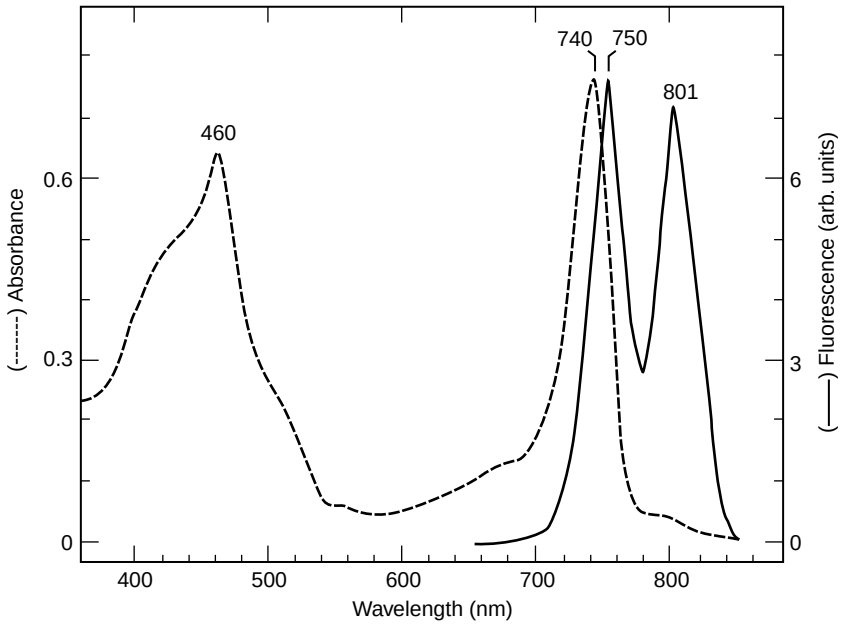

FIGURE 3 Absorption and fluorescence emission spectra of F-chlorosomes. Fluorescence was excited at 460 nm. Adapted from Brune *et al.* (1990). *Photosynth. Res.* **24**, 253–263 with permission of Kluwer Academic Publishers.

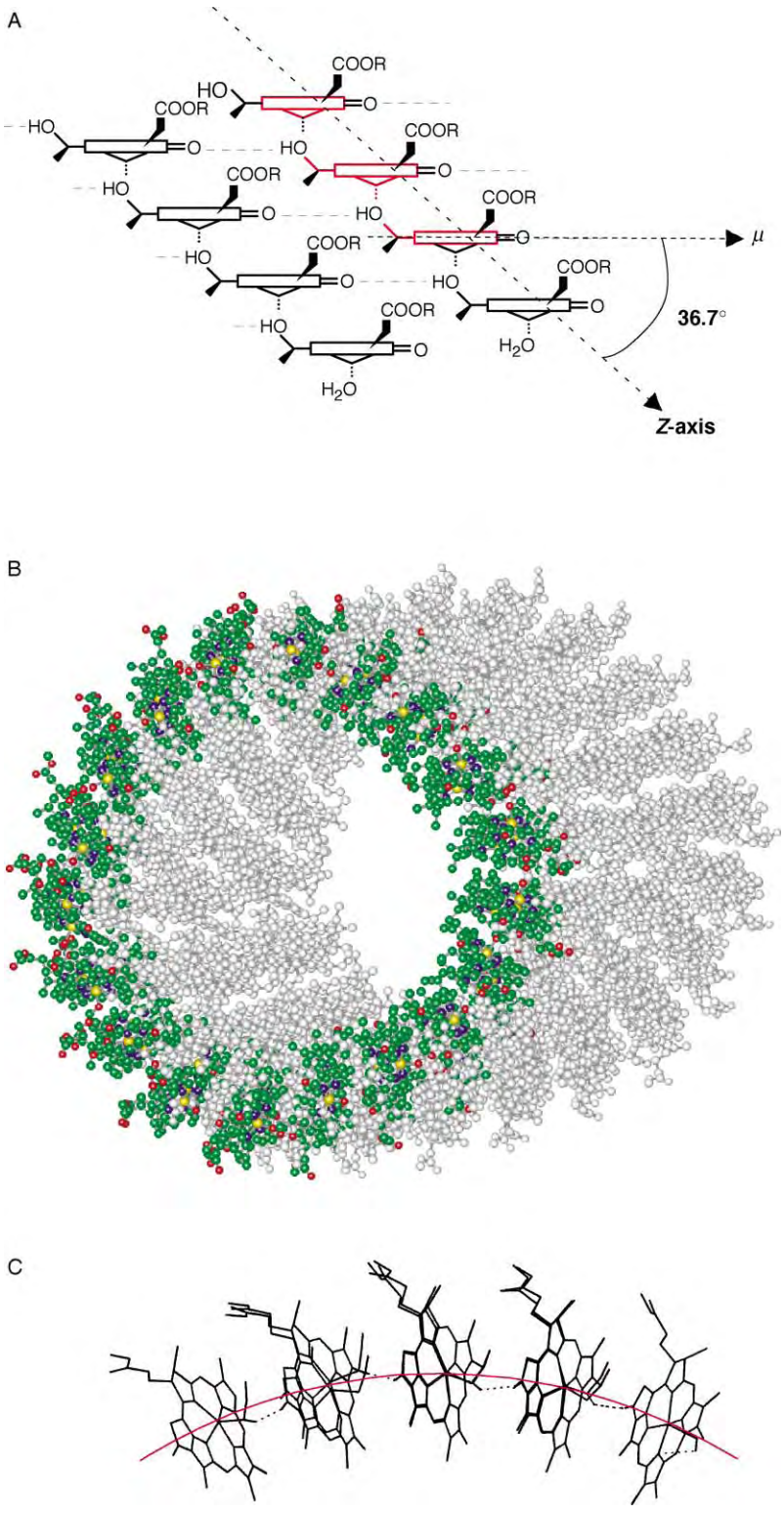

FIGURE 4 (A) The arrangement of chlorosome chlorophylls in a stack. The dashed *Z*-axis connects the Mg atoms of the chlorophylls in a single stack. (B) Space view of the tubular chlorophyll aggregate obtained by molecular modeling. The farnsyl groups, pointing to the outside of the rod, are not shown. (C) Arrangement of chlorophyll molecules at the outside edge of the chlorosome. Reproduced from Prokhorenko, V. I., Steensgaard, D. B., and Holzwarth, A. R. (2000). Exciton dynamics in the chlorosomal antennae of the green bacteria *Chloroflexus aurantiacus* and *Chlorobium tepidum*. *Biophys. J.* **79**, 2105–2120 with permission of the Biophysical Society.

2. The chlorophyll molecules also exhibit long-range order with their Q_y transitions parallel to the long axis of the chlorosome.

3. The 13^1-carbonyl of each chlorophyll molecule interacts with a functional group on another chlorophyll molecule.

4. The 3^1-hydroxyethyl group is coordinated directly to a Mg atom in a second chlorophyll molecule and is H-bonded to the 13^1-carbonyl of a third chlorophyll molecule.

5. Essentially all the Mg atoms in the chlorophyll molecules are five-coordinate.

Using computer modeling, Prokhorenko, Steensgaard, and Holzwarth (2000) have developed the useful model of chlorophyll organization shown in Figure 4. The large-scale structure is a tube with a diameter of 4.6 nm (with respect to Mg atoms), corresponding to the diameter of the rod elements in F-chlorosomes. The chlorophyll macrocycles are perpendicular to the surface of the tube, and the hydrocarbon tails (not shown) are oriented toward the outside of the tube.

Energy Transfer

The overall pathway of excitation energy transfer upon irradiation of filamentous bacteria with red or far-red light can be written as follows:

BChl *c* (chlorosome) → BChl *a* (chlorosome)
→ BChl *a* (membrane proteins) → BChl*a* (RC)

The membrane proteins are labeled B806–866 in Figure 2A. In sulfur bacteria the FMO protein replaces the membrane proteins as shown in Figure 2B. Energy transfer between chlorosome chlorophyll molecules takes place by a relatively fast exchange mechanism, while energy transfer between chlorosome chlorophyll and BChl *a* in the chlorosome takes place by a relatively slow Förster mechanism. The chlorosome light-harvesting system is an example of an energy funnel in which each successive pigment pool has progressively red-shifted absorption and fluorescence emission spectra. The descending energy levels thus provide an excitation gradient into the RC.

Energy transfer in the green sulfur bacteria is regulated by the redox potential *in vivo*. Under oxidizing conditions the overall energy transfer efficiency drops from ~100% to 10% or less. Redox titration of fluorescence in isolated chlorosomes gives a midpoint potential of −146 mV at pH 7.0. (This regulation is mediated by the quinone in the chlorosomes.) The formation of flourescence quenchers at high redox potentials may protect the bacteria from lethal photo-oxidation reactions such as superoxide formation resulting from the reduction of ferredoxin in the presence of oxygen. These redox effects are largely missing from the green filamentous bacteria, whose RCs do not reduce ferredoxin.

Evolutionary Considerations

The presence of chlorosomes in both green filamentous bacteria and green sulfur bacteria is the only justification for lumping them together as green bacteria. Although the two types of chlorosomes (F and S) show differences in size and rod element morphology, the organization of the chlorosome chlorophylls appears to be basically similar, and the *csmA*/CsmA genes and proteins appear to be homologous. This suggests the F- and S- chlorosomes are descended from a common ancestor coded for by an ancestral "genome" containing the *csmA* gene.

See Also the Following Articles

Chlorophylls and Carotenoids • Green Bacteria: Secondary Electron Donor (Cytochromes) • Green Sulfur Bacteria: Reaction Center and Electron Transport • Photosynthesis • Photosynthetic Carbon Dioxide Fixation

Glossary

chemoheterotroph An organism that requires organic compounds and a chemical source of energy.

excitonic interaction An interaction in which the excited state is shared by more than one molecule.

Förster energy transfer Nonradiative resonance transfer.

heliobacteria Photosynthetic bacteria that contain BChl *g* and an iron–sulfur-type RC similar to those found in green sulfur bacteria and photosytem I of cyanobacteria and chloroplasts.

homologue A molecule that is identical to another molecule except for one substituent.

photoautotroph An organism that requires light and inorganic carbon.

proteobacteria A subgroup of Gram-negative bacteria that includes purple photosynthetic bacteria.

Further Reading

Blankenship, R. E., and Matsuura, K. (2003). Antenna complexes from green photosynthetic bacteria. In *Light-Harvesting Antennas* (B. R. Green and W. W. Parsons, eds.), pp. 195–217. Kluwer, Dordrecht.

Blankenship, R. E., Olson, J. M., and Miller, M. (1995). Antenna complexes from green photosynthetic bacteria. In *Anoxygenic Photosynthetic Bacteria* (R. E. Blankenship, M. T. Madigan and C. E. Bauer, eds.) pp. 399–435. Kluwer, Dordrecht.

Ke, B. (2000). The green bacteria: I. The light-harvesting complex, the chlorosomes. In *Photosynthesis: Photochemistry and Photobiophysics*, pp. 147–158. Kluwer, Dordrecht.

Oelze, J., and Golecki, J. R. (1995). Membranes and chlorosomes of green bacteria. In *Anoxygenic Photosynthetic Bacteria* (R. E. Blankenship, M. T. Madigan and C. E. Bauer, eds.) pp. 259–278. Kluwer, Dordrecht.

Olson, J. M. (1998). Chlorophyll organization and function in green photosynthetic bacteria. *Photochem. Photobiol.* **67**, 61–75.

Prokhorenko, V. I., Steensgaard, D. B., and Holzwarth, A. R. (2000). Exciton dynamics in the chlorosomal antennae of the green bacteria *Chloroflexus aurantiacus* and *Chlorobium tepidum*. *Biophys. J.* **79**, 2105–2120.

Biography

John M. Olson is adjunct Professor of Biochemistry and Molecular Biology at the University of Massachusetts. He retired in 1994 after 12 years as Professor of Photosynthesis at Odense University in Denmark. His main research interest over the last 40 years has been the function of chlorophyll in green sulfur bacteria, and in 1962 he discovered the Fenna–Matthews–Olson BChl *a* protein, the first chlorophyll protein to have its structure determined by X-ray diffraction. He has also written several articles on the evolution of photosynthesis.

Green Sulfur Bacteria: Reaction Center and Electron Transport

Günter A. Hauska and Thomas Schödl
Universität Regensburg, Regensburg, Germany

Green bacteria comprise two distant taxonomic groups, the green sulfur bacteria (GSB) – *Chlorobiaceae*, and the filamentous green "nonsulfur" bacteria – *Chloroflexaceae*. Both are photosynthetic taxa, which are exceptional in two ways. They share a most efficient light capturing apparatus, the chlorosomes, and they do not assimilate CO_2 via ribulose-bisphosphate carboxylase (Rubisco) and the Calvin cycle. GSB use the reductive tricarboxylic acid cycle (TCA), while *Chloroflexaceae* carboxylate acetyl CoA, employing a vitamin B_{12}-dependent pathway via methyl malonate. Otherwise the two groups have little in common. The reaction center (RC) of *Chloroflexaceae* is of the Q-type, closely related to the RCs found in the purple bacteria *Rhodospirillaceae* and in plant PSII, the RC of *Chlorobiaceae* is of the FeS-type and represents a simplified version of the PSI-RC in plants. Instead of a heterodimeric core with two similar, but different proteins, it is homodimeric built from two identical proteins. The only other photosynthetic taxon with such a simple FeS-type RC are the gram-positive *Heliobacteria*. All other phototrophic organisms contain heterodimeric RCs. The recent annotation of the complete genome of *Chlorobium tepidum* further documents the peculiarities of GSB, and this article will focus on them.

Light Capture

Chlorosomes

Chlorosomes were first reported by Cohen-Bazire *et al.* in 1964 as organelles attached to the inner surface of the cytoplasmic membrane of green sulfur bacteria (GSB). They are surrounded by a lipid–protein monolayer, and contain thousands of bacteriochlorophylls *c*, *d*, or *e*, depending on the bacterial species, stacked in tubular arrangement (Figure 1). Among photosynthetic organisms only the green bacteria, *Chlorobiaceae* and *Chloroflexaceae*, process this special organization of light-harvesting antennae which is responsible for efficient absorption in dim light. *Heliobacteria*, which live closer to the water surface, lack chlorosomes. Monomeric bacteriochlorophyll (BChl) *c*, *d*, and *e* absorb at 660–670 nm, but the stacking of the tetrapyrrol rings shifts the absorption to 720–750 nm. The excitation energy in these stacks is transferred via Bchl *a*-species in the baseplate and in the FMO protein absorbing around 800 nm, finally to the reaction center (RC) in the membrane. This energy transfer is quenched under aerobic conditions preventing damage by oxygen. This redox control may be mediated by chlorobiumquinone (1′-oxomenaquinone-7) and FeS centers of proteins, which are present in the chlorosome envelope (Csm proteins). The chlorosomes also contain carotenoids which participate in energy transfer and protection from photodamage.

The FMO Protein

This chlorophyll protein was the first to be crystallized and structurally resolved to atomic resolution in 1979, lending itself to detailed laser spectroscopic studies. It is a water-soluble, trimeric protein with seven BChl *a* molecules per 40 kDa monomer, which is largely of β-sheet structure. The seven BChl *a* molecules can be distinguished by low-temperature spectroscopy. FMO is located on the cytoplasmic surface of the cell membrane in *Chlorobiaceae*, between the chlorosomes and the RC (Figure 1). It is absent from *Chloroflexaceae*. Energy transfer from the FMO protein to the RC also is under redox control, as is the one from the chlorosomes; however, even under anaerobic conditions it has been found to be surprisingly low in isolated membranes. However, a new crystal structure for the FMO, which was obtained from isolated RC, reveals the presence of an eighth chlorophyll per monomer, which may bridge the gap to the RC *in vivo* (see Figure 2C).

The Homodimeric P840-Reaction Center — Composition, Structure, and Electron Transfer

Energy transfer to the RC of GSB leads to charge separation in the RC, across the membrane. The formation

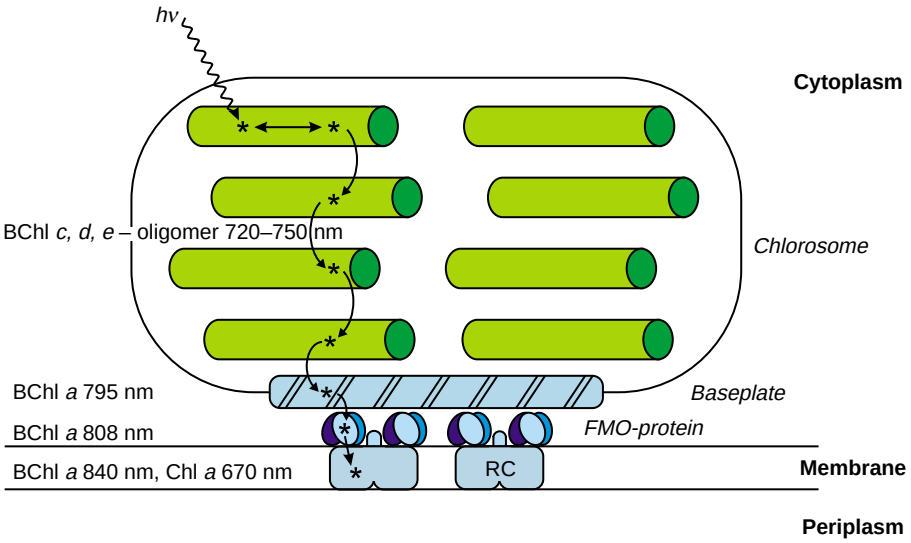

FIGURE 1 Excitation transfer in green sulfur bacteria. Numbers following the designations of the pigments indicate the wavelengths of the absorption maxima.

of P840* results in bleaching at 840 nm. A functionally competent P840-RC, free of chlorosomes, can be isolated from the membranes of various GSB species with the help of detergents, with and without retention of FMO trimers. The core of the P840-RC consists of four subunits. A large hydrophobic PscA protein (82 kDa) which is homologous to the subunits PsaA and PsaB of the FeS-type P700-RC in PSI of plants and cyanobacteria. It contains 11 putative transmembrane helices like these, binds all pigments and four redox centers (see Figure 3). These are (1) the primary electron donor P840, an electronically coupled, special pair of Bchl *a* molecules ($E_0' = 240$ mV), (2) the primary acceptor A_0, a pair of chlorophyll (Chl) *a* molecules, (3) the secondary electron acceptor A_1 which is menaquinone-7, and (4) F_X, the first of three

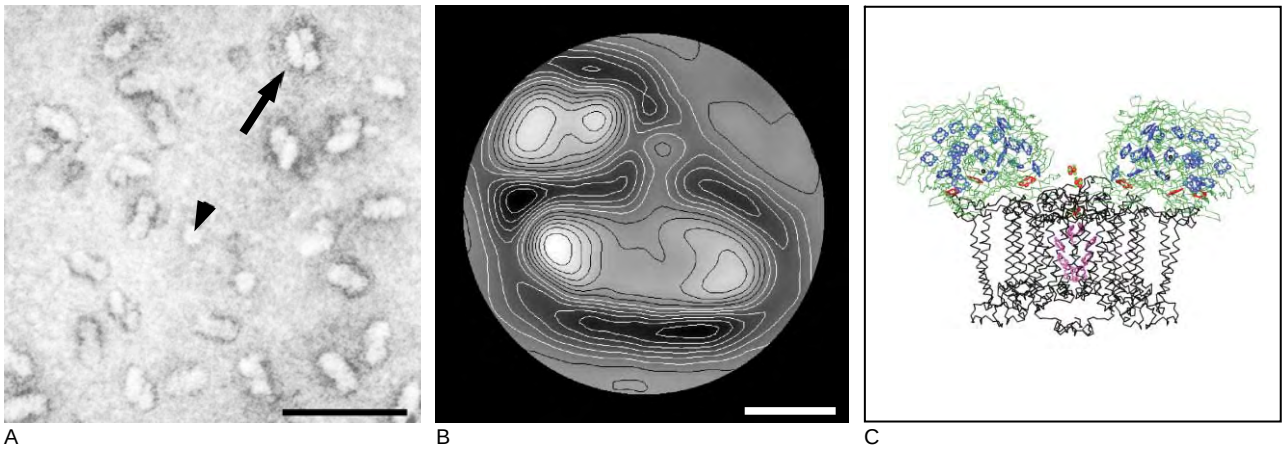

FIGURE 2 Structural representations of the FMO/P840-RC complex. Parts (A) and (B) are taken from Remigy, H-W., Hauska, G., Müller, S.A., and Tsiotis, G. (2002). The reaction center from green sulfur bacteria: Progress towards structural elucidation. *Photosynth. Res.* **71**, 91–98; (A) is a scanning transmission electron micrograph of the particle mixture, with free FMO trimers (arrowhead), P840-RC with two bound FMO trimers (arrow), a dominant proportion of RCs with one FMO trimer and some RCs without FMO; the bar represents 20 nm. Part (B) shows a projection of the RC with one bound FMO trimer in side view after imaging; the bar represents 5 nm. Part (C) is taken from Ben-Shem, A. *et al.* (2004). Evolution of photosystem I – from symmetry to pseudosymmetry to asymmetry. *FEBS lett.*, **564**(3): 274–80, and presents a high-resolution structural model for the P840-RC with two bound FMO trimers; The homodimeric core was constructed from two PsaB proteins from the RC of PSI, showing the Cα-backbone with the 22 transmembrane helices in black; the six Chl *a* molecules forming P700 and A_0, plus the two A_1-phylloquinones are depicted in magenta, and the three cubic 4Fe4S centers F_X, F_B, and F_A are printed in red for the irons and in green for the sulfurs; the Cα-backbone of PsaB protein, which carries F_B and F_A, is left out. The folding of the Cα-backbone of the two FMO trimers is printed in green with the 3×7 BChl *a* originally identified in blue, and the three newly detected chlorophylls, one per FMO protein in red (courtesy Adam Ben-Shem).

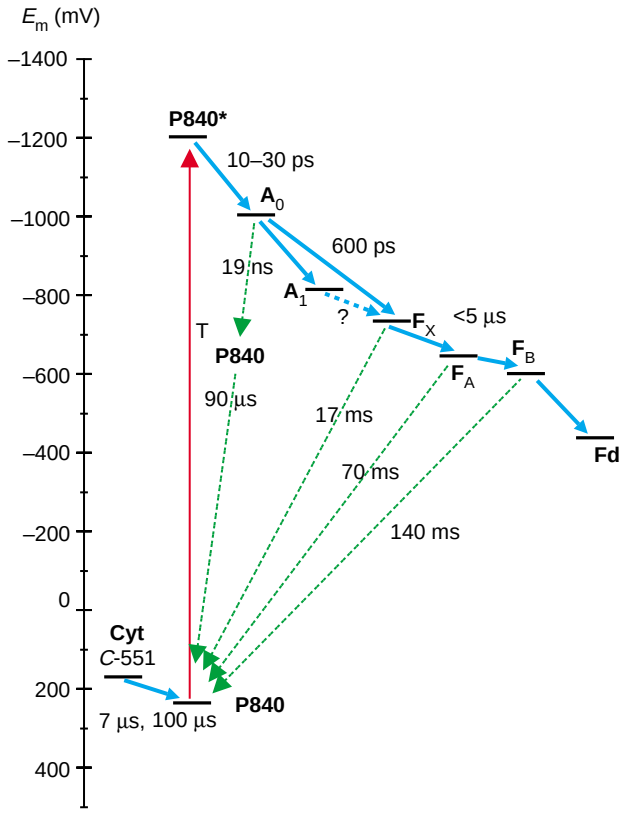

FIGURE 3 Electron transfer within the P840 reaction center in the redox potential diagram. The rates are given for isolated RCs at RT; abbreviations are explained in the text.

4Fe4S centers. In PSI these four redox centers are bound to the heterodimer PsaA/PsaB in pseudosymmetric arrangement across the membrane. P700 and F_X are bound between PsaA and PsaB, each contributing half of the ligand residues, while A_0 and A_1 – a phylloquinone in PSI – occur as a double set in the two subunits. The second subunit in the P840-RC is the FeS protein PscB (24 kDa), which resembles PsaC from PSI, carrying F_A and F_B, the two terminal 4Fe4S centers that reduce ferredoxin. The third subunit PscC is the secondary electron donor cyt *c*-551 (23 kDa, +180 mV), and the fourth is PscD (15 kDa), which lacks a redox center. The gene for PscA is associated with the gene for PscB in a transcription unit and occurs only once in the genome of *C. tepidum*. Therefore, since by analogy to PsaA/PsaB of PSI, PscA contributes only half of the binding sites for P840 and F_X, the core of the P840-RC in GSB must be a homodimer, probably with strictly symmetric transmembrane arrangement of the redox centers, as depicted in Figure 4. A similar argumentation led to the conclusion that the P798-RC of *Heliobacteria* is homodimeric in structure. This reaction center may even be simpler, because an equivalent for PscB, with the two peripheral FeS centers escaped detection so far.

A preparation of the RC core only consisting of PscA and PscB, but fully functional in charge separation has been isolated from *Prostecochloris aestuarii*. Its spectra at RT and at low temperature in the visible region are shown in Figure 5, as well as those of the RC core of *C. tepidum*, which retains cyt *c*-551 (see the small peak at 551 nm in Figure 5 B and D, marked by an arrow). The P840-RC is much less pigmented than the P700-RC of PSI. Per RC monomer only eight BChl *a* molecules are present. Their absorptions between 780 and 840 nm are resolved into distinct bands at low temperature. In addition, two Chl *a* molecules are present which absorb at 670 nm (second arrow in Figure 5). It is noteworthy that while the primary electron donor P840 is built by two BChl *a* molecules the primary electron acceptor A_0 consists of Chl *a*. Unlike the P700-RC, in which both are formed by Chl *a*, the P840-RC allows for photoselection of A_0. Also in *Heliobacteria*, A_0 is a derivative of Chl *a*, while the bulk of the pigments is BChl *g*, and the occurrence of Chl *a*-types as the primary acceptors in these two taxa with "primitive" homodimeric RCs is intriguing with respect to the evolution of the chlorophyll pigments.

The photosynthetic unit in *C. tepidum* comprises 16 BChl *a*, 4 Chl *a* molecules and 1 carotenoid in the P840-RC, 48 BChl *a* in the 2 FMO-trimers, and ~2000 BChl *c*, carotenoids, and some additional BChl *a* in the chlorosomes.

A_1-menaquinone-7 is more loosely bound in the P840-RC than A_1-phylloquinone in PS1, and may actually not be an obligatory intermediate in the electron transfer, but rather on a side path, in exchange with free menaquinone-7 in the membrane (see Figures 3 and 4). In accordance with looser binding the hydrophilic dipeptide SR in PscA replaces YW in the quinone-binding pockets of PsaA and PsaB, oriented toward the inner surface of the cytoplasmic membrane, after transmembrane helix 10.

A scanning transmission electromicrograph of P840-RC preparation from *C. tepidum* is shown in Figure 2A which predominantly consists of particles with RC cores bound to one FMO trimer. A side projection of this structure after imaging is shown in Figure 2B. The preparation depicted in Figure 2A also contains free FMO trimers (arrowhead) and occasionally particles with two trimers are seen (arrow). This structure, which probably represents the *in vivo* organization in the membrane, has been modeled recently by Ben-Shem *et al.*, as shown in Figure 2C. In this model the new structure for the FMO trimer with the additional chlorophylls in red is combined with a homodimer constructed from two PsaB subunits of the P700-RC in PS1.

An energy diagram of the charge transfer steps in the P840-RC, with approximate life times, and including recombination reactions is presented in Figure 3,

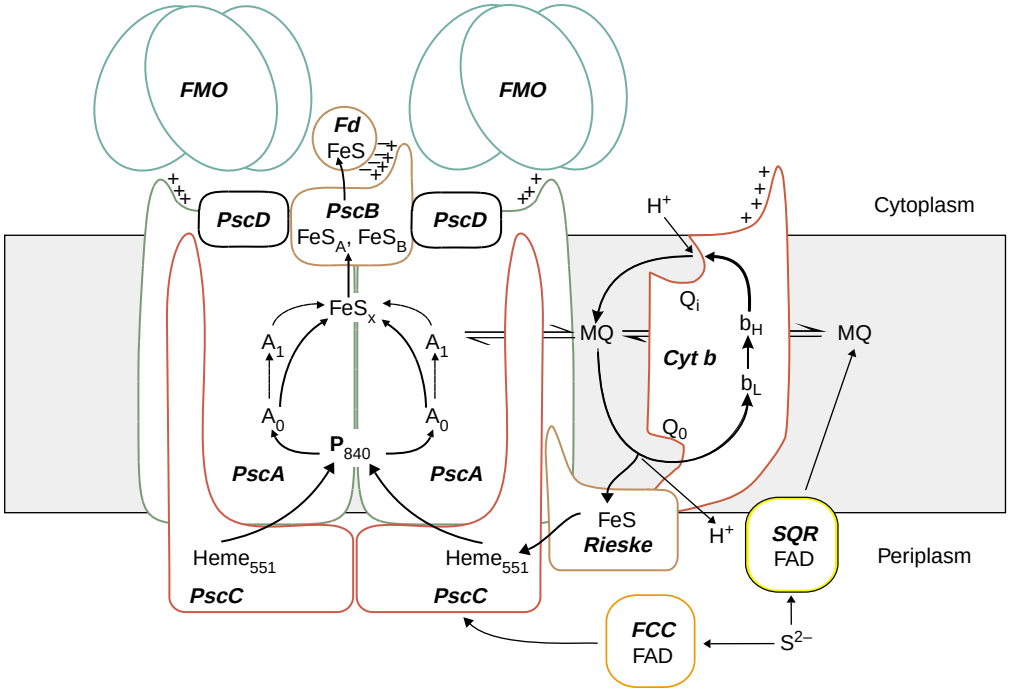

FIGURE 4 Membrane topography of the P840 reaction center and other electron transport components in green sulfur bacteria. The abbreviations are explained in the text; positively charged parts of the proteins PscA, PscB and cyt *b*, detected in the corresponding genes and exposed to the cytoplasmic surface are indicated; MQ stands for menaquinone; b_H and b_L denote high potential and low potential heme *b*, respectively.

which is similar to the scheme for the RC of PSI, but shows some quantitative differences. In particular, electron transfer from A_0 to the first FeS center F_X is 20–300 times faster in the P840-RC, which may reflect a shorter distance, and also the loser binding of A_1.

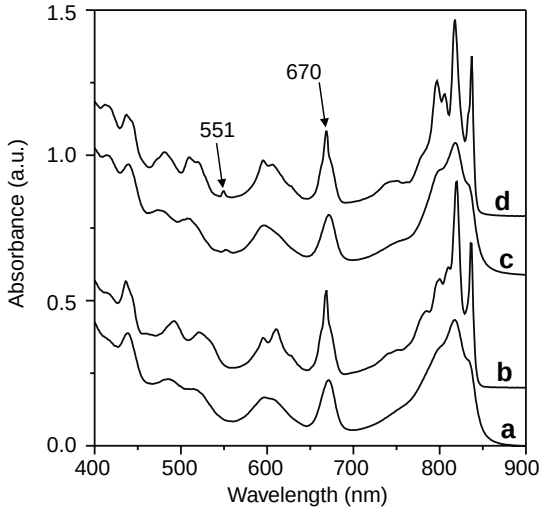

FIGURE 5 Absorption spectra of reaction center cores from green sulfur bacteria. The figure is a modified version of Figure 3 from Permentier, H. P., Schmidt, K.A., Kobayashi, M., Akiyama, M. Hager-Braun, C., Neerken, S., Miller, M., and Amesz, J. (2000). Composition and optical properties of the recation centre complexes from the bgreen ulfue bacteria *Prosteocochloris aestuarii* and *Chlorobium tepidum*. *Photosynth. Res.* **64**, 27–39, and shows the spectra at RT and at 6 K for *Prostecochloris aestuarii* (a,b) and *Chlorobium tepidum* (c,d); the arrows indicate absorption peaks of cyt *c*-551 and of the primary acceptor A_0, which is Chl *a* (670 nm).

Secondary Electron Donors and Acceptors

Figure 4 presents a scheme for the topographical arrangement of the homodimeric P840-RC in the membrane of GSB, together with prominent other components of electron transport (ET) from sulfide to ferredoxin. Electrons from sulfide enter the system at the periplasmic side in two ways, either via sulfide-quinone reductase (SQR) into the menaquinone pool of the membrane, or are transferred by flavocytochrome *c* (FCC) to cyt *c*-551. SQR and the flavoprotein moiety of FCC belong to the phylogenetic family of disulfide oxidoreductases, together with glutathion reductase and lipoamide dehydrogenase. The path via SQR is coupled to ATP formation, because menaquinol oxidation by the Rieske FeS center of the cyt *bc* complex, in the so-called Q-cycle translocates protons, and the resulting proton gradient drives an ATP synthase. The bifurcation of electron transport during the Q-cycle, at the site of quinol oxidation Qo manifests itself as "oxidant-induced reduction" of cyt *b*, which has been observed in membranes of *Chlorobium*. Among the family of the quinol oxidizing cyt *bc* complexes the one in GSB is interesting in two ways. The menaquinol oxidizing

2Fe2S cluster of the Rieske protein has a lowered redox potential (+150 mV), and the cyt *b* shows a mixture of the characteristics for the mitochondrial cyt bc_1 and the plastidal cyt b_6f complexes.

Multiple genes for soluble ferredoxins, six for 2(4Fe4S) and two for 2Fe2S–proteins, have been identified in the genome of *C. tepidum*. Three of the 2(4Fe4S)-types are reducible by PscB in isolated P840-RC (Figure 4), and two of them are involved in CO_2 fixation in the reductive TCA cycle. One of them reduces $NAD(P)^+$ via a ferredoxin-$NAD(P)^+$ reductase (FNR), which is not related to FNR from plants, but to thioredoxin reductase.

Further Genes For Electron Transport Components

The complete sequence of the genome from *C. tepidum* revealed many more genes for ET components, some of them unexpected and several of them in multiple forms, for which physiological functions have been documented only in part so far. The rest will have to be identified by deletion studies. Noteworthy, several of the genes document a closer relation of the GSB to cyanobacteria and plants than to other bacteria.

Next to the eight genes for ferredoxins mentioned above, three for rubredoxins are present. Together with an uptake Ni–Fe hydrogenase they may be involved in using hydrogen for photoautotrophic growth. An operon of 11 genes codes for subunits of a type-1 NADH dehydrogenase. Since the further genes are lacking, it may be linked to this Ni–Fe hydrogenase, or may be involved in cyclic ET around the RC, and not to NADH oxidation. The presence of on CydABCD operon for a cyt *bd* quinol oxidase came as a surprise. It may provide yet another mechanism for protection from oxygen damage, together with superoxide dismutase and other enzymes dealing with oxygen radicals. The genes necessary for nitrogen fixation, and for sulfur metabolism in addition to sulfide oxidation are also found. Interestingly, although CO_2 is fixed by the reductive TCA cycle, a gene related to Ribulose bisphosphate carboxylase/oxygenase (Rubisco) is present. Its expression product is not active as Rubisco, however, but is somehow participating in sulfur metabolism. This may be a hint toward the evolution of CO_2 fixation by the Calvin cycle.

See Also the Following Articles

Cytochrome bc_1 Complex (Respiratory Chain Complex III) • Ferredoxin • Ferredoxin-$NADP^+$ Reductase • Green Bacteria: Secondary Electron Donor (Cytochromes) • Green Bacteria: The Light-Harvesting Chlorosome

Glossary

energy transfer The transfer of the excitation energy among pigment molecules by the Förster–Dexter mechanism.

FMO protein The water soluble BChl *a* protein occurring in GSB, characterized by Fenna, Mathews, and Olson; it was the first chlorophyll protein elucidated by X-ray crystallography.

photosynthetic unit The total of pigment molecules associated with one reaction center, and is synonymous to "photosystem."

Q-type and FeS-type RCs RCs are distinguished according to their terminal electron acceptors, which are either quinones or FeS clusters; since the RCs of plant PSI is of the FeS-type and of PSII is of the Q-type, the synonymous denotations type-1 and type-2 are also in use.

Further Reading

Ben-Shem, A. *et al.* (2004). Evolution of photosystem I – from symmetry to pseudosymmetry to asymmetry. *FEBS lett.*, **564**(3): 274–280.

Blankenship, R. E., Madigan, M. T., and Bauer, C. E. (eds.) (1995). *Advances in Photosynthesis*, *Vol 2*, *Anoxygenic Photosynthetic Bacteria*. Kluwer Academic, Dordrecht, The Netherlands.

Bryant, D. A. (1994). Gene nomenclature recommendations for green photosynthetic bacteria and heliobacteria. *Photosynth. Res.* **41**, 27–28.

Friegaard, N.-U., Chew, A.G.M., Li, H., Maresca, J.A., and Bryant, D.A. (2003). *Chlorobium tepidum*: Insights into the structure, physiology, and metabolism of a green sulfur bacterium derived from the complete genome sequence. *Photosynth. Res.* **78**, 93–117.

Hauska, G., Schoedl, T., Remigy, H., and Tsiotis, G. (2001). The reaction center of the green sulfur bacteria. *Biochim. Biophys. Acta* **1507**, 260–277.

Heathcote, P. (guest editor) (2001). Type I photosynthetic reaction centers (Special issue). *Biochim. Biophys. Acta* **1507**, 1–310.

Permentier, H. P., Schmidt, K.A., Kobayashi, M., Akiyama, M., Hager-Braun, C., Neerken, S., Miller, M., and Amesz, J. (2000). Composition and optical properties of the recation centre complexes from the green sulfur bacteria *Prosteocochloris aestuarii* and *Chlorobium tepidum*. *Photosynth. Res.* **64**, 27–39.

Remigy, H.-W., Stahlberg, H., Fotiadis, D., Muller, S.A., Wolpensinger, B., Engel, A., Hauska, G., and Tsiotis, G. (1999). The reaction center complex from the green sulfur bacterium *C. tepidum*: A structural analysis by scanning transmission electron microscopy. *J. Mol. Biol.* **290**, 851–858.

Remigy, H.-W., Hauska, G., Müller, S.A., and Tsiotis, G. (2002). The reaction centre from green sulfur bacteria: Progress towards structural elucidation. *Photosynth. Res.* **71**, 91–98.

Schütz, M., Brugna, M., Lebrun, E., Baymann, F., Huber, R., Stetter, K.O., Hauska, G., Toci, R., Lemesle-Meunier, D., Tron, P., Schmidt, C., and Nitschke, W. (2000). Early evolution of cytochrome bc complexes. *J. Mol. Biol.* **300**, 663–675.

Seo, D., and Sakurai, H. (2002). Purification and characterization of ferredoxin-$NAD(P)^+$ reductase from the green sulfur bacterium *Chlorobium tepidum*. *Biochim. Biophys. Acta* **1597**, 123–132.

Theissen, U. Hoffmeister, M., Grieshaber, M., and Martin, W. (2003). Single eubacterial origin of eukaryotic sulfide: Quinone oxidoreductase, a mitochondrial enzyme conserved from early evolution of eukaryotes during anoxic and sulfidic times. *Mol. Biol. Evol.* **20**, 1564–1574.

Biography

Günter Hauska is a Professor of Cell Biology and Plant Physiology at the Institute of Botany, in the Department of Biology at the University of Regensburg, Germany. He obtained his Ph.D. in chemistry at the University of Vienna in 1967. Subsequently he served as postdoctoral fellow in the biochemistry department of the Cornell University before qualifying as Dozent for biochemistry at the Ruhr-Universität in Bochum, Germany. His research interest is in energy transduction by membrane protein complexes of electron transport chains, especially in quinol oxidation by cytochrome *bc* complexes and in photosynthetic reaction centers. His recent interest has been in flavoproteins. He is a member of the German Society for Biochemistry and Molecular Biology.

Thomas Schödl graduated from the University of Regensburg and finished his Ph.D. in biochemistry. He is studying the structure and redox reactions of flavoproteins, in particular of sulfide quinone reductases from bacteria and eukaryotes.

G_s Family of Heterotrimeric G Proteins

Susanne M. Mumby
University of Texas Southwestern Medical Center, Dallas, Texas, USA

Members of the G_s family of heterotrimeric G proteins stimulate the activity of the adenylyl cyclase enzyme. This enzyme is responsible for producing the intracellular second-messenger, cyclic AMP (cAMP), which in turn triggers a cascade of biochemical changes that ultimately bring about an alteration in cellular behavior.

G Protein-Mediated Signal Transduction

In order to function and survive, cells must respond to signals in their environment including chemical messengers dispatched from other parts of the body (such as hormones and neurotransmitters) and external stimuli (such as light and odorants). Typically, messengers do not enter target cells, but instead they are transduced by conveyance of information through intermediaries that form a chemical switchboard (Figure 1). This is a common biological strategy to regulate cellular behavior.

A major form of signal transduction is initiated at the plasma membrane by G protein-coupled receptors that function as antennas or discriminators (Figure 1). The process of signal transduction is initiated by binding of a primary messenger (an agonist, such as a hormone or neurotransmitter) to a specific receptor at the cell surface. The stimulated, transmembrane receptor activates the G protein, which is tucked just inside the plasma membrane. The G protein in turn modulates the activity of an effector (such as an enzyme or ion channel) that performs as an amplifier to produce second-messengers inside the cell. Second-messengers trigger a specific cascade of additional biochemical events, that cause a change in behavior characteristic of a particular cell type.

G proteins are heterotrimeric in structure, composed of α-, β-, and γ-subunits, but are usually defined by the identity of their α-subunits. Sixteen distinct genes encode α-subunits in mammals and 20 or more proteins are synthesized through alternative splicing of mRNA. The family of α-subunits is commonly divided into four subfamilies based on their amino acid sequence, which roughly correlates with their function: G_s, G_i, G_q, and G_{12}. The G_s subfamily is comprised of proteins named G_s and G_{olf}. Members of the G_s subfamily stimulate adenylyl cyclase, an enzyme that catalyzes the conversion of ATP to the second-messenger, cyclic AMP (cAMP).

Discovery

Appreciation of G protein-mediated signal transduction began with the characterization of hormone-sensitive adenylyl cyclase. The model that evolved for regulation of adenylyl cyclase proved to be the general paradigm for a large number of signaling pathways and impelled the award of the 1994 Nobel Prize in Medicine or Physiology to Rodbell and Gilman. Rodbell first promulgated the notion of a transducer acting as an intermediary between receptors and adenylyl cyclase. He and his colleagues established that receptor agonist (first messenger) was not sufficient to activate the enzyme, but in addition the guanine nucleotide, GTP, was required. Gilman and colleagues purified the first G protein, G_s, by reconstituting hormone-stimulated adenylyl cyclase activity in membranes from a mutant cell line lacking the G protein. Later, an additional G protein, G_i (a member of a distinct family of G proteins), was discovered to transduce negative regulation from inhibitory receptors (such as the muscarinic receptor) to adenylyl cyclase, as depicted in Figure 2. G_i and other families of heterotrimeric proteins are described in additional articles within this volume.

Regulation of G Proteins by Guanine Nucleotides

G proteins are so named because they bind guanine nucleotides. Figure 3 shows a current model for the

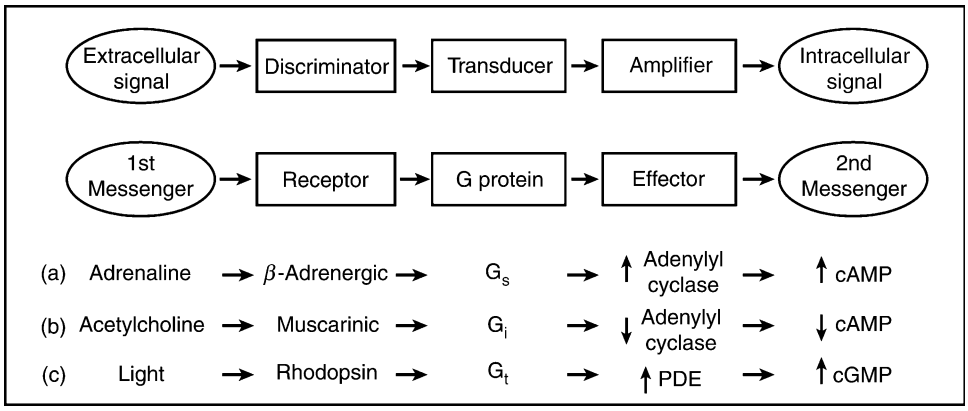

FIGURE 1 Relay diagram of G protein signaling. Line 1 is based on Rodbell's early concept of informational processing, which is restated in biochemical terms in line 2. The lettered subheadings below line 2 are specific examples of signaling relays for hormone sensitive adenylyl cyclase and the visual transduction systems. The horizontal arrows indicate the direction of the flow of information. The upward pointing arrows indicate increases in effector activity or levels of second messenger. The downward pointing arrows indicate decreases in effector activity or levels of second messenger. Reprinted from Mumby, S.M. (2000). G proteins I: G_s and G_i. In *GTPases* (A. Hall, ed.) pp.1–27. With permission of Oxford University Press, New York.

mechanism of G protein-mediated signal transduction in which nucleotide-driven conformational changes in the α-subunit drive interactions with an upstream receptor or downstream effector. Two cycles are superimposed in this model: GTP binding/hydrolysis and subunit dissociation/reassociation. In the basal state, (Figure 3A) the ligand-binding site of the receptor is unoccupied, the three G-protein subunits form an oligomer, and GDP is bound to the α-subunit. Activation is triggered when agonist binds to the receptor, which acts as a guanine nucleotide exchange factor (Figure 3B). The liganded receptor binds to its cognate G protein and promotes release of GDP from Gα (the rate limiting step), thus allowing this subunit to bind the more abundant guanine nucleotide in the cell, GTP. A conformational change in Gα accompanies binding of GTP and leads to the dissociation of Gα from receptor and the high-affinity complex of β- and γ-subunits (Figure 3C). These liberated subunits are competent to modulate the activity of effectors. In the example shown in Figure 3C, α-GTP interacts with the effector (although $\beta\gamma$ also can modulate some effectors). The intrinsic GTPase activity of Gα acts as a molecular clock to terminate the signal by returning this subunit to the inactive GDP bound state with increased affinity for G$\beta\gamma$. Reassociation of Gα-GDP with G$\beta\gamma$ restores the system to the basal state to await a new cycle of activation.

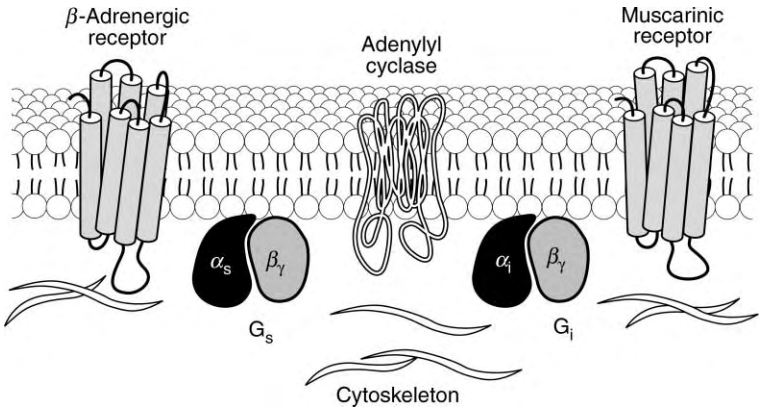

FIGURE 2 Schematic view of plasma membrane components that participate in the hormone-sensitive adenylyl cyclase system. G protein-coupled receptors have a similar structure that includes seven putative transmembrane helices and regions of homology in the cytoplasmic loops. Lipid modifications (not shown) promote interactions of G proteins with the inner surface of the plasma membrane. Adenylyl cyclases presumably span the membrane twelve times, with the active site oriented on the cytoplasmic side of the membrane. Reprinted from Mumby, S. M. (2000). G proteins I: G_s and G_i. In *GTPases* (A. Hall, ed.) pp.1–27. With permission of Oxford University Press, New York.

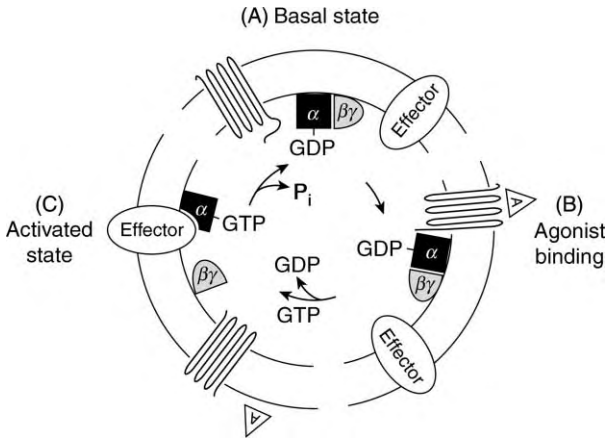

FIGURE 3 Simple mechanistic model of G protein-mediated signal transduction. The circular parallel lines represent the plasma membrane. The receptor is represented by the serpentine lines spanning the membrane seven times and agonist is shown as the letter A surrounded by a triangle. The two superimposed cycles of GTP-binding/hydrolysis and G protein subunit dissociation/reassociation described in the text. Reprinted from Mumby, S. M. (2000). G proteins I: G_s and G_i. In *GTPases* (A. Hall, ed.) pp.1–27. With permission of Oxford University Press, New York.

Members of the Family

Members of the G_s family include various isoforms of G_s and G_{olf} (listed in Table I). The hallmark of these proteins is that they stimulate the activity of adenylyl cyclase. This stimulation increases the production of cAMP, which is an important second-messenger for many physiological processes including growth and development, regulation of the force and rate of cardiac contraction, learning and memory, perception of odorants and endocrine functions including those of the thyroid, pituitary, and parathyroid glands. Table II lists a sampling of physiological processes that are regulated by members of the G_s family.

$G\alpha_S$

The Long and Short of it

G_s is a ubiquitous G protein. Variations in splicing of G_s mRNA leads to the production of short and long isoforms of αs, which are both produced in most cell types. The relative proportions of the variants change under a wide range of metabolic conditions such as cellular differentiation, development, aging, and various adaptive processes. The physiological explanation for existence of multiple isoforms is not known. Functional differences have been reported for cells or isolated membranes that display different proportions of short and long $G\alpha_s$, but it is not known if additional differences in the samples also may have influenced functional output. *In vitro* experiments with purified proteins have documented that long and short isoforms vary in their relative rates of GDP dissociation and specificity of interaction with different combinations of $\beta\gamma$ isoforms.

$G\alpha_sXL$

Alternative promoter usage and splicing of mRNA produces an extra long form of $G\alpha s$. Conventional $G\alpha_s$ shares exon 2–13 with $G\alpha_sXL$. Exon 1 encodes 47 residues for conventional α_s compared to 367 residues for $G\alpha_sXL$. The XL isoform is expressed in the Golgi complex and plasma membrane of neuroendocrine cells, suggesting a role for the protein in regulated secretion. $G\alpha_sXL$ does not interact with G_s-coupled receptors, but does bind $G\beta\gamma$ and can stimulate adenylyl cyclase.

$G\alpha_{olf}$

$G\alpha_{olf}$ is so named because it was originally considered to be strictly an olfactory-neuron-specific G protein involved in odorant signal transduction. $G\alpha_{olf}$ differs from the short splice variant of $G\alpha_s$ *a* in 80 amino acids, with the majority of the differences being localized in the

TABLE I

Properties of the Mammalian G_s Family of α-Subunits

Subfamily/subunit	Molecular mass (kDa)	Distribution in tissue	Representative receptors[a]
$G\alpha_{s(S)}$[b]	44	Ubiquitous	βAR
$G\alpha_{s(L)}$[b]	46	Ubiquitous	Glucagon, TSH
$G\alpha_sXL$[b]	94	Brain, adrenal, pituitary	Secretion?
$G\alpha_{olf}$	45	Olfactory neuroepithelium, brain, heart, pancreas, male germ cell	Odorant, D1, A2a

[a] Receptor abbreviations: βAR, β-adrenergic; TSH, thyroid-stimulating hormone; D1, dopamine, A2a, adenosine.
[b] Splice variations: $G\alpha_{s(S)}$ = short forms of $G\alpha_s$; $G\alpha_{s(L)}$ = long forms of $G\alpha_s$.

TABLE II

Sampling of Physiological Effects Mediated by G_s Family Members

Primary messenger	Cell type	G protein	Effect
Adrenaline (epinephrine)	Heart cells	G_s	Increased rate and force of contraction
Adrenaline, glucagon	Liver cells	G_s	Breakdown of glycogen
Adrenaline, glucagon	Fat cells	G_s	Breakdown of fat
Luteinizing hormone	Ovarian follicles	G_s	Increased synthesis of estrogen and progesterone
Antidiuretic hormone	Kidney cells	G_s	Conservation of water
Odorants	Neuroepithelial cells in nose	G_{olf}	Sensation of odorants

α-helical domain of the protein (domain structure described below). Studies with the $G\alpha_{olf}$ knockout mouse showed that this G protein is involved in the perception of floral, fruity, minty, and putrid odorants. These findings fit to data showing that such odorants activate adenylyl cyclase in olfactory cilia. Greater than 75% of the G_{olf} mutant mice are unable to nurse and die within 2 days after birth; surviving homozygous ones also exhibit hyperactive behaviors. This behavioral phenotype and additional data suggest that G_{olf} may also play an essential role more centrally in the brain. More thorough analysis of the expression of $G\alpha_{olf}$ suggests functions for this G protein in heart, pancreas, and male germ cell development as well.

Structure

Heterotrimeric G proteins are related to the so-called small GTPases, including Ras, Rho, Rab, Arf, and Ran. Although there is substantial sequence diversity among members of the GTPase superfamily, structural and biochemical studies have demonstrated a common core architecture that is embodied in Ras.

Nucleotide-Bound Protein

X-ray crystallographic structures of G proteins complexed with nucleotide reveal a Ras-like architecture with four inserted substructures. The largest insert is a helical domain connected to the Ras-like domain by two linkers (which are absent from Ras). The helical domain covers the nucleotide completely and prevents its release. By sequestering the nucleotide, the helical domain slows nucleotide release 5–50 fold compared with rates observed for Ras. The ligand-bound receptor is likely responsible for separation of the two domains to allow release of GDP, entry of GTP, and activation of the G protein. Although not present in the recombinant proteins used to generate crystal structures, lipids covalently modify the peptide backbone of G proteins *in vivo*.

Covalent Modifications

G-protein α-subunits are acylated at or near their amino termini by fatty acids, myristate and/or palmitate. These lipid modifications facilitate protein–protein and protein–membrane interactions of $G\alpha$. G_s is the only α-subunit that is known to be modified by palmitate through two different linkages: via a thioester bond (reversible and common to most α-subunits) and via a stable amide at the amino terminal glycine residue (unique). The turnover of palmitate in the thioester linkage is regulated by a receptor agonist. The presence of this palmitate residue is thought to regulate interaction of $G\alpha_s$ with lipids and certain proteins present in cellular membranes.

Many G proteins are modified by ADP-ribosylation, which is catalyzed pathologically by the action of toxins. Cholera toxin selectively modifies the multiple forms of $G\alpha_s$ on a particular arginine residue (201 in the numbering of the long form of $G\alpha_s$). This modification irreversibly inhibits the GTPase activity of $G\alpha_s$, thus locking the protein in an active form.

G_s Dysfunction in Human Disease

Either activating or inactivating defects in G-protein α-subunits can give rise to diseases in humans. Examples of G_s-associated pathology include the effects of bacterial toxins and genetic mutations.

Cholera

The activity of $G\alpha_s$ is increased in intestinal epithelial cells of patients with secretory diarrhea caused by infection with *Vibrio cholerae*. The bacteria secrete an oligomeric protein exotoxin composed of an A subunit and five B subunits. The B oligomer is responsible for toxin binding to the cell surface. Following entry into the cell and processing by proteolysis and reduction, the A component catalyzes the ADP ribosylation of $G\alpha_s$ to drastically reduce GTPase activity. The persistent production of cAMP that ensues ultimately leads to

the devastating fluid and electrolyte loss that causes the diarrhea.

Genetic Mutations

Pseudohypoparathyroidism

Pseudohypoparathyroidism (PHP) is a dramatic example of decreased G_s function. For one subtype of the disease, PHP 1a, affected subjects show resistance not only to parathyroid hormone but also to several other hormones such as thyroid-stimulating hormone and gonadotropins whose actions are mediated by receptors coupled to G_s. Affected individuals also show phenotypic features including obesity, short stature, and skeletal abnormalities, which are collectively called Albright hereditary osteodystrophy.

McCune–Albright Syndrome

The McCune–Albright syndrome is characterized by hyperfunction of one or more endocrine glands (pituitary somatotrophs, adrenal cortex, thyroid, and gonads) coupled with cafe-au-lait skin hyperpigmentation and bone deformity (polyostotic fibrous dysplasia). Missense mutation of arginine 201 (the site of ADP ribosylation by cholera toxin) is one of the constitutively activating mutations identified in patients with McCune–Albright syndrome. Patients express mutations in a mosaic pattern that correlates with the cellular abnormalities observed. The spectrum of affected tissues may be determined by the time in development that the mutations occur. Timing may range from early in embryogenesis leading to a wide distribution with pleiotropic, potentially severe manifestations to those occurring as later monofocal events and leading to localized manifestations such as growth hormone-secreting pituitary tumors.

Tumors

A subset of pituitary adenomas are characterized by elevated cAMP levels and growth hormone (GH) production. Cells from these tumors are relieved of the requirement for GH-releasing hormone to stimulate adenylyl cyclase, growth hormone secretion, and proliferation of normal pituitary somatotrophs. In some GH-releasing hormone independent tumors, $G\alpha_s$ is constitutively activated by a point mutation in either of two residues: arginine 201 (the ADP-ribosylation site) or glutamine 227, which is equivalent to glutamine 61 of Ras, a frequent site of GTPase-inhibiting mutations in the Ras proteins. Some autonomously functioning thyroid adenomas have similar mutations.

See Also the Following Articles

Adenylyl Cyclases • G_{12}/G_{13} Family • G_i Family of Heterotrimeric G Proteins • G_q Family • Ras Family • Small GTPases

Glossary

effector Intracellular second-messenger-producing enzyme or ion channel.

G protein A heterotrimeric protein comprised of α-, β- and, γ-subunits that binds and hydrolyzes GTP and transduces signals from outside to the inside of the cell.

G_{olf} A heterotrimer composed of $G\alpha_{olf}$ and any isoforms of β- and γ-subunits.

G_s The heterotrimer composed of any isoform of $G\alpha_s$, β-, and γ-subunits.

GTPase An enzyme that binds and hydrolyzes GTP. The superfamily of GTPases includes "small" members such as Ras, as well as heterotrimeric G proteins.

receptor A plasma membrane-spanning protein that specifically recognizes an extracellular signal and when agonist is bound transmits information to the cell interior.

signal transduction Transmission of information from outside to inside a cell, thus causing a change in cellular behavior.

Further Reading

Farfel, Z., Bourne, H. R., and Irir, T. (1999). The expanding spectrum of G protein diseases. *New England J. Med.* **340**, 1012–1020.

Kaziro, Y., Itoh, H., Kozasa, T., Nakafuku, M., and Satoh, T. (1991). Structure and function of signal-transducing GTP-binding proteins. *Annu. Rev. Biochem.* **60**, 349–400.

Mumby, S. M. (2000). G proteins I: G_s and G_i. In *GTPases* (A. Hall, ed.) pp. 1–27. Oxford University Press, New York.

Neves, S. R., Ram, P. T., and Iyengar, R. (2002). G protein pathways. *Science* **31**, 1636–1639.

Sprang, S. R. (1997). G protein mechanisms: Insights from structural analysis. *Annu. Rev. Biochem.* **66**, 639–678.

Biography

Susanne M. Mumby is an Associate Professor in the Department of Pharmacology at the University of Texas Southwestern Medical Center at Dallas. She holds a Ph.D. in Biochemistry from the University of Washington and her principal research interests are in the structure and function of lipid modifications of signal-transducing G proteins. Dr. Mumby serves as director of the Antibody Laboratory of the Alliance for Cellular Signaling, a multi-institutional research collaboration to study and model G protein-mediated and related signaling systems (www.signaling-gateway.org).

Heat/Stress Responses

Davis T. W. Ng
Pennsylvania State University, University Park, Pennsylvania, USA

All cells from simple bacteria to highly differentiated animal cells maintain specialized mechanisms to monitor and respond to changes in their local environments. Unfavorable circumstances that threaten cellular homeostasis will elicit one or more *stress response* programs in an effort to preserve viability of the organism. The many forms of cellular stress include temperature variation, exposure to toxic compounds, oxidative and reductive stress, ionizing radiation, hypoxia, aging, mechanical injury, and the invasion of pathogens. Mounting the correct response can insure cell survival or initiate an apoptotic program depending on the severity of the stress. Stress responses are also activated in numerous disease states and deficient responses are etiological for afflictions including Parkinson's and Alzheimer's diseases. More recently, stress-regulated genes were intimately linked to aging and shown to be required for the extension of life in model organisms. As a general rule, stress responses remodel relevant cellular pathways to counteract specific effects of the insult.

The Stress of Unfolded Proteins

Proteins are the class of molecules that perform most cellular functions. First synthesized as chains of amino acids encoded by genes, nascent proteins must fold into their correct three-dimensional structures to be active. The folded state is labile and dependent on the thermodynamic nature of each molecule. Fully mature proteins are the product of unique amino acid sequences that specify numerous noncovalent interactions within each molecule. Abrupt changes can create unfavorable local environments that weaken such interactions or prevent their correct formation. Conditions that cause the unfolding or disrupt the proper synthesis of proteins are major forms of cellular stress. Left unchecked, the inherent toxicity of unfolded proteins or their loss of function could leave cells irreversibly damaged.

The Heat Shock Response

The first stress response to unfolded proteins was reported over forty years ago. Examination of fruit fly salivary chromosomes revealed morphological puffs along their lengths after treatment by heat, dinitrophenol, or sodium salicylate. Termed the heat shock response (HSR), it was later shown that the puffs signified activation of genes encoding heat shock proteins (Hsps). For virtually all organisms, exposure to 5–10°C above the optimal growth temperature leads to a robust HSR. Within the cell, an increase of this magnitude can have many deleterious effects including increased membrane fluidity and the partial unfolding of proteins.

Inputs

The HSR can be activated by a wide variety of conditions beyond temperature change. A few examples include exposure to ethanol, heavy metals, amino acid analogues, mechanical damage, and conditions of hypoxia, ischemia, and osmotic stress. As with temperature increases, these conditions are believed to increase the concentration of unfolded proteins. In addition, the nonstress conditions of cells undergoing rapid proliferation or differentiation also induce the HSR. Here, the physiological need is to boost the capacity for protein synthesis.

Stress Detection and Response

The HSR relies on the activity of "molecular chaperone proteins" to detect stress. Chaperones bind to unfolded proteins and facilitate folding by preventing inappropriate interactions. Chaperones also bind irreversibly misfolded proteins to neutralize their toxicity and promote their destruction. As stress conditions increase the concentration of unfolded proteins, the available pool of free chaperones diminishes. Specialized sensor proteins can detect the change and initiate a response. In the eukaryotic HSR (prokaryotes employ a different mechanism), the heat shock factor (HSF) plays both stress sensor and transcription activator for the response output. In metazoan organisms, the inert state of HSF is a monomer that is maintained through associations with the chaperones Hsp70, Hsp90, and Hsp40 (Figure 1). As the demand for chaperones increases, release from chaperone complexes permits conversion of HSF to a homotrimer (and translocation into the nucleus if found in the cytosol). This form of HSF can bind to heat shock

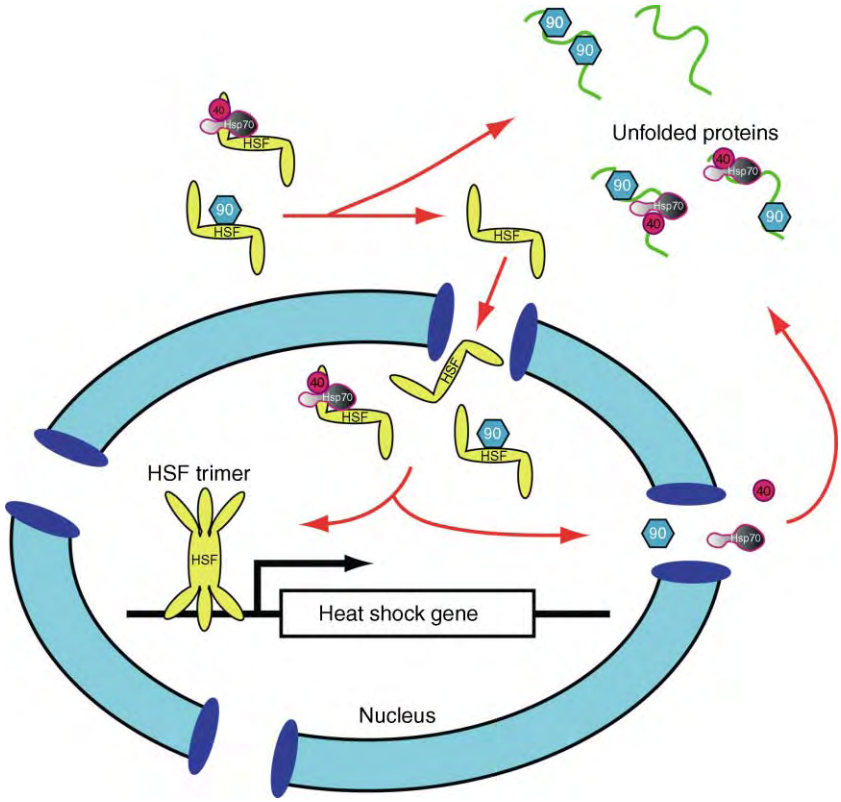

FIGURE 1 Activation of the HSR is a multistep mechanism. The increase of unfolded proteins stimulates the binding of cytosolic chaperones and reduces the free chaperone pool (upper right, Hsp90 and Hsp40 proteins labeled "90" and "40," respectively). The reduction in chaperone binding to HSF monomers promotes assembly into HSF trimers (and nuclear localization of cytosolic HSF). Initial binding of trimeric HSF to heat-shock promoters is in the inert state. Transcriptional activation of the target gene requires HSF phosphorylation. In yeast, HSF is similarly regulated except that it always exists as a trimer.

elements of heat shock genes but does so in the inert state. Transcriptional activation requires HSF phosphorylation and a conformational change. Subsequently, a dramatic but transient rise in the synthesis of Hsps is accompanied by a reduction in overall protein synthesis.

The HSR Output

Protein Repair and Preservation

The most notable output of the HSR is the induction of chaperone genes. Chaperones are well adapted to resist stress. Beyond their established role in the folding of most newly synthesized proteins, direct biochemical analyses have shown that some chaperones disaggregate and refold misfolded proteins. Organisms harboring mutations in chaperone genes are less tolerant to various forms of stress. Taken together, the evidence supports the view that chaperones protect cells from stress by maintaining the folded states of proteins and repairing those that are damaged.

Degradation of Aberrant Proteins

Since they can be toxic, damaged proteins that cannot be repaired must be destroyed. Fittingly, the HSR regulates key factors of protein degradative pathways. For example, another facet of chaperone function is their requirement in the degradation of misfolded proteins. In eukaryotes, offending proteins are conjugated with ubiquitin, a highly conserved 76 amino acid protein. Poly-ubiquitin chains serve as signals for the 26S proteasome, which degrades the attached protein. The factors responsible for the recognition and modification of substrates belong to two large enzyme families that include the ubiquitin conjugating enzymes (E2s) and the ubiquitin ligases (E3). The role of protein degradation pathways in stress tolerance is well established. For example, yeast strains that lack two heat shock genes, *UBC4* and *UBC5* (E2s), are hypersensitive to elevated temperatures and other forms of stress. Recent studies have shown that increasing the cellular capacity to degrade damaged proteins is likely the major role of the HSR in stress tolerance.

The Environmental Stress Response

The development of DNA microarray technology has made analysis of whole genome expression patterns possible. The application of this technology revealed that the transcriptional output of the HSR is remarkably broad. Although the HSR has its own molecular signature, a large subset of its genes is regulated

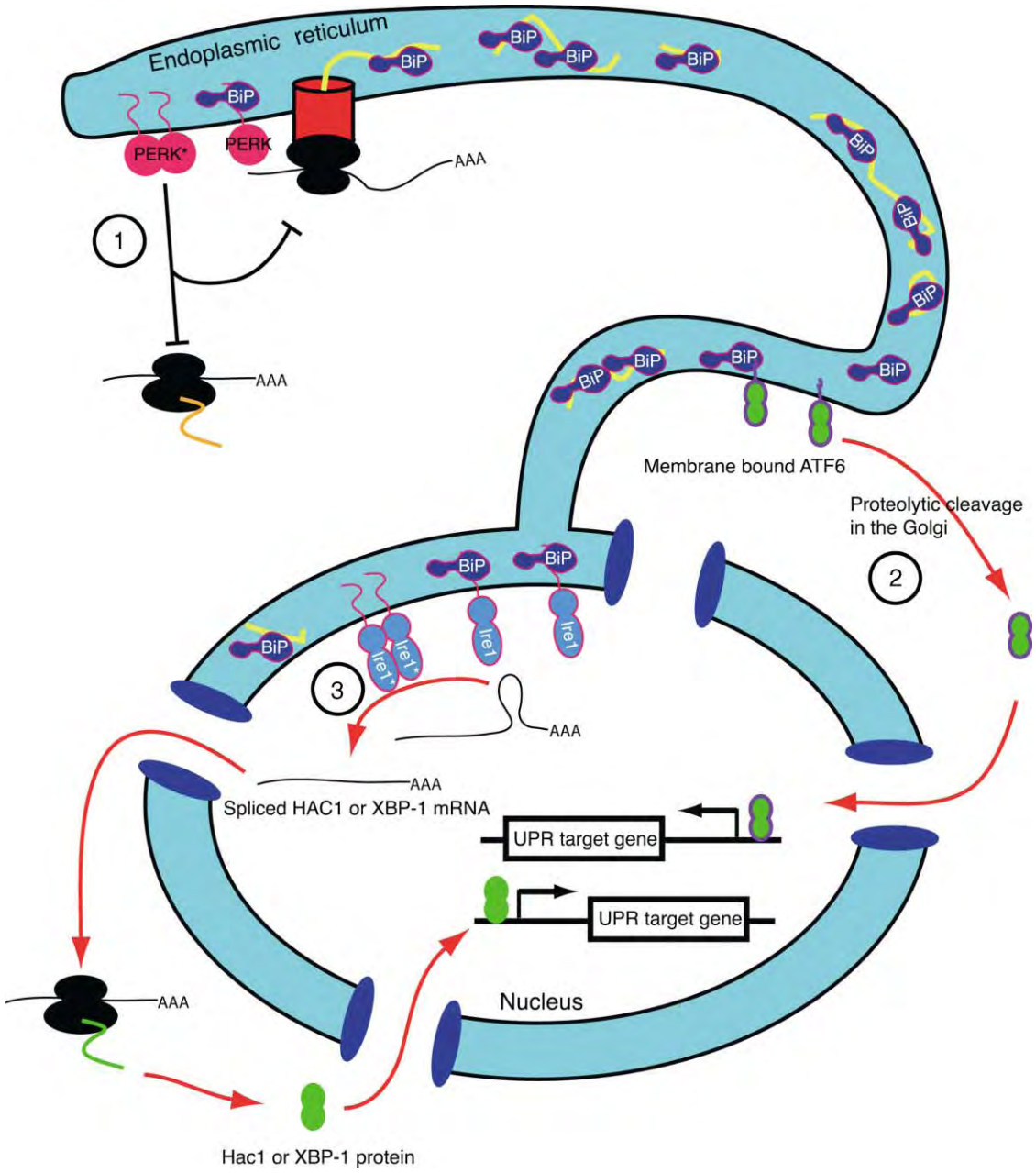

FIGURE 2 Activation of the UPR. The accumulation of unfolded proteins in the ER reduces the free pool of BiP and activates three distinct UPR sensor/transducers. (1) PERK dimers form following the reduction of BiP bound to their lumenal domains. Activated PERK phosphorylates eIF2α resulting in the temporary attenuation of general translation. (2) The reduction of BiP binding to ATF6 lumenal domains stimulates their relocalization to the Golgi apparatus where the transcription factor is released by intramembrane proteolysis. Soluble ATF6 translocates to the nucleus where it activates expression of a subset of UPR target genes. (3) The release of BiP derepresses Ire1 by promoting its dimerization and transphosphorylation. The activated ribonuclease domain cleaves introns of messages encoding UPR-specific transcription factors. Newly synthesized Hac1 (yeast) or XBP-1 (metazoans) activates the transcription of UPR target genes. In yeast, mechanism 3 is the only known UPR pathway. Asterisks indicate activated forms of enzymes.

similarly among disparate environmental stress conditions. These genes, comprising the environmental stress response (ESR), represent many stress-related functions and a variety of metabolic pathways. Thus, any specific stress response can be thought of as comprising the ESR plus additional outputs tailored to their specific circumstances.

The Unfolded Protein Response

The HSR primarily monitors the state of the cytosol and nucleoplasm. For the endomembrane system of the secretory pathway, the health of proteins in the endoplasmic reticulum (ER) is monitored by the unfolded protein response (UPR). Circumstances leading to ER

disequilibrium and activation of the UPR include exposure to reducing agents, incomplete protein glycosylation, glucose deprivation, excess nitrogen, calcium depletion, and proteasome dysfunction. The UPR is a signal transduction pathway that relays information on the condition of the ER lumen to regulatory networks of the nucleus and cytosol.

Stress Sensors and Transmembrane Signaling

As with the HSR, increasing unfolded proteins in the ER reduce the free pool of lumenal chaperones. However, since these chaperones are physically separated from downstream regulatory mechanisms, the UPR employs strategies distinct from the HSR to monitor stress. The key sensor, found in all eukaryotes, is Ire1 (Figure 2). Ire1 is a transmembrane protein with three functional domains. Binding of the ER chaperone BiP to the lumenal domain keeps Ire1 in the inactive monomeric state. Under stress, increased demand for BiP reduces its occupancy on Ire1. Free Ire1 dimerizes and activates two enzyme domains oriented to the cytosolic/nucleoplasmic side of the membrane. The kinase domain transphosphorylates Ire1, and the nuclease domain splices mRNAs encoding UPR-specific transcription factors. In budding yeast, splicing enables *HAC1* mRNA to be translated. In metazoans, the Ire1 target is *XBP-1*. Spliced *XBP-1* directs the expression of a functional UPR transcription factor that is larger and more stable from the version synthesized from the unspliced transcript. Metazoan organisms also have additional levels of UPR regulation. A membrane-bound transcription factor, ATF6 (α- and β-isoforms), is released by regulated intramembrane proteolysis upon ER stress. Soluble ATF6 then translocates into the nucleus to activate UPR target genes. A third sensor is the ER transmembrane protein PERK. Like Ire1, PERK contains a kinase that is regulated by BiP occupancy of its lumenal domain. By contrast, PERK targets the translation factor eIF2α under ER stress. Phosphorylation of eIF2α attenuates general translation.

Outputs of the UPR

The transcriptional program of the UPR shows functional similarities to the HSR but it is customized for the secretory pathway. Cells lacking an intact UPR are hypersensitive to ER stress. Under stress, such cells fail to properly fold and modify secretory proteins, trafficking functions are shut down, and misfolded proteins accumulate unabated. Accordingly, the UPR program is complex with nearly half the regulated genes having functions throughout the secretory pathway. Similar to the HSR, the deployment of chaperone proteins preserves the integrity of existing proteins, aids the folding of new proteins, and promotes the degradation of misfolded proteins. Misfolded secretory and membrane proteins are degraded by a specialized arm of ubiquitin/proteasome pathway called ER-associated protein degradation (ERAD). The ERAD pathway serves to recognize, translocate, and ubiquitylate proteins for degradation. Studies have shown that all levels of the ERAD pathway are regulated by the UPR and this regulation plays an essential role in ER stress tolerance. In metazoans, the three ER sensors appear to act coordinately to resist stress. The activity of PERK is the first line of defense. Activation of ATF6 is similarly rapid and precedes the mobilization of XBP-1. The available data indicate that key chaperone genes are ATF6-regulated while key genes of the ERAD pathway are regulated by XBP-1. Thus, a model has emerged (Figure 2) that has PERK rapidly attenuating general translation to decease the load of unfolded proteins in the ER. This gives the existing machinery in the ER an opportunity to begin restoring homeostasis. Those efforts are augmented by the increased synthesis of chaperone proteins directed by ATF6. If stress persists, the ERAD pathway is upregulated by the activity of XBP-1. This serves to clear those proteins that cannot be refolded in the initial response. In cells experiencing stress that cannot be ameliorated, ER-associated apoptotic pathways are activated to sacrifice afflicted cells.

See Also the Following Articles

Chaperones for Metalloproteins • Chaperones, Molecular • Chaperonins • Endoplasmic Reticulum-Associated Protein Degradation • Proteasomes, Overview • 26S Proteasome, Structure and Function • Secretory Pathway • Ubiquitin-Like Proteins • Unfolded Protein Responses

Glossary

endoplasmic reticulum First organelle of the secretory pathway. All secreted and resident proteins of the pathway are first synthesized in this membrane-bound compartment.

kinase Enzyme that transfers phosphate groups, usually from ATP, to target substrates. For protein substrates, phosphate is usually added to the hydroxyl group of serine, threonine, or tyrosine side chains.

molecular chaperone These molecules function by preventing inappropriate interactions of other molecules. Chaperones play many cellular roles including protein folding, protein translocation, signal transduction, and protein degradation.

proteasome Large multisubunit protein complex that degrades proteins modified by poly-ubiquitin.

transcription factor Proteins that regulate the synthesis of mRNA at gene promoter elements.

ubiquitin A highly conserved 76 amino acid protein that functions through covalent conjugation of proteins (either a target or another ubiquitin molecule) to lysyl side chains via an isopeptide bond. Ubiquitin plays roles in protein degradation, regulation of protein activity, and protein localization.

Further Reading

Glickman, M. H., and Ciechanover, A. (2002). The ubiquitin-proteasome proteolytic pathway: Destruction for the sake of construction. *Physiol. Rev.* **82**, 373–428.

Harding, H. P., Calfon, M., Urano, F., Novoa, I., and Ron, D. (2002). Transcriptional and translational control in the Mammalian unfolded protein response. *Annu. Rev. Cell Dev. Biol.* **18**, 575–599.

Morimoto, R. I. (1998). Regulation of the heat shock transcriptional response: Cross-talk between a family of heat shock factors, molecular chaperones, and negative regulators. *Genes Dev.* **12**, 3788–3796.

Parsell, D. A., and Lindquist, S. (1993). The function of heat-shock proteins in stress tolerance: Degradation and reactivation of damaged proteins. *Annu. Rev. Genetics* **27**, 437–496.

Patil, C., and Walter, P. (2001). Intracellular signaling from the endoplasmic reticulum to the nucleus: The unfolded protein response in yeast and mammals. *Curr. Opin. Cell Biol.* **13**, 349–355.

Spear, E., and Ng, D. T. W. (2001). The unfolded protein response: No longer just a special teams player. *Traffic* **2**, 515–523.

Biography

Davis Ng is an Associate Professor of Biochemistry and Molecular Biology at Pennsylvania State University, University Park. His research interests include cellular stress tolerance mechanisms, the quality control of protein folding, and the physiology of the unfolded protein response. He received his Ph.D. from Northwestern University and was a postdoctoral fellow at the University of California, San Francisco.

Hematopoietin Receptors

Barbara A. Miller and Joseph Y. Cheung
The Pennsylvania State University College of Medicine, Hershey, Pennsylvania, USA

Hematopoietin receptors comprise a superfamily of glycoproteins with structural similarities including single transmembrane spanning domains. They are activated by the binding of specific hematopoietic growth factors or cytokines, initiating a signaling cascade which results in stimulation of cell proliferation, differentiation, or enhancement of survival. Conserved domains in their extracellular region include cysteine pairs and a tryptophan-serine-x-tryptophan-serine (WSXWS) motif, which are important in ligand binding. Their cytoplasmic domains are diverse but have some limited similarities in membrane proximal regions known as box 1 and box 2. Box 1 and 2 are essential for transducing mitogenic signals, and for association with and activation of Janus family (JAK) kinases. No intrinsic kinase or enzyme motif has been identified in the cytoplasmic domains of hematopoietin receptor superfamily members. Instead, signal transduction through these receptors is regulated by their interaction with kinases of the JAK family, other cytosolic kinases, and protein messengers. Cytokine receptor signaling for all of these factors is initiated by ligand binding to the receptor, resulting in receptor oligomerization; some receptors form homodimers while others are active as hetero-oligomers. Following receptor oligomerization, the receptor-associated JAKs transphosphorylate, activating each other. They subsequently phosphorylate tyrosines on the associated receptor, which then serve as docking sites for other signal transducers including the signal transducer and activator of transcription (STAT) proteins, initiating a signaling cascade.

Classification

Members of the hematopoietin receptor superfamily, also referred to as the cytokine receptor superfamily, can be separated into Class I and Class II receptors based on structural features. Class I includes (1) receptors consisting of a single subunit which forms homodimers including those of erythropoietin, thrombopoietin, G-CSF, growth hormone, and prolactin; (2) receptors consisting of two subunits, a unique α-subunit and a common β-subunit including those of the IL-3 (GM-CSF, IL-5) family and IL-6 family; and (3) receptors for several interleukins which share the IL-2 γ-chain and consist of two to three subunits, α, β, and γ. A schematic representation of Class I hematopoietin receptors is presented in Figure 1. Class II consists of receptors for the interferons, interleukin-10, and tissue factor, important in coagulation. Soluble forms of cytokine receptors are formed by limited proteolysis of membrane-bound receptors or alternative mRNA splicing. These can form a complex with specific cytokines and act antagonistically or agonistically depending on the complex involved. A second group of receptors through which hematopoietic growth factors signal, unrelated to the hematopoietin receptor family, is called the receptor tyrosine kinase gene family. This group of receptors have intrinsic tyrosine kinase activity. Examples include c-kit, the receptor for stem cell factor which acts synergistically in culture with many other hematopoietic growth factors, and the M-CSF receptor, which is critical for monocyte/macrophage growth. This family will not be discussed here. Representative members of the hematopoietin receptor family will be presented as model systems for signaling of other members. Hematopoietin receptor family members share many intracellular signaling molecules, and exact mechanisms responsible for signaling specificity remain uncertain.

Single Subunit Hematopoietin Receptors

Erythropoietin Receptor

Expression

Erythropoietin (Epo) is the primary regulator of erythropoiesis and promotes the survival, proliferation, and differentiation of erythroid cells. Epo is synthesized primarily in the kidney, but also in the liver, and its level is regulated by the arterial oxygen tension. It mediates its effects by interaction with its receptor, Epo-R, a 66 kDa protein expressed on the surface of progenitor and precursor cells committed to the erythroid lineage. The essential function of Epo-R is demonstrated by the severe anemia and death at 11–15 days gestation following homozygous deletion of the Epo or Epo-R genes in mice. The earliest cell in the erythroid lineage, the burst-forming unit erythroid (BFU-E), has only low

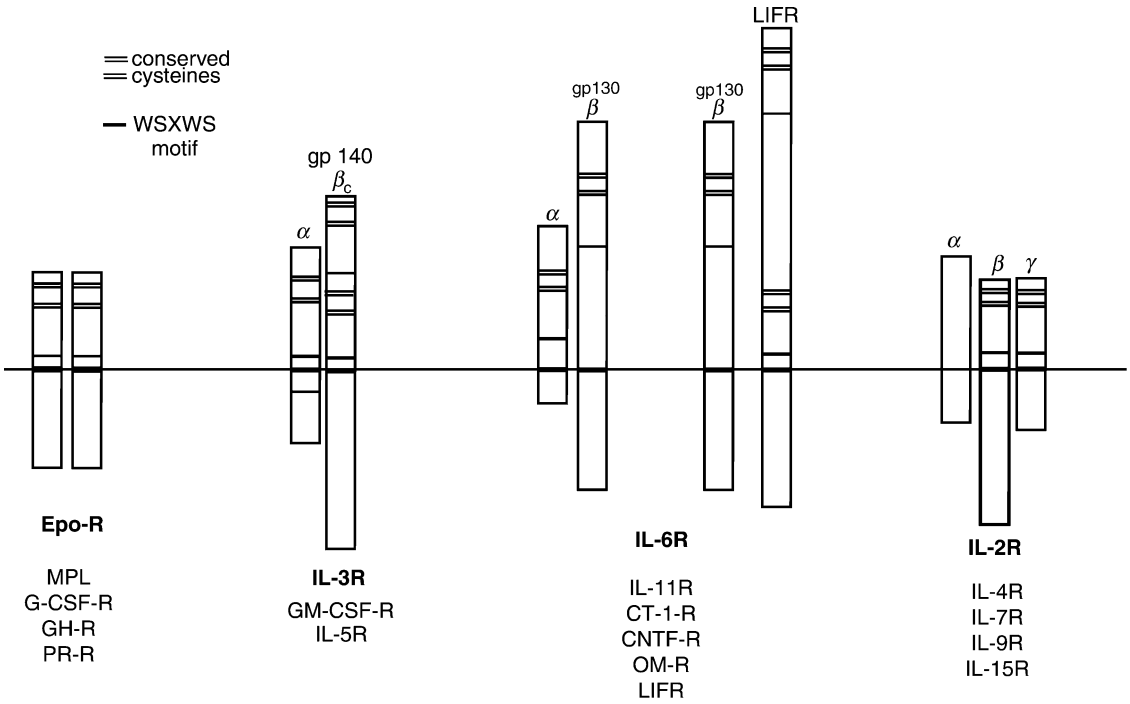

FIGURE 1 Class I hematopoietin receptor families. A schematic representation of the single-chain receptor (receptors for erythropoietin, thrombopoietin, G-CSF, growth hormone, and prolactin), multiple chain IL-3, IL-6, and IL-2 receptor families are shown.

numbers of Epo-R. Epo-R expression peaks at the later erythroid progenitor (colony-forming unit erythroid, CFU-E) and proerythroblast stage, followed by a decline during maturation to undetectable levels in mature erythroid cells. Epo-R is also expressed on megakaryocytes and several nonhematopoietic cells including endothelial cells, myoblasts, and neuronal cells. In these nonhematopoietic cells, the biological significance of receptor expression has not been clarified.

Signaling Pathways Activated by Epo

Epo-R consists of a single subunit which forms a homodimer in the presence or absence of Epo. Other members of the hematopoietin receptor family which form homodimers are receptors for thrombopoietin, G-CSF, growth hormone, and prolactin. These receptors transduce signals for a specific cytokine but do not cross react with other ligands of the same family. Epo binding results in a conformational change in Epo-R, allowing two JAK2, a tyrosine kinase associated with the cytoplasmic domain of Epo-R, to come into close proximity with each other. JAK2 is activated by transphosphorylation of its active site, and subsequently phosphorylates some or all of the eight tyrosine residues in the intracellular domain of Epo-R. The essential role of JAK2 in red blood cell production has been demonstrated in knockout mice. Phosphorylation of tyrosine residues on Epo-R provides docking sites for intracellular proteins to bind to Epo-R via SH2 domains, and many of these are then tyrosine phosphorylated. However, for both Epo-R and other hematopoietin receptors, the physiologic role of tyrosines in the cytoplasmic domain in regulation of proliferative, differentiating, and survival signals requires further definition. A representation of major signaling pathways activated following Epo-R stimulation are shown in Figure 2. One of the pathways activated by Epo is STAT5. STAT5 binds to phosphorylated Epo-R, and is phosphorylated by JAK2. Phosphorylated STAT5 dissociates from Epo-R and forms dimers through SH2-phosphotyrosine interactions. These dimers then translocate to the nucleus and bind specific promoter elements to activate expression of target genes. Epo-R activation by its receptor also results in activation of Ras through several pathways. Through a number of signal adapters and transducers including Grb2, Shc, GAB1, a Ras guanine nucleotide exchange factor called SOS, and/or a hematopoietic specific protein with Ras/GDP/GTP nucleotide exchange activity called Vav, Ras is activated by increased exchange of GDP with GTP. Epo stimulation also results in inhibition of GTPase-activating protein (GAP) by Epo-induced tyrosine phosphorylation. Following Ras activation, a downstream cascade proceeds including phosphorylation and activation of Raf-1, and of mitogen-activated protein kinases

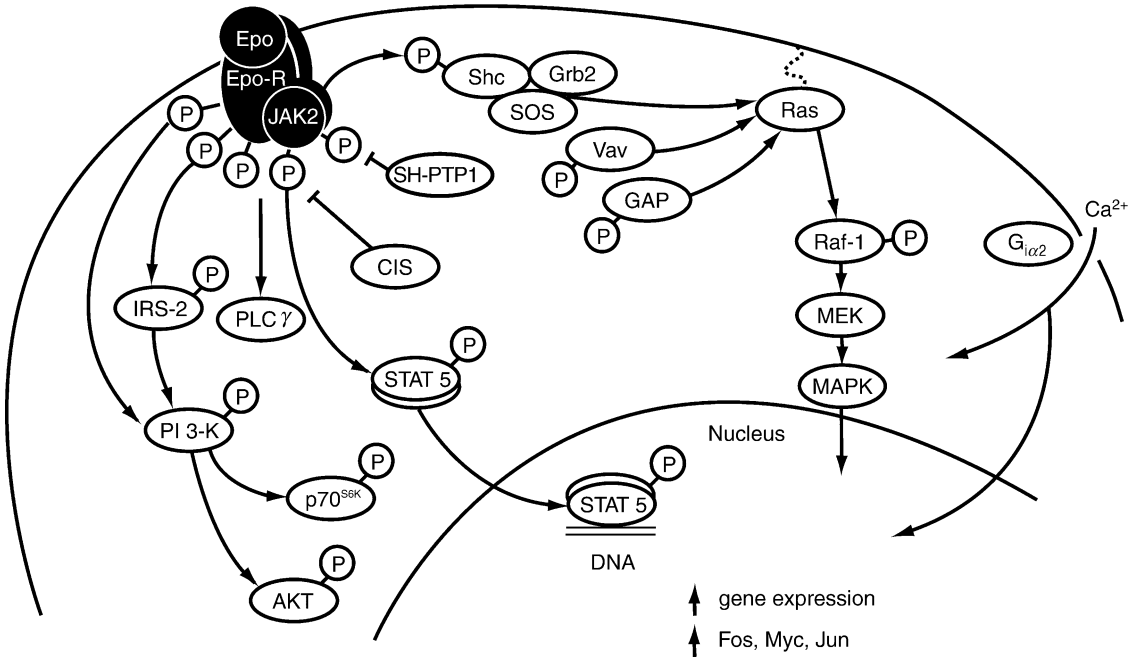

FIGURE 2 Pathways in erythropoietin receptor signaling. Erythropoietin binding leads to activation of associated JAK2 by autotransphosphorylation. Activated JAK2 phosphorylates tyrosines in the cytoplasmic region of Epo-R as well as associated proteins. This leads to activation of STAT5, Ras/Raf/MAPK, and PI 3-kinase pathways, leading to transcription and activation of genes involved in cell cycling, differentiation, and survival.

(MAPKs), with subsequent induction of immediate early genes including c-fos, c-myc, and c-jun. Phosphatidylinositol 3-kinase (PI 3-kinase) is another important kinase activated by Epo-R, either through direct association of the SH2 domain of the 85 kDa PI 3-kinase subunit with activated Epo-R or by binding to Epo-R through IRS-2 (insulin receptor substrate-2). PI 3-kinase can activate downstream targets including Akt, a kinase with important antiapoptotic activity, and $p70^{s6k}$, a kinase which phosphorylates ribosomal protein S6 and plays an important role in transcription, translation, and cell cycle progression. Ligand binding of Epo-R also results an increase in intracellular calcium, a universal second messenger, which influences many cell functions. Activation of tyrosine phosphorylation in erythroid cells is down-modulated by the hematopoietic protein tyrosine phosphatase SH-PTP1 (SHP1), which acts as a negative regulator. SH-PTP1 is recruited via its SH2 domains to tyrosine phosphorylated Epo-R, dephosphorylates JAK2 and terminates proliferative signals. Natural mutations in the negative regulatory region of cytoplasmic domain of Epo-R have been identified in benign erythrocytosis. Negative regulation is also mediated through suppressors of cytokine signaling (SOCS) proteins. One example is the SOCS protein CIS (cytokine-inducible SH2) containing protein, which may compete with STAT5 for binding sites on Epo-R and through this mechanism modify JAK/STAT signaling. CIS is also ubiquitinated and may promote Epo-R degradation. A number of other nonreceptor protein kinases, phosphatases, and phospholipases have also been shown to have important roles in Epo-R signal transduction, as well as additional adapters and transducers, including phospholipase Cγ, Cbl, and SHIP. Together, these pathways influence the expression and activity of a variety of proteins including transcription factors (GATA-1, NF-E2, SCL, NF-κB) and proto-oncogenes which participate in regulation of cell survival, proliferation, and differentiation.

Thrombopoietin Receptor

Expression

Thrombopoietin (Tpo) is the primary physiological hormone, which regulates all aspects of megakaryocyte and platelet development. Tpo interacts with its receptor, Mpl, on the cell surface of megakaryocyte precursors, mature megakaryocytes, and platelets to stimulate megakaryocyte progenitor proliferation and maturation, megakaryocyte polyploidy, and induction of platelet specific proteins. The biological activity of the Mpl receptor is not limited to the megakaryocytic lineage. Unlike Epo or G-CSF, thrombopoietin exerts profound effects on the proliferation of primitive hematopoietic cells through expression of Mpl on hematopoietic stem cells of all lineages.

Signaling Pathways Activated by Thrombopoietin

Upon binding of thrombopoietin to its receptor, Mpl, a number of signaling events are triggered which are very similar to those of activated Epo-R. Binding of thrombopoietin to Mpl induces the formation of an active dimer, enabling the associated JAK2 kinases to transphosphorylate each other. Activation of JAK2 results in phosphorylation of two of five tyrosines in the cytoplasmic region of Mpl. Proteins recruited to these sites include STAT3 and STAT5, Shc, Grb2, SOS, and Vav. Signaling pathways which are activated include those of Ras, MAPKs, and PI 3-kinase/Akt, as well as negative regulatory pathways through tyrosine phosphatases including SH-PTP1 and the SOCS family. The distinction between intracellular signals of Tpo which promote hematopoietic stem cell expansion versus megakaryocyte development and platelet production are unknown. Defective Mpl expression is thought to be the cause of congenital amegakaryocytic thrombocytopenia, a severe inherited thrombocytopenia in infants with absent megakaryocytes in bone marrow and severely low circulating platelet counts.

G-CSF Receptor

Expression

The receptor for G-CSF, G-CSF-R, regulates the proliferation and differentiation of myeloid progenitors to form neutrophilic granulocytes, enhances the effector functions of mature neutrophils, and promotes their survival. G-CSF-R is expressed on myeloid progenitor cells, mature neutrophils, monocytes, and platelets. G-CSF-R expression increases with neutrophil differentiation. G-CSF-R is also expressed on endothelial cells, where it is thought to induce proliferation as well as migration.

Signaling Pathways Activated by G-CSF

G-CSF-R binds G-CSF as a homodimer. Unlike the other single-chain cytokine receptors, G-CSF-R activates multiple JAK kinases including JAK1, JAK2, and TYK2. Once activated, the JAK kinases induce phosphorylation of receptor tyrosines, which become docking sites for multiple SH2-containing signaling proteins as well as STAT1, STAT3, and STAT5. Pathways activated by G-CSF-R include those leading to activation of Ras, and MAPKs. Negative regulation occurs through the phosphatase SH-PTP1 and through SOCs. Experiments with G-CSF-R lacking one or more of the four cytoplasmic tyrosines suggest that pathways which regulate proliferation, differentiation, or survival differ, and characterization of these differences has important implications for understanding disorders of granulopoiesis.

GM-CSF/IL-3/IL-5 Receptors

Expression

The granulocyte/macrophage colony-simulating factor (GM-CSF), interleukin-3 (IL-3), and IL-5 receptors are a subfamily of Class I hematopoietin receptors. They have unique ligand-binding alpha(α)-chains but share a common beta-chain (β_c), also called gp140. Many factors contribute to specificity in signaling between these receptors, and one of these is that they are differentially expressed. Both the GM-CSF-R and the IL-3R are expressed on hematopoietic stem cells, and on the progenitors/precursors of neutrophils, macrophages, erythrocytes, megakaryocytes, and eosinophils. The IL-3R is expressed earlier in myeloid development than the GM-CSF-R. IL-3 promotes the expansion of the $CD34^+$ multipotential hematopoietic progenitors to a greater extent than GM-CSF, and promotes the development of a greater range of lineages that GM-CSF including basophils and lymphoid cells. In contrast, IL-5R is restricted to expression in eosinophils, basophils, and mouse B cells.

Signal Transduction through the GM-CSF/IL-3/IL-5 Receptor

The common β_c-subunit does not bind ligand by itself. Instead, β_c executes two critical functions following ligand binding. It enhances the ligand-α receptor binding from a low-affinity to a high-affinity interaction, and it functions as a major signaling component. The α-chain may preassociate with β_c, but increased association occurs in the presence of ligand. Ligand binding increases oligomerization, creating clusters of 2 α and 2 β_c chains, the functional complex, or even larger complexes. Ligand binding facilitates formation of a disulfide linkage between α and β_c, not observed with the single-chain receptors. The β_c-subunit elicits many signaling events, although the α-chain is also required for signal transduction. There are eight tyrosine residues present on human β_c, and proteins with SH2-binding domains which bind to the phosphorylated tyrosine residues largely determine the function of different receptor regions. The membrane proximal cytoplasmic region of β_c constitutively or inducibly associates with JAK kinases, predominantly JAK2, and is involved in induction of proliferation. The mid region is necessary for promotion of viability, and the distal region is involved in growth inhibition. Receptor binding results in rapid activation/tyrosine phosphorylation of JAK2, the β_c, and other JAK substrates. Downstream pathways activated include multiple STATs (1,3,5,6), Src kinases, Ras, MAPKs, PI 3-kinase, and Akt. Differences in signaling which result in the stimulation of different lineages, and proliferation versus differentiation or survival signals are still being defined.

Receptors in the IL-6 Subfamily

Receptors for IL-6, IL-11, cardiotropin-1 (CT), ciliary neurotrophic factor (CNTF), oncostatin M (OM), and leukemia inhibitory factor (LIF) represent another Class I hematopoietin subfamily. They have major roles in hematopoiesis and in acute-phase and immune responses. They consist of a unique, ligand-binding α-subunit and a common β-chain called gp130, which oligomerize in response to ligand binding to initiate signaling. While gp130 is ubiquitiously expressed, the types of cells which respond to a specific IL-6 family cytokine is limited by the restricted and tightly regulated expression of the α-receptor subunit. IL-6R and IL-11R have their own α-subunits which complex with gp130, whereas other IL-6 subfamily cytokine receptor complexes signal through different combinations of gp130, LIFR, and OM-R. Similar to the common IL-3 β_c and the IL-2R γ-subunit, the shared gp130 subunit enhances the affinity of receptor binding and serves as a major signaling component. Like other members of the hematopoietin family, these receptors signal through JAK/STAT, Ras, MAPK, and PI 3-kinase cascades, and terminate or modulate signals through tyrosine phosphatases, the SOCS, and PIAS (protein inhibitors of activated STAT) proteins.

Receptors in the IL-2 Subfamily

The IL-2 family cytokines play a critical role in the development of the immune system and in modulation of lymphocyte activation. The IL-2 receptor subfamily includes receptors for IL-2, IL-4, IL-7, IL-9, IL-15, and IL-21, which share the γ-chain of IL-2R. Receptors for IL-4, IL-7, and IL-9 consist of two subunits, a unique α-subunit in addition to γ. Receptors for IL-2 and IL-15 have three subunits, a unique α-subunit and shared IL-2Rβ and γ. The α-subunit acts as the ligand-binding subunit, whereas the β- and γ-subunits function to enhance receptor affinity and in signal transduction. Many of the signal transducers utilized by these receptors are the same as for other hematopoietin receptors, except that this subfamily is one of the few to utilize JAK3. Mutations of γ have been shown to be the cause of X-linked severe combined immunodeficiency (SCID). All mutant receptors are defective in activation of JAK3.

The Class II Receptor Family

Interferons (IFN) receptors have been divided into several major groups including Type I (for IFN-αs, IFN-β, and IFN-ω), which are vital for cells to initiate an antiviral response; Type II (for IFN-γ and IL-10), which are involved in regulation of specific immune responses; and tissue factor, which is important in coagulation. The structure of type I IFN receptors is not yet fully understood. An example of type II receptors, IFN-γ binds to ligand binding IFNγR1 subunits, followed by recruitment of IFNγR2 subunits to initiate signal transduction events through activation of associated JAKs. The active IFN-γ receptor consists of two IFNγR1 and two IFNγR2 subunits. IFN receptors signal through distinct combinations of JAKs and STATs, although many of the pathways leading to specificity of response need to be defined.

See Also the Following Articles

Cytokines • JAK-STAT Signaling Paradigm • Mitogen-Activated Protein Kinase Family • Phospholipase C

Glossary

colony stimulating factor (CSF) A factor that stimulates hematopoietic progenitor/precursor cells. The prefix denotes the hematopoietic lineage stimulated by the factor, e.g., G-CSF stimulates granulocyte colony formation; GM-CSF stimulates granulocyte and macrophage/monocyte colony formation.

cytokine An extracellular signaling peptide or protein that mediates cell–cell communication, activating a signaling cascade after interaction with a cell surface receptor.

hematopoiesis The process of development of mature blood cells from stem cells or precursors cells committed to blood cell formation.

interleukin (IL) One of a number of secreted peptides or proteins, produced by lymphocytes or monocytes, that are involved in regulation of the immune system or leukocyte interactions. The number behind IL is the designation of that particular interleukin, e.g., IL-3.

Further Reading

Cheung, J. Y., and Miller, B. A. (2001). Molecular mechanisms of erythropoietin signaling. *Nephron* **87**, 215–222.

Geddis, A. E., Linden, H. M., and Kaushansky, K. (2002). Thrombopoietin: A pan-hematopoietic cytokine. *Cytokine Growth Factor Rev.* **13**, 61–73.

Heinrich, P. C., Behrmann, I., Haan, S., Hermanns, H. M., Muller-Newen, G., and Schaper, F. (2003). Principles of Interleukin (IL)-6-type cytokine signalling and its regulation. *Biochem. J.* **374**, 1–20.

Hermans, M. H. A., van de Geijn, G.-J., Antonissen, C., Gits, J., van Leeuwen, D., Ward, A. C., and Touw, I. P. (2003). Signaling mechanisms coupled to tyrosines in the granulocyte colony-stimulating factor receptor orchestrate G-CSF-induced expansion of myeloid progenitor cells. *Blood* **101**, 2584–2590.

Kotenko, S. V., and Pestka, S. (2000). Jak-Stat signal transduction pathways through the eyes of cytokine class II receptor complexes. *Oncogene* **19**, 2557–2565.

Lin, J.-X., and Leonard, W. J. (2000). The role of Stat5a and Stat5b in signaling by IL-2 family cytokines. *Oncogene* **19**, 2566–2576.

Reddy, E. P., Korapati, A., Chaturvedi, P., and Rane, S. (2000). IL-3 signaling and the role of Src kinases, JAKs, and STATs: A covert liaison unveiled. *Oncogene* **19**, 2532–2547.

Biography

Barbara A. Miller is Four Diamonds Professor and Vice-Chairman of Research in Pediatrics, The Pennsylvania State University College of Medicine, Hershey, Pennsylvania. Her major research interests are in hematopoietic proliferation and differentiation, and in abnormalities that result in leukemia. She holds an M.D. from the Pennsylvania State University College of Medicine and received postdoctoral training at Duke and Harvard Universities. Her research has focused on erythropoietin signal transduction.

Joseph Y. Cheung is Professor of Cellular and Molecular Physiology and Medicine, The Pennsylvania State University College of Medicine, Hershey, Pennsylvania. His major research interests are in regulation of calcium in cardiac and hematopoietic cells, and in exercise physiology. He received a Ph.D. from the Pennsylvania State University College of Medicine, an M.D. from Duke University, and postdoctoral training at Harvard University.

Heme Proteins

Johannes Everse
Texas Tech University Health Sciences Center, Lubbock, Texas, USA

The class of proteins known as heme proteins includes all proteins that contain a heme moiety as a prosthetic group, which may or may not be covalently bound to the protein. The class encompasses proteins with a wide range of functions. Based on their properties, they may be separated into the following three subclasses:

1. Proteins that bind oxygen reversibly. These proteins are designed to transport and/or store oxygen among or within various body tissues.

2. Proteins that bind oxygen and "activate" it. These proteins serve as enzymes, capable of catalyzing an extensive list of reactions. This group also includes the enzymes that react with hydrogen peroxide.

3. Proteins that are unable to bind oxygen, and serve as electron carriers or transporters.

Structural Properties of Heme Proteins

Heme proteins are strongly colored proteins, usually reddish-brown, which is due to the presence of the heme moiety. The heme moiety consists of a substituted protoporphyrin ring, containing a liganded iron atom. In many mammalian heme proteins, the protoporphyrin ring is protoporphyrin IX, shown in Figure 1. Chelated iron, whether ferrous or ferric iron, preferentially forms six liganded structures. In the heme proteins four of these ligands are formed with the nitrogen atoms of the four pyrroles in the protoporphyrin ring. The fifth ligand, often referred to as the proximal ligand, is formed by an amino acid residue of the protein. This residue is a histidine residue in the oxygen-carrying proteins – myoglobin and hemoglobin, where the bond with the oxygen molecule forms the sixth or distal ligand. In heme proteins that serve as enzymes, the fifth ligand may be formed by a histidine, cysteine, methionine, or tyrosine residue. In the electron-carrying cytochromes, both fifth and sixth ligands are occupied by amino acid residues.

Heme Proteins that Serve as Oxygen Carriers

Several heme proteins are specifically designed to bind oxygen reversibly. In higher animals these proteins are hemoglobin and myoglobin. The function of hemoglobin is to take up oxygen in the lungs, and transport it to the various tissues in the body. Myoglobin, present in muscle tissues, takes up the oxygen from the hemoglobin and stores it until it is needed for the production of ATP in the mitochondria.

One oxygen molecule binds to the iron atom of the heme moiety at the sixth position which is vacant in the deoxygenated form of these proteins. The nature of the Fe–oxygen bond has been the subject of many investigations, and is still a matter of some controversy. At the present time it appears that the properties of the oxygenated forms of hemoglobin and myoglobin are best explained by assuming that the bond between the oxygen molecule and the heme iron is a biradical bond, stabilized by d–p orbital overlap.

Myoglobin

Function

Myoglobin serves as an oxygen storage protein in muscle tissues, where it also aids in the diffusion of oxygen into the tissues. Together with the cytochromes, it is responsible for the red-brown color of muscle. The protein is abundant in the heart and skeletal muscles of animals; and it is especially abundant in the muscles of diving mammals, such as whales and seals, where a high capacity for the storing of oxygen is essential.

Structure

The protein is a monomeric heme protein, consisting of a single chain of 153 amino acids, and a non-covalently bound heme moiety. The structure is that of a compact, globular protein, consisting of eight helices, with the heme moiety located in a cleft formed between helices C, E, and F (Figure 2). The fifth ligand to the heme iron is donated by the imidazole nitrogen of histidine residue

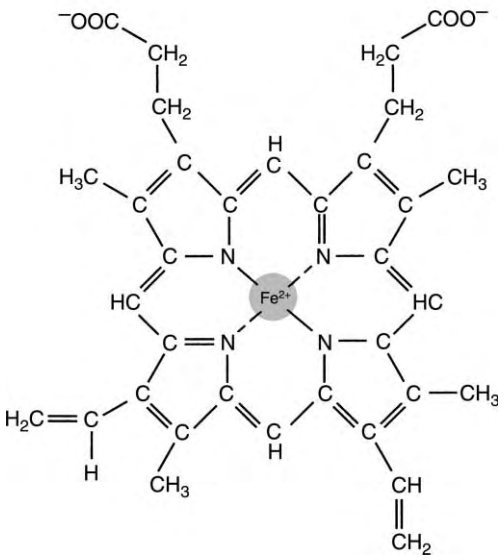

FIGURE 1 Chemical structure of iron-protoporphyrin IX (hemin).

F8 of the F helix. The sixth ligand is formed by the bound oxygen, whereas in deoxymyoglobin the sixth ligand is vacant.

The iron atom in myoglobin is in the ferrous state. Oxidation of the iron to the ferric form yields metmyoglobin, which is unable to bind oxygen, and is therefore no longer functional.

Oxygen Binding

Myoglobin has a high affinity for oxygen, as shown in Figure 3. This fact allows muscle tissues to extract oxygen from the bloodstream.

Hemoglobin

Structure

Hemoglobin is one of the most widely studied proteins. Its structure consists of four subunits, normally an $\alpha_2\beta_2$ tetramer, and each containing a heme moiety with the iron in the ferrous state.

Each α chain consists of 141 amino acid residues, and the β chains have 146 residues each. The three-dimensional structure of the individual subunits is very similar to that of myoglobin, although the amino acid compositions are very different.

Oxygen Binding

Allosteric Effects The tetrameric structure of the molecule is crucial to its biological function. Oxygen does not have a high affinity for deoxy-hemoglobin. However, binding of a molecule of oxygen to one of the hemes causes the Fe atom, which is normally located somewhat above the plane of the heme ring, to be drawn into the plane, a distance of 0.04 nm. This relatively slight movement triggers a change in the protein conformation that is transmitted to the adjacent subunits, which in turn dramatically enhances the affinity of their heme groups for oxygen. The result is that the oxygen saturation curve of hemoglobin has a sigmoidal form, as shown in Figure 3. This strong cooperative effect among the four subunits assures that almost total oxygenation occurs when the hemoglobin passes through the lungs, and that the oxygen is effectively released in the body tissues. A similar change in the position of the heme iron occurs in myoglobin upon the binding of an oxygen molecule; in myoglobin, however, this change in position appears to be non-consequential.

Bohr Effect The affinity for oxygen is also dependent on pH. Lower pH decreases the affinity for oxygen. This is known as the Bohr effect. This effect causes a better unloading of the oxygen in tissues with a high metabolic rate. Such tissues usually have a lower pH, because of the presence of acidic products, such as lactate, citrate, and malate.

Regulation by 2,3-Diphosphoglycerate Oxygen binding to hemoglobin is also regulated by the metabolite 2,3-diphosphoglycerate (2,3-DPG). 2,3-DPG is present in erythrocytes at a concentration similar to that of hemoglobin. Hemoglobin binds one molecule of 2,3-DPG per tetramer. Its regulatory effect on oxygen binding by hemoglobin is most evident when there is a change in altitude. At higher altitudes, where the partial pressure of oxygen is lower, 2,3-DPG binding compensates by shifting the oxygen saturation curve to the right.

Interaction with Other Compounds

In addition to oxygen, other compounds bind to the heme iron of hemoglobin and myoglobin, Among them are the notorious compounds carbon-monoxide and cyanide. Both compounds bind to the heme iron much more strongly than oxygen, thus preventing oxygen from binding. This is the basis for the high toxicity of these compounds, even at low concentrations.

Methemoglobin Formation

The oxygen in oxy-hemoglobin promotes a spontaneous oxidation of the ferrous hemoglobin to ferric hemoglobin or methemoglobin, which is unable to bind oxygen. During this reaction the oxygen is reduced to the superoxide radical, which subsequently dismutates to hydrogen peroxide:

$$\text{Hemoglobin-Fe}^{++} + O_2 \rightarrow \text{Hemoglobin-Fe}^{+++} + O_2^{-\cdot}$$

$$2O_2^{-\cdot} + 2H^+ \rightarrow O_2 + H_2O_2$$

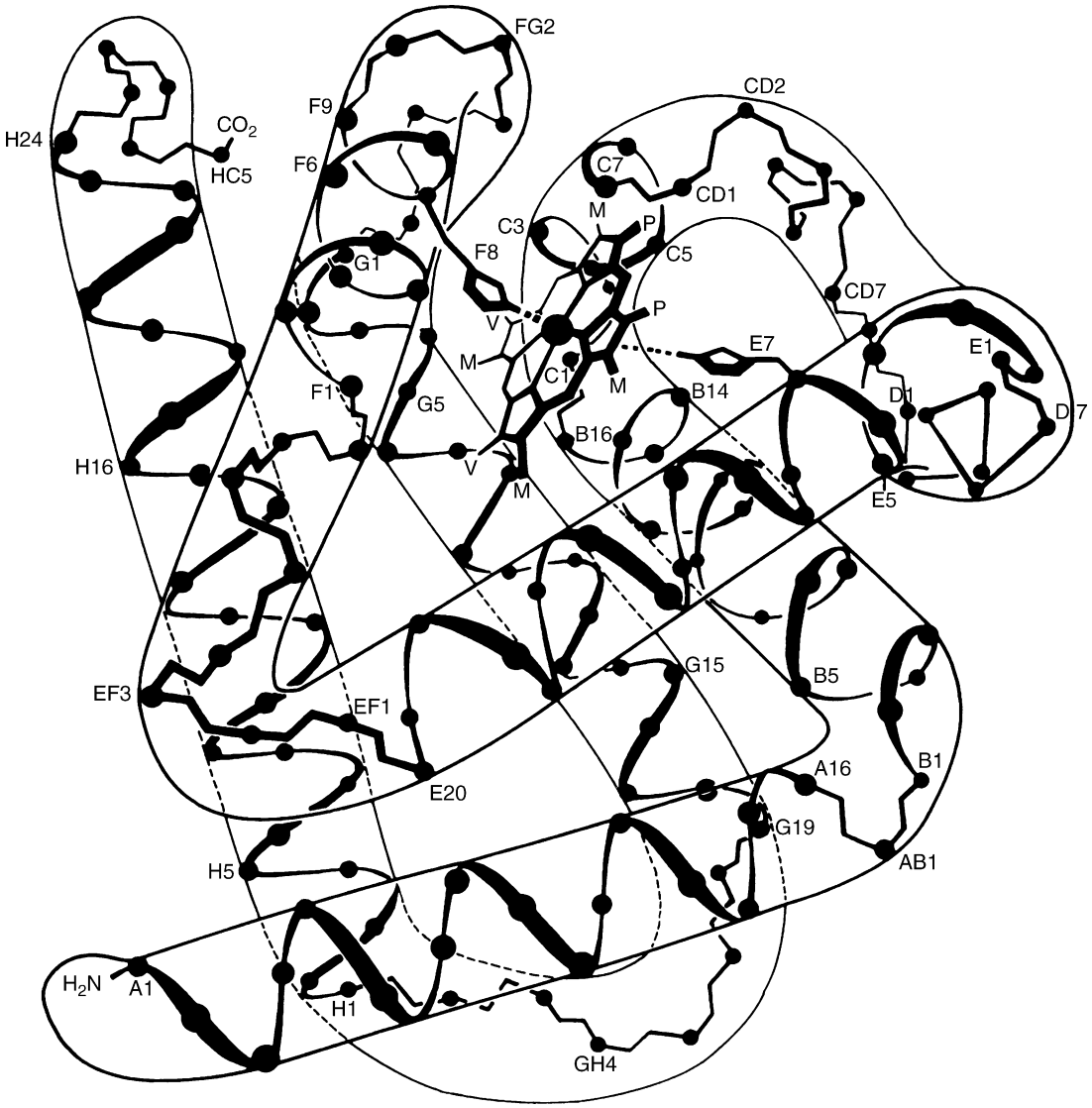

FIGURE 2 Molecular structure of myoglobin. The polypeptide chain consists of eight helices, designated by the letters A through H, linked by short, unordered regions. Amino acids are numbered by their relative position in the chain. Reprinted form Dickenson, R. E. *The Proteins*, 2nd Edition, Vol. II, p. 634, 1964, with permission from Elsevier.

Fortunately, an enzyme present in red cells, methemoglobin reductase, reduces the methemoglobin back to normal hemoglobin, whereas catalase, which is also abundant in erythrocytes, catalyzes the dismutation of hydrogen peroxide to oxygen and water. This mechanism, together with the fact that the oxidation to methemoglobin is rather slow, assures that under normal conditions the amount of methemoglobin present in the red cell is only a few percent of the total hemoglobin present.

Hemoglobin Mutants

Fetal Hemoglobin A large number of mutant hemoglobins are known to exist, most of which are harmless modifications. Several, however, are of physiological importance. Most important among them is fetal hemoglobin or hemoglobin F (HbF), which contains two γ chains instead of two β chains. Its tetrameric constitution is thus $\alpha_2\gamma_2$, instead of the $\alpha_2\beta_2$ configuration of normal hemoglobin (HbA). The γ chain differs from the β chain in that a serine residue is present at position 143 instead of a histidine. This one amino acid substitution causes a shift in the oxygen affinity curve to the left, especially at the upper portion of the curve. Thus, HbF has a higher affinity for oxygen than HbA. This allows the fetus to extract oxygen from its mother's blood in the placenta. HbF is gradually replaced by HbA during the first several months after birth.

Sickle Cell Hemoglobin Another well-known hemoglobin mutant is HbS, or sickle cell hemoglobin. In HbS the amino acid residues at position 6 in the β chains are valines rather than glutamic acid residues. This change causes the deoxy-form of HbS to aggregate

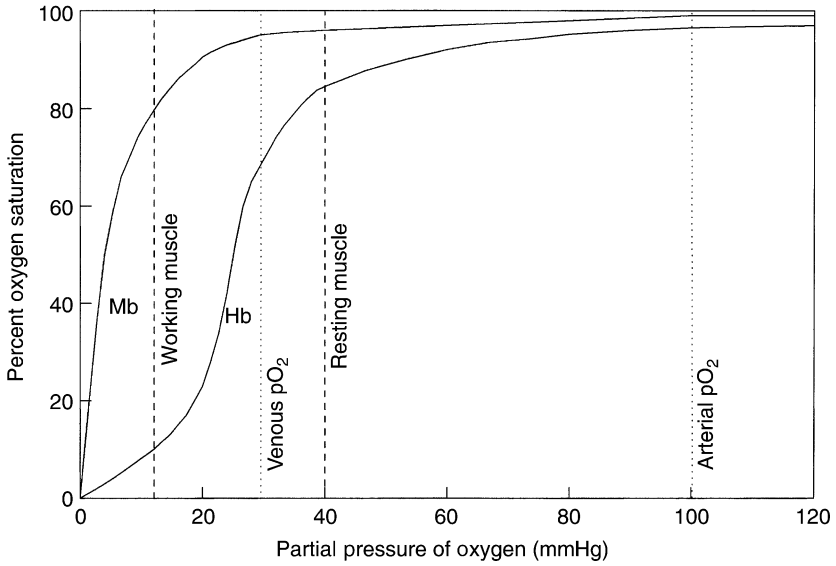

FIGURE 3 Oxygen saturation curves of hemoglobin (Hb) and myoglobin (Mb).

into insoluble fibers. The presence of these fibers distorts the shape of the erythrocytes from a disk-shaped into a sickle-shaped cell. Sickle cells are considerably more fragile than normal erythrocytes, which accounts for the observed anemia in sickle cell patients.

It is estimated that in the USA about three million people suffer from the disease, mostly people of African descent. The reason for the high survival rate of the mutant gene is that HbS provides protection against the malaria parasite, the greatest killer of all times. This parasite spends part of its life cycle in human erythrocytes. However, the HbS is apparently much less suitable for the proper development of the parasite than HbA, thus protecting the sickle cell patients when malaria epidemics occur.

Blood Substitutes

A considerable amount of research has been done recently on the modification of human and bovine hemoglobins in order to produce a suitable product to serve as a blood substitute. This requires a covalent crosslinking of the α and β chains in order to prevent dissociation of the tetramer. Initial clinical trials, however, revealed that hemoglobin can be quite toxic when it is present in large quantities in the circulation outside the confines of the red cell.

Heme Proteins that Serve as Enzymes

A considerable number of heme proteins are found in nature that serve as enzymes. These include most peroxidases and catalases, as well as a large group of monooxygenases generally referred to as the cytochrome P_{450} enzymes. In addition, a few oxidases, hydrolases, and dioxygenases are heme enzymes. Peroxidases and catalases use hydrogen peroxide as the oxidizing agent. The cytochrome P_{450} enzymes, as well as the other enzymes catalyze oxidizing reactions that involve molecular oxygen, of which either one or both atoms are incorporated into a substrate.

Peroxidases

Structure and Function

Peroxidases are a group of enzymes that catalyze the oxidation of a substrate by hydrogen peroxide or an organic peroxide. Most peroxidases are ferric heme proteins; one notable exception being the glutathione peroxidase, which is a selenium-containing enzyme. They are present in virtually all living species.

Most peroxidases are able to oxidize a variety of substrates of widely different structures, varying from halide ions to hydroquinones to aromatic azo compounds. A binding site for the substrate to be oxidized is therefore virtually absent in most of these enzymes. In fact, simple molecules consisting of 8–12 amino acids and a covalently linked heme moiety, with a histidine residue forming the proximal ligand, have considerable peroxidase activity. These compounds are known as microperoxidases. Furthermore, methemoglobin and metmyoglobin can effectively function as peroxidases, having about 5–10% of the activity of horseradish peroxidase.

Mechanism of Action

The mechanism of action of the heme peroxidases is shown in Figure 4. The first step involves an oxidation

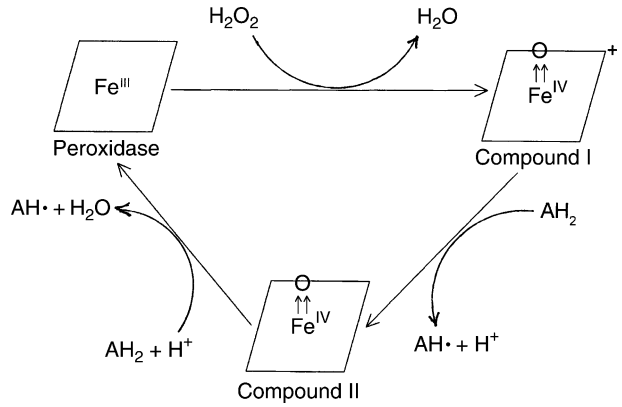

FIGURE 4 Mechanism of action of peroxidases. The two arrows in compounds I and II represent the two unpaired electrons in the biradical bond between the iron and the oxygen atom. The " + " mark in compound I represents the positive charge on the porphyrin ring. AH_2 and $AH^{\cdot}$ represent the substrate and the radical product, respectively.

of the enzyme by the peroxide, leading to the formation of a ferryl (Fe^{IV}) heme moiety and the removal of an electron from either the porphyrin ring or an amino acid residue of the protein. This intermediate is commonly referred to as Compound I. Compound I can then react with a suitable substrate and promote a one-electron oxidation of the substrate. A one-electron oxidation of the substrate (such as the oxidation of a hydroquinone to a semiquinone) converts the enzyme to Compound II, in which the heme is still in the ferryl form, but the original structure of the porphyrin ring or the amino acid residue is restored. Transfer of a second electron from Compound II to a substrate restores the native ferric enzyme.

Of the plant peroxidases, the enzyme from horseradish is perhaps the most studied. It is a 40 kDa monomeric enzyme, with a histidine residue as the proximal ligand. The functions of the peroxidases in plants appear to be the generation of free radical intermediates that promote the polymerizations and crosslinkings necessary to form the cell wall structures in plants. Enzymes present in the roots of plants are thought to protect the host against invading fungi and other microorganisms.

In mammals, the most studied peroxidases are myeloperoxidase present in neutrophils, eosinophil peroxidase present in eosinophils, thyroid peroxidase present in the thyroid gland, and lactoperoxidase present in milk and saliva. Except for the thyroid peroxidase, the function of all these peroxidases seem to involve a defense against invading microorganisms. The function of the thyroid peroxidase is the iodination of tyrosine residues during the synthesis of the hormone thyroxine.

Haloperoxidases

The mechanism by which myeloperoxidase exerts its anti-microbial activity has been largely elucidated by Seymour Klebanoff and his colleagues. The phagocytosis of a microorganism by a neutrophil activates a membrane-bound NADPH oxidase, that excretes large amounts of hydrogen peroxide into the phagosome. The myeloperoxidase reacts with the H_2O_2 to form a Compound I-type structure, which in turn oxidizes a chloride ion to hypochlorite (HOCl) in a reaction involving a two-electron transfer, similar to that of catalase. The hypochlorite formed is lethal to the microorganism. Lactoperoxidase uses a similar mechanism to kill bacteria present in milk or saliva; however, it uses either iodide or isocyanate as the ion to be oxidized. *In vitro*, these enzymes exert a cytolytic activity against most cells, prokaryotic as well as eukaryotic.

Other peroxidases that are capable of oxidizing halide ions include chloroperoxidase present in certain molds. This enzyme carries out organic chlorination reactions, presumably through the formation of an intermediate enzyme-bound form of hypochlorite.

Reactive Oxygen Species

An increasing number of the heme enzymes have recently attracted attention, because of their alleged involvement in the generation of reactive oxygen species (ROSs). ROSs are implicated in causing damage to DNA, RNA, lipids, and proteins, and may be directly or indirectly involved in the initiation of cancer, as well as diseases such as Alzheimers, Parkinsons, multiple sclerosis, and other diseases involving tissue degeneration and cell death. ROSs include superoxide, hydrogen peroxide, the hydroxyl radical, singlet oxygen, and ozone.

It should be clear from the above description that peroxidases are enzymes specifically designed to generate free radical products. Compounds I and II have oxidative energies comparable to that of the hydroxyl radical, and the products generated by these enzymes often are free radicals. These products in turn can promote polymerization reactions of proteins and lipids. Furthermore, it is known from *in vitro* experiments that most if not all peroxidases are able to exert cytolytic activities under appropriate conditions. It is also known that both myeloperoxidase and chloroperoxidase are able to generate singlet oxygen. These observations support the hypothesis that peroxidases may be involved in at least some of the tissue damage that is presently ascribed to the actions of ROSs.

CATALASES

Structure and Function

Catalases are enzymes designed to neutralize the hydrogen peroxide that is formed *in vivo* by various

oxidases and other enzymes. The enzyme catalyzes the dismutation of two moles of hydrogen peroxide into one mole of oxygen and one mole of water:

$$2H_2O_2 \rightarrow 2H_2O + O_2$$

Catalases are found in all aerobic cells; in fact, in some bacteria catalase may account for as much as 1% of their total dry weight. High concentrations are also present in erythrocytes, where it serves to neutralize the hydrogen peroxide formed during the autoxidation of oxy-hemoglobin to methemoglobin. Catalases are among the enzymes with the highest turnover rates known: under optimal conditions each subunit can dismutate 2×10^5 mol of hydrogen peroxide per second.

Catalases in eukaryotes are tetramers, each subunit containing a ferric heme and a bound molecule of NADPH. The reason for the presence of this coenzyme is still unclear at this time. In the catalases, a tyrosine residue forms the proximal ligand to the heme iron.

Mechanism of Action

Their mechanism of action is somewhat similar to that of the peroxidases. Upon binding of a mole of H_2O_2, a Compound I-type intermediate is formed, and a mole of water is released. The enzyme then reacts with a second mole of H_2O_2 to form a mole of oxygen and the native enzyme is regenerated (Figure 5). No radical intermediates are formed by catalases.

Oxygenases

Oxygenases are a group of heme enzymes that catalyze the oxidation of various substrates by molecular oxygen. Certain oxygenases catalyze the incorporation of both oxygen atoms into the substrate; these are referred to as dioxygenases. Others catalyze the incorporation of one atom of oxygen into the substrate, while the other atom is reduced to water. This group constitutes the monooxygenases.

Almost all of the dioxygenases do not contain heme; non-heme iron sulfur groups form their active center. An example of a heme-containing dioxygenase is tryptophan dioxygenase.

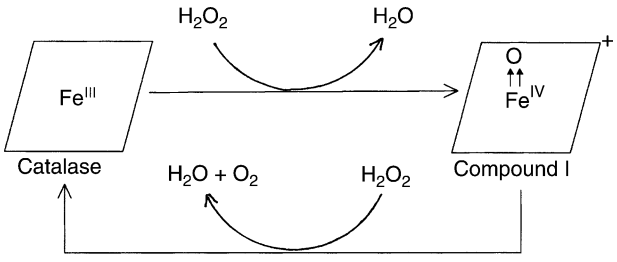

FIGURE 5 Mechanism of action of catalases.

Monooxygenases are also referred to as mixed-function oxygenases or hydrolases. In addition to molecular oxygen, this group of enzymes requires the presence of a co-substrate capable of donating a pair of electrons to reduce the second atom of oxygen to water. A typical monooxygenase reaction is the hydroxylation of an alkane to an alcohol:

$$CH_3-(CH_2)_n-CH_3 + O_2 + RH_2 \rightarrow CH_3-(CH_2)_n-CH_2OH + H_2O + R$$

in which R represents the co-substrate. Many compounds can serve as a co-substrate for the monooxygenases; these include the pyridine nucleotides, flavins, ferredoxins, hydroquinones, ascorbate, and others.

Cytochromes P_{450} Enzymes

The cytochrome P_{450} enzymes are a special group of monooxygenases, all of which use NADPH as the co-substrate. The name of this group of enzymes is associated with their discovery, when it was noted that, in the presence of carbonmonoxide, their absorption spectrum resembles that of the known cytochromes, with the maximum absorbance of the Soret band located at about 450 nm. Functionally, however, they are not related to the group of proteins normally known as cytochromes.

Occurrence

The cytochrome P_{450} family of enzymes are present in all living species. They have been isolated from bacteria, yeasts, plants, insects, as well as from vertebrate animals, where they are present in a large number of tissues. In fact, a list of the sequences of 325 different cytochrome P_{450}'s is presented in Ortiz de Montellano's book "Cytochrome P450" (see Further Reading), and many more have been identified since then.

Functions

The cytochromes P_{450} comprise a large group of enzymes that are able to incorporate one of the two atoms of an oxygen molecule into a broad variety of substrates, with the concomitant reduction of the other oxygen atom to water. Members of the family are known to catalyze hydroxylations, epoxidations, N-oxidations, N-, S-, and O-dealkylations, sulfoxidations, dehalogenations, and other reactions.

The two main functions of the cytochrome P_{450} enzymes appear to include first the control of the steady-state level of endogenous effectors of growth and differentiation. As such, they are important in the metabolism of numerous physiological substrates, including prostaglandins, steroids, cytokines, bile

acids, fatty acids, and biogenic amines. Second, they metabolize a wide range of foreign chemicals, including environmental pollutants, drugs, various natural plant products, and many other foreign materials that enter the body.

Mechanism of Action

The enzymes contain a heme moiety with iron in the ferric state, and with a cysteine residue as the proximal ligand. Oxygen binds as the sixth ligand. The principal catalytic cycle of the cytochrome P_{450} enzymes for a hydroxylation reaction is shown in Figure 6. The first step involves a binding of the substrate XH to the enzyme. In step 2 the ferric enzyme is reduced to the ferrous form with an electron obtained from the co-substrate NADPH. The ferrous enzyme then binds a molecule of oxygen in step 3. In step 4 a second electron from NADPH is used to reduce the oxygen molecule, which leads to the uptake of two protons, the release of a molecule of water, and the formation of a Compound I-type ferryl enzyme. In the final step the oxygen atom of Compound I is incorporated into the substrate, and the product is released. Steps 4 and 5 probably constitute a series of individual steps; however, they occur so fast that they cannot be observed with present-day's techniques.

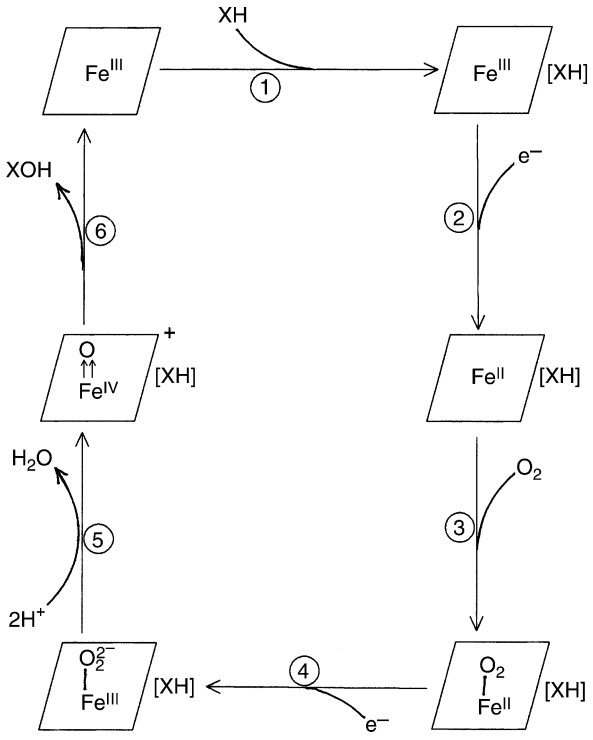

FIGURE 6 Principal catalytic cycle of cytochrome P_{450} enzymes. XH, substrate; XOH, product.

Heme Proteins that Serve as Electron Carriers

Cytochromes

Function

The cytochromes, with the exception of the members of the cytochrome P_{450} family, are heme proteins, designed for the transport of individual electrons. Their heme moiety is normally enveloped by the protein portion, excluding it from contact with the outside solvent. The transport of individual electrons is facilitated by an oscillation of the heme iron between the ferrous and the ferric forms. The flow of electrons from the outer edge of the cytochrome to the heme iron may involve the participation of one or more amino acid residues (e.g., tyrosines). The driving force for the movement of electrons is provided by the differences in redox potential between the electron donor and the acceptor.

Cytochromes are identified by the type of heme moiety present (a, b, c, or d), and the wavelength of maximal absorbance of the Soret band, e.g., cytochrome b_{559}. The four heme moieties differ in the structure of the side chains of the porphyrin ring.

Cytochromes c

c-Type cytochromes are found in animals, plants, and eukaryotic microorganisms. They are the only type cytochrome that is water-soluble. They are monomeric proteins, containing a heme c moiety, with the proximal and distal ligands formed by histidine and methionine residues. They usually contain a single heme per molecule; however, molecules containing up to 8 heme residues are found in certain photosynthetic bacteria. The best-known and most-studied member of this group is the mitochondrial cytochrome c, which transports electrons from Complex II to Complex III in the electron transport system.

Cytochromes b

b-Type cytochromes are widely distributed. They are present in bacteria, chloroplasts, and mitochondria. The mitochondrial b-type cytochromes are normally embedded in membranes as part of Complex II of the electron transport system. They contain a protoheme with histidine in both the proximal and distal ligand positions. The function of all b-type cytochromes appears to be to transport electrons from dehydrogenases to cytochrome c-type proteins or to iron–sulfur proteins.

Cytochromes a

The a-type cytochromes in mitochondria are an important part of the electron transport chain. They form an integral part of Complex III, where they take up electrons from cytochrome c and pass them on to the copper ions and the bound oxygen in the cytochrome oxidase system.

See Also the Following Articles

Cytochrome *c* • Cytochrome P-450 • Hematopoetin Receptors • Heme Synthesis • Iron–Sulfur Proteins

Glossary

biradical bond A chemical bond characterized as a biradical, three-center four-electron bond.

prosthetic group A chemical compound present in and an integral part of an enzyme or protein that is not composed of amino acid residues.

singlet oxygen An oxygen molecule having one electron in an excited state. Chemical notation: $O_2(^1\Delta g)$.

Soret band The most intense absorption band in heme proteins. Also referred to as the γ band.

Further Reading

Alayash, A. I. (2000). Hemoglobin-based blood substitutes and the hazards of blood radicals. *Free Radic. Res.* **33**, 165–175.

Alayash, A. I., Patel, R. P., and Cashon, R. E. (2001). Redox reactions of hemoglobin and myoglobin: Biological and toxicological implications. *Antioxid. Redox Signal* **3**, 313–327.

Brunori, M. (2000). Structural dynamics of myoglobin. *Biophys. Chem.* **86**, 221–230.

Everse, J. (1998). The structure of heme proteins compounds I and II: Some misconceptions. *Free Rad. Biol. Med.* **24**, 1338–1346.

Everse, J., Everse, K. E., and Grisham, M. B. (eds.) (1991). *Peroxidases in Chemistry and Biology*, Vols I and II, CRC Press, Baton Rouge, FL.

Everse, J., Vandegriff, K. D., and Winslow, R. M. (eds.) (1994). *Hemoglobins Methods in Enzymology*, Vols 231 and 232, Academic Press, San Diego, CA.

Garrett, R. H., and Grisham, C. M. (1994). *Biochemistry.* Saunders College Publishing, Orlando, FL.

Ortiz de Montellano, P. R. (ed.) (1995). *Cytochrome P450; Structure, Mechanism, and Biochemistry.* Plenum Press, New York.

Ortiz de Montellano, P. R., and De Voss, J. J. (2002). Oxidizing species in the mechanism of cytochrome P450. *Nat. Prod. Rep.* **19**, 477–493.

Biography

Johannes Everse is a Professor in the Department of Cell Biology and Biochemistry at the Texas Tech University Health Sciences Center in Lubbock, Texas. His principal research interests are in the mechanisms of action and biological functions of heme proteins, and in the utilization of immobilized enzymes in industry and medicine. He holds a Ph.D. from the University of California, San Diego. He has co-edited six books, including two on peroxidases, and two on hemoglobin.

Heme Synthesis

Gloria C. Ferreira
University of South Florida, Tampa, Florida, USA

Heme, a four-ring organic compound with a central iron atom, plays multiple roles in cellular processes. For example, it is the crucial component in hemoglobin, a red blood cell protein responsible, in vertebrates, for the transport of oxygen from the lungs to the different tissues and the transport of carbon dioxide from the tissues to the lungs. It is heme that gives the characteristic red color to blood. Given its importance in many vital functions in organisms ranging from bacteria to man, it is not surprising that most cells synthesize heme. However, in humans, differentiating erythrocytes represent the major site of heme production due to the synthesis of hemoglobin, which accounts for ~85% of the total heme.

Heme Structure

The observation that hemoglobin can be split into two components, with the smaller unit corresponding to the compound which today is recognized as heme, was made by L. R. LeCanu in 1837. While the correct structure of heme was initially proposed by Kuster in 1912, it only received general acceptance 16 years later upon its chemical synthesis. The Nobel Prize winning organic chemist Hans Fischer developed syntheses leading to the assembly of four rings, or pyrroles, into a macrocyclic structure with a purple-red color, which he appropriately named porphyrin (from the Greek porphuros, meaning purple). The chemically synthesized porphyrin, which had properties identical to those of the "natural porphyrin" (derived from heme upon the release of the iron atom), was designated protoporphyrin IX. Thus, heme consists of four rings (pyrroles), composed of carbon, nitrogen, and hydrogen atoms, linked together in a cyclic array and containing an atom of iron in its center (Figure 1).

Heme is now recognized as a member of a larger family of metalated tetrapyrroles, which are essential for life on Earth. They include chlorophylls, cobalamin (vitamin B_{12}), siroheme, and coenzyme F_{430}. Chlorophylls trap the light energy required in photosynthesis. Cobalamin-containing enzymes catalyze intramolecular rearrangements, methylations, and reduction of ribonucleotides to deoxyribonucleotides. Siroheme is an essential component of enzymes involved in sulfur and nitrogen metabolisms. Coenzyme F_{430}, present in methanogenic bacteria, functions in methane formation. While the central metal ions in these tetrapyrroles differ – Fe^{2+} in the case of heme and siroheme, Mg^{2+} in chlorophyll and bacteriochlorophyll, Co^{2+} in cobalamin, and Ni^{2+} in coenzyme F_{430} – the unifying feature is the presence of a complexed metal ion, which promotes a remarkable number of different biochemical reactions. Further, the protein scaffold binding the metalloporphyrin modulates the chemistry (redox state and coordination properties) of the metal ion, such that the spectrum of the reactions expands beyond the normal properties of the metal ion. It is this interplay between the protein moiety and the metalloporphyrin that provides the plethora of functions associated with metalloporphyrin-containing proteins.

The Heme Biosynthetic Pathway

Formation of 5-Aminolevulinate

The biosynthesis of tetrapyrroles is initiated from simple molecules and comprises only a few enzymatic steps (Figure 2). The first committed precursor, 5-aminolevulinic acid (ALA), is synthesized from either succinyl-CoA or glutamate, and thus the names C4 and C5 (based on the number of carbon atoms in the precursor), for the two ALA biosynthetic pathways evolved in nature. In most non-photosynthetic eukaryotes and a few prokaryotes (i.e., the α-proteobacteria), ALA results from the condensation between glycine and succinyl CoA (C4 pathway), while in plants and most bacteria, ALA is derived from glutamate (C5 pathway). The C4 pathway requires a single enzyme, ALA synthase (ALAS); in contrast, three enzymes are involved in the conversion of glutamate into ALA. Specifically, glutamyl-tRNA synthetase converts glutamate to glutamyl-tRNA, which is reduced by glutamyl-tRNA reductase to glutamyl-1-semialdehyde (GSA); this product is then transformed by GSA aminomutase or GSA aminotransferase (GSA-AT) to ALA. Pyridoxal 5′-phosphate, a vitamin B_6-derivative, is an essential component (cofactor) of both ALAS and GSA-AT, as these enzymes cannot function relying solely on the protein moiety. Among prokaryotes, ALAS is only

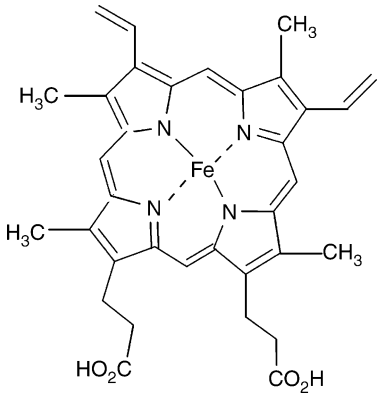

FIGURE 1 Iron–protoporphyrin IX, which is commonly designated as heme. Iron–protoporphyrin IX (or heme) has an iron ion complexed with the conjugated, aromatic porphyrin ring and an asymmetrical side-chain substitution. Note the $-CH_3$ (methyl), $-CH{=}CH_2$ (vinyl), and $-CH_2-CH_2-COOH$ (propionate) groups as side chains.

found in the α-proteobacteria, which are considered to be the most closely related, free-living organisms to the ancestral progenitor of the mitochondrion. Thus, it is conceivable that eukaryotic ALASs were acquired from a free-living α-proteobacterium during its transformation, first to an endosymbiont and subsequently to a mitochondrion.

From ALA to Uroporphyrinogen III

In eukaryotes, the first and three final enzymatic steps of heme biosynthesis occur within mitochondria, while the intervening four occur in the cytosol (Figure 2). Once ALA is made and transported to the cytosol, through a yet unidentified mechanism, two molecules of ALA are asymmetrically condensed to form the monopyrrole porphobilinogen (PBG) by PBG synthase (PBGS; also known as ALA dehydratase). PBG constitutes

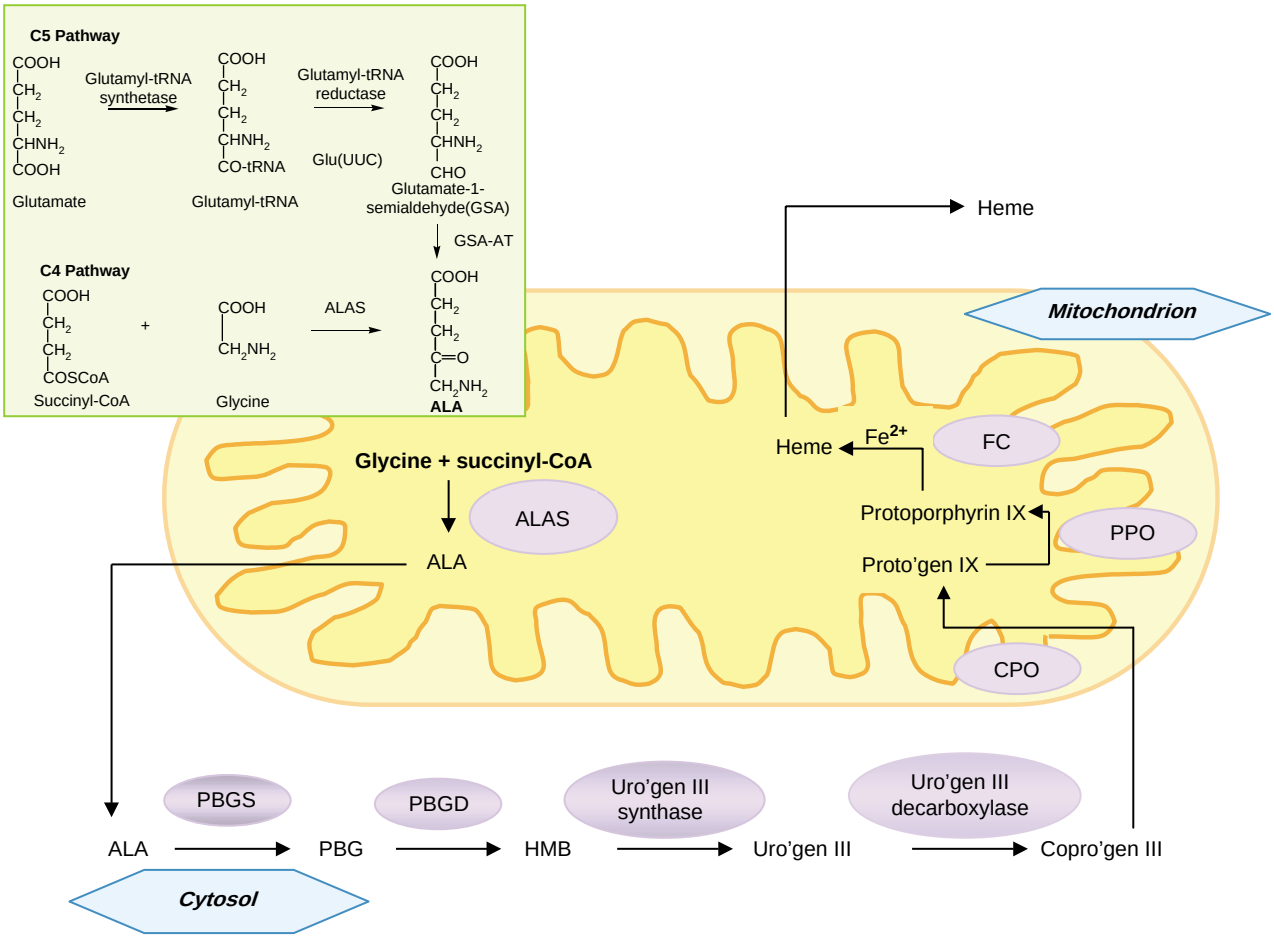

FIGURE 2 Diagrammatic representation of the heme biosynthetic pathway in eukaryotic animal cells. ALA, 5-aminolevulinate; ALAS, ALA synthase; PBG, porphobilinogen; PBGS, PBG synthase; PBGD, PBG deaminase; HMB, hydroxymethylbilane; Uro'gen III, uroporphyrinogen III; copro'gen III, coproporphyrinogen III; CPO, coproporphyrinogen III oxidase; proto'gen IX, protoporphyrinogen IX; PPO, protoporphyrinogen IX oxidase; FC, ferrochelatase. Inset: The two paths to ALA.

the building unit of tetrapyrroles and hence eight molecules of ALA are required to form one heme molecule. Crystal structures of PBGSs from different species have confirmed the presence of two distinct binding sites for each ALA molecule, termed A and P to distinguish the two ALA substrate molecules. The A-side of ALA forms the acetyl half of PBG, leaving its amino group intact, while the P-side of ALA forms the propionyl half of PBG with the amino group becoming part of the PBG ring. PBGS has a homo-octomeric structure composed of four dimers, and each subunit contains an active site metal ion (zinc or magnesium and/or potassium depending on the species) and in many cases an allosteric metal ion (magnesium). The next step in heme biosynthesis involves the deamination and stepwise polymerization of four PBG molecules by PBG deaminase to give the linear tetrapyrrole 1-hydroxymethylbilane. Then, uroporphyrinogen III synthase catalyzes the cyclization of the linear tetrapyrrole, whereby the D ring of hydroxymethylbilane is inverted to generate the asymmetrical macrocycle, uroporphyrinogen III. In the absence of uroporphyrinogen III synthase, 1-hydroxymethylbilane cyclizes into the non-physiological relevant tetrapyrrole, uroporphyrinogen I. The incredible acrobatics that must occur with the flipping of the D ring and closure of hydroxymethylbilane speak for the importance of uroporphyrinogen III synthase in making uroporphyrinogen III synthesis reaction. In fact, disastrous consequences emerge with the malfunction of uroporphyrinogen III synthase, as observed in patients with the blood disorder porphyria cutanea tarda, who typically have high levels of uroporphyrinogen I and derivatives thereof.

From Uroporphyrinogen III to Protoporphyrinogen IX

For most eukaryotes, the last cytosolic step is the sequential decarboxylation of the four acetate side chains of uroporphyrinogen III to methyl groups by uroporphyrinogen decarboxylase (Figure 2). This enzyme is a $(\alpha/\beta)_8$ barrel protein, which appears to be functional as a homodimer and not to require prosthetic groups or cofactors. The uroporphyrinogen decarboxylase-catalyzed reaction gives coproporphyrinogen III, which is the substrate of coproporphyrinogen oxidase (CPO). The oxidative decarboxylation of the propionate side chains of the rings A and B of coproporphyrinogen III yields protoporphyrinogen IX. While eukaryotic CPO activity depends on oxygen, prokaryotic organisms, under anaerobic conditions, use alternative electron acceptors in the oxidative decarboxylation reaction. Hence, oxygen-independent CPOs (HemN and HemZ, i.e., the products of the *hemN* and *hemZ* genes) are found in bacteria; indeed, facultatively anaerobic bacteria, such as *Escherichia coli*, possess both oxygen-dependent CPO (HemF) and oxygen-independent CPO (HemN). Recently, it has been found that HemN contains an iron–sulfur center ([4Fe–4S]), which is essential for the activity of the enzyme in conjunction with NAD(P)H and *S*-adenosyl-L-methionine (SAM). As one would expect, the enzyme appears to have a distinct reaction mechanism with the involvement of SAM in the formation of a radical, and thus HemN has been aptly identified as a "radical SAM enzyme." As far as the subcellular location of the oxygen-dependent CPO goes, it seems to vary! In mammals and other higher eukaryotes, it appears to be associated with the inner side of the mitochondrial outer membrane, whereas in the yeast *Saccharomyces cerevisiae* and bacteria it is found in the cytosol.

From Protoporphyrinogen IX to Heme

In the penultimate step, protoporphyrinogen oxidase (PPO) catalyzes the complete aromatization of protoporphyrinogen IX ring into protoporphyrin IX, which involves a six-electron oxidation (Figure 2). Similar to CPO, anaerobic and facultative anaerobic bacteria have an oxygen-independent PPO; however, in contrast to CPO, facultative anaerobic bacteria possess solely an oxygen-independent PPO (and not in complementation with an oxygen-dependent PPO). All other organisms appear to have PPOs, which use oxygen as the terminal electron acceptor. Ferrochelatase catalyzes the terminal step of the heme biosynthetic pathway, the insertion of ferrous iron into the protoporphyrin IX macrocyclic ring. Eukaryotic ferrochelatases associate with the inner side of the mitochondrial inner membrane, and vertebrate enzymes have a [2Fe–2S] cluster (although this is not an exclusive structural feature of vertebrate ferrochelatases). The mechanism of the ferrochelatase reaction involves an out-of-plane distortion of the porphyrin, which facilitates the reaction by exposing the pyrrole nitrogens to the incoming ferrous iron substrate.

Regulation of the Heme Biosynthetic Pathway/ Heme Biosynthesis

There is not a single ubiquitous regulatory mechanism for heme biosynthesis, and so the discussion in this entry will focus solely on the regulation of the pathway in mammalian cells. Considering that heme is predominantly synthesized in bone marrow (i.e., in erythroblasts and reticulocytes that still contain mitochondria) and

liver cells, most of the studies on regulation have focused on these two types of cells. Predominance of heme synthesis in bone marrow and liver cells reflects the greater demands due to the syntheses of the heme-containing proteins, hemoglobin, and cytochrome P-450 enzymes, respectively. The major regulatory and rate-limiting step of the pathway corresponds to the reaction catalyzed by ALAS, the first enzyme of the pathway. Two genes, located in two different chromosomes in humans, encode the two ALAS forms of the enzyme (or isozymes): ALAS1 and ALAS2. The gene encoding ALAS1 is expressed in every cell, whereas that for ALAS2 is specifically expressed in erythroid cells. Importantly, the regulatory mechanisms for the expression of the two ALAS genes and the post-transcriptional events seem to be distinct in differentiating erythrocytes from those in non-erythroid cells. ALAS1 controls the production of heme for basic cellular functions and is feedback-regulated by heme through inhibition of (1) transcription of the ALAS1 gene, (2) translation of the ALAS1 message, (3) import of the cytosolic precursor form of the enzyme into mitochondria, and (4) enzymatic activity. In contrast, certain drugs and hormones induce liver cells to make more ALAS, and consequently heme and cytochrome P-450, by activating transcription of the ALAS1 gene.

In differentiating erythroid cells, the syntheses of heme and globin need to be coordinated, as the production of hemoglobin requires that neither the protein (globin) component nor the non-protein component (heme) will be in excess. And indeed, identical transcriptional elements have been identified in the genes of ALAS2 and globin. Another level of regulation of the erythroid heme biosynthetic pathway is centered at the stage of translation, which responds to the cellular iron levels. This response is mediated through specific interactions between an iron-responsive element (IRE), present in the ALAS2 mRNA, and IRE-binding proteins, such that under iron limitation, the translation of ALAS2 mRNA is inhibited, while the presence of iron above the cellular threshold relieves the repression caused by IRE-binding proteins. The essential requirement for ALAS2 in heme biosynthesis and erythropoiesis was clearly demonstrated with targeted disruption of ALAS2 in the mouse, which led to no hemoglobin in cells, the accumulation of iron (albeit in the cytoplasm and not in mitochondria) and, ultimately, embryonic death.

Heme Function

The known roles of heme are many and variable, and most probably many other functions await discovery. As referred to above, heme is a prosthetic group of proteins involved in oxygen transport such as hemoglobins and myoglobins, which are the major blood and muscle proteins, respectively. In addition, heme participates in other cellular processes including anaerobic and aerobic respiration, sensing of diatomic gases (e.g., nitric oxide and carbon monoxide), detoxification of foreign substances (e.g., drugs) by oxidative metabolism, and signal transduction. Some of these functions might also be coupled with the regulatory roles of heme in gene transcription, translation, mitochondrial protein import, protein stability, and differentiation. Recently, a transcription factor that regulates the mammalian biological clock was discovered to use heme as a cofactor to sense, and react to, changes in the cell, thus linking cellular metabolism with the biological clock. Another area of research has led to the emergence of a new proposal that heme deficiency or dysregulation is intimately associated with the aging process, including neural decay.

Disorders of the Heme Biosynthetic Pathway

Malfunction of the heme biosynthetic pathway can have disastrous consequences, and in humans it can be

TABLE I

Heme Biosynthesis-Associated Disorders

Disorder	Defective enzyme
X-linked sideroblastic anemia	5-Aminolevulinate synthase (erythroid)
ALA dehydratase, or Doss, porphyria	Porphobilinogen synthase (or ALA dehydratase)
Acute intermittent porphyria	Porphobilinogen deaminase
Congenital erythropoietic porphyria	Uroporphyrinogen III synthase
Porphyria cutanea tarda	Uroporphyrinogen decarboxylase
Coproporphyria	Coproporphyrinogen oxidase
Variegate porphyria	Protoporphyrinogen oxidase
Erythropoietic protoporphyria	Ferrochelatase

manifested in porphyrias. Briefly, porphyrias are disorders that result from inherited or acquired defects in the heme biosynthetic pathway. The first reports of porphyrias were in 1874. Since then, seven types of porphyrias associated with defects in each of the seven enzymes beyond the first step of the pathway have been identified (Table I), and depending on the major site of expression of the enzymatic defect, they have been classified into hepatic or erythropoietic porphyria. Although the molecular mechanisms behind the clinical manifestations are not well understood, the two major symptoms include cutaneous photosensitivity and central nervous system disturbances, and thus the other classification of either photosensitive or neurological porphyrias. Some porphyrias, however, manifest overlapping symptoms. Photosensitivity is a result of porphyrin accumulation, which occurs when the defective enzyme is anywhere in the pathway beyond the third step of the pathway (i.e., the PBG deaminase-catalyzed reaction), whereas the neurologic manifestations are associated with overproduction of ALA and PBG. Since the 1980s, many of the genetic mutations responsible for the enzymatic defects have been identified and mouse models, targeted to correct the defective enzyme, have been developed by engineering functional enzyme expression in bone marrow cells. Finally, mutations in the gene encoding for the erythroid ALAS are associated with X-linked sideroblastic anemia (Table I), a blood disorder characterized by mitochondrial iron accumulation due to a reduction in heme biosynthesis destined for hemoglobin production in erythroblasts.

See Also the Following Articles

Hematopoetin Receptors • Heme Proteins • Porphyrin Metabolism

Glossary

erythroblast Erythroid cell precursor; nucleated cell in bone marrow that develops into an erythrocyte.

erythrocyte A red blood cell; non-nucleated, disk-shaped blood cell that contains hemoglobin.

erythroid Erythrocyte-related.

erythropoiesis Formation and production of erythrocytes.

tetrapyrrole A general term that refers to molecules with four rings of the pyrrole type, most often linked together by single-atom bridges between the α-positions of the five-membered pyrrole rings. The arrangement of the four rings is macrocyclic in porphyrins.

Further Reading

Ferreira, G. C. (1999). 5-Aminolevulinate synthase and mammalian heme biosynthesis. In *Iron Metabolism. Inorganic Biochemistry and Regulatory Mechanism* (G. C. Ferreira, J. G. Moura and R. Franco, eds.) pp. 15–34. Wiley-VCH, Weinheim, Germany.

Kadish, K. M., Smith, K. M., and Guilard, R. (2000). *The Porphyrin Handbook*. Academic Press, San Diego, CA.

Lee, G. R., Foerster, J., Lukens, J., Paraskevas, F., Greer, J. P., and Rodgers, G. M. (1999). *Wintrobe's Clinical Hematology*. William and Wilkins, Baltimore, MD.

Panek, H., and O'Brian, M. R. (2002). A whole genome view of prokaryotic haeme biosynthesis. *Microbiology* **148**, 2273–2282.

Ponka, P. (1999). Cell biology of heme. *Am. J. Med. Sci.* **318**, 241–256.

Rodgers, K. R. (1999). Heme-based sensors in biological systems. *Curr. Opin. Chem. Biol.* **3**, 158–167.

Biography

Dr. Gloria C. Ferreira is a Professor in the Department of Biochemistry and Molecular Biology at the University of South Florida College of Medicine in Tampa. Her major research interest is on heme biosynthesis, including the reaction mechanisms of the enzymes of the mammalian heme biosynthetic pathway and their regulation. She holds a Ph.D. from the University of Georgia and served as a postdoctoral fellow at The Johns Hopkins University School of Medicine. She has authored and edited texts in the fields of heme and iron metabolisms and was Chair of the 2002 Gordon Research Conference on the Chemistry and Biology of Tetrapyrroles.

Hepatocyte Growth Factor/Scatter Factor Receptor

Selma Pennacchietti and Paolo M. Comoglio
University of Turin, Turin, Italy

Hepatocyte growth factor/scatter factor (HGF/SF) receptor is the prototype of a distinct tyrosine kinase receptor family, which also includes Ron, and is encoded by the c-*Met* proto-oncogene. Its ligand, HGF/SF, is a mesenchymal cytokine which belongs to the scatter factor protein family and is responsible for activating a genetic program that includes cell detachment, repulsion, protection from apoptosis, invasiveness of extracellular matrices, and proliferation. This pleiomorphic response is defined as "invasive growth," a process which accounts for morphogenetic cell movements through the matrix and for ordered building of epithelial tubules. Dysfunctions in invasive growth cause enhanced proliferation, uncontrolled migration into surrounding tissues, and failure to differentiate, all events that foster tumor growth and metastasis.

Hepatocyte Growth Factor/Scatter Factor

Hepatocyte growth factor (HGF) and scatter factor (SF) were discovered independently for their abilities to induce the proliferation of primary hepatocytes and dissociation/motility of epithelial cells (scattering), respectively. After biochemical purification and cDNA cloning, the two proteins were shown to be the same molecule. Later it became clear that both the mitogenic action and the scatter effect are different facets of a complex biological response that follows activation of the same receptor.

Scatter Factor Family

HGF/SF belongs to a family of structurally related soluble molecules, named scatter factors, consisting of HGF/SF and its homologue macrophage stimulating protein (MSP).

Structure

HGF/SF is a heparin-binding glycoprotein consisting of a 62-kDa α-chain linked to a 32/34-kDa β-chain by a disulfide bond. The α-subunit is characterized by the presence of an N-terminal 'hairpin' loop and by four repeated domains, named kringles (80 amino acids forming double-looped structures stabilized by three internal disulfide bridges), homologous to those found in plasminogen. Kringles are protein–protein interaction motifs and contain the binding sites for both the high-affinity receptor—Met tyrosine kinase, and the low-affinity receptor—heparin sulfate proteoglycans. The latter, being membrane bound, allows accumulation of HGF/SF in the proximity of target cells. The β-chain of HGF/SF is highly homologous to serine proteases of the blood-clotting cascade, but lacks enzymatic activity due to the replacement of critical amino acids in the catalytic site (Figure 1).

Activation of pro-HGF

The heterodimeric HGF/SF derives from a biologically inactive single-chain precursor (pro-HGF), which is secreted and stored by coupling to proteoglycans. In the extracellular environment, pro-HGF is converted to its bioactive form by a single proteolytic cleavage between R^{494} and V^{495}. A number of proteases have been reported to perform this cleavage *in vitro*, including urokinase-type (uPA) and tissue-type plasminogen activators; coagulation factor XII and one homologous serine-protease (XII-like factor).

HGF/SF Receptor

The high-affinity receptor for HGF/SF is a tyrosine kinase encoded by the *c-Met* proto-oncogene. It was originally identified as a transforming sequence derived from a chromosomal rearrangement, induced by a chemical carcinogen *in vitro*, between *5′* sequences derived from translocated promoter region (Tpr), encoding a leucine zipper-dimerization motif, and the cytoplasmic domain of Met, excluding the juxta-membrane region. Later, Tpr-Met was also found to be a product of chromosomal translocation in rare,

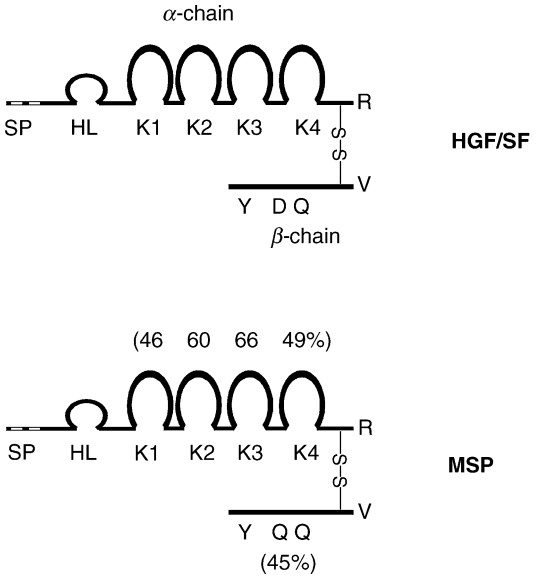

FIGURE 1 A diagram of the structure of scatter factors HGF/SF and MSP. Both are heterodimers consisting of a heavy α-chain and a light β-chain held together by a disulfide bond. The mature heterodimer is formed by proteolytic digestion at a specific dibasic arginine–valine (R–V) site. Starting from the amino-terminal signal peptide (SP), the α-chain contains a hairpin loop (HL) followed by four kringles (K), whereas the β-chain contains a serine-protease-like structure. The lack of proteolytic activity in the HGF/SF molecule is due to the replacement of the histidine and serine residues lying within the catalytic site of conventional serine proteases with glutamine (Q) and tyrosine (Y), respectively. The same substitutions, together with replacement of an aspartate (D) with glutamine (Q), are present in MSP. The percentage of homology of individual kringles as well as the β-chain between the two molecules is also specified.

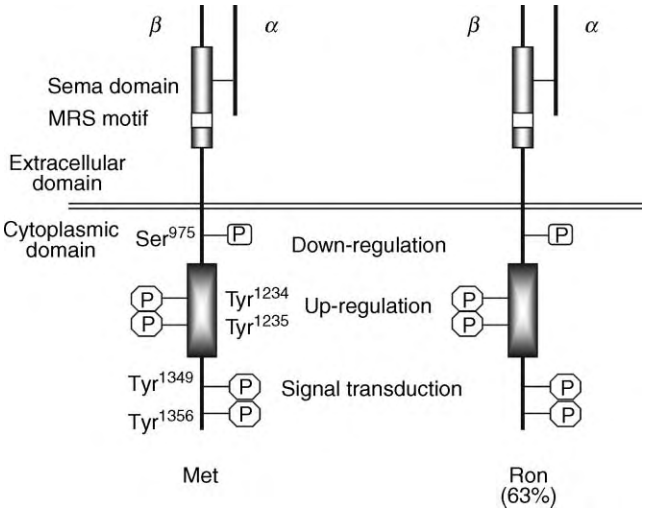

FIGURE 2 The tyrosine kinase family of scatter factor receptors. The HGF/SF receptor, Met, and the MSP receptor, Ron, share a 63% overall percentage homology. Met and Ron are disulfide-linked heterodimeric proteins formed by an extracellular α-chain and by a β-chain, that spans the plasma membrane and contains the tyrosine kinase domain (box in the cytoplasmic domain). The extracellular domains of Met and Ron include the Sema domain (common to the signaling molecules semaphorins and to their receptors' plexins) and the Met-related sequence (MRS). In the cytoplasmic domain, residues endowed with regulatory and transduction activity are conserved in both receptors. In the HGF/SF receptor, upon phosphorylation, a serine in the juxta-membrane region (Ser^{975}) down-regulates the kinase activity. Two phosphotyrosines in the kinase domain (Tyr^{1234} and Tyr^{1235}) up-regulate the kinase activity in an autocatalytic fashion. Finally, phosphotyrosines in the C-terminal tail (Tyr^{1349} and Tyr^{1356}) form a multifunctional docking site that recruits the full spectrum of signal transducers required to induce invasive growth.

naturally occurring cancers. In the intracellular fusion protein, Tpr provides stable dimerization that mimics the effect of the natural ligand and induces constitutive activation of the Met kinase.

Structure

The HGF/SF receptor Met is the prototypic member of a distinct family of protein tyrosine kinases sharing a highly homologous structure. The MSP receptor, encoded by the *Ron* proto-oncogene, is another member of this receptor family, while the product of the *Sea* proto-oncogene, once listed as a third member of the family, has recently been recognized as the avian counterpart of *Ron*. These receptors are single-pass cell membrane glycoproteins with unique structural features: they are dimeric molecules composed of a 50-kDa α-chain disulfide-linked to a 145-kDa β-chain in an α/β complex of 190 kDa. The α-chain is exposed at the cell surface and the β-chain spans the plasma membrane (Figure 2). The HGF/SF receptor, synthesized as a large precursor (pr170) that includes both the α-chain and the β-chain, undergoes cotranslational glycosylation and is further cleaved by proteases of the furin family to form the mature subunits. Both the α-subunit and the β-subunit are necessary for biological activity.

The extracellular moiety of the β-chain contains distinctive features, namely a cysteine-rich motif called Met-related sequence (MRS) which is embedded in a larger region (Sema domain); both are present also in the signaling molecules, semaphorins, and in their receptors, plexins. The intracellular portion of the HGF/SF receptor can be divided into three functional domains: a juxtamembrane domain, a tyrosine kinase catalytic domain, and a C-terminal tail.

The juxtamembrane domain is endowed with a negative regulatory role: phosphorylation of a serine residue (S^{975}) by either protein kinase C or Ca^{2+}/calmodulin-dependent kinases results in a strong inhibitory effect on receptor activity.

The tyrosine kinase catalytic domain contains the major phosphorylation site, represented by tyrosine residues Y^{1234} and Y^{1235} (conserved in *Ron*) which are essential for full activation of the enzyme. Following ligand-induced dimerization, transphosphorylation of

these residues causes the up-regulation of the enzymatic activity of the Met kinase in an autocatalytic fashion.

The C-terminal tail domain of the HGF/SF receptor is crucial for its biological activity; the tail comprises of a short sequence containing two tyrosines that are phosphorylated on HGF/SF binding and are responsible for mediating high-affinity interactions with multiple signal transducers containing Src homology-2 (SH2) domains, phosphotyrosine-binding (PTB) domains, or a peculiar Met-binding domain (MBD).

Signal Transduction

The HGF/SF C-terminal domain is unique among receptor tyrosine kinases because it contains a single, multifunctional docking site, made of a tandemly arranged degenerate sequence Y^{1349}*VHV*NATY^{1356}*VNV*, responsible for the bulk of receptor-signaling activity. While the majority of tyrosine kinase receptors use different phosphotyrosines to recruit distinct signal effectors, this sequence is able, alone, to recruit multiple signal transducers and adaptors, triggering a pleiotropic response. When phosphorylated, these two tyrosines interact with Grb2, p85/phosphatidylinositol 3-kinase (PI3K), phospholipase C-γ (PLC-γ), stat-3, Shc, SHP2 phosphatase and the large adaptor protein Gab1. Grb2, which has a strong requirement for asparagines in the $+2$ position specifically interacts only with the sequence Y^{1356}VNV.

The multifunctional docking site is an absolute requirement for Met signaling. When the two tyrosines are substituted with phenylalanines, cells become completely unresponsive to HGF/SF *in vitro*, even when the receptor's intrinsic catalytic activity is activated by oncogenic point mutations, and transgenic mice that express this mutant display a lethal phenotype that resembles the one observed in *Met*-knock-out animals. In mirror experiments, artificial insertion of this sequence into other receptor tyrosine kinases allows them to switch their conventional biological responses into promotion of invasive growth.

The components of the signal transduction machinery implicated in individual Met-mediated biological responses have been partially elucidated. Coupling of the receptor to the Ras-mitogen-activated protein kinase (MAPK) pathway is both essential and sufficient for proliferation. Conversely, activation of PI3K as well as the Ras/Rac/Rho pathways is required to induce motility. Activation of stat3 and PLC-γ is required for cell polarization and formation of branched tubular structures. The simultaneous activation of the Ras cascade, which promotes growth, and the PI3K pathway, which promotes motility and suppresses apoptosis, leads to efficient cell dissociation, invasion of the extracellular matrix, and metastasis, whereas isolated activation of either pathway does not. Moreover, the morphogenetic response, which is specifically induced by the HGF/SF receptor and cannot be elicited by other receptor tyrosine kinases, involves Gab1 and Stat3.

Biological Activity

HGF/SF Receptor Induces Invasive Growth

Although originally identified as a mediator of growth and motility, it is now clear that the HGF/SF-Met receptor system promotes a highly integrated biological program, referred to as invasive growth, which leads to proliferation, dissociation and migration, invasion of extracellular matrix, prevention of apoptosis, cell polarization, and tubule formation. The best example of how these apparently independent effects are, indeed, part of a single complex phenomenon is the formation of tubular structures in response to HGF/SF (Figure 3). This event strongly resembles the branching morphogenesis occurring during embryonal organogenesis.

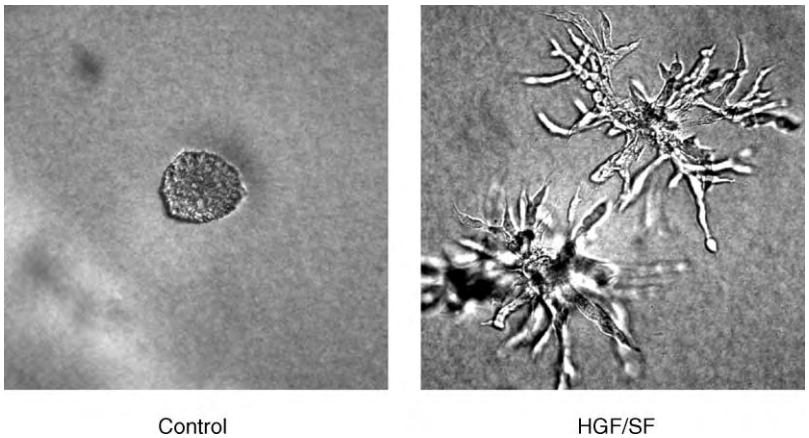

FIGURE 3 HGF/SF-induced branching morphogenesis on epithelial liver progenitor cells (MLP29). Tubule formation was observed culturing the cells within a collagen matrix for 2–3 days in the presence of 20 ng ml^{-1} recombinant factor.

Several epithelial cell lines derived from liver, mammary gland, kidney, prostate, and lung can form spheroid-like structures when grown in collagen gels. Upon HGF/SF stimulation, the cells which form these structures dissociate from each other by disrupting the cell–cell junctions, degrade the extracellular matrix, acquire transient migratory and invasive properties, and finally polarize to form differentiated tubular structures.

Morphogenetic Role in Embryogenesis

During gastrulation, HGF/SF and its receptor are both selectively expressed in the endoderm and in the mesoderm. Subsequently, the expression of HGF/SF becomes limited to the mesenchymal cells, while that of the receptor is induced in the surrounding ectoderm. At this stage (approximately E13), HGF/SF contributes to the development of several epithelial organs (e.g., lungs, liver, and gut) and induces the migration of specific myogenic precursor cells. HGF/SF, in fact, is expressed in the limb mesenchyme and can thus provide the signal for migration, which is received by *c-Met* expressing myogenic precursors.

Illuminating observations concerning the role of the HGF/SF receptor in embryogenesis came from the analysis of transgenic mice, where factor or receptor genes had been targeted. Complete knock-out embryos die *in utero* due to hyponutrition, caused by a reduction of the labyrinth layer of the placental trophoblast, which is normally responsible for controlling the invasion of maternal tissues to expand the placenta. Moreover, these embryos display impaired development of the liver and lack skeletal muscles deriving from long-range migrating precursors.

Several observations indicate that HGF/SF and its receptor play an important role in the process of epithelial morphogenesis. One of the best examples is given by the formation of kidney tubules from metanephric tissue and ureteric bud. Metanephric mesenchymal cells secrete HGF/SF whereas epithelial cells of the ureteric bud express the HGF/SF receptor. When the latter contact the metanephros, they form branching tubules; in turn, some of the metanephric cells start to express the receptor for HGF/SF and, stimulated by the autocrine loop, undergo a process known as "mesodermic–epithelial transition." They acquire epithelial features, form cell–cell junctions, polarize, and eventually form tubules. The mammary gland is a good example of an organ that undergoes major morphological changes after birth and in which branching development takes place during pregnancy and lactation. This program of differentiation relies on sequential stimulation of the epithelium by HGF/SF and neuregulin, which are secreted by the mesenchyme in different developmental stages. HGF/SF is expressed at puberty and promotes branching of the ductal tree, whereas neuregulin is responsible for alveolar budding and production of milk during pregnancy and lactation.

Trophic Role in Adult Life

In adult animals, HGF/SF has been found to stimulate regeneration of organs such as liver, kidney, and lungs after injury, and to promote cell survival in the presence of pro-apoptotic cytokines or drugs. Other than stimulating development and regeneration of epithelial organs, HGF/SF is a potent angiogenic factor, and is able to induce remodeling of cartilage and bone, by stimulating both proliferation and motility. HGF/SF is also a hematopoietic factor, produced by the bone marrow stroma. It stimulates growth and differentiation of multipotent and erythroid precursors, modulating their adhesive contacts with the surrounding stroma and promoting the spread of differentiated cells into the bloodstream.

Finally, the HGF/SF receptor plays a role in the development of neurons, as predicted by detection of expression of both factor and its receptor in the mouse nervous system. HGF/SF promotes survival of sensory and sympathetic neurons and stimulates the outgrowth of their axon, an invasive process restricted to a single part of the cell.

The HGF/SF Receptor in Human Tumors

The *Met* oncogene is associated with, and in some cases directly responsible for, a wide variety of human cancers. The most convincing evidence for the involvement of the HGF/SF receptor in human cancer arose from analysis of patients affected by hereditary papillary renal carcinoma (HPRC), a form of inherited cancer, characterized by the presence of multiple, bilateral tumors. These patients bear germ-line missense mutations of the HGF/SF receptor that are also found in somatic cells of patients affected by sporadic renal carcinomas or childhood hepatocellular carcinoma. Some mutations are homologous to those found in the oncogenes *Ret* or *Kit*, which are responsible for inherited multiple endocrine neoplasia (type 2) or for hematological disorders, respectively. *In vitro* studies show that these mutated forms of Met display an increased tyrosine kinase activity, are transforming, and confer to cells in nude mice the ability to form tumors and to overcome apoptosis. Unexpectedly, it has been demonstrated that tumorigenesis is dependent on stimulation by the ligand and is abolished in the presence of HGF/SF-specific inhibitors. Conceivably, the onset of HPRC depends both on the presence of inherited Met mutations and on availability of HGF/SF. Furthermore, it has been reported that somatic

mutations of *Met* are selected during metastatic spread of head and neck squamous carcinoma.

Met overexpression is the most common alteration found in human tumors of epithelial origin, in stringent association with metastatic tendency and poor prognosis. In the case of colorectal carcinoma, amplification of the *Met* gene, associated with protein overexpression, confers a selective advantage for acquiring metastatic potential to the liver.

Tumorigenesis can also be associated with ectopic expression of the HGF/SF receptor, as in aggressive osteosarcomas, melanomas, and glioblastomas. Aberrant expression of Met in human tumors of mesenchymal origin is often associated to the secretion of HGF/SF by the same cells, causing formation of autocrine loops which provide invasive properties. The autocrine circuit can sustain not only the persistent activation of the receptor, but also its overexpression, since HGF/SF stimulates *Met* transcription.

See Also the Following Articles

Cell Death by Apoptosis and Necrosis • Mitogen-Activated Protein Kinase Family

Glossary

apoptosis Programmed cell death, the body's normal method of disposing of damaged, unwanted, or unneeded cells.

knock-out The excision or inactivation of a gene within an intact organism or even animal (e.g., "knock-out mice"), usually carried out by a method involving homologous recombination.

src homology 2 (SH2) domains Protein segments able to recognize and bind to phosphorylated tyrosines embedded in specific consensus sequences. They are present in several intracellular proteins acting as signal transducers.

tyrosine kinases Enzymes able to transfer the terminal γ-phosphate groups from ATP to tyrosines that reside in intracellular substrates.

Further Reading

Birchmeier, C., and Gherardi, E. (1998). Developmental roles of HGF/SF and its receptor, the c-Met tyrosine kinase. *Trends Cell Biol.* **8**, 404–410.

Birchmeier, W., Brinkmann, V., Niemann, C., Meiners, S., DiCesare, S., Naundorf, H., and Sachs, M. (1997). Role of HGF/SF and c-Met in morphogenesis and metastasis of epithelial cells. In *Plasminogen-related growth factors* (G. R. Bock and J. A. Goode, eds.) 1st edition, Ciba Found. Symp. 212, pp. 230–240. Wiley, Chichester, England.

Chirgadze, D. Y., Hepple, J., Byrd, R. A., Sowdhamini, R., Blundell, T. L., and Gherardi, E. (1998). Insights into the structure of hepatocyte growth factor/scatter factor (HGF/SF) and implications for receptor activation. *FEBS Lett.* **430**, 126–129.

Comoglio, P. M., and Boccaccio, C. (2001). Scatter factors and invasive growth. *Semin. Cancer Biol.* **11**, 153–165.

Trusolino, L., and Comoglio, P. M. (2002). Scatter-factor and semaphorin receptors: Cell signalling for invasive growth. *Nat. Rev. Cancer* **4**, 289–300.

Van der Voort, R., Taher, T. E., Derksen, P. W., Spaargaren, M., van der Neut, R., and Pals, S. T. (2000). The hepatocyte growth factor/Met pathway in development, tumorigenesis, and B-cell differentiation. *Adv. Cancer Res.* **79**, 39–90.

Biography

Paolo Comoglio is full Professor at the University of Torino Medical School and Scientific Director of the Institute for Cancer Research and Treatment -IRCC- in Candiolo, near Turin. He holds an M.D. from the University of Torino. His postdoctoral studies in immunology were carried out at Washington University in St. Louis. His main interests are the molecular mechanisms of invasive growth under both physiological and pathological conditions, focusing on the role of scatter factors and semaphorins in epithelial morphogenesis and carcinoma progression.

Hexokinases/Glucokinases

Emile Van Schaftingen
University of Louvain, Louvain-la-Neuve, Belgium

Hexokinases are intracellular enzymes that phosphorylate glucose, mannose, and fructose to the corresponding hexose 6-phosphates. These can then be broken down to pyruvate by glycolysis or utilized for various biosyntheses. Glucokinase is, strictly speaking, a form of hexokinase that specifically acts on glucose, and such enzymes indeed exist in microorganisms. The name glucokinase is, however, commonly (and improperly) used to designate mammalian hexokinase IV, an isoenzyme that displays a low affinity for glucose and can therefore play an important role in glucose-sensing.

Role of Phosphorylation in Sugar Utilization

In order to be utilized by cells, monosaccharides need to be transported across the plasma membrane and phosphorylated. In many bacteria, transport of glucose and other sugars is coupled to their phosphorylation by complex systems utilizing the high-energy phosphoryl donor phospho*enol*pyruvate. By contrast, transport and phosphorylation – in this case, at the expense of ATP – are catalyzed by separate proteins in eukaryotic cells and also to some extent in bacteria. Sugars are most often phosphorylated on their last carbon (glucose to glucose 6-phosphate; D-ribose to ribose 5-phosphate; etc.), though in some cases, phosphorylation takes place on the first carbon (D-galactose, L-fucose, fructose in liver).

Phosphorylation provides several advantages: it is an exergonic process, capable of concentrating metabolites inside the cells; it prevents leakage of metabolites across the plasma membrane and intracellular membranes; it increases the potential binding energy of substrates to enzymes, thereby facilitating catalysis. The name hexokinase (from hexose and the Greek word, "κινεειν," to move) was coined by Otto Meierhof to designate the enzyme that activates glucose, making it ready for fermentation by muscle extracts. Kinase was to become the word used to designate all ATP-dependent phosphorylating enzymes.

Reaction Catalyzed by Hexokinases

Hexokinases (EC 2.7.1.1) are defined as enzymes phosphorylating glucose and other closely related sugars (mannose, 2-deoxyglucose, glucosamine, fructose) on their sixth carbon. Glucokinases (2.7.1.2) catalyze the same reaction but with only glucose as a substrate. Glucokinases using ADP or polyphosphate as phosphoryl donor have been described in archaebacteria (*Pyrococcus furiosus* and *Thermococcus litoralis*); these are not discussed further here.

Hexokinases and glucokinases catalyze the transfer of the terminal phosphoryl group of ATP to the oxygen borne by the sixth carbon of glucose. As with other kinases, the true phosphoryl donor is the ATP–Mg complex. Except for ITP, other triphosphonucleotides are usually much poorer substrates than ATP. ADP is generated in the reaction, as well as a hexose 6-phosphate. The reaction is highly exergonic ($\Delta G^{o\prime} \sim -16.7\,\mathrm{kJ\,mol^{-1}}$), which means that in practical terms it is irreversible, most particularly under intracellular physiological conditions ($\Delta G < -30\,\mathrm{kJ\,mol^{-1}}$). However, reversibility of the reaction can be demonstrated *in vitro* provided the generated ATP and glucose are continuously consumed.

The reaction mechanism involves the formation of a ternary complex and an in-line transfer of the phosphoryl group from the donor to the acceptor without formation of an enzyme-bound covalent intermediate. Many studies have been devoted to the determination of the order of substrate addition and product release, without any emerging consensus. It is likely that most hexokinases and glucokinases may bind the substrates in any order to produce a reactive ternary complex, though some enzymes at least definitely display a preferred order (e.g., glucose before ATP in the case of mammalian hexokinase IV).

Diversity of Hexokinases and Glucokinases

Eukaryotes usually have several hexokinases. The yeast *Saccharomyces cerevisiae* has two hexokinases

TABLE I

Some Well-Studied Hexokinases and Glucokinases

	Approximate subunit size (kDa)	Number of subunits	K_m for glucose	Inhibitor	Tissular distribution
Mammals					
Hexokinase I (A)	100	1	~10 μm	Glucose 6-phosphate	Brain, erythrocytes (all tissues)
Hexokinase II (B)	100	1	~100 μm	Glucose 6-phosphate	Heart, skeletal muscle, adipocytes
Hexokinase III (C)	100	1	~1 μm	Glucose 6-phosphate Glucose	(Liver, lung, spleen)
Hexokinase IV (D) (glucokinase)	50	1	~8 mM	Glucose regulatory protein (fructose 6-phosphate)	Liver, β- and α-cells of pancreatic islets, hypothalamic neurons
Invertebrates					
Asterias amurensis (starfish) Hexokinase	50	1	~50 μm	Glucose 6-phosphate	
S. cerevisiae					
Hexokinase A (or PI)	50	2	~100 μm	Trehalose 6-phosphate	
Hexokinase B (or PII)	50	2	~100 μm	Trehalose 6-phosphate	
Glucokinase	50	(aggregates)	~30 μm		

(P_I and P_{II} or A and B) as well as a glucokinase (Table I). All three enzymes have subunits of 50 kDa, the two hexokinases being dimers of 100 kDa. The two hexokinases share ~75% sequence identity with each other and only ~37% sequence identity with glucokinase from the same species. All three enzymes display hyperbolic saturation curves for their substrates and a K_m for glucose < 1 mM. Both hexokinases A and B are inhibited by trehalose 6-phosphate, an intermediate in the formation of trehalose, which appears to play the role of a feedback inhibitor for this enzyme (equivalent to the role of glucose 6-phosphate with mammalian hexokinases).

Mammals have four distinct hexokinases (called I, II, III, and IV, or A, B, C, and D). Hexokinases I to III are ~100 kDa monomeric proteins, which resulted from the duplication of an ancestral gene encoding a 50-kDa hexokinase. They are characterized by low K_m values for glucose (< 0.2 mM) and by their sensitivity to inhibition by physiological concentrations of glucose 6-phosphate. Hexokinase III has an extremely low K_m for glucose and is inhibited by high concentrations of this substrate. Only the C-terminal half of hexokinase I (and probably of hexokinase III) appears to be catalytically active, whereas both amino and carboxyl halves of hexokinase II are endowed with catalytic activity.

Hexokinase IV or D is a ~50-kDa protein that has a low affinity for glucose, a sigmoidal saturation curve for this substrate and is not inhibited by physiological concentrations of glucose 6-phosphate. It is, however, inhibited by a regulatory protein. It does catalyze the phosphorylation of hexoses other than glucose, but due to its low affinity for all hexoses (including glucose), its physiological action is restricted to the most concentrated one, glucose, which is also its best substrate. Furthermore, there is ample evidence that hexokinase D plays the role of a glucose sensor. This may explain the popularity of its designation as "glucokinase," which however does not mean that this enzyme is closer to true (microbial) glucokinases than to hexokinases. As a matter of fact, hexokinase IV is closer to mammalian low K_m hexokinases than to any other hexokinases or glucokinases.

Distinct hexokinase isozymes are also found in insects (e.g., in *Drosophila melanogaster*) and plants. The starfish enzyme is a 50-kDa protein that is inhibited by physiological concentrations of glucose 6-phosphate, indicating that this property is not limited to the 100-kDa enzymes.

Prokaryotes typically contain a series of specific hexokinases that each act on one hexose, normally glucose, mannose, or fructose. They are often composed of two subunits with a smaller size (20–35 kDa) than the eukaryotic enzymes. There are, however, examples of true hexokinases in bacteria (e.g., the hexokinase of the archaebacterium *Thermoproteus tenax*) or of enzymes catalyzing the phosphorylation of two hexoses but not glucose (e.g., mannofructokinase).

Classification and Evolution of Hexokinases

Sugar kinases can be classified into three distinct families (the hexokinase, ribokinase, and galactokinase families)

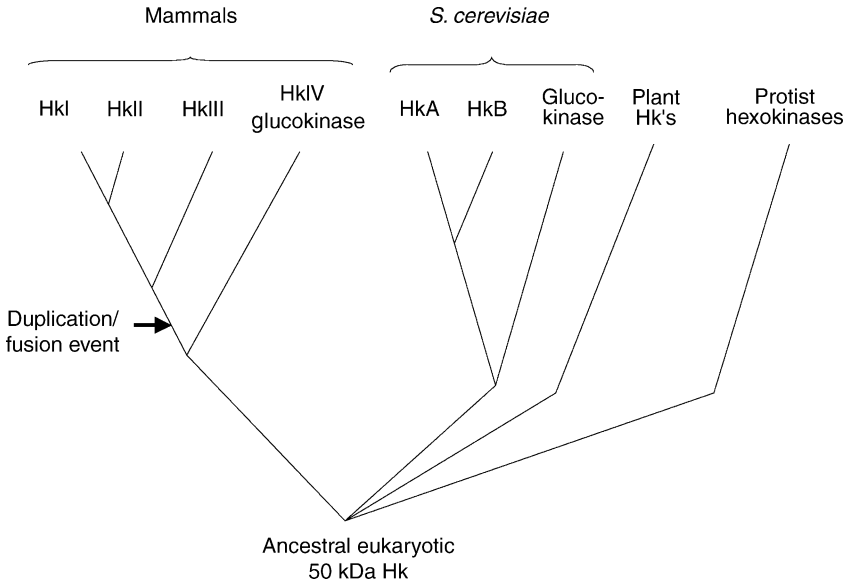

FIGURE 1 Evolutionary relationship between some eukaryotic hexokinases and glucokinases (Hk, hexokinase).

of enzymes that differ in their three-dimensional structures and show no significant similarity. In the hexokinase family, the eukaryotic enzymes form a distinct subfamily of enzymes sharing $>30\%$ sequence identity. The hexokinase family also comprises bacterial enzymes acting on various substrates (hexokinases, glucokinases, mannokinases, fructokinases, and N-acetylmannosamine kinases) that are very distantly related to eukaryotic hexokinases.

The ancestral eukaryotic hexokinase was probably a 50-kDa protein (Figure 1). Early and late duplication events in the fungi lineage led to the appearance of yeast glucokinase and of the more closely related hexokinases A and B. In vertebrates, hexokinase IV (glucokinase) separated from hexokinases I–III before the gene duplication and fusion event that led to the 100-kDa enzyme. Hexokinase III branched off earlier than the duplication event that led to hexokinases I and II, consistent with the closer kinetic properties of the latter two enzymes compared to hexokinase III.

Three-Dimensional Structure

Yeast hexokinase A and B structures were among the first such structures determined during the 1970s. Yeast hexokinase has a bilobar structure with a large (primarily C-terminal) and a small (primarily N-terminal) lobe that are connected by a hinge region. Both domains are made of β-sheets of similar topologies, flanked by α-helices (Figure 2). These are more abundant and larger in the C-terminal domain, accounting for its larger size. Between the two lobes is a deep crevice where the catalytic site resides. The enzyme exists under two distinct conformations, described as open and close, which differ by the dihedral angle between the two lobes.

The glucose-binding site comprises side chains of extremely conserved residues of the hinge region (Asp211 in hexokinase B), the large lobe (Asn237, Glu269, Glu302) and of the small lobe (Ser158, Thr172, Arg173). Binding of glucose to the large lobe induces closure of the catalytic cleft, allowing glucose to contact also the small lobe. The conformational change induced by this substrate is thought to facilitate the subsequent phosphoryl group transfer, being a nice illustration of the induced-fit theory. This theory is also supported by the observation that lyxose, a 5-carbon substrate analogue lacking the hydroxymethyl group that normally serves as phosphoryl acceptor, stimulates by $\sim$30-fold the hydrolysis of ATP to ADP and Pi catalyzed by yeast hexokinase.

Until now, no hexokinase has been crystallized with ATP. The location of the binding site for this substrate, nearby the glucose-binding site, has been inferred – and confirmed by site-directed mutagenesis – from structural analogy of hexokinase with glycerokinase, HSP-ATPase and actin, enzymes that have a similar bilobar architecture as hexokinase.

The crystal structures of human hexokinase I and the enzyme from *Schistosoma mansoni* (*S. mansoni*), a glucose 6-phosphate sensitive enzyme, have been determined recently. They are fundamentally similar to the structure of yeast hexokinase, repeated twice in the case of the mammalian enzyme. The human and *S. mansoni* enzymes were also crystallized as complexes with glucose 6-phosphate, showing that the binding site for this inhibitor overlaps with the putative ATP-binding site.

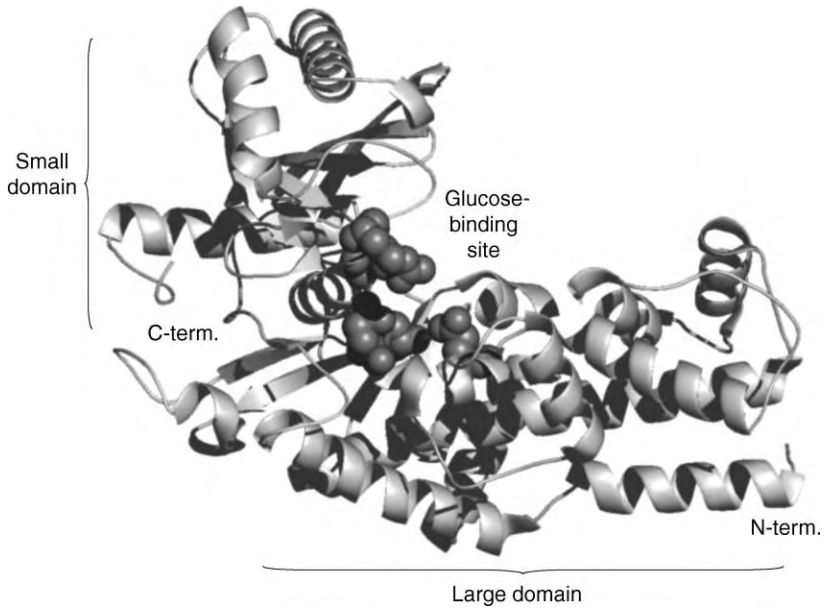

FIGURE 2 Three-dimensional structure of yeast hexokinase. The structure shown is that of the *Saccharomyces cerevisiae* B (P-II) isozyme in its open conformation. Glucose-binding residues are shown as space-filling models. Modified from Kuser, P. R., Krauchenco, S., Antunes, O. A., and Polikarpov, I. (2000) The high resolution crystal structure of yeast hexokinase PII with the correct primary sequence provides new insights into its mechanism of action. *J. Biol. Chem.* **275**, 20814–20821, courtesy of J. F. Collet.

Mammalian Low-K_m Hexokinases

The activity of the low K_m hexokinases cannot be regulated by the glucose concentration in tissues or cell types (human erythrocytes) where the glucose concentration is well above their K_m. In other cell types (e.g., the adipocytes), their activity may well be controlled by the glucose concentration and therefore by glucose transport. There is, however, still a large degree of uncertainty as to the glucose concentration and the rate-limiting aspect of glucose transport in several cell types.

Inhibition by Glucose 6-Phosphate

Hexokinases I–III are inhibited by glucose 6-phosphate in a noncompetitive manner with respect to glucose, but competitive versus ATP. Inhibition by glucose 6-phosphate takes place at physiological concentrations, which argues for its physiological significance. It is antagonized by inorganic phosphate in the case of hexokinase I, but not of hexokinase II. This inhibition involves a site distinct from the glucose-binding site, as indicated by the finding that the phosphorylation product (mannose 6-phosphate, 2-deoxyglucose 6-phosphate) of several good substrates for hexokinase I are poor inhibitors compared to glucose 6-phosphate. At one time, it was thought that the (catalytically inactive) aminoterminal half of hexokinase contained the glucose 6-phosphate allosteric site, but the realization that the isolated carboxyterminal half of the enzyme, as well as starfish hexokinase (a 50-kDa enzyme), were sensitive to glucose 6-phosphate inhibition argued against this hypothesis. Structural studies indicate that glucose 6-phosphate binds to the two halves of hexokinase I, in positions that overlap the putative ATP-binding sites. This agrees with the fact that the inhibition by glucose 6-phosphate is competitive versus ATP but not versus glucose. Site-directed mutagenesis experiments suggest, however, that the binding of glucose 6-phosphate to both sites may contribute to inhibition in hexokinase I.

Subcellular Localization of Mammalian Hexokinases

Hexokinases are cytosolic enzymes, but hexokinases I and II bind to mitochondria, through an N-terminal hydrophobic region that interacts with a porin. This proximity with the mitochondrial pore implies that hexokinases I and II are closer to the main source of ATP and to the main sink for ADP, thus facilitating diffusion. Binding of hexokinase I to mitochondria also decreases the affinity for the inhibitor glucose 6-phosphate.

Hexokinase IV (Glucokinase)

Sigmoidal Kinetics

One intriguing aspect of glucokinase, a monomeric enzyme, is that it displays a sigmoidal saturation curve

for glucose, with a Hill coefficient of 1.6. This is not due to the presence of a second, allosteric binding site for glucose on the glucokinase monomer, but to the existence of two distinct conformations, with low and high affinity for glucose, that equilibrate slowly (as assumed in models designated mnemonical model and slow transition model). If the hypothesis is made that the low-affinity conformation predominates in the absence of glucose, raising the glucose concentration will increase not only the binding of substrate to each of the two forms, but also the proportion of enzyme in the high-affinity conformation. This model is supported by the finding that, in glucokinase crystallized in its free form, the structure of the small domain differs markedly from what it is in low K_m hexokinases, or in glucokinase crystallized as a complex with glucose and an allosteric activator (see below).

Another intriguing aspect of glucokinase is its low affinity for glucose. As all glucose-binding residues found in low K_m hexokinases are conserved in this enzyme, the low affinity must be the result of local or global conformational differences compared to the low K_m hexokinases, most probably the presence of the relatively stable low-affinity state postulated above. This agrees with the finding that mutations of a few selected residues outside the catalytic site may convert glucokinase to a low-K_m enzyme and with the recent discovery of agents – bearing no structural relationship with glucose – that increase the affinity of glucokinase for glucose by binding to an allosteric site in the hinge region.

Liver Glucokinase and its Regulatory Protein

One of the main sites of glucokinase expression is the liver. This is in relation to the ability of this organ to store glucose as glycogen. Glucose transport across the plasma membrane of liver parenchymal cells, carried out by GLUT-2, is extremely rapid. Glucokinase may therefore play a regulatory role and indeed the low affinity that glucokinase displays for glucose is one of the mechanisms by which glucose uptake can be regulated by glucose concentration. In addition to this, glycogen metabolism is under the direct control of glucose, which binds to glycogen phosphorylase, thereby affecting the phosphorylation state of this enzyme as well as of glycogen synthase.

Hepatic glucokinase is controlled by a glucokinase regulatory protein (GKRP), which binds to glucokinase and inhibits it in a competitive manner with respect to glucose. Association of the two proteins is stimulated by fructose 6-phosphate, a GKRP ligand, which behaves therefore as an inhibitor of glucokinase, and antagonized by fructose 1-phosphate, another GKRP ligand. Regulation by GKRP makes, therefore, that glucokinase in intact liver cells has a lower affinity for glucose than the purified enzyme, and that low concentrations of fructose stimulate glucose utilization by the liver.

Quite surprisingly, GKRP appears also to control the subcellular localization of glucokinase: this enzyme is predominantly in the nucleus at low concentration of glucose and in the absence of fructose, but moves to the cytosol when the glucose concentration increases or if fructose is added. The physiological meaning of glucokinase translocation is not known, but it may be to protect glucokinase against degradation by cellular proteases. This would be consistent with the finding that mice devoid of GKRP have lower amounts (and total activities) of glucokinase than wild-type mice.

Role of Glucokinase in β-Cells

The low affinity that this enzyme displays for glucose (half-saturation is observed at 8 mM with the human enzyme), the sigmoidal saturation curve, and the lack of inhibition by physiological concentrations of glucose 6-phosphate make that this enzyme is well suited to respond to changes in glucose concentration and to act thereby as a "glucose sensor." This role is well established in the case of the insulin-secreting cells (β-cells) of pancreatic islets. Glucose appears to be one of the main fuels for β-cells. Raising the glycolytic flux (e.g., by raising the glucose concentration) leads to an increase in the cytosolic [ATP]/[ADP] ratio, which in turn results in closure of a nucleotide-sensitive K^+ channel. The ensuing depolarization of the plasma membrane causes an increase in the cytosolic Ca^{2+} concentration, which triggers insulin secretion. Metabolic analyses indicate that glucokinase, not glucose transport or a step beyond glucose phosphorylation, plays a major role in the control of this system. Accordingly, a form of diabetes known as maturity-onset diabetes of the youth type 2 is due to glucokinase mutations resulting in decreased enzymatic activity. The disease is dominantly inherited, which means that a mutation in one copy of the gene (resulting in at most a 50% decrease in glucokinase activity) is sufficient to perturb the "glucose-sensing apparatus of the pancreas." Conversely, glucokinase mutations that increase the activity (mostly by increasing the affinity for glucose) may result in familial hypoglycemia.

See Also the Following Article

Glucose/Sugar Transport in Mammals

Glossary

glucokinase Hexokinase that acts specifically on glucose; also mammalian hexokinase IV.

hexokinase Enzyme catalyzing the ATP-dependent phosphorylation of glucose and related hexoses (mannose, 2-deoxyglucose, fructose) to their 6-phospho-derivative.

mnemonical and slow transition models Kinetic models allowing one to explain the non-hyperbolic saturation curve of some monomeric enzymes, most particularly the sigmoid saturation curve of mammalian glucokinase. These models assume the existence of two conformations with distinct affinities for the substrate and that they interconvert slowly. Only the high-affinity conformation is endowed with catalytic activity in the mnemonical model.

Further Reading

Aleshin, A. E., Zeng, C., Bartunik, H. D., Fromm, H. J., and Honzatko, R. B. (1998). Regulation of hexokinase I: crystal structure of recombinant human brain hexokinase complexed with glucose and phosphate. *J. Mol. Biol.* **282**, 345–357.

Cárdenas, M. L., Cornish-Bowden, A., and Ureta, T. (1998). Evolution and regulatory role of the hexokinases. *Biochim. Biophys. Acta* **1401**, 242–264.

Grimsby, J., Sarabu, R., Corbett, W. L., Haynes, N. E., Bizzarro, F. T., Coffey, J. W., Guertin, K. R., Hilliard, D. W., Kester, R. F., Mahaney, P. E., Marcus, L., Qi, L., Spence, C. L., Tengi, J., Magnuson, M. A., Chu, C. A., Dvorozniak, M. T., Matschinsky, F. M., and Grippo, J. F. (2003). Allosteric activators of glucokinase: Potential role in diabetes therapy. *Science* **301**, 370–373.

Kamata, K., Mitsuya, M., Nishimura, T., Eiki, J., and Nagata, Y. (2004). Structural basis for allosteric regulation of the monomeric allosteric enzyme human glucokinase. *Structure (Camb.)* **12**, 429–438.

Kuser, P. R., Krauchenco, S., Antunes, O. A., and Polikarpov, I. (2000). The high resolution crystal structure of yeast hexokinase PII with the correct primary sequence provides new insights into its mechanism of action. *J. Biol. Chem.* **275**, 20814–20821.

Matschinsky, F. M. (2002). Regulation of pancreatic beta-cell glucokinase: From basics to therapeutics. *Diabetes* **51**, S394–S404.

Mulichak, A. M., Wilson, J. E., Padmanabhan, K., and Garavito, R. M. (1998). The structure of mammalian hexokinase-1. *Nat. Struct. Biol.* **5**, 555–560.

Van Schaftingen, E., Detheux, M., and Veiga da Cunha, M. (1994). Short-term control of glucokinase activity: Role of a regulatory protein. *FASEB J.* **8**, 414–419.

Wilson, J. E. (1995). Hexokinases. *Rev. Physiol. Biochem. Pharmacol.* **126**, 65–198.

Biography

Emile Van Schaftingen is a Researcher at the Christian de Duve Institute of Cellular Pathology in Brussels (ICP) and a Professor of Biochemistry at the Faculty of Medicine of the Université Catholique de Louvain (UCL). His principal research interests are the regulation of glucose metabolism in mammalian cells and more recently the repair of glucose-induced damage to proteins. He has authored or co-authored more than 120 research publications. He holds an M.D. from UCL and received a Ph.D. from the same university under the supervision of Prof. Henri-Géry Hers.

Histamine Receptors

Stephen J. Hill and Jillian G. Baker
University of Nottingham, Nottingham, UK

Histamine (a basic amine) is a hormone secreted by a number of cell types (e.g., mast cells, basophils, and nerve cells). Its normal physiological function is to act as a local hormone (i.e., one that is secreted and acts on neighboring cells rather than entering the bloodstream) or a neurotransmitter (which acts on neighboring cells following release from nerve endings in response to electrical impulses). For example, histamine is secreted from mast cells in the stomach where it is involved in the normal regulation of gastric acid secretion. Histamine is also an important contributor to the pathophysiological processes of allergic inflammatory reactions. Upon exposure to an allergen or antigen, histamine is released from mast cells which exist throughout the body. The reaction may be localized, as in a minor insect bite or, rarely, generalized to become life-threatening anaphylaxis (e.g., ingestion of penicillin in a penicillin-allergic individual, where histamine release is so widespread that it enters the bloodstream and causes catastrophic reactions).

The actions of histamine are mediated by the binding of extracellular histamine to one of four different G-protein-coupled receptors (GPCRs; namely, H_1, H_2, H_3, H_4). These are, like all GPCRs, embedded in the cell surface plasma membrane. They have seven membrane-spanning domains that are connected together by six loops of amino acids (three outside and three inside the cell; see Figure 1). They also have a string of amino acids at the N terminus that are on the outside of the cell and a string at the C terminus that hang inside the cell. Once activated, each type of histamine receptor interacts with a specific class of heterotrimeric G proteins, which in turn alter levels of intracellular second messengers (e.g., cyclic AMP and Ca^{2+} ions). These second messengers then trigger a variety of intracellular processes.

Histamine H_1-Receptor

The human histamine H_1-receptor is a 487 amino acid protein and is encoded by a gene on chromosome 3. It has a very large third intracellular loop (208 amino acids; through which it mediates interactions with the $G_{q/11}$ family of G proteins) and a relatively short (17 amino acids) intracellular C-terminal tail. As with all $G_{q/11}$-coupled receptors, stimulation of the receptor–$G_{q/11}$ protein complex results in activation of the enzyme phospholipase Cβ. This leads to the formation of the intracellular second messengers inositol 1,4,5-triphosphate (IP_3) and diacylglycerol. IP_3 is released into the cytosol and then stimulates the release of intracellular free Ca^{2+} ions (which, for example, can result in smooth muscle contraction), while diacylglycerol can activate protein kinase C and mediate responses such as cell proliferation and the activation of the trasncription of pro-inflammatory genes.

Histamine H_1-receptors are found throughout the body. Activation of H_1-receptors in smooth muscle leads to contraction in the walls of the airways, gastrointestinal tract, and in blood vessels. In endothelial cells (cells that line the inside of blood vessels), H_1-receptor activation increases vascular permeability (which is responsible for the characteristic "wheal" response seen in the skin after, e.g., insect bites) and leads to the synthesis and release of vascular smooth muscle relaxants (e.g., prostacyclin and nitric oxide). Activation of H_1-receptors also stimulates the release of catecholamines (noradrenaline (norepinephrine) and adrenaline (epinephrine)) and enkephalins from chromaffin cells in the adrenal medulla. In neurons, histamine H_1-receptor stimulation activates peripheral sensory nerve endings leading to itching. Via an axonal reflex, peptide neurotransmitters are subsequently released from nearby collateral nerve endings leading to a surrounding vasodilatation (flare). In the brain, H_1-receptors are present in the cerebral cortex, hippocampus, nucleus accumbens, thalamus, and posterior hypothalamus, activation of which stimulates an increase in neuronal activity.

A very similar H_1-receptor is found in other animal species and contains 491 (bovine), 486 (rat), 488 (guinea pig), and 489 (mouse) amino acids.

H_1 Agonists

Besides histamine itself, there are several histamine derivatives that also bind to and activate (i.e., are agonists of) the histamine H_1-receptor. N-methylhistaprodifen, 2-(3-(trifluoromethyl)phenyl)-histamine,

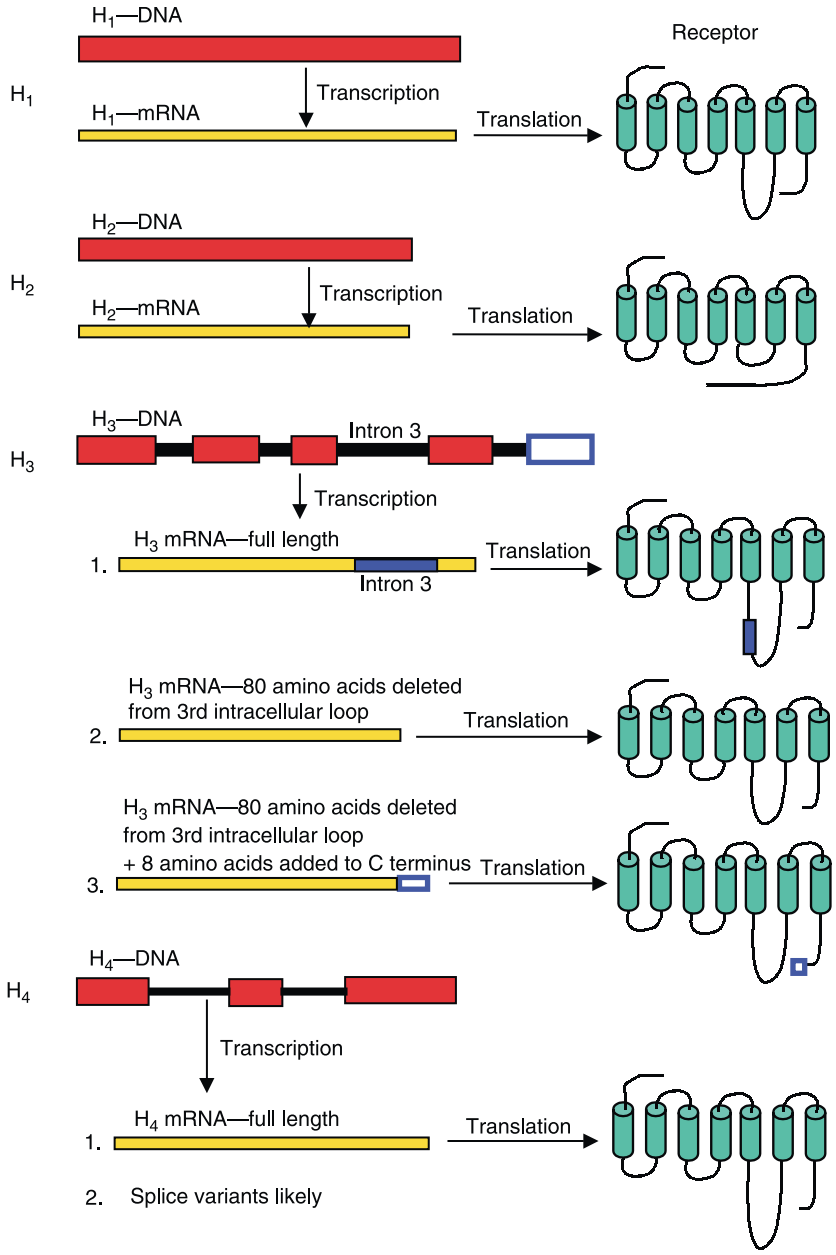

FIGURE 1 Transcription and translation of histamine receptors.

2-(3-bromophenyl)-histamine, and histaprodifen are all more potent than histamine itself and bind better to H_1-receptors (i.e., are more selective) than to other types of histamine receptors. There is no therapeutic indication for H_1-receptor agonists, but these compounds are important for fundamental research into the physiological and pathophysiological roles of histamine H_1-receptors.

H_1-Antagonists

Classical H_1-receptor antagonists, including mepyramine, chlorpheniramine, promethazine, diphenhydramine, and cyproheptadine, are used as systemic and/or topical preparations in the management of allergic reactions (i.e., hay fever, allergic rhinitis, insect bites, and anaphylactic reactions). However, at therapeutic doses, many of these H_1-antagonists cross the blood–brain barrier, antagonize CNS H_1-receptors, and lead to a decrease in neuronal activity and hence sedation. This "side effect" has been exploited in the development of several preparations marketed as sleeping aids (e.g., diphenhydramine or promethazine). A second generation of H_1-antagonists has been developed which is much less able to cross the blood–brain barrier and hence is much less sedating (e.g., cetirizine, loratidine, fexofenadine, terfenadine, and astemizole).

H_1-antagonists are also used in the management of non-allergic urticaria, e.g., hydroxyzine, cyproheptadine, and promethazine. Many H_1-receptor antagonists also possess marked muscarinic receptor antagonist properties (e.g., cyclizine, promethazine, and diphenhydramine) and this "side effect" is exploited for the treatment of nausea and motion sickness. Several other classes of drugs, such as the antidepressant drugs doxepin, amitriptyline, and mianserin, are also potent H_1-antihistamines and hence are sedating.

Interestingly, some of the H_1-antagonists in current use, e.g., chlorpheniramine, loratidine, and cetirizine, are actually inverse agonists of the H_1-response. That is, upon binding to the receptor, instead of just blocking histamine-binding and hence histamine-activation of the receptor, they actively turn off the response (i.e., produce an opposite effect to agonists) and hence decrease the basal response of the cell.

Recently, two second-generation H_1-antihistamines (terfenadine and astemizole) have been associated with an increased incidence of cardiac arrhythmias. This appears to be due to an ability to directly block cardiac HERG1 K^+ channels and has led to the withdrawal of terfenadine and astemizole in a number of countries. A number of other second-generation antihistamines (e.g., cetirizine and loratidine), however, do not share this property.

Histamine H_2-Receptors

The human histamine H_2-receptor contains 359 amino acids and is encoded by a single exon on chromosome 5. Unlike the H_1-receptor, the histamine H_2-receptor has a short third intracellular loop (30 amino acids), a much longer C-terminal tail (70 amino acids), and couples to G_S proteins to stimulate the enzyme adenylyl cyclase. This leads to the synthesis of the intracellular second messenger cyclic AMP, which activates protein kinase A, and in turn stimulates cellular responses. In gastric parietal cells, histamine activation of H_2-receptors stimulates gastric acid secretion in the stomach. In the heart, H_2-receptor activation and subsequently an elevation in cAMP production leads to an increase in both the rate and force of contraction, whereas in smooth muscle (in the airways and in blood vessels) the H_2-receptor-mediated increase in cAMP produces relaxation. H_2-receptors are also present in lymphocytes where histamine activation inhibits antibody synthesis, T-cell proliferation, and cytokine production. However, in some cell types (particularly gastric parietal cells), there is increasing evidence that H_2-receptor stimulation can also release calcium from intracellular stores leading to an increase in intracellular Ca^{2+} concentrations. Finally, H_2-receptor activation in the brain usually results in a decrease of neuronal activity, except in hippocampal neurons where the long-lasting after-hyperpolarization is blocked and excitatory stimuli potentiated.

Very similar H_2-receptor structure and function has been observed in other animal species, including dog, guinea pig, mouse (all have 359 amino acids), and rat (358 amino acids).

H_2-Receptor Agonists

A number of very selective potent agonists (including impromidine, arpromidine, dimaprit, and amthamine) are available for the histamine H_2-receptor, although as with the H_1-receptor, none are used clinically. In the case of impromidine and arpromidine, the compounds are 48 and 100 times more potent, respectively, than histamine itself. However, although acting as agonists at the H_2-receptor, some of these compounds are antagonists at other histamine receptors (see Table I).

H_2-Receptor Antagonists

H_2-receptor antagonists are widely used in the management of gastric and duodenal ulcers and in gastro-esophageal reflux disease. The development of specific antagonists for the H_2-receptor is a classic example of rationale drug design for which Sir James Black won the Nobel prize. Burimamide was the first compound that demonstrated selectivity for H_2- over H_1-receptors. It reduced gastric acid secretion and reduced the blood pressure response to histamine. However, with the discovery of the H_3-receptor, burimamide was subsequently found to be a more potent H_3-receptor antagonist. Cimetidine was developed directly from burimamide and is an effective agent in the treatment of gastric and duodenal ulceration because of its ability to inhibit basal and gastrin-stimulated gastric acid secretion. Several other highly selective H_2-receptor antagonists, including ranitidine, famotidine, and nizatidine, are also available now and are in regular clinical use.

Burimamide is a neutral antagonist, i.e., it binds to the H_2-receptor and therefore blocks histamine activation of the receptor. Cimetidine and ranitidine block histamine activation and are also inverse agonists, i.e., upon binding to the H_2-receptor, they actively turn off the receptor and thus decrease basal cAMP in cells.

Histamine H_3-Receptors

The human histamine H_3-receptor (445 amino acids) and the gene encoding this receptor has been localized to chromosome 20. It has a long third intracellular loop (142 amino acids) and a short C-terminal tail (29 amino acids). The receptor couples to the $G_{i/o}$ family of G proteins that can inhibit adenylyl cyclase activity, thus upon histamine activation of the receptor intracellular

TABLE I

Pharmacology of Histamine Receptor Subtypes

	H_1	H_2	H_3	H_4
Human gene (amino acids)	487	359	445	390
Introns	No	No	Yes	Yes
Chromosome	3	5	20	18
G protein	$G_{q/11}$	G_s	$G_{i/o}$	$G_{i/o}$
Cellular response	Ca^{2+}/IP_3	Increase in cAMP	Decrease in cAMP Inhibition of neurotransmitter release	Decrease in cAMP
Agonists	Histamine Histaprodifen N-methylhistaprodifen	Histamine Arpromidine Impromidine Amthamine dimaprit	Histamine Imetit Immepip R-α-methylhistamine	Histamine Imetit Immepip Clozapine[a] Thioperamide (weak)
Antagonists	Meyramine[a] Chlorpheniramine[a] Promethazine[a] Cyproheptidine[a] Cetirizine[a] Loratidine[a] Fexofenadine[a] Cyclizine[a] Terfenadine Astemizole Arpromidine	Cimetidine[a] Titotidine Famotidine[a] Nizatidine[a] Ranitidine[a] Mifentidine	Thioperamide Iodophenpropit Clobenpropit Ciproxifan Iodoproxyfan Impentamine Proxyfan	Clobenpropit

[a] Drugs in clinical use.

cAMP is decreased. The histamine H_3-receptor was first identified as a presynaptic autoreceptor which can inhibit the synthesis and release of more histamine from the same and surrounding histaminergic nerves in the CNS. The small number of neurons that use histamine as a neurotransmitter in the brain have their cell bodies in the posterior hypothalamus, but their axons extend to innervate most areas of the forebrain. H_3-receptors, however, are also found on the terminals of other neurons, e.g., those that use acetylcholine, 5-HT, dopamine, and noradrenaline as neurotransmitters. This is also true for peripheral neurons, where H_3-receptor activation leads to the inhibition of the release of sympathetic neurotransmitters in human saphenous vein, heart, bronchi, and trachea.

Splice Variants of the H_3-Receptor

Unlike the genes for H_1- and H_2-receptors, the gene that encodes the H_3-receptor contains introns. These are areas of DNA that are not transcribed into the finished mRNA (and not therefore translated into protein). During transcription, these areas are skipped and the coding regions either side are joined up to make the continuous strand of mRNA. The H_3-receptor has three of these introns (and therefore four coding regions or exons, see Figure 1). This means that, as a consequence of the coding sequences either side of an intron being joined together at different points within the overall receptor-coding region, multiple forms of the H_3-receptor can be produced from the single H_3-receptor gene. This is called alternative splicing, and the resulting isoforms of the receptor formed are called splice variants. So far, several isoforms of the H_3-receptor have been detected in different species. In the guinea pig, two isoforms have been identified that differ by a 30 amino acid stretch within the third intracellular loop of the receptor. In the rat, three functionally active H_3-receptor isoforms have been identified: a full-length version and two that lack either 32 or 48 amino acids in the middle of the third intracellular loop of the receptor. Each of these three H_3-receptor isoforms has a different distribution with the CNS and signals with different efficacy to inhibit adenylyl cyclase and other signaling pathways. In the human at least six distinct isoforms have been identified, of which three (including the full-length receptor) are functionally active H_3-receptor proteins. One of the active human isoforms lacks 80 amino acids contained entirely within the third intracellular loop. The other has this 80 amino acid deletion

as well as a novel eight amino acid C terminus. As several different H_3-splice variants exist with different signal transduction capabilities, this splicing mechanism offers a way for tightly regulating the biological actions of the H_3-receptor in different tissues.

H_3-Receptor Agonists and Antagonists

Although it is clear that human H_3-receptors are involved in neurotransmission, and potential therapeutic indications for clinical intervention have been identified (e.g., for the treatment of Alzheimer's disease, Parkinson's disease and the maintenance of wakefulness), no drugs are in current clinical use. Nevertheless, agonists and antagonists have been developed for scientific purposes. Agonists with good selectivity for H_3-receptors (relative to H_1- and H_2-receptors) include R-α-methylhistamine, imetit, and immepip. H_3-receptor antagonists include thioperamide, clobenpropit, iodoproxyfan, ciproxifan, and impentamine which all have higher affinity for H_3-receptor than for H_1- and H_2-receptors.

Constitutive H_3-Receptor Activity and Inverse Agonism

The H_3-receptor appears to be naturally expressed in a constitutively active form in the CNS. That is, the mere presence of the H_3-receptor itself causes a substantial intracellular response (in this case decrease in cAMP or inihibiton of neurotransmitter release) in the absence of agonist. Other GPCRs have been artificially mutated in the third intracellular loop to make them constitutively active and these engineered sequences are very similar to those naturally occurring in the H_3-receptor. This naturally occurring constitutive activity means that there is potential for developing inverse agonists (to turn off the receptor) as well as agonists (for activating the receptor) and neutral antagonists (that just stop other drugs binding, whether they are agonists or inverse agonists). Many of the compounds developed as H_3-receptor antagonists have been shown to behave as inverse agonists in cell lines expressing recombinant H_3-receptors. These include thioperamide, clobenpropit, and iodophenpropit. Neutral antagonists (e.g., proxyfan) have also been identified.

Histamine H_4-Receptors

The human H_4-receptor (390 amino acids) is encoded by a gene on chromosome 18. Like the H_3-receptor it has a genomic structure consisting of introns and exons suggesting that splice variants may also occur (see Figure 1). It too has a long third intracellular loop (111 amino acids) and a short C terminus (28 amino acids). Again like the H_3-receptor, the H_4-receptor couples to the $G_{i/o}$ family of G proteins and therefore activation results in an inhibition of adenylyl cyclase activity. The H_4-receptor is found primarily in cells of the immune system (e.g., in bone marrow, neutrophils, eosinophils, spleen, and mast cells). The H_4-receptors from rat, mouse (both 391 amino acids long), and guinea pig (389 amino acids) have also recently been cloned.

Ligands for the H_4-Receptors

Currently, there are no drugs undergoing clinical trials that are designed to specifically interact with the histamine H_4-receptor, although their rather selective localization within the immune system will surely see the development of H_4-immune-modifying drugs in future. Imetit and immepip are high-affinity H_4-receptor agonists that are used in scientific research. Clobenpropit also binds with high affinity to the H_4-receptor but has weak H_4-agonist activity. R-α-methylhistamine (a weak H_4-agonist) and thioperamide (an H_4-antagonist) also bind to the H_4-receptor but with less affinity than the H_3-receptor. Some data also suggest that thioperamide may have inverse agonist activity on the H_4-receptor. The atypical antipyschotic drug clozapine is also an H_4-agonist.

See Also the Following Articles

Adenylyl Cyclases • G Protein-Coupled Receptor Kinases and Arrestins • G_i Family of Heterotrimeric G Proteins • Phospholipase C

Glossary

agonist A drug that binds to a receptor and turns on the processes that lead to a functional response (i.e., it binds to the receptor and has positive efficacy).

constitutive receptor activity Occurs when GPCRs in a cell spontaneously associate with a G protein and increase the basal response even when there is no agonist present.

inverse agonist A drug that binds to a receptor and actively turns off the receptor activation process (i.e., it binds to the receptor and has negative efficacy). It therefore has the opposite effect to an agonist. Thus, when there is constitutive receptor activity (in the absence of an agonist), inverse agonists will reduce the basal response.

neutral antagonist A drug that binds to a receptor and prevents the binding of agonists or inverse agonists (i.e., it binds to the receptor and has no efficacy).

Further Reading

Hill, S. J. (1990). Distribution, properties and functional characteristics of three classes of histamine receptor. *Pharmacol. Rev.* **42**, 45–83.

Hill, S. J., Ganellin, C. R., Timmerman, H., Schwartz, J. C., Shankley, N. P., Young, J. M., Schunack, W., Levi, R., and Haas, H. L. (1997). International union of pharmacology XIII classification of histamine receptors. *Pharmacol. Rev.* **49**, 253–278.

Hough, L. B. (2001). Genomics meets histamine receptors: New subtypes, new receptors. *Molecul. Pharmacol.* **59**, 415–419.

Leurs, R., Watanabe, T., and Timmerman, H. (2001). Histamine receptors are finally "coming out". *Trends Pharmacol. Sci.* **22**, 337–339.

Leurs, R., Church, M. K., and Taglialatela, M. (2002). H_1-antihistamines: Inverse agonism, antiinflammatory actions and cardiac effects. *Clin. Exp. All.* **32**, 489–498.

Van der Goot, H., and Timmerman, H. (2000). Selective ligands as tools to study histamine receptors. *Eur. J. Med. Chem.* **35**, 5–20.

Biography

Stephen J. Hill is a Professor of Molecular Pharmacology in the Institute of Cell Signalling at the University of Nottingham, United Kingdom. His principal research interests are in the molecular pharmacology of G-protein-coupled receptors. He holds a Ph.D. from the University of Cambridge where he also undertook his postdoctoral training.

Jillian G. Baker is a Wellcome Trust Clinical Scientist Fellow and Registrar in Respiratory and General Internal Medicine. Her current research interest is the study of the effect of G-protein-coupled receptor activation on gene transcription. She obtained her Medical Degree and Ph.D. from the University of Nottingham.

HIV Protease

Ben M. Dunn
University of Florida College of Medicine, Gainesville, Florida, USA

HIV protease is a proteolytic enzyme and is part of the protein component of the human immunodeficiency virus (HIV). HIV protease plays a critical role in the life cycle of the virus and for this reason has become an important target for drug development in the battle against HIV infection. HIV protease is a member of the aspartic protease family of proteolytic enzymes and discoveries in the general field have provided clues to effective drug design. Subsequently, HIV protease has become one of the most thoroughly studied proteins and most likely has been studied by structural analysis more than any other protein.

Human Immunodeficiency Virus (HIV)

Human immunodeficiency virus (HIV) is an enveloped virus with RNA as the molecule used for storage of genetic information. HIV is a retrovirus, which means that the RNA is converted into a DNA copy that becomes integrated into the genomic DNA of a host cell. The genomic DNA is transcribed into RNA by the normal cellular machinery and this RNA is used as both messenger RNA for production of proteins by cellular ribosomes and as daughter RNA for assembly into new viral particles. HIV infects cells of the human immune system, leading to death of the cell and, thus, depletion of the immune constituents of the bloodstream with a consequent fall in immune function. Hence, the name of the disease caused by HIV is acquired immunodeficiency syndrome (AIDS). This disease is a scourge upon humankind and, as of early 2000s, has killed millions worldwide and infected as many as 40 million more.

Proteins of HIV

Gag Proteins

Translation of the gag/pol messenger RNA of HIV leads to the production of two proteins: Gag and Gag/Pol. The Gag polyprotein has a molecular weight of ~55 kDa and is called a polyprotein because it contains several proteins connected head-to-tail. Three of the proteins of the Gag polyprotein (Figure 1) are important constituents of the new viral particles: matrix, or MA, a 17-kDa protein that forms a spherical shell around other proteins, thus providing one level of packaging for the viral particle; capsid, or CA, a 24-kDa protein that forms conical structure within the matrix shell and contains the daughter RNA, providing a second layer of protection; and nucleocapsid, or NC, a 7-kDa protein that binds to the RNA to provide a third level of packaging. When the new viral particle buds off from an infected cell, it takes some of the cell envelope along with it to complete the packaging of the new virion.

Pol Proteins

The *Pol* gene, which is the second part of the Gag/Pol fusion protein, codes for a polyprotein containing three enzymatic functions: reverse transcriptase (RT), which copies the viral RNA into DNA; protease (PR), which acts to cleave the Gag and Gag/Pol proteins into their separate pieces; and integrase (IN), which catalyzes the insertion of the DNA copy of the viral genetic information into the host cell genome.

Structure of HIV Protease

HIV protease begins as a component of the Gag/Pol fusion polyprotein. As a single molecule, the Gag/Pol-embedded protease is inactive, because dimer formation is required to create the active site and catalytic machinery.

Gag/Pol Polyprotein and Viral Assembly

Following ribosomal synthesis, Gag/Pol fusion proteins become myristolated and assemble on the inner surface of the cell membrane. This concentration of the protein leads to dimerization at several points along the polyprotein, including the HIV protease. The dimerization of two protease components of the polyprotein may be assisted by prior assembly of other regions of the protein, such as the proteins in the Gag portion.

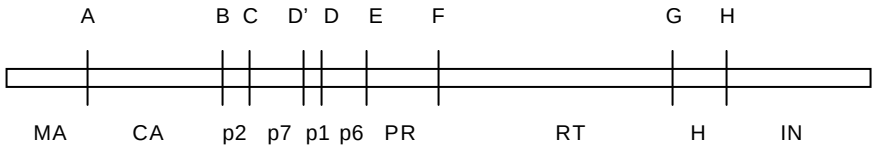

FIGURE 1 Diagram illustrating the arrangement of the Gag–Pol polyprotein. The letters above the boxes indicate the cleavage sites within the Gag–Pol polyprotein. The codes below the boxes indicate the designations for the protein products of the cleavages.

The viral particle, or virion, buds off from the cell, taking some of the plasma membrane along. At this point, the virus is immature and non-infectious. Upon a change in conditions, possibly caused by an influx of protons into the virion with concomitant decrease in pH, the protease begins its function of cutting apart Gag and Gag/Pol fusion proteins. Little is known about the structure of the Gag/Pol fusion protein in the immature virion. It has been demonstrated that the cleavage of the viral polyprotein into smaller units proceeds by a series of steps that could be controlled by the organization of the polyprotein or by the selectivity of the protease for the different cleavage site junctions.

Structure of HIV Protease as an Isolated Entity

Once released from attachment to the other components of the viral Gag/Pol polyprotein, or when expressed from the 297 bp gene encoding the sequence, HIV protease can be isolated and crystallized. The three-dimensional structure reveals a molecule with structural similarities to other members of the aspartic protease family, but with some significant differences. The enzyme is a dimer of two identical 99 residue monomers and has a folding pattern that contains all the elements seen in the pepsin-like aspartic proteases, including a deep active site cleft on one side of the molecule (Figure 2) with both monomers contributing contact sites for bound substrates or inhibitors. Each monomer provides one aspartic acid residue and the carboxylic acid side chains of each of these come together at the bottom of the active site and bind a water molecule, which completes the catalytic machinery. This machinery catalyzes the attack of the water molecule upon the peptide bond of a bound substrate.

Inhibitor Binding

Due to the desire to create potent and selective inhibitors of the HIV protease, many different laboratories, in pharmaceutical companies, in government institutes, and at universities have studied complexes of HIV protease with small molecule inhibitors. In fact, HIV protease was the first case where structural biology provided key insights that were used to design new, effective compounds. To date, the FDA has approved seven drugs for use in humans and these have had an enormous impact on therapy of AIDS patients. The approved compounds provide a longer life span and an improved quality of life. However, problems with the development of resistant variants dampen the success.

Mode of Inhibitor Binding

Inhibitors bind within the active site cavity of HIV protease, similar to what has been shown for binding of inhibitors against other members of the aspartic protease family. The compounds are arranged in an extended conformation (Figure 3) with hydrogen bonding to backbone atoms of the protease and with interactions between groups of the inhibitor and hydrophobic regions of the active site cleft. These interactions provide the specificity and potency of binding necessary to have a compound that will not cause harm to the aspartic proteases of the human host. The FDA-approved drugs all meet these criteria; however, some have side effects that are not completely understood at this time.

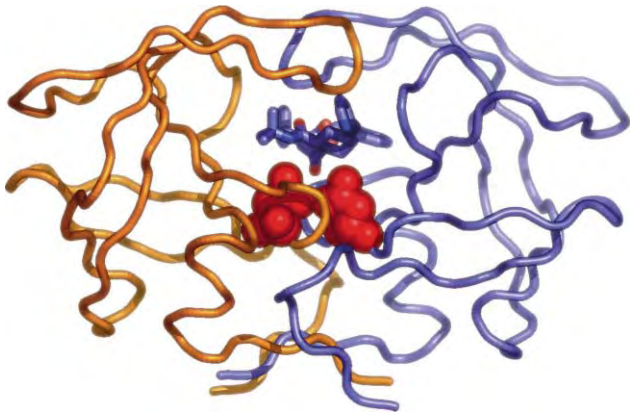

FIGURE 2 Representation of the three-dimensional structure of HIV protease. Two identical domains are shown in orange (left monomer) and blue (right monomer). Each domain contributes one aspartic acid residue to the catalytic machinery at the bottom of the active site cleft. These are shown in space-fill representation near the center of the figure. A bound inhibitor is shown above the two aspartic acids and directly in the middle of the active site cleft. Above the inhibitor, one can see the two prominent beta-hairpin "flaps," one from each monomer. The flaps cover the inhibitor in the bound state depicted here.

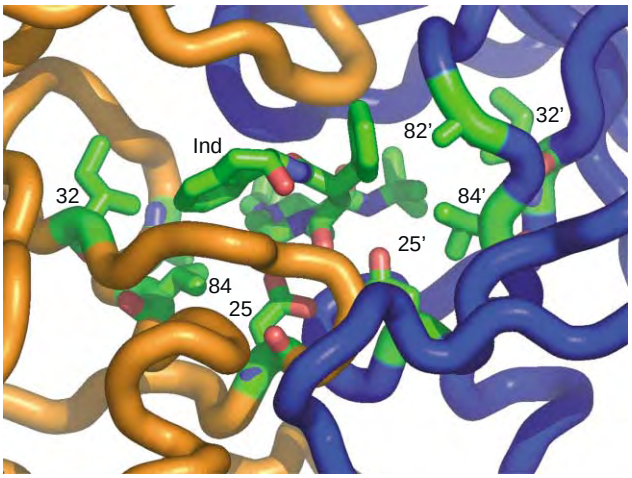

FIGURE 3 Close-up view of a bound inhibitor (shown in capped-sticks representation at the center of the picture) within the active site cleft of HIV protease. The two catalytic aspartic acids are seen just below the inhibitor. Several amino acids of the HIV protease are shown around the inhibitor. Each monomer contributes several amino acids that make hydrophobic interactions with the bound inhibitor. This view shows a drug-resistant form of HIV-1 protease, with Val32Ile, Val82Ala, and Ile84Val mutations shown in this view.

Development of Resistant HIV Protease Variants

As a retrovirus, replication of the virus begins with the creation of a DNA copy of the viral RNA genome. The enzyme that performs this reaction, HIV RT, is coded for by the virus and is present in the infectious virion particle. The process does not take place until the virion enters a new cell and the four different barriers protecting the viral RNA are stripped off. HIV RT makes errors while copying the viral genetic information and, unlike DNA polymerases of human cells, HIV RT does not have a proof-reading function. This results in nucleotide changes during replication, so that the progeny virus will contain variations on the sequence of the infecting virus. On an average, one nucleotide is altered in each round of replication of virus. As replication takes ~2 days, the number of mutations that can arise over a 6-month period is quite large. Some of these nucleotide alterations will not change the amino acid (silent mutations), but some will. What will be the properties of the new viral protein? In some cases, the progeny virus will be defective and noninfectious, as function could be affected by the mutations. In other cases, the new virus will have favorable properties. This is how drug-resistant variants arise during therapy, especially if the patient does not follow the drug regimen prescribed. Virus that is sensitive to the drug will be killed off, but virus that has properties that include decreased sensitivity to the effects of the antiviral drugs will survive and multiply.

The Spectrum of Drug-Resistant Variants

Out of the 99 amino acid HIV PR, as many as 25–30 amino acids can change without losing catalytic activity. In many cases, the efficiency of the enzyme is reduced, but as long as a threshold of activity is maintained (believed to be ~10% of starting level), the virus can survive and continue to replicate. Some of the mutations that occur are within the active site cleft and this can change the binding of inhibitors to reduce the effectiveness of antiviral therapy. Discovering new drugs that do not lead to the development of resistance remains a major research objective in antiviral therapy. On the other hand, knowledge of the genetic drift of the virus population into sequences that are resistant to a certain therapeutic regimen can predict when the patient could be switched to another set of antiviral drugs.

Structure of HIV PR Variants

In addition to studies of the structure of HIV protease from laboratory strains of the virus, with the discovery of drug-resistant forms of the virus it became important to discover how the amino acid substitutions, coded for by the altered forms of the viral genetic information, altered the activity of the protein. Thus, considerable effort has been expended to study the structure of drug-resistant forms of HIV protease. In general, it can be stated that changes in the enzyme structure are small, with obvious changes in the size of an amino acid that interacts with a bound inhibitor in the "wild-type" enzyme, leading to an obvious hole or protrusion, depending on the direction of the change. Even subtler are changes that occur when amino acids outside of the active site cleft occur, leading to an enhancement of resistance in some cases. A picture is emerging from studies of variant forms of HIV protease that the enzyme is very "plastic" or malleable, meaning that changes at any single position can be transmitted throughout the enzyme to have an impact on binding within the active site cleft and enzymatic function.

HIV PR as a Model System for Analysis of Protein Structure/Function

The classical history of protein biochemistry has involved studies of a few key proteins: the oxygen binding proteins, hemoglobin and myoglobin, the proteolytic enzymes trypsin and chymotrypsin, and the nucleic acid degrading enzymes, ribonuclease and staphylococcal nuclease. In the 1990s, HIV protease became a new classical protein that proved to be

amenable to detailed analysis. The protein is relatively easy to produce by recombinant means and purify, it has a robust activity and can be analyzed by several different methods, and variants can be created by current methods of molecular biology. Consequently, the HIV protease has been studied by nearly every method of analysis available to the protein chemist. Due to its small size, computational approaches have been applied and HIV protease has become an excellent system for theoretical studies of protein structure/function.

See Also the Following Articles

DNA Polymerases: Kinetics and Mechanisms • Reverse Transcriptase and Retroviral Replication

Glossary

AIDS Acquired immunodeficiency syndrome, a devastating disease caused by the HIV.

enveloped virus A virus that has an outer covering consisting of lipid and protein derived from host cells.

Gag polyprotein A 55-kDa protein produced by translation of HIV messenger RNA.

HIV Human immunodeficiency virus.

myristolation The addition of a fatty acid chain to the amino terminus of a protein, altering the properties of the protein.

polyprotein A protein that contains several functional elements attached head-to-tail, which must be separated in order to express their function.

progeny virus New viral particles produced as a result of replication within an infected cell.

protease An enzyme that cuts other proteins into pieces.

retrovirus A virus containing RNA as the genetic element and which must be converted into a DNA copy as part of the replicative cycle.

virus The simplest form of life, a virus depends on host cells in order to reproduce and continue infection.

Further Reading

Dunn, B. M. (ed.) (1999). *Proteases of Infectious Agents*. Academic Press, San Diego, CA.

Kuo, L. C., and Shafer, J. A. (eds.) (1994). *Retroviral Proteases*, Vol. 241, Academic Press, San Diego, CA.

Levy, J. A. (ed.) (1994). *The Retroviridae*, 3 vols, Plenum Press, New York.

Wlodawer, A., and Vondrasek, J. (1998). *J. Annu. Rev. Biomol. Struct.* **27**, 249–284.

Biography

Ben M. Dunn is a Distinguished Professor of Biochemistry and Molecular Biology at the University of Florida College of Medicine. He began his career at Florida after earning a B.S. in chemistry at Delaware in 1967 and a Ph.D. at the University of California, Santa Barbara in bio-organic chemistry, two years of postdoctoral work in protein chemistry and one year as a Staff Fellow at the NIH. His laboratory studies the enzymatic function of proteases, using kinetics and biophysical techniques including X-ray crystallography.

HIV-1 Reverse Transcriptase Structure

Kalyan Das, Stefan G. Sarafianos and Eddy Arnold
CABM and Rutgers University, Piscataway, New Jersey, USA

Stephen H. Hughes
National Cancer Institute, National Institutes of Health, Frederick, Maryland, USA

The reverse transcriptase (RT) of retroviruses, including HIV, is a multifunctional enzyme responsible for the conversion of the single-stranded viral RNA genome into double-stranded DNA (dsDNA). The dsDNA subsequently permanently integrated into the host genome. RT has two enzymatic activities: a DNA polymerase that can copy either RNA or DNA templates and a ribonuclease H (RNase H) that cleaves the RNA strand in RNA:DNA hybrids. HIV-1 RT is a heterodimer consisting of p66 and p51 subunits. Both subunits share a common N terminus; p51 lacks the C-terminal RNase H domain present in p66. Because of its pivotal role in the HIV type 1 (HIV-1) life cycle, HIV-1 RT is a primary target for the development of antiretroviral agents. Currently, 11 out of 19 approved anti-AIDS drugs are RT inhibitors. These drugs can be divided into two classes: nucleoside analogue reverse transcriptase inhibitors (NRTIs) and non-nucleoside reverse transcriptase inhibitors (NNRTIs). Extensive biochemical and structural studies have contributed to the understanding mechanisms of DNA polymerase catalysis, drug inhibition, and development of drug resistance.

Structural Studies on Reverse Transcriptase

HIV-1 reverse transcriptase (RT) structure has a right hand-like conformation for the p66 subunit, having "fingers," "palm," "thumb," and "connection" subdomains (Figure 1). While both p66 and p51 subunits contain these subdomains, the arrangement of the subdomains is different in p66 and p51. The p51 subunit is not directly involved in DNA polymerization. It is, however, essential for RT activity presumably because it plays a structural role and forms part of the nucleic-acid-binding cleft that extends from the polymerase active site to the RNase H active site. The non-nucleoside reverse transcriptase inhibitors (NNRTIs) bind in a hydrophobic pocket adjacent to the RT polymerase active site. The polymerase and RNase H active sites have each three catalytic carboxylates that are required for Mg^{2+}-dependent phosphotransferase activity (D110, D185, and D186 for polymerase and D443, D498, and D549 for RNAse H activity; the RNase H active site also includes E478). The two active sites are separated by ~17 DNA bp. The dsDNA substrate has B-form geometry at the polymerase active site and A-form geometry at the RNase H active site. Transition between the two forms occurs over a stretch of 4 bp in a segment of the DNA that is bent (~40°) and interacts with the p66 thumb subdomain.

In the past 11 years, significant progress has been made toward understanding the function of HIV-1 RT at the atomic level. Several structures of RT in complexes with inhibitors or substrates representing different steps in the mechanism of DNA polymerization are now available. The RT structures may be broadly categorized into four distinct groups (Figure 1): (I) apo HIV-1 RT (in absence of any bound substrate or inhibitor) and apo HIV-2 RT, (II) RT/nucleic acid binary complexes, (III) RT/nucleic acid/nucleotide triphosphate ternary complexes, and (IV) RT/NNRTI complexes. There are important differences in the structure and conformation of the enzyme in the various RT structures. Some of the structural changes are discussed in the context of the function(s) of the enzyme.

Functional Implications of RT Structures

In the unliganded (apo-) structures of HIV-1 (Figure 1, structure I) and HIV-2 RT, the p66 thumb subdomain folds over into the nucleic-acid-binding cleft. In nucleic-acid-bound RT structures (Figure 1, structure II), the p66 thumb moves out of the nucleic-acid-binding cleft and helps position the template primer. The NNRTI-binding site is near the hinge of the p66 thumb and p66

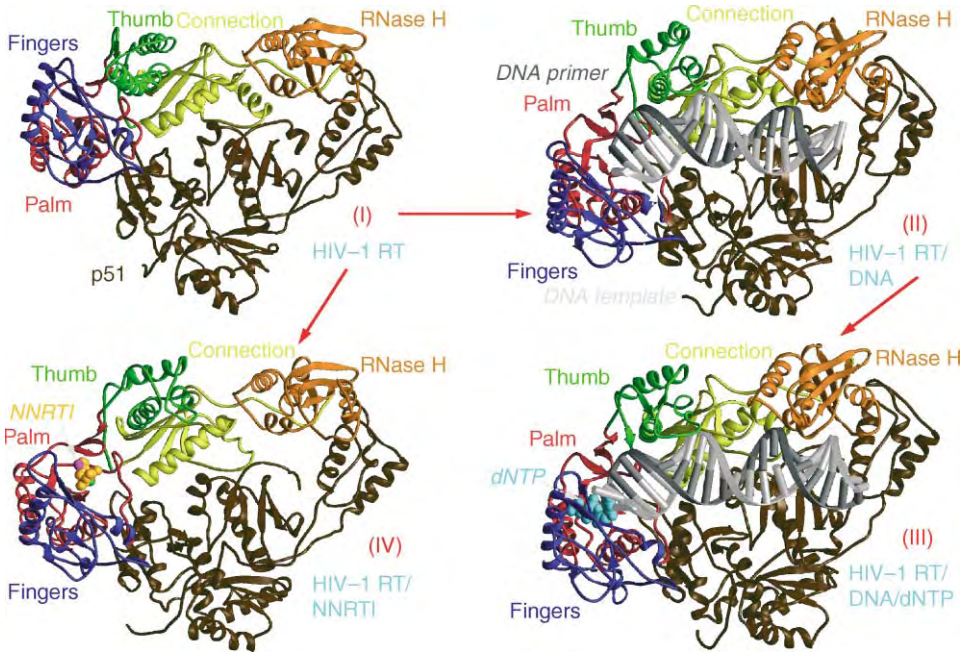

FIGURE 1 Four types of HIV-1 RT structures. Structure I of RT (apo-RT) contains no substrate or inhibitor. The subdomains of the p66 subunit are color-coded: fingers in blue, palm in red, thumb in green, connection in yellow, and RNase H in orange. The p51 subunit is shown in dark brown. Structure II corresponds to a binary complex of RT with nucleic acid (dark gray primer and light gray template) in which the thumb subdomain is displaced from the nucleic-acid-binding cleft to accommodate the nucleic acid. Structure III shows the ternary RT/DNA/dNTP complex (dNTP in cyan). Structure IV is a representative RT/NNRTI complex. The bound NNRTI, 8-Cl TIBO, is represented by a gold-colored CPK model.

palm subdomains; NNRTI binding locks the p66 thumb at an upright position (IV).

The structure of the RT/DNA complex (Figure 1, structure II) revealed details of nucleic acid recognition by HIV-1 RT and identified the structural elements of RT that interact with dsDNA including the "template grip," the "primer grip," and the p66 thumb subdomain. This structure inspired numerous biochemical studies that led to further characterization of the enzyme. The structure of RT complexed with an RNA:DNA led to the identification of the "RNase H primer grip," a set of amino acids that interact with the DNA primer strand and help to determine the specificity of RNase H cleavage. The RNA:DNA duplex in the crystal structure contained a polypurine sequence, known as the polypurine tract (ppt), that is not cleaved by RNase H. During viral replication, the ppt serves as a primer for the synthesis of the second strand of DNA. Analysis of the RT/RNA:DNA structure suggested that the RNase H cleavage specificity is controlled by the width of the minor groove and the trajectory of the RNA:DNA duplex. An unusual unzipping of the base pairs in the ppt may also play a role in determining the specificity of RNase H cleavage.

To obtain a structure of a ternary complex of RT with dsDNA and dNTP (Figure 1, structure III) the groups of Stephen Harrison and Greg Verdine at Harvard University developed a technique that covalently linked the dsDNA to the protein. A disulfide link was formed between and an engineered cysteine at residue 258 of the αH-helix in the p66 thumb subdomain and a thiol tether linked at N2 position of an adjacent DNA-template base. Comparison of the structures of RT/DNA/dNTP and RT/DNA complexes revealed a repositioning of the p66 fingers subdomain in the ternary complex. An analogous movement occurs in many other DNA polymerases (such as klentaq DNA polymerase I, murine leukemia virus RT, T7 RNA polymerase, etc.) and with the RNA-dependent RNA polymerases of poliovirus, hepatitis C virus, rabbit hemorrhagic disease virus, reovirus, and bacteriophage ϕ6. The structural and functional characteristics of these enzymes are useful in understanding the general mechanism of nucleic acid polymerization. The RT/DNA cross-linking technique was also subsequently used to obtain crystals of RT in complex with AZT-terminated DNA trapped before, and after, the DNA translocation step. Structural differences between the two complexes suggest that the conserved YMDD loop that contains two catalytically essential aspartates (D185 and D186) is also involved in translocation, acting as a springboard that helps to move the end of the primer after incorporation of a nucleotide.

TIBO and nevirapine are the first NNRTIs discovered by screening libraries of compounds for RT-inhibition activity. NNRTIs are highly specific inhibitors of HIV-1 RT; most do not inhibit HIV-2 RT. Three NNRTIs (nevirapine, delavirdine, and efavirenz) have been

approved for treating HIV-1 infections. The structure of HIV-1 RT in a complex with nevirapine, from Thomas Steitz and co-workers was the first structure of RT bound to an NNRTI. Since then, a large number of crystal structures of RT/NNRTI complexes have been determined independently by several groups including ours and that of David Stammers and David Stuart. Included among the structures are RT in complex with NNRTIs including α-APA, TIBO, delavirdine, efavirenz, HBY 097, HEPT, and PETT. All these structures belong to type IV in Figure 1. Variations in the shape and size of non-nucleoside inhibitor-binding pocket (NNIBP) correlate with differences in the size and shapes of the bound NNRTIs. Despite strong similarities in all RT/NNRTI structures (IV), specific details in inhibitor-protein interactions, binding modes of NNRTIs, shapes and sizes of NNIBP have provided valuable information that has implications for structure-based design of potent NNRTIs.

Analysis of RT/NNRTI structures helped in understanding the mechanism of RT inhibition by NNRTIs. NNRTIs are noncompetitive inhibitors that do not appear to interfere with binding of either nucleic acid or nucleoside substrates. No predefined NNIBP exists in the structures of RT that do not contain a bound NNRTI. Opening of the NNIBP involves large torsional displacements of the aromatic side chains of Y181 and Y188 and a rotation of the $\beta12-\beta13-\beta14$ sheet that moves the "primer grip" away from the polymerase active site. Once bound, an NNRTI restricts the flexibility of the enzyme, particularly, the relative positioning of the "primer grip" (which is responsible for translocation of the nucleic acid substrate and for positioning the 3′-end of the DNA-primer strand) with respect to the YMDD-motif at the polymerase active site. Restriction of the conformational mobility of the YMDD-motif may be another factor contributing to the NNRTI inhibition mechanism.

Structural Basis of HIV-1 RT Drug Resistance

The most effective strategies for reducing viral loads and keeping them at undetectable levels in HIV-1 infected patients are currently based on combinations of drugs (under the treatment strategy called highly active antiretroviral therapy, HAART) that usually include one or two RT inhibitors and one inhibitor of the viral protease. Despite the early success of combination therapies, treatment failure and severe side effects affect a growing proportion of patients receiving therapy. An increasing number of treatment failures are linked to the emergence of drug-resistant HIV strains. Resistant strains emerge because of the virus' rapid rate of replication and high rate of mutation. Amino acid residues that confer drug resistance are clustered in specific regions of Amino acid. Most of the sites where mutations are associated with drug resistance have potential to influence directly or indirectly the binding of the drug or specific functional steps of RT. In a number of cases, structural studies in combination with biochemical and clinical results have helped explain the molecular basis of drug resistance.

A single mutation (M184I/V) results in strong resistance to lamivudine (3TC), a nucleoside analogue that contains a β-L-pseudo-ribose-ring. The structure of RT/DNA/dNTP and the structure of the lamivudine-resistant M184I mutant RT in complex with nucleic acid is suggested that replacement of methionine at position 184 with a β-branched amino acid residue (V, I, or T) causes resistance to lamivudine by a steric hindrance mechanism, a proposal that is supported by biochemical experiments. Structures of HIV-1 RT were used to create a structural model of hepatitis B (HBV) polymerase. This model has been used to interpret the available biochemical and clinical data describing the susceptibility and resistance of HBV polymerase to nucleotide analogues such as lamivudine and adefovir (PMEA).

AZT treatment frequently selects a set of RT mutations (M41L, D67N, K70R, T215F/Y, and K219Q) that confer resistance to AZT. However, recombinant HIV-1 RT containing these mutations remained susceptible to inhibition by AZTTP in conventional polymerase assays. RT structures showed that these mutations would not directly affect the binding of a dNTP substrate or its analogue. The longstanding mystery about the molecular mechanism of RT resistance to AZT was solved in part when Dr. Michael Parniak and colleagues proposed that RT performs a pyrophosphate-mediated excision of AZTMP after the drug has been incorporated. Dr. Walter Scott and co-workers suggested that the pyrophosphate donor in the *in vivo* excision reaction is ATP. However, these proposals did not fully explain the mechanism of resistance. We developed a model for the excision reaction based on structural and biochemical data. In this model, several of the mutations associated with AZT resistance act primarily to enhance the binding of ATP; AZTMP is preferentially excised because of steric clashes involving the azido group. The model is strongly supported by crystal structures of RT in a complex with AZTMP-terminated DNA, trapped either in a pre- or a post-translocation state. The excision reaction is similar to reverse of polymerization reaction. RT uses its polymerase active site to cleave the AZTMP (from the DNA primer strand). This reaction requires that the AZTMP be located at the active site (pre-translocation state). Normally, when a dNTP or a nucleoside analogue is incorporated by HIV-1 RT, it is translocated and the next incoming dNTP binds. This would prevent excision. However, the azido

group of AZTMP interferes with the formation of a stable closed complex with the incoming dNTP. This gives an AZTMP-terminated primer good access to the active site where it can be excised.

In contrast to nucleoside analogues, NNRTIs bind to a well-defined hydrophobic pocket (NNIBP). Structural studies have shown that NNRTI-resistance mutations are located in and around the NNIBP. Commonly observed resistance mutations in NNRTI-treated patients include K103N, Y181C, L100I, Y188L, and G190A; these can be present singly or in combination. Structural studies of NNRTI-resistant RTs with and without bound NNRTI have provided clues for understanding the roles of resistance mutations in NNRTI binding. Structural studies, supported by clinical and biochemical data, suggest that different sets of mutations have different mechanisms. The Y181C and Y188L mutations appear to cause decreased NNRTI binding by the loss of aromatic ring interactions with inhibitors (by "loss of contact" mechanism); L100I and G190A/S are likely to cause steric hindrance with NNRTIs; and the K103N mutation appears to have effect on the entry of an NNRTI into the NNIBP; however, it may also favor binding of certain NNRTIs like TMC125-R165335 (etravirine).

RT Structures in Drug Design

Variations in RT sequence and emergence of drug-resistant strains present serious challenges for developing potent anti-AIDS drugs. Potent anti-AIDS drugs should be able to overcome the effects of commonly observed drug resistance mutations. A structural understanding of the target enzyme, mode of drug action, and effects of drug resistance can aid the design of potent anti-AIDS drugs. Together with Dr. Paul Janssen and colleagues, we have used systematic structural and molecular modeling studies of HIV-1 RT/NNRTI complexes to design new NNRTIs that are potent against a broad spectrum of resistant strains. Conformational flexibility and compactness of the new NNRTIs, including the diarylpyrimidine derivatives TMC120-R147681 (dapivirine) and TMC125-R165335, appear to be favorable design features that can offset the effects of resistance mutations and allow binding of the drugs to wild-type and a variety of mutant RTs. This concept may have broader implications for designing drugs against other rapidly evolving targets.

Crystallographic studies have played a crucial role in characterizing the molecular interactions of drugs with HIV-1 RT. We believe that structural approaches will become increasingly important in understanding existing and emerging multidrug resistance and in using that information to design improved anti-AIDS drugs and to develop new treatment strategies.

See Also the Following Articles

HIV Protease • Reverse Transcriptase and Retroviral Replication

Glossary

excision Reverse of the polymerization reaction by which the RT catalyzes the removal of the nucleotide at the DNA primer terminus.

non-nucleoside RT inhibitors (NNRTIs) Inhibitors that bind in a hydrophobic pocket near the polymerase active site and block DNA polymerization. Nevirapine, delavirdine, and efavirenz are three clinically approved NNRTI drugs for treating HIV-1 infection.

nucleoside RT inhibitors (NRTIs) Analogues of normal nucleosides, which lack a 3′-OH and act as terminators of DNA elongation. AZT (zidovudine) and 3TC (lamivudine) are among the approved NRTI drugs for treatment of HIV-infected patients.

resistance mutation A change in amino acid sequence that reduces susceptibility of the enzyme to an inhibitor.

reverse transcriptase (RT) An enzyme that converts single-stranded RNA to double-stranded DNA.

Further Reading

Coffin, J. M., Hughes, S. H., and Varmus, H. E. (1997). *Retroviruses*. Cold Spring Harbor Laboratory Press, Plainview, NY.

Das, K., Clark, Jr., A. D., Lewi, P. J., Heeres, J., de Jonge, M. R., Koymans, L. M. H., Vinkers, H. M., Daeyaert, F., Ludovici, D. W., Kukla, M. J., De Corte, B., Kavash, R. W., Ho, C. Y., Ye, H., Lichtenstein, M. A., Andries, K., Pauwels, R., de Béthune, M.-P., Boyer, P. L., Clark, P., Hughes, S. H., Janssen, P. A. J., and Arnold, E. (2004). Roles of Conformational and Positional Adaptability in Structure-Based Design of TMC125-R165335 (Etravirine) and Related Non-nucleoside Reverse Transcriptase Inhibitors that are Highly Potent and Effective against Wild-Type and Drug-Resistant HIV-1 Variants. *J. Med. Chem.* **47**, 2550–2560.

Huang, H., Chopra, R., Verdine, G. L., and Harrison, S. C. (1998). Structure of a covalently trapped catalytic complex of HIV-1 reverse transcriptase: Implications for drug resistance. *Science* **282**, 1669–1675.

Jacobo-Molina, A., Ding, J., Nanni, R. G., Clark, A. D., Jr., Lu, X., Tantillo, C., Williams, R. L., Kamer, G., Ferris, A. L., Clark, P., Hizi, A., Hughes, S. H., and Arnold, E. (1993). Crystal structure of human immunodeficiency virus type 1 reverse transcriptase complexed with double-stranded DNA at 3.0Å resolution shows bent DNA. *Proc. Natl. Acad. Sci. USA* **90**, 6320–6324.

Jaeger, J., and Pata, J. D. (1999). Getting a grip: Polymerases and their substrate complexes. *Curr. Opin. Struct. Biol.* **9**, 21–28.

Kohlstaedt, L. A., Wang, J., Friedman, J. M., Rice, P. A., and Steitz, T. A. (1992). Crystal structure at 3.5Å resolution of HIV-1 reverse transcriptase complexed with an inhibitor. *Science* **256**, 1783–1790.

Ren, J., Esnouf, R., Garman, E., Somers, D., Ross, C., Kirby, I., Keeling, J., Darby, G., Jones, Y., Stuart, D., and Stammers, D. K. (1995). High resolution structures of HIV-1 RT from four RT-inhibitor complexes. *Nat. Struct. Biol.* **2**, 293–302.

Sarafianos, S. G., Das, K., Ding, J., Boyer, P. L., Hughes, S. H., and Arnold, E. (1999). Touching the heart of HIV-1 drug resistance: The fingers close down on the dNTP at the polymerase active site. *Chem. Biol.* **6**, R137–R146.

Sarafianos, S. G., Clark, A. D., Jr., Das, K., Tuske, S., Birktoft, J. J., Ilankumaran, P., Ramesha, A. R., Sayer, J. M., Jerina, D. M., Boyer, P. L., Hughes, S. H., and Arnold, E. (2002). Structures of HIV-1 reverse transcriptase with pre- and post-translocation AZTMP-terminated DNA. *EMBO J.* **21**, 6614–6624.

Tantillo, C., Ding, J., Jacobo-Molina, A., Nanni, R. G., Boyer, P. L., Hughes, S. H., Pauwels, R., Andries, K., Janssen, P. A. J., and Arnold, E. (1994). Locations of anti-AIDS drug binding sites and resistance mutations in the three-dimensional structure of HIV-1 reverse transcriptase: Implications for mechanisms of drug inhibition and resistance. *J. Mol. Biol.* **243**, 369–387.

Biography

Kalyan Das is an Associate Research Professor of Chemistry and Chemical Biology and a Research Faculty Member at the Center for Advanced Biotechnology and Medicine. His research is primarily focused on application of structural and molecular modeling studies in understanding drug resistance and in structure-based drug design aiming at HIV-1 reverse transcriptase and other viral targets.

Stefan Sarafianos is an Associate Research Professor of Chemistry and Chemical Biology. His research at the Center for Advanced Biotechnology and Medicine is focused on mechanisms of enzyme function and drug resistance in HIV reverse transcriptase and other DNA and RNA polymerases.

Eddy Arnold is a Professor of Chemistry and Chemical Biology at Rutgers University and a Resident Faculty Member at the Center for Advanced Biotechnology and Medicine in Piscataway, New Jersey. His laboratory uses structural biology to design drugs and vaccines against AIDS and other infectious diseases with a special emphasis on targeting antiviral resistance.

Stephen Hughes is Chief of Retroviral Replication Laboratory in the HIV Drug Resistance Program at the NIH National Cancer Institute in Frederick, MD. Dr. Arnold and Dr. Hughes have collaborated on studies of HIV-1 RT structure, function, and resistance since 1987 and have published more than 50 papers together on the subject.

Homologous Recombination in Meiosis

Nancy M. Hollingsworth
State University of New York, Stony Brook, New York, USA

During meiosis, homologous chromosomes undergo a reciprocal exchange of DNA in a process called recombination or "crossing over." Meiotic crossing over serves two important functions: (1) it creates a physical connection between homologous chromosomes that is necessary for proper segregation at the first meiotic division (MI) and (2) it generates new combinations of alleles. Like meiosis, the process of meiotic recombination is highly conserved between organisms as diverse as yeast and humans. Recombination is highly regulated during meiosis, such that crossovers occur between homologues and not sister chromatids. Furthermore, crossovers are distributed so that every pair of homologues receives at least one crossover. The molecular mechanism of meiotic recombination has been elucidated primarily by research using fungi.

Meiosis

Sexually reproducing organisms face a daunting challenge: for the chromosome number of the species to remain constant, the gametes (germ cells) used for reproduction must contain only half the number of chromosomes as the diploid parent. This reduction in chromosome number is achieved by a specialized cell division, meiosis, in which two rounds of chromosome segregation follow a single round of chromosome duplication. After DNA replication produces pairs of sister chromatids (step 1, Figure 1), homologous chromosomes align and undergo a reciprocal exchange of DNA specifically between non-sister chromatids (step 2, Figure 1). At the first meiotic division, also known as meiosis I (MI), homologues segregate to opposite poles (step 3, Figures 1–3). In contrast, at the second meiotic division, or meiosis II (MII), sister chromatids are segregated (step 4, Figure 1). As a result, a single diploid cell can produce four haploid gametes (step 5, Figure 1).

The Role of Recombination in Meiosis

In addition to independent assortment, crossing over between homologous chromosomes produces new combinations of alleles that provide the grist for evolution.

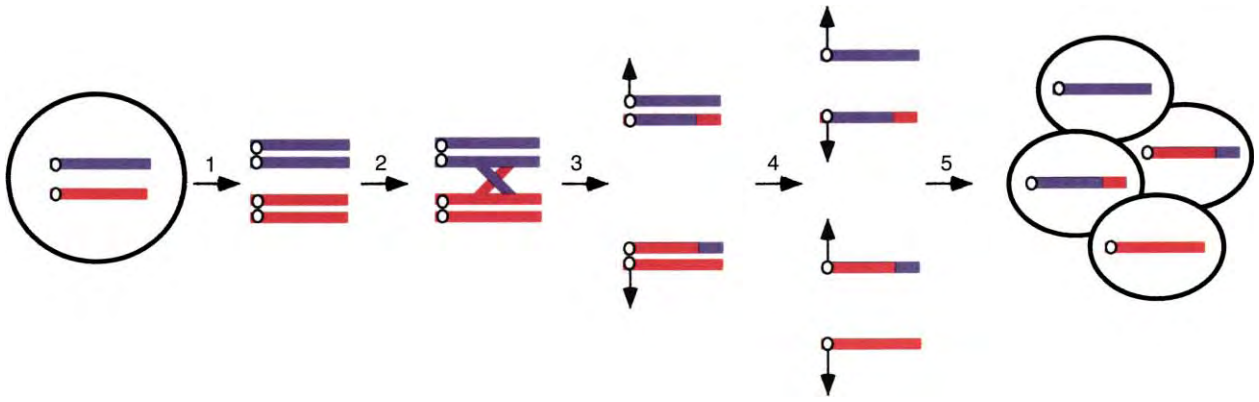

FIGURE 1 Chromosome behavior during meiosis. A diploid cell containing a pair of homologous chromosomes (one blue and one red) is shown. Small white circles represent the centromeres to which spindle fibers attach. Arrows connected to centromeres indicate the direction of segregation. (1) Chromosomes replicate to form sister chromatids. (2) Reciprocal recombination, or crossing over, connects homologous chromosomes, enabling their proper alignment prior to MI. (3) Homologues segregate to opposite poles at MI. (4) Sister chromatids segregate to opposite poles at MII. (5) Four haploid products are packaged into gametes. In yeast, these gametes are called spores.

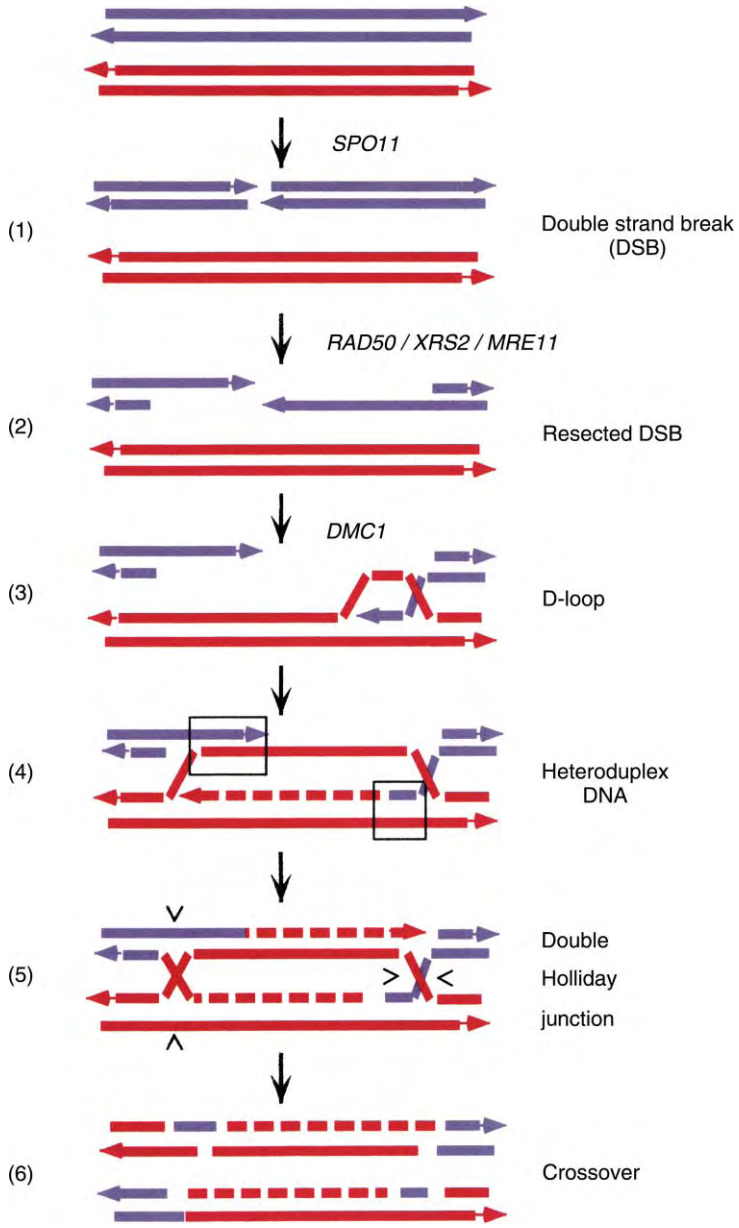

FIGURE 2 The double-strand break repair model for meiotic recombination. The double strands of DNA from one chromatid of each homologue (one blue and one red) are shown. Arrows on the DNA indicate the 3′ ends. Dashed lines indicate newly synthesized DNA. Karats indicate sites of nicking and religation used for Holliday junction resolution. Boxes indicate sites of heteroduplex DNA. (1) A DSB is introduced into one chromatid by Spo11. (2) Resection of the 5′ end on each side of the break produces two 3′ SS tails. (3) With the help of Dmc1, a 3′ SS tail invades the DNA of the homologous chromatid. (4) DNA synthesis extends the D-loop until it can anneal with the 3′ tail on the other side of the break. (5) Ligation of the invading strand creates an intermediate in which the chromatids are connected by two Holliday junctions. (6) Resolution of the Holliday junctions in opposite directions creates a crossover chromosome.

Recombination also plays a critical mechanical role in meiosis by creating a physical connection between homologues that is crucial for proper MI segregation (step 2, Figure 1). In the absence of recombination, chromosomes segregate randomly, thereby creating gametes with too few or too many chromosomes. Meiotic recombination is therefore, critical to fertility and the production of healthy offspring.

A Molecular Model for Meiotic Recombination

Initiation

The double-strand break repair (DSBR) model for recombination was first proposed in 1983 based on genetic data from meiotic studies using a number of

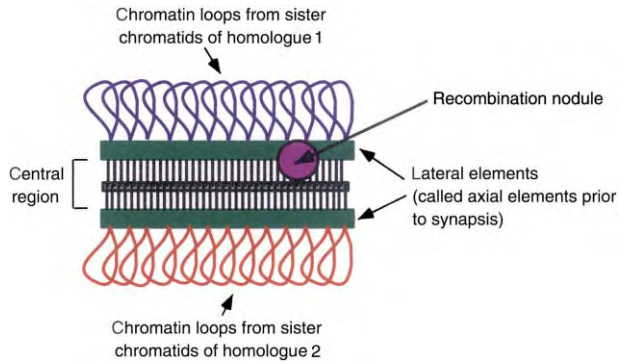

FIGURE 3 The synaptonemal complex. Synapsis of two homologous chromosomes (one blue and one red) is shown.

different fungi. Since that time, many of the molecular intermediates predicted by the DSBR model have been observed experimentally and the model has gained wide acceptance. The DSBR model proposes that meiotic recombination is initiated by the introduction of a double-strand break (DSB) on one of the four chromatids of a pair of homologues (step 1, Figure 2). The formation of DSBs is catalyzed by a meiosis-specific protein called Spo11. Spo11 breaks DNA by forming a transient covalent bond between the protein and the DNA. Yeast cells lacking the Spo11 protein fail to make breaks, undergo no recombination, and exhibit high levels of chromosome missegregation. Meiotic defects resulting from mutation of Spo11 have also been observed in fruit flies, worms, and mice, indicating that the mechanism for initiating meiotic recombination is evolutionarily conserved.

Resection

After a DSB is made, the 5′ ends on each side of the break are resected to produce 3′ single-stranded (SS) tails (step 2, Figure 2). In budding yeast, resection requires a highly conserved protein complex containing Rad50, Xrs2, and Mre11. While the absence of any one of these proteins prevents DSB formation, specific mutant versions of the proteins exhibit DSBs, but the breaks remain unprocessed because Spo11 remains covalently bound to the 5′ end of the break. Therefore, DSB formation and 5′ end processing are coupled together by these proteins.

Invasion

After resection, a 3′ SS tail from one side of the break invades the duplex of the homologous chromosome, thereby displacing the strand of like polarity to form a displacement loop (D-loop) (step 3, Figure 2). Strand invasion is facilitated by Dmc1, a highly conserved protein which is a member of the RecA family of strand transferases. The Dmc1 protein is produced only during meiosis and it specifically promotes invasion of the 3′ tail into the homologous chromosome, as opposed to the sister chromatid. This bias is important, as intersister-recombination events do not facilitate MI chromosome segregation.

Double Holliday Junction Formation

After strand invasion, DNA synthesis extends the invading strand, thereby increasing the size of the D-loop until the displaced single strand can complementary base pair with the 3′ tail on the other side of the break (step 4, Figure 2). A recombination intermediate containing two cross-shaped structures called Holliday junctions (HJs) is then created (step 5, Figure 2). To separate the two recombining chromatids from each other, each HJ must be resolved by nicking of the two strands of like polarity, followed by religation. To generate a crossover, the two HJs must be resolved in opposite directions (step 6, Figure 2). Proteins exhibiting HJ resolvase activity have been identified in bacteria but, so far, attempts to discover a nuclear HJ resolvase used for meiosis have been unsuccessful.

Gene Conversion

Mendel's first law states "alleles segregate equally into gametes." Therefore, when a diploid that contains two different alleles of a gene (+/−) is put through meiosis, half of the gametes should contain the "+" allele and half should contain the "−" allele (indicated by 2^{+}:2^{-}). The ability in fungi to analyze all four products from a single meiosis (called spores) led to the discovery that for a small percentage of the time Mendel's first law is broken. In these cases, meiosis produces spores in a ratio of 3^{+}:1^{-} or 1^{+}:3^{-} by a process called gene conversion.

Gene conversion changes the sequence of one allele precisely to the sequence of the other allele in the cell. This transfer of sequence information can happen due to the formation of heteroduplex DNA during recombination. Heteroduplex DNA results when a strand of DNA from one homologue complementary base pairs with a strand of DNA from the other homologue. According to the DSBR model, there are two times when heteroduplex is formed – after the initial strand invasion and after the displaced single strand of DNA in the D-loop anneals to the 3′ end on the other side of the break (step 4, Figure 2). Because the DNA sequences of homologous chromosomes, while highly similar, are not necessarily identical, base pair mismatches can occur in heteroduplex DNA. These mismatches are then corrected by a highly conserved mismatch repair machinery. A mismatch can be corrected so that the original base pair is restored,

thereby producing 2^+:2^- spores or it can be corrected, so that the sequence of one allele is changed to the sequence of the other allele (3^+:1^- or 1^+:3^-). Gene conversion has been proposed to play an important role in maintaining the sequence homogeneity of multi-gene families.

The Meiotic Recombination Checkpoint

The introduction of DSBs into chromosomes by Spo11 puts the cell in grave peril. Proceeding ahead through MI with unrepaired DSBs would be fatal, as pieces of broken chromosomes would become irrevocably separated from each other. Once recombination is initiated, the process is carefully monitored such that MI occurs only after recombination is complete. This surveillance process has been called the meiotic recombination checkpoint or the pachytene checkpoint. For example, budding yeast lacking Dmc1 arrests recombination prior to MI. Examination of the DNA indicates that DSBs are made and resected, but because there is no Dmc1 to promote strand invasion into the homologue, recombination cannot proceed and the meiotic recombination checkpoint is triggered. The cells remain arrested, waiting for the break to be repaired.

Genetic Interference

It is critical that each pair of homologues receives at least one crossover to prevent missegregation at MI. Because in many organisms there is a finite number of crossovers in each meiosis, crossovers must be distributed so that large chromosomes do not sustain a disproportionate number of crossovers at the expense of small chromosomes. This distribution is accomplished by a phenomenon known as genetic interference. Interference was first observed at the beginning of the twentieth century when fruit fly geneticists were mapping genes on the same chromosomes. These geneticists observed that the presence of a crossover in one interval decreased the chance that a second crossover would occur nearby. Mutation of genes required for interference in budding yeast increases MI missegregation, especially of small chromosomes. Despite intense research, the mechanism by which the cell distributes crossovers through interference remains obscure.

The Synaptonemal Complex

A unique feature of meiosis is the physical association of homologous chromosomes by a meiosis-specific structure called the synaptonemal complex (SC) that is formed by a process called synapsis (Figure 3). After DNA replication, sister chromatids condense along protein cores called axial elements (AEs) that are comprised, at least in part, of meiosis-specific proteins. AEs from homologous chromosomes then become "glued" together by insertion of the central region to form SCs. In the context of the SC, AEs are referred to as lateral elements. Associated with SCs are densely staining bodies called recombination nodules (RNs). RNs are thought to contain the proteins that mediate recombination. The relationship between the SC and meiotic recombination varies depending upon the organism. In worms and fruit flies, SC formation is necessary, but not sufficient for recombination, whereas in yeast and mammals, recombination is a prerequisite for SC formation. In budding yeast, loss of the central region has little effect on crossing over, but interference is abolished, suggesting that the SC may be important for distributing crossovers. In contrast, the absence of AEs greatly decreases the frequency of both gene conversion and crossing over, demonstrating that there is an important connection between meiotic chromosome structure and recombination.

Mitotic versus Meiotic Recombination

Meiotic recombination exhibits a number of important differences from mitotic recombination. First, meiotic recombination is several orders of magnitude more frequent. This is due, in part, to the induction of meiosis-specific recombination proteins such as Spo11. In mitotically dividing cells, recombination is used to repair lesions in DNA and therefore recombination events occur rarely and are located randomly along the chromosomes. In meiotic cells there are "hot spots" of recombination – these are places on chromosomes where Spo11 prefers to act. In mitotic cells recombination occurs most frequently between sister chromatids, which act as a template for DNA repair. In contrast, crossing over in meiotic cells is targeted between homologues. This bias is key because only interhomologue crossovers promote proper segregation at MI. Finally, meiotic recombination occurs between homologous chromosomes that are physically associated by a meiosis-specific structure, the SC.

See Also the Following Articles

Chromosome Organization and Structure, Overview • DNA Mismatch Repair and Homologous

Recombination • Meiosis • Mitosis • Non homologous Recombination: Bacterial Transposons • Non homologous Recombination: Retro transposons • Recombination: Heteroduplex and Mismatch Repair *in vitro*

Glossary

alleles Alternative forms of the same gene that vary in DNA sequence.

homologues Chromosomes with highly similar, but not necessarily identical, DNA sequences.

recombination Includes both crossing over, which is the reciprocal exchange of segments of DNA between homologous chromosomes, and gene conversion, the process by which the sequence of one allele is changed to the sequence of the other allele in the cell.

sister chromatids Two identical copies of a chromosome created by DNA replication.

synapsis The physical association of homologous chromosomes during meiosis by the formation of the synaptonemal complex.

Further Reading

Hassold, T., and Hunt, P. (2001). To err (meiotically) is human: The genesis of human aneuploidy. *Nat. Rev.* **2**, 280–291.

Keeney, S. (2001). Mechanism and control of meiotic recombination initiation. *Curr. Topics Dev. Biol.* **52**, 1–53.

Roeder, G. S., and Bailis, J. M. (2000). The pachytene checkpoint. *Trends Genet.* **16**, 395–403.

Smith, K. N., and Nicolas, A. (1998). Recombination at work for meiosis. *Curr. Opin. Genet. Devel.* **8**, 200–211.

Villeneuve, A. M., and Hillers, K. J. (2001). Whence meiosis? *Cell* **106**, 647–650.

Biography

Nancy M. Hollingsworth is an Associate Professor in the Department of Biochemistry and Cell Biology at the State University of New York at Stony Brook. Her principal research interest is understanding the molecular basis by which chromosomes recombine, synapse, and segregate during meiosis. She holds a Ph.D. in genetics from the University of Washington and has received postdoctoral training both at the Fred Hutchinson Cancer Research Center in Seattle and the University of California, San Francisco.

HPLC Separation of Peptides

James D. Pearson
Pfizer, Portage, Michigan, USA

High-performance liquid chromatography (HPLC) is a separation method based on partitioning between a coated silica solid phase and a liquid phase. The term high-performance (also known as "high-pressure") refers to the speed and superior separation compared to agarose "soft gel" particles that were the mainstay of pre-1970s column-chromatography separations. The main type of HPLC used today to separate peptides is called reversed-phase HPLC (RP-HPLC or simply RPLC). This separation mode is based on nonpolar adsorption of peptides onto the stationary phase within the column. The peptides are then differentially released from the stationary phase as a function of increasing organic component in the liquid phase.

Historical

The earliest high-performance liquid chromatography (HPLC) peptide separations were done in the 1970s using reversed-phase. Other separation modes have been developed since and will be discussed, but RPLC remains the most popular mode for peptide separations. Two key observations were made in the early 1980s that dramatically increased the use of RPLC for peptide separations. First, it was found that increasing the pore size of silica particles from ~100 to ~300Å had a dramatic effect on improving the separation of peptide fragments generated from enzymatic or chemical digests of proteins. Second, researchers replaced phosphoric acid with trifluoroacetic acid (TFA) as the ion-pairing agent in RPLC peptide separations. TFA often resulted in better peptide separations and, importantly, it was volatile. This simplified the process for preparing isolated peptide fragments for amino acid analysis and Edman gas-phase protein sequencing during the mid-1980s. Another key to the early acceptance of TFA as the IPA of choice was its commercial availability as a highly purified protein-sequencing reagent. The lack of impurities afforded sensitive UV detection at 214 nm. By the late 1980s, RPLC using TFA in the mobile phase and 300Å pore diameter silica particles was the standard for peptide separations. During this time period, advances in peptide RPLC purification enabled advances in protein sequencing. Gas-phase N-terminal Edman sequenators were introduced around this time, and the ability to purify peptide samples by RPLC reduced background noise during sequence cycles in these instruments.

The widespread use of RPLC for peptide separations during the late 1980s encouraged vendors to develop the next generation of HPLC instruments. Gas-phase protein sequenators were in wide use during the early 1990s and chromatographers needed more sensitive HPLCs to conduct microscale peptide purifications. By the early 1990s, separation scientists realized that reducing the column internal diameter (ID) from 4.6 to 1 mm increased peptide detection tenfold. At the time of this observation, HPLC systems were designed to generate and deliver reproducible gradients in the 300–500 μl min^{-1} range. HPLC instrument companies were challenged to design and deliver HPLCs that could generate gradient flows down to 50 μl min^{-1} with low dead volumes for 1 mm ID columns. These instruments became widely available by the mid-1990s. The driving force for increasing detection sensitivity then began to shift from gas-phase protein sequencing technology to RPLC coupling to ion-trap electrospray ionization (IT-ESI) mass spectrometers. HPLC separations today are routinely conducted on $\leq$0.2 mm ID columns flowing at "nano-flow" nl ml^{-1} rates and directly coupled to MS/MS instruments. These automated LC/MS systems process raw spectral data using specialized software and output-automated peptide identifications. This high-throughput ability to separate peptide by RPLC, generate ion fragment data by MS, and identify the original proteins using translated genomic database software is collectively referred to as Proteomics.

Reversed-Phase Supports

Origin of the "Reversed-Phase" Term

In the early 1900s, standard partitioning chromatography was routinely done with a polar stationary phase and a less-polar mobile phase. In 1928, Holmes and McKelvey separated a series of fatty acids in this

fashion using silica gel as the stationary phase with a toluene mobile phase. They found that when nonpolar carbon adsorbent and polar water were used, the order of fatty acid adsorption was reversed. In 1950, Howard and Martin described this partitioning process as "reversed phase" to distinguish it from conventional partitioning chromatography. From the 1950s to the 1970s, this separation mode had various names such as salting-out, hydrophobic interaction, hydrophobic salting-out, solubilization, and solvophobic chromatography. Under these various names the technique was increasingly used, especially during the late 1970s when n-alkyl groups bonded to silica and packed into HPLC columns replaced n-alkyl linked agarose soft-gel columns. Although the concept of reversed phase as originally described by Howard and Martin in 1950 seems archaic today, it is the term that survived and flourished during the 1980s to become a part of commonly used scientific lexicon today.

Reversed-phase columns are used for most HPLC separations today because they offer a higher degree of sample fractionation per unit of gradient time compared to other modes of HPLC. RPLC fractions also avoid the high salt content usually found in other HPLC modes. The avoidance of desalting procedures makes RPLC fractions ideal for drying and continuing directly on to other analyses such as immunocharacterization or mass spectrometry for analysis.

Types of Reversed-Phase Columns

RPLC supports are usually made of silica particles that contain silanol groups that are reacted with n-alkylchlorosilanes. These n-alkyl chains are usually in the form of n-butyl (C4), n-octyl (C8), or n-octadecyl (C18) stationary phases. The C4 phase is preferred for protein recovery, especially when sub-microgram amounts are chromatographed. The C18 phase is favored for peptides and is recommended for tryptic digest peptide separations. C18 columns are preferred to separate small, early eluting peptides compared to C4 columns. The C8 column is a good compromise for users who do not want to switch back and forth between C4 and C18 columns. N-alkyl phases from C1 to C22 have been compared in the past for peptide and protein separation selectivity. C1 to C3 coatings perform similar to the C4 type for protein separations, but column life tends to be less because shorter chains are not as well protected against siloxane hydrolysis compared to C4 and longer n-alkyl coatings. C10 to C22 coatings yield similar results for peptide separations and manufacturers gravitated towards the C18 chain for optimization in the early 1980s. The silylation reagent n-octadecyltrichlorosilane also happened to be the least expensive n-alkychorosilane available in the early 1980s.

Alternative Reversed-Phase Supports

Nonporous materials are alternatives to porous silica supports when fast separation times are critical. These columns are typically packed with 1.5 μm particles that increase the efficiency of the separation. There are two disadvantages for these materials. First, the column back pressure is substantially higher than for macroporous supports, which can lead to faster system failure if the column inlet gets clogged with debris. This can be mitigated by using a shorter column. Second, the loading capacity is sharply decreased, which can impact sample identity efforts when a fraction is subjected to additional HPLC separation steps prior to mass spectrometry characterization. The use of nanoflow LC/MS systems compensate for this deficiency. A compromise material is "superficially" porous particles, which consists of nonporous silica core particles covered with a layer of 300Å pores (such as Aligent's "Poroshell"^{TM} supports). These 5 μm diameter materials are packed in short columns and are designed to reduce peak broadening at high linear flow mobilephase rates. Separations in 6 min or less are common, which is one-tenth the time required for conventional macroporous support separations. Advantages of these superficially coated supports over nonporous materials include the following: (1) lower back pressure due to larger particle size; (2) enhanced loading capacity because of increased support surface area; and (3) less column failure as a result of flow plugging. These materials are also desirable for nanoflow LC/MS applications, where shortened separation times save data processing time and hence data storage space.

Silica dissolves at pH 12 and readily degrades at pH 9; so high-pH mobile phases are a problem for silica-based HPLC columns. Even at pH 7.5 (a common condition for anion exchange separations), column supports degrade over time. To address this degradation problem vendors have developed "pH stable" supports that have a pH 1.5–10 workable range. To avoid basic pH silica support degradation altogether, polystyrene divinylbenzene (PSDVB) supports have been developed since the mid-1980s. These supports are not as resilient to high back pressure surges compared to rigid silica supports, but they can be used at both high and low pH extremes to test diverse mobile phase conditions. PSDVB also has an advantage when coupled to sensitive mass spectrometer detection. The gradual leeching of silanolic alkyl phase in silica-based supports into the mobile phase is avoided in PSDVB supports.

Supports for Small Tryptic Peptide Separations

Recently, specialized columns for small (<20 aa) tryptic peptide separations have been commercialized.

These supports utilize ~90Å pores that are suitable for chromatography of small peptides, and offer higher loading capacities compared to 300Å supports. The higher column loading capacity is a function of increased surface area of the 90Å pores supports compared to macroporous materials. Supports with ~300Å pores remain optimal for RPLC separations of larger polypeptides and proteins.

Ion-Pairing Agents

Types and Uses

RPLC peptide separations require an organic component in the gradient and an ion-pairing agent (IPA). The actual choice or organic mobile phase is generally not as critical as the choice of IPA for optimizing peptides separations. In the early days of peptide RPLC, the favored IPA for superior peptide separations was 10 mM phosphate at pH 2. TFA is the most popular IPA used today, others include triethylammonium phosphate (TEAP), citrate, acetic acid, formic acid, and phosphate. Since TFA is the overwhelming IPA of choice for optimal RPLC separations a few words on its use will follow. The TFA concentration is usually 0.1% (v/v) in both solvents of a gradient system and it is used with an acetonitrile gradient. At sensitive UV detection levels (210–220 nm), the TFA concentration in the eluting solvent is commonly lowered slightly to 0.09% to minimize the upward UV-baseline drift. When an HPLC is directly coupled with electrospray ionization mass spectrometry (ESI-MS), the TFA concentration can be lowered to 0.01% to reduce ion current signal suppression, but a noticeable loss in peptide separation is observed below 0.05%. To address this problem of resolution loss at lower TFA concentrations, HPLC suppliers have introduced low-TFA supports. These HPLC columns are made with specially coated supports that improve separations when the TFA concentration is below 0.1%.

Another feature of TFA as the IPA of choice is that it is an excellent peptide solubilizer. Peptides that are refractory to 0.1% TFA solubility can sometimes be solubilized in higher TFA concentrations. The simple procedure is to use a high enough TFA concentration to solubilize the peptides, and then dilute the concentration back to $<2\%$ TFA before injection onto the HPLC column. For extremely hydrophilic peptides that do not adsorb to reversed-phase supports in TFA-based systems, heptafluorobutyric acid (HFBA) is an alternative that enhances adsorption for gradient elution.

Controlling Silanophilic Effects

Free silanol groups are present even after the silica surface is reacted with n-alkylcholorosilanes to form the reversed-phase coating. This is due to steric hindrance during the coating process. Therefore, an acidic IPA is also important to add to the mobile phase to control these undesirable stationary phase effects. These "silanophilic" interactions between peptide and accessible free silanol groups introduce a dual adsorption mode. A low-pH mobile phase helps to suppress these undesirable negatively charged siloxyl groups (SiO^-) on the support by converting them to neutral silanol (SiOH) groups. Acidic IPAs, such as TFA, acetic acid, or formic acid are used to achieve this effect, otherwise peptide resolution is compromised. Manufacturers have addressed the problem of unreacted silanol groups by a process developed by Klaus Unger in the mid-1970s. Supports are reacted with trimethylchlorosilnae (TMCS) after the n-alkyl phase has been bonded to the silica. This process results in RPLC columns that significantly deactivate these free silanol groups and are referred to as "encapped" columns. Free silanolic groups can also be minimized by n-alkylchlorosilane polymeric coating procedures. These supports are especially useful for enhancing separations of small molecules containing free amino groups.

Mass Spectrometry Applications

The underlying technological rational for increasing detection sensitivity of HPLC peptide separations shifted from gas-phase Edman sequencing to mass spectrometry applications in the early 1990s. During this time manufacturers developed packing methods to deliver efficient HPLC columns with significantly reduced column diameters. HPLC peptide separations today are routinely conducted on μm ID columns flowing at nl min^{-1} rates, directly coupled to tandem MS/MS instruments that deliver automated peptide identifications. Interestingly, the many attributes of TFA that revolutionized peptide RPLC for gas-phase Edman sequencing sample preparation during the 1980s had a fault in the 1990s. TFA suppressed peptide ionization signals in electrospray mass spectrometers. Therefore, most nanospray LC/MS/MS applications today use formic acid or acetic acid instead of TFA as the IPA to increase ionization sensitivity. Although 0.1% TFA is superior for peptide separations compared to the typical 1% formic acid or 2–5% acetic IPAs used today, modern LC/MS systems and software allow for automated multiple peptide identifications within a single fraction. Thus, advancements in mass spectrometry instrumentation have altered what is considered optimal for HPLC peptide separation sensitivity. Instead of using TFA for a superior RPLC peptide separation, less resolved profiles using formic or acetic acid as the IPA suffice because peaks containing multiple peptides can be readily deconvoluted and identified by mass detectors.

Organic Solvents for Gradients

Acetonitrile is the organic eluant of choice for peptide separations, while isopropanol, ethanol, and methanol are used to a lesser extent. It is desirable to make the starting solvent of the gradient system ~2% organic to reduce spontaneous gas bubble formation otherwise seen in mixing pure aqueous with organic solvents. Most peptides elute within the 5–80% acetonitrile concentration window in TFA-based gradients, therefore an elution solvent made of 90% acetonitrile is used often. In the case where peptides are extremely hydrophobic, isopropanol can be substituted for acetonitrile and the peptides will elute at a lower-percentage organic during the gradient. The drawback with isopropanol is that it has a significantly higher viscosity compared to acetonitrile. This causes a higher column back pressure, which may lead to premature column failure. Methanol does not have a viscosity problem, but since it is not as elutropic as acetonitrile it may not release extremely hydrophobic peptides from the column. Ethanol is usually not the best solvent for optimizing peptide separations; it is mainly used for process scale purification protocols, where regulatory agencies favor its use because of safety issues. In the research laboratory, setting gradients are usually run in the linear mode for about an hour to optimize the separation. Gradients longer than 2 h usually result in only incremental increases in resolution at the cost of diluting the eluted peptides. As a rule of thumb, gradient rates below 0.2% min^{-1} organic do not offer enhanced peptide resolution, but are preferred to isocratic elution.

Column Length and Diameter, Flow Rates, and Support Size

HPLC columns come in lengths ranging from ~5 to 25 cm. The column diameter dictates the flow rate and there is a commonly used lexicon for these column diameter/flow rate systems. Analytical HPLC is the term used for 4.1–4.6 mm ID columns with 0.6–1 ml min^{-1} flow rates and optimal resolution for loads up to several hundred micrograms. Narrowbore HPLC signifies ~2 mm ID columns used at 50–200 μl min^{-1} flow rates and loads up to 50 μg of peptide. Microbore HPLC refers to 1 mm ID columns with 10–50 μl min^{-1} flow rates and loads up to 10 μg. Capillary HPLC means 0.3–0.5 mm ID columns and 2–10 μl min^{-1} flow rates with loads up to 1–2 μg. Nanoflow HPLC refers to ≤0.2 mm ID columns with nl min^{-1} flow rates and loads below 1 μg. Capillary and nanoflow HPLC require specially designed HPLC plumping and low-volume detection systems.

Five-micron supports give the overall best resolution in microbore, narrowbore, and analytical HPLC. These are the mainstay columns used in biological research laboratories. Smaller 3 μm particles can yield slightly better resolution, but are not used that often because they generate a significantly higher back pressure, which can lead to faster column failure. Semipreparative columns refer to columns packed with 5 or 10 μm particles in 10 mm diameter columns. Preparative columns are packed with 10 μm particles in ~20 mm diameter columns. Process columns are packed with 10–15, 15–20, or 20–30 μm particles in columns 3–10 cm in diameter. The practical loading capacity of these larger ID columns depends on the complexity of the sample and the location(s) of the desired peak(s) of interest.

Guard Columns

The degree of peptide profile resolution offered by HPLC erodes as a function of the number of crude biologic samples applied to the column. It is expensive to use a fresh HPLC column every week so a short "guard column" placed in series before the separation column is sometimes used. Instead of replacing the HPLC column, the guard column that collects debris is changed periodically. Before the invention of guard columns, chromatographers used to unscrew the column inlet, remove the first several millimeters of dirty brown silica support and replace it with fresh support. The advent of guard columns simplified the column rejuvenation process. There are several sound reasons to use guard columns for many applications, but it is important to know what these devices actually do before using them on a routine basis. When a sample is injected onto an adsorptive HPLC support material such as reversed-phase or ion exchange, the peptides stick at the head of the column and then a gradient is used to elute the peptides to effect the separation. The important point here is that the actual separation is in the first several millimeters of the HPLC column. That is why the column head must be debris free. It has been shown by several groups that columns 1 cm in length can separate polypeptides almost as well as a 25 cm column. The lesson here is that the integrity of the first several millimeters of the column inlet are the most important. It must be clean and contain the same support material as the rest of the column. If not, the separation will be influenced by different adsorption–desorption characteristics. This principle is the reason why a guard column must contain the same support material as the HPLC column, since the head of the guard column is critical to the success of the overall separation. In capillary HPLC, clogging the column inlet with debris is especially problematic, but there is a different remedy.

Since the length of the column has a limited effect on the separation, experts usually dispense with guard columns and simply break off a few millimeters of the capillary column inlet for rejuvenation.

RPLC Applications (CNBr, Trypsin, and V8 Protease Protein Digestions)

In the 1970s large cyanogen bromide (CNBr) cleavage fragments (>30 aa) were notoriously difficult to separate by RPLC because they tend to be very surface hydrophobic. The advent of large-pore-sized RPLC columns in the early 1980s allowed researchers to readily purify these large polypeptides. This was a timely chromatographic advance since cocurrent advancements in gas-phase Edman microsequencing technology enabled longer N-terminal sequence determinations of the large CNBr fragments. Tryptic peptides tend to be smaller and less hydrophobic compared to CNBr fragments, so tryptic HPLC separation profiles generally resulted in more highly resolved peaks, but shorter partial N-terminal sequence determinations.

Recent advances in LC-MS/MS technology have readily automated the process of protein identification using tyrptic digestion. By the early 1990s the use of CNBr chemical cleavage to generate peptide fragments for RPLC separations was not used that often by analytical core facilities. Tyrptic digestion offered smaller, more reproducible peptide separation profiles, while CNBr chemical cleavage required safety handling precautions and less-resolved HPLC peptide separations. Today the standard is tyrptic digestion and to a lesser extent *S. aureus* V8 protease digestion. This separation process is known as peptide mapping. Trypsin cleaves peptide bonds C-terminally after basic lysyl and arginyl residues, while V8 protease cleaves after acidic aspartyl and glutamyl residues. Therefore, V8 protease fragmentation is ideal for generating peptide fragments from low pI proteins.

Other HPLC Peptide Separation Modes

Ion Exchange

RPLC is the preferred method for separating peptides, but there are cases where ion exchange can result in superior separations. Ion exchange can be either cation or anion exchange; both processes involve electrostatic interactions between charged amino acid side chains on the peptide and the stationary phase. For example, deamidated peptides can sometimes be better separated from their nonmodified counterparts using sulfonic-acid-based strong cation exchange as opposed to RPLC. Peptides with a low pI can be separated from other components in a mixture using weakcation exchange supports. Salt gradients of KCl, NaCl, $NaClO_4$, and NH_4SO_4 are commonly used with 10–50 mM Tris, bis-Tris, triethanolamine, or L-histidine buffering systems. Adding small amounts of acetonitrile (~5%) can also increase resolution of peptides. Temperature does not effect ion-exchange peptide separations as much as it does in RPLC separation, but it does effect protein separations. This is because proteins have tertiary structure that can be altered by temperature. When salts are used in an HPLC gradient system, extra care must be taken if stainless steel is exposed to the mobile phase. Corrosion will occur if exhaustive water-washing steps are not used after the separation procedure.

Weak anion-exchange HPLC columns usually contain diethylaminoethyl (DEAE) groups, quaternary amine functionalities (referred to as "Q"), n-propylamine chains, or polyethyleneimine (PEI) polymers adsorbed onto silica. Anion-exchange HPLC columns are also used for protein purifications and the salt gradient is usually in the pH 5–9 range. Weak cation exchangers are based on support materials with a carboxylic acid (COOH) function group and salt gradients in the pH 2–7 range. Commonly used buffering systems in order of increasing pK_a include phosphate (pK_a 2.1), formate, acetate, MES, phosphate (pK_a 7.2), and HEPES.

Ion exchange is increasingly being used before RPLC for two-dimensional HPLC separations. Examples include the multidimensional protein identification technology (MudPIT) method of Yates for complex protein identifications. In this example, a yeast ribosome preparation was first digested with trypsin; then the peptide fragments were fractionated into pools using strong-cation exchange; and finally the peptide pools were separated and identified by ion-trap electrospray LC-MS/MS. The common theme of this and other two-dimensional HPLC procedures is that salt, which is required for ion-exchange separations, is removed during the two-dimensional RPLC separation step. This makes the final factions ideal for mass spectrometry analysis.

Size Separation

Size exclusion chromatography (SEC) is the HPLC name for classical gel-permeation chromatography (GPC). In both cases macromolecules are eluted in order of size from largest to smallest. The key to this type of separation is minimizing interactions of the polypeptides with the stationary phase. This will allow the macromolecules to sieve down the column and be separated as a function of size only. Salt-based mobile phases are used to minimize the interactions of polypeptides with

support material during this sieving or permeation process. SEC is usually used to separate proteins over a broad molecular mass range, typically 10–200 kDa. Applications for peptide separations are limited because they are all relatively small (<10 kDa), although such separations can sometimes be achieved ~30% acetonitrile is added to the mobile phase.

See Also the Following Articles

Affinity Chromatography • Oligosaccharide Analysis by Mass Spectrometry

Glossary

ion-pairing reagent A chemical added to both solvent components of an RPLC gradient to control pH and improve peptide elution profiles.

peptide A short amino acid polymer consisting of ~20 or less residues. Longer chains are referred to as polypeptides or proteins and contain tertiary structure.

RPLC or **RP-HPLC** Reversed-phase high-performance liquid chromatography. A mode of HPLC where peptides are applied to hydrophobic coating support, and then selectively eluted using an organic mobile phase.

stationary phase The coating on a HPLC support surface that determines the mode of peptide separation used for elution.

support Particles that are coated with a stationary phase and packed into a column.

Further Reading

Gelpí, E. (1995). Biomedical and biochemical applications of liquid chromatography-mass spectrometry. *J. Chromatogr. A* **703**, 59–80.

Issaq, H. J. (2001). The role of separation science in proteomics research. *Electrophoresis* **22**(17), 3629–3638.

Liu, H., Lin, D., and Yates, J. R. III (2002). Multidimensional separations for protein/peptide analysis in the post-genomic era. *Biotechniques* **32**(4), 898.

Lubman, D. M., Kachman, M. T., Wang, H., Gong, S., Yan, F., Hamler, R. L., O'Neil, K. A., Zhu, K., Buchanan, N. S., and Barder, T. J. (2002). Two-dimensional liquid separations-mass mapping of proteins from human cancer cell lysates. *J. Chromatogr. B: Analyt. Technol. Biomed. Life Sci.* **782**(1–2), 183–196.

Biography

James D. Pearson is a member of the Molecular Technologies Department at Pfizer Global Research and Development, Ann Arbor, Michigan. He developed RPLC peptide and protein columns in the early 1980s, micropreparative-HPLC purification techniques in the late 1980s, 2-D gel separation systems in the 1990s, and is currently working in the areas of ribosomal and mitochondrial proteomics. He received a B.S. degree at the University of California at Davis, and a Ph.D. at Purdue University with Prof. Fred Regnier.

Imaging Methods

György Szabadkai and Rosario Rizzuto
University of Ferrara, Ferrara, Italy

The currently widely used imaging techniques evolved from the necessity of following the results of molecular biology (with the isolation of cDNA, and ensuing identification of the macromolecular components of living organisms), with the goal of clarifying where the different gene products are located, and how they act and interact (i.e., how they affect the different parameters and functions of the cell). In biochemistry and cell biology applications, the most developed imaging techniques work at the light microscopy level, but contemporary new techniques emerge to explore the exact nature of complex macromolecular interactions at the subcellular level and intercellular communication at the organ/organism level.

Objectives of Imaging Methods

The two main uses of cellular imaging are either to define the exact spatial localization of a given object or to quantitatively assess a given cellular parameter. Accordingly, the user interfaces of the digital imaging systems generally differentiate between morphological (focusing on three-dimensional (3-D) spatial data, utilizing either fixed or living samples) and quantitative (focusing of intensity measurements, generally in time dimension in living samples) applications.

Physical Optics and Microscopy

Image Formation Characteristics

The image formation of the light microscope (Figure 1) is based on a compound lens system comprising an objective with very short focus distance and high magnification power, and an ocular lens with longer focus and usually lower magnification. The sample is positioned slightly out of the focal distance of the objective, and thus an intermediate, magnified, reversed image is formed inside the focal distance of the ocular (eyepiece). The final, virtual, magnified, direct image can be observed by eye through the ocular or by detectors after collecting the divergent light by additional lens systems. Modern microscopes, by utilizing motorized objectives that can be focused axially in successive focal planes, allow the examination of specimen in three dimensions. Besides its magnification power, the most important characteristics of the microscope is its resolution power (i.e., its ability to distinguish between two adjacent points), which is limited by the diffraction of the light and determined by the properties of light and the objective (wavelength, λ; numeric aperture, NA). Based on these inherent physical properties, a maximum of 190 nm resolution is achievable observing green ($\lambda \sim 550$ nm) light emission and 130 nm at UV ($\lambda = 365$ nm) emission. This resolution limit can be greatly enhanced (more than 10^3 times, below nm scale) by the use of electron microscopes, using accelerated electrons instead of photons. Electrons can be focused by electromagnets on the (very thin) specimen where part of electrons will scatter on dense elements (salts or heavy metal labels), and the remaining ones will form an image on a phosphorus screen and a light detector. The main obstacle of electron microscopy is the rough fixation and drying necessary for sample preparation (consequently positioned in very high vacuum), which makes the observation of physiological elements very difficult.

Specialized Light Microscopy Techniques

Living or fixed cells visualized by traditional bright-field microscopy (using homogenous illumination by transmitted light) generally give images which are poor in contrast, because cellular components cause only very small amplitude difference of the transmitted light. The human eye is sensitive only to the colors of the visible spectrum (variations in light frequency) or to differing levels of light intensity (variations in wave amplitude). However, different cellular components may have quite large optical path difference (which is the function of object thickness and refractive index, relative to the neighboring substance) causing modulation of the phase of the diffracted light at object boundaries. To render these phase differences visible, several contrast-enhancing techniques using different illumination and image formation methods have been introduced. The most widely used phase contrast microscopy separates the direct and diffracted light and creates destructing interference between them. This results in the details

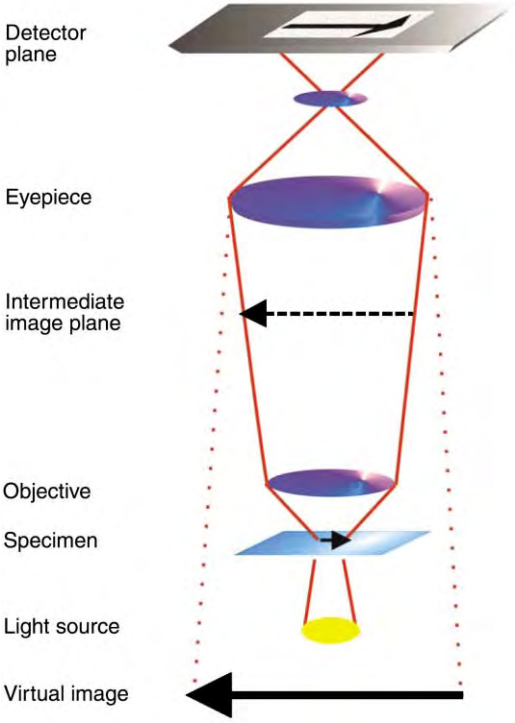

FIGURE 1 Schematic representation of image formation of the compound microscope.

of the image appearing darker against a lighter background. Differential interference contrast (DIC, DIC-Nomarski) microscopy appears to be the most powerful (but rather expensive) method to render subcellular details clearly visible only by optical means. This technique applies two polarized light beams perpendicular to each other, to detect edges of cellular components and converts them either in intensity or color difference with high lateral and axial resolution, giving a pseudo-3D appearance of the image.

Fluorescence Microscopy

Another solution for rendering subcellular details visible is to label cellular components by light-absorbing chemical substances (contrast enhancing and colored dyes), i.e., to increase the amplitude modulation of the transmitted light leading to increased contrast of the generated image. However, the revolution of cellular imaging stems from the introduction of fluorescent labels, which allows the visualization of virtually any desired object even in living specimens with exclusive sensitivity and selectivity. Fluorescent light emission is the result of selective excitation of electron state in particular chemical substances, generally polyaromatic hydrocarbons or heterocycles, followed by the return of the excited electron to its basal energy value after a few nanoseconds lifetime (Figure 2A). An inherent property of the light emission cycle is that the exciting photon has

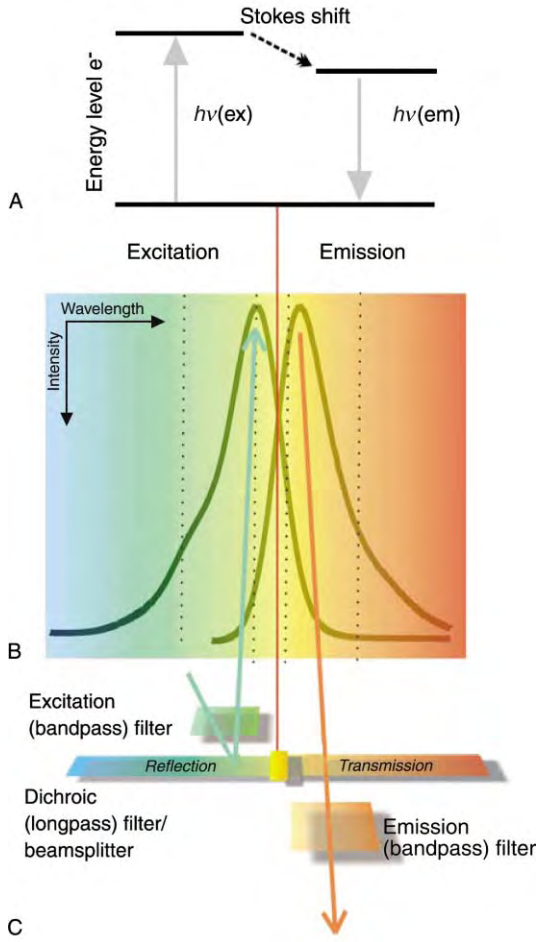

FIGURE 2 Principles of fluorescence: (A) formation of emitted light after excitation of the electron state in a fluorescent substance, (B) absorption and emission spectra of the fluorescent substance, and (C) optical filter set.

higher energy ($h\nu = h1/\lambda$), and therefore lower wavelength than the emitted photon. Thus, the absorption and emission spectra (Figure 2B) of a given fluorophor can be well separated. This allows the separation of the two different wavelengths in the illumination and detection optical path of the microscope by using a series of optical filters (Figure 2C). The core of color separation is the dichroic filter or beamsplitter, which, depending on its wavelength, either reflects or transmits the incident light. Additionally, to obtain specific excitation light and to detect a given range of emitted wavelengths, bandpass, lowpass, or highpass filters are applied. In multicolor or ratiometric-timelapse applications, in order to quickly change the excitation and emission wavelengths, filter wheels or even faster monochromators are used.

Electronic Light Detectors

The type of detector used is a critical parameter in cellular imaging techniques, since it determines the

sensitivity and spatial resolution of the obtained image. The two general solutions to electronically detect emitted, reflected, or transmitted light are the use of photomultiplier tubes and photodiodes, which in itself does not give spatial information or video imagers/area detectors, designed to directly provide spatially resolved images (tube type: vidicon; solid-state detectors: charge coupled device (CCD) and complementary metal oxide semiconductor (CMOS) cameras). These devices generate an analog voltage signal in function of light intensity, which must be digitized for image display and storage.

Photomultiplier Tubes

Photomultiplier tubes (PMTs) are useful for light detection of very weak signals, because they work by amplifying the electrons generated by a photocathode exposed to the incident photons. Among imaging applications, confocal microscopes combine high spatial resolution scanning and PMT in order to gauge light intensity and spatial information. Besides the high sensitivity, an important feature of PMT applications is their ability to record extremely fast events with very high signal-to-noise ratio ($>10^6$), since they respond to changes in input light fluxes within a few nanoseconds and exhibit extremely low dark current.

CCD Sensors

CCDs are silicon-based integrated circuits consisting of a dense matrix of photodiodes (determining picture elements, pixels of the chip), which operate by converting photon energy to an electronic charge. The accumulated charge is then transferred to a common output (through horizontal and vertical registers), amplified and digitized by an A/D converter located either in the camera or in the computer card (frame grabber). The main characteristics of CCD sensors, which determine the choice of camera type for a specialized imaging application, areas follows: (1) The number of electrons that can accumulate in the potential well of each pixel is referred to as well depth, that determines the upper limit of the dynamic range of the CCD. (2) The quantum efficiency (QE) defined as the number of electron–hole pairs created and successfully read out by the device for each incoming photon. It is the function of wavelength and standard sensors are usually more sensitive to wavelengths in the 500–800 nm range than they are to blue light (400–500 nm). (3) Image noise, by influencing signal to noise ratio (S/N), also determines the lower limit of chip sensitivity and dynamic range. Dark noise is a result of thermic generation of electron–hole pairs in the absence of illumination and can be reduced by cooling of the CCD (up to -50°C; a 20°C decrease in temperature reduces the dark current of the CCD tenfold). Readout noise is generated by collecting, amplifying, and digitizing the signal. (4) Spatial resolution and contrast depends on both the microscope optics and CCD architecture. The resolution and performance of an optical microscope can be characterized by a quantity known as the modulation transfer function (MTF), which is a measurement of the microscope's ability to transfer the spatial frequency of different contrast elements of the specimen to the image plane. This function is often utilized by optical manufacturers to incorporate resolution and contrast data into a single specification. On the other hand, the resolution of a CCD is a function of the number of its pixels and their individual size, thus increase in pixel number and decrease in pixel size will increase the resolution power of the CCD array. However, even if small pixels improve spatial resolution, they also limit the dynamic range of the device. Spatial resolution and sensitivity can be changed by unifying (clocking) multiple pixel charges in both the horizontal and vertical direction into a single larger charge. This procedure is called binning, which inherently leads to the increase of the sensitivity to incident light, but in parallel leads to the loss of spatial resolution. (5) Transfer speed of an image from the camera to the memory or screen of the computer depends on the CCD-readout rate (the time required to digitize a single pixel, pixel/sec), frame rate (the time needed for the CCD to acquire an image and then completely read that image out, frame/sec, fps), and the parameters of the computer utilized.

Three different CCD architectures, varying in their basic abilities, are currently in use to adapt CCD cameras to different applications. Full frame CCDs utilize their whole high-density pixel arrays to produce high-resolution images. In this configuration, the image transfer rates are lower, and can be increased by subdividing the CCD array into smaller, but identical subregions, which can then be read separately. The CCD array of frame transfer cameras is divided into the light-sensitive image array, where image data are collected; then the data are quickly (in 100 microseconds range) shifted to the storage array for the final readout by the serial shift register. Thus, during readout, the CCD is able to capture the next image, allowing for faster frame rates, but preserving high resolution and sensitivity. A potential drawback of frame-transfer CCDs is the presence of image "smear" at high frame rates, which occurs because acquisition and transfer to the storage array occur simultaneously. Interline CCD architecture is composed of a separate photodiode and an associated parallel storage and readout region into each pixel element. During the period in which the parallel storage array is being read, the image array is busy acquiring the next image frame, similar to the operation of the

frame-transfer CCD. This composition allows very fast image transfer rates but has lower sensitivity due to a decrease of the photosensitive area. This drawback, however, can be partially overcome by incorporation of microlenses on the photodiode array to increase the amount of light reaching each element.

CMOS Image Sensors

CMOS image sensors are similar to CCDs, but each active-pixel image sensor of a CMOS contains not only the photodetector element but also an active transistor circuitry, which works as an amplifier and serves for readout of the pixel signal, allowing random access to each image pixel and thus fast readout, and thereby rendering the acquired image extremely flexible to digital processing as compared to the sophisticated approaches necessarily used in CCDs. Another great advantage of CMOS sensors is their low cost since they can be produced in standard manufacturing facilities, producing standard semiconductor chips like computer microprocessors and memory chips. Further technological improvement to increase the sensitivity of these detectors will most likely lead to their introduction also into scientific imaging.

High-End Imaging Technologies to Increase Detection Sensitivity

Three different technologies have been applied to increase the sensitivity of CCDs: (1) The standard front illumination of the CCD array result in ~60% loss of quantum efficiency, due to the fact that the light must pass through the silicon layer covering the photodiode. The use of back-illuminated CCDs overcame this problem leading to an increase ~100% quantum efficiency at visible and infrared light and to 50% in UV detection. In this architecture, light arrives at the back of the CCD in a region that has been thinned to be transparent (thickness: 10–15 μm). Manufacturing these CCDs is significantly more difficult, resulting in a much higher cost of these detectors. (2) Amplification of the incoming photons by PMT-like devices has been integrated in specialized intensified cameras. The available technical solutions are ranging from several generations of microchannel plate-electron multipliers combined with a phosphorescent output screen to the recently introduced electron-bombarded charge-coupled device (EBCCD), which is a combination of the image intensifier and the CCD camera. The advantages of these devices over a cooled, slow-scan (low noise) CCD are the additional gain and accompanying speed. However, their noise levels are very high and their spatial resolution and dynamic range is significantly lower. (3) Very recently, on-chip amplification devices (amplifying signal before readout, thus reducing readout noise) have also been introduced, which, in combination with back-illuminated CCD architecture, may further increase the speed and sensitivity of imaging detectors.

Three-Dimensional (3D) Imaging

In order to visualize objects in three dimensions, images must be acquired and resolved along the z-axis (z stacks). An inherent problem of bright field and fluorescence microscopy is that images formed always contain out-of-focus light (haze). Two fundamentally different solutions emerged to overcome this problem: (1) 3-D deconvolution, to remove out-of-focus haze by computational methods from a series of optical section images acquired by digital microscopy, and (2) confocal imaging, to optically subtract light which does not arrive from the focal plane of the objective.

3D Deconvolution

The 3D distribution of out-of-focus light can be mathematically modeled as a point spread function (PSF). Deconvolution algorithms are designed to invert the blurring effect of the point spread function in order to restore the image contrast. Simplest solutions, like no- and nearest neighbor algorithms work by deblurring one 2D image, utilizing a subtraction of the blurred form of the adjacent slices and are particularly useful for fast deconvolution of high-intensity/contrast images. The term blind deconvolution is used when deblurring algorithms are based on theoretical PSFs. This method may give better results when additional algorithms are used to adopt PSF to the actual z image series. Still, the most powerful approaches utilize measured PSFs, which contain the actual aberrations inherent of the microscope configuration in use; thus, the deconvolution process can apply an efficient correction of the sum of these errors occurring in the nondeconvolved original image (Figure 3).

Confocal Laser Scanning Microscopy

In the excitation path of the confocal laser scanning microscopy (CLSM), an expanded laser light beam, focused on the specimen, is used to scan a given area in the $x-y$ space, and then the emitted fluorescent light passes through the dichroic mirror in the direction of the photomultiplier. A confocal aperture (pinhole) is placed in front of the photodetector (PMT), such that the emitted light from points on the specimen that are not within the focal plane (out-of-focus light) will be largely

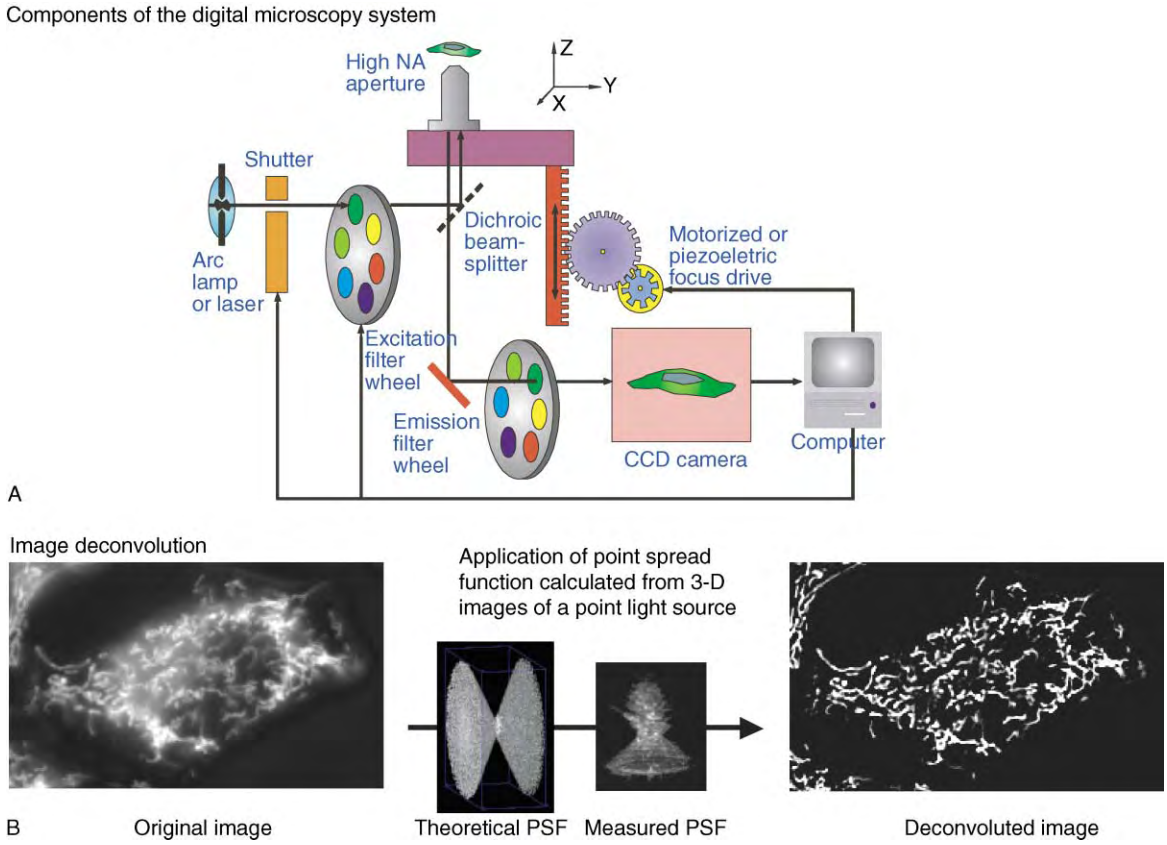

FIGURE 3 3-D microscopy: (A) basic components used for image acquisition and (B) image processing by 3D deconvolution.

blocked outside of the pinhole. Thus, the great advance of the use of CLSM is that the resulting image will be formed only from a slice of the sample with a given thickness, which is the function of the diameter of the aperture. The cost paid for this result is the relatively slower integration (scanning) time and higher illumination intensity needed, compared to high-sensitivity CCD detectors. This may lead to photobleaching of the fluorescent probe and damage of a living specimen. This phenomenon is greatly reduced in multiphoton confocal applications, where coincidence of two or more photons (with double or triple wavelength) is used to excite the probe only in the focal plane; thus, the specimen is illuminated with less intensity and less damaging (longer wavelength) light.

The images acquired either by 3D deconvolution of digital microscopy images or by the use of CLSM are usually visualized using volume rendering and surface rendering 3D reconstruction methods. In volume rendering, the pixel intensity information from a z series of 2D images is combined to generate voxels, volume elements. In surface rendering, only the surface pixels are utilized, and the interior structure is not visible because of the surface opacity.

Digital Image Characteristics

A 2D digital image is usually presented as a rectangular grid of individual pixels (picture elements). A fundamental characteristic of each pixel and thus of the whole image is its bit-depth, i.e., the scale of different colors or gray shades it may have (Table I). The sensitivity of the human eye is about 16–32 shades in gray and about two million shades in color; thus an image published in 8-bit grayscale or 24-bit color (true color) is more than sufficient. The resolution of the displayed image is defined as a number of pixels in a given distance (dot/inch dpi or sometimes dot/cm). The different output devices of the computer have different resolution ranging from 72 dpi of the monitor screen to 1200 dpi of laser printers. However, one should always keep in mind that the quality of the published image depends primarily on the resolution of the acquired image. The most commonly used color model is the additive RGB (red, green, blue) on-screen model, based on the three different phosphors on the monitor screen, excited at different intensities (usually an 8-bit range for each color, for 256 intensities per color, for a total of 24 bit possible color combinations). Color printing typically

TABLE I
Digital Image Characteristics

Number of colors/shades in gray scale	Bit depth
2	2^1
32	2^4
256	2^8
4096	2^{12}
65 536	2^{16}
16 777 216	2^{24}

uses a subtractive color model called CYM (cyan, yellow, magenta) or CYMK (with black added), which however cannot reproduce a range of colors as large as the RGB model. The most popular alternative color-space model is the hue, saturation, and intensity (HSI) color space, which represents color in an intuitive way (the manner in which humans tend to perceive it). Instead of describing characteristics of individual colors or mixtures, as with the RGB color space, the HSI color space is modeled on the intuitive components of color. For example, the hue component controls the color spectrum (red, green, blue, yellow, etc.), while the saturation component regulates color purity, and the intensity component controls how bright the color appears. Grayscale digital images can be rendered in pseudocolor by assigning specific gray level ranges to particular color values. This technique is useful for highlighting particular regions of interest in gray-scale images, because the human eye is better able to discriminate between different shades of color than between varying shades of gray. Pseudocolor imaging is widely employed in fluorescence microscopy to display merged monochrome images obtained at different wavelengths utilizing multiply stained specimens.

Another important consideration for the published images is the file format used. For scientific images, the most frequently used format is tagged image file format (TIFF), which supports 8- or 16-bit grayscale as well as 24-bit color, and lossless (LZW) compression, most often used on web pages, not suitable for most scientific images. A relatively new and very convenient format that is not widely supported yet is PNG (portable network graphics), which supports up to 48-bit color and 16-bit grayscale with lossless compression. In contrast, the JPEG and GIF formats, widely used on web pages, are generally not suitable for scientific images either because of their low bit-depth or lossy compression methods.

See Also the Following Articles

HPLC Separation of Peptides • Oligosaccharide Analysis by Mass Spectrometry • PCR (Polymerase Chain Reaction) • Two-Dimensional Gel Electrophoresis • X-Ray Determination of 3-D Structure in Proteins

Glossary

digitalization Process done by an analog/digital converter, during which a continuous signal (voltage or current) is transformed into discrete values. The range and step size of these discrete values is dependent on the number of bits used in digitalization.

numeric aperture (NA) Feature of the microscope objective defining its resolution power, function of the half of angular aperture (α) of the objective lens and the refractive index (n) for the medium through which the light passes ($NA = n\sin\alpha$).

photobleaching Irreversible destruction of the excited fluorophore, which happens usually under high-intensity illumination conditions. Photobleaching originates from a third excited state created from the singlet state and some pathways leading to photobleaching may include reactions between dye molecules.

quantum efficiency (QE) Number of electron–hole pairs created and successfully read out by a charge coupled device (CCD) for each incoming photon, describing the sensitivity of the light detector.

resolution (1) Distance between two adjacent points which can be imaged separately; and (2) number of picture elements (pixels) in a given distance of a digitally displayed image.

Further Reading

Centonze, V. E. (2002). Introduction to multiphoton excitation imaging for the biological sciences. In *Cell Biological Applications of Confocal Microscopy* (B. Matsumoto, ed.) 2nd edition, Vol 70, pp. 129–148. Methods in Cell Biology, Academic Press, New York.

Gerlich, D., and Ellenberg, J. (2003). 4D imaging to assay complex dynamics in live specimens. *Nat. Cell Biol.*, S14–S9.

Isenberg, G. (ed.) (1998). *Modern Optics, Electronics, and High Precision Techniques in Cell Biology (Principles and Practice Series)*. Springer, Berlin, Germany.

Miyawaki, A. (2003). Fluorescence imaging of physiological activity in complex systems using GFP-based probes. *Curr. Opin. Neurobiol.* **13**, 591–596.

Rizzuto, R., Carrington, W., and Tuft, R. A. (1998). Digital imaging microscopy of living cells. *Trends Cell Biol.* **8**, 288–292.

Tsien, R. Y. (2003). Imagining imaging's future. *Nat. Rev. Mol. Cell. Biol.*, SS16–SS21.

http://micro.magnet.fsu.edu/primer/index.html – M. W. Davidson, Florida State University.

Biography

Rosario Rizzuto is a Professor of General Pathology at the University of Ferrara. He developed a new method for measuring Ca^{2+} concentration in specific cell domains, based on the targeting of the Ca^{2+}-sensitive photoprotein aequorin and applied 3D microscopy to show close contact between the endoplasmic reticulum and mitochondria. His research interest is the role of calcium ions as intracellular second messengers, with special emphasis on the mechanism and functional role of mitochondrial Ca^{2+} homeostasis.

György Szabadkai is a Research Assistant at the Telethon Center for Cellular Imaging, University of Ferrara. His main interest is the study of intraorganellar Ca^{2+} signaling in mitochondria and endoplasmic reticulum, and determining its role in different forms of apoptosis and neuronal cell death.

Immunoglobulin (Fc) Receptors

Mark Hogarth
Austin Research Institute, Melbourne, Australia

Immunoglobulin Fc receptors (FcRs) are cell surface molecules that bind the Fc portion of immunoglobulin. Receptors have been identified for all immunoglobulin classes and subclasses with the exception of IgD. These should not be confused with microbial proteins that bind the Fc portion of immunoglobulin.

General Comments

When antibodies contact their specific antigen, they form an immune complex and in the case of most pathogens, many antibodies will coat a single macromolecule or pathogen fragment leading to the formation of oligovalent immune complexes. These complexes can then interact with specific cell surface Fc receptors (FcRs) and this interaction subsequently initiates signaling cascades inside cells.

The affinity of the interaction between the different Ig subclasses and specific FcRs varies enormously, ranging from low-micromolar affinity for some of the IgG receptors to high-femtomolar affinity for the high-affinity IgE receptors. Such a vast range of affinities have specifically evolved to suit the biological activities of particular receptor types.

The nomenclature of FcRs is as the name suggests, based on the capacity to bind the Fc portion of a particular class of antibody (e.g., IgM, Fcμ; IgG, Fcγ), the letter R designates the receptor and a Roman numeral designates a particular subtype of FcR e.g., FcγRII. There are further subclassifications by letters a, b, c, etc. e.g., FcγRIIa.

The vast majority of FcRs are found on leukocytes where they are involved in the regulation of cellular activity by antibody. For the most part, this is the activation of cells, but a discrete and unique class of FcR is able to down-regulate leukocyte activity following their binding of immune complexes.

Whilst the vast majority of FcRs are found on leukocytes and have been the principal subject of most research, several other FcRss have been identified, present on epithelial and endothelial cells, with specific functions related to transport and recovery of immunoglobulins.

Leukocyte Fc Receptors

Most leukocyte FcR are multisubunit complexes requiring a ligand-binding chain noncovalently associated with a signaling chain and in some cases with an additional signal amplifying subunit (Figures 1 and 2). The biochemical and functional characteristics of the most-frequently studied FcR of leukocytes is detailed below.

IgE Fc Receptors

The high-affinity IgE receptor FcεRI binds monomeric IgE with an affinity of 10^{10} M^{-1} and is found principally on mast cells and basophils and in a modified form on eosinophils and monocytes. The binding of IgE to this receptor and the subsequent cross-linking of the bound IgE by antigen induces one of the most potent pharmacological responses in biology. In adverse situations, this results in a classic type-I hypersensitivity reaction clinically manifest as allergy e.g., hay fever, penicillin or food allergies. Unlike the high-affinity IgE receptor, the FcεRII binds IgE with a lower affinity (10^{7} M^{-1}). This is a type-II membrane glycoprotein with lectin-like activity and is found on many leukocytes including T-cells, B-cells, and monocytes. Its function appears largely to regulate activity of immune responses.

These receptors are biochemically distinct, FcεRI is a transmembrane glycoprotein and is a member of the Ig superfamily with two extracellular domains, each of which belongs to the Ig superfamily. By contrast FcεRII is a type-II membrane glycoprotein with lectin-like activity.

IgG Receptors

There are three main classes of leukocyte IgG Fc receptors – FcγRI, FcγRII, and FcγRIII (Figures 2 and 3A and 3B). These are widespread with every leukocyte with the exception of lymphocytes bearing one or more of these receptors. They can be distinguished by both amino acid sequence and by the use of specific monoclonal antibodies and also by differences in affinities for IgG. FcγRI is the high-affinity receptor for

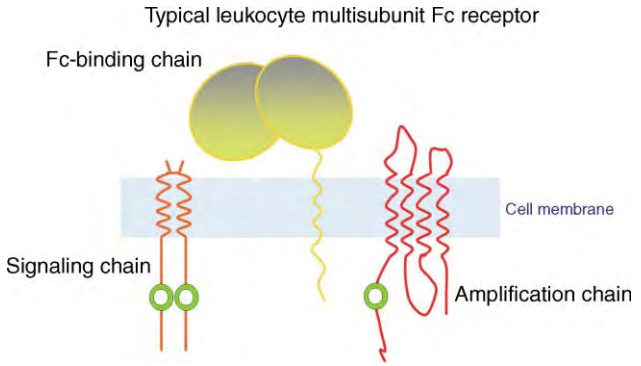

FIGURE 1 Schematic representation of a typical multisubunit Fc receptor. The typical components of many FcR found on leukocytes. A ligand-binding chain usually a Type-1 transmembrane glycoprotein is noncovalently associated with other subunits: a signaling chain, often the FcR-γ chain, which is a 24 kDa covalent homodimer wherein each monomer contains an ITAM, a specialized tyrosine-containing signaling motif (green annulus). In at least two cases, the ligand-binding chain is further associated with a tetra transmembrane signal-amplifying chain.

IgG ($10^8\ M^{-1}$) and is restricted largely to monocytes, macrophages, and neutrophils. FcγRII is composed of two major subtypes: FcγRIIa and FcγRIIb that are separate gene products and are biochemically distinct. Both bind IgG with very low affinity (1 μM) as monomeric immunoglobulins have a very rapid on and off rate, however, as these low-affinity receptors are present on the cell membrane they can effectively and very avidly bind oligovalent complexes of antigen and antibody.

FcγRIII also has two principal subtypes: FcγRIIIa and FcγRIIIb. Both are low-affinity receptors though they bind with IgG with tenfold higher affinity than the FcγRII low-affinity receptors. FcγRIIa is found on virtually every leukocyte including platelets. Similarly, FcγRIIb is found on virtually every leukocyte including B-cells but not platelets. FcγRIIIa is found on natural killer cells and macrophages, and monocytes, whereas FcγRIIIb is found only on neutrophils.

All of these FcRs belong to the Ig superfamily. Each has two extra cellular Ig-like domains with the exception of FcγRI, which has three (Figure 2). Another interesting difference is that whilst FcγRIa, FcγRIIa, and FcγRIIIa are transmembrane glycoproteins, FcγRIIIb is a GPI-anchored receptor (Figure 2).

IgA and IgM Fc Receptors

A single leukocyte receptor specific for IgA has been defined – FcαRI, which is found on neutrophils and monocytes (Figure 3C). The affinity for IgA is $\sim 10^7\ M^{-1}$ but immune complexes of IgA binding to FcαRI are potent inducers of cell activation. A receptor that is able to bind both IgA and IgM has also been defined though there has been relatively little characterization of this.

Sites of Interaction with Ig Ligands

The Ig-binding sites of FcεRI, FcγRI, FcγRII, and FcγRIII are located in similar regions in these structurally related but functionally distinct receptors (Figures 3A and 3B). The binding site largely involves the second domain together with sequences at the junction of the first and second domains. The stoichiometry of FcR:IgG interaction for these receptors is 1:1 (Figure 3A). For FcαRI, the IgA-binding site is located on the extreme tip of the first domain, which allows it to form a rather unique two to one stoichiometry with IgA (Figure 3C). The head groups of the triple helix of FcεRII interact with IgE in a 1:1 stoichiometry.

Receptor-Binding Sites in Immunoglobulin

FcγRI, FcγRII, and FcγRIII interact with sequences in the lower hinge and adjacent areas of Cγ2 of the IgG Fc (Figure 3A). Differences in the nature and extent of these

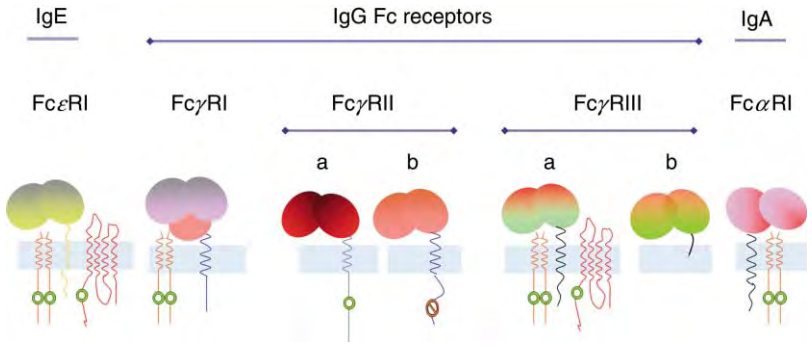

FIGURE 2 Schematic representation of leukocyte FcR showing configuration of signaling competent receptor complexes. FcγRII (not shown). ITAMS shown as green annulus; the FcγRIIb ITIM as a red crossed circle.

interactions explain the differences in affinity of FcR:Ig interaction. FcεRI interacts with a sequence between Cε2 and Cε3, which is distinct from the area of the sites of interaction of FcεRII. The nature of these interactions clearly define the stoichiometry. FcαRI interacts with the area between Cα2 and Cα3. Currently, there is no information on the interactions of Fc$\alpha\mu$R and IgA or M.

Signal Transduction Complexes

With the exception of FcεRII there has been a great deal of investigation of the signal transduction by leukocyte FcRs, which have become one of the most widely studied groups of receptors. The binding of antibody or immune complexes to these can be a potent inducer of biochemical signals, but FcγRIIa and FcγRIIb have additional unique biochemistry. The related leukocyte receptors – FcεRI, FcγRI, FcγRIIIa, and FcαRI all signal by very similar mechanisms involving the immuno-receptor tyrosine activation motif (ITAM), which is recognized by the *syk* and *src* family protein tyrosine kinases. To signal, these receptors must form multi subunit signaling complexes composed minimally of the Ig-binding chain, (all of which are the Ig superfamily members), non-covalently associated with a low-molecular-weight hetero- or homodimeric signaling chain – the common FcR-γ chain or in the case of FcγRIIIa and in NK cells the TCR-ζ chain (Figures 1 and 2).

The ITAM motif that is necessary for recognition by *syk* and *src* kinases is contained in these associated low-molecular homodimers. Cross-linking of the FcR by immune complexes or by antigen binding to cell-bound Ig, aggregates the receptors leading to phosphorylation of tyrosine in the ITAMs and the subsequent induction of the signaling cascades. Similar mechanisms of leukocyte activation are well described for the antigen receptors of T and B lymphocytes.

FcγRIIa stands out as an exception to the multi subunit paradigm for ITAM-dependent immunoreceptor signaling (Figures 2 and 3B). Whilst aggregation of this receptor leads to *syk* and *src* kinase activation, this receptor does not require association with the common FcR-γ chain or other FcR molecules as the ITAMs are contained within its cytoplasmic tail. Indeed FcγRIIa is one of the few immunoreceptors to have the signaling motifs contained in the ligand-binding chain. Furthermore, this receptor forms a unique dimer on the cell surface that juxtaposes the ITAM motifs for signal transduction (Figure 3B).

FcγRIIb is not an activating FcR; indeed its role is to inhibit and regulate the activities of other ITAM-containing activating FcRs and the antigen receptor of B cells. The cytoplasmic tail of FcγRIIb contains an immunoreceptor tyrosine inhibitory motif (ITIM), which on "coaggregation" with ITAM-containing activating receptors, recruits phosphatases, which in turn down-regulate or eliminate ITAM-dependent signal transduction. Its best-characterized role is its co-engagement with the antigen receptor of B lymphocytes where it regulates B-cell activation by antigen.

Other Leukocyte FcRs

In recent years especially with the output of the human and mouse genome projects, new cell surface molecules with FcR-like activity have been described though they are currently poorly characterized. Nonetheless, for the sake of completeness, these are included here. The most advanced characterizations have involved the leukocyte in receptor cluster, which is a large family of cell surface molecules present on leukocytes, and some of these show immunoglobulin-binding activity. Biochemically these molecules include members with multiple Ig-like domains and with tissue distributions ranging from the highly restricted to the very broad. The precise biochemical characterization and biological roles are as yet poorly understood but will no doubt be revealed in time.

Non-Leukocyte FcRs

Two major non-leukocyte FcRs have been defined. The poly Ig receptor (Poly IgR) and FcRn.

The poly Ig receptor is responsible for the binding and transport of secretory immunoglobulins – sIgA and sIgM. It is found on secretory epithelium, notably in the lactating breast, as well as mucosal surfaces. This is a cell surface molecule composed of five domains: the IgA and IgM-binding sites occur in the first two domains, which when attached to sIgA or sIgM are cooperatively cleaved from the receptor and thereby form the so-called secretory component associated with secretory IgA and IgM.

FcRn is biochemically distinct from all other leukocyte and non-leukocyte Fc receptors. It is a transmembrane glycoprotein but it is more structurally related to the major histocompatibility molecules (MHC Class I) whose principal function is antigen presentation to T-cells (Figure 3D). However, it is sufficiently biochemically different from these, which makes it unable to be involved in that process. The main function of FcRn in humans is the recycling of immunoglobulins in the circulation, which ensures the prodigious half-life of IgG. Intact, and undenatured IgG, which is taken into endothelial cells by pinocytosis is recycled to the circulation following its attachment to FcRn in the acidifying pinocytotic vesicle, where it undergoes acid-dependent attachment to FcRn, recycling to the endothelial cell surface and release at the neutral pH of the circulation.

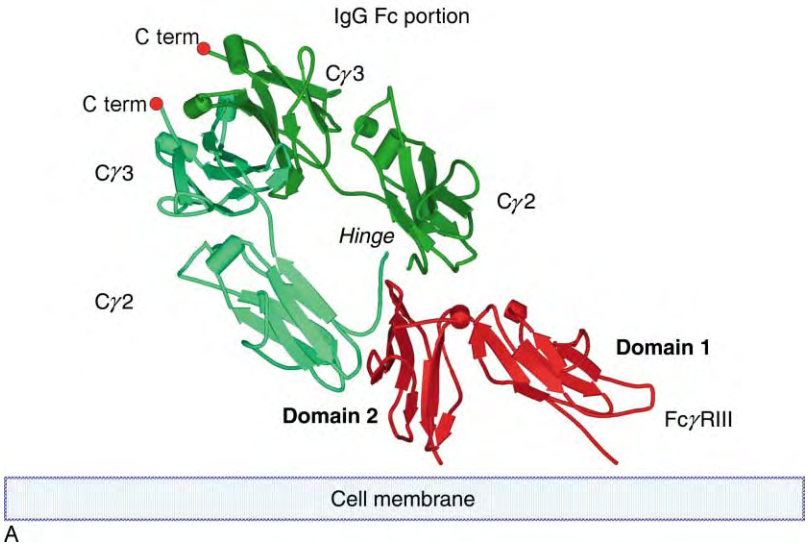

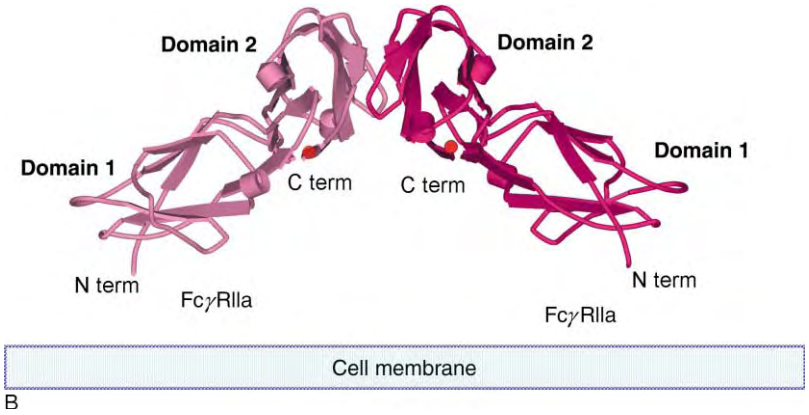

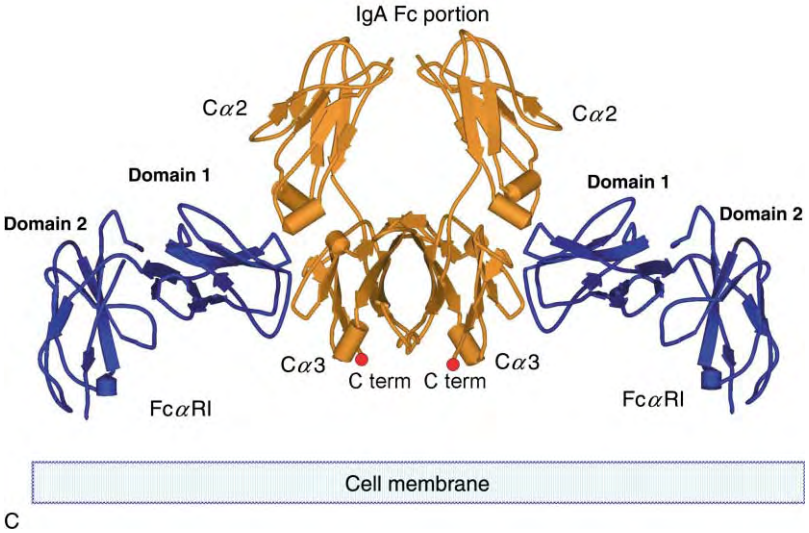

FIGURE 3 Alpha-carbon backbones of selected Fc receptors and ligands. (A) Complex of FcγRIIIa and IgG. From the Data Base:(PDB, 1E4K). The receptor's second domain and interdomain region interact with the lower hinge region of the IgG Fc giving the characteristic 1:1 stoichiometry. (B) FcγRIIa (PDB 1FCG). This receptor is unique as it forms a non-covalent homodimer. Details of the interaction with IgG are not known but interaction as seen for FcγRIII IgG (Figure 3(A) is not possible with this dimer because steric clashes between the dimer and Cγ2 prevent proper interaction of domain 2 with the lower hinge of IgG. (C) Complex of FcγRI and IgA (PDB, 1OW0). Interaction between the "tip" of the first domain of FcαRI and the Cα2/Cα3 junction of each Fc chain gives the 2:1 stoichiometry.(D) Structure of FcRn and IgG complex (PDB, 1I1A).

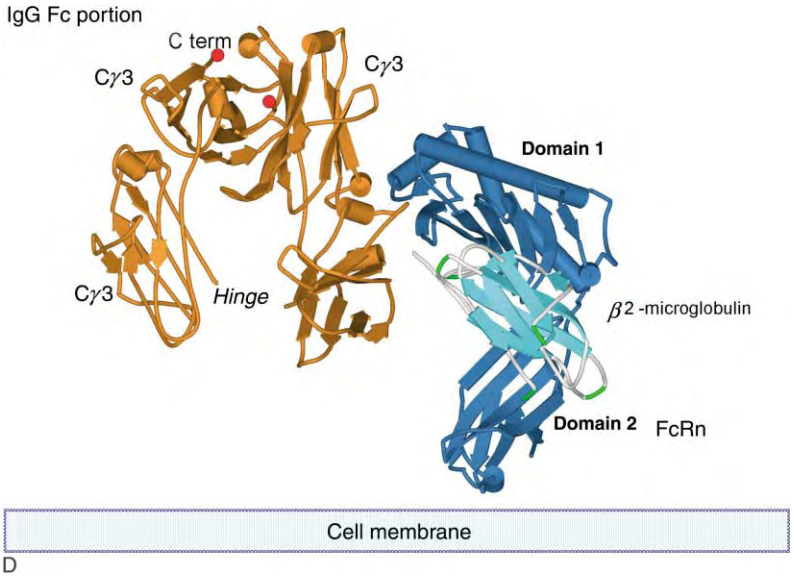

FIGURE 3 (*continued*)

Biological Role of Leukocyte Fc Receptors

These receptors participate in a range of normal biological functions, most of which are associated with the activation of leukocytes, which then lead to specialized functions associated with difference cell types, e.g., the degranulation of mast cells and the release of inflammatory mediators caused by co-engagement of the high-affinity IgE receptor. However, for the most part, FcγRI, FcγRII, and FcγRIII appear to be mostly concerned with antibody dependent of leukocyte function rather than the historical view that Fc receptors on cells such as macrophages, dendritic cells, and other phagocytes serve the principal role for the phagocytic removal of immune complexes.

It is now in the more modern view that these receptors play a far more active and sensitive role rather than one of simply garbage disposal, which in humans is largely filled by the complement system and in particular CR-1 on erythrocytes.

This capacity to bind immune complexes, though not in itself pathogenic, can in the presence of aberrant immune complexes, such as autoantibody, lead to the potent and continuous stimulation of leukocytes, leading in turn to pathological inflammation and tissue destruction. This is clearly the case in diseases such as systemic lupus erythromatosus (SLE), rheumatoid arthritis, glomerulonephritis, allergies. Attempts to interfere with the interaction of immune complexes with FcRs are now forming the basis of novel approaches to the treatment of those diseases.

Key Events in the Analysis of FcR

The existence of specific receptors for immune complexes was noted in the early 1970s by Metzger and by Basten and their co-workers. The observation by Metzger and Bevan that engagement of these receptors could induce a measurable intracellular biochemical event was an exciting observation of importance, not only for Fc receptors but for immunologically important receptors generally. There have been several major milestones in the application of new technologies to the characterization of Fc receptors – Jay Unkeless produced the first monoclonal antibody defining an Fc receptor and Hibbs and colleagues defined first function-associated genetic polymorphis using monoclonal antibodies. The genetics revolution led to the first cloning in the mid 1980s of FcR gene simultaneously and independently by Hibbs, Ravetch, Mellman, and Kinet. By the early 1990s Ierino and co-workers had established that blockade of FcR may provide useful

Interaction of the FcRn first domain with amino acids in the junction of Cγ2 and Cγ3 of a single Fc chain. The β2-microglobulin typically associated with MHC class I molecules is shown associated with FcRn ectodomains. All chains are represented as α-carbon backbones; strands as arrows and α-helices as barrels. The C terminus of each polypeptide chain is shown in red. Constant regions of IgA or IgG are indicated – Cα or Cγ and the position of the hinge is shown. Orientation of the polypeptides to the membrane is assumed.

therapeutic approaches for the treatment of disease. Finally in more recent times the three-dimensional structures of FcR have become available for the first time through the work of Maxwell and Powell, Jardetzky, Sun, Sondermann, and others.

Conclusion

The Fc receptors are a large family of immunoregulatory molecules that play crucial roles in antibody effector systems, leading in normal immune responses to the activation or regulation of leukocytes.

See Also the Following Articles

Cytokines • Fibroblast Growth Factor Receptors and Cancer-Associated Perturbations

Glossary

autoimmune disease Diseases where the immune system attacks the hosts' tissues and/or organs. Examples include rheumatoid arthritis, systemic lupus erythematosus.

hypersensitivity Powerful and frequently destructive inflammatory reaction often induced by antibodies in autoimmune diseases.

leukocyte White blood cell including eosihophil, polymorphonuclear leukocyte or neutrophil, macrophage, monocyte, mast cell, basophil, lymphocyte.

phagocyte Cell that actively ingests particles, typically macrophage or neutrophil.

phagocytosis Process, distinct from pinocytosis, by which particles are taken into the cell. Unlike pinocytosis, considerable intracellular and membrane reorganization is required for the uptake of the particle.

pinocytosis Process by which cells sample small amounts of fluid from their surrounding environment. This usually involves internalization of small vesicles formed from the invagination of the cell membrane.

Further Reading

Ierino, F., Powell, M. S., McKenzie, I. F. C., and Hogarth, P. M. (1993). Recombinant soluble human FcγRII: Production, characterization and inhibition of the arthus reaction. *J. Exp. Med.* **178**, 1617–1628.

Metzger, H. (1999). It's spring and thoughts turn to…allergies. *Cell* **97**, 287–290.

Ravetch, J. V., and Bolland, S. (2001). IgG Fc Receptors. *Ann. Rev. Immunol.* **19**, 275–290.

Van de Winkel, J. G. S., and Hogarth, P. M. (eds.) (1998). *The Immunologlobulin Receptors and Their Physiological and Pathological Roles in Immunity.* Kluwer Academic, Dordrecht.

Biography

Mark Hogarth, Director of the Austin Research Institute in Melbourne, has a long-standing interest in the biochemistry, immunology, and genetics of cell surface molecules. He has made seminal discoveries in the study of FcRs for antibodies – including some of the first monoclonal antibodies, molecular cloning, and X-ray structure analysis of this family and recently in the development of potential new therapeutic entities for the treatment of autoimmune disease and inflammation.

Inorganic Biochemistry

Robert J. P. Williams
University of Oxford, Oxford, UK

All organisms require a limited, selected number of chemical elements. The requirement includes obviously the nonmetal elements H, C, N, O, P, and S which provide the vast majority of elements in organic compounds in every cell. Other elements which are necessary for organisms include Na, K, Mg, Ca, Mn, Fe, (Co), (Ni), (Cu), Zn, Mo or W, Cl, B, and Se. Those in parentheses are essential for most organisms. Inorganic biochemistry therefore includes the modes of uptake, the ways of incorporation, and the functional value of these essential elements. It also includes consideration of elements as poisons and as valuable drugs in medical practice.

Introduction

A glance at the periodic table, Figure 1, shows that of the 18 groups in the table, elements have been selected by organisms from 15 groups, indicating that life is based on almost the full diversity of the chemistry of the periodic table. Absent are elements from groups 4, 13, and 18. There are also organisms which use F, Si, Sr, Ba, V, Cd, and possibly Sn. Thus of the common elements there are only a few that are not found in some living system, e.g., Al and Ti, while most of the uncommon elements, i.e., elements heavier than Zn, are absent. This gives rise to the possibility for the use by man in attacking medical and agricultural problems of several inorganic elements as accidental or deliberate poisons or medicines. Examples are Be, Al, Br, Pt, Hg, Au, Sb, Bi, and Pb. It is the study of all the elements, often but not always in combination with the elements of organic chemistry that is called "inorganic chemistry," and when applied in a living system it is called "inorganic biochemistry" or "biological inorganic chemistry." In what follows, attention is drawn to the value of certain of these elements starting from the most common in all organisms, but it is clear that together organic and inorganic elements, some 15–20 in all, created life as we know it.

Electrolytes

All cells are required to manage the ions of those elements which are highly available in the environment and are mainly free, namely, Na^+, K^+, Mg^{2+}, Ca^{2+} and Cl^-. Especially Na^+, K^+, and Cl^- are rarely combined with organic or inorganic molecules or anions. These five elements have always dominated the sea as electrolytes but have been and are present at much lower concentrations in all freshwater. All cells need to control the uptake of these ions for they are serious components of the ionic strength and osmotic pressure inside as well as outside cells and they are major units in electrolytic charge balance in all natural fluids. It is found that cells have, possibly universally, a free ion cytoplasmic concentration of Na^+ (10^{-2} M), K^+ (10^{-1} M), Mg^{2+} (10^{-3} M), Ca^{2+} ($<10^{-6}$ M), Cl^- (10^{-3} M). Clearly life in the sea rejects Na^+, Mg^{2+}, Ca^{2+} and Cl^- while taking in K^+ but life in freshwater, which evolved later, has to take in all five elements. The above functional value of Na^+, K^+, and Cl^-, the most available and which bind the least to organic matter, evolved from the use in simple electrolyte balances to include employment in bioenergetic exchanges across membranes and more recently to dominate electrolytic messages. Here particularly Na^+, K^+, Cl^-, and now including Ca^{2+} are the only simple ionic current carriers of such cells as nerves and muscles and are essential components of the functioning of the brain. Text books on physiology to a great degree concern mainly these five elements.

Calcium is the most strongly rejected of all five but also functions as a bound element especially in cell activation of higher cellular organisms. Magnesium is not rejected strongly from any cell and is an essential weak acid catalyst. It is present in most of the reactions of phosphates including ATP^{4-}, which is ~50% $MgATP^{2-}$ in cells. Examples of its functions are kinases and it is a vital structural component of RNA and DNA. Mg^{2+} and Ca^{2+} together help to stabilize cell membranes and walls and are present in most biological minerals such as shells and bones.

Magnesium has a quite exceptional additional function in chlorophyll, the light-harvesting and light-activating factor of virtually all plant life.

Iron

The next most common metal element is iron. It is very largely bound to proteins not free in cells. It was very

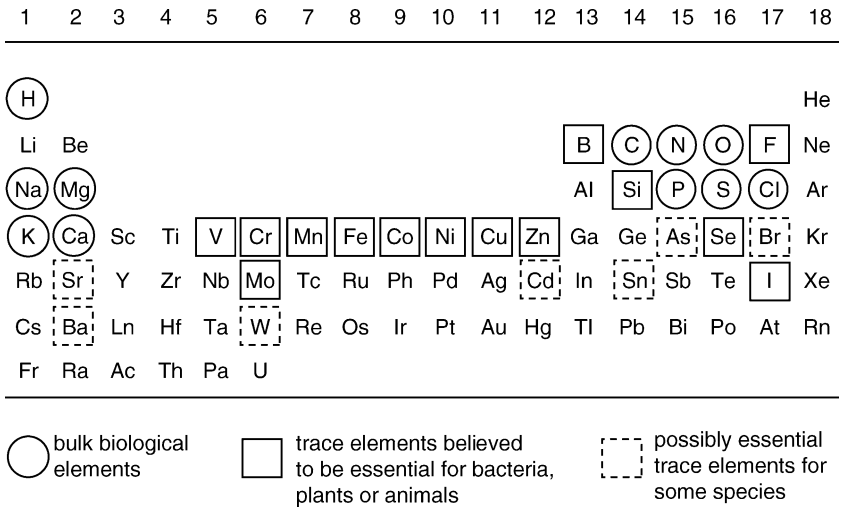

FIGURE 1 The periodic table of the elements showing those essential for most organisms and those required by some organisms. Note the distribution of required elements within the periodic table.

readily available from the primitive reducing sea as ferrous ion but, as oxygen pressure rose more than two billion years ago, iron became ferric ions in solution which precipitated and availability became very reduced. As a consequence all aerobic organisms have cleverly devised scavenging systems for iron. The essential nature of the element derives from its use as a catalyst. In its protein combinations it is found bound in iron–sulfur proteins, in heme proteins, and in proteins bound simply to nitrogen and oxygen side chains. These proteins are largely engaged in oxidation or reduction catalysts, in the transport of electrons, as carriers (hemoglobin and myoglobin), as sensors for CO, NO, and O_2, in DNA synthesis from RNA, and as storage buffers for iron. There is in fact a very extensive network of iron proteins essential in all cells but very noticeable in the bioenergetics of both chloroplasts and mitochondria. There is for this metal element a series of concentration controls linked through transcription factors to DNA. It may be that the overall expression of many functional parts of a cell are linked to the concentration of free ferrous ions in the cell cytoplasm. However, the storage of iron is in a ferric ion precipitate bound in a protein, ferritin.

Zinc

Next to iron in importance amongst trace elements is zinc. Unlike iron it was restricted in its availability to primitive life since it has an insoluble sulfide. As sulfur, in the form of H_2S, became oxidised to sulfate, so zinc was liberated, and it is now quite a common element in the sea. Zinc is not like iron in its functions. It does not take part in oxidation or reduction reactions but is a good acid catalyst. Hence it finds use in organic chemistry as well as in organisms. In cells its acidic function is used not only in a wide range of degradative enzymes – peptidases, nucleases, and saccharases, and in hydration reactions – but also in RNA/DNA synthetases. Zinc has a distinct role in the nucleus of eukaryotes in proteins called zinc fingers, which act as transcription factors especially involving sterol, thyroxine, retinoic acid, and related hormones. Thus, it is important in homeostasis and in organism metamorphic transformations such as the transition through puberty. There is now strong evidence that free zinc, normally very low in cells, is used at considerable concentrations in certain parts of the brain as a transmitter and in the reproductive tract of males. As is the case for iron there may be no life without zinc.

Copper

Copper is probably not a universal requirement for life. The sulfides of copper are extremely insoluble and primitive anaerobic archaea probably did not use it. Later oxidation of sulfide generated available copper and in general aerobes employ it as an oxidative catalyst. This use is mainly confined to extracellular or periplasmic compartments of cells since free copper itself is very poisonous internally, where it is probably no more than 10^{-15} M. The locations of the sites of action of copper proteins contrast strongly with those of iron as seen in the different cell compartments in which the two are used. A particular function of copper is in the cross-linking of extracellular matrices which helps to stabilize multicellular organisms e.g. the final forms of collagen, lignin, and chitin. The homeostasis of copper in cells

appears to be managed by a class of proteins, metallothineins, which also control the levels of free zinc. Uptake and rejection of copper requires cellular pumps and several disadvantageous inherited conditions arise from mutations in these pumps.

Cobalt

The requirement for cobalt in organisms is unusually distributed. It is most commonly found in vitamin B_{12}, yet advanced plants do not have this compound – a vitamin in higher animals and also essential in primitive anaerobes. Apart from its function in some ribonucleotide reductases vitamin B_{12} is required in several enzymes controlling rearrangement reactions especially of sugars. This vitamin is needed in smaller amounts than any of the other vitamins.

Manganese

The requirement for manganese, a relatively abundant trace element, is due to its major involvement in two kinds of enzymes, glycosylases and oxygen production units. The production of oxygen is confined to plants but it was the evolution of this reaction, initially in single cell anaerobes to obtain hydrogen from water, which caused the major steps of biological advancement over billions of years. The present-day level of some 20% oxygen in the atmosphere is entirely due to the activity of manganese enzymes. Some enzymes stated to require manganese may in fact be magnesium proteins *in vivo* since manganese readily replaces magnesium functions *in vitro*.

Nickel

Nickel, although it is available, is a rare element in all organisms being most common in primitive anaerobes. There it occurs in hydrogenases as a multimetal complex with iron and in the coenzyme F-430 which like heme, chlorophyll, and vitamin B_{12} is synthesized from uroporphyrin. Although nickel is used in urease, especially in plants, it has no functional protein coded in the DNA of higher animals such as man. Even so nickel is required in man since it is utilized by some of the lower organisms which inhabit the digestive tract of man where they aid degradation. A feature of evolution is the decline in the use of nickel and cobalt with a steady use of iron and an ever-increasing involvement of zinc and copper.

Molybdenum

Molybdenum is present in the sea in considerable concentration. It would appear that it is essential for all life except some very primitive anaerobes where its function is replaced by tungsten. The most obvious use of molybdenum is in nitrogen fixing bacteria, symbiots of plant life. Plants and animals cannot fix nitrogen gas. In these higher organisms molybdenum is required in a variety of oxygen-atom transfer reactions including enzymes for nitrate, sulfate, and carboxylate substrates. Note that the requirement for molybdenum for fixation of nitrogen gas and for reduction of nitrate implies that virtually all sources of the element nitrogen for organic synthesis in cells are dependent upon this element. The fact that these enzymes are found in prokaryotes, not higher organisms, stresses the nature of life as belonging to an ecosystem. Many diseases are associated with deficiency of the element especially in cattle.

Selenium

The importance of this element in all organisms is often missed despite the fact that it is the only heavy element which is part of a coded amino acid, seleno-methionine. This nonmetal is also found in seleno-cysteine. The functions of selenium are very different in anaerobes where it acts as a metal ligand from those in higher organisms where it is part of a powerful antioxidant – peroxidase. The switch in function follows the change of availability of the element from hydrogen selenide in primitive seas to selenate today, compare the chemical change of sulfur. It is thought that low levels of selenium in the human diet are responsible for many diseases, for example, of the heart. Selenium is now added as a supplement in some foods and to some soils.

Iodine

Iodine is found in the hormone, thyroxide, which is a hormone responsible for some features of growth control. The use of the element appears later in evolution. Iodine deficiency is a well-known genetic disease associated with goitre. Once again iodine is not used in lower organisms. Note that bromine and fluorine are little used in any organism so that iodine, fluorine, and bromine are quite unlike chlorine as chloride in biological organisms.

Rare Uses of Inorganic Elements

There are a variety of organisms in which minerals contain metals other than calcium and nonmetals other than carbonate (shells), phosfate (bone), or oxalate in plants. They include strontium and barium sulfates, which because of their density cause cells to settle in water and are useful as gravity sensors; calcium fluoride

in krill; various iron oxides in teeth and in magnetic sensors; and silica especially in diatoms and some plants.

Suggestive evidence is now available showing that cadmium may well be essential in a few lowly organisms and increasingly it is believed that chromium may be a factor in combating diabetes. There is clear evidence for the requirement of arsenic, boron, vanadium, and questionable evidence concerning some heavier elements, in selected organisms.

Inorganic Elements in Medicines and Poisons

Apart from the obvious uses in poisons and drugs of the above essential elements in organic derivatives unknown to living systems, there are many uses of other inorganic elements as both medicines and poisons. Of course, we must be careful with the use of these words, "drugs" and "poisons," since the use of medical drugs is dependent on dose where excess of a drug becomes a poison. Historically in medical practice inorganic elements were in fact used extensively before they were thought to do more harm than good. The uses of mercury, even mercury amalgam in teeth fillings, were considerable but mercury compounds are not recommended today. However, today, surprisingly, there are medicines using amongst other elements lithium, platinum, gold, and bismuth as well as technecium in diagnostics. It is anticipated that there will be many more uses of nonessential as well as those of essential elements in the not too distant future. In agricultural procedure several antifungal agents contain copper or mercury to this day.

The Selection of Elements by Cells

Given that only a limited number of elements are required and must be accumulated by organisms from a free condition in the environment, many unwanted elements must be screened against or have to be rejected since they are poisons, e.g., Al, while many have to be somewhat rejected but used, Na, Cl, Ca, Cu, Ni, and Co, for example, while some have to be concentrated, for example, C, N, P, S, Se, and K and others from organisms living in fresh water. Selection is therefore required at cell membranes by outwardly or inwardly directed pumps and also by binding. The principles of selection are well understood chemically. Such activity requires energy and here one other element is of dominant interest, hydrogen as the proton, in the form of H^+ gradients which make ATP for use in pumps for uptake and rejection of elements, and generally in many biological activities such as synthesis and mechanical action.

Conclusion

Today it is clearly obvious that living systems are not just composed of organic chemicals although the major bulk of them are of the conventional light nonmetals. Other elements, mainly metals, are involved in essential roles from maintaining cell stability and in communication networks to catalysis. The interaction of the system life/environment is therefore extremely complicated.

See Also the Following Articles

Chloroplasts • Heme Proteins • Heme Synthesis • Iron–Sulfur Proteins • Vitamin B_{12} and B_{12}-Proteins • Zinc Fingers

Glossary

abundance The quantitative amount of an element in the universe or on the surface of Earth.

availability A measure of the quantity of elements to which organisms have access ranging from easily available such as sodium and potassium to available with difficulty such as iron today.

essential Describing or referring to a requirement for an element without which the organism would show extreme abnormality or even not exist.

Further Reading

Bertini, I., Gray, H. B., Lippard, S. J., and Valentine, J. S. (1994). *Bioinorganic Chemistry*. University Science Books, Mill Valley, California.

Fraústo da Silva, J. J. R., and Williams, R. J. P. (2001). *The Biological Chemistry of The Elements*. 2nd edition. Oxford University Press, Oxford.

Kaim, W., and Schwederski, B. (1994). *Bioinorganic Chemistry: Inorganic Elements in the Chemistry of Life*. Wiley, Chichester.

Lippard, S. J., and Berg, J. M. (1994). *Principles of Bio-Inorganic Chemistry*. University Science Books, Mill Valley, California.

Messerschmidt, A., Huber, R., Poulos, T., and Wieghardt, K. (eds.) (2001). *Handbook of Metalloproteins*, Vols 1 and 2, Wiley, Chichester.

Biography

R. J. P. Williams is an Emeritus Professor at Oxford University, UK. He is sometimes referred to as the "grandfather" of bioinorganic chemistry, because he initiated the detailed study of the selective interaction of inorganic elements with organic compounds. His major work has been on heme-, zinc-, and copper-containing enzymes as well as on the use of calcium and magnesium in cells. He proposed the use of proton gradients in the synthesis of ATP.

Inositol Lipid 3-Phosphatases

Gregory S. Taylor and Jack E. Dixon
University of California, San Diego, California, USA

Phosphoinositides are lipid-signaling molecules that are essential for a wide variety of cellular processes including cell growth, apoptosis, membrane trafficking, vesicular transport, cytoskeletal regulation, cell motility, and control of gene expression. To facilitate the organization of such a striking array of signaling tasks within a cell, inositol lipids serve multifunctional roles including acting as docking modules for recruiting phosphoinositide-binding proteins to specific sites within a cell, allosteric regulators of enzyme activity/function, and also function as sorting signals and spatial landmarks during intracellular trafficking. In light of the multitude of cellular functions in which they are involved, it is not surprising that the levels of phosphoinositides within a cell are stringently regulated. To accomplish this, cells must carefully balance the relative rates of phosphoinositide biosynthesis and degradation. Phosphoinositides are derived from phosphatidylinositol (PI) by the actions of phosphoinositide kinases, which create and interconvert the various phosphoinositides via addition of phosphoryl groups to the inositol headgroup of PI. The actions of these kinases are opposed by phospholipases, which hydrolyze and remove the phosphoinositide acyl moieties and/or the inositol headgroup, and phosphoinositide phosphatases, which remove phosphoryl groups from the inositol ring. Phosphoinositide phosphatases can be loosely categorized by their structural and enzymatic properties into three groups, which include the protein tyrosine phosphatase-like PTEN and myotubularin phosphatases, SAC domain-containing phosphatases, and inositol 5′-phosphatases. This article, will focus on the structure and function of PTEN and myotubularin lipid phosphatases, the human disease states that are associated with their dysfunction, and discuss potential regulatory mechanisms for these enzymes.

Phosphoinositides as Signaling Molecules

The extensive use of phosphoinositides as cell signaling molecules in eukaryotes is likely to have arisen from the diversity of second messengers that can be derived from a single PI molecule simply by changing its phosphorylation state. As shown in Figure 1, seven different phosphoinositide signaling molecules can be generated through successive phosphorylation events by phosphoinositide kinases at the D3, D4, and D5 positions of the inositol ring of PI. Although they are relatively scarce, constituting less than 10% of the total cellular lipid content, phosphoinositides are distributed to compartments and membrane structures throughout the cell where their functions are required. One important function of phosphoinositides is to serve as ligands for inositol lipid-binding motifs that include the ENTH (epsin N-terminal homology), FERM (band 4.1, ezrin, radixin, moesin), FYVE (Fab1p, YOTB, Vps27p, EEA1), PH (pleckstrin homology), and PX (Phox homology) domains. Proteins that contain these lipid-binding motifs are recruited to form complexes on membranes where their specific target phosphoinositides are localized and concentrated. Once formed, these protein complexes can perform their specialized function(s) in membrane trafficking and intracellular transport tasks. Thus, the temporal and spatial regulation of phosphoinositide levels is a critical factor in determining when, where, and how these complexes form and carry out their functions. In addition to their roles as docking sites for phosphoinositide-binding domains, inositol lipids can also function as allosteric regulators of enzymatic activity. In this role, these lipids act as "on/off" switches for enzymes that contain specific lipid recognition/binding motifs. Whether they function as targeting sites for protein complex formation or as allosteric activators, it is clear that cellular phosphoinositides must be carefully regulated so that the downstream processes they control are also properly synchronized. In this capacity, phosphoinositide phosphatases can function to oppose and attenuate the signals generated by phosphoinositide kinases by removing phosphoryl groups from the D3, D4, and D5 positions of the inositol headgroup.

Protein Tyrosine Phosphatases

Protein tyrosine phosphatases (PTPs) are an extremely diverse family of enzymes that are characterized by a catalytic core of ~200 amino acids encompassing a highly conserved Cys-x_5-Arg (Cx_5R) active site motif. PTPs employ a common catalytic mechanism during

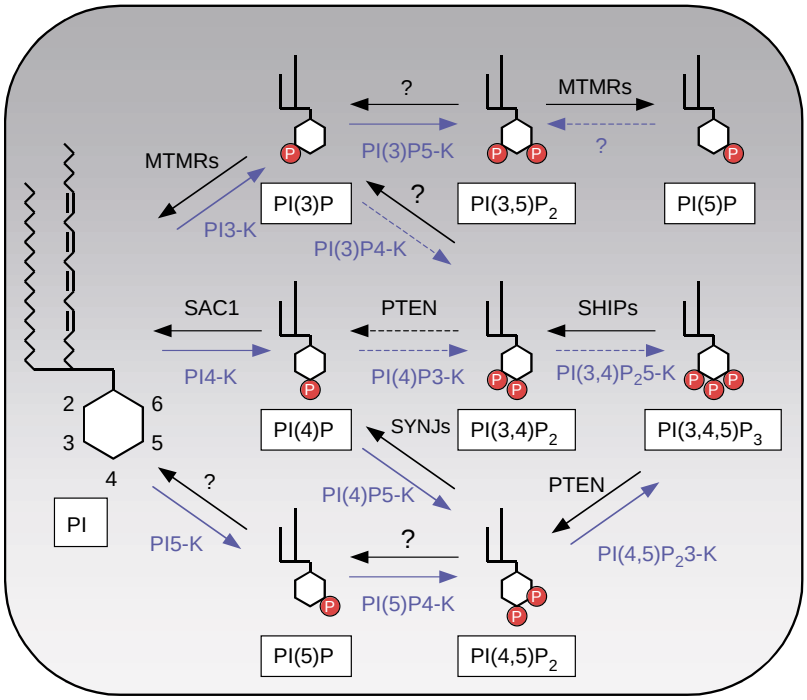

FIGURE 1 Mammalian phosphoinositide pathways. The seven different phosphoinositides are produced via successive phosphorylation (left to right) by phosphoinositide kinases starting with phosphatidylinositol (PI). The phosphoinositide kinases and the respective steps they catalyze are shown in blue. The substrates dephosphorylated by PTEN (PTEN), myotubularin-family (MTMRs), SH2-containing inositol 5′-phosphatases (SHIPs), synaptojanin-family (SYNJs), and SAC1 (SAC1) enzymes are indicated with black arrows. Steps denoted by "dashed arrows" represent the minor pathways of biosynthesis or conversion and "question marks" indicate that no phosphatase or kinase has yet been identified that regulates that particular inositol lipid. PI(5)P in the "upper right corner" of this diagram represents the product of PI(3,5)P_2 dephosphorylation by myotubularin family phosphatases.

hydrolysis of phosphomonoesters. During catalysis, the Cys residue within the Cx_5R motif functions as the reaction nucleophile to attack the phosphate phosphorous atom, forming an enzyme thio-phosphoryl intermediate. The conserved Arg residue helps to position the substrate phosphate for in-line attack by the Cys nucleophile. A conserved aspartic acid ~30–50 residues N-terminal to the Cx_5R sequence functions as a general proton donor to facilitate hydrolysis of the enzyme phosphoryl intermediate and substrate release. In addition to the hallmark Cx_5R sequence, PTPs also contain a wide variety of noncatalytic motifs that are important for subcellular localization and regulation of phosphatase activity. Based on their structural features and substrate specificity, PTPs can be categorized into tyrosine-specific, dual-specificity, low-molecular weight, Cdc25, RNA triphosphatase, and phosphoinositide phosphatase subgroups. As might be expected from their names, the tyrosine-specific PTPs exclusively dephosphorylate protein phosphotyrosine residues, whereas the dual-specificity enzymes can hydrolyze phosphotyrosine, phosphoserine, or phosphothreonine residues. Low-molecular weight tyrosyl phosphatases exhibit a preference for phosphotyrosine-containing substrates. Cdc25-related PTPs are unique cell cycle regulatory dual-specificity phosphatases that are specific for cyclin-dependent kinases. The RNA triphosphatases remove mRNA 5′-phosphate group(s) and function to regulate the mRNA capping process, nuclear export, and stability. The phosphoinositide phosphatase PTP-like enzymes consist of the PTEN and myotubularin families. These enzymes are specific for D3-phosphorylated inositol lipid substrates and will be the focus of this article.

PTEN and Myotubularin: PTP-Like Phosphoinositide Phosphatases

The phosphoinositide phosphatase subfamily of PTP-like enzymes consists of the PTEN and myotubularin lipid phosphatases. Both PTEN and myotubularin family lipid phosphatases contain PTP-like catalytic domains with active site Cx_5R motifs and employ a catalytic mechanism similar to that of other PTPs. However, PTEN and myotubularin phosphatases are unique among the PTPs in that they utilize D3-phosphorylated phosphoinositides as their principle physiologic substrates.

PTEN

PTEN as a Tumor Suppressor

The *PTEN* (phosphatase and tensin homologue) gene was initially identified by virtue of its localization on human chromosome 10q23.3, a region frequently deleted in brain, breast, and prostate cancers. Also known as mutated in multiple advanced cancers (*MMAC*) and TGFβ-regulated and epithelial cell-enriched phosphatase 1(*TEP1*), the *PTEN* gene was found to encode a protein with significant similarity to the cytoskeletal/focal adhesion protein, tensin, and protein tyrosine phosphatases. To date, numerous loss-of-function mutations in the *PTEN* gene including missense, nonsense, frameshift, deletion, and insertion mutations have been associated with human cancer and provide strong evidence for its role as a tumor suppressor gene. Germline mutations in the *PTEN* gene have also been associated with Bannayan–Zonana syndrome, Cowden syndrome, juvenile polyposis syndrome, and Lhermitte–Duclos disease. These disorders are characterized by hamartomatous polypoid growths as well as a predisposition toward certain types of cancer. Based on these observations, it was initially thought that PTEN might function as a tumor suppressor by dephosphorylating tyrosine-phosphorylated or serine/threonine-phosphorylated proteinaceous substrates. However, PTEN was found to possess exceedingly poor protein phosphatase activity when tested against a variety of artificial protein and peptide substrates. In fact, PTEN exhibited almost undetectable phosphatase activity toward proteinaceous substrates with the exception of an extremely acidic synthetic phosphopeptide substrate (poly-Glu_4Tyr).

PTEN Dephosphorylates the Phosphoinositide Second Messenger, PI(3,4,5)P_3

The key to understanding PTEN function as a human tumor suppressor was its identification as a phosphoinositide-specific phosphatase. The pathology of human diseases associated with PTEN mutations strongly supported its role as a tumor suppressor. However, its poor protein phosphatase activity and preference for highly acidic substrates suggested the possibility that PTEN might actually utilize a nonproteinaceous substrate as its physiologic target. Phosphoinositides were considered as possible alternatives to proteinaceous substrates for PTEN because of their involvement in cell survival signaling as well as the fact that their strong acidity fit the profile of PTEN preference for anionic substrates. The discovery that PTEN specifically dephosphorylated D3 position of the inositol signaling lipid, PI(3,4,5)P_3 (PIP_3) provided the first clear correlation between loss of PTEN activity and tumorigenesis. At this time, PIP_3 was known to promote cell survival and growth signaling through the Akt serine/threonine protein kinase as illustrated in Figure 2. In the Akt survival pathway, activation of receptor tyrosine kinases by mitogens results in the recruitment and activation of type I PI 3-kinase, which then phosphorylates PI(4,5)P_2 to produce PI(3,4,5)P_3. The plasma membrane-localized PIP_3 can then recruit and activate a phosphoinositide-dependent Ser/Thr protein kinase (PDK1) via its PH domain. PDK1 phosphorylates and activates Akt, which has also been recruited to the plasma in a PH domain-dependent manner via PIP_3 and/or PI(3,4)P_2. Activated Akt then functions to restrain apoptotic signaling and promote cell survival and growth by phosphorylating and negatively regulating proapoptotic factors including the Ser/Thr kinase GSK3β, cyclin-dependent kinase inhibitors $p21^{WAF1}$ and $p27^{KIP1}$, Forkhead transcription factors, Bad, and Caspase-9. PTEN antagonizes survival signaling by preventing the accumulation of PIP_3, thereby inhibiting the membrane-association of PDK1 and subsequent phosphorylation and activation of Akt. Its identification as a PIP_3-specific phosphoinositide phosphatase provided the first clear connection between loss-of-function PTEN mutations and human cancer. It is of note that PTEN orthologues in the nematode worm, *Caenorhabditis elegans*, and fruitfly, *Drosophila melanogaster*, also regulate PIP_3-dependent signaling through Akt and function to control cell size and development in these organisms.

PTEN Structure

The X-ray crystal structure of PTEN has provided significant insight into the molecular basis underlying its function as a phosphoinositide phosphatase and tumor suppressor. PTEN consists of an N-terminal phosphatase catalytic domain that contains the conserved Cx_5R active site motif and a C-terminal C2 domain. Although it is quite similar in overall topology to the catalytic core structures of other dual specificity and tyrosine-specific PTPs, the catalytic domain of PTEN is unique with respect to the architecture surrounding its active site. Specifically, the PTEN active site pocket is much wider and not as deep as those of dual specificity or tyrosine-specific enzymes. This structural feature of PTEN is essential for its ability to accommodate the inositol headgroup of PIP_3, which is much larger and more highly charged than the substrate phosphoserine, phosphothreonine, or phosphotyrosine residues targeted by other PTPs. Within the active site of PTEN, the Cx_5R sequence adopts a conformation similar to that observed for the P-loops of other PTPs, placing the Cys nucleophile and phosphate-binding Arg residues in the orientation required for efficient catalysis. The PTEN structure also points to a critical function for the C2 domain at its C terminus. C2 domains are found in a

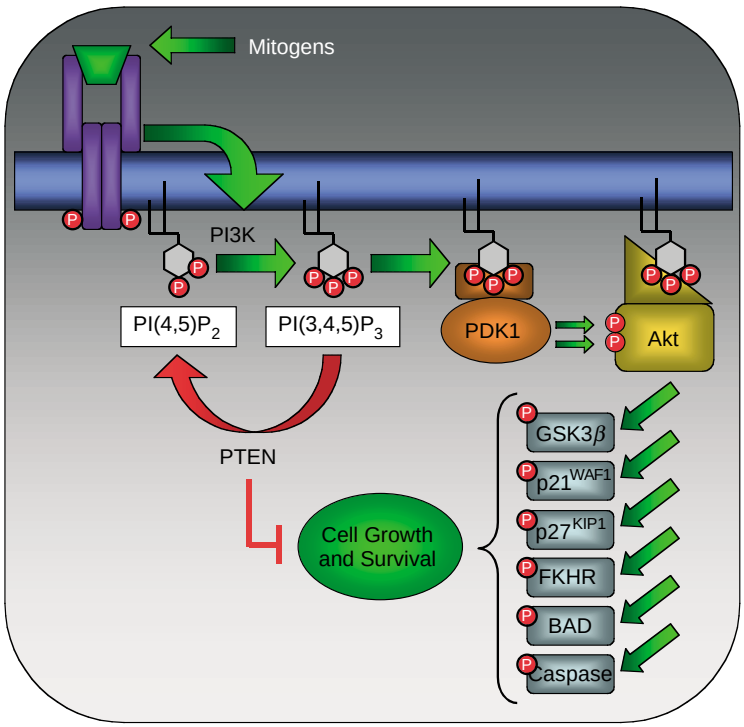

FIGURE 2 PTEN negatively regulates Akt signaling via PIP_3. Stimulation of growth factor receptor tyrosine kinases by extracellular mitogens results in the translocation and up-regulation of type I PI 3-kinase (PI3K) and production of $PI(3,4,5)P_3$. PIP_3 recruits the phosphoinositide-dependent (PDK1) and Akt (*Akt*) kinases to the plasma membrane where Akt is activated by PDK1-dependent phosphorylation. Activated Akt promotes cell growth and survival by phosphorylating and negatively regulating downstream proapoptotic factors including the Ser/Thr kinase (*GSK3β*), cyclin-dependent kinase inhibitors ($p21^{WAF1}$, $p27^{KIP1}$), forkhead transcription factors (*FKHR*), Bcl2 family member (*BAD*), and protease (*Caspase-9*). PTEN antagonizes mitogenic/survival signaling by preventing the accumulation of PIP_3 and subsequent activation of PDK1 and Akt.

number of membrane-associated proteins and function to regulate membrane recruitment. The C2 domain of PTEN most closely resembles the calcium-independent C2 domain subtype and can associate with lipid bilayers *in vitro*, suggesting it plays a role in targeting PTEN to cellular membranes where PIP_3 is located. The PTEN catalytic and C2 domains share an extensive hydrophobic interface and many PTEN disease mutations are localized to this interface. Moreover, PTEN C-terminal missense and truncating mutations that directly affect the C2 domain but not the catalytic domain are associated with human disease. Together, these observations demonstrate the requirement for a functional C2 domain and underscore the necessity for proper subcellular localization in addition to lipid phosphatase activity for maintaining PTEN function.

PTEN Regulation

PTEN function can be regulated by a number of different mechanisms. PTEN contains a C-terminal PDZ-binding motif, which can control its entry into PDZ-protein complexes. The PDZ domain is a protein motif of ~90 amino acids named for the postsynaptic density protein, PSD-95, *Drosophila* septate junction protein, Discs Large, and the tight junction protein, ZO-1. PDZ-domains are among the most abundant metazoan protein domains and serve as molecular scaffolds to assemble macromolecular protein signaling complexes. PTEN can physically associate with PDZ complexes via its PDZ-binding sequence. The exact function(s) of these complexes are not known, but they may function to stabilize the PTEN protein and help it to localize to specific sites within cells where its lipid phosphatase activity is required. PTEN function is also regulated by reversible protein phosphorylation. PTEN undergoes Ser/Thr phosphorylation within the extreme C-terminal region. Phosphorylation of sites within its C-terminus leads to an increase in the stability of the PTEN protein. PTEN contains a consensus PEST degradation sequence that overlaps these sites and may be masked via phosphorylation. PTEN C-terminal phosphorylation also appears to inhibit its association with PDZ complexes, suggesting that multiple modes of regulation are mediated through its C-terminal region.

MYOTUBULARIN

Myotubularins in Neuromuscular Disease

Myotubularin (MTM1) is mutated in X-linked recessive myotubular myopathy, a serious neonatal disorder in

which muscle cell development/maturation is dysfunctional. The muscle cells of affected individuals exhibit abnormal centrally located nuclei, perinuclear halos, and the persistence of fetal forms of vimentin and desmin. In severe cases, death often occurs from respiratory failure in early infancy. The myotubularin gene, *MTM1*, is localized to chromosome Xq28 and encodes a protein with significant similarity to dual specificity PTPs. MTM1 is the archetypical member of one of the largest families of dual specificity PTP-like phosphatases yet identified. As shown in Figure 3, the myotubularin-related (MTMR) phosphatase family includes eight catalytically active forms and at least six forms that are enzymatically inactive due to germ line substitutions in residues required for catalysis. The MTMR proteins can be further categorized into subgroups based on sequence similarity and the presence and arrangement of non-catalytic domains (Figure 3). Loss-of-function mutations in a second MTMR gene, *MTMR2*, cause the autosomal-recessive peripheral demyelinating neuropathy, type 4B Charcot-Marie-Tooth (CMT) syndrome. Type 4B CMT is characterized by focally folded myelin in the peripheral nerves and is thought to result from improper Schwann cell maturation. Mutations in a third MTMR gene, *MTMR13*, have also been shown to cause type 4B CMT. This is of particular interest because MTMR13 is a catalytically inactive MTMR. Although their precise roles in the onset and progression of human neuromuscular diseases are not known, the association of MTMR mutations with these disorders suggests that phosphoinositide regulation is critical for proper cellular development and maintenance in these tissues.

MTMRs Dephosphorylate 3-Phosphorylated Phosphoinositides

Like PTEN, myotubularin was originally thought to function as a dual-specificity PTP based on its protein sequence. Moreover, myotubularin also exhibited very poor phosphatase activity when tested against artificial protein and peptide substrates. The connection between myotubularin and lipid phosphatase activity was established following the observation that its Cx_5R active site motif resembled the corresponding sequence

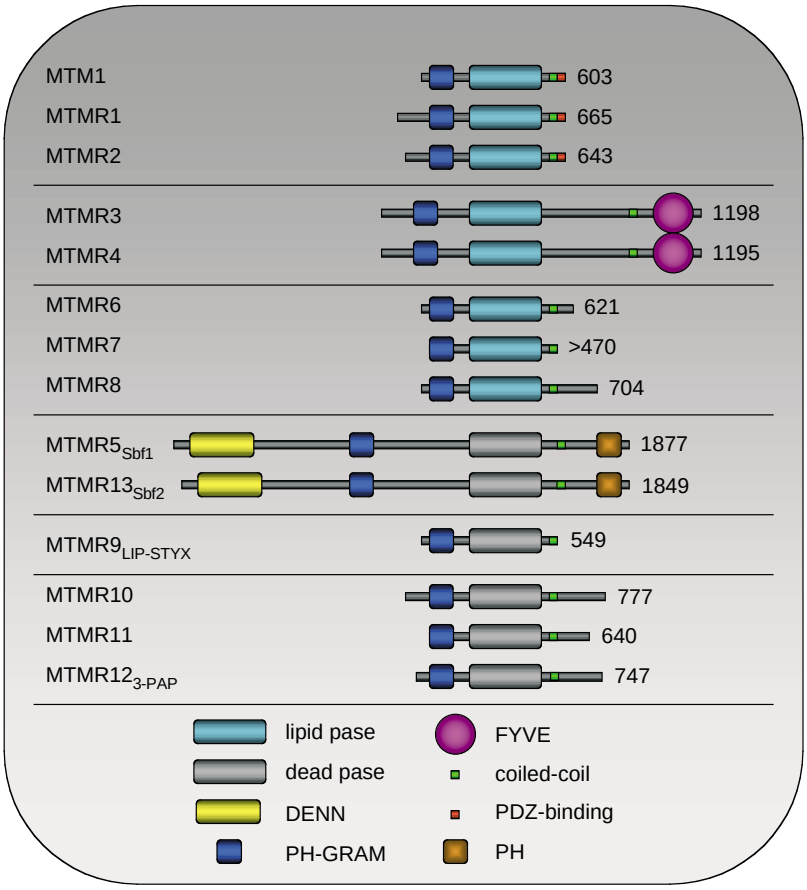

FIGURE 3 Structural diversity among myotubularin-family proteins. The structural features of myotubularin-related (MTMR) proteins are illustrated. MTMR subgroups classified based on sequence similarity and domain organization are separated by 'black lines." A legend denoting each of the protein domains/motifs pictured is shown at the "bottom." The number of amino acid residues in each MTMR protein are shown to the "right" of each structural diagram. Although more than one splicing variant may exist, only a single form is shown for each MTMR.

in the budding yeast inositol lipid phosphatase, Sac1p. This enzyme was known to dephosphorylate monophosphorylated phosphoinositides and to play a critical role in regulating trafficking through the yeast secretory pathway. Initial analyses revealed that MTM1 was highly active against the inositol lipid, PI(3)P. This lipid is the principal target of the FYVE and PX phosphoinositide-binding domains and is an important regulator of vesicular trafficking processes. Since the initial discovery of MTM1 as an inositol lipid-specific phosphatase, the catalytically active MTMR proteins, MTMR1, MTMR2, MTMR3, MTMR6, and MTMR7 have also been shown to dephosphorylate PI(3)P, suggesting that it is a common substrate of all the active MTMRs. Myotubularin family phosphatases have recently been found to dephosphorylate the D3 position of PI(3,5)P_2. Produced by phosphorylation at the D5 position of PI(3)P by PI(3)P 5-kinase, PI(3,5)P_2 is crucial for vesicular transport and plays an important role in regulating cellular responses to stress conditions. The exact mechanism(s) by which these lipids participate in cell signaling during neuromuscular development remain unknown. However, their role as substrates for MTMR family phosphatases demonstrates that regulation of PI(3)P and PI(3,5)P_2 is essential and points to trafficking defects as a possible underlying cause for myotubular myopathy and type 4B CMT.

MTMR Regulation

An emerging paradigm for MTMR regulation involves the physical interaction between catalytically active and inactive MTMR proteins. Active and inactive MTMRs can form heterodimeric complexes. To date, interactions have been demonstrated between MTM1/MTMR12, MTMR2/MTMR5, and MTMR7/MTMR9 active/inactive pairs. It has been proposed that heterodimer formation can affect both the lipid phosphatase activity and the subcellular localization of the complex, however, the specific physiologic function(s) of these complexes remain to be elucidated. It is of note that mutations in both MTMR2 and MTMR13 result in type 4B CMT disease. MTMR13, a catalytically inactive MTMR, is highly similar to MTMR5, which has previously been shown to associate with MTMR2. Although a physical association between MTMR2 and MTMR13 remains to be demonstrated, it is intriguing to speculate that an MTMR2/MTMR13 heterodimeric complex might be essential for proper Schwann cell development.

See Also the Following Articles

Inositol Phosphate Kinases and Phosphatases • Phosphatidylinositol Bisphosphate and Trisphosphate • Phosphatidylinositol-3-Phosphate • Phosphoinositide 4- and 5-Kinases and Phosphatases • Phosphoinositide-Dependent Protein Kinases

Glossary

kinase An enzyme that catalyzes the addition of phosphoryl groups.

phosphatase A hydrolytic enzyme that catalyzes the removal of phosphoryl groups.

phosphoinositide A more highly phosphorylated form of the phospholipid, phosphatidylinositol.

PTP Protein tyrosine phosphatase, a large family of enzymes that catalyze the hydrolysis of phosphomonoesters and contain a highly conserved Cys-x5-Arg active site motif.

tumor suppressor A protein that functions to repress cell growth and proliferation.

Further Reading

Lemmon, M. A. (2003). Phosphoinositide recognition domains. *Traffic* **4**, 201–213.

Maehama, T., Taylor, G. S., and Dixon, J. E. (2001). PTEN and myotubularin: Novel phosphoinositide phosphatases. *Ann. Rev. Biochem.* **70**, 247–279.

Pendaries, C., Tronchere, H., Plantavid, M., and Payrastre, B. (2003). Phosphoinositide signaling disorders in human diseases. *FEBS Lett.* **546**, 25–31.

Simonsen, A., Wurmser, A. E., Emr, S. D., and Stenmark, H. (2001). The role of phosphoinositides in membrane transport. *Curr. Opin. Cell. Biol.* **13**, 485–492.

Sulis, M. L., and Parsons, R. (2003). PTEN: From pathology to biology. *Trends Cell Biol.* **13**, 478–483.

Tronchere, H., Buj-Bello, A., Mandel, J. L., and Payrastre, B. (2003). Implication of phosphoinositide phosphatases in genetic diseases: The case of myotubularin. *Cell. Mol. Life Sci.* **60**, 2084–2099.

Wishart, M. J., and Dixon, J. E. (2002). PTEN and myotubularin phosphatases: From 3-phosphoinositide dephosphorylation to disease. *Trends Cell Biol.* **12**, 579–585.

Biography

Gregory S. Taylor received his Ph.D. from Purdue University and has been a postdoctoral research fellow in Dr. Jack Dixon's laboratory at the University of Michigan and at the University of California, San Diego. Dr. Taylor's research has focused on understanding the structure and function of inositol lipid phosphatases including PTEN and myotubularin, as well as their relation to human disease. Dr. Taylor is currently seeking a faculty position in academia.

Jack E. Dixon is a Professor of pharmacology, cellular and molecular medicine, and chemistry and biochemistry, and is also the Dean for Scientific Affairs at the University of California, San Diego. Dr. Dixon's research has focused on two principal areas of interest: protein tyrosine phosphatase structure and function, and mechanisms of bacterial pathogenesis. Dr. Dixon received his Ph.D. from the University of California, Santa Barbara, and completed a postdoctoral research fellowship at the University of California, San Diego. Dr. Dixon is currently a member of the American Academy of Arts and Sciences and the National Academy of Sciences.

Inositol Phosphate Kinases and Phosphatases

Stephen B. Shears
Laboratory of Signal Transduction, NIEHS/NIH/DHHS, Research Triangle Park, North Carolina, USA

A novice attempting to access the literature concerning inositol phosphate kinases and phosphatases is confronted by a list of participants that is intimidating in its size, and a sometimes bewildering terminology to distinguish between them. In an effort to ease the pain, herein is provided an hospitable guide to the nomenclature describing inositol phosphates and the enzymes that metabolize them.

Information transfer in biological systems requires sensor proteins to detect and respond to regulatory input from other proteins and small molecules. The ability of a sensor to perceive an effector is frequently dependent upon a recognition pattern generated by the presence or absence of phosphate groups. When one or more of these phosphate groups are added (phosphorylation) or removed (dephosphorylation) from the effector, such a process acts as a molecular switch that determines whether the regulator is "on" or "off." Inositol (Figure 1) is an example of a small molecule that is functionally modified in this manner. Each of the six hydroxyl groups that are attached to the carbons of the *myo*-inositol ring (Figure 1A) are sites for phosphorylation. Enzymes that add phosphate groups to the inositol moiety are known as inositol phosphate kinases. A separate family of enzymes, the inositol phosphate phosphatases, removes phosphate groups from the inositol ring. Phosphate-transfer reactions catalyzed by these phosphatases and kinases are networked in serial and parallel configurations, permitting the cell to add and subtract phosphate groups in a combinatorial manner, so generating an array of inositol phosphate molecules. Recognition patterns, that arise from specific arrangements of phosphate groups around the inositol ring, endow certain inositol phosphates with biologically important functions. Thus, inositol phosphate kinases and phosphatases control the synthesis and metabolism of important effector molecules.

Inositol Phosphate Nomenclature

In order to appreciate the nature of phosphate recognition patterns around the inositol ring, it is necessary to understand the nomenclature which distinguishes the different carbons that comprise the inositol moiety. Fortunately, Agranoff's turtle provides us with a timeless, visual mnemonic. In this *aide mémoire*, the hydrogens are conveniently ignored and the inositol ring is depicted in its thermodynamically stable so-called "chair" conformation (Figure 1B). The structure's resemblance to a turtle is then apparent (Figure 1C). As a consequence of deliberations by International Nomenclature Committees, the turtle's appendages are numbered in an anticlockwise direction (when viewed from above), commencing with the front right flipper. The 2-hydroxyl (the turtle's head) is axial to the plane of the ring, whereas the other five hydroxyls (the four flippers and the tail) are equatorial (i.e., approximately in the same plane as the ring). This numbering system allows us to readily and unambiguously specify the location of phosphate groups that are added to the inositol ring. Ins(1,4,5)P_3, for example (see Figure 2), is an abbreviation that describes the addition of three single phosphate groups (P_3) to the inositol (Ins) ring, at positions 1, 4, and 5. Ins(1,2,3,4,5,6)P_6 describes the molecule in which all six of the carbons are attached to single phosphate groups, but since this feature makes the numbering superfluous, InsP_6 is the acceptable definition (Figure 2). This particular inositol phosphate is also widely known as phytic acid. Some inositol phosphates contain diphosphate (i.e., PP) groups (Figure 2). One of the diphosphates added to InsP_6 is known to be at the 5-position, but till date, the positions of all of the diphosphate groups have not been determined.

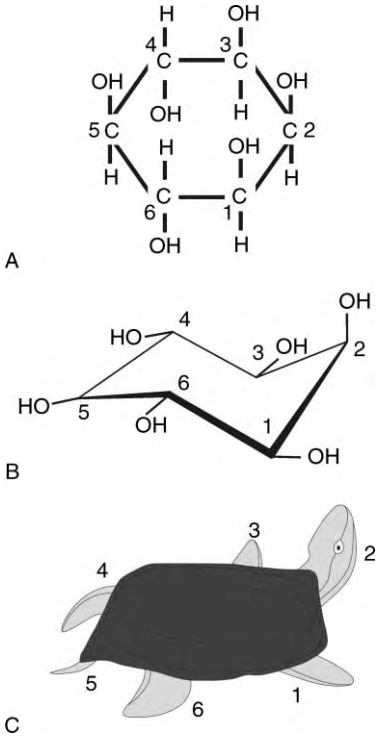

FIGURE 1 Inositol ring nomenclature. (A) full chemical structure of inositol; (B) naturally occurring conformation of inositol, *sans* hydrogens; (C) the numbering of the turtle's appendages in an anticlockwise direction (beginning with its right flipper) provides an *aide mémoire* for inositol phosphate nomenclature.

Enzyme Nomenclature and Metabolic Interrelationships

Figure 2 provides a metabolic map showing the participation of those inositol phosphate kinases and phosphatases that are most commonly found across the phylogenetic spectrum. Ideally, these enzymes ought to be named in a manner that is both universally accepted, and unambiguously describes their function(s). In its simplest form, it is possible to designate some of these enzymes according to both the nature of the substrate(s), and the position(s) on the inositol ring that is modified. Thus, the Ins(1,3,4,5,6)P_5 2-kinase phosphorylates Ins(1,3,4,5,6)P_5 to InsP_6 (see Figure 2). One problem with this approach is that almost all of the inositol phosphate kinases and phosphatases metabolize more than one substrate. For example, a single enzyme removes the 5-phosphate from both Ins(1,4,5)P_3 and Ins(1,3,4,5)P_4. Unfortunately, "inositol polyphosphate 5-phosphatase," is a popular terminology for this enzyme, despite the fact that this exaggerates its promiscuity, by erroneously implying the enzyme removes the 5-phosphate from other inositol phosphates. The preferred, unambiguous nomenclature for this enzyme is Ins(1,4,5)P_3/Ins(1,3,4,5)P_4 5-phosphatase (Figure 2). Nevertheless, such a systematic approach

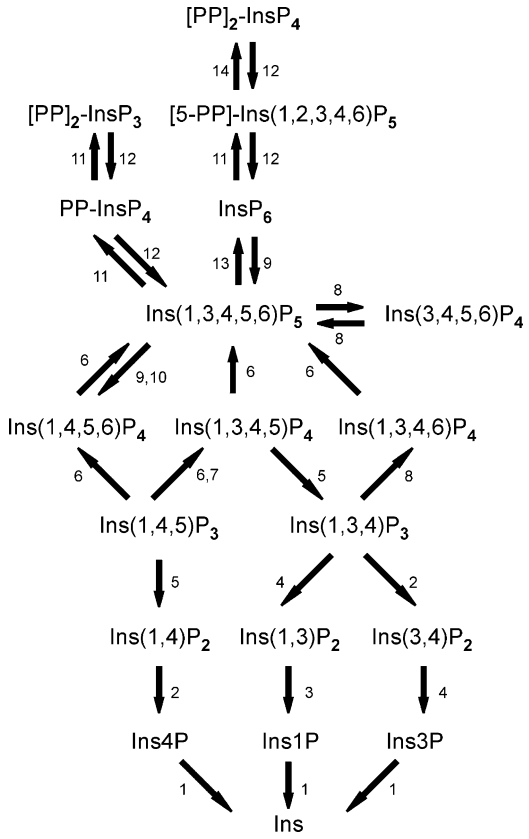

FIGURE 2 Metabolic interrelationships of inositol phosphate kinases and phosphatases. This figure provides a metabolic map showing the participation of some important inositol phosphate kinases and phosphatases that are widely distributed across the phylogenetic spectrum. The numbers associated with each arrow represent the following enzymes: 1, Inositol monophosphatase; 2, Ins(1,4)P_2/Ins(1,3,4)P_3 1-phosphatase; 3, Ins(1,3)P_2 3-phosphatase; 4, Ins(3,4)P_2/Ins(1,3,4)P_3 4-phosphatase; 5, Ins(1,4,5)P_3/Ins(1,3,4)P_3 5-phosphatase; 6, inositol phosphate multikinase; 7, Ins(1,4,5)P_3 3-kinase; 8, Ins(1,3,4)P_3 6-kinase/Ins(3,4,5,6)P_4 1-kinase/Ins(1,3,4,5,6)P_5 1-phosphatase; 9, multiple inositol polyphosphate phosphatase; 10, PTEN (for *p*hosphatase and *ten*sin homologue, deleted on chromosome *ten*); 11, inositol hexakisphosphate kinase; 12, diphosphoinositol polyphosphate phosphohydrolase; 13, Ins(1,3,4,5,6)P_5 2-kinase; 14, diphosphoinositol polyphosphate kinase.

does become unwieldy when a single enzyme metabolizes three or more substrates, especially when the positional specificity of the enzyme varies with the nature of the substrate. For example, there is a single kinase that adds a 3-phosphate to Ins(1,4,5)P_3, a 6-phosphate to Ins(1,3,4,5)P_4, a 5-phosphate to Ins(1,3,4,6)P_4 and a 3-phosphate to Ins(1,4,5,6)P_4. For brevity, this protein is simply known as the "inositol phosphate multikinase" (Figure 2). Equally, the phosphatase that specifically removes the 3-phosphate from Ins(1,3,4,5,6)P_5 and the 6-phosphate from Ins(1,4,5,6)P_4 is also capable of removing any of the phosphate groups from InsP_6; this enzyme is known as the "multiple inositol polyphosphate phosphatase." Finally, the names of some enzymes will occasionally

not specifically address their ability to metabolize an inositol phosphate, as in the case of the Ins(1,3,4,5,6)P_5 3-phosphatase activity of PTEN (see Figure 2). The reason the latter protein's name does not illuminate its function is because it was christened prior to a complete understanding of its range of catalytic activities.

Regulatory Input into the Inositol Phosphate Pathway

There are two separate metabolic routes which feed into the pathway shown in Figure 2. The first is by enzymatic conversion of glucose-6-phosphate into Ins3P. The second is synthesis of Ins(1,4,5)P_3. The latter is initially attached through its 1-phosphate (i.e., its front right flipper, Figure 1C) to the lipid material that represents the bulk phase of cellular membranes. This attachment is severed by a specialized enzyme – a phospholipase C – that is stimulated when a hormone or neurotransmitter binds to appropriate receptor on the cell surface. The Ins(1,4,5)P_3 released by phospholipase C has the role of liberating cellular stores of calcium, which in turn regulates many calcium-dependent cellular processes. The efficacy of Ins(1,4,5)P_3 depends upon its intracellular concentration, which in turn is dictated by a dynamic balance between competing rates of Ins(1,4,5)P_3 synthesis (by phospholipase C) and metabolism (by inositol phosphate kinases and phosphatases; Figure 2). Hormones and neurotransmitters also use cell-surface receptors to activate the synthesis of many other intracellular chemical messengers, and these can lead to changes in the activities of several inositol phosphate kinases and phosphatases. In this way, the cell can carefully regulate metabolic flux through specific areas of the inositol phosphate pathway, thereby manipulating levels of inositol phosphates which are themselves intracellular signals.

See Also the Following Articles

Phosphatidylinositol Bisphosphate and Trisphosphate • Phospholipase C

Glossary

diphosphoinositol polyphosphate A type of inositol phosphate which has either one or two diphosphate ("pyrophosphate") groups.

inositol phosphate A compound with a six-member carbon ring structure to which single phosphates (and sometimes diphosphates) are attached at various positions.

inositol phosphate kinase An enzyme that transfers a phosphate group from adenosine triphosphate to the inositol ring.

inositol phosphate phosphatase An enzyme that removes a phosphate group from the inositol ring.

intracellular signal/messenger One member of what is usually a functionally coupled series of molecules or ions that together comprise a chemical pathway which conveys and amplifies a cell's biological response to a specific extracellular stimulus, such as a hormone or neurotransmitter.

phospholipase C A specialized enzyme that releases Ins(1,4,5)P_3 from its membrane tether.

phytic acid The nonsystematic but widely used alternate name for $InsP_6$; the molecule formed by filling all six carbons of the inositol ring with single phosphate groups.

turtle A marine reptile that provides a visual mnemonic for easy recall of the nomenclature for numbering the carbon atoms that comprise the inositol ring.

Further Reading

Agranoff, B. W. (1978). Textbook errors: cyclitol confusion. *Trends Biochem. Sci.* **3**, N283–N285.

Albert, C., Safrany, S. T., Bembenek, M. E., Reddy, K. M., Reddy, K. K., Falck, J. R., Bröker, M., Shears, S. B., and Mayr, G. W. (1997). Biological variability in the structures of diphosphoinositol polyphosphates in *Dictyostelium discoideum* and mammalian cells. *Biochem. J.* **327**, 553–560.

Caffrey, J. J., Darden, T., Wenk, M. R., and Shears, S. B. (2001). Expanding coincident signaling by PTEN through its inositol 1,3,4,5,6-pentakisphosphate 3-phosphatase activity. *FEBS Lett.* **499**, 6–10.

Fisher, S. K., Novak, J. E., and Agranoff, B. W. (2002). Inositol and higher inositol phosphates in neural tissues: Homeostasis, metabolism and functional significance. *J. Neurochem.* **82**, 736–754.

Ho, M. W. Y., and Shears, S. B. (2002). Regulation of calcium-activated chloride channels by inositol 3,4,5,6-tetrakisphosphate. In *Current Topics in Membranes* (C. M. Fuller, ed.) Vol 53, pp. 345–363. Academic Press, London.

Irvine, R. F., and Schell, M. (2001). Back in the water: The return of the inositol phosphates. *Nat. Rev. Molecul. Cell Biol.* **2**, 327–338.

Biography

Steve Shears leads the Inositol Signaling Group at the National Institute of Environmental Health Sciences. His long-standing and continuing interests in inositol phosphate function began under the tutorship of Prof. Bob Michell at the University of Birmingham, United Kingdom. Dr. Shears obtained his Ph.D. from the University of York, United Kingdom. He has authored over 100 articles and reviews, and he serves as an editor of several international scientific journals.

Insulin- and Glucagon-Secreting Cells of the Pancreas

Franz M. Matschinsky
University of Pennsylvania School of Medicine, Philadelphia, Pennsylvania, USA

Alpha and beta cells are the predominant cell types in microscopic endocrine organs called the islets of Langerhans, which are scattered throughout the exocrine pancreas and produce, store, and secrete the hormones glucagon and insulin, respectively. Secretion of these hormones is regulated by fuels (glucose, amino acids, and fatty acids) or through neuroendocrine input. Insulin and glucagon in turn regulate the metabolism of these fuels. Loss of beta cells by autoimmune destruction or impairment of their function by poorly understood mechanisms are the causes of type I or type II diabetes mellitus (T1DM or T2DM), respectively. Individuals with T1DM require insulin substitution therapy for survival, and those with T2DM can manage their disease with diet restrictions, exercise, and a variety of drugs with different mechanisms of action. It is thus of critical importance to develop a comprehensive understanding of insulin- and glucagon-producing cells of the pancreas.

Introduction

Pancreatic alpha and beta cells play the predominant role in maintaining glucose homeostasis in humans and many laboratory animals and keep the blood glucose in the narrow range of 5 to 8 mM in response to the demands of feeding and fasting. Both cells have a threshold of approximately 5 mM glucose for stimulation of hormone release. The alpha cell is triggered to release glucagon when the glucose falls below this level, whereas the beta cell is activated to secrete insulin when this level is exceeded. Expressed differently, the inhibitory glucose dependency curve for alpha cells and the stimulatory glucose dependency curve for beta cells have their crossover point at 5 mM, which is the setpoint of the system for glucose homeostasis. (Note that alpha-cell deinhibition with falling glucose manifests itself most clearly when these cells are also under the influence of physiological stimuli, e.g., amino acids, a condition that is met *in situ*.) Auxiliary neuroendocrine mechanisms involving acetylcholine, catecholamines, glucagon-like peptide 1 (GLP-1), and gastric inhibitory peptide (GIP) enhance or blunt the response of the pancreatic endocrine cells to fuel stimulation. The other two fuel classes, amino acids (AA) and fatty acids (FA), stimulate insulin release in a strictly glucose-dependent manner. AA are the most effective fuel stimulant of alpha cells at biologically relevant concentrations (e.g., 3.5 to 7.0 mM of the physiological mixture of 20 AA enhances glucagon release markedly when glucose falls below 5.0 mM).

This entry focuses on the mechanisms of glucose-stimulated insulin release (GSIR) because this issue is central to beta-cell function and because knowledge of this aspect of beta-cell biology and glucose homeostasis is well established, much less tenuous or controversial than current understanding of how the other fuels act on alpha and beta cells. However, when important and possible, how glucose and other fuels or neuroendocrine factors interact with these two types of pancreatic endocrine cells is discussed.

The Beta-Cell Glucokinase Glucose Sensor and the Threshold for GSIR

The glucokinase glucose sensor concept and the threshold concept for GSIR explain a great deal about beta cells and the nature of glucose homeostasis in humans and most laboratory animals. Glucokinase (GK) serves as the beta cell's cytosolic glucose-sensing device and contributes a critical element to the regulatory feedback loop or signaling chain that interconnects blood glucose, the beta cell, the hormone insulin, and the major insulin target tissues (i.e., the liver, muscle, and adipose tissue). The kinetic characteristics of GK are ideally suited for this purpose: the k_{cat} for glucose phosphorylation is about 60 s^{-1}; the glucose $S_{0.5}$ (i.e., the glucose concentration resulting in half-maximal enzymatic activity) is about 8.0 mM; the glucose dependency curve of GK action is sigmoidal as indicated by a Hill coefficient (n_h) of 1.7; the ATP K_m is about 0.4 mM, indicating that the enzyme operates *in vivo* near saturation with its second substrate; finally, there is no feedback inhibition by glucose-6-P in contrast to

the highly effective inhibition of other hexokinases by this metabolite. Of great theoretical interest and practical importance is the recent recognition of an allosteric activator site on GK that explains the mechanism of action and efficacy of a newly discovered class of antidiabetic agents (GK activators [GKAs]; see following discussion). Beta-cell GK is inducible by glucose (maximally 5- to 10-fold compared to basal levels at 1.0 mM glucose) through mechanisms yet to be fully clarified. Note that hepatic GK is induced by insulin in a glucose-independent manner and is also activated by GKAs. Note also that hepatic GK is regulated by the inhibitory GK regulatory protein (GKRP), which sequesters the enzyme to the nuclear compartment from which GK is released by glucose during hyperglycemia. In contrast, GKRP seems to be of little importance for beta-cell GK function. Differential expression control of islet and hepatic GK is explained by the presence of two tissue-specific promoters in one single gene. Due to these characteristic features, GK determines the rate of beta-cell glycolysis with a control strength approaching unity, outperforming all other metabolic steps. Glycolytic flux of beta cells is therefore a function of substrate pressure rather than of energy demand, which determines glucose use of many other tissues, including brain and muscle.

These features are a prerequisite for the glucose sensor role of GK; they do not, however, explain the 5 mM setpoint for glucose homeostasis and threshold for GSIR. This threshold is a function of the biophysical characteristics of the K^+ and Ca^{2+} channels of the beta-cell membrane (Figure 1). The K-ATP channel is a hetero-octamer composed of four subunits each of the Kir6.2 inward rectifier and the drug target SUR-1 and is regulated by the phosphate potential of the beta cells. Important for physiology, it is inhibited by ATP^{4-} and activated by $MgADP^{2-}$ such that a decrease of the cytosolic ATP/ADP ratio determines K^+ conductivity and consequently the membrane potential. Enhanced glucose metabolism increases this ratio and depolarizes the beta cell. Alterations of the membrane potential are transmitted to the voltage-sensitive L-type Ca^{2+} channel. Depolarization stimulates Ca^{2+} influx and leads to elevation of the free intracellular calcium ($[Ca^{2+}]_i$). The combination of high ATP and $[Ca^{2+}]_i$ elicits insulin release. Important for understanding the threshold phenomenon for GSIR is the fact that the decrease of the K^+ conductivity is a graded function of glucose metabolism (i.e., the GK rate), whereas the L-type Ca^{2+}channel has a well-defined triggering potential of -60 to 50 mV, which happens to be reached when GK or glycolysis operates at 25–30% of its normal capacity, i.e., at 5.0 mM glucose. Note that extra- and intracellular glucose are virtually identical at all times as a result of high-capacity glucose transport by Glut-2. This basic signaling pathway from glucose to insulin release as previously outlined is termed the triggering pathway (TPW). It is complemented by the so-called augmentation pathway (APW), which potentiates glucose action, but the molecular basis of the latter remains to be defined in detail.

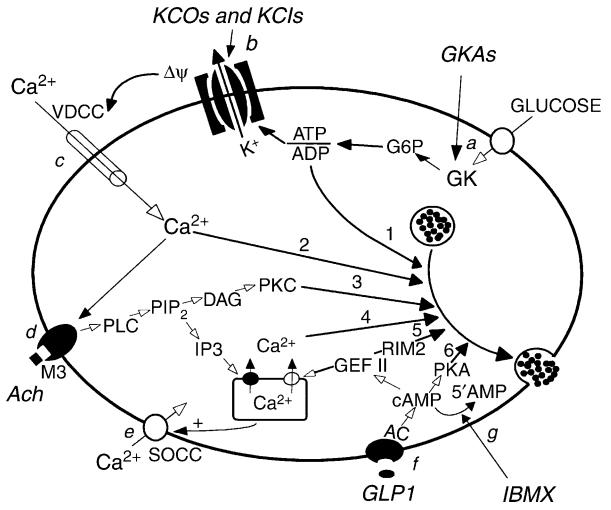

FIGURE 1 Signaling pathways in pancreatic beta cells. Six distinct signaling pathways in pancreatic beta cells are depicted (1–6). Abbreviations are as follows, with a–g identifying initial or other critical steps for these pathways: GK, glucokinase (a); the K_{ATP} channel complex, consisting of ATP-sensitive K^+ channels and sulfonyl urea receptor type 1 (SUR-1) subunits (b); VDCC, voltage-dependent Ca^{2+} channel or L-channels (c); acetylcholine (Ach) and muscarinic receptor type 3 (m3) (d); SOCC, store-operated calcium channels (e); GLP-1, glucagon-like peptide-1 and receptor (f); IBMX, 3-isobutyl-1-methylxanthine, a phosphodiesterase inhibitor (g). Other abbreviations are as follows: AC, adenylate cyclase; cAMP, cyclic AMP; PKC, protein kinase C; PKA, protein kinase A; DAG, diacylglyceride; IP3, inositol triphosphate; GEFII, cAMP-guanidine nucleotide exchange factor (or Epac2); $\Delta\Psi$, change of cell membrane potential. Additional abbreviations are explained in the text. Modified from Doliba, N. M., Qin, W., Vatamaniuk, M. Z., Li, C., Zelent, D., Najafi, H., Buettger, C. W., Collins, H. W., Carr, R. D., Magnuson, M. A., and Matschinsky, F. M. (2004). Restitution of defective glucose-stimulated insulin release of sulfonylurea type 1 receptor knockout mice by acetylcholine. *Am. J. Physiol. Endocrinol. Metab.* **286**(5); E834–843 (Epub 2004 Jan 21), (electronic publication) with permission of The American Physiological Society.

Model Experiments to Illustrate the Operation of the TPW and the APW

The APW comes into play when $[Ca^{2+}]_i$ and ATP/ADP are elevated by the TPW and when the beta cells are activated in addition by acetylcholine, GLP-1, or GIP. Model experiments with perifused islets isolated from control mice and from mice lacking functional K^+ channels (i.e., from SUR-$1^{-/-}$ knockout [KO] mice) illustrate many of the points discussed in the preceding

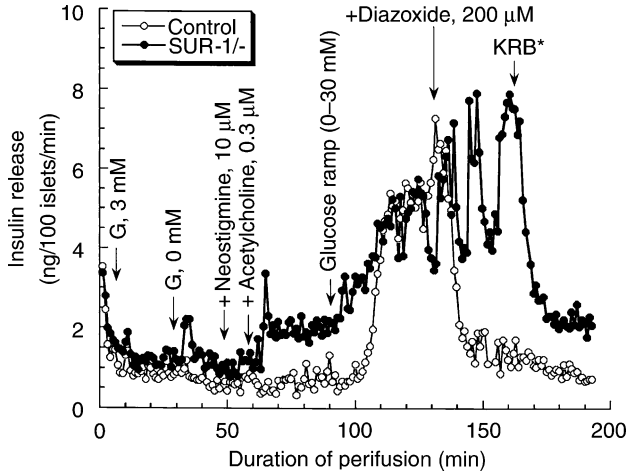

FIGURE 2 Experimental dissection of signaling pathways in glucose-stimulated insulin release (GSIR). Acetylcholine increases the insulin release in SUR-$1^{-/-}$ islets in the absence of glucose, demonstrating marked hypersensitivity to the transmitter compared to controls. Acetylcholine also restitutes defective GSIR by these islets. After stable insulin secretion rates were achieved at 30 min, islets were perifused in the absence of glucose for 60 min (t-30 to t-90). Following addition of neostigmine (a cholinesterase inhibitor) and acetylcholine, a glucose ramp (from 0 to 30 mM with an 0.8 mM increment per min) was applied for 37.5 min to control and SUR-$1^{-/-}$ islets, and glucose was then maintained constant at 30 mM for about 30 min longer in the continued presence of acetylcholine (t-90 to t-160). The experiment was completed by perifusing islets with KRB solution lacking glucose and drugs. The rise in the glucose concentration in the perfusate led to an increase in hormone secretion in SUR-$1^{-/-}$ islets as well as in the controls. However, note the different patterns of the release profiles. Also appreciate that in the absence of acetylcholine and neostigmine, SUR-$1^{-/-}$ islets did not respond to glucose in contrast to the controls (not shown). Diazoxide, a K_{ATP} channel activator, immediately decreased insulin release to baseline in control but was unable to block hormone release in SUR-$1^{-/-}$ islets. Reproduced from Doliba, N. M., Qin, W., Vatamaniuk, M. Z., Li, C., Zelent, D., Najafi, H., Buettger, C. W., Collins, H. W., Carr, R. D., Magnuson, M. A., and Matschinsky, F. M. (2004). Restitution of defective glucose-stimulated insulin release of sulfonylurea type 1 receptor knockout mice by acetylcholine. *Am. J. Physiol. Endocrinol. Metab.* **286**(5); E834–843 (Epub 2004 Jan 21), (electronic publication) with permission of The American Physiological Society.

paragraph (Figure 2). First, beta cells from SUR-$1^{-/-}$ do not show GSIR when acetylcholine is absent because the TPW is blocked in contrast to controls. Second, the distinctly different secretion profiles for GSIR evoked in control and SUR-$1^{-/-}$ islets in the presence of low acetylcholine illustrate that the glucose response caused by the combined TPW and APW in the control has a clear threshold and is blocked by diazoxide (a potassium channel opener [KCO]) as expected, whereas that of the APW alone as seen in the SUR-$1^{-/-}$ islets is clearly graded (lacking a threshold) and is not blocked by diazoxide, again as expected. Both signaling pathways operate during a meal and result in the robust, threshold-based GSIR as mimicked by the experiment shown in Figure 2 for control islets.

Amino Acids and Fatty Acids as Glucose-Dependent Stimuli of Beta Cells

Stimulation of insulin release by a physiological mixture of 20 amino acids (20-AASIR) is biologically highly relevant but less well understood than GSIR. It is established, though, that 20-AASIR of normal islets has an absolute glucose requirement, i.e., at least 2.5 mM. It is not clear which signaling pathways are involved, but it is likely that the TPW as sketched in the preceding discussion plays a role. Assuming a major role for metabolism in 20-AASIR, it must be postulated that transport into the cell and subsequent transdeamination are efficient processes. AA metabolism requires transamination as the first step, generating glutamate and alanine as the major products, followed by oxidative deamination of glutamate with glutamate dehydrogenase (GDH) to form NAD(P)H, which is converted to ATP. The need for the alpha-ketoacids, alpha-ketoglutarate and pyruvate as acceptors for the transamination reaction may explain, at least in part, the absolute requirement for glucose. It is also possible that AA metabolism generates metabolic coupling factors in addition to energy, with glutamate and glutamine as possibilities. It is indeed remarkable that more than half of the stimulatory effect of 20 AA can be attributed to glutamine, which contributes only 15% to the mixture. Studies of leucine-stimulated insulin release have been very extensive but have resulted in much controversy. It is now understood that leucine has two actions: it is converted to acetyl-CoA and acetoacetate, serving as direct fuel stimulant, or it stimulates GDH allosterically, thus enhancing glutaminolysis with the production of alpha-ketoglutarate, NAD(P)H, and ammonia. However, beta cells respond to this indirect allosteric effect of leucine only when GDH is sensitized, that is, when it is not fully inhibited by GTP (or ATP) as a result of enhanced glucose metabolism. 20-AASIR may also be mediated, at least in part, by depolarization due to increased Na^+ entry involving Na^+-dependent transporters, a possibility that has received little attention. Some of this discussion is illustrated in studies with isolated perifused islets by the differential effect that "energy run down" has on stimulation of insulin release by glucose, leucine, and alpha-ketoisocaproate (Figure 3). Isolated rat islets that had been cultured in 10 mM glucose and perifused with 2 mM glutamine show a remarkable change of chemosensitivity of their beta cells as a function of energy depletion with time. They respond well to glucose and alpha-ketoisocaproate at an early time point when they are totally blind to leucine, but as energy depletion proceeds they respond briskly to all three stimuli. Fatty acids (FA)

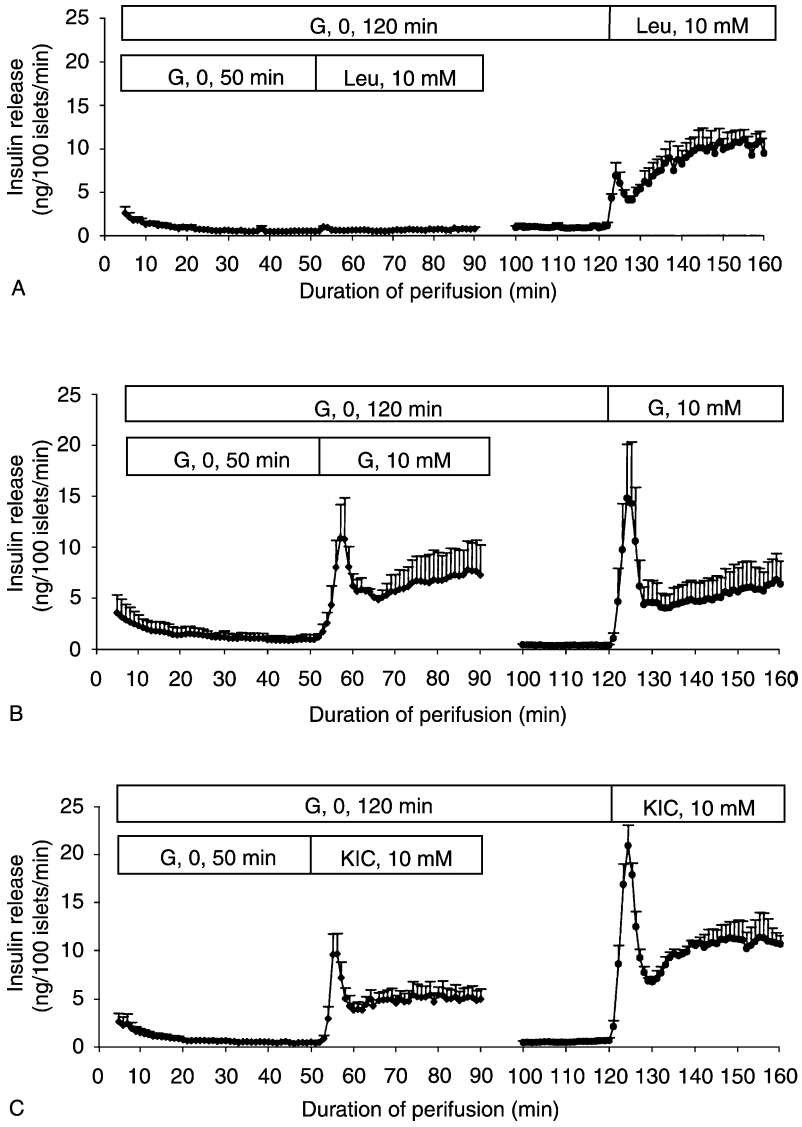

FIGURE 3 Effect of energy run-down on islet chemosensitivity. Isolated rat islets were cultured with 10 mM glucose for 3 days and then perifused with 2 mM glutamine in the absence of glucose for energy run-down periods of 50 min (diamonds) or 120 min (circles) prior to stimulation with (A)10 mM leucine (Leu), (B)10 mM glucose (G), and (C)10 mM alpha-ketoisocaproate (KIC). Values represent the means ± SE for 100 islets from three separate perifusions. Reproduced from Li, C., Najafi, H., Daikhin, Y., Nissim, I. B., Collins, H. W., Yudkoff, M., Matschinsky, F. M., and Stanley, C. A. (2003). Regulation of leucine-stimulated insulin secretion and glutamine metabolism in isolated rat islets. *J. Biol. Chem.* **278**, 2853–2858 with permission of The American Society for Biochemistry & Molecular Biology.

are effective glucose-dependent stimuli of insulin release (FASIR). It is now widely believed that specific metabolic products of FA metabolism play a more important role as signals or coupling factors for secretion than increased generation of ATP by their catabolism. For example, long-chain acyl-CoA and/or diacylglycerol may serve as activators of protein kinase C (PKC). This idea has been expanded, and it is proposed that these and possibly other lipid-derived metabolic coupling factors are critical for GSIR as well. This notion is captured by speaking of the "essentiality of FA for GSIR."

Neuroendocrine Modification of Fuel-Stimulated Insulin Release

Eating and digestion of food results in the production of the enterohormones GLP-1 and GIP and also enhances vagal activity, all of which augments fuel-stimulated insulin release. Catecholamines, on the other hand, block secretion very effectively. Recall that neuroendocrine stimulation of beta cells requires glucose. The signaling pathways are well established (Figure 1). The effects are quantitatively very marked, resulting in

a left shift and increased magnitude of the fuel dose–response curves for activators and a right shift and decreased magnitude for inhibitors. It is not surprising then that the pharmaceutical industry is making great strides in taking advantage of these pathways therapeutically.

A Brief Note on Alpha-Cell Function

AA and catecholamines are powerful physiological stimulators of glucagon release from alpha cells, and glucose inhibits these actions. The signaling pathways that operate here are not well understood but may involve steps similar to those described for beta cells, including nucleotide-controlled K^+ channels and L-type Ca^{2+} channels. Much controversy exists about the mechanism(s) of glucose inhibition of glucagon secretion. It has not been determined whether the glucose effects are direct or are mediated by the paracrine actions of insulin, GABA, Zn^{2+}, or other signals. The probable reason for this scanty knowledge lies in the great difficulties that hinder metabolic and other functional studies of alpha cells.

Glucokinase Disease and GDH or K^+ Channel-Linked Hypoglycemia

The biochemical genetic characterization of GK-linked hyper- and hypoglycemia syndromes (collectively termed glucokinase disease) and of GDH or K^+ channel-linked hyperinsulinemic hypoglycemia has strongly reinforced basic scientific concepts about the role of GK as glucose sensor and other crucial steps in GSIR and AASIR. Nearly 200 GK mutations have been discovered in patients with GK disease, usually inherited as an autosomal dominant trait. Activating mutations cause hyperinsulinemic hypoglycemia because the threshold for GSIR is left shifted as expected, while inactivating mutations cause a mild form of DM in the case of haploinsufficiency due to a right shift of the glucose threshold. However, severe ketotic permanent neonatal DM (PNDM) ensues when both alleles are strongly affected. In the latter case, beta cells seem to be totally nonfunctional, and the patients require full insulin replacement therapy right after birth. The syndromes of GK disease are nature's compelling proof of the GK glucose sensor concept. Activating mutations of GDH, usually explained by loss of GTP (ATP) inhibition of the enzyme, cause hyperinsulinemic hypoglycemia because beta-cell glutaminolysis is enhanced. These patients are also leucine hypersensitive, in agreement with the findings of basic research (see model experiment in Figure 3). Inactivating mutations of one of the subunits of the K^+ channel are a frequent cause of autosomal recessive hyperinsulinemic hypoglycemia. These mutations depolarize the beta cells and result in elevated $[Ca^{2+}]_i$, rendering them supersensitive to AA stimulation and neuroendocrine activation. The hyperresponse to protein meals as observed in these patients is reproduced in isolated perifused islets of SUR-$1^{-/-}$ mice that are stimulated by a physiological 20 AA mixture, in contrast to control islets that are refractory to this stimulus in the absence of glucose. There is also increasing support for the view that the highly common E23K polymorphism of the Kir6.2 channel causes a predisposition for the development of T2DM. The E23K mutation increases K^{2+} conductivity and hyperpolarizes beta cells, rendering them less sensitive to physiological stimuli. These examples illustrate how basic and clinical sciences cooperate in their quest to understand glucose homeostasis and its disturbances.

Beta-Cell Therapy in T2DM and Hyperinsulinemia

Our knowledge of physiological chemistry and biochemical genetics of the beta cell has its corollary in beta-cell-based therapeutics of T2DM and hyperinsulinemic hypoglycemia, which contributes substantially to our understanding of islet cell function and glucose homeostasis. The following drugs will be discussed in brief: K^+ channel inhibitors and activators (KCIs and KCOs), GK activators (GKAs), GLP-1, GIP, methylxanthines, and muscarinic agonists (see Figure 1). KCIs (i.e., sulfonyl urea derivatives and other chemicals that inhibit the K^+ channel) reduce K^+ conductivity, depolarize the beta cell, and sensitize it to all known physiological stimuli. For decades they have been the drugs of choice for the treatment of T2DM. KCOs (e.g., diazoxide) hyperpolarize beta cells and have been useful in the treatment of mild forms of hyperinsulinemic hypoglycemia (e.g., due to mutations of GK or GDH). GKAs have been discovered only recently and hold considerable promise for a new approach to the treatment of T2DM. They have effects very similar to those of activating mutations of GK, and it seems that they act by binding to an allosteric activator site of the enzyme (Figure 4). They cause a left shift of the concentration dependency curve of GSIR and have the additional advantage that they activate hepatic GK and augment glycogen synthesis. It is hoped that ongoing trials in humans will demonstrate the clinical usefulness and safety of this novel, theoretically very attractive approach to treatment of T2DM. GLP-1 and GIP are obvious candidates for antidiabetic agents as is apparent from Figure 1, and promising trials are underway. M3 agonists that could reproduce the effects of

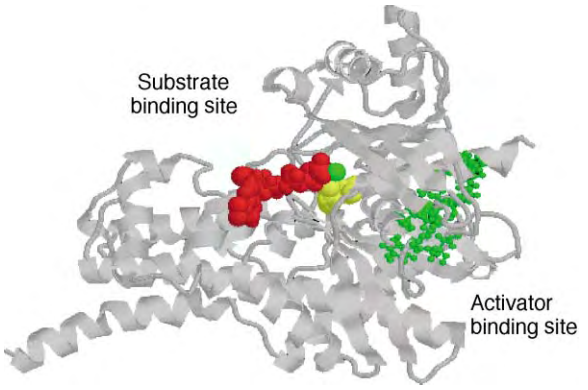

FIGURE 4 Allosteric activator site of the glucokinase glucose sensor molecule: ribbon drawing of the model structure of GK, with the N-terminal to the left and the C-terminal to the right. Glucose, ATP, and Mg^{2+} are located in the substrate cleft of the enzyme, and the allosteric activator site is indicated by several amino acids. The mutation of any one of these (e.g., V62M, I211A, Y214C, M235A, V455M, and A456V) activates the enzyme markedly. Glucokinase activators bind to this site.

acetylcholine, although potentially useful, have not been explored, most likely because lack of beta-cell specificity might become an issue. Phosphodiesterase inhibitors (e.g., IBMX) are powerful potentiators of fuel-stimulated insulin release, but here again it is apparently difficult to design a beta-cell-specific drug. Note that drug treatment of beta cells seems to reduce the diabetes-associated hyperfunction of the glucagon-producing alpha cells as well, thus indirectly enhancing the benefit of antidiabetic drugs with beta-cell action.

Conclusion

This entry illustrates that experimental work and mutually corrective or reinforcing dialog between biochemists, geneticists, pharmaceutical chemists, pharmacologists, and the practicing diabetologists has resulted in a deep understanding of the role that pancreatic endocrine cells play in glucose homeostasis and the pathogenesis of diabetes mellitus and how various therapies might ameliorate the dysfunction of these cells. This remarkable track record bodes well for the future, holding great promise for even deeper insights and the development of new antidiabetic agents and drugs that combat severe hyperinsulinemia.

See Also the Following Articles

Diabetes • Fatty Acid Oxidation • Fatty Acid Receptors • Fatty Acid Synthesis and its Regulation • Glucagon Family of Peptides and their Receptors • Hexokinases/Glucokinases • Insulin Receptor Family • Protein Kinase C Family

Glossary

beta cell threshold for glucose-stimulated insulin release The level of glucose required to initiate insulin release, i.e., about 5 mM. This beta-cell threshold is the critical determinant of the glucose setpoint of the body.

glucokinase (GK) disease Hypo- and hyperglycemia syndromes in humans caused by activating and inactivating mutations of glucokinase. This "experiment of nature" is the most compelling evidence for the glucokinase glucose sensor concept and its importance in understanding glucose homeostasis.

glucokinase glucose sensor Glucokinase (also known as hexokinase IV or D) phosphorylates D-glucose using ATP, forming glucose-6-phosphate. The enzyme serves as a glucose sensor of the pancreatic beta cells because it is rate limiting for glucose metabolism (i.e., glycolysis and oxidation), which is an absolute prerequisite for the triggering of insulin secretion.

glucose setpoint of the body Blood glucose level maintained precisely by the fine tuning of opposing processes that either produce or consume glucose. In humans, this setpoint is close to 5 mM.

Further Reading

Grimsby, J., Sarabu, R., Corbett, W. L., Haynes, N. E., Bizzarro, F. T., Coffey, J. W., Guertin, K. R., Hilliard, D. W., Kester, R. F., Mahaney, P. E., Marcus, L., Qi, L., Spence, C. L., Tengi, J., Magnuson, M. A., Chu, C. A., Dvorozniak, M. T., Matschinsky, F. M., and Grippo, J. F. (2003). Allosteric activators of glucokinase: Potential role in diabetes therapy. *Science* **301**, 370–373.

Matschinsky, F. M. (1996). Banting Lecture 1995: A lesson in metabolic regulation inspired by the glucokinase glucose sensor paradigm. *Diabetes* **45**, 223–241.

Matschinsky, F. M. (2002). Regulation of pancreatic beta-cell glucokinase: From basics to therapeutics. *Diabetes* **51 Suppl. 3**, 394–404.

Newgard, C B., and Matschinsky, F. M. (2001). Substrate control and insulin release. In *Handbook of Physiology* (L. Jefferson and A. Cherrington, eds.) Vol 2, pp. 125–151. Oxford University Press, Oxford.

Prentki, M., and Matschinsky, F. M. (1987). Ca^{2+}, cAMP and phospholipids derived messengers in coupling mechanisms of insulin secretion. *Physiol. Rev.* **67**, 1185–1248.

Biography

Franz M. Matschinsky is the current Benjamin Rush Professor of Biochemistry and Biophysics at the University of Pennsylvania School of Medicine. His research focuses on the role of pancreatic alpha and beta cells in glucose homeostasis, the role of glucokinase as glucose sensor, the biochemical genetics of glucokinase disease, and drug therapy of diabetes mellitus using glucokinase activators. He received medical training in Freiburg and Munich, Germany, and postdoctoral training at Washington University in St. Louis. He was Professor of Pharmacology at that institution from 1972 to 1978.

Insulin Receptor Family

Paul F. Pilch
Boston University Medical School, Boston, Massachussetts, USA

Jongsoon Lee
Joslin Diabetes Center, Harvard Medical School, Boston, Massachussetts, USA

The mammalian insulin receptor family is composed of three members: the insulin receptor (IR), the insulin-like growth factor I receptor (IGF1R) and the insulin receptor-related receptor (IRR). All are ligand-activated tyrosine kinases, i.e., members of the large receptor tyrosine kinase (RTK) superfamily. The IR family members share ~55% overall sequence homology with each other, and have many similar biochemical and functional characteristics. The IRR is an orphan receptor lacking a physiological ligand, and its knockout in the mouse has no gross phenotype. Consequently, there is very little to say about the IRR. Because of its critical role in metabolic regulation, the insulin receptor is one of the most-studied RTKs and the details of its structure, function, and mechanism of action will be emphasized. The biochemically similar IGF1R serves as a mitogen receptor and does not normally acutely regulate nutrient metabolism.

IR Family Ligands and Their Specificity

The ligands for the insulin receptor family also comprise a family of related peptides, namely, insulin, IGF1 and IGF2, the latter two being mitogens. These peptides are synthesized with a cleavable signal sequence for secretion and have three inter/intra-chain disulfide bonds. Insulin alone is further processed by an endoprotease, which results in the excision of an internal 33-amino acid "connecting" or C peptide from the proinsulin precursor and produces mature insulin in the form of disulfide-linked 21- and 30-amino acid A and B chains, respectively. Insulin and IGF1 bind only their cognate receptors with high affinity, whereas IGF2 can bind both these receptors with reasonable (physiological) affinity. However, there exists another high-affinity IGF2 receptor, also called the cation-independent mannose-6-phosphate receptor that has no signaling function but serves to clear IGF2 (and other molecules) from circulation.

Receptor Structure/Function

Composition and Biosynthesis

Figure 1 depicts a two-dimensional cartoon for the structure of the insulin (numbered without exon 11) and IGF1 receptors. The mature receptors are $\alpha_2\beta_2$ heterotetramers in which the two extracellular α-chains are linked to each other and to a β-subunit through disulfide bridges (horizontal lines, Figure 1). Both α- and β-subunits (respectively, 719 and 624 aas) of the insulin (IGF1) receptor are heavily glycosylated and have approximate molecular weights of 130 and 95 kDa, respectively, as assessed by gel electrophoresis. The α-subunits are totally extracellular and are responsible for ligand recognition. The β-subunits have three topographically distinct regions: the extracellular, transmembrane (TM), and cytosolic domains. The cytosolic tyrosine kinase domain, which shares the most similarity among family members, has an ATP-binding site and three clusters of tyrosine residues located in the juxtamembrane region, the kinase activating loop, and the C terminus. These tyrosines are phosphorylated upon ligand binding to α-subunits (*vide infra*).

Both receptor subunits are encoded in a single gene, which is composed of 22 exons for IR and 23 exons for IGF1R in humans. The initial translation product of IR family members is a single polypeptide proreceptor precursor, a type 1 transmembrane protein with its N terminus having an extracellular topography. The proreceptor is glycosylated and dimerized in the endoplasmic reticulum, transported into the Golgi, and then proteolytically cleaved by the endoprotease furin, into mature $\alpha_2\beta_2$ receptors. While the IGF1R has a single isoform, the IR has two isoforms produced by alternative splicing of exon 11 (12-amino acids) at the C terminus of α-subunits. Several studies show that there are differences between the two isoforms in tissue distribution, ligand-binding specificity and relative expression levels among diabetes patients. However, a definitive physiological significance for the separate isoforms is still uncertain.

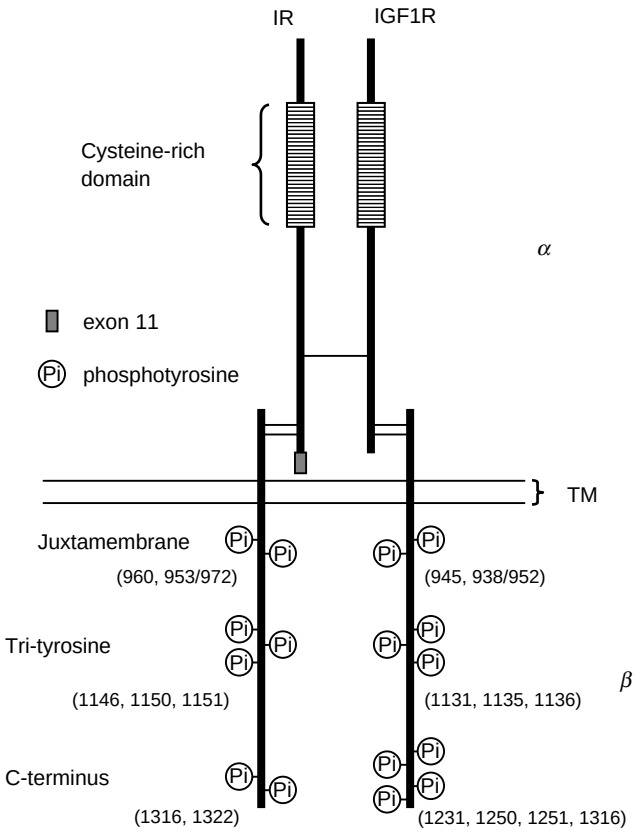

FIGURE 1 Two-dimensional representation of IR (left side) and IGF1R (right side) structural/biochemical features. The IR is numbered without Exon 11 (12 aas). The extracellular α-subunits are linked to each other and to β-subunits by disulfide bridges (horizontal lines). The α-subunits contain the ligand-recognition sequences including the cysteine-rich domain. The β-subunits span the lipid bilayer via their transmembrane (TM) domains and have three clusters of tyrosine residues whose phosphorylation has functional consequences (see the text).

Ligand Binding

Affinity labeling of the insulin receptor using bifunctional cross-linking agents and photo-activatable insulin analogues first documented the α-subunit, including the cysteine-rich region shown in Figure 1, as the site of insulin (IGF1)-receptor contact. Insulin/IGF1-binding studies with various mutant receptor constructs as well as domain-swapping studies between IR and IGF1R confirmed these biochemical data and also identified exons 2 and 3 (aas 16-286, including the cysteine-rich region) as sequences that govern ligand-binding specificity between insulin and IGF1.

However, while residues in the α-subunit govern ligand recognition, there is role for the β-subunit in ligand affinity. Insulin and IGF1-binding studies support the notion that only one ligand molecule binds the holoreceptor with high affinity, whereas each $\alpha\beta$ half-receptor can bind one ligand molecule, albeit with low affinity. Kinetic analysis of ligand binding to the holoreceptor reveal it to exhibit negative cooperativity, whereby one ligand molecule binds with high affinity and a second binds with much less affinity. Mutational analysis has shown that soluble versions of the insulin receptor containing $\alpha-\alpha$ disulfide linkages have low insulin-binding affinity and a stoichiometry of one insulin/α-subunit. The high-affinity state can be recapitulated by bringing the α-subunits into their proper orientation relative to one another by including the transmembrane sequence of the β-subunit, a leucine zipper domain or parts of an immunoglobulin protein. Various cellular and biochemical studies confirm that binding of one insulin molecule to the holoreceptor is the normal situation at physiological concentrations of insulin and this is sufficient to activate the receptor and its signaling pathway. The conclusion from all these studies is that both α-subunits participate in the formation of the high-affinity ligand-binding site. The molecular details of this await X-ray crystallography studies of the holoreceptor-ligand complex. Indeed, X-ray crystal structures have been determined for the N terminus of IGF1R α-subunit and for the kinase domain of the IR. Recently, a structure of the IR based on three-dimensional electron microscopy and adopting coordinates from the X-ray structure of IGF1R N terminus has been proposed, and has provided new information concerning the overall shape of the IR. However, these results are of too low resolution to reveal the details of ligand-receptor interaction.

Autophosphorylation and Kinase Activation

Ligand binding to the insulin receptor causes a transmembrane conformational change that results in autophosphorylation and activation of exogenous tyrosine kinase activity in the receptor's β-subunit. Evidence supporting conformational changes includes the differential recognition of site-specific anti-receptor antibodies for activated versus inactive insulin receptor, differential susceptibility to proteases, changes in intrinsic fluorescence of the insulin receptor during receptor activation and the different X-ray structural configuration of the isolated kinase domain comparing activated (tyrosine phosphorylated) versus basal states. Taken together, these studies provide evidence that conformational changes occur during each step of receptor activation: insulin binding, ATP binding, and kinase activation by phosphorylation. However, the exact molecular nature and sequence of the conformational changes by which ligand binding activates the kinase domains and mediates transmembrane signaling are not fully understood.

It is known that activation of IR/IGF1R receptor kinase occurs in trans, that is; one kinase domain

phosphorylates the other. The IR contains two identical kinase domains and two sets of phosphorylation sites and both must be active for exogenous tyrosine kinase activity, i.e., substrate phosphorylation, to occur. Biochemical studies of the photo-labeled IR as well as studies of receptor chimeras consisting of half kinase-active and half kinase-dead receptors document asymmetric IR autophosphorylation. For the photo-labeled holoreceptor, autophosphorylation is initially asymmetric and the insulin-linked receptor half is 50% less phosphorylated than the other half. Thus, initially only one β-subunit is phosphorylated, but at the later time points, both subunits become phosphorylated and in a given ligand-bound receptor, autophosphorylation is a stochastic process.

There are 13 and 15 tyrosine residues, respectively, in the cytoplasmic domain of IR and IGF1R, and phosphopeptide mapping analysis and/or site-directed mutagenesis has revealed three clusters (Figure 1) that can be phosphorylated upon receptor binding. Phosphorylation of tyrosines at the activation loop (Tyr1146, 1150 and 1151 for IR, Tyr1131, 1135 and 1136 for the IGF1R) is critical for kinase activity. The non-phosphorylated activation loop of the receptor blocks the ATP-binding site in the basal state. Ligand binding allows the tyrosine phosphorylation of these residues and moves the activation loop away from the opening of the ATP-binding site, thus allowing access so that the kinase can phosphorylate exogenous substrates such as the insulin receptor substrate (IRS) family relevant to the IR and IGF1R. Mutation of the activation loop tyrosines to phenylalanine abolishes kinase activation and insulin-signaling cascades.

The physiological role of tyrosine phosphorylation at the other sites is less clear. Mutation of Tyr960 of the IR to Phe does not change insulin-stimulated autophosphorylation and kinase activation, but it does abolish phosphorylation of IRS1, hence signaling, as deduced from transfection experiments. The phosphorylated NPE(X)Y-motifs (Tyr960 of IR and Tyr945 IGF1R) can serve as docking sites for IRS proteins via their phosphotyrosine binding (PTB) domains and this may be necessary for signal propagation. On the other hand, peptide mapping of the autophosphorylated receptor demonstrates that the juxtamembrane region is rather minimally phosphorylated, although this does occur to a significant extent with the isolated kinase domain. Phosphorylation of tyrosines at the C terminus of the IR (residues 1316 and 1322) accounts for 30–40% of total phosphorylation of β-subunits. However, deletion/substitution of the residues has produced conflicting results in different labs as to the effects, if any, of these manipulations, and consequently, there is no clear physiological role yet for these sites.

Postreceptor Signaling

Physiological Effects of Insulin and IGF1

These are too numerous to elaborate, so the emphasis of this section will be IR-regulated glucose metabolism. Glucose is a primary energy source for various tissues including the brain, and insulin maintains the circulating blood glucose concentration within narrow limits. Glucose homeostasis is coordinately regulated by insulin in liver, fat, and muscle. Pancreatic β-cells play an obvious role in insulin production. Liver maintains basal glucose levels between meals by producing glucose through two mechanisms: *de novo* glucose synthesis (gluconeogenesis) and breakdown of glycogen (glycogenolysis). Muscle, and to a lesser degree fat, lowers postprandial glucose levels by increasing glucose uptake (transport) and its storage as glycogen and lipid. Insulin, produced and secreted from β-cells in response to changes in circulating glucose levels after meals, regulates all these processes. Glucose homeostasis is achieved by insulin-dependent suppression of hepatic glucose production and by enhanced glucose uptake and storage in muscle and fat. Enhanced glucose uptake is achieved by the insulin-dependent movement of a glucose transport protein Glut4, from an intracellular reservoir to the cell surface (Figure 2). On the other hand, IGF1 promotes cell growth, differentiation, and survival as largely studied in cell culture. Its signaling pathway closely resembles that of insulin but its role *in vivo* is not as well defined compared to insulin.

Signaling Cascades

Once the insulin or IGF1 receptor is activated by autophosphorylation, it phosphorylates one or more of the IRS proteins noted above. Six IRS family members have been identified and they are all adaptor proteins, that upon tyrosine phosphorylation, bind and activate a number of effector molecules through their src homology 2 (SH2 domains). IRS-1 and -2 have been implicated as the major signaling components directly downstream of the IR and IGF1R. The major event following IRS phosphorylation is the activation of the p110 (Figure 2) catalytic subunit of phosphoinositol-3-kinase (PI3-K) by binding of the p85 subunit of PI3-K to tandem pYMXM sequence motifs of an IRS molecule. The formation of the lipid PIP_3 by PI3-K causes the activation of the *p*hosphoinositide-*d*ependent serine/threonine *k*inase, PDK1, and, in turn, it phosphorylates and activates Akt/PKB (protein kinase B) and PKCλ/ζ, each of which may affect glucose transport (Figure 2).

Akt is the serine/threonine kinase that appears to be the key regulatory enzyme in insulin/IGF1 signaling that

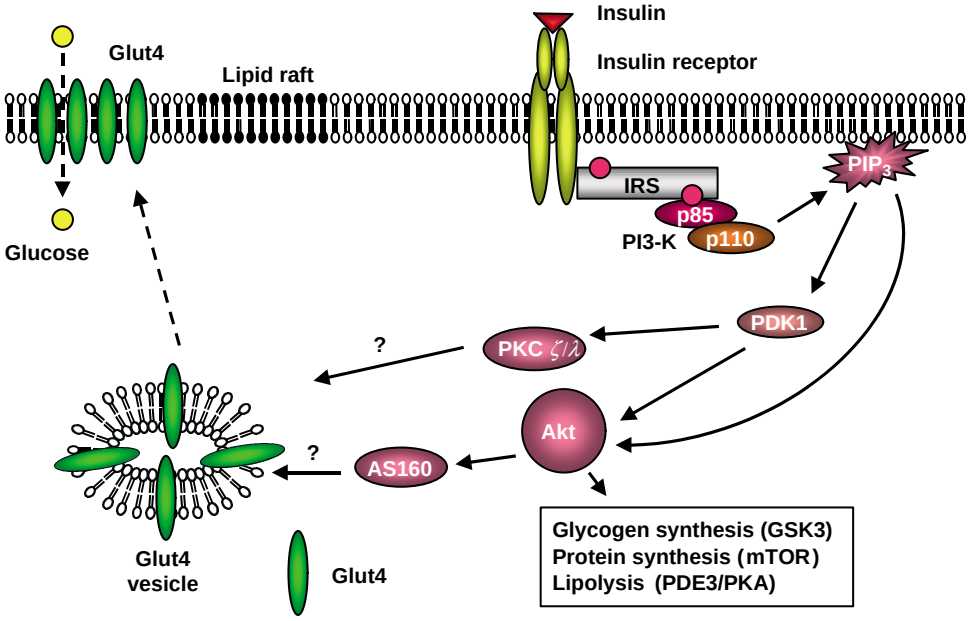

FIGURE 2 The insulin receptor signaling cascade that activates glucose transport. The solid arrows indicate the signaling pathway, the dashed arrows indicate movement and the question mark, an unknown or uncertain biochemical event. Refer to the text for a description of the known biochemical events in the pathway from the receptor to the Glut4 vesicle. Note that the size of the proteins depicted in the cartoon is not to scale relative to one another.

impacts different physiological end points of metabolism such as gluconeogenesis and glycogenolysis in liver, glucose transporter (Glut4) trafficking in muscle and fat, and β-cell survival. Thus, mice lacking the Akt2 isoform of this enzyme have a diabetic phenotype and show metabolic abnormalities in the processes just noted. That is, they have impaired suppression of hepatic glucose output, deficient glucose uptake in fat and muscle, and abnormal islets. At the molecular level in liver, Akt phosphorylates the transcription factor Foxo1, that regulates expression of gluconeogenic enzymes. AS160, for Akt substrate of 160 kDa, is a recently described protein that may link the canonical PI3-K pathway to Glut4 translocation but "exactly how?" remains unknown. A second pathway by which insulin-dependent Glut4 translocation may occur in adipocytes has been proposed. Insulin-signaling, independent of PI3-K, is postulated to emanate from subdomains of the plasma membrane called lipid rafts and causes cyto-skeletal changes that bring Glut4 to the plasma membrane. The physiological relevance of this second pathway remains to be established.

"Genetics" and IR-IGF1R Comparisons

On a biochemical level, signaling pathways from the IR and IGF1R appear to be identical yet they clearly serve different functions *in vivo*. The phenotypes of knockout (KO) mice for these receptors and their ligands have further revealed this diversity of function. Although there is minor compensation between the two pathways, it is evident that insulin regulates glucose/lipid metabolism and IGF1 (IGF2) mediates growth/development. Thus, while IR and IGF1R knockouts are lethal in mice, the former is due to hyperglycemia and the latter lack of muscle development. The reasons for these differences are highly complex and beyond the scope of this article. However, it is worth noting that unlike mice, humans lacking functional insulin receptors live for at least a short time after birth, probably due to IGF1R compensation.

To determine physiological roles of the IR in specific insulin responsive cell types, tissue-specific insulin receptor KO-mouse models have been made including in muscle, liver, fat, and β-cells. These tissue-specific mouse models generally show mild insulin resistance short of diabetes. Because insulin resistance leading to diabetes is a total body disease, disruption of insulin signaling, hence glucose metabolism, in individual tissues may not be sufficient for the development of this pathological state. Further genetic studies including multiple "knockout" and "knockin" mouse models, the latter with specific receptor mutations, should increase our understanding of development of insulin resistance and diabetes. Subsequent biochemical and cellular studies will provide us with the details of the molecular mechanisms underlying the IR and IGF1R signaling pathways.

See Also the Following Articles

Diabetes • Glucose/Sugar Transport in Mammals • Insulin- and Glucagon-Secreting Cells of the Pancreas

Glossary

glycosylated Referring to or describing protein modified by the covalent attachment to/of carbohydrate molecules.
ligand A molecule such as a hormone that binds to a receptor.
mitogen A molecule that stimulates cell growth and division.
phosphorylation Covalent modification of a molecule (here protein) by the attachment of a phosphate residue.

Further Reading

De Meyts, P., and Whittaker, J. (2002). Structural biology of insulin and IGF1 receptors: Implications for drug design. *Nat. Rev. Drug Discov.* **1**, 769–783.

Kim, J. J., and Accili, D. (2002). Signaling through IGF-I and insulin receptors: Where is the specificity? *Growth Horm IGF Res.* **12**, 84–90.

Kitamura, T., Kahn, C. R., and Accili, D. (2003). Insulin receptor knockout mice. *Annu. Rev. Physiol.* **65**, 313–332.

Lee, J., Pilch, P. F., Shoelson, S. E., and Scarlata, S. F. (1997). Conformational changes of the insulin receptor upon insulin binding and activation as monitored by fluorescence spectroscopy. *Biochemistry* **36**, 2701–2708.

Sano, H., Kane, S., Sano, E., Miinea, C. P., Asara, J. M., Lane, W. S., Garner, C. W., and Lienhard, G. E. (2003). Insulin-stimulated phosphorylation of a Rab GTPase-activating protein regulates GLUT4 translocation. *J. Biol. Chem.* **278**, 14599–14602.

Whiteman, E. L., Cho, H., and Birnbaum, M. J. (2002). Role of Akt/protein kinase B in metabolism. *Trends Endocrinol. Metab.* **13**, 444–451.

Biography

Paul Pilch is a Professor of Biochemistry at Boston University School of Medicine who since long ago has evinced keen interest in insulin/IGF1 receptors and the metabolic consequences of activating their signaling pathway(s).

Jongsoon Lee is an Instructor at the Joslin Diabetes Center, Harvard Medical School, who shares the same interest. Separately and together, they have published extensively on these topics.

Integrin Signaling

Lawrence E. Goldfinger and Mark H. Ginsberg
Scripps Research Institute, La Jolla, California, USA

Integrins are heterodimeric transmembric receptors expressed on virtually all cells in multicellular organisms. They mediate attachment of cells to the extracellular matrix and to other cells. In addition to, and participation with their adhesive function, integrins are conduits of bidirectional signaling between the extracellular environment and the cell interior. Through "outside-in" integrin signaling, binding of ligands to integrin extracellular domains initiates intracellular signaling pathways which regulate such processes as protein phosphorylation, gene expression, proliferation, apoptosis and differentitation. These signals are initiated by conformational changes in the integrin structure propagated from the extracellular "head" domains, through the transmembrane regions and terminating at the cytoplasmic "tail" domains. Conformational changes in the tails subsequently affect the binding and signaling properties of intracellular signaling molecules. Conversely, conformational activation of integrin head domains to promote ligand binding is regulated by intracellular signaling pathways, in a process called "inside-out" integrin signaling. Cytoplasmic proteins associate with integrin tails, leading to allosteric rearrangements in the extracellular head domains to effect a switch from low to high affinity ligand binding. This process of inside-out integrin signaling is crucial to hemostasis and the maintenance of normal tissue integrity. Furthermore, ligand binding to integrins can be regulated by avidity modulation by which integrin clustering promotes increased binding to ligands. Thus, intricate regulation of outside-in and inside-out signaling and integrin avidity plays key roles in numerous cellular phenotypes.

Integrins are transmembrane receptors that promote cellular attachment to the extracellular matrix (ECM) and to counter receptors on the surfaces of neighboring cells. Integrins are responsible for mediating cell adhesion and migration, and for maintaining tissue integrity. They are expressed at the surface of virtually all multicellular animal cells as noncovalent heterodimers of α- and β-subunits. Integrins are named based on their α- and β-subunit composition, e.g., $\alpha_1\beta_1$, $\alpha_{IIb}\beta_3$.

The integrin family in humans consists of 18 α- and 8 β-subunits, which each are encoded by unique genes. Each α-subunit pairs with a restricted set of β-subunits, resulting in a total of 24 known functional integrin heterodimers. Each pairing, in turn, is expressed on a limited array of cell types. Thus, each cell has its own particular repertoire of integrins. Since different integrins display distinct ligand-binding preferences, these repertoires specify adhesive preferences of different cell types. In some cases, multiple integrins can recognize the same ligand. For example, many integrins bind to the ECM protein, fibronectin. Even within the same ECM protein, integrins can vary in recognition specificity. Integrin $\alpha_V\beta_3$, for example, binds to an Arg-Gly-Asp (RGD) motif in fibronectin, while integrin $\alpha_4\beta_1$ binds to a Leu-Asp-Val (LDV) motif present in a different part of fibronectin. Furthermore, these short peptide motifs can occur in evolutionarily unrelated proteins, where they can serve as recognition sites for many different integrins. The RGD motif occurs in many proteins and can bind to many integrins (e.g., $\alpha_{IIb}\beta_3$, $\alpha_v\beta_3$, $\alpha_v\beta_5$, $\alpha_5\beta_1$). This integrin-binding motif interaction is conserved in phylogeny; for example, the *Drosophila* PS2 integrin recognizes an RGD sequence in tiggrin, a matrix protein. The occurrence of integrin-binding motifs, such as RGD, is an example of convergent evolution dictated by the recognition specificity of adhesion receptors.

All integrin subunits possess a single transmembrane domain, which separates the large extracellular, N-terminal ligand-binding domain from the typically short (less than 60 amino acids) C-terminal cytoplasmic domain, or cytoplasmic tail. Besides acting as cellular glue to support adhesion, and feet to facilitate migration, integrins initiate transmembrane signals, which regulate processes such as embryogenesis, cell development, proliferation, apoptosis, and the immune response.

General Features of Integrin Signaling

Integrins derive their name from their role of integrating the ECM with the insoluble cellular skeleton (cytoskeleton). Binding of ligands to the extracellular portion of integrins leads to both conformational changes in the receptors and to receptor clustering. This combination

of events initiates intracellular signals such as protein tyrosine phosphorylation, activation of small GTPases, and changes in phospholipid biosynthesis. This process is commonly referred to as outside-in signaling. In addition, integrins are subject to so-called inside-out signaling. Integrins can fluctuate between three functional states: an active state that manifests high affinity for binding ligands, a high-affinity state that is bound to ligand, or in a distinct "inactive" state, which has a low affinity for ligands. Inside-out signaling is defined as modulation of the functional state of integrins via intracellular signaling processes. It is frequently mediated by interactions of intracellular components with the integrins' cytoplasmic tails. Furthermore, signals from one integrin can regulate the activation state of another in a phenomenon referred to as integrin transregulation or cross talk. Through transregulation, multiple integrins can be linked via a combination of both outside-in and inside-out signaling.

Inside-Out Signaling

Modulation of integrin function can occur by changes in ligand-binding affinity or by changes in the clustering of these receptors. The former mechanism is often referred to as integrin activation and the latter as a change in avidity. These functional changes can be caused by signaling pathways initiated by agonist-receptor interactions at the plasma membrane. The appropriate regulation of integrin activation is required for the formation and maintenance of normal tissue architecture.

Physiological Roles of Inside-Out Signaling

Integrin Activation in Hematopoietic Cells

Integrin activation plays a crucial role in the biology of blood cells. For example, the platelet integrin, $\alpha_{IIb}\beta_3$, is usually maintained in the inactive state, with very low affinity for its extracellular ligands, fibrinogen, fibronectin, and von Willebrand factor. Upon platelet stimulation, the integrins are quickly activated, leading to fibrinogen binding and consequent platelet aggregation, an early step in hemostasis. Thus, the loss of $\alpha_{IIb}\beta_3$ integrin activation impairs hemostasis. Conversely, platelet aggregation is central in arterial thrombosis that is responsible for the majority of heart attacks and strokes. Pharmacological blockade of activation of integrin $\alpha_{IIb}\beta_3$ by agents such as aspirin or ticlopidine is therefore often used to treat patients at risk for these diseases. Similarly, rapid activation of dormant integrins on leukocytes allows these cells to attach firmly to the endothelial vessel wall and resist strong shear forces from the flowing blood. This step is essential for their migration into sites of inflammation. For this reason, loss of leukocyte integrin activation can lead to enhanced susceptibility to infections and its blockade may be useful in anti-inflammatory therapies.

Integrin Activation in Tissues

For adherent cells in tissues, such as fibroblasts or epithelial cells, stable cellular attachment to the ECM is necessary for maintaining tissue integrity. Many of the best-studied integrins in these cells, such as the α_5, α_v, and α_6 integrins, are indispensable components of cell-substrate attachment structures: focal adhesions, hemidesmosomes, and podosomes. In addition to attaching to the ECM, integrins participate in formation and remodeling of the ECM. Activation of tissue integrins can regulate the assembly and structure of the ECM and control the stability of integrin–matrix attachments. In addition, the migration of these cells in tissues is regulated by the ability of integrins to become activated. Furthermore, integrin activation may be topographically localized across the basal cell surface. For example, activated $\alpha_v\beta_3$ integrins are preferentially localized to the leading edge of endothelial cells during cell migration and neurite outgrowth.

Integrin Activation

The switch from an inactive to an active state is the result of alterations in the conformation of the integrin extracellular domains. These conformational changes can be triggered by protein–protein interactions at the integrin cytoplasmic face. These protein–protein interactions are regulated by different signaling pathways in different cells. However, in many contexts, activation of key intermediates such as the GTPase Rap1, or protein kinase C, promote increased integrin affinity. Conversely, activation of Raf-1 kinase often suppresses integrin activation. Whatever the upstream events, it is likely that the final common events involve changes in interactions at the integrin cytoplasmic domain (Figure 1).

Contribution of Cytoplasmic Domains

Tail-Binding Proteins Numerous cytoplasmic integrin-binding proteins have been described, and several have been reported to contribute to activation through binding to the integrin tails. The best-characterized example is the cytoskeletal linker protein talin, which promotes integrin activation by binding to a subset of integrin β-subunit tails at a highly conserved NPxY motif. Mutational evidence suggests that integrin α–β-subunit tail interactions inhibit activation. The ability of talin to activate the integrins has

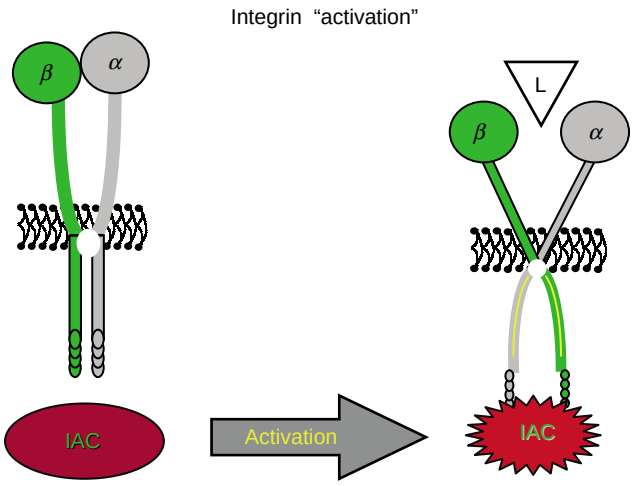

FIGURE 1 Inside-out signaling activates integrins. Binding of an integrin-activating complex (IAC) to the cytoplasmic tails of an integrin heterodimer produces conformational changes in the extracellular head domains, leading to activation and high-affinity binding to ligand (L).

been attributed to competition with the α-subunit for β-tail binding.

Membrane Proximal Residues Deletion of the tail sequences adjacent to the putative transmembrane regions in either the α- or β-tail can activate integrins, indicating that these residues are essential for maintaining integrins in an inactive state. One model for activation entails a breaking of a salt bridge in this region that holds the tails together, leading to an "opening" of the tails via a scissor-like mechanism (Figure 1). This leads to an allosteric rearrangement in the extracellular domain and a shift to the active state.

Extracellular Domain Conformational Changes

Precise conformational shifts at the ligand-binding face of integrins result in high-affinity binding to ligands. Integrin–ligand interactions require an essential Asp or Glu residue in the integrin recognition sequence in the ligand, as well as the presence of a divalent cation. Some of the integrin α-subunits have an "inserted", or I/A domain near the N-terminus; these integrins contact ligand solely through the α-subunit, although the β-subunit plays an accessory role. The I/A domain manifests a metal ion-dependent adhesion site (MIDAS). Key residues in the ligand cooperate with the MIDAS to coordinate the cation and allow integrin–ligand interaction. Conformational changes in the MIDAS during cation coordination and ligand binding subsequently result in secondary changes in the rest of the integrin, including a downward shift of a α-helix C-terminal to the I/A domain, thereby switching the integrin from the "closed" inactive state into the "open" active state. For integrins with a α-subunit that does not contain an I/A domain, the I/A-like domain in the β-subunit cooperates with the α-subunit in a somewhat different fashion to mediate ligand interaction, but also through coordination of a divalent cation.

Avidity Modulation

In addition to affinity modulation through conformational changes in individual integrin molecules, cell adhesion can also be enhanced by increasing the density of ligand-binding sites through integrin clustering, via an affinity-independent mechanism known as avidity modulation. Many integrin ligands are multivalent; thus, integrin clustering can promote adhesion through cooperative ligand binding. In many cases, a combination of affinity and avidity modulation both contribute to the regulation of cell adhesion.

Outside-In Signaling

Occupancy of integrins leads to conformational changes that can propagate over long distances in the extracellular domain. It has been proposed that these allosteric rearrangements can be transmitted across the plasma membrane, changing the interactions of the α and β cytoplasmic domains with each other and thus, the integrin's interactions with intracellular signaling molecules. Furthermore, occupancy leads to integrin clustering, which can also change the physical relationships of the integrin cytoplasmic domains with each other. This combination of occupancy and clustering is believed to initiate signals from integrins. These signals regulate the formation and strengthening of adhesion sites, the dynamics of cytoskeletal structure, cell shape and size, and cell polarity and cell migration. In addition to controlling the physical activities of cells, signaling through integrins also regulates gene expression, cell proliferation and apoptosis, and many integrins are required for the development of particular lineages.

Integrins in Adhesion Sites

Most integrins are physically linked to the actin cytoskeleton via interactions of the β-tail with actin-binding proteins such as α-actinin, talin, and filamin. $\alpha_6\beta_4$ integrins associate with the intermediate filament cytoskeleton through other linker proteins: BP180 (BPAG2), BP230 (BPAG1), and plectin. By connecting the ECM with the cytoskeleton, clustered integrins form the essential core of complexes of structural and signaling molecules such as focal complexes and adhesions (contacts), hemidesmosomes (specific to

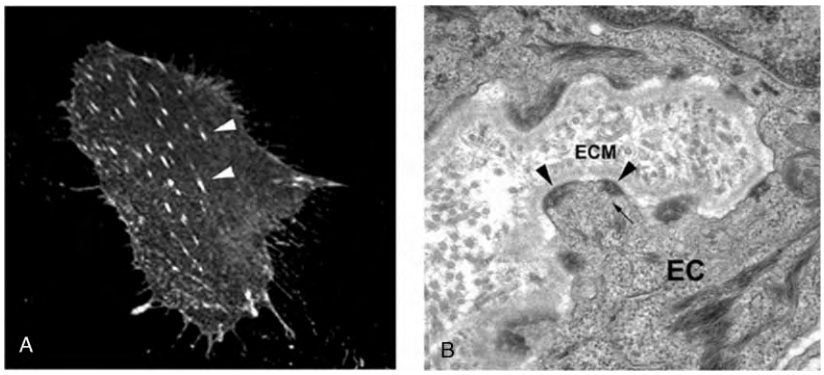

FIGURE 2 Focal contacts and hemidesmosomes. Two types of integrin–ECM contacts are shown. (A) Focal contacts are visualized by labeling $\alpha_{IIb}\beta_3$ integrin clusters in a fibroblast expressing $\alpha_{IIb}\beta_3$ attached to fibrinogen. Arrowheads indicate two focal contacts. (B) Transmission electron micrograph of a cross section of bovine tongue. Hemidesmosomes (arrowheads) are seen as electron-dense structures at the basal surface of the tongue epithelial cells (EC), connecting the intermediate filaments (arrow) to the ECM. Image courtesy of Gregory W. deHart and Jonathan C.R. Jones.

epithelial cells, they contain $\alpha_6\beta_4$ integrin and are linked to intermediate filaments), and osteoclast structures called podosomes (which have many of the same protein components as focal adhesions) (Figure 2).

Formation of Adhesion Sites

Ligand binding and integrin clustering nucleate nascent cell adhesion sites. Numerous cytoskeletal adapters and signaling molecules are subsequently recruited to the clustered integrin tails. These complexes serve as the initiation points for signaling by integrins to affect cellular phenotypes. Focal complexes "mature" to become focal adhesions (focal contacts) as more integrins and signaling molecules associate, thereby strengthening cellular attachments to the ECM.

Regulation of Adhesion Dynamics

Adhesion sites are dynamic structures which undergo remodeling to fit the needs of the cell or of the region of the cell in contact with the ECM. Focal complexes form at the leading edges of lamellipodia and of filopodia in migrating cells, where they mediate new attachments, but do not mature to focal adhesions. Instead, these smaller complexes are subject to rapid turnover, as the cell continues to extend protrusions in the direction of migration. Concomitantly, integrins in focal adhesions at the rear of the cell are recycled to the front via a treadmill-like mechanism. Focal adhesions, hemidesmosomes, and podosomes break apart and reform by severing and re-establishing integrin–ECM contacts, under conditions in which cells are motile, such as during development and in wound healing.

Contributions to Cellular Phenotypes

Effects on the Cytoskeleton

By connecting the ECM to the intracellular cytoskeleton, integrins also act as mechanosensors, transmitting information about the physical state of the ECM into the cell and altering cytoskeletal dynamics. Integrin ligation can activate key signaling components, such as the small GTPases Rho, Cdc42, and Rac, which promote cytoskeletal rearrangements leading to the formation of actin stress fibers, filopodia, and lamellipodia, respectively. Within focal adhesions, integrins can activate kinases important for downstream signaling, such as focal adhesion kinase (FAK) and Src tyrosine kinases. Activation of these enzymes results from signals initiated at the integrin cytoplasmic tails. Integrin tails also affect cytoskeletal rearrangements through other mechanisms, e.g., activation of Syk tyrosine kinase through its direct binding to the β3-tail, which promotes Vav1-induced GTP loading of Rac and subsequent lamellipodial formation. Through such mechanisms, integrins regulate cell polarity, migration, shape, and size.

Connections to Intracellular Signaling Pathways

Although integrins themselves do not manifest any catalytic activity, they transmit signals through binding partners such as integrin-associated protein (IAP, CD47), integrin-linked kinase (ILK), and members of the tetraspanin transmembrane protein family. Integrin ligation activates members of the Ras family of GTPases, and can also lead to activation of kinases such as JNK, PAK, and ERK/MAP (microtubule-associated proteins) kinase—the latter two are localized to integrin-rich adhesion sites. These enzymes

can subsequently regulate the expression of genes involved in cell proliferation and differentiation. Furthermore, integrins play a role in the inhibition of detachment-induced apoptosis, called "anoikis," through regulation of the PI3-kinase/Akt signaling pathway.

Integrin Cross Talk

Ligand binding to one subtype of integrins can affect the activation state of another integrin subtype on the same cell, by modulating the ligand-binding affinity and/or avidity of that integrin. For example, outside-in signaling through ligand binding of $\alpha_4\beta_1$ integrin can affect $\alpha_L\beta_2$-dependent lymphocyte adhesion and migration by regulating signaling through $\alpha_L\beta_2$. Furthermore, integrins are involved in cooperative signaling with other non-integrin receptors, such as the Epidermal Growth Factor (EGF) receptor and the T-cell receptor complex.

See Also the Following Articles

Actin-Related Proteins • Desmosomes and Hemidesmosomes • Epidermal Growth Factor Receptor Family • Focal Adhesions • Hematopoetin Receptors • Integrin Signaling • Protein Kinase C Family • Small GTPases

Glossary

cytoplasmic tail Intracellular portion (20–60 amino acids) of integrins involved in signaling.

cytoskeleton Structural network of actin microfilaments, keratin intermediate filaments and tubulin microtubules in mammalian cells.

extracellular matrix (ECM) Dense array of fibrillar proteins, enzymes and other molecules that provides a scaffold for cells and tissues, and contains binding sites for integrins.

focal adhesion Dash-like cell–matrix adhesion site consisting of a cytoplasmic multiprotein complex surrounding a core of clustered integrins.

integrin ligand ECM protein that binds the extracellular head domain of integrins.

MIDAS Metal ion-dependent adhesion site—array of key residues in some integrin head domains which coordinates a divalent cation during ligand binding.

NPxY Conserved sequence in most integrin β-tails that serves as a docking site for signaling molecules.

Further Reading

Beckerle, M. C. (2001). *Frontiers in Molecular Biology: Cell Adhesion*. Oxford University Press, New York.

Hughes, P. E., and Pfaff, M. (1998). Integrin affinity modulation. *Trends Cell Biol.* **8**, 359–364.

Hynes, R. O. (2002). Integrins: Bidirectional, allosteric signaling molecules. *Cell* **110**, 673–687.

Schoenwalder, S. M., and Burridge, K. (1999). Bidirectional signaling between the cytoskeleton and integrins. *Curr. Op. Cell Biol.* **11**, 274–286.

Schwartz, M. A., Schaller, M. D., and Ginsberg, M. H. (1995). Integrins: Emerging paradigms of signal transduction. *Annu. Rev. Cell Biol.* **11**, 549–599.

Biography

Mark H. Ginsberg is a Professor in the Departments of Vascular and Cell Biology at the Scripps Research Institute, La Jolla, California. He was awarded an M.D. summa cum laude from SUNY Downstate Medical Center, and performed his internship, residency, and post-doctoral fellowship at the University of Chicago. He played an important role in the discovery and analysis of integrins, and has authored over 245 scientific publications, largely devoted to integrins. He has served on the editorial boards of many scientific journals and has received numerous awards.

Lawrence E. Goldfinger obtained a B.S. in Biology from Carnegie Mellon University and a Ph.D. in Cell Biology from Northwestern University Medical School. His research focuses on integrin-mediated intracellular signaling and the roles of integrins in cell adhesion, migration, and vascular remodeling.

Interferon Receptors

Christopher P. Elco and Ganes C. Sen
Cleveland Clinic Foundation and Case Western Reserve University, Cleveland, Ohio, USA

Interferons (IFNs) are a family of cytokines, or protein hormones, which modulate the immune response and provide resistance to viral infection. The effects of IFN are mediated through cell surface receptors, which recognize extracellular IFN and activate cellular signaling pathways, ultimately leading to gene induction and repression. IFNs are divided into two classes, type-I and type-II IFNs. There are multiple members of the type-I IFN family, including IFN-α and IFN-β, whereas IFN-γ is the only known type-II IFN. The two types of IFN bind to two distinct receptors and have very different cellular outcomes. Type-I IFN receptors predominantly activate an antiviral, innate immune response. Signaling through type-II IFN receptors, on the other hand, is involved in modulating the adaptive immune response. Both types of receptors share in common the ability to directly and quickly induce new gene transcription through the activation of JAK/STAT signaling pathways.

IFN receptors are classified as type-II cytokine receptors. Both type-I and type-II cytokine receptors have extracellular and intracellular domains connected by a single transmembrane domain. The extracellular domains of cytokine receptors contain a conserved tandem fibronectin type-III (FNIII) motif, which is distinguished by unique cystine pairings at both ends of the domain. Type-II cytokine receptors lack an additional conserved Trp-Ser-X-Trp-Ser motif, found in the extracellular domain of type-I receptors. Ligand binding to the receptor leads to receptor oligomerization and activation of a signaling cascade. In addition to type-I and type-II IFN receptors, the receptors for tissue factor and the cytokine IL-10 belong to this class. The IFN receptors and the IL-10 receptor are composed of two different subunits, both of which are required for proper functioning of the receptors.

IFN-γ Receptors

Expression of IFN-γ and Its Receptor

Expression of the IFN-γ receptor is common to almost all cell types with the exception of mature red blood cells. Two genes, IFN-γR1 and IFN-γR2, encode the receptor components.

The human IFN-γR1 gene is located on the long arm of chromosome 6. Expression of IFNγ-R1 mRNA is not regulated by any known stimuli, but appears to be under standard housekeeping controls. Although the IFN-γ receptor functions on the cell surface, a large intracellular reserve of IFN-γR1 is present in some cells at levels up to 2–4 times the amount of receptor present on the cell surface. This reserve serves to keep the surface level of IFN-γR1 constant.

The human gene for IFN-γR2 is located on chromosome 21. The mouse gene for IFN-γR2 is on chromosome 16. Study of the mouse gene promoter has revealed that it contains binding sites for a number of activated transcription factors, suggesting that unlike IFN-γR1, IFN-γR2 expression can be regulated. Both proteins must be expressed on the cell surface and associate in order for IFN-γ signaling to occur, but there is evidence that some T cells control their responsiveness to IFN-γ by modulating the cell surface expression of IFN-γR2.

Unlike the receptors, IFN-γ is expressed only in response to stimulus by antigen and only in cells of lymphoid origin, in particular, natural killer cells, macrophages, and some T cells. Once synthesized, IFN-γ is secreted and signals as a homodimer.

Receptor Structure

Both IFN-γR1 and IFN-γR2 have extracellular and intracellular domains, along with a single transmembrane domain, common to all type-II cytokine receptors. The sequences of extracellular domains can vary greatly among species causing highly species-specific IFN-γ binding. In contrast, intracellular domains of the IFN-γ receptor subunits are more conserved among species, and can be substituted freely. The intracellular domains mainly serve as a scaffolding structure for the interaction of downstream-signaling proteins and contain no enzymatic activity of their own. The IFN-γR1 is a 90 kDa glycoprotein consisting of 472 amino acid residues. The first 228 residues of the protein comprise the extracellular domain. IFN-γR1 has a 24 amino acid transmembrane domain and an intracellular domain that spans the C terminus from residues 252–472.

IFN-γR2 is a 62 kDa, 315 amino acid residue protein. Both the extracellular and transmembrane domains of IFN-γR2 are comparable in length to those of IFN-γR1. Residues 1–226 form the extracellular domain and 227–250 are the transmembrane domain. At only 65 amino acid residues, the intracellular domain of IFN-γR2 is much smaller than that of IFN-γR1.

The crystal structure of a soluble, truncated version of the extracellular domain of human IFN-γR1 is known. It contains two distinct domains, both consisting of two β-sheets and displaying FBNIII topology. An 11 amino acid linker connects the two domains. Binding of ligand is accomplished through the interaction of both domains.

Ligand Binding

IFN-γ binds to the extracellular domain of IFN-γR1 only. In the absence of IFN-γR1, IFN-γR2 cannot bind IFN-γ. However, the presence of IFN-γR2 does strengthen the association of IFN-γ and IFN-γR1 threefold, though the two subunits of the receptor do not associate in the absence of IFN-γ. Further, IFN-γR2 is vital for IFN-γ signal transduction, and for this a highly specific interaction must occur between the extracellular domains of IFN-γR1 and IFN-γR2.

An active signaling complex consists of an IFN-γ homodimer and two chains each of IFN-γR1 and IFN-γR2. Each subunit of the IFN-γ homodimer binds an IFN-γR1 chain, which in turn binds IFN-γR2. In the absence of IFN-γR2, IFN-γR1 molecules bound to an IFN-γ homodimer are separated by over 27Å and, therefore, are unable to interact with each other.

Signal Transduction

Janus tyrosine kinase (Jak)/Signal transducer and activator of transcription (STAT) signaling is carried out through a series of tyrosine phosphorylation events, at the receptor, mediated by members of the Jak family. Signaling culminates with the activation and nuclear translocation of STAT proteins, where they function to induce new mRNA synthesis. The IFN receptors serve as docking sites for both Jaks and STATs. With the formation of IFN-receptor complex, Jak proteins are brought into close proximity, which enables them to transphosphorylate and thereby activate each other. Independent of IFN binding to the extracellular domain of the receptor, the Jak proteins Jak1 and Jak2 associate with the intracellular domains of IFN-γR1 and IFN-γR2, respectively (Figure 1A). Upon the formation of a receptor complex with IFN-γ, Jak2 transphosphorylates Jak1 (Figure 1B). Jak1 then transphosphorylates Jak2 and either Jak phosphorylates IFN-γR1 at Tyr440 (Figure 1C). Phosphorylation of IFN-γR1 in turn leads to the recruitment and binding of a STAT1 protein to each IFN-γR1 chain. Bound STAT1 proteins are phosphorylated by the Jaks, disassociate from the receptor and form a homodimer (Figure 1D). This complex then translocates to the nucleus where it can induce the transcription of many genes.

STAT-dependent signaling is the best-studied IFN-γ signaling pathway, but there is evidence that STAT1-independent signaling pathways can also be activated by IFN-γ through IFN-γR1 and IFN-γR2. In cell lines lacking STAT1, activation of the IFN-γ receptor by IFN still causes the induction of a set of genes.

In order for signal transduction to occur normally, two regions of the intracellular domain of IFN-γR1 and one region of the intracellular domain of IFN-γR2 are required. The association of Jak1 with IFN-γR1 requires the amino acid residues from 266 to 269, LPKS, located in the membrane proximal region. Distal to the membrane at amino acids 440–444, YDKPH comprise the STAT1-binding site. Within the intracellular domain of IFN-γR2 a proline-rich 12 amino acid sequence P^{263}PSIPLQIEEYL^{274} is needed for Jak2 binding. Disruption of any of these three regions abolishes normal signaling.

Upon the binding of IFN-γ, the receptor complex is internalized. Internalized receptor–ligand complex is trafficked to an acidic compartment. IFN-γ disassociates from the receptor, goes to the lysosome, and is degraded, whereas the IFN-γR1 subunit of the receptor is recycled into the cytoplasmic reserve. Mutation of either Leu 270 or Ile 271 inhibits the internalization of the receptor, leading to the accumulation of IFN-γ ligand–receptor complexes on the surface of the cell.

Effects of Signaling Through the IFN-γ Receptor

IFN-γ can be thought of as the antimicrobial interferon. Signaling through type-II IFN receptors has pro-inflammatory effects and antibacterial effects. Mice lacking type-II IFN receptors have a much higher susceptibility to infection by bacteria and intracellular microbes. The antibacterial effects of IFN-γ are mediated through multiple pathways. IFN-γ leads to the activation of neutrophils, natural killer cells and in particular macrophages by increasing their ability to recognize, kill, and digest foreign material or microbes. In T cells, IFN-γ promotes the maturation of cytotoxic CD8 + T cells, as well as the T_H1 subset of CD4 + T cells. IFN-γ also enhances the humoral immune response by up-regulating genes such as class-I and class-II major histocompatibility complex (MHC) molecules, along with cell surface adhesion molecules. Together these effects serve to augment the adaptive immune response to pathogens.

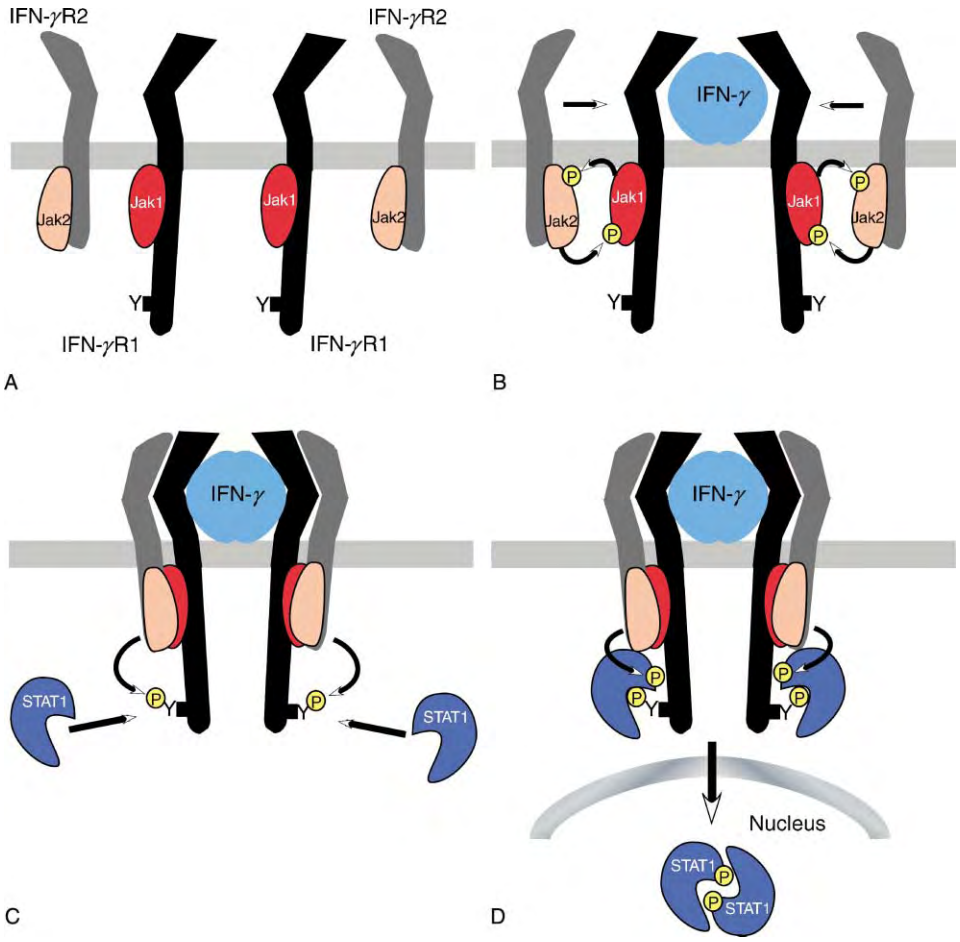

FIGURE 1 Kinetics of the IFN-γ signaling cascade ((A)–(D)), showing the proteins and tyrosine phosphorylation events involved in signal transduction by the IFN-γ receptor.

As would be expected, loss of the IFN-γ receptor genes leads to increased susceptibility to infection by microbes. Mice lacking the IFN-γ receptor genes are affected much more severely by infections with lysteria and mycobacteria. Otherwise, the receptor knockout mice display no developmental defects, have normal T cell responses and are no more susceptible to most viral infections than wild-type mice. These effects are seen in humans as well. Children susceptible to infections with weakly pathogenic mycobacteria species such as *M. avium* were found to have mutations in the IFN-γ receptor genes. The susceptibility was mycobacteria specific, as these children did not have increased difficulties fighting off infections from other bacteria, viruses, or fungi.

An unexpected consequence of IFN-γ receptor loss is an increased susceptibility to tumor development. IFN-γ receptor knockout mice develop tumors at a much higher frequency than their IFN-γ responsive counterparts. Compared to IFN-γ responsive tumors, IFN-γ unresponsive tumors are less prone to rejection when transplanted into immunocompetent wild-type mice. Studies of human carcinomas have revealed that loss of responsiveness to IFN-γ is not uncommon. Taken together, these facts suggest that loss of IFN-γ signaling enables tumors to evade the normal surveillance mechanisms of the immune system. Normal expression of the IFN-γ receptor proteins is therefore important in preventing the development of cancer.

The IFN-α/β Receptor

Expression of IFN-α/β and Their Receptor

Like the IFN-γ receptor, the IFN-α/β receptor is composed of two polypeptides encoded by two genes. Both IFN-α/β receptor genes, IFN-αR1 and IFN-αR2, are clustered on human chromosome 21 (or chromosome 16 in mice) with IFN-γR2 and IL-10R2 (also a member of the class-II cytokine family). Expression of

the receptor proteins is thought to be ubiquitous, but it can also be modulated.

The gene encoding IFN-αR1 is 32 kb and contains 11 exons. The second through ninth exons encode the extracellular domain of the protein, while the last two exons encode the transmembrane and intracellular domains.

In the case of IFN-αR2, there are three splice variants of the protein encoded by a nine-exon gene. The 515 aa, IFN-αR2c, encoded by a 4.5 kb mRNA, is the only functional splice variant and has an extended intracellular domain compared to the other two variants. IFN-αR2b has a shorter cytoplasmic domain and cannot signal through the Jak-STAT pathway, and IFN-αR2a is a secreted form of the extracellular domain of the receptor only. Studies in mice, which express only homologues of the 2a and 2c splice variants, have shown that the 2a variant is expressed in greater abundance in most tissues, except that of lymphoid origin where the two isoforms are expressed in a 1:1 ratio. It is not clear if the truncated splice variants play a functional role in modulating responsiveness to IFN; however, IFN-αR2a can act as a dominant-negative inhibitor for type-I IFN signaling.

There are many members of the type-I IFN family. The most well-known are IFN-α and IFN-β, which share little structural homology with each other. IFN-β was first isolated from fibroblasts, while IFN-α was discovered in lymphoid cells. Within the IFN-α family alone, there are over 13 subtypes encoded by different genes. The proteins they synthesize can vary in size from 15 to 21 kDa, and contain different degrees of posttranslational modification. Despite the apparent diversity in type-I IFNs, they all bind to the same receptor composed of IFN-αR1 and IFN-αR2c. There is, however, variation in the type and degree of response generated.

Receptor Structure

The extracellular domain of IFN-αR1 spans the first 409 aa residues of the protein, and the intracellular domain contains the final 100 residues from amino acid 431 to 530. IFN-αR1 is unique among class-II cytokine receptors in that its extracellular domain contains four tandem fibronectin type-III domains, compared to the two contained by other IFN receptor proteins. When compared to IFN-αR1, the 217 amino acid extracellular domain of IFN-αR2 is relatively short. In contrast, the intracellular domain of IFN-αR2c is much longer than that of IFN-αR1, covering the C-terminal 251 amino acids. There is not nearly as much known about the structure of IFN-α/β receptors as IFN-γ receptors.

Ligand Binding

Both IFN-αR1 and IFN-αR2 bind type-I IFNs, cooperatively. This is different from the IFN-γ receptor where only IFN-γR1 had ligand-binding activity. Also, the signaling complex for the α/β-receptor consists of a single pair of receptor proteins as opposed to the two pairs that compose the γ-receptor complex.

Another feature of the IFN-α/β receptors is their ability to bind multiple ligands. Unlike IFN-γ receptors, which only bind IFN-γ, the α/β-receptors can bind all subspecies of IFN-α, along with IFN-β and other type-I IFN species. Ligand-receptor interactions for the different classes of IFN are unique. By mutating residues in the extracellular portion of either receptor protein it is possible to generate mutants, which bind and respond to IFN-β, but not all IFN-α species. The exact structural mechanism for how the differences in ligand binding translate into differences in downstream signaling effects is still unknown.

Signal Transduction

Signaling again occurs principally through the Jak-STAT pathway, but involves different members of the two families of proteins. Independent of ligand binding, Tyk2 a member of the Jak family associates with IFN-αR1, while Jak1, STAT1, and STAT2 associate with IFN-αR2c (Figure 2A). The binding of ligand brings both receptor subunits into close proximity with each other. This allows Jak1 to transphosphorylate Tyk2 (Figure 2B). Tyk2 in turn phosphorylates Jak1 along with Tyr466 of IFN-αR1. The phosphorylation of Tyr466 of IFN-αR1 allows STAT2 to bind to it instead of IFN-αR2c. The IFN-αR1-bound STAT2 is phosphorylated on Tyr690 (Figure 2C). This leads to the STAT2-dependent phosphorylation of STAT1 on Tyr701. STAT1 and STAT2 dissociate from the receptor and form a heterodimer. The STAT1-STAT2 dimer associates with p48, or IRF9, a member of the interferon regulatory factor family, to form the transcription complex interferon-stimulated gene factor 3 (ISGF3). ISGF3 translocates to the nucleus, binds to interferon-stimulated regulatory element (ISRE) sequences present in the promoters of IFN-stimulated genes (ISGs) and induces transcription.

The binding sites for Jak and STAT proteins on IFN-α/β receptors have not been characterized as well as their IFN-γ receptor counterparts. Tyr 466 of IFN-αR1 along with surrounding residues is needed for STAT2 binding to the subunit. In the case of IFN-αR2c, the constitutive STAT2 binding site has been mapped to between amino acids 404 and 462. Further, multiple tyrosine residues throughout the intracellular domain of the IFN-αR2c are required for full signaling activation, but their precise role is still not fully known.

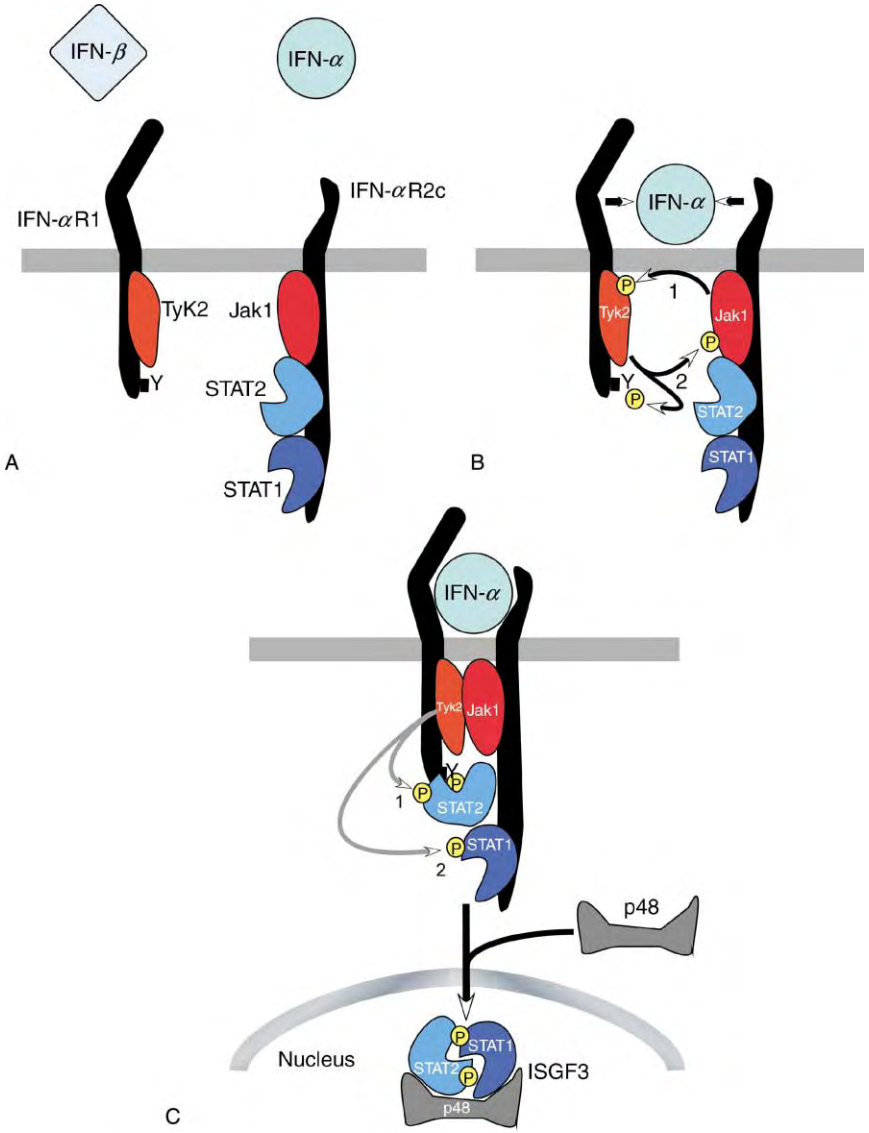

FIGURE 2 Signal transduction through the IFN-α/β receptor, showing the protein–protein associations and tyrosine phosphorylation steps involved. Numbers indicate the order in which tyrosine phosphorylation events (P) occur.

Effects of Signaling Through the IFN-α/β Receptor

Type-I IFNs are considered to be antiviral interferons. They provide a vital signal for cells to mount a state of antiviral defense. The antiviral state is achieved through the diverse actions of newly translated proteins made in response to the induction of hundreds of interferon stimulated genes by IFN signaling. ISGs encode proteins that have effects ranging from cell cycle arrest to the inhibition of translation and RNA degradation. Together these effects serve to make the cell a very unfavorable environment for viral replication. Not surprisingly, cell lines and mice defective in type-I IFN receptors are much more susceptible to viral infection.

See Also the Following Articles

Cytokines • JAK-STAT Signaling Paradigm

Glossary

cytokine receptor A cell surface protein that binds to a distinct extracellular polypeptide hormone and induces a response within the cell.

interferon Cytokines involved in regulating antiviral and immune responses.

kinase An enzyme that phosphorylates (adds a phosphate group to) a protein.

signal transduction The conversion of an extracellular signal to an intracellular response.

transphosphorylation The reaction by which one protein causes the addition of a phosphate group to another protein.

Further Reading

Abbas, A. K., Lichtman, A. H., and Pober, J. S. (1997). Cytokines. In *Cellular and Molecular Immunolgy*, 3rd edition, pp. 250–277. W.B. Saunders, Philadelphia.

Bach, E. A., Aguet, M., and Schreiber, R. D. (1997). The IFNγ receptor: A paradigm for cytokine receptor signaling. *Ann. Rev. Immunol.* **15**, 563–591.

Ikeda, H., Old, L. J., and Schreiber, R. D. (2002). The roles of IFNγ in protection against tumor development and cancer immunoediting. *Cytokine Growth Fact. Rev.* **13**, 95–109.

Mogensen, K. E., Lewerenz, M., Reboul, J., Lutfalla, G., and Uze, G. (1999). The type I interferon receptor: Structure, function, and evolution of a family business. *J. Interferon Cytokine Res.* **19**, 1069–1098.

Sen, G. C. (2001). Viruses and interferons. *Annu. Rev. Microbiol.* **55**, 255–281.

Stark, G. R., Kerr, I. M., Williams, B. R., Silverman, R. H., and Schreiber, R. D. (1998). How cells respond to interferons. *Ann. Rev. Biochem.* **68**, 227–264.

Biography

Ganes C. Sen is a member of the Professional Staff in the Department of Molecular Biology at the Cleveland Clinic Foundation, and Professor of Physiology and Biophysics, and Biochemistry at the Case Western Reserve School of Medicine. His principal research interests are in the role of the interferon system in host–virus interactions and in the tissue-specific functions of the angiotensin-converting enzyme. He received his Ph.D. from McMaster University, Canada and his postdoctoral training at Yale University. His research has made seminal contributions to the understanding of the modes of induction and the functions of many interferon-inducible genes.

Intermediate Filament Linker Proteins: Plectin and BPAG1

Peter Fuchs and Gerhard Wiche
University of Vienna, Vienna, Austria

Plectin and bullous pemphigoid antigen 1 (BPAG1) are among the best-characterized members of an emerging family of sequence-related cytoskeletal linker proteins (cytolinkers), referred to as plakins or plakin protein family. Originally, both proteins were identified on the basis of their association with intermediate filaments (IFs) or IF-anchoring structures, such as adhesive cell junctions. By anchoring IFs to themselves, to junctional complexes, and to the other major cytoskeletal networks of actin filaments and microtubules, both cytolinkers play crucial roles in maintaining cell and tissue integrity, and orchestrating dynamic changes in cytoarchitecture and cell shape. Plectin and BPAG1 are encoded by large genes that give rise to many different isoforms, each with unique functions and varying capacities to link different cytoskeletal systems. Due to their multi-domain structure and enormous size (300–800 kDa) these proteins bridge large distances and can serve as scaffolding platforms for the assembly, positioning, and regulation of complex protein machineries required for signaling and motor protein-based trafficking. Both proteins are involved in diseases affecting the skin, neuronal tissues, and skeletal as well as cardiac muscle.

Plectin

The first identification of plectin as an interaction partner of IFs was made in cultured cells. In fact, the choice of its name (from $\pi\lambda\varepsilon\kappa\tau\eta$, the ancient Greek word for network or meshwork) was motivated by its microscopic visualization as a dense cytoplasmic network array in cells.

Gene Locus and Isoform Diversity

In humans, the plectin gene is located on chromosome 8 (position q24), the murine orthologue on chromosome 15 (position 44.0 cM). The exon–intron organization of the plectin gene has been determined for man, mouse, and rat. Several plectin isoforms could be identified differing in their amino termini. In the case of the mouse gene alternative splicing of 11 different first exons into one common exon (exon 2) gives rise to a multiplicity of plectin variants (Figure 1). Additional alternative splicing in the 5′ area within the region coding for the actin-binding domain (ABD) increases the number of possible plectin isoforms. In rat tissues, plectin transcript variants were identified that lack a single large exon encoding almost the entire α-helical coiled coil rod domain of the molecule. Plectin isoforms are named after their alternative starting exons (plectin 1, plectin 1a, …, plectin 1j); however, the exact composition of the subsequent exons transcribed in each of the very large plectin mRNAs, especially in their very complex 5′ part, has not yet been determined with absolute certainty.

Expression and Subcellular Localization

With the exception of certain neurons, plectin has been found to be expressed in all mammalian cells investigated so far. It decorates different types of IFs, shows codistribution with their plasma membrane attachment sites, and colocalizes with actin structures, primarily in peripheral areas of cells. It is associated with Z-lines of striated muscle, dense plaques of smooth muscle, intercalated discs of cardiac muscle, the basal cell surface membrane (specifically hemidesmosomes) of keratinocytes, desmosomes of epithelial cells, and focal adhesion contact sites of cells in culture. Plectin has also been identified in cell layers separating tissues from fluid-filled cavities like liver bile canaliculi, gut villi, kidney glomeruli, and endothelial cells of blood vessels. The expression patterns of plectin isoforms can vary considerably among different tissues and cell types. The quantitation of mRNAs isolated from different organs of the mouse revealed low expression levels of plectin isoforms 1, 1e, 1g, 1h, 1i, and 1j, intermediate levels of plectin 1f, and high levels of plectin 1a, 1b, 1c, and 1d. In the majority of these preparations all plectin isoforms could be identified, except for plectin 1d, found predominantly in skeletal muscle and heart, and plectin 1c, which is more or less restricted to neuronal tissues

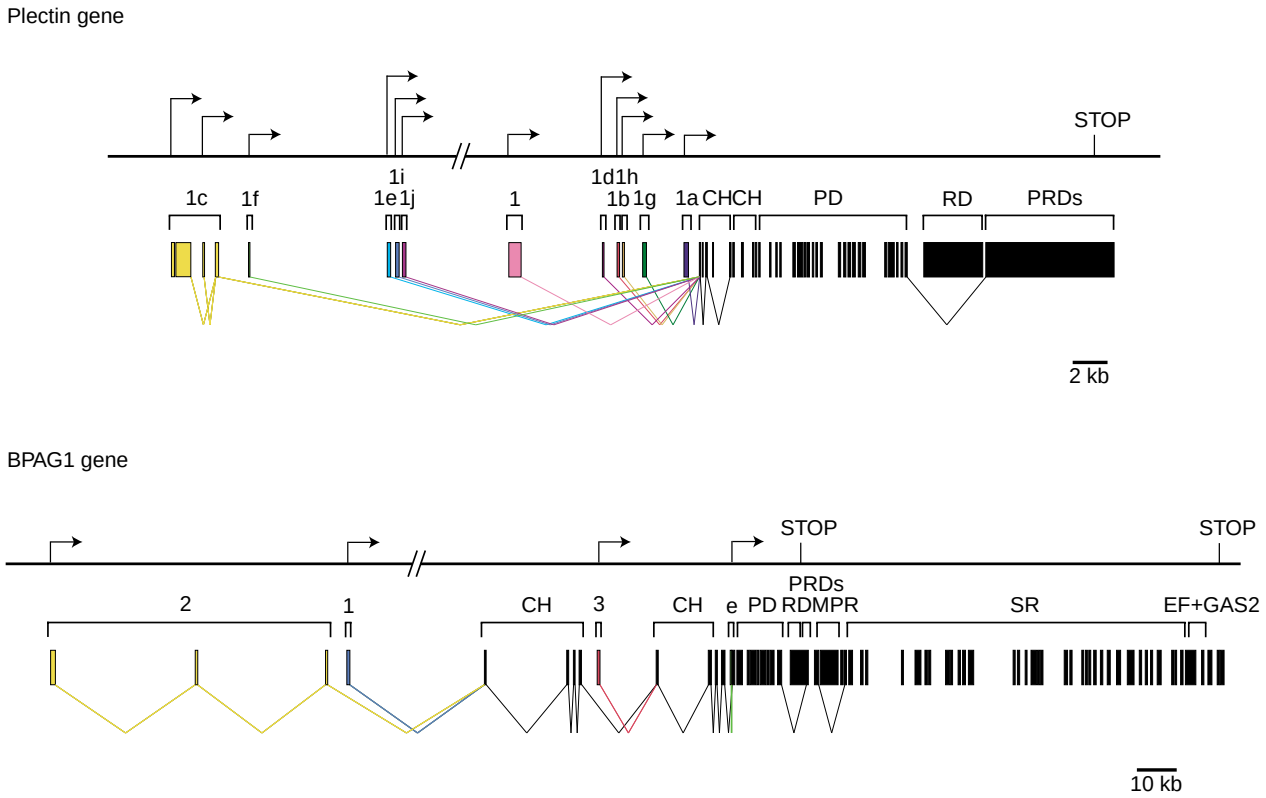

FIGURE 1 Plectin and BPAG1 gene structure and alternative splicing. Schematics shown represent murine plectin and human BPAG1 species (BPAG1, modified from Röper, K., Gregory, S. L., and Brown, N. H. (2002). The "Spectraplakins": cytoskeletal giants with characteristics of both spectrin and plakin families, *J. Cell Sci.* **115**, 4215–4225, with permission of The Company of Biologists Ltd). Alternative transcriptional start sites (arrows) and stop codons are indicated. Alternative starting exons are shown as colored boxes, other exons as black boxes. Splicing is indicated by bended lines for alternative starting exons or when exons are bypassed. Alternative single first exons and combinations of starting exons are designated with numbers and/or small letters, protein domains with capital letters. CH, calponin-homology domains forming the ABD; PD, plakin domain; RD, coiled-coil rod domain; PRDs, plakin repeat domains; MPR, modules of plectin repeats; SR, spectrin repeats; EF + GAS2, EF-hand domains and GAS2 domain. Note that in the case of plectin isoform 1c two transcriptional start sites at the beginning of non-coding exons are used with only one 1c-specific coding exon in front of the subsequent exon common to all plectin isoforms.

and skin. In cultured keratinocytes the two major isoforms expressed, plectin 1a and plectin 1c, were found differentially distributed to hemidesmosomes and to microtubules.

Structural Properties

Considering just full-length versions of the protein, plectin has a molecular mass of 506–535 kDa depending on its first coding exon (Figure 2). The molecule has been visualized by electron microscopy as a dumbbell-shaped structure composed of a central rod domain flanked by two large globular domains. In these structures two plectin polypeptide chains most likely are arranged in parallel forming an α-helical coiled-coil central rod. The so-called plakin domain, the defining feature of plakin protein family members, and an ABD of the "classical" CH1-CH2-type (i.e., containing two calponin-homology domains) reside within the N-terminal part of each chain, preceding the rod-forming segment. The C-terminal part of plectin comprises six tandemly arranged so-called plakin-repeat domains, each containing a globular core structure, or module, and a surface-exposed linker domain. Plectin modules, similar to those of other plakins, consist of four complete and one incomplete tandem copies of a 38 residues-long sequence motif, referred to in databases as plectin repeat. Forming a β-hairpin followed by two antiparallel α-helices, the plectin repeat structurally resembles a motif called ankyrin repeat, which is found in a large number of proteins. It should be noted that plectin isoforms that are encoded by transcripts starting with non-coding first exons, such as plectin 1h, 1i, and 1j, contain only truncated versions of plectin's ABD (Figure 2).

Molecular Interactions

Plectin binds to cytoplasmic IFs of different types via direct interaction with their subunit proteins, including vimentin, desmin, GFAP, neurofilament proteins, and cytokeratins; binding has also been demonstrated to

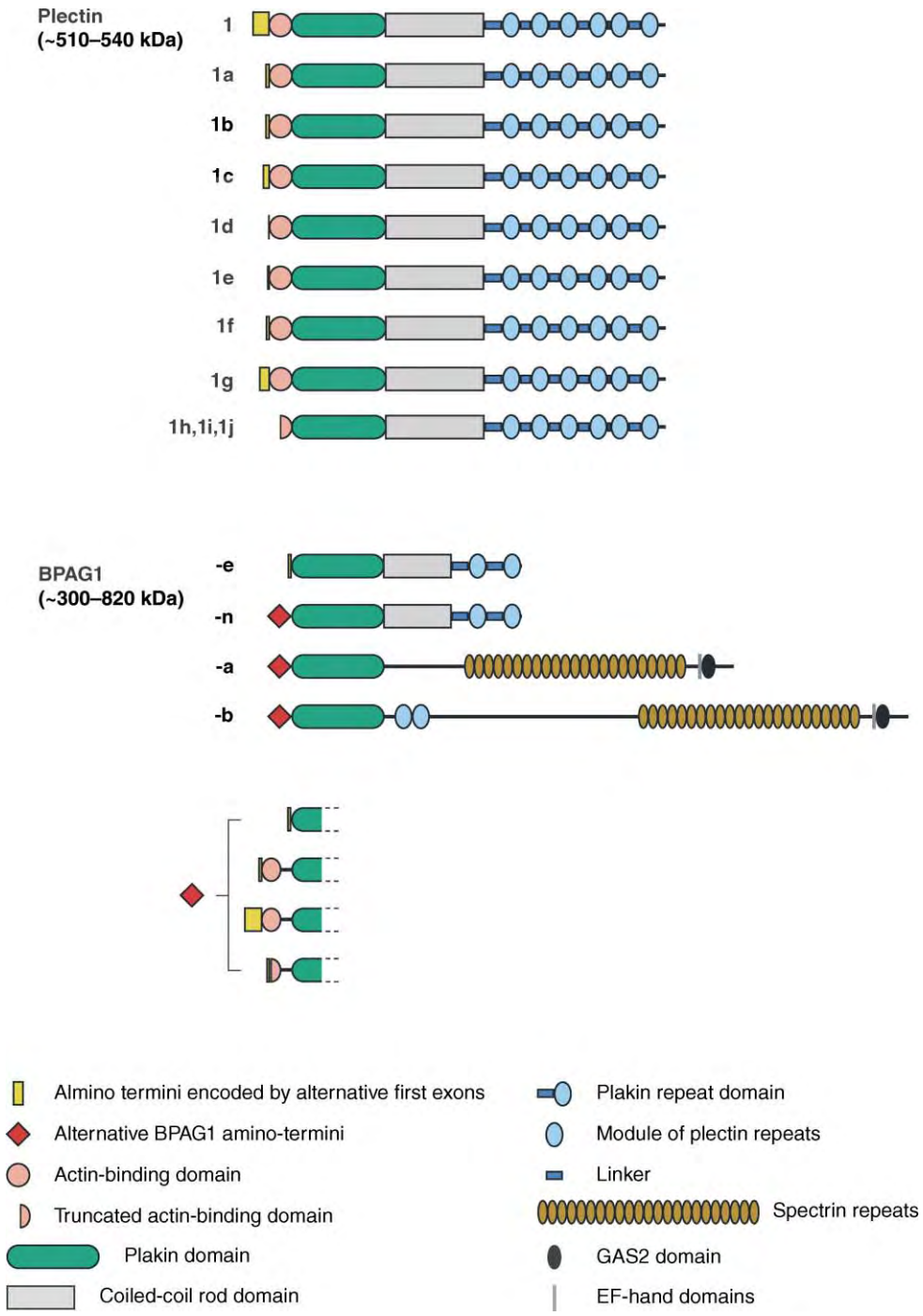

FIGURE 2 Schematic diagram of plectin and BPAG1 protein isoforms. Designation of isoforms (e.g., plectin 1a, BPAG1-e) and approximate molecular weight are given (drawings are at scale). The diamond (red) in front of BPAG1-n, -a, and -b stands for the four possible alternative amino termini shown underneath; in the case of BPAG1-n one of these possibilities is already presented as BPAG1-e. Note that in some variants of both proteins the ABD, typically consisting of two calponin-homology domains, can be truncated due to alternative splicing, resulting in only one calponin-homology domain to be present in certain BPAG1 isoforms. The plakin domain is an interaction domain organized into α-helical bundles showing structural similarities to spectrin repeats. The plakin repeat domains each contain a globular module and a linker domain. Modules consist of four complete and one incomplete plectin repeats forming a complex globular domain. Linkers are considered as surface-exposed interaction domains, such as the IF binding site of plectin. The GAS2 domain was named after the growth-arrest-specific protein 2 and is suggested to mediate microtubule binding.

the nuclear IF protein lamin B. The major binding site for IF subunit proteins has been mapped to a short sequence in the linker segment between modules 5 and 6 in plectin's C-terminal domain. The ABD in plectin's N-terminal globular domain is fully functional, as demonstrated *in vitro* and *in vivo*. Whether this is true also for plectin isoforms expressing only truncated versions of this domain remains to be shown. In addition to its actin-binding function, the ABD serves as docking site for the β4 subunit protein of the hemidesmosomal $\alpha 6\beta 4$ integrin receptor and for the signaling molecule PIP2. Furthermore, it dimerizes by self-interaction. Additional integrin β4 binding sites have been ascribed to plectin's plakin domain and to its C-terminal globular domain. The plakin domain of plectin harbors also a binding site for BPAG2/BP180, another hemidesmosomal protein. There is broad consent about plectin having the capacity to bind to microtubules. In fact, a direct interaction of the protein with microtubule-associated proteins (MAPs) has been demonstrated, although the molecular domain(s) involved need to be identified. Plectin also interacts with the subplasma membrane skeleton proteins α-spectrin and fodrin and with the desmosomal protein desmoplakin. In line with the emerging concept that cytolinkers act as a platform for the assembly of complex protein machineries required for intracellular signaling and trafficking, plectin has been shown to be a target for a variety of serine/threonine kinases, including mitotic $p34^{cdc2}$ kinase, and to interact, via its plakin domain, with the non-receptor tyrosine kinase Fer. The question whether the isoform-specific protein sequences located at the aminoterminus of plectin variants can select for distinct binding partners or influence the affinities of other binding sites remains to be answered.

Plectin Deficiency in Man and Mouse

In humans, mutations in the plectin gene lead to the autosomal recessive disease epidermolysis bullosa simplex with muscular dystrophy (EBS-MD). Patients affected suffer from severe skin blistering and late-onset muscular dystrophy. In all the cases described, plectin expression is missing or substantially attenuated. The autosomal-dominant disease epidermolysis bullosa simplex Ogna (EBS-O), first described for a family from the Norwegian municipality of Ogna, is due to a site-specific mutation causing the exchange of a single amino acid residue (W to R) in plectin's long-rod domain. In this case, patients suffer from generalized skin fragility but show no muscular symptoms. Disruption of the plectin gene in the mouse using knockout strategies results in a phenotype similar to EBS-MD, except that plectin knockout mice die 2–3 days after birth, probably due to their severe skin blistering. In addition, already at this early stage they show an increase in the number of necrotic fibers and abnormal Z-lines in skeletal muscle.

Bullous Pemphigoid Antigen 1

Bullous pemphigoid antigen 1 (BPAG1) was originally identified in a search for antigens with immunoreactivity to autoantibodies of patients suffering from bullous pemphigoid, an autoimmune subepidermal skin blistering disease. The murine orthologue is also called dystonin, in consideration of the fact that mutations in this gene cause sensory neuron degeneration in the mouse mutant *dystonia musculorum* (*dt*).

Gene Locus and Isoform Diversity

The BPAG1 gene is localized in humans on chromosome 6 at position p12-p11. In mice, where in genebanks it is referred to as dystonin, it has been mapped to chromosome 1 at position 16.5 cM. In both species, multiple exons in the BPAG1 gene are the basis of several protein isoforms generated by alternative splicing of transcripts. Amongst many possibly expressed isoforms, four major variants (BPAG1-a, -b, -e, and -n) were specified, showing clear differences in length and structure (Figure 1). It should be noted, however, that the two large isoforms BPAG1-a and -b were identified only recently, and that the missing level of awareness concerning these proteins may have led to some incorrect conclusions regarding BPAG1-e and -n in the older literature. Moreover, similar to plectin, the exact composition of exons transcribed in some of the very large BPAG1 mRNAs has yet to be defined.

Expression and Subcellular Localization

The major isoform of the BPAG1 gene, BPAG1-e, is expressed in basal epithelial cells where it is primarily located at hemidesmosomes. BPAG1-a is expressed at high levels in the nervous system, especially in dorsal root ganglia and spinal cord, while BPAG1-n/dystonin, previously thought to be the dominant isoform in this tissue, seems to be minor compared to BPAG1-a. The BPAG1-b isoform has been found in developing mouse embryos to be restricted to heart, skeletal muscle, and bone cartilage of the vertebrae.

Structural Properties

The molecular mass of the BPAG1 isoforms characterized to date is 302 kDa for BPAG1-e, 344 kDa for BPAG1-n, 615 kDa for BPAG1-a, and 824 kDa for BPAG1-b (Figure 2). All four isoforms show clear structural divergence. BPAG1-e contains a coiled-coil

rod domain flanked by an amino-terminal plakin domain and a carboxy-terminal region comprising two plakin-repeat domains. BPAG1-n is similar to BPAG1-e, but contains an additional amino-terminal ABD of the CH1-CH2-type. It is truncated in one variant, however, and contains only one calponin-homology domain. BPAG1-a, starting with an ABD followed by a plakin domain, resembles BPAG1-n at its amino terminus, but differs regarding the rest of the molecule. Its rod domain consists of 23 spectrin repeats and its carboxy-terminal domain contains EF-hand Ca^{2+}-binding motifs followed by a region including the so-called GAS2 domain. BPAG1-b comprises structural features similar to BPAG1-a, except for an additional pair of closely adjoining plectin repeat modules located between the plakin domain and the spectrin repeats.

Molecular Interactions

The large size and the structural diversity of BPAG1 isoforms suggest not only a variety of interaction partners but also different sets of binding partners for each isoform. Via the CH1-CH2-type ABD at their amino-terminal ends, BPAG1 isoforms can associate with filamentous actin. However, one of the BPAG1-n isoforms of BPAG1, which due to alternative splicing within the ABD contains only one of the two calponin-homology domains, lacks this ability (Figure 2). This truncation has been suggested to activate a microtubule-binding site located within the plakin domain of BPAG1 that otherwise remains cryptic. Since the tail regions of BPAG1-a and -b contain a GAS2-related domain, suggested to be involved in microtubule binding, it has been proposed that these BPAG1 variants possess an alternative microtubule-binding domain close to their carboxy terminus. The location of IF-binding sites within the carboxy-terminal plakin-repeat domains of BPAG1-e and -n has been confirmed for keratin and neuronal IFs. Additional binding partners of BPAG1's plakin domain are BPAG2 (*alias* BP180 or type XVII collagen), a transmembrane protein found in hemidesmosomes, and ERBIN, a specific Erb-B2 tyrosine kinase receptor-binding protein. Whether the carboxy-terminal Ca^{2+}-binding motifs of BPAG1-a and -b are functional remains to be shown.

BPAG1 Deficiency in Mouse

In mice, deletions in the BPAG1 gene cause an autosomal recessive neuropathy called *dystonia musculorum* (*dt*). At the age of 1–2 weeks homozygous *dt* mice display progressive loss of limb coordination caused by degeneration of sensory neurons. Dorsal root ganglia axons exhibit disorganization of neuronal IFs and microtubule networks accompanied by abnormal axonal myelination and axonal swelling(s). It has been suggested that this axonal swelling results from defective axonal transport caused by microtubule disorganization. In addition, defects in the functions of Schwann cells and muscle have been reported for these mice. Not all *dt* mouse strains, however, lack the BPAG1-e isoform. Independent of the *dt* mice most of which carry spontaneously arisen BPAG1 mutations, a BPAG1-defective mouse strain was generated using gene targeting techniques. This mutation eliminates the exons encoding the plakin domain of BPAG1 (common to all four isoforms) and therefore is considered as null allele. Besides the phenotype already described for *dt* mice, these knockout mice show fragility of skin upon mechanical stress. Based on these findings it is assumed that BPAG1-e is responsible for the observed skin abnormalities, the absence of BPAG1-a accounts for the neuronal deficits and the lack of BPAG1-b could be the reason for muscle defects. No known human disease has been linked to mutations in the BPAG1 gene to date. The role of autoantibodies against BPAG1 in patients suffering from bullous pemphigoid remains obscure.

See Also the Following Articles

Actin-Related Proteins • Intermediate Filaments • Keratins and the Skin • Microtubule-Associated Proteins

Glossary

alternative splicing Mechanism to create different proteins (protein isoforms) from the same mRNA transcript by splice events using different exons or exon combinations.

cytoskeleton Network of protein filaments in eukaryotic cells that determines and influences cell shape and enables movement. Main components are actin filaments, microtubules, and intermediate filaments.

knock-out mouse Mutated mouse line generated by the use of embryonic stem (ES)-cell technology in combination with genetic methods. Knock-out mice normally harbor one or more defined mutations in genes leading to inactivation of the gene product.

plakin protein family The plakin protein family, also referred to as the plakins, to date comprises plectin, BPAG1, desmoplakin, envoplakin, periplakin, and epiplakin. Plakins are structurally and functionally related proteins connecting cytoskeletal elements to each other and to the plasma membrane. Common to all family members is the presence of at least one of two structurally highly conserved protein domains, the so-called plakin domain and the PRD. An alternative designation suggested for plakins, i.e., cytolinkers (an abbreviation for cytoskeletal linker protein), is now being used to more broadly specify proteins with functions similar to those of plakins independently of sequence homology.

protein isoforms Variant forms of protein products stemming from a single gene brought about by, for example, alternative splicing.

Further Reading

Coulombe, P. A. (2002). A new fold in an old story: Attachment of intermediate filaments to desmosomes. *Nat. Struct. Biol.* **9**, 560–562.

Fuchs, E., and Karakesisoglou, I. (2001). Bridging cytoskeletal intersections. *Genes Develop.* **15**, 1–14.

Janda, L., Damborsky, J., Rezniczek, G. A., and Wiche, G. (2001). Plectin repeats and modules: Strategic cysteines and their presumed impact on cytolinker functions. *BioEssays* **23**, 1064–1069.

Leung, C. L., Green, K. J., and Liem, R. K. (2002). Plakins: A family of versatile cytolinker proteins. *Trends Cell Biol.* **12**, 37–45.

Röper, K., Gregory, S. L., and Brown, N. H. (2002). The "Spectraplakins": Cytoskeletal giants with characteristics of both spectrin and plakin families. *J. Cell Sci.* **115**, 4215–4225.

Steinböck, F., and Wiche, G. (1999). Plectin: A cytolinker by design. *Biolog. Chem.* **380**, 151–158.

Wiche, G. (1998). Role of plectin in cytoskeleton organization and dynamics. *J. Cell Sci.* **111**, 2477–2486.

Biography

Gerhard Wiche is a Professor and Chair of the Department of Biochemistry and Molecular Cell Biology at the University of Vienna, in Vienna, Austria. His principal research interest is in the mammalian cytoskeleton and its role in cellular morphogenesis, signaling and disease. He holds a Ph.D. from the University of Vienna Medical School. He received his postdoctoral training at the former Roche Institute of Molecular Biology in Nutley, New Jersey, and at the University of California, Berkeley. He has authored many papers on cytolinker proteins, including key publications on plectin, such as first identification, cloning and sequencing, identification of human mutations, and gene ablation in mice.

Peter Fuchs is a Senior Postdoctoral Fellow in G.W.'s laboratory at the University of Vienna.

Intermediate Filaments

Kelsie M. Bernot and Pierre A. Coulombe
The Johns Hopkins University School of Medicine, Baltimore, Maryland, USA

Intermediate filaments (IFs) are intracellular fibrous polymers that became a prominent constituent of the cytoskeleton coinciding with the appearance of multicellular life. They are readily distinguishable from actin microfilaments (6–8 nm) and microtubules (25 nm) by virtue of their diameter (10–12 nm). In mammals, >67 genes encode proteins able to self-assemble into IFs. A small subset of these encode lamins, the building blocks of the nuclear lamina, whereas all others encode cytoplasmic proteins. A major function shared by all IFs is to endow cells and tissues with a unique ability to resist trauma – this contribution is important in structures (e.g., axons and nuclei), cells, and tissues exposed to significant stress. Additional important functions are manifested in a sequence- and context-specific manner.

Features of Intermediate Filament Proteins

As a group, IF proteins are very heterogeneous in size (40–240 kDa), charge, and various other properties (Table I). The property of self-assembly is hard-wired into the characteristic tripartite domain structure shared by all IF proteins (Figures 1A and 1B). The central domain, an extended α-helix featuring long-range heptad repeats interrupted at three conserved locations, is the main determinant of self-assembly. This "rod" domain comprises 310 and 352 amino acids in cytoplasmic and nuclear IF proteins, respectively, and is bordered by invariant, signature ~15-mer sequences. Flanking sequences at the N and C termini of the rod domain are key in conferring each IF protein its individuality. Most IFs are heteropolymeric *in vivo*, although several IF proteins can *de facto* self-assemble into filaments as homopolymers *in vitro*.

Almost all metazoans (animals) contain both nuclear and cytoplasmic IFs, with the notable exception of arthropods, which contain only lamins. The presence of an exoskeleton, along with an increased density of microtubules in cells subjected to stress, may account for the absence of cytoplasmic IFs in arthropods. Phylogenetic analyses suggest that IFs initially appeared in the nucleus and later moved to the cytoplasm during evolution. IFs have not been found in plants, fungi, or protists. Most IFs are intracellular proteins; rare exceptions are the hagfish IFs, which are secreted polymers.

Assembly, Structure, and Regulation of Intermediate Filaments

Assembly and Structure

Owing to the long-range heptad repeats present within their central α-helical domain, IF proteins readily dimerize through coiled-coil interactions. In the dimer, individual rod domains are aligned in parallel (due to specific electrostatic interactions) and in register (owing to controlled nucleation by a "trigger motif") (Figure 1B). Nuclear and cytoplasmic IFs differ in the formation of tetramers. Lamin dimers associate in a head-to-tail fashion to form thin longitudinal strands, several of which laterally associate with an antiparallel orientation to form mature filaments. Dimers of cytoplasmic IFs, on the other hand, interact along their lateral surfaces with an antiparallel orientation to form compact tetramers. These tetramers continue to favor lateral interactions as they further polymerize to form ~60 nm long "unit-length filament" (ULF). Annealing of ULFs produces mature 10–12 nm filaments whose length can reach >10 μm (Figure 1C). Mature IFs lack an obvious structural polarity (see Figure 1B), reflecting the antiparallel orientation of dimers within them. While models for "idealized IFs" usually include 32 monomers per filament cross-section, determinations of mass per unit length revealed that, in actuality, this number can vary depending on the source and type of IFs. This heterogeneity is still unexplained. There is as yet no satisfactory model for the high-resolution structure of IFs.

Unlike actins and tubulins, IF proteins do not bind or metabolize nucleotides. They do not require an external input of energy or cofactor for assembly *in vitro*. They readily assemble into filaments when ectopically expressed in virtually any cell type in culture, suggesting that the process does not require specialized factors *in vivo*. Cytoplasmic IF networks often extend from the perinuclear area to the cell periphery, although there are

TABLE I

The Intermediate Filament Protein Family

IF type	Protein name	No. genes	Protein (kDa)	Assembly group[a]	Tissue distribution	Association with human disease[b]
I	Keratins (acidic)	>25	40–64	A	Epithelia	Multiple skin fragility diseases
						Oral and cornea fragility diseases
						Hair disorders
						Inflammatory bowel disease[c]
						Cryptogenic cirrhosis[c]
II	Keratins (basic)	>24	52–68	A	Epithelia	Nearly identical to type I keratins
III	Vimentin	1	55	B	Mesenchyme (esp early develop.)	None known
	Desmin	1	53	B	Muscle	Distal myopathy; cardioskelet. myop.
	GFAP	1	50–52	B	Astrocytes/Glia	Alexander's disease
	Peripherin	1	54	B	PNS neurons	None known
	Syncoilin	1	54	B	Muscle	None known
IV	NF-L	1	62	B	CNS neurons	Charcot-Marie-tooth disease
	NF-M	1	102	B	CNS neurons	Parkinson's disease[d]
	NF-H	1	110	B	CNS neurons	Amyotrophic lateral sclerosis
	α-Internexin	1	66	B	CNS neurons	None known
V	Lamin A/C	1	72/62	C	Differentiated tissue (nucleus)	Muscular dystrophy variants ($n = 2$)
						Dilated cardiomyopathies ($n = 2$)
						Familial partial lipodystrophy
						Mandibular acrodysplasia
						Charcot-Marie-tooth disease
						Premature aging conditions ($n = 2$)
	Lamin B1	1	65	C	Ubiquitous (nucleus)	
	Lamin B2	1	78	C	Ubiquitous (nucleus)	
Orphan	Nestin	1	240	B	Heterogeneous	None known
	Synemin	1	182	B	Muscle	None known
	Desmuslin	1	140	B	Muscle	None known
	Phakinin/CP49	1	46	D	Lens	Juvenile and congenital cataracts
	Filensin/CP115	1	83	D	Lens	None known

[a] Within each group proteins heteropolymerize in either an obligatory or facultative fashion to form filaments.
[b] Mutations affecting IF coding sequences are causative in the diseases listed unless indicated otherwise.
[c] Mutations in either K8 or K18 have been identified as risk factors for these conditions.
[d] Association needs to be confirmed in additional patients.

many instances in which IFs are concentrated in specialized regions of the cell. Such is the case for keratins in polarized epithelial sheets, desmin in myocytes, and neurofilaments in axons. In the cytoplasm, IFs can interact with F-actin, microtubules, and specific adhesion-mediating complexes. While the relative importance of these interactions varies between IF proteins and cell types, their dominant influence on IF organization has been established though experiments in which these other cytoskeletal complexes were disrupted.

Regulation

Both nuclear and cytoplasmic IFs are disassembled and/or profoundly reorganized during mitosis. Both of them can also be dynamically remodeled under steady-state conditions in non-cycling cells. *In vivo* experiments utilizing green fluorescent protein (GFP)-tagged vimentin or keratin suggest that filament formation is initiated at the cell periphery, whereas the subunit exchange fueling steady-state dynamics possibly occurs along the filament wall. More information about

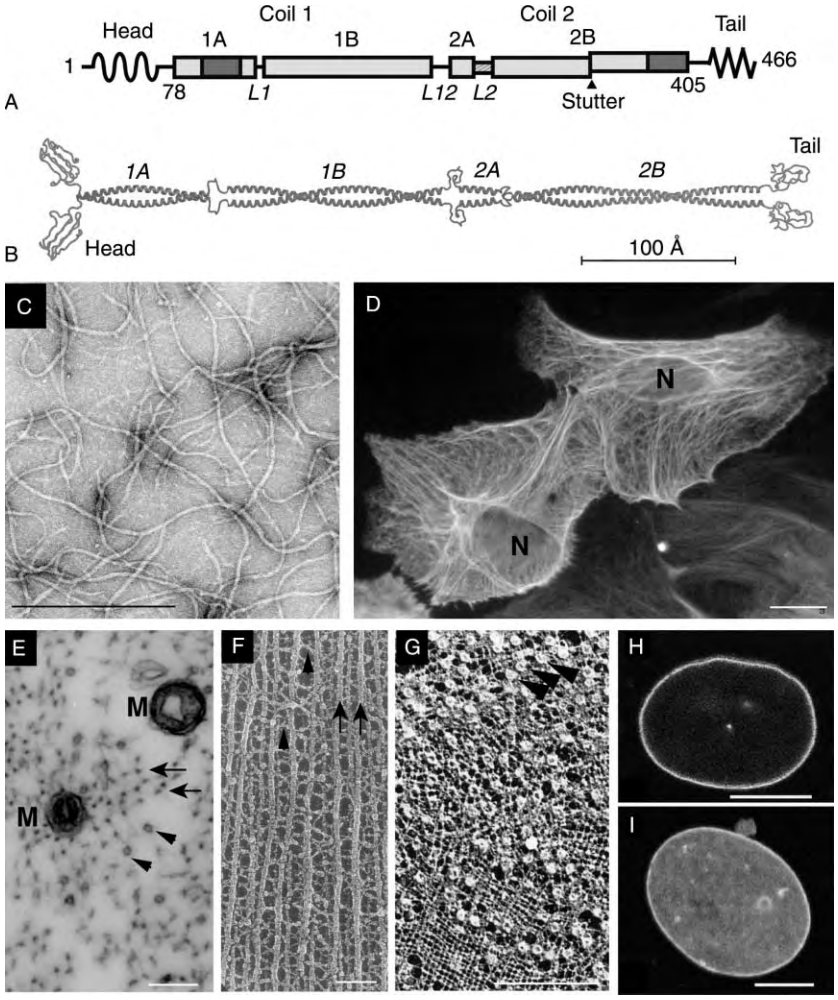

FIGURE 1 (A) Diagram illustrating the domain substructure of IF proteins. Rectangles depict central α-helical rod domain (1A, 1B, 2A, 2B) separated by short, non-helical linkers (L1, L12, L2). The rod domain is flanked by non-helical head and tail domains. Two highly conserved regions critical for the nucleation of coiled-coil dimer formation ("trigger motifs") are darkly shadowed. The numbers represent amino acid residues in human vimentin. (From Strelkov, S. V., Herrmann, H., and Aebi, U. (2003). Molecular architecture of intermediate filaments. *Bioessays* **25**, 243–251, with permission of John Wiley & Sons, Inc.) (B) Diagram illustrating the architecture of the human vimentin dimer, as determined by X-ray crystallography (1A and 2B subdomains, dark gray) or modeling (light gray). (From Strelkov, S. V., Herrmann, H., and Aebi, U. (2003). Molecular architecture of intermediate filaments. *Bioessays* **25**, 243–251, with permission of John Wiley & Sons, Inc.) (C) Keratin IFs reconstituted *in vitro* from purified proteins and visualized by negative staining and electron microscopy. These filaments appear as smooth-surfaced, apolar, flexible polymers of ~11 nm in width and several micrometers in length. Bar equals 250 nm. (D) Visualization of keratin IFs by indirect immunofluorescence in primary cultures of mouse skin keratinocytes. The filaments form a network extending from the surface of the nucleus (N) to the cytoplasmic periphery in these two cells. Bar equals 30 μm. (E and F) Visualization of neurofilaments in axon processes. (E) Thin-section transmission electron microscopy, showing neurofilaments viewed in cross-section. Neurofilaments (arrows), microtubules (arrowheads), and mitochondria (M) can be distinguished. Bar equals ~250 nm. (F) Quick-freeze deep-etch electron microscopy of axoplasm along its main axis. Neurofilaments (arrows) fill the axoplasm, and numerous cross-bridges (arrowheads) between the filaments can be seen. Bar equals 100 nm. (From Hirokawa, N., Glicksman, M.A., and Willard, M.B. (1984). Organization of mammalian neurofilament polypeptides within the neuronal cytoskeleton. *J. Cell. Biol.* **98**, 1523–1536, with permission of The Rockefeller University Press.) (G–I) Visualization of lamins in the nucleus. (G) Native nuclear lamina of *Xenopus* oocytes. Preparation of Triton X-100-extracted nuclear envelope by freeze-dried/metal-shadowing reveals the meshwork "basket weave" of the nuclear lamina and the array of nuclear pore complexes (arrowheads). Bar equals 1 μm. (From Aebi, U., Cohn, J., Buhle, L., and Gerace, L. (1986). The nuclear lamina is a meshwork of intermediate-type filaments. *Nature* **323**, 560–564, with permission.) (H and I) GFP-tagged Lamin B (H) or A (I) was introduced into mouse embryonic fibroblasts. Live cells in interphase show bright fluorescence around the nuclear rim while a fainter "veil" of fluorescence is visible in the nucleoplasm. Bar equals 10 μm. (From Moir, R.D., Yoon, M., Khuon, S., and Goldman, R.D. (2000). Nuclear lamins A and B1: different pathways of assembly during nuclear envelope formation in living cells. *J. Cell. Biol.* **151**, 1155–1168, with permission of The Rockefeller University Press.)

these crucial aspects of IF biology is needed. Posttranslational modifications play a key role toward the regulation of the assembly and disassembly of IFs *in vivo*, and of their interaction with associated proteins. Thus, all IF proteins are subject to phosphorylation, and the kinase, target site(s) and significance have been deciphered in many instances. The molecular basis of steady-state polymer dynamics, which have been tied to nucleotide

metabolism for F-actin and microtubules, remain unresolved for IFs. Possibly, rapid cycles of IF protein phosphorylation–dephosphorylation could enact the reversible conformational change needed. In addition, specific IF proteins have been shown to be O-glycosylated or modified in other ways, although the underlying significance is unclear. Lamins undergo lipid modification and enzymatic processing of their C terminus, reflecting their association with the inner nuclear membrane.

Dissecting the IF Superfamily

Most of the >67 genes forming the IF superfamily can be easily classified to one of five sequence types based on gene structure and nucleotide homology over the central α-helical domain. Individual members within each sequence type are often related in their tissue distribution. The remaining sequences defy classification and have been assigned to a sixth, orphan group of sequences.

Type I and Type II Keratins

Type I and type II IFs are part of the keratin (or cytokeratin) family of proteins found in all epithelia. The human and mouse genomes have >50 functional keratin genes, with a slightly larger number of type I keratin genes (see Table I). Type I keratins (K9-K21, K23, Ha1-8) are smaller and acidic compared to the larger, neutral-basic type II keratins (K1-K8, Hb1-6). Keratin assembly proceeds strictly from type I–type II heterodimers, accounting for the duality of sequences as well as their pairwise regulation *in vivo*. While any combination of purified type I and type II keratin proteins yields a fibrous polymer *in vitro*, specific pairs are coregulated in a fashion directly related to epithelial tissue type and/or differentiation state *in vivo*. In mammals, specific type I–type II gene pairings occur in simple (e.g., liver, GI tract), complex (e.g., skin, oral mucosa) and hard epithelia (e.g., hair, nail), with little overlap. Quite remarkably, moreover, specific type I–type II gene pairs are differentially and sequentially expressed in progenitor (mitotically active), early, and late differentiation stages in a host of epithelia. The conservation of keratins in terms of primary structure and distribution suggests an important role in epithelial diversity – this role has yet to be defined and does not lie in the execution of differentiation.

Type III Intermediate Filaments

The type III group consists of vimentin, desmin, GFAP, peripherin, and syncoilin (Table I). Vimentin is widely expressed during development, but typically gives way to other IF proteins during differentiation. Accordingly vimentin, which is assembly competent on its own, is usually found in co-polymers with other type III, type IV, or orphan sequences in mature cell types. Vimentin persists as the dominant cytoplasmic IF protein in fibroblasts, endothelial cells, adipocytes, macrophages, lymphocytes, and neutrophils. Desmin is found in the cytoplasm of smooth muscle and is concentrated at the Z lines of skeletal and cardiac muscle. Several variants of glial fibrillary acidic protein (GFAP) arise from a single precursor mRNA, and occur in the astrocytes of the central nervous system and in Schwann cells of the peripheral nervous system (PNS). Peripherin occurs in the post-mitotic neurons of the PNS, whereas syncoilin is an intrinsic component of the dystrophin-associated protein complex in skeletal and cardiac muscle.

Type IV Neurofilaments

This group occurs specifically in neurons and consists of the neurofilament triplet proteins NF-L, -M, and -H, and α-internexin. NF-L (light), NF-M (medium) and NF-H (heavy) co-polymerize obligatorily in a 5:3:1 ratio to form filaments with a core diameter of 10–12 nm and unusual side arms projecting >20 nm away (Figure 1E). These side arms represent the extended C-terminal tails of NF-M and NF-H, which feature a large number of Lys-Ser-Pro repeats that adopt an elongated shape when stoichiometrically phosphorylated. Neurofilament proteins are synthesized in the cell body of neurons and transported to the axon, where they contribute to the determination of axon caliber owing to their side arm projections (Figure 1F). α-Internexin, on the other hand, is expressed at an earlier stage of neuronal differentiation, and homopolymerizes into IFs that may thereafter scaffold the assembly of NF-L, M, and H, synthesized late during differentiation.

Type V Lamins

Nuclear lamins constitute type V IFs. Consistent with their unique distribution within the cell, lamin proteins contain a canonical nuclear localization signal within their C-terminal tail, and a CAAX-box at their C terminus which, after farnesylation and carboxylmethylation, mediates membrane anchorage. The C terminus of lamin A is a novel β immunoglobulin-like fold that acts as a docking site for several lamin-associated proteins, and its alteration causes disease (Table I). In addition, lamins feature six extra heptad repeats within the α-helical subdomain 1B of the rod, the significance of which is unclear. The presence of these six extra heptads in the cytoplasmic IF proteins of invertebrates has lent strong support to a proposal that the ancestral IF gene was lamin-like in character.

There are two major types of lamins, designated A and B. B-type lamins, which are essential in all species tested to date, are found in all somatic and germ cells.

The mammalian *Lmna* locus yields four distinct proteins; the two major ones, A (664 a.a.) and C (573 a.a.), are identical over residues 1-566 and differ at their C termini owing to alternative splicing of a common precursor mRNA. The *Lmna* products occur preferentially in differentiated cells. Lamins form a meshwork structure called the nuclear lamina just beneath the inner nuclear membrane (Figure 1G), where they interact with several key constituents of that membrane. In addition, lamins also occur in the nucleoplasm, with a mixed organization as a diffuse network and in focal clusters (Figures 1H and 1I).

Orphan IFs

Several orphan IFs exist that do not easily fit into any other group (Table I). These tend to show a very restricted tissue distribution. Exclusive to differentiated lens fiber cells, phakinin (also called CP115) and filensin (also called CP49) coassemble in a 3:1 molar ratio to produce a unique structure called beaded filaments, where 20 nm wide "beads" decorate the otherwise 8 nm wide filament in a regularly spaced pattern. Nestin was originally discovered as a marker of neuroepithelial stem cells, but is now known to exhibit a broader distribution including various multipotent progenitor cells. It is incorporated into filaments at very low stoichiometry compared to others IF proteins. Synemin, desmuslin, and paranemin coassemble with type III IFs (notably desmin) in muscle, with varying stoichiometry. Just like NF-M and NF-H, nestin, synemin, and paranemin have unusually long C-terminal tail domains that influence interaction between IFs and with other elements of the cytoskeleton.

Functions of Intermediate Filaments, and Their Involvement in Disease

Resistance to Stress

A major, family-wide function of IFs is to endow cells and tissues with a resilient and yet flexible scaffold needed to withstand mechanical, and in some cases non-mechanical, stresses. This concept first came to light from studies in which transgenic mice expressing a mutant epidermal keratin developed severe epidermal blisters. Subsequent analysis of DNA from patients with epidermolysis bullosa simplex, an epidermal blistering disease, revealed mutations in epidermal keratins, confirming the link between mutant IF proteins and inability of cells to withstand mechanical stress. Since then, the importance of IFs and resistance to various trauma has been extended to a variety of cell types including myocytes, fibroblasts, astrocytes, and trophoblasts. In the absence of stress, these cells usually tolerate the expression of a mutated, defective IF protein even though it may lead to disorganization of their IF network. In the event of shear stress, however, the intracellular rupture of such mutant-expressing cells reveals their unusual fragility. These features can also be observed in the absence of one or more keratins, as is evidenced by the fragility of the oral mucosa in Krt6α/β null mice (Figures 2A and 2B) and disruption of the keratin intermediate filament network in cultured primary keratinocytes form these mice (Figures 2C and 2D). Evolving studies of the mechanical properties of IF assemblies *in vitro* and in live cells in culture showed that they exhibit properties that are uniquely suited to fulfill this crucial role, and that inherited mutations compromise these properties. The diversity of IF sequences and their differential expression may serve, at least in part, the purpose of achieving the right compromise between properties of pliability and resilience given the context-specific demands placed upon a cell or its constituents.

Insight from Laminopathies

Nuclear lamins offer tantalizing clues for additional functions. Multiple lines of evidence, adeptly reviewed in recent texts, show that the nuclear lamina participates in determining the shape, size, and integrity of the nucleus, along with the number and positioning of nuclear pores. For example, *Lmna* null mice exhibit severe growth retardation and features of muscular dystrophy (Figures 2E–H). Inherited mutations in the *Lmna* gene are now known to give rise to a variety of clinical disorders (Table I), which from a bird's eye view seem very distinct from one another. Premature aging conditions such as Hutchinson–Gilford progeria syndrome (HGPS) and atypical Werner syndrome are the most recent entries in the world of laminopathies. While fragility of the nuclear envelope could possibly account, at least in part, for the pathogenesis of the muscle-based laminopathies, other mechanisms must be invoked for the premature aging conditions and related disorders. Among the likely possibilities are alterations in the control of gene expression and perturbations in the composition and function of the endoplasmic reticulum, which extends into and communicates with the nuclear envelope. An impact on gene expression could result from lamins' potential involvement in basic nuclear processes such as chromatin organization, DNA replication, RNA processing, and nucleocytoplasmic exchange.

Apoptosis

The possibility exists that just like their nuclear counterpart, cytoplasmic IFs evolved the ability to organize, through scaffolding, proteins and factors involved in signaling and other metabolic processes. Such interactions,

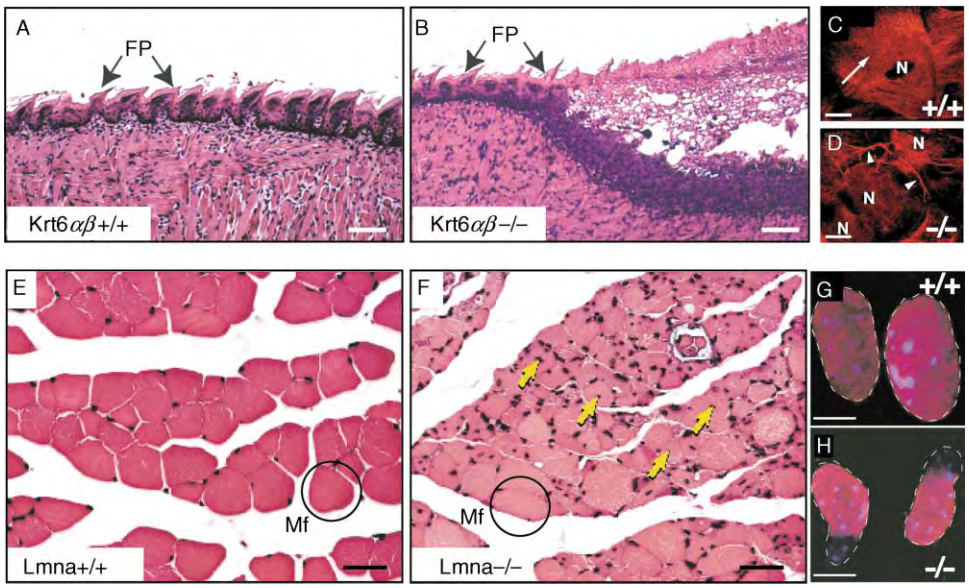

FIGURE 2 (A and B) Hematoxylin-eosin stained, paraffin-embedded section of wild-type (A) and K6α/K6β double null (B) mouse tongues. Tissue is oriented along its anterior–posterior axis. In the absence of the K6 proteins α and β, the posterior region of the tongue epithelium develops severe blistering owing to the fragility of filiform papillae (FP). Bar equals 200 μm. (From Wong, P., Colucci-Guyon, E., Takahashi, K., Gu, C., Babinet, C., and Coulombe, P.A. (2000). Introducing a null mutation in the mouse k6 alpha and k6 beta genes reveals their essential structural role in the oral mucosa. *J. Cell. Biol.* **150**, 921–928, with permission of The Rockefeller University Press.) (C and D) Visualization of keratin IF networks by indirect immunofluorescence in primary culture of skin keratinocytes from wild-type (C) and K6α/K6β null mice (D). Several null cells (−/−) feature disrupted keratin IF networks (see arrowheads). Bar equals 50 μm. (From Wong, P., and Coulombe, P.A., (2003). Loss of keratin 6 (k6) proteins reveals a function for intermediate filaments during wound repair. *J. Cell. Biol.* **163**, 327–337, with permission of The Rockefeller University Press.) (E and F) Aberrant localization of nuclei in muscle from *Lmna* null mice. (E) Hematoxylin-eosin stained, paraffin-embedded sections through wild-type perivertebral muscle show the peripheral localization of the nuclei in the muscle fibers. (F) In *Lmna* null muscle, myofibrils (Mf) are irregularly sized, and there is an increase in the number of nuclei, many of which are centrally located within the muscle fibers (arrows). Bar equals ~15 μm. (From Sullivan, T., Escalante-Alcade, D., Bhatt, H., Anver, M., Bhatt, N., Nagashima, K., Stewart, C.L., and Burke, B. (1999). Loss of A-type lamin expression compromises nuclear envelope integrity leading to muscular dystrophy. *J. Cell. Biol.* **147**, 913–920, with permission of The Rockefeller University Press.) (G and H) Immunohistochemical analysis of wild-type and *Lmna* null mouse embryonic fibroblasts in culture. After fixation with 3% paraformaldehyde, the nuclei were labeled with DAPI (blue), and indirect immunofluorescence of Lamin B (red). Note the uniform distribution of this protein in wild-type nuclear envelopes (G), but its loss from one pole of the irregularly shaped nuclei in the *Lmna* null cells (H). Dashed line indicates boundary of nucleus. Bar equals ~10 μm. (From Sullivan, T., Escalante-Alcade, D., Bhatt, H., Anver, M., Bhatt, N., Nagashima, K., Stewart, C.L., and Burke, B. (1999). Loss of A-type lamin expression compromises nuclear envelope integrity leading to muscular dystrophy. *J. Cell. Biol.* **147**, 913–920, with permission of The Rockefeller University Press.)

for instance, clearly modulate the response of various types of cells to pro-apoptotic signals. Absence or disruption of one or more IFs in several cell types (simple epithelial cells lacking K8, keratinocytes lacking K17, and neurons containing peripherin aggregates) renders cells significantly more likely to undergo apoptosis in response to TNFα or Fas. In simple epithelial cells lacking K8, this occurs in part because K8/18 IFs contribute to the targeting of Fas receptors to the cell surface, and bind to the cytoplasmic tail domain of TNFR2, and to death domain-containing proteins such as TRADD and DEDD. In addition to influencing the decision to undergo apoptosis, IF proteins are also key in its proper execution through their caspase-mediated degradation.

Spatial Organization

Recent evidence points to a role for IFs toward spatial organization within the cell. Keratin IFs can influence the sorting events leading to the organization of the apical pole in polarized epithelial cells, and vimentin IFs promote the association of the sodium-glucose cotransporter SGLT1 with lipid rafts, and its activity, in renal tubular cells. The contribution of neurofilaments toward the radial growth of neurons, itself a crucial determinant of conduction velocity, represent another example of how IFs can promote an asymmetric cytoarchitecture. The notion that cytoplasmic IFs promote some form of spatial organization is quite surprising given their nonpolar character – the spatial code required might be provided by site-specific, dynamic phosphorylation events, and regulated interactions with associated proteins. Future efforts should lead to a broader appreciation of the many metabolic processes influenced by IFs and underlying mechanisms of how inherited IF mutations cause disease.

See Also the Following Articles

Cell Death by Apoptosis and Necrosis • Intermediate Filament Linker Proteins: Plectin and BPAG1 •

Keratins and the Skin • Neuronal Intermediate Filaments • Nuclear Envelope and Lamins

Glossary

intermediate filament (IF) Filaments of 10–12 nm width and several micrometers in length found in the nucleus and the cytoplasm, where they form the cytoskeleton along with actin microfilaments and microtubules.

nuclear lamina A scaffold-like network of lamin intermediate filaments apposed against the inner membrane of the nuclear envelope.

trigger motif Small group of amino acids required for stabilization of an α-helix and nucleation of dimmer formation through coiled coil interactions

unit length filament (ULF) Late stage intermediate during the assembly of cytoplasmic IFs, which are ~60 nm in length and consists of eight tetramers (32 monomers) annealed laterally.

Further Reading

Aebi, U., Cohn, J., Buhle, L., and Gerace, L. (1986). The nuclear lamina is a meshwork of intermediate-type filaments. *Nature* **323**, 560–564.

Cassidy, A. J., Lane, E. B., Irvine, A. D., and McLean, W. H. I (2002). "The Human Intermediate Filament Mutation Database." http://www.interfil.org.

Coulombe, P. A., Bousquet, O., Ma, L., Yamada, S., and Wirtz, D. (2000). The 'ins' and 'outs' of intermediate filament organization. *Trends Cell Biol.* **10**, 420–428.

Erber, A., Riemer, D., Bovenschulte, M., and Weber, K. (1998). Molecular phylogeny of metazoan intermediate filament proteins. *J. Mol. Evol.* **47**, 751–762.

Fuchs, E., and Cleveland, D. W. (1998). A structural scaffolding of intermediate filaments in health and disease. *Science* **279**, 514–519.

Fuchs, E., and Weber, K. (1994). Intermediate filaments: Structure, dynamics, function, and disease. *Ann. Rev. Biochem.* **63**, 345–382.

Helfand, B. T., Chang, L., and Goldman, R. D. (2003). The dynamic and motile properties of intermediate filaments. *Annu. Rev. Cell Dev. Biol* **19**, 445–467.

Hesse, M., Magin, T. M., and Weber, K. (2001). Genes for intermediate filament proteins and the draft sequence of the human genome: Novel keratin genes and a surprisingly high number of pseudogenes related to keratin genes 8 and 18. *J. Cell Sci.* **114**, 2569–2575.

Hirokawa, P., Glicksman, M.A., and Willard, M.B. (1984). Organization of mammalian neurofilament polypeptides within the neuronal cytoskeleton. *J. Cell. Biol.* **98**, 1523–1536.

Moir, R.O., Yoon, M., Khuon, S., and Goldman, R.O. (2000). Nuclear lamins A and B1: different pathways of assembly during nuclear envelope formation in living cells. *J. Cells. Biol.* **151**, 1155–1168.

Mounkes, L., Kozlov, S., Burke, B., and Stewart, C. L. (2003). The laminopathies: Nuclear structure meets disease. *Curr. Opin. Genet. Dev* **13**, 223–230.

Omary, M. B., Ku, N. O., Liao, J., and Price, D. (1998). Keratin modifications and solubility properties in epithelial cells and *in vitro*. In *Subcellular Biochemistry: Intermediate Filaments* (H. Herrman and J. R. Harris, eds.) Vol 31, pp. 105–140. Plenum Press, New York.

Strelkov, S. V., Herrmann, H., and Aebi, U. (2003). Molecular architecture of intermediate filaments. *Bioessays* **25**, 243–251.

Sullivan, T., Escalante-Alcade, O., Bhatt, H., Anver, M., Bhatt, N., Nagashima, K., Stewart, C.L., and Burke, B. (1999). Loss of A-type lamin expression compromises nuclear envelope integrity leading to muscular dystrophy. *J. Cell. Biol.* **147**, 913–920.

Wong, P., and Coulombe, P.A (2003). Loss of keratin 6 (k6) proteins reveals a function for intermediate filaments during wound repair. *J. Cell. Biol.* **163**, 327–337.

Wong, P., Colucci-Guyon, E., Takahashi, K., Gu, C., Babinet, C., and Coulombe, P.A. (2000). Introducing a null mutation in the mouse k6 alpha and k6 beta genes reveals their essential structural role in the oral mucosa. *J. Cell. Biol.* **150**, 921–928.

Biography

Pierre A. Coulombe is a Professor in the Department of Biological Chemistry at the Johns Hopkins University School of Medicine in Baltimore, Maryland. He holds a Ph.D. from Université de Montréal in Canada and received his postdoctoral training at the University of Chicago. At that time, he and Dr. Elaine Fuchs discovered that mutations in keratins can elicit epithelial fragility in transgenic mice and individuals suffering from inherited blistering diseases. He continues to explore the properties and function of keratin genes and proteins in epithelial cells and tissues.

Kelsie M. Bernot is a native of Pennsylvania and a student in the biochemistry, cellular and molecular biology graduate training program at Hopkins. Her thesis research focuses on the properties and function of keratin 16, which is up-regulated during wound repair and in chronic hyperproliferative skin disorders.

Intracellular Calcium Channels: cADPR-Modulated (Ryanodine Receptors)

Antony Galione
University of Oxford, Oxford, UK

Ca^{2+} mobilization from intracellular stores constitutes an important mechanism for producing Ca^{2+} signals within cells. Two major families of intracellular Ca^{2+} release channels have been characterized and are predominantly expressed in the endoplasmic reticulum/sarcoplasmic reticulum (ER/SR). The first is termed the inositol 1,4,5 trisphosphate receptor and is gated by the ubiquitous second messenger inositol 1,4,5 trisphosphate (IP_3). This messenger is generated through the activation of cell surface receptors coupled to the activation of phospholipase C and subsequent hydrolysis of the membrane lipid, phosphatidylinositol 4,5 bisphosphate. The other major family of channels are termed ryanodine receptors. These were first characterized in skeletal and cardiac muscle as proteins which bind the plant alkaloid ryanodine with high affinity. Later they were shown to comprise the major pathway for Ca^{2+} release from the sarcoplasmic reticulum during excitation–contraction coupling. However, it has emerged that ryanodine receptors are ubiquitously expressed throughout cells of the animal and plant kingdom.

Ryanodine Receptors

Ryanodine receptors are encoded by three genes in mammals and genes from a number of non-mammalian species have been sequenced. They are very large proteins with subunits typically of ~560 kDa. Functional channels are usually homotetrameric, comprising of four identical subunits. The large cytoplasmic domains of each subunit provide enormous scope for regulation through interactions with proteins and low-molecular-weight molecules. In skeletal muscle, ryanodine receptors are regulated mainly by direct coupling to voltage-sensor proteins termed dihydropyridine receptors in plasma membrane invaginations called t-tubules. In other cells, direct interactions with plasma membrane proteins are not widely observed for ryanodine receptors, prompting questions about how these proteins are regulated by extracellular stimuli.

Cyclic Adenosine Diphosphate Ribose

Recent evidence has emerged that ryanodine receptors, like IP_3 receptors, too may be gated by a small phosphorylated second messenger called cyclic adenosine disphosphate ribose (cADPR). This molecule is a metabolite of the pyridine nucleotide nicotinamide adenine dinucleotide (NAD^+) and is generated in many cells through the activation of enzymes termed ADP ribosyl cyclases, the best characterized being CD38, expressed at plasma and internal membrane systems. Although it may seem paradoxical that an ectoenzyme such as CD38 may regulate intracellular levels of cADPR, studies from CD38 knockout mice have implicated CD38 in the regulation of cellular cADPR levels during calcium signaling during secretion in both endocrine and exocrine pancreas, as well as in neutrophil chemotaxis. However, in brain, for example, other enzymes may be involved in cADPR synthesis based on similar studies from CD38 knockout mouse.

In an important study, Lee and his colleagues reported in 1987 that not only the established Ca^{2+} mobilizing messenger IP_3 released Ca^{2+} from internal stores in sea urchin egg homogenates, but so also did the two pyridine nucleotides, NAD^+ and NADP. However, NAD^+ was found not to be a Ca^{2+} mobilizing agent *per se*. The active principle was subsequently identified as cADPR, synthesized from NAD^+ in the egg homogenates. A contaminant of NADP, $NAADP^+$, was later shown to be a potent Ca^{2+} mobilizing molecule too. cADPR, at nanomolar concentrations, was shown directly to release Ca^{2+} from intracellular stores by microinjection into intact sea urchin eggs in the absence of extracellular Ca^{2+}. Subsequent pharmacological analysis of cADPR-induced Ca^{2+} release indicated that it was not activating IP_3 receptors since its release was

not blocked by the IP_3 receptor antagonist, heparin. Furthermore, when sea urchin egg homogenates were desensitized to release by IP_3, cADPR was still able to initiate a full Ca^{2+} release. Importantly, Ca^{2+} release by cyclic ADP ribose was found to be selectively blocked by ryanodine receptor inhibitors such as ryanodine itself, ruthenium red, and procaine. In addition, substituted analogues of cADPR were synthesized and found to act as selective antagonists of cADPR but not IP_3-induced Ca^{2+} release.

cADPR has now been implicated in the control of Ca^{2+} release via ryanodine receptors in many different cell types. It is now thought that in many cells cADPR acts in concert with IP_3 to generate the complex Ca^{2+} signaling patterns widely observed in cells. An important property of Ca^{2+} release through ryanodine receptors is that they are modulated by Ca^{2+} itself. This positive feedback mechanism is termed Ca^{2+}-induced Ca^{2+} release (CICR) and is known to be important in excitation–contraction coupling in cardiac muscle and for amplifying local Ca^{2+} signals in many different cell types. This phenomenon is also thought to be critical in determining the complex patterns of Ca^{2+} signals widely observed in cells such as Ca^{2+} spiking and Ca^{2+} waves. cADPR is thought to sensitize ryanodine receptors to their activation by Ca^{2+}.

Cyclic ADP Ribose Receptors

The mechanisms by which cADPR activates ryanodine receptors are not well understood. The possibility exists that cyclic ADP ribose may bind directly to ryanodine receptors or to accessory proteins, which in turn modulate ryanodine receptor openings. High-affinity specific binding of [^{32}P] cADPR has been demonstrated in sea urchin egg microsomes and longitudinal smooth muscle. The photoaffinity compound [^{32}P]-8-azido-cADPR labels distinct 100 and 140 kDa proteins in sea urchin egg extracts. However, these proteins have not been characterized further but are smaller than ryanodine receptor subunits. Two important accessory proteins which are known to bind to ryanodine receptors have both been implicated in cADPR-induced Ca^{2+} release are calmodulin and FKBP-binding proteins. A feature of cADPR-induced Ca^{2+} release from sea urchin egg microsomes is the requirement for a soluble protein factor. This protein was subsequently identified as calmodulin. Calmodulin appears to confer cADPR sensitivity on the microsomes, an effect that is direct and does not rely on enzyme activities. The desensitization phenomenon observed with multiple applications of cADPR is due to the dissociation of calmodulin following the cADPR-induced activation of Ca^{2+} release. Calmodulin is a known accessory protein of ryanodine receptors and its binding sites to this protein have been mapped. The immunophilin FKBP12.6 is a binding protein for immunosuppressant drugs such as FK-506 and binds to ryanodine receptors. In mammalian systems, cADPR has been proposed to induce Ca^{2+} release via ryanodine receptor openings by promoting the dissociation of FKBP12.6 from the channels. cADPR also modulates [^{3}H]ryanodine binding in a number of systems. cADPR enhances [^{3}H]ryanodine binding to cardiac SR vesicles and to T cell membranes. In contrast, in parotid cells, cADPR competes with [^{3}H]ryanodine for its binding sites. The most direct evidence for the investigation of cADPR interaction with ryanodine receptors has come from studying the effects of cADPR on the effects of reconstituted ryanodine receptors in lipid bilayers. These data are often confusing with evidence for and against direct gating of channel openings by cADPR for each of the three isoforms of this Ca^{2+} release channel in mammalian systems. cADPR activation of ryanodine receptors reconstituted into lipid bilayers has been observed with proteins derived from sea urchin eggs, cardiac myocytes, and coronary smooth muscle. In the last case, FKBP12.6 is required to reveal the effects of cADPR on the open probability of the channels.

In addition, three other effects of cADPR have been proposed. In cardiac myocytes, cADPR has been suggested to stimulate SERCA pumps of the sarcoplasmic reticulum (SR), thereby increasing Ca^{2+} loading of this organelle. In colonic smooth muscle cells cADPR has been proposed to stimulate plasma membrane-based calcium removal mechanisms, whilst a modulatory site modulated by high concentrations of cADPR at IP_3 receptors has also been demonstrated.

cADPR and Activation of Different RYR Isoforms

Based largely on pharmacological evidence, the majority of calcium release studies have implicated ryanodine receptors as the major intracellular target for cADPR action. In terms of cADPR selectivity for different RYR isoforms, there are several reports, both positive and negative, of regulation of each of the three different mammalian isoforms of RYRs by cADPR. These reports are based not only on isolated channels in lipid bilayers, but also in intact cells predominantly expressing one type of native or recombinant ryanodine receptor. However, as stated before, it is still unclear whether cADPR binds directly to ryanodine receptors or modulates ryanodine receptor openings through its interaction with accessory proteins.

cADPR-Mediated Calcium Signaling

The development of 8-substituted analogues of cADPR as potent antagonist of cADPR action have been crucial in unraveling stimuli that signal through cyclic ADP ribose action. Phenomena that are blocked by antagonists by 8-amino-cADPR or 8-Br-cADPR include cardiac contractility enhanced by β-adrenergic agonists, abscisic acid-induced stomatal closures, and gene expression in plants, CCK and acetylcholine-evoked fluid secretion in pancreatic acinar cells, nitric oxide mediated long-term depression in brain slices, fertilization in sea urchin eggs, and T cell receptor activation as well as neurotransmitter release from nerve terminals. 8-Br-cADPR, which is membrane permeant, is gaining widespread usage as a membrane permeant antagonist of cADPR action. The use of this analogue has been used to implicate cADPR in the control of long-term depression in rat hippocampus, hypoxia-mediated vasoconstriction in pulmonary smooth muscle, cardiac contractility and smooth muscle contraction. In the generation of many intracellular Ca^{2+} signals both IP_3- and cADPR-sensitive mechanisms are involved in determining the Ca^{2+} signaling patterns. In sea urchin eggs, for example, both IP_3 and cADPR mechanisms can independently produce Ca^{2+} waves and are both produced by the fertilizing sperm. Similar results were found in dopaminergic neurons in mammalian CNS where activation of metabotropic glutamate receptors induces Ca^{2+} mobilization by intracellular stores through the activation of both IP_3 and cyclic ADP ribose/ryanodine receptor mechanisms.

Measurement of cADPR Levels in Tissues and Cells

The development of a number of sensitive and selective assays for measuring cyclic ADP ribose in mammalian tissues has led to the identification of cellular stimuli that are coupled to cADPR synthesis in cells. These studies have complemented those employing selective cADPR antagonists, as outlined earlier. The major cADPR assays are a radio-receptor assay based on the ability of endogenous cADPR to displace [^{32}P]cADPR binding to sea urchin egg microsomes and a novel cycling assay for cyclic ADP ribose with a nanomolar sensitivity. The principle of this cycling assay is that NAD^+ can be generated by from cADPR by the reversal of the ADP-ribosyl cyclase enzyme. NAD produced after initially depleting cell extracts of endogenous NAD is then coupled to cycling assays involving alcohol dehydrogenase and diaphorase generating a fluorescent product.

cADPR synthesis has been shown to be coupled through G protein-coupled receptors including muscarinic cholinergic receptors and α_1-adrenoceptors as well as tyrosine-kinase-linked receptors such as the T cell receptor. In addition, the second messenger cyclic GMP, may through its cyclic GMP-dependent protein kinase, directly activate the ADP ribosyl cyclase through phosphorylation. In addition, intermediary metabolism through modulation of NAD^+/NADH levels may be coupled to cADPR synthesis. Chronic changes in cyclic ADP ribose levels may be associated also with changes in the levels of ADP ribosyl cyclase enzymes. For example, retinoic acid and oestrogen increase expression of ADP ribosyl cyclases, resulting in chronic elevations in cyclic ADP ribose levels. Now that assays exist for the measurement of cADPR in cells, it has been found that cellular stimuli generally elevate cyclic ADP ribose for prolonged periods, as long as a number of minutes, in contrast to the more transient elevations of IP_3. These data indicate that cADPR may act as a long-term modulator of Ca^{2+} release from intracellular stores.

See Also the Following Articles

Calcium Signaling: Calmodulin-Dependent Phosphatase • Calcium Signaling: Cell Cycle • Calcium Signaling: Motility (Actomyosin–Troponin System) • Calcium Signaling: NO Synthase • G Protein-Coupled Receptor Kinases and Arrestins • Intracellular Calcium Channels: $NAADP^+$-Modulated • IP_3 Receptors • The Neuronal Calcium Signal in Activity-Dependent Transcription • Phosphatidylinositol Bisphosphate and Trisphosphate • Phosphatidylinositol-3-Phosphate • Store-Operated Membrane Channels: Calcium

Glossary

Ca^{2+}-induced Ca^{2+} release A phenomenon where a modest rise in intracellular Ca^{2+} activates Ca^{2+} release channels, amplifying and globalizing Ca^{2+} signals.

Ca^{2+} release channel A channel on intracellular organelles, usually the endoplasmic reticulum, that when opened releases stored Ca^{2+}.

Ca^{2+} signal Changes in the intracellular levels of free Ca^{2+} often manifested as complex Ca^{2+} spikes and propagating regenerative waves.

NAD Nicotinamide adenine dinucleotide, a ubiquitous coenzyme found in all cells.

ryanodine receptor Ca^{2+} release channel found in muscle and other cells that is modulated by the plant alkaloid ryanodine. It is a large homotetrameric protein each consisting of four large subunits.

second messenger An intracellular molecule that mediates the effects of extracellular stimuli.

Further Reading

Berridge, M., Lipp, P., and Bootman, M. (2000). The versatility and universality of calcium signalling. *Nat. Mol. Cell Biol. Rev.* **1**, 11–21.

Clapper, D. L., Walseth, T. F., Dargie, P. J., and Lee, H. C. (1987). Pyridine nucleotide metabolites stimulate calcium release from sea urchin egg microsomes desensitized to inositol trisphosphate. *J. Biol. Chem.* **262**, 9561–9568.

Fill, M., and Copello, J. A. (2002). Ryanodine receptor calcium release channels. *Physiol. Rev.* **82**, 893–922.

Galione, A., and Churchill, G. (2000). Cyclic ADP-ribose as a calcium mobilizing messenger. *Science STKE*, 1–6. www.stke.org/cgi/content/full/OC_sigtrans;2000/41/pe1.

Leckie, C., Empson, R., Becchetti, A., Thomas, J., Galione, A., and Whitaker, M. (2003). The NO pathway acts late during the fertilization response in sea urchin eggs. *J. Biol. Chem.* **278**, 12247–12254.

Lee, H. C. (2001). Physiological functions of cyclic ADP-Ribose and NAADP as calcium messengers. *Annu. Rev. Pharmacol. Toxicol.* **41**, 317–345.

Morgan, A. J., and Galione, A. (2002). Sensitizing Ca^{2+}-induced Ca^{2+} release. Role of cADPR as an endogenous modulator. In *Cyclic ADP-Ribose and NAADP. Structures, Metabolism and Functions* (H. C. Lee, ed.) pp. 167–197. Kluwer, Dordrecht.

Patel, S., Churchill, G. C., and Galione, A. (2001). Coordination of Ca^{2+} signalling by NAADP. *Trends Biochem. Sci.* **26**, 482–489.

Tang, W. X., Chen, Y. F., Zou, A. P., Campbell, W. B., and Li, P. L. (2002). Role of FKBP12.6 in cADPR-induced activation of reconstituted ryanodine receptors from arterial smooth muscle. *Am. J. Physiol.* **282**, H1304–H1310.

Thomas, J. M., Summerhill, R. J., Fruen, B. R., Churchill, G. C., and Galione, A. (2002). Calmodulin dissociation mediates desensitization of the cADPR-induced Ca^{2+} release mechanism. *Curr. Biol.* **12**, 2018–2022.

Biography

Antony Galione is a Professor of Pharmacology in the Department of Pharmacology at the University of Oxford, UK and a senior research fellow of the Wellcome Trust, UK. His principal research interests are Ca^{2+} mobilization from intracellular stores by novel Ca^{2+}-mobilizing messengers cADPR and NAADP. He holds a Ph.D. from the University of Cambridge and received his postdoctoral training at University College, London and Johns Hopkins University.

Intracellular Calcium Channels: $NAADP^+$-Modulated

Armando A. Genazzani and Marcella Debidda
University of Cambridge, Cambridge, UK

It is well established that inositol 1,4,5-trisphosphate (IP_3) and Ca^{2+} are able to mediate signal transduction by opening intracellular Ca^{2+}-channels located on intracellular membranes. These messengers do this by activating IP_3 and ryanodine receptors, respectively. Nonetheless, in recent years evidence has emerged that other molecules may mediate intracellular Ca^{2+}-release, either by the modulation of these two channels, or via the activation of further, previously unknown, channels. Derivatives of NAD and NADP have been shown to be able to induce Ca^{2+}-release via both mechanisms. In particular, cyclic ADP ribose (cADPR) acts on particular subtypes of the ryanodine receptor, while nicotinic acid adenine dinucleotide phosphate (NAADP) releases Ca^{2+} via a novel and distinct mechanism.

Structure of NAADP

NAADP is a pyridine nucleotide similar to NADP, except for the amide group of the nicotinamide ring, which in the NAADP molecule is replaced by a carboxyl group (Figure 1). Despite this small difference, in sea urchin eggs (the model system used to characterize this molecule), NADP is devoid of any Ca^{2+}-release efficacy, suggesting that the binding site specifically recognizes this region of the molecule as a discriminator and that NAADP is not just a cellular surrogate for NADP.

NAADP-Induced Ca^{2+}-Release in Invertebrates and Plants

Although the chemical existence of NAADP was reported by Bernofsky in 1980, the possibility that NAADP could be a putative intracellular messenger was hypothesized by Lee and co-workers. In 1987, they described the presence of a contaminant in commercially available NADP that could release Ca^{2+} in sea urchin eggs. Only in 1995, this contaminant was shown to be NAADP. NAADP has now been found to be a potent Ca^{2+}-releasing agent in various invertebrate systems including starfish, sea snails, and sea squirts (see Table I). Furthermore, NAADP has also been shown to release Ca^{2+} from microsomes prepared from plant preparations. Although the NAADP receptor has not yet been cloned, it presumably is a Ca^{2+}-channel distinct from those described to date, as indicated by numerous biochemical evidences. Nonetheless, in a few systems, such as the skeletal muscle, NAADP might also use the ryanodine receptor as a mediator of its effect. In sea urchin eggs, the best characterized model to date, NAADP releases Ca^{2+} via an intracellular channel that is distinct from those that are responsive to inositol 1,4,5-triphosphate (IP_3) and cyclic ADP ribose (cADPR). NAADP-induced Ca^{2+}-release does not exhibit any cross-desensitization with the other two mechanisms. Furthermore, it is not sensitive to heparin, ruthenium red or high concentrations of ryanodine, antagonists of the IP_3, and ryanodine channels. According to the concentrations, Ca^{2+} can both activate and inhibit IP_3 and ryanodine receptors, providing a means of modulation of the channel independent of ligands. A major difference between the NAADP mechanism and the other two is the insensitivity of the NAADP-induced Ca^{2+}-release to both cytosolic and vesicular Ca^{2+}-concentrations. Furthermore, other differences exist in the channels in regard to the pH sensitivity, ion dependency, endogenous modulators, and kinetic features. Finally, specific NAADP-binding sites, insensitive to IP_3 and cADPR, have been shown in sea urchin egg microsomes.

All the efforts done to characterize the pharmacology have failed so far to produce a valid antagonist of the NAADP-sensitive mechanism. In echinoderms, it has been shown that L-type Ca^{2+}-channel antagonists (and BayK8644, an agonist) are able to inhibit NAADP-induced Ca^{2+}-release, but this occurs just at concentrations, which are approximately 100-fold higher than those able to inhibit voltage-operated Ca^{2+}-channels. Nonetheless, it has been found that NAADP itself can be used as an antagonist since in sea urchin eggs subthreshold concentrations of this nucleotide are able to completely abrogate the calcium release caused by

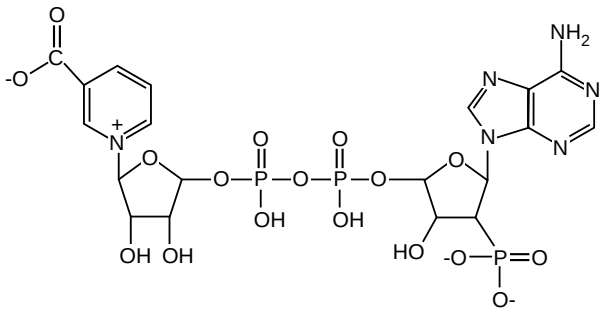

FIGURE 1 Structure of nicotinic acid adenine dinucleotide phosphate.

further NAADP elevations. Neither IP_3 nor cADPR are regulated by this mechanism and so far the significance of this process is unknown.

In sea urchin eggs, the NAADP sensitive channel does not appear to reside on the same intracellular organelles compared to IP_3 and ryanodine receptors, as shown by membrane separation experiments. To support this, while IP_3- and cADPR-induced Ca^{2+}-release are completely abolished by pretreatment of homogenates with thapsigargin, a poison of the Ca^{2+}-pump that is responsible for the accumulation of Ca^{2+} in the endo(sarco)plasmic reticulum, NAADP-induced Ca^{2+}-release appears to be unaffected. Recently, it has been shown that, at least in this system, the organelle on which the mechanism might reside is the reserve granule, the egg equivalent to lysosomes. Whether this will be a general feature of this mechanism across species remains to be established.

In sea urchins, starfish, and sea squirts (invertebrate systems) where the properties of NAADP on Ca^{2+}-release have been investigated in intact cells, it has been shown that this Ca^{2+}-release mechanism does not act in isolation from the others, but instead appears to work in concert to elicit specific responses. For example, in starfish NAADP-induced Ca^{2+}-release appears to be partially inhibited by the co-injection of IP_3 and ryanodine receptor antagonists, suggesting that the NAADP-induced cytosolic calcium elevations are due to both release from the NAADP channel and to amplification through IP_3 and ryanodine receptors. The extent and the manner of the cross-talk appears to be different from one system to another, but it is

TABLE I

Models Described to be Responsive to NAADP Between 1995 and 2002

Species	Model	NAADP effect
Sea urchin	Intact egg,	Inactivation (<1 nM, IC_{50} 200 pM) Agonist (>3 nM, EC_{50} 25 nM)
	Microsomes	Inactivation (<1nM, IC_{50} 200 pM) Agonist (>3 nM, EC_{50} 25 nM)
Starfish	Intact egg	Agonist (1–2 μM)
Sea squirt	Intact oocyte	Agonist (EC_{50} 30 nM)
Sea snail ganglia	Pre-synaptic neuron	Agonist (10–50 μM)
Red Beet	Microsomes	Agonist (96 nM)
Cauliflower	Microsomes	Agonist (1 μM) Inactivation (3 nM)
Frog neuromuscular junction	Nerve terminal	Agonist (10 μM–1 nM; liposomal delivery)
Human β pancreatic cells	Intact cells	Agonist (100 nM) Inactivation (10 μM)
Human T-lymphocytes	Intact cells	Agonist (max 100 nM) Inactivation (10 μM)
Mouse pancreatic acinar cells	Intact cells	Agonist (50 nM) Inactivation (1–100 μM)
Rat pulmonary smooth muscle cells	Intact cells	Agonist (10 nM) Inactivation (100 μM)
Rat fibroblast cells	Microsomes	Agonist (10 μM)
Rat brain	Microsomes	Agonist (EC_{50} 1 μM)
Rabbit heart	Microsomes	Agonist (EC_{50} 320 nM)
Rat mesangial kidney cells	Microsomes	Agonist (EC_{50} 4 μM)
A7r5, HL-60, H9c2 cell lines	Microsomes	Agonist (10 μM)

one of the conserved features of NAADP signaling through evolution, since it has been observed also in vertebrate systems.

NAADP-Induced Ca^{2+}-Release in Vertebrates

Both microsomal and intact systems from vertebrate models have been shown to respond to NAADP (Table I). Furthermore, binding sites with nanomolar affinity for NAADP have been described in brain and cardiac tissues. In similar fashion to what is observed in invertebrate systems, NAADP-induced Ca^{2+}-release is distinct from the IP_3 and ryanodine-mediated mechanisms when it is investigated in microsomal preparations, while in intact systems there appears to be a high degree of overlap. One of the differences observed between vertebrates and invertebrates is that the unusual desensitization property observed in sea urchin eggs does not seem to have been conserved in vertebrates. Instead, in many of the systems described (e.g., pancreatic acinar and β-cells, T-lymphocytes), NAADP appears to release Ca^{2+} in an inverted bell-shaped curve, with high concentrations unable to have any effect. Observations of cross-talk between NAADP-induced Ca^{2+}-release and IP_3 and ryanodine receptors in pancreatic acinar cells and T-lymphocytes have led to the hypothesis that NAADP might act as a trigger by releasing enough Ca^{2+} to induce and/or sensitize the other two mechanisms to amplify its signal. This cross-talk means that cells might encode signals via increasing to different levels the three-second messengers, instead of having the option to modulate just one messenger to different levels. The net outcome of this could be the possibility to use Ca^{2+} to specifically and unambiguously encode a higher number of intracellular messages.

At present, no extracellular message has been linked unequivocally with NAADP signaling. Nonetheless, the capacity of high concentrations of NAADP to block the release mechanism has been used experimentally to suggest that NAADP might be involved, among other functions, in colecystokinin-mediated signaling in pancreatic acinar cells, in insulin signaling in β-cells, and in the T cell receptor/CD3 signaling.

Metabolism of NAADP

It has been shown that cADPR, a derivative of NAD, in which the nicotinamide has been cleaved and the terminal ribose is cyclized with the adenine group at the N1 position, can be synthesized by a subfamily of NAD^+ glycohydrolases. Members of this family have been characterized in *Aplysia* and in mammalian systems. These enzymes are peculiar since they are able to catalyze both the cyclization and the degradation of cADPR. Surprisingly, in the presence of nicotinic acid, these enzymes are also capable of catalyzing a base-exchange reaction that replaces the nicotinamide on NADP with nicotinic acid to produce NAADP. Therefore, it is likely that these enzymes are central to calcium signaling, since they can catalyze the production of two signaling molecules with two distinct targets, as well as the degradation of one of these. For this mechanism to produce diversity it could be hypothesized that the different reactions should be modulated differently by intracellular pathways. Recent evidence suggests that this might be the case. First, the base-exchange reaction seems to be favored over the cyclization in acidic conditions, although substantial amounts of NAADP are generated at physiological pH. Second, both the laboratories led by Lee and by Galione have separately shown that cyclic nucleotides can differentially regulate the production of cADPR and NAADP. In particular, in sea urchin eggs elevations of cAMP appear to favor NAADP production while elevations of cGMP favor production of cADPR. Nonetheless, this could be due to either a differential modulation of the same enzyme or to modulation of two separate enzymes. Among the enzymes described to date that can catalyze these reactions, the mammalian members, the most important of which is the lymphocyte antigen CD38, are membrane-bound ectoenzymes, with extracellular catalytic activity. Although there are some descriptions of CD38 present on intracellular membranes such as the nuclear envelope or the mitochondrion, it is likely that other members of this family will be described in the future that possess intracellular activity. Alternatively, the group led by De Flora has postulated a mechanism by which the extracellularly produced messengers can be internalized.

NAADP degradation has been shown to occur in both invertebrate and vertebrate cells. The mechanism by which this occurs is at present unknown, although it has been recently postulated that in mouse tissues a Ca^{2+}-dependent phosphatase, via conversion to NAAD, might be involved in the termination of signaling by NAADP.

In most systems evaluated to date, NAADP induces Ca^{2+}-release at low nanomolar concentrations, making its detection extremely difficult. It has recently been shown that sea urchin sperm contain micromolar levels of NAADP, together with a membrane-bound high capacity enzyme for its synthesis. It is likely that these observations will be extended to other systems with the characterization of more sensitive detection methods.

See Also the Following Articles

Phosphatidylinositol-3-Phosphate • Intracellular Calcium Channels: cADPr-Modulated (Ryanodine Receptors) • IP_3 Receptors • Phosphatidylinositol Bisphosphate and Trisphosphate • Phospholipase C • Voltage-Sensitive Ca^{2+} Channels

Glossary

cADPR An intracellular messenger derived from NAD^+ acting on the ryanodine receptor as an agonist or a modulator.

IP_3 A second messenger derived from the cleavage of PIP_2 (phosphatidylinositol 4,5-bisphosphate) by Phospholipase C which interacts with IP_3-sensitive Ca^{2+} channels causing calcium release.

NAADP An intracellular messenger derived from $NADP^+$ acting on a yet unknown intracellular Ca^{2+}-release channel.

second messenger An intracellular molecule whose concentration is regulated in response to binding of a specific ligand to an extracellular receptor to transduce information.

Further Reading

Cancela, J. M., Van Coppenolle, F., Galione, A., Tepikin, A. V., and Petersen, O. H. (2002). Transformation of local Ca^{2+} spikes to global Ca^{2+} transients: The combinatorial roles of multiple Ca^{2+} releasing messengers. *EMBO J.* **21**, 909–919.

Churchill, G. C., Okada, Y., Thomas, J. M., Genazzani, A. A., Patel, S., and Galione, A. (2002). NAADP mobilizes Ca^{2+} from reserve granules, lysosome-related organelles, in sea urchin eggs. *Cell* **111**, 703–708.

Clapper, D. L., Walseth, T. F., Dargie, P. J., and Lee, H. C. (1987). Pyridine nucleotide metabolites stimulate calcium release from sea urchin egg microsomes desensitized to inositol trisphosphate. *J. Biol. Chem.* **262**, 9561–9568.

Genazzani, A. A., and Billington, R. A. (2002). NAADP: An atypical Ca^{2+}-release messenger? *Trends Pharmacol. Sci.* **23**, 165–167.

Lee, H. C. (2002). *Cyclic ADP-ribose and NAADP Structures, Metabolism and Functions*. Kluwer, Boston.

Patel, S., Churchill, G. C., and Galione, A. (2001). Coordination of Ca^{2+} signalling by NAADP. *Trends Biochem. Sci.* **26**, 482–489.

Biography

Armando Genazzani is an Associate Professor at the University of Piemonte Orientale, Novara, Italy. His major interests include intracellular Ca^{2+} release mechanisms and the understanding of Ca^{2+}-induced gene expression in neurons. He holds an M.D. from the University of Catania, Italy and a Ph.D. from the University of Oxford. He received postdoctoral training at the University of Oxford and at the Swiss Federal Institute of Technology (ETH) in Zurich and has been University lecturer and BBSRC David Phillips Fellow at the University of Cambridge, UK.

Marcella Debidda holds a Ph.D. from the University of Sassari, Italy. She received postdoctoral training at the University of Cambridge (UK) and is currently a postdoctoral fellow in the division of Experimental Hematology at Cincinnati Children's Hospital Medical Center.

Ion Channel Protein Superfamily

William A. Catterall
University of Washington, Seattle, Washington, USA

Electrical signals control contraction of muscle, secretion of hormones, sensation of the environment, processing of information in the brain, and output from the brain to peripheral tissues. In excitable cells, electrical signals also have an important influence on intracellular metabolism and signal transduction, gene expression, protein synthesis and targeting, and protein degradation. In all these contexts, electrical signals are conducted by members of the ion channel protein superfamily, a set of more than 140 structurally related pore-forming proteins. In addition, members of this protein family are crucial in maintaining ion homeostasis in the kidney and in many different cell types and participate in calcium signaling pathways in nonexcitable cells. In this article, the founding members of each family of ion channel proteins that are structurally related to the voltage-gated ion channels are introduced and an overview of their structure, function, and physiological roles is presented. References are given to one or two recent review articles on each channel family to provide a broad introduction to the literature.

Voltage-Gated Sodium and Calcium Channels

The founding member of this superfamily in terms of its discovery as a separate protein is the voltage-gated sodium channel. These channels are specialized for electrical signaling and are responsible for the rapid influx of sodium ions that underlies the rising phase of the action potential in nerve, muscle, and endocrine cells. Neurotoxin labeling, purification, and functional reconstitution showed that sodium channels from mammalian brain contain voltage-sensing and pore-forming elements in a single protein complex of one principal α-subunit of 220–260 kDa and one or two auxiliary β-subunits of ~36 kDa. The α-subunits of sodium channels contain four homologous domains that each contain six hydrophobic, probable transmembrane segments. A membrane-reentrant loop between the fifth and sixth (S5 and S6) transmembrane segments forms the narrow extracellular end of the pore while the S6 segments form the intracellular end (Figure 1, red). The pore is formed in the center of a pseudosymmetric array of the four domains, and a single α-subunit containing four domains is able to receive voltage signals and activate its intrinsic pore. The channel responds to voltage by virtue of its S4 segments (Figure 1, green), which contain repeated motifs of a positively charged amino acid residue followed by two hydrophobic residues, and move outward under the influence of the membrane electric field to initiate a conformational change that opens the pore. Drugs that block the pore of sodium channels are important as local anesthetics, antiarrhythmic drugs, and antiepileptic drugs. The four β-subunits consist of an amino-terminal extracellular immunoglobulin-like domain, a single transmembrane segment, and a short intracellular segment. They both modulate the gating of the α-subunits and serve as cell adhesion molecules by interaction with extracellular matrix, membrane, and cytoskeletal proteins. Nine voltage-gated sodium channel α-subunits, designated $Na_v1.1$–1.9 have been functionally characterized. They comprise a single family of proteins with greater than 70% amino acid sequence identity in their transmembrane segments. One additional related α-subunit, which defines a second subfamily, $Na_v2.1$, is known but is apparently not voltage-gated.

Voltage-gated calcium channels are the key signal transducers of electrical signaling, converting depolarization of the cell membrane to an influx of calcium ions that initiates contraction, secretion, neurotransmission, and other intracellular regulatory events. Skeletal muscle calcium channels first identified by drug labeling, purification, and functional reconstitution have a principal $\alpha1$-subunit of 212–250 kDa, which is similar to the sodium channel α-subunit but is associated with auxiliary $\alpha2\delta$, β, and γ-subunits that are unrelated to the sodium channel auxiliary subunits. cDNA cloning and sequencing showed that the $\alpha1$-subunit of calcium channels is analogous to the sodium channel α-subunits in structural organization (Figure 1) and is ~25% identical in amino acid sequence in the transmembrane regions. As for the sodium channel α-subunit, the calcium channel $\alpha1$-subunit is sufficient to form a voltage-gated calcium-selective pore by itself. Ten functional calcium channel $\alpha1$-subunits are known in vertebrates, and they fall into three subfamilies that

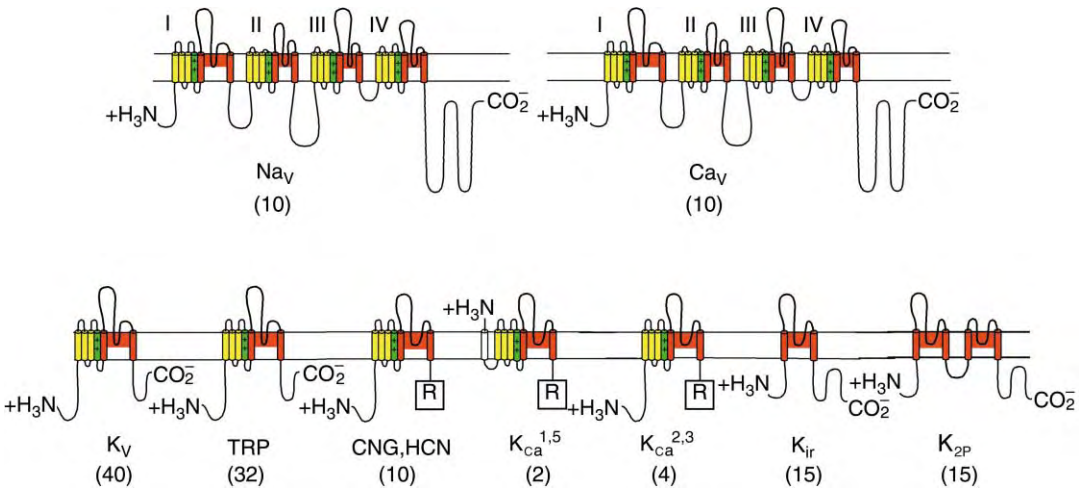

FIGURE 1 The voltage-gated ion channel protein family. The different members of the ion channel protein family structurally related to the voltage-gated ion channels are illustrated as transmembrane folding diagrams in which cylinders represent probable transmembrane alpha-helices. Red, S5–S6 pore-forming segments; green, S4 voltage sensor, yellow, S1–S3 transmembrane segments; R, regulatory domain that binds intracellular second messengers. The numbers of family members in the human genome are given in parentheses.

differ in function and regulation. The Ca_v1 family ($Ca_v1.1–1.4$) conducts L-type calcium currents that initiate contraction, endocrine secretion, and synaptic transmission at the specialized ribbon synapses involved in sensory input in the eye and ear. L-type calcium currents also are important regulators of gene expression and other intracellular processes. Blockers of $Ca_v1.2$ channels are important in the therapy of cardiovascular diseases including hypertension, cardiac arrhythmia, and angina pectoris. The Ca_v2 family of calcium channels ($Ca_v2.1–2.3$) conducts N-, P/Q- and R-type calcium currents that initiate fast synaptic transmission at synapses in the central and peripheral nervous systems and are blocked specifically by peptide neurotoxins from spider and cone snail venoms. The Ca_v3 family of calcium channels ($Ca_v3.1–3.3$) conducts T-type calcium currents that are important for repetitive action potential firing of neurons in the brain and in the pacemaker cells of the sino-atrial node in the heart. The functional and regulatory properties and protein–protein interactions of these channels are adapted to their different roles in electrical signaling and cellular signal transduction.

Voltage-Gated Potassium Channels

Voltage-gated potassium channels are activated by depolarization, and the outward movement of potassium ions through them repolarizes the membrane potential to end action potentials, hyperpolarizes the membrane potential immediately following action potentials, and plays a key role in setting the resting membrane potential. In this way, potassium channels control electrical signaling and regulate ion flux and calcium transients in nonexcitable cells. The first voltage-gated potassium channels were cloned from *Drosophila* based on a mutation that causes the *Shaker* phenotype. They are composed of four transmembrane subunits, each of which is analogous to a single domain of the principal subunits of sodium or calcium channels (Figure 1). The voltage-gated potassium channels are remarkable for their diversity. They include 40 different channels that are classified into 12 distinct groups based on their amino acid sequence homology (Kv1 to Kv12). These α-subunits can assemble into homo- and hetero-tetramers, leading to a wide diversity of different channel complexes. The Kv1 channels also associate with Kvβ-subunits, which are intracellular proteins. The Kv4 subunits associate with KChiPs, intracellular calmodulin-like calcium-binding proteins that regulate channel gating. Some of the Kv7 and Kv11 α-subunits associate with single membrane-spanning subunits (minK, MiRP1, MiRP2), which regulate their gating properties. The diversity of potassium channels allows neurons and other excitable cells to precisely tune their electrical signaling properties by expression of different combinations of potassium channel subunits.

Second Messenger-Gated and Sensory Ion Channels

In addition to the voltage-gated sodium, calcium, and potassium channels, the voltage-gated ion channel family includes additional members that are gated by a combination of voltage and binding of second

messengers, including calcium, cyclic nucleotides, and lipid messengers. These channels have six transmembrane segments and a generally similar structure to voltage-gated potassium channels, but contain in addition a regulatory domain attached at their carboxy terminus.

Calcium-activated potassium channels ($K_{Ca}1-5$) have an ion channel domain attached to an intracellular calcium-dependent regulatory domain in their C terminus. They are activated by a combination of depolarization and binding of calcium ions. For the $K_{Ca}1$, and $K_{Ca}5$ channels, calcium binding to a regulatory domain in the C terminus (R, Figure 1) enhances activation of the channels by depolarization, resulting in synergistic gating of channel activity by voltage and intracellular calcium concentration. $K_{Ca}1$ channels have an extra transmembrane segment at the N terminus (S0) and associate with $K_{Ca}\beta$-subunits, which are 2-TM intrinsic membrane proteins. For $K_{Ca}2$ or $K_{Ca}3$ channels, calcium binds to a constitutively associated calmodulin molecule bound to the C-terminal regulatory domain and activates the channels without a voltage stimulus. All of the K_{Ca} channels serve to repolarize excitable cells following single-action potentials or trains of action potentials, during which calcium entry increases cytosolic calcium levels and activates them. One of their prominent roles is to define the length of action potential trains in neurons by activating in response to calcium influx through voltage-gated calcium channels and thereby repolarizing and hyperpolarizing the cell. Similarly, in smooth muscle cells they hyperpolarize the membrane and relax the smooth muscle.

The structurally related cyclic nucleotide-gated ion channels (CNG, six family members) and hyperpolarization-activated, cyclic nucleotide-gated ion channels (HCN, four family members) are composed of four subunits that each have a 6-TM voltage-gated ion channel domain attached to an intracellular cyclic nucleotide-binding domain at their C terminus. These channels were first purified and cloned from retinal rods, where they conduct the dark current that underlies visual signal transduction. Upon capture of photons by rhodopsin, activation of a G-protein-signaling pathway leads to activation of a cyclic nucleotide phosphodiesterase that hydrolyzes cGMP. Reduction in the cGMP concentration in the rod outer segment closes these "dark-current" channels, causing hyperpolarization and initiation of visual signal transduction to the neural cells of the retina. Closely related cyclic nucleotide-gated channels are responsible for olfactory signal transduction in the nasal epithelium. The more distantly related HCN channels are involved in cyclic nucleotide-regulated pacemaking in cells that generate repetitive action potentials, like the sino-atrial node pacemaker cells of the heart and the persistently firing neurons of the thalamus in the brain. They are also involved in sensation of sour tastes in taste buds. Remarkably, they are activated by hyperpolarization (rather than depolarization) via their S4 voltage sensor, and their opening by hyperpolarization is greatly enhanced by simultaneous binding of cAMP and/or cGMP.

The transient receptor potential (trp) channels were discovered first in *Drosophila*, where the founding member is the site of mutations that cause the trp phenotype that alters visual signal transduction in the eye. Subsequent to that work, a family of 32 related channels, which can be divided into six subfamilies, have been defined in mammals. These channels are weakly voltage-sensitive, are either calcium-selective or non-selective cation channels that conduct calcium, and are activated by a range of signals including heat, cold, and intracellular lipid messengers. The TRPC subfamily of channels is most closely related to the classical *Drosophila* trp channel. The TRPV subfamily of channels is most closely related to the "vanilloid receptor," a channel protein that serves as a receptor for the hot chili pepper ingredient capsaicin, a vanilloid compound. It also responds to heat and mediates noxious thermal pain sensations. The TRPM subfamily is most closely related to melastatin, first discovered as a tumor marker in melanoma. TRPM7, the first member of this family to be functionally expressed, is slightly calcium-selective and contains an intrinsic protein kinase domain that may autophosphorylate to activate its ion channel domain. The PKD, CatSper, and mucolipin subfamilies of ion channel subunits are also distantly related to trp. CatSper plays an essential (but still unknown) role in calcium signaling in sperm. PKD channels are involved in sensing fluid transport in the kidney and other epithelial tissues. Mucolipin channels may be involved in auditory signaling in the ear and in calcium transport regulating lysosome function.

Inwardly Rectifying Potassium Channels and their Relatives

The inwardly rectifying potassium channels (K_{ir}) are the structurally simplest ion channels, containing four subunits that each have two transmembrane segments and a membrane-re-entrant pore loop between them (Figure 1). As their name implies, they conduct potassium more effectively inward than outward, but their outward conductance of potassium is physiologically important to repolarize cells near the resting membrane potential. They are structurally related to the S5 and S6 segments of the voltage-gated ion channels, and their pore loop forms the extracellular end of the pore as in that family of proteins. The two transmembrane segments and the pore loop of a related bacterial potassium channel have been shown directly by X-ray crystallography to form an ion-selective

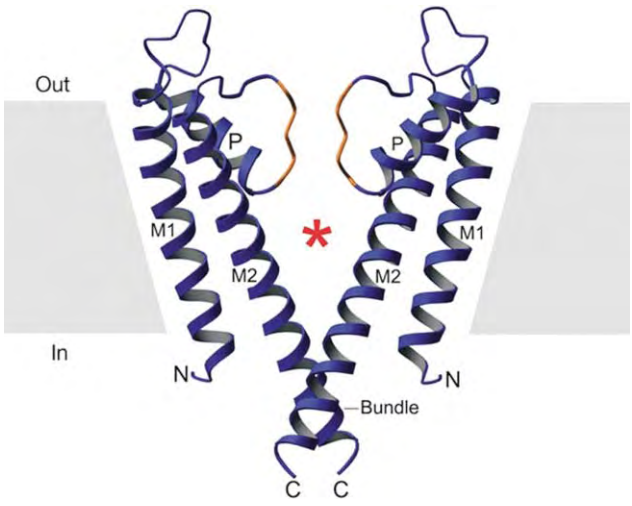

FIGURE 2 Structure of the pore of a bacterial potassium channel. The structures of two of the four subunits of a bacterial potassium channel related to the inwardly rectifying potassium channels are illustrated. Orange marks the backbone carbonyls that form the narrow ion selectivity filter. Red asterisk indicates the water-filled cavity in the ion permeability pathway where a potassium ion is located in the X-ray structure.

pore (Figure 2). Many inwardly rectifying potassium channels are gated by intracellular divalent cations that bind in their pore, including Mg, spermine, and spermidine. The X-ray structure of a related vertebrate inwardly rectifying potassium channel reveals an extended pore region that projects into the cytoplasm and contains divalent cation-binding sites that may control ion flow through the pore. Other K_{ir} channels are gated by direct binding of G protein $\beta\gamma$-subunits and inositol phospholipid messengers. Remarkably, ATP-sensitive potassium channels are composed of an inwardly rectifying potassium channel core in association with the much larger sulfonylurea receptor (SUR) protein, a member of the ABC transporter family that binds ADP and ATP and regulates the function of the inwardly rectifying potassium channel. These channels are crucial regulators of insulin secretion from pancreatic beta cells controlled by intracellular glucose and ATP levels, and SUR is the molecular target for the sulfonylurea drugs used in treatment of diabetes.

Two-Pore-Motif Potassium Channels

The most recently discovered family of ion channels are potassium channels that have two repeats of the inward rectifier pore motif and are designated K_{2P} (Figure 1). The channels function as "open rectifiers," that is, they are constitutively open and constantly drive the membrane potential toward the potassium equilibrium potential by mediating outward potassium conductance. They are thought to be important for setting the resting membrane potential of excitable cells at a negative value near the equilibrium potential for potassium of $\sim$80 mV. Although they are not regulated by physiological mechanisms that have been described to date, they may be an important target for the actions of inhalation anesthetics, which activate these channels and thereby could prevent action potential firing in the brain during general anesthesia.

Structure and Function

Viewed from the perspective of the entire ion channel protein family, the functions of these proteins can be divided into three complementary aspects: ion conductance, pore gating, and regulation. All members of the family share a common pore motif, with variations appropriate to determine their different ion selectivity. It is likely that this pore motif first evolved in the bacterial ion channels that resemble inward rectifiers. The X-ray crystal structure of one of these channels has shown that the narrow outer mouth of the pore is formed by the pore loops between the M1 and M2 segments that are analogous to the S5 and S6 transmembrane segments of the 6-TM family members while the length of the pore is formed by a tilted bundle, "inverted teepee" arrangement of the M2 segments (Figure 2). This structure suggests that the pore is closed at its intracellular end and discriminates ions at the narrow ion selectivity filter at its extracellular end. This model of pore formation fits well with a wealth of structure–function data on the voltage-gated ion channels and the cyclic nucleotide-gated channels. The closure of the pore at the intracellular end suggests that this is the site of pore gating. Support for this idea comes from classical biophysical studies and from more recent work. The structure of a calcium-activated bacterial potassium channel with calcium bound shows that the crossing of the M2 segments at the intracellular end of the pore is opened by bending of the helix, consistent with the hypothesis that this is the mechanism of pore opening.

The different protein families within the ion channel superfamily are regulated by different mechanisms. The simplest family members, the inwardly rectifying potassium channels, are gated extrinsically by divalent cations binding in the pore or by binding of other regulators. The cyclic nucleotide-gated ion channels and the calcium-activated potassium channels are gated by ligand binding to their carboxy-terminal regulatory domains. These ligand-induced conformational changes are thought to exert a torque on the connected S6 segments and force the opening of the pore bundle of S6 helices. In addition, the HCN channels and the

$K_{Ca}1$ channels are also gated synergistically by changes in membrane potential and are highly sensitive to small voltage changes. The voltage-gated sodium, calcium, and potassium channels are primarily gated by changes in membrane potential. Their regulation depends on the S1 to S4 segments of these channels, which can be viewed as an evolutionary addition to the pore-forming segments. The detailed mechanism of voltage-dependent gating is unknown. However, there is clear structure–function evidence for an outward and rotational movement of the positively charged S4 segments during the gating process, and it is assumed that the conformational change accompanying this outward movement exerts a torque on the bundle of four S6 segments at the intracellular end of the pore forcing the bundle to open. Voltage-dependent gating of the sodium and calcium channels is also modulated by binding of calcium/calmodulin and G proteins to the C-terminal domain, suggesting that these interactions may also exert a torque on the S6 segments and thereby alter the energetics of gating.

Conclusion

The voltage-gated ion channel superfamily is one of the largest families of signaling proteins, following the G protein-coupled receptors and the protein kinases in the number of family members. The family is likely to have evolved from a 2-TM ancestor like the modern inwardly rectifying potassium channels and bacterial potassium channels. Modular additions of intracellular regulatory domains for ligand binding and a 4-TM transmembrane domain for voltage gating have produced extraordinarily versatile signaling molecules with capacity to respond to voltage signals and intracellular effectors and to integrate information coming from these two types of inputs. The resulting signaling mechanisms control most aspects of cell physiology and underlie complex integrative processes like learning and memory in the brain and coordinated movements of muscles. The evolutionary appearance and refinement of these signaling mechanisms is one of the hallmark events allowing the development of complex multicellular organisms.

See Also the Following Articles

G Protein Signaling Regulators • Voltage-Dependent K^+ Channels • Voltage-Sensitive Ca^{2+} Channels • Voltage-Sensitive Na^+ Channels

Glossary

gating The intrinsic regulatory process through which ion channels are opened and closed by conformational changes of the ion channel protein.

ion channel A transmembrane protein that forms a pore through which ions move down their electrochemical gradients into or out of cells or intracellular organelles.

rectifying An ion channel in which ion flow is favored in one direction – e.g., inwardly rectifying potassium channels that conduct potassium ions inward more readily than outward, even though outward potassium movement is that physiologically relevant direction.

voltage-gated Ion channels whose gating is regulated by changes in transmembrane voltage.

Further Reading

Catterall, W. A. (2000a). From ionic currents to molecular mechanisms: The structure and function of voltage-gated sodium channels. *Neuron* **26**, 13–25.

Catterall, W. A. (2000b). Structure and regulation of voltage-gated calcium channels. *Annu. Rev. Cell Dev. Biol.* **16**, 521–555.

Goldstein, S. A., Bockenhauer, D., O'Kelly, I., and Zilberberg, N. (2001). Potassium leak channels and the KCNK family of two-P-domain subunits. *Nat. Rev. Neurosci.* **2**, 175–184.

Jan, L. Y., and Jan, Y. N. (1997). Cloned potassium channels from eukaryotes and prokaryotes. *Annu. Rev. Neurosci.* **20**, 91–123.

Matulef, K., and Zagotta, W. N. (2003). Cyclic nucleotide-gated ion channels. *Annu. Rev. Cell Dev. Biol.* **19**, 23–44.

Montell, C. (2001). Physiology, phylogeny, and functions of the TRP superfamily of cation channels. Sci STKE, RE1.

Patel, A. J., Lazdunski, M., and Honore, E. (2001). Lipid and mechano-gated 2P domain K^+ channels. *Curr. Opin. Cell Biol.* **13**, 422–428.

Reimann, F., and Ashcroft, F. M. (1999). Inwardly rectifying potassium channels. *Curr. Opin. Cell Biol.* **11**, 503–508.

Vergara, C., Latorre, R., Marrion, N. V., and Adelman, J. P. (1998). Calcium-activated potassium channels. *Curr. Opin. Neurobiol.* **8**, 321–329.

Zhou, Y., Morais-Cabral, J. H., Kaufman, A., and MacKinnon, R. (2001). Chemistry of ion coordination and hydration revealed by a potassium channel–Fab complex at 2.0 A resolution. *Nature* **414**, 43–48.

Biography

William Catterall is Professor and Chair of Pharmacology at the University of Washington. His interests are neurobiology and molecular pharmacology, with research focus on ion channel proteins. He received his Ph.D. in Physiological Chemistry from Johns Hopkins University and was postdoctoral Fellow and Staff Scientist in the Laboratory of Biochemical Genetics, NHLBI, NIH. He is a member of the National Academy of Sciences, Institute of Medicine, and American Academy of Arts and Sciences.

IP_3 Receptors

Colin W. Taylor
University of Cambridge, Cambridge, UK

Edward Morris and Paula da Fonseca
Imperial College, London, UK

Inositol 1,4,5-trisphosphate (IP_3) is an intracellular messenger. It is produced from a lipid in the plasma membrane by enzymes (phospholipases C) that are stimulated in response to activation of many different receptors in the plasma membrane. IP_3 is released into the cytosol where it can bind to its own receptor, a very large intracellular Ca^{2+} channel, and stimulate release of Ca^{2+} from intracellular stores. The Ca^{2+} released by IP_3 receptors also regulates their activity and this contributes to the complex changes in cytosolic Ca^{2+} concentration that follow activation of receptors that stimulate phospholipase C.

A Brief History

For more than a century, beginning with Sidney Ringer in 1883 serendipitously discovering that Ca^{2+} was required for contraction of frog hearts, increases in intracellular Ca^{2+} concentration have been known to regulate cellular activity. Such Ca^{2+}-regulated events begin at fertilization, continue through development and cell death, and include many responses of differentiated cells, such as contraction, secretion, and metabolism. In short, changes in cytoplasmic Ca^{2+} concentration provide an ubiquitous link between extracellular stimuli (hormones, neurotransmitters, etc.) and the regulation of intracellular processes. The first suggestion that turnover of phosphoinositides, a minor class of lipids with a phosphorylated inositol headgroup (Figure 1), might provide a common link between extracellular stimuli and physiological responses came from work by the Hokins in the 1950s. But it was a hefty review from Bob Michell some 20 years later that developed the idea that receptor-stimulated phosphoinositide hydrolysis might be causally linked to changes in intracellular Ca^{2+} concentration. For years, it was disputed whether Ca^{2+} signals were the result, or the cause, of the phosphoinositide hydrolysis, a dispute that was fuelled by the observation that the enzymes responsible for the hydrolysis (phospholipases C) are stimulated by Ca^{2+}. Experiments with the salivary gland of the humble blowfly were instrumental in resolving the dispute and establishing that increases in intracellular Ca^{2+} concentration result from receptor-stimulated hydrolysis of phosphatidylinositol 4,5-bisphosphate to produce inositol 1,4,5-trisphosphate (IP_3) and diacylglycerol (Figure 1). Both products are intracellular messengers. The latter regulates the activity of certain proteins kinase C and it can also be metabolized to additional signaling molecules. The signaling properties of IP_3 were demonstrated exactly a century after Ringer's discovery in a seminal paper from Mike Berridge, Robin Irvine, and their colleagues. They showed that IP_3 stimulates release of Ca^{2+} from intracellular stores (later shown to be largely within the endoplasmic reticulum). As expected of an intracellular signaling molecule, IP_3 is rapidly metabolized to products that cannot stimulate release of Ca^{2+} from stores. Within months, the ability of IP_3 to stimulate Ca^{2+} release was confirmed in countless cell types, and the signaling pathway illustrated in Figure 1 was shown to be almost ubiquitously expressed and to provide the essential link between many different receptors and the release of Ca^{2+} from intracellular stores. Later work has established the roles of IP_3 receptors in generating complex intracellular Ca^{2+} signals and has begun to address how the structure of IP_3 receptors underlies their function.

Structure of IP_3 Receptors

IP_3 receptors are big proteins. Each receptor has four subunits arranged around a central Ca^{2+}-permeable pore that opens when the receptor is activated. When purified IP_3 receptors are reconstituted into artificial lipid membranes, addition of IP_3 causes a large cation-permeable channel to open. This confirms that the tetrameric IP_3 receptor complex is all that is required to produce an IP_3-gated channel. Other proteins are intimately associated with IP_3 receptors in native cells, but their roles are modulatory: the assembly of four IP_3 receptor subunits is sufficient to form a functional,

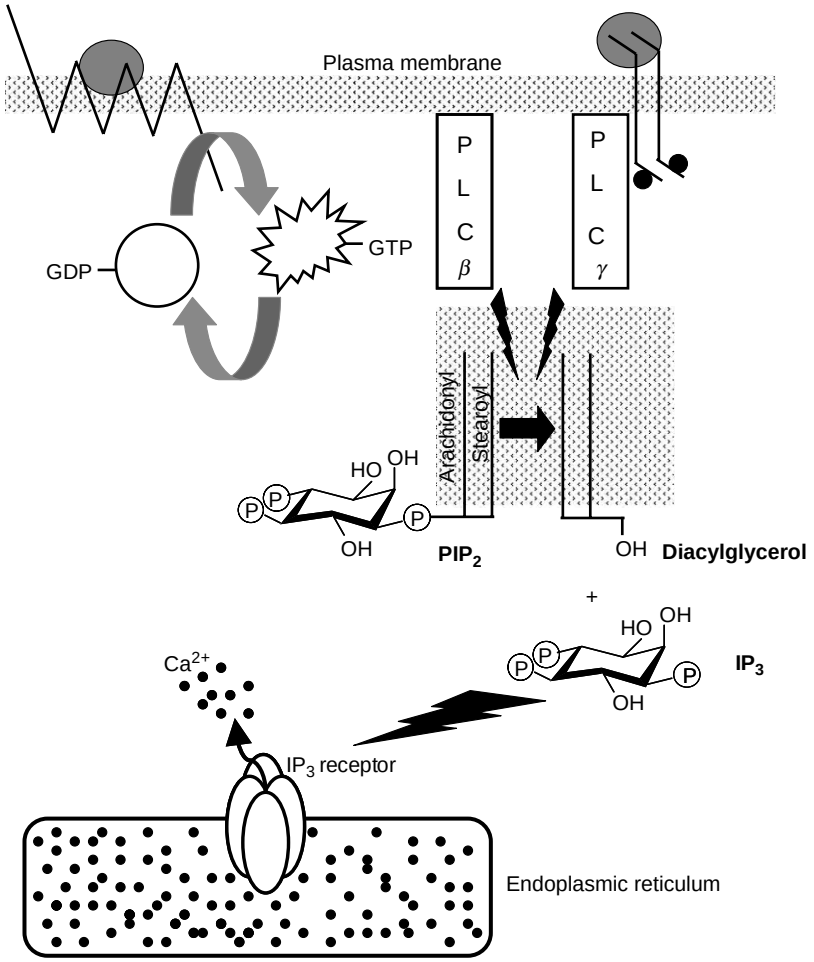

FIGURE 1 Receptor-stimulated Ca^{2+}mobilization. Two different families of phosphopliase C, PLCβ and PLCα, are regulated by different classes of receptor. The former are stimulated by the dissociated subunits of G proteins, which are themselves activated by receptors with a structure that includes seven-membrane-spanning segments. PLCα is activated when it associates with and becomes phosphorylated by receptors with either intrinsic or associated protein tyrosine kinase activity. Both families of PLC catalyze hydrolysis of phosphatidylinositol 4,5-bisphosphate (PIP2) in the plasmamembrane to give diacylglycerol and IP_3. The latter then stimulates release of $Ca^{2+}$from intracellular stores via IP_3 receptors.

IP_3-sensitive, Ca^{2+} channel. Most eukaryotic cells express IP_3 receptors and the genes that encode the subunits are closely related in species as diverse as man and the insect, *Drosophila*. The structural basis of IP_3 receptor function is therefore likely to be similar in all eukaryotes. In mammals, there are three closely related genes for IP_3 receptor subunits, each encoding a protein of ~2700 amino acid residues. This protein sequence can be divided into three functional regions (Figures 2A and 2B): an N-terminal cytoplasmic region that binds IP_3, a cytoplasmic regulatory region, and a channel region containing the transmembrane segments close to the C-terminus. The tetrameric receptor is some 20 nm across and extends more than 10 nm from the membrane of the endoplasmic reticulum (ER) into the cytoplasm as shown in a recent three-dimensional analysis of electron microscope images of the receptor (Figure 2C). This analysis combined with biochemical data suggest a model in which the primary amino-acid sequence of each subunit is assigned to specific positions within the three-dimensional map (Figures 2A–2C). A recent X-ray crystallographic analysis of the IP_3-binding region of the receptor (residues 224-604) shows IP_3 bound in a cleft between two domains which form an L-shaped structure (Figure 2D). The N-terminal domain consists of a globular barrel made up of 12 β-strands, while the C-terminal domain consists of a bundle of eight α-helices. IP_3 is coordinated by residues from each of the domains. Each receptor (with its four subunits) has four IP_3-binding sites and it is likely that each must bind IP_3 before the channel can open.

There is as yet no high resolution structure for the remaining 87% of the receptor, although it is clear that towards the C-terminal end of each subunit there are six-transmembrane segments that span the ER membrane and form the pore of the channel (Figures 2A and 2B). Each of the IP_3 receptor subunits contributes to the pore, which is formed by

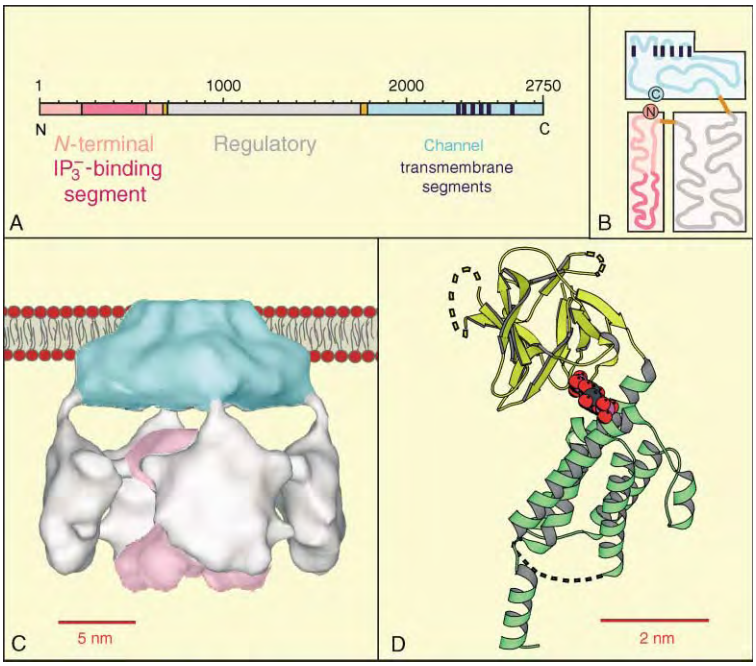

FIGURE 2 Structure of IP_3 receptors. (A) Functional regions of the IP_3 receptor are shown mapped onto the primary sequence. (B) Proposed spatial organization of the functional domains. (C) Three-dimensional reconstruction of an IP_3 receptor purified from brain derived from analysis of images from electron microscopy. The channel region (blue) embedded in the lipids of the ER membrane is connected by thin strands to four outer domains (gray) which are thought to form the regulatory region. Four inner domains (pink) are thought to include the IP_3-binding sites. (D) X-ray crystallographic structure of the IP_3-binding region of the type 1 IP_3 receptor. The protein backbone is shown as a ribbon diagram with the N-terminal β-barrel domain (yellow) uppermost and the C-terminal α-helical bundle domain (green) at the bottom. The IP_3 molecule (red) lying in the cleft between the two domains is represented as space-filling spheres.

the last two of the transmembrane segments and the intervening loop. This pore region shares considerable similarities with many other cation channels, suggesting a conserved structural organization. Comparison of the intermediate resolution structure of the IP_3 receptor with other cation channels suggests that conservation of structural organization may also extend to other regions. We do not yet have a sufficient understanding of IP_3 receptor structure to know how binding of IP_3 at one end of the amino acid sequence of each subunit leads to opening of a pore formed by residues lying at the opposite end of the primary sequence.

Because analyses of receptor function often depend upon selective agonists and antagonists, briefly highlighted are the relative paucity of such ligands for IP_3 receptors. Heparin and decavanadate are membrane-impermeant competitive antagonists of IP_3; and Xestospongin, caffeine, and 2-aminoethoxydiphenyl borane (2-APB) are membrane-permeant noncompetitive antagonists. Each drug lacks specificity. Many inositol phosphates are agonists of IP_3 receptors (although none is better than IP_3), but a fungal product (now synthesized), adenophostin, is an agonist of IP_3 receptors with an affinity some 10 times greater than that of IP_3.

IP_3 Receptors are Regulated by IP_3 and Ca^{2+}

IP_3 provides the link between receptors in the plasma membrane and release of Ca^{2+} from intracellular stores (Figure 1), but all IP_3 receptors are also regulated by cytosolic Ca^{2+}. Indeed considerable evidence suggests that binding of both IP_3 and Ca^{2+} are required before the channel can open: IP_3 and Ca^{2+} should be regarded as coagonists of the receptor. The effects of Ca^{2+} are more complex, however, because many studies have shown that modest increases in Ca^{2+} concentration potentiate the effects of IP_3 (consistent with the need for both IP_3 and Ca^{2+} to bind for channel opening), while more substantial increases are inhibitory. These biphasic effects of Ca^{2+} on IP_3 receptor function are important in mediating interactions between IP_3 receptors and between IP_3 receptors and other Ca^{2+} channels. Whether these effects of Ca^{2+} result from Ca^{2+} binding directly to the IP_3 receptor or to associated Ca^{2+}-binding proteins is not resolved. It is, however, clear that binding of IP_3 regulates the Ca^{2+}-binding site, so that the sensitivity of the IP_3 receptor to Ca^{2+} is regulated by IP_3.

The Ca^{2+} signals recorded from intact cells are often complex: they may remain spatially restricted to only parts of a cell allowing local regulation of Ca^{2+}-sensitive processes, or they may propagate regeneratively across the cell as Ca^{2+} waves allowing global regulation of Ca^{2+}-sensitive processes. The interplay between IP_3 and Ca^{2+} in regulating IP_3 receptors is crucial in determining whether Ca^{2+} signals propagate. Ca^{2+} released by active IP_3 receptors (or by other Ca^{2+} channels) is thought to ignite the activity of more distant IP_3 receptors by providing the Ca^{2+} they need to open. This regenerative process has been described as Ca^{2+}-induced Ca^{2+} release. The much higher Ca^{2+} concentration in the immediate vicinity of active IP_3 receptors is thought to restrain this potentially explosive positive feedback by inhibiting IP_3 receptors.

IP_3 Receptors and Ca^{2+} Entry

Receptors that stimulate IP_3 formation typically cause both release of Ca^{2+} from intracellular stores and enhanced Ca^{2+} entry across the plasma membrane. Cells express a variety of Ca^{2+}-permeable channels regulated by different products of the phosphoinositide pathway, but store-regulated (also known as "capacitative") Ca^{2+} entry is the most widely expressed pathway. Here, emptying of intracellular Ca^{2+} stores (by IP_3) generates a signal (it has not yet been identified) that causes activation of a Ca^{2+}-permeable channel in the plasma membrane. There is therefore an inextricable link between store emptying (mediated by IP_3) and Ca^{2+} entry, and as the stores refill (when IP_3 is no longer produced) then so capacitative Ca^{2+} entry is also switched off. Under physiological conditions, where IP_3 links receptors in the plasma membrane to emptying of intracellular Ca^{2+} stores, IP_3 receptors are clearly required for activation of capacitative Ca^{2+} entry. But they may also play a more direct role because there is evidence, albeit controversial, that IP_3 receptors may be physically coupled to the Ca^{2+} channels in the plasma membrane and may thereby serve as the link between the stores and capacitative Ca^{2+} entry.

See Also the Following Articles

Calcium Waves • Intracellular Calcium Channels: $NAADP^+$-Modulated • Phosphatidylinositol Bisphosphate and Trisphosphate • Phosphatidylinositol-3-Phosphate • Phospholipase C • Protein Kinase C Family

Glossary

agonist A substance that binds to a receptor to cause its activation.

antagonist A substance that binds to a receptor to prevent its activation.

phosphoinositides Account for about 10% of cellular phospholipids. A glycerol backbone attached to two fatty acids (stearoyl at position 1, arachidonyl at position 2) and inositol (linked by a phosphodiester bond at position 3). The inositol headgroup can also be further phosphorylated.

phospholipase C An enzyme (there are many forms) that catalyses cleavage of the diacylglycerol-phosphate bond of a glycerophospholipid. In the context of this article, the important phospholipases C are those that cleave phosphatidylinositol 4,5-bisphosphate to diacylglycerol and IP_3.

positive feedback A situation where the output of a process (e.g., Ca^{2+} from an IP_3 receptor) provides the stimulus for that process (e.g., channel opening).

receptor A signal-transducing protein that can be activated by specific agonists, the actions of which can be selectively blocked by appropriate antagonists.

Further Reading

Barritt, G. J. (1992). *Communication within Animal Cells*. Oxford University Press, Oxford.

Berridge, M. J. (1997). Elementary and global aspects of calcium signalling. *J. Physiol.* **499**, 291–306.

Berridge, M. J., and Irvine, R. F. (1989). Inositol phosphates and cell signalling. *Nature* **341**, 197–205.

Bosanac, I., Alattia, J.-R., Mal, T. K., Chan, J., Talarico, S., Tong, F. K., Tong, K. I., Yoshikawa, F., Furuichi, T., Iwai, M., Michikawa, T., Mikoshiba, K., and Ikura, M. (2002). Structure of the inositol 1,4,5-trisphosphate receptor binding core in complex with its ligand. *Nature* **420**, 696–701.

da Fonseca, P. C. A., Morris, S. A., Nerou, E. P., Taylor, C. W., and Morris, E. P. (2003). Domain organisation of the type 1 inositol 1,4,5-trisphosphate receptor as revealed by single particle analysis. *Proc. Acad. Nat. Sci (USA)* **100**, 3936–3941.

Michell, R. H. (1975). Inositol phospholipids and cell surface receptor function. *Biochim. Biophys. Acta* **415**, 81–147.

Putney, J. W. Jr. (1997). *Capacitative Calcium Entry*. R.G. Landes Co. Austin, Texas, USA.

Streb, H., Irvine, R.F., Berndge, M. J., and Schulz, I. (1983).Release of Ca^{2+} from a nonmitochondrial store of pancreatic acinar cells by inositol-1,4,5-triphosphate. *Nature* **306**, 67–69.

Taylor, C. W., and Laude, A. J. (2002). IP_3 receptors and their regulation by calmodulin and cytosolic Ca^{2+}. *Cell Calcium* **32**, 321–334.

Biography

Colin W. Taylor is a Professor of Cellular Pharmacology in the Department of Pharmacology, University of Cambridge. He holds Ph.D. and Sc.D. degrees from the University of Cambridge, and pursued postdoctoral studies at the Medical College of Virginia. His major research interests are in the structure and function of IP_3 receptors and in the regulation of Ca^{2+} entry pathways.

Edward Morris is a Senior Lecturer in the Division of Biomedical Sciences, Imperial College London. He holds a Ph.D. from the University of London. His research focuses on the structural biology of membrane proteins.

Paula C. A. da Fonseca is a Postdoctoral Research Associate in the Division of Biomedical Sciences, Imperial College London. After her first degree in biochemistry at the University of Lisbon, she obtained a Ph.D. at the University of London. Her research interests include the structure and function of membrane proteins.

Iron–Sulfur Proteins

Helmut Beinert
University of Wisconsin, Madison, Wisconsin, USA

Jacques Meyer
Commissariat á l'Energie Atomique, Grenoble, France

Roland Lill
University of Marburg, Marburg, Germany

Iron–sulfur (Fe–S) proteins contain iron ligated by inorganic sulfide and/or at least two cysteines (Cys) as ligands. Fe–S active sites are required for or involved in electron transfer, mostly in the range of low oxidation–reduction potentials. They also can serve as active sites of enzymes and as sensing and regulating agents. Fe–S active sites are perhaps the most ancient cofactors, and Fe–S compounds may have been essential reactants of prebiotic chemistry.

Iron–Sulfur Clusters

Properties

Structure

Nomenclature and Shorthand Designations The conventions for the nomenclature of Fe–S clusters and Fe–S proteins are found in the 1989 recommendations of the Nomenclature Committee of the International Union of Biochemistry (IUB). The components of the cluster core are placed into brackets and the oxidation level of the core (not including that of ligands) is given as a superscript $[2Fe–2S]^{2+}$. The possible oxidation states of the species that can be formed are indicated as shown: $[2Fe–2S]^{2+,+}$. If the kind of ligands to this cluster is to be specified, the alternative designation $[Fe_2S_2(RS)_2(L_2)]^{2-}$ should be used.

Structures In the great majority of Fe–S proteins the iron is present in clusters, with the irons linked by sulfides. The [4Fe–4S] cluster is the predominant species. The simplest Fe–S protein and also the simplest building block of Fe–S proteins is the mononuclear thiolate complex $[Fe(Cys)_4]^{2-,-}$ as it occurs in rubredoxins (Rd). The cluster types are shown in Figure 1. The coordination is tetrahedral throughout. As evident from the figure, the S–S distances are ~1.3 times longer than the Fe–Fe distances, which produces the distorted cubic structure typical for [4Fe–4S] clusters. The 3Fe cluster can be considered as a 4Fe cluster with one Fe missing. The cluster structures shown are to some extent interconvertible and the 3Fe-cluster is central to all cluster interconversions. By partial denaturation of the protein it can also be converted to a linear form: $(Cys)_2FeS_2FeS_2Fe(Cys)_2$. The 3Fe cluster can serve as starting material for producing heterometal clusters with metals such as Zn, Ni, Co, Cd, Ga, Tl, Mo; however, such clusters are not found in nature. Those that occur have modified structures and are formed by specific synthetic systems. The 4Fe to 3Fe cluster conversion is also used in nature to condition clusters for use as active sites in enzymes and for sensing functions.

Stability

Sulfur is a weak ligand, allowing the iron to remain in the high-spin state, which makes the ligands relatively labile as compared to strong ligands such as cyanide. As evident from the cluster interconversions and distortions mentioned above, Fe–S clusters are rather malleable, and from high-resolution X-ray structures it is apparent that they can be further distorted by influences from the protein and can be adapted for various conditions and functions. Fe–S clusters are sensitive toward oxidants such as oxygen and its reduction products and toward NO, and also to an excess of their own constituents, namely S^{2-} and RS^-, to dithiothreitol and dithionite and toward hydrolysis at high or low pH. As mentioned above, Cys ligands belonging to protein frameworks are required for the formation of stable clusters. Replacement of one Cys with another functional residue is allowed in some clusters; however, the only clusters that are known to be stable with two non-Cys ligands are those with two histidine (His) ligands, as they occur naturally in the so-called "Rieske" proteins. While polypeptide chains are mandatory for the stabilization

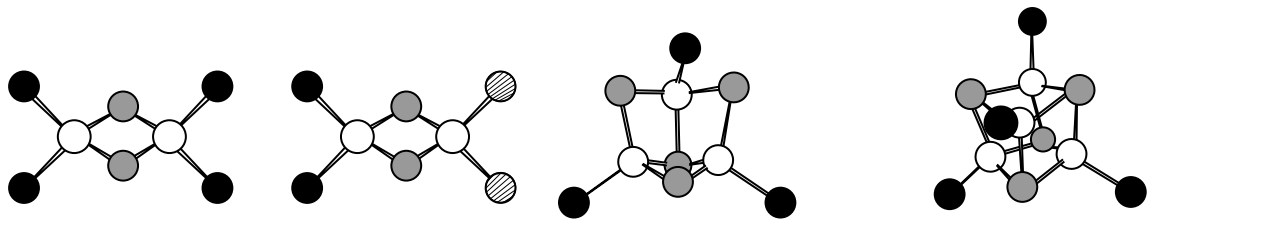

FIGURE 1 Models for structures of 2Fe, 3Fe, and 4Fe clusters. White: Fe; black: cysteine, and gray sulfide sulfurs; hatched: histidine nitrogens. Adapted with permission from Holm, R. H., Kennepohl, P., and Solomon, E. I. *Chem. Rev.* (1996). Structural and functional aspects of metal sites in biology. **96**, 2239–2314.

of Fe–S clusters, their protecting effect is very variable: the lifetime of Fe–S proteins in air may vary from seconds to weeks. As naturally occurring Fe–S clusters require protein-ligands for support, their functions are considered in the section titled 'Iron–Sulfur Proteins' below.

Electronic Structure and Magnetism

The electronic charge in Fe–S clusters is concentrated at their sulfides and Cys ligands. It has been shown by X-ray near-edge spectroscopy (XANES), that all bonds involving sulfur are highly covalent, with those involving sulfide exhibiting 2–3 times the covalency of the thiolate bonds. On the contrary, the unpaired spin density resides primarily on the irons. Fe–S clusters owe many of their characteristic properties to the ordering of their spin-systems. This ordering is dominated by three forces: first, the tendency to pair the spins antiparallel, which is expressed in the magnitude of the spin coupling parameter J; second, the tendency to pair the spins parallel, expressed in the parameter B, the resonance integral (this tendency arises when an extra electron is present, leading to spin-dependent electron delocalization (SDD)); and third, the dynamic trapping energy, arising through vibronic coupling with groups in the neighborhood. On one-electron reduction of $[2Fe–2S]^{2+}$ (2 Fe^{III}) clusters the trapping energy leads almost invariably to antiparallel coupling and localization of the electron at one Fe ($1Fe^{III}$, $1Fe^{II}$) so that the system spin $S = 5/2 - 4/2 = 1/2$. In $[4Fe–4S]^{2+}$ clusters there are two pairs of parallel-coupled (according to SDD) mixed valence (mv) irons ($2Fe^{II}$, $2Fe^{III}$) both with $S = 5/2 + 4/2 = 9/2$, which then couple antiparallel to $S = 0$. On addition of an electron there will be one mv pair and two Fe^{II}, thus: $S = 9/2 - 2 \times 4/2 = 1/2$, i.e., paramagnetism. If instead one electron is removed from the 2 + level to form $[4Fe–4S]^{3+}$ ($3Fe^{III}$,$1Fe^{II}$), there are one mv pair and two Fe^{III}, thus $S = 2 \times 5/2 - 9/2 = 1/2$ and paramagnetism. The $[4Fe–4S]^{3+}$ level has been first observed in so-called high potential iron protein (HiPIP); however, these proteins are now counted among ferredoxins (Fd) with high redox potentials. Occasionally $[4Fe–4S]^{+}$ clusters with an $S = 3/2$, a mixed 1/2 and 3/2, or even higher ground-state spins have been observed.

Iron–Sulfur Proteins

Structure

Nomenclature

Small proteins containing only the mononuclear $[Fe(Cys)_4]$ complex are called rubredoxin (Rd), and those containing one or two [2Fe–2S] or [4Fe–4S] clusters are called ferredoxin (Fd). Many Fe–S clusters occur in large and sometimes membrane-bound proteins, together with other prosthetic groups and/or metal cofactors. These proteins are designated as complex Fe–S proteins.

Primary Structure

In many Fe–S proteins the Cys ligands of the active sites occur in characteristic sequence patterns. For instance, the Fe-ion in Rd is ligated by two $-C-x_2-C-$ motifs (x standing for residues other than Cys) separated by 20–30 residues. In plant- and mammalian-type [2Fe–2S] Fds, the pattern is $-C-x_{4,5}-C-x_2-C-x_n-C-$, with $n \approx 30$. In Rieske-type [2Fe–2S] proteins the two Cys ligands of one iron and the two His ligands of the other one occur in a $-C-x-H-x_{15-17}-C-x_2-H-$ pattern. These proteins are found in membrane-bound enzymes in conjunction with *b*-type cytochromes in mitochondria (bc_1, or complex III) and chloroplasts (b_6f), as well as in soluble bacterial dioxygenases. In [4Fe–4S] Fds the canonical pattern is $-C-x_2-C-x_2-C-x_n-C-$, with $n \approx 20–40$. This pattern is duplicated in Fds containing two [4Fe–4S] clusters. The patterns containing the ligands in Rd and Fd were initially found in small 50–100 residue sequences, but they have now been observed in the larger sequences of many redox enzymes. Significant diversification has occurred, particularly among Fd patterns, through

insertions or deletions of up to several tens of residues. In addition to these canonical sequences, an increasing number of novel Cys patterns are found to furnish ligands to [2Fe–2S] and [4Fe–4S] sites.

Secondary and Tertiary Structure

Many three-dimensional structures of Fe–S proteins have now been determined by X-ray crystallography. At an early stage, the structures of the small Rds and Fds revealed characteristic folds, each specific of a given Fe–S structural framework. The Rd molecule is composed of a three-stranded pleated sheet and two loops that bear a $-C-x_2-C-$ ligand pair each. These two loops are related by a pseudo-twofold symmetry axis passing through the iron atom. Some zinc-finger modules in which the zinc ion has four Cys ligands are structurally very similar to Rd. Plant- and mammalian-type [2Fe–2S] Fds assume a structure named β-grasp, of which the main framework is a five-stranded antiparallel β-sheet with an α-helix lying on top of it. The remainder of the structure consists of short secondary elements and loops. Prominent among the latter is a surface loop including three of the four Cys ligands of the cluster. Another type of [2Fe–2S] Fd has a structure closely related to that of thioredoxin. The protein fold of Rieske proteins around their [2Fe–2S] active site is superimposable on the Rd fold; the His-ligated iron is the one closest to the protein surface. In 2[4Fe–4S] Fds, the two [4Fe–4S] clusters are surrounded by two pairs of antiparallel β-strands on one side, and two α-helices on the other. The structure displays a conspicuous twofold symmetry as a consequence of the sequence duplication. In high-potential Fd (HiPIP), a sizeable part (40%) of the structure is composed of hairpin turns while the remainder consists of several short strands and helices. Thereby, the [4Fe–4S] cluster is deeply buried in a hydrophobic cavity that stabilizes its oxidized 3+ state. The structural frameworks of the [2Fe–2S] Fd and low-potential [4Fe–4S] Fd are ubiquitous, and occur not only in small soluble Fds, but also in subunits and domains of many redox enzymes. The low-potential [4Fe–4S] Fd-fold is particularly versatile, and insertions and deletions inferred from sequence alignments have been substantiated by crystal structures. In addition to variations in sequence length, cases of cluster modification or loss have been observed.

Higher-Order Structures

While the canonical Fe–S protein folds described above have long dominated the landscape, numerous novel folds are revealed by the rapid growth of structural databases. It was predictable that polypeptide chains can fold in many different ways to position Cys residues appropriately for the binding of [2Fe–2S] or [4Fe–4S] active sites. Indeed, for the accommodation of [4Fe–4S] clusters alone, well over ten distinct protein folds have now been structurally characterized. There are even cases of [4Fe–4S] clusters held in proteins between two subunits, each of which provide two of the four Cys ligands as in nitrogenase and photosystem I.

Complex Fe–S Proteins with Clusters of High Nuclearity and Hetero-Metal Clusters

A yet higher level of complexity is displayed by proteins containing large metalloclusters which in several cases belong to the Fe–S family. Some of these "superclusters" can be roughly described as juxtapositions of two [4Fe–4S] clusters without (e.g., P clusters of nitrogenase) or with (e.g., FeMo-co clusters of nitrogenase) a metal atom other than Fe (Mo or V). Others are derived from a single [4Fe–4S] cluster by addition of one or two transition metal atoms (Fe, Ni). In the majority of these large metalloclusters, protein ligands other than Cys (His, Ser, peptidyl-N) or nonprotein ligands (homocitrate, dithiols, CO, CN^-) are also involved. Protein frameworks that accommodate these large clusters are generally bigger and more sophisticated than those of the usual Fe–S clusters. Nevertheless, it is noted that a number of them are assemblages of smaller substructures (e.g., Rossman folds).

Structural Flexibility and Relations to Function

Even though non-Cys ligation of Fe–S active sites is relatively rare, it is functionally important as a means of modulating chemical reactivity or redox potential. Several crystal structures of Fe–S active sites with His, Ser, or carboxylate ligands have now been determined. In some of these, non-Cys ligands are naturally present, in others they have been introduced by site-directed mutagenesis.

Atomic resolution (1.2Å or better) X-ray crystallography has become more accessible through technical improvements (synchrotron radiation, low temperature) and allows the detection of minute structural deviations that are imposed by the polypeptide chain or occur upon redox transitions. Crystal structures may convey the misleading impression that proteins are rigid structures; however, Fe–S proteins have malleable metal sites associated with flexible polypeptide chains. While essential functions of Fe–S proteins, electron transfer in particular, are indeed optimized through minimization of structural flexibility, as in Fd, many other functions require structural reorganizations of the polypeptide chain and metal cluster. Such modifications have long been known to occur upon degradation (oxidative denaturation, loss of iron) of some Fe–S proteins. Those kinds of structural fluctuations are difficult to monitor by X-ray crystallography. A notable

exception is the 3Fe/4Fe interconversion, which may occur with minimal protein reorganization. Other modifications of cluster nuclearity are expected to be associated with significant protein movements, since the Cys ligand sets of the [1Fe], [2Fe–2S], and [4Fe–4S] sites have very different spatial distributions. More recently, the functional relevance of structural changes in Fe–S proteins has moved to front-stage. Indeed, flexibility of both the metal site and the polypeptide chain are a necessity in proteins committed to sensing and transducing signals which may depend on redox state or metal concentration. Such structural changes may be classified in two main groups, according to whether it is the polypeptide chain (protein-driven reorganization of the metal site) or the metal site (cluster-driven protein movements) that assumes the leading role. Examples of the latter, where polypeptide chain movements are driven by the avidity of Fe–S clusters for Cys ligands, have been structurally characterized.

Functions

Electron Transfer

Obviously the principal function of Fe–S proteins is electron transfer. Thus, the oxidation–reduction potentials of the various possible redox couples in simple and complex Fe–S proteins are of interest. There are several reasons for the wide redox potential range ($\sim$1 V) covered by Fe–S proteins, the first of which is the electronic structure peculiarity of each type of Fe–S framework. Second, as each iron ion can be in either the Fe(III) or Fe(II) state, clusters of n Fe atoms are in principle endowed with $n - 1$ redox transitions. While this is observed in nature only in the case of the [4Fe–4S] clusters (3+/2+ and 2+/+ transitions), it allows the latter clusters to cover a range of $\sim$1 V on their own. Third, the redox potentials of Fe–S clusters can be modified by several parameters that are adjustable by the polypeptide chain. These include cluster ligation (sulfur, nitrogen, or oxygen), polarity of the medium, and neighboring charges. Studies of synthetic analogues and proteins, native as well as mutated ones, have shown that variations of each of these parameters can cause redox potential shifts larger than 50 mV. For instance, in Rieske-type proteins, the presence of two His ligands on the same Fe raises the redox potential of this Fe sufficiently so that it becomes reducible at a much higher potential than that of all-Cys ligated [2Fe–2S] active sites (Figure 1). The development of algorithms aimed at computing redox potentials of Fe–S clusters from charge and dipole distributions in their vicinity is an active area of research. Redox potentials reported in other compendia have been collected and the maximal and minimal values observed for various types of Fe–S proteins are summarized in Figure 1. Fe–S proteins can participate in more complex oxidation–reduction reactions, in which any component of the cluster or groups of the protein are also involved.

Reduction of Disulfide Bonds During the enzymatic reduction of some disulfide bonds as, e.g., in plant thioredoxin reductase, an extension of the coordination sphere of one of the iron ions occurs such that the cluster transitionally assumes the $[4Fe–4S]^{3+}$ level, as indicated by electron paramagnetic resonance (EPR), and its sulfides or Cys ligands may act as nucleophiles attacking disulfide bonds.

Initiation of Radical Chain Reactions There are a number of enzymes that use free-radical chemistry supported by adenosylmethionine to achieve substitutions on unactivated carbon atoms. In these enzymes a $[4Fe–4S]^{+}$ cluster with only three Cys ligands splits adenosylmethionine by transferring an electron and generating the adenosyl radical, which in turn initiates a radical chain reaction.

Generation of Unusual Reducing Power In a number of enzymes a reduced 4Fe cluster in conjunction with the hydrolysis of MgATP is used to achieve reductions of substrates by more than 1 V, such as required for the reduction of aromatic compounds or of dinitrogen. In these enzymes the 4Fe cluster is formed between two subunits of a protein with each contributing two Cys ligands. In such a structural arrangement conformational energy can be derived from MgATP binding and hydrolysis and then be made available for reduction of a substrate.

Functions not Involving Net Electron Transfer

The influence of the mere presence of Fe–S clusters or of rearrangements within clusters on adjacent groups or cofactors must also be considered. Fe–S clusters may polarize charges on adjacent groups or may serve as a reservoir capable of donating or absorbing charge. For such functions it is essential for Fe–S clusters to interact with their environment via any of their constituents, iron, sulfide, and the Cys ligands.

Fe–S Clusters as Active Sites of Enzymes The prime example, as to how one of the Fe-ions of a cluster can be used as active site of an enzyme is aconitase, in which there are only three Cys ligands to its Fe–S cluster. Thus, the unique iron is able to extend its coordination from four- to six-coordinate and bind the substrates, citrate or isocitrate. It can thus serve as a Lewis acid in the dehydration of the substrate to *cis*-aconitate and the rehydration to the alternate substrate with inversion of the positions of the H and OH substituents.

Similar changes in coordination of one of the iron ions are observed in reactions of other enzymes which contain a 4Fe cluster with only three Cys ligands.

Stabilization of Structures In some enzymes the network of ligands around an Fe–S cluster is used to stabilize specific structures.

Sensing and Regulatory Functions Fe–S clusters are labile toward oxygen, some of its reduction products and toward nitric oxide, and iron is required for their synthesis. Fe–S clusters can, therefore, also be used in nature as signaling or regulatory agents. While the Fe–S clusters of proteins that belong to this group may undergo one electron oxidation or complete oxidative destruction, the ensuing regulatory function involves specific interactions with DNA (SoxR, FNR) or RNA (IRP), which either require the presence (SoxR, FNR) or complete absence (IRP) of the Fe–S cluster. Examples of this are the [2Fe–2S] SoxR and [4Fe–4S] FNR protein in bacteria and the iron regulatory protein (IRP) in eukaryotes. SoxR is a sensor for the superoxide anion that binds to DNA upstream of the *soxS* gene. Its oxidation–reduction potential is such that it normally occurs in the reduced 1+ form in bacteria. Upon oxidation to the 2+ level by the superoxide anion, a structural modification of the SoxR–*soxS* nucleoprotein complex triggers expression of *soxS* and induction of the synthesis of defensive enzymes such as superoxide dismutase and other proteins. The FNR protein acts as oxygen sensor. Its 4Fe cluster is rapidly destroyed in the presence of oxygen and therewith its ability to induce the synthesis of enzymes required for anaerobic respiration with fumarate or nitrate as oxidants instead of oxygen. IRP of eukaryotes, on the contrary, is unable to serve as iron-regulator unless its cluster-binding site (3Cys) is unoccupied and contains free thiols. However, when it acquires an Fe–S cluster as [4Fe–4S] protein it takes on the function of a cytoplasmic aconitase. Both cytoplasmic and mitochondrial aconitases are only active in their 4Fe-form and are inactivated by loss of the unique iron that lacks a Cys ligand. As the 3Fe cluster is relatively stable it has been proposed that the switch between 4Fe (active) and 3Fe (inactive) enzyme is used in nature to protect the Fe–S cluster from irreversible further oxidation and for metabolic control, because aconitase is necessary for the functioning of the tricarboxylic acid cycle. As nitric oxide reacts with Fe–S clusters, with the main product formed being the dinitrosyl–iron complex (DNIC), NO has to be considered as an alternative messenger in the mentioned sensing pathways. In intact cells the Fe–S clusters can eventually be rebuilt in all the cases mentioned above. The interrelation of the pathways for sensing iron, oxygen, or its reduction products, and nitric oxide represents an interesting example of crossroads in natural signaling systems.

Methods for Obtaining Information on Fe–S Proteins

While gross information on Fe–S proteins is available from chemical approaches such as analysis for sulfide, iron, protein, and amino acids, spectroscopic methods have furnished a wealth of information on the more detailed and subtle properties of these fascinating, multipurpose tools of nature. Historically EPR was the first decisive method. It was soon followed by a considerable arsenal of diverse methods. Many of them probe the electronic and magnetic properties of the metal site in various ways that render them complementary to each other and to EPR. The most important of these are Mössbauer, magnetic circular dichroism (MCD), nuclear magnetic resonance (NMR), and electron-nuclear double resonance (ENDOR) spectroscopies. Other methods, such as resonance Raman and X-ray absorption spectroscopy (EXAFS, XANES), provide specific information relevant to the structural framework of the metal site. Computational approaches have been of great help for unraveling details of the electronic and magnetic structures of Fe–S clusters. The master tool of structural investigation, X-ray crystallography, has been implemented on small Rds and Fds at a very early stage, and is now successfully used for the determination of structures of large Fe–S enzymes and complexes. Very high resolution ($\leq$1Å) now allows the description of Fe–S active sites with a precision nearly matching that achieved with small synthetic molecules.

Biogenesis of Iron–Sulfur Proteins

General Overview

Methods for the *in vitro* assembly of Fe–S clusters on apoproteins were devised in the 1960s, while the chemical synthesis of Fe–S clusters in the absence of protein was also pursued and eventually developed to a high degree of specificity. However, it was around the late 1990s that the biosynthesis of Fe–S clusters in a living cell became a major field of interest and experimentation. It is clear now that these biochemical processes require the assistance of complex assemblies of proteins. At present, three different biogenesis systems have been identified. The most general one appears to be the ISC assembly machinery present in α-, β-, and γ-proteobacteria as well as in mitochondria of eukaryotes. The NIF system is specialized for the assembly of the complex Fe–S protein nitrogenase and consequently is found in several nitrogen-fixing bacteria, but also in nondiazotrophic ε-proteobacteria. The most

recently discovered system is the SUF machinery, which is found in a wide range of bacteria, archaea, and plastids of plants. In some organisms, either the ISC or the SUF system is responsible for assembly of cellular Fe–S proteins, whereas in other species they are present in parallel and may be responsible for the assembly of different subsets of Fe–S proteins.

Biogenesis of Fe–S Proteins in Bacteria

The Bacterial ISC Assembly Machinery

In prokaryotes the ISC assembly machinery is encoded by the *isc* (*i*ron–*s*ulfur *c*luster) gene cluster. This operon comprises genes encoding the proteins IscS, IscU, IscA, HscA, HscB, and Fdx. In addition to these proteins directly required for biogenesis, IscR is involved in the regulation of the *isc* gene expression. Biogenesis starts with the production of a sulfane sulfur from cysteine by the cysteine desulfurase IscS (Figure 2). The sulfur remains transiently bound to IscS and is covalently attached as a persulfide at a conserved cysteine residue. Upon interaction of IscS with the dimeric form of IscU the sulfur moiety is transferred to IscU, where it is also bound as a persulfide. The binding of ferrous iron to IscU leads to the formation of a [2Fe–2S] cluster, which then can give rise to the generation of a [4Fe–4S] cluster. Thus, IscU provides a scaffold for assembly of iron and sulfide ions. The molecular details of these reactions are still under investigation. IscU interacts with two chaperones, the ATP-dependent Hsp70/DnaK homologue HscA and the Hsp70/DnaJ homologue HscB. The interaction strongly stimulates the ATPase activity of HscA, but the precise function of these two proteins remains to be elucidated. Fe–S cluster assembly depends on the transfer of electrons from the [2Fe–2S] ferredoxin Fdx. The reactions which need the input of electrons are not known yet, but may involve the release of sulfur from cysteine by IscS and the dissociation of the Fe–S cluster from IscU. IscA is thought to function as an alternative scaffold protein to facilitate the assembly of Fe–S clusters. A [2Fe–2S] cluster can be assembled on IscA and subsequently transferred to a Fe–S protein such as Fdx. Presently, it is not known how the dissociation of the cluster from the scaffold proteins is triggered and which components may participate in cluster transfer to apoproteins.

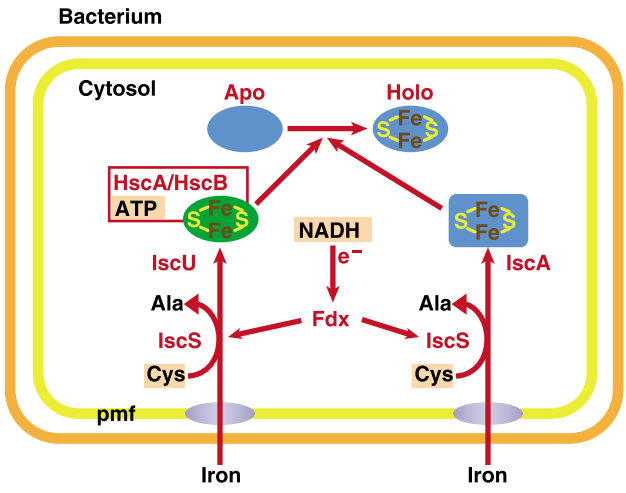

FIGURE 2 A working model for biosynthesis of Fe–S proteins in bacteria. For details see text. pmf, proton motive force.

The Bacterial SUF Machinery

The existence of a biogenesis system for Fe–S proteins in addition to the ISC assembly machinery has been noted only recently. When the *isc* operon is deleted in *E. coli*, Fe–S proteins are assembled at an efficiency of only 2–10% of that in wild-type cells. The residual assembly activity is due to the *suf* (mobilization of *sulf*ur) operon which contains the proteins SufA, SufB, SufC, SufD, SufS, and SufE. Many organisms contain only a subset of the *suf* genes. Overexpression of the *suf* gene cluster can restore Fe–S protein assembly in an *isc* deletion mutant. The *suf* operon is induced under iron-limiting conditions and repressed by the iron-sensing repressor protein Fur. Further, the *suf* operon is regulated by the transcription factor OxyR that senses oxidative stress conditions. This suggests that the SUF system is crucial under iron-limiting and oxidative stress conditions. The Suf proteins, homologues of Fdx and NifU, and an Fdx reductase are also present in apicoplasts, a plastid-like organelle of Apicomplexa such as Plasmodium and Toxoplasma.

SufS and SufA are homologues of IscS and IscA, respectively and may serve similar functions in liberating sulfur from cysteine, in scaffolding, and in cluster assembly. SufC is an atypical ATPase which forms a complex with SufB and SufD. SufE accepts sulfur from SufS and acts synergistically with the SufBCD complex to stimulate the cysteine desulfurase activity of SufS. This regulation of SufS activity may be important for limiting sulfur release during oxidative stress conditions. In addition, SufS has been assigned a function as a selenocysteine lyase in *E. coli*.

The Bacterial NIF Machinery for Assembly of Nitrogenase

Studies on nitrogen-fixing bacteria have identified the *nif* (*ni*trogen *f*ixation) operon as being responsible for maturation of the complex Fe–S protein nitrogenase. This enzyme consists of two oxygen-labile metalloproteins, the MoFe protein (NifKD) and the Fe protein (NifH). The latter contains a [4Fe–4S] cluster, whereas

the MoFe protein is associated with two unique superclusters: the P cluster and the iron–molybdenum cofactor (FeMo-co). The *nif* operon-encoded proteins NifS and NifU are involved in cluster biosynthesis by performing similar functions as their homologues IscS and IscU, respectively. The N terminus of NifU is homologous to IscU and provides a scaffold for assembly of transiently bound clusters, whereas the middle part of NifU contains a permanent [2Fe–2S] cluster that may carry out a redox function. Further, a homologue of IscA termed ^{Nif}IscA is thought to be an alternative scaffold for cluster assembly. Central components in the biosynthesis of FeMo-co are NifN and NifE, which form a hetero-tetramer and serve as a scaffold for cluster assembly before transfer to NifKD apoproteins. Further components needed for FeMo-co assembly are the *nif* operon-encoded proteins NifQ (Mo processing), NifV (homocitrate synthase), NifB (sulfur and iron donor) as well as NifH and NifX, the functions of which are unknown.

Biogenesis of Fe–S Proteins in Eukaryotes

The Mitochondrial ISC Assembly Machinery

In eukaryotes mitochondria are central for biogenesis of cellular Fe–S proteins. In keeping with their bacterial origin, these organelles contain homologues of the bacterial ISC assembly machinery. All proteins of the mitochondrial ISC assembly machinery are encoded by nuclear DNA and are imported after translation in the cytosol. The mitochondrial ISC assembly machinery consists of a few more proteins as compared to that in bacteria. Nevertheless, the mechanistic principles underlying biosynthesis might be rather similar. For instance, the cysteine desulfurase Nfs1 and the two highly homologous proteins Isu1 and Isu2 execute similar functions in elemental sulfur production and scaffolding as bacterial IscS and IscU, respectively (Figure 3). Formation of the transiently bound Fe–S cluster on the Isu proteins depends on the ferredoxin reductase Arh1 and the ferredoxin Yah1, which form an electron transfer chain using NADH as a reducing agent. In addition, Yfh1 acts as an iron donor during Fe–S cluster synthesis by directly interacting with the Isu/Nfs1 complex. Its human homologue, termed frataxin, is depleted in patients of Friedreich's ataxia, a neurodegenerative disease. The dissociation of the transiently bound Fe–S cluster from the Isu proteins and/or its insertion into apoproteins requires the mitochondrial glutaredoxin Grx5 and the two chaperones Ssq1 and Jac1 (Figure 3). The function of the IscA homologues Isa1 and Isa2 is still unclear, but possibly they provide an Isu protein-independent scaffolding function for the assembly of Fe–S clusters. Nfu1 genetically interacts with Ssq1 and Isu1, but its biochemical role in mitochondrial Fe–S protein assembly is not understood to date.

The Mitochondrial ISC Export Machinery

The mitochondrial ISC assembly machinery is not only responsible for the assembly of mitochondrial Fe–S proteins, but also plays an essential function in the maturation of Fe–S proteins outside mitochondria. To date, four components have been identified that are specifically needed for maturation of extra-mitochondrial, but not of mitochondrial Fe–S proteins (Figure 3). The first-known protein of the so-called ISC export machinery is the mitochondrial ABC transporter Atm1. The other components are the sulfhydryl oxidase Erv1 of the intermembrane space and glutathione (GSH). To date, not much is known about this export pathway on a biochemical level. For instance, the substrate of Atm1 is not known and the precise roles of Erv1 and GSH are unclear. Since virtually all components of the mitochondrial ISC assembly machinery are involved in the maturation of extra-mitochondrial Fe–S proteins, it is assumed that Atm1 exports an Fe–S cluster or a derivative thereof to the cytosol for transfer onto apoproteins. Mutation of the human homologue of Atm1, termed ABC7, gives rise to the iron storage disease X-linked sideroblastic anemia and cerebellar ataxia (XLSA/A). Finally, biogenesis of cytosolic Fe–S proteins requires Cfd1, a cytosolic P-loop ATPase that is conserved in

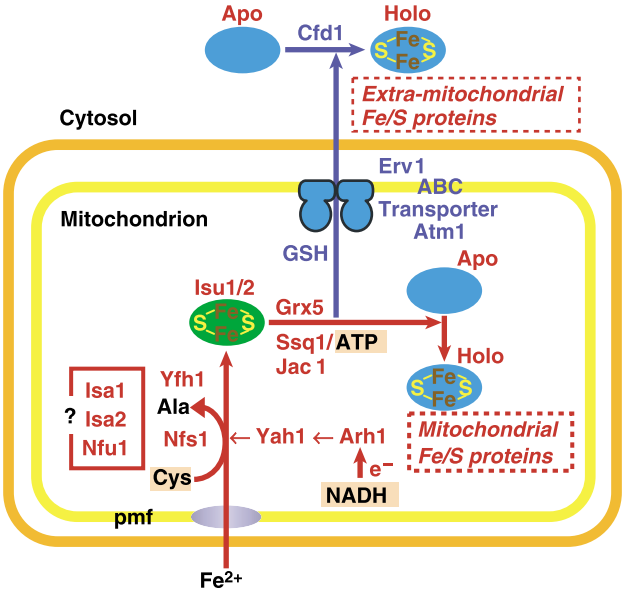

FIGURE 3 A working model for biosynthesis of Fe–S proteins in yeast. For details see text. pmf, proton motive force.

all eukaryotes. The protein may assist in Fe–S cluster insertion into cytosolic apoproteins.

Many components of the ISC machineries are essential for viability of yeast cells (e.g., Nfs1, Yah1, Arh1, Jac1, Erv1, and Cfd1) which demonstrates the importance of Fe–S protein biogenesis. Essential Fe–S proteins are known to be present in the yeast cytosol, but not in mitochondria. Hence, mitochondria appear to be essential organelles because they perform crucial steps in the biosynthesis of cytosolic Fe–S proteins.

Biogenesis of Fe–S Proteins in Chloroplasts

For more than a decade it has been clear that isolated chloroplasts can assemble Fe–S proteins suggesting that they contain their own assembly machinery. To date, we know a few components of this system. Homologues of IscS, IscA, and NifU have been located in plastids suggesting that a system homologous to the ISC assembly machinery is responsible for Fe–S protein biogenesis in these organelles. Further support for this notion comes from studies in cyanobacteria which are believed to be the evolutionary ancestors of chloroplasts. They contain several homologues of the ISC assembly machinery. Two members of the IscS family and NifU have been shown experimentally to perform functions similar to bacterial IscS and NifU. Strikingly, there is no member of the IscU family present in cyanobacteria suggesting that, in contrast to mitochondria, Fe–S cluster assembly does not involve Isu-like proteins but rather NifU and IscA as scaffolding proteins.

See Also the Following Articles

Disulfide Bond Formation • Ferredoxin • Ferredoxin-$NADP^+$ Reductase • Photosystem I: F_X, F_A, and F_B Iron–Sulfur Clusters

Glossary

Fe–S active sites Sites in proteins containing iron ligated to inorganic sulfides and/or cysteines.

iron–sulfur clusters The form in which irons and sulfides are organized in Fe–S proteins.

iron–sulfur proteins Proteins that contain iron and sulfur, active mostly (even if not exclusively) in electron transfer.

Further Reading

Beinert, H., and Kiley, P. J. (1999). Fe–S proteins in sensing and regulatory functions. *Curr. Opin. Chem. Biol.* **3**, 152–157.

Beinert, H., Kennedy, M. C., and Stout, C. D. (1996). Aconitase as iron–sulfur protein, enzyme, and iron-regulatory protein. *Chem. Rev.* **96**, 2335–2373.

Bertini, I., Zhou, H. X., Gori-Savellini, Luchinat, C., Mauk, A. G., Moore, G., Gunner, M. R., Alexov, E., Torres, E., Lipovaca, S., Gábor, N. S., Armstrong, F. A., Warshel, A., Papazyan, A., and Muegge, I. (1996). Determinants of reduction potentials in metalloproteins. *J. Biol. Inorg. Chem.* **2**, 108–152.

Cammack, R., and Sykes, A. G. (eds.) (1992). *Advances in Inorganic Chemistry*, Vol 38, Iron–Sulfur Proteins. Academic Press, San Diego, CA.

Craig, E. A., and Marszalek, J. (2002). A specialized mitochondrial molecular chaperone system: A role in formation of Fe/S centers. *Cell. Mol. Life Sci.* **59**, 1658–1665.

Frazzon, J., and Dean, D. R. (2003). Formation of iron–sulfur clusters in bacteria – An emerging field in bioinorganic chemistry. *Curr. Opin. Chem. Biol.* **7**, 166–173.

Gerber, J., and Lill, R. (2002). Biogenesis of iron–sulfur proteins in eukaryotes: Components, mechanism and pathology. *Mitochondrion* **2**, 71–86.

Johnson, M. K. (1994). Iron–sulfur proteins. In *Encyclopedia of Inorganic Chemistry* (R. B. King, ed.), Vol 4, pp. 1896–1915. Wiley, Chichester, UK.

Meyer, J. (2001). Ferredoxins of the third kind. *FEBS Lett.* **509**, 1–5.

Mühlenhoff, U., and Lill, R. (2000). Biogenesis of iron–sulfur proteins in eukaryotes: A novel task of mitochondria that is inherited from bacteria. *Biochim. Biophys. Acta* **1459**, 370–382.

Palmer, G., and Reedijk, J. (1991). Committee of the International Union of Biochemistry, Non-Heme Iron Proteins, in "Nomenclature of Electron-Transfer Proteins". *Eur. J. Biochem.* **200**, 599–611.

Rees, D. C. (2002). Great metalloclusters in enzymology. *Annu. Rev. Biochem.* **71**, 221–246.

Sykes, A. G., and Cammack, R. (eds.) (1999). *Advances in Inorganic Chemistry*, Vol. 47, Iron–sulfur proteins. Academic Press, San Diego, CA.

Biography

Helmut Beinert holds the degree of Doctor of Natural Sciences from the University of Leipzig, Germany. He was a postdoctoral Fellow at the Institute for Enzyme Research at the University of Wisconsin, Madison, where he is now a Professor Emeritus. His interests are mainly in enzymes of biological oxidation and metal-proteins.

Jacques Meyer studied at the École Supérieure de Physique et Chimie of Paris, earned a doctoral degree of Natural Sciences from the University of Grenoble and now holds a permanent research position at the CEA at Grenoble. His interest is in structure and function of Fe–S proteins.

Roland Lill holds a degree of Doctor of Natural Sciences from the University of München, Germany, received postdoctoral training at the University of California at Los Angeles, USA, and currently is a Professor of Cell Biology at the University of Marburg, Germany. His interest is in the biogenesis and function of Fe–S proteins.

JAK-STAT Signaling Paradigm

Edward Cha and Christian Schindler
College of Physicians and Surgeons, Columbia University, New York, USA

The janus kinases (JAKs) and their downstream signal transducers and activators of transcription (STATs) comprise a remarkably direct signaling pathway. Cytokines that transduce signals through this pathway play a critical role in cellular development, differentiation, and immune response. This article discusses how the scheme works, what factors are involved, and the biological functions JAKs and STATs play.

Introduction

The JAK-STAT pathway was first discovered through an investigation into the mechanism by which a subfamily of cytokines, the interferons (IFNs), rapidly induced the expression of new genes. Subsequent studies demonstrated that this pathway is not restricted to IFNs, but encompasses a ~50 member subset of the cytokine family known as hematopoietins (see Table I). These hematopoietins are particularly important in the development and activity of leukocytes and so were given the name interleukin (IL). When these hematopoietins bind to their specific cognate cell surface receptors, a member of the STAT family is activated by tyrosine phosphorylation to become a potent transcription factor that translocates to the nucleus and rapidly induces the expression of specific target genes. Because hematopoietin receptors lack catalytic activity, their cytoplasmic domains associate with members of the JAK family to acquire tyrosine kinase activity. Table I provides a list of the members of the hematopoietin family and the JAKs and STATs through which they transduce signals. These hematopoietins are divided into subgroups based on the five structurally and functionally related receptor subfamilies to which they bind.

The Signaling Paradigm

The prototypical JAK-STAT signaling pathway, illustrated in Figure 1, consists of a series of sequential tyrosine phosphorylation events that culminate in the induction of target genes. When a cytokine binds to its corresponding receptors, it promotes a conformational change, bringing receptor-associated JAK kinases into close proximity. The kinases then activate each other by transphosphorylation and subsequently phosphorylate specific tyrosine residues on the cytoplasmic tail of the receptor. The STAT Src homology 2 (SH2) domain (see Figure 2) recognizes these specific receptor phosphotyrosine motifs (a phosphotyrosine and four adjacent amino acids), effecting its recruitment to the receptor. Once at the receptor, the STATs are phosphorylated on a single tyrosine residue (Figure 2), in a JAK-dependent manner. The activated STATs then dissociate from the receptor and dimerize through a classical phosphotyrosine-SH2 interaction. Only then are STATs truly competent for rapid nuclear translocation and DNA binding to members of the gamma-activated sequence (GAS) family of enhancers.

JAK Kinases

There are four mammalian members of the JAK family: Jak1, Jak2, Jak3, and Tyk2. They are over 1000 amino acids in length and range in size from 120 to 130 kDa. All but Jak3 are expressed ubiquitously, the latter being found only in cells of myeloid and lymphoid lineages. JAKs consist of seven conserved Jak homology (JH) domains (Figure 2). The carboxy-terminal JH1 constitutes the tyrosine kinase domain and JH2 the pseudokinase domain, which has all the structural features of a tyrosine kinase except catalytic activity and appears to regulate JH1 activity. The amino-terminal JH domains, JH3–JH7, constitute a FERM (four point one, ezrin, radixin, moesin) domain and mediate association with receptors. Specifically, JAKs associate with proline-rich, membrane proximal box1/box2 domain of these receptors. Each receptor subgroup is linked to a particular pair of JAKs by these domains. Consistent with that, Jak gene targeting studies have identified characteristic signaling defects.

Jak1 associates with the IFN-α receptor, gp130, and the common γ (γC) receptor chain families. Knockout mice die perinatally due to a neurological defect attributed to a loss in gp130 signaling. Jak1$^{-/-}$ mice also exhibit reduced lymphocyte counts due to a lack of T and NK cells. Consistent with biochemical studies,

TABLE I

Hematopoietin-Dependent JAK-STAT Signaling

Ligands	JAKs	STATs
gp130 family[a]		
IL-6	**Jak1**, (Jak2)	**Stat3**, Stat1
IL-11	Jak1	**Stat3**, Stat1
OSM	Jak1, (Jak2)	**Stat3**, Stat1
LIF	**Jak1**, (Jak2)	**Stat3**, Stat1
CNTF	Jak1, (Jak2)	**Stat3**, Stat1
NNT-1/BSF-3	Jak1, (Jak2)	**Stat3**, Stat1
G-CSF	Jak1, (Jak2)	**Stat3**
CT-1	Jak1, (Jak2)	**Stat3**
Leptin	Jak2	**Stat3**
IL-12	**Tyk2**, Jak2	**Stat4**
IL-23	?	**Stat4**
IL-27	?	Stat4
γC family[b]		
IL-2	**Jak1**, **Jak3**	**Stat5**, (Stat3)
IL-7	**Jak1**, **Jak3**	**Stat5**, (Stat3)
TSLP[c]	?	Stat5
IL-9	Jak1, Jak3	**Stat5**, Stat3
IL-15	**Jak1**, Jak3	**Stat5**, (Stat3)
IL-21	Jak3, (Jak1)	Stat3, Stat5, (Stat1)
IL-4	**Jak1**, **Jak3**	**Stat6**
IL-13[c]	Jak1, Jak2	**Stat6**, (Stat3)
IL-3 family		
IL-3	**Jak2**	**Stat5**
IL-5	**Jak2**	**Stat5**
GM-CSF	**Jak2**	**Stat5**
Single-chain family		
Epo	**Jak2**	**Stat5**
GH	Jak2	**Stat5**, (Stat3)
Prl	Jak2	**Stat5**
Tpo	**Jak2**	**Stat5**
IFN/IL-10 family[d]		
IFN-γ (Type II)	**Jak1**, **Jak2**	**Stat1**, (Stat5)
IFN, Type I[e]	**Jak1**, Tyk2	**Stat1**, **Stat2**, (Stats3–6)
IL-28a (IFN-λ1)	Jak1, Tyk2	Stat1, Stat2, Stat3
IL-28b (IFN-λ2)	Jak1, Tyk2	Stat1, Stat2, Stat3
IL-29 (IFN-λ3)	Jak1, Tyk2	Stat1, Stat2, Stat3
IL-10	**Jak1**, Tyk2	**Stat3**, Stat1
IL-19	?	?
IL-20	?	Stat3
IL-22	**Jak1**, Tyk2	Stat3, (Stat5)
IL-24	?	Stat3
IL-26	?	Stat3
IL-28a (IFN-λ1)	Jak1, Tyk2	Stat1, Stat2, Stat3
IL-28b (IFN-λ2)	Jak1, Tyk2	Stat1, Stat2, Stat3
IL-29 (IFN-λ3)	Jak1, Tyk2	Stat1, Stat2, Stat3

Hematopoietins transduce their signals through specific sets of JAKs and STATs as indicated. Assignments for which there is the most confidence (i.e., based on knockout and biochemical studies) are shown in boldface; those with less confidence are shown in lightface; and those with the least confidence are shown in parentheses.

[a] As indicated, this family is divided into two subfamilies.

[b] As indicated, this family is divided into two subfamilies.

[c] Bind to a related but γC-independent receptor.

[d] As indicated, this family is divided into three subfamilies.

[e] In humans this family consists of 12 IFN-αs, IFN-β, IFN-ω, Limitin, and, most distantly, IFN-λs.

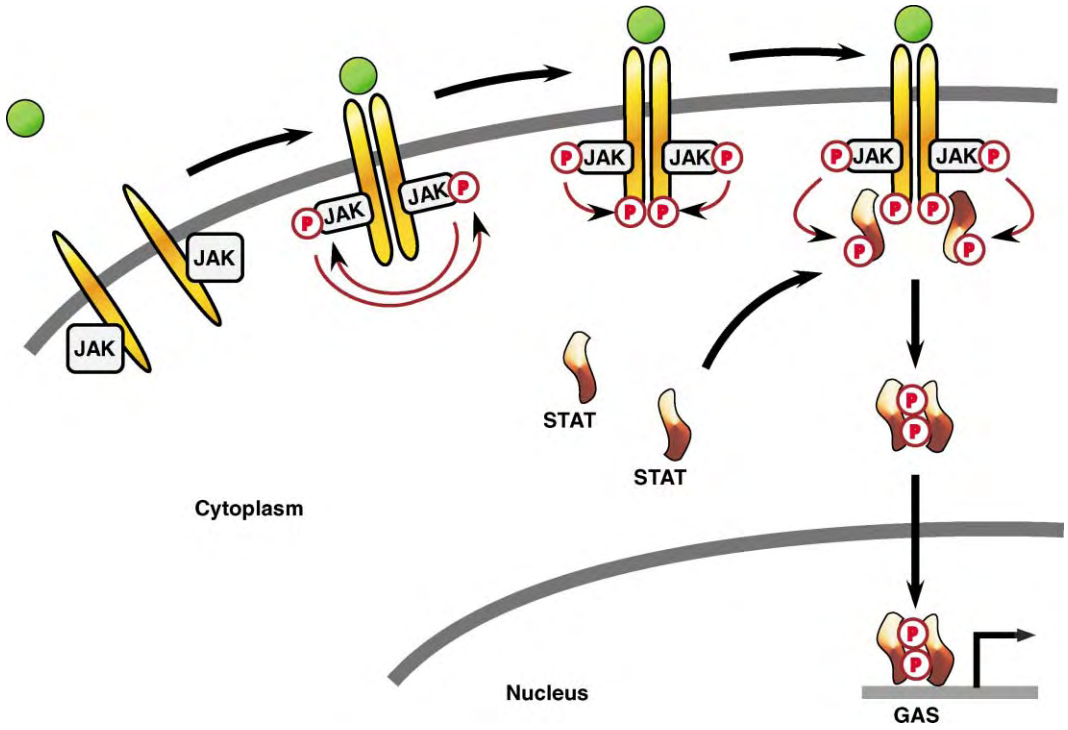

FIGURE 1 The JAK-STAT signaling pathway. Upon binding ligand, receptor-associated JAKs become activated and phosphorylate specific receptor tyrosine residues. STAT SH2 domains recognize the receptor phosphotyrosines, effecting their recruitment to the activated receptor complex. STATs are then tyrosine-phosphorylated. The activated STATs are released from the receptor, dimerize, translocate to the nucleus, and bind to members of the gamma activation site (GAS) family of enhancers.

cells collected from Jak1$^{-/-}$ mice fail to respond to cytokines from the gp130, γC, and IL-10 families.

Jak2-deficient mice exhibit an embryonic lethal phenotype, dying at embryonic day 12.5 due to failure in definitive erythropoiesis, analogous to what has been observed in the erythropoietin knockout mice. Tissues collected from Jak2 knockout mice fail to respond to IFN-γ and most of the cytokines from the IL-3 and single-chain (excluding G-CSF) cytokine receptor families (see Table I).

Jak3 expression is limited to hematopoietic cells, where it exclusively associates with the γC chain. Hence, the Jak3 knockout mice exhibit a severe combined immunodeficiency (SCID) syndrome, with impaired lymphopoiesis, which is also analogous to the defect seen in γC-deficient hosts.

Biochemical studies have implicated Tyk2 in the biological response to type I IFNs, IL-10 and IL-12, and have shown that Tyk2 associates with the corresponding receptors. Moreover, Tyk2 was originally identified in a genetic screen designed to identify components mediating the biological response to IFN-α. Yet Tyk2 knockout mice exhibit only relatively subtle defects in their response to IFN-α/β and IL-10 responses. They do,

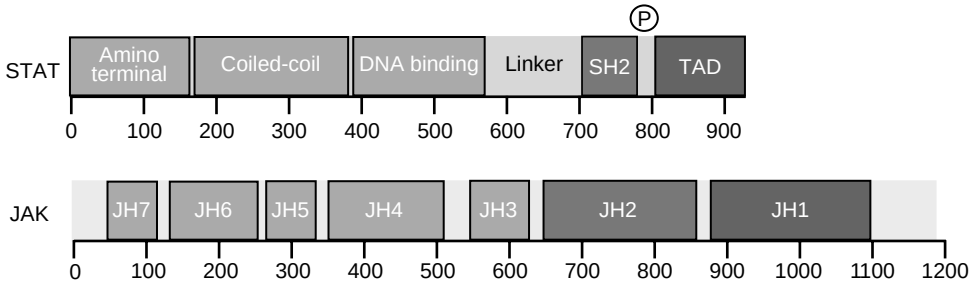

FIGURE 2 Schematic representation of JAK and STAT structures. JAKs can be divided into seven homology regions, JH1–JH7. JH1 encodes the kinase; JH2 encodes the pseudokinase domain, which regulates catalytic kinase activity; JH3–JH7 encode the FERM domain, which mediates receptor interactions. STAT proteins can also be divided into seven structurally and functionally conserved domains, including the amino-terminal, coiled-coil, DNA-binding, linker, SH2, tyrosine activation site, and transcriptional activation domains.

however, exhibit significant defects in their response to IL-12 and profound defects in their responses to LPS. How Tyk2 pertains to LPS activation in macrophages remains an important area of inquiry.

The STATs

There are seven mammalian STATs (Stats 1, 2, 3, 4, 6, and two Stat5 genes) ranging in size from 750 to 900 amino acids. They contain seven structurally and functionally conserved domains: amino-terminal, coiled-coil, DNA-binding, linker, SH2, tyrosine activation, and transcriptional activation domains (TADs) (Figure 2).

The amino-terminal ~125 amino acids represent an independently folded and stable moiety, which is well conserved but functionally not fully characterized. Several studies have implicated this domain in promoting cooperativity in DNA binding, in homotypic dimerization, in regulating nuclear translocation, and in promoting interactions with other proteins. The coiled-coil domain (amino acids ~135 to ~315) consists of a four-α-helix bundle that protrudes about 80 Å laterally from the core structure. This domain provides a largely hydrophilic surface that promotes interactions with a number of potentially important regulatory modifiers, such as IRF9 and StIP1. It has also been implicated in nuclear export.

The DNA-binding domain (amino acids ~320 to ~480) is a β-barrel with an immunoglobulin fold that recognizes the GAS family of enhancers. The dissociation constant lies in the nanomolar range, so cooperativity in DNA binding is likely important in establishing an effective transcriptional activity. Interestingly, like the upstream coiled-coil domain, the DNA-binding domain appears to regulate nuclear export. In contrast to all other STATs and despite a well-conserved DNA-binding domain, Stat2 is unable to bind DNA directly. The adjacent linker domain (amino acids ~480 to ~580) is important in ensuring the appropriate conformation of the DNA binding motif in activated STAT dimers. This domain also appears to regulate nuclear export in resting cells.

Not surprisingly, the SH2 domain (amino acids ~575 to ~680) is the most highly conserved motif and mediates both receptor attachment and STAT dimerization. It consists of an antiparallel β-sheet flanked by two α-helices, which form a pocket. At the base of the pocket lies an absolutely conserved arginine that mediates the interaction with the conserved phosphorylated tyrosine motif of the dimerization partner. This short tyrosine activation motif is located near residue 700. All STATs except Stat2 form stable homodimers *in vivo*. Finally, the carboxy terminus carries a TAD, which is conserved between species for each STAT (e.g., murine and human Stat1) but varies considerably between different STAT family members (e.g., Stat1 vs Stat2). Once again, Stat2 is the exception. Its TAD domain varies considerably in sequence between the murine and human homologues.

STAT dimers bind to a palindromic GAS element ($TTCN_{2-4}GAA$). The spacing between the palindromic half sites determines preferential binding specificity. For instance, Stat1 binds to an element with a canonical n = 3 spacing, while Stat3 and Stat6 favor n = 2 and n = 4, respectively. Cooperative binding to neighboring sites of two or more STAT dimers has also been well documented for a number of target genes. Again, however, Stat2 is the exception. Upon activation, Stat2 forms a heterodimer with Stat1 that exhibits no DNA-binding activity. Rather, it associates with IRF9 and binds to the IFN-stimulated response element (ISRE; AGTTTNNNTTTCC), a member of the IRF family of enhancers.

Stat1 is critical for both type I (IFN-$\alpha/\beta/\lambda$) and type II (IFN-γ) interferon signaling. Stat1 homodimerizes in response to activation by IFN-γ or heterodimerizes with Stat2 in response to activation by IFN-α/β. Biochemical and genetic studies have also suggested that Stat1 contributes to the biological response to gp130 receptors along with Stat3.

Stat2 is the most unique member of the STAT family. As previously indicated, it only transduces signals for type I IFNs, but can neither form homodimers nor bind to DNA directly. Rather, it heterodimerizes with its obligate partner Stat1 to translocate to the nucleus, where it associates with IRF9 to form the ISGF-3 and to bind to ISRE elements. In ISGF-3, IRF9 constitutes the core DNA-binding component, and Stat1 promotes contact with the additional flanking nucleotides. Finally, there is a surprising level of divergence between murine and human Stat2.

Stat3 transduces signals for a large number of cytokines, most notably members of the gp130 and IL-10 families. Pointing back to its evolutionary origins as a critical regulator of development, Stat3 knockout mice display an early (i.e., day 6.5–7.5) embryonic lethal phenotype. However, tissue-specific deletions of the Stat3 gene have confirmed the critical role Stat3 plays in transducing signals for the gp130 and IL-10 families of hematopoietin receptors.

Stat4 is predominantly involved in signaling for the small IL-12 family, which includes IL-12, IL-23, and IL-27. IL-12, whose response has been studied most extensively, is a potent inducer of IFN-γ production in both T-cells and NK cell. It also plays an important role in driving polarization of naive $CD4^+$ T-helper cells into the Th1 effector subset.

Stat5a and Stat5b are encoded by two tightly linked and highly homologous genes (~96% amino acid identity). All members of the IL-3 receptor and single-chain receptor families (e.g., GH, PRL, and EPO) transduce signals through these isoforms of Stat5.

The γC receptors (i.e., the IL-2, IL-7, IL-9, IL-15, and IL-21 receptors) have also been shown to transduce important signals through Stat5. Yet the defect in Stat5a knockout is almost exclusively toward PRL, and the defect in Stat5b is almost exclusively toward GH. Mice deficient in both feature notable defects in their response to PRL, GH, EPO, IL-2, and members of the IL-3 family.

Stat6 transduces signals for IL-4 and the closely related IL-13. IL-4 plays an important role in the development of the Th2 subset of T-helper cells. Thus, Stat4 and Stat6 serve as protagonists in maintaining the important balance between the Th1 and Th2 subsets of effector T-cells. IL-4 is also important for B-cell maturation. Consistent with this, Stat6 knockout mice fail to proliferate, up-regulate MHC II expression, or secrete IgE in response to IL-4.

Regulation of JAK-STAT Signaling

STAT-dependent gene induction is both rapid and transient. The brisk activation phase entails both rapid nuclear translocation and robust DNA-binding activity. This nuclear translocation is mediated by karyopherins (e.g., importin-α5) and Ran-GTPase. (This process is distinct from low levels of basal nuclear import/export that have been reported for several STATs.) However, identification of a canonical STAT nuclear localization signal (NLS) sequence remains elusive. Although putative NLS sequences have been reported for several STATs (e.g., in the DNA-binding domain), they fail to mediate the nuclear import of reporter proteins.

STAT-dependent signal decay, which is typically initiated within hours of stimulation, is also carefully regulated. This process entails phosphatases (nuclear and cytoplasmic), nuclear export, and one or more families of regulatory proteins. Recent studies indicate that STAT nuclear export is tightly coupled with dephosphorylation, possibly mediated by TC-PTP, but the molecular events regulating this appear complex. For example, several leucine-rich nuclear export sequence (NES) motifs, which drive the GTP-dependent nuclear export, have been identified in the coiled-coil and DNA-binding domains of Stat1 and Stat3. Other phosphatases, including SHP1 and CD45, dephosphorylate the JAKS and receptors, where the signal was initiated.

Signaling is also negatively regulated by SH2-containing SOCS (suppressors of cytokine signaling) proteins, whose expression is directly induced by STAT-dependent signals, completing a classical negative feedback loop. $SOCS1^{-/-}$ mice, for example, die between the second and third week of life with a disorder marked by nonspecific T-cell activation, inflammation, and liver necrosis. These findings have been attributed to unchecked IFN-γ–Stat1- and IL-4–Stat6-dependent inflammation. $SOCS3^{-/-}$ mice die during embryogenesis from a placental defect. However, specific tissues exhibit prolonged and abnormal gp130-dependent signaling. SOCS1 and SOCS3 are believed to exert their negative effect by binding to phosphorylated tyrosine residues in the activation loop of Jak2 and the gp130 receptor, respectively. SOCS family members may also promote protein degradation by directly facilitating the addition of ubiquitin to target proteins.

Another group of proteins implicated in the negative regulation of STATs is the PIAS (protein inhibitors of activated STATs) family, which was initially suggested to mediate their negative effects by binding directly to activated STAT dimers. However, the recent recognition that PIAS proteins are SUMO (small ubiquitin-related modifiers) E3 ligases has raised the possibility that they may exert their negative regulation by promoting the covalent addition of SUMO adducts. Studies indicating that some nuclear pore proteins may SUMOylate target proteins, and that Stat1 is SUMOylated, suggest a potential role in the regulation of STAT nuclear import and export.

In closing, it should be noted that some STAT modifications serve to integrate STAT signal transduction with that of other signaling pathways, potentiating STAT activity. For example, JNK/MAP kinase-dependent pathways have been shown to promote the phosphorylation of specific serine residues (Ser727 in Stat1 and Stat3) within the TAD, thereby enhancing the expression of some, but not all, target genes. These observations raise the question of whether other types of covalent modification (e.g., acetylation or methylation) will be found to similarly regulate and integrate STAT signals.

See Also the Following Articles

Cytokines • Hematopoetin Receptors • Interferon Receptors • SUMO Modification

Glossary

gamma activation site (GAS) A specific enhancer element that is recognized by most activated STAT homodimers. It was first identified as an IFN-γ response element.

hematopoietins A subset of cytokines, which are secreted peptide ligands, that mediate potent biological responses in target cells. They are predominantly involved in regulating inflammation and immunity. Examples include IFN-α, IFN-γ, IL-2, IL-3, IL-4, PRL, GH, EPO, G-CSF, and GM-CSF.

IFN-stimulated response element (ISRE) A specific enhancer that is recognized by ISGF-3, an IFN-α-activated transcription factor consisting of Stat1, Stat2, and IRF-9.

janus kinase (JAK) Tyrosine kinase that associates with cytokine receptors and provides catalytic activity that is essential to initiate signal transduction.

protein tyrosine kinases Catalytic function measures the ability of the enzyme to phosphorylate itself or its substrates.

protein tyrosine phosphorylation Posttranslational modification required of tyrosine residues that can modulate catalytic function as well as mediate protein–protein interactions.

receptors Transmembrane-spanning proteins that specifically bind extracellular ligands to mediate a biological response. Examples include the IFN receptor (IFNAR), the IF-γ receptor, gp130, and γC.

signal transducers and activators of transcription (STATs) A family of latent cytoplasmic transcription factors that transduce signals for cytokines.

Src homology 2 (SH2) The domain that mediates protein–protein interactions by binding to sites of tyrosine phosphorylation.

Src homology 3 (SH3) The domain that mediates protein–protein interactions by binding to proline-rich motifs with a core sequence of Pro-X-X-Pro.

tyrosine kinase A kinase that phosphorylates protein substrates on tyrosine residues.

Further Reading

Kisseleva, T., Bhattacharya, S., Braunstein, J., and Schindler, C. W. (2002). Signaling through the JAK/STAT pathway, recent advances and future challenges. *Gene* **285**, 1–24.

Levy, D. E., and Darnell, J. E. Jr. (2002). Stats: Transcriptional control and biological impact. *Nat. Rev. Mol. Cell. Biol.* **3**, 651–662.

O'Shea, J. J., Gadina, J., and Schreiber, R. D. (2002). Cytokine signaling in 2002: New surprises in the Jak/Stat pathway. *Cell* **109**, S121–S131.

Schindler, C. (2002). JAK-STAT signaling in human disease. *J. Clin. Invest.* **109**, 1133–1137.

Biography

Ed Cha earned his Bachelor's degree from Princeton University and is currently an M.D.–Ph.D. student at Columbia University's Medical Scientist Training Program.

Christian Schindler earned his Bachelor's degree from the University of Pennsylvania, and his M.D. and Ph.D. degrees from New York University School of Medicine. After a residency in internal medicine at Jacobi Hospital/Albert Einstein Medical Center, he became an Endocrinology Fellow at the Cornell/Memorial Sloan Kettering/Rockefeller University program. This training culminated in a postdoctoral fellowship in James Darnell's laboratory, where he purified and cloned the first two STAT proteins. Since 1992 he has been a Faculty Member in the Departments of Medicine and Microbiology at Columbia University.

Keratins and the Skin

Pierre A. Coulombe and Kelsie M. Bernot
The Johns Hopkins University School of Medicine, Baltimore, Maryland, USA

Keratins are among the most abundant proteins in epithelial cells, in which they occur as a cytoplasmic network of 10–12 nm wide intermediate filaments. They are encoded by a large multigene family in mammals, with over 49 individual genes partitioned into two major sequence types. A strict requirement for the heteropolymerization of types I and II keratin proteins during filament assembly underlies the pair wise transcriptional regulation of keratin genes. Modulation of keratin expression also depends upon both the type and stage of differentiation in epithelia. A major function fulfilled by keratin filaments is to act as a resilient yet pliable scaffold, which endows epithelial cells with the ability to sustain mechanical and nonmechanical stresses. Reflecting this crucial role as structural scaffolds, inherited mutations altering the coding sequence of keratins are responsible for a large number of epithelial fragility disorders. Additional functions, manifested in a sequence- and context-dependent fashion, have been identified.

Keratin Classification

Keratins belong to the superfamily of intermediate filament (IF) proteins. They are heterogeneous in size (400–644 amino acid residues) and charge (pI ~ 4.7–8.4), and notoriously insoluble owing to their primary structure. Keratin nomenclature originally was based upon protein separation by both charge and size via two-dimensional electrophoresis. Type I keratins tend to be smaller (40–64 kDa) and acidic (pI ~ 4.7–6.1) compared to type II, which are larger (52–68kDa) and basic-neutral (pI ~5.4–8.4) in charge. Comparison of either amino acid sequence (Figure 1A) or gene substructure (number and position of introns) reveals two distinct groups of approximately equal numbers of keratin members, designated type I (K9–K23; Ha1–Ha8; Irs1–4) and type II (K1–K8; Hb1–Hb6; K6irs1–4) IF proteins.

Keratin Gene Clusters Reflect Tissue Expression: Implications for Keratin Evolution

The coordinated regulation of the two distinct types of keratin-like genes, along with the obligatory heteropolymerization of their products to form 10–12 nm wide filaments, is present as far back as primitive chordates. In *Homo sapiens*, functional type I and type II keratins genes are clustered on the long arms of chromosomes 17 and 12, respectively (Figures 1B and 1C). There is a notable exception to this principle, in that the type I keratin 18 (K18) locus is located next to K8 at the telomeric boundary of the type II cluster (Figure 1C). K8 and K18 exhibit a very tight coregulation in both embryonic and adult simple epithelia, and likely are the direct descendants of the ancestral pair of keratin genes. The key molecular features of individual keratin genes (e.g., size and number of introns/exons) and those of the genomic clusters they form (e.g., transcriptional orientation, position relative to other family members) are perfectly conserved in human and mouse, and in many other species of mammals as well. This conservation has direct implications for the evolution of keratin genes and points to the existence of locus control elements simultaneously affecting the regulation of several neighboring genes.

Comparing the primary structure of human keratins also reveals the existence of distinct subfamilies within each of the two keratin types (Figure 1A), and provides additional insight into the mechanisms presiding over their evolution. Groupings of individual genes within each of the two major clusters correspond to similar patterns of expression in specific types of epithelial cells or tissues. This situation applies for most genes expressed in simple epithelia (K7, K8, K18, K20), "soft" complex epithelia (K1–K6; K9–K17), "hard" epithelia such as hair shaft and nail (Ha1–Ha8; Hb1–Hb6), and even the highly restricted inner root sheath compartment of hair follicles (K6irs-1–4; Irs1–4). In addition to these intriguing features, the clustering of keratin genes is mirrored by a corresponding clustering of related protein products as revealed by phylogenetic analysis. This striking equivalence, highlighted by the color scheme employed in Figure 1, implies a hierarchical pattern of gene duplication and specialization during evolution.

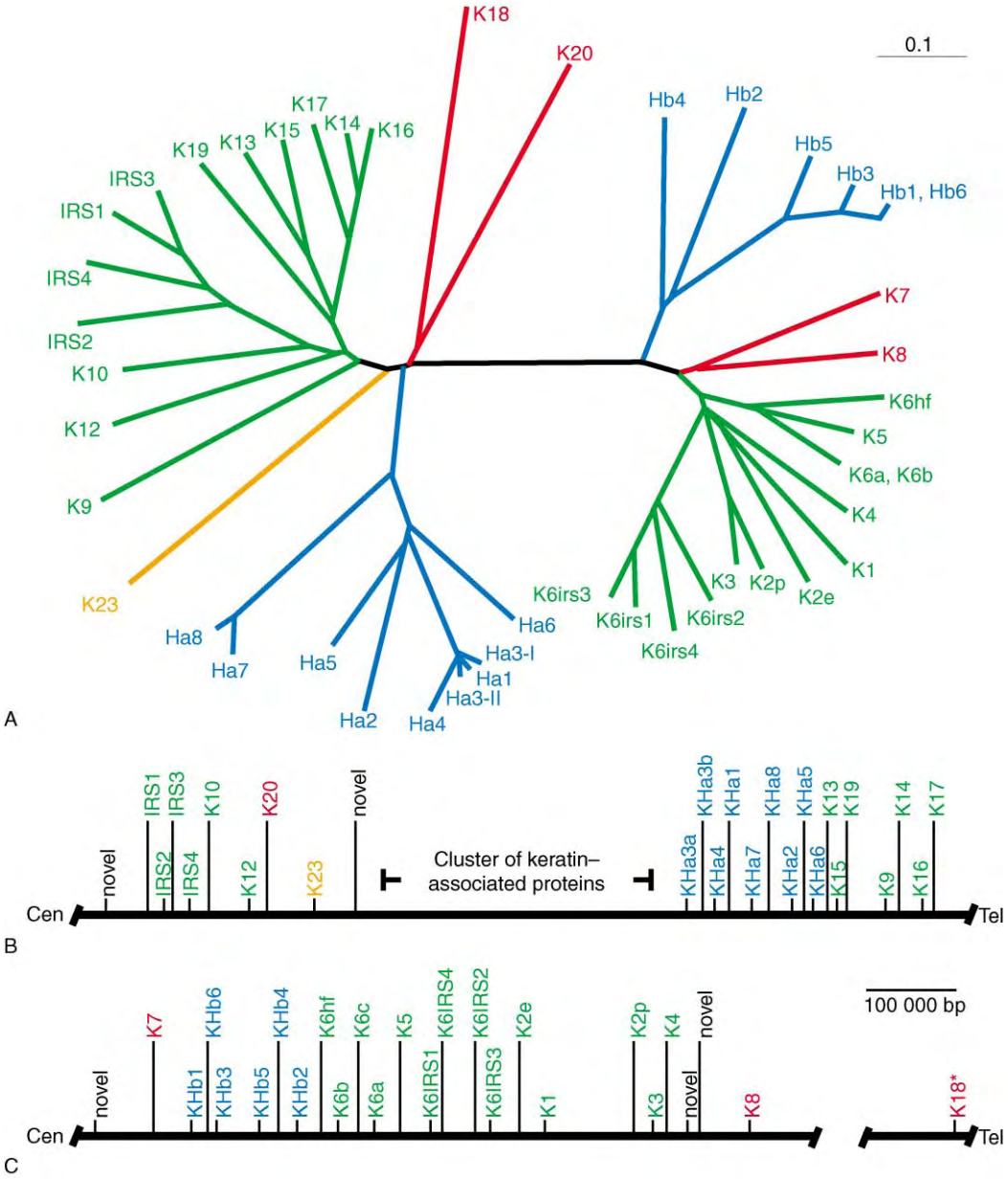

FIGURE 1 The human keratin family *circa* 2003. (A) Comparison of the primary structure of human keratins using the publicly available ClustalW and TreeView software. Sequence relatedness is inversely correlated with the length of the lines connecting the various sequences, and to the number and position of branch points. This comparison makes use of the sequences from the head and central rod domain for each keratin. A few keratins were left out for purposes of clarity. Two major branches are seen in this tree display, corresponding exactly to the known partitioning of keratin genes into type I and type II sequences. Beyond this dichotomy each subtype is further segregated into major subgroupings. (B) Organization of functional type I keratin genes in the human genome. All functional type I keratin genes are clustered on the long arm of human chromosome 17. The only exception is K18 (asterisk), which is located at the telomeric (Tel) boundary of the type II gene cluster (Cen = centromere). Transcriptional orientation is from Tel to Cen for all genes. (C) All functional type II keratin genes are clustered on the long arm of human chromosome 12. The *K8* and *K18* genes are separated by 450 000 bp. Comments on A–C: As highlighted by the color code, individual type I and type II keratin genes belonging to the same subgroup, based on the primary structure of their protein products, tend to be clustered in the genome. Moreover, very highly related keratins are often encoded by neighboring genes (e.g., *K5* and *K6* paralogues; also, *K14*, *K16*, and *K17*), further emphasizing the primary role of gene duplication in generating keratin diversity. These features of the keratin family are virtually identical in mouse (not shown).

Keratin Proteins Form the Intermediate Filament Network of Epithelial Cells

Features of Keratin Proteins

Despite sequence differences, all keratins display the tripartite domain structure that is typical of intermediate filament-forming proteins (Figure 2A). The central domain consists of an extended α-helix featuring long-range heptad repeats that mediate coiled-coil dimerization. This "rod" domain is invariably 310 amino acids long and is flanked by highly variable sequences at the N-terminal head and C-terminal tail domains. Neither terminal domain exhibits known functional motifs other than the poorly understood glycine loops seen in epidermal keratins. The head and tail domains are protease- and kinase-accessible and thus must be exposed at the surface of the filament, where they can foster interactions with neighboring filaments, other proteins, and serve as substrates for posttranslational modifications involved in their regulation. Given the notion that they are very heterogeneous in size and primary structure among keratins, the head and tail domains are clearly key to the differential function and regulation of these proteins *in vivo*.

Keratin Proteins Self-Assemble into 10–12 nm Wide Filaments

The central rod domain of keratins is the main determinant of polymerization, with an additional contribution provided by the head domain, whereas the tail domain is largely dispensable for this purpose. Polymerization of keratins begins with the formation of heterodimers in which the α-helical rod domains of type I and II keratins are aligned in parallel and perfect register. These heterodimers then interact along their lateral surfaces and then in an end-to-end fashion to give rise to the 10–12 nm wide filaments. The extraordinary stability of heterodimers (some of them resist 10 M urea!) and heterotetramers underscores the tightness of the interactions between type I and type II rod domains. Not surprisingly, most of the intracellular pool of keratin proteins is in the polymerized form (>95%).

Organization and Regulation of Keratin Filaments *in vivo*

The abundance and organization of keratin IFs *in vivo* varies according to the epithelium considered. Keratins are particularly abundant (from 10 to 80% of total cellular proteins) in surface-exposed stratified epithelia (e.g., epidermis, oral mucosa, cornea, etc.). In cells of these tissues, keratin IFs are organized in a pan-cytoplasmic network extending from the surface of the nucleus to the cytoplasmic periphery, where they associate with membrane-spanning cell–cell or cell–matrix attachment complexes such as desmosomes and hemidesmosomes (Figure 2C). In simple epithelia (e.g., liver, gut, pancreas, etc.), keratins remain a major fraction of proteins even though they are less abundant (from 1 to 5% of total cellular proteins). Such tissues are made up of polarized epithelial cells that often contain asymmetrically organized keratin IFs, concentrated mostly at the cytoplasmic periphery and particularly at the apical pole. A number of associated proteins interact with and contribute to the organization of keratin IFs in these various settings. Some directly promote the bundling of keratin IFs (e.g., filaggrin, trichohyalin), their association with microtubules and microfilaments (e.g., plectin, BPAG isoforms), and/or with desmosomes or hemidesmosomes (desmoplakin, plakophilin, BPAG isoforms, etc.).

Keratin Posttranslational Modification

The organization of keratin filaments *in vivo* is also regulated through phosphorylation. All keratin proteins are phosphoproteins. Their phosphorylation by a variety of kinases occurs in a very dynamic and reversible fashion, usually on Ser/Thr residues, and involves multiple sites on the nonhelical head domain and, to a lesser extent, on the tail domain. Circumstances in which keratin IFs are reorganized in a rapid fashion, such as mitosis or cellular stress, invariably correlates with increased phosphorylation of specific residues located in the end domains. The head domains of at least some keratins are also substrates for ubiquitination (which mediates their degradation) and O-glycosylation (whose significance has yet to be ascertained). As is the case for microtubules and actin microfilaments, the assembly and organization of keratin IFs is thus regulated though a variety of mechanisms in epithelial cells, and undoubtedly represents a key determinant of their function *in vivo*.

Keratin Gene Expression Mirrors Epithelial Differentiation: The Case of Skin

Skin provides a beautiful example of the tight relationship that has evolved between keratin gene regulation and epithelial differentiation. More than half of all keratin genes are expressed in mature mammalian skin tissue (Figure 2 and Table I). The architectural complexity of adult skin epithelia is

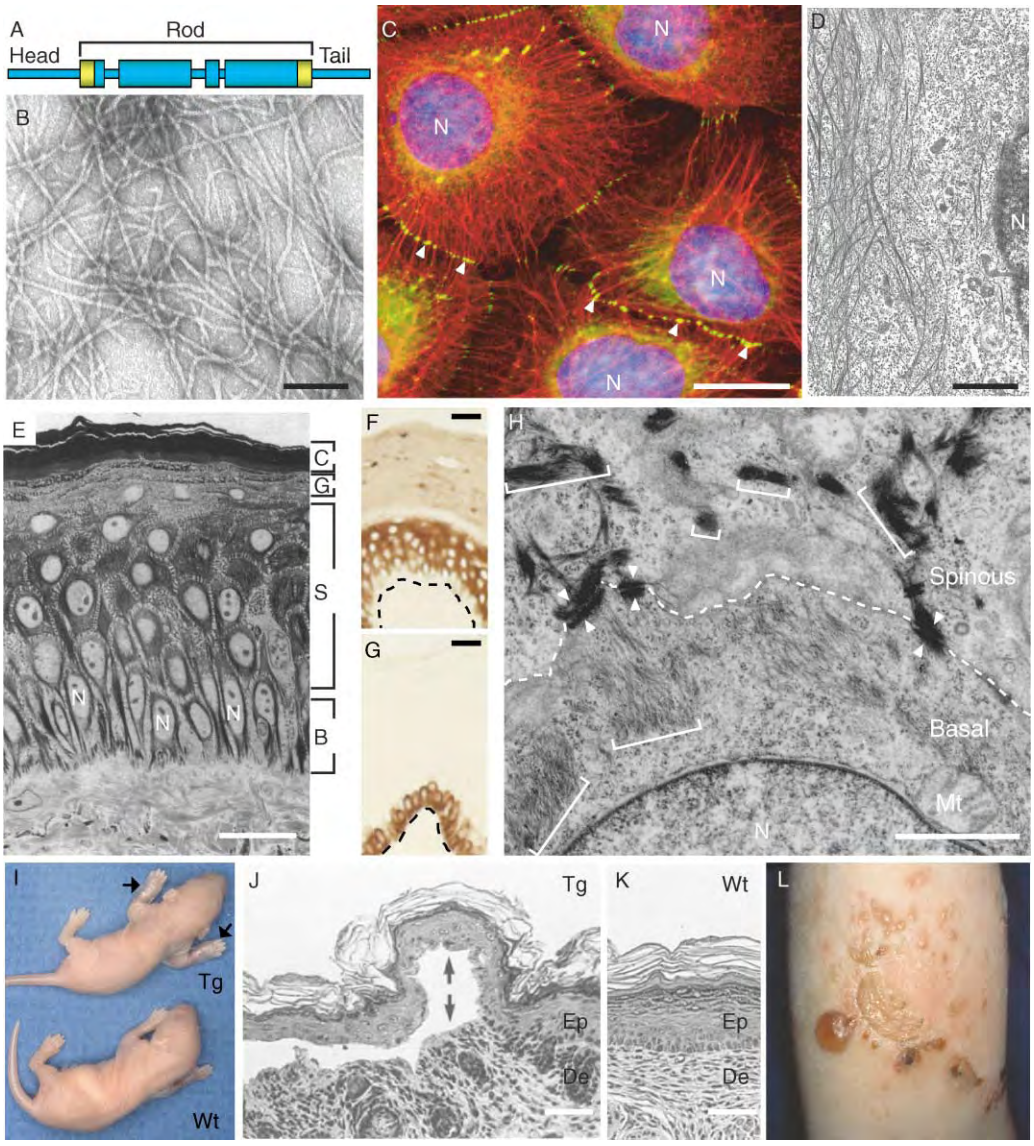

FIGURE 2 Attributes, differential regulation, and disease association of keratin. (A) Schematic representation of the tripartite domain structure shared by all keratin and other intermediate filament proteins. A central α-helical "rod" domain acts as the major determinant of self-assembly and is flanked by nonhelical "head" and "tail" domains at the N and C termini, respectively. The ends of the rod domain contain 15–20 amino-acid regions (yellow) highly conserved among all intermediate filaments. (B) Visualization of filaments, reconstituted *in vitro* from purified K5 and K14, by negative staining and electron microscopy. Bar equals 125 nm. (C) Triple-labeling for keratin (red chromophore) and desmoplakin, a desmosome component (green chromophore) and DNA (blue chromophore), by indirect immunofluorescence of epidermal cells in culture. Keratin filaments are organized in a network that spans the entire cytoplasm and are attached at points of desmosomal cell–cell contacts (arrowheads) between cells. Bar equals ~30 μm. N, nucleus. (D) Ultrastructure of the cytoplasm of epidermal cells in primary culture, as visualized by transmission electron microscopy. Keratin filaments are abundant and tend to be organized in large bundles of loosely packed filaments in the cytoplasm. (E) Histological cross-section of resin-embedded human trunk epidermis, revealing the basal (B), spinous (S), granular (G), and stratrum corneum (C) compartments. Bar equals ~50 μm. N, nucleus. (F) and (G) Differential distribution of keratin epitopes on human skin tissue cross-sections (similar to frame E) as visualized by an antibody-based detection method. K14 occurs in the basal layer, where the epidermal progenitor cells reside. K10, on the other hand, is primarily concentrated in the differentiating, suprabasal layers of epidermis. Dashed line indicates the basal lamina. Bar equals ~100 μm. (H) Ultrastructure of the boundary between the basal and suprabasal cells in mouse trunk epidermis, as seen by routine transmission electron microscopy. The sample, from which this micrograph was taken, is oriented in the same manner as frame E. Organization of keratin filaments as loose bundles (see brackets in basal cell) correlates with the expression of K5–K14 in basal cells, whereas the formation of much denser and electron-dense filament bundles (see brackets in spinous cell) reflects the onset of K1–K10 expression in early differentiating cells. Arrowheads point to desmosomes connecting the two cells. Bar equals 1 μm. N, nucleus (I) Newborn mouse littermates. The top mouse is transgenic (Tg) and expresses a mutated form of K14 in its epidermis. Unlike the control pup below (Wt), this transgenic newborn shows extensive blistering of its front paws (arrows). (J) and (K) Hematoxylin/eosin-stained histological cross-section through paraffin-embedded newborn mouse skin (similar to those shown in frame I). Compared to the intact skin of a control littermate (K, Wt), the epidermis of the K14 mutant expressing transgenic pup (J, Tg) shows intra-epidermal cleavage at the level of the basal layer, where the mutant keratin is expressed (see opposing arrows).

TABLE I

Distribution of Keratins in the Major Compartments of Skin Epithelia

Skin compartment	Cell type	Keratin expression (mRNA level)
Interfollicular epidermis	Basal keratinocytes	K5, K14; also, K15
	Early differentiating keratinocytes	K1, K10
	Late differentiating keratinocytes	K2e
	Merkel cells (in basal layer)	K8, K18, K20
Palmar/plantar epidermis	Basal keratinocytes	K5, K14; also, K15, K17, K19
	Early differentiating keratinocytes	K1, K9, K10; K6, K16
	Late differentiating keratinocytes	K2e
Hair follicles	Outer root sheath	K5, K14, K17; also, K15 and K19
	Companion layer	K6a, K16 and K6hf, K17
	Inner root sheath	Irs1–4, K6irs1–4; also, K7
	Hair shaft: cuticle & cortex	Ha and Hb keratins
	Hair shaft: medulla	K6hf, K17
Sebaceous glands (apocrine)	Glandular epithelium	K14; others unknown
	Cambial cells	K5, K14, K17
Sweat glands (eccrine)	Glandular epithelium	K8, K18?
	Myopithelium	K5, K7, K14, K17
	Duct	K5, K14; K7, K17; K6, K16
Nail	Matrix	K5, K14, K17
	Nail plate	Ha and Hb keratins
	Nail bed	K5, K14; K7, K17; K6, K16
	Proximal nail fold	K5, K14; K1, K10; K6, K16
	Hyponychium (upper layers)	K5, K14; K17; K6, K16

achieved through a temporally and spatially regulated sequence of simple decisions, resulting in progressive restriction of fate determination and reflected by specific changes in keratin gene regulation. In the clinical setting, "keratin typing" is often exploited in diagnosing cancer type, its differentiation status (and therefore prognosis), as well as the origin of the cells forming metastatic foci. This strategy is also applied for diseases other than cancer.

Keratin Gene Expression in Thin Epidermis

In thin epidermis, mitotically active cells of the basal layer act as progenitors, and consistently express K5 and K14 as their main keratin pair (Figure 2F), along with lower levels of K15. Onset of differentiation coincides with the appearance of the K1/K10 pair through a robust transcriptional induction that occurs at the expense of K5/K14. Accordingly, K1/K10 proteins are readily detectable in the lowermost suprabasal layer of epidermis (Figure 2G). The appearance of K1 and K10 correlates with a sudden and dramatic shift in the organization of cytoplasmic keratin filaments, which now exhibit significant bundling (Figure 2H). Another type II keratin gene, *K2e*, is expressed at a later stage of differentiation.

Keratin Gene Expression in Thick Epidermis

The epidermis of palm and sole skin is significantly thicker, owing to its specialization for resisting larger amounts of stress. This function is reflected in its architecture of alternating stripes of primary and secondary ridges, and specific changes in keratin expression. In the thick, stress-bearing, primary ridges, the major differentiation-specific type I K9 is presumed to foster a more resilient cytoskeleton. In the thinner secondary ridges, postmitotic cells preferentially express the type II K6a and type I K16 and K17. Relative to K1, K9, and K10, the properties

Bar equals 100 μm. (L) Leg skin in a patient suffering from the Dowling-Meara form of epidermolysis bullosa simplex. Characteristic of this severe variant of this disease, several skin blisters are grouped in a herpetiform fashion.

of K6a, K16, and K17 are believed to foster greater cellular pliability, thereby providing flexible "hinge" regions in-between the more rigid, K1/K9-rich primary ridges. While it remains to be supported by experimentation, this attractive notion is consistent with the dramatic up-regulation of K6a, K6b, K16, and K17 that occurs in keratinocytes recruited from wound margins to participate to the restoration of the epidermal barrier following injury.

Keratin Gene Expression in Hair Follicles

Consistent with its greater complexity, a larger number of keratin genes are transcribed in the pilosebaceous unit (Table I). A mature hair follicle houses eight distinct epithelial layers segregated into three histological compartments organized in concentric circles along its main axis. These compartments are, from inside out, the hair shaft proper; the inner root sheath (IRS); and the outer root sheath (ORS), an epithelium that wraps around the follicle and is contiguous with the epidermis. The regulation of ~27 keratin genes expressed in hair follicles is detailed in Table I. Key features are highlighted here. The *Ha1–Ha8* and *Hb1–Hb6* genes are unique to the hair shaft and related hard epithelia (e.g., nail). These keratin genes exhibit a stage-specific regulation during the differentiation of matrix progenitors in the bulb region to hair cortex keratinocytes. The cysteine-rich head and tail domains of the "hard" keratin proteins form disulfide bridges which, along with the γ-glutamyl cross-links catalyzed by transglutaminases, foster the organization of very large bundles of densely packed keratin filaments. This organization endows hair (and nail) with its unique structural features, shape, and resilience. Irs1–4 and K6irs1–4 are found in the inner root sheath compartment. The outer root sheath epithelium, on the other hand, expresses several of the keratins genes expressed in the epidermis, with the notable exception of the differentiation-specific K1, K2e, and K10 (Table I). By the time an epidermal or hair cortex keratinocyte has completed differentiation, more than 80% of its protein content is keratin. This extreme situation is reminiscent of globin gene expression in erythrocytes, another highly specialized cell type, and underscores the fundamental importance of keratin proteins to surface epithelia.

Functions of Keratin Filaments

Structural Support

The properties typifying keratin filaments collectively point to an important structural role. Evidence for this function came from transgenic mouse studies in which a mutated form of K14 capable of dominantly disrupting filament assembly and organization was targeted to the basal layer of epidermis *in vivo*. Unlike controls, mutant-expressing animals exhibited massive intracellular lysis of the basal cells in response to modest mechanical trauma to the skin (Figure 2I–2K). This mouse phenotype mimicked key aspects of a group of dominantly inherited epidermal disorders known as epidermolysis bullosa simplex (EBS, Figure 2L), and it was shown shortly thereafter that the human condition arises from mutations in either K5 or K14. EBS turned out to be a very useful paradigm. We now know that keratin IFs fulfill a similar function in all complex epithelia, ranging from the surface of the eye (cornea) to hair tissue. *In vitro* studies showed that keratin IFs exhibit unique viscoelastic properties that support their involvement in a structural capacity, and that disease-causing mutations significantly decrease the strength of keratin assemblies subject to mechanical strain. Likewise, biophysical studies of live cells in culture showed that keratin IFs account for a substantial fraction of their viscoelastic properties, and that disrupting keratin cytoplasmic organization causes cells to soften considerably. Demonstration of a structural support role has been comparatively more difficult for simple epithelial tissues, but strong evidence to that effect now exists for liver hepatocytes as well as trophoblast giant cells.

Scaffolding Components of Signaling Pathways and Other Functions

Transgenic mouse studies that focused on adult liver and extraembryonic tissue revealed that simple epithelial keratins 8/18 play an important cytoprotective role against chemical insults and in modulating the response to pro-apoptotic signals. In liver hepatocytes, interestingly, the function of cytoprotection requires phosphorylation of K8/K18. In regard to apoptosis, studies showed that K8/K18 filaments can bind to, and either organize or sequester key intracellular effectors of the signaling machinery downstream from engagement of the TNF-α and fas receptors. Of note, the presence of K17 is also required the survival of matrix epithelial cells in mature hair follicles. It appears likely that keratin IFs will be found to influence additional basic metabolic processes in the cell. In that regard, recent studies have shown that an intact K8/K18 filament network is required for the proper sorting of specific membrane proteins in polarized simple epithelial cells. Determining how nonpolar assemblies are adapted to foster spatial organization in the cell promises to reveal additional keratin properties and functions.

TABLE II

Disorders Associated with Mutations in Keratin Genes

Disease	Main target tissue	Gene mutated
Diseases for which mutations are causative		
Epidermolysis bullosa simplex	Basal cells/epidermis	K5, K14
Epidermolytic hyperkeratosis	Differ. cells/epidermis	K1, K10
Ichtyosis bullosa of Siemens	Differ. cells/epidermis	K2e
Meeman's corneal dystrophy	Cornea	K3, K12
Monilethrix	Hair cortex	Hb1, Hb6
Oral white sponge nevus	Oral mucosa	K4, K13
Pachyonychia congenita		
Type 1 (Jadhasson–Lewandowsky)	Nail; other appendages	K6a, K16
Type 2 (Jackson–Lawler)	Nail; other appendages	K6b, K17
Palmoplantar keratoderma		
Epidermolytic	Palmar/plantar epidermic	K9
Non-epidermolytic	Palmar/plantar epidermic	K1, K16
Steatocystoma multiplex	Sebaceous glands	K17
Diseases for which mutations are a risk factor		
Cryptogenic cirrhosis, hepatitis	Liver	K8, K18
Inflammatory bowel disease	Gut	K8, K18

Keratin Involvement in Disease

The role of keratin mutations in causing several epidermal, oral, ocular, and hair-related diseases is well established (Table II). These diseases are genetically well defined and typically inherited in an autosomal-dominant fashion, although recessive inheritance is occasionally seen. The vast majority of genetic lesions consists of missense mutations, although premature stop codons, small deletions, and mutations affecting mRNA splicing occur with some frequency. In general, disease severity correlates with the location and nature of the mutation within the keratin backbone. A keratin mutation database is being maintained at the University of Dundee and can be accessed online (http://134.36.196.124/interfilwlcm.htm).

For most of the disorders listed in Table II, mutations are causative for the disease and act through their ability to compromise the role of keratin IFs toward structural support. Mutations causing severe outcomes tend to affect amino acid residues that are highly conserved at either end of the central rod domain (Figure 1A), and often lead to the appearance of large aggregates of mispolymerized keratins in the cytoplasm of affected cells. In such instances, the aggregates appear to exacerbate the effect of the loss of a functional keratin IF network, and contribute to disease pathogenesis. Other types of mutations may also elicit alternative mechanisms of disease pathogenesis. Examples include mutations that could either affect keratin degradation during apoptosis or directly modulate keratin phosphorylation by introducing or removing a potential phosphorylation site. In contrast with other keratins, mutations affecting the simple epithelial keratins K8/K18 appear to predispose to, rather than cause disease per se (Table II). Again, this notion is supported by studies involving transgenic mice. Many of the diseases listed in Table II are characterized by a clinical heterogeneity that cannot be entirely accounted for through the position and nature of the mutation along the keratin chain. For instance, the same missense allele of K17, $Arg_{94} \rightarrow Cys$, can cause either type 2 pachyonychia congenita (which affects primarily the nail) or steatocystoma multiplex (a glandular disorder with minimal if any nail alterations) in different kindreds. Together with studies involving gene manipulation in mice, this finding points to a sometimes dramatic impact of the genetic background on disease expression.

See Also the Following Articles

Cell Death by Apoptosis and Necrosis • Intermediate Filaments

Glossary

apoptosis Orderly process of programmed cell death by which a cell commits suicide.

coiled-coil Tertiary structure of a protein motif mediating oligomerization in which two alpha-helices wrap around each other forming a hydrophobic core with characteristic interdigitation of side chains between neighboring helices, known as knob-in-hole packing.

complex epithelia One to several layers of cells in which nuclei are present on several planes covering either internal or external surfaces of the body.

desmosome Junction formed between adjacent cells in order to form a tissue.

hemidesmosome Junction that anchors cells to the basement membrane.

intermediate filaments Nonpolar, 10–12 nm wide filamentous proteins of the cytoskeleton that provide structural support to the cell.

pilosebaceous unit Composed of a hair follicle, sebaceous gland attached to it, and arrector pili muscle.

simple epithelium Single layer of cells attached to a basal lamina, in which all nuclei are aligned in a single plane often covering an internal surface of the body.

Further Reading

Cassidy, A. J., Lane, E. B., Irvine, A. D., and McLean, W. H. I. (2002). *The Human Intermediate Filament Mutation Database*. http://www.interfil.org.

Coulombe, P. A., and Omary, M. B. (2002). "Hard" and "soft" principles defining the structure, function, and regulation of keratin intermediate filaments. *Curr. Opin. Cell Biol.* **14**, 110–122.

Coulombe, P. A., Bousquet, O., Ma, L., Yamada, S., and Wirtz, D. (2000). The "ins" and "outs" of intermediate filament organization. *Trends Cell Biol.* **10**, 420–428.

Erber, A., Riemer, D., Bovenschulte, M., and Weber, K. (1998). Molecular phylogeny of metazoan intermediate filament proteins. *J. Mol. Evol.* **47**, 751–762.

Fuchs, E. (1995). Keratins and the skin. *Annu. Rev. Cell Dev. Biol.* **11**, 123–153.

Fuchs, E., and Cleveland, D. W. (1998). A structural scaffolding of intermediate filaments in health and disease. *Science* **279**, 514–519.

Hesse, M., Magin, T. M., and Weber, K. (2001). Genes for intermediate filament proteins and the draft sequence of the human genome: Novel keratin genes and a surprisingly high number of pseudogenes related to keratin genes 8 and 18. *J. Cell Sci.* **114**, 2569–2575.

Moll, R., Franke, W. W., Schiller, D. L., Geiger, B., and Krepler, R. (1982). The catalog of human cytokeratins: Patterns of expression in normal epithelia, tumors and cultured cells. *Cell* **31**, 11–24.

Omary, M. B., Ku, N. O., Liao, J., and Price, D. (1998). Keratin modifications and solubility properties in epithelial cells and *in vitro*. In *Subcellular Biochemistry: Intermediate Filaments* (H. Herrman and J. R. Harris, eds.) Vol 31, pp. 105–140. Plenum Press, New York.

Oshima, R. G. (2002). Apoptosis and keratin intermediate filaments. *Cell Death Differ.* **9**, 486–492.

Biography

Pierre A. Coulombe is a Professor in the Department of Biological Chemistry at the Johns Hopkins University School of Medicine in Baltimore, Maryland. He holds a Ph.D. from Université de Montréal in Canada and received his postdoctoral training at the University of Chicago. At that time, he and Dr. Elaine Fuchs discovered that mutations in keratins can elicit epithelial fragility in transgenic mice and individuals suffering from inherited blistering diseases. He continues to explore the properties and function of keratin genes and proteins in epithelial cells and tissues.

Kelsie M. Bernot is a native of Pennsylvania and a student in the biochemistry, cellular, and molecular biology graduate training program at Hopkins. Her thesis research focuses on the properties and function of keratin 16, which is up-regulated during wound repair and in chronic hyperproliferative skin disorders.

Ketogenesis

Janos Kerner and Charles L. Hoppel
Case Western Reserve University School of Medicine, Louis Stokes VA Medical Center, Cleveland, Ohio, USA

Ketogenesis is a process in which acetyl-CoA produced by fatty acid oxidation is converted to acetoacetate or D-3-hydroxybutyrate. These compounds, referred to as ketone bodies, are water-soluble equivalents of fatty acids and serve as important metabolic fuels for many peripheral tissues, particularly heart and skeletal muscle. During starvation, ketone bodies become the major fuel source for the brain.

Background

Ketogenesis becomes significant under conditions of food (carbohydrate) deprivation. Provision of peripheral tissues, such as skeletal muscle and heart, with ketone bodies as an alternative fuel for energy production results in glucose sparing for organs depending on glucose as an energy source. The brain then can use ketones as well as glucose, and the red blood cells continue to use glucose. The enhanced gluconeogenesis associated with ketogenesis further eases the glucose need, thus potentiating the glucose-sparing effect.

The liver plays a central role in switching from a carbohydrate to a fatty acid-based metabolism such as occurs physiologically in fasting. Under normal dietary conditions, hepatic production of ketone bodies, acetoacetate, and D-3-hydroxybutyrate is minimal and the concentrations of these compounds in blood is low. However, during food deprivation the synthesis of ketone bodies is greatly enhanced, and the circulating concentration of ketone bodies can reach values of approximately 5 mM. Thus, liver responds uniquely by enhancing its capacity to convert incoming fatty acids into ketone bodies, which then serve as fuel for energy production in peripheral tissues and thus conserve glucose for the central nervous system and for erythrocytes. For example, in the liver, the major metabolic fate of acetyl-CoA produced by the β-oxidation of fatty acids during starvation is ketone body formation, and practically all fatty acids oxidized by the liver are diverted into ketone body synthesis. It has been estimated that under saturating concentrations of acetyl-CoA, the liver has the capacity to synthesize its own weight of acetoacetate in 48 h. Although fatty acids are by far the major carbon donors for ketone body synthesis, the catabolism of some (ketogenic) amino acids also provides carbon atoms for ketogenesis, either via acetyl-CoA or directly by yielding acetoacetate.

Hepatic Fatty Acid Oxidation

The provision of acetyl-CoA by fatty acid β-oxidation is the main factor determining the rate of ketone body synthesis. Fatty acids are activated by long-chain acyl-CoA synthetase present in the mitochondrial outer membrane. Activated fatty acids are then transported into the mitochondria via the mitochondrial carnitine transport system and are sequentially chain-shortened, yielding acetyl-CoA and reducing equivalents. However, the major fate of acetyl-CoA is not oxidation in the citric acid cycle and electron transport chain to CO_2 and H_2O, but rather the formation of acetoacetate and D-3-hydroxybutyrate for export and use by peripheral tissues for energy production. It has been estimated that in fasting adult humans, brain and muscle each use at approximately equal rates 40–45% of the ketone bodies produced. Under ketogenic conditions the oxidation of palmitate to acetyl-CoA consumes 14 atoms of oxygen, whereas its complete oxidation to CO_2 and H_2O via the citric acid cycle and electron transport chain requires 46 atoms. Thus, about threefold as much palmitate must undergo β-oxidation to yield the same amount of ATP. This helps to explain the high rates of ketogenesis required to supply ATP for gluconeogenesis.

Synthesis of Ketone Bodies

The first committed step of hepatic ketone body synthesis is the condensation of two acetyl-CoA molecules to yield acetoacetyl-CoA (Figure 1). This reaction is catalyzed by acetyl-CoA acetyltransferase, an enzyme present both in the cytosol and mitochondria. The mitochondrial isoform serves in ketone body synthesis, while the cytosolic enzyme is involved in cholesterol synthesis. The mitochondrial enzyme exists

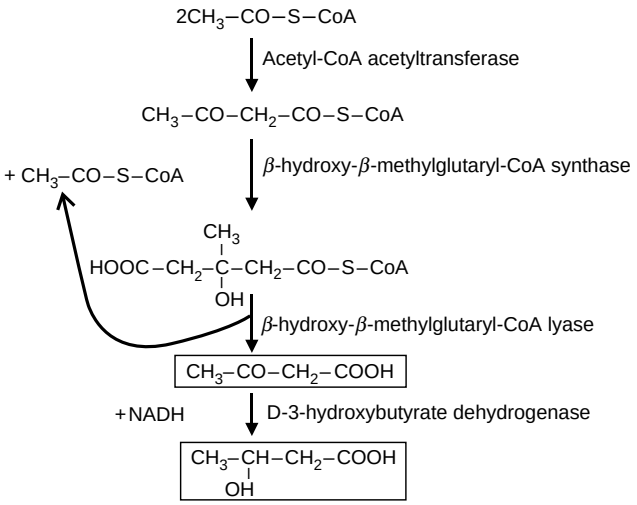

FIGURE 1 Pathway enzymes of hepatic ketogenesis.

in two isoforms, both of which are different from the cytosolic form.

The second step in the pathway is the formation of 3-hydroxy-3-methylgluratyl-CoA catalyzed by the enzyme 3-hydroxy-3-methylgluratyl-CoA synthase (HMG-CoA synthase). In liver there are two HMG-CoA isoforms, one in the cytosol and one in the mitochondria. The former takes part in cholesterol synthesis, whereas the mitochondrial form catalyzes the formation of HMG-CoA for ketone body formation. HMG-CoA synthase represents the rate-limiting enzyme of the ketogenic pathway. Consequently, overexpression of mitochondrial HMG-CoA synthase in transgenic mice caused hepatic hyperketogenesis, and hepatocytes in primary cultures from transgenic mice showed a threefold increase in acetoacetate and D-3-hydroxybutyrate in the medium. Short-term regulation of enzyme activity is achieved by succinylation. Succinylation by succinyl-CoA inhibits the activity and the enzyme is reactivated by desuccinylation.

Completion of ketone body synthesis is achieved by the action of 3-hydroxy-3-methylgluratyl-CoA lyase (HMG-CoA lyase), resulting in the formation of acetoacetate and acetyl-CoA. This enzyme is present in the mitochondrial matrix. No regulatory properties of HMG-CoA lyase have been described, and the activity of this enzyme is thought to be sufficient to effect the rapid conversion of HMG-CoA to acetoacetate.

In mitochondria some of the acetoacetate is then reduced to D-3-hydroxybutyrate by the enzyme D-3-hydroxybutyrate dehydrogenase. This enzyme is tightly bound to the matrix side of the mitochondrial inner membrane and maintains 3-hydroxybutyrate and acetoacetate concentrations that reflect the mitochondrial matrix NADH/NAD ratio. The ratio of these two ketone bodies in liver, as well as in blood, has been used as an indication of mitochondrial redox potential. Some acetoacetate is spontaneously decarboxylated to acetone in a nonenzymatic reaction.

Ketone Body Utilization

Acetoacetate and D-3-hydroxybutyrate produced in the liver are released and carried by the bloodstream to the peripheral tissues for use as alternative fuel. There, the ketone bodies are converted to two acetyl-CoA as outlined in Figure 2 for further oxidation in the citric acid cycle and electron transport chain to CO_2 and H_2O. The first reaction in ketone body utilization in peripheral tissues is the oxidation of D-3-hydroxybutyrate to acetoacetate catalyzed by D-3-hydroxybutyrate dehydrogenase. The rates of D-3-hydroxybutyrate utilization and of acetoacetate production are proportional to D-3-hydroxybutyrate concentration. Acetoacetate is then converted to its CoA ester, acetoacetyl-CoA, by the enzyme 3-ketoacyl-CoA transferase (succinyl-CoA:3-ketoacid CoA transferase). 3-ketoacyl-CoA transferase is the key enzyme of ketone body utilization. Hereditary deficiency of this enzyme is an inborn error of ketone body utilization, characterized by intermittent ketoacidotic crises and persistent ketosis. It is detected in all tissues except liver, with highest activities found in heart. The activity is decreased in hindlimb muscle of diabetic rats and might contribute to the development of diabetic ketoacidosis. The last step in ketone body utilization is the thiolytic cleavage of acetoacetyl-CoA to two acetyl-CoAs by the enzyme acetyl-CoA acetyltransferase.

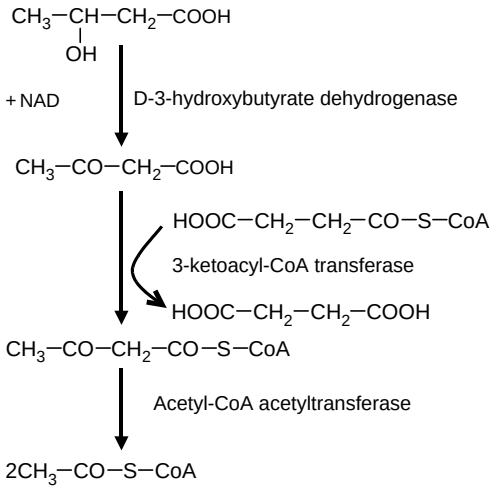

FIGURE 2 Reactions of ketone body utilization.

Regulation of Ketone Body Metabolism

Active ketogenesis requires an increased delivery of nonesterified fatty acids to the liver and an increase in hepatic fatty acid oxidation. These requirements are met by increased lipolysis due to a decrease in circulating insulin, an elevation of the glucagon/insulin ratio, resulting in activation of fatty acid oxidation. As in peripheral tissues, liver mitochondrial uptake of activated fatty acids is absolutely dependent on carnitine and requires all three enzymes of the mitochondrial carnitine transport system. The site of regulation resides at the reaction catalyzed by CPT-I, thus committing the activated fatty acids toward oxidation in the mitochondria. The mechanism by which CPT-I exerts its control is achieved through changes in concentrations of the enzyme's physiological regulator, malonyl-CoA, and through changes in the sensitivity of CPT-I to inhibition by malonyl-CoA. Thus, transition back and forth between normal and ketotic states is accompanied by changes in malonyl-CoA content and also by marked shift in the sensitivity of CPT-I to the inhibitor. Significant control of ketogenesis is exerted at another intramitochondrial site distal to CPT-I, more specifically, HMG-CoA synthase. Short-term regulation of HMG-CoA synthase is achieved by succinylation/desuccinylation of the enzyme. Thus, HMG-CoA synthase is succinylated and inactivated in the starved–fed transition and in high carbohydrate/low-fat weaned rats; it is substantially desuccinylated under ketogenic conditions such as starvation, fat feeding, diabetes, and lactation.

Both regulatory enzymes CPT-I and HMG-CoA synthase are also regulated at the transcriptional level. Thus, the developmental patterns of gene expression of CPT-I and HMG-CoA synthase in rat liver are very similar. Furthermore, mRNA and protein levels and enzyme activities for hepatic CPT-I and HMG-CoA synthase are increased during starvation, dibutyryl cAMP treatment, fat feeding, and diabetes. Opposite changes in these parameters for both enzymes are observed upon refeeding and insulin treatment, respectively.

In conclusion, changes in hepatic mitochondrial CPT-I and HMG-CoA synthase activities occur in the same direction. Control of hepatic ketogenesis may thus be exerted in a coordinated fashion at these two major regulatory sites.

See Also the Following Articles

Fatty Acid Oxidation • Fatty Acid Receptors • Fatty Acid Synthesis and its Regulation • Muscarinic Acetylcholine Receptors • Nicotinic Acetylcholine Receptors

Glossary

coenzyme A (CoA) A cosubstrate of numerous enzymes central to energy metabolism.

ketogenesis Synthesis of acetoacetate and 3-hydroxybutyrate (ketone bodies) from acetyl-CoA produced by oxidation of long-chain fatty acid in liver mitochondria.

mitochondria Eukaryotic organelles surrounded by an inner and an outer membrane that are the sites of energy production.

Further Reading

Eaton, S. (2002). Control of mitochondrial β-oxidation flux. *Prog. Lipid Res.* **41**, 197–239.

Guzman, M., and Geelen, M. J. H. (1993). Regulation of fatty acid oxidation in mammalian liver. *Biochim. Biophys. Acta* **1167**, 227–241.

Hegardt, F. G. (1999). Mitochondrial 3-hydroxy-3-methylglutaryl-CoA synthase: A control enzyme in ketogenesis. *Biochem. J.* **338**, 569–582.

Kerner, J., and Hoppel, C. (2000). Fatty acid import into mitochondria. *Biochim. Biophys. Acta* **1486**, 1–17.

McGarry, J. D., and Brown, N. F. (1997). The mitochondrial carnitine palmitoyltransferase system. *Eur. J. Biochem.* **244**, 1–14.

McGarry, J. D., and Foster, D. W. (1980). Regulation of hepatic fatty acid oxidation and ketone production. *Ann. Rev. Biochem.* **49**, 395–420.

Williamson, D. H., and Whitelaw, E. (1978). Physiological aspects of the regulation of ketogenesis. *Biochem. Soc. Symp.* **43**, 137–161.

Biography

Charles Hoppel graduated from Gonzaga University and St. Louis University School of Medicine. He is Professor of Pharmacology, Medicine and Oncology at Case Western Reserve University, Co-Director of the Center for Inherited Disorders of Energy Metabolism at CWRU, and Associate Director, Research in the Geriatric Research, Education, and Clinical Center at the Louis Stokes VA Medical Center. His research interests are in mitochondrial structure and function, mitochondrial fatty acid oxidation, and regulation of carnitine palmitoyltransferase-I.

Janos Kerner graduated from Humboldt University and held a faculty position in the Department of Biochemistry at Medical University of Pecs (Hungary) until 1994. He was a visiting faculty member in the Department of Biochemistry at Michigan State University and joined the Department of Nutrition at Case Western Reserve University in 1995. His research interest is mitochondrial fatty acid oxidation and its regulation by malonyl-CoA.

Kinesin Superfamily Proteins

Nobutaka Hirokawa and Reiko Takemura
University of Tokyo, Tokyo, Japan

Kinesin was first identified biochemically as microtubule-dependent motor protein responsible for transport of membranous organelles in the axon. It is now recognized that microtubule-dependent motor proteins form a large gene family, kinesin superfamily proteins (KIFs). The human genome contains 45 KIF genes. KIFs have high homology at the so-called "motor domain," which is a globular domain responsible for moving along microtubules by hydrolysis of ATP. Outside the motor domain, the sequence is unique to each member. The motors bind to the "cargoes," the molecule to be transported, at this domain. KIFs transport many different types of cargoes including membrane-enclosed vesicles, macromolecular complexes, cytoskeletal proteins, and mRNAs. They play important roles in a wide variety of intracellular transport, such as transport from Golgi to plasma membrane pathways involved in exocytosis and endocytosis, axonal transport, transport in dendrites, and special transport called intraflagellar transport. They also play important roles in mitosis. Functions and/or dysfunctions of KIF motors underlie some diseases. KIFs also play important roles in the early event of mammalian embryonic development, namely the formation of the left–right axis.

Introduction

The study of axonal transport provided the first clue that there is a microtubule-dependent motor protein that is not related to dynein. It has been known for quite some time that various membranous organelles and proteins are transported within axon, but the rails and motors were not known. Experimental evidence then suggested that long-distance transport within the axon is microtubule-dependent. Quick-freeze deep-etch electron microscopy revealed that short cross-bridges were present between membranous organelles and microtubules, and these were likely to be a candidate for motor proteins (Figure 1). In mid-1980s, "conventional kinesin (KIF5)" was first isolated biochemically as motor protein responsible for the transport of membranous organelles in the direction of cell body to synapse. Conventional kinesin has a rod-like structure composed of two globular heads (10 nm in diameter), a stalk, and a fanlike end, with a total length of 80 nm (Figure 2). The globular heads bind to microtubules and have an ATP-binding sequence and a microtubule-binding sequence. A systematic molecular biological search of kinesin superfamily genes coding for proteins containing similar ATP-binding and microtubule-binding sequences led to the discovery of a group of motors, which is now called kinesin superfamily proteins, KIFs (Figures 2 and 3). Human genome contains 45 KIF genes. KIFs in the human and mouse genomes are presented in a phylogenic tree along with those in *S. cerevisiae*, *Drosophila melanogaster*, and *Caenorhabditis elegans* in Figure 4. KIFs identified in mouse are named as KIF1–KIF26, and KIFC1–KIFC3. KIFs identified in other species have various names. For clarity, the nomenclature in the mouse was used as much as possible. However, for some KIFs other names were used.

Although all members of KIFs share a highly homologous domain having ~350 amino acids containing a site for ATP binding and one for microtubule binding, they are quite divergent outside the motor domain. This seems to allow the binding of KIF to various cargoes, including membrane-enclosed vesicles, macromolecular complexes, and mRNAs, and they play important roles in various transport processes including axonal transport, transport in dendrite, intracellular vesicular trafficking such as pathways involved in endocytosis and exocytosis, and special transport called intraflagellar transport (Table I). For most of the KIFs, the motor domain resides at the N-terminal portion of the molecule (N-kinesin), but the motor domain could be in the C-terminal (C-kinesin) or the middle of the molecule (M-kinesin) (Figure 3). The range of the size of typical KIF molecule is from 600–1800 amino acids (Figure 3). Different KIFs take various forms (Figure 2). Some are homodimer with or without associated light chains; some are monomeric; some are heterodimer with associated protein; some are homotetramer forming bipolar minifilaments. Some KIFs bind their cargo directly, and some do so via light chains or associated proteins discussed individually in this article.

Microtubule has a polarity. It has a fast-growing plus-end, and opposite minus-end. In the nerve cell axons, the microtubules are unipolar, the plus-end

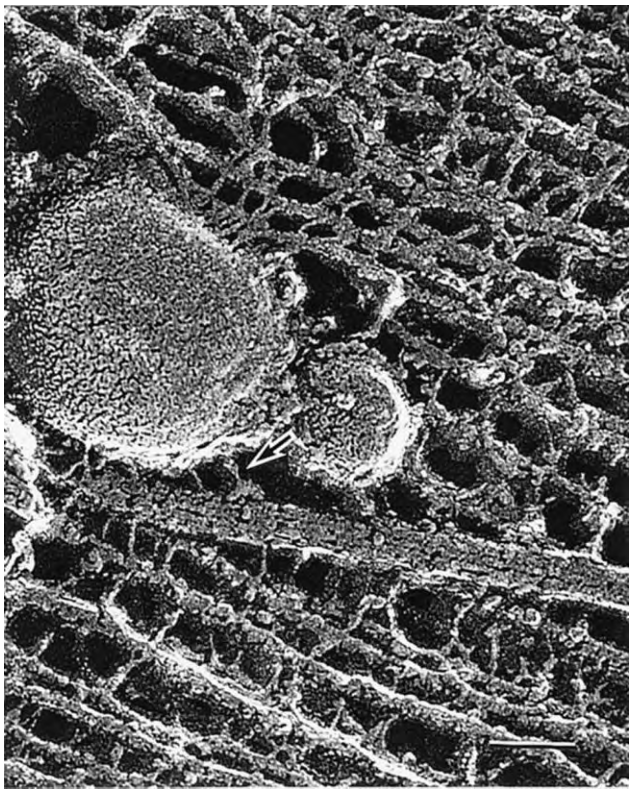

FIGURE 1 Quick-freeze deep-etch electron micrographs showing short cross-bridges between membranous organelles and microtubules that are structural candidates for KIFs. Bar 50 nm. (Reproduced, with permission, from Hirokawa, N. (1998). Kinesin and dynein superfamily proteins and the mechanism of organelle transport. *Science* **279**, 519–526.)

pointing to the direction of synapse (Figure 5A). However, in dendrites microtubules have mixed polarity in proximal region, while they are oriented like in axon in the distal region. In interphase cells, microtubules are in radial array with the minus-end pointing the cell center, and the plus-end pointing the cell periphery (Figure 5B). The direction of transport and velocity of each motor can be assessed in the so-called "*in vitro* motility assay." Most of the KIFs are plus-end directed motors, including conventional KIFs. Some KIFs are minus-end directed motor, but the minus-end directed transport is also carried out by cytoplasmic dynein (Figures 5A and 5B). In general, N-kinesin and M-kinesin are plus-end directed, and C-kinesin are minus-end directed. The typical velocity is within the range of 0.1–1.5 $\mu m\ s^{-1}$. In comparison, microtubules minus-end directed motors dyneins, which are one of the fastest motor, have velocity of $\sim 14\ \mu m\ s^{-1}$. The direction obtained from *in vitro* assay generally agree with that predicted from *in vivo* study. However, one may need some caution in interpreting the velocity of in vitro assay, because, for some KIFs, the condition of *in vitro* motility assay may not be optimal.

The characteristics of some KIFs, whose functions are relatively well characterized, are summarized in Table I. Cargoes and physiological roles of some well-characterized KIF are described next.

N-Kinesin

N-kinesin holds by far the largest number of members and it consists of 11 classes, N-1 through N-11 (Figure 4). Some classes have more than one family.

N-1 Kinesins (The KIF5 Family)

Conventional kinesin corresponds to KIF5. KIF5 forms tetramers consisting of two kinesin heavy chains (120 kDa) and two light chains (64 kDa). Light chains are unrelated in sequence to kinesin. They are a rod-like structure composed of two globular heads, a stalk, and a fanlike end, in which the light chains reside (Figure 2). KIF5 is a plus-end directed motor with the velocity of $\sim 0.5\ \mu m\ s^{-1}$. KIF5 is relatively abundantly expressed in both nervous tissue and other tissues, and transports an amazingly wide variety of cargoes including vesicles containing amyloid precursor protein (APP), GAP43, ApoE2, the receptor for the Reelin ligand, or the AMPA-type glutamate receptor GluR2, mitochondria, and lysosomes, (Figures 5A and 5B). KIF5 could also convey mRNA complexes, tubulin oligomers and intermediate filament, vimentin protein complexes. Recently the direct interactions between KIF5 and some of the cargoes have been shown (Figure 6). KIF5 may interact with certain cargoes via light chains, and yet with other cargoes via heavy chain. Moreover, whether KIF5 interacts via light chains or heavy chains may determine the destination. Glutamate receptor interacting protein 1 (GRIP1) binds to the tail domain of kinesin heavy chain and transports AMPA-type glutamate receptor (GluR2)-containing vesicles to dendrites, while JIP1,2 steers ApoER2 containing vesicles to axons through its interaction with light chains (Figure 6).

N-3 Kinesins

The Unc104/KIF1 Family

KIF1A and KIF1Bβ are plus-end directed motors of ~ 190 kDa, which are relatively abundantly expressed in the axon and transport precursors of synaptic vesicles. They are monomeric motors, which is rather unique compared to other KIFs (Figure 2). They are also one of the fastest KIF ($\sim 1.5\ \mu m\ s^{-1}$) (Table I). Unc104 is a homologue of mouse KIF1A. The knockout mice of KIF1A and KIF1Bβ show aberrant neuronal functions due to the defect in the transport of precursors of synaptic vesicles. Further study showed that patients

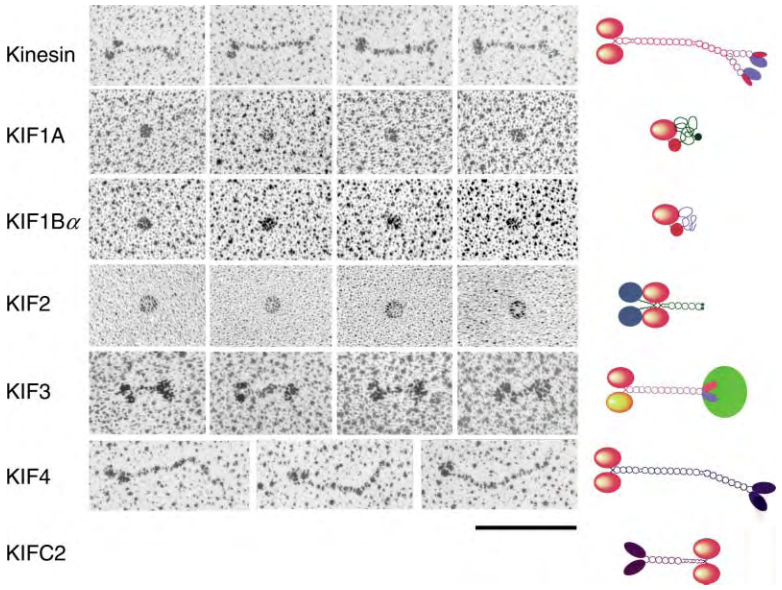

FIGURE 2 Left: Panels showing main KIFs functioning in intracellular transport, as observed by low-angle rotary shadowing EM. Scale bar, 100 nm. Right: Schematic illustration of the same KIFs based on EM studies or predicted from analysis of primary structures. (Reproduced, with permission, from Hirokawa, N. (1998). Kinesin and dynein superfamily proteins and the mechanism of organelle transport. *Science* **279**, 519–526.)

with Charcot-Marie-Tooth disease type 2A carry a loss-of-function mutation in the motor domain of the *kif1b* gene. This was the first clear indication that impaired transport due to dysfunction of KIF motors underlie the cause of neurodegenerative disease. KIF1Bα is a plus-end directed motor ($\sim 0.5\ \mu m\ s^{-1}$) expressed ubiquitously and transports mitochondria.

The KIF13 Family

KIF13A is a plus-end directed motor with the velocity of $0.1–0.3\ \mu m\ s^{-1}$ and transports vesicles containing the mannose-6-phosphate receptor from the trans-Golgi network to the plasma membrane (Figure 5B). The interaction of KIF13A with the vesicle is mediated via direct interaction between KIF13A tail and β-1-adaptin, a subunit of the AP-1 adaptor complex (Figure 6).

N-4 Kinesins

The KIF3 Family

The KIF3 forms a heterotrimeric complex, in which a heterodimer of KIF3A (80 kDa) and KIF3B ($\sim$95 kDa) interact at its tail domain with a nonmotor protein, kinesin superfamily-associated protein 3 (KAP3, $\sim$100 kDa) (Figure 2). The KIF3 complex is plus-end directed with the velocity of $\sim 0.3\ \mu m\ s^{-1}$. KIF3 is relatively abundantly expressed in the axon and other tissues, and functions in axonal transport, intracellular transport, and in the intraflagellar transport (IFT). In the axon, the complex transports vesicles that carry fodrin and choline acetyltransferase, a soluble protein. In melanophore, it disperses pigment organelles called melanosomes. In cilia and flagellar, the KIF3 complex transports macromolecular protein complexes, called IFT particles, from the bottom to the distal tip, which is important in formation and maintenance of cilia and flagella.

An interesting aspect of the involvement of KIF3 in cilium formation is that it also plays a significant role in the determination of the left–right axis in early mouse development. During mouse development, there is a monocilium at the nodal cell that rotates to produce unidirectional leftward flow of extraembryonic fluid. This nodal flow could generate concentration gradients of putative secreted morphogen, which could switch on a gene cascade leading to left–right asymmetry. In *kif3A* (−/−) or *kif3B* (−/−) mouse, nodal cilia cannot be formed, nodal flow is absent, and the left–right axis formation is fundamentally impaired.

In retinal photoreceptor cells, the KIF3 complex is localized in the connecting cilium, which is located between the outer and inner segment. KIF3 complex participates in the transport of opsin from the inner to the outer segment at the connecting cilium; the impairment of this transport process could be one of the causes of retinitis pigmentosa.

The KIF17 Family

KIF17 is localized to the dendrites and transports vesicles containing N-methyl-D-aspartate (NMDA)-type

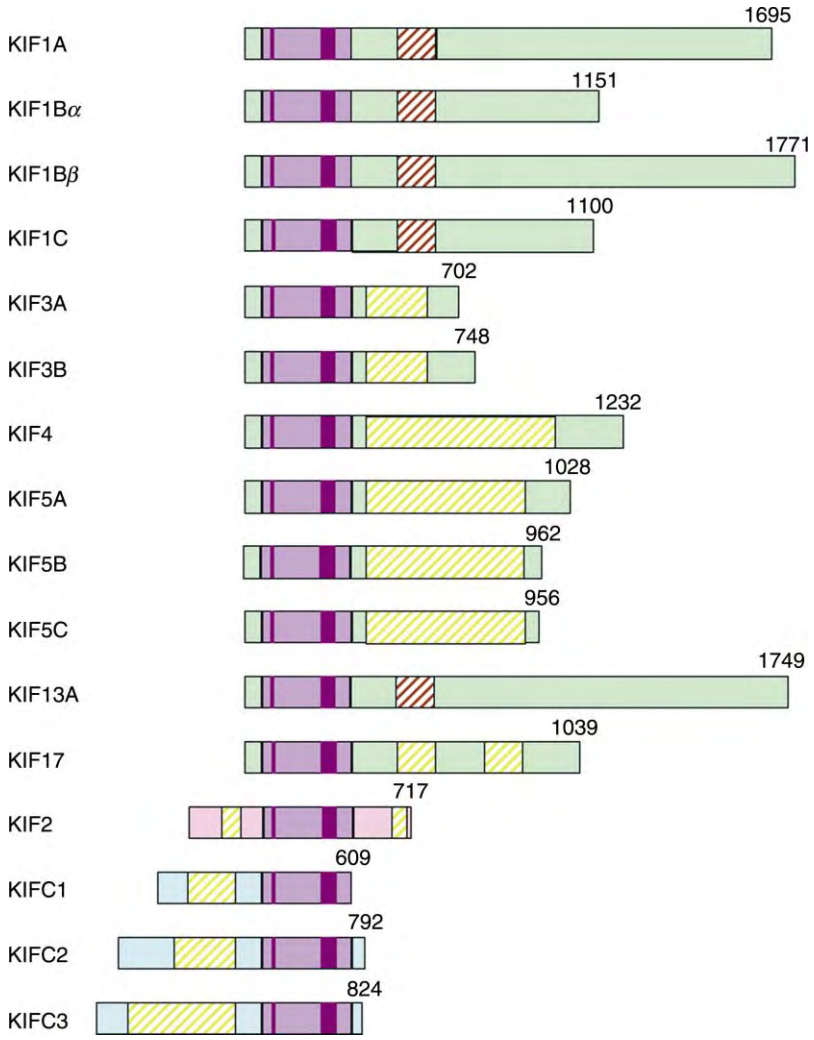

FIGURE 3 Structure of cDNAs from murine kinesin superfamily proteins (KIFs). Purple, motor domain; thin red line, ATP-binding consensus sequence; thick red line, microtubule-binding consensus sequence. (Reproduced from Hirokawa, N., and Takemura, R. (2003). Kinesin superfamily proteins. In *Molecular Motors* (M. Schliwa, ed.) pp. 79–109. Wiley-VCH, Weinheim, with permission.)

glutamate receptor 2B towards the microtubule plus end to the postsynaptic site, where the receptor plays an important role in synaptic plasticity (Figure 5). The large protein complex containing mLin-10, mLin-2, mLin7, and NR2B mediates the attachment of KIF17 to the vesicle (Figure 6). The tail domain of KIF17 interacts directly with the PDZ domain of mLin-10. Transgenic mice overexpressing KIF17 increase synthesis of KIF17 and NR2B and enhance spacial and working memories.

Other N-Kinesins

For the rest of the N-kinesin members, the physiological function has been elucidated to the varying degrees. The members of N-2 kinesins, *H. sapiens* Eg5 or *C. elegans* BimC form bipolar tetramer and participate in mitosis. They localize at the midzone of interpolar microtubules, where microtubules run in antiparallel orientation. They crosslink microtubules and allow their sliding against each other. N-5 and N-6 kinesins are involved in both mitosis and vesicle transport. N-7 and N-8 kinesins are involved primarily in mitosis. N-11 class includes the Costal 2, which is a part of the hedgehog-signaling cascade.

M-Kinesins

M-kinesins have a motor domain at the center of the molecule. There is only one family in this group, namely the KIF2 family, which is composed of *kif2a*, *kif2B*, and *kif2c* genes. KIF2 family has functional roles in vesicle transport, mitosis, and regulation of microtubule

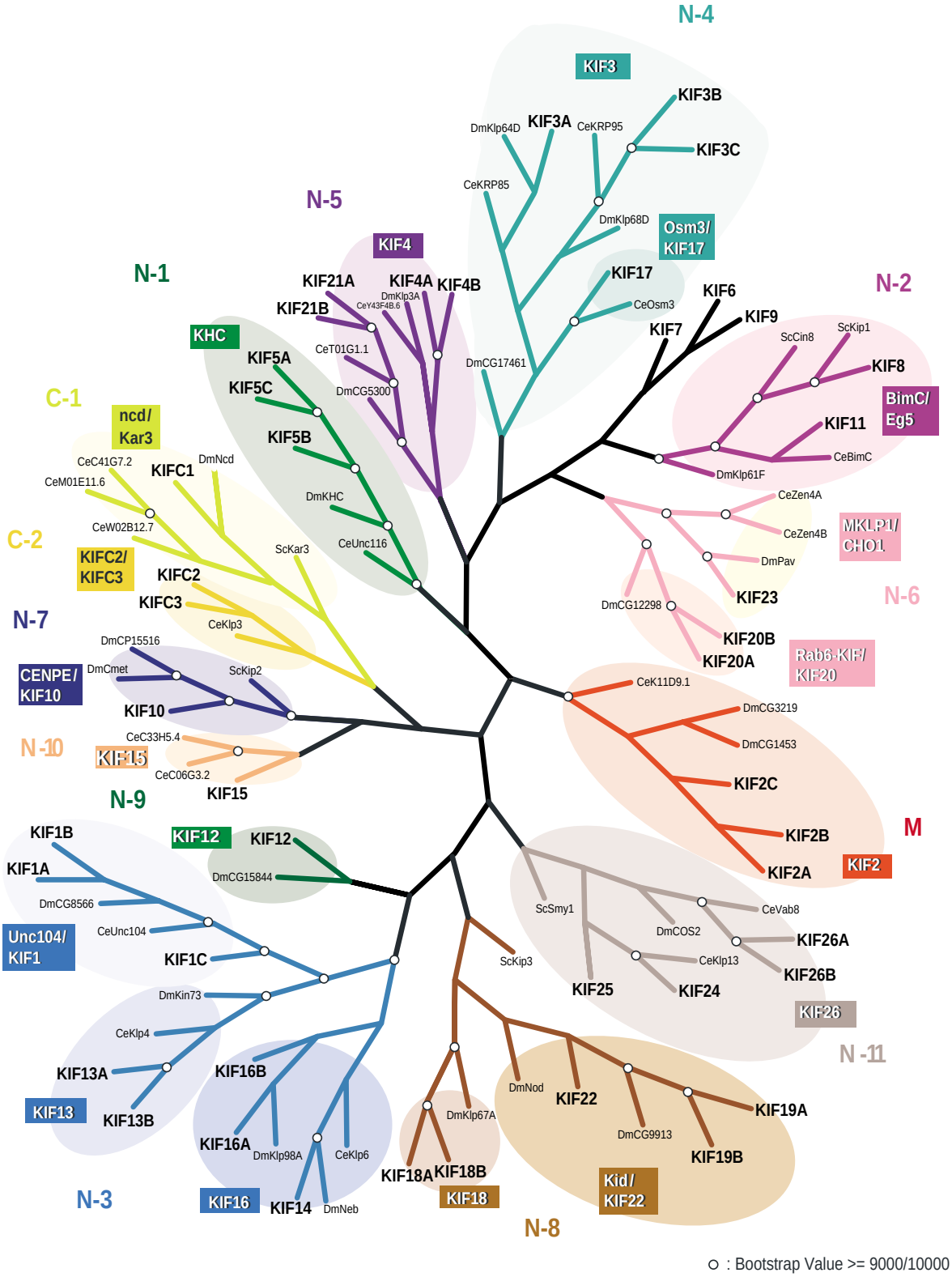

FIGURE 4 Phylogenetic analysis of all KIFs expressed in mouse/human, *D. melanogaster*, *C. elegans*, and *S. cerevisiae*. Amino acid sequences were aligned using maximum parisomy. (Reproduced from Miki, H., Setou, M., Kaneshiro, K., and Hirokawa, N. (2001). All Kinesin superfamily protein, KIF, genes in mouse and human. *Proc. Natl Acad. Sci. USA* **98**, 7004–7001, with permission.)

TABLE I

Some Members of KIF and their Properties

Class	Name	Subunit structure	Direction of transport, velocity	Functions	Cargo
N-kinesin					
N-1	KIF5 (conventional kinesin)	Homodimer plus two light chains	Microtubule plus-end $\sim 0.5\ \mu m\ s^{-1}$	Axonal transport	Vesicles containing APP and GAP43, or ApoE2, tubulin oligomers
				Dendritic transport	Vesicles containing AMPA-type glutamate receptor
				Intracellular transport	Mitochondria, Lysosomes, Vimentin protein mRNA complexes
N-2	*H. sapiens* Eg5, *C. elegans* BimC	Bipolar homotetramer	Microtubule plus-end	Mitosis	Microtubule (crosslinking and sliding of antiparallel interpolar microtubules at midzone, producing expanding force)
N-3	KIF1A, KIF1Bβ	Monomer	Microtubule plus-end $\sim 1.5\ \mu m\ s^{-1}$	Axonal transport	Precursors of synaptic vesicles
	KIF1Bα	Monomer	Microtubule plus-end $\sim 0.5\ \mu m\ s^{-1}$	Axonal and intracellular transport	Mitochondria
	KIF13		Microtubule plus-end $0.1-0.3\ \mu m\ s^{-1}$	Intracellular transport (endocytic, exocytic pathway)	Vesicles containing mannose-6-phosphate receptor
N-4	KIF3	Heterodimer plus associated protein (KIF3A/3B-KAP3)	Microtubule plus-end $\sim 0.3\ \mu m\ s^{-1}$	Axonal transport	Vesicle containing fodrin, Choline acetyltransferase
				Intracellular transport	Melanosomes
				Intraflagellar transport (IFT)	IFT particles
	KIF17	Homodimer	Microtubule plus-end $0.7-1.2\ \mu m\ s^{-1}$	Dendritic transport	NMDA-type glutamate receptor
M-kinesin					
M	KIF2	Homodimer	Microtubule plus-end $\sim 0.5\ \mu m\ s^{-1}$	Axonal transport	Vesicles containing IGF-1
				Intracellular transport	Lysosomes
	Xenous XKCM1			Mitosis	Microtubule (depolymerizing kinetochore microtubules at the kinetochore)
C-kinesin					
C-1	Ncd		Microtubule minus-end	Mitosis	Microtubules (crosslinking and sliding of antiparallel interpolar microtubules at midzone, opposing the effect of N-2 kinesins)
C-2	KIFC2	Homodimer		Dendritic transport	Multivesicular body-like membranous organelles
	KIFC3		Microtubule minus-end $\sim 4.5\ \mu m\ s^{-1}$	Intracellular transport	Vesicles containing annexin XIIb containing vesicles

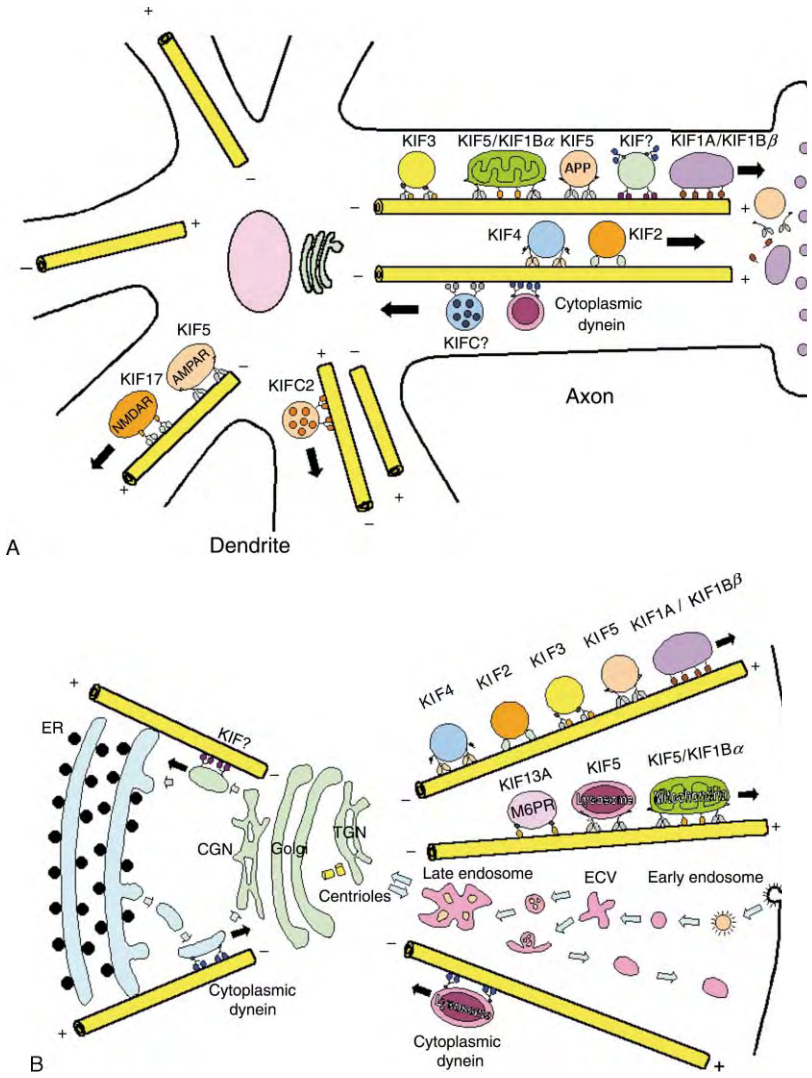

FIGURE 5 Scheme of KIFs and their cargo organelles in neurons (A) and in cells in general (B). In (B), neuron-specific KIFs and ubiquitous KIFs are illustrated in the same cell. CGN, cis-Golgi network; TGN, trans-Golgi network; ECV, endosomal carrier vesicle. Black arrows indicate the direction of transport. (Reproduced from Hirokawa, N., and Takemura, R. (2003). Kinesin superfamily proteins. In *Molecular Motors* (M. Schliwa, ed.) pp. 79–109. Wiley-VCH, Weinheim, with permission.)

dynamics. *Xenopus* XKCM1 has a microtubule-destabilizing activity, and depolymerizes microtubules at the kinetochore and promotes chromosome segregation.

C-Kinesins

C-1 Kinesins (The KIFC1 Family)

Drosophila Ncd crosslinks and slides antiparallel spindle microtubules in relation to another, pulling them apart, opposing the effect of bipolar plus-end-directed motors.

C-2 Kinesins (The KIFC2/KIFC3 Family)

KIFC2 transports multivesicular body-like membranous organelles in dendrites (Figure 5A). It has not been rigorously demonstrated, but it is presumed that KIFC2 acts as a minus-end-directed motor.

KIFC3 is a minus-end-directed microtubule motor protein that exists in kidney epithelial cells and other types of cell. In epithelial cells, microtubule organization is different from that in other types of cell; microtubule minus ends run towards the apical surfaces of the cell. KIFC3 accumulates on the apical surface of epithelial cells and transports vesicles associated with annexin

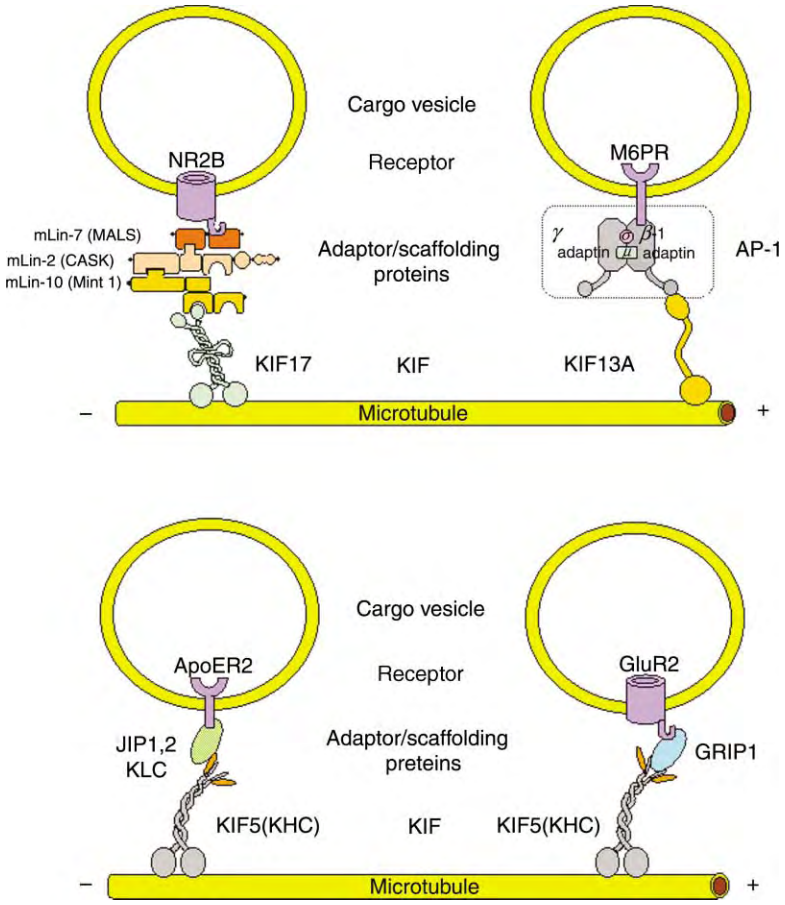

FIGURE 6 Scheme of how KIFs recognize and bind cargoes. (Reproduced from Hirokawa, N., and Takemura, R. (2003). Kinesin superfamily proteins. In Molecular Motors (M. Schliwa, ed.) pp. 79–109. Wiley-VCH, Weinheim, with permission.)

XIIIb, a previously characterized membrane protein for apically transported vesicles.

Perspectives

Cargoes of KIFs; Specificity and Redundancy

As mentioned earlier KIFs convey various types of cargo. In some cases, a single KIF transports several distinct cargoes. How the same KIF can transport different cargoes is an interesting and important question that needs to be addressed.

At the same time, KIFs sometimes redundantly convey similar cargoes. KIF1Bα transports mitochondria, while mitochondria have another redundant motor KIF5. KIF1A's cargo is a synaptic vesicle precursor, whereas KIF1Bβ also conveys synaptic vesicle precursors. Another example is lysosomes that have at least two microtubule plus-end motors, kinesin and KIF2Aβ. This redundancy could be a cause of subtle phenotypes of knockout mice in which some *kif* genes have been knocked out.

Recognition and Binding to Cargoes

To address the question of how specificity and redundancy are controlled, it is important to understand how KIFs recognize and bind to their own cargoes. As discussed earlier, some of the interactions of KIFs and cargoes are beginning to be uncovered.

In terms of how KIFs recognize and bind cargoes, several forms can be categorized (Figure 6).

1. *KIF tail – scaffolding protein(s) or adaptor protein(s) – membrane protein*. This is applicable to KIF17-mLin10-mLin2-mLin7-NR2B, KIF13A-β1adaptin-AP-1adaptor complex-M6PR, KLC-JIP1/JIP2-ApoE2, the reelin receptor, and KIF5 (KHC)-GRIP1-GluR2.

2. *KIF tail – membrane protein*. Kinesin was reported to bind directly to membrane proteins through its interaction with KLC. Sunday Driver (also called JSAP1 and JIP3) and APP were proposed to be membrane proteins that bind to directly kinesin through KLC, while it needs to be studied further if Sunday Driver (JSAP1 ad JIP3) is indeed a membrane protein.

It is only now being understood how KIFs recognize and bind to their specific cargoes, but thus far what was only known was that rather complex mechanisms are involved in these events. This may be related to how the association and dissociation between KIFs and cargoes are regulated. Another question is how KIFs recognize and bind to protein complexes such as tubulin and intermediate filament proteins, chromosomes, and mRNAs. These are obviously significant questions that need to be answered in the near future.

How to Determine Directions of Transport

Another intriguing question is how a cell regulates direction of transports, e.g., axon versus dendrites. In the case of KIF5, whether KIF5 binds to cargoes via heavy chain or light chain seems to determine the direction of transport, and JIP1.2 and GRIP1 are functioning as drivers (Figure 6). There are motors that transport cargoes mainly to dendrites. KIF17 conveys NMDA receptors mainly to dendrites and KIFC2 transports new multivesicular body-like organelles to dendrites. KIF21B was also proposed to be a motor for dendritic transport. How differential transports are performed is clearly the fundamental question that needs to be solved in the near future. The mechanism is probably not simple and could involve several distinct events.

Thus, cells use interestingly many KIFs and very precisely control the direction and velocity of transport of various distinct cargoes that are fundamental in cellular basic functions. This field is obviously very important and rapidly advancing. Further studies need to be carried out to understand the entire mechanism of intracellular transport.

See Also the Following Articles

Dynein • Kinesins as Microtubule Disassembly Enzymes • Microtubule-Associated Proteins • Mitosis

Glossary

axonal and transport Axons transmit the signal from the cell body to the synaptic terminal. Because axons lack ribosomes, i.e., the protein synthetic machinery, most of the proteins needed in the axon and synaptic terminal need to be synthesized at the cell body and transported. The transport in the direction from the cell body to synapse is called the anterograde transport. Some molecules are transported in the opposite direction (retrograde transport). The proximal part of the dendrite contains ribosomes, although the number reduces at the distal region.

cilia and flagella Cilia and flagella contain microtubules in the "9 + 2" axonemal configuration (9 doublets and central pair of microtubules). The microtubules in the doublets slide along one another by the stroke of axonemal dynein, which bridges neighboring doublets.

dynein Minus-end directed microtubule motor. It forms a massive multisubunit complex composed of two–three heavy chains (~530 kDa), which have motor domains, and variable numbers of associated intermediate and light chains. There are two classes, axonemal and cytoplasmic. Axonemal dyneins are attached to microtubule doublets in cilia and flagellar, and slide against microtubules producing the beating movement. Cytoplasmic dyneins are expressed in most eukaryotic cells and important in vesicle trafficking and cell division.

microtubule Filament of 25 nm diameter assembled from α- and β-tubulin subunits (55 kDa). Microtubules, microfilaments (actin filaments), and intermediate filaments are the major cytoskeletal filaments. In addition to the structural role, microtubules serve as rails for the long-distance transport, and microfilaments serve as rails for the short-distance transport. Microtubules are also reorganized as mitotic spindle during mitosis, and play an important role in cell division.

mitosis Replicated chromosomes are separated into two daughter cells, by a complex cytoskeletal machine called mitotic spindles. The process proceeds as prophase, prometaphase, metaphase, anaphase, and telophase. Several different classes of KIFs and the cytoplasmic dynein participate in the complex movement of mitotic spindles.

Further Reading

Alberts, B., Johnson, A., Lewis, J., Raff, M., Roberts, K., and Walter, P. (2002). *Molecular Biology of the Cell*, 4th edition. Garland Publishing, New York.

Grafstein, B., and Forman, D. S. (1980). Intracellular transport in neurons. *Physiol. Rev.* **60**, 1167–1283.

Heald, R. (2000). Motor function in the mitotic spindle. *Cell* **102**, 399–402.

Hirokawa, N. (1998). Kinesin and dynein superfamily proteins and the mechanism of organelle transport. *Science* **279**, 519–526.

Hirokawa, N. (2000). Stirring up development with the heterotrimeric kinesin KIF3. *Traffic* **1**, 29–34.

Hirokawa, N., and Takemura, R. (2004). Biochemical and molecular characterization of diseases linked to motor proteins (submitted).

Hirokawa, N., and Takemura, R. (2003). Kinesin superfamily proteins. In *Molecular Motors* (M. Schliwa, ed.) pp. 79–109. Wiley-VCH, Weinheim.

Hirokawa, N., Noda, Y., and Okada, Y. (1998). Kinesin and dynein superfamily proteins in organelle transport and cell division. *Curr. Opin. Cell Biol.* **10**, 60–73.

Schliwa, M. (2003). *Molecular Motors*. Wiley-VCH, Weinheim.

Tanaka, Y., and Hirokawa, N. (2002). Mouse models of Charcot-Marie-Tooth disease. *Trends Genet.* **18**, S39–S44.

Terada, S., and Hirokawa, N. (2000). Moving on to the cargo problem of microtubule-dependent motors in neurons. *Curr. Opin. Neurobiol.* **10**, 566–573.

Verhey, K. J., and Rapoport, T. A. (2001). Kinesin carries the signal. *Trends Biochem. Sci.* **26**, 545–550.

Biography

Nobutaka Hirokawa is Professor and Chair of the Department of Cell Biology and Anatomy, and Dean of the School of Medicine, University of Tokyo. His principal research interests are organization of cytoskeletal structures in neurons and molecular motors involved in the axonal transport. He holds an M.D. and a Ph.D. from University of Tokyo. He developed the quick-freeze, deep-etch electron microscopy with John Heuser, and did pioneering work in elucidating the neuronal cytoskeleton in molecular detail. He was also one of the first to tackle the analysis of kinesin motor molecules, clone multiple kinesin superfamily proteins from mammalian brain and point out the importance of this motor protein family.

Kinesins as Microtubule Disassembly Enzymes

Susan L. Kline-Smith and Arshad Desai
University of California, San Diego, California, USA

Kinesins are an important class of proteins that were discovered on the basis of their ability to couple ATP hydrolysis to translocation along microtubule polymers. Microtubules are hollow cylindrical polymers assembled from α/β-tubulin heterodimers that are found in all eukaryotes and function in many different biological contexts. Microtubules exhibit structural polarity, with the α/β-tubulin heterodimers oriented in a uniform head-to-tail fashion within the polymer lattice. β-tubulin points toward the faster polymerizing "plus" end and α-tubulin toward the slower polymerizing "minus" end of the microtubule. The defining member of the kinesin superfamily, referred to as conventional kinesin, is a well-characterized, processive plus end-directed motor protein. Sequences homologous to the catalytic domain responsible for the motor activity of conventional kinesin have been discovered in a large number of proteins, and the complete genomic complement of kinesins is known for the many eukaryotes with sequenced genomes.

Although motility was the defining activity of kinesins, recent work has revealed that the catalytic domain is used in a subset of kinesins to drive microtubule disassembly rather than motor activity. Physiologically, the regulation of microtubule dynamics by kinesins is likely to be of great significance in cellular organization, division, and differentiation. Here, we first briefly review the work that led to the recognition of specific kinesins acting as microtubule disassembly enzymes. We then discuss progress toward understanding the mechanism by which the catalytic domain is used to drive a very different biochemical activity and finally comment on the physiological relevance of this nonmotile activity.

Kinesins as Regulators of Microtubule Dynamics: A Brief Historical Overview

The kinesin superfamily has been subdivided based on catalytic domain sequence homology and placement of the catalytic domain within the primary sequence (Figure 1). Conventional kinesin, the first discovered kinesin, has its catalytic domain at the N terminus and is a fast, plus end-directed motor protein (Figures 1 and 2). All kinesins with N-terminal catalytic domains (Kin Ns) that have been subsequently analyzed *in vitro* exhibit plus end-directed motility. In contrast, slow minus end-directed movement has been observed for Kin C kinesins, which have their catalytic domain at the C terminus (Figures 1 and 2).

Kinesins were assumed to move along the microtubule lattice without significantly influencing their dynamic properties. Consistent with this assumption, the motility of kinesin-coated microspheres was found to have no effect on the parameters of microtubule dynamics in quantitative studies. The first hint for the involvement of kinesins in regulation of microtubule dynamics came from *in vitro* analysis of Kar3, a budding yeast member of the Kin C subfamily. *In vitro*, the catalytic domain of Kar3 translocated slowly toward the minus end and also increased depolymerization from minus ends of microtubules stabilized with the drug paclitaxel (Figure 2). A role for Kar3 in promoting microtubule disassembly was also supported by the ability of microtubule-destabilizing drugs to suppress Kar3 mutations. While this work was suggestive, compelling evidence for kinesins acting as microtubule-disassembly enzymes came from analysis of the Kin I kinesin subfamily, whose members have an internal catalytic domain (Figures 1 and 2). When a *Xenopus* member of the Kin I subfamily was inactivated in egg extracts, microtubule polymerization was dramatically increased. This increase was attributed to a reduction in the transition from microtubule polymerization to depolymerization (termed microtubule catastrophe). Subsequently, purified Kin I kinesins were shown to be sufficient for microtubule disassembly, and the majority of studies on kinesins as microtubule disassembly enzymes has been focused on members of this subfamily.

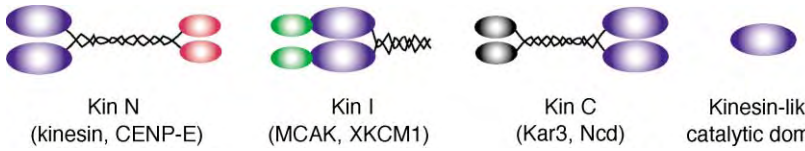

FIGURE 1 Kinesin superfamily domains. Proteins that share sequence homology in the kinesin-like catalytic domain (shown in purple) are defined as members of the kinesin superfamily. The placement of the catalytic domain within the primary sequence of the proteins further subdivides the family into Kin N (N-terminal catalytic domain), Kin I (Internal catalytic domain), and Kin C (C-terminal catalytic domain) subfamilies. Examples of proteins belonging to each subfamily are listed.

Kin I Kinesins: Motors or Disassembly Enzymes?

The presence of a kinesin-like catalytic domain in Kin I kinesins suggested that they are motor proteins. Consistent with this expectation, a neuron-specific member of this subfamily was reported to be a fast plus end-directed motor. However, the dramatic increase in microtubule polymerization upon inhibition of a Kin I kinesin in *Xenopus* egg extracts suggested that these kinesins promote microtubule disassembly. One obvious hypothesis to accommodate both views was that Kin I kinesins do not themselves act as depolymerases, but instead deliver a destabilizing factor to microtubule plus ends. However, *in vitro* analysis of purified Kin I kinesins contradicted this hypothesis and clearly demonstrated that microtubule disassembly is an intrinsic activity of members of this subfamily. Particularly compelling evidence came from the observation that depolymerization occurred at both microtubule ends, inconsistent with the unidirectional motility that has been demonstrated for all other kinesins with motor activity. In addition, *Xenopus* Kin I kinesins preferentially targeted to both microtubule ends over the microtubule lattice, even in the presence of the nonhydrolyzable ATP analogue AMP-PNP. These findings for *Xenopus* Kin Is have been replicated successfully for mammalian and invertebrate members of this subfamily, and it is now generally accepted that Kin I kinesins use their catalytic domain to depolymerize microtubules rather than to translocate along the microtubule lattice. The first study reporting motility for a Kin I kinesin is most likely explained by the presence of a contaminant in the assayed protein preparation, as none of the subsequent studies have been able to demonstrate motor activity.

Kin I Kinesins: Mechanism of Action

Multiple *in vitro* studies have demonstrated that Kin Is are able to catalytically depolymerize microtubules from both their plus and minus ends. Mechanistic studies concerning Kin Is largely used stabilized microtubule substrates: a necessity for studying intermediary steps in the microtubule disassembly process. Kin Is are able to depolymerize microtubules stabilized using the drug paclitaxel as well as microtubules stabilized with a slowly hydrolyzable analogue of GTP, called GMP-CPP, which mimics a stable GTP-like microtubule lattice. With respect to dynamic microtubules assembled from purified tubulin, the more physiologically relevant substrate, Kin I kinesins have been shown to promote microtubule catastrophes, but whether they influence the rates of polymerization and depolymerization or the transition from depolymerization to polymerization (termed microtubule rescue) is not known.

Negative stain electron microscopy of GMP-CPP stabilized microtubules has demonstrated that Kin Is destabilize microtubules at both ends of the polymer by

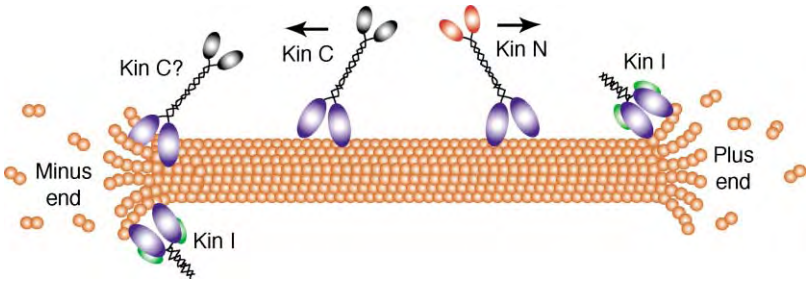

FIGURE 2 Kinesin–microtubule interactions. Kinesin-like proteins exhibit various interactions with the microtubule polymer, including plus end-directed motor activity (Kin Ns), minus end-directed motor activity (Kin Cs), and depolymerization of microtubules from both ends of the microtubule (Kin Is). A Kin C from budding yeast has also been shown to weakly destabilize the minus ends of microtubules.

inducing protofilaments to peel backwards. In dynamic microtubules, the bulk of the polymer is made up of GDP-associated tubulin, with the newly added tubulin heterodimers still bound to GTP. It is thought that the GTP-bound dimers (referred to as the GTP "cap") constrain the rest of the polymer to maintain a straight conformation as opposed to the preferred curved conformation of the GDP-bound protofilaments. Interestingly, Kin Is do not induce protofilament curvature by stimulating hydrolysis of the tubulin-bound nucleotide, suggesting that their binding results in a destabilizing conformational change at microtubule ends. A direct preference of Kin Is for microtubule ends versus the side lattice has been demonstrated using fluorescence microscopy to visualize the accumulation of Kin I molecules on the peeling protofilaments at the end of depolymerizing GMP-CPP microtubules. In addition, the depolymerization rate of Kin Is saturates at a very low ratio of Kin I:tubulin, suggesting that Kin I activity is restricted to microtubule ends.

The preferential targeting of Kin Is to microtubule plus and minus ends is consistent with their ability to depolymerize either end, although the mechanism by which Kin Is target ends is not known. Interestingly, Kin Is display a much higher on-rate for microtubule ends than the on-rate of conventional kinesin for the microtubule lattice, suggesting that the process of end-targeting might be more directed than simple diffusion of the Kin I molecules. Recent data demonstrating one-dimensional diffusion of Kin Is along the lattice of GMP-CPP microtubules have led to the hypothesis that this mechanism enables Kin Is to quickly reach either end of the microtubule. However, Kin Is can target to ends and induce protofilament peeling in the presence of AMP-PNP, which inhibits one-dimensional diffusion of other kinesins. The effect of AMP-PNP on the one-dimensional diffusion of Kin Is along the microtubule lattice is an important issue to address in future work.

Quantitative ATPase assays have provided additional evidence that Kin Is act at microtubule ends; however, the precise coupling between the ATPase and microtubule disassembly cycles is controversial. In the presence of AMP-PNP, Kin I kinesins accumulate at and cause peeling of GMP-CPP microtubule ends without disassembling the entire stabilized polymer. Thus, it was initially proposed that ATP hydrolysis occurs after dissociation of the Kin I–tubulin complex from the microtubule, thereby recycling the Kin I for multiple depolymerization cycles (Figure 3A). Consistent with this observation, Kin Is have been shown to bind tubulin subunits and exhibit tubulin-stimulated ATPase activity. In contrast, ATPase analyses have also suggested that Kin Is may act processively at GMP-CPP microtubule ends, with each Kin I causing disassembly of several tubulin subunits without dissociation of the Kin I molecule from the microtubule end (Figure 3B). Further work is necessary to reconcile these opposing viewpoints.

Specialized microtubule substrates have been used to determine how Kin Is bind microtubules to induce protofilament peeling. Two possible mechanisms of inducing the curved conformation at the end of a microtubule are: (1) the Kin I binds between two protofilaments, splaying them apart, or (2) the Kin I binds a single protofilament, inducing a kink in the conformation of that protofilament, which would then lead to destabilization of the microtubule lattice. *In vitro* analyses support the latter hypothesis, as Kin Is can still depolymerize zinc-induced macrotubes, which are 250 nm tubes (tenfold larger diameter than microtubules) made up of protofilaments that have opposing polarity. Thus, in a zinc macrotube the side-by-side

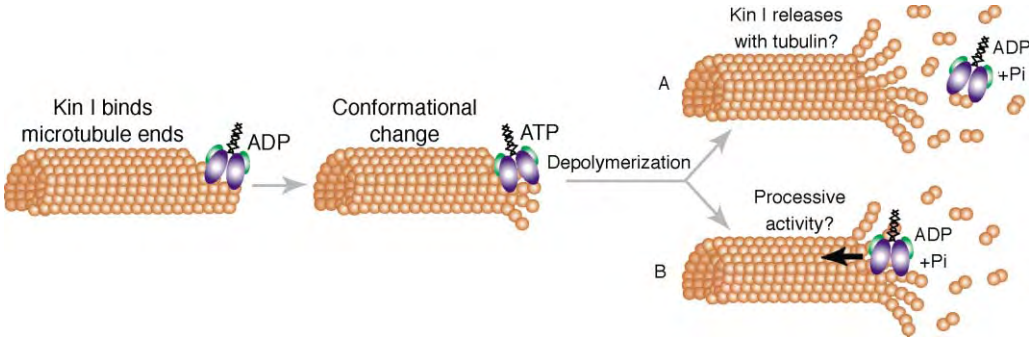

FIGURE 3 Kin I ATPase and microtubule disassembly cycles. Although Kin Is can bind and depolymerize both microtubule ends, only one end is illustrated for simplicity. As with other kinesin-like proteins, Kin Is are thought to bind microtubules in an ADP-bound state. Microtubules act as nucleotide exchange factors, resulting in ATP-bound Kin Is, which initiate a conformational change in the lattice at microtubule ends. This conformational change leads to depolymerization of the microtubule polymer. Two proposed models suggest different functions for ATP hydrolysis in this cycle. (A) After initiating depolymerization of the microtubule, Kin Is use ATP hydrolysis to be released from tubulin heterodimers, allowing the Kin I to participate in another depolymerization cycle. (B) Alternatively, ATP hydrolysis may allow Kin Is to processively depolymerize microtubules, with each Kin I molecule removing multiple tubulin dimers before dissociating from the microtubule lattice.

protofilaments alternate between the luminal face and the external face of protofilaments in a normal microtubule. If Kin Is bound between two protofilaments, the protofilament would be required to have the same directionality. Current structural studies are focusing on how Kin Is dock onto protofilaments and how the conformations of both the Kin I and the microtubule change during the cycle of Kin I activity.

Kin Is are homodimeric proteins, largely through interactions in the α-helices of the short C-terminal stalk of the protein. However, Kin Is are still able to depolymerize microtubules in their monomeric form both *in vitro* and *in vivo*. In most systems, the internal kinesin-like catalytic domain (which includes microtubule binding and ATP hydrolysis domains) is sufficient only to bind microtubules. To reconstitute the activity of microtubule depolymerization, Kin Is require the catalytic domain plus a small section of the N terminus called the "neck," which is just proximal to the catalytic domain. In conventional kinesin, the neck is responsible for the power stroke that allows one head to "step" in front of the other head on the microtubule lattice. In Kin Is, the neck must be positively charged for microtubule destabilization to occur, presumably because the positively charged neck interacts with the negatively charged microtubule polymer. Interestingly, Kin Is are unable to depolymerize microtubules treated with the drug subtilisin, which cleaves the negatively charged C terminus of β-tubulin known to interact with other motile kinesins, suggesting a degree of conservation in the mechanism of interaction between diverse kinesins and microtubule polymer.

Overall, biochemical and microscopic studies are improving our understanding of the mechanism of Kin I-induced microtubule depolymerization; however, many questions still remain regarding microtubule end targeting, coupling of the Kin I ATPase cycle with microtubule disassembly, and the structural requirements for Kin I binding to the microtubule. In addition, defining the extent to which these results can be applied to dynamic microtubules is perhaps the most important future goal.

Physiological Roles of Microtubule-Depolymerizing Kinesins

During interphase, Kin Is exist as a soluble pool in the cytoplasm and nucleus of cells. Inhibition of the cytoplasmic pool suggests that Kin Is help to regulate microtubule dynamics by stimulating the catastrophe frequency and suppressing the rescue frequency of microtubules. During mitosis, Kin Is display a complex localization at centromeres, spindle poles, and in the cytoplasm of somatic cells and embryonic extracts (Figure 4). Truncation assays have demonstrated that the globular N-terminal domain of Kin Is aids in centromere localization of the protein. It is unclear how Kin Is localize to spindle poles during mitosis, although this enrichment does appear to require microtubules.

Inhibition assays suggest that Kin Is regulate different aspects of mitotic spindle formation and function. Immunodepletion of a *Xenopus* Kin I from embryonic egg extracts completely inhibits spindle formation due to a huge increase in microtubule polymerization as a result of decreased catastrophe frequency of microtubules (Figure 5B). Similarly, inhibition of Kin Is in somatic cells leads to increases in microtubule spindle polymer, delayed centrosome separation, and delayed mitosis. Thus, regulation of global microtubule dynamics in the mitotic spindle appears to be a conserved activity of Kin I kinesins. These findings, however, demonstrate the defects due to overall inhibition of Kin Is, and do not distinguish between the roles for Kin Is specifically localized to the centromere or the spindle poles. Interestingly, studies designed to specifically inhibit the centromeric portion of Kin Is in embryonic extracts and in mammalian somatic cells have shown that Kin Is are required to properly align and segregate chromosomes on the mitotic spindle (Figure 5C). Although the exact mechanism for how centromere-bound Kin Is are functioning to regulate chromosome positioning is not known, cellular studies implicate Kin Is in regulating

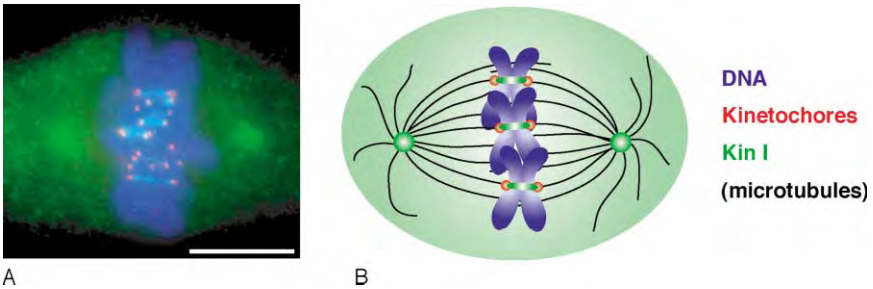

FIGURE 4 Kin I localization during mitosis. (A) This mammalian epithelial (PtK2) cell immunostained for DNA (blue), kinetochores (red), and Kin I (green) shows that Kin Is are in the cytoplasm with enrichment at centromeres and spindle poles during mitosis. (B) Kin I localization is illustrated here to show the placement of mitotic spindle microtubules (black) which are not immunostained in (A). Scale bar for (A) is 10 μm. Image provided by Susan Kline-Smith.

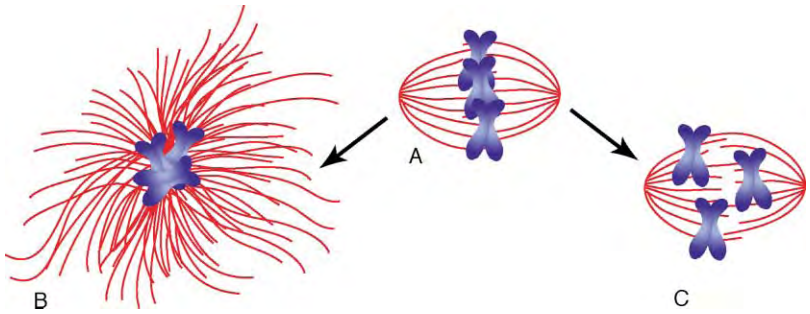

FIGURE 5 Kin I kinesins regulate microtubule dynamics and chromosome positioning during mitosis. (A) Normal spindle assembly in *Xenopus* egg extracts is illustrated here with microtubules in red and chromosomes in blue. (B) Upon immunodepletion of Kin Is, spindle assembly is inhibited due to a dramatic increase in microtubule polymerization. (C) When Kin Is are disrupted only at the centromere, however, chromosomes are unable to align despite the presence of a normal bipolar spindle.

both the dynamic properties of kinetochore-associated microtubules and the precise binding and orientation of these microtubule attachments.

In fungi, Kip3 subfamily kinesins (Kip3 in budding yeast and Klps 5/6 in fission yeast) have *in vivo* activities similar to Kin I kinesins. However, these proteins exhibit different sequence features and general domain organization from Kin Is in higher eukaryotes. These kinesins may represent a highly divergent class of Kin Is and may use a distinct mechanism for microtubule destabilization. *In vitro* microtubule depolymerization assays are necessary to test whether these kinesins are intrinsic depolymerases and whether their mechanism of action bears resemblance to Kin I kinesins in higher eukaryotes.

Overall, the biochemical analyses of Kin I kinesins have demonstrated use of the kinesin catalytic domain to control microtubule polymerization dynamics. Understanding the mechanism by which the catalytic domain was adapted to this non-motile function should give insight into the flexible design of this important protein superfamily. In addition, analysis of the physiological functions of microtubule-depolymerizing kinesins will be relevant to understanding the role of the microtubule cytoskeleton in many diverse processes including cell division and differentiation.

See Also the Following Articles

Centromeres • Centrosomes and Microtubule Nucleation • Intermediate Filaments • Kinesin Superfamily Proteins • Microtubule-Associated Proteins • Tubulin and its Isoforms

Glossary

centromere The primary constriction of a mitotic chromosome that connects the two sister chromatids.

centrosome The primary organizing center for microtubules in cells. During mitosis, a centrosome forms each of the two poles of the mitotic spindle.

kinetochore The complex, proteinaceous structure that assembles onto each side of the centromere, allowing for chromosome attachment to and movement on the microtubules of the mitotic spindle.

protofilament Formed by longitudinally associated tubulin heterodimers. Protofilaments associate laterally to form the microtubule polymer.

Further Reading

Cassimeris, L., and Spittle, C. (2001). Regulation of microtubule-associated proteins. *Int. Rev. Cytol.* **210**, 163–226.

Desai, A., and Mitchison, T. J. (1997). Microtubule polymerization dynamics. *Annu. Rev. Cell Develop. Biol.* **13**, 83–117.

Goldstein, L. S., and Philp, A. V. (1999). The road less traveled: Emerging principles of kinesin motor utilization. *Annu. Rev. Cell Develop. Biol.* **15**, 141–183.

Kreis, T., and Vale, R. (1999). *Guidebook to the Cytoskeletal and Motor Proteins*, 551 pp. Oxford University Press, Oxford.

Ovechkina, Y., and Wordeman, L. (2003). Unconventional motoring: An overview of the kin C and kin I kinesins. *Traffic* **4**, 367–375.

Vale, R. D., and Fletterick, R. J. (1997). The design plan of kinesin motors. *Annu. Rev. Cell Develop. Biol.* **13**, 745–777.

Biography

Susan Kline-Smith received her Ph.D. in cell biology from Indiana University Bloomington. She is currently a postdoctoral Fellow with Dr. Desai.

Arshad Desai holds a Ph.D. in Cell Biology from the University of California, San Francisco and received his postdoctoral training at the European Molecular Biology Laboratory (Heidelberg, Germany) and the Max Planck Institute for Cell Biology and Genetics (Dresden, Germany). He is currently an Assistant Member of the Ludwig Institute for Cancer Research, La Jolla and an Assistant Professor in the Department of Cellular and Molecular Medicine, University of California, San Diego. The principal focus of his laboratory is to understand the mechanisms by which the replicated genome is accurately segregated during cell division.

Kinetic Isotope Effects

Justine P. Roth and Judith P. Klinman
University of California, Berkeley, California, USA

Isotopes are atoms that have identical numbers of protons and different numbers of neutrons in their nuclei. Because the electron distributions of molecules composed of isotopic atoms are identical, they exhibit identical chemical reactivity patterns. In reactions where bonds to isotopically labeled atoms are made and broken, rates are affected in proportion to the masses of the reacting bonds. Ratios of rates for such reactions are termed kinetic isotope effects (KIEs). KIEs are largest when bonds are made and broken at the site of isotopic substitution (a primary effect) but also are seen when significant reorganization occurs peripheral to a site that undergoes a change in bonding (a secondary effect). Both types of KIEs reflect the nature of the energy barrier to a fundamental chemical reaction. Primary hydrogen KIEs typically vary between two and eight, while the largest secondary hydrogen effects are <1.5. Thus, secondary KIEs often require the use of competitive methods and highly sensitive techniques to analyze product distributions whereas primary KIEs can be detected using non-competitive and less accurate techniques.

Physical Origin of Kinetic Isotope Effects

Primary KIEs have mostly been determined for reactions of carbon, nitrogen, and oxygen atoms bonded to the isotopes of hydrogen: protium (^{1}H), deuterium (^{2}H), and tritium (^{3}H). Such processes which include proton, hydrogen atom, and hydride transfer have been studied extensively in enzymes, solution phase and to a lesser extent in the gas phase. The observation of a primary KIE is conventionally understood using a semi-classical model. The model is semi-classical because it takes into account the quantization of energy in chemical bonds but does not explicitly deal with the dual wave/particle nature of the constituent atoms.

Chemical Bonds as Harmonic Oscillators

A chemical bond can be described as two massive bodies attached to a spring. The particles experience a restoring force that is proportional to their displacement (x) by the force constant (F). Hooke's law (eqn. [1]) relates the frequency of motion (ν) of the atoms undergoing oscillation (eqn. [2]) and the force constant characteristic of the bond. Force constants are the same for isotopic bonds and changes in vibration frequency result from changes in μ. The largest perturbation in ν is caused by changes in μ upon substituting deuterium or tritium for protium:

$$\nu = \frac{1}{2\pi}\sqrt{\frac{F}{\mu}} \qquad [1]$$

$$\mu^{-1} = (m_1 + m_2)^{-1} \qquad [2]$$

The oscillations of atoms from their equilibrium positions can be approximated by a harmonic function. The energy of a bound particle ($h\nu$) is defined by the harmonic-oscillator approximation according to eqn. [3], where h is Planck's constant ($h = 6.626 \times 10^{-34}$ J s) and vibrational energy levels are designated n_{vib}. The zero-point energy ($n_{\text{vib}} = 0$) is the lowest vibrational energy level of a harmonic oscillator. These zero-point energies dominate the origin of kinetic isotope effects within a semi-classical picture:

$$E_{\text{vib}} = (n_{\text{vib}} + 1/2)h\nu, \quad n_{\text{vib}} = 0, 1, 2, \ldots \qquad [3]$$

Wave/Particle Dualism

Particles also have wavelengths, with this property dependent on the mass (m) and velocity (v) of the particle. At constant energy, the wavelengths of unbound particles follow from the de Broglie equation (eqn. [4]):

$$\lambda = h/m\text{v} \qquad [4]$$

Defining the unbound particle kinetic energy as $E_{\text{k}} = (\frac{1}{2}m\text{v}^2)$ allows de Broglie wavelengths to be calculated (Table I). The arbitrarily assigned kinetic energies are characteristic of barrier heights encountered in many (C, N or O)–H cleavage reactions. According to eqn [3], $E_{\text{k}} \sim 4$ kcal mol^{-1} approximates the potential energy present in (C, N or O)–H bonds ($\nu \sim 3000$ cm^{-1}) at 0 K. When the electron is compared to the proton and

TABLE I

de Broglie Wavelengths as a Function of Mass and Kinetic Energy

Particle	e^-	^1H	^2H	^3H	^{12}C	^{16}O	^{80}Br
Mass ($\times 10^{27}$ kg)	0.000 911 0	1.661	3.321	4.982	19.93	26.57	132.8
λ (Å), $E_k = 4$ kcal mol^{-1}	29.40	0.69	0.49	0.40	0.20	0.17	0.077
λ (Å), $E_k = 10$ kcal mol^{-1}	18.60	0.44	0.31	0.25	0.13	0.11	0.049

then to an oxygen nucleus, there is an extremely large variation in the quantum wavelengths ranging from ~29.40Å to ~0.69Å to ~0.17Å, respectively. The values indicate that the de Broglie wavelengths for the electron and hydrogen are comparable to the distances traversed by these particles in chemical reactions, consistent with experimental findings that indicate a dominance of their reactivity by quantum mechanical behavior.

KIEs as Mechanistic Probes

KIE measurements are routinely used for the elucidation of reaction mechanisms. The reaction coordinate represents the three-dimensional motion of all nuclei along the lowest-energy path that interconverts reactants and products. The reaction coordinate may represent the displacement of atoms within a chemical bond and/or the reorientation of surrounding solvent molecules. Regardless of the nature of the reaction coordinate, isotope substitution does not change the electronic potential energy surface for the reaction. Reaction rates vary with isotopic perturbation due to changes in vibrations that directly or indirectly couple to the reaction coordinate and by a decrease in wavelength for heavier atoms.

Activation Energy and Transition State Theory

In the year 1889, Svante Arrhenius documented the observation that chemical reaction rates vary as a function of temperature, predating the discovery of the first isotope, deuterium, in 1932. The Arrhenius equation (eqn. [5]) expresses a rate constant (k) as an exponential function of thermal activation energy (E_{act}). Together the temperature (T) and the gas constant (R) define the population of states that, as the result of molecular collisions, have sufficient E_{act} for reaction. The A term, originally referred to as a frequency factor, reflects the rate at which an activated complex (one possessing E_{act}) decomposes to product:

$$k = A \exp(-E_{act}/RT) \quad [5]$$

The transition-state theory (TST) developed separately by Eyring and by Evans and Polanyi (ca. 1935) is the preeminent model for interpretation of energy barriers to chemical reactions. TST gives the rate of reaction in terms of the molecular-level properties of an activated complex or transition state. Unlike the phenomenological Arrhenius equation, TST defines the energy difference between reactant and transition state using translational, rotational, vibrational, and electronic (gas phase) partition functions. The reaction coordinate is treated classically and separated from all of the other classical and quantum modes. The transition state occupies the dividing surface separating reactants from products and contains all degrees of freedom orthogonal to the reaction coordinate. The fundamental assumption of classical TST is that reactants do not re-cross the dividing surface and products are formed with the frequency of a bond vibration or solvent fluctuation once the transition-state configuration is attained. This assumption is relaxed in the semi-classical expression given by eqn. [6], where the rate constant is expressed in terms of an equilibrium constant for the formation of the transition state from the reactant state $\{K^{\ddagger} = \exp(-\Delta G^{\ddagger}/RT)\}$ and a frequency factor ($\kappa(k_B T/h)$). In the pre-exponential term, k_B is Boltzmann's constant and κ appears as a correction factor for the non-unit probability that products will form each time the reactants attain the energy of the transition state:

$$k = \kappa \frac{k_B T}{h} \exp(-\Delta G^{\ddagger}/RT) \quad [6]$$

Figure 1 shows a curve-crossing diagram for a molecule of methane reacting with atomic chlorine. The transition state is denoted by "double dagger" and represents a configuration for H atom transfer where the C–H bond is stretched and there is an attractive force between the Cl and H atoms. Thus, the reaction coordinate is the stretching of the bond. This situation is depicted further in Figure 2, where reaction occurs when an energy barrier is surmounted that converts the stretching motion of a C–H

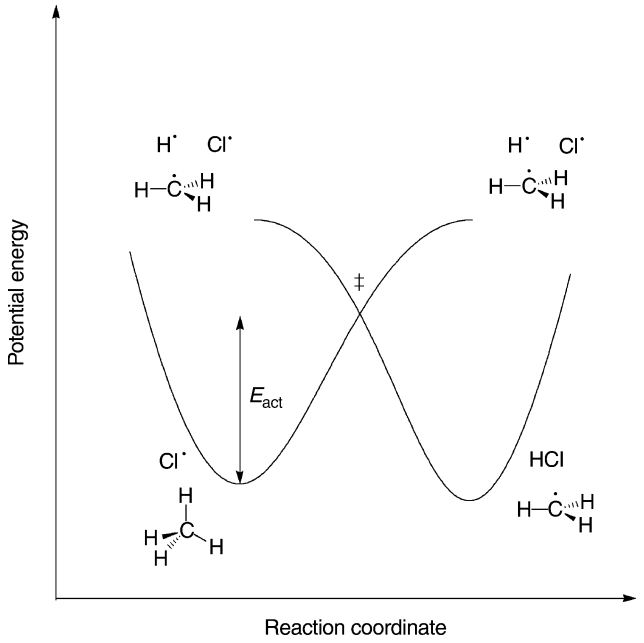

FIGURE 1 Reaction coordinates for H· abstraction from methane by Cl· depicting the transition state as the intersection of potential energy surfaces for stretching C–H and H–Cl bonds.

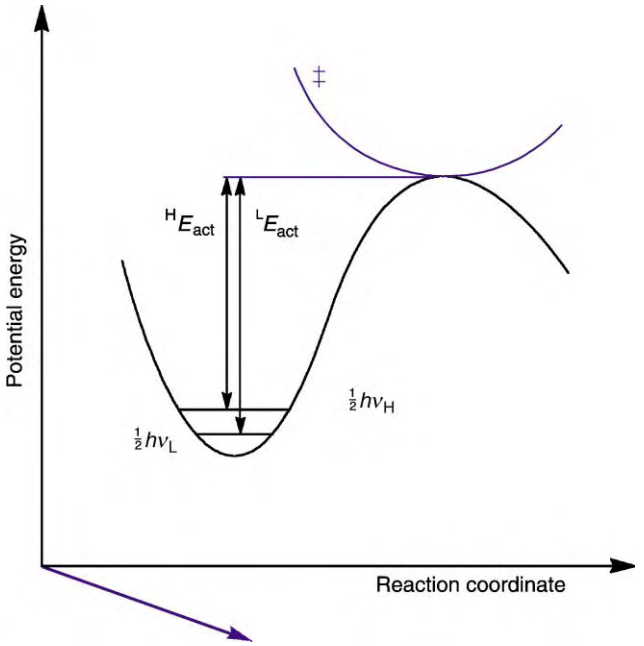

FIGURE 2 Energy diagram representing the origin of KIE on cleaving a C–H or C–L bond (H = ^{1}H, L = ^{2}H or ^{3}H). In this picture, a stretching mode in the reactant has been converted to a translational mode in the transition state.

(or C–L, where L = ^{2}H or ^{3}H) bond to a translational degree of freedom.

Although the nature of the reaction coordinate is not specified in the original derivation of TST, diagrams akin to Figure 2 have been used extensively for pedagogical reasons. The transition state is not an intermediate and has no detectable lifetime. The curvature of the reaction coordinate in the transition state region is defined by an imaginary frequency for the C–^{1}H or C–L vibration that is lost. Clearly this formulation of a bond-stretching reaction coordinate is an oversimplification when frequencies are high. When $\hbar\nu \gg k_B T$, the reacting bonds are essentially frozen and should not contribute much to the activation energy for reaction.

Isotope Effects from Zero-Point Energies

According to the Born–Oppenheimer approximation, the mass disparity between an electron and a nucleus allows the timescale for electronic motion to be separated from the much slower nuclear motion. It follows that reduced mass differences cause the zero-point energies to follow the trend C–^{1}H > C–^{2}H > C–^{3}H, as shown in Figure 2. Neglecting differences for reactions of isotopic molecules due to their quantum wavelengths, KIEs can be calculated from activation energies.

In the simplest case, the reaction coordinate involves conversion of a ground-state stretch to a translation and, hence, neglects isotopic zero-point energies in the transition state. The differences in the zero-point levels of the reactant state give the upper limit to the primary KIE through eqn. [7], where the subscript L designates either of the heavier isotopes of hydrogen. From the stretching frequencies of C–^{1}H ($\nu = 3000\ \text{cm}^{-1}$), C–^{2}H ($\nu = 2200\ \text{cm}^{-1}$), and C–^{3}H bonds ($\nu = 1800\ \text{cm}^{-1}$), KIEs of 7 and 18 are estimated for $k_{^1H}/k_{^2H}$ and $k_{^1H}/k_{^3H}$ at 298 K, respectively:

$$\frac{k_{^1H}}{k_L} = \exp[(h\nu_H - h\nu_L)/2RT] \qquad [7]$$

The Melander–Westheimer principle (ca. 1960) models the parabolic variation of primary KIEs in terms of a linear transition state for hydrogen transfer (cf Figure 1). The symmetry of the transition state depends on the overall reaction thermodynamics. Asymmetry increases as the transition state becomes more reactant-like (or earlier along the reaction coordinate) for exothermic reactions or more product-like (later) in an endothermic reaction. For real molecules that contain multiple degrees of vibrational freedom, compensating vibrations that are isotopically sensitive will reduce the size of the isotope effect from its peak at a symmetric transition state.

Deviations from Predicted Values

In general, observed primary KIEs are less than the upper limit set by eqn. [7]. Observations of values larger than those predicted by eqn. [7] have been observed and tentatively attributed to an insufficient description of the reaction coordinate. For instance, KIEs may appear inflated when isotope labels in secondary positions contribute to differences in E_{act}. As discussed in the monograph by Melander and Saunders (see Further Reading), KIEs may be up to threefold larger because of restricted transition-state geometries wherein bending vibrations present in the reactant state have been lost.

In contrast to effects ascribable to the ratio of reactant and transition state partition functions, non-Boltzmann effects such as nuclear tunneling may also give rise to large isotope effects. Tunneling has historically been treated as a correction, with the dominant contribution to the rate constant viewed as the activation energy associated with distortion of the reacting bond. However, there has been a resurgence of attention to quantum phenomena in the chemical and biochemical literature. New models for proton, hydrogen atom and hydride transfer reactions are being developed which presuppose tunneling mechanisms and formulate reaction coordinates in terms of the collective low-frequency motions of heavy atoms and the surrounding solvent molecules or protein. It is important to realize that a wide range of KIEs with values *both larger and smaller* than those predicted by eqn. [7] are consistent with mechanisms of tunneling, where reactants do not need to have the activation energy required to reach the transition state and reaction may occur by passing through rather than over the potential energy barrier.

KIEs as Mechanistic Probes during Enzyme Catalysis

By virtue of being a catalyst, an enzyme accelerates a chemical reaction without changing the overall thermodynamics. The term catalysis frequently refers to a multi-step reaction such as the oxidation of glucose to gluconolactone and reduction of O_2 to H_2O_2 as it occurs in the glucose oxidase reaction (eqn. [8]). Additionally, the term catalysis may refer specifically to a single chemical step that is accelerated by lowering or circumventing an energy barrier.

To understand the role of an enzyme during a catalytic transformation, the substrate-binding step and chemical step, where reactants are converted to products, must be analyzed separately. Assessment of barrier-lowering effects requires comparison of the enzymic reaction to a solution-phase reaction, both referenced to some standard state:

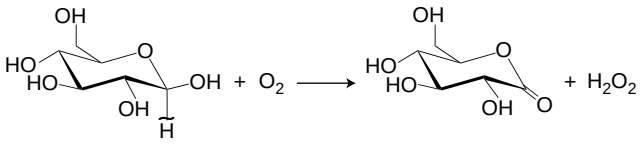

[8]

Experimental Considerations

Primary, secondary, and solvent KIEs can be used to elucidate the extent to which a change in bonding occurs in or before the rate-determining step. Primary effects are invariably normal, that is, the light isotope reacts faster than the heavy one. Secondary effects may show inverse behavior when the reaction is characterized by an increase in bonding and the difference in zero-point energies in the transition state is greater than in the reactant state. Primary effects are typically measured for reactions where protium is exchanged for deuterium and/or tritium, but isotope labeling of the heavy atoms may also give rise to measurable effects.

The largest effects are predicted upon isotopic substitution of protium because of the sizable perturbation to the zero-point energy levels as discussed earlier. Because reactions involving the transfer of protium and its isotopes give rise to the largest effects, experiments performed non-competitively, using the pure labeled substrates in separate reaction solutions, require high isotopic enrichment in addition to chemical purity. Isotopic purity becomes crucial when KIEs are >10 and only 5% contamination of the heavy isotope by the light isotope will cause an apparent deflation of the KIE by a factor of >1.4.

Secondary KIEs are typically much smaller and are, therefore, most often measured by competitive techniques. While isotope purity is not required, sensitive methods such as scintillation counting of radiolabeled products or mass-spectrometric analysis of chemically labeled products are necessary. Intra-molecular measurements can be more informative than inter-molecular measurements, as spurious isotope discrimination due to differential binding effects is absent. However, the determination of intra-molecular primary isotope effects on enzymatic reactions is, most generally, precluded by the inherent stereoselectivity imparted by the protein.

An Example from Glucose Oxidase Catalysis

Glucose oxidase mediates the oxidation of glucose and other simple six-carbon sugars. Enzymes isolated from fungi have been the subjects of extensive mechanistic studies due in large part to their robustness under a variety of temperature and pH conditions. The active enzyme is a homodimer that contains one

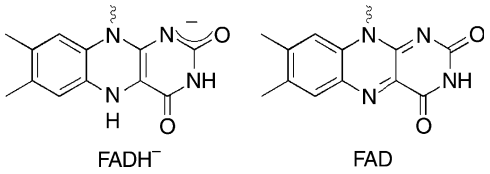

FIGURE 3 The isoalloxazine rings of oxidized (FAD) and reduced ($FADH^-$) flavin adenine dinucleotide.

non-covalently bound flavin adenine dinucleotide cofactor (Figure 3) per subunit. The flavin adenine dinucleotide (FAD) is reduced by simple sugars in the reductive half-reaction to produce $FADH^-$, which is oxidized by molecular O_2 in the oxidative half-reaction. A ping-pong type kinetic mechanism has been demonstrated for glucose oxidase wherein the first substrate binds, gets converted to product, and is then released prior to the reaction of the second substrate (Figure 4).

The mechanisms advanced for the reactions of sugars with glucose oxidase involve cleavage of the anomeric C–H in the rate-determining step (eqn. [8]). The main evidence is the significant primary KIEs observed upon isotope labeling of this position in glucose and in the alternative, slower-reacting substrate 2-deoxyglucose. Under steady-state conditions at pH 5 and 298 K, the second-order rate for the reaction of substrate (k_{cat}/K_M) is 3–4 times faster for [1-^{1}H]-glucose than for [1-^{2}H]-glucose (Table II). The k_{cat}/K_M values for [1-^{1}H] and [1-^{2}H] 2-deoxyglucose are 860 and 120 $M^{-1}\,s^{-1}$, respectively revealing a primary kinetic isotope effect of ~7. The rates are an order of magnitude slower than for the glucose [1-^{1}H] and [1-^{2}H] for which k_{cat}/K_M is 8200 and 2600 $M^{-1}\,s^{-1}$. The difference in the KIEs shows how C–H cleavage in the slower substrate has a greater contribution than substrate binding to its second order rate constant. The reasoning is consistent with the observation that the unimolecular rate constant that controls turnover (k_{cat}) is more than order of magnitude faster for glucose (1200 s^{-1}) than for 2-deoxyglucose (50 s^{-1}) under the same conditions.

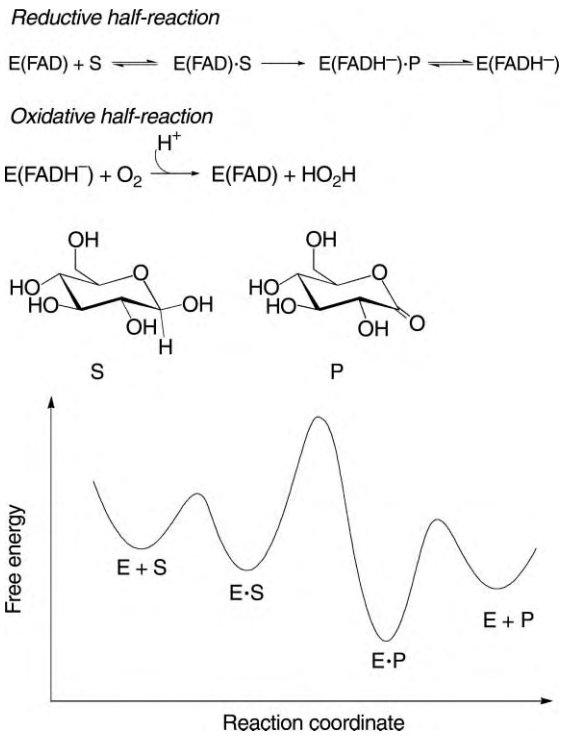

FIGURE 4 Ping-pong kinetic scheme and energy landscape for the reductive half-reaction of glucose oxidase. The E·S and E·P are arbitrarily defined as being more stable than separated reactants and products.

The degree to which bond cleavage limits the rate of sugar oxidation may vary with pH and with temperature depending on relative heights of energy barriers along the potential energy landscape. For oxidation of 2-deoxyglucose by glucose oxidase, the commitment to catalysis defined by Northrop as the ratio of the product-forming rate constant to the rate constant for substrate dissociation (see Further Reading) appears to be low and independent of pH. At pH 5, non-competitive measurements with pure [1-^{1}H] and [1-^{2}H] 2-deoxyglucose has allowed a direct comparison of k_{cat} to k_{cat}/K_M effects; these show that the isotope effect on k_{cat}/K_M approaches the intrinsic isotope effect on k_{cat} (^{1}H versus ^{2}H) ~8. Thus, the rate-determining step in both the first- and second-order kinetic processes includes the cleavage of the bond to the anomeric carbon (the E·S to E·P step in Figure 4). Similar results at pH 9.0, where [1-^{1}H] 2-deoxyglucose reacts with $k_{cat}/K_M = 580\ M^{-1}\,s^{-1}$ and exhibits ^{1}H versus ^{2}H kinetic isotope effects on both k_{cat}/K_M and k_{cat} of ~7, indicate that bond cleavage represents the highest point on the energy landscape (Figure 4). This result has been confirmed by highly accurate kinetic isotope effects measured using radiolabeled substrates under competitive conditions. Here the KIEs correspond to differential reactivity of isotopically labeled substrates in the same reaction solution. Isotope effects on k_{cat}/K_M for 2-deoxyglucose at pH 9.0 and 298 K reveal that the ^{3}H substrate reacts 15.9 (0.5) times slower than the ^{1}H substrate and 2.44 (0.04) times slower than the ^{2}H substrate. From the above data, the calculated ^{1}H versus ^{2}H isotope effect on k_{cat}/K_M is found to be 6.5 (0.5) close to the value derived from the non-competitive measurements. Based on observed KIEs under a variety of conditions, it can be concluded that the observed k_{cat} reflects the free-energy barrier associated with the chemical step wherein sugar is transformed to lactone.

The kinetics of $FADH^-$ oxidation by O_2 has also been analyzed using isotope effects. Solvent KIEs and heavy-atom KIEs on k_{cat}/K_M for O_2 have been determined for high- and low-pH forms of glucose oxidase. The latter measurements were determined competitively

TABLE II

Rate Constants and Isotope Effects Under Air Saturation at 298 K

Substrate	k_{cat}/K_M ($M^{-1}s^{-1}$)	L (k_{cat}/K_M)	k_{cat} (s^{-1})	L (k_{cat})
[1-^{1}H] glucose (pH 5)	$8.2\ (1.9) \times 10^3$	3–4	$1.2\ (0.3) \times 10^3$	~6
[1-^{2}H] glucose (pH 5)	$2.6\ (0.6) \times 10^3$		$2.0\ (0.5) \times 10^2$	
[1-^{1}H] 2-deoxyglucose (pH 5)	$8.6\ (0.8) \times 10^2$	~7	$4.4\ (1.2) \times 10^1$	~8
[1-^{2}H] 2-deoxyglucose (pH 5)	$1.2\ (0.4) \times 10^2$		5.7 (0.1)	
[1-^{1}H] 2-deoxyglucose (pH 9)	$5.8\ (0.2) \times 10^2$	6.5	$2.6\ (1.0) \times 10^1$	~7
[1-^{2}H] 2-deoxyglucose (pH 9)	$8.8\ (0.2) \times 10^1$		3.5 (0.6)	
[1-^{3}H] 2-deoxyglucose (pH 9)	$3.6\ (0.2) \times 10^1$	2.4	N/A	

L represents ^{2}H or ^{3}H.

by using isotope ratio mass spectrometry to follow the enrichment of ^{18}O in natural abundance O_2 as a function of reaction. The ratio of k_{cat}/K_M for $^{16,16}O_2$ to $^{16,18}O_2$ ranges from 1.027(3) to 1.028(4) for the two enzyme forms. The KIE is close to the equilibrium isotope effect estimated using the Bigeleisen approach, which employs gas-phase partition functions for O_2 and O_2^-, the reactant and product of the rate-determining step. Solvent isotope effects accompanying O_2 reduction were found to be close to unity, showing that electron transfer, and not proton transfer, limits $k_{cat}/K_M(O_2)$. In addition, the observed isotope effects aid a direct comparison of rate constant for the enzymatic reduction of O_2 and the non-enzymatic reaction which in turn allows the extent of barrier-lowering (catalysis) in the chemical step to be addressed.

Various types of kinetic isotope effects have been used to elucidate the chemical mechanisms of glucose oxidase catalysis. The observed KIEs indicate that the rate of the chemical step can be extracted from the steady-state measurements using the slowly reacting substrate 2-deoxyglucose. The observed KIEs demonstrate rate-determining C–H cleavage in the reductive half-reaction and a rate-determining change in oxygen bond order upon electron transfer in the oxidative half-reaction. In addition to exposing which steps limit catalysis, KIE probes have been invaluable in demonstrating the role of the protein environment in facilitating catalysis.

See Also the Following Articles

Flavins • Substrate Binding, Catalysis, and Product Release

Glossary

commitment to catalysis The rate constant for the conversion of ES to EP divided by the rate constant for the return of ES to E + S.

intrinsic isotope effect The isotope effect when the bond cleavage or bond reorganization event completely limits the reaction rate.

nuclear tunneling A process whereby an atomic nucleus, because of its wave-mechanical nature, is able to penetrate rather than surmount an energy barrier.

zero-point energy The potential energy present in a bond at 0 K.

Further Reading

Bell, R. P. (1980). *The Tunnel Effect in Chemistry*. Chapman and Hall, New York.

Bright, H. J., and Gibson, Q. H. (1967). The oxidation of 1-deuterated glucose by glucose oxidase. *J. Biol. Chem.* **242**, 994–1003.

Cook, P. F. (ed.) (1991). *Enzyme Mechanism from Isotope Effects*. CRC Press, Boca Raton, FL.

McQuarrie, D. E. (1983). *Quantum Chemistry*. University Science Books, Mill Valley, CA.

Melander, L., and Saunders, W. H. Jr. (1980). *Reaction Rates of Isotopic Molecules*. Wiley-Interscience, New York.

Northrop, D. B. (1981). The expression of isotope effects on enzyme-catalyzed reactions. *Annu. Rev. Biochem.* **50**, 103–131.

Roth, J. P., and Klinman, J. P. (2003). Catalysis of electron transfer during O2 activation by the flavoprotein glucose oxidase. *Proc. Nat. Acad. Sci. USA* **100**, 62–67.

Steinfeld, J. I., Francisco, J. S., and Hase, W. L. (1989). *Chemical Kinetics and Dynamics*. Prentice-Hall, Englewood Cliffs, New Jersey.

Biography

Judith Klinman is a Professor in the Departments of Chemistry and Molecular and Cell Biology at the University of California, Berkeley, where she has been teaching and conducting research since 1978. She has had a long-standing interest in protein structure and function and was one of the earliest investigators to recognize the power of kinetic isotope effects to elucidate mechanisms of enzyme action.

Justine Roth was a Postdoctoral Fellow in the laboratory of Judith P. Klinman and received her Ph.D. (from Professor James Mayer) at the University of Washington in inorganic chemistry. She is currently an Assistant Professor of chemistry at Johns Hopkins University pursuing studies at the interface of chemistry and biology.

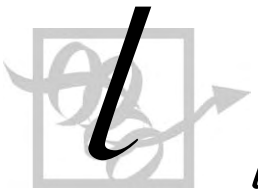

lac Operon

Liskin Swint-Kruse and Kathleen S. Matthews
Rice University, Houston, Texas, USA

All living organisms must respond to their environment. To this end, they must sense a variety of exogenous and endogenous stimuli and use this information to regulate when and where specific genes are expressed as proteins. Until the middle of the twentieth century, when DNA was identified as the genetic material, variation in gene expression could only be ascertained by visible effects on the organism (phenotype). Once the central pathway for genetic expression was established (DNA encodes mRNA encodes protein), opportunity arose to understand gene regulation on the molecular level. The first control mechanism was elucidated for a region in the *Escherichia coli* genome termed the *lac* operon. The *lac* operon regulatory system responds to external lactose (milk sugar) and glucose concentrations, and the *lac* metabolic genes that transport and metabolize lactose are therefore expressed only under specific environmental conditions. Such regulation conserves energy for the organism, avoiding costly production of enzymes that are not useful when substrate is unavailable, and simultaneously providing a rapid and robust response to environmental opportunity. More recently, this highly effective regulatory system has been exploited to control selected expression of a wide variety of proteins in prokaryotes as well as eukaryotes. In addition, this system has been modified to screen for mutation types/rates in higher organisms (e.g., BigBlue® is a mouse system in which mutation in either LacI or LacO can be detected as a screen for mutagens).

Historical Perspective

In the post-World War II years at the Pasteur Institute in France, Jacques Monod and Francois Jacob were examining the ability of bacteria to "adapt" to different sources of carbon as their energy source. They discovered that enzymes that metabolize lactose were present at very low levels when lactose was absent from the growth medium. When lactose was added, enzyme production increased ~1000-fold, a phenomenon termed "induction." The sugar lactose is chemically similar to other sugars that are collectively called galactosides. By varying the molecular structure of these sugars and comparing growth and *lac* enzyme activity for *E. coli* variants, they established that the function of inducing the metabolic enzymes was separate from the capacity of these enzymes to utilize lactose. (The DNA regions that encode the three enzymes of the *lac* operon have historically been called "structural genes;" however, we use the term "metabolic genes" in describing these regions to distinguish them from later studies of the *lac* repressor and CRP protein structures.) However, the mechanism by which galactosides induced the metabolic enzymes was not elucidated for several more years. In the early 1960s, Jacob and Monod found that the role of an "inducer" sugar was to "relieve" transcription repression of the metabolic genes. Therefore, the inducer must act through another agent, which was finally identified as the lactose repressor protein, LacI. When the LacI protein was inactivated in the bacteria, the metabolic enzymes were always expressed at high levels, whether or not an inducer sugar was present. From these experiments, Jacob and Monod demonstrated that enzyme (or other protein) production can be negatively controlled. This phenomenon is termed "repression."

Further experimental observations indicated that this simple view of modulating *lac* operon expression by LacI alone did not encompass the entire pattern of gene regulation. Specifically, significant induction of *lac* enzymes by lactose does not occur when glucose is abundantly available. From the cellular perspective, direct glucose utilization provides a more efficient energy source than converting lactose to glucose and galactose (and then galactose to glucose). Thus, an additional regulatory mechanism must contribute to determining the level of *lac* enzyme expression. Two different mutations were discovered in the late 1960s/early 1970s that illuminated this issue. In fact, the *lac* operon was used in a cell-free system to demonstrate that the protein CRP (cAMP receptor protein, also referred to as the catabolite activator protein, CAP) was disrupted by one of these mutations. CRP binds the signaling molecule cAMP, which in turn is produced by the other protein identified in these mutagenesis experiments, adenlyate cyclase, which is inhibited by high glucose concentrations. Together, these proteins provide a means to alter transcription by "sensing" glucose levels via detection of cAMP. In contrast to the high specificity of the *lac* repressor (which only regulates the *lac* operon),

the CRP glucose sensor *activates* transcription of numerous systems in *E. coli* in its cAMP-bound form.

lac Operon

The entire region of the *E. coli* genome involved in lactose metabolism and control of *lac* gene expression is termed the *lac* operon. This region of DNA comprises sequences that contain several types of information—open reading frames for two classes of proteins (enzymatic and regulatory), binding sites for RNA polymerase (promoter regions), and binding sites for regulatory proteins. In sequence within the genome (Figure 1), the elements of the *lac* operon include the following:

1. the promoter for initiating transcription of LacI; the *lacI* gene, which encodes the *lac* repressor protein (LacI);
2. the promoter for the *lac* metabolic genes involved in transporting and metabolizing lactose;
3. DNA-binding sites for *lac* repressor (LacO) and CRP that overlap this promoter; and
4. the genes for the *lac* metabolic enzymes.

The latter encode proteins required for the transport and metabolism of lactose: β-galactosidase (LacZ), lactose permease (LacY), and thiogalactosidase transacetylase (LacA). Further discussion will focus on the functions and structures of the two regulatory proteins, LacI, and CRP.

Lactose Repressor Protein

LacI Function

The role of LacI is to inhibit mRNA production for proteins encoded by the *lac* operon. Transcription is not completely eliminated, but *lacZYA* mRNA is transcribed

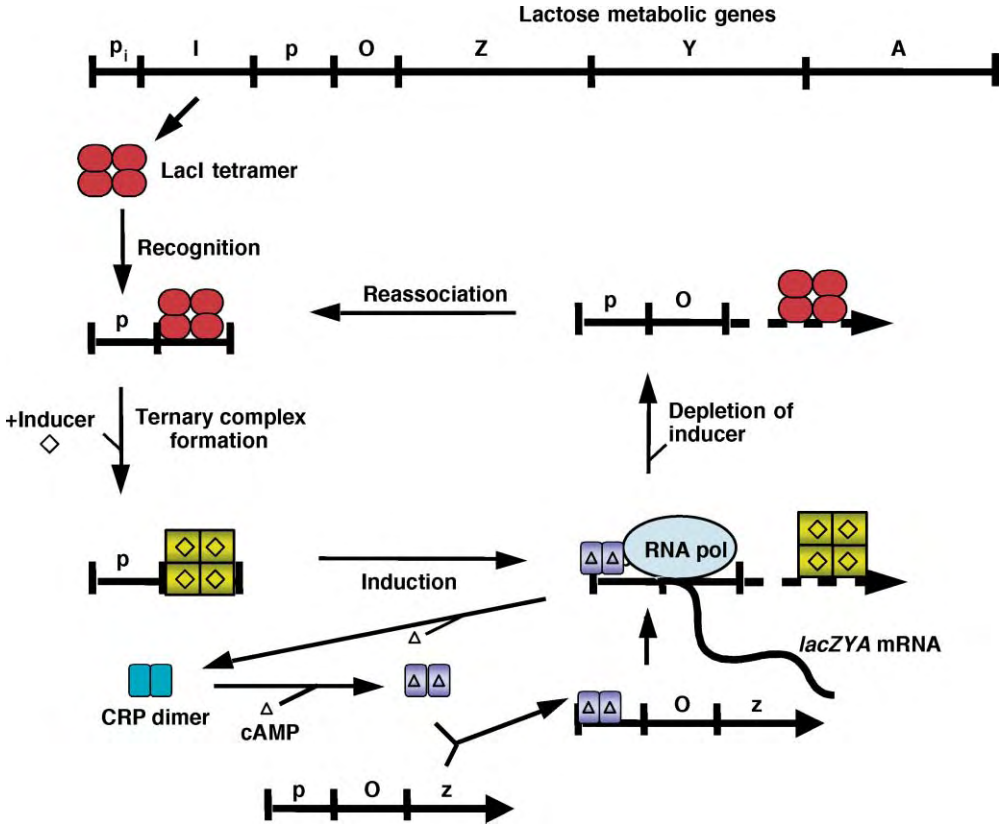

FIGURE 1 Schematic of the *lac* operon. The top sequence of DNA (horizontal bar) indicates the positions of the promoter (p_i) for the tetrameric lactose repressor (*lacI* gene, "I"), the promoter (p) for the metabolic enzymes, the operator sequence LacO (O site for LacI binding), and the metabolic enzyme genes (*lacZYA*, "Z," "Y," and "A"). The cartoon of the functional cycle represents LacI tetramer binding to operator, association with inducer (◇), dissociation from operator (induction), RNA polymerase (RNA pol) binding and transcription, and subsequent reassociation with the operator when sugar levels diminish. Shown at the bottom of the figure is the dimeric structure of CRP, its association with cAMP (triangle), and binding within the promoter region to facilitate RNA polymerase binding and transcription. CRP dissociates from the promoter when glucose levels increase and cAMP levels fall. Substitution of the *lac* metabolic genes by other protein coding sequences (prokaryotic or eukaryotic) allows effective control of specific protein expression using inducer/cAMP levels.

only at very low levels. This function is accomplished by specific binding of LacI protein to the *lac* operator DNA sequence to inhibit transcription via a variety of mechanisms. Since the *lac* operator (LacO) overlaps the promoter, LacI binding directly competes with RNA polymerase for binding this region. LacI can also impede transcription initiation and/or block elongation of mRNA. The LacI·LacO association and consequent transcription repression occur when no lactose is available to serve as the substrate of the *lac* metabolic proteins.

When lactose is available as a carbon source, the low levels of metabolic enzymes allow a small amount of this sugar to be transported into the bacterium by LacY. Next, residual LacZ metabolizes lactose to glucose and galactose, which produces energy for the bacterium. Notably, this catalytic process also generates low levels of allolactose (a rearrangement of the β-1,4 linkage between glucose and galactose to a β-1,6 linkage; Figure 2). The by-product allolactose binds to LacI and elicits a conformational change in the protein that results in release of the operator DNA sequence (induction). Consequently, RNA polymerase is freed to generate numerous copies of mRNA encoding the *lac* enzymes. When translated into proteins, these enzymes allow the bacterium to transport and metabolize large quantities of lactose as its carbon energy source, taking advantage of environmental opportunity. One result of the studies by Jacob and Monod was the discovery that a variety of non-natural galactoside sugars (e.g., IPTG; Figure 2) can induce LacI and relieve transcription repression of *lacZYA*.

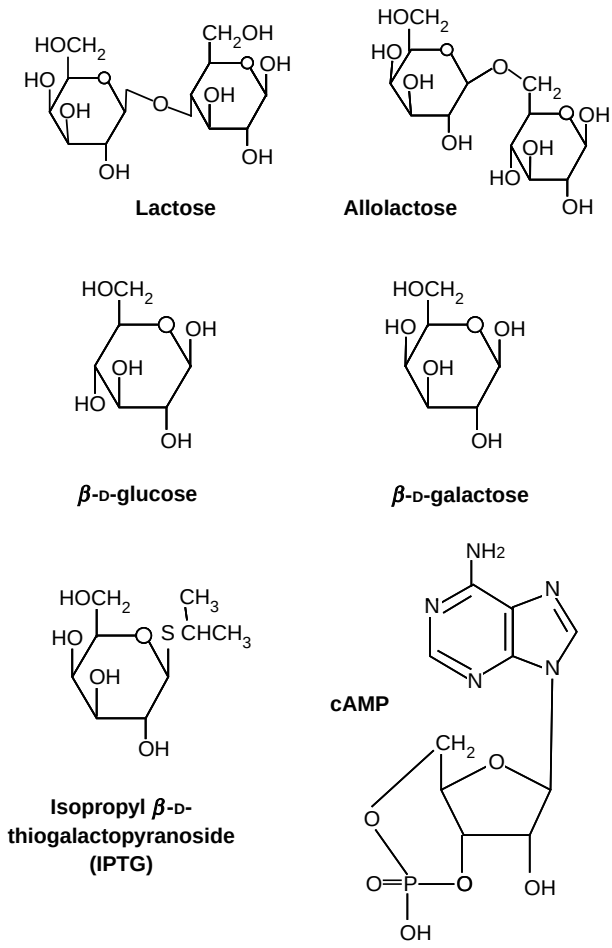

FIGURE 2 Chemical structures for lactose, allolactose (the natural inducer), the sugar components of lactose (glucose and galactose), the gratuitous inducer IPTG, and cAMP.

LacI Structural Characteristics

Structural detail of the LacI protein has provided insight into the atomic-level mechanism by which this protein performs its functions. LacI is a multimeric, multi-domain protein, an arrangement now known to be typical for genetic regulatory proteins. LacI has four, identical polypeptide chains (Figure 3A). Each polypeptide folds into distinct regions that have specific functions, and the monomers associate to form tetrameric LacI. A very interesting feature is that specific regions of LacI (called the hinge helices) are folded *only* in the presence of the operator DNA target sequence. Thus, protein folding is integral to the regulatory cycle.

Folded protein domains can usually be isolated from the intact protein and maintain function and structure that are highly similar to the intact protein. For LacI, the N-terminal domain and hinge helix comprise the DNA-binding site, and this region can be isolated as monomeric units by proteolysis. Note that the LacI *dimer* is the DNA-binding unit (two DNA-binding sites/tetramer). The DNA-binding site comprises one helix from each N-terminal domain, which associates with bases in the DNA major groove, and the hinge helices, which insert into the minor groove and elicit a bend in the DNA. (Note that the LacO site is highly, but imperfectly, symmetric in sequence, therefore accommodating the two identical DNA-binding domains.) The LacI core domain, which can be isolated by proteolysis as a tetramer, encompasses two subdomains that flank the sugar-binding site. Each monomer is able to bind an inducer molecule (four sugars/tetramer). (Note that the N- and C-subdomains within the core domain are interconnected by multiple strands and *cannot* be cleaved to produce distinct functional units.) When the inducer-binding site is occupied, structural changes in the N-subdomain affect the DNA-binding domain (Figure 3B). These shifts result in hinge helix unfolding, an event that appears crucial for dissociation of the protein from the operator DNA site. The final domain of LacI is the C-terminal tetramerization domain that connects the four subunits via an antiparallel four-helix bundle (Figure 3A).

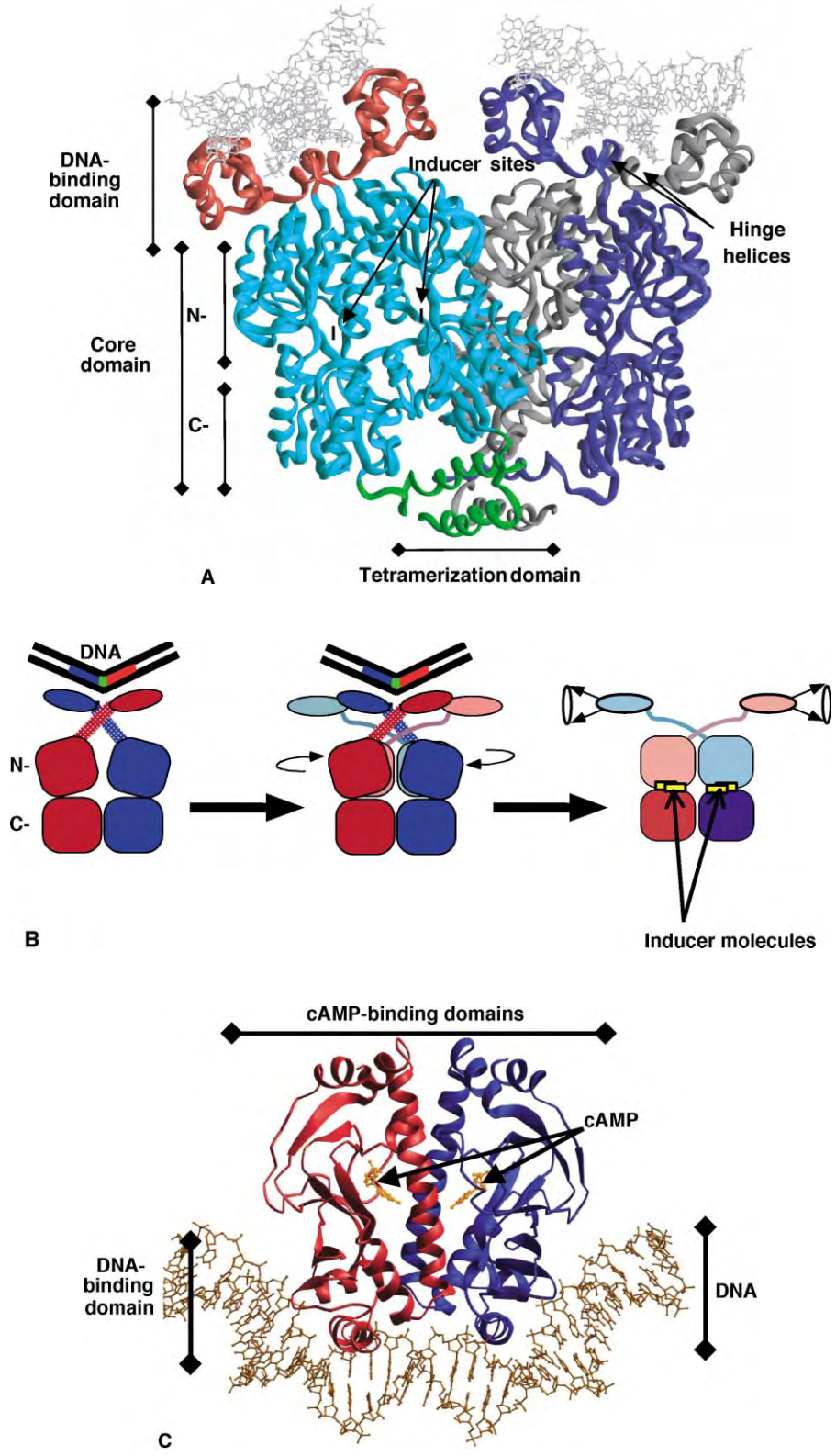

FIGURE 3 Structures of LacI and CRP. (A) The tetrameric structure of the lactose repressor is shown in ribbons format. (Note that this view does not show all atoms of the protein.) The right dimer is colored to show the subunits, and the left dimer shows the binding sites. DNA is shown at the top of the figure in ball-and-stick format (which depicts all nonhydrogen atoms of this molecule). Note that the dimer is the DNA-binding unit, whereas the monomer is the inducer-binding unit. (B) Cartoon depicts the conformational change of a LacI dimer when it binds inducer. (C) The dimeric structure of CRP is shown with the sites for cAMP- and DNA-binding indicated. The structure of unbound CRP has not been derived; thus, the nature of the conformational change for this protein is not explicitly known.

Multiple Sites/Multiple Targets – DNA Looping

Early studies indicated that additional "pseudo-operator" sequences were present within the *lac* operon sequence and contribute to repression. The DNA sequences of the pseudo-operators are very similar, but not identical, to LacO and are bound by LacI more weakly. The presence of two DNA-binding sites in LacI protein tetramer suggests a mechanism by which pseudo-operators could enhance repression—one LacI tetramer could bind two separate operators and generate a looped DNA structure (Figure 4). Experimental evidence for DNA looping has been obtained from a variety of laboratories. These structures are highly stabilized, accounting for the significant repression of *lacZYA* expression observed in bacterial cells. Indeed, DNA containing multiple operator sequences and with the supercoiling density characteristic of *E. coli* exhibits a half-life for the complex that exceeds two days. However, even these looped complexes respond rapidly (in less than 30 s) to the presence of inducer sugars, allowing quick adaptation to an external lactose source that may be transient.

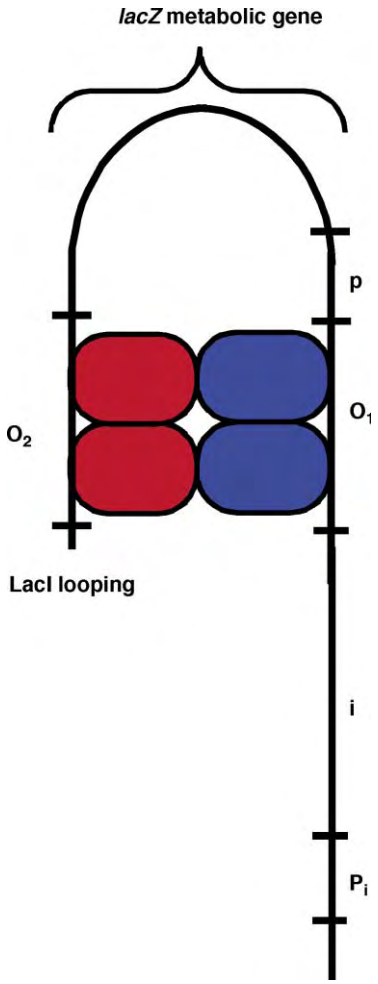

FIGURE 4 Looped DNA structure. The pseudo-operator sequence (O_2) located within the *lacZ* gene can interact with LacI bound to the primary operator sequence (O_1) that overlaps the promoter sequence for the *lacZYA* metabolic genes. This structure "loops" the DNA and generates a complex with very high stability. The dimers interacting with O_1 and O_2 are shown in different colors.

Catabolite Repressor Protein

CRP Function

CRP measures glucose levels in the bacterium through detecting cAMP levels, a signaling molecule created by another protein called adenylate cyclase. Since adenylate cyclase is inhibited by high glucose, levels of glucose and cAMP are inversely related. As glucose levels decrease, cAMP levels rise, and cAMP binds to CRP, causing a conformational shift. This form of CRP has high affinity for specific target sequences within the bacterial genome (Figure 1). Note that cAMP enhances DNA binding by CRP, whereas with LacI, sugar binding decreases the DNA binding. One of the DNA target sequences for cAMP·CRP is found within the promoter for the *lac* structural proteins upstream of the *lac* operator sequence (Figure 1). In the absence of glucose (elevated cAMP), the cAMP·CRP complex binds and *enhances* RNA polymerase transcription of *lacZYA* mRNA. Thus, the enzymes for lactose utilization are expressed at high levels only when environmental glucose is low and lactose levels are high.

CRP Structural Characteristics

Like LacI, CRP is multimeric and has multiple domains (Figure 3C). In this case, CRP structure is dimeric, and each monomer comprises two domains. The N-terminal domain facilitates dimer formation and binds at least one molecule of cAMP (two/dimer). The C-terminal domain binds DNA through a helix-turn-helix motif, now known to be common in regulatory proteins. Protein binding again elicits a bend in the target DNA-binding site. Each monomer only binds to one-half of the DNA-binding site, which is symmetric through the center of the sequence. The *lac* operon regulatory sites signaled that symmetry of these DNA-binding sites would be a common feature, going hand-in-hand with the generally multimeric natures of these proteins.

Implications for Complex Organisms

This "simple" bacterial regulatory system illustrates the complexity that can be generated with only two "on/off" switches. In fact, the response of this system is more analogous to a rheostat. Since the two protein switches

respond to different signals, graded response occurs at intermediate ratios of glucose/lactose. Gene regulation in response to specific signals—whether environmental availability of substrate or other signaling molecule—has a twofold advantage. The organism conserves energy/resources under conditions where gene expression would be useless (and expensive), but maintains selective response to a variety of input information. This type of regulatory control—DNA binding modulated either negatively or positively by interaction with a small ligand or with another protein or biomolecule—underlies the incredibly complex pathways by which gene expression is fine-tuned to create specific temporal, spatial, and environmental patterns in higher organisms.

See Also the Following Articles

DNA Supercoiling • RNA Polymerase Reaction in Bacteria • RNA Polymerase Structure, Bacterial

Glossary

activation Process that enhances transcription to boost cellular levels of regulated proteins.

conformational change A significant rearrangement of atoms within a protein molecule in response to binding a specific small molecule (e.g., sugar binding by LacI).

genome The entire DNA complement composing the genetic material of an organism.

inducer A sugar that elicits LacI conformational rearrangement that releases operator DNA.

induction The increase in *lac* enzyme production triggered by the presence of an inducer sugar.

mRNA A "copy" of the DNA sequence that is used as a template for protein translation.

operator The DNA sequence to which the repressor protein binds and thus inhibits RNA polymerase transcription.

operon A region of bacterial DNA that is regulated as a unit, e.g., the entire region encoding the *lac* repressor, metabolic enzymes, and regulatory regions.

promoter The DNA sequence recognized by RNA polymerase for transcription initiation; in bacteria this region frequently contains a binding site for the catabolite repressor protein (CRP).

repression The inhibition of transcription to maintain low levels of metabolic proteins/enzymes in the absence of appropriate conditions, such as lack of substrate for a metabolic pathway.

repressor The protein that mediates inhibition of transcription by binding to a specific DNA sequence (see *operator*).

Further Reading

Busby, S., and Ebright, R. H. (1999). Transcription activation by catabolite activator protein (CAP). *J. Mol. Biol.* **293**, 199–213.

Emmer, M., deCrombrugghe, B., Pastan, I., and Perlman, R. (1970). Cyclic AMP receptor protein of *E. coli*: Its role in the synthesis of inducible enzymes. *Proc. Natl Acad. Sci. USA* **66**, 480–487.

Harman, J. G. (2001). Allosteric regulation of the cAMP receptor protein. *Biochim. Biophys. Acta* **1547**, 1–17.

Jacob, F., and Monod, J. (1961). Genetic regulatory mechanisms in the synthesis of proteins. *J. Mol. Biol.* **3**, 318–356.

Kolb, A., Busby, S., Buc, H., Garges, S., and Adhya, S. (1993). Transcriptional regulation by cAMP and its receptor protein. *Annu. Rev. Biochem.* **62**, 749–795.

Lewis, M., Chang, G., Horton, N. C., Kercher, M. A., Pace, H. C., Schumacher, M. A., Brennan, R. G., and Lu, P. (1996). Crystal structure of the lactose operon repressor and its complexes with DNA and inducer. *Science* **271**, 1247–1254.

Matthews, K. S., and Nichols, J. C. (1998). Lactose repressor protein: Functional properties and structure. *Prog. Nucl. Acid Res. Mol. Biol.* **58**, 127–164.

Miller, J. H., and Reznikoff, W. S. (eds.) (1980). *The Operon*, 2nd edition. Cold Spring Harbor Laboratory, New York.

Müller-Hill, B. (1996). *The lac Operon: A Short History of a Genetic Paradigm*. Walter de Gruyter, Berlin, New York.

Zubay, G., Schwartz, D., and Beckwith, J. (1970). Mechanism of activation of catabolite-sensitive genes: A positive control system. *Proc. Natl Acad. Sci. USA* **66**, 104–110.

Biography

Liskin Swint-Kruse is a Research Scientist in Biochemistry and Cell Biology at Rice University. She received her B.S. from Baylor University and her Ph.D. from the University of Iowa. She has been a Fellow of the Keck Center for Computational Biology (National Library of Medicine). In her postdoctoral studies, she pursued computational, biophysical, and genetic studies of LacI structure and function. Her long-term goals are to define determinants for functional distinction within the large, closely related family of LacI proteins.

Kathleen S. Matthews is Dean of Natural Sciences and Stewart Memorial Professor of Biochemistry and Cell Biology at Rice University. She received her Ph.D. from the University of California, Berkeley, and postdoctoral training at Stanford University. Her research interests are structure/function studies of genetic regulatory proteins, and she has had a long-term interest in understanding the structural determinants of function in LacI protein.

Lectins

Nathan Sharon and Halina Lis
Weizmann Institute of Science, Rehovot, Israel

Lectins are a class of proteins that bind carbohydrates specifically and reversibly. They occur widely in animals, plants, and microorganisms, where their main function is to serve as cell recognition molecules. Their main use is for the detection, isolation, and characterization of glycoconjugates in solution and on cells.

Lectins (from Latin, *legere*, to select or choose) are proteins that combine with mono- and oligosaccharides reversibly and with high specificity, but are devoid of catalytic activity and, in contrast to carbohydrate-binding antibodies, are not products of an immune response. They are found in all classes of organisms, from viruses and bacteria to higher animals, including humans (Table I) and occur in different shapes and forms (Figure 1). Hundreds of lectins have been isolated by affinity chromatography on immobilized carbohydrates, as well as by recombinant DNA techniques. The richest source of these proteins are plants, from the seeds of which several of the long-known proteins of this class – such as concanavalin A, phytohemagglutinin (PHA), and soybean agglutinin (SBA) – have been obtained. Most lectins are bi- or oligovalent with respect to carbohydrate binding; therefore, when they combine with sugars on the surface of cells, such as erythrocytes, they cause cross-linking of the cells and their subsequent precipitation, a phenomenon referred to as cell agglutination. The erythrocyte-agglutinating, or hemagglutinating, activity of lectins is a major attribute of these proteins and is used routinely for their detection and characterization. Lectins also possess the ability to precipitate polysaccharides or glycoproteins from solution; these reactions are inhibited by the sugars for which the lectins are specific.

Carbohydrate Specificity

Lectins are classified primarily into five specificity groups, according to the monosaccharide for which they exhibit the highest affinity: mannose, galactose/*N*-acetylgalactosamine, *N*-acetylglucosamine, fucose, and *N*-acetylneuraminic acid (sugars are of the D-configuration except for fucose which is L). Relevant for the biological functions of lectins is the fact that, of the numerous monosaccharides found in nature, these six are typical constituents of surfaces of eukaryotic cells. Some lectins specific for mannose also bind glucose, which differs from mannose in the configuration of the 2-hydroxyl, but only in rare cases they react with galactose, which differs from glucose in the configuration of the 4-hydroxyl. Lectins of the same specificity group may differ markedly in affinity for oligosaccharides or cells, while a few of them recognize only oligosaccharide derivatives of the above monosaccharides. Specificity for other sugars has been rarely encountered. The affinity of lectins to monosaccharides is usually weak, with association constants in the millimolar range, whereas that to oligosaccharides is often much higher, up to three orders of magnitude.

Molecular Properties

In general, lectins are oligomeric proteins of diverse structure and molecular size. They differ in primary, secondary, and tertiary structure, number of subunits and subunit assembly (Figure 2), metal requirement, as well as in the constitution of carbohydrate-binding sites. The polypeptide chains often consist of several molecular domains, only one of which is the carbohydrate recognition domain (CRD). Lectins belong to distinct protein families or superfamilies that share sequence homologies and similar tertiary and quaternary structures. These families are often of the same phylogenetic origin (e.g., the cereal lectins), although they sometimes cross phylogenetic barriers (as in the case of the structurally similar legume lectins that belong to different specificity groups and the galectins, animal lectins that bind exclusively β-galactosides, such as lactose and *N*-acetyllactosamine [Galβ(1–4)GlcNAc]). The C-type (Ca^{2+}-requiring) lectins are members of a superfamily of diverse specificities that includes endocytic lectins, collectins, and selectins, many of which are membrane bound. In collectins, the CRD is linked to a collagen-like region, whereas in selectins–E-selectin, P-selectin, and L-selectin–it is attached to an epidermal growth-factor-like domain and several short repeating

TABLE I

Representative Lectins

Source	Organism or lectin name	Specificity	Mol. wt. kDa	No. of subunits
Viruses	Influenza A	NeuAc	225	3
Bacteria	*Escherichia coli* type 1	Man		Multi
	Escherichia coli P	Galα4Gal		Multi
	Pseudomonas aeruginosa	Fuc	47	4
Protozoa	*Entamoeba histolytica*	Gal/GalNAc	260	2
Plants	*Arachis hypogaea* (Peanut) (PNA)	Gal	110	4
				4
	Artocarpus integrifolia (Jackfruit)	Gal	66	2
		Glc/Man		
	Canavalia ensiformis (Jackbean) (Con A)	Glc/Man	106	4
	Erythrina corallodendron (Coral tree)	Gal/GalNAc	57	2
	Galanthus nivalis (Snowdrop) (GNA)	Man	50	4
	Glycine max (Soybean) (SBA)	Gal/GalNAc	120	4
	Lotus tetragonolobus (Asparagus pea)	Fuc	110	4
	Ricinus communis (Castor bean)			
	Toxin	Gal/GalNAc	60	2
	Lectin	Gal/GalNAc	120	4
	Sambucus nigra (Elderberry) (SNL)	NeuAcα2,6Gal	240	4
	Triticum vulgare (Wheat) (WGA)	GlcNAc	36	2
Invertebrates	*Anguilla anguilla* (Eel) (AAA)	Fuc	50	3
	Helix pomatia (Garden snail)	GalNAc	100	6
	Limulus polyphemus (Horseshoe crab)	NeuAc	400	
Vertebrates	Galectin-1	Gal	28	2
	Mammalian hepatic binding protein (HBP)	Gal/GalNAc	130–190	3–4
	Macrophage mannose receptor (MMR)	Man	175	1
	Mannose-binding lectin A (MBL-A)	Man	200–600	6–18
	Selectins E, P and L	Sialyloligosach.	90–140	1
	Man-6-P receptors	Man6P	90–300	1–2
	Siglec-1	NeuAcα2,3Gal	185	1
	Calnexin	Glcα3Man	65	1

units related to complement-binding protein (Figure 1). The siglecs are a family of sialic-acid-specific cell surface lectins with variable numbers of extracellular immunoglobulin-like domains and are thus members of the immunoglobulin superfamily. Bacterial lectins are typically in the form of fimbriae (or pili), hair-like submicroscopic appendages, consisting of an assembly of several different types of subunits, only one of which has carbohydrate-binding activity, e.g., for mannose (in type 1 fimbriae of *Escherichia coli* and *Klebsiella pneumoniae*) or galabiose, Galα(1–4)Gal (in P fimbriae of *E. coli*).

High-resolution X-ray crystallography of lectins in complex with their ligands and site-directed mutagenesis allowed the identification of the chemical groups on the protein and on the carbohydrate that interact with each other and of the types of bonds formed. These studies have shown that, like other carbohydrate-binding proteins, lectins combine with their ligands primarily by a network of hydrogen bonds and hydrophobic interactions; in rare cases, electrostatic interactions (or ion pairing) and coordination with metal ions also play a role. One or more water molecules sometimes mediate the bonding. Although in a single lectin a limited set of residues contribute to the formation of the bonds with the ligand, overall almost all kinds of amino acids participate in ligand binding.

Functions

Lectins express numerous biological activities, nearly all of which are based on their ability to recognize and bind carbohydrates specifically (Table II). In other words, as a result of their unusual capacity to decode the information encoded in carbohydrates, they act as recognition determinants in diverse

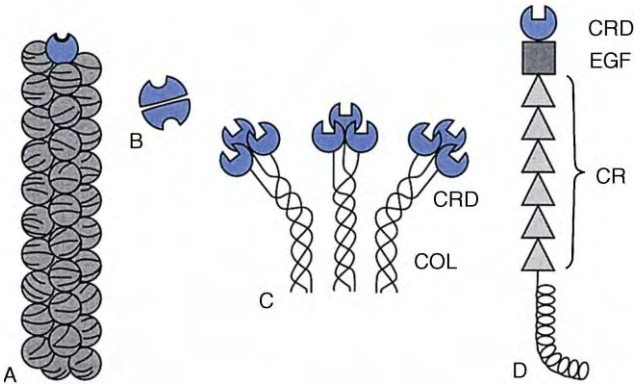

FIGURE 1 Schematic representation of the overall structure of lectins from different sources. (A) Part of fimbriae of *Escherichia coli*. The fimbriae are an assembly of different types of subunits, only one of which (blue) contains a carbohydrate-binding site. (B) A dimeric legume lectin (e.g., from lentils or peas). (C) Mammalian soluble mannose-binding lectin, a collectin. (D) E-selectin; the coil represents the membrane-spanning and cytoplasmic domains. COL, collagenous region; CR, complement regulatory repeats; EGF, epidermal growth factor-like domain; CRD, carbohydrate recognition domain. The indentations represent binding sites. Reproduced from Sharon, N., and Lis, H. (1995) *Essays in Biochemistry* 30, 59–75. Copyright The Biochemical Society.

biological processes. Thus, they function in cell–cell, cell–molecule, or molecule–molecule recognition. Influenza virus hemagglutinin A, a lectin specific for *N*-acetylneuraminic acid (or hemagglutinin C specific for 9-*O*-acetyl-*N*-acetylneuraminic acid), as well as bacterial surface lectins, mediate the binding of the pathogens to host cells, a prerequisite for initiation of infection. Inhibitors of bacterial lectins protect animals against experimental infection by the lectin-carrying organisms, providing a basis for attempts to develop anti-adhesion therapy of microbial infections. In some cases the bacterial lectins are responsible for the attachment to sugar residues on phagocytic cells, permitting the latter cells to kill the bacteria in the absence of serum factors, in a process designated lectinophagocytosis.

In plants, lectins may serve as defense agents against different kinds of phytopathogenic fungi and insects, as well as predatory invertebrates and vertebrates. They may also be involved in the establishment of symbiosis between nitrogen-fixing bacteria, mainly rhizobia, and leguminous plants, a process of cardinal importance both in the nitrogen cycle of terrestrial life and in agriculture.

The galectins are believed to function in cell adhesion. Their elevated levels on the surfaces of metastatic cancer cells may be responsible for the adhesion of these cells to target organs, a step necessary for metastasis formation. The mannose-6-phosphate (Man-6-P) receptors target lysosomal enzymes into the lysosomes. A defect in the synthesis of the Man-6-P marker on these enzymes results in I-cell disease (mucolipidosis II or MLII). This is an inherited lysosomal storage disease, characterized by a lack of enzymes in the lysosomes that normally carry the marker, resulting in accumulation in these subcellular organelles of undigested glycoconjugates.

The endocytic lectins are responsible for the clearance from the circulatory system of glycoproteins (e.g., ceruloplasmin and α_1-acid glycoprotein) from which terminal sialic acid has been removed, and possibly of cells too (e.g., aged erythrocytes or bacteria). A prominent representative is the mammalian asialoglycoprotein receptor (or hepatic-binding protein) found on hepatocytes, specific for galactose and *N*-acetylgalactosamine. The mannose-specific lectin present on the surface of macrophages (MMR) has been implicated in antimicrobial innate immunity. It binds infectious organisms that expose mannose-containing glycans on their surface, leading to their killing. The soluble mannose-binding lectins (MBLs) of mammalian serum and liver and pulmonary surfactant proteins A and D (SP-A and SP-D), all members of the collectin family, also function in innate immunity. MBL deficiency syndrome is associated with recurrent, severe bacterial infections in infants; it is caused by a mutation of a single amino acid in the collagen-like domain of the lectin.

The selectins mediate the adhesion of circulating leukocytes to endothelial cells, a prerequisite for their extravasation into other tissues. They thus control the migration (homing) of lymphocytes to specific lymphoid organs and of leukocytes to sites of inflammation, where they act to eliminate bacteria and other foreign intruders. Individuals unable to synthesize oligosaccharides recognized by the selectins, such as sialyl-Le^x [NeuAcα(2–3)Galβ(1–4)[Fucα(1–3)]GlcNAc] (as seen, for example, in cases of leukocyte deficiency type II (LADII)), suffer from recurrent microbial infections. The mechanism that helps leukocytes to break the endothelial barrier as a step in the fulfillment of their infection-fighting duties, is also responsible for their undesirable accumulation in tissues where they do not belong (e.g., joints), thereby causing damage, swelling, and pain. In reperfusion injury, which may happen after heart infarct or cerebral stroke, the accumulated leukocytes destroy tissues that have been damaged by temporary lack of oxygen. As shown in experimental animals, sialyl-Le^x attenuates myocardial necrosis after myocardial ischemia and reperfusion, another example of the great potential of antiadhesion therapy. In addition to their involvement in inflammation, the selectins may play a role in the attachment of the human blastocyst to the uterine lining and in the spread of cancer cells from the main tumor throughout the body to form metastases. The

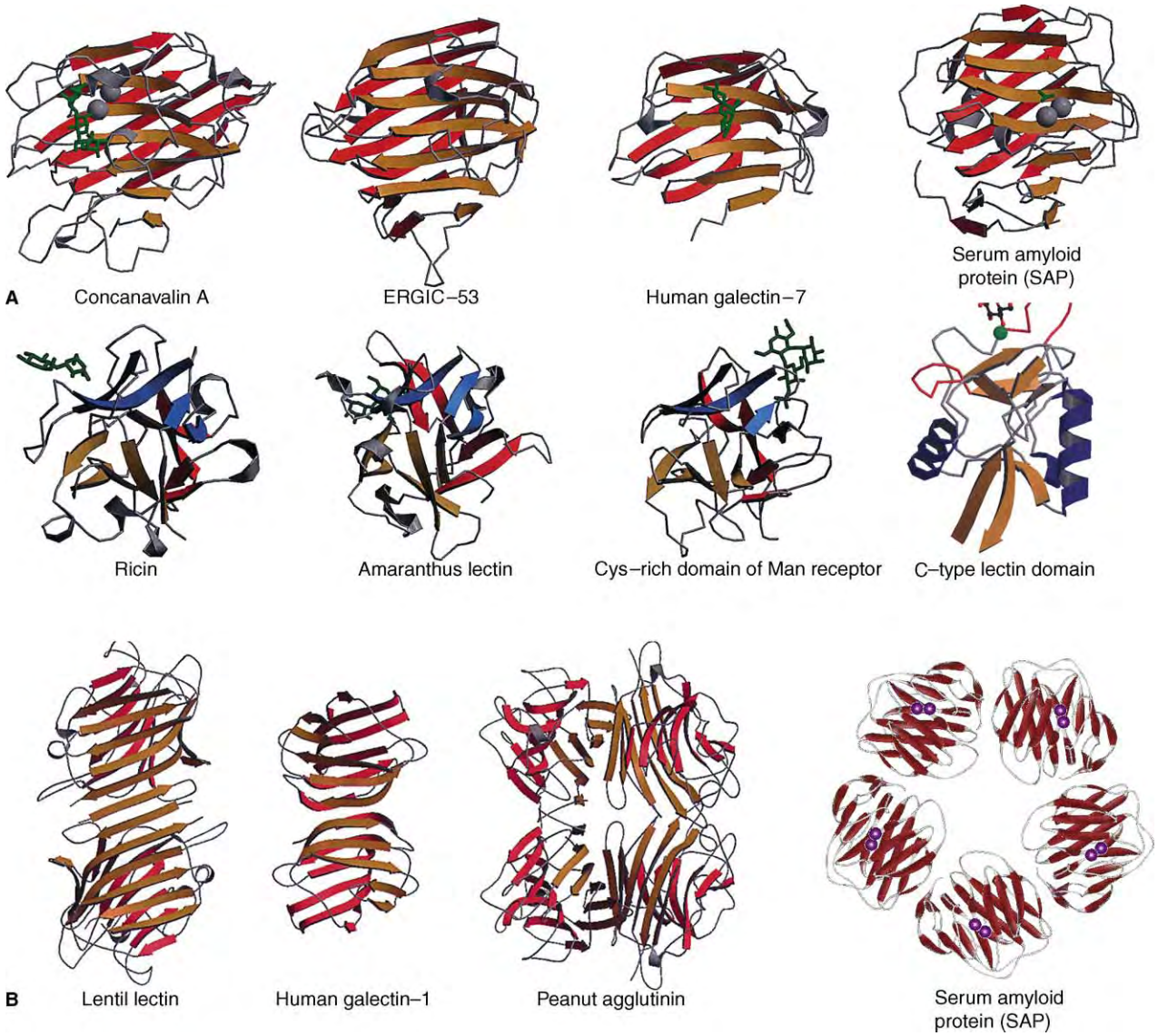

FIGURE 2 Structures of different lectins represented as ribbon diagrams. (A) Upper row shows monomers of lectins from different sources that share the jelly roll or lectin fold. First three lectins (from left) in the lower row all exhibit the β-trefoil fold. (B) Variations in quaternary lectins structures. The gray spheres represent metal ions; bound carbohydrate is shown in ball-and-stick representation. All diagrams, except for that of SAP, reprinted from Loris, R. (2002). Principles of structures of animal and plant lectins. *Biochim. Biophys. Acta* **1572**, 198–208. The diagram of SAP is from PDB entry sac.

siglecs have been implicated in cell–cell interactions in the immune system and in the process of myelination. Intracellular lectins such as calnexin, calreticulin, and ERGIC-53 participate in the control of glycoprotein biosynthesis.

Applications

Lectins, mainly those from plants, are invaluable tools for detection, isolation, and structural and functional investigation of complex carbohydrates, especially glycoproteins. In immobilized form, e.g., covalently bound to Sepharose, they are indispensable for purification and isolation by affinity chromatography of glycoproteins, glycopeptides, and oligosaccharides. Lectins are also useful as histochemical and cytochemical reagents: derivatized with fluorescent dyes, gold particles, or enzymes they serve for the detection of glycoconjugates in tissue sections and on cells, as well as on and in subcellular organelles, mainly for examination of changes that occur on cell surfaces and in cells during physiological and pathological processes, from differentiation to cancer.

A few lectins are employed in blood typing, e.g., those of the seeds of *Lotus tetragonolobus* and *Ulex europaeus*

TABLE II

Lectin Functions

Functions	Examples of lectins involved
Microorganisms	
Infectivity	*Escherichia coli* fimbriae; *Entamoaeba histolytica* Gal/GalNAc-specific lectin; influenza virus hemagglutinin
Plants	
Defense	Snowdrop lectin, jacalin, wheat germ aglutinin
Symbiosis with nitrogen-fixing bacteria	Pea lectin
Animals	
Clearance of glycoproteins from circulation	Asialoglycoprotein receptor
Control of lymphocyte migration	Selectins
Control of glycoproteins biosynthesis	Calnexin, calreticulin, ERGIC-53
Innate immunity	
Complement activation	MBLs
Lectinophagocytosis	MMR, SP-A
Modulation of cell–cell and cell–substratum interactions	Galectins
Modulation of signal transduction by B lymphocytes	Siglec-2
Neuronal myelination and regeneration	Siglec-4a and -4b
Targeting of glycoproteins to lysosomes	Man6P receptors
Tumor metastases	Galectins-1, -3, and -8; selectins

for the identification of type O cells, and of secretors of blood group substances. PHA and concanavalin A are potent *in vitro* T lymphocyte mitogens, while another lectin, pokeweed mitogen (PWM), stimulates both T and B cells. Mitogenic stimulation by lectins provides a simple means to assess the immunocompetence of patients and to monitor the effects of immunosuppressive and immunotherapeutic treatments, as well as for preparation of chromosome maps for karyotyping, sex determination, and detection of chromosome defects.

Selective agglutination by PNA permits the facile separation of mouse and human cortical (immature) thymocytes from the medullary (mature) ones. Treatment with SBA removes mature T cells from human bone marrow and affords a fraction enriched in stem cells. Lectin-purged bone marrow of haplo-identical donors serves routinely for transplantation into children born with severe combined immune deficiency (bubble children) with close to 70% success. The method is also used experimentally in bone marrow transplantation of leukemia patients. Knowledge of the properties of lectins was essential for the development of enzyme replacement therapy for the treatment of Gaucher disease, and there is hope for lectin replacement therapy for patients with defects in innate immunity.

A major application of toxic lectins, such as ricin, is for selection of resistant animal cell lines. These cell lines provide access to glycoproteins with modified glycan structures and to novel glycosyltransferases. They are useful tools for investigation of the mechanism of protein glycosylation and for large-scale production of therapeutic glycoproteins with desired carbohydrate structures.

See Also the Following Articles

Galectins • Protein Glycosylation Inhibitors • Siglecs

Glossary

glycan Any compound consisting of a few or many monosaccharides in free form or attached to another substance; a carbohydrate or saccharide.

glycoconjugate A substance that consists of one or more glycans covalently attached to a noncarbohydrate constituent, typically protein (to give a glycoprotein) or lipid (forming a glycolipid).

innate immunity A form of defense of animals and other organisms that acts against infection in the first minutes or hours. It is different from acquired or adaptive immunity that takes days or weeks to develop.

mitogen A substance that stimulates cell division, especially of lymphocytes.

Further Reading

Crocker, P. (ed.) (2001). *Mammalian Carbohydrate Recognition Systems*, Vol. 33, Results Problems Cell Differ, Springer, Berlin, 252pp.

Gabius, H.-J. (1997). Animal lectins. *Eur. J. Biochem.* **243**, 543–576.

Goldstein, I. J., Winter, H. C., and Poretz, R. D. (1997). Plant lectins: Tools for the study of complex carbohydrates. In *Glycoproteins II*

(J. Montreuil, J. F. G. Vliegenthart and H. Schachter, eds.) pp. 403–474. Elsevier, Amsterdam.

Kilpatrick, D. C. (2002). Mannan-binding lectin: Clinical significance and applications. *Biochim. Biophys. Acta* **1572**, 401–413.

Ley, K. (2003). The role of selectins in inflammation and disease. *Trends Molecular Med.* **9**, 263–268.

Loris, R. (2002). Principles of structures of animal and plant lectins. *Biochim. Biophys. Acta* **1572**, 198–208.

Sharon, N., and Lis, H. (1993). Carbohydrates in cell recognition. *Sci. Am.* **268**(1), 82–89.

Sharon, N., and Lis, H. (2003). *Lectins*, 2nd edition. Kluwer Academic, Dordrecht, The Netherlands, 457pp.

Sharon, N., and Ofek, I. (2000). Safe as mother's milk: Carbohydrates as future anti-adhesion drugs for bacterial diseases. *Glycoconjugate J.* **17**, 659–664.

Taylor, M. E., and Drickamer, K. (2003). *Introduction to Glycobiology.* Oxford University Press, Oxford, UK, 207pp.

Van Damme, E. J. M., Peumans, W. J., Barre, A., and Rougé, P. (1998a). Plant lectins: A composite of several distinct families of structurally and evolutionary related proteins with diverse biological roles. *Crit. Rev. Plant Sci.* **17**, 575–692.

Biography

Nathan Sharon and Halina Lis have been collaborating in research on lectins since 1960. Their numerous publications on the subject include many reviews and two books. Sharon received his Ph.D. from the Hebrew University, Jerusalem, in 1953. He then joined the Weizmann Institute, became a Professor in 1968 and Head of the Department of Biophysics in 1974, and Emeritus in 1990. He was a visiting professor at different institutions in Europe and the US, and is the recipient of many awards and honors, among them the Israel Prize in Biochemistry and Medicine, and membership of the Israel Academy of Sciences and Humanities and of EMBO.

Halina Lis received her Ph.D. in 1957 from the University of Uppsala, moved to Weizmann in 1960 and became an Associate Professor in 1986.

Leptin

Thomas W. Gettys
Pennington Biomedical Research Center, Baton Rouge, Louisiana, USA

Leptin is a 16 kDa peptide hormone released from adipose tissue that regulates the balance between energy intake and energy utilization by binding to hypothalamic receptors and modulating appetite control centers in the brain. Occupancy of central leptin receptors also increases activity of the sympathetic nervous system, which stimulates energy expenditure in peripheral target tissues through a process called adaptive thermogenesis. Through coordinated regulation of these two systems, leptin functions to match rates of energy expenditure with energy intake. Leptin also functions to preserve energy reserves during starvation by lowering body temperature, basal metabolic rate, and limiting hypothalamic support for reproductive function. As such, leptin is a peripheral signal that acts centrally to integrate a complex array of behavioral and metabolic systems that function to maintain energy homeostasis when food supplies are adequate and ensure survival when they are not.

Historical Perspective of Leptin Discovery

The search for the primary genetic defect giving rise to the obese/diabetic syndrome of *ob/ob* mice (Figure 1) was guided by the early work of Douglas Coleman, who postulated that *ob/ob* mice were missing a circulating satiety signal. To test this hypothesis, he surgically joined *ob/ob* mice with lean littermates, *ob/ob* mice with *db/db* (diabetes) mice, and lean mice with *db/db* mice so that the parabiotic pairs shared blood supplies. *db/db* mice were included in his experiments because they also developed morbid obesity after weaning, but differed from *ob/ob* mice in that the *db/db* mutation resides on a different chromosome. This landmark experiment showed that the obesity syndrome of *ob/ob* mice, but not *db/db* mice, was corrected by a circulating factor from lean mice. The obesity syndrome of *ob/ob* mice was also reversed by parabiotic pairing with *db/db* mice, but in this case, the *ob/ob* mouse in each pair eventually died from starvation. The results indicated that *ob/ob* mice were missing a satiety factor but retained the ability to respond to the missing factor. In contrast, *db/db* mice were unresponsive to the satiety factor, but apparently produced it in abundant quantities. Some 30 years later, the missing factor (and receptor) inferred from the work of Coleman was identified by Jeffrey Friedman at Rockefeller University with the cloning of the *ob* gene in late 1994. The cloning of the *ob* receptor by Louis Tartaglia followed soon thereafter. The product of the *ob* gene was named leptin, from the Greek "leptos," meaning thin.

Obesity Syndrome Produced by Leptin Absent in *ob/ob* Mice

The cloning of the *ob* gene identified leptin as the "lipostat" which regulates the balance between energy intake and utilization to maintain body weight equilibrium. Adipocytes of *ob/ob* mice do not produce leptin, and its absence produces a complex metabolic syndrome characterized by hyperphagia, morbid obesity, and diabetes. Hypertrophy of adipose tissue is noted prior to the hyperphagia that develops post weaning in *ob/ob* mice, and obesity occurs even when *ob/ob* mice are pair-fed with lean littermates. Thus, their thriftiness is a significant component of their propensity to become obese. Treatment of *ob/ob* mice with exogenous leptin corrects their obesity, and part of the weight loss can be accounted for by reductions in food intake. However, when differences in food intake between saline and leptin-injected *ob/ob* mice are controlled, leptin-injected mice still lose more weight. These results illustrate that an important component of leptin's physiological actions are to regulate energy expenditure.

Central Mechanisms of Leptin Action

Leptin is a key component of the neuroendocrine circuitry that regulates food intake and energy utilization, and its activation of the sympathetic nervous system (SNS) is now recognized as the primary efferent limb of the circuit regulating peripheral energy utilization. Leptin activates the SNS by increasing cocaine

FIGURE 1 *ob/ob* mouse and lean littermate (+/?) 12 weeks after weaning.

amphetamine-related transcript (CART) and α-melanocyte stimulating hormone (α-MSH) release from leptin-responsive neurons within the arcuate nuclei, and these peptides increase sympathetic outflow by binding to melanocortin and CART receptors on preganglionic neurons of the SNS. The resulting increase in sympathetic stimulation of muscle and adipose tissue promotes fat oxidation through targeted effects on futile energy cycles in the respective tissues. A second population of leptin-responsive neurons in the hypothalamus coexpress neuropeptide Y (NPY) and agouti-related peptide (AGRP), and expression of these orexigenic peptides is decreased by leptin. Thus, it is through reciprocal regulation of these two populations of hypothalamic nuclei that leptin produces its full effect on energy homeostasis (see Figure 2).

Adipose Tissue as a Target of the SNS

Mitochondrial oxidation of fatty acids creates a proton electrochemical gradient that is used to drive the conversion of ADP to ATP via ATP synthase. Brown adipose tissue (BAT) mitochondria possess an alternative pathway that allows protons to re-enter the mitochondrial matrix without coupling to ATP synthesis, and this pathway is mediated by "uncoupling protein 1" (UCP1). UCP1 transforms electrochemical energy into heat, enabling small mammals to survive exposure to cold. The sympathetic nervous system and UCP1 are essential components of this thermogenic response system. The conventional wisdom has been that UCP1 expression is restricted to brown adipocytes, but recent evidence has clearly established that sympathomimetics can induce

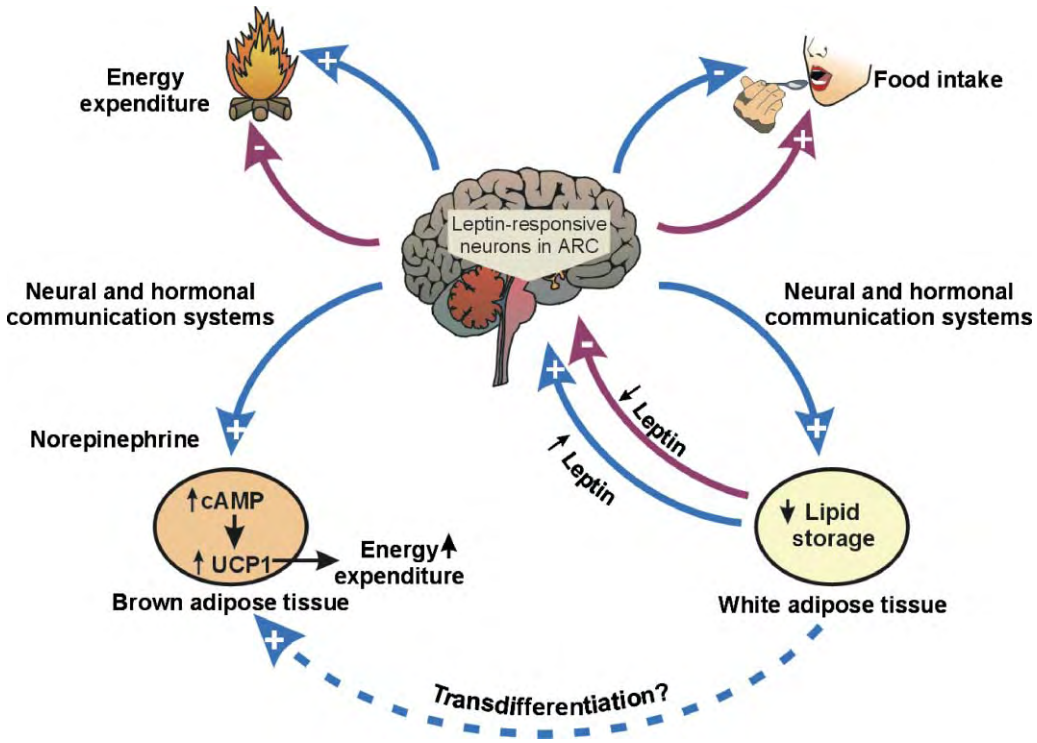

FIGURE 2 Model of leptin regulation of energy balance. Leptin regulates its own expression in white adipose tissue and thermogenesis in brown adipose tissue through central modulation of sympathetic nervous system outflow to adipose tissue.

ectopic expression of UCP1 in white adipose tissue (WAT) depots. The origin of the UCP1-expressing cells was originally a mystery, but evidence has emerged to support the concept that mature adipocytes are capable of significant functional plasticity, and readily transdifferentiate between cell types whose primary function is to store triglyceride (WAT) and multilocular, mitochondria-rich adipocytes capable of significant fat oxidation (BAT). It is clear that intense SNS stimulation can also promote the differentiation of preadipocytes within white depot sites into brown adipocytes. The unexpected appearance of UCP1 in WAT was originally observed in mice, where cold exposure caused a population of cells within the depot to transdifferentiate from unilocular white adipocytes to multilocular, mitochondria-rich brown adipocytes. Cold exposure produces these responses through increased sympathetic outflow to adipose tissue, and induces the transcriptional program of transdifferentiation in WAT through a norepinephrine, β-adrenoceptor, and cAMP-dependent mechanism. SNS stimulation of adipose tissue is also subject to regulation by leptin. In this case, modulation of SNS outflow is used to match rates of energy utilization to energy intake through the process of adaptive thermogenesis. A consensus has emerged to support the view that transdifferentiation of white adipocytes is an important component of the adaptive thermogenic response, and that leptin is a key mediator of the process.

The potential for transdifferentiation is depot-site specific and has a strong genetic component in both mice and humans. The significance of this process was demonstrated in elegant studies analyzing backcrosses of parental mouse strains with widely varying ability of WAT to transdifferentiate. Using UCP1 as a BAT-specific indicator, Leslie Kozak showed that recombinant inbred strains from the crosses reduced fat deposition after adrenergic stimulation in direct proportion to their induction of UCP1 in convertible WAT depots. These findings indicated that the relative ability of a mouse strain to resist obesity is a function of the ability of WAT to increase UCP1 in response to adrenergic stimulation. Thus, an important component of leptin's ability to regulate energy utilization in peripheral tissues is conferred by its ability to induce UCP1 expression and enhance fat oxidation in adipose tissue. Some WAT depots do not respond to SNS stimulation with an increase in UCP1 expression and *in situ* fat oxidation. In this case, SNS stimulation activates lipolysis, and mobilizes lipid for transport to more oxidatively active sites.

Regulation of Leptin Expression

Well before the discovery of leptin, George Bray proposed that most obesities known are low in sympathetic activity (MONA-LISA Hypothesis). This hypothesis stemmed in part from the observation that *ob/ob* mice were cold intolerant, but after leptin and its receptor were cloned, it was noted that leptin mRNA was significantly up-regulated in adipose tissue from both models. This indicated the absence of an efferent signal from the SNS in both models which was important in regulating leptin expression. Circulating leptin concentrations are the product of transcriptional regulation of the gene and release of the expressed protein from adipocytes. Work in the author's laboratory established that leptin secretion from isolated adipocytes was inhibited by activation of β_3-adrenoceptors in parallel to the activation of cAMP-dependent protein kinase. The SNS also regulates leptin expression. Figure 3 illustrates that mice lacking the gene which converts dopamine into norepinephrine (dopamine β-hydroxylase) were unable to down-regulate leptin mRNA expression after treatment with exogenous leptin. Thus, the SNS is the efferent arm of a feedback system which negatively regulates leptin expression and release.

Leptin is positively regulated by insulin and glucocorticoids. Both hormones produce rapid increases in leptin secretion from adipose tissue in conjunction with a coordinated increase in transcription of the gene. These hormonal and neurotransmitter-dependent pathways represent acute regulatory systems that are superimposed onto a diurnal pattern of leptin secretion which in humans, produces lowest concentrations at night and highest during the day. Serum leptin levels are also strongly correlated to percentage body fat and body mass index, but the relationship is dichotomous between male and female patients. For instance, as body mass

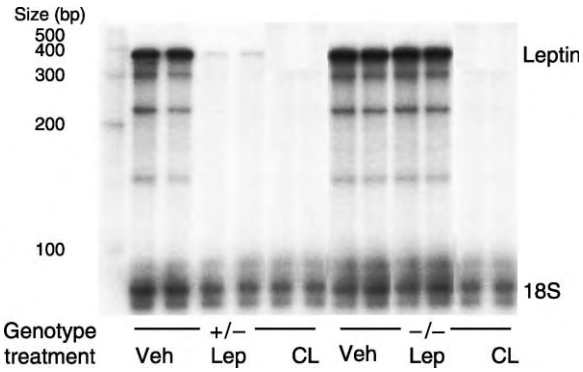

FIGURE 3 Ribonuclease protection assay of leptin mRNA in total RNA from EWAT of control (*Dbh* $^{+/-}$) and dopamine β-hydroxylase (Dbh$^{-/-}$) knockout mice injected with either saline, leptin, or the β3-adrenergic receptor agonist, CL-316,243 for 3 days. The blot shows that the ability to synthesize catecholamines is required for leptin to down-regulate its own expression in white adipose tissue. Reproduced from Commins, S. P., Marsh, D. J., Thomas, S. A., Watson, P. M., Padgett, M. A., Palmiter, R. D., and Gettys, T. W. (1999). Norepinephrine is required for leptin effects on gene expression in brown and white adipose tissue. *Endocrinology* **140**, 4772–4776.

index increases serum leptin levels increase threefold faster in females than males. Testosterone inhibits leptin expression and likely explains the gender difference in circulating leptin between males and females. Considered together, leptin expression and release are regulated by a complex network of hormonal and autonomic inputs, which are integrated to regulate transcription of the leptin gene and secretion of expressed protein into the bloodstream.

Leptin Resistance and Obesity

A factor common to diet-induced obesity in mice and humans is insensitivity to leptin. This conclusion is supported by the observation that most cases of rodent and human obesity are characterized by high-circulating leptin levels. In addition, treatment with exogenous leptin is minimally effective. Leptin resistance was originally thought to result from reduced transport of serum leptin into the cerebrospinal fluid. Short isoforms of the leptin receptor mediate this transport process across the blood–brain barrier (BBB), but the evidence is unconvincing that expression of this receptor isoform is altered during states of leptin resistance. It is also possible that elevation of serum leptin in dietary obesity saturates the transport system, making it unresponsive to subsequent changes in circulating leptin. To test this concept, leptin transport across the BBB was measured after injecting *db/db* and *ob/ob* mice with radiolabeled leptin. Despite great differences in endogenous circulating leptin in these two models, leptin transport into the hypothalamus did not differ between them. Evidence supporting defective transport comes mainly from studies where ICV injection produces responses in mice where peripheral leptin is ineffective. However, recent work has clearly established that the efficacy of ICV leptin to activate the first step of the signaling cascade (signal transducers and activators of transcription 3; STAT3) was diminished in mice that were also unresponsive to peripherally injected leptin. These findings support the alternative interpretation that decreased sensitivity of leptin-responsive nuclei make the mouse unresponsive to peripherally injected leptin without any change in transport kinetics. Such a mechanism would involve signal deamplification downstream of the leptin receptor.

Two potential mechanisms of signal deamplification have been proposed and both involve inhibition of leptin-dependent Janus kinase 2 (JAK2) activation. The first mechanism involves a member of the suppressors of cytokine signaling (SOCS) family called SOCS-3 that blocks leptin receptor-dependent phosphorylation and activation of JAK2. However, while SOCS-3 may have a role in mediating leptin resistance in yellow obese mice (i.e., A^y mice), no evidence has been found to support its involvement in the leptin resistance of mouse models of diet-induced obesity. The second mechanism of leptin signal deamplification involves protein tyrosine phosphatase 1B (PTP1B), which inhibits leptin signaling by dephosphorylating JAK2. JAK2 is a receptor-associated kinase which becomes active upon leptin receptor occupancy, and initiates the leptin signal by phosphorylating STAT-3. A model of how PTP1B functions in leptin signal deamplification in pro-opiomelancortin containing (POMC) neurons neurons of the arcuate nuclei is presented in Figure 4.

Interestingly, PTP1B activity and expression are both regulated by insulin, and expression of PTP1B is increased in peripheral tissues in insulin resistant states. It is unclear whether hypothalamic expression is upregulated in insulin-resistant obese states, but deletion of the PTP1B gene does produce leaner mice with increased energy expenditure and enhanced insulin sensitivity. It is also worth noting that the mice are resistant to diet-induced obesity and exquisitely sensitive to exogenous leptin.

The second step in central leptin signal transduction is translating STAT3 phosphorylation in hypothalamic target nuclei into activation of the SNS. Leptin activates the SNS by increasing α-MSH release from POMC neurons within the arcuate nuclei, and these peptides increase SNS outflow by binding to melanocortin receptors (MCR3, MCR4) on preganglionic neurons of the SNS. The MCR3 and MCR4 receptors are canonical seven-membrane spanning receptors, which signal by activating the stimulatory G protein, $G_s\alpha$ and increasing cAMP. Therefore, the transmission of the leptin signal from first order neurons (NPY/AGRP, POMC) to second order neurons (preganglionic SNS) is another step subject to alteration during the development of leptin resistance. For instance, it is now evident that posttranslational processing of POMC modifies the generation of sympathoexcitatory (α-MSH) versus sympathoinhibitory

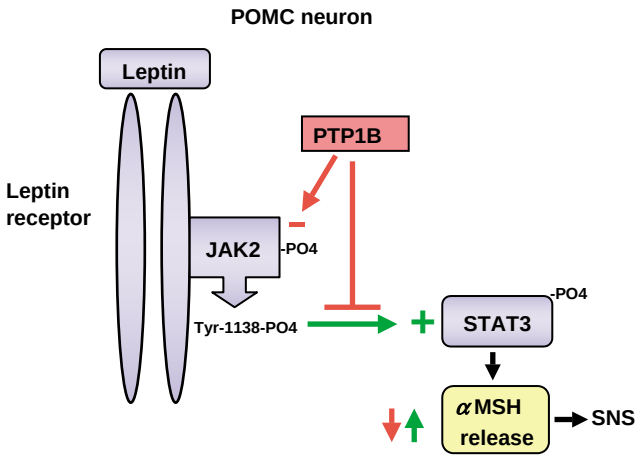

FIGURE 4 Schematic model showing deamplification of leptin signaling in POMC neurons by protein phosphatase 1B.

(β-endorphin) ligands from leptin-sensitive POMC neurons. Second, high-fat diets transform the sympathetic response to ICV leptin from excitatory to inhibitory in Wistar rats. These findings provide a framework to propose that high-fat diets modify the processing of POMC in a manner which alters the translation of the leptin signal and alters its ability to regulate downstream responses and enhance peripheral energy utilization.

The third component of leptin signal transduction is SNS outflow to adipose tissue, where activation of β-adrenoceptors initiates the transcriptional program of adaptive thermogenesis in a cAMP-dependent manner. Analysis of the promoter structure of genes transactivated during this response shows that the nuclear receptor, peroxisome proliferator activated receptor γ (PPARγ) is an essential component of the transcriptional complex. Although the endogenous ligand for this receptor has yet to be identified, *in vitro* studies have shown that long-chain-polyunsaturated fatty acids and their metabolites can act as partial agonists. The relevance of PPARγ to adaptive thermogenesis is apparent from work with obesity prone strains of mice, where it is known that high-fat diets compromise the ability of sympathetic stimulation to initiate thermogenic responses in adipose tissue. Remarkably, simultaneous provision of synthetic PPARγ agonists with sympathomimetics rescues the compromised adaptive thermogenic response of obesity-prone mice and produces a significant loss of WAT. Coadministration of PPARγ agonists with sympathomimetics is not required in obesity-resistant mice, as high-fat diets do not compromise their adaptive thermogenic responses. Although the underlying mechanism is not yet known, high-fat diets accentuate leptin resistance by altering the requirement for endogenous PPARγ agonists to support transcriptional activation of genes involved in adaptive thermogenesis. The consensus at present is that changes in dietary fat content and composition alter synthesis of the endogenous ligands for PPARs in a manner that produces coordinated, integrated transcriptional responses in and among metabolically active target organs. Collectively, the PPARs are viewed as a lipid-based nutrient sensing system. In the case of adipose tissue, the productive integration of signaling inputs from leptin-induced SNS outflow and lipid-sensitive PPAR activation are required for a full and effective adaptive thermogenic response. A better understanding of the signaling systems, which interact to regulate and limit leptin signaling is an important missing component in our overall understanding of the mechanisms of energy homeostasis.

See Also the Following Articles

Fatty Acid Oxidation • JAK-STAT Signaling Paradigm • Neuropeptide Y Receptors • Uncoupling Proteins

Glossary

brown adipocyte Adipose cell type with large number of mitochondria whose primary function is to conduct fat oxidation that is uncoupled from ATP synthesis via mitochondrial protein UCP1.

energy homeostasis Physiological state when energy intake and energy utilization are matched to produce stable body weight.

leptin 16 kDa hormone secreted by adipose tissue that regulates the balance between food intake and energy utilization.

obesity Excessive fat storage resulting from chronic positive energy balance.

sympathomimetic Endogenous or synthetic agonist of adrenoceptors.

transdifferentiation A programmatic change in gene expression in white adipocytes which transforms their morphology and functionality from fat storage to fat oxidation.

uncoupling protein 1 Specialized mitochondrial protein that short circuits the proton gradient across the mitochondrial matrix, uncouples oxidative phosphorylation, and transforms electrochemical energy into heat energy.

Further Reading

Bates, S. H., Stearns, W. H., Dundon, T. A., Schubert, M., Tso, A. W., Wang, Y., Banks, A. S., Lavery, H. J., Haq, A. K., Maratos-Flier, E., Neel, B. G., Schwartz, M. W., and Myers, M. G. (2003). STAT3 signalling is required for leptin regulation of energy balance but not reproduction. *Nature* **421**, 856–859.

Bray, G. A. (1991). Obesity, a disorder of nutrient partitioning: The MONA LISA hypothesis. *J. Nutr.* **121**, 1146–1162.

Commins, S. P., Marsh, D. J., Thomas, S. A., Watson, P. M., Padgett, M. A., Palmiter, R. D., and Gettys, T. W. (1999). Norepinephrine is required for leptin effects on gene expression in brown and white adipose tissue. *Endocrinology* **140**, 4772–4776.

Considine, R. V. (1999). An overview and update of the physiology of leptin in humans. *J. Clin. Ligand Assay* **22**, 233–235.

Friedman, J. M. (1997). The alphabet of weight control. *Nature* **385**, 119–120.

Friedman, J. M. (1999). Leptin and the regulation of body weight. *Harvey Lect.* **95**, 107–136.

Friedman, J. M. (2002). The function of leptin in nutrition, weight, and physiology. *Nutr. Rev.* **60**, S1–S14.

Gettys, T. W., Harkness, P. J., and Watson, P. M. (1996). The β_3-adrenergic receptor inhibits insulin-stimulated leptin secretion from isolated rat adipocytes. *Endocrinology* **137**, 4054–4057.

Guerra, C., Koza, R. A., Yamashita, H., Walsh, K., and Kozak, L. P. (1998). Emergence of brown adipocytes in white fat in mice is under genetic control – effects on body weight and adiposity. *J. Clin. Invest.* **102**, 412–420.

Halaas, J. L., Gajiwala, K. S., Maffei, M., Cohen, S. L., Chait, B. T., Rabinowitz, D., Lallone, R. L., Burley, S. K., and Friedman, J. M. (1995). Weight-reducing effects of the plasma protein encoded by the *obese* gene. *Science* **269**, 543–546.

Zhang, Y., Proenca, R., Maffei, M., Barone, M., Leopold, L., and Friedman, J. M. (1994). Positional cloning of the mouse obese gene and its human homologue. *Nature* **372**, 425–432.

Biography

Dr. Thomas W. Gettys is Professor of Adipocyte Signaling and Chief of the Experimental Obesity Division at the Pennington Biomedical Research Center. His principal research interests are in central and peripheral leptin signaling mechanisms, with special emphasis on the signaling mechanisms linking β-adrenoceptors to the transcriptional program of transdifferentiation in adipose tissue. He earned his Ph.D. in nutrition at Clemson University and completed postdoctoral training at Vanderbilt University in the Howard Hughes Medical Institute with Dr. Jackie Corbin.

LexA Regulatory System

Veronica G. Godoy, Penny J. Beuning and Graham C. Walker
Massachusetts Institute of Technology, Cambridge, Massachusetts, USA

The LexA regulon, also known as the SOS response, is a genetic system that responds to exogenous and endogenous DNA damage by inducing the expression of a number of genes whose products are responsible for maintaining the integrity of the genetic information in the chromosome. It has been widely studied in *E. coli*, and sequencing of a number of bacterial genomes has allowed the identification of genes that belong to this regulon in a wide variety of organisms. Comparison with the organization of the *E. coli* regulon indicates common and unique pathways in those organisms to protect the DNA against damage.

The LexA Regulatory System in *E. coli*

The central elements of the control system for the LexA regulon are the gene products of the *recA* and *lexA* genes. RecA protein is involved in the sensing of DNA damage and LexA is the repressor of the regulon. The LexA protein binds as a dimer to sequences located close to the promoters of the genes that it regulates, interfering with their transcription. Therefore, the expression of these genes occurs only under conditions that cause DNA damage in the cell. Such damage leads to the production of single stranded DNA (ssDNA), which is often generated by the replication machinery's failed attempts to replicate the damaged DNA. The RecA protein readily binds the ssDNA, forming a protein–DNA complex known as the RecA:ssDNA nucleoprotein filament. LexA binds deep in the groove of the nucleoprotein filament, which then acts as a coprotease to facilitate autocleavage of LexA between residues Ala84–Gly85. This cleavage inactivates LexA so it can no longer act as a repressor. The decreased intracellular concentration of LexA leads to expression of the LexA-regulated genes (Figure 1).

LexA Crystal Structure and Insights into Repressor Function

The autocleavage of LexA is catalyzed by a Ser-Lys dyad related to those found in signal peptidases. The crystal structures of several mutant forms of LexA have revealed that the loop containing the Ala-Gly cleavage site can adopt two conformations relative to the Ser-Lys dyad. In the "noncleavable" conformation, the cleavage site is quite distant from the Ser-Lys dyad that catalyzes cleavage, while in the cleavable conformation, the cleavage site lies proximal to the active site dyad, apparently poised for cleavage (Figure 2). This switch from a noncleavable to a cleavable conformation appears to form part of the basis for regulation of the cleavage reaction. It has been proposed that the RecA:ssDNA filament facilitates LexA cleavage by binding preferentially to the cleavable conformation. Cryoelectron microscopy experiments suggest that the RecA:ssDNA filament stabilizes the higher energy, cleavable form of LexA by binding LexA in the filament groove.

There is also a chemical barrier regulating LexA cleavage by preventing autodigestion. In the Ser-Lys active site dyad, the ϵ-amino group of Lys156 deprotonates Ser119, but the ϵ-amino group of Lys156 is solvent-exposed and likely protonated in the noncleavable conformations of LexA. The energetic cost of burying the charged ϵ-amino group of Lys156, which is required for cleavage, provides another layer of regulation of LexA cleavage and helps to prevent autodigestion.

LexA Binding Site

LexA, the repressor, exerts its regulatory effects by binding to palindromic sequences located near the promoter of the genes it regulates; the consensus sequence for the *E. coli* LexA binding site is $CTGtN_{10}$ aCAG (see Table I). LexA binds with different affinities to the variants of this sequence located upstream of the different SOS genes thereby enabling differential regulation of the LexA-regulated genes. Interestingly, both the *recA* and *lexA* genes are regulated by LexA. Upon DNA damage one of the first genes to be induced is *recA*.

LexA Autoregulation

LexA autoregulation sets the basal level of LexA; so the system is stable without DNA damage, but the response can easily be modulated. DNA damage results in the formation of RecA:ssDNA filaments, which in turn

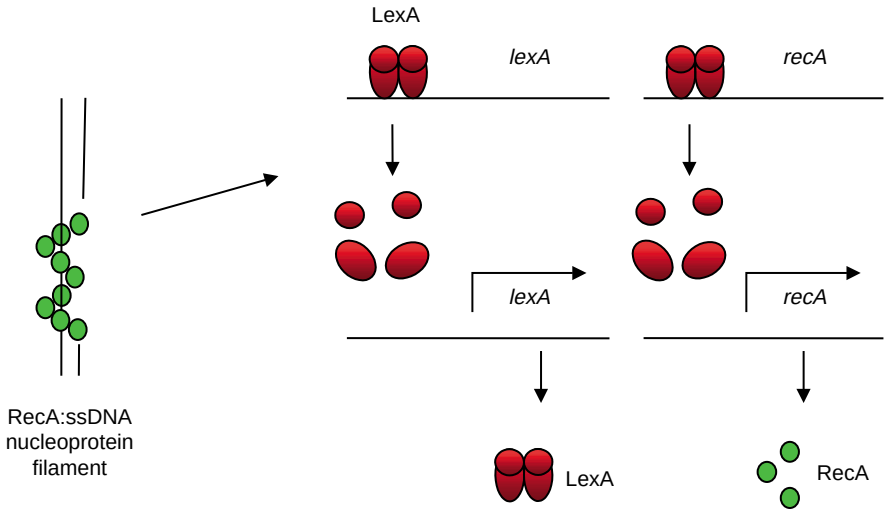

FIGURE 1 Induction of the SOS response. Shown are two of the operons under LexA control, including LexA itself. After DNA damage, RecA polymerizes on single-stranded DNA (ssDNA), forming a RecA:ssDNA nucleoprotein filament. This facilitates LexA cleavage, which inactivates it as a repressor and thus induces the SOS Response.

facilitate LexA cleavage, thereby inducing the expression of LexA-repressed genes.

The LexA Regulon

In *E. coli*, recent microarray experiments indicate that there are approximately 43 genes in the genome that are LexA-regulated. Thus, ~1% of *E. coli*'s genes (4402 ORFs) are induced in a concerted fashion in response to DNA damage.

LexA Mutants and their Phenotype

The elucidation of the major pathways involved in the response to DNA damage was initiated by the genetic analysis of both *recA* and *lexA* mutants. One of the first mutations analyzed that blocks induction of SOS genes was found to be a *lexA*[Ind$^-$] allele that results in a noncleavable LexA. Mutations in *lexA* that make cells constitutively express SOS genes [termed *lexA*(Def)] have been isolated as well. Such *lexA*(Def) mutations are lethal unless the cells also carry a mutation in the LexA-regulated *sulA* gene. Since *sulA* encodes a cell division checkpoint protein that blocks septation, its constitutive expression blocks cell division and results in cell death. Thus, mutations that inactivate the *sulA* gene permit *lexA* mutants that constitutively express SOS genes to carry out cell division and hence to be viable.

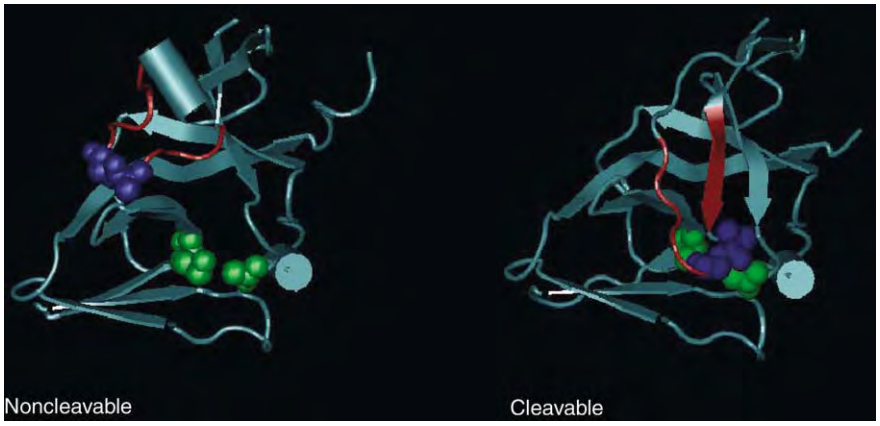

FIGURE 2 Conformational switch regulating LexA cleavage. Shown are the noncleavable (left) and cleavable (right) forms of the C terminus of LexA. The cleavage site Ala84–Gly85 is shown in blue spheres, while the Ser119–Lys156 catalytic dyad are shown in the green spheres. The red portion is the loop that displays a large conformational change in the noncleavable versus cleavable conformations. Figure prepared with VMD – Visual Molecular Dynamics. (Humphrey, W., Dalke, A., and Schulten, K. (1996). VMD: Visual molecular dynamics. *J. Molec. Graphics* **14**, 33–38.)

TABLE I

***Escherichia coli* Genes with their Respective LexA Box Sequence Compared to the Consensus Sequence**

Known genes	LexA box sequence
ysdAB	taCTGtttatttataCAGta
umuDC	taCTGtatataaaaaCAGta
sbmC	taCTGtatataaaaaCAGta
pcsA	aaCTGtatataaataCAGtt
recN no. 1	taCTGtatataaaacCAGtt
dinQ	taCTGtatgattatcCAGtt
urvB	aaCTGtttttttatcCAGta
dinI	acCTGtataaataacCAGta
hokE	caCTGtataaataaaCAGct
recA	taCTGtatgctcataCAGta
sulA	taCTGtacatccataCAGta
uvrA	taCTGtatattcattCAGgt
ssb	acCTGaatgaatataCAGta
yebG	taCTGtataaaatcaCAGtt
lexA/dinF no. 2	aaCTGtatatacaccCAGgg
ydjQ	caCTGgatagataacCAGca
lexA/dinF no. 1	tgCTGtatatactcaCAGca
ruvAB	cgCTGgatatctatcCAGca
yjiW	taCTGatgatatataCAGgt
molR	aaCTGgataaaattaCAGgg
dins	agCTGtatttgtctcCAGta
uvrD	atCTGtatatataccCAGct
recN no. 2	taCTGtacacaataaCAGta
ding	taTTGgctgtttataCAGta
yigN	aaCTGgacgtttgtaCAGca
ydjM1	taCTGtacgtatcgaCAGtt
ftsK	tcCTGttaatccataCAGca
dinB	caCTGtatactttacCAGtg
recN no. 3	taATGgtttttcataCAGga
ydjM2	caCTGtataaaaatcCTAta
ybfE	aaCTGattaaaaaccCAGcg
polB	gaCTGtataaaaccaCAGcc
Consensus	taCTGtatatatataCAGta

Modified from Courcelle, J., Khodursky, A., Peter, B., Brown, P. O., and Hanawalt, P. C. (2001). Comparative gene expression profiles following UV exposure in wild-type and SOS-deficient *Escherichia coli*. *Genetics* **158**, 41–64.

Defining the LexA Regulon

The first experiment showing that the SOS response is a global genomic response to DNA damage was performed by Kenyon and Walker. By first isolating transcriptional *lacZ* fusions located randomly in the genome they were able to screen for genes whose expression is induced after DNA damage. The identities of these *din* (*d*amage *in*ducible) genes indicated that the SOS response to DNA damage helps *E. coli* preserve the integrity of its DNA. Characterization of these *din* damage-inducible genes allowed the definition of the 20-base pair LexA binding site, which in turn led to the identification of additional genes belonging to the LexA regulon. Many of the *din* genes found this way are still intensely studied, since understanding their particular functions is yielding insights into the molecular mechanisms underlying this sophisticated global response to DNA damage.

The advent of transcriptional profiling technology (DNA microarrays), in which it is possible to test simultaneously the genome-wide expression of genes involved in a given process, has allowed nearly definitive identification of each of the genes regulated by LexA. Comparing the gene expression profiles in wild-type vs. *lexA*(Ind$^-$) (LexA noncleavable, non-SOS-inducible) strains allowed determination of the genes that are up-regulated in response to DNA damage specifically in a LexA-dependent manner. In this way, 43 genes were classified as part of the LexA regulon, including 17 previously unknown ones, and the kinetics of their induction were determined. For example, *recA*, *recN*, *sulA*, and *dinD* are nearly fully induced within 5 min following UV irradiation, and their transcripts persist throughout the time course (60 min). In contrast, *uvrA* induction occurs within the first 5 min following UV irradiation, but then the levels decrease almost immediately. There are also several genes whose transcripts decreased in a LexA-dependent manner, suggesting a role for LexA in reducing the expression of certain genes. It should be noted that with this technique it is impossible to differentiate between a decrease in transcription or an increase in mRNA degradation. Notably, some genes that are not part of the LexA regulon exhibit a similar expression profile as the LexA-dependent genes after UV irradiation. Some of the genes with this behavior include genes involved in carbon metabolism, lipid synthesis, and the response to osmotic stress. Therefore, it seems that this response is part of a larger, concerted stress response network.

Other Bacterial LexA Regulatory Systems

The sequencing of a number of microbial genomes (96 bacterial and 16 species of archaebacteria) has shown that some bacteria lack homologues of LexA. However, in those species that are known to exhibit the SOS response, it functions analogously to that of *E. coli*. The general SOS response is characterized by a LexA homologue binding to a consensus DNA-binding site on the promoter regions of the genes it regulates. The major differences between species are the set of genes repressed by LexA and the consensus sequence of the binding site. While the role of LexA as a repressor of genes involved in the cellular response to DNA damage is widely conserved across bacteria exhibiting the SOS response, there are idiosyncrasies.

An interesting example is that of *Rhodobacter sphaeroides* in which LexA has an unusual role – acting as both a transcriptional repressor and an activator. It achieves this by apparently interacting differently with both the DNA and the RNA Polymerase depending on the LexA concentration. At high concentrations of LexA, transcription of a LexA-regulated promoter is repressed because RNA polymerase gets trapped at the promoter in such a fashion that it cannot reach the open complex conformation, and hence cannot initiate transcription. When LexA concentrations are lower, transcription from a LexA-regulated promoter (e.g., RecA promoter) is increased due to enhanced open complex formation. In both cases, LexA increases binding of RNA polymerase to the promoter region. This is fundamentally different than the mechanism of LexA repression in *E. coli*, in which LexA sterically blocks RNA polymerase from binding initially to the promoter.

Summary

The SOS system is a concerted response to DNA damage, encompassing ~1% of *E. coli*'s genes, and it is seemingly part of an even larger stress response network. The LexA protein, the repressor that binds as a dimer with different affinities to an inverted repeat (SOS box) on the promoters of the genes it regulates, negatively controls the expression of the SOS genes. The LexA protein switches from a noncleavable to a cleavable form upon binding to the groove of the RecA:ssDNA nucleoprotein, which is the sensing element of the SOS response, that accumulates after DNA damage. Cleavage inactivates LexA – so it can no longer function as the repressor – leading in turn to the expression of the LexA-regulated genes. The LexA protein is autoregulated such that the response to DNA damage might be easily modulated. The SOS system and LexA's function as a repressor, although there are idiosyncrasies, appear widely conserved among bacteria. While many insights have been gained in the understanding of the SOS response, there is still much to know about the molecular mechanisms underlying this sophisticated global response to DNA damage.

See Also the Following Articles

Cell Cycle: DNA Damage Checkpoints • DNA Damage: Alkylation • DNA Mismatch Repair and the DNA Damage Response • DNA Mismatch Repair: *E. coli* Vsr and Eukaryotic G–T Systems

Glossary

autoregulation The same gene product regulates the expression of its gene.

DNA microarrays A surface carrying an array of DNA oligonucleotides corresponding to genes of interest, which is probed with RNA isolated from cells under a given condition.

promoter Sequence located upstream of a gene that is recognized by RNA polymerase and is used to initiate transcription.

regulon Group of genes whose expression is synchronized by common regulator(s).

repressor Gene product that binds a site near the promoter of a gene that regulates by sterically interfering with the binding of the RNA polymerase to its promoter.

transcriptional fusions A fusion that places the expression of a reporter gene (e.g., *lacZ*) under the transcriptional control of another gene.

Further Reading

Brent, R., and Ptashne, M. (1981). Mechanism of action of the *lexA* gene product. *Proc. Natl. Acad. Sci. USA* **78**, 4204–4208.

Courcelle, J., Khodursky, A., Peter, B., Brown, P. O., and Hanawalt, P. C. (2001). Comparative gene expression profiles following UV exposure in wild-type and SOS-deficient *Escherichia coli*. *Genetics* **158**, 41–64.

David, J., Bittner, M., Chen, Y., Meltzer, P., and Trent, J. M. (1999). Expression profiling using cDNA microarrays. *Nat. Genet. Suppl.* **21**, 10–14.

Friedberg, E. C., Walker, G. C., and Seide, W. (1995). *DNA Repair and Mutagenesis*. The American Society for Microbiology, Washington, DC.

Kenyon, C. J., and Walker, G. C. (1980). DNA-damaging agents stimulate gene expression at specific loci in *Escherichia coli*. *Proc. Natl. Acad. Sci. USA* **77**, 2819–2823.

Koch, W. H., and Woodgate, R. (1998). The SOS response. In *DNA Damage and Repair* (J. A. Nickoloff and M. F. Hoekstra, eds.) Vol 1, pp. 107–134. Humana Press, Totowa, New Jersey.

Little, J. W., Mount, D. W., and Yanisch-Perron, C. R. (1981). Purified *lexA* protein is a repressor of the *recA* and *lexA* genes. *Proc. Natl. Acad. Sci. USA* **78**, 4199–4203.

Sutton, M. D., Smith, B. T., Godoy, V. G., and Walker, G. C. (2000). The SOS response: Recent insights into *umuDC*-dependent mutagenesis and DNA damage tolerance. *Annu. Rev. Genet.* **34**, 479–497.

Biography

Veronica G. Godoy obtained her Ph.D. from the Department of Molecular Biology and Microbiology at Tufts Medical School in Boston. During her graduate research she studied a bacterial pathogen, and became interested in how bacteria mutate in response to environmental stress. Upon graduation she investigated possible mechanisms of bacterial mutability under non-lethal conditions of selection with Dr. Maurice Fox at MIT. This led to her current interest in DNA damage tolerance in Dr. G. Walker's lab, where she is currently a senior scientist.

Penny J. Beuning received her B.A. from Macalester College (St. Paul, MN) and her Ph.D. in Chemistry from the University of Minnesota, Twin Cities. She studied enzyme-substrate recognition in aminoacyl-tRNA synthetases, as well as amino acid editing, during her graduate work. This led to her interest in how organisms maintain genetic fidelity. She is a postdoctoral researcher studying DNA repair and DNA damage tolerance in bacteria. She is also a representative on the

MIT Postdoctoral Scholars Advisory Council and is involved in Graduate Women in Science.

Graham C. Walker is an American Cancer Society Research Professor and an HHMI Professor in the Department of Biology at the Massachusetts Institute of Technology. Prior to joining MIT, he did his Hons. B.Sc. at Carleton University in Ottawa, Ontario, obtained his Ph.D. from the University of Illinois, Champaign-Urbana, Illinois, and did postdoctoral work at the University of California, Berkeley. He has worked on cellular responses to DNA damage and on mutagenesis and DNA repair. He has also studied the *Rhizobium*–legume symbiosis and its relationship to chronic pathogenesis. He has served as the Editor-in-Chief of *Journal of Bacteriology*. Dr. Walker has been deeply involved in undergraduate education throughout his career.

Ligand-Operated Membrane Channels: Calcium (Glutamate)

Elias K. Michaelis
University of Kansas, Kansas City, Kansas, USA

The mammalian central nervous system has a great capacity to adapt to many stimuli and perturbations of normal physiological function and this adaptability or plasticity is crucial in coding, storing, and retrieving information. Over the past decade, it has become clear that transient elevation of intracellular calcium (Ca^{2+}) in neurons represent the key signals used by nerve cells to alter their molecular structure and function and to produce long-lasting changes in cell function. These Ca^{2+}-activated molecular events are crucial not only for such phenomena as learning and memory but also for determining neuronal survival or damage. Key regulators of Ca^{2+} entry into neurons are the receptors for the excitatory neurotransmitter L-glutamic acid.

Calcium Signaling in Neurons

Adaptation of brain function to incoming stimuli or to altered behavioral states is a well-demonstrated phenomenon. Such adaptation is thought to involve long-lasting alterations in the sensitivity of select neuronal networks or select synapses of individual neurons. The phenomenon of long-lasting changes in synaptic activity in neurons is, in part, the result of altered gene transcription and protein synthesis and changes in the concentration of free intracellular calcium (Ca^{2+}) brought about either through influx into nerve cells or release from intracellular stores are considered to be the major signals for such adaptive changes in neurons. Under normal physiological conditions in unstimulated neurons, the concentration of free intracellular Ca^{2+} ($[Ca^{2+}]_i$) is maintained at $\sim$45–75 nM, i.e., a concentration that is $\sim$10 000-fold lower than that in the extracellular environment of neurons. Following stimulation of neurons, either through synaptic activation, primarily of glutamate receptors but also of other receptors, such as nicotinic acetylcholine receptors (AchRs), or direct electrical stimulation, the intracellular levels of free Ca^{2+} can change quite rapidly and substantially, as will be described next (Figure 1).

The low free $[Ca^{2+}]_i$ is maintained through buffering mechanisms that are dependent on the activity of both Ca^{2+}-transport systems and Ca^{2+}-binding proteins present in neurons. Both of these Ca-buffering processes are important in re-establishing low free $[Ca^{2+}]_i$ following perturbations of the concentrations after synaptic activation and membrane depolarization of neurons. Among the buffering mechanisms, the transport carriers either pump Ca^{2+} out of the intracellular environment, such as the plasma membrane ($Ca^{2+} + Mg^{2+}$)-ATPase (PMCA) and the sodium Na^+–Ca^{2+} exchange carriers (NCX), or sequester Ca^{2+} in intracellular compartments, such as the endoplasmic reticulum, through the activity of the sarcoplasmic/endoplasmic reticulum Ca-ATPase (SERCA), and the mitochondria, through the activity of the mitochondrial Ca^{2+} uniporter (Figure 1). Calcium-binding proteins (Ca^{2+} BP) that have been shown to buffer intracellular Ca^{2+} include parvalbumin and calbindin as the primary Ca^{2+}-buffering proteins in neurons, as well as many other Ca^{2+}-binding proteins, such as, calmodulin, calcyphosine, neurocalcin, hippocalcin, and visinin-like protein 3.

Electrical stimulation of neurons with a stimulus of sufficient magnitude to depolarize the cell membrane from the normal electrical potential of ~ -70 mV internal negative to a potential that is 10–20 mV or more, less negative internally, can trigger the initiation of a regenerative, self-propagating form of membrane depolarization that usually starts in the region where the axon process of a neuron emerges from the cell body and travels down to the fine terminal branching points of the axon (Figure 2). This self-propagating depolarization, known as an action potential, depends on the rapid opening of voltage-gated sodium channels (VGSCs).

Depolarization of the nerve terminal region of a neuronal axon by an action potential leads also to the opening of voltage-gated Ca^{2+} channels (VGCCs) in the axon terminal region. VGCCs allow for the rapid entry of Ca^{2+} from the extracellular environment, an event that is crucial for the first step in the transformation of the electrical event that has traveled down the axon to a chemical signaling event, that is, the release of chemical

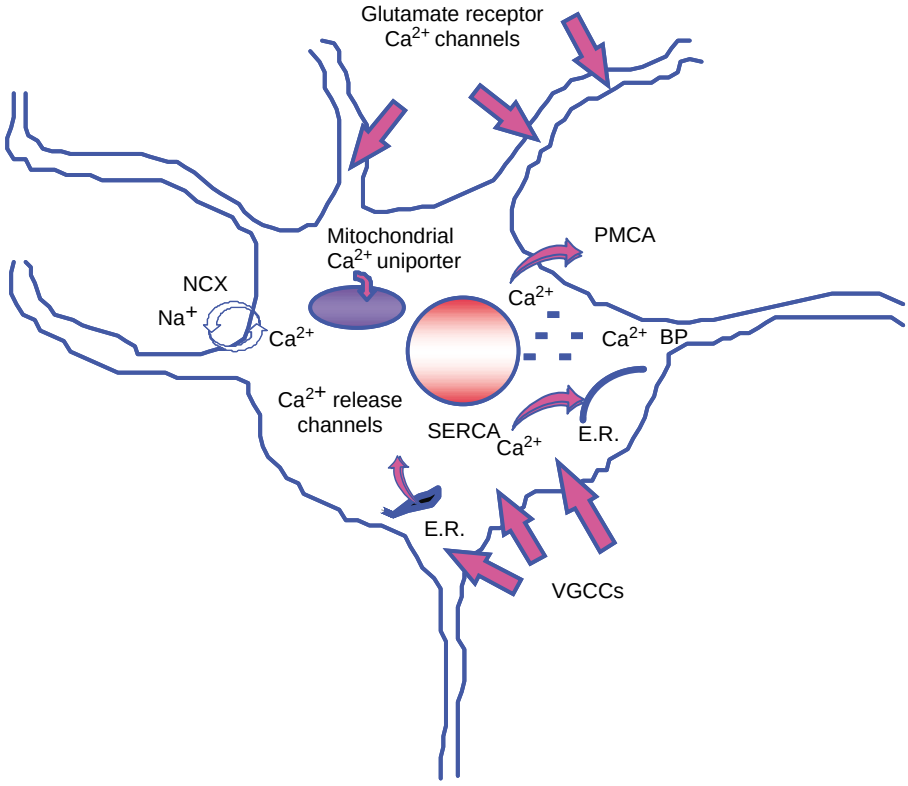

FIGURE 1 Pathways of Ca^{2+} entry, extrusion, and sequestration in neurons.

transmitters. The molecular events that lead to Ca^{2+}-induced exocytosis of transmitter molecules stored within synaptic vesicles at the nerve terminal are progressively being defined through biochemical, biophysical, and genetic studies but will not be discussed further here.

Action potentials initiated at the beginning of the axon as it exits the cell body spread in two directions,

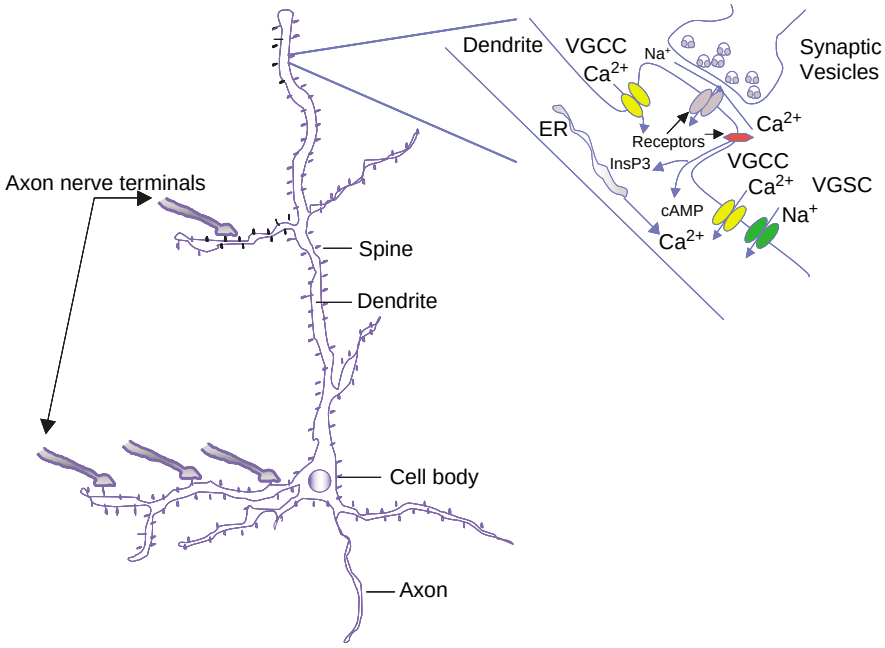

FIGURE 2 Diagrammatic representation of a large neuron that might be found in the neocortex or hippocampus of the brain. The structures of dendrites, dendritic spines, and axon terminals are highlighted.

toward the axon terminal as described above, as well as toward the cell body and the other processes emanating from the cell body of a neuron, the dendrites (Figure 2). Dendrite processes are considered to be the primary site for the reception of chemical information transmitted by means of neurotransmitters released from hundreds or thousands of axon terminals impinging upon the dendrites or the soma of a single neuron. The contacts that nerve terminals make with either dendrites or the soma of a neuron are, of course, the synapses across which chemical neurotransmission takes place. Most synapses on dendrites of brain neurons occur through close approximation of nerve terminals with specialized, small processes protruding from the main shaft of a dendrite (Figure 2). These knob-like protrusions are referred to as dendritic spines and represent a specialized compartment in a neuronal dendrite. The signals initiated by Ca^{2+} entry through transmitter receptor-ion channels and back-propagating action potentials in a spine differ from those initiated in the main body of a dendrite. Therefore, integration of signals that lead to long-lasting changes in neuronal responses to incoming stimuli and to changes in gene transcription and protein synthesis is determined by signals initiated in spines as well as those in dendrites.

The narrowness of the neck of spines that connects them to the respective dendrite is thought to delay diffusion and equilibration of intra-spine Ca^{2+} with that in the dendrites. Thus, the levels of free $[Ca^{2+}]_i$ within the head of a spine are determined not only by the amount of Ca^{2+} entering the spine through receptor-activated and voltage-gated ion channels but also through the kinetics of diffusion out of the spine and the Ca-buffering capacity within the spine. Action potentials initiated in axons and invading the cell body and dendrites produce "supralinear" increases in free $[Ca^{2+}]_i$ in dendrites when they are coincident with synaptic activation of neurotransmitter receptor-associated Ca^{2+} channels. Supralinear increases in $[Ca^{2+}]_i$ are defined as increases that exceed the sum of net increases in free $[Ca^{2+}]_i$ brought about by the simultaneous activation of both neurotransmitter receptor channels and VGCCs. Free $[Ca^{2+}]_i$ in spines following the activation of back-propagating action potentials has been estimated to reach levels as high as 2 μM. If back-propagating potentials are coupled to neurotransmitter activation of receptors that allow the influx of Ca^{2+} into neurons, such as glutamate receptors, then the levels are estimated to be more than tenfold higher, i.e., 26 μM.

The coincidence of glutamate receptor-mediated and action potential-induced Ca^{2+} signals plays a crucial role in the phenomenon known as synaptic plasticity, i.e., the long-term change in the magnitude of responses across a synapse following a series of activating stimuli delivered to a set of synapses in a neuron. Synaptic plasticity is fundamental to the processes of learning and memory and to the adaptive brain changes described above. Long-term increases in synaptic responses to a given stimulus are known as long-term potentiation (LTP), and long-term decreases in such responses are known as long-term depression (LTD). At the center of the molecular events that lead to synaptic plasticity are glutamate receptors, VGCCs, and intraneuronal Ca^{2+} signaling.

Glutamate Receptors in the Mammalian Central Nervous System: Structure and Function

Physiological and Pharmacological Properties of Glutamate Receptors

L-Glutamic acid is the most prevalent excitatory neurotransmitter in the vertebrate nervous system. Glutamate receptor activation is one of the stimuli for neuronal migration and synapse formation in the developing central nervous system (CNS), causes the elongation of neuritic processes and enhances the survival of some neurons. However, excessive stimulation of glutamate receptors by moderately high concentrations of L-glutamate and several of its analogues, such as *N*-methyl-D-aspartate (NMDA), leads to delayed neuronal damage through the activation of apoptosis. Stimulation of glutamate receptors by even higher concentrations of L-glutamate or NMDA leads to acute toxicity through necrosis. Both the phenomena of synaptic plasticity and neuronal damage are dependent on the entry of Ca^{2+} into neurons but they differ, of course, in the magnitude and duration of the changes in free $[Ca^{2+}]_i$.

Before proceeding with a discussion of the regulation of Ca^{2+} signaling in neurons by glutamate receptors, it is important to define the various types of glutamate receptors present in the mammalian CNS. The classification is based on pharmacological and physiological properties of neuronal glutamate receptors (Table I). On the basis of functional characteristics, two general categories of glutamate receptors have been identified, the ion channel-forming receptors, or ionotropic receptors, and the receptors linked to the activation of phospholipase C (PLC) or the inhibition of adenylyl cyclases (AC), known as the metabotropic receptors. Metabotropic receptors that activate PLC also stimulate phospolipase D. Ionotropic receptors fall into three categories, those that are activated by NMDA, those that respond to kainic acid (KA), and those that are

TABLE I

Classification of L-Glutamate Receptor Subtypes Found in the Mammalian Central Nervous System

Receptor classes	Ionotropic			Metabotropic
Receptor subtype	NMDA	AMPA	Kainate	Quisqualate, L-AP4
Selective agonists	NMDA	AMPA	Kainate, (2S, 4R)-4-methylgutamic acid	1S3RACPD, L-AP4 LCCG1, DCG IV, ACPT III
Functional characteristics	Activation of channels for Na^+, and K^+, and Ca^{2+}	Activation of channels for Na^+ and K^+	Activation of channels for Na^+ and K^+	Activation of PLC; Activation of PLD; Inhibition of AC
	Slow excitation	Fast excitation	Fast excitation	
Other agonists	Ibotenate, L-HCA, Quinolinate	Quisqualate, Kainate, Domoate, Willardine	Domoate, Acromelic acids A and B	Quisqualate, L-serine-O-phosphate, Ibotenate, CCG
Allosteric modulators	Glycine, D-serine, Spermine	Aniracetam, Benzothiazides, CX164 (AMPAkine)	Concanavalin A (Con A)	
Competitive antagonists	2-AP5, 2-AP7, CPP, CPP-ene, CGP39653, CGS19755, biphenyl	CNQX, NBQX, DNQX	GAMS, γ-D-glutamyl-glycine	Phenylglycine analogs (3HPG, 4CPG, 4C3HPG, MCPG)
Antagonists at modulator sites	5,7-diCl-Kyn, HA-966, CNQX, L-689560	2,3-Benzodiazepines (GYKI52466), SYM2206		
Ion channel inhibitors	PCP, MK-801, Ketamine	JST, Barbiturates		

Abbreviations used: AC, adenylyl cyclase; ACPD, 1-aminocyclopentane-1,3-dicarboxylate; Aniracetam, 1-(4-methoxybenzoyl)-2-pyrrolidinone, L-AP4, L-2-amino-4-phosphonobutanoic acid; 2-AP5, D-2-amino-5-phosphonopentanoic acid; 2-AP7, D-2-amino-7-phosphonoheptanoic acid; CCG, 2-carboxycyclopropylglycine; CGP39653, (±)-(E)-2-amino-7-amino-4-propyl-5-phosphonopentenoic acid; CGS19755, [[(±)-2-carboxy-piperidin-4-yl]methyl]-phosphonic acid; 4C3HPG, (*S*)-4-carboxy-3-hydroxy-phenylglycine; CNQX, 6-cyano-7-nitroquinoxaline-2,3-dione; 4CPG, (*S*)-4-carboxy-phenylglycine; CPP, [3-[(±)-carboxypiperazin-4-yl]prop-1-yl]-phosphonic acid; CPP-ene. [3-[(±)-2-carboxypeprazin-4-yl]-propen-1-yl]-phosphonic acid; CX614, 2H,3H,6aH-pyrrolidino[2″,1″_3′,2′]1,3-oxazino[6′,5′-5,4]benzo[*e*]1,4-dioxan-10-one; 5,7-di-Cl-Kyn, 5,7-dicholorokynurenic acid; DNQX, 6,7-dinitroquinoxaline-2,3-dione; GAMS, γ-D-glutamylamino-methylsulfonate; HA-966, 3-amino-1-hydroxy-2-pyrrolidone; 3HPG, (*S*)-3-hydroxy-phenylglycine; JST, Joro spider toxin; L-689,650, *trans*-2-carboxy-5,7-dichloro-4-phenylamino-carbonylamino-1,2,3,4-tetrahydroquinoline MCPG, (+)-α-methyl-4-carboxy-5,7-dichloro-4-phenylaminocarbonylamino-1,2,3,4-tetrahydroquinoline MCPG, (+)-α-methyl-4-carboxy-phenylglycine; MK-801, (+)-5-methyl-10,11-dihydro-5H-dibenzo[*a*,*d*]cyclohepten-5,10-imine; NBQX, 2,3-dihydroxy-6-nitro-7-sulphamoyl-benzo-(F)-quinoxaline; PLC, phospholipase C; SYM 2206, (±)-4-(4-aminophenyl)-1,2-dihydro-1-methyl1-2-propylcarbamoyl-6,7-methylenedioxyphthalazine.

activated by α-amino-3-hydroxy-5-methyl-4-isoxazole-propionic acid (AMPA) (Table I). Metabotropic glutamate receptors are subdivided into Group I, II, and III based on their sensitivity to various agonists and antagonists, as well as their effects on either PLC or adenylyl cyclases.

KA and AMPA receptors (KARs and AMPARs) are the primary receptors for rapid excitatory transmission in the CNS. The receptor-associated ion channels activated by AMPA or KA are primarily permeable to Na^+ and K^+. However, some AMPARs as well as some KARs form ion channels that are permeable to Ca^{2+}. AMPARs in brain neurons are activated by both AMPA and KA, but AMPA is the more potent agonist. AMPARs can be distinguished from KARs on the basis of the effects that selective allosteric modulators, the benzothiazides and AMPAkines, and selective non-competitive inhibitors, the 2,3-benzodiazepines, have on AMPARs but not on KARs (Table I). Some of the selective modulators of AMPARs, such as the AMPAkines, are currently being explored as agents that might enhance memory formation in diseases that produce decrements in memory, such as the dementia of Alzheimer's disease.

NMDA receptors (NMDARs) respond to glutamate more slowly than either KARs or AMPARs. The slow response of NMDARs is thought to be due to the fact that they are tonically inhibited by Mg^{2+}. Mg^{2+} inhibition of NMDARs is a voltage-dependent phenomenon and membrane depolarization relieves such blockade. Thus, the rapid activation of KARs and AMPARs by glutamate and the subsequent depolarization of the membrane diminishes the inhibition of NMDARs by Mg^{2+} and leads to the activation of these receptors by glutamate. In neuronal synapses on dendritic spines, both AMPA- and NMDA-sensitive

receptors are proximal to each other. Back-propagating action potentials in dendrites or action potentials generated within spines and dendrites also relieve the Mg^{2+}-induced inhibition of NMDAR channels.

The opening of NMDAR ion channels increases the permeability of the membrane to Na^+, K^+, and Ca^{2+}. A unique feature of NMDARs is the requirement for the presence of nanomolar to micromolar concentrations of a coagonist, glycine, in order to be fully activated (Table I). Because of the multiplicity of sites that activate or inhibit NMDAR ion channels, antagonists for NMDARs fall under four categories (Table I), antagonists that compete for the recognition sites of L-glutamate and NMDA (e.g., 2-AP5, 2-AP7), those that block the binding sites for the coagonist glycine (e.g. 5,7-diCl-kynurenic acid), those that inhibit the allosteric enhancement of agonist activation by the polyamines (e.g. ifenprodil) and those that inhibit the receptor-associated ion channel (e.g. dizocilpine or MK801).

Metabotropic glutamate receptors (mGluRs) are localized primarily in what is known as the perisynaptic region of dendritic spines, i.e., not within the synapse as AMPARs, KARs, or NMDARs do. These receptors are apparently not activated by the release of neurotransmitter glutamate following single-action potentials but rather following repeated, high-frequency stimulation of axons and their nerve endings. Of particular interest with regard to Ca^{2+} signaling in neurons is the fact that group I mGLuRs produce two types of neuronal depolarization, a rapid, transient depolarization related to the release of Ca^{2+} from intracellular stores, and a prolonged and larger depolarization resulting from activation of transient receptor potential (TRP) Ca^{2+} channels (TRPCs). The release of Ca^{2+} from intracellular stores is the result of inositol-1,4,5-triphosphate ($InsP_3$) formation and the activation of $InsP_3$ receptor-ion channels on endoplasmic reticulum membranes. This transient elevation in intracellular Ca^{2+} causes propagating increases in free $[Ca^{2+}]_i$ and elicits changes in the activity of CNS neurons that are dependent on protein synthesis, i.e., it has some of the characteristics of long-term changes associated with synaptic plasticity. In addition, these Ca^{2+} transients can produce supralinear increases in free $[Ca^{2+}]_i$ in dendrites and spines of CNS neurons if they occur at the same time as back-propagating action potentials.

Molecular Structure of Glutamate Receptors

The cloning of the cDNAs for glutamate receptors has revealed a great complexity in the structure of these receptors (Table II and Figures 3 and 4). The size of all glutamate receptor proteins represented by the cDNAs for GluR1, NMDAR1, mGluR1, and their homologues (95–163 kDa) is considerably larger than that for other neurotransmitter receptor proteins, both ion channel-forming receptors and G protein-coupled receptors (Table II and Figures 3 and 4). Based on the amino acid sequence of the proteins for the ionotropic receptors and the relative hydrophobicity of various domains in the proteins, it was predicted that each ionotropic receptor protein cloned had a large extracellular amino terminal region and three transmembrane domains. One of the hydrophobic domains, the second domain or M2, forms a loop at the opening of the ion channel but does not traverse the membrane bilayer. The carboxyl terminal of the ionotropic receptor proteins is on the intracellular domain (Figure 5). Structurally, the ion channel-forming region of KARs, AMPARs, and NMDARs exhibits high homology to voltage-gated K^+ channels, especially the M2 loop described above that forms a hairpin loop at the opening of the ion channel. Single amino acid substitutions in the hairpin loop at the opening of the ion channels of glutamate receptors affect dramatically the permeability of the channel to Ca^{2+}.

AMPA Receptor Genes and Protein Structure

With regard to the structure of native AMPARs, homomers of any of the proteins GluR1-4 form ion channels that are activated by both AMPA and kainate and exhibit the characteristics of neuronal AMPARs. GluR1-4 receptor proteins are expressed broadly throughout the CNS. Forms of AMPARs that are derived from alternatively spliced exonic sequences in the respective mRNAs are also expressed in the CNS (Figure 3). With regard to Ca^{2+} permeability of the ion channels associated with AMPARs, the key subunit is the GluR2 subunit. When this subunit is present in a receptor complex, then the AMPARs exhibit a linear relationship between voltage applied to the membrane and the current conducted through the receptor channels and have very low permeability to Ca^{2+}, i.e., they resemble most native AMPA receptors of CNS neurons. Homomeric complexes made of the GluR1, GluR3, or GluR4 proteins form channels that are permeable to Ca^{2+}. The restriction of Ca^{2+} permeability imparted to receptor complexes by the presence of the GluR2 subunit is dependent on a critical Arg586 (R586) in the M2 loop of this subunit. The corresponding residue in GluR1 is Gln582 (Q582) (Figure 5), and mutation of this Gln residue to Arg abolishes the Ca^{2+} permeability of channels formed by homomeric expression of the GluR1 protein. GluR3 and GluR4 also have Gln residues in the hairpin loop.

TABLE II

Characteristics of the Cloned Glutamate Receptors, Including some Putative Receptors, from Mammalian and Amphibian Brain

Subunits	Receptor type	Protein size (kDa)	Protein assembly	Functional properties
GluR1	AMPA (KA)	99.8	GluR1–4; most native receptors contain GluR 2	Glutamate, AMPA, KA-activated channels; low Ca^{2+} permeability
GluR2		96.4		
GluR3		98		
GluR4		101		
GluR5	KA	102.8	GluR5–7 with KA1, KA2	Glutamate and KA-activated channels; rapidly desensitizing
GluR6		93.9		
GluR7		100		
KA1		105		
KA2		109		
KBP-chick	KA binding	51.8	Single subunit	No channel function
KBP-frog		52.5		
δ1	Orphan receptor	110.4	Unknown	No channel function
δ2		113.2		
NMDAR1a	NMDA	103.5	NR-1 with	NMDA-activated channels;
NMDAR2A		163.3	NR-2 subunits	glycine a co-agonist high Ca^{2+}
NMDAR2B		162.9		permeability, MK-801 and
NMDAR2C		133.5		ketamine block; voltage-
NMDAR2D		140.6		dependent Mg^{2+} block
NMDAR3A		124.5	NR-1 with	Glycine-activated excitatory
NMDAR3B		109	NR-3 subunits	responses; NA^{+}, K^{+} channels; not permeable to Ca^{2+}; no Mg^{2+} blockade
GBP	NMDAR-like complex	57	Complex of GBP,	Reconstituted NMDA-activated
Gly/TCP-BP		52.7	Gly/TCP-BP, CPP-BP,	ion channels; glycine a co-agonist;
CPP-BP		78.3	and a 36 kD protein as purified from brain	MK-801 and ketamine block; low sensitivity to Mg^{2+}
mGluR1a	Metabotropic GluRs	133.2	Single protein receptor;	mGluR1, mGluR5: Activation
mGluR2		95.8	coupled to G proteins	of PLC and PLD; mGluR2,
mGluR3		99		mGluR3, mGluR4, mGluR6,
mGluR4a		101.8		mGlurR7, mGluR8: Inhibition
mGluR5a		128.3		of adenylyl cyclases
mGluR6		95.1		
mGluR7		102.2		
mGluR8		97.5		

The Arg residue in M2 of GluR2 is the result of RNA editing. The gene codon for the amino acid at this position is CAG for Gln, not CGG for Arg. The pre-messenger RNAs (pre-mRNA) are edited by an adenosine deaminase whose activity depends on the presence of the double stranded RNA (dsRNA) structure between exon 11 and intron 11 of the GluR2 pre-mRNA. The adenosine in the CAG codon is deaminated to inosine, thus forming the CIG codon for Arg. This dsRNA deaminase is expressed in brain and other tissues and edits with very high efficiency (~90%) and selectivity GluR2 pre-mRNA. In the disease amyotrophic lateral sclerosis, editing of GluR2 is significantly less complete and leads to the expression of AMPARs in spinal neurons that are highly permeable to Ca^{2+}. This increased permeability to Ca^{2+} may cause neuronal death during the lifespan.

KA Receptor Genes and Protein Structure

Homomers of GluR5 or GluR6 form channels that resemble KARs in brain neurons. On the other hand, GluR7, KA1, and KA2 fail to form channels when each protein is expressed by itself but the coexpression of GluR5–7 and KA1 and KA2 proteins in different

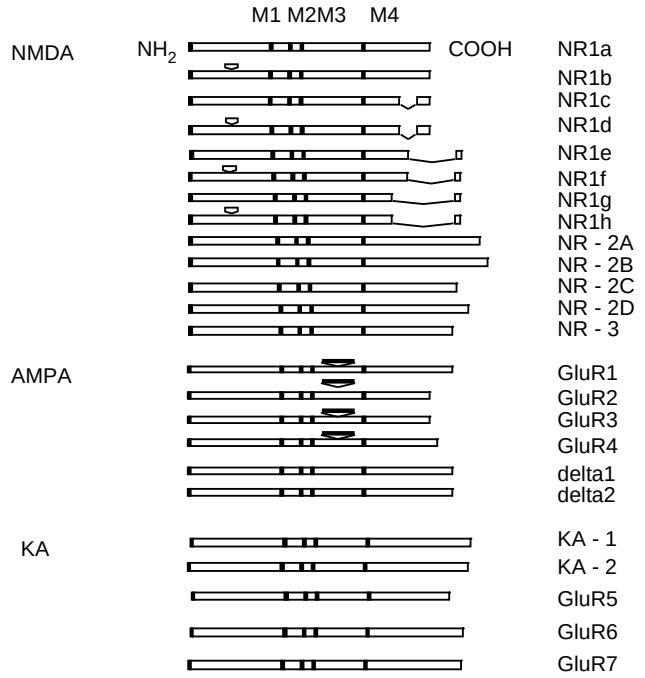

FIGURE 3 Linear representation of the structure of the cloned ionotropic glutamate receptor proteins. Shown are the NMDA, AMPA, and KA receptor proteins, as well as some of the orphan receptor proteins and the variant forms of NMDAR1 that result from alternative RNA splicing. Such alternative splicing leads to the addition or deletion of amino acid residues at either the amino (NH_2) or carboxyl (COOH) terminal of the protein. All proteins are shown to contain four hydrophobic domains designated M1–M4 (black boxes). For the proteins GluR1–4, the presence of the "flip" and "flop" splice variants in the region between M3 and M4 is indicated by boxes above the diagram of each receptor protein.

combinations of pairs of proteins leads to the formation of channels with unique properties that resemble, for the most part, neuronal KARs. In addition, the transfer of the likely ion channel domain of GluR7 into either GluR1 or GluR6 leads to the formation of receptor proteins that are fully functional as homomeric

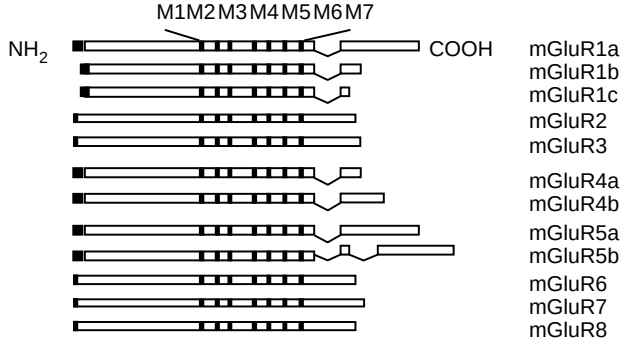

FIGURE 4 Linear representation of the structure of the cloned metabotropic glutamate receptor proteins mGluR1–8, including several splice variants. The seven hydrophobic domains considered as the likely transmembrane regions of the proteins are designated as M1 to M7 and are shown as black boxes.

receptor-ion channels. The same is not true, though, for two other genes, δ1 and δ2. The expressed proteins from these genes lack function either as homomeric or heteromeric receptor complexes and are therefore designated as orphan receptors. Based on these observations, GluR5–7 and KA1 and KA2 are considered to be the subunits of neuronal KARs. Different sets of neurons in the brain express these KAR receptor proteins and some of them, for example those in the CA3 field of the hippocampus, are some of the most vulnerable brain neurons to KA-induced neurotoxicity (neurotoxic KARs) as well as to seizure-induced neuronal damage.

The RNA for GluR5 and GluR6 is also edited leading to a Gln to Arg change in the M2 domain. However, the efficiency of editing (35% and 75%, respectively) is lower than that observed for GluR2. For the GluR6 receptor protein, the permeability of the channel for Ca^{2+} is controlled not only by the editing of the Gln residue in the M2 domain but also by the editing of two other residues in the first transmembrane domain, M1, of the protein.

Ionotropic glutamate receptors are macromolecular complexes composed of either four or five subunits. Identification of the ligand-binding sites of the GluR and KA subunits has been achieved by analysis of chimeras made of GluR3, an AMPAR protein, and GluR6, a KAR protein. The last 150 amino acids before the M1 domain and the amino acids right after M3 in the loop between M3 and M4 are the most critical ones in determining ligand-binding selectivity in the GluR3/GluR6 proteins. These two domains are referred to as the S1 and S2 domains and a bi-lobed structure is formed by the two regions of the protein (Figure 4). This structure of the ligand-binding domain has recently been confirmed by X-ray crystallographic analysis of the extracellular domains of the GluR1 protein.

NMDA Receptor Genes and Protein Structure

Expression of the NMDAR2 subunits by themselves does not lead to the formation of functional NMDARs, but the coexpression of the NMDAR2 subunits together with NMDAR1 leads to the formation of ion channels that have conductances very similar to those of NMDA receptors in neurons. The expression of NMDAR3 together with NMDAR1 and NMDAR2 subunits leads to receptor-ion channels with lower conductance levels than those of NMDAR1/NMDAR2 receptor ion channels and decreased Ca^{2+} permeability. In the NMDAR1 protein, the amino acid present in the corresponding position as Arg586 in GluR2 is Asn598. The channels formed by these subunits of NMDARs are highly permeable to Ca^{2+}. Finally, each of the combinations

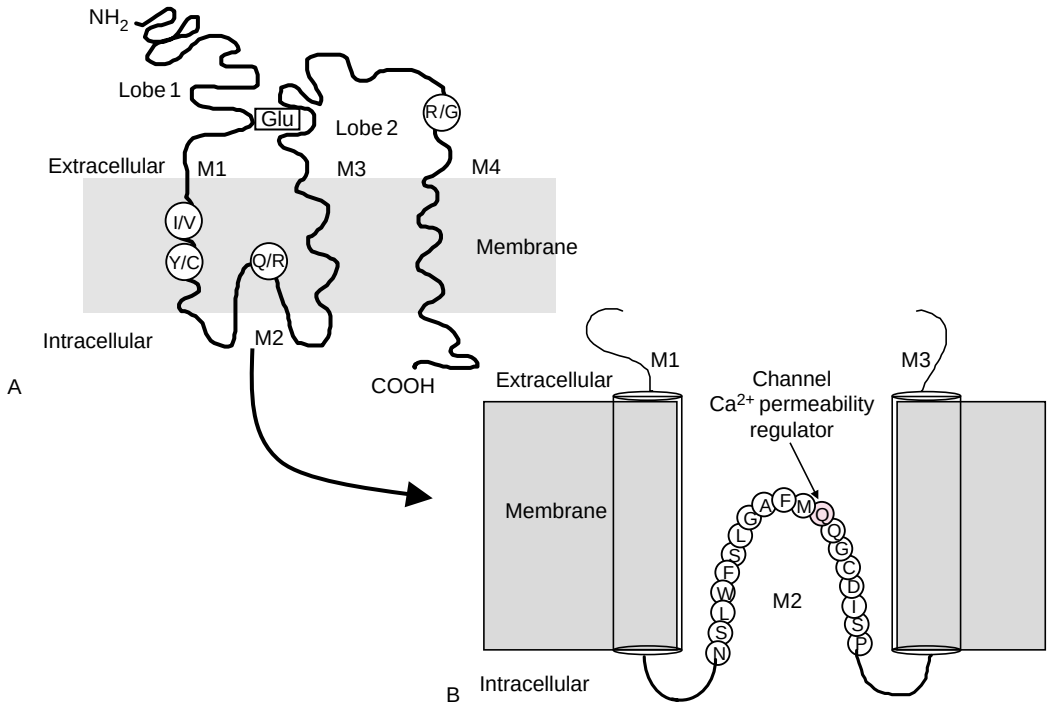

FIGURE 5 A representation of the distribution of different domains of the AMPA receptor (GluR proteins) in the neuronal membrane (A) and an enlarged view of the formation of a hairpin loop at the inner opening of the ion channel by the M2 domain. The formation of a glutamate-binding site by the two lobes of the protein projecting to the extracellular environment is also shown.

of NMDAR1 and one of the NMDAR2 subunits exhibit different degrees of sensitivity to the coagonist glycine, the competitive antagonist 2-AP5, and the channel inhibitor Mg^{2+}.

The glycine-binding site of NMDARs is in the NMDAR1 subunit and is formed by domains equivalent to the S1 and S2 domains of GluR1–4. This predicts a very similar molecular structure to the bi-lobed formation of the ligand binding sites in the GluR proteins. The primary glutamate/NMDA-binding site of NMDA receptors is localized on the corresponding extracellular domains of the NMDAR2 subunits. In addition to the six isoforms of NMDARs, there are eight splice variant forms of NMDAR1 (NMDAR1a-h, Figure 3). These splice variant forms exhibit clearly distinguishable sensitivities to agonists, antagonists, Zn^{2+}, and polyamines. Thus, a wide array of receptor complexes with differing affinities for ligands may be expressed in neurons through different combinations of the NMDAR1/R2 subunits, as well as the NMDAR1 splice variants. Differential expression and localization of the NMDAR1 subunits in various brain regions or even within a single neuron, e.g., cell body versus dendrites, could influence the responses of neurons to synaptically released L-glutamic acid.

Most synaptic NMDARs are formed by a combination of NMDAR1/R2A/R2B. Localization of the NMDAR proteins in synaptic regions is determined by the carboxyl-terminal region of the NMDAR1 and NMDAR2 subunits (NMDAR2A and 2B). Mice lacking one of the NMDAR2 subunits (NMDAR2A) have diminished NMDA receptor channel activity and a reduction in the process of induction of LTP in CNS neurons.

Neuronal toxicity produced by NMDA also depends on the specific combination of subunits that form the receptors in neurons. Cells of the human embryonic kidney cell line 293, for example, die when they are transiently transfected with the NMDAR1 and NMDAR2 subunits and such toxicity is greatest when NMDAR1 and NMDAR2A are coexpressed, less if NMDAR2B is coexpressed with NMDAR1, and it is not apparent when the NMDAR2C subunit is coexpressed with NMDAR1.

mGluR Genes and Proteins

Eight forms of mGLUR genes have been identified (Figure 4). Group I are the mGluR1 and mGluR5, group II are the mGluR2 and mGluR3, and group III are mGluR4 and mGluR6–8. The activation of PLC by mGluR1 and 5 appears to involve transduction of the signal through coupling of the receptor proteins with either the Gi–Go family of GTP-activated proteins (G proteins) or the Gq family. All of the group II and III mGluR proteins appear to be coupled to the Gi–Go

family of G proteins. All mGluR proteins have a large extracellular amino terminal domain, which contains a region that is homologous to bacterial periplasmic binding proteins. It is likely that the glutamate-binding sites on mGluRs are within this extracellular domain. Insertions or deletions due to alternative mRNA splicing are confined to the carboxyl-terminal region and do not disrupt the amino terminal domain of mGluRs.

Glutamate Receptors, Ca^{2+}-Signaling, and Synaptic Plasticity

Coincidence of action potentials in spines and dendrites with synaptic activation of glutamate receptors, primarily NMDARs, can enhance Ca^{2+} entry into neurons and produce long-lasting changes in synaptic activity. The timing of the two events, action potentials, and synaptic activation of receptor-induced Ca^{2+} influx, appears to be crucial. If receptors are activated after an action potential invades dendrites, it produces LTD. If it precedes or is coincident with the action potential it produces LTP. Activation of Ca^{2+} influx seems to be a key event in the expression of synaptic plasticity and neuronal adaptation but such increases in free $[Ca^{2+}]_i$ frequently work in a cooperative manner with other signaling events, such as the formation of cyclic AMP (cAMP) and the activation of cAMP-dependent protein kinase A (PKA). For example, the establishment of LTP in some neurons is strengthened by the concurrent activation of neurotransmitter receptors that activate adenylyl cyclases, such as, dopamine, muscarinic acetylcholine, and β-adrenergic receptors.

The entry of Ca^{2+} into neurons following glutamate receptor activation, especially activation of NMDA receptors, or the opening of VGCCs leads to altered gene transcription, mRNA splicing, mRNA translation, and protein synthesis. These effects are, to a substantial degree, dependent on the stimulation of several kinases, including Ca^{2+}/calmodulin (CaM)-dependent kinases (CaMK), protein kinase C (PKC), extracellular signal-regulated kinase or mitogen-activated kinase (ERK or MAPK), MAPK-ERK kinase (MEK), stress-activated protein kinase, aurora kinase and protein tyrosine kinases such as proline-rich tyrosine kinase and src kinase (Figure 6). However, not all types of Ca^{2+} influx into a cell lead to the same level of activation of gene transcription, even when the levels of $[Ca^{2+}]_i$ achieved are the same. There is clear compartmentalization of Ca^{2+} arriving at synaptic junctions as opposed to those received following generalized depolarization of a neuron. Ca^{2+} that enters following activation of either a receptor-ion channel or a VGCC apparently remains very close to the internal mouth of the channel

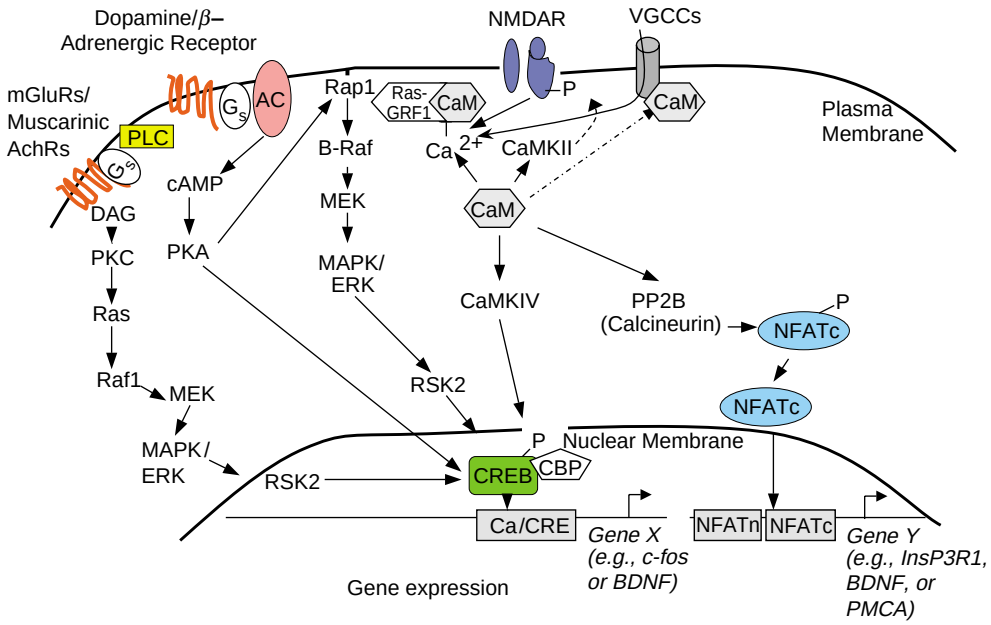

FIGURE 6 Regulation of transcription in neurons by Ca^{2+} following activation of NMDARs or VGCCs, and the interaction with pathways of gene transcription regulation following stimulation of G protein-coupled receptors. Shown is the Ca^{2+}-induced and cAMP or diacylglycerol (DAG)-induced stimulation of kinases that phosphorylate CREB and cause activation of gene transcription. Also shown is the activation by Ca^{2+} and CaM of the protein phosphatase 2B (PP2B) or calcineurin and the subsequent dephosphorylation of NFAT, the translocation of NFAT into the nucleus and the regulation of gene transcription in neurons. More details are presented in the text. CBP: CREB binding protein.

(~100 nM radius). Even if all other free Ca^{2+} in dendrites and cell bodies of neurons is chelated, the localized Ca^{2+} near ion channels still functions as an intracellular signal. Most likely readout of Ca^{2+} signaling is that of changes in the frequency of transient Ca^{2+} elevations and the most likely sensor of such frequency modulations is CaMKII. It is important to note that the mRNA for CaMKIIα is selectively transported to the dendritic region of neurons and that activation of NMDARs leads to polyadenylation of CaMKIIα mRNA and initiation of its translation through a process dependent on aurora kinase stimulation.

Stimulation of protein phosphorylation is pivotal in the activation of signal transduction cascades that lead to altered transcriptional regulation (Figure 6). A transcription factor that is sensitive to activation by several incoming stimuli and that regulates the expression of as many as 100 other genes, is the cAMP response element (CRE) binding protein (CREB). A key gene whose transcription is regulated by CREB is that for brain-derived nerve growth factor (BDNF), a gene that is known to influence the establishment of LTP. CREB activation is dependent on phosphorylation of crucial Ser residues. CaMKIV, when directly activated by Ca^{2+} and CaM in the nucleus, phosphorylates CREB. But Ca^{2+} entering neurons through NMDA and VGCCs also leads to CREB phosphorylation through the activation of MAPK/ERK and RSK2 kinases (Figure 6). Activation of the small GTPase Rap 1 follows binding of the Ca^{2+}-CaM complex to a guanine-nucleotide exchange factor, Ras guanine-nucleotide-releasing factor (Ras-GRF1, Figure 6). The same cascade of kinases can also be activated by cAMP and PKA and by diacylglycerol (DAG) and PKC, thus leading to the potential strengthening of signal transduction by Ca^{2+} following coincident activation of receptors coupled to adenylyl cyclases (AC) or those coupled to PLC (Figure 6).

Ca^{2+} entry following NMDAR or VGCC activation also leads to the stimulation of the Ca^{2+} plus calmodulin-activated phosphatase PP2B (calcineurin) and as a consequence of that, to the activation of the transcription factor nuclear factor of activate T cells (NFAT). The transcription of some 34 genes is thought to be either up- or down-regulated by NFAT in neurons. A prominent gene whose transcription is up-regulated is the $InsP_3$ receptor-ion channel (Figure 6). The activation of kinases following stimulation of glutamate receptors is thought to be a key step in the formation of LTP and memory formation, whereas the activation of calcineurin following weak stimulation of glutamate receptors is thought to cause primarily LTD. It is noteworthy also that phosphorylation of NMDARs by PKC, CaMKIIα, or protein tyrosine kinases leads to increases in the response to agonists whereas activation of calcineurin or protein tyrosine phosphatases diminishes their response. Given the importance of NMDARs in synaptic plasticity and neuronal adaptation, it is not surprising to find such complex orchestration of protein modifications by kinases and phosphatases and of the consequent alterations in the activity of the receptors.

Glutamate Receptors, Ca^{2+}, and Neurodegeneration

Excessive activation of glutamate receptors leads to neuronal degeneration in the mammalian brain, such as that occurring during ischemia, anoxia, hypoglycemia, epileptic seizures, and chronic neurodegenerative diseases, for example, Alzheimer's disease. The entry of Ca^{2+} into neurons increases the activity of the calmodulin-activated form of nitric oxide synthase (NOS). Activation of these two enzymes leads to the generation of intracellular nitric oxide radical ($NO^{\cdot}$) and superoxide anion ($O_2^{\cdot -}$), both of which appear to play a role in delayed neurotoxicity. The entry of Ca^{2+} through NMDA receptors also leads to the activation of proteases, such as Ca^{2+}-activated calpain, and enhanced proteolytic activity. Also, Ca^{2+} entry after activation of populations of non-synaptic NMDA receptors is the primary contributor to alterations in mitochondrial Ca^{2+} handling and the initiation of neuronal apoptosis.

See Also the Following Articles

Allosteric Regulation • Calcium Oscillations • Calcium Signaling: Calmodulin-Dependent Phosphatase • Calcium Signaling: Cell Cycle • Calcium Signaling: NO Synthase • Calcium, Biological Fitness of • Cyclic Nucleotide-Regulated Cation Channels • Glutamate Receptors, Ionotropic • Glutamate Receptors, Metabotropic • Ligand-Operated Membrane Channels: GABA • Neuronal Calcium Signal

Glossary

ionotropic glutamate receptors This general class of glutamate receptors represents ligand-gated, ion channel-forming receptor complexes in neuronal membranes. Channel activation occurs following the application of L-glutamate or one of its analogues. This class of receptors is further subdivided into three families of receptor-ion channels based on their sensitivity to select agonists.

long-term depression (LTD) Synaptic plasticity that occurs following low-frequency stimulation of synapses and which manifests itself as a decreased response to a subsequent single stimulus applied to the same synapses.

long-term potentiation (LTP) Synaptic plasticity that occurs following high frequency stimulation of synapses and which manifests itself as an increased response to a subsequent single stimulus applied to the same synapses.

metabotropic glutamate receptors A class of G protein-coupled glutamate receptors in neuronal membranes. These receptors may either activate phospholipase C or they may inhibit adenylyl cyclases, and they do not directly activate ion channels. This class of receptors is further subdivided into three groups, referred to as Group I–III, based on their sensitivity to select agonists and antagonists.

synaptic plasticity The adaptive changes in neurotransmission across synapses occurring as a result of repeated stimulation of a set of synapses. The changes in the electrical response of a set of synapses to a single stimulus applied after the delivery of a series of high frequency, repetitive stimuli can last for many hours or many days. These changes in synaptic efficacy are accompanied by alterations in gene transcription, protein synthesis and enzyme, ion channel, and receptor activity.

Further Reading

Cullen, P. J., and Lockyer, P. J. (2002). Integration of calcium and Ras signaling. *Nat. Rev.* **3**, 339–348.

Genazzani, A. A., Carafoli, E., and Guerini, D. (1999). Calcineurin controls inositol 1,4,5-trisphosphate type I receptor expression in neurons. *Proc. Nat. Acad. Sci. (USA)* **96**, 5797–5801.

Hollmann, M., and Heinemann, S. (1994). Cloned glutamate receptors. *Ann. Rev. Neurosci.* **17**, 31–108.

Johansen, T. N., Greenwood, J. R., Frydenvang, K., Madsen, U., and Krogsgaard-Larsen, P. (2003). Stereostructure-activity studies on agonists at the AMPA and kainite subtypes of ionotropic glutamate receptors. *Chirality* **15**, 167–179.

Kuner, T., Seeburg, P. H., and Guy, H. R. (2003). A common architecture for K+ channels and ionotropic glutamate receptors? *Trends Neurosci.* **26**, 27–32.

Madden, D. R. (2002). The inner workings of the AMPA receptors. *Curr. Opin. Drug Discov. Dev.* **5**, 741–748.

Michaelis, E. K. (1998). Molecular biology of glutamate receptors in the central nervous system and their role in excitotoxicity, oxidative stress, and aging. *Progr. Neurobiol.* **54**, 369–415.

Pin, J.-P., and Duvoisin, R. (1995). Neurotransmitter receptors I: The metabotropic glutamate receptors: Structure and functions. *Neuropharmacology* **34**, 1–26.

West, A. E., Griffith, E. C., and Greenberg, M. E. (2002). Regulation of transcription factors by neuronal activity. *Nat. Rev.* **3**, 921–931.

Yasuda, R., Sabatini, B. L., and Svoboda, K. (2003). Plasticity of calcium channels in dendritic spines. *Nat. Neurosci.* **6**, 948–955.

Biography

Elias K. Michaelis is University Distinguished Professor and Chair of Pharmacology and Toxicology and the Director of the Higuchi Biosciences Center, University of Kansas. His research program is focused on the neurochemistry, molecular neurobiology, and neuropharmacology of excitatory neurotransmission in the brain, the cell and molecular biology of alcoholism and of neuronal oxidative stress, and the molecular and cell biology of aging and neuro-degeneration.

Ligand-Operated Membrane Channels: GABA

F. Minier and Erwin Sigel
University of Bern, Bern, Switzerland

γ-Aminobutyric acid (GABA) is the major inhibitory neurotransmitter in the central nervous system. GABA is synthesized in GABAergic neurons by decarboxylation of glutamate and released in the synaptic cleft in response to an action potential. There it acts at two receptors: the ionotropic $GABA_A$ receptors (which form chloride-selective ion channels) and the metabotropic $GABA_B$ receptors (which couple to G-proteins). The $GABA_A$ receptor is an integral membrane protein and consists of five protein subunits that surround a central ion pore. Binding of the neurotransmitter GABA triggers a conformational change in the receptor leading to the opening of the pore. Clinically used benzodiazepines promote this opening. As a consequence, further electrical activity of the neuron will be suppressed. This article deals with the synthesis, transport, and degradation of GABA, the $GABA_A$ receptor and its binding site for benzodiazepine-type drugs.

Handling of the Neurotransmitter GABA: Biosynthesis, Transport, and Degradation

γ-Aminobutyric acid (GABA) is synthesized from glutamate in the cytosol of GABAergic neurons by two types of glutamic acid decarboxylase (GAD), namely, GAD65 and GAD67, according to their molecular weights (Figure 1). GAD65 is important for the local control of GABA synthesis at the synaptic sites, whereas GAD67, more widely distributed in the cell, is responsible for maintaining GABA baseline levels. Presynaptic membrane depolarization triggers release of GABA into the synaptic cleft. After the activation of $GABA_A$ and $GABA_B$ receptors, GABA is taken up in surrounding neuronal and glial cells by high-affinity GABA transporters (GATs). This re-uptake may contribute to the termination or modulation of GABA neuronal transmission. GABA transporters belong to a superfamily of Na^+/Cl^--dependent neurotransmitter transporters. Four GABA transporters have been cloned: GAT-1, GAT-2, GAT-3, and BGT-1. They are expected to be 12 transmembrane domain proteins with both intracellular N and C termini, and an extracellular loop between transmembrane domains 3 and 4. Each of these transporters displays specific features: GAT-1 seems to be highly expressed throughout the brain at a neuronal presynaptic localization, while GAT-2 is mainly extraparenchymal and found in the meninges. GAT-3 displays a similar macroscopic distribution as GAT-1. It is expressed both in presynaptic neurons and astrocytes. BGT-1 is weakly expressed throughout the brain in postsynaptic neuronal cells. The GABA degradation pathway, called GABA shunt, is one of the energy synthetic pathways in the brain. This pathway is composed of consecutive actions of three enzymes. The mitochondrial enzyme GABA-transaminase (GABA-T) catabolizes GABA to succinic semialdehyde (SSA). Then, SSA is converted either to succinic acid (a substrate for the Krebs cycle) by succinic semialdehyde dehydrogenase (SSADH) or to γ-hydroxybutyrate (GHB) by succinic semialdehyde reductase (SSAR). All these pathways are summarized in Figure 1.

Early $GABA_A$ Receptor Biochemistry

Indirect evidence suggested a close relation of the $GABA_A$ receptor and the benzodiazepine-binding site. The benzodiazepine drugs are widely used for their sedative, anxiolytic, muscle relaxant, and anticonvulsant action. Affinity chromatography directed at the benzodiazepine-binding site led to the isolation of a pure protein complex with binding properties expected for the $GABA_A$ receptor and for its chloride pore. This demonstrated the presence of benzodiazepine-binding sites within the $GABA_A$ receptor. The subunits of the complex had a molecular mass of 49–58 kDa and the entire complex of ~250 kDa.

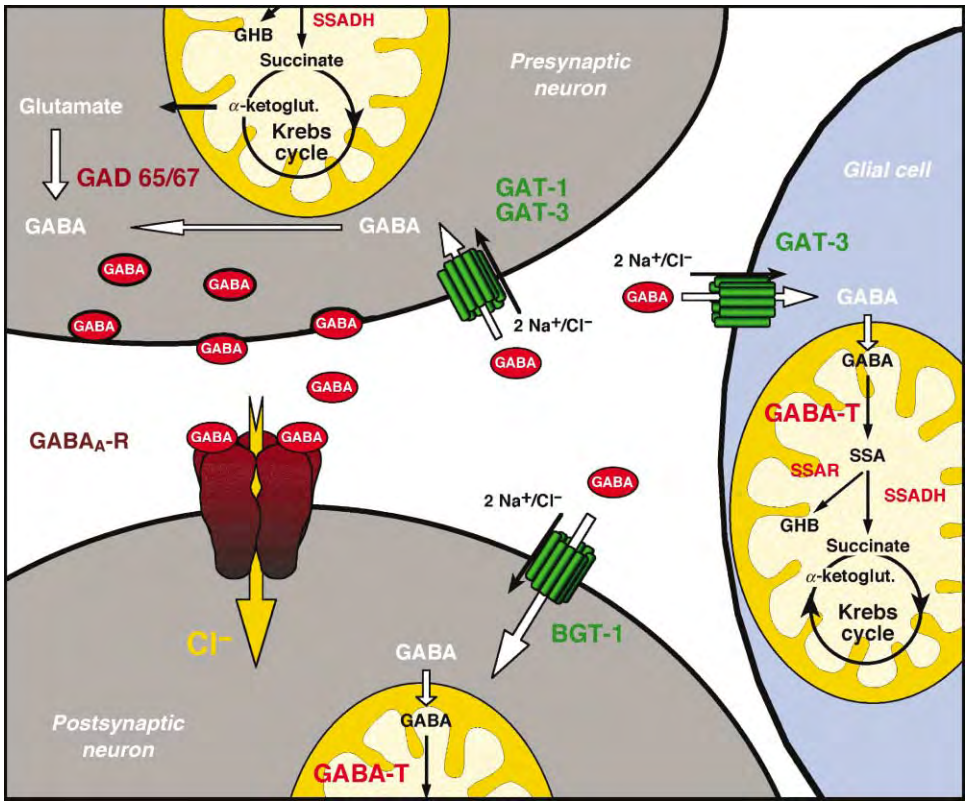

FIGURE 1 GABAergic synapse and main GABA metabolic pathways. GABA is synthesized from glutamate by the enzyme glutamate decarboxylase (GAD). Glutamate itself is synthesized from α-ketoglutarate (α-ketoglut.). The end of its action is determined by the GABA transporters of the GAT type or BGT-1 (for betaine/GABA transporter) and intracellular degradation by GABA transaminase (GABA-T) to succinic semialdehyde (SSA) and subsequently by succinic semialdehyde reductase (SSAR) to γ-hydroxybutyrate (GHB) or by succinic semialdehyde dehydrogenase (SSADH) to succinate, which is part of the Krebs cycle. Succinate in turn is converted to α-ketoglutarate.

Later it became clear that five subunits surround the central ion pore.

Molecular Biology of the $GABA_A$ Receptor

Two $GABA_A$ receptor subunits were initially cloned. Hydrophobicity analysis indicated the presence of four membrane spanning regions (Figure 2B). The second transmembrane segment of each of the five subunits contributes to the ion pore. Initial cloning was quickly followed by cloning of closely related subunits α_{1-6}, β_{1-3}, γ_{1-3}, δ, ε, θ, π. At the genomic level these subunits are organized on chromosomes in clusters, raising the possibility of a cluster specific regulation of expression (Table I). If the degree of amino acid sequence identity was $>80\%$ subunits were grouped under the same Greek letter, if it was lower a new Greek letter was used. In both cases subunits share predicted topology and there are many conservative substitutions of amino acid residues. With a sequence identity of $\sim 20\%$, the subunits are also homologous to subunits of the other members of the channel family including the nicotinic acetylcholine receptor, the glycine receptor, and the 5HT3 receptor. Thus, 16 subunits of the $GABA_A$ receptor are available and frequently many of them are coexpressed in the same cell. On the other hand, only five subunits can be accommodated in a single channel. It is today not known how many different $GABA_A$ receptors exist and what their subunit composition is, but this diversity of subunits indicates that there may exist a large variety of $GABA_A$ receptors. The major adult $GABA_A$ receptor isoform is likely to be composed of $2\alpha_1$, $2\beta_2$, and $1\gamma_2$ subunits. Attempts to demonstrate coassembly of different subunit isoforms into a common pentamer have included immunoprecipitation and subsequent analysis of the precipitate, a type of approach heavily relying on excellent quality antibodies.

It is a major challenge for basic research to bring order in this subunit chaos, to establish the subunit composition of $GABA_A$ receptors really existing *in vivo* and most importantly to find drugs that selectively modulate their function.

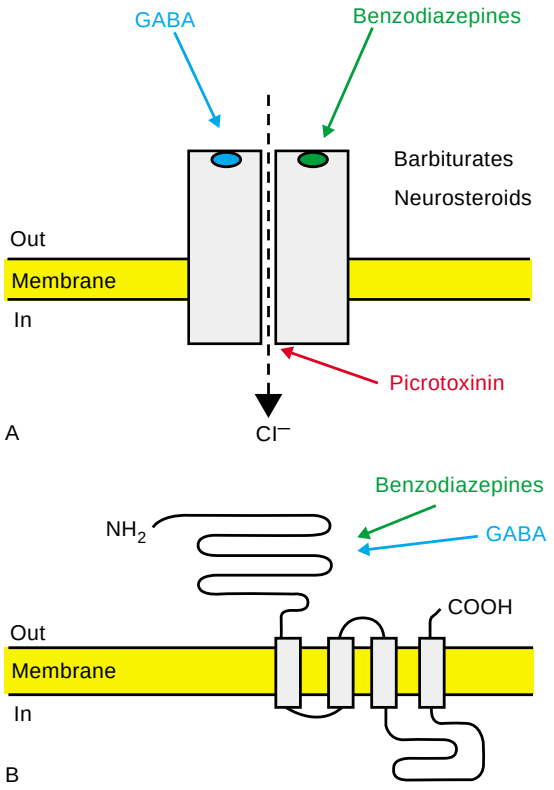

FIGURE 2 (A) The $GABA_A$ receptor is built of five membrane protein subunits that surround a central chloride selective channel. Opening of this ion channel is caused by a conformational change in the protein occurring as a consequence of the binding of the channel agonist GABA. Various drugs (benzodiazepines and neurosteroids) modify channel opening and picrotoxinin blocks the pore. (B) Topology of a subunit characterized by a large N-terminal extracellular domain carrying the drug-binding sites. The second transmembrane domain lines the ion channel. The large loop between transmembrane segments 3 and 4 carries sites for posttranslational modification (phosphorylation).

TABLE I

At Genomic Level $GABA_A$ Receptor Subunits are Organized in Gene Clusters Whose Chromosomal Location is Given for the Human Species

Subunits	Locus
δ	1p
α_2, α_4, β_1, γ_1	4p14–p12
α_1, α_6, β_2, γ_2, π	5q31–q35
α_5, β_3, γ_3	15q11–q13
α_3, ε, θ	Xq28

Physiological Function

In Situ Studies

GABA induces a conformational change in the receptor protein, such as to allow chloride ion flux. This ion flux may be measured as current flowing through the membrane by using electrophysiological techniques. Current amplitude depends on the concentration of GABA applied. While it is thought that the synaptic cleft is briefly flooded with GABA during activation of the synapse and as a consequence receptors on the postsynaptic membrane are maximally activated, a graded response may be obtained in artificial systems. As a consequence of chloride channel opening the membrane potential of the corresponding neuron will tend to move towards the chloride equilibrium potential which is about −75 mV in mature neurons. In case the $GABA_A$ receptor has a postsynaptic localization, this opening of chloride ion channels following neurotransmitter release from the presynaptic neuron will be brief (~50 ms) and transient. These receptors mediate fast synaptic inhibition. GABA will then partially diffuse out of the synaptic cleft and trigger opening of extrasynaptic receptors. In this case opening will be prolonged and a tonic inhibition will result.

Modulation

Benzodiazepines, neurosteroids, and barbiturates modulate the ion flux, while picrotoxinin inhibits it by blocking the pore and bicuculline, a plant alkaloid, acts at the GABA site as competitive inhibitor. Modulation by benzodiazepines will be briefly summarized here. On their own classical benzodiazepines (such as diazepam) do not induce opening of the ion pore. If they are co-applied with the agonist GABA, they lead to an increase in the current (Figure 3) through an allosteric increase of the affinity of the receptor for GABA. At the single channel level this stimulation is evident as an increase in channel open frequency, at least when GABA is applied at submaximal concentrations. These benzodiazepines are therefore called positive allosteric modulators. There exist competitive antagonists (such as Ro 15-1788) and negative allosteric modulators as illustrated here with the β-carbolines (Figure 3). The picture is complicated by the fact that there exists a continuum of partial positive and negative allosteric modulators.

In Vitro Studies

Heterologous expression has been used to identify subunit isoforms that can form together a functional pentamer. This has been possible in cases where a certain subunit isoform confers to the receptor distinct functional properties. Such studies established, for example, that the combination of α- and β-subunits produces GABA-gated currents, but coexpression of a γ-subunit is required for benzodiazepine sensitivity of the expressed receptors. It has also been possible to exclude many theoretically possible subunit combinations.

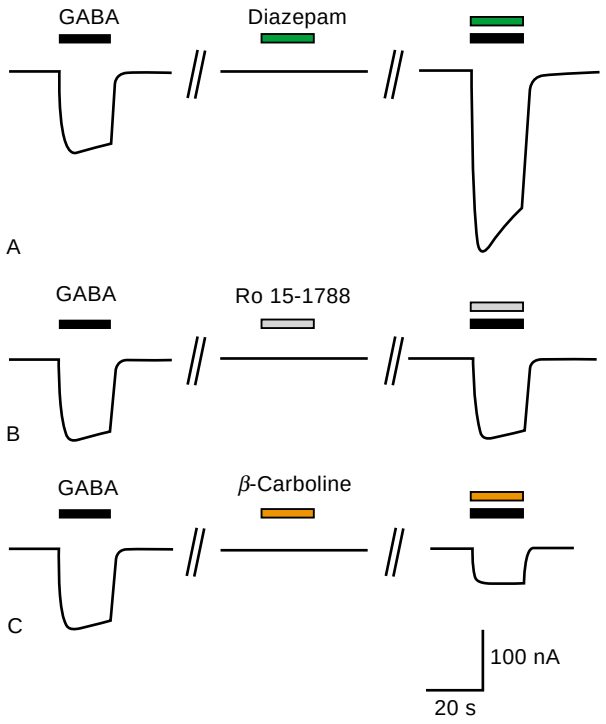

FIGURE 3 (A) Superfusion of a cell expressing $GABA_A$ receptors with GABA induces an ion current that is measured using the two-electrode voltage clamp technique. Superfusion of the same cell with the positive-allosteric modulator diazepam (prototype of benzodiazepines) does not elicit any current response while combined application of GABA and diazepam elicits a much bigger response than GABA alone. (B) Analogous experiments with the benzodiazepine antagonist Ro 15-1788, which binds with high affinity to the benzodiazepine binding site but fails to alter the current responses. (C) Analogous experiment with a negative allosteric modulator of the β-carboline class, leading to a decrease in the current response.

Transgenic Mice

Transgenic mice either lacking a subunit isoform or carrying a diazepam-insensitive subunit isoform have been used to assign function or drug effects to an individual subunit isoform. Such studies have shown that α_1 is mainly responsible for the sedative effects and α_2 for anxiolysis induced by diazepam and α_5 is involved in memory functions.

Binding Sites

Following techniques have contributed to the description of amino acid residues involved in the interaction with the channel agonist GABA, its competitive antagonists, for ligands of the benzodiazepine-binding site and for picrotoxinin: photoaffinity labeling, point mutation combined with either ligand-binding studies or functional characterization, cysteine point mutant water accessibility as determined by covalent modification by a cysteine reactive reagent and its protection by the corresponding ligand. The binding sites of other drugs such as neurosteroids and barbiturates are still characterized to a lesser extent. Amino acid residues located in the N-terminal extracellular part of both the β_2- and α_1-subunits are taking part in the formation of the agonist-binding site, while residues on the α_1- and γ_2-subunits are taking part in the formation of the benzodiazepine-binding site in the major isoform of the $GABA_A$ receptor. Both binding sites are thus located at subunit interfaces. Interestingly, both sites show a high degree of homology to each other, but only at the structural level and not at the functional level, as GABA can and benzodiazepines cannot open the channel. It should be noted that the benzodiazepine-binding site not only accepts benzodiazepines as allosteric modulators, but also some drugs with β-carboline, imidazopyridine, triazolopyridazine, and cyclopyrrolone structures.

Recently, an acetylcholine-binding protein homologous to the N-terminal extracellular portion of the nicotinic acetylcholine receptor has been crystallized. The $GABA_A$ receptor shares structural and to a small extent sequence homology with the crystallized protein. The crystallized protein in its native state is able to bind acetylcholine and a cavity putatively binding this ligand has been identified. As the agonist-binding sites of the ligand-gated ion channel family have been conserved and as the binding pocket for benzodiazepines is homologous to the agonist site, this cavity must then be homologous to the binding pocket for benzodiazepines. The binding site is located in a cleft between two subunits. This fits very well with the data obtained using classical methods, which indicated importance of the corresponding amino acid residues on α_1 and γ_2 which participate in the formation of the binding site. Thus, in $\alpha_1\beta_2\gamma_2$ $GABA_A$ receptors the binding pocket for benzodiazepines is located in a subunit cleft between γ_2- and α_1-subunits in a position homologous to the agonist-binding site for GABA that is located between α_1- and β_2-subunits (Figure 4).

Subtly Altered Receptor Subunits Cause Diseases

In two different cases human point mutations in the γ_2-subunit have been shown to occur in families with inherited forms of epilepsy. In both cases the mutation has been tightly linked to the disease and in both cases chloride ion flux is decreased, leading to a reduced state of neuronal inhibition. It can be anticipated for the future that many other diseases will be linked to isoforms of this important receptor. The $GABA_A$

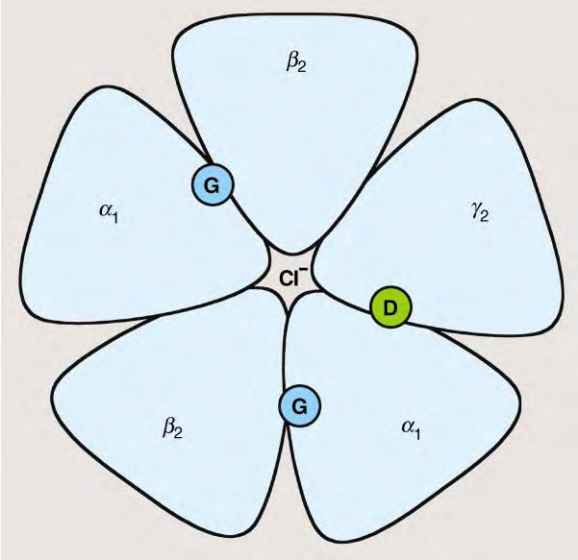

FIGURE 4 Subunit arrangement of the major isoform of the $GABA_A$ receptor showing the arrangement of subunits around the central ion channel as seen from the synaptic cleft. The benzodiazepine-binding site (D) is located at the $\gamma_2\alpha_1$-subunit interface in a homologous position to the two GABA (G) binding sites located at $\beta_2\alpha_1$-subunit interfaces.

receptor has especially been implicated in pathological anxiety, insomnia, and epilepsy.

Architecture

The structure of the acetylcholine-binding protein has given an idea of how the extracellular domain of the $GABA_A$ receptor could look like. The availability of a crystal structure of a protein homologous to the binding domain has also allowed establishment of the steric orientation of the subunits. From the study of covalently linked subunits, it has been concluded that the arrangement of subunits of the major $GABA_A$ receptor isoform is $\beta\alpha\gamma\beta\alpha$. However, this still allows for a clockwise or counterclockwise arrangement. Figure 4 shows the correct arrangement as viewed from the synaptic cleft taking in account the information provided by the crystallization study.

See Also the Following Articles

$GABA_B$ Receptor • Neurotransmitter Transporters • Nicotinic Acetylcholine Receptors

Glossary

chloride equilibrium potential Membrane potential at which opening of chloride ion selective channel mediates no net ion flux due to the concentration gradient of the corresponding ion.

conservative substitution Replacement of an amino acid residue by a residue with similar chemical properties.

heterologous expression Introduction of genetic information in the form of cDNA or cRNA is introduced into a foreign cell where the encoded protein is synthesized.

hydrophobicity analysis Scan of an amino acid residue sequence predicted by the coding cDNA is scanned for the average hydrophobicity of succeeding amino acid residues. A longer hydrophobic stretch is indicative of a transmembrane sequence in the protein.

voltage clamp Imposition of a desired membrane potential on a cell using electrophysiological techniques.

Further Reading

Barnard, E. A., Skolnick, P., Olsen, R. W., Mohler, H., Sieghart, W., Biggio, G., Braestrup, C., Bateson, A. N., and Langer, S. Z. (1998). International union of pharmacology: XV. Subtypes of gamma-aminobutyric acid A receptors: Classification on the basis of subunit structure and receptor function. *Pharmacol. Rev.* **50**, 291–313.

Borden, L. A. (1996). GABA transporter heterogeneity: Pharmacology and cellular localization. *Neurochem. Int.* **29**, 335–356.

Macdonald, R. L., and Olsen, R. W. (1994). $GABA_A$ receptor channels. *Annu. Rev. Neurosci.* **17**, 569–602.

Moss, S. J., and Smart, T. G. (2001). Constructing inhibitory synapses. *Nat. Rev. Neurosci.* **2**, 240–250.

Rabow, L. E., Russek, S. J., and Farb, D. H. (1995). From ion currents to genomic analysis, recent advances in $GABA_A$ receptor research. *Synapse* **21**, 189–274.

Rudolph, U., Crestani, F., and Möhler, H. (2001). GABA(A) receptor subtypes: Dissecting their pharmacological functions. *Trends Pharmacol. Sci.* **22**, 188–194.

Sieghart, W., Fuchs, K., Tretter, V., Ebert, V., Jechlinger, M., Hoger, H., and Adamiker, D. (1999). Structure and subunit composition of GABA(A) receptors. *Neurochem. Int.* **34**, 379–385.

Sigel, E., and Buhr, A. (1997). The benzodiazepine binding site of $GABA_A$ receptors. *Trends Pharmacol. Sci.* **18**, 425–429.

Biography

Erwin Sigel is an Associate Professor at the Department of Pharmacology at the University of Bern, Switzerland. His principal research interests are the $GABA_A$ receptors. He holds a Ph.D. from the Swiss Federal Institute of Technology (ETH), Zürich and received his first postdoctoral training at the Imperial College of Science and Technology, London. He has biochemically isolated the $GABA_A$/benzodiazepine receptor and later studied its binding sites.

Frédéric Minier obtained his Ph.D. in Neurosciences from the Pierre & Marie Curie University (Paris VI). His main research interest focuses on epilepsies and structural and functional studies of $GABA_A$ receptors. He is currently a postdoctoral fellow in the laboratory of Dr. Sigel.

Light-Harvesting Complex (LHC) I and II: Pigments and Proteins

Stefan Jansson
University of Umeå, Umeå, Sweden

Light-harvesting systems are present in the photosynthetic apparatus of all photosynthetic organisms. These systems are not necessary for the photosynthetic reaction but they increase the capacity for harvesting light and, in addition, have important regulatory functions. Light-harvesting systems typically have a very high pigment/protein ratio and are thus a cost-efficient way of maximizing light-harvesting capacity. The protein components serve as backbones that organize the light-harvesting pigments in a way that ensures that the absorbed light energy is efficiently transferred from the pigment first excited into the photosynthetic reaction center, where charge separation takes place.

Heterogeneity of Light-Harvesting Systems

Different taxa of photosynthetic organisms have organized light-harvesting systems in different ways, i.e., have rather different light-harvesting proteins and pigments. In fact, phylogenetic grouping of photosynthetic organisms is often based on their light-harvesting pigments. Green sulfur bacteria get their color from bacteriochlorophyll *c*, *d*, or *e* in the chlorosome complex, red algae from phycoerythrin, and cyanobacteria from phycocyanin in their phycobilisomes. Green algae and higher plants have chlorophyll (chl) *a* and *b* in their LHC I and LHC II. The antenna proteins from these phylogenetic groups complexes share no sequence homology and light-harvesting systems are therefore likely to have evolved several times in contrast to photosynthetic reaction centers that seem to have only evolved once. The LHC systems of all higher plants (angiosperms, gymnosperms) as well as ferns, mosses, and green algae are, however, homologous structures and have a lot in common and these antenna systems will be described using examples from angiosperms, whose antennas are best studied.

The Higher Plant Light-Harvesting Antenna

The higher plant LHC proteins bind, via noncovalent bonds, the antenna pigment chl *a*, chl *b*, and a set of xanthophylls (carotenoids). The LHC proteins of most plants bind the same set of xanthophylls, lutein, violaxanthin (that can get photoconverted), and neoxanthin, although some plant species may contain unusual light-harvesting carotenoids. Since the excited state of chl *b* has a higher energy as compared to that of chl *a*, the preferred energy transfer path is from chl *b* to chl *a*. This energy transfer is supposed to take place through the Förster mechanisms, i.e., excitation energy can jump between electrons in neighboring pigment molecules by a dipole–dipole mechanism. The chl molecules bound to the LHC proteins are, however, in different chemical environments and have thus different excitation energies, so some chl *a* molecules have slightly lower energy than the others. The differences in energy levels in general are typically small, so the energy transfer direction is not unidirectional and many jumps between antenna pigments could occur before it ends up in the reaction centers that have the lowest energy levels. Other light-harvesting systems are, however, organized slightly differently. In phycobilisomes of cyanobacteria and red algae, peripheral pigments have considerably higher energy levels than those closer to the reaction center so energy transfer there is unidirectional.

The Protein Components

The Lhca and Lhcb Proteins

There are ten major LHC proteins in angiosperms, whose genes are designated Lhca1–4 and Lhcb1–6. The Lhca genes code for LHC proteins associated with photosystem I, whereas the Lhcb3–6 proteins associate with PS II. Lhcb1 and Lhcb2 serve as antenna for both photosystems. Although all these proteins share a common secondary structure with three

membrane-spanning regions, embedded in the thylakoid membrane of the chloroplasts, their tertiary structure differ. Lhcb1, Lhcb2 that typically are much more abundant than the others, form together with Lhcb3 trimeric complexes, the Lhcb4–6 (commonly named CP29, CP26, and CP24) proteins are monomeric, and the Lhca proteins seem to form dimers. This organization is not static, for example, Lhcb1 and Lhcb2 can monomerize and Lhcb5 can form trimers. The true molecular weight of each protein varies only slightly between different plants, although the apparent mobilities change considerably both with plant species and gel systems used, but they all fall within the range of 20–30 kDa. Since several of the proteins typically comigrate, identification solely based on molecular weight is often not possible.

Structure of the LHC Complexes

In the monomeric structure, two homologous membrane-spanning regions form the core of the complex. Closely associated with these are two carotenoid molecules that in the case of LHC II are lutein. A third membrane-spanning region is located more peripheral in the complex, and a short C-terminal helix, not spanning the membrane, is located on the lumenal side of the complex. Fourteen chlorophyll molecules (eight chl *a* and six chl *b*) are bound to each monomer, with the head groups in the interior of the complex and the phytol tails protruding toward the surrounding membrane.

Organization of LHC II

The organization of the LHC proteins around PS II in the so-called "PS II supercomplex" is shown in Figure 1. The monomeric CP29 and CP26 proteins associate most closely with the core complex, and CP24 sits next to CP29. LHC II trimers (consisting of trimers of Lhcb1, Lhcb2, and Lhcb3 in different combinations) attach to the monomeric proteins, which thus form a bridge between the trimeric proteins and the core. In the "supercomplex," only three trimers could attach to each PS II center. In low light conditions, there are more trimers functionally attached to each PS II, but the positions of these are not yet known. A larger complex of seven trimers has been observed, but it is not known to what extent such complexes exist *in vivo* and to what they are associated.

Organization of LHC I

The subunit position in LHC I is not fully understood, but the proteins seem to bind to only one side of the PS I complex. Lhca1 and Lhca4 form a heterodimer, named LHCI-730 after its characteristic low-temperature fluorescence emission peak, and Lhca2 and Lhca3 may perhaps also form heterodimers. The latter two proteins are also based on the fluorescence emission of isolated complexes, named LHCI-680, although it is likely that they, in the purified forms, have lost chlorophylls emitting at long wavelengths that *in vivo* associate with the complexes, so the name is actually misleading. The long-wavelength emitting chlorophylls make up a small portion of the total pool of LHC I pigments. These are kept in a chemical environment that results in an absorption shifted to longer (red) wavelengths and their role seems to be to allow use of wavelengths just outside of the visible spectrum to excite PS I, despite the fact that they have lower energy than that of the PS I reaction center. In addition to the LHC I subunits, a fraction of the LHC II trimers associate with PS I. The attachment site for these seems to be opposite to that of LHC I, so excitation energy presumably transfers directly from the trimers to the PS I core, not via LHC I.

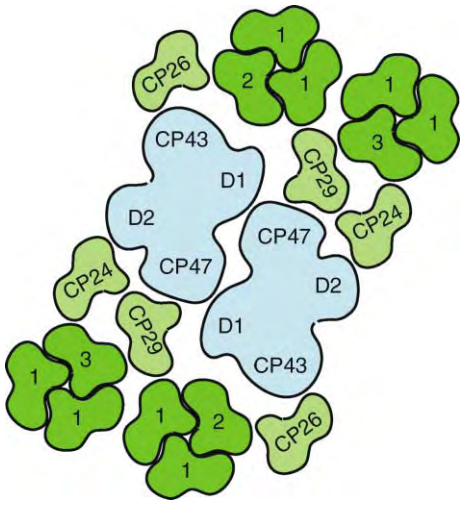

FIGURE 1 Schematic representation of the photosystem II dimer including the peripheral antenna. D1 and D2 are reaction center polypeptides, CP43 and CP47 core antenna proteins, CP24, CP26, and CP29 are monomeric LHC proteins, and 1, 2, and 3 denote tentative positions of Lhcb1, Lhcb2, and Lhcb3 proteins, respectively, in the peripheral LHC II trimers.

The Pigment Components

The pigment/protein stoichiometry of the LHC proteins has been surprisingly hard to determine and is still somewhat uncertain. The LHC II trimer is the most "pigment dense" complex and may bind in total 24 chl *a*, 18 chl *b*, 6 lutein, 3 neoxanthin, and 3 violaxanthin molecule. CP29 may bind 7 chl *a*, 2 chl b, and one each of the three carotenoids, and CP26 one additional chl *b*. The individual Lhca proteins, on the other hand, may associate with about 14 chlorophylls, one or two luteins, a small amount of violaxanthin and perhaps also trace amounts of β-carotene, a nonxanthophyll carotenoid. The functions of the carotenoids are more complex than

those of the chlorophylls. Carotenoids are indeed antenna pigments, also harvesting lights at wavelengths (~500 nm) where the chlorophylls have a low absorptivity, enabling plants to efficiently utilize daylight, although the chlorophylls mainly absorb in the red and blue regions of the spectrum. In addition, they have an equally important function in photoprotection against excess light. Photoprotective processes are necessary in the antenna systems if the excitation energy is not able to quickly enter into the reaction centers but stays in the antenna system for prolonged times. This could, for example, happen if the energy-consuming reactions downstream of the photosynthetic light reaction are not able to utilize the energy in the same speed as it is generated, for example, if the system is at low temperature when enzymatic reactions are slow. This creates a block in electron flow away from the reaction centers that will not be able to accept another energy package from the antenna. Excited chlorophyll molecules can, via a triplet state, under such circumstances produce singlet oxygen molecules that are highly reactive and thus dangerous for the system.

Mechanisms of Photoprotection

The molecular details behind the roles of carotenoids in photoprotection are not fully understood, but it involves both direct effects (quenching of reactive oxygen species) and an indirect effect, namely, an increase in energy dissipation in the antenna resulting in loss of excitation energy. This process, named "feedback de-excitation" or "qE type of nonphotochemical quenching," is mediated by PsbS, a protein related to the LHC proteins. Feedback de-excitation is triggered (within seconds) when the lumenal pH drops below a certain point, as a result of photosynthetic proton pumping over the thylakoid exceeding the backflow through the ATP synthase complex. The PsbS protein is then protonated but the low pH does also bring about a change in the photosynthetic xanthophylls (the xanthophyll cycle), violaxanthin is converted to zeaxanthin via antheraxanthin by the enzyme violaxanthin de-epoxidase, activated by the low lumenal pH. Zeaxanthin accumulates in the antenna and is also found free in the thylakoid membrane. Zeaxanthin could protect directly against oxygen radicals, but when zeaxanthin is bound to protonated PsbS, a conformational change takes place resulting in the creation of a highly quenching species (perhaps a chl *a* dimer) that relieves the excitation pressure from the system into heat, and thus contributes to photoprotection. Only a small fraction of the zeaxanthin formed is, however, associated with PsbS; most of the other LHC proteins can also have zeaxanthin bound to them, but whether this also contributes to photoprotection is not clear. Zeaxanthin is backconverted to violaxanthin when the light level drops.

Other Regulatory Roles

LHC II is also involved in another regulatory process, referred to as state transitions based upon the different "states" of chl fluorescence that can be obtained by treating the plant with light of different quality. If the plant is exposed to light preferentially absorbed by PS I (wavelengths >680 nm) or "normal" light, the fraction of LHC II trimers functionally associated with the photosystems can change in order to create an even excitation pressure of the photosystems. Overcapacity of PS II leads to over-reduction of the interphotosystem electron carriers that, subsequently, leads to the induction of an LHC II kinase. Phosphorylation of LHC II results in a reduction of the PS II antenna size, releasing the system from the imbalance. There is a connection between light quality and quantity, LHC II phosphorylation, LHC II migration between the different thylakoid regions and the amount of *grana* stacking, but the details are not yet fully understood. In any case, the reversible phosphorylation takes place on a Thr or Ser residue close to the N terminus of the protein, which protrudes into the stroma. The phosphorylation leads presumably to a conformational change that, in turn, changes the properties of the complex.

The amount of LHC proteins varies considerably in different light regimes. Higher light results in decreased amounts of LHC and, as a consequence, since chl *b* is confined to the LHC proteins, an increased chl *a*/*b* ratio of the plant. Hence, this ratio is an indicator of the amount of antenna protein and, thus, antenna size of the plant. This is an acclimation to the conditions when light harvesting is not limiting for photosynthesis. However, the different LHC proteins do not decrease simultaneously: the quantity of Lhcb1 and Lhcb2 (making up the bulk of the trimers) is most variable; but at full sunlight, Lhcb1 and Lhcb2 quantities are low, and the other LHC proteins also decrease in abundance.

See Also the Following Articles

Chlorophylls and Carotenoids • Photosynthesis • Photosystem I, Structure and Function • Photosystem II Light Harvesting System: Dynamic Behavior • Photosystem II: Assembly and Turnover of the D1 Protein • Photosystem II: Protein Components • Photosystem II: Water Oxidation, Overview

Glossary

LHC I The light-harvesting system containing proteins and pigments, associated with PS I.

LHC II The light-harvesting system containing proteins and pigments, associated with PS II.

xanthophyll cycle The light-dependent conversions of the three xanthophylls – violaxanthin, antheraxanthin, and zeaxanthin. It plays a significant role in photoprotection.

Further Reading

Bassi, R., Giuffra, E., Croce, R., Dainese, P., and Bergantino, E. (1996). Biochemistry and molecular biology of pigment binding proteins. In *Light as an Energy Source and Information Carrier in Plant Physiology* (R. C. Jennings, G. Zucchelli, F. Ghetti and G. Colombetti, eds.) pp. 41–63. Plenum Press, New York.

Horton, P., Ruban, A. V., and Walters, R. G. (1996). Regulation of light harvesting in green plants. *Annu. Rev. Plant Physiol. Plant Molecul. Biol.* **47**, 655–684.

Jansson, S. (1994). The light-harvesting chlorophyll *a/b* binding-proteins. *Biochim. Biophys. Acta – Bioenergetics* **1184**, 1–19.

Jansson, S. (1999). A guide to the Lhc genes and their relatives in Arabidopsis. *Trends Plant Sci.* **4**, 236–240.

Niyogi, K. K. (1999). Photoprotection revisited: Genetic and molecular approaches. *Annu. Rev. Plant Physiol. Plant Molecul. Biol.* **50**, 333–359.

Young, A. J., and Britton, G. (1993). *Carotenoids in Photosynthesis*. Chapman and Hall, London.

Biography

Stefan Jansson, a Professor of Plant Cell and Molecular Biology at Umeå University in Sweden, has studied the light-harvesting antenna of higher plants using a variety of methods. He has used gene technology to create plants lacking the different LHC components, and the analysis of these has given data on the functions of the individual polypeptides.

Lipases

Howard L. Brockman
University of Minnesota, Austin, Minnesota, USA

Lipases are water-soluble, ester hydrolases that are traditionally defined by their marked preference for apolar, water-insoluble ester substrates. This group of enzymes also includes species referred to as cholesterol esterases. Lipases and cholesterol esterases are distinguished from phospholipases that catalyze the hydrolysis of acyl ester bonds of highly amphipathic phospholipids having an *sn*-glycero-3-phospho-X moiety and from carboxylesterases that hydrolyze polar, water-soluble esters. These distinctions are relative, however, because some lipases exhibit activity toward phospholipids or soluble esters. Typical natural lipase substrates include, in order of amphipathicity, long aliphatic chain acyl esters of cholesterol (cholesteryl esters), triacyl esters of glycerol (triacylglycerols), acyl esters of long chain alcohols (wax esters), diacyl esters of glycerol (diacylglycerols) and monoacyl esters of glycerol. Because lipase substrates tend to be oily and only weakly amphipathic, they reside primarily in a bulk oil phase in preference to the aqueous phase or to the interface, i.e., monomolecular surface phase that separates the bulk oil and aqueous phases. It follows, because lipases are water-soluble enzymes, that the site of lipolysis is the quasi-two-dimensional interface. The focus of basic research on lipases has been to understand how a reaction involving such a change in dimensionality can occur and how it is regulated. Medically, lipases are targets for therapeutic intervention in the treatment of obesity. The focus of applied research with lipases has been to exploit the unusual properties of lipolytic systems for the production of chiral pharmaceuticals, improved detergents, and designer fats.

Roles of Lipases

In times of abundant energy supply cells accumulate triacylglycerols or wax esters as energy storage depots. This is exemplified by adipose tissue in animals and by the formation of seed oils in plants. Cholesteryl ester storage provides a potential reservoir of cholesterol for steroidogenic tissues. Triacylglycerol and cholesteryl ester accumulation also provides a mechanism of cellular defense by ameliorating the toxic effects of excess fatty acids and cholesterol. Most notable in this regard is the accumulation of cholesteryl esters in the arterial endothelium during atherogenesis. The mobilization of these bulk lipid inclusions intra- and extracellularly is catalyzed by lipases and cholesterol esterases. Once the ester bond is split, the more amphipathic hydrolysis products can be used metabolically or mobilized, in higher organisms, for transport among tissues. Because of the requirement, for hydrolysis for transport, lipases are key enzymes in maintaining lipid homeostasis in multi-organ animals and plants. For example, in mammals there are secreted gastric and pancreatic lipases for digesting dietary lipids. From the resulting hydrolysis products, long-chain fatty acids and monoacylglycerols, triacylglycerols are resynthesized in the intestinal wall. These circulate in the form of lipoproteins that are then subjected to hydrolysis by lipoprotein lipase for entry into peripheral tissues and by hepatic lipase for entry into the liver, respectively. Within peripheral tissues, e.g., adipose tissue, triacylglycerols are resynthesized and, when needed, are mobilized by hormone-sensitive lipase/cholesterol esterase. The resulting fatty acids re-enter the circulation for transport back to the liver for re-esterification or to organs like muscle and heart for energy generation.

Hydrolysis Mechanism and Specificity

The catalytic domain of lipases contains both lipid binding determinants and the active site. The core structure of the catalytic domain is an α/β-hydrolase fold, a motif common to other classes of hydrolases, that consists of β-sheets connected by α-helices. This supports a Ser–His–Glu/Asp catalytic triad resembling that of serine proteases and other hydrolytic enzymes. The active site serine is contained in a consensus sequence of Gly–X–Ser–X–Gly that forms a tight turn exposing the serine hydroxyl group to the scissile ester bond of the substrate. The general mechanism of the reaction catalyzed by lipases is shown in Figure 1.

Substrate specificity among various lipases is variable because of the long flexible hydrocarbon-like groups that must be accommodated by the active site. This is in contrast to carboxylesterases that act on more soluble

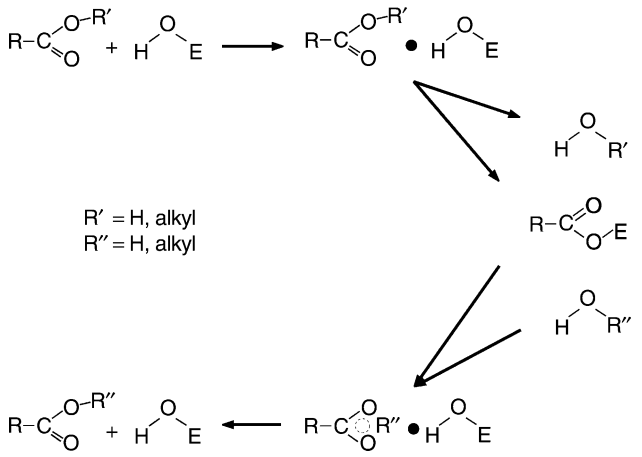

FIGURE 1 Lipolysis mechanism. E–O–H represents the active site serine which forms the acyl-enzyme intermediate in catalysis. The interchangeability of H, R′, and R″ shows that lipases readily catalyze ester synthesis, ester hydrolysis, and acyl exchange, depending on the activity of water in the system, and the circular bond in the lower right structures indicates that the carboxyl oxygen atoms become randomized during the catalytic cycle.

substrates and tend to have much more restrictive sites to accommodate a particular substrate. Lipases that have relatively restricted substrate access to the active site, e.g., pancreatic triacylglycerol lipase, tend to be specific for esters of primary alcohols, whereas others readily catalyze hydrolysis of esters of secondary alcohols as well, e.g., *Candida rugosa* lipase. These latter enzymes are also more likely to exhibit activity against phospholipids and other nonconventional substrates. The list of atypical substrates includes peptides, simple amides, Schiff bases, (lyso)phospholipids, percarboxylic acids and polyesters.

In addition to differing specificities for acyl and alkyl size, some lipases, e.g., *Rhizomucor miehei* lipase, show pronounced stereospecificity, whereas others, e.g., porcine pancreatic triacylglycerol lipase, do not. Interestingly, stereospecificity extends to prochiral molecules, e.g., trioleoylglycerol, in which the lipid substrate is symmetrical but the product of the reaction following removal of an acyl group from position 1 or 3 is chiral. Overall, there is interplay among the various types of specificity in lipases so that generalizations are difficult and specificity must be determined on a substrate-by-substrate basis. Also, the presentation of the substrate to the lipase can affect measured specificity. For pharmaceutical and other fine chemical applications, there have been extensive efforts to engineer lipases to carry out particular reactions with high stereospecificity.

Although lipases are defined and function *in vivo* as hydrolytic enzymes, they are increasingly employed industrially for *de novo* ester synthesis and acyl exchange. Most globular proteins, including lipases, will irreversibly denature if confronted with an interface between an aqueous phase and a highly apolar phase, e.g., hydrocarbon-like. However, if water is removed from the enzyme to the extent that its chemical activity is reduced to very low levels, e.g., by freeze drying, the enzymes are stable and potentially active in an apolar medium. While this is true of many enzymes, it is particularly advantageous with lipases. This is because water is a reactant in the system (Figure 1) and because the substrates are nonpolar. The absence of water shifts the equilibrium of the reaction from ester hydrolysis to ester synthesis and the reactants are compatible with or can even serve as their own apolar solvent. This enables the synthesis of esters in high yield or the exchange of one ester acyl group for another (Figure 1).

Lipolysis Regulation

Physiochemical Importance of Interfaces

Lipases are classically defined as enzymes, generally monomeric and water-soluble, that catalyze the hydrolysis of ester substrates that are apolar and, therefore, generally water-insoluble. Although this definition indicates what lipases do, it does not reveal how they do it. The key to understanding how lipases work is to appreciate the role of the interface between the oil and water phases as an enabler of catalysis. This is shown schematically in Figure 2. Having ester functional groups, lipase substrates are more polar than simple hydrocarbons and have some tendency to partition between the bulk oil phase and the interface. Likewise, lipases will also partition to an oil-water interface from the aqueous phase. The consequence of these partitioning reactions is to orient and concentrate the substrate and enzyme together in a quasi-two-dimensional phase. This phenomenon is known as the "substrate theory" of why lipases are more active on insoluble substrates than soluble ones. In this view of lipolysis the interface assumes part of the role played by classical enzyme-substrate binding in solution, but in a nonspecific way. The most important consequence of enzyme and reactant partitioning is that the instantaneous rate of lipolysis depends on the two-dimensional concentrations of enzyme and reactants in the interface rather than their concentrations in either of the bulk phases.

This sequential scheme for lipolysis has other consequences as well. For a substrate, it means that its amphipathicity, together with its bulk concentration in the oil phase, will contribute to its two-dimensional concentration in the interface. Simplistically, if one had an equimolar mixture of glycerides in an oil phase their interfacial concentrations would be in the relative order monoacylglycerols $>$ diacylglycerol $\gg$ triacylglycerol. Measuring initial rates of hydrolysis for this mixture using a hypothetical lipase with no positional specificity

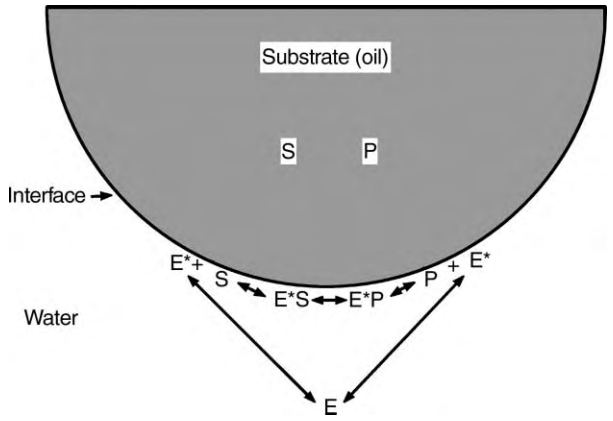

FIGURE 2 The interfacial nature of lipolysis. The substrate (S) is initially present in or as an oil droplet (shaded) whereas the lipase (E) is in the aqueous phase. Catalysis requires that both E and S partition to the interface. Partitioning of E involves a conformational change with the bound species noted as E*. Reaction products (P) will remain in the interface or partition to the oil phase, depending on their amphipathicity.

and normalizing for the number of ester bonds available would show this same apparent order leading, incorrectly, to the conclusion that the lipase is specific for monoacylglycerols. Another consequence of the interfacial nature of lipolysis is that the reaction products will accumulate in the interface, unless they are removed by partitioning into the oil phase or are solubilized in the aqueous phase. With respect to the latter, albumin or cyclodextrins are often used *in vitro* to trap fatty acids and monoacylglycerols in the aqueous phase during the hydrolysis of tri- or diacylglycerols. When it occurs, the accumulation of reaction products in the interface enriches the interface in more amphipathic molecules, greatly complicating the measurement of specificity and interpretation of kinetic data. Product accumulation also can have the effect of slowing the reaction due to fatty acid accumulation while at the same time causing the area of the interface to expand. Area expansion will have the opposite effect by favoring the partitioning of more lipase to the interface. Thus, once lipolysis is initiated in a system having a bulk oil phase as well as an aqueous phase, the regulation of lipolysis rate and extent becomes extremely complex. It is for this reason that researchers have utilized simpler systems, like mono-molecular lipid films, in efforts to understand lipase regulation.

That lipolysis is heterogeneous was unequivocally demonstrated by the P. Desnuelle group in 1965. They showed that if the same insoluble substrate was presented to a lipase as coarse and fine dispersions in buffer, the apparent Michaelis constant for the reaction, i.e., the three-dimensional concentration of substrate at which the hydrolysis rate was half maximal, was lower for the fine dispersion. However, if the rate data were analyzed as a function of total substrate particle surface area rather than bulk substrate concentration, the constant was the same for both dispersions. This occurred because the two-dimensional concentration of substrate at the particle interface was actually the same for the coarse and fine dispersions and the observed saturation of reaction rate with increasing substrate dispersion reflected saturation of lipase partitioning to that surface with increasing interfacial area. Despite the complexity of lipolysis kinetics arising from the interfacial nature of the process, it has been possible to develop kinetic schemes for analyzing lipase kinetics, at least for simple experimental systems, e.g., where reaction products are removed from the interface when formed. These are valuable for screening potential lipase inhibitors to determine the efficiency at which each step of the reaction, i.e., partitioning or interfacial catalysis, contributes to the observed inhibition.

Structural Adaptation of Lipases at Interfaces

It might be presumed that lipases would possess a high affinity for lipid–water interfaces, i.e., that they would be highly amphipathic. However, their affinities toward interfaces dominated by amphipathic lipids, like phospholipids, is often no higher than that of other water-soluble globular proteins. Indeed, many lipases can be isolated as soluble monomeric proteins that do not show a propensity to aggregate. However, if exposed to a surface of a pure substrate, like triacylglycerol, lipases bind with high affinity. Related to this observation is their ability to efficiently catalyze the hydrolysis of insoluble substrates, but not soluble substrates. To explain this observation, it was proposed early on that lipases somehow became activated at interfaces. In the 1990s the determination of lipase structures under varying conditions revealed the physical basis of this phenomenon (Figure 3). In aqueous solution the active site of most lipases is not exposed to the medium but lies in the interior of the protein under a "lid" or "flap" structure. This keeps soluble ester substrates away from the catalytic triad. As implied by its name, the lid can open to reveal the active site and, simultaneously, to create and expose a large area comprised of hydrophobic amino acids. Whereas, this open conformation is energetically unfavorable in the aqueous phase, it may be induced or trapped by the presence of an apolar surface. The lipase then binds with high affinity to the interface, the active site is accessible for diffusion of substrate molecules into it and catalysis can proceed. It is the conformation of this open form of the enzyme that determines specificity for particular substrates. The changing of conformation by lipases in the vicinity of an interface is known as the "enzyme theory" of why lipases are more active on insoluble substrates than

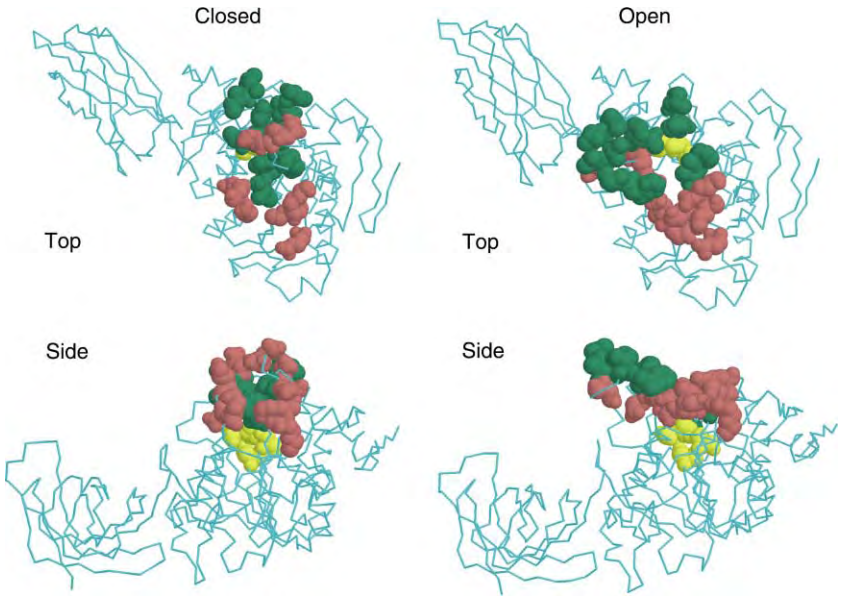

FIGURE 3 Closed and open conformations of pancreatic triacylglycerol lipase. The backbone structure of the lipase is shown in light blue-green with the C2 regulatory domain on the left and the catalytic domain on the right. Nonpolar (green) and polar/charged (red) residues in the vicinity of the catalytic triad (yellow) are shown space filled. Note that in the closed conformation, presumed to exist in solution (left) and designated E in Figure 2, mostly polar/charged residues are exposed to water and the catalytic triad is shielded from water. In the closed conformation, presumed to exist at the interface and designated E^* in Figure 2, a large, apolar surface is exposed on the top of the molecule as shown and the catalytic triad becomes accessible from the top. This surface presumably interacts with the substrate-containing oil droplet. The closed structures were drawn from coordinates kindly provided by Dr. C. Cambillau and the open structure from the Protein Data Base, file 1LPA.pdb.

soluble ones. It should be noted that the enzyme theory of lipolysis and the substrate theory of lipolysis described above are not mutually exclusive.

A still unresolved question is what kind of a surface a lipase needs for surface binding in the open conformation. Natural interfaces tend to be dominated by phospholipids and proteins. These are necessary to emulsify the apolar lipid substrate, i.e., to stabilize it in a dispersed state with high surface area, but tend to inhibit lipase binding to the interface. Research suggests that lipases need a defect or a patch free of binding inhibitor in the interface to initiate lipolysis. Once bound, the generation of lipolysis proceeds and its reaction products increase the number of binding sites and more lipase molecules can bind. Thus, lipolysis often appears to be autocatalytic in the presence of inhibitory phospholipids or proteins, i.e., there is an initial lag in lipolysis followed by a burst. Overcoming the inhibition of lipases by amphipathic lipids and proteins is important not only to understanding their roles and regulation *in vivo*, but also their applications, e.g., improve the efficiency of detergents.

Lipase Regulatory Domains

Many lipases, like gastric lipase, consist of a single protein domain but others have a second domain connected to the catalytic domain by a flexible linker. The most studied of these are members of the lipase gene family, exemplified by pancreatic triacylglycerol lipase (Figure 3), lipoprotein lipase, and hepatic lipase. These have a C2 domain, a motif common to other peripheral (also called amphitrophic) proteins, i.e., proteins that reside in solution but translocate to and function at a lipid–water interface in response to a signal. The C2 domain framework is an eight-stranded, antiparallel β-sandwich with connecting loops. In lipases having C2 domains one of these loops exposes hydrophobic amino acid side chains, like leucine, tyrosine, and tryptophan. These confer an amphipathic character to the domain and, depending on assay conditions, can be essential for lipase activity to be expressed. Given the large hydrophobic surface created near the active site of the catalytic domain by the opening of the lid, such dependence on a C2 domain for initiating lipolysis suggests that it is needed to associate the enzyme with a substrate-containing interface long enough for catalytic domain to open and "lock" the enzyme on the interface.

Lipase Cofactors

Two members of the lipase gene family, pancreatic triacylglycerol lipase and lipoprotein lipase, utilize cofactor proteins for carrying out efficient lipolysis. As noted above, lipase-interface-binding tends to be inhibited by those molecules that help create and

stabilize interfaces, like phospholipids. Cofactor proteins facilitate the initiation of lipolysis at such interfaces. The traditional view of cofactors has been that they are amphipathic proteins that simply bind both the interface and the lipase and thereby anchor the lipase to the interface. However, the comparable affinities of lipases and their cofactors for protected interfaces suggest that they do more. Structural studies of the complex between pancreatic lipase and its protein cofactor, colipase, show that the cofactor may facilitate the opening of the lid through protein–protein interactions with the open conformation of the catalytic domain of the enzyme. Another role has been suggested by comparison of the ability of the cofactor to bind to interfaces with different compositions. Specifically, if a phospholipid-rich interface also contains the substrates and products of lipolysis, colipase binding is strengthened. This occurs because the colipase molecules tend to laterally concentrate the non-phospholipid molecules in their vicinity. In this way they help to create a nanometer-sized region from which phospholipid tends to be excluded. This facilitates lipase binding by a combination of lipid–protein and protein–protein interactions and thereby helps initiate lipolysis. Another speculative role for lipase cofactors is that their preference for binding to substrate-containing surfaces acts to target lipase to those surfaces in preference to interfaces that do not contain substrate.

See Also the Following Articles

Cholesterol Synthesis • Fatty Acid Oxidation • Fatty Acid Receptors • Fatty Acid Synthesis and its Regulation • Lipid Bilayer Structure • Lipid Modification of Proteins: Targeting to Membranes • Lipoproteins, HDL/LDL

Glossary

amphipath A molecule that contains both polar, hydrophilic (water-loving) and apolar, hydrophobic (water-avoiding) groups that are spatially distinct, conferring a tendency to localize at and stabilize interfaces between water and oil phases.

designer fat Dietary fats or fat substitutes that have been *de novo* synthesized or modified, either chemically or enzymatically, to achieve desired intestinal absorption ability, taste, thermal or rheological properties.

interface A quasi-two-dimensional phase between two bulk phases in which the physical environment of the molecules that comprise the region is distinct from the bulk phases.

interfacial activation The process by which an enzyme increases its activity in the presence of an interface. For lipases it results from the combination of enzyme and substrate being oriented and concentrated at interfaces as a consequence of their amphipathic nature (the substrate theory) and from the conformational transition of the lipase to an open conformation as it binds to the interface (the enzyme theory).

Further Reading

Brockman, H. L. (2000). Kinetic behavior of the pancreatic lipase–colipase–lipid system. *Biochimie* **82**, 987–995.

Fojan, P., Jonson, P. H., Petersen, M. T. N., and Petersen, S. B. (2000). What distinguishes an esterase from a lipase: A novel structural approach. *Biochimie* **82**, 1033–1041.

Kraemer, F. B., and Shen, W.-J. (2002). Hormone-sensitive lipase: Control of intracellular tri-(di-)acylglycerol and cholesteryl ester hydrolysis. *J. Lipid Res.* **43**, 1585–1594.

Lombardo, D. (2001). Bile salt-dependent lipase: Its pathophysiological implications. *Biochim. Biophys. Acta* **1533**, 1–28.

Miled, N., Canaan, S., Dupuis, L., Roussel, A., Rivière, M., Carrière, F., De Caro, A., Cambillau, C., and Verger, R. (2000). Digestive lipases: From three-dimensional structure to physiology. *Biochimie* **82**, 973–986.

Panaiotov, I., and Verger, R. (2000). Enzymatic reactions at interfaces: Interfacial and temporal organization of enzymatic lipolysis. In *Physical Chemistry of Biological Interfaces* (A. Baszkin and W. Norde, eds.) pp. 359–400. Marcel Dekker, New York.

Biography

Dr. Howard Brockman is a Professor at the Hormel Institute, a research branch of the University of Minnesota in Austin, Minnesota. His principal research interest is in the regulation of interfacial enzymatic reactions with emphasis on the role of the lateral distribution of interfacial constituents in controlling bulk-interface partitioning and substrate accessibility. He holds a Ph.D. from Michigan State University and received postdoctoral training at the University of Chicago. He has developed novel methodologies for studying interfacial reactions and has contributed to the mechanistic understanding of their regulation.

Lipid Bilayer Structure

Erwin London
State University of New York, Stony Brook, New York, USA

Natural biological membranes consist of a lipid bilayer in which membrane proteins are embedded. As such, the bilayer is the underlying structural unit of the membrane. Understanding bilayer structure, and properties is critical to an understanding of membrane function.

Chemical Structure of Bilayer-Forming Lipids

Lipid bilayers are composed primarily of polar lipids. Glycerophospholipids and sphingolipids are usually the predominant polar lipids in natural membranes. Unlike dietary lipids (fats), these molecules possess a highly polar headgroup in addition to (two) nonpolar (i.e., hydrophobic) tails (Figure 1).

The hydrophobic tails consist of the hydrocarbon chain portions of fatty acids and/or the base sphingosine. Hydrocarbon chains are linear in eukaryotic organisms, but sometimes have branching methyl groups in bacteria.

The polar headgroups of the lipids can have various chemical structures. Often they contain phosphate to which a polar or charged alcohol derivative is attached. In other cases they contain carbohydrates. The polar headgroup can be electrically neutral, zwitterionic, or negatively charged.

In eukaryotes, sterols such as cholesterol are also major components of the bilayer. Sterols differ from other polar lipids in having a simple, small hydroxyl group as their polar portion. This hydroxyl group is attached to four fused aliphatic hydrocarbon rings. In addition, they contain a branched hydrocarbon chain that is attached to the end of the rings opposite the hydroxyl.

Organization of Lipids in Bilayers

In bilayers lipids orient such that their polar groups are in contact with the aqueous environment and their hydrocarbon segments face each other (Figure 1). As a result, the polar groups in each half of the bilayer (called a monolayer or leaflet) face away from one another. As one moves from the aqueous solution to the bilayer center, a somewhat ill-defined gradient of decreasing polarity is encountered.

The formation of the bilayer is driven by the hydrophobic effect, which is conventionally thought of as primarily a decrease in water free energy that occurs when the clustering of hydrophobic groups allows them to avoid contact with water molecules. Because of the shape of polar lipids, they usually form topologically closed bilayers, e.g., a spherical or elliptical shell. Such closed structures eliminate direct contact between lipid hydrocarbon and water. They contain an internal aqueous lumen separated from the external aqueous solution by the bilayer. Artificially formed bilayers of this type are called liposomes. The bilayer plus the internally trapped aqueous solution is known as a vesicle (Figure 2). Vesicles can contain one lipid bilayer, in which case they are said to be unilamellar vesicles, or multiple bilayers each separated by thin layers of aqueous solution, in which case they are called multilamellar vesicles. Flattened stacks of bilayers with the internal aqueous solution largely squeezed out can also be prepared.

Membrane Proteins and Bilayers

Natural membranes are associated with numerous proteins. Those proteins that span the lipid bilayer are said to be transmembraneous (Figure 2). Non-transmembraneous proteins associated with the polar surface of the bilayer are also present (Figure 2). Proteins can have a significant influence on membrane structure. For example, they are likely to be responsible for the distortion of natural membranes into more complex shapes than those observed for pure lipid bilayers. Familiar examples are the membranes of red blood cells and the variable-shape membranes surrounding amoeba. On the other hand, it is clear that natural membranes contain bilayers that have physical properties similar to those of pure lipid bilayers. The fact that the lipid-facing amino acid residues of membrane proteins form hydrophobic surfaces that match lipid

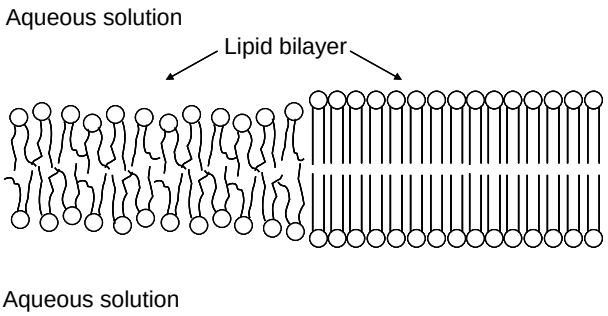

FIGURE 1 Schematic representation of cross-section through a lipid bilayer composed of a single type of phospholipid or sphingolipid. Polar headgroups are illustrated as circles and hydrocarbon tails are shown as lines. Notice each lipid has one headgroup and two tails. A bilayer composed of both a disordered liquid domain (left) and an ordered gel domain (right) is illustrated.

dimensions is no doubt an important factor explaining this behavior. Nevertheless, the physical properties of the hydrophobic segments of membrane proteins are very different than those of lipids and the consequences of these differences remain to be fully explored.

Bilayer Dimensions

Experiments on liposomes show that the diameter of spherical lipid bilayers can be any value upwards from 250Å. Bilayer width (thickness) is determined by the length of the nonpolar tails of the polar lipids and sterols. This can range from 16 to 24 carbon atoms for the hydrocarbon chains of phospholipids and sphingolipids. Combined with the effects of lipid state and double bonds (see below), this results in a hydrocarbon core of the bilayer that is ~30Å in width. Total width including the lipid headgroups is on the order of 45–50Å, but the exact value depends on the structure of the lipid polar headgroups, which can be very large in some cases.

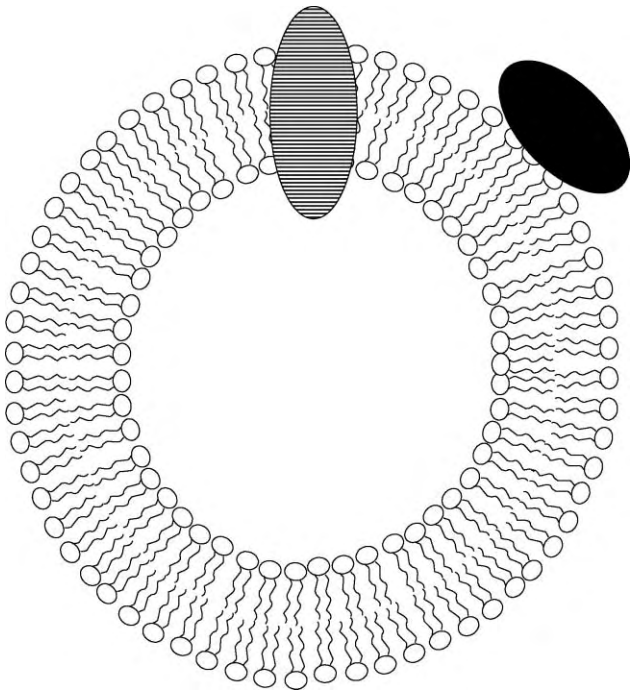

FIGURE 2 A unilamellar lipid vesicle formed by a lipid bilayer and containing one transmembrane protein (striped) and one protein associated with the lipid polar headgroups (filled).

Relationship between Bilayer Form and Bilayer Function

The properties of bilayers are admirably suited to their biological function. The closed structure of the bilayer allows biological membranes to completely encase cellular contents (such as nucleic acids, proteins, sugars, and amino acids) in a hydrophobic barrier that prevents them from escaping into the surrounding solution.

The width of the bilayer is such that proteins of ordinary size are able to span the lipid bilayer. This allows membrane proteins to maintain contact with both the internal and external aqueous milieu. As a result, membrane proteins can carry out functions such as the transport of molecules across bilayers. Such abilities are central to membrane function. A bilayer that was much wider than that formed by natural lipids, i.e., one formed by much longer fatty acid chains, would require the metabolically wasteful synthesis of extra-large transmembrane proteins as well as that of longer lipids. A bilayer that was significantly thinner than that formed by natural lipids would not be stable.

Physical State of Bilayer Lipids

Another important property of lipid bilayers is their ability to exist in different physical states (or phases). At low temperatures bilayers often exist in a relatively solid-like state called the gel or Lβ state or phase. At higher temperatures gel-state bilayers undergo a melting transition and the gel state is replaced by a more disordered, liquid-like state, variously designated as the liquid crystalline, liquid disordered, or Lα state. Melting temperatures (or if temperature is decreased, freezing temperatures) depend on the structure of both the hydrophobic tails and the polar headgroups of the individual lipid molecules. The melting temperature of lipids with linear saturated tails, which contain only single bonds connecting carbon atoms to each other, are much higher than those of lipids with unsaturated tails, which have *cis* double bonds, as well as single bonds. Because sphingolipids tend to contain hydrocarbon

chains lacking *cis* double bonds, they tend to have much higher melting temperatures than glycerophospholipids, which tend to have more highly unsaturated hydrocarbon chains.

Bilayers containing sterols can exist in a third lipid state called the liquid ordered or Lo state. This state is observed most frequently in mixtures of sterols with relatively saturated chain polar lipids. The Lo state has properties that are intermediate between the disordered liquid and gel states.

Studies in synthetic lipid bilayers show that in a single bilayer, different regions (known as domains) can exist in different physical states (Figure 1). It is believed that the disordered liquid state is by far the most common state present in biological membranes. However, in eukaryotic cells it is now thought that ordered liquid-state domains can coexist with disordered liquid domains. Lo state domains in cell membrane, called lipid rafts, are rich not only in sphingolipids and sterols, but also in special subsets of membrane proteins. Rafts appear to have a specialized role in a number of important biological processes.

The Effect of Lipid State upon Lateral Organization of Lipid Molecules

Lipid bilayers in different physical states differ in a number of properties. One is the degree of lateral interaction between various bilayer lipids. In the disordered liquid-like state, bilayers are believed to exist as a more-or-less random mixture of various lipid species. In other words, there are few or no cases in which tight associations between two different lipid molecules occur. As spacial constraints tend to be much more restrictive in solids, a much higher degree of lateral organization is likely to exist in a gel-state bilayer containing a mixture of different lipids. This is little studied except to the extent that it appears that separate gel-phase domains with different lipid compositions can coexist in a single bilayer. The nature of lateral interactions between different lipids in the liquid-ordered state is being actively studied, but remains unclear. There may be specific arrangements of sterol molecules relative to the other polar lipids present in the bilayer, and various liquid-ordered domains with different compositions may be able to coexist in a single bilayer.

Interactions between each of the monolayers within a single bilayer is also poorly understood in most cases. Under some conditions certain combinations of hydrocarbon chain lengths allow interdigitation of hydrocarbon chains from opposite monolayers.

Influence of Physical State on Lipid Conformation and Lateral Diffusion

The conformation of individual lipid molecules within a bilayer is also dependent upon lipid state. In all states, the hydrocarbon chains of the lipids tend to align parallel to one another and perpendicular to the surface. A high degree of parallel alignment characterized by the presence of tightly packed lipids occurs in the gel- and liquid-ordered states. In contrast, in the disordered liquid state, lipids are more loosely packed and the degree of alignment is reduced because carbon-carbon single bonds can twist a manner that results in bending of the hydrocarbon chains. This also results in the bilayer being thinner than in other states (Figure 1). The relatively random location of such bends within a hydrocarbon chain results in increased disorder as one moves from the bilayer surface toward the bilayer center. There is also a contribution to disorder from the presence of double bonds. These are usually in the form of *cis* double bonds, which form permanent bends in hydrocarbon chains.

Headgroup conformation, and its dependence on lipid state, are more poorly characterized in most cases.

Another property of bilayers that depends on lipid state is lateral diffusion. This refers to random sliding motions of lipids within the plane perpendicular to the average direction of the hydrocarbon tails. Lateral motions are rapid in both the liquid-disordered and liquid-ordered state, but much reduced in the gel state. It should be emphasized that the ability to undergo relatively rapid lateral motions is an important feature of biological membranes. It allows membrane components to rearrange within the lipid bilayer such that they can form and break functionally important complexes.

Transverse Lipid Movements

Lipids can also undergo transverse movement, in which they move (or flip) from one monolayer of the bilayer to the opposite one. For good reason this motion is many orders of magnitude slower than lateral diffusion. Transverse flipping requires that the polar/charged portions of lipids transiently dissolve within the hydrophobic core of the bilayer. This is very unfavorable energetically. However, it should be noted that in natural membranes specific flippase proteins are believed to catalyze rapid flipping events in some cases. Furthermore, it appears that spontaneous flipping is more rapid for sterol molecules, which have a headgroup that is very small and not excessively

polar, than it is for most phospholipids and sphingolipids, although this remains an area of some controversy.

Effect of Lipid Bilayers on Local Aqueous Environment

Finally, it is important to remember that lipid bilayers can also affect the structure of their immediate aqueous environment. When a significant fraction of lipids in a bilayer is anionic, they tend to attract significant numbers of cations while repelling anions. As a result a special double layer of solution depleted in anions and enriched in cations surrounds the bilayer. This layer can alter the structure and function of membrane proteins.

See Also the Following Articles

Fatty Acid Synthesis and its Regulation • Flippases • Lipid Modification of Proteins: Targeting to Membranes • Lipid Rafts • Phospholipid Metabolism in Mammals • Phospholipid Synthesis in Yeast • Sphingolipid Biosynthesis • Sphingolipid Catabolism

Glossary

biological membranes A thin shell surrounding either internal compartments in cells or the entire cell. Composed of special proteins and lipids.

lipids Small biomolecules with hydrophobic characteristics.

polar headgroup The portion of a lipid molecule that interacts with aqueous solution; fusually contains several chemical groupings that can hydrogen bond with water.

Further Reading

Brown, D. A., and London, E. (2000). Structure and function of sphingolipid- and cholesterol-rich rafts. *J. Biol. Chem.* **275**, 17221–17224.

Gennis, R. B. (1989). *Biomembranes: Molecular Structure and Function*. Springer, New York.

Jain, M. K. (1988). *Introduction to Biological Membranes*. Wiley, New York.

Koynova, R., and Caffrey, M. B. (1998). Phases and phase transitions of the phosphatidylcholines. *Biochim. Biophys. Acta* **1376**, 91–145.

Lee, A. G. (1977). Lipid phase transitions and phase diagrams. *Biochim. Biophys. Acta* **472**, 237–281.

Biography

Erwin London is a Professor in the Department of Biochemistry and Cell Biology, and in the Department of Chemistry, of Stony Brook University. His expertise is in characterization of the organization of proteins and lipids in membranes. He holds a Ph.D. from the Cornell University (Ithaca) and received postdoctoral training at the Massachusetts Institute of Technology.

Lipid Modification of Proteins: Targeting to Membranes

Marilyn D. Resh
Memorial Sloan-Kettering Cancer Center, New York, USA

Lipid modification refers to the covalent attachment of hydrophobic groups to specific amino acids in proteins. All proteins contain a polypeptide chain backbone consisting of various combinations of amino acids linked via amide bonds. In addition, some proteins are modified by the attachment of other chemical structures directly to one or more amino acids. These modifying groups are diverse and include phosphate, methyl groups, sugars, as well as lipids. Three different types of lipid moieties are typically found attached to proteins: fatty acids, isoprenoids, and glycosylphosphatidyl inositol (GPI) anchors (Figure 1, Table I). Linkage of each of these groups occurs within different protein sequences and is catalyzed by different enzymes. The attachment of hydrophobic groups to proteins modifies their structure, intracellular localization, and/or function.

Lipid Modification of Proteins

Fatty Acylation

Two types of fatty acids are typically found attached to fatty acylated proteins: myristate or palmitate. In addition, some proteins are dually fatty acylated, i.e., they contain both myristate and palmitate.

Myristoylation

Myristate is a 14-carbon saturated fatty acid that is directly linked to the N terminus of select proteins in a process known as N-myristoylation. In eukaryotes ~0.5% of all proteins are modified in this manner; in humans this corresponds to ~150 proteins. Nearly all N-myristoylated proteins begin with the sequence: Met-Gly. During protein translation, the initiating methionine is removed by the enzyme methionine aminopeptidase, exposing glycine at the N terminus. The fatty acid is then linked to the protein via an amide bond between myristate and the N-terminal glycine residue. Additional amino acids near the N terminus are important for determining whether a protein becomes N-myristoylated. An algorithm is available on the Web (http://mendel.imp.univie.ac.at/myristate/) that allows one to predict with high accuracy whether a particular protein sequence is N-myristoylated. The high stability of the amide linkage makes N-myristoylation an essentially irreversible protein modification.

N-myristoylation is catalyzed by the enzyme N-myristoyl transferase (NMT). Most organisms have one or two NMT genes, and NMT has been shown to be an essential gene product that is required for the growth of yeast, flies, and plants. The N-myristoylation reaction occurs in a co-translational manner, i.e., while the newly translated polypeptide is still attached to the ribosome. The preferred fatty acid substrate for NMT is myristoyl-CoA, an activated form of myristate. Fatty acids that are shorter or longer than myristate are generally not transferred from their respective fatty acyl-CoAs to proteins. However, NMT will transfer unsaturated 14 carbon fatty acids to proteins, a process that occurs primarily in the retina.

Palmitoylation

Several hundred eukaryotic proteins are posttranslationally modified by covalent attachment of the 16-carbon fatty acid palmitate. The fatty acid is generally attached to one or more cysteine residues within the protein through a thioester linkage. Palmitoylation can occur within five types of protein sequences: (1) at or near the transmembrane domain of a membrane protein; (2) near a C-terminal prenylated cysteine; (3) near the N or C terminus; (4) adjacent to or near an N-terminal myristoylated glycine; and (5) at an N-terminal cysteine via an amide bond. The rules that govern the choice of the palmitoylation site(s) are not well-understood. Eukaryotic cells contain multiple palmitoyl acyl transferases that are located in many different subcellular sites. In addition to palmitate, longer fatty acids such as stearate or arachidonate may be transferred to proteins. Palmitoylation is a reversible reaction; palmitate is removed from proteins by palmitoyl protein thioesterases. The reciprocal action of transferases and thioesterases sets up a dynamic

balance of palmitoylation/depalmitoylation reactions in the cell.

Prenylation

Prenyl groups are built from 5-carbon building blocks known as isoprene. Protein prenylation involves the attachment of two types of isoprenoid groups, 15-carbon farnesyl or 20-carbon geranylgeranyl, via thio-ether linkage to a cysteine residue at or near the C terminus. Most prenylated proteins contain a "CAAX" (C = Cys, A = aliphatic amino acid, X = any amino acid) box sequence at their C terminus. The identity of the C-terminal amino acid determines whether the protein is recognized by farnesyl transferase (FTase) (X = met,ser) or geranylgeranyl transferase I (GGTase I) (X = leu). Following prenylation, two additional modifications occur. The three C-terminal amino acids are cleaved by the endoprotease hRce1, and the prenylated C-terminal cysteine is carboxymethylated by the carboxymethyltransferase pcCMT/Icmt. A third prenyl transferase, Rab GGTase or GGTase II, attaches geranylgeranyl to Rab proteins that terminate with -CC, CXC, CCX or CCXX sequences. Rab proteins must be bound to Rab Escort protein (REP) in order to be prenylated by GGTase. Genetic mutations in REP cause choroideremia, a disease characterized in humans by retinal degeneration and blindness.

GPI Anchors

GPI anchors are complex structures that consist of ethanolamine phosphate, three mannoses, N-acetyl-glucosamine, and phosphatidylinositol (PI). At least 20 enzymes are involved in the synthesis and attachment of GPI anchors, a process that occurs in the endoplasmic reticulum. A C-terminal hydrophobic region in the target protein serves as a signal for GPI anchor attachment and is then cleaved from the modified protein, leaving the GPI anchor at the C terminus. The modified protein is transported through the Golgi apparatus and ultimately to the extracellular leaflet of the plasma membrane.

Detection of Lipid Modified Proteins

Mass spectroscopy analysis provides definitive identification of the modifying group on proteins. Alternatively, fatty acylated and prenylated proteins are detected by radiolabeling cells with ^{3}H or ^{125}I labeled fatty acids or isoprenoid precursors, followed by isolation of the protein with a specific antibody and autoradiographic analysis. A hallmark of GPI-anchored proteins is that they are released from the cell surface by *in vitro* cleavage with PI-specific phospholipase C; this process occurs *in vivo* for certain GPI-anchored proteins (e.g., alkaline phosphatase) (Figure 1, Table I).

Membrane Targeting of Lipid Modified Proteins

Lipid modifications play important roles in promoting interaction of proteins with membranes. The nature of the lipid group determines how tightly a protein will bind to a membrane and which membrane it will bind to.

Myristoylated and Farnesylated Proteins

The hydrophobicity of myristate or farnesyl is not sufficient to stably anchor a protein to the membrane. N-myristoylated and farnesylated proteins therefore use a second signal to promote membrane binding. The second signal is either a cluster of basic amino acids (lysine or arginine) contained within the protein or covalently bound palmitate. The positively charged basic cluster provides electrostatic interaction with negatively charged lipids on the cytoplasmic surface of the plasma membrane, whereas palmitate enhances hydrophobic interactions with the interior of the phospholipid bilayer. The two signals together promote specific targeting of the modified proteins to the cytoplasmic face of the plasma membrane. Examples of lipid modified proteins that use two signals

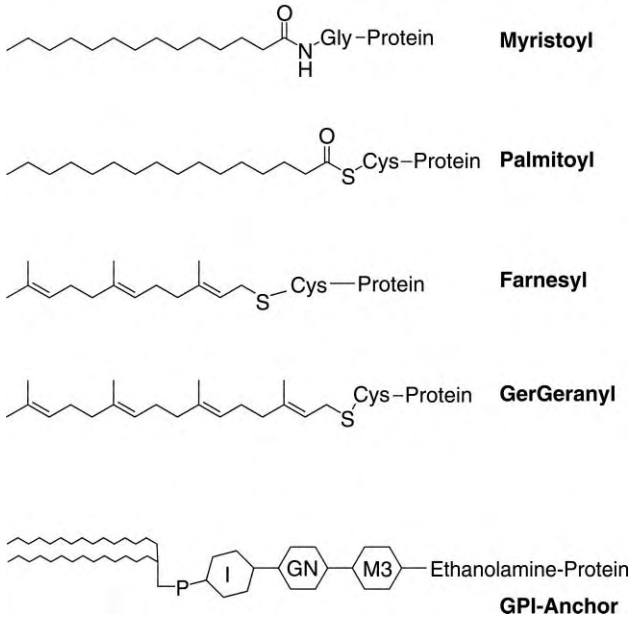

FIGURE 1 Structures of Lipid Modifying Groups on Proteins. Structures of the different lipid modifying groups and their linkages to proteins are depicted. For the GPI anchor, I = inositol, GN = N-acetylglucosamine, M3 = 3 mannoses.

TABLE I

Examples of Lipid Modified Proteins

Fatty acylated	Prenylated	GPI-anchored
Myristate	*Farnesyl*	Alkaline phosphatase, CD55 (DAF),
Src family kinases, Gα subunits, Arf, recoverin, MARCKS, mammalian retroviral Gag proteins, calcineurin B, eNOS	H-Ras, K-Ras, Lamins	5′-nucleotidase, Thy-1, PrP^c prion, trypanosomal VSG
Palmitate	*Geranylgeranyl*	
Transferrin receptor, CD4, caveolin-1, β2 adrenergic receptor, H-Ras, Gα subunits, GAP43, PSD-95, Src family kinases, eNOS	Gγ subunits, Rho family proteins, Rab proteins	

for membrane binding include Src (myristate + basic) and H-Ras (prenyl + palmitate).

Palmitoylated, Geranylgeranylated, and GPI-Anchored Proteins

The presence of a molecule of palmitate, geranylgeranyl, or a GPI-anchor is sufficient for membrane binding of the modified protein. The final destination of these modified proteins is dictated by several factors. The site where palmitoylation occurs often determines protein localization. This is the case for dually fatty acylated members of the Src family of tyrosine kinases, which are palmitoylated by a plasma membrane localized palmitoyl transferase, and remain bound to the plasma membrane. Other proteins are modified in internal membranes, but traffic through the classical secretory pathway and are thereby specifically delivered to the plasma membrane (e.g., farnesylated H-Ras and GPI-anchored proteins). A third consideration is protein–protein interactions, which influence the ultimate destination of a modified protein. Finally, in polarized cells such as epithelial cells, the plasma membrane is divided into two distinct domains – apical and basolateral – that differ in protein and lipid composition. The GPI-anchor provides a sorting signal that directs the modified protein to the apical surface in most epithelial cells.

Reversible Membrane Binding

Several mechanisms exist *in vivo* to regulate membrane-binding of lipid-modified proteins. The first is removal of the modifying group, e.g., depalmitoylation by palmitoyl thioesterases. Myristoylated and prenylated proteins contain stable lipid–protein linkages and are thus not subject to this mode of regulation. Instead, exposure of the modifying group can be regulated, either via interactions with the modified protein itself (intramolecular) or with other proteins (intermolecular). For example, recoverin and Arf are N-myristoylated proteins whose membrane-binding is regulated by an intramolecular myristoyl switch. These proteins exist in two conformations. In one conformation, myristate is hidden within a hydrophobic pocket inside the protein, and the protein is cytosolic. Binding of ligand triggers the myristoyl switch: a conformational change results in exposure of myristate and promotion of membrane-binding. Intermolecular interactions also regulate membrane localization. When geranylgeranylated RhoA is bound to its inhibitor, RhoGDI, the isoprene unit is sequestered within a hydrophobic cleft of RhoGDI and the complex is cytosolic. Activation of RhoA causes it to be released from RhoGDI and localize to the plasma membrane.

Targeting to Membrane Rafts

Membrane rafts are small subdomains of the plasma membrane that are enriched in cholesterol and sphingolipids. The lipids in rafts predominantly contain saturated fatty acid chains, which promotes tight packing and formation of a specialized region of the membrane bilayer known as a "liquid ordered" domain. Proteins modified by saturated fatty acids or GPI anchors preferentially localize to rafts. Myristoylated and palmitoylated proteins localize to the cytoplasmic side of plasma membrane rafts, while GPI-anchored proteins are sorted into rafts in the trans Golgi network and then trafficked to the exoplasmic leaflet of the raft membrane. Raft localization of these proteins enhances protein–protein interactions and is important for propagating efficient signal transduction by growth factor and immune cell receptors.

Membrane Targeting and Protein Function

Membrane targeting is essential for the function of many types of lipid-modified proteins. Localization of proteins to a membrane increases their local concentration, and

amplifies the efficiency of interaction with other membrane-bound substrates and targets. When lipid modification is inhibited, the affected proteins are mislocalized within the cell and no longer function effectively. Drugs that interfere with N-myristoylation (2-OH-myristate), palmitoylation (2-bromopalmitate) and prenylation (farnesyl transferase inhibitors (FTIs)) have been developed. There is great clinical interest in FTIs, which have been shown to inhibit farnesylation of Ras and reduce the growth of Ras-induced human tumors.

See Also the Following Articles

Fatty Acid Oxidation • Fatty Acid Receptors • Fatty Acid Synthesis and its Regulation • Glycosylphosphatidylinositol (GPI) Anchors • Lipid Bilayer Structure • Lipid Rafts • Phospholipase C • Protein N-Myristoylation • Protein Palmitoylation

Glossary

fatty acylation The process whereby fatty acids are covalently attached to proteins.

GPI anchor A complex structure consisting of ethanolamine phosphate, three mannoses, N-acetylglucosamine, and phosphatidylinositol.

isoprenylation The process whereby isoprenoid groups are covalently attached to proteins.

rafts Membrane regions that are enriched in cholesterol and sphingolipids.

Further Reading

Bijlmakers, M. J., and Marsh, M. (2003). The on-off story of protein palmitoylation. *Trends Cell Biol.* **13**, 32–42.

Casey, P. J. (1995). Protein lipidation in cell signaling. *Science* **268**, 221–225.

Farazi, T. A., Waksman, G., and Gordon, J. I. (2001). The biology and enzymology of protein N-myristoylation. *J. Biol. Chem.* **276**, 39501–39504.

Resh, M. D. (1999). Fatty acylation of proteins: New insights into membrane targeting of myristoylated and palmitoylated proteins. *Biochim. Biophys. Acta* **1451**, 1–16.

Takeda, J., and Kinoshita, T. (1995). GPI-anchor biosynthesis. *Trends Biochem. Sci.* **20**, 367–371.

Biography

Marilyn D. Resh is a member in the Cell Biology Program at Memorial Sloan-Kettering Cancer Center and is a Professor in the Cell Biology and Biochemistry Graduate Departments at the Weill Graduate School of Medical Sciences of Cornell University. Her research focuses on understanding how lipid modification regulates protein structure and function. She holds a Ph.D. from Harvard University, where she also received her postdoctoral training. She discovered the two-signal mechanism of membrane binding utilized by Src and the HIV-1 Gag protein, and was one of the first to demonstrate that Src family tyrosine kinases are palmitoylated.

Lipid Rafts

Deborah A. Brown
State University of New York, Stony Brook, New York, USA

Lipids do not always mix uniformly in membranes, but can cluster to form microdomains. A certain class of these microdomains has been named "lipid rafts." These are enriched in cholesterol and sphingolipids. Rafts probably exist in membranes in the liquid-ordered phase or a phase with similar properties. Increasing evidence suggests that phospholipid-rich liquid-crystalline phase domains and sphingolipid-rich liquid-ordered phase domains (rafts) can exist in equilibrium in biological membranes, especially the plasma membrane. Preferential partitioning of membrane proteins into rafts can affect function. Among the proteins that are targeted to rafts are those anchored in the outer leaflet of the membrane through covalent attachment to a special glycolipid, glycosyl phosphatidylinositol (GPI). Other proteins that are linked to saturated acyl chains, such as those that are directly acylated with two or more palmitate chains, or a palmitate and a myristate chain, are also targeted to rafts. Targeting of GPI-anchored proteins and other proteins to rafts plays a role in signal transduction, especially in hematopoietic cells, and possibly also in sorting in intracellular membranes and regulation of cell-surface proteolysis in other mammalian cells.

Physical Properties

The fact that membrane lipids have such heterogeneous structures suggests that they may mix nonrandomly in the bilayer to form lipid microdomains. However, despite much interest in the subject, good evidence that lipids cluster in cell membranes has been slow to emerge. We will discuss one type of microdomain that has recently been described in cell membranes. These are rich in cholesterol and sphingolipids, and probably exist in membranes in the liquid-ordered (l_o) phase or a phase with similar properties. These domains have also been called rafts. The fact that rafts are in the l_o phase gives them a surprising but technically useful property; they are resistant to solubilization by non-ionic detergents such as Triton X-100 in the cold. Thus, after extraction of cells in detergent, insoluble rafts can be separated from fully-solubilized non-raft proteins and lipids, and isolated for further analysis. We will use the term raft to refer to the domain in the intact membrane, and the term DRM to refer to the structure isolated by detergent insolubility.

Certain proteins, including those anchored in membrane by GPI and those linked to dual saturated acyl chains such as palmitate and myristate, are targeted to rafts. We will discuss GPI-anchorage, an unusual form of membrane anchorage, in detail, covering synthesis and the types of proteins that are GPI-anchored. We will also discuss the functions of GPI-anchorage, focusing on the ability of this modification to target proteins to lipid rafts (Figure 1).

Lipid Phase Behavior

Since rafts are probably in a separate phase from the rest of the bilayer, we briefly review membrane lipid phase behavior. Artificial bilayers consisting of one pure phospholipid species exist in a "frozen," ordered, gel phase at low temperatures. Acyl chains of gel-phase lipids are extended and packed tightly together, and lipids have low rates of rotational mobility and diffusion in the bilayer. These frozen acyl chains have a melting temperature (T_m) that is characteristic of each phospholipid species. Above this temperature, the bilayer is present in a phase, termed liquid-crystalline (l_c) or liquid-disordered (l_d), in which the lipid acyl chains are fluid and disordered. In the l_c phase, the acyl chains are disordered and do not pack tightly together. They also have high rates of rotational and lateral mobility in the bilayer. Binary mixtures of phospholipids with different T_m can be examined at temperatures between the T_m of the two lipids. When one component is present at low levels, the mixture is uniform, and generally remains in the phase favored by the major component. Above a threshold concentration of one component, cooperative phase separation occurs, and gel and l_c phase domains can coexist. In these two-phase systems, the gel phase is enriched in the high-T_m lipid, and the l_c phase is enriched in the low-T_m lipid. Phase separation in these mixtures is affected by temperature; high temperatures favor the l_c phase, while low temperatures favor the gel phase. Whenever two phases are present, the lipid composition of each phase remains constant. Thus, as the lipid composition and the temperature are changed, only

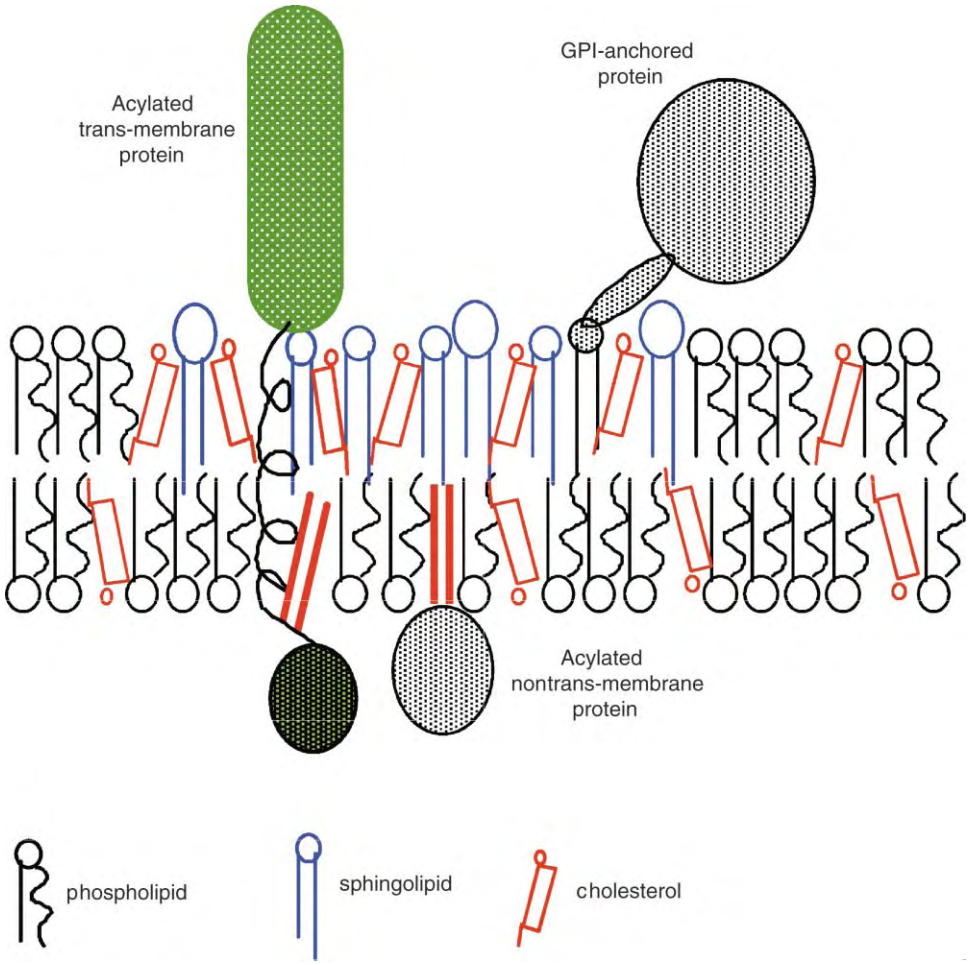

FIGURE 1 Diagram of a membrane raft. Rafts form in membranes rich in cholesterol or other sterols (red) and sphingolipids (blue). Rafts are enriched in these lipids, and relatively depleted in phospholipids (black). Most phospholipids in biological membranes contain one unsaturated acyl chain (curvy line). Lipids can form rafts spontaneously in model membranes, though proteins may affect raft formation in cell membranes. Most sphingolipids are present in the outer leaflet of the plasma membrane. The lipid composition of inner leaflet rafts is not known. Proteins with a high affinity for the ordered lipid environment present in rafts can concentrate there. These include GPI-anchored proteins (whose phosphatidyl inositol moieties generally contain two saturated acyl chains), acylated cytoplasmic proteins such as Src-family tyrosine kinases and alpha subunits of heterotrimeric G proteins, and some acylated transmembrane proteins (which are generally modified with palmitate chains). Saturated acyl chain lipid modifications on proteins are diagrammed as thick red lines.

the relative amount of the two different phases in the membrane changes.

Eukaryotic cell membranes contain mixtures of glycerolipids (in mammalian cells, all phospholipids except sphingomyelin), sphingolipids, and sterols. Biological glycerolipids generally have very low T_m, while sphingolipids (especially glycosphingolipids) have much higher T_m. This disparity has suggested that phase separation between glycerolipid- and sphingolipid-rich domains (possibly in the l_c and gel phases, respectively) might occur in membranes in cells. Because lipids in the gel phase are insoluble in detergent, DRMs might be gel-phase domains. However, although phase separation between l_c and gel phases has been well-characterized in model membranes, the gel phase does not appear to exist in biological membranes, except in unusual cases. In addition, DRMs are rich in cholesterol, making it unlikely that they are present in the gel phase. However, another type of phase separation has also been described in model membranes. This is phase separation between two fluid phases in binary mixtures of a saturated-chain phospholipid (which has a high T_m) and cholesterol. In this case, above the T_m of the phospholipid, a liquid-ordered (l_o) phase can separate from the l_d phase as the amount of cholesterol is increased. Acyl chains of lipids in the l_o phase have properties that are intermediate between those of the gel and l_d phases. They are extended, ordered, and tightly packed together, as in the gel phase, but have high lateral mobility in the bilayer, as in the l_d phase. Phase separation between the l_d and l_o phases also occurs in model membranes containing ternary mixtures of high- and low-T_m lipids

and cholesterol, although the process is more complex. In particular, l_c/l_d phase separation occurs at 37°C in mixtures of phospholipids, sphingolipids, and cholesterol in proportions similar to those found in the plasma membrane. This result is important because it shows that formation of l_o phase domains in the plasma membrane is plausible from a biophysical standpoint.

DRMs are in the L_O Phase

Several studies suggest that DRMs isolated from cells exist in intact membranes as domains in the l_o phase. First, DRMs are in the l_o phase when they are isolated. Second, controlled experiments have addressed the possibility of detergents introducing artifacts. One such artifact is that lipids in membranes might be in a uniform phase, with a concentration of sphingolipids (high-T_m lipids) too low to induce phase separation. However, detergent might preferentially extract low-T_m phospholipids first. As phospholipids are gradually removed, the concentration of sphingolipids in the membrane might gradually increase. This process might eventually lead to phase separation when a threshold concentration of sphingolipids is reached. Detergents do not act in this manner, as shown by model membrane experiments. A series of liposomes whose phase behavior is known from methods independent of detergent extraction is made. Some of these liposomes contain sphingolipids and cholesterol, but at levels too low for phase separation. When these liposomes are extracted with detergent, no DRMs are produced. This shows that detergent does not rearrange membrane lipids to induce DRM formation.

Two different models of raft formation have been proposed. The first, supported by most data, suggests that rafts form by phase separation. Thus, structural features of lipids that affect T_m and promote phase separation will promote raft formation. One key difference between phospholipids and sphingolipids is the length and saturation of their acyl chains. Lipid head-groups can also contribute to T_m by altering the way lipids pack together. According to our model, acyl chain packing plays a key role in raft formation. Head group interactions might also be important, although these interactions may affect raft formation indirectly by affecting acyl chain packing. Cholesterol is recruited to rafts through its ability to pack tightly with lipids of high T_m when the l_o phase is formed. Another group has proposed a different model for raft structure. According to this model, rafts are primarily clusters of glycosphingolipids held together through hydrogen-bonding or other interactions between glycosphingolipid head groups. Because cholesterol has a small head group, it is recruited to rafts because it fits well in the gaps between bulky-headed glycosphingolipids.

Proteins in DRMs

The physiological significance of raft formation is likely to stem from the preferential partitioning of certain proteins into rafts. It has been known for several years that proteins anchored in membranes by GPI are detergent-insoluble and are present in DRMs. Acylated proteins, which are covalently linked to fatty acids, can also be targeted to DRMs. In both cases, this is likely to occur through partitioning of order-preferring lipid modifications into rafts. Thus, proteins that have an affinity for an ordered lipid phase will partition into rafts.

GPI-anchorage can target proteins to rafts. It has become clear in the last few years that targeting to rafts is an essentially universal property of GPI-anchored proteins in mammalian cells. Proposed function(s) of this targeting, which are still being elucidated, include sorting in polarized epithelial cells, signal transduction, and regulation of cell-surface hydrolytic activity. GPI-anchored proteins have long been known to be insoluble in non-ionic detergents such as Triton X-100 in the cold. The basis of this property was not understood until recently. Integral membrane proteins are generally detergent-soluble unless they are linked to cytoskeleton. However, GPI-anchored proteins do not have access to cytoskeleton, as they are located in the outer leaflet of the plasma membrane. Detergent-insoluble GPI-anchored proteins are enriched in DRMs. This finding led us to postulate that partitioning of the saturated acyl chains on GPI-anchored proteins into the l_o phase targets the proteins to rafts. Alternatively, protein–protein contacts might be required for detergent-insolubility of GPI-anchored proteins. To test these possibilities, we purified a GPI-anchored protein, placental alkaline phosphatase (PLAP), and incorporated it into SCRL liposomes that (as discussed above) probably contain both detergent-soluble l_d and detergent-resistant l_o phase domains. When we incorporated PLAP into these liposomes, subjected them to detergent extraction, and separated DRMs and the Triton-soluble fractions, we found that PLAP associated with the DRMs. This result shows that the protein interacts directly with lipids in the l_o-phase. Other GPI-anchored proteins behave the same way, while a control transmembrane protein is fully solubilized.

Functions of Rafts

Rafts have been proposed to form in the *trans*-Golgi network, and to function during sorting of apical and basolateral proteins into separate transport vesicles in polarized epithelial cells. In what appears to be an analogous process, rafts have also been implicated in

axonal versus dendritic sorting of proteins in neurons. Rafts are also required for infection of mammalian cells by a number of viruses, including HIV, measles, and Ebola virus. Rafts are required for both entry of viruses into target cells and budding of mature virions from infected cells. However, the best-characterized functions of rafts are in signaling, especially in hematopoietic cells, and in membrane pits called caveolae, as described next.

Signaling in Hematopoietic Cells

Signaling through the antigen receptors in both T cells and basophils also occurs in rafts. For instance, in T cells, the T-cell receptor, associated kinases Lck and Fyn, the downstream adaptor protein LAT, and the costimulatory protein CD28 are present in rafts during signaling. Mutations in Lck and LAT that prevent association of these proteins with rafts affect signaling through the TCR, as do agents that disrupt rafts. These results show that rafts play an important role in signaling in T cells. This novel mechanism of regulating interactions between proteins by selective partitioning into membrane domains is unlikely to be restricted to one cell type. Further work is likely to demonstrate the importance of rafts in signaling in other cell types as well.

Caveolae

Caveolae are 50–100 nm pits in the plasma membrane of most mammalian cells. The membrane protein caveolin-1 plays an important structural role in caveolae, and can induce their formation when expressed in cells that lack caveolae. Unlike clathrin-coated pits, whose formation is induced by transient recruitment of soluble clathrin and adaptor complex coat to membranes, caveolin-1 is an integral membrane protein, and remains embedded in the membrane. Caveolin-1 (22 kDa) forms high-molecular-weight oligomers (400–600 kDa). These oligomers associate with each other in the plane of the membrane in caveolae. Several pieces of evidence show that lipid rafts are concentrated in caveolae. For instance, GPI-anchored proteins have a high affinity for caveolae and will cluster there when cross-linked by antibodies. Gangliosides, acidic glycosphingolipids that are important components of lipid rafts, show similar behavior. Caveolin-1 itself has a high affinity for rafts, and is enriched in DRMs.

Several functions have been ascribed to caveolae. They appear to be signaling centers, where a number of signaling proteins are concentrated. A role for caveolae in intracellular cholesterol transport has also been proposed. Caveolin-1 is a cholesterol-binding protein, which may contribute to a role in cholesterol homeostasis. Caveolae can also internalize from the cell surface. In endothelial cells, caveolae may participate in transport of albumin across the cell monolayer. At least some pathogens have co-opted this pathway. SV40 virus and some pathogenic *Escherichia coli* (*E. coli*) bacteria enter mammalian cells through caveolae during infection.

See Also the Following Articles

Fat Mobilization: Perilipin and Hormone-Sensitive Lipase • Glycosylphosphatidylinositol (GPI) Anchors • Lipid Bilayer Structure • Src Family of Protein Tyrosine Kinases • V-ATPases • Vitamin D

Glossary

caveolae 50–100 nm plasma membrane pits coated with tightly packed oligomers of caveolin-1 and/or other caveolin proteins.

ganglioside Acidic glycosphingolipid containing one or more sialic acid moieties.

glycosphingolipid Sphingolipid with one or more sugars as a head group.

GPI-anchored protein Protein anchored on the outside of the plasma membrane by covalent linkage to glycosyl phosphatidylinositol.

lipid raft Membrane microdomain in the liquid-ordered (l_o) phase; in cell membranes, rich in sterol and sphingolipids.

sphingolipid Membrane lipid with a ceramide backbone consisting of a sphingoid base backbone and a long saturated acyl chain, and a polar head group.

Further Reading

Brown, D. A., and London, E. (1998). Structure and origin of ordered lipid domains in biological membranes. *J. Membr. Biol.* **164**, 103–114.

Harder, T. (2001). Raft membrane domains and immunoreceptor functions. *Adv. Immunol.* **77**, 45–92.

Jacobson, K., and Dietrich, C. (1999). Looking at lipid rafts? *Trends Cell Biol.* **9**, 87–91.

Mukherjee, S., and Maxfield, F. R. (2000). Role of membrane organization and membrane domains in endocytic lipid trafficking. *Traffic* **1**, 203–211.

Simons, K., and Ikonen, E. (1997). Functional rafts in cell membranes. *Nature* **387**, 569–572.

Smart, E. J., Graf, G. A., McNiven, M. A., Sessa, W. C., Engelman, J. A., Scherer, P. E., Okamoto, T., and Lisanti, M. P. (1999). Caveolins, liquid-ordered domains, and signal transduction. *Mol. Cell Biol.* **19**, 7289–7304.

van der Goot, F. G., and Harder, T. (2001). Raft membrane domains: from a liquid-ordered membrane phase to a site of pathogen attack. *Semin. Immunol.* **13**, 89–97.

Biography

Deborah A. Brown is a full Professor in the Department of Biochemistry and Cell Biology at the State University of New York at Stony Brook. In collaboration with Dr. Erwin London, she developed the prevailing model for lipid raft structure, demonstrating that raft lipids exist in membranes as liquid-ordered phase domains. Her principal research interests are in the structure and function of membrane rafts, and membrane trafficking. She obtained a Ph.D. from Stanford University. She received postdoctoral training at Yale University School of Medicine.

Lipoproteins, HDL/LDL

Fayanne E. Thorngate and David L. Williams
State University of New York, Stony Brook, New York, USA

Lipoproteins are large complexes of lipids and proteins that allow the transport of nonpolar lipids through the aqueous plasma. Lipoproteins allow the uptake and transport of dietary fat, fat-soluble vitamins, and cholesterol to peripheral sites to provide energy (skeletal muscle) or for storage (adipose tissue). They consist of a core of nonpolar triglycerides (TG) and cholesteryl ester (CE) surrounded by a monolayer of phospholipids (PL), free cholesterol, and protein. The apolipoproteins are necessary for maintaining the structure of the particles and often serve as ligands or cofactors for receptors and enzymes involved in lipid metabolism. The two major classes of lipoproteins circulating in humans are high-density lipoprotein (HDL) and low-density lipoprotein (LDL), often referred to as "good" cholesterol and "bad" cholesterol, respectively, because of their relative roles in the development of cardiovascular disease.

Structure and Classification

The density at which they float in density-gradient ultracentrifugation defines lipoproteins. The more lipid the particle contains, the lighter its buoyant density. Figure 1 shows the basic structure of the lipoproteins as well as the major size classes. They are also sometimes classified by their complement of apolipoproteins.

Lipoprotein Structure

The cross-section of the chylomicron (CM) in Figure 1 shows the basic structure shared by all of the lipoprotein classes. They are spheres with a core composed of the neutral lipids triglyceride (TG) and cholesterol fatty acid ester (CE). A monolayer of phospholipid (PL), free cholesterol, and apolipoproteins surrounds and solubilizes the water-insoluble core lipids. PLs have polar head groups and hydrophobic acyl tails, which allow them to act as a detergent to solubilize the hydrophobic core lipids.

Apolipoproteins

The apolipoproteins are amphipathic proteins. They have one face that is hydrophobic and interacts with the lipoprotein lipids and one face that is hydrophilic and interacts with the aqueous plasma. Because of their amphipathic properties, the apolipoproteins act as detergents to keep the lipids in solution as microemulsion particles.

Amphipathic α-helix

A fundamental biochemical feature of the amphipathic character is that it is due to protein secondary structure and not to the primary amino acid sequence. The exchangeable apolipoproteins evolved from a common ancestor, and have a structure composed of variable numbers of 11 or 22 amino acid repeat units that form amphipathic α-helices. Thus, when the amino acid chain assumes an α-helical configuration, one face of the helix has hydrophobic amino acid side chains and interacts with lipids and one face of the helix has hydrophilic amino acid side chains and interacts with water. Figure 2 shows a space filling model of apoliprotein A1 (apoA1) as a helical ring, with the lighter colored hydrophobic amino acids on the inside of the ring. The 10 amphipathic α-helices are numbered.

Apolipoprotein Functions

All of the apolipoproteins, except for apolipoprotein B (apoB) are exchangeable and can dissociate and transfer to other particles. They serve as structural components of the lipoprotein and, depending on the apolipoprotein, act as ligands for receptors, activators of enzymes involved in lipid metabolism, or as inhibitors. The overall complement of apolipoproteins on a particle directs its metabolic fate. Table 1 is a list of the major apolipoproteins and some of their basic characteristics.

Metabolism

Apolipoprotein B Lipoprotein Metabolism

CM, secreted by the intestine, have apoB48 as their primary apolipoprotein. The liver secretes very low density lipoprotein (VLDL) with apoB100 as its

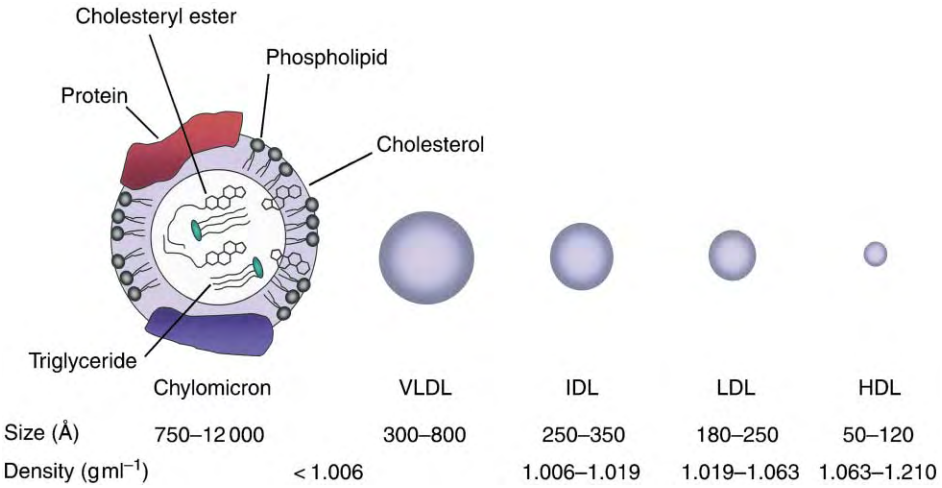

FIGURE 1 Basic physical and structural characteristics of lipoproteins (sizes are not to scale). All lipoproteins are spherical complexes with the sizes and buoyant densities shown beneath. The largest particle, the chylomicron, is shown in cross-section to illustrate its composition; the other particles have similar basic structures, differing in the amount of each component. VLDL, very low density lipoprotein; IDL, intermediate-density lipoprotein; LDL, low-density lipoprotein; HDL, high-density lipoprotein.

primary apolipoprotein. The products of VLDL metabolism in the circulation are intermediate-density lipoprotein (IDL) and low-density lipoprotein (LDL). The apoB lipoproteins carry TG, cholesterol, and fat-soluble vitamins through the circulation to peripheral tissues.

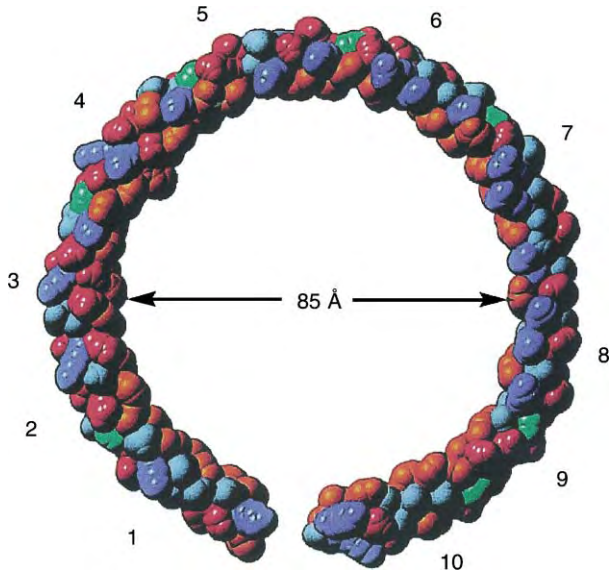

FIGURE 2 A top view of the interfacial surface of apoAI, shown as a space filling model. The lighter shaded, hydrophobic, residues are on the inner face. The ten tandem repeat amphipathic α-helices are numbered. The inner diameter of the structure is 85 Å and the outer diameter is 105 Å. (Reproduced from Segrest, J. P., Jones, M. K., Klon, A. E., Sheldahl, C. J., Hellinger, M., De Loof, H., and Harvey, S. C. (1999). A detailed molecular belt model for apolipoprotein A–I in discoidal high density lipopoprotein. *J. Biol. Chem.* **274**, 31755–31758.)

Dietary Absorption and Chylomicrons

Dietary fat, TG, is broken down in the intestine to fatty acids and glycerol. These fatty acids and dietary cholesterol are taken up by enterocytes, reesterified to TG and CE, and packaged into CM. CMs require apoB48 for formation and carry apoAI, apoAII, and apoIV on their surface as well. The intestine secretes the CM into the lymph and they subsequently enter the circulation where CMs are rapidly catabolized. As shown in Figure 3, lipoprotein lipase (LPL) bound to heparin sulfate proteoglycans on the capillary lumen hydrolyzes the CM–TG. Apo CII is required to activate LPL, and both apoCI and apoCIII inhibit LPL activity. The fatty acids generated are then taken up by muscle as an energy source or by adipocytes and reesterified to form TG for storage as fat. The remaining CM remnants lose the apoA's and acquire apolipoprotein E (apoE) and apolipoprotein C's (apoC's) from the circulation. ApoE serves as a ligand for all of the LDL receptor family members, and mediates clearance of the CM remnants by receptors primarily on the liver. This part of the lipoprotein metabolic pathway is referred to as the extrinsic pathway, as it deals with lipid coming from external sources.

Lipoproteins Produced by the Liver

The liver can also package and secrete lipids, either from remnant catabolism or endogenous synthesis. ApoB100 is essential for the formation of VLDL, which are smaller than CM, but carry significant amounts of TG and CE. This branch of the metabolic pathway is the intrinsic pathway, since it involves endogenous lipids.

TABLE I

Physical and Functional Characteristics of the Apolipoproteins

Apolipoprotein	Molecular mass (Da)	Site of synthesis	Lipoprotein association	Function
ApoAI	28 400	Liver, intestine	HDL, CM	Maintains HDL structure, activates LCAT
ApoAII	17 414	Liver, intestine	HDL, CM	Not well characterized
ApoAIV	46 465	Intestine	HDL, CM	Not well characterized
ApoAV	~39 000	Liver	HDL	Modulates circulating triglyceride levels
ApoB48	241 000	Intestine	CM	Maintains CM structure
ApoB100	512 000	Liver	VLDL, IDL, LDL	Maintains VLDL, IDL, LDL structure, ligand for LDL receptor
ApoCI	6 630	Liver	CM, VLDL, IDL, HDL	Inhibits uptake of CM and VLDL, inhibits lipases
ApoCII	8 900	Liver	CM, VLDL, IDL, HDL	Activates lipoprotein lipase
ApoCIII	8 900	Liver	CM, VLDL, IDL, HDL	Inhibits uptake of CM and VLDL, inhibits lipases
ApoE	34 145	Primarily liver and steroidogenic tissues, many sites	CM, VLDL, IDL, HDL	Ligand for CM and VLDL remnant clearance, binds to all LDL receptor family members
Apo(a)	Varies	Liver	VLDL, IDL, LDL	Unknown, procoagulant

The table lists the most common plasma apolipoproteins, giving their size in Da, their sites of biosynthesis, their respective lipoprotein associations, and some of their major functions. Apolipoproteins, Apo; lecithin cholesterol acyltransferase, LCAT.

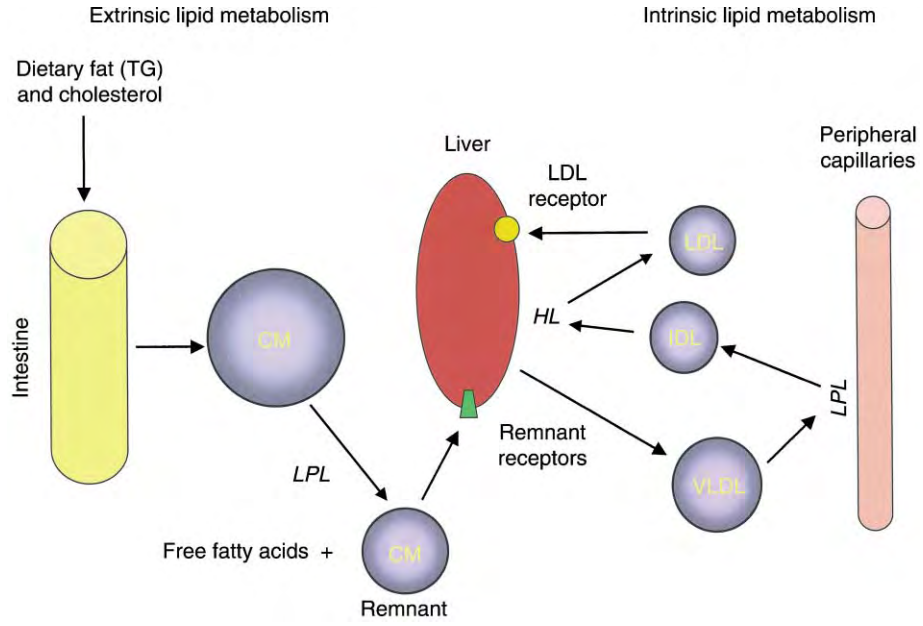

FIGURE 3 Apolipoprotein B (ApoB)-containing lipoprotein metabolism. Enzyme names are shown in italics. In the extrinsic pathway, the small intestine absorbs fats (triglycerides, TG) and cholesterol and resecretes them in chylomicrons (CMs). CMs in the circulation are acted on by lipoprotein lipase (LPL), which hydrolyzes TG and releases fatty acids. One of several remnant receptors on the liver takes up the remaining CM remnants. In the intrinsic pathway, the liver repackages the remnant lipids and secretes them as very low density lipoproteins (VLDL). LPL in the periphery breaks down the VLDL-TG for local energy use. The resulting smaller particles, intermediate-density lipoproteins (IDL), can then either be cleared by liver remnant receptors, or further hydrolyzed by hepatic lipase (HL) at the liver. LDL receptors on the liver or elsewhere take up the final metabolic product, low-density lipoprotein (LDL).

As shown in the right-half of Figure 3, VLDL is lipolyzed by LPL in the periphery, similar to CM. In the circulation, it picks up apoE's and apoC's that modulate its metabolism. Liver remnant receptors clear the VLDL remnants by binding to apoE on the lipoprotein and internalizing the particle. Alternatively, VLDL remnants remain in the circulation for further catabolism. Hepatic lipase (HL), localized to heparin sulfate proteoglycans on the liver, hydrolyzes both TG and PL. IDL is a product of VLDL lipid digestion in the circulation; further metabolism of the particles produces LDL. LDL loses most of the exchangeable apolipoproteins and has mainly apoB100 that is now a ligand for the LDL receptor. In a fasted state, LDL contains most of the circulating cholesterol. Mutations in the LDL receptor can cause familial hypercholesterolemia, characterized by very high plasma cholesterol levels and the development of premature atherosclerosis and heart disease, demonstrating how crucial the receptor is for normal lipoprotein metabolism. Apo(a) is a complex of Lp(a), a protein similar to plasminogen, covalently linked to apoB100 in LDL. The plasma concentrations of apo(a) vary widely from person to person. Lp(a) interferes with clearance of the particles, and interferes with plasminogen action, making it prothrombotic.

HDL Metabolism and Reverse Cholesterol Transport

The apoB-containing lipoproteins provide cholesterol and TG to peripheral tissues. HDL, with apoAI as its primary apolipoprotein provides a way to remove excess cholesterol from tissues and transport it back to the liver for excretion as bile acids and in the bile. This process is called reverse cholesterol transport, and is the only way most tissues can dispose of excess cholesterol.

Production of HDL

Unlike CM or VLDL, HDL is formed in the circulation. The liver secretes apoAI and apoAII either as lipid-free proteins or bound to a few PL. As shown in Figure 4, these complexes circulate as apolipoprotein–PL disks, and not as spherical particles. They can have various combinations of apoA's, but apoAI is predominant. An alternate source of lipid-poor apoAI and apoAIV is from the surface of CM as they are metabolized. These disks can interact with several systems to pick up lipids and mature into spherical HDL. Lipid-poor apolipoproteins can bind to the recently characterized protein, ATP-binding cassette protein type A1 (ABCA1). Most cell types express ABCA1 on their surface. ABCA1 mediates the transfer of PL and cholesterol from the cell surface to the apolipoprotein. When this occurs in peripheral tissues, it is the first step of reverse cholesterol transport; however, most apoAI is probably lipidated by ABCA1 in the liver.

Interestingly, mutations in ABCA1 cause a syndrome that is one of the first genetically caused lipoprotein disorders described. Tangiers disease is characterized by very low or no circulating apoAI and HDL, and accumulation of cholesterol in macrophage rich tissues, such as the tonsils. Only recently the genetic cause has been determined. The apoAI gene and its expression are normal in this syndrome, but without ABCA1 to transfer lipid to apoAI, the kidneys rapidly catabolize the apoAI.

With apoAI as an activator, the enzyme lecithin cholesterol acyltransferase (LCAT) can transfer an acyl group from a PL to the cholesterol, generating CE. The CE is nonpolar so it moves to form a core within the disk, generating a spherical HDL. These particles can also accept free cholesterol passively desorbing from the cell surface, a process facilitated by the HDL receptor, scavenger receptor class B type I (SR-BI). Free cholesterol efflux from cells is another mode of reverse cholesterol transport.

Lipid Transfer Proteins

There are two lipid transfer proteins involved in HDL metabolism in the plasma. Phospholipid transfer protein (PLTP) can transfer excess surface PL, generated during the metabolism of remnant lipoprotein core lipids to HDL. It also can facilitate the fusion of HDL particles, generating large HDL and lipid-poor apolipoproteins. Cholesteryl ester transfer protein (CETP) catalyzes the transfer of CE from HDL to VLDL and LDL, which can then be cleared by liver receptors for excretion. This is one way to complete reverse cholesterol efflux.

HDL Delivery of CE to Tissues

The only tissues capable of catabolizing cholesterol are the liver and steroid hormone producing organs (adrenal, ovaries, testes). The liver converts cholesterol to bile acids and excretes them through the intestine. The steroidigenic organs convert cholesterol to steroid hormones (cortisol, estrogen, testosterone, etc.). These tissues have an abundance of the HDL receptor, SR-BI, which in addition to facilitating cholesterol efflux from cells allows the uptake of CE by cells. HDL binds to the receptor and selectively transfers the CE core to the cell, without the degradation of the particle as a whole. Selective uptake differs from the LDL receptor uptake pathway, in which the whole lipoprotein is internalized and degraded. HL found on the surface of the liver and adrenal gland hydrolyzes the PL and TG left in the CE depleted HDL, releasing lipid-poor apoAI. Probably the major path for the loss of cholesterol from the body is the loss of cholesterol with epidermal cells shed from the skin. However, the SR-BI mediated transfer of CE to the

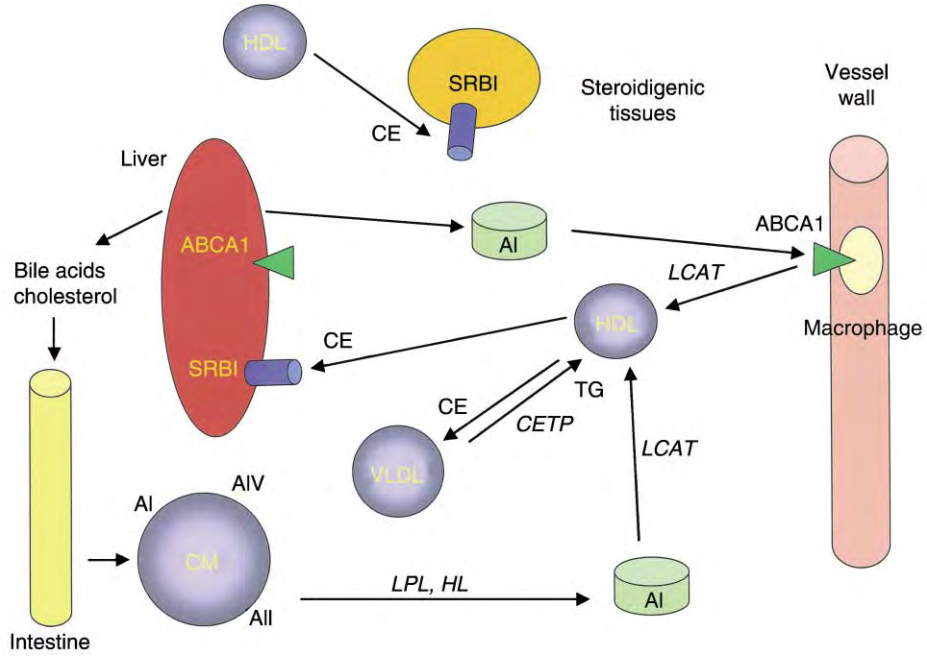

FIGURE 4 High-density lipoprotein (HDL) metabolism and reverse cholesterol transport. Lipolytic enzyme and transfer protein names are shown in italics. Apolipoprotein AI (AI) enters the circulation either by secretion from the liver as a lipid-poor apolipoprotein or on CM secreted by the intestine. Lipoprotein lipase (LPL) and hepatic lipase (HL) hydrolyze CM lipids, releasing lipid-poor apoA's from the remnant surface. The lipid-poor apoAI-phospholipid (PL) disks (shown as disks instead of spheres) can interact with peripheral ATP binding cassette transporter type A1 (ABCA1) and pick up PL and cholesterol. Lecithin cholesterol acyltransferase (LCAT) can then esterify the cholesterol in the outer monolayer of the disks, producing cholesteryl ester (CE) that moves to form a lipid core; all of these activities result in larger, spherical HDL. These CE-enriched HDLs can then deliver the CE to the liver or steroidigenic tissues via interaction with scavenger receptor type BI (SR–BI). In addition, cholesteryl ester transfer protein (CETP) can mediate the exchange of CE from HDL for triglyceride (TG) from VLDL or remnants with the subsequent clearance of the remnants by the liver. The liver converts cholesterol delivered to it to bile acids, or secretes the cholesterol with the bile into the intestine for excretion.

liver is critical for removing cholesterol from internal tissues and completing reverse cholesterol transport.

Pathologies of Lipoprotein Metabolism

The primary metabolic contributor to the development of atherosclerosis (deposition of cholesterol in the artery wall with subsequent vascular, inflammatory and thrombotic dysfunction) is elevated LDL cholesterol. There is a strong epidemiological evidence that elevated LDL cholesterol correlates with cardiovascular disease, as does decreased HDL cholesterol. Several natural human mutations elevate LDL levels and lead to atherosclerotic vascular disease, implicating elevated LDL levels as a requisite cause of this disease. More recently, studies with LDL lowering drugs demonstrate reduced disease risk. Additionally, a wealth of studies in numerous animal models demonstrates that LDL, IDL, and CM remnants can cause atherosclerotic disease. Atherosclerosis is one of the major contributors to cardiovascular disease, leading to heart attacks and stroke. Disorders of lipoprotein metabolism may also contribute to obesity, type 2 diabetes, and renal disease, all of which are becoming more prevalent in our aging population.

Disruption of any step in these pathways can lead to imbalances in plasma lipids, by either increased production or decreased catabolism, and clearance. There are many syndromes stemming from mutations in proteins involved in lipoprotein metabolism. A classical example is familial hypercholesterolemia, mentioned above. In this syndrome LDL receptors are not functional, severely inhibiting LDL clearance, leading to accumulation of LDL cholesterol in the circulation. This can lead to death from heart attacks as young as the early teens. The Further Reading selections describe other pathologies of lipoprotein metabolism.

A great deal has been learned about the components and interactions of these systems, spurred on recently by the development of transgenic and knockout mouse models. However, it is critical that we expand our understanding of these systems, especially in view of the dramatic increases in diseases linked to disruptions of lipoprotein metabolism.

See Also the Following Articles

Cholesterol Synthesis • Endocytosis • Fat Mobilization: Perilipin and Hormone-Sensitive Lipase • Fatty Acid Oxidation • Fatty Acid Receptors • Fatty Acid Synthesis and Its Regulation

Glossary

apolipoproteins The major protein components of lipoproteins. They stabilize the structure of the lipoproteins. In addition, some serve as ligands for lipoprotein receptors and some are activators or inhibitors of enzymes and transfer proteins involved in lipoprotein metabolism.

ATP cassette binding protein type A1 A recently characterized apolipoprotein binding protein. It mediates the transfer of phospholipid and cholesterol from cells to lipid-poor apolipoproteins.

LDL receptor family A family of related cell-surface receptors critical for lipoprotein uptake into cells. All of the receptors bind apoE, and the definitive member; the LDL receptor also binds apoB and is critical for LDL uptake. Loss of LDL receptor function causes familial hypercholesterolemia.

reverse cholesterol transport The removal of cholesterol from peripheral tissues and its clearance and excretion, mainly by the liver. This process protects the vessel wall from accumulating cholesterol and becoming atherosclerotic.

scavenger receptor class B type I A HDL receptor that facilitates efflux of free cholesterol from cells to HDL. It also mediates the selective uptake of CE from HDL for clearance by the liver or steroid hormone synthesis in the adrenal gland, ovaries, and testes.

Further Reading

Betteridge, D. J., Illingworth, D. R., and Shepherd, J. (eds.) (1999). *Lipoproteins in Health and Disease*. Arnold, London.

DeWinter, M. P. J., and Hofker, M. H. (2002). New mouse models for lipoprotein metabolism and atherosclerosis. *Curr. Opin. Lipidol.* **13**, 191–197.

Knowles, J. W., and Maeda, N. (2000). Genetic modifiers of atherosclerosis in mice. *Arterioscler. Thromb. Vasc. Biol.* **20**, 2336–2345.

Scriver, D. R., Sly, W. S., Childs, B., Beaudet, A. L., Valle, D., Kinzler, K. W., and Vogelstein, B. (2002). *The Metabolic and Molecular Bases of Inherited Disease* 8th edition, Chapters 114–123. McGraw-Hill, New York.

Segrest, J. P., Jones, M. K., Klon, A. E., Sheldahl, C. J., Hellinger, M., De Loof, H., and Harvey, S. C. (1999). A detailed molecular belt model for apolipoprotein A–I in discoidal high density lipopoprotein. *J. Biol. Chem.* **274**, 31755–31758.

Singh, B. K., and Mehta, J. L. (2002). Management of dyslipidemia in the primary prevention of coronary heart disease. *Curr. Opin. Cardiol.* **17**, 503–511.

Biography

Fayanne E. Thorngate is a research instructor of pharmacological sciences in the School of Medicine at the State University of New York at Stony Brook. Her research interests are the mechanisms of atherosclerotic disease development, cholesterol and lipoprotein metabolism, with an emphasis on the use of mouse models of disease. Dr. Thorngate received her Ph.D. in biochemistry and nutrition from the University of North Carolina at Chapel Hill where she was a National Science Foundation fellow in biochemistry. She did postdoctoral work in lipoprotein metabolism at the University of Tennessee Health Sciences Center in Memphis, and at the State University of New York at Stony Brook.

David L. Williams is a Professor of Pharmacological Sciences in the School of Medicine at the State University of New York at Stony Brook. His research interests are in the areas of atherosclerotic disease processes, cholesterol, and lipoprotein metabolism, and in the cell biology of lipoprotein receptors. Dr. Williams received his Ph.D. in cell biology from the University of Illinois at Urbana and did postdoctoral work in molecular biology at the University of California at San Francisco. He was among the first investigators to apply molecular biological approaches to the study of lipoproteins and the first to establish the tissue sites of apolipoprotein E expression in humans and animal models.

Low Barrier Hydrogen Bonds

Perry A. Frey
University of Wisconsin, Madison, Wisconsin, USA

Proteins contain mainly weak, conventional hydrogen bonds; however, a few enzymes have low barrier hydrogen bonds (LBHBs) in transition state analogue complexes. Hydrogen bonds display variations in physicochemical properties including length, spectroscopic characteristics, and strength. Three classes of hydrogen bonds have been defined – weak (2–8 kcal mol^{-1}), strong (10–20 kcal mol^{-1}), and very strong (24–40 kcal mol^{-1}). In a weak hydrogen bond, the proton is bonded to one heteroatom by a dipolar covalent bond and engages in a weak electrostatic attraction with another heteroatom. In a strong hydrogen bond, or LBHB, the heteroatoms are closer than a van der Waals contact, the covalent bond to the proton is elongated, and the contact between the proton and the second heteroatom is significantly shorter than in a weak hydrogen bond. In a very strong, or single-well hydrogen bond, the heteroatoms are much closer than a van der Waals contact, and the proton is nearly centered between them. LBHBs in proteins and small molecules are characterized by their spectroscopic and thermodynamic properties, deuterium fractionation factors, and crystallographic structures. LBHBs have been identified in transition state analogue complexes of a few enzymes and are postulated to stabilize the transition states in catalysis.

The Nature of Hydrogen Bonds

Hydrogen bonds were controversial throughout the 20th century. By mid-20th century, the weak conventional hydrogen bonds were reasonably well understood and widely accepted. Unlike covalent bonds, which vary in strength within a factor of ~4 (30–120 kcal mol^{-1}), hydrogen bonds are much less constrained in their geometry and physical properties, and they vary in strength by a factor of at least 20-fold (2–40 kcal mol^{-1}). Very few strong hydrogen bonds had been documented before the mid-20th century, principally the very strong hydrogen bond in hydrogen difluoride $[F\cdots H\cdots F]^-$ (40 kcal mol^{-1}). Such strong hydrogen bonds were thought to be limited to crystalline states. In the latter half of the century, strong hydrogen bonds were discovered in several classes of organic molecules in crystals and aprotic liquid phases and characterized by crystallographic, spectroscopic, and chemical methods.

Weak, Strong, and Very Strong Hydrogen Bonds

The distinctions among hydrogen bonds can be illustrated by the differences among their energy profiles, as shown in Figure 1. Figure 1A is the energy profile for a weak hydrogen bond, that in Figure 1B is for a strong or LBHB, and that in Figure 1C is for a single-well or very strong hydrogen bond. The three classes are sometimes referred to as weak, moderate, and strong hydrogen bonds. Most hydrogen bonds in proteins and nucleic acids involve oxygen or nitrogen as the heteroatoms. For that reason, the hydrogen bonding properties delineated below refer to N or O as heteroatoms. Larger or smaller heteroatoms such as sulfur or fluorine display analogous properties with physical parameters outside the ranges for N and O.

Weak Hydrogen Bonds

As illustrated in Figure 1A, the hydrogen (or deuterium) is confined to covalent bonding with one heteroatom by the fact that their zero point vibrational energies are much lower than the barrier separating the heteroatoms. The covalent bond linking the electronegative atom to a hydrogen is dipolar, with a partial positive charge on the proton and a partial negative charge on the heteroatom. The electrostatic attraction between the proton and another partially negative heteroatom is a weak hydrogen bond. The strengths of weak hydrogen bonds range between 2 and 8 kcal mol^{-1}, depending on the type of heteroatoms, their electrostatic charge, the distance separating them, and the dielectric medium. Because they are weak, conventional hydrogen bonds easily undergo exchange with protons of water, with enthalpies of activation on the order of 2–3 kcal mol^{-1}.

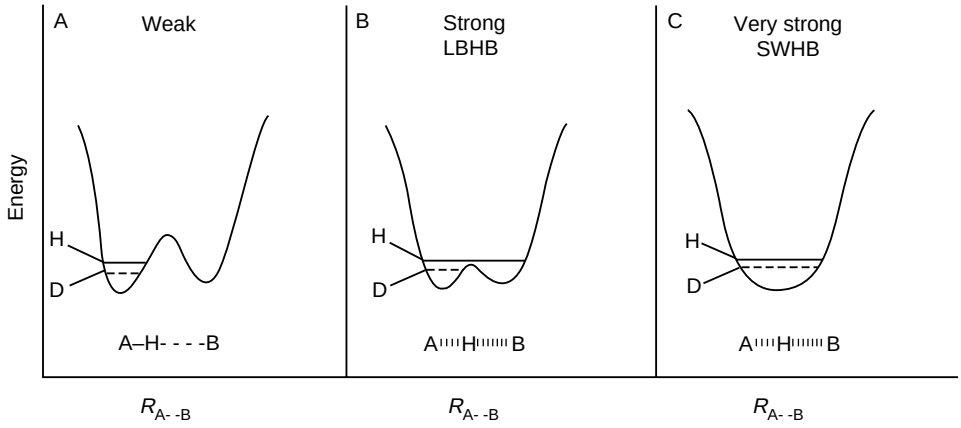

FIGURE 1 In (A), the double well potential for a proton covalently bonded to heteroatom A and weakly hydrogen bonded to heteroatom B is illustrated. The zero point energies for H and D are both well below the barrier, and both are strictly covalently bonded to A. In (B) for an LBHB, the heteroatoms are drawn close together in violation of van der Waals contact distance, the proton is moved toward B and away from A, and the barrier is lowered to near the zero point energy of H. The zero point energy of D is lower, so that deuterium is less attracted to B. In (C) for a single-well hydrogen bond, the heteroatoms are even closer together, and the proton is nearly centered between them. In the LBHB and SWHB the bonding of the proton to heteroatom B is partially covalent.

LBHBs—Strong Hydrogen Bonds

In an LBHB (Figure 1B) the heteroatoms are closer together and separated by significantly less than the van der Waals contact distance. As a consequence, the energy barrier between them is lowered to the range of the zero point vibrational energy for hydrogen, so that the hydrogen feels increased attraction to the other heteroatom and is drawn away from the first heteroatom, A···H in Figure 1B. Deuterium, feels less attraction to the second heteroatom, owing to its lower zero point energy. Because of this difference, an LBHB displays deuterium and tritium isotope effects. LBHBs are stronger (10–20 kcal mol^{-1}) than weak hydrogen bonds because of the partial covalency between hydrogen and the second heteroatom, H···B in Figure 1B. As they are strong, LBHBs undergo exchange with protons of water less readily than weak hydrogen bonds. In an LBHB the proton is strongly held, and the activation enthalpy for exchange with the protons of water is much higher than the $\sim$3 kcal mol^{-1} for a weakly hydrogen bonded proton. For LBHBs in proteins, the activation enthalpies for exchange are typically 10–19 kcal mol^{-1}.

Single-Well or Very Strong Hydrogen Bonds

In a single-well hydrogen bond the heteroatoms are so close together that the zero point energies of both hydrogen and deuterium lie above the barrier, as in A···H···B of Figure 1C. The proton is almost equally bonded between the heteroatoms and is nearly centered between them. Perfectly symmetrical, single-well hydrogen bonds are the strongest, 24–40 kcal mol^{-1}, and are observed in very few small molecules. Such hydrogen bonds have not been detected in proteins.

Physicochemical Properties

Bond Lengths

Weak Hydrogen Bonds

The covalent bond length (O, N–H) is about 0.95Å, the length of the electrostatic contact with the second heteroatom is $\geq$ 1.7Å, and the separation between the heteroatoms is $\geq$ 2.6Å for O···O, $\geq$ 2.7Å for O···N, and $\geq$ 2.8Å for N···N. Distances separating the heteroatoms can vary from the minima quoted above to as much as 3.5Å.

LBHBs

In an LBHB (Figure 1B) the covalent bond is elongated to 1.05–1.1Å, and the distance to the second heteroatom is shortened, e.g., to 1.4–1.5Å. The separation between heteroatoms is shortened to $\leq$2.6Å for O···O, $\leq$2.7Å for O···N, and $\leq$2.8Å for N···N. A short contact distance between heteroatoms is necessary but not sufficient for an LBHB. To be an LBHB, the hydrogen must be positioned in alignment with the heteroatoms. If the hydrogen is out of alignment, the hydrogen bond will be weak. In the strongest LBHBs, the proton affinities of the heteroatoms are similar or identical. The p*K*a of the conjugate acid of a heteroatom is a measure of proton affinity, and heteroatoms in functional groups with similar or identical values of p*K*a form the strongest hydrogen bonds.

Single-Well Hydrogen Bonds

The hydrogen lies nearly equidistant from the heteroatoms and is approximately equally shared. The hydrogen is 1.2–1.3Å from each heteroatom, depending on whether it is O or N. Perfectly symmetrical hydrogen bonds are rare and so far observed only in small molecules incorporating special structural constraints that favor single-well hydrogen bonding. Single-well hydrogen bonds range in strength from 24 to 40 kcal mol^{-1} and are the strongest hydrogen bonds. They are formed between heteroatoms of functional groups with identical values of p*K*a, in molecules or lattices in which the groups are held in close proximity.

Spectroscopic Properties

Weak Hydrogen Bonds

The NMR chemical shift of the proton ranges between 9 and 11 ppm and does not display an isotope effect (isotope shift) upon replacement with deuterium or tritium.

LBHBs

Due to the elongated bond to the hydrogen, A···H in Figure 1B, the proton is substantially deshielded from the nonbonding electrons of the heteroatom. Consequently, the NMR signal for an LBHB involving O or N is downfield in the range of 18–20 ppm on the chemical shift scale. In the absence of an internal magnetic effect, such as complexation with a paramagnetic metal ion, a downfield chemical shift is a strong indicator of an LBHB or single-well hydrogen bond. In an LBHB as in Figure 1B, the zero point energy difference between hydrogen and deuterium leads to deuterium and tritium isotope effects on the NMR signal, with that for deuterium falling upfield by up to 0.6 ppm from that for hydrogen.

As the proton in an LBHB interacts with both heteroatoms to a greater degree than a deuteron, there is an isotope effect on the infrared stretching frequency. The ratio of stretching frequencies ν_{OH}/ν_{OD} for and O–H and O–D engaged in an LBHB differs from the ratio typical of weak hydrogen bonds. For weak hydrogen bonds $\nu_{OH}/\nu_{OD} = 1.4$ and represents the mass difference between hydrogen and deuterium. For an LBHB, $1.0 \leq \nu_{OH}/\nu_{OD} < 1.4$ in small molecules. This is because of the greater strength of the LBHB with H than with D, and the difference in strength arises because of the differential interactions of H and D with the barrier in Figure 1B. This property of LBHBs in small molecules has been extensively documented. Among the physicochemical properties that have been used in characterizing LBHBs, the deuterium isotope effect on the infrared stretching frequencies is the only one that has not been applied to LBHBs in proteins.

Single-Well Hydrogen Bonds

Single-well hydrogen bonds display downfield NMR signals at 21–22 ppm when the heteroatoms are O or N. Because the zero point energies of both H and D lie above the barrier in Figure 1C, single-well hydrogen bonds do not display deuterium or tritium isotope effects on NMR signals. They also do not display deuterium isotope effects on infrared stretching frequencies, that is, $\nu_{OH}/\nu_{OD} = 1.4$.

Deuterium Fractionation Factors

Weak Hydrogen Bonds

Weakly hydrogen bonded protons display deuterium fractionation factors Ψ of about 1.0–1.2. The fractionation factor is the equilibrium constant for the exchange of hydrogen bonded protons with deuterons in deuterium oxide. A fractionation factor of 1.0 means that deuterons and protons are bound with equal affinities.

LBHBs

In an LBHB, hydrogen is more strongly bonded than deuterium because of the effect illustrated in Figure 1B. Therefore, the deuterium fractionation factor Ψ for an LBHB is less than 1.0, typically 0.3–0.7.

Single-Well Hydrogen Bonds

In a single-well hydrogen bond, the zero point energies of both H and D lie above the barrier, so that they interact similarly with both heteroatoms. Therefore, the fractionation factor is generally ~1.0.

LBHBs in Enzymes

Serine Proteases

An LBHB was first assigned to the proton bridging His57 and Asp102 in chymotrypsin at low pH and in transition state analogue complexes of chymotrypsin. The assignment was based initially on the downfield NMR chemical shift for this proton of 18.0 ppm for chymotrypsin at low pH and 18.9 ppm for chymotrypsin a transition state-analogue complex, and on the close contact between His57 and Asp102 (<2.6Å) in crystal structures of transition state analogue complexes. The LBHB was postulated to stabilize the transition state and facilitate its formation. It was shown in this connection to increase the basicity of His57. The characterization of this LBHB in several transition state analogue complexes was completed by measurements of its fractionation factor of 0.3–0.4, its enthalpy of activation for exchange

of 14–19 kcal mol^{-1}, and the deuterium and tritium isotope effects on its NMR chemical shifts. The role of the LBHB in catalyzing the formation of the acyl-chymotrypsin intermediate in the action of chymotrypsin is illustrated in Figure 2. In resting chymotrypsin, His57 is not protonated and is engaged in weak hydrogen bonding with Asp102. His57 abstracts the proton from Ser195 as it attacks the acyl carbonyl group of a substrate to form the tetrahedral intermediate. In the transition state for proton abstraction, His57 becomes protonated on His57-Nε2, and the LBHB is formed between His57-Nδ1 and Asp102. The resulting LBHB stabilizes the transition state and tetrahedral adduct and thereby facilitates the formation of the metastable intermediate. The LBHB maintains the basicity of His57 with a p*K*a of 10.6 to 12, intermediate between that of Ser195 (13.4) and that of the amino terminus (9.2) of the peptide leaving group. Thus, the LBHB makes His57 an optimal acid/base catalyst for the acylation of Ser195 by a peptide substrate.

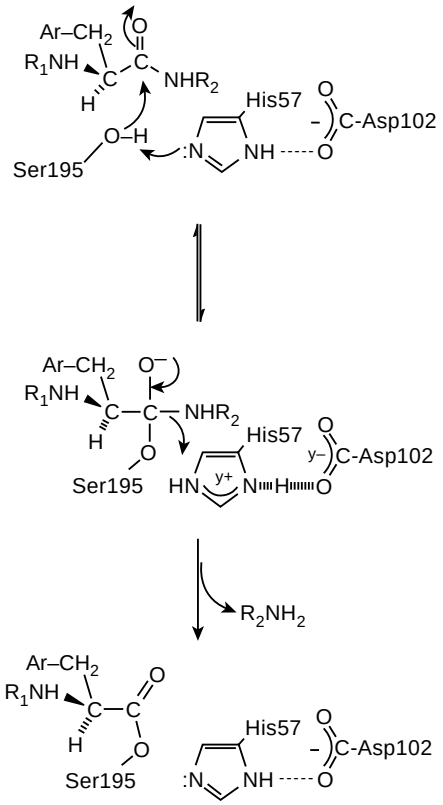

FIGURE 2 The role of the LBHB in the mechanism of acylation of serine proteases. In the Michaelis complex, the active site histidine (His57 in chymotrypsin numbering) is neutral and weakly hydrogen bonded to Asp201. In the first step, His57 abstracts a proton from Ser195 as it undergoes nucleophilic addition to the substrate carbonyl group. As His57-Nε2 becomes protonated, the hydrogen bond between His57-Nδ1 and Asp-Oδ2 becomes a strong LBHB, and this increases the basicity of His57 as it enters the transition state. The LBHB stabilizes the transition state and transient tetrahedral intermediate. In the second step, His57-Nε2 donates the proton to the N-terminal amino group of the leaving peptide.

Evidence, similar to but less extensive than that above, for chymotrypsin has been obtained for other serine proteases, especially trypsin and subtilisin. The crystal structure of subtilisin at 0.78Å resolution shows electron density for hydrogen in the LBHB linking His64 and Asp32. The electron density for the proton places it 1.2Å from His57-Nδ1 and 1.5Å from Asp32-Oδ2. ^{15}N NMR analysis of the LBHB in a transition state analogue complex of subtilisin indicates that the proton, 20–30%, is transferred toward Asp32. Both the crystallography and NMR spectroscopy verify that this is an LBHB and support its catalytic role as originally postulated in the action of chymotrypsin.

Serine Esterases

Serine esterases have catalytic triads similar to serine proteases and function by a similar mechanism. Extensive NMR analysis of the hydrogen bond, linking the active site histidine with the active site glutamate, document the presence of an LBHB.

Δ^5-3-Ketosteroid Isomerase

The isomerization requires the enolization of the 3-keto group of the substrate to form a homoenolate anion as a metastable intermediate. The homoenolate is within hydrogen bonding distance of Tyr14, and the p*K*a of the homoenol is similar to that of tyrosine or phenol. The phenolic inhibitor dihydroequilinen forms an LBHB with Tyr14 in analogy with a putative LBHB in the complex of the metastable homoenolate with Tyr14. The LBHB displays the properties including a downfield NMR signal, low deuterium fractionation factor, and close contact in the crystal structure. The LBHB is postulated to stablize the homoenolate and thereby facilitate its formation in the catalytic mechanism.

See Also the Following Articles

Kinetic Isotope Effects • Substrate Binding, Catalysis, and Product Release

Glossary

deuterium ractionation factor The equilibrium constant for exchange of a proton with the deuterons in D_2O.

isotope shift The upfield perturbation of an NMR signal of an atom when a heavy isotope is substituted for it.

transition state analogue A stable molecule that has nearly all of the structural features of a transition state.

Further Reading

Choi, G., Ha, N. C., Kim, S. W., Kim, D. H., Park, S., Oh, B. H., and Choi, K. Y. (2000). Asp-99 donates a hydrogen bond not to Tyr-14 but to the steroid directly in the catalytic mechanism of Delta 5-3-ketosteroid isomerase from Pseudomonas putida biotype B. *Biochemistry* **39**, 903–909.

Cleland, W. W. (1992). Low-barrier hydrogen bonds and low fractionation factor bases in enzymatic reactions. *Biochemistry* **31**, 317–3199.

Cleland, W. W., and Kreevoy, M. M. (1994). Low-barrier hydrogen bonds and enzymic catalysis. *Science* **264**, 1887–1890.

Frey P. A., Whitt S. A., Tobin J. B. (1994). A low-barrier hydrogen bond in the catalytic triad of serine proteases. *Science* **264**, 1927–1930.

Gerlt, J. A., and Gassman, P. M. (1993). Understanding the rates of certain enzyme-catalyzed reactions: proton abstraction from carbon acids, acyl-transfer reactions, and displacement reactions of phosphodiesters. *Biochemistry* **32**, 11943–11952.

Halkides, C. J., Wu, Y. Q., and Murray, C. J. (1996). A low-barrier hydrogen bond in subtilisin: 1H and 15N NMR studies with peptidyl trifluoromethyl ketones. *Biochemistry* **35**, 15941–15948.

Hibbert, F., and Emsley, J. (1990). Hydrogen bonding and chemical reactivity. *Adv. Phys. Org. Chem.* **26**, 255–379.

Jeffrey, G. A. (1997). *An Introduction to Hydrogen Bonding*. Oxford University Press, New York.

Kuhn, P., Knapp, M., Soltis, S. M., Ganshaw, G., Thoene, M., and Bott, R. (1998). The 0.78Å structure of a serine protease: Bacillus lentus subtilisin: *Bacillus lentus Subtilisin*. *Biochemistry* **37**, 13446–13452.

Lin, J., Cassidy, C. S., and Frey, P. A. (1998). Correlations of the basicity of His 57 with transition state analogue binding, substrate reactivity, and the strength of the low-barrier hydrogen bond in chymotrypsin. *Biochemistry* **37**, 11940–11948.

Lin, J., William, M., Westler, W., Wallace Cleland, Markley, J. L., and Frey, P. A. (1998). Fractionation factors and activation energies for exchange of the low barrier hydrogen bonding proton in peptidyl trifluoromethyl ketone complexes of chymotrypsin. *Proc. Natl. Acad. Sci.* **95**, 14664–14668.

Massiah, M. A., Viragh, C., Reddy, P. M., Kovach, I. M., Johnson, J., Rosenberry, T. L., Mildvan, A. S. (2001). Short, strong hydrogen bonds at the active site of human acetylcholinesterase: proton NMR studies. *Biochemistry* **40**, 5682–5690.

Mildvan, A. S., Harris, T. K., and Abeygunawardana, C. (1999). Nuclear magnetic resonance methods for the detection and study of low-barrier hydrogen bonds on enzymes. *Methods Enzymol.* **308**, 219–245.

Neidhart, D., Wei, Y., Cassidy, C., Lin, J., Cleland, W. W., and Frey, P. A. (2001). Correlation of low-barrier hydrogen bonding and oxyanion binding in transition state analogue complexes of chymotrypsin. *Biochemistry* **40**, 2439–2447.

Westler, W. M., Frey, P. A., Lin, J., Wemmer, D. E., Morimoto, H., Williams, P. G., and Markley, J. L. (2002). Evidence for a strong hydrogen bond in the catalytic dyad of transition-state analogue inhibitor complexes of chymotrypsin from proton-triton NMR isotope shifts. *J. Am. Chem. Soc.* **124**, 4196–4197.

Zhao, Q., Abeygunawardana, C., Talalay, P., and Mildvan A. S. (1996). NMR evidence for the participation of a low-barrier hydrogen bond in the mechanism of 5-3-ketosteroid isomerase. *Proc. Natl. Acad. Sci.* **93**, 8220–8224.

Biography

Perry A. Frey is the Robert H. Abeles Professor of Biochemistry at the University of Wisconsin-Madison. His main research interest is the elucidation of enzymatic and coenzymatic reaction mechanisms. He holds a Ph.D. in biochemistry from Brandeis University and was a postdoctoral fellow in Chemistry at Harvard University. He has authored a textbook in biochemistry and is a life-time member of the National Academy of Sciences.

Luft's Disease

Salvatore DiMauro
Columbia University, New York, USA

Luft's disease is an extremely rare human disorder characterized by loose coupling of mitochondrial oxidative phosphorylation in skeletal muscle, that is, loss of the control normally exerted by ATP on the rate of respiration of muscle mitochondria. Although described only in two patients, Luft's disease is of great historical importance because it was the first example of organellar medicine and it opened the field of mitochondrial diseases, which has expanded into a large and complex area involving all subspecialties of medicine.

Clinical Considerations

Both patients were women, one from Sweden, the other from Jordan, without any family history of similar disorders. The clinical hallmark was hypermetabolism, with fever, heat intolerance, profuse perspiration, polyphagia, polydipsia, and tachycardia at rest. Although both patients suffered from exercise intolerance, weakness was mild. The Jordanian patient also had diffuse erythema of the legs due to capillary proliferation, maybe an attempt by the body to create a radiator to facilitate heat dispersion. The initial diagnosis was hyperthyroidism, but Rolf Luft, an endocrinologist at the Karolinska Institute in Stockholm, ruled out this possibility and astutely suggested that mitochondrial dysfunction of skeletal muscle, the most abundant tissue in the body, could underlie this condition. A muscle biopsy confirmed that mitochondria were excessively numerous and morphologically abnormal, and polarographic studies of isolated mitochondria showed loose coupling. The paper describing these findings is a classic of clinical investigation, which amply justifies the eponym.

Onset of symptoms had been in childhood in both patients, and the course was slowly but relentlessly progressive: both women died, in their middle ages, of respiratory failure. Autopsies were not performed, but clinical evidence strongly suggests that the disease is confined to skeletal muscle, as heart function was normal and there were no symptoms of central nervous system (CNS) involvement.

Electromyography (EMG) was compatible with myopathy.

Therapy

In 1971, Haydar employed a naïve but pioneer approach to gene therapy in the second patient with Luft's disease,

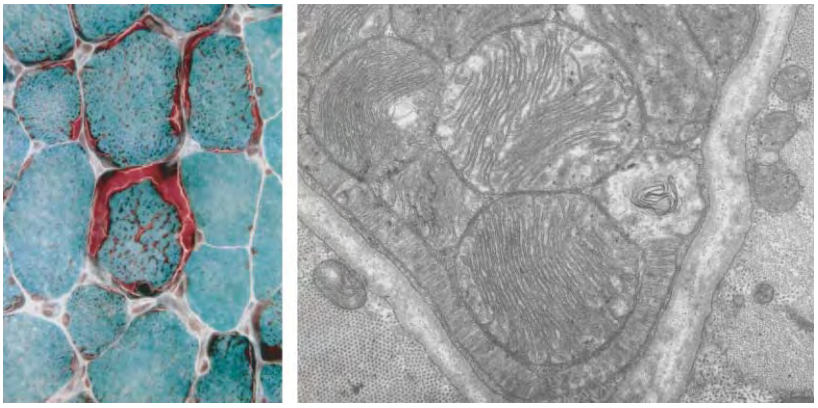

FIGURE 1 Morphology of a muscle biopsy from the second patient with Luft's disease. The left panel shows the histochemical stain of a frozen section with the modified Gomori trichrome, which reveals abnormal accumulations of mitochondria as reddish blotches (ragged-red fibers). The right panel is an electron micrograph showing a portion of one fiber (bottom) with normal morphology. The adjacent fiber (top) shows massive accumulation of mitochondria under the cell membrane. The accumulated mitochondria are greatly enlarged and have tightly packed cristae.

who was given chloramphenicol to inhibit mitochondrial protein synthesis and reduce her basal metabolic rate. During the first trial, some reduction of the basal metabolic rate was achieved and was accompanied by mild subjective improvement, but the second trial had to be interrupted because of drug toxicity.

Thus, the molecular basis of the prototypical mitochondrial myopathy remains obscure 40 years after Luft described the first patient, a situation made more difficult by the fact that only one other patient with Luft's disease has been identified; both patients are deceased, and no tissues are available, except fibroblasts from the second patient.

Muscle Biopsy

Morphology

In both women, there was massive proliferation of mitochondria, documented with the modified Gomori trichrome histochemical stain by the presence of ragged-red fibers (RRFs) in the second patient, and by electron microscopy in both patients. Ultrastructurally, there were large pools of mitochondria, predominantly under the sarcolemma. Many of the mitochondria were greatly enlarged and contained tightly packed cristae, some also contained abnormal osmiophilic inclusions (Figure 1). Intramuscular capillaries were overabundant.

A skin biopsy in the second patient was normal, except for capillary proliferation.

Biochemistry

Polarographic studies of isolated skeletal muscle, mitochondria showed maximal oxygen consumption (respiratory rate) even in the absence of ADP, indicating that respiratory control was lost, although phosphorylation capacity was normal (Figure 2). Spectra and content of cytochromes were normal, and the activities of individual enzymes of the respiratory chain were also normal. However, basal ATPase activity was greatly increased and poorly stimulated by the uncoupler 2,4-dinitrophenol (DNP).

In 1976, DiMauro *et al*. found in the second patient that the rate of energy-dependent calcium uptake by isolated mitochondria was normal, but the amount of calcium accumulated decreased, and intramitochondrial calcium could not be retained and was quickly released into the medium. A vicious cycling of calcium uptake and release was proposed as a mechanism to explain the waste of electrochemical energy as heat.

Genetics

The lack of maternal inheritance, the apparent muscle specificity of the disease, and the lack of large-scale rearrangements of mitochondrial DNA (mtDNA) in the second patient are circumstantial evidence that Luft's disease may be due to a nuclear DNA (nDNA) defect.

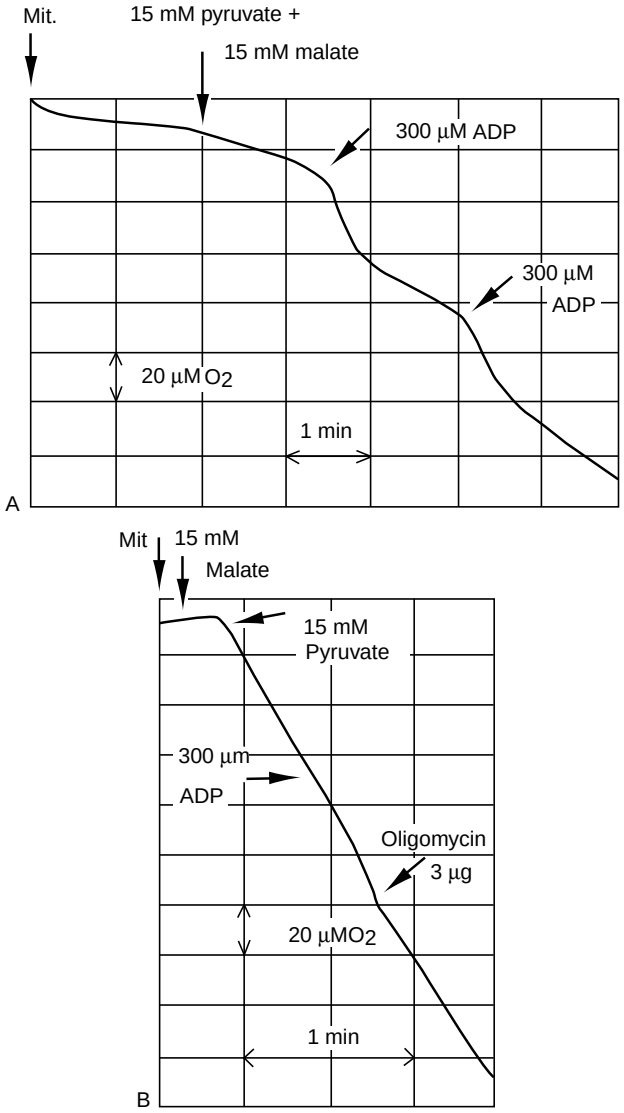

FIGURE 2 Polarographic tracings of isolated muscle mitochondria from the second patient with Luft's disease (B) and from a normal individual (A). Note how addition of micromolar amounts of ADP stimulate oxygen uptake in normal mitochondria, but not in the patient's mitochondria, whose rate of respiration is maximal after the addition of substrates (pyruvate + malate). This high rate of respiration is neither stimulated by ADP nor inhibited by oligomycin. This condition, in which ATP is formed normally but does not control the rate of respiration, is defined "loose coupling" of oxidation and phosphorylation.

See Also the Following Articles

Mitochondrial DNA • Mitochondrial Genome, Overview

Glossary

erythema Redness of the skin due to capillary dilatation or proliferation.

hypermetabolism A condition of enhanced metabolic activity in one or more tissues, resulting in increased heat production by the body, typically associated with hyperthyroidism.

polydipsia Prolonged excessive thirst and excessive intake of liquids.

polyphagia Excessive eating.

tachycardia Rapid beating of the heart, usually above 90 beats min^{-1}.

Further Reading

DiMauro, S., and Schon, E. A. (2003). Mitochondrial respiratory-chain diseases. *New England J. Med.* **348**, 2656–2668.

DiMauro, S., Bonilla, E., Lee, C. P., Schotland, D. L., Scarpa, A., Conn, H., and Chance, B. (1976). Luft's disease. Further biochemical and ultrastructural studies of skeletal muscle in the second case. *J. Neurol. Sci.* **27**, 217–232.

Haydar, N. A., Conn, H. L., Afifi, A., Wakid, N., Ballas, S., and Fawaz, K. (1971). Severe hypermetabolism with primary abnormality of skeletal muscle mitochondria. *Annu. Intern. Med.* **74**, 548–558.

Luft, R., *et al.* (1962). *J. Clin. Invest.* **41**, 1176–1804.

Pon, L. A., and Schon, E. A. (eds.) (2001). *Mitochondria.* Academic Press, San Diego, CA.

Biography

Dr. Salvatore DiMauro is the Lucy G. Moses Professor of Neurology at Columbia University College of Physicians & Surgeons. His main interests are inborn errors of metabolism, especially defects of the mitochondrial respiratory chain. He holds an M.D. from the University of Padova, Italy. He and his collaborators have pioneered the study of mtDNA in human disease.

Lysophospholipid Receptors

Gabor J. Tigyi
University of Tennessee Health Sciences Center, Memphis, Tennessee, USA

The lysophospholipids (LPLs) include lysophosphatidic acid (radyl-lyso-glycerophosphate, LPA), 2,3-cyclic phosphatidic acid, 1-alkyl-2-acetyl-glycero-3-phosphate, sphingosine-1-phosphate (S1P), dihydro-sphingosine-1-phosphate, sphingosylphosphorylcholine (lysosphingomyelin, SPC), and lysophosphatidylcholine (LPC). LPLs exert many of their biological effects through specific plasma membrane and/or intracellular receptors. LPLs are abundantly present in biological fluids and many of them are generated through stimulus-coupled activation of biochemical pathways. With only very few exceptions (e.g. RH7777 hepatoma, Sf9 insect and *Sacchromyces cerevisiae* yeast cells), most cells are responsive to one or more LPLs, indicating a widespread expression of their receptors. LPLs promote cell survival, exert mitogenic/antimitogenic regulation of the cell cycle, affect cell shape and enhance/inhibit cell motility, regulate organotypic differentiation, modulate immunological responses, and regulate calcium homeostasis. In a pathological context, LPLs have been shown to play a role in tumor cell invasion, angiogenesis, neointima formation, development of the heart ventricles, chemotherapeutic and radiation resistance, facial dysmorphism, nociception, and suckling behavior. The current understanding of lysophospholipid biology is very limited and the present understanding of their role in disease is rudimentary.

Sphingolipid Receptors

Plasma Membrane Receptors

Receptors for sphingolipids form three clusters, two of which show considerable homology with receptors for the glycerolipids lysophosphatidic acid (LPA) and lysophosphatidylcholine (LPC). In the order of discovery, the first cluster belongs to the endothelial differentiation gene (EDG) family. Five receptors of the eight-member EDG family recognize sphingosine-1-phosphate (S1P), dihydro-S1P, and to a lesser degree sphingosylphosphorylcholine (SPC), which include $S1P_1$ (formerly EDG1), $S1P_2$ (EDG5, H218, AGR16), $S1P_3$ (EDG3), $S1P_4$ (EDG6), and $S1P_5$ (EDG8). Whereas $S1P_1$, $S1P_2$, $S1P_3$ are expressed in many tissues and often coexpressed with at least one other EDG-family receptor in the same cell, $S1P_4$ expression is restricted to the hematopoietic cells and the lung; $S1P_5$ expression is restricted to the nervous tissue. Knockout (KO) mice for $S1P_1$ show embryonic lethality around embryonic day 12.5 due to a defect in vascular wall maturation hallmarked by a failure of smooth muscle cells surrounding the primitive capillaries, which leads to bleeding and death.

$S1P_2$ KO mice show no obvious phenotypic alteration but a slightly smaller litter size in homozygous matings on C57BL/6N background. $S1P_2$ KO mice on C57BL/6 albino background have been noted to suffer seizures leading to epileptic death, which was not found in the KO in the C57BL/6N background. $S1P_2$ mice showed slightly diminished adenylyl cyclase inhibition and severely impaired Rho activation in response to S1P stimulation. $S1P_3$ KO mice show no phenotypic abnormalities but embryonic fibroblasts display decreases in PLC activation, Ca responses, slight decreases in adenylyl cyclase inhibition, and no change in Rho activation.

Embryonic fibroblasts taken from double KO mice for $S1P_2$/$S1P_3$ display a complete loss of Rho activation, and a significant decrease in PLC activation and Ca mobilization without diminished inhibition of adenylyl cyclase. These double KO mice display decreased litter sizes and suffer increased perinatal lethality.

Another cluster of receptors that include OGR1(GPR68), GPR4, and G2A have been reported to be activated by SPC and LPC. However, the original claim that these receptors respond to LPLs has been disputed as these receptors have been shown to be activated by changes in pH. A related gene to this cluster, TDAG8, encodes a receptor to psychosine, a glycosphingolipid, which inhibits adenylyl cyclase in a pertussis toxin-independent mechanism, mobilizes Ca and leads to the formation of multinuclear cells.

A third cluster of lysosphingolipid receptors includes GPR3, GPR6, and GPR12. The closest relatives of this cluster include the anandamide and melanocortin receptors and the EDG family. These receptors are activated by S1P but also possess high intrinsic activity stimulating adenylyl cyclase and also couple to $G_{i/o}$. The thalamus and the caudate nucleus are the sites of the highest expression for these receptors in the nervous system; whereas in the periphery the thymus, stomach, and small intestine show high levels of mRNA

expression, and the kidney, heart, spleen, and pancreas show low levels of mRNA expression. Related to this cluster, GPR63 also recognizes dihydro-S1P and dioleoyl phosphatidic acid. GPR12 shows a preference for SPC over S1P as well as for the D-erythro-SPC stereoisomer. This receptor is presumed to play a role in the differentiation and postmitotic maturation of neurons. Antagonists of S1P receptors are in their early stages of development.

Intracellular Receptors

S1P is generated intracellularly from sphingosine by sphingosine kinase (SK). SK activity and consequent elevation in S1P have been linked to cell proliferation, survival, motility, and Ca mobilization. There is reasonable evidence for S1P's role in releasing Ca from endoplasmic reticulum in a mechanism independent of the inositol trisphosphate-gated release mechanism. The molecular targets of S1P remain obscure with the exception of the Ca^{2+} channel SCAMPER. In addition, S1P and SPC have been shown to modulate the properties of the ryanodine receptor.

Glycerolipid Receptors

Plasma Membrane Receptors

The GPR63 receptor for dioleoyl-PA is also activated by sphingolipids as discussed in the previous section. There are three clusters of GPCR that mediate LPA responsiveness.

The LPA_1 (EDG2), LPA_2 (EDG4), and LPA_3 (EDG7) receptors are close relatives of the EDG-family S1P receptors. LPA_1 is widely distributed, whereas LPA_2 mRNA is expressed in the nervous system, kidney, lung, and the prostate. LPA_3 is abundantly expressed in the testis and prostate and at a lower level in the heart, brain, lung, and kidney. LPA_1 and LPA_2 couple to $G_{i/o}$, G_q, and G_{13}, whereas LPA_3 couples to G_i and G_q heterotrimeric G proteins. LPA_1 KO animals have minimal phenotypes that include facial dysmorphism and altered suckling behavior, which leads to increased perinatal mortality. The impaired suckling behavior might be due to cortical developmental problems and/or alteration in the olfactory bulb. LPA_2 KO animals are without major phenotypic alterations but show a modest attenuation in LPA-induced PLC activation. Some of the LPA_1/LPA_2 double KO animals develop perinatal cranial hematomas in the frontal region of the brain. In embryonic fibroblasts isolated from these mice phospholipase C activation, Ca mobilization, adenylyl cyclase activation, proliferation, Jnk activation, Akt activation, and stress fiber formation, are absent or severely reduced.

The LPA_1, LPA_2, and LPA_3 receptors are all activated by either stereoisomer of LPA, alkyl-LPA, alkenyl-LPA, and cyclic phosphatidic acid. LPA_1 and LPA_2 do not show a preference between *sn1* and *sn2* localization of the fatty acyl chain, however, LPA_3 shows a preference for LPA with *sn2* over *sn1* fatty acids. All three receptors show a slight preference for LPA containing unsaturated fatty acids. Dioctylglycerol pyrophosphate has been identified as an inhibitor of $LPA_3 > LPA_1$ receptors without any effect on LPA_2. VPC12249 is an antagonist with a slight preference for LPA_1 over LPA_3 and without any effect on LPA_2. VPC31143 is an agonist selective for LPA_1. Short chain fatty alcohol phosphates show receptor-selective agonist and antagonist properties; the decanyl analogue is an LPA_2-selective agonist, whereas the dodecanyl analogue is an LPA_3-selective antagonist.

The *Xenopus* PSP24 α (GPR45) and β (GPR63) genes, when over-expressed in Xenopus oocytes augment the LPA but not the cyclic-PA and alkenyl-GP response. These receptors, which are abundant in the nervous system are also present in other tissues. The mammalian orthologues do not seem to respond to LPA when expressed in mammalian cells. However, recent evidence shows that mammalian orthologue of GP63 is a receptor for dioleoyl-PA and S1P. Interestingly, the mammalian GPR63 lacks a glutamine residue that is present in the *Xenopus* orthologue of GPR45 and which has been found essential for LPA recognition.

LPA_4 (GPR23, P2Y9Y) is a GPCR, distant from the EDG cluster, sharing only 20–24% amino acid identity and is a member of the purinergic receptor cluster. LPA_4 is abundantly expressed in the ovary and shows a ligand preference 18:1 > 18:0 > 16:0 > 14:0 > alkyl > alkenyl LPA.

Intracellular Receptors

The peroxisome proliferator activated receptor γ (PPARγ) is a transcription factor that heterodimerizes with the retinoic acid receptor and binds to specific DNA sequences known as peroxisome proliferator-activated receptor response element (PPRE). PPARγ is an intracellular receptor for LPA and alkyl-GP but not for cPA. The LPA-induced activation of PPARγ might be an important step in the regulation of adipogenesis, macrophage function, neointima formation, and atherogenesis because the scavenger receptor CD36 and the adipocyte fatty acid binding protein aP2 both have PPREs in their promoters.

See Also the Following Articles

Adenylyl Cyclases • Peroxisome Proliferator-Activated Receptors • Sphingolipid Biosynthesis • Sphingolipid Catabolism

Glossary

lysophospholipid A phosphate-containing lipid that causes cell lysis at high concentrations (>mM) due to its detergent-like properties.

receptor A protein that binds with a high degree of selectivity a ligand and upon binding elicits a biological response thorough the activation of signal transduction pathways.

Further Reading

Cavalli, A. L., O'Brien, N. W., Barlow, S. B., Betto, R., Glembotski, C. C., Palade, P. T., and Sabbadini, R. A. (2003). Expression and functional characterization of SCaMPER: A sphingolipid-modulated calcium channel of cardiomyocytes. *Am. J. Physiol. Cell Physiol.* **284**, C780–C790.

Fischer, D. J., Nusser, N., Virag, T., Yokoyama, K., Wang, D., Baker, D. L., Bautista, D., Parrill, A. L., and Tigyi, G. (2001). Short-chain phosphatidates are subtype-selective antagonists of lysophosphatidic acid receptors. *Mol. Pharmacol.* **60**, 776–784.

Heise, C. E., Santos, W. L., Schreihofer, A. M., Heasley, B. H., Mukhin, Y. V., Macdonald, T. L., and Lynch, K. R. (2001). Activity of 2-substituted LPA analogs at LPA receptors: Discovery of a LPA_1/LPA_3 receptor antagonist. *Mol. Pharmacol.* **60**, 1173–1180.

Ignatov, A., Lintzel, J., Hermans-Borgmeyer, I., Kreienkamp, H. J., Joost, P., Thomsen, S., Methner, A., and Schaller, H. C. (2003). Role of the G-protein-coupled receptor GPR12 as high-affinity receptor for sphingosylphosphorylcholine and its expression and function in brain development. *J. Neurosci.* **23**, 907–914.

McIntyre, T. M., Pontsler, A. V., Silva, A. R., St Hilaire, A., Xu, Y., Hinshaw, J. C., Zimmerman, G. A., Hama, K., Aoki, J., Arai, H., and Prestwich, G. D. (2003). Identification of an intracellular receptor for lysophosphatidic acid (LPA): LPA is a transcellular PPARgamma agonist. *Proc. Natl Acad. Sci. USA* **100**, 131–136.

Niedernberg, A., Tunaru, S., Blaukat, A., Ardati, A., and Kostenis, E. (2003). Sphingosine 1-phosphate and dioleoylphosphatidic acid are low affinity agonists for the orphan receptor GPR63. *Cell Signal* **15**, 435–446.

Sharma, C., Smith, T., Li, S., Schroepfer, G. J., Jr and Needleman, D. H. (2000). Inhibition of Ca^{2+} release channel (ryanodine receptor) activity by sphingolipid bases: mechanism of action. *Chem. Phys. Lipids* **104**, 1–11.

Tigyi, G., and Parrill, A. L. (2003). Molecular mechanisms of lysophosphatidic acid action. *Prog. Lipid Res.* **42**, 498–526.

Uhlenbrock, K., Gassenhuber, H., and Kostenis, E. (2002). Sphingosine 1-phosphate is a ligand of the human gpr3, gpr6 and gpr12 family of constitutively active G protein-coupled receptors. *Cell Signal* **14**, 941–953.

Virag, T., Elrod, D. B., Liliom, K., Sardar, V. M., Parrill, A. L., Yokoyama, K., Durgam, G., Deng, W., Miller, D. D., and Tigyi, G. (2003). Fatty alcohol phosphates are subtype-selective agonists and antagonists of LPA receptors. *Mol. Pharm.* **63**, 1032–1042.

Zhang, C., Baker, D. L., Yasuda, S., Makarova, N., Balazs, L., Johnson, L. R., Marathe, G. K., Mclntyre, T. M., Xu, Y., Prestwich, G. D., Byun, H.-S., Bittman, R., and Tigyi, G. (2004). Lysophosphatidic acid induces neointima formation through PPARγ activation. *J. Exp. Med.* **199**, 763–774.

Biography

Gabor Tigyi is a Professor in the Department of Physiology at the University of Tennessee Health Science Center in Memphis. He holds an M.D. from the Medical University of Pecs and a Ph.D. from the Hungarian Academy of Sciences in Budapest. He has made seminal contributions to the identification of LPA-like ligands, the development of LPA receptor-selective antagonists, and the role of LPA in neointima formation.

MDR Membrane Proteins

Nathan C. Rockwell
University of California at Berkeley, California, USA

Multidrug resistance (MDR) membrane proteins are integral membrane proteins belonging to the ABC transporter family that extrude drugs from mammalian cells. These proteins are implicated in the phenomenon of MDR, in which cancers treated with one drug in the course of chemotherapy will acquire resistance not only to that drug but also to a number of others that have not been used in treatment. The most familiar example of such a protein is MDR1, but related proteins can also confer resistance to multiple drugs beyond the compound used in selection, and thus can also be considered as MDR transporters in a broader sense.

MDR1 and the Clinical MDR Phenotype

The Discovery of MDR1

In the treatment of cancer patients by chemotherapy, chemical compounds preferentially more toxic to cancer cells are administered to the patient. Chemotherapy often fails or offers only a brief respite, and there are a number of mechanisms for such failure. In one such mechanism, cancer cells may express proteins that export the drug from the cell, preventing its accumulation to effective concentrations. The genetic instability of cancer cells permits them to alter expression of proteins or to develop mutated forms of proteins during the course of the disease, and the use of chemotherapy is in essence a selection for those cancer cells which are able to resist the drug or drugs used, such that the resistant cells will come to dominate the population of cancer cells over time.

One can study this by taking mammalian cells in tissue culture and selecting for cells which are able to resist a given drug. In the laboratory of Victor Ling, cells selected for resistance to the chemotherapeutic drug colchicine were shown to have simultaneously gained cross-resistance to a number of other compounds with no obvious overlap in chemical structure. This cross-resistance was shown to correlate with the expression of P-glycoprotein or Mdr1, an integral membrane protein subsequently shown to be encoded by the *MDR1* gene through the work of Michael Gottesman and others. Later studies have established that Mdr1 is an ATP-dependent pump that binds to drug molecules and extrudes them from the cell.

Clinical Relevance of MDR1

In the years since the discovery of MDR1, much research has focused on its role in the clinical outcomes of patients. The idea behind this work can be summarized in the form of two questions: (1) Does expression of MDR1 actually correlate with the results of treatment? (2) Does blocking MDR1 function alter the results of treatment for the better?

The answer to the first question has proven complex. For certain types of cancer, there is clear evidence that MDR1 is a significant factor in the outcome of treatment. However, evidence for a role for MDR1 in other types of cancer is much weaker, even in more recent studies. Complications arise in answering this question, such as the role of other transporters in MDR, individual genetic variation in the level of MDR1 present, and similar variation in the presence of any mutations in the MDR1 sequence. Nonetheless, at this point it seems clear that MDR1 is a clinically relevant factor in treating certain cancers, and new genetic screening approaches are being developed to permit a finer diagnosis of whether MDR1 might be a complication in treating other cancers in particular individuals.

Obtaining any answer to the second question has proven frustrating. Some studies have reported that blocking MDR function can improve the results of treatment, but other studies have argued that such inhibition has no effect. Factors which lead to these disparate results include the frequent lack of surrogate assays ensuring that MDR1 is truly being inhibited, the lack of examination of other transporters in the patient sample populations, and the observation that blocking MDR1 can increase the toxicity of chemotherapeutic drugs to the patient and thereby alter the outcome of chemotherapy indirectly. Studies which take all of these factors into account are only now underway.

Biochemical Behavior of MDR1

Good progress has been made toward understanding how MDR1 actually works to extrude drug substrates from cells. Like most ABC transporters, MDR1 hydrolyzes ATP at the conserved ATP-binding cassettes (ABCs, also known as ABC domains, nucleotide-binding domains (NBDs)). This hydrolysis is directly coupled to transport of drugs out of the cell. Thus, MDR1 is a direct active transporter, able to work against a concentration gradient without the aid of other gradients by coupling ATP hydrolysis to vectorial transport.

The Conundrum of MDR1: Broad Specificity with High Affinity

A very wide range of compounds can serve as substrates for MDR1, without obvious structural motifs that distinguish substrates from nonsubstrates (Figure 1). In spite of this, MDR1 is able to transport these compounds with seemingly high affinity (low K_M). Paradoxically, conventional enzymology dictates that high affinity is achieved via extensive interactions between enzyme and substrate and thus of necessity is accompanied by stringent specificity.

More recent studies indicate that the apparently high affinity of MDR1 for its substrates is misleading. The hydrophobic nature of MDR1 substrates causes them to accumulate to very high concentrations in biomembranes, and it is this population of membrane-bound substrates that is recruited for transport (Figure 1). Thus, the actual affinity of MDR1 for its substrates is probably much lower than had been thought. This allows a suitably hydrophobic binding pocket to accommodate many substrates in slightly different binding modes with modest affinity and without making extensive enzyme-substrate contacts. It is perhaps best to view MDR1 as a polyspecific transporter, meaning that it has very broad specificity but does actually recognize specific features of its substrates.

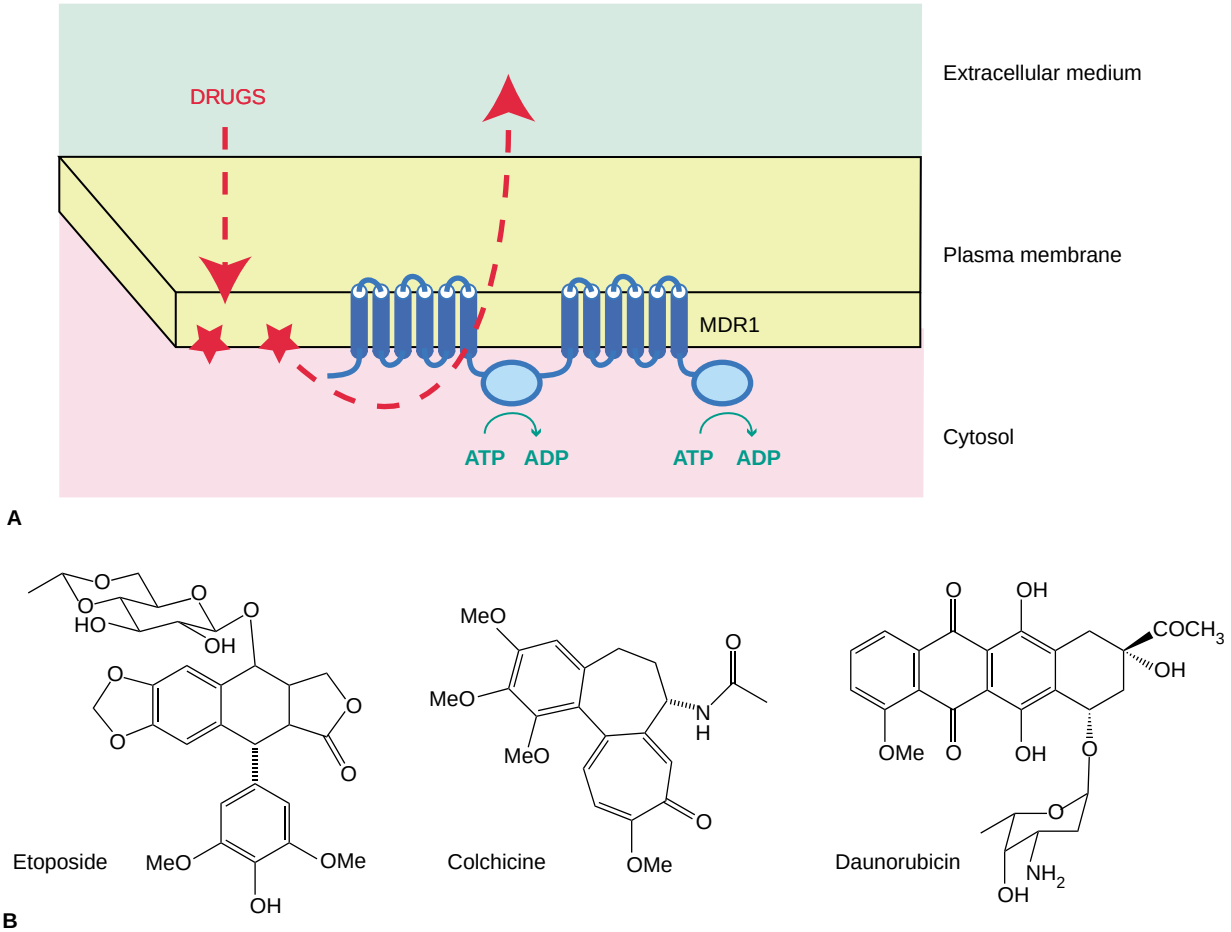

FIGURE 1 MDR1 function in drug export. (A) A cartoon schematic of the MDR1 transporter in the plasma membrane (yellow) is shown, with the transmembrane segments as vertical cylinders and the ABC domains as ovals. Drug molecules transiting the plasma membrane (red stars) are recruited by MDR1 and then exported from the cell, concomitant with ATP hydrolysis at the cytosolic ABC domains. (B) Structures of selected drugs known to be MDR1 substrates are shown.

ATP Hydrolysis and the Catalytic Cycle of MDR1

MDR1 has the four canonical domains of an ABC transporter: two membrane-spanning domains each containing six transmembrane segments and two ABC domains. It is known that ATP derivatives can photo-cross-link to the ABC domains of MDR1 and other ABC transporters, while transport substrates such as drugs instead cross-link to the membrane-spanning domains. The affinity for drugs changes during the catalytic cycle. Kinetic analysis of ATP hydrolysis by MDR1 leads to the idea that the two ATPase active sites alternate during transport, but the exact stoichiometry of ATP hydrolysis to transport is not yet known. Recent medium-resolution structural studies of the MDR1 catalytic cycle from the laboratory of Chris Higgins indicate that major conformational changes take place upon ATP binding, and this may mean that ATP hydrolysis actually occurs after transport and simply serves to reset the transporter.

The ABC domains dimerize on the cytosolic face of the protein. The exact mode of dimerization for the ABC domains in any ABC transporter has been the subject of intense speculation. Much other evidence supports the most recent model, based on the crystal structure of Rad50 from *E. coli*. This model is also consistent with the crystal structure of the intact BtuCD transporter. However, less is known about how the membrane-spanning domains of MDR1 are organized, as there is much less conservation of these domains among the different subfamilies of ABC transporters.

Other MDR Transporters

MRP1

MDR protein 1 (MRP1) or *ABCC1* was isolated by Susan Cole and Roger Deeley as a protein implicated in multidrug resistance in lung cancer cells. It is a member of a different subfamily of ABC transporters (Figure 2). Whereas MDR1 transports drugs without the need for any chemical modification, MRP1 frequently transports drugs that have first been chemically conjugated to glutathione. Exceptions to this rule are sometimes cotransported with unlinked glutathione molecules. As with MDR1, the presence of MRP1 correlates with clinical outcome for certain cancers. The development of specific inhibitors and surrogate assays for MRP1 is underway.

ABCG2

ABCG2 (also called MXR or BCRP) was isolated by several labs as a transporter implicated in drug-resistance in breast cancer cells. It belongs to a third subfamily of ABC transporters (Figure 2). The specificity of ABCG2 seems more narrow than that of MDR1 or MRP1, but chemical conjugation of drugs is

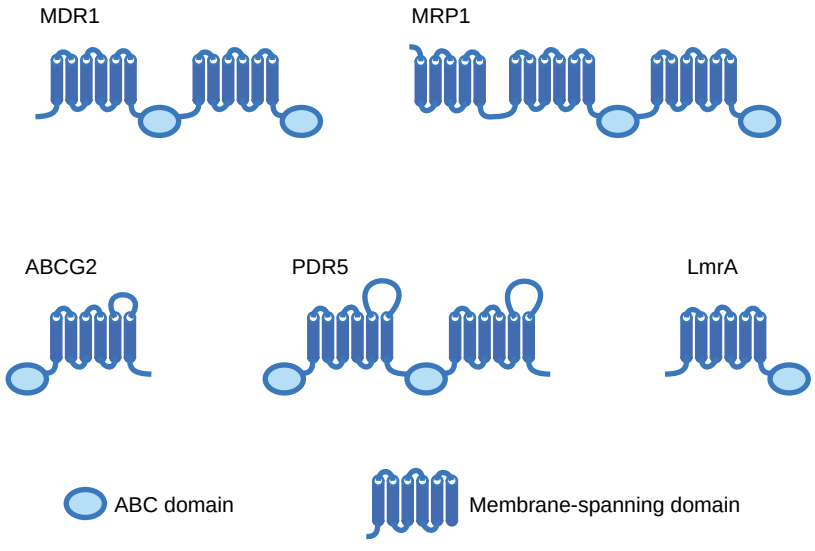

FIGURE 2 Cartoon schematics of ABC transporters implicated in cross-resistance. MDR1, MRP1, and ABCG2 are all MDR transporters, while Pdr5 and LmrA have similar functions in different organisms. MDR1 is a classic ABC transporter with all four domains in a single open reading frame, while MRP1 has an N-terminal extension with an additional five transmembrane segments. ABCG2 is a "half-transporter" which is thought to form a homodimer to constitute the active transporter. Pdr5 is a complete transporter with the relative order of the four domains in the open reading frame reversed relative to MDR1, while LmrA is a "half-transporter" known to be active as a homodimer. Throughout, membrane-spanning domains are shown as clusters of vertical blue cylinders, and ABC domains are shown as blue ovals.

not required. Clinical trials to assess the importance of ABCG2 in human cancer are still in the early stages.

Homologous Transporters not Associated with Drug Resistance

Each transporter associated with clinical drug resistance has close relatives not associated with such resistance. For instance, the two closest relatives of MDR1 are MDR3 (encoded by the *ABCB4* gene) and BSEP (encoded by *ABCB11*). Although both proteins exhibit modest drug-efflux activity *in vitro*, neither one has been clinically implicated in drug resistance, possibly because their ability to export drugs is too weak. Similarly, the closest relative to MRP1 is MRP3, which again can confer weak drug resistance when overexpressed but has not been convincingly linked to drug resistance in human cancers. Another relative, MRP2, may play a role in clinical drug resistance, because it can be amplified in cell lines selected for resistance to cisplatin and has been detected in clinical samples, but it is not yet clear whether it plays a true role in the MDR phenotype.

Physiological Functions of MDR Transporters

The Physiological Role of MDR1

MDR1 is found in the gut, kidney, liver, and blood–brain barrier, and *mdr1–/–* knockout mice have altered ability to withstand and excrete toxic compounds known to be MDR1 substrates. This is consistent with the idea that MDR1 is primarily responsible for extrusion of toxic metabolites or xenotoxins from certain cells to allow facile excretion from the body, thereby protecting the rest of the organism (or, in the case of the blood–brain barrier, forming a "safe haven" within the organism). However, MDR1 is also expressed in cells of the adrenal gland, so it is possible that MDR1 may have some role in the proper function of this tissue in the absence of toxins.

The Physiological Role of MRP1

As with MDR1, at least one physiological role of MRP1 is the removal of various toxins from the body. Unlike MDR1, MRP1 expression is quite widespread. This protein also has a physiological role in the secretion of leukotrienes, and this has been shown to have implications for response to bacterial lung infections.

The Physiological Role of ABCG2

ABCG2 is expressed in intestine and placenta as well as in a side population of hematopoietic stem cells. It is likely to play a role in detoxification in the intestine, but its functions in placenta and stem cells are not yet clear.

The Physiological Functions of Homologous Transporters

MDR3 and BSEP (the two closest homologues of MDR1) are both implicated in proper function of the liver; MDR3 is an outward-directed transporter for the lipid phosphatidylcholine, and BSEP is a bile salt exporter. Mutations in these two proteins interfere with proper secretion of bile and are associated with different subtypes of progressive familial intrahepatic cholestasis (PFIC).

There are a number of homologues for MRP1. Its closest relative, MRP3, may play a role in cholestasis in the liver, or it may be another detoxification protein, while MRP2 is the pump responsible for exporting a wide range of anionic conjugates across the apical membrane of polarized cells. There are also several homologues of ABCG2, but the only ones whose functions are known are ABCG5 and ABCG8, which are important in exporting plant sterols from the cells of the intestine.

Analogous Systems in Other Organisms

The phenomenon of MDR is by no means unique to mammalian cells. The ABC transporter family is ubiquitous, and every eukaryotic organism examined to date has its own cohort of these proteins, at least some of which are involved in drug resistance or detoxification. Examples include *AtMRP* proteins from *Arabidopsis thaliana*, Pdr5 from *Saccharomyces cerevisiae*, and PGPA from *Leishmania*. Nor is this phenomenon unique to eukaryotes; the bacterium *Lactococcus lactis* expresses an MDR1 homologue, LmrA, which is able to complement the loss of MDR1 function in mammalian cells. Thus, MDR transporters are a special case of a general theme in biology: removal of a wide variety of toxic compounds from the cell via a small number of polyspecific ABC transporters.

The observation that such transporters have close homologues not responsible for significant drug transport is also a general one. For instance, the two closest homologues of Pdr5 in the *Saccharomyces* genome are Pdr10 and Pdr15, neither of which is implicated in drug resistance. It is thus possible that MDR transporters and their analogues in other organisms evolved from related transporters several times in several subfamilies of ABC transporters.

See Also the Following Articles

ABC Transporters • Prostaglandins and Leukotrienes

Glossary

cross-resistance The general phenomenon whereby a cell selected for resistance to one toxin simultaneously acquires resistance to other toxins not presented to the cell; MDR is a special case of cross-resistance.

homologue A protein with significant sequence similarity to another protein, either across its entire length or in certain regions or domains.

photo-cross-link To covalently link a molecule (usually a protein) with a substrate or ligand bound to the protein *in vitro* and then excited by ultraviolet light to react with the protein.

polyspecific Having very broad specificity, with minimal overlap in chemical structure.

Further Reading

Ambudkar, S. V., Kimchi-Sarfaty, C., Sauna, Z. E., and Gottesman, M. M. (2003). P-glycoprotein: From genomics to mechanism. *Oncogene* **22**, 7468–7485.

Bates, S. E. (2003). Solving the problem of multidrug resistance: ABC transporters in clinical oncology. In *ABC Proteins: From Bacteria to Man* (I. B. Holland, S. P. C. Cole, K. Kuchler and C. F. Higgins, eds.) pp. 359–391. Academic Press/Elsevier Science, London, UK.

Deeley, R. G., and Cole, S. P. C. (2003). Multidrug resistance protein 1 (ABCC1). In *ABC Proteins: From Bacteria to Man* (I. B. Holland, S. P. C. Cole, K. Kuchler and C. F. Higgins, eds.) pp. 393–422. Academic Press/Elsevier Science, London, UK.

Hopfner, K. P., Karcher, A., Shin, D. S., Craig, L., Arthur, L. M., Carney, J. P., and Tainer, J. A. (2000). Structural biology of Rad50 ATPase: ATP-driven conformational control in DNA double-strand break repair and the ABC-ATPase superfamily. *Cell* **101**, 789–800.

Locher, K. P., Lee, A. T., and Rees, D. C. (2002). The E. coli BtuCD structure: a framework for ABC transporter architecure and mechanism. *Science* **296**, 1091–1098.

Linton, K. J., Rosenberg, M. F., Kerr, I. D., and Higgins, C. F. (2003). Structure of ABC transporters. In *ABC Proteins: From Bacteria to Man* (I. B. Holland, S. P. C. Cole, K. Kuchler and C. F. Higgins, eds.) pp. 65–80. Academic Press/Elsevier Science, London, UK.

Rosenberg, M. F., Velarde, G., Ford, R. C. Martin, C., Berridge, G., Kerr, I. D., Callaghan, R., Schmidlin, A., Wooding, C., Linton, K. J., and Higgins, C. F. (2001). Repacking of the transmembrane domains of P-glycoprotein during the transport ATPase cycle. *EMBO J.* **20**, 5615–5625.

Van Veen, H. W., and Callaghan, R. (2003). Substrate-binding sites in ABC transporters. In *ABC Proteins: From Bacteria to Man* (I. B. Holland, S. P. C. Cole, K. Kuchler and C. F. Higgins, eds.) pp. 81–105. Academic Press/Elsevier Science, London, UK.

Biography

Nathan Rockwell is conducting postdoctoral research in the laboratory of Professor Jeremy Thorner at the University of California, Berkeley. His research focuses on the physiological roles of ABC transporters in the absence of cytotoxic drugs, using the yeast *Saccharomyces cerevisiae* as a model system. He holds a Ph.D. from Stanford University.

Meiosis

Neil Hunter
University of California, Davis, California, USA

Meiosis is the specialized type of cell division by which gametes are produced. This process achieves the remarkable feat of halving the chromosome complement of a cell, typically from diploid to haploid. Meiosis thereby allows the diploid state to be restored when two gametes fuse during fertilization to form a zygote. Reduction of ploidy occurs during meiosis because a single round of DNA replication is followed by two successive rounds of chromosome segregation. During the first round, sister chromatids remain associated while homologues (pairs of sisters) are segregated. As prerequisites to their accurate segregation, homologues must pair and undergo crossing-over, a reciprocal exchange of chromosome arms. Homologue pairing and crossing-over both involve homologous recombination, which occurs by the programmed formation and repair of DNA double-strand breaks. Crossing-over is a critical aspect of meiosis that underlies the fundamental laws of heredity: first, crossovers are essential for genetic transmission because they convert connections between sister chromatids into connections between homologues, called chiasmata. These connections permit proper orientation of the homologues on the segregation apparatus (the spindle), and thereby facilitate their orderly segregation. Second, crossovers produce new combinations of alleles on which genetic selection can act. Through its effect on chromosome segregation, defective crossing-over is linked to infertility, miscarriage, and genetic disease in humans.

The Sexual Life Cycle

In sexually reproducing organisms, successive generations maintain a constant number of chromosomes. This is because syngamy, the fusion of two gametes to form a zygote (which gives rise to a new individual), is alternated with meiosis, which halves the cellular chromosome number. Without meiosis, syngamy would result in a catastrophic doubling of the chromosome content with each successive generation. Thus, the alternation of diploid (two copies of each chromosome) and haploid (one copy of each chromosome) generations of cells is a fundamental feature of sexually reproducing organisms. In metazoans, syngamy is typically followed by extensive cell proliferation, by mitosis, and the development of a new individual. Meiosis in metazoans occurs in the germ-line cells of the gonads.

Mitotic and Meiotic Chromosome Cycles

Understanding how meiosis achieves the remarkable feat of halving the cellular chromosome number first requires an appreciation of how cells segregate chromosomes during mitotic cell division (Figure 1).

Mitosis

During mitosis, copies of both maternal and paternal chromosomes are distributed to two daughter cells. Replication first produces two identical copies of each chromosome called sister chromatids (Figure 1Aii). Microtubules of the spindle apparatus attach to the chromatids via structures called kinetochores, which assemble at regions called centromeres (Figure 1Aiii). Chromatids are then pulled apart to opposite poles of the cell, which then divides (Figure 1Aiv). The result is two identical daughter cells each containing two complete (maternal and paternal) sets of chromosomes. Two interdependent features ensure that chromosome segregation is an accurate process: (1) connections between sister chromatids and (2) a mechanism that senses the tension created when each pair of chromatids becomes attached to microtubules emanating from both poles of the spindle. Connections between sister chromatids, called sister-chromatid cohesion, form during replication and hold the sister chromatids together until they are ready to be segregated. When the two kinetochores of a sister-chromatid pair attach to microtubules emanating from opposite poles of the cell, the pulling forces of the spindle are resisted by the cohesion between sister centromeres. The resulting tension stabilizes microtubule attachments. When all chromatid pairs have achieved this biorientation on the spindle, sister-chromatid cohesion is destroyed and chromatids are pulled to the cell poles.

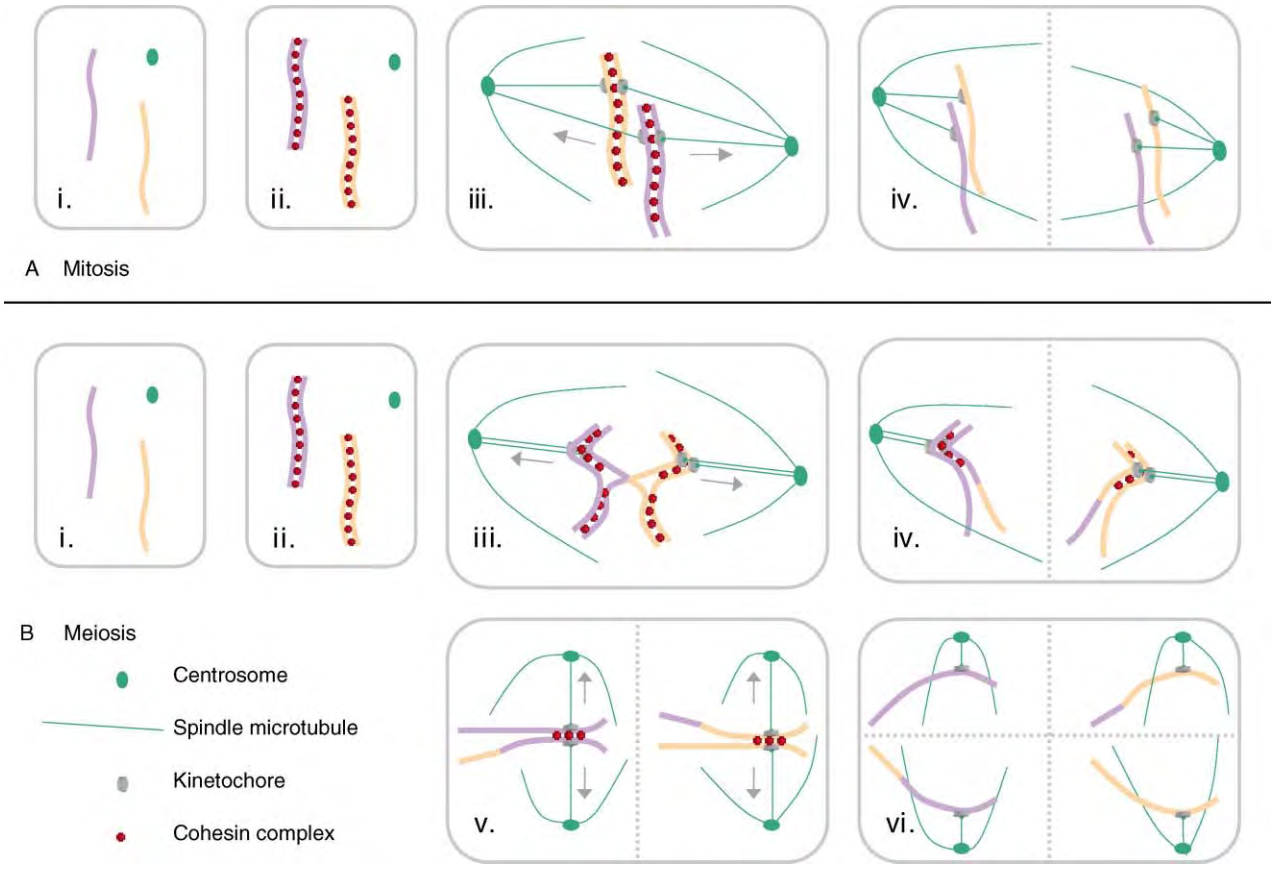

FIGURE 1 Comparison of mitotic and meiotic chromosome cycles. Centrosomes are cell organelles that produce microtubules. These structures duplicate, migrate to opposite poles of the cell, and grow the microtubules that form the spindle. Arrows indicate directions of the pulling forces generated by microtubules. Dashed lines indicate the planes of cell division. See text for details.

MEIOSIS

Meiosis, like mitosis, begins with replication to produce pairs of sister chromatids connected by cohesion (Figure 1Bii). Then, in contrast to mitosis, a single copy of every chromosome must be accurately distributed to four different nuclei. Meiosis achieves this in the only logical way: via two successive rounds of nuclear division, first segregating homologues (the maternal and paternal chromatid pairs) and then segregating sister chromatids, as in mitosis. Regular homologue segregation is unique to meiosis and requires the following four modifications of the mitotic chromosome cycle:

1. Maternal and paternal homologues pair and become connected by structures known as chiasmata (Figures 1Biii and 2). A chiasma results from a reciprocal exchange between a maternal and a paternal chromatid. Chiasmata hold the homologues together by virtue of the sister-chromatid cohesion, which was established as the chromosomes were replicated. Chiasma formation is the physical basis of genetic crossing-over.

2. The kinetochores of sister chromatids are modified such that they are unable to attach to microtubules emanating from different poles. Thus, the two sister kinetochores of a homologue behave like the kinetochore of a single sister chromatid in mitosis. This monopolar property allows the interconnected homologue pair to biorient on the spindle, but in this case, spindle forces are resisted by the combination of chiasma and distal sister-chromatid cohesion (Figure 1Biii). The monopolar modification of sister kinetochores is reversed in preparation for the second meiotic division in order to allow sister chromatids to be segregated (Figure 1Bv).

3. The cohesion between the chromosome arms is destroyed prior to the first division, whereas cohesion between sister centromeres is protected until the second round of segregation ensues. This modification allows homologues to be segregated at the first meiotic division, while leaving sufficient cohesion to facilitate sister segregation at the second division (Figure 1Biii–v).

4. The two meiotic divisions occur without an intervening round of replication.

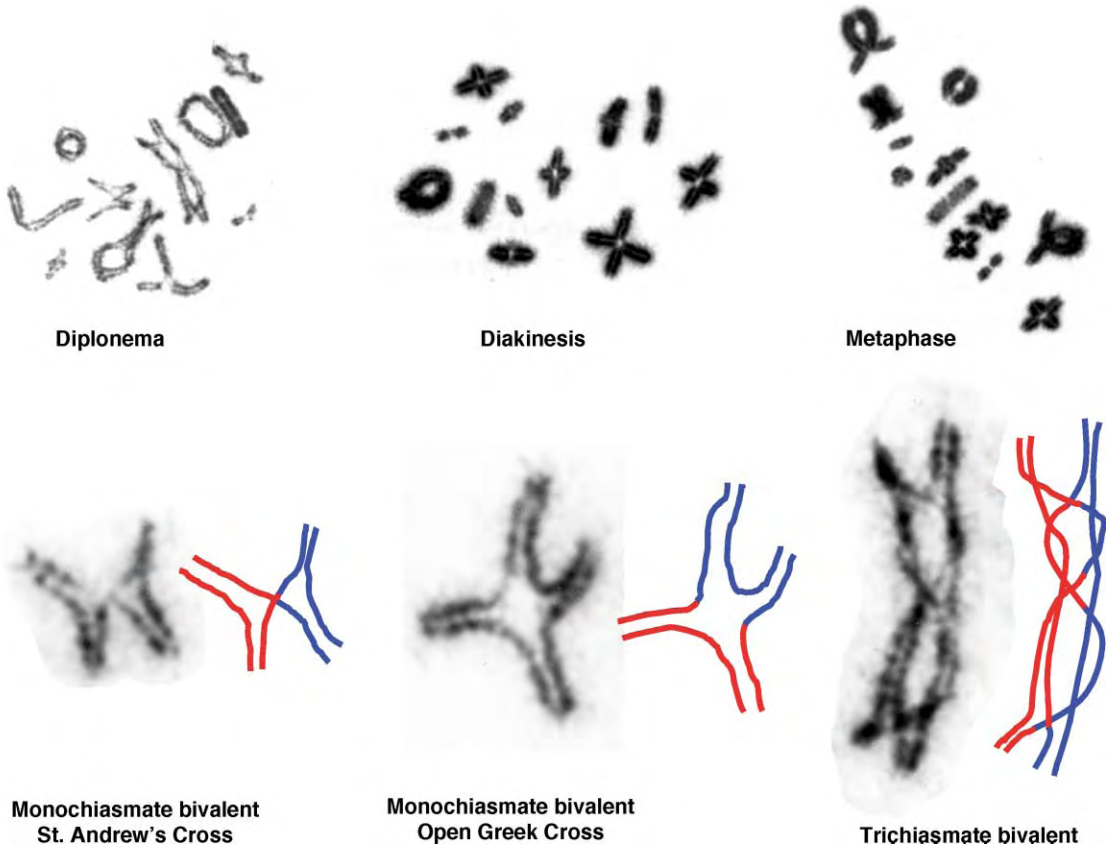

FIGURE 2 Chiasmata in the migratory locust, *Locusta migratoria*. Top: Chiasmata are observed during three distinct stages of meiotic prophase I, after which the homologues are segregated. Bottom: enlargements of individual homologue pairs; cartoons show the topological relationships between chromosomes and the points of exchange. Images kindly provided by Professor Gareth Jones, Birmingham University.

Meiotic Prophase I

The first meiotic division is preceded by an extended prophase during which the chromosomes are paired and chiasmata are formed. This period is divided into the following five stages, defined by the appearance of the chromosomes under the light microscope (Figure 3):

1. Leptonema (adjective = leptotene; from the Greek *lepto*, meaning "thin"). During leptonema, which follows chromosome replication, chromosomes are first visible as long thin strands.
2. Zygonema (adjective = zygotene; from the Greek *zygo*, meaning "yoke," Old English for "couple" or "unite"). Homologues begin to closely associate during zygonema. The extent of association increases throughout this stage.
3. Pachynema (adjective = pachytene; from the Greek *pachy*, meaning "thick"). Homologues are associated along their entire lengths and thus appear as thick, morphologically indistinguishable entities.
4. Diplonema (adjective = diplotene; from the Greek *diplo*, meaning "double"). Diplonema is usually preceded by the diffuse stage during which chromosomes are indistinct. When they reappear at diplonema, homologues are no longer associated along their lengths, but are visibly connected by chiasmata (Figure 2). In female animals, meiosis typically arrests after diplonema, and oocytes move into a quiescent dictyate stage in which the chromosomes are less condensed. In most vertebrates, the first meiotic division is completed only in response to hormonal stimulation.
5. Diakinesis (from the Greek *dia*, meaning "across," and *kinesis*, meaning "movement"). During diakinesis, the nuclear membrane begins to break down, and spindle microtubules develop and connect to the monopolar kinetochores of the homologues. The homologue pairs condense dramatically, becoming progressively shorter and thicker, and they move towards the equator of the cell (Figures 2 and 3).

After Prophase I

Following the events of prophase I, the cell prepares the chromosomes for segregation and then segregates them via two additional stages, which are the meiotic counterparts of the final stages of mitosis (Figure 3).

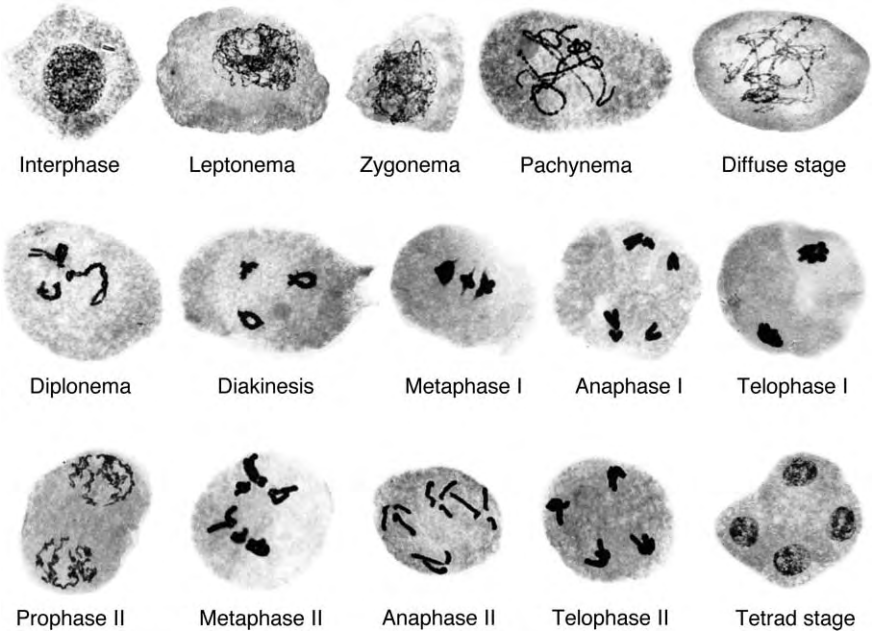

FIGURE 3 Classical stages of meiosis in *Crepis capillaris*, a flowering plant of the family *Compositae*. The cells of the tetrad eventually differentiate into pollen. Images kindly provided by Professor Gareth Jones, Birmingham University. Reprinted with permission from: Funcham, J.R.S. (1983) *Genetics*, Jones & Bartlett Publishers, Sudbury, MA.

1. Metaphase I (from the Greek *meta*, meaning "between, with, beside, after" and *phasis*, meaning "appearance"). At metaphase I, the condensed chromosomes are aligned along the equator of the spindle, typically at the central plane of the cell. This configuration is the consequence of stable biorientation of the homologue pairs on the spindle (Figures 2 and 3).

2. Anaphase I (from the Greek *ana*, meaning "up, throughout, according to" and *phases*, meaning "appearance"). At anaphase I, cohesion between chromosome arms is destroyed, and the homologues are pulled toward the poles of the spindle.

3. Telophase I and interphase I (from the Greek *telos*, meaning "end"; and from the Latin *inter*, meaning "between, among" and the Greek *phasis*, meaning "appearance"). Telophase is the last phase of mitosis, in which the segregated chromosomes decondense and are enclosed in a new nuclear membrane. Interphase is any period or stage between two successive mitotic divisions. These stages are not a general feature of meiosis and in many cases are skipped as the cell proceeds directly to the second meiotic division. In oocytes, cell division is asymmetric, resulting in the production of a small polar body plus a large oocyte cell.

4. Meiosis II. During prophase II, the chromosomes recondense, spindle microtubules develop, and the sister chromatid pairs biorient, and then congress at the equational plane of the spindle at metaphase II. The oocytes of vertebrates arrest for a second time at metaphase II, where they remain until fertilization. Typically, the plane of the meiosis II spindles is perpendicular to that of the meiosis I spindle. Sister chromatids are pulled apart at anaphase II, and new nuclear envelopes form during telophase II.

5. Gametogenesis. At this stage, the products of meiosis are known as meiocytes. The differentiation of meiocytes then produces gametes that are characteristic of the specific organism, e.g., sperm, pollen, and spores.

Meiotic Chromosome Structure and the Synaptonemal Complex

Loops and Axes

Meiotic chromosomes have a well-defined loop-axis structure (Figures 4A–4C), which is revealed by ultrastructural studies using the electron microscope. The loops are loops of chromatin that vary in size from ~20 kb in simple eukaryotes such as yeast to ~2500 kb in grasshopper, an organism with particularly large chromosomes. Thus, the large differences in genome size between different organisms are accommodated in large part by changes in chromatin loop size, such that meiotic chromosome length does not vary linearly with genome size. The loops of every pair of chromatids are connected at their bases, in a linear arrangement, along a rod-like axis or core, i.e., one axis = two chromatids = one homologue. Protein constituents of the homologue axes included those involved in sister-chromatid cohesion. The basic loop-axis structure is thought to be organized by the cohesion proteins; this then serves as a platform

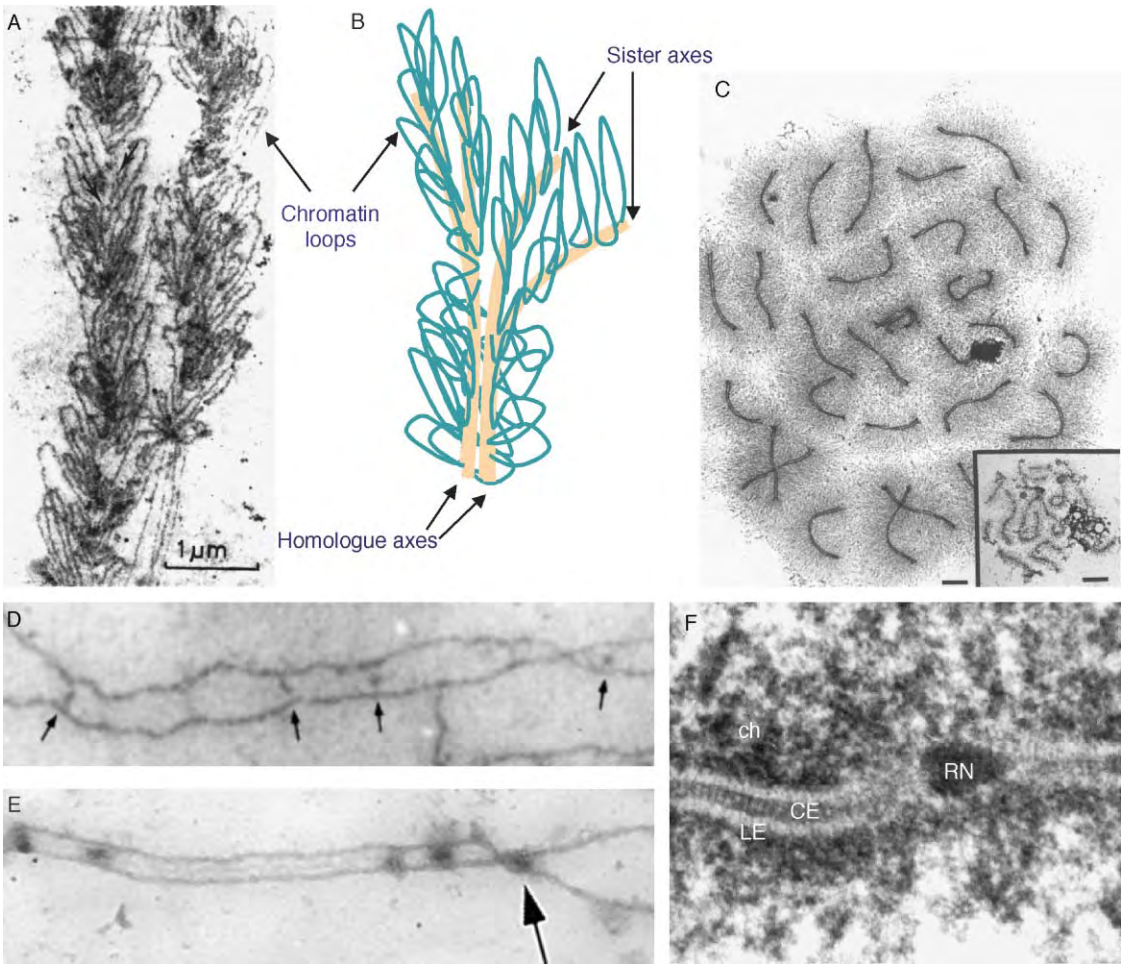

FIGURE 4 Chromosome structure in meiotic prophase. (A) Late pachytene stage chromosomes from the midge, *Chironomus*. Reprinted from Keyl, H. G. (1975). Lampbrush chromosomes in spermatocytes of *Chornomous*. *Chromosoma* **51**, 75–91 with permission of Springer-Verlag. (B) Cartoon rendering of loop-axis structure showing that each distinct homologue axis comprises two conjoined sister axes. (C) Spread chromosomes from the moth, *Hyalophora columbia*, and baker's yeast, *Saccharomyces cerevisiae* (inset; bars = 2 μm); note the large difference in chromatin loop size. Reprinted from Moens, P. B., and Pearlman, R. E. (1988). Chromatin organization at meiosis. *Bioessays* **9**, 151–153 with permission of John Wiley & Sons, Inc. (D) Part of a spread chromosome pair in early zygonema from the onion, *Allium cepa*, showing early recombination nodules at the sites of axial association (indicated by arrows). Reprinted from Albini, S. M., and Jones, G. H. (1987). Synaptonemal complex spreading in *Allium cepa* and *A. fistulosum*. I. The initiation of pairing. *Chromosoma* **95**, 324–338 with permission of Springer-Verlag. (E) Part of a spread chromosome pair in mid-late zygonema from the tree tomato, *Cyphomandra betacea*, showing SC-associated early recombination nodules. Arrow highlights an early nodule at the junction of synapsed and unsynapsed axes. Reprinted from Anderson, L. K., Hooker, K.D., and Stack, S. M. (2001). The distribution of early recombination nodules on zygotene bivalents from plants. *Genetics* **159**, 1259–1269. (F) SC longitudinal section from the beetle, *Blaps cribrosa*, with associated late recombination nodule. Abbreviations: LE, lateral element; CE, central element; RN, recombination nodule; ch, chromatin. Reprinted from Shmekel, K., and Daneholt, B. (1988). Evidence for close contact between recombination nodules and the central element of the synaptonemal complex. *Chromosome Res*. **6**, 155–159 with permission of Springer-Verlag.

for the binding of additional proteins that gives rise to the distinct axes detected by electron microscopy (Figures 4C–4F).

Synaptonemal Complexes

Meiotic chromosome pairing culminates with formation of synaptonemal complexes (SCs), prominent proteinaceous structures that form between homologues, along their entire lengths. SC morphology, as defined by ultrastructural studies, is remarkably conserved between different organisms (Figure 4C, F): two dense lateral elements flank a central region, which contains a less dense central element. The lateral elements correspond to the homologue axes. Transverse filaments lie across the central region to create a striated, zipper-like appearance. Central region proteins (putative transverse filaments) share a broadly similar secondary structure: a long coiled coil flanked by globular C and N termini. Coiled-coil lengths of ~70–90 nm fit the prediction that these

proteins span the 100 nm central region in a head-to-head configuration. SCs are thought to assemble by a two-step process: nucleation, by installing central region proteins at sites where homologue axes are very closely paired, followed by polymerization between and along the homologue axes. SCs are important for the normal formation of chiasmata.

Prophase I Stages at the Ultrastructural Level

The homologue axes develop and become distinct during leptonema. The homologues progressively pair, eventually becoming coaligned along their lengths at a distance of ~400 nm. During this presynaptic alignment, axes closely associate at several sites along each pair of homologues. These axial associations are the sites where DNA molecules are interacting via homologous recombination and are often associated with densely staining nodular structures that contain recombination proteins (Figures 4D and 4E.). During zygonema, the polymerization of SCs is nucleated at a subset of these sites, as well as at the chromosome ends. Cells enter pachynema when SCs extend along the lengths of every pair of homologues, and a second type of nodular structure develops that is typically larger, denser, rounder, and much less numerous than that observed during zygonema (Figure 4F). These late recombination nodules mark the sites where chiasmata will appear following the breakdown of SCs and entry into diplonema.

Homologous Recombination during Meiosis

Homologous recombination is the use by a broken or damaged chromosome of a homologous chromosome as a template for its repair. Each recombination event has one of two potential outcomes: a crossover (reciprocal exchange of chromosome arms), or a non-crossover (local transfer of genetic information without exchange of chromosome arms). Studies of chromosome structure have used organisms with large, readily visualized chromosomes. In contrast, much of our understanding of the molecular processes of meiotic homologous recombination comes from studies using the single-celled eukaryote, baker's yeast *Saccharomyces cerevisiae*, which has a genome ~250 times smaller than that of a human. These studies reveal that homologous

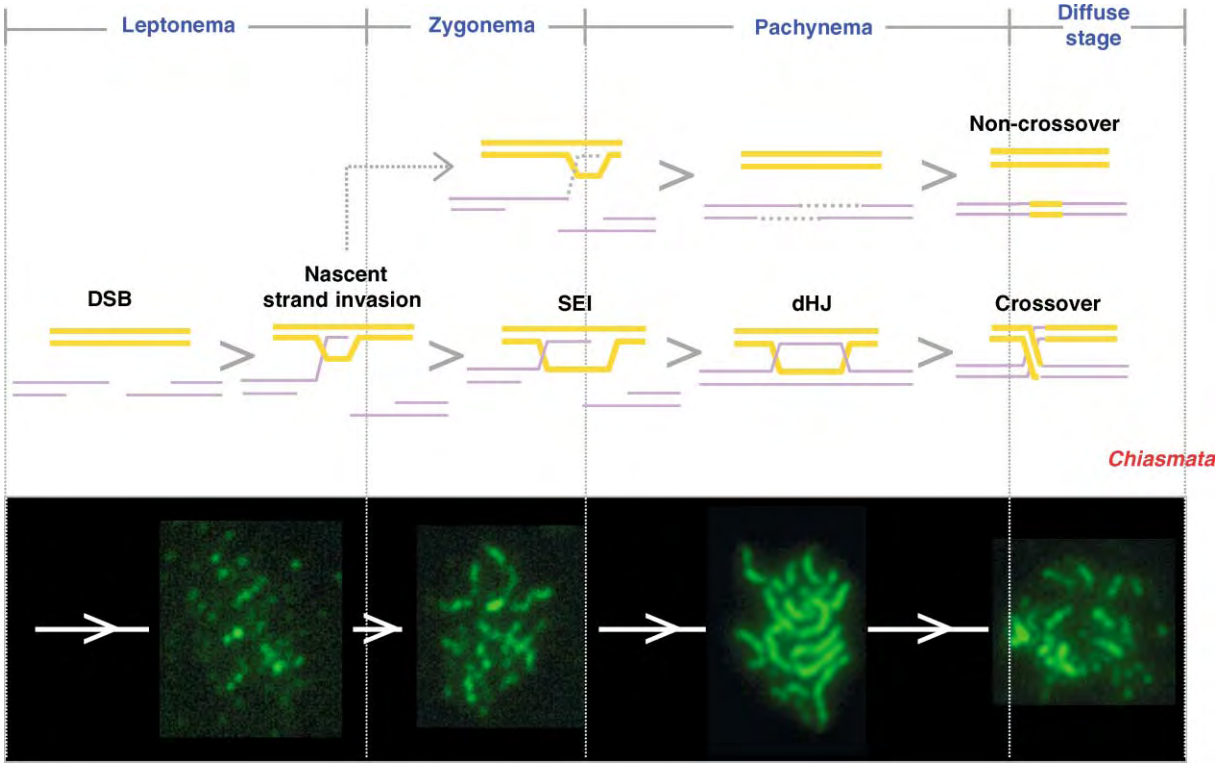

FIGURE 5 Relative timeline of the DNA events of recombination and the cytological stages of meiosis. Top row: the stages of meiotic prophase I. In mammals, this period occupies about 4 weeks; in a simple eukaryote such as yeast, it takes just 5 hours. Middle row: relative timing and molecular details of meiotic recombination. Each pair of lines represents a DNA duplex. Only the two chromatids involved in the recombination event are shown. See text for details. Bottom row: synaptonemal complex formation in baker's yeast, *Saccharomyces cerevisiae*. Spread meiotic chromosomes were stained with fluorescent antibodies to a synaptonemal complex protein.

recombination plays two successive roles during meiosis: (1) close pairing of homologues during leptonema/zygonema; and (2) connection of homologues via chiasmata from diplonema through to anaphase I.

Mechanism and Regulation of Meiotic Recombination

Meiotic recombination is initiated by the programmed formation of DNA double-strand breaks (DSBs) in chromosomes during leptonema (Figure 5). In yeast and similarly in mouse and humans, it can be inferred that ~250 double-strand breaks are formed per meiotic cell. Such a large number of recombination events is required to bring homologues into close register and facilitate the formation of SCs. Only a subset of DSBs (~5–30%, depending on the organism) go on to produce crossovers. DSBs are processed to give long single-stranded tails, which load proteins related to the bacterial recombinase RecA. These RecA homologues have the amazing ability to coat a single strand of DNA and then rapidly locate and pair with an identical DNA sequence anywhere in the genome. Meiotic chromosomes use this homologous pairing activity to recognize and pair with their homologous partner during leptonema.

A key aspect of meiotic recombination is its regulation. Most importantly, the cell must ensure that every pair of homologues receives at least one chiasma, as required for successful segregation at anaphase I. This means that the decision as to whether a DSB will eventually produce a crossover or a non-crossover is not random and must be actively imposed. It is not known how this decision is made, but its timing and molecular consequences are now becoming clear. The crossover or non-crossover decision is made at an early step in the recombination pathway, at the transition into zygonema. At this stage, DSBs that have been designated to become crossovers begin to exchange DNA strands with the homologous chromosome. Exchange at the two DSB ends occurs sequentially to form first a single-end invasion (SEI) and then a double-Holliday junction (dHJ; named after Robin Holliday, who proposed the existence of these strand-exchange structures during homologous recombination) (Figure 5). dHJs form during pachynema and are resolved toward the end of this stage by a nick and ligation mechanism, giving crossovers. DSBs that are not designated as crossovers are repaired primarily by a process called synthesis-dependent strand annealing (SDSA), which involves first copying DNA sequences from the homologous chromosome and then annealing the two DSB ends to seal the break. SDSA does not appear to involve stable, long-lived strand-exchange intermediates such as SEIs and dHJs.

See Also the Following Articles

Cell Cycle: Mitotic Checkpoints • Chromosome Organization and Structure, Overview • DNA Mismatch Repair and Homologous Recombination • Homologous Recombination in Meiosis • Metaphase Chromosome • Mitosis • Nucleoid Organization of Bacterial Chromosomes

Glossary

chiasma The point where homologous chromosomes exchange arms; the cytological manifestation of crossing-over.

crossing-over A reciprocal exchange between two DNA molecules; occurs essentially via a reciprocal breakage and rejoining process.

sister-chromatid cohesion The connections that hold newly replicated chromosome pairs together until they are ready to be distributed into daughter cells.

synaptonemal complexes Proteinaceous structures, resembling zippers or railroad tracks, that assemble between homologous chromosomes during meiosis. They hold chromosomes together during the pachytene stage and promote the formation of chiasmata.

Further Reading

Allers, T., and Lichten, M. (2001). Differential timing and control of noncrossover and crossover recombination during meiosis. *Cell* **106**, 47–57.

Hassold, T., and Hunt, P. (2001). To err (meiotically) is human: The genesis of human aneuploidy. *Nat. Rev. Genet.* **2**, 280–291.

Hunter, N., and Kleckner, N. (2001). The single-end invasion: An asymmetric intermediate at the double-strand break to double-holliday junction transition of meiotic recombination. *Cell* **106**, 59–70.

Jones, G. H. (1984). The control of chiasma distribution. *Symp. Soc. Exp. Biol.* **38**, 293–320.

Kleckner, N. (1996). Meiosis: How could it work? *Proc. Natl. Acad. Sci. USA* **93**, 8167–8174.

Page, S. L., and Hawley, R. S. (2003). Chromosome choreography: The meiotic ballet. *Science* **301**, 785–789.

Petronczki, M., Siomos, M. F., and Nasmyth, K. (2003). Un menage a quatre: The molecular biology of chromosome segregation in meiosis. *Cell* **112**, 423–440.

Roeder, G. S. (1997). Meiotic chromosomes: It takes two to tango. *Genes Dev.* **11**, 2600–2621.

Zickler, D., and Kleckner, N. (1999). Meiotic chromosomes: Integrating structure and function. *Annu. Rev. Genet.* **33**, 603–754.

Biography

Neil Hunter is an assistant professor in the section of microbiology at the University of California at Davis. He holds a Ph.D. from Oxford University and performed his postdoctoral studies at Harvard University. His research focuses on the mechanism and control of homologous recombination during meiosis. He has developed specialized DNA assays to monitor the molecular events of recombination in cells undergoing meiosis.

Melanocortin System

Roger D. Cone
Oregon Health and Science University, Portland, Oregon, USA

The melanocortins are a family of peptides defined by their ability to modulate the activity of a family of five related G protein-coupled receptors, called the melanocortin receptors (MC1-R, also called the melanocyte stimulating hormone receptor; MC2-R, also called the adrenocorticotropin receptor; and MC3-R, MC4-R, and MC5-R). The name is derived from the two original physiological activities identified for the family of peptides, stimulation of melanin synthesis and deposition, and stimulation of glucocorticoid synthesis and release by the adrenals. Four major melanocortin agonist peptides (α-MSH, β-MSH, γ-MSH, and ACTH) are encoded by a single gene, the proopiomelanocortin (POMC) gene. Major sites of POMC gene expression include the pituitary, hypothalamus, brainstem, and skin. The melanocortin system is quite unique in that specific receptor antagonists, called agouti and agouti-related protein, also exist. Together, these melanocortin agonists and antagonists regulate a remarkably diverse array of physiological processes, including the pigmentation of hair and skin, production of glucocorticoids, energy homeostasis, natriuresis, secretion of diverse exocrine gland products, and erectile function.

Melanocortin Ligands and Receptors

Elements of the melanocortin system are encoded by eight genes. Peptide agonists are encoded by a single gene, the POMC preprohormone precursor. This gene is expressed primarily in the anterior and intermediate lobes of the pituitary, the arcuate nucleus of the hypothalamus and the nucleus of the solitary tract of the brainstem, and in skin and a handful of peripheral sites where the peptides are thought to act in a paracrine or autocrine fashion. Melanocortin peptides are cleaved from three different regions of POMC to yield γ-MSH (amino terminal), ACTH, and α-MSH (overlapping peptides from the central portion), and β-MSH (carboxy-terminal end) peptides. Specific patterns of cleavage occur in different tissues, so, for example, the 39 amino acid peptide encoding ACTH is produced in the anterior pituitary by the peptidase PC1. A peptidase expressed in the intermediate lobe, PC2, makes a second cleavage to yield α-MSH, derived from the first 13 amino acids of ACTH. Melanocortin peptides derived from any of the three regions of POMC contain a His-Phe-Arg-Trp amino acid motif; this peptide motif is required for high-affinity binding of these peptides to the melanocortin receptors.

In addition to peptide melanocortin agonists derived from POMC, two genes, agouti and agouti-related protein (AGRP), encode small secreted antagonists of the melanocortin receptors. Agouti is a 131 amino acid protein with ten disulfide-bonded cysteine residues related in structure to small peptide toxins like the conotoxins and plectotoxins, produced by cone snails, and spiders, respectively. Agouti is produced by hair follicle cells, where it acts on adjacent follicular melanocytes to antagonize the MC1-R and switch the cell from eumelanin (brown-black) to pheomelanin (yellow-red) pigment synthesis. AGRP, also 131 amino acids in length, shares sequence similarity with agouti in the cysteine-rich carboxyterminal domain, and is an endogenous antagonist of the MC3-R and MC4-R. AGRP is expressed in the adrenal gland and in the arcuate nucleus of the hypothalamus; in this latter site AGRP is co-expressed with neuropeptide Y in a set of neurons adjacent but distinct from POMC arcuate neurons. In the brain, the AGRP gene is significantly up-regulated by fasting.

The melanocortin receptors, MC1-R through MC5-R, are encoded by a family of five independent genes; each receptor amino acid sequence is found in a single coding exon. The receptors are in the 7-membrane spanning G protein-coupled receptor class, and all five receptors couple, via Gs, to activation of adenylyl cyclase. With the exception of the MC2-R, all of the melanocortin receptors bind multiple species melanocortin peptide species. The MC2-R binds only the ACTH peptide, and the MC3-R is the only receptor that exhibits high-affinity γ-MSH binding. Much of the physiological specificity of melanocortin peptide action derives from the unique tissue distribution of the five receptor subtypes (Table I).

Pigmentation

The genetic study of coat colors in mice led to the identification of over 60 genes involved in pigmentation.

TABLE I

The Melanocortin Receptors and their Known Functions

Receptor subtype	Site of action	Ligand	Biological function
MC1-R	Melanocyte	α-MSH = β-MSH = ACTH > γ-MSH > $ACTH_{4-10}$ Antagonists – Agouti ($IC_{50} \sim 1$ nM)	Pigmentation
MC2-R	Adrenal cortex	ACTH	Steroidogenesis
MC3-R	CNS, stomach, duodenum, placenta, and pancreas	γ_1-MSH = γ_2-MSH = α-MSH = β-MSH = ACTH Antagonists – AGRP ($\sim$2 nM)	Inhibitory autoregulation of MC4-R system; natriuresis
MC4-R	Adult CNS, spinal cord, fetal brain, spinal cord, autonomic nervous system	α-MSH (EC_{50} = 0.2–1.5 nM) = β-MSH = ACTH > $ACTH_{4-10}$ = γ-MSH > $ACTH_{4-10}$ Antagonists – AGRP ($IC_{50} \sim 2$ nM)	Energy homeostasis
MC5-R	Exocrine glands	α-MSH > β-MSH = ACTH > γ-MSH > $ACTH_{4-10}$	Synthesis and secretion of exocrine gland products

These genes encode proteins involved in all stages and aspects of the process by which melanocytes migrate from the neural crest, populate skin and hair follicles, and synthesize and secrete melanin or pigment granules. The biochemically complex melanin polymers can be divided into two classes, the yellow-red pheomelanins and brown-black eumelanins. The regulation of enzyme activities leading to these two pigment classes is termed the eumelanin-pheomelanin switch. Genetic studies of pigmentation in the mouse and a variety of other mammalian species led to the identification of two gene loci primarily involved in the regulation of the eumelanin/pheomelanin switch, "agouti" and "extension." The "extension" locus encodes the melanocyte stimulating hormone receptor, or MC1-R, while "agouti" encodes an endogenous MC1-R antagonist expressed in skin and hair follicle. Mutations inactivating the MC1-R lead to yellow or red coat color, while mutations inactivating agouti lead to dark black coat colors. Loss-of-function mutations in the human MC1-R are one cause of red hair color and type I skin pigmentation in humans. In many mammals in the wild, up-regulation of agouti expression during a brief period of synthesis of a hair shaft leads to blockade of MC1-R activity, and results in deposition of a pheomelanin band along the otherwise darkly pigmented hair, known as the wild-type agouti pigmentation pattern.

Adrenocortical Steroidogenesis

The ACTH receptor, or MC2-R, is expressed almost exclusively in the cortex of the adrenal glands, where it regulates synthesis and release of glucocorticoids in response to release of adrenocorticotropic hormone (ACTH) by the pituitary gland. ACTH also has long-term effects on the growth and differentiation of the cells of the adrenal cortex. ACTH is a 39 amino acid melanocortin peptide cleaved from proopiomelanocortin in the anterior lobe of the pituitary. ACTH release, in turn, is regulated by production of corticotropin releasing hormone, a hypothalamic releasing factor produced in response to a wide variety of stressors. These factors, in concert, constitute what is widely known as the hypothalamic–pituitary–adrenal (HPA), or stress axis, which functions to allow organisms to adapt to internal and external challenges to homeostasis. Glucocorticoids serve many functions, but in general serve an adaptive role in coping with challenges to the organism by mobilizing carbohydrate energy stores and suppressing the immune system. Glucocorticoids are also essential for development. A rare syndrome of ACTH resistance resulting from loss-of-function mutations in the MC2-R, known as familial adrenocorticotropic hormone resistance, often presents with neonatal hypoglycemia, hepatitis, hyperpigmentation of skin due to elevated ACTH, and in some cases severe septic events.

Energy Homeostasis and Other CNS Actions

The cloning of the MC1-R (MSH-R) and MC2-R (ACTH-R) genes led to the identification of three additional GPCRs that were highly related in primary amino acid sequence and also were high-affinity receptors for melanocortin peptides. Since these receptors had, at the time, unknown physiological roles, they were termed MC3-R, MC4-R, and MC5-R. Remarkably, a novel mutation in the agouti gene that caused not only yellow coat color but also an obesity syndrome in the mouse ultimately led to the discovery that the MC3-R and MC4-R play a role in the central control of energy homeostasis. The "lethal yellow" allele of agouti results from a promoter rearrangement that causes ubiquitous expression of the agouti gene, in contrast to its normal expression limited to the hair

follicle, where it normally serves to block eumelanin synthesis. Aberrant expression of agouti in the brain results in blockade of the brain MC4-R, resulting in the agouti obesity syndrome. Discovery of AGRP identified an endogenous hypothalamic antagonist of the central MC3-R and MC4-R that has a physiological role in the regulation of the central melanocortin system. Both pharmacological blockade of the MC4-R and deletion of the gene in knockout mice also reproduce the agouti obesity syndrome. In humans, haploinsufficiency of the MC4-R, i.e., loss-of-function mutations in one allele, appears to be responsible for as much as 5% of cases of severe obesity, making the MC4-R the most common genetic cause of severe obesity known. Less is known regarding the MC3-R; however, it is expressed in a majority of arcuate POMC neurons where it appears to function as an inhibitory autoreceptor.

The central melanocortin system is defined as the hypothalalmic POMC and AGRP neurons that originate in the arcuate nucleus, brainstem POMC neurons originating in the nucleus of the solitary tract, and their target MC3-R- and MC4-R-expressing neurons, found throughout the CNS, in ~200 discrete locations (Figure 1). Central administration of melanocortin agonists both inhibits food intake and increases energy expenditure. These data, and the fact that blockade of MC4-R signaling causes obesity, argue that the POMC neurons tonically inhibit food intake and energy storage. The melanocortin system does this through effects on both food intake and on autonomic outflow to metabolically important tissues in the periphery. POMC neurons express receptors for the adipostatic hormone leptin, and play an important role in sensing and responding to the leptin signal from adipose tissue that informs the brain of long-term energy stores. POMC neurons also appear to be important for sensing and responding to acute satiety and hunger signals. The central melanocortin system affects autonomic outflow to a wide variety of tissues; melanocortins also have effects on blood pressure, heart rate, natriuresis, inflammatory response, and the male erectile response. Therapeutic applications of melanocortins may include obesity, diabetes, cachexia, and erectile dysfunction.

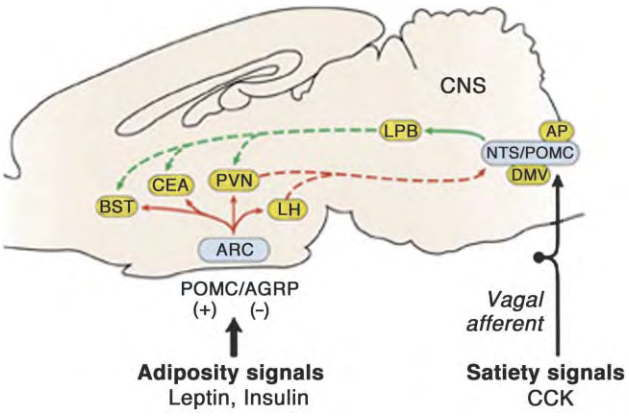

FIGURE 1 Integration of long-term adipostatic signals and acute satiety signals by the central melanocortin system. Blue: nuclei containing POMC neurons and AGRP neurons; yellow: nuclei containing MC4-R neurons that may serve to integrate adipostatic and satiety signals; red arrows: adipostatic signaling; green arrows: satiety signaling; BST, bed nucleus of the stria terminalus; CEA, central nucleus of the amygdala; PVN, paraventricular nucleus of the hypothalamus; LH, lateral hypothalamic area; LPB, lateral parabrachial nucleus; AP, area postrema; DMV, dorsal motor nucleus of the vagus. Reprinted from Fan, W., Ellacott, K. L. J., Halatchev, I., Takahashi, K., Yu, P., and Cone, R. D. (2004). Role for the brainstem melanocortin system in CCK-mediated satiety. *Nat. Neuroscience* 7, 335–336, with permission.

Exocrine Gland Function and Other Peripheral Actions

The MC5-R is expressed at high levels in a diverse array of exocrine glands, such as the sebaceous, lacrimal, preputial, and Harderian glands of the mouse. The receptor appears to stimulate the production and release of exocrine gland products from these tissues. For example, a knockout mouse specifically lacking the MC5-R gene was found to produce reduced amounts of certain lipids normally secreted by sebaceous glands onto the coat of the animal, thus reducing the ability of the coat to repel water. Male MC5-R knockout mice also exhibit a defect in initiating aggressive behavior relative to their wild-type counterparts, which has been attributed to defects in the secretion of pheromones by glands like the preputial, known to express high levels of the receptor. Little is known regarding the actual physiological roles of the MC5-R in the various exocrine tissues. For example, it is not clear whether the source of ligand for the MC5-R is the predominant serum melanocortin, ACTH, or whether this receptor is regulated by yet uncharacterized paracrine sources of POMC. If the former is the case, the system would provide a mechanism for stress-induced stimulation of exocrine gland function.

The MC3-R is also expressed in a handful of peripheral tissues, although little is know regarding its actions. The MC3-R and γ-MSH appear to be involved in the regulation of natriuresis; the reflex natriuresis that occurs after unilateral nephrectomy requires the MC3-R, and MC3-R knockout mice exhibit salt-sensitive hypertension.

See Also the Following Articles

Adenylyl Cyclases • Diabetes • Leptin

Glossary

adrenocorticotropin ACTH, a 39 amino acid peptide cleaved from POMC in the anterior pituitary, that is secreted into the bloodstream and regulates the synthesis and release of the glucocorticoid class of steroid hormones.

agouti proteins Agonti and agouti-releated proteins (AGRPs) are two small secreted proteins that bind to and antagonize melanocortin receptors.

energy homeostasis The process by which the brain detects long term energy reserves, stored in adipocytes in the form of fat, and regulates food intake and metabolic processes so as to keep reserves constant.

melanocortin A peptide derived from the proopiomelanocortin gene containing a -His-Phe-Arg-Trp- motif within its sequence that binds to and activates one or more of a family of five melanocortin receptors.

melanocyte A cell type populating skin and hair follicles that pigments hair and skin by secreting a variety of forms of melanin.

Further Reading

Chen, W., Opitz-Arraya, and Cone, R. D. (1997). Exocrine gland dysfunction in MC5-R deficient mice: Evidence for coordinated regulation of exocrine gland function. *Cell* **91**, 789–798.

Clark, A. J., Metherell, L., Swords, F. M., and Elias, L. L. (2001). The molecular pathogenesis of ACTH insensitivity syndromes. *Ann. Endocrinol (Paris)* **62**, 207–211.

Cone, R. D. (ed.) (2000). *The Melanocortin Receptors*. Humana Press, Totowa, New Jersey.

Cone, R. D. (ed.) (2003). The melanocortin system. In *Annals of the New York Academy of Science*, Vol 994. New York Academy of Science, New York.

MacNeil, D. J., *et al.* (2002). The role of melanocortins in body weight regulation: Opportunities for the treatment of obesity. *Eur. J. Pharmacol.* **440**, 141–157.

Rees, J. L. (2000). The melanocortin 1 receptor (MC1R): More than just red hair. *Pigment Cell Res.* **13**, 135–140.

Biography

Roger Cone is Director of the Center for the Study of Weight Regulation and Associated Disorders and a Senior Scientist within the Vollum Institute at the Oregon Health and Science University. His principal research interest is in the control of energy homeostasis by the central nervous system, and in the physiological processes regulated by the melanocortin system. He holds a Ph.D. from the Massachussetts Institute of Technology.

Membrane Fusion

Joshua Zimmerberg and Leonid V. Chernomordik
The National Institute of Child Health and Human Development, National Institutes of Health, Bethesda, Maryland, USA

Membrane fusion occurs when two cellular membranes attach, meld components, and become one membrane with preservation of sidedness and contents. This transformation seems somewhat miraculous, given that in everyday life only liquids with clean interfaces spontaneously fuse. So it is the hallmark of eukaryotic life that huge numbers of fusion reactions occur each second in an individual cell. Life begins with the fusion of the sperm membrane to the egg membrane, which allows the parental genes to mix together without any leakage into the extracellular space. So, relatively leak-free fusion is absolutely required for safe sex. Plasma membranes also fuse during the cell–cell fusion that directly causes the development of syncytia of several tissues, such as myotubes of muscle, trophoblastic syncytia of placenta, and the multinucleate giant cells of granuloma. In the development of *Caenorhabditis elegans*, where each cell can be traced, about one-third of the cells fuse.

But by far the most frequent site of membrane fusion is in the organization of intracellular membranes and the secretory pathway. For about half of a cell's genes are membrane proteins, and after their synthesis into the membrane of the endoplasmic reticulum, they must be delivered to their appropriate site of action, whether it is the membrane of the cell surface, or the membrane of an intracellular organelle. This protein trafficking is mediated by membrane fusion, as vesicles pinch one compartment, move through the cell, and then fuse to another compartment, often in one cycle after another before reaching their destination. Even then, proteins are taken up again into vesicles during their recycling, to fuse either to staging compartments or to degradation compartments. And it is not only membrane proteins that are trafficked in this manner, but vesicle fusion also delivers soluble proteins to the lumen of these compartments. This constant maintenance function of fusion is called constitutive fusion, to distinguish itself from the specifically regulated fusion events that must occur at the right time.

Arguably the most important regulated, or triggered fusion event for a human is the release of neurotransmitters such as acetylcholine, glutamate, and neuropeptides from synaptic vesicles during synaptic signal transmission. This class of fusion of intracellular secretory vesicles to the plasma membrane is called exocytosis, since the contents of the secretory vesicle are topologically in a space that becomes continuous with the outside of the cell, and never sees the cytoplasm. It is the triggered, regulated exocytosis that mediates many extremely important physiological events. The secretory vesicles are also called granules when their contents are seen as dense in traditional thin-section electron microscopy. Insulin, thyroid hormone, growth hormone, antidiuretic hormone, adrenaline, norepinephrine, follicle stimulating hormone, leutinizing hormone, and ACTH are just a few examples of hormones stored in secretory granules awaiting the proper signal for their coordinated and rapid secretion by fusion into the extracellular space for transport via the blood stream. Exocrine glands are also arranged for vectorial synthesis of digestive enzymes, such as trypsin and chymotrypsin, which are condensed into storage granules, whose membrane fuses to the luminal membrane of the glandular acinus. It has been clear that calcium is the intracellular messenger that triggers secretion in many systems. In other systems the intracellular messenger is not yet fully elucidated.

In addition, some exocytotic fusions are also constitutive, and provide the basis for most of the tissue organization of multicellular life. Thus collagen, fibronectin, proteoglycans, and other skeletal macromolecular elements are secreted via this constitutive secretory pathway. In addition, immunoglobulins are constitutively released from immune system cells throughout life, as are many cytokines and chemokines. It is worth noting that even the constitutive pathway is not devoid of control, as cytokines and chemokines are regularly up- and down-regulated at the levels of the control of gene and protein expression. The mast cell and the granulocytic series of white blood cells also rely upon fusion for their exocytosis of the mediators of inflammation and their release of compounds that kill invading pathogens. This is an essential part of the host response to disease.

It is impossible to overstress the importance of membrane fusion in the development, function, and

maintenance of tissues, organs, and organism. Since the extracellular space has no genome, all gene expression needed for the coordinated structure and function of tissues is a result of secretion of gene products through exocytosis, sometimes in response to requirements known by signaling to cell surface receptors or by internalization of informative macromolecules that in turn traffic to their targets by membrane fusion. In addition, new experiments suggest that stem cells in adult animals can remodel their cellular organization by fusing to adult cells. This points to membrane fusion as critical to the regeneration of tissues and organs.

Unfortunately, much of human suffering over the ages also derives in part from membrane fusion. Intracellular parasites use membrane fusion to enter cells and to evade the immune system. Over half the strains of human pathogenic viruses are encased in an envelope, a biological membrane, that must fuse to cellular membranes for the virus' internal genes to gain access to their intracellular destinations. And enveloped viruses are on the top of lists of human pathogens causing death and disease. HIV, the cause of AIDS, influenza, the cause of the flu (grippe), the viruses of rabies, measles and SARS, respiratory syncytial virus, and hepatitis C virus are just a few of these pathogens. Luckily for scientists studying fusion, the viral envelope often has only one major membrane protein, which causes membrane fusion and is easy to identify (e.g., the hemagglutinin of the influenza virus (HA)). So studies of viral fusion have led to many discoveries about the proteins and ultimately the mechanism of membrane fusion.

Proteins and Lipids

Proteins

From this diversity of membranes which fuse, are there any structural motifs that are common to the proteins that foment fusion? A definitive answer to this question is hindered by uncertainty about the identity of such proteins, a paucity of structural information on those that are identified, and the fact that most of the structural data derives from the same family of viral envelope proteins. Nevertheless, some generalizations can be made.

All viral fusogenic proteins characterized to date are anchored in the envelope by one or more transmembrane domains. While there is some latitude in the specific amino acid sequence of the transmembrane domains supporting fusion, the general mechanism by which the fusogenic protein is attached to the membrane is of importance for its activity and, in particular, for the late stages of fusion. As a rule, viral fusion proteins, as most viral envelope proteins, are homo- or hetero-oligomers. The importance of this for their fusogenic activity remains to be clarified. However, at least in some cases the stability of these oligomers appears to be crucial for fusion.

Specific triggering events start a major restructuring of viral fusion proteins from their initial conformation to fusion-competent forms. For viruses that invade cells by an endocytotic pathway, the binding and fusion functions of envelope proteins appear to be well separated, and the trigger for conformational change is acidification. Other viruses, such as HIV, enter cells by fusing with the target cell plasma membrane. Here binding of the fusogenic protein to specific receptors at the surface of the target cell triggers the subsequent cascade of conformational change. For still other viruses, such as the Rous Sarcoma virus, receptor binding primes the fusion protein for subsequent triggering by acidification.

One of the most important features of this trigger-dependent restructuring of viral fusion proteins is exposure of an amphiphilic, highly-conserved stretch of $\sim$10–30 amino acid residues that is critical for fusion. This "fusion peptide" is hidden from the aqueous environment in the initial conformation of the protein. It inserts into membrane after activation. The HA fusion peptide, the amphiphilic stretch of $\sim$20 amino acid residues at the NH2-terminus of the HA2 subunit of HA, is highly conserved; mutations here have deleterious effects on fusion activity. In general, fusion peptides spontaneously insert into membranes and disturb the structure of lipid bilayers. Based on the dependence of the fusogenic activity of HA on the sequence of the fusion peptide, fusion appears to require membrane-insertion of the fusion peptide in a boomerang-like conformation.

Similar aminoterminal peptides are found in the fusion proteins of a number of other viruses such as HIV, Sendai, and hepatitis B. There are also many viruses where the fusion peptide is found in the midst of the amino acid sequence of membrane-anchored glycoproteins (for instance, Semliki Forest, tick-borne encephalitis and rabies viruses). While fusion peptides, one or more per protein, undoubtedly play a key role in all well-characterized fusion machines, their specific role in fusion requires clarification. The prevailing model suggests that the fusion peptide, when inserted into the target membrane, both destabilizes the membrane and serves as a handle allowing the fusion protein to bend this membrane towards the viral membrane. It has been also hypothesized that the fusion peptide inserts into, destabilizes, and bends the viral rather than target membrane. In addition, the functional role of some of the protein regions identified as fusion peptides may not be limited to direct interaction with membranes and may involve directing the refolding of the activated protein by supporting or destabilizing certain conformations.

Many fusion proteins, named class 1 (e.g., HA and HIV *env*), have a stage of proteolytic cleavage which

liberates the N terminus of the fusion peptide from other domains. Final conformations of the proteins of this class share a common hairpin arrangement with a central α-helical coiled-coil domain surrounded by an outer layer of polypeptide chains. Class 2 proteins (e.g., fusion proteins of flaviviruses, E) have an internal fusion peptide, and here proteolytic cleavage of an accessory protein leads to the mature conformation of the fusion protein itself. Class 2 proteins are not predicted to form coiled-coils and contain predominantly β-strand secondary structure.

In spite of much diversity in their initial structures, fusion proteins of the two classes apparently share an important feature of the final conformations of these viral fusion proteins: close proximity of the fusion peptide and transmembrane domain. In addition, for diverse fusion proteins the triggering event not only starts a cascade of conformational changes of individual proteins, but also initiates lateral protein–protein interactions. These interactions are detected as cooperativity of both conformational change and membrane fusion as well as formation of multiprotein complexes of activated fusion proteins.

The identification and characterization of the proteins that mediate intracellular membrane fusion is much more complex and controversial, and mechanistic studies lag behind. There are slews of interesting proteins that are important for the regulation, binding, docking, priming, and execution of membrane fusion, most identified through a genetic screen for mutants in secretion in yeast. In general, it is thought that small GTP-binding proteins mediate recognition of pairs of membranes destined to fuse together with the SNARE proteins. There are some excellent reviews on SNARE proteins and their role in fusion.

Exocytosis is the best-studied type of intracellular fusion. A collection of proteins known as the exocyst complex is involved in the binding of vesicles to the plasma membrane. Priming of the bound and docked proteins involves the phosphorylation of a specific inositol lipid, PIP2, and other ATP-dependent processes. Some of the rates of vesicle mobilization, binding, docking, and priming are dependent upon the local intracellular free calcium ion concentration. In regulated exocytosis *in vivo*, it is almost always this divalent ion that triggers fusion. Synaptotagmins, annexins, and calmodulin have been implicated as the calcium-binding partner in triggering exocytosis in different systems. The SNARE proteins are the leading candidates for the protein that mediates the membrane fusion event itself, but their generality and mechanism of action is still a controversial question in the field. In particular, it is not clear how much their interaction energy contributes to overcoming the barriers to membrane fusion. To estimate those barriers, the role of lipids and the pathway of membrane fusion needs to be considered.

Lipids

Since ultimately fusion proteins must act on the lipid bilayer of membranes, it is no surprise that protein-mediated fusion is sensitive to lipid composition. A distinction between physiological requirements and experimental effects of lipids must be made. As an example of the physiological lipid requirements, fusion mediated by Semliki Forest Virus is strictly dependent on the presence of sphingolipid and cholesterol in the target membrane: the former (optimum at ~ 5 mol%) is needed for the actual fusion event and the latter (optimum at 30 mol%) is required for the low-pH-dependent conformational change in the fusion protein and membrane insertion of its fusion peptide. A second example is the triggered exocytosis of chromaffin cells that requires specific polyphosphoinositides.

In contrast to physiological lipid requirements, usually specific for different systems, non-bilayer lipids that change the propensity of lipid monolayers to bend have effects on fusion that are strikingly universal. These effects depend on both the effective shape of the lipids, and the monolayer to which they are added. Inverted cone lipids such as lysophosphatidylcholine, when added to the contacting monolayers of fusing membranes, inhibit membrane merger in disparate biological fusion reactions. Lysolipids inhibit virtually all systems that have access to the contacting leaflet, irrespective of the specific fusion proteins and the triggering agent. In contrast, cone-shaped lipids such as phosphatidylethanolamine and *cis*-unsaturated fatty acids (e.g., oleic and arachidonic acids) promote fusion. In addition to this early stage of fusion that is sensitive to the composition of the "contacting" membrane monolayers, there is also a later stage that is sensitive to the composition of the "noncontacting" monolayers of the fusing membranes: inverted-cone shaped amphiphiles added to these distal monolayer of the fusing membranes promote fusion. These stages likely involve the actual merger of the lipid bilayers.

Mechanistic Pathways

At the time of the writing of this article, there are many open questions for research on the mechanism of membrane fusion. One theme, however, that is common to many of the disciplines studying fusion, is that at the center of biological membrane fusion is a fundamental rearrangement of lipid bilayer topology that follows the same pathway as does the fusion of synthetic lipid bilayers. For any pathway in biology, we need to identify the intermediate structures, the relative energy of each intermediate, and the driving forces that propel the membranes to fuse. After binding, lipid bilayer membranes that are to fuse first exchange the lipids of the

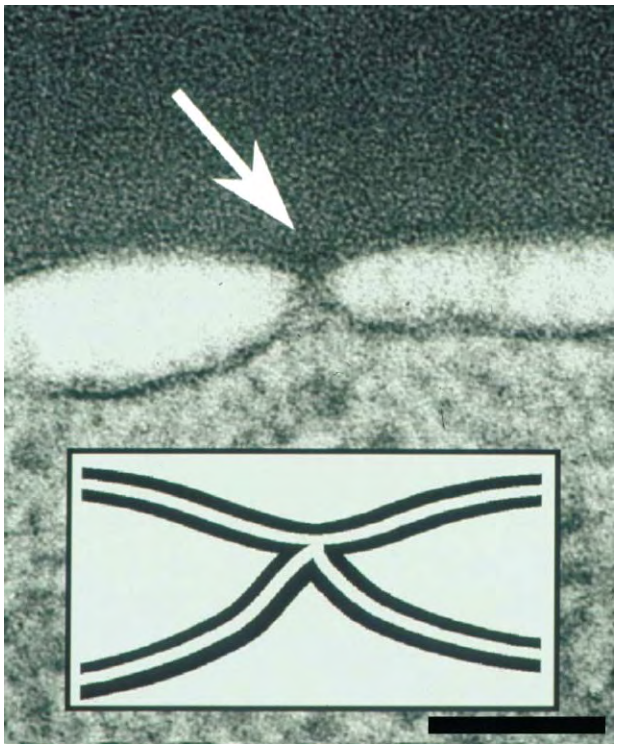

FIGURE 1 The contact site between a red cell membrane (top) and a fibroblast expressing the influenza hemagglutinin (HA) mutated to delete the transmembrane domain and attach the ectodomain of HA to a glycerol phosphoinositol lipid. The membranes were activated for fusion after binding with a pulse of low pH. After 20 min, the cells were frozen into vitreous ice by slamming them against a copper block cooled with liquid nitrogen. After freeze-substitution and thin sectioning, electromicrographs were taken at two tilt angles, and analyzed with stereo viewing. The drawing illustrates the view from stereography. Bar = 100 nm.

contacting monolayers (hemifuse), then form small aqueous pores that transiently open and close. Complete fusion ensues only when tension is applied to the fusing lipid bilayer membranes.

Biological membrane fusion offers constraints on the spontaneous fusion of lipid bilayers by dint of the regulated activities of the fusion proteins. Studies on mast cell exocytosis show that the tension propelling fusion must be exerted locally by proteins rather than through swelling of the vesicles. Studies on fusion mediated by influenza HA show that the early hemifusion intermediate is reversible, and converts into a small pore (the fusion pore) when the distal monolayers merge. In electron micrographs of thin sections of cells frozen into vitrious ice, then freeze-substituted, both the contact site and the fusion pore can be visualized (Figure 1). Since the outer diameter of the contact site ranges between 10 and 50 nm, there is not much expansion of the stalk before the initial pore is formed, which is ~1 nm internal aqueous diameter. This initial fusion pore, which can only be detected by electrophysiological assay, is usually spontaneously reversible, giving a flickering pore phenotype observed both for viral fusion and exocytosis. Opening of one or several of these early pores is followed by an expansion of at least one of them to complete fusion. Progress through the pathway, and perhaps alternate pathways, is dependent upon the density of the fusogenic protein. At lower densities of HA, one observes either small non-expanding fusion pores or hemifusion phenotypes. Only at optimal conditions of high density of activated HAs and physiological temperature, fusion reaction

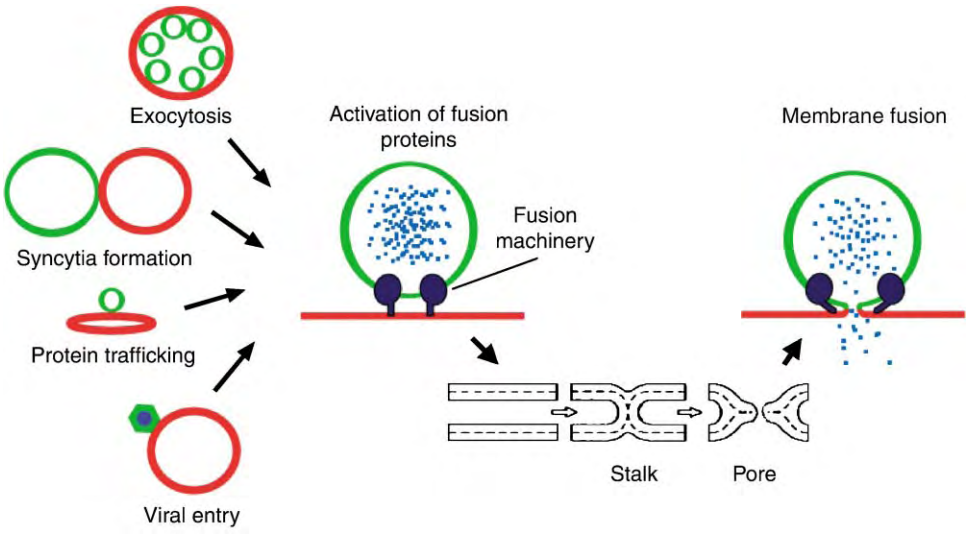

FIGURE 2 Diverse biological processes that feature membrane fusion apparently converge to a common stalk-pore pathway of lipid bilayers, after activation of different specific fusogenic proteins by specific triggers (e.g., Ca^{2+}, H^{+}, and GTP), or by receptor binding (e.g., CD4 in HIV). Both stalk- and pore-intermediates are generated by protein-mediated bending of membrane lipid monolayers. Dashed lines show the boundaries of the hydrophobic surfaces of two monolayers in each membrane and in hypothetical intermediates.

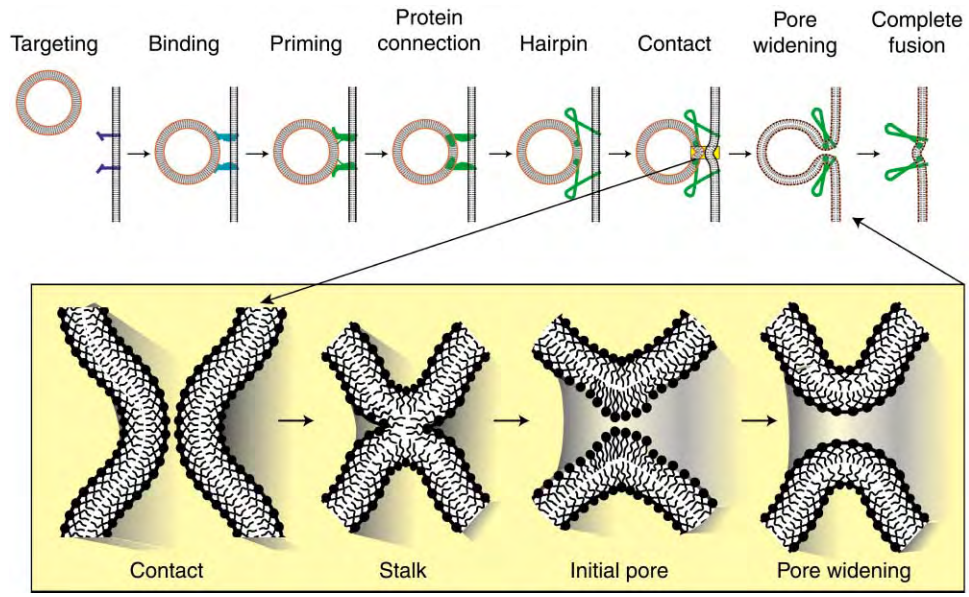

FIGURE 3 A schematic representation of the many steps in protein-mediated membrane fusion, abstracted from research on many different proteins and systems. Top: The delivery of vesicles to their fusion partner may be highly organized and targeted, as in intracellular trafficking, or random, as in viral infection. Binding of the two membranes is mediated through the attachment of the fusion protein to its receptor in the partner membrane, which can be either a protein or a lipid. In many systems there next are priming reactions such as covalent bond modifications involving either cleavage of part of the fusogenic protein, interaction with co-receptors, or phosphorylation of lipids with ATP. At this stage the system is ready for any trigger that may be needed to regulate fusion. In the case of influenza HA, this trigger leads to insertion of the fusion peptide into the target membrane, and a protein now connects both membranes' bilayers. Next protein conformational change, often to a hairpin configuration, leads to contact between the two membranes at discrete spots where the bilayers are deformed. Spontaneous rearrangement of contacting lipids can lead to stalk formation and then the opening of the initial fusion pore. After pore widening, contents can be released or mixed.

yields an expanding fusion pore that fully mixes both lipids and aqueous contents.

The current synthesis of results on biological fusion, along with experimental and theoretical work on fusion of synthetic lipid bilayers, suggests that membrane rearrangement in cellular membrane fusion can be considered as a sequence of local bending deformations. First, contacting monolayers of the two bilayers merge to form a local hemifusion connection referred to as a stalk and then after some expansion, small pores form in the hemifusion junction. With tension, fusion is completed by formation and expansion of the pore. Two key intermediates, stalk and pore, are both formed by strongly bent lipid monolayers. However the net curvature of these intermediates is opposite. In the stalk there is less room for the polar heads of the lipids than for the lipid tails. In the pore, it is just the opposite. Also, while the stalk is formed by contacting monolayers, the pore is formed by the distal monolayers of the membranes that came into contact only after hemifusion. The universal effects of nonbilayer lipids for both purely lipid bilayer membranes and for a variety of cellular fusion systems (Figure 2) suggest that these disparate processes all revolve around stalk-pore rearrangements of their membrane bilayers.

We can summarize membrane fusion with a pathway of the current working hypothesis of many groups (Figure 3). Essentially, cell biologists, lipid physical chemists, and membrane biophysicists have converged their views: in biological membrane fusion, as in many biological processes, proteins act to accelerate fusion by lowering the energy barriers for unfavorable intermediates of the spontaneous fusion pathway of lipid bilayer membranes. The specific mechanisms by which proteinaceous fusion machines break and reseal the continuous and tight bilayer structures of biological membranes remain to be understood.

See Also the Following Articles

Lipid Bilayer Structure • MDR Membrane Proteins

Glossary

fusion pore An early aqueous connection between compartments joined by fusion.

fusion protein Specialized protein that catalyzes merger of two membrane bilayers into one.

hemifusion The coalescence of the contacting monolayers of the two bilayers with their distal monolayers to remain distinct. In many cases hemifusion allows diffusion of a lipid dye originally only in

the outer leaflet of one cell or vesicle to another, without any diffusion of an aqueous dye originally in the lumen of the cell (the cytosol) or a vesicle.

stalk intermediate Hypothetical local hemifusion connection between contacting monolayers at early fusion stages.

Further Reading

Blumenthal, R., Clague, M. J., Durell, S. R., and Epand, R. M. (2003). Membrane fusion. *Chem. Rev.* **103**, 53–70.

Chernomordik, L. V., and Kozlov, M. M. (2003). Protein–lipid interplay in fusion and fission of biological membranes. *Annu. Rev. Biochem.* **72**, 175–207.

Cohen, F. S., and Melikyan, G. B. (1998). Methodologies in the study of cell–cell fusion. *Methods* **16**, 215–226.

Hernandez, L. D., Hoffman, L. R., Wolfsberg, T. G., and White, J. M. (1996). Virus–cell and cell–cell fusion. *Annu. Rev. Cell Dev. Biol.* **12**, 627–661.

Jahn, R., Lang, T., and Sudhof, T. C. (2003). Membrane fusion. *Cell* **112**, 519–533.

Lentz, B. R., Malinin, V., Haque, M. E., and Evans, K. (2000). Protein machines and lipid assemblies: Current views of cell membrane fusion. *Curr. Opin. Struct. Biol.* **10**, 607–615.

Rothman, J. E. (2003). The machinery and principles of vesicle transport in the cell. *Nat. Med.* **8**, 1059–1062.

Shemer, G., and Podbilewicz, B. (2003). The story of cell fusion: Big lessons from little worms. *Bioessays* **25**, 672–682.

Skehel, J. J., and Wiley, D. C. (2000). Receptor binding and membrane fusion in virus entry: The Influenza Hemagglutinin. *Annu. Rev. Biochem.* **69**, 531–569.

Tamm, L. K., Crane, J., and Kiessling, V. (2003). Membrane fusion: A structural perspective on the interplay of lipids and proteins. *Curr. Opin. Struct. Biol.* **13**, 453–466.

Zimmerberg, J., and Chernomordik, L. V. (1999). Membrane fusion. *Adv. Drug Deliv. Rev.* **38**, 197–205.

Biography

Joshua Zimmerberg, Chief of the Laboratory of Cellular and Molecular Biophysics, received his M.D. and Ph.D. from the Albert Einstein College of Medicine of Yeshiva University, working with Fredric S. Cohen under the mentorship of Alan Finkelstein in the Galvani Institite of Electromembranology, and did his postdoctoral work with V. Adrian Parsegian at the NIH. His principal contributions have been in the discoveries of the requirement of tension in membrane fusion, the fusion pore, the pathway of fusion in exocytosis and viral fusion, and the lipidic nature of the apoptotic pore.

Leonid V. Chernomordik, Chief of the Section on Membrane Biology in the Laboratory of Cellular and Molecular Biophysics, received his Ph.D. in electrochemistry from the Frumkin Institute of Electrochemistry, Russian Academy of Sciences in 1979 and his Doctor of Sciences in biophysics degree from the Moscow State University in 1991. His principal contributions have been in developing the stalk-pore hypothesis of membrane fusion first for synthetic lipid bilayers and then for biological membranes.

Membrane Transport, General Concepts

Stanley G. Schultz
University of Texas Medical School, Houston, Texas, USA

The term membrane transport refers to processes that bring about the movement of solutes and water across the barrier, or envelope that surrounds all living cells in the animal and plant kingdoms. These processes are responsible for two ubiquitous characteristics of living cells, namely: (1) the ability to maintain constant, or near constant, intracellular compositions that differ from the extracellular environment, containing the highly specialized molecules essential for metabolism and replication; and at the same time, (2) the ability to selectively exchange matter and energy with that environment.

All cell membranes consist of a double layer of phospholipids oriented so that their electrically charged, hydrophilic (or water-loving) head projects into the interior and exterior of the cells, respectively, and their lipid tails, which are hydrophobic (or water-fearing), project inward and form an oily core. Floating in this oily structure are surface or peripheral proteins that do not extend through the thickness of the bilayer, and integral proteins that span the bilayer and provide pathways for direct communication between the intracellular and extracellular compartments. This lipoprotein bilayer model, which consists of large expanses of lipid studded here and there with protein, is illustrated in Figure 1.

Exchange of solutes and water across the lipoprotein barrier takes place through the lipid as well as through integral proteins and can be classified as (1) simple diffusion; (2) diffusion through pores or channels; and (3) carrier-mediated transport. The latter may be subdivided into facilitated diffusion (or facilitated transport), primary active transport, and secondary active transport.

Simple Diffusion

The simplest form of membrane transport was recognized more than a century ago by Overton, who noted that the ease with which a large variety of molecules cross plant cell membranes is proportional to their solubility in lipids; indeed, it is the observation that first suggested that the membranes were composed of lipids. In essence he suggests that the molecule simply dissolves in the lipid across one surface, passes through this oily barrier, and exits at the other side. The rate of this process is given by a modification of a law derived by Fick in 1855:

$$J_i = k_i D_i \Delta C_i$$

where J_i is the rate of diffusion of solute i across the membrane (in amount of solute per unit time), k_i is a measure of the solubility of the solute i in oil compared to water (oil:water partition coefficient), D_i is the diffusion coefficient of i or the mobility of i in the lipid, and ΔC_i is the concentration difference of i across the membrane. The product $k_i D_i$ is often abbreviated as the permeability coefficient P_i.

Overton demonstrated a linear relation between J_i and k_i in plant cells and this relation, now referred to as Overton's law, has been confirmed repeatedly.

Diffusion through Pores or Channels (Restricted Diffusion)

Lipid membranes are essentially impermeable to ions and are only slightly permeable to water. It is now clear that these highly hydrophilic molecules traverse cell membranes through integral proteins that form water-filled pores or channels that span the bilayer. Although the presence of "holes" in membranes had been speculated as early as the 1850s and were strongly suggested by the pioneering work of Hodgkin, Huxley, and Keynes on the squid axon in the 1950s, they were established beyond doubt, more recently, by Hille, Armstrong, and MacKinnon.

Although some use the terms pore and channel interchangeably, others prefer to employ the word pore for integral proteins that are continually open to the two aqueous compartments on both sides of the membrane (using the analogy of an open pipe) and reserve the word channel for a pore that has a "gate" that determines how

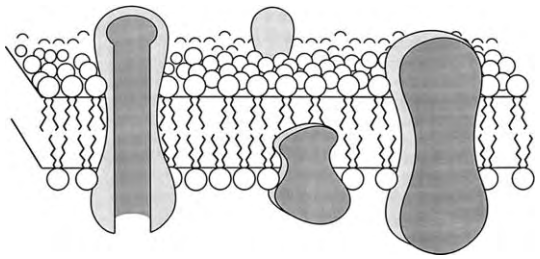

FIGURE 1 Illustration of phospholipid bilayer with peripheral proteins adhering to the surfaces and integral proteins spanning the thickness of the membrane. One integral protein is portrayed as a channel. The charged head groups of the phospholipids are represented as circles and the lipophilic fatty tail groups as the wavy lines forming the core of the bilayer.

long it will be in the fully open state and how long it will be closed (the analogy being a pipe with shutter).

In general, then, channels have gates that determine the probability that they will be in the open state at any time (open-time probability) and how long they will stay open (mean open time). The properties of these gates may be influenced by the electrical potential difference across the membrane (voltage-gated channels), the binding of one or more ligands (ligand gated channels) or both. In addition, they possess "filters" that confer selectivity on the channel; the structural characteristics of ion channels that result in a high preference for one ion over other have recently been unraveled for potassium channels.

Movement of an ion through an open channel obeys a form of Ohm's law for current flow caused by a conductance driven by an electrochemical potential difference. Thus,

$$i_{\mathrm{i}} = g_i(V_{\mathrm{m}} - E_{\mathrm{i}})$$

where i_{i} is the rate of flow of the ion through a single open channel given in electrical terms of amperes (this is analogous to J_i), and g_i is the conductance of the channel (analogous to P_i). V_{m} is the electrical potential difference across the membrane, E_{i} is the Nernst equilibrium potential for the ion so that the difference, $(V_{\mathrm{m}} - E_{\mathrm{i}})$, is the displacement of the ion from equilibrium in electrical terms and is thus the driving force for flow. More than one million ions may traverse a single channel per second so that single channel currents may be readily recorded using a variety of techniques. The ionic current through an ensemble of such channels is $I_{\mathrm{i}} = i_{\mathrm{i}} N_{\mathrm{i}} p_{\mathrm{o}}$, where N_{i} is the total number of channels and p_{o} is the open probability.

Carrier-Mediated Transport

Carrier-mediated transport differs from diffusion through lipid phase, pores, or channels in that after entering the integral protein the transported solute(s) bind to a specific site(s) on this protein which then undergoes some translocation that exposes and/or releases them to the other side. Unlike pores or channels, carriers are not open to both sides of the membrane simultaneously. Because conformational changes are necessary for carriers to function, the number of molecules transported per second is orders of magnitude less than pores. In this sense, carriers may be viewed as enzymes that do not chemically alter the transported species (substrate) but, instead, catalyze a change in their location. For this reason, the terms permeases and translocases are used in some instances as synonymous with carriers. Indeed, one characteristic of carrier-mediated transport is that it displays Michaelis–Menten saturation kinetics, marked by a maximum transport velocity (J_m) and a solute concentration needed to achieve a half-maximal transport velocity (K_t), and often obeys the simple relation

$$J_{\mathrm{S}} = \left\{ [S] J_{\mathrm{m}} / K_{\mathrm{m}} + [S] \right\}$$

where J_{S} is the rate of transport and $[S]$ is the concentration of the transported solute (Note: this relation describes the initial rate of transport when there is solute present on one side of the membrane only).

Facilitated Diffusion

The earliest recognized and simplest form of carrier-mediated transport is facilitated diffusion, often called facilitated transport, in which an otherwise impermeant solute binds to a site on an integral protein (carrier) from one side of the membrane and then undergoes a translocation that provides the solute access to the other side. The classic example of facilitated diffusion is glucose transport across the membranes of cells such as erythrocytes, muscle, adipocytes, etc. The carriers that mediate this transport have been cloned and sequenced and fall into a group of proteins that have 12 membrane spanning segments called GLUT. Urea is transported across the membranes of many cells by a facilitated transporter called UT.

It must be emphasized that because these carriers are not directly or indirectly coupled to a supply of energy, they cannot perform osmotic work, i.e., they cannot transport a neutral solute against a concentration difference (e.g., from lower to higher concentration) or a charged solute against a combined electrochemical potential difference. Thus, like diffusion, facilitated diffusion carriers bring about equilibration; transport ceases when intrinsic thermodynamic driving forces are abolished.

Active Transport

Active transport is the term reserved for transport processes that result in the movement of a solute uphill or against its natural direction. For the case of a neutral solute (at constant temperature and pressure), this resolves into movement against a concentration difference; for a charged solute, it is movement against the combination of concentration and electrical potential differences. This is work (e.g., charging a battery) and it therefore requires the investment of energy.

There are two groups of carrier-mediated active transport processes: those where the coupling to energy is direct and those where the coupling to energy is indirect.

Primary Active Transport

Primary active transport processes are capable of coupling energy directly to the uphill movement of the transported species. By far the most abundant, and well understood, primary active transporters are the retinylidene proteins or, more commonly called, rhodopsins, capable of coupling light energy to ion transport. Bacteriorhodopsins found in *Archaea*, *Circhaea,* and some eukaryotic and prokaryotic cells pump protons out of these cells, thereby establishing a "proton-motive force" across the membrane. Holophilic bacteria possess a form referred to as halorhodopsin that pumps Cl^- into cells. These transporters have been studied extensively using high-resolution crystallography and all possess seven membrane spanning segments attached to a chromophore.

In higher animals, all primary active transporters are ATPases, that derive the energy for moving the transported solute against a thermodynamic driving force (i.e., uphill) from ATP hydrolysis. The most prevalent is the Na–K pump found in virtually all cells from higher animals and responsible for pumping three Na^+ ions out of the cell and two K^+ ions into the cell for every ATP hydrolyzed. This pump is responsible for the fact that these cells have a lower intracellular Na^+ concentration and higher intracellular K^+ concentration than the concentrations of these ions in the surrounding extracellular fluid. As will be discussed below, the extrusion of Na^+ from the cell establishes a "natrio-motive" force across the membrane analogous to the "proton-motive" force established by light-driven proton pumps in lower life forms. The detailed mechanism of action of the Na–K pump is not well established except for the fact that it is a member of a superfamily of ATPases referred to as E_1–E_2 ATPases or P-type ATPases, because the operation of the pump involves cycling between two configurations of the protein driven by phosphorylation and dephosphorylation reactions.

Other ATPases that perform primary active transport include the Ca^{2+} ATPase found in muscle and responsible for regulation of the Ca^{2+} activity of the cytoplasm, the H^+–K^+ ATPase of gastric parietal cells responsible for secreting protons into the gastric juice in response to appropriate stimuli, and the H^+ ATPase that is responsible for acidifying intracellular organelles such as lysosomes, endosomes, etc.

Secondary Active Transport

Secondary active transport processes bring about the uphill transport of one or more solutes but do not derive the necessary energy from direct coupling to a source of metabolic energy. Instead, these transport processes are energized by coupling those movements to the downhill movement of another solute.

Cotransport (symport) The uphill or secondary active transport of a large number of solutes into cells of higher animals is coupled to the downhill movement of Na^+. Thus, the carrier protein binds both the transported solute and Na^+ from the extracellular solution. Inasmuch as the Na^+ concentration in the intracellular solution is lower than that in the extracellular solution, because of the action of the Na^+–K^+ pump as discussed, this coupling permits the downhill movement of Na^+ and provides the energy for the uphill movement of the coupled solute. In essence, the energy invested into the Na^+–K^+ pump by the hydrolysis of ATP has set up an Na^+-gradient or natrio-motive force across the membrane that can be deployed to energize the secondary active transport of solutes whose translocation across the membrane is coupled to that of Na^+.

In many lower forms of life, secondary active cotransport is energized by the H^+ gradient or proton-motive force across the membrane established and maintained by light-driven primary active extrusion of protons, as discussed above.

Countertransport (antiport) Coupling to the downhill movement of Na^+ into cells can also serve to energize the uphill or secondary active transport of solutes out of cells. Important examples of counter-transporters are the Na^+–H^+ exchanger (NHE) responsible for extruding H^+ from cells and the regulation of cell pH and the Na^+–Ca^{2+} exchanger (NCX) responsible for extruding Ca^{2+} from many cells.

Na^+-coupled co- and counter-transport processes are very diverse and are beautiful examples of bioenergetic economy where a single primary active transport process directly coupled to the hydrolysis of ATP can establish a transmembrane ion (Na^+) gradient that can, in turn, be utilized to energize a wide variety of secondary active transport processes.

See Also the Following Articles

ER/SR Calcium Pump: Function • ER/SR Calcium Pump: Structure • Membrane Transporters: Na^+/Ca^{2+} Exchangers • Plasma-Membrane Calcium Pump: Structure and Function • P-Type Pumps: Copper Pump • P-Type Pumps: H^+/K^+ Pump • P-Type Pumps: Na^+/K^+ Pump • P-Type Pumps: Plasma Membrane H^+ Pump

Glossary

active transport Transport of a solute against a chemical (concentration) and/or electrical potential difference that is directly (primary) or indirectly (secondary) driven by metabolic energy.

carrier Integral proteins that span the membrane phospholipid bilayer and are capable of binding a solute(s) and catalyzing translocation from one side of the membrane to the other.

channel Integral proteins that span the membrane phospholipid bilayer and provide water-filled passage ways (pores) for the diffusion of solutes.

diffusion Flow of a solute from a region of higher to a region of lower chemical (concentration) and/or electrical potential driven solely by thermal random motion of solute particles.

facilitated diffusion Carrier-mediated transport processes that are not coupled to a supply of metabolic energy and thus can only result in the equilibration of a transport solute across the membrane.

Further Reading

Bretscher, M. S. (1985). The molecules of the cell membrane. *Sci. Am.* **253**(4), 100–108.

Doyle, D. A., Cabral, J. M., Pfuetzner, R. A., Kuo, A., Gulbis, J. M., Cohen, S. L., Chait, B. T., and MacKinnon, R. (1998). The structure of the potassium channel: Molecular basis of K^+ conductance and selectivity. *Science* **280**, 69–77.

Hille, B., Armstrong, C. M., and MacKinnon, R. (1999). Ion channels: From idea to reality. *Nat. Med.* **5**, 1105–1109.

Schultz, S. G. (1980). *Basic Principles of Membrane Transport*. Cambridge University Press, Cambridge.

Schultz, S. G. (2003). Membrane transport. In *Essential Medical Physiology* (L. R. Johnson, ed.) 3rd edition, pp. 37–70. Elsevier, USA.

Spudich, J. L., Yang, C.-S., Jung, K.-H., and Spudich, E. N. (2000). Retinylidene proteins: Structures and functions from Archaea to humans. *Ann. Rev. Cell Dev. Biol.* **16**, 365–392.

Biography

Dr. Stanley G. Schultz is Professor and Vice-chair of the Department of Integrative Biology and Pharmacology, and Interim Dean of the University of Texas Medical School in Houston; he is also holder of the Fondren Family Chair in Cellular Signaling. He was previously Chairman of the Department of Physiology and Cell Biology at that institution. Dr. Schultz holds an M.D. from The New York School of Medicine. His principal research interest is in epithelial, particularly, small intestinal, transport and he has authored and edited seminal papers and texts in the area of membrane transport physiology and biophysics. He is past President of the American Physiological Society.

Membrane Transporters: Na^+/Ca^{2+} Exchangers

Jonathan Lytton
University of Calgary, Calgary, Alberta, Canada

The Na^+/Ca^{2+} exchanger is a plasma membrane protein that can bind and transport both Na^+ and Ca^{2+} ions. The exchanger is reversible, and the direction in which it moves Ca^{2+} depends upon the relative gradients of Na^+ and Ca^{2+} across the membrane, the membrane potential, and the number of ions that bind and are transported. Under normal physiological conditions in eukaryotic cells, the Na^+/Ca^{2+} exchanger extrudes Ca^{2+} from the cytoplasm in exchange for Na^+ entry, and thus participates in Ca^{2+} homeostasis in a variety of cellular environments, most notably heart, brain, and kidney. The Na^+/Ca^{2+} exchanger is encoded by a family of structurally and functionally related gene products that have distinct patterns of expression in different tissues. There are two major branches to the family, one that encodes Na^+/Ca^{2+} exchangers that transport Na^+ ions in exchange for only Ca^{2+} ion (NCX), and one in which Na^+ ions are exchanged for both Ca^{2+} and K^+ (NCKX). The NCX branch has three known members, NCX1 (*SLC8A1*), NCX2 (*SLC8A2*), and NCX3 (*SLC8A3*), while the NCKX branch has five known members, NCKX1 (*SLC24A1*) through NCKX5 (*SLC24A5*). Only NCX1 and NCKX1 proteins have been studied extensively in their endogenous environment (cardiac myocytes and retinal rod photoreceptor outer segments, respectively). The remaining members of the family have been defined through cloning or bioinformatic tools, and the unique contributions they each make to cellular Ca^{2+} homeostasis is an active area of investigation.

Cellular Ca^{2+} Homeostasis

Ca^{2+} ion is one of the most ubiquitous intracellular second messengers. Changes in the concentration of Ca^{2+} control a variety of cellular processes ranging from fertilization through proliferation and differentiation, the specific functions of different mature adult cells and tissues, all the way to programmed cell death. The coordination of such a diverse set of functions is thought to be achieved through Ca^{2+}-binding events that are sensitive to complex spatial and temporal patterns of intracellular Ca^{2+} concentration. Unlike other second messenger systems, Ca^{2+} cannot be metabolized, and its concentration is controlled primarily by transport across membranes that bound intracellular compartments (such as the sarco- or endoplasmic reticulum and the mitochondrion) and the cell periphery (the plasma membrane). Cells possess a complex array of different Ca^{2+} transporting mechanisms, and the process of Na^+/Ca^{2+} exchange has emerged as a major contributor to Ca^{2+} efflux across the plasma membrane. The unique and precise nature and arrangement of different Ca^{2+} transport protein molecules in different cells is generally thought to provide a major component of control over complex Ca^{2+} dynamics. When this carefully orchestrated homeostasis goes awry, and Ca^{2+} concentrations are dys-regulated, the repercussions are usually extreme, resulting in cell damage and death which are a prelude to the pathological consequences of diseases such as stroke, neuro-degeneration, and heart disease.

Discovery of the Na^+/Ca^{2+} Exchanger

A competitive relation between the effects of extracellular Na^+ and Ca^{2+} on intracellular Ca^{2+} and contraction in cardiac, skeletal, and smooth muscle was first noted over 50 years ago. Then in the late 1960s three different groups (Reuter, Baker, and DeLuca), working on three different tissue preparations (mammalian cardiac muscle, squid axon, and mammalian intestinal epithelium), concluded that the coupled counter-transport of Na^+ for Ca^{2+} across the plasma membrane – so called Na/Ca exchange – could explain the apparent competitive relation between Na^+ and Ca^{2+}. This finding established the physiological importance of Na^+/Ca^{2+} exchanger as a mechanism contributing to the control of Ca^{2+} homeostasis, and launched the search for a protein molecule underlying the activity.

The development of biochemical measurements of Na^+/Ca^{2+} exchanger function in membrane preparations and effective solubilization and reconstitution procedures allowed several groups to partially purify

Na^+/Ca^{2+} exchange activity. Aided by immunological approaches, Philipson's group provided strong evidence that a 120 kDa protein of canine cardiac sarcolemmal membranes, and its 70 kDa proteolytic product, corresponded to the Na^+/Ca^{2+} exchanger. At the same time, recombinant expression cloning techniques were being developed, which led to the seminal molecular cloning work from Philipson's laboratory, published in *Science* in 1990, that confirmed the identity of the canine cardiac Na^+/Ca^{2+} exchanger.

During the 1980s, studies on visual adaptation in mammalian retinal rod photoreceptors also provided evidence for a Na^+/Ca^{2+} exchange mechanism responsible for controlling cytosolic Ca^{2+} in that environment. Further biochemical studies of rod Na^+/Ca^{2+} exchange revealed an obligate dependence on K^+, and demonstrated that the rod Na^+/Ca^{2+} exchanger catalyzed the exchange of Na^+ for both Ca^{2+} and K^+. As with the cardiac exchanger, solubilization and reconstitution studies allowed purification of the bovine rod photoreceptor $Na^+/Ca^{2+} + K^+$ exchanger, which was identified as a ~220 kDa protein. Immunological tools were then used to clone the molecule in 1992 by Cook's laboratory. Surprisingly, despite the mechanistic similarity and a broadly similar topology pattern (Figure 1) the cardiac and rod exchangers share sequence similarity in only two short stretches, which were subsequently termed the α-repeats (Figure 2).

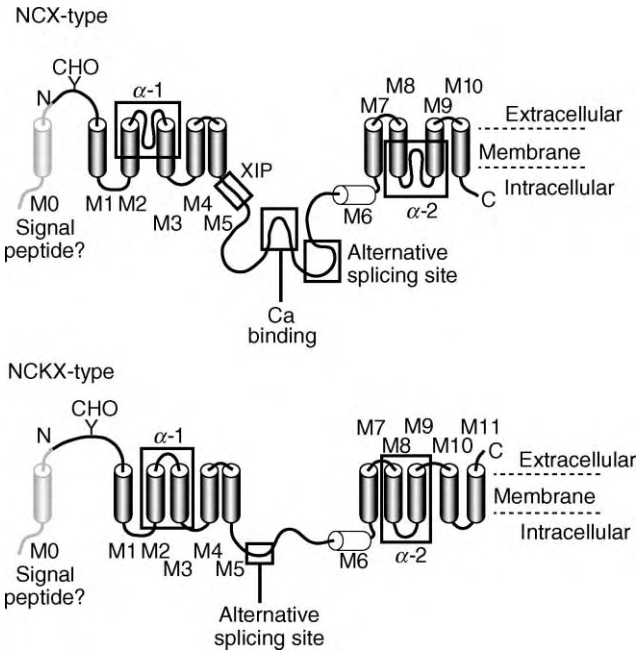

FIGURE 1 Topology models for Na^+/Ca^{2+}exchangers (NCX-type) and $Na^+/Ca^{2+} + K^+$ exchangers (NCKX type). The predicted folding of each class of protein with respect to the membrane, based on hydropathy analysis and experimental data, is shown. The cylinders labeled M0 (putative signal peptide, removed co- or posttranslationally) to M11 indicate transmembrane helices, with the exception of M6, which was originally proposed to span the membrane, but later modeled to be cytoplasmic. The conserved α-repeat regions (α-1 and α-2) are boxed and labeled. The N terminus (N) and C terminus (C) of the mature protein, as well as sites of glycosylation (CHO), alternative splicing, calcium binding, and the exchange inhibitory peptide (XIP) sequence are also indicated.

An Expanding Gene Family

Cloning of the canine cardiac Na^+/Ca^{2+} exchanger (NCX1 – gene *SLC8A1*) and the bovine rod photoreceptor $Na^+/Ca^{2+} + K^+$ exchange (NCKX1 – gene *SLC24A1*) opened the exchanger field to molecular analysis. NCX1 was subsequently cloned from heart, brain, and kidney of several different animal species. In the course of these studies, it became evident that the NCX1 gene gave rise to a complex set of alternatively spliced mRNA transcripts whose protein products differed in one relatively small region of the protein (Figure 1). The power of molecular cloning was also harnessed to uncover the existence of structurally related gene products, revealing that NCX1 is a member of a gene family that includes two other members, NCX2 (*SLC8A2*) and NCX3 (*SLC8A3*) whose products display ~70% amino acid identity with one another. NCX3 is also subject to alternative splicing, in a similar location as NCX1.

Advances in the molecular analysis of the NCKX family was not so rapid, but by the end of the 1990s a second member, NCKX2 (*SLC24A2*), had been identified. At the turn of the millennium, information contributed to the databases from random sequencing efforts and from the various animal genome projects had turned the identification of homologous genes from a bench experiment into a computer search. The discovery of NCKX3 (*SLC24A3*), NCKX4 (*SLC24A4*), and most recently NCKX5, followed rapidly.

During the early phase of homologous gene discovery, it was recognized that NCX1 contains two regions of paired internal similarity, suggesting an ancient gene-duplication event. One pair is found flanking the site of Ca^{2+} binding in the cytoplasmic loop of the protein (the β-repeat) and the other pair resides, one member within each hydrophobic membrane spanning domain (the α-repeat; see Figure 1). As indicated above, the α-repeats contain the only regions of similarity between NCX and NCKX exchangers. Moreover, a database search with the α-repeat motif identifies a large number of genes in species ranging from higher vertebrates to flies, worms, plants, yeast, and bacteria. The deduced proteins of these database hits contain two sequences homologous to the α-repeat, each within a relatively hydrophobic region, suggesting that these proteins are all membrane transporters, although in most cases the function of the gene products has not been determined

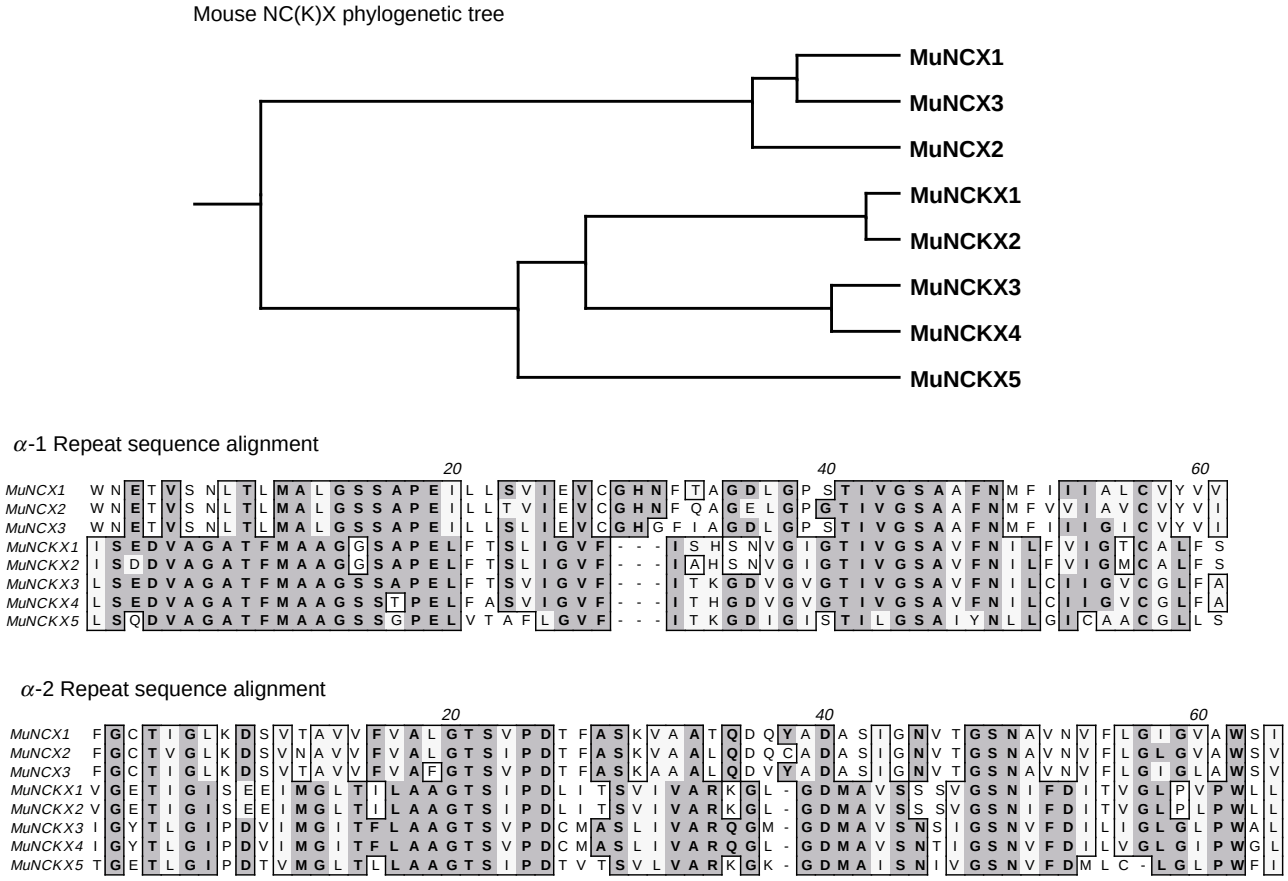

FIGURE 2 Phylogenetic relation and sequence alignment. The evolutionary relation between the different murine NC(K)X molecules is shown as a phylogenetic tree based on the combined similarities of the two α-repeat regions. A qualitatively similar pattern is obtained if the entire protein sequence from each isoform is used for the analysis. The sequences corresponding to the two α-repeats are shown aligned. Amino acids that are identical in five or more of the sequences are shown boxed, dark shaded, and highlighted in bold; chemically similar amino acids are boxed and light shaded.

directly. In some cases, the degree of sequence identity extends beyond the α-repeats, and these genes are likely to be orthologues of known mammalian NCX or NCKX exchanger genes. In other cases, the sequences are quite divergent, and the function of the encoded protein is not clear, but is presumed to involve cation exchange, for example Ca^{2+}/H^+ or Mg^{2+}/H^+ exchange.

Expression of NCX and NCKX in Mammals

NCX1 is ubiquitously expressed in almost all mammalian tissues, with the highest level of expression found in heart, brain, and kidney. The predominant NCX1 transcript in each of these three tissues corresponds to a different alternatively spliced species. The expression of NCX2 and NCX3 is highly restricted, with NCX2 present at high levels in the brain, but not at significant levels elsewhere, while NCX3 is present in skeletal muscle and at lower levels in selected brain regions, but is not significantly expressed in other tissues. The NCX1 protein has been localized mainly to the T-tubules in cardiomyocytes, to axonal and dendritic processes of neurons, and the basolateral membrane of distal convoluted tubule connecting segment cells in the kidney. Studies on the NCX2 and NCX3 proteins are less well developed.

NCKX1, originally defined in rod photoreceptors, is expressed almost exclusively in the eye, where the protein is present in the outer segments of rods. NCKX2 was originally found to be expressed at high abundance in neurons throughout the brain, but only at much lower levels elsewhere. Subsequently, this molecule was found to be present in the cone photoreceptors. Both NCKX3 and NCKX4 are abundant in brain but, in contrast to NCKX1 and NCKX2, are also broadly distributed in a number of tissues, including those rich in smooth muscle. NCKX5 has been identified only through database searches thus far, and so little information is available concerning the pattern of expression of this molecule. Aside from NCKX1, very

little is known about the expression of the NCKX family members at the protein level.

Structural Properties

Broadly speaking, all the Na^+/Ca^{2+} exchanger protein family members have a similar overall architecture (Figure 1). A hydrophobic signal peptide at the N terminus is cleaved off co- or posttranslationally, directing the glycosylated N-terminal region of the mature protein to the extracellular space. Two hydrophobic regions, each modeled as a cluster of transmembrane spanning segments, are separated by a large cytoplasmic loop. Within each branch of the family (i.e., NCX and NCKX), the length and sequence of each hydrophobic segment is well conserved, especially in the α-repeat regions (Figure 2). A comparison of these regions of clear homology can be used to generate a phylogenetic tree, illustrating the evolutionary relation between the different genes (Figure 2). In contrast to the hydrophobic regions, the sequence of both extracellular and intracellular loops are quite variable between different family members.

The arrangement of transmembrane spans within each hydrophobic region, originally based solely on hydropathy analysis, has recently been tested experimentally in several different labs using cysteine-scanning mutagenesis and antibody epitope insertion. The data from those experiments revealed that the hydrophobic region originally called M6 is not buried in the membrane, and that the α-repeat regions are oriented on opposite sides of the membrane (Figure 1). In the case of NCX1, both α-repeats are suggested to form re-entrant loop structures that come into close physical proximity with one another in the intact protein. Mutagenesis studies also revealed the importance for transport function of many of the conserved amino acids in the α-repeats, reinforcing the concept that these regions line the ion-binding and translocation pathway. Studies on the NCKX family have confirmed much of these data. However, there is no clear evidence for a re-entrant loop in the NCKX2 α-2 repeat, and the C terminus of the mature NCKX2 protein appears to be extracellular, while that of NCX1 is intracellular.

The large cytoplasmic loop of NCX1 contains several structural features thought to contribute to regulation of exchange function. At the extreme N-terminal region of the loop, an amphipathic sequence (XIP) reminiscent of a calmodulin-binding domain was noted. Exogenous addition of a peptide corresponding to this sequence inhibits Na^+/Ca^{2+} exchange. Near the center of the loop, two clusters of acidic amino acids contribute to a Ca^{2+}-binding site or sites that are critical for NCX function. Just C terminal to the Ca^{2+}-binding motifs lies the site of diversity introduced by alternative splicing. Two mutually exclusive exons, one expressed primarily in cardiomyocytes and neurons, and the other in nonexcitable cells, are combined with several cassette-type exons to form tissue-specific isoforms.

The large cytoplasmic loop of the NCKX family has not been investigated in so much detail, largely because there is no clear evidence for regulation. NCKX1, but not the other family members, has an unusually long loop as a consequence of a simple tandem repeat structure. Though this motif is present in NCKX1 molecules from various animal species, the sequence and extent of the repeat is different in each. Several of the NCKX family members are subject to alternative splicing that changes a short region toward the N-terminal end of the cytoplasmic loop. The consequences of these differences on transport function are currently not known.

Functional Properties

As their name implies, all Na^+/Ca^{2+} exchangers couple the movement of Na^+ ions in one direction to Ca^{2+} ions in the other. An extensive collection of experimental data supports a simple model where the transporter has a single set of ion-binding and transport sites that can be occupied by either Na^+ ions or a Ca^{2+} ion (and in the case of NCKX exchangers, a K^+ ion as well), but cannot be occupied by both Na^+ and Ca^{2+} ions simultaneously. The ion-binding sites on the exchanger must be fully occupied in order for their aqueous accessibility to shift across the membrane barrier (Figure 3). The exchanger can thus catalyze Na^+/Na^+ exchange, Ca^{2+}/Ca^{2+} (or in the case of NCKX, $(Ca^{2+} + K^+)/(Ca^{2+} + K^+)$) exchange, as well as Na^+/Ca^{2+} exchange. The direction of net ion flux is determined by the relative electrochemical ion gradients across the membrane, and the number of ions that bind to the transporter. For NCX1, the ion-binding stoichiometry has been a subject of intense investigation, but remains somewhat controversial, with most flux studies suggesting $3Na^+{:}1Ca^{2+}$, while most ionic current studies suggest $4Na^+{:}1Ca^{2+}$. For NCKX1 and NCKX2, the stoichiometry has been established as $4Na^+{:}1Ca^{2+} + 1K^+$. The stoichiometry of the other NCX and NCKX family members has not been determined, but is likely to be similar to their paralogous family members.

Although the direction of flux is dictated by thermodynamic considerations, the magnitude of the flux is determined by the intrinsic rate of the enzyme, the relative occupancy of the ion-binding sites, and various regulatory factors. For NCX1, which has a very high turnover rate, the enzyme is limited by the concentration of cytosolic Ca^{2+}, which is normally well below the concentration for half-maximal occupancy of the transport sites. NCX1 activity is also regulated in a complex

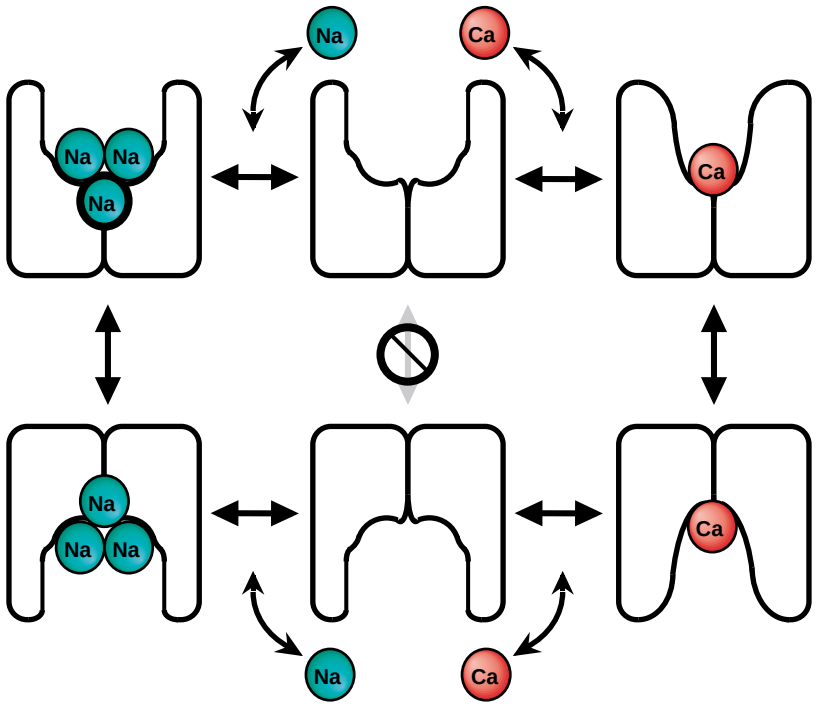

FIGURE 3 The Na^+/Ca^{2+} exchanger reaction cycle. A simple six-state model is shown, where either three Na^+ ions or a single Ca^{2+} ion can bind to the transport site from either side of the membrane in a competitive fashion. Only fully loaded transporter can re-orient the aqueous accessibility of the ion-binding sites across the membrane. Note that, in the case of $Na^+/Ca^{2+} + K^+$ exchanger, four Na^+ ions bind instead of three, and K^+ binds and is transported together with Ca^{2+}.

fashion through the central cytosolic loop. Intracellular Ca^{2+} activates the exchanger, while high concentrations of Na^+ cause inactivation. Acidic phospholipids, and ATP through phosphorylation of phosphatidyl-inositol, also activate the exchanger. These events are mediated via the identified Ca^{2+}-binding sites and the XIP region of the loop, although the mechanism is not well understood. Modulation of various kinase pathways has a modest effect on Na^+/Ca^{2+} exchange activity, but there is little convincing evidence for direct phosphorylation of NCX1. Though not studied in as much detail, it appears the other NCX family members function in an analogous manner.

The rod photoreceptor exchanger, NCKX1, appears to turn over more slowly than NCX1. On the other hand, NCKX1 has a higher apparent affinity for cytosolic Ca^{2+} and should theoretically be able to drive Ca^{2+} down to very low levels. That this does not happen in rod photoreceptors, suggests that other kinetic or regulatory factors may influence the activity of the molecule. One good candidate for such regulation is the rod cyclic nucleotide-gated channel, which interacts functionally via Ca^{2+} cycling and also physically associates with NCKX1. Neither Ca^{2+} nor Na^+ appear to regulate NCKX exchangers as they do the NCX branch of the family. Little else is known regarding regulation of the NCKX family of exchangers.

Physiological Relevance

In the case of heart, it is clearly established that NCX1 plays a critical role in relaxation by removing Ca^{2+} that enters during the early phase of systole. NCX1 probably also plays a role in excitation–contraction coupling, although the magnitude of its contribution remains somewhat controversial. During the early phase of the cardiac action potential, as the membrane depolarizes and ion gradients change, NCX1 probably contributes to Ca^{2+} entry. Furthermore, as NCX1 switches to Ca^{2+} extrusion later in systole, it creates a depolarizing current that can significantly modulate the shape of the action potential. Normally these contributions of NCX1 to cardiac excitation–contraction coupling are integrated into overall Ca^{2+} homeostasis. However, during pathological circumstance, the expression pattern of Ca^{2+} channels and transporters changes, and ion concentrations and gradients are altered dramatically. Under these conditions, changes in NCX1 activity may be maladaptive, and so may contribute to, rather than protect against, deleterious consequences.

In the kidney very high levels of NCX1 are found on the basolateral aspect of a selected population of distal nephron cells. In this environment, NCX1 contributes to the control of extracellular, systemic, Ca^{2+} homeostasis by driving the active trans-cellular reabsorption of Ca^{2+}.

NCX1 is also present in brain neurons and astrocytes, where it presumably plays a role in Ca^{2+} extrusion. Its precise role in this environment and the contribution made by NCX2 and NCX3 expression are less clearly understood.

The unique and specialized role that NCX1 plays in controlling Ca^{2+} flux and homeostasis in heart and kidney is also reflected in the fact that this gene is expressed under the control of three different, and tissue-specific promoters. One promoter is used essentially exclusively in heart, one exclusively in kidney, while the third is used widely in various tissues. This arrangement provides the opportunity for expression of the heart and kidney NCX1 molecules to be regulated independently and in response to the specialized requirements of these tissues for Ca^{2+} homeostasis.

In the rod photoreceptors, NCKX1 is thought to play a critical role in maintaining Ca^{2+} homeostasis, especially in the dark when cyclic-nucleotide-gated channels are open and so the membrane is depolarized, the Na^+ gradient is low, and Ca^{2+} flux is high. Under these circumstances, the thermodynamic power derived from the $4Na^+:1Ca^{2+} + K^+$ coupling ratio is necessary to allow continued Ca^{2+} efflux. While this argument makes some sense in the retinal photoreceptors, it is less clear as to why NCKX family members are also expressed quite broadly, especially in the brain.

Elucidating the unique individual physiological roles for the expanding family of NCX and NCKX protein molecules is an active area of research that is likely to provide exciting novel insights.

See Also the Following Articles

Calcium Sensing Receptor • Calcium Signaling: Cell Cycle • Calcium Transport in Mitochondria • Calcium, Biological Fitness of • Membrane Transport, General Concepts • Plasma-Membrane Calcium Pump: Structure and Function • Store-Operated Membrane Channels: Calcium

Glossary

alternative splicing A process in which the individual expressed regions of a gene (exons) are arranged in different patterns to produce different mRNA molecules that often encode different proteins.

excitation–contraction coupling The process by which an electrical signal generated in the plasma membrane of a muscle cell results in movement of the muscle fiber proteins, and contraction of the cell.

Na^+/Ca^{2+} exchanger A plasma membrane protein that couples the movement of Na^+ ions in one direction with Ca^{2+} ions in the other.

plasma membrane The membrane that surrounds every cell, separating inside from outside.

α-repeat A short stretch of amino acids identified within the Na^+/Ca^{2+} exchanger that is conserved among a large superfamily of membrane proteins. Two copies of this conserved sequence are present in each Na^+/Ca^{2+} exchanger, which are modeled to interact to form the ion-binding and translocation pocket.

retinal rod photoreceptors Long, cylindrically shaped, cells in the retina of the eye that respond to changes in low levels of light.

Further Reading

Berridge, M. J., Bootman, M. D., and Lipp, P. (1998). Calcium – A life and death signal. *Nature* **395**, 645–648.

Bers, D. M. (2002). Cardiac excitation–contraction coupling. *Nature* **415**, 198–205.

Blaustein, M. P., and Lederer, W. J. (1999). Sodium/calcium exchange: Its physiological implications. *Physiol. Rev.* **79**, 763–854.

Lytton, J., Schnetkamp, P. P. M., Hryshko, L. V., and Blaustein, M. P (eds.) (2002). *Cellular and Molecular Physiology of Sodium–Calcium Exchange*. Proceedings of the fourth international conference. Annu. NY Acad. Sci., Vol 976. New York Academy of Sciences, New York.

Nicoll, D. A., Longoni, S., and Philipson, K. D. (1990). Molecular cloning and functional expression of the cardiac Na,Ca-exchanger. *Science* **250**, 562–565.

Philipson, K. D., and Nicoll, D. A. (2000). Sodium–calcium exchange: A molecular perspective. *Annu. Rev. Physiol.* **62**, 111–133.

Reiländer, H., Achilles, A., Friedel, U., Maul, G., Lottspeich, F., and Cook, N. J. (1992). Primary structure and functional expression of the Na/Ca,K-exchanger from bovine rod photoreceptors. *EMBO J.* **11**, 1689–1695.

Shigekawa, M., and Iwamoto, T. (2001). Cardiac Na^+–Ca^{2+} exchange: Molecular and pharmacological aspects. *Circ. Res.* **88**, 864–876.

Biography

Dr. Jonathan Lytton is a Professor of biochemistry and molecular biology at the University of Calgary, Canada. His principal research interests are in the molecular biology and physiology of calcium transport proteins. He holds a Ph.D. from Harvard University and did postdoctoral training at the University of Toronto. His work has been instrumental in the molecular cloning and characterization of SERCA Ca^{2+} pump isoforms, Na^+/Ca^{2+} exchanger isoforms, and novel $Na^+/Ca^{2+} + K^+$ exchanger gene products expressed in brain.

Membrane-Associated Energy Transduction in Bacteria and Archaea

Günter Schäfer
University of Lübeck, Lübeck, Germany

Archaea and bacteria represent the two prokaryotic branches of the universal tree of life. Their plasma membranes host protein complexes specialized in primary and secondary energy-transducing mechanisms. Common to bacteria and archaea is the underlying principle of primary energy conservation, the chemiosmotic mechanism generating an electrochemical potential of ions across the membrane on expense of the energy derived from membrane-associated fermentative, redox- or light-driven processes. In evolution, two of these, oxygen respiration and oxygenic photosynthesis, were transferred to eukaryotes by endosymbiontic uptake of putative ancient bacteria, the precursors of mitochondria and chloroplasts. Archaea differ from bacteria not only by genetic and taxonomic markers, membrane structure, specialized metabolic functions, and archaetypical coenzymes but also by their extremophilic life styles regarding thermo-, pH-, and salinity-tolerance. Several energy-transducing processes are confined to the archaeal domain such as methanogenesis and rhodopsin-dependent photosynthesis. Chlorophyll-dependent photosynthesis does not exist in the archaeal domain. Secondary membrane-associated energy transduction like the synthesis of ATP from ADP and various active transport systems are consumers of the primarily generated electrochemical ion gradient. The ions coupling primary and secondary energy transduction are predominantly hydrogen ions; in several bacteria and archaea sodium ions are also used.

Membranes

The matrix of polar lipids in plasma membranes serves as the environment for associated and membrane-spanning proteins. In bacteria glycerol diester phospho- and glycolipids form a liquid–crystalline bilayer into which the energy-transducing membrane–protein complexes are inserted. The hydrophobic properties and fluidity of the core are determined by the fatty acid hydrocarbon chains; the permeability properties are additionally determined by the polar head groups. The lipid profile can serve as a taxonomic marker. Archaea, in contrast, contain unique lipids consisting of derivatives of diphytanylglycerol diethers and of di-biphytanyl-diglycerol-tetraethers. Consistently, besides bilayer structures, these membranes are composed of membrane-spanning lipid monolayers conferring extremely high stability, especially to the hyperthermophilic genera of the archaeal domain. The diether- and tetraether-derived lipids include phospholipids, glycolipids, and sulfoglycolipids. Generally, these lipids are glycosylated with the carbohydrate groups facing the plasma membrane outside. The unique lipid composition clearly delineates the archaea from all other organisms. Also the cell envelopes of archaea are distinct from those of bacteria. Murein and lipopolysaccharide containing outer membranes are not found in archaea. The quasi-crystalline surface layers of archaea are high-molecular-weight glycoproteins and have mainly form-stabilizing function and in most cases are the only envelope layer outside the plasma membrane.

Energy-Transducing Functions

Membrane-associated energy transduction proceeds by linking an exergonic process catalyzed by a membrane-residing enzyme (or protein complex) to the simultaneous vectorial translocation of charge (electrons or ions) across this membrane by the same enzyme. This principle is common to bacteria and archaea (Figure 1). Typical processes can be metabolic substrate conversions like redox reactions or decarboxylation, respiratory electron transport from a low-potential donor to a high-potential acceptor (respiratory chains), or the decay from an energized state of a molecule generated by absorption of light to the low-energy ground state.

Fermentation

Fermentations are anaerobic redox processes in which ATP is usually generated by substrate-level

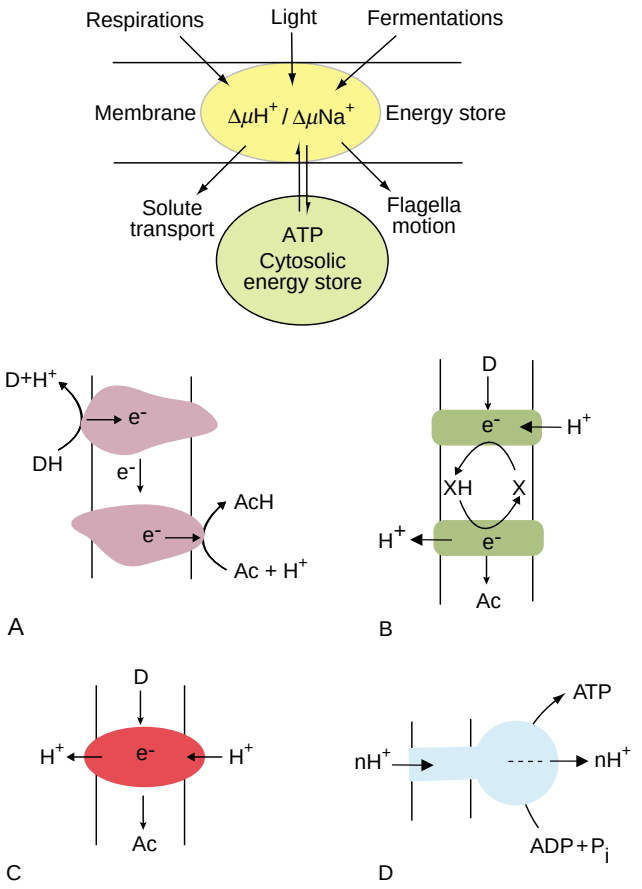

FIGURE 1 Schematic illustration of energy-conserving principles used by bacteria and archaea for the generation of an electrochemical potential of ions ($\Delta\mu Na^+$ or $\Delta\mu Na^+$) across their plasma membrane. (A) symbolizes $\Delta\mu H^+$ generation by scalar or so-called "chemical" protons consumed or liberated on opposite sides of the membrane; only electrons are transduced through the membrane. (B) and (C) illustrate pumps; (B) functions via the intermediary quinol pool (x), (C) integrates pumping and electron transport within the same protein module like cytochrome-*c* oxidases; (D) symbolizes the universal ATP synthetase; its vectorial action and orientation is consistently opposite to that of the primary pumps.

phosphorylation. In some special cases, partial reactions of fermentative pathways are catalyzed by membrane-residing enzymes, and the free-energy change of the reaction is coupled to the generation of an electrochemical-ion gradient. Examples are the biotin-dependent methylmalonyl-CoA decarboxylase of *Propionigenium modestum*, the oxaloacetate decarboxylase involved in citrate fermentation, or the glutaconyl-CoA decarboxylase involved in glutamate fermentation; they generate a $\Delta\mu Na^+$. By means of H^+/Na^+ exchange transporters the sodium gradient can be coupled to a proton gradient, or the $\Delta\mu Na^+$ can directly drive ATP synthesis by a Na^+-translocating ATP synthetase. In methanogenic archaea methyl-group transfer from an N atom to an SH group drives a sodium pump and generates also a $\Delta\mu Na^+$. The above examples demonstrate that in anaerobic fermentations also non-redox reactions can play an important role in membrane associated energy transduction.

Anaerobic Respiration

Many organotrophic and chemolithotrophic bacteria and archaea can conserve energy by means of membrane-residing electron transport chains employing terminal acceptors other than oxygen. This group of obligately or facultatively anaerobic microbes uses electron acceptors like nitrate, nitrite, fumarate, sulfur, ferric ion, carbon dioxide, sulfate or even organic chlorocompounds for oxidation of organic molecules or hydrogen. Energy is conserved as a $\Delta\mu H^+$. Example reactions are given in Table I.

Denitrification

Denitrification is a typical example of anaerobic respiration and is found in over 40 genera; in archaea only in some extreme halophiles. However, nitrate is reduced in four steps to N_2 via $NO_2^- \rightarrow NO \rightarrow N_2O \rightarrow N_2$. The enzymes are integrated into the plasma membrane or located in the periplasm. Oxygen represses their synthesis. Nitrate reductase is a molybdopterin dinucleotide-containing enzyme associated with an iron–sulfur protein (4 FeS clusters) and a membrane spanning *b*-type cytochrome. Energy from NO_3^- reduction is conserved by release of protons from the reductant, ubiquinone, or menaquinone, at the membrane outside, whereas protons for water formation are

TABLE I

Standard Free Energy Changes of Anaerobic and Aerobic Respiratory Reactions

Chemical reaction	ΔG (kJ mol^{-1})
$S^0 + 2[H] \Rightarrow H_2S$	−33.5
$SO_4^{2-} + 8[H] + 2H^+ \Rightarrow H_2S + 4H_2O$	−151.7
$2NO_3^- + 5H_2 + 2H^+ \Rightarrow 6H_2O + N_2$	−959.8
$2NO + 2H^+ + 2e^- \Rightarrow N_2O + H_2O$	−305.9
$CO + H_2O \Rightarrow CO_2 + 2H^+ + 2e^-$	−492
$[H]_2\text{–}X + 1/2O_2 \Rightarrow H_2O + X$	−219.0
$2H_2 + O_2 \Rightarrow 2H_2O$	−472.5
$2S^0 + 2H_2O + 3O_2 \Rightarrow 2H_2SO_4$	−1014.0
$2FeS_2 + H_2O + 7O_2 \Rightarrow 2FeSO_4 + 2H_2SO_4$	−1498.4
$2CO + O_2 \Rightarrow 2CO_2$	−504.9
$4Fe^{2+} + O_2 + 4H^+ \Rightarrow 4Fe^{3+} + 2H_2O$	−17.7

The block on top gives examples for electron accepting reactions in anaerobic respirations, the lower block examplifies electron donor reactions used by organotrophic and chemolithotrophic oxygen respiration. $[H]_2$–X symbolizes an organic hydrogen-donating molecule, e.g., NADH or succinate.

taken up from the cytosol. NO reductase displays analogy to heme/Cu oxidases but hosts Fe instead of Cu in the binuclear reaction center; in contrast to the latter, it does not pump protons. Denitrifying pathways are widespread in Gram-negative proteobacteria (e.g., *Paracoccus*, *Alcaligenes*, *Pseudomonas*, *Thiobacillus*). Associated with denitrification is ammonification, which saves NH_4^+ by reduction of NO_2^- with NAD(P)H. Ammonification is a cytosolic process catalyzed by a siroheme/[4Fe4S] containing enzyme.

Fumarate Respiration

In *Wolinella*, nitrate reduction can be achieved with molecular hydrogen or with formate as electron donors. It involves fumarate respiration (Figure 2), as an alternative mechanism to generate a proton motive force. H^+ is released at the outer side of the membrane by oxidation of hydrogen or formate, whereas proton uptake and reduction of fumarate occurs at the inner side. The dehydrogenases as electron donors and the fumarate reductase as acceptor are interacting via *b*-type cytochromes and the menaquinone pool in the membrane ($E_0' = -100$ mV). The reduction of fumarate to succinate is catalyzed by an enzyme similar to nitrate reductase, but molybdopterin is replaced by FAD. The enzyme is structurally and evolutionarily related closely to succinate dehydrogenases of aerobic organisms which catalyze the reverse reaction using ubiquinone ($E_0' = +60$ mV), or in thermoacidophilic archaea caldariella quinone ($E_0' = +106$ mV), as primary electron acceptor.

Sulfur Respiration

Some bacteria and archaea perform sulfur respiration. *Wolinella succinogenes* is an example. Instead of insoluble elemental sulfur polysulfide ($^-S{-}S_n^-$) serves as electron acceptor. The electron transport chain involves three membrane-residing enzymes with their substrate binding sites facing the periplasm: formate dehydrogenase or hydrogenase, and polysulfide reductase. In contrast to fumarate respiration, a quinone is not involved in electron transfer. The reduction of sulfur to H_2S is coupled to generation of $\Delta\mu H^+$ at a low H^+/e^- ratio by a hitherto unknown mechanism.

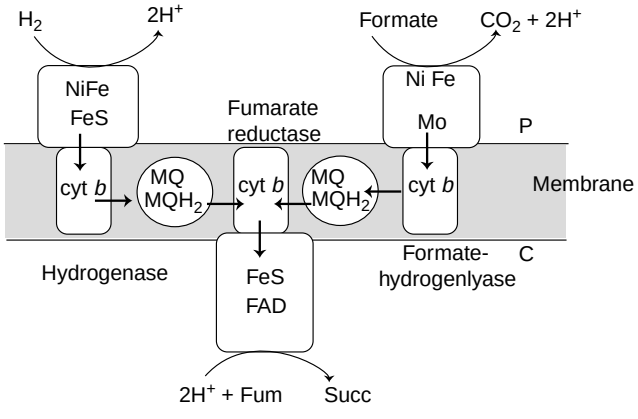

FIGURE 2 Scheme of an anaerobic respiration. Fumarate respiration is taken as an example with two possible electron-donating systems (MQ = menaquinone P = periplasm, C = cytosol). The type of energy conservation corresponds to principle A in Figure 1.

Ferric Ion Reduction

Members of the genera *Clostridium*, *Escherichia*, and *Bacillus* among others are able to reduce ferric to ferrous ions. It has not been shown unequivocally that the reaction is coupled to energy conservation. Though the couple $Fe^{3+/2+}$ has a high redox potential ($E_0' = +770$ mV) similar to oxygen, organisms using Fe^{3+} as terminal electron acceptor have to cope with its extreme insolubility, except in a strongly acidic environment.

Oxygen Respiration

Aerobic Organotrophs

Oxygen is a superior electron acceptor for aerobic microbes that use reduced substrates or even molecular hydrogen as donors of reducing equivalents. Organotrophes deliver electrons into a respiratory chain (Figure 3) via ubi- or mena-quinone reducing membrane anchored or integral membrane protein complexes. A major complex is the FMN-dependent type-I NADH dehydrogenase (complex I), composed of 14 different polypeptides (e.g., *Paracoccus*, *Escherichila coli*). It couples the translocation of (probably four) protons to the reduction of quinone and consists of a peripheral substrate oxidizing subcomplex facing the cytosol, a membrane integral transducer subcomplex with several FeS centers, and a receiver subcomplex transferring electrons to the quinone. Alternatively, in many bacteria and in archaea, type-II NADH dehydrogenases are found; these have less complex composition and cannot couple ion translocation to substrate oxidation. Several alkaline-adapted bacteria couple the translocation of Na^+ instead of protons to NADH oxidation. As another quinone-reductase succinate dehydrogenase (complex-II) is found in the plasma membranes of all aerobic microbes. The small change in free energy of this reaction is insufficient to drive energy-conserving ion translocation. The reoxidation of reduced quinones is either catalyzed directly by heme/Cu-type quinol oxidases as, for example, in *E. coli*, *Paracoccus denitrificans*, and *Rhodobacter sphaeroides*, or by a second energy-conserving module of respiratory chains, the bc_1 complex (complex-III). The essential redox catalysts of this module are an [$2Fe_2S$] iron–sulfur

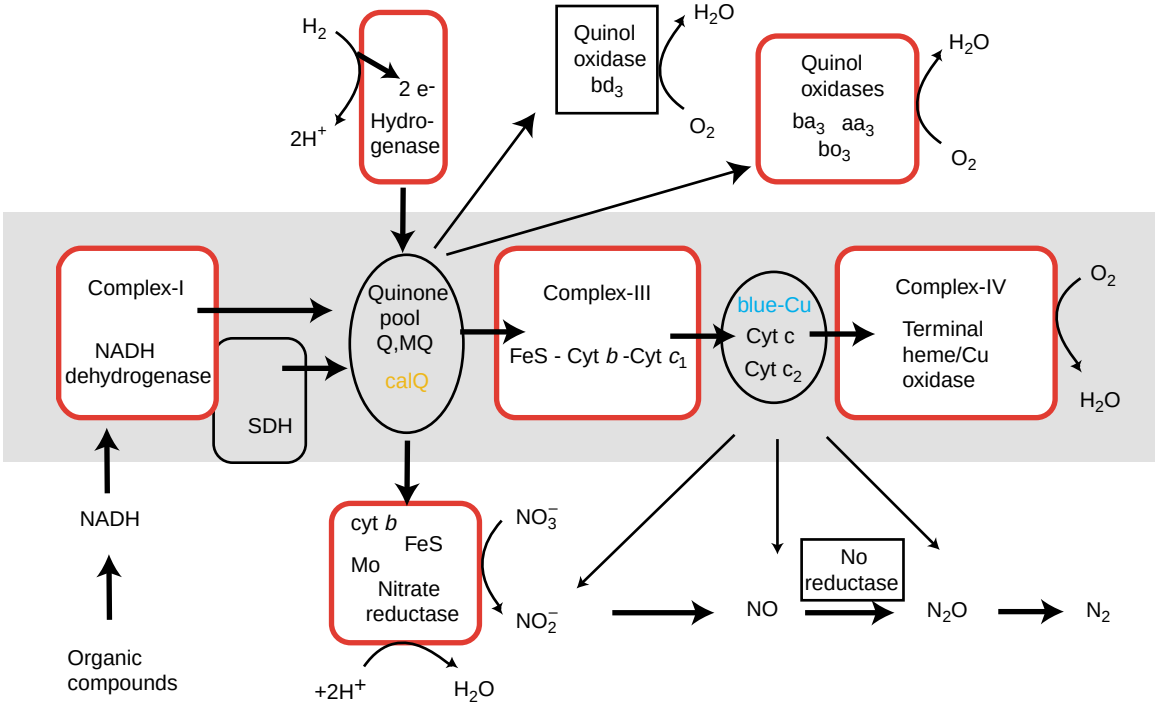

FIGURE 3 Illustration of the diversity of energy-transducing membrane systems in bacteria and archaea. All boxed or encircled components are membrane-integral or membrane-associated. All red boxes are proton pumps acting according to principles B and C of Figure 1. The scheme depicts the situation in *P. denitrificans*. The shaded block from left to right symbolizes a regular and complete aerobic respiratory chain as present, for example, in purple bacteria and also in eukaryotic mitochondria. The linear arrows indicate the direction of electron flux between donor and acceptor complexes or compounds. The symbols aa_3, ba_3, bo_3 in the box Quinoloxidases indicate the species-dependent variability of observed heme-compositions; calQ (caldariella quinone) applies to some archaea, as does the blue-Cu protein instead of c-type cytochromes. (SDH = succinate dehydrogenase, complex II.)

protein (Rieske protein), a diheme *b*-type cytochrome, and a *c*-type cytochrome c_1. Complex-III couples the stepwise reoxidation of QH_2 to the transport of $2H^+$ across the membrane for each electron transduced to cytochrome c_1. The complex reaction mechanism is known as Q-cycle. The mobile redox carrier cytochrome *c* associated with the outer surface of the plasma membrane accepts electrons from cytochrome c_1 and serves as the connector to the terminal oxidase module, the heme/Cu-type cytochrome *c* oxidase (⇒). All oxygen-reducing heme/Cu oxidases are proton pumps. The path of electrons from NADH to oxygen can thus conserve the energy equivalent to $12H^+$ pumped across the membrane per [H_2]. Depending on the genetic disposition, either one of the energy-transducing complexes can be missing, except a terminal oxidase. The modular structure of microbial respiratory chains allows a variety of special adaptations. Besides an aerobic respiratory chain, all modules for denitrification and even several terminal oxidases can be present in parallel (e.g., Figure 3); their individual contribution to energy transduction is usually regulated via the expression of the respective genes in response to nutritional and environmental conditions.

Aerobic Chemolithotrophs

A large variety of bacteria, the chemolithotrophs, can derive energy from oxidation of inorganic electron donors such as hydrogen, carbon monoxide, sulfur and nitrogen compounds, or divalent cations (e.g., Fe^{2+}, Mn^{2+}). Many of these use molecular oxygen as oxidant. The mechanisms of energy transduction in chemolithotrophs are essentially the same as in organotrophs, i.e., the electrons are channeled into a cytochrome chain and flow down to the terminal oxidase enabeling a number of proton translocating redox loops. Examples are given in Table I. The acidophile *Thiobacillus ferrooxidans* uses a periplasmic Fe^{2+} oxidase transferring electrons via cytochrome *c* and the Cu-protein rusticyanin to a heme/Cu-terminal oxidase, which reduces oxygen on the plasma membrane inside. The reaction generates a proton motive force by scalar consumption of H^+ on the inside in addition to proton pumping by the aa_3-type terminal oxidase. So-called "Knallgas" bacteria comprising a large group of Gram-negative and Gram-positive bacteria which can oxidize molecular hydrogen. Essential for the mechanism is a Ni–Fe hydrogenase dimer (e.g., in *Alcalignes eutrophus*) in the cytoplasmic membrane. It transfers electrons from hydrogen via

the bimetallic reaction center, several Fe–S clusters, and a *b*-type cytochrome to the respiratory electron transport chain. By this process scalar protons are produced outside in addition to protons pumped by the respiratory chain. Several "Knallgas" bacteria contain a second, cytoplasmic hydrogenase which is used for the reduction of NAD^+ via FMN by an enzyme with homology to NADH:ubiquinone oxidoreductase (complex-I).

Phototrophic Bacteria

The utilization of light by cyanobacteria, phototrophic purple, and green bacteria follows the same principles as in algae and higher plants. Also the light absorbing pigments, other cofactors and their hosting membrane proteins are essentially similar. Both, oxygenic and anoxygenic photosynthesis, are found; the latter is restricted to purple, green, and heliobacteria.

Pigments of Energy Transducers

Absorption of light energy and transduction of energized states is mediated by antenna complexes. These contain the cyclic tetrapyrrol derivatives chlorophyll and bacteriochlorophyll, carotenoids, and in cyanobacteria open-chain tetrapyrrols (phycobillins). The conjugated polyene compounds absorb light from the near-UV to the near-IR and are non-covalently bound to membrane-integral and membrane-associated proteins in arrays. They transduce the excited state to the reaction centers (RCs) proper. The ratio is about 25–30 mol antenna chlorophyll per mol RC. In purple bacteria and heliobacteria (e.g., *Rhodobacter*, *Rhodopseudomonas*, *Chromatium*, *Heliobacillus*) the antenna complexes are integrated within the cytoplasmic membrane. In green bacteria (e.g., *Chlorobium*, *Chloroflexus*) the antenna complexes are organized as chlorosomes, i.e., vesicles attached to the inner side of the plasma membrane.

Anoxygenic Photosynthesis

Anoxygenic photosynthesis produces an electrochemical proton gradient across the membrane which drives ATP synthesis and other energy consuming processes. Excitation energy is transfered from antennas to the RC within ~50 ps. In the RC, the energy is utilized to generate a charge separation ($\Delta\Psi$) across the membrane. It occurs by electron transfer between the primary donor, a special pair of chlorophylls, localized towards the cytosolic side of the membrane and secondary acceptors at the opposite side. These can be quinones (type-II RC) or Fe–S clusters (type-I RC). From there the electrons flow back to cytochrome c_2 and the special pair via a quinone pool and through the bc_1 complex, as it is also used for respiratory energy conservation; a $\Delta\mu H^+$ is produced. Thus, anoxygenic photosynthesis can occur as a cyclic process. Production of reducing equivalents is not coupled to anoxygenic photosynthesis. In facultatively phototrophic/chemotrophic bacteria (*Rhodobacter*, *Rhodospirillum*) photosynthesis and respiration are competing for the bc_1 complex depending on the environmental conditions (oxygen tension, light intensity).

Oxygenic Photosynthesis

Cyanobacteria (*Synechococcus*, *Synechocystis*, *Anacystis*) perform oxygenic photosynthesis. It employs two photosystems in sequence in its membrane (PS-I, PS-II). PS-I is essentially equivalent to the RC of anoxgenic phototrophic bacteria but channels the electrons to ferredoxin as terminal acceptor. Ferredoxin serves as reductant for $NADP^+$, thus generating reducing equivalents for the cell. The reaction center PS-II is an H_2O:plastoquinone oxidoreductase and couples the reduction of the primary e^--donor, the special pair of chlorophylls, to the oxidation of water by a Mn-enzyme associated with PS-II at the periplasmic surface. The water-splitting Mn-enzyme liberates molecular oxygen and H^+. The reducing equivalents are passed on to PS-I via the plastoquinone quinone pool, the b_6f-complex, and the Cu-protein plastocyanin. The b_6f-complex is functionally and structurally analogous to the bc_1 complex. It is composed of a diheme cytochrome *b*, a Rieske Fe–S protein, and the mono-heme cytochrome *f*. b_6f acts as a proton pump performing a Q-cycle ($\Rightarrow$). The photosynthetic apparatus of cyanobacteria is localized in thylacoids; the antenna systems are organized as phycobillisomes attached to the thylacoid membranes. These structures largely resemble the structure of eukaryotic organelles. Also respiratory enzymes (NADH dehydrogenase, cytochrome *c* oxidase) are localized in the thylacoid and partially also in the plasma membrane of cyanobacteria.

Special Mechanisms in Archaeal Energy Transduction

Methanogenesis from one- or two-carbon atom compounds and light-driven energy conservation by bacteriorhodopsins are mechanisms restricted to archaea. Methanogens comprise the genera *Methanosarcina*, *Methanolobus*, *Methanobacterium*, *Methanotrix*, *Methanothermus*, *Methanococcus*, and others among about 50 known species. Examples for the best-investigated genera of extreme halophilic archaea are *Halobacterium*, *Haloferax*, *Haloarcula*, *Halococcus*, and *Natronomonas*.

Methanogenesis

Methanogenesis is a reductive process under strictly anaerobic conditions. It involves reduction of C_1 compounds (CO_2, CO, CH_3OH, CH_3NH_2) mainly by H_2, but also the disproportionation of acetate, formiate, or methanol. Many of the methanogenic archaea are extremely thermophilic (growth at $\approx 100\,^{\circ}C$). For example, the change in free energy of the reaction $CO_2 + 4H_2 \Rightarrow CH_4 + 2H_2O$ is $\Delta G = -131\ kJ\ mol^{-1}$ and is comparable to CH_4 formation from other sources; that of acetate disproportionation is only $-36\ kJ\ mol^{-1}$. Both reactions can drive chemiosmotic ATP synthesis by linking membrane-associated partial reactions to generation of ion gradients ($\Delta\mu H^+$, $\Delta\mu Na^+$). The reactions involve unusual coenzymes, not found in bacteria or eukaryotic organisms. These are the fluorescent 5-deazaflavin F_{420}, methanofuran, methanopterin (H_4MPT), coenzyme-M (mercaptoethanesulfonate), a Ni-tetrapyrole F_{430}, 5-hydroxybenzimidazolyl-cobamide, and methanophenazine as a substitute for membrane-residing quinones. For details of pathways the reader is referred to specialized publications. Important for membrane-associated energy transduction are electron transport chains involved in methanogenesis, as illustrated in Figure 4. The ion-translocating redox chains involve heterodisulfide reductase, two *b*-type cytochromes, methanophenazine, and Ni-hydrogenase or another donor of reducing equivalents. Redox cycling of methanophenazine with asymmetric uptake and release of protons can act as a proton pump with $H^+/e^- = 1$. Hydrogen can also be provided from ferredoxin:methanophenazine oxidoreductase, or from F_{420} dehydrogenase, depending on the individual organisms and the C_1 carbon source used for methanogenesis. Whether the latter functions as proton pump is under debate; the observed total H^+/e^- ratios of 3–4, are higher than calculated for the methanophenazine cycle alone. Hydrogenases and F_{420} dehydrogenase display structural similarities to proton-translocating respiratory NADH dehydrogenases and are bearing subunits with several $[Fe_n–S_n]$ clusters. Also heterodisulfide reductase contains two [4Fe–4S] clusters. Apart from proton motive electron transport chains, all methanogens have a primary Na^+ pump, the membrane integral methyl-H_4MPT:CoM- methyltransferase. This enzyme contains the above-mentioned cobamide cofactor and a [4Fe–4S] cluster. The reaction proceeds in two steps: first, the transfer of the methyl group to the corrin cofactor, second, methyltransfer to

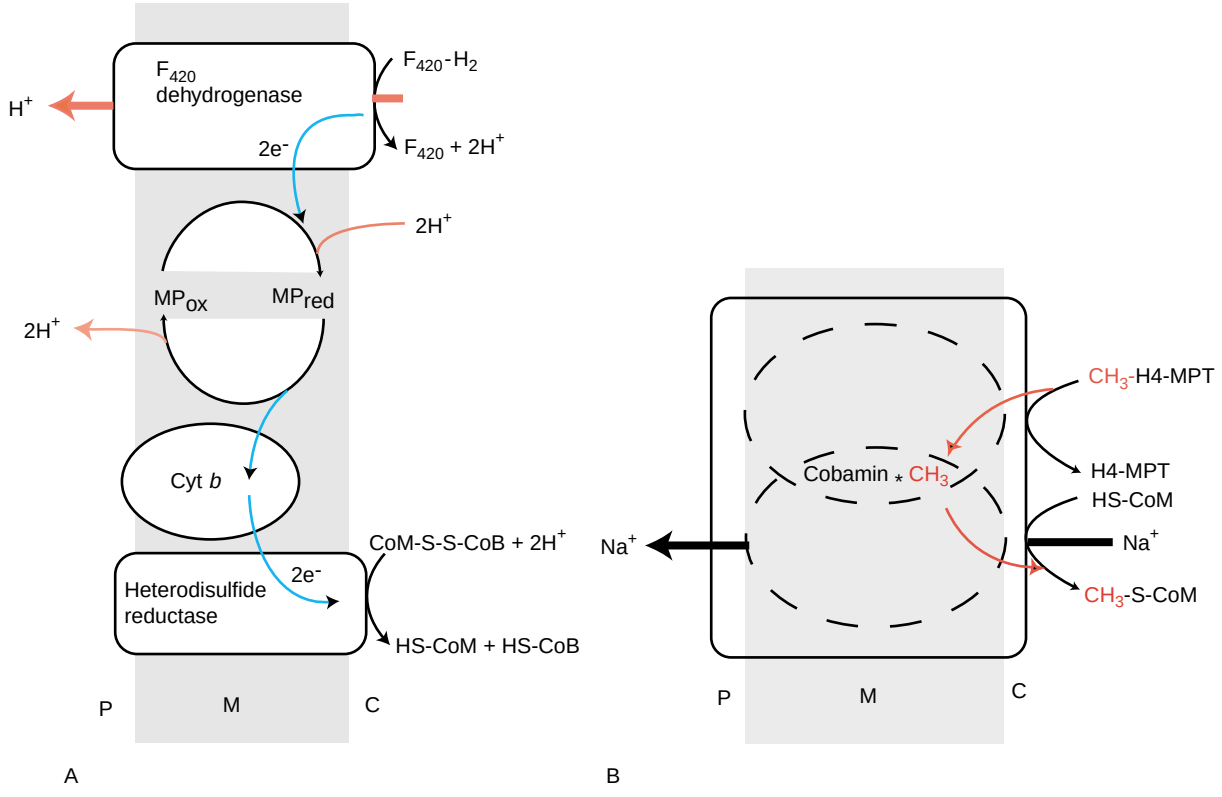

FIGURE 4 (A) Illustration of chemiosmotic energy conservation in methanogenic archaea. The example combines mechanisms (B) and (C) of Figure 1; (P = periplasmic space, M = membrane, C = cytosol, MP = methanophenazine, CoM = coenzyme M). (B) Energy transduction by a non-redox reaction in archaeal methanogenesis. The sodium pump is driven by the energy change of the transmethylation reaction (H4-MPT = tetrahydro-methanopterin). The mechanism is thought to involve conformational coupling between the group-transferring and the ion-transferring modules; similar mechanisms apply to the sodium pumps driven by decarboxylation reactions.

the cytosolic cofactor HS–Coenzyme M. Sodium pumping is associated with the second partial reaction producing a Na^+ gradient equivalent to a -60 mV membrane potential. The sodium pump consists of 6–8 polypeptides (species dependent). The central pathway of methanogenesis is reversible. Accordingly, the enzyme acts as a sodium pump during methanogenesis from CO_2 or acetate but drives the reverse reaction by means of a sodium potential in methanogenesis from methyl group containing C_1 compounds.

Utilization of Light

Photosynthetic apparatuses as found in phototrophic bacteria and eukaryotes do not exist in archaea. However, the aerobic extreme halophiles like *H. salinarum* can synthesize a light-driven proton pump under conditions of low-oxygen tension composed of a single integral-membrane protein bacteriorhodopsin (BR). BR spans the membrane with seven α-helical domains enclosing the chromophore retinal, which is bound as protonated Schiff's base to a lysine in the hydrophobic core of the protein. Absorption of light induces an all-*trans* to 13-*cis* isomerization of retinal accompanied by a deprotonation of the Schiff's base with concommitant release of the proton on the periplasmic membrane surface via a channel delineated by a series of protonable aminoacid residues and water molecules. The light-triggered reaction is accompanied by conformational changes of the protein and initiates a photocycle of the chromophore that relaxes through 5–6 consecutive steps to the all-*trans* ground state. In that phase reprotonation of the Schiff's base from the cytosolic side of the plasma membrane is attained. The proton pumping power-stroke corresponds to about -50 kJ mol^{-1} and can generate a proton-motive potential of about 300 mV. The light-induced proton gradient $\Delta\mu H^+$ can drive ATP synthesis, the flagellar motor, or a Na^+/H^+ antiporter to drive sodium out of the cell. Besides BR, three other archaeal rhodopsins were found. Halorhodopsin (HR) has a similar structure but acts as an inwardly directed chloride pump. The two other so-called sensory rhodopsins (SR 1 + 2) are photoreceptors that trigger the flagellar motor (phototactic/photophobic) via conformational coupling of membrane-associated transducer units (Figure 5). As such they are basic models for the large variety of seven-helix membrane receptors. All four archaeal rhodopsins have striking similarity regarding protein structure, the retinal chromophore and its photocycle. However, the ion-transducing BR and HR perform fast photocycles in the millisecond range, whereas SR 1 + 2 are comparativelty slow (~100 ms).

Respiratory Complexes

The euryarchaeota *Halobacteria*, *Thermoplasma*, and many species of the crenarchaeota comprising genera as *Sulfolobus*, *Acidianus*, *Metallosphera*, or *Pyrobaculum* are obligate or facultative aerobes. Their respiratory systems essentially resemble modular components of respiratory chains as found in oxygen-respiring bacteria. A significant difference is the lack of a proton translocating NADH:quinol oxidoreductase. Instead, type-II NADH dehydrogenases were found, whereas complex-II analogous succinate dehydrogenases are

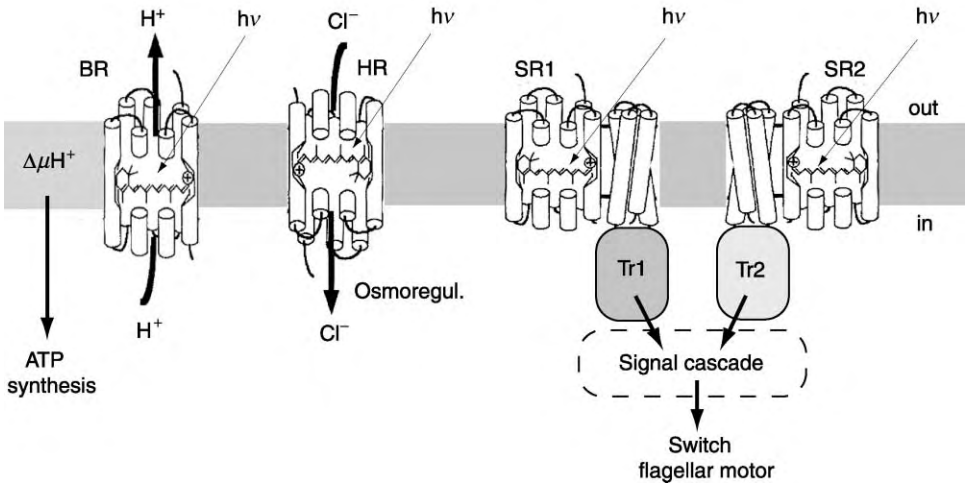

FIGURE 5 Illustration of energy transduction and sensory functions of rhodopsins in the extreme halophilic archaea. BR bacteriorhodopsin, HR halorhodopsin, SR1 and SR2 are sensory rhodopsins. Only BR and HR are ion pumps. The homodimeric transducer complexes Tr1, 2 are conformationally coupled to SR1, SR2, and transfer the conformational signal via their cytoplasmatic domains to a signaling cascade controlling the rotational direction of the flagella motor. The orientation of vectorial reactions is indicated with "in" symbolizing the cytosolic side of the plasma membrane.

present in all aerobic archaea. Two groups of enzymes can be distinguished: one group resembles the properties of SDHs from bacteria and mitochondria, and the other represents a novel class with unusual iron–sulfur clusters, as well as additional ones in a subunit with homology to methanobacterial heterodisulfide reductase, suggesting a novel electron pathway to the quinone pool. In *Halobacteria*, menaquinone and ubiquinone function as membrane-integral electron acceptors; in *Thermoplasma* and thermoacidophilic crenarchaeota like *Sulfolobales*, these are replaced by caldariella quinone and a variety of similar sulfur-containing thiopheno-benzoquinones. Several archaea like *A. ambivalens* contain only fragmentary respiratory chains established from NADH- and succinate-quinone reductases and a heme/Cu-type quinol oxidase as terminal electron acceptor; the latter serves as the only energy-conserving proton pump. Rieske Fe–S proteins are present in *Halobacteria*, *Sulfolobales*, and *Pyrobaculum* for example, but cytochrome *c* and regular quinol:cytochrome *c* reductases are absent in many species. Instead, analogous functions are replaced by alternate membrane protein assemblies, e.g., the SoxLN complex of *S. acidocaldarius*, using different electron acceptors as, for example, a mono-heme *b*-type cytochrome and/or blue copper proteins like sulfocyanine from various *Sulfolobus* species, or halocyanines from *Natronomonas* or *Halobacterium salinarum*. The proton pumping terminal heme/Cu-type oxidases are organized as supercomplexes in some thermoacidophilic creanarchaeota that combine features of quinol- and cytochrome *c* oxidases. The best-investigated examples are the SoxM complex and the SoxABCD complex from *Sulfolobus*.

Secondary Energy Transducers

ATP synthetases (⇒) are the most important universal secondary energy transducers integrated into plasma membranes. Bacterial ATP synthetases and those of mitochondria and chloroplasts are of the F_0F_1-type (⇒). Functionally, the ATP synthases are reversible ion-transporting ATPases driving the reaction ADP + Pi → ATP + H_2O by dissipation of a $\Delta\mu H^+$ or $\Delta\mu Na^+$ across the membrane. F_1 extends to the cytosol and bears the substrate binding sites; F_0 is the membrane integral ion-conducting subcomplex. Archaea contain A_0A_1-type ATP synthetases that structurally resemble the eukaryotic vacuolar V-type ATPases (⇒) but, in contrast to the latter, function as ATP synthetases driven by an ion-motive $\Delta\mu H^+$ or $\Delta\mu Na^+$ according to the rotational reaction mechanism of F_0F_1. The peripheral substrate binding A_1 moiety has been identified from many *Halobacteria*, *Sulfolobales*, and *Methanobacteria*. The only integrated A_0A_1-complex was isolated from the methanogen *Methanococcus jannashii*.

Evolutionary Links

In the evolution of higher organisms, cyanobacteria are the most likely precursor of chloroplasts which originated from an endosymbiotic uptake of such a prokaryotic phototroph into a precursor form of a eukaryotic cell. Likewise, the mitochondria have been derived from aerobic prokaryotes similar to the recent purple bacteria by endosymbiosis. The recipient might have been an archaebacterium.

See Also the Following Articles

Bioenergetics: General Definition of Principles • Chemolithotrophy • Cytochrome bc_1 Complex (Respiratory Chain Complex III) • Cytochrome Oxidases, Bacterial • Energy Transduction in Anaerobic Prokaryotes • F1–F0 AT Synthase • Green Sulfur Bacteria: Reaction Center and Electron Transport • Purple Bacteria: Photosynthetic Reaction Centers • Respiratory Chain Complex I • Respiratory Chain Complex II and Succinate: Quinone Oxidoreductases • Respiratory Chain Complex IV

Glossary

archaea The prokaryotic domain consists of two branches of the phylogenetic tree of life, one occupied by the bacterial domain and the other by the archaeal domain. The latter splits into the euryarchaeota and the crenarchaeota. Both archaeal sub-branches are host to many extremophilic genera. The methanogens belong to the euryarchaeota, the thermoacidophiles with a few exceptions to the crenarchaeota.

chemolithotrophs Prokaryotes assimilating carbon dioxide as sole carbon source and extracting energy from inorganic redoxreactions (in contrast to organotrophs which use reduced organic substrates as their carbon and/or nitrogen source).

chromophore Usually, a colored organic molecule bound to a protein and functioning as a cofactor in catalysis. Hemes are chromophores of cytochromes and host Fe ions in the core of a porphyrin ring; other tetrapyrrol derivatives like chlorophyll host Mg or Co. Chlorophylls and carotenoids in reaction centers or antenna systems, and retinal in rhodopsins, are light-energy transducers.

endosymbiosis Uptake of an originally independent free living organism into cells of a host organism, where it can reproduce under the control of the host organism and share metabolic functions (the energy-transducing organelles of eukaryotes originated by permanent transfer of genetic material from the endosymbiont to the host genome).

prokaryotes Unicellular microbes without a cell nucleus (in contrast to the eukaryotes which are located on a distinct branch of the universal phylogenetic tree of life, the eukaryotic domain).

thermoacidophiles Prokaryotes with a lifestyle adapted to hyperthermophilic conditions (75–110 °C) as well as to extremely low environmental pH (3.5–0.5). Most of them belong to the archaea.

vacuoles Membrane encapsulated compartments within eukaryotic cells, in most cases, filled with liquid of low pH; their membrane contains an ATP driven proton pump, the V-type ATPase.

Further Reading

Anthony, Ch. (ed.) (1988). *Bacterial Energy Transduction*. Academic Press, New York.

Driessen, A. J. M., Rosen, B. P., and Konings, W. N. (2000). Diversity of transport mechanisms: common structural principles. *TIBS* **25**, 397–401.

Harold, F. M. (1986). *The Vital Force: A Study of Bioenergetics*. Freeman, New York.

Kates, M., Kushner, D. J., and Matheson, A. T. (eds.) (1993). *The Biochemistry of Archaea*. Elsevier, Amsterdam.

Lengeler, J. W., Drews, G., and Schlegel Hans, G. (eds.) (1999). In *Biology of the Prokaryotes*. Thieme Verlag, Stuttgart, Germany.

Lolkema, J. S., Speelmans, G., and Konings, W. N. (1994). Na^+-coupled versus H^+-coupled energy transduction in bacteria. *Biochim. Biophys. Acta* **1187**, 211–215.

Schäfer, G. (2004). Respiratory systems of the Archaea: From minimal structures to supercomplexes. In *Progress in Photosynthesis and Respiration* (D. Zanoni, ed.) Kluwer, New York.

Schäfer, G., Engelhard, M., and Müller, V. (1999). Bioenergetics of the archaea. *Microbiol. Molecul. Biol. Rev.* **63**, 570–620.

Schäfer, G. (series ed.) (2004). Extremophilic archaea and bacteria: New insights into their roles in membrane transport and other bioenergetic functions (Minireview Series). *J. Bioenerg. Biomemb.* **36**, 3–159.

Biography

Günter Schäfer is a Professor Emeritus since 2002 and former Chair of the Institute of Biochemistry at the University of Lübeck, Germany. His principal research interest is in the entire field of bioenergetics including ATPases and electron transport systems of mitochondria, chloroplasts and microorganisms. He holds a Ph.D. in chemistry from the Technical University of Munich, Germany. In his recent research he specialized in bioenergetics of archaea and extremophiles as well as the structural basis of hyperthermostable archaeal proteins.

Metabolite Channeling: Creatine Kinase Microcompartments

Uwe Schlattner and Theo Wallimann
Institute of Cell Biology, Swiss Federal Institute of Technology (ETH), Zürich, Switzerland

Subcellular microcompartments, consisting of multienzyme complexes embedded within the cellular, highly viscous matrix, associated with the cytoskeleton, or situated along membranes, are operating according to exclusion principles and favor preferred pathways of intermediates. This process, called metabolite or substrate channeling, is defined as transfer of intermediates between sequential enzymes without equilibration of these metabolites with the surrounding bulk solution. Such an association between two or more sequential enzyme- or transport reactions in a microcompartment, forming a distinct functional pool of intermediates, is also called functional coupling. It can be considered as a general mechanism to increase efficiency of sequential reactions in a metabolic pathway. Since metabolite channeling leads to segregation of a metabolic pathway from other cellular reactions, it represents a specific kind of metabolic compartmentation similar to that operating within membrane-separated organelles or by restricted two-dimensional diffusion at surface boundary layers. Here, metabolite channeling is described with special emphasis on high-energy phosphate channeling by creatine kinase (CK), the phosphocreatine circuit or shuttle, and the mitochondrial CK isoenzyme.

Subcellular Microcompartments and Mechanisms of Metabolite Channeling

Life most likely originated autotrophically *de novo* in metabolic complexes organized on FeS_2 (pyrite) mineral surfaces, the earliest form of microcompartments. Likewise, a cell is by no means represented best by a well-mixed bag of enzymes, behaving in complete equilibrium according to solution kinetics. Because of the intricate structural and functional organization of living cells, enzymes and metabolites do not behave as if they were freely diffusible in solution. Instead, they may form structurally, functionally, and temporally defined subcellular microcompartments, either via strong static, or via fickle, dynamic interactions with other enzymes, proteins, or subcellular structures. Such a structural organization of pathway components is a general prerequisite for metabolite channeling. It may involve (1) huge covalently linked enzyme-complexes (or multifunctional enzymes) such as fatty acid synthase (FAS), (2) kinetically stable multienzyme complexes like pyruvate dehydrogenase (PDH) or bacterial and plant tryptophan synthase (TS), (iii) more dynamic, reversibly associating enzymes such as glycolytic complexes containing glyceraldehyde phosphate dehydrogenase (GAPDH) or glycerol phosphate dehydrogenase (GPDH), or (4) colocalization on subcellular particles. These associations allow the transfer of intermediates between the channeling components by different mechanisms: (1) sequential covalent binding to very close active sites in the reaction sequence (e.g., PDH), (2) physical hindrance or electrostatic effects prevent mixing with bulk solution and drive a directed diffusion (e.g., TS), (3) transfer of noncovalently bound intermediates between active sites (e.g., NADH dehydrogenase), (4) transfer in an unstirred surface layer. These mechanisms can be fulfilled in both, static and dynamic enzyme associations. However, while static associations allow for an almost perfect or "tight" channeling of metabolites, dynamic channeling is often only partial or "leaky."

Advantages of Metabolite Channeling

Sequestering of intermediates in a microcompartment through channeling provides kinetic and regulatory advantages for not only the reaction sequence itself (see Figure 1), but also for cellular metabolism. In general: (1) enzyme reaction rates and equilibria are controlled by local and enzyme bound substrates, rather than bulk phase substrate concentrations, (2) for a readily reversible reaction, local supply of substrate and removal of product may drive the reaction in the desired direction, (3) sequestered intermediates are present at high local concentrations and an apparently low K_m for

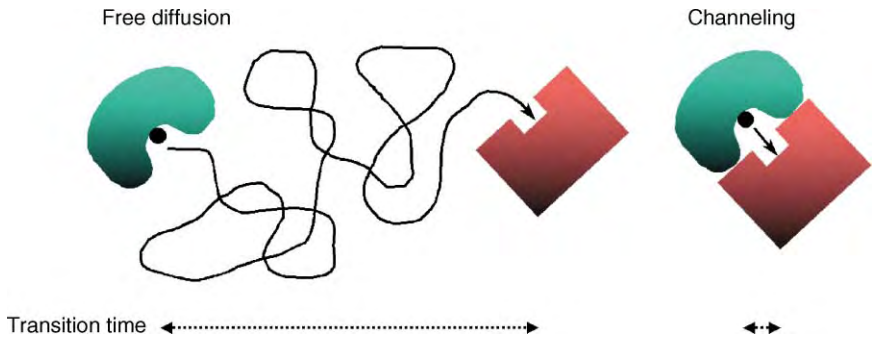

FIGURE 1 Free diffusion versus metabolite channeling. Compartmentation of a reaction sequence without equilibration with bulk solution leads to shorter transition times and further advantages (see text).

these intermediates can be observed with the channeling complex compared to the nonchanneling situation measured with isolated components, (4) metabolites are isolated from competing reactions, e.g., between anabolic and catabolic pathways, (5) the life-time of the intermediate in the solvent phase is shortened relative to free diffusion, which may be essential in case of unstable intermediates, (6) in certain cases, the unfavorable energetics of desolvating the substrate that precedes binding to the enzyme is avoided, (7) channeling components can be regulated by modulators that affect enzyme associations, and (8) a larger degree of metabolic control of the over-all-flux of the reactions can be achieved, e.g., via feed-back regulatory mechanisms such as substrate activation, product inhibition, and cooperativity.

Subcellular Targeting of Glycolytic Multienzyme Complexes

In muscle, glycolytic enzymes are targeted to the actin-containing thin filaments at the sarcomeric I-band region where they form highly complex metabolons. The I-band in *Drosophila* flight muscle contains a multi-enzyme complex consisting of GDPH-1, aldolase, and GAPDH. By elegant experiments with transgenic *Drosophila* expressing GDPH-3 instead of GDPH-1, it could be shown that all three glycolytic enzymes no longer colocalize in the I-band to form a microcompartment. Even though the full complement of active glycolytic enzymes was still present, their failure to colocalize in the sarcomer resulted in the inability to fly. Thus, correct targeting and formation of multienzyme complexes that lead to functionally coupled microcompartments and substrate/product channeling seem to be a prerequisite for proper function of glycolysis and ultimately for correct muscle function. In mammalian cells, CK is also participating in the glycolytic metabolon.

Compartmentation of Creatine Kinase Isoenzymes and Channeling of High-Energy Phosphates

The Creatine Kinase/Phosphocreatine Circuit or Shuttle

One fundamental requirement of life is energy supply. Cellular energy demand and supply are balanced, and tightly regulated for economy and efficiency of energy use. CK is a major enzyme of higher eukaryotes that copes with high and fluctuating energy demands to maintain cellular energy homeostasis in general and to guarantee stable, locally buffered ATP/ADP ratios in particular.

The enzyme catalyzes the reversible phosphoryl transfer from ATP to creatine (Cr) to generate ADP and phosphocreatine (PCr). Thus, CK is able to conserve energy in the form of metabolically inert PCr and vice versa, to use PCr to replenish global as well as local cellular ATP pools. Since PCr can accumulate to much higher cellular concentrations than ATP, the CK/PCr-system constitutes an efficient and immediately available cellular "energy buffer." In addition, tissue-specific CK isoenzymes are located in the cytosol (dimeric muscle-type MM-CK and brain-type BB-CK) and the mitochondrial intermembrane space (sarcomeric sMtCK and ubiquitous uMtCK, both forming octamers and dimers). CK isoenzymes are often associated with sites of ATP supply, where they generate PCr, or with sites of ATP consumption, where they regenerate ATP by using PCr. Thus, together with the faster diffusion rate of PCr as compared to ATP, the CK/PCr system also supports an intrinsic energy transfer system (CK/PCr-circuit or -shuttle), coupling sites of energy generation (oxidative phosphorylation or glycolysis) with sites of energy consumption (Figure 2). This circuit is particularly important in large and/or polar cells, such as spermatozoa where diffusional limitations of adenine nucleotides, especially ADP, along the sperm tail become especially apparent.

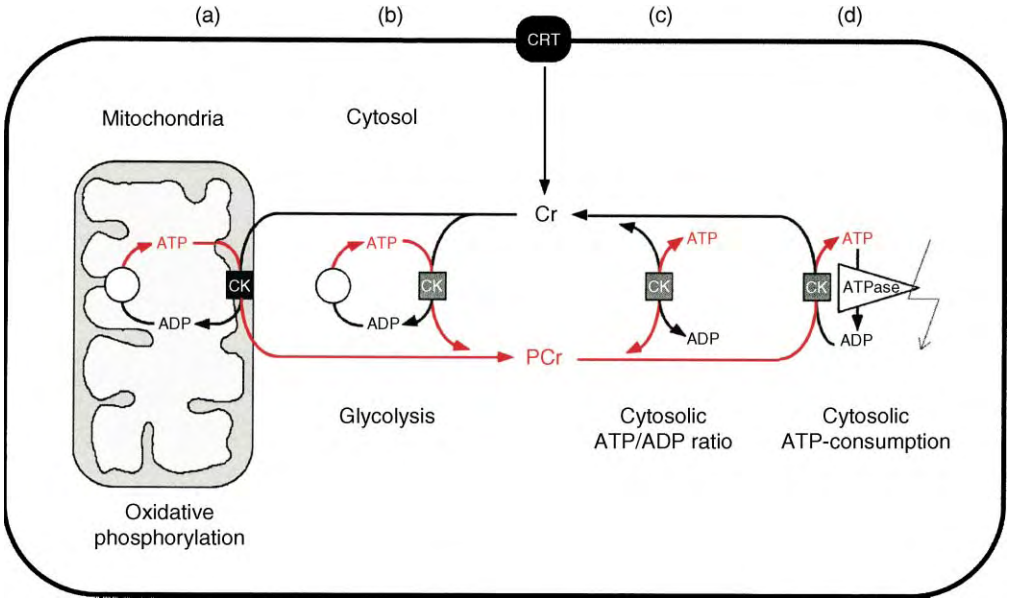

FIGURE 2 The creatine kinase (CK)/phosphocreatine (PCr) system. Isoenzymes of CK are found in different compartments like mitochondria (a) and cytosol (b–d) in soluble form (c) or associated to a different degree to ATP-delivering (a,b) or -consuming processes (d). A large cytosolic PCr pool up to 30 mM is built up by CK using ATP from oxidative phosphorylation like in heart (a) or glycolysis like in fast-twitch glycolytic muscle (b). PCr is then used to buffer global (c) and local (d) ATP/ADP ratios. In cells that are polarized and/or have very high or localized ATP consumption, these CK isoenzymes, together with easily diffusible PCr, also maintain an energy shuttle between ATP-providing or -consuming processes (a,d). Metabolite channeling occurs where CK is associated with ATP-providing or -consuming transporters, pumps or enzymes (a,b,d). Creatine (Cr) is synthesized in only few cell types (e.g., liver and kidney) and has to be taken up from the blood stream by a specific Cr transporter (CRT).

Channeling with Cytosolic CK

Cytosolic CK is only partially soluble. A significant fraction is structurally and functionally associated or co-localized with different, structurally bound ATPases or ATP-regulated processes. These include (1) different ion pumps in the plasma membrane, (2) the sarcomeric M-band of the myofibrils in muscle, (3) the calcium pump of the muscular sarcoplasmic reticulum, and (4) the ATP-gated K^+-channel. In all these cases, PCr is used for the local regeneration of ATP, which is directly channeled from CK to the consuming ATPase without major dilution by the surrounding bulk solution. Only in some cases, the physical basis for the metabolite channeling is known. For example, MM-CK uses a "charge clamp" consisting of four lysine residues to specifically bind to partner molecules, myomesin and M-protein in the M-band,

Cytosolic CK is structurally associated with the key regulatory enzyme of glycolysis, phosphofructokinase (PFK), which itself is regulated by ATP, Likewise, structural and functional interaction of cytosolic CK with the PAR-1 receptor of the thrombin-signaling pathway and with the ATP-gated K^+-channel, respectively, has been demonstrated. A tight functional coupling of CK to ATPases, e.g., acto-myosin ATPase and ion pumps, such as the K^+/Na^+-ATPase or the Ca^{2+}-ATPase, has the advantage (1) that product inhibition of the ATPase by ADP and H^+ is avoided, since the latter are both substrates of the CK reaction ($PCr + ADP + H^+ \leftrightarrow Cr + ATP$) and (2) that the high free energy of ATP hydrolysis (ΔG_{ATP}) at sites of ATP hydrolysis is preserved by keeping locally very high ATP/ADP ratios due to coupling of CK with those ATPases *in situ* and thus preventing energy dissipation caused by transport of ATP and mixing it with the bulk surrounding. Interestingly, the strongest phenotype of CK double knockout mice, which no longer express cytosolic MM-CK and mitochondrial MtCK in muscle, is characterized by significant difficulties with intracellular calcium handling and muscle relaxation, emphasizing the physiological importance of the CK system for the energetics of intracellular calcium homeostasis in general and the delivery of ATP to the energetically demanding Ca^{2+}-ATPase, in particular.

Channeling in Energy Transducing Mitochondrial Microcompartments

MtCK forms mainly large, cuboidal octamers (Figure 3) that are present (1) between the outer and inner mitochondrial membrane (the so-called "intermembrane space" of mitochondria) and preferentially localized at the so-called "mitochondrial contact sites" between

outer and inner mitochondrial membrane, as well as (2) in the "cristae space" (see Figure 3 inset). The kinase catalyzes the direct transphosphorylation of intramitochondrial produced ATP and Cr from the cytosol into ADP and PCr. ADP enters the matrix space to stimulate oxidative phosphorylation, giving rise to mitochondrial recycling of a specific pool of ATP and ADP, while PCr is the primary "high energy" phosphoryl compound that leaves mitochondria into the cytosol. The molecular basis for such directed metabolite flux is channeling between the large, cuboidal MtCK octamer and two transmembrane proteins, adenine translocator (ANT) and mitochondrial porin or voltage-gated anion channel (VDAC). ANT is an obligatory antiporter for ATP/ADP exchange across the inner mitochondrial membrane, while VDAC is a nonspecific, potential-dependent pore in the outer mitochondrial membrane. The MtCK-linked metabolite channeling is based on (1) colocalization, (2) direct interactions, and (3) diffusion barriers. MtCK tightly binds to cardiolipin, an acidic phospholipid that is specific for the mitochondrial inner membrane. Since ANT is situated in a cardiolipin patch, this leads to colocalization and metabolite channeling between both proteins in cristae and intermembrane space (Figure 3). MtCK in the intermembrane space further interacts with outer membrane phospholipids and VDAC, thus virtually

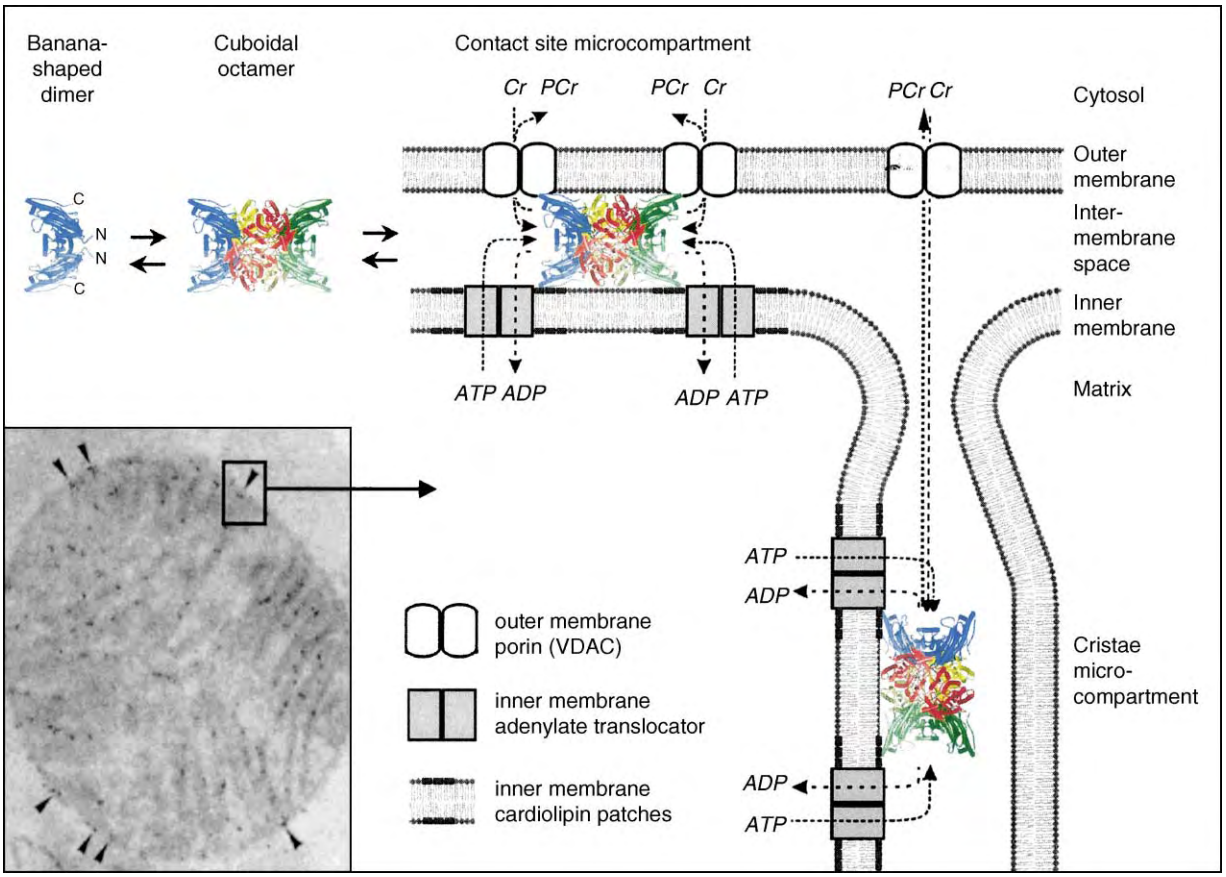

FIGURE 3 Inset: Dual localization of mitochondrial CK by electron microscopy. Post-embedding immuno-gold labeling of MtCK in a mitochondrion from photoreceptor cells of chicken retina, showing localization of MtCK in the peripheral intermembrane space (arrows) and along the cristae membranes. Scheme: Microcompartments and metabolite channeling of mitochondrial CK. After the import of nascent MtCK over the mitochondrial outer membrane and cleavage of the targeting sequence, MtCK first assembles into dimers. Dimers rapidly associate into octamers (top left), and although this reaction is reversible, octamer formation is strongly favored by high MtCK concentrations and MtCK binding to acidic phospholipids. MtCK is then found in two locations; (1) in the so-called mitochondrial contact sites associated with ANT and VDAC (top center), and (2) in the cristae associated with ANT only (at right). In contact sites, MtCK simultaneously binds to inner and outer membrane due to the identical top and bottom faces of the octamer. Binding partner in the inner membrane is the twofold negatively charged cardiolipin, which allows a functional interaction with adenine nucleotide translocator that is situated in cardiolipin membrane patches. In the outer membrane, MtCK interacts with other acidic phospholipids and, in a calcium-dependent manner, directly with VDAC. Substrate and product fluxes between MtCK and the associated proteins are depicted as arrows. In contact sites, this substrate channeling allows for a constant supply of substrates and removal of products at the active sites of MtCK. In cristae, only ATP/ADP exchange is facilitated through direct channeling to the MtCK active site, while Cr and PCr have to diffuse along the cristae space to reach VDAC.

cross-linking inner and outer membrane and contributing to the "mitochondrial contact sites." Increasing the external calcium concentrations strengthens the interaction of MtCK with VDAC, which may improve channeling under cytosolic calcium overload as occurring at low cellular energy state. Some studies suggest that only the membrane-bound, octameric form of MtCK is able to maintain the metabolite channeling described above. Finally, the limited permeability of VDAC and thus of the entire outer membrane creates a dynamic microcompartmentation of metabolites in the intermembrane space that contributes to MtCK-linked channeling and separate mitochondrial ATP- and ADP pools. Similar to MtCK, hexokinase is able to use intramitochondrially produced ATP by binding to VDAC from the cytosolic mitochondrial surface at contact sites containing only ANT and VDAC. The direct functional coupling of MtCK to oxidative phosphorylation can be demonstrated with oxygraph respirometry on skinned muscle fibers from normal and transgenic mice lacking MtCK.

Oxidative damage of MtCK, induced by reactive oxygen and nitrogen species, generated under cellular stress situations, e.g., in infarcted heart or under chemotherapeutic intervention by anthracyclines lead to inactivation and dimerization of MtCK, as well as to dissociation of the enzyme from the mitochondrial inner membrane. Thus, important prerequisites for efficient channeling of high-energy phosphates by MtCK are negatively affected. These events contribute to cardiac energy failure and specific anthracycline cardiotoxicity.

FIGURE 4 Intramitochondrial inclusions in patients with mitochondrial myopathies consist of mitochondrial MtCK. Immuno-electron histochemistry of human intra-mitochondrial crystalline "railway-track" inclusions seen in patients with mitochondrial myopathies showing "ragged-red" skeletal fibers as a hallmark of the disease. Note the grossly enlarged mitochondrion, here from a patient with Kearns-Sayre syndrome, displaying the typical regularly spaced intra-cristae inclusions (dark) surrounded by mitochondrial inner cristae membranes. The section has been stained by rabbit anti-MtCK antibodies, followed by colloidal gold-conjugated second antibody (in collaboration with Dr. A. M. Stadhouders, Nijmegen, The Netherlands). Note that the dark inclusion bodies are heavily and specifically stained by the small 10 nm gold particles, indicating a high propensity of MtCK at these locations. Isolation of such inclusions, plus image processing of sections through them revealed that they consist mainly of crystalline MtCK octamers, which crystallize in sheet-like structures.

Mitochondrial CK, Intramitochondrial Inclusions, and Low Cellular Energy State

MtCK is an indicator for cellular low-energy stress, that is, the expression of this enzyme is highly up-regulated in patients with mitochondrial myopathies in the so called "ragged-red" skeletal muscle fibers, where mitochondrial volume and size are markedly increased and where characteristic intra-mitochondrial "railway-track inclusions" are observed as a hallmark of pathology. The latter were shown to consist of crystalline sheets of MtCK (see Figure 4). Similar MtCK inclusions can also be induced in animal by chronic Cr depletion leading to cellular low-energy state, Even more generally, cellular low-energy stress, be it chronic endurance training, fasting, Cr depletion, or pathologies in ATP generation like mitochondrial dysfunction seen in patients with mitochondrial cytopathies, induces a coordinated induction of "energy gene expression" to compensate for impaired energy supply and transport. In case of MtCK, one of the most prominent among these genes, overexpression is such that it leads to crystallization of the enzyme in a pathological state as described above.

Mitochondrial CK and the Mitochondrial Permeability Transition Pore

MtCK, together with its substrate Cr, has been recently implicated in regulation of the mitochondrial permeability transition pore that is crucially involved in triggering apoptosis, This seems to be due to metabolite channeling in the MtCK/ANT microcompartment also, which maintains high ADP concentrations in the matrix space that are inhibitory for permeability transition. Thus, the CK-system and its substrates seem to exert additional effects that are not necessarily directly coupled to improving cellular energetics. This may explain the remarkable cell- and neuro-protective effects of Cr that have been reported.

See Also the Following Articles

Free Radicals, Sources and Targets of: Mitochondria • Mitochondrial Channels • Mitochondrial Membranes, Structural Organization • Mitochondrial Metabolite Transporter Family • Mitochondrial Outer Membrane and the VDAC Channel • P-Type Pumps: Na^+/K^+ Pump

Glossary

metabolite channeling Local transfer of metabolic intermediates between sequential enzyme or transport reactions without equilibration with bulk solution.

metabolic compartmentation Segregation of intermediates and enzymes of a metabolic pathway by membranes, binding to a specific surface or direct interaction in protein complexes allowing metabolite channeling.

microcompartment Structural unit allowing metabolic compartmentation, also called "metabolon."

mitochondrial contact sites Close adhesions of inner and outer mitochondrial membrane that can be observed by electron microscopy and can be isolated as a separate microcompartment. Contact sites consist of multi-lipid/protein complexes with variable composition and are involved in energy transduction (e.g., containing ANT/VDAC or ANT/MtCK/VDAC) or protein import.

mitochondrial permeability transition pore A multienzyme complex, probably composed of VDAC, ANT, Bax, cyclophilin, MtCK and others, that is crucially involved in early events that trigger apoptosis like release of cytochrome *c* and other apoptosis-inducing factors into the cytosol.

Further Reading

Agius, L., and Sherratt, H. S. A. (eds.) (1997). *Channelling in Intermediary Metabolism*. Research Monograph IX, Portland Press, London, GB.

Dolder, M., Walzel, B., Speer, O., Schlattner, U., and Wallimann, T. (2003). Inhibition of the mitochondrial permeability transition by creatine kinase substrates. Requirement for microcompartmentation. *J. Biol. Chem.* **278**, 17760–17766.

Jacobus, W. E., and Lehninger, A. L. (1973). Creatine kinase of rat heart mitochondria. Coupling of creatine phosphorylation to electron transport. *J. Biol. Chem.* **248**, 4803–4810.

Kay, L., Nicolay, K., Wieringa, B., Saks, V., and Wallimann, T. (2000). Direct evidence for the control of mitochondrial respiration by mitochondrial creatine kinase in oxidative muscle cells in situ. *J. Biol. Chem.* **275**, 6937–6944.

Ovádi, J. (1995). *Cell Architecture and Metabolic Channeling*. Springer, Heidelberg.

Ovádi, J., and Srere, P. A. (2000). Macromolecular compartmentation and channeling. *Int. Rev. Cytol.* **192**, 255–280.

Schlattner, U., Forstner, M., Eder, M., Stachowiak, O., Fritz-Wolf, K., and Wallimann, T. (1998). Functional aspects of the X-ray structure of mitochondrial creatine kinase: a molecular physiology approach. *Mol. Cell. Biochem.* **184**, 125–140.

Srere, P. A., and Knull, H. R. (1998). Location-location-location. *Trends Biochem. Sci.* **23**, 319–320.

Srivastava, D. K., and Bernhard, S. A. (1986). Metabolite transfer via enzyme–enzyme complexes. *Science* **234**, 1081–1086.

Wallimann, T., Wyss, M., Brdiczka, D., Nicolay, K., and Eppenberger, H. M. (1992). Intracellular compartmentation, structure and function of creatine kinase isoenzymes in tissues with high and fluctuating energy demands: the 'phosphocreatine circuit' for cellular energy homeostasis. *Biochem. J.* **281**, 21–40.

Biography

Uwe Schlattner is Docent at the Institute of Cell Biology, Swiss Federal Institute of Technology (ETH), Zürich, Switzerland. He received his masters in biology at the University of Freiburg, Germany, and his Ph.D. in Natural Science at the University of Geneva, Switzerland. His research interest is in cellular energetics, in particular the molecular structure and physiology of kinases involved in regulating the cellular energy state.

Theo Walliman is a Professor at the Institute of Cell Biology at Swiss Federal Institute of Technology (ETH) in Zürich, Switzerland, where he also received his Ph.D. After a postdoctoral stay in Prof. Andrew G. Szent-Györgyi's laboratory at Brandeis University, Boston, from 1975 to 1981, he returned to ETH-Zürich. His research interests are in cellular energetics, especially creatine kinases and AMP-activated protein kinases, as well as creatine supplementation in health and diseases.

Metalloproteases

David S. Auld
Harvard Medical School, Boston, Massachusetts, USA

Metalloproteases are a class of enzymes that use protein-bound metal ion(s) and a coordinated water molecule to catalyze the addition of water to a peptide bond. Proteases are necessary for the survival of all living creatures, and are encoded by ~2% of the genes in all kinds of organisms. They are an exceptionally important group of enzymes in biology, medical research, and biotechnology.

Functional Classification

Scientists who work in the general area of proteolytic enzymes have given much latitude to the naming of such enzymes. At present they are frequently referred to as proteases, proteinases, and peptidases, in an interchangeable manner. Some of the terms used are more illustrative of their function. Exopeptidases cleave one or a few amino acids from the N or C terminus of a polypeptide, while endoproteases act internally on the polypeptide chain. Aminopeptidases and carboxypeptidases act on the N and C terminus of the polypeptide, respectively, usually cleaving off one amino acid at a time, but some are capable of removing two (dipeptidyl peptidases) or three (tripeptidyl peptidases) amino acids at a time. These enzymes are often classified according to their general mechanism type as structural/functional information becomes available. This classification results in four major types: aspartic, cysteine, metallo-, and serine, each named for a critical component of the active site. In the case of metalloproteases, the metal most frequently found is zinc. However, manganese, cobalt, and iron are also observed for some specific cases. Proteases are often named according to a specific physiological substrate that they hydrolyze. Angiotensin I converting enzyme (ACE) is a zinc metalloprotease that cleaves the C-terminal dipeptide from angiotensin I to produce the potent vasopressor, octapeptide, angiotensin II and inactivates bradykinin by the sequential removal of two dipeptides from its C terminus. The role of this enzyme in blood pressure control and water and salt metabolism was identified through the use of potent inhibitors of its action. It is also defined as a zinc dipeptidyl carboxypeptidase. Tumor necrosis factor-alpha (TNF-alpha) is a cytokine that induces protective inflammatory reactions and kills tumor cells. Soluble TNF-alpha is released from its membrane-bound precursor by a membrane-anchored proteinase, identified as a multidomain metalloproteinase called TNF-alpha-converting enzyme (TACE). This enzyme is also named as *a d*isintegrin-like *a*nd *m*etalloproteinase *s*ite (ADAMS) 17 endopeptidase for a classification based on structural considerations. Frequently, such a substrate-based classification requires a very general term when the substrate specificity is only known in general terms, such as matrix metalloproteinase (MMP).

Structural Classification

During the past decade, the advent of sequencing the protein through its gene and the ability to obtain three-dimensional (3D) structures on proteins allowed the recognition of metalloprotease families. These studies permit several different classifications based, for example, on the type of metal site present and/or similarity in overall protein fold and/or amino acid sequence similarities.

Metal Sites

The metal that is found in most metalloproteases is zinc. The function of these enzymes is therefore related to the chemistry of zinc, which is quite versatile. It has a remarkably adaptable coordination sphere that allows it to accommodate a broad range of coordination numbers and geometries when forming complexes. If the zinc retains a positive charge after ligating to protein side chains, it can act as a Lewis acid in catalysis. If a zinc–bound water is converted to hydroxide, the zinc site can act as a base or nucleophile in catalysis. In this sense the catalytic zinc sites are amphoteric. The oxidation/reduction properties of its neighboring transition metals is a major cause of their ligand exchange rates, amphoteric properties, and coordination geometries. Since zinc has a filled *d*-shell, it does not have oxidation/reduction properties, thus providing a stable metal ion species in a biological medium whose redox potential is in constant flux. There are now about six dozen X-ray diffraction and NMR structures of individual metalloproteases. These structures provide standards of

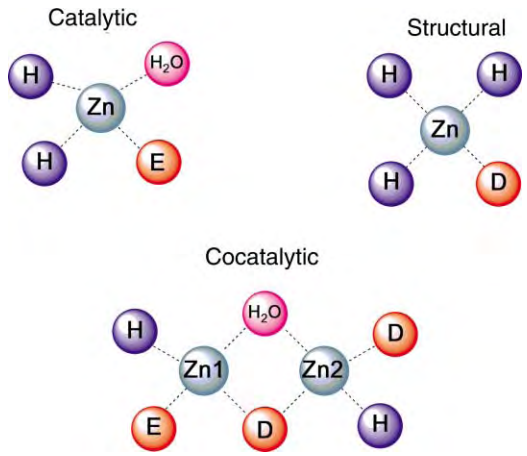

FIGURE 1 Zinc-binding sites in metalloproteases. Schematic shown is for a *catalytic* site, represented by carboxypeptidase A, the *structural* site for the matrix metalloproteases, and the *cocatalytic* site of Aeromonas aminopeptidase.

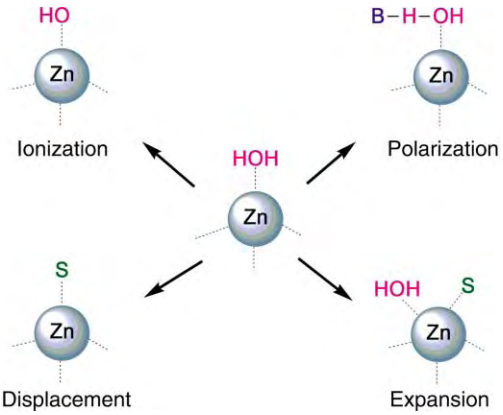

FIGURE 2 The role of the metal and bound water in catalysis. The water can ionize either (1) without or (2) with the help of the adjacent base supplied by an amino acid residue. The zinc–bound water can also (3) be displaced by substrate or (4) the coordination sphere be expanded upon interaction with substrate.

reference for the identity and nature of zinc ligands in other proteins, for which only the primary structure is known, and thus allow formation of metalloprotease families. Three types of distinct zinc-binding motifs emerge from these analyses: *catalytic*, *cocatalytic*, and *structural* sites (Figure 1). In zinc metalloenzymes the most common amino acids that supply ligands to these sites are His, Glu, Asp, and Cys. Thus far, Cys has been found as a ligand in only one metalloprotease.

Catalytic Sites

3D structures of the catalytic sites of about five dozen metalloproteases show that zinc forms complexes with any three nitrogen (His) and oxygen (Glu or Asp) donors, with His being the predominant amino acid chosen by a ratio of ~2:1 over Glu plus Asp. Histidine (usually the Nε2 nitrogen) may be chosen because of its capacity to disperse charge through H-bonding of its non-ligating nitrogen. The carboxylate anion of Glu and Asp ligands will reduce the charge on the metal, making it more difficult for the metal–bound water to ionize and for the metal to act as a Lewis acid catalyst. The first two metal ligands are separated by a short amino acid spacer with the third ligand being supplied by a longer spacer. In catalytic zinc sites of proteases the ligands are generally supplied from within an α-helix or a β-sheet that places restraints on the coordination of the metal by the side chains of the amino acids. The overall length of such sites can be as small as 11 amino acids, as is observed in the astacin super family of zinc proteases.

Catalytic zinc sites are usually four or five coordinate in metalloproteases and the geometry in the free state is frequently distorted-tetrahedral or trigonal-bipyramidal. Water is always a ligand to these sites. In principle, the zinc and its bound water molecule can be involved in catalysis by a number of different means (Figure 2). Metalloproteases generally have a Glu or His residue within H-bonding distance of the zinc–bound water that could play the role of a general acid/base catalyst or may stabilize the transition state of a tetrahedral intermediate. Alternatively, the direct ionization of the metal–bound water can lead to nucleophilic catalysis by zinc hydroxide, while displacement of water or expansion of the coordination sphere can result in Lewis acid catalysis by the catalytic zinc atom. The three protein ligands, their spacing, and secondary interactions with neighboring amino acids in conjunction with the vicinal properties of the active center created by protein folding, are all critical to the mechanisms through which zinc is involved in catalysis.

Structural Sites

Metalloproteases frequently use either disulfides or calcium ions to aid in stabilizing the structure of the enzyme. Structural metal sites have four protein ligands and no metal–bound water molecule. Cys ligands, followed by His, are the preferred ligands in such sites in zinc metalloenzymes. However, only one Cys containing zinc site is observed in the class of metalloproteases. Human picornavirus endoprotease 2A binds one zinc to three Cys and one His in the sequence $Cx_1Cx_{57}Hx_1C$. One other metal site that fits the criteria for a structural zinc site has been observed in the matrix metalloproteases and has a signature of $Hx_1Dx_{12}Hx_{12}H$ (Figure 1). This site may indirectly affect the activity of the enzyme. The amino acids adjacent to the third and fourth His ligands to the structural zinc site provide a number of hydrophobic residues that border a catalytic Glu residue. These residues could provide a hydrophobic environment for the Glu carboxylate group and thus raise its pK_a and allow it to play a role in stabilizing the transition state in catalysis. The zymogen form of the

MMPs has a Cys ligand in place of the zinc-bound water in the catalytic zinc site, thus having the properties of a structural zinc site.

Cocatalytic Sites

These sites in metalloenzymes contain two or three metals in close proximity with two of the metals bridged by a side-chain moiety of a single amino acid residue, such as Asp, Glu, His, or a carboxylated lysine, LysCO, and sometimes a water/hydroxide molecule (Figure 1). Thus far, structures for amino- and carboxy- and a tripeptidase have been reported. Asp and Glu and sometimes an additional water molecule are the preferred bridging ligands for these sites. The distance between the metals is dictated by the type of bridging ligand, 2.8–3.6 Å, for the carboxylate. No Cys ligands have been reported for these sites.

The bridging amino acids and H_2O could have critical roles in catalysis. Thus, their dissociation from either or both metal atoms during catalysis could change the charge on the metal promoting its action as a Lewis acid or allowing interaction with an electronegative atom of the substrate. Alternatively, the bridging ligand might participate transiently in the reaction as a nucleophile or general acid/base catalyst. In this manner the metal atoms and their associated ligands would play specific roles in each step of the reaction that works in concert to bring about catalysis.

The ligands to these sites often come from nearly the entire length of the protein. The metals may therefore be important to the overall fold and stability of the protein as well as catalytic function. The secondary structural elements α-helices and β-sheets again play a strong role in supplying the ligands. However, in contrast to the catalytic zinc sites, the ligands often reside one or two amino acids from the N or C terminus of an α-helix or a β-sheet. These positions should allow more flexibility in forming the cocatalytic site.

Some of the cocatalytic sites contain metal ions other than zinc ions. The *E. coli* methionine aminopeptidase-1, MetAP-1, the hyperthermophile *Pyrococcus furiosus* methionine aminopeptidase-2 and human methionine aminopeptidase-2 have been isolated as dicobalt enzymes and the *E. coli* proline aminopeptidase as the dimanganese enzyme. The physiological metal for these enzymes is still not certain. Zinc works as well as cobalt in the yeast aminopeptidase-1 and recent studies of the *E. coli* MetAP-1 indicate that it functions as an Fe(II) enzyme.

Genetic Origin and Ligand Nature

The identification of the ligands to these metal sites and the spacing characteristics in combination with modern sequencing techniques has led to further classifications of the metalloproteases. An excellent source of information on proteolytic enzymes is the *Handbook of Proteolytic Enzymes* and its associated website of MEROPS (http://merops.sanger.ac.uk/index.htm). This protease database groups peptidases into three levels – clans, families, and an individual peptidase. A clan contains all the peptidases that are believed to have diverged from a single evolutionary origin. In terms of the metalloproteases, they may have similar catalytic metal sites and overall folds. The clans can be further divided into families of proteases that show significant similarities in amino acid sequence. Finally, a member of a family is an individual peptidase. The Release 6.6(March, 2004) of MEROPS gives information on 6349 sequences of metallopeptidases and groups them into 16 clans, 52 families, and 657 metallopeptidases.

Physiological Function

These enzymes are important to a wide range of physiological processes too numerous to cover completely herein. Carboxypeptidase A (CPD A), was the first zinc protease and second zinc enzyme discovered. The zinc exopeptidases, CPD A and B compliment the action of the serine endoproteases, trypsin, and pepsin, in the degradation of food proteins. The serine proteases cleave proteins internally either at positions of basic amino acids such as Lys or Arg (trypsin) or hydrophobic aromatic amino acids such as Phe or Trp (pepsin). The zinc exopeptidases then liberate the essential amino acids Lys and Phe from the C terminus of the peptides generated by the endoproteases. The combination of structural and functional studies on these metalloproteases have revealed the presence of other members of this family that are important to hormone processing, immune/inflammatory activity and blood-clotting functions. Information on the active sites of CPD A led to the development of specific inhibitors of angiotensin-converting enzyme decades before a crystal structure was known for it, based on the proposition that both enzymes contained a zinc–bound water. Drugs for control of hypertensin were identified by these means. Methionyl aminopeptidases, MetAP, remove the N-terminal methionine residue from newly transcribed polypeptides. The physiological importance of these enzymes is underscored by the lethal nature of the removal of the MetAP gene from a number of bacterial sources. The "Handbook of Proteolytic Enzymes" along with its associated MEROPS website is an excellent source for detailed information on metalloproteases.

Metalloprotease Inhibition

The crucial nature of these enzymes to physiological processes has led to considerable research efforts on

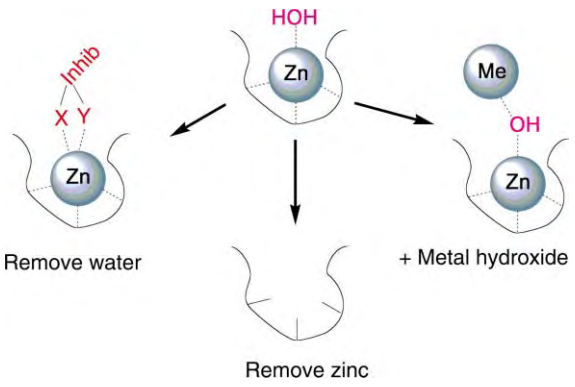

FIGURE 3 Inhibition of zinc proteases is accomplished by either (1) removing the water, (2) removing the metal, or (3) binding a metal hydroxide complex.

discovering natural inhibitors of them that could be involved in their regulation. The MEROPS website contains a good compilation of such inhibitors. The importance of the metal and its bound water are the key to inhibiting the metalloproteases (Figure 3). Inhibition can be accomplished by one of the three ways – (1) displace the water by an inhibitor binding to the metal, (2) remove the metal, or (3) bind a metal hydroxide complex to the catalytic metal and an active site residue.

Displacement of the Metal-Bound Water

The importance of zinc proteases in both normal and pathological processes makes them targets for drug design. The fact that zinc can readily form four-, five-, and six-coordinate complexes has led to the design of a number of synthetic inhibitors that act by displacing the metal–bound water. These studies have shown that the strength of the chelator–metal interaction increases the potency of the agent as a drug. The inhibitors are designed to have both structural specificity for the active site and a "war head" that will bind to the catalytic metal. Specificity is incorporated on either side of the metal-binding ligand. Popular warheads are hydroxamates, thiolates, and phosphoryl groups as chelating ligands. Carboxyalkyl and phosphinic acid groups are used as transition state or tetrahedral intermediate mimics.

Catalytic Chelators

It should also be possible to inhibit zinc proteases by removing the metal. This is often not very specific and many common chelators, such as ethylenediamine tetra-acetic acid (EDTA), are ineffective. However, D-penicillamine, a drug used to treat Wilson's disease and rheumatoid arthritis, has been shown to catalyze the release of zinc from CPD A. In the presence of a second scavenger chelator, such as EDTA or the physiological chelator, thionein (apo-metallothionein), the inhibition is quite potent. From a physiological perspective, such a mechanism of inhibition would be essentially irreversible, given the low levels of free zinc believed to be present in the body.

Inhibition by Metal Hydroxide Complexes

Many zinc proteases are inhibited by adding zinc to the assays. In the case of the exopeptidase, CPD A, and the endoprotease, thermolysin a combination of kinetic and structural studies have shown this inhibition is due to zinc hydroxide binding the ionized carboxylate of an active site glutamate residue which then bridges to the catalytic zinc by displacing its bound water. In the case of CPD A, both zinc and lead inhibit in the form of M(OH)Cl with sub-micromolar-inhibition constants. If multidentate ligands interact with the inhibitory metal and the enzyme-active site, significantly stronger inhibition is anticipated. Inhibition by such metal hydroxide complexes could be important to regulatory and/or toxicological processes of zinc proteases.

See Also the Following Articles

Aminopeptidases • Angiotensin Receptors • Aspartic Proteases • Cysteine Proteases • Cytokines • Proteases in Blood Clotting

Glossary

aminopeptidase Protease catalyzing the cleavage of amino acids from the N terminus of polypeptides.

carboxypeptidase Protease catalyzing the cleavage of amino acids from the C terminus of polypeptides.

dipeptidyl peptidase Protease that removes two amino acids at a time from the N or C terminus of the polypeptide.

endoprotease Protease that acts internally on a polypeptide chain.

protease or proteinase Enzyme catalyzing the hydrolysis of peptide bonds in proteins.

Further Reading

Auld, D. S. (2001a). Zinc coordination sphere in biochemical zinc sites. *BioMetals* **14**, 271–313.

Auld, D. S. (2001b). Zinc sites in metalloenzymes and related proteins. In *Handbook on Metalloproteins* (I. Bertini, A. Sigel and H. Sigel, eds.) pp. 881–959. M. Dekker, New York.

Auld, D. S. (2004). Cocatalytic zinc sites. In *The Handbook of Metalloproteins* (A. Messerschmidt, W. Bode and M. Cygler, eds.) Vol. 3, pp. 416–431, Wiley, Chichester.

Barrett, A. J., and Rawlings, N. D. (2004). MEROPS the peptidase database (http://merops.sanger.ac.uk/index.htm).

Barrett, A. J., Rawlings, N. D., and Woessner, J. F. (eds.) (2004). Metallopeptidases. In *Handbook of Proteolytic Enzymes*. 2nd edition, pp. 268–288, Academic Press, London.

Lowther, W. T., and Matthews, B. W. (2000). Structure and function of the methionine aminopeptidases. *Biochim. Biophys. Acta* **1477**, 157–167.

Vendrell, J., Querol, E., and Aviles, F. X. (2000). Metallocarboxypeptidases and their protein inhibitors – Structure, function and biomedical properties. *Biochim. Biophys. Acta* **1477**, 284–298.

Woessner, J. F., and Nagase, H. (2000). *Matrix Metalloprotinases and TIMPS*. Oxford University Press, Oxford.

Biography

David S. Auld is an Emeritus Associate Professor in the Department of Pathology and Research Associate Professor in the Department of Biology at Boston College in Chestnut Hill, Massachusetts. His principal research interests are in the biochemistry of zinc and the mechanism of action of metalloproteases. He holds a Ph.D. from Cornell University.

Metalloproteinases, Matrix

Hideaki Nagase
Imperial College, London, UK

Gillian Murphy
University of Cambridge, Cambridge, UK

Matrix metalloproteinases (MMPs), also called matrixins, are a group of structurally related proteolytic enzymes containing a zinc ion in the active site. They are secreted from cells or bound to the plasma membrane and hydrolyze extracellular matrix (ECM) and cell surface molecules. The first MMP to be identified was collagenase in the tadpole tail undergoing metamorphosis, exemplifying the importance of ECM-degrading proteinases in tissue remodeling. Numerous lines of evidence have now shown that they play key roles in embryonic development, organ morphogenesis, ovulation, embryo implantation, nerve growth, bone remodeling, wound healing, angiogenesis, and apoptosis. Under such physiological conditions MMP activities are regulated in accordance with matrix synthesis at the level of transcription, activation of the precursor zymogens, interaction with ECM and cell surface molecules, and inhibition by endogenous inhibitors. Many cell types have the ability to synthesize MMPs but their production is tightly controlled by growth factors, cytokines, physical stress to the cell, oncogenic transformation, hormones, cell–cell and cell–ECM interactions. Aberrant activities of MMPs are often associated with the progression of diseases such as cancer, arthritis, cardiovascular disease, nephritis, neuro-degenerative diseases, periodontal disease, skin ulceration, gastric ulcer, corneal ulceration, liver fibrosis, emphysema, fibrotic lung, and many others.

MMP Family

MMPs are found in vertebrates, fruit flies (*Drosophila melanogaster*), nematodes (*Caenorhabditis elegans*), sea urchins (*Paracentrotus lividus*), hydras (*Hydra vulgaris*), and plants (e.g., *Arabidopsis thaliana*, *Glycine max*). The human genome has 24 MMP genes. There are two genes in *Drosophila*, six genes in *C. elegans*, and five genes in *Arabidopsis*. They are classified as the matrixin subfamily of metalloprotease family M10 in the MEROPS database (http://www.merops.co.uk/merops/merops.htm). Vertebrate matrixins are assigned with MMP numbers and trivial names in many cases (Table I). MMP numbers missing in the list (i.e., MMP-4, -5, -6, and -22) were found to be identical to one of the other MMPs. Expression of individual MMPs varies depending on cell types (Figure 1).

Most MMPs consist of a prodomain, a catalytic domain, a hinge (or linker), and a hemopexin domain.

The signatures to assign proteinases to the MMP family are the cysteine switch motif with amino acid sequence PRCGXPD in the propeptide and the zinc-binding motif HEXGHXXGXXH in the catalytic domain, where the three histidines coordinate the zinc ion (Zn^{2+}). The primary structure of the catalytic domain is homologous to collagenase 1 (MMP-1). On the basis of substrate specificity sequence similarity and domain organization, MMPs are divided into six subgroups (Table I, Figure 2).

Collagenases

Collagenase 1 (MMP-1), collagenase 2 (MMP-8), collagenase 3 (MMP-13), and collagenase 4 in *Xenopus* (MMP-18) belong to this subgroup. The characteristic feature of these enzymes is their ability to cleave native fibrilar collagen types I, II, and III into $\frac{3}{4}$ and $\frac{1}{4}$ fragments. Some members of other MMP subgroups also degrade fibrilar collagen (e.g., MMP-2 and MMP-14). Collagenases also digest other ECM and non-ECM proteins (Table I).

Gelatinases

Gelatinase A (MMP-2) and gelatinase B (MMP-9) are in this subgroup. They have three repeats of fibronectin type II motifs attached to the catalytic domain, which distinguishes them from other MMPs. These repeats interact with collagens, gelatins, and laminin. Both MMPs readily digest denatured collagens, i.e., gelatins, and a number of ECM molecules (Table I). MMP-2, but not MMP-9, cleaves collagen I, II, and III into $\frac{3}{4}$ and $\frac{1}{4}$ fragments.

TABLE 1

Substrates of Mammalian MMPs

Enzyme	MMP	Human chromosome	Substrates
Soluble-types			
Collagenases			
Interstitial collagenase (collagenase 1)	MMP-1	11q22–q23	Collagens I, II, III, VII, VIII, X, and XI, gelatin, entactin, tenascin, aggrecan, fibronectin, myelin basic protein, IGFBP-3, α_1PI, IL-1β
Neutrophil collagenase (collagenase 2)	MMP-8	11q21–q22	Collagens I, II, and III, α_1PI, substrate P
Collagenase 3	MMP-13	11q22.3	Collagens I, II, III, IV, IX, X, and XIV, gelatin, collagen telopeptides, fibronectin, aggrecan
Collagenase 4 (*Xenopus*)	MMP-18	–	Collagen I
Gelatinases			
Gelatinase A	MMP-2	16q13	Gelatin, collagens I, II, III, IV, V, VII, and X, fibronectin, laminin, aggrecan, elastin, tenascin, decorin, myelin basic protein, α_1PI, IL-1β, IGFBP-3, MCP-3
Gelatinase B	MMP-9	20q12.2–q13.1	Gelatin, collagens IV, V, XI, XIV, elastin, aggrecan, decorin, laminin, entactin, myelin basic protein, α_1PI, IL-1β
Stromelysins			
Stromelysin 1	MMP-3	11q23	Collagens III, IV, V, IX, X, and XI, telopeptides of collagens I and II, gelatin, aggrecan, fibronectin, laminin, entactin, tenascin, decorin, myelin basic protein, α_1PI, IL-1β, IGFBP-3, activation of proMMP-1, proMMP-3, proMMP-8, proMMP-9
Stromelysin 2	MMP-10	11q22.3–q23	Collagen III, IV, and V, gelatin, fibronectin, elastin, aggrecan, activation of proMMP-1, proMMP-7, proMMP-8, proMMP-9
Stromelysin 3	MMP-11	22q11.2	α_1PI (mouse MMP-11 has weak activities on collagen IV, gelatin, fibronectin, laminin, aggrecan)
Matrilysins			
Matrilysin 1	MMP-7	11q21–q22	Collagen IV, gelatin, aggrecan, elastin, fibronectin, vitronectin, laminin, SPARC, entactin, decorin, myelin basic protein, tenascin, fibulin, α_1PI, proTNFα, activation of proMMP-1, proMMP-2, proMMP-9
Matrilysin 2	MMP-26	11p15	Fibronectin, fibrinogen, vitronectin, gelatin, α_1-PI
Others			
Metalloelastase	MMP-12	11q22.2–q22.3	Elastin, collagen IV, gelatin, fibronectin, vitronectin, laminin, entactin, aggrecan, myelin basic protein, α_1PI, proTNFα
(No name)	MMP-19	12q14	Collagen IV, laminin, entactin, tenascin, fibronectin, gelatin, aggrecan, COMP
Enamelysin	MMP-20	11q22.3	Amerogenin, COMP
(No name)	MMP-21	10	Gelatin, α_1PI
CA-MMP	MMP-23*	1p36.3	Gelatin
(No name)	MMP-27	11q24	–
Epilysin	MMP-28	17q21.1	Casein
Membrane-types			
Transmembrane			
MT1-MMP	MMP-14	14q11–q12	Collagens I, II, and III, gelatin, fibronectin, vitronectin, laminins 1 and 5, entactin, aggrecan, fibrin, α_1PI, decorin, proTNFα, CD44, activation of proMMP-2 and proMMP-13
MT2-MMP	MMP-15	8q21	ProMMP-2, laminin, fibronectin, tenascin, entactin, aggrecan, perlecan, proTNFα
MT3-MMP	MMP-16	15q13q21	ProMMP-2, collagen III, fibronectin
MT5-MMP	MMP-24	20q11.2	ProMMP-2, proteoglycans, gelatin
GPI-anchored			
MT4-MMP	MMP-17	12q24.3	Fibrinogen, fibrin, proTNFα
MT6-MMP	MMP-25	16p13.3	Collagen IV, gelatin, fibrinogen, fibrin, fibronectin

*two identical genes are found head to head arrangement in chromosome 1.

α_1-PI, α_1-proteinase inhibitor; TNFα, tumor necrosis factor α; IGFBP-3, insulin-like growth factor binding protein 3; MCP-3, monocyte chemoattractant protein 3; SPARC, secreted protein acidic and rich in cysteine (also known as osteonectin or BM40); COMP, cartilage oligomeric matrix protein; IL-1, interleukin 1.

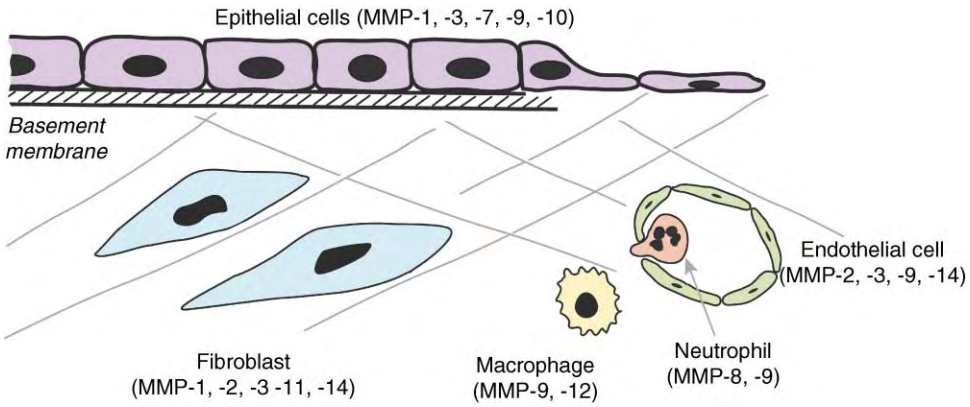

FIGURE 1 Tissue expression of MMPs. Representative MMPs produced by various cell-types are shown. The production of these MMPs is usually transcriptionally controlled by stimulatory factors.

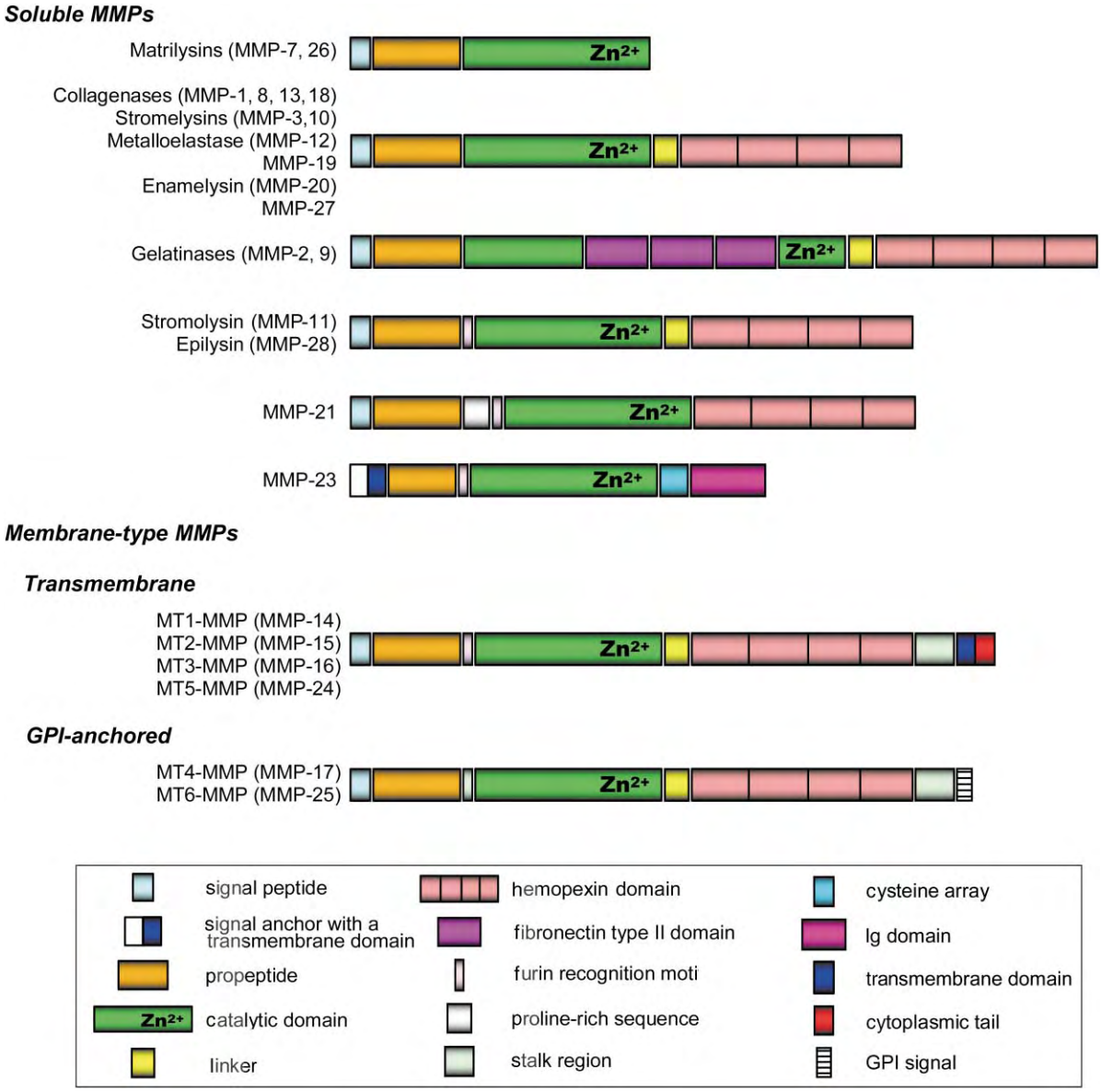

FIGURE 2 Domain arrangements of vertebrate MMPs.

Stromelysins

Stromelysin 1 (MMP-3), stromelysin 2 (MMP-10), and stromelysin 3 (MMP-11) are assigned to this subgroup. While MMP-3 and MMP-10 have similar enzymatic properties including their abilities to cleave various ECM molecules and activate several other MMPs (Table I), MMP-11 has a more divergent amino acid sequence and substrate specificity. Human MMP-11 does not cleave ECM components. Alternative splicing and promoter usage generates an intracellular form of MMP-11.

Matrilysins

Matrilysin 1 (MMP-7) and matrilysin 2 (MMP-26) are assigned to this subgroup. They consist of a pro-domain and the catalytic domain only (Figure 2). MMP-7 is produced in epithelial cells and secreted apically. Besides digesting ECM molecules, it processes pro-α-defensin, Fas ligand, protumor necrosis factor α, and E-cadherin from the cell surface. MMP-26 digests several ECM molecules (Table I).

Membrane-Type MMPs (MT-MMPs)

There are six MT-MMPs in humans. They are numerically assigned from MT1-MMP to MT6-MMP; four are type I transmembrane proteins (MMP-14, MMP-15, -16, and -24) and two are glycosylphosphatidylinositol (GPI)-anchored proteins (MMP-17 and MMP-25). The catalytic domain and the hemopexin domain are exposed on the cell surface. With the exception of MT4-MMP (MMP-17), MT-MMPs activate proMMP-2 as well as digest ECM components. MT1-MMP, MT2-MMP, and MT3-MMP digest fibrilar collagens to varying degrees, and MT1-MMP activates proMMP-13. While MT1-MMP is expressed in many cell-types, MT5-MMP is expressed in brain, mainly in the cerebellum, and MT6-MMP in leukocytes.

Other MMPs

Seven MMPs do not belong to the above subgroups. Metalloelastase (MMP-12) is primarily expressed in macrophages. It digests elastin and other proteins, and it is essential for macrophage migration. MMP-19 is expressed in liver, skin, and mononuclear cells. Enamelysin (MMP-20) is mainly expressed in newly formed tooth enamel. It processes amelogenin, and resulting products are essential for tooth enamel formation. MMP-21 is expressed in various fetal and adult tissues and in several invasive cancer cells. It digests gelatin and α_1-proteinase inhibitor. MMP-23 is mainly expressed in reproductive tissues. Two identical copies of the MMP-23 gene are located in human chromosome 1p36 loci in a head to head arrangement. The enzyme is a type II transmembrane protein with a membrane-anchoring sequence located in the N-terminal end of propeptide. The propeptide is removed by a proprotein converting proteinase and therefore it is secreted from the cell as an active enzyme. The enzyme lacks both the cysteine switch motif in the propeptide domain and a hemopexin domain. The latter is replaced by a cysteine array and an immunoglobulin domain. MMP-27 is an orthologue of chicken MMP (originally assigned as MMP-22). The enzymatic properties of MMP-27 have not been characterized. Epilysin (MMP-28) is expressed in keratinocytes, and its expression increases during wound healing.

Structural Chemistry

The propeptide domain plays a key role in maintaining the MMPs in their zymogen forms (proMMPs) by blocking the active site. It has ~80 amino acids and consists of three α-helices and extended peptides including the cysteine switch motif (Figure 3A). The residues in the cysteine switch interact with the substrate-binding cleft in the catalytic domain by forming β-structure-like hydrogen bonds in a manner similar to a substrate, but in the opposite direction. The cysteine residue coordinates with the catalytic Zn^{2+} to maintain the latency of the enzyme.

The catalytic domain has ~170 amino acids including the zinc-binding motif (HEXGHXXGXXH) and a conserved methionine that forms a unique "Met-turn" structure. The domain consists of three α-helices, a five-stranded β sheet, and bridging loops (Figure 3B). It contains two zinc ions (Zn^{2+}); one is essential for catalysis, and the other together with three calcium ions stabilizes the structure. The overall polypeptide folds, including the Met-turn, are similar to those of astacins, reprolysins, ADAMs, and bacterial proteinase serralysins, which together constitute the metzincins.

The hemopexin domain consists of ~190 amino acids and forms a four-bladed β-propeller structure arranged almost symmetrically around a central axis, and each blade is comprised of a four-stranded anti-parallel β sheet (Figure 3A). The domain is stabilized by a calcium ion and a disulfide bond between blades I and IV.

The catalytic domain and the hemopexin domain are connected by a "hinge" (also called "linker") region of variable length, which does not have a specific structure.

The fibronectin type II motif found in MMP-2 and MMP-9 consists of two double-stranded anti-parallel β-sheets and two large loops (Figure 3A). Each β-sheet has one disulfide bond.

Several MMPs are glycoproteins. In particular, proMMP-8, proMMP-9, and proMMP-23 are highly glycosylated, with ~20–45% of their molecular mass being carbohydrate.

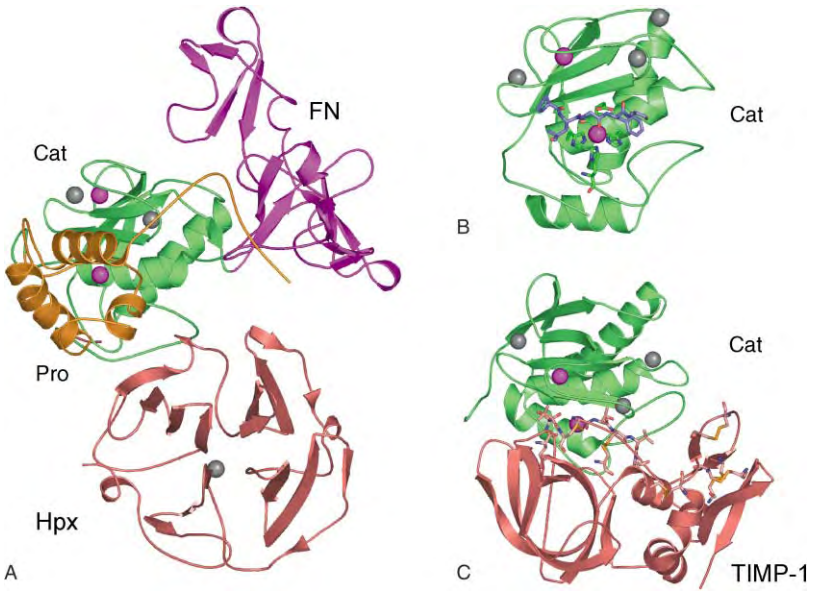

FIGURE 3 Three-dimensional structure of MMPs and TIMPs. (A) Ribbon diagram of proMMP-2. The propeptide (pro) is shown in orange; the catalytic (cat) domain in green; the fibronectin (FN) domain in pink; and the hemopexin (Hpx) domain in red. Zinc ions and calcium ions are in pink and grey, respectively. (B) The catalytic domain of MMP-1 with a peptide substrate (stick representation) bound to the active site. (C) The complex of TIMP-1 and the catalytic domain of MMP-3.

Mechanism of Peptide Bond Hydrolysis

The active site of MMPs consists of the catalytic Zn^{2+} bound to three imidazoles of histidines in the HEXGH XXGXXH motif and the glutamate in the motif. A proposed mechanism of peptide bond hydrolysis by MMPs is shown in Figure 4. In an active MMP, one water molecule is bound to the catalytic Zn^{2+}. Upon binding of a peptide substrate to the active site of the enzyme, the carbonyl group of the P1 residue interacts with the catalytic Zn^{2+} and the water molecule is displaced towards the carboxyl group of the glutamate. This polarizes the water molecule and promotes its nucleophilic attack on the carbonyl carbon of the scissile bond, resulting in formation of a hemiketal intermediate and the subsequent hydrolysis of the peptide bond. The glutamate functions as a general acid/base during catalysis. Mutation of the glutamate to aspartate reduces the enzymatic activity to less than 1% and mutation to alanine reduces activity to 0.01% of the wild-type.

Activation of proMMPs

MMPs are synthesized as pre-pro-MMPs and many are secreted from cells as zymogens (proMMPs) which need to be activated outside the cell. The major activation pathways are proteolytic processes.

Activation by Proteinases

The six MT-MMPs and MMP-11, -21, -23, and -28 contain a furin-like proprotein converting proteinase recognition sequence at the C-terminal end of the propeptide-domain. Most of them are therefore activated within the cell and secreted or bound to the membrane as the active form.

Other MMPs are secreted from cells as proMMPs in the tissue, proMMPs are likely to be activated by tissue or plasma proteinases or opportunistic bacterial proteinases. Figure 5 illustrates activation pathways that are involved in pericellular ECM hydrolysis. The urokinase-type plasminogen activator/plasmin system initiates the activation of many proMMPs near the cell surface. Unlike many other MMPs, proMMP-2 is not readily activated by plasmin or other proteinases, but activated on the cell surface by MT1-MMPs. This activation process is assisted by binding to a TIMP-2-MT1-MMP complex which presents proMMP-2 to an adjacent active MT1-MMP. ProMMP-13 is also activated by MT1-MMP, but this does not require TIMP-2 (Figure 5).

Activation by Chemical and Physical Means

One biochemical property unique to matrixins is that proMMPs can be activated *in vitro* by SH-reactive agents (e.g., 4-aminophenylmercuric acetate, iodoacetamide, oxidized glutathione), chaotropic agents

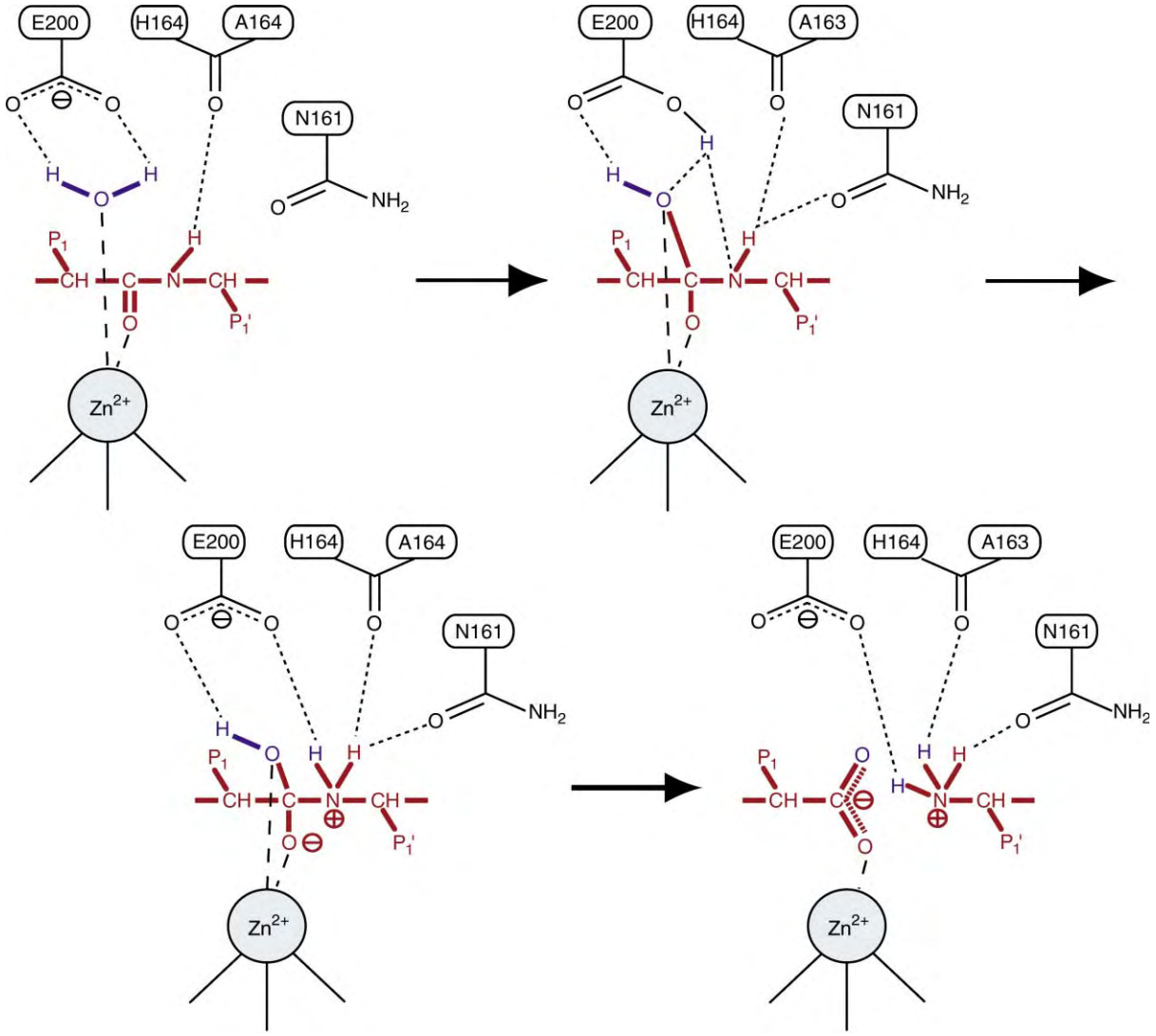

FIGURE 4 A proposed mechanism of action of MMPs. A peptide substrate and a water molecule that are involved in hydrolysis are shown red and blue, respectively. The residues shown are in MMP-1. See text for details.

(e.g., urea, SCN^-, I^-), sodium dodecylsulfate, reactive oxygen, low pH and heat treatment. This is due in part to the disruption of the cysteine–zinc interaction formed between the propeptide and catalytic domains and subsequent removal of the propeptide by autoproteolysis. Oxidation may activate some proMMPs, but it may also destroy the enzyme.

Activity and Substrate Specificity

MMPs exhibit optimal proteolytic activities at around pH 7.0–8.0 for most substrates but in some cases they exhibit a broader pH range. An exception is human stromelysin 1 which has optimal activity at around pH 5.5–6.0 with a shoulder of activity at pH 7.5–8.0.

MMPs degrade ECM and non-ECM proteins (see Table I for representative substrates). The potential substrates of more recently discovered MMPs (higher numbers) have not been well characterized. In general the substrate needs to be six amino acids or longer, and the enzymes have a strong preference for hydrophobic residues at the P1′ site (the residue located on the right of the cleaved peptide bond) such as Leu, Ile, Met, Phe or Tyr, but the amino acid at the P1 site (the residue on the left of the cleaved peptide bond) is not important. Non-catalytic domains greatly influence substrate specificity for some MMPs when substrates are extracellular macromolecules; e.g., fibronectin domain repeats of MMP-2 and MMP-9 play an important role in expressing the activity on type IV collagen, gelatin, and elastin; and the hemopexin domain of collagenases is essential for the collagenolytic activity.

MMPs are inhibited by chelating agents such as EDTA, 1,10-phenanthroline, cysteine, and dithiothreitol. Based on substrate specificity, numerous synthetic inhibitors of MMPs, many aimed at therapeutic

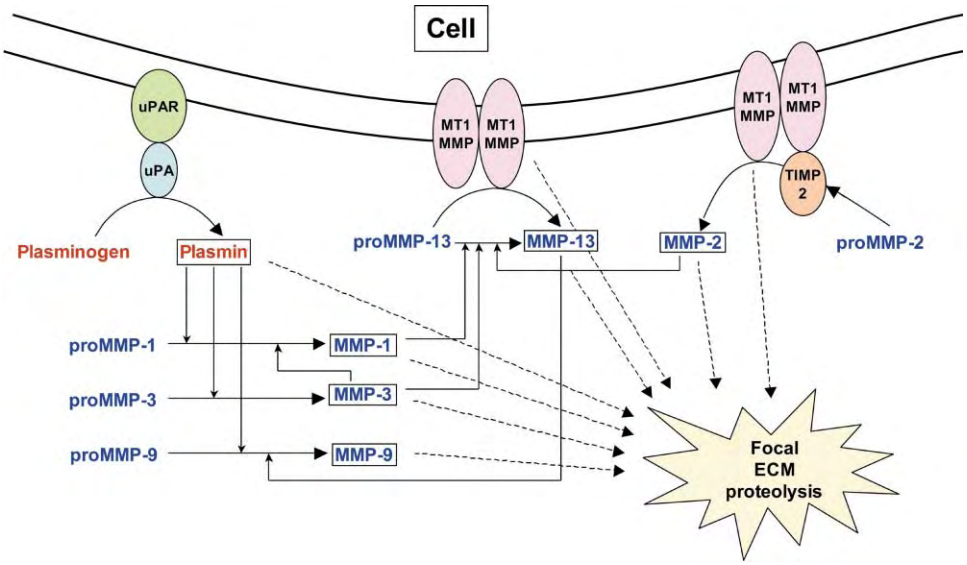

FIGURE 5 Activation pathways of proMMPs involved in pericellular ECM proteolysis. Urokinase-like plasminogen activator (uPA) bound to uPA receptor (uPAR) activates plasminogen to plasmin, which in turn activates a number of proMMPs. MT1-MMP activates proMMP-2; this process is assisted by binding to the TIMP-2-MT1-MMP complex which presents proMMP-2 to an adjacent active MT1-MMP. Activation of proMMP-13 by MT1-MMP does not require TIMP-2. Activated MMPs also participate in the activation of other proMMPs. Active enzymes are boxed.

purposes, have been designed. They commonly contain a zinc-chelating moiety such as a hydroxamic acid, a carboxyl, a thiol, or a phosphorus group. Some selective inhibitors for specific MMPs have been generated, but many broadly inhibit MMPs and other metalloproteinases. Phosphoramidon is not inhibitory. Tissue inhibitors of metalloproteinases (TIMPs), α2-macroglobulins and ovomacroglobulins (ovostatins) are the known natural protein inhibitors.

Endogenous Inhibitors of MMPs

α2-Macroglobulins

Human α2-macroglobulin is a plasma glycoprotein of 725 kDa consisting of four identical subunits of 180 kDa. It inhibits most endopeptidases by a trap mechanism: the interaction with a proteinase is initiated by the proteolytic cleavage in the middle of the subunits, causing a conformational change in the macroglobulin, hence entrapping the proteinase molecule. The active site of the trapped proteinase is not blocked, but its access to large protein substrates is sterically hindered. Related macroglobulins in other species including ovomacroglobulins (ovostatins) have a similar inhibition mechanism.

TIMPs

TIMPs are structurally related proteins which inhibit matrixins with a 1:1 molar stoichiometry. The human genome has four TIMP genes and there are two genes in *C. elegans* and one in *Drosophila*. The four human isoforms (TIMP-1 to -4) consist of 184–194 amino acids, sub-divided into N-terminal and C-terminal domains, each having three disulfide bonds. The N-terminal domain is the inhibitory domain and it binds to the active site of the MMPs. ProMMP-2 and proMMP-9 zymogens of MMPs bind to TIMPs via interaction between the C-terminal non-inhibitory domain of TIMP and the C-terminal hemopexin domain of proMMP. These complexes act as MMP inhibitors since the N-terminal inhibitory domain of TIMPs is not blocked. TIMP-3 is unique among four TIMPs as it also inhibits ADAMs and ADAMTSs, metalloproteinases containing a disintegrin domain.

Inhibition Mechanism

The inhibitory domain of TIMPs has an OB-fold structure with a reactive ridge formed by the N-terminal segment Cys^{1}-Thr-Cys-Val^{4} and the Ser^{68}-Val-Cys^{70} (residues are in TIMP-1) where Cys^{1} and Cys^{70} are disulfide linked. This ridge structure slots into the active site cleft of the MMPs (Figure 3C). The nitrogen of the N-terminal NH_2-group and the carbonyl oxygen of Cys^{1} bidentately chelate the Zn^{2+} in the active site of the enzyme. MMPs do not form covalent bonds with TIMPs nor cleave TIMPs, but form tight complexes with inhibition constants in the subnanolar range.

Other Biological Activities of TIMPs

TIMP-1 and TIMP-2 have erythroid potentiating and cell growth promoting activities. TIMP-3 binds to

vascular endothelial growth factor (VEGF) receptor-2 and blocks angiogenesis induced by VEGF.

These biological activities are independent of their MMP-inhibitory activity. TIMP-3 induces apoptosis of several cancer cells and vascular smooth muscle cells possibly by blocking the proteolytic release of cell death receptors such as tumor necrosis factor α receptor, Fas, TNF-related apoptosis-inducing ligand receptor 1. TIMP-1 and TIMP-2 exhibit anti-apoptotic activity in some *in vitro* cell studies.

Biological Activities of MMPs

The main function of MMPs is considered to be removal of ECM macromolecules from the tissues, but they also alter the function of ECM molecules by specific proteolysis and express new biological functions of these molecules. MMPs can also release growth factors bound to ECM and from carrier proteins, or inactivate inflammatory cytokines and chemokines, which then influence cellular behavior. For example, the cleavage of type I collagen is associated with keratinocyte migration during wound healing, activation of osteoclasts during bone remodelling and induction of apoptosis of amnion epithelial cells before the onset of labor. Cleavage of laminin 5 and CD44 by MMPs promotes cell migration. The expression of MT1-MMP and activation of proMMP-2 occur in invasive tumour cells and endothelial cells at the migratory front and promotes cells to migrate and invade by cleaving and shedding these ECM and cell surface molecules. The release of transforming growth factor β and VEGF from the matrix by MMPs modulates ECM synthesis and angiogenesis, respectively, which are key events in development, morphogenesis, reproduction, tissue remodeling and repair. Inactivation of monocyte chemoattractant proteins or interleukin 1β by MMP reduces inflammation.

Human Genetic Disorders and DNA Polymorphisms

Unregulated MMP activities are implicated in the progression of a variety of diseases characterized by aberrant breakdown of ECM molecules. In many cases their activities are controlled at the cellular level by various stimulatory factors. In addition, a few inherited human disorders associated with the MMP and TIMP genes have been described.

Mutations in human MMP-2 resulting in the absence of active MMP-2 are linked to a rare autosomal recessive genetic disorder, multicentric osteolysis, which causes destruction of the affected bones and joints. A mutation in the coding region for MMP-13 is associated with spondyloepimetaphyseal dysplasia, a dwarfism resulted from abnormal development of the vertebrae and extremities. Amelogenin imperfecta, a genetic disorder caused by defective enamel formation, is due to mutation at MMP-20 cleavage sites.

Mutations in the coding region of the *TIMP3* gene leading to the presence of an extra Cys in the C-terminal region of the expressed protein cause the rare autosomal dominant Sorsby's fundus dystrophy, a form of blindness characterized by death of the retinal pigment epithelium.

Various DNA polymorphisms in MMP genes are associated with a number of diseases. In many cases polymorphic sites are found in the promoter regions of MMP genes: polymorphisms in the *MMP1* gene are associated with coronary heart disease, rheumatoid arthritis, periodontitis, and cancers (e.g., cervix, ovary, colon, kidney, lung, and skin); in the *MMP2* gene with the risk of developing lung cancer; in the *MMP3* gene with coronary heart disease, coronary aneurysms and cancers (colon and breast); in the *MMP9* gene with coronary heart disease, aneurysms, nephropathy, and preterm prenatal rupture of the fetal membrane; and in the *MMP12* gene with coronary atherosclerosis.

See Also the Following Articles

Collagenases • Collagens

Glossary

ADAM Abbreviation for type I transmembrane proteins with *a* *d*isintegrin *a*nd *m*etalloprotease domain, some of which are involved in shedding of cell surface molecules and have some overlapping properties shared with MMPs. While the primary structures of the metalloprotease domain are homologous to each other, about half of the members of this family do not contain the strictly conserved zinc-ion-binding motif, and so they are probably proteolytically inactive.

ADAMTS Abbreviation for proteins with *a* *d*isintegrin *a*nd *m*etalloprotease domain with type I *t*hrombospondin motifs. The metalloproteinase domains are homologous to ADAMs, but they do not possess a transmembrane domain.

α_2-macroglobulin A glycoprotein in blood of 720 kDa consisting of four identical subunits. It inhibits most endopeptidases regardless of their catalytic mechanism by physical entrapment of the enzyme molecule upon proteolytic attack on the macroglobulin.

extracellular matrix A complex network of secreted extracellular macromolecules (e.g., collagens, proteoglycans, glycoproteins, fibronectin, complex carbohydrates etc.) which provides an organized lattice and helps to hold cells and tissues together in multicellular organisms.

metzincin Metalloproteinases that contain the zinc-ion-binding motif HEXXHXXGXXH and a conserved methionine that forms a unique "Met-turn" structure, e.g., matrix metalloproteinases, astacins, reprolysins, ADAMs, ADAMTSs, pappalysins, serralysins, and leishmanolysin.

MMP Abbreviation for *m*atrix *m*etallo*p*roteinases that are secreted from cells or bound to the cell surface and degrade extracellular matrix molecules.

proteinase Proteolytic enzymes, also known as proteases or endopeptidases, that hydrolyze internal peptide bonds of proteins and polypeptide chains; cf. exopeptidase, enzymes that hydrolyze one or a few amino acids from the N- or C-terminus of polypeptides.

TIMP An acronym for *t*issue *i*nhibitors of *m*etallo*p*roteinases with molecular masses of 22–30 kDa that inhibit MMPs.

Further Reading

Barrett, A. J., Rawlings, N. D., and Woessner, J. F. (2004). *Handbook of Proteolytic Enzymes*, 2nd edition. Academic Press/Elsevier Science, London.

Parks, W. C. (1998). *Matrix Metalloproteinases*. Academic Press, San Diego.

Rawlings, N. D., O'Brien, E. A., and Barrett, A. J. (2002). MEROPS: The protease database. *Nucleic. Acid Res.* **30**, 343–346.

Sternlicht, M. D., and Werb, Z. (2001). How matrix metalloproteinases regulate cell behaviour. *Annu. Rev. Cell Dev. Biol.* **17**, 463–516.

Woessner, J. F. Jr., and Nagase, H. (2000). *Matrix Metalloproteinases and TIMPs*. Oxford Univesity Press, Oxford.

Biography

Hideaki Nagase is the Head of Matrix Biology Department at the Kennedy Institute of Rheumatology Division, Imperial College London, UK. His principal research interest is in the structure and function of matrix metalloproteinases and TIMPs. He holds a Ph.D. from the University of Miami and received his postdoctoral training at Stangeways Research Laboratory, Cambridge, UK and Dartmouth Medical School. He elucidated the inhibition mechanism of TIMPs in collaboration with Professor Wolfram Bode and Professor Keith Brew.

Gillian Murphy is the Chair of Cancer Cell Biology at the Department of Oncology, University of Cambridge, Cambridge, UK. Her principal research interests are in the biochemistry, biology, and pathology of metalloproteinases and their inhibitors. She holds a Ph.D. from the University of Birmingham. She received her postdoctoral training at Max-Planck Institut für Biochemie, Munich, Germany and Strangeways Research Laboratory, Cambridge, UK. She pioneered the elucidation of the activation mechanisms and domain functions of matrix metalloproteinases and their implications in biology and pathology.

Metaphase Chromosome

Sharron Vass and Margarete M. S. Heck
University of Edinburgh, Edinburgh, UK

The metaphase chromosome is a transient entity—one that reflects the moment in mitosis when the DNA in each chromosome is maximally condensed. In higher eukaryotes, the length of DNA may be compacted up to 10 000-fold to ensure that the sister chromatids can be separated far enough from one another to avoid entrapment by the ingressing cleavage furrow late in mitosis. This metaphase chromosome has formed only after essential checkpoints early in the cell cycle have been properly navigated, so that the genome is replicated completely and at the right time and any damage fully and accurately repaired. In addition, the metaphase chromosome contains elaborate kinetochore structures, which can "read" whether each centromere of a sister chromatid pair is attached via microtubules to opposing spindle poles. Finally, the chromosome serves a crucial function in regulating precisely where the cleavage furrow will form during cytokinesis. Such strict control over genome packaging and partitioning is clearly essential for the maintenance of a normal diploid state, and the avoidance of aneuploidy through chromosome gain, loss, or fragmentation.

Background

The majority of cells within an organism will ultimately face one of three potential fates: to divide, to differentiate, or to die. In order to divide successfully, the cell must possess the ability first to replicate, then to package, and finally to partition its entire genome to two new daughter cells. The genomic DNA must be accurately replicated in S phase to form an exact copy of itself, thus resulting in two identical single chromatids, both of which must be held in close proximity to one another to permit DNA repair. The process of cell division requires the DNA to be condensed into ordered, yet highly dynamic structures. This appears to happen as a two-stage process, with most condensation resulting in distinct chromosomes occurring even before nuclear envelope breakdown. The condensed chromosomes are only resolved into two discernible chromatids late in prophase. Following bipolar attachment to the mitotic spindle in metaphase, sister chromatids are separated from each other and actively moved to the two spindle poles in anaphase. It is absolutely critical that chromosomes are accurately condensed and resolved prior to the metaphase to anaphase transition. Inadequate resolution could result in chromatid bridging in anaphase. If chromosomes are not condensed enough, they may be caught and cleaved by the ingressing cleavage furrow. Likewise, it is essential that chromatid separation occurs at the right time, otherwise aneuploidy could result from the unequal partitioning of chromatids to the two daughter cells. Finally, the chromosomes must be decondensed to the right degree to facilitate transcription and replication in a subsequent cell cycle. The consequences of failures in any of these processes would indeed be dire for the life of cells.

Brief Historical Perspective

The choreography of mitosis is without question esthetic, and has captivated the attention of cell biologists for over a century. Flemming originally described cell division in his book of 1882, coining the word "mitosis" (from Greek for thread) to emphasize the central role played by the thread-like chromosomes in the process. In his drawings of dividing salamander cells, he even diagrammed the longitudinal splitting of chromosomes into separate chromatids, thus taking the nuclear events of mitosis to a level higher than mere pinching in half. The affinity of nucleohistone for assorted bright-field stains ensured that mitosis was accessible to analysis, in a range of organisms, even in the absence of sophisticated microscopy, biochemistry, or molecular biology. What has become apparent with the current level of scrutiny possible is the extensive degree to which the molecular players are conserved. Thus, our understanding of chromosome structure has advanced through the use of diverse experimental approaches that may each enjoy distinct cytological, biochemical, or genetic advantages.

The Physical Chromosome

All organisms, prokaryotic or eukaryotic, single-celled or metazoan, must compact their genomes. There is simply too much DNA, and it has too high a negative charge to be squeezed into any sort of compartment without the aid of particular proteins. Even bacterial genomic DNA will

be on the order of 150 μm in length – while the cell itself may be less than 1 μm in size! It is exciting, and particularly humbling, that even in an age when newly completed genome sequences appear at an astounding pace, we do not understand all there is to know about making that DNA sequence work to produce anything from a simple bacterium to a thinking, feeling human being. Exactly how the cell manages to organize its genetic material has been the focus of much research and remains curiously enigmatic.

Interphase

The degree of structural engineering required to accomplish the packaging of the genome is quite staggering when one considers that the naked DNA of a typical diploid human cell, if stretched end-to-end, would measure ~2 m in length. This length of DNA 2 nm in diameter is packaged into a cell's nucleus typically measuring only 5–10 μm in diameter. What has so far been clearly demonstrated is that the naked DNA molecule wraps twice around a core octamer of positively charged histone subunits (two proteins each of H2A, H2B, H3, and H4) to form a disk-shaped structure called the nucleosome. Under nonphysiological low salt conditions, the nucleosomal fiber takes on a "beads-on-string" appearance when viewed by electron microscopy. This initial level of organization gives rise to a sixfold compacted DNA strand ~10 nm thick. The linker histone protein (H1, or variants) facilitates organization of the fiber into a shorter, thicker fiber of 30 nm—a 40-fold level of DNA compaction. One of the most debated issues relates to the path of the 10 nm nucleosomal fiber in the 30 nm fiber: is it a relatively ordered helical solenoid, a twisted helical ribbon, or even a random zig-zag aggregation of nucleosomes? The fragility of the chromatin fiber upon isolation from cells has so far precluded detailed resolution of its structure.

The 30 nm fibers are organized into large (10–100 kb) loops by intermittent anchoring, at spots that may or may not be determined by DNA sequence. This basic level of compaction appears to be similar in both interphase and mitotic chromatin. It is also fairly well accepted that chromosomes occupy distinct domains or territories within interphase nuclei, in contrast to a bowl of intertwined spaghetti strands! These domains reflect gene density, transcriptional activity, and/or replication timing. In general, the more transcriptionally silent chromosomes are later replicating and localized closer to the nuclear envelope.

Mitosis

The compaction of DNA described above cannot account for the final condensation observed in metaphase chromosomes of eukaryotic cells. The level of packaging required to produce a metaphase chromosome is nearly 10 000-fold (~250 times greater than in interphase)! Why should such an extreme level of compaction be required? As a generic human cell may be only 20–30 μm in diameter, a chromosome clearly has to be less than half that size in order to have cleared the midzone of the cell before the cleavage furrow ingresses during cytokinesis. Indeed, human metaphase chromosomes range in size from 2 to 10 μm. Any less compaction could result in chromosome cleavage and likely death. Strikingly, if cells are arrested in mitosis, chromosomes continue to condense even further—demonstrating that the genome is not usually condensed as much as it could be.

It is by no means completely accepted how the 30 nm fiber is organized in the metaphase chromosome. While it has also been demonstrated that histones H1 and H3 become hyperphosphorylated during mitosis, a causal role for this in chromosome condensation remains unestablished. Therefore, although numerous factors and processes contributing to the formation of mitotic chromosomes have been identified, many intriguing and unanswered questions remain.

How Is the Metaphase Chromosome Structured?

Teasing Apart Mitotic Chromosomes

The purpose of mitotic chromosome condensation is clearly to create a robust package that can survive the rigorous forces of mitosis to maintain the genomic DNA in an intact state. This extensive compaction is precisely what has hindered the elucidation of mechanisms or components essential for generating condensed chromosomes. Electron microscopy, while invaluable for the study of subcellular architecture, allowed disappointingly little insight into the architecture of intact mitotic chromosomes. Early micrographs by DuPraw in the 1960s showed extremely dense structures, from which one could occasionally glimpse loops of chromatin at the periphery—but no information about underlying organization.

Just as the folding of the 10 nm fiber within the 30 nm fiber has been controversial, so has the precise organization of the 30 nm fiber within the metaphase chromosome. Clearly, more extreme approaches were needed, as intact, unperturbed chromosomes were unlikely to give up their secrets. Models for the organization of chromatin in metaphase ranged from random folding of the 30 nm fiber to successive hierarchies of helical coiling, to a model whereby specific nonhistone proteins tethered particular DNA sequences to form chromatin loops.

A radical, though incredibly insightful, approach pioneered by Laemmli and colleagues depended on

techniques they developed in the 1970s for the isolation of highly purified mitotic chromosomes from synchronized mitotic cells. As histones comprise a third of the metaphase chromosome by mass (as does the DNA), removal of these proteins should provide a significant enrichment for the nonhistone proteins that comprise the final third of the chromosome. When Laemmli and co-workers extracted histones (and the majority of nonhistone proteins) from metaphase chromosomes by high salt or negatively charged polyanions, they observed something truly remarkable. Electron micrographs of the residual structures clearly showed clouds of naked DNA looping out from a proteinaceous "scaffold"-like structure that resembled the size and shape of the native chromosome. When examined more closely, there appeared to be very few loose DNA ends, instead these large loops of DNA appeared to emanate from and return to the same region of the "scaffold."

These stunning images led to the "radial loop model," or "scaffold hypothesis," to explain mitotic chromosome architecture. Large loops of chromatin were proposed to attach to a nonhistone proteinaceous scaffold, thus providing a framework for the final levels of chromosome condensation. Further evidence to support this hypothesis resulted from the discovery of scaffold attachment regions (SARs) or matrix attachment regions (MARs) that contain specific DNA sequences displaying a high affinity for the scaffold and thereby thought to facilitate the tethering of chromatin loops. Perhaps even more striking was the discovery that the composition of the residual "scaffold" fraction was not only surprisingly simple, but also remarkably reproducible independent of the protocol used to obtain it. Nevertheless, this model for chromosome architecture was controversial, with skeptics distrustful of the harsh biochemical procedures utilized to obtain "scaffolds."

DNA Topoisomerase II in Chromosome Architecture

SDS-PAGE analysis revealed that purified scaffolds were composed of two prominent bands at 170 and 135 kDa (named Sc1 and Sc2, respectively) and a number of minor proteins. Through immunocytochemical approaches, Sc1 was identified in the 1980s as DNA topoisomerase II, a homodimeric enzyme capable of making a double-stranded break in the DNA, and passing a strand through this break before religating the cleaved strand of DNA. Such an enzyme would clearly be necessary to decatenate duplicated and entwined DNA strands, such as would arise following replication of genomic DNA loops. A logical place to position a protein capable of decatenation would be at the base of chromatin loops, precisely where it appeared to be found in both chicken and human cells. Gratifyingly, at a similar time, genetic analyses of yeast topoisomerase II mutations showed that cells died in the absence of this protein, specifically during mitosis as cells tried unsuccessfully to segregate their entangled chromosomes. Immunocytochemical and genetic avenues had converged to reach the same critical conclusion about this crucial enzyme.

DNA topoisomerase II has long been a chemotherapeutic target in the fight against cancer. Understanding its role in chromosome architecture in dividing cells helps to make sense as to why it may be an effective target, and furthermore, suggests that other proteins with similar critical roles in chromosome structure and behavior may also be possible chemotherapeutic targets in the future.

Identification of Other Proteins Playing Roles in Chromosome Dynamics

Another powerful system that began to be exploited in the 1980s was the use of concentrated cytosolic extracts prepared from *Xenopus laevis* eggs. Depending on the manipulation of the collected eggs, "interphasic" or "mitotic" extracts could be generated and then utilized to study DNA replication, cell cycle enzymatic machinery, spindle assembly, and also, chromosome condensation. The incredible stockpiling of components essential for the first rapid cleavage divisions of embryogenesis meant that exogenous DNA (e.g., plasmid, phage, demembranated *Xenopus* sperm, or human nuclei) added to such extracts could be remodeled into mitotic chromosome-like structures—with the subsequent identification of newly associated proteins.

Using this approach, a "condensin" complex was identified by Hirano and colleagues. This was a complex of five proteins: a heterodimer of large 115–165 kDa proteins associated with three additional, putative regulatory subunits. The heterodimeric proteins appeared to each contain five structural domains: an N-terminal globular domain with a Walker-A (NTP binding) motif, a C-terminal globular domain with a Walker-B (NTP-hydrolysis) motif, and two long (200–450 amino acids) internal coiled coils separated by a globular "hinge" region. This complex was associated with assembled chromosomes and was also shown to be essential for chromosome condensation *in vitro*. Similar complexes have since been identified biochemically in human and *Drosophila* cells.

A second serendipitous convergence of results arose from the comparison of the genes for the heterodimeric proteins in *Xenopus* condensin with genes identified from screens in yeast for proteins essential for the stability of mini chromosomes by Koshland and colleagues. The yeast *SMC1* gene bore a striking resemblance in organization to the heterodimeric proteins mentioned above. Based on this, SMC was

redefined as "structural maintenance of chromosomes." It is now apparent that all eukaryotes, from microsporidia to man, contained such genes that could be phylogenetically grouped into six subfamilies. Biochemically, these subfamilies of SMC proteins comprise at least three different heterodimeric complexes (along with non-SMC subunits), involved in sister chromatid cohesion (SMCs1/3), chromosome condensation (SMCs2/4), dosage compensation, and DNA repair (SMCs5/6). It should come as no surprise that the vertebrate Sc2 protein was identified as none other than SMC2 of the condensin complex.

While biochemical analysis using *Xenopus* extracts demonstrated that the condensin complex was required for chromosome condensation *in vitro*, paradoxically, the same did not appear to be true *in vivo*. Genetic mutation or dsRNA-mediated depletion in *Drosophila* cultured cells of SMC and non-SMC condensin subunits showed that chromosomes could indeed condense—but exhibited extreme difficulties in chromosome segregation in anaphase, apparently because resolution into individual chromatids was impaired. A similar defect was observed when the Sc2/SMC2 protein was lost from cultured chicken cells. Informatively, in this case, the clearly condensed mitotic chromosomes were missing a large number of additional "scaffold" components, implicating condensin in the proper assembly and structural integrity of mitotic chromosomes. These results clearly emphasized the need to examine and compare many different experimental systems with their own strengths and weaknesses.

Future prospects in this field are extremely exciting, as there now appear to be two distinct condensin complexes (I and II)—sharing SMCs2/4, but possessing different sets of non-SMC subunits. It has long been known that embryonic chromosomes are often longer and more flexible than those found in later somatic cells. Varying the ratio of condensin I to condensin II at different times of development may be one way to alter higher-order chromosome architecture.

How Is the Metaphase Chromosome Held Together?

Clearly the replicated sister chromatids must be held together until the metaphase to anaphase transition when they can be segregated to the two spindle poles. Close apposition is essential to allow for repair of any DNA damage using a sister chromatid as template, and to ensure that each new daughter cell gets a full diploid complement of the chromosomes. Cohesion between sister chromatids is established coincident with replication to facilitate appropriate alignment, and this is maintained until sisters are separated. One factor involved is the cohesin complex containing SMCs1/3 and non-SMC subunits.

Intriguing mechanistic differences between lower and higher eukaryotes have been observed. Proteolytic cleavage of a non-SMC cohesin subunit is responsible for the lengthwise separation of sister chromatids in yeast, but the process is more complicated in higher eukaryotes. Enzymatic phosphorylation of the cohesin complex is required to remove the bulk of these proteins from the length of the chromatid arms during condensation—perhaps facilitating resolution of sister chromatids, but the final separation of sisters at the centromere occurs as it does in yeast—with the cleavage of a non-SMC subunit. Clearly, the activity of cohesin and condensin, along with topoisomerase II, must be coordinated in some way as cells enter mitosis. A variant of cohesin is found in meiosis, presumably reflecting the requirement for sister chromatids to stay together through meiosis I, with only homologues separating from one another.

How to Control Chromosome Dynamics During the Cell Cycle: Checkpoints

The appropriate cohesion and condensation of chromosomes is of no use if it does not happen at the right time. The coordination of the chromosomal events of mitosis with the rearrangement of the cytoskeleton is critical if chromosomes are to be partitioned accurately. In order for a cell to achieve this, "checkpoints" must be navigated ensuring that a previous event, upon which a subsequent process is dependent, has occurred with high fidelity. The checkpoints that a cell must pass through include:

1. ensuring that DNA has been fully replicated once and only once in the cell cycle,
2. ensuring that any damage to the DNA has fully and accurately repaired, and
3. ensuring that the two kinetochores of each chromosome are not only attached to microtubule fibers, but that they are connected to opposing poles.

Only when each checkpoint has been satisfied can the cell proceed to the next stage, culminating finally in the precise distribution of genetic material to two new daughter cells. How the structural elements discussed in this article interface with checkpoint machinery is still to be understood.

Reversing the Process: Postsegregation Decondensation

After chromosome segregation and nuclear envelope reformation, the extreme condensation reached during

metaphase must be reversed to facilitate transcription and DNA replication in actively cycling cells. As a corollary, terminally differentiated cells that are not transcriptionally active or cycling (e.g., erythrocytes in certain species) have highly condensed nuclei. How the chromatin is decondensed, and how active this process is, remains unclear. DNA topoisomerase II is proteolytically degraded at the end of mitosis, and the mitosis-specific phosphorylation of histone H3 is removed. Indeed, certain proteins essential for DNA replication, though dispersed during metaphase, are assembled back onto chromosomes during anaphase. While correlated, these events are not necessarily causal to the process of chromosome decondensation. Probably other structural proteins (e.g., subunits of the condensin complex) are also degraded or regulated through differential localization or post-translational modification.

Listening to the Metaphase Chromosome

Hitching a Ride: The Chromosome Passengers

Naïvely, it is easy to think of the metaphase chromosome as an isolated, almost inert entity—likened by Mazia in 1961 to the corpse at a funeral: the reason for the proceedings, but hardly taking an active part in them! We know that there is very little, if any, transcription during mitosis—so in terms of gene expression, the mitotic chromosome is mute. However, with regard to the dynamic structural events occurring during mitosis, the chromosome has a lot to say.

In the 1980s, Earnshaw and colleagues discovered a very interesting class of proteins among polypeptides fractionating with the insoluble chromosome scaffold. The founding member of this class of "chromosome passengers" (INCENP—for inner centromere protein) exhibited a localization all along chromosome arms early during chromosome condensation, and then became restricted to the region between centromeres prior to the separation of sister chromatids. Dramatically the chromosome passengers then transfer to the spindle midzone during anaphase, before finally being discarded in the mitotic trashcan (the midbody) at the end of cell division. There are now at least three other proteins exhibiting this striking localization, two of them (survivin and aurora B kinase) residing in a complex with INCENP. Why should this complex track along chromosome arms to the inner centromere, only to then transfer to the microtubules? The localization presumably reflects the assorted substrates that must be phosphorylated at different times of mitosis (e.g., early—histone H3, late—regulatory light chain of myosin). In addition, localization of the chromosome passengers reflects a demonstrated role in orchestrating cytokinesis. One of the surest ways to place these proteins at the point of the future cleavage furrow is to have them mark the precise site of chromosome segregation—exactly where the cleavage furrow should ingress without entrapping chromosomes during cytokinesis.

Mitotic Chromosome Architecture Is Coordinated with DNA Replication and Repair

The ability to perform a cytological analysis in an organism amenable to genetic analysis allows the examination of mutations that visibly affect the process of chromosome condensation and segregation. Such an analysis is possible in *Drosophila* as the chromosomes are big enough to observe easily by light microscopy in diploid, mitotically active cells at different times of development. While genetic analysis in yeast is highly sophisticated, the cells themselves are extremely small and it is difficult to visualize native chromosome structure. Therefore, work in *Drosophila* has complemented biochemical approaches in *Xenopus*, genetic analyses in yeast, and cytological analysis in higher eukaryotic cultured cells.

Specifically, the identification of *Drosophila* mutations disrupting mitotic chromosome structure has significantly highlighted a cell's need to coordinate the accurate duplication and repair of chromosomes with subsequent mitotic condensation. *A priori*, one might expect that mutations in replication proteins might result solely in an S phase arrest. However, mutations of three subunits of the origin recognition complex result not only in replication defects as expected, but also in unexpectedly irregularly condensed chromosomes during metaphase. The regions that are inadequately condensed have replicated abnormally late, suggesting that the factors or machinery required for condensation may somehow be "templated" during S phase. ORC may act as a landing pad for factors other than those essential for DNA replication. In addition, mutations in RFC4 (replication factor C, subunit 4) result in pulverized or prematurely separated (albeit properly condensed) chromosomes, in addition to anticipated replication defects. These observations make sense when one takes into account that there are at least three different "RFC" complexes. While sharing a core of four small subunits, the large subunit can be exchanged thereby resulting in different complexes essential for DNA replication, DNA repair, and cohesion between sister chromatids. Thus, novel roles have been elucidated for proteins identified initially for their functions in DNA replication and repair.

Concluding Comments and Future Prospects

This article has highlighted the importance of diverse experimental approaches to the identification of proteins and analysis of mitotic chromosome dynamics and behavior. State-of-the-art genomics and proteomics avenues are currently supplementing genetic, cell biological, and biochemical approaches to expand the identification of components essential for the formation and function of the metaphase chromosome. How these proteins may be regulated during the normal development of an organism or during the progression of disease states are provocative questions to be addressed in the next decades.

See Also the Following Articles

Cell Cycle: Control of Entry and Progression Through S Phase • Cell Cycle: DNA Damage Checkpoints • Cell Cycle: Mitotic Checkpoint • Centromeres • Chromatin Remodeling • Chromatin: Physical Organization • Chromosome Organization and Structure, Overview • DNA Topoisomerases: Type II • Mitosis • Nuclear Organization, Chromatin Structure, and Gene Silencing • Telomeres: Maintenance and Replication

Glossary

chromatid Once a chromosome has replicated, it is composed of two identical sister chromatids, which are held together until the metaphase to anaphase transition when each chromatid of a pair is pulled via microtubules to opposing spindle poles.

chromosome A linear, stable fragment of the genome with one centromere and telomeres at each end. The genomic DNA of a eukaryotic organism is divided into a number of individual chromosomes (from one in the jumper ant *Myrmecia pilosula* to more than 600 in the fern *Ophioglossum reticulatum*). In contrast, prokaryotic genomes generally are found in a single piece of DNA.

chromosome passenger Term for the extremely dynamic localization during mitosis of a number of proteins (many of which are found in a common complex). While these proteins localize to chromosome arms early in mitosis, they are then restricted to the region between the centromeres of sister chromatids. At the metaphase to anaphase transition, they leave the chromosome only to associate with the microtubules, presaging formation of the cleavage furrow.

cohesin A complex of two different SMC proteins (of the SMC1 and SMC3 subfamilies) along with non-SMC subunits that appear to have regulatory roles. The function of the complex in chromatid cohesion is differentially regulated in lower (proteolytic cleavage of one non-SMC subunit) and higher eukaryotes (regulation by phosphorylation in addition to cleavage).

condensin A complex of two different SMC proteins (of the SMC2 and SMC4 subfamilies) along with non-SMC subunits that appear to have regulatory roles. The complex has been implicated in chromosome condensation *in vitro*, and in chromosome resolution and structural integrity *in vivo*.

DNA topoisomerase II An ATP-dependent homodimeric enzyme capable of making a double-stranded break in the DNA, and passing a strand through this break before religating the cleaved strand of DNA. Such activity is required for the decatenation or separation of replicated and entwined sister chromatids.

SMC Abbreviation for "structural maintenance of chromosomes." While prokaryotes have a single SMC gene responsible for forming a homodimer, eukaryotes have six subfamilies of these genes. Different combinations of heterodimers are important for sister chromatid cohesion (SMCs1/3), chromosome condensation (SMCs2/4), dosage compensation, and DNA repair (SMCs5/6). These proteins, when dimerized, have ATPase activity by virtue of bringing together N (NTP binding) and C termini (NTP hydrolysis). The intervening part of the molecule contains two extended coiled-coils separated by a globular hinge.

Further Reading

Cobbe, N., and Heck, M. M. S. (2004). The evolution of SMC proteins: Phylogenetic analysis and structural implications. *Mol. Biol. Evol.* **21**, 332–347.

Nasmyth, K. (2001). Disseminating the genome: Joining, resolving, and separating sister chromatids during mitosis and meiosis. *Ann. Rev. Genetics* **35**, 673–745.

Pollard, T. D., and Earnshaw, W. C. (2002). *Cell Biology*. Saunders, Philadelphia.

Sumner, A. T. (2003). *Chromosomes: Organization and Function*. Blackwell Publishing, Oxford.

Swedlow, J. R., and Hirano, T. (2003). The making of the mitotic chromosome: Modern insights into classical questions. *Mol. Cell* **11**, 557–569.

Biography

Margarete Heck is a Wellcome Trust Senior Research Fellow at the University of Edinburgh, Wellcome Trust Centre for Cell Biology, Scotland. She was awarded her Ph.D. from Johns Hopkins University and performed her postdoctoral work at the Carnegie Institute of Washington. Her principal research interests focus on chromosome organization and dynamics, predominantly utilizing *Drosophila* as a model organism. The Heck laboratory has exploited both "forward" and "reverse" genetic technologies to identify gene products that are essential for normal chromosome structure and function in *Drosophila*; intriguing human orthologues are examined further.

Sharron Vass has been working as a Research Associate and Ph.D. student in the Heck laboratory; her research is focused on cohesion of sister chromatids during the cell cycle.

Methyl-CpG-Binding Proteins

David G. Skalnik
Indiana University, Indianapolis, Indiana, USA

The development of multicellular organisms requires the generation of a variety of terminally differentiated cell types from a common set of totipotent stem cells. Integral to this process is the phenomenon of cell memory (e.g., a liver cell gives rise to progeny liver cells upon cell division, rather than kidney or spleen cells). At the molecular level, cell memory derives from distinct patterns of gene expression that are correlated with each type of cell lineage. However, nearly all somatic cells in a multicellular organism contain the same genome. The term epigenetics refers to heritable patterns of gene expression that occur in the absence of altered DNA sequence, and represents the underlying molecular mechanism for cell memory. The CpG dinucleotide represents an important regulatory component of mammalian genomes. The cytosine of this dinucleotide serves as the target of DNA methyltransferases, which catalyze the formation of 5-methylcytosine, a critical epigenetic modification of DNA. Methylated DNA is associated with transcriptionally inactive genes and is generally tightly packaged as heterochromatin, while actively expressed genes are generally hypomethylated and present in a more open euchromatin configuration. Methyl-CpG-binding proteins contribute to both the formation of heterochromatin and the repression of transcription.

Epigenetic Regulation of Gene Expression

The DNA of higher eukaryotes is found tightly associated with proteins *in vivo*. In fact, at least 50% of the mass of a chromosome is contributed by proteins. Although originally thought to provide primarily a packaging function, it is now appreciated that chromatin structure is highly dynamic, and plays a critical function in the epigenetic regulation of gene expression. It is necessary to understand the nature of chromatin structure to appreciate the function of methyl-CpG-binding proteins.

Nucleosomes

The primary level of chromatin structure is the nucleosome, in which a DNA double helix is wrapped twice around a core octamer of eight histone protein molecules (two copies each of histone H2a, H2b, H3, and H4). Nucleosomes are separated by short linkers of DNA, and ~200 base pairs of DNA are present in each nucleosome repeat. Chromatin in this configuration is referred to as a "bead-on-a-string" structure, or euchromatin, and can be transcriptionally active. Additional packaging of nucleosomes into a 30 nm helical array is found in heterochromatin, which is transcriptionally inactive, and is also tightly associated with another species of histone (H1).

Histone Code

Determination of the structure of the nucleosome revealed that the amino terminus of each histone molecule extends away from the octamer core. These histone tails are sites of covalent modification, such as phosphorylation, acetylation, and methylation. At least 30 distinct sites of histone covalent modification have been identified, and many of these are associated specifically with either euchromatin or heterochromatin (Figure 1). The sum of histone modifications found in chromatin is referred to as the histone code, and provides important regulatory information with respect to chromatin structure and ultimately gene expression. For example, acetylated histones are found preferentially in euchromatin. The net acetylation state of a specific region of chromatin is the result of balance between the action of histone acetyltransferases (HATs) and histone deacetylases (HDACs). Similarly, methylated lysine 4 of histone H3 is found in euchromatin, while heterochromatin preferentially contains methylated lysine 9 of histone H3. Lysine residues in histone proteins can be mono-, di-, or trimethylated. Posttranslationally modified histone molecules can also serve as binding sites for proteins implicated in the control of chromatin structure. For example, methylated lysine 9 of histone H3 serves as a binding site for the heterochromatin-associated protein HP1, which recruits a histone methyltransferase to the chromatin. This leads to the methylation of adjacent histone H3-lysine 9 residues, formation of additional HP1-binding sites, and spreading of the heterochromatin configuration.

Histone H2A	Histone H2B	Histone H3	Histone H4
Ser 1, P	Lys 5, Ac	Arg 2, Me	Ser 1, P
Lys 5, Ac	Lys 12, Ac	Lys 4, Me	Arg 3, Me
Lys 9, Ac	Lys 15, Ac	Lys 9, Me	Lys 5, Ac
Lys 119, Ub	Lys 20, Ac	Ser 10, P	Lys 8, Ac
	Lys 24, Ac	Lys 14, Ac	Lys 12, Ac
	Lys 123, Ub	Arg 17, Me	Lys 16, Ac
		Lys 18, Ac	Lys 20, Me
		Lys 23, Ac	
		Arg 26, Me	
		Lys 27, Me	
		Ser 28, P	
		Lys, 36, Me	
		Lys 79, Me	

FIGURE 1 Covalent modifications of histones. Thirty covalent modifications that contribute to the histone code are summarized. For each species of histone protein, the amino acid residue, position, and type of modification are presented. Me, mono-, di-, or trimethylation; P, phosphorylation; Ub, ubiquitation; Ac, acetylation.

Cytosine Methylation

Another covalent modification associated with heterochromatin and repression of gene expression is cytosine methylation, which occurs in the DNA double helix in the context of the 5′-CpG-3′ dinucleotide (where p denotes the phosphodiester linkage between the cytosine and guanine nucleotides). In mammalian genomes ~75% of the CpG motifs found are methylated, and these are concentrated in areas of repetitive DNA sequences. This dinucleotide is the target of DNA methyltransferase proteins, which catalyze the addition of a methyl group to the C5 position of the cytosine ring. DNA methyltransferase 1 is the major maintenance methyltransferase. It exhibits high affinity for hemi-methylated DNA (the immediate product of semi-conservative DNA replication), and catalyzes the addition of a methyl group to the CpG cytosines within the newly synthesized DNA strand. DNA methyltransferases 3a and 3b are *de novo* DNA methyltransferases that are responsible for establishing specific patterns of cytosine methylation during gametogenesis and early development. The mechanisms by which appropriate patterns of cytosine methylation are initially established are not well understood.

Functions of Cytosine Methylation

Appropriate patterns of cytosine methylation within DNA are essential for numerous biological processes. This is clearly reflected in the finding that mice lacking DNA methyltransferase gene(s) die prior to or shortly after birth.

Regulation of Gene Expression

As mentioned above, cytosine methylation is associated with heterochromatin and repressed gene expression. Because the majority of 5-methylcytosine is found in repetitive DNA elements, this may provide a defense mechanism against expression of parasitic DNA. Indeed, loss of appropriate cytosine methylation results in the induction of repetitive DNA expression. Maintenance of repetitive elements in heterochromatin configuration may also be important for chromosome stability by preventing homologous recombination between repetitive element sequences.

X-Chromosome Inactivation

X-chromosome inactivation refers to the irreversible inactivation during early embryonic development of one of the X-chromosomes present in each cell of a female. The inactive X-chromosome becomes heavily methylated at CpG motifs and takes on a heterochromatin configuration.

Genomic Imprinting

Distinct patterns of cytosine methylation are established throughout the genome during spermatogenesis and oogenesis, leading to parent-of-origin epigenetic marks that distinguish maternally derived from paternally derived gene alleles. Such genomic imprinting results in a uni-allelic pattern of gene expression. Genomic imprinting is essential for normal development, as zygotes carrying two sets of paternal or two sets of maternal alleles fail to develop normally, even though they carry an appropriate diploid complement of the DNA genome. To date ~50 mammalian genes have been identified that exhibit genomic imprinting.

Cancer

A large number of DNA mutations in oncogenes and tumor suppressor genes have been identified in cancer cells. More recently, it has been recognized that cancer cells also exhibit epigenetic aberrations, including global cytosine hypomethylation, as well as hypermethylation of CpG motifs specifically within the promoters of tumor suppressor genes.

Methyl-CpG-Binding Proteins

The function of methylated CpG motifs is mediated in part by methyl-CpG-binding proteins, which specifically bind to DNA at sites of methyl-CpG and affect transcription rates and local chromatin structure. A small family of proteins share a common DNA-binding domain, the methyl-CpG-binding domain (MBD) (Figure 2).

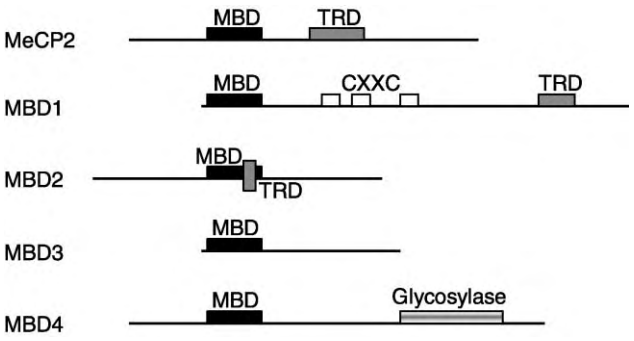

FIGURE 2 Schematic comparison of the MBD family of proteins. The conserved methyl-CpG binding domains (MBD) present in each protein are aligned. TRD, transcriptional repression domain.

MeCP2

MeCP2 is the founding member of the MBD protein family. It localizes to heterochromatin *in vivo*, and represses transcription via a carboxyl terminus transcriptional repression domain (TRD). MeCP2 also contains an amino terminus MBD DNA-binding domain. One mechanism for MeCP2-mediated transcriptional repression appears to be regulation of chromatin structure, as the TRD of MeCP2 interacts with a co-repressor that contains an HDAC. Disruption of the X-chromosome-linked MeCP2 gene in mice leads to premature death, and mutations in the human MeCP2 gene causes Rett syndrome, a progressive neurodegenerative disease found nearly exclusively in girls. The severity of symptoms in Rett syndrome depends on the exact nature of mutation present in the MeCP2 gene (most of which alter the sequence of the MBD or TRD domains), and the mosaic pattern of mutant gene expression resulting from random X-chromosome inactivation.

MBD1

Similar to MeCP2, MBD1 contains an amino terminus MBD DNA-binding domain and a carboxyl terminus TRD, although the TRD exhibits no sequence similarity to the MeCP2 TRD. MBD1 binds methylated DNA targets and represses gene expression. Various isoforms of MBD1 produced by differential RNA splicing additionally contain two or three CXXC domains, a cysteine-rich motif also found in DNA methyltransferase 1, human trithorax (HRX), and CpG-binding protein (CGBP). The CXXC domain constitutes the DNA-binding domain of CGBP, and is responsible for that factor's binding specificity for unmethylated CpG motifs. Similarly, HRX also binds unmethylated-CpG motifs, and the third CXXC domain of MBD1 is responsible for this factor's ability to bind unmethylated target sequences and repress transcription. The significance of the CXXC domain for MBD1 function is unclear, as it is not required for binding to sites of methyl-CpG motifs.

MBD2 AND MBD3

MBD2 and MBD3 are the most structurally related members of the MBD family, sharing 75% similarity over the entire length of MBD3, the shortest member of the family. MBD2 contains an additional 140-amino acid amino terminus extension. Despite this structural similarity, these MBD proteins exhibit quite dissimilar properties. MBD2 binds to methylated DNA and represses transcription via overlapping MBD and TRD domains. MBD2 interacts with HDAC1, and is a component of the methyl-DNA-binding complex MeCP1. The ability of MBD2 to repress transcription is sensitive to inhibitors of HDAC activity, suggesting a mechanism for cross-talk between cytosine methylation and chromatin structure. Surprisingly, mice lacking the MBD2 gene are viable despite lacking the MeCP1 complex. In contrast, MBD3 contains a divergent MBD domain and fails to interact directly with methylated DNA. However, similar to MeCP2, MBD3 is a component of a co-repressor complex. The importance of MBD3 is illustrated by the finding that mice lacking an MBD3 gene fail to develop to birth.

MBD4

MBD4 is an unusual member of the MBD protein family, as it apparently plays no role in transcriptional repression. Rather, it functions as a DNA-repair protein. Cytosine exhibits a propensity to spontaneously deaminate to form uracil (Figure 3). Cells contain DNA-repair enzymes (e.g., -uracil DNA glycosylase) that recognize a uracil base in DNA as a site of damage, and excise this nucleotide to permit replacement with cytosine. This may explain the presence of thymidine in DNA rather than uracil, as it would be more difficult for a cell to recognize a site of cytosine deamination if uracil were a normal nucleotide used for encoding genetic information in DNA. However, deamination of 5-methylcytosine leads to the formation of thymidine. It is this rate of spontaneous deamination that leads to the relative rarity of the CpG dinucleotide in mammalian genomes (only 5–10% of the expected frequency). Conversely, CpG motifs near widely expressed genes are usually unmethylated, and hence avoid this mutagenic pressure. This is hypothesized to explain the clustering of unmethylated CpG motifs in CpG islands near the promoters of ~50% of mammalian genes. The MBD domain of MBD4 binds with highest affinity to methylated CG/TG mismatched sequences, and the protein also contains a glycosylase activity in its carboxyl terminus which is able to remove the

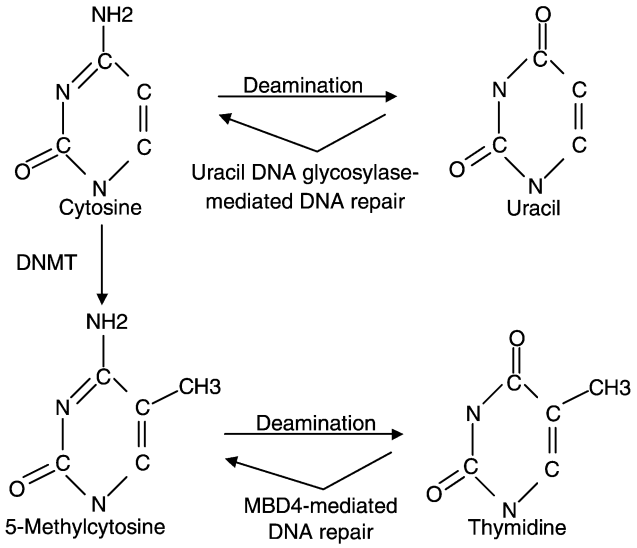

FIGURE 3 Summary of chemical relationships between cytosine, 5-methylcytosine, uracil, and thymidine, including how these species inter-convert *in vivo*. DNMT, DNA methyltransferases.

mismatched thymidine base from DNA to permit replacement with cytosine. The biological significance of this enzymatic activity is illustrated by an elevated rate of mutation at CpG motifs and increased tumorigenesis in mice lacking MBD4.

Cross-Talk between DNA Methylation and Chromatin Structure

The nature of epigenetic modifications associated with transcriptionally active or inactive genomic loci is now well established. Current investigations are focused on the regulation of these modifications. How does a cell choose which regions of DNA to methylate and/or assemble into heterochromatin? Recently, it has become clear that DNA methylation and chromatin structure are highly interdependent epigenetic processes. For example, perturbations of the cellular machinery responsible for nucleosome remodeling or histone modifications also result in aberrations in the pattern of cytosine methylation. Conversely, the association of MBD family members with chromatin-modifying enzymes (e.g., -HDACs) suggests a mechanism whereby cytosine methylation may provide an epigenetic mark that permits targeted recruitment of chromatin-remodeling enzymes to specific genomic loci. Hence, cytosine methylation patterns and the histone code may represent mutually reinforcing processes that lead to the stable maintenance of chromatin packaging and gene expression patterns characteristic of cellular memory.

See Also the Following Articles

Chromatin: Physical Organization • Nuclear Organization, Chromatin Structure, and Gene Silencing

Glossary

CpG island Region of DNA containing a cluster of unmethylated CpG dinucleotides, usually found near promoters of actively expressed genes.

epigenetics Heritable patterns of gene expression that occur in the absence of altered DNA sequence.

euchromatin Open form of chromatin associated with transcriptionally active genes.

genomic imprinting Phenomenon whereby maternally derived and paternally derived alleles of a gene exhibit distinct expression patterns as a result of distinct epigenetic modifications established during gametogenesis.

heterochromatin Highly compact form of transcriptionally inactive chromatin.

Further Reading

Ballestar, E., and Wolffe, A. P. (2001). Methyl-CpG-binding proteins: Targeting specific gene repression. *Euro. J. Biochem.* **268**, 1–6.

Felsenfeld, G., and Groudine, M. (2003). Controlling the double helix. *Nature* **421**, 448–453.

Jaenisch, R., and Bird, A. (2003). Epigenetic regulation of gene expression: How the genome integrates intrinsic and environmental signals. *Nat. Genet.* **33**, 245–254.

Jorgensen, H. F., and Bird, A. (2002). MeCP2 and other methyl-CpG-binding proteins. *Mental Retardation and Developmental Disabilities Rev. Res.* **8**, pp. 87–93.

Nakao, M. (2001). Epigenetics: Interaction of DNA methylation and chromatin. *Gene* **278**, 25–31.

Wade, P. A. (2001a). Methyl CpG-binding proteins and transcriptional repression. *Bioessays* **23**, 1131–1137.

Wade, P. A. (2001b). Methyl CpG binding proteins coupling chromatin architecture to gene regulation. *Oncogene* **20**, 3166–3173.

Biography

Dr. David G. Skalnik is a professor of pediatrics and biochemistry and molecular biology at the Indiana University School of Medicine. His principal research interest is the epigenetic regulation of chromatin structure and gene expression during mammalian development. He holds the Ph.D. from Stanford University and received his postdoctoral training at The Children's Hospital, Harvard Medical School. His laboratory group cloned CpG-binding protein, which binds to unmethylated CpG motifs and is required for early development and maintenance of normal patterns of cytosine methylation.

Microtubule-Associated Proteins

Nobutaka Hirokawa
University of Tokyo, Tokyo, Japan

Reiko Takemura
Okinaka Memorial Institute for Medical Research, Tokyo, Japan

Microtubules are formed by polymerization of α- and β-tubulin. They are intrinsically in dynamic turnover state, subject to treadmilling and dynamic instability. Microtubule-associated proteins (MAPs) are a heterogeneous group of proteins that have microtubule-binding domains. MAPs are abundantly expressed in the brain, and historically MAPs (e.g., MAP1, MAP2, and tau) derived from the brain have been studied extensively. MAP4 is ubiquitously expressed. These classical MAPs are filamentous proteins of various lengths, ranging from 50 to 185 nm. They have microtubule-binding domain and the projection domain that extends as filamentous structure. By binding along the side of microtubules, they stabilize microtubules. In addition, by extending the projection domain from the microtubule surface, they produce microtubule bundles of various densities. Tau and MAP2C predominantly expressed in the axon produce microtubule bundles of ~20 nm distances. MAP2 predominantly expressed in the dendrite produces microtubule bundles of ~65 nm distances. The microtubule bundles produced by tau/MAP2C and MAP2 resemble microtubule domains in axons and dendrites, respectively. These microtubule bundles are extended from the cell as axon- or dendrite-like processes. Therefore, MAPs serve as determinants of microtubule organization within the cell, particularly in neurons. There are some other groups of newly identified MAPs, and some of them destabilize microtubules. Binding of MAPs to microtubules is regulated by phosphorylation. In some neurodegenerative diseases including Alzheimer's disease, hyperphosphorylated tau precipitates as filaments on its own and may be one of the important factors to determine the progress of the disease.

Classical Microtubule-Associated Proteins

Microtubules are formed by polymerization of α- and β-tubulin. Microtubules play important roles in organizing and maintaining the shape of the cell, and also act as tracks for the transport of membranous organelles and macromolecules. So-called motor proteins (kinesin superfamily proteins and dynein superfamily proteins) are involved in the transport processes and they use the energy derived from the hydrolysis of ATP. Microtubule-associated proteins (MAPs) bind to microtubules without a requirement for nucleotide involvement, and organize the spatial arrangement of microtubules within the cell; they also regulate the polymerization of microtubules. Historically, MAPs have been isolated from the mammalian brain by their property that they remain bound to microtubules through repeated cycle of polymerization and depolymerization. The quick-freeze, deep-etch microscopy reveals that in neurons, there are abundant filamentous structures of various length associated with microtubules. These filamentous structures were proven to be mainly composed of MAPs (Figures 1 and 2). These MAPs have been studied extensively, and we term these well-characterized MAPs as classical MAPs. The major part of this article will be spent on these classical MAPs. Some other MAPs have been known and some new MAPs have been identified recently. These will be dealt with in relevant places. Classical MAPs include MAP1A, MAP1B, MAP2A, MAP2B, MAP2C, and tau (from mammalian brains) and MAP4 (found ubiquitously) (Table I). All these MAPs are fibrous molecules of different lengths, ranging from 50 to 185 nm, and form filamentous projections from the microtubule surface. First, the basic biochemical properties and their expression patterns will be described for each of the classical MAPs.

MAP1A and MAP1B

MAP1A and MAP1B are high-molecular-weight, heat-labile, filamentous proteins of ~350 and 320 kDa on SDS-PAGE. MAP1A and MAP1B are transcribed from the separate genes. MAP1B has also been called MAP1x or MAP5. The protein originally called MAP1C turned out to be cytoplasmic dynein. Therefore, it is not usually included in MAPs. MAP1A encodes protein of 2774 amino acid residues, and MAP1B encodes protein of

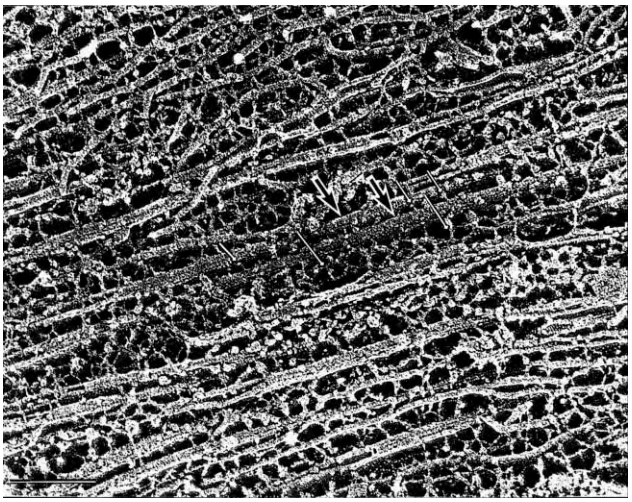

FIGURE 1 Axonal cytoskeleton observed by quick-freeze, deep-etch electron microscopy. Between microtubules (thick black arrows), short crosslinkers (short arrows) and longer crosslinkers are found. Reproduced from Hirokawa, N. (1991). Molecular architecture and dynamics of the neuronal cytoskeleton. In *Neuronal Cytoskeleton* (R. D. Burgoyne, ed.) pp. 5–74. With permission of Wiley-Liss, Inc., New York.

2464 amino acid residues. Rotary-shadowing electron microscopy reveals that MAP1A and MAP1B are highly elongated, flexible molecule of ~150–185 nm in length. Both MAP1A and MAP1B have associated light chains. Interestingly, the light chains, LC2 and LC1, are encoded at the C-terminal portion of MAP1A and MAP1B molecules, respectively. At the N-terminal portion of both MAP1A and MAP1B molecules, there is a domain

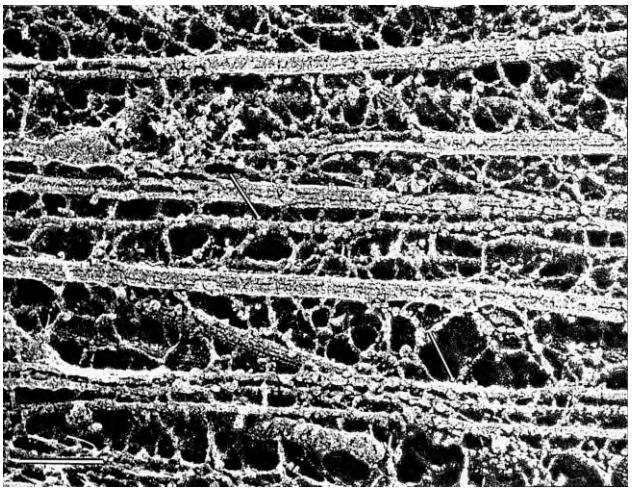

FIGURE 2 Dendritic cytoskeleton observed by quick-freeze, deep-etch electron microscopy. Between microtubules, and between microtubules and neurofilaments (arrows), long crosslinkers are found. Reproduced from Hirokawa, N. (1991). Molecular architecture and dynamics of the neuronal cytoskeleton. In *Neuronal Cytoskeleton* (R. D. Burgoyne, ed.) pp. 5–74. With permission of Wiley-Liss, Inc., New York.

enriched in the positively charged amino acids and contains the short motif (KKEX), repeated 11 and 21 times in MAP1A and MAP1B (Table I and Figure 3). This domain serves as microtubule-binding domain, and interacts with C terminus of tubulin, which has a large number of acidic residues. Both MAP1A and MAP1B form filamentous structures associated with microtubules in neurons.

MAP1A and MAP1B are predominantly expressed in neuron, although a smaller amount may be expressed in other tissues as well. There is a developmental regulation in the expression of MAP1. MAP1A is more abundantly expressed in the adult, and MAP1B is more abundantly expressed in the developing nervous system. In fact, the expression of these two proteins appears to be complementary to each other. In the rat brain development, the level of MAP1B expression is highest at the first few postnatal days, when many neurons are extending their axons. Thereafter, the expression of MAP1B declines. In contrast, the expression of MAP1A is very low at this period, but the level of its expression increases thereafter, and reaches its maximal level in adults. There is a spatial difference in the expression of MAP1B and MAP1A. MAP1B is predominantly expressed in the developing axon, although smaller amount is found in the dendrite of juvenile and mature neurons. In contrast, MAP1A is abundantly expressed in the mature dendrites, with the smaller amount of expression at the axons.

MAP2A, MAP2B, AND MAP2C

MAP2A and MAP2B were identified as high-molecular-weight, filamentous protein of ~280 and 270 kDa on SDS-PAGE. MAP2A and MAP2B have been known to be heat stable, which is rather unique considering the high molecular weight of these proteins. MAP2B encodes proteins of 1828 amino acid residues; MAP2A is a splice variant having additional exon of 83 amino acid residues in the middle of the molecule. Rotary-shadowing electron microscopy revealed that MAP2A and MAP2B are highly elongated, flexible molecules of ~100 nm in length. Subsequent study revealed that there is additional low-molecular-weight form, MAP2C, which is ~70 kDa on SDS-PAGE. In MAP2C, the N- and C-terminal ends are joined, resulting in the protein of 467 amino acid residues. The unique characteristic of MAP2 is that they have binding domain for the regulatory subunit of type II cyclic AMP-dependent kinase on the N terminus. The C-terminal portion of the MAP2 forms the microtubule-binding domain (Table I and Figure 3). The sequence of this region does not have homology to MAP1, but it has unique imperfect tandem repeats of 31–32 amino acids; similar repeats of 18 amino acids joined by less-conserved, variable "spacers" of

TABLE I

Characteristics of Classical MAPs

MAPs	App. mol. weight on SDS-PAGE (KDa)	# of amino acids	Length of isolated molecule (nm)	Distance in microtubule bundles (nm)	Microtubule-binding domain	Developmental and topological expression pattern
MAP1A[a]	350	2774	150–185		N-terminal KKEX repeats	Abundant in mature dendrite
MAP1B[a]	320	2464	150–185		Same as above	Abundant in developing axon
MAP2A[b]	280	1911	~100	~65	C-terminal tandem repeats	Specific to developing dendrite
MAP2B[b]	270	1828	~100	~65	Same as above	Specific to developing and mature dendrite
MAP2C[b]	70	467		~20	Same as above	Abundant in developing axon and dendrite
tau[c]	55–65	352–441	~50	~20	Same as above	Abundant in developing and mature axon
MAP4	210	1072			Same as above	Ubiquitously expressed

[a] MAP1A and MAP1B are transcribed from separate genes.
[b] MAP2A, MAP2B, MAP2C are splice variants.
[c] Six isoforms of tau are splice variants.

13–14 amino acids. These repeats bind to the C-terminal ends of tubulin. These imperfect tandem repeats are also used in the microtubule-binding domain of tau and MAP4, which also reside in the C-terminal part of the molecule. Each molecule has three or four repeats. The central portion of the MAP2A and MAP2B molecule corresponds to the extended arm. Lacking this arm portion, MAP2C is revealed as

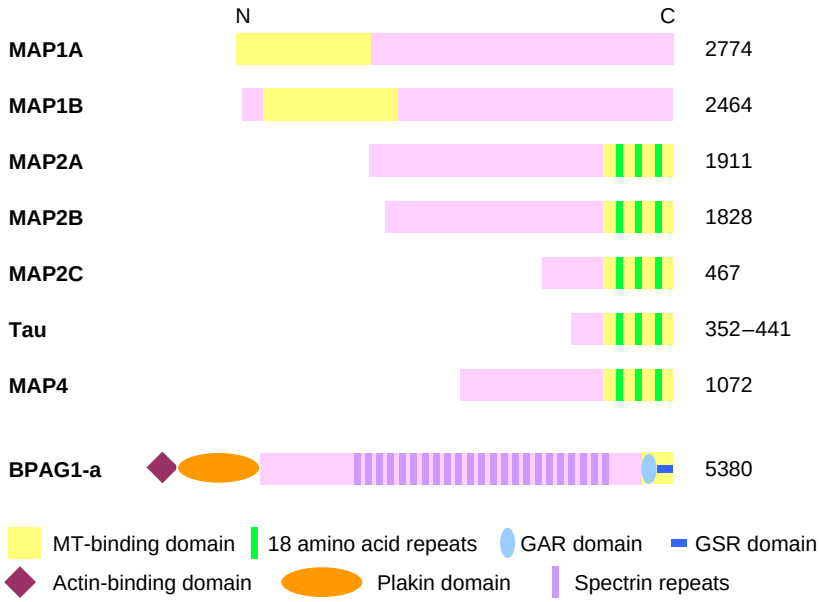

FIGURE 3 Schematic diagram of representative MAPs. Domain structures of MAP1A, MAP1B, MAP2A, MAP2B, MAP2C, tau, MAP4, and BPAG1-a are shown. Numbers of amino acids of representative molecules are shown on the right. MAP1A and MAP1B have a microtubule-binding domain on the N-terminal portion, which is a domain enriched in the positively charged amino acids and contains the short motif (KKEX), repeated 11 and 21 times in MAP1A and MAP1B, respectively. C-terminal portion serves as a projection domain. MAP2A, MAP2B, MAP2C, tau, and MAP4 have a microtubule-binding domain on the C-terminal portion, which is a unique imperfect tandem of three or four basic repeats of 31–32 amino acids, similar repeats of 18 amino acids joined by less conserved, variable "spacer" of 13–14 amino acids, and is quite well preserved among these MAPs. Molecules with three repeats are depicted in the drawing. BPAG-1a, one of the new MAPs, has actin-binding domain, plakin domain, spectrin-repeat-containing rod domain, GAR domain, and GSR domain. The GAR and the GSR domain together constitute the microtubule-binding domain in BPAG1-a as well as in MCAF. In plakin, which is not depicted here, GAR domain is missing and GSR domain at the C-terminal portion can associate with microtubules. Not drawn to scale.

filamentous molecule ~50 nm in length by the rotary-shadowing electron microscopy.

MAP2 is almost exclusively expressed in neurons. Importantly, MAP2A and MAP2B are specifically localized to the dendrites. It is often used as markers for dendrites. There is a developmental regulation of MAP2 expression. MAP2C is expressed in juvenile neuron; it is found in cell bodies, dendrites, and axons. MAP2A is expressed in the adult, and MAP2B is expressed throughout the developmental stage.

Tau

Tau was the first MAP purified from the brain. It is heat stable, consists of several bands of 55–65 kDa on SDS-PAGE. It is now known that tau consists of six isoforms (ranging from 352 to 441 amino acid residues), which are splice variants of single tau gene. In the C-terminal half of the molecule, tau has three or four tandem repeats of 31 or 32 amino acids, as described above, which serves as the microtubule-binding domain (Table I and Figure 3). In rotary-shadowing electron microscopy, tau forms filaments of ~50 nm in length. Tau forms ~20 nm short filamentous structures associated with microtubules. It is known that in the peripheral nervous system, additional isoform of 110 kDa is expressed. However, this isoform is less well characterized.

There is a developmental regulation of expression of tau isoforms. In the juvenile brain, only the three repeat isoforms are expressed, and in the adult brain, tau isoforms with both three and four repeats are expressed. Tau is posttranslationally modified by phosphorylation. A part of the heterogeneity of the tau bands on the SDS-PAGE results from phosphorylation. When antibodies that recognize all tau isoforms are used, tau is predominantly localized in the axon, with some expression in cell bodies and dendrites.

MAP4

Although MAP1, MAP2, and tau are rather abundantly expressed in the nervous system, their expression outside the nervous system is limited. MAP4 is a major MAP found outside the nervous system. It is a protein of 210 kDa on SDS-PAGE. MAP4 encodes protein of 1072 amino acid residues. It is composed of an N-terminal projection domain and a C-terminal microtubule-binding region, which has homology to the microtubule-binding domain of tau and MAP2 (Table I and Figure 3).

Control of Microtubule Dynamics

Microtubules are dynamic and unstable. By binding along the sides of the microtubules, MAPs control microtubule dynamics *in vitro* and *in vivo*. Many MAPs, including classical MAPs, stabilize microtubules. Classical MAPs were usually expressed predominantly in the nervous system. Microtubules in the neuron are usually much more stable than those in most interphase cells. Therefore, it is not surprising that one important function of classical MAPs is the stabilization of microtubules against disassembly. As described above, tau, MAP2, and MAP4 share conserved C-terminal three or four pseudorepeats, which serves as microtubule-binding domain. In tau, it is shown that one of these repeats bind to the tubulin C-terminal end, and other repeats bind to another internal site of tubulin. Therefore, these tandem repeats are likely to bind to microtubule in such a way to crosslink adjacent tubulin subunits and stabilize microtubules against disassembly. These bindings are controlled by phosphorylation. Both tau and MAP2 have many residues, which can be phosphorylated.

There are other modes of regulation of microtubule dynamics by MAPs. Microtubule is usually disassembled in the cold temperature. Stable tubule-only polypeptide

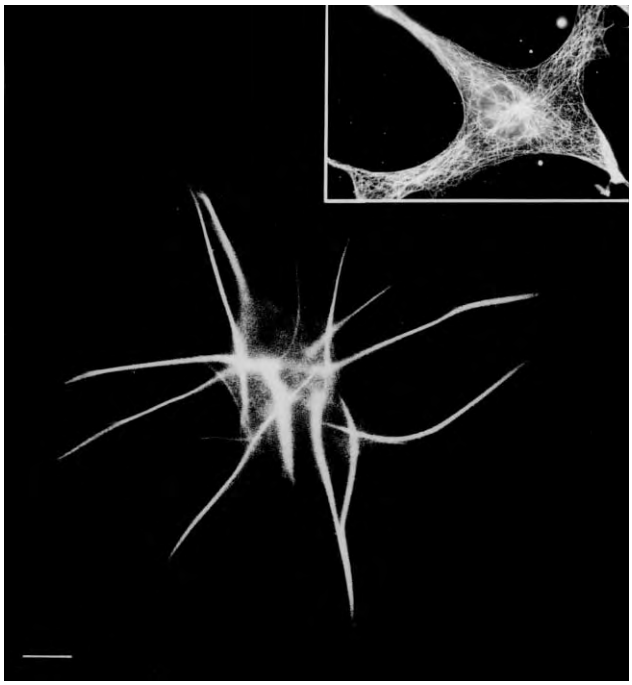

FIGURE 4 Microtubule bundle formation in fibroblasts transfected with tau cDNA. Immunofluorescence using anti-tubulin antibody. Long processes are formed and microtubule bundles extend into the processes. Upper right corner is the immunofluorescence of nontransfected control fibroblasts stained with antitubulin antibody. Microtubules radiate in various direction from the microtubule-organizing center near the nucleus. Reproduced from Kanai, Y., Takemura, R., Oshima, T., Mon, H., Ihara, Y., Yanagisawa, M., Masaki, T., and Hirokawa, N. (1989). Expression of multiple tau iso-forms and microtubule bundle formation in fibroblasts transfected with a single tau cDNA. *J. Cell Biol.* **109**, 1173–1184 with permission of The Rockefeller University Press.

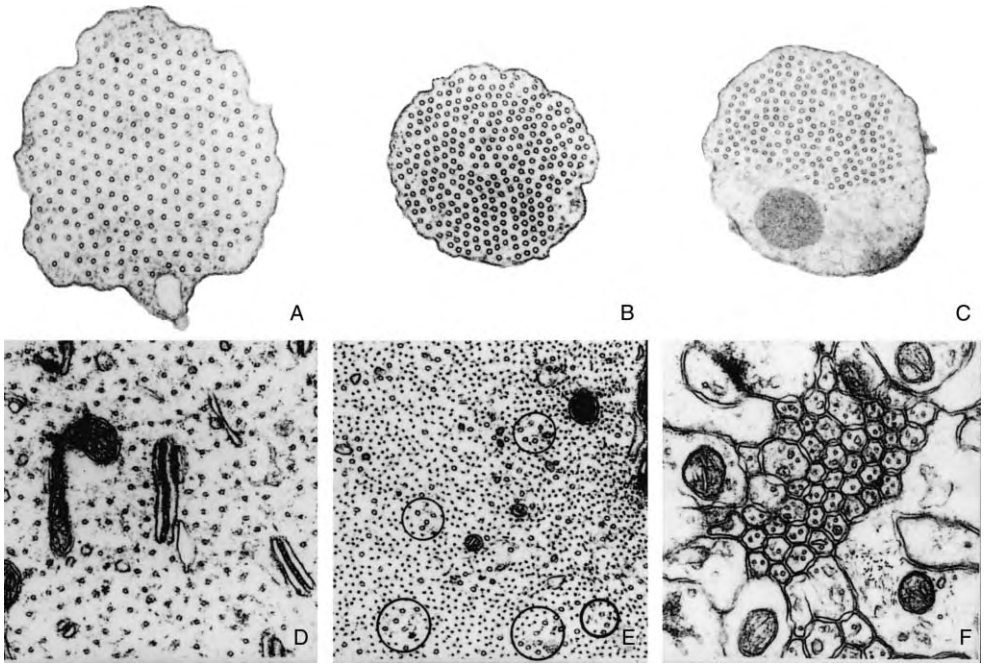

FIGURE 5 Cross-section electron micrographs of processes induced by transfection of MAP2 (A), MAP2C (B), and tau (C) into Sf 9 cells. Each MAP2 forms microtubule bundles, but the organization is different. When MAP2 is transfected, wall-to-wall distance between nearest adjacent microtubules is ~65 nm, which is similar to the microtubule organization of Purkinje cell dendrite in the cerebellum (D). In contrast, when MAP2C or tau are transfected, the distance between microtubules is ~20 nm, which is similar to the microtubule organization of large myelinated axons in the spinal cord (inside the circle in (E)) or parallel fiber axons in the cerebellum (F). Reproduced from Chen, J., Kanai, Y., Cowan, N. J., and Hirokawa, N. (1992). Projection domains of MAP2 and tau determine spacings between microtubules in dendrites and axons. *Nature* **360**, 674–677 with permission of Nature.

(STOP) is a MAP known to stabilize microtubules against cold temperature. A few MAPs are also known to destabilize microtubules, including katanin, Op18, and stathmin. In addition to structural MAPs, some of the kinesin superfamily proteins belonging to KIF2 class also destabilize microtubules.

Bundling of Microtubules: MAPs and Neurite Outgrowth

Neuron extends axon and dendrites from the cell body. In the axon and dendrites, microtubules run in parallel, in longitudinal array. In the quick-freeze, deep-etch electron microscopy, it can be shown that microtubules are highly crosslinked by meshwork of fine filamentous structures in axons and dendrites (Figures 1 and 2). MAPs form these crosslinkers. Moreover, MAPs induce microtubule bundle formation and outgrowth of processes from the cell. When classical MAPs are transfected and overexpressed in the cells, such as fibroblast or Sf9 cells, unusual microtubule bundles are formed, and long processes very much like neurites can be induced (Figures 4 and 5).

In addition, MAPs determine the spacing between neighboring microtubules to be axon like or dendrite like. Namely, MAPs expressed in the axon, such as tau and MAP2C, produce microtubule bundles similar to those seen in the axon (wall-to-wall distance of neighboring microtubules, ~20 nm), and MAPs expressed in the dendrites, such as MAP2A and MAP2B, produce microtubule bundles similar to those seen in the dendrites (wall-to-wall distance of neighboring microtubules, ~65 nm) (Figure 5). Therefore, in addition to the stabilization of microtubules, projection domains of MAPs induce microtubule bundle formation, induce process outgrowth, and determine the spacing between microtubules.

Analysis of Transgenic and Knockout Mice: Relation of MAPs to Neurodegenerative Diseases

Recently, genetically altered mice gave some insights to the role of individual MAPs *in vivo*. In general, lack of MAP produces the expected effect, but the overall effect is rather limited. This implies that there is certain

overlap in the function of MAPs. In fact, when the double knockout mice were formed in the combination of two MAPs, the expected effect is much more severely observed. For example, in *tau* $^{-/-}$ mice, an effect on the microtubule stabilization and bundle formation in the axon was observed, but the effect is evident mainly in the small caliber axon. Likewise, in *MAP2* $^{-/-}$ mice, an effect on microtubule organization in dendrite is evident, but the effect is somewhat limited. However, when both tau and MAP1B, or both MAP1B and MAP2 are deleted, impaired microtubule bundle formation and outgrowth of axon or dendrite was markedly observed.

Tau has been implicated in the pathogenesis of certain cognitive neurodegenerative diseases. The diseases are sometimes grouped as tauopathies, which comprise a heterogeneous group of age-dependent cognitive disorders, including Alzheimer's disease. In these diseases, abnormally hyperphosphorylated tau forms filamentous aggregates within the cell. The aggregates do not contain microtubules, and the formation of aggregates is independent of microtubules. There is a loss of neurons in the affected brain area. In 1998, tau gene mutations were identified in patients with dementia and parkinsonism linked to chromosome 17 (FTDP-17). Transgenic mice with these mutations have been developed for an analysis.

New MAPs

Recently, a family of proteins of a very high molecular weight, plakin family, has been identified as crosslinker proteins that connect different cytoskeletal filaments. Some of the members, such as plectin, Bullous pemphigoid antigen 1 (BPAG1), and microtubule-actin crosslinking factor (MACF), have microtubule-binding domain, and they are likely to crosslink microtubule to intermediate filaments, or actin filaments. Microtubule-binding domain used in the plakin family proteins are of two kinds: Gas2-related (GAR) domain in BPAG1 and MACF; and glycine-serine-arginine (GSR) domain in plakin, BPAG1, and MACF (Figure 3). That these new crosslinkers play an important physiological role is suggested by the fact that mutations in these proteins cause neurological defects *in vivo*. For example, mutations in BPAG1 cause degeneration of sensory neurons, and mutation in MCAF cause deficits in axon outgrowth and dendritic sprouting.

See Also the Following Articles

Centrosomes and Microtubule Nucleation • Kinesins as Microtubule Disassembly Enzymes • Kinesin Superfamily Proteins

Glossary

axon Structure that transmits the signal from the cell body to the synaptic terminal. Single axon extends from the cell body. Microtubules and neurofilaments are major components of the axonal cytoskeleton. Microtubules in the axons are organized more densely than in the dendrites.

dendrite Structures that receive signals and transmit them to the direction of the cell body. Usually, multiple dendrites emanate from the cell body in "dendritic" shape. Microtubules are the major components of the dendritic cytoskeleton, and microtubules in the dendrites are organized more loosely than in the axon.

microtubule Filament of 25 nm diameter. Assembled from α- and β-tubulin subunits (55 kDa), it is actually a hollow cylinder (hence tubule) composed of 13 protofilaments. During mitosis, it forms a mitotic spindle. Compared to intermediate filaments (10 nm diameter), microtubules turn over much more dynamically. New subunits are added at the "plus" end, while subunits dissociate from the "minus" end (treadmilling). In addition, microtubules show the property called "dynamic instability," in which individual microtubules are either growing or shrinking and they stochastically switch between the two states.

Further Reading

Alberts, B., Johnson, A., Lewis, J., Raff, M., Roberts, K., and Walter, P. (2002). *Molecular Biology of the Cell.* Garland Publishing, New York.

Chen, J., Kanai, Y., Cowan, N. J., and Hirokawa, N. (1992). Projection domains of MAP2 and tau determine spacings between microtubules in dendrites and axons. *Nature* **360**, 674–677.

Desai, A., and Mitchison, T. J. (1997). Microtubule polymerization dynamics. *Annu. Rev. Cell Develop. Biol.* **13**, 83–117.

Garcia, M. L., and Cleveland, D. W. (2001). Going new places using an old MAP: tau, microtubules and human neurodegerative disease. *Curr. Opin. Cell Biol.* **13**, 41–48.

Hirokawa, N. (1991). Molecular architecture and dynamics of the neuronal cytoskeleton. In *Neuronal Cytoskeleton* (R. D. Burgoyne, ed.) pp. 5–74. Wiley-Liss, New York.

Hirokawa, N. (1994). Microtubule organization and dynamics dependent on microtubule-associated proteins. *Curr. Opin. Cell Biol.* **6**, 74–81.

Homma, N., Takei, Y., Tanaka, Y., Nakata, T., Terada, S., Kikkawa, M., Noda, Y., and Hirokawa, N. (2003). Kinesin superfamily protein 2A (KIF2A) functions in suppression of collateral branch extension. *Cell* **114**, 229–239.

Houseweart, M. K., and Cleveland, D. W. (1999). Cytoskeletal linkers: New MAPs for old destinations. *Curr. Biol.* **9**, R864–R866.

Hyams, J. S., and Lloyd, C. W. (1994). *Microtubules.* Wiley-Liss, New York.

Kanai, Y., Takemura, R., Oshima, T., Mori, H., Ihara, Y., Yanagisawa, M., Masaki, T., and Hirokawa, N. (1989). Expression of multiple tau isoforms and microtubule bundle formation in fibroblasts transfected with a single tau cDNA. *J. Cell Biol.* **109**, 1173–1184.

Leung, C. L., Green, K. J., and Liem, R. K. H. (2002). Plakins: A family of versatile cytolinker proteins. *Trends Cell Biol.* **12**, 37–45.

Takei, Y., Teng, J., Harada, A., and Hirokawa, N. (2000). Defects in axonal elongation and neuronal migration in mice with disrupted tau and map1b genes. *J. Cell Biol.* **150**, 989–1000.

Teng, J., Takei, Y., Harada, A., Nakata, T., Chen, J., and Hirokawa, N. (2001). Synergistic effects of MAP2 and MAP1B knockout in neuronal migration, dendritic outgrowth, and microtubule organization. *J. Cell Biol.* **155**, 65–76.

Biography

Nobutaka Hirokawa is Professor and Chair of Department of Cell Biology and Anatomy, and Dean of the School of Medicine, University of Tokyo. His principal research interests are organization of cytoskeletal structures in neurons and molecular motors involved in the intracellular transport. He holds an M.D. and Ph.D. from University of Tokyo. He developed the quick-freeze, deep-etch electron microscopy with Dr. John Heuser, and did pioneering work in elucidating the neuronal cytoskeleton in molecular detail, including the analysis of MAPs. He was also one of the first to tackle the analysis of kinesin motor molecules, and the first to clone multiple kinesin superfamily proteins from mammalian brain and to point out the importance of this motor protein family in mammalian intracellular transport.

Mitochondrial Auto-Antibodies

Harold Baum
King's College London, London, UK

Auto-antibodies are antibodies that bind specifically to self-constituents, and so would seem to be an anomaly of a system geared to respond to foreign molecules and be tolerant to self. The antigens that they may recognize encompass the spectrum from tissue specific to being common to all cell types. They may be pathogenic, disease-specific, and diagnostic, or of no clear significance. Auto-antibodies against mitochondrial components are illustrative of this range of characteristics, even to the extent that diseases characterized by them may be very specifically tissue localized. They have been extensively studied, and in the case of primary biliary cirrhosis (PBC) they have become a paradigm in the study of autoimmune diseases. A consideration of the mitochondrial auto-antibodies (AMA) characteristic of PBC is the major focus of this article.

Detection of Mitochondrial Auto-antibodies

Auto-antibodies (AMAs) have been detected by immunofluorescence (IFL) (where they are visualized as bright granular staining in cell types with high mitochondrial content), or by applying complement fixation tests (CFTs), enzyme-linked immunosorbant assays (ELISAs) or Western immunoblotting (IB) to tissue extracts, purified subcellular constituents or specific, recombinant mitochondrial species. Proof that mitochondria were the target of antibodies detected by such methods was provided in early studies, such as the landmark paper of Walker *et al.*, by the specific absorption of serum reactivity using preparations of mitochondria. It was subsequently recognized that AMAs recognizing different mitochondrial antigens might characterize different clinical conditions. The molecular identity of many, but not all, of these antigens is now established. Not all of these AMAs are detectable by all of the above methodologies. The preferred test in general diagnostic laboratories is IFL on a composite substrate of rodent tissues. In the research laboratory however, and where specific AMAs are under investigation, the preferred assays are ELISAs and IB, using purified or recombinant antigens, or synthetic peptides.

The M-Classification of AMAs

In the early 1980s an arbitrary classification of AMAs, as anti-M1-9, was developed, mainly by Berg's group in Tübingen, on the basis of patterns of IFL and/or properties of target antigens as determined by various assay procedures. It is noteworthy that in all these cases the AMAs are not species specific. Whilst this M-classification is now somewhat obsolete, and does not include all known mitochondrial targets for AMAs, it is still sufficiently in common use for it to be helpful in listing reactivities (Table I).

Anti-M1 AMAs and Cardiolipin

The M1 pattern of IFL is exhibited exclusively with sera of patients with untreated secondary syphilis. The reaction is abolished completely by absorption of sera with cardiolipin, the characteristic phospholipid of the mitochondrial inner membrane. However, the simple conclusion that anti-M1 antibodies are specific for cardiolipin is complicated by another observation. The earlier diagnostic test for syphilis, the Wasserman reaction, is based on CFTs against cardiolipin. However, not all sera positive in this test show an M1 pattern of IFL. Moreover, Wasserman-positive sera that are negative for M1 give a strongly positive ELISA reaction against purified cardiolipin, whereas anti-M1 AMAs are scarcely detectable by ELISAs using purified cardiolipin, whilst they react strongly in ELISAs against sub-mitochondrial particles. Interestingly, M1-negative, Wasserman positive sera are frequently false positives for syphilis and may instead reflect collagen disorders such as systemic lupus erythmatosus (SLE). It seems likely that these anomalies reflect antibodies to different epitopes in cardiolipin, the different assay systems exposing different conformations of the same molecule. (Indeed some of the anti-cardiolipin antibodies in M1-negative sera of SLE patients may be detected as antibodies against nucleic acids, cross-reactivity arising by virtue of the similarity between the glycerol phosphate arrays in cardiolipin arrays and the ribose phosphate backbone of nucleic acids.) Anti-M1 AMAs probably recognize a more native form of the

TABLE I

The M-Classification of Specificities of Mitochondrial Auto-Antibodies

Antigen	Occurrence of auto-antibodies
M1	Secondary syphilis
M2	PBC
M3	Phenopyrazone-induced pseudolupus syndrome
M4	PBC (prognostic indicator? "mixed form"?)
M5	Subgroup of systemic lupus; anti-phospholipid syndrome
M6	Iproniazid-induced hepatitis
M7	Cardiomyopathies
M8	PBC (prognostic indicator?)
M9[a]	PBC (prognostic indicator?)

[a] NB. In fact this antigenic specificity is not mitochondrial (see text).

lipid, as it exists in the intact mitochondrial membrane (and may arise from immunological cross-reactivity with a membrane constituent of the agent of syphilis, *Treponema pallidum*).

Anti-M2 AMAs

The most important mitochondrial auto-antibodies, anti-M2 AMAs, exhibit a characteristic pattern of IFL and were initially defined both by their disease specificity and by properties of the antigen that they recognized. This was shown to be trypsin sensitive and associated with (but detachable from) the inner surface of the inner membrane of all mitochondria tested, from human to fungal. Anti-M2 antibodies were also shown to cross-react with several bacteria, anti-mitochondrial activity, for example, being absorbed out of PBC sera by *E. coli*.

Association with Primary Biliary Cirrhosis

Primary biliary cirrhosis (PBC) is a chronic, cholestatic liver disease, predominantly affecting middle-aged women. It is characterized by spontaneous inflammatory damage to the epithelial cells of the bile duct (BEC). Whilst the clinical presentation and disease progression are variable, and the disease may be virtually asymptomatic for many years, the end stage is cirrhotic liver failure, and the disease is the second most frequent reason for liver transplantation in the developed World. Although the most clinically significant pathology relates to the liver, PBC is actually a multi-system disorder, and may feature lachrymal salivary and pancreatic hyposecretion. The paper by Walker, referred to earlier, and many subsequent studies, demonstrated clearly that PBC is characterized by high and persistent titers of AMAs of a kind not seen in normal subjects or other diseases. Since the description of this close association, the detection of this class of AMAs, designated as anti-M2, has acted as a powerful diagnostic tool. Anti-M2 antibodies (both IgG and IgM) are found in up to 98% of PBC patients, the precise figure depending on the sensitivity of the assay used. Interestingly, these AMAs are not restricted to serum, being found in the bile, saliva, and urine of patients with PBC. Moreover anti-M2 AMAs have turned out to be predictors for the disease; asymptomatic subjects, accidentally having been identified as being positive for anti-M2 AMAs, are frequently found to develop the disease subsequently.

Identity of M2 Antigens

Western IB soon revealed that M2 actually consists of a "family" of up to seven co-purifying peptides of differing molecular weight, encompassing a spectrum from around 75 to 36 kDa. Different PBC sera demonstrated different patterns of reactivity against these (see Table II), but virtually all recognized a predominant peptide that was eventually identified as being the E2 component (dihydrolipoamide acetyltransferase) of the pyruvate dehydrogenase complex. Thereafter, it soon became clear that the other M2 antigens were also constituents of one or other of the 2-oxo-acid dehydrogenase multienzyme complexes (OADCs): pyruvate, 2-oxoglutarate and branched-chain 2-oxo acid dehydrogenase complexes (PDC, OGDC, and BCOADC, respectively). Each of the three complexes occupies a key position in energy metabolism in aerobic cells. Each consists of multiple copies of at least three enzymes (E1, E2, and E3), which are encoded by genes in the nucleus and separately imported into mitochondria for assembly into high molecular weight multimers localized to the matrix aspect of the inner membrane. The structural core of these complexes is provided by E2 (the acyltranferase), to which multiple copies of E1

TABLE II

Frequency of Occurrence of Anti-M2 AMA to Specific Antigens in PBC

Complex	Subunit	Apparent M_r (kD[a])	AMA-positive (%)[a]
PDC	E1α	41	53
PDC	E1β	34–36	4
PDC	E2	70–74	96
PDC	E3BP (X)	50–56	96
OGDC	E2	48–50	74
BCOADC	E1α	46	50
BCOADC	E2	50–52	56
All	E2's		50
At least one	E2		98

[a] Approximate average of published data using defined antigens.

(the decarboxylating dehydrogenase) and E3 (dihydrolipoamide dehydrogenase) are noncovalently bound. The E2 enzymes are notably homologous in structure as between different complexes and different species (e.g., there is 52% similarity in sequence as between rat PDC-E2 and OGDC-E2 of *E. coli*). E3 is common to all three complexes, whereas E1 and E2 are unique to each complex. PDC contains a fourth polypeptide with a structural role, the E3-binding protein (E3BP), once termed protein X. This contains a lysine-linked lipoate moiety, located in a domain that is strongly homologous to corresponding domains in PDC-E2.

In view of this latter homology, it is not surprising that all sera recognizing PDC-E2 also bind E3BP, and that the antibodies to the two peptides are cross-reactive. The other members of the M2 "family" were shown to include the E2's of OGDC and BCOADC. However, notwithstanding the general similarity between the respective E2's, there seems only to be a limited degree of antibody cross-reactivity between them and only about 50% of PBC sera recognize all three. (On the other hand AMA against a particular E2 recognize that peptide in mitochondria of all species tested.) About half of all PBC sera also recognize the α-subunit of PDH-E1, (with the β-subunit being rarely recognized). Additionally, human auto-antibodies, specific for BCOADC-E1α, were found, in a more recent study, in the sera of almost half of the PBC patients tested. A summary of frequency of occurrence of AMAs to individual members of the M2 "family" is given in Table II. The E3 component, a common subunit of all three complexes, is not listed in this table. This is because, whilst specifically anti-mammalian E3 antibodies are found in PBC, these are in relatively low amount and are not totally disease specific.

Enzyme Inhibition by Anti-M2 AMAs

A notable characteristic of AMAs in PBC sera is their capacity to block the catalytic function of the 2-OAD multienzyme complexes *in vitro*. For example, sera with AMAs recognizing PDC-E2 rapidly inhibit PDC at dilutions of 1/500–1/5000, much of this inhibitory activity being removed by pre-absorption of the sera with recombinant PDC-E2. Similarly, affinity-purified antibody against PDC-E1α also specifically inhibits PDC reactivity.

Possible Target for Anti-M2 AMAs on Bile Duct Cells

What may be a key fact relating to the occurrence and disease association of AMAs in PBC is the reactivity that has been observed of anti-M2 AMAs (and of selected monoclonal antibodies against PDC-E2) with some component at the surface of a subset of BEC in livers of PBC patients. Conflicting views are that this antigen is an inappropriately localized component of PDC, or that it is a different molecule with a sequence similarity to a dominant B-cell epitope. In view of the potentially fundamental significance of the presence of a disease specific antigen at the site of tissue damage, it is regrettable that no definitive identification has yet been made.

Cross-Reactivity of Anti-M2 AMAs Against Bacteria

Early reports of cross-reactivity of PBC-specific AMAs against a variety of bacterial species were confirmed in studies of reactivity against individual microbial E2's of the three OADC complexes. (There is no homology between microbial and corresponding mitochondrial E1's; neither is there reactivity of E1-specific AMAs against bacteria.) Further evidence of cross-reactivity is that antibodies raised in rabbits, against bacterial mutants having fragile cell walls, were reported to react with a typical M2 pattern on IB against mitochondria. However, detailed absorption/elution and other studies have led to a current view that, whilst there is indeed some cross-reactivity between corresponding enzymes, PBC sera contain distinct sets of antibodies against mitochondrial and microbial OADCs respectively.

Anti-M2 AMAs and Chronic Bacterial Infection

In a study of women with asymptomatic recurrent bacteriuria, a majority of the patients were found to be weakly positive for antibodies to PDC-E2 by immunoblot, in the absence of evidence of liver disease. AMAs were also detected by ELISAs and IB in 43% of patients with active pulmonary tuberculosis and in patients with leprosy. However, it is not clear whether what is being detected in these cases are "true" AMAs or antibodies against corresponding microbial enzymes that are partially cross-reactive against mitochondrial peptides.

Epitopes Recognized by Anti-M2 AMAs

Most studies on B-cell epitopes in PBC have focused on the E2 antigens. Here it is clear that the main immunogenic regions are the lipoyl domains. Short peptides (e.g., of around 20 residues in length) encompassing the lipoyl-binding site are rather weakly antigenic, and full immunological reactivity is only seen for much longer peptides. Thus, for PDC-E2, the 93-residue sequence, 128–221, of the inner lipoyl domain is required for maximal antibody binding. The outer lipoyl domain, although containing a highly homologous region around the lysine residue that is bound to lipoate, is only weakly antigenic. These and other findings suggest that the overall epitopes are conformational

ones, but centered on the lipoyl-binding sites. The strong homologies between these domains among the three OADCs, and between mitochondrial and microbial enzymes, may account for partial cross-reactivities, with extended flanking regions being responsible for specificity and full reactivity. There is some disagreement as to whether lipoyl residues themselves are necessary for full reactivity, but corresponding peptides not containing lipoate are undoubtedly antigenic.

Stimulus for Anti-M2 AMAs Production in PBC

There is good evidence that B-cell clones producing AMAs are maximally stimulated, and it is noteworthy that the dominant epitopes of the $CD4^+$ T-cells, that provide the help for antibody production, are short peptides of the lipoyl-binding domain. (Similar peptides are also the dominant epitopes of the cytotoxic $CD8^+$ T-cells that infiltrate the bile ducts in this disease.) What then is the antigenic drive in PBC? It cannot be a secondary response to tissue damage, since M2 AMAs are not detectable in many other destructive diseases of the liver.

As mentioned earlier, chronic microbial infection may be characterized by low titers of anti-M2 AMAs. There is also epidemiological evidence of association between recurrent urinary tract infection (UTI) and PBC. Moreover, UTI is particularly common in middle-aged women, the group in which PBC most commonly occurs. So it is suggested that the initial stimulus for an immune reaction directed specifically at the E2's of the OADCs, (and E3BP of PDC), is chronic exposure, in the context of co-stimulatory signals (and perhaps a particular genetic background), to microbial peptides that share strong sequence similarities with the lipoyl-binding domains at the core of the dominant epitopes. Expansion of reactivity and specificity to incorporate the entire domain, and then also to recognize E1 subunits, would be by epitope-spreading. Such "microbial mimics" might not necessarily be the homologous OADCs. A number of other bacterial and viral peptides have been identified with strong sequence similarities to the "core" peptidyl epitope of PDC-E2, and have been shown, by ELISAs, to react specifically with PBC sera, the antibodies being cross-reactive with that "core peptide."

One other important fact needs bearing in mind in any speculation about antigenic drive. Once it is established, it persists. Even after liver transplantation high titers of anti-M2 AMAs are still found.

Role of AMAs in the Pathogenesis of PBC

Anti-M2 AMAs are so focused in specificity and so disease specific that it has to be assumed that they are relevant to disease pathogenesis, but most workers have concluded that it is T-cells rather than the antibodies themselves that are the direct cause of tissue damage. For example, high titers of AMAs can be raised in experimental animals, e.g., by immunization with recombinant human PDC-E2, with no evidence of liver damage even after a prolonged period, and only a minority of patients exhibit unambiguous recurrence of PBC following liver transplantation, despite the persistence of AMAs. However in the former case, fine specificities of the AMAs may not be identical to those of the PBC-specific antibodies, and in the latter immunosuppressive drugs may be protective. If the AMAs were to be directly cytotoxic, it might be by inhibition of mitochondrial function following uptake into BEC. Such uptake might be mediated by binding to the elusive antigen that might be the primary recognition target at the surface of BEC.

Anti-M3 AMAs and Pseudolupus Syndrome

Some time ago it was recognized that there was an association between the taking of the drug phenopyrazone, for cardiovascular disease, and a disorder designated as pseudolupus syndrome (PLE). This syndrome was characterized by AMAs that could be demonstrated by IFL, CFTs, and ELISAs, but not by IB. The antigen, classified as M3, was shown to be associated with the outer mitochondrial membrane, and was not organ specific. High titers of anti-M3 were detectable during the acute phase of the disease, but they declined on cessation of treatment with phenopyrazone, a drug that has since been withdrawn. No further cases of PLE have been reported, and the M3 antigen has not been further characterized. However, it has been speculated that it might be a drug-metabolizing enzyme such as monoamine oxidase (MAO), rendered immunogenic through tight binding to the drug.

Anti-M4 AMAs and Sulfite Oxidase

In addition to anti-M2, another complement-fixing antibody has been shown to be closely associated with PBC. The target antigen in this case, designated as M4, was found to co-purify with the outer mitochondrial membrane and be insensitive to trypsin. It was identified as being sulfite oxidase, an enzyme of the intermembrane space, a precursor of which binds to the outer membrane. Sulfite oxidase in an evolutionarily highly conserved enzyme, also found in bacteria, but enzyme activity does not seem to be inhibited by M4-positive PBC sera and the identity of the antigen is now in some doubt. The clinical significance of the detection of anti-M4 in addition to anti-M2 AMA is controversial. There have been claims that anti-M4 AMAs reflect a "mixed form" pathology of PBC with histological

features of chronic active hepatitis, and/or that their detection is an indicator of poorer prognosis towards the end stage of the disease. However, other workers have questioned their specificity in relation to PBC, suggesting that these, and anti-M8/M9, are nonspecific indicators of high serum levels of IgG.

Anti-M5 AMAs and Phospholipid

Mention has been made that false Wasserman-positive tests may reflect a different conformation of cardiolipin than that recognized by the M1-positive, syphilis-specific pattern of IFL, and are frequently associated with SLE. Such false-positive reactions often correlate with a characteristic IFL pattern, designated as M5. This pattern is seen both with a subset of SLE and patients with antiphospholipid syndrome, characterized by thrombocytopenia and recurrent fetal loss. Whilst anti-M5 reactivity may be absorbed out by inner mitochondrial membranes, no specific reactivities have been detected against any mitochondrial proteins, and it is concluded that M5 is some form of phospholipid, although the reactivity is not absorbed out by cardiolipin liposomes or cardiolipin–glycoprotein complexes.

Anti-M6 AMAs and Immuno-Allergic Hepatitis

Anti-M6 AMAs have been detected, by a characteristic pattern of IFL, in sera of patients who had developed acute hepatitis associated with taking the anti-depressive drug iproniazid. The M6 antigen could be detected by CFTs and ELISAs, was partially tissue specific (liver–kidney), and was associated with the inner membrane. The antigen has now been identified as MAO-B and the activity of this enzyme against substrates such as tyramine is inhibited by these AMAs. As MAO-B is irreversibly inhibited by iproniazid, the stimulus for AMA production may arise from metabolite/enzyme haptenization as also suggested, above, in the case of anti-M3.

Anti-M7 AMAs and Flavoenzymes

Around 60% of patients with acute myocarditits and 30% of patients with cardiopathy of unknown etiology exhibit a class of AMAs designated as anti-M7. The antibodies in acute myocarditis are predominantly of the IgM class and disappear on recovery, whilst in chronic disease they are IgG and persist. Such antibodies are not seen in coronary artery conditions and have been considered as reflecting infective disease. The target antigen was originally reported as being heart specific and tightly associated with the inner mitochondrial membrane, but it is now recognized that this class of AMA is directed generally against flavoenzymes. Hence, in heart mitochondria a dominant target is the flavoprotein of succinate dehydrogenase, whilst in liver it includes sarcosine dehydrogenase and dimethylglycine dehydrogenase.

Anti-M8 AMAs and Anti-M9 "AMAs" in PBC

Two other sets of AMAs have been claimed to be specific to PBC, and like anti-M4, important in prognosis of disease progression. One of these recognizes a mitochondrial target categorized as M8. This is an outer membrane, nonorgan-specific, trypsin-sensitive antigen, detectable by CFTs and ELISAs but not by IB. To date M8 is defined only by the protocol for its preparation. The other specificity, categorized as M9, was defined in terms of a trypsin-insensitive constituent of the inner membrane of liver mitochondria. However, it has since been identified as the nonmitochondrial, cytoplasmic enzyme, glycogen phosphorylase, which presumably co-purifies with inner-membrane fragments on ultracentrifugation. Hence, anti-M9 antibodies can no longer be considered as AMAs.

Other AMAs

Naturally Occurring Anti-Mitochondrial Antibodies

Sensitive detection methods reveal that sera of healthy individuals exhibit a spectrum of naturally occurring anti-mitochondrial antibodies (NOMAs), perhaps reflecting an arm of the normal immunoregulatory network, and/or a history of exposure to microbial antigens with structures that "mimic" those of mitochondrial constituents. Where NOMA reactivities against particular antigens have been studied, their fine specificities have been shown to differ from those of disease-associated AMAs recognizing the same molecular species. Interestingly, it has been reported that there is a relative lack of NOMA in patients with PBC, which might be a clue to their normal role in immune regulation.

AMAs Arising from Tissue Damage

Following acute myocardial infarction, many patients demonstrate the short-term production of AMAs against human heart mitochondria. These cross-react against mitochondria from human skeletal muscle, but not with heart mitochondria of other species. Similarly, synovial B-cells in rheumatoid arthritis have been reported as producing AMAs, the finding being interpreted as reflecting local tissue destruction. Such an interpretation

may also apply to the demonstration, in insulin-dependent diabetes, of auto-antibodies against the mitochondrial enzyme of pancreatic β-islet cells, glycerophosphate dehydrogenase.

Pathogenetic AMAs against the Adenine Nucleotide Transporter

Myocarditis and dilated myocarditis are diseases related to viral infection, and (independently of the anti-M7 AMAs described above) are characterized by the production of organ-specific AMAs directed at the mitochondrial ADP/ATP carrier. These antibodies are cytotoxic when tested against guinea pig ventricular myocytes, and in mouse heart, where the transport activity of the carrier has been shown to decline in a manner related to the decrease of cardiac function. The production of these AMAs declines over a period of 2–3 months, and it has been speculated that the underlying mechanism might involve "molecular mimicry" with a viral constituent. However, they may arise as a secondary response to virally induced tissue injury.

See Also the Following Articles

Biliary Cirrhosis, Primary • Phospholipid Metabolism in Mammals • Pyruvate Dehydrogenase

Glossary

CD4$^+$-T cell T-lymphocyte, with a receptor recognizing a specific short peptide, derived from an antigen and presented by an antigen-presenting cell, and thereafter primed to help B-cells that also present that peptide to secrete antibodies against the antigen.

epitope The specific target recognized by a T-cell or antibody.

immunofluorescence A technique for detecting antibodies that bind to specific structures on tissue sections, by treatment with a fluorescently labeled, anti-immunoglobulin antibody.

lipoyl residue The amide of 6,8-dithio octanoic acid, the oxidized, disulfide form of which is reductively acylated in the catalytic cycle of the 2-oxoacid dehydrogenase complexes.

molecular mimicry Similarity in structure, either accidental or evolutionarily selected, between two antigens, leading to immunological cross-reactivity.

Further Reading

Bogdanos, D. P., Baum, H., Sharma, U. C., *et al.* (2001). Antibodies against homologous microbial caseinolytic proteases P characterize primary biliary cirrhosis. *J. Hepatol.* **36**, 14–21.

Gershwin, M. E., Ansari, A. A., Mackay, I. R., *et al.* (2000). Primary biliary cirrhosis: An orchestrated immune response against epithelial cells. *Immunol. Rev.* **174**, 210–225.

Haydon, G. H., and Neuberger, J. (2000). PBC: An infectious disease? *Gut* **47**, 586–588.

Mackay, I. R., Whittingham, S., Fida, S., *et al.* (2000). The peculiar autoimmunity of primary biliary cirrhosis. *Immunol. Rev.* **174**, 226–237.

Van de Water, J., Ishibashi, H., Coppel, R. L., *et al.* (2001). Molecular mimicry and primary biliary cirrhosis: Premises not promises. *Hepatology* **33**, 771–775.

Walker, J. G., Daniach, D., Roitt, I. M., and Sherlock, S. (1965). Serological tests in diagnosis of primary biliary cirrhosis. *Lancet* **39**, 827–831.

Yeaman, S. J., Kirby, J. A., and Jones, D. E. (2000). Autoreactive responses to pyruvate dehydrogenase complex in the pathogenesis of primary biliary cirrhosis. *Immunol. Rev.* **174**, 238–249.

Biography

Harold Baum is Emeritus Professor of Biochemistry and visiting professor in Immunology at King's College London, where he was previously Head of the School of Life, Basic Medical and Health Sciences. His current research is on mechanisms of autoimmune disease, but much of his earlier research was on mitochondrial bioenergetics. His Ph.D. was in chemistry from the University of Birmingham, United Kingdom, but he moved into Biochemistry following a postdoctoral year at the Institute for Enzyme Research in Madison, Wisconsin, where he was subsequently a visiting professor. In addition to his normal research output he is also known for having set metabolic pathways to traditional melodies in "The Biochemists' Songbook."

Mitochondrial Channels

M. Catia Sorgato and Alessandro Bertoli
University of Padova, Padova, Italy

Eukaryotic cells are living organisms surrounded by a surface membrane, which also house other membranes that define intracellular organelles. Membranes are lipidic structures impermeable to hydrophilic molecules (polar or charged); that is why they harbor proteins, called ion channels and carriers, catalyzing the life-requiring exchange of material between a cell and the external space, and between organelles and the cytoplasm. At variance from carriers, ion channels form aqueous pores crossing the lipid bilayer that allow the highly selective transmembrane passage of charged species, namely inorganic ions (e.g., Na^+, K^+, Ca^{2+}, Cl^-), with high potency (10^5–10^8 ions per second are transported by a single molecule); they also possess regulatory domains that open and close the pore upon specific stimuli (electric or chemical). Mitochondria are organelles composed of two membranes; channels may be present in either of the membranes. However, while channels in the outer membrane are justified by their overall high permeability, the presence of these entities in the inner membrane was unexpected in view of its implication in the process of oxidative phosphorylation that imposes an extremely controlled permeability to ions. After the initial phenomenological description, substantial advances in the functional (if not molecular) identification of several mitochondrial channels, disclose the possibility that they take part in crucial schemes of mitochondrial functionality, as well as in dramatic cell events.

Channels and Carriers in Mitochondrial Bioenergetics

According to the chemiosmotic principles, the energy-requiring synthesis of ATP, indispensable for the life of the cell, is driven by the inner membrane (IM)-spanning ATP-synthase complex that utilizes a high electrochemical proton gradient generated by the active proton translocation (from the inner compartment (matrix) outwardly) of other IM-enzyme complexes during substrates oxidation. As intuitively expected, mitochondria need to avoid dissipation of the proton gradient by uncontrolled fluxes of protons, and ions in general, toward the negatively charged matrix. Accordingly, such movements have been restricted to tightly regulated processes proceeding at a much lower rate than ions through channels, i.e., catalyzed by enzymes or carriers such as (1) the ATP-synthase; (2) the H^+-carrier that physiologically dissipates energy as heat in brown fat; and (3) carriers driving the accumulation of metabolic anion substrates, or aimed at counterbalancing the influx of positive charges, for example, carried by Ca^{2+} and K^+. A different reasoning applies to the outer membrane (OM) that houses no energy transducing apparatus, and hence develops no proton gradient. This excludes conceptual barriers for its ion permeability properties, and indeed the electric features of OM channels, the first to be identified in mitochondria, have led to assume that, rather than classical ion conducting elements, they act as principal regulated pathways for the intense exchange of molecules (with molecular mass up to 6–8 kDa) connecting the IM with the rest of the cell.

Functional and Molecular Aspects of Mitochondrial Channels

OM Channels

The voltage-dependent anion channel (VDAC, or mitochondrial porin) is one of the few mitochondrial channels with known primary structure. Its presence in all eukaryotes examined so far speaks in favor of a key role pertaining to this protein, and a single case of human pathology, plausibly linked to VDAC malfunction, has been reported. Extensive electrophysiologic studies (carried out by incorporating the purified protein in planar bilayers) have revealed that VDACs from different species have amazingly conserved biophysical properties. Paradigmatic is the symmetrical closure upon raising the transmembrane electric field, in that the large conductive (maximally open) state adopted by VDAC at low applied voltages (roughly between ± 10 mV) (Table I) is drastically reduced (albeit not nullified) as voltage is increased on both directions (positive and negative). Attainment of the lower conducting states, nicknamed "closed," parallels the change of the ionic selectivity from slightly anionic to cationic.

TABLE I

Main Mitochondrial Channels

Location	Maximal conductance (pS) (150 mM salt)	Putative role
Outer membrane		
VDAC	600–750 (1)[a]	Transport of metabolites
		Apoptosis
Unknown	~100–300 (2,3)	Transport of metabolites (?)
Tom40	1000 (1,2)	Protein import
MAC	2500 (2)	Apoptosis
Inner membrane		
K_{ATP}	9.7 (4)	Matrix volume regulation
mCS	107 (4)	
MCC (TIM)	1000 (2)	Protein import

[a] Used techniques: (1) lipid bilayers; (2) patch clamping of proteoliposomes; (3) patch clamping of intact mitochondria; and (4) patch clamping of mitoplasts.

Note. Table I does not include the PTP complex of the IM, likely to be involved in apoptosis, has not yet been conclusively identified neither electrophysiologically nor at the molecular level. However, from the permeability properties detected in intact mitochondria, PTP open state allows the translocation of molecules with mass up to 1.5 kDa.

Such features, in particular the voltage-dependent permeability, and other biochemical, and genetically based findings, have thus frequently suggested that, by acting as a molecular sieve, the protein regulates the cell metabolism, if not the process of oxidative phosphorylation.

Intriguingly, VDACs from different organisms show little conservation of the amino acid sequence. The almost overlapping electric picture has thus suggested that all VDACs acquire similar secondary structures. Indeed, prediction algorithms have proposed a general feature of the pore's wall formed by antiparallel β-sheets, with the hydrophilic amino acids expectedly facing the internal aqueous ion conducting space. A large body of electron microscopic data of fungal, and mammalian, VDAC crystals have also suggested that the channel crosses the membrane as a hollow cylinder, or with an oval structure, respectively, with an internal (lumen) 1.7–2.8 nm diameter that correlates well with the high conductances described in reconstituted systems. Yet, there are instances that may contradict the above hypothesis. For example, the yeast VDAC2 isoform (in yeast, as in other organisms, there is a VDAC-related multigene family), which can functionally replace VDAC1 in VDAC1-knockout cells, is apparently unable to form channels in planar bilayers.

Because VDAC is the most abundant OM protein, its conserved electric pattern in planar membranes was surprisingly never detected when applying a patch clamp electrode to intact mitochondria. Instead of the typical bell-shaped curve, the response of the macroscopic current (i.e., of the entire membrane) to positive and negative voltages was asymmetrical, while in no case was the behavior of analyzed single channels reminiscent of VDAC properties (Table I). Clearly, the picture emerging from *in situ* experiments suggests that either channels different from VDAC are the major contributors to the OM electric behavior, or that VDAC in native membranes is under the control of OM or intermembrane regulators that get lost in reconstitution experiments. As yet, the physiology and molecular structure of most of such channels are still missing, although, consistent with the OM concept, they are most likely to transport metabolites rather than only small ions. Finally, the only attempt to analyze mitochondria in its cellular context (at the presynaptic terminals of large neurons) has demonstrated that, especially during synapse activation, the OM displays intense electrical activities, which, however, do not resemble that of VDAC.

The electrophysiologic analysis of OM- (or IM-) containing proteoliposomes, and of some membrane components (in planar bilayers), has eventually proven the long-lasting hypothesis that most (~99%) mitochondrial proteins, nuclear-encoded and cytosolic-synthesized, reach their final destination by passing through large permeation pathways of mitochondrial membranes. Specifically, it has been found that both the purified multisubunit translocase of the OM (TOM) (which does not include VDAC), and the TOM component putatively involved in translocation, Tom40, form a pore with a large full open state (of around 1000 pS) and a slight preference for cations (Table I). These features, which are *per se* consistent with a role of TOM pore in allowing permeation of unfolded polypeptides, have been further substantiated by the disturbance provoked by cationic peptides mimicking the mitochondrial targeting domain of several proteins, possibly reflecting transient occlusions of the pore during the peptide translocation.

IM Channels

The *in situ* electric recording of the IM of isolated, intact mitochondria demands that the OM be removed first; this allows the expansion of the IM invaginations, and the formation of a vesicle (mitoplast) sufficiently large to be patch clamped. Except for one type of conductance (called mitochondrial mega (MMC) or multiconductance channel (MCC)) showing huge and unselective fluxes of ions, this strategy has been instrumental for the description of two main kinds of channels, distinguishable by several criteria, not the least by discrete conductance values (Table I). One channel, of around 10 pS, with no clear voltage dependence, translocates only K^+ (K_{ATP}), and is

modulated by physiologic effectors (it is active only at low matrix ATP). The other channel, of around 100 pS (named mitochondrial Centum pico-Siemens, mCS), is preferentially permeated by anions. Although several molecules apparently modulate the channel (nucleotides, Ca^{2+}, etc.), its most prominent feature is the voltage dependence that opens the channel at nonphysiologic (positive) matrix voltages, while it renders it inoperative (closed) at those high negative potentials normally sustained by mitochondria. Parenthetically, it is the powerful activity of mCS channels (found in many mammalian tissues), which accounts for the electric pattern of the entire IM, while most of the other described conductances, in the 15–130 pS range, may be rather safely attributed to mCS substates, or to experimentally induced variations of the K_{ATP} channel conductance.

To search for the role of IM channels, much experimentation has followed the concept that the IM transport of small ions may guarantee fundamental aspects of mitochondrial physiology, such as osmotic stability. Insight into such routes has been provided particularly by monitoring the osmotic swelling of isolated mitochondria that, under the used conditions, is the direct consequence of the ability of a specific solute to cross the IM. Several carrier-mediated pathways have been described, two of which are of interest in the context of ion channels' theme: the selective pathway for K^+ (K^+ uniport), and the pathway allowing the permeation of anions different from metabolites, adenine nucleotides, or phosphate (inner membrane anion channel, IMAC). The extensive biochemical and pharmacological characterization of these proteins (initially denominated channels for their high translocation rate, not because of their, as yet unknown, molecular nature) has led to the proposition that both are implicated in maintaining mitochondrial volume homeostasis. In fact, the similar action of physiologic (ATP) and drug molecules has sustained the functional identity between the K^+ uniport and K_{ATP} channels. With regard to their physiology, the enhancement of K^+ influx under the stressed condition of low-matrix ATP content renders the channel suitable at serving in the K^+ cycle-based volume regulatory mechanism, especially within the proposed control of mitochondrial oxidation rate by matrix volume changes. In addition, it has been shown that the same drugs, opening (cromakalin, diazoxide) or closing (glibenclamide, 5-hydroxydecanoate) mitochondrial K_{ATP} channels, enhance or abolish, respectively, the beneficial effects of ischemic preconditioning, a phase that protects the heart from ischemic injuries. These findings thus point to a cardioprotective role of K_{ATP} channels, although the actual means by which this is achieved have not yet been clarified.

Also in the case of IM anion permeation, accurate electrophysiological reinvestigations of mCS single channels, and of the entire IM, have provided substantial evidence for the functional homology of IMAC and mCS channels; both conduct anions of different valence, are active at alkaline internal (matrix) pH (i.e., such pH renders mCS channels operative also at negative matrix potentials), and are equally blocked by specific drugs. The particular conditions of IMAC activation in intact mitochondria have suggested that it mediates efflux of matrix anions, as part of the mechanism designed to protect against excessive swelling. However, more recently, by relying on pharmacological tests on isolated intact cardiomyocytes, it has been proposed that the opening of IMAC/mCS channels may trigger metabolic oscillations, observed when cells are deprived of substrates, which, at the mitochondrial level, give rise to periodic, redox-state transitions, and a continuous switching between dissipation and re-establishment of the proton gradient. As this phenomenon (if uncontrolled) is likely to provoke a whole set of excitability disturbances in the heart, including arrhythmias, mCS channels may thus become important targets of pharmacological heart treatments.

Similar to the TOM machinery, the reconstituted translocase of the IM (TIM) forms pores with that large conductance (of ~1000 pS) expected for protein transport (Table I). Complemented by immunologic approaches, this study has also suggested the functional (and molecular) identity of the MCC, originally described by patch clamping mitoplasts, with the TIM pore.

Involvement of Mitochondrial Channels in Cell Death Mechanisms

In the recent years, there have been increasing suggestions for a mitochondrial implication in regulating the life and death of the cell through the apoptotic process. Apoptosis is a naturally occurring programmed cell death essential for normal embryonic development and tissue homeostasis in adults. Expectedly, the process is controlled by a variety of factors, including members of the Bcl-2 family (e.g., the pro- and anti-apoptotic Bax and Bcl-2, respectively), and mitochondrial proteins of the intermembrane space (cytochrome *c*, endonuclease G, and others) released in the cytosol. By necessity, passage of these high mass molecules across the OM calls for a further increase of the already large membrane permeability. Accordingly, data have been presented involving either an enhancement of VDAC permeability by Bax, for example, or the capacity of Bax itself to form autonomous protein translocating pores. The latter may be identifiable with extremely large single-channel conductances (named mitochondrial apoptosis-induced channel, MAC) (Table I), recently observed by patch

clamping OM-containing proteoliposomes, especially because such activities are dependent on Bax presence, while rendered silent by Bcl-2 overexpression. However, several other observations point to a direct involvement of the mitochondrial IM, in that a dramatic increase of its permeability leads to loss of mitochondrial osmotic stability by excessive ions intake; in turn, this event provokes matrix swelling, OM disruption by the expanded IM, and release of intermembrane proteins. Such process, reported in isolated organelles and in cells challenged with apoptotic stimuli, is apparently caused by the opening of a huge and unselective IM pathway, known as the permeability transition pore (PTP), formed by a multisubunit complex that may include proteins located in both the IM and OM, e.g., cyclophilin D and the adenine nucleotide translocator, and VDAC, respectively. MMC (or MCC) has also been proposed as a PTP subunit, but its recent identification as a TIM component renders such candidacy unlikely.

See Also the Following Articles

Cell Death by Apoptosis and Necrosis • Chemiosmotic Theory • Mitochondrial Outer Membrane and the VDAC Channel

Glossary

conductance G Expressed in siemens (S = ampere/volt (A/V)) is the ratio between the electric current and the applied voltage. At 100 mV (10^{-1} V), a G of 10 pS (10^{-11} S) corresponds to a current of 1 pA (10^{-12} A) generated by about six million monovalent ions per second.

electrochemical proton gradient Generated by the H^+-pump activity of mitochondrial inner membrane (IM) enzyme complexes, it is commonly expressed in millivolts (mV) as proton motive force ($\Delta p = \Delta\mu_{H^+}/F = \Delta\psi - 60\Delta pH$). $\Delta\psi$ defines the difference in charges, and ΔpH that in H^+ concentrations, between the matrix and the aqueous phase external to the IM. A Δp of 180–200 mV (matrix negative) is normally found, with $\Delta\psi$ contributing for 150–180 mV.

lipid bilayer Allows the recording of electric activities from artificial planar membranes fused with vesicles obtained from native membranes, or reconstituted with purified proteins.

mitochondria Organelles composed of an outer membrane (OM), an intermembrane space, and an invaginated IM delimiting a matrix space that houses crucial metabolic routes.

patch clamp By means of fine electrodes, it records ionic currents directly from the membrane of isolated cells or organelles, as well as from large lipid vesicles reconstituted with channel-containing membrane fractions (proteoliposomes).

Further Reading

Borecky, J., Jezek, P., and Siemen, D. (1997). 108 pS channel in brown fat mitochondria might be identical to the inner membrane anion channel. *J. Biol. Chem.* **272**, 19282–19289.

Kroemer, G., and Reed, J. C. (2000). Mitochondrial control of cell death. *Nat. Med.* **6**, 513–519.

O'Rourke, B. (2000). Pathophysiological and protective roles of mitochondrial ion channels. *J. Physiol.* **529**, 23–36.

Sakmann, B., and Neher, E. (eds.) (1995). *Single Channel Recording*. Plenum Press, New York.

Sorgato, M. C., and Moran, O. (1993). Channels in mitochondrial membranes: Knowns, unknowns and prospects for the future. *Crit. Rev. Biochem. Mol. Biol.* **18**, 127–171.

Truscott, K. N., Brandner, K., and Pfanner, N. (2003). Mechanisms of protein import into mitochondria. *Curr. Biol.* **13**, R326–R337.

Biography

M. Catia Sorgato is a Professor of Medical Chemistry at the Faculty of Veterinary Medicine, University of Padova. After graduating in biology, she worked at the Biochemistry Department, Oxford University (UK) on energy transduction processes, and then at the Max-Planck-Institute, Göttingen (Germany), where she accomplished the first electrophysiologic analysis of mitochondrial inner membranes. Her actual research interest is the physiopathology of prion proteins.

Alessandro Bertoli graduated in physics and holds a Ph.D. in biochemistry and biophysics. He is currently a research fellow at the Department of Biological Chemistry, University of Padova. His past experience dealt with the electrophysiology of mammalian cell, and yeast mitochondrial channels, while his actual interest is the biology of neurodegenerative disorders.

Mitochondrial DNA

Gottfried Schatz
Swiss Science and Technology Council, Bern, Switzerland

Mitochondria, the eukaryotic organelles of oxidative phosphorylation, contain their own DNA genome. This genome is much smaller than that in the nucleus and encodes only ~1% of the mitochondrial proteins. Yet it is essential for the formation of fully functional mitochondria.

Discovery of Mitochondrial DNA

Some concepts take the scientific world by storm, but others conquer it only after many skirmishes. The discovery of mitochondrial DNA (mtDNA) belongs to this second category. Biochemists, histologists, and electron microscopists had seen DNA in mitochondria for years, but most of them were not ready for the idea that the DNA really belonged there. This may explain why textbook accounts of mtDNA almost never tell how this DNA was discovered.

After the basic building plan of the eukaryotic cell had been revealed in the early 1950s by the electron micrographs of Palade, Sjöstrand, and others, biochemists embraced de Duve's dogma that every macromolecule had one, and only one, intracellular location. In the analysis of cell fractions, cytochrome oxidase was taken as a marker for the mitochondria, NADPH–cytochrome *c* reductase for the endoplasmic reticulum, and DNA for the nucleus. Given this frame of mind, it is easy to understand why the presence of DNA in mitochondrial fractions was generally attributed to contamination by nuclear fragments. Histochemical DNA stains, such as the Feulgen reaction, also stained the kinetoplasts of *Trypanosomes* and the "*Nebenkern*" of insect spermatozoa, but at that time it was not yet recognized that these structures were, in fact, unusual mitochondria. Massive amounts of extranuclear DNA were also detected in the cytoplasm of amphibian oocytes, but it took many years to realize that this DNA was, in fact, mtDNA whose abundance reflected the enormous amount of mitochondria in these large cells. In 1961, at the Fifth Annual Meeting of the American Society of Cell Biology in Chicago, Hans Ris showed electron micrographs of mitochondria with inclusions resembling the DNA-containing nucleoids of bacteria and made the heretical proposal that mitochondria (and also chloroplasts) contain their own DNA. In a paper that appeared in the following year, Ris and Walter S. Plaut further documented and expanded these observations. Soon thereafter, biochemical and morphological evidence from several groups confirmed the presence of DNA in chloroplasts.

The discovery of chloroplast DNA made biochemists take a fresh look at early findings by Margaret Mitchell and Boris Ephrussi that certain mutations affecting mitochondrial function in the mold *Neurospora crassa* and the yeast *Saccharomyces cerevisiae* were not inherited according to Mendel's laws. It seemed tempting to speculate that the unknown "extrachromosomal factors" implicated in these mutations were, in fact, mtDNA.

By 1962, the ground for the concept of mtDNA was thus well prepared, but the concept itself was not generally accepted. In retrospect it seems that the scientific community was waiting for convincing studies that documented the existence of mtDNA by several diverse methods.

One of these studies came from the electron microscopists Margit M. K. Nass and Sylvan Nass, who were then working at the Wenner Gren Institute of the University of Stockholm. They showed that the matrix of osmium-fixed chick embryo mitochondria contained thread-like inclusions whose appearance after different fixation procedures closely paralleled that of the histone-free DNA nucleoid of bacteria: after fixation with osmium tetroxide, the inclusions appeared clumped and as bars with a diameter of ~400Å; fixation of the tissues with osmium tetroxide followed by treatment with uranyl acetate before dehydration made them appear as 15–30Å thin fibers. Even more convincing evidence for the presence of DNA in these inclusions was the observation that the inclusions could be removed by treating the lightly fixed embryonic tissue with DNase. Treatment with pepsin, with RNase, or with DNase-free buffer controls was ineffective. The clarity of these electron micrographs and the careful controls that were included had a compelling impact on cell biologists. M. M. K. Nass and S. Nass published their work in two back-to-back papers in a 1963 issue of the *Journal of Cell Biology*. At that time, however, cell biology and biochemistry were still rather

different disciplines and most biochemists did not peruse journals devoted to cell biology. It therefore took a while before the findings by M. M. K. Nass and S. Nass entered the consciousness of the biochemical community.

At about the same time, Ellen Haslbrunner, Hans Tuppy, and Schatz at the Biochemistry Institute of the University of Vienna were trying to find a biochemical basis for the extrachromosomal mutations that abolished respiratory function in the yeast *S. cerevisiae*. In the early 1960s, many biochemists were still reluctant to consider the "respiratory granules" of yeast as *bona fide* mitochondria, which placed the research by Haslbrunner *et al.* well outside the mainstream of mitochondrial biochemistry in the United States and elsewhere.

To look for DNA in mitochondria, a biochemical approach was chosen. Yeast mitochondria were purified by the best methods available, and their DNA content was measured by the time-honored "Diesche" color reaction. A few years before, de Duve and co-workers had shown that centrifuging subcellular fractions to equilibrium in a density gradient often gave a clean separation of different organelles. Surprisingly, the usual sucrose gradients did not separate yeast mitochondria from nuclear fragments, but when sucrose was replaced with the X-ray contrasting agent "Urografin," the mitochondria formed an extremely sharp band, and DNA was present in only two fractions: most was at the bottom of the centrifuge tube, and a very small amount, but discrete peak coincided exactly with that of the mitochondria. The DNA in the bottom fraction was easily digested by DNase and apparently represented nuclear DNA. The DNA in the mitochondrial fraction was not readily digested by DNase unless the organelles were first disrupted with trichloroacetic acid; presumably, it represented DNA enclosed by the mitochondrial membranes. Its concentration was very constant between different experiments – between 1 and 4 μg per mg mitochondrial protein. Urografin – purified mitochondria from rat liver, rat kidney, and bovine heart – contained almost 10 times less DNA, between 0.2 and 0.6 μg DNA per mg protein. The typical mammalian mitochondrion was calculated to contain 3×10^{-17} g DNA. Assuming that the DNA was double-stranded, it could encode no more than 1.2 MDa of polypeptide chains. This result was considered important, because it firmly excluded the possibility that mtDNA encoded all of the mitochondrial proteins. Today, this early calculation by Haslbrunner *et al.* could be challenged on several grounds, yet it came remarkably close to reality: the 13 polypeptides encoded by mammalian mtDNA have a total mass of 0.423 MDa, and the remainder of the coding potential is largely accounted for by genes for ribosomal – and transfer RNAs, as well as the by fact that mitochondria usually have more than one copy of their DNA genome.

Properties of mtDNA

Soon thereafter, several laboratories showed that mtDNA from several organisms had a different base composition and sometimes also a different buoyant density in cesium chloride gradients than the corresponding nuclear DNA. Particularly, striking was the observation that mtDNA from mammals was a small double-stranded circle. Late in 1964, the existence of DNA in mitochondria was generally accepted, and efforts focused on its function. Its identity with the "extrachromosomal factors" affecting respiratory function in *S. cerevisiae* was established by the observations that mtDNA was either altered or missing in the corresponding mutants. Several laboratories then showed that mitochondria from yeast and *N. crassa* synthesized the three large subunits of cytochrome oxidase, the heme-carrying subunit of the cytochrome bc_1 complex, and at least one membrane-bound subunit of the ATP synthase complex.

Sequence and Gene Content

In 1981, Fred Sanger and co-workers published the complete sequence of the 16,569 nucleotides of human mtDNA. This seminal paper provided the first complete sequence of a eukaryotic genome and identified the mitochondrial genes. Subsequent work by others then showed that the size of mtDNA can vary dramatically between different species (Table I). There are also considerable differences in gene content. Whereas mtDNA from humans and most mammals encodes 13 proteins and 24 RNAs (Figure 1 and Table II), that from the freshwater protozoon *Reclinomonas americana*

TABLE I

Sizes of mtDNAs from Different Species

Species	Kilo-base pairs
Mammals	16.5
Fungi	
Saccharomyces cerevisiae	78
Schizosaccharomyces pombe	17
Aspergillus nidulans	32
Plants	
Zea mays	570
Muskmelon	2500

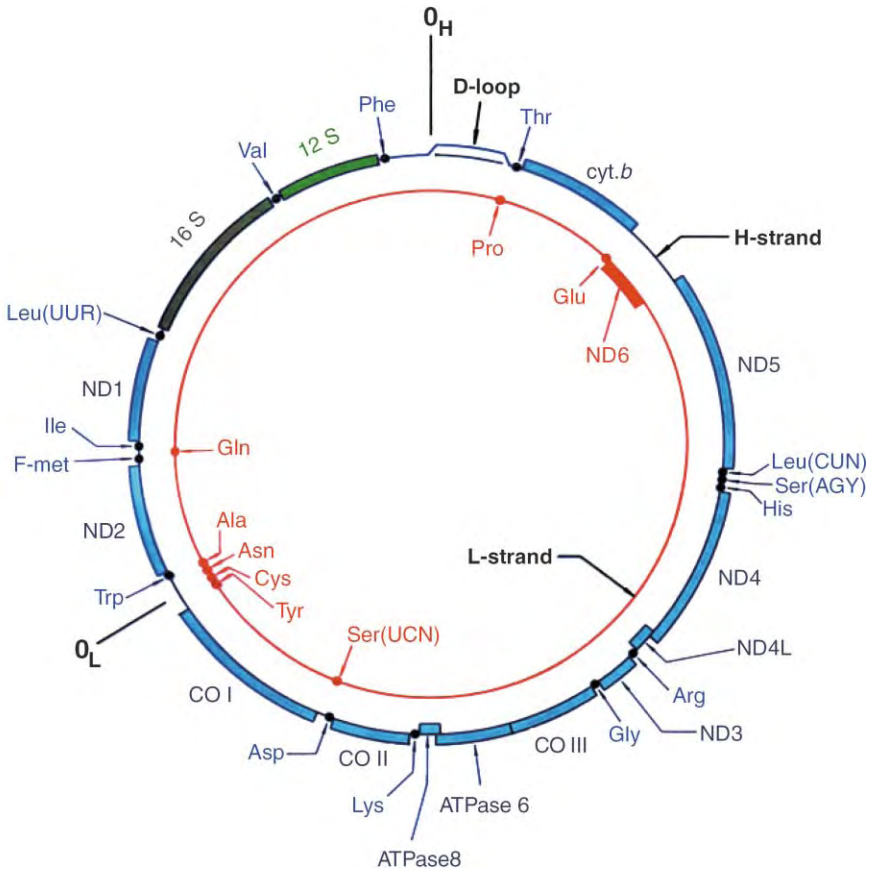

FIGURE 1 Genes on human mtDNA. 12S, 16S: rRNA of small and large ribosomal subunit; ND1–6 and ND4L: subunits of NADH dehydrogenase; CO I–III, subunits 1–3 of cytochrome oxidase; cyt. *b*, cytochrome *b* subunit of cytochrome bc_1 complex; ATPase 6 and 8: subunits of ATP synthase complex; amino acids designate the corresponding tRNAs; D-loop, highly variable gene-free region; O(H) and O(L), sites previously proposed by some as strand-specific replication origins. Reproduced from Attardi, G. (1986). The elucidation of the human mitochondrial genome: A historical perspective. *Bioassays* **5**, 34–39.

TABLE II

Genes on Human mtDNA

Function	Molecule(s)	Number
Protein synthesis	rRNAs	2
	tRNAs	22
Electron transport	Cytochrome oxidase	3
	NADH dehydrogenase	7
	Cytochrome bc_1 complex	1

carries no fewer than 97 genes. Sequence comparisons between some of the genes and the corresponding polypeptide products also uncovered the astounding fact that the genetic code of mtDNA differs slightly but significantly from that of nuclear DNA (Table III). For example, the codon UGA defines "stop" in the nucleus, but "tryptophan" in mtDNA from mammals, yeast, and many other species. This unexpected finding explained why so many earlier attempts to identify the protein products of mtDNA by coupled transcription/translation in *Escherichia coli* or reticulocyte lysates had failed.

Outlook

There is no end to the fascinating properties of the mitochondrial genome, and many of these properties still beg an explanation. Why is the mitochondrial genome of mammals one of the most compact genomes known, whereas that of plants and yeast spreads its genes luxuriously over five, ten, or even hundreds of times more DNA? Why has the genetic code diverged from the "standard" one that is used in the nucleus? Why does mtDNA mutate ~10 times faster than the corresponding nuclear DNA? Why have some mitochondria dozens of copies of their genome? Most importantly, why does mtDNA exist at all? Maintaining its few protein-coding genes from one generation to the next keeps hundreds of nuclear genes occupied, which

TABLE III

Unusual Codon Usage in mtDNAs

Codon	"Universal" usage	Mitochondrial usage	Species
CUA	Leucine	Threonine	Yeast
UGA	Stop	Tryptophan	Most species, not plants
AUA	Isoleucine	Methionine	Most species, not plants
AG(A,G)	Arginine	Stop	Mammals
		Serine	Insects
		Arginine	Yeast

seems highly uneconomical. Evolution provides the answer: it is now generally accepted that today's mitochondria are descendants of free-living prokaryotes that entered into symbiosis with other cells and transferred most of their genome to the nucleus of their host. The mtDNA is the small remnant of the genome of these endosymbionts.

Since a typical somatic cell has only two copies of a nuclear gene, but as many as a thousand copies of each mitochondrial gene, mtDNA has become a favorite tool for genetic fingerprinting and evolutionary studies. Also, it is now well established that mutations in mtDNA can cause a host of devastating maternally-inherited diseases, such as blindness, deafness, muscular degeneration, diabetes, and severe neuro-degenerative syndromes. A possible involvement of mtDNA in aging and cancer is under intense investigation. There is also mounting evidence that mutations of mtDNA may impair mammalian fertility and the success of *in vitro* fertilization experiments. Indeed, many of the most exciting functions of mtDNA may yet await discovery.

See Also the Following Articles

Cytochrome bc_1 Complex (Respiratory Chain Complex III) • Cytochrome Oxidases, Bacterial • Mitochondrial DNA • Mitochondrial Genes and their Expression: Yeast • Mitochondrial Genome, Evolution • Mitochondrial Genome, Overview

Glossary

cytochrome bc_1 complex A multi-subunit complex of the respiratory chain that transfers electrons from ubiquinone to cytochrome *c*.

cytochrome oxidase A multi-subunit green heme protein of the respiratory chain reducing oxygen gas to water.

endosymbiont Organism living symbiotically inside another organism.

kinetoplast The single, giant mitochondrion of a trypanosome cell.

nebenkern Spiral-like single mitochondrion wrapped around the flagellum of certain spermatozoa.

Further Reading

Andersen, S., Bankier, A. T., Barrell, B. G., de Bruijn, M. H., Coulson, A. R., Drouin, J., Eperon, I. C., Nierlich, D. P., Rae, B. A., Sanger, F., Schreier, P. H., Smith, A. J., Staden, R., and Young, I. G. (1981). Sequence and organization of the human mitochondrial genome. *Nature* **290**, 457–465.

Attardi, G., and Schatz, G. (1988). Biogenesis of mitochondria. *Annu. Rev. Cell Biol.* **4**, 289–333.

Attardi, G., Yoneda, M., and Chomyn, A. (1995). Complementation and segregation behavior of disease-causing mitochondrial DNA mutations in cellular model systems. *Biochim. Biophys. Acta.* **1271**, 241–248.

Chomyn, A., and Attardi, G. (2003). MtDNA mutations in aging and apoptosis. *Biochem. Biophys. Res. Commun.* **304**, 519–529.

Clayton, D. A. (1991). Replication and transcription of vertebrate mitochondrial DNA. *Annu. Rev. Cell. Biol.* **7**, 453–478.

Grivell, L. A. (1983). Mitochondrial DNA. *Sci. Am.* **248**, 78–89.

Nass, M. M. K., and Nass, S. (1963). Intramitochondrial fibers with DNA characteristics II. *J. Cell Biol.* **19**, 613–629.

Nass, S., and Nass, M. M. K. (1963). Intramitochondrial fibers with DNA characteristics I. *J. Cell Biol.* **19**, 593–612.

Schatz, G., Haslbrunner, E., and Tuppy, H. (1964a). Deoxyribonucleic acid associated with yeast mitochondria. *Biochem. Biophys. Res. Commun.* **15**, 127–132.

Schatz, G., Haslbrunner, E., and Tuppy, H. (1964b). Intramitochondriale Deoxyribonukleinsäure in Säugetierzellen. *Monatshefte f. Chemie* **95**, 1135–1140.

Scheffler, I. E. (1999). *Mitochondria*, 364pp. Wiley, New York.

Scheffler, I. E. (2000). A century of mitochondrial research: achievements and perspectives. *Mitochondrion* **1**, 3–31.

Wallace, D. C. (1997). Mitochondrial DNA in aging and disease. *Sci. Am.* **277**, 40–47.

Biography

Gottfried Schatz obtained his Ph.D. in biochemistry in 1961 in Austria. He then worked as an Assistant Professor at the University of Vienna, as postdoctoral fellow with Efraim Racker at New York, and as a Professor of Biochemistry at Cornell University in Ithaca. In 1974 he joined the Biozentrum at the University of Basel. Upon retiring as a Professor in 1999, he was elected President of the Swiss Science and Technology Council.

Mitochondrial Genes and their Expression: Yeast

Piotr P. Slonimski
Centre de Génétique Moléculaire du Centre National de la Recherche Scientifique (CNRS), Gif-sur-Yvette, France

Giovanna Carignani
University of Padova, Padova, Italy

Mitochondria possess their own genome, which encodes a small part of the proteins that make up the organelle. The remaining proteins, i.e. the majority, are encoded by the nuclear genome. Mitochondrial life thus depends on the coordinated expression and interaction of nuclear genes and genes present on the organellar genome (mtDNA) itself. Although mtDNA encodes very few subunits of the energy-transducing complexes of the inner mitochondrial membrane, these subunits constitute the key elements of the overall process: cytochrome *b* for the reductase activity, cytochrome *c* oxidase subunit 1 for the oxidative activity, and Atp6 for the synthetase activity. The genes coding for these three subunits are always located in the mtDNA in all eukaryotes, whether fungi, protists, animals, or plants. The mtDNA is supposed to be a remnant of a prokaryotic genome that would have originated from a symbiotic event between different cellular species. As the majority of the prokaryotic genes would, however, in the course of evolution, have migrated to the nucleus of the new cell, it is surprising that even today a mitochondrial genome exists. A plausible reason might reside in the compulsory evolution of the formation mechanism of the enzymatic complexes of the inner mitochondrial membrane. This might depend on a topological constraint of the expression and assembly of the different subunits, some of which are very hydrophobic and have to be transcribed, translated, inserted, and assembled from inside the organelle. It follows then that these key genes are present inside the mitochondrion. This would also explain the persistence of mtDNA and its complex machinery of expression for a billion years since the original symbiotic event.

The knowledge of the conjoint expression of both the mitochondrial and nuclear genes involved in energy transduction is best advanced in the study of baker's yeast, essentially due to the extraordinary power of molecular genetics both *in vivo* and *in vitro*.

Yeast as a Model Organism for the Study of Mitochondrial Biogenesis and Function

The facultative anaerobic yeast *Saccharomyces cerevisiae* has provided the main information about mitochondrial biogenesis, from the discovery of petite mutants by Boris Ephrussi and Piotr Slonimski and their collaborators in the 1950s. This was followed by the exhaustive analysis of mitochondrial genetics in the 1970s in the laboratory of Gif-sur-Yvette and by the identification of mtDNA by Gottfried Schatz, and still remains an excellent experimental organism, owing to its capacity of surviving in the absence of competent mitochondria, to the facility of isolation or construction of mutants (several thousand have already been characterized) and to the possibility of mitochondrial transformation. The search for nuclear genes involved in mitochondrial biogenesis and function is constantly carried out in this organism and the results continually lead to the isolation of functionally homologous human genes. In particular, many mitochondrial disease genes have been identified in this way.

Mitochondrial life depends on the coordinated expression and interaction of nuclear genes and genes present on the organellar genome (mtDNA) itself. The mitochondrial genetic system is required for the synthesis of a limited number of proteins, in particular in yeast of seven highly hydrophobic subunits of the energy-transducing complexes of the inner membrane (Figure 1).

All the processes necessary to the expression of these genes (i.e., transcription, RNA processing, and translation), as well as those required for mtDNA maintenance and integrity, take place in the same

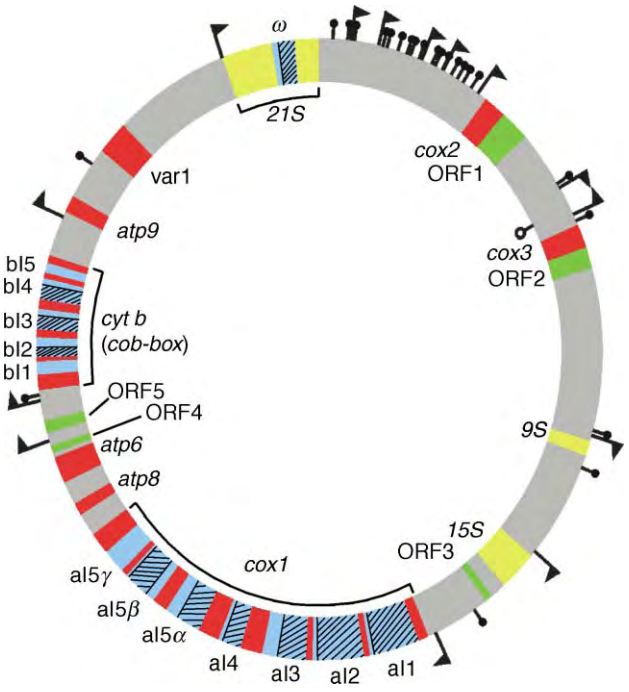

FIGURE 1 The mitochondrial genome of *Saccharomyces cerevisiae*. The circular map is in agreement with the genetic results and with the observation that mtDNA replicates by the rolling-circle mode. Different yeast strains contain mtDNA molecules of different lengths (comprised between 70 and 85 bp). These differences are essentially due to the presence/absence of introns and hypothetical open reading frames (ORFs 1–5 in this representation). Yeast mtDNA encodes seven highly hydrophobic subunits of the energy-transducing complexes of the inner membrane, i.e., apocytochrome *b* (encoded by the *cyt b*, or *cob-box*, gene), three subunits of cytochrome c oxidase (encoded by the *cox1*, *cox2*, and *cox3* genes) and three subunits of ATP synthase (encoded by the *atp6*, *atp8*, and *atp9* genes). The *cytb*, *cox1*, and *21S rRNA* genes contain introns, some of which are translated, independently or in frame with their upstream exons, to produce maturases (e.g., the bI2 intron of the *cytb* gene, see Figure 3) or site-specific endonucleases (the *ω* intron of the *21S rRNA* gene); others encode complex proteins with multiple functions, i.e., maturases, reverse transcriptases, endonucleases (e.g., the aI1 intron of the *cox1* gene). Red: exons of protein-coding genes; blue: introns (aI1–aI5; bI1–bI5; *ω*); hatched blue: intron-encoded ORFs; green: hypothetical ORFs; yellow: 9S, 15S, and 21S RNAs; solid circles: tRNAs. Flags indicate the transcription initiation sites and their orientation. The orientation of all the transcription units is clock-wise, with the exception of the $tRNA^{thr1}$ gene (open circle), which is transcribed from the opposite strand.

compartment, the mitochondrion itself, as they occur in a bacterium, the hypothetical mitochondrial ancestor. Also, the different processes are functionally linked, frequently through the activity of proteins exhibiting multiple roles.

Expression of Mitochondrial Genes

Mitochondrial gene expression requires the coordinated interaction of mitochondrial and nuclear encoded factors: the mitochondrial genome (Figure 1) participates in the process with the genes encoding the RNA-subunit of mitochondrial RNase P (9S RNA), the 21S and 15S rRNAs, a complete set of tRNAs, and one protein of the small mitoribosomal subunit, Var1; in addition some introns encode proteins necessary for RNA splicing (RNA maturases). The nuclear genome encodes all other factors necessary for mitochondrial genome maintenance and expression, as well as all other mitochondrial proteins (~500 yeast proteins located in the organelle were currently listed in the Yeast Proteome Database, YPD, in 2001, but predictions indicate about 700). These are translated in the cytoplasm, and then imported into different compartments of mitochondria using protein-specific import mechanisms. A mitochondrial targeting sequence, often present at the amino terminus of translated precursors, allows their interaction with the mitochondrial receptor–translocator TOM–TIM, followed by maturation of the precursor and its localization in mitochondria. Also, recent results point out that nuclear-encoded mitochondrial proteins of bacterial origin are synthesized on polysomes associated with the mitochondrion, while those of eukaryotic origin are generally translated on free cytosolic polysomes, thus promoting speculations about organelle origins.

General Features of Simple and Mosaic Genes

(To describe the expression of yeast mitochondrial genes, we distinguish between simple genes and mosaic genes, i.e., genes containing introns and thus subject to a more complicated expression pathway.)

Transcription

The yeast mitochondrial genome is ~4 times larger than mammalian mitochondrial genomes, although they contain approximately the same number of genes. The difference is due to the lengths of intergenic regions and to the presence of introns in some of the yeast genes. Whereas the 16,000 base-pair mammalian mitochondrial genome is transcribed by two opposite promoters (one for each strand), genes on the 80,000 base-pair yeast mtDNA are transcribed, singly or in clusters, from several promoters (14 active promoters have been identified, see Figure 1). The consensus sequence of mitochondrial promoters is a nonanucleotide 5′ATATAAGTA 3′, whose last A is the +1 position of the transcript, and termination of transcription is indicated by the dodecanucleotide consensus 5′AAUAAUAUUCUU3′ (see Figure 2).

As in the case of bacterial transcription, all mitochondrial genes are transcribed by the same RNA

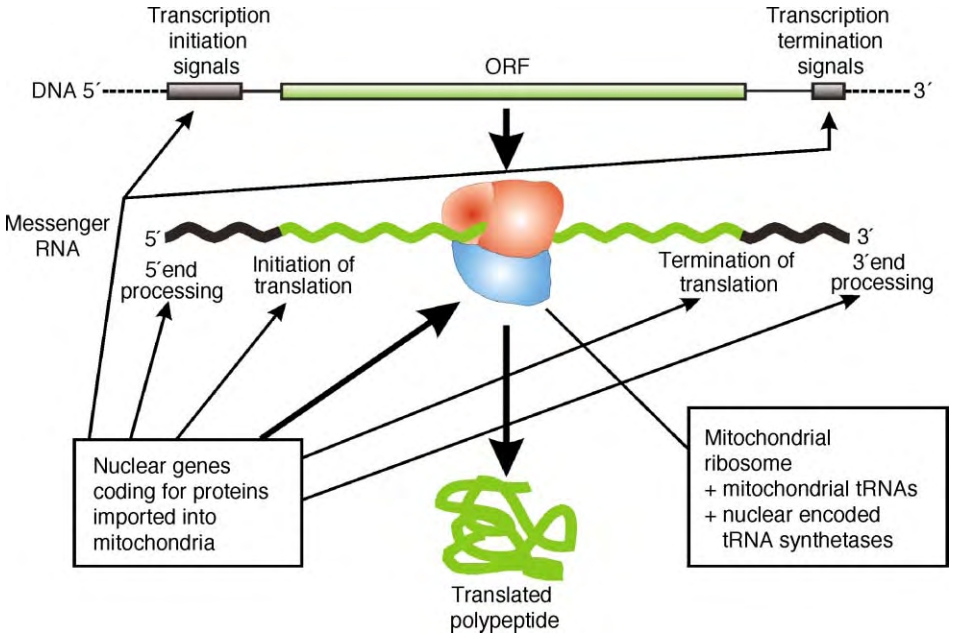

FIGURE 2 Main features of the expression of a "simple" mitochondrial protein-coding gene. The open reading frame (ORF) of the gene located in the mtDNA is transcribed into messenger RNA and translated into a polypeptide chain according to the general principles of molecular biology. However, most of the elements of these two machines derive their information from a different cellular compartment than the one where these processes take place. The genes coding for the transcriptional machinery as well as those involved in the processing or stability of mRNA are located in the nucleus, the proteins synthesized in the cytoplasm and imported inside the mitochondrion where they recognize specific signals, i.e., mtDNA or mtRNA sequences or structures indicating the beginning and the end of DNA transcription or RNA processing (e.g., Mtf1, Nam1). The next step of gene expression is even more complex, since in addition to numerous nuclear genes coding for proteins involved in initiation/termination of translation, as well as the translation process itself (more than seventy ribosomal proteins, e.g., Nam9, all translation factors, e.g., Cbp1, and all specific mitochondrially located tRNA synthetases), a number of genes located in the mitochondrial genome participate in the process. They encode essentially the catalytic RNAs: the two, large and small, rRNAs, the complete set of tRNAs and a subunit of RNAse P. As a result of this double inheritance scenario, a mutational lesion in any one of the elements (e.g., the nuclear encoded leucine tRNA synthetase by gene NAM2 or a mtDNA encoded tRNA) will ineluctably and irreversibly abolish the expression of all the genes located in mtDNA.

polymerase. This is composed of only two nuclear encoded subunits, a core RNA polymerase, Rpo41, which is similar to the very simple T-odd phages RNA polymerases, and the mitochondrial transcription factor, Mtf1, which is required for the recognition of the promoter by the holoenzyme and is released when Rpo41 enters into the elongation mode, as happens for sigma factors of bacterial RNA polymerases. Mtf1 in fact shares sequence similarity with regions 2 and 3 of bacterial sigma factors, but, unexpectedly, crystal structure of Mtf1 has revealed clear similarity to the family of RNA and DNA methyltransferases and one of the two human homologues of Mtf1 has been proved to methylate a conserved stem-loop in bacterial 16S rRNA and human mitochondrial 12S RNA. This is one of the several evidences (the incessant definition of protein crystal structures is currently revealing novel cases) where the structure/function relationship of a present day protein indicates that it might have evolved from a multifunctional ancestor or from a protein with a different function.

RNA Processing: 5′ and 3′ Processing

Mitochondrial transcription units are unusual as they are characterized by the presence of mRNAs interspersed with tRNA and rRNAs. In human mtDNA tRNAs genes "punctuate" the very long principal transcription unit and their processing at both ends "release" the majority of other RNAs. In yeast the mitochondrial transcription units are shorter but also contain various combinations of RNAs. tRNAs precursors are processed at 5′ end by mitochondrial RNAse P and at 3′ end by a specific endonuclease (successively tRNAs are matured by CCA addition and nucleotide modifications). The processing of mRNAs at their 5′ end, assisted by nuclear encoded factors (e.g., Cbp1 for the cytochrome *b* transcript) consists in a cleavage to generate mature mRNA at a position specific for each transcript. In some transcription units the transcript is first released by the 3′ end processing of a preceding tRNA or mRNA. Processing at 3′ end of mRNAs is done near the conserved dodecamer sequence 5′AAUAAUAUUCUU3′, which is protected by a

complex of three proteins before cleavage by a probably specific endonuclease. All these processes are assisted by several nuclear encoded proteins with a gene-specific or a more general role (see Figure 2).

Processing of Mosaic Genes is More Complex: RNA Splicing

A typical feature of yeast mtDNA, which is not shared by human mtDNA (but is common to many mtDNA from plants, fungi, and protists), is that some of its genes are split by introns. In *S. cerevisiae* these are the *21S rRNA*, *cytb* (*cob-box*) and *cox1* genes. Splicing of these introns is catalyzed by the intron itself (catalytic RNA), and depends on the formation of a conserved RNA three-dimensional structure, which enables them to undergo self-splicing *in vitro*, albeit inefficiently and under non-physiological conditions. *In vivo*, however, splicing requires the presence of specific proteins that function to promote a stable and active RNA conformation. Furthermore, some yeast mitochondrial introns behave as mobile genetic elements, as they can be inserted into an intronless version of the gene at the same position it already occupies in the intron-containing version (intron homing) or to a novel location (intron transposition). Mitochondrial introns belong to two classes, group I and II, based on the secondary and tertiary structure of the intron transcript and on the mechanism of splicing. The mechanism of splicing of group II introns has suggested that they might be progenitors of nuclear pre-messenger introns and of the spliceosome-catalyzed splicing process, with group II intron domains having evolved into small nuclear RNAs (snRNAs).

Several features of mitochondrial introns have been uncovered in the laboratory at Gif-sur-Yvette in the late 1970s, among these some encode proteins, i.e., RNA maturases, which assist the splicing of the intron itself and sometimes also of a different intron (see Figure 3), and also promote intron mobility. Intron encoded proteins also belong to two groups. Group I proteins are members of the LAGLI-DADG family of DNA endonucleases and, besides the endonuclease activitiy required for intron mobility via DNA (as happens for prokaryotic transposons), some of them have high-affinity RNA-binding properties necessary for their role in splicing. Mobile group II introns (e.g., intron aI1 of the *cox1* gene) encode multifunctional proteins, endowed with maturase and DNA endonuclease activity, but also encode reverse transcriptases that bind specifically to the intron RNAs to promote both intron mobility and RNA splicing. In the case of group II introns, transposition occurs via RNA, the procedure adopted by eukaryotic nuclear retrotransposons and retroviruses. Some of the mitochondrial intron encoded proteins are translated in-frame with the upstream exon and subsequently processed to mature proteins by various proteases. This process shows how the different events of mitochondrial gene expression (in this case splicing and translation) are strictly interconnected and also enlightens a peculiarity of mitochondrial translation, that it starts immediately after transcription, as in prokaryotes, however before RNA processing, an occurrence unique to this system.

In vivo self-splicing of yeast mitochondrial introns is thus assisted by proteins that, in general, have the role to promote the folding of the catalytic core of the intron, inducing the formation of nucleotide interactions required for catalytic activity. These proteins are the maturases encoded by the intron itself and other proteins, encoded in the nuclear genome, that concur in assisting the splicing event. Numerous of these proteins have been identified as suppressors of splicing-defective mitochondrial mutations and most of them are proteins that, besides their role in mitochondrial splicing, have also other functions. An example is the mitochondrial enzyme leucyl-tRNA synthetase, Nam2, which is also necessary for the splicing of the group I intron bI4. Actually, recent interesting results indicate that the tyrosyl-tRNA synthetase of *Neurospora crassa* interacts with group I introns by recognizing conserved tRNA-like structural features of the intron RNA, thus suggesting that this might be the case for other tRNA synthetases as well. Also the Mrs2 protein, which assists splicing of group II introns, seems to be implicated in a more general function, as a mitochondrial Mg^{2+} transporter. A particularly interesting protein is Nam1, that is involved in the removal of introns from the *cytb* and *cox1* transcripts and in overall translation capacity, and is also responsible of coupling these processes to transcription, through direct interaction with the amino terminus of mitochondrial RNA polymerase, Rpo41.

Translation

Translation of mitochondrial mRNAs resembles more closely its prokaryotic than eukaryotic counterpart with respect to the spectrum of antibiotics inhibiting mitochondrial translation. Also, mitochondrial mRNAs are uncapped and lack the poly(A) tail, as prokaryotic mRNAs. However mitochondrial translation has unique features, e.g., the use of an alternative genetic code and the composition of mitochondrial ribosomes. These are made up of nuclearly encoded proteins (with the exception of Var1), the majority of which have no recognizable homology to known proteins, i.e., are unique. It has been suggested that these proteins have more specialized functions connected with the coupling of the translation process to the inner mitochondrial membrane, where the seven hydrophobic mtDNA-encoded proteins have to be assembled.

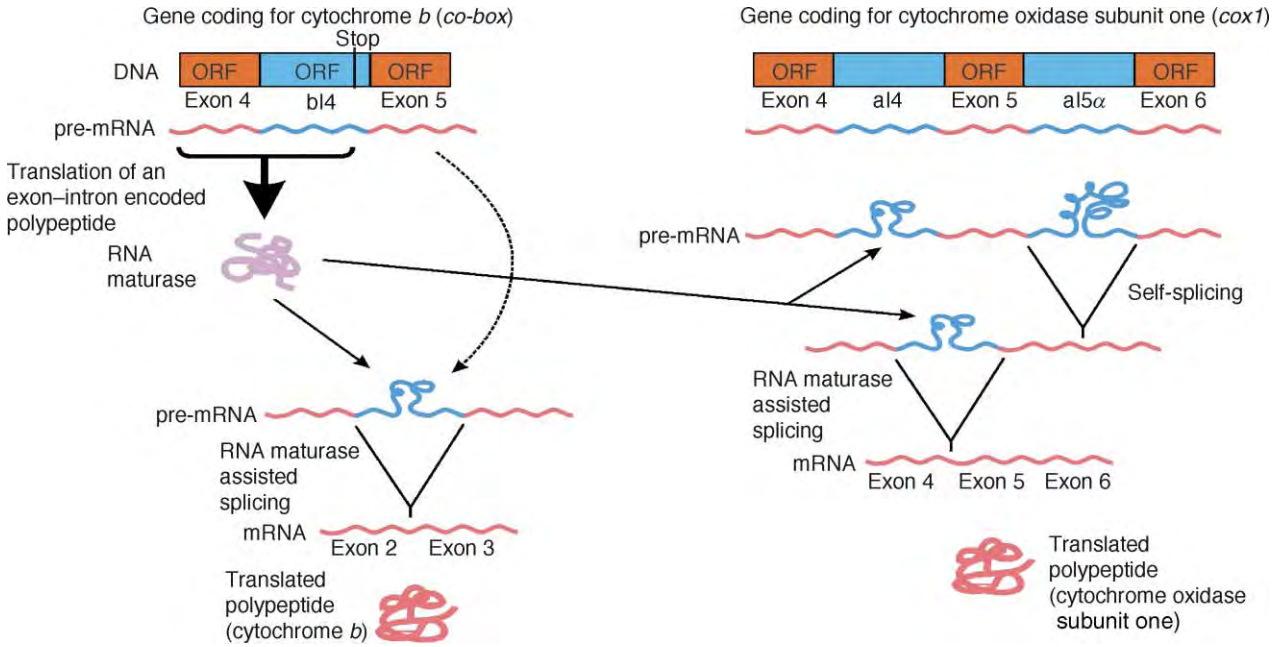

FIGURE 3 Specific features of the expression of a "mosaic" mitochondrial protein-coding gene. Several yeast mitochondrial genes contain introns and some of these introns contain ORFs (see Figure 1). The expression of such "mosaic" genes occurs in two successive steps supplementary to the general features of expression of "simple" genes (see Figure 2). The primary, unspliced RNA transcript (pre-mRNA) for apocytochome *b* acts as a messenger for a protein translated from the upstream exon ORF of cytochrome *b* and the ORF of the successive intron. This fusion protein, mRNA maturase (in the example shown referred to as the bI4 RNA maturase) promotes catalytically the excision of the intervening sequence from the pre-mRNA and ligation of cytochrome *b* exonic RNA leading to the formation of cytochrome *b* mRNA. The maturase recognizes specific structures of the intervening sequence, helps the productive folding and facilitates the activity of the ribozyme. At the same time the maturase activity destroys the RNA which codes for itself and thus exerts a negative feedback for its own biosynthesis. In consequence the amount of maturase in the organelle is very low, and the protein can be detected only when its splicing function is impaired. Generally, the maturases act selectively on the introns which encode them. A notable exception is the maturase shown in the example, i.e., the maturase encoded by the fourth intron of the cytochrome *b* gene (bI4): its activity is essential also for the splicing of the fourth intron (aI4) of a different gene, *cox1*, which encodes the subunit one of cytochrome *c* oxidase. In this manner the expression of the key catalysts of the electron transfer cascade may be coordinated.

The 5′-untranslated leader sequences (UTLs) of mitochondrial mRNAs contain sequence or structural signals that indicate the translation initiation site and that are recognized by mRNA-specific activator proteins (e.g., Cbs1, Cbs2, and Cbp1 for *cytb*, Pet309 for *cox1*, Pet 111 for *cox2* mRNA). Some of the translational activators, that mediate mRNA interactions with mitochondrial ribosomes, are organized on the surface of the inner mitochondrial membrane in a way that facilitates assembly of the inner membrane complexes. Assembly of these complexes necessitates also other proteins, e.g., Oxa1 is necessary for the correct assembly of cytochrome *c* oxidase and the ATP synthase complex.

The recent observed interaction of some membrane-bound specific activators with two proteins, Nam1 and Sls1, that, besides being involved in posttranscriptional events and in translation, are able to bind the amino-terminal domain of mitochondrial RNA polymerase, suggests that expression of mtDNA-encoded genes involves a complex series of interactions that localize active transcription complexes to the inner membrane, in order to coordinate translation with transcription.

In this way synthesis of the mitochondrially encoded proteins is coordinated with their assembly into multimeric respiratory complexes. On the other hand, the posttranslational targeting mechanism of nuclear encoded subunits seems to be preceded by mRNA localization in cytoplasmic ribosomes tightly associated with the organelles, thus facilitating the localization of proteins. This suggests a topological coordination between translation of the mitochondrial and nuclear-encoded subunits and their assembly into higher order complexes.

See Also the Following Articles

Adrenergic Receptors • Mitochondrial DNA • Mitochondrial Inheritance • mRNA Polyadenylation in Eukaryotes • mRNA Processing and Degradation in Bacteria • Pre-tRNA and Pre-rRNA Processing in Bacteria • Pre-tRNA and Pre-rRNA Processing in Eukaryotes

Glossary

self-splicing The intrinsic ability of some introns to remove themselves and link together the two adjacent RNA exons, by transesterification reactions.

spliceosome The large RNA–protein body upon which splicing of nuclear mRNA precursors occurs.

suppressor gene A gene which, by mutation, is able to eliminate the effects of a mutation in another gene.

TOM–TIM Proteins forming receptor complexes that are needed for tanslocation of proteins across the mitochondrial outer (TOM) or inner (TIM) membrane.

Further Reading

Barrientos, A. (2003). Yeast models of human mitochondrial diseases. *IUBMB Life* **55**, 83–95.

Belfort, M. (2003). Two for the price of one: A bifunctional intron-encoded DNA endonuclease–RNA maturase. *Genes Dev.* **17**, 2860–2863.

Bolduc, J. M., Spiegel, P. C., Chatterjee, P., Brady, K. L., Downing, M. E., Caprara, M. G., Waring, R. B., and Stoddard, B. L. (2003). Structural and biochemical analyzes of DNA and RNA binding by a bifunctional homing endonuclease and group I intron splicing factor. *Genes Dev.* **17**, 2875–2888.

Chen, X. J., and Clark-Walker, G. D. (2000). The petite mutation in yeasts: 50 years on. *Int. Rev. Cytol.* **194**, 197–238.

Contamine, V., and Picard, M. (2000). Maintenance and integrity of the mitochondrial genome: A pletora of nuclear genes in the budding yeast. *Microbiol. Mol. Biol. Rev.* **64**, 281–315.

Dieckmann, C. L., and Staples, R. R. (1994). Regulation of mitochondrial gene expression in *Saccharomyces cerevisiae*. *Int. Rev. Cytol.* **152**, 145–181.

Dujon, B., Colleaux, L., Jacquier, A., Michel, F., and Monteilhet, C. (1986). Mitochondrial introns as mobile genetic elements: The role of intron-encoded proteins. *Basic Life Sci.* **40**, 5–27.

Grivell, L. A. (1995). Nucleo-mitochondrial interactions in mitochondrial gene expression. *Crit. Rev. Biochem. Mol. Biol.* **30**, 121–164.

Lazowska, J., Jacq, C., and Slonimski, P. P. (1980). Sequence of introns and flanking exons in wild-type and box3 mutants of cytochrome b reveals an interlaced splicing protein coded by an intron. *Cell* **22**, 333–348.

Michel, F., and Ferat, J. L. (1995). Structure and activities of group II introns. *Annu. Rev. Biochem.* **64**, 435–461.

Neupert, W., and Brunner, M. (2002). The protein import motor of mitochondria. *Nat. Rev. Mol. Cell. Biol.* **3**, 555–565.

Sylvestre, J., Vialette, S., Corral Debrinski, M., and Jacq, C. (2003). Long mRNAs coding for yeast mitochondrial proteins of prokaryotic origin preferentially localize to the vicinity of mitochondria. *Genome Biol.* **4**, R44.

Biography

Giovanna Carignani obtained her degree in pharmacy in 1960 at the University of Trieste (Italy). She is an Assistant Professor of Molecular Biology of the Faculty of Medicine of the University of Padova (Italy).

Piotr P. Slonimski obtained his M.D. degree in 1947 at the University of Cracow (Poland) and soon after he joined the Centre National de la Recherche Scientifique (CNRS), Laboratory of Boris Ephrussi, in Paris. He became Director of the CNRS Laboratory of Physiological Genetics in 1960, then Director of the CNRS Center of Molecular Genetics of Gif-sur-Yvette until 1992. He was Professor of Molecular Genetics at the Sorbonne, at the University Pierre et Marie Curie (Paris VI) and Guest Professor at several American and European universities. He was in charge of the first French government Genome Project (Groupement de Recherches et d'Etudes sur les Genomes, GREG) and is active now, as Emeritus Professor, in the field of genome bioinformatics.

Mitochondrial Genome, Evolution

B. Franz Lang, Dennis V. Lavrov and Gertraud Burger
Université de Montréal, Montréal, Québec, Canada

Mitochondria, the energy-producing organelles of the eukaryotic cells, evolved from an endosymbiotic α-Proteobacterium, more than one billion years ago. These organelles contain their own genetic system, which is a remnant of the endosymbiont's genome. Mitochondrial DNA (mtDNA) varies considerably in size, structure, and coding capacity throughout eukaryotes. The ~5–100 genes contained in mtDNA code for mitochondrial components with functions in oxidative phosphorylation, protein synthesis, protein transport and maturation, RNA processing, and, in rare instances, transcription. Mitochondrion-encoded proteins make up only a small fraction of the mitochondrial proteome. The majority of mitochondrial proteins is encoded by nuclear genes, most of which are thought to have originally resided in mtDNA, and migrated to the nucleus in the course of eukaryotic evolution.

Origin and Evolution of Mitochondria

Eubacterial Ancestry of Mitochondria

Two decades of research in mitochondrial biogenesis and genomics unequivocally confirms the eubacterial ancestry of mitochondria (Figure 1). This ancestry is strikingly obvious in mitochondrial genomes of minimally derived eukaryotes, such as the recently described bacterivorous freshwater flagellate *Reclinomonas americana* (Table I). Among other eubacteria-like features, the mtDNA of this jakobid protist and its relatives has putative ribosome-binding motifs (Shine–Dalgarno sequences) upstream of protein-coding genes typical for bacterial systems, and codes for a eubacteria-like multisubunit RNA polymerase not found in mtDNA of other eukaryotic groups.

Phylogenetic analyses based on mitochondrial protein sequences show that mitochondria originated only once from within α-Proteobacteria, a bacterial assembly that includes free-living species such as *Magnetospirillum* and *Rhodobacter*, facultative symbionts/pathogens of plants like *Rhizobium* and *Agrobacter*, and intracellular, obligatory animal pathogens of the *Rickettsia* group including the causative agents of typhus and spotted fever. The closest living relatives of mitochondria appear to be within the *Rickettsiae*. However, this conjecture needs to be considered with caution, because available phylogenetic methods tend to group together species with highly accelerated evolutionary rates (such as mitochondria and *Rickettsia*), irrespective of their true evolutionary relationships. Whether or not they are sister groups, mitochondria and rickettsial bacteria are most likely the product of independent reductive evolution from a common (most likely free-living) bacterial ancestor, as indicated by differences in energy metabolism, and the lack of shared derived traits (e.g., gene order).

Nature of the Host Cell

A most controversial issue is, whether the host of the endosymbiotic symbiont that gave rise to the mitochondrion was a nucleus-containing amitochondriate eukaryote resembling extant anaerobic protists, or rather an archaebacterium; i.e., it is unclear whether the distinctive features of eukaryotic cells existed before this endosymbiotic event, or arose subsequently. Although accumulating molecular evidence suggests that all known amitochondriate eukaryotes once harbored mitochondria that were lost secondarily, the question remains whether primitively amitochondriate eukaryotes ever existed; and if so, to what extent their cellular organization featured the characteristics of present-day eukaryotes. The inference of the nature of eukaryotic ancestors (e.g., presence or absence of a cytoskeleton and a nucleus), and of the contribution of mitochondrial endosymbiosis to the evolution of the eukaryotic cell, will require additional massive genomic information, particularly from minimally derived eukaryotes.

Genome Size Reduction and Accelerated Evolution in Early Mitochondrial History

Early steps in the evolutionary history of mitochondria were likely governed by similar principles as those observed in present-day intracellular bacterial pathogens and symbionts, as briefly discussed in the following.

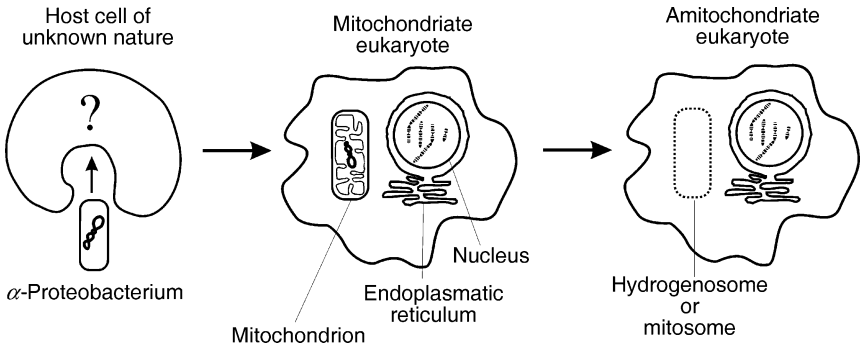

FIGURE 1 Evolution of the mitochondrion. Hypothesis describing the origin of the mitochondrion via endosymbiosis of an α-Proteobacterium with a host cell of undefined nature. Amitochondriate eukaryotes are believed to have lost mitochondria secondarily, often leaving behind relict organelles, such as hydrogenomes or mitosomes.

Bacteria that reside inside eukaryotic cells benefit from an environment rich in nutrients, which renders a large set of their biosynthetic and metabolic genes obsolete. These superfluous genes are usually lost in obligate intracellular bacteria, together with genes involved in DNA repair, recombination, lateral gene transfer among bacteria, and propagation of phages and other mobile sequence elements. Loss of these genes, in conjunction with a radically different selective pressure within the host cell, are likely responsible for the accelerated sequence evolution and changes in nucleotide composition (decrease of G + C content), observed in strictly intracellular bacteria. The gene loss is massive and progressive. For example, the obligate intracellular leprosy bacillus *Mycobacterium leprae* possesses a relatively large genome for a pathogen (3.27 mbp) with 1604 identifiable protein coding genes, 1116 pseudogenes, ~50% noncoding sequence, and a G + C content of 57.7%. In contrast, the genomes of the more derived, obligate endosymbiotic/endoparasitic bacteria *Rickettsia*, *Wigglesworthia* and *Buchnera* (symbionts of insects), and *Wolbachia* (parasite of arthropods and nematods) have genomes sizes of ~1 mbp only, and code for as few as 583 protein coding genes with an overall G + C content as low as 26.3%.

Transition from an Autonomous Bacterium to a Subcellular Organelle

Gene migration from the mtDNA to the nucleus, and the acquisition of a unique mitochondrial protein import machinery, were pivotal steps in the transformation of the proto-mitochondrion into an integrated, subcellular organelle. However, not all genes lost from mtDNA have necessarily moved to the nucleus; mitochondrial genes may have also been substituted by either genuinely nuclear genes, or genes from other (unknown) sources. An example for the latter case is the replacement of the original multisubunit bacteria-like RNA polymerase (inherited from the proto-mitochondrial ancestor) by a bacteriophage T3/T7-like RNA polymerase. This secondarily acquired RNA polymerase directs mitochondrial transcription in all contemporary eukaryotes, except in the minimally derived jakobid flagellates.

There is currently much controversy about the proportion of mitochondrial genes that reside in the nuclear genome. In yeast, some 400–630 nuclear genes (close to 10% of the genome) are considered to code for mitochondrial proteins. However, only a minority of these proteins can be traced to an α-proteobacterial origin on the basis of phylogenetic analysis. We would argue that yeast, with its highly accelerated rate of gene evolution and a considerably reduced gene set, is not an appropriate organism for such estimations. We expect that nuclear genomes of little-derived protists harbor a substantially higher number of genes of clearly identifiable mitochondrial origin.

Ongoing Gene Transfer to the Nucleus

Mitochondrion-to-nucleus gene migration is an ongoing process. For example, in leguminous plants, the active gene specifying cytochrome oxidase subunit 2 (*cox2*) resides in the nucleus in some species, but in the mitochondrion in others (as in all nonleguminous plants). Even more intriguingly, in soybean, an inactive mitochondrial *cox2* gene copy exists in addition to an active nuclear one. In this particular example, there is strong evidence that the transfer to the nucleus proceeded via an mRNA → cDNA intermediate. Nevertheless, direct transfer of genomic DNA appears to be an alternative avenue: nuclear genomes of plants and animals (including human) often contain large insertions of mtDNA, some even of full length. Finally, a surprisingly high rate of gene transfer from the

TABLE I

Features of Mitochondrial Genomes from Representative Eukaryotes

Organismal group	Genome size and structure[a]	Protein genes[b]	RNA genes[c]	Translation code[d]	Introns[e]
Metazoa (animals)					
Homo sapiens (human)	16.6 (circular)	13	24	**UGA(W), AUA(M)**[f]	
Metridium senile (sea anemone)	17.4 (circular)	13	4	**UGA(W)**	2
Fungi					
Hyaloraphidium curvatum (chytrid)	30.0 (linear)	14	9	Standard	1
Saccharomyces cerevisiae (baker's yeast)	85.8 (circular)	8	27	**UGA(W), AUA(M), CUN(T)**	13
Schizosaccharomyces pombe (fission yeast)	19.4 (circular)	8	28	Standard[g]	3
Spizellomyces punctatus (chytrid)	58.8; 1.4; 1.1 (3 circular DNAs)	14	10	**UAG(L)**	12
Plants					
Marchantia polymorpha (liver wort)	186.6 (circular)	38	30	Standard	32
Arabidopsis thaliana (thale cress)	366.9 (circular)	31	21	Standard	23
Photosynthetic protists					
Chlamydomonas reinhardtii (green alga)	15.8 (linear)	7	5	Standard	
Prototheca wickerhamii (green alga[h])	55.3 (circular)	31	29	Standard	5
Ochromonas danica (golden alga)	41.0 (linear)	30	27	Standard	
Porphyra purpurea (red alga)	63.7 (circular)	22	26	Standard	2
Nonphotosynthetic protists					
Acanthamoeba castellanii (amoeba)	41.6 (circular)	34	18	**UGA(W)**	3
Monosiga brevicollis (choanoflagellate)	76.6 (circular)	26	27	**UGA(W)**	4
Phytophthora infestans (oomycete)	38.0 (circular)	35	27	Standard	
Reclinomonas americana (jakobid flagellate)	69.0 (circular)	64	31	Standard	1

[a] Size in kbp, rounded values; "circular" stands for "circular mapping," i.e., the major portion of these mtDNAs occurs as long linear concatamers, not as monomeric circles. "Linear" stands for "monomeric linear."

[b] The number of identified genes is indicated. The basic set of protein-coding genes typically found in animals and fungi are, *cob* (apocytochome b), *cox1,2,3* (cytochrome oxidase subunits), *atp6,8,9* (ATPase subunits), and *nad1,2,3,4,4L, 5, 6* (NADH dehydrogenase subunits). The *M. senile* mtDNA contains an additional gene with similarity to bacterial *mutS*, and protists, fungi and plants contain additional hypothetical protein genes (ORFs).

[c] Genes for *rns, rnl* (small and large subunit rRNAs) occur in all mtDNAs, whereas genes coding for *rrn5* (5S rRNA), and RNase P RNA, might be absent. The number of mtDNA-encoded tRNAs varies. Duplicated genes are counted only once.

[d] Deviations from the standard bacterial translation code are indicated in bold.

[e] Total number of introns, the two mitochondrial intron classes "I" and "II" are not distinguished.

[f] Further codon reassignments include the use of AGA and AGG as stop codons, and additional translation initiation codons other than AUG and GUG.

[g] In *S. pombe*, one UGA(Trp) is present in *rps3*, and two in intronic ORFs.

[h] *Prototheca* belongs to green algae, but has secondarily lost its capacity for photosynthesis.

mtDNA to the nucleus ($\sim 10^{-5}$ per generation) has been experimentally determined in yeast.

Limitation of Gene Transfer to the Nucleus

Not a single eukaryote is known in which all genes have been relocated to the nucleus. All eukaryotes that lack mtDNA are unable to produce ATP via oxidative phosphorylation, and frequently contain degenerated mitochondria (hydrogenosomes or mitosomes).

Two major hypotheses have been proposed to explain why certain mitochondrial genes are much more rarely transferred to the nucleus than others. It has been reasoned that import of gene products into mitochondria may be hampered if these are highly hydrophobic (e.g., Cox1 and Cob), or very large (ribosomal RNAs), and thus counteract the transfer of the corresponding genes to the nucleus. Another theory invokes control of transcription initiation of mitochondrial genes by changes in redox potential inside mitochondria. This would require sensor genes to reside on

mtDNA, a mechanism described for chloroplasts. Both interpretations are consistent with the observed hierarchy of mitochondrial gene loss in different eukaryotic lineages, and may well apply in concert.

Mitochondrial Genome Diversity in Extant Eukaryotes

Over the past two decades, >500 complete mitochondrial genome sequences have been determined. Here, we will only summarize the distinctive features of mtDNAs from the major eukaryotic groups. Figure 2 depicts the maps of some selected mitochondrial genomes, demonstrating the diversity of mtDNA size, gene organization, and gene content.

Animal mtDNAs

To date, complete mtDNA sequences of more than 400 animals have been deposited in public databases. Animal mtDNAs are typically small (14–17 kbp in size) and carry intronless genes that are compactly arranged on both DNA strands. Mitochondrial genes code for the small and large subunit ribosomal RNAs, 13 proteins,

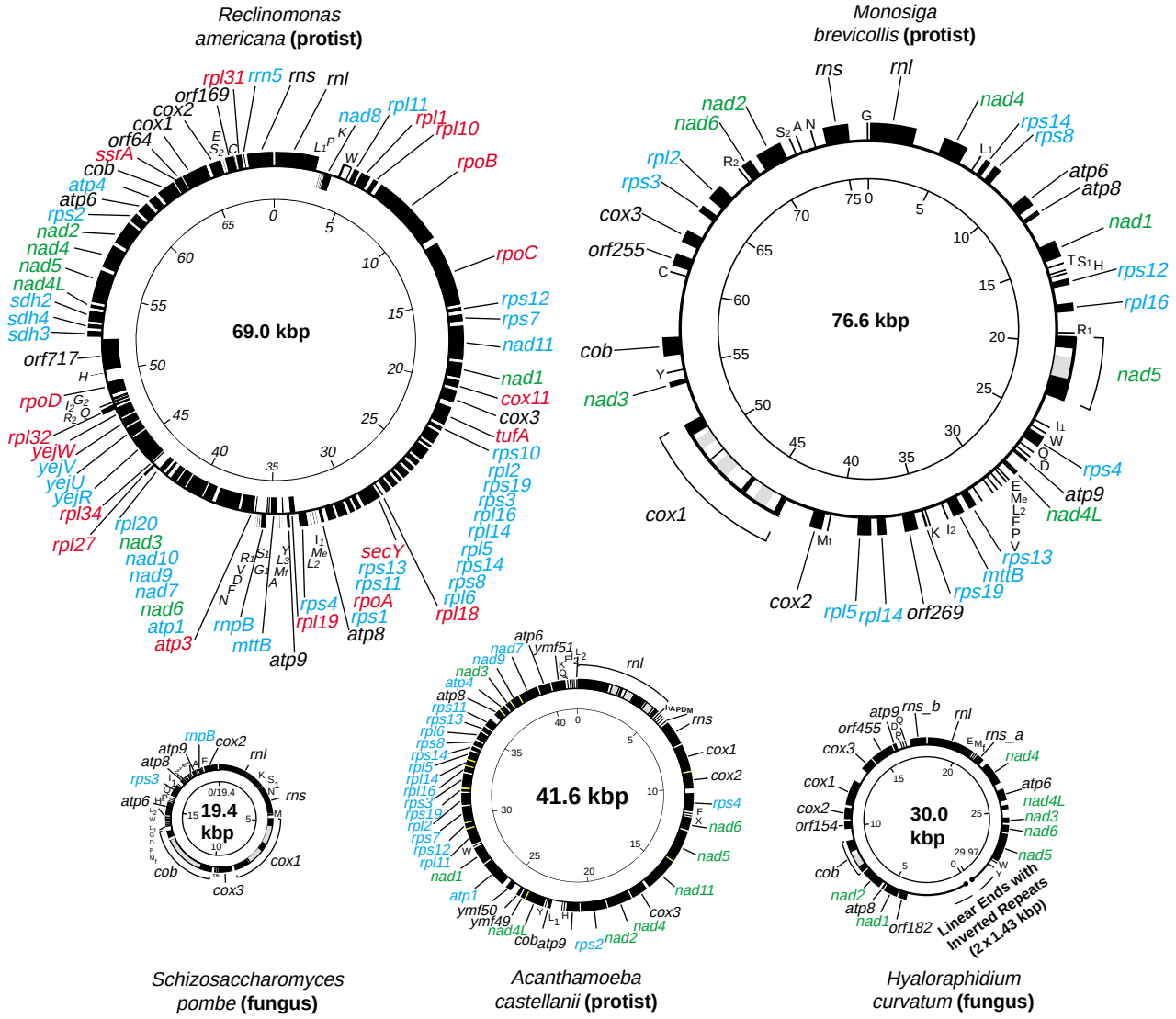

FIGURE 2 Diversity of mitochondrial genomes from various eukaryotic groups. Genetic maps of mtDNAs from protists and fungi, demonstrating the wide range of coding capacity, size, and organization (the mtDNA of *Hyaloraphidium* is linear, but is depicted as a circle to facilitate comparisons). Outer ring, transcription is clockwise; black rectangles, genes; white rectangles with gray-shaded sections, introns and intronic open reading frames. Gene names in black are genes of the basic gene complement common to all fungal and animal mtDNAs, and unidentified open reading frames (ORFs); green, extended gene set common to fungi and animals (and most other eukaryotes); blue, extra genes common to most protists; red, extra genes only found in jakobid flagellates.

and up to 22 tRNAs (Table I). Genes are arrayed in an order that is well conserved within and, to a lesser degree, among animal phyla. Exceptions are found among corals and sea anemones (phylum Cnidaria), which are the only animals whose mitochondrial genes contain introns, and which have lost all but two tRNA genes. In addition, all animals studied to date use modified mitochondrial translation codes, and tRNA and rRNA structures are highly reduced and derived compared to bacterial systems.

Animal phylogenies, even when using complete sets of mitochondrial proteins, often fail to generate wellsupported tree topologies. This lack of support results from the unusually high evolutionary rate of most animal mtDNAs. In contrast, rearrangements in animal mitochondrial genomes are exceptionally rare events, which allows the use of mitochondrial gene order data for inferring evolutionary relationships in animals.

Fungal mtDNAs

Currently, completely sequenced mtDNAs are available from 22 fungal taxa, including representatives of all four major divisions of this kingdom: Ascomycota, Basidiomycota, Zygomycota, and Chytridiomycota. Fungal mtDNAs are highly variable in terms of size, structure, and content of genes and introns. For instance, in two groups of Ascomycota, all seven genes for subunits of the NADH dehydrogenase typically encoded by the mtDNA are absent. The chytridiomycete *Rhizophydium136* contains as many as 37 introns whereas other members of this group (e.g., *Harpochytrium* species) contain none. Several fungi encode highly reduced sets of only 7–9 mitochondrial tRNAs. Additional differences in coding content include unidentified reading frames and plasmid-encoded polymerases, which are quite common in filamentous fungi.

Despite this variability, the basic set of fungal mitochondrial genes resembles that of animals (Table I), apparently a result of independent events of gene loss in the two lineages.

Plant mtDNAs

Mitochondria of land plants have the largest known mtDNAs, with sizes from 180 to 2400 kbp. Despite ~100-fold increase in genome size, the number of mitochondrial genes of plants is not even twice as high as in animals, and lower than in most protists (Table I). The few sequenced plant mitochondrial genomes suggest that the increase in size is due to a progressive accumulation of noncoding DNA. Although mtDNAs of angiosperms have generally high rates of genome rearrangements and frequently contain insertions of chloroplast and nuclear DNA, the evolutionary rate of mitochondrial genes is exceptionally low relative to nuclear genes.

Protist mtDNAs

Protists are a heterogeneous group of eukaryotes that are negatively defined as not belonging to the animal, fungal, or plant kingdoms. Based on ultrastructural characteristics, several dozen protist phyla are distinguished, but the evolutionary relationships among these phyla are mostly contentious. Many protist mitochondrial genomes are more bacteria-like, and encode a substantially larger set of genes than those of animals and fungi (Table I). However, mtDNA of several parasitic protists exhibit novel and puzzling features. For instance, the linear mtDNA (6 kbp) of the malaria parasite *Plasmodium falciparum* carries only five genes. Its rRNAs are encoded by many small gene pieces. Another oddity is found in trypanosomatid parasites, whose mtDNA consists of a network of thousands of concatenated minicircles and a few dozen maxicircles. The RNAs transcribed from maxicircle genes undergo massive RNA editing through nucleotide insertions and deletions to generate translatable mRNAs.

Conclusion

Protists comprise more biological diversity than animals, plants, and fungi together. Without a doubt, investigations of mtDNAs from poorly studied protist groups will lead to further discoveries of novel genome structures and molecular mechanisms, and provide insights into the evolutionary forces that have brought about the eukaryotic cell as we know it today.

See Also the Following Articles

Mitochondrial DNA • Mitochondrial Genes and their Expression: Yeast • Mitochondrial Genome, Overview • Mitochondrial Inheritance

Glossary

Archaebacteria (Archaea) One of the three domains of life besides eukaryotes and eubacteria.

oxidative phosphorylation The generation of ATP driven by the electron flow to oxygen in bacteria and mitochondria.

phylogeny Evolutionary relationships among organisms. Molecular phylogeny is based on DNA and protein sequences (or other molecular characters).

Proteobacteria Group of Gram-negative eubacteria that are subdivided into α, β and γ.

RNA editing The programmed modification of primary transcript sequence, including substitutions, as well as insertions and deletions.

Further Reading

Boore, J. L. (1999). Animal mitochondrial genomes. *Nucleic Acids Res.* **27**, 1767–1780.

Gray, M. W., Burger, G., and Lang, B. F. (1999). Mitochondrial evolution. *Science* **283**, 1476–1481.

Gray, M. W., Burger, G., and Lang, B. F. (2001). The origin and early evolution of mitochondria (reviews). *Genome Biol.* **2**, 1018.1–1018.5.

Lang, B. F., Burger, G., O'Kelly, C. J., Cedergren, R., Golding, G. B., Lemieux, C., Sankoff, D., Turmel, M., and Gray, M. W. (1997). An ancestral mitochondrial DNA resembling a eubacterial genome in miniature. *Nature* **387**, 493–497.

Lang, B. F., Gray, M. W., and Burger, G. (1999). Mitochondrial genome, evolution and the origin of eukaryotes. *Annu. Rev. Genetics* **33**, 351–397.

Leigh, J., Seif, E., Rodriguez, N., Jacob, Y., and Lang, B. F. (2003). Fungal evolution meets fungal genomics. In *Handbook of Fungal Biotechnology* (D. Arora, ed.) 2nd edition. Marcel Dekker, New York, pp. 145–161.

Martin, W., Hoffmeister, M., Rotte, C., and Henze, K. (2001). An overview of endosymbiotic models for the origins of eukaryotes, their ATP-producing organelles (mitochondria and hydrogenosomes), and their heterotrophic lifestyle. *Biol. Chem.* **382**, 1521–1539.

Roger, A. J., and Silberman, D. J. (2002). Mitochondria in hiding. *Nature* **418**, 827–829.

Wernegreen, J. J. (2002). Genome evolution in bacterial endsymbionts of insects. *Nat. Rev. Genetics* **3**, 850–861.

Biography

B. Franz Lang and G. Burger are both Professors in the biochemistry department at the Université de Montréal, Canada. Their principal research interests are in the fields of comparative genomics, molecular evolution, and bioinformatics. They are best known for their work on organellar genome evolution and a publicly accessible organelle database. Dr. Lang holds a Ph.D. from the University of Munich, Germany. He has been Fellow of the Canadian Institute for Advanced Research (CIAR) for over 10 years. Dr. Burger also holds a Ph.D. from the University of Munich. She is a CIAR associate, and leader of the bioinformatics programs at the Université de Montréal.

Dennis Lavrov obtained his Ph.D. from the University of Michigan and is currently a postdoctoral fellow at the Canadian Institute of Health Research, with BFL.

Mitochondrial Genome, Overview

Douglas C. Wallace
University of California, Irvine, California, USA

The mitochondrial genome is the sum of the genes that are required to assemble a mitochondrion. These genes are distributed between a DNA molecule located in the mitochondrion, the mitochondrial DNA (mtDNA), and the nuclear DNA (nDNA). Whereas the genes encoded by the mtDNA vary between different species, essentially all mtDNAs code for three or more essential proteins of the mitochondrial energy-generating process of oxidative phosphorylation (OXPHOS), plus the small and large ribosomal RNAs (rRNAs) for the mitochondria-specific ribosomes. The rest of the genes necessary to assemble a mitochondrion reside in the nDNA.

Structure, Biology, and Origins

Mitochondria are present in virtually all eukaryotic cells (cells with a nucleus), and each eukaryotic cell contains multiple mitochondria that generate most of the cellular energy by oxidative phosphorylation (OXPHOS). The mitochondria became a component of the eukaryotic cell about 2 billion years ago through a symbiotic association between a motile nucleated cell and the α-proteobacterium, a *Rickettsia*-like oxidative bacterium. Because the mitochondrion was a bacterial cell, it had (and still retains) a complete information storage and retrieval system, based on the mtDNA. The mtDNA is replicated within the mitochondrion and transcribed into structural RNAs (rRNAs and tRNAs) and messenger RNAs (mRNA), and the mRNAs are translated into proteins on chloramphenicol (CAP)-sensitive mitochondrial ribosomes.

While the actual physiological interactions that stabilized the original symbiosis are unknown, one scenario is that the protomitochondrion, which carried the mitochondrial antioxidant enzyme manganese superoxide dismutase (MnSOD), provided protection to the host cell against the increasing toxicity of the global atmospheric oxygen that was being generated by the cyanobacteria during photosynthesis. Later, the host cell invented the adenine nucleotide (ADP/ATP) translocator (ANT), which permitted it to extract ATP from the mitochondrion in exchange for spent cytosolic ADP. This established the energetic interrelationship between the host and symbiont that still exists today.

As the symbiotic relationship evolved, most of the original genes of the bacterial genome were either lost or transferred to the nDNA, where they were scattered across the various chromosomes. Chromosomal mitochondrial genes are now transcribed using nuclear RNA polymerase; the mRNAs are then translated on 80S cytosolic ribosomes. The resulting proteins destined for the mitochondrion contain specific amino-terminal or internal mitochondrial-targeting sequences, permitting them to bind to the mitochondrion and to traverse the outer and inner mitochondrial membranes through the transport across the outer (TOM) and transport across the inner (TIM) complexes. These mitochondrial proteins first interact with the 70 kDa heart shock protein (HSP) and the mitochondrial import-stimulating factor (MSF); then they bind to one of two receptors (Tom20 + Tom22 or Tom37 + Tom70). These receptors interact with the general insertion pore of the TOM complex composed of Tom40, 22, 5, 6, and 7 polypeptides. Those polypeptides that are targeted to the matrix then interact with the TIM complex composed of Tim33, 23, 17, and 11 polypeptides. As the polypeptide traverses the inner membrane, it interacts with Tim44 and mitochondrial HSP70; the amino-terminal peptide is cleaved off by the mitochondrial-processing peptidase and, in some cases, the mitochondrial intermediate peptidase. By contrast, hydrophobic mitochondrial carrier proteins destined for insertion in the mitochondrial inner membrane are complexed in the intermembrane space by either the Tim9,10 or the Tim8,9,13 polypeptide complexes. These proteins are then delivered into the inner membrane by the 300 kDa TIM complex composed of the Tim54, 22, 12, 10, and 9 proteins.

Different protist genera harbor a wide variety of mtDNA structures and gene complements. Common mtDNA-encoded genes include the small and large rRNA, one subunit (cytochrome b [cytb]) of respiratory complex III (bc_1 complex), two or three subunits (COI, COII, COIII) of cytochrome c oxidase (COX or complex IV) and one or more subunits (ATP6, ATP8, ATP9) of complex V (ATP synthase [ATPsyn]). The most complex mtDNA genome analyzed to date is that of *Reclinomonas americana*. This mtDNA encodes eubacteria-like 23S, 16S, and 5S rRNA genes; a nearly

complete set of tRNA genes employing the standard genetic code; and 62 protein coding genes, including subunits for a bacteria-like RNA polymerase, multiple ribosomal proteins, additional subunits of complexes I, II, and V, etc. Modern human and vertebrate mtDNAs encode a 12S and 16S rRNA; 22 tRNAs; and 13 proteins: ND1, 2, 3, 4L, 4, 5, and 6 of the roughly 46 polypeptides of complex I, cytb of the 11 subunits of complex III, COI, II, and III of the 13 subunits of complex IV, and ATP6 and 8 of the ~17 polypeptides of complex V (Figure 1).

Some mtDNAs can have altered genetic codes. For example the mtDNA lineage leading from fungi to mammals encompasses a progression of codon changes. The earliest change, found in all fungal and animal mtDNAs, was an alteration in the tryptophan anticodon that suppressed the opal stop codon. The tryptophan codon 5′-UGG-3′ is read by the anticodon 3′-ACC-3′. Since C cannot pair with the terminal A in the adjacent opal codon (5′-UGA-3′), this is a stop codon. However, in fungal and animal mtDNAs, the tryptophan anticodon is converted to 3′-ACU-5′, and the U can pair with A, converting the opal stop codon to a tryptophan codon. Other changes include expansion of the number of methionine codons and alteration of the isoleucine codons. Finally, in the transition from *Xenopus* to mammals, the tRNA that interprets the arginine codons 5′-AGA-3′ and 5′-AGG-3′ was deleted, rendering these stop codons. Possibly these genetic code changes became established to reduce the inadvertent translation of mRNAs in the wrong compartment. The use of 5′-UGA-3′ as tryptophan in the mitochondrion would mean that mtDNA mRNAs would prematurely terminate in the cytosol. Similarly, the loss of the tRNA for the arginine AGA and AGG codons would mean that the cytosolic mRNAs could not be translated in the mitochondrion. By blocking erroneous crosstalk between the mitochondrial matrix and the cytosol, this system would increase the efficiency of protein synthesis in both compartments. However, it also means that functional

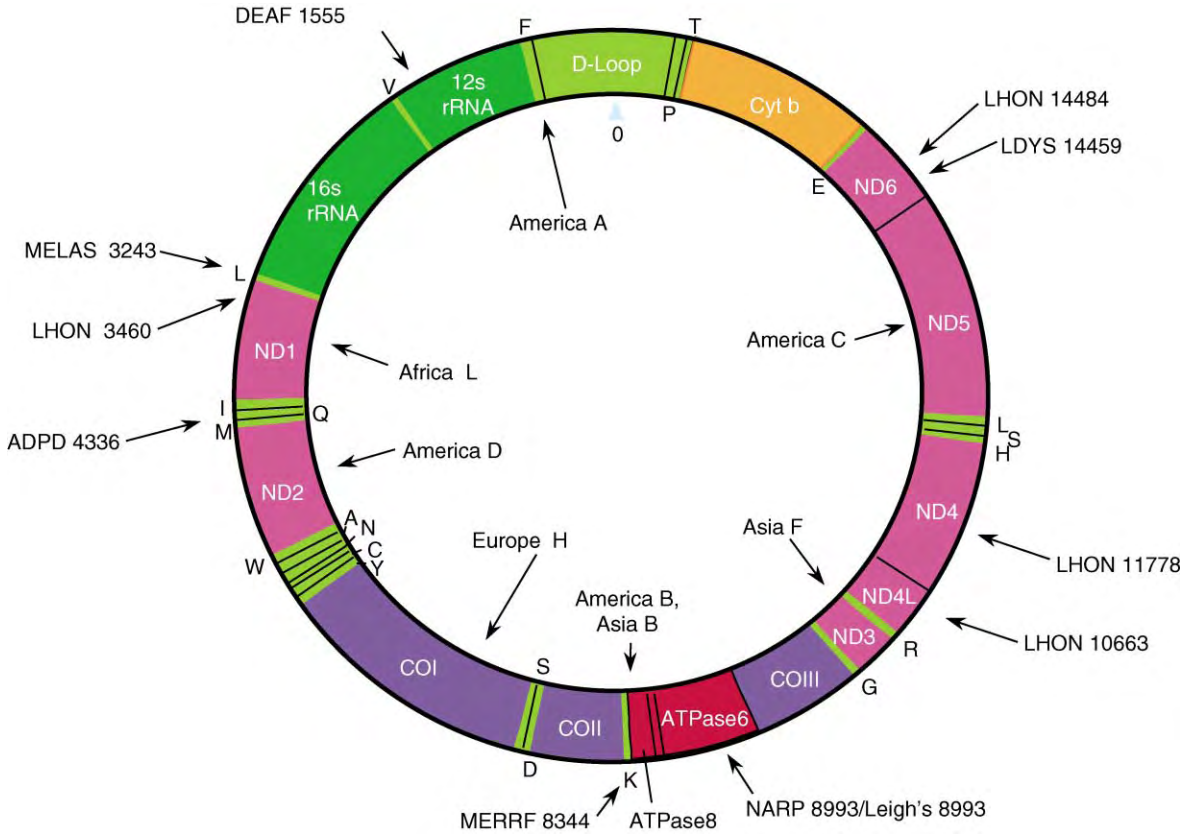

FIGURE 1 Human mitochondrial DNA map. D-loop = control region. Letters around the outer perimeter indicate cognate amino acids of the tRNA genes. Other gene symbols are defined in the text. Arrows leading from continent names and associated letters on the inside of the circle indicate the position of defining polymorphisms of selected region-specific mtDNA lineages. Arrows leading from abbreviations followed by numbers around the outside of the circle indicate representative pathogenic mutations; the number indicates the nucleotide position of the mutation. Abbreviations: DEAF, deafness; MELAS, mitochondrial encephalomyopathy, lactic acidosis, and stroke-like episodes; LHON, Leber's hereditary optic neuropathy; ADPD, Alzheimer's and Parkinson's disease; MERRF, myoclonic epilepsy and ragged red fiber disease; NARP, neurogenic muscle weakness, ataxia, retinitis pigmentosum; LDYS, LHON + dystonia. From http://www.mitomap.org.

mtDNA genes can no longer be incorporated into the nDNA. Hence, the mtDNA gene complement has been substantially conserved from fungi to humans.

All mitochondria generate energy via OXPHOS (Figure 2). OXPHOS burns hydrogen derived from carbohydrates and fats with oxygen to generate water (H_2O). In endotherms such as humans, the energy that is released is used to maintain body temperature and to generate ATP. The reducing equivalents (electrons) from dietary calories are collected by the tricarboxylic acid (TCA) cycle and transferred to either NAD^+ to generate NADH or FAD to give $FADH_2$. The electrons are then oxidized by the electron transport chain (ETC). The ETC collects electrons from NADH through complex I (NADH dehydrogenase) or from succinate in the TCA cycle through complex II (succinate dehydrogenase) and transfers them to ubiquinone (coenzyme Q_{10}, or CoQ) to generate ubisemiquinone (CoQH·) and then ubiquinol ($CoQH_2$). From $CoQH_2$, the electrons are transferred to complex III, then cytochrome c, then complex IV, and finally to ½ O_2 to give water. The energy that is released during electron transport is used to pump protons from the matrix out across the mitochondrial inner membrane to create an electrochemical gradient ($\Delta P = \Delta\Psi + \Delta\mu^{H+}$). This biological capacitor serves as a source of potential energy to drive complex V to condense ADP + Pi to give ATP. The mitochondrial ATP is then exchanged for cytosolic ADP by the ANT. The efficiency by which ΔP is converted to ATP is known as the coupling efficiency. Tightly coupled OXPHOS generates the maximum ATP and minimum heat, whereas loosely coupled OXPHOS generates less ATP but more heat.

As a toxic by-product of OXPHOS, the mitochondria generate most of the reactive oxygen species (ROS), or oxygen radicals, generated within eukaryotic cells. This results from the misdirection of electrons from the early stages of the ETC surrounding CoQH· directly to O_2 to generate superoxide anion ($O_2^{\cdot-}$). Superoxide anion is highly reactive but can be detoxified by MnSOD

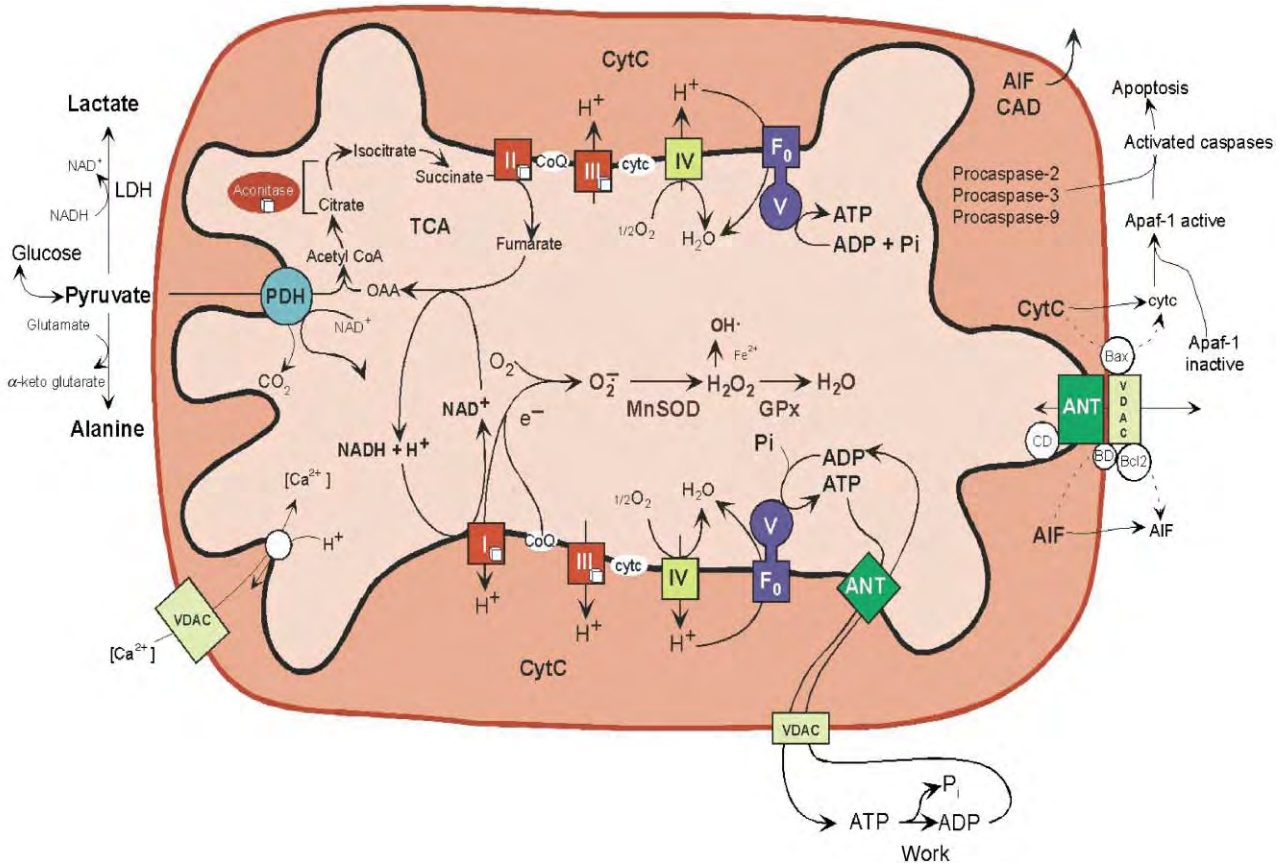

FIGURE 2 Three features of mitochondrial metabolism relevant to the pathophysiology of disease: (1) energy production by oxidative phosphorylation (OXPHOS), (2) reactive oxygen species (ROS) generation as a toxic by-product of OXPHOS, and (3) regulation of apoptosis through activation of the mitochondrial permeability transition pore (mtPTP). Abbreviations: I, II, III, IV, and V, OXPHOS complexes I–V; ADP, adenosine diphosphate; ATP, adenosine triphosphate; ANT, adenine nucleotide translocator; cytc, cytochrome c; GPx, glutathione peroxidase-1; LDH, lactate dehydrogenase; MnSOD, manganese superoxide dismutase or SOD2; NADH, nicotinamide adenine dinucleotide; TCA, tricarboxylic acid cycle; VDAC, voltage-dependent anion channel.

to generate hydrogen peroxide (H_2O_2). Hydrogen peroxide is relatively stable. In the presence of transition metals, however, it can be reduced to hydroxyl radical ($^{\cdot}OH$), which is the most toxic ROS. Consequently, H_2O_2 is reduced to water by glutathione peroxidase (GPx1) or catalase (Figure 2). ROS damage mitochondrial proteins, lipids, and nucleic acids, which inhibit OXPHOS and further exacerbate ROS production. Ultimately, the mitochondria become so energetically impaired that they malfunction and must be removed from the tissue.

Cells with faulty mitochondria are removed by programmed cell death (apoptosis) through the activation of the mitochondrial permeability transition pore (mtPTP). The mtPTP is thought to be composed of the outer membrane voltage-dependent anion channel (VDAC) proteins, the inner membrane ANT, the pro- and antiapoptotic Bcl2-Bax gene family proteins, and cyclophilin D. This complex senses changes in mitochondrial ΔP, adenine nucleotides, ROS, and Ca^{2+}, and when these factors get sufficiently out of balance, the mtPTP becomes activated and opens a channel between the cytosol and the mitochondrial matrix, depolarizing ΔP and causing the mitochondrion to swell. Proteins from the mitochondrial intermembrane space are then released into the cytosol. Among these is cytochrome c, which activates cytosolic Apaf-1 to convert procaspases 2, 3, and 9 to active caspases that degrade cellular and mitochondrial proteins. Apoptosis-initiating factor (AIF) and caspase-activated DNase (CAD) are transported to the nucleus, where they degrade the nDNA. As a consequence, the cell with faulty mitochondria is removed from the tissue so that its energetic failure dose not compromise the normal cells of the tissue and organ (Figure 2).

MtPTP-induced apoptosis means that only cells with optimally functioning mitochondria are retained in the tissue. However, postmitotic tissues have a finite number of cells, generally enough for the organ to function optimally until postreproductive age. Cell loss due to mitochondrial decline results in organ failure and the symptoms we call aging. Thus, the pathophysiology of degenerative diseases and aging results from the interplay between three central mitochondrial processes: energy production via OXPHOS, ROS generation and oxidative stress, and mtPTP activation initiating apoptosis.

Because of its extrachromosomal location, the mtDNA has unique genetics. In vertebrates, the mtDNA is inherited exclusively through the mother. However, each cell can harbor thousands of copies of the mtDNA, which can be pure normal (homoplasmic wild-type), a mixture of mutant and normal (heteroplasmic), or homoplasmic mutant. The percentage of mutant mtDNAs determines the relative energy deficiency of the cell and thus the probability of apoptosis. The tissues most sensitive to the adverse effects of mitochondrial decline are the central nervous system, heart, muscle, and renal and endocrine systems, the tissues most affected by aging.

Because of its chronic exposure to ROS, mammalian mtDNAs have a very high mutation rate. Hence, even though the human mtDNA is small, mtDNA diseases are common. Germline mtDNA mutations result in maternally inherited diseases. However, mtDNA mutations also accumulate in postmitotic somatic tissues, resulting in tissue decline.

Mitochondrial Variation and Human Origins

Because of its exclusive maternal inheritance and high mutation rate, human mtDNA variation has been used to reconstruct the ancient origins and migrations of women (Figure 3). These studies revealed that humans arose in Africa approximately 150,000 to 200,000 years before present (YBP), with sub-Saharan African mtDNAs radiating into four African-specific lineages: L0, L1, L2, and L3. The most ancient mtDNA lineages are found among the Khoisan Bushmen. About 65,000 YBP, L3 gave rise to two new lineages in northeastern Africa, designated M and N. Only M and N left Africa to colonize the rest of the world. One group migrated along the southeastern Asian coast to colonize Australia, while others bearing M and N radiated into Eurasia. In Europe, lineage N gave rise to the European-specific lineages H, I, J, K, T, U, V, W, and X. In Asia, both M and N radiated to generate a plethora of Asian-specific mtDNA lineages, including A, B, and F from N and C, D, and G from M. Among all of the Asian mtDNA lineages, only A, C, and D successfully occupied arctic Chukotka in northeastern Siberia. When the Bering land bridge appeared, individuals bearing these mtDNAs moved into the Americas about 20,000 YBP. Subsequently, a coastal migration brought lineage B to mix with A, C, and D about 12,000–15,000 YBP, thus generating the final Paleo-Indian mtDNA complement. Another migration across the arctic brought the European haplogroup X to the Great Lakes region of North America approximately 15,000 YBP. A migration from around the Sea of Okhotsk about 7,000–9,000 YBP brought a modified A to found the Na-Dene. Finally, a migration bringing A and D mtDNAs gave rise to the Eskimos and Aleuts.

MtDNA Variation and Human Adaptation to Cold

One geographical constraint that could have acted on mtDNA variation is climate. The mitochondria utilize

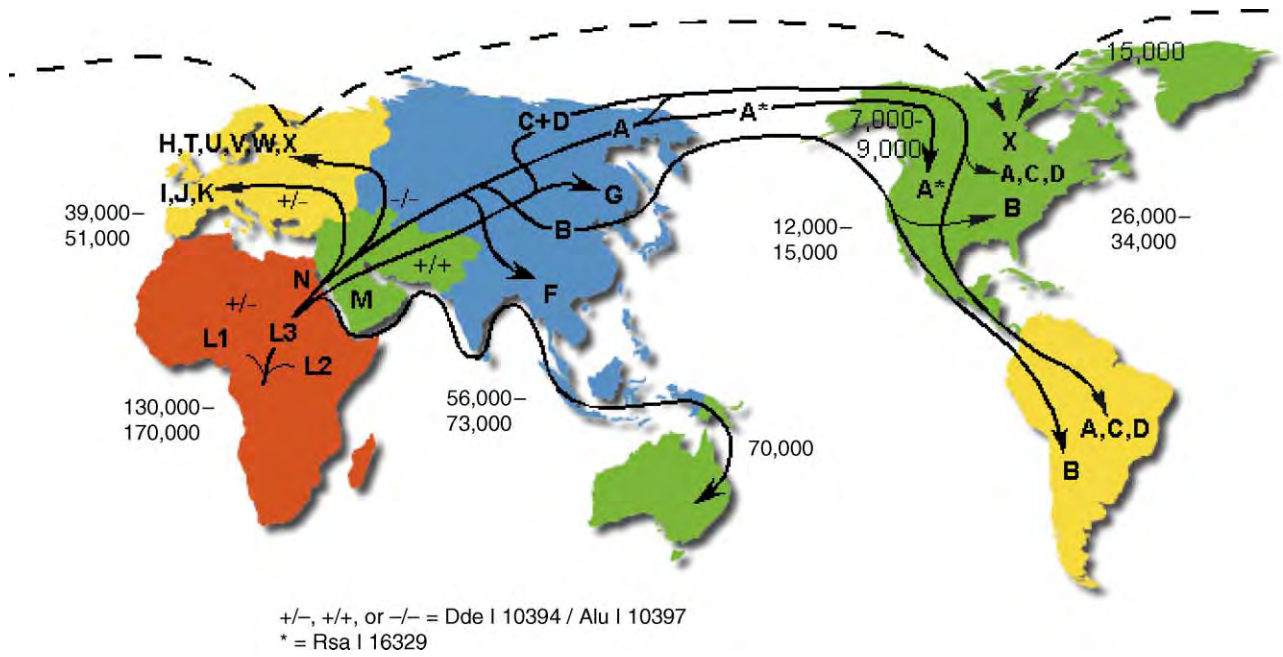

FIGURE 3 Global radiation of mtDNA types showing the regional association of mtDNA types. Capital letters represent major region groups of related haplotypes (haplogroups). In sub-Saharan Africa, haplogroup L0, which arose between 150,000 and 200,000 years before present (YBP), radiated into haplogroups L1, L2, and L3. At about 65,000 YBP, haplogroup L3 gave rise to haplogroups M and N in northeastern Africa. M and N then left Africa in two directions. A southeastern migration moved through Southeast Asia, ultimately giving rise to Australian mtDNAs. A northeastern migration colonized Eurasia, with haplogroup N giving rise to the European mtDNA haplogroups H, I, J, K, T, U, V, W, and X and to the Asian haplogroups A, B, F, etc. Haplogroup M radiated into Asia to give rise to Asian haplogroups C, D, G, etc. Haplogroups A, C, and D became enriched in northeastern Siberia and crossed the Bering land bridge between 20,000 and 30,000 YBP to found the Paleo-Indians. Haplogroup B migrated along the Asian and Bering coasts to mix with Native American haplogroups A, C, and D about 12,000–15,000 YBP. European-like haplogroup X arrived in Central North America about 15,000 YBP; derivatives of haplogroup A crossed the Bering Strait about 7,000–9,000 YBP to generate the Na-Dene; and derivatives of haplogroups A and D crossed the Bering Strait approximately 3,000–5,000 YBP to give rise to the Eskimos and Aleuts. The +/+, +/−, −/− represent important diagnostic restriction sites. The ages were calculated using the empirically determined mtDNA sequence evolution rate of 2.2–2.9%/million years (MYR). From http://www.mitomap.org.

dietary calories not only to synthesize ATP but also to generate heat to maintain body temperature. Individuals in the tropics would need tightly coupled mitochondria to maximize ATP production and minimize heat production, while individuals from the arctic would need uncoupled mitochondria to increase heat production at the expense of ATP generation.

This concept is supported by the nonrandom distribution of mtDNA gene amino acid substitutions. The mtDNA ATP6 protein sequence is hypervariable in the arctic Siberians and North Americans but conserved in the tropical Africans and temperate zone Europeans. The cytb protein sequence is hypervariable in temperate Europeans but conserved in the Africans and Siberians. COI is most variable in Africans, and so on. A detailed study of the sequences of more than 1000 mtDNAs from around the world permitted the assembly of a global human mtDNA phylogenetic tree, in which every mutation was positioned according to the relative time that it occurred. This revealed that ancient conserved amino acid substitution mutations occurred at the base of many of the temperate and arctic zone mtDNA lineages. These mutations appear to reduce OXPHOS coupling efficiency by reducing the efficiency of either proton pumping by the ETC or ATP generation by the ATP synthase. Hence, as people moved north, mtDNA lineages from the warmer climates were excluded, while mtDNA lineages with new mutations that reduced coupling efficiency and increased heat production survived and expanded into the colder latitudes.

These same nodal mutations have been found to correlate with longevity and protection against neurodegenerative diseases. European lineages J and K, which harbor cytb mutations in the inner and outer CoQ-binding sites, are protective for Alzheimer's or Parkinson's disease and also are associated with increased longevity. Mutations in the CoQ-binding sites would inhibit the Q cycle of complex III and thus reduce the efficiency of proton pumping. Because uncoupled mitochondria would oxidize more electrons, fewer would be available to generate ROS. Hence, cold-adapted mtDNAs would be associated with less

oxidative stress, thus increasing the longevity of postmitotic cells. Thus, ancient adaptive mtDNA variants are affecting individual predisposition to degenerative diseases and aging today.

Diseases of the mtDNA

The high mtDNA mutation rate that generated the ancient adaptive polymorphisms also results in a high frequency of pathogenic mutations today. Pathogenic base substitution and rearrangement mutations are both common in the human mtDNA. Base substitution mutations can alter proteins. For instance, the ND4 missense mutation (R340H) at nucleotide pair (np) 11778 causes Leber's hereditary optic neuropathy (LHON), a form of sudden-onset, midlife blindness. mtDNA mutations can also change protein synthesis genes, tRNAs, or rRNAs. For example, a $tRNA^{Lys}$ mutation at np 8344 causes myoclonic epilepsy and ragged red fiber disease (MERRF). Rearrangement mutations can occur throughout the mtDNA and result in multisystem disorders such as chronic progressive external ophthalmoplegia (CPEO), the Kearns-Sayre syndrome, or the Pearson's marrow pancreas syndrome. A plethora of pathogenic mutations in the mtDNA have now been described and are catalogued at www.mitomap.org. These diseases involve the following: the central nervous system, affecting vision, hearing, movement, balance, and memory; muscle, causing progressive weakness; heart, leading to hypertrophic and dilated cardiomyopathy; the endocrine system, including diabetes mellitus; and the renal system. Hence, it is now clear that mitochondrial defects represent one of the most common forms of human inborn errors of metabolism.

The pathogenicity of mildly deleterious mutations can also be augmented by the mtDNA lineage on which the mutation occurred. LHON can be caused by a number of mtDNA point mutations in the ND genes. The more biochemically severe mutations can cause LHON independent of the background mtDNA. However, the milder ND mutations cause LHON only when they co-occur on the European mtDNA lineage J. Hence, the diminished ATP production of partially uncoupled haplogroup J mtDNAs must augment the energetic defect of the mild ND mutations.

Somatic mtDNA Mutations in Aging

One of the most distinctive features of mitochondrial diseases is that they have a delayed onset and a progressive course. Because known mtDNA mutations can cause all of the same symptoms as seen in the elderly, it has been suggested that the accumulation of mtDNA mutations provides the aging clock. The age-related decline of mitochondrial function and an associated accumulation of somatic mtDNA mutations have been documented in a variety of animal species, with the level of mtDNA damage being proportional to lifespan, not absolute time. The accumulation of mtDNA deletions is observed in most tissues, but the

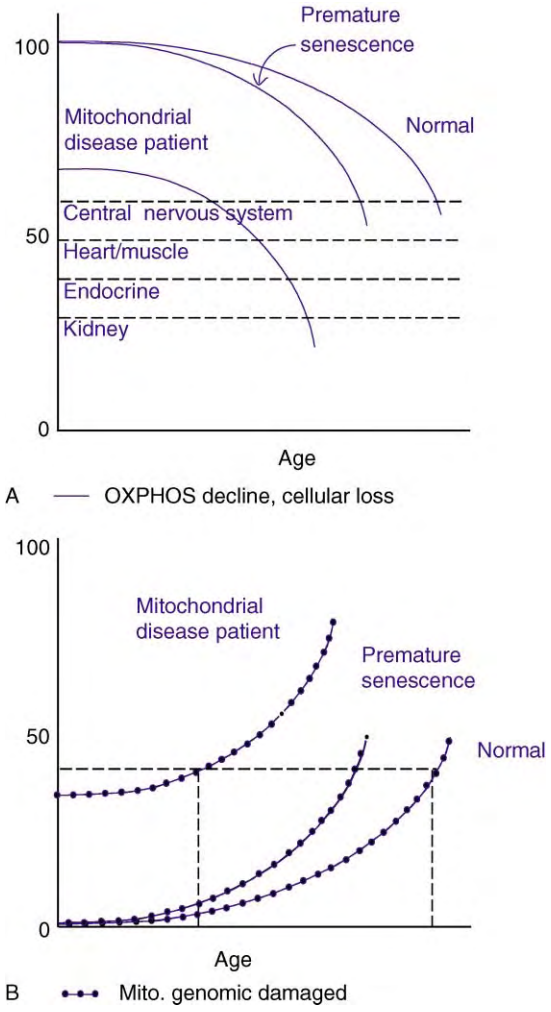

FIGURE 4 Hypothesis for the role of mitochondrial energetic decline and mitochondrial nDNA and mtDNA gene mutations in aging and degenerative disease. (A) Relationship between mitochondrial energy-generating capacity and age. (B) Relationship between defective mitochondrial genes and age. The initial energetic capacity (A) is determined by the inherited mitochondrial genotype (B), with some individuals having a lower proportion of deleterious mitochondrial variants and thus a higher initial energetic output than others. However, as individuals age they accumulate somatic mtDNA mutations in their postmitotic tissues (B) that causes the erosion of their mitochondrial energetic capacity (A). Ultimately, the sum of the inherited genetic defects plus the acquired somatic mtDNA defects cause the mitochondrial energetic capacity to fall below the minimum levels necessary for normal tissue function. If this occurs early in life, it is called disease, whereas if it occurs late in life, it is called senescence.

age-related accumulation of somatic mtDNA point mutations has been observed in the control region and appears to be tissue specific.

Aging is also the most significant risk factor for developing cancer, which implicates somatic mtDNA mutations in cancer as well. Consistent with this concept, somatic mtDNA mutations have been identified in a variety of cancers, including an ND1 intragenic deletion in a renal adenocarcinoma, base substitutions and small deletions in colon carcinomas, various point mutations in bladder, head, and neck, and lung primary tumors.

Therefore, mitochondrial diseases, aging, and cancer can be envisioned as related processes, differing only in their time course (Figure 3). Each individual starts life with a particular energetic capacity determined by his inherited mtDNA and nDNA mitochondrial variants. If the individual inherits a robust mitochondrial genotype, he starts high on the energetic scale. If he harbors one or more partially deleterious variants in the mitochondrial genome, however, he starts lower on the energetic scale (Figure 4). As the individual ages, he accumulates somatic mtDNA mutations that further erode his cellular mitochondrial function and thus tissue integrity and function. Eventually, cellular loss results in organ failure and symptoms. If thresholds are crossed early, it is called mitochondrial disease; if they are crossed late, it is known as aging.

See Also the Following Articles

Cell Death by Apoptosis and Necrosis • Cytochrome *c* • Cytochrome Oxidases, Bacterial • Free Radicals, Sources and Targets of: Mitochondria • Mitochondrial DNA • Mitochondrial Genes and their Expression: Yeast • Mitochondrial Inheritance

Glossary

apoptosis A process of programmed cell death resulting in the activation of caspase enzymes and degradation of cellular proteins that can be initiated via the mitochondrion through the activation of the mitochondrial permeability transition pore (mtPTP) in response to energy deficiency, increased oxidative stress, excessive Ca^{2+}, and/or other factors.

mitochondrial DNA (mtDNA) The portion of the mitochondrial genome that resides in the matrix of the mitochondrion, often as a circular DNA molecule containing the mitochondrial rRNA genes, some tRNA genes, and at least three cytochrome *b* and cytochrome *c* oxidase subunits I and III (COI and COIII) mitochondrial protein genes.

mitochondrion Cellular organelle of endosymbiotic origin residing in the cytosol of most nucleated (eukaryotic) cells that produces energy by oxidizing organic acids and fats with oxygen by the process of oxidative phosphorylation (OXPHOS).

oxidative phosphorylation (OXPHOS) The process by which the mitochondrion generates energy through oxidation of organic acids and fats with oxygen to create a capacitor [electron chemical gradient ($\Delta P = \Delta\Psi + \Delta^{pH}$)] across the mitochondrial inner membrane and uses this stored potential energy to generate adenosine triphosphate (ATP), transport substrates or ions, or produce heat.

reactive oxygen species (ROS) Toxic by-products [primarily superoxide anion ($O_2^{\cdot-}$), hydrogen peroxide (H_2O_2), and hydroxyl radical ($^{\cdot}OH$)], commonly referred to as oxygen radicals, that are generated by oxidative phosphorylation, which damages the mitochondrial and cellular DNA, proteins, lipids, and other molecules causing oxidative stress.

Further Reading

Gray, M. W., Burger, G., and Lang, B. F. (1999). Mitochondrial evolution. *Science* **283**, 1476–1481.

Michikawa, Y., Mazzucchelli, F., Bresolin, N., Scarlato, G., and Attardi, G. (1999). Aging-dependent large accumulation of point mutations in the human mtDNA control region for replication. *Science* **286**, 774–779.

Mishmar, D., *et al.* (2003). Natural selection shaped regional mtDNA variation in humans. *Proc. Natl. Acad. Sci. USA* **100**, 171–176.

Ruiz-Pesini, E. E., Mishmar, D., Brandon, M., Procaccio, V., and Wallace, D. C (2004). Effects of purifying and adaptive selection on regional variation in human mtDNA. *Science*, **303**(5655): 223–226.

Wallace, D. C. (1992). Mitochondrial genetics: A paradigm for aging and degenerative diseases? *Science* **256**, 628–632.

Wallace, D. C. (1999). Mitochondrial diseases in man and mouse. *Science* **283**, 1482–1488.

Wallace, D. C. (2001). Mouse models for mitochondrial disease. *Am. J. Med. Gen.* **106**, 71–93.

Wallace, D. C., Brown, M. D., and Lott, M. T. (1999). Mitochondrial DNA variation in human evolution and disease. *Gene* **238**, 211–230.

Wallace, D. C., Lott, M. T., Brown, M. D., and Kerstann, K. (2001). In *The Metabolic and Molecular Basis of Inherited Disease* (C. R. Scriver, A. L. Beaudet, W. S. Sly and D. Valle, eds.) Mitochondria and neuro-ophthalmologic diseases. pp. 2425–2512. McGraw-Hill, New York.

Wallace, D. C., and Lott, M. T. (2002). In *Emery and Rimoin's Principles and Practice of Medical Genetics* (D. L. Rimoin, J. M. Connor, R. E. Pyeritz and B. R. Korf, eds.) Mitochondrial genes in degenerative diseases, cancer and aging. pp. 299–409. Churchill Livingstone, London.

Biography

Douglas C. Wallace received his B.S. degree from Cornell University in 1968 and Ph.D. from Yale University in 1975 in microbiology and human genetics. He was Assistant Professor of Genetics at Stanford University from 1976 to 1983 and Professor of Biochemistry and Genetics at Emory University from 1983 to 2002. In 2002 he joined the University of California, Irvine as Donald Bren Professor of Molecular Medicine and Director, Center for Molecular and Mitochondrial Medicine and Genetics.

Mitochondrial Inheritance

Eric A. Shoubridge
McGill University, Montréal, Québec, Canada

Mitochondria are small cellular organelles whose primary function is the provision of cellular energy by the process of oxidative phosphorylation. They are surrounded by a double membrane and are about the size of the bacteria from which they were derived by endosymbiosis more than a billion years ago. Mitochondria contain their own DNA that codes for a relatively small number of proteins and RNAs. The size of the mitochondrial genome varies enormously in the biological world, and it generally exists as multiple copies per organelle, with tens to thousands of copies per cell. Mitochondrial genomes do not obey Mendelian laws of segregation and independent assortment. Allelic variants of mitochondrial DNA segregate during mitosis and meiosis, and even in postmitotic cells as mitochondria turn over. This results from the lack of stringent control on mitochondrial DNA replication, and on the random partitioning of mitochondrial genomes to daughter mitochondria. Mitochondrial DNA is uniparentally transmitted in nearly all organisms, in most cases through the female germ line.

Mitochondrial Structure and Function

Mitochondria are cytoplasmic organelles of $\sim 0.5-1.0\ \mu M$ in diameter. They are bounded by a double membrane: an outer membrane that is permeable to small molecules, and an impermeable inner membrane, across which an electrochemical proton gradient formed by electron transport is used to drive ATP synthesis. The inner membrane is a specialized structure, rich in cardiolipin, containing the respiratory chain complexes and carriers that move metabolites in and out of the matrix compartment. This membrane is highly convoluted into folds called cristae, which act to increase the surface area of this membrane. The matrix space bounded by the inner membrane contains soluble enzyme components required for the myriad other functions of mitochondria including the tricarboxylic acid cycle, heme biosynthesis, urea cycle, iron-sulfur cluster biosynthesis, fatty acid oxidation, and amino acid metabolism. It also contains the mitochondrial genome and the machinery necessary for its replication, transcription and translation. It is thought that mitochondria cannot be made *de novo*, but only from other mitochondria. Although mitochondria are often depicted in textbooks as small spherical bodies, they can in fact take on a variety of shapes from simple spheres to large interconnected reticular networks. Mitochondria actively move within the cell and are in a dynamic equilibrium that involves fusion and fission of individual organelles.

Structure of Mitochondrial Genomes

The mitochondrial genomes of all eukaryotes are generally much smaller than bacterial genomes, most of the genes in the original endosymbiont having been transferred to the nucleus during the course of evolution. All animal mitochondrial genomes that have been studied are less than 20 kbp in size, and the majority of these are circular. Mammalian mitochondrial genomes contain only 13 protein-coding genes and the 22 tRNAs and 2 rRNAs necessary to translate these proteins in the mitochondrial matrix. There are no introns, and few noncoding bases outside of the control regions that contain sequences essential for replication and transcription of the genome. Some animal mitochondrial genomes do not contain a full complement of tRNAs and these must therefore be imported. The mitochondrial genomes of the fungi are generally 20–100 kbp in size. They often contain fewer genes than animal mitochondrial genomes, the larger size being attributable to the presence of introns and other large pieces of noncoding DNA. Flowering plants have the largest mitochondrial genomes; most are a few to several hundred kbp in size. These circular genomes contain large direct-repeat sequences that actively recombine to produce large full-length genomes and families of smaller subgenomic circles. Plant mitochondrial genomes often contain sequences derived from the chloroplast genome, the other organellar genome in plants. Many plant mitochondrial genomes contain coding

sequences for chimeric proteins that are responsible for cytoplasmic male sterility.

Mitochondrial DNA is complexed with proteins in the mitochondrion in a structure called the nucleoid, which may be physically associated with the inner mitochondrial membrane.

Genetic Code

The mitochondrial genetic code in animals and fungi is different from the universal genetic code. For instance, the universal stop codon UGA specifies tryptophan in the mitochondrial code, preventing the translation of full-length mitochondrial polypeptides on cytosolic ribosomes. The mitochondrial (and chloroplast) genetic code in flowering plants is the same as the universal code. Transfer of functional genes from the mitochondrial genome to the nucleus thus can and does still occur in plants.

Heteroplasmy and the Segregation of Mitochondrial DNA

New mutations in mitochondrial DNA, which can arise in somatic or germ cells, lead to a situation in which more than one mitochondrial DNA sequence variant (allele) is present in the cell. This generally transient state is referred to as mitochondrial DNA heteroplasmy. Segregation of the different alleles eventually returns the system to the homoplasmic state in which there is no allelic variation. Mitochondrial DNA does not obey the Mendelian laws that apply to the segregation and independent assortment of chromosomal DNA in the nucleus. Although the copy number of mitochondrial DNA is regulated according to the cellular requirements for mitochondrial function, the stringent control that the cell exerts over the replication of nuclear DNA, in which only one copy of each chromosome can be made at each cell cycle, does not exist for mitochondrial DNA. Like some bacterial plasmids, replication of mitochondrial DNA is relaxed and not linked to the cell cycle; the only control is over the copy number. Thus, individual templates may replicate more than once or not at all during mitochondrial proliferation and division. In a dividing cell, mitochondrial DNAs will partition randomly to the daughter cells. In the absence of selection for one allele or another, the relative proportion of the different alleles will be subject to random genetic drift. The rate of genetic drift depends on the copy number and half-life of mitochondrial DNA in the cell. Genetic drift will be fastest in cells containing few copies of mitochondrial DNA with a short half-life. The unit of inheritance of mitochondrial DNA, which determines the effective mitochondrial DNA copy number, is likely to be larger than the genome itself, as multiple genomes can exist per nucleoid and multiple nucleoids populate a mitochondrion.

Transmission of Mitochondrial DNA between Generations

In most organisms, mitochondrial genomes are inherited from one parent, usually, but not universally, the female. The mitochondrial DNA copy number is usually larger in oocytes than in somatic cells. There are 100,000–200,000 copies of mitochondrial DNA in a mammalian oocyte, distributed as ~one per organelle. Despite this large copy number, new allelic variants have been observed to segregate rapidly between generations, with complete fixation often occurring in a few generations. This apparent paradox is the result of a mitochondrial bottleneck that occurs in oogenesis. The number of mitochondria changes dramatically during early embryogenesis and oogenesis. After fertilization, mitochondrial DNA replication does not resume until implantation of the early mammalian embryo. This effectively reduces the copy number of mitochondrial DNA per cell by a factor of ~1000, returning it to that typical of a somatic cell. In the early embryo, a small population of cells is set aside called primordial germ cells. These cells will give rise to all of the gametes that will eventually colonize the gonads. Ultrastructural analyses show that these cells contain only about ten mitochondria, and this is where the bottleneck for transmission occurs. The number of mitochondria increases to ~200 in the oogonia, the migratory cells that populate the genital ridge, and then to a few thousand in the primary oocyte of primordial follicles. A nearly 100-fold amplification of mitochondrial DNA is associated with maturation of the pre-ovulatory oocyte. Thus, although the oocyte contributes at least 100,000 mtDNAs to the zygote in mammals, the effective number of mitochondrial DNA molecules that are transmitted between generations is determined by the relatively small number of mitochondrial DNAs, perhaps as few as ten, which pass through the primordial germ cells. This accounts for the rapid segregation of allelic variants of mitochondrial DNA between generations. Transmission of different alleles through the female germline is, however, a stochastic process. The proportion of a particular allelic variant varies considerably among offspring because of the bottleneck, but the mean proportion in all offspring is similar to that in the mother. In other words, the level of heteroplasmy for an allelic variant in an individual is just as likely to have increased or decreased compared to that of the mother.

Uniparental Inheritance

Uniparental inheritance may be achieved passively by simple dilution of mitochondrial genomes in organisms where the sizes of the two gametes are unequal, or by active processes that exclude or eliminate the contribution from one parent. Examples of active processes include exclusion of organelles from gametes or zygotes, degradation of organelles in the gamete or zygote, and exclusion of organelles from embryonic tissue. The largest variety of active mechanisms is found in plants, where uniparental inheritance of the chloroplast genome (sometimes from a different parent) is also the rule. In mammals, sperm mitochondria, which contain ~100 copies of mitochondrial DNA, enter the zygote, but they are actively eliminated with the sperm remnants during early embryogenesis. Male leakage of mtDNA has been observed in interspecific crosses in mice, suggesting that the factors controlling the elimination of paternal mitochondria are species-specific. Male transmission of mtDNA appears to be extremely rare in humans, a single case having been reported. The fact that uniparental inheritance of organellar genomes is so pervasive suggests that there has been strong selection for this trait throughout evolution. Such a system may have evolved to prevent the spread of mitochondrial genomes with a replicative advantage, but without significant coding-gene content (selfish genomes) in a population. Such genomes have been identified in yeast. Uniparental inheritance would confine selfish genomes to the particular lineage in which they arose.

Mitochondrial Diseases

Diseases resulting from pathogenic mutations in human mitochondrial DNA occur with a frequency of about 1 in 8500 live births and are thus relatively frequent causes of genetic disease. They produce a wide variety of clinical phenotypes with prominent involvement of muscles and nerves. Most mitochondrial DNA mutations exist in a heteroplasmic state because homoplasmy for the severe mutations would be lethal. There are marked tissue-specific differences in the segregation patterns of pathogenic mutations, suggesting that pathogenic mutations are under differing selective pressures in different tissues. The segregation pattern is also influenced by the particular mutation. Generally, a high proportion (85–90%) of mitochondrial DNAs carrying the pathogenic mutation must accumulate in the cell for expression of a pathological biochemical and clinical phenotype. This phenomenon is referred to as threshold expression. It results from intraorganellar genetic complementation in which the products of wild-type mitochondrial DNAs are able to functionally rescue the products of the mutant genomes. Mitochondrial DNAs carrying pathogenic mutations are transmitted to the next generation in a largely stochastic fashion, implying that there is weak selection for mitochondrial respiratory chain function during oogenesis, embryogenesis or fetal life.

The best-studied mitochondrial disease of flowering plants is cytoplasmic male sterility because of its agricultural importance in hybrid seed production. It results from the presence of a chimeric gene in mitochondrial DNA that usually consists of an unidentified open reading frame, fused in frame with a fragment of a mitochondrial protein-coding gene. The product of this gene specifically disrupts the production of fertile pollen. Nuclear restorer genes have been identified that suppress this phenotype.

Glossary

genetic bottleneck (mitochondrial) A restriction in the number of mitochondria and mitochondrial DNAs that occurs in mammalian oogenesis, decreasing the effective number of mitochondrial DNAs that contribute to the next generation.

heteroplasmy A state in which more than one allelic variant of mitochondrial DNA exists in a cell.

homoplasmy A state in which all copies of mitochondrial DNA in the cell have the same sequence.

mitochondrial DNA The mitochondrial genome.

nucleoid A structure containing mitochondrial DNA complexed with protein that associates with the inner mitochondrial membrane.

relaxed replication Mitochondrial DNA can be replicated at any stage during the cell cycle and individual templates can be copied more than once or not at all.

segregation (mitochondrial) The process by which different alleles of mitochondrial DNA are separated when mitochondria proliferate. This happens during mitosis, meiosis, and in postmitotic cells.

threshold expression Refers to notion that a certain proportion of mutant mitochondrial DNA must be present in the cell for an abnormal phenotype to be expressed.

Further Reading

Birky, Jr. C. W. (1994). Relaxed and stringent genomes: Why cytoplasmic genes don't obey Mendel's laws. *J. Hered.* **85**, 355–365.

Birky, Jr. C. W. (1995). Uniparental inheritance of mitochondrial and chloroplast genes: Mechanisms and evolution. *Proc. Natl. Acad. Sci. USA* **92**, 11331–11338.

Chinnery, P. F., and Schon, E. A. (2003). Mitochondria. *J. Neurol. Neurosurg. Psychiatry* **74**, 1188–1199.

Gillman, N. W. (1994). *Organelle Genes and Genomes*. Oxford University Press, New York.

Jansen, R. P. S. (2000). Germline passage of mitochondria: Quantitative considerations and possible embryological sequelae. *Hum. Reprod.* **15**(suppl. 2), 112–128.

Shoubridge, E. A. (2000). Mitochondrial DNA segregation in the developing embryo. *Hum. Reprod.* **15**(suppl. 2), 229–234.

Biography

Eric A. Shoubridge is a Professor in the Department of Neurology and Neurosurgery and the Department of Human Genetics at the Montreal Neurological Institute of McGill University. His principal research interests are in mammalian mitochondrial genetics and mitochondrial diseases. He holds a Ph.D. from the University of British Columbia and received his postdoctoral training at Oxford University. He is an International Scholar of the Howard Hughes Medical Institute and a Senior Investigator of the Canadian Institutes for Health Research.

Mitochondrial Membranes, Structural Organization

Carmen A. Mannella
Wadsworth Center, New York State Department of Health, Albany, New York, USA

The mitochondrion is the organelle in eukaryotic cells that is the primary generator of ATP, the molecule that fuels most of the cell's machinery. The chemiosmotic mechanism of ATP production involves establishment of an electrochemical gradient across the mitochondrial inner membrane by the respiratory chain complexes. The free energy in this gradient is coupled to phosphorylation of ADP by the F_1F_0 ATP synthase on the inner membrane. Since chemiosmosis entails very rapid fluxes of ions and metabolites between the mitochondrial interior and the cytosol, the shape as well as the permeability properties of the energy-transducing inner membrane can be expected to affect mitochondrial function.

Electron Microscopy and the Structure of Mitochondria

Pioneering work of Palade, Sjostrand and others in the 1950s led to the first high-quality electron microscopic images of mitochondria. Controversies ensued, partly due to the inherent difficulty of interpreting images of plastic sections that were too thin (80 nm) to convey three-dimensional (3-D) structure. Conversely, this section thickness imposed a lower limit on resolution in the axial direction (parallel to the electron beam) in these images. Thus, despite the general acceptance of a model by the early 1960s (Figure 1), work on determining the structure of mitochondria has been a work in progress. An important advance was the development of electron tomography in the 1990s, in which numerous micrographs of a serially tilted specimen are combined to yield a 3-D image. Using high-voltage electron microscopes, this technique has provided actual 3-D images of mitochondria in thick sections (200–1000 nm) with axial resolution on the order of 5 nm (Figure 2). Moreover, with computer-controlled cryo-electron microscopes, it is possible to image intact, frozen-hydrated mitochondria, rapidly frozen in aqueous buffer, without the chemical fixatives or metal stains employed with plastic sections (Figure 3).

Mitochondrial Membranes and Compartments

The mitochondrion is formed by two nested membranes, which define three classes of compartments.

Outer Membrane

The mitochondrial outer membrane is the interface between the organelle and the cytosol. It excludes proteins and other macromolecules, but is thought to be permeable to most solutes below a molecular weight of ~2000 since it carries many copies of a pore-forming protein called VDAC (voltage-dependent, anion selective channel) or mitochondrial porin.

Inner Membrane

The inner membrane is the site of the respiratory chain, the ATP synthase, and numerous carrier proteins such as ANT, the adenine nucleotide transporter that exchanges ADP and ATP.

Intermembrane Space

The space between the outer and inner membranes is called the intermembrane (or peripheral) space. Its protein content, which is much lower than that of the matrix, includes kinases (for interconversion of phosphorylated metabolites) and cytochrome *c* (involved in both electron transfer and apoptosis).

Matrix Space

The space enclosed by the inner membrane is occupied by a very dense, largely protein matrix. This compartment contains a variety of enzymes, particularly those of the Krebs cycle, along with several copies of the circular mitochondrial genome and numerous mitochondrial ribosomes. (Mitochondria synthesize a small number of respiratory chain proteins; 90% of the mitochondrial protein mass is imported from the cytosol.)

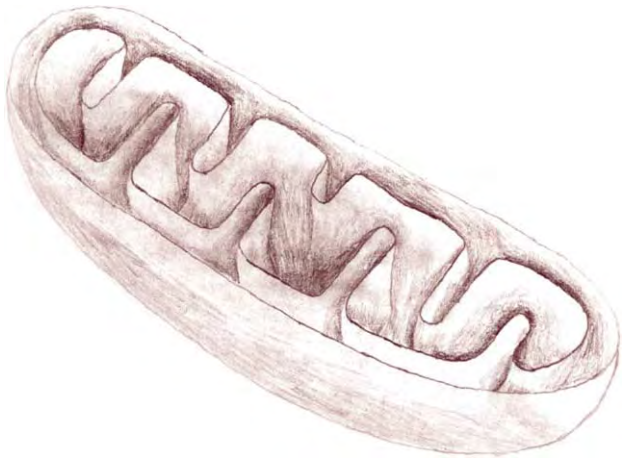

FIGURE 1 The conventional model for mitochondrial structure From Philomena Sculco, Wadsworth Center.

Cristae

The inner membrane has a much larger surface area than the outer membrane, typically by a factor of 2.5–10. There is a correlation between the energy demand in a particular tissue and the inner membrane surface, e.g., heart mitochondria have more inner membrane (and so more ATP generating capacity) than liver mitochondria. The inner membrane is contained by the smaller outer membrane because it is invaginated or involuted. The internal compartments defined by the infoldings of the inner membrane are called cristae and the space they enclose is the intracristal space. The intracristal space connects to the intermembrane space through the openings of the cristae in the peripheral region of the inner membrane.

Mitochondrial Inner Membrane Topology

The early model of mitochondrial structure portrayed the cristae as baffle-like folds in the inner membrane (Figure 1). Three-dimensional images provided by electron tomography of a wide variety of mitochondria, isolated and *in situ*, indicate a different internal architecture. The inner membrane comprises numerous pleiomorphic compartments, which are connected to each other and to the periphery of the inner membrane by narrow (20–30 nm diameter) tubular segments (Figure 2). These tubular connecting regions (called cristae junctions) can vary in length from a few tens to several hundred nanometers.

Functional Implications of the Cristae Junctions

The fact that cristae open into the intermembrane space through narrow, sometimes very long tubular segments suggests that diffusion of solutes between the internal compartments of mitochondria might be restricted. This was not a concern with the early structural model, which depicted the baffle-like cristae with wide, slot-shaped

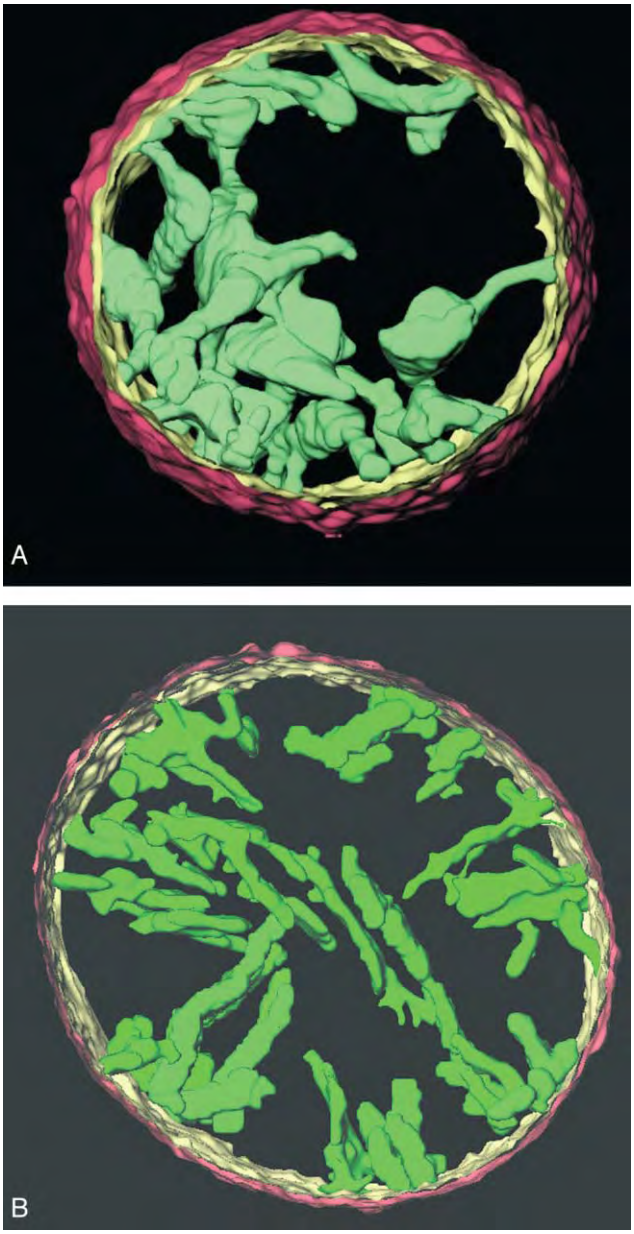

FIGURE 2 Tomographic reconstruction of membranes in isolated rat liver mitochondria in (A) condensed and (B) orthodox conformations. Mitochondria were chemically fixed, plastic-embedded and stained by conventional procedures. Approximate dimensions: (A) 1500 nm diameter, 500 nm thick, and (B) 500 nm diameter, 200 nm thick. (A) Adapted with permission from Mannella *et al.* (2001), Figure 1a.

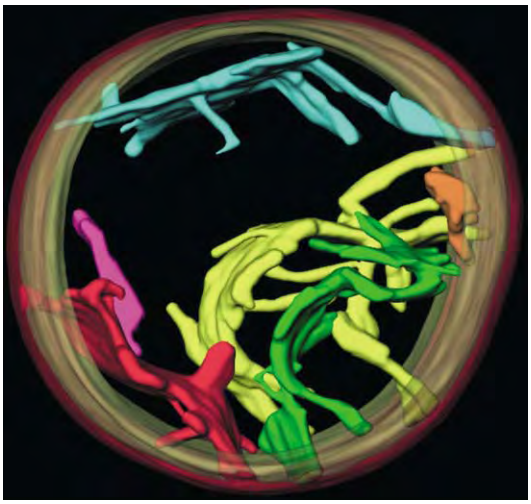

FIGURE 3 Tomographic reconstruction of membranes in an intact, frozen-hydrated rat liver mitochondrion, prepared with no chemical fixatives or stains. Approximate dimensions: 700 nm diameter, 450 nm thick. Adapted with permission from Mannella *et al.* (2001), Figure 4b.

openings into the intermembrane compartment. Computer simulations indicate that diffusion of ADP between the intermembrane and intracristal compartments via long, narrow tubes (the cristae junctions) can cause depletion of ADP in the intracristal space and locally diminished ADP phosphorylation. Thus, the topology of the mitochondrial inner membrane may directly influence the efficiency of ATP generation by the organelle.

Cristae Junctions Form Spontaneously

Tubular cristae junctions appear to be a highly conserved feature of the mitochondrial inner membrane. If they are functionally important (as implied above), it is expected that their formation would be spontaneous or energetically favored. This has been demonstrated with yeast mitochondria. Tubular connections between cristae and the peripheral region of the inner membrane form spontaneously in membranes, which initially lack cristae due to extreme osmotic swelling of the mitochondria. (Osmotic effects on mitochondrial structure are discussed in detail below.)

Changes in Mitochondrial Inner Membrane Topology

Although the mitochondrial inner membrane has a high protein-to-lipid ratio and encases a dense protein matrix, it is very flexible. The morphology of this membrane in isolated mitochondria changes readily in response to osmotic and metabolic conditions.

Osmotic Adjustments in Inner Membrane Topology

Tedeschi and Harris showed in the 1950s that mitochondria behave as "perfect osmometers" over a range of osmotic conditions. The matrix volume adjusts to changes in osmotic conditions (external solute concentration) by expanding (water influx) or shrinking (water efflux). Isolated mitochondria with a shrunken matrix (caused by water efflux in response to hyper-osmotic external conditions) are said to be in the condensed conformational state (Figure 2A). Mitochondria with a more expanded matrix (exposed to iso-osmotic or slightly hypo-osmotic conditions) are said to be in the orthodox (cell-like) state (Figure 2B). Exposure of mitochondria to very hypo-osmotic media causes extreme matrix swelling, and can lead to rupture of the outer membrane. (The latter is considered osmotically inactive due to its permeability to small solutes.)

Changes in Inner Membrane Topology Associated with Metabolic State

In the 1960s, Hackenbrock demonstrated that isolated mitochondria could reversibly switch between orthodox and condensed conformations during respiration. When ADP is added, respiring mitochondria change from orthodox to condensed conformation, then back to orthodox as ADP runs out. Condensed mitochondria tend to have larger internal compartments with longer cristae junctions, which can limit ADP diffusion into the cristae (above). Thus, the switch to orthodox conformation (smaller internal compartments, shorter tubular junctions) as ADP levels drop may prevent intracristal depletion of ADP and so maintain more efficient ATP production. Note that cellular ADP levels are normally low and mitochondria are usually in the orthodox conformation.

Inner Membrane Fusion and Fission

Comparison of 3-D images of condensed and orthodox mitochondria suggest an important role for membrane fusion and fission in regulation of inner membrane topology. Condensed mitochondria have large cristae with multiple tubular connections (cristae junctions) to the periphery of the inner membrane (Figure 2A). Conversely, orthodox mitochondria have predominantly narrower cristae with single peripheral connections (Figure 2B). Interconversion of these two membrane topologies cannot be achieved by simple unfolding and refolding of the inner membrane.

The topologies can be reconciled by postulating that large cristae with multiple tubular segments form by fusion of individual narrower cristae which make contact during matrix contraction. Likewise, matrix expansion and associated stress on the inner membrane may trigger fissioning of larger cristae into individual tubular membranes. Support for this mechanism is provided by tomographic images of frozen-hydrated mitochondria, in which large cristae clearly appear to be composed of fused tubular membranes (Figure 3). Dynamin-like proteins such as Mgm-1 and Drp-1 are involved in fusion and fission of mitochondria during organelle biogenesis and transport. These or other related proteins may regulate inner membrane fusion and fission during conformational changes as well.

Unusual Inner Membrane Topologies

While cristae in mitochondria from many animal, plant, and fungal cells have a more or less common appearance, there are numerous exceptions. For example, mitochondria in steroidogenic tissues like adrenal glands have cristae that are arranged in parallel tubular arrays. Densely packed cristae in some muscle mitochondria are arranged concentrically. Other specialized tissues (in gastropods and insects, for example) have cristae with triangular or square cross-sections. Several examples of unusual inner membrane topologies appear to be associated (at least in part) with abnormal inner membrane fusion or fission.

Cubic Paracrystalline Inner Membrane

Mitochondria in protists tend to have randomly arranged tubular cristae. In the amoeba, chaos carolinensis, fasting induces a dramatic change in inner membrane topology to an interconnected labyrinth of internal compartments with threefold (cubic) paracrystalline order. Deng and co-workers have shown that this structural transition is associated with several metabolic changes in the organism, including increased free radical production (oxidative stress). Conversion of the normally tubular inner membranes to a continuous membrane network implies induction of large-scale fusion. The highly symmetric shape of the membranes further implies that a change in membrane composition has occurred that imposes constant curvature everywhere.

Vesicular Cristae

Cristae that do not connect with the peripheral region of the inner membrane have been observed in several types of mitochondria, including muscle mitochondria from patients with a rare disorder called Senger's syndrome. This appears to be a case in which either the cristae junctions are unstable or inner membrane fission has become dominant over fusion. The specific genetic defect is unknown in Senger's syndrome, but research carried out by Huizing and co-workers suggests a tentative association with decreased ANT content.

Cytochrome *c* Release During Apoptosis

The process of apoptosis, or programmed cell death, in many cell types requires release of mitochondrial factors, including cytochrome *c*, to activate caspases involved in cellular degradative reactions. This process of mitochondrial protein release involves members of the Bcl-2 family of proteins. A key event is migration of Bax from cytosol to the mitochondrial surface, where it oligomerizes and causes protein release across the outer membrane. The trigger for this event is the truncated form of the protein Bid (tBid). Scorrano, Korsmeyer and co-workers have recently shown that tBid alone induces a dramatic change in topology of the mitochondrial inner membrane that correlates with increased accessibility of cytochrome *c* to the intermembrane space. After tBid exposure, the cristae have reversed curvature and appear to be fused into a continuum, not unlike the paracrystalline inner membrane of the fasting amoeba. Importantly, the openings of the cristae into the peripheral region of the inner membrane are considerably wider (55 nm versus 20 nm), which may account for improved diffusion of soluble proteins between compartments.

See Also the Following Articles

ATP Synthesis in Plant Mitochondria: Substrates, Inhibitors, Uncouplers • ATP Synthesis: Mitochondrial Cyanide-Resistant Terminal Oxidases • Cell Death by Apoptosis and Necrosis • Cytochrome *c* • DNA Replication, Mitochondrial • Mitochondrial DNA • Mitochondrial Genome, Evolution • Mitochondrial Genome, Overview • Mitochondrial Inheritance • Mitochondrial Outer Membrane and the VDAC Channel • Nuclear Genes in Mitochondrial Function and Biogenesis • Protein Import into Mitochondria

Glossary

cristae The complex internal compartments of mitochondria that are formed by invagination of the inner membrane.

cristae junctions Tubular regions of the inner membrane that connect the internal cristae compartments to the region of the membrane along the mitochondria periphery.

electron tomography A technique involving computation of a three-dimensional density map from scores of images recorded in an electron microscope of a serially tilted specimen.

mitochondria The organelle in eukaryotic cells, composed of an outer and inner membrane, that uses the free energy of substrate oxidation for ATP production.

Further Reading

Frey, T. G., and Mannella, C. A. (2000). The internal structure of mitochondria. *Trends Biochem. Sci.* **25**, 319–324.

Mannella, C. A (2003). Downloadable video clip of a 3-D model of a frozen-hydrated rat-liver mitochondrion. http://www.wadsworth.org/databank/electron/cryomito_dis2.html.

Mannella, C. A., Buttle, K., and Marko, M. (1997). Reconsidering mitochondrial structure: New views of an old organelle. *Trends Biochem. Sci.* **22**, 37–38.

Mannella, C. A., Pfeiffer, D. R., Bradshaw, P. C., Moraru, I. I., Slepchenko, B., Loew, L. M., Hsieh, C., Buttle, K., and Marko, M. (2001). Topology of the mitochondrial inner membrane: Dynamics and bioenergetic implications. *IUBMB Life* **52**, 93–100.

Munn, E. A. (1974). *The Structure of Mitochondria*. Academic Press, London.

Nicastro, D., Frangakis, A. S., Typke, D., and Baumeister, W. (2000). Cryo-electron tomography of Neurospora mitochondria. *J. Struct. Biol.* **129**, 48–56.

Perkins, G., Renken, C., Martone, M. E., Young, S. J., Ellisman, M., and Frey, T. (1997). Electron tomography of neuronal mitochondria: Three-dimensional structure and organization of cristae and membrane contacts. *J. Struct. Biol.* **119**, 260–272.

Rasmussen, N. (1995). Mitochondrial structure and the practice of cell biology in the 1950s. *J. History Biol.* **28**, 381–429.

Biography

Carmen A. Mannella is a research scientist and Director of the Division of Molecular Medicine at the Wadsworth Center, New York State Department of Health in Albany, NY. His main research interests are in mitochondrial membrane structure and permeability. He holds a Ph.D. from the University of Pennsylvania and received his postdoctoral training at Roswell Park Cancer Institute and St. Louis University. As co-director of the Wadsworth Center's Resource for the Visualization of Biological Complexity (a NIH NCRR biomedical technology resource center), he participates in the development of electron tomography and its application to a wide range of biological problems.

Mitochondrial Metabolite Transporter Family

Ferdinando Palmieri
University of Bari, Bari, Italy

Martin Klingenberg
University of Munich, Munich, Germany

The mitochondrial transporters are a family of nuclear-coded, membrane-embedded proteins that, with one exception, are found in the inner membranes of mitochondria and catalyze the translocation of solutes across the membrane. Since mitochondria and cytosol cooperate in a large number of metabolic cellular processes, a continuous and highly diversified flux of metabolites, nucleotides, and cofactors into and out of the mitochondria is needed. Functional studies in intact mitochondria have indicated the presence of more than 20 carrier systems for the transport of metabolites involved in the citric acid cycle, oxidative phosphorylation, fatty acid oxidation, gluconeogenesis, lipogenesis, transfer of reducing equivalents, urea synthesis, amino acid degradation, and other functions shared between cytosol and mitochondria. The central role of some mitochondrial carriers in cell metabolism is illustrated in this entry.

Purification

Eleven carrier proteins have been purified to homogeneity from mitochondria using a procedure that, with very few exceptions, involved chromatographic steps on hydroxyapatite and celite. Purification and subsequent reconstitution of pure protein into phospholipid vesicles (liposomes) was useful for identification, functional characterization, and some structural studies.

Structure

Early studies elucidated the primary structure of six purified and biochemically well-characterized mitochondrial-carrier proteins. These are the ADP/ATP carrier (AAC, in fact the first metabolite transporter to be sequenced), the uncoupling protein (UCP), and the carriers for phosphate (PiC), oxoglutarate (OGC), citrate (CIC), and carnitine/acylcarnitines (CAC) (Figure 1). Their primary structures were derived by sequencing the full-length peptide chain, or by molecular biological techniques initiated with partial amino acid sequence information. A unique feature of these six mitochondrial carriers is their tripartite sequence structure, i.e., they consist of three tandemly repeated homologous domains ~100 amino acids in length. Each domain contains two hydrophobic stretches, which are thought to span the membrane as α-helices. All carriers contain, in at least one of the repeats, the characteristic sequence motif P-h-D/E-X-h-K/R-X-R/K-(20–30 residues)-D/E-G-(4 residues)-a-K/R-G, where "h" represents a hydrophobic and "a" represents an aromatic residue. Therefore, they all belong to the same protein family.

A generally accepted two-dimensional model of mitochondrial carriers is illustrated in Figure 2 based on the sequence features described above and on the accessibility of carriers to impermeable reagents, proteolytic enzymes, and peptide-specific antibodies. According to this model, the typical mitochondrial carrier monomer has six helices traversing the membrane connected by hydrophilic loops with both the N and C termini on the cytosolic side of the inner mitochondrial membrane. The matrix loops of the AAC, CAC, and UCP have been proposed to protrude into the membrane between the transmembrane segments of the protein, based on observations that residues located in the hydrophilic matrix region of these carriers react with membrane-impermeable reagents applied from the cytosolic side. It should also be noted that the transmembrane segments IV of CIC and OGC have been shown to be in α-helical structure using spin labels on engineered single-Cys residues.

Most of the isolated carrier proteins are shown to be homodimers and this may apply to all members of the mitochondrial carrier family (MCF). The evidence is based on direct MW determination of isolated proteins, on chemical, and recombinant cross-linking. The role of the homodimers in the transport mechanism, involving,

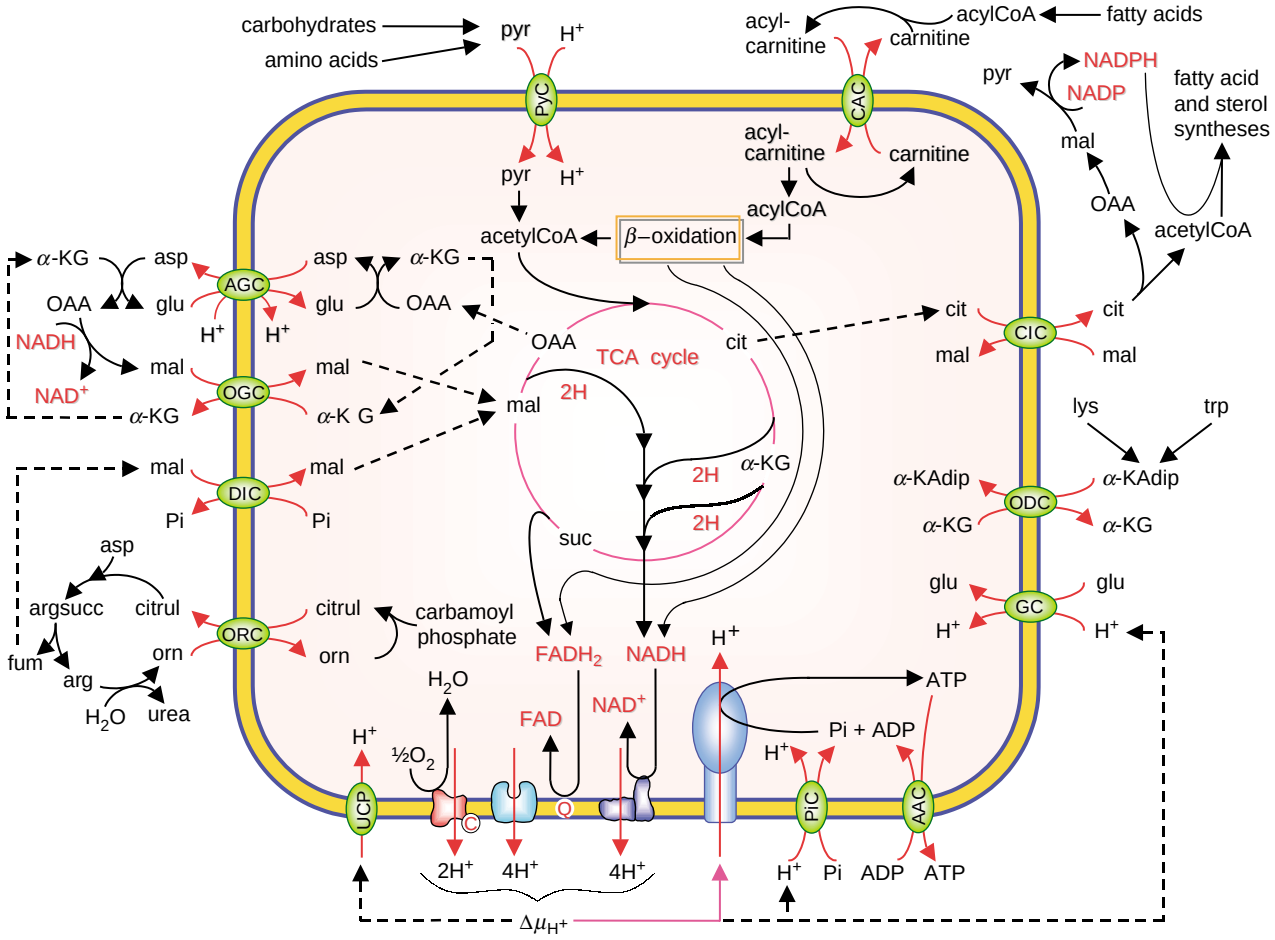

FIGURE 1 Metabolic roles of mitochondrial carriers. The scheme shows 12 carriers catalyzing metabolite transport through the inner mitochondrial membrane. These carriers are involved in oxidative phosphorylation (AAC, PiC, UCP), in oxidation/reduction pathways (AGC, OGC, DIC, CIC, CAC, PyC), and, with partial overlap, in amino acid metabolism (AGC, ORC, GC, ODC). The scheme does not include all of the carriers listed in Table I and does not show all the metabolic pathways in which individual carriers are involved (see Table I).

for example, a central channel or cooperative interactions between the monomers is still being elucidated.

Extension of the Mitochondrial Carrier Family

With the availability of DNA banks, the characteristic sequence features of the MCF were used to search for carriers of unknown function within the same family. Thus, a subfamily of UCPs (UCP 1–5) has been discovered with a wide variety of functions such as thermogenesis, oxygen radical suppression, regulation of fatty acid oxidation, immune response, and insulin secretion. The *Saccharomyces cerevisiae* genome contains 35 MCF members, and the human one presumably more. In this context, a breakthrough was achieved when the bovine OGC was overexpressed in *Escherichia coli*. The recombinant OGC, accumulated as inclusion bodies in the bacteria, was solubilized with sarkosyl and functionally reconstituted into liposomes. This was the first eukaryotic membrane protein to be produced in *E. coli* and recovered in active form. Using this strategy, i.e., gene expression and transport assays in the reconstituted system, the nucleotide and amino acid sequences of eight new mitochondrial carriers in *S. cerevisiae*, four in plants, and nine in man (including isoforms) have so far been identified (see Table I). The transporters identified first in yeast are the carriers for dicarboxylates (DIC), succinate/fumarate (SFC), ornithine (ORC), oxaloacetate/sulfate (OAC), oxodicarboxylates (OAC), thiamine pyrophosphate (TPC), and adenine nucleotides (ANT). The main function of DIC in yeast is to import succinate (produced by the glyoxylate cycle in the cytosol) or other dicarboxylates into mitochondria, whereas SFC directs the carbon skeleton of succinate to gluconeogenesis. The yeast OAC

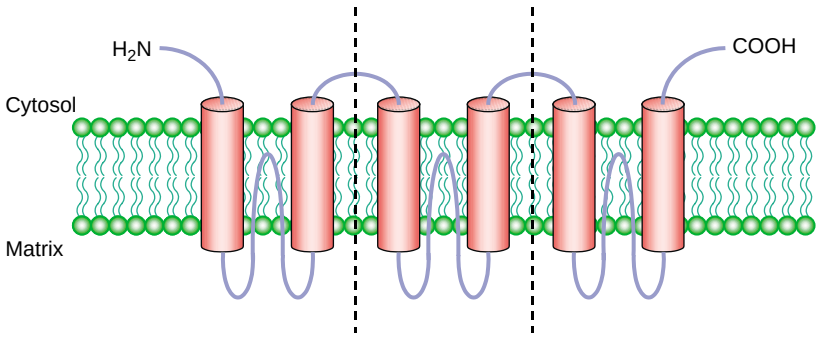

FIGURE 2 Suggested folding pattern of the mitochondrial solute carriers. Six helices traverse the inner mitochondrial membrane with the C and N termini facing the cytosol. The whole sequence is divided into three similar domains each with two transmembrane helices. Within each domain the two helices are connected by a long hydrophilic matrix loop (A, B, C respectively) which is assumed to protrude into the membrane space.

has also an anaplerotic role, as the *S. cerevisiae* pyruvate carboxylase is cytoplasmic. The main function of ORC in yeast is to export ornithine in exchange for H^+ to the cytosol, where it is converted into arginine and polyamines. The yeast ODC transports oxoadipate in exchange for oxoglutarate or malate from the mitochondria to the cytosol where it is converted into Lys. The essential cofactor thiamine pyrophosphate, produced in the cytosol, is transported into mitochondria by TPC. The peroxisomal ANT transports ATP, ADP, and AMP and its function is to transport cytosolic ATP into the peroxisomal lumen in exchange for AMP generated in the activation of fatty acids (in yeast fatty acid β-oxidation occurs in the peroxisomes). It differs from the mitochondrial AAC because it transports AMP and is unaffected by the AAC inhibitors CATR and BK. ANT is the first member of the MCF found to be located in a nonmitochondrial membrane, and it is the first peroxisomal protein proven to perform a transport function.

Other carriers were identified first in man. Among them, the human DNC transports dNDPs and dNTPs (in exchange for ADP or, more likely, ATP and pyrophosphate) into mitochondria for mDNA synthesis. Interestingly, DNC can transport dideoxynucleotides efficiently, which explains the toxic side effects of nucleoside analogues in the treatment of viral illnesses including AIDS. Other examples are the aspartate/glutamate carrier (AGC), which had previously been purified but not sequenced, and the glutamate/H^+ carrier (Table I).

Driving Forces for Transport

The majority of mitochondrial carriers catalyze strict solute exchange reactions. Those mediating H^+-compensated unidirectional substrate flux may also fall into the above category, because at least PiC has been shown to function in a phosphate/OH^- antiport mode. CAC has an unusual dual function mediating both unidirectional transport of carnitine and carnitine/acylcarnitine exchange, whereas UCP catalyzes uniport as exclusive transport mode.

Mitochondrial carriers can be divided into electrogenic (or electrophoretic) and electroneutral transporters. So far, three well-characterized carriers have been shown to be electrophoretic. AAC and AGC catalyze exchanges that result in a charge imbalance because they transport ADP^{3-} for ATP^{4-} and $aspartate^-$ for $glutamate^- + H^+$, respectively, across the mitochondrial membrane. The third, UCP, catalyzes the unidirectional transport of H^+. Electroneutral balance can be achieved by cotransport (symport) of solutes, countertransport of solutes, and uniport of electroneutral metabolites. The carriers for Pi, glutamate, pyruvate, and in yeast for oxaloacetate/sulfate facilitate the transport of anions together with an equivalent amount of H^+ (anion/H^+ symport) or in exchange for OH^- (anion/OH^- antiport). Other carriers catalyze an exchange of anions or cations. OGC, for example, transports $oxoglutarate^{2-}$ for $malate^{2-}$ and ORC ornithine for lysine, arginine, or H^+. In some cases electroneutrality is imposed by simultaneous carrier-mediated H^+ movement. CIC, for example, transports H-$citrate^{2-}$ against $malate^{2-}$ and the human ORC can transport $ornithine^+$ against citrulline and H^+.

The mitochondrial carriers utilize, as their driving force, the concentration gradient of the solutes and/or the H^+ electrochemical potential generated across the inner mitochondrial membrane by the functioning of the respiratory chain. Since the electrical component of $\Delta\mu H^+$ is rather high, the electrical nature of AAC and AGC provides a powerful means of ejecting ATP and aspartate against the concentration gradient from the mitochondrial matrix to the cytosol. In cases of H^+ symport or H^+ exchange, the transmembrane pH gradient regulates the distribution of anionic and

TABLE I

Mitochondrial Transporters

Carrier	Symbol	Isoforms	Main substrates	Mode of transport	Metabolic role
A					
ADP/ATP	AAC	3	ADP, ATP	Exchange	Energy transfer, oxidative phosphorylation
UCP	UCP	5[a]	H^+	Uniport	Uncoupling for thermogenesis (UCPI) and for regulation of some specific cellular events (UCP2 to 5)
Phosphate	PiC	2[b]	Phosphate	H^+ symport	Energy transfer, oxidative phosphorylation, counter-ion for malate
Oxoglutarate	OGC		Oxoglutarate, malate	Exchange	Malate/asparate shuttle, isocitrate/oxoglutarate shuttle, nitrogen metabolism, gluconeogenesis from lactate
Citrate	CIC		Citrate, malate, phosphoenolpyruvate isocitrate, *cis*-anconitate	Exchange	Fatty acid and sterol biosyntheses, gluconeogenesis from lactate, isocitrate/oxoglutarate shuttle
Carnitine	CAC		Carnitine, acylcarnitines	Exchange and uniport	Fatty acid oxidation
B					
Dicarboxylate	DIC		Malate, succinate, phosphate, sulfate, thiosulfate	Exchange	Anaplerosis, gluconeogenesis from pyruvate (and amino acids), urea synthesis, sulfur metabolism
Fumarate/succinate (y)	SFC		Fumarate, succinate	Exchange	Gluconeogenesis
Ornithine	ORC	2	Ornithine, lysine, citrulline	Exchange/H^+ symport	Urea synthesis
Oxaloacetate/sulfate (y)	OAC		Oxaloacetate, sulfate, thiosulfate	H^+ symport	Anaplerosis, sulfur metabolism, transfer of reducing equivalents
Folate	MFT		Folates	?	Cofactor
Deoxynucleotide	DNC		dNDPs, dNTPs, ADP, ATP	Exchange	Mitochondrial DNA synthesis

(*continues*)

TABLE I

Continued

Oxodicarboxylate	ODC	2[c]	Oxoadipate, oxoglutarate	Exchange	Lysine, tryptophan and hydroxylysine catabolism
Aspartate/glutamate	AGC	2	Aspartate, glutamate, cysteinesulfinate	Exchange	Malate/aspartate shuttle urea synthesis, gluconeogenesis, cysteine metabolism
Adenine nucleotide[d]	ANTI		ATP, ADP, AMP	Exchange	Peroxisomal fatty acid β-oxidation
Coenzyme A			Coenzyme A	?	Cofactor
Glutamate	GC	2	Glutamate	H^+ symport	Urea synthesis, nitrogen metabolism
Dicarboxylate/ tricarboxylate (p)	DTC	2[e]	Oxoglutarate, oxaloacetate, malate, citrate, isocitrate	Exchange	Fatty acid and isoprenoid syntheses, redox shuttle in photorespiration, nitrogen assimilation
Thiamine pyrophosphate (y)	TPC		Thiamine pyrophosphate, thiamine monophosphate	Exchange/H^+ symport	Matrix thiamine-dependent reactions
Basic amino acid (p)	BAC	2	Arginine, lysine, ornithine, hystidine	Exchange/H^+ antiport	Basic amino acids metabolism
C					
ATP-Mg^{2+}/Pi			ATP-Mg^{2+}, phosphate	Exchange	Matrix adenine nucleotide content
Pyruvate	PYC		Pyruvate, other monocarboxylates	H^+ symport	Citric acid cycle, glyconeogenesis, ketone bodies
Branched-chain α-ketoacid			α-ketoisocaproate, α-ketoisovalerate	H^+ symport	Branched-chain amino acid catabolism
Glutamine	GLC		Glutamine, asparagine	Uniport	Glutamine degradation

A carriers functionally identified and sequenced after purification. *B* carriers functionally identified upon expression of their genes. *C* carriers proposed from transport studies in mitochondria. y (yeast) and p (plants) indicate the species where the carrier has so far been identified. All the other carriers have been identified also or only in man.

[a] UCP3 and UCP5 exist as two splicing variants (short and long forms).

[b] Isoforms generated by alternative splicing.

[c] Isoforms present in yeast but not in man.

[d] Localized in the peroxisomal membrane.

[e] Isoforms present in *Nicotiana tabacum*.

cationic solutes across the membrane. For example, with a higher pH inside, the carrier-mediated H^+-compensated uptake of Pi or glutamate is stimulated, as well as the efflux of cationic solutes such as the export of ornithine.

Functional Models for Mitochondrial Exchange Carriers

Two models of transport have been proposed for mitochondrial exchange carriers. According to the "single site gated pore" mechanism, suggested for the AAC, the transporter has only one binding site which is exposed alternately to the two different sides of the membrane (Figure 3A). On binding the substrate to one side, the carrier–substrate complex undergoes a conformational change and the binding site becomes exposed to the opposite side. The transported substrate now has to leave the transport site before another substrate to be transported in the opposite direction is bound. In the alternative hypothesis, the "double site gated pore" mechanism, two binding sites are exposed on the opposite sides of the membrane at the same time and both have to be occupied by the exchanging substrates before the conformational change and the substrate translocation occurs (Figure 3B). For AAC, the reorientation of the binding is well documented at carrier protein level since high-affinity inhibitor ligands exist which bind to the carrier either on the cytosolic side (atractyloside, ATR) or on the matrix side (bongkrekate, BK). These ligands remove ADP or ATP and their binding is mutually exclusive, indicating a single reorienting binding site.

The second possibility is supported by kinetic analysis of several carriers. Two-reactant initial-velocity studies varying both the internal and external substrate concentrations have conclusively shown that the reconstituted AGC, OGC, CIC, DIC, PiC, ORC, and possibly AAC function according to a simultaneous (sequential) mechanism, implying that one internal and one external substrate molecule form a ternary complex with the

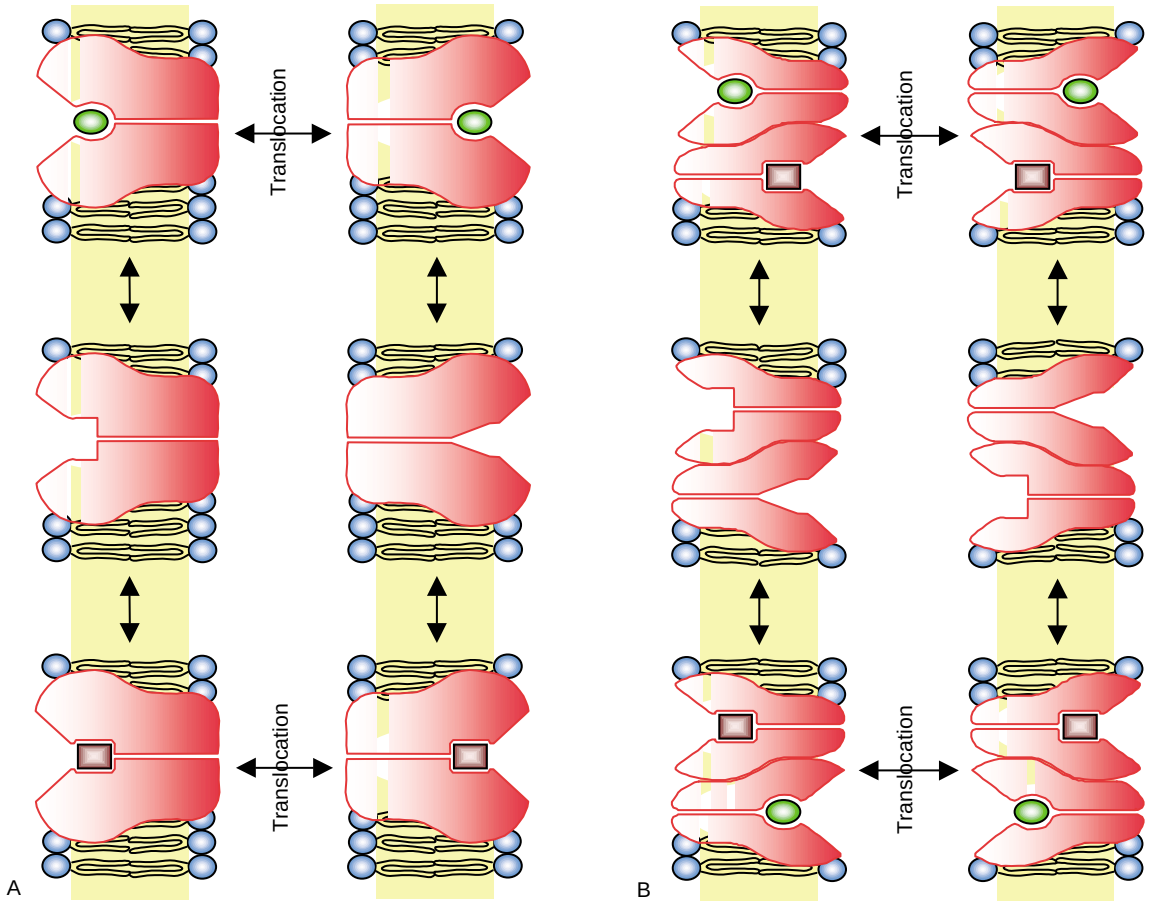

FIGURE 3 Functional models for mitochondrial exchange carriers. (A) The single site gated pore model of translocation corresponding to a ping-pong kinetic mechanism of exchange. The transport pathway is assumed to be formed between the two monomers. (B) The double site gated pore model of translocation corresponding to a simultaneous kinetic mechanism of exchange. Two separate and coordinated substrate translocation pathways are assumed, one in each monomer.

carrier before transport occurs, in agreement with the "double site gated pore" mechanism. The CAC differs from the other mitochondrial carriers analyzed so far, since it follows a ping-pong mechanism indicating only binary carrier–substrate complexes according to the existence of a single binding site. As CAC mediates uniport besides exchange of substrates, it is likely that the activation energy barrier for the reorientation of the unloaded carrier form is much lower for the CAC than for exchange carriers. As the uniport function is essential in a transport system like the carnitine carrier, the common sequential mechanism has apparently been changed into a ping-pong type of mechanism.

Channel-Like Properties

Unidirectional, partially unspecific transport can be induced in exchange-type carriers by various influences. A general effect is the induction of uniport by mercurials in various exchange carriers. In this state the transport can approach open channel-like characteristics. For AAC a slow specific uniport can be induced by phosphate and Mg^{2+} which prestages a wide unspecific channel induced by Ca^{2+}. This "megachannel" plays a central role in mitochondrial pore transition (MPT). The specific AAC ligands ADP and BK inhibit, while ATR sustains, MPT. The pore can also be induced by pro-oxidants at low Ca^{2+} and seems to be a major target of oxygen radical damage. Very important is the formation of this pore and thus of AAC as an early trigger of apoptosis by inducing the release of cytochrome *c*.

The appearance of channel-like functions reveals an intrinsic property of the MCF, i.e., the presence of an unspecific channel within the carrier protein which is normally hidden by appropriate gates. This model, which can in principle be reconciled with a gated pore mechanism, has of course to be substantiated by further studies leading to a molecular description of the putative channel pathway.

Structure and Function Studies: The Use of Mutant Proteins

Recombinant expression of the mitochondrial carriers in yeast and in *E. coli* enabled site-directed mutagenesis for structure–function studies. The mutation of Cys to Ser, one at a time or all together, evidenced the absence of essential cysteines in several carriers, although transport could be inhibited by SH reagents. Thus, the cysteine reagents may cause sterical hindrance or conformational changes. Inversely, by systematically substituting single amino acids with Cys, essential residues could be identified, e.g., G183, R190, and Q198 in transmembrane segment IV (TMSIV) of OGC, and R181 and R189 in TMSIV of CIC.

In AAC, three types of charged residues have been probed by mutagenic charge neutralization: positively charged residues located within TMSs (K38A, R96A, R204L, and R294A) and within the matrix loops (K48A, R152A, K179I, K182I, R252I, R253I, and R254I); and negatively charged residues at the end of TMSI, TMSIII, and TMSV (E45G, D149S, D249S). By comparing the *in vivo* (yeast aerobic growth) and *in vitro* effects (reconstituted transport), these residues could be assigned to transport or structure maintenance to varying degrees. Using a regain-of-function approach in yeast, in second site mutations negatively charged residues were affected, which evidenced ion-pair interactions R294-E45, K38-E45, R152-E45, R152-D149, and D149-R252 and indicated an arrangement where TMSI and TMSVI are in vicinal and skewed position.

Using the *E. coli* expression system, R90 and R98 in TMSII, R190 in TMSIV, and R288 in TMSVI of OGC, mutated into Leu, and R181 and R189 in TMSIV of CIC, mutated into Cys, were found to be essential for activity. A positive charge either from Arg or from Lys sufficed for transport activity at all positions, except at positions 98 and 190 of OGC where the guanidinium moiety of Arg was indispensable. Furthermore, by a combination of Cys-scanning mutagenesis, spin-labeling, and chemical modification studies, a water-accessible face of helix IV in both CIC and OGC has been identified and suggested to line part of the substrate translocation pathways through these proteins.

In PiC H32 in TMSI, E126 and E137 in TMSIII, and D39 and D236 at the matrix ends of the first and fifth TMS were found to be indispensable for normal growth in yeast and transport function. The six charged residues (H32, E126, and E137 of both subunits) are proposed to form the proton cotransport channel within the homodimer. An inhibitory disulfide formation under oxidizing conditions between the two Cys-28 residues (also located in the TMSI) of two PiC molecules is in agreement with this model.

A direct involvement of charged residues in proton transport pathway through UCP1 has been demonstrated. D27 within TMSI and the H145/H147 unit within loop B are thought to function as proton donor/acceptors, respectively, in the channel and the matrix-side entrance of the H^+ transport pathway. Further mutagenesis studies carried out on charged residues positioned in TMSII (R83 and E129), TMSIV (R182), TMSVI (R276), and in the TMSV at the cytosolic interface (H214) suggested that the three arginines are part of the purine-nucleotide-binding site and H214 and E190 act as pH sensors for the control of access of the phosphate moiety of the nucleotide to its binding cleft. Deletion of F267-K268-G269 in the

matrix loop C, as well as analogous deletions in loops A and B, caused loss of nucleotide regulation, suggesting a gating function of the three hydrophilic matrix loops in the regulation of UCP by purine nucleotides.

Diseases

At least four autosomal-recessive diseases are caused by defects in a specific mitochondrial carrier gene. Mutations in the human gene SLC25A20 coding the carnitine carrier are responsible for the Stanley syndrome (MIM 212138). The fatty acid β-oxidation and carnitine carrier activity are very low or absent in patients' fibroblasts. The disease generally presents with acute, potentially life-threatening episodes of hypoglycemic coma induced by fasting. Defects in the gene SLC25A13 coding isoform 2 of the aspartate/glutamate carrier (the only isoform present in liver) cause type II citrullinemia (MIM 215700). The lack of AGC2-mediated aspartate supply to the cytosol of liver cells causes: (1) deficiency of arginosuccinate synthetase, an enzyme of the urea cycle and (2) deficiency of the malate/aspartate shuttle leading to an increased NADH/NAD ratio in the cytosol that inhibits glycolysis and gluconeogenesis from reduced substrates.

The hyperornithine-hyperammone-homocitrullinemia (HHH) syndrome (MIM 23970) is caused by alterations of the ornithine carrier (isoform 1, gene SLC25A15) that catalyzes the exchange between cytosolic ornithine and mitochondrial citrulline, an important step in the urea cycle. The main features are homocitrullinuria, hyperammonemia, and consequent symptoms. Amish microcephaly (MIM 607196) is associated with mutant deoxynucleotide carrier (gene SLC25A19) and is characterized by severe congenital microcephaly and premature death. Although the molecular defect(s) responsible for 2-oxoadipate acidemia have not yet been characterized, this disease has been suggested to be due to defective oxodicarboxylate carrier or oxoadipate dehydrogenase (the two enzymes that transport into mitochondria and oxidize 2-oxoadipate, respectively). Finally, one of the three distinct loci involved in autosomal-dominant progressive external ophthalmoplegia (adPEO) (MIM 103220) includes the heart and skeletal muscle specific isoform of the ADP/ATP carrier (gene SLC25A4).

See Also the Following Articles

Fatty Acid Oxidation • Free Radicals, Sources and Targets of: Mitochondria • Protein Import into Mitochondria • Urea Cycle, Inborn Defects of

Glossary

electrogenic, electrophoretic transport The movement of a net electrical charge across the membrane coupled to the transport of metabolites. It is driven by the membrane potential.

exchange carriers Carriers that facilitate transport only by coordinated counter exchange of solutes across the membrane.

mitochondrial carriers Proteins primarily located in the inner mitochondrial membrane which catalyze transport of metabolites between cytosol and mitochondrial matrix space.

Further Reading

Kaplan, R. S. (2001). Structure and function of mitochondrial anion transport proteins. *J. Membr. Biol.* **179**, 165–183.

Klingenberg, M., and Echtay, K. S. (2001). Uncoupling proteins: The issue from a biochemist point of view. *Biochim. Biophys. Acta* **1504**, 128–143.

Krämer, R., and Palmieri, F. (1992). Metabolite carriers in mitochondria. In *Molecular Mechanisms in Bioenergetics* (L. Ernster, ed.) pp. 359–384. Elsevier Science, Amsterdam.

Palmieri, F., and van Ommen, B. (1999). The mitochondrial carrier protein family. In *Frontiers in Cellular Bioenergetics* (S. Papa, F. Guerrieri and J. M. Tager, eds.) pp. 489–519. Kluwer Academic/Plenum, New York.

Walker, J. E. (1992). The mitochondrial transporter family. *Curr. Opin. Struct. Biol.* **2**, 519–526.

Biography

Ferdinando Palmieri is a Professor in the Department of Pharmaco-Biology of the University of Bari. His principal research interests are in the field of biochemistry and molecular biology of mitochondrial transporters and related diseases.

Martin Klingenberg is Professor Emeritus at the University of Munich. His principal interest in recent years has been in the field of characterizing the mechanism of mitochondrial carriers.

Mitochondrial Outer Membrane and the VDAC Channel

Marco Colombini
University of Maryland, College Park, Maryland, USA

Mitochondria are organelles found in virtually all eukaryotic cells. They are composed of two membranes. The inner membrane is highly convoluted and of quite variable morphology. The outer membrane forms the boundary between the mitochondrial spaces and the cytosol. It contains membrane channels, called VDAC, that allow metabolites to cross this membrane while restricting the passage of proteins.

Origin and Structure of the Outer Membrane

Mitochondria have most likely evolved from endosymbiotic bacteria. The outer membrane may have originated as an endosomal membrane that engulfed the original endosymbiotic bacterium or may be related to the bacterial outer membrane. Whatever its origin, structurally it is a relatively simple limiting membrane forming a continuous boundary (Figure 1). It seems to limit the boundary of the mitochondrial space and, unlike the inner membrane, maintains a fairly constant total mitochondrial volume.

Further aspects of mitochondrial structure and function vary depending on the source and thus most of what will be presented applies to mammalian sources.

The outer membrane interacts intimately with neighboring membranes. Rivet-like connections between the outer and inner membranes often exist and are referred to as contact sites. These are mechanically sturdy as they interfere with the experimental separation of the outer and inner membranes. These contacts are proposed to serve a number of functions including the formation of macromolecular complexes between transporters and enzymes to expedite metabolic flow. The outer membrane also interacts closely with the endoplasmic reticulum and this close apposition may be the reason for preferential transfer of Ca^{2+} from the endoplasmic reticulum to the mitochondrial matrix compartment. This has been especially well studied in the heart where changes in Ca^{2+} level on a beat-by-beat basis alter dehydrogenase activity matching cellular energy consumption. If specialized docking structures are involved in this interaction with the endoplasmic reticulum, they must be more labile than the contact sites because isolation of mitochondria from endoplasmic reticulum is quite easy.

Functions of the Outer Membrane

The outer membrane of isolated mitochondria is highly permeable to metabolites due to the presence in this membrane of large aqueous channels formed by the protein called voltage-dependent anion-selective channel (VDAC). Their similarity to channel-forming proteins in bacterial outer membranes collectively referred to as porins has led some to refer to VDAC as mitochondrial porin. Although the permeability characteristics conferred to the outer membrane by VDAC are rather complex, physical size is a major factor. Thus, under normal conditions the outer membrane is essentially impermeable to molecules larger than 5 kDa. This allows proteins to be sequestered in the intermembrane space, the compartment between the outer and inner membranes. This sequestration serves at least two functions. First, it localizes proteins that could diffuse away to the site where they are needed. For example, the soluble protein, cytochrome *c*, is a member of the electron transport chain and must transmit electrons between complex III and IV so that respiration may proceed. Second, the sequestration prevents pro-apoptotic proteins from being released into the cytosol as this would initiate programmed cell death (apoptosis). Cytochrome *c* is also an example of a sequestered proapoptotic protein. The permeability barrier to pro-apoptotic proteins and others of similar size is lifted under some conditions that lead to cellular apoptosis.

The permeability of the outer membrane to small molecules can be regulated resulting in the outer membrane limiting metabolite flux and consequently the level of metabolic activity. This regulation is probably critical to changes in cell function.

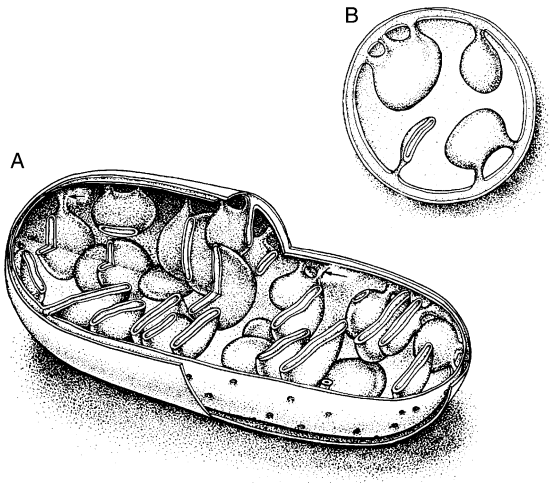

FIGURE 1 A drawing of the membranes and compartments of a typical small mitochondrion. (A) shows the mitochondrion with portions of the membranes cut out so as to reveal inner structure and compartmentation. (B) Illustrates a cross-section. Reproduced from Lea, P. J., and Hollenberg, M. J. (1989). Mitochondrial structure revealed by high-resolution scanning electron microscopy. *The American Journal of Anatomy* **184**, 245–257. Drawings made by Karen Visser. With permission of Wiley-Liss, Inc., a Subsidary of John Wiley & Sons, Inc.

Most mitochondrial proteins and RNA molecules are synthesized in the cytosol and imported into mitochondria. The Tom complex is responsible for much of the protein import through the outer membrane. Leader sequences on the proteins are recognized by Tom and the protein is treaded through a pore in the complex and delivered to the intermembrane space where it is picked up by the Tim complex in the inner membrane for translocation through that membrane. The processing of outer membrane proteins by this complex is less clear.

Mitochondria are usually found in the portion of cells where they are needed. For example, to minimize diffusion limitations they are located close to sites of high-energy dissipation. Sometimes they need to be delivered to distal sites in a cell (e.g., from cell body to nerve terminal of a neuron or to the reproductive bud of a yeast cell). Motors located either on microtubules or actin filaments move mitochondria from one location in the cell to another. The outer membrane must provide sites of attachment for the motors that perform the translocation.

Composition

The composition of the outer membrane varies somewhat depending not only on the species but also the tissue from which it was isolated. With that caveat, it can be said that there are a number of similarities between the constituents of the outer membrane and the endoplasmic reticulum. For example, the presence of cytochromes b and b_5, antimycin-insensitive NADH-cytochrome c reductase, and ceramide synthase. Yet there are also many differences and the enzymes present in the two locations are usually different isoforms. Thus, the similarity may reflect similar origins but certainly these two membranous compartments are distinct.

The outer membrane also contains enzymes involved in fatty acid and phospholipid metabolism and an amine oxidase. The liver mitochondria contain a peripheral benzodiazepine receptor whose role is unclear. The membrane can also bind some kinases that are typical soluble enzymes and the binding is thought to accelerate energy transduction.

The outer membrane has a higher lipid content than the inner membrane, one more typical of other cell membranes. The lipid composition is also drastically different from that of the inner membrane, the outer membrane being rich in sterol, while the inner has higher levels of cardiolipin.

VDAC Channels in the Outer Membrane

VDAC Structure

Mitochondria from all eukaryotic kingdoms contain VDAC channels in their outer membrane. These are formed by a single polypeptide of approximately 30 kDa and form a single large aqueous pore. In some plant and fungal mitochondria, VDAC channels form two-dimensional crystals (Figure 2), which upon further analysis reveal fundamentally cylindrical proteins forming water-filled transmembrane pathways. The wall of the channel is almost certainly a single layer of protein mainly consisting of a beta structure. Experimental evidence leads to the conclusion that the transmembrane portion consists of 1 α-helix and 13 β-strands. The surface domains (yellow regions in Figure 2) likely act as binding sites for a variety of proteins that bind or interact with the channel.

VDAC Function and Dynamics

The primary role of mitochondria is metabolism that is closely integrated with the metabolism occurring in the cytosol. This requires the continuous and rapid exchange of metabolites between these two major compartments. VDAC channels in the outer membrane can exist in conformational states that either favor or hinder metabolite flux. The state that favors metabolite flux, the open state, does so by having an electrostatic environment that favors anions. In addition, the charge distribution in the lining of the channel is

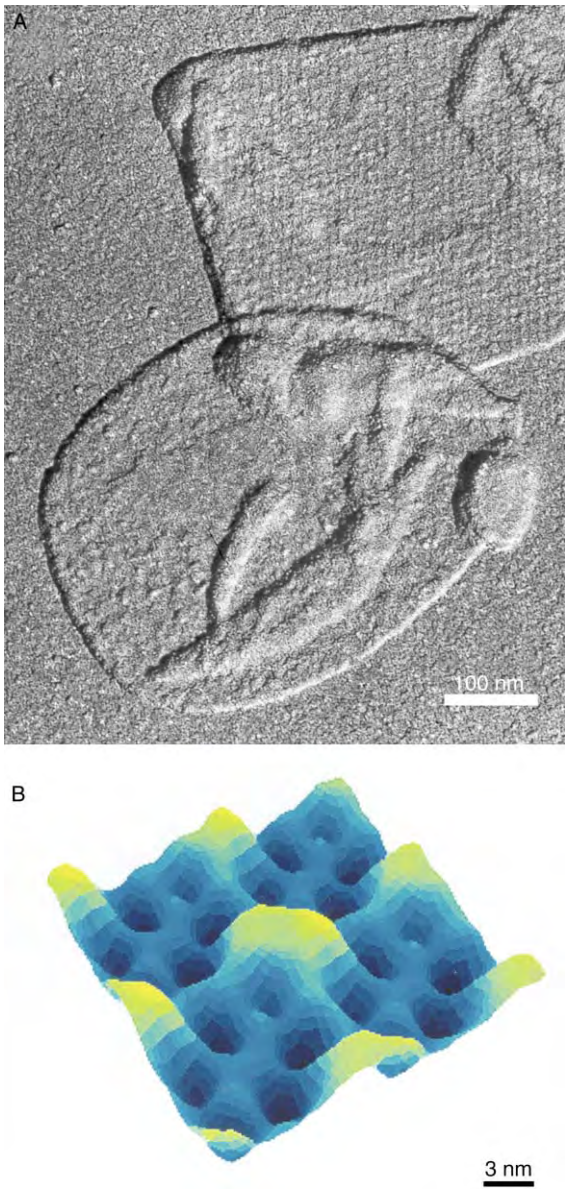

FIGURE 2 Views of mitochondrial outer membranes and the ubiquitous VDAC channels in these membranes. Panel (A) shows electron micrographs of freeze-dried mitochondrial outer membranes with two-dimensional crystals of VDAC channels (membrane with squared edges and ordered array of particles) and without such crystals (smooth membrane with rounded edges). Outer membrane vesicles isolated from mitochondria are dried down on a surface and they form collapsed sacs. Panel (B) shows a surface view of the VDAC channels obtained after computer filtration and averaging of multiple micrographs containing images of two-dimensional crystals. The yellow shows regions of elevation and the dark blue areas are the openings of the pores (holes) that are formed through the membrane. These allow the metabolites to cross the outer membrane. This figure was assembled from the work of Dr. Lorie Thomas. Adapted from Thomas, L., Kocsis, E., Colombini, M., Erbe, E., Trus, B.L., and Steven, A.C. (1991). Surface topography and molecular stoichiometry of the mitochondrial channel, VDAC, in crystalline arrays. *Journal of Structural Biology* **106**, 161–171.

such that it favors the translocation of ATP over that of anions of similar size and charge. In the closed states, the water-filled channel is somewhat narrower (the pore size decreases from 2.5 nm in the open state to 1.8 nm in the larger of the population of closed states) but, most importantly, the electrostatic nature is such that it hinders the flow of anions. A positively charged region lining the channel in the open state is translocated out of the channel resulting in a pathway with a net negative charge. This excludes ATP and drastically reduces the permeability of other anionic metabolites. At the same time this change favors the flux of cations.

This gating of VDAC is voltage dependent and thus the channels can respond to changes in the voltage across the outer membrane. An electrical potential across this membrane may arise from the presence of different charged macromolecules in the aqueous compartments (Donnan potential) and/or differential metabolite flux responding to metabolic rates. In addition, numerous factors influence this gating process including cytosolic NADH levels and specific proteins in the cytosol and intermembrane space. The importance of this regulation is indicated by its remarkable conservation of VDAC from all species tested (including all eukaryotic kingdoms). The diversity of influences on the gating of VDAC indicates that VDAC may integrate the influence of a variety of cellular factors and thus tune mitochondrial activity appropriately.

VDAC's ability to bind with cytosolic hexokinase and intermembrane space creatine kinase has been proposed to result in organized structures that increase the efficiency of energy transduction.

The Outer Membrane and Apoptosis

Apoptosis, programmed cell death, is a process by which a cell repackages itself to be ingested by other cells, generally macrophages. The outer membrane separates proteins that once combined initiate an amplification cascade leading to "full blown" apoptosis. The leakage of proteins from the intermembrane space into the cytosol is sufficient to cause apoptosis. Even injecting just one of these proteins, cytochrome c, into the cytosol is sufficient.

How the outer membrane becomes permeable to proteins is an area of intense investigation. The proteins that cross this membrane can be as large as 50–100 kDa. Proteins of the Bcl-2 family partition between the cytosol and the outer membrane. They can exist both as soluble proteins and intrinsic membrane proteins capable of generating ion channels.

Some of these are pro-apoptotic and others are anti-apoptotic. Some anti-apoptotic proteins are often associated with the outer membrane under normal conditions, i.e., cells functioning normally, and may favor normal mitochondrial function. Others translocate to the outer membrane at the early stages of apoptosis, perhaps forming the protein efflux pathways. The sphingolipid, ceramide, can also be produced in mitochondria early in the apoptotic process and has been shown to be able to form channels large enough for protein flux.

Under some conditions of apoptosis induction, exchange of nucleotides between mitochondria and the cytosol is greatly inhibited. The outer membrane becomes poorly permeable to ATP and ADP and other anionic metabolites. This phase precedes the release of intermembrane space proteins and in this phase cells can be rescued. This gives the outer membrane the role of deciding between life and death.

Emerging Importance of the Outer Membrane

Once considered relatively unimportant, the mitochondrial outer membrane is emerging as a site for control of overall mitochondrial function and a location where the fate of the entire cell is decided. Despite its deceptively simple appearance, this membrane performs a variety of vital functions. By hindsight, its location at the frontier between the cytosol and the mitochondrial spaces makes it an ideal site for control of the flux of matter and transduction of information.

See Also the Following Articles

Cell Death by Apoptosis and Necrosis • Cytochrome *c* • Mitochondrial Membranes, Structural Organization

Glossary

apoptosis A self-destruct process present in cells of multi-cellular organisms that eliminates cells that are no longer needed.

mitochondrion An organelle occurring in the vast majority of eukaryotic cells that is critical for energy transduction and metabolism. It is also semiautonomous with its own DNA and independent reproductive rate.

VDAC Voltage-dependent anion-selective channel, protein found in the outer membrane of all mitochondria. It forms large channels in this membrane allowing metabolites to cross.

Further Reading

Colombini, M., Blachly-Dyson, E., and Forte, M. (1996). VDAC, a channel in the outer mitochondrial membrane. In *Ion Channels* (T. Narahashi, ed.) Vol 4, pp. 169–202. Plenum, New York.

Gordon, D. M., Dancis, A., and Pain, D. (2000). Mechanisms of mitochondrial protein import. *Essays Biochem.* **36**, 61–73.

Lea, P. J., and Hollenberg M. J. (1989). Mitochondrial structure revealed by high-resolution scanning electron microscopy. *Amer. J. Anatomy* **184**, 245–257.

Thomas, L., Kocsis, E., Colombini, M., Erbe, E., Trus, B. L., and Steven, A. C. (1991). Surface topography and molecular stoichiometry of the mitochondrial channel, VDAC, in crystalline arrays. *J. Struct. Biol.* **106**, 161–171.

Tyler, D. D. (1992). *The Mitochondrion in Health and Disease*. VCH Publishers, currently Wiley-VCH Verlag GmbH and Co., Wiley, Somerset, NJ.

Waterhouse, N. J., Ricci, J., and Green, D. R. (2002). And all of a sudden it's over: mitochondrial outer-membrane permeabilization in apoptosis. *Biochimie* **84**, 113–121.

Biography

Dr. Marco Colombini is a Professor in the Department of Biology at the University of Maryland in College Park. His research is in the area of membrane biophysics with specific focus on channels in the mitochondrial outer membrane. He was part of the group that originally discovered and named the outer membrane channel called VDAC. Research from his laboratory continues to yield new insights into the structure and molecular mechanisms of mitochondrial channels and their role in regulation of mitochondrial function.

Dr. Colombini holds a Ph.D. from McGill University and is an active member of the Biophysical Society.

Mitogen-Activated Protein Kinase Family

Hidemi Teramoto and J. Silvio Gutkind
National Institute of Dental and Craniofacial Research, Bethesda, Maryland, USA

Mitogen-activated protein kinases (MAPKs) are a group of protein kinases that play an essential role in signal transduction by modulating gene transcription in the nucleus in response to changes in the cellular environment. MAPKs also play a key role in intracellular communication, and their activating pathways have been conserved throughout evolution, from plants, fungi, nematodes, insects, to mammals. In humans, there are at least 11 members of the MAPK superfamily, which can be divided into 6 groups: the extracellular signal-regulated protein kinases (ERK1 and ERK2); c-Jun N-terminal kinases (JNK1, JNK2, JNK3); p38s (p38α, p38β, p38γ, p38δ); ERK5 (ERK5); ERK3s (ERK3, p97 MAPK, ERK4); and ERK7s (ERK7, ERK8). Each group of MAPKs can be stimulated by a separate signal transduction pathway in response to different extracellular stimuli. In turn, MAPKs exhibit distinct substrate specificities. Thus, individual extracellular stimuli can lead to the differential activation of each MAPK and the consequent phosphorylation of a distinct set of MAPK substrates. Whereas components of some of these biochemical routes are now well established, others are still poorly understood. The specificity of the molecular mechanisms by which each MAPK can be activated ensures that cells mount an appropriate response to extracellular stimulation, as the resulting pattern of gene expression will depend on the integration of the combinatorial signals provided by the temporal activation of each of these groups of MAPKs.

ERK Family

ERK1 and ERK2

The extracellular signal-regulated protein kinase (ERK) group of MAPK includes ERK1 and ERK2. In certain cells their activation contributes to normal and aberrant growth, including malignant transformation, while in other cells this pathway can promote cell survival or initiate differentiation processes in others. The enzymatic activity of ERK1 and ERK2 is enhanced by dual phosphorylation on Thr and Tyr residues within a short sequence that forms the "activation loop", located close to the kinase active site, by a group of dual-specificity protein kinases (MAPK kinases; MAPKKs), represented by MEK1 and MEK2. Each MAPK family exhibits a distinct phosphor–acceptor motif in their activation loop (Figure 1), which provides specificity for the MAPKK–MAPK interactions. This phosphorylation leads to conformational changes in ERKs, thereby promoting their activation and nuclear localization. Subsequently, ERK activity is terminated by dephosphorylation on either Thr or Tyr by a Ser/Thr or Tyr phosphatase. This dephosphorylation can be mediated also by a dual specificity MAPK phosphatase. Similarly, the mammalian MAPKK, such as MEK1 and MEK2, are activated by phosphorylation mediated by MAPK kinase kinases (MAPKKK), which includes the Ras effector, Raf. Thus, the Raf group of MAPKKK that includes A-Raf, B-Raf, and c-Raf-1, plays an important role in the coupling of ERK MAPK activation to the Ras signaling pathway (see Figure 2).

The discovery of the Ras-Raf-MEK-ERK signaling route represented a breakthrough in cancer biology, and emerged as the product of the conversion of a large number of research efforts in a variety of otherwise poorly connected fields. Indeed, a large body of information was derived from genetic analyses of model organisms including *Drosophila*, *Saccharomyces cerevisiae*, and *Caenorhabditis elegans*, in addition to biochemical and biological studies in mammalian cells. They, collectively, led to the identification of Ras as a key downstream component of the pathway initiated by polypeptide growth factor receptors, and to the realization that this small GTPase acts subsequently as a master switch initiating the activity of a cascade of cytoplasmic kinases that culminate with the activation of the ERK1 and ERK2. ERKs, in turn direct the activities of many nuclear transcription factors, thus regulating gene expression. These findings provided a better understanding of the molecular basis for the transduction of proliferative signals, as well as the first clue as to how the aberrant function of Ras proteins may contribute to the malignant conversion of cancer cells.

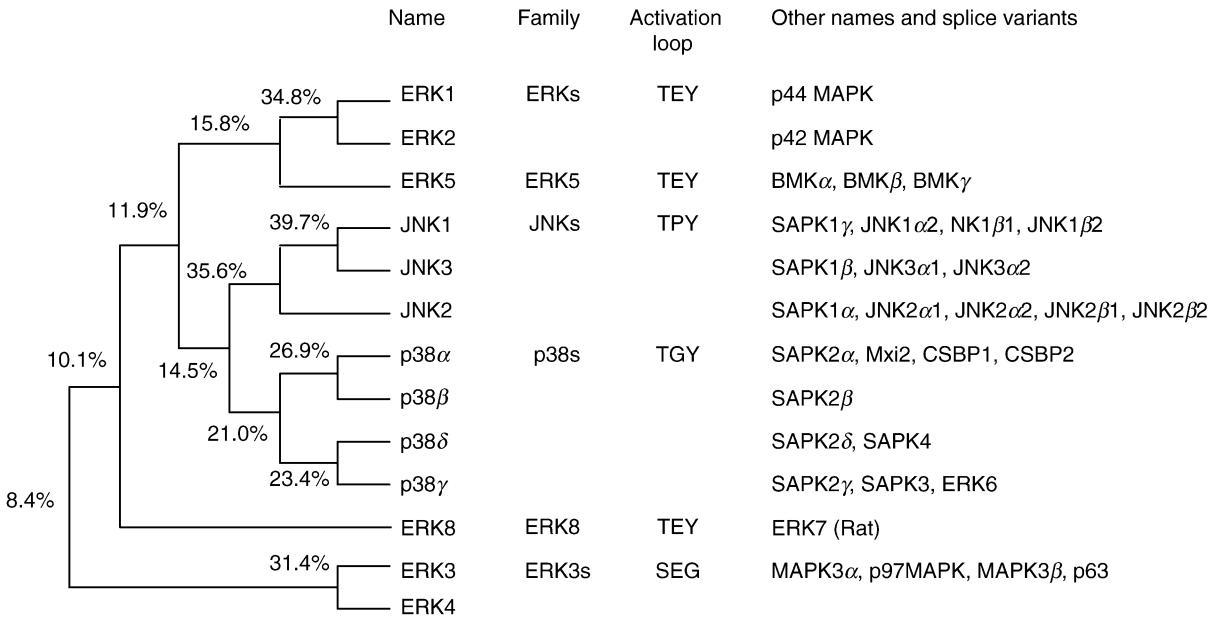

FIGURE 1 Phylogenetic tree of human MAPKs. A computer-generated phylogenetic tree of the MAPKs. The GenBank accession numbers are human ERK1 (X60188), human ERK2 (M84489), human ERK3 (S23429), human p97 (X80692), human ERK4 (P31152), human ERK5(U25278), human BMK (U29725), Rat ERK7 (AF078798), human ERK8 (AY065978), human JNK1 (U34822), human JNK2 (U34821), human JNK3 (U34820), human Mxi2 (U19775), CSBP1 (S52419), CSBP2 (S52420), human p38β (U53442), and human p38γ (U66243).

c-Jun N-Terminal Kinases (JNK1, JNK2, JNK3)

JNK was initially discovered by its ability to phosphorylate the N-terminal transactivating domain of the transcription factor c-Jun. As its activity was stimulated primarily by cellular stress rather than by mitogens, contrary to ERKs, it was also termed stress-activated protein kinase (SAPK). It is now known that there are three members of the JNK family, JNK1–3, and that they play numerous biological roles in response to a large variety of cell surface receptors as well as physical and chemical stresses. Whereas the JNK1 and JNK2 genes and their alternatively spliced variants are expressed ubiquitously, generating a total of eight JNK isoforms, the JNK3 gene has a more restricted expression pattern, being its two alternative spliced transcripts expressed the highest in brain and testis. Studies of mammalian cells demonstrated that JNK is required for neuroexcitatory stress-induced neuronal apoptosis, as well as for certain inflammatory responses and for the survival and malignant transformation of specific cell types (e.g., B cells).

Following the distinct pattern of activation of ERK and JNK by cellular receptors, an unexpected discovery was that whereas Ras regulates ERKs, two members of the Rho family of GTPases, Rac1 and Cdc42, initiate an independent kinase cascade regulating JNK activity. These findings provided direct evidence of a role for Rho GTPases in transcriptional regulation, thus expanding previous efforts addressing the function of these Rho related proteins, which were primarily focused on the molecular dissection of the mechanism(s) involved in their ability to control the dynamic assembly and remodeling of actin-containing cytostructures. Components of this pathway include several MAPKKKs: MEKK1, MEKK2, MEKK3, and MEKK4, apoptosis-stimulated kinase 1 (ASK1), mixed-lineage kinase 3 (MLK3), tumor progression locus 2, also known as Cot (TPL2), TGF-β-activated kinase (TAK), MAPK upstream kinase (MUK), germinal center kinase (GCK), and PAK, which can all contribute to activation of JNKs, apparently through two MAPKKs, MKK4 (also called Sek or JNKK1), and MKK7. Substrates for JNK include transcription factors of the c-Jun family, as well as other transcription factors, including Elk-1 and Elk-2, serum response factor accessory protein-1 (Sap-1), nuclear factor of activated T cells 4 (NFAT4), and activating transcription factor 2 (ATF2).

p38s (p38α, p38β, p38γ, p38δ)

The family of p38 kinases has expanded over the past few years, including now four members known as p38α (or CSBP-1), p38β, p38γ (also known as SAPK3 or ERK6) and p38δ (or SAPK4), and in some cases their corresponding splice variants. These MAPKs share a Thr-Gly-Tyr phosphorylation motif in their activation loop, and are

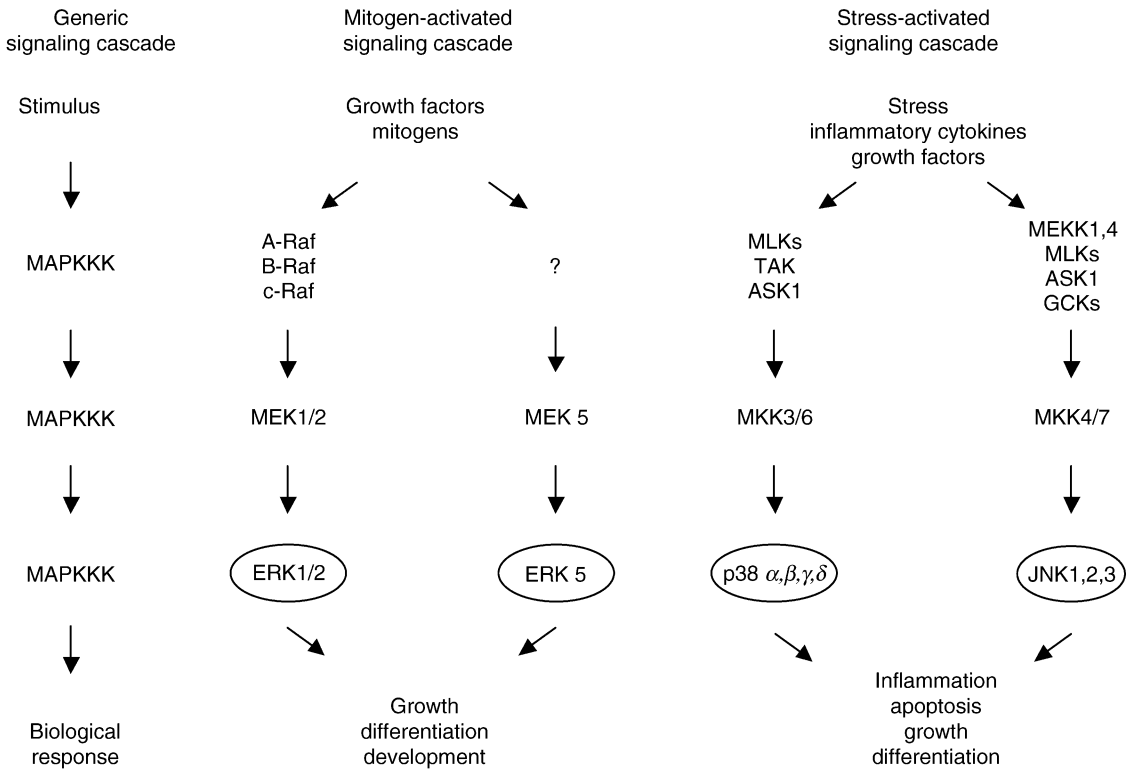

FIGURE 2 MAPK signaling cascades. Schematic representation of generic (left), mitogen activated (center), and stress activated (right) signaling cascades. Separate signal transduction pathways initiated by different extracellular stimuli activate each group of MAPKs that, in turn, exhibit distinct substrate specificities.

stimulated by receptors and environmental stresses similar to those provoking the activation of JNKs. These enzymes are particularly sensitive to their stimulation by exposure of cells to endotoxins, including bacterial lipopolysaccharides. Evidence of their role in transducing stress signals can be found as far philogenetically as in yeast, where genetic analysis indicates that the Hog1p MAPK, the yeast homologue of p38, is required for the response to osmotic stress that involves the enhanced expressions of genes participating in the biosynthetic pathway of the osmotic stabilizer glycerol.

As for the ERKs, p38s are activated by dual phosphorylation on Thr and Tyr residues by MKK3 and MKK6, the latter being a general stimulator for p38s, and the former exhibiting certain preference for p38α. The immediate upstream activators for these kinases are not yet well defined, and include the potential p38 MAPKKKs known as ASK1 and TAK1. The specific transcription factors that can be regulated by p38s include cAMP-responsive element-binding protein (CREB), activating transcription factor 1 (ATF1), ATF2, Max, C/EBP homologous protein (CHOP), and MEF2C. In addition, these MAPKs can also trigger the activation of other serine-threonine kinases such as Mnk1 (MAPK-interacting kinase 1) and Mnk2 and MAPKAPKs (MAPK-activated protein kinases).

ERK5

ERK5, also known as big mitogen-activated protein kinase (BMK1), is distantly related to ERK1 and ERK2. Although it contains a Thr-Glu-Tyr motif in its activation loop, similar to that of ERK1 and ERK2, ERK5 is larger than any other known MAPK ($\sim$80 kDa) and is selectively activated by MEK5 but not by MEK1 or MEK2. This kinase can be stimulated by oxidative stress, and can play a role in early gene expression triggered by EGF and serum by the direct phosphorylation of the transcription factors MEF2C or c-Myc, thereby participating in cell proliferation and progression through the cell cycle. Although information on this MAPK is still limited, evidence supporting its role in cell growth is also provided by its ability to cooperate with the activated Raf or MEK, which act on ERK1 and ERK2, to promote neoplastic transformation. The physiological function of ERK5 is nevertheless still unclear, and further studies are required to establish the biological role of this MAPK signaling pathway.

Others (ERK3, ERK4, ERK7, and ERK8)

Novel member of the MAPK family, ERK 7 (61 kDa) and ERK8 also contain a Thr-Glu-Tyr activation motif. ERK8 was cloned using the rat ERK7 cDNA to screen a human multiple tissue cDNA library and share an overall amino acid sequence identity of 69%. In contrast to rat ERK7, ERK8 does not display significant constitutive kinase activity, does not phosphorylate c-Fos, and is activated in response to stimulation by Src or serum. ERK3 contains a Ser-Glu-Gly activation motif, with gly in place of the tyr. The ERK3 subfamily of MAPKs is composed of two functional genes, MAPK6 (p97 MAPK) and MAPK4 (ERK4), and several pseudogenes. Upstream activators of ERK3 are still poorly defined, and this kinase is not present in yeast or *C. elegans*. None of the currently known MEK family members is able to phosphorylate and activate ERK3 and no physiological substrates of ERK3 have been found. ERK3 is localized constitutively to the nucleus without a conventional nuclear localization sequences.

Specificity and Fidelity in Nuclear Signal Transmission by MAPK Signaling Pathways

Protein kinases typically interact with their substrates by recognizing primary sequence determinants that surround the phosphorylation site(s). In the case of MAPK, the minimum general primary sequence required to be a substrate for protein phosphorylation is the presence of a Ser or Thr residue followed by Pro. Additionally, most MAPKs also appear to interact with their substrates by binding to a second site. This "docking" interaction is required for substrate phosphorylation by MAPK *in vitro* and is likely to be a relevant mechanism for the selection of high affinity substrates by these kinases *in vivo*. The current view is that for substrate recognition, MAPKs first dock to the substrate through a binding interaction at one site leading to phosphorylation of the substrate at a second site at one or more Ser/Thr-Pro motifs. Recent studies demonstrate that the selective interaction of MAPK with substrates may influence the physiological regulation of MAPK targets *in vivo*. Examples of such docking interactions include the interaction of ERK or JNK with the transcription factor Elk-1. Furthermore, there is substantial evidence that the normal function of MAPK signaling modules requires the proper organization of their components within the cell.

Of interest, in the past decade, scaffolding proteins have emerged as general regulatory mechanisms ensuring the fidelity of intracellular pathways. These proteins bind components of signaling routes, physically organizing them to enable rapid physiological responses. The prototypical signaling scaffold is the yeast protein Ste5p which binds the components of the yeast MAPK cascade leading to the mating response after activation of the pheromone receptor, thus maintaining the signaling fidelity of this cascade. Several scaffold-binding components of MAPK cascades have now been described in multicellular organisms, including Kinase Suppressor of RAS (KSR) and c-Jun Terminal Kinase Interacting Protein family (JIPs). Their role is to maintain the integrity of biochemical routes connecting cell surface receptors to the nucleus. For example, the JIP family of scaffolding proteins consists of three mammalian homologues JIP/IB-1, -1b, and -2. These molecules bind members of the mixed-lineage group of MAPKKK's (MLK) that have been reported to activate both JNK and p38. In addition, both IB1/JIP1 and IB2/JIP-2 have been found to bind the JNK MAPKK, MKK7, while IB2/JIP-2 has also been reported to bind MLK3 and p38γ. An emerging concept derived from recent studies is that these scaffold proteins are organizers and keepers of signal specificity and fidelity. Indeed, it may be as important to keep signals separate between closely related MAPK cascades, as it is to integrate them in a coordinated response, particularly in gene expression control.

The activation of MAPK-mediated signaling pathways is often initiated by stimuli acting at the cell surface. However, many of the transcription factors that act as MAPK substrates are located in the nucleus, thus suggesting the existence of mechanisms by which the signals can be transmitted from the cytoplasm to the nucleus. This has been extensively investigated for the ERK1/2 pathway. For example, the activated forms of Raf (MAPKKK) are present at the plasma membrane, while activated MEK1 and MEK2 (MAPKK) are located in the cytoplasm, due to the presence of a nuclear export signal (NES) in the protein. Thus, the final step in signal transmission from the cytoplasm to the nucleus appears to be directly mediated by ERK1/2. Indeed, these ERKs are located in the cytoplasm of quiescent cells but in the nucleus of activated cells. The mechanism by which activation promotes the translocation of ERKs to the nucleus is still unclear. It has been suggested that ERKs may be actively sequestered in the cytoplasm by inactive MEK1/2, and upon their activation by Raf, MEK1 and MEK2 may dissociate from ERK1 and ERK2, which may then be able to migrate to the nucleus as homodimers. Whereas available evidence supports this model, it is still unclear whether the release of ERKs from their MAPKK, MEK1 and MEK2, is sufficient to promote the nuclear

accumulation of ERKs or whether additional processes are involved. Furthermore, whether other MAPKs use similar or distinct mechanisms to ultimately phosphorylate nuclear proteins is also poorly understood, and under current intense investigation.

Regulation of Gene Expression through MAPK Signaling Pathways

Although MAPKs can phosphorylate cytoplasmic substrates, most MAPK signaling pathways ultimately converge in the nucleus to regulate gene expression, either by acting at the pretranscriptional, transcriptional, and posttranscriptional level. The most widely used mechanism by which MAPKs regulate gene expression is the phosphorylation of transcription factors, thereby enhancing their activity. For example, phosphorylation of the transcriptional activation domains of ATF2, CHOP, Elk-1, and c-Jun causes increased transcription. As studied in detail for the transcription factor CREB, transcription factor phosphorylation can cause changes in the interaction with coactivator molecules, including CBP and p300, which function, in part, through the regulation of the chromatin structure by acetylating histones.

Less frequent cases are found where MAPKs negatively regulate transcription factors by promoting their retention in the cytoplasm upon phosphorylation, and active dephosphorylation of these factors is then needed for their migration to the nucleus to stimulate gene transcription. As examples, phosphorylation of the transcription factors SMAD1 and NFAT4 by ERK1/2 and JNK, respectively, causes their cytoplasmic retention and therefore the inhibition of their transcriptional activity. Whether instead the phosphorylation by MAPKs of cytoplasmic transcription factors may cause their nuclear translocation is still unclear. Regulation of the DNA-binding activity is also a mechanism employed by MAPKs to control transcription factor activity. An example is the transcription factor Elk-1, which is phosphorylated by ERK, JNK, and p38 MAPKs leading to increased DNA binding.

Regulation of translation represents a fourth mechanism of regulation of gene expression by MAPKs. The best example is the translational regulation of cytokine expression observed in macrophages exposed to endotoxin. In this case, p38 MAPK acts on a *cis*-acting element in the TNFα mRNA to regulate its translation. Modulation of mRNA processing and nuclear export has not been described, although these biosynthetic steps also represent potential sites for intervention by MAPK.

The final mechanism employed by MAPK to regulate gene expression is the regulation of protein degradation. This is exemplified by the short-lived transcription factor c-Jun, which is rapidly degraded by the ubiquitin–proteasome pathway. Phosphorylation of c-Jun by JNK inhibits the ubiquitination of c-Jun and, therefore, its rapid degradation. Consequently, JNK activation prolongs the half-life of c-Jun, leading to the accumulation of the c-Jun protein. The regulation of protein stability by MAPK therefore contributes to the regulation of gene expression mediated by these signaling pathways.

See Also the Following Articles

Muscarinic Acetylcholine Receptors • Ras Family • Src Family of Protein Tyrosine Kinases

Glossary

extracellular signal-regulated protein kinase (ERK) One class of MAPKs.

GTPases Molecular switches that control cellular responses by exchanging GDP (inactive form) for GTP (active form) in response to a variety of stimuli. In the GTP-bound form they interact with effector molecules. Subsequently, they hydrolyze GTP to GDP, thereby returning to their inactive state.

mitogen-activated protein kinases (MAPKs) A group of serine/threonine protein kinases that play an essential role in signal transduction in response to changes in the cellular environment.

protein kinases Phosphotransferases that catalyze the transfer of a phosphate group from ATP, or in some cases from GTP, to a protein substrate. Most protein kinases phosphorylated serine or threonine residues (serine-threonine protein kinases) or tyrosine residues (protein tyrosine kinases).

Ras A small GTPase that controls the activation of the ERK kinase cascade, as well as other downstream targets.

Further Reading

Cano, E., and Mahadevan, L. C. (1995). Parallel signal processing among mammalian MAPKs. *Trends Biochem. Sci.* **20**(3), 117–122.

Chang, L., and Karin, M. (2001). Mammalian MAP kinase signaling cascades. *Nature* **410**(6827), 37–40.

Gutkind, J. S. (2000). Regulation of mitogen-activated protein kinase signaling networks by G protein-coupled receptors. *Sci. STKE* **40**, RE1.

Johnson, G., and Lapadat, R. (2002). Mitogen-activated protein kinase pathways mediated by ERK, JNK, and p38 Protein Kinases. *Science* **298**, 1911–1912.

Kultz, D. (1998). Phylogenetic and functional classification of mitogen- and stress-activated protein kinases. *J. Mol. Evol.* **46**, 571–588.

Ono, K., and Han, J. (2000). The p38 signal transduction pathway: Activation and function. *Cell Signal* **12**(1), 1–13.

Pearson, G., Robinson, F., Beers Gibson, T., Xu, B. E., Karandikar, M., Berman, K., and Cobb, M. H. (2001). Mitogen-activated protein (MAP) kinase pathways: Regulation and physiological functions. *Endocr. Rev.* **22**(2), 153–183.

Weston, C. R., and Davis, R. J. (2002). The JNK signal transduction pathway. *Curr. Opin. Genet. Dev.* **12**(1), 14–21.

Biography

Hidemi Teramoto is a visiting scientist at Cell Growth Regulation Section, Pharyngeal Cancer Branch, National Institute of Dental and Craniofacial Research, National Institutes of Health. He holds M.D. and Ph.D. degrees from University of Tottori in Japan.

J. Silvio Gutkind is the Chief of the Oral and Pharyngeal Cancer Branch, National Institute of Dental and Craniofacial Research, National Institutes of Health. He holds a Ph.D. degree from University of Buenos Aires in Argentina.

Their principal research interest is in the molecular basis of cancer, which they have addressed by studying normal and aberrant functions of molecules involved in the transduction of proliferative signals. The laboratory has made seminal contributions to the field, and helped elucidate some of the basic molecular mechanisms whereby cell surface receptors regulate the nuclear expression of growth promoting genes.

Mitosis

Patricia Wadsworth and Nasser M. Rusan
University of Massachusetts, Amherst, Massachusetts, USA

Mitosis is the phase of the cell division cycle when the duplicated chromosomes are equally partitioned into two daughter cells. Chromosome motion occurs on the mitotic spindle, a dynamic structure that is assembled at the beginning of mitosis and subsequently disassembled. Mitosis is followed by cytokinesis, the division of the cytoplasm. Together, mitosis and cytokinesis constitute cell division and result in the generation of a pair of daughter cells.

The Cell Cycle

Dividing mammalian cells experience an ~24 h long cell cycle, during which the cells grow, replicate their DNA, and divide into two daughter cells. The cell cycle is composed of interphase, which lasts ~22 h, and mitosis, which is completed in ~2 h. Interphase can be subdivided into three parts. During S phase or synthetic phase of interphase, DNA is synthesized, or replicated. The interval between the end of mitosis and the beginning of S phase is called first gap (G1) phase. During G1, cells grow in preparation for division. However, if nutrients or growth signals are lacking, cell cycle progression can be slowed, or stopped. The phase after DNA replication and before the initiation of cell division is called gap 2 (G2). During G2, cells evaluate DNA replication; if damaged, or unreplicated, DNA is detected, the cell cycle is delayed. If no DNA damage is detected, cells progress through G2, and enter mitosis.

Spindle Structure

The mitotic spindle at metaphase is a bilaterally symmetric, microtubule-based structure with chromosomes aligned in the middle. The spindle is bipolar: the two spindle poles define the spindle axis and are the sites to which the chromatids are moved during anaphase (Figure 1). In many animal cells, a centrosome, composed of a pair of centrioles and associated pericentriolar microtubule-nucleating material, is present at the spindle poles (Figure 1). The major structural elements of the spindle are microtubules, dynamic cytoskeletal filaments that radiate from the two spindle poles. Microtubules attach chromosomes to the spindle and are essential for chromosome motion. Spindle microtubules are classified by their location in the spindle (Figure 1). Interpolar microtubules extend from each spindle pole and overlap in the middle of the spindle. Kinetochore microtubules have one end embedded in a specialized attachment site on the chromosome, the kinetochore. The third class of spindle microtubules, astral microtubules, extend away from the centrosomes toward the cell cortex. Astral microtubules contribute to spindle positioning and in defining the position of the contractile ring at cytokinesis.

Considerable variation in spindle structure exists among diverse cells. In cells of higher plants, the spindle pole lacks centrioles and is broad, not focused. Plant spindles are also anastral, lacking astral microtubules. In yeasts, which undergo closed mitosis inside of an intact nuclear envelope, a spindle pole body is present at the two ends of the spindle. The spindle pole body, a trilaminar plaque-like structure embedded in the nuclear envelope, nucleates microtubules that radiate into the nucleus and cytoplasm. The number of spindle microtubules also varies among cell types. Yeasts have a simple spindle, and a single microtubule links each kinetochore to the spindle pole body. In contrast, ~20 microtubules are associated with each kinetochore in a typical animal cell and hundreds of microtubules are present in each half-spindle. Despite these differences in spindle structure, in all cases, mitosis accomplishes the accurate segregation of the replicated genetic material into the two daughter cells.

Phases of Mitosis

Prophase

Chromosome Condensation

Prior to mitosis, during the S phase of interphase, each chromosome is replicated, resulting in two identical sister chromatids that are bound together by protein complexes called cohesions. The sister chromatids are very long strands of DNA and must be compacted for division. This process, called chromosome condensation, occurs as specialized proteins called condensins

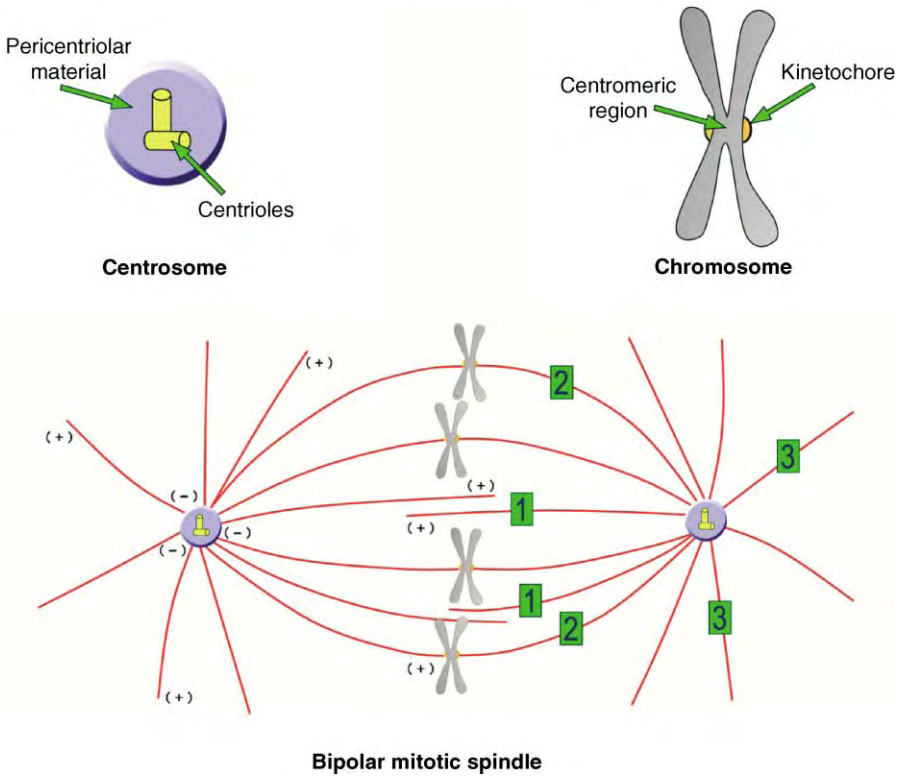

FIGURE 1 Highly schematic diagram of a mammalian mitotic spindle at metaphase of mitosis. Microtubules are depicted as red lines; interpolar, kinetochore, and astral microtubules are labeled 1, 2, and 3, respectively. The plus and minus ends of the microtubules are marked. Inset, upper left, shows a schematic diagram of a centrosome consisting of pericentriolar material, purple, and centrioles, yellow. Inset, upper right, shows a diagram of a chromosome; the centromeric region and the kinetochore are shown.

coil the DNA into loops. As prophase progresses, the chromosomes become increasingly visible in the nucleus, first as threads or strands and later as highly condensed rod-like structures called chromosomes, each of which is composed of two chromatids (Figure 2). The term mitosis comes from the Greek word *mito* meaning thread, referring to the appearance of thread-like structures in the prophase nucleus.

Kinetochore Assembly

In order for the chromatids to be accurately segregated into the two daughter nuclei, they must be attached to, and later moved by, the spindle machinery. Mitotic chromosomes are characterized by an indentation, or primary constriction, called the centromere (Figure 1). The centromere is a region of highly repeated DNA sequences that serves as the assembly site for a plate-like structure called the kinetochore. The kinetochore functions to link each chromatid to the spindle via kinetochore microtubules and also functions as a signaling device that regulates progression through the cell cycle. Kinetochores of sister chromatids are arranged back-to-back so that the binding sites for spindle microtubules face in opposite directions to facilitate the association of each chromatid with microtubules from opposite spindle poles.

Centrosome Separation

In animal cells, the centrosome is also duplicated during S phase of interphase, and the two daughter centrosomes remain adjacent to one another. Centrosome duplication ensures that two centrosomes are present at the beginning of mitosis to form the spindle poles and guarantees that each daughter cell inherits one centrosome. In prophase, the duplicated centrosomes separate and begin moving to opposite sides of the nucleus to establish a bipolar spindle. The microtubule nucleating capacity of each centrosome also increases dramatically at prophase.

PROMETAPHASE

Nuclear Envelope Breakdown

In cells with an open mitosis, the breakdown of the nuclear envelope marks the beginning of prometaphase.

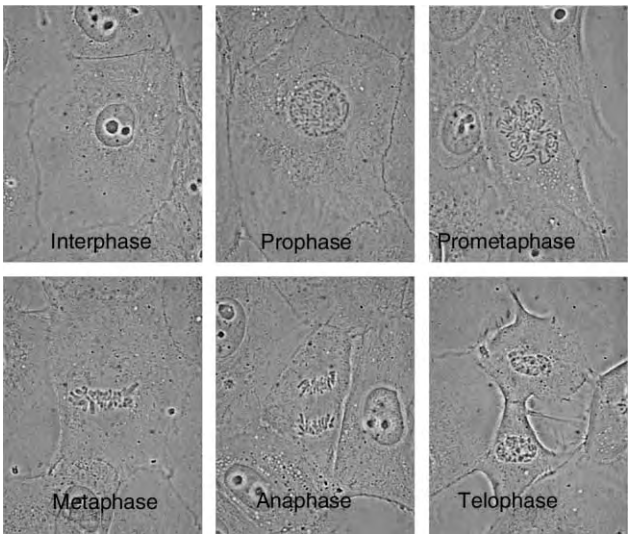

FIGURE 2 Phase contrast light micrographs of living LLCPK1 mammalian cells in mitosis. Each panel shows a different cell at the indicated stage of mitosis.

Microtubules assist nuclear envelope breakdown resulting in the fragmentation of the nuclear membrane into small vesicles and consequently releasing the chromosomes into the cytoplasm.

Spindle Assembly

Spindle assembly requires dynamic microtubules. Because microtubules are polar polymers, their two ends have different dynamic properties. The less dynamic end, called the minus end, is associated with the spindle pole material; the more dynamic end, called the plus end, extends outward toward the cell periphery (Figure 1). Microtubule plus ends display a behavior called dynamic instability, in which they switch stochastically between phases of assembly and disassembly. The result of dynamic instability behavior is that microtubule plus ends continually probe the cytoplasm as they grow and shorten. Microtubules in mitotic cells are more dynamic than microtubules in interphase cells because they switch from growing to shortening more frequently and shorten further before resuming growth. The result is a population of relatively short, highly dynamic microtubules that radiate from each spindle pole. At nuclear envelope breakdown, chromosomes are released into the cytoplasm and dynamic microtubules can interact with each kinetochore. Once a connection between a microtubule and kinetochore is established, the microtubule becomes less dynamic in order to maintain the connection. Cells monitor the attachment of chromosomes to the mitotic spindle and mitosis is delayed if even a single chromosome is unattached. This regulatory system is called the spindle assembly checkpoint, or metaphase checkpoint.

Microtubule motor proteins, which utilize the energy of ATP hydrolysis to perform work in cells, are also important for spindle assembly. The type and properties of the motor protein govern the direction of motion, either toward the minus end or the plus end of the microtubule. Multifunctional motors or motor protein complexes can exert force on microtubules by cross-linking neighboring microtubules and sliding them relative to one another or by binding to one microtubule while walking along an adjacent one. Alternatively, the nonmotor region of the motor protein can bind to a tethered structure, the cell cortex for example, while the motor region of the protein applies a pulling force on the microtubule. Motor proteins are present at the kinetochores, between interpolar microtubules, along kinetochore microtubules and at the cell cortex.

Motor proteins contribute to various motions during mitosis. During centrosome separation in prophase, motors located between the antiparallel, interpolar microtubules contribute to the separation of the two spindle poles. At the kinetochores, motors contribute to the initial bipolar attachment of chromosomes to spindle microtubules. Motors also contribute to congression, the movement of the chromosomes to the spindle equator, or metaphase plate, following initial attachment. In the assembled spindle, a balance of the activities of oppositely directed motor proteins maintains spindle length; some motors tend to pull the poles together, and this is resisted by motors that act to push the poles apart. Motor proteins also contribute to spindle positioning in mitotic cells, and to the dynamic turnover of mitotic microtubules.

Spindle assembly can also occur in the absence of centrosomes. In this situation, microtubules assemble in the vicinity of chromosomes and are subsequently sorted into a bipolar array by the activity of motor proteins. In both the presence and absence of centrosomes, dynamic microtubules and motor proteins contribute to spindle formation.

Metaphase

The cell is in metaphase when all of the duplicated chromosomes are aligned midway between the two spindle poles (Figures 2 and 3), a location referred to as the metaphase plate or spindle equator. Spindle length remains relatively constant at metaphase, but the spindle microtubules are not static. Rather, they undergo a behavior called spindle flux, in which spindle microtubules continually assemble at their plus ends and disassemble at the minus ends, coupled to poleward translocation of the polymer. As a result of flux, marks placed on spindle microtubules are observed to move slowly toward the poles during metaphase and anaphase of mitosis.

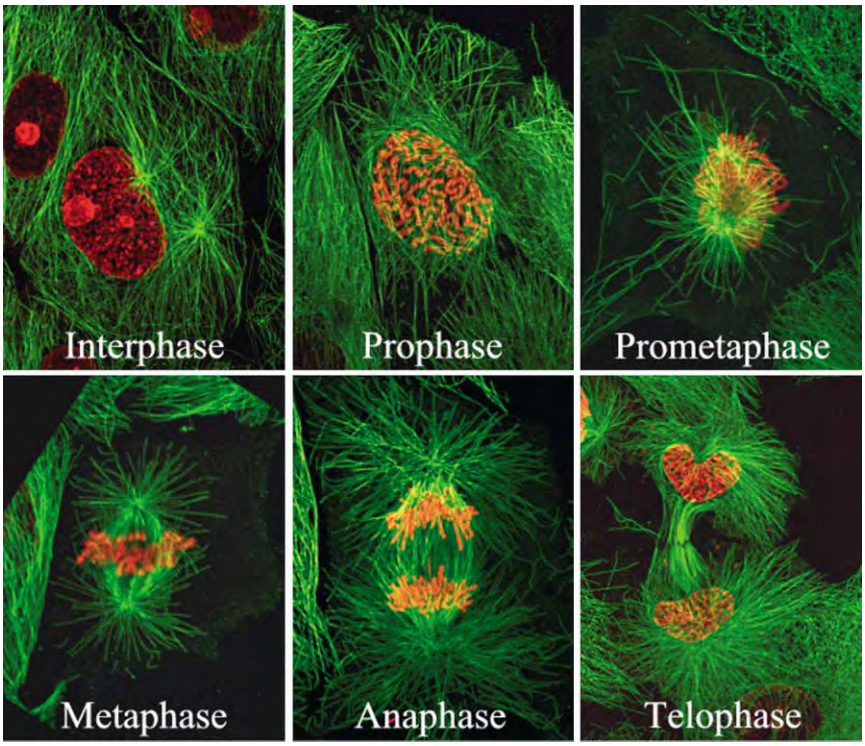

FIGURE 3 Distribution of microtubules and DNA throughout mitosis. Fluorescence light micrographs of cells that have been fixed and stained with antibodies to tubulin, to label microtubules, and propidium iodide, to stain DNA. Microtubules are shown in green and DNA in red. Images are maximum projections of deconvolved image stacks taken with a spinning disc confocal microscope.

Not only are microtubules dynamic at metaphase, the chromosomes are also active, oscillating towards and away from each spindle pole. Chromosomes are also under tension, ready for subsequent movement in anaphase. If the connection between one sister chromatid and the pole is severed at metaphase, the chromosome moves to the pole to which it remains attached, demonstrating that the metaphase position results from a balance of pole directed forces acting on the chromosomes.

Anaphase

During anaphase, sister chromatids separate and move to the spindle poles (Figures 2 and 3). Anaphase consists of two phases, anaphase A and B. During anaphase A, the chromosomes move to the poles and kinetochore fiber microtubules shorten; during anaphase B, the spindle poles move apart as interpolar microtubules elongate and slide past one another. Many cells undergo both anaphase A and B motions, but in some cases one or the other motion dominates.

Separation of the paired sister chromatids is required for poleward motion in anaphase. Chromatid separation results from the proteolytic degradation of components that link the chromatids at the centromere. Degradation is triggered by the activity of the anaphase-promoting complex, which regulates cell cycle progression. Chromatid separation is not the result of tugging by microtubules and motor proteins, and can be observed even in the absence of microtubules.

Although the motion of the chromosomes to the spindle poles in anaphase has fascinated biologists for many years, the molecular basis for this motion remains controversial and incompletely understood. During anaphase A, kinetochore microtubules must shorten as the chromosomes move poleward. Measurements of spindle flux show that subunit loss from microtubules occurs at the spindle poles during anaphase. In many cells, however, the rate that chromosomes move exceeds the rate of subunit loss at the pole, and thus subunit loss must also occur at the kinetochore.

Pioneering studies of mitosis in living embryonic cells demonstrated that assembly and disassembly of microtubule polymers result in chromosome motion. This work led to the hypothesis that microtubule disassembly drives chromosome motion. Later work identified molecular motors at the kinetochore, leading to the alternative hypothesis that forces generated by molecular motors drive chromosome motion. One possibility is that molecular motors power chromosome motion, but the rate of chromosome motion is limited by kinetochore microtubule disassembly. Alternatively,

disassembly may be responsible for chromosome motion, and motors may tether the chromosomes to the shortening fiber. The presence of potentially redundant mechanisms for chromosome motion may reflect the fact that mitotic fidelity is of utmost importance.

Telophase

In telophase, the chromosomes decondense, and the nuclear envelope begins to reform around them (Figures 2 and 3), returning the cell to the interphase condition. The short dynamic microtubules of the spindle are replaced with the less dynamic microtubules of the interphase array that extend to the cell periphery (Figure 3). During telophase the contractile ring assembles midway between the spindle poles in preparation for cytokinesis.

Cytokinesis

Cytokinesis is the process of constricting the cytoplasm between the two forming daughter nuclei resulting in the formation of two cells. Cytokinesis is achieved by a contractile ring, or belt, composed of filaments of the cytoskeletal polymer, actin, and the molecular motor protein, myosin II, which provides the force for cytokinesis. The contractile ring is tethered to the cell membrane, and its contraction creates a cleavage furrow, or indentation of the plasma membrane, during cytokinesis. The contractile ring assembles midway between the two spindle poles in telophase, and disassembles when cytokinesis is completed. The signals that determine the location of contractile ring formation in the cell cortex have yet to be identified, but microtubules are involved in their delivery to the cortex. In some cells, radiating astral microtubules that overlap midway between the spindle poles dictate the site of contractile ring formation. In other cases, interzonal microtubules located between the separating chromosomes play an important role in specifying the location of furrow formation. The completion of cytokinesis marks the end of mitosis and the birth of two completely independent daughter cells in interphase of their cell cycle.

See Also the Following Articles

Cell Cycle: Mitotic Checkpoint • Centrosomes and Microtubule Nucleation • Chromosome Organization and Structure, Overview • Cytokinesis • Metaphase Chromosome • Nucleoid Organization of Bacterial Chromosomes • Septins and Cytokinesis

Glossary

centrosome Structure present at the spindle poles in many animal cells that is composed of a pair of centrioles and associated pericentriolar material.

congression The motion of chromosomes to the midplane, or equator, of the spindle during prometaphase.

kinetochore Structure located at the centromere of each chromatid that functions to link each chromatid to the spindle. The kinetochore is also the location of components of the spindle assembly checkpoint.

microtubule Polar, cytoskeletal polymer composed of tubulin dimers that are a major structural element of the mitotic spindle and are required for chromosome motion.

spindle flux Poleward motion of microtubule polymers that occurs during metaphase and anaphase of mitosis.

Further Reading

Compton, D. A. (2000). Spindle assembly in animal cells. *Annu. Rev. Biochem.* **69**, 95–114.

Inoue, S., and Salmon, E. D. (1995). Force generation by microtubule assembly/disassembly in mitosis and related movements. *Mol. Biol. Cell.* **6**, 1619–1640.

Karsenti, E., and Vernos, I. (2001). The mitotic spindle: A self-made machine. *Science* **294**, 543–547.

McIntosh, J. R., and McDonald, K. L. (1989). The mitotic spindle. *Sci. Am.* **261**, 48–56.

Nicklas, R. B. (1997). How cells get the right chromosomes. *Science* **275**, 632–637.

Rieder, C. L., and Khodjakov, A. (2003). Mitosis through the microscope: Advances in seeing inside live dividing cells. *Science* **300**, 91–96.

Scholey, J. M., Brust-Mascher, I., and Mogilner, A. (2003). Cell division. *Nature* **422**, 746–752.

Wittman, T., Hyman, A., and Desai, A. (2001). The spindle: A dynamic assembly of microtubules and motors. *Nat. Cell Biol.* **3**, E28–E34.

Biography

Dr. Patricia Wadsworth is a Professor in the Department of Biology at the University of Massachusetts, Amherst. Her principal research interests are in the area of mitosis and the cytoskeleton, with particular focus on the dynamic behavior of microtubules. She received a Ph.D. from Dartmouth College and was a post-doctoral fellow at the University of North Carolina, Chapel Hill.

Nasser M. Rusan is a Ph.D. candidate in molecular and cellular biology at the University of Massachusetts, Amherst. His research interest is in the cytoskeleton, with particular emphasis on microscopy and digital imaging technology.

mRNA Polyadenylation in Eukaryotes

Mary Edmonds
University of Pittsburgh, Pittsburgh, Pennsylvania, USA

Polyadenylation is a process used by all cells to generate the polyA sequence on the 3′ end of messenger RNA (mRNA). The restriction of this modification to mRNAs is achieved through two conserved sequences in the 3′ non-coding region of the RNA polymerase transcript. These sequences direct four multisubunit cleavage complexes to these sites for a specific endonucleolytic cleavage that produces the hydroxyl group on which the polyA tail is generated by a polyA polymerase along with a polyA binding processivity factor.

An unexpectedly large number of proteins are needed for this simple two step enzymatic reation. Additional roles for these specific proteins within the cleavage complexes account in part for this complexity. Some regulate levels of mRNA and even choice of specific mRNA from transcripts with multiple polyA sites. Others interact with processing complexes for 5′ end capping and intron removal. Still others couple RNA processing to transcription through binding of cleavage complexes to the C-terminal domain of RNAP11. Along with capping and splicing complexes a dynamic complex linking RNA processing to transcription results which persists through all phases of transcription up to termination where cleavage factors play a decisive role.

Polyadenylation is a cellular process that generates the poly A sequence on the 3′ end of mRNA. A nuclear poly A polymerase (PAP) adds AMP units from ATP to the 3′ hydroxyl group at the 3′ end of mRNA and processively elongates the sequence to ~200 nucleotides (nts) in mammals and 60 in *Saccharomyces cerevisiae*. A critical feature that bestows specificity on the process is the selection of the site in the mRNA to be polyadenylated. Rather than addition to the 3′ end of the transcript produced by RNA polymerase II (RNAP II), a specific site within this precursor mRNA transcript is created by endonucleolytic cleavage. The site is defined in mammals by a conserved hexanucleotide upstream of the cleavage site and by a less conserved site 10–50 nts downstream of the cleavage site.

A large number of proteins is needed to achieve this cleavage specificity. Most exist within two large cleavage complexes, one of which binds to an upstream site and the other to a downstream site. Two other less well-understood complexes are essential only for cleavage, while PAP and a poly A-binding protein, add AMPs processively to the 3′ hydroxyl group at the 3′ end of the upstream cleavage product.

Although the major RNA processing reactions of 5′ capping, splicing, and polyadenylation occur independently *in vitro*, mutual stimulation of one processing reaction on another is common, i.e., polyadenylation and terminal exon splicing and 5′ capping and polyadenylation. These mutual effects are now understood to result from the coordination of RNA processing with transcription through a dynamic assembly of processing factors with the C-terminal domain (CTD) of the large subunit of RNAP II.

The role of the poly A sequence long remained a mystery in spite of its potential effects either on mRNA stability, nuclear export, or translation. Poly A is now known to participate in each of these processes, often serving as an anchor for a poly A-binding protein that interacts with components of each of these reactions in a manner that modulated gene expression.

Sequences Required for Polyadenylation

Sequences Upstream of the Poly A Site

Point mutations of the AAUAAA signal result in greatly extended nascent RNAP II transcripts. This finding led to the prediction that the poly A addition site was created by cleavage rather than by transcription termination. A high degree of conservation of AAUAAA was evident when about 90% of 250 sequenced mRNAs had an AAUAAA sequence (with 10% as AUUAAA) near their 3′ ends.

More recent analyses of several thousand human expressed sequence tags (ESTs) showed a higher incidence of alternative hexanucleotide signals as only 60% were AAUAAA with 12% AUUAAA. Biological evidence for more extensive use of alternative signals is

most clearly seen in male germ cells where frequencies of AAUAAA resemble those from the EST data, raising the possibility of tissue-specific polyadenylation. A variant cleavage stimulation factor CstF subunit (CstF-64) of the male germ cells but not present in HeLa cells CstF may recognize an alternative poly A signal. Experimental data indicate that AAUAAA functions in a single-stranded form, a finding compatible with the limited number of folded structures examined thus far.

Sequences Downstream of the Poly A Site

Correct 3′ end processing requires a sequence 10–50 nts downstream of the cleavage site that is far less conserved than AAUAAA. This sequence is often a 5nt UMP-rich element (U_4N) and less commonly a 5nt 2(GU)N sequence. However, ~20% of human pre-mRNAs have a downstream sequence that differs somewhat from both of these elements, emphasizing the lack of conservation of downstream elements. Spacing between upstream and downstream elements is crucial for the interaction between cleavage polyadenylation specificity factor (CPSF), bound to AAUAAA and CstF bound to $U_4(N)$ downstream that initiates cleavage.

Proteins of Cleavage/ Polyadenylation

mRNA 3′ end formation and polyadenylation (Figure 1) is deceptively simple. However, as shown in Table I, four multisubunit complexes are required for cleavage along with the polymerase and a poly A-binding protein. Together, at least 14 polypeptides are involved in the reaction. Most have been cloned and sequenced and several expressed as recombinant forms. Table I summarizes features and general functions of the core components responsible for 3′ end formation.

CPSF

CPSF is a complex of 160, 100, 73, and 30 kDa subunits that binds to the AAUAAA poly A signal through the 160 kDa subunit. Binding is stabilized by the other subunits including the 30 kDa protein that binds to pre-mRNA. Little is known of the roles of the 100 and 73 kDa proteins, although these two proteins share 23% sequence identity. The 30 kDa protein has been proposed to be the nuclease for cleavage based on a marked sequence similarity to a 30 kDa *Drosophila* endonuclease, although CPSF-30 lacks such activity, as do all the core proteins.

In vivo CPSF is recruited to the transcript promoter by the TFIID transcription factor where it binds to the CTD of RNAP II. Upon initiation of transcription it interacts cooperatively with the CstF complex, which also binds to the CTD. CPSF remains bound as RNAP II transcribes the gene up to and beyond the poly A site to the termination site.

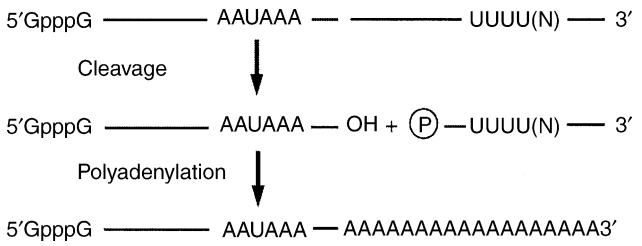

FIGURE 1 The two steps in mRNA 3′ end processing. Endonucleolytic cleavage between the AAUAAA sequence and the downstream element shown as an oligo U-rich sequence generates an upstream fragment with a 3′ OH group and a downstream fragment with a 5′ phosphate group. The upstream fragment is polyadenylated and the downstream fragment is degraded. (Reproduced from Wahle, E., and Keller, W. (1996). The Biochemistry of Polyadenylation. *Trends Biochem. Sci.* **21**, 247.

Cleavage Stimulation Factor

CstF is a trimeric complex needed only for cleavage. The 77 kDa subunit bridges the 64 and 50 kDa subunits of CstF and the trimer interacts cooperatively with CPSF most likely through a strong interaction between CstF-77 and CPSF-160.

CstF-77 is homologous to a suppressor protein of *Drosophila* implicated in the regulation of poly A site

TABLE I

Mammalian Cleavage and Polyadenylation Factors

Factor	Subunits (kDa)	Function
CPSF	160 100 73 30	Cleavage and polyadenylation binds AAUAAA
CstF	77 64 50	Cleavage; binds downstream element
$CF1_m^a$	25 (72, 68, 55)[b]	Cleavage; binds RNA
$CF11_m^a$	47	Cleavage
PAP	82	Cleavage and polyadenylation; catalyzes AMP polymerization
PABP2	33	Poly A extension; stimulates PAP; controls poly A length
RNA pol II (large subunit)	200	Cleavage; binds CPSF and CstF

[a] One of these three interacts with the 25 kDa subunit to give a functional heterodimer.

[b] Mammalian.

choice. However, it is CstF-64 that has been assigned this role in human and chicken cells. Increased levels of CstF-64 favor the use of weak poly A sites normally underused relative to stronger sites. If such sites are in different coding exons, proteins with different sequences will be produced that may have different functions. This occurs during differentiation of β cells into antibody-secreting plasma cells. In undifferentiated β cells the use of a stronger downstream poly A site generates an mRNA for the immunoglobulin heavy chain that codes for a membrane-bound protein, while a weaker upstream polyA site is more active in plasma cells, and leads to a shorter mRNA coding for a secreted immunoglobulin heavy chain. The switch from membrane mRNA to the secreted form is correlated with large increases of CstF-64 while levels of other subunits of CstF remain unchanged. Other activators and inhibitors of the switch are known that may increase upon cytokine stimulation of differentiation.

The CstF-50 subunit is characterized by a seven WD-40 repeat of 40 amino acids that are also in the transducin repeats of the β-subunit of tripartite G proteins. CstF-50 forms a complex with the nuclear protein, BARD1, which is known to associate *in vivo* with the breast cancer tumor suppressor BRCA1. This complex inhibits polyadenylation *in vitro*. Both CstF-50 and BARD1 interact with the CTD of RNAP II leading to speculations that BARD1 may prevent inappropriate 3′ end formation.

$CF1_M$ and $CF11_M$ Cleavage Factors

Both are required for cleavage. CF1 has subunits of 68, 59, and 25 kDa; however, a dimer of the 68 and 25 kDa proteins can replace CF1 *in vitro*. CF1 binds to CPSF at an early stage of assembly of the cleavage complex. CF11 has only been partially purified, but has a subunit of 47 kDa that is homologous to the yeast 3′ end-processing factor, Clp1. CF11-47 interacts with CPSF and $CF1_m$.

Poly A Polymerase

PAP was characterized initially by its specificity for ATP but it lacked specificity for an RNA primer. Specificity for mRNA is now known to be conferred by CPSF. Two functional isoforms, PAP I (77 kDa) and PAP II (82 kDa) are generated by alternative splicing of a mouse gene with 22 introns. Although PAP II is more common, both have identical activities and specificities. The highly conserved amino two-thirds of the molecule has the catalytic site while the C-terminal regions contain an RNA-binding domain and two nuclear localization signals as well as serine/threonine-rich phosphorylation sites.

Crystals of calf and yeast PAPs both show a cylindrical U-shaped molecule with the N-terminal catalytic site spread along one wall of the cavity. The locus of the RNA-binding site awaits analysis of RNA:protein cocrystals.

PABP2

The nuclear 33 kDa poly A-binding protein (PAB2) is responsible for processive elongation by the polymerase and for control of poly A tail length.

RNAP II

RNAP II has recently been recognized as the engine of an RNA machine that carries RNA processing complexes including CPSF and CstF on the CTD of its large subunit. CTD is a separate domain of heptad repeats of seven amino acids repeated 52 times in mammals and 26 times in yeast where two of its serines undergo phosphorylation after transcription is initiated.

Transcription Termination and Polyadenylation are Linked

Evidence for a link between mRNA 3′ end formation and transcription was first seen with point mutations of the AAUAAA poly A signal that resulted in greatly elongated nascent transcripts. This was also seen *in vivo* in a transcript from a thalessemia patient with a point mutation in the AAUAAA signal of the α-globin gene. Defining a mechanism for this linkage of transcription termination to 3′ end processing was difficult until the dependence of mRNA 3′ end processing on an intact CTD of RNAP II was established. The binding of cleavage/polyadenylation complexes CPSF and CstF to the CTD occurs prior to initiation of transcription, and they can remain affiliated with the polymerase up to sites of termination. This finding has stimulated new analytical approaches emphasizing accumulation of nascent transcripts, especially the highly unstable downstream cleavage products.

It is now clear that transcription termination occurs before cleavage as RNAP II moves far beyond the cleavage site producing uncleaved nascent transcripts. The fact that this requires a functional poly A site, usually hundreds of nucleotides upstream of the termination site, suggests a model in which the nascent RNA is looped out between the CTD bound cleavage/polyadenylation factors and the RNA exit channel of RNAP II. The identification of specific sequences including pause sites in this 3′ flanking region and termination factors that may interact with

cleavage/polyadenylation factors to drive mRNA 3′ end formation has introduced a new level of complexity into the nature of this coupling.

Polyadenylation in Yeast

The mechanism of mRNA 3′ end formation in yeast generally resembles that of mammals, although the length of the poly A tail is only ~50–70 nts. The yeast poly A polymerase N-terminal half is essentially identical to that of the N terminus of the mammalian enzyme. Yeast mRNAs have two poorly conserved poly A signals including an upstream U-rich site and an A-rich site downstream but both are upstream of the poly A addition site. Two large multisubunit complexes required for cleavage have subunits homologous to those of CPSF and CstF emphasizing their shared evolutionary history.

A role for poly A in translation has been established with a yeast extract. The poly A tail of mRNA serves as an anchor for a poly A-binding protein that binds to a translation initiation factor, eIF4G to which a 5′ cap-binding protein is also bound at a distinct site. This complex brings 5′ and 3′ ends of mRNA together to initiate translation.

Role of Polyadenylation in Regulating Gene Expression

The type and level of mRNA expressed from nascent transcripts can affect cell growth, differentiation, or function. Like other RNA modifications, polyadenylation can be critical for regulating functional mRNA levels beginning with nuclear export. This occurs in influenza virus-infected cells that produce a viral protein that inhibits cellular mRNA 3′ end formation by binding both cleavage and polyadenylation factors leading to accumulation of non- or underpolyadenylated cellular mRNAs in the nucleus while polyadenylated viral mRNAs processed by a different mechanism exit to the cytoplasm.

Early evidence for a poly A function in the regulation of mRNA activity was seen in maturing oocytes and zygotes where activation of cytoplasmic dormant mRNAs became translationally active upon 3′ end polyadenylation. This activation depended on an intact AAUAAA poly A signal and a specific U-rich sequence in the 3′ untranslated region of a restricted set of mRNAs to which specific proteins bind. A specific cytoplasmic polymerase with unique properties has recently been reported in *Caenorhabditis elegans* suggesting that cytoplasmic polyadenylation may also occur in mammals, a likely possibility that needs to be re-examined.

The regulated choice between two functional poly A sites in different coding exons of a pre-mRNA can produce two mRNAs coding for proteins with different biological functions. One well-studied example is the immunoglobulin heavy chain in β cells where a switch in poly A site usage occurs during β cell differentiation into plasma cells. The role of the 64 kDa subunit of CstF cleavage complex in this switch has already been described. Another involves the calcitonin gene transcript that codes for the Ca^{2+}-activated protein that is produced in most tissues, but not in neuronal cells where an mRNA with two additional exons is processed at a poly A site farther downstream leading to the production of a larger protein, the calcitonin gene-related protein with several neurotrophic activities. The restriction of this choice to neuronal tissues was originally attributed to activator or inhibitor proteins not present in other tissues, while use of the upstream poly A site to produce calcitonin was considered the default mechanism. Surprisingly a novel mechanism for stimulating cleavage and polyadenylation at this upstream poly A site involved an enhancer sequence in the downstream adjacent intron. This enhancer sequence includes partial 5′ and 3′ splice sites that bind a splicing factor that interacts with the cleavage complex at the poly A site of the upstream exon to stimulate polyadenylation. Factors in neuronal tissue that may over-ride this intron enhancer mechanism have not yet been identified.

Finally phosphorylation:dephosphorylation of the serine/threonine-rich C-terminal domain of poly A polymerase can regulate its enzymatic activity *in vivo* and *in vitro*. This is under the control of the cell cycle as a hyperphosphorylated PAP accumulates during mitosis reducing its enzymatic activity that coincides with a general shutdown of RNA and protein synthesis while hypophosphorylation of PAP is characteristic of other phases of the cell cycle.

See Also the Following Articles

RNA Polymerase II Elongation Control in Eukaryotes • RNA Polymerase II Structure in Eukaryotes • Spliceosome • Transcription Termination

Glossary

5′ mRNA capping Addition of a 7-methyl guanosine to the 5′ phosphorylated end of a nascent mRNA transcript that creates a 5′–5′ triphosphate linkage.

3′ mRNA polyadenylation The processive addition by a poly A polymerase of AMP units from ATP to the 3′ end of mRNA. The site for poly A addition is created by cleavage of a specific phosphodiester bond within the 3′ region of the precursor mRNA that provides the site of the 3′ hydroxyl group for poly A addition.

splicing A coupled two-step process for removing noncoding intervening sequences (introns) from precursor mRNA and for

joining the two resulting adjacent coding sequences (exons) to produce a translatable mRNA sequence.

Further Reading

Calvo, O., and Manley, J. (2003). Strange bedfellows: Polyadenylation factors at the promoter. *Genes Dev.* **17**, 1321–1327.

Edmonds, M. (2002). A history of poly A sequences: From formation to factors to function. *Prog. Nucleic Acid Res. Mol. Biol.* **71**, 268–389.

Proudfoot, N., Furger, A., and Dye, M. (2002). Integrating mRNA processing with transcription. *Cell* **108**, 501–512.

Wahle, E., and Keller, W. (1996). The biochemistry of polyadenylation. *Trends Biochem. Sci.* **21**, 247.

Zhao, J., Hyman, L., and Moore, C. (1999). Formation of mRNA 3′ ends in eukaryotes. *Microbiol. Mol. Biol. Rev.* **63**, 405–455.

Biography

Mary Edmonds is a Professor Emerita in the Department of Biological Sciences at the University of Pittsburgh. Her research has been in the area of RNA processing beginning with the discovery of poly A polymerases and polyadenylated pre-mRNAs and messenger RNA in human cells. Later with John Wallace, a graduate student they discovered branched polyadenylated nuclear RNAs that are key intermediates in the splicing reaction that removes introns from nascent RNA transcripts.

mRNA Processing and Degradation in Bacteria

Deborah A. Steege
Duke University, Durham, North Carolina, USA

Messenger RNA molecules in bacteria are subject to cleavage by ribonucleases (RNases) and to extension by addition of A residues to their 3′-terminal ends. In a few instances, the function of RNase digestion is the processing of precursor mRNAs during biosynthesis to generate the mature ends found on the mRNAs translated by ribosomes. However, the primary function of RNase action on mRNA is to effect its degradation and make the nucleotide units available for use in synthesis of new mRNAs. This enables bacterial cells to modulate the levels of particular mRNAs in response to changes in the environment. The defining feature of mRNA at the time of its discovery during the 1960s was instability. At any one time in a bacterial cell mRNA represents a substantial fraction of the RNA being made by RNA polymerase, but it is degraded quickly. Only a few enzymes are required to degrade mRNA, several of which are coordinated in a large complex termed the degradosome. During the steps of degradation, stable RNA structures in mRNAs pose strong barriers to decay. In these instances, addition of a stretch of single-stranded A residues (a poly(A) tail) to the 3′ end of the mRNA facilitates continued degradation of the mRNA molecule.

Ribonucleases that Mediate mRNA Degradation in the Bacterium *Escherichia coli*

In bacteria, mRNA is degraded by the sequential action of endonucleases and exonucleases (Figure 1). The only bacterial species for which sufficient information about mRNA decay pathways is available for discussion is *Escherichia coli* (*E. coli*). RNases are defined by two properties: (1) whether they act on internal phosphodiester bonds within an RNA chain (endonuclease) or on an end of an RNA chain (exonuclease); and (2) whether the exonuclease degrades from the 3′ or the 5′ end of an RNA chain. In bacteria only 3′ to 5′ exonucleases have been found. The combined action of endonuclease cleavage and 3′ to 5′ exonuclease digestion on an mRNA generally produces an apparent 5′ to 3′ wave of degradation intermediates. Only six of some 20 RNases identified in *E. coli* are currently known or implicated to function in mRNA decay (Table I). Three are endonucleases and three are 3′ to 5′ exonucleases. The principal endonuclease that initiates decay is the large enzyme RNase E, which is specific for single-stranded regions in mRNA. This enzyme has the unique property of preferring as substrates the monophosphorylated 5′ ends on the downstream products of mRNA cleavage. This feature, in combination with the direction of ribosome movement on an mRNA, probably accounts for the apparent 5′ to 3′ directionality of decay observed for many mRNAs. The other two endonucleases have many fewer substrates on mRNAs than RNase E. RNase G is homologous to the N-terminal catalytic domain of RNase E and shares the other properties of RNase E. RNase III is specific for double-stranded regions of mRNAs and often makes staggered cleavages on opposite strands of the stem in an RNA stem-loop. The exonuclease RNase II, which accounts for the bulk of exonucleolytic activity on mRNA in *E. coli*, is a hydrolytic enzyme that removes nucleoside 5′ monophosphates from RNA 3′ ends. The exonuclease polynucleotide phosphorylase (PNPase), by contrast, acts in a phosphorolytic manner using inorganic phosphate to produce nucleoside 5′ diphosphates. A puzzling feature of these two enzymes is that they both have difficulty digesting through stable stem-loop structures on RNA 3′ ends. Such structures are a characteristic feature of the 3′ ends of many bacterial mRNAs. Another property of these two exonucleases is that they digest the limit products of mRNA decay very inefficiently. The small fragments remaining from mRNA, 2–5 nt long, are in fact degraded by oligoribonuclease, an exonuclease conserved across a wide range of organisms. Overall, the RNases for mRNA decay define a small group of genes, most of which are required either alone or in combination for viability of the bacterial cell.

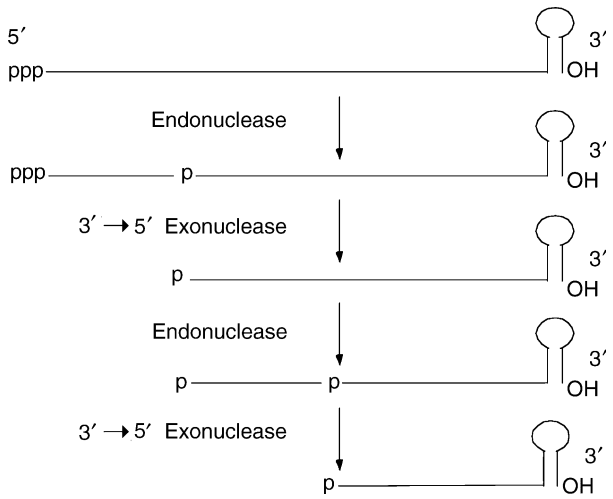

FIGURE 1 mRNA is degraded by the sequential action of endonucleases and 3′ to 5′ exonucleases. A triphosphorylated mRNA synthesized by RNA polymerase and terminated beyond a stem-loop is shown. The products of endonucleolytic cleavage bear monophosphates on their 5′ ends and hydroxyl groups on their 3′ ends.

Control of Gene Expression by RNase III Processing

Although the major function of RNase III in the bacterial cell is synthesis of mature ribosomal RNAs from their large precursors, RNase III is also known to process a number of mRNA species. Processing of mRNA generally functions to alter the stability of one or more coding regions on mRNAs encoding multiple genes, or to regulate the efficiency with which a gene is translated. An example of translational regulation is provided by the well-studied *E. coli* virus lambda. This virus selects one of two modes of growth when it first enters the bacterial cell. If the cells are growing in a rich medium that permits a high rate of growth, the virus multiplies and releases progeny into the medium. In poor media, cell growth rates are much lower. Under these conditions the incoming viral DNA molecule simply integrates into the bacterial chromosome and is then replicated by the host machinery until intracellular conditions become more suitable for production of new viruses. The cellular sensor of physiological conditions is the endonuclease RNase III. Expression of the gene encoding RNase III is regulated by growth rate, with the result that the intracellular concentration of RNase III is a direct function of growth rate. When lambda enters the bacterial cell, one of the first viral genes expressed is N, which is located at the 5′ end of an mRNA transcript encoding many genes (Figure 2). Just upstream of the initiator AUG codon for N gene translation (position 223) lies a hairpin stem that is a substrate for a pair of RNase III cleavages on opposite sides of the stem. When RNase III is abundant, this hairpin is cleaved, and the remaining lower half of the stem unfolds to make the mRNA more accessible for ribosome binding. The result of RNase III cleavage is thus to increase the efficiency of N gene translation. The protein product of the N gene is part of a complex that permits RNA polymerase to read through transcription termination sites at several positions downstream from the N gene on lambda DNA. When N protein is abundant, the genes downstream of the N gene are transcribed and translated, and virus production can proceed. When RNase III is scarce, the RNase III-sensitive hairpin is left uncleaved, less N protein is translated, and little transcription of downstream genes takes place. This is the signal indicating that growth conditions do not favor virus production. Lambda DNA accordingly enters the quiescent state as part of the bacterial chromosome. Thus, mRNA processing in this case plays a critical role in regulating the appropriate choice between the two possible modes of viral development.

TABLE I

***E. coli* RNases in mRNA Decay**

Enzyme	Gene	Monomer size (kDa)
Endoribonucleases		
RNase E	*rne*	118
RNase G	*rng*	55
RNase III	*rnc*	25
3′ → 5′ Exoribonucleases		
RNase II	*rnb*	72.5
Polynucleotide phosphorylase	*pnp*	77
Oligoribonuclease	*orn*	20.7

The Degradosome, a Multiprotein Complex for RNA Degradation

Once many of the decay RNases were purified and characterized, evidence began to appear that at least two of the RNases were associated with other enzymes in a high molecular weight complex that has come to be called the degradosome. At minimum, the purified degradosome contains two RNases: the endonuclease RNase E and the exonuclease PNPase. Present as well are two additional proteins, the ATP-dependent RNA helicase RhlB and the glycolytic enzyme enolase. Polyphosphate kinase is seen in substoichiometric amounts in some degradosome preparations. A functional degradosome containing only RNase E, PNPase, and RhlB assembles spontaneously *in vitro* and shows ATP-activated degradation of an mRNA substrate that is indistinguishable from the activity observed with

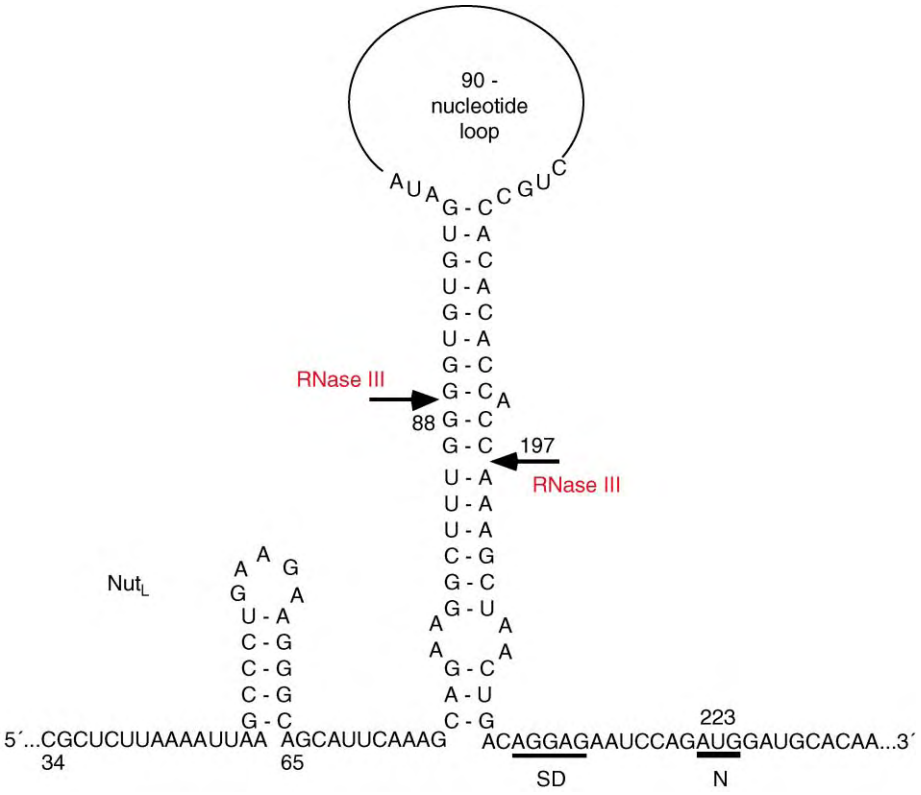

FIGURE 2 Structure of the leader region preceding the translational start of the lambda N gene. Nucleotides are numbered from the 5′ end of the transcript. Nut_L, the site at which RNA polymerase can be modified so as to read through transcription terminators; SD, Shine–Dalgarno sequence in the N gene ribosome binding site; RNase III, sites of cleavage by RNase III.

purified degradosomes. It is evident that the C-terminal half of the RNase E protein functions as the scaffold for association of the other degradosome components because the degradosome complex does not form in a mutant RNase E strain missing the C-terminal half of the protein. The discovery of RNase E, PNPase, and RhlB in a complex immediately raised the possibility that the degradosome might coordinate endo- and exonucleolytic digestion and the unwinding of RNA secondary structure. Evidence from studying the degradation of structured mRNA substrates supports this idea. The stoichiometry of degradosome components remains uncertain, but size estimates for degradosome preparations are indicative of a complex of $(1.5–2.4) \times 10^6$ Da. This is a large enough size that degradosomes can be seen by electron microsopy at the outer edge of the bacterial cell near the inner membrane.

The question of whether the bacterial degradosome is related to any of the high molecular weight complexes observed in the eukaryotic cell has recently taken a very interesting turn with the publication of an X-ray crystal structure for a bacterial PNPase. Whereas comparisons of the mRNA decay pathways in bacteria and eukaryotes have until now indicated few similarities, the bacterial PNPase structure revealed the presence of two repeats per monomer unit of a motif found in the phosphorolytic *E. coli* exonuclease RNase PH. This indicates that the degradosome contains multiple copies of homologues to RNase PH. Similar homologues of RNase PH are found in the exosome, a macromolecular complex present in the eukaryotic cell. A plausible prediction is that the central structure of the two complexes may prove to be quite similar. A second similarity emerging between bacteria and eukaryotes is that these high molecular weight machines are involved in processing and degradation of all three types of RNA: mRNA, rRNA, and small stable RNAs.

Polyadenylation Maintains the Momentum of mRNA Decay

Polyadenylation in bacteria, rediscovered during the 1990s, plays a significant role in the degradation of mRNA. Polyadenylation also appears to function in cellular quality control by removing defective rRNA and tRNA precursors from the cell. Poly(A) tails on bacterial mRNAs are short (10–40 nt), and the extent to which any given mRNA species is polyadenylated is low. Most poly(A) tails are synthesized by poly(A) polymerase I

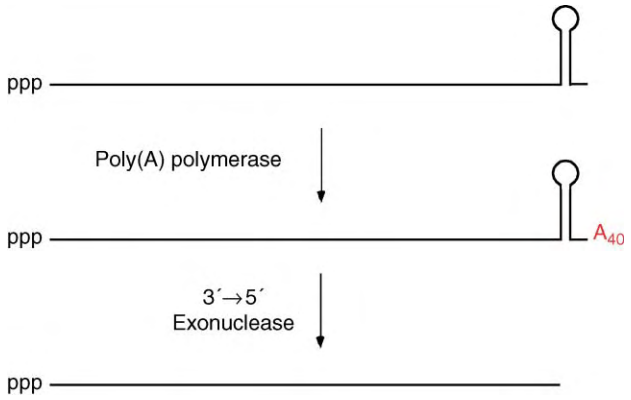

FIGURE 3 Polyadenylation of an mRNA facilitates exonuclease digestion through structural barriers.

(PAP I), an enzyme that is not required for viability of the cell. However, a residual level of polyadenylation is observed in the absence of PAP I and is due to PNPase working in the biosynthetic direction. In contrast to eukaryotic poly(A) tails, which function as stability determinants, addition of a poly(A) tail to a bacterial mRNA stimulates its degradation by exonuclease digestion (Figure 3). This can be understood in light of the difficulty PNPase and RNase II have in digesting through structured regions within and at the ends of mRNA. By providing a single-stranded region of A residues at the 3′ end of an mRNA, the poly(A) tail serves as a toehold for tight binding of the exonucleases as they establish a processive mode of digestion. Thermodynamically stable structures appear to require repeated steps of adding single-stranded poly(A) extensions followed by exonuclease digestion to complete exonucleolytic degradation through highly structured decay intermediates. Thus, polyadenylation appears to be a dynamic process which maintains the momentum of 3′ to 5′ exonucleolytic decay through structural barriers. The question of when, during the lifetime of an mRNA, polyadenylation takes place has recently been resolved. Although polyadenylation was believed to function as the initiating step of decay, it is now clear from following the decay of specific mRNAs over time that PAP I only slowly accesses the 3′ ends of mRNAs. In general, polyadenylation is a later rather than the initiating step of decay, although there certainly are some mRNAs or decay intermediates that require polyadenylation for degradation even to begin.

Decay Pathways Vary with the Position of the Initiating Cleavage

The extent to which molecular models for mRNA decay can be formulated using currently known enzymes is limited (Figure 4). It is relatively straightforward using

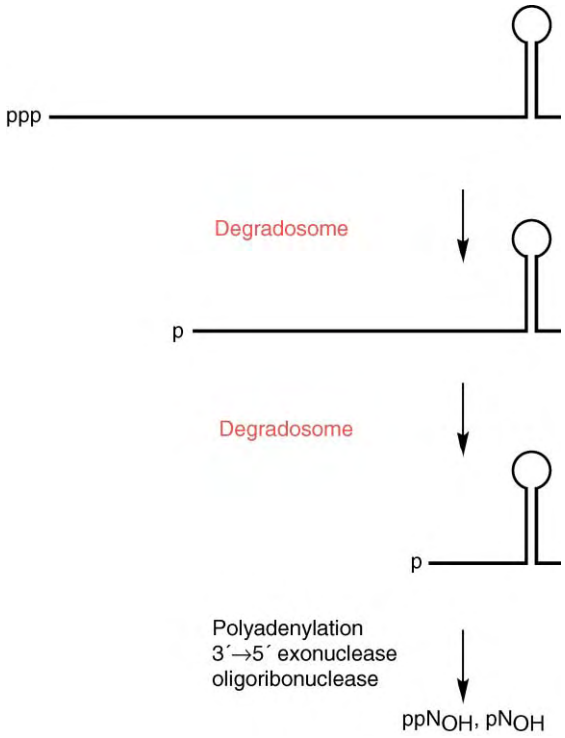

FIGURE 4 General model for mRNA decay based on current knowledge.

mutants deficient in RNase E or RNase III to assign which endonuclease initiates decay. In most cases, decay is initiated by RNase E in the degradosome. Since oligoribonuclease shows specificity for the limit products of mRNA decay, this enzyme can be placed at the end of the decay pathway. By contrast, assigning PNPase or RNase II to the exonucleolytic steps of a decay pathway is often difficult, although it is likely that PNPase in the degradosome digests the upstream fragments produced by endonuclease cleavage. The fact that excess PNPase is present in free form in the cell as well will complicate determining whether degradosome-bound PNPase is in fact responsible for degradation of such products. A similar problem is posed by the existence of at least two mechanisms (polyadenylation and unwinding by the RhlB helicase) for clearing the barriers presented by RNA secondary structure. At present the lack of mutant strains without RhlB activity precludes monitoring decay in the absence of RhlB, so it is not known under what conditions which mechanism is operating to unwind RNA structure. These problems aside, it is abundantly clear that multiple pathways for decay exist. In large part the mode of decay and overall appearance of a pathway is governed by the position of the initiating cleavage. This position must be determined empirically for each mRNA through a combination of *in vivo* experiments and *in vitro* biochemical studies. From in-depth study of

several mRNAs, it appears that if the initiating cleavage is near the 5′ end of an mRNA, the wave of endonucleolytic decay may move in the 5′ to 3′ direction, followed by rapid exonucleolytic degradation of the upstream products. If instead the initiating endonucleolytic cleavage serves to remove the terminator structure at the 3′ end of an mRNA, decay may show a predominantly 3′ to 5′ exonucleolytic mode which may be accelerated by additional RNase E cleavages within the body of the mRNA. A third alternative is that the initiating cleavage occurs at an internal position within an mRNA. Cleavage at this position gives two products that undergo further degradation at a rate determined by the extent to which structural barriers impede exonuclease digestion on each intermediate. Whatever the mode of decay, it is likely that RhlB helicase activity and polyadenylation cooperate to minimize the number of rounds of polyadenylation required for complete degradation of highly structured mRNA decay intermediates.

See Also the Following Articles

DNA Polymerase I, Bacterial • Exonucleases, Bacterial

Glossary

degradosome A large complex of proteins that coordinates the processing of transfer RNAs and ribosomal RNAs as well as the enzymatic degradation of mRNAs and ribosomal RNAs.

endoribonuclease RNase that cleaves internal phosphodiester bonds in an RNA chain.

exoribonuclease RNase that removes nucleotides from one end of an RNA.

mRNA degradation Enzymatic RNA cleavage and nucleotide addition steps that bring about degradation of mRNAs to recycle the nucleotides for new gene expression.

mRNA processing RNA cleavage events on precursor mRNAs that bring about their maturation to the functional forms translated by ribosomes.

polyadenylation Enzymatic addition of ~40 A residues to the 3′-terminal ends of mRNA molecules and decay intermediates to generate a poly(A) tail.

Further Reading

Carpousis, A. J., Vanzo, N. J., and Raynal, L. C. (1999). mRNA degradation: A tale of poly(A) and multiprotein machines. *Trends Genet.* **15**, 24–28.

Kushner, S. R. (2002). mRNA decay in *Escherichia coli* comes of age. *J. Bacteriol.* **184**, 4658–4665.

Régnier, P., and Arraiano, C. M. (2000). Degradation of mRNA in bacteria: Emergence of ubiquitous features. *Bioessays* **22**, 235–244.

Steege, D. A. (2000). Emerging features of mRNA decay in bacteria. *RNA* **6**, 1079–1090.

Symmons, M. F., Williams, M. G., Luisi, B. F., Jones, G. H., and Carpousis, A. J. (2002). Running rings around RNA: A superfamily of phosphate-dependent RNases. *Trends Biochem. Sci.* **27**, 11–18.

Biography

Dr. Deborah Steege is a Professor in the Department of Biochemistry at Duke University. Her principal research interests are molecular mechanisms in gene expression, in particular those steps that take place after RNA polymerase has synthesized an mRNA. She holds a Ph.D. from Yale University and served as a postdoctoral fellow at the same institution. She has authored research papers for 30 years in several areas of the broad field of RNA biology.

Mucin Family of Glycoproteins

Juan Perez-Vilar
University of North Carolina at Chapel Hill, North Carolina, USA

Robert L. Hill
Duke University, Durham, North Carolina, USA

Mucins are glycoproteins found in epithelial membranes and as components of the mucus secretions that cover the epithelial cells in the gastrointestinal, urogenital, tracheobronchial, ocular, and auditory systems of all vertebrates and the epidermis of amphibians. Mucins are not exclusive of vertebrates, and they can be found in almost all eukaryotes. Mucus production is considered to be a critical feature for multi-cellular organisms to survive the presence of noxious agents that are part of their environment. All members of the mucin family are rich in carbohydrates and many of them are among the largest proteins known, with complex structures and different protein domains.

General Features

Definitions

Mucins are structurally diverse but share similar structural features. One region of the polypeptide backbone of mucins has an amino acid sequence rich in threonine and/or serine residues that is repeated several times. O-linked oligosaccharide chains are covalently bound to these residues, resulting in the formation of highly glycosylated domains, known as the tandem repeat domains, O-glycosylated domains, or just mucin domains. Because proline residues are commonly found in the mucin domains, they are also known as PTS domains. The term mucin domain is preferred because it is not in conflict with the existence of nonglycosylated repeated domains in many mucins, O-glycosylated regions in the polypeptide chains of many glycoproteins, and mucins (e.g., MUC2) with either serine or threonine residues, but not both, in their mucin domains.

Mucin Members

The exact number of mucins in humans or other vertebrates is unknown. Proteins with well-characterized biological activities that contain mucin domains in their structures are not considered members of the mucin family. In these cases, the functional, rather than structural, properties prevail. This is the case of many membrane receptors that have mucin domains that help to expose their ligand-binding domains. However, 17 potential human mucin genes have been reported, 12 of which (*MUC1*, *MUC2*, *MUC3A*, *MUC3B*, *MUC4*, *MUC5AC*, *MUC5B*, *MUC6*, *MUC7*, *MUC9*, *MUC13*, and *MUC15*) are fully sequenced. The others (*MUC8*, *MUC11*, *MUC12*, *MUC16*, and *MUC17*) are only partially sequenced. Human mucin proteins and genes are designated by the notation MUC and *MUC*, respectively, followed by a number that indicates the specific mucin. The notation for animal mucins is similar but includes upper/lower case letters (Muc and *Muc* for protein and genes, respectively) and an additional lower case letter for designating the particular species (e.g., mMuc1 and *mMuc1* indicate the mouse mucin homologous to MUC1 and *MUC1*, respectively). However, it is common to find in the literature that many animal mucins are designated following the name of the tissue in which they are predominant (e.g., porcine gastric mucin). In many of these cases, biochemical studies started prior to the cloning of their corresponding genes. For instance, porcine submaxillary mucin (pMuc5b) was the focus of many biochemical studies years before its gene was sequenced.

Mucin Subtypes

Mucins can be divided into membrane and secreted mucins based on the presence or absence of a transmembrane domain-encoding sequence in their genes. Membrane mucins are anchored to the apical side of epithelial cells by a transmembrane domain, whereas secreted mucins, which do not have such a domain, are secreted into the extracellular space. However, some membrane mucins (e.g., MUC1 and MUC4) are partially proteolytically cleaved during their biosynthesis, resulting in formation of membrane-attached and soluble subunits. Because these two subunits can be anchored in the membrane as a noncovalent complex, the term

membrane-tethered or tethered mucins can be found in the literature. In addition, splicing of some membrane mucin genes (e.g., *MUC1*) may lead to synthesis of variants lacking transmembrane domains.

Structural subtypes within membrane and secreted mucins can be recognized by comparing the primary sequences of the nonmucin domains. Though the mucin domains in all mucins have similar amino acid composition (e.g., threonine and/or serine rich), they do not share significant protein sequence similarities when compared.

Membrane Mucins

In general, membrane mucins have short cytoplasmic regions at their C-terminal end while their extracellular regions are much larger and contain the mucin domains. Their sizes vary from 334 amino acid residues (MUC15) to more than 6000 amino acid residues (MUC4). *E*pidermal *g*rowth *f*actor (EGF)-, *s*ea-urchin/*e*nterokinase/*a*grin (SEA)-, von Willebrand factor D (D)-, and/or nidogen (NIDO)-like domains can be found in membrane mucin polypeptides. Because MUC3A, MUC3B, MUC12, MUC13, and MUC17 all have EGF- and SEA-like domains, whereas MUC4 lacks SEA-like domains, the former set of mucins likely represent a functional subgroup within membrane mucins. MUC1 and MUC15 are relatively short membrane mucins lacking EGF-, SEA-, D-, and NIDO-like domains.

Secreted Mucins

All secreted mucins, except MUC7 and MUC9, have polypeptide chains with thousands of amino acid residues. These large mucins – including MUC2, MUC5AC, MUC5B, and MUC6 – are known as secreted, gel-forming mucins, because they are found in mucus secretions and endow mucus with their viscoelastic and adhesive properties. Moreover, they all share a similar structural organization that includes nonmucin domains homologous to protein domains found in human von Willebrand factor (e.g., B-, C-, CK-, and D-domains), a protein essential for blood clotting. MUC6, however, lacks B-, C-, and one of the four D-like domains found in the others. In addition, MUC2, MUC5AC, and MUC5B have several copies of a domain, known as the Cys subdomain or CS-domain, which is scattered along their corresponding mucin domains. Similar domains are also found repeated in oikosin-1 (a mucous protein found in certain tunicates) and human cartilage intermediate protein (a cartilage protein of unknown function), but not in von Willebrand factor. MUC7 and MUC9, also known as oviductin or oviductal glycoprotein 1, are secreted mucins not related to gel-forming mucins. MUC7 is a small mucin present in the oral cavity and likely involved in the clearance of bacteria that bind to it. MUC9 is a 678 amino acid residues mucin found exclusively in the oviduct, where it may have a function in fertilization and early embryo development.

Mucin Genes

In general, mucin genes consist of large central exons encoding the entire mucin domains. Alleles of some mucin genes (e.g., *MUC1, MUC2, MUC4*, and *MUC6*) differ in the number of tandem repeats encoded by the central exons, a feature known by the acronym VNTR (*v*ariable *n*umber of *t*andem *r*epeats), although polymorphism due to nucleotide changes has been reported as well. Sequences encoding other domains and regions in the mucin polypeptides are usually constituted by short exons interrupted by large introns. The genes for structurally related mucins are located in specific chromosomal regions. Thus, *MUC3A, MUC3B, MUC11*, *MUC12*, and *MUC17* are located in 7q22, whereas *MUC2, MUC5AC, MUC5B*, and *MUC6* are positioned at 11p15. However, their promoter sequences have little overall homologies and, in general, contain elements for tissue-specific expression and regulation.

Mucin Cell and Tissue Distribution

In general, membrane mucins are secreted by several types of epithelial cells, whereas gel-forming mucins are predominantly synthesized in and secreted from epithelial and submucosal goblet/mucous cells. Each organ/tissue is characterized by the synthesis of a set of mucins with one or two major ones, although a given mucin is usually found in more than one tissue/organ (Table I).

Roles in Health and Diseases

Because of their large size, extent of glycosylation, and locations, mucins protect epithelial cells from dehydration, noxious agents and physical injury, as well as aid the passage of materials through a tract. However, the roles of mucins in mucosal homeostasis likely are more important and complex than previously anticipated. For instance, MUC1 and MUC4 may be involved in cell signaling. The fact that mucin production is regulated in mammals by mechanisms operating at different levels attests to the central role of these glycoproteins. Thus, the number and differentiation state of the cells producing mucin/mucus, the rate of mucin secretion, and the activities of mucin genes are all responsive to bacterial and viral compounds, chemicals and inflammatory mediators.

Many mucin genes have been described but gene deletion studies to assess mucin function are not yet

TABLE I

Tissue Distribution of Human Mucins

MUC1	Widely distributed among epithelial cells. Present in some nonepithelial cells (e.g., fibroblasts) and body fluids (e.g., urine)
MUC2	Colon and small intestine (goblet cells), salivary gland ducts, inferior turbinates, conjunctival epithelium
MUC3A	Colon and small intestine (goblet and absorptive cells)
MUC3B	Colon and small intestine (goblet and absorptive cells)
MUC4	Bronchus, colon, conjuctival epithelium, middle ear
MUC5AC	Bronchus (superficial goblet cells and submucosal mucus cells), colon (goblet cells), superficial stomach epithelium, endocervical epithelium, inferior turbinates, conjunctival epithelium, middle ear
MUC5B	Bronchus (submucosal mucus cells, salivary glands, submandibular glands, gall bladder epithelium, endocervical epithelium, inferior turbinates (submucosal glands), colon (goblet cells), middle ear
MUC6	Gastric epithelium (mucus neck cells; antral mucus cells) small intestine (goblet cells), colon, gall bladder epithelium, seminal vesicle, pancreas (centroacinar cells and ducts), endocervical epithelium, endometrial epithelium, biliary epithelial cells, middle ear
MUC7	Salivary glands (mucus cells), bronchus (submucosal glands), conjunctival epithelium, middle ear
MUC8	Bronchus (submucosal glands), middle ear, urogenital system
MUC9	Oviduct, middle ear
MUC11	Colon, bronchus, middle ear
MUC12	Colon, middle ear
MUC13	Colon and small intestine (columnar and goblet cells), bronchus, kidney, small intestine, conjunctival epithelium, lymphoid cells
MUC15	Widely distributed among epithelial cells. Expressed in some nonepithelial cells
MUC17	Intestine (absorptive cells), colon, gastric epithelium, conjunctival epithelium

completed. However, lack of functional mucins is expected to have profound effects of mucosal homeostasis. Thus, mMuc2-deficient mice develop colorectal cancer in contrast to normal littermates. Conversely, overproduction of mucins/mucus is a serious and sometime devastating feature in several chronic lung diseases, including chronic obstructive pulmonary disease, chronic bronchitis, asthma, bronchiectasis, and, especially, cystic fibrosis. An excess of mucus accumulation can lead to excessive sputum production, respiratory infections, and airways obstruction, and ultimately contribute to the morbidity and mortality associated with these diseases.

Structural Features

Signal Peptides

Both membrane and secreted mucins have short signal peptides at their N-terminal ends that allow them to be synthesized and processed along the organelles involved in the secretory pathway. In general, these sequences are rich in hydrophobic residues but do not have significant homologies among different mucins.

Mucin Domains

Characteristically, the mucin domains are centrally located in the mucin polypeptide backbone (Figure 1). These domains are constituted by a repeated Ser/Thr-rich sequence together with degenerate repeats and unique Thr/Ser-rich sequences at both ends of the repeated regions. The sequence, length, and number of the Thr/Ser-rich repeats vary among mucins. In general, there are as many repeated sequences as mucins described. Some mucins (e.g., MUC3A, MUC3B, and MUC4) have two different mucin domains, each one with different repeated sequences. Only a few kinds of amino acids, in addition to threonine and serine, are found in the mucin domains, with proline and glycine among the most common.

Major Nonmucin Domains in Secreted Mucins

D-Like Domains

Gel-forming mucins contain three homologous N-terminal D-domains (designated D1, D2, and D3) and, all but MUC6, a fourth domain, D4, at the C-terminus. A partial D-domain, D′, is between D2 and D3 in all secreted mucins. Each D-like domain has 325–400 amino acid residues and contains up to 30 cysteines. The D-like domains have several conserved N-glycosylation acceptor motifs and are N-glycosylated when expressed in cultured cells. The available data indicate that the D1-, D2-, and D3-like domains are involved in the assembly of disulfide-linked mucinmultimers.

CK (Cystine Knot)-Like Domains

The CK-like domain is 90–100 amino acid residues long, cysteine-rich domain, located at the C terminus of gel-forming mucins. This domain is homologous to the cystine knot domain in several growth factors and norrin. The CK-like domain is N-glycosylated when expressed in cultured cells. The CK-domain is involved in the assembly of disulfide-linked mucin multimers.

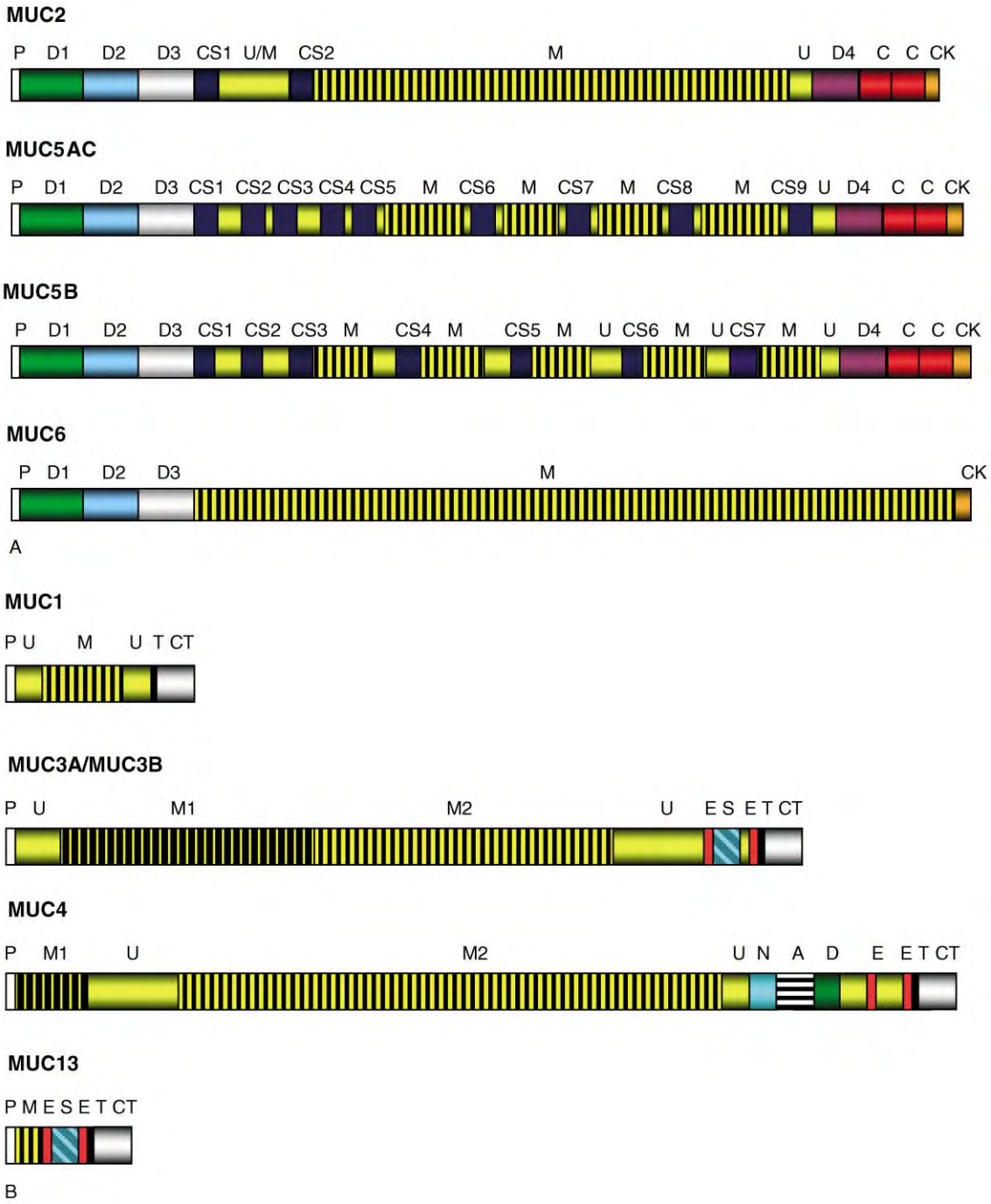

FIGURE 1 Domains in the polypeptide chains of some mucins. Comparisons of the protein domains in secreted (gel-forming) mucins (*A*) and four membrane mucins (*B*), respectively. The length of the corresponding domains is approximately proportional to the number of amino acid residues. *A* and *B* are not drawn to the same scale. P, signal peptide; U, unique sequences (usually Ser/Thr-rich); M, mucin domains; D, D-domains; CS, Cys subdomains; C, C-domains; CK, CK (cystine-knot)-like domain; T, transmembrane domains; CT, cytoplasmic domain; E, EGF-like domains; S, SEA-like domains; N, NIDO (nidogen)-like domain; A, AMOP (adhesion-associated domain in MUC4 and other proteins)-like domain.

CS (Cys Subdomain)-Domains

The CS-domains, also known as the Cys subdomains, are short (100 amino acid residues long) cysteine-rich domains that are scattered along the mucin domains of MUC2, MUC5AC, and MUC5B. Nine, seven, and two CS-domains are found in MUC5AC, MUC5B, and MUC2, respectively. All CS-domains have one C-mannosylation acceptor motif (WXXW) at their

N-terminal side. C-Mannosylation has been reported in recombinant CS-domains expressed in cultured cells. The role of the CS domains is unclear at present.

Major Nonmucin Domains in Membrane Mucins

Transmembrane and Cytoplasmic Domains

The transmembrane domain in mucins comprises a short stretch of hydrophobic amino acid residues. The mucin cytoplasmic domains are short (20–79 amino acid residues long) and contain tyrosine and serine residues that can be phosphorylated.

EGF-Like Domains

EGF-like domains are 45–60 amino acids long domains located between the transmembrane domains and the mucin domains in MUC3A, MUC3B, MUC4, MUC12, MUC13, and MUC17 (Figure 1). They have six cysteine and two glycine residues conserved. The roles of these domains have not been clearly established, but recent studies suggest that they might be involved in cell signaling.

SEA-Like Domains

The SEA-like domain is an 85–110 amino acids long domain found conserved in many extracellular proteins. It is located between the transmembrane and mucin domains in MUC3A, MUC3B, MUC12, MUC13, and MUC17 (Figure 1). The role of the SEA-like domains is not yet defined, but they contain the GSVVV peptide motif that may be cleaved during the biosynthesis of these mucins.

Other Domains

Other protein domains in mucins are the *A*dhesion-associated domain in *M*UC4 and *O*ther *P*roteins (AMOP) and the *nido*gen (NIDO)-like domains that are found in MUC4. Their functions are not yet established, but similar domains are also present in extracellular or surface proteins involved in cellular adhesion.

O- and N-Linked Oligosaccharide Chains

O-linked oligosaccharides in the mucin domains comprise up to 90%, but not less than 50%, of the weight of the native mucins. They decisively contribute to formation of an extended mucin structure by limiting the rotation around peptide bonds, and by the repulsion generated among the neighboring, negatively charged oligosaccharide and sulfate groups. Such long, extended molecules have a much greater solution volume than native or denatured proteins with little or no carbohydrate, and endow aqueous solutions of mucins a high viscosity.

N-linked oligosaccharides are not present in the mucin domains but in many of the nonmucin, cysteine-rich, domains. They may have a role during folding of the nascent mucin polypeptide in the endoplasmic reticulum.

Sulfation

Several monosaccharides in mucin N- and O-linked oligosaccharide chains, especially galactose, N-acetyl-galactosamine, and N-acetyl-glucosamine, are sulfated. Sulfation contributes to the stiffness of the mucin domains by increasing the negative charges of their O-linked oligosaccharide chains, which, as mentioned above, is critical for their viscoelastic properties. In addition, sulfation protects oligosaccharide chains from bacterial glycosidases.

Biosynthesis

Mucin biosynthesis occurs along the endoplasmic reticulum and the Golgi complex and involves folding, N- and O-glycosylation, sulfation, proteolytic processing, and, in the case of secreted gel-forming mucins, covalent assembly.

Membrane Mucins

Like other membrane proteins, membrane mucins are synthesized and N-glycosylated in the endoplasmic reticulum. Some membrane mucins (e.g., MUC1 and MUC4) may be cleaved while inside this organelle. This produces two subunits that can form a noncovalent complex and, ultimately, secretion of soluble forms of these mucins. The cleavage motif in MUC1 (GSVVV) is also found in the SEA-like domains of MUC3A, MUC3B, MUC12, and MUC17. Membrane mucins are O-glycosylated and sulfated in the Golgi complex, but, contrary to gel-forming mucins (see below), they do not form interchain disulfide bond oligomers/multimers.

Secreted (Gel-Forming) Mucins

Except for MUC7 and likely MUC9, the rest (MUC2, MUC5AC, MUC5B, and MUC6) are assembled to disulfide-linked oligomers/multimers prior secretion.

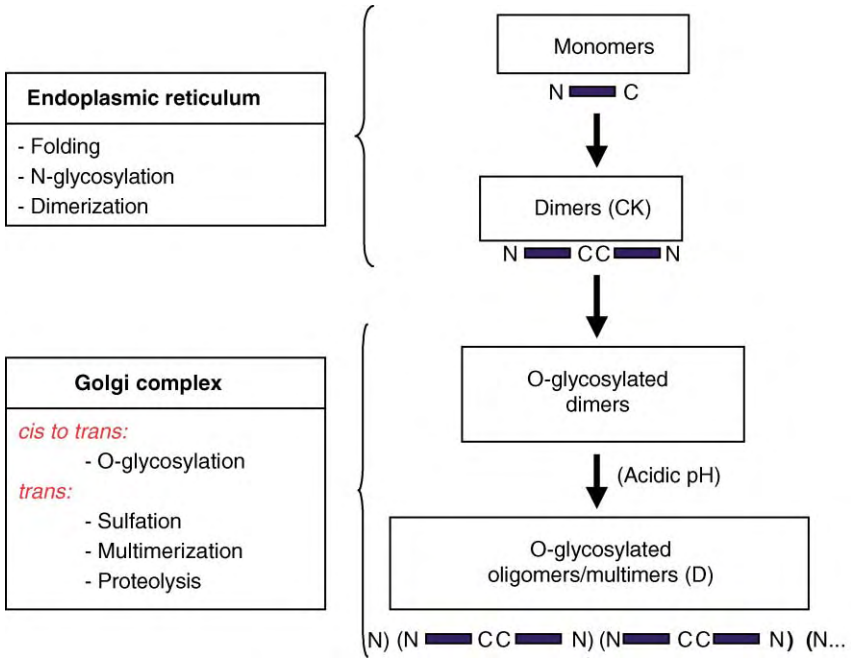

FIGURE 2 Biosynthesis and assembly of secreted, gel-forming mucins. Mucin polypeptide chains are synthesized and translocated into the endoplasmic reticulum. Folding and N-glycosylation of the nascent polypeptide chain is followed by rapid formation of disulfide bonds between the C-terminal CK-like domains in two mucin monomers. Thereafter, dimeric mucins are transported to the Golgi complex where O-glycosylation of the mucin domains and unique Thr/Ser-rich sequences takes place, starting in the *cis*-Golgi compartment and finishing in the late, *trans*-Golgi compartments. In the later compartments, mucins are sulfated and the dimeric forms are assembled into disulfide-bonded oligomers/multimers through their N-terminal D-domains.

Endoplasmic Reticulum

Nascent mucin polypeptides are N-glycosylated and, perhaps, C-mannosylated in their respective NXS/T and WXXW peptide motifs. Mucin assembly starts by formation of dimers via interchain disulfide bonds connecting the CK-domains in two mucin monomers (Figure 2). The CXCC peptide motifs in these domains are critical for dimerization.

Golgi Complex

Mucin dimers are O-glycosylated and sulfated along different compartments of the Golgi complex by resident glycosyltransferases and sulfotransferases. Glycosylated dimers are then assembled into oligomers/multimers via disulfide linkages connecting their NH_2-terminal D-domains (Figure 2). This step likely occurs just before secretion, in the late, acidic, compartments of the Golgi complex and/or beyond. The thiol/disulfide oxido/reductase motifs (CGLC) in the D1 and D3 domains and the CXWXYXPCG sequence in the D3 domains seem to be critical for proper mucin assembly. While light scattering and electron microscopic studies indicate that mucin multimers form linear structures, recent studies suggest the existence of branched polymers as well.

In the *trans*-Golgi compartment, some mucins, including MUC2 and likely MUC5B, may be processed by proteases recognizing the GSDS peptide motif at their corresponding C-terminal regions.

Storage and Secretion

Fully processed gel-forming mucins are stored in high amounts in large secretory vesicles, known as mucous or mucin granules, which occupy the majority of the cytoplasm in goblet/mucous cells. High calcium content and acidic pH are thought to be critical for mucin packing. Mucins are secreted constitutively, which may involve steady exocytosis of mucous granules, small vesicles, or both, or, alternatively, via a regulated pathway involving exocytosis of mucous granules. Regulated secretion is activated by a variety of physiological agents, including cytokines/chemokines, bacterial exoproducts, nucleotides, neurotransmitters, and proteases.

See Also the Following Articles

Disulfide Bond Formation • Oligosaccharide Chains: Free, *N*-Linked, *O*-Linked • Glycoprotein Folding and Processing Reactions • Golgi Complex • Mucins in

Embryo Implantation • *N*-Linked Glycan Processing Glucosidases and Mannosidases • Protein Glycosylation, Overview • Secretory Pathway

Glossary

glycoproteins Proteins with oligosaccharide (carbohydrate) chains covalently attached to their polypeptide backbones.

mucus Viscous aqueous secretions produced by epithelial cells mainly composed by mucins, ions, and water.

***N*- and *O*-linked oligosaccharides** Oligosaccharide chains linked to serine or threonine and aparagine residues in glycoproteins, respectively.

peptide motif Peptide sequence that has a critical function during the biosynthesis, processing, or assembly of a protein (e.g., the CXCC motif is required for dimerization via the mucin CK-like domains), or for the role of a protein.

protein domain A region in the polypeptide chain of a protein that has a specific function (e.g., the CK-like domain in gel-forming mucins is a dimerization domain).

secretory pathway Biosynthetic pathway taken by mucins and other glycoproteins that involves different organelles, e.g., endoplasmic reticulum and Golgi complex, and many consecutive co-/post-translational modifications, including folding, N-/O-glycosylation, disulfide bond formation, sulfation, etc.

Further Reading

Gendler, S. J., and Spicer, A. P. (1995). Epithelial mucin genes. *Annu. Rev. Physiol.* **37**, 607–634.

Perez-Vilar, J., and Hill, R. L. (1999). The structure and assembly of secreted mucins. *J. Biol. Chem.* **274**, 31751–31754.

Strous, G., and Dekker, J. (1992). Mucin-type glycoproteins. *Crit. Rev. Biochem. Mol. Biol.* **27**, 57–92.

Velcich, A., Yang, W., Heyer, J., Fragale, A., Nicholas, C., Viani, S., Kucherlapati, R., Lipkin, M., Yang, K., and Augenlicht, L. (2002). Colorectal cancer in mice genetically deficient in the mucin Muc2. *Science* **295**, 1726–1729.

Biography

Juan Perez-Vilar is an Assistant Professor of Medicine at the Cystic Fibrosis/Pulmonary Research and Treatment Center, University of North Carolina at Chapel Hill, North Carolina. His research interests are in the biochemistry and cellular biology of airway mucins and their roles in obstructive lung diseases. He graduated from the University of Seville in Spain and did postdoctoral studies with Professor Robert L. Hill at Duke University.

Robert L. Hill is a James B. Duke Professor of Biochemistry at the Duke University Medical Center, Duke University, Durham, North Carolina. His research interests since the 1950s have centered around the structure/function relationship of proteins, including enzymes and more recently, complex glycoproteins.

Mucins in Embryo Implantation

Daniel D. Carson
University of Delaware, Newark, Delaware, USA

Mucin glycoproteins are defined as proteins heavily substituted with oligosaccharides in O-glycosidic linkage between N-acetylgalactosamine and S/T residues. Carbohydrates can account for 50–90% of the mucin molecular weight and greatly influence the physical properties of these molecules. Mucins also are predominant constituents of the apical surfaces of reproductive tract epithelia. In many species, uterine mucin expression changes dynamically during the reproductive cycle and in preparation for embryo attachment. This article will summarize current knowledge of factors controlling the expression and function of uterine mucins with particular emphasis on MUC1 and the process of embryo implantation.

The Implantation Process

The process of embryo implantation (Figure 1) into the uterine wall involves complex interactions between embryonic- and uterine-derived factors. These factors include secreted signals as well as cell-surface recognition events. In regard to the latter, a number of cell-surface components have the ability to support embryo attachment and are located at sites of embryo uterine attachment. These include integrins, proteoglycans, and cadherins. The failure of gene knockouts of any of these receptors to prevent the initial events in implantation indicates that there is considerable redundancy in function. This is consistent with *in vitro* studies demonstrating the ability of embryos to attach to a wide variety of cell types and substrates via different cell-surface receptor systems as well as the ability of trophoblast to modulate their cell-surface expression of such receptors in response to the extracellular matrix they encounter.

In spite of the highly invasive nature of blastocysts and trophoblast, the uterus displays the remarkable ability to limit both embryo and tumor cell attachment and invasion. Only during a well-defined "window" in time does the uterus permit attachment to and penetration of the endometrium. This control appears to be primarily exerted at the first point of encounter, namely the apical surface of the lumenal epithelium. In response to ovarian steroid influences, the uterus develops through a series of stages that may be defined as prereceptive, receptive, and postreceptive with regard to the ability to support embryo attachment. The end of the ovarian cycle is marked by a fall in steroid hormone levels and resetting of the uterine clock to begin another cycle of receptivity. In menstruating species, the endometrium is largely sloughed and new tissue formed; however, in most species menstruation does not occur and the endometrium is restructured via processes involving controlled apoptosis and cell proliferation as well as extracellular matrix remodeling. If implantation occurs, steroid hormone levels are maintained and the endometrium not only remains, but also differentiates further in many species in a process called the decidual response.

During the receptive phase, the uterine epithelium also displays remodeling evident by electron microscopy as well as light microscopy if staining for specific markers is used. While there are many species-specific variations on the theme, there are features of this process that are well-conserved across species. These include retraction of apical microvilli and reorganization of the cortical actin filaments, the transient appearance of large membrane protrusions (pinopods or uterodomes), and alterations in the apical glycocalyx. Much of the apical glycocalyx is composed of large, heavily glycosylated glycoproteins identified as mucins. The article will briefly summarize our current knowledge of the function and expression of mucins in the context of the embryo implantation process.

Mucins

Functions

As a general principle, mucins heavily coat the lumenal surfaces of epithelia where they provide the first line of defense against infectious agents as well as degradative enzymes. Consistent with this role, mucin glycoproteins are highly resistant to proteolytic attack and require the actions of multiple glycosidases to remove their constituent carbohydrates. While mucins provide a barrier to infection, it is clear that many bacteria and viruses bind well to mucins. Thus, the concept emerges that these molecules serve as "traps" for the infectious agents

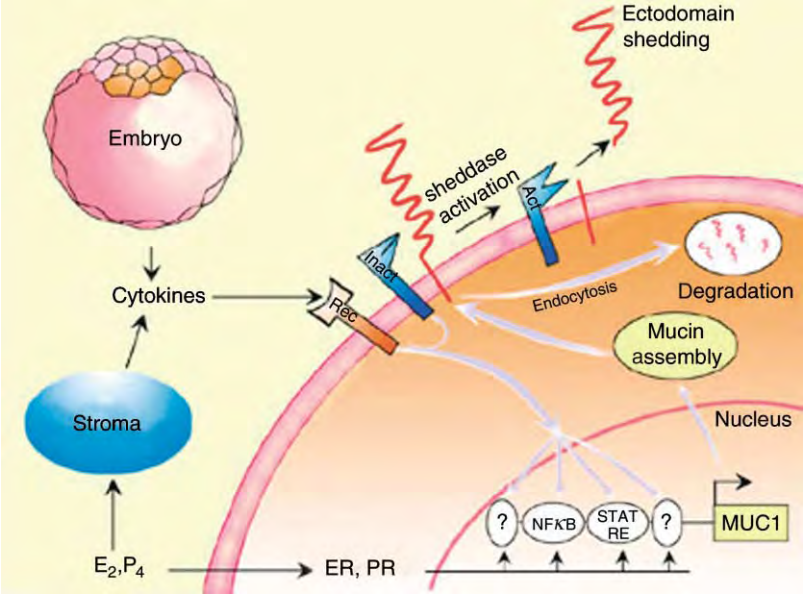

FIGURE 1 Mucin dynamics during embryo implantation. Uterine epithelial cells produce mucins, including transmembrane mucins like MUC1 (represented by the squiggly lines in the figure). In general, these mucins are believed to be a barrier to embryo attachment that must be removed to create access to the apical surface of the uterine epithelium. In some cases, mucin gene expression can be regulated by ovarian steroids, estrogen (E_2) and progesterone (P_4) that may act through their nuclear receptors (ER and PR) directly or indirectly on the MUC1 promoter. Cytokines, produced by neighboring stromal cells or the embryo, bind to cell surface receptors (Rec) on uterine epithelia also can regulate MUC1 gene expression via NFκB and STAT binding. These same elements also may be downstream of steroid hormone actions. Cytokines also can trigger loss of mucin protein by causing increased expression or conversion of latent (Inact) cell-surface proteases or sheddases to active forms (Act) that catalyze mucin ectodomain release. Mucins also may be removed by endocytosis and intracellular degradation pathways.

that interact with them before they can establish contact with the plasma membrane of the host epithelium. A number of mucins occur as transmembrane proteins (see Table I). MUC1 is an example of a transmembrane mucin glycoprotein and experiments with MUC1 null mice demonstrate that these animals are much more prone to bacterial infection and inflammation than their wild-type counterparts. Thus, a paradox arises over how a glycoprotein that can promote attachment of an infectious agent simultaneously serves to protect against the microbe. As discussed below, the host may be able to recognize attachment and shed the ectodomains of transmembrane mucins in response. This process then would convert the shed mucins into a soluble mucin trap removing the potential pathogen from the cell surface.

In the context of embryo implantation, mucins also appear to be antiadhesive. Polarized uterine epithelia of rodents are constitutively nonreceptive *in vitro* and abundantly express mucins. Selective, enzymatic removal of mucins or genetic ablation of Muc1 converts these cells to a functionally receptive state. Moreover, transfection and overexpression of MUC1 into cells that normally adhere well to blastocysts markedly reduces their adhesive activity. In contrast, under some conditions, mucins can carry selectin ligands and, thereby, potentially support cell attachment. Recent studies indicate that this occurs at the fetal–maternal interface and may contribute to aspects of trophoblast binding.

In addition to being abundantly expressed at the apical surface of uterine epithelia, mucins are physically very large with individual molecules being hundreds of nanometers in length. In contrast, typical cell-surface receptors extend 10–30 nm from the cell surface. Due to their heavily glycosylated nature, individual mucins have large hydration spheres. In addition, mucins often form complex aggregates or gels. Consequently, the mucin coat presents a large, formidable matrix that must be somehow traversed or removed in order for molecules or cells to establish contact with the plasma membrane. The size of the ectodomains is an important determinant of transmembrane mucin function as an anti-adhesive molecule. Truncation mutations of the ectodomains of both MUC1 and MUC4 demonstrate that these mucins must extend more than 50 nm from the cell surface to be effective. This would extend well beyond the distance spanned by most cell-surface receptors.

Other interesting functions associated with mucins include immunosupression and association with intracellular signal-transducing molecules. In the former case, the mechanism of action is not clear although effects on several cell types involved in cell-mediated immunity have been reported. In the case of signal transduction, MUC1 has been shown to be associated

TABLE I

Uterine Mucin Expression

Mucin	Type[a]	Found in endometrium?	Species[b]	References
MUC1	TM, Sec	Yes	Hu, Pri, Sh, Bov, Por, Rab, Rat, Mu	Reviewed in Thathiah and Carson (2002)
MUC2	Sec	No	Hu	Gipson *et al.* (1993)
MUC3	TM, Sec	No	Hu	Gipson *et al.* (1997), Ho *et al.* (1993)
MUC4	TM, Sec	Yes	Rat	Carraway and Iddris (2001)
MUC5AC	Sec	No	Hu	Gipson *et al.* (1997)
MUC5B	Sec	No	Hu	Gipson *et al.* (1997)
MUC6	Sec	Yes	Hu	Gipson *et al.* (1997)
MUC7	Sec	No	Hu	Gipson *et al.* (1997)
MUC8	Sec	Yes	Hu	D'Cruz *et al.* (1996)
MUC9	Sec	Yes	Ham	Martoglio and Kan (1996),
		No	Rab	Yong *et al.* (2002)
MUC10	Sec	ND[c]		
MUC11	TM	ND		
MUC12	TM	ND		
MUC13	TM	ND		
MUC15	TM	ND		
MUC16	TM[d]	Yes	Hu	Hamilton *et al.* (2002)
MUC17	TM	ND		
MUC18	TM	ND		

[a] Transmembrane (TM) or secreted (Sec); some can be either depending on alternative mRNA splicing.
[b] Human (HU), Primates (Pri), Sheep (Sh), Cattle (Bov), Swine (Por), Rabbits (Rab), Rats (Rat), Mice (Mu), Hamster (Ham).
[c] Not Determined (ND).
[d] Predicted by cDNA sequence.

with β-catenin, Grb2, and EGF receptor. Furthermore, tyrosine phosphorylation of the cytoplasmic tail is stimulated when ligand is added to cells expressing a fusion protein consisting of a ligand binding extracellular domain and the MUC1 cytoplasmic tail. The physiological significance of these interactions has not been demonstrated although EGF treatment appears to both increase MUC1 association with EGF receptor and activated EGF receptor can tyrosine-phosphorylate the cytoplasmic tail of MUC1, an event suggested to increase MUC1:β-catenin association.

Expression

To date 18 mammalian mucin genes have been identified. The predicted protein structures indicate that the protein cores fall into two classes, soluble and transmembrane. As discussed below, even transmembrane mucins may be shed from the cell surface and so may contribute to the pool of soluble mucins. As a general principle, much of the core protein structure is composed of tandemly repeated sequences rich in serine, threonine, and proline, thereby capable of carrying many O-linked oligosaccharide chains. Secreted mucins also usually contain multiple cysteine-rich regions that participate in disulfide bond formation and the assembly of mucin gels. A hallmark feature is the presence of a large number of O-linked oligosaccharides that can constitute 50–90% of the molecular weight of the glycoprotein. A number of mucin oligosaccharide structures have been determined and considerable information on the glycosyltransferases that assemble these structures is available. The oligosaccharides are branched, can be reasonably complex, and carry a net negative charge due to the presence of sialic acid and/or sulfate residues.

The structures of reproductive tract mucin oligosaccharides change during the cycle under the influence of ovarian steroids. Consistent with this are studies showing that glycosyltransferase activities in endometrium also change in parallel. Expression of mRNA encoding certain mucin core proteins also changes during the cycle; however, only changes in the expression of MUC1 and MUC4 have been studied in any detail, in this regard (see Table I). In rodents, estrogen strongly stimulates MUC1 expression. Progesterone alone has no effect on MUC1 expression, but antagonizes this estrogen action. Both the actions of estrogen and progesterone on MUC1 expression are mediated by their corresponding nuclear receptors. The murine MUC1 promoter contains a number of sequences that are good candidates for estrogen receptor

as well as progesterone receptor-binding sites; however, none of these sites appear to be functional with regard to estrogen receptor-α or -β. Thus, estrogen actions are likely to be indirect and may be mediated in a paracrine fashion by estrogen-regulated growth factors or cytokines. Consistent with this is the conservation of a functional STAT-binding site in the mouse and human MUC1 promoter. Proinflammatory cytokines strongly stimulate MUC1 expression in mammary epithelium by recruiting STAT1α to this site. Synergy with other cytokines has been observed, notably TNFα. In this case, co-operativity with p65 and a corresponding NFκB-binding site appears to further enhance MUC1 transcription. It is noteworthy that these cytokines are highly expressed in the mouse uterus at times when MUC1 levels are high as well, e.g., estrus and day 1–2 *post coitum*, most likely in response to the microbial challenge associated with coitus. Thus, this response may help protect the reproductive tract from infections that would trigger implantation failure or abortion.

Hormonal regulation of reproductive tract mucin expression is observed in other species as well, although in many cases progesterone stimulates mucin expression. Potential progesterone receptor-binding sites are found in the mouse and human MUC1 promoters; however, it is not clear if these are functional. In rats, MUC4 expression also is strongly regulated by progesterone and estrogen. In addition, TGF-β down-regulates MUC4 expression in both mammary and uterine epithelium. Nonetheless, mucin expression changes differently in different parts of the female reproductive tract in response to steroid hormone influences. Thus, regulation of these genes is tissue-specific and complex. MUC1 appears to be differentially spliced as well since forms lacking the extracellular tandem repeats or the cytoplasmic tail also can be detected in certain cell types. It is not clear what fraction of the total MUC1 pool are contributed by these splice variants or exactly what functions these forms play in the implantation process. Other mucins including MUC3 and MUC4 also undergo alternative splicing to generate transmembrane or soluble variants.

Transport and Metabolism

Mucin assembly involves synthesis and transit of the core protein from the rough endoplasmic reticulum through the Golgi apparatus where most of the glycosylation occurs. Subsequently, the fully assembled mucin is transported to the cell surface. The entire process described above takes 60–90 min for the average mucin molecule in several cell types. Both MUC1 and MUC4 are synthesized from a single mRNA, but are proteolytically cleaved during their biosynthesis resulting in the formation of stable heterodimers of their respective ectodomains and transmembrane/cytoplasmic tail domains. While the exact nature of the association is not clear, in the case of MUC1 the complex is not dissociable by a number of agents including urea, heating, high salt, or reducing agents; however, it is readily dissociable by sodium dodecyl sulfate in a variety of normal cells and tumor-derived cell lines.

After arriving at the cell surface, MUC1 undergoes one of the three fates – (1) it can be recycled and further sialylated intracellularly and returned to the cell surface, or (2) it may be endocytosed and degraded in acidic compartments, presumably lysosomes, or (3) the ectodomains may be released or shed from the cell surface. Although the process of mucin shedding has been recognized for many years, the identity of the "sheddases" mediating this release has remained elusive. Recent evidence indicates that TACE/ADAM17 is one such sheddase. Other studies indicate that additional activities are involved as well. Mucin shedding is a property of both normal and tumor cells and, indeed, serum levels of shed ectodomains are used as markers of tumor burden in certain cancers. Shedding also may be stimulated by physiologically relevant agents, e.g., cytokines, as well as other compounds, e.g., phorbol esters. In the context of embryo implantation, stimulation of mucin shedding may be the key method to create cell-surface access to embryo receptors in certain species, e.g., rabbits and humans. In other species, shedding may be coupled with decreased mucin expression to clear the apical cell surface in preparation for embryo attachment.

Summary and Future Directions

The process of embryo implantation is under the control of the actions of ovarian steroids that coordinate the development of the embryo with the maturation of the endometrium. A panorama of receptors and binding factors may participate in a redundant fashion to promote embryo–uterine interactions during implantation. Nonetheless, the thick mucin-coat that covers the apical surface of the uterine epithelium under most conditions not only serves as a protective barrier to infection and enzymatic digestion, but also as a barrier to embryo attachment. This barrier must be removed in order for embryo attachment to occur. In many species, the same ovarian steroids that coordinate the implantation process also control mucin expression leading to the loss of the mucin coat at the time of implantation. In other species, including humans, ovarian steroids do not down-regulate mucin expression. Rather, localized activation of mucin-shedding at the cell surface has been proposed as a mechanism to create access to the apical cell surface of the uterine epithelium. Identification of factors responsible for regulation of mucin gene

expression as well as shedding may provide novel avenues to promote fertility as well as improve protection of the reproductive tract from infectious agents. In addition, recent, surprising findings that certain transmembrane mucins interact with intracellular signal transducing molecules suggest novel roles for these complex glycoproteins in sensing and triggering responses to the extracellular environment.

See Also the Following Articles

Oligosaccharide Chains: Free, *N*-Linked, *O*-Linked • Glycosylation in Cystic Fibrosis • JAK-STAT Signaling Paradigm • Mucin Family of Glycoproteins

Glossary

embryo implantation The process by which the mammalian embryo binds to and implants into the uterine wall.

mucin Any member of a class of glycoproteins that contain a large number of oligosaccharides linked through the hydroxyl groups of serine or threonine via N-acetylgalactosamine.

MUC1 The first transmembrane mucin glycoprotein to be completely molecularly cloned.

uterus The upper portion of the female reproductive tract into which the mammalian embryo normally implants and in which the fetus develops.

Further Reading

Bowen, J. A., Bazer, F. W., and Burghardt, R. C. (1996). Spatial and temporal analyses of integrin and Muc-1 expression in porcine uterine epithelium and trophectoderm *in vivo*. *Biol. Reprod.* **55**, 1098–1106.

Carson, D. D., Bagchi, I., Dey, S. K., Enders, A. C., Fazleabas, A. T., Lessey, B. A., and Yoshinaga, K. (2000). Embryo implantation. *Develop. Biol.* **223**, 217–237.

D'Cruz, O. J., Dunn, T. S., Pichan, P., Hass, G. G. Jr., and Sachdev, G. P. (1996). Antigenic cross-reactivity of human tracheal mucin with human sperm and trophoblasts correlates with the expression of mucin 8 gene messenger ribonucleic acid in reproductive tract tissues. *Fertil. Steril.* **66**, 316–326.

DeSouza, M. M., Surveyor, G. A., Price, R. E., Julian, J., Kardon, R., Zhou, X., Gendler, S., Hilkens, J., and Carson, D. D. (1999). MUC1/episialin: A critical barrier in the female reproductive tract. *J. Reprod. Immunol.* **45**, 127–158.

Gendler, S. J. (2001). MUC1, the renaissance molecule. *J. Mammary Gland Biol. Neoplasia* **6**, 339–353.

Gipson, I. K., Ho, S. B., Spurr-Michaud, S. J., Tisdale, A. S., Zhan, Q., Torlakovic, E., Pudney, J., Anderson, D. J., Toribara, N. W., and Hill, J. A. 3rd. (1997). Mucin genes expressed by human female reproductive tract epithelia. *Biol. Reprod.* **56**, 999–1011.

Hamilton, J. A., Iles, R. K., Gunn, L. K., Wilson, C. M., Lower, A. M., and Grudzinskas, J. G. (2002). High concentrations of CA 125 in uterine flushings: influence of cause of infertility and menstrual cycle day. *Gynecol. Endocrinol.* **16**, 19–25.

Hild-Petito, S., Fazleabas, A. T., Julian, J., and Carson, D. D. (1996). Mucin (Muc-1) expression is differentially regulated in uterine luminal and glandular epithelia of the baboon (Papio anubis). *Biol. Reprod.* **54**, 939–947.

Hoffman, L. H., Olson, G. E., Carson, D. D., and Chilton, B. S. (1998). Progesterone and implanting blastocysts regulate Muc1 expression in rabbit uterine epithelium. *Endocrinology* **139**, 266–271.

Lagow, E. L., and Carson, D. D. (2002). Synergistic stimulation of MUC1 expression in normal breast epithelia and breast cancer cells by interferon-gamma and tumor necrosis factor-alpha. *J. Cell Biochem.* **86**, 759–772.

Martoglio, A. M., and Kan, F. W. (1996). Immunohistochemical localization of oviductin in the endometrial lining of the golden hamster (*Mesocricetus auaratus*) during the estrous cycle and early gestation. *Histochem. J.* **28**, 449–459.

Pimental, R. A., Julian, J., Gendler, S. J., and Carson, D. D. (1996). Synthesis and intracellular trafficking of Muc-1 and mucins by polarized mouse uterine epithelial cells. *J. Biol. Chem.* **271**, 28128–28137.

Surveyor, G. A., Gendler, S. J., Pemberton, L., Das, S. K., Chakraborty, I., Julian, J., Pimental, R. A., Wegner, C. C., Dey, S. K., and Carson, D. D. (1995). Expression and steroid hormonal control of Muc-1 in the mouse uterus. *Endocrinology* **136**, 3639–3647.

Thathiah, A., and Carson, D. D. (2002). Mucins and blastocyst attachment. *Rev. Endocr. Metabol. Disord.* **3**, 87–96.

Thathiah, A., Blobel, C. P., and Carson, D. D. (2003). Tumor necrosis factor-alpha converting enzyme/ADAM 17 mediates MUC1 shedding. *J. Biol. Chem.* **278**, 3386–3394.

Yong, P., Gu, Z., Luo, J. P., Wang, J. R., and Tso, J. K. (2002). Antibodies against the C-terminal peptide of rabbit oviductin inhibit mouse early embryo development to pass 2-cell stage. *Cell Res.* **12**, 69–78.

Biography

Daniel Carson is the Trustees Distinguished Professor and Chairman of the Department of Biological Sciences at the University of Delaware. His principal research interests are in the area of cell surface and extracellular matrix biology with particular emphasis on reproduction and development. He holds a Ph.D. from Temple University Medical School and served as a postdoctoral fellow at Johns Hopkins University and a faculty member at the M.D. Anderson Cancer Center in Houston, Texas. He has authored many primary research and review articles and is a member of several professional societies including the American Society for Molecular Biology and Biochemistry, the Society for the Study of Reproduction, the American Society for Cell Biology, the Society for Developmental Biology, and the American Society for Matrix Biology.

Multiple Sequence Alignment and Phylogenetic Trees

Russell F. Doolittle
University of California, San Diego, California, USA

The alignment of macromolecular sequences is a computer-assisted procedure for gathering information about the evolutionary relatedness of nucleotide or amino acid sequences. Algorithms of various kinds can then be used to analyze the alignments in a way that reflects similarities or differences among the individual sequences. Phylogenetic trees depict these relationships graphically. Phylogenetic trees constructed from nucleotide or amino acid sequences have provided remarkable insights, both with regard to the evolution and relationships of life forms, and to the evolution and functions of the macromolecules themselves.

The two kinds of macromolecule, nucleic acids and proteins, present somewhat different challenges for alignment. Nucleic acids usually involve only four character states (A, G, C, and T/U), whereas protein sequences involve, with rare exception, 20 character states (the 20 amino acids). (Formally, "characters" are the positions in a sequence and the "character states" are the bases or amino acids that occupy them.) In either case the problem involves distinguishing chance matches from those due to common ancestry.

Alignment implies adjusting one or the other character strings by the insertion of gaps. The gaps are justified because, it is known that the insertion or deletion of nucleotides can occur in genetic material. Still, some limit needs to be imposed on the number of gaps, or any two strings of characters could be made virtually identical simply by skipping along until a match is found. Accordingly, a system is usually employed that has appropriate rewards for matches and penalties for gaps. The penalty for a gap can also be set to be dependent on the length of the gap, although gap length is seldom a major concern.

The quality (reliability) of an alignment will depend on how dissimilar the two sequences are. As two proteins or nucleic acids continue to diverge, a point will eventually be reached where it will not be possible to distinguish common ancestry from chance matching on the basis of sequence comparison alone. No matter what kind of scoring scheme is employed, there is no sharp cut-off. Because of the intrinsic variance of the process, there will always be a nebulous region referred to as the "twilight zone." For a pair of sufficiently long amino acid sequences, say a hundred residues or more, the region of uncertainty is usually thought to be between 15 and 25% identity (Figure 1). When shorter sequences are compared, chance matches will be an even bigger concern. A measure of confidence about common ancestry can be obtained by comparing the alignment scores of randomized sequence pairs of the same lengths and compositions, as the two sequences under study.

Binary Alignment

Nucleotide Sequences

The alignment of two strings of characters with a computer depends on pre-determined criteria. In the simplest case, only identities are tallied, i.e., a match involves having exactly the same character state. The use of matched non-identities can provide much information, however, especially when highly divergent sequences are involved. For example, in nucleic acids, transitions (A/G and C/T or C/U) occur much more frequently than do transversions (A/T and G/T or A/U and G/U), and are much more common when corrected for what would be expected from random occurrence. As a result, matches that are the apparent result of transversions may weigh more heavily in order to compensate for the likelihood of multiple transitions at a single site.

As might be expected, interchanges between similar amino acids are much more common than between those with very different structures and properties. Alignment schemes that use substitution tables (matrices) can be constructed that take account of the favored likelihood of such matches and weigh their occurrences accordingly.

Ribosomal RNA

The alignment of ribosomal RNA sequences, and the phylogenetic inferences made from them was the original basis for dividing all of life into three realms,

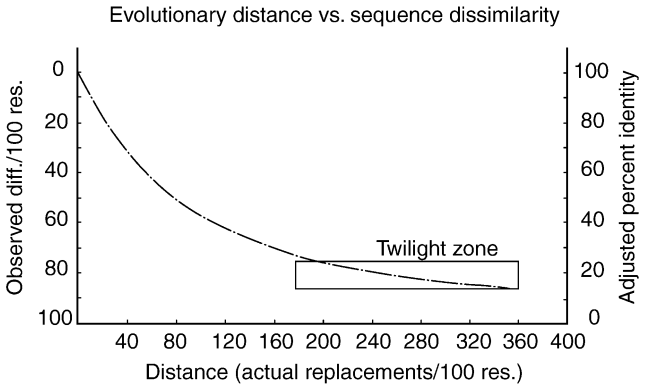

FIGURE 1 Partly as a result of back mutations and multiple mutations at the same site, the divergence of two sequences from a common ancestral sequence follows the course of a negative exponential. Other factors, including the favored likelihood of certain interchanges over others, also contribute. See glossary and text for explanation of twilight zone.

an observation since borne out by many other considerations. Since then, various kinds of ribosomal RNA sequences (5S, small subunit and large subunit) from thousands of different organisms have been determined and used to a great advantage in charting phylogenetic relationships. For these purposes, computer alignments are often limited to certain sets of preferred sites that are well calibrated with regard to their propensity for change.

Mitochondrial DNA

Phylogenetic studies of eukaryotes have been greatly aided by the now routine determination of complete mitochondrial DNA sequences. Generally speaking, these sequences change at a faster rate than nuclear DNA, making mitochondrial DNA sequences especially useful for determining relationships between closely related organisms.

Amino Acid Sequences

The simplest and arguably most informative expression of resemblance for two amino acid sequences is their percent identity. Even so, sequence alignments can be greatly improved by the use of substitution tables that provide scores for every possible amino acid interchange. A substitution table provides a weight for each interchange relative to what would be expected if those interchanges only occurred by chance and were not favored by genetic or structural considerations. Typically, these matrices give weights to each of the 20 sets of (matched) identical residues, as well as to the 190 possible interchanges. Many such tables have been devised, each based on some logical premise. Among the most commonly used are the accepted point mutation 250 (PAM250) matrix and blocks substitution matrix 62 (BLOSUM62) (Figure 2). In these two tables, interchanges with positive scores are more likely to occur than expected by chance, and those with negative scores less likely.

PAM matrices are generated in a sophisticated manner and take into account not only the frequencies of the individual amino acids but also their propensities for change. The suffix attached to the acronym, as in PAM120 or PAM250, denotes how many cycles of calculated mutation were conducted to generate a particular matrix. For example, PAM250 implies 250 rounds of change, and is most useful for rather dissimilar sequences.

An alternative set of tables can be constructed simply on the basis of amino acid frequencies in the individual columns of block alignments. Block alignments are prepared from ungapped segments of large numbers of homologous sequences. Scores for all possible interchanges can be calculated simply by comparing the observed frequency of an interchange with the frequency expected on the basis of the overall occurrences of the two amino acids. These BLOSUM tables have proved surprisingly effective. Suffices are used here to indicate how dissimilar the sequences were in the blocks from which values were calculated. In BLOSUM62, for example, all of the sequences in the block alignment were less than 62% identical.

Global versus Local Alignments

A global alignment ordinarily involves an entire protein sequence, whereas a local alignment involves only a portion of a sequence. The popular searching program basic local alignment search tool (BLAST) finds the highest scoring matching segments within two sequences. The Smith–Waterman algorithm also searches for best matching subsets for two sequences.

In contrast, the Needleman–Wunsch algorithm is designed to find the best global alignment between two amino acid sequences. It is also, well suited for accommodating any kind of substitution matrix and allows for suitable penalties for gaps.

Multiple Alignments

Considerably more information accrues when several homologous sequences are available for alignment. Such alignments can aid the protein scientist in determining the most essential residues in a protein, to the point that given enough divergent sequences, the active site of an enzyme may be inferred even without experimental data. More commonly, the evolutionary history of organisms or proteins is the target. Multiple alignments

	C	S	T	P	A	G	N	D	E	Q	H	R	K	M	I	L	V	F	Y	W	
	9	–1	–1	–3	0	–3	–3	–3	–4	–3	–3	–3	–3	–1	–1	–1	–1	–2	–2	–2	C
		4	1	–1	1	0	1	0	0	0	–1	–1	0	–1	–2	–2	–2	–2	–2	–3	S
C	12		5	–1	0	–2	0	–1	–1	–1	–2	–1	–1	–1	–1	–1	0	–2	–2	–2	T
S	0	2		7	–1	–2	–2	–1	–1	–1	–2	–2	–1	–2	–3	–3	–2	–4	–3	–4	P
T	–2	1	3		4	0	–2	–2	–1	–1	–2	–1	–1	–1	–1	–1	0	–2	–2	–3	A
P	–3	1	0	6		6	0	–1	–2	–2	–2	–2	–2	–3	–4	–4	–3	–3	–3	–2	G
A	–2	1	1	1	2		6	1	0	0	1	0	0	–2	–3	–3	–3	–3	–2	–4	N
G	–3	1	0	–1	1	5		6	2	0	–1	–2	–1	–3	–3	–4	–3	–3	–3	–4	D
N	–4	1	0	–1	0	0	2		5	2	0	0	1	–2	–3	–3	–2	–3	–2	–3	E
D	–5	0	0	–1	0	1	2	4		5	0	1	1	0	–3	–2	–2	–3	–1	–2	Q
E	–5	0	0	–1	0	0	1	3	4		8	0	–1	–2	–3	–3	–3	–1	2	–2	H
Q	–5	–1	–1	0	0	–1	1	2	2	4		5	2	–1	–3	–2	–3	–3	–2	–3	R
H	–3	–1	–1	0	–1	–2	2	1	1	3	6		5	–1	–3	–2	–2	–3	–2	–3	K
R	–4	0	–1	0	–2	–3	0	–1	–1	1	2	6		5	1	2	1	0	–1	–1	M
K	–5	0	0	–1	–1	–2	1	0	0	1	0	3	5		4	2	3	0	–1	–3	I
M	–5	–2	–1	–2	–1	–3	–2	–3	–2	–1	–2	0	0	6		4	1	0	–1	–2	L
I	–2	–1	0	–2	–1	–3	–2	–2	–2	–2	–2	–2	–2	2	5		4	–1	–1	–3	V
L	–6	–3	–2	–3	–2	–4	–3	–4	–3	–2	–2	–3	–3	4	2	6		6	3	1	F
V	–2	–1	0	–1	0	–1	–2	–2	–2	–2	–2	–2	–2	2	4	2	4		7	2	Y
F	–4	–3	–3	–5	–4	–5	–4	–6	–5	–5	–2	–4	–5	0	1	2	–1	9		11	W
Y	0	–3	–3	–5	–3	–5	–2	–4	–4	–4	0	–4	–4	–2	–1	–1	–2	7	10		
W	–8	–2	–5	–6	–6	–7	–4	–7	–7	–5	–3	2	–3	–4	–5	–2	–6	0	0	17	

FIGURE 2 Two different substitution matrices. BLOSUM62 is shown in the upper right, and the PAM250 in the lower left. Matches or interchanges with positive scores are more likely to occur than expected by chance, and those with negative scores less likely.

can also be used to construct "profiles" or "patterns" that are then used to search databases for more distantly related sequences.

Various methods of multiple sequence alignments may vary subtly. The mathematically optimal alignment of multiple sequences may differ significantly from the real history of events leading to the sequences, and these alignments may differ from those based on three-dimensional structure information. Because it is usually history that is being sought, and because the biological processes of interest operate in a binary fashion (species divergences and gene duplications), the preferred clustering process begins with the most similar pair of sequences, progressively incorporating more distant relatives. More weight is accorded to the more similar pairs, the logic being that those are the more reliable data.

Constructing Phylogenetic Trees

Many different ways of constructing phylogenetic trees from aligned sequences have been developed, and numerous programs are available that perform the operations automatically. Although some procedures actually construct the alignment and the tree simultaneously, in most cases the alignment is made first, after which the tree is calculated from it. One of the most important caveats for all molecular phylogenists is embodied in the slogan "Bad alignment, bad tree." Thus, many workers submit a set of sequences to some computerized regimen and accept the emergent tree, together with some formulized set of statistics allegedly providing some measure of confidence in it. It is always prudent to examine the alignment first. One common shortcoming becomes evident when one or more of the sequences being aligned are significantly shorter than the others. Long unmatched stretches will distort the relative global resemblances. Similar problems will occur with mosaic proteins in which only parts of the sequences are homologous or in which segments have been interchanged. The worst outcomes are the results of including sequences that are not homologous.

Phylogenetic trees can be dissected into two components, the branching order and the branch lengths.

Sometimes cladograms are made that make no attempt to quantify branch lengths, concentrating only on the grouping (branching order) of the entries. On another note, there is always the problem of determining the root of a phylogenetic tree. Ordinarily, accessory information over and beyond that contained in the sequences is needed to establish the root with any confidence.

Distance Methods

Distance methods depend on a table of pairwise distances being derived from the scores accumulated during the alignment process. In the simplest case, the number of differences between each pair of sequences can be used. More commonly, scores determined with a substitution matrix are transformed into units of evolutionary distance. Once the distance matrix has been constructed, the tree can be calculated by a clustering algorithm. These often involve the method of least squares, an effort being made to reconcile the individual pairwise distances with the smaller number of constituent branch lengths in a global tree.

Maximum Parsimony

Maximum parsimony strives to find the tree that can be constructed from the smallest number of mutations. There are numerous versions of the procedure, the most common of which attempt to minimize the overall tree length. In these procedures the individual positions in the sequences are considered column by column, in contrast to the overall pairwise distances used in distance matrix methods.

Maximum Likelihood

Maximum likelihood involves an evaluation procedure based on the probabilities of interchange at different nodes in the tree. In this case one starts with a model tree, and tests it for the probabilities of observed character matches and interchanges based on the character states that exist at neighboring nodes. The probabilities for all nodes are summed, and the most probable tree is the one with the highest total likelihood score.

Summary

The tremendous power of multiple sequence alignment procedures stems directly from the fact that all life forms descend from a common ancestor (or a small number of forms that could freely exchange genes). That most of biology and biochemistry is the result of the duplication and modification of a set of primitive genes seems beyond dispute. During evolution, an enormous binomial expansion of homologous sequences has occurred, the radiation of species on the one hand leading to orthologous genes with the same function in different organisms, and gene duplications on the other allowing for diversification of function within species by parologous genes. When sufficient data are available, properly constructed phylogenetic trees can distinguish between these two. Occasionally, sequence entries may occur on phylogenetic trees in unexpected positions, the result of genes having been transferred laterally between species. In any case, the relatively slow rate of change in many genes is what has made possible the enlightened reconstruction of ancient events.

See Also the Following Articles

mRNA Polyadenylation in Eukaryotes • mRNA Processing and Degradation in Bacteria • Pre-tRNA and Pre-rRNA Processing in Bacteria • Pre-tRNA and Pre-rRNA Processing in Eukaryotes • Ribosome Assembly • Ribosome Structure

Glossary

BLOSUM (BLOcks SUbstitution Matrix) A table of values reflecting the frequencies of amino acids at the same positions in a series of block alignments.

bootstrap A method for determining the confidence level for a branching order in a phylogenetic tree.

homologue A sequence related to another by common ancestry.

indel An insertion or deletion of characters in a macromolecular sequence leading to a gap in the alignment.

orthologue A homologous sequence reflecting a pair of gene products related by direct (orthologous) descent.

PAM A pronounceable acronym for an Accepted Point Mutation that has led to an amino acid replacement.

paralogue A homologous sequence reflecting a pair of genes related as a result of a gene duplication.

twilight zone The region of low similarity for pairs of sequences for which the distinction between common ancestry and chance matching is difficult.

Further Reading

CLUSTAL (for aligning sequences and tree construction) http://www.ebi.ac.uk/clustalw.

Feng, D. F., and Doolittle, R. F. (1987). Progressive sequence alignment as a perequisite to correct phylogenetic trees. *J. Mol. Evol.* **25**, 351–360.

Fitch, W. M., and Margolish, E. (1967). Construction of phylogenetic trees. *Science* **155**, 279–284.

Henikoff, J. G., and Henikoff, S. (1996). Blocks database and its applications. *Meth. Enzymol.* **266**, 88–105.

Higgins, D. G., Thompson, J. D., and Gibson, T. J. (1996). Clustal using CLUSTAL for multiple sequence alignments. *Meth. Enzymol.* **266**, 383–402.

Needleman, S. B., and Wunsch, C. D. (1970). A general method applicable to the search for similarities in the sequences of two proteins. *J. Mol. Biol.* **48**, 443–453.

Phylip (for tree construction) http://evolution.genetics.washingtonu.edu/phylip.html.

Phylodendron (for tree construction) http://iubio.bio.indiana/treeapp/.
Ribosomal sequence alignments: www.rna.iomb.utexas.edu/.
Saitou, N. (1996). Reconstruction of gene trees from sequence data. *Meth. Enzymol.* **266**, 427–449.
Schwartz, R. M., and Dayhoff, M. O. (1978). Matrices for detecting distant relationships. In *Atlas of Protein Sequence and Structure* (M. O. Dayhoff, ed.) pp. 353–358. National Biomed. Res. Found, Washington, DC.

BIOGRAPHY

Russell F. Doolittle is a Research Professor at the Center for Molecular Genetics, University of California, San Diego. His principal research interests center around the evolution of protein structure and function. He has a Ph.D. in biochemistry from Harvard (1962) and did post-doctoral work in Sweden. He was an early advocate of using computers to study amino acid sequences as an aid to characterizing proteins.

Muscarinic Acetylcholine Receptors

Neil M. Nathanson
University of Washington, Seattle, Washington, USA

Acetylcholine (ACh) is an important neurotransmitter in both the central and peripheral nervous systems. ACh is synthesized in the cytoplasm of nerve terminals by the enzyme choline acetyltransferase, and is then transported into synaptic vesicles. Depolarization of the nerve terminal causes an influx of calcium into the nerve terminal and evokes the release of ACh into the synaptic cleft; the release of ACh can be blocked by botulinum toxin. The actions of ACh are terminated by the enzyme ACh-sterase, which hydrolyzes ACh. The activity of ACh-sterase can be inhibited by drugs such as neostigmine and the nerve gas agent sarin.

ACh is released from a nerve terminal and binds to a receptor on the cell surface of a target cell to allow transfer of information across a chemical synapse. Sir Henry Dale in 1914 divided receptors for ACh into two classes based on their distinct pharmacological properties, nicotinic and muscarinic. Muscarinic ACh receptors (mAChR) are present on central and peripheral neurons, and in such target organs of the parasympathetic nervous systems as cardiac and smooth muscle, and many exocrine glands. The binding of ACh to mAChR can be blocked by antagonists such as atropine.

The Muscarinic Acetylcholine Receptor Gene Family

While pharmacological and biochemical analyses suggested for many decades after Dale's classification that there was only a single type of muscarinic receptor, drugs were eventually developed that distinguished between muscarinic receptors in different tissues. For example, gallamine was an antagonist at nicotinic receptors that selectively blocked muscarinic receptors in the heart compared to other tissues, while pirenzepine blocked muscarinic acetylcholine receptor (mAChR) in certain neurons with higher affinity than in the heart. These studies indicated that there were multiple pharmacologically distinct muscarinic receptors. In the 1980s, mAChR were purified from both heart and brain, which allowed the isolation of cDNA and genomic clones encoding the mAChR. There are five subtypes of mAChR, termed M_1, M_2, M_3, M_4, and M_5, which are encoded by distinct genes and differentially expressed in various organs and parts of the nervous system (Table I).

Muscarinic Receptor-Mediated Signal Transduction

Muscarinic Receptors Signaling Utilizes G Proteins

While nicotinic acetylcholine (ACh) receptors are ligand-gated ion channels (i.e., the same protein both binds ACh and acts as an ion channel), mAChR are members of the G protein-coupled-receptor (GPCR) superfamily. G proteins are a family of GTP-binding heterotrimeric proteins (they consist of three non-identical subunits) and they couple receptors to various effector proteins, such as adenylyl cyclase, phospholipase C, and ion channels. In the inactive state, GDP is bound to the α-subunit. The binding of ACh to mAChR promotes the dissociation of GDP and the binding of GTP to the α-subunit. This in turn causes the dissociation of the α-subunit from the $\beta\gamma$-subunits; both the α- and $\beta\gamma$-subunits can interact with effector proteins to regulate their activity. The α-subunits have GTPase activity which can be increased by the action of regulator of G protein signaling (RGS) proteins. This hydrolysis of GTP to GDP promotes the reassociation of the α- and $\beta\gamma$-subunits and terminates signaling unless ACh is still present to reinitiate the signaling cycle.

Muscarinic Receptor-Mediated Regulation of Second Messenger Pathways

The mAChR can be divided into two groups on the basis of both sequence similarities and functional responses. The M_1, M_3, and M_5 receptors preferentially couple to the Gq family of G proteins, whose α-subunits can activate phospholipase C (PLC). PLC activity produces two intracellular second messenger, inositol trisphosphate, which causes release of calcium from intracellular stores, and diacylglycerol, which activates protein

TABLE I

Subtypes of Muscarinic Receptors

Subtype	Number of amino acids	G-protein family	Some tissues with high expression
M_1	460	G_q	Cortex, hippocampus, striatum
M_2	466	G_i/G_o	Heart, cerebellum
M_3	590	G_q	Exocrine glands, smooth muscles cortex, thalamus
M_4	479	G_i/G_o	Striatum
M_5	532	G_q	Hippocampus, ventral tegmentum

The table shows the number of amino acids in the five human mAChR subtypes, the G-protein family to which each receptor preferentially couples, and representative tissues which express the various subtypes.

kinase C. The increased intracellular calcium in turn can produce many potential effects, such as activation of protein kinases, activation or inhibition of adenylyl cyclase, activation of phoshodiesterases, and activation of nitric acid synthetase, which can result in increased intracellular cGMP levels. The M_2 and M_4 receptors preferentially couple to the Gi family of G proteins to inhibit adenylyl cyclase activity, thus lowering intracellular cAMP levels. The types of signals produced by any mAChR can depend on both the level of receptor expression and the particular complement of signaling proteins expressed in a given cell.

Ion Channels

Many of the physiological responses mediated by the activation of mAChR on excitable cells are due to the regulation of the activity of ion channels. Regulation of ion channel activity can occur by many different mechanisms. Modulation of ion channel activity can occur due to protein phosphorylation. For example, activation of protein kinase C or decreased activity of cAMP-dependent protein kinase (due to inhibition of adenylyl cyclase activity) can lead to decreased activity of sodium and calcium channels, respectively. Activation of tyrosine kinases can regulate potassium channel activity.

Another mechanism is the regulation of ion channel activity directly by intracellular second messengers. Increased intracellular calcium can increase the activity of calcium-activated potassium channels, and increased cyclic GMP can activate cyclic nucleotide-gated ion channels. In addition, $\beta\gamma$-subunits released following activation of Gi-family G protein can interact with and regulate ion channel activity. For example, inwardly rectifying potassium channels in the heart are activated in this manner following M_2 mAChR activation.

Mitogen-Activated Protein Kinase (MAPK) and Related Pathways

Muscarinic receptors can mediate regulation of a series of protein kinase cascades implicated in a wide variety of processes, including cell growth, differentiation, and apoptosis. These protein kinase cascades lead to activation of the MAPKs Erk1 and Erk2, p38 kinase, and c-Jun terminal kinase. The particular cascades which are regulated, the mechanisms responsible for this regulation, and whether there is activation or inhibition of a particular kinase pathway depend both on the specific subtype of mAChR and the cell type the receptor is expressed in.

Structural Studies

Transmembrane Topology

Like other members of the GPCR superfamily, the muscarinic receptors are heptahelical, that is, they have seven helical transmembrane domains, with the amino-terminal extracellular and the carboxyl-terminal intracellular. The amino-terminal domains of the various mAChR subtypes contain asparagine residues which are sites for N-linked glycosylation. Based on the crystal structure determined for the prototypical GPCR rhodopsin and on mutagenesis and structural analyses of both the mAChr and other GPCR, it is likely that the transmembrane helices are arranged in a bundle.

Ligand Binding to the mAChR

ACh binds to the mAChR by interacting in a crevice with multiple transmembrane domains in the plane of the membrane. A negatively charged aspartic acid residue in the third transmembrane domain interacts with the positively charged ammonium group of ACh. Mutagenesis experiments have also implicated specific residues in the second, fifth, sixth, and seventh transmembrane domains in the binding of cholinergic ligands.

Regions of the mAChR Involved in Coupling to G Proteins

The binding of ACh to the mAChR induces a conformational change in the receptor which allows it to activate the appropriate G protein(s). The regions responsible for determining the specificity of coupling of the mAChR to G proteins has been determined primarily by construction of chimeric receptors between two mAChR, such as M_2 and M_3, which couple to different G proteins. The membrane proximal portions of the third cytoplasmic loop are the main determinants of the specificity of G protein coupling, although other regions such as the second intracellular domain may also play a role in mAChR-G protein interactions.

Muscarinic Receptor Actions *in vivo*

Muscarinic Receptor Actions in the Periphery

Muscarinic receptors are present in many target organs of the autonomic nervous system. A generalization based on pharmacological and molecular genetic approaches is that the M_2 receptors are present in heart, while the M_3 receptor is present in smooth muscles and exocrine glands, however, this generalization must be tempered by the presence of additional subtypes of mAChR present in low abundance in both cardiac and smooth muscles and by the possibility of differences in subtype expression between different animal species. Muscarinic receptors decrease the rate and force of contraction of the heart, and increase the tone and motility of the gastro-intestinal and urinary tracts. Muscarinic receptors increase secretions from salivary and sweat glands, and cause bronchoconstriction and increased bronchial secretions. Intravenous administration of ACh causes vasodilation. This is due not to activation of mAChR on the smooth muscle cells but to activation of the mAChR on the endothelial cells in the blood vessel. mAChR activation results in the production of NO, which then diffuses out of the endothelial cells and into the smooth muscle cells, resulting in relaxation of the blood vessel.

Muscarinic Receptor Actions in the Central Nervous System

Muscarinic receptors play an important role in the central nervous system. Many studies have implicated mAChR in learning and memory. Administration of muscarinic antagonists interfere with performance in many learning and memory tests, and the decreased cognition in patients with Alzheimer's disease is thought to be due in part to impaired muscarinic transmission. Both pharmacological and genetic experiments have implicated the M_1 mAChR in memory and learning, although it is likely that multiple muscarinic receptor subtypes play a role in these processes.

Muscarinic receptors in the spinal cord and at supraspinal sites (i.e., the brain) can mediate an analgesic response. Genetic studies in mice show that both the M_2 and M_4 receptors are involved in this anti-nociceptive effect.

Muscarinic receptors have been implicated in many other processes as well. For example, muscarinic receptors regulate the function of the basal ganglia, where multiple subtypes of muscarinic receptors modulate dopaminergic signaling. M_5 receptors are present in the ventral tegmentum and are involved in drug reward mechanisms.

Pharmacological analyses carried out over many years have led to the development of a number of drugs which produce their therapeutic actions by either activating or blocking muscarinic receptors. The increased understanding of the actions of individual mAChR subtypes should be a great aid in the development of drugs with increased therapeutic actions while decreasing effects at undesired mAChR subtypes.

See Also the Following Articles

Mitogen-Activated Protein Kinase Family • Nicotinic Acetylcholine Receptors • Phospholipase C

Glossary

agonist A drug which binds to a receptor and mimics the actions of a natural transmitter.

antagonist A drug which binds to a receptor and blocks the action of an agonist.

G-proteins A family of proteins which bind GTP and which couple receptors to signaling proteins such as ion channels, adenylyl cyclase, and phospholipase C.

neurotransmitter Chemical signal released by a neuron.

Further Reading

Anagnostaras, S. G., Murphy, G. G., Hamilton, S. E., Mitchell, S. L., Rahnama, N. P., Nathanson, N. M., and Silva, A. J. (2003). Selective cognitive dysfunction in acetylcholine M1 muscarinic receptor mutant mice. *Nature Neurosci.* **6**, 51–58.

Birdsall, N. J. M., Nathanson, N. M., and Schwarz, R. D. (2001). Muscarinic receptors: It's a knockout. *Trends Pharmacol. Sci.* **22**, 215–219.

Caulfield, M. P., and Birdsall, N. J. M. (1998). International union of pharmacology: XVII. Classification of muscarinic receptors. *Pharmacol. Rev.* **50**, 279–290.

Duttaroy, A., Gomeza, J., Gan, J. W., Siddiqui, N., Basile, A. S., Harman, W. D., Smith, P. L., Felder, C. C., Levey, A. I., and Wess, J. (2002). Evaluation of muscarinic agonist-induced analgesia in muscarinic acetylcholine receptor knockout mice. *Mol. Pharmacol.* **62**, 1084–1093.

Gutkin, J. S. (1998). The pathways connecting G protein-coupled receptors to the nucleus through divergent mitogen-activated protein kinase cascades. *J. Biolog. Chem.* **273**, 1839–1842.

Levey, A. I. (1996). Muscarinic ACh receptor expression in memory circuits: Implications for treatment of Alzheimer disease. *Proc. Natl. Acad. Sci. USA* **93**, 13541–13546.

Nathanson, N. M. (1987). Molecular properties of the muscarinic acetylcholine receptor. *Annu. Rev. Neurosci.* **10**, 195–236.

Nathanson, N. M. (2000). A multiplicity of muscarinic mechanisms: Enough signaling pathways to take your breath away. *Proc. Natl. Acad. Sci. USA* **97**, 6245–6247.

Wess, J. (1996). Molecular biology of muscarinic acetylcholine receptors. *Crit. Rev. Neurobiol.* **10**, 69–99.

Biography

Neil M. Nathanson is a Professor in the Department of Pharmacology, University of Washington School of Medicine. He received the Ph.D. in Biochemistry from Brandies University, and carried out postdoctoral training at the National Institutes of Health and the University of California, San Francisco. His research interests are focused on the regulation of signaling and expression of muscarinic receptors and receptors for neurotrophic factors.

Myosin Motors

Roy E. Larson
University of Sao Paulo, Sao Paulo, Brazil

Movement is a fundamental property of living matter. Specialized molecules with mechano-chemical properties are responsible for cellular motility and its macroscopic manifestations, such as muscle contraction. The myosins make up a large family of molecular motors that feature a conserved mechano-chemical domain, capable of transforming the chemical energy of ATP hydrolysis into the generation of force and movement along filamentous actin tracks. Although first characterized as the molecular power generator of muscle contraction, myosins are now known to be ubiquitous in virtually all mammalian cell types as well as widely distributed amongst eukaryotic organisms, both in plants and animals. They have multifunctional roles in many cellular processes, ranging from cytokinesis and pseudopodia extension to pigment granule transport and cytoplasmic streaming. Over the past 15 years, researchers have identified ~150 myosin genes, making up ~18 distinct structural classes, referred to as myosins I–XVIII, within what is now called the myosin superfamily of molecular motors. Although structural variations amongst the myosins reflect their specific cellular type and function, and also their phylogeny, there is a basic architectural plan followed by these motors.

Overall Molecular Architecture

The protein structure of myosins can be divided into three principal structural and functional domains. The highly conserved, mechano-chemical generator, usually referred to as the "head domain," is almost universally positioned at the amino terminal portion of the protein and contains the actin-binding and adenosine triphosphate (ATP) hydrolysis sites (Figure 1). The crystal structures have been determined from at least five myosins, widely distant on the evolutionary scale (vertebrate skeletal and smooth muscle myosin, slime mold myosin, scallop muscle myosin, and vertebrate class V myosin), which revealed very similar atomic structures amongst them, indicating that the basic machinery for movement has been highly conserved. Immediately following the head domain is an elongated, α-helical region to which calmodulin and/or calmodulin-like light chains bind, forming the regulatory or "neck domain" (Figure 1). This domain acts as a lever arm to amplify small movements in the head domain. In several myosins the neck domain inhibits the mechano-chemical cycle and thus acts as the regulatory element that triggers the mechano-chemical events when this inhibition is released by factors, such as calcium binding to or phosphorylation of the light chains. The rest of the molecule is referred to as the "tail domain" and is the most structurally diverse part, varying extensively between classes, yet maintaining significant homology within a class. The tail domains are regions of interaction with lipid membranes, proteins, and signaling molecules, important for site recognition, receptor binding, and specific functions. Many myosins are dimerized via the formation of intertwined α-helices, referred to as coiled coils (Figure 2). The prime example is skeletal muscle myosin II whose tail domain is completely composed of a coiled-coil motif, which aligns and joins together with other tail domains to form the bipolar thick filaments of the sarcomere. The myosin II class is often referred to as "conventional" myosin due to its historical identification and characterization. However, it is now viewed as being quite unique in that no other class within the myosin superfamily is known to organize into filaments. Clearly the myosins II have been refined by evolution, culminating in their role in the generation of macroscopic force and velocity of skeletal muscle contraction. The tail domains of all other myosins have globular regions, and are without the propensity for filament formation, although they may or may not form coiled coils and, thus, can exist as monomeric or dimeric structures (Figure 2).

Evolutionary Diversity and Phylogenic Classification

With the advent of DNA sequencing, ~18 classes of myosin genes have been identified based on comparisons of the amino acid sequences of the head domains, even though this domain is highly conserved across the board for the myosin superfamily. On the other hand, the tail domains are quite unique for each myosin class,

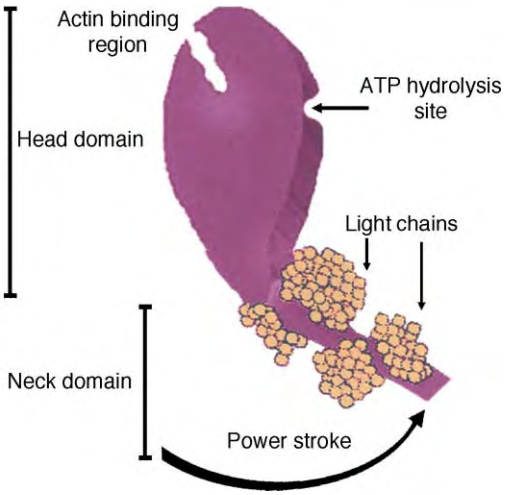

FIGURE 1 Schematic diagram of the head and neck domains of myosin showing the relative positions of the actin-binding region to the ATP site and to the light chains in the neck domain. The rotation of the neck domain which represents the power stroke is indicated as a curved arrow. (Drawn by Silvia Andrade.)

indicating that evolution selected a tail-domain design for the specific cellular function(s) of that particular myosin class. Phylogenetic analysis of the head sequences also indicated that myosins diversified quite early in eukaryotic evolution. Curiously, myosin precursors have not been identified in prokaryotes. It is tempting to speculate that the appearance of myosin motors with their diversity of tails was an evolutionary innovation that furnished impetus for eukaryotic cells to experiment and gain new niches.

Mechano-Chemical Features and Regulation

A description of the molecular mechanism of energy transduction by mechanoenzymes has been a challenge for workers in the field for half a century. The determination, during the last decade, of the atomic structures of myosin in several conformational states with nucleotide derivatives bound has brought this goal close to realization. An overall description of the molecular events taking place during the mechano-chemical cycle, which lead to movement and force generation, is given here. There are three elements to keep in mind: first, ATP binds to the myosin head domain at an active site capable of hydrolyzing it to adenosine diphosphate (ADP) and inorganic phosphate (Pi); second, myosin binds to filamentous actin (F-actin) either strongly or weakly depending on the molecular conformation of the myosin; third, conformational changes in myosin structure occur depending on the nucleotide occupying the active site. Beginning with the binding of ATP to the nucleotide-binding site in the head domain of myosin, this event puts the myosin in a weak F-actin-binding conformation, i.e., most of the myosin is not bound to F-actin. Myosin quickly hydrolyzes the ATP; however, the hydrolysis products, ADP and Pi, are only slowly released from the active site. The energy of ATP binding and hydrolysis is conserved in the high-energy conformation of the myosin at this point, which is considered to be the fully cocked state. The slow release of products from the active site dissipates this conformational energy and puts myosin into its lowest energy state, ready for the binding of another ATP molecule. In the absence of F-actin the energy of this conformational change from the high to low energy state is dissipated as heat. However, when F-actin is bound to myosin, the rate of release of ADP and/or Pi dramatically increases, while the myosin is converted to its strong F-actin-binding conformation. Thus, when F-actin is present, the conformational change in the myosin molecule associated with product release occurs simultaneously with tight coupling to F-actin and, rather than being immediately dissipated as heat, is now converted to tension development and work. The exact conformational change that occurs, referred to as the "power stroke," is a rotation of ~90° of the myosin neck domain relative to the F-actin orientation (see Figure 1). Thus, for native muscle myosin with the neck domain connected to its tail domain that, in turn, is embedded in a thick filament, the power stroke will move the thick filament relative to the actin filament. A return to the weak binding state and disassociation of myosin from F-actin occurs with the rebinding of ATP to the nucleotide site, thus initiating a new cycle. In summary, the mechano-chemical cycle results from the tight coupling of protein conformational energy in the myosin head and neck domains with chemical energy (ATP binding and hydrolysis) and cyclic transitions between strong and weak binding between myosin and F-actin. As presented, this cycle will continue as long as myosin can contact actin and a steady

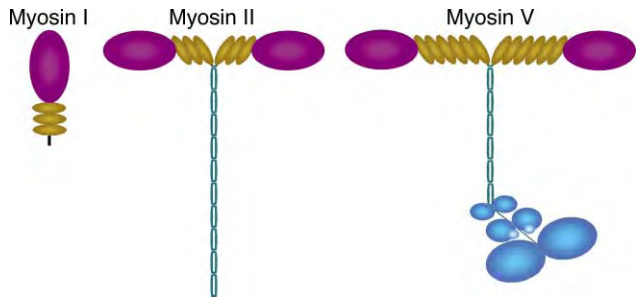

FIGURE 2 Schematic diagram of three typical myosins representing classes I, II, and V. The tear-drop structures (light gray) represent the head domains; the small oblong structures (dark gray) represent the light chains; the stippled circles represent globular regions of the tail domain. The coiled coil is represented by intertwined lines. (Drawn by Silvia Andrade.)

supply of ATP is maintained. (n.b. *Rigor mortis* results from the interruption of the metabolic supply of ATP that comes with death and represents the strong binding, low-conformational energy state of the actomyosin in muscle at the end of the power stroke).

As with any motor, it is desirable to be able to turn the myosin mechano-chemical cycle on and off, depending on need. There are several mechanisms to do this, most of which use calcium ion as the triggering element. For example, in striated muscles a calcium-sensitive system of regulator proteins decorates F-actin and sterically blocks access of the myosin head to the actin sites. Calcium relieves this blockage, such that an increase in its intracellular concentration determines actomyosin activation. For molluscan myosin and vertebrate smooth muscle myosin, regulation is myosin-based, in that an inhibitory effect of the neck domain can be relieved by calcium binding to a light chain or by calcium-activated phosphorylation. For other myosins the mechanisms of regulation are less well understood, although calcium and/or phosphorylation most likely play a role.

A Multitude of Cellular Functions

Simplistically, myosins have two functional ends: the motor end, which generates force and movement on actin filaments, and the tail end, which links it to its cargo or, as in the special case of muscle, to itself forming bipolar filaments. Surprisingly, in spite of their highly conserved structure, the myosin heads differ in a fundamental property related to their mechano-chemical cycle, which affects their cellular function. Individual myosin II molecules bind to actin for only a small fraction of the cycle duration. This property is essential for the smooth sliding of myosin filaments in muscle with their arrays of many heads interacting with the organized actin filaments of the sarcomere. On the other hand, at least two myosins (a class V and a class VI myosin) have the property of "processivity," i.e., they are able to move as individual molecules along actin filaments for some distance without losing contact. Present evidence indicates that these two-headed myosins walk in a "hand-over-hand" manner along the actin filament, each head binding to actin for more than 50% of the cycle duration. This property, therefore, allows these myosins, acting alone, to carry cargo without losing a grip on the actin track.

The tail domain determines the enormous diversity of function within the myosin superfamily and dictates the specific function of each myosin. To exemplify this diversity, it is noted that in a single vertebrate cell type – the human intestinal epithelial cell – there have been identified at least 12 myosins, representing 6 classes. Sorting out the specific functions of individual myosins and myosin classes has been a formidable challenge to researchers in the field. The involvement of myosins in three general areas has been described: membrane-associated movements, intracellular vesicle and particle transport, and intracellular signaling. Besides their role in contraction of muscle cells, myosins are involved in amoeboid movements, pseudopodia extensions, phagocytosis, exocytosis, cytokinesis, cell gliding over a surface, and other manifestations of plasma membrane dynamics. The myosins of class II, which include the muscle myosins, are one of the principal actors in these processes, due in part to their tail's ability to form bipolar filaments and thus generate constrictive forces. Also, however, the single-headed, class I myosins are involved in membrane interactions due to the phospholipid-binding regions in their tail domains, thus giving them the ability to orient force generation directly toward membranes.

Many examples of intracellular vesicle and organelle transport that depend on myosin motors have been found. The dramatic cytoplasmic streaming in plants is a good example. This process involves class XI myosins, one of only two classes found in plants (the other is class VIII). Mutations in class V myosins result in defective distribution of pigment granules in melanocytes of vertebrates and of membrane vesicles in dividing yeast. Several linker proteins have been described that connect myosin motors to their cargo, such as melanophilin and Rab27a, which link pigment granules to myosin V, and Vac17p, a key component of the myosin receptor on yeast vacuoles. The demonstration in squid axoplasm of translocation of moving vesicles from microtubule tracks to actin filaments suggested that organelle transport involves cooperative interactions between microtubule- and actin-based systems. These examples serve to illustrate that myosin motors have important roles in the transport of membrane delimited organelles, but attention has been given to recent evidence that myosins also transport macromolecular complexes. Myo4p, a class V myosin in yeast, is directly involved, together with at least two other proteins, in the transport of a specific mRNA, encoding a transcription factor, to the daughter cell of budding yeast, thus playing an essential role in regulation of differential gene expression in these organisms.

Being molecular effectors, one may expect that myosins are end-targets for cell signaling. As previously discussed, myosins bind to calmodulin and are indeed activated or modulated by ionic calcium and protein kinases, all of which are important intracellular messengers for signal transduction pathways. However, it is noteworthy that myosins also seem to participate in the signaling pathways themselves, as a kind of motorized signaling devise. Evidence for this first appeared upon analysis of the tail sequences, where sequence motifs related to cell signaling pathways, such as the SH3, PDZ, and PH motifs, were recognized in several distinct

myosin classes. These motifs are signals for protein–protein and protein–phosphoinositide binding that participate in the assembly of signaling complexes, although the functional role of myosins containing these signal motifs is still not clear. The tail domain of myosins IX has a region with homology to GTPase-activating proteins (GAPs), which act as molecular switches in the organization of the actin cytoskeleton, particularly in the formation of cell–matrix focal adhesions. Overexpression of a myosin IX in HeLa cells caused the cells to lose actin filament organization and substrate contact, resulting in their rounding up and release from the substrate. These examples illustrate that myosins are not only final targets for cellular signaling, but potential intermediate players in the signaling cascades. Myosins are involved in other cell processes in ways not well understood, such as mitotic spindle orientation in yeast, phototransduction in *Drosophila* retina and auditory function of the vertebrate inner ear. There is much to be learned about the functional roles of myosin motors throughout the biosphere.

Myosins in Disease

The human genome has ~40 myosin genes, composing 12 classes. As described above, myosins are fundamentally important in many cellular processes and thus would be expected to underlie cellular dysfunction in human disease. In fact, several myosins have been identified as the causes of hereditary diseases. A major cause of familial hypertrophic cardiomyopathy lies in mutations of the head domain of cardiac muscle myosin II. Usher syndrome, the most common cause of inherited deaf–blindness in children, has been linked to mutations in myosin VII. Also, mutations in myosin XV have been identified in human nonsyndromic deafness; and in myosin VI in the Snell's Waltzer mouse, which suffers from deafness due to degeneration of the sensory neuroepithelia in the inner ear. Thus, different myosin classes have important roles that converge in the auditory system. In Griscelli syndrome, where children exhibit hair hypopigmentation, linked to severe immunological and neurological deficits that frequently lead to early death, mutations have been identified in myosin V or Rab27a, a protein that links myosin V to organelles. It is likely that more connections will be made between human disease and myosin function as genetic probes and analyses increase.

See Also the Following Articles

Actin Assembly/Disassembly • Calcium/Calmodulin-Dependent Protein Kinase II • DNA Sequence Recognition by Proteins

Glossary

α-helix The specific helical arrangement of a polypeptide chain formed by hydrogen bonding between atoms of peptide bonds separated by four amino acids along the chain.

calmodulin A calcium-binding protein, found ubiquitously in eukaryotic cells, that acts as a calcium-sensitive regulator of many enzymes.

focal adhesions Sites of attachment of cells to underlying substratum involving specialized protein complexes linking the intracellular actin cytoskelton to the extracellular matrix.

sarcomere The functional contractile unit of muscle cells consisting of interdigitating actin and myosin filaments.

Further Reading

Alberts, B., Johnson, A., Lewis, J., Raff, M., Roberts, K., and Walter, P. (2002). *Molecular Biology of the Cell*. Garland Science, New York.

Cooper, G., and Hausman, R. (2003). *The Cell. A Molecular Approach*. ASM Press, Washington.

Lodish, H., Berk, A., Matsudeira, P., Kaiser, C., Kreiger, M., Scott, M., Zipursky, S., and Darnell, J. (2003). *Molecular Cell Biology*. Freeman, New York.

Kendrick-Jones, J. (2003). The Myosin Home Page. MRC Laboratory of Molecular Biology. www.proweb.org/myosin.

Pollard, T., and Earnshaw, W. (2002). *Cell Biology*. Saunders, Philadelphia.

Sellers, J., and Goodson, H. (1995). Motor proteins 2: Myosin. *Protein Profiles* **2**(12), 1323–1423.

Biography

Roy E. Larson is a Professor and Chairman of the Department of Cellular and Molecular Biology and Pathogenic Bioagentes at the Faculdade de Medicina de Ribeirao Preto, Universidade de Sao Paulo, Brazil. He holds a Ph.D. in molecular biology from the University of Pennsylvania and received his postdoctoral training at Yale University. His principal research interests are in cytoskeletal dynamics. He initially purified and identified myosin V from vertebrate brain and was instrumental in its biochemical and structural characterization.

Editors-in-Chief

William J. Lennarz

State University of New York at Stony Brook, Stony Brook, New York, USA

Section: Lipids, Carbohydrates, Membranes and Membrane Proteins

WILLIAM J. LENNARZ received his B.S. in Chemistry from Pennsylvania State University and a Ph.D. in Organic Chemistry from the University of Illinois. Subsequently he carried out postdoctoral work at Harvard with Konrad Bloch on fatty acid biosynthesis. In 1962 he was appointed Assistant Professor at Johns Hopkins in the Department of Physiological Chemistry. After promotion to Associate Professor in 1967, and full Professor in 1971, he remained at Hopkins until 1983. At that time, he was appointed Robert A. Welch Professor and Chair of the Department of Biochemistry and Molecular Biology at the University of Texas Cancer Center, M.D. Anderson Hospital. In 1989 he became a Leading Professor and Chair of the Department of Biochemistry and Cell Biology at SUNY at Stony Brook. In 1990 he founded and became Director of the Institute for Cell and Developmental Biology at Stony Brook.

Dr. Lennarz has served on many national and international committees. He has served as President of the Biochemistry Chairman's Organization, President of the American Society for Biochemistry and Molecular Biology and President of the Society for Glycobiology. He was a member of the Executive Committee of the International Union of Biochemistry and Molecular Biology for almost a decade.

He has presented special lectures at the University of Notre Dame, the NIH, the University of West Virginia, Johns Hopkins University, Florida State University, the University of California at San Diego, the University of Arkansas, Indiana University and the Medical College of Virginia.

He is a member of the National Academy of Sciences. The focus of his early work was on lipids and bacterial cell surfaces. More recent efforts have been in the structure, biosynthesis and function of cell surface glycoproteins. The biosynthesis studies initially were carried out in liver and oviduct, but these efforts now are focused in yeast. The functional studies have concentrated on the role of cell surface glycoproteins in fertilization and early development in the sea urchin and, more recently, the frog. For over 30 years Dr. Lennarz' research has been supported by federal sources, primarily the National Institutes of Health. Recently he was appointed Distinguished Professor and Chair of his department.

M. Daniel Lane

The Johns Hopkins University, School of Medicine, Baltimore, Maryland, USA

Section: Metabolism, Vitamins and Hormones

M. DANIEL LANE received B.S. and M.S. degrees in 1951 and 1953 from Iowa State University and a Ph.D. in 1956 from the University of Illinois. He was a Senior Postdoctoral Fellow with Professor Feodor Lynen at the Max-Planck Institute Fur Zellchemie in Munich. Following faculty positions at Virginia Polytechnic Institute and New York University School of Medicine, he joined the faculty at the Johns Hopkins University School of Medicine in 1969 and served as DeLamar Professor and Director of the Department of Biological Chemistry from 1978 to 1997. He is presently Distinguished Service Professor at Johns Hopkins. In 2002 he received an honorary degree, Doctor of Humane Letters, from Iowa State University.

Dr. Lane was elected to membership in the National Academy of Sciences (in 1987) and was elected as a Fellow of the American Academy of Arts and Sciences (in 1982) and of the American Society of Nutritional Sciences (in 1996). He received the Mead Johnson Award from the American Society for Nutritional Sciences in 1966 for his research on biotin-dependent enzymes and in 1981, the William C. Rose Award from the American Society for Biochemistry and Molecular Biology for his work on the insulin receptor. In 1990–1991 Lane served as President of the American Society of Biochemistry and Molecular Biology. He has presented many named lectureships (including the

Feodor Lynen Lecture in Germany in 1999) and served on numerous editorial boards including the Journal of Biological Chemistry and the Annual Reviews of Biochemistry. Currently he is Associate Editor for Biochemical and Biophysical Research Communications.

Dr. Lane has published 280 research papers in major scientific journals. His early work focused on various enzymatic CO_2 fixation reactions, notably the mechanisms by which the B-vitamin, biotin, functions in enzymes to catalyze carboxylation. Dr. Lane's work on the regulation of acetyl-CoA carboxylase, the key regulatory enzyme of fatty acid synthesis, led him to his present interests which are to understand the basic mechanisms of lipogenesis, adipogenesis and the consequence of aberrations in these processes, most notably obesity. Research currently underway in his laboratory focuses on: (1) the genes that signal stem cell "commitment" to the adipocyte lineage and subsequent differentiation into adipocytes, and (2) the mechanisms by which the region of the brain, known as the hypothalamus, monitors and controls the drive to eat.

Associate Editors

Ernesto Carafoli

Università degli Studi di Padova, Padova, Italy
Section: Bioenergetics

ERNESTO CARAFOLI earned his M.D. degree at the University of Modena in Italy in 1957. After postdoctoral studies in the Laboratory of Albert L. Lehninger at Johns Hopkins University in the mid 1960s he returned to his home institution in Italy where he worked until 1973, when he was appointed Professor of Biochemistry at the Swiss Federal Institute of Technology (ETH) in Zurich. He returned to Italy in 1998 as a Professor of Biochemistry at the University of Padova, where he now also directs the newly founded Venetian Institute of Molecular Medicine (VIMM).

Dr. Carafoli became interested in calcium as a signaling agent during his post-doctoral days at Johns Hopkins. When he arrived there his main interests were in mitochondrial bioenergetics and it was thus natural for him to expand them to the newly discovered area of mitochondrial calcium transport. He was involved in most of the early discoveries in the field, and he continued to work on mitochondria and calcium after his return to Italy and until he moved to the ETH. There his interests still remained focused on calcium, but the emphasis shifted to the proteins that transport it across membranes and to those that process its signal. His favorite object of study became the calcium pumps, especially that of the plasma membrane, an enzyme which is essential to the regulation of calcium homeostasis and thus to the well being of cells. His contributions on the enzyme, especially after he purified it in 1979, have helped establishing most of its properties and have clarified important problems of mechanism, regulation and structure.

Dr. Carafoli has authored or co-authored about 450 peer-reviewed articles and reviews, and has edited or co-edited about 20 books. He has served on the Editorial or Advisory Boards of several periodicals and has organized about 30 International Workshops and Symposia. He has been featured as a plenary or honorary lecturer at numerous events ranging from specialized Workshops to International Symposia and Congresses. Dr. Carafoli's honors and awards include several international prizes and medals, memberships in several Academies, and three honorary degrees.

Don W. Cleveland

University of California, San Diego, La Jolla, CA, USA
Section: Cell Architecture and Function

DON W. CLEVELAND has been a longstanding contributor to the elucidation of regulation of assembly of mitotic spindles and chromosome movement and how errors in these contribute to the chromosome loss characteristic of human tumors. He discovered the tubulin gene families encoding the major subunits of microtubules and the first mammalian example of control of gene expression through regulated RNA instability. He identified components required for microtubule nucleation and anchoring during spindle assembly. He identified the first human centromeric protein (CENP-B). He then discovered CENP-E, the centromere-associated, microtubule-motor that he showed to be essential for chromosome attachment and for activation and silencing of the mitotic checkpoint, the cell cycle control mechanism that prevents errors of chromosome segregation in mitosis.

Dr. Cleveland has also been a leading force in dissecting the disease mechanism for major human neurodegenerative disorders. He initially purified and characterized tau, the microtubule-associated protein that assembles aberrantly in human dementias including Alzheimer's disease and Pick's disease. He established that the extreme asymmetry of neurons acquired during development is achieved with a deformable array of interlinked neurofilaments, microtubules and actin. He showed that disorganization of neurofilament arrays caused selective death of motor neurons in mice and humans. He also demonstrated that neuronal death could also arise by a toxicity of mutant superoxide dismutase unrelated to its normal activity, thereby uncovering the mechanism underlying the major genetic form of amyotrophic lateral sclerosis. He showed that this toxicity could be

sharply ameliorated by lowering the content of neurofilaments.

Dr. Cleveland is currently Head, Laboratory for Cell Biology in the Ludwig Institute for Cancer Research and Professor of Medicine, Neurosciences and Cellular and Molecular Medicine at the University of California at San Diego. He is also the Editor of the Journal of Cell Biology and Current Opinion in Cell Biology.

Jack E. Dixon

University of California, San Diego School of Medicine,
La Jolla, CA, USA
Section: Protein/Enzyme Structure, Function, and Degradation

JACK E. DIXON earned his Ph.D. in Chemistry at the University of California, Santa Barbara in 1971 and did his postdoctoral training in Biochemistry at the University of California, San Diego.

Dr. Dixon is a pioneer and leader in the structure and function of the protein tyrosine phosphatases (PTPases). He demonstrated that the unique catalytic mechanism of the PTPases proceeds via a novel cysteine-phosphate intermediate. He discovered the first dual-specificity phosphatase, which led to the identification of the cell cycle protein, $p80^{cdc25}$, as a phosphatase. He also showed that the bacteria responsible for the plague or "black death" harbor the most active PTPase ever described. He and his colleagues went on to demonstrate that this PTPase gene product is essential for the pathogenesis of the bacteria. Dr. Dixon and his colleagues determined X-ray structures for both tyrosine and dual specificity phosphatases. Dr. Dixon also found that sequences outside of the PTPase catalytic domain could function to direct the subcellular localization of the PTPases and to restrict their substrate specificity. This is now a widely acknowledged regulatory paradigm for the PTPases. Recently, his laboratory demonstrated that the tumor suppressor gene, PTEN, which shares sequence identity with the PTPases, catalyzes the dephosphorylation of a lipid second messenger, phosphatidylinositol 3,4,5-trisphosphate (PIP3). This represents the first example of a PTPase dephosphorylating a lipid second messenger. PIP3 activates the protein kinase, AKT, which plays a critical role in controlling the balance between apoptosis and cell survival. The loss of the PTEN gene elevates PIP3 levels leading to constitutive activation by AKT and oncogenesis. Recently, Dr. Dixon in collaboration with Nikola Pavletich determined the X-ray structure of PTEN. Their structure–function studies explain the PIP3 substrate specificity of PTEN and also provide a rationale for many of the mutations seen in human cancers. Earlier in his career, Dr. Dixon adopted the tools of molecular biology as they became available in the 1970s, and his laboratory was among the first to use synthetic oligonucleotides to isolate and extensively characterize cDNAs encoding peptide hormones.

Dr. Dixon is Professor of Pharmacology, Cellular and Molecular Medicine and Chemistry and Biochemistry and Dean of Scientific Affairs at the University of California, San Diego. He is a member of the National Academy of Sciences, the Institute of Medicine and the American Academy of Arts and Sciences. Dr. Dixon was the recipient of the 2003 William C. Rose Award from the American Society for Biochemistry and Molecular Biology.

John H. Exton

Howard Hughes Medical Institute, Vanderbilt University School of Medicine, Nashvillie, TN, USA
Section: Signaling

JOHN H. EXTON was born and educated in New Zealand where he received his medical training and a Ph.D. in Biochemistry from the University of Otago in 1963. He did postdoctoral work at Vanderbilt University under Charles R. Park and Earl W. Sutherland, and became an Investigator of the Howard Hughes Medical Institute in 1968 and Professor of Physiology in 1970. He is presently Professor of Molecular Physiology and Biophysics, Professor of Pharmacology and a Hughes Investigator at Vanderbilt.

Dr. Exton's research initially focused on the changes in carbohydrate metabolism in liver during diabetes and treatment with various hormones using the perfused rat liver as the experimental system. His work concentrated on gluconeogenesis and identified the enzymatic reactions that were under control by insulin, epinephrine (adrenaline), glucagon and glucocorticoids, and demonstrated the importance of cyclic AMP in the regulation of these reactions. The role played by the supply of substrates, especially of alanine, was also shown.

Dr. Exton then turned his attention to the action of epinephrine (adrenaline) and demonstrated that many of its actions were not mediated by cyclic AMP but by calcium ions. This led to study of the breakdown of inositol phospholipids by phospholipase C that underlay the increase in calcium. Later this resulted in the discovery of G_q, a novel G protein that activated phospholipase C. Further studies demonstrated that agonists caused the breakdown of another phospholipid (phosphatidylcholine) by another phospholipase (phospholipase D). Current work is focused on the physiological role of phospholipase D.

Dr. Exton has authored over 350 scientific articles and is presently an Associate Editor of the Journal of Biological Chemistry. He has served on many scientific review groups and as a reviewer for many journals. He has won numerous awards, most notably the Lilly

Award of the American Diabetes Association, Fellow of the American Association for the Advancement of Science and election to membership in the National Academy of Sciences.

Paul Modrich

Duke University Medical Center, Durham, NC, USA
Section: Molecular Biology

PAUL MODRICH is an Investigator of the Howard Hughes Medical Institute and James B. Duke Professor of Biochemistry at Duke University Medical Center. He received his undergraduate degree from M.I.T. and his Ph.D. in Biochemistry from Stanford University. His current research addresses the mechanisms of DNA repair. He has served on the editorial boards of the Journal of Biological Chemistry, Biochemistry, Proceedings of the National Academy of Sciences, and DNA Repair. His honors include election to National Academy of Sciences and the Institute of Medicine, the Pfizer Award in Enzyme Chemistry, the General Motors Mott Prize in Cancer Research, and the Pasarow Foundation Award in Cancer Research.

Preface

Biological Chemistry is defined as the chemistry of the compounds and processes that constitute living organisms. The ultimate goal, of course, is to understand and define biology at a mechanistic level. This was aptly stated in an historical treatise on the founding of the *Journal of Biological Chemistry*, where John Edsall quoted a statement in a letter from J. L. Loeb (in Berkeley), "The future of biology lies with those who attack its problems from a chemical point of view." What was an emerging field in 1900 with its origins in physiology, nutrition and chemistry has broadened and expanded to include numerous other fields including mechanistic enzymology, molecular biology, structural biology, cell biology, genomics, proteomics, bioinformatics, metabolomics and others, that were not defined as discrete fields at that time.

Modern biochemistry (biological chemistry) began with the accidental discovery by Eduard Buchner in 1897 that a cell-free yeast extract could carry out fermentation of glucose to alcohol and CO_2 *in the absence of intact cells*. He named the dissolved substance responsible for this process zymase, the substance(s) we now refer to as enzymes. Importantly, Buchner recognized the significance of his discovery. This ended the dogma of the time, perpetuated by Pasteur, the concept of *vitalism*; i.e., that fermentation (and presumably other complex biological phenomena) required the action of intact cells. Thus, serendipity and a prepared mind ushered in a new era of discovery. Now it became possible to dissect complex physiological processes and to study them with preparations free of the constraints of intact cells. Once a metabolic pathway/process was established, it became possible to purify the enzymes, cofactors and substrates involved, to reconstitute the process with purified components and to characterize the components chemically. What followed was an information explosion in the field of biochemistry and progression through a series of trends, each "in vogue" in its time. The identification of the dietary essentials, the hunt for the vitamins/cofactors, the hormones, identification of metabolic pathways and the enzymes involved, oxidative phosphorylation, protein synthesis, molecular biology—each developed as a primary focus.

The need to associate chemistry with function came early and was evident in the naming of departments and journals. Over time names changed from Agricultural Chemistry to Physiological Chemistry to Biochemistry to Biological Chemistry. An example is the Department of Biochemistry at the University of Wisconsin, which began in 1883 as the Department of Agricultural Chemistry.

Where are we headed? We have reached the point where the borders of these areas have become blurred. What constitutes cell biology, molecular biology/genetics, developmental biology, physiology, immunology—ultimately reduces to chemistry. To understand these processes we must know what the molecules are and understand how they interact, i.e. the basic chemistry. That is what this encyclopedia is about.

The breadth of content of this encyclopedia aims to cover major topics of modern biochemistry, each authored by an expert in the area. We feel that the coverage is broad and we have been inclusive in choice of topics. The encyclopedia is a reference work encompassing four volumes containing over 500 articles with more than 750 authors or coauthors. Each article/topic covers an important area of the field which reflects the point of view of the authors. Together the articles cover virtually every aspect of biology for which we have "mechanistic" information. For those who wish to probe more deeply into a topic, references to further readings are included at the end of each article. The editorial board that made decisions on coverage consists of seven members, each an expert representing a major area in the field of biochemistry. A dedicated effort was made to provide coverage that is as complete as possible. The content is presented at a level that we hope will be interpretable to interested individuals with some background in chemistry and biology. It is intended for such individuals rather than specialists with extensive scientific backgrounds in specific areas. It is aimed at the generalist as opposed to the specialist.

Finally, we would like to single out Gail Rice and Dr. Noelle Gracy for their enormous contribution in putting this encyclopedia together. They, in fact, were a driving force that brought this major work to completion.

Notes on the Subject Index

Abbreviations used in subentries without explanation:

CoA	coenzyme A
DAG	diacylglycerol
ELISA	enzyme-linked immunosorbent assay
ERK	extracellular-signal regulated kinase
GlcNAC	N-Acetylglucosamine
HPLC	high-pressure liquid chromatography
IP_3	inositol 1,4,5-triphosphate
MAP	mitogen-activated protein
MMP	matrix metalloproteinase
mtDNA	mitochondrial DNA
NADPH	nicotinamide-adenine dinucleotide phosphate
PFK-2/ FBPase-2	6-phosphofructo-2-kinase/fructose-2,6-bisphosphatase
PI3K	phosphatidylinositol 3-kinase
PIP_2	phosphatidylinositol 4,5-bisphosphate
PIP_3	phosphatidylinositol-3,4,5-triphosphate
PPAR	peroxisome proliferator-activated receptor
RPLC	reversed-phase high-performance liquid chromatography

Volume 1

ABC Transporters, Pages 1-5, Andre Goffeau, Benoit De Hertogh and Philippe V. Baret

Abscisic Acid (ABA), Pages 6-11, Ramanjulu Sunkar and Jian-Kang Zhu

Actin Assembly/Disassembly, Pages 12-18, Henry N. Higgs

Actin-Capping and -Severing Proteins, Pages 19-26, Sankar Maiti and James R. Bamburg

Actin-Related Proteins, Pages 27-33, R. Dyche Mullins

Adenosine Receptors, Pages 34-39, Lauren J. Murphree and Joel Linden

Adenylyl Cyclases, Pages 40-45, Ronald Taussig

Adrenergic Receptors, Pages 46-50, David B. Bylund

Affinity Chromatography, Pages 51-56, Pedro Cuatrecasas and Meir Wilchek

Affinity Tags for Protein Purification, Pages 57-63, Joseph J. Falke and John A. Corbin

A-Kinase Anchoring Proteins, Pages 64-67, Lorene K. Langeberg and John D. Scott

Allosteric Regulation, Pages 68-73, Barry S. Cooperman

Alternative Splicing: Regulation of Fibroblast Growth Factor Receptor (FGFR), Pages 74-77, Mariano A. Garcia-Blanco

Alternative Splicing: Regulation of Sex Determination in Drosophila melanogaster, Pages 78-84, Jill K. M. Penn, Patricia Graham and Paul Schedl

Amine Oxidases, Pages 85-89, Giovanni Floris and Alessandro Finazzi Agro

Amino Acid Metabolism, Pages 90-95, Luc Cynober

Aminopeptidases, Pages 96-98, Ralph A. Bradshaw

Amyloid, Pages 99-104, Ronald Wetzel

Anaplerosis, Pages 105-110, Raymond R. Russell, III and Heinrich Taegtmeyer

Angiotensin Receptors, Pages 111-115, Tadashi Inagami

ara Operon, Pages 116-119, Robert F. Schleif

ARF Family, Pages 120-122, Gustavo Pacheco-Rodriguez, Joel Moss and Martha Vaughan

Aspartic Proteases, Pages 123-127, Ben M. Dunn

ATP Synthesis in Plant Mitochondria: Substrates, Inhibitors, Uncouplers, Pages 128-132, Kathleen L. Soole and R. Ian Menz

ATP Synthesis: Mitochondrial Cyanide-Resistant Terminal Oxidases, Pages 133-137, James N. Siedow

Autophagy in Fungi and Mammals, Pages 138-143, Daniel J. Klionsky and Ju Guan

B12-Containing Enzymes, Pages 145-151, Vahe Bandarian and Rowena G. Matthews

Bax and Bcl2 Cell Death Enhancers and Inhibitors, Pages 152-154, David L. Vaux

B-Cell Antigen Receptor, Pages 155-158, Thomas M. Yankee and Edward A. Clark

Bile Salts and their Metabolism, Pages 159-163, Ulrich Beuers and Thomas Pusl

Biliary Cirrhosis, Primary, Pages 164-169, Marshall M. Kaplan

Bioenergetics: General Definition of Principles, Pages 170-173, David G. Nicholls

Biotin, Pages 174-178, Steven W. Polyak and Anne Chapman-Smith

Biotinylation of Proteins, Pages 179-181, Ronald A. Kohanski

Bradykinin Receptors, Pages 182-185, Ronald M. Burch

Branched-Chain -Ketoacids, Pages 186-191, David T. Chuang

Brassinosteroids, Pages 192-197, Steven D. Clouse

Cadherin Signaling, Pages 199-204, David B. Sacks and Jonathan M. G. Higgins

Cadherin-Mediated Cell-Cell Adhesion, Pages 205-211, Frauke Drees and W. James Nelson

Calcitonin Gene-Related Peptide and Adrenomedullin Receptors, Pages 212-216, Debbie L. Hay, Alex C. Conner and David R. Poyner

Calcitonin Receptor, Pages 217-220, Samia I. Girgis, Niloufar Moradi-Bidhendi, Lucia Mancini and Iain MacIntyre

Calcium Buffering Proteins: Calbindin, Pages 221-225, Willi Hunziker and Igor Bendik

Calcium Buffering Proteins: ER Luminal Proteins, Pages 226-230, Jody Groenendyk and Marek Michalak

Calcium Oscillations, Pages 231-234, Marisa Brini

Calcium Sensing Receptor, Pages 235-240, Jacob Tfelt-Hansen and Edward M. Brown

Calcium Signaling: Calmodulin-Dependent Phosphatase, Pages 241-245, Claude Klee, Hao Ren and Shipeng Li

Calcium Signaling: Cell Cycle, Pages 246-249, Luigia Santella

Calcium Signaling: Motility (Actomyosin-Troponin System), Pages 250-255, Takeyuki Wakabayashi and Setsuro Ebashi

Calcium Signaling: NO Synthase, Pages 256-260, Zhi-Qiang Wang and Dennis J. Stuehr

Calcium Transport in Mitochondria, Pages 261-266, Rosario Rizzuto and Marisa Brini

Calcium Waves, Pages 267-269, Lionel F. Jaffe

Calcium, Biological Fitness of, Pages 270-273, Robert J. P. Williams

Calcium/Calmodulin-Dependent Protein Kinase II, Pages 274-280, Andy Hudmon and Howard Schulman

Calcium/Calmodulin-Dependent Protein Kinases, Pages 281-286, J. Robison and Roger J. Colbran

Calcium-Binding Proteins: Cytosolic (Annexins, Gelsolins, C2-Domain Proteins) , Pages 287-293, Joachim Krebs

Calcium-Modulated Proteins (EF-Hand), Pages 294-299, Robert H. Kretsinger

Calpain, Pages 300-306, Hiroyuki Sorimachi and Yasuko Ono

Carbohydrate Chains: Enzymatic and Chemical Synthesis, Pages 307-313, Thomas J. Tolbert and Chi-Huey Wong

Carnitine and -Oxidation, Pages 314-318, Janos Kerner and Charles L. Hoppel

Caspases and Cell Death, Pages 319-327, Don W. Nicholson, Pierluigi Nicotera and Gerry Melino

Cell Cycle Controls in G1 and G0, Pages 328-331, WengeShi and Steven F. Dowdy

Cell Cycle: Control of Entry and Progression Through S Phase, Pages 332-337, Susan L. Forsburg

Cell Cycle: DNA Damage Checkpoints, Pages 338-344, Jean Y. J. Wang

Cell Cycle: Mitotic Checkpoint, Pages 345-351, Tim J. Yen

Cell Death by Apoptosis and Necrosis, Pages 352-355, Pierluigi Nicotera

Cell Migration, Pages 356-361, J. Victor Small and Emmanuel Vignal

Cell-Matrix Interactions, Pages 362-366, Janet A. Askari and Martin J. Humphries

Centromeres, Pages 367-371, Beth A. Sullivan

Centrosomes and Microtubule Nucleation, Pages 372-376, Reiko Nakajima, Ming-Ying Tsai and Yixian Zheng

c-fes Proto-Oncogene, Pages 377-382, Thomas E. Smithgall and Robert I. Glazer

Chaperones for Metalloproteins, Pages 383-386, Valeria C. Culotta and Edward Luk

Chaperones, Molecular, Pages 387-392, Sue Wickner and Joel R. Hoskins

Chaperonins, Pages 393-398, Arthur L. Horwich, Wayne A. Fenton and George W. Farr

Chemiluminescence and Bioluminescence, Pages 399-404, Thomas O. Baldwin

Chemiosmotic Theory, Pages 405-412, Keith D. Garlid

Chemokine Receptors, Pages 413-418, Ann Richmond and Guo-Huang Fan

Chemolithotrophy, Pages 419-424, Alan B. Hooper

Chemotactic Peptide/Complement Receptors, Pages 425-429, Eric R. Prossnitz and Larry A. Sklar

Chlorophylls and Carotenoids, Pages 430-437, Hugo Scheer

Chloroplast Redox Poise and Signaling, Pages 438-445, John F. Allen

Chloroplasts, Pages 446-450, Nicoletta Rascio

Cholesterol Synthesis, Pages 451-455, Peter A. Edwards

Chromatin Remodeling, Pages 456-463, Eric Kallin and Yi Zhang

Chromatin: Physical Organization, Pages 464-468, Christopher L. Woodcock

Chromosome Organization and Structure, Overview, Pages 469-474, Elena Gracheva and Sarah C. R. Elgin

Coenzyme A, Pages 475-477, M. Daniel Lane

Collagenases, Pages 478-481, Kenn Holmbeck and Henning Birkedal-Hansen

Collagens, Pages 482-487, Darwin J. Prockop

Cyclic AMP Receptors of Dictyostelium, Pages 488-493, Dale Hereld and Peter N. Devreotes

Cyclic GMP Phosphodiesterases, Pages 494-500, Sharron H. Francis and Jackie D. Corbin

Cyclic Nucleotide Phosphodiesterases, Pages 501-505, Vincent C. Manganiello and Eva Degerman

Cyclic Nucleotide-Dependent Protein Kinases, Pages 506-511, Sharron H. Francis and Jackie D. Corbin

Cyclic Nucleotide-Regulated Cation Channels, Pages 512-515, Martin Biel and Franz Hofmann

Cysteine Proteases, Pages 516-520, David J. Buttle and John S. Mort

Cytochrome b6f Complex, Pages 521-527, Gunter A. Hauska and Thomas Schodl

Cytochrome bc1 Complex (Respiratory Chain Complex III), Pages 528-534, Bernard L. Trumpower

Cytochrome c, Pages 535-538, Hans Tuppy and Gunther Kreil

Cytochrome Oxidases, Bacterial, Pages 539-543, Peter Brzezinski and Pia Adelroth

Cytochrome P-450, Pages 544-549, Rita Bernhardt

Cytokines, Pages 550-555, Andrea L. Wurster and Michael J. Grusby

Cytokinesis, Pages 556-561, Masanori Mishima and Michael Glotzer

Cytokinin, Pages 562-567, Thomas Schmulling

Desmosomes and Hemidesmosomes, Pages 569-576, Rachel L. Dusek, Jonathan C. R. Jones and Kathleen J. Green

Detergent Properties, Pages 577-581, Darrell R. McCaslin

Diabetes, Pages 582-592, David W. Cooke

Diacylglycerol Kinases and Phosphatidic Acid Phosphatases, Pages 593-597, Stephen M. Prescott and Matthew K. Topham

Disulfide Bond Formation, Pages 598-602, Hiram F. Gilbert

DNA Base Excision Repair, Pages 603-608, Hilde Nilsen and Tomas Lindahl

DNA Damage: Alkylation, Pages 609-613, Anton B. Guliaev and B. Singer

DNA Glycosylases: Mechanisms, Pages 614-617, Daniel J. Krosky and James T. Stivers

DNA Helicases: Dimeric Enzyme Action, Pages 618-623, Timothy M. Lohman

DNA Helicases: HexamericEnzyme Action, Pages 624-631, Smita S. Patel

DNA Ligases: Mechanism and Functions, Pages 632-636, Alan E. Tomkinson and John B. Leppard

DNA Ligases: Structures, Pages 637-643, C. Kiong Ho, Mark Odell and Dimitar B. Nikolov

DNA Methyltransferases, Bacterial, Pages 644-651, Albert Jeltsch and Richard I. Gumport

DNA Methyltransferases, Structural Themes, Pages 652-659, Sanjay Kumar

DNA Methyltransferases: Eubacterial GATC, Pages 660-664, Martin G. Marinus

DNA Mismatch Repair and Homologous Recombination, Pages 665-670, Ivan Matic and Miroslav Radman

DNA Mismatch Repair and the DNA Damage Response, Pages 671-674, Guo-Min Li and Steven R. Presnell

DNA Mismatch Repair Defects and Cancer, Pages 675-681, Richard D. Kolodner

DNA Mismatch Repair in Bacteria, Pages 682-686, A-Lien Lu

DNA Mismatch Repair in Mammals, Pages 687-690, James T. Drummond

DNA Mismatch Repair: E. coli Vsr and Eukaryotic G-T Systems, Pages 691-693, Margaret Lieb

DNA Oxidation, Pages 694-697, Arthur P. Grollman and Dmitry O. Zharkov

DNA Photolyase, Pages 698-702, Carrie L. Partch and Aziz Sancar

DNA Polymerase, Eukaryotic α, Pages 703-707, Teresa S. -F. Wang

DNA Polymerase, Eukaryotic β, Pages 708-712, William A. Beard and Samuel H. Wilson

DNA Polymerase, Eukaryotic δ, Pages 713-715, Antero G. So and Kathleen M. Downey

DNA Polymerase, Eukaryotic ε, Pages 716-719, Yasuo Kawasaki and Akio Sugino

DNA Polymerase I, Bacterial, Pages 720-725, Catherine M. Joyce

DNA Polymerase II, Bacterial, Pages 726-728, Judith L. Campbell

DNA Polymerase III, Bacterial, Pages 729-733, Hisaji Maki

DNA Polymerases: Kinetics and Mechanism, Pages 734-739, Kenneth A. Johnson

DNA Replication Fork, Bacterial, Pages 740-744, Nancy G. Nossal

DNA Replication Fork, Eukaryotic, Pages 745-748, Lori M. Kelman, Jerard Hurwitz and Zvi Kelman

DNA Replication, Mitochondrial, Pages 749-752, David A. Clayton

DNA Replication: Eukaryotic Origins and the Origin Recognition Complex, Pages 753-760, Melvin L. DePamphilis and Cong-jun Li

DNA Replication: Initiation in Bacteria, Pages 761-766, Jon M. Kaguni

DNA Restriction and Modification: Type I Enzymes, Pages 767-771, David T. F. Dryden

DNA Restriction and Modification: Type II Enzymes, Pages 772-777, Darren M. Gowers and Stephen E. Halford

DNA Restriction and Modification: Type III Enzymes, Pages 778-781, Desirazu N. Rao and S. Srivani

DNA Secondary Structure, Pages 782-787, Albino Bacolla and Robert D. Wells

DNA Sequence Recognition by Proteins, Pages 788-793, Arabela A. Grigorescu and John M. Rosenberg

DNA Supercoiling, Pages 794-797, Tao-shih Hsieh

DNA Topoisomerases: Type I, Pages 798-805, James J. Champoux

DNA Topoisomerases: Type II, Pages 806-811, Renier Velez-Cruz and Neil Osheroff

DNA Topoisomerases: Type III-RecQ Helicase Systems, Pages 812-816, Rodney Rothstein and Erika Shor

Dopamine Receptors, Pages 817-822, Kim A. Neve

Dynactin, Pages 823-826, Trina A. Schroer

Dynein, Pages 827-831, K. Kevin Pfister

Volume 2

EF-G and EF-Tu Structures and Translation Elongation in Bacteria, Pages 1-5, Poul Nissen and Jens Nyborg

Eicosanoid Receptors, Pages 6-9, Richard M. Breyer and Matthew D. Breyer

Elastin, Pages 10-12, Judith Ann Foster

Endocannabinoids, Pages 13-15, Daniele Piomelli

Endocytosis, Pages 16-19, Julie G. Donaldson

Endoplasmic Reticulum-Associated Protein Degradation, Pages 20-23, Maurizio Molinari

Energy Transduction in Anaerobic Prokaryotes, Pages 24-30, Gottfried Unden

Enzyme Inhibitors, Pages 31-37, Vern L. Schramm

Enzyme Kinetics, Pages 38-44, Irwin H. Segel

Enzyme Reaction Mechanisms: Stereochemistry, Pages 45-50, Ming-Daw Tsai, Li Zhao and Brandon J. Lamarche

Epidermal Growth Factor Receptor Family, Pages 51-55, Denis Tvorogov and Graham Carpenter

ER/SR Calcium Pump: Function, Pages 56-60, Giuseppe Inesi

ER/SR Calcium Pump: Structure, Pages 61-65, Chikashi Toyoshima and Yuji Sugita

Exonucleases, Bacterial, Pages 66-72, Susan T. Lovett

F1-F0 ATP Synthase, Pages 73-79, Donata Branca

FAK Family, Pages 80-84, Steven K. Hanks

Fat Mobilization: Perilipin and Hormone-Sensitive Lipase, Pages 85-89, Constantine Londos and Alan R. Kimmel

Fatty Acid Oxidation, Pages 90-94, Horst Schulz

Fatty Acid Receptors, Pages 95-98, Christer Owman and Bjorn Olde

Fatty Acid Synthesis and its Regulation, Pages 99-103, Steven D. Clarke and Manabu T. Nakamura

Ferredoxin, Pages 104-106, Giuliana Zanetti and Vittorio Pandini

Ferredoxin-NADP+ Reductase, Pages 107-111, Giuliana Zanetti and Alessandro Aliverti

Fibroblast Growth Factor Receptors and Cancer-Associated Perturbations, Pages 112-117, Marko Kornmann and Murray Korc

Flavins, Pages 118-122, Barrie Entsch and David P. Ballou

Flippases, Pages 123-127, Charles J. Waechter

Focal Adhesions, Pages 128-133, Eli Zamir and Benjamin Geiger

Free Radicals, Sources and Targets of: Mitochondria, Pages 134-142, Alberto Boveris and Enrique Cadenas

Friedreich's Ataxia, Pages 143-145, Paul E. Hart and Anthony H. V. Schapira

G Protein Signaling Regulators, Pages 147-151, John H. Exton

G Protein-Coupled Receptor Kinases and Arrestins, Pages 152-157, Jeffrey L. Benovic

G12/G13 Family, Pages 158-161, Stefan Offermanns

GABAA Receptor, Pages 162-166, Richard W. Olsen and Gregory W. Sawyer

GABAB Receptor, Pages 167-170, S. J. Enna

Galectins, Pages 171-174, R. Colin Hughes

Genome-Wide Analysis of Gene Expression, Pages 175-180, Karine G. Le Roch and Elizabeth A. Winzeler

Gi Family of Heterotrimeric G Proteins, Pages 181-185, Maurine E. Linder

Giant Mitochondria (Megamitochondria), Pages 186-188, Bernard Tandler and Charles L. Hoppel

GlcNAc Biosynthesis and Function, O-Linked, Pages 189-192, Kaoru Sakabe and Gerald W. Hart

Glucagon Family of Peptides and their Receptors, Pages 193-196, Laurie L. Baggio and Daniel J. Drucker

Gluconeogenesis, Pages 197-203, Richard W. Hanson and Oliver E. Owen

Glucose/Sugar Transport in Bacteria, Pages 204-207, Lan Guan and H. Ronald Kaback

Glucose/Sugar Transport in Mammals, Pages 208-212, Silvia Mora and Jeffrey Pessin

Glutamate Receptors, Ionotropic, Pages 213-219, Derek B. Scott and Michael D. Ehlers

Glutamate Receptors, Metabotropic, Pages 220-223, P. Jeffrey Conn

Glutathione Peroxidases, Pages 224-228, Fulvio Ursini and Matilde Maiorino

Glycation, Pages 229-236, Suzanne R. Thorpe and John W. Baynes

Glycine Receptors, Pages 237-243, Bodo Laube and Heinrich Betz

Glycogen Metabolism, Pages 244-248, Peter J. Roach

Glycogen Storage Diseases, Pages 249-254, George H. Sack, Jr.

Glycogen Synthase Kinase-3, Pages 255-260, James R. Woodgett

Glycolipid-Dependent Adhesion Processes, Pages 261-265, Senitiroh Hakomori

Glycolysis, Overview, Pages 266-271, Robert A. Harris

Glycoprotein Folding and Processing Reactions, Pages 272-276, Armando J. Parodi

Glycoprotein-Mediated Cell Interactions, O-Linked, Pages 277-282, Robert S. Haltiwanger

Glycoproteins, N-Linked, Pages 283-292, Mark A. Lehrman

Glycoproteins, Plant, Pages 293-296, Carolyn J. Schultz

Glycosylation in Cystic Fibrosis, Pages 297-301, Andrew D. Rhim, Thomas F. Scanlin and Mary Catherine Glick

Glycosylation, Congenital Disorders of, Pages 302-307, Hudson H. Freeze

Glycosylphosphatidylinositol (GPI) Anchors, Pages 308-311, Anant K. Menon

Golgi Complex, Pages 312-315, Mark Stamnes

Gq Family, Pages 316-320, Wanling Yang and John D. Hildebrandt

Green Bacteria: Secondary Electron Donor (Cytochromes), Pages 321-324, Hirozo Oh-oka and Robert E. Blankenship

Green Bacteria: The Light-Harvesting Chlorosome, Pages 325-330, John M. Olson

Green Sulfur Bacteria: Reaction Center and Electron Transport, Pages 331-336, Gunter A. Hauska and Thomas Schodl

Gs Family of Heterotrimeric G Proteins, Pages 337-341, Susanne M. Mumby

Heat/Stress Responses, Pages 343-347, Davis T. W. Ng

Hematopoietin Receptors, Pages 348-353, Barbara A. Miller and Joseph Y. Cheung

Heme Proteins, Pages 354-361, Johannes Everse

Heme Synthesis, Pages 362-366, Gloria C. Ferreira

Hepatocyte Growth Factor/Scatter Factor Receptor, Pages 367-371, Selma Pennacchietti and Paolo M. Comoglio

Hexokinases/Glucokinases, Pages 372-377, Emile Van Schaftingen

Histamine Receptors, Pages 378-383, Stephen J. Hill and Jillian G. Baker

HIV Protease, Pages 384-387, Ben M. Dunn

HIV-1 Reverse Transcriptase Structure, Pages 388-392, Kalyan Das, Stefan G. Sarafianos, Eddy Arnold and Stephen H. Hughes

Homologous Recombination in Meiosis, Pages 393-397, Nancy M. Hollingsworth

HPLC Separation of Peptides, Pages 398-403, James D. Pearson

Imaging Methods, Pages 405-410, Gyorgy Szabadkai and Rosario Rizzuto

Immunoglobulin (Fc) Receptors, Pages 411-416, Mark Hogarth

Inorganic Biochemistry, Pages 417-420, Robert J. P. Williams

Inositol Lipid 3-Phosphatases, Pages 421-426, Gregory S. Taylor and Jack E. Dixon

Inositol Phosphate Kinases and Phosphatases, Pages 427-429, Stephen B. Shears

Insulin- and Glucagon-Secreting Cells of the Pancreas, Pages 430-435, Franz M. Matschinsky

Insulin Receptor Family, Pages 436-440, Paul F. Pilch and Jongsoon Lee

Integrin Signaling, Pages 441-445, Lawrence E. Goldfinger and Mark H. Ginsberg

Interferon Receptors, Pages 446-451, Christopher P. Elco and Ganes C. Sen

Intermediate Filament Linker Proteins: Plectin and BPAG1, Pages 452-457, Peter Fuchs and Gerhard Wiche

Intermediate Filaments, Pages 458-464, Kelsie M. Bernot and Pierre A. Coulombe

Intracellular Calcium Channels: cADPR-Modulated (Ryanodine Receptors), Pages 465-468, Antony Galione

Intracellular Calcium Channels: NAADP+-Modulated, Pages 469-472, Armando A. Genazzani and Marcella Debidda

Ion Channel Protein Superfamily, Pages 473-477, William A. Catterall

IP3 Receptors, Pages 478-481, Colin W. TaylorEdward Morris and Paula da Fonseca

Iron-Sulfur Proteins, Pages 482-489, Helmut Beinert

JAK-STAT Signaling Paradigm, Pages 491-496, Edward Cha and Christian Schindler

Keratins and the Skin, Pages 497-504, Pierre A. Coulombe and Kelsie M. Bernot

Ketogenesis, Pages 505-507, Janos Kerner and Charles L. Hoppel

Kinesin Superfamily Proteins, Pages 508-516, Nobutaka Hirokawa and Reiko Takemura

Kinesins as Microtubule Disassembly Enzymes, Pages 517-521, Susan L. Kline-Smith and Arshad Desai

Kinetic Isotope Effects, Pages 522-527, Justine P. Roth and Judith P. Klinman

lac Operon, Pages 529-534, Liskin Swint-Kruse and Kathleen S. Matthews

Lectins, Pages 535-540, Nathan Sharon and Halina Lis

Leptin, Pages 541-545, Thomas W. Gettys

LexA Regulatory System, Pages 546-550, Veronica G. Godoy, Penny J. Beuning and Graham C. Walker

Ligand-Operated Membrane Channels: Calcium (Glutamate), Pages 551-561, Elias K. Michaelis

Ligand-Operated Membrane Channels: GABA, Pages 562-566, F. Minier and Erwin Sigel

Light-Harvesting Complex (LHC) I and II: Pigments and Proteins, Pages 567-570, Stefan Jansson

Lipases, Pages 571-575, Howard L. Brockman

Lipid Bilayer Structure, Pages 576-579, Erwin London

Lipid Modification of Proteins: Targeting to Membranes, Pages 580-583, Marilyn D. Resh

Lipid Rafts, Pages 584-587, Deborah A. Brown

Lipoproteins, HDL/LDL, Pages 588-593, Fayanne E. Thorngate and David L. Williams

Low Barrier Hydrogen Bonds, Pages 594-598, Perry A. Frey

Luft's Disease, Pages 599-601, Salvatore DiMauro

Lysophospholipid Receptors, Pages 602-604, Gabor J. Tigyi

MDR Membrane Proteins, Pages 605-609, Nathan C. Rockwell

Meiosis, Pages 610-616, Neil Hunter

Melanocortin System, Pages 617-620, Roger D. Cone

Membrane Fusion, Pages 621-626, Joshua Zimmerberg and Leonid V. Chernomordik

Membrane Transport, General Concepts, Pages 627-630, Stanley G. Schultz

Membrane Transporters:Na+/Ca2+ Exchangers, Pages 631-636, Jonathan Lytton

Membrane-Associated Energy Transduction in Bacteria and Archaea, Pages 637-645, Gunter Schafer

Metabolite Channeling: Creatine Kinase Microcompartments, Pages 646-651, Uwe Schlattner and Theo Wallimann

Metalloproteases, Pages 652-656, David S. Auld

Metalloproteinases, Matrix, Pages 657-665, Hideaki Nagase and Gillian Murphy

Metaphase Chromosome, Pages 666-671, Sharron Vass and Margarete M. S. Heck

Methyl-CpG-Binding Proteins, Pages 672-675, David G. Skalnik

Microtubule-Associated Proteins, Pages 676-682, Nobutaka Hirokawa and Reiko Takemura

Mitochondrial Auto-Antibodies, Pages 683-688, Harold Baum

Mitochondrial Channels, Pages 689-692, M. Catia Sorgato and Alessandro Bertoli

Mitochondrial DNA, Pages 693-696, Gottfried Schatz

Mitochondrial Genes and their Expression: Yeast, Pages 697-702, Piotr P. Slonimski and Giovanna Carignani

Mitochondrial Genome, Evolution, Pages 703-708, B. Franz Lang, Dennis V. Lavrov and Gertraud Burger

Mitochondrial Genome, Overview, Pages 709-715, Douglas C. Wallace

Mitochondrial Inheritance, Pages 716-719, Eric A. Shoubridge

Mitochondrial Membranes, Structural Organization, Pages 720-724, Carmen A. Mannella

Mitochondrial Metabolite Transporter Family, Pages 725-732, Ferdinando Palmieri and Martin Klingenberg

Mitochondrial Outer Membrane and the VDAC Channel, Pages 733-736, Marco Colombini

Mitogen-Activated Protein Kinase Family, Pages 737-742, Hidemi Teramoto and J. Silvio Gutkind

Mitosis, Pages 743-747, Patricia Wadsworth and Nasser M. Rusan

mRNA Polyadenylation in Eukaryotes, Pages 748-752, Mary Edmonds

mRNA Processing and Degradation in Bacteria, Pages 753-757, Deborah A. Steege

Mucin Family of Glycoproteins, Pages 758-764, Juan Perez-Vilar and Robert L. Hill

Mucins in Embryo Implantation, Pages 765-769, Daniel D. Carson

Multiple Sequence Alignment and Phylogenetic Trees, Pages 770-774, Russell F. Doolittle

Muscarinic Acetylcholine Receptors, Pages 775-777, Neil M. Nathanson

Myosin Motors, Pages 778-781, Roy E. Larson

Volume 3

Natriuretic Peptides and their Receptors, Pages 1-5, Lincoln R. Potter

N-End Rule, Pages 6-10, Alexander Varshavsky

Neoglycoproteins, Pages 11-15, Y. C. Lee and Reiko T. Lee

Neuronal Calcium Signal, Pages 16-20, Hilmar Bading

Neuronal Intermediate Filaments, Pages 21-25, Ronald K. H. Liem

Neuropeptide Y Receptors, Pages 26-31, Eric M. Parker

Neurotensin Receptors, Pages 32-36, William Rostene, Patrick Kitabgi and Didier Pelaprat

Neurotransmitter Transporters, Pages 37-40, Aurelio Galli, Randy D. Blakely and Louis J. DeFelice

Neurotrophin Receptor Signaling, Pages 41-45, Jennifer J. Gentry and Bruce D. Carter

Nicotinamide Nucleotide Transhydrogenase, Pages 50-56, Jan Rydstrom

Nicotinic Acetylcholine Receptors, Pages 57-61, Nivalda O. Rodrigues-Pinguet and Henry A. Lester

Nitric Oxide Signaling, Pages 62-65, Michael A. Marletta

N-Linked Glycan Processing Glucosidases and Mannosidases, Pages 46-49, Linda O. Tremblay and Annette Herscovics

Non-Homologous End Joining, Pages 66-70, Penny A. Jeggo

Nonhomologous Recombination: Bacterial Transposons, Pages 71-79, Bao Ton Hoang and Michael G. Chandler

Nonhomologous Recombination: Retrotransposons, Pages 80-86, Siew Loon Ooi and Jef D. Boeke

Nuclear Compartmentalization, Pages 87-91, Kelly P. Smith and Jeanne B. Lawrence

Nuclear Envelope and Lamins, Pages 92-95, Bryce M. Paschal

Nuclear Factor kappaB, Pages 96-99, Thomas D. Gilmore

Nuclear Genes in Mitochondrial Function and Biogenesis, Pages 100-104, Alexander Tzagoloff and Carol L. Dieckmann

Nuclear Organization, Chromatin Structure, and Gene Silencing , Pages 105-108, Lori L. Wallrath, John R. Danzer, Oya Yazgan and Pamela K. Geyer

Nuclear Pores and Nuclear Import/Export, Pages 109-114, Anita H. Corbett

Nucleoid Organization of Bacterial Chromosomes, Pages 115-118, Charles J. Dorman

Nucleolus, Overview, Pages 119-122, Thoru Pederson

Nucleotide Excision Repair and Human Disease, Pages 123-129, James E. Cleaver

Nucleotide Excision Repair in Eukaryotes, Pages 130-133, Laura A. Lindsey-Boltz and Aziz Sancar

Nucleotide Excision Repair, Bacterial: The UvrABCD System, Pages 134-142, Bennett Van Houten and Lawrence Grossman

Nucleotide Excision Repair: Biology, Pages 143-147, Errol C. Friedberg

Olfactory Receptors, Pages 149-154, Sigrun I. Korsching

Oligosaccharide Analysis by Mass Spectrometry, Pages 155-160, Andrew J. Hanneman and Vernon N. Reinhold

Oligosaccharide Chains: Free, N-Linked, O-Linked, Pages 161-164, Tadashi Suzuki

Oncocytes, Pages 165-166, Bernard Tandler and Charles L. Hoppel

Opioid Receptors, Pages 167-171, P. Y. Law and Horace H. Loh

Ornithine Cycle, Pages 172-177, Malcolm Watford

Oxygenases, Pages 178-182, Osamu Hayaishi

P2X Purinergic Receptors, Pages 183-187, Annmarie Surprenant

P2Y Purinergic Receptors, Pages 188-191, George R. Dubyak

p53 Protein, Pages 192-195, Jamie Hearnes and Jennifer Pietenpol

p70 S6 Kinase/mTOR, Pages 196-200, Christopher G. Proud

Parathyroid Hormone/Parathyroid Hormone-Related Protein Receptor, Pages 201-207, Thomas J. Gardella

PCR (Polymerase Chain Reaction), Pages 208-210, Michael J. Brownstein

Pentose Phosphate (Hexose Mono Phosphate) Pathway, Pages 211-215, Bernard R. Landau

Pentose Phosphate Pathway, History of, Pages 216-225, John F. Williams

Peptide Amidation, Pages 226-230, Mark J. Niciu, Richard E. Mains and Betty A. Eipper

Periplasmic Electron Transport Systems in Bacteria, Pages 231-238, David J. Richardson, Gary Sawers and Rob J. M. Van Spanning

Peroxisome Proliferator-Activated Receptors, Pages 239-245, Mary C. Sugden, Edward A. Sugden and Mark J. Holness

Peroxisomes, Pages 246-250, Suresh Subramani

Phage Display for Protein Binding, Pages 251-255, Henry B. Lowman

Pheromone Receptors (Yeast), Pages 256-261, James B. Konopka and Jeremy W. Thorner

PHO Regulon, Pages 262-265, Bengt L. Persson

Phosphatidylinositol Bisphosphate and Trisphosphate, Pages 266-271, Alex Toker

Phosphatidylinositol-3-Phosphate, Pages 272-276, Joseph V. Virbasius and Michael P. Czech

Phosphofructokinase-2/Fructose Bisphosphatase-2, Pages 277-280, Daniel M. Raben

Phosphoinositide 3-Kinase, Pages 281-286, Khatereh Ahmadi and Michael Waterfield

Phosphoinositide 4- and 5-Kinases and Phosphatases, Pages 287-291, Shawn F. Bairstow, Matthew W. Bunce and Richard A. Anderson

Phosphoinositide-Dependent Protein Kinases, Pages 292-296, Nick R. Leslie and C. Peter Downes

Phospholipase A2, Pages 297-300, Timothy R. Smith and Edward A. Dennis

Phospholipase C, Pages 301-305, Fujio Sekiya, Yeun Ju Kim and Sue Goo Rhee

Phospholipase D, Pages 306-313, Mary M. LaLonde and Michael A. Frohman

Phospholipid Metabolism in Mammals, Pages 314-320, Claudia Kent

Phospholipid Synthesis in Yeast, Pages 321-325, Gil-Soo Han and George M. Carman

Photoreceptors, Pages 326-329, King-Wai Yau

Photosynthesis, Pages 330-335, Richard C. Leegood

Photosynthetic Carbon Dioxide Fixation, Pages 336-341, Matthew J. Paul

Photosystem I, Structure and Function, Pages 342-347, Petra Fromme

Photosystem I: FX, FA, and FB Iron-Sulfur Clusters, Pages 348-356, Mikhail L. Antonkine and John H. Golbeck

Photosystem II Light Harvesting System: Dynamic Behavior, Pages 357-362, Peter Horton and Alexander Ruban

Photosystem II: Assembly and Turnover of the D1 Protein, Pages 363-366, Eira Kanervo and Eva-Mari Aro

Photosystem II: Protein Components, Pages 367-374, James Barber

Photosystem II: Water Oxidation, Overview, Pages 375-380, Fabrice Rappaport and Pierre Joliot

Plant Signaling: Peptides, Pages 381-384, Clarence A. Ryan and Gregory Pearce

Plasma-Membrane Calcium Pump: Structure and Function, Pages 385-389, Emanuel E. Strehler

Plastocyanin, Pages 390-393, Elizabeth L. Gross

Platelet-Activating Factor Receptor, Pages 394-398, Katherine M. Howard and Merle S. Olson

Platelet-Derived Growth Factor Receptor Family, Pages 399-406, Marina Kovalenko and Andrius Kazlauskas

Polysialic Acid inMolecular Medicine, Pages 407-414, Frederic A. Troy, II

Porphyrin Metabolism, Pages 415-419, Mark Shepherd and Harry A. Dailey

Pre-tRNA and Pre-rRNA Processing in Bacteria, Pages 420-424, Sidney R. Kushner

Pre-tRNA and Pre-rRNA Processing in Eukaryotes, Pages 425-431, Hendrik A. Raue

Prions and Epigenetic Inheritance, Pages 432-436, Reed B. Wickner

Prions, Overview, Pages 437-440, Cedric Govaerts and Fred E. Cohen

Processivity Clamps in DNA Replication: Clamp Loading, Pages 441-446, Megan J. Davey and Mike O'Donnell

Propionyl CoA-Succinyl CoA Pathway, Pages 447-451, Wayne A. Fenton

Prostaglandins and Leukotrienes, Pages 452-456, William L. Smith and Robert C. Murphy

Proteases in Blood Clotting, Pages 457-463, John D. Kulman and Earl W. Davie

Proteasomes, Overview, Pages 464-468, Martin Rechsteiner

26S Proteasome, Structure and Function, Pages 469-473, Peter Zwickl and Wolfgang Baumeister

Protein Carboxyl Esterification, Pages 474-477, Shilpa G. Lalchandani and Jeffry B. Stock

Protein Data Resources, Pages 478-483, Philip E. Bourne

Protein Degradation, Pages 484-492, Tomo ari and Alfred L. Goldberg

Protein Folding and Assembly, Pages 493-499, David P. Goldenberg

Protein Glycosylation Inhibitors, Pages 500-503, Alan D. Elbein

Protein Glycosylation, Overview, Pages 504-509, Natasha E. Zachara and Gerald W. Hart

Protein Import into Mitochondria, Pages 510-515, Johannes M. Herrmann and Walter Neupert

Protein Kinase B, Pages 516-522, Bettina A. Dummler and Brian A. Hemmings

Protein Kinase C Family, Pages 523-526, Alexandra C. Newton

Protein N-Myristoylation, Pages 527-531, Erica Dutil Sonnenburg and Jeffrey I. Gordon

Protein Palmitoylation, Pages 532-535, Robert J. Deschenes

Protein Tyrosine Phosphatases, Pages 536-542, David J. Pagliarini, Fred L. Robinson and Jack E. Dixon

Proteinase-Activated Receptors, Pages 543-548, Kristina K. Hansen and Morley D. Hollenberg

Proteoglycans, Pages 549-555, Sara K. Olson and Jeffrey D. Esko

Pteridines, Pages 556-560, S. Colette Daubner and Paul F. Fitzpatrick

P-Type Pumps: Copper Pump, Pages 561-564, Ilia Voskoboinik and James Camakaris

P-Type Pumps: H+/K+ Pump, Pages 565-570, Jai Moo Shin and George Sachs

P-Type Pumps: Na+/K+ Pump, Pages 571-576, Peter L. Jorgensen

P-Type Pumps: Plasma-Membrane H+ Pump, Pages 577-581, A. Brett Mason and Carolyn W. Slayman

Purple Bacteria: Electron Acceptors and Donors, Pages 582-585, Evaldas Katilius and Neal W. Woodbury

Purple Bacteria: Photosynthetic Reaction Centers, Pages 586-594, C. Roy D. Lancaster

Pyridoxal Phosphate, Pages 595-599, David E. Metzler

Pyrimidine Biosynthesis, Pages 600-605, Monika Loffler and Elke Zameitat

Pyruvate Carboxylation, Transamination, and Gluconeogenesis, Pages 606-610, Sarawut Jitrapakdee and John C. Wallace

Pyruvate Dehydrogenase, Pages 611-615, Sam A. Johnson and James G. McCormack

Pyruvate Kinase, Pages 616-619, Kosaku Uyeda

Quinones, Pages 621-627, Giorgio Lenaz and Maria Luisa Genova

Rab Family, Pages 629-634, Mary W. McCaffrey and Andrew J. Lindsay

Ran GTPase, Pages 635-639, Mary Shannon Moore

Ras Family, Pages 640-644, Lawrence A. Quilliam

Recombination: Heteroduplexand Mismatch Repair in vitro, Pages 645-648, Leroy Worth

Recombination: Strand Transferases, Pages 649-653, Floyd R. Bryant

Recombination-Dependent DNA Replication, Pages 654-659, Kenneth N. Kreuzer

recQ DNA Helicase Family in Genetic Stability, Pages 660-664, Mary A. Risinger and Joanna Groden

Regulated Intramembrane Proteolysis (Rip), Pages 665-670, Jin Ye, Michael S. Brown and Joseph L. Goldstein

Respiratory Chain and ATP Synthase, Pages 671-675, David G. Whitehouse and Anthony L. Moore

Respiratory Chain Complex I, Pages 676-680, Ulrich Brandt

Respiratory Chain Complex II and Succinate: Quinone Oxidoreductases, Pages 681-687, C. Roy D. Lancaster

Respiratory Chain Complex IV, Pages 688-694, Hartmut Michel

Respiratory Processes in Anoxygenic and Oxygenic Phototrophs, Pages 695-699, Roberto Borghese and Davide Zannoni

Retinoblastoma Protein (pRB), Pages 700-703, Nicholas Dyson and Maxim Frolov

Retinoic Acid Receptors, Pages 704-707, Martin Petkovich

Reverse Transcriptase and Retroviral Replication, Pages 708-713, Laura Tarrago-Litvak, Marie-Line Andreola and Simon Litvak

Rho GTPases and Actin Cytoskeleton Dynamics, Pages 714-718, Priam Villalonga and Anne J. Ridley

Ribosome Assembly, Pages 719-724, John L. Woolford

Ribosome Structure, Pages 725-732, Brian T. Wimberly

Ribozyme Mechanisms, Pages 733-737, John Hsieh and Carol A. Fierke

Ribozyme Structural Elements: Group I Introns, Pages 738-742, Barbara L. Golden

Ribozyme Structural Elements: Hairpin Ribozyme, Pages 743-746, Adrian R. Ferre-D'Amare

Ribozymes and Evolution, Pages 747-752, Niles Lehman

RNA Editing, Pages 753-758, Charles E. Samuel

RNA Polymerase I and RNA Polymerase III in Eukaryotes, Pages 759-762, Robert J. White

RNA Polymerase II and Basal Transcription Factors in Eukaryotes, Pages 763-765, Joan Weliky Conaway and Ronald C. Conaway

RNA Polymerase II Elongation Control in Eukaryotes, Pages 766-769, David H. Price

RNA Polymerase II Structure in Eukaryotes, Pages 770-774, Patrick Cramer

RNA Polymerase Reaction in Bacteria, Pages 775-780, Arkady A. Mustaev and Alexander D. Goldfarb

RNA Polymerase Structure, Bacterial, Pages 781-784, Michael Anikin, Dmitri Temiakov and William T. McAllister

Volume 4

Secondary Structure in Protein Analysis, Pages 1-6, George D. Rose

Secretases, Pages 7-10, Robert L. Heinrikson

Secretory Pathway, Pages 11-16, Karen J. Colley

Selenoprotein Synthesis, Pages 17-21, August Bock

Septins and Cytokinesis, Pages 22-26, Makoto Kinoshita and Christine M. Field

Serine/Threonine Phosphatases, Pages 27-32, Thomas S. Ingebritsen

Serotonin Receptor Signaling, Pages 33-37, Paul J. Gresch and Elaine Sanders-Bush

Siglecs, Pages 38-40, Ajit Varki

Sigma Factors, Pages 41-44, John D. Helmann

Sliding Clamps in DNA Replication: E. coli -Clamp and PCNA Structure, Pages 45-47, Eric R. Goedken and John Kuriyan

Small GTPases, Pages 48-54, Adam Shutes and Channing J. Der

Somatostatin Receptors, Pages 55-60, Agnes Schonbrunn

Spastic Paraplegia, Pages 61-66, Elena Irene Rugarli and Andrea Ballabio

Spectrophotometric Assays, Pages 67-75, Britton Chance

Sphingolipid Biosynthesis, Pages 76-81, Martina Leipelt and Alfred H. Merrill

Sphingolipid Catabolism, Pages 82-87, Akira Abe and James A. Shayman

Spliceosome, Pages 88-92, Timothy W. Nilsen

Src Family of Protein Tyrosine Kinases, Pages 93-98, Jonathan A. Cooper

Starvation, Pages 99-110, Oliver E. Owen and Richard W. Hanson

Steroid/Thyroid Hormone Receptors, Pages 111-116, Ramesh Narayanan and Nancy L. Weigel

Store-Operated Membrane Channels: Calcium, Pages 117-122, Indu S. Ambudkar

Substrate Binding, Catalysis, and Product Release , Pages 123-126, W. Wallace Cleland

Sugar Nucleotide Transporters, Pages 127-129, Carlos B. Hirschberg

SUMO Modification, Pages 130-134, Frauke Melchior and Andrea Pichler

Superoxide Dismutase, Pages 135-138, Irwin Fridovich

Syk Family of Protein Tyrosine Kinases, Pages 139-145, Andrew C. Chan

T7 RNA Polymerase, Pages 147-151, Rui Sousa

Tachykinin/Substance P Receptors, Pages 152-157, Mark D. Richardson and Madan M. Kwatra

Taste Receptors, Pages 158-161, John D. Boughter, Jr. and Steven D. Munger

T-Cell Antigen Receptor, Pages 162-168, Andrea L. Szymczak and Dario A. A. Vignali

Tec/Btk Family Tyrosine Kinases, Pages 169-173, Shuling Guo and Owen N. Witte

Telomeres: Maintenance and Replication, Pages 174-179, Alessandro Bianchi and David Shore

Thyroid-Stimulating Hormone/Luteinizing Hormone/Follicle-Stimulating Hormone Receptors, Pages 180-186, Deborah L. Segaloff, Dario Mizrachi and Mario Ascoli

Tight Junctions, Pages 187-189, Shoichiro Tsukita

Title, Pages, Authors

Toll-Like Receptors, Pages 190-194, Himanshu Kumar, Kiyoshi Takeda and Shizuo Akira

Transcription Termination, Pages 195-199, Thomas J. Santangelo and Jeffrey W. Roberts

Transcriptional Silencing, Pages 200-203, Ann Sutton and Rolf Sternglanz

Transcription-Coupled DNA Repair, Overview, Pages 204-208, Isabel Mellon

Transforming Growth Factor-β Receptor Superfamily, Pages 209-213, Mark de Caestecker

Translation Elongation in Bacteria, Pages 214-223, Oliver Vesper and Knud H. Nierhaus

Translation Elongation in Eukaryotes, Pages 224-229, William C. Merrick and Anton A. Komar

Translation Initiation in Bacteria: Factors and Mechanisms, Pages 230-236, Cynthia L. Pon and Claudio O. Gualerzi

Translation Initiation in Eukaryotes: Factors and Mechanisms, Pages 237-241, Tatyana V. Pestova and Christopher U. T. Hellen

Translation Termination and Ribosome Recycling, Pages 242-246, Nadja Koloteva-Levin and Mick F. Tuite

Translesion DNA Polymerases, Eukaryotic, Pages 247-250, Alexandra Vaisman and Roger Woodgate

Trehalose Metabolism, Pages 251-255, Alan D. Elbein

Tricarboxylic Acid Cycle, Pages 256-262, Richard L. Veech

tRNA Synthetases, Pages 263-266, Karla L. Ewalt and Paul Schimmel

trp Operon and Attenuation, Pages 267-271, Paul Gollnick

Tubulin and its Isoforms, Pages 272-276, Eva Nogales

Tumor Necrosis Factor Receptors, Pages 277-283, Karen G. Potter and Carl F. Ware

Two-Dimensional Gel Electrophoresis, Pages 284-289, Gerhard Schmid, Denis Hochstrasser and Jean-Charles Sanchez

Two-Hybrid Protein-Protein Interactions, Pages 290-293, Ilya Serebriiskii and Erica A. Golemis

Tyrosine Sulfation, Pages 294-297, Denis Corbeil and Wieland B. Huttner

Ubiquitin System, Pages 299-303, Aaron Ciechanover and Michael H. Glickman

Ubiquitin-Like Proteins, Pages 304-307, Edward T. H. Yeh

UmuC, D Lesion Bypass DNA Polymerase V, Pages 308-312, Zvi Livneh

Uncoupling Proteins, Pages 313-318, Daniel Ricquier and Frederic Bouillaud

Unfolded Protein Responses, Pages 319-325, David Ron

Urea Cycle, Inborn Defects of, Pages 326-330, Marsha K. Fearing and Vivian E. Shih

Vacuoles, Pages 331-336, Christopher J. Stefan and Scott D. Emr

Vascular Endothelial Growth Factor Receptors, Pages 337-342, Kenneth A. Thomas

Vasopressin/Oxytocin Receptor Family, Pages 343-348, Michael J. Brownstein

V-ATPases, Pages 349-353, Michael Forgac

Vitamin A (Retinoids), Pages 354-359, Joseph L. Napoli

Vitamin B12 and B12-Proteins, Pages 360-366, Bernhard Krautler

Vitamin C, Pages 367-371, Robert B. Rucker and Francene Steinberg

Vitamin D, Pages 372-377, Hector F. DeLuca and Margaret Clagett-Dame

Vitamin D Receptor, Pages 378-383, Diane R. Dowd and Paul N. MacDonald

Vitamin E, Pages 384-388, Ute C. Obermuller-Jevic and Lester Packer

Vitamin K: Biochemistry, Metabolism, and Nutritional Aspects, Pages 389-393, J. W. Suttie

Vitamin K: Blood Coagulation and Use in Therapy, Pages 394-398, Matthew D. Stone and Gary L. Nelsestuen

Voltage-Dependent K+ Channels, Pages 399-404, Ramon Latorre and Francisco J. Morera

Voltage-Sensitive Ca2+ Channels, Pages 405-408, Harald Reuter

Voltage-Sensitive Na+ Channels, Pages 409-415, William J. Brammar

Von Hippel-Lindau (VHL) Protein, Pages 416-418, Ronald C. Conaway and Joan Weliky Conaway

XPV DNA Polymerase and Ultraviolet Damage Bypass, Pages 419-421, Alan R. Lehmann

X-Ray Determination of 3-D Structure in Proteins, Pages 422-428, Martha L. Ludwig

Yeast GAL1-GAL10 System, Pages 429-433, Dennis Lohr and Ralph Bash

Zinc Fingers, Pages 435-439, Mark Isalan

Lipids, Carbohydrates, Membranes and Membrane Proteins

Carbohydrate Chains: Enzymatic and Chemical Synthesis; Vol.1 - Pages 307-313, Thomas J. Tolbert and Chi-Huey Wong

Cell–Matrix Interactions; Vol.1 - Pages 362-366, Janet A. Askari and Martin J. Humphries

Detergent Properties; Vol.1 - Pages 577-581, Darrell R. McCaslin

Endocytosis; Vol.2 - Pages 16-19, Julie G. Donaldson

Flippases; Vol.2 - Pages 123-127, Charles J. Waechter

Galectins; Vol.2 - Pages 171-174, R. Colin Hughes

GlcNAc Biosynthesis and Function, O-Linked; Vol.2 - Pages 189-192, Kaoru Sakabe and Gerald W. Hart

Glycation; Vol.2 - Pages 229-236, Suzanne R. Thorpe and John W. Baynes

Glycolipid-Dependent Adhesion Processes; Vol.2 - Pages 261-265, Senitiroh Hakomori

Glycoprotein Folding and Processing Reactions; Vol.2 - Pages 272-276, Armando J. Parodi

Glycoprotein-Mediated Cell Interactions, O-Linked; Vol.2 - Pages 277-282, Robert S. Haltiwanger

Glycoproteins, N-Linked; Vol.2 - Pages 283-292, Mark A. Lehrman

Glycoproteins, Plant; Vol.2 - Pages 293-296, Carolyn J. Schultz

Glycosylation in Cystic Fibrosis; Vol.2 - Pages 297-301, Andrew D. Rhim, Thomas F. Scanlin and Mary Catherine Glick

Glycosylation, Congenital Disorders of; Vol.2 - Pages 302-307, Hudson H. Freeze

Glycosylphosphatidylinositol (GPI) Anchors; Vol.2 - Pages 308-311, Anant K. Menon

Ion Channel Protein Superfamily; Vol.2 - Pages 473-477, William A. Catterall

Lectins; Vol.2 - Pages 535-540, Nathan Sharon and Halina Lis

Lipases; Vol.2 - Pages 571-575, Howard L. Brockman

Lipid Bilayer Structure; Vol.2 - Pages 576-579, Erwin London

Lipid Rafts; Vol.2 - Pages 584-587, Deborah A. Brown

Lipoproteins, HDL/LDL; Vol.2 - Pages 588-593, Fayanne E. Thorngate and David L. Williams

MDR Membrane Proteins; Vol.2 - Pages 605-609, Nathan C. Rockwell

Membrane Fusion; Vol.2 - Pages 621-626, Joshua Zimmerberg and Leonid V. Chernomordik

Mucin Family of Glycoproteins; Vol.2 - Pages 758-764, Juan Perez-Vilar and Robert L. Hill

Mucins in Embryo Implantation; Vol.2 - Pages 765-769, Daniel D. Carson

Neoglycoproteins; Vol.3 - Pages 11-15, Y. C. Lee and Reiko T. Lee

N-Linked Glycan Processing Glucosidases and Mannosidases; Vol.3 - Pages 46-49, Linda O. Tremblay and Annette Herscovics

Oligosaccharide Chains: Free, N-Linked, O-Linked; Vol.3 - Pages 161-164, Tadashi Suzuki

Phospholipid Metabolism in Mammals; Vol.3 - Pages 314-320, Claudia Kent

Phospholipid Synthesis in Yeast; Vol.3 - Pages 321-325, Gil-Soo Han and George M. Carman

Prostaglandins and Leukotrienes; Vol.3 - Pages 452-456, William L. Smith and Robert C. Murphy

Protein Glycosylation Inhibitors; Vol.3 - Pages 500-503, Alan D. Elbein

Proteoglycans; Vol.3 - Pages 549-555, Sara K. Olson and Jeffrey D. Esko

Secretory Pathway; Vol.4 - Pages 11-16, Karen J. Colley

Siglecs; Vol.4 - Pages 38-40, Ajit Varki

Sphingolipid Biosynthesis; Vol.4 - Pages 76-81, Martina Leipelt and Alfred H. Merrill, Jr.

Sphingolipid Catabolism; Vol.4 - Pages 82-87, Akira Abe and James A. Shayman

Sugar Nucleotide Transporters; Vol.4 - Pages 127-129, Carlos B. Hirschberg

Trehalose Metabolism; Vol.4 - Pages 251-255, Alan D. Elbein

Metabolism, Vitamins and Hormones

Amino Acid Metabolism; Vol.1 - Pages 90-95, Luc Cynober

Anaplerosis; Vol.1 - Pages 105-110, Raymond R. Russell, III and Heinrich Taegtmeyer

Bile Salts and their Metabolism; Vol.1 - Pages 159-163, Ulrich Beuers and Thomas Pusl

Biliary Cirrhosis, Primary; Vol.1 - Pages 164-169, Marshall M. Kaplan

Branched-Chain -Ketoacids; Vol.1 - Pages 186-191, David T. Chuang

Carnitine and -Oxidation; Vol.1 - Pages 314-318, Janos Kerner and Charles L. Hoppel

Cholesterol Synthesis; Vol.1 - Pages 451-455, Peter A. Edwards

Diabetes; Vol.1 - Pages 582-592, David W. Cooke

Fat Mobilization: Perilipin and Hormone-Sensitive Lipase; Vol.2 - Pages 85-89, Constantine Londos and Alan R. Kimmel

Fatty Acid Oxidation; Vol.2 - Pages 90-94, Horst Schulz

Fatty Acid Synthesis and its Regulation; Vol.2 - Pages 99-103, Steven D. Clarke and Manabu T. Nakamura

Gluconeogenesis; Vol.2 - Pages 197-203, Richard W. Hanson and Oliver E. Owen

Glucose/Sugar Transport in Bacteria; Vol.2 - Pages 204-207, Lan Guan and H. Ronald Kaback

Glucose/Sugar Transport in Mammals; Vol.2 - Pages 208-212, Silvia Mora and Jeffrey Pessin

Glycogen Metabolism; Vol.2 - Pages 244-248, Peter J. Roach

Glycogen Storage Diseases; Vol.2 - Pages 249-254, George H. Sack, Jr.

Glycolysis, Overview; Vol.2 - Pages 266-271, Robert A. Harris

Hexokinases/Glucokinases; Vol.2 - Pages 372-377, Emile Van Schaftingen

Insulin- and Glucagon-Secreting Cells of the Pancreas; Vol.2 - Pages 430-435, Franz M. Matschinsky

Ketogenesis; Vol.2 - Pages 505-507, Janos Kerner and Charles L. Hoppel

Ornithine Cycle; Vol.3 - Pages 172-177, Malcolm Watford

Pentose Phosphate (Hexose Mono Phosphate) Pathway; Vol.3 - Pages 211-215, Bernard R. Landau

Pentose Phosphate Pathway, History of; Vol.3 - Pages 216-225, John F. Williams

Phosphofructokinase-2/Fructose Bisphosphatase-2; Vol.3 - Pages 277-280, Daniel M. Raben

Photosynthesis; Vol.3 - Pages 330-335, Richard C. Leegood

Photosynthetic Carbon Dioxide Fixation; Vol.3 - Pages 336-341, Matthew J. Paul

Porphyrin Metabolism; Vol.3 - Pages 415-419, Mark Shepherd and Harry A. Dailey

Propionyl CoA–Succinyl CoA Pathway; Vol.3 - Pages 447-451, Wayne A. Fenton

Pyruvate Carboxylation, Transamination, and Gluconeogenesis; Vol.3 - Pages 606-610, Sarawut Jitrapakdee and John C. Wallace

Pyruvate Dehydrogenase; Vol.3 - Pages 611-615, Sam A. Johnson and James G. McCormack

Pyruvate Kinase; Vol.3 - Pages 616-619, Kosaku Uyeda

Starvation; Vol.4 - Pages 99-110, Oliver E. Owen and Richard W. Hanson

Tricarboxylic Acid Cycle; Vol.4 - Pages 256-262, Richard L. Veech

Urea Cycle, Inborn Defects of; Vol.4 - Pages 326-330, Marsha K. Fearing and Vivian E. Shih

Vitamin A (Retinoids); Vol.4 - Pages 354-359, Joseph L. Napoli

Vitamin B12 and B12-Proteins; Vol.4 - Pages 360-366, Bernhard Krautler

Vitamin C; Vol.4 - Pages 367-371, Robert B. Rucker and Francene Steinberg

Vitamin D; Vol.4 - Pages 372-377, Hector F. DeLuca and Margaret Clagett-Dame

Vitamin E; Vol.4 - Pages 384-388, Ute C. Obermuller-Jevic and Lester Packer

Vitamin K: Biochemistry, Metabolism, and Nutritional Aspects; Vol.4 - Pages 389-393, J. W. Suttie

Vitamin K: Blood Coagulation and Use in Therapy; Vol.4 - Pages 394-398, Matthew D. Stone and Gary L. Nelsestuen

Cell Architecture and Function

Actin Assembly/Disassembly; Vol.1 - Pages 12-18, Henry N. Higgs

Actin-Capping and -Severing Proteins; Vol.1 - Pages 19-26, Sankar Maiti and James R. Bamburg

Actin-Related Proteins; Vol.1 - Pages 27-33, R. Dyche Mullins

Autophagy in Fungi and Mammals; Vol.1 - Pages 138-143, Daniel J. Klionsky and Ju Guan

Bax and Bcl2 Cell Death Enhancers and Inhibitors; Vol.1 - Pages 152-154, David L. Vaux

Cadherin-Mediated Cell–Cell Adhesion; Vol.1 - Pages 205-211, Frauke Drees and W. James Nelson

Caspases and Cell Death; Vol.1 - Pages 319-327, Don W. Nicholson, Pierluigi Nicotera and Gerry Melino

Cell Cycle Controls in G1 and G0; Vol.1 - Pages 328-331, WengeShi and Steven F. Dowdy

Cell Cycle: Control of Entry and Progression Through S Phase; Vol.1 - Pages 332-337, Susan L. Forsburg

Cell Cycle: DNA Damage Checkpoints; Vol.1 - Pages 338-344, Jean Y. J. Wang

Cell Cycle: Mitotic Checkpoint; Vol.1 - Pages 345-351, Tim J. Yen

Cell Migration; Vol.1 - Pages 356-361, J. Victor Small and Emmanuel Vignal

Centromeres; Vol.1 - Pages 367-371, Beth A. Sullivan

Centrosomes and Microtubule Nucleation; Vol.1 - Pages 372-376, Reiko Nakajima, Ming-Ying Tsai and Yixian Zheng

Chaperones for Metalloproteins; Vol.1 - Pages 383-386, Valeria C. Culotta and Edward Luk

Chaperones, Molecular; Vol.1 - Pages 387-392, Sue Wickner and Joel R. Hoskins

Chaperonins; Vol.1 - Pages 393-398, Arthur L. Horwich, Wayne A. Fenton and George W. Farr

Chromosome Organization and Structure, Overview; Vol.1 - Pages 469-474, Elena Gracheva and Sarah C. R. Elgin

Cytokinesis; Vol.1 - Pages 556-561, Masanori Mishima and Michael Glotzer

Desmosomes and Hemidesmosomes; Vol.1 - Pages 569-576, Rachel L. Dusek, Jonathan C. R. Jones and Kathleen J. Green

Dynactin; Vol.1 - Pages 823-826, Trina A. Schroer

Dynein; Vol.1 - Pages 827-831, K. Kevin Pfister

Endoplasmic Reticulum-Associated Protein Degradation; Vol.2 - Pages 20-23, Maurizio Molinari

Focal Adhesions; Vol.2 - Pages 128-133, Eli Zamir and Benjamin Geiger

Golgi Complex; Vol.2 - Pages 312-315, Mark Stamnes

Heat/Stress Responses; Vol.2 - Pages 343-347, Davis T. W. Ng

Inositol Lipid 3-Phosphatases; Vol.2 - Pages 421-426, Gregory S. Taylor and Jack E. Dixon

Intermediate Filament Linker Proteins: Plectin and BPAG1; Vol.2 - Pages 452-457, Peter Fuchs and Gerhard Wiche

Intermediate Filaments; Vol.2 - Pages 458-464, Kelsie M. Bernot and Pierre A. Coulombe

Keratins and the Skin; Vol.2 - Pages 497-504, Pierre A. Coulombe and Kelsie M. Bernot

Kinesin Superfamily Proteins; Vol.2 - Pages 508-516, Nobutaka Hirokawa and Reiko Takemura

Kinesins as Microtubule Disassembly Enzymes; Vol.2 - Pages 517-521, Susan L. Kline-Smith and Arshad Desai

Meiosis; Vol.2 - Pages 610-616, Neil Hunter

Metalloproteinases, Matrix; Vol.2 - Pages 657-665, Hideaki Nagase and Gillian Murphy

Microtubule-Associated Proteins; Vol.2 - Pages 676-682, Nobutaka Hirokawa and Reiko Takemura

Mitosis; Vol.2 - Pages 743-747, Patricia Wadsworth and Nasser M. Rusan

Myosin Motors; Vol.2 - Pages 778-781, Roy E. Larson

N-End Rule; Vol.3 - Pages 6-10, Alexander Varshavsky

Neuronal Intermediate Filaments; Vol.3 - Pages 21-25, Ronald K. H. Liem

Nuclear Compartmentalization; Vol.3 - Pages 87-91, Kelly P. Smith and Jeanne B. Lawrence

Nuclear Envelope and Lamins; Vol.3 - Pages 92-95, Bryce M. Paschal

Nuclear Pores and Nuclear Import/Export; Vol.3 - Pages 109-114, Anita H. Corbett

Peroxisomes; Vol.3 - Pages 246-250, Suresh Subramani

26S Proteasome, Structure and Function; Vol.3 - Pages 469-473, Peter Zwickl and Wolfgang Baumeister

Protein Glycosylation, Overview; Vol.3 - Pages 504-509, Natasha E. Zachara and Gerald W. Hart

Rho GTPases and Actin Cytoskeleton Dynamics; Vol.3 - Pages 714-718, Priam Villalonga and Anne J. Ridley

Septins and Cytokinesis; Vol.4 - Pages 22-26, Makoto Kinoshita and Christine M. Field

SUMO Modification; Vol.4 - Pages 130-134, Frauke Melchior and Andrea Pichler

Tight Junctions; Vol.4 - Pages 187-189, Shoichiro Tsukita

Transcriptional Silencing; Vol.4 - Pages 200-203, Ann Sutton and Rolf Sternglanz

Tubulin and its Isoforms; Vol.4 - Pages 272-276, Eva Nogales

Unfolded Protein Responses; Vol.4 - Pages 319-325, David Ron

Vacuoles; Vol.4 - Pages 331-336, Christopher J. Stefan and Scott D. Emr

Protein/Enzyme Structure Function and Degradation

Allosteric Regulation; Vol.1 - Pages 68-73, Barry S. Cooperman

Aminopeptidases; Vol.1 - Pages 96-98, Ralph A. Bradshaw

Amyloid; Vol.1 - Pages 99-104, Ronald Wetzel

Aspartic Proteases; Vol.1 - Pages 123-127, Ben M. Dunn

B12-Containing Enzymes; Vol.1 - Pages 145-151, Vahe Bandarian and Rowena G. Matthews

Biotin; Vol.1 - Pages 174-178, Steven W. Polyak and Anne Chapman-Smith

Biotinylation of Proteins; Vol.1 - Pages 179-181, Ronald A. Kohanski

Calpain; Vol.1 - Pages 300-306, Hiroyuki Sorimachi and Yasuko Ono

Chemiluminescence and Bioluminescence; Vol.1 - Pages 399-404, Thomas O. Baldwin

Coenzyme A; Vol.1 - Pages 475-477, M. Daniel Lane

Collagenases; Vol.1 - Pages 478-481, Kenn Holmbeck and Henning Birkedal-Hansen

Collagens; Vol.1 - Pages 482-487, Darwin J. Prockop

Cysteine Proteases; Vol.1 - Pages 516-520, David J. Buttle and John S. Mort

Disulfide Bond Formation; Vol.1 - Pages 598-602, Hiram F. Gilbert

Elastin; Vol.2 - Pages 10-12, Judith Ann Foster

Enzyme Inhibitors; Vol.2 - Pages 31-37, Vern L. Schramm

Enzyme Kinetics; Vol.2 - Pages 38-44, Irwin H. Segel

Enzyme Reaction Mechanisms: Stereochemistry; Vol.2 - Pages 45-50, Ming-Daw Tsai, Li Zhao and Brandon J. Lamarche

Flavins; Vol.2 - Pages 118-122, Barrie Entsch and David P. Ballou

Heme Proteins; Vol.2 - Pages 354-361, Johannes Everse

HIV Protease; Vol.2 - Pages 384-387, Ben M. Dunn

Kinetic Isotope Effects; Vol.2 - Pages 522-527, Justine P. Roth and Judith P. Klinman

Lipid Modification of Proteins: Targeting to Membranes; Vol.2 - Pages 580-583, Marilyn D. Resh

Low Barrier Hydrogen Bonds; Vol.2 - Pages 594-598, Perry A. Frey

Metalloproteases; Vol.2 - Pages 652-656, David S. Auld

Peptide Amidation; Vol.3 - Pages 226-230, Mark J. Niciu, Richard E. Mains and Betty A. Eipper

Phage Display for Protein Binding; Vol.3 - Pages 251-255, Henry B. Lowman

Prions, Overview; Vol.3 - Pages 437-440, Cedric Govaerts and Fred E. Cohen

Proteases in Blood Clotting; Vol.3 - Pages 457-463, John D. Kulman and Earl W. Davie

Proteasomes, Overview; Vol.3 - Pages 464-468, Martin Rechsteiner

Protein Carboxyl Esterification; Vol.3 - Pages 474-477, Shilpa G. Lalchandani and Jeffry B. Stock

Protein Degradation; Vol.3 - Pages 484-492, Tomo ari and Alfred L. Goldberg

Protein Folding and Assembly; Vol.3 - Pages 493-499, David P. Goldenberg

Protein N-Myristoylation; Vol.3 - Pages 527-531, Erica Dutil Sonnenburg and Jeffrey I. Gordon

Protein Palmitoylation; Vol.3 - Pages 532-535, Robert J. Deschenes

Pteridines; Vol.3 - Pages 556-560, S. Colette Daubner and Paul F. Fitzpatrick

Pyridoxal Phosphate; Vol.3 - Pages 595-599, David E. Metzler

Regulated Intramembrane Proteolysis (Rip); Vol.3 - Pages 665-670, Jin Ye, Michael S. Brown and Joseph L. Goldstein

Secretases; Vol.4 - Pages 7-10, Robert L. Heinrikson

Selenoprotein Synthesis; Vol.4 - Pages 17-21, August Bock

Substrate Binding, Catalysis, and Product Release; Vol.4 - Pages 123-126, W. Wallace Cleland

Two-Hybrid Protein–Protein Interactions; Vol.4 - Pages 290-293, Ilya Serebriiskii and Erica A. Golemis

Tyrosine Sulfation; Vol.4 - Pages 294-297, Denis Corbeil and Wieland B. Huttner

Ubiquitin System; Vol.4 - Pages 299-303, Aaron Ciechanover and Michael H. Glickman

Ubiquitin-Like Proteins; Vol.4 - Pages 304-307, Edward T. H. Yeh

Zinc Fingers; Vol.4 - Pages 435-439, Mark Isalan

Bioenergetics

ABC Transporters; Vol.1 - Pages 1-5, Andre Goffeau, Benoit De Hertogh and Philippe V. Baret

Amine Oxidases; Vol.1 - Pages 85-89, Giovanni Floris and Alessandro Finazzi Agro

ATP Synthesis in Plant Mitochondria: Substrates, Inhibitors, Uncouplers; Vol.1 - Pages 128-132, Kathleen L. Soole and R. Ian Menz

ATP Synthesis: Mitochondrial Cyanide-Resistant Terminal Oxidases; Vol.1 - Pages 133-137, James N. Siedow

Bioenergetics: General Definition of Principles; Vol.1 - Pages 170-173, David G. Nicholls

Calcium Buffering Proteins: Calbindin; Vol.1 - Pages 221-225, Willi Hunziker and Igor Bendik

Calcium Buffering Proteins: ER Luminal Proteins; Vol.1 - Pages 226-230, Jody Groenendyk and Marek Michalak

Calcium Oscillations; Vol.1 - Pages 231-234, Marisa Brini

Calcium Sensing Receptor; Vol.1 - Pages 235-240, Jacob Tfelt-Hansen and Edward M. Brown

Calcium Signaling: Calmodulin-Dependent Phosphatase; Vol.1 - Pages 241-245, Claude Klee, Hao Ren and Shipeng Li

Calcium Signaling: Cell Cycle; Vol.1 - Pages 246-249, Luigia Santella

Calcium Signaling: Motility (Actomyosin–Troponin System); Vol.1 - Pages 250-255, Takeyuki Wakabayashi and Setsuro Ebashi

Calcium Signaling: NO Synthase; Vol.1 - Pages 256-260, Zhi-Qiang Wang and Dennis J. Stuehr

Calcium Transport in Mitochondria; Vol.1 - Pages 261-266, Rosario Rizzuto and Marisa Brini

Calcium Waves; Vol.1 - Pages 267-269, Lionel F. Jaffe

Calcium, Biological Fitness of; Vol.1 - Pages 270-273, Robert J. P. Williams

Calcium/Calmodulin-Dependent Protein Kinase II; Vol.1 - Pages 274-280, Andy Hudmon and Howard Schulman

Calcium-Binding Proteins: Cytosolic (Annexins, Gelsolins, C2-Domain Proteins); Vol.1 - Pages 287-293, Joachim Krebs

Calcium-Modulated Proteins (EF-Hand); Vol.1 - Pages 294-299, Robert H. Kretsinger

Cell Death by Apoptosis and Necrosis; Vol.1 - Pages 352-355, Pierluigi Nicotera

Chemiosmotic Theory; Vol.1 - Pages 405-412, Keith D. Garlid

Chemolithotrophy; Vol.1 - Pages 419-424, Alan B. Hooper

Chlorophylls and Carotenoids; Vol.1 - Pages 430-437, Hugo Scheer

Chloroplast Redox Poise and Signaling; Vol.1 - Pages 438-445, John F. Allen

Chloroplasts; Vol.1 - Pages 446-450, Nicoletta Rascio

Cytochrome b6f Complex; Vol.1 - Pages 521-527, Gunter A. Hauska and Thomas Schodl

Cytochrome bc1 Complex (Respiratory Chain Complex III); Vol.1 - Pages 528-534, Bernard L. Trumpower

Cytochrome c; Vol.1 - Pages 535-538, Hans Tuppy and Gunther Kreil

Cytochrome Oxidases, Bacterial; Vol.1 - Pages 539-543, Peter Brzezinski and Pia Adelroth

Cytochrome P-450; Vol.1 - Pages 544-549, Rita Bernhardt

Energy Transduction in Anaerobic Prokaryotes; Vol.2 - Pages 24-30, Gottfried Unden

ER/SR Calcium Pump: Function; Vol.2 - Pages 56-60, Giuseppe Inesi

ER/SR Calcium Pump: Structure; Vol.2 - Pages 61-65, Chikashi Toyoshima and Yuji Sugita

F1–F0 ATP Synthase; Vol.2 - Pages 73-79, Donata Branca

Ferredoxin; Vol.2 - Pages 104-106, Giuliana Zanetti and Vittorio Pandini

Ferredoxin-NADP+ Reductase; Vol.2 - Pages 107-111, Giuliana Zanetti and Alessandro Aliverti

Free Radicals, Sources and Targets of: Mitochondria; Vol.2 - Pages 134-142, Alberto Boveris and Enrique Cadenas

Friedreich's Ataxia; Vol.2 - Pages 143-145, Paul E. Hart and Anthony H. V. Schapira

Giant Mitochondria (Megamitochondria); Vol.2 - Pages 186-188, Bernard Tandler and Charles L. Hoppel

Glutathione Peroxidases; Vol.2 - Pages 224-228, Fulvio Ursini and Matilde Maiorino

Green Bacteria: Secondary Electron Donor (Cytochromes); Vol.2 - Pages 321-324, Hirozo Oh-oka and Robert E. Blankenship

Green Bacteria: The Light-Harvesting Chlorosome; Vol.2 - Pages 325-330, John M. Olson

Green Sulfur Bacteria: Reaction Center and Electron Transport; Vol.2 - Pages 331-336, Gunter A. Hauska and Thomas Schodl

Heme Synthesis; Vol.2 - Pages 362-366, Gloria C. Ferreira

Intracellular Calcium Channels: cADPR-Modulated (Ryanodine Receptors); Vol.2 - Pages 465-468, Antony Galione

Intracellular Calcium Channels: NAADP+-Modulated; Vol.2 - Pages 469-472, Armando A. Genazzani and Marcella Debidda

IP3 Receptors; Vol.2 - Pages 478-481, Colin W. TaylorEdward Morris and Paula da Fonseca

Iron–Sulfur Proteins; Vol.2 - Pages 482-489, Helmut Beinert, Jacques Meyer and Roland Lill

Ligand-Operated Membrane Channels: Calcium (Glutamate); Vol.2 - Pages 551-561, Elias K. Michaelis

Ligand-Operated Membrane Channels: GABA; Vol.2 - Pages 562-566, F. Minier and Erwin Sigel

Light-Harvesting Complex (LHC) I and II: Pigments and Proteins; Vol.2 - Pages 567-570, Stefan Jansson

Luft's Disease; Vol.2 - Pages 599-601, Salvatore DiMauro

Membrane Transport, General Concepts; Vol.2 - Pages 627-630, Stanley G. Schultz

Membrane Transporters:Na+/Ca2+ Exchangers; Vol.2 - Pages 631-636, Jonathan Lytton

Membrane-Associated Energy Transduction in Bacteria and Archaea; Vol.2 - Pages 637-645, Gunter Schafer

Metabolite Channeling: Creatine Kinase Microcompartments; Vol.2 - Pages 646-651, Uwe Schlattner and Theo Wallimann

Mitochondrial Auto-Antibodies; Vol.2 - Pages 683-688, Harold Baum

Mitochondrial Channels; Vol.2 - Pages 689-692, M. Catia Sorgato and Alessandro Bertoli

Mitochondrial DNA; Vol.2 - Pages 693-696, Gottfried Schatz

Mitochondrial Genes and their Expression: Yeast; Vol.2 - Pages 697-702, Piotr P. Slonimski and Giovanna Carignani

Mitochondrial Genome, Evolution; Vol.2 - Pages 703-708, B. Franz Lang, Dennis V. Lavrov and Gertraud Burger

Mitochondrial Genome, Overview; Vol.2 - Pages 709-715, Douglas C. Wallace

Mitochondrial Inheritance; Vol.2 - Pages 716-719, Eric A. Shoubridge

Mitochondrial Membranes, Structural Organization; Vol.2 - Pages 720-724, Carmen A. Mannella

Mitochondrial Metabolite Transporter Family; Vol.2 - Pages 725-732, Ferdinando Palmieri and Martin Klingenberg

Mitochondrial Outer Membrane and the VDAC Channel; Vol.2 - Pages 733-736, Marco Colombini

Neuronal Calcium Signal; Vol.3 - Pages 16-20, Hilmar Bading

Nicotinamide Nucleotide Transhydrogenase; Vol.3 - Pages 50-56, Jan Rydstrom

Nuclear Genes in Mitochondrial Function and Biogenesis; Vol.3 - Pages 100-104, Alexander Tzagoloff and Carol L. Dieckmann

Oncocytes; Vol.3 - Pages 165-166, Bernard Tandler and Charles L. Hoppel

Oxygenases; Vol.3 - Pages 178-182, Osamu Hayaishi

Periplasmic Electron Transport Systems in Bacteria; Vol.3 - Pages 231-238, David J. Richardson, Gary Sawers and Rob J. M. Van Spanning

Phosphatidylinositol-3-Phosphate; Vol.3 - Pages 272-276, Joseph V. Virbasius and Michael P. Czech

Photosystem I, Structure and Function; Vol.3 - Pages 342-347, Petra Fromme

Photosystem I: FX, FA, and FB Iron–Sulfur Clusters; Vol.3 - Pages 348-356, Mikhail L. Antonkine and John H. Golbeck

Photosystem II Light Harvesting System: Dynamic Behavior; Vol.3 - Pages 357-362, Peter Horton and Alexander Ruban

Photosystem II: Assembly and Turnover of the D1 Protein; Vol.3 - Pages 363-366, Eira Kanervo and Eva-Mari Aro

Photosystem II: Protein Components; Vol.3 - Pages 367-374, James Barber

Photosystem II: Water Oxidation, Overview; Vol.3 - Pages 375-380, Fabrice Rappaport and Pierre Joliot

Plasma-Membrane Calcium Pump: Structure and Function; Vol.3 - Pages 385-389, Emanuel E. Strehler

Plastocyanin; Vol.3 - Pages 390-393, Elizabeth L. Gross

Protein Import into Mitochondria; Vol.3 - Pages 510-515, Johannes M. Herrmann and Walter Neupert

P-Type Pumps: Copper Pump; Vol.3 - Pages 561-564, Ilia Voskoboinik and James Camakaris

P-Type Pumps: H+/K+ Pump; Vol.3 - Pages 565-570, Jai Moo Shin and George Sachs

P-Type Pumps: Na+/K+ Pump; Vol.3 - Pages 571-576, Peter L. Jorgensen

P-Type Pumps: Plasma-Membrane H+ Pump; Vol.3 - Pages 577-581, A. Brett Mason and Carolyn W. Slayman

Purple Bacteria: Electron Acceptors and Donors; Vol.3 - Pages 582-585, Evaldas Katilius and Neal W. Woodbury

Purple Bacteria: Photosynthetic Reaction Centers; Vol.3 - Pages 586-594, C. Roy D. Lancaster

Pyrimidine Biosynthesis; Vol.3 - Pages 600-605, Monika Loffler and Elke Zameitat

Quinones; Vol.3 - Pages 621-627, Giorgio Lenaz and Maria Luisa Genova

Respiratory Chain and ATP Synthase; Vol.3 - Pages 671-675, David G. Whitehouse and Anthony L. Moore

Respiratory Chain Complex I; Vol.3 - Pages 676-680, Ulrich Brandt

Respiratory Chain Complex II and Succinate: Quinone Oxidoreductases; Vol.3 - Pages 681-687, C. Roy D. Lancaster

Respiratory Chain Complex IV; Vol.3 - Pages 688-694, Hartmut Michel

Respiratory Processes in Anoxygenic and Oxygenic Phototrophs; Vol.3 - Pages 695-699, Roberto Borghese and Davide Zannoni

Spastic Paraplegia; Vol.4 - Pages 61-66, Elena Irene Rugarli and Andrea Ballabio

Store-Operated Membrane Channels: Calcium; Vol.4 - Pages 117-122, Indu S. Ambudkar

Superoxide Dismutase; Vol.4 - Pages 135-138, Irwin Fridovich

Uncoupling Proteins; Vol.4 - Pages 313-318, Daniel Ricquier and Frederic Bouillaud

V-ATPases; Vol.4 - Pages 349-353, Michael Forgac

Voltage-Dependent K+ Channels; Vol.4 - Pages 399-404, Ramon Latorre and Francisco J. Morera

Voltage-Sensitive Ca2+ Channels; Vol.4 - Pages 405-408, Harald Reuter

Voltage-Sensitive Na+ Channels; Vol.4 - Pages 409-415, William J. Brammar

Molecular Biology

Alternative Splicing: Regulation of Fibroblast Growth Factor Receptor (FGFR); Vol.1 - Pages 74-77, Mariano A. Garcia-Blanco

Alternative Splicing: Regulation of Sex Determination in Drosophila melanogaster; Vol.1 - Pages 78-84, Jill K. M. Penn, Patricia Graham and Paul Schedl

ara Operon; Vol.1 - Pages 116-119, Robert F. Schleif

Chromatin Remodeling; Vol.1 - Pages 456-463, Eric Kallin and Yi Zhang

Chromatin: Physical Organization; Vol.1 - Pages 464-468, Christopher L. Woodcock

DNA Base Excision Repair; Vol.1 - Pages 603-608, Hilde Nilsen and Tomas Lindahl

DNA Damage: Alkylation; Vol.1 - Pages 609-613, Anton B. Guliaev and B. Singer

DNA Glycosylases: Mechanisms; Vol.1 - Pages 614-617, Daniel J. Krosky and James T. Stivers

DNA Helicases: Dimeric Enzyme Action; Vol.1 - Pages 618-623, Timothy M. Lohman

DNA Helicases: HexamericEnzyme Action; Vol.1 - Pages 624-631, Smita S. Patel

DNA Ligases: Mechanism and Functions; Vol.1 - Pages 632-636, Alan E. Tomkinson and John B. Leppard

DNA Ligases: Structures; Vol.1 - Pages 637-643, C. Kiong Ho, Mark Odell and Dimitar B. Nikolov

DNA Methyltransferases, Bacterial; Vol.1 - Pages 644-651, Albert Jeltsch and Richard I. Gumport

DNA Methyltransferases, Structural Themes; Vol.1 - Pages 652-659, Sanjay Kumar

DNA Methyltransferases: Eubacterial GATC; Vol.1 - Pages 660-664, Martin G. Marinus

DNA Mismatch Repair and Homologous Recombination; Vol.1 - Pages 665-670, Ivan Matic and Miroslav Radman

DNA Mismatch Repair and the DNA Damage Response; Vol.1 - Pages 671-674, Guo-Min Li and Steven R. Presnell

DNA Mismatch Repair Defects and Cancer; Vol.1 - Pages 675-681, Richard D. Kolodner

DNA Mismatch Repair in Bacteria; Vol.1 - Pages 682-686, A-Lien Lu

DNA Mismatch Repair in Mammals; Vol.1 - Pages 687-690, James T. Drummond

DNA Mismatch Repair: E. coli Vsr and Eukaryotic G–T Systems; Vol.1 - Pages 691-693, Margaret Lieb

DNA Oxidation; Vol.1 - Pages 694-697, Arthur P. Grollman and Dmitry O. Zharkov

DNA Photolyase; Vol.1 - Pages 698-702, Carrie L. Partch and Aziz Sancar

DNA Polymerase α, Eukaryotic; Vol.1 - Pages 703-707, Teresa S. -F. Wang

DNA Polymerase β, Eukaryotic; Vol.1 - Pages 708-712, William A. Beard and Samuel H. Wilson

DNA Polymerase δ, Eukaryotic; Vol.1 - Pages 713-715, Antero G. So and Kathleen M. Downey

DNA Polymerase ε, Eukaryotic; Vol.1 - Pages 716-719, Yasuo Kawasaki and Akio Sugino

DNA Polymerase I, Bacterial; Vol.1 - Pages 720-725, Catherine M. Joyce

DNA Polymerase II, Bacterial; Vol.1 - Pages 726-728, Judith L. Campbell

DNA Polymerase III, Bacterial; Vol.1 - Pages 729-733, Hisaji Maki

DNA Polymerases: Kinetics and Mechanism; Vol.1 - Pages 734-739, Kenneth A. Johnson

DNA Replication Fork, Bacterial; Vol.1 - Pages 740-744, Nancy G. Nossal

DNA Replication Fork, Eukaryotic; Vol.1 - Pages 745-748, Lori M. Kelman, Jerard Hurwitz and Zvi Kelman

DNA Replication, Mitochondrial; Vol.1 - Pages 749-752, David A. Clayton

DNA Replication: Eukaryotic Origins and the Origin Recognition Complex; Vol.1 - Pages 753-760, Melvin L. DePamphilis and Cong-jun Li

DNA Replication: Initiation in Bacteria; Vol.1 - Pages 761-766, Jon M. Kaguni

DNA Restriction and Modification: Type I Enzymes; Vol.1 - Pages 767-771, David T. F. Dryden

DNA Restriction and Modification: Type II Enzymes; Vol.1 - Pages 772-777, Darren M. Gowers and Stephen E. Halford

DNA Restriction and Modification: Type III Enzymes; Vol.1 - Pages 778-781, Desirazu N. Rao and S. Srivani

DNA Secondary Structure; Vol.1 - Pages 782-787, Albino Bacolla and Robert D. Wells

DNA Sequence Recognition by Proteins; Vol.1 - Pages 788-793, Arabela A. Grigorescu and John M. Rosenberg

DNA Supercoiling; Vol.1 - Pages 794-797, Tao-shih Hsieh

DNA Topoisomerases: Type I; Vol.1 - Pages 798-805, James J. Champoux

DNA Topoisomerases: Type II; Vol.1 - Pages 806-811, Renier Velez-Cruz and Neil Osheroff

DNA Topoisomerases: Type III–RecQ Helicase Systems; Vol.1 - Pages 812-816, Rodney Rothstein and Erika Shor

EF-G and EF-Tu Structures and Translation Elongation in Bacteria; Vol.2 - Pages 1-5, Poul Nissen and Jens Nyborg

Exonucleases, Bacterial; Vol.2 - Pages 66-72, Susan T. Lovett

HIV-1 Reverse Transcriptase Structure; Vol.2 - Pages 388-392, Kalyan Das, Stefan G. Sarafianos, Eddy Arnold and Stephen H. Hughes

Homologous Recombination in Meiosis; Vol.2 - Pages 393-397, Nancy M. Hollingsworth

lac Operon; Vol.2 - Pages 529-534, Liskin Swint-Kruse and Kathleen S. Matthews

LexA Regulatory System; Vol.2 - Pages 546-550, Veronica G. Godoy, Penny J. Beuning and Graham C. Walker

Metaphase Chromosome; Vol.2 - Pages 666-671, Sharron Vass and Margarete M. S. Heck

Methyl-CpG-Binding Proteins; Vol.2 - Pages 672-675, David G. Skalnik

mRNA Polyadenylation in Eukaryotes; Vol.2 - Pages 748-752, Mary Edmonds

mRNA Processing and Degradation in Bacteria; Vol.2 - Pages 753-757, Deborah A. Steege

Non-Homologous End Joining; Vol.3 - Pages 66-70, Penny A. Jeggo

Nonhomologous Recombination: Bacterial Transposons; Vol.3 - Pages 71-79, Bao Ton Hoang and Michael G. Chandler

Nonhomologous Recombination: Retrotransposons; Vol.3 - Pages 80-86, Siew Loon Ooi and Jef D. Boeke

Nuclear Organization, Chromatin Structure, and Gene Silencing; Vol.3 - Pages 105-108, Lori L. Wallrath, John R. Danzer, Oya Yazgan and Pamela K. Geyer

Nucleoid Organization of Bacterial Chromosomes; Vol.3 - Pages 115-118, Charles J. Dorman

Nucleolus, Overview; Vol.3 - Pages 119-122, Thoru Pederson

Nucleotide Excision Repair and Human Disease; Vol.3 - Pages 123-129, James E. Cleaver

Nucleotide Excision Repair in Eukaryotes; Vol.3 - Pages 130-133, Laura A. Lindsey-Boltz and Aziz Sancar

Nucleotide Excision Repair, Bacterial: The UvrABCD System; Vol.3 - Pages 134-142, Bennett Van Houten and Lawrence Grossman

Nucleotide Excision Repair: Biology; Vol.3 - Pages 143-147, Errol C. Friedberg

PHO Regulon; Vol.3 - Pages 262-265, Bengt L. Persson

Pre-tRNA and Pre-rRNA Processing in Bacteria; Vol.3 - Pages 420-424, Sidney R. Kushner

Pre-tRNA and Pre-rRNA Processing in Eukaryotes; Vol.3 - Pages 425-431, Hendrik A. Raue

Prions and Epigenetic Inheritance; Vol.3 - Pages 432-436, Reed B. Wickner

Processivity Clamps in DNA Replication: Clamp Loading; Vol.3 - Pages 441-446, Megan J. Davey and Mike O'Donnell

Recombination: Heteroduplexand Mismatch Repair in vitro; Vol.3 - Pages 645-648, Leroy Worth, Jr.

Recombination: Strand Transferases; Vol.3 - Pages 649-653, Floyd R. Bryant

Recombination-Dependent DNA Replication; Vol.3 - Pages 654-659, Kenneth N. Kreuzer

recQ DNA Helicase Family in Genetic Stability; Vol.3 - Pages 660-664, Mary A. Risinger and Joanna Groden

Reverse Transcriptase and Retroviral Replication; Vol.3 - Pages 708-713, Laura Tarrago-Litvak, Marie-Line Andreola and Simon Litvak

Ribosome Assembly; Vol.3 - Pages 719-724, John L. Woolford

Ribosome Structure; Vol.3 - Pages 725-732, Brian T. Wimberly

Ribozyme Mechanisms; Vol.3 - Pages 733-737, John Hsieh and Carol A. Fierke

Ribozyme Structural Elements: Group I Introns; Vol.3 - Pages 738-742, Barbara L. Golden

Ribozyme Structural Elements: Hairpin Ribozyme; Vol.3 - Pages 743-746, Adrian R. Ferre-D'Amare

Ribozymes and Evolution; Vol.3 - Pages 747-752, Niles Lehman

RNA Editing; Vol.3 - Pages 753-758, Charles E. Samuel

RNA Polymerase I and RNA Polymerase III in Eukaryotes; Vol.3 - Pages 759-762, Robert J. White

RNA Polymerase II and Basal Transcription Factors in Eukaryotes; Vol.3 - Pages 763-765, Joan Weliky Conaway and Ronald C. Conaway

RNA Polymerase II Elongation Control in Eukaryotes; Vol.3 - Pages 766-769, David H. Price

RNA Polymerase II Structure in Eukaryotes; Vol.3 - Pages 770-774, Patrick Cramer

RNA Polymerase Reaction in Bacteria; Vol.3 - Pages 775-780, Arkady A. Mustaev and Alexander D. Goldfarb

RNA Polymerase Structure, Bacterial; Vol.3 - Pages 781-784, Michael Anikin, Dmitri Temiakov and William T. McAllister

Sigma Factors; Vol.4 - Pages 41-44, John D. Helmann

Sliding Clamps in DNA Replication: E. coli -Clamp and PCNA Structure; Vol.4 - Pages 45-47, Eric R. Goedken and John Kuriyan

Spliceosome; Vol.4 - Pages 88-92, Timothy W. Nilsen

T7 RNA Polymerase; Vol.4 - Pages 147-151, Rui Sousa

Telomeres: Maintenance and Replication; Vol.4 - Pages 174-179, Alessandro Bianchi and David Shore

Transcription Termination; Vol.4 - Pages 195-199, Thomas J. Santangelo and Jeffrey W. Roberts

Transcription-Coupled DNA Repair, Overview; Vol.4 - Pages 204-208, Isabel Mellon

Translation Elongation in Bacteria; Vol.4 - Pages 214-223, Oliver Vesper and Knud H. Nierhaus

Translation Elongation in Eukaryotes; Vol.4 - Pages 224-229, William C. Merrick and Anton A. Komar

Translation Initiation in Bacteria: Factors and Mechanisms; Vol.4 - Pages 230-236, Cynthia L. Pon and Claudio O. Gualerzi

Translation Initiation in Eukaryotes: Factors and Mechanisms; Vol.4 - Pages 237-241, Tatyana V. Pestova and Christopher U. T. Hellen

Translation Termination and Ribosome Recycling; Vol.4 - Pages 242-246, Nadja Koloteva-Levin and Mick F. Tuite

Translesion DNA Polymerases, Eukaryotic; Vol.4 - Pages 247-250, Alexandra Vaisman and Roger Woodgate

tRNA Synthetases; Vol.4 - Pages 263-266, Karla L. Ewalt and Paul Schimmel

trp Operon and Attenuation; Vol.4 - Pages 267-271, Paul Gollnick

UmuC, D Lesion Bypass DNA Polymerase V; Vol.4 - Pages 308-312, Zvi Livneh

XPV DNA Polymerase and Ultraviolet Damage Bypass; Vol.4 - Pages 419-421, Alan R. Lehmann

Yeast GAL1–GAL10 System; Vol.4 - Pages 429-433, Dennis Lohr and Ralph Bash

Signaling

Abscisic Acid (ABA); Vol.1 - Pages 6-11, Ramanjulu Sunkar and Jian-Kang Zhu

Adenosine Receptors; Vol.1 - Pages 34-39, Lauren J. Murphree and Joel Linden

Adenylyl Cyclases; Vol.1 - Pages 40-45, Ronald Taussig

Adrenergic Receptors; Vol.1 - Pages 46-50, David B. Bylund

A-Kinase Anchoring Proteins; Vol.1 - Pages 64-67, Lorene K. Langeberg and John D. Scott

Angiotensin Receptors; Vol.1 - Pages 111-115, Tadashi Inagami

ARF Family; Vol.1 - Pages 120-122, Gustavo Pacheco-Rodriguez, Joel Moss and Martha Vaughan

B-Cell Antigen Receptor; Vol.1 - Pages 155-158, Thomas M. Yankee and Edward A. Clark

Bradykinin Receptors; Vol.1 - Pages 182-185, Ronald M. Burch

Brassinosteroids; Vol.1 - Pages 192-197, Steven D. Clouse

Cadherin Signaling; Vol.1 - Pages 199-204, David B. Sacks and Jonathan M. G. Higgins

Calcitonin Gene-Related Peptide and Adrenomedullin Receptors; Vol.1 - Pages 212-216, Debbie L. Hay, Alex C. Conner and David R. Poyner

Calcitonin Receptor; Vol.1 - Pages 217-220, Samia I. Girgis, Niloufar Moradi-Bidhendi, Lucia Mancini and Iain MacIntyre

Calcium/Calmodulin-Dependent Protein Kinases; Vol.1 - Pages 281-286, J. Robison and Roger J. Colbran

c-fes Proto-Oncogene; Vol.1 - Pages 377-382, Thomas E. Smithgall and Robert I. Glazer

Chemokine Receptors; Vol.1 - Pages 413-418, Ann Richmond and Guo-Huang Fan

Chemotactic Peptide/Complement Receptors; Vol.1 - Pages 425-429, Eric R. Prossnitz and Larry A. Sklar

Cyclic AMP Receptors of Dictyostelium; Vol.1 - Pages 488-493, Dale Hereld and Peter N. Devreotes

Cyclic GMP Phosphodiesterases; Vol.1 - Pages 494-500, Sharron H. Francis and Jackie D. Corbin

Cyclic Nucleotide Phosphodiesterases; Vol.1 - Pages 501-505, Vincent C. Manganiello and Eva Degerman

Cyclic Nucleotide-Dependent Protein Kinases; Vol.1 - Pages 506-511, Sharron H. Francis and Jackie D. Corbin

Cyclic Nucleotide-Regulated Cation Channels; Vol.1 - Pages 512-515, Martin Biel and Franz Hofmann

Cytokines; Vol.1 - Pages 550-555, Andrea L. Wurster and Michael J. Grusby

Cytokinin; Vol.1 - Pages 562-567, Thomas Schmulling

Diacylglycerol Kinases and Phosphatidic Acid Phosphatases; Vol.1 - Pages 593-597, Stephen M. Prescott and Matthew K. Topham

Dopamine Receptors; Vol.1 - Pages 817-822, Kim A. Neve

Eicosanoid Receptors; Vol.2 - Pages 6-9, Richard M. Breyer and Matthew D. Breyer

Endocannabinoids; Vol.2 - Pages 13-15, Daniele Piomelli

Epidermal Growth Factor Receptor Family; Vol.2 - Pages 51-55, Denis Tvorogov and Graham Carpenter

FAK Family; Vol.2 - Pages 80-84, Steven K. Hanks

Fatty Acid Receptors; Vol.2 - Pages 95-98, Christer Owman and Bjorn Olde

Fibroblast Growth Factor Receptors and Cancer-Associated Perturbations; Vol.2 - Pages 112-117, Marko Kornmann and Murray Korc

G Protein Signaling Regulators; Vol.2 - Pages 147-151, John H. Exton

G Protein-Coupled Receptor Kinases and Arrestins; Vol.2 - Pages 152-157, Jeffrey L. Benovic

G12/G13 Family; Vol.2 - Pages 158-161, Stefan Offermanns

GABAA Receptor; Vol.2 - Pages 162-166, Richard W. Olsen and Gregory W. Sawyer

GABAB Receptor; Vol.2 - Pages 167-170, S. J. Enna

Gi Family of Heterotrimeric G Proteins; Vol.2 - Pages 181-185, Maurine E. Linder

Glucagon Family of Peptides and their Receptors; Vol.2 - Pages 193-196, Laurie L. Baggio and Daniel J. Drucker

Glutamate Receptors, Ionotropic; Vol.2 - Pages 213-219, Derek B. Scott and Michael D. Ehlers

Glutamate Receptors, Metabotropic; Vol.2 - Pages 220-223, P. Jeffrey Conn

Glycine Receptors; Vol.2 - Pages 237-243, Bodo Laube and Heinrich Betz

Glycogen Synthase Kinase-3; Vol.2 - Pages 255-260, James R. Woodgett

Gq Family; Vol.2 - Pages 316-320, Wanling Yang and John D. Hildebrandt

Gs Family of Heterotrimeric G Proteins; Vol.2 - Pages 337-341, Susanne M. Mumby

Hematopoietin Receptors; Vol.2 - Pages 348-353, Barbara A. Miller and Joseph Y. Cheung

Hepatocyte Growth Factor/Scatter Factor Receptor; Vol.2 - Pages 367-371, Selma Pennacchietti and Paolo M. Comoglio

Histamine Receptors; Vol.2 - Pages 378-383, Stephen J. Hill and Jillian G. Baker

Immunoglobulin (Fc) Receptors; Vol.2 - Pages 411-416, Mark Hogarth

Inositol Phosphate Kinases and Phosphatases; Vol.2 - Pages 427-429, Stephen B. Shears

Insulin Receptor Family; Vol.2 - Pages 436-440, Paul F. Pilch and Jongsoon Lee

Integrin Signaling; Vol.2 - Pages 441-445, Lawrence E. Goldfinger and Mark H. Ginsberg

Interferon Receptors; Vol.2 - Pages 446-451, Christopher P. Elco and Ganes C. Sen

JAK-STAT Signaling Paradigm; Vol.2 - Pages 491-496, Edward Cha and Christian Schindler

Leptin; Vol.2 - Pages 541-545, Thomas W. Gettys

Lysophospholipid Receptors; Vol.2 - Pages 602-604, Gabor J. Tigyi

Melanocortin System; Vol.2 - Pages 617-620, Roger D. Cone

Mitogen-Activated Protein Kinase Family; Vol.2 - Pages 737-742, Hidemi Teramoto and J. Silvio Gutkind

Muscarinic Acetylcholine Receptors; Vol.2 - Pages 775-777, Neil M. Nathanson

Natriuretic Peptides and their Receptors; Vol.3 - Pages 1-5, Lincoln R. Potter

Neuropeptide Y Receptors; Vol.3 - Pages 26-31, Eric M. Parker

Neurotensin Receptors; Vol.3 - Pages 32-36, William Rostene, Patrick Kitabgi and Didier Pelaprat

Neurotransmitter Transporters; Vol.3 - Pages 37-40, Aurelio Galli, Randy D. Blakely and Louis J. DeFelice

Neurotrophin Receptor Signaling; Vol.3 - Pages 41-45, Jennifer J. Gentry and Bruce D. Carter

Nicotinic Acetylcholine Receptors; Vol.3 - Pages 57-61, Nivalda O. Rodrigues-Pinguet and Henry A. Lester

Nitric Oxide Signaling; Vol.3 - Pages 62-65, Michael A. Marletta

Nuclear Factor kappaB; Vol.3 - Pages 96-99, Thomas D. Gilmore

Olfactory Receptors; Vol.3 - Pages 149-154, Sigrun I. Korsching

Opioid Receptors; Vol.3 - Pages 167-171, P. Y. Law and Horace H. Loh

P2X Purinergic Receptors; Vol.3 - Pages 183-187, Annmarie Surprenant

P2Y Purinergic Receptors; Vol.3 - Pages 188-191, George R. Dubyak

p53 Protein; Vol.3 - Pages 192-195, Jamie Hearnes and Jennifer Pietenpol

p70 S6 Kinase/mTOR; Vol.3 - Pages 196-200, Christopher G. Proud

Parathyroid Hormone/Parathyroid Hormone-Related Protein Receptor; Vol.3 - Pages 201-207, Thomas J. Gardella

Peroxisome Proliferator-Activated Receptors; Vol.3 - Pages 239-245, Mary C. Sugden, Edward A. Sugden and Mark J. Holness

Pheromone Receptors (Yeast); Vol.3 - Pages 256-261, James B. Konopka and Jeremy W. Thorner

Phosphatidylinositol Bisphosphate and Trisphosphate; Vol.3 - Pages 266-271, Alex Toker

Phosphoinositide 3-Kinase; Vol.3 - Pages 281-286, Khatereh Ahmadi and Michael Waterfield

Phosphoinositide 4- and 5-Kinases and Phosphatases; Vol.3 - Pages 287-291, Shawn F. Bairstow, Matthew W. Bunce and Richard A. Anderson

Phosphoinositide-Dependent Protein Kinases; Vol.3 - Pages 292-296, Nick R. Leslie and C. Peter Downes

Phospholipase A2; Vol.3 - Pages 297-300, Timothy R. Smith and Edward A. Dennis

Phospholipase C; Vol.3 - Pages 301-305, Fujio Sekiya, Yeun Ju Kim and Sue Goo Rhee

Phospholipase D; Vol.3 - Pages 306-313, Mary M. LaLonde and Michael A. Frohman

Photoreceptors; Vol.3 - Pages 326-329, King-Wai Yau

Plant Signaling: Peptides; Vol.3 - Pages 381-384, Clarence A. Ryan and Gregory Pearce

Platelet-Activating Factor Receptor; Vol.3 - Pages 394-398, Katherine M. Howard and Merle S. Olson

Platelet-Derived Growth Factor Receptor Family; Vol.3 - Pages 399-406, Marina Kovalenko and Andrius Kazlauskas

Protein Kinase B; Vol.3 - Pages 516-522, Bettina A. Dummler and Brian A. Hemmings

Protein Kinase C Family; Vol.3 - Pages 523-526, Alexandra C. Newton

Protein Tyrosine Phosphatases; Vol.3 - Pages 536-542, David J. Pagliarini, Fred L. Robinson and Jack E. Dixon

Proteinase-Activated Receptors; Vol.3 - Pages 543-548, Kristina K. Hansen and Morley D. Hollenberg

Rab Family; Vol.3 - Pages 629-634, Mary W. McCaffrey and Andrew J. Lindsay

Ran GTPase; Vol.3 - Pages 635-639, Mary Shannon Moore

Ras Family; Vol.3 - Pages 640-644, Lawrence A. Quilliam

Retinoblastoma Protein (pRB); Vol.3 - Pages 700-703, Nicholas Dyson and Maxim Frolov

Retinoic Acid Receptors; Vol.3 - Pages 704-707, Martin Petkovich

Serine/Threonine Phosphatases; Vol.4 - Pages 27-32, Thomas S. Ingebritsen

Serotonin Receptor Signaling; Vol.4 - Pages 33-37, Paul J. Gresch and Elaine Sanders-Bush

Small GTPases; Vol.4 - Pages 48-54, Adam Shutes and Channing J. Der

Somatostatin Receptors; Vol.4 - Pages 55-60, Agnes Schonbrunn

Src Family of Protein Tyrosine Kinases; Vol.4 - Pages 93-98, Jonathan A. Cooper

Steroid/Thyroid Hormone Receptors; Vol.4 - Pages 111-116, Ramesh Narayanan and Nancy L. Weigel

Syk Family of Protein Tyrosine Kinases; Vol.4 - Pages 139-145, Andrew C. Chan

Tachykinin/Substance P Receptors; Vol.4 - Pages 152-157, Mark D. Richardson and Madan M. Kwatra

Taste Receptors; Vol.4 - Pages 158-161, John D. Boughter, Jr. and Steven D. Munger

T-Cell Antigen Receptor; Vol.4 - Pages 162-168, Andrea L. Szymczak and Dario A. A. Vignali

Tec/Btk Family Tyrosine Kinases; Vol.4 - Pages 169-173, Shuling Guo and Owen N. Witte

Thyroid-Stimulating Hormone/Luteinizing Hormone/Follicle-Stimulating Hormone Receptors; Vol.4 - Pages 180-186, Deborah L. Segaloff, Dario Mizrachi and Mario Ascoli

Toll-Like Receptors; Vol.4 - Pages 190-194, Himanshu Kumar, Kiyoshi Takeda and Shizuo Akira

Transforming Growth Factor-β Receptor Superfamily; Vol.4 - Pages 209-213, Mark de Caestecker

Tumor Necrosis Factor Receptors; Vol.4 - Pages 277-283, Karen G. Potter and Carl F. Ware

Vascular Endothelial Growth Factor Receptors; Vol.4 - Pages 337-342, Kenneth A. Thomas

Vasopressin/Oxytocin Receptor Family; Vol.4 - Pages 343-348, Michael J. Brownstein

Vitamin D Receptor; Vol.4 - Pages 378-383, Diane R. Dowd and Paul N. MacDonald

Von Hippel-Lindau (VHL) Protein; Vol.4 - Pages 416-418, Ronald C. Conaway and Joan Weliky Conaway

Techniques and Methodology

Affinity Chromatography; Vol.1 - Pages 51-56, Pedro Cuatrecasas and Meir Wilchek

Affinity Tags for Protein Purification; Vol.1 - Pages 57-63, Joseph J. Falke and John A. Corbin

Genome-Wide Analysis of Gene Expression; Vol.2 - Pages 175-180, Karine G. Le Roch and Elizabeth A. Winzeler

HPLC Separation of Peptides; Vol.2 - Pages 398-403, James D. Pearson

Imaging Methods; Vol.2 - Pages 405-410, Gyorgy Szabadkai and Rosario Rizzuto

Inorganic Biochemistry; Vol.2 - Pages 417-420, Robert J. P. Williams

Multiple Sequence Alignment and Phylogenetic Trees; Vol.2 - Pages 770-774, Russell F. Doolittle

Oligosaccharide Analysis by Mass Spectrometry; Vol.3 - Pages 155-160, Andrew J. Hanneman and Vernon N. Reinhold

PCR (Polymerase Chain Reaction); Vol.3 - Pages 208-210, Michael J. Brownstein

Polysialic Acid inMolecular Medicine; Vol.3 - Pages 407-414, Frederic A. Troy, II

Protein Data Resources; Vol.3 - Pages 478-483, Philip E. Bourne

Secondary Structure in Protein Analysis; Vol.4 - Pages 1-6, George D. Rose

Spectrophotometric Assays; Vol.4 - Pages 67-75, Britton Chance

Two-Dimensional Gel Electrophoresis; Vol.4 - Pages 284-289, Gerhard Schmid, Denis Hochstrasser and Jean-Charles Sanchez

X-Ray Determination of 3-D Structure in Proteins; Vol.4 - Pages 422-428, Martha L. Ludwig

ENCYCLOPEDIA OF
Biological Chemistry

Editors
William J. Lennarz
M. Daniel Lane

Natriuretic Peptides and their Receptors

Lincoln R. Potter
University of Minnesota, Minneapolis, Minnesota, USA

Natriuretic peptides are an ancient family of hormones/paracrine factors that regulate blood pressure, cardiovascular homeostasis, and bone growth. The mammalian family consists of atrial natriuretic peptide, brain natriuretic peptide, and C-type natriuretic peptide. All three peptides are derived from separate genes, but share a common 17-amino-acid disulfide ring that is required for biological activity. A family of three cell surface receptors mediates their cellular effects: two are receptor guanylyl cyclases, enzymes that catalyze the synthesis of the intracellular second messenger, cGMP, whereas one is a decoy receptor that lacks enzymatic activity. In this article, the structure, function, and regulation of each hormone and receptor are discussed.

Natriuretic Peptides

Atrial Natriuretic Peptide

The first natriuretic peptide to be identified was atrial natriuretic peptide (ANP), which was originally called atrial natriuretic factor (ANF) because of its unknown structure. It was discovered by de Bold and co-workers in 1981. They found that intravenous infusion of atrial, but not ventricular, homogenates into rats caused a rapid and dramatic increase in renal sodium and water excretion that was accompanied by reduced blood pressure. Subsequently, a smooth muscle relaxing activity was shown to cofractionate with the natriuretic activity. The peptide responsible for both blood pressure lowering properties was purified and sequenced from multiple species by several laboratories. The structure of the polypeptide precursor of the mature peptide was derived from cDNA sequence, which like the peptide sequence was obtained from a number of different species by several different laboratories.

All natriuretic peptides are synthesized as preprohormones. Human preproANP is 151 amino acids in length. Proteolytic removal of the amino-terminal signal sequence yields a 126 residue proANP peptide, which is the predominant storage form found in dense atrial granules. Upon secretion, proANP is cleaved by corin, a transmembrane serine protease, to a 98 residue amino-terminal peptide and a 28 residue carboxyl-terminal peptide. Both fragments circulate in the plasma and are elevated under conditions where vascular volume is increased, such as congestive heart failure. The carboxyl terminal 28 amino-acid peptide is the mature biologically active form of ANP that mediates the known biological effects associated with the ANP gene (Figure 1).

The majority of ANP gene expression occurs in the cardiac atria, but there is low-level expression in extra-atrial tissues, e.g., central nervous system, adrenal gland, kidney, and ventricles. Expression in the latter tissue is generally only observed in early life or during ventricular hypertrophy. Hence, ANP mRNA expression has become a universal marker for ventricular remodeling that results from prolonged hypertension or other forms of cardiovascular insult. Differential processing of ANP in the kidney produces a variant containing four additional amino-terminal amino acids called urodilatin. It has been reported to be more potent than ANP, possibly because it is less sensitive to proteolytic degradation by neutral endopeptidases (NEPs). Atrial-wall stretch, reflecting increased intravascular volume, is the dominant stimulus for ANP release. However, several hormones and neurotransmitters – such as endothelin, arginine vasopressin, and catecholamines – also stimulate its secretion.

In addition to stimulating natriuresis, diuresis, and vasorelaxation, ANP also inhibits renin, vasopressin, and aldosterone release. It decreases cell proliferation and hypertrophy as well. Hence, ANP's short-term (natriuresis, diuresis, vasorelaxation) and long-term (antimitogenesis) effects are generally considered beneficial.

Transgenic mice exhibiting lifelong elevated plasma ANP levels display reduced blood pressure and heart size. In contrast, mice lacking ANP are hypertensive. The initial report describing these animals suggested that ANP regulates blood pressure in a salt-sensitive manner, but a subsequent communication indicated that these same mice were also hypertensive when fed a very low

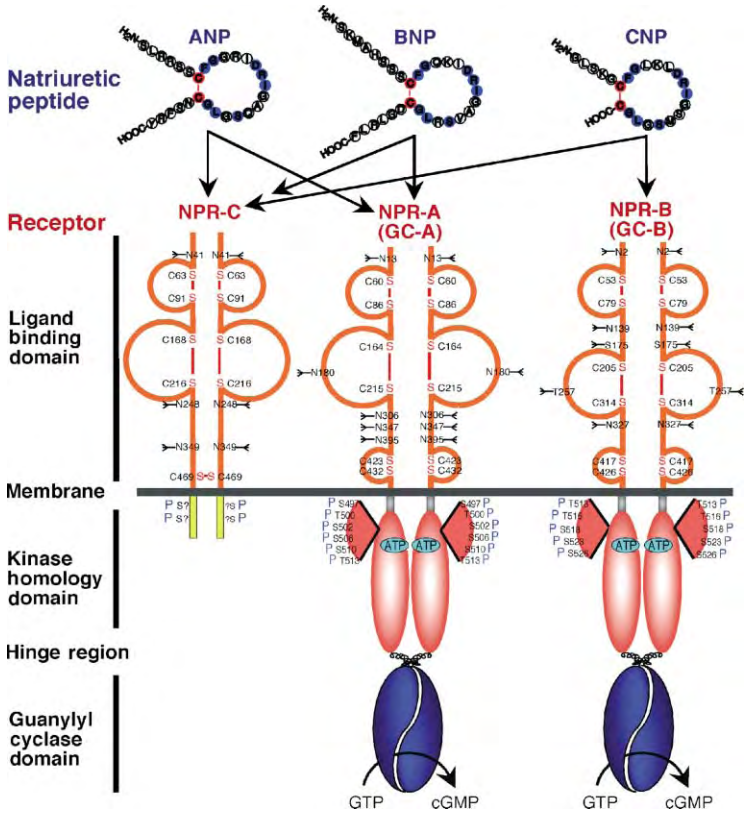

FIGURE 1 Schematic representation of natriuretic peptides and their receptors. Black arrows indicate which receptors each natriuretic peptide binds. Note that each peptide can bind more than one receptor. Blue circles in natriuretic peptide structures indicate conserved residues. Red lines indicate disulfide bonds. Black branched lines indicate N-linked glycosylation sites. Blue Ps indicate phosphorylation sites. ANP, atrial natriuretic peptide; BNP, brain natriuretic peptide; CNP, C-type natriuretic peptide; cGMP, cyclic guanosine monophosphate; GC-A, guanylyl cyclase A; GC-B, guanylyl cyclase B; GTP, guanosine triphosphate; NPR-A, natriuretic peptide receptor A; NPR-B, natriuretic peptide receptor B; NPR-C, natriuretic peptide receptor C.

salt diet (0.008% NaCl), consistent with ANP mediating its effects independently of body sodium chloride levels.

ANP is degraded outside and inside the cell by extracellular proteases and NPR-C-dependent internalization and degradation, respectively. The extracellular NEP 24.11 is a metallopeptidase that degrades all three natriuretic peptides. Recently, compounds have been developed that inhibit both angiotensin converting enzyme (ACE) and NEP. Omapatrilat, the most studied of these so-called vasopeptidase inhibitors, has the combined benefit of prolonging the blood pressure decreasing effects of natriuretic peptides while inhibiting the blood pressure increasing effects of the angiotensin system. Although early indications from clinical trials suggested that these drugs are beneficial to some patients with hypertension and/or congestive heart failure, very recent studies indicate that patients receiving vasopeptidase inhibitors experience more angioedema than patients treated with ACE inhibitors. Therefore, further development is needed before vasopeptidase inhibitors are viable alternatives to current therapies.

Brain Natriuretic Peptide

Although brain natriuretic peptide (BNP) was originally isolated from porcine brain, it was subsequently found to be more abundant in cardiac ventricles. Of all the natriuretic peptides, the amino-acid sequence of BNP varies most among species. For instance, in human, pig, and rat, mature BNP is 32, 26, and 45 amino acids in length, respectively.

Human BNP cDNA encodes a 132 amino-acid preprohormone that is processed to a 105-residue prohormone by removal of the signal peptide. Both corin and the endopeptidase, furin, have been shown to cleave the prohormone into the 32 amino-acid mature peptide. In the myocyte, BNP mRNA levels are regulated transcriptionally and posttranscriptionally in response to increased ventricular filling pressures or mechanical stretch. BNP is functionally similar to ANP

with respect to its vasorelaxant, natriuretic, and diuretic properties, but normal plasma BNP levels are only one-seventeenth of ANP levels. In contrast to ANP, ventricular BNP is not stored in secretory granules, instead it is released in a constitutive fashion following synthesis. Transgenic mice overexpressing BNP exhibited reduced blood pressure and cardiac weight accompanied by an elevation of plasma cGMP concentrations. They also exhibit increased long bone growth that most likely results from cross-activation of NPR-B. BNP null mice have normal blood pressures, but display pressure-sensitive cardiac fibrosis, proliferation of interstitial fibroblasts, and elevated ventricular extracellular matrix proteins. Hence, BNP's main function may be to regulate the cardiac ventricles.

BNP release is directly proportional to ventricular volume expansion and pressure overload. Although ANP is elevated in patients with congestive heart failure, BNP levels correlate more closely with left ventricular pressure, amount of dyspnea, and the state of neurohormonal modulation. Therefore, BNP, more than ANP, is an excellent indicator of heart failure. A rapid, whole-blood BNP assay (Triage BNP Test, Biosite Inc., San Diego, CA) that allows quick evaluation of patient plasma BNP levels was recently approved by the US Food and Drug Administration. Normal human plasma levels of BNP are <40 pg ml^{-1} and levels greater than 100 pg ml^{-1} are highly correlated with congestive heart failure. The high negative predictive value of this measurement suggests that it may be extremely useful in ruling out cardiac abnormalities in patients with dyspnea.

Recombinant B-type natriuretic peptide, whose clinical and trade names are Nesiritide and Natrecor, respectively, mimics the actions of endogenous BNP. It has been studied in more than 1700 patients with acute decompensated heart failure and has been shown to cause potent, dose-related vasodilation that is rapid in onset and sustained for the duration of drug infusion. It was approved for the treatment of acute decompensated congestive heart failure by the Food and Drug Administration in 2001.

C-Type Natriuretic Peptide

Like BNP, C-type natriuretic peptide (CNP) was first isolated from porcine brain. It is the most highly expressed natriuretic peptide in this tissue. Similarly in cerebrospinal fluid, CNP is $\sim$2 pM, which is about tenfold higher than ANP or BNP. BNP is also found at high concentrations in cytokine-treated endothelial cells and bone tissue. Because it is barely detectable in plasma, CNP is expected to signal primarily in a paracrine manner.

The primary structure of CNP is similar to ANP and BNP, but it lacks a C-terminal tail (Figure 1). It has higher amino-acid identity between species than ANP and BNP. For example, the structures of CNP from humans, pigs, and rats are identical. The 103 amino acid CNP propeptide is processed to either 53 or 22 amino acid forms. Furin, but not corin, has been suggested to mediate this final cleavage step. Both the 53 and 22 amino acid forms have been identified *in vivo* and the 22-amino-acid peptide predominates in the central nervous system, anterior pituitary, kidney, vascular endothelial cells, and plasma. Unlike ANP, CNP is not stored in granules. Instead, it is regulated at the level of transcription by various signaling molecules, such as transforming growth factor-β, tumor necrosis factor-α, and shear stress.

CNP relaxes vascular smooth muscle and is a more potent dilator of veins than ANP or BNP. It is not a potent inducer of diuresis and natriuresis. Like ANP, CNP has been shown to inhibit the proliferation of various cultured cell lines. A potential clinical benefit of this antimitogenic property was demonstrated in a rodent model when CNP treatment was shown to dramatically inhibit the normal vascular intimal thickening that accompanies balloon angioplasty.

Homozygous deletion of the gene-encoding CNP in mice caused more than half of the offspring to die during postnatal development. Surviving animals exhibited shortened body length and defects in endochondral bone development, which is analogous to human dwarfism. Importantly, cGMP-dependent protein kinase II (PKGII) knockout mice also develop dwarfism as a result of impaired endochondral ossification, suggesting that PKGII mediates the CNP-dependent skeletal effects. Consistent with a linear CNP/cGMP/PKGII pathway, the targeted expression of CNP in growth plate chondrocytes cannot increase the longitudinal bone growth or chondrocytic proliferation and hypertrophy in PKGII knockout mice.

Natriuretic Peptide Receptors

There are three known natriuretic peptide receptors. Natriuretic peptide receptor A (NPR-A) (also known as guanylyl cyclase A (GC-A)) and natriuretic peptide receptor B (NPR-B) (also known as guanylyl cyclase B (GC-B)) are receptor guanylyl cyclases, whereas the natriuretic peptide clearance receptor (NPR-C) does not possess any known enzymatic activity. Instead, NPR-C controls the local concentration of natriuretic peptides that are available to bind NPR-A and NPR-B through receptor-mediated internalization and degradation.

Guanylyl Cyclase-Linked Natriuretic Peptide Receptors

The ligand selectivity for NPR-A is ANP > BNP ≫ CNP, whereas the ligand selectivity for NPR-B is CNP ≫ ANP > BNP. Mice lacking NPR-A are hypertensive and develop cardiac hypertrophy and ventricular fibrosis. In addition, they are completely unresponsive to the renal and vasorelaxing effects of ANP and BNP, consistent with NPR-A being the sole signaling receptor for these peptides. A promoter mutation resulting in reduced transcription of the human NPR-A gene was recently identified and shown to be highly correlated with essential hypertension or ventricular hypertrophy.

Both NPR-A and NPR-B consist of an ~450-amino-acid extracellular ligand-binding domain, a 21-residue hydrophobic membrane-spanning region, and a 566- or 568-amino-acid intracellular domain, respectively (Figure 1). The latter can be divided into a ~250-amino-acid kinase homology domain (KHD), a 41-amino-acid hinge-dimerization region, and a 250-amino-acid C-terminal guanylyl cyclase catalytic domain. Like adenylyl cyclases and soluble guanylyl cyclases, a dimer is believed to be the minimal catalytic unit for both NPR-A and NPR-B.

The NPR-A extracellular domain contains three intramolecular but no intermolecular disulfide bonds (Figure 1). Similar Cys are conserved in the extracellular domain of NPR-B. Both NPR-A and NPR-B are highly glycosylated, and several studies suggest that glycosylation is required for proper receptor folding and/or transport of the receptor to the cell surface, but is not required for hormone binding. The crystal structure of the glycosylated, unliganded, dimerized hormone-binding domain of NPR-A has been solved at 2.0Å resolution. It reveals that the monomer consists of two interconnected subdomains, each encompassing a central β-sheet flanked by α-helices and the dimerization results from juxtaposition of 2×2 parallel helices that bring the two protruding C termini in close proximity. The crystal structure of an ANP–NPR-A complex has not been solved.

Activation of the guanylyl-cyclase-linked natriuretic peptide receptors is incompletely understood. Both receptors are homooligomers in the absence and presence of their respective ligands, indicating that receptor activation does not simply result from ligand-dependent dimerization. However, ANP binding does cause a conformational change in NPR-A that brings the extracellular juxtamembrane regions of each monomer closer together. In addition to natriuretic peptides, ATP is also required to maximally activate these receptors in broken cell preparations. Since receptors lacking the kinase homology domain are constitutively active and are not further stimulated by ATP, it has been suggested that the ATP binding to the kinase homology domain may relieve the basal repression of the guanylyl cyclase domain. No direct binding data have been presented to confirm this hypothesis, but ATP has been shown to modulate ANP binding and cyclase activity in purified receptor preparations, which is consistent with a direct binding model. On the other hand, the ATP effect observed with purified preparations is significantly less than that seen in crude membranes, which is consistent with a hypothesis where membranes contain an ATP-binding factor that is only partially removed during the purification procedure.

In the resting state, both NPR-A and NPR-B are highly phosphorylated on serines and threonines within their KHD domains. NPR-A isolated from resting 293 cells is phosphorylated on Ser497, Thr500, Ser502, Ser506, Ser510, and Thr513, which are located within a 17-residue stretch that contains the glycine-rich elbow and putative ATP-binding region of its KHD. Mutation of any of these phosphorylated residues to alanine in order to mimic a dephosphorylated serine or threonine results in decreased ANP-dependent guanylyl cyclase activities. Furthermore, receptors containing alanine substitutions at four or more phosphorylation sites are completely unresponsive to hormone. NPR-B is phosphorylated on Thr513, Thr51, Ser518, Ser523, and Ser526 in a similar region of its KHD. Four of these five sites are conserved between NPR-A and NPR-B. Phosphorylation of NPR-B is also required for ligand-dependent activation.

With respect to the mechanism by which an activated receptor is turned off, a process commonly referred to as desensitization, a number of theories have been put forth. Initial *in vitro* data suggested that direct phosphorylation of NPR-A by protein kinase C mediated its desensitization, but subsequent studies conducted in live cells indicated that desensitization in response to chronic natriuretic peptide exposure (homologous desensitization) or activators of protein kinase C results in the loss of phosphate from NPR-A and NPR-B. The role of phosphorylation/dephosphorylation in the regulation of these receptors was later clarified when mutations that mimic phosphorylated or dephosphorylated receptors were shown to be active or inactive, respectively. These experiments revealed for the first time a clear positive correlation between the phosphorylation state and enzymatic activity of NPR-A and NPR-B.

In contrast to the protein phosphorylation, the role of ligand-dependent internalization and degradation of NPR-A is unclear. Pandey and co-workers have reported many times that NPR-A undergoes this process, whereas Maack and co-workers contend that NPR-A is a constitutively membrane resident protein that is not internalized.

The Natriuretic Peptide Clearance Receptor

In addition to NPR-A and NPR-B, all three natriuretic peptides bind to a third receptor called the natriuretic peptide clearance receptor (NPR-C). NPR-C migrates as a 60 and 120 kDa protein when fractionated by reducing or nonreducing SDS-PAGE, respectively. It is found on the cell surface as a disulfide-linked homodimer. NPR-C has a large amino-terminal extracellular ligand-binding domain, a single transmembrane domain, and an intracellular domain that contains only 37 amino acids and possesses no known enzymatic activity (Figure 1). It binds ANP, BNP, and CNP with similar affinities, but it can also bind tightly to several smaller carboxyl-terminal and ring-deleted peptide analogues that do not bind well to NPR-A or NPR-B. C-ANF, the prototypical form of these peptides, is sometimes used to distinguish NPR-C from NPR-A in both binding and cGMP stimulation assays. The crystal structure of both the apo form and CNP bound form of NPR-C has been determined. In contrast to the 2:2 stoichiometry that was suggested for the ANP–NPR-A complex, the stoichiometry of binding of CNP to NPR-C was determined to be 1:2.

NPR-C is the most abundant natriuretic peptide receptor on the cell surface, and its primary function is to remove natriuretic peptides from the circulation via receptor mediated internalization and degradation, thereby controlling the local concentrations of the natriuretic peptides that are available to bind NPR-A and NPR-B. Like many nutrient receptors, NPR-C internalization is constitutive, i.e., it is not increased by natriuretic peptide binding. In addition to its clearance role, NPR-C has also been implicated in signaling, possibly in a G-protein-dependent manner. However, mice lacking NPR-C displayed a reduced ability to clear ^{125}I-ANP from the circulation, but no reduction in known signaling functions. In fact, pathways activated by NPR-A and NPR-B, blood pressure, and bone growth, respectively, are increased in these animals. Nonetheless, it remains possible that NPR-C may signal as yet unidentified processes.

See Also the Following Articles

Aminopeptidases • Calcium/Calmodulin-Dependent Protein Kinase II • Metalloproteases • Protein Kinase C Family • Vasopressin/Oxytocin Receptor Family

Glossary

cyclic GMP A cyclic mononucleotide of guanosine that acts as an intracellular second messenger for hormones, such as natriuretic peptides, guanylin, and nitric oxide.

guanylyl cyclase An enzyme that catalyzes the synthesis of cyclic GMP and pyrophosphate from guanosine triphosphate.

natriuresis Urinary sodium excretion.

protein phosphorylation Covalent addition of a phosphate molecule to the side chain of an amino acid, usually serine, threonine, or tyrosine in mammalian cells.

Further Reading

Levin, E. R., Gardner, D. G., and Samson, W. K. (1998). Natriuretic peptides. *N. Engl. J. Med.* **339**, 321–328.

Potter, L. R., and Hunter, T. (2001). Guanylyl cyclase-linked natriuretic peptide receptors: Structure and function. *J. Biol. Chem.* **276**, 6057–6060.

Schreiner, G. F., and Protter, A. A. (2002). B-type natriuretic peptide for the treatment of congestive heart failure. *Curr. Opin. Pharmacol.* **2**, 142–147.

Biography

Lincoln Potter earned his B.S. in biology/chemistry from David Lipscomb University in Nashville. He received his Ph.D. under the direction of David Garbers from Vanderbilt University in 1994 and then conducted postdoctoral studies with Tony Hunter at the Salk Institute in San Diego. In the fall of 1999, he joined the Department of Biochemistry, Molecular Biology and Biophysics at the University of Minnesota as a tenure-track assistant professor, which is his current position.

N-End Rule

Alexander Varshavsky
California Institute of Technology, Pasadena, California, USA

The N-end rule relates the *in vivo* half-life of a protein to the identity of its N-terminal residue The N-end rule stems from the activity of a universally present proteolytic pathway called the N-end rule pathway.

Proteolysis

Proteolysis, or protein degradation, is a set of processes that result in the hydrolysis of one or more of the peptide bonds in a protein. Proteolysis is a part of protein turnover, in which the molecules of specific proteins are first made through ribosome-mediated translation, and are eventually destroyed, in ways and at rates that are specific for the protein in question and depend on the state of an organism. The *in vivo* half-lives of intracellular proteins vary from a few seconds to many days. Two major functions of intracellular proteolysis are the selective destruction of damaged or otherwise abnormal proteins, and the regulated destruction of normal proteins whose concentrations must vary depending on the cell's state. Metabolic instability (a short *in vivo* half-life) is a property of many regulatory proteins. These proteins evolved not only to carry out their primary functions, for example, those of a phosphokinase or a repressor of transcription, but also to be rapidly destroyed *in vivo*. A short half-life of a regulator provides a way to generate its spatial gradients and allows for rapid adjustments of its concentration through changes in the rate of its synthesis. A protein can also be conditionally unstable, i.e., long-lived or short-lived depending on the state of molecular circuit of which the protein is a part. This fact, and also a faster (in general) destruction of the newly formed molecules of a protein in comparison to older, conformationally mature molecules of the same protein result in complex degradation kinetics, so that a single "half-life" of specific protein is at best an approximation of its actual decay curve *in vivo* (Figure 1).

The Ubiquitin System

A major set of pathways that target and destroy specific intracellular proteins is the ubiquitin (Ub) system, also called the Ub-proteasome system. In eukaryotes, the N-end rule pathway (Figure 2) is one pathway of the Ub system. Ub, a highly conserved 76-residue protein, is conjugated to ε-amino groups of lysine residues of other proteins (including other Ub molecules) through the action of three enzymes, E1, E2, and E3. The selectivity of ubiquitylation is determined by E3, which recognizes a substrate's degradation signal (degron). The term "Ub ligase" denotes either an E2–E3 complex or its E3 component. A ubiquitylated protein substrate bears a covalently attached poly-Ub chain, which mediates the binding of substrate to the 26S proteasome, an ATP-dependent protease that processively destroys the bound protein, yielding short peptides. The rate of degradation of specific proteins is regulated through modulation of the structure or steric exposure of their degrons, and also through the control of activity of Ub ligases. Physiological functions of the Ub system encompass enormous range: the regulation of cell differentiation, cell cycle, embryogenesis, apoptosis, signal transduction, DNA transcription, replication, repair and recombination, transmembrane and vesicular transport, stress responses (including the immune response), functions of the nervous system, and many other processes.

The N-End Rule Pathway

The multiple proteolytic pathways of the Ub system have in common their dependence on Ub conjugation and the proteasome, and differ largely through their utilization of distinct E2–E3 complexes. The Ub ligase of the N-end rule pathway targets proteins bearing specific (destabilizing) N-terminal residues (Figure 2). The corresponding degron, called the N-degron, consists of a substrate's destabilizing N-terminal residue and an internal lysine residue, the latter being the site of formation of a substrate-linked poly-Ub chain. Because an N-degron must be produced through a proteolytic cleavage that yields a destabilizing N-terminal residue, a nascent N-end rule substrate contains a cryptic N-degron, called pro-N-degron. In the yeast *Saccharomyces cerevisiae*, the two substrate-binding

Residue X	Half life of X-βgal	
	E. coli	*S. cerevisiae*
Arg	2 min	2 min
Lys	2 min	3 min
Phe	2 min	3 min
Leu	2 min	3 min
Trp	2 min	3 min
Tyr	2 min	10 min
His	> 10 h	3 min
Ile	> 10 h	30 min
Asp	> 10 h	3 min
Glu	> 10 h	30 min
Asn	> 10 h	3 min
Gln	> 10 h	10 min
Cys	> 10 h	> 30 h
Ala	> 10 h	> 30 h
Ser	> 10 h	> 30 h
Thr	> 10 h	> 30 h
Gly	> 10 h	> 30 h
Val	> 10 h	> 30 h
Pro	> 10 h	> 30 h
Met	> 10 h	> 30 h

FIGURE 1 The N-end rules of the prokaryote *E. coli* and the eukaryote (yeast) *S. cerevisiae*. Approximate *in vivo* half-lives of X-β-galactosidase (X-βgal) test proteins in *E. coli* at 36°C and in *S. cerevisiae* at 30°C. The N-end rule pathway is Ub-dependent in eukaryotes, and is also present in prokaryotes, which lack the Ub system.

sites of the 225-kDa Ub ligase UBR1 recognize (bind to) primary destabilizing N-terminal residues of two types: basic (type 1: Arg, Lys, His) and bulky hydrophobic (type 2: Phe, Trp, Leu, Tyr, Ile) (Figure 2B). Several other N-terminal residues function as tertiary (Asn, Gln) and secondary (Asp, Glu) destabilizing residues, in that they are recognized by UBR1 only after their enzymatic conjugation to Arg, a primary destabilizing residue (Figure 2). In the case of N-terminal Asn and Gln, the conjugation of Arg is preceded by enzymatic deamidation, to yield N-terminal Asp and Glu. In animals (but not in fungi such as *S. cerevisiae*), N-terminal Cys is yet another tertiary destabilizing residue, in that the arginylation of Cys is preceded by its oxidation. These covalent modification/conjugation reactions of N-terminal residues are required for the "downstream" step of Ub conjugation to N-end rule substrates that bear N-terminal Asn, Gln, Asp, Glu, or Cys (Figure 2A).

The UBR1 Ub ligase of the N-end rule pathway contains yet another, third substrate-binding site that recognizes a specific internal (non-N-terminal) degron in pathway's substrates. The only physiological substrate of this class that had been identified thus far is the 35-kDa homeodomain transcriptional repressor CUP9 of *S. cerevisiae*. Among the genes repressed by CUP9 is *PTR2*, which encodes a di- and tripeptide transporter. CUP9 is a short-lived protein targeted by the N-end rule pathway through an internal degron near the C terminus of CUP9. Dipeptides with destabilizing N-terminal residues allosterically activate UBR1, leading to accelerated *in vivo* degradation of CUP9 and the resulting induction of PTR2 expression (Figure 3). Through this positive feedback, *S. cerevisiae* can sense the presence of extracellular peptides and react by accelerating their uptake. Thus, the type 1 and type 2 sites of UBR1 function not only as substrate-binding sites, but also as nutritional sensors, making possible the adaptive regulation of peptide import (Figure 3). The mechanism of activation by dipeptides involves a conformational transition in UBR1, induced by the binding of dipeptides, that exposes the previously inactive (sterically inaccessible) CUP9-binding site of UBR1.

Another function of the *S. cerevisiae* N-end rule pathway is the maintenance of chromosome stability. At the metaphase–anaphase transition, the *ESP1*- encoded protease, called separase, cleaves SCC1, a subunit of cohesin complexes that hold together sister chromatids of replicated chromosomes. The resulting 33-kDa C-terminal fragment of SCC1 bears N-terminal Arg and is rapidly degraded by the N-end rule pathway. A failure to degrade this fragment of SCC1 in *ubr1*Δ cells (which lack the pathway's Ub ligase) results in a greatly increased frequency of chromosome loss, presumably because the retention of cohesin's fragment perturbs the assembly of intact cohesin complexes in subsequent cell cycles. Thus, the type 1 binding site of the UBR1 Ub ligase has a dual function of both a dipeptide-binding nutritional sensor (Figure 3) and a site that recognizes proteins with destabilizing N-terminal residues, targeting these proteins for Ub-dependent degradation.

Methionine aminopeptidases (MetAPs), the proteases that are specific for N-terminal Met (every nascent protein bears N-terminal Met), would remove this Met residue if, and only if, the second residue after Met is a stabilizing residue in the N-end rule. The only exceptions, in the mammalian N-end rule, are destabilizing residues Cys, Ala, Ser, and Thr (Figure 2A). Other destabilizing residues can be exposed at the N termini of proteins only through cleavage by proteases other than MetAPs. One such protease is separase, which cleaves the SCC1 subunit of cohesin, as stated before. A large class of proteases that can also produce, *in vivo*, a destabilizing residue at the N terminus of a protein are deubiquitylating enzymes (DUBs). One reaction catalyzed by these proteases is the cleavage of a linear Ub-X-polypeptide fusion at the Ub-X junction; this cotranslational cleavage can take place irrespective of the identity of a residue X at the junction, proline being a single exception. A method, called the Ub fusion technique, that takes advantage of

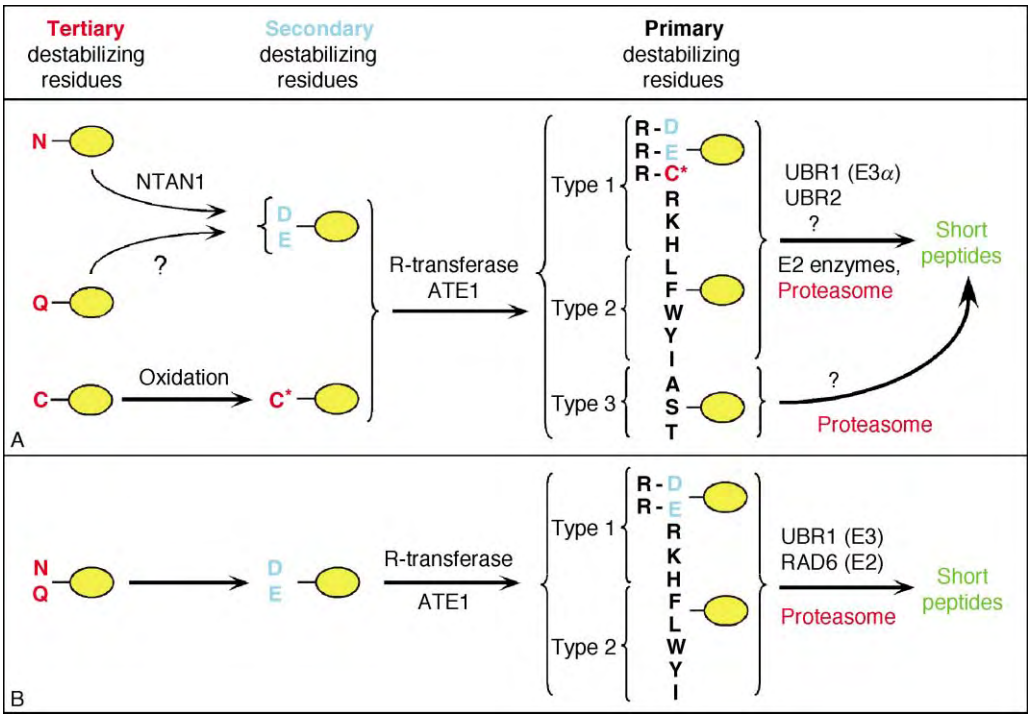

FIGURE 2 The N-end rule pathway in mammals (A) and the yeast *S. cerevisiae* (B). N-terminal residues are indicated by single-letter abbreviations. The ovals denote the rest of a protein substrate. In mammals (A), the Asn-specific N-terminal amidase NTAN1 converts N-terminal Asn into Asp. N-terminal Gln is deamidated by another (unidentified) amidase. N-terminal Asp, Glu, and Cys are conjugated to Arg by Arg-tRNA-protein transferases (R-transferases), encoded by the *ATE1* gene. N-terminal Cys is arginylated after its oxidation to either sulfinic or cysteic acid (A), a reaction that does not take place in yeast (B). The primary destabilizing N-terminal residues Arg, Lys, His (type 1 residues), as well as Phe, Leu, Trp, Tyr, and Ile (type 2 residues) are recognized in yeast (B) by the UBR1 E3, in a complex with the RAD6 E2 enzyme. In mammals (A), the same residues are recognized by UBR1 and UBR2, and by another Ub ligase that remains to be identified. In mammals but not in yeast, Ala (A), Ser (S), and Thr (T) are primary (type 3) destabilizing residues, recognized by a distinct Ub ligase that remains to be characterized.

this property of DUBs, has made it possible to produce different residues at the N termini of otherwise identical test proteins *in vivo*, and led, in 1986, to the discovery of the N-end rule.

Besides CUP9 and SCC1, several other proteins were also found to be substrates of the N-end rule pathway. These proteins include Sindbis virus RNA polymerase (and homologous polymerases of other alphaviruses), the integrase of the human immunodeficiency virus (HIV), a bacterial protein p60, which is secreted by *Listeria monocytogenes* into the cytosol of infected mammalian cells, the mammalian GTPase-activating proteins (GAP) RGS4 and RGS16, the *S. cerevisiae GPA1*-encoded Gα protein, and the encephalomyocarditis (EMC) virus 3C protease. Physiological functions, if any, of the degradation of these proteins by the N-end rule pathway are either unknown or have not been established definitively.

The N-end rule pathway of multicellular eukaryotes is organized similarly to that in *S. cerevisiae*, with several additional features. Among them is the presence of at least three functionally overlapping Ub ligases that target pathway's substrates, in contrast to a single such ligase, UBR1, in *S. cerevisiae* (Figure 2). Molecular genetic analyses in the mouse have demonstrated, through the deletion of *ATE1*, which encodes Arg-tRNA-protein transferases (R-transferases), that the arginylation branch of the mammalian N-end rule pathway (Figure 2A) is essential for cardiovascular development. It was also discovered that the mammalian N-end rule pathway is essential for meiosis in spermatocytes: in the absence of UBR2 (one of the pathway's Ub ligases), spermatocytes fail to form synaptonemal complexes and die, rendering the male *UBR2* $^{-/-}$ mice infertile. The corresponding molecular circuits, as well as physiological N-end rule substrates whose metabolic stabilization causes the cardiovascular and meiotic phenotypes in these mutants are unknown. Yet another function of the N-end rule pathway is regulation of apoptosis (programmed cell death) in the fruit fly *Drosophila melanogaster*. Specifically, the activated caspases (specific proteases that mediate apoptosis) cleave DIAP1, the inhibitor of apoptosis, producing a large C-terminal fragment of DIAP1 that bears Asn, a tertiary destabilizing residue in the N-end rule (Figure 2A). The degradation of this fragment by the N-end rule pathway down-regulates

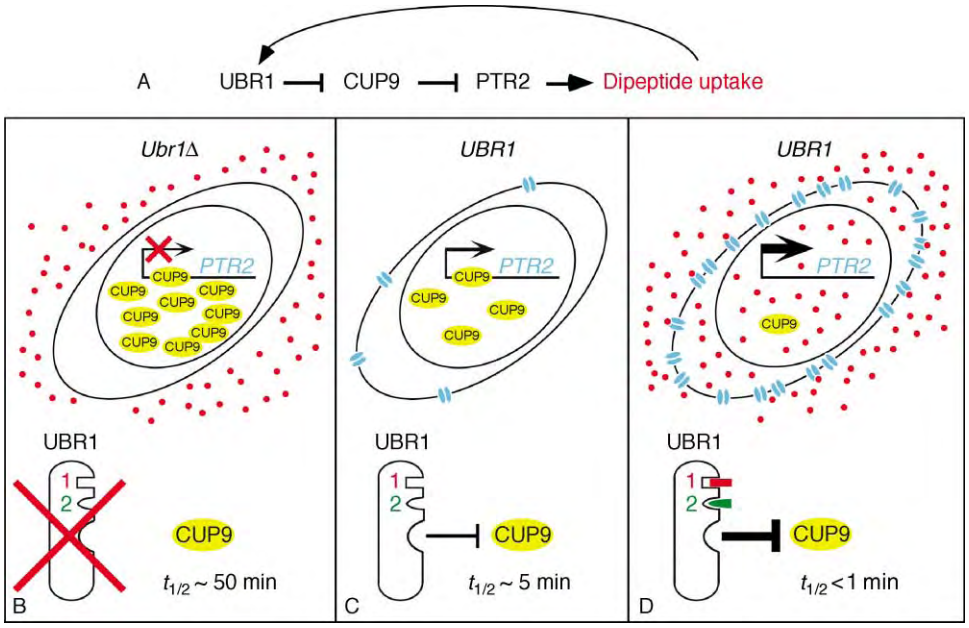

FIGURE 3 Ubiquitin-dependent activation of peptide import in *S. cerevisiae*. (A) Genetic diagram of the peptide transport circuit. (B) UBR1 is required for dipeptide uptake. In the absence of UBR1 (*ubr1*Δ), the transcriptional repressor CUP9 is long-lived, accumulates to high levels, and extinguishes the expression of peptide transporter, encoded by *PTR2*. *ubr1*Δ cells cannot import dipeptides (small dots). (C) In a *UBR1* cell growing in the absence of extracellular dipeptides, UBR1 targets CUP9 for degradation ($t_{1/2}$ ~ 5 min), resulting in a lower steady-state concentration of CUP9 and weak but significant expression of the PTR2 transporter (double ovals). (D) In *UBR1* cells growing in the presence of extracellular dipeptides some of which bear destabilizing N-terminal residues, the imported dipeptides bind to the basic (type 1) or hydrophobic (type 2) residue-binding sites of UBR1. These peptides are denoted as a rectangle and a wedge, respectively. Binding of either type of dipeptide to UBR1 allosterically increases the rate of UBR1-mediated degradation of CUP9. The resulting decrease of the half-life of CUP9 from ~5 min to less than 1 min leads to a further decrease in CUP9 levels, and consequently to a strong induction of the PTR2 transporter.

the apoptosis in *Drosophila*, presumably through the concomitant destruction of DIAP1-associated activators of apoptosis. The set of proteases that produce physiological N-end rule substrates is unlikely to be confined to MetAPs, caspases, and separases. For example, the cleavage specificity of calcium-activated proteases called calpains and the properties of other, less well-characterized cytosolic and/or nuclear proteases suggest that they, too, may function as upstream components of the N-end rule pathway. Although many functions of the N-end rule pathway remain to be discovered, the functions that have already emerged – peptide import, chromosome stability, cardiovascular development, meiosis, and apoptosis – are strikingly diverse. The broad functional range of the N-end rule pathway thus resembles, in a microcosm, the vastly greater span of the Ub system at large.

See Also the Following Articles

Aminopeptidases • Proteasomes, Overview • Ubiquitin System • Ubiquitin-Like Proteins

Glossary

degrons, or degradation signals Features of proteins that confer metabolic instability (short *in vivo* half-lives) on these proteins.

polyubiquitin chain A chain of covalently linked Ub moieties in which the C-terminal Gly residue of one moiety is conjugated to a specific lysine residue (usually, but not always, Lys-48) of adjacent Ub moieties. Protein-linked poly-Ub chains of different topologies (mediated by different, but unique for a given chain, lysine residues of Ub) underlie distinct roles of the Ub system, including its nonproteolytic functions. Poly-Ub can also exist as linear, head-to-tail chains of DNA-encoded Ub repeats produced through the ribosome-mediated translation. Such chains, the natural precursors of mature Ub, are called linear poly-Ub.

spermatocytes Germ cells in the testes of animals that are engaged in meiosis.

synaptonemal complex Two chromosome-length, closely apposed structures that mediate the pairing of two homologous chromosomes in meiosis.

ubiquitin ligase A complex of E2 and E3 enzymes, or an E3 enzyme alone.

ubiquitylation Conjugation of Ub to other proteins, including other Ub molecules. Ub whose C-terminal (Gly-76) carboxyl group is covalently linked to another compound is called the *ubiquityl* moiety.

Further Reading

Bachmair, A., Finley, D., and Varshavsky, A. (1986). *In vivo* half-life of a protein is a function of its N-terminal residue. *Science* **234**, 179–186.

Ditzel, M., Wilson, R., Tenev, T., Zachariou, A., Paul, A., Deas, E., and Meier, P. (2003). Degradation of DIAP1 by the N-end rule pathway is essential for regulating apoptosis. *Nat. Cell Biol.* **5**, 467–473.

Du, F., Navarro-Garcia, F., Xia, Z., Tasaki, T., and Varshavsky, A. (2002). Pairs of dipeptides activate the binding of substrate by ubiquitin ligase through dissociation of its autoinhibitory domain. *Proc. Natl. Acad. Sci. USA* **99**, 14110–14115.

Hershko, A., Ciechanover, A., and Varshavsky, A. (2000). The ubiquitin system. *Nat. Med.* **6**, 1073–1081.

Kwon, Y. T., Kashina, A. S., Davydov, I. V., Hu, R.-G., An, J. Y., Seo, J. W., Du, F., and Varshavsky, A. (2002). An essential role of N-terminal arginylation in cardiovascular development. *Science* **297**, 96–99.

Kwon, Y. T., Xia, Z., An, J. Y., Tasaki, T., Davydov, I. V., Seo, J. W., Sheng, J., Xie, and Varshavsky, A. (2003). Female lethality and apoptosis of spermatocytes in mice lacking the UBR2 ubiquitin ligase of the N-end rule pathway. *Mol. Cell. Biol.* **23**, 8255–8271.

Rao, H., Uhlmann, F., Nasmyth, K., and Varshavsky, A. (2001). Degradation of a cohesin subunit by the N-end rule pathway is essential for chromosome stability. *Nature* **410**, 955–960.

Turner, G. C., Du, F., and Varshavsky, A. (2000). Peptides accelerate their uptake by activating a ubiquitin-dependent proteolytic pathway. *Nature* **405**, 579–583.

Varshavsky, A. (1996). The N-end rule: Functions, mysteries, uses. *Proc. Natl. Acad. Sci. USA* **93**, 12142–12149.

Varshavsky, A. (2003). The N-end rule and regulation of apoptosis. *Nat. Cell Biol.* **5**, 373–376.

Biography

Alexander Varshavsky is Smits Professor of Cell Biology at the California Institute of Technology, in Pasadena. He is a member of the US National Academy of Sciences, and has received a number of scientific awards, including the Gairdner Award, the Lasker Award, the Sloan Prize, the Merck Award, the Wolf Prize, the Horwitz Prize, the Max Planck Prize, the Pasarow Award, the Massry Prize, and the Wilson Medal.

Neoglycoproteins

Y. C. Lee and Reiko T. Lee
The Johns Hopkins University, Baltimore, Maryland, USA

The term neoglycoproteins refers to proteins modified with chemical or enzymatic means to acquire structurally defined carbohydrates. The carbohydrates can be monosaccharides, oligosaccharides, or even polysaccharides.

Preparation

Direct Coupling of Oligosaccharides to Proteins

The easiest method is to attach naturally available oligosaccharides to the amino groups of proteins. This process does not require any chemical manipulations other than the conjugation process by reductive amination. Some of the readily available di- and oligosaccharides are: lactose, maltose, cellobiose, melibiose, N-acetyl-lactosamine, di-N-acetyl-chitobiose, and a number of milk oligosaccharides. An example of coupling of lactose by reductive amination to protein using sodium cyanoborohydride or pyridine borane as reducing agent, which preferentially reduces aldimine (Schiffs base) over aldehyde, is shown in Figure 1. This method relies on the fact that reducing sugars in acyclic aldehydo form, although present in a very minor proportion, are in equilibrium with the cyclic forms. As the aldehydo form of oligosaccharide is consumed, more will become available by conversion from the cyclic forms. However, the conjugation by this simple method is a very slow process, requiring several days or longer, because of the low concentration of the aldehyde form of oligosaccharide in solution.

The reductive amination converts the primary amino groups of N terminus and lysine side chains to secondary amines initially, and eventually to tertiary amines (with two sugar groups attached to a single nitrogen), if both oligosaccharide and reducing agent are present in excess. It is important to note that after such a reaction, the reducing terminal sugar of the oligosaccharide will become acyclic, and for this reason, conjugation with monosaccharide is meaningless. The shortcoming of this approach, in addition to long reaction time mentioned above, is the limited availability of suitable oligosaccharides. However, the number of commercially available oligosaccharides that are naturally derived or synthetically prepared has been steadily increasing.

Using Synthetic Carbohydrate Derivatives

Neoglycoproteins prepared by direct conjugation of oligosaccharides sometimes can be disadvantageous, due to sugar residues that are recognition target being too close to the protein surface. Synthetic carbohydrate derivatives would expand the scope of neoglycoprotein considerably both in terms of sugar structure and its disposition on the protein surface. The procedures can be totally synthetic or can be chemical modifications of naturally available glycans either in a free sugar form or linked to a group such as peptide. A few of the popular procedures are presented below.

Aromatic Glycosides

Commercially available *p*-aminophenyl glycosides are convenient derivatives for making neoglycoproteins either by diazo-coupling to tyrosine side chains or via transformation into isothiocyanate (reaction with thiophosgen), which then reacts with amino groups. *p*-Nitrophenyl glycosides, commonly used chromogenic glycosides, are available in even wider variety, and can be easily reduced to the corresponding *p*-aminophenyl glycosides. A shortcoming of these derivatives is that they can increase the hydrophobicity of product neoglycoprotein considerably and consequently may alter the nature of protein and give anomalous results in the probing of carbohydrate function.

Nonaromatic Glycosides

The problem of excessive hydrophobicity can be alleviated by the use of derivatives which do not contain aromatic rings and are not as hydrophobic as aromatic glycosides (e.g., Figure 2). Some of these derivatives are thioglycosides, which have the advantage of being more resistant to most exoglycosidases and also specifically cleavable with mercuric salts. Examples shown in Figure 2 are: (A) sugar imidate reacting with amino groups of protein to produce amidino-type (AI)

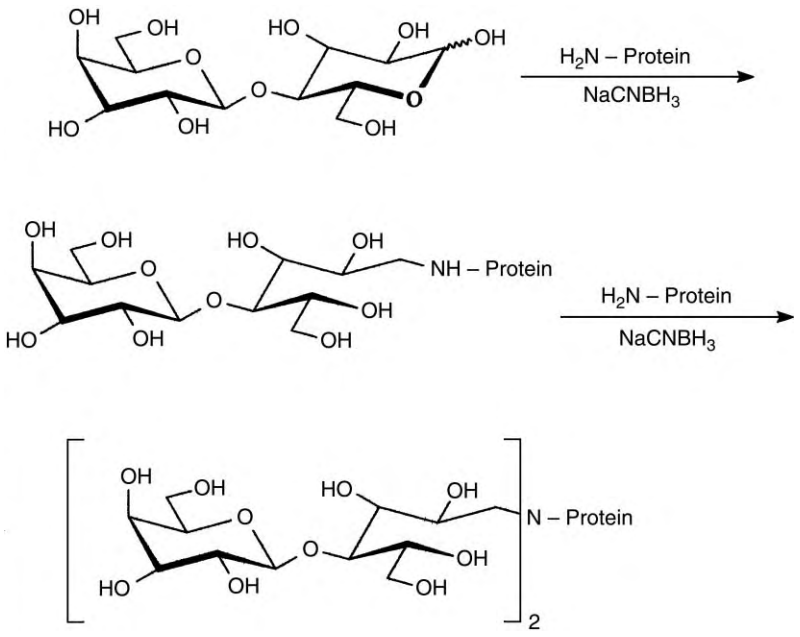

FIGURE 1 Conjugation of lactose via reductive amination.

neoglycoproteins; (B) an ω-aldehydo glycoside being coupled to protein via reductive amination; and (C) an ω-aminoalkyl glycosides converted to squaric acid derivative which can react with amino groups of protein. In both (B) and (C), the length of a glycon can be varied.

Reduced and Periodate-Oxidized Natural Oligosaccharides

Synthesis of oligosaccharides having complex structure is still a tedious and difficult task. Therefore, it is prudent sometimes to utilize naturally isolable oligosaccharides, if the quantity of neoglycoprotein needed is not too large. Natural oligosaccharides, pre-existing or obtained from natural glycoconjugates by enzymatic cleavage, can be made more reactive by first reducing them with sodium borohydride (to convert the reducing sugar residue into acyclic alditol) followed by mild periodate oxidation (e.g., 10 mM $NaIO_4$ for 10 min at room temperature), which will preferentially oxidize acyclic glycols to generate aldehydo group(s) without affecting the rest of the cyclic sugar residues. The newly generated aldehyde can be used in the reductive amination reaction as described above.

Using Other Functional Groups of Proteins

Most of the conjugation methods described above utilize amino groups of proteins for conjugation, which are often abundant and reactive because of the distance from the protein backbone. However, other functional groups such as phenolic, sulfhydryl, and carboxyl groups can also be used for conjugation. Diazo coupling of aryl glycosides to tyrosine side chain has been mentioned earlier. Thiol groups of protein are easy target for oligosaccharide attachment, since chemically mild, thiol-specific reactions are readily available. For example, a heterobifunctional linker with an amino-reacting group on one end and a maleimido or iodoacetamido group on the other end is reacted first to an Asn-oligosaccharide (or other glycopeptide) via its amino terminus, which is then reacted with protein thiol groups to produce neoglycoprotein in high yield. Bovine serum albumin has a single sulfhydryl group which can be utilized in this way to produce a neoglycoprotein carrying a single oligosaccharide chain of defined structure. An interesting approach is to react glycosylthiol with protein thiol group to form a disulfide bond. This will result in a product quite similar in structure to the natural N-glycosylated protein in terms of linkage length.

Use of Glycosyl Transferases

As the number of glycosyl transferases available commercially increases steadily, these enzymes have become a powerful synthetic tool in neoglycoprotein synthesis. The advantage of glycosyl transferases, is their exquisite specificity for anomeric configuration as well as the position of attachment. Thus, these enzymes are especially suited for modifying a pre-existing glycan structure (even a monosaccharide) at a specific position. Attachment of terminal α-L-fucosyl group or sialic acid group is a prime example. The enzymatic reaction can be carried out on the oligosaccharide before conjugation or after the conjugation to proteins.

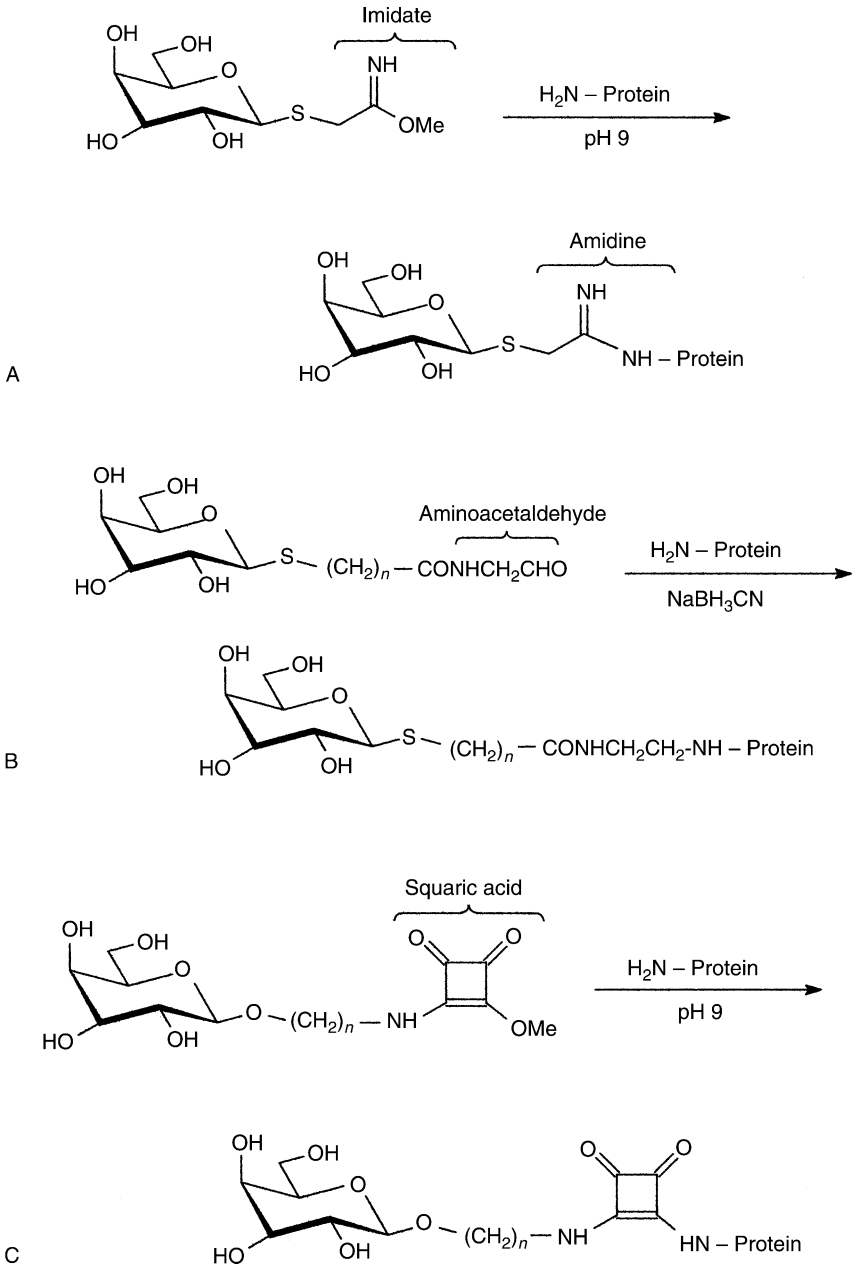

FIGURE 2 Example of synthetic methods for neoglycoprotein preparations.

Conjugation of Glycopeptides

For the conjugation of glycan structures from glycoprotein, sometimes it is easier to generate glycopeptide than to generate reducing oligosaccharide. A heterobifunctional crosslinker with a hydrazide and an acetal groups at two ends of molecule was devised to react first with amino groups of glycopeptide (or any other amino-terminated carbohydrate derivatives) via azide reaction, which is followed by generation of aldehydo function and then coupling to protein via reductive amination.

In all of these reactions, the level of sugars on neoglycoproteins can be controlled either by the ratio of reagent to protein or by the length of reaction. It should be borne in mind that these modifications generally produce a distribution of different sugar substitution in terms of both position and number. However, the ability to vary the degree of substitution turned out to be a great advantage for probing of carbohydrate function in many biological systems that is not readily available in natural glycoproteins. This is because recognition of carbohydrates often requires multivalency (Glycoside Clustering Effect) in order to manifest its function unequivocally. Neoglycoproteins can readily provide multivalency and thus are powerful ligands for carbohydrate binding.

In addition, neoglycoproteins can be radioiodinated (using the tyrosine side chain) or modified with fluorescent groups, such as fluorescein (using available ε-amino group) for easy monitoring.

Applications

Carbohydrate Receptor Analyses

Using neoglycoproteins, one can easily survey sugar-binding receptors (or lectins) in biological specimen. For example, a series of neoglycoproteins have been used to determine that alligator hepatic receptor has binding specificity for mannose and L-fucose. The binding of tagged neoglycoproteins (e.g., ^{125}I-labeled) to receptors can be probed both in solution phase and solid phase. Properly labeled neoglycoproteins can be used as cytochemical markers.

Affinant for Isolation

Neoglycoproteins can serve as effective affinant for isolation of lectins and receptors. For such a purpose, a neoglycoprotein can be conveniently immobilized to a suitable solid phase (e.g., Sepharose). In an alternate case, a protein (such as BSA) is immobilized first and then modified with one of the reagents mentioned above to form neoglycoproteins on solid phase.

Substrates for Enzymes

Neoglycoproteins can be used as convenient substrate for enzymes. For example, GlcNAc-BSA adsorbed on microtiter wells was used conveniently as substrate to assay β-galactosyl transferase with great sensitivity, which in turn can be used to assay α-fucosyl transferase.

Targeting Device

Neoglycoproteins can be used to target drugs and other materials to specific organs. For example, Gal- or GalNAc-containing neoglycoproteins, when properly conjugated to drug or anti-sense materials, can be used to target such materials to mammalian liver.

Examination of Glycoprotein Structure/Function Relationship

Carbohydrate chains of glycoprotein can have biological and biochemical function unrelated to specific sugar–lectin interaction. One of the better documented cases is the glycan in the Fc domain of IgG, which is required for interaction with Fc receptor. Neoglycoproteins were prepared by disulfide formation between Cys (in lieu of Asn) in the Fc domain and glycosylthiols of various structures to examine the effect of glycan structure on Fc receptor binding activity. Moreover, if the amino acid sequence and X-ray structure are known, one can place a Cys at different surface locations by genetic engineering, which would provide more latitude in examination of the role of carbohydrates on glycoproteins.

See Also the Following Articles

DNA Ligases: Mechanism and Functions • DNA Ligases: Structures • DNA Mismatch Repair and the DNA Damage Response • Glycoprotein Folding and Processing Reactions • Glycoproteins, N-linked • Glycosylation, Congenital Disorders of • Immunoglobulin (Fc) Receptors • Nonhomologous Recombination: Bacterial Transposons • Nonhomologous Recombination: Retrotransposons • Glycoprotein-Mediated Cell Interactions, O-Linked • Protein Glycosylation Inhibitors • Protein Glycosylation, Overview • Protein Kinase C Family

Glossary

BSA Bovine serum albumin.

glycoside clustering effect When glycosides are bundled together at proper distances, the total effect can be much greater ($>10^6$-fold) than the simple sum of individual glycoside.

neoglycoconjugates The original term of neoglycoproteins has now been expanded, and the term neoglycoconjugates has been introduced to encompass all the glyco-modified materials.

Further Reading

Lee, R. T., and Lee, Y. C. (1997). Neoglycoproteins. In *Glycoproteins II* (J. Montreuil, J. F. G. Vliegenthart and H. Schachter, eds.) pp. 601–620. Elsevier, Amsterdam, The Netherlands.

Lee, Y. C., and Lee, R. T. (1994). *Methods in Enzymology, Vol. 247. Neoglycoconjugates: Part A. Synthesis*. Academic Press, San Diego, CA.

Lee, Y. C., and Lee, R. T. (1994). *Methods in Enzymology, Vol. 242. Neoglycoconjugates: Part B. Biomedical Applications*. Academic Press, San Diego, CA.

Lee, Y. C., and Lee, R. T. (1994). *Neoglycoconjugates: Preparation and Applications*. Academic Press, San Diego, CA.

Macindoe, W. M., Van Oijen, A. H., and Boons, G. J. (1998). A unique and highly facile method for synthesizing disulfide linked neoglycoconjugates: A new approach for remodelling of peptides and proteins. *Chem. Commun.* **7**, 847–848.

Monsigny, M., Midoux, P., Mayer, R., and Roche, A. C. (1999). Glycotargeting: Influence of the sugar moiety on both the uptake and the intracellular trafficking of nucleic acid carried by glycosylated polymers. *Biosci. Rep.* **19**, 125–132.

Monsigny, M., Mayer, R., and Roche, A. C. (2000). Sugar–lectin interactions: Sugar clusters, lectin multivalency and avidity. *Carbohydr. Lett.* **4**, 35–52.

Biography

Y. C. Lee is Professor of Biology at the Johns Hopkins University in Baltimore, Maryland. He received his Ph.D. from the University of Iowa. His principal research interests are chemistry and biochemistry of glycoconjugates, especially biological interactions involving carbohydrates. He developed the field of neoglycoproteins as well as discovered glycoside clustering effect. He has published nearly 400 papers and book chapters, and received the Claude Hudson Award of the American Chemical Society in 2001.

Reiko Lee also received her Ph.D. from University of Iowa and is a Research Scientist in Biology Department of the Johns Hopkins University. She has coedited several volumes of books on the topics of neoglycoconjugates and recognition of carbohydrates in biological systems.

Neuronal Calcium Signal

Hilmar Bading
University of Heidelberg, Heidelberg, Germany

Neurons initiate many changes in gene expression in response to a synaptic or electrical stimulus. Calcium is the principal second messenger bridging the gap between the synapse and the nucleus. To couple synaptic events to specific genomic responses, neurons exploit the spatial diversity of calcium signals associated with the stimulus. Dendritic calcium signals, activating the MAP kinase (extracellular signal-regulated kinase, ERK1/2) signaling cascade, stimulate gene expression mediated by the serum response element. Calcium signals in the cell nucleus activate the transcription factor CRE-binding protein (CREB) and the coactivator CREB-binding protein (CBP). Nuclear calcium may, in particular, initiate and govern gene-expression-dependent forms of neuronal adaptations, including survival, learning, and memory.

Calcium Ions, Key Regulators of Electrical-Activity-Dependent Gene Expression

The generation of calcium signals following electrical activation is a fundamental property of neurons that controls many processes in the developing and the adult nervous system. Activity-induced increases in the intracellular calcium concentration result from calcium entering neurons from the extracellular space through ligand- and/or voltage-gated ion channels; these calcium transients can be amplified through calcium release from intracellular calcium stores. The N-methyl-D-aspartate (NMDA) receptor, a calcium permeable, glutamate-gated ion channel, plays a particularly important role in the mammalian central nervous system. Calcium entry through NMDA receptors, triggered by electrical activity, stimulates mechanisms that affect synaptic connectivity and neuronal network behavior leading to information storage; NMDA receptor-mediated calcium entry can also promote neuronal survival or cause cell death. For the consolidation of these activity-induced responses it is important that calcium signals, generated initially at the plasma membrane, are transduced to the cell nucleus where they stimulate the expression of particular genes. Thus, neurons use calcium ions to couple electrical signals to specific genomic events. Among the target genes of calcium signaling are neurotrophic factors, cytoskeletal proteins, and transcription factors (see below).

Spatial Calcium Signaling in Synapse-to-Nucleus Communication

The use of calcium as a universal signal mediator raises the issue of specificity: what mechanism allows neurons to use a single second messenger to convert a diverse range of electrical stimuli into distinct gene expression responses? Neurons appear to achieve this by using a calcium code: a given electrical stimulus is transformed into a calcium signal with particular spatial and temporal properties. Thus, an activity-induced neuronal calcium signal is a signature of the stimulus; it functions as its intracellular representation and links the stimulus to a gene expression response. The amplitude and the duration of the calcium signal, two features that transcriptional regulators decode, primarily control the magnitude of the increase in transcription. The site of calcium entry also matters; indeed, calcium entry through synaptic NMDA receptors and through extrasynaptic NMDA receptors has opposing effects on the activation of a crucial transcription factor (see below). However, most importantly, the genomic response depends on which part of the neuron is invaded by the calcium transient (Figure 1). For example, a weak synaptic input may generate a calcium signal that is confined to the submembranous space in the immediate vicinity of the site of calcium entry; following a stronger stimulus, calcium increases may reach further into the dendritic tree. Under certain conditions the calcium signal can invade the cell body and the nucleus. It is important for the specification of the gene expression response exactly which subcellular compartment (i.e., submembranous space, dendritic tree and somatic cytoplasm, and cell nucleus) undergoes a change in the calcium concentration. Thus, the "dialogue between genes and synapses" (to use a phrase from Eric Kandel) exploits the spatial and temporal diversity of calcium

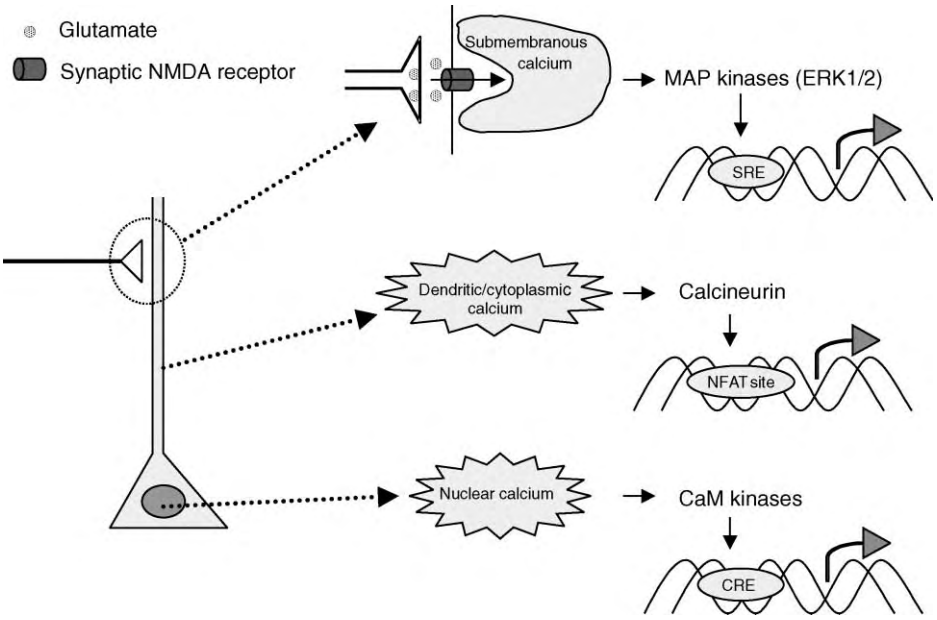

FIGURE 1 Schematic drawing of a neuron and the intracellular signaling pathways that mediate the induction of gene expression following neuronal activity. Three spatially distinct calcium signals (submembranous, cytoplasmic, and nuclear) are illustrated. Each type of calcium signal couples to a specific effector mechanism with distinct genomic targets. The decoding, by transcriptional regulators, of spatial information contained in activity-induced calcium transients allows neuronal impulse patterns to specify gene expression responses.

transients associated with electrical activation. Transcriptional regulation and the neuronal responses depend on how calcium enters the neurons, the amplitude of the signal, how long the signal lasts and what subcellular compartment it invades.

Regulators of Calcium-Induced Gene Expression

Much knowledge of the mechanisms of electrical-activity-dependent gene expression comes from studies of the *c-fos* gene. This gene is induced, without the need for new protein synthesis, within minutes after the stimulation. The *c-fos* gene encodes a DNA binding protein; together with members of the Jun transcription factor family it forms the AP-1 complex that is involved in the regulation of many genes. *c-fos* was the first gene found to be induced by membrane depolarization and calcium influx into excitable cell lines and primary neurons.

SRE AND CRE

Analysis of the *c-fos* promoter revealed that calcium influx-induced gene transcription is mediated by two distinct DNA regulatory elements: the cAMP response element (CRE) and the serum response element (SRE). The CRE and the SRE were previously known to mediate gene induction upon increasing intracellular levels of cAMP or following the addition of serum to serum-starved fibroblasts, respectively. Analysis of calcium regulation of SRE-dependent and CRE-dependent transcription uncovered the importance of the intracellular localization of the calcium signal: an increase in cytoplasmic calcium activates gene expression mediated by the SRE; in contrast, activation of the CRE and the CRE-binding protein (CREB) require increases in the nuclear calcium concentration. Thus, a single second messenger can, depending on its intracellular localization, induce distinct responses.

NFAT AND DREAM

Calcium-responsive regulators of transcription, other than the SRE and CREB, include the Nuclear Factor of Activated T-cells (NFAT) and the downstream regulatory element (DRE)-binding protein, DREAM (DRE-Antagonist Modulator). NFAT is important in the immune system; it mediates in activated T-cells the induction of interleukin-2 expression, a critical step in the response to antigen stimulation. DREAM is a multifunctional calcium-binding protein that can act as a repressor of gene transcription. The importance of spatial calcium signaling in the regulation of the SRE, the CRE, NFAT, and DREAM is outlined in the following section.

Calcium Signals in Different Subcellular Compartments

Calcium brings about biological responses through activating effector molecules such as protein kinases or protein phosphatases. Exactly which calcium-regulated molecule is stimulated depends on the subcellular localization of the calcium transient.

Submembranous Calcium Signals

A calcium microdomain restricted to the submembranous space near synaptic NMDA receptors serves as the "on-switch" of the MAP kinase (ERK1/2) cascade following synaptic activity. This signaling pathway is a major route for intracellular communication. The actions of MAP kinases (ERK1/2), both in the vicinity of calcium entry sites and in the nucleus, are involved in controlling many different brain functions ranging from learning to neuronal survival and light-induced shifts in the circadian rhythm.

One important target of the MAP kinase (ERK1/2) cascade is the nucleus. The MAP kinase (ERK1/2) signal propagates to the nucleus independently of global (i.e., cell-wide) increases in the calcium concentration and stimulates gene expression mediated by the SRE. It can also lead to the phosphorylation of CREB on its activator site, serine 133. Although this phosphorylation is necessary for inducing CREB-mediated transcription, it is not sufficient; a second regulatory event is required that involves stimulation of the activity of the CREB coactivator CBP by nuclear calcium and nuclear calcium/calmodulin (CaM)-dependent protein kinases. Nevertheless, the MAP kinase (ERK1/2) cascade acts as an auxiliary pathway that promotes at least one of several activating steps that control CREB-dependent gene expression. CREB target genes include *c-fos* and the brain-derived neurotrophic factor (BDNF).

Dendritic/Cytoplasmic Calcium Signals

The second calcium pool with a role in transcription regulation by neuronal activity is localized to the dendrites and the cytoplasm of the cell body. One of the targets of dendritic/cytoplasmic calcium is calcineurin (CaN). CaN is a cytoplasmic serine/threonine phosphatase that, upon activation by calcium/CaM, catalyzes the dephosphorylation of NFAT, which unmasks a NFAT nuclear localization signal. The activated CaN/NFAT complex is subsequently imported into the nucleus to activate gene transcription. Possible target genes of the CaN/NFAT signaling module are genes involved in regulating calcium homeostasis; this includes the IP_3 receptor and plasma membrane calcium ATPases (calcium pumps).

Once calcium concentrations have returned to basal levels, the NFAT/CaN complex dissociates, NFAT is exported from the nucleus and transcription is rapidly shut off. Thus, the magnitude of the transcriptional response is a function of the duration of the calcium signal; only prolonged increases in intracellular calcium efficiently activate NFAT-mediated gene expression. In addition, increases in nuclear calcium are required to maintain NFAT in the nucleus and to sustain transcription. Such calcium signals (i.e., elevated calcium plateaus in the cytoplasm and the nucleus) are typically seen in antigen-stimulated T-cells that require NFAT activation for the immune response (see above). In neurons, synaptic activity often generates only transient increases in intracellular calcium that may induce a less robust NFAT activation.

Nuclear Calcium Signals

The third player in electrical-activity-dependent gene expression is nuclear calcium. Synaptically evoked calcium transients can be amplified by calcium release from intracellular stores and are propagated, possibly in the form of a regenerative wave, to the nucleus. Nuclear calcium is a central regulator of neuronal gene expression. It activates nuclear calcium/CaM-dependent protein kinases and is the principal regulator of gene expression by the CREB/CBP complex. Activation of gene expression by CREB/CBP requires at least two regulatory events: phosphorylation of CREB on its activator site serine 133, which allows CBP to be recruited to CREB. The second event is the stimulation of CBP activity. The first regulatory step can be catalyzed by several protein kinases, including kinases of the MAP kinase (ERK1/2) signaling pathway (triggered by submembranous calcium; see above) and nuclear calcium-induced CaM kinases. Induction of CBP activity, however, depends upon increases in the nuclear calcium concentration and the activation of nuclear CaM kinases.

The only other second messenger known to stimulate CBP activity and to increase CREB/CBP-mediated gene expression is cAMP. Global increases in the intracellular concentration of cAMP stimulate the cAMP-dependent protein kinase (PKA); upon binding of cAMP to the PKA regulatory subunit, the catalytic subunit of PKA translocates to the cell nucleus to activate the CREB/CBP complex. A large body of literature suggests that cAMP and PKA are important for certain long-term, gene-expression-dependent forms of plasticity and learning in *Aplysia californica* and *Drosophila melanogaster*. Mammalian neurons are also capable of increasing intracellular levels of cAMP

following synaptic activity through a process that involves calcium/CaM-dependent adenylyl cyclases. However, electrical activity does not appear to elevate global levels of cAMP sufficiently high to stimulate the CREB/CBP complex, although it may increase cAMP and PKA activity locally leading to the phosphorylation of neurotransmitter receptors or other proteins in the post-synaptic space. Thus, the cAMP-PKA system may be important for localized dendritic signaling in the mammalian nervous system, but the stimulation of CREB/CBP-dependent gene expression following synaptic activity appears to be controlled by nuclear calcium signals.

CBP is a coactivator of CREB, but it also interacts with several other DNA-binding proteins, thereby conferring calcium inducibility. One example is the transcription factor c-Jun that can function as a calcium-regulated activator. Thus, control of CBP activity by nuclear calcium and nuclear CaM kinases provides a general mechanism through which electrical activity regulates an entire class of transcription factors and, consequently, many genes. This may be important in activity-dependent neuronal adaptation including information storage and memory that are likely to require up-regulation (or down-regulation) of many genes. Indeed, CREB (presumably as a CREB/CBP complex) has been implicated in synaptic plasticity and learning-related event in *Aplysia californica*, *Drosophila melanogaster*, and mice. Nuclear calcium may be essential for these processes.

A second type of transcriptional regulation by nuclear calcium involves DREAM. Rather than being controlled by calcium/CaM-dependent enzymes, the ability of DREAM to modulate transcription is directly controlled by nuclear calcium. DREAM is a calcium-binding protein that, in the absence of calcium, interacts with the DRE and represses transcription. Increases in nuclear calcium lead to the formation of a calcium/DREAM complex; calcium-bound DREAM dissociates from the DNA, allowing transcription to take place. Potential DREAM-binding sites are present in many different genes; the involvement of DREAM is best documented for the prodynorphin gene.

CREB Shut-Off Pathway

The genomic responses (and their effects on survival and plasticity programs) induced by calcium flux through synaptic NMDA receptors are antagonized by a signaling pathway stimulated by the addition of glutamate to the extracellular medium. Bath glutamate application stimulates both synaptic and extrasynaptic NMDA receptors as well as other types of glutamate receptors. Pharmacological experiments revealed that calcium flux through extrasynaptic NMDA receptors is responsible for this nuclear signaling mechanism that negatively regulates gene expression; this pathway also couples to neuronal cell death. The target transcription factor inactivated following calcium entry through extrasynaptic NMDA receptors is CREB; the CREB shut-off is brought about by a rapid dephosphorylation of CREB on its activator site, serine 133.

Extrasynaptic NMDA Receptors Antagonize Nuclear Calcium Signaling and BDNF Gene Expression

After calcium entry through extrasynaptic NMDA receptors, one of the consequences of the CREB shut-off is the suppression of BDNF gene expression. BDNF, a neurotrophic factor, activates intracellular signaling pathways through binding to TrkB, a receptor tyrosine kinase; BDNF also acts as a fast neurotransmitter and can rapidly depolarize neurons. BDNF has many functions in neuronal plasticity and cell survival. BDNF gene transcription is electrical-activity-dependent and controlled, antagonistically, by two calcium signaling pathways: calcium flux through synaptic NMDA receptors (or through L-type voltage-gate calcium channels) stimulates BNDF gene transcription; in contrast, calcium flux through extrasynaptic NMDA receptors antagonizes increases in BDNF expression. The BDNF gene's promoter is complex and provides binding sites for many transcription factors; however, a key factor is CREB, which may explain the opposing action of synaptic and extrasynaptic NMDA receptors on influencing BDNF gene transcription. Activation of synaptic NMDA receptors (or L-type voltage-gate calcium channels) strongly promotes CREB activity, whereas CREB function is shut off following activation of extrasynaptic NMDA receptors. Thus, the dialogue between the synapse and the nucleus is modulated by extrasynaptic NMDA receptors; those receptors trigger a CREB shut-off signal and antagonize increases in BDNF transcription induced by calcium entry through synaptic NMDA receptors. This underscores the importance of the intracellular localization of the calcium signal for the specification of the neuronal response.

See Also the Following Articles

Chaperones, Molecular • Proteasomes, Overview • Ubiquitin System • Ubiquitin-Like Proteins

Glossary

calcium Principal second messenger in the control of gene expression by electrical activity in neurons.

CBP (CREB binding protein) Transcriptional coactivator regulated by cAMP and calcium signaling pathway; interacts with CREB and many transcription factors thereby conferring calcium- and cAMP-inducibility.

CRE (cAMP response element) DNA regulatory element present in the promoter of many genes.

CREB (CRE binding protein) CRE-interacting transcription factor that is a target of cAMP and calcium signaling pathways; mediates gene induction upon synaptic activity and nuclear calcium transients.

MAP kinases/extracellular signal-regulated kinases (ERK 1/2) Important intracellular signaling pathway; activated by electrical activity-induced submembranous calcium signals.

spatial calcium signaling Electrical activity can induce calcium signals in different intracellular compartments; submembranous, cytoplasmic, and nuclear calcium activate gene expression through different mechanisms and have distinct genomic targets.

SRE (serum response element) DNA regulatory element regulated by signaling pathway, activated by growth factors, serum, or calcium; nuclear target of MAP kinases (ERK 1/2) signaling pathway.

Further Reading

Bading, H. (2000). Transcription-dependent neuronal plasticity: The nuclear calcium hypothesis. *Eur. J. Biochem.* **267**, 5280–5283.

Carafoli, E., and Klee, C. B. (1999). *Calcium as a Cellular Regulator.* Oxford University Press, New York.

Hardingham, G. E., and Bading, H. (2003). The yin and yang of NMDA receptor signalling. *Trends Neurosci.* **26**, 81–89.

Kandel, E. R. (2001). The molecular biology of memory storage: A dialogue between genes and synapses. *Science* **294**, 1030–1038.

West, A. E., Griffith, E. C., and Greenberg, M. E. (2002). Regulation of transcription factors by neuronal activity. *Nat. Rev. Neurosci.* **3**, 921–931.

Biography

Hilmar Bading is Professor of Neurobiology and Director of the Neurobiology Institute at the Interdisciplinary Center for Neurosciences at Heidelberg University, Germany. He holds an M.D. from Heidelberg University, received postdoctoral training at the Max Plank Institute in Berlin and Harvard Medical School, and was a staff scientist at the MRC Laboratory of Molecular Biology, Cambridge, United Kingdom. His principal research interest is neuronal calcium signaling and how this affects gene regulation and plasticity. His work highlighted the spatial aspects of calcium signals and the importance of nuclear calcium in governing activity-dependent gene expression in neurons.

Neuronal Intermediate Filaments

Ronald K. H. Liem
Columbia University College of Physicians and Surgeons, New York, USA

Neuronal intermediate filaments (IFs) are 10–12 nm filaments that are expressed in the nervous system. IF proteins belong to a large gene family and the expression of different IF proteins is tissue specific. In the nervous system, different neuronal IFs are expressed in neuroepithelial stem cells, the central nervous system (CNS) and peripheral nervous system (PNS). In addition, the expression patterns of these neuronal IFs are developmentally regulated. There are six neuronal IFs that will be described in this section. These are the three neurofilament triplet proteins (NFTPs), α-internexin, peripherin, and nestin.

Introduction

The cytoskeleton of most eukaryotic cells is composed of microtubules, microfilaments, and IFs. Microtubules are 25 nm in diameter and are composed of two subunit proteins called α- and β-tubulin, as well as a number of associated proteins, microfilaments are 6–8 nm in diameter and made up of a protein called actin. IFs are intermediate in size between the microtubules and microfilaments. All IF proteins contain a central α-helical rod domain flanked by nonhelical N-terminal head and C-terminal tail domains. The rod domain contains hydrophobic repeats (called heptad repeats) that mediate dimerization by allowing two α-helices to wrap around each other forming a "coiled coil." Subsequent polymerization into filaments involves the formation of tetramers and higher-order structures for which the N-terminal head domain is particularly important. Based on their protein sequence similarities and their gene structure, the IF protein family is separated into six or seven types. In the nervous system, IFs are expressed in both neurons and glial cells. In the CNS, astroglial cells express the glial fibrillary acidic protein (GFAP), whereas oligodendrocytes appear to be one of the few cell types that express no cytoplasmic IFs. In the PNS, Schwann cells express the more ubiquitous IF protein vimentin. Vimentin and GFAP are quite similar in sequence and gene structure and are part of a subfamily of IFs called type III IFs.

Neuronal IFs are the major and most visible filamentous structures in the axons. The number of neuronal IFs is correlated with axon diameter and they are believed to be primary determinants of axonal diameter. The NFTPs are the most ubiquitous IF proteins in neurons; they are present in both central and peripheral nerves. The NFTPs and α-internexin are more closely related to each other than to other IF proteins and are classified together as a subfamily called type IV IFs. The expression of peripherin predominates in the PNS. Although peripherin is expressed exclusively in neurons, based on its protein sequence homologies and its gene structure, peripherin is more similar to vimentin and GFAP and is therefore considered a type III IF. Nestin is the IF protein found in neuroepithelial stem cells, as well as muscle progenitor cells. The protein sequence of nestin is quite unique and nestin is sometimes considered to be a separate type VI IF. However, on the basis of its gene structure, it resembles the other type IV neuronal IFs.

One of the hallmarks of a number of neurodegenerative diseases is the accumulation of neuronal IFs in the form of axonal spheroids. These axonal spheroids have been observed in amyotropic lateral sclerosis (ALS, also called Lou Gehrig's disease) as well as other neuropathies. A number of recent studies from transgenic mice have indicated that the disorganization of neuronal IFs, especially in the forms of axonal spheroids, can lead to neurodegeneration. The relationship between the various neuronal IF proteins and neurodegeneration will be discussed below.

The Neurofilament Triplet Proteins

The NFTPs are composed of three proteins called NFL, NFM, and NFH for neurofilament light, medium, and heavy chain. NFTPs have been identified in all mammals and birds. The identification of the NFTPs was first done on the basis of studies on the transport of proteins in the axon. To study the transport of particular proteins, early studies used radioactive amino acids to label the newly synthesized proteins, and the nerves were then analyzed to determine the rates at which different proteins move. The slowest moving fraction moved at 0.1–1 mm per day and were believed to be the structural components. There were five major proteins, α- and β-tubulin and three

proteins with apparent molecular weights of 68, 145, and 200 kDa. Since actin, the component of the microfilaments, moved somewhat faster than these five proteins, the three unidentified proteins were identified as the subunits of the other structural element, the neurofilaments. Biochemical verification came when neurofilaments were purified and isolated and the contaminating astroglial filaments were removed. Each subunit was purified and the ability of the purified proteins to assemble *in vitro* was determined and assayed by examining the assembled filaments under the electron microscope. These *in vitro* assembly studies showed that the 68 kDa protein, later called NFL, was necessary and sufficient for IF formation. The 145 kDa (NFM) and 200 kDa (NFH) proteins coassembled with NFL and their long C-terminal tails appeared to form the links that can be observed between filaments in the electron microscope. The actual sequences of each of these proteins were determined by protein sequencing and later by cDNA cloning. They are shown schematically in Figure 1. Like all other IFs they contain a central α-helical rod domain flanked by nonhelical N-terminal head and C-terminal tail. The rod domain contains α-helical segments that are represented as cylinders. The rod domain of NFL can be divided into three separate segments (1A, 1B, and 2), whereas those of NFM and NFH are separated into two segments. The NF proteins have variable size C-terminal tails. The lengths of the C-terminal tails determine the ultimate sizes of the three proteins.

The tails of NFM and NFH contain multiple lysine-serine protein (KSP) repeats (shown as yellow circles), which are sites for phosphorylation as described below. As mentioned above, NFL is necessary for filament formation. Using various assays to study protein–protein interactions, it has been demonstrated that NFL can form homodimers and heterodimers with NFM and NFH. These results are consistent with the earlier observations from *in vitro* assembly studies that NFL can form a filament, whereas the other two proteins require NFL to assemble into filaments. Interestingly, transfection studies have shown that rat or mouse NFL needed either NFM or NFH to form a filamentous network *in vivo*, indicating that rodent neurofilaments are obligate heteropolymers. Human NFL can self-assemble in the transfected cells, but this assembly is not very efficient. The other neuronal IF proteins, peripherin, and α-internexin are able to self-assemble into homopolymers *in vitro* and *in vivo*, although NFM appears to have an inhibitory effect on the ability of peripherin to assemble into a filamentous network.

Neurofilaments have been suggested to play a role in regulating axonal caliber and thereby influencing axonal conduction velocity. This role has been confirmed by studies of the Japanese *quiver* quail, which has a premature termination codon in its NFL gene and consequently no neurofilaments in its axons. Normal radial growth is severely inhibited in the large caliber fibers. When the NFL gene was deleted in NFL knockout mice, no visible IFs were observed and there was axonal hypotrophy. There was also a substantial decrease in NFM and NFH in the NFL knockout mice, presumably because they were unstable, since they could not polymerize into filaments. Curiously, in spite of this hypotrophy, the NFL deficient mice developed normally and showed no obvious neurological problems. NFM and NFH knockouts have an even less severe phenotype. NFM knockouts also resulted in some reduction of the caliber of large axons and some axonal loss, whereas NFH knockouts resulted in an even more modest reduction in axonal caliber. Overexpression of NFL and either NFH or NFM in transgenic mice resulted in an increase in the number of neurofilaments as well as axonal caliber, consistent with the role of neurofilaments in regulating axonal calibers.

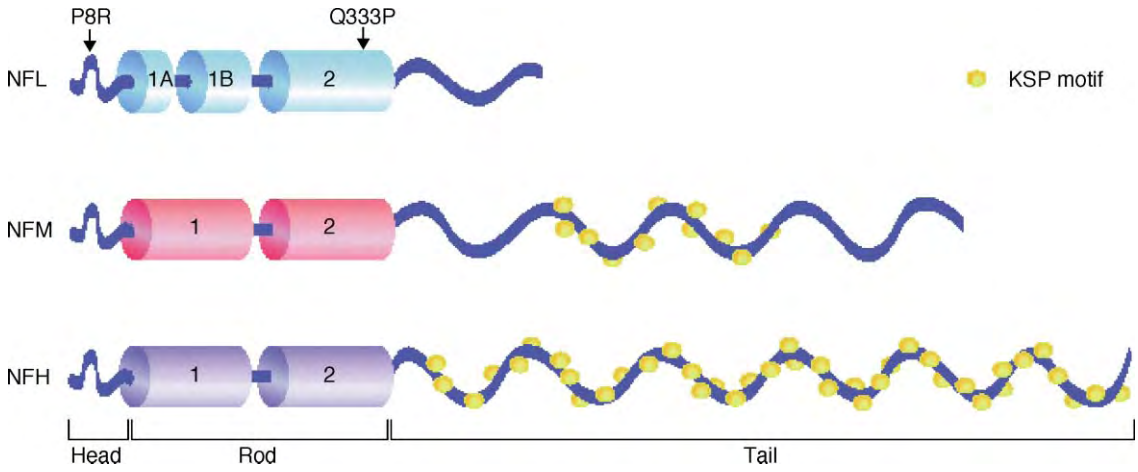

FIGURE 1 Diagrammatic representation of the NFTPs. Note that the size of the proteins are dependent on the lengths of the C-terminal tails. The a-helical rod regions are shown as cylinders. The KSP phosphorylation sites in the tail regions are shown as yellow circles. The first two mutations linked to CMT disease in NFL are indicated.

NFs are characterized by their phosphorylation, a post-translational mechanism that is thought to regulate their functions. NFM and NFH are phosphorylated mainly in the (KSP) repeats located in their C-terminal tail domains. These phosphorylation sites are depicted in the tail domains seen in Figure 1. NFH has 44–51 KSP residues, whereas NFM has 5–14 of these residues, depending on species. Phosphorylation of NFs induces extension of their side arms from the filament backbone, apparently increasing the spacing between individual filaments and ultimately the axonal caliber. Phosphorylated NFs are found in axons, while the nonphosphorylated forms are found in neuronal cell bodies and dendrites. A number of different kinases have been shown to phosphorylate the KSP residues of NFM and NFH. Phosphorylation of the KSP residues has been proposed to be important for the increase of the radial growth of axons by increasing the nearest neighbor distances between the neurofilaments, possibly through electrostatic repulsion between the neurofilament sidearms. The evidence for this proposal came from electron microscopy studies that showed that dephosphorylated neurofilaments were more closely spaced together than phosphorylated neurofilaments. In the dysmyelinated *Trembler* mouse mutant, there is a decrease in neurofilament phosphorylation and smaller axonal diameter. When segments of *Trembler* sciatic nerves were grafted onto control nerves, the *Trembler* segments still maintained their smaller diameters and dephosphorylated neurofilaments, whereas adjacent regions showed normal diameters and neurofilament phosphorylation. These studies were considered as strong evidence that phosphorylation of neurofilaments (especially of NFH) is a determinant of axonal diameter. It therefore came as a surprise that the NFH knockout mice showed only a slight decrease in nearest neighbor spacing of neurofilaments and did not change the axon caliber, indicating that NFH phosphorylation may be less important for the determination of axonal caliber than was predicted. To test this particular property of NFH more rigorously, the NFH gene was replaced in transgenic mice with one deleted in the NFH tail. The results showed that the loss of the NFH tail and all of its phosphorylation sites did not affect the interfilament spacing of the neurofilaments. In contrast, the NFM tail and its state of phosphorylation may be more important for radial growth, even though it contains considerably fewer phosphorylation sites.

As described before, neurofilament proteins are synthesized in the cell body and have been found to move down the axon as part of the slow component of axonal transport with a velocity of $\sim 0.1–1$ mm day^{-1}. The initial hypothesis was that the entire axoplasm moved as a coherent block, but more recent work has shown that the entire axoplasm in its totality does not move. Neuronal IFs are now thought to move as monomeric and polymeric units. Studies using proteins tagged with green fluorescent protein and live-video microscopy have demonstrated that neuronal IFs undergo rapid, intermittent, and nonsynchronous transport in both directions, with predominance of the anterograde transport and long pauses in between movements along the axons. These studies indicate that slow transport is actually the result of fast motions interrupted by long pauses. This fast transport is likely to utilize one of the many motors that have been identified for fast transport. These motor proteins could also be responsible for some of the cross-links observed between IFs and microtubules. Other potential cross-linkers are members of the plakin family of proteins that were first identified in junctions in epithelial cells. Recent studies have indicated that some plakins are also expressed in the nervous system. Plakins have distinct domains that include microtubule, microfilament, and IF-binding domains and could therefore be important in the formation of cross-links between these cytoskeletal elements. The phosphorylation of the side chains of the neurofilaments described above has also been considered to be important for the regulation of transport of neurofilaments through axons. Two recent studies have provided different conclusions regarding the role of NFH side arm phosphorylation in neurofilament transport. In one study, all the potential phosphorylation sites of NFH were mutated either to preclude phosphorylation or mimic permanent phosphorylation of the NFH side arms. These mutants displayed altered rates of transport in a bulk transport assay. The mutant mimicking permanent phosphorylation spent a higher proportion of time pausing than one that could not be phosphorylated, indicating that NFH phosphorylation slows neurofilament transport. In contrast, in transgenic mice, where the endogenous NFH was replaced by a tailless NFH, there were no changes in the rate of bulk transport. These studies indicate that the mouse studies are not always consistent with the studies in cultured cells, in part due to additional compensatory mechanisms that may exist in the mouse. In any case, some of these aspects of neurofilament transport will become clearer when the specific motors that move neurofilaments are identified.

Overexpression of neuronal IFs in transgenic mouse models results in the formation of mislocalized protein aggregates, which affect neuronal function and survival. This has been shown in the case of human NFH, mouse NFL, peripherin, and rat α-internexin. The relationship between misexpression, disrupted transport, and mislocalization of neuronal IFs to neurodegeneration is also apparent from the appearance of axonal neurofilamentous accumulations in a number of neurodegenerative diseases. In particular, aggregation of IFs in motor neurons and alteration in their axonal transport has been reported in amyotrophic lateral sclerosis (ALS).

It appears likely that mutations in neurofilament proteins would also lead to neurodegeneration. When an assembly disrupting NFL mutant was produced in a transgenic mouse model, the mutant NFL caused massive degeneration of motor nerves. Recently, several mutations have been identified in neurofilament proteins that lead to neurodegenerative diseases. Deletions and insertions in the tail domain of NFH have been reported in 1–2% of patients with sporadic ALS. More strikingly, a number of mutations in the NFL gene have now been linked to Charcot-Marie-Tooth neuropathy type 2E. Two of these mutations (P8R and Q333P) are shown in Figure 1. When these same mutations are introduced in an NFL cDNA and the mutant NFL constructs are expressed in cultured cells, defects in assembly and transport of NFL are observed. It appears therefore that these mutations in NFL might alter axonal transport, which in turn would cause neurodegeneration. This notion is consistent with the hypothesis that alterations in axonal transport (in which neuronal IFs could be directly or indirectly involved) play a role in the pathogenesis of other neurodegenerative diseases.

α-Internexin

α-Internexin was first isolated from optic nerve and spinal cord and found to be particularly abundant in the developing nervous system. α-Internexin has an apparent molecular weight of 66 kDa and is therefore a little smaller than the NFTPs. Although it is present in both the CNS and PNS early in development, it is mainly CNS specific in the mature mammalian nervous system. Consistent with its expression early in development in the absence of other IFs, α-internexin has been shown to be able to self-assemble both *in vitro* and in transfected cells. α-Internexin is closely related to the NFTPs and is therefore also classified as a type IV IF protein. α-Internexin is the first neuronal IF expressed in neurons after they are committed to the neuronal lineage. The expression of α-internexin is high early in development and then decreases after the axon matures. In the PNS, the level of α-internexin decreases significantly in adulthood, although it persists especially in thinner unmyelinated axons. In the CNS, α-internexin expression is also lower after the axon matures. Of particular interest is the fact that α-internexin is the only neuronal IF expressed in some neurons, e.g., the granule cell neurons in the cerebellum. The axons of these neurons are thinner in diameter than the ones that express the NFTPs suggesting that α-internexin is not important for maintaining axonal diameter. The early expression of α-internexin led to the suggestion that it might be important for axon outgrowth. Although this idea was supported by antisense inhibition experiments in cultured cells, the α-internexin knockout mice have no obvious phenotype. No compensatory changes in the levels of other neuronal IFs were observed and it appears that α-internexin is not necessary for axon outgrowth in these mice. Unfortunately, these knockout studies tell us little about other potential functions of this protein. Overexpression of α-internexin in transgenic mice results in the formation of cerebellar torpedoes. These torpedoes are swellings in Purkinje cell axons. The presence of these torpedoes results in the degeneration and ultimate death of the Purkinje cell. There is a dysfunction of the cell as determined behaviorally from the transgenic mice before the cells die.

Peripherin

Peripherin was first identified as an IF protein from neuroblastoma and its cDNA was cloned from a cell line that can be induced to grow neuronal processes by the addition of nerve growth factor, called PC12 cells. Peripherin has a molecular weight of 57 kDa and belongs to the type III IF proteins, which also consists of vimentin, the glial specific GFAP, and the muscle specific IF protein called desmin. Peripherin is therefore the only type III neuronal IF protein, since all the other neuronal IFs are in the type IV category. The significance of this difference is not known. Like all the other type III IFs, peripherin can self-assemble into a filamentous network. Peripherin can also coassemble with other neuronal IFs. Peripherin is predominantly found in the PNS (hence its name), but some CNS neurons also express peripherin. As described above, peripherin was identified as a gene that was increased in PC12 cells upon stimulation by nerve growth factor. Peripherin has also been shown to be up-regulated following axonal injury. These studies suggested that peripherin may play a role in axon outgrowth and elongation. Peripherin depletion experiments with anti-sense technologies yielded conflicting results: initial studies showed that anti-sense oligonucleotides did not inhibit neurite outgrowth, whereas more recent studies using small interfering RNAs (siRNAs) showed that peripherin siRNA inhibits the initiation, extension and maintenance of neurites in PC12 cells. The reason for this discrepancy is not clear. Peripherin knock-out mice have normal caliber axons and show no axonal loss. Some interesting observations have led to the possibility that misexpression of peripherin can lead to neurodegenerative disease. Peripherin has been found in axonal spheroids in patients with ALS. Furthermore, overexpression of peripherin by four to seven fold in transgenic mice leads to late onset progressive motor neuron disease, which is accelerated in mice that lack NFL.

Nestin

Nestin was first described as a marker of neuroepithelial stem cells. Subsequent cDNA cloning showed that a large IF protein encoded this marker. Nestin has the basic hallmarks of an IF protein with a α-helical rod, capable of forming coiled coil dimers, a very short head domain and a very long tail domain. Nestin has little homology to the other mammalian IF proteins, but its genomic structure is similar to the NFTPs and α-internexin. As a result, nestin is placed either as a separate type of IF (type VI), or as a type IV IF along with the NFTPs and α-internexin. During early development, nestin is expressed in neuroepithelial cells and muscle progenitor cells. Transgenic mouse studies have indicated that different regulatory elements in the nestin gene are responsible for directing gene expression in developing muscle and neural precursor cells, respectively. Nestin is not able to self-polymerize, but requires vimentin to form a filamentous network. There have been no published reports of a nestin knockout mouse.

See Also the Following Articles

Actin Assembly/Disassembly • Actin-Capping and -Severing Proteins • Actin-Related Proteins • Intermediate Filament Linker Proteins: Plectin and BPAG1 • Intermediate Filaments • Microtubule-Associated Proteins • Rho GTPases and Actin Cytoskeleton Dynamics • Tubulin and its Isoforms

Glossary

axonal spheroids Accumulations of protein aggregates in axons, usually containing neurofilamentous structures.

axonal transport The movements of vesicles, mitochondria, and other cytoplasmic structures down the axon, necessitated by the fact that most protein synthesis occurs in the axon and the proteins must sometimes travel long distances to reach the end of the axon. This transport generally occurs by way of motor proteins along microtubules and microfilaments.

Charcot–Marie–Tooth (CMT) disease An inherited neurological disorder that affects the peripheral nerves. It is named after the three physicians who described it. CMT patients slowly lose the normal use of their limbs as the nerves to the extremities degenerate. There are a large number of different causes for the disease, including the recently identified neurofilament mutations.

cytoskeleton A network of interconnected cytoplasmic filaments that consists of microtubules, microfilaments and IFs.

transgenic mouse A mouse that has been genetically altered to express a gene that is not normally expressed or to have a gene deleted (also called a knockout mouse).

Further Reading

Coulombe, P. A., Ma, L., Yamada, S., and Wawersik, M. (2001). Intermediate filaments at a glance. *J. Cell Sci.* **114**, 4345–4347.

Helfand, B. T., Chang, L., and Goldman, R. D. (2003). The dynamic and motile properties of intermediate filaments. *Annu. Rev. Cell Dev. Biol.* **19**, 445–467.

Lariviere, R. C., and Julien, J. P. (2004). Functions of intermediate filaments in neuronal development and disease. *J. Neurobiol.* **58**, 131–148.

Leung, C. L., and Liem, R. K. H. (2003). Neuronal intermediate filament overexpression and neurodegeneration in transgenic mice. *Exp. Neur.* **184**, 3–8.

Leung, C. L., Flores, R. G., and Liem, R. K. H. (1998). The complexity of intermediate filaments in the nervous system. In *Intermediate Filaments* (H. Herrmann and R. Warton, eds.) pp. 497–526. Plenum Press.

Leung, C. L., Green, K. J., and Liem, R. K. H. (2002). Plakins: A family of versatile cytolinker proteins. *Trends Cell Biol.* **12**, 37–45.

Shah, J. V., and Cleveland, D. W. (2002). Slow axonal transport: Fast motors in the slow lane. *Curr. Opin. Cell Biol.* **14**, 58–62.

Biography

Ronald K. H. Liem is a Professor of Pathology and Anatomy and Cell Biology at Columbia University College of Physicians and Surgeons. Dr. Liem's primary research interest is in the cell and molecular biology of the neuronal cytoskeleton and its involvement in neurodegenerative diseases. His contributions include the biochemical identification of the neurofilament triplet proteins, the first identification and cDNA cloning of α-internexin and the characterization of the plakins, the major cytoskeletal linker proteins in the nervous system.

Neuropeptide Y Receptors

Eric M. Parker
Schering-Plough Research Institute, Kenilworth, New Jersey, USA

Neuropeptide Y (NPY) is a 36 amino acid neuropeptide that is widely distributed in both the central and peripheral nervous systems. NPY is a member of the pancreatic polypeptide family, which also includes the structurally related peptides peptide YY (PYY) and pancreatic polypeptide (PP). Neurons containing NPY typically coexpress and cosecrete classical neurotransmitters and/or other neuropeptides (e.g., norepinephrine, γ-aminobutyric acid, somatostatin, corticotrophin releasing hormone); hence, NPY probably acts in concert with other neurotransmitters and neuropeptides in either a cotransmitter or modulatory role. As expected from its ubiquitous distribution and colocalization with other neurotransmitters and neuropeptides, NPY has been implicated in a wide variety of physiological effects, including the regulation of body weight, neuronal excitability, circadian rhythms, mood, ethanol consumption, nociception, cognition, endocrine function, cardiovascular function, gastrointestinal function, and bone formation. The effects of NPY on energy homeostasis have been most extensively studied in recent years. NPY increases body weight via stimulation of food intake and reduction of energy expenditure and also induces metabolic abnormalities associated with obesity, including hyperinsulinemia, hyperglycemia, and hypercortisolemia.

Neuropeptide Y (NPY) produces its physiological effects by interacting with at least six distinct G-protein-coupled receptors designated Y_1, Y_2, Y_3, Y_4, Y_5, and y_6. With the exception of the Y_3 receptor, genes and/or cDNAs encoding each of these receptors have been cloned. Pharmacological tools that activate (agonists) or inhibit (antagonists) each of the NPY receptors have also been identified (Table 1, Figure 1). Although all the NPY receptors are G-protein-coupled receptors with high affinity for NPY, their primary sequences are not highly related to one another (Figure 2). Site-directed mutagenesis studies suggest that NPY, NPY-related peptides, and nonpeptide NPY receptor antagonists have overlapping (although not entirely identical) binding sites, composed primarily of residues in the extracellular domains and in the extracellular side of the transmembrane domains.

The NPY Y_1 Receptor

The NPY Y_1 receptor is pharmacologically characterized by its high affinity for [Pro^{34}]NPY and [D-Arg^{25}]NPY; its low affinity for N-terminally truncated NPY analogues; and its high affinity for nonpeptide antagonists such as 1229U91, BIBP3226, and BIBO3304 (Table 1, Figure 1). Structurally, the receptor is related to the NPY Y_4 and NPY y_6 receptors (Figure 2). NPY Y_1 receptor mRNA is expressed at highest levels in brain (especially cortex, hippocampus, thalamus, and hypothalamus), vascular smooth muscle, heart, kidney, spleen, skeletal muscle, lung, testis, adrenal gland, placenta, bone marrow, and gastrointestinal tract. NPY Y_1 receptor protein distribution mirrors mRNA distribution fairly closely with the notable exception that low levels of receptor are detected in most hippocampal regions. The NPY Y_1 receptor is coupled to multiple signal transduction pathways via pertussis toxin sensitive G proteins (G_i and/or G_o), including reduction of cyclic AMP (cAMP) formation, an increase in intracellular calcium, an increase in MAP kinase activity, and activation of GIRK K^+ channels and L-type Ca^{2+} channels. The NPY Y_1 receptor mediates several biological effects of NPY, including contraction of vascular smooth muscle, stimulation of food intake and body weight gain, inhibition of insulin secretion, anxiolytic and antidepressant effects, regulation of pituitary hormone secretion (reduction of growth hormone and thyroid stimulating hormone secretion, stimulation of luteinizing hormone secretion), regulation of ethanol consumption, nociception, and neurogenic inflammation. Activation of the NPY Y_1 receptor acutely stimulates food intake and body weight gain, and acute treatment with NPY Y_1 receptor antagonists often has the opposite effect. As expected from acute experiments, mice lacking the NPY Y_1 receptor are hypophagic, hyperinsulinemic and have slightly reduced NPY- and deprivation-induced food intake. However, NPY Y_1 receptor-deficient mice are also obese, perhaps due to hyperinsulinemia, reduced locomotor activity, and/or reduced metabolic rate.

TABLE 1

Potencies of Standard Agonist and Antagonist Ligands for the Known NPY Receptors

Peptide	Y_1	Y_2	Y_3	Y_4	Y_5	y_6
NPY	0.14	1.2	1.8	>1000	0.96	1.9
PYY	0.70	0.58	7200	>1000	1.0	0.8
NPY (2–36)	3.4	1.6		>1000	1.2	1.4
NPY (3–36)	110	2.4		>1000	2.8	4.9
NPY (13–36)	300	2.2		>1000	20	16.1
[Pro^{34}] PYY	0.37	>1000		6.0	1.3	
Human PP	150	>1000		0.037	1.4	>1000
Rat PP	>1000	>1000		0.060	170	>1000
[D-Arg^{25}]NPY	0.2	28.1		577	118	
1229U91	**0.063**	**> 1000**		**3**	**> 1000**	**0.8**
BIBP3226	**5.1**	**> 1000**	**> 1000**	**> 1000**	**> 1000**	**> 1000**
BIBO3304	**0.38**	**> 1000**		**> 1000**	**> 1000**	
BIIE0246	**> 1000**	**15**		**> 1000**	**> 1000**	
[D-Trp^{32}]NPY	>1000	>1000		>1000	43	164
[D-Trp^{34}]NPY	363	>1000		525	15	186
[Ala^{31}, Aib^{32}]NPY	>1000	>1000		>1000	29	
CGP-71684A	**> 1000**	**> 1000**		**> 1000**	**0.72**	**> 1000**

EC_{50} (nM) (Agonists; normal text) or **K_i (nM) (Antagonists; bold text)**.

The NPY Y_2 Receptor

The NPY Y_2 receptor is structurally quite distinct from the other NPY receptors (Figure 2) and is pharmacologically characterized by its high affinity for N-terminally truncated NPY analogues, its low affinity for [Pro^{34}]NPY, and its high affinity for the nonpeptide antagonist BIIE0246 (Table 1). The NPY Y_2 receptor is localized primarily in the brain, but is also expressed at low levels in the gastrointestinal tract and peripheral nerve terminals. In the brain, highest levels of NPY Y_2 receptor mRNA are found in hippocampus, piriform cortex, olfactory tubercle, hypothalamus, thalamus, inferior olive, and lateral reticular nucleus. NPY Y_2 receptor protein is detected at highest levels in subfornical organ, thalamus, hypothalamus, substantia nigra, and area postrema. NPY-containing neurons in the brain express the NPY Y_2 receptor and the NPY Y_2 receptor antagonist BIIE0246 increases depolarization-evoked NPY release from brain slices, suggesting that the NPY Y_2 receptor acts as an autoreceptor. Similarly, pharmacological studies have shown that the receptor is localized on sympathetic, parasympathetic, and sensory nerve terminals where it functions as both an autoreceptor and a heteroreceptor to regulate neurotransmitter/neuropeptide release. The NPY Y_2 receptor couples to pertussis toxin-sensitive G proteins (G_i and/or G_o) leading to a reduction of cAMP formation, an increase in intracellular calcium mediated by activation of phospholipase C, an increase in MAP kinase activity, an activation of K^+ channels (e.g., Kv4, GIRK, and Ca^{2+} activated K^+ channels), and an inhibition of voltage-gated (N and P/Q type) Ca^{2+} channels. The NPY Y_2 receptor also apparently increases intracellular calcium via a phospholipase C-independent pathway that utilizes a pertussis-toxin insensitive G protein. The NPY Y_2 receptor is involved in several physiological processes, including reduction of neuronal excitability and seizure activity, regulation of circadian rhythms, regulation of body weight and energy metabolism, improvement in learning and memory, regulation of ethanol consumption, reduction of bone formation, reduction of gastrointestinal motility, intestinal secretory activity and stimulation of angiogenesis and wound healing. The precise role of the NPY Y_2 receptor in the regulation of body weight is currently unclear. Selective NPY Y_2 receptor peptide agonists do not alter food intake, suggesting that this receptor does not mediate the orexigenic effects of NPY. In fact, the NPY Y_2 receptor peptide agonist PYY3-36, which is released postprandially, actually decreases food intake and body weight in humans. Variable effects of genetic deletion of the NPY Y_2 receptor in mice have been reported. Further studies are needed to definitively determine the role of the NPY Y_2 receptor in the regulation of body weight.

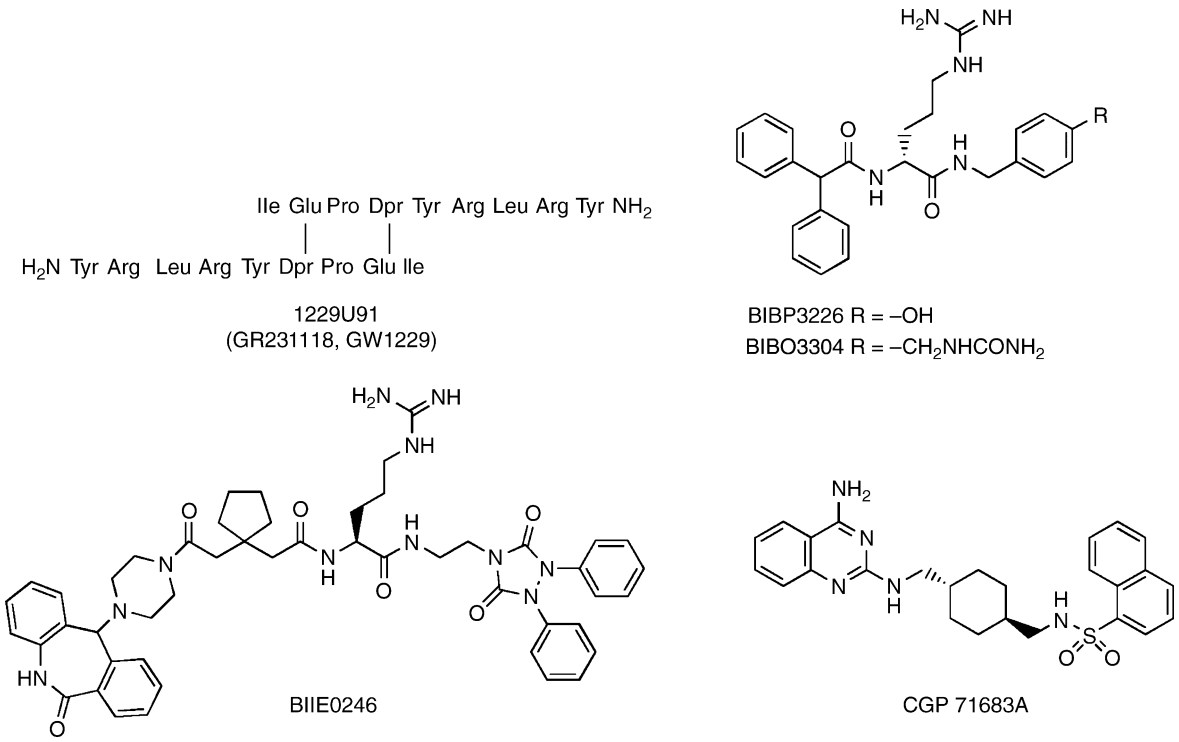

FIGURE 1 Structures of standard NPY receptor antagonists.

The NPY Y_3 Receptor

The NPY Y_3 receptor has been pharmacologically characterized in bovine adrenal chromaffin cells and in the rat heart, colon, lung, hippocampus, and brainstem. The distinguishing pharmacological feature of this receptor is its higher affinity for NPY than for PYY. Activation of the NPY Y_3 receptor has been shown to decrease cAMP formation and increase intracellular calcium concentration. Application of NPY to the brainstem decreases blood pressure and heart rate, effects that may be mediated by activation of the NPY Y_3 receptor. Although pharmacological evidence supports the existence of this receptor in rats and cows, there is no evidence that this receptor exists in humans, and a gene or cDNA encoding the receptor has not been cloned. Molecular characterization of the NPY Y_3 receptor is required to unequivocally validate its existence and determine its physiological role.

The NPY Y_4 Receptor

The NPY Y_4 receptor is structurally related to the NPY Y_1 and NPY y_6 receptors (Figure 2), but has distinct pharmacological properties (Table 1). Specifically, the NPY Y_4 receptor has high affinity for human and rat pancreatic polypeptide (PP), but has low affinity for NPY (Table 1). Indeed, this receptor would be more accurately classified as a PP receptor rather than as an NPY receptor. Interestingly, the rat and human NPY Y_4 receptors display some significant pharmacological differences, perhaps due to the fact that these species orthologues are only 75% identical to one another. Very low levels of NPY Y_4 receptor mRNA are expressed in the brain, primarily in the brainstem and hypothalamus. There are also species differences in the expression pattern of the NPY Y_4 receptor in the periphery. In rat, the receptor is expressed primarily in testis and lung, whereas in human the receptor is expressed primarily in colon, small intestine, prostate, and pancreas. Activation of the NPY Y_4 receptor decreases cAMP formation and increases intracellular calcium. Pharmacological studies have shown that, the NPY Y_4 receptor mediates the ability of PP to increase pancreatic secretion and increase intestinal motility. Mice lacking the NPY Y_4 receptor suggest that this receptor is involved in aggressive behavior and in maintaining sympathetic nervous system activity. In addition, genetically obese *ob*/*ob* mice lacking the NPY Y_4 receptor have improved fertility relative to *ob*/*ob* mice with an intact NPY Y_4 receptor, suggesting that this receptor mediates at least some of the negative effects of NPY and/or PP on fertility and on the hypothalamic–pituitary–gonad axis.

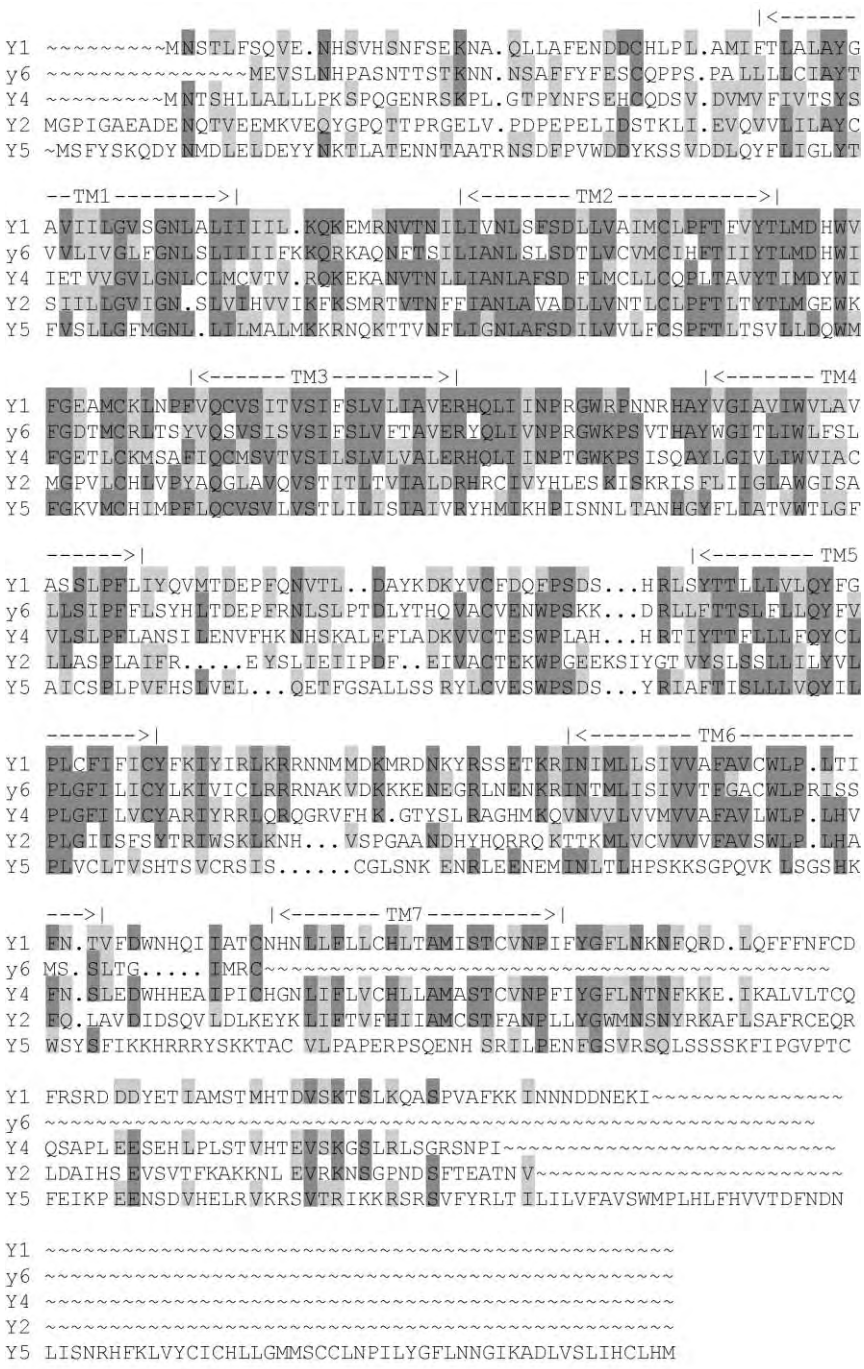

FIGURE 2 Alignment of the primary sequences of the NPY receptors. Amino acids that are identical in ≥3 NPY receptors are shaded dark while conservative amino acid substitutions in >3 NPY receptors are shaded light. The approximate location of the seven transmembrane domains is indicated over the sequences.

The NPY Y_5 Receptor

The NPY Y_5 receptor is a structurally and pharmacologically unique NPY receptor (Figure 2) characterized by high affinity for N-terminally truncated NPY analogues [Pro^{34}]NPY, [D-Trp^{32}]NPY, [D-Trp^{34}]NPY, and [Ala^{31}, Aib^{32}]NPY (Table 1). This receptor also has high affinity for several recently disclosed nonpeptide antagonists such as CGP-71684A (Figure 1). The NPY Y_5 receptor is discretely localized in brain, primarily in hypothalamus, hippocampus, piriform cortex, and olfactory tubercle. Interestingly, NPY Y_5 receptor mRNA is almost always localized in neurons that also express NPY Y_1 mRNA. Since the

genes encoding the NPY Y_1 and Y_5 receptors overlap on chromosome 4q31, this may reflect a regulatory mechanism inherent to this gene locus. In the periphery, NPY Y_5 receptor mRNA has been detected in testis, spleen, pancreas, gastrointestinal tract, vascular smooth muscles, and cardiomyocytes. Like the other NPY receptors, the NPY Y_5 receptor couples to multiple G protein-mediated pathways (primarily pertussis toxin-sensitive G proteins G_i and/or G_o) to decrease cAMP formation, increase intracellular calcium concentration, and activate MAP kinase pathways. There is evidence that the NPY Y_5 receptor utilizes a somewhat different signaling pathway to activate MAP kinase than do the other NPY receptors. Evidence suggests that this receptor is involved in the regulation of body weight (stimulation of food intake and reduction of energy expenditure), control of glucose homeostasis, regulation of pituitary hormone secretion (stimulation of adrenocorticotropin secretion, inhibition of thyroid stimulating hormone secretion, inhibition of luteinizing hormone secretion), regulation of ethanol consumption, control of neuronal excitability and seizure activity, circadian rhythms, diuresis, and natriuresis. Although selective NPY Y_5 receptor peptide agonists have been shown to stimulate food intake and decrease energy expenditure, selective NPY Y_5 receptor antagonists generally do not affect food intake, energy expenditure, or body weight. Furthermore, mice lacking the NPY Y_5 receptor have normal food intake, energy expenditure, and body weight. Thus, the role of the NPY Y_5 receptor in the regulation of body weight remains unclear.

The NPY y_6 Receptor

The NPY y_6 receptor is structurally related to the NPY Y_1 and Y_4 receptors. It is pharmacologically very similar to the NPY Y_1 receptor, although it tends to bind N-terminally truncated NPY analogues with somewhat higher affinity than the NPY Y_1 receptor. The NPY y_6 receptor couples to G_i and inhibits cAMP formation. Interestingly, a functional NPY y_6 receptor is found in mice and rabbits, but not in rats and primates. In the case of rats, a gene encoding the NPY y_6 gene cannot be detected, whereas in primates the gene is a nonfunctional pseudogene. The lack of a functional NPY y_6 receptor in primates has resulted in the adoption of a lower case designation for this receptor. In mice, NPY y_6 receptor mRNA has been detected in kidney, testis, and brain, particularly in the hypothalamus. Although the NPY y_6 receptor clearly does not contribute to the effects of NPY in humans, this receptor must be taken into account when considering the physiological effects of NPY in mice. To date, however, no physiological effect of NPY in mice has been linked to activation of the NPY y_6 receptor.

Regulation of NPY Receptors

As is the case for most G-protein-coupled receptors, NPY receptors are subject to various mechanisms of regulation. The NPY Y_1, Y_2, and Y_5 receptors have recently been shown to exist as homodimers in the plasma membrane, although the extent of homodimerization was not affected by the binding of NPY to the receptors or by the coupling of the receptors to G proteins. NPY receptors have also been shown to be subject to both homologous and heterologous desensitization. These desensitization processes are typically mediated by phosphorylation of the receptor and subsequent association of the phosphorylated receptor with arrestins. Over a longer period of time, receptors can internalize and be recycled or degraded. Changes in receptor gene expression can also occur. NPY Y_1 receptors rapidly desensitize after NPY treatment by phosphorylation of the receptor and rapid internalization of the receptor via clathrin coated pits. Conversely, NPY Y_2 receptors are internalized very slowly. The NPY Y_1, Y_2, Y_4, and Y_5 receptors also associate with β-arrestin 2, with the Y_1 receptor again showing the most rapid association rate and NPY Y_2 receptors showing the slowest association rate. With respect to heterologous desensitization, NPY Y_2 receptors have been shown to desensitize after exposure of LN319 cells to bradykinin.

See Also the Following Articles

G Protein-Coupled Receptor Kinases and Arrestins • Neurotensin Receptors • Neurotransmitter Transporters • Phospholipase C

Glossary

G protein A heterotrimeric GTP binding protein consisting of α-, β-, and γ-subunits. G proteins link G-protein-coupled receptors to a wide variety of effector molecules in signal transduction pathways by alternately binding and hydrolyzing GTP in response to receptor and effector activation.

G-protein-coupled receptors (GPCRs) A family of ~500 neurotransmitter and neuropeptide receptors (as well as several hundred odorant receptors) that are structurally characterized by seven transmembrane domains, an extracellular amino terminus, and a cytoplasmic carboxy terminus. This receptor family is functionally characterized by the ability to bind and activate G proteins upon binding of their cognate ligand.

Further Reading

Berglund, M. M., Hipskind, P. A., and Gehlert, D. R. (2003). Recent developments in our understanding of the physiological

role of PP-fold peptide receptor subtypes. *Exp. Biol. Med.* **228**, 217–244.

Parker, E., van Heek, M., and Stamford, A. (2002). Neuropeptide Y receptors as targets for anti-obesity drug development: perspective and current status. *Eur. J. Pharmacol.* **440**, 173–187.

Thorsell, A., and Heilig, M. (2002). Diverse functions of neuropeptide Y revealed using genetically modified animals. *Neuropeptides* **36**, 182–193.

Biography

Eric Parker is Group Director of Central Nervous System Research at the Schering-Plough Research Institute. His research interests include the molecular pathogenesis of Alzheimer's disease and neuropeptide and neurotransmitter receptors involved in the etiology of obesity and psychiatric disease. He holds a Ph.D. in pharmacology from the University of North Carolina at Chapel Hill.

Neurotensin Receptors

William Rostène, Patrick Kitabgi and Didier Pélaprat
INSERM, Paris, France

Peptides are now well-recognized as important modulators of central and peripheral functions. Among the considerable number of peptides which has been discovered in various species, neurotensin (NT) has been found to play an essential role in specific brain and neuroendocrine functions and more recently in cancer. These effects of NT have been related to an interaction of this 13 aminoacid peptide with receptors belonging to the family of G protein-coupled receptors (GPCRs) with seven transmembrane domains. Very recently a new NT receptor with a single transmembrane domain has been discovered. Cloning of these receptors has permitted to develop agonists and antagonists for NT, the more recent developments being focused on the potential therapeutical usefulness of nonpeptide and peptido-mimetic substances able to cross the blood–brain barrier.

Neurotensin

The discovery of Neurotensin (NT), a 13 aminoacid peptide, occurred during the isolation of another peptide, substance P, from bovine hypothalamus, by Susan Leeman and Robert Carraway in 1973. It was the simple observation of a characteristic vasodilatation occurring around the face and ears after intravenous injection of the isolated material which allowed the purification of NT. Rapidly after its primary structure in aminoacids was known, antibodies were raised, a strategy used for several peptides in order to develop sensitive radio-immunoassays and immunocytochemical approaches which provided useful information on the physiology, content, distribution, and anatomical localization of NT in fluids and tissues. Though NT was first found in the brain, 90% of the peptide is located in the gut.

The main *in vivo* biological activities of NT following peripheral administration include a strong vasodilatation and hypotension, an increase in vascular permeability via histamine released by the mast cells, a hyperglycemia involving glucagon, insulin and histamine, inhibition of gastric acid and pepsin secretion and of gastric motility. Strong neuroendocrine effects on the release of pituitary hormones such as ACTH, LH, FSH, GH, and prolactin have been particularly evidenced. Central injection of NT induced hypothermia, release of the neurotransmitter dopamine (DA), inhibition of feeding in fasted animals, and analgesic effects which are not mediated by opiates. Finally, high-fat meal and drugs affecting the brain DA systems have been reported to produce strong release of NT in plasma and brain, respectively.

Neurotensin Receptors

The relatively simple amino acid sequence of NT allowed structure-activity studies which showed that the C-terminal part (aa 8–13) of the peptide contained the whole activity of NT. Thus, design of small peptide molecules and modifications both in the N- and C-terminal portions of NT rapidly led to NT analogues which could be labeled with tritium or iodine in order to carry out binding studies. Such experiments demonstrated that high affinity NT binding sites could be observed in several tissues and various cell lines including human cancer cells. From these binding studies, it became obvious that NT could bind to several receptors as already shown for other neuropeptides.

Up to now indeed, three NT receptors – NTS1, NTS2, and NTS3 – have been identified and their biochemical and pharmacological properties recently reviewed. We will thus briefly outline their main characteristics (Table I).

NTS1

NTS1 has been cloned from rat and human and belongs to the family of G protein-coupled receptors (GPCRs) with seven transmembrane domains. It seems to be involved in the majority of the physiological effects of NT reported so far. NTS1 is a Gq-preferring receptor suggesting that binding of NT to NTS1 induces activation of phospholipase C, increase in inositol phosphate, and intracellular calcium concentration. In parallel, in transfected cell systems, NTS1 has been also reported to be linked to Gi/o or Gs, leading to inhibition or stimulation of cyclic AMP production, respectively, and to stimulation of more distal transduction pathways such as mitogen-activated protein kinases. Interestingly, the most recent data indicate that different intracellular

TABLE I

Characteristics of Cloned Neurotensin Receptors

Receptor subtype	Structure	Signal transduction pathway	Protein size amino acids	Agonists	Antagonists
NTS1	7 transmembrane domains	G_q/G_{11}, calcium mobilization	418 (h[a])	Neurotensin	SR 48692
		G_S, increase cAMP	424 (r[b])	NL-69L	SR 142948A
NTS2	7 transmembrane domains	Calcium mobilization	410 (h)	SR 48692 SR 142948A	Neurotensin Levocabastine
			416 (r)	Neurotensin SR 48692 Levocabastine	
NTS3 also termed sortilin	A single transmembrane domain	Unknown	831 (h) 825 (m[c])		

[a] Human.
[b] Rat.
[c] Mouse.

domains of the receptor are involved in coupling to the various G-proteins and suggest the existence of multiple agonist-selective conformations, which may lead to the preferential activation of either of the corresponding signaling pathways. These results open the possibility of designing agonists selective for one of the pathways associated with a given NTS receptor.

Although the development of selective NT agonists may be important for a better understanding of the physiological relevances of this peptide, random screening and chemical optimization led to the achievement of nonpeptide antagonists, which have proved extremely useful to study the role of endogenous NT associated with NTS1. The first nonpeptide antagonist, SR 48692, developed by Sanofi-Synthelabo, as well as the recent development of knock-out mice for NTS1 confirmed that most of the NT effects reported above can be attributed to NTS1. More recently, another nonpeptide NTS1 antagonist, SR 142948A, but with less selectivity for NTS1 than SR 48692, has been described.

Elegant strategies of mutagenesis and modeling of NTS1 have provided useful information about the molecular determinants of NT and SR 48692 binding sites on NTS1 demonstrating that on the 424 aminoacid protein sequence of rat NTS1, the third extracellular domain and residues in the sixth and seventh transmembrane domains were essential for both NT and SR 48692 binding. Some residues such as Trp339, Phe344, and Tyr347 (all of them aromatic aminoacids) located in the third extracellular loop of NTS1 are implicated in NT binding, Tyr324, Tyr351, Thr354, Phe358, and Tyr359 are involved in antagonist binding only, and Met208, Phe331, and Arg327 interact with both agonist and antagonist. The third intracellular loop of the NTS1 and the first half of the C-terminal intracellular domain are involved in Gq and Gi/o coupling respectively, whereas the C terminus is essential for NT-induced NTS1 internalization, an observation important for NT targeting, as it will be discussed later (Figure 1).

NTS2

NTS2 which is also a GPCR shares 60% sequence similarity with NTS1. It has been cloned from mouse, rat, and human, and corresponds to the low NT affinity sites originally described and able to bind the nonpeptide histamine H1 antagonist levocabastine. Most of the physiolological implications of NTS2 are unknown, but several arguments suggest that it mediates the analgesic effect of NT reported in the mouse. Surprisingly, depending on the species studied, NT, SR 48692, and levocabastine behave differently on transduction signaling pathway activation. In summary, SR 48692, an antagonist of the NTS1, behaves as a potent agonist on NTS2, whereas NT or levocabastine have no effect or antagonize the effect of SR 48692, for instance, on inositol phosphate production. These results suggest that an endogenous activator for NTS2 other than NT may exist and remains to be discovered. Though mutagenesis studies have not been carried out as extensively for NTS2 as that for NTS1, it was recently reported that a single tyrosine residue in position 237 in the third intracellular loop of the mouse and human NTS2 was responsible for receptor phosphorylation and essential for receptor recycling.

NTS3

In contrast to both NTS1 and NTS2, this more recently discovered NT receptor subtype belongs to the family of proteins characterized by a single-transmembrane domain, a cystein-rich domain, a signal peptide, a furin cleavage site, and a short cytoplasmic C-terminal

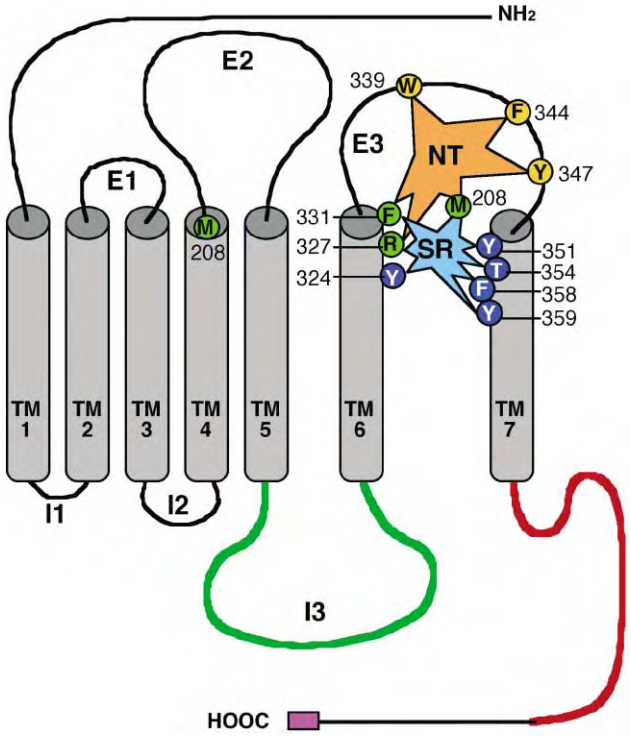

FIGURE 1 Molecular properties of the rat NTS1 (color illustration). The rat NTS1 is a 424 amino acid proteins with seven transmembrane (TM) domains. The SR 48692 (SR, light blue) and NT (orange) binding domains were established by mutagenesis and modeling studies. The residues that play a role in agonist and antagonist binding can be grouped in three categories: Met208, Phe331, Arg327 that interact with both NT and SR 48692 (green); Tyr324, Tyr351, Thr354, Phe358, and Tyr359 that are involved in antagonist binding only (blue); and Trp339, Phe344, and Tyr347 in extracellular loop 3 (E3) that interact with NT only (yellow). The C terminus of the NTS1 (magenta box) is essential for agonist-induced receptor internalization. Intracellular loop 3 (I3, in green) and the first half of the C-terminal intracellular domain (in red) are involved in Gq and Gi/o coupling, respectively.

tail. This 100 kDa protein shares 100% with sortilin, a protein involved in molecule sorting between the cell surface and intracellular compartments. Thus, it was recently observed that NTS3 could interfere with NT-induced intracellular trafficking of NTS1. Brain distribution of NTS3 demonstrates an extensive overlap of NTS3 with NTS1 and NTS2 subtypes, suggesting that NTS3 might interact with the other NT receptors to mediate central effects of NT. Recent evidence suggests that NT3 can mediate the effect of NT on microglial migration.

Receptor-Mediated Physiological Effects of NT

Although NT has been implicated in several central and peripheral effects as reported above, studies have been extensively focused on two main orientations. On the one hand, the brain involvement of NT in the regulation of central dopaminergic systems. On the other hand, in the periphery, its implication in cancer.

The main conclusions of these studies and their potential implication in therapeutics are reported here.

Neurotensin Receptor Implication in Brain Functions

Neurotensin and Dopamine Interaction

More than twenty years ago, it was observed that some behavioral and biochemical effects of centrally administered NT were similar to those exhibited by antipsychotic drugs, and that these drugs stimulated NT expression in brain regions where there are mesocorticolimbic and nigrostriatal DA neuronal projections. These observations led to the hypothesis that NT may act as an endogenous neuroleptic, and stimulated the research on NT–DA interactions. Moreover, autoradiographic binding studies showing that central DA neuronal pathways could be mapped using radiolabeled NT further suggested that NT could regulate DA transmission.

Subsequent studies confirmed that NT compounds targeting NTS1 might represent a new class of antipsychotic drugs. However, there is still a debate as to whether an NTS1 agonist or an antagonist such as SR 48692 would be more suitable as an antipsychotic and have fewer side effects than the antipsychotic drugs used in clinics. Such controversial issue has recently been addressed in two complementary reviews.

Part of the discrepancies is based on the fact that NT exerts opposite effects on DA transmission depending on the site of injection in the brain. Administered into the nucleus accumbens where the mesolimbic DA system projects, NT produced a neuroleptic-like effect. By contrast, injection of the peptide in the ventral tegmental area, the region of the mesolimbic DA cell bodies, elicits psychostimulant-like effects. Similarly, though several data demonstrate that NT facilitates DA synthesis and DA transmission (an effect blocked by SR 48692), suggesting a psychostimulant action of NT, the observation that SR142948A disrupted acquisition of latent inhibition in rat, an animal model of schizophrenia, is in favor of NT mediating the effects of antipsychotic drugs. Finally, a pseudopeptide analogue of NT able to cross the blood brain barrier, NL-69L, was recently reported to exhibit antipsychotic-like effects after peripheral administration in rat.

Overall, final answer to whether an NT agonist or antagonist may be useful for the treatment of psychotic disorders such as schizophrenia will need clear-cut results in human trials.

Another field in which interaction between NT and DA has been proved to be potently and clinically

interesting is the treatment of stress and drug abuse. On the one hand, SR48692 has been shown to blunt stress-induced DA release and stimulation of the hypothalamo-pituitary adrenal axis; on the other hand, very recent data clearly report that NT neurons play a key role in the modulation of DA mesolimbic system in reward, blockade of NTS1 by SR 48692 inducing an inhibition of both amphetamine and cocaine-induced increase in locomotor activity and addiction.

NT and Pain Modulation

Whereas NTS1 seems to be implicated in NT–DA interaction, strong evidence suggests the involvement of NTS2 in the mediation of NT antinociceptive effects. Pharmacological studies have demonstrated that the NT antagonist SR 142948A does not distinguish between NTS1 and NTS2, blocks NT-induced nociception, whereas the NTS1-specific antagonist SR 48692 does not. Recent data on NTS1 and NTS2 knockout mice suggest the implication of NTS2 in the analgesic effects of NT. Supporting this, levocabastine and NTS2 antisense oligonucleotides were both found to inhibit the antinociceptive effects of intracerebroventricular administration of NT. Furthermore, brain structures associated with every single sensory system, in particular those implicated in the descending control of nociceptive inputs (e.g., the periaqueductal gray or raphe nuclei), contain a strong NTS2 immunoreactivity. However, since the distribution of brain NTS2 largely exceeds that of NT terminal fields, it suggests that NT may not be the only endogenous ligand for this receptor subtype. More work has to be done to clarify the pharmacology and physiological relevance of NTS2 in that context.

Neurotensin Receptor Implication in Cancer

Increasing evidence demonstrates that proNT and NTS1 are deregulated in several human cancers such as colon, pancreatic, prostate, and lung cancer, suggesting that NT may exert an autocrine activation of its own NTS1 receptor in cancer. Thus, the use of NT receptor antagonists to block the proliferative effect of NT on cancer cells is one of the promising prospects in cancer therapy. In this respect, it has been recently reported that SR 48692 could inhibit NT-stimulated growth of human colon, pancreatic, and lung cancer cell lines and, when administered alone to nude mice grafted with human NTS1-expressing colon cancer cells, could induce a reduction in tumor volume. It also seems that the proliferative effect of NT can be mediated not only by NTS1 but also by NTS3 since several of the cancer cells coexpressed both receptor subtypes. Selective NTS3 antagonists may thus be of particular interest in cancer therapy.

Not only NT antagonists but also NT agonists may be useful in cancer. Since NT receptors can be overexpressed in cancer tissues, this property can be used positively to target NTS-expressing cancer cells. Like most GPCRs, NTS1 undergoes internalization of the agonist into the target cell. Because NTS1-agonist complexes readily internalize, radiolabeled NT analogues targeting NTS1-expressing cancer cells have been recently developed. Pseudopeptide NT 8–13 stable analogues radiolabeled with 99mTechnecium have been developed for diagnostic purpose in cancer. Recently a strategy using the simultaneous detection of an antigen specifically expressed on cancer cells, carcinoembryonic antigen, with NTS1 using an 111Indium labeled NT hapten-bearing analogue has been shown to be an extremely promising approach to enhance selectivity to target tumor cells as compared to cells only expressing the cell surface receptor. This approach could allow the development of radiopharmaceuticals labeled with isotopes suitable not only for diagnostic but also for radiotherapy.

See Also the Following Articles

Dopamine Receptors • G Protein-Coupled Receptor Kinases and Arrestins • Neuropeptide Y Receptors

Glossary

antipsychotic and **psychostimulant drugs** Synthetic molecules which affect brain dopamine transmission. Neuroleptics are antipsychotics and psychostimulant drugs of abuse.

dopamine A neurotransmitter synthesized in specific cells from tyrosine, by means of a rate-specific enzyme, tyrosine hydroxylase. Dopamine is implicated in motor activity, mood behavior, and emotion. It is considered as a "pleasure" molecule.

EISAI, NT-69-L, JMV 449, JMV 431 NT analogues used for the characterization of NTS.

GPCR G protein-coupled receptors, receptor family of heptahelical transmembrane proteins that trigger intracellular signaling cascade via G proteins when stimulated by a variety of stimuli including light, odorant molecules, neurotransmitters, hormones, and peptides. They represent targets for more than 40% of all marketed drugs and around 10% of the human genome.

levocabastine A nonpeptide histamine H1 antagonist that binds NTS2; developed by Janssen Laboratories, Beerse, Belgium.

neuropeptides Peptides that work as neurotransmitters or neuromodulators on brain and neuroendocrine functions. More than 100 have been described so far.

neurotensin A 13 amino acid peptide found mainly in both the brain and the gut. Synthetized as part of a precursor protein (pro-NT) from which it is excised by prohormone convertases in the regulated secretory pathway of neuroendocrine cells. Its primary structure is: pGlu-Leu-Tyr-Glu-Asn-Lys-Pro-Arg-Arg-Pro-Tyr-Ileu-Leu.

SR 48692 and SR 142948A Synthetic molecules which are nonpeptide antagonists of NTS1 and agonists of NTS2 developed by Sanofi Synthelabo, France.

Further Reading

Bérod, A., and Rostène, W. (2002). Neurotensin: An endogenous psychostimulant? *Curr. Opin. Pharmacol.* **2**, 93–98.

Betancur, C., Azzi, M., and Rostène, W. (1997). Nonpeptide antagonists of neuropeptide receptors: Tools for research and therapy. *Trends Pharmacol. Sci.* **18**, 372–386.

Dal Farra, C., Sarret, P., Navarro, V., Botto, J. M., Mazella, J., and Vincent, J. P. (2001). Involvement of the neurotensin receptor subtype NTR3 in the growth effect of neurotensin on cancer cell lines. *Int. J. Cancer* **92**, 503–509.

Hillairet De Boisferon, M., Raguin, O., Thiercelin, C., Dussaillant, M., Rostene, W., Barbet, J., Pelegrin, A., and Gruaz-Guyon, A. (2002). Improved tumor selectivity of radiolabeled peptides by receptor and antigen dual targeting in the neurotensin receptor model. *Biocong. Chem.* **13**, 654–662.

Kitabgi, P. (2002). Targeting neurotensin receptors with agonists and antagonists for therapeutic purposes. *Curr. Opin. Drug Discov. Develop.* **5**, 764–776.

Kinkead, B., and Nemeroff, C. B. (2002). An endogenous antipsychotic? *Curr. Opin. Pharmacol.* **2**, 99–103.

Martin, S., Vincent, J. P., and Mazella, J. (2003). Involvement of the neurotensin receptor-3 in the neurotensin-induced migration of human microglia. *J. Neurosci.* **23**, 1198–1205.

Rostène, W., and Alexander, M. J. (1997). Neurotensin and neuroendocrine regulation. *Front Neuroendocrinol* **18**, 115–173.

Sarret, P., Gendron, L., Kilian, P., Nguyen, N. H., Gallo-Payet, N., Payet, M. D., and Beaudet, A. (2002). Pharmacology and functional properties of NTS2 neurotensin receptors in cerebellar granule cells. *J. Biol. Chem.* **277**, 36233–36243.

Vincent, J. P., Mazella, J., and Kitabgi, P. (1999). Neurotensin and neurotensin receptors. *Trends Pharmacol. Sci.* **20**, 302–309.

Biography

William Rostène is Research Director at INSERM, France. He was head of the INSERM Unit 339 in Paris (1991–2002). He qualified as a neuroendocrinologist and was President of the French Society for Neuroendocrinology (1997–2000). He is one of the pioneers in the development of autoradiography and image analysis for neuropeptide receptors and has carried out extensive work on two neuropeptides, neurotensin and VIP.

Patrick Kitabgi is Research Director at INSERM, France. He is currently Head of INSERM E0350 in Paris. He has devoted most of his scientific career to the study of neurotensin starting in 1974 in the laboratory of Susan Leeman who discovered neurotensin.

Didier Pélaprat is Research Director at INSERM, France. He qualified as an organic chemist and then a neurobiologist. His work particularly focused on functional consequences of ligand–receptor interactions and modulation of dopaminergic systems by neuropeptides such as cholecystokinin and neurotensin.

Neurotransmitter Transporters

Aurelio Galli, Randy D. Blakely and Louis J. DeFelice
Vanderbilt University, Nashville, Tennessee, USA

Neurotransmitters are chemical messengers that neurons use to communicate with each other. Timely removal of neurotransmitters from the synaptic cleft is critical for synaptic neurotransmission. If released neurotransmitter molecules remain in the synaptic cleft, the synapse would become nonresponsive due to continued exposure of neurotransmitter. Removal of neurotransmitter from the synaptic cleft occurs by three mechanisms: diffusion, enzymatic degradation, and reuptake. Transporter proteins localized in nerve and glial cell membranes mediate high affinity reuptake for the released neurotransmitters, and under many circumstances reuptake is the dominant mechanism for the termination of synaptic signaling. This mechanism not only serves to clear extracellular neurotransmitter, but it also recaptures transmitter molecules for possible reuse. In addition, significant ionic currents are associated with transport, and these may contribute substantially to the excitability of the cell.

Neurotransmitter transporters utilize the electrochemical energy derived from the inward movement of ions, particularly sodium, to drive the intracellular accumulation of neurotransmitter. Neurotransmitter transporters are thus designated as cotransporters. In the early 1990s, several of these membrane proteins were cloned and two broad families have been identified. The first, which includes the norepinephrine (NE), dopamine (DA), γ-aminobutyric acid (GABA) and serotonin (5HT) transporters, shares no significant sequence homology with the second, which includes transporters for glutamate. After the "cloning" decade, several intriguing and exiting questions related to their structure and function are being raised: What is the molecular mechanism of transport? How does the protein structure define these mechanisms? What are the cellular signals and determinants that regulate transporter expression and function? Are there disease states related to neurotransmitter transporter dysfunction? This article will be restricted to GABA transporters and the monoamine transporters; discussion of vesicular transporters, glutamate transporters and sodium-dependent glucose transporters will be omitted.

Mechanisms of Transport

Reuptake

Neurotransmitter transporters operate by coupling the transmembrane translocation of substrate to the movement of driving ions down pre-established electrochemical gradients (cotransport). Members of this family include the membrane carriers for dopamine (DAT), serotonin (SERT), norepinephrine (NET), and γ-aminobutyric acid (GAT1–3). The most widely held concept of how cotransporters function is founded on the "alternating access model," in which the binding sites for substrates and cosubstrates are alternately exposed to extracellular or cytoplasmic environments via conformational changes in the transporter protein. The thermodynamic work of the transporter is accomplished by coupling the flux of substrate to the movement of cotransported ions down their electrochemical gradients. The stoichiometry inferred from radiolabeled transport studies on neurotransmitter transporter-expressing cells and membrane vesicles is two Na^+, one Cl^-, and one molecule of substrate for DAT and GAT1. For NET the proposed stoichiometry is one Na^+, one Cl^-, and one molecule of NE. With the exception of mammalian SERT, which is proposed to be electroneutral due to additional counter ion flow, the neurotransmitter transporter process is electrogenic meaning that the transport cycle moves net charges across the plasma membrane. Indeed, in cell lines stably transfected with the cDNA of neurotransmitter transporters, it is possible to record electrical currents generated by their activity using the patch clamp technique in the whole-cell configuration. However, these currents are generally too large to be explained entirely by fixed stoichiometry models (see Figure 1).

Recent electrophysiological studies of both native and cloned neurotransmitter transporters revealed that transporters can have brief and rare channel-like openings comparable to those generated by ligand-gated ion channels. Models for this exiting mode of the neurotransmitter transporters have been established, in which substrate, Na^+ and Cl^- induce the carrier to transport in the alternating access mode (Figure 1A, 1B), and rarely switching to a channel-like mode (Figure 1C). The alternating access model assumes that the substrate permeation occurs through a state transition (A ↔ B) and results in the transport of a single neurotransmitter molecule (Figures 1A and 1B). The channel-like mode (Figure 1C) is a low probability event that consists of hundreds of ions

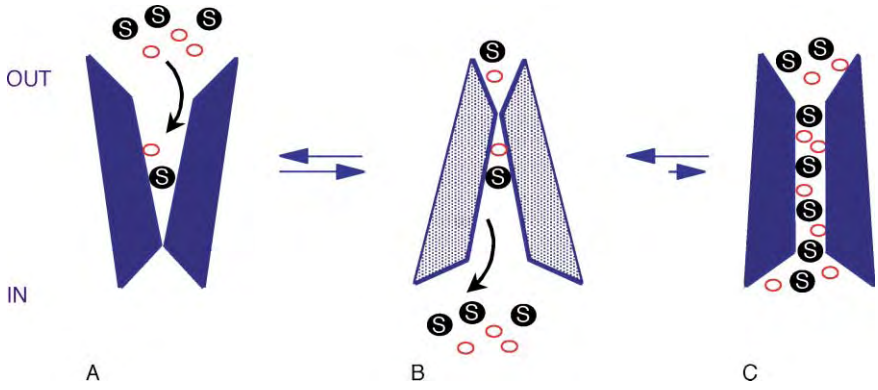

FIGURE 1 Model for neurotransmitter transporter function.

crossing the membrane (using a transporter pore), down their electrochemical gradients. These models have been recently refined and expanded based on new data.

Efflux

In addition to mediating the reuptake of neurotransmitter into nerve terminals, transporters can also cause non-Ca^{2+}-mediated efflux of the transmitter from the nerve terminal. There are essentially two mechanisms by which to elicit reverse transport from neurons: first, by changing the transmembrane ion gradients and voltage; and, second, for monoamine transporters, via the actions of pharmacological compounds such as amphetamine that may stabilize an efflux competent conformation, modulate ion gradients or both. In the case of glutamate transporters, nonvesicular neurotransmitter release is thought to play a role in pathophysiological conditions causing membrane depolarization such as epilepsy, or excitotoxicity such as stroke.

Structure and Function

A milestone in the advancement of knowledge of neurotransmitter transporters was achieved in 1990 when the first cDNAs encoding the GABA transporters were cloned and sequenced. As a consequence neurotransmitter transporters cDNAs for NET and SERT were soon cloned, and the list grew. The gene products of the Na^+/Cl^- neurotransmitter transporter family are highly conserved. Monoamine and GABA transporters show a common structure of a predicted 12 transmembrane (TM) domains with a single large loop in the external side of the plasma membrane with potential glycosylation sites. Each TM domain contains predominantly hydrophobic amino acid residues. The TM domains are connected by extracellular or intracellular loops located on either side of the plasma membrane in which the residues are mostly hydrophilic. Because high-resolution structures, such as the ones obtained by X-ray crystallography, are difficult to gain for integral membrane proteins, most of the structural information for neurotransmitter transporters obtained in recent years has been obtained by chemical modification with labeling reagents. In particular, the cysteine accessibility method (SCAM) has been used to gather information on the topology and the mechanism of transport. With this technique, a particular residue in the sequence is replaced usually with a cysteine residue. Then, chemical modifications of the cysteine are performed to measure its accessibility by evaluating, for example, changes in transporter function induced by the chemical modification. Cysteines are well tolerated as a replacement for a particular amino acid in the sequence of most membrane transporter proteins. By using different types of reagents, and, depending on the reagent used, the accessibility of a residue may provide information about its location and function. Use of these methodologies allowed researchers to measure the level of exposure of predicted extracellular loops in SERT, DAT, and other neurotransmitter transporters. Because the kinetics of reactivity for cysteine substitutions in TM domains and loops are expected to be different, SCAM can also provide information on the location of the end and the beginning of a particular transmembrane domain. Furthermore, cysteine substitutions whose chemical reactions result in a robust modification in transporter activity can elucidate the relationship between structure and function. For example, if the change in transporter activity resulting from the chemical modification of a cysteine can be altered by the presence of an inhibitor or a substrate, there is the possibility that this cysteine is part of the substrate-inhibitor binding site. With this experimental strategy, Rudnick and co-workers suggested that the Ile in position 172 and Tyr in position 176 of the TM domain 3 of the rat

SERT are in proximity to the binding site for 5-HT and cocaine. A relevant transporter (lactose permease of *Escherichia coli*) structure from another gene family has recently appeared.

Regulation

It is not surprising that molecules regulating the spatial and temporal dimension of synaptic events are tightly regulated. Several reports have shown that various signaling molecules can rapidly regulate many of the neurotransmitter transporters. Regulators of neurotransmitter transporter activity include G protein-coupled receptors such as the D_2 and mGluR5 receptors, kinases such as protein kinase C, phosphatidylinositol 3-kinase, tyrosine kinase, and Ca^{2+}/calmodulin kinase, protein kinase B, protein kinase C, and neurotrophic factors. In addition to transporter rates, many studies suggested that the regulation of neurotransmitter transport capacity might originate from a change in their cell surface expression. In this context, it is important to point out that transporter interacting proteins finely control plasma membrane expression level of neurotransmitter transporters. For example, in addition to PKC and other signaling pathways, cell surface expression and activity of GAT1 and NET are regulated by syntaxin 1A, a protein involved in synaptic vesicle fusion to the plasma membrane. Similarly, DAT surface expression can be influenced by its PDZ-mediated protein–protein interaction with PICK1, a PKC-binding protein. Although it is still not clear whether this transporter family shares common regulating factors, it is becoming evident that the trafficking of neurotransmitter transporters represents a new paradigm by which neurons control their ability to reuptake neurotransmitter. Other regulators of DAT and SERT cell surface expression include psychostimulants such as AMPH and cocaine.

The general process of transporter trafficking, that involves endocytosis, intracellular sorting, and exocytosis of these membrane proteins, is acquiring great interest for neuroscientists. Indeed, researchers studying transporter cell surface redistribution are envisioning the possibility of discovering new cellular targets to cure specific neurological disorders.

Relationships Between Disease States and Neurotransmitter Transporters

The ability of the neurotransmitter transporters to regulate normal synaptic signaling implies that functional modification of transporter activity might contribute to the etiology of multiple neurobiological diseases. Indeed, many studies have suggested for years, largely on the basis of pharmacology, that the monoamine transporters NET, DAT, and SERT play an important role in regulating mood, learning, and motor activity, while GABA transporters have been implicated in neuronal excitability dysfunction such as epilepsy. Indeed, a decade of innovative pharmacology resulted in the development of compounds that, by targeting neurotransmitter transporters, alleviate the symptoms of neurological diseases such as drug abuse and attention deficit/hyperactivity disorder. New hopes for the cure of these conditions are coming from studying the gene organization and polymorphisms of these membrane proteins. It has been shown that variations in the human neurotransmitter transporter sequences, known as polymorphisms, may alter transporter expression level, activity, or regulation that ultimately may influence the levels of extracellular neurotransmitter. The cloning of the neurotransmitter transporter genes has provided the tool for examining transporter genetic variations and possibly to correlate them to human diseases. This is particularly true for the monoamine transporters (SERT, DAT, NET) each encoded by a single gene. Therefore, the impact of polymorphisms could have far-reaching consequences due to a limited opportunity for compensation from other genes. Finding an association of a polymorphism with disease is clearly the first of many steps toward understanding how genetics shape the neurobiological diseases. A recent example of such an effort is the identification of a NET coding variant, A457P, in subjects with orthostatic intolerance.

See Also the Following Articles

Calcium/Calmodulin-Dependent Protein Kinase II • Calcium/Calmodulin-Dependent Protein Kinases • Dopamine Receptors • $GABA_A$ Receptor • $GABA_B$ Receptors • Protein Kinase C Family • Serotonin Receptor Signaling

Glossary

neurotransmitters Message chemicals released from one neuron at the presynaptic nerve terminal.

polymorphism A genetic variance that appears at least in 1% of the population.

synaptic cleft A gap between the pre-and postsynaptic membranes.

Further Reading

Abramson, J., Smirnova, I., Kasho, V., Verner, G., Kaback, H. R., and Iwata, S. (2003). Structure and mechanism of the lactose permease of *Escherichia coli*. *Science* **301**, 610–615.

Beckman, M. L., and Quick, M. W. (1998). Neurotransmitter transporters: Regulators of function and functional regulation. *J. Membr. Biol.* **164**, 1–10.

Chen, J. G., Sachpatzidis, A., and Rudnick, G. (1997). The third transmembrane domain of the serotonin transporter contains residues associated with substrate and cocaine binding. *J. Biol. Chem.* **272**, 28321–28327.

DeFelice, L. J., and Galli, A. (1998). Fluctuation analysis of norepinephrine and serotonin transporter currents. *Methods Enzymol.* **296**, 578–593.

Guastella, J., Nelson, N., Nelson, H., Czyzyk, L., Keynan, S., Miedel, M. C., Davidson, N., Lester, H. A., and Kanner, B. I. (1990). Cloning and expression of a rat brain GABA transporter. *Science* **249**, 1303–1306.

Jardetzky, O. (1966). Simple allosteric model for membrane pumps. *Nature* **211**, 969–970.

Javitch, J. A. (1998). Probing structure of neurotransmitter transporters by substituted-cysteine accessibility method. *Methods Enzymol.* **296**, 331–346.

Rudnick, G. (1998). Bioenergetics of neurotransmitter transport. *J.Bioenerg. Biomembr.* **30**, 173–185.

Saunders, C., Ferrer, J. V., Shi, L., Chen, J., Merrill, G., Lamb, M. E., Leeb-Lundberg, L. M. F., Carvelli, L., Javitch, J. A., and Galli, A. (2000). Amphetamine-Induced Loss of Human Dopamine Transporter Activity: An Internalization-Dependent and Cocaine-Sensitive Mechanism. *Proc. Natl Acad. Sci. USA* **97**, 6850–6855.

Shannon, J. R., Flattem, N. L., Jordan, J., Jacob, G., Black, B. K., Biaggioni, I., Blakely, R. D., and Robertson, D. (2000). Orthostatic intolerance and tachycardia associated with norepinephrine-transporter deficiency. *N. Engl. J. Med.* **342**, 541–549.

BIOGRAPHY

Aurelio Galli received his Ph.D. from the University of Milan in 1994. He is now a faculty member in the Department of Molecular Physiology and Biophysics at Vanderbilt University in Nashville, Tennessee. His principal research interest is to study the regulation by psychostimulants of neurotransmitter transporter function.

Randy Blakely received his doctorate in Neuroscience from the Johns Hopkins School of Medicine and then pursued postdoctoral studies at Yale University. Following a faculty position at Emory University, he became the Alan D. Bass Professor of Pharmacology at Vanderbilt. His major interest is in the molecular regulation of neurotransmitter transporter.

Louis J. DeFelice received his Ph.D. in Physics in Calgary, Alberta, Canada in 1967. He is now a Professor of Pharmacology and Neuroscience at Vanderbilt University. His principal research interest is the molecular mechanism of ion tansport across membranes, including ion channels and co-transporters.

Neurotrophin Receptor Signaling

Jennifer J. Gentry and Bruce D. Carter
Vanderbilt University, Nashville, Tennessee, USA

The purification of nerve growth factor (NGF) during the 1950s, based on its ability to promote the survival of sensory and sympathetic neurons, led to the discovery of a family of related trophic factors referred to as the neurotrophins. The members of the neurotrophin family include NGF, brain-derived neurotrophic factor (BDNF), neurotrophin 3 (NT3), and neurotrophin 4 (NT4), and each is essential for the survival of specific, but overlapping, populations of neurons during development. Given that nearly half of the neurons generated during mammalian ontogenesis undergo programmed cell death, it is clear that the neurotrophins have a major role in determining the ultimate population size for a given group of neurons. Moreover, the neurotrophins not only promote survival, but also regulate differentiation, axon guidance, synaptogenesis and neurite branching, and elongation; thus, this family of trophic factors has a wide spectrum of actions that are key for the proper sculpting of the mammalian nervous system. In addition to their role in development, this family of proteins also has important effects on maintenance of the nervous system, including such processes as learning and memory, neurogenesis in the adult and response to injury. This article will focus on the molecular-signaling mechanisms activated by the binding of neurotrophins to their receptors, with particular emphasis on the regulation of cell viability.

Introduction

The diversity in neurotrophin function is likely a reflection of the variety of signaling pathways that are influenced by activation of their receptors. The neurotrophin receptors consist of a family of tyrosine kinase receptors, the Trks, and a member of the tumor necrosis factor receptor family, p75NTR. Neurotrophin binding to the Trks promotes survival and differentiation while activation of p75NTR can also enhance cell viability or, paradoxically, induce apoptosis. Although activation of the Trks or p75NTR can initiate discrete signal transduction pathways, the two receptor types are frequently coexpressed on a given cell. Thus, it is the complex interactions between these receptors and crosstalk between their signaling pathways that ultimately determines the fate of the cell. In addition, a number of other receptors are modulated by the neurotrophins or can regulate neurotrophin signaling, either through interaction between receptors or cross talk between signaling pathways.

Neurotrophin Activation of Trk Receptors

The most well-studied actions of neurotrophins are mediated through activation of a family of tyrosine kinase receptors, the Trks. There are three members of the Trk family, TrkA, TrkB, and TrkC. Each receptor binds to specific members of the neurotrophin family preferentially with nerve growth factor (NGF) having the highest affinity for TrkA, BDNF, and NT4/5 for TrkB, and NT-3 for TrkC. Binding of a neurotrophin, which exist as dimers, to a Trk receptor triggers receptor dimerization and activation of intrinsic tyrosine kinase activity. Like other tyrosine kinase receptors, autophosphorylation of specific residues within the intracellular domain of the receptor leads to the recruitment of a wide variety of signaling molecules (Figure 1). In particular, these phosphotyrosines serve as docking sites for proteins containing Shc homolog 2 (SH2) or phosphotyrosine-binding (PTB) domains, including phospholipase C-γ (PLC-γ) and the adaptor proteins Shc, Frs-2, rAPS and SH2-B. These receptor-binding proteins initiate several signal transduction cascades.

Association of Trk with PLC-γ activates this enzyme, resulting in cleavage of phosphatidylinositol (4,5) bisphosphate to release the second messengers inositol-1,4,5-triphosphate (IP3) and diacylglycerol (DAG). DAG activates a number of isoforms of protein kinase C (PKC) while IP3 triggers the release of Ca^{2+} from intracellular stores, which activates a variety of pathways, including calmodulin kinases and Ca^{2+} regulated isoforms of PKC. The maintenance of calcium homeostasis has been well documented as key for regulating neuronal survival. Indeed, a role for PKC in prosurvival effects of the neurotrophins has been suggested; however, recent data suggests that this pathway has a more significant role in regulating spatial learning and

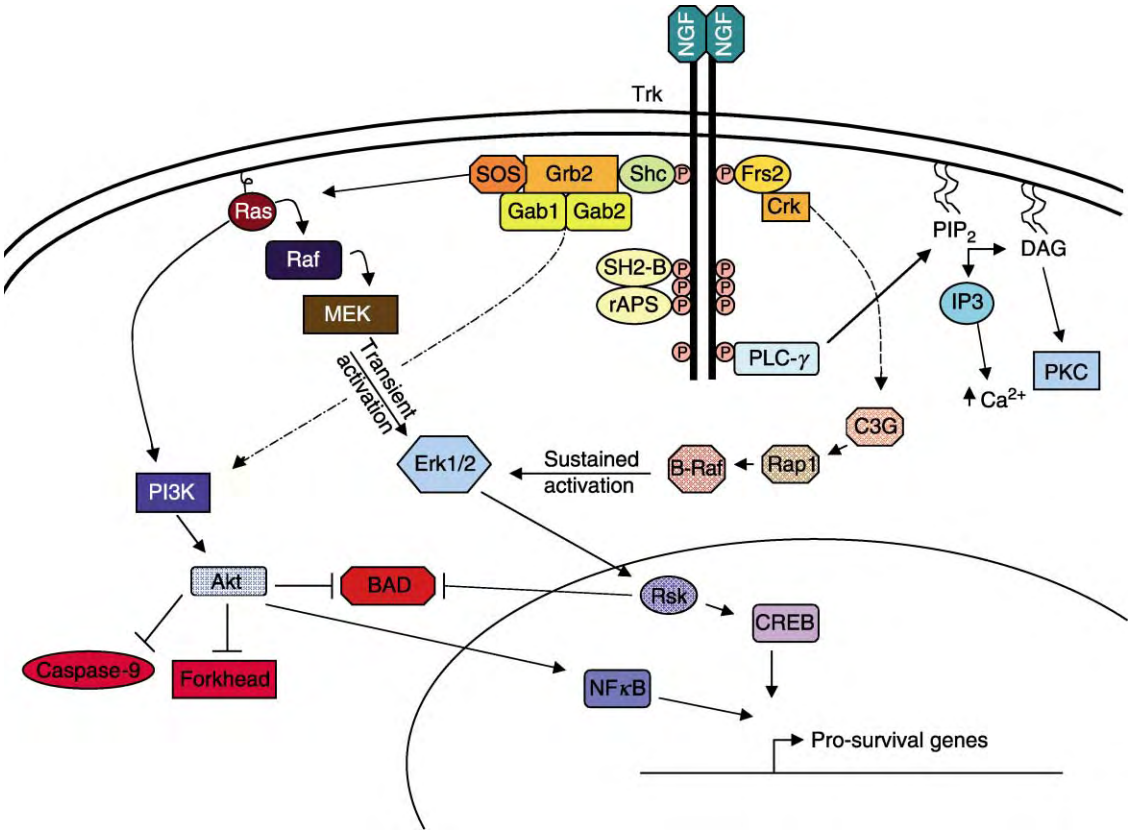

FIGURE 1 Neurotrophin signaling through the Trk receptor.

memory. Analysis of transgenic, knock-in mice lacking the docking site for PLC-γ on the TrkB receptor has not revealed any defects in neuronal survival, but the animals do display deficiencies in hippocampal long-term potentiation (LTP), which is a model for spatial memory.

Another signaling cascade activated by the Trk receptors is the Ras–MAP kinase pathway (Figure 1). The phosphorylation of the membrane proximal tyrosine (Y490 on TrkA) recruits the protein Shc, leading to docking of the adaptor proteins Gab1, Gab2, and Grb2. Grb2 associates with the guanine-nucleotide-exchange factor SOS, which facilitates activation of Ras, an activator of several pathways. The activated, GTP-bound form of Ras recruits the serine/threonine kinase Raf to the plasma membrane, thereby facilitating its activation. Raf then phosphorylates MEK1 and/or MEK2 and these kinases phosphorylate the MAP kinases Erk1 and 2. The activated Erks translocate into the nucleus where they phosphorylate a variety of substrates, including the kinase Rsk, which can phosphorylate and inactivate the proapoptotic protein Bad. Rsk also phosphorylates the transcription factor CREB, resulting in its activation and the subsequent up-regulation of downstream genes such as the prosurvival gene Bcl-2. In addition, the Ras–MAP kinase pathway is also important for neurotrophin mediated differentiation, including the induction of neurite outgrowth. For example, expression of activated Raf, in the absence of neurotrophin, induced neurite elongation in sensory neurons and constitutively active MEK up-regulated p35, leading to cdk5 activation, which increases neurite extension.

The ability of neurotrophins to promote differentiation appears, in part, to depend on prolonged Erk1/2 activation, as opposed to the transient activation of the kinases induced by other growth factors such as EGF. The longer kinetics are a result of phospho-Trk associating with the adaptor, Crk, through interaction with the fibroblast growth factor receptor substrate-2 (Frs2). Crk binds to the nucleotide-exchange factor C3G, thereby stimulating the small GTP-binding protein Rap1. The kinase B-Raf is then activated by Rap1, resulting in sustained Erk1/2 activation (Figure 1).

The activation of Ras also leads to activation of the lipid kinase, phosphatidylinositol 3 kinase (PI3K). In addition, PI3K can be activated independent of Ras through Grb2 binding to the adaptor Gab1/2, which facilitates Trk stimulation of the kinase. PI3K produces phosphatidylinositides phosphorylated on the third position of the inositol and these serve to indirectly

activate the serine/threonine kinase Akt. Akt acts on a number of signaling proteins that are critical regulators of cellular survival. The kinase activity of Akt leads to activation of the transcription factor NFκB, which can serve as a prosurvival factor in the nervous system, and inhibition of the proapoptotic proteins Bad, Forkhead, GSK3β, and caspase 9. Numerous studies have demonstrated a requirement for the PI3K-Akt pathway in neurotrophin mediated survival; however, this pathway also promotes protein translation and neurite branching (Figure 1).

Adding to the complexity of Trk signaling is the presence of several splice variants of all of these receptors. Among these isoforms, both Trk B and Trk C exist as truncated receptors lacking the intracellular kinase domain. While there is evidence that loss of the kinase domain can function to abrogate Trk signaling by competitively binding the available neurotrophin or forming inactive complexes with full length receptor, there is also evidence that these truncated Trks may function to display bound neurotrophin to adjacent cells. In addition, recent findings suggest that the truncated receptors can initiate signaling within astrocytes, leading to IP3-dependent calcium release. A second type of splice variant observed for all of the Trks is a form of the receptor lacking a small portion of the extracellular domain in the juxtamembrane region. Expression of these isoforms more stringently restricts the responsiveness of a given Trk for its cognate neurotrophin and may be one mechanism to insure the elimination of neurons making connections to an inappropriate target tissue.

One important aspect of neurotrophin signaling that needs to be considered is the spatial limitations of a neuron. Typically, it is the axonal tip that encounters the neurotrophins, while the regulation of survival involves transcriptional activity; hence, the signal must be retrogradely transported some distance back to the neuron soma. Although it has long been known that neurotrophins are retrogradely transported, it was only recently demonstrated that it is essential that the factor be transported with the active receptor, although this requirement has been contended by Campenot and colleagues. TrkA and NGF are not transported alone, rather, an entire complex of signaling proteins associated with an internalized vesicle, referred to as a signalosome, has been shown to undergo transport from neuronal endings back to the cell body.

Neurotrophin Activation of the p75NTR Receptor

While p75NTR was the first neurotrophin receptor identified and the founding member of the TNF receptor family, only recently has its importance for neurotrophin action been appreciated. With that appreciation, a wave of research highlighting both the mechanisms and functional consequences of its signal transduction pathway has been generated. p75NTR is important for neuronal development through its regulation of programmed cell death. In addition, accumulating evidence indicates that p75NTR also plays an important role in injury response within the nervous system.

Like many members of the TNF receptor family, p75NTR can activate the transcription factor NFκB and the stress activated kinase JNK (c-Jun N-terminal kinase) (Figure 2). The activation of NFκB by p75NTR has been shown to promote survival, thus providing a mechanism by which this receptor can function together with Trk to keep cells alive. In contrast, the activation of JNK is a proapoptotic signal in many contexts. For example, p75NTR-mediated apoptosis has been demonstrated to play a role in the normal elimination of neurons during development of the mouse retina, spinal cord, basal forebrain, and sympathetic ganglia. One of the major roles for cell death induced by this receptor may be after nerve injury. Following a spinal cord lesion in rodents, oligodendrocytes undergo p75NTR-dependent apoptosis. Similarly, pilocarpine-induced seizures cause mouse hippocampal neurons to die through a process dependent on p75NTR. Given that p75NTR is highly up-regulated following a large number of insults, it is likely that future studies will continue to reveal a role for this receptor in the associated cell death.

In addition to its activation of NFκB and JNK, p75NTR has been shown to regulate the small GTP-binding proteins Rac and Rho (Figure 2). Rac has been suggested as an upstream activator for JNK, thus playing an essential role in the apoptotic signal; however, Rac and Rho are best known for their ability to alter the cytoskeletal architecture. It is through modulation of these G proteins that p75NTR alters neurite extension, either promoting it following binding of neurotrophin, or causing growth cone collapse upon association with ligand-bound Nogo receptor.

Although the downstream signals activated by p75NTR are similar to other members of the TNF receptor family (NFκB and JNK), the receptor-proximal mechanisms used appear to be somewhat different. This is not entirely surprising given that p75NTR is the only member of the TNF receptor family that is activated by a dimeric ligand, rather than the trimeric ligands (e.g., TNFα and Fas ligand) that create trimeric receptor complexes and recruit trimeric adaptor proteins. Recently, much effort has been focused on understanding the transduction mechanism of this unique pathway. This work has resulted in the identification of a large number of p75NTR interacting factors whose sheer

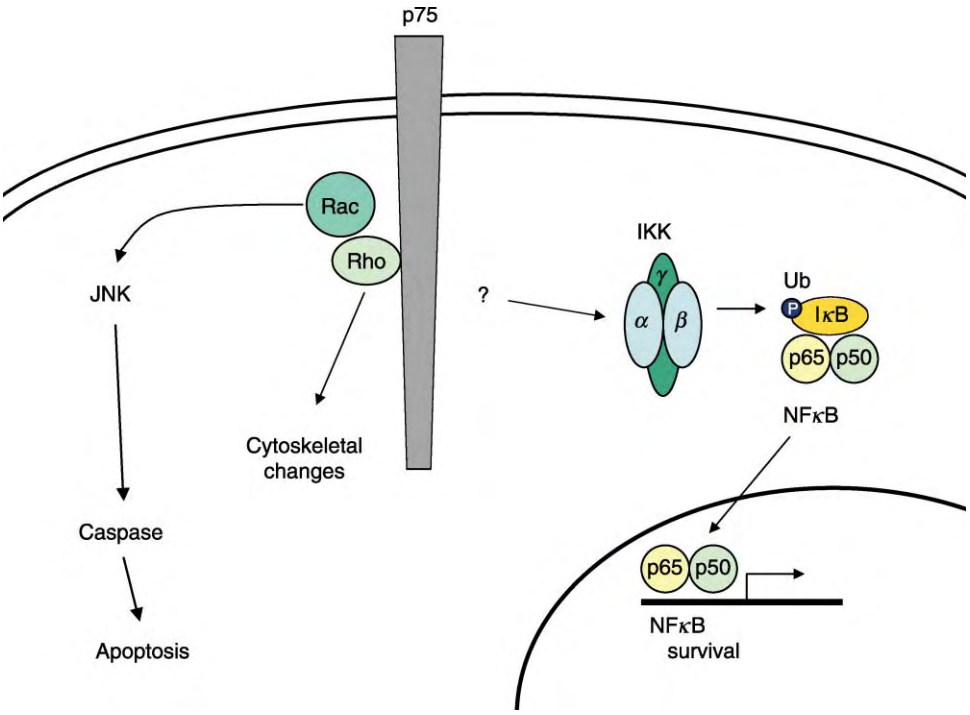

FIGURE 2 Neurotrophin signaling through p75NTR. Neurotrophin binding to this receptor activates the stress kinase JNK, the transcription factor NFκB, and regulates the GTP-binding proteins Rac and Rho. Not depicted are the numerous receptor-binding proteins that have been reported, since how they participate in p75NTR signaling has yet to be elucidated.

numbers will require some time to sort through to understand how they fit into p75NTR signaling under various conditions.

A long-standing conundrum in understanding the physiological role of p75NTR has been the high levels of neurotrophin needed to activate the receptor. *In vivo*, the neurotrophins are typically found at very low levels, usually at or below the K_D for p75NTR. Recently, the group of B. Hempstead made an important discovery that may resolve this dilemma. They found that the unprocessed, proform of the neurotrophins bind p75NTR with high affinity and activate downstream pathways more effectively than the mature neurotrophins. Hence, a mechanism exists for selective activation of p75NTR, since the proneurotrophins do not bind or activate the Trks. This discovery has renewed interest in studying the regulation of neurotrophin processing and release, as these are likely to be key for modulating neuronal survival during development and after injury.

Crosstalk Between p75NTR and the Trks

It is clear that neurotrophin binding to either p75NTR or members of the Trk family of receptors can initiate distinct signal transduction pathways, but these receptors are often coexpressed in the same cells. When both neurotrophin receptors are present, they interact to form a very selective, high-affinity complex. Given the limiting quantities of neurotrophin present in typical target tissues, such a binding site provides neurons expressing both receptors, in the proper ratio, with a competitive advantage during development. Moreover, the interaction between p75NTR and Trk leads to enhanced Trk tyrosine kinase activity and more robust activation of downstream survival signals. The binding of mature neurotrophin to the p75NTR–Trk complex also represses the p75NTR apoptotic signal; for example, Trk activation of Ras has been shown to inhibit p75NTR activation of JNK. Thus, the two receptors synergize to increase neuronal viability. A lack of the p75NTR–Trk receptor interaction has been proposed to explain the significant loss of sensory neurons in the p75NTR −/− mice.

Interaction Between p75NTR and the Nogo Receptor

Although p75NTR responds to binding of the neurotrophins, this receptor can also be activated by an additional group of ligands typically expressed on central nervous system myelin, including Nogo, myelin associated glycoprotein (MAG) and oligodendrocyte

myelin glycoprotein (OMgp). These myelin proteins inhibit neurite outgrowth and are, in part, responsible for preventing regeneration of CNS axons after nerve injury. They all bind to a GPI-linked receptor referred to as the Nogo receptor (NgR), which interacts with p75NTR. Association of NgR with p75NTR results in activation of Rho, which causes changes in the actin-cytoskeleton resulting in growth cone collapse. Interestingly, the association of NgR with p75NTR activates Rho and inhibits Rac, while the binding of neurotrophin to p75NTR has the opposite effects on these G proteins. The mechanisms by which these opposing signals are generated have yet to be fully resolved.

Crosstalk Between Trk and Non-Neurotrophin Receptors

The Trk receptors also interact with a number of non-neurotrophin receptors, although this is primarily an indirect interaction. Several G protein-coupled receptors can transactivate Trk and thereby stimulate downstream signaling pathways. For example, the adenosine receptor and the pituitary adenylate cyclase activating polypeptide (PACAP) receptor can induce phosphorylation of TrkA through a mechanism that does not involve neurotrophins. Such crosstalk is likely involved in the neuroprotective effects of these ligands.

Alternatively, neurotrophin binding to Trk can cross-stimulate the tyrosine kinase c-Ret, a component of the receptor complex for the glial cell line-derived neurotrophic factor (GDNF) family. Although c-Ret is normally activated by GDNF family members, it can also be phosphorylated in mature sympathetic neurons following NGF binding to TrkA. This indirect activation of c-Ret is required for these neurons to maintain their metabolic status and somal size. Similarly, BDNF stimulation of TrkB can transactivate a subunit of the NMDA receptor, which is essential for the formation of LTP. Since BDNF is known to enhance LTP, Trk-NMDA receptor crosstalk may be the mechanism underlying this effect.

See Also the Following Articles

Caspases and Cell Death • Neurotransmitter Transporters • Nuclear Factor kappaB • Phospholipase C

Glossary

neurotrophin A member of a family of homologous growth factors that promote the survival and differentiation of neurons.

nuclear factor kappa B (NFκB) A transcription factor.

phosphatidyl-inositol 3 kinase (PI3K) Kinase that phosphorylates inositol lipids on the third position of the sugar.

PLC-γ An enzyme that cleaves phosphatidyl inositol (4,5) bisphosphate to release inositol-3-phosphate (IP3) and diacylglycerol (DAG).

p75NTR The 75 kDa neurotrophin receptor.

Trk The tyrosine kinase neurotrophin receptor.

Further Reading

Chao, M. V. (2003). Neurotrophins and their receptors: A convergence point for many signalling pathways. *Nat. Rev. Neurosci.* **4**, 299–309.

Dechant, G., and Barde, Y. A. (2002). The neurotrophin receptor p75(NTR): Novel functions and implications for diseases of the nervous system. *Nat. Neurosci.* **5**, 1131–1136.

Ginty, D. D., and Segal, R. A. (2002). Retrograde neurotrophin signaling: Trk-ing along the axon. *Curr. Opin. Neurobiol.* **12**, 268–274.

Hempstead, B. L. (2002). The many faces of p75NTR. *Curr. Opin. Neurobiol.* **12**, 260–267.

Huang, E. J., and Reichardt, L. F. (2001). Neurotrophins: Roles in neuronal development and function. *Annu. Rev. Neurosci.* **24**, 677–736.

Huang, E. J., and Reichardt, L. F. (2003). Trk receptors: Roles in neuronal signal transduction. *Annu. Rev. Biochem.* **72**, 609–642.

Lee, F. S., Rajagopal, R., and Chao, M. V. (2002). Distinctive features of Trk neurotrophin receptor transactivation by G protein-coupled receptors. *Cytokine Growth Factor Rev.* **13**, 11–17.

Biography

Dr. Bruce Carter is an Associate Professor of Biochemistry in the School of Medicine at Vanderbilt University. His principal area of research is on the mechanisms by which the neurotrophins regulate neuronal survival. He holds a Ph.D. degree from the University of Michigan and received postdoctoral training at the Max Planck Institute in Munich, Germany and at Cornell Medical School.

Dr. Jennifer Gentry received her Ph.D. from Vanderbilt University and is currently a postdoctoral Fellow at Harvard Medical School.

Nicotinamide Nucleotide Transhydrogenase

Jan Rydström
Göteborg University, Göteborg, Sweden

Membrane-bound nicotinamide nucleotide is located in the bacterial plasma membrane and mitochondrial inner membrane and catalyzes the reversible reduction of $NADP^+$ by NADH. The reaction is linked to the electrochemical proton gradient across the membrane, generating NADPH essential for, e.g., detoxification of peroxides. In its isolated form the enzyme is a proton pump where proton translocation is driven by the catalytic reaction, mediated by conformational changes. Extensive investigations of the structure–function relationships especially of the substrate-binding domains have established their structures and roles. The membrane domain, in which the proton channel resides, has been structurally predicted, but remains to be determined structurally at the atomic level. Models for the molecular proton translocation mechanism are therefore beginning to emerge.

Introduction

Proton-pumping nicotinamide nucleotide transhydrogenase (E.C. 1.6.1.2) is an integral membrane protein found in most species except some yeasts, plants, and certain bacteria. It is located in the inner membrane of mitochondria and in the plasma membrane of bacteria. The enzyme catalyzes the reversible reduction of $NADP^+$ by a hydride ion, donated by NADH, which is linked to proton translocation across the membrane according to the reaction

$$H^+_{out} + NADH + NADP^+ \rightleftharpoons H^+_{in} + NAD^+ + NADPH \quad [1]$$

In the absence of an electrochemical proton gradient (Δp), the reaction from left to right (the forward reaction) is approximately fivefold slower than the reverse reaction. Under these nonphysiological conditions, the overall reaction proceeds to an equilibrium constant of close to 1. In the presence of a Δp, i.e., under more physiological conditions, the forward reaction is increased five- to tenfold and the apparent equilibrium constant is increased to ~ 500, with one proton translocated per NADPH formed. The net effect of the transhydrogenase (TH) reaction is therefore probably to provide NADPH at the expense of NADH and Δp. Thus, this suggests important roles of TH in mitochondrial/cellular redox regulation including biosynthesis, detoxication (via the glutathione/thioredoxin systems), and apoptosis. TH is globally expressed in eukaryotes, e.g., human, mouse, and *C. elegans*.

Proton-translocating THs from eukaryotes are homodimeric proteins with a relatively large hydrophilic domain composed of the NAD(H)-binding domain I (dI) and the NADP(H)-binding domain III (dIII); part of dI is homologous to alanine dehydrogenase (Figure 1). The hydrophobic part of the enzyme containing the proton channel, denoted domain II (dII), is composed of a variable number of transmembrane helices depending on species. The *Escherichia coli* TH is composed of an α-subunit and a β-subunit, the former subunit containing dI and helices 1–4 of dII and the latter subunit containing dIII and helices 6–14 of dII. Intact *E. coli* TH has the composition $\alpha_2\beta_2$, i.e., it is a tetramer in which $\alpha+\beta$ corresponds to the mitochondrial single polypeptide. dI and dIII can be expressed separately and purified in an active state and, when combined, show catalytic activity. In order to elucidate the coupling mechanism of TH, the enzyme mainly from bovine, human, and *E. coli* has been extensively studied in the purified forms, in cytosolic (plasma membrane) vesicles, as well as reconstituted in liposomal membranes. dI and dIII from bovine, human, and *Rhodospirillum rubrum*, as well as a complex between dI and dIII, have been structurally determined using X-ray crystallography and NMR.

Structure–Function of the Substrate-Binding Domains

Recent advances in structural resolution of the hydrophilic dI and dIII by X-ray crystallography and NMR spectroscopy have dramatically increased our

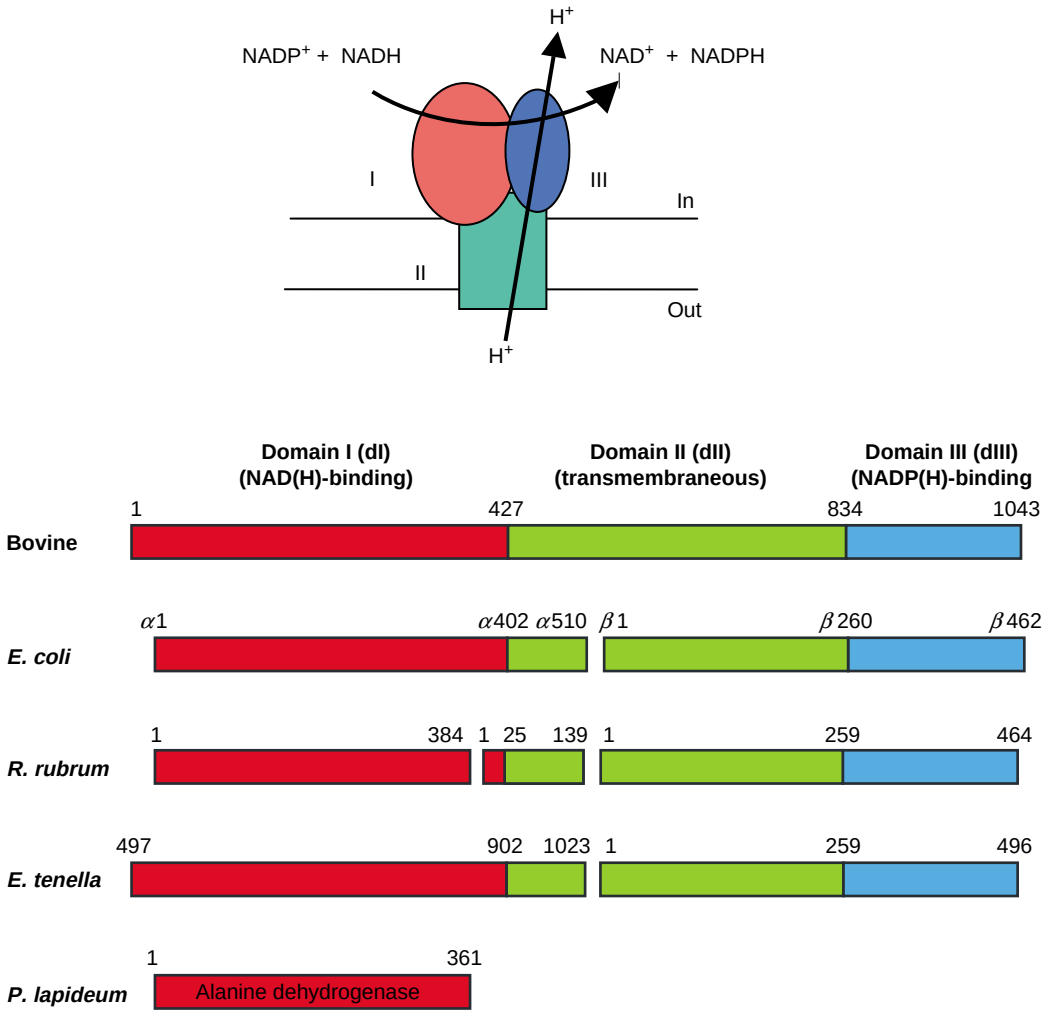

FIGURE 1 Structural organization of proton pumping THs.

knowledge about the structure–function relationships of these domains and their interactions. Thus, the crystal structure of the NAD^+ form of dI from *Rhodospirillum rubrum* solved by Jackson and coworkers and, in the NADH form from the same source later by Hatefi and coworkers, shows that it involves a dimer of a 40 kDa subunit, denoted A and B. Each subunit comprises two subdomains, dI.1 and dI.2, both of which have a Rossmann nucleotide-binding fold composed of a sheet of parallel β-strands flanked by α-helices. The two domains are arranged on the sides of a deep cleft. However, in the crystal structure of the dimer only dI.2(A) contains bound NAD^+ positioned so that its nicotinamide moiety is exposed in the cleft. In contrast, dI.2(B) site contains disordered NAD^+ or no ligand. The arrangement of the monomers in the dimer is such that the nucleotide-binding sites in dI.2(A) and dI.2(B) are pointing away from each other. The potential nucleotide-binding sites in dI.1 (A) and dI.1(B) have no known ligands. It is obvious that in the dI dimer, dI.2(A) and dI.2(B) must have different conformations, since only dI.2(A) contains well-ordered NAD^+. In a dimeric structure of dI with bound NADH, other minor but significant structural changes are observed.

Human and bovine dIII have been structurally resolved by Jackson and co-workers, and Hatefi and coworkers, respectively, using X-ray crystallography. These are structurally close to identical. The structures involve an alternating α/β-structure with a central β-sheet core, and a Rossmann fold in which $NADP^+$ is tightly bound at the C-terminal end of the β-sheet. The molecular mass of dIII is 20 kDa, it is a monomer, and it is isolated with predominantly tightly bound $NADP^+$; the K_d of the NADP(H) bound is in the nM–μM range. A striking difference, however, as compared with other NAD(P)-binding enzymes is that the $NADP^+$ bound to dIII is turned approximately 180°, i.e., the nicotinamide ring is close to α-helix 3 in *E. coli* dIII (corresponding to α-helix B in *R. rubrum* dIII) (Figure 2). A number of

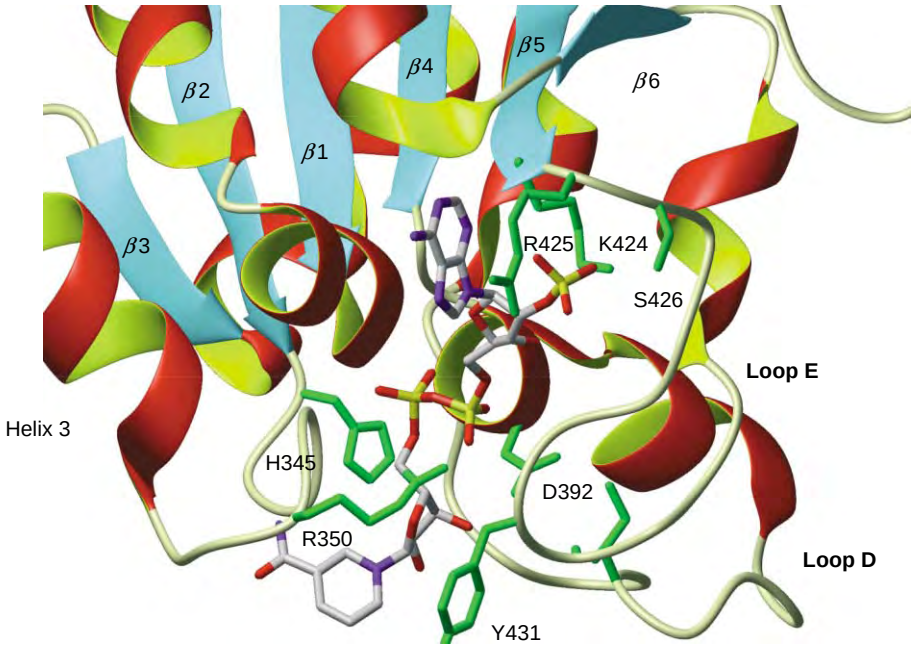

FIGURE 2 The NADP(H)-binding region of dIII. Amino acid residues and loops indicated are directly or indirectly essential in binding NADP(H).

hydrogen bonds stabilize NADP(H) in its binding site, involving, for example, Asp392, Lys424, Arg425, and Ser426. Loops D and E may indeed contribute to the binding and have been proposed to be involved in the Δp-dependent release of NADPH. Interactions between dI and dIII and their regulation by NADP(H)/NAD(H) have been investigated thoroughly by Karlsson and coworkers using NMR spectroscopy.

A crystal structure of a heterotrimer dI_2–dIII complex from *R. rubrum* showed that the dI and dIII structures are essentially identical to those determined separately. However, the dI_2–dIII structure revealed that dIII interacts with the dI.2(B), i.e., the NAD(H)-binding site that contains disordered NAD^+ rather than well-ordered NAD^+. This may be interpreted as indicating that when dIII (with bound $NADP^+$) is interacting with dI_2, it binds the dI.2(B) that has a disorganized NAD^+, not the dI.2(A) that has a well-ordered NAD^+. However, a complicating fact is that, even though an NAD(H) molecule could be modeled in the dI.2(B) site, the two nicotinamide rings are still separated by some 4–6Å, making direct hydride transfer difficult. A possible mechanistic solution to this problem is that the nicotinamide ring of the modeled NAD(H) is changed from an *anti* to a *syn* conformation, leading to a more open exposure of the nicotinamide ring in the cleft, and a direct interaction with the nicotinamide ring of $NADP^+$. Indeed, this rotation may be the very reason why NAD^+ is more mobile in dI.2(B). An additional factor influencing the interaction between dI and dIII, and thus hydride transfer, is the amino acids that make up the interface between the domains. One of these, Gln132 in dI, appears to be essential for activity because it works as a "tether" during the catalytic cycle, holding both NAD(H) and NADP(H) together in the right conformation through H-bonds.

Mechanism of Hydride Transfer

Transfer of the hydride ion between the 4A-hydrogen (*pro-R*) of NADH and the 4B (*pro-S*)-hydrogen of $NADP^+$, while the two substrates are bound to dI and dIII, respectively, occurs directly without any known intermediate and without exchange with bulk protons. Even though NAD^+/NADH are rapidly exchanging with the NAD(H)-binding site in dI throughout the reaction cycle, NADH especially shows different affinities in the open (ordered, high affinity) and closed (disordered, low affinity) states. These affinity changes, and the associated *anti/syn* transitions of NAD(H), are apparently induced by subtle conformational changes in the dI dimer. However, several pieces of evidence together indicate that regulation of hydride transfer by, for example, an electrochemical proton gradient, Δp, occurs mainly at the level of dIII, rather than dI. Essential information in this context was derived from the fact that separately expressed and purified dIII contains tightly bound NADP(H) which, due to a limiting release of the product NADP(H), catalyzes an ~2 orders of

magnitude slower reverse and forward reactions in the presence of purified dI than the wildtype enzyme. Isolated dIII also catalyzes a very fast so-called cyclic reaction, i.e., reduction of 3-acetyl-pyridine-NAD^+ (an NAD^+ analogue) by NADH, mediated by the bound NADP(H). This reaction involves reduction of bound $NADP^+$ by NADH, release of the NAD^+ formed, binding of 3-acetyl-pyridine-NAD^+, reduction of 3-acetyl-pyridine-NAD^+ by the bound NADPH, and release of 3-acetyl-pyridine-NADH. Indeed, it was reasonable to assume that the properties of the isolated dIII reflected an intermediate, the "occluded" state, in the reaction cycle of the intact transhydrogenase (TH). In reaction [1], this is interpreted to indicate that the activity of the forward reaction is limited by NADPH release, a limitation that is alleviated by Δp, allowing the enzyme to be catalytically fully active.

A general reaction scheme for forward reaction catalyzed by the *E. coli* TH may be outlined as follows (Figure 3). Starting with the resting state (state A), $NADP^+$ binds to dIII in the β-subunit generating state B, in which the proton channel and the protonatable group X2 become accessible to the periplasmic space; in state C, the enzyme is protonated at X2, and the β-subunit subsequently changes conformation to state D. In state D the proton moves from X2 to X1 concomitant with hydride transfer from NADH to $NADP^+$, generating state E. States D and E correspond to the "occluded" state. Following a conformational change in dIII, an opening of dIII, and a less tight NAD(H) (state F), the proton dissociates on the cytosolic side generating state G. After dissociation of NADPH, the enzyme returns to the resting state A. During the entire cycle NAD(H) can freely bind to and dissociate from dI. X3 indicates a group on dI that may be regulated by the cytosolic pH.

As further discussed below, at any given time, only half of the sites in the active dimeric enzyme (in the *E. coli* enzyme, $\alpha_2\beta_2$) seem to be available for, for example, NADP(H) binding and reaction with dicyclohexylcarbodiimide. In a recent modification of this principle, an alternating site mechanism has been proposed in which the two dIIIs alternate between an open and a closed ("occluded") state.

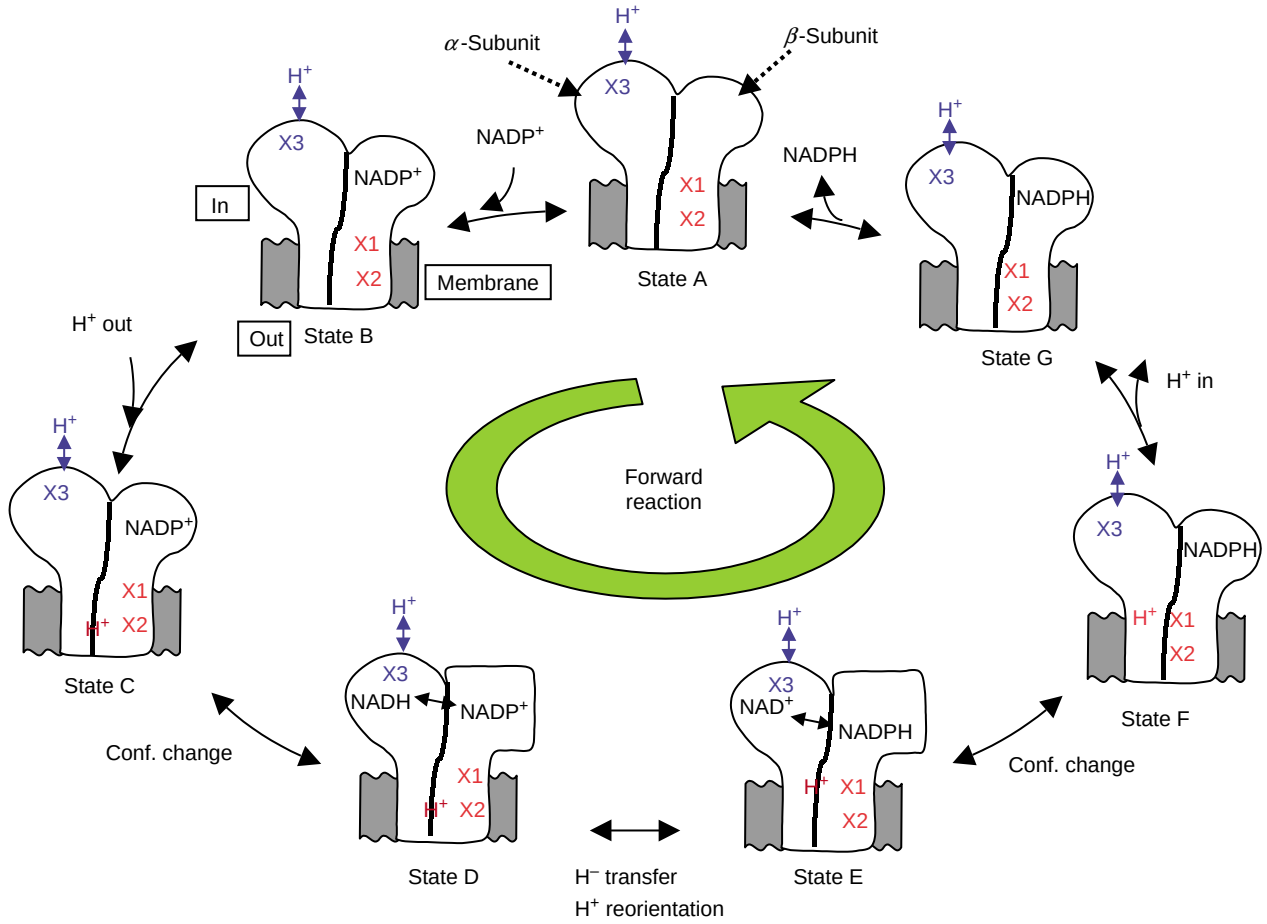

FIGURE 3 Reaction cycle of the forward TH reaction. X1 and X2 denote two protonatable residues in dII, possibly His91 and Asn222, respectively. X3 is a protonatable group in dI unrelated to the proton channel.

Membrane Topology and Helix Packing of the Membrane Domain

dII of the mitochondrial TH was early predicted to be composed of 14 transmembrane α-helices, whereas dII of the *E. coli* TH has been shown to be composed of 13 transmembrane α-helices (Figure 4). However, in contrast to the mitochondrial enzyme, *E. coli* TH consists of two subunits, the α- and β-subunits, which both contribute to dII. For some time, the membrane topology of the *E. coli* enzyme was unclear, especially regarding the region in dII where the two subunits interact. Subsequently, it was shown that the α- and β-subunits can be fused at the gene level, generating a mitochondrial-like TH, provided that the peptide linker is long enough, i.e., as long as the extra helix peptide in the mitochondrial TH; shorter linkers lead to truncated proteins with diminished activities. The C terminus of the α-subunit and the N terminus of the β-subunit are therefore located on different sides of the membrane (Figure 4).

Despite the obvious importance of dII in the overall transhydrogenase reaction, the structure of this domain has subsequently received comparatively little attention. However, a systematic effort to elucidate the packing of dII of the *E. coli* enzyme using cysteine crosslinking of double cysteine mutants in the cysteine-free background has been carried out, with one cysteine located in the α-subunit and the other at various positions in the β-subunit. The results show that, within the $\alpha+\beta$ unit, helices 2 and 4 are close to helix 6, and helix 3 and the C terminus of the α-subunit are close to helix 7. In the $\alpha_2\beta_2$, helices 2 and 4, as well as helix 6, are close to the same helices in the second subunit.

The Proton Channel

Being a proton pump, the membrane domain of THs must contain at least one proton channel, and considering the symmetry of the active $\alpha_2\beta_2$ structure, most likely two identical channels, one in each β-subunit. That the channel resides in the β-subunit is obvious due to the lack of suitable conserved protonatable residues in the α-subunit. However, residues in the α-subunit may contribute to the proton channel. DII of the *E. coli* TH contains few conserved protonatable amino acids, which may form part of a proton channel. Based on the properties of especially the positively charged H91K and N222R mutants (mimicking protonated His91 and Asn222, respectively), located in helix 9 and helix 13 (Figure 4), Bragg and coworkers made the important discovery that these mutants contain tightly bound NADP(H), reminiscent of isolated dIII. Indeed, this was the first piece of evidence indicating that dII not only communicates with dIII, but that the degree of protonation of specific residues, i.e., His91 and Asn222, in dII

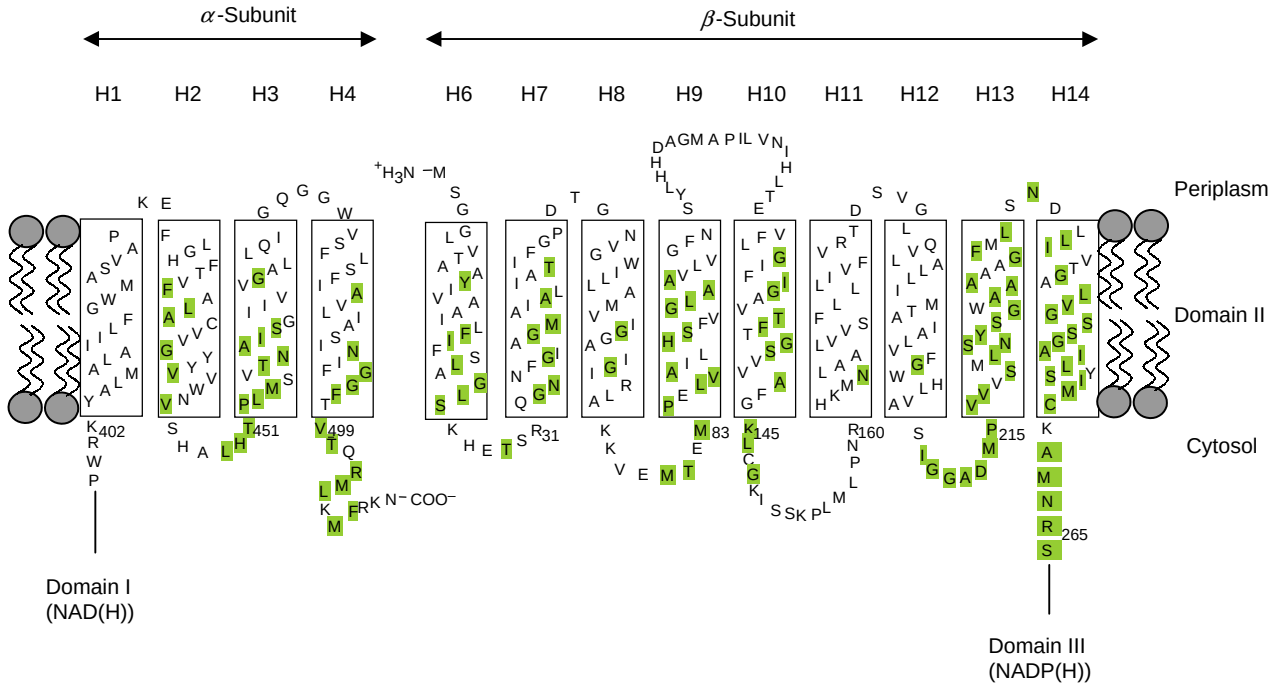

FIGURE 4 Membrane topology of *E. coli* TH. The topology was determined as described by Meuller, J., and Rydström, J. (1999). The membrane topology of proton-pumping *Escherichia coli* transhydrogenase determined by cysteine labeling. *J. Biol. Chem.* **274**, 19072–19080. Residues in green background are at least 80% conserved among 61 THs.

induces conformational changes that affect the dissociation constant for binding of NADP(H) to dIII. Ser139 is another potential component of the proton channel, with Glu85, Asp213, and Glu124 being possible peripheral residues of the channel, located close to the membrane surfaces.

Some mutants of the conserved His91, Asn222, and Ser139 residues still catalyze proton pumping although at reduced rates. This may be due to a compensatory effect of the remaining protonatable residues in the channel. In this context it should be stressed that a proton channel *per se* does not require protonatable residues. It would be sufficient with a chain of bound water molecules in a channel across the membrane to allow protons to "jump" from one water molecule to another. Protonation/deprotonation of protonatable amino acids in the channel induces conformational changes in the channel which link proton passage through the channel to catalytic events in often distantly located domains.

Coupling Mechanism

One of the main mechanistic challenges in past and present TH research is to understand how a Δp can be converted into a high [NADPH][NAD^+]/[NADH][$NADP^+$] ratio and conversely, how a high [NADPH][NAD^+]/[NADH][$NADP^+$] (or a [$NADP^+$][NADH]/[NADPH][NAD^+]) ratio can drive proton pumping. Since the difference in standard redox potential between the NADPH/$NADP^+$ and NADH/NAD^+ pairs is negligible, the main contribution to the redox potential/free energy is derived from the above substrate/product ratios. Because of the water-soluble nature of the TH substrates, and the apparently large distance between the substrate-binding sites and the membrane, it has been generally accepted that some kind of conformational coupling is involved. Such a mechanism is often described as resembling that of ATPase/synthase in which conformationally dependent binding changes are essential. This was also experimentally demonstrated earlier by extensive Δp-dependent changes of Km values for especially NAD(H). As described in the previous section, the single most important finding in this context was that mutating His91 and Asn222 to more positive amino acids lead to tightly bound NADP(H) in the intact mutant enzyme. An important contribution was also the demonstration of tightly bound NADP(H) in isolated dIII, which was assumed to represent an intermediate in the reaction cycle of TH, denoted the "occluded" state, which led to the proposal that both directions of the TH reaction, but especially the Δp-stimulated forward reaction, is limited by dissociation of NADP(H). The term "binding change" mechanism is frequently used in order to stress the role of dissociation/binding of NADP(H).

Despite the known crystal structures of dI, dIII, and the dI–dIII complex, the interface between dII and dI+dIII is unknown, i.e., little is known regarding the communication between dII and dIII. Most cytosolic loops of dII are poorly conserved, which makes it unlikely that dII–dIII signaling occurs via the surfaces of these domains. However, the peptide linking the C-terminal end of dII with dIII is quite conserved, and is highly mobile during catalysis as indicated by the NADP(H)-dependent increased trypsin sensitivity of Arg265 close to transmembrane helix 14 (Figure 4), indicating that this region is potentially important. Subsequently, Arg265 has been suggested to form a functional-salt bridge with Asp213, constituting an essential component ("hinge" region) of a new coupling mechanism. However, communication between this proposed salt bridge and the NADP(H)-binding site remains unknown, although loops D and E close to the NADP(H)-binding site in dIII may be important. Proton-translocating THs, which are all dimers, may work according to an alternate-site-binding change mechanism. According to this mechanism, only half of the intact TH is catalytically active at any given time.

Physiological Role

In 1959 Klingenberg and Slenczka found that the mitochondrial redox level of NADP(H) was at least 90%, and that of NAD(H) ~50–60%. The forward TH reaction (reaction [1]), driven by Δp, is largely responsible for this high redox level of NADPH which, as expected, is sensitive to uncouplers. This also explains the fact that NADPH-dependent detoxification (through glutathione peroxidase) of organic peroxides in intact mitochondria is more effective with NADH-linked substrates than with NADPH-linked substrates. Thus, endogenous $NADP^+$ together with NADH (generated by the added substrate, e.g., β-hydroxybutyrate) provides a higher redox level of NADPH through TH than NADPH-linked substrates. A high level of NADPH is important because it generates reduced glutathione essential for, for example, glutathione peroxidase. NADPH also regulates the redox levels of thioredoxin and protein-bound thiols. Organic peroxides lead to a rapid oxidation of mitochondrial reduced glutathione through the glutathione peroxidase system, which in turn leads to a massive release of Ca^{2+} ions, presumably through the mitochondrial permeability transition pore (MPTP). MPTP may, in turn, contain redox-sensitive protein thiols. Therefore, the high mitochondrial redox level of NADP(H), maintained by TH, is of crucial importance for detoxification, Ca^{2+} homeostasis, cell thiol regulation, and biosynthesis. In liver, but probably not in heart, TH-generated NADPH in the

mitochondrion contributes to cytosolic NADPH through transport in the form of (iso)citrate generated by the NADP-dependent isocitrate dehydrogenase (NADP–ICDH).

A different hypothesis for the physiological role of TH involves a regulation of the citric acid cycle, especially the NAD and the NADP-dependent isocitrate dehydrogenases. The NAD enzyme (NAD–ICDH) is irreversible and strongly regulated by, for example, ADP, whereas NADP–ICDH is reversible and apparently unregulated. Oxidative decarboxylation of isocitrate to α-ketoglutarate, carbon dioxide, and NADH by the NAD–ICDH can be linked to the NADP–ICDH by a reductive carboxylation of α-ketoglutarate, carbon dioxide, and NADPH back to isocitrate. The NADH generated by the NAD–ICDH, together with $NADP^+$, is thus used by TH and Δp to generate NADPH that drives the NADP–ICDH. This nonproductive cycle uses one proton/cycle to slow down or regulate the flux through this step in the citric acid cycle. However, there is no obligatory simultaneous occurrence of TH and NADP-isocitrate dehydrogenase in some species, which casts some doubt on this potentially important regulatory system.

Theoretically, a reversal of reaction [1] can also be used to generate a Δp under, e.g., ischemic conditions. However, it is generally believed that unless a continuous source of $NADP^+$-reducing substrates as well as NAD^+-oxidizing substrates are available, the Δp generated would be transient and short-lived.

See Also the Following Article

Glutathione Peroxidases

Glossary

membrane protein A membrane-associated protein, in this context an integral membrane protein spanning the membrane.

NAD(H) Oxidized (NAD^+) and reduced (NADH) nicotinamide adenine dinucleotide, a common cofactor in cell metabolism, especially catabolism.

NADP(H) Oxidized ($NADP^+$) and reduced (NADPH) nicotinamide adenine dinucleotide phosphate, a common cofactor in cell metabolism, especially anabolism.

proton pump A group of membrane proteins catalyzing a translocation of protons across the membrane, driven either by redox energy, an ion gradient, or ATP.

transhydrogenases A group of enzymes composed of two subgroups: a soluble flavine-containing type and a membrane-bound and proton-translocating type. Both catalyze the transfer of a hydride ion between NAD(H) and NADP(H).

Further Reading

Bergkvist, A., Johansson, C., Johansson, T., Rydstrom, J., and Karlsson, B. G. (2000). Interactions of the NADP(H)-binding domain III of proton-translocating transhydrogenase from *Escherichia coli* with NADP(H) and the NAD(H)-binding domain I studied by NMR and site-directed mutagenesis. *Biochemistry* **39**, 12595–12605.

Bizouarn, T., Fjellström, O., Meuller, J., Axelsson, M., Bergkvist, A., Johansson, C., Karlsson, B. G., and Rydström, J. (2000). Proton translocating nicotinamide nucleotide transhydrogenase from *E. coli*. Mechanism of action deduced from its structural and catalytic properties. *Biochim. Biophys. Acta* **1457**, 211–228.

Bizouarn, T., Althage, M., Pedersen, A., Tigerström, A., Karlsson, J., Johansson, C., and Rydström, J. (2002). The organization of the membrane domain and its interaction with the NADP(H)-binding site in proton-translocating transhydrogenase from *E. coli*. *Biochim. Biophys. Acta* **1555**, 122–127.

Bragg, P. D., and Hou, C. (1999). Mutation of conserved polar residues in the transmembrane domain of the proton-pumping pyridine nucleotide transhydrogenase of *Escherichia coli*. *Biochim. Biophys. Acta* **363**, 182–190.

Buckley, P. A., Jackson, J. B., Schneider, T., White, S. A., Rice, D. W. and Baker, P. J. (2000). Protein–protein recognition, hydride transfer and proton pumping in the transhydrogenase complex. *Structure* **8**, 809–815.

Cotton, N. P., White, S. A., Peake, S. J., McSweeney, S., Jackson, J. B. (2001). The crystals structure of an asymmetric complex of the two nucleotide binding components of proton-translocating transhydrogenase. *Structure* **9**, 165–176.

Glavas, N. A., and Bragg, P. D. (1995). The mechanism of hydride transfer between NADH and 3-acetylpyridine adenine dinucleotide by the pyridine nucleotide transhydrogenase of *Escherichia coli*. *Biochim. Biophys. Acta* **1231**, 297–303.

Hatefi, Y., and Yamaguchi, M. (1996). Nicotinamide nucleotide transhydrogenase: A model for utilization of substrate binding energy for proton translocation. *FASEB J.* **10**, 444–452.

Hoek, J. B., and Rydström, J. (1988). Physiological roles of nicotinamide nucleotide transhydrogenase. *Biochem. J.* **254**, 1–10.

Jackson, J. B., White, S. A., Quirk, P. G., and Venning, J. D. (2002). The alternating site, binding change mechanism for proton translocation by transhydrogenase. *Biochemistry* **41**, 4173–4185.

Meuller, J., and Rydström, J. (1999). The membrane topology of proton-pumping *Escherichia coli* transhydrogenase determined by cysteine labeling. *J. Biol. Chem.* **274**, 19072–19080.

Prasad, G. S., Wahlberg, M., Sridhar, V., Sundaresan, V., Yamaguchi, M., Hatefi, Y., and Stout, C. D. (2002). Crystal structures of transhydrogenase domain I with and without bound NADH. *Biochemistry* **41**, 12745–12754.

Biography

Professor Jan Rydström is Head of Biochemistry and Biophysics, Department of Chemistry, Göteborg University, Sweden. His research interests are focused on structure–function relationship of membrane proteins, especially transport proteins, and biochemical toxicology.

Nicotinic Acetylcholine Receptors

Nivalda O. Rodrigues-Pinguet and Henry A. Lester
California Institute of Technology, Pasadena, California, USA

Ion channels are classified by their gating (opening) mechanisms. Mechano-sensitive channels are activated directly by forces applied to the channel proteins. The superfamily of voltage-gated channels responds to changes in the membrane potential. The ligand-gated or agonist-gated receptors open as they bind specific molecules. The nicotinic acetylcholine receptor (nAChR) is a well-studied member of the superfamily of ligand-gated ion channels (LGICs). The nAChR is the prototype LGIC since its sequence and structure strongly resemble that of glycine, serotonin 5-HT3$_A$, γ-aminobutyric acid (GABA$_A$), and invertebrate glutamate-gated chloride (GluCl) receptors. Since the early twentieth century, researchers have worked to unravel some of the mysteries of this cylindrically shaped macromolecule embedded in the membrane at vertebrate nerve–muscle synapses, at invertebrate nicotinic synapses, and in the vertebrate central nervous system. To date, several nAChR subtypes have been successfully isolated, cloned, purified, imaged, expressed, and unitary currents have been recorded from these channels. There is now a clear picture of the nAChR architecture and function. However, efforts are still underway to understand key functional aspects of this receptor as well as its role in addiction and disease.

Structure

Nigel Unwin and colleagues have resolved the muscle nicotinic acetylcholine receptor (nAChR) structure from *Torpedo* electric organ, which is derived from muscle, to 4Å resolution. The structure of the neuronal nAChR has not been resolved. Yet one expects that many details, certainly including its membrane topology, are identical to the muscle receptor. From Unwin's work, it is now known that the entire muscle nicotinic receptor complex is ~150Å tall (Figure 1A). Biochemical and electron microscopic studies reveal that nicotinic receptors, in peripheral organs (e.g., muscle) and in the central nervous system, are heteromers composed of five subunits that assemble into a barrel-like structure around a central ion pore. The receptor has three main parts: a region found outside of the cell (extracellular), a region located within the membrane (transmembrane), and an intracellular portion (cytoplasmic).

Subunits

Steve Heinemann, Norman Davidson, Shosaku Numa, Jim Patrick, Jim Boulter, and others cloned the nAChR subunits. To date, ten α-subunits and seven β-, γ-, δ-subunits have been cloned. However, additional subunit genes probably await discovery. Each of the five nicotinic subunits is composed of (from N–C terminus) an extracellular domain, four transmembrane domains (referred to as M1–M4) 19–27 amino acids in length, a cytoplasmic loop, and an extracellular C terminus consisting of ~20 amino acid residues (Figure 1A). The fetal or denervated muscle nAChR is a heteromeric pentamer composed of two α-subunits and one β-, γ-, and δ-subunit. In most adult nAChRs, the δ-subunit is replaced with an ε-subunit. Central nicotinic receptors can be either homomeric or heteromeric pentamers composed of α-subunits or, α- and β-subunits, respectively.

The Extracellular Domain

The extracellular domain protrudes ~60Å away from the membrane and has several characteristic structural elements shared by other members of the ligand-gated ion channels (LGICs) superfamily. In 2001, Titia Sixma and co-workers crystallized the acetylcholine-binding protein (AChBP) from a mollusc. Most of the nAChR N-terminal features deduced from X-ray crystallographic, biochemical, and physiological studies have been confirmed with the 2.7Å resolution structure of AChBP. This protein has ~20% homology to the extracellular domain of nicotinic receptors, and it lacks transmembrane, cytoplasmic, and C-terminal domains. Yet Sixma's AChBP crystal structure has given researchers a clearer image of the extracellular region of the nAChR. There are six loops, named with the letters A–F, involved in ligand binding. This region also contains a disulfide bond within loop C and another disulfide bond (the signature loop) located between cysteine residues 123 and 136. Sixma's AChBP crystal structure suggests that the signature disulfide loop present in the nAChR is located at the bottom of the binding domain, where it can interact directly with

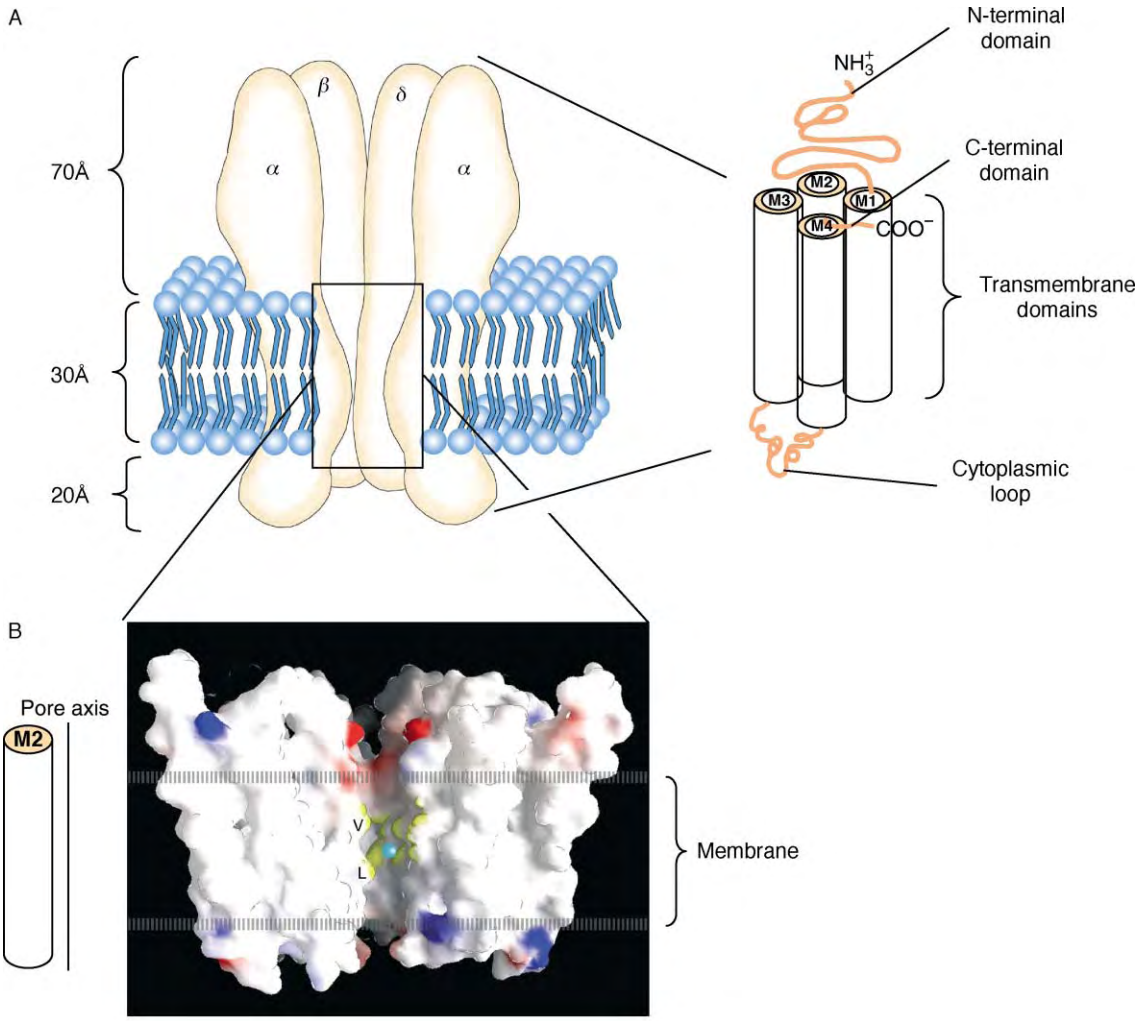

FIGURE 1 (A) The structure of the muscle nicotinic receptor embedded in the plasma membrane (blue), with the front subunit removed. Each subunit is composed of an N-terminal domain, four transmembrane domains (M1–4), a cytoplasmic loop, and a C-terminal domain. (B) The nAChR pore is mostly lined by M2 α-helices. Gray lines represent the plasma membrane, red and blue areas correspond to negative and positive charges, respectively. The channel's gate is expected to be located in hydrophobic regions within the pore (shown in yellow). The blue sphere in the channel represents a sodium ion. (Reproduced from Miyazawa, A., Fujiyoshi, Y., and Unwin, N. (2003). Structure and gating mechanism of the acetylcholine receptor pore. *Nature* **423** (6943), 949–955, with permission from Nature.)

other parts that reside within the membrane, possibly coupling agonist binding with channel opening.

The Agonist Binding Site

The endogenous ligand for the nAChR is acetylcholine (ACh). The open state of the channel is much more likely to be associated with two bound agonist molecules than with a single bound molecule. ACh specifically binds to amino acids at the subunit interface of the extracellular region, within loops A, B, and C in the α-subunit and D, E, and F in the non-α-subunit. The binding site resembles a box that is lined by aromatic amino acid residues (tyrosine and tryptophan) (Figure 2). The positively charged ACh molecule binds to its target site partially via cation–π interactions. In this type of interaction the cation (or positively charged moiety) interacts with the electron density at the face of an aromatic side chain.

The Pore

The nicotinic receptor's pore lies within the membrane ~50Å below the ACh binding site. The central ion channel is mostly lined by the M2 α-helices from the five nicotinic subunits (Figure 1B). Parts of the M1 transmembrane domain from each subunit also protrude into the pore. The M2 domains approach each other most closely midway through the membrane creating a gate, which prevents ions from permeating the channel in the closed conformation. Sliding, rotating, and/or tilting of the M2 α-helices during nearly symmetrical transitions of the pentameric bundle remove this constriction. Once the receptor opens, three rings of

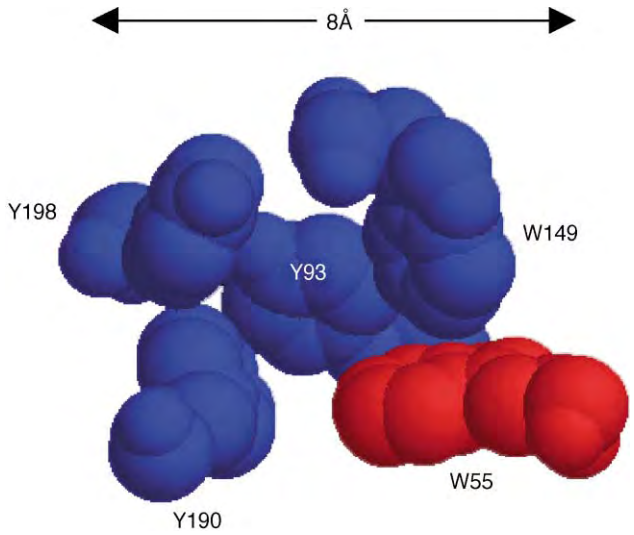

FIGURE 2 The agonist binding site resembles a box lined with five aromatic amino acid residues. Amino acids shown in blue and red are located in the α- and the non-α-subunits, respectively.

negatively charged amino acids within the pore allow the receptor to conduct positively charged sodium, potassium, and calcium ions.

The Cytoplasmic Loop

The M3–M4 cytoplasmic loop in the nAChR varies in both length and sequence among the nicotinic receptor subunits. However, the sequences of the cytoplasmic loops contain consensus phosphorylation sites for various kinases including protein kinase A, C, tyrosine kinase, casein kinase, calmodulin dependent kinase II, and cyclin dependent kinase 5. The M3–M4 loop also contains endoplasmic reticulum retention and export motifs as well as endocytosis motifs. In addition to having phosphorylation sites and targeting motifs, the M3–M4 loop of the muscle nAChR binds to a protein called rapsyn. The muscle nicotinic receptor is anchored to the membrane through its association with this protein.

Channel Activation

The nicotinic acetylcholine receptor has various conformational states including a resting, an active (open channel), and at least two desensitized (non-conducting) states. Upon binding two molecules of ACh in the extracellular region, the receptor undergoes a poorly known conformational change that places the M2 α-helices in the open, cation-conducting state. The channel remains open, or opens several times in succession, for only a few thousandths of a second before one or both agonist molecules dissociate from the binding pocket and the channel closes. If agonist remains present and binds repeatedly, the channel enters a desensitized state.

The Function of nAChRs *in vivo*

Neuromuscular Junction

After the motor nerve muscle is stimulated, the nerve action potential reaches the presynaptic terminal, where it evokes release of prepackaged vesicles containing ACh. The ACh released into the synaptic cleft binds and activates nicotinic receptors located on the postsynaptic muscle membrane. Once the postsynaptic cell is depolarized, voltage-gated sodium channels open, propagating the action potential, and consequently leading to muscle twitches. Presynaptically released ACh remains in the synapse for only about a millisecond before it is broken down by acetylcholinesterase or, more slowly, diffuses away.

Central Nervous System

Researchers have begun by studying the structure and function of the muscle nicotinic receptor. However, the diversity and function of the neuronal nicotinic receptors is being appreciated only now. Despite good efforts, researchers have still not clearly described the various neuronal nAChRs' precise subunit composition, assembly, regulation, and the significance of their heterogeneity.

Neuronal nAChR Composition

Researchers believe that many central nicotinic receptors are heteropentamers composed of at least two α- and three other (α- or β-) subunits. The α7-, α8-, and α9-subunits can form functional homopentameric receptors. There are eight α-subunit (α2–α7, α9, and α10) and three β-subunit (β2–β4) genes expressed in the vertebrate nervous system. An additional α8-subunit gene has been identified in avian species. However, β-, γ-, δ-, and ε-subunits are not expressed in the brain. Although there are literally thousands of different theoretical subunit combinations, only a handful of these produce functional receptors with distinct pharmacological and biophysical properties. Heterologous expression of nAChRs in *Xenopus* oocytes and in mammalian cells has revealed which specific α/β combinations produce functional receptors. The α2-, α3-, and α4-subunits can each form heteropentamers with either β2 or β4. α6β4 receptors express successfully, but similar to the α5- and β3-subunits, α6 expresses best in combination with two other types of subunits. Although the α7-, α8-, and α9-subunits can form functional homopentameric receptors, they can also

form heteropentamers (i.e., $\alpha 7\alpha 8$ and $\alpha 9\alpha 10$ receptors). Evidence for the precise subunit composition of native neuronal receptors is still scant. Although a few major subtypes have been identified (i.e., $\alpha 7$ homopentamers, $\alpha 4\beta 2$, and $\alpha 3\beta 4$), future studies will probably discover other subtypes and perhaps more complex subunit combinations.

The Role of Neuronal nAChRs

Previous work using *in situ* hybridization techniques and radiolabeled ligands shows that nicotinic receptors are present in various brain structures, including the thalamus, cortex, hippocampus, hypothalamus, and cerebellum. Although many neuronal nAChRs are found on the presynaptic terminal, some are located postsynaptically. Brain nAChRs are thought to presynaptically modulate, rather than directly mediate, chemical synaptic transmission. In the retina and striatum, cholinergic (ACh containing) interneurons release ACh and activate nAChRs located on the presynaptic cell. Presynaptic nicotinic receptor activation can positively or negatively affect the release of various neurotransmitters including GABA, glutamate, dopamine, and noradrenaline.

Nicotinic Receptor Agonists and Antagonists

Agonists

In addition to ACh, other compounds can activate nicotinic receptors. In fact, nAChRs are offensive or defensive targets for various organisms. For instance, nicotine, an alkaloid product from tobacco, is the prototypic agonist for nAChRs. Additionally, epibatidine, a powerful analgesic that is purified from the skin of the South American tree frog, *Epipedobates tricolor*, is the most potent nAChR agonist discovered. Other naturally occurring nAChR agonists include choline, cytisine, anabaseine, and (+)-anatoxin A. In an effort to provide greater subtype selectivity and therapeutic efficacy, researchers have also developed a wide range of synthetic compounds that can activate nAChRs. Keep in mind that the muscle and the various neuronal nicotinic receptor subtypes have distinct pharmacological profiles for different natural and synthetic agonists.

Antagonists

Nicotinic receptor inhibitors stabilize the closed-channel conformation and, in the case, of competitive inhibitors, prevent agonist binding. D-tubocurarine (d-TC) is a classic competitive nAChR inhibitor that does not discriminate well between the various types of nicotinic receptors. South American Indians commonly used this poison found in the shrubs of *Chondodendron tomentosum* to coat the tip of their arrows. More selective than d-TC, dihydro-β-erythroidine is an alkaloid that is mostly used to inhibit $\alpha 4\beta 2$ receptors. α-Bungarotoxin (α-Bgt) is a well-established selective competitive nAChR antagonist found in the venom of the Taiwanese banded krait (*Bungarus multicintus*). α-Bgt inhibits muscle nAChRs and $\alpha 7$ homomers, as well as receptors containing $\alpha 8$- and $\alpha 9$-subunits. It does not appear to interact with α/β heteropentamers. Other nAChR noncompetitive inhibitors include α-conotoxins, mecamylamine, steroids, local anesthetics, and such therapeutic agents as MK 801, carbamazepine, buproprion, and chlorpromazine.

Nicotinic Receptors and Disease

Congenital Myasthenic Syndrome

Nicotinic receptors have been implicated in a number of diseases. At the neuromuscular junction, 26 mutations have been identified in the extracellular, transmembrane, and cytoplasmic domains of the nAChR that lead to different forms of congenital myasthenic syndrome (CMS). CMS are presynaptic, synaptic, and postsynaptic in origin. Postsynaptic CMS mutations are divided into two categories, depending on their effects at the endplate region of the muscle membrane. CMS mutations are classified as either slow- or fast-channel syndromes. The slow-channel mutations enhance agonist affinity or gating efficiency. The fast-channel syndrome mutations reduce agonist affinity for the open channel or impair gating. Work from Andrew Engel, Christopher Gomez, Steven Sine and Anthony Auerbach has contributed to the molecular pathophysiology of CMS. Furthermore, their biophysical analyses of the CMS mutations have provided us with some basic insights into the relationship between the structure and function of nAChRs.

Epilepsy

Nicotinic receptors appear to be linked to several forms of inherited epilepsy. Autosomal-dominant nocturnal frontal lobe epilepsy (ADNFLE) is a monogenic disease presently linked to three $\alpha 4$ and two $\beta 2$ mutations. All five of these mutations lie within (or immediately adjacent to) M2 and produce similar clinical symptoms. To date, the mechanism(s) by which these mutations lead to the onset of a partial epileptic seizure remains to be elucidated. However, two effects common to all of the mutations have been identified. (1) The ADNFLE mutants reduce the nAChR's sensitivity to changes in extracellular calcium and (2) the mutations enhance the receptor's sensitivity to ACh. Studies on mouse

models of ADNFLE may be the most appropriate tactic for understanding the pathophysiology of these partial seizures.

Alzheimer's Disease (AD)

AD is a neuro-degenerative disease characterized by the progressive deterioration of higher cognitive functions, including memory loss. Since nicotinic receptors play a critical role in learning and memory, it is not surprising that AD patients lose the cholinergic pathways from the basal forebrain to the hippocampus and the cortex. Moreover, the brains of AD patients have a reduced number of cholinergic cells and presynaptic nAChRs. Since low levels of ACh are believed to lead to the cognitive decline observed in patients, cholinesterase inhibitors (such as tacrine, donepezil, and rivastigmine) are currently used to treat AD.

Parkinson's Disease (PD)

Patients with PD, another neuro-degenerative disorder, have difficulty initiating and sustaining smooth muscle movements. Although loss of dopaminergic neurons defines PD, patients also lose cholinergic cells in the basal forebrain and their high affinity nAChRs. In fact, the reduction in cortical nAChRs correlates well with the degree of dementia. Furthermore, researchers have correlated tobacco use with a lower incidence of PD.

Other Diseases

Nicotinic receptors have also been implicated in other diseases such as schizophrenia, Tourette's syndrome, anxiety, and depression. However, the precise role of the nAChR in the pathology of these diseases remains to be determined.

See Also the Following Articles

Calcium/Calmodulin-Dependent Protein Kinase II • Calcium/Calmodulin-Dependent Protein Kinases • Disulfide Bond Formation • Muscarinic Acetylcholine Receptors • Neurotransmitter Transporters • Protein Kinase C Family

Glossary

acetylcholinesterase The enzyme that breaks down acetylcholine into choline and acetate.

disulfide bond The covalent bond between two thiol groups (S–S) of cysteine residues.

endplate The surface of the muscle fiber at the junction where the motor nerve terminal meets the muscle.

neurotransmitter A chemical released from neurons across the synapse.

postsynaptic Located after the synapse.

presynaptic Located before the synapse.

synapse The extracellular space between the presynaptic and postsynaptic neurons.

Further Reading

Brejc, K., van Dijk, W. J., Klaassen, R. V., Schuurmans, M., van Der Oost, J., Smit, A. B., and Sixma, T. K. (2001). Crystal structure of an ACh-binding protein reveals the ligand-binding domain of nicotinic receptors. *Nature* **411**, 269–276.

Bertrand, D., Picard, F., Le Hellard, S., Weiland, S., Favre, I., Phillips, H., Bertrand, S., Berkovic, S. F., Malafosse, A., and Mulley, J. (2002). How mutations in the nAChRs can cause ADNFLE epilepsy. *Epilepsia* **43**, 112–122.

Engel, A. G., Ohno, K., and Sine, S. (2002). The spectrum of the congenital myasthenic syndromes. *Mol. Neurobiol.* **26**, 347–367.

Hille, B. (2001). Ligand-gated channels of fast chemical synapses. In *Ion Channels of Excitable Membranes*, 3rd edition, pp. 169–199. Sinauer Associates, Massachusetts.

Miyazawa, A., Fujiyoshi, Y., and Unwin, N. (2003). Structure and gating mechanism of the acetylcholine receptor pore. *Nature* **423**, 949–955.

Paterson, D., and Nordberg, A. (2000). Neuronal nicotinic receptors in the human brain. *Prog. Neurobiol.* **61**, 75–111.

Rodrigues-Pinguet, N., Jia, L., Li, M., Figl, A., Klaassen, A., Truong, A., Lester, H. A., and Cohen, B. (2003). Five ADNFLE mutation reduce the Ca^{2+} dependence of the mammalian $\alpha 4\beta 2$ acetylcholine response. *J. Physiol.* **550**, 11–26.

Sharples, C. G. V., and Wonnacott, S. (2001). Neuronal nicotinic receptors. *Tocris Rev.* **19**, 1–12.

Steinlein, O. K. (2002). Channelopathies can cause epilepsy in man. *Eur. J. Pain* **6**(suppl. A), 27–34.

Unwin, N. (2002). Structure of the acetylcholine-gated channel. *The Roy. Soc.* **355**, 1813–1829.

Wonnacott, S. (1997). Presynaptic ACh receptors. *Trends Neurosci.* **20**, 92–98.

Biography

Nivalda O. Rodrigues-Pinguet obtained her Ph.D. in Biomedical Sciences at the University of California, Riverside. She is currently a post-doctoral scholar with Drs. Bruce N. Cohen and Henry A. Lester at the California Institute of Technology. During her graduate tenure, Dr. Rodrigues-Pinguet studied the functional effects of nicotinic receptor mutations linked to autosomal dominant nocturnal frontal lobe epilepsy (ADNFLE).

Henry A. Lester is the Bren Professor of Biology at the California Institute of Technology. He obtained his Ph.D. in Biophysics from Rockefeller University and pursued his postdoctoral training with Dr. Jean-Pierre Changeux, at the Institut Pasteur in Paris, France. Dr. Lester received formal training in physics but has also embraced biochemistry, molecular biology, and neurogenetics. He has worked on nicotinic receptors for 30 years and is an authority on ion channels and molecular neuroscience.

Nitric Oxide Signaling

Michael A. Marletta
University of California, Berkeley, California, USA

The basic components of nitric oxide (NO) signaling involve nitric oxide synthase (NOS) to synthesize NO and the soluble isoform of guanylate cyclase (sGC) to trap NO. Once activated by NO, sGC converts GTP to guanosine 3′5′-cyclic monophosphate (cGMP), leading to cGMP-dependent physiological responses such as vasodilation. Termination of the cGMP signal involves a cyclic nucleotide phosphodiesterase (PDE). There are multiple PDE isoforms, and selective inhibition of specific isoforms has proven to be clinically useful (for example, sidenifil [Viagra] in the treatment of erectile dysfunction). sGC must also be turned off; however, the *in vivo* mechanism for this remains unknown. Catalytic activity of constitutive NOS isoforms involved in signaling is controlled by Ca^{2+} and calmodulin via receptor-mediated events that trigger Ca^{2+} release from intracellular stores or uptake from external sources.

Biological Processes Controlled by Nitric Oxide

First defined as EDRF (endothelium-derived relaxing factor), the biological effects of nitric oxide (NO) have now been definitively characterized in a number of tissues. Smooth muscle is often the target of NO action, leading to vasodilation in blood vessels (Figure 1) and penile erection via NO synthesis in the corpus cavernosum, two well-established functions. Smooth muscle relaxation in the gut is another important function for NO, playing a key role in gastrointestinal tract motility. NO synthesis in the brain is also well established, though the exact role in learning and memory is still under debate. In the CNS, NO acts as a somewhat atypical neurotransmitter in that it is not synthesized and stored and then released with the appropriate signal, but is synthesized on demand. Constitutive nitric oxide synthases (NOSs) are involved in all of these responses and are under the control of Ca^{2+} and calmodulin. Receptor-mediated events that trigger Ca^{2+} release or uptake turn on the specific NOS isoform in the tissue. NOS has also been found in skeletal muscle, in the myocardium, and in many other cells, suggesting that it will play an even more extensive role in physiological control than is currently established. The function of NO in the myocardium is particularly complex, although it appears that novel therapeutics will be an outcome of sorting out the complexity.

Nitric Oxide Synthase

The catalytic activity of the NOS isoforms (constitutive) involved in signaling is controlled by Ca^{2+} and calmodulin (CaM). After stimulation by the appropriate external signal, an increase in intracellular-free Ca^{2+} occurs, which then leads to a Ca^{2+}–calmodulin complex. Each of the four EF hands of calmodulin binds one Ca^{2+}, and then this Ca^{2+}–CaM complex binds to NOS, thereby activating NOS to synthesize NO. The NOS reaction is shown in Figure 2. The enzyme converts L-arginine to citrulline and NO. Co-substrates for the reaction include NADPH and O_2. NOS is composed of two domains: a reductase domain with homology to cytochrome P450 reductase and a heme domain. The reductase domain contains two bound flavins, FAD and FMN, and with analogy to P450 reductase, the electron transfer route is from NADPH to FAD and then to FMN. The heme domain contains a cytochrome P450-type heme (ferric protoporphyrin IX coordinated to cysteine thiol), one equivalent of 6(R)-tetrahydro-L-biopterin (H_4B), and the L-arginine binding site. Crystal structures of the heme domain show it to be dimeric with a tetra-thiolate zinc center at the dimeric interface using two cysteines from each subunit. Catalytic chemistry at the heme domain is dependent on electron transfer from the flavins in the reductase domain, which is triggered by binding of the Ca^{2+}–CaM complex to NOS.

The catalytic chemistry takes place at the P450 heme site; in fact, structures of the oxygenase domain that have been solved in the presence of L-arginine show the substrate positioned over the heme. H_4B also participates in electron transfer at the heme site, using unprecedented one-electron chemistry. The exact details of the involvement of this required bound cofactor are still emerging. As shown in Figure 2, L-arginine is first converted to NHA (N^G-hydroxy-L-arginine) and then NHA is converted to citrulline

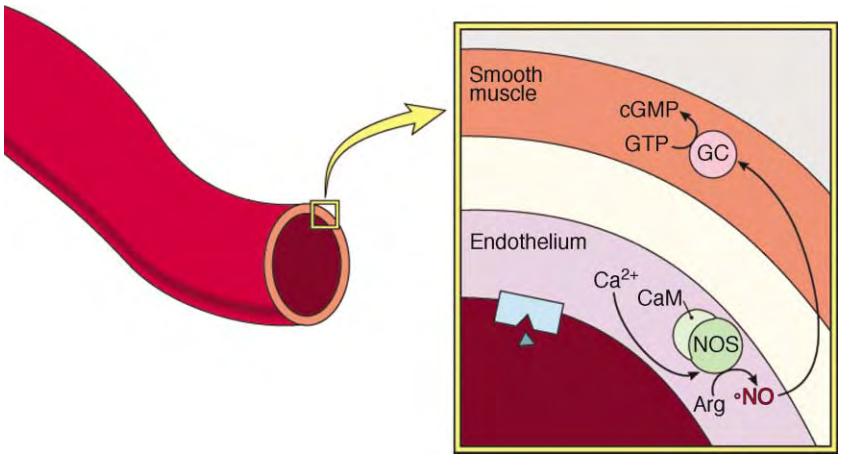

FIGURE 1 Nitric oxide function in blood vessel dilation. In response to a receptor-mediated event (shown schematically), endothelial NOS is activated by Ca^{2+} and calmodulin, leading to the synthesis of NO. NO then diffuses into the adjacent smooth muscle and activates the soluble isoform of guanylate cyclase and the synthesis of cGMP. cGMP, through a signaling cascade, then leads to smooth muscle relaxation.

and NO. NADPH and O_2 are required in both steps of the reactions, as is H_4B. The mechanism of the reaction is complicated and not fully understood, but clearly involves oxidative chemistry at the P450 heme with participation of H_4B.

The Ca^{2+}–CaM complex exerts control over the NOS reaction catalyzed by the constitutive cell-signaling isoforms, eNOS (endothelial NOS) and nNOS (neuronal NOS) by controlling electron transfer from the reductase domain to heme domain. Without this required process, the reaction does not take place, therefore, Ca^{2+}–CaM exerts complete control over the reaction. NO is toxic, and so it is absolutely crucial in NO signaling to strictly control the amount of NO that is made. Tight regulation over Ca^{2+} concentrations in the cell provides this required level of control. In general, nM concentrations of NO are synthesized by the generator cell, and pM concentrations act in the target cell. iNOS (inducible NOS) was first described as a Ca^{2+}–CaM-independent isoform, but subsequent studies showed that Ca^{2+}–CaM co-purified with this isoform. It is, therefore, "constitutively" active. Because the function of iNOS is in the host response to infection, a NOS isoform that is constitutively active and produced at the site of infection conforms to this biological role.

A number of inhibitors of NOS have been developed. The initial molecules were simple derivatives of the substrate L-arginine; however, other non-arginine-related structures were later found that were derived largely from library screens in the pharmaceutical industry, and some demonstrate significant isoform selectivity.

Chemistry of NO

NO is unstable in aqueous, aerobic solution. The stable end products of NO decomposition are nitrite (NO_2^-) and nitrate (NO_3^-). The reaction sequence that leads to these products is shown in Figure 3. This solution chemistry consumes NO as it traverses a path from the generator cell to the target cell, hence the amount that

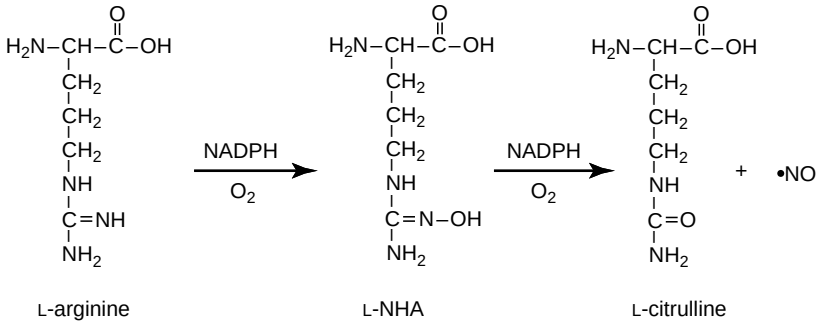

FIGURE 2 The reaction catalyzed by nitric oxide synthase. The substrate for the reaction is the amino acid L-arginine, which is converted to L-NHA and then to citrulline and ·NO. Although it has never been shown, it is assumed that the stereochemistry of citrulline at the α-carbon remains unchanged.

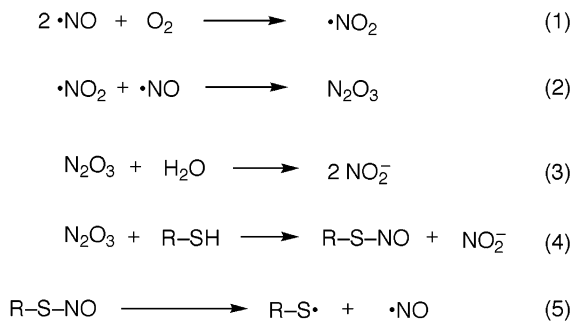

FIGURE 3 Relevant solution chemistry of nitric oxide. NO reacts with O_2 in aqueous solution to produce nitrogen dioxide ($\cdot NO_2$) (Eq. 1). ·NO2 then reacts with another molecule of ·NO to produce dinitrogen trioxide (N_2O_3) (Eq. 2). N_2O_3 can then hydrolyze to yield NO_2^- (Eq. 3) or react with protein or low molecular weight thiols to make the S-nitroso derivative (Eq. 4). The S-nitrosated protein or small molecule is capable of homolytically cleaving to generate the thiol radical and ·NO (Eq. 5).

arrives at the target cell is always lower. An intermediate along the reaction pathway is dinitrogen trioxide (N_2O_3). N_2O_3 can react with water as shown to produce NO_2^- or react with other cellular nucleophiles. The reaction with cysteine residues in proteins or with small cellular sulfur nucleophiles such as glutathione leads to the formation of S-nitrosated species as shown in Figure 3. S-Nitrosated proteins and small molecules are known to decompose to the sulfur radical and NO in a so-called homolytic cleavage (Figure 3); certain biological conditions can accelerate the reaction. The significance of this chemistry is discussed below. NO has 11 valence electrons and, therefore, has one unpaired electron. The radical nature of NO dictates other chemistry, such as the facile reaction of NO with superoxide to give peroxynitrite ($^-$OONO), which then converts very quickly to NO_3^-, and the reaction with oxyhemoglobin to give methemoglobin and NO_3^-, again with the intermediacy of $^-$OONO. Peroxynitrite is a potent oxidant and has been shown to be important in various types of tissue damage associated with the formation of high levels of NO. The decomposition of relatively high concentrations of NO in tissue that occurs under inflammatory conditions leads to nitration chemistry, most frequently seen on tyrosine residues.

Guanylate Cyclase

The soluble isoform of guanylate cyclase (sGC) is the receptor for NO in target cells. Activation of sGC leads to the formation of cGMP, and then through a cascade involving cGMP-dependent kinases, a lowering of intracellular Ca^{2+} occurs, leading to effects such as smooth muscle relaxation (e.g., vasodilation). sGC is a heterodimeric protein composed of two subunits. The best characterized is the physiologically occurring $\alpha1\beta1$ heterodimer, first isolated from lung tissue. The β-subunit contains a unique ferrous heme cofactor that is the receptor for NO. This porphyrin, despite having the same ligation as the globins, does not bind oxygen; rendering it ideally suited to bind NO is the presence of a high competing concentration of oxygen. Upon binding of NO, sGC is activated 300-fold over the basal activity, and a burst of cGMP is produced. cGMP then acts through cGMP-dependent kinases to bring about physiological responses such as vasodilation and other smooth muscle relaxation responses.

Tools to manipulate sGC are emerging and include ODQ (1H-[1,2,4]oxadiazole[4,3-a]quinoxalin-1-one), which inhibits sGC by oxidation of ferrous porphyrin to the ferric oxidation, and a family of activators based on the structure of YC-1 (3-(5′-hydroxymethyl-2′-furyl)-1-benzyl indazole). This compound is a weak activator of sGC; however, YC-1 and CO activate sGC to the same level as NO, and YC-1 acts synergistically with NO. A class of activators based on the YC-1 structure that directly activate and are more potent than YC-1 are entering clinical trials.

Non-cGMP NO-Signaling Pathways

As mentioned previously, N_2O_3 is an intermediate that forms during the aerobic solution decomposition of NO. N_2O_3 is a potent nitrosating agent that reacts with the ω-amino group of lysine and the thiol of cysteine. Formation of S-nitrosated cysteines in proteins can cause a change in the biological activity of the protein. Although increasing studies are directed toward understanding the chemistry and biological activity of the S–NO bond and the formation of these bonds with small molecule thiols and protein thiols, critical aspects remain to be determined. For example, the formation of R–S–NO could occur via the solution reaction of N_2O_3 with the thiol or by an enzyme-catalyzed process. The former path would appear to be too inefficient, and an enzyme to catalyze the latter path has not been isolated. Other hypotheses advanced involve the reversible formation of R–S–NO, where again the R group could be either a low molecular weight species or a protein similar to phosphoryl transfer. The kinase and phosphatase equivalents have yet to be isolated. Confounding all these hypotheses is the chemical reaction of R–SH with N_2O_3, which would be facilitated much beyond what would be expected to occur when nonbiological concentrations of NO are used.

There is another important outcome from the formation of S-nitrosated proteins and low molecular

weight compounds like glutathione. The S-nitroso bond is known to homolytically fragment, forming NO and a thiyl radical. The NO so derived can then function to activate sGC as described above. This mode of generating NO is attractive in that it represents a semi-stable form of this signaling agent and could be a way to store, transport, and deliver NO. There is no question that the decomposition of NO in aerobic aqueous solution will lead to S-nitrosation; rather, the issue is whether the amounts formed *in vivo* are physiologically significant.

See Also the Following Articles

Calcium Signaling: NO Synthase • Flavins • Heme Proteins • Heme Synthesis • Neurotransmitter Transporters

Glossary

domain A compact region of protein structure that is a stable entity.
heterodimer A protein composed of two nonidentical subunits.
kinase An enzyme that transfers a phosphoryl group from a donor (typically ATP) to an acceptor (often a protein in cell signaling pathways).
neurotransmitter A chemical messenger released or synthesized at a synapse.
phosphatase An enzyme that removes a phosphoryl group.
radical A chemical species with an unpaired electron.

Further Reading

Bredt, D. S., and Snyder, S. H. (1994). Nitric oxide: A physiologic messenger molecule. *Annu. Rev. Biochem.* **63**, 175–195.

Denninger, J. W., and Marletta, M. A. (1999). Guanylate cyclase and the NO/cGMP signaling pathway. *Biochim. Biophys. Acta* **1411**, 334–350.

Marletta, M. A. (1994). Nitric oxide synthase: Aspects concerning structure and catalysis. *Cell* **78**, 927–930.

Marletta, M. A. (2001). Another activation switch for endothelial nitric oxide synthase: Why does it have to be so complicated? *Trends Biochem. Sci.* **26**, 519–521.

Moncada, S., Palmer, R. M., and Higgs, E. A. (1991). Nitric oxide: Physiology, pathophysiology, and pharmacology. *Pharmacol. Rev.* **43**, 109–142.

Biography

Michael A. Marletta is the Aldo DeBenedictis Distinguished Professor of Chemistry in the Department of Chemistry, and Professor of Biochemistry in the Department of Molecular and Cell Biology at the University of California, Berkeley. His research interests on protein structure and function relationships have an emphasis on enzymatic catalysis and redox biochemistry. He holds a Ph.D. from the University of California, San Francisco. He is a Fellow of AAAS and was elected to the American Academy of Arts and Sciences and the Institute of Medicine.

N-Linked Glycan Processing Glucosidases and Mannosidases

Linda O. Tremblay and Annette Herscovics
McGill University, Montréal, Québec, Canada

Endoplasmic reticulum (ER) and Golgi glucosidases and mannosidases trim the asparagine-linked glycans (*N*-glycans) attached to newly formed glycoproteins within the secretory pathway. The sequential action of these enzymes yields the substrate(s) required for the biosynthesis of hybrid and complex *N*-glycans which mediate cell–cell interactions during embryogenesis, development, tumor metastasis, lymphocyte trafficking, leukocyte recruitment in inflammation, and many other biological interactions. In addition, the glycosidases participate in glycoprotein folding and quality control.

Abrogation of mammalian glycosidase functions as a consequence of genetic defects in humans or of targeted gene ablation in the mouse results in developmental and multisystemic abnormalities due to anomalous *N*-glycan biosynthesis. Herein the structure, function, and physiological roles of mammalian ER and Golgi processing glucosidases and mannosidases are reviewed, including pertinent studies of yeast and filamentous fungi enzymes.

Glucosidases

Glucosidase I

Glucosidase I is a type-II ER transmembrane protein of 92 kDa that cleaves the terminal α1,2-linked glucose residue of $Glc_3Man_9GlcNAc_2$ immediately following its transfer to nascent polypeptide chains. This inverting glycosidase has been conserved during eukaryotic evolution and, based on sequence similarity, it belongs to glycosylhydrolase family 63. Recently, missense mutations were identified in the human glucosidase I gene of a severely ill neonate that perished shortly after birth (Table I), showing that removal of the terminal glucose residue of $Glc_3Man_9GlcNAc_2$ is essential for human development and viability.

Glucosidase I is inhibited by castanospermine, 1-deoxynojirimycin and its N-methyl and N-butyl-deoxynojirimycin derivatives. These compounds prevent exit of some glycoproteins from the ER. As a result, they affect processes such as myoblast fusion to myotubes, transformation induced by glycoprotein oncogenes, cell surface expression of glycoprotein receptors, and also act as antiviral agents.

Glucosidase II

ER glucosidase II removes the two inner α1,3-linked residues (Figure 1). This glycosidase (glycosylhydrolase family 31) consists of a soluble catalytic α-subunit ($\sim$110 kDa) and a β-subunit ($\sim$80 kDa) which contains the ER retrieval signal HDEL. Glucosidase II is affected by the same inhibitors as glucosidase I, as well as by bromoconduritol.

Endo α-Mannosidase

Endo α-mannosidase is a 52-kDa enzyme present in the intermediate compartment and in the Golgi. It provides an alternate pathway independent of ER glucosidases for glucose removal from $Glc_{1-3}Man_{4-9}GlcNAc_2$, the preferred substrate being $Glc_1Man_9GlcNAc_2$ (Figure 1). Endo α-mannosidase expression is cell-specific and restricted to the chordate phylum; thus, it is likely to have appeared late in evolution. It does not share homology with any other known proteins. Upregulation of endo α-mannosidase was suggested to partially compensate for the glucosidase I deficiency described in the aforementioned patient.

Classification and Properties of Processing α-Mannosidases

Processing mannosidases have been classified into two distinct groups based on their amino acid sequences, different enzymatic mechanisms, and sensitivity to inhibitors. Class-I α1,2-mannosidases (glycosylhydrolase family 47) are inverting enzymes that have been conserved through eukaryotic evolution. They require calcium for activity and are inhibited by 1-deoxymannojirimycin and kifunensine, but not by

TABLE I

Human Glycosidase Genetic Defects and Mouse Glycosidase Gene Ablation Phenotypes

Glycosidase gene	Phenotype
Human diseases	
Glucosidase I	Generalized hypotonia, hypomotility, dysmorphic features, hepatomegaly, hypoventilation, seizures, neonatal lethality
Mannosidase II	Congenital dyserythropoietic anemia (HEMPAS), jaundice, hepatosplenomegaly, diabetes and gallstones
Mouse gene ablations	
Mannosidase II	Dyserythropoietic anemia, splenomegaly, autoimmune disease similar to systemic lupus erythematosus
Mannosidase IIx	Male infertility, hypospermatogenesis, decreased testis size, diminished spermatogenic cell adhesion to Sertoli cells

swainsonine. In contrast, class-II α-mannosidases (glycosylhydrolase family 38) are retaining enzymes that are inhibited by swainsonine, but not by 1-deoxymannojirimycin or kifunensine. The class-II enzymes are involved in *N*-glycan biosynthesis as well as in degradation, and with the exception of the Drosophila Golgi α-mannosidase II, they do not require divalent cations for activity.

Class-I α1,2-Mannosidases

α1,2-Mannosidase Subgroups

The class-I family consists of three subgroups of proteins sequestered by their sequence similarity and distinguished by their enzymatic activity. Subgroup (1) contains yeast and mammalian ER α1,2-mannosidase I that primarily form $Man_8GlcNAc_2$ isomer B; subgroup (2) includes mammalian Golgi α1,2-mannosidases IA, IB and IC as well as filamentous fungi α1,2-mannosidases that readily form $Man_5GlcNAc_2$ from $Man_9GlcNAc_2$ through $Man_8GlcNAc_2$ isomers A and/or C as intermediates; subgroup (3) consists of a group of proteins with amino acid sequence similarity to α1,2-mannosidases, such as mammalian EDEM and yeast Htm1p/Mnl1p, that have no apparent α1,2-mannosidase activity. This latter subgroup of proteins has been implicated in the degradation of misfolded glycoproteins as described in various articles in this encyclopedia.

ER α1,2-Mannosidase I

ER α1,2-mannosidase I is a type-II transmembrane protein of about 80 kDa that absolutely requires calcium for activity. It is the only processing α1,2-mannosidase in the yeast *Saccharomyces cerevisiae*. X-ray crystallographic studies of the yeast catalytic domain as an enzyme–product complex showed that it consists of a novel $(\alpha\alpha)_7$ barrel with one side of the barrel plugged by a β-hairpin forming a cavity of $\sim$15Å. The active site consisting of essential acidic residues and calcium is located at the bottom of the barrel. The structure of the human enzyme in complex with the inhibitors 1-deoxymannojirimycin and kifunensine was also determined. It shows that calcium coordinates with conserved acidic residues and the O2′ and O3′ hydroxyls of the six-membered rings of the inhibitors stabilized in a $^1C_4$ conformation. Although ER α1,2-mannosidase I primary trims the terminal middle arm α1,2-linked mannose residue of $Man_9GlcNAc_2$ to form $Man_8GlcNAc_2$ isomer B (Figure 1), recent studies revealed that ER α1,2-mannosidase I is capable of removing additional mannose residues from $Man_8GlcNAc$, *in vitro* and *in vivo*.

Class-I Golgi α1,2-Mannosidases

There are three mammalian class-I Golgi α1,2-mannosidases, IA, IB, and IC, derived from different genes on different chromosomes. They are type-II transmembrane proteins of about 70 kDa. These enzymes trim the α1,2-linked mannose residues from $Man_8GlcNAc_2$ isomer B to form $Man_5GlcNAc_2$ (Figure 1). When $Man_9GlcNAc_2$ is used as substrate, they readily form $Man_6GlcNAc_2$, but remove the last α1,2-linked mannose residue much more slowly. Their specificity is complementary to that of ER α1,2-mannosidase I since the last residue cleaved from $Man_9GlcNAc_2$ by the Golgi enzymes is the mannose preferred by ER α1,2-mannosidase I. There are small differences in the order of mannose removal by the different Golgi α1,2-mannosidases. X-ray crystallographic and modeling studies of a fungal α1,2-mannosidase with the same specificity as the mammalian Golgi orthologues revealed that the overall protein fold and topology of the active site is identical to that of ER α1,2-mannosidase I, and that the different specificities of these enzymes is determined by the space within the barrel. The fungal enzyme barrel permits binding of multiple oligosaccharide conformations of all three $Man_8GlcNAc_2$ isomers, whereas only a single conformation of $Man_8GlcNAc_2$ isomer B is accommodated by ER α1,2-mannosidase I.

The major difference between the three mammalian Golgi α1,2-mannosidases is their tissue- and cell-specific expression as determined by Northern blots of murine and human tissues and by immunolocalization studies in the male rat reproductive system.

The organization of the three human and murine Golgi α1,2-mannosidase genes is highly conserved with the location of the intron–exon boundaries being nearly identical. Thus, late evolutionary gene duplication is

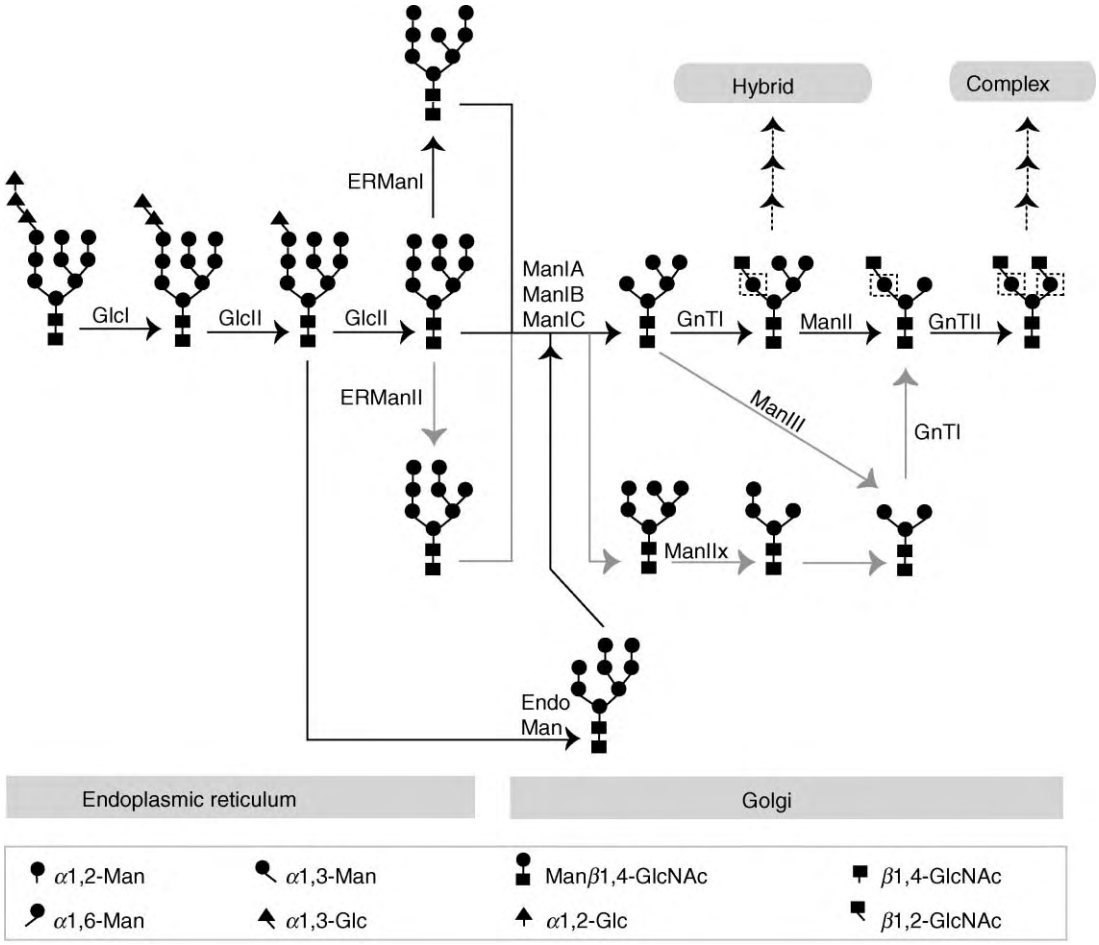

FIGURE 1 Role of glycosidases in mammalian *N*-glycan processing. The $Glc_3Man_9GlcNAc_2$ precursor oligosaccharide attached to asparagine residues of nascent chains (within Asn-X-Ser/Thr where X is any amino acid except Pro) is sequentially modified by processing glycosidases and glycosyltransferases, beginning in the endoplasmic reticulum and continuing in the Golgi. Trimming by α-glucosidases and α1,2-mannosidases is essential for the formation of complex and hybrid *N*-glycans initiated by GnTI. Additional enzymes add other GlcNAc residues to the boxed core mannose residues. Subsequently, glycosyltransferases further elaborate the structures by linking galactose, fucose, and sialic acid. Gray arrows indicate the suggested role of ERManII and the proposed ManIIx- and ManIII-mediated alternate pathways independent of Golgi α-mannosidase II. GlcI, α1,2-glucosidase I; GlcII, α1,3-glucosidase II; ERManI, ER α1,2-mannosidase I; ERManII, ER α1,2-mannosidase II; ManIA, IB, IC, Golgi α1,2-mannosidase IA, IB, IC; Endo Man, endo-α-mannosidase; ManII, IIx, III, α-mannosidase II, IIx, III; GnTI, II, N-acetylglucosaminyltransferase I, II. (Modified from Tremblay, L.O., PhD Thesis, McGill University 2002).

likely to have produced the Golgi α1,2-mannosidase gene family. However, the organization of the Golgi α1,2-mannosidase genes differs from that of the other two class-I α1,2-mannosidase subgroups, suggesting that the genes of the three subgroups may have arisen independently.

Class-II Processing α-Mannosidases

Class II Golgi α-Mannosidases

Golgi α-mannosidase II trims the terminal α1,3- and α1,6-linked mannose residues of $GlcNAc_1Man_5GlcNAc_2$, thus providing the substrate for complex *N*-glycan biosynthesis (Figure 1). It is absolutely dependent upon prior action of N-acetylglucosaminyltransferase I (GnTI) that initiates the first N-acetyllactosamine branch of complex *N*-glycans. The enzyme is a type-II membrane protein of ~130 kDa. The crystal structure of the Drosophila Golgi α-mannosidase II revealed that the active site is on the planar side of the hemi-oval-shaped catalytic domain comprised of an N-terminal α/β-domain, a bundle of three helices, and a C-terminal β-domain. The conformation is stabilized by disulfide bonds and the coordination of a zinc ion. The zinc ion participates directly in the catalytic mechanism and contributes to substrate binding. The terminal GlcNAc of the substrate is anchored in a binding pocket near the active site and is postulated to serve as an anchor

point for substrate rotation within the active site leading to the sequential trimming of the α1,6- and α1,3-linked mannose residues with minimal conformational change.

Ablation of the mouse α-mannosidase II gene indicated that this enzyme plays an important role in the biosynthesis of glycoproteins that maintain erythrocyte membrane integrity. This phenotype resembles congenital dyserythropoietic anemia type II, a rare human disease also known as HEMPAS, caused by a defect in the human Golgi α-mannosidase II gene (Table I). Mice lacking α-mannosidase II also progressively develop autoantibodies indicating that proteins bearing the atypical *N*-glycans produced in these mice can evade self-tolerance. These α1,2-mannosidase II null mice thus provide a model for lupus erythematosus in humans. The fact that complex *N*-glycan biosynthesis occurs in many tissues of mice lacking α-mannosidase II revealed the existence of an alternate biosynthetic pathway mediated by a cobalt-dependent enzyme called α-mannosidase III (Figure 1). However, a gene or cDNA encoding this activity has not yet been identified.

The human and mouse genomes also encode α-mannosidase IIx, a protein that has significant amino acid similarity to α-mannosidase II. The exact specificity of this enzyme remains to be definitively established. However, targeted gene ablation of mouse α-mannosidase IIx indicated that it is required for the biosynthesis of complex *N*-glycans that mediate spermatogenic cell interactions with Sertoli cells in the testis (Table I).

ER α1,2-Mannosidase II

The existence of mammalian ER α1,2-mannosidase II has been proposed from studies with intact cells and membrane preparations, but remains to be confirmed. This activity is distinct from ER α1,2-mannosidase I, since it yields a different $Man_8GlcNAc_2$ isomer (Figure 1) and is inhibited by swainsonine and 1-deoxymannojirimycin but not by kifunensine. Its substrate specificity and sensitivity to inhibitors are similar to those of a class-II cytosolic α-mannosidase involved in glycoprotein degradation. In addition, ER α1,2-mannosidase II cross-reacts with antibodies generated towards the cytosolic α-mannosidase. The existence of a distinct cDNA or gene encoding ER α1,2-mannosidase II has not been described.

In conclusion, the enzymatic specificities and properties of mammalian glycosidases that are involved in *N*-glycan biosynthesis have been well characterized. Current studies are elucidating their functions in glycoprotein folding and in ERAD, but their physiological roles and involvement in genetic diseases remain to be elucidated by further gene ablation studies.

See Also the Following Article

Glycoprotein Folding and Processing Reactions

Glossary

inverting glycosidase Glycosidase that catalyzes hydrolysis with inversion of the anomeric configuration.

retaining glycosidase Glycosidase that catalyzes hydrolysis with retention of the anomeric configuration.

Further Reading

Coutinho, P. M., and Henrissat, B. (1999). Carbohydrate-active enzymes: An integrated database approach. In *Recent Advances in Carbohydrate Bioengineering* (H. J. Gilbert, B. Davies, B. Henrissat and B. Svensson, eds.) pp. 3–12. The Royal Society of Chemistry, Cambridge. http://afmb.cnrs-mrs.fr/CAZY/index.html.

Helenius, A., and Aebi, M. (2001). Intracellular functions of N-linked glycans. *Science* **291**, 2364–2369.

Herscovics, A. (2001). Structure and function of class I α1,2-mannosidases involved in glycoprotein synthesis and endoplasmic reticulum quality control. *Biochimie* **83**, 757–762.

Lobsanov, Y. D., Vallée, F., Imberty, A., Yoshida, T., Yip, P., Herscovics, A., and Howell, P. L. (2002). Structure of *Penicillium citrinum* α1,2-mannosidase reveals the basis for differences in specificity of the ER and Golgi class I enzymes. *J. Biol. Chem.* **277**, 5620–5630.

Moremen, K. W. (2002). Golgi α-mannosidase II deficiency in vertebrate systems: Implications for asparagine-linked oligosaccharide processing in mammals. *Biochim. Biophys. Acta* **1573**, 225–235.

Parodi, A. (2000). Protein glucosylation and its role in protein folding. *Annu. Rev. Biochem.* **69**, 69–93.

Schachter, H. (2001). Congenital disorders involving N-glycosylation of proteins. *Cell Mol. Life Sci.* **58**, 1085–1104.

Tremblay, L. O (2002). *Characterization of Human Class I α1,2 Mannosidases Involved in N-Glycan Biosynthesis and the Role of Murine α1,2-Mannosidase 1B in Embryogenesis and Development*. Thesis, McGill University.

Vallée, F., Lipari, F., Yip, P., Sleno, B., Herscovics, A., and Howell, P. L. (2000). Crystal structure of a class I α1,2-mannosidase involved in *N*-glycan processing and endoplasmic reticulum quality control. *EMBO J.* **19**, 581–588.

Vallée, F., Karaveg, K., Herscovics, A., Moremen, K. W., and Howell, P. L. (2000). Structural basis for catalysis and inhibition of *N*-glycan processing class I α1,2-mannosidases. *J. Biol. Chem.* **275**, 41287–41298.

Biography

Dr. Linda O. Tremblay recently obtained her Ph.D. from McGill University. The focus of her dissertation was on the cloning and characterization of mammalian α1,2-mannosidases.

Dr. Annette Herscovics is a Professor at the McGill Cancer Centre and in the Departments of Medicine, Biochemistry, and Oncology at McGill University. Her main research interests are concerned with the structure and function of enzymes required for eukaryotic glycosylation. She holds a Ph.D. from McGill University and is a Fellow of The Royal Society of Canada.

Non-Homologous End Joining

Penny A. Jeggo
University of Sussex, Brighton, UK

The process of DNA non-homologous end joining (NHEJ) is one of several mechanisms that function to repair DNA double strand breaks (DSBs) in DNA. NHEJ represents the major mechanism for DSB repair in G1 phase cells. If unrepaired, a DSB can lead to loss of genomic material which is likely to result in cell death; a misrepaired DSB can cause genomic rearrangements, a potential initiating event for carcinogenesis. NHEJ, therefore, represents an important mechanism for maintaining genomic stability. Paradoxically, NHEJ also functions during immune development to help create genetic diversity.

Nature of the Rejoining Process

Three mechanisms for DSB rejoining have been described. Homologous recombination (HR) uses an undamaged homologue as a template to repair a DSB and to restore any genetic information lost at the site of the break. Single strand annealing (SSA) uses short direct repeat sequences to hold the broken ends together and then rejoins the two closely located DNA nicks. NHEJ, in contrast, requires no homology or, at most, a few base pairs of microhomology to achieve DSB rejoining. HR has the potential to be highly accurate even if sequence information is lost at the break site. SSA annealing is inherently inaccurate leading to deletions at the break site. The level of accuracy achieved by NHEJ is still unclear. However, cells lacking NHEJ components show increased levels of misrepair observable either as chromosomal rearrangements or in specific assays aimed at detecting misrepair.

Proteins that Function in NHEJ

Six proteins required for NHEJ have been identified in mammalian cells (see Table I). The first component identified was Ku, a heterodimer consisting of two subunits, Ku70 and Ku80. Ku has strong double-strand DNA end-binding activity. Once bound to a DNA end, Ku recruits a large protein kinase to form a complex called the DNA-dependent protein kinase (DNA-PK). The catalytic component of this complex is called the DNA-PK catalytic subunit (DNA-PKcs). A complex of two further proteins, XRCC4 and DNA ligase IV, are required for the rejoining step of NHEJ. More recently, "artemis" has been identified as an additional protein required for some aspects of NHEJ. In the yeasts, *Saccharomyces cerevisciae* and *Schizosaccharomyces pombe*, some additional proteins are required for NHEJ but either homologues of these proteins have not been identified in mammalian cells or the identified homologues do not appear to be required for the process (see Table I). It is noteworthy that there are differences in the requirements for these additional proteins even between the two yeasts. The roles of Sir2, 3, and 4 and Nej1p are regulatory.

The Ku Protein

In addition to being a strong DNA end-binding protein, Ku is able to translocate along the DNA, leading to a DNA substrate with multiple bound Ku molecules. The crystal structure of Ku resembles a basket-shaped structure with two pillars and a handle. A double-stranded DNA end is able to fit through the cavity in the structure allowing Ku to encircle the DNA. The C-terminal region of Ku80 is required for interaction with DNA-PKcs.

DNA-PKcs

DNA-PKcs is a member of a subfamily of phosphoinositol (PI) 3-kinases called PI 3-K-like kinases (PIKKs). This subfamily has protein kinase activity, in contrast to the lipid kinase activity of the PI 3-Ks. DNA-PKcs at 460 kDa is one of the largest PIKKs and other family members include ataxia telangiectasia mutated protein (ATM) and ataxia telengiectasia and Rad 3-like protein (ATR). PI 3-Ks have a conserved kinase domain at the C terminus and PIKKs in addition have a small region at the extreme C terminus that is required for protein kinase activity. Although *in vitro*, DNA-PK can phosphorylate many of the proteins phosphorylated by ATM and ATR, *in vivo*, the three PIKKs have distinct functions. The *in vivo* substrates of DNA-PK have not

TABLE I

Proteins Required for NHEJ in Different Model Systems

	Mammalian cells	*S. cerevisiae*	*S. pombe*
Ku70, Ku80	+	+	+
DNA ligase IV	+	+ (Lig4p)	+ (Lig4p)
XRCC4	+	+ (Lif1p)	+ (Lif1p)
DNA-PKcs	+	No homologue identified	No homologue identified
Artemis	+	No homologue identified	No homologue identified
Mre 11/Rad50/Xrs2	Not required	+	+
Nej1p	No homologue identified	+	No homologue identified
Sir 2, 3, and 4	No homologue identified	+	No role identified

been identified although artemis and XRCC4 are likely substrates. DNA-PK also undergoes autophosphorylation, which is essential for its function in NHEJ. It has been suggested that one role of DNA-PKcs is to regulate the process by phosphorylating NHEJ components. In line with this, autophosphorylation of DNA-PKcs results in release of the protein from the Ku–DNA complex.

XRCC4-DNA Ligase IV

DNA ligase IV has a conserved ligase domain at its N terminus and two BRCT domains at its C terminus. The region between the two BRCT domains is required for interaction with its partner protein, XRCC4. The crystal structure of XRCC4 and the interacting region with DNA ligase IV shows that XRCC4 consists of a globular head domain and a helical tail. A single ligase chain binds to an XRCC4 dimer leading to unwinding of the coiled coil that forms in the uncomplexed molecule. XRCC4 stimulates but is not essential for DNA ligase IV's activity. However, XRCC4 is essential for NHEJ and cells lacking either XRCC4 or DNA ligase IV have identical phenotypes. Ku bound to DNA can recruit the DNA ligase IV-XRCC4 complex, thereby stimulating ligation.

Artemis

Artemis is a member of the metallo-β-lactamase superfamily and, when unphosphorylated, has $5'-3'$ exonuclease activity. Artemis forms a complex with and is phosphorylated by DNA-PKcs, which changes the specificity of its nuclease activity so that it acquires endonucleolytic activity as well as the ability to cleave hairpin structures. A hairpin intermediate is generated during the process of V(D)J recombination and artemis cleaves this hairpin allowing V(D)J recombination to proceed. Consequently, cells and patients lacking artemis are unable to rejoin the coding junctions during V(D)J recombination leading to severe combined immunodeficiency.

Model for NHEJ

Figure 1 presents a model for NHEJ based on a range of biochemical, biophysical, cellular, and molecular studies. The first step of the process is the binding of the Ku heterodimer to DNA ends followed by recruitment of DNA-PKcs and activation of DNA-PK activity. Recruitment of DNA-PKcs causes inward translocation of Ku on the DNA molecule and potentially synapsis of the DNA ends. DNA-PK phosphorylates artemis, which activates its hairpin cleavage activity, a step essential for V(D)J recombination. The specificity of artemis nuclease activity may also be modulated by phosphorylation allowing it to cleave ends that are not amenable to direct ligation. DNA-PKcs may also undergo autophosphorylation enabling it to be released from DNA-bound Ku. Ku then recruits the DNA ligase IV-XRCC4 complex to the DNA end. Subsequent rejoining ensues with the release of the DNA ligase IV-XRCC4 complex.

Roles of NHEJ

Rodent cell lines lacking NHEJ components, as well as the SCID mouse and SCID cell line, have provided invaluable tools to evaluate the function of NHEJ. Complementation analysis of the rodent cells led to the classification of the defective genes as X-ray cross complementing (XRCC). This classification was made prior to cloning, resulting in some of the genes having dual nomenclature (for example, Ku80 is also XRCC5). This nomenclature and the rodent cell lines studied are given in Table II. More recently, mice knocked out for each of the NHEJ components have been generated. The phenotypes observed in the cell lines and mice are shown in Table III. Some phenotypes may represent roles of the proteins separate from their role in NHEJ. For example, Ku70 and 80 knockout mice are growth retarded, die early, and show a severe combined immunodeficient (SCID) phenotype. The latter phenotype reflects the role

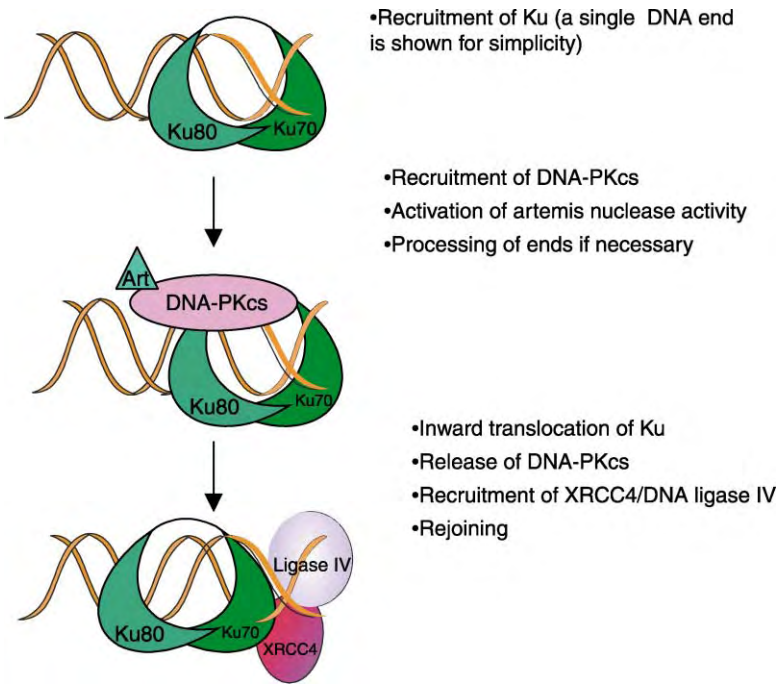

FIGURE 1 Model for DNA NHEJ. Proposed steps involved in the process.

of NHEJ in V(D)J recombination whilst the growth retardation and early senescence are most likely caused by a role of Ku in telomere maintenance, which may be distinct from its role in NHEJ. Mice lacking XRCC4 or DNA ligase IV are embryonic lethal displaying extensive neuronal apoptosis. It is currently unclear whether these differences represent roles for XRCC4 and DNA ligase IV in a process distinct from NHEJ or whether some rejoining can occur in the absence of the other NHEJ components. It has also been suggested that the uncoordinated binding of Ku to DNA ends prevents alternative DSB rejoining mechanisms taking place.

Repair of Radiation Induced DSBs

A DNA DSB is the most biologically significant lethal lesion induced by ionizing radiation. Consequently, all cell lines lacking components of the NHEJ machinery display pronounced radiosensitivity demonstrating that NHEJ represents a major mechanism for the repair of radiation-induced DSBs. Another characteristic feature of Ku, DNA-PKcs, XRCC4, and DNA ligase IV-deficient cells is impaired DSB rejoining monitored by the technique of pulse field gel electrophoresis. Interestingly, artemis-deficient cells repair the majority of their DSBs normally demonstrating that its role is distinct from the other NHEJ components. It is currently unclear if artemis functions downstream of the break rejoining process, for example to relay to the cell that the break has undergone rejoining, or possibly functions to repair a critical subset of breaks that are not detected by the pulse field gel electrophoresis technique. Cytological studies have shown that NHEJ-deficient cells display, not only increased gaps and breaks after irradiation

TABLE II

Nomenclature of Genes Involved in NHEJ and Characterized Cell Lines

Gene	XRCC nomenclature	Rodent cell lines	Human patients
Ku80	XRCC5	xrs 1-6; XRV15-B; XRV9B; sxi-3	None identified
Ku70	XRCC6	sxi-1	None identified
DNA-PKcs/SCID	XRCC7	SCID mouse cell line; V3; M059J glioma cell line; XR-C1; SX9; irs-20	None identified
XRCC4	XRCC4	XR-1	None identified
DNA ligase IV (LIG4)		SX10	LIG4 syndrome
Artemis		None identified	RS-SCID

TABLE III

Phenotypes of Cell Lines and Mice Defective in NHEJ Components

	Cell line deficiency			
Phenotype	**Ku70/Ku80**	**XRCC4/DNA ligase IV**	**DNA-PKcs**	**Artemis**
Cultured cell lines				
Radiosensitivity	Marked sensitivity	Marked sensitivity	Marked sensitivity	Slighly milder sensitivity
DSB rejoining	Defective	Defective	Defective	Normal or mild defect
DNA end-binding activity	Defective	Normal	Normal	Normal
DNA-PK activity	Defective	Normal	Defective	Normal
V(D)J recombination				
Coding joins	Major defect	Major defect	Major defect	Major defect
Signal joins	Major defect	Major defect	Minor defect	No defect
Primary cell lines				
Spontaneous breakage	Increased (also in heterozygotes)	Increased (also in heterozygotes)	Normal	Normal
Mice				
Immunodeficiency	SCID	SCID	SCID	SCID
Growth/viability	Growth retarded senesce early	Embryonic lethal	Normal	Normal
T cell lymphomas	Increase in Ku70−/− mice; no lymphomas in Ku80−/− mice	Mice not viable	Small increase	Increase in patients with hypomorphic mutations

Many of the phenotypes of Ku70-/- and Ku80-/- cell lines and mice are similar and so they have been grouped together. Similarly for XRCC4/DNA ligase IV deficient mice.

indicative of failed rejoining, but also increased chromosomal rearrangements, indicative of misrejoining. Whilst this finding does not address the fidelity of NHEJ, it does suggest that in its absence, there is increased misrejoining. Finally, NHEJ-deficient cells show normal ability to effect cell-cycle checkpoint responses after irradiation demonstrating that the defect lies primarily in the rejoining process rather than in the signalling responses to DSB induction.

Role During Immune Development

In germ line cells, the variable (V), diversity (D), and joining (J) segments are arranged on the DNA as contiguous sequences which become rearranged into distinct V(D)J units during T- and B-cell differentiation via a process called V(D)J recombination. Each V, D, or J segment, termed a coding sequence, is associated with a semi-conserved signal sequence. The initiating event for the recombination process is the generation of a site-specific DSB by two recombination-activating gene proteins (RAG1 and 2). The breaks form between a pair of coding sequences and their adjacent signal sequences and rejoining ensues to create coding and signal junctions from the rejoining of two coding and signal sequences, respectively. A number of additional processes serve to create deletions or insertions at the coding junctions, adding to the diversity of junctions generated. There are distinctions between the rejoining of coding and signal junctions. RAG-mediated cleavage generates hairpin coding ends in contrast to blunt-ended signal ends and the requirements for rejoining of the two ends can be distinguished genetically; coding joint formation requires all six NHEJ components whereas signal joint formation does not require artemis and has only a partial requirement for DNA-PKcs. Current evidence has shown that artemis is the nuclease that cleaves the hairpin end and is activated by DNA-PKcs, providing an explanation for these differences.

Changes in antibody isotype (IgM to IgG/IgA/IgE), an essential feature of the immune response, is achieved by class switch recombination (CSR). Since CSR takes place after V(D)J recombination, it cannot be readily monitored unless V(D)J recombination has taken place. Nonetheless, several novel approaches using transgenes have provided evidence that CSR requires the introduction of a DSB as well as components of the NHEJ machinery.

Role in Maintaining Genomic Stability

Cells constantly incur endogenous DNA damage from reactive oxygen species (ROS) generated as metabolic by-products. DSBs can arise indirectly from ROS following the processing of oxidative damage. DSBs also arise during replication. Current evidence suggests that breaks at the replication fork are repaired

by homologous recombination. Nonetheless, studies of primary cells lacking NHEJ components or even primary cells heterozygous for these proteins have shown elevated chromosome breaks demonstrating that NHEJ also functions to repair endogenously generated damage.

Contribution to Human Disease

Two hereditary syndromes have been shown to be caused by defects in components of the NHEJ machinery. LIG4 syndrome is characterized by pancytopaenia, developmental and growth delay. Hypomorphic mutations in DNA ligase IV have been found in LIG4 syndrome patients, all of which markedly impact upon the protein function. One of the five patients identified developed leukaemia and showed dramatic clinical radiosensitivity. However, the small number of patients precludes an assessment of whether LIG4 syndrome is associated with cancer predisposition.

RS-SCID patients display severe combined immunodeficiency with no additional clinical features. Cell lines derived from the patients show pronounced radiosensitivity. RS-SCID has been shown to be caused by mutations in artemis, many examples of which are loss of function mutational changes. Hypomorphic mutations in artemis have also been described in patients with partial T and B lymphocyte immunodeficiency and a predisposition to EBV-associated lymphomas.

The clinical differences between RS-SCID compared to LIG4 syndrome patients highlights the differing roles of artemis and DNA ligase IV during neuronal development.

See Also the Following Articles

DNA Ligases: Mechanism and Functions • DNA Ligases: Structures • DNA Mismatch Repair and the DNA Damage Response • Homologous Recombination in Meiosis • Immunoglobulin (Fc) Receptors • Nonhomologous Recombination: Bacterial Transposons • Nonhomologous Recombination: Retrotransposons • Protein Kinase C Family

Glossary

DNA damage response mechanisms A number of distinct processes that function to maintain genomic stability. They include pathways of DNA repair and signaling mechanisms that effect cell-cycle checkpoint control and/or apoptosis.

DNA-dependent protein kinase A complex involving Ku, the DNA targeting component, and DNA-PKcs, the catalytic component.

DNA end-binding activity A protein that can bind to double-strand DNA ends. This is normally monitored by electrophoretic mobility shift assays (EMSAs).

genomic rearrangement Joining of two genetic sequences that are not linked in a normal genome. Often visualized cytogentically.

hairpin DNA end A DNA molecule that does not have 5′ and 3′ ends but a continuous looped sequence to the opposite strand. Normally the hairpin involves some unpaired bases.

phenotype The characteristic features of a cell or animal. Contrasts to genotype which describes the genetic status of a cell or animal.

V(D)J recombination A process of recombination that occurs during differentiation of immunoglobulin and T cell receptor genes and serves to enhance their genetic diversity.

Further Reading

Alt, F. W., Oltz, E. M., Young, F., Gorman, J., Taccioli, G., and Chen, J. (1992). VDJ recombination. *Immunol. Today* **13**, 306–314.

Featherstone, C., and Jackson, S. P. (1999). DNA double-strand break repair. *Curr. Biol.* **90**, 759–761.

Jackson, S. (2002). Sensing and repairing DNA double strand breaks. *Carcinogenesis* **23**, 687–696.

Lieber, M. R. (1999). The biochemistry and biological significance of non-homologous DNA end joining: An essential repair process in multicellular eukaryotes. *Genes Cells* **4**, 77–85.

Pastink, A., Eeken, J. C., and Lohman, P. H. (2001). Genomic integrity and the repair of double-strand DNA breaks. *Mutat. Res.* **480-481**, 37–50.

Rouse, J., and Jackson, S. P. (2002). Interfaces between the detection, signaling, and repair of DNA damage. *Science* **297**, 547–551.

Biography

Dr. Penny A. Jeggo is a Senior Scientist and Group Leader at the Genome Damage and Stability Centre, University of Sussex, UK. She holds a Ph.D. from the National Institute of Medical Research, London which she undertook in Dr. Robin Holliday's laboratory. Dr. John Cairns was another significant mentor. Dr. Jeggo played a key role in identifying the first components of the NHEJ machinery. She now has broader interests in damage response mechanisms and the contribution of these processes to human disease.

Nonhomologous Recombination: Bacterial Transposons

Bao Ton Hoang and Michael G. Chandler
Laboratory of Molecular Genetics and Microbiology CNRS, Toulouse, France

Transposable genetic elements (TEs) are small functional segments of DNA capable of translocation into DNA sites within and between genomes and play an important role in horizontal gene transfer. A major division between TEs is whether they translocate via RNA or DNA intermediates. Prokaryotic TEs are probably exclusively limited to those that move using DNA intermediates. They are capable of sequestering and transmitting a variety of genes involved in accessory cell functions such as resistance to antimicrobial agents, catabolism of unusual compounds, and pathogenicity, virulence, or symbiotic functions. They also promote deletions and inversions and their insertion can activate or extinguish gene expression. TEs can constitute an important fraction of bacterial genomes (both chromosomes and plasmids). For example, one class of transposon, bacterial insertion sequences, represents ~7% of the 4 Mbp *Bordetella pertussis* chromosome and ~40% of the 220 kbp *Shigella flexnerii* virulence plasmid pWR100.

Structural Similarities and Diversity

All TEs encode a cognate transposase (Tpase) or recombinase, which recognizes their ends and catalyzes the individual DNA cleavages and strand transfer events necessary for transposition. In bacteria the term transposon (Tn) is limited to elements that carry genes specifying additional functions to those involved in transposition. The large number of TEs which do not include a distinct phenotypic trait are known as insertion sequences (ISs).

Definition of Transposases

Different types of elements can be defined by the nature of their cognate recombinases. In transposition reactions, these enzymes are known as transposases (Tpases). The majority fall into a class generally called DDE transposases because of the presence of three key amino acids, two aspartate residues and a glutamate, as part of the active site. Although DDE enzymes represent the majority of known Tpases, at least three additional types of Tpases have been identified. One class is similar to rolling circle replicases used by certain bacteriophages and plasmids. These are known as Y2 transposases since their catalytic mechanism involves two highly conserved tyrosine residues. The other two classes are members of the site-specific recombinase families. However, while these Tpases show site-specificity for the ends of the donor transposon, they appear more flexible than classic site-specific recombinases in the target DNA sequences they recognize and use. They are known as Y-Tpases and S-Tpases to distinguish them from tyrosine and serine recombinases. A fifth class, which catalyzes sequence-specific integration but does not resemble any of the above groups is represented by a newly discovered class of elements.

Types of Transposable Elements

Insertion Sequences

The smallest autonomous elements known are the bacterial ISs. These have been detected in almost all eubacterial and archaebacterial genomes. They are genetically compact, between 750 bp and 2500 bp in length, are generally flanked by two partially identical and inverted sequences (terminal inverted repeats: IRs) and encode only functions involved in their mobility. The Tpase gene is composed of one or two open reading frames (*orf*s) occupying almost the entire length of the IS (Figure 1A). The IR proximal to the Tpase promoter is defined as IRL. In many ISs with two *orf*s, Tpase is produced as a fusion protein using a programmed −1 translational frameshift between the *orf*s similar to that observed in generating the pol polyprotein in some retro-viruses.

Over 1000 bacterial ISs are known. These have been divided into ~20 groups or families defined by their genetic organization, similarities in their IRs and Tpase sequences, and their preference for given target DNA

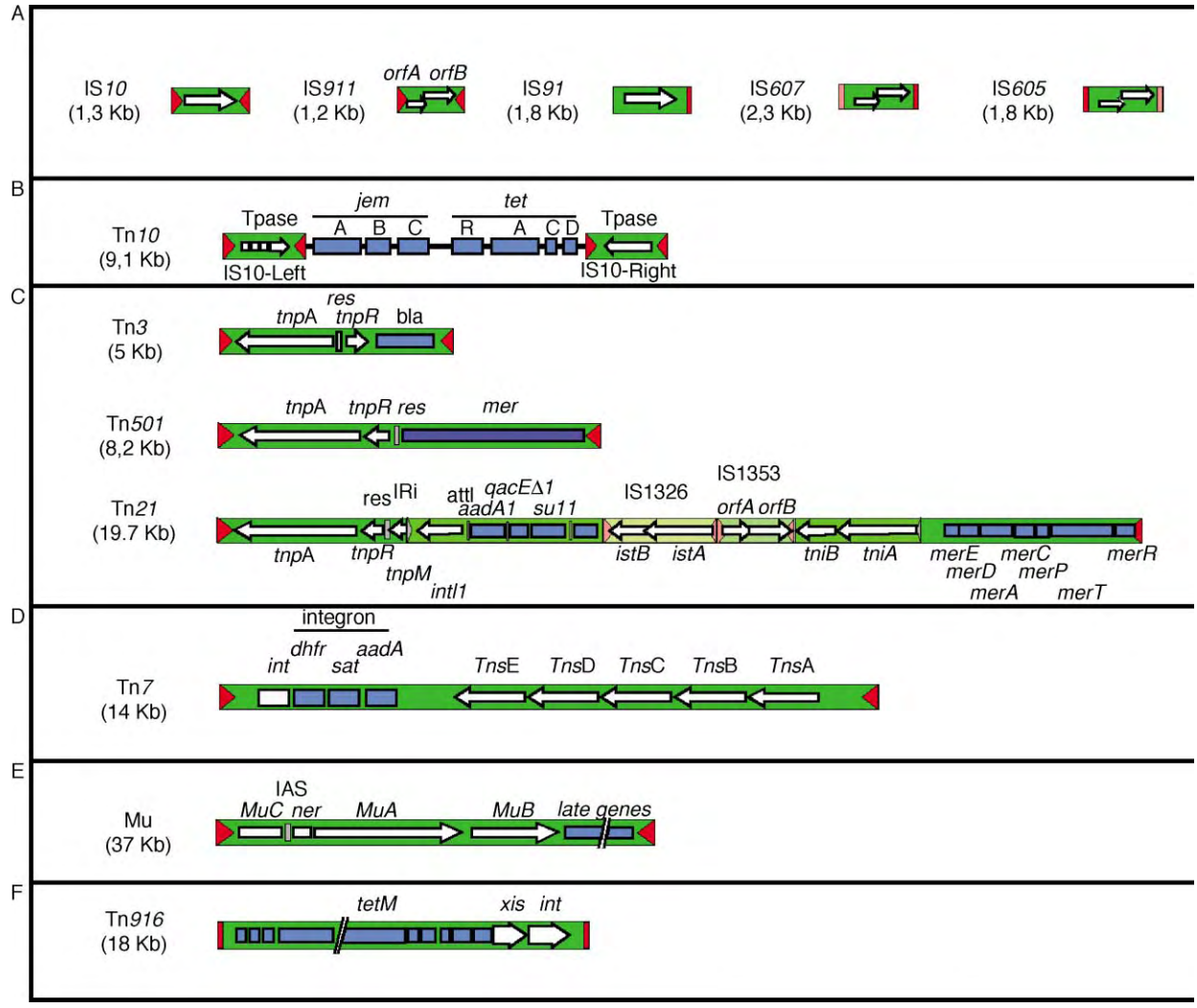

FIGURE 1 Diversity of bacterial transposable elements. The organization of different types of bacterial TE is shown. Terminal repeats (red triangles), transposon ends (red boxes in the case of IS*91*, IS*605*, IS*607* and Tn916 to indicate that they are not inverted repeats), genes whose products are involved in transposition, site-specific integration or recombination (int, xis, R) functions (white boxed arrows), resistance genes and accessory genes (conjugative transfer or phage functions) (blue boxes) are indicated. Grey boxes indicate recombination sites for resolution of cointegrates (*res*) or integron capture of gene cassettes (*att*). *bla*: resistance to β-lactams; *tet*: resistance to tetracycline; *mer*: mercury resistance.

sequences (www-IS.biotoul.fr). The majority (17/20) of these families encode a DDE Tpase, one (IS*91*) encodes a Y2 enzyme, a third (IS*607*) encodes an S-Tpase while a fourth (IS*605*/IS*608*) specifies an enzyme whose mechanism of catalysis is at present unknown (Figure 1A). This classification will undoubtedly continue to evolve as more are characterized.

Miniature Inverted Repeat Transposable Elements

Several bacterial genomes harbor many copies of small DNA segments. Depending on the bacterial species, these are variously called *Rep*, *Box*, *Rup*, or *Correia*. Some resemble ISs, which have been deleted for the transposase. Interestingly, the ends often resemble those of members of the IS*630* family and like these elements are flanked by a directly repeated TA dinucleotide. These were first described in eukaryotic systems.

Compound Transposons

Antibiotic resistance genes in bacteria were often found to be flanked by a pair of similar IS elements. Flanking ISs are capable of mobilizing any interstitial DNA segment. These structures are known as compound transposons. They are widespread and can include resistance to many different antibacterials, to genes involved in bacterial–host interactions as well as to other "accessory" genes, which are important to the host under some conditions of growth. Classical examples are tetracycline resistance transposon, Tn*10*

(flanked by two IS*10* elements in inverse repeat) (Figure 1B), the neomycin resistance transposon, Tn*5* (flanked by two IS*50* elements in inverted repeat) and the chloramphenicol resistance transposon, Tn*9* (flanked by two copies of IS*1* in direct repeat). In some cases the autonomy of the flanking ISs may be reduced in various ways to favor transposition of the entire structure.

Unit Transposons

Another class of bacterial transposons are the unit transposons such as members of the Tn*3* family (Figure 1C). Here, additional genes are contained within the transposable element itself. Large numbers of such transposons have been described carrying antibiotic resistance genes or genes involved in catabolism of unusual substances (including xenobiotics). Tn*3*-family transposons share very similar IRs (~40 bp) and carry highly related DDE transposase genes. They carry a specific site (*res*) and encode a site-specific recombinase (*tnp* R), which promotes recombination in the cointegrate between the two elements at their *res* sites. This leads to separation of donor and target molecules and leaves a single copy of the transposon embedded in each. Many variations on this basic structure have been observed. They include derivatives, which encode only the Tpase with no additional genes and therefore might be included within the IS group.

Tn*3*-family elements can accommodate and accumulate additional genes. For example Tn*21* (Figure 1C) evolved by insertion of a now defective transposon into an ancestral mercury resistance transposon, which has additionally acquired two ISs. Tn*21* also carries a genetic trap, which permits the acquisition of additional genes: the integron system. Integrons include an integrase gene, related to the Y-recombinase of bacteriophage λ. It also carries a flanking site equivalent to the λ attachment site, *att*, at which integration occurs. The acquired genes are generally promoterless and are located on small cassettes, which integrate site-specifically into the *att* site where a resident promoter is appropriately located to drive expression.

Tn*7*

Transposon Tn*7* (Figure 1D) is unusual in that it encodes five proteins necessary for its transposition and uses two transposition pathways: a site-specific insertion pathway and a more random pathway, which recognizes aspects of DNA structure in the target. One of the transposition enzymes (TnsB) is a DDE transposase while a second (TnsA) shows similarity to restriction endonucleases. Two additional proteins (Tns D and E) are involved in target choice for each of the two pathways while the fifth (TnsC) provides a bridge between target protein and the transposase. Tn*7* also carries an integron system, which has permitted it to acquire resistance to trimethoprim among other antibiotic resistances. Other members of this group including different resistance genes have also been described.

Transposable Bacteriophage

The first example of this type to be described was the temperate mutator phage Mu (Figure 1E), so-named because it inserts in a relatively random way and generates mutations during infection. Many different examples of mutator phages have been identified either as phage particles or during annotation of bacterial genome sequences. They are extremely large (>40 kbp) and relatively complex since they must encode for the enzymes and structural proteins involved in the bacteriophage lifestyle. They transpose using DDE enzymes.

Conjugative Transposons

These were first discovered in gram-positive bacteria as elements capable of transmitting tetracycline resistance from cell to cell and between bacterial species. Although they have been called transposons (Ctns for conjugative transposons), they use a site-specific recombination reaction for integration and excision. The enzymes are generally Y-transposases, similar to the site-specific recombinases used by phage λ or the integrons. However, whereas λ and integrons show pronounced sequence specificity for integration, conjugative transposons are much less exacting in their choice of integration sites. They are large and, in addition to the genes involved in integration and excision and in antibiotic resistance, they carry genes required for conjugative transfer. Tn*916* (Figure 1F) and Tn*1545* are the best-characterized transposons of this type. Several examples of Ctns encoding S-transposases have also been described.

Mechanism

DDE Enzymes

Transposition requires precise cleavage at the transposon ends and their coordinated transfer into a target molecule. This is achieved through the assembly of a nucleo-protein complex of defined architecture: the transpososome. This structure involves the Tpase, the transposon ends and target DNA. The signals for recognition and processing by Tpase are located in the transposon ends. Most bacterial ISs carry relatively simple IRs with a single Tpase-binding site. Other transposons show a complex constellation of sites often arranged differently at each end (e.g., phage Mu and Tn*7*).

The majority of known Tpases are structurally related and carry a conserved triad of acidic amino acids, the DDE motif, which coordinate two divalent metal ions central to catalysis. Cleavage at the 3′ ends of the element by an attacking nucleophile (generally H_2O) occurs to expose a free 3′OH group (Figure 2A). This nucleophile then attacks a 5′ phosphate group in the target DNA in a single-step transesterification reaction

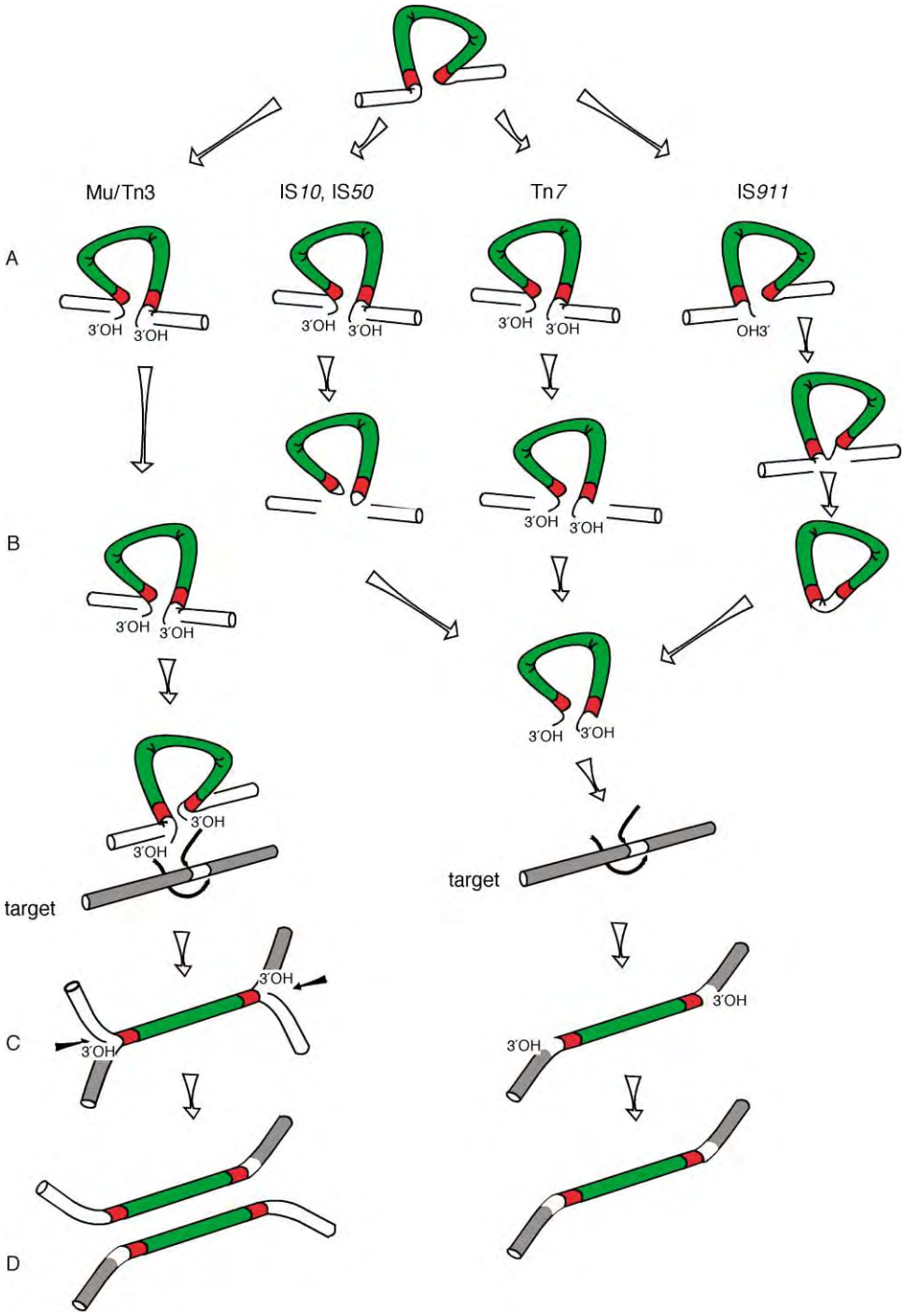

FIGURE 2 Transposition mechanism of DDE elements. Transposon, inverted repeats, and flanking sequences are shown as green, red, and white respectively. In target DNA (grey), direct repetitions (DR) are shown in white. Liberated 3′OH groups involved in subsequent strand joining reactions are shown (A and B). Left column: Replicative transposition as the result of single strand cleavage and transfer to create a replication fork (C). 2nd column: In the IS*10* (IS*50*) reaction pathways the 3′OH liberated in the initial hydrolysis attacks the opposite strand to generate a hairpin intermediate, liberating the transposon from its flanking donor DNA (A). A second hydrolysis regenerates the 3′OH (B). 3rd column: Double strand cleavage using two enzymes (e.g.Tn*7*). 4th column: For members of the IS3 family (e.g., IS*911*), the 3′OH from a single-end hydrolysis directs a strand transfer reaction to the same strand to the other end of the element (A). The branched single-strand circle is resolved into a transposon circle by the host. Single-strand hydrolysis at each 3′end (B) generates a linear transposon, which can integrate in a target.

(Figure 2B). The reaction, analyzed in detail for bacteriophage Mu, HIV, and IS*10*, has been shown to occur as an in-line nucleophilic attack with chiral inversion of the phosphate group. The two metal ions are thought to act respectively as a Lewis acid and base in the reaction.

Concerted transfer of both transposon ends into the target site, while maintaining the correct strand polarity, results in joining each transposon strand to opposite target strands. Since the position of attack in target DNA is generally staggered, this generates short, complementary single strand regions flanking the newly inserted element (Figure 2C). Repair by the appropriate host machinery generates a short duplication (direct repeat or DR) of defined length in the flanking target DNA (Figure 2D). The reactions do not require an external energy source nor do they involve a covalently linked enzyme-substrate intermediate. The donor transposon strand performs the cleavage-ligation steps in the target DNA and no cleaved target molecule is detected in the absence of strand transfer.

DDE enzymes cleave only one of the two DNA strands. An important feature of the transposition reaction is therefore the way in which the 5′ end (second strand) is processed. Some transposons do not process the second strand and are therefore not separated from the donor molecule. Strand transfer generates a structure, which can be used as a replication fork. "Replicative integration" generates cointegrates or replicon fusions where the donor and target replicons are fused and separated at each junction by a directly repeated copy of the element (e.g., bacteriophage Mu, the Tn*3* family; Figure 2 left column). Other elements shed their donor DNA prior to insertion. For some elements, the 3′OH generated by the first hydrolysis attacks the second strand to generate a hairpin form which then undergoes hydrolysis to regenerate an active 3′OH (e.g., IS*10* and IS*50*; Figure 2 second column). Others possess a second enzyme dedicated to cleavage of the second strand (e.g., Tn*7*; Figure 2 third column). For members of several bacterial IS families (e.g., IS*3*, IS*21*, and IS*30*) the 3′OH liberated at one end of the IS attacks the other end on the same strand generating a form in which one IS strand is circularized. The entire transposon is then resolved into a free transient circular form by replication or recombination of the second strand. The transposon circle then undergoes efficient integration after single-strand cleavage at each end (Figure 2 fourth column).

Non-DDE Transposases

The mechanism of transposition mediated by the other classes of transposase is less well detailed than that of the DDE transposases.

Y2 Transposases

The Y2 transposases, at present limited to the IS*91* family, show significant identity to the rolling circle replicases of phage and plasmids in the regions covering their active sites. The characteristics of transposition are strikingly different from those of DDE-mediated events. ISs of this type do not exhibit terminal IRs, do not generate flanking direct repeats and insert into a conserved tetranucleotide, which is required for further transposition events. The right (but not the left) end and the tetranucleotide are essential for transposition. Moreover, deletion of the left end can result in one-ended transposition. In this case, the inserted fragment of donor DNA is flanked at one end (constant end) by the right end and at the other end by a conserved tetranucleotide sequence present elsewhere in the donor plasmid (variable end). In addition, circular single-stranded derivatives of IS*91* have been observed and may represent transposition intermediates. While these data clearly support a polarized rolling circle mechanism, little is known about the strand transfer, which would assure transfer from donor to target site.

Y- and S-Transposases

Again, although site-specific recombination reactions directed by S- and Y- recombinases are known in exquisite detail, the activities of the corresponding transposases remain largely uninvestigated. By analogy, and in contrast to the DDE enzymes, it is assumed that catalysis involves the formation of a covalent enzyme substrate intermediate (Figure 3). In both cases, the element is excised precisely from the donor molecule.

For the Y-transposases, this would involve nucleophilic attack of the target phosphodiester bond by the active site tyrosine to generate a 3′-phosphotyrosyl bond exposing a 5′OH (Figure 3A, left column). In a second step, the 5′OH attacks the phosphotyrosine bond at the opposite end to promote strand exchange (Figure 3B, left column). Note that the reaction of only one strand is shown here. Sequential reactions of cleavage and transfer on the opposite strand would then generate a circular intermediate (Figure 3C, left column). Insertion is thought to occur by reversal of these reactions (Figure 3D, left column).

For the S-transposases recombination occurs by a concerted four strand cleavage (Figure 3A, right column) in which a catalytic serine residue attacks the target phosphodiester bond to generate a 5′ phosphoserine bond and to expose a 3′OH (Figure 3B, right column). Strand transfer to generate a circular intermediate would occur by nucleophilic attacks of the covalent DNA-enzyme bonds by the 3′ hydroxyl ends generated by cleavage (Figure 3C, right column). A second round of similar recombination reactions (Figure 3D, right column)

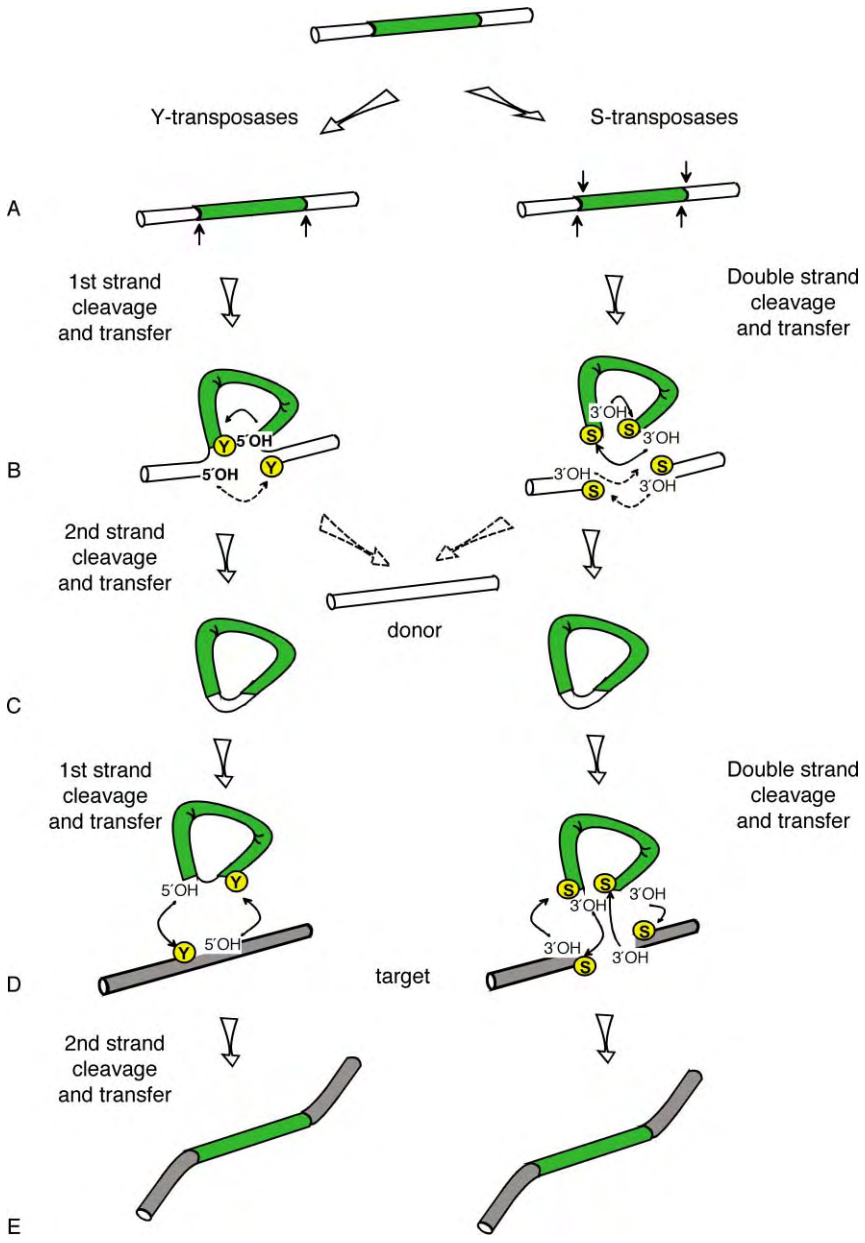

FIGURE 3 Reaction mediated by Y- transposase and S-transposases. Left column: Transposon and flanking sequences are shown as green and white respectively. The active site residue Y or S is shown within a yellow circle. Y-transposase nicks one transposon strand (here on bottom strand) at both ends (A) and forms covalent 3′ phosphotyrosine intermediates (B). The liberated 5′ OH attacks the phosphotyrosine linkage at the other end (arrows) to circularize one transposon strand (B). The same reaction is performed on the top strand to regenerate the donor and a circular intermediate (C). Further cleavage and transfer (D) is presumed to result in an insertion into target DNA (E). In contrast to site-specific recombination, the Y-transposase exhibits low sequence specificity for the target site. Right column: S-transposase catalyzes concerted double-strand breaks at both ends (A), forming covalent 5′ phosphoserine intermediates (B). After a switch of strands, the 3′ OHs attack the phosphoserine bonds in the opposite end (B), resulting in a circular intermediate (C). The same process (D) permits insertion of the element in a target (E). For both pathways, strand transfers reconstituting donor molecule (B and C) are shown by dotted arrows.

would then lead to insertion of the circular transposition intermediates (Figure 3E).

Target Choice

The choice of an insertion site can have important implications both for the transposon and for the host. Insertion into a specific target DNA sequence can provide a secure refuge for the transposon. For example, by using a specific sequence in a highly conserved gene in such a way that insertion does not disrupt the gene, transposon Tn*7* is assured an insertion site, which does not affect the fitness of the host and occurs in many bacterial species. On the other hand, in excluding insertions into other DNA sequences, this strategy precludes the capacity of

the element to generate mutations or to activate or sequester genes and thus to generate genetic diversity. Different transposons exhibit a variety of different strategies for selecting a target. On a genome scale, most transposons appear to insert "randomly". However, when analyzed at the nucleotide level, most show some degree of target preference. Insertion can be sequence-specific, with target sequence lengths varying from a few to many nucleotides, or show regional preferences, for example GC or AT rich DNA segments, probably reflecting more global parameters such as local DNA structure. Other factors which have also been implicated are: the degree of supercoiling, DNA replication, transcription, direction of conjugative transfer, and protein-mediated targeting to, or exclusion from, transcriptional control regions. In addition, some transposons show a preference for insertion close to sequences resembling the transposon end. Others exhibit the converse behavior: exclusion of insertions close to a resident end. This phenomenon, transposition immunity, can act over many kilobases of DNA. For Tn*7* and Mu it has been shown that this is accomplished by a second transposon-encoded protein (in both cases a DNA dependant ATPase), which binds target DNA. Briefly, for phage Mu, the transposase MuA, is capable of stimulating dissociation of the DNA-dependent ATPase, MuB from DNA. Thus, MuA bound to a transposon end resident in the target molecule is thought to provoke disassembly of MuB from neighboring DNA with a probability, which decreases as the distance increases.

Clearly, many insertion preferences must reflect constraints in the architecture of the synaptic complexes formed between the transposon ends, the target DNA and the transposase.

Regulation

Transposable elements are very highly regulated and have evolved a variety of perspicacious regulatory mechanisms. Apart from the temperate transposable bacteriophages, which possess a highly efficient transposition mechanism during their lytic development, transposition is not an efficient event. A given transposable element generally possesses an ensemble of regulatory mechanisms, which can differ in detail from even closely related elements.

Regulation can be at the gene expression level or at the level of Tpase activity. A combination of weak promoters and poor ribosome-binding sites can limit transcription and translation while secondary structures, which sequester translation initiation sites and involve RNA sequences upstream and downstream of the Tpase promoter can be present to prevent accidental activation by impinging transcription (IS*10*, IS*5*). Some elements produce a small antiRNA also capable of sequestering translation initiation signals, which acts as a negative control component (IS*10*). Another mechanism to control transposition activity has been documented in elements whose transposition involves a circular or a dimeric intermediate (IS*911*, IS*2*, IS*30*, IS*21*). Here, the weak endogenous promoter can provide low levels of transposase to enable low frequency formation of the transposon circle. However, the IR–IR junction formed in both transposon dimers and circles creates a strong promoter by virtue of a -10 promoter element oriented inward at one IR and a -35 element oriented outward in the other. This boosts transposase synthesis resulting in cleavage, disassembly of the junction promoter and insertion of the transposon, which then again assumes a low level of Tpase expression from the indigenous promoter. Transcription termination signals within the Tpase *orf* or posttranslational processing might also regulate Tpase expression, although these mechanisms have not been investigated in detail. Another relatively common regulatory mechanism involves programmed translational frameshifting (IS*1* and IS*3* families). Here, the Tpase is distributed over two consecutive *orf*s and frameshifting serves to generate a fusion protein including the products of the upstream *orf*, which generally carries DNA-binding and multimerization functions, and the downstream *orf*, which can include the catalytic site. The product of the upstream frame in these cases generally serves a regulatory role. For certain elements, posttranslational proteolysis might also be used to generate small regulatory proteins. IS*50* also generates a protein, Inh, using a second promoter located downstream from the Tpase promoter and representing an N-terminal truncated derivative of the Tpase. Inh acts as a transposase inhibitor.

Regulation can also occur at the level of transposase activity. The differential arrangement of Tpase-binding sites at each of phage Mu and Tn*7* (and perhaps members of the IS*21* family) permits a functional distinction and presumably favors the use of one left and one right end *in vivo*. Moreover, in many cases, Tpase bound at one end catalyzes strand cleavage at the partner end. This "trans" cleavage assures that the correct complex has been assembled before transposition can take place. For Tn*7*, the cleavage and strand transfer reactions require the presence of the target DNA molecule.

An additional level of control of Tpase activity is reflected in the observation that these enzymes often prefer to act on the copy of the element from which they are synthesized. In other words, they exhibit a preference for activity *in cis*. Several nonexclusive explanations for this behavior are apparent and *cis* activity is likely to involve a combination of different effects. One invokes a, yet untested, cotranslational-binding model in which a nascent Tpase protein is

capable of correctly folding its DNA-binding domain and binding to transposon ends before synthesis of the entire protein is accomplished. A second model invokes Tpase stability and it has been demonstrated in at least one case, IS*903*, that the ion protease plays a crucial role *in cis* activity.

Other host factors can also intervene at different regulatory levels. DAM methylase is involved in regulating Tpase expression and the recombination activity of the ends both IS*10* and IS*50*. DNA architectural proteins such as IHF, Fis and Hu have also been implicated in assuring the correct assembly of the transpososome. Moreover, IHF has been implicated in driving the molecular transitions leading to strand cleavage in IS*10*. Other factors such as RecBC, DnaA, Acyl carrier protein, and ribosomal protein L29 have also been implicated in the transposition behavior of various elements but the exact details remain to be elaborated.

Eukaryotic Transposons

Although this section is devoted to prokaryotic elements, it is important to note that eukaryotes generally carry large numbers of both intact and truncated transposable elements. These constitute over 40% of the human genome and somewhat less in Arabidopsis. There are many similarities between prokaryotic and eukaryotic elements. A major group is the Tc/mariner superfamily whose members are similar to bacterial ISs. They carry terminal inverted repeats and encode a DDE, or in this case, a DDD group transposase and resemble the IS*630* family of bacterial elements. Many eukaryotic genomes, especially those of plants, harbor extremely high numbers of truncated derivatives, similar to those found in bacteria, in which the transposase gene appears to have been deleted leaving both IRs. These elements have been also called miniature inverted repeat transposable elements (MITES) and can presumably be mobilized by the full length copies of the elements located elsewhere in the genome.

Another major group, which is limited to eukaryotes are the retro-viruses and LTR-retro-transposons, which pass through an RNA intermediate during their (viral) life cycle. Integration into the host genome occurs through a double-stranded cDNA intermediate and uses DDE group integrase (IN).

The immunoglobulin V(D)J recombination system represents another important element in vertebrates. Here, rearrangements involve two host proteins, RAG1 and RAG2. The RAG1 recombinase is related to DDE transposases. An interstitial DNA segment (signal sequence) is excised to permit the rejoining of two flanking sequences (coding sequence). In a similar way to IS*10* and IS*50*, recombination involves the formation of a hairpin intermediate. In this case, however, the hairpin is generated on the flanking DNA rather than on the excised fragment.

A third large family of eukaryotic elements is the hAT superfamily. Although the nature of their transposase is not clear and little work has yet been undertaken concerning their transposition (which includes *hobo* and *Hermes* from insects, Ac and Tam3 from plants) it seems probable that they have adopted a V(D)J-type of recombination mechanism.

Eukaryotes also harbor other families of IS-like elements including the P element of *D. melanogaster* whose mode of transposition has received much attention due to its use in mutagenesis, the CACTA family, which includes the plant transposons Tam1 and Tam1, and the En/Spm family.

Other newly recognized classes of eukaryotic elements are the helitrons, which resemble rolling circle transposons of the IS*91* family, and Cryptons, DIRS1, and kangaroo elements, which appear to encode Y-transposases.

In addition to eukaryotic elements, which transpose using a DNA intermediate including the retro-viruses, a large class of transposons, which transpose by a completely novel mechanism have also been identified. These are the target-primed (TP) retro-transposons in which an RNA intermediate is copied into its DNA target via reverse transcription.

See Also the Following Article

Nonhomologous Recombination: Retrotransposons

Glossary

DDE transposases Transposases in which the catalytic site includes two aspartate (D) and one glutamate (E) amino acid residue.

S transposases Transposases that resemble serine (S) site-specific recombinases.

transposases Enzymes that catalyze transposition.

Y transposases Transposases that resemble tyrosine (Y) site-specific recombinases.

Y2 transposases Transposases that resemble rolling circle replicases and in which the catalytic site includes two tyrosine (Y) amino acid residues.

Further Reading

Chandler, M., and Fayet, O. (1993). Translational frameshifting in the control of transposition in bacteria. *Mol. Microbiol.* 7(4), 497–503.

Craig, N. L. (1997). Target site selection in transposition. *Annu. Rev. Biochem.* **66**, 437–474.

Craig, N. L., Craigie, R., Gellert, M., and Lambowitz, A (2002). *Mobile DNA II*. ASM press, Washington DC.

Curcio, M. J., and Derbyshire, K. M. (2003). The outs and ins of transposition: from mu to kangaroo. *Nat. Rev. Mol. Cell Biol.* **4**, 865–877.

Hallet, B., and Sherratt, D. J. (1997). Transposition and site-specific recombination: Adapting DNA cut-and-paste mechanisms to a variety of genetic rearrangements. *FEMS Microbiol. Rev.* **21**(2), 157–178.

Haren, L., Ton-Hoang, B., and Chandler, M. (1999). Integrating DNA: Transposases and retroviral integrases. *Annu. Rev. Microb.* **53**, 245–281.

Mizuuchi, K. (1992). Polynucleotidyl transfer reactions in transpositional DNA recombination. *J. Biol. Chem.* **267**(30), 21273–21276.

Mizuuchi, K. (1997). Polynucleotidyl transfer reactions in site-specific DNA recombination. *Genes Cells* **2**(1), 1–12.

Rice, P., Craigie, R., and Davies, D. R. (1996). Retroviral integrases and their cousins. *Curr. Opin. Struct. Biol.* **6**(1), 76–83.

Biography

Bao Ton Hoang is a Research Scientist with the Centre National de Recherche Scientifique (CNRS) in Toulouse, France. She obtained her Ph.D. from the Université Paul Sabatier and received her postdoctoral training at the Institut National de Recherche Agronomique, Auzeville and the Ecole Veterinaire, Toulouse, France.

Michael Chandler is a Research Director with the CNRS in Toulouse. He obtained his Ph.D. from the University of Leicester (England) and received his postdoctoral training at the University of Geneva (Switzerland). The principal interest of both authors is in genome plasticity and horizontal gene transfer.

Nonhomologous Recombination: Retrotransposons

Siew Loon Ooi and Jef D. Boeke
The Johns Hopkins University School of Medicine, Baltimore, Maryland, USA

Transposons are segments of DNA that can move from one chromosomal locus to another locus on the same or different chromosomes within one cell. DNA transposons transpose via a DNA intermediate, while retrotransposons transpose via an RNA intermediate. Retrotransposons use its own reverse transcriptase protein to make a copy of its DNA from RNA, and the newly-made DNA is then inserted into a new chromosomal location. In this sense, the life cycle of retrotransposons closely resembles that of HIV virus. DNA transposons exist in both prokaryotes and eukaryotes, while retrotransposons are only found in eukaryotes. Interestingly, retrotransposons make up a significant portion of our genome and may play a role in shaping our genome by providing plasticity for evolution.

Genes are typically considered static entities that stably reside at identical loci of chromosomes in the same species. For the most part, this assumption is correct. However, in the 1940s, while studying the genetic basis of variegated pigmentation pattern of maize (Indian corn) kernels (Figure 1), Barbara McClintock proposed that some genes can change position and move from one locus to another locus on the same or different chromosomes, changing the pigmentation patterns of the kernels. She termed these genetic entities that could move into and back out of genes "controlling elements". When a controlling element moves into a gene required for pigment color formation, it disrupts the function of the gene, thus giving rise to a cell that has no color. McClintock's discovery of transposable sequences was ~30 years ahead of its time and was largely ignored mainly because it contradicted the then accepted concept that genes resided at fixed spots on chromosomes. It was not until the 1970s, when transposons were discovered in bacteria, that the general scientific community became more receptive to the concept of transposons.

Transposons

Transposons exist in all forms of life ranging from simple unicellular prokaryotes (e.g., the gut bacterium *Escherichia coli*) and eukaryotes (e.g., yeast *Saccharomyces cerevisiae*) to more complex multicellular eukaryotes including worms, insects, and mammals. Transposons are defined as segments of DNA that can move from one chromosomal locus to another locus on the same or different chromosomes within one cell, without any sequence homology to the insertion site. Transposons are also known as transposable genetic elements, insertion sequences (IS), mobile elements, jumping genes, and nomadic elements. For clarity, the parental copy of the transposon, located in one site of the host genome, is defined as the donor copy (Figure 2A). The new chromosomal site into which the transposon transposes is termed the target site and the new copy of transposon at the target site is termed the newly transposed copy (Figure 2A).

Almost all transposons acquire their abilities to mobilize themselves from the gene(s) encoded in their DNA such as transposase, integrase, and reverse transcriptase. The bacterial IS*50* element is a simple bacterial DNA transposon. IS*50* elements encode transposase required to carry out the transposition reaction and a repressor protein that represses transposition. IS*50* is flanked by a 9 base pair (bp) inverted repeat sequence required for protein binding and recognition by its transposase. Retro transposons are a type of transposon that makes a new copy of itself by copying or "reverse transcribing" an RNA copy of itself. In this way, the life cycle of retro transposons closely resembles that of retro-viruses. Yeast *Ty1*, a long terminal repeat (LTR) retro transposon, is an example of retro transposon (Figure 3A). *Ty1* contains ~340 bp direct LTR repeat that flanks both ends of the retro transposon and its two open reading frames (ORFs) or genes (Figure 3A). The first ORF encodes *GAG*, a structural protein that packages the *Ty1* RNA into a virus-like particle. The second ORF encodes *POL*, a catalytic protein containing activities such as integrase, protease, and reverse transcriptase required for transposition.

FIGURE 1 The discovery of transposons. By studying genetic entities important for pigment formation in maize, Barbara McClintock discovered maize DNA transposons, which can transpose into and out of genes involved in pigment formation and cause corn kernels to have segments with different colors.

Features of Transposons

The size and orientation of repeat elements and the size of the target site duplication are characteristic of individual types of transposons.

Direct Versus Inverted Repeat Elements

Most transposons are flanked by repeat elements ranging in length from a few to more than 300 bp. The 9 bp near-perfect inverted repeat in IS*50* serves as a binding site for the IS*50*-encoded transposase while in *Ty1*, the 340 bp repeat element is required for proper reverse transcription and integrase binding. Repeat elements can exist in either the direct or inverted orientations (Figure 2B). The orientation of the repeat elements is significant because it affects the type of chromosomal rearrangement product resulting from recombination of the repeat sequences. Interestingly, even those transposons flanked by direct repeats such as LTRs are also flanked by short inverted repeats. That is, each LTR itself contains a terminal inverted repeat sequence – in the case of *Ty1* this sequence is TG … CA. Inverted repeat sequences are also known as palindromes. However, palindromes in the "language" of DNA differ from the English palindromes (Figure 2B).

Target Site Duplication

The target site duplication (TSD) is the short "host" DNA sequence that flanks the transposon (Figure 4). For each individual copy of a transposon, the sequence of the TSD will be different, but typically its length is the same. During transposition, the target site is cleaved on both strands by transposase (or for LTR retro transposons, the integrase) followed by insertion of the transposon, resulting in a transposition intermediate structure that must be repaired by DNA synthesis. These repaired gaps that flank both ends of the transposon are identical in sequence, and form the new TSD. Note that TSD is a direct repeat sequence. The size of the TSD is defined by the distance between the two cleavage sites created by the transposase and is unique to each transposon.

"Cut-and-Paste" versus "Copy-and-Paste" Transposition

During conservative transposition, practiced by many but not all DNA transposons, the transposon excises

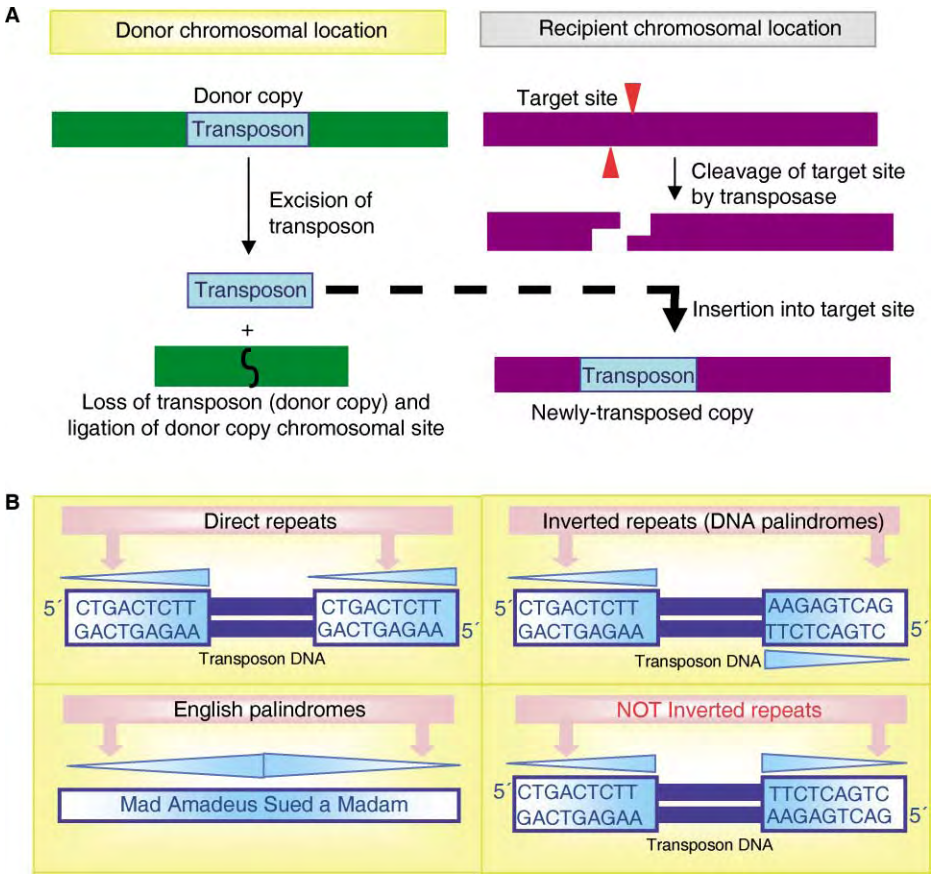

FIGURE 2 (A) Transposition. During transposition, the transposon (donor copy) is first excised from its donor chromosomal location by transposase. Next, transposase cleaves both strands of the DNA at the target site, defined as the chromosomal location into which the transposon will transpose. The transposon inserts itself into the target site, creating a "newly-transposed copy" of the transposon. The yellow background depicts events occurring at the donor chromosomal location while the gray background events occurring at the target site. In this case, the transposon transposes via the "cut-and-paste" mechanism, thus the donor copy of the transposon is lost at the donor chromosomal location. (B) Direct versus inverted repeats. Due to the double-stranded nature of DNA, direct repeats have the same DNA sequence encoded on the same strand, while inverted repeats have the same DNA sequence encoded on opposite strands. Inverted repeats are DNA palindromes, which differ from English palindromes (Reprinted by permission of David R. Godine, from "Mad Amadeus Sued A Madam," by Allan Miller).

itself from the donor site and reinserts itself into the target site. This is also known as "cut-and-paste" transposition. In contrast, retro transposons do not cut themselves out of the donor site. Rather, they copy themselves into RNA (using the cellular RNA polymerase) and then copy that RNA sequence back into DNA using reverse transcriptase. The newly made DNA copy is then inserted into a new site and this process is known as "copy-and-paste" transposition.

RNA- versus DNA-Mediated Transposition: Retro- versus DNA-Transposon

DNA transposons transpose via a DNA intermediate. Transcription of DNA transposons is only needed as a means of expressing the transposon-encoded proteins. In contrast, retro transposons transpose via an RNA intermediate, and transcription of retro transposon is important both for (1) the translation of the retro transposon-encoded proteins and (2) making a full-length RNA copy of its own genome to serve as the template for retro-transposition.

Retrotransposons

In summary, retro transposons differ from DNA transposon mainly because retrotransposons transpose via an RNA intermediate and the "copy-and-paste" mechanism. In addition, retro transposons are only found in eukaryotes including microbes, plants, and animals. Retro transposons can be categorized into long terminal repeats (LTRs) and non-LTR types (Figure 3). They differ primarily in the 5′ and 3′ end structure and in their transposition mechanisms.

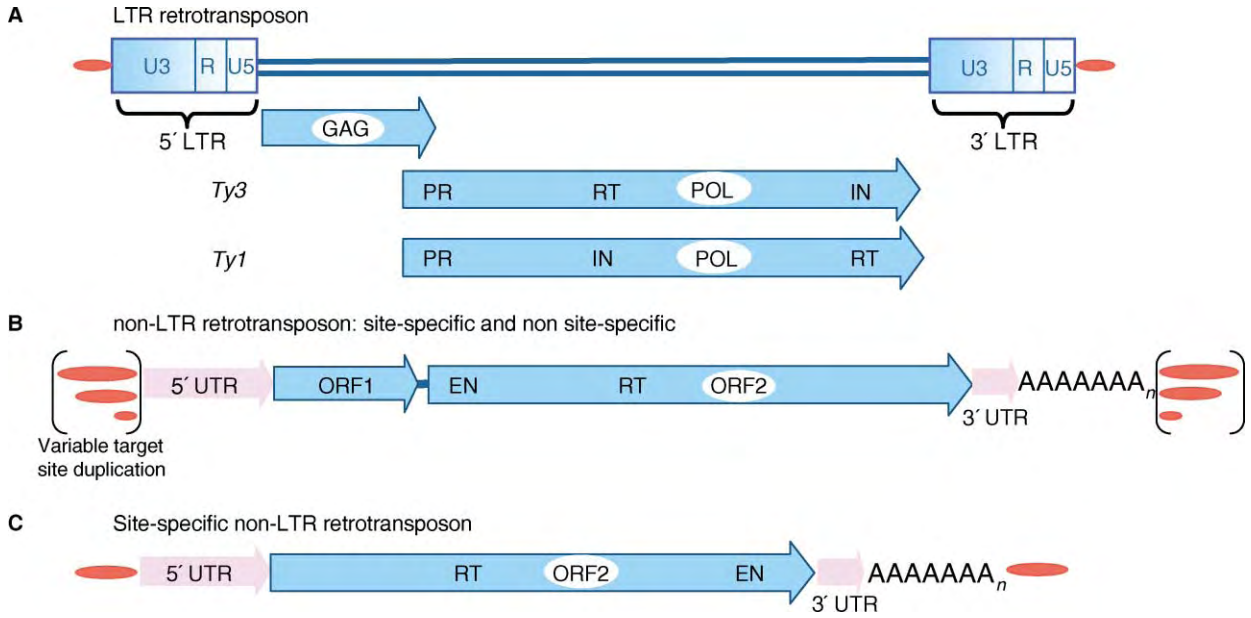

FIGURE 3 Structure of retrotransposons. (A) The long terminal repeat (LTR) of LTR retrotransposon is a few hundred base pair in length and is made up of three distinct segments termed U3, R, and U5. The transposon encodes two ORFs: GAG and POL. In *Ty3*, POL encodes protease (PR), reverse transcriptase (RT) followed by integrase (IN). In *Ty1* POL, the IN domain precedes the RT domain. (B) Non-LTR retrotransposon lacks repeat elements, instead, its 3′ end always ends in stretches of polyA sequences. Non-LTR retrotransposons encode two ORFs: ORF1 and ORF2. ORF1 contains RNA binding activity, while ORF2 encodes for endonuclease (EN), reverse transcriptase (RT) and other unknown functions. (C) Some site-specific non-LTR retrotransposons encode for only one ORF. The red oval denotes the target site duplication, which is variable in length for non-LTR retrotransposons.

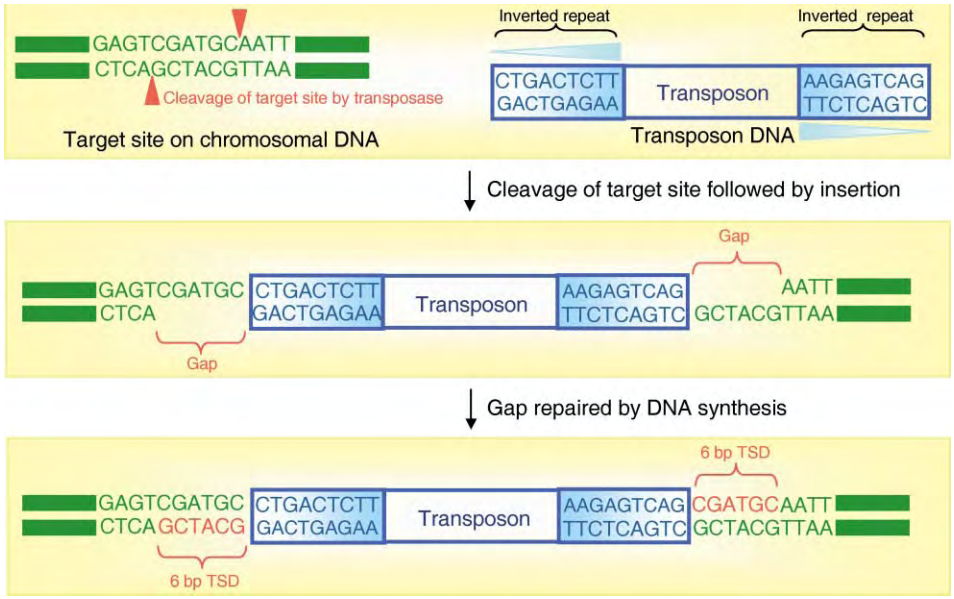

FIGURE 4 The generation of target site duplication (TSD). During transposition, transposase cleaves both strands of the DNA at the target site. The transposon, together with its terminal inverted repeats (arrows) can then insert itself into the new genomic locus. The insertion creates a gap that is usually repaired by DNA synthesis. Once repaired, the 6 bp flanking the transposon is identical in sequence, and is thus termed target site duplication (TSD). The distance between these two cleavage sites defines the size of the TSD. Genomic sequence, transposon and newly synthesized DNA are depicted in green, blue and red respectively.

Long Terminal Repeat (LTR) Retrotransposons

LTR retro transposons resemble retro-viruses such as HIV both in their basic structure and life cycle (Figure 5). Both their DNA structures begin and end with long terminal repeats several hundred bp long and they have similar *Gag* and *Pol* gene structures. The *Pol* gene encodes protease, reverse transcriptase, and integrase (the integrase functions similarly to the transposase of DNA transposons, effecting the reaction outlined in Figure 4). The major difference between LTR retro transposons and retro-viruses is that retro-viruses have a retro-virus-specific *Env* gene, encoding an envelope protein that can bind to receptors on host cells, conferring on retro-viruses the ability to shuttle from cell to cell and thus their infectivity. Retrotransposon life cycles take place within a single host cell, and they are not infectious. Retro-viruses are believed by most scientists to have evolved from the simpler LTR retro transposons.

Non-LTR Retrotransposons

Mammalian genomes contain an additional class of retro transposons that do not have LTRs, suggesting that these retro transposons are quite different from retro-viruses. In human cells for example, the long-interspersed nuclear element (LINE-1 or L1) element is a 6 kilobase (kb) long non-LTR retro transposon. LINE-1 retro transposon consists of a 900 bp 5′ untranslated region (UTR) containing an internal promoter; ORF1, encoding an RNA-binding protein; ORF2, encoding a large protein containing endonuclease, reverse transcriptase and possibly other functions, and a 3′ UTR (Figure 3B). In contrast to LTR retro transposons, the 3′ end of LINE-1 (and similar elements found in other host species) ends in a polyA tail ranging in size from a few nucleotides to ~100 bp long. LINE-1 and related elements lack not only LTRs, but any type of terminal repeats, suggesting a fundamentally different type of insertion mechanisms. Finally, the target site duplication length is variable rather than fixed in LINE-1 retro transposon.

Site-Specific Non-LTR Retrotransposons

Some non-LTR retro transposons such as the insect R1, R2, TRAS1, and SART1 elements are defined as site-specific retro transposons, because they have preferred target sites in the genome. For non-LTR retro transposons, the target site preference is usually defined by a specific host DNA sequence that is repetitive in nature and one that can be recognized and cleaved by the endonuclease encoded by each type of element. R1 and R2 elements target different sequences in ribosomal

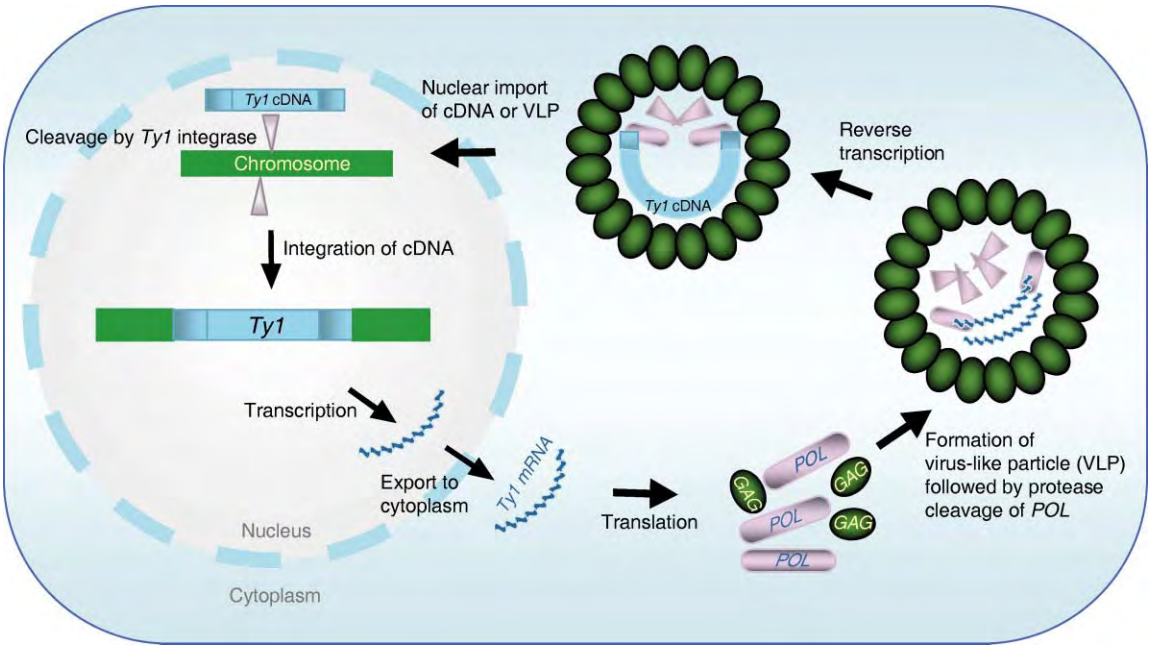

FIGURE 5 The life cycle of *Ty1*. The *Ty1* full length RNA is transcribed in the nucleus and exported to the cytoplasm, which leads to translation of Ty1 protein: *GAG* and *POL*. Full length *Ty1* RNA, together with *GAG* and *Ty1* reverse transcriptase and integrase, is then packaged into a virus-like particle (VLP). *Ty1* protease cleaves *POL* protein into the RT and IN peptides within the VLP. Reverse transcription most likely occurs within the VLP. The newly made *Ty1* cDNA is then imported into the nucleus, and with the help of integrase, which nicks the DNA at the target site, is inserted into a new chromosomal locus to create a new copy of the *Ty1* retrotransposon.

DNA (hundreds of copies per host genome) and TRAS and SART elements target opposite strands of the telomeric repeat sequence (present in hundreds to thousands of copies per host genome). Since the targets are repetitive in nature, such retro transposon insertions are unlikely to harm the host.

Alu Elements

Alu elements are ~300 nucleotide long interspersed elements found only in primate genomes, including the human genome. There are ~1.4 million copies of *Alu* in the human genome, comprising more than 10% of the human genome. Like LINE-1 elements, *Alu*s have 20–100 base pair long polyA tails. *Alu*s elements are too short to encode for proteins required for their transposition. *Alu*s most likely use the transposition machinery of LINE-1 for mobilization, as their 3′ end structures resemble those of LINE-1. Thus, *Alu*s are considered nonautonomous retrotransposons.

Significance

Retrotransposons Make up a Significant Portion of the Human Genome

DNA encodes genetic information required to specify an organism, however, surprisingly, only 2% of the human genome encodes for protein sequences. About 36% of the human genome is comprised of repetitive DNA, of which ~17% are LINE-1 retro transposons and 10% are *Alu* elements. About 8% are LTR elements, and the rest are DNA transposons or unclassified. The genome of multicellular organisms such as primates, fly, and worms contains a very high percentage of noncoding DNA, while the genome of unicellular organism such as yeast and bacteria has a higher percentage of coding DNA. This raises the question of why so much of our genome encodes DNA that does not seem to do anything obvious for the organism.

Are Retrotransposons Selfish DNA or are they One of the Shapers of our Genomes?

Transposon DNAs are often disparaged as junk or selfish DNA since it is not clear what they are doing in our genome. Transposons may have spread simply because they can multiply independently of the host genome. In this view, transposons are purely genomic parasites, selfish DNA that often has detrimental effects on the host. Deleterious insertions are removed from the host species by selection. Elements required for the survival of a species will be selected for. Transposons could play positive evolutionary roles by shaping the genome of host organisms, including our genome, serving as a source of plasticity. LINE-1 sequences sometimes move "chunks" of host genes around in the genome, shuffling gene segments to form new combinations. Their ability to transpose, copy, and rearrange DNA sequences allows the host opportunities to restructure their genome to survive and to adapt to a new environment. There is good evidence that transposons can spread because they confer selective advantages to the cells. Perhaps an organism's ability to evolve and compete effectively directly depends on the flexibility provided by "junk" DNA.

Transposons are Agents of Mutation

If left unchecked, in theory, transposons can colonize an entire genome. To survive, an organism needs to have mechanisms to down-regulate transposition. Full-length human LINE-1 RNA is expressed at very low levels. Worms apparently use RNA interference (RNAi) as one mechanism to defend their genome from transposon invasion by down-regulating transposon RNA expression. Other organisms including mammals may use similar mechanisms. Most of the time, transposons do not cause any detectable phenotypic changes. However, if a transposon inserts itself into coding regions, it can have detrimental effects on the host. There are examples of hemophilia A and other human diseases caused by insertion of LINE-1 sequences into human genes. In *Drosophila*, many spontaneous mutations with visible phenotypes result from insertions of transposable elements.

See Also the Following Article

Nonhomologous Recombination: Bacterial Transposons

Glossary

coding DNA DNA sequence that encodes for protein: the exons of mRNA.

host The organism in whose genome a transposon or retro transposon resides.

integrase A protein required for retro-transposition, in order to make a cleavage in the template DNA so that transposon can insert itself into a new chromosomal locus; analogous to transposase in DNA transposons.

noncoding DNA DNA sequence that does not encode for proteins or any functional RNAs. This includes the promoter element, introns and 3′ untranslated region of mRNAs as well as intergenic regions, which can be extensive.

protease An enzyme that recognizes specific amino acid sequences within a protein and cleaves the protein via hydrolysis of the peptide bonds.

retrotransposon Transposon that transposes via an RNA intermediate using reverse transcriptase.

reverse transcriptase A protein required for retro-transposition and retro-virus multiplication, which uses single stranded RNA as

template to make a double stranded DNA termed complementary DNA (cDNA).

RNA interference (RNAi) A mechanism used by eukaryotes to degrade mRNA via a double stranded RNA intermediate.

target site The DNA sequence in the host genome that the transposon inserts into.

target site duplication (TSD) A short host sequence flanking a transposon that was duplicated during the insertion process.

transposition Movement of a transposon to a new, nonhomologous target site.

transposon Segment of DNA that can move from one chromosomal locus to another locus on the same or different chromosomes within one cell without having any sequence homology to the insertion site.

Further Reading

Boeke, J. D., and Stoye, J. P. (1997). Retrotransposons, endogenous retroviruses, and the evolution of retroelements. In *Retroviruses* (J. M. Coffin, S. H. Hughes and H. E. Varmus, eds.) pp. 343–435. Cold Spring Harbor Laboratory Press, Plainview, NY.

Boeke, J. D., Garfinkel, D. J., Styles, C. A., and Fink, G. R. (1985). Ty elements transpose through an RNA intermediate. *Cell* **40**, 491–500.

Dewannieux, M., Esnault, C., and Heidmann, T. (2003). LINE-mediated retrotransposition of marked Alu sequences. *Nat. Genetics* **35**, 41–48.

Kazazian, Jr. H. H., Wong, C., Youssoufian, H., Scott, A. F., Phillips, D. G., and Antonarakis, S. E. (1988). Haemophilia A resulting from de novo insertion of L1 sequences represents a novel mechanism for mutation in man. *Nature* **332**, 164–166.

Moran, J. V., DeBerardinis, R. J., and Kazazian, Jr. H. H. (1999). Exon shuffling by L1 retrotransposition. *Science* **283**, 1530–1534.

Biography

Jef D. Boeke is a Professor of molecular biology and genetics, Professor of oncology, and Director of the High Throughput Biology Center at the Johns Hopkins University School of Medicine in Baltimore, Maryland. His principal research interests are in retro-transposition, chromatin structure, and yeast genetics and genomics. He holds a Ph.D. from the Rockefeller University and received his postdoctoral training at the Whitehead Institute at the Massachusetts Institute of Technology.

Siew Loon Ooi was a graduate student with Dr. Boeke.

Nuclear Compartmentalization

Kelly P. Smith and Jeanne B. Lawrence
University of Massachusetts Medical School, Worcester, Massachusetts, USA

The eukaryotic nucleus must somehow accommodate diverse tasks ranging from DNA replication to the selective transcription, processing, and transport of different classes of RNA, each requiring its distinct macromolecular machinery. On a gross morphological level the nucleus is composed of a bilayered nuclear envelope, separating the nuclear contents from the cytoplasm, the nucleolus, devoted largely to rRNA metabolism, and the nucleoplasm, which contains the bulk of the genome and the myriad factors essential to its maintenance, replication, and expression. It has now become evident that the nucleoplasm is further differentiated into a number of non-membrane bound "compartments" in which distinct subsets of macromolecules concentrate, presumably for a common function. Despite the significant amount of investigation into these compartments, their functions remain elusive and controversial. Although the list of nucleoplasmic compartments or bodies is incomplete, this article elucidates the current state of knowledge of the most studied of these nucleoplasmic structures, the splicing factor domains, PML nuclear bodies, Cajal bodies and Gemini of Cajal bodies.

Splicing Factor Compartments, "Speckles," or SC35 Domains

In the eukaryotic nucleus, the distribution of pre-mRNA splicing factors is not uniform, but is markedly concentrated at 20–40 sites, with lower levels of factors diffuse throughout the nucleoplasm (Figure 1). Variously referred to as "speckles," "SC35 domains," or "splicing factor compartments (SFCs)," these irregular but discrete domains are most frequently visualized with an antibody directed against the spliceosome assembly factor SC35. Each domain, 0.5–3.0 μm in diameter, corresponds largely, if not entirely, to ultrastructures termed interchromatin granule clusters (IGCs). In addition to spliceosome assembly factor SC35, these domains contain numerous splicing factors and SR proteins, as well as poly(A) RNA, poly(A) RNA-Binding Protein II, hyperphosphorylated RNA polymerase II, lamins, and factors implicated in RNA export. These components are also more diffusely distributed throughout the nucleus. Although the positions of the domains themselves are relatively immobile, they are dynamic structures in that factors within them are in rapid flux dependent upon their phosphorylation state. It is likely that ~150 different proteins localize, at least transiently, to these domains.

As they show relatively little label with uridine incorporation, one hypothesis is that they do not contain mRNA or pre-mRNA but are storage sites of excess splicing components. These components are then "recruited" to nearby active genes, where splicing occurs. However, several active genes have been shown to position directly at the periphery of domains, and RNAs from highly expressed genes have been found within them. The organization of these genes with domains is locus specific and cell-type specific. Evidence now suggests that most, if not all, splicing factor domains associate with numerous genes and contain mRNAs derived from them. The placement of specific genes near these concentrated domains of RNA metabolic factors suggests a specific nuclear organization to the gene relative to the domain which would facilitate the rapid reassembly and use of large RNA metabolic complexes for highly expressed and complex genes (see Figure 2).

PML Nuclear Bodies, ND10

Mammalian nuclei contain 10–30 spherical structures termed PML nuclear bodies (PML NBs) (also termed PODs, ND10 or Kremer bodies) (Figure 3). These 0.3–1 μm bodies were first observed by electron microscopy (EM) and later found to contain the PML protein. Interest in this nuclear body, and nuclear structure in general significantly increased with the discovery that the gene encoding PML is fused to the retinoic acid receptor gene in the t(15;17) translocation of acute promyelocytic leukemia (APL). The resulting PML-retinoic acid receptor fusion protein causes a breakdown of PML domains, a major hallmark of APL. PML bodies are also targeted by many DNA viruses in early infection, and are the site of viral transcription initiation. Subsequently, the viral early proteins localize to and eventually disrupt PML NBs.

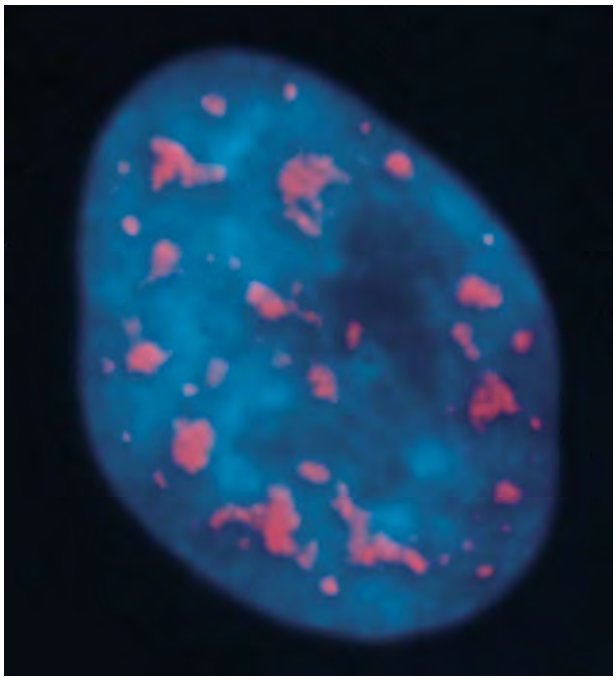

FIGURE 1 Splicing factor rich SC35 domains. Human fibroblast nucleus immunostained using an antibody to the spliceosome assembly factor SC35 (red). The nucleus is stained blue using the DNA stain 4′,6-diamidino-2-phenylindole (DAPI).

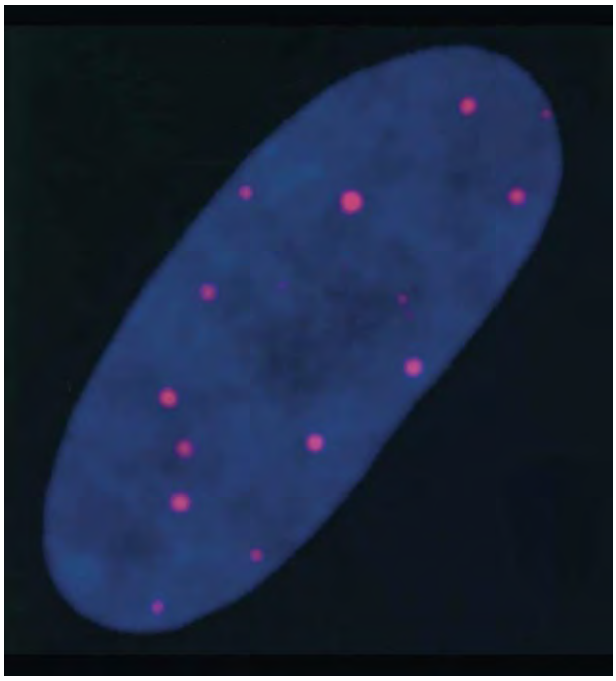

FIGURE 3 PML Nuclear Bodies. Human fibroblast nucleus stained with DAPI (blue) has numerous PML nuclear bodies visualized with an anti-PML antibody (red).

The lynchpin of the PML NB is the PML protein, essential for PML body formation. The PML protein occurs in numerous alternatively spliced isoforms and contains a RING finger, B-box coiled coil (RBCC) motif. This domain allows PML to interact with many of the PML NB proteins (Table I), as well as some proteins such as HDAC that are not concentrated in the PML body, some in an isoform specific manner. The PML NB proteins are involved in a number of different cellular processes including tumor suppression, growth control, apoptosis, immune response, and transcription regulation. A few of the over 40 proteins found within PML NBs are present under all conditions, but many others localize under a variety of conditions such as cell cycle and transient overexpression (see Table I). All of these factors are found at lower levels in the nucleoplasm in addition to the concentrations in PML NBs. Some proteins do not colocalize with all PML NBs or in all cell types, suggesting that different PML NBs may have distinct functions.

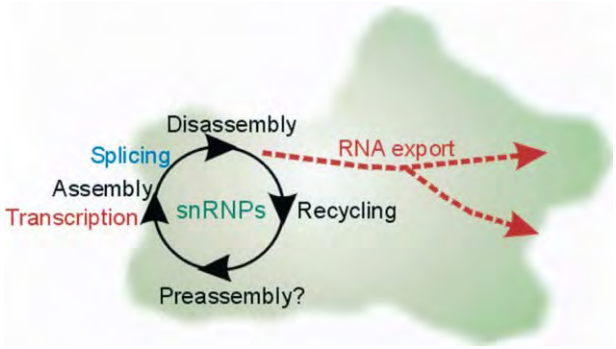

FIGURE 2 SC35 domain model. Domains may function by coupling the completion of mRNA maturation and release for mRNA export with the recycling/preassembly of factors. Because the RNA metabolic machinery requires interaction of such a large number of different factors, their concentration at a site would facilitate recycling and a rapid rate of reuse for expression of adjacent genes. Adapted from Johnson, C. V., Primorac, D., McKinstry, M., McNeil, J., Rowe, D., and Lawrence, J. B., (2000). Tracking COL1A1 RNA in osteogenesis imperfecta. Splice-defective transcripts initiate transport from the gene but are retained within the SC35 domain. *J. Cell Biol.* **150**, 417–431 with permission.

The sheer variety of proteins found in PML bodies has made attribution of a single function almost impossible. The dynamic and diverse nature of these bodies has led to the theory that PML NBs are "nuclear depots" in which numerous proteins are recruited and/or released in response to stimuli such as viral attack or other cell stress. Additionally, PML NBs could be sites for degradation of some nuclear proteins. However, PML NBs may also play a more specific, though indirect, role in transcription, by sequestration and/or modification of transcription factors. Recently, reports have asserted that PML NBs can associate with specific genes such as the p53 locus TP53. Other evidence suggests that, contrary to earlier reports, PML NBs contain newly synthesized RNA. These results are suggestive of a more direct role for PML NBs in gene expression.

TABLE I

Partial List of PML Nuclear Body Components

Component	Function	PML interaction[a]	Conditional association[b]
PML	Essential for NB formation; transcription activator? repressor?	Y	
Transcription			
pRB	Tumor suppressor, transcription factor	Y	Y
p53	Tumor suppressor, transcription factor	Y	Y
CBP	Histone acetylase	Y	Y
Daxx	Transcription regulation, apoptosis	Y	
Sp 100	Transcription factor		
Sp 140	Transcription factor		Y
Sp 110	Transcription factor		
Translation initiation			
eIF-4	Recruits ribosomes to mRNA	Y	Y
INT-6	Promotes ribosomes binding to mRNA		Y
Protein modification			
SUMO-1	Protein modifier	Y	
HAUSP	De-ubiquitination		Y
Ubiquitin	Protein modifier, not with all PML NBs		
Immune response			
PA28	Activates immunoproteasome		
ISG20	Exonuclease, antiviral activity		Y
DNA repair			
BLM	DNA helicase, genome stability		

[a] Factors known to interact with the PML protein.
[b] Factors shown to interact with PML NBs under certain conditions such as cell cycle or interferon treatment.

Cajal (Coiled) Bodies and Gems

First described in 1903 as nucleolar accessory bodies, the Cajal (coiled) bodies (CBs) are usually seen as roughly spherical 0.1–2.0 μM structures numbering one to five per nucleus (see Figure 4A), varying in number and size during the cell cycle and in different cell types. The Cajal bodies are not seen in all cells or tissues, but are especially prominent in highly proliferative cells such as cancer cells or metabolically active cells like neurons. The neuronal CBs, as originally identified, are not round nucleoplasmic bodies, but are found capping the nucleolus as seen in Figure 4B. This localization illustrates the close association between the nucleolus

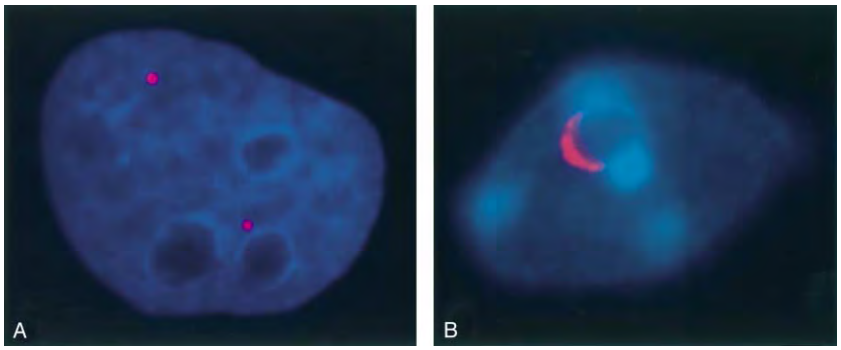

FIGURE 4 Heterogeneity of Cajal Bodies. Cajal bodies, seen using an anti-coilin antibody (red) can appear as round nucleoplasmic bodies in highly proliferative cultured cells like the cervical carcinoma cell HeLa (A) or can be found to cap the nucleolus in mouse brain neurons (B). DNA in nuclei is stained with DAPI.

and the CBs. Whether the CBs capping the nucleolus are functionally distinct from the nucleoplasmic bodies most often seen in cultured cells is unknown.

The coilin protein was first identified using human autoimmune serum and has become the marker most often used to visualize CBs. Although relatively little is known about the function of coilin, studies have indicated that it is the link between CBs and the nucleolus. In addition to coilin, numerous snRNAs and proteins of both nuclear and nucleolar origin are enriched in the CBs. These include factors involved in transcription and/or processing of mRNAs, snRNAs, histone mRNAs, and rRNA (see Table II). CBs have been shown to spatially associate with several U snRNA and histone gene loci, all of which have unusual 3′ processing, suggesting that CBs could have relationship to expression and nuclear metabolism of specific types of RNAs. The CBs contain U7RNA involved in histone RNA processing and have been shown to contain pre-U2RNA, implicating them in snRNA modification or transport. More recent studies have found small Cajal body-specific RNAs (scaRNAs) which catalyze the methylation and pseudouridylation of snRNAs within Cajal bodies.

Like PML bodies, recent work has linked loss of CBs to leukemia. ELL is an RNA polymerase II (pol II) transcriptional elongation factor that interacts with a protein called EAF1. Both ELL and EAF1 are components of Cajal bodies. In acute myeloid leukemia, the (11;19) (q23;p13.1) translocation results in the formation of a chimeric MLL-ELL fusion protein. This fusion mislocalizes ELL and causes the disruption of the Cajal bodies in leukemic cells. The role of ELL in CB formation is unknown.

TABLE II

Reported Coiled Body Components

Component	Function
p80-coilin	Shuttling protein? Interacts with many CB components
mRNA splicing factors	
snRNAs	
U1, U2, U4, U5, U6	General pre-mRNA splicing
U11, U12	Splicing of minor class of introns
U7	3′ processing of histone pre-mRNAs
Sm core proteins	pre-mRNA splicing
U2AF	Splice site selection
SART3/p110	snRNP reassembly after splicing
snRNA modification	
scaRNAs: U85 U93	Modification of spliceosomal snRNAs
Nucleolar factors	
Fibrillarin	rRNA processing, pre-rRNA modification
Nopp 140	Transcription regulation? Nucleolus-cytoplasmic shuttling
Ribosomal protein S6	Ribosome function
Gar1p	pre-rRNA processing
NAP 57	rRNA processing, ribosome assembly
snoRNAs	
U3	Processing of pre-18S ribosomal RNA
U8	Cleavage of pre-rRNA to 5.8S and 28S rRNAs
Transcription factors	
ELL, EAF1	RNA pol II transcription elongation factors
cdk7, cyclin H, MAT1, p62	Subunits of general transcription factor TFIIH
p220(NPAT)	Histone gene transcription factor
PTF	snRNA transcription factor

SMN "Gems" and CBs

Modification of snRNAs may not be the sole function of CBs. The disease Spinal Muscular Atrophy results from deletion of a gene encoding the "survival of *m*otor *n*euron" (SMN) protein. This protein is consistently enriched in foci termed SMN gemini of Cajal bodies (gems), since in the cell line in which they were discovered, gems were often very closely associated or even coincident with CBs (see Figure 5A). However, subsequently in many cultured cells studied, SMN and coilin staining appear to be coincident in CBs (Figure 5B). The SMN protein complexes with a number of other factors, termed gemins. Currently there are six identified geminus, 2–7, in this complex. The SMN complex has been implicated in snRNP assembly, supporting the idea that gems and CBs may be involved in the recycling and/or biogenesis of splicing factors. An extension of this hypothesis is that CBs are sites of preassembly of pols I, II, and III transcription/RNA processing complexes or "transcriptosomes."

The Compartmentalized Nucleus

While this article has focused on some of the most-studied non-nucleolar compartments in the nucleus, there is evidence for the existence of numerous other compartments about which little is known. These include the perinucleolar compartment, Sam68 bodies, cleavage bodies, paraspeckles, and OPT domains. In addition to these compartments, some portions of the genome can form dense, transcriptionally inert regions in the nucleus, often referred to as the heterochromatic compartment. While the nuclear compartments described here all have different components and seemingly different functions, they all do seem to have certain traits in common. First, they are all dynamic structures, varying in composition in different conditions. Additionally, they all appear to associate with specific gene loci. Lastly, PML bodies, CBs, and splicing

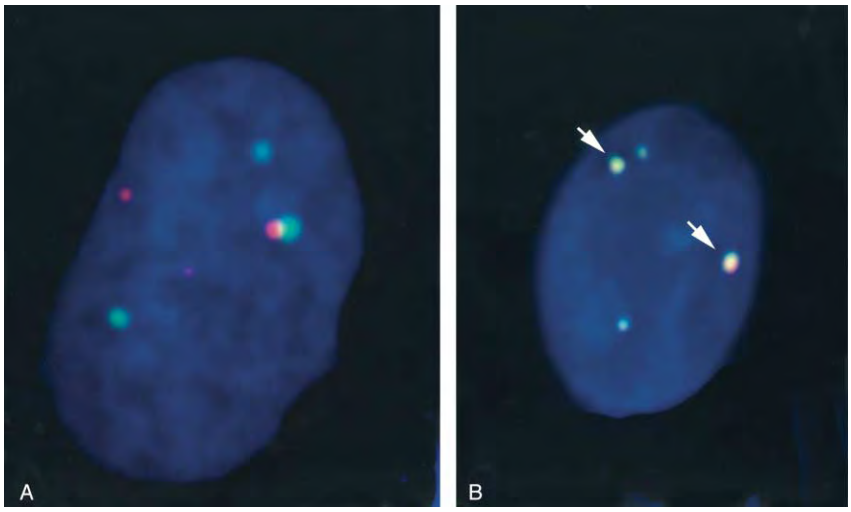

FIGURE 5 SMN gems differ in their association with CBs. By dual staining with anti-SMN antibody (red) and anti-coilin antibody (green), we see that SMN gems are separate from, but often associated with, CBs in some cells such as HeLa (A), but are most often found to be completely coincident with CBs (arrows) as seen in the breast cancer cell HCC1937 (B). Nuclei are stained with DAPI.

factor compartments appear to associate with one another. These commonalities reveal a compartmentalized, functionally integrated nucleus.

See Also the Following Articles

Chromosome Organization and Structure, Overview • mRNA Polyadenylation in Eukaryotes • Nuclear Envelope and Lamins • Nuclear Organization, Chromatin Structure, and Gene Silencing • Nucleolus, Overview

Glossary

Cajal bodies Spherical nuclear bodies (1–5/nucleus) enriched in mRNA, rRNA, and snRNA processing factors.

nuclear compartment A non-membrane-bound subnuclear structure in which a variety of factors accumulate to facilitate specific nuclear processes.

nucleus A membrane-bound cellular structure containing DNA which controls the cell's growth, metabolism, and replication.

PML nuclear bodies Spherical nuclear structures (10–30/nucleus) rich in a variety of factors, many of which are involved in transcription regulation.

SC35 domains 20–40 irregular "speckles" in the nucleus in which numerous factors required for mRNA metabolism accumulate.

SMN gems Nuclear bodies enriched in survival of motor neurons (SMN) protein and other factors involved in snRNP assembly. Gems often associate or coincide with Cajal bodies.

Further Reading

Borden, K. L. (2002). Pondering the promyelocytic leukemia protein (PML) puzzle: Possible functions for PML nuclear bodies. *Mol. Cell Biol.* **22**, 5259–5269.

Gall, J. G. (2000). Cajal bodies: The first 100 years. *Annu. Rev. Cell Develop. Biol.* **16**, 273–300.

Jady, B. E., Darzacq, X., Tucker, K. E., Matera, A. G., Bertrand, E., and Kiss, T. (2003). Modification of Sm small nuclear RNAs occurs in the nucleoplasmic Cajal body following import from the cytoplasm. *EMBO J.* **22**, 1878–1888.

Johnson, C. V., Primorac, D., McKinstry, M., McNeil, J., Rowe, D., and Lawrence, J. B. (2000). Tracking COL1A1 RNA in osteogenesis imperfecta. Splice-defective transcripts initiate transport from the gene but are retained within the SC35 domain. *J. Cell Biol.* **150**, 417–431.

Meister, G., Eggert, C., Fischer, U. (2002). SMN-mediated assembly of RNPs: A complex story. *Trends Cell Biol.* **12**, 472–478.

Misteli, T. (2000). Cell biology of transcription and pre-mRNA splicing: nuclear architecture meets nuclear function. *J. Cell Sci.* **113**, 1841–1849.

Negorev, D., and Maul, G. G. (2001). Cellular proteins localized at and interacting within ND10/PML nuclear bodies/PODs suggest functions of a nuclear depot. *Oncogene* **20**, 7234–7242.

Polak, P. E., Simone, F., Kaberlein, J. J., Luo, R. T., and Thirman, M. J. (2003). ELL and EAF1 are Cajal body components that are disrupted in MLL-ELL leukemia. *Mol. Biol. Cell* **14**, 1517–1528.

Zhong, S., Salomon, P., and Pandolfi, P. P. (2000). The transcriptional role of PML and the nuclear body. *Nat. Cell Biol.* **2**, E85–E90.

Biography

Jeanne B. Lawrence is a Professor of Cell Biology at the University of Massachusetts Medical School in Worcester, Massachusetts. Her research interests bridge the basic cell and developmental biology of nuclear organization with human genetics. She holds an M.S. in Human Genetics and Genetic Counseling from Rutgers University and a Ph.D. in Developmental Biology from Brown University. Dr. Lawrence is a pioneer in the development of fluorescence *in situ* hybridization technology for detection of individual genes and nuclear RNAs.

Nuclear Envelope and Lamins

Bryce M. Paschal
University of Virginia, Charlottesville, Virginia, USA

The nucleus is a prominent cytological feature of eukaryotic cells that is enclosed within a specialized double membrane termed the nuclear envelope. Because of this arrangement, the nuclear envelope provides a physical boundary that separates nuclear processes such as DNA replication and RNA synthesis from cytoplasmic processes such as protein synthesis. Other important functions of the nuclear envelope are mediated by macromolecular structures that are physically integrated into the membrane. Nuclear pore complexes, which are elaborate channels that span the double membrane, provide the passages for transport between the nucleus and the cytoplasm. The nuclear lamina, a meshwork of proteins just beneath the membrane, acts as a scaffold that contributes to nuclear architecture and to the regulation of gene expression. The importance of the nuclear lamina in human biology is underscored by the discoveries of genetic disorders that are caused by mutations in lamina proteins.

Structure of the Nuclear Envelope

The first descriptions of the nuclear envelope were provided by 19th century biologists, notably Fleming, who used light microscopy to examine the nuclei of plants and protozoa. A century later, the application of electron microscopy to the analysis of a variety of intracellular organelles revealed the unique structure and organization of the nuclear envelope. The nuclear envelope consists of two membranes, an inner membrane and an outer membrane, each of which is a bilayer of lipids and proteins (Figure 1). The intermembrane space, or lumen, is a site of calcium storage in the cell, and special channels in the membrane facilitate calcium release and re-uptake upon physiological stimulation. Since the outer nuclear membrane is continuous with the rough endoplasmic reticulum membrane, there is continuity between the lumen of the nuclear envelope and the rough endoplasmic reticulum.

Structure of the Nuclear Lamina

In 1966, Fawcett published a seminal electron microscopy study showing the presence of a "fibrous lamina on the inner aspect of the nuclear envelope" in several cell types. The organization of the lamina as a meshwork of 10 nm diameter filaments adjacent to the inner nuclear membrane was later revealed in samples prepared from frog oocyte nuclei (Figure 1).

Composition of the Lamina

The development of biochemical procedures for isolating nuclei from cells and for preparing the lamina-nuclear pore complex fraction from nuclei set the stage for identifying proteins that comprise the lamina.

Lamins

The major proteins of the nuclear lamina, termed lamins, are members of the intermediate filament protein superfamily. The molecular weights of lamins range from 60–70 kDa depending on the isoform, and all lamins have related primary and secondary structures. The amino- and carboxyl-terminal domains of lamins are globular, the latter encoding a nuclear localization signal. Like other members of the intermediate filament superfamily, lamin proteins contain a central rod domain composed of four α-helical segments that mediate coiled-coil interactions resulting in the formation of lamin dimers (Figure 2). Lamin dimers assemble into tetramers, which, in turn, assemble into 10 nm diameter filaments that comprise the nuclear lamina. The approximately orthogonal arrangement of lamin filaments observed by electron microscopy implies the presence of proteins that mediate inter-filament crosslinks, however, the proteins and interactions that establish and maintain this higher order structure have not yet been identified.

Lamin Genes

Lamins are classified as A-type and B-type. The B-type lamins are expressed in most cell types, whereas A-type lamins, which include lamin C, are generally expressed in differentiated tissues. There is a single lamin A gene (*LMNA*) in mammals that, through alternative

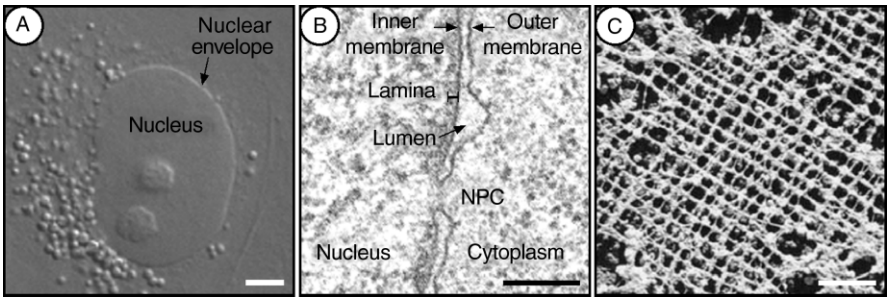

FIGURE 1 The nuclear membrane viewed by light and electron microscopy. (A) Differential interference contrast microscopy of a cell showing the nuclear envelope (scale bar, 5 μm). (B) Thin section electron microscopy showing a small region of the nuclear envelope and associated structures (scale bar, 0.2 μm). (C) Metal-shadowed nuclear lamina from a frog oocyte viewed by electron microscopy (scale bar, 0.5 μm). (Part (C) is modified from Aebi, U., Cohn, J., Buhle, L., and Gerace, L. (1986). The nuclear lamina is a meshwork of intermediate-type filaments. *Nature* **323**, 560–564.

splicing, produces transcripts for two lamin A isoforms and two lamin C isoforms. There are two lamin B genes (*LMNB1* and *LMNB2*) that together encode three lamin isoforms. The phylogenetic distribution of lamins extends to invertebrates, but lamins are absent from plants and fungi.

Lamin-Associated Proteins

A group of integral membrane proteins, which are unique to the inner nuclear membrane, bind directly to nuclear lamins and play critical roles in modulating lamina structure and function. This group includes LAP2, Emerin, Man1, and LBR. These proteins are anchored in the inner nuclear membrane by hydrophobic, membrane-spanning segments, while the rest of the protein projects into the nucleoplasm, where it contacts the lamina. Lamin-associated proteins also interact with DNA-binding proteins such as BAF and GCL that mediate chromatin-attachment to the nuclear membrane.

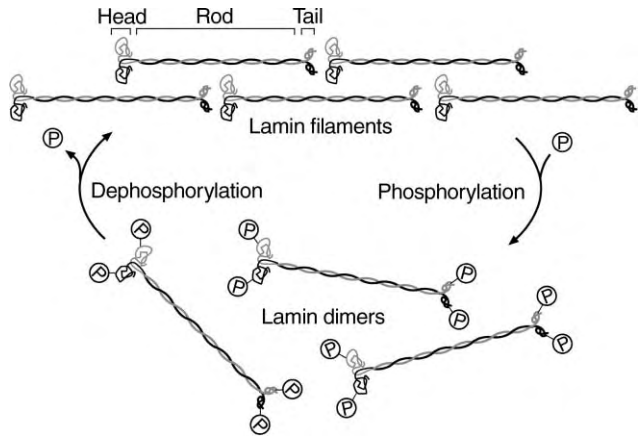

FIGURE 2 Structure of the nuclear lamina is regulated by phosphorylation. Lamin filaments undergo phosphorylation by kinases in mitosis, causing disassembly into lamin dimers. At the end of mitosis, the lamins are dephosphorylated by phosphatases, which return the lamins to an assembly competent state.

Functions of the Lamina

The nuclear lamina performs both structural and regulatory functions. These functions are not mutually exclusive, since alterations in structure can change the capacity of the nuclear lamina to regulate nuclear functions. Characterization of the regulatory functions of the nuclear lamina is a relatively recent area of investigation, and this knowledge base should expand dramatically in the next several years.

Nuclear Envelope Assembly after Mitosis

Disassembly of the nuclear envelope and lamina occurs at prometaphase, a period of the mitotic cell cycle that precedes chromosome segregation. The nuclear envelope fragments into membrane vesicles, and the lamin filaments are disassembled into lamin dimers. Near the end of mitosis in late anaphase, the nuclear envelope-derived vesicles and lamin proteins are reassembled around the chromosomes of the two new daughter cells. The reassembly pathway involves multiple steps, beginning with the binding of lamins and vesicles to the surface of chromosomes. The vesicles then fuse to generate membranes. The incorporation of lamins into the lamina continues after membrane formation by virtue of nuclear import of lamins through newly formed nuclear pore complexes.

Nuclear Size

Experimental manipulation of the nuclear reassembly pathway has shown that lamins and lamina-associated proteins are necessary for the several-fold increase in volume of the nucleus during the cell cycle. The lamina is, therefore, a critical regulator of nuclear size.

Nuclear Shape and Rigidity

The lamina forms a cage-like structure within the nucleus and is tethered to the inner nuclear membrane. As such, the lamina plays a major role in defining nuclear shape. A striking example of how lamins determine the shape of the nucleus is lamin B3, a lamin isoform that was shown by Furukawa and Hotta in 1993 to be responsible for the unusual hook-shape of nuclei in spermatocytes. The lamina also provides rigidity that resists deformation and aids in restoration of shape following deformation. Nuclei from the nematode *Caenorhabditis elegans,* rendered lamin-deficient, show little resistance to deformation, and a failure to restore nuclear shape.

Positioning of Nuclear Pore Complexes

Nuclear pore complexes span both the inner and outer nuclear membranes. Integration of nuclear pore complexes into the membrane is mediated by GP210, an integral membrane protein. The relative spacing of nuclear pore complexes in the two-dimensional plane of the nuclear envelope is maintained by the nuclear lamina. B-type lamins mediate this spacing through direct interactions with nuclear pore complexes. Loss of this functionality results in a failure to maintain the proper distribution of nuclear pore complexes in the nuclear envelope.

Regulation of Gene Expression

Lamins can have a positive or negative influence on gene expression, depending on the context. Lamins and lamina-associated proteins bind to chromatin, resulting in the attachment of a subset of chromatin to the inner nuclear membrane which can be observed by microscopy. Because there is a strong correlation between localization of chromatin at the nuclear periphery and gene silencing, the nuclear lamina has historically been viewed as a scaffold for anchoring transcriptionally inactive heterochromatin. Lamin B is highly concentrated at the inner nuclear membrane, and, together with several DNA-binding proteins that repress transcription, mediates the negative influence on transcription at the nuclear periphery. In contrast, it has been shown that lamin A can turn on expression of muscle-specific genes, a clear indication of positive effects on transcription. Lamin A is found at both the inner nuclear membrane and throughout the nucleoplasm, and the latter pool is thought to promote transcription. Thus, whether lamins influence transcription positively or negatively is dependent on the particular lamin protein, and its subnuclear distribution.

Regulation of DNA Replication

Lamins play an important role in DNA replication by facilitating the recruitment of proteins needed for initiation of replication. The original link between lamins and DNA replication was made by Newport and colleagues in 1990, using a system that reconstitutes nuclear assembly *in vitro*. Depletion of lamin B from the system resulted in small nuclei that failed to initiate DNA synthesis. Subsequent experiments have implicated lamina-associated proteins in DNA replication as well.

Posttranslational Modification of the Lamina

The lamin proteins are subject to modifications that profoundly affect function.

Phosphorylation

Gerace and Blobel showed in 1980 that phosphorylation is used as a molecular switch to control the assembly properties of lamins. Disassembly of lamin filaments at prometaphase is driven by lamin phosphorylation (Figure 2). Lamin disassembly occurs specifically at prometaphase because the kinase that mediates lamin phosphorylation is activated during the mitotic phase of the cell cycle. The phosphorylated lamins are subsequently dephosphorylated by phosphatases, rendering them competent for reassembly into filaments in late anaphase and telophase.

Isoprenylation

A cysteine-containing motif in the carboxyl terminus of lamin B, called a CaaX box, is the site for attachment of an isoprenyl group. This lipid moiety inserts into the inner nuclear membrane, and mediates the stable membrane attachment of lamin B. During mitosis, lamin B remains stably associated with nuclear-envelope-derived vesicles. The isoprenylated carboxyl terminus is cleaved from Lamin A, and Lamin C protein lacks this modification altogether because the CaaX box is not encoded in Lamin C transcripts.

Proteolysis

Lamins are regulated by proteolysis in two functionally distinct pathways. After translation, the carboxyl-terminal 18 amino acids of lamin A are removed by proteolytic cleavage. This cleavage reaction removes the site of isoprenylation and the capacity of lamin A to associate directly with membranes.

During apoptosis, lamins are cleaved by a group of proteases called caspases. Lamin cleavage is a critical step in disassembly and fragmentation of the nucleus, and is commonly used as a biochemical indicator of apoptosis.

Lamins in Human Disease

Certain mutations in lamin A, or in the lamin-associated protein Emerin, cause Emery-Dreifuss muscular dystrophy. Patients display tendon contractures, degeneration of skeletal muscle, and electrical conduction problems in cardiac muscle. Lamin A mutations are also linked to familial partial lipodystrophy, which causes partial loss of fat tissue and late-onset insulin-resistant diabetes. These and other human disorders caused by mutations in the lamin A gene are referred to as laminopathies.

The clinical severity of a particular lamin A mutation often varies, even among members of a given family. This indicates that penetrance of the phenotype can be highly dependent on the genetic background. A major unanswered question is how laminopathies are manifest in specific tissues since lamins are expressed in all cell types. Currently there are two hypotheses addressing the tissue-specific basis of laminopathies. The structural hypothesis proposes that muscular dystrophies result from fragile nuclei that are susceptible to muscle contraction-induced physical damage. The gene expression hypothesis is based on the concept that lamin deficiencies alter nuclear architecture in a manner that changes the pattern of gene expression.

See Also the Following Articles

Chromatin: Physical Organization • Imaging Methods • Metaphase Chromosome • Mitosis • Nuclear Pores and Nuclear Import/Export

Glossary

chromatin Complex of DNA, histones, and nonhistone proteins contained within the nucleus of eukaryotic cells. Heterochromatin is transcriptionally inactive.

electron microscopy A type of microscopy that resolves fine structural details of cells by using a focused beam of electrons to penetrate the specimen.

integral membrane protein Membrane-bound protein containing one or more regions that span the hydrophobic core of the phospholipid bilayer.

lamina Fibrous network of lamins and associated proteins on the inner surface of the nuclear envelope. Lamins are not related to extra-cellular proteins laminins.

nuclear envelope Double membrane structure that surrounds the nucleus.

nuclear pore complex Specialized channels that span the nuclear envelope which are responsible for bidirectional transport of macromolecules between the nucleus and the cytoplasm.

Further Reading

Aebi, U., Cohn, J., Buhle, L., and Gerace, L. (1986). The nuclear lamina is a meshwork of intermediate-type filaments. *Nature* **323**, 560–564.

Burke, B., and Stewart, C. (2002). Life at the edge: The nuclear envelope and human disease. *Nat. Rev. Molecul. Cell Biol.* **3**, 575–585.

Hutchison, C. J. (2002). Lamins: Building blocks or regulators of gene expression? *Nat. Rev. Molecul. Cell Biol.* **3**, 848–858.

Pollard, T. D., and Earnshaw, W. C. (2002). *Cell Biology.* Saunders Press, Philadelphia.

Biography

Bryce M. Paschal is an Associate Professor of Biochemistry and Molecular Genetics in the Center for Cell Signaling at the University of Virginia in Charlottesville. His principal research interests are the mechanisms of transport through the nuclear pore complex. He holds a Ph.D. from the University of Massachusetts Medical School and received his postdoctoral training at The Scripps Research Institute in La Jolla, California. Using biochemical and cell biological approaches, Dr. Paschal has identified several proteins that play major roles in intracellular transport.

Nuclear Factor kappaB

Thomas D. Gilmore
Boston University, Boston, Massachusetts, USA

Nuclear factor kappaB (NFκB) is a family of structurally related DNA-binding proteins that act as transcription factors to regulate the expression of a wide variety of genes involved in many key cellular and organismal processes. The discovery of mammalian NFκB is generally attributed to Ranjan Sen and David Baltimore, who were studying the regulation of expression of a specific immunoglobulin gene; however, it is now clear that earlier researchers studying a viral oncoprotein (v-Rel) and a protein (Dorsal) required for the establishment of *Drosophila* embryonic polarity were also studying an NFκB activity. This entry focuses primarily on the vertebrate NFκB system, although most of the discussion is also applicable to the NFκB system in insects. NFκB activity is controlled by a multicomponent signal transduction pathway, such that in most cells. NFκB is inactive until any of several inducers initiates the signaling pathway that ultimately activates NFκB as a nuclear, DNA-binding protein. Misregulation of NFκB activity has been implicated in a number of human diseases, including several chronic inflammatory diseases and cancer, and the NFκB pathway is modulated by or used by several viruses as part of their pathology or replication. As such, the NFκB pathway is the subject of intense focus for pharmacological intervention.

NFκB Proteins and Protein Structure

The nuclear factor kappaB (NFκB) family is comprised of several evolutionarily conserved proteins that are related through a domain, usually called the Rel homology domain (RHD), which has sequences required for DNA binding, dimerization, and nuclear localization (Figure 1A). In *Drosophila*, there are three known NFκB proteins (Dorsal, Dif, and Relish), whereas in vertebrates, the NFκB protein family is comprised of five proteins: p50/p105, p52/p100, c-Rel, RelA (also called p65), and RelB. There is also an avian retroviral oncoprotein, v-Rel, that is a member of this family. All NFκB proteins contain the ~300 amino acid RHD towards their N termini; however, NFκB proteins can be subdivided into two distinct groups based on sequences C terminal to the RHD. One group (including p50/p105, p52/p100, and Relish) contains C-terminal sequences that fold back to inhibit the RHD, and thus these C-terminal sequences must be removed to release the active DNA-binding protein (i.e., p50 or p52 from the precursors p105 and p100, respectively). A second group (c-Rel, RelA, RelB, Dorsal, Dif) contains C-terminal sequences that are not cleaved and that activate transcription.

NFκB proteins bind to 9–10 bp DNA sites, usually called κB sites, located in the regulatory regions of many cellular and viral promoters. To bind DNA, NFκB proteins must form dimers. These dimers can, with few exceptions, be any combination of homodimer or heterodimer, although the most common NFκB dimer in many cells is a p50–RelA dimer (Figure 1B). The affinity of the various NFκB subunits for one another and the affinity of the various dimers for specific target DNA sites can vary greatly. These considerations provide an array of diversity in the NFκB dimers that are found in different cells, in the DNA sites that can be recognized by different NFκB dimers, and in the genes (and consequently cellular responses) that these dimers regulate.

Regulation of NFκB Activity

In most cells, NFκB is present in the cytoplasm in an inactive state, due to interaction with a family of inhibitor proteins, termed inhibitor of κB (IκB) proteins. IκB proteins include IκBα, IκBβ, IκBϵ, Bcl-3, and the C-terminal sequences of the NFκB precursor proteins p105 and p100. Through a series of ~30 amino acid repeats (called ankyrin repeats), a single IκB protein binds directly to sequences in the RHD of an NFκB dimer. Binding of an IκB to NFκB inhibits the activity of the dimer in two ways: it causes NFκB to be in the cytoplasm and it blocks NFκB DNA binding.

A variety of inducers (Table I), including many cytokines, cell stress, and viral or bacterial infections, can activate NFκB. In almost all cases, NFκB activity is induced through activation of a cellular kinase complex called IκB kinase (IKK). IKK is composed of three subunits: two related kinases (IKKα and IKKβ) and a

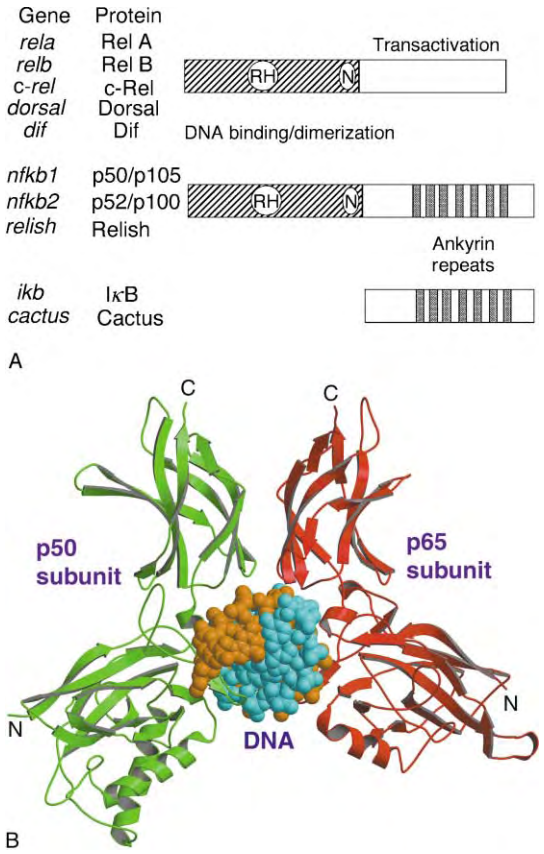

FIGURE 1 NFκB proteins. (A) Shown are the generalized structures, protein names, and genes encoding the two classes of NFκB proteins and the IκB proteins. RH, Rel Homology domain; N, nuclear localization signal; vertical bars, ankyrin repeats. (B) X-ray crystal structure of the NFκB p50–RelA (p65) dimer on DNA. N, N terminus; C, C terminus. Figure provided courtesy of Gourisankar Ghosh.

sensing or scaffold protein called IKKγ. Activation of the IKK complex generally requires phosphorylation of residues in the activation loop of the IKKα or IKKβ kinase, and probably also phosphorylation of IKKγ. Activated IKK then phosphorylates the IκB protein, which in turn signals the IκB sequences for degradation by the ubiquitin–proteasome pathway. The liberated NFκB complex can then enter the nucleus, bind to DNA, and activate specific target gene expression. In many cases, activation of NFκB is transient (perhaps lasting no more than 30 min) primarily because one of the target genes for NFκB is the gene encoding IκB. Therefore, newly synthesized IκB can cause NFκB to be resequestered in an inactive form in the cytoplasm, thus returning the pathway to its original state.

Although the overall pathway of activation is similar (as in Figure 2), there are actually two distinct pathways to activation of NFκB, depending on the nature of the IκB protein and IKK involved. In one pathway, a separate IκB molecule, such as IκBα bound to p50–RelA, is phosphorylated by the IKKβ subunit, which leads to the complete proteolysis of IκBα. In a second activation pathway involving a complex such as p100–RelB, a C-terminal site in p100 is phosphorylated by IKKα, which then leads to the partial proteolysis of the C-terminal ankyrin repeat sequences of p100, ultimately yielding an active p52–RelB dimer, which can also translocate to the nucleus to regulate gene expression.

However, a variety of recent evidence suggests that the NFκB pathway is regulated by mechanisms in addition to interaction with IκB proteins. For example, NFκB proteins can undergo posttranslational modifications

TABLE I

Some Inducers of NFκB Activity

General category	Examples
Bacteria	*Salmonella*, *Staphylococcus*, Lipopolysaccharide
Viruses	HTLV-1, Epstein–Barr virus, hepatitis B virus
Cytokines	Interleukins, tumor necrosis factor
Oxidative stress	Hydrogen peroxide, reperfusion ischemia
Growth factors/ hormones	Platelet-derived growth factor, epidermal growth factor, insulin, transforming growth factor
Drugs	Various chemotherapeutic agents

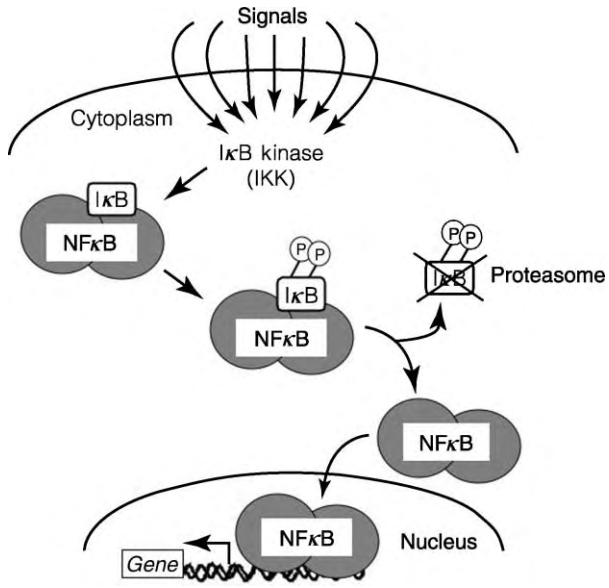

FIGURE 2 The NFκB signal transduction pathway. Under most circumstances, NFκB dimers (e.g., p50–RelA) are located in the cytoplasm of cells bound to inhibitory IκB proteins. Upon receiving an inducing signal, an IκB kinase (IKK) is activated. Active IKK phosphorylates IκB, and phosphorylated IκB then serves as a substrate for the ubiquitin–proteasome degradation pathway. Free NFκB can then enter the nucleus to increase or decrease specific target gene transcription. The system is eventually returned to its resting state through an auto-regulatory system, in that NFκB turns on expression of the gene encoding IκB, and newly synthesized IκB then resequesters NFκB in the cytoplasm.

(such as phosphorylation and acetylation) that affect their activity, they can interact with a variety of other proteins (including many other transcription factors), and the IKK proteins may also have effects on chromatin-binding proteins to affect gene expression from κB site-containing promoters.

Genes and Biological Processes Regulated by NFκB

Normal Biological Roles for NFκB

There are over 300 genes whose transcription is known to be regulated by NFκB activity, and these genes are involved in a multitude of biological processes (Table II). However, a variety of genetic and cellular studies have established that one of the key roles of NFκB is in regulating the innate immune response. In *Drosophila*, the activities of Dorsal, Dif, and Relish are induced to enter the nucleus by bacterial and fungal pathogens. These fly NFκB proteins then bind upstream and increase the expression of a family of genes called cecropins, which encode antifungal and antibacterial peptides. In mammals, it is also clear that many genes that encode antibacterial peptides, cytokines, and interferons are rapidly induced after infection with various pathogens. Moreover, mice in which individual genes for c-Rel, RelB, p50, and p52 are disrupted ("knockout mice") have severe defects in T- and B-cell-mediated immune responses. For example, c-*rel* knockout mice have B cells with greatly reduced survival and proliferation in response to antigen stimulation.

NFκB proteins are, however, also involved in the control of several other genes and processes that are not directly related to immunity. These include certain developmental processes, apoptosis, cell growth, and cell stress. In terms of development, NFκB activity (as directed by Dorsal) is required for the proper establishment of dorsal-ventral polarity in the early *Drosophila* embryo. In mammals, NFκB activity appears to be involved in proper limb development, due to the regulation of a gene called *Twist*.

NFκB transcription factors also regulate cell survival in many contexts, either by promoting or, more often, by inhibiting apoptosis. For example, RelA is required to protect liver cells from apoptosis induced by tumor necrosis factor, and RelA knockout mice die embryonically due to massive liver degeneration. Thus, the genes encoding several inhibitors of apoptosis are activated by NFκB.

TABLE II

Some Biological Processes and Relevant Genes Regulated by NFκB

Biological process	Relevant NFκB target genes
Angiogenesis	Vascular endothelial growth factor (VEGF)
Apoptosis	Bcl-X1, Bfl/A1, Bcl-2, IAP, TRAF, Fas
Cell adhesion	ICAM-1, VCAM-1
Cell growth	Cyclin D1, c-Myc
Stress	Cyclooxygenase, superoxide dismutase, nitric oxide synthetase
Innate immunity	Interleukins, interferon, tumor necrosis factor
Viral promoters	HIV-1, cytomegalovirus

NFκB and Disease

Aberrant NFκB activity has been implicated in several human diseases (Table III), most notably certain cancers and chronic inflammatory diseases, such as inflammatory bowel disease, asthma, and arthritis.

Many cancer cells have constitutively active, nuclear NFκB activity. In certain B-cell lymphomas, notably diffuse large B-cell lymphomas and Hodgkin's lymphomas, NFκB activity is dysregulated due to either amplification of the c-*rel* gene or mutations that inactivate the gene encoding Iκ B. Furthermore, several oncogenic human viruses, such as Epstein-Barr virus (lymphomas, nasopharyngeal carcinomas), HTLV-1 (T-cell leukemias), and Hepatitis B virus (liver cancer), encode proteins that activate NFκB. However, in many other cancers one finds chronic nuclear NFκB activity, which is usually made up of p50–RelA dimers, in the apparent absence of mutations in the NFκB signaling pathway or associated viral infection. That increased NFκB activity is important for the growth and survival of several cancers is emphasized by studies showing that inhibition of NFκB activity often either causes the tumor cells to die (undergo apoptosis) or to become more sensitive to apoptosis-inducing agents.

Because NFκB controls the expression of many cytokines, it is also consistently active in many situations involving acute or chronic inflammation. Moreover, in several animal model systems inhibition of NFκB activity can reduce inflammation. Furthermore, mice with knockouts in the genes encoding p50 or c-Rel are resistant to experimentally induced arthritis.

TABLE III

Some Diseases Associated with Chronic NFκB Activation

Arthritis
Asthma
Cancer
Diabetes
Inflammatory bowel disease
Ischemia/reperfusion damage
Sepsis

Pharmacological Regulation of NFκB Activity

Because of the role played by NFκB in inflammatory diseases and cancer, it has received much attention as a molecular target for pharmacological intervention. As a multicomponent pathway, NFκB activation can be inhibited at a variety of levels, including activation of IKK, IKK-mediated phosphorylation of IκB, ubiquitination and proteasome-mediated degradation of IκB, nuclear translocation of NFκB, and DNA-binding and transactivation by NFκB. Indeed, NFκB inhibitors that act at each of these steps have been described (partial list in Table IV). Nevertheless, to date, most research effort has focused on identifying NFκB inhibitors that target the IKK complex, due to its central role in controlling the NFκB pathway and to successes in identifying specific kinase inhibitors in other systems.

Several natural products with anticancer or anti-inflammatory activities have been shown to inhibit activation of NFκB. Among many others, these natural NFκB inhibitors include gold compounds (anti-arthritis), green tea (anticancer), curcumin (anticancer, anti-inflammation), and various plant extracts (anti-inflammation). In addition, some commonly used anti-inflammatory compounds, such as glucocorticoids, ibuprofen, and aspirin, have been reported to have anti-NFκB activity in experimental model systems. However, in these cases, it is not clear if their biological effects in people are exerted through inhibition of NFκB, due to the fact that doses lower than those required to inhibit NFκB are often still effective in reducing inflammation in humans.

Because NFκB is constitutively active in many cancers, clinical trials are underway with several compounds known to inhibit NFκB. Early clinical trials have reported promising results in the use of a small-molecule inhibitor of the proteasome for the treatment of multiple myeloma, an NFκB-dependent B-cell cancer. Such compounds inhibit activation of NFκB by blocking proteasome-mediated degradation of IκB.

TABLE IV

Some Inhibitors of NFκB Signaling

Inhibitor	Molecular target
Aspirin (high doses)	IKK
Curcumin	IKK
Glucocorticoids	Re1A
Green tea compounds	IKK
PS-341	Proteasome
Sulindac	IKK

See Also the Following Articles

Cell Death by Apoptosis and Necrosis • Cytokines • Proteasomes, Overview • Ubiquitin System • Ubiquitin-Like Proteins

Glossary

apoptosis A programmed cell death pathway that is used by an organism to eliminate unwanted cells or maintain organ size.

cytokines Factors that regulate the growth and activity of blood cells and lymphocytes.

proteasome A cellular complex composed of several proteases that degrades ubiquitinated proteins.

protein kinase An enzyme that can add a phosphate group onto specific residues in a target protein, which then affects the activity of the target protein.

signal transduction A molecular process by which a signal (often an extracellular compound) effects a cellular response. Often this is a multicomponent step-wise intracellular pathway that involves binding of a ligand to a cell-surface receptor, which initiates a cascade of cytoplasmic enzymatic activities that ultimately leads to the activation of a transcription factor that then regulates the expression of a biologically-relevant set of target genes.

transcription factor A protein or protein complex that binds to specific DNA sequences to regulate (increase or decrease) the rate of transcription of a gene.

ubiquitin A small (~8.6 kDa) polypeptide chain that can be conjugated to substrate proteins, which often targets them for degradation by the proteasome.

Further Reading

Beyaert, R. (ed.) (2003). *Nuclear Factor-κB: Regulation and Role in Disease*. Kluwer Academic, The Netherlands.

Ghosh, S., May, M. J., and Kopp, E. B. (1998). NF-κB and rel proteins: Evolutionarily conserved mediators of immune responses. *Annu. Rev. Immunol.* **16**, 225–260.

Gilmore, T. D. (ed.) (1999). NF-κB. *Oncogene*. **18**, 6841–6964.

Gilmore, T. D (2003). Rel/NF-κB transcription factors. http://www.nf-kb.org.

Gilmore, T. D., and Ip, Y. T. (2003). Signal transduction pathways in development and immunity: Rel pathways. In *Nature Encyclopedia of Life Sciences*, Nature Publishing Group, London, ([doi: 10.1038/npg.els.0002332] http://www.els.net).

Karin, M., Cao, Y., Greten, F. R., and Li, Z-W. (2002). NF-κB in cancer: From innocent bystander to major culprit. *Nat. Rev. Cancer* **2**, 301–310.

Silverman, N., and Maniatis, T. (2001). NF-κB signaling pathways in mammalian and insect innate immunity. *Genes and Dev.* **15**, 2321–2342.

Biography

Thomas D. Gilmore is a Professor in the Department of Biology at Boston University. His general research area is in the molecular basis of cancer. He holds a Ph.D. from the University of California (Berkeley) and received postdoctoral training at the University of Wisconsin (Madison). He has authored many research papers and review articles on the role of Rel/NF-κB transcription factors in leukemia and lymphoma, and recently his laboratory was the first to show that human c-Rel has oncogenic activity.

Nuclear Genes in Mitochondrial Function and Biogenesis

Alexander Tzagoloff
Columbia University, New York, USA

Carol L. Dieckmann
University of Arizona, Tucson, Arizona, USA

Only a small fraction of the protein constituents of mitochondria are encoded in the small vestigial genome of the organelle. Most of the genes governing the biogenesis of mitochondria reside in the chromosomal DNA of the nucleus. Referred to as *PET* genes, they represent a sizeable fraction of the total genetic information in the nucleus. *PET* genes code for the enzymes making up the different metabolic pathways housed in mitochondria, for the substrate and protein transport systems, and for the transcriptional and translational machineries involved in expression and regulation of mitochondrial genes.

Historical Background

All life depends on ATP, the universal currency of biological energy. The chemical energy inherent in the structure of this molecule is used to support a large variety of phenomena including chemical, osmotic, electrical, and mechanical work. Most of the ATP in eukaryotic organisms is supplied by the mitochondrion, a complex cellular organelle composed of two membranes (outer and inner) and two soluble compartments (intermembrane space and matrix). Biogenesis of mitochondria occurs by replenishment and addition of newly synthesized proteins and phospholipids to the preexisting organelle. In dividing cells there is a net increase of mitochondrial mass, which is distributed among the progeny. This process is aided by the ability of mitochondria to undergo fusion and fission. Mitochondria, therefore, are not synthesized *de novo* but rather serve as a template for their own faithful replication. The genetic determinants of mitochondria are located in two physically separate compartments of the cell. Most of the information is provided by the *PET* genes of the nucleus, but a small number of genes present in mitochondrial DNA (mtDNA) also play an important role.

The discovery of an extranuclear genetic element (*rho*) in yeast by Boris Ephrussi, and the later demonstration by Gottfried Schatz that this factor corresponds to a unique DNA present in mitochondria, were the foundations for much of the subsequent work aimed at understanding the function of this genome. Despite large variability in the organization, mode of expression, and gene compositions of mtDNA among different members of the plant and animal kingdoms, some general statements can be made nonetheless. More than 100 different mtDNAs have so far been sequenced. In all instances, at least some components of the mitochondrial translational apparatus, such as the genes for the endogenous ribosomal RNAs and tRNAs, are encoded in mtDNA. Another important attribute of this genetic system is that it codes for a small number of mitochondrial proteins that are important for the respiratory and ATP-generating capacities of the organelle. In most organisms, the protein-coding genes of mtDNA specify several subunits of cytochrome oxidase, cytochrome *b*, and one or more subunits of the proton-translocating ATP synthetase/hydrolase. The *rho* zero mutants lacking this set of genes produce mitochondria that are defective in respiration and oxidative phosphorylation because they lack the genes for catalytically important components of the respiratory chain, ATP synthetase, and the ribosomal RNA and tRNAs needed for translation of the endogenous mRNAs.

A much larger share of the information essential for maintaining the structural and functional integrity of mitochondria is contributed by *PET* genes, which are located in the chromosomal DNA of the nucleus.

Origin of Nuclear Gene Products with Functions in Mitochondria

The endosymbiont hypothesis, first proposed by Lynn Margulis in 1968, was a landmark advance in our thinking about how cells evolved in response to major changes in their environment. According to this

hypothesis, many organelles of modern-day eukaryotic cells, including mitochondria and chloroplasts, are stripped down products of what originally were free-living bacteria. In the case of mitochondria, a nucleated cell dependent on glycolysis as its sole source of ATP was invaded by a bacterium with an aerobic mode of energy metabolism. Such a union was advantageous to the host and became fixed during evolution. There is compelling evidence to support the bacterial origin of subcellular structures that inhabit eukaryotic cells. Most notable is the presence in mitochondria and chloroplasts of autonomously replicating genomes, and of all the enzymatic machinery needed to transcribe the organellar genes and translate the resulting RNAs into the encoded protein products. Significantly, the transcriptional and translational machineries of mitochondria and chloroplasts are more closely related to their bacterial counterparts than to those operating in the cytoplasm of eukaryotic cells.

The extent to which the mitochondrial genome contributes towards the propagation of the organelle has been severely reduced due to a continual transfer of genetic information to the host's nuclear DNA. Today, the existence of mitochondria relies in large measure on the expression of gene products encoded in nuclear DNA. The loss of mitochondrial autonomy is clearly evident from the properties of cells that have been depleted of mtDNA. Such genome-less variants termed *rho* zero mutants have been created in yeast and mammalian (e.g., human) cells. Despite the complete absence of mitochondrial DNA, *rho* zero mutants contain subcellular structures with the characteristic morphology and most of the metabolic pathways of mitochondria. These observations point to the nonessentiality of mtDNA for the perpetuity of mitochondria, but do not minimize the importance of this genome for their functional competence.

Number of Mitochondrially Related Nuclear Genes

The number of distinct proteins in mitochondria is still not known precisely but based on currently available data of the unicellular yeast, *Saccharomyces cerevisiae*, a reasonable estimate is in the range of 700–800. This corresponds to ~10–12% of the different proteins known to exist in this organism. Of course, this number will vary in more complex eukaryotes, where depending on their tissue of origin, mitochondria may have specialized and have less complex functions. For example, in mammals, mitochondria of organs like heart and muscle have simpler metabolic profiles than those of liver and consequently are simpler in their protein composition.

Yeast as a Model for Mitochondrial Studies

For practical reasons, *S. cerevisiae* has become an important model for the study of *PET* genes. A vast arsenal of genetic and biochemical tools is directly applicable to the analysis of mitochondria in this organism. Also available are the complete sequences of the 16 nuclear chromosomes and of mtDNA. Finally, because of its status as a facultative anaerobe, this yeast is able to tolerate most mutations that impair mitochondrial function as long as it is supplied with a fermentable source of carbon and energy.

Most of what we presently know about *PET* genes stems from three different sources. An important body of information has been derived from traditional studies of the intermediary metabolism carried out by mitochondria. In some instances, such studies have predated the discovery of mitochondria as the cellular repository of the pathways in question. Genetic analysis has played an equally important role. Respiratory defective mutants of yeast have been instrumental in defining many nuclear genes that impinge on all aspects of mitochondrial function and biogenesis. More recently, the high-throughput proteomic approach has further augmented the list of mitochondrially related gene products, whose functions are yet to be understood.

Gene Functions

Based on the phenotype of the respective mutants, *PET* genes can be either essential or nonessential. Nonessential genes, which make up the larger class, are defined by *pet* mutants. Such strains are viable, but because of their genetic lesions are unable to produce ATP by means of oxidative phosphorylation. The products of *PET* genes have functions that are related either directly or indirectly to mitochondrial metabolism, but not to the continuity of mitochondria as a structural compartment of the cell. The second, less abundant, class consists of essential genes needed for the survival of the cell. Their products provide functions relevant to the structural integrity of mitochondria or to some essential aspect of metabolism. Mutations in the latter prevent growth on both fermentable and nonfermentable substrates.

Nonessential *PET* Genes

These genes encompass a wide range of mitochondrial functions. The most important, from a quantitative point of view, are involved in the expression of the products encoded in mtDNA (Figure 1). They consist of proteins that function in replication of mtDNA, transcription and processing of mitochondrial RNA.

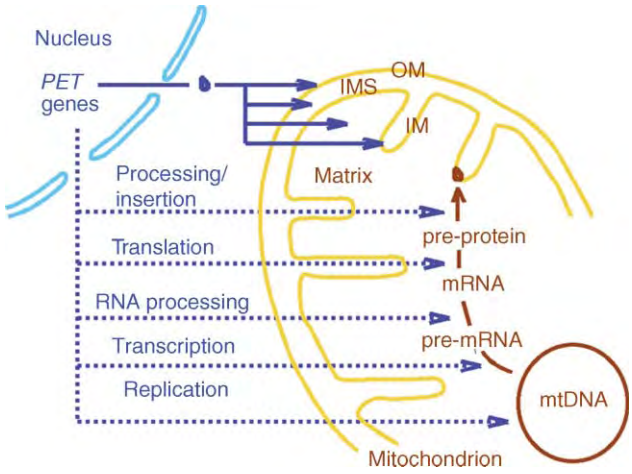

FIGURE 1 Dependence of mitochondrial gene expression on products of *PET* genes. The dashed blue arrows show some of the functions contributed by nuclear DNA for expression of the mitochondrially encoded subunits of the ATPase and respiratory enzymes. In yeast, the pre-mRNAs can be multi-genic transcripts that are matured by excision of intronic sequences and endonucleolytic cleavages. Some proteins are synthesized as precursors (pre-protein) with amino-terminal sequences that are removed by specific proteases. The solid blue arrows denote *PET* gene products targeted to the outer membrane (OM), intermembrane space (IMS), inner membrane (IM), and internal matrix compartment.

They also code for all except one of the mitochondrial ribosomal proteins, as well as most of the tRNA synthetases and translation initiation, elongation, and termination factors. A second important group of genes code for proteins that catalyze most of mitochondrially based metabolism. This includes enzymes of the tricarboxylic acid cycle (TCA cycle), fatty acid metabolism, some aspects of amino acid biosynthesis, and a number of other pathways needed for the synthesis of important cofactors such as hemes A and B, coenzyme Q, and lipoic acid.

The ATP synthetase/hydrolase as well as the enzymes making up the respiratory chain (Figure 2) are all hetero-oligomeric proteins, with more than a dozen different subunit polypeptides in most cases. Assembly of the subunits into the final holoenzymes is a complex process that requires the assistance of nuclearly encoded factors. Some of the chaperones act by facilitating a topologically correct insertion of specific subunits into the inner membrane, by preventing nonproductive interactions of hydrophobic proteins, or by still other unknown mechanisms. Because these chaperones target specific subunits, they represent a substantial fraction of the total number of mitochondrial proteins. For example, some dozen nuclear mutants have been reported to be cytochrome oxidase deficient due to mutations in proteins that affect late events in assembly of this single enzyme. Finally, many *PET* genes, coding for novel proteins still lack functions that can be assigned at this time.

Essential *PET* Genes

The highly regulated metabolism of eukaryotic cells depends on the sequestration of the enzymes making up the various pathways in their appropriate compartments. Proteins translated in the cytoplasm but destined to function in one of the internal compartments of mitochondria are imported and sorted by means of complex

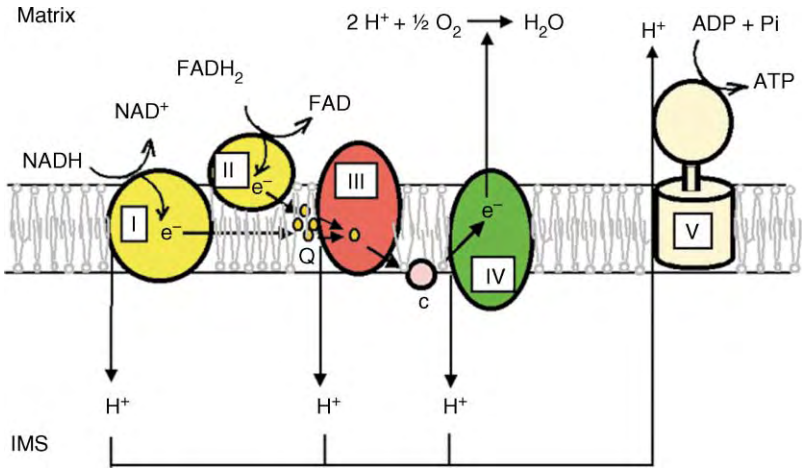

FIGURE 2 Schematic representation of the respiratory complexes and ATP synthetase in the mitochondrial inner membrane. The four complexes of the respiratory chain are: NADH-coenzyme Q reductase or complex I (yellow), succinate-coenzyme Q reductase or complex II (yellow), coenzyme QH_2-cytochrome *c* reductase or complex III (red), and cytochrome *c* oxidase or complex IV (green). Coenzyme Q is denoted by the small orange circles and cytochrome *c* by the pink circle. The ATP synthetase/hydrolase or complex V is shown with the F_1 ATPase protruding into the matrix compartment. In addition to catalyzing the transfer of electrons from NADH and $FADH_2$ to oxygen, three of the complexes promote the vectorial transfer of protons from the matrix to the intermembrane space (IMS). Protons are recycled by the ATP synthetase during synthesis of ATP from ADP and inorganic phosphate.

machines such as the TOM and TIM translocases of the outer and inner membranes, respectively. Mutations in components of either of these protein transport systems are lethal to the cell for several reasons. An immediate effect of the transport defect is a mislocalization of proteins in the cytoplasm. This abrogates the accretion of newly synthesized material by mitochondria, resulting in their eventual disappearance.

Mitochondria house proteins that function in pathways essential for the overall economy of the cell. For example, certain steps of heme B biosynthesis occur in mitochondria. Since heme B is a prosthetic group of enzymes (e.g., P450 hydroxylases) other than those involved in respiration, cells unable to produce heme B are not viable. This also applies to certain enzymes of amino acid biosynthesis located in mitochondria. In animals, carbamoyl synthetase and ornithine transcarbamylase, two important enzymes of arginine biosynthesis, catalyze their respective reactions in the mitochondrial matrix.

In certain instances, nuclear genes may code for proteins that are apportioned in the cytoplasm and mitochondria. This is true for some tRNA modification enzymes and for aminoacyl-tRNA synthetases. In yeast, six mitochondrial aminoacyl-tRNA synthetases are expressed from nuclear genes that also code for the same cytoplasmic enzymes. Therefore, mutations in these essential genes result in cell lethality.

Regulation

Many *PET* genes of yeast are regulated at the level of transcription by oxygen and carbon source. Oxygen stimulates the synthesis of heme in mitochondria mainly at later steps of the pathway catalyzed by oxygenases. Heme activates the binding of the Hap1 transcriptional activator to the upstream activation sites of some genes for respiratory chain proteins such as cytochrome *c*, thereby activating their transcription. Glucose has the opposite effect. It suppresses transcription of genes involved in alternative fuel usage by means of a complex regulatory pathway called catabolite repression. In the absence of glucose, repression is relieved and transcription of glucose-responsive genes is enhanced by the Hap2/3/4/5 transcriptional activator complex.

Mitochondrial gene expression is regulated primarily at the posttranscriptional level by products of *PET* genes. Mitochondrial RNA polymerase recognizes a simple promoter and there is little regulation of its activity except that it is more abundant in the absence of glucose and the presence of oxygen. Most mitochondrial genes are transcribed as long multigenic RNAs. Points of regulation include processing of 5′ and 3′ ends of RNA to the mature length, excision of introns and RNA stability. Initiation of translation is regulated by factors that attract ribosomes to the correct internal translational start sites of mitochondrial mRNAs. Posttranslation modification and assembly of the constituent subunits of the respiratory and ATP synthetase complexes also depend on the intervention of factors encoded by *PET* genes subject to these regulatory systems.

Human Disorders

A growing list of human pathologies has been related to mitochondrial defects and the responsible mutations mapped to RNA and protein-coding genes of mtDNA. Such mutations manifest a wide range of clinical phenotypes including encephalomyopathies, cardiomyopathy, deafness, diabetes, optic neuropathy, and dystonia. Similar presentations are elicited by mutations in nuclear DNA that affect mitochondrial metabolism either directly through lesions in the structural genes for enzymes of the TCA cycle, fatty acid oxidation, and mtDNA integrity; or indirectly by interfering with metabolite and protein import, assembly of respiratory chain complexes, metal homeostasis, and protein turnover. In view of their central role in oxidative metabolism, the list of currently known mitochondrially related diseases will undoubtedly be increased in the future.

See Also the Following Articles

Chaperones, Molecular • Cytochrome bc_1 Complex (Respiratory Chain Complex III) • DNA Replication, Mitochondrial • Mitochondrial DNA • Mitochondrial Genome, Evolution • Mitochondrial Genome, Overview • Mitochondrial Inheritance • The Cytochrome b_6f Complex • Tricarboxylic Acid Cycle

Glossary

ATP synthetase/hydrolase An enzyme of the inner membrane able to form ATP from ADP and inorganic phosphate by utilizing the energy of the proton gradient generated during the oxidation reactions catalyzed by the respiratory chain complexes. It can also form a proton gradient by hydrolyzing ATP to ADP and inorganic phosphate.

chaperones Proteins that promote the folding or unfolding of proteins. In the present context they also facilitate association of subunit polypeptides into hetero-oligomeric proteins.

eukaryotes Organisms with cells having a nucleus enclosed by a membrane.

organelle A structure or membrane enclosed compartment of a cell.

***pet* mutants** Viable mutants able to derive ATP from glycolysis but not from oxidative phosphorylation.

proteome Term used to denote all of the proteins of an organism or compartment of the cell.

respiration In the biochemical sense, the process by which the electrons and protons extracted from reduced fuels such as carbohydrates, fats, and proteins are transferred to oxygen.

***rho* zero mutants** Mutants devoid of mitochondrial DNA.

TIM complex An organized assembly of proteins that mediates the translocation of proteins from the TOM complex to the inner membrane or matrix of mitochondria.

TOM complex An organized assembly of proteins that mediates the translocation of a protein from the cytoplasm to the intermembrane space of mitochondria.

Further Reading

Alberts, B., Bray, D., Lewis, J., Raff, M., Roberts, K., and Watson, J. D. (1994). *Molecular Biology of the Cell*, 3rd edition. Garland Publishing, New York.

Ernster, L., and Schatz, G. (1981). Mitochondria: A historical review. *J. Cell. Biol.* **91**, 227s–255s.

Margulis, I. (1981). *Symbiosis in Cell Evolution*. W. H. Freeman, New York.

Neupert, W., and Brunner, M. (2002). The protein import motor of mitochondria. *Nat. Rev. Mol. Cell Biol.* **3**, 555–565.

Scheffler, I. E. (1999). *Mitochondria*. Wiley-Liss, New York.

Tzagoloff, A., and Dieckmann, C. L. (1990). *PET* genes of *Saccharomyces cerevisiae*. *Microbiol. Rev.* **54**, 211–225.

Biography

Alexander Tzagoloff is a Professor in the Department of Biological Sciences at Columbia University. He received a Ph.D. from Columbia University and postdoctoral training at the Enzyme Institute of the University of Wisconsin. He has used genetics and biochemical approaches to study the roles of mitochondrial and nuclear genes in biogenesis of yeast mitochondria.

Carol L. Dieckmann is a Professor in the Department of Biochemistry and Molecular Biophysics at the University of Arizona. She received a Ph.D. from the University of California, San Diego, and did postdoctoral training at Columbia University. She has used a combination of genetics, molecular biology, and biochemistry to study the regulation of mitochondrial gene expression.

Nuclear Organization, Chromatin Structure, and Gene Silencing

Lori L. Wallrath, John R. Danzer, Oya Yazgan and Pamela K. Geyer
University of Iowa, Iowa City, Iowa, USA

Gene silencing is the process whereby a gene is inactivated due to its chromosomal position. Chromosomal rearrangements that move a gene from a transcriptionally permissive location to a transcriptionally nonpermissive location result in gene silencing. This loss of gene expression is not due to a mutation in a gene itself, but due to the placement of a gene into a chromatin environment that is not favorable for transcription. Chromatin packaging influences whether a chromosomal location will support transcription or result in gene silencing. Eukaryotic genomes are packaged into two types of chromatin, euchromatin and heterochromatin. Euchromatin is represented by single copy, gene-rich DNA sequences located between centromeres and telomeres. These regions are packaged with acetylated histones that foster gene expression. In contrast, heterochromatin is represented by repetitive, gene-poor DNA sequences located near centromeres and telomeres. These regions are packaged with hypoacetylated histones and can cause gene silencing.

The regulation of gene expression involves complex interactions between DNA sequences and protein factors. One mechanism for regulating access of transcription factors to DNA is through chromatin packaging. Double-stranded DNA is wound twice around a histone octamer, forming the fundamental packaging unit, the nucleosome. Nucleosomal DNA is further folded into higher-order chromatin structures that differentiate euchromatin from heterochromatin. A second mechanism for regulating access of transcription factors to DNA involves the spatial positioning of genes within the nucleus. Increasing evidence supports the notion that the nucleus is not a homogenous mixture of DNA and proteins, but is a highly organized environment. For example, chromosome labeling techniques show that certain chromosomes reproducibly localize to specific positions within the nucleus, termed chromosome territories (Figure 1). Thus, a given gene might have a specific address within the nucleus.

Nuclear zones are superimposed on chromosome territories (Figure 1). A zone is defined as a region of the nucleus that is enriched in a particular class of transcription factors. There are two types of zones, those enriched for silencing factors that do not support transcription (inactive zones), and those enriched for activating factors that do support transcription (active zones). Entire chromosomes can be located within a zone, such as the case for the inactive X chromosome (Barr body) of mammalian females that localizes to an inactive zone along the nuclear periphery. Alternatively, smaller regions along a chromosome can attract transcription factors and form a local zone (Figure 1). In addition, regions of similar transcription activity on different chromosomes can come together to form a zone. Thus, regulation of gene expression can occur at many levels involving the local chromatin environment, chromosomal territories, and the nuclear zones.

Establishing a Zone

Zones are established by increasing the local concentrations of transcriptional regulatory factors within an area of the nucleus. This nonuniform distribution of factors occurs by mechanisms involving protein–protein and protein–DNA interactions. As an example, heterochromatin protein 1 (HP1) can direct silent chromatin into the inactive zone at the nuclear periphery. The amino terminal chromo domain of HP1 interacts with a histone modification that is enriched in heterochromatin and the carboxy chromo shadow domain of HP1 interacts with a component of the nuclear envelope. These protein–protein interactions promote the accumulation of heterochromatin and HP1 at the nuclear periphery. The role of protein–DNA interactions is illustrated by studies of yeast telomeres. Repetitive DNA sequences found at yeast telomeres attract the DNA-binding protein Rap1. This protein interacts with Sir proteins that are involved in gene silencing. Through this interaction, the concentration of Sir proteins increases at the nuclear periphery relative to the interior of the nucleus. The concentration gradient of Sir proteins within the nucleus can be "sensed" by reporter transgenes containing Sir-responsive DNA sequences. When such a reporter transgene is

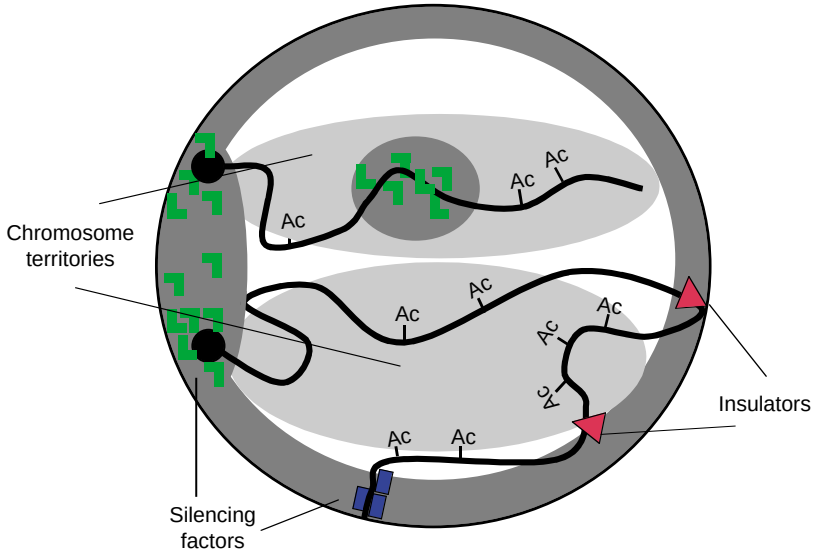

FIGURE 1 Diagram of organization within the nucleus. A nucleus is depicted with chromosome territories (light gray) and silencing zones (dark gray). Histone acetylation (Ac) is shown over active chromatin. Hypoacetylation is associated with inactive chromatin, such as that found at centromeres (black circle) and telomeres. Small domains within a chromosome can acquire properties similar to heterochromatin and form a silencing zone (shaded circle). Silencing factors (green and blue shapes) are involved in chromatin compaction, gene silencing, and tethering to the nuclear periphery. Insulator elements (red triangles) partition chromosomes into transcriptonally related domains and assist in organizing chromatin into zones.

placed at positions close to the telomere, gene silencing is strong. When the same transgene is positioned further from the telomere, gene silencing is weak. Overexpression of Sir proteins produces silencing at internal sites, presumably due to increased levels of Sir proteins within the interior of the nucleus. These studies demonstrate that gene silencing can be modulated by the position of a gene within the nucleus, as well as, the local concentration of regulatory factors.

Organizing DNA into Zones

What mechanisms ensure that chromosome domains remain independent? Specialized DNA elements called insulators may be responsible for maintaining domain autonomy. These DNA elements, 0.2–3 kb in length, associate with specific proteins that limit the scope of regulatory interactions. An insulator located between an enhancer and promoter blocks activated gene expression. Insulator elements flanking a gene "insulate" it from neighboring positive and negative regulatory elements. Several models have been proposed to explain the mechanism of insulator action. One model states that attachment of insulators to the nuclear envelope could result in the formation of looped domains that compartmentalize gene activity (Figure 1). Physical associations with architectural components of the nucleus could serve to anchor chromosomal sites leading to spatial positioning of insulated domains within a zone.

Changes in Gene Expression Correlate with Shifting Zones

The nucleus is a highly dynamic environment in which protein factors and chromosomal domains can change positions within seconds. This mobility allows gene expression to be regulated by shifting zones. Studies on the expression and localization of lymphocyte specific genes demonstrate this point. A set of lymphocyte-specific genes in mice associate with Ikaros, a zinc-finger DNA-binding protein that also associates with centric heterochromatin. When these genes are silenced they localize to discrete foci within B-cell nuclei that correspond to the location of centromeres. Expression of these genes correlates with movement away from the centric foci. A direct role for Ikaros in this process was demonstrated by examining cells that had low levels of Ikaros. In such cells, these genes do not colocalize with centromeres when silenced. These data suggest that Ikaros is not required for silencing but plays a critical role in directing silent genes to an inactive zone. However, it appears that in these examples movement into an inactive zone is not the cause of gene silencing. Therefore, positioning a gene within a silent zone might be a consequence of silencing or assist in the maintenance of the silent state.

Additional studies correlating nuclear position with gene expression have focused on the *brown* gene in the fruit fly *Drosophila*. The *brown* gene is normally positioned at a site distant from centric heterochromatin.

A mutant allele designated *brown*^{Dominant} contains an insertion of a large block of heterochromatin (>1 Mb) in the coding region. Heterochromatin proteins associate with the insertion and are involved in positioning *brown*^{Dominant} near centric heterochromatin. Surprisingly, the wild-type brown allele also becomes silenced. This occurs due to a process called "*trans*-silencing" that results from homologous pairing along the length of *Drosophila* chromosome arms. Silencing of the wild-type *brown* gene demonstrates the impact of positioning within an inactive zone.

In some cases it appears that localization within an inactive zone occurs as the default state. Studies using a mouse *β-globin* transgene demonstrate that a complete enhancer element is required for both gene expression and localization away from inactive zones. Point mutations within the enhancer element that disrupt binding of a transcription factor eliminate gene expression and cause the *β-globin* transgene to localize to inactive zones near centromeres. Interactions between factors bound at enhancer elements and the transcriptional machinery housed within the interior of the nucleus might be responsible for localization within an active zone. Alternatively, factors that bind to enhancer elements might recruit chromatin remodeling machines and/or histone acetyltransferases, generating a chromatin environment that disrupts interactions with silencing proteins in the inactive zone.

Multiple Determinants for Establishing the Activity State of a Gene

The emerging picture is that both nuclear zones and local chromatin structure play essential roles in establishing the transcriptional state of a gene. Silencing at the yeast mating type locus *HMR-E* is dependent upon the recruitment of specific *trans*-acting factors. Deletion of some of their binding sites generates a defective silencer, leading to transcriptional derepression. Tethering an *HMR-E* with a defective silencer to the nuclear periphery restores gene silencing. However, tethering an *HMR-E* in which all binding sites had been removed has no effect on gene expression. These experiments demonstrate that the local chromatin structure, not just the position within a nuclear zone, is necessary to establish the transcriptionally inactive state.

Effects of local chromatin structure and nuclear positioning were further demonstrated by studies involving chromosomal translocations in *Drosophila*. A stock possessing a reporter gene inserted within a region associated with heterochromatin-silencing factors was subjected to X-rays and translocations were recovered. The degree of silencing of the reporter gene was dependent on the location of the translocation breakpoints. Rearrangements that placed the transgene closer to centric heterochromatin showed increased levels of gene silencing. In contrast, rearrangements that placed the transgene at sites distant from centric heterochromatin resulted in decreased gene silencing. Contrasting observations were made when a stock containing the same transgene inserted within a chromosomal region that normally does not associate with heterochromatic silencing factors was subjected to X-rays. Resulting translocations did not alter the expression of the reporter gene, even when the transgene localized near centric heterochromatin. The transgene appeared to be insensitive to positioning in the nucleus. These data suggest that local chromatin structure can influence the response of a gene to placement within a particular nuclear zone.

Nuclear Zones and Human Disease

Studies in model organisms, such as yeast and fruit flies, have clearly demonstrated that nuclear positioning affects gene expression. There is growing evidence in humans that some diseases might result from misregulation of gene expression due to translocations that place a disease-causing gene into an inappropriate zone. Examples include cases of aniridia (absence of the iris), autism, and Burkitt's lymphoma. In these cases the disease-related gene is not damaged by the translocation, in fact, the breakpoints of the translocation map several kilobases or megabases from the gene affected. It is hypothesized that altered expression of the disease gene is due to placement in an inappropriate nuclear zone as a consequence of the translocation. Therefore, understanding the rules of gene regulation has become a three-dimensional problem that will require sophisticated detection of gene expression coupled with high-resolution nuclear imaging.

See Also the Following Articles

Chromatin: Physical Organization • Chromosome Organization and Structure, Overview • Nucleoid Organization of Bacterial Chromosomes • Transcriptional Silencing

Glossary

boundary elements DNA elements that bind specialized nuclear complex that attach to nuclear substructure to delimit chromosome domains.

chromosome territory An area within the nucleus that is occupied by a specific chromosome.

euchromatin Regions of the genome that contain mostly single copy DNA sequence and are relatively gene-rich. These regions replicate early in S phase and decondense during interphase.

heterochromatin Regions of the genome, frequently located near centromeres and telomeres, that contain repetitive DNA sequences and are relatively gene-poor. These regions replicate late in S phase and remain condensed throughout the cell cycle.

histones Small, highly conserved, basic proteins that form a nucleosome.

insulators Specialized DNA sequences that block the effect of enhancers or silencers when placed between a promoter and the regulatory element. When flanking both ends of a gene, they block position effects that arise from neighboring regulatory elements.

nucleosome The fundamental unit of chromatin packaging containing eight histones and ~165 bp of double stranded DNA.

somatic pairing Pairing of two homologous chromosomes during interphase in somatic cells.

Further Reading

Brown, K. E., Guest, S. S., Smale, S. T., Hahm, K., Merkenschlager, M., and Fisher, A. G. (1997). Association of transcriptionally silent genes with Ikaros complexes at centromeric heterochromatin. *Cell* **91**, 845–854.

Cryderman, D. E., Morris, E. J., Biessmann, H., Elgin, S. C. R., and Wallrath, L. L. (1999). Silencing at Drosophila telomeres: Nuclear organization and chromatin structure play critical roles. *EMBO J.* **18**, 3724–3736.

Dernberg, A. F., Broman, K. W., Fung, J. C., Marshall, W. F., Philips, J., Agard, D. A., and Sedat, J. W. (1996). Perturbation of nuclear architecture by long-distance chromosome interactions. *Cell* **85**, 745–759.

Gasser, S. M. (2001). Positions of potential: Nuclear organization and gene expression. *Cell* **104**, 639–642.

Ishii, K., Arib, G., Lin, C., Van Houwe, G., and Laemmli, U. K. (2002). Chromatin boundaries in yeast: The nuclear pore connection. *Cell* **109**, 551–562.

Kleinjan, D.-J., and van Heyningen, V. (1998). Position effect in human genetic disease. *Human Mol. Genet.* **7**, 1611–1618.

Kuhn, M. J., and Geyer, P. K. (2003). Genomic insulators: Connecting properties or mechanism. *Curr. Opin. Cell Biol.* **15**, 259–265.

Mahy, N., Perry, P. E., and Bickmore, W. A. (2002). Gene density and transcription influence the localization of chromatin outside of chromosome territories detectable by FISH. *J. Cell Biol.* **159**, 753–763.

Sass, G. L., and Henikoff, S. (1999). Pairing-dependent mislocalization of a Drosphila *brown* gene reporter to a heterochromatic environment. *Genetics* **152**, 595–604.

Williams, R. R. E. (2003). Transcription and the territory: The ins and outs of gene positioning. *Trends Genet.* **19**, 298–302.

Biography

Lori L. Wallrath and Pamela K. Geyer are faculty members in the Department of Biochemistry at the University of Iowa. Their principal research interest is chromatin structure and gene expression. Dr. Wallrath's research is focused on the molecular mechanisms of gene silencing. Dr. Geyer's research is focused on the role of genomic insulators in gene expression.

John Danzer is a senior Ph.D. student in the Molecular Biology Program, working on the molecular mechanism of heterochromatin spreading.

Dr. Oya Yazgan is a Postdoctoral Fellow researching the role of proteins that associate with insulators.

Nuclear Pores and Nuclear Import/Export

Anita H. Corbett
Emory University School of Medicine, Atlanta, Georgia, USA

The hallmark of a eukaryotic cell is the presence of the nucleus, which separates the chromosomes that encode the genetic information from the protein translation machinery in the cytoplasm. This physical separation requires nuclear transport (import and export) machinery, which is capable of moving macromolecules such as proteins and RNAs rapidly but selectively into and out of the nucleus. There are many processes in eukaryotic cells that require macromolecular exchange between the nucleus and the cytoplasm. The most obvious example is the expression of a gene where the DNA is transcribed to messenger RNA (mRNA) within the nucleus and this mRNA must be transported to the ribosomes, the cytoplasmic protein translation machinery, to be decoded and translated into protein. In addition, many proteins that are created by the cytoplasmic translation machinery enter the nucleus to function in essential nuclear processes such as DNA replication, transcription, DNA repair, and many others. Thus, there is a great deal of traffic between the cytoplasm and the nucleus and these transport events are critical for the proper functioning of a eukaryotic cell.

Nuclear Pores

All transport between the nucleus and the cytoplasm occurs through large protein channels that are embedded in the nuclear membrane. These channels, which are called nuclear pore complexes (NPCs), are composed of proteins referred to as nucleoporins.

Structure

NPCs are large (~30 MDa in yeast and ~60 MDa in vertebrates) structures that span the double membrane, which surrounds the nucleus to provide a transport channel for very large macromolecular cargoes. Many different studies have led to a model for the structure of the NPC (Figure 1). The core of the NPC consists of a cylinder with eightfold rotational symmetry, which spans the nuclear envelope and surrounds a central channel. In addition to this central channel, there are filaments that extend into the cytoplasm and a basket structure that extends into the nucleoplasm. Cargoes that move through the nuclear pores probably interact first with the peripheral structures, move through the central channel, and are then released into their target compartment.

Composition

Sophisticated biochemical studies have revealed the identity of the nucleoporin proteins that make up the NPC. Surprisingly, these studies reveal that both the yeast and vertebrate nuclear pores are composed of only approximately 30 distinct proteins. The pore is large because most of these pore components are present in 16–32 copies per NPC. Many of these nucleoporins contain a characteristic repeat sequence of phenylalanine glycine repeats (FG). These FG-repeat nucleoporins line the central channel of the pore and probably provide the conduit for movement of macromolecules through the pore complex.

Transport Mechanisms: Protein Trafficking

Transport through nuclear pores occurs in both directions, from the nucleus to the cytoplasm and from the cytoplasm to the nucleus. The desired direction of transport generally depends on the cargo to be transported. The cell has developed sophisticated mechanisms to mark cargoes for transport and regulate the direction of the transport processes.

Targeting Signals

As with most intracellular targeting mechanisms, trafficking between the nucleus and the cytoplasm depends on amino acid sequences within the protein cargoes to be transported. However, unlike other targeting mechanisms, such as mitochondrial and ER targeting, nucleocytoplasmic trafficking signals are not

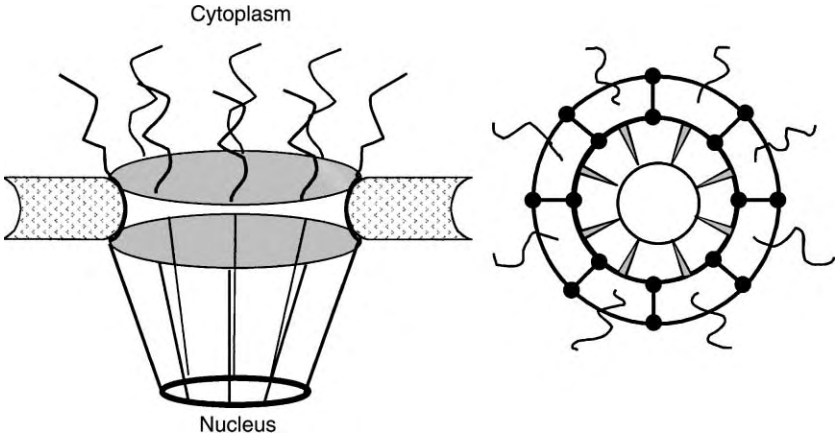

FIGURE 1 Schematic of the nuclear pore complex (NPC). Left: A schematic of the pore in the plane of the membrane is shown. The schematic shows the cytoplasmic filaments and the nuclear basket. Right: A schematic view of the pore looking down from the cytoplasmic face. The eightfold rotational symmetry of the pore is evident.

cleaved and remain an integral part of the protein. This mechanism can allow the cargo proteins to undergo multiple rounds of import and/or export. The nuclear targeting signal within the cargo protein generally mediates a physical interaction with a soluble nuclear transport receptor, which targets the cargo to the nuclear pore for transport.

Canonical signals for both nuclear protein import and nuclear protein export have been identified and studied in some detail. Nuclear import signals are generally termed nuclear localization signals (NLS), while signals that target proteins for export from the nucleus are termed nuclear export signals (NES). The classical NLS consists of either a single cluster of basic amino acid residues (monopartite) or two clusters of basic amino acid residues separated by a 10–13 amino acid linker sequence (bipartite). The monopartite NLS sequence is typified by the NLS found in the simian virus 40 (SV40) large T antigen (PKKKRKV), whereas the bipartite NLS is typified by the nucleoplasmin NLS (**KR**PAATKKAGQA**KKKK**). The classical NES is comprised of a series of hydrophobic amino acids, generally leucine, isoleucine, or valine. Numerous variations on this theme have been identified and thus far the best consensus sequence for an NES is LxxxLxxLxL, where the spacing between the leucines can vary, and, in fact, the leucines can be substituted with virtually any hydrophobic amino acid. Although classical NLS and NES signals are typically identified through computer searches of proteins sequences, it is essential that their function be verified through experimental methods.

Transport Receptors

Targeting signals within cargo proteins are recognized by soluble receptors that direct those cargoes to the nuclear pore for transport. These receptors form a family of structurally related molecules that are generally referred to as importins (for import receptors), exportins (for export receptors), or generally as transport receptors or karyopherins. The family of related receptors is generally referred to as the importin β or karyopherin β-family. One feature of these transport receptors is that they are modulated in such a way that they bind tightly to their cargo in the compartment where the cargo needs to be picked up. However, following the translocation through the NPC to the compartment where the cargo needs to be delivered, the transport receptor undergoes a conformational change that leads to the efficient release and delivery of the cargo. This switch in binding to the cargo is regulated by the small GTPase Ran.

Although most transport cargoes bind directly to their cognate transport receptor, there are examples where an adaptor protein mediates this interaction. The best example of this occurs in nuclear protein import of cargoes that contain a classical NLS sequence. The NLS within these cargoes is recognized by an adaptor protein called importin α or karyopherin α. The importin/karyopherin α recognizes and binds to the cargo and then binds directly to the transport receptor to form a trimeric import complex. This complex is then translocated through the nuclear pore into the nucleus and the NLS cargo is delivered.

Once cargo is released from the transport receptors within the delivery compartment, all the receptors are recycled for another round of transport. Import receptors are recycled back to the cytoplasm and export receptors are recycled back to the nucleus. This recycling of receptors assures that a single receptor can mediate multiple rounds of transport.

The Ran GTPase Cycle

The small GTPase Ran, serves as a molecular switch that modulates the directionality of nuclear transport. As with other GTPases, Ran can exist in two forms, either bound to GDP (RanGDP) or bound to GTP (RanGTP). It is the compartmentalization of these two distinct forms of Ran that regulates cargo/receptor interactions to impart directionality on nuclear transport. This compartmentalization is achieved through the intracellular separation of the two important regulators of the Ran GTPase cycle. The Ran GTPase-Activating Protein (RanGAP), which enhances Ran-mediated GTP hydrolysis, is located in the cytoplasm and the Ran Guanine Nucleotide Exchange Factor (RanGEF), which facilitates exchange of GDP for GTP on Ran, is located in the nucleus. As shown in Figure 2, with the RanGAP in the cytoplasm, any RanGTP that enters the cytoplasm is rapidly converted to RanGDP. Thus, in the cytoplasm the level of RanGDP exceeds the level of RanGTP. In contrast, within the nucleus in the presence of the RanGEF, RanGDP is rapidly converted to RanGTP. Thus, in the nucleus the level of RanGTP is high compared to the level of RanGDP. Due to the asymmetric localization of the Ran regulators, high levels of RanGTP serve as a marker for the nucleus and high levels of RanGDP serve to identify the cytoplasmic compartment.

The different nucleotide bound states of Ran regulate the flow of protein cargoes into and out of the nucleus by regulating the assembly of the import and export complexes (Figure 3). Cargoes to be transported into the nucleus bind to their cognate import receptors in the cytoplasm. These complexes are translocated into the nucleus through NPCs. Once they reach the nucleus, where levels of RanGTP are elevated, RanGTP binds to the import receptor causing a conformational change that releases the import cargo into the nucleus. In contrast, export cargoes bind to their export receptors only in the presence of RanGTP. Export complexes are trimeric complexes that consist of the export receptor, the export cargo, and RanGTP. As with import, the export complex is translocated through NPCs to the cytoplasm. In the cytoplasm, the export complex encounters the RanGAP and the bound RanGTP is converted to RanGDP. This disassembles the export complex and leads to the release of the export cargo into the cytoplasm.

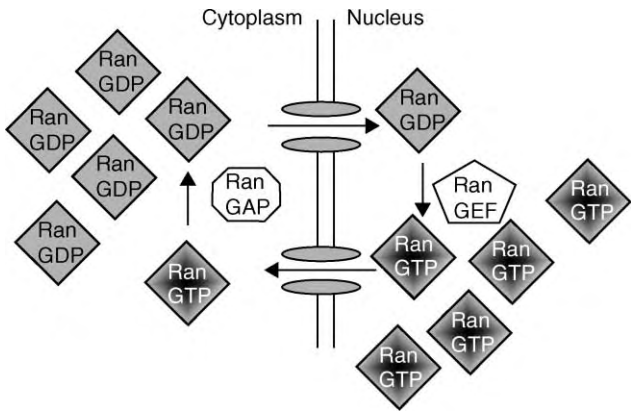

FIGURE 2 The RanGTP gradient. The compartmentalization of the RanGAP to the cytoplasm and the RanGEF to the nucleus results in localized concentrations of RanGDP and RanGTP. In the cytoplasm where the RanGAP enhances the Ran-mediated GTP hydrolysis, levels of RanGDP are high. In the nucleus where the RanGEF facilitates the exchange of GTP for GDP on Ran, the levels of RanGTP are high. This compartmentalization is critical for the identification of the nuclear and cytoplasmic compartments in nuclear transport and in other cellular processes.

Classical NLS-Mediated Protein Import

The best understood nuclear transport process is the import of protein cargoes that contain a classical basic NLS (Figure 4). Thus, this process can be used most readily to illustrate the steps that occur when a transport cargo is moved into or out of the nucleus. Historically, nuclear protein import was divided into two steps, docking at the nuclear pore, an energy-independent step, and translocation into the nucleus, an energy-dependent step. Advances in our understanding of the process and the players now lead us to define at least five distinct steps for import of a cargo that contains a classical NLS: (1) recognition and binding of the NLS cargo to the α/β heterodimeric-import receptor in the cytoplasm; (2) targeting to the nuclear pore through interactions between the importin/karyopherin β nuclear transport receptor and the nuclear pore; (3) translocation through the pore through transient interactions between importin/karyopherin β and the FG-repeat containing nucleoporins; (4) delivery into the nucleus where RanGTP binds to importin/karyopherin β to cause a conformational change that releases α and the NLS cargo; and (5) recycling of importin/karyopherin α to the cytoplasm in a heterotrimeric complex with an importin/karyopherin α export receptor and RanGTP and importin/karyopherin β presumably in complex with RanGTP. Note that the only energy expenditure in this process occurs when the karyopherin proteins are recycled to the cytoplasm and the accompanying RanGTP is hydrolyzed.

Transport Mechanisms: RNA Trafficking

Multiple classes of RNAs, including mRNAs, tRNAs, and U snRNAs are transcribed and processed within

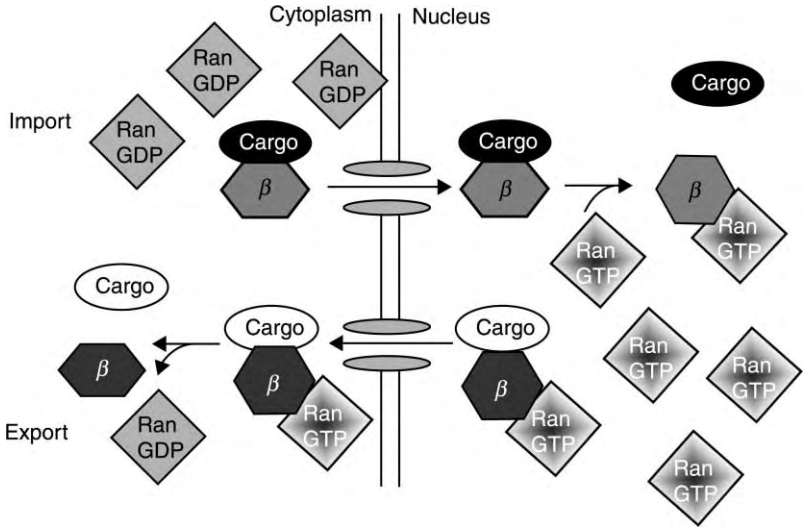

FIGURE 3 Ran regulates the assembly of import and export complexes. Top: For transport into the nucleus (Import), cargoes are recognized in the cytoplasm by an importin/karyopherin β receptor to form an import complex. Once this complex is translocated into the nucleus, it encounters the nuclear RanGTP, which binds tightly to the importin/karyopherin β receptor and causes a conformational change that releases the import cargo. Bottom: For transport out of the nucleus (Export), cargoes are recognized in the nucleus by an importin/karyopherin β receptor. However, in contrast to the import complex, the export complex can only form in the presence of RanGTP. Thus, export complexes are obligate trimeric complexes that consist of the export cargo, the importin/karyopherin β export receptor, and RanGTP. Once the export complex is translocated to the cytoplasm, it encounters the RanGAP. In the presence of the RanGAP, the RanGTP within the complex is converted to RanGDP and the complex dissociates resulting in the release of the export cargo into the cytoplasm. Hence, by controlling complex assembly and disassembly, the different forms of Ran confer directionality on the nuclear transport machinery.

the nucleus and then transported to their sites of action in the cytoplasm. As compared with proteins, RNAs require extensive processing before they reach their mature form and are ready to exit the nucleus. This means that RNA export is intimately linked to RNA processing within the nucleus.

Export of RNA via Classical Nuclear Transport Receptors

The export of tRNA, U snRNA, and rRNA follows pathways analogous to nuclear protein export. For example, tRNA is recognized directly by the importin/karyopherin β family nuclear transport receptor, exportin-t/Los1p and is exported as a complex with RanGTP. As for any classical export process, this trimeric complex is disassembled in the cytoplasm when RanGTP is hydrolyzed to RanGDP. Preferential export of mature tRNAs seems to be achieved at least in part by the specificity of exportin-t for the mature processed, modified, and appropriately aminoacylated tRNAs. U snRNAs are synthesized in the nucleus, transported to the cytoplasm where they associate with protein components of mature small nuclear ribonucleoproteins (snRNPs), and are then reimported to the nucleus where they function in mRNA splicing. Although this export depends on Ran, it is controversial whether Ran plays a direct role in export or whether its activity may be essential for the import of components required for RNP assembly.

mRNA Export

Export of poly (A)+ mRNA remains the least well understood of the RNA export mechanisms. mRNAs are not exported to the cytoplasm as naked nucleic acids, but rather as RNP complexes, and it is generally agreed that the export machinery recognizes signals within the proteins of these complexes rather than the RNA itself. For example, export of intron-containing HIV transcripts from the nucleus is mediated by the HIV protein Rev through its binding to the classical NES receptor, CRM1/exportin. While the HIV virus exploits this mechanism, none of the classical nuclear transport receptors play a central role in cellular mRNA export.

Although the mechanistic details of mRNA export have not yet been fully elucidated, it appears that there are two classes of proteins that are required to achieve export of mature messages. First, there is a family of evolutionarily conserved heterogeneous nuclear ribonucleoproteins (hnRNPs) that interact with poly (A)+ RNA *in vivo*. A number of these hnRNP proteins shuttle between the cytoplasm and the nucleus and escort the poly(A)+ RNAs as they are exported through the NPC. Current models suggest that at least some of the hnRNP proteins may be involved in RNA processing steps that occur cotranscriptionally. The hnRNPs that remain bound to the maturing messages may serve as markers that the different processing steps have been successfully accomplished. The second class of proteins consists of

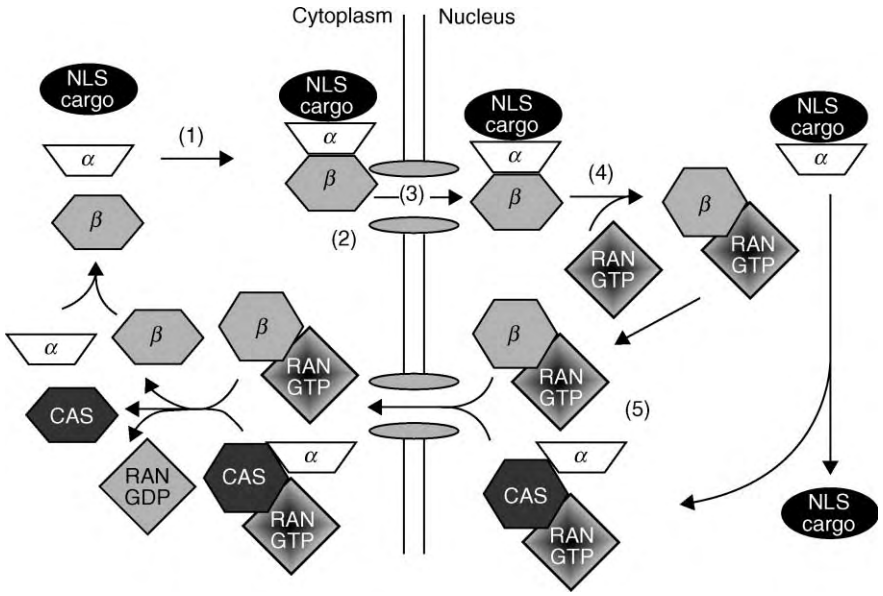

FIGURE 4 Model for classical NLS-mediated protein import into the nucleus. The best-understood transport mechanism is that of classical nuclear protein import mediated by importin/karyopherin β and the NLS binding adapter, importin/karyopherin α. This process can be divided into at least five distinct steps as shown in the model: (1) recognition and binding of the NLS cargo to the α/β heterodimeric import receptor in the cytoplasm; (2) targeting to the nuclear pore through interactions between the importin/karyopherin β nuclear transport receptor and the nuclear pore; (3) translocation through the pore through transient interactions between importin/karyopherin β and the FG-repeat containing nucleoporins; (4) delivery into the nucleus where RanGTP binds to importin/karyopherin β to cause a conformational change that releases α and the NLS cargo; and (5) recycling of importin/karyopherin α to the cytoplasm in a heterotrimeric complex with an importin/karyopherin α export receptor and RanGTP and importin/karyopherin β presumably in complex with RanGTP.

those proteins that have been implicated more directly in the export process; including a helicase, Sub2p/UAP56, and the heterodimeric-export receptor, Mex67p/Mtr2p (TAP/p15 in humans). TAP/Mex67p shuttles between the cytoplasm and the nucleus, and in complex with p15/Mtr2p, binds both to mRNA and to nucleoporins. Thus, it could potentially target bound RNAs directly to the NPC for export.

See Also the Following Articles

mRNA Polyadenylation in Eukaryotes • mRNA Processing and Degradation in Bacteria • Neurotransmitter Transporters • Ran GTPase • RNA Editing

Glossary

cargo Macromolecular substrate to be transported between the nucleus and the cytoplasm.

GTPase Protein that binds to and hydrolyzes the nucleotide GTP.

heterogeneous nuclear ribonucleoprotein (hnRNP) Abundant non-specific poly(A)+ RNA binding protein.

HIV Human immunodeficiency virus.

messenger RNA (mRNA) Class of RNA that carries the information from the DNA to the cytoplasm and serves as the informational blueprint for protein synthesis.

nuclear export signal (NES) An amino acid sequence within a protein that targets that protein for export from the nucleus.

nuclear localization signal (NLS) An amino acid sequence within a protein that targets that protein for import into the nucleus.

nuclear pore complex (NPC) The large proteinaceous channel through which macromolecular cargoes are transported in and out of the nucleus.

nucleoporins Proteins that make up the NPC.

Ran A small GTPase that regulates the directionality of nuclear transport.

RanGAP Cytoplasmic protein that enhances the GTPase activity of Ran.

RanGEF Nuclear protein that facilitates the nucleotide exchange on Ran.

ribosomal RNA (rRNA) Class of RNA that serves as a structural and catalytic component of ribosomes.

transfer RNA (tRNA) Class of RNA that is charged with amino acids to decode the mRNA for protein synthesis.

transport receptor/karyopherin/importin/exportin The receptors that bind to and recognize protein and RNA cargoes that are transported into or out of the nucleus.

U snRNA Small RNAs that participate in splicing.

Further Reading

Damelin, M., Silver, P. A., and Corbett, A. H. (2002). Nuclear protein transport. *Methods Enzymol.* **351**, 587–607.

Dasso, M. (2002). The ran GTPase: Theme and variations. *Curr. Biol.* **12**, R502–R508.

Gorlich, D., and Kutay, U. (1999). Transport between the cell nucleus and the cytoplasm. *Annu. Rev. Cell Develop. Biol.* **15**, 607–660.

Lei, E. P., and Silver, P. A. (2002). Protein and RNA export from the nucleus. *Develop. Cell.* **2**, 261–272.

Quimby, B. B., and Corbett, A. H. (2001). Nuclear transport mechanisms. *Cell Mol. Life Sci.* **58**, 1766–1773.

Rout, M. P., and Aitchison, J. D. (2000). Pore relations: Nuclear pore complexes and nucleocytoplasmic exchange. *Essays Biochem.* **36**, 75–88.

Strom, A. C., and Weis, K. (2001). Importin-beta-like nuclear transport receptors. *Genome Biol.* **2**, Epub 2001 Jun 05.

Suntharalingam, M., and Wente, S. R. (2002). Peering through the pore: Nuclear pore complex structure, assembly, and function. *Develop. Cell.* **4**, 775–789.

Weis, K. (2002). Nucleocytoplasmic transport: Cargo trafficking across the border. *Curr. Opin. Cell Biol.* **14**, 328–335.

Biography

Anita H. Corbett, Ph.D., is an Associate Professor of biochemistry at the Emory University School of Medicine. Her principal research interest is in the area of macromolecular trafficking between the cytoplasm and the nucleus. She utilizes the budding yeast, *Saccharomyces cerevisiae* as a model system for most of her studies. Dr. Corbett holds a Ph.D. in biochemistry from Vanderbilt University. She completed a postdoctoral fellowship at Harvard Medical School before moving to Emory in 1997.

Nucleoid Organization of Bacterial Chromosomes

Charles J. Dorman
Trinity College, Dublin, Ireland

Bacteria do not possess a nuclear membrane, and so have no clearly defined nucleus in the eukaryotic sense. It is for this reason that they are classed as prokaryotes. The term nucleoid is used to describe that part of the bacterial cytoplasm that is occupied by the genetic material. This has been the subject of investigation for several decades now, yet despite intensive study, many details of nucleoid structure and function remain obscure. It seems ironic that our understanding of these so-called "simple" organisms continues to lag behind that of cells in higher organisms in this respect. This article will describe those features of the bacterial nucleoid over which there is general agreement. Much of the material comes from work with *Escherichia coli*, the best-studied prokaryote, and encompasses the organization of the genetic material within the nucleoid and its interactions with those DNA-binding proteins that are thought to impart structure to it.

Organization of DNA in the Nucleoid

When considering the nucleoid, one of the first issues to be confronted concerns the problem of how to package a circular DNA molecule measuring ~1.5 mm in circumference within a cylindrical container with hemispherical ends (the cell) that measures 2 μm in length × 1 μm diameter. Any solution to this problem must take into account the persistence length of the molecule, which for B-DNA is 50 nm (150 bp). This imposes on the circular chromosome a tendency to adopt a disordered globular configuration, resulting in a ball of DNA measuring 10 000 nm in diameter. This structure is at least 10 times too large to fit in the cell. Since bacterial chromosomes clearly do fit in cells, organization at some level must be imposed on this otherwise chaotic arrangement. Organization is also required so that the DNA can participate in transactions such as gene transcription. It seems that this organization occurs at least on two levels. The first concerns an effect on the shape of the DNA itself that is imparted through negative supercoiling, whereas the second involves the interaction of the DNA with so-called nucleoid-associated proteins. Each of these aspects will be considered in turn.

DNA Supercoiling

As with DNA in other types of cells, bacterial DNA is maintained in a negatively supercoiled state. This arises because the double helix in the cell has a deficiency of helical turns; in other words, it is in an under-wound state. The molecule is thus placed in a thermodynamically unfavorable state due to torsional stress. This difficulty is resolved by a structural transition to an energetically more favorable form. In practice, this involves adopting a shape (or topology) that we call supercoiled, in which an already-coiled molecule (the DNA duplex) itself becomes coiled (Figure 1). Supercoiling creates writhing of the DNA helical axis and this results in a more compact molecule. The compaction can arise due to adoption by the DNA of a plectomenic (braided) or a toroidal (doughnut-like) configuration. Depending on how supercoiled the DNA becomes, the structure can also form branches, leading to further compaction. This reduces the diameter of the DNA ball to a value that can be accommodated within the confines of the cell.

The foregoing description of DNA supercoiling and its effects on DNA compaction is highly qualitative. It is possible to treat DNA supercoiling in a quantitative manner, making accurate measurements of how supercoiled DNA molecules are under particular conditions. This is desirable since it allows one to calculate the energetic consequences for DNA of different levels of supercoiling. The under-winding of the DNA duplex that is a characteristic of negatively supercoiled molecules imparts free energy to the DNA, and this energy is available to drive the major transactions in which DNA participates, such as gene transcription. Knowledge of the minimum energy requirements of a particular transaction can be used to estimate the level

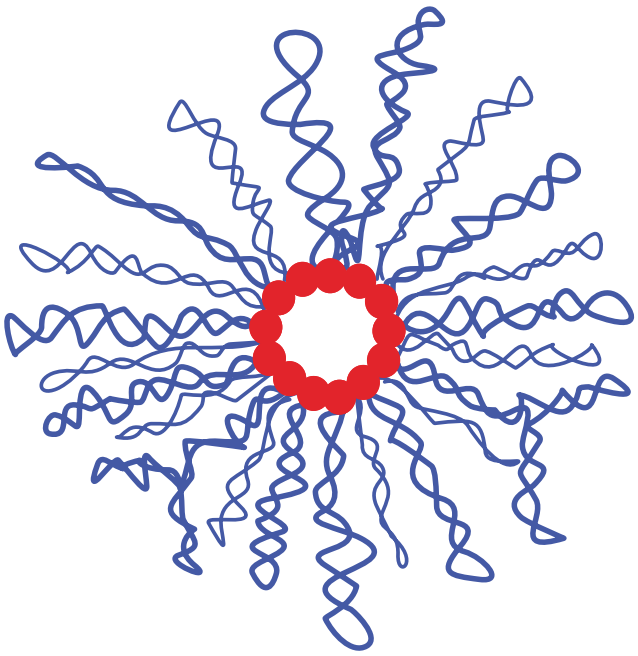

FIGURE 1 Organization of the bacterial nucleoid. A representation of the nucleoid liberated from the cell is shown. The red spheres at the core represent the nucleoprotein complexes that define the ends of the supercoiled domains. These complexes are thought to be composed of nucleoid-associated proteins and possibly topoisomerases. The blue ribbons represent the DNA making up the supercoiled domains. A typical nucleoid from *E. coli* has between 50 and 100 of these.

to which DNA has become supercoiled. When used in conjunction with physical methods based on electrophoretic mobility of covalently closed circular DNA or its sedimentation rates, one can obtain robust measurements of DNA supercoiling.

DNA can be described in terms of three topological parameters: linking number (L), twist (T), and writhe (W). The linking number is a measure of the number of times the two strands of the DNA duplex link with one another. Twist measures the turning of the DNA strands about the helical axis, whereas writhe measures the winding of the helical axis about itself. These properties are related as follows: $L = T + W$ and $\Delta L = \Delta T + \Delta W$. This means that a change in linking number is distributed between the other two parameters, resulting in a change that is manifest: (1) only as altered twist, (2) only as altered writhe, or (3) as a change in both twist and writhe. For very large DNA molecules, such as bacterial chromosomes, measurements of L are cumbersome and largely impractical. Here one employs a parameter such as the superhelical density, σ. This is the average number of superhelical turns per helical turn of DNA:

$$\sigma = 10.5\tau/N$$

where τ is the number of measurable supercoils, N is the number of base pairs in the molecule, and 10.5 refers to the number of base pairs per helical turn in B DNA. The importance of the energetics of supercoiling for DNA-based processes was referred to above. The free energy of supercoiling is related to the change in DNA linking number as follows: $\Delta G = (1050\ RT/N)\ (\Delta L)^2$, where R is the gas constant, T is the temperature in kelvin, and N is the size of the molecule in base pairs. The important point to note about this relationship is that the free energy varies in proportion to the square of the change in the linking number (L). Put qualitatively, this means that even modest changes in the linking number can result in significant variances in the energy imparted to the DNA.

Control of DNA Supercoiling

The level of DNA supercoiling in the bacterial nucleoid is established and maintained largely by the action of specialist enzymes called topoisomerases (Table I). Bacterial DNA gyrase is a type II ATP-dependent topoisomerase that introduces negative supercoils into DNA, reducing its linking number in steps of two. It can also remove positive supercoils using the same enzymatic mechanism. The activity of gyrase is opposed in the cell by DNA topoisomerase I, a type I topoisomerase that removes supercoils from negatively supercoiled DNA by a "swivelase" mechanism, increasing the linking number of the molecule in steps of one. It acts independently of ATP, using the energy stored in the supercoiled DNA molecule to drive the reaction. *E. coli* has two other topoisomerases, III and IV (Table I) that can relax negatively supercoiled DNA, although their main role *in vivo* seems to be to act as decatenases. The promoters of the genes coding for gyrase (*gyrA*, *gyrB*) and topoisomerase I (*topA*) are controlled, *inter alia*, by DNA supercoiling. This provides a useful feedback loop that controls the supply of these proteins. The *gyr* promoters are activated by DNA relaxation (loss of negative supercoiling), whereas the *topA* promoter is repressed by negative supercoiling. An important link between gyrase activity and cellular physiology concerns the dependence of this enzyme on ATP and the fact that gyrase is inhibited by ADP. In this way the major source of negative supercoiling is directly responsive to the energy charge of the cell.

The Domain Structure of the Nucleoid

Physical analysis has indicated that the chromosome within the cell is subdivided into ~50–100 independently supercoiled domains (Figure 1). Evidence comes from experiments in which chemical agents were used to

TABLE I

DNA Topoisomerases of *E. coli*

Enzyme	Gene	Molecular mass (kDa)	Remarks
Topoisomerase I	*topA*	97	Type I enzyme; relaxes negatively supercoiled DNA; cuts one strand of DNA and binds to cut site via a 5′-phospho-tyrosine covalent bond; Mg^{2+} dependent
DNA gyrase (Topoisomerase II)	*gyrA* *gyrB*	105 (GyrA) 95 (GyrB)	Type II enzyme; negatively supercoils relaxed DNA (requires ATP); relaxes positively supercoiled DNA; makes a transient double-stranded cut in DNA and binds via a 5′-phosphotyrosine bond Mg^{2+} dependent
Topoisomerase III	*topB*	73.2	Type I enzyme; can relax negatively supercoiled DNA; decatenase; Mg^{2+} dependent
Topoisomerase IV	*parC* *parE*	75 (ParC) 70 (ParE)	Type II enzyme; with strong sequence homology to gyrase; decatenase; relaxes negative supercoils but cannot create them; requires ATP and Mg^{2+}

nick the DNA. If the chromosome consisted of one continuous domain, a nick anywhere along its length would allow all supercoils to be lost through DNA relaxation. Since 50–100 nicks must be introduced to relax the DNA fully, it has been concluded that subdomains must exist. The possibility that these domains might be supercoiled to different values of σ is an attractive idea since it would allow gene promoters at different locations on the chromosome to experience different degrees of negative superhelicity. This in turn might contribute to differential expression of genes at different locations. However, experiments in which supercoiling-sensitive promoters were placed at different locations in the genome provided no support for this proposal. Therefore, it seems likely that on average each domain of the nucleoid is supercoiled to a similar value of σ.

An important and unresolved issue concerns the nature and locations of the boundaries of the chromosomal domains. Some evidence obtained by promoting long-range interactions in the genome leading to DNA recombination indicates that these boundaries are not fixed in their locations. They may have a transient existence, being dismantled to permit processes such as replication of the DNA to proceed. A favorite hypothesis to explain the nature of the boundaries envisages a role for nucleoid-associated DNA-binding proteins, perhaps acting in combination with topoisomerases (Figure 1).

Nucleoid-Associated Proteins

Bacteria possess DNA-binding proteins that have been described both as "histone-like" and "nucleoid-associated." The former term reflects their function rather than any strong structural similarity to the histones of eukaryotes. The latter name implies that they have a role to play in the organization of the nucleoid. These proteins typically have a low molecular mass, are basic in amino acid composition, and have DNA-binding activity. Depending on the protein, on binding to DNA it can bend or wrap the DNA around itself. DNA wrapping results in the constraining of supercoils. If the DNA is nicked in the absence of the protein, the supercoils are lost; if the protein has wrapped the DNA around itself, the DNA in association with the protein has its supercoils preserved. Measurements of σ for *E. coli* indicate that at any given time ~50% of the DNA in the cell is associated with such proteins while the remainder is in the form of plectonemic supercoils. This is in sharp contrast to the situation in eukaryotes where interaction with histones is the norm. It means that in the bacteria the impact of changes in σ can have more immediate consequences for DNA transactions in these protein-free regions.

The bacteria possess a wide array of histone-like proteins. In *E. coli* the most important include HU, IHF, H-NS, and Fis (Table II). Of these, HU and H-NS are characterized by a lack of a consensus sequence for DNA binding. Instead, they interact with structures in the DNA, such as four-way junctions (HU) or intrinsically curved DNA (H-NS). IHF has a similar amino acid sequence to HU (Fis, HU, and H-NS are structurally distinct) but binds to a clearly defined consensus sequence where it introduces a DNA bend of up to 180°. This gives it a powerful role in local structural organization within the nucleoid, although its action is confined to regions that contain a copy of its binding site. It may also act in conjunction with DNA gyrase to maintain supercoiling at strategically important sites. Fis binds to a rather degenerate consensus sequence and is characterized by having an expression profile that is

TABLE II

Major Nucleoid-Associated Proteins of *E. coli*

Protein	Gene	Molecular mass (kDa)	Remarks
Fis	*fis*	11.2	Fis: factor for inversion stimulation; homodimeric DNA-binding protein; binds to degenerate consensus sequence; bends DNA by between 40° and 90°; organizes local DNA topology; multifunctional and is involved in transcription, DNA replication, recombination, and transposition. Strong growth phase regulation varies protein number/cell over 200–100 000 range
H-NS	*hns*	15.6	H-NS: histone-like nucleoid structuring; oligomeric DNA-binding protein; lacks a consensus sequence for DNA binding but has an affinity for curved DNA; compacts DNA and constrains supercoils; important transcription regulator (usually a repressor); estimated to be 20 000–60 000 H-NS monomers/cell
HU	*hupA* *hupB*	9.5 9.5	HU: heat unstable; abundant heterodimeric DNA-binding protein; 60 000 dimers/cell; lacks a consensus sequence for DNA binding; can constrain DNA supercoils
IHF	*ihfA* *ihfB*	11.2 10.6	IHF: integration host factor; heterodimeric DNA-binding and -bending protein; homologue of HU but binds to well-conserved consensus sequence; bends DNA by up to 180°; between 17 000 and 34 000 monomers/cell

tightly linked to the growth phase of the cell. It is highly abundant in cells exiting lag phase but is present in miniscule amounts in cells in late logarithmic growth. The Fis protein plays a direct role in nucleoid organization by acting as a transcription repressor at the promoters of *gyrA* and *gyrB*, the genes coding for gyrase. It also binds preferentially to DNA with intermediate values of σ and preserves their topology in the face of attempts by topoisomerases to alter σ. Finally, DNA supercoiling controls the supply of Fis at the level of *fis* gene transcription, providing a feedback loop linking expression of this protein to the topological state of the nucleoid. In *E. coli*, the subunit composition of HU and its activities vary with growth phase as the relative amounts of each subunit change in the cell. H-NS is expressed roughly at a constant level throughout growth, but it forms hetero-oligomers with a paralogous protein called StpA at certain periods in the growth cycle and this may alter its properties. IHF also shows a growth-phase-dependent pattern of expression, being most abundant as the cell approaches the stationary phase of growth. This dynamism in the expression of the nucleoid-associated proteins can be expected to have an impact on the structure of the nucleoid as the cell grows and may be reflected in the location and number of domain boundaries and the compactness of the nucleoid.

See Also the Following Articles

Chromosome Organization and Structure, Overview • DNA Supercoiling • DNA Topoisomerases: Type I • DNA Topoisomerases: Type II • Nuclear Organization, Chromatin Structure, and Gene Silencing

Glossary

decatenase An enzyme that unlinks interlinked circular DNA molecules.

par protein A protein involved in DNA partitioning at cell division.

persistence length The average length over which a polymer maintains a straight trajectory when subject to Brownian motion.

Further Reading

Dorman, C. J., and Deighan, P. (2003). Regulation of gene expression by histone-like proteins in bacteria. *Curr. Opin. Genet. Dev.* **13**, 179–184.

Pettijohn, D. E. (1996). The nucleoid. In *Escherichia coli and Salmonella, Cellular and Molecular Biology* (F. C. Neidhardt, R. Curtiss III, J. L. Ingraham, E. C. C. Lin, K. B. Low, B. Magasanik, W. S. Reznikoff, M. Riley, M. Schaechter and H. E. Umbarger, eds.) 2nd edition, Vol 1, pp. 158–166. American Society for Microbiology Press, Washington, DC.

Sinden, R. R. (1994). *DNA Structure and Function.* Academic Press, San Diego.

Trun, N. J., and Marko, J. F. (1998). Architecture of a bacterial chromosome. *ASM News* **64**, 276–283.

Biography

Charles J. Dorman is Professor of Microbiology at the Department of Microbiology, Moyne Institute for Preventive Medicine, University of Dublin, Trinity College. His principal research interest is the regulation of bacterial gene expression by nucleoid-associated proteins and DNA topology. He holds a Ph.D. from the University of Dublin and was a Royal Society Research Fellow in Biochemistry at the University of Dundee. He is editor-in-chief elect of the journal *Microbiology.*

Nucleolus, Overview

Thoru Pederson
University of Massachusetts Medical School, Worcester, Massachusetts, USA

Nucleoli are specialized structures within the nuclei of most eukaryotic cells and are the sites of ribosomal RNA synthesis and the assembly of ribosomes. Nucleoli form around the genes for ribosomal RNA (rRNA), and their structural organization is thought to be a manifestation of ongoing rRNA synthesis and ribosome assembly. The nucleoli are not separated from the rest of the nuclear interior by a membrane, and there is a rapid and diverse traffic of various RNAs and proteins in and out of nucleoli (in addition to the overall export of new ribosomes). There is increasing evidence that nucleoli are involved in functions in addition to ribosome synthesis.

Background

The nucleolus was one of the earliest intracellular structures (and the first within the nucleus) to be observed by microscopy, around 1860. Throughout the early twentieth century, cytologists were struck by the consistent presence of nucleoli inside the nuclei of virtually all cells examined, although the number and shape of nucleoli were quite variable (Figure 1). In the 1930s, it was discovered that the formation of the nucleolus is determined by a distinct genetic locus. This genetic element, termed "the nucleolus organizer," was found in the 1960s to consist of repeated genes for rRNA. It is an interesting historical fact that the rRNA genes were not only the first ones from eukaryotes to be observed at high resolution in the electron microscope, but also they were the first genes to be physically isolated, well before the advent of recombinant DNA techniques.

Although a considerable amount of cytochemical and ultrastructural research had been done on nucleoli up through the 1950s, a major advance occurred when they were first isolated by cell fractionation in the mid-1960s. This opened the door to the investigation of their protein and RNA components, and accelerated the study of rRNA synthesis and processing.

Structure

Although the ultrastructural (electron microscopic) appearance of nucleoli is highly variable, a tripartite organization is generally observed. Fibrillar centers (FCs) are one or more rather small foci within a nucleolus that have a distinctive appearance. Each of these FCs is surrounded (in three dimensions) by a typically much larger zone, called the "dense fibrillar component" (DFC). The remainder of the nucleolus, or at least most of the remainder, displays a distinctly more granular appearance, and is thus called the granular component (GC).

Functional Organization

The tripartite ultrastructural landscape of the nucleolus has been functionally defined (Figure 2). The FCs are the zones where the active rRNA genes themselves are located. The nascent transcripts of pre-rRNA extend out into the juxtaposed DFC, which also contains intermediate RNA species in the rRNA processing pathway. Also present in the DFC are numerous (100–200 or more) small RNA species (and their associated proteins) that serve as guide RNAs for the site-specific modification (2′-*O*-ribose methylation and pseudouridine formation) of many internal nucleotides in pre-rRNA. The GC consists of more mature, assembled ribosomal particles. It is not yet entirely clear whether certain stages of ribosome maturation are sharply restricted to the DFC or the GC or instead have some degree of overlap between them.

Amplified Nucleoli and Missing Nucleoli

One of the most dramatic aspects of the biology of the nucleolus is its selective amplification in the oocytes of certain organisms. In these cells, the rRNA genes are amplified into a large number (typically thousands) of extrachromosomal copies, which form supernumerary nucleoli. Through their activity, the growing oocyte builds up a large reservoir of maternal ribosomes to sustain early embryonic development. Amplified nucleoli are found in the oocytes of several phyletic

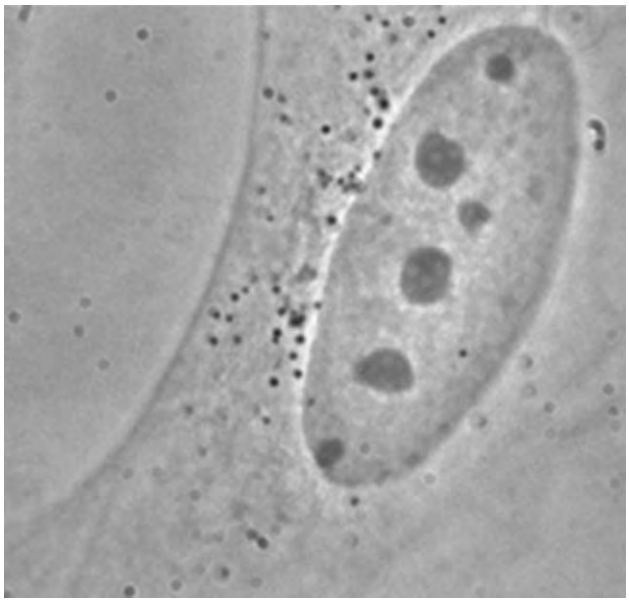

FIGURE 1 Phase contrast micrograph of a portion of a living HeLa (human cervical carcinoma) cell. The dark, spherical objects within the nucleus are the nucleoli. This micrograph was taken by Laura Lewandowski in the author's laboratory. Magnification approx. 3,000x.

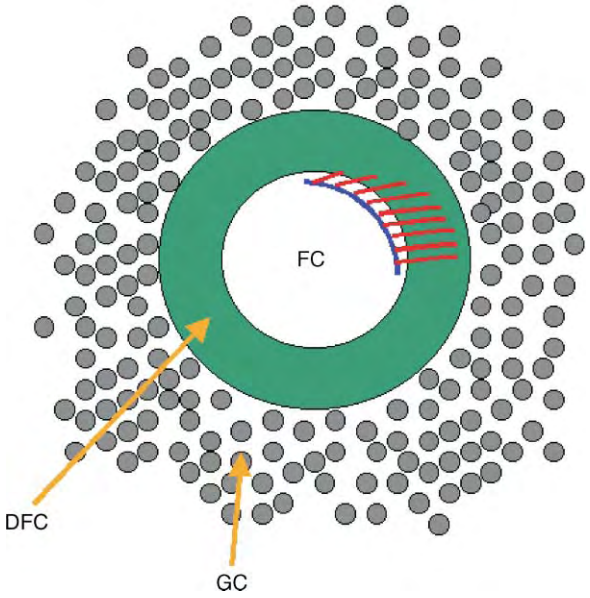

FIGURE 2 A schematic diagram illustrating the relationships of the three major components of the nucleolus. An FC contains the active rRNA genes (blue) with the nascent transcripts of pre-rRNA (red) extending into the surrounding DFC, embedded in the GC. See text for further details. Reproduced with permission from Huang, S. (2002). Building an efficient factory: Where is pre-rRNA synthesized in the nucleolus? *J. Cell Biol.* **157**, 739–741, with copyright permission from the Rockefeller University Press and with the kind consent of the author.

groups, but have been most extensively studied in urodele and anuran Amphibia (salamanders and frogs).

One of the ways the function of the nucleolus in ribosome synthesis was first revealed was by an elegant experiment that involved a frog mutant in which one chromosomal set of rRNA genes is missing. Half the oocytes of females that are heterozygous for this mutation have no rRNA genes whatsoever and, consequently, cannot form amplified nucleoli, nor can anucleolate embryos descended from them synthesize new ribosomes. Accordingly, these embryos die at a time during development when the maternal supply of ribosomes becomes limited. This experiment is one of the classics in the field of eukaryotic gene expression.

Clinical Connections

Two aspects of the nucleolus are significant clinically. For many years pathologists have used nucleolar morphology and number as an important guide in the diagnostic classification of certain malignancies. In addition, a specialized structure called the perinucleolar compartment (PNC) sits as a cap-like disk on the surface of the nucleoli in most malignant cells (both tumor cell lines and actual patient biopsies). The PNC seems to be involved in RNA metabolism, and contains a set of small RNAs that are transcribed by RNA polymerase III. However, its relationship to malignancy is not known.

The Plurifunctional Nucleolus

Since the 1990s a number of clues have begun to suggest that the nucleolus may have functions beyond ribosome synthesis. One line of evidence consists of the observation in nucleoli of various molecules that have no known connection with ribosome biosynthesis. For example, several proteins related to mitogenic cell signaling and cell cycle progression have been found in nucleoli, although these various observations have not yet been drawn together into a coherent framework. In budding yeast, the nucleolus of interphase cells contains a complex that is released and promotes a late stage of mitosis after the nucleolus breaks down, but whether this complex has some role within the interphase nucleolus as well is not known. The RNA subunit of the ribonucleoprotein enzyme telomerase appears to shuttle between the chromosomes and the nucleolus in some cells but, again, the functional meaning of this observation is not clear. The fact that so many of the various ribosome-unrelated molecules and complexes that are increasingly being observed in the nucleolus are related to cell growth is quite intriguing, and this is an important area for future work.

It has also become clear that the life cycle of certain viruses involves the nucleolus in some way. For example, in the replication of the human immunodeficiency virus, certain forms of viral messenger RNAs are associated with the nucleolus during a particular stage in the infectious cycle. However, the functional significance of this and other observations of viral connections with the nucleolus is not presently known.

A third nonribosomal function of the nucleolus is its likely participation in the biosynthesis of the signal recognition particle (SRP). The SRP is an RNA–protein complex that ensures the topologically correct synthesis of membrane and secreted proteins. Both the RNA component of the SRP and some of the SRP's protein components are present in the nucleolus in yeast, amphibian oocytes (i.e., in the amplified nucleoli), and

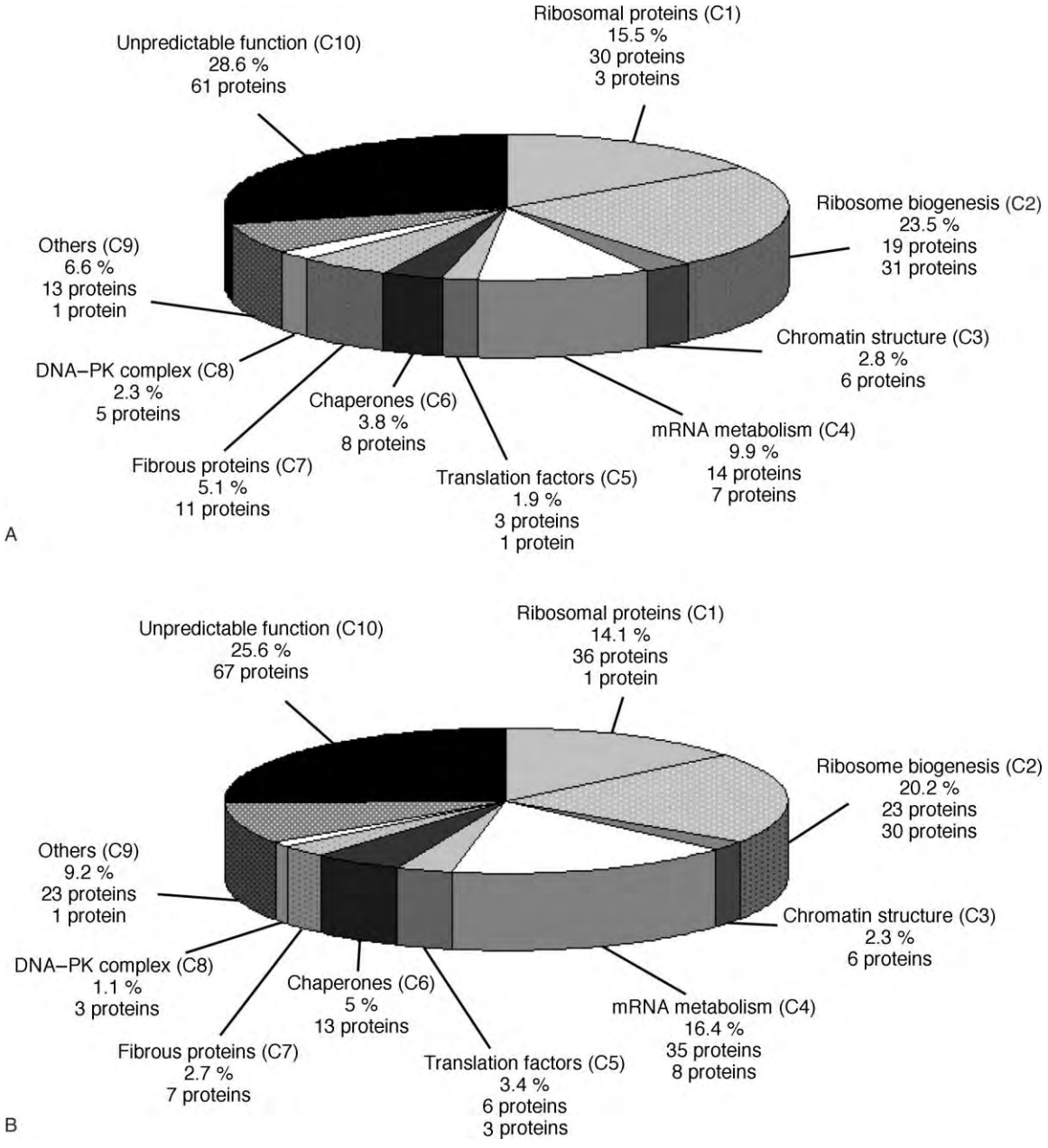

FIGURE 3 Relative occurrence of various classes of proteins in nucleoli purified from HeLa cells, as determined by proteomics. The two panels present the results from two independent studies. Panel A shows the results from Scherl, A., Coute, Y., Deon, C., Calle, K., Kindbeiter, K., Sanchez, J.-D., Greco, A., Hochstrasser, D., and Diaz, J. J. (2002). Functional proteomic analysis of human nucleolus. *Mol. Biol. Cell* **13**, 4100–4109. Panel B shows the results from Andersen, J. S., Lyon, C. E., Fox, A. H., Leung, A. K., Lam, Y. W., Steen, H., Mann, M., and Lamond, A.I. (2002). Directed proteomic analysis of the human nucleolus. *Current Biol.* **12**, 1–12. The figure is reproduced from Scherl, A., Coute, Y., Deon, C., Calle, K., Kindbeiter, K., Sanchez, J.-D., Greco, A., Hochstrasser, D., and Diaz, J.J. (2002). Functional proteomic analysis of human nucleolus. *Mol. Biol. Cell* **13**, 4100–4109, with copyright permission from the American Society for Cell Biology and with the kind consent of the authors. For further details see also Pederson, T. (2002). Proteomics of the nucleolus: more proteins, more functions? *Trends Biochem. Sci.* **27**, 111–112.

mammalian cells, suggesting that this translation-related RNA–protein complex originates in the nucleolus, as do the ribosomes themselves.

Current Trends and Conclusion

At the present time, studies on the nucleolus are being conducted by nucleolar specialists on the one hand, and by an increasing number of cell biologists on the other, who are encountering a nucleolar connection in their work. A nucleolar protein has been implicated in the biology of embryonic stem cells, and a reorganization of the nucleolus in donor somatic cell nuclei appears to be a key factor in the cloning of mammalian animals. Meanwhile, on the analytical front, proteomics studies of purified human nucleoli have identified ~350 proteins that are highly enriched in the isolated fraction (Figure 3). Many of these proteins have no obvious relationship to ribosome biosynthesis. One interesting possibility is that perhaps all of these apparently nonribosome related nucleolar components are indeed related to ribosome biosynthesis after all, not in the constitutive pathway of ribosome synthesis itself (the classical model), but as regulatory components of cellular growth control circuits that intersect in the nucleolus and thus with the biogenesis of the protein synthesis machinery (a neoclassical model).

See Also the Following Articles

Ribosome Assembly • Ribosome Structure • Translation Termination and Ribosome Recycling

Glossary

nucleolus organizer A genetic locus containing genes for ribosomal RNA.

perinucleolar compartment A discoid, cap-like structure situated on the surface of nucleoli in most malignant cells.

proteomics An emergent field of protein sequence determination in complex mixtures, based on a high-resolution analytical method in which the protein components of a subcellular complex or organelle, first separated by electrophoresis or liquid chromatography, is proteolytically cleaved (usually by trpysin) into fragments that are then resolved by matrix-assisted, laser desorption ionization time-of-flight mass spectrometry.

Further Reading

Andersen, J. S., Lyon, C. E., Fox, A. H., Leung, A. K., Lam, Y. W., Steen, H., Mann, M., and Lamond, A. I. (2002). Directed proteomic analysis of the human nucleolus. *Current Biol.* **12**, 1–12.

Brown, D. D., and Gurdon, J. B. (1964). Absence of rRNA synthesis in the anucleolate mutant of *X. laevis*. *Proc. Natl Acad. Sci. USA* **51**, 139–146.

Hernandez-Verdun, D., Roussel, P., and Gebrane-Younes, J. (2002). Emerging concepts of nucleolar assembly. *J. Cell Sci.* **115**, 2265–2270.

Huang, S. (2002). Building an efficient factory: Where is pre-rRNA synthesized in the nucleolus? *J. Cell Biol.* **157**, 739–741.

Olson, M. O., Dundr, M., and Szebeni, A. (2000). The nucleolus: An old factory with unexpected capabilities. *Trends Biochem. Sci.* **10**, 189–196.

Pederson, T. (1998). The plurifunctional nucleolus. *Nucleic Acids Res.* **17**, 3871–3876.

Pederson, T. (2002). Proteomics of the nucleolus: more proteins, more functions? *Trends Biochem. Sci.* **27**, 111–112.

Pederson, T., and Politz, J. C. (2000). The nucleolus and the four ribonucleoproteins of translation. *J. Cell Biol.* **148**, 1091–1095.

Scherl, A., Coute, Y., Deon, C., Calle, K., Kindbeiter, K., Sanchez, J.-D., Greco, A., Hochstrasser, D., and Diaz, J. J. (2002). Functional proteomic analysis of human nucleolus. *Mol. Biol. Cell* **13**, 4100–4109.

Biography

Thoru Pederson is the Vitold Arnett Professor in the Department of Biochemistry and Molecular Pharmacology at the University of Massachusetts Medical School. He received his Ph.D. from Syracuse University and was a Postdoctoral Fellow in Cell Biology at the Albert Einstein College of Medicine. He was at the Worcester Foundation for Biomedical Research throughout his initial career. His research is centered on RNA processing, RNA–protein interactions, and the functional organization of the cell nucleus.

Nucleotide Excision Repair and Human Disease

James E. Cleaver
University of California, San Francisco, California, USA

Nucleotide excision repair, the mechanism of repair of large DNA adducts, has a key role in the development of every organism. This article discusses the types and mechanisms of nucleotide excision repair, and the clinical consequences associated with its deficiencies.

Introduction

DNA repair is an important set of cellular processes that maintain the integrity of the genomes of every organism. Repair genes are found in every sequenced genome, and repair systems are dynamically interrelated to each other and with normal cell metabolism. The mechanism of repair of large DNA adducts especially those produced by ultraviolet (UV) light, known as nucleotide excision repair (NER), plays an important part in the development of the subject. The first connection between repair, specifically NER, and human disease has been found in xeroderma pigmentosum (XP) and details of the disease are in the website – www.xpmutations.org (Table I). XP is predominantly due to a failure of NER in cells that contain UV-induced photoproducts in their DNA (Figure 1). When these photoproducts are unrepaired-replication errors and cytosine deamination leads to characteristic C to T mutations, including especially CC to TT mutations, that are found at very high frequencies in sun-exposed skin and UVB (between 280 and 320 nm wavelength)-induced skin cancers.

Transcribed genes and their transcribed strands are more rapidly repaired than the rest of the DNA in a cell. A specific branch of NER has therefore been named "transcription coupled repair (TCR)" to distinguish it from repair of the remainder of the genome, called "global genome repair (GGR)" (Figure 2). Several components of the basal transcription factor, TFIIH, are also NER enzymes, indicating close integration of the transcription apparatus with repair.

Although in prokaryotes many DNA repair enzymes are inducible in response to damage, in eukaryotes a different strategy appears to predominate. Most of the eukaryotic repair genes are constitutively expressed, except for a small number in human cells that are p53-responsive such as *XPC*, *DDB2*, and *GADD45*. Modification of enzyme activity by phosphorylation, however, represents a major strategy by which eukaryotic cells regulate their response to cellular and DNA damage.

Types of Damage Repaired by NER

The NER system recognizes and repairs DNA damage that consists of UV-induced photoproducts and large DNA adducts. These include the cyclobutane [5–5], [6–6] pyrimidine dimers (CPDs) and the [6–4] pyrimidine pyrimidinone dimers ([6–4]PDs) that can involve T and C pyrimidines (Figure 1). The [6–4]PD can further photoisomerase to the Dewar photoproduct at longer UV wavelengths. Cytosine in dimers has an increased propensity to deaminate causing C to T mutagenesis. Chemical adducts include those produced by N-acetoxy-N-acetyl aminofluorene (AAAF), benzo[a]pyrene, 7,12-dimethyl-1,2-benz[a]anthracene (DMBA) aflatoxin, photoactivated psoralens, and *cis*-platinum. An oxidative purine product, 5′,8-purine cyclodeoxynucleoside, also requires the NER system for repair. The NER system can even recognize DNA triplexes formed by the binding of short oligonucleotides to double-stranded DNA.

Other kinds of damage involving smaller modifications to DNA bases (radiation and oxidative products, alkylations) or DNA breakage require a different suite of enzymes, some of which are involved with immunoglobulin rearrangements and developmental processes. The distinctions between the various repair systems are not absolute, however, and there are overlaps in the substrate specificity of these various repair systems and variations in the efficiencies and sites of action on DNA in differing metabolic states.

TABLE I

The Main Genes and Functions of the NER System

Gene	Chrom location[a]	Protein	Function	Partner(s)	CNS[b]
XPA	9q34.1	273aa	DNA damage binding	RPA	+
XPB	2q21	782aa	3′-5′ helicase	TFIIH	+
XPC	3p25.1	940aa	DNA damage binding	HR23B	−
XPD	19q13.2	760aa	5′-3′ helicase	TFIIH	+
XPE	11p11-12	427aa	DNA damage binding (DDB2)	DBB1(p127)	−
XPF	16p13.3	916aa	Endonuclease 5′ to damage	ERCC1	−
XPG	13q32-33	1186aa	Endonuclease 3′ to damage	Thymine glycosylase (nth)	+
XPV	6p21	713aa	Low fidelity DNA polymerase (pol η)	PCNA	−
CSA	5q11.2	396aa	WD protein, ubiquitination of RNA pol II		+
CSB	10q23	1493aa	DNA dependent ATPase, ubiquitination of RNA pol II		+

[a] For further details on chromosome locations and sequence see www.ensembl.org and for mutations in the genes see www.xpmutations.org.
[b] The presence of central nervous system (CNS) disorders in the majority of the patients in the group is indicated by a " + ," complete absence by a " − ".

Recognition of Damage in Transcriptionally Inactive and Active Regions of the Genome

The initial damage recognition factors uniquely required for GGR are the XPC and XPE DNA binding proteins (Figure 2). XPC is found in association with a cofactor HR23B, one of the two human homologues of the yeast Rad23 gene product. The XPC/HR23B complex is the earliest damage detector to initiate NER in nontranscribed DNA with highest affinity for the [6–4]PD. In XP-C cells that lack this complex, repair is confined to small transcriptionally active islands of the genome, where repair occurs at normal rates, surrounded by oceans of unrepaired transcriptionally silent DNA. The constitutive level of expression of *XPC* is controlled by p53, and the protein can be induced by UV irradiation.

The *XPE* gene product involves a dimeric protein having subunits of 127 kDa (DDB1) and 48 kDa (DDB2) and mutations that are diagnostic for XP-E patients are located in the DDB2 subunit. The XPE protein is mainly involved in repair of mutagenic UV-induced photoproducts.

CPDs are excised more rapidly from actively transcribed genes, especially from the DNA strand used as the template for transcription. The initial damage recognition mechanism for TCR may be the stalled RNA Pol II, itself, although a potentially large number of gene products play a role in mediating the increased rate of repair. Excision can be slow where binding proteins interact with the promoter but increases immediately after the ATG start site for transcription.

Two genes, *CSA* & *CSB*, are involved specifically in TCR. CSA contains WD-repeat motifs that are important for protein–protein interactions. CSB contains an ATPase, helicase motifs, and a nucleotide binding domain, but only the latter is essential for TCR, and CSB does not function as a helicase. Cells lacking either CSA or CSB are unable to ubiquitinate the C-terminal domain of RNA Pol II, that may influence its ability to dissociate or back away from stalling lesions.

The Core Excision Process Common to GGR and TCR

The individual factors of NER associate sequentially and independently on UV photoproducts, *in vivo*, without preassembly of a "repairosome" complex (Figure 2).

Damage Verification

After damage recognition, the initial proteins are replaced by another damage binding complex, XPA and replication protein A (RPA) that acts as a foundation on which many of the other components of the NER process assemble.

DNA Unwinding

The damaged site is unwound by the 3′-5′ (XPB) and 5′-3′ (XPD) helicases of TFIIH and stabilized by the XPA–RPA binding complex.

Excision of the Damaged Strand

An oligonucleotide, 27–29 nucleotides long, containing the photoproduct is excised by enzymatic cleavages, 5 nucleotides on the 3′ side of the photoproduct, and

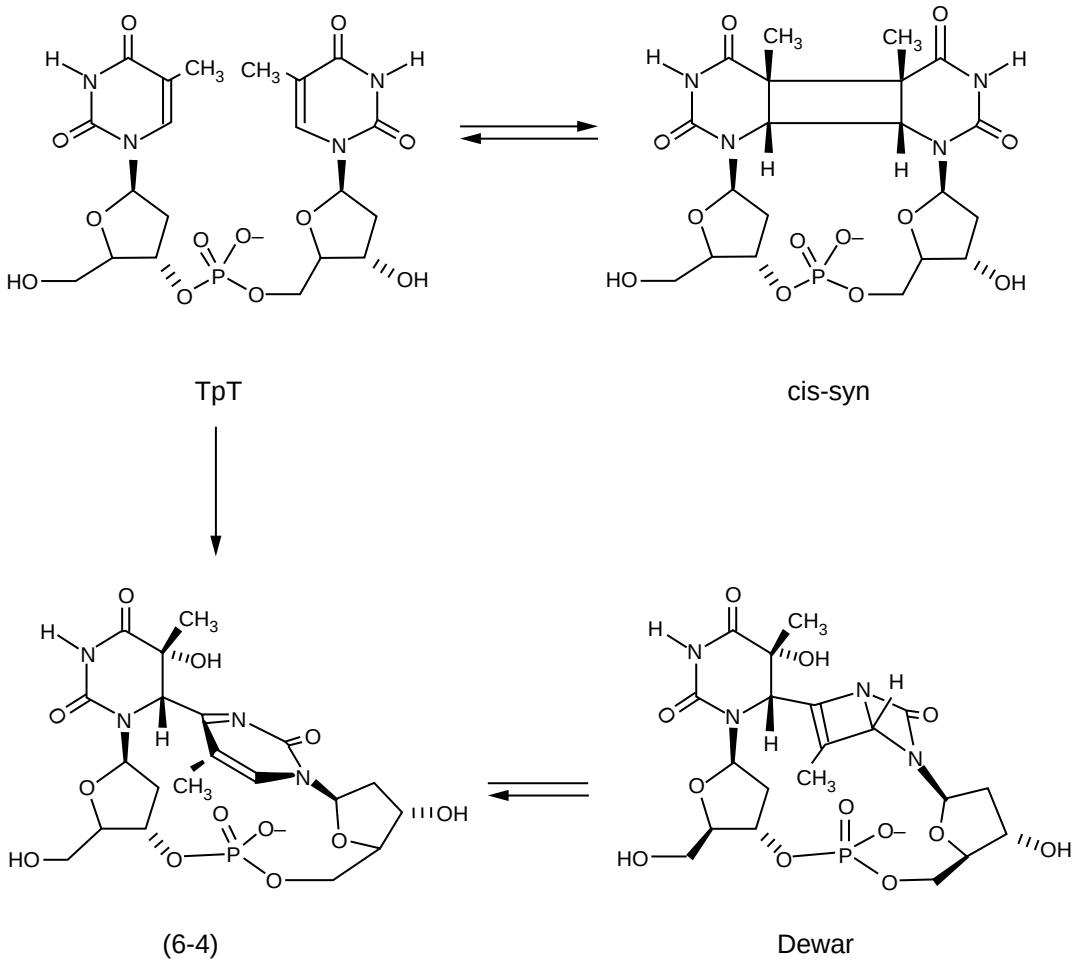

FIGURE 1 Photochemical reactions in a dipyrimidine DNA sequence leading to the formation of a cis-syn CPD (top right) or a [6–4]PD (bottom left) and its photolytic derivative, the Dewar pyrimidine (bottom right). (Reproduced from Cleaver J. E., and Mitchell D. L. (2003). Ultraviolet radiation carcinogenesis. In *Cancer Medicine*, 6th edition, Chap. 20, with permission of B. C. Dekker, London.)

24 nucleotides on the 5′ side. The structure-specific cleavage pattern is determined by binding of RPA to the unwound damaged site, and the excised fragment is close in size to the footprint of RPA on DNA. The XPG nuclease cleaves first on the 3′ side of the damage and interacts with the XPC–HR23B complex and with TFIIH; the XPF–ERCC1 heterodimer then binds to XPA through ERCC1 and cleaves on the 5′ side of the damaged site.

Synthesis of the Repair Patch

The excised region is replaced by the action of a complex similar to that involved in normal DNA replication. Proliferating cell nuclear antigen (PCNA) is loaded onto the DNA by the 5 subunit replication factor C (RFC) complex which then anchors the replicative DNA polymerases, Pol δ or Pol ε. The final closure of the repaired site occurs with DNA ligase I.

Replication of Damaged DNA

NER can remove DNA damage before DNA replication begins, and consequently plays a major role in reducing the amount of damage that becomes fixed as mutations during replication. DNA photoproducts, however, are blocks to the replicative DNA polymerases – alpha, delta and epsilon (Pol α, δ, ε, respectively). Replicative bypass of these photoproducts is achieved instead by damage-specific polymerases with relaxed substrate specificity, now defined as the low-fidelity class Y polymerases. These polymerases have larger active sites that allow them to read-through noninformative sequence information resulting from DNA damage. One adverse consequence of this relaxed specificity is that these polymerases have high error rates of the order of 1% when assayed *in vitro*, and this property must be controlled *in vivo*, otherwise the results would be catastrophic to the cell.

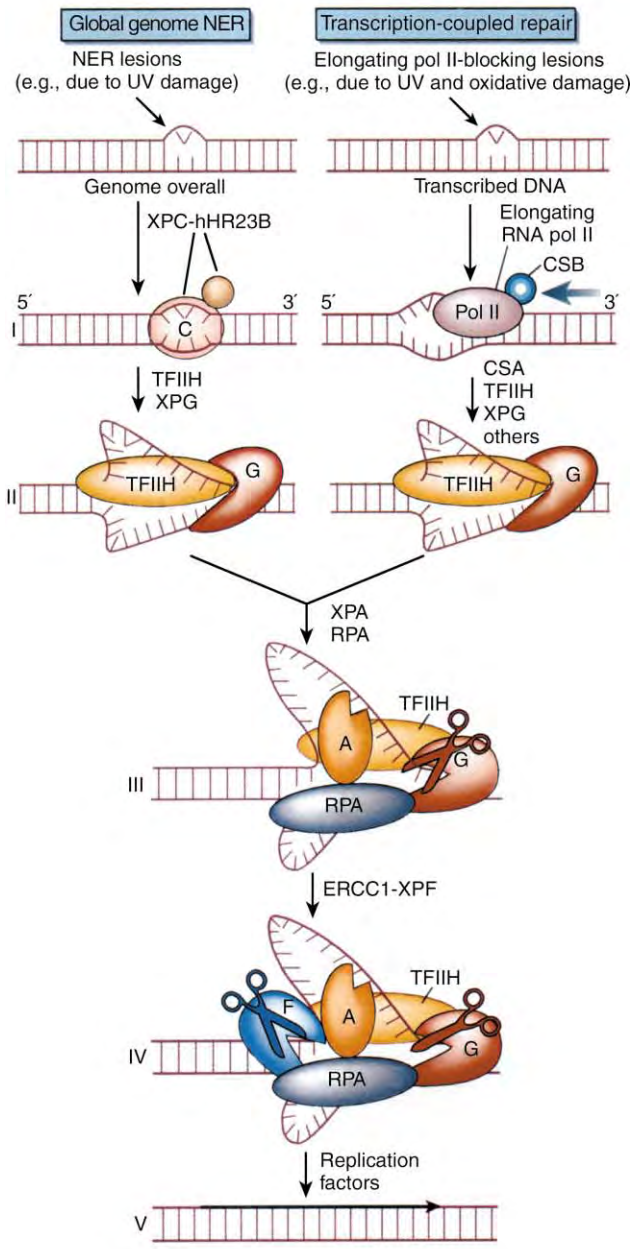

FIGURE 2 The sequence of steps involved in nucleotide excision repair (global genome repair and transcription coupled repair) from damage recognition, verification, unwinding, excision, polymerization and ligation. I, damage recognition; II, DNA unwinding; III, cleavage 3′ to the damaged site; IV, cleavage 5′ to the damaged site; V, repair replication. (Reproduced from Hoeijmakers J.H.J. (2001) Genome maintenance mechanisms for preventing cancer, with permission of Nature.)

Three class Y polymerase genes have been identified in the mammalian genome, *Pol* η, ι, and κ. *Pol* η and ι are close homologues, unique to mammalian cells, and only a single *Pol* η gene is found in yeast. Mutations in *Pol* η result in similar clinical symptoms to those seen in the NER-defective XP patients. Pol η and ι are involved in replication of UV damage but Pol κ replicates other kinds of damage or extends a DNA strand from mis-matched 3′ termini. Pol η preferentially inserts adenines across from thymine-containing photoproducts, resulting in accurate replication of a T-T CPD. Pol ι preferentially inserts guanines across from cytosine-containing photoproducts, resulting in accurate replication of a T–C CPD or [6–4]PD.

Pol η acts distributively to extend nascent DNA chains by one or two bases across from CPDs, and there may be a role for editing by a separate exonuclease. Chain extension then requires the activity of Pol ζ or Pol κ. Pol η is uniformly distributed in the nucleus, and excluded from the replication fork until replication is stalled by UV damage. Pol η then traffics into the nucleus and accumulates with a large number of other proteins in microscopically visible foci at the replication fork. This requires specific sequence motifs in the protein for translocation and for binding to PCNA.

Clinical Consequences of NER Deficiencies – Cancer

Mutations in NER genes are found in XP, and in other cancer, developmental or neurodegenerative diseases such as Cockayne syndrome (CS), trichothiodystrophy (TTD), and Cerebro-Oculo-Facio-Skeletal (COFS) syndrome. These represent only about 10 of the possible 30 genes involved in NER. The other genes are probably essential and mutations are likely to be inconsistent with viability, as has been demonstrated for *ERCC1* and *HR23B*.

XP manifests as a multigenic, multiallelic autosomal-recessive disease but heterozygotes are unaffected. The frequency in the United States is about 1:250 000, but higher in Japan and the Mediterranean, and possibly Central American areas. The disease begins in early life with the first exposures to sunlight, the median age of onset being 1–2 years of age, with skin rapidly exhibiting the signs associated with years of sun exposure. Pigmentation is patchy, and skin shows atrophy and telangiectasia with progressive degeneration of sun-exposed regions of the skin and eyes, usually leading to various forms of cutaneous malignancy (melanoma and nonmelanoma). Cancer incidence for those individuals under 20 years of age is 2000 times that seen in the general population. There may be a reduction in life span associated with the progression of cancer or neurologic degeneration, but a specific effect on aging itself has not been observed. In areas with poor health care, malignant disease may compound other life-threatening conditions (malnutrition, infections etc), but stringent protection from sun-exposure can minimize the development of symptoms dramatically.

The nonmelanoma skin cancers that develop in XP patients contain mutations in the *p53* gene (squamous carcinomas) or *patched* (basal cell carcinoma) that are mainly C to T transitions at dipyrimidine sequences, characteristic of the UV photoproducts that are the substrates for NER (Figure 1). Melanomas are also found at higher frequency in XP patients with a similar body distribution to those in non-XP patients, but UV-specific mutations in relevant genes (*p16*, *BRAF*) have not yet been found.

Clinical Consequences of NER Deficiencies – Neurodegeneration

Progressive neurologic degeneration occurs in a significant number of patients, with NER deficiencies (Table I). Most of these patients have mutations in subset of XP and CS genes, especially those associated with TCR. These include *XPA*, *XPB*, *XPD*, and *XPG*, and the *CSA* and *CSB* genes. Several of these also regulate repair of oxidative damage in transcriptionally active genes. Whether the neurodegeneration and other developmental disorders are due to defects in transcription of critical genes, or defects in repair of oxidative damage in these genes is therefore debatable. Both possibilities may have an element of truth.

In Japan a large fraction of the *XPA* mutations occur at the same splice site, and patients present a fairly uniform neurological disorder involving loss of walking ability and sensoneural deafness.

Patients with one of their *XPA* mutations in exon VI outside the DNA binding region of the gene have much less neurodegeneration. Tunisian patients have a common mutation in this region and have relatively mild symptoms despite their sun exposure. Some neurological dysfunction may, however, appear late in life.

XPD is a particularly complex gene in which mutations can give rise to various diseases and mixed symptoms that correspond to either XP, XP/CS syndrome, XP/TTD, or COFS. Many of these mutations occur in the DNA or RNA helicase "box" regions of the gene or in the 3′ terminal region. Inactivating mutation are lethal, hence all patients so far studied have at least one missense mutation resulting in a change of function, and occasional haplo-insufficiency. Similar XP/CS symptoms are seen in the small number of patients reported with mutations in *XPB*.

TTD is a rare autosomal-recessive disorder characterized by sulfur-deficient brittle hair and ichthyosis. Hair shafts split longitudinally into small fibers, and this brittleness is associated with levels of cysteine/cystine in hair proteins that are 15–50% of those in normal individuals. The hair has characteristic "tiger-tail" banding visible under polarized light. The patients often have an unusual facial appearance, with protruding ears and a receding chin. Mental abilities range from low normal to severe retardation. Several categories of the disease can be recognized on the basis of cellular responses to UV damage and the affected gene. Severe cases have low NER and mutations in *XPB* or *D* as described above. A third category involves another unidentified gene called *TTDA* and lacks major UV sensitivity, but has an unstable TFIIH.

COFS is a particularly severe developmental and neurological expression of mutations in *XPD*, *XPG*, and *CSB*. The disease leads to brain microcephaly and atrophy with calcifications, cataracts, microcornea, optic atrophy, progressive joint contractures, and growth failure.

The XPG nuclease has a particularly complex range of activities, and mutations in *XPG* are often associated with both XP and CS diseases. One patient with a mutation that permits a significant level of repair has been reported who is much milder and has no neurological dysfunction. XPG is an endonuclease in the FEN-1 family that is capable of strand-specific cleavage of a range of DNA substrates that may arise during DNA replication, repair, and recombination. The XPG gene product also interacts with RNA Pol II and facilitates efficient transcription elongation, thereby providing an explanation for the complex symptoms of some XPG patients that show both XP and CS symptoms. XPG is also a cofactor required for the activity of thymine glycosylase (*nth* gene) and is thereby linked to repair of oxidative damage that may also be important in maintaining neural functions that fail in CS.

CS is an autosomal-recessive disease characterized by cachectic dwarfism, retinopathy, microcephaly, deafness, neural defects, and retardation of growth and development after birth. They have a typical facial appearance with sunken eyes and a beaked nose and projecting jaw. CS patients are sensitive to the sun but do not develop cancers, setting this disease apart from XP. Patients who only have CS have mutations in one of two genes, *CSA* and *CSB*, the former being the more common. Cells from CS patients are only defective in TCR. The excision of DNA photoproducts from total genomic DNA of CS cells is normal, but repair of transcriptionally active genes is reduced. Clinically, however, the disease has been classified into type I, II, and others, but no detailed correlation has been made between these classifications and the mutations in *CSA* and *CSB*.

Mouse Models of NER Deficiencies

A series of mouse strains have been developed in which the *XP* or *CS* genes have been knocked out (http://webpath.swmed.edu/mutation/). The knockouts,

in general, exhibit increased cancer rates from treatment with UVB or chemical carcinogens, as expected from their human counterparts.

Xpa and Xpc knockouts, for example, are very sensitive to skin cancer induction. Strikingly, though, mouse knockouts have tended to exaggerate the cancer risks and minimize the neurodegeneration as compared to the corresponding human patients. $Xpa^{-/-}$, $Csa^{-/-}$, $Csb^{-/-}$ mice, for example, show increased skin carcinogenesis from UV light or chemical carcinogens, but have negligible neurodegeneration, whereas the corresponding patients are often severely affected neurologically. Mice that are $Xpa^{-/-}$ or $Csb^{-/-}$ are very sensitive to toxic effects of DMBA, but $Xpc^{-/-}$ survive much better, even though they show increased mutation rates. The severity of the neurological phenotype is greatly enhanced in crosses between Xpa and Csb knockouts, and the double homozygote shows early postnatal ataxia and abnormal cerebellar development.

Homozygous knockouts of the *Xpb* and *Xpd* genes are lethal very early in embryonic cell division because these genes are part of the essential transcription factor TFIIH. Mice with a human TTD mis-sense mutation in the *Xpd* gene are viable and have many of the same symptoms as TTD patients. These TTD mice show increased UVB-induced skin cancer and age prematurely, although TTD patients do not exhibit a corresponding increase in cancer.

Mice lacking Xpg are very severely affected, and exhibit postnatal growth failure and neurological dysfunction especially loss of purkinje cells and early death. Although both Xpg and Xpa mice lack repair completely, Xpa knockouts have a near normal lifespan suggesting important differences in Xpa and Xpg during development.

These studies indicate important differences between the clinical presentation of human patients and corresponding mouse models. One obvious cause is that patients have a variety of mis-sense, chain-terminating, splice site, and deletion mutations, which would not necessarily lead to the same phenotypes as complete knockouts. Another cause may be the difference in NER between human and rodents in the function of the XPE heterodimer. A consensus DNA-binding site for p53 is present in the promoter region of human p48 (DDB2) but the sequence has diverged in the mouse homologue, and is methylated in the hamster. UV-induced expression of DDB2 consequently occurs through p53 transactivation in human, but not mouse or hamster cells. The inactivation of the p53 response element provides a partial explanation for early observations that excision repair was low in some mouse strains and hamster cell strains. Therefore re-expression of DDB2 in mice might confer a phenotype that more closely resembles the human disorders.

Differentiation and Tissue-Specific Expression of DNA Repair Genes

As cells differentiate to a nondividing state their capacity for NER of UV damage declines. The major loss is in the capacity for repair of transcriptionally inactive genes or regions of the genome. Specific down-regulation of repair has been described in the testis due to reduced expression of XPA, rendering testicular tumors more sensitive to cis-platin chemotherapy. In the basal layer of the skin, a small fraction of cells seem to be specifically defective in repair of UV and carcinogen damage and retain photoproducts for long times after irradiation. This represents down-regulation of repair in a few cells distributed among a large population of repair-competent cells.

Polymorphisms in DNA Repair Genes

Polymorphisms that are not directly associated with the XP disease phenotype have been described for many of the NER and other repair genes. Polymorphisms have been found in the *XPA*, *XPC*, and *D* genes. Many of these polymorphisms result in nonconservative amino acid changes that could have an impact on NER function and disease. A large number of alleles present at low frequency individually could combine to create variation in disease frequency in the overall population.

See Also the Following Articles

DNA Helicases: Dimeric Enzyme Action • DNA Helicases: Hexameric Enzyme Action • Nucleotide Excision Repair in Eukaryotes • Nucleotide Excision Repair, Bacterial: The UvrABCD System • Nucleotide Excision Repair: Biology • Transcription-Coupled DNA Repair, Overview • Ubiquitin System • Ubiquitin-Like Proteins

Glossary

DNA damage Any chemical or radiation damage to the bases, deoxyribose and phosphodiester bonds in DNA that interferes with its normal functions.

helicase An enzyme that can unwind double-stranded RNA or DNA in a strand-specific direction.

nucleotide excision repair The process of recognition, removal and resynthesis of a damaged region of DNA.

polymerase An enzyme that copies DNA into RNA (RNA polymerase) or duplicates DNA (DNA polymerase).

polymorphisms Different nucleotides in one position of a gene that give rise to changes in sequence without major alterations in function.

ubiquitin A short peptide that is enzymatically attached to a protein by a set of conjugating enzymes to modify its function or mark it for degradation.

ultraviolet light The wavelengths of solar and artificial light between 240 and 280 nm (UVC), and 280 and 320 nm (UVB) that are strongly absorbed in nucleic acids.

xeroderma pigmentosum A human disease in which hereditary mutations in nucleotide excision repair result in a very high incidence of sunlight-induced skin cancers.

Further Reading

Batty, D. P., and Wood, R. W. (2000). Damage recognition in nucleotide excision repair of DNA. *Gene* **241**, 193–204.

Berg, R. J., Rebel, H., van der Horst, G. T., van Kranen, H. J., Mullenders, L. H., van Vloten, W. A., and de Gruijl, F. R. (2000). Impact of global genome repair versus transcription-coupled repair on ultraviolet carcinogenesis in hairless mice. *Cancer Res.* **60**, 2858–2863.

Bohr, V. A. (1991). Gene specific DNA repair. *Carcinogen.* **12**, 1983–1992.

Bootsma, D., Kraemer, K. H., Cleaver, J. E., and Hoeijmakers, J. H. J. (1998). Nucleotide excision repair syndromes: Xeroderma pigmentosum, Cockayne syndrome, and trichothiodystrophy. In *The Genetic Basis of Human Cancer* (B. Vogelstein and K. W. Kinzler, eds.) pp. 245–274. McGraw-Hill, New York.

Cleaver, J. E., and Mitchell, D. L. (2003). Ultraviolet radiation carcinogenesis. In *Cancer Medicine*, 6th edition, Chap. 20. B. C. Dekker, London.

Cleaver, J. E. (1968). Defective repair replication in xeroderma pigmentosum. *Nature* **218**, 652–656.

Cleaver, J. E., and Mitchell, D. L. (1997). Ultraviolet radiation carcinogenesis. In *Cancer Medicine* (J. F. Holland, R. C., Jr., Bast, D. L. Morton, E. Frei, III, D. W. Kufe and R. R. Weichselbaum, eds.) Vol 1, pp. 307–318. Williams and Wilkins, Baltimore.

Friedberg, E. C., Walker, G., and Siede, W. (1995). *DNA Repair and Mutagenesis*. ASM Press, Washington, DC.

Kraemer, K. H., Lee, M. M., and Scotto, J. (1987). Xeroderma pigmentosum: Cutaneous, ocular and neurological abnormalities in 830 published cases. *Archiv. Dermatol.* **123**, 241–250.

Sancar, A. (1994). Mechanisms of DNA excision repair. *Science* **266**, 1954–1956.

Schaeffer, L., Roy, R., Humbert, S., Moncollin, U., Vermeulen, W., Hoeijmakers, J. H. J., Chambon, P., and Egly, J. M. (1993). DNA repair helicase: A component of BTF2 (TFIIH) basic transcription factor. *Science* **260**, 58–63.

Trincao, J., Johnson, R. E., Escalante, C. R., Prakash, S., Prakash, L., and Aggarwal, A. K. (2001). Structure of the catalytic core of *S. cerevisiae* DNA polymerase η: Implications for translesion synthesis. *Molecul. Cell* **8**, 417–426.

Wood, R. D., Mitchell, M., Sgouros, J., Lindahl, T. (2001). Human D.N.A. repair genes. *Science* **291**, 1284–1289.

Biography

James E. Cleaver is a Professor of dermatology and pharmaceutical chemistry, former Associate Director in the Laboratory of Radiobiology and Environmental Health, and presently Head of the Cutaneous Oncology Program of the UCSF Cancer Center, University of California, San Francisco. His principal research interest is in the field of DNA repair, and he is best known for discovering the repair defect in the human disease xeroderma pigmentosum that linked repair to human cancer. He holds a B.A. and Ph.D. from the University of Cambridge, UK. He has authored over 350 publications and was elected to the National Academy of Sciences in 1999.

Nucleotide Excision Repair in Eukaryotes

Laura A. Lindsey-Boltz and Aziz Sancar
University of North Carolina School of Medicine, Chapel Hill, North Carolina, USA

Eukaryotes possess several repair mechanisms to provide defense against a large variety of DNA alterations. One of these mechanisms, nucleotide excision repair, is responsible for repairing bulky DNA lesions, which if left unrepaired, can result in oncogenesis, developmental abnormalities, and cellular lethality. Humans with hereditary defects in nucleotide excision repair suffer from diseases including xeroderma pigmentosum, Cockayne syndrome, and trichothiodystrophy, with symptoms including elevated sun sensitivity and skin cancers, neurological degeneration, and developmental delays.

Substrates

Two major carcinogens produce the bulky, DNA helix-distorting lesions which are repaired by the nucleotide excision repair system. UV light produces cyclobutane pyrimidine dimers and (6-4) photoproducts, and cigarette smoke produces benzo[a]pyrene-guanine adducts. However, the nucleotide excision repair system is not limited to the repair of bulky DNA lesions. It removes virtually all base lesions tested, including thymine glycols and 8-oxoguanine which are not bulky. Because of the wide substrate range, it is unlikely that the nucleotide excision repair system recognizes the specific chemical groups that make up the lesion, but rather recognizes the changes in the conformation of the phosphodiester backbone created by the damage.

Nucleotide Excision Repair Factors

In eukaryotes, nucleotide excision repair is carried out by six repair factors containing eighteen polypeptides (Table I). The six human nucleotide excision repair factors are RPA, XPA, XPC, TFIIH, XPG, and XPF-ERCC1. With the exception of XPA and XPG, each repair factor consists of 2–9 polypeptides that are in tight complexes, and these complexes are considered to be the subunits of the nucleotide excision repair enzyme (excision nuclease). All eukaryotic organisms whose genomes have been sequenced to date have homologues of the six nucleotide excision repair factors. However, only in the case of human and the budding yeast, *S. cerevisiae*, the excision nuclease has been reconstituted with the purified factors.

The nucleotide excision repair factors were primarily identified by genetic studies in cell lines derived from humans with xeroderma pigmentosum (XP) and UV-sensitive rodent cell lines. Thus, the repair genes have been named *XPA*, *XPB*, etc. or excision repair cross complementary group 1 (*ERCC1*), etc., depending on whether they were cloned by complementing human XP mutants or repair-defective rodent cell lines. In addition to the seven XP proteins, two multifunctional, multi-subunit factors, RPA and TFIIH, have been shown to be required for nucleotide excision repair. Replication protein A(RPA) is a complex of three proteins, and was originally identified and named for its role in replication. TFIIH, a complex of nine proteins, was originally identified as one of the six general transcription factors required for optimal transcription by RNA polymerase II. TFIIH consists of a core complex of proteins containing XPB, XPD, p62, p52, p44, and p34; and the cdk-activating kinase (CAK) subcomplex, consisting of cdk7, cyclinH, and Mat1 (Table I). Only the TFIIH core complex is required for nucleotide excision repair *in vitro*.

Mechanism of Nucleotide Excision Repair

The three basic steps of nucleotide excision repair in eukaryotes are: (1) dual incisions bracketing the lesion in a 24–32 nt-long oligomer; (2) repair synthesis to fill in the resulting gap; and (3) ligation of the newly synthesized DNA (patch) to the old DNA (Figure 1). Of these three steps, the last two are carried out by replication and recombination enzymes, and thus the dual incision (excision) step might be considered the repair reaction proper. Assays for detecting DNA–protein complexes (gel mobility shift and DNAaseI and

TABLE I

The Six Human Nucleotide Excision Repair Factors Consisting of Eighteen Proteins

Factor	Proteins (yeast homolog)	Activity	Role in repair
XPA	XPA/p31 (Rad14)	DNA binding	Damage recognition
RPA	p70	DNA binding	Damage recognition
	p34		
	p11		
XPC	XPC/p125 (Rad4)	DNA binding	• Damage recognition
	HHR23B/p58 (Rad23)		• Stabilization of preincision complex and protection from degradation
TFIIH	XPB/ERCC3/p89 (Rad25)	• DNA-dependent ATPase	• Formation of preincision complex
	XPD/ERCC2/p80 (Rad3)	• Helicase	• Transcription-repair coupling
	p62 (Tfb1)	• General transcription factor	
	p52 (Tfb2)	• Cdk-activating kinase activity	
	p44 (Ssl1)		
	p34 (Tfb4)		
	Cdk7/p41 (Kin28) } CAK sub-complex		
	CyclinH/p38(Ccl1) } CAK sub-complex		
	Mat1/p32 (Tfb3) } CAK sub-complex		
XPF	XPF/ERCC4/p112 (Rad1) ERCC1/p33 (Rad10)	Nuclease	5′ incision
XPG	XPG/ERCC5/p135 (Rad2)	Nuclease	3′ incision

permanganate footprinting) have led to the identification of three high-specificity and high-stability intermediates along the assembly pathway of the excision nuclease. These three intermediates are called preincision complexes (PIC) 1, 2, and 3 and are described in detail below.

Preincision Complex 1

PIC1 consists of DNA, RPA, XPA, XPC, and TFIIH. ATP is required for the formation of this complex. It is hydrolyzed by two helicases in TFIIH, XPB and XPD, which have 3′ to 5′ and 5′ to 3′ helicase activities, respectively. These helicases unwind the DNA by about 20 bp around the lesion in an asymmetric manner with about 15 bp unwound on the 5′ side and 5 bp unwound on the 3′ side of the damage. The overall direction of unwinding with respect to the damaged strand was determined to be 5′ to 3′ based on data with substrates containing an interstrand cross-link.

Preincision Complex 2

XPG enters to form the second complex, which is much more stable than PIC1. As in the case of PIC1, the formation of PIC2 is also dependent on ATP hydrolysis by the XPB and XPD subunits of TFIIH. Interestingly, when the composition of PIC2 was analyzed by gel mobility shift assays it seemed to lack XPC. It appears that XPC leaves the complex after helping to recognize the damage and unwind the duplex, which then enables XPG to enter. The replacement of XPC in PIC1 by XPG in PIC2 is consistent with the findings that TFIIH makes relatively tight complexes with XPC and XPG. Apparently, the binding surfaces of these two factors on TFIIH overlap and therefore the entry of one into the complex is concomitant with the exit of the other. Thus, the composition of PIC2 is RPA XPA XPG TFIIH-DNA.

Preincision Complex 3

Finally, with the entry of XPF ERCC1 into PIC2, the PIC3 forms the complex composed of RPA XPA XPG TFIIH XPF ERCC1-DNA. Within this complex the 3′ incision is made by XPG and the 5′ incision is made by XPF-ERCC1. Following the dual incisions, the excised 24–32 nt-long oligomer carrying the damage is released, and the excision nuclease is dissociated. Replication Factor C (RFC) loads the PCNA trimeric circle onto the DNA, and PCNA recruits DNA Pol δ or Pol ε to fill in the gap in the DNA. Repair is completed by ligation by DNA ligase I.

Damage Recognition and Transcription-Coupled Repair

Recognition of the DNA damage is most likely the rate-limiting step in nucleotide excision repair. The DNA

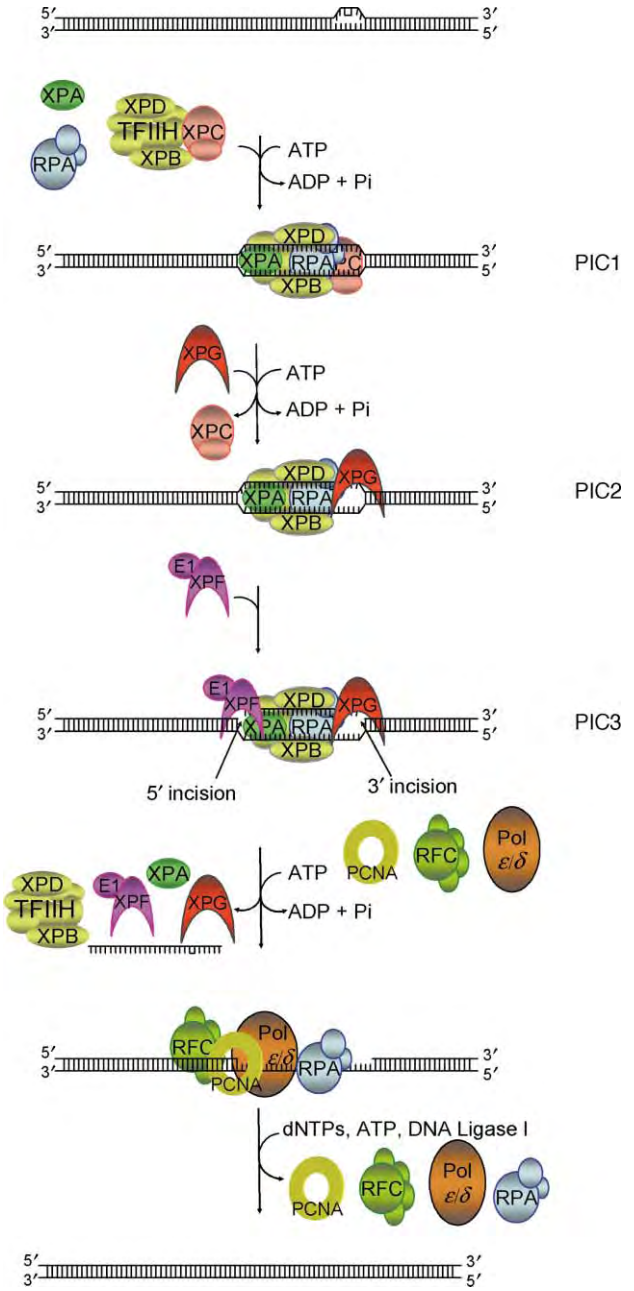

FIGURE 1 Model for nucleotide excision repair in humans. The DNA lesion is bound by RPA, XPA, and TFIIH XPC to form preincision complex (PIC) 1. ATP is hydrolyzed by the XPB and XPD helicase subunits of TFIIH to locally unwind the DNA. XPG enters and XPC exits in the next step which requires ATP hydrolysis by XPB and XPD to form PIC2. After XPF enters to form PIC3, the two endonucleases make incisions in the strand containing the lesion; the 3′ incision is made by XPG and the 5′ incision is made by XPF-ERCC1. Repair synthesis then fills in the single-stranded gap.

lesions must be located among the 3 billion base pairs present in the human genome. The damage recognition factors of the human excision nuclease are RPA, XPA, and XPC. All three proteins are DNA-binding proteins with some preference for damaged DNA, and all three apparently play a role in low-discriminatory damage recognition independent of ATP. However, the precise order of assembly has been difficult to establish with kinetic experiments, resulting in conflicting studies wherein one study concluded that RPA and XPA are the repair factors which make the initial contact, and another study found that XPC makes the initial contact. Nucleotide excision repair appears to operate somewhat differently on DNA that is transcriptionally active (transcription-coupled repair) from that which is transcriptionally silent (global genome repair). Transcribed DNA is repaired at a faster rate than nontranscribed DNA, and this is most likely due to recognition of the RNA polymerase stalled at the damage. In addition to the nucleotide excision repair factors, transcription-coupled repair depends on the CSA and CSB gene products in humans. *In vivo* data indicate that in humans, but not in yeast, XPC is dispensable for transcription-coupled repair. It is thought that the transcription bubble 3′ to the lesion which impedes the progression of RNA polymerase creates a unique damaged DNA structure which can be recognized in the absence of XPC. Indeed, when a cyclobutane thymine dimer is placed adjacent to a 10 nt bubble in a synthetic substrate, it is recognized and excised efficiently in the absence of XPC. Transcription-coupled repair has not been reconstituted *in vitro*, and therefore the mechanism in eukaryotes is currently not known.

See Also the Following Articles

DNA Helicases: Dimeric Enzyme Action • DNA Helicases: Hexameric Enzyme Action • Nucleotide Excision Repair and Human Disease • Nucleotide Excision Repair: Biology

Glossary

Cockayne's syndrome (CS) Human disease caused by defects in proteins involved in coupling transcription to nucleotide excision repair; symptoms include mental retardation, dwarfism, neurological defects, and moderate sensitivity to UV light.

endonuclease Protein that cleaves bonds within a nucleic acid chain, e.g., XPF and XPG.

excision nuclease Enzyme that removes damaged bases by dual incisions bracketing the lesion in the damaged strand.

helicase Protein that uses the energy of ATP hydrolysis to unwind a nucleic acid duplex, e.g., XPB and XPD.

trichothiodystrophy (TTD) Human disease caused by mutations in XPB and XPD which results in defects in both transcription and nucleotide excision repair; symptoms include brittle hair and nails, mental retardation and skeletal abnormalities.

xeroderma pigmentosum (XP) Human disease caused by reduced level of nucleotide excision repair; symptoms include mental retardation, ataxia, deafness, and predisposition to skin cancer caused by sunlight exposure.

Further Reading

Bessho, T., and Sancar, A. (1998). Nucleotide excision repair in man. In *Nucleic Acids and Molecular Biology*, (F. Eckstein and D. M. J. Lilley, eds.) Vol 12, pp. 141–155. Springer, Berlin, Heidelberg.

Cleaver, J. E., and Kraemer, K. H. (1989). Xeroderma pigmentosum and cockayne syndrome. In *The Metabolic and Molecular Bases of Inherited Disease* (C. R. Scriver, A. L. Beaudet, W. S. Sly and D. Valle, eds.) 7th edition, pp. 4393–4419. McGraw-Hill, New York.

Hanawalt, P. C. (1994). Transcription-coupled repair and human disease. *Science* **266**, 1457–1458.

Sancar, A. (1995). Excision repair in mammalian cells. *J. Biol. Chem.* **270**, 15915–15918.

Sancar, A. (1996). DNA excision repair. *Annu. Rev. Biochem.* **65**, 43–81.

Wood, R. D. (1996). DNA repair in eukaryotes. Annu. *Rev. Biochem.* **65**, 135–167.

Biography

Laura Lindsey-Boltz is a Postdoctoral Fellow in Dr. Aziz Sancar's laboratory, and she holds a Ph.D. from Duke University.

Aziz Sancar is a Kenan Professor in the Department of Biochemistry and Biophysics at the University of North Carolina, Chapel Hill. His principal research interests are in the fields of DNA repair, DNA damage checkpoints, and circadian photoreceptors. He holds an M.D. from Istanbul University School of Medicine and a Ph.D. from the University of Texas at Dallas.

Nucleotide Excision Repair, Bacterial: The UvrABCD System

Bennett Van Houten
National Institute of Environmental Health Sciences, Research Triangle Park, North Carolina, USA

Lawrence Grossman
The Johns Hopkins University, Baltimore, Maryland, USA

DNA repair is intrinsic to the evolution of life, and organisms have evolved a large number of complex systems to ensure the integrity of their heredity material. DNA constantly undergoes chemical modification as a result of its intrinsic chemical instability, as well as, endogenous and environmental stresses. The most versatile DNA repair mechanism is nucleotide excision repair (NER), first discovered in *Escherichia coli* in 1964 independently by Setlow and Carrier and Boyce and Howard-Flanders. This bacterial system, like its eukaryotic counterpart, has a very broad spectrum of damage recognition and operates according to the same basic principles in all organisms: (1) repair proteins form macromolecular assemblies in order to locate and activate damage utilizing a number of ATP-hydrolysis-driven nucleoprotein rearrangements; (2) the DNA is incised on both sides of damage; and (3) the incised fragment is displaced with concomitant resynthesis followed by ligation. NER is coupled to other cellular processes, notably, transcription. The sequencing of the complete genomes of over 20 different bacterial species indicates that the NER system is a highly conserved process.

UvrABC Endonuclease

The nucleotide excision repair (NER) pathway consists of five basic steps: damage recognition, incision, excision, repair synthesis, and ligation. In most bacteria the first steps of this process are carried out by an ensemble of three proteins encoded by the *uvrA*, *uvrB*, and *uvrC* genes in an ATP-dependent series of reactions. During the initial characterization of these proteins, the name of this system was shortened to "UvrABC endonuclease" which makes both the 5′ and 3′ incisions to a lesion in a "dual incision" reaction (Figure 1). The UvrABC endonuclease possesses a broad spectrum of substrate specificity and is capable of acting on a wide variety of unrelated DNA damage (Table I).

Genetics and Evolutionary Conservation of *uvr* Genes

It was photobiologists who discovered NER from analyses of ultraviolet radiation (UV) survival curves in some bacterial, most notably *E. coli*. Rather than observing a first-order decline in survival of cells as a function of UV dose there was a shoulder in the survival curves at lower doses. Some *E. coli* mutants, which lacked this shoulder, were sensitive to low doses of UV, and were isolated. All these mutants map at one of three loci on the *E. coli* chromosome designated *uvrA* (92 min), *uvrB* (17 min), and *uvrC* (41.5 min), and are hence, unlinked genes. In species of *Bacillus*, the *uvrA* and *uvrB* genes are within 50 bp of each other on the chromosome.

The *uvr* genes were first cloned, sequenced, and amplified from *E. coli*, which led to a greater understanding of the roles of three proteins in the process of damage recognition and incision. Subsequently, large-scale sequencing efforts have revealed that *uvr* genes are highly conserved among the bacterial species

uvrA

uvrA is one of a series of genes collectively referred to as SOS genes, which are induced to increased levels of transcription by agents that cause DNA damage. A specific binding site for the LexA repressor protein specific for the operator promoter region of the *uvrA* gene (the so-called LexA box or SOS box) has been identified. Sequence analyses reveal that the *uvrA* gene (2.82 kbp) translates into 940 amino acids (Mr = 103,874 Da) and contains two ATP-binding motifs, two zinc-finger motifs and a helix-turn-helix motif.

uvrB

The *uvrB* gene is also a member of the SOS regulon and is inducible by DNA damage. The gene is transcribed

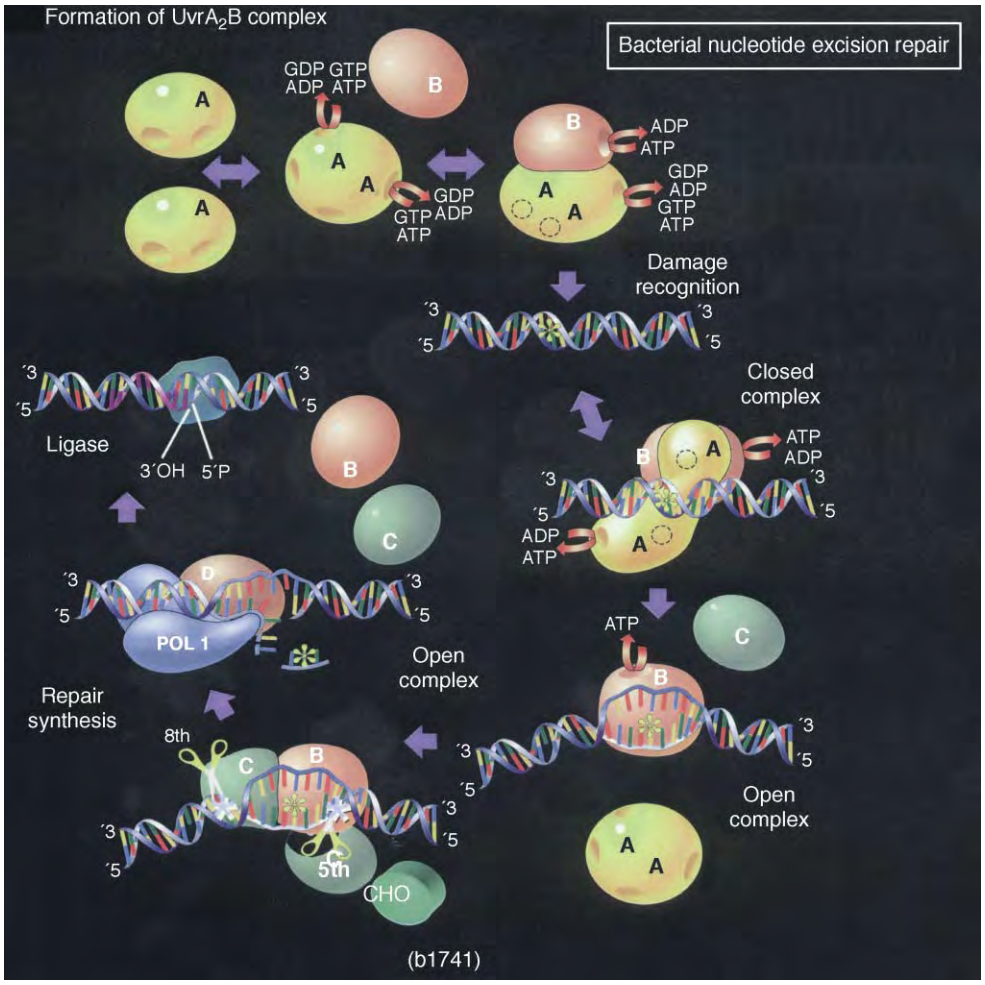

FIGURE 1 Nucleotide excision repair pathway in bacteria. $UvrA_2$ interacts with UvrB, and this $UvrA_2B_1$ complex translocates to the damaged sites. UvrA dissociates and UvrC binds to the UvrB—DNA complex at a damaged site. Dual incision is catalyzed by UvrC. The N-terminal domain is involved in the 3′ incision and the C-terminal domain performs the 5′ incision. UvrD displaces UvrC and an oligonucleotide containing the damage. DNA polymerase I fills the single stranded gap, and DNA ligase seals the nick.

from two overlapping promoters called P1 and P2. A LexA protein-binding site is present in the P2 promoter region. Transcription from P2 is inhibited by LexA repressor protein while that from P1 is unaffected. Sequence analysis revealed that the *uvrB* gene is 2,019 bp, which translates into 673 amino acids (76.6 kDa). The *uvrB* gene product has a consensus Walker-type A nucleotide-binding motif, helicase motifs II–VI as well as coiled-coils consensus sequences.

uvrC

In contrast to *uvrA* and *uvrB*, *uvrC* is not inducible by DNA damage and is not a member of the SOS regulon, although its cellular location is altered during SOS. The sequence analysis shows that the size of *uvrC* is 1,830 bp encoding a polypeptide of 610 amino acids (66 kDa).

Cho

It was quite surprising that a new uvrC homologue, Cho, could be discovered in an organism for which the complete genome sequence was known since 1997. The gene encoding Cho was found to be UV-inducible by Hanawalt and Brown using a high density DNA microarray. Careful inspection of this gene revealed homology to the Tev-homing endonucleases and also the N terminus of uvrC. Goosen and co-workers cloned and overexpressed the Cho protein, and found that the Cho protein will incise a DNA adduct at the tenth phosophodiester bond 3′ to the damaged site. This cutting at a distance was shown to help incise at bulky lesions, which might otherwise block the normal uvrC 3′ incision. They also found that uvrC can complete the incision process by efficient cleavage 5′ to the 3′ incised adduct. Cho is rather rare in the bacterial kingdom (Figure 2).

TABLE I

Range of Substrates of the Bacterial NER UvrABC System

Type	Lesion	UvrABC	ΔM_r	Properties
Single base modification	Thymine glycol	++	+34	
	Dihydrothymine	0	+2	
	Benzo[*a*]pyrene adduct	+++	+171	T_M lowered
	Anthramycin adduct	+++	+191	T_M elevated
	Cross-linked triple strand	+ [72]	~ + 3000	
	O^4-alkyl thymine	+	+14	
	O^6-methyl guanine	+	+14	
	N^6-methyl adenine	0	+14	
	Psoralen adduct	+++	+185	Positive kink
	Base removed (AP site)	+	~ − 130	
Cross-links, intra-strand	*cis*-Pt adduct	+++	+227	Negative kink
	Pyrimidine dimer	++	0	
	6–4 photoproduct	+++	0	
Cross-links, inter-strand	*cis*-Pt adduct	++	+227	
	Nitrogen mustard adduct	+	+69	
	Psoralen bisadduct	+++	+185	Unwound
Natural bases	dsDNA	0	0	
	A-tracts	0	0	Bent
	Mismatches, loops	0[a]	0	
Noncovalent modifications	Caffeine complex	−	+194	Intercalator
	Ditercalinium complex	++[b]	+500	Bisintercalator

[a] Some mismatches are recognized with very low efficiency (<1%).
[b] Futile cycle of spurious repair and subsequent formation of the complex at another site.

A selection of DNA lesions illustrates the lack of a single common property that determines the response of UvrABC to DNA damage. The relative rate of incision for a particular lesion (neglecting the influence of sequence context) by the UvrABC system is indicated by +, ++, and +++; 0 indicates no incision, − indicates inhibition. ΔM_r, change in molecular weight due to the modification.

Properties of UvrA, UvrB, and UvrC Proteins

UvrA

The UvrA protein is a DNA-independent ATPase that binds DNA and is a member of the ABC transporter superfamily characterized by dual ATP binding sites. Soon after UvrA was sequenced, it was noticed that the gene probably arose through multiple duplication events in which a four-cysteine zinc finger was placed between the Walker type A and B nucleotide-binding motifs. Site-directed mutagenesis studies show directly that UvrA has an ATPase activity located in a region centered at lysine residues of two Walker type A nucleotide-binding motifs. UvrA also hydrolyzes GTP. ATPase activity of UvrA is modulated by DNA. High concentrations of UvrA protein and the binding energy of ATP (or poorly hydrolyzable ATP-γ-S) favor dimerization of the protein. UvrA dimers are DNA-binding species. The binding of UvrA to undamaged DNA is $10^3 \sim 10^4$-fold weaker than to the damaged one. The specificity for damaged DNA is abolished by ATP-γ-S, while it enhances nonspecific binding. The dissociation rate for UvrA from damaged sites is fast in the presence of ATP. ATP hydrolysis increases the specificity of binding to the damaged DNA, but lowers the equilibrium binding constant by stimulating dissociation. UvrA contains two zinc atoms per molecule, at least one of which is required for DNA binding. Consistently, C-terminal zinc-finger of UvrA is absolutely essential for nonspecific DNA binding, while N terminal is dispensable. The helix-turn-helix motif as well as C-terminal glycine-rich region appears to contribute into damage recognition by UvrA.

UvrB

The purified protein has no detectable ATPase activity, although it binds ATP with a $K_d \sim 1$ mM. However, ATPase activity is observed when UvrB interacts with UvrA in the presence of DNA. This dramatic appearance is due to activation of the cryptic ATPase when UvrB forms an UvrAB–DNA complex. When UvrB is proteolyzed in a specific region of the C terminus, the resulting ~70 kDa protein is referred to as UvrB*. The "cryptic UvrB ATPase" functional in UvrB*

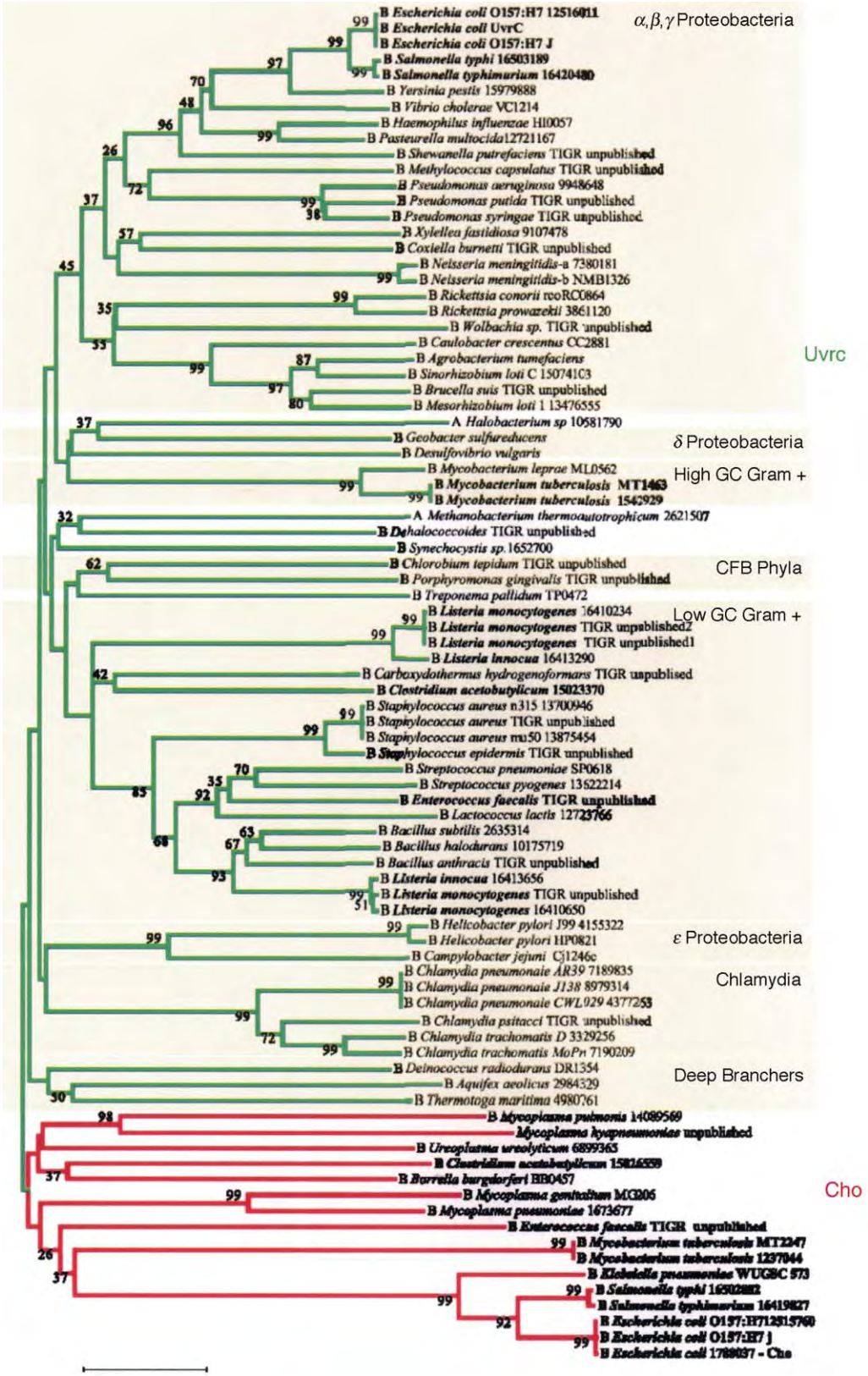

FIGURE 2 Phylogenetic tree of UvrC and Cho in various bacterial species. Phylogenetic tree of UvrC and Cho homologues. Homologues were identified in complete or nearly complete genomes by blastp or blastx searches. Protein sequences were aligned using clustalx. Boostrap values, a measure of statistical support for particular groupings of genes to the right of the number, are shown on the tree when greater than 40%. Reprinted from Van Houten, B., Eisen, J. A., and Hanawalt, P. C. (2002). A cut above: discovery of an alternative excision repair pathway in bacteria. *Proc. Natl Acad. Sci. USA* **99**(5), 2581–2583, with permission of the National Academy of Sciences, U.S.A.

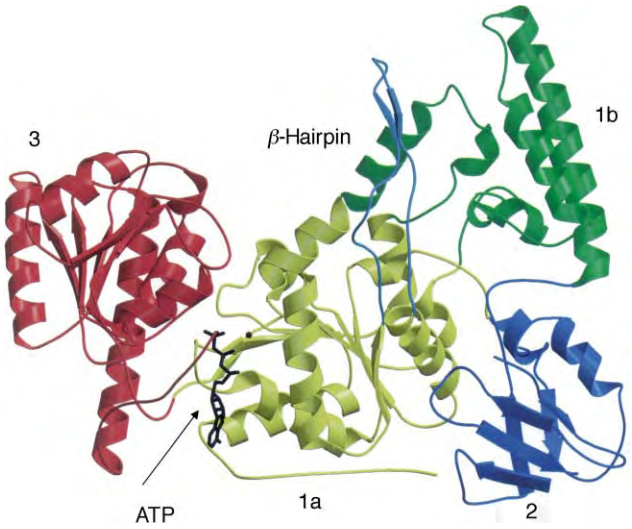

FIGURE 3 Structure of UvrB. Domains 1a, 1b, 2, and 3 are shown in yellow, green, purple and red, respectively. The β-hairpin bridging the gap between domains 1a and 1b is shown in cyan. The ATP molecule bound at the interface between domains 1 and 3 is indicated. (Reprinted from Theis, K., Chen, P. J., Skorvaga, M., Van Houten, B., and Kisker, C. (1999). Crystal structure of UvrB Provides insight into the mechanism of nucleotide excision repair. *EMBO J.* **18**(24), 6899–6907, with permission of Oxford University Press.)

is activated by single stranded DNA or chaotropic salts. UvrB can bind to double stranded DNA only in the presence of UvrA, and binds to single-stranded DNA with a K_d in the micromolar range. The amino acid sequence of the UvrB protein shows homology with two limited stretches of the sequence of the UvrC protein. Three groups have independently solved the crystal structure of UvrB. The structure has revealed that UvrB is folded into four separate domains (Figure 3). Domain 1a includes four helicase motifs: Ia, Ib, II, and III that are required for ATPase activity. Domain two is important for UvrA interaction and domain 3 contains helicase motifs, IV, V, and VI. Sandwiched between domains 1a and 1b is an important β-hairpin motif which is believed to provide important DNA contacts. Further details of the UvrB structure and how it provides function is discussed below.

UvrC

UvrC is a single-strand DNA-binding protein and binds to it with a relatively high affinity. UvrC is a catalytic subunit of the UvrABC endonuclease. Mutations in the C-terminal region of UvrC are extremely sensitive to UV and defective in 5′-incision activity. The 314 C-terminal amino acids of UvrC are sufficient to support dual incision of damaged DNA by the UvrABC endonuclease. UvrC protein associates with a UvrB–DNA complex at damaged site. Recently, the C-terminal part of UvrC was solved by multidimensional NMR and shown to consist of two helix-hairpin-helix (HhH) motifs as predicted previously. Kaptein and co-workers found that this C-terminal region of the protein bound avidly to double-strand/single-strand junctions like those found in bubble substrates containing more than six unpaired bases. Interestingly this is exactly the number of base pairs believed to be unwound during the formation of the UvB–DNA complex.

Damage Recognition and Incision

The broad substrate specificity of the UvrABC endonuclease is achieved through a complex molecular mechanism (Figure 1) identifying some general changes in DNA conformation and dynamics rather than chemically modified bases *per se*.

Molecular Mechanism of Damage Recognition

Molecular recognition proceeds through a series of coordinated Uvr protein–protein and nucleoprotein intermediates characterized by different composition and architecture.

UvrA Dimerization

UvrA forms a dimer in solution with apparent $K_d \sim 10^{-8}$ M. Nucleotide (ATP) binding to UvrA drives UvrA dimerization, whereas the hydrolysis of ATP or the presence of ADP drives monomerization. The UvrA dimer is the active form in binding to undamaged or damaged DNA. Formation of a dimer results in a conformational change of the UvrA protein. UvrA is believed to recognize overall changes in the structure of the DNA helix.

$UvrA_2B_1$ Complex in Solution

The purified UvrA protein associates in solution with UvrB protein (domain 2) in an ATP-dependent manner. The N-terminal 230 amino acids of UvrA are involved in this interaction. UvrB has two UvrA-binding sites: one within amino acids 115–250 and another within C-terminal amino acids 573–673. However, $UvrB^*$ which lacks these C-terminal amino acids can also bind UvrA in solution. The apparent stochiometry of the UvrA–UvrB complex in solution is $UvrA_2UvrB_1$.

$UvrA_2$–DNA Binding

The UvrA dimer binds both damaged and undamaged DNA. ADP decreases the UvrA-binding affinity two- to

threefold and ATP is not required for the specific binding to a damaged site. ATP-γ-S quantitatively inhibits the specific binding while enhancing nonspecific binding. The equilibrium constant for nonspecific binding of UvrA is $(0.7–2.9) \times 10^5\ M^{-1}$. The apparent binding affinity of $UvrA_2$ to damaged DNA is in the range $0.07 \sim 1.0 \times 10^9\ M^{-1}$, depending on the damage type. However, affinity of $UvrA_2$ to damage does not generally correlate with the efficiency of the entire incision reaction.

$UvrA_2B_1$–DNA Complex

This complex provides for more productive damaged DNA-binding intermediates than UvrA dimer. Binding of $UvrA_2B_1$ to DNA results in locally unwound undamaged-DNA between 180° and 220°. Furthermore, it has been proposed that the DNA is wound around the UvrB molecule. The formation of the $UvrA_2B_1$–DNA complex results in a multifold stimulation of ATPase activity apparently through activation of a "cryptic" ATPase of UvrB. Using atomic force microscopy, Goosen and co-workers have recently suggested that UvrA and UvrB can form $UvrA_2UvrB_2$ complex on DNA. Once the UvrAB complex actively engages the damage, UvrA (and possible one molecule of UvrB) dissociate leaving a long-lived salt stable UvrB–DNA complex.

Formation of the UvrB–DNA Intermediate

Previous work by Grossman and co-workers have suggested that the UvrAB complex can track along the DNA helix using a limited helicase activity to create waves of negative and positive supercoiling behind and in front of the damaged site, respectively. This is consistent with the helicase fold of UvrB (shown in Figure 3). However, work from both the Rupp and Van Houten laboratories have argued that the UvrAB complex cannot dissociate damaged DNA strands even as small as 26 bases, and that formation of the UvrB–DNA complex leads to a destabilization of the DNA helix. However, neither UvrB by itself or in complex with UvrA can unwind long tracks of DNA, which is a typical property of proteins with true helicase activity.

Damage-Sensing Mechanism: Padlock Model of Damage Recognition by UvrB

The UvrABC endonuclease does not recognize a specific chemical group or structure in the damaged nucleotide nor does it, in all likelihood, solely recognize a specific backbone deformity in the duplex induced by the varied and unrelated genotoxic chemicals (Table I). Initial damage recognition may occur through direct UvrA–DNA interactions. This triggers structural changes of the preceding $UvrA_2B_1$–DNA complex, so that $UvrA_2$ dissociates, while UvrB is loaded onto a damaged site. Even though the cocrystal structure of the UvrB–DNA complex has not yet been solved, this complex has been observed in footprinting experiments by electron microscopy and gel mobility shifts and the complex is isolated by gel filtration. The formation of this complex requires ATP hydrolysis by both UvrA and UvrB and occurs after the recognition of a damage site by the UvrAB complex. As noted above, Goosen and co-workers have shown that the formation of the UvrB pre-incision complex at damaged sites results in a conformational change of both UvrB and DNA. The DNA molecule in this complex is kinked and the DNA wrapped around the UvrB molecule. Helicase motifs and the β-hairpin motif of UvrB seem to play a role in UvrB–DNA binding at damaged sites (Figure 4). The rate of UvrB loading to DNA is low ($k_{on} = 6–10^{-4}\ M\ s^{-1}$), suggesting that this step may be limiting for damage-specific incision of DNA. Kisker and co-workers have proposed a padlock model of UvrB binding to DNA to help reconcile the earlier helicase-unwinding model of Grossman with the known helicase fold of UvrB. In this model the UvrAB complex uses the UvrB ATPase to make limited motion along the DNA, causing transient opening and closing of the DNA, in which it is believed that the β-hairpin is inserted through the helix. If a DNA lesion is encountered by UvrB, there is a conformational change in the protein–DNA complex leading to the release of UvrA. In this precision complex, UvrB is believed to lock down the nondamaged between the β-hairpin and the wall of domain 1B (Figure 4). In this locked padlock model, the damaged strand wraps in front of the β-hairpin and the hydrophobic tyrosine side-changes at the base of the β-hairpin are believed to bind to or facilitate the damaged nucleotide to flip out of the DNA helix. In this locked down conformation, ATP binding is believed to lead to a large motion of domain 3 which clamps down on the DNA resulting in further deformation of the DNA helix leading to strained structure that is recognized by UvrC.

Dual Incision

The binding of UvrC to the pre-incision UvrB–DNA complex results in the incision of DNA on both sides of the lesion in the damaged strand. DNA sequence context and the type of damage affect the precise location of the 5′ and 3′ incision sites. Usually, it occurs at the 8th phoshodiester bond 5′ to the damage and 4th or 5th phoshodiester bond 3′ to the damage. The C-terminal coiled-coil motif of UvrB (amino acids 636–668) and the N-terminal homologous regions of UvrC (amino acids 214–239) are required for the

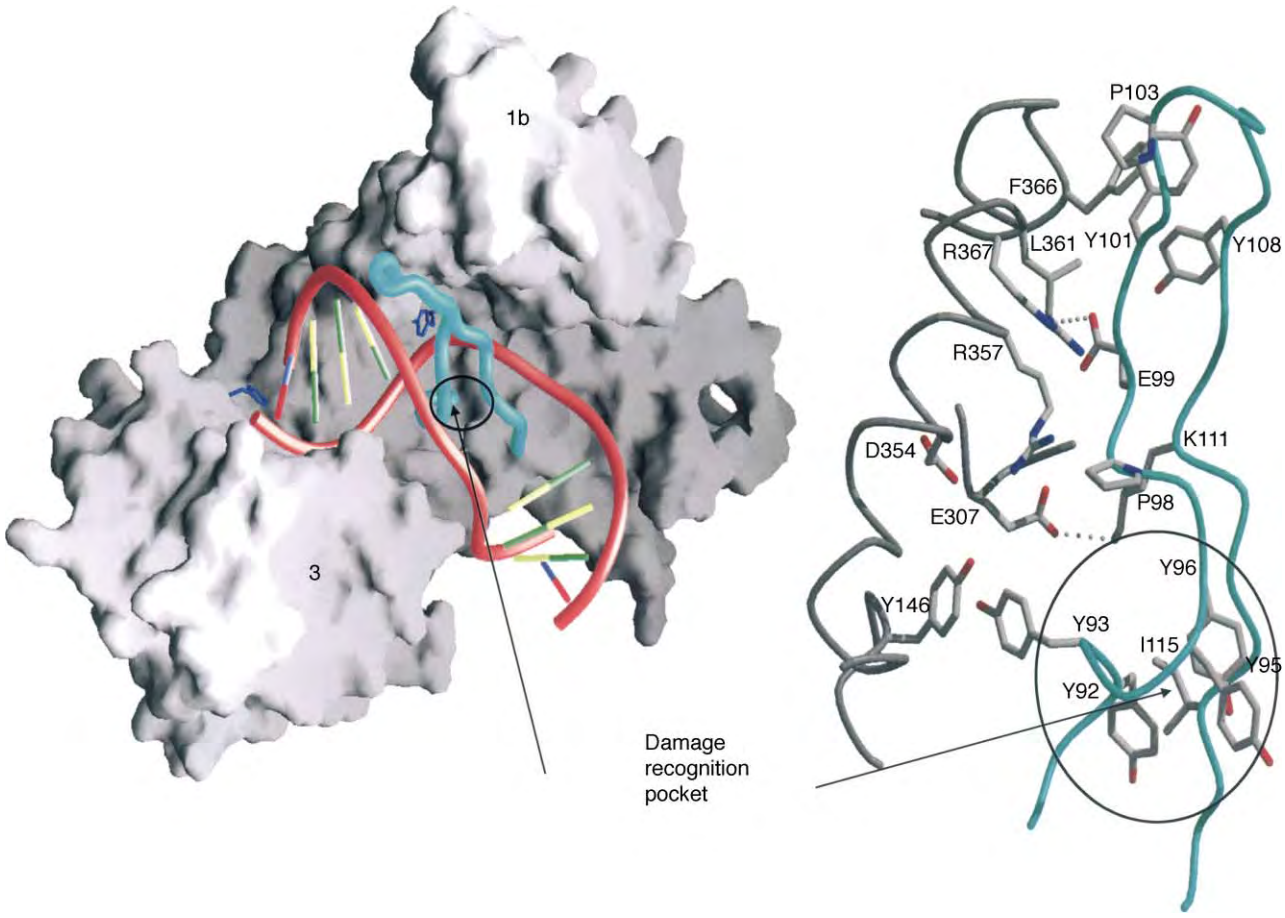

FIGURE 4 Hypothetical model of UvrB–DNA complex showing proposed damage recognition pocket. Left panel, hypothetical model of the UvrB–DNA pre-incision complex. Domains 1b and 3 are indicated. The proposed conformation of DNA is shown as phosphate backbone in red with the undisrupted base pairs shown as spokes. The β-hairpin is depicted in cyan. (Reprinted from Theis, K., Chen, P. J., Skorvaga, M., Van Houten, B., and Kisker, C. (1999). Crystal structure of UvrB Provides insight into the mechanism of nucleotide excision repair. *EMBO J.* **18**(24), 6899–6907, with permission). Right Panel, the β-hairpin and its proposed role in binding to DNA. A Ca-trace of the β-hairpin of bcUvrB cyan and neighboring residues of domain 1b in gray. Hydrophobic residues (Tyr 95–96) believed to be involved in damage recognition are circled. (Modified from Theis, K., Skorvaga, M., Machius, M., Nakagawa, N., Van Houten, B., and Kisker, C. (2000). The nucleotide excision repair protein UvrB, a helicase-like enzyme with a catch. *Mutat. Res.* **460**(3–4), 277–300, with permission from Elsevier.)

formation of UvrBC complex. Site-directed mutagenesis of the UvrC and UvrB proteins has led to the conclusion that the incision process is not a concerted one. The 3′ incision is affected by the N terminus of the UvrC protein, and this incision precedes the 5′ nicking, catalyzed by the C terminus of UvrC protein. There is a conformational change of UvrBC–DNA complex following 3′-incision. The C-terminal region of UvrC (amino acids 555–610) is involved in DNA binding and 5′-incision. Dual incision *per se* does not require ATP hydrolysis; ATP-γ-S can substitute ATP during this step.

Postincision Steps

Following dual incision, the UvrBC complex remains bound to damaged DNA. As a result of the stability of the postincision complex, UvrABC endonuclease does not turnover in an *in vitro* system, which is biochemically reconstituted with only Uvr proteins. Restoration of the DNA primary structure and integrity as well as turnover of the Uvr proteins is accomplished in a series of postincision steps, which require products of two additional genes, uvrD and polA.

UvrD

Its gene maps at 84 min of *E. coli* chromosome. UvrD + is a part of the SOS regulon and is induced by DNA damage. The product of this gene is a 3′–5′ DNA helicase II – a 75 kDa protein which is a DNA-dependent ATPase. DNA helicase II is required for removal of incised damage as a 12–13-mer oligonucleotide fragment. It also effects release of UvrC protein, but not UvrB from the postincision complex.

PolA

Its gene maps at 85 min of *E. coli* genetic map. It encodes a 109 kDa protein, DNA polymerase I. The UvrB protein is not displaced by DNA helicase II and remains bound to gapped DNA. In the presence of deoxyribonucleoside-5′-triphosphates, DNA polymerase I catalyzes repair synthesis, resulting in the filling in of the gap and displacement of the UvrB protein. The size of *in vitro* repair patch is usually ~12 nucleotides in length. Molecular interactions of Uvr proteins, DNA helicase II, and DNA polymerase I during postincision events are not presently known. *E. coli* strains, deficient in uvrD + and polA + are usually significantly less sensitive to the killing effects of UV radiation than Uvr-deficient strains, indicating their auxiliary role in repair. DNA ligase completes NER by catalyzing joining of the last 3′-nucleotide of the patch with the rest of polynucleotide chain.

Transcription-Coupled Repair

Transcription-repair coupling (TRC) allows cells to select some regions of the genome for NER in preference to others. In *E. coli*, as a consequence of a 436-fold induction of β-galactosidase operon, 70% of the UV-induced pyrimidine dimers are removed from the transcribed strand of the induced operon within 5 min, whereas only 50% of dimers are removed from the nontranscribed strand after 20 min of repair. This selective removal of pyrimidine dimers from the transcribed strand of a gene is abolished in the absence of significant levels of transcription. The mechanism of TRC in *E. coli* is a complex one, and may include several subpathways. In one of them, TRC is achieved through the action of transcription-repair coupling factor (TRCF). TRCF is a product of mfd + (for mutation frequency decline) gene, which maps at 25 min on the *E. coli* chromosome. The cloned mfd + gene is translated into a 1148 amino acids protein of ~130 kDa. The Mfd protein has consensus Walker type A nucleotide-binding motif, and, indeed, is a relatively weak ATPase. The Mfd protein can nonspecifically bind dsDNA (and less efficiently ssDNA) in an ATP binding-dependent manner, the ATP hydrolysis promoting its dissociation. The amino acid sequence of Mfd reveals motifs, which are characteristic of a number of DNA and RNA helicases. However, *in vitro* purified Mfd does not show either DNA or RNA helicase activity. The N-terminal 1–378 residues of Mfd, having 140 amino acid region of homology with UvrB, bind UvrA protein. The Mfd protein can also bind different forms of *E. coli* RNA polymerase (RNAP). Amino acids 370–571 of Mfd are involved in this binding. *In vitro*, transcription inhibits NER of damage in a transcribed strand, while it has no effect on the coding strand. This inhibition is thought to result from RNAP stalled at the site of damage. Mfd is able to release stalled RNAP in an ATP hydrolysis-dependent manner. Moreover, Mfd actually stimulates NER on the transcribed strand, so that it becomes faster than on the nontranscribed one. Based on all these observations, it is concluded that TRCF-Mfd carries out preferential repair of the transcribed strand by (1) releasing RNAP stalled at damaged site, and (2) recruiting the $UvrA_2B_1$ complex to damaged site through the high-affinity interaction with UvrA protein. The TRC in *E. coli* is influenced by the rate and conditions of growth as well as the level of gene

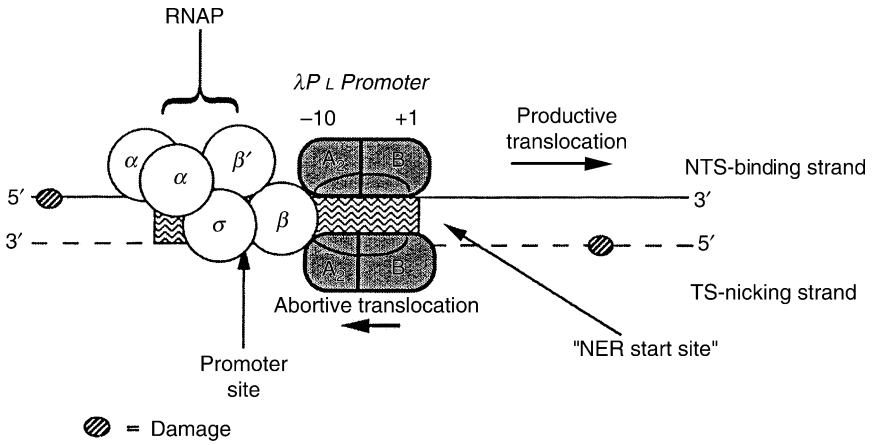

FIGURE 5 Model for strand selectivity by UvrAB helicase. RNA polymerase provides the UvrAB complex a preferred binding site at transcription bubble region via the physical interaction of RNAP with the UvrAB complex. Once the UvrAB complex binds to the promoter region, a competent nucleoprotein complex for helicase action is formed. The UvrAB complex may translocate along the non-transcribed strand in an ATP hydrolysis-dependent reaction. During tanslocation, the DNA damage recognition domain of the UvrA subunit of the UvrAB complex senses damaged sites on the complementary strand. (Reprinted from Ahn, B., and Grossman, L. (1996). RNA polymerase signals UvrAB landing sites. *JBC.* **271**(35), 2153–2161, with permission of The American Society for Biochemistry and Molecular Biology.)

transcription. In the LacZ gene the Mfd-dependent mechanism of preferential repair dominates at basal levels of transcription, while Mfd-independent mechanisms prevail at induced transcription levels. It was shown that in the presence of RNAP, $UvrA_2B_1$ complex is able to specifically bind promoter regions and translocate unidirectionally along coding strand while sensing damage in a transcribed strand. This strand specificity is dictated by the $5'-3'$ directionality of the $UvrA_2B_1$ helicase which can translocate only on the coding strand because the RNAP interferes with that directionality on the transcribed strand (Figure 5). Nicking occurs only on the strand opposite to the strand, along which the $UvrA_2B_1$ complex translocates. Hence, it is the transcribed strand, which is initially repaired. This mechanism could account for the observed Mfd-independent TRC *in vivo*. The Mfd-dependent mode of preferential repair seems to operate at those RNAP molecules which escaped binding of $UvrA_2B_1$ complex at the promoter region and was subsequently stalled at a damaged site.

Conservation of Nucleotide Excision Repair from Bacteria to Man

Nucleotide excision repair (NER) of bacterial, yeast, and mammalian cells have been reconstituted *in vitro* with purified proteins and defined damaged DNA substrates. While it would appear that it takes some 25 proteins in a human cell to complete the process achieved by six bacterial proteins, there is a high degree of conservation of function from bacteria to eukaryotes. Thus NER system of bacteria will certainly serve as a primary model for structure–function studies for years to come.

See Also the Following Articles

DNA Damage: Alkylation • DNA Helicases: Dimeric Enzyme Action • DNA Helicases: Hexameric Enzyme Action • DNA Polymerase I, Bacterial • Zinc Fingers

Glossary

DNA polymerase A protein or protein complex which synthesizes a daughter strand of DNA using a sparental strand as a template.

helicase A protein, which actively separates the two strands of DNA using the energy of ATP hydrolysis.

nucleotide excision repair (NER) A highly conserved multistep process in which several protein machines identify and remove bulky damage from DNA using a dual incision mechanism.

SOS response A number of DNA metabolism genes controlled by the LexA repressor, which is cleaved during genotoxic stress.

***uvr* genes** Genes encoding subunits of NER proteins, which confer sensitivity to killing by UV light.

Zinc Finger A DNA-binding motif consisting of a molecule of zinc bound to four cys found in many DNA-repair proteins.

Further Reading

Friedberg, E. C., Walker, G. C., and Siede, W. (1995). *DNA Repair and Mutagenesis*. ASM Press, Washington, DC.

Goosen, N., and Moolenaar, G. F. (2001). Role of ATP hydrolysis by UvrA and UvrB during nucleotide excision repair. *Res. Microbiol.* **152**(3–4), 401–409.

Goosen, N., Moolenaar, G. F., Visse, R., and van de Putte, P. (1998). Functional domains of the *E. coli* UvrABC proteins in nucleotide excision repair. In *Nucleic Acids and Molecular Biology* (F. Eckstein and D. M. J. Lilley, eds.) Vol 12. Springer, Berlin.

Grossman, L., and Thiagalingam, S. (1993). Nucleotide excision repair, a tracking mechanism in search of damage. *J. Biol. Chem.* **268**, 16871–16874.

Grossman, L., Lin, C.-I. G., and Ahn, B. (1998). Nucleotide excision repair in *Escherichia coli*. In *DNA Damage and Repair* (J. A. Nickoloff and M. F. Hoekstraeds, eds.) Vol 1, pp. 11–27. Humana Press, Totowa, NJ.

Mellon, I., and Hanawalt, P. C. (1989). Induction of the *Escherichia coli* lactose operon selectively increases repair of its transcribed DNA strand. *Nature* **342**, 95–98.

Sancar, A. (1996). DNA excision repair. *Annu. Rev. Biochem.* **65**, 43–81.

Sancar, A., and Rupp, W. D. (1983). A novel repair enzyme: UVRABC excision nuclease of *Escherichia coli* cuts a DNA strand on both sides of the damaged region. *Cell* **33**, 249–260.

Skorvaga, M., Theis, K., Kisker, C., and Van Houten, B. (2002). β-hairpin motif of UvrB is essential for DNA binding, damage processing and UvrC mediated-incisions. *J. Biol. Chem.* **277**(2), 1553–1559.

Theis, K., Chen, P. J., Skorvaga, M., Van Houten, B., and Kisker, C. (1999). Crystal structure of UvrB Provides insight into the mechanism of nucleotide excision repair. *EMBO J.* **18**(24), 6899–6907.

Theis, K., Skorvaga, M., Machius, M., Nakagawa, N., Van Houten, B., and Kisker, C. (2000). The nucleotide excision repair protein UvrB, a helicase-like enzyme with a catch. *Mutat. Res.* **460**(3–4), 277–300.

Van Houten, B. (1990). Nucleotide excision repair in *Escherichia coli*. *Microbiol. Rev.* **54**, 18–51.

Van Houten, B., Eisen, J. A., and Hanawalt, P. C. (2002). A cut above: discovery of an alternative excision repair pathway in bacteria. *Proc. Natl Acad. Sci. USA* **99**(5), 2581–2583.

Biography

Bennett (Ben) Van Houten works at the National Institute of Environmental Health Sciences. His principle research interest is in the structure and function of DNA repair enzymes, and the consequences of mitochondrial DNA damage. He holds a Ph.D. from the University of Tennessee and completed postdoctoral training at the University of North Carolina, and has received the Burroughs Wellcome Toxicology Scholar award.

Lawrence (Larry) Grossman is the University Distinguished Service Professor of Biochemistry in the Department of Biochemistry and Molecular Biology in the Johns Hopkins Bloomberg School of Public Health. His research interests included the chemistry, biochemistry, and enzymology of damaged nucleic acids. He holds a Ph.D. from the University of Southern California and has been a Guggenheim Fellow as well as a Commonwealth Fund Fellow.

Nucleotide Excision Repair: Biology

Errol C. Friedberg
University of Texas Southwestern Medical Center, Dallas, Texas, USA

Nucleotide excision repair (NER) is a fundamental DNA repair process that is ubiquitously distributed from bacteria to man. The process is essential for the enzyme-catalyzed removal of various types of base damage from the nuclear genome, typically those that result in significant distortion of the helical structure of DNA. This article discusses the overview and biology of NER.

The name nucleotide excision repair derives from the fact that during this process damaged bases are excised from the genome as oligonucleotide fragments. This distinguishes nuclear excision repair (NER) from other types of excision repair such as base excision repair (BER), during which damaged bases are excised as free bases, and mismatch excision repair (MMR), during which mismatched nucleotides are removed from the genome as mononucleotides. The oligonucleotide fragments are generated by specific incision of the damaged DNA strand on either side of sites of base damage (bimodal incision) (Figure 1). The gaps (~30 nucleotides in length) generated by oligonucleotide excision are filled in by repair synthesis (Figure 1), using the intact opposite strand as an informational template. When the last nucleotide is inserted, the remaining nick is sealed by DNA ligase (Figure 1).

Modes of Nucleotide Excision Repair

Nucleotide excision repair (NER) transpires in cells in various subforms. Its operation on transcriptionally silent regions of the genome and on the non-transcribed strand of transcriptionally active genes is often referred to as global NER, to distinguish it from NER that specifically operates on the transcribed strand of transcriptionally active genes, so-called transcription-coupled NER (TC-NER). Additionally, both global NER and TC-NER are characterized by incision of the affected DNA strand on either side of sites of base damage (Figure 1), some lower eukaryotes support a form of NER that involves a single incision 5′ to the site of base damage. This process is referred to as specialized NER.

The Biology of NER

Distribution in Nature

As we ascend the evolutionary ladder and encounter increasingly more complex organisms, our information about the cellular biology of NER becomes less precise, even though paradoxically our biochemical understanding has taken leaps and bounds in recent years. Several aspects of the cell biology of higher cells contribute to this paucity of information. Perhaps most importantly, both the structure and organization of the eukaryotic genome is much more complex than that of prokaryotes. Eukaryotic genomes are considerably larger, and the requirements for packaging such large amounts of DNA into the limited confines of the cell nucleus have led to a complex structural organization. A consideration of the distribution of DNA damage in eukaryotes must take into account that nuclear DNA exists in intimate association with both histones and nonhistone chromosomal proteins, and that the structure of chromosomes reflects various levels of folding and coiling of the basic chromatin structural unit, the nucleosome.

Our present understanding of how chromosome structure and nucleosome conformation influence the enzymology of DNA incision and of postincision events during NER in eukaryotes is still scanty. It is certain that structural elements do in fact limit the access of repair enzymes to sites of base damage, and that specific perturbations of chromatin structure are necessary to facilitate NER.

Conventional NER involving the bimodal incision of damaged DNA is operationally and fundamentally similar in all organisms, from bacteria to man. However, there are significant biochemical differences between NER in prokaryotes and eukaryotes. Additionally, the biochemistry of global NER and TC-NER differ in important details during the initial stage of the process. Specifically, during global NER particular proteins are required for the recognition of base damage in DNA. In contrast, during TC-NER the process of arrested RNA polymerase II transcription is believed to provide the mechanism of damage recognition.

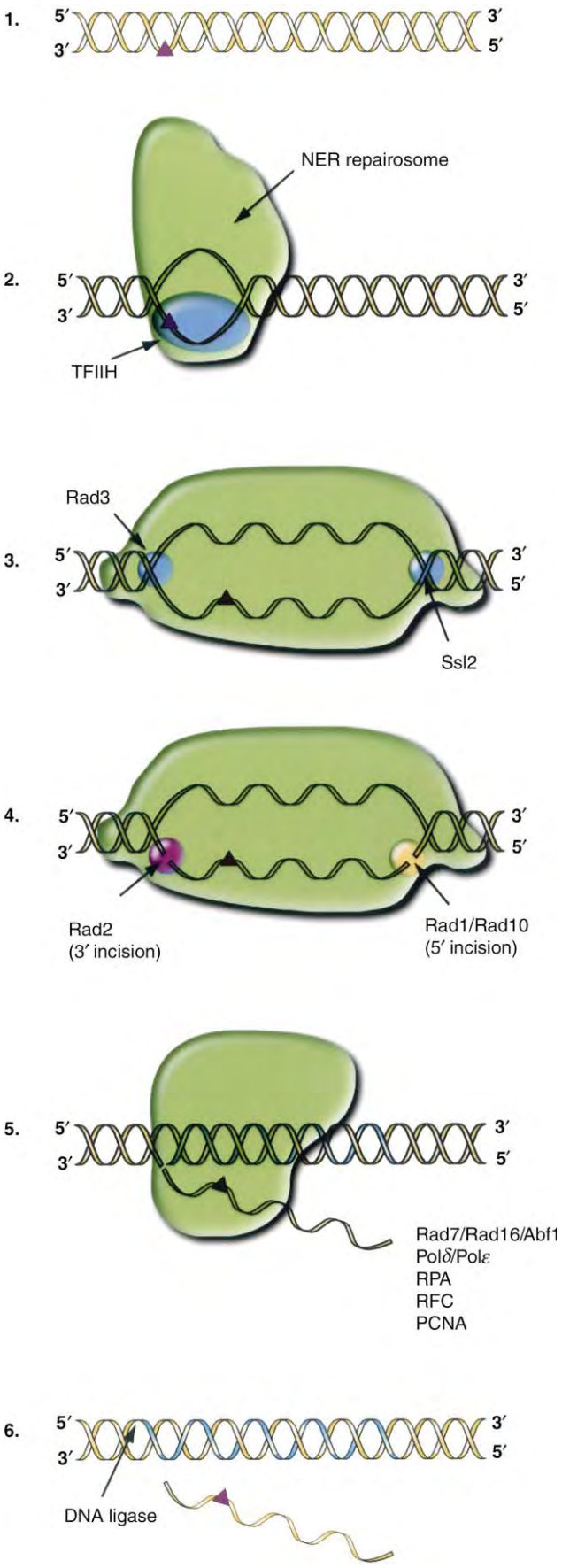

The NER Machinery

NER operates through the assembly of a multiprotein complex. In bacteria this complex comprises about six polypeptides. However, in both lower and higher eukaryotes as many as 30 proteins are required for NER. These comprise proteins that participate in (1) the recognition of base damage, (2) bimodal incision of DNA, (3) oligonucleotide fragment incision, (4) repair synthesis of the gap generated in DNA, and (v) DNA ligation. (Figure 1). In eukaryotes the RNA polymerase II, basal transcription factor IIH (TFIIH) is an integral component of the NER machinery. As noted below, mutations in some of the genes encoding TFIIH subunits can result in disease states with transcription defects.

Substrate Specificity

NER operates primarily on types of base damage that generate conformational distortion of the DNA helical structure. The so-called (6–4) photoproduct, a highly distortive type of base damage in DNA that results from exposure to UV light (Figure 2), as well as cyclobutane pyrimidine dimers (Figure 2), are premier examples of substrates for NER. The NER machinery does not recognize small loops or mismatches in DNA, and small chemical adducts such as those produced by methylation and the oxidation of bases are preferentially recognized by the BER process. The precise mechanism of substrate recognition during NER in eukaryotes remains to be determined.

Detection of NER *in vivo* and *in vitro*

Studies on NER in mammalian cells have historically utilized a variety of increasingly refined experimental strategies and techniques, many of which have been adapted from methods initially developed for studies

FIGURE 1 The general mechanism of nucleotide excision repair (NER) in eukaryotes. In the figure yeast is used as an example. The red triangle represents some type of base damage that is recognized by the transcription-independent NER system. The binding of multiple proteins at or near the site of base damage in an ordered step-wise fashion generates a large multiprotein complex, the NE repairosome, that includes the RNA polymerase II basal transcription factor TFIIH. Two DNA helicase subunits in TFIIH (Rad 3 and Ssl2 in yeast) facilitate the generation of a bubble in the DNA that is ~30 nucleotides in length and that flanks the site of base damage. The double-stranded/single-stranded DNA junctions are then recognized by two structure-specific endonucleases (Rad2 and Rad1/10). These cut the DNA duplex only on the damaged strand, generating an oligonucleotide fragment ~30 nucleotides in length. The Rad7/Rad16/Abf1 protein complex then facilities displacement of the oligonucleotide as a free DNA fragment carrying the damaged base. Replicative DNA polymerases (d and/or e) together with accessory proteins (RPA, RFC, PCNA) fill in the gap formed and DNA ligase seals the damaged DNA strand to restore complete covalent integrity.

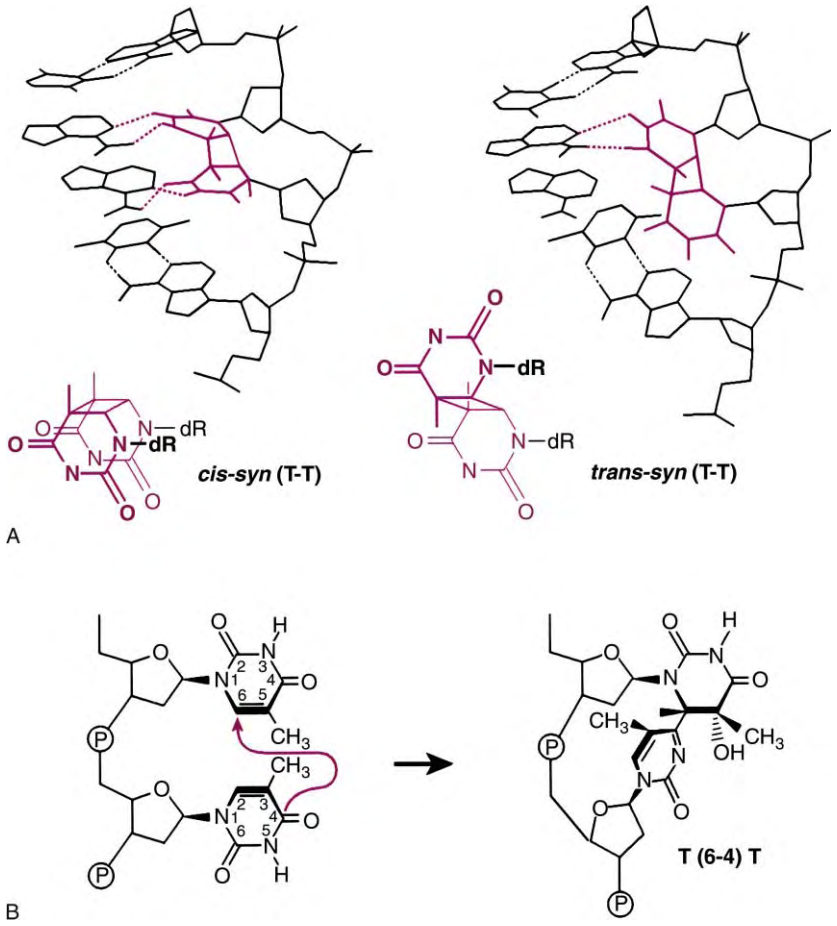

FIGURE 2 Chemical structures of cyclobutane pyrimidine dimers (CPD) (A) and [6–4] photoproducts (B). Both of these photoproducts are generated in large amounts when DNA is exposed to UV light, including sunlight.

with bacteria. Some of these procedures measure the damage-specific incision of DNA, either directly or indirectly. Others measure the physical excision of damaged nucleotides, repair synthesis of DNA, or the rejoining of strand breaks (DNA ligation). A particularly widely used technique for monitoring NER in living cells is referred to as the unscheduled DNA synthesis (UDS) assay, that identifies repair synthesis of DNA. In this procedure cells in monolayer culture are exposed to a DNA damaging agent such as UV radiation and the medium is supplemented with a radiolabeled precursor for DNA synthesis. Repair synthesis of DNA associated with NER is identified by a delicate autoradiographic stippling of nuclei in cells that are outside the S phase of the cell cycle (hence UDS) (Figure 3).

Kinetics of NER

While the application of many of the experimental procedures mentioned above supports the existence of NER in higher organisms, the relative kinetics of specific events associated with NER, such as DNA incision, the excision of specific lesions from high-molecular-weight DNA, and repair synthesis in mammalian cells, are still controversial. In part these controversies have arisen from the use of different experimental procedures, which, though designed to measure the same biological end points, sometimes have optimal reliabilities at different extents of DNA damage and under different experimental conditions, and hence may not be strictly comparable. Nonetheless, some of these apparent "experimental inconsistencies" may actually reflect real distinctions in NER associated with different cell types, different functional states of cells, particular regions of the genome, and different types of DNA damage. It is generally acknowledged that (6–4) photoproducts are removed from the genome of human, and in particular rodent cells, more rapidly than are pyrimidine dimers. It can take many hours before the latter lesions are fully cleared from the genome.

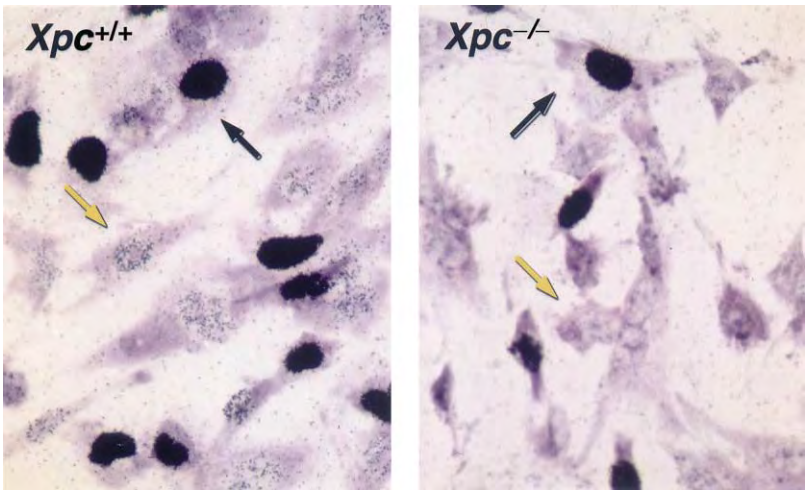

FIGURE 3 The identification of repair synthesis during NER in mammalian cells. The repair synthesis step shown in Figure 1 can be monitored in mammalian cells in monolayer culture. Mouse wild-type ($Xpc^{+/+}$) and NER-defective ($Xpc^{-/-}$) cells are exposed to UV radiation and allowed to incubate in the presence of [^{3}H] thymidine. Cells in S phase of the cell cycle undergo intense autoradiographic labeling by incorporating the radiolabled thymidine (black arrows). However, cells undergoing repair synthesis during NER incorporate much less label which can be identified as a delicate autoradiographic stippling (yellow arrow, $Xpc^{+/+}$). These grains are greatly reduced or absent in the NER-defective $Xpc^{-/-}$ cells.

Defective NER and Human Disease

Several human hereditary diseases have been identified that result from defective NER. The so-called classical xeroderma pigmentosum (XP) is an autosomal-recessive disease that results from defects in both global NER and TC-NER. Affected individuals are extremely sensitive to sunlight and have a markedly increased risk of developing skin cancers. A clinically indistinguishable form of XP called the XP variant form, derives from mutations that affect a different biological response to UV radiation-induced DNA damage. Individuals with mutations in genes required for both NER and RNA polymerase II transcription can develop the clinical features of both XP and a different disease called Cockayne syndrome (CS). Pure CS (unaccompanied by XP) arises from defects in the *CSA* or *CSB* genes that encode proteins required for TC-NER. Unlike XP, CS does not lead to an increased risk of skin cancer in human subjects. Defects in subunits of TFIIH can result in a spectrum of diseases characterized by developmental and neurological defects with or without defective NER, the disease trichothiodystrophy (TTD) being a notable example.

Mouse Models for Defective NER

Mouse models for each of the human hereditary diseases mentioned above have been generated by conventional targeted gene replacement, and sometimes by more refined strategies. In general these mice have proven to mimic the human disease well and have provided much valuable information about the relationships between defective NER and cancer predisposition and pathogenesis.

See Also the Following Articles

DNA Helicases: Dimeric Enzyme Action • DNA Helicases: Hexameric Enzyme Action • RNA Polymerase I and RNA Polymerase III in Eukaryotes • RNA Polymerase II and Basal Transcription Factors in Eukaryotes • RNA Polymerase II Elongation Control in Eukaryotes • RNA Polymerase II Structure in Eukaryotes • Transcription-Coupled DNA Repair, Overview

Glossary

damaged DNA DNA in which the covalent structure, nucleotide sequence, or conformation has been altered.

DNA repair A collection of cellular processes whereby damaged DNA is restored to its normal chemistry, nucleotide sequence, conformation, and function.

eukaryotes One of the kingdoms of life, more highly evolved than bacteria, the cells of which contain a defined nucleus.

oligonucleotides Fragments of one or two DNA strands that can be of any size.

transcriptionally active genes Genes that are in the active process of being transcribed into RNA.

Further Reading

Batty, D. P., and Wood, R. D. (2000). Damage recognition in nucleotide excision repair of DNA. *Gene* **241**, 193–204.

de Boer, J., and Hoeijmakers, J. H. J. (2000). Nucleotide excision repair and human syndromes. *Carcinogenesis* **21**, 453–460.

Friedberg, E. C. (2001). How nucleotide excision repair protects against cancer. *Nat. Rev. Cancer* **1**, 22–33.

Friedberg, E. C., Walker, G. C., and Siede, W. (1995). *DNA Repair and Mutagenesis*. ASM Press, Washington DC.

Norbury, C. J., and Hickson, I. D. (2001). Cellular responses to DNA damage. *Annu. Rev. Pharmacol. Toxicol.* **41**, 367–401.

Biography

Errol C. Friedberg is Professor and Chair in the Department of Pathology, University of Texas Southwestern Medical Center at Dallas. He is the senior author of the textbook *DNA Repair and Mutagenesis* and has published over 300 papers on these topics.

Olfactory Receptors

Sigrun I. Korsching
University of Cologne, Germany

Olfactory receptors mediate the primary interaction of the olfactory brain with the external world. Any odor stimulus is initially represented as activation of one to many different olfactory receptors. Vice versa, anything that binds and activates an olfactory receptor, is as per definition an odor, or odorant, as the single compounds are often called. Olfactory receptors constitute one of the largest families of G protein-coupled receptors. Many large and small clusters of olfactory receptors are distributed throughout the genome. Olfactory receptors are expressed in a highly specific manner and monogenic expression is the general rule, i.e., one neuron–one receptor. The molecular receptive range has been analyzed for several olfactory receptors. Generally, olfactory receptors have been found to exhibit a somewhat relaxed specificity towards ligands. However, some receptors, in particular those for pheromones, show very high specificity. Olfactory receptors signal through specialized trimeric G proteins to open calcium-permeable nonspecific cation channels.

Olfactory Receptors are G Protein-Coupled Heptahelical Receptors

From a modest origin in simple eukaryotes like yeast, G protein-coupled heptahelical receptors (Figure 1) have evolved into the largest superfamily known. As the name indicates, signaling occurs through (trimeric) G proteins, with particular families making use of different G proteins. These receptors transmit biological effects of many hormones, neurotransmitters, chemokines, and diverse sensory stimuli. Chemosensation constitutes an ancient function for this family. Already in yeast a dichotomy between sensing nutrients and sensing pheromones is found.

Whereas simple animals like nematodes possess a single chemosensory sense, in higher animals several specialized systems have evolved, using olfactory and gustatory receptors, respectively. Olfactory receptors may recognize volatile or water-soluble odorants, depending on the species (e.g., mammals versus fish), and the defining difference to taste receptors appears not to be the nature of the ligand, but the outreach of the system. Taste is generally considered to be a contact sense, whereas olfaction delivers long-range information.

Olfactory Receptors Segregate in Several Highly Divergent Groups

Thirteen years ago, the first higher eukaryote chemosensory receptors – mammalian odorant receptors proper (OR) – have been identified. Linda Buck, then a postdoctoral fellow in Richard Axel's laboratory, used short motifs conserved in previously known heptahelical receptors to amplify a group of rat odorant receptors from nasal cDNA via polymerase chain reaction. Like all heptahelicals, odorant receptors exhibit the canonical seven-transmembrane domain structure (Figure 1) and the G protein-interaction motif. Peculiar are the relatively short N and C termini. OR are a highly divergent group, and amino acid homologies below 20% have been reported within one species. Between phyla, homologies have been so low as to be undetectable. Thus, insect and nematode chemosensory receptors have not been identified via homology searches, but by looking for orphan heptahelical receptors in either single cell libraries or genomic databank searches.

Two classes of distantly related receptors have been found in the mid-1990s. They are designated V1R and V2R family, after their occurrence in the mammalian vomeronasal or accessory olfactory system. V1R receptors share the short N and C termini with the OR receptors, whereas the V2R exhibit a large extracellular N-terminal domain, and show some sequence homology to the Ca^{2+}-sensing receptor and the metabotropic glutamate receptor, a neurotransmitter receptor. In mice the V2R family comprises ~100 genes and the V1R family contains ~150 genes, which segregate into 12 subfamilies designated V1Ra, V1Rb etc. Humans and other hominoids have nearly no VR receptors as their accessory olfactory system is derelict and their VR genes suffer ongoing pseudogenization. No intact human V2R is remaining and less than a handful of intact *V1R* genes have been identified in extensive genome searches.

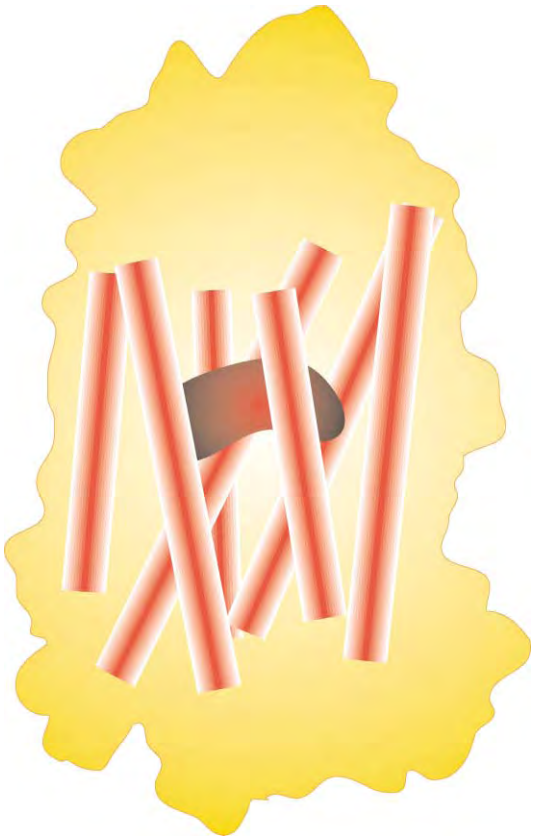

FIGURE 1 Schematical representation of an olfactory receptor. No crystallographical data are available for olfactory receptors. It is assumed that their structure is analogous to that of rhodopsin and the adrenergic receptor, which are more extensively studied. This is supported by some mutational analysis and molecular dynamics modeling. The scheme shown here is based on the structure of rhodopsin, whose crystal structure has been solved in 2000. Seven-transmembrane regions are depicted as cylinders. The binding site for ligands is centrally situated, between several transmembrane domains.

It is commonly assumed but not rigorously shown that OR deal with common odors whereas VR are specialized for detecting pheromones – odors which are relevant in a social context as in kin recognition and mating.

It should be mentioned that there may be another, radically different group of olfactory receptors, a type of membrane-bound guanylate cyclases with a single transmembrane domain. Members of this family are expressed in specific subsets of olfactory receptor neurons. However, no ligands have been identified for them so far.

Gene Structure and Genomic Arrangement of Olfactory Receptors

Vertebrate OR and V1R feature an intronless coding region of ~1 kb that may be preceded by one to several noncoding introns. Alternative splicing is a frequent phenomenon for odorant receptors. Insect olfactory receptors and vertebrate V2R contain several introns within the coding region, as is common for other G protein-coupled receptors.

The OR family size approaches 1300 identified genes in mouse, a species with a completely sequenced genome. About one-fifth are pseudo-genes, a high percentage, which has people speculating about a putative role of the pseudo-genes in the evolution of the gene family. The human OR gene family is of similar size; however, the percentage of pseudo-genes is much higher, so that only ~350 odorant receptors appear functional in humans. Clusters of related genes are a frequent feature and indicate recent expansions of the respective gene lineages. Sometimes other genes may be interspersed, a notable example being the intercalation of MHC genes with odorant receptors reported for the mouse (but not for the human) genome. Overall, olfactory receptors are widely spread throughout the genome, asserting the ancient origin of this gene family.

Family sizes are smaller for lower vertebrates and insects – for *Drosophila* 60 receptor genes have been identified in the complete genome, mosquitoes possess ~80 olfactory receptor genes. For fish estimates range ~100 different OR. However, the occurrence of (smaller) clusters and the overall widespread distribution of receptor genes are equivalent to higher vertebrates. Surprisingly, the nematode *Caenorhabditis elegans* boasts ~1100 different chemosensory receptor genes (including 30% pseudogenes).

Monogenic and Monoallelic Expression of Olfactory Receptor Genes

Nematode chemosensory neurons, like taste receptor cells, express many different receptor genes per cell. Such bundling of receptors may be efficient if many different chemicals should lead to very few behavioral outcomes – mainly the choice between "stay here" and "get out of here" or "swallow this" and "spit it out," respectively. As soon as a chemical sense is used for more sophisticated distinctions, it is imperative that more selective means of expression are used.

Accordingly, the expression of vertebrate and insect olfactory receptors is highly regulated. One particular olfactory receptor neuron expresses only a single type of OR gene or VR gene (Figure 2). This very restricted expression has been christened monogenic expression. In fact, for rodents it has been shown that expression is restricted even to one allele of a particular *OR* or

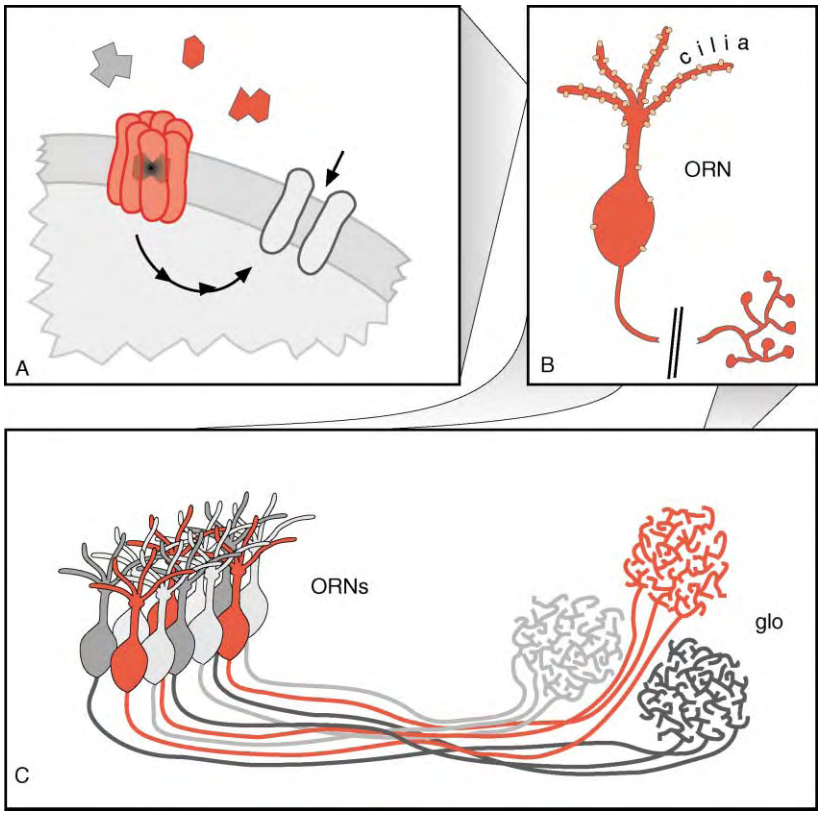

FIGURE 2 Olfactory receptors are part of the olfactory information processing pathway. (A) Olfactory receptors bind odorants and initiate a several step signal processing cascade. As endpoint various channels are opened, leading to depolarization of the olfactory receptor neuron. (B) The olfactory receptors are mainly expressed on the cilia (or microvilli, not shown) of olfactory receptor neurons. These neurons generate action potentials in their axons and propagate them towards their terminals in the so-called glomeruli (glo). Glomeruli are neuropil structures and constitute the first relay station (synapse) in the olfactory processing pathway. (C) Ciliated olfactory receptor neurons expressing the same odorant receptor are distributed within the sensory surface, but converge onto a common glomerulus. Microvillar receptor neurons such as those expressing the *V1R* and *V2R* genes converge onto several microglomeruli (not depicted here).

*VR*gene, reminiscent of the monoallelic expression of immunoglobulin genes.

Some exceptions occur to the rule of one neuron–one gene. Notably a particular insect olfactory receptor, OR83b, has been found to be coexpressed in about two-thirds of all olfactory receptor neurons. This receptor is also highly unusual in that it is strongly conserved between many insect species. It is suspected that such atypical receptors may not have a role in odor detection, but serve another, so far unknown function.

Olfactory Receptor Gene Expression is Regulated by Proximal and Distal Control Regions

A stringent test for specificity of expression relies on the convergence of olfactory receptor neurons expressing the same receptor gene into a single glomerulus at a roughly fixed position (Figure 2). In several cases such a restricted expression pattern could be reproduced faithfully by reporter gene constructs containing variable segments of DNA flanking the coding region. It has been possible to narrow-down control elements to regions of one to a few kilobases, but specific enhancer sites, transcription factors, or combinations thereof are just beginning to be identified. In some cases all control elements appear to be situated close to the gene, whereas for other OR essential regulatory elements have been found in distances of ~100 kb from the coding region.

Selection of an odorant receptor gene for expression is a multilevel process. First, a choice is made for a particular subgroup of genes. Such subgroups feature spatially or temporally limited expression. In a second step, a particular odorant receptor is selected in a stochastic manner and then exerts negative feedback regulation onto all other OR. Thus, monogenic expression of odorant receptors is ensured.

Ligand Spectra have been Established for a Handful of Olfactory Receptors

Although hundreds of olfactory receptors have been cloned to date, ligands are only known for a small percentage of them. The difficulty of guessing potential ligands from among the enormous pool of potential odorants has been a major problem. Also, correct expression in heterologous systems has turned out to be unusually complicated, and has only been possible for some receptors. Most of the receptor molecules synthesized in heterologous systems are not transported to the plasma membrane, but remain in the endoplasmatic reticulum, possibly because some unknown auxiliary molecules are missing. Indeed, for nematode chemosensory receptors a chaperone has been shown to be essential for proper protein translocation and V2R receptors are coexpressed with MHC class 1b molecules that appear to serve as escort molecules. For two OR genes it has been possible to use a viral transfection method to express the recombinant odorant receptor in olfactory receptor neurons. In several cases knockouts of particular olfactory receptors have served to identify receptor ligands, as first shown for the *C. elegans* ODR10 diacetyl receptor. The binding of ligands is not measured directly, but evaluated by a downstream parameter such as a change in membrane potential, or, more commonly, a rise in intracellular calcium levels.

Usually olfactory receptors respond best to a small group of highly related compounds and with lower sensitivity to further odorants. Often a particular functional group is preferred, but in some cases ligands with other functional groups may also activate the same receptor. Many strong ligands identified so far contain an aldehyde or keto group. The most extensive ligand analysis has been performed for the rat odorant receptor I7, which has *n*-octanal as main ligand. Hydrocarbon chain length is another molecular feature that influences ligand efficacy. In the vast majority of cases longer hydrocarbon chains result in more avid binding. From psychophysical experiments it is known that also the shape and rigidity of the ligand molecule determine the olfactory sensation. Enantiomers of known ligands often, but not always, show differential responses. Taken together, a particular olfactory receptor requires a particular combination of molecular features in its cognate ligand/s.

Combinatorial versus Monospecific Representation of Odorants

Due to the monogenic expression of olfactory receptors, the ligand specificity of the olfactory receptor determines the odor responses of the corresponding olfactory receptor neurons (Figure 2). Due to the convergence of olfactory neurons expressing the same receptor in single glomeruli (Figure 2) the ligand specificity of the olfactory receptor determines the odor responses in these glomeruli. This results in a rather direct map of the ligand specificities of the olfactory receptor repertoire on a two-dimensional surface in the corresponding brain region (the olfactory bulb in mammals, the antennal lobe in insects). Interestingly mammalian odorant receptors influence the choice of a target glomerulus of olfactory receptor neurons as shown by gene swap experiments. Insect olfactory receptors, on the other hand, appear not to be involved in selection of the proper target site.

Two complementary principles of odorant representation emerged from ligand binding studies *in situ* and in heterologous systems. Firstly, many odorants activate a small subset of the large repertoire of odorant receptors. Vice versa, any particular OR gets activated by a handful of different compounds, not just by a single compound. This results in a unique combination of activated receptors for each individual odor compound (Figure 3). The theoretical coding capacity of such a combinatorial representation is immense and much higher than needed – even for millions of different odors. In fact, the neuronal representation is sparse – the large majority of receptors does not respond to any given odorant – and thus suboptimal with respect to coding capacity. Nevertheless, humans (trained perfumers, that is) can distinguish and identify several thousand different odors, more than tenfold the number of the functional human OR repertoire.

An alternative principle of neuronal representation seems to be realized for a smaller group of chemicals, including many pheromones. The high sensitivity and specificity of several such olfactory receptors (observed in mammals, fish and insects) appears to indicate a monospecific interaction. A well-known example is the male/female attraction in silk moth, *Bombyx mori* (Figure 3). To integrate labeled line coding with hard-wired behavior appears straightforward. The coding capacity of such a system is low – it equals the number of different olfactory receptors devoted to this strategy – but sufficient for the limited number of potential pheromones. An example for a receptor/ligand pair is the mouse V1Rb2 receptor that specifically recognizes 2-heptanone.

Signal Transduction of Olfactory Receptors

All heptahelical olfactory receptors signal through trimeric G proteins. A controversy surrounding the

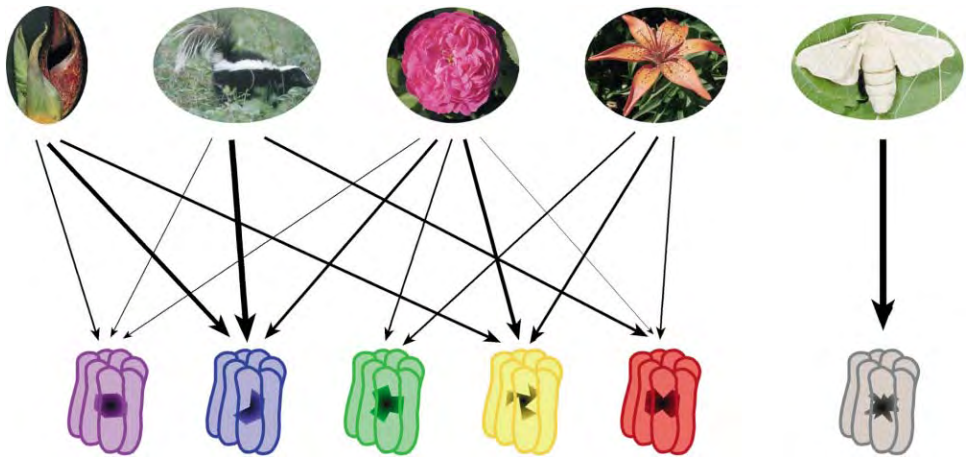

FIGURE 3 Two types of olfactory processing: combinatorial versus monospecific. To the left the combinatorial representation of odorants is depicted. Different odors – here symbolized by various odor sources (skunk cabbage, skunk, rose, lily) – activate overlapping, but distinctive combinations of olfactory receptors. This is also valid for the individual odor components, the odorants. Each odorant activates a particular subset of all olfactory receptors and thus each odorant generates a unique, if overlapping "fingerprint" of olfactory receptor activation. To the right monospecific representation of odorants is shown. A single compound activates a highly specific receptor very selectively, as is often observed for pheromones. Depicted here is a female silk moth, source of an attractive pheromone that is detected with extremely low threshold by the male of that species.

signal transduction by OR has been more or less resolved. Vertebrate OR signal through G_{olf}, a specialized α-subunit, which in turn activates adenylate cyclase type III (Figure 4). The resulting cAMP activates a cyclic nucleotide-gated channel that is a rather nonselective cation channel. Such channels are widespread in the nervous system, their particular gating properties are set by the subunit composition (A2A4B1b in the case of the mammalian olfactory channel). A considerable portion of inward current is carried by calcium (Figure 4). The resulting influx of calcium opens a calcium-gated chloride channel, resulting in chloride efflux, i.e., in further depolarization and thus amplification of the signal (mammals, amphibians, and fish). Finally, the odor-induced signal is switched off by G protein-coupled receptor kinase 3 (GRK3) and binding of arrestin-related molecules to the phosphorylated odorant receptor (Figure 4). Even with a constant odor stimulus the olfactory sensation is down-regulated within seconds, in part due to the peripheral mechanisms mentioned here.

The signal transduction cascade has not been worked out as well in invertebrates. Insects appear to also use cAMP as second messenger. Lobster may additionally employ IP3 as a second signal transduction system that

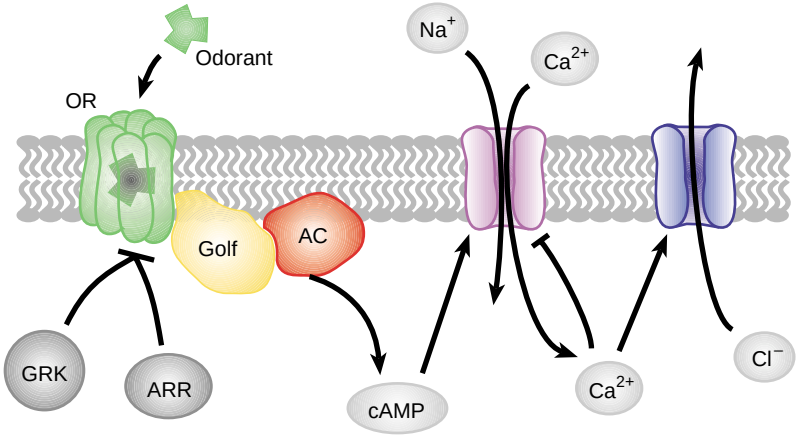

FIGURE 4 Signal transduction and termination of odor responses. A schematical representation of the main signaling pathway. AC, adenylate cyclase type III; ARR, β-arrestin-related molecules; G_{olf}, an α-subunit somewhat specific for the olfactory nervous system; GRK, G protein-coupled receptor kinase; OR, odorant receptor. The cyclic nucleotide-gated channel is permeable for sodium and calcium, but gets blocked by calcium. GRKs phosphorylate the odorant receptor, which subsequently binds β-arrestin, leading to a complete stop of the signal transduction cascade.

opens IP3-gated channels situated in the plasma membrane. Such channels have been described in olfactory receptor neurons of many species, including fish and rodents, but appear to be a minor constituent compared to the number of cyclic nucleotide-gated channels. The effects described for IP3 on olfactory signal transduction in mammals and fish may reflect a modulatory role of this second messenger, conceivably in setting the basal activity level of olfactory receptor neurons. When all the evidence is weighed, a completely independent second signaling pathway for odorant receptors appears not plausible.

Signal transduction for olfactory receptors of the VR type differs both from OR and between V1R and V2R. The emerging picture is that V1R signal via the G_{i2} α-subunit and V2R via the G_o α-subunit. Finally, a transient receptor potential channel, TRP2, is activated by diacylglycerol and allows the influx of cations including calcium.

See Also the Following Articles

Cyclic Nucleotide-Regulated Cation Channels • G Protein-Coupled Receptor Kinases and Arrestins • Taste Receptors

Glossary

chemosensation Any chemical sense, such as olfaction or taste. Very ancient, occurs already in bacteria where it is used for chemotaxis.

glomeruli Globular neuropil, comprises synapses of olfactory receptor neurons.

heptahelical A receptor with seven-transmembrane helices, often, but not exclusively a G protein-coupled receptor.

odorant A chemically pure odor, i.e., a single compound that activates an odorant receptor.

olfactory code The neuronal representation of odors insofar as it is relevant to the encoding of these odors. Often confused with the neuronal representation, which is more commonly studied.

pheromone An odorant that mediates intraspecies communication, eliciting neuroendocrine changes and stereotyped behavioral repertoires.

Further Reading

Breer, H. (2003). Olfactory receptors: Molecular basis for recognition and discrimination of odors. *Anal. Bioanal. Chem.* **377**, 427–433.

Crasto, C., Singer, M. S., and Shepherd, G. M. (2001). The olfactory receptor family album. *Genome Biol.* **2**, 1027.

Halpern, M., and Martinez-Marcos, A. (2003). Structure and function of the vomeronasal system: An update. *Prog. Neurobiol.* **70**, 245–318.

Keller, A., and Vosshall, L. B. (2003). Decoding olfaction in drosophila. *Curr. Opin. Neurobiol.* **13**, 103–110.

Kim, J., and Carlson, J. R. (2002). Gene discovery by E-genetics: Drosophila odor and taste receptors. *J. Cell Sci.* **115**, 1107–1112.

Korsching, S. (2002). Olfactory maps and odor images. *Curr. Opin. Neurobiol.* **12**, 387–392.

Nagao, H., Yamaguchi, M., Takahash, Y., and Mori, K. (2002). Grouping and representation of odorant receptors in domains of the olfactory bulb sensory map. *Microsc. Res. Tech.* **58**, 168–175.

Ronnett, G. V., and Moon, C. (2002). G proteins and olfactory signal transduction. *Annu. Rev. Physiol.* **64**, 189–222.

Touhara, K. (2002). Odor discrimination by G protein-coupled olfactory receptors. *Microsc. Res. Tech.* **58**, 135–141.

Young, J. M., and Trask, B. J. (2002). The sense of smell: Genomics of vertebrate odorant receptors. *Hum Mol. Genet.* **11**, 1153–1160.

Biography

Sigrun Korsching is a Professor at the Institute of Genetics at the University of Cologne in Germany. Her principal research interest is in the field of sensory neurobiology, in particular the sense of smell. She holds a Ph.D. from the Ludwig-Maximilian-Universität in Munich, Germany and received her postdoctoral training at the California Institute of Technology, California. She has authored influential texts in the fields of neurotrophic interactions and olfactory encoding.

Oligosaccharide Analysis by Mass Spectrometry

Andrew J. Hanneman and Vernon N. Reinhold
University of New Hampshire, Durham, New Hampshire, USA

Glycosylation is important for cellular regulation and recognition activities and oligosaccharide structural details are essential determinants of function. In contrast to other biopolymers that are joined by identically positioned functional groups, an oligosaccharide chain is commonly branched, with multiple positions for linkage. The monomer units themselves may exist as isomeric ring conformers (pyrans, furans), with differing spatial orientation of hydroxyl groups. When these hydroxyl groups are involved in linkage between residues (anomers), additional isomeric complexity is introduced. As a consequence, oligosaccharide structure elucidation can be a complicated problem requiring a number of different analytical approaches. Most of the techniques currently available for oligosaccharide analysis are based on mass spectrometry (MS) and we summarize in this report the details of composition, sequence, branching, and inter-residue linkage that can be obtained using small amounts of sample material.

Important Classes of Oligosaccharides

Glycoprotein Glycans

Glycoprotein glycans are branched oligomers having ~5–20 monosaccharides that are added to proteins co- or posttranslationally. Protein glycosylation is primarily based upon two main structural motifs: (1) *N*-linked glycans are linked through the amide bond of asparagine at an amino acid sequence called the consensus site: asparagine-x-serine/threonine (where x can be any amino acid except proline); and (2) *O*-linked glycans, which have no known consensus sequence and are linked through glycosidic bonds to serine and threonine residues on the protein. For both glycan types there are constant core structures proximal to the protein backbone, although numerous variations are known.

Glycosphingolipid Glycans

Glycosphingolipids represent a diverse set of amphipathic molecules comprised of an outer glycan portion linked to a ceramide lipid tail. In glycosphingolipids the ceramide lipid serves as an anchor to the cell membrane and the carbohydrate can present a hydrophilic surface for cell–cell recognition.

Glycosaminoglycans

Glycosaminoglycans (GAGs) are linear carbohydrate chains consisting of repeating disaccharide units, often rich in sulfate groups (e.g., heparin), that make up the carbohydrate portion of high molecular weight protein/carbohydrate assemblages known as proteoglycans. Tissue-specific proteoglycans are inserted into plasma membranes, excreted into the extracellular matrix, or stored in intracellular compartments where they are involved in adhesion, lubrication, and regulatory functions.

Methods and Instrumentation

Obtaining and Preparing Glycans for Mass Spectrometry

Carbohydrates, being less polar, are generally more difficult to ionize than other classes of biological molecules, a feature that is compounded when in the presence of salts and peptides. Consequently, judicious purification steps are required for effective MS analysis of carbohydrates. Purification, including desalting, is often accomplished online using high pressure liquid chromatography (HPLC) prior to electrospray mass spectrometry (ESI). Changing the physical characteristics by derivatization has also proven to be successful, and this is discussed below.

Glycan Release and Purification

Prior to mass spectrometry glycoproteins can be enzymatically cleaved using trypsin or other proteases

resulting in a peptide/glycopeptide mixture; however, glycopeptides ionize poorly within such mixtures and subfractionation is usually advantageous. Consequently, glycans are often enzymatically or chemically released from proteins first and then purified. This approach, however, loses an important feature of structure: the location of the glycan and its consensus sequence on a peptide. Most *N*-linked glycans are conveniently released from proteins using the endoglycosidase enzymes PNGase F or PNGase A. Analogous enzymes for general release of *O*-linked glycans, however, are not known and *O*-linked glycans are typically released using chemical methods including base-release (beta-elimination) and anhydrous hydrazine at low temperature. Hydrazinolysis at higher temperatures is well suited for *N*-linked glycan release, however, at high temperature significant degradation of *O*-glycans is observed.

Glycolipids are obtained from biological materials by extraction with organic solvents, including chloroform: methanol:water (CMW). Glycolipids can be isolated from other lipids using ion exchange or silica gel chromatography and may then be analyzed directly or the oligosaccharide chains are enzymatically or chemically released and extracted.

GAGs are chemically released from proteoglycans and subjected directly to MS analysis or may first be broken down into smaller subunits using GAG-chain-specific enzymes including chondroitinases and heparinases.

Derivatization and Adduction for Ionization

Lacking very polar functional groups many oligosaccharides are not easily ionized. In the positive ion mode naturally occurring oligosaccharides are typically observed as adducts with cations such as sodium or potassium, although numerous cations can be used. Derivatization is another strategy for improving ionization to enhance MS signal. Some of the common derivatization strategies were originally developed to improve the volatility of carbohydrates for gas chromatographic analysis. Complete methylation of hydroxyl groups improves volatility and also assists purification by organic solvent extraction, providing sensitivity enhancement when analyzed by electrospray ionization (ESI) or matrix-assisted laser desorption ionization (MALDI)-MS. Permethylation is also advantageous when structural details are pursued. Other procedures involve covalent attachment of an ionizable functional group such as an amine to the oligosaccharide-reducing end. Some aminated derivatives may include a chromophore or fluorophore to enhance UV/vis or fluorescence detection.

Instrumentation for Glycoconjugate Mass Spectrometry

Mass spectrometry is a gas-phase analytical technique originally limited for use with small molecules that had to be thermally vaporized prior to ionization. The molecular weight obstacle has since been overcome by techniques that combine vaporization and ionization in a single step; these include ESI and MALDI. Both techniques have been interfaced with a variety of mass analyzers, and high-molecular-weight samples now provide no barrier using these techniques.

Gas-phase ions are a long way from detailed structural understanding, thus the recent challenges in mass spectrometry relate to disassembly of large structures within the mass spectrometer. Notwithstanding recent developments, composition analysis of depolymerized oligosaccharides by GCMS has remained an important tool for structure determination.

Ionization Methods for Mass Spectrometry

Electron Impact and Chemical Ionization Electron-impact ionization (EI) and chemical ionization (CI) were the first ionization methods to be widely applied to carbohydrate samples. EI and CI are gas-phase techniques that are readily interfaced with a gas chromatograph (GC) enabling complex mixtures to be efficiently separated by GC with subsequent component identification by MS. EI imparts high energy to the sample resulting in extensive fragmentation. The fragments serve to guide structure determination. Excessive energy and resultant fragmentation in EI often precludes molecular weight determination leaving structural ambiguity if the parent ion is lost from the spectrum. This limitation led to the development of the softer ionization technique CI. CI is an extension of EI wherein energetic electrons are initially directed toward ionizing a gaseous molecule such as methane. The gas-phase analyte is ionized by interaction with the gas (by proton transfer in the case of methane). CI generates a robust molecular ion signal but lacks the information that can be obtained following fragmentation. Modern MS approaches are tailored toward soft ionization to obtain a molecular ion followed by fragmentation step(s) for subsequent structural characterization.

Electrospray Ionization (ESI) Electrospray induces vaporization concurrent with soft ionization making it an extremely useful technique for analysis of biopolymers in solution, including HPLC eluates. Electrospray exploits a high electric field to aerosolize analyte-containing solutions creating a fine mist of charge-dense droplets. A bath gas at ambient pressure serves to vaporize solvent from droplet surfaces reducing their

size and increasing the surface charge density. Electrostatic repulsion ultimately disrupts the droplet surface leading to production of small charged droplets and eventual ejection of gas-phase analyte ions into a high vacuum region for mass analysis.

Matrix-Assisted Laser Desorption Ionization (MALDI) MALDI is a solid-state ionization method that, like ESI, combines ionization and vaporization into a single step thereby providing another convenient interface for biopolymer analysis. In MALDI the sample is dissolved in a matrix solution, spotted onto a stainless steel "target" and dried. The matrix molecules provide a UV-chromophore with an absorbance spectrum tuned to the laser-irradiation source. Laser ablation of the target spot under vacuum results in flash vaporization and ionization of the matrix and embedded sample molecules that can be subsequently directed into the mass analyzer region. In contrast with ESI, which may produce multiply charge ions, MALDI ions are typically singly-charged.

Mass Analyzers

In a mass spectrometer the ionization sector (e.g., ESI, MALDI) is coupled to a mass analyzer. The earliest mass analyzers used magnetic and/or electric sectors to separate ions by their mass-to-charge ratio (*m/z*); more recent instruments use a variety of new designs to accomplish the same task; these include the ion trap (IT), quadrupole mass filter, time-of-flight (TOF) tube, as well as hybrid instruments consisting of a combination of mass analyzers arranged in series for tandem or sequential mass spectrometry.

Complete Structure Elucidation by Mass Spectrometry

Oligosaccharide structure elucidation generally follows an approach consisting of determining the monosaccharide composition, defining monomer sequence and branch points, identifying inter-residue linkage positions, and specifying the anomeric configuration of glycosidic bonds.

Obtaining an MS Profile

After using a specific release, extraction, and cleanup procedure, an oligosaccharide sample is typically profiled by single-stage MS (MALDI, ESI, or HPLC-ESI) to profile the molecular weight(s) of constituent oligosaccharides. With molecular weight in hand, a general composition of monomers may be assigned to each oligosaccharide, i.e., hexose, deoxyhexose, N-acetyl hexosamine, but without indication of specific isomers. When combined with knowledge about the source material, release and purification method, and a composition analysis, a significant component of sequence information can be hypothesized based on the MS profile; however, it remains fraught with holes for potential incorrect assignments. Further characterization is mandatory to accurately assign sequence, branching, and linkage details.

Composition Analysis by GCMS

MALDI and ESI allow most oligosaccharides to be analyzed intact; however, GCMS-based composition analysis has remained a useful method for quantitative determination of monosaccharide composition, offering valuable complementary information. GCMS involves depolymerization into constituent monomers by hydrolysis or methanolysis, followed by volatility-enhancing derivatization. Both the GC retention time and the mass spectrum are used to identify and quantify the constituent monomers. A variety of derivatization or combined depolymerization/derivatization schemes, involving methylation, acetylation, and/or trimethylsilylation are used in composition analyses.

Linkage Analysis

Linkage analysis is used to determine inter residue linkage and branch points. This methodology is an extension of composition analysis wherein the oligosaccharide is permethylated prior to hydrolysis. Following hydrolysis the partially methylated monomers are reduced and acetylated, placing acetyl groups at all the positions opened by hydrolysis and reduction. The resulting alditol acetates have mixed methylation/acetylation substitution patterns depending upon their position in the original polymer, and reduction decreases anomeric heterogeneity in the gas chromatograms. The GC retention times and electron impact fragmentation patterns of partially methylated alditol acetates (PMAA) are used to indicate the type of linkages associated with specific monomers. Because the method involves depolymerization, however, the information that connects one monomer with another is lost making it challenging to use linkage analysis with mixtures.

Tandem Mass Spectrometry (MS/MS) and Sequential Mass Spectrometry (MS^N)

When collision-induced dissociation (CID) is performed on isolated parent ions the fragments produced provide an important strategy for understanding structure. Tandem mass spectrometry is commonly

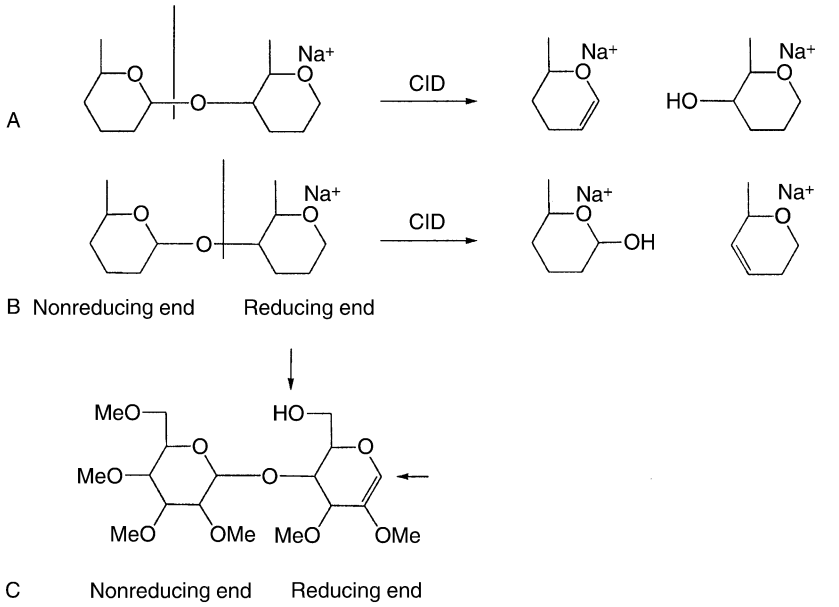

FIGURE 1 (A) and (B) Glycosidic bond cleavages for sodium adducted oligosaccharides. Sodiated fragments representing the reducing and nonreducing ends are observed for breaks on both sides of the glycosidic bond. (C) A branch point fragment; arrows identify the broken bonds.

used in this manner to sequence linear polymers. This straightforward approach has been applied with remarkable success to characterization of peptides but is limited when applied to oligosaccharides. Oligosaccharides are replete with isomeric possibilities that require further decomposition not available by tandem MS.

In order to fully characterize branching and obtain complete understanding of sequence and linkage, sequential steps of collision-induced dissociation must

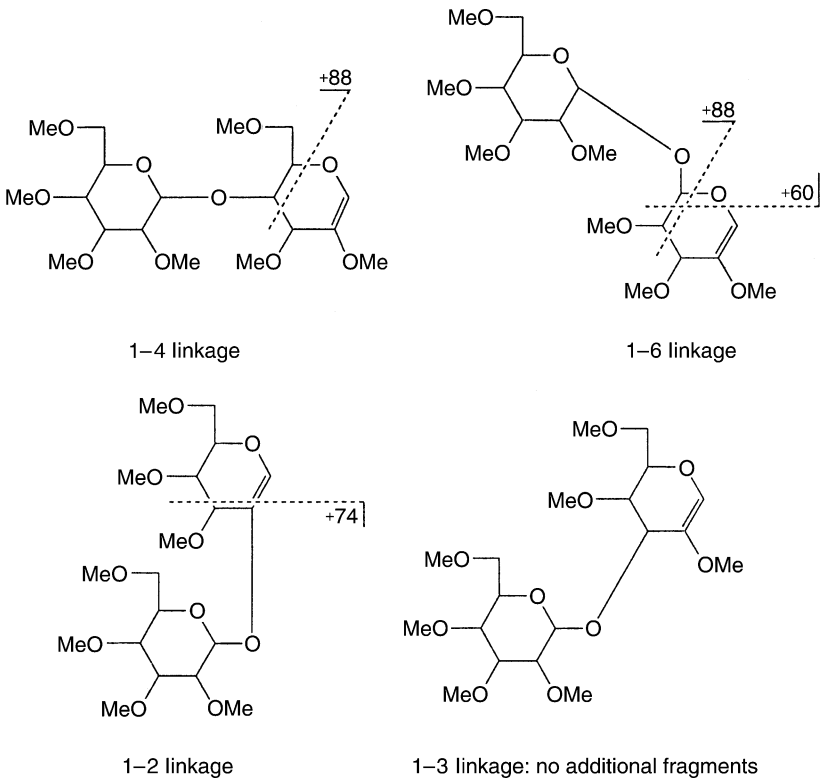

FIGURE 2 Use of cross-ring cleavages in MS^n to identify linkage position on hexoses in permethylated glycans.

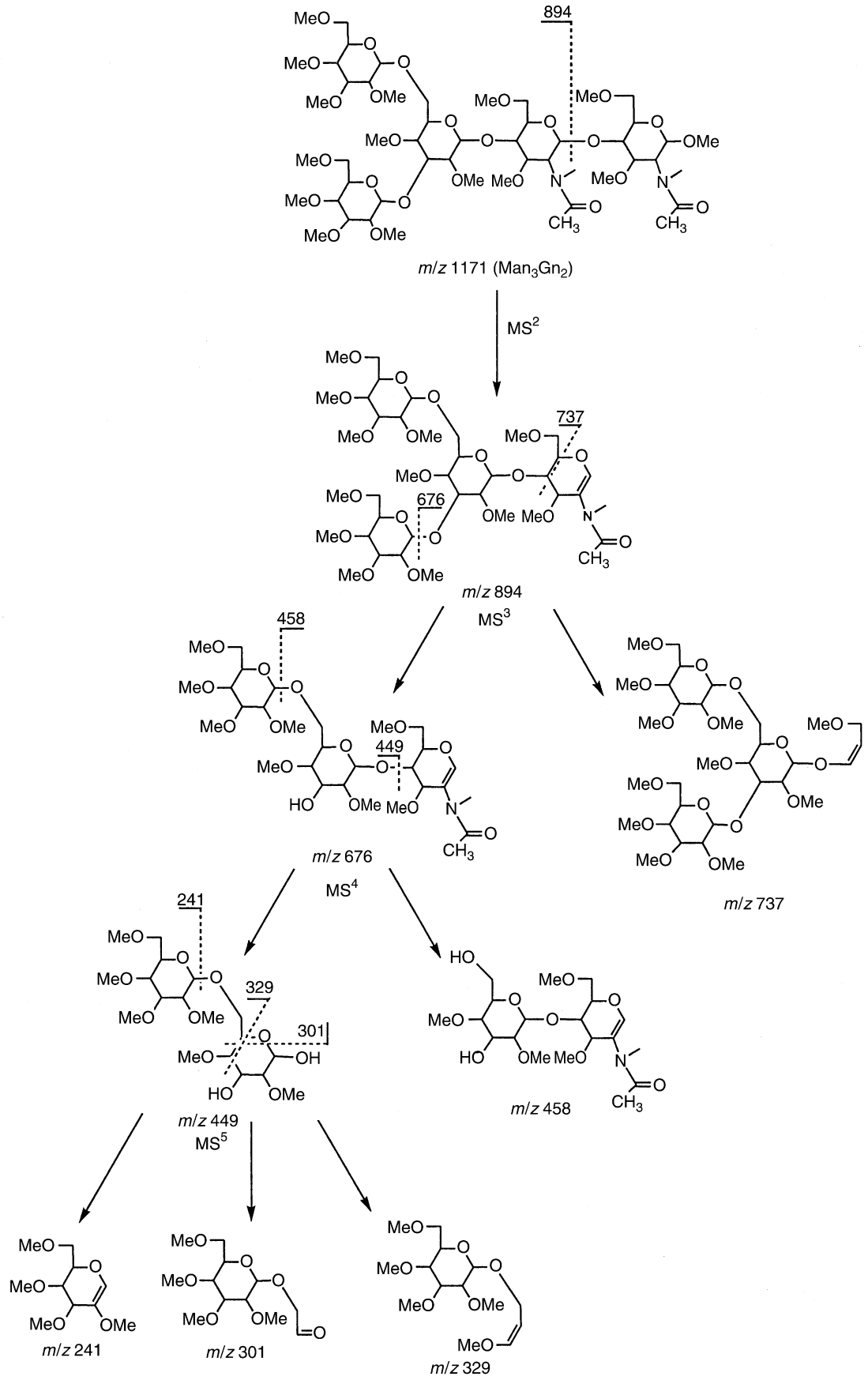

FIGURE 3 Use of MS^n to dissect a typical *N*-linked glycan. Selected CID pathways are shown through MS^5.

be performed using ion trap mass spectrometry (IT-MS). In ion trapping the molecular ion is maintained in a stable oscillatory trajectory within an ion trap via application of electrical fields. Ion trap instruments are programmed to perform sequential rounds of ion isolation sweeping the trap free of all other products. The generated fragments are released from the trap by resonance activation and mass measured, or single product ions may be re-isolated in the same manner and fragmented again. Fragmentation on any isolated ion is accomplished by low-energy collision-induced dissociation (CID) using a neutral gas.

Using MS^n to Identify Oligosaccharide Branching: Glycosidic Bond Rupture

Glycosidic bonds are easily ruptured by CID and fragments representing a single cleavage on either side of the glycosidic oxygen are observed with a mass difference of 18 Da (Figures 1 (A) and 1(B)). Methylation prior to MS analysis uniquely provides identity to reducing and nonreducing termini, as well as an indication of branching when MS peaks appearing at 14 Da lower intervals indicate hydroxyl group exposed during CID (Figure 1 (C)).

Using MS^n for Linkage Analysis: Cross-Ring Cleavages

Monomers within an oligosaccharide sequence are linked through C-1 of a nonreducing end monomer to any one of four hydroxyl groups (2, 3, 4, or 6) on the adjoining reducing end monomer. These subtleties in structure can be identified in an MS/MS spectrum through minor fragment ions in the mass spectrum appearing above the abundant ions indicating glycosidic ruptures. The increment is a consequence of cross-ring fragmentation around the linkage position (88 Da, 4-linkage; 74 Da, 2-linkage; 88 & 60 Da, 6-linkage), (Figure 2). Cross-ring cleavages are not typically observed for 1–3 glycosidic linkages. Diagnostic cleavages observed during MS^n for the *N*-linked glycan Man_3Gn_2 are shown in Figure 3.

Complementary Techniques

Mass spectrometry is typically used to define all oligosaccharide features except for the configuration of anomeric glycosidic bonds. When used in conjunction with MS, anomericity can be approached using enzymes with known activity for specific glycosidic bonds. The enzymes may be employed sequentially or in parallel array and MS and MS^n spectra from before and after treatment are compared to indicate which monomers were lost.

See Also the Following Articles

Glycoprotein-Mediated Cell Interactions, O-Linked • Glycoproteins, N-linked • HPLC Separation of Peptides • Oligosaccharide Chains: Free, *N*-Linked, *O*-Linked • Proteoglycans • Sphingolipid Biosynthesis • Sphingolipid Catabolism

Glossary

glycoside bond An acetal bond linking the monosaccharides in a polymeric carbohydrate chain; originates from carbon-1 of a nonreducing end sugar and may be linked to any of a number of hydroxylated positions on a reducing end sugar.

molecular ion The ion indicating the molecular weight of an intact molecule.

monosaccharide The poly-alcohol units comprising a carbohydrate polymer. In biopolymers monosaccharides are present in the ring-closed form.

oligosaccharide A carbohydrate polymer comprised of a relatively small number of monosaccharides.

reducing end The end of a glycan having a hemi-acetal linkage that can be reduced to an alcohol using a reducing agent. As such, the reducing end is capable of forming linkages to proteins, as in glycoproteins; or with lipids, as in glycolipids.

Further Reading

Cheng, H. S., and Her, G. R. (2002). Determination of linkages of linear and branched oligosaccharides using closed-ring chromophore labeling and negative ion trap mass spectrometry. *J. Am. Soc. Mass Spectrom* **13**, 1322–1330.

Harvey, D. J. (1999). Matrix-assisted laser desorption/ionization mass spectrometry of carbohydrates. *Mass Spec. Rev.* **18**, 349–451.

Reinhold, V. N., and Reinhold, B. B. (1999). Carbohydrate mass spectrometry, a characterization of sequence, linkage and branching using ES-MS and CID. In *Fundamentals and Applications of Gas Phase Ion Chemistry* (K. R. Jennings, ed.) pp. 181–200. Kluwer Academic Publishers, Netherlands.

Sheeley, D. M., and Reinhold, V. N. (1998). Structural characterization of carbohydrate sequence, linkage and branching in a quadrupole ion trap mass spectrometer: Neutral oligosaccharides and N-linked glycans. *Anal. Chem.* **70**(14), 3053–3059.

Varki, A., Cummings, R., Esko, J., Freeze, H., Hart, G., and Marth, J. (eds.) (1999). In *Essentials of Glycobiology.* Cold Springs Harbor Press, Cold Springs Harbor, NY.

Viseux, N., Hoffmann, E. de, and Domon, B. (1998). Structural assignment of permethylated oligosaccharide subunits using sequential tandem mass spectrometry. *Anal. Chem.* **70**, 4951–4959.

Weiskopf, A. S., Vouros, P., and Harvey, D. J. (1997). Characterization of oligosaccharide composition and structure by quadrupole ion trap mass spectrometry. *Rapid Comm. Mass Spectrometry* **11**, 1493–1504.

Biography

Reinhold is a Professor of Chemistry and Biochemistry at the University of New Hampshire in Durham New Hampshire, and Director of the University of New Hampshire Center for Structural Biology (UNH-CSB).

Hanneman is a Bioanalytical Chemist in the Reinhold laboratory.

Oligosaccharide Chains: Free, *N*-Linked, *O*-Linked

Tadashi Suzuki
Osaka University, Osaka, Japan

There is growing evidence that *N*-linked glycans play pivotal roles in protein folding and intra- and intercellular trafficking of *N*-glycosylated proteins. It has been known that during the *N*-glycosylation of proteins, significant amounts of free oligosaccharides (free OSs) are generated in the lumen of the endoplasmic reticulum (ER), possibly by the action of oligosaccharyltransferase. Free OSs are also formed in the cytosol by enzymatic deglycosylation of misfolded glycoproteins, which are destined to be destroyed by a cellular system called ER-associated degradation. Although the precise fate of intracellular free OSs remains obscure, recent biochemical studies have revealed that a novel cellular machinery enables them to be catabolized in a sophisticated manner that involves pumping free OSs from the ER to the cytosol where further processing occurs, followed by their entry into the lysosomes.

Free Oligosaccharides Formed in the Endoplasmic Reticulum

N-Glycosylation is one of the most common co- and posttranslational modifications of eukaryotic proteins occurring in the lumen of the endoplasmic reticulum (ER). During the translocation of proteins in the ER, an enzyme complex called oligosaccharyltransferase (OST) transfers an oligosaccharide (OS) moiety from the dolichol-linked donor substrate to asparagine residues located within the consensus sequence -Asn-Xaa-Ser/Thr- (where Xaa is any amino acid except Pro) to form *N*-linked glycans on the nascent polypeptide chains. Although the biosynthesis of lipid-linked OSs, as well as processing of *N*-linked glycan chains on glycoproteins, is understood in outline, certain aspects of phenomena occurring during *N*-glycosylation reaction remain largely unknown. For instance, biochemical studies have shown that a significant pool of free OSs does occur in the lumen of the ER. It has been proposed that, in the absence of sufficient acceptor sequences, the OST exhibits hydrolytic activity and transfers OSs ($Glc_3Man_9GlcNAc_2$ in most organisms) on dolichol to water, presumably to control the amount of donor substrates when fewer acceptor molecules are around. The OSs formed by OST bear di-*N*-acetylchitobiose (GlcNAcβ1-4GlcNAc) at their reducing termini. Whether there are any other enzyme activities responsible for the release of free oligosaccharides in the lumenal side of the ER is still controversial and has not been unequivocally demonstrated in any organism.

Free Oligosaccharide Transport System from the Endoplasmic Reticulum to the Cytosol

Although it is not known whether free OSs have a physiological role in the ER, one could easily envisage that the accumulation of vast amount of free OSs in the ER could interfere with the quality-control system involving the recognition of the folding state of proteins, export of misfolded lumenal and transmembrane proteins into the cytosol, and degradation of them by the 26S proteasome (see later discussion). Therefore, it is not surprising that cells have machinery to eliminate free glycans from the ER lumen. Using permeabilized mammalian cells, it has been demonstrated that free OSs formed in the ER are, after rapid deglucosylation, exported from the ER into the cytosol. A transporter responsible for the export of free OSs from the ER membrane has not been identified, although biochemical studies show that the export is an ATP- and Ca^{2+}-dependent process. The OS export is also effectively blocked by the addition of low concentrations of mannose and its derivatives, but not by other sugars, suggesting that the transport machinery for free OSs recognizes the mannosyl residues at the nonreducing end, but not the GlcNAc residues at their reducing termini. The main structure of free OSs released from the ER to the cytosol has been shown to be $Man_{8\sim9}GlcNAc_2$ (Figure 1).

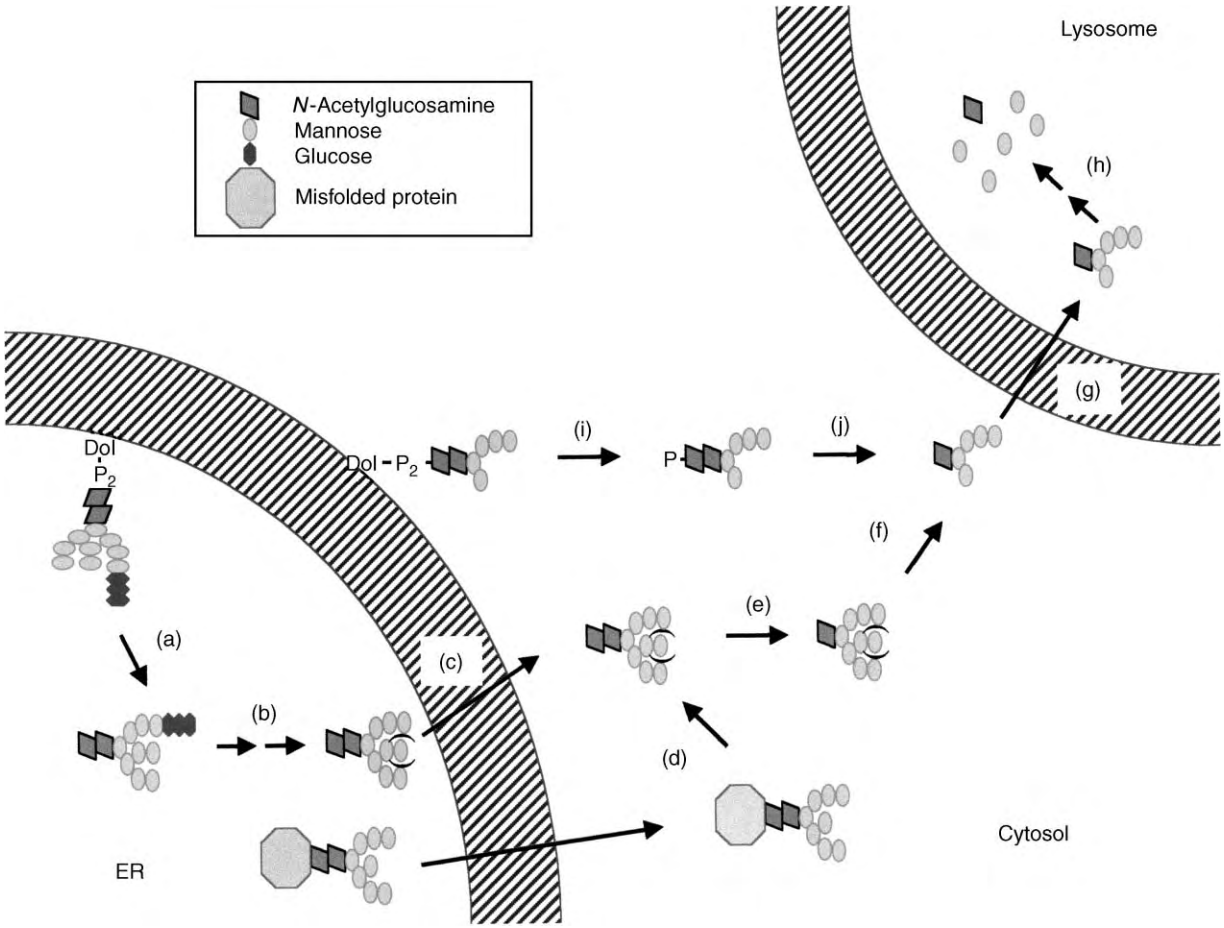

FIGURE 1 Model for the fate of free oligosaccharides generated in and outside of the ER in mammalian cells. Step (a), Free OSs generated in the lumen of the ER by the hydrolytic activity of OST bear di-*N*-acetylchitobiose (two GlcNAc residues) at their reducing termini. Step (b), After quick deglucosylation by α-glucosidase I and II (and sometimes ER α-mannosidase I), (c) $Man_{8\sim9}GlcNAc_2$ is transported into the cytosol by a putative transporter. Step (d), In the cytosol, PNGase removes *N*-linked glycan (most likely a $Man_8GlcNAc_2$ structure because action of an ER α-mannosidase I is prerequisite for the efficient export of misfolded glycoproteins from the ER to the cytosol) from misfolded glycoproteins and thereby releases free OSs bearing di-*N*-acetylchitobiose. Step (e), Once in the cytosol, ENGase (or, in some cases, a chitobiase) forms a free OS with a single GlcNAc at the reducing termini ($Man_{8\sim9}GlcNAc$). Step (f), The free OS with a single GlcNAc is now susceptible to the action of a cytosolic α-mannosidase, giving rise to a $Man_5GlcNAc$ structure. This structure is identical to the last dolichol intermediate present in the cytosolic face. Step (g), The $Man_5GlcNAc$ is transported into the lysosomes by a specific transporter. Step (h), In lysosome, the $Man_5GlcNAc$ is hydrolyzed into monomers (Man and GlcNAc) by lysosomal α- and β-mannosidases. Step (i), Putative pyrophosphatase, whose activity is reported in the cytosolic face of the ER membrane, can also release free OSs from the dolichol-linked OSs (presumably with the structure of $Man_5GlcNAc_2$) in the cytosol. Step (j), probably, this OS-phosphate will be processed by ENGase to give rise to $Man_5GlcNAc$, which is readily transported into lysosome. Note that this scheme cannot be applied to other organisms; for example, *Saccharomyces cerevisiae* does not possess ENGase, so there must be a distinct path.

Free Oligosaccharides Formed in the Cytosol: Its Connection with Endoplasmic-Reticulum-Associated Degradation

Recent evidence clearly shows that the ER has quality-control machinery that differentiates between misfolded (glyco)proteins and correctly folded ones, so that only the latter move from the ER to the Golgi. In this system, proteins that fail to fold or form subunit structures are retained in the ER and interact with various lumenal chaperones that allow them to mature into their native structure before they exit the ER. When proteins consistently fail to acquire the correct state, they eventually are degraded by the mechanism called ER-associated degradation(ERAD). It is now clear that this degradation process involves the retro-translocation of the defective (glyco)proteins from the ER to the cytosol, followed by their degradation in the cytosol by the action of proteasome. Recent growing

evidence shows that glycan chains on glycoproteins play critical roles in monitoring the folding state of glycoproteins in the ER that involves various intracellular lectins.

When the misfolded glycoproteins are retrotranslocated to the cytosol for degradation, protein is ultimately degraded by the action of the 26S proteasome. However, it is reasonable to assume that for glycoproteins to be degraded efficiently by the proteasome, bulky modifications of polypeptide side chains such as *N*-glycan chain may be removed prior to precessive proteolysis by the proteasome. The removal of glycan is achieved by the action of peptide:*N*-glycanase (PNGase), releasing free OSs in the cytosol (Figure 1). PNGase cleaves the amide bond between glycosylated asparagine residues and the proximal GlcNAc residues (Figure 2), and under physiological pH ammonia is released, generating free OSs bearing a di-*N*-acetylchitobiose unit at the reducing termini. The cytosolic PNGase occurs widely from yeast to mammalian cells, and the gene encoding this enzyme has been identified.

Another enzyme that can generate free OSs in the cytosol is a pyrophosphatase that releases OS-phosphate moieties from dolichol-linked OSs (Figure 1). Such cytosol-oriented enzyme activity has been detected in mammalian cells. Another possibility is the action of endo-β-*N*-acetylglucosaminidase (ENGase), which cleaves the glycoside bond in the di-*N*-acetylchitobiose structure, giving rise to free OSs with a single GlcNAc remaining at the reducing termini (Figure 2). This cytoplasmic enzyme is also known to occur widely, but not in yeasts such as *Saccharomyces cerevisiae* or *Schizosaccharomyces pombe*. It is not known whether the cytoplasmic ENGase can directly generate free OSs either from dolichol-linked OS or from glycoproteins *in vivo*.

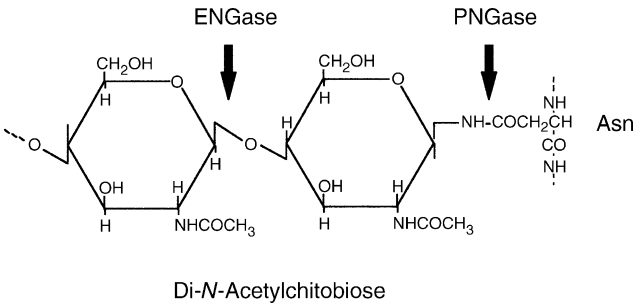

FIGURE 2 Reaction sites for two deglycosylating enzymes acting on *N*-glycosylated peptide. PNGase hydrolyzes the asparaginyl amide bond to give an aspartic acid-containing polypeptide chain and 1-amino-*N*-acetylglucosaminyl oligosaccharide; the latter is subsequently hydrolyzed under neutral pH to *N*-acetylglucosaminyl oligosaccharides and ammonia. On the other hand, ENGase hydrolyzes the glycoside bond in the di-*N*-acetylchitobiose moiety of the core region of *N*-linked glycan, leaving a single *N*-acetylglucosamine on the core peptide.

Cytosolic Processing of Free Oligosaccharides

Irrespective of their source, cytosolic OSs must be further catabolized, possibly to maximize the reuse of the component sugars. In the cytosol, two enzymes mainly contribute to the catabolism of free OSs: β-*N*-acetylglucosaminidase and α-mannosidase. For β-*N*-acetylglucosaminidase, so far two distinct enzyme activities have been reported; one is ENGase and the other is a cytosolic, neutral chitobiase. Although a chitobiase catalyses the same reaction with ENGase, it acts only if the reducing termini of the free OSs are di-*N*-acetylchitobiose, releasing a single GlcNAc from their reducing termini. Therefore, the chitobiase can be called a reducing-end exoglycosidase. Although the gene encoding cytoplasmic ENGase has been identified quite recently, the molecular nature of the cytosolic chitobiase is not known.

It has been shown that the action by a cytosolic α-mannosidase requires that free OSs bear only a single GlcNAc at the reducing ends. The trimming of free OSs by the cytosolic α-mannosidase (α1-2,3,6 mannosidase) results in a different Man_5 structure, yielded by the action of Golgi α-mannosidase I (α1-2 mannosidase), but in the same isomeric conformation with that is present in the dolichol-OS intermediate (Figure 1). The end product of ENGase (or chitobiase) and α-mannosidase in the cytosol, $Man_5GlcNAc$, is then transported into the lysosomes, where further degradation by α- and β-mannosidase can occur (Figure 1). The transporter on the lysosomal membrane seems to be specific to $Man_5GlcNAc$ structure, is ATP-driven, and is inhibited by *N*-acetylglucosamine but not by mannose. The last observation suggests that the reducing terminal structure of free OSs, in sharp contrast to the ER transporter, is crucial for recognition of free OSs by the lysosomal transporter. The molecular nature of the transporter remains to be identified.

Concluding Remarks

Cells possess a variety of enzymes and transporters to handle free OSs generated by several distinct mechanisms. Free OSs collected in the cytosol are processed by ENGase (or a chitobiase) and α-mannosidase before being incorporated into the lysosomes for degradation into monomeric sugars. Why this rather complicated pathway (ER to cytosol to lysosome) is

used for free OS catabolism is a mystery. One notion is that this trafficking route enables them to be removed quickly from the ER, thereby preventing them from interfering with the efficient glycan-dependent quality-control machinery for newly synthesized glycoproteins in the ER. However, it is still possible that a particular free OS itself may play a role in certain cellular processes. Indeed, intracellular free OS derivatives of *N*-glycan chains are known to play a role in the growth, senescence, and ripening of fruits in plants. Although similar bioactivity in other organisms still remains to be detected, the identification of molecules involving the formation, modification, and transport of free OS should provide us with more insight into the mechanism and function of this novel pathway.

See Also the Following Articles

Chaperones, Molecular • Endoplasmic Reticulum-Associated Protein Degradation • Proteasomes, Overview

Glossary

chaperones Molecules that, by associating with substrates, prevent them from aggregation and facilitate their acquiring the correct folding state.

di-*N*-acetylchitobiose A dimer of *N*-acetylglucosamine with β1-4 linkage.

***N*-linked glycan** An oligosaccharide linked by asparagines in the protein/peptide, a common modification in all eukaryotic proteins that go through the secretory pathway.

proteasome A cytoplasmic gigantic protease complex involved in various cellular processes, including the degradation of misfolded proteins and antigen processing.

quality-control machinery A system that maintains the quality of product (i.e., newly synthesized proteins in the endoplasmic reticulum).

Further Reading

Cacan, R., and Verbert, A. (1999). Transport of free and N-linked oligomannoside species across the rough endoplasmic reticulum membranes. *Glycobiology* **10**, 645–648.

Helenius, A. (2001). Quality control in the secretory assembly line. *Philos. Trans. Royal Soc. London B Biol. Sci.* **356**, 146–150.

Moore, S. E. H. (1999). Oligosaccharide transport: Pumping waste from the ER into lysosomes. *Trends Cell Biol.* **9**, 441–446.

Moore, S. E. H., Bauvy, C., and Codogno, P. (1995). Endoplasmic reticulum-to-cytosol transport of free polymannose oligosaccharides in permeabilized HepG2 cells. *EMBO J.* **14**, 6034–6042.

Saint-Pol, A., Bauvy, C., Codogno, P., and Moore, S. E. H. (1997). Transfer to free polymannose-type oligosaccharides from the cytosol to lysosomes in cultured human hepatocellular carcinoma hepG2 cells. *J. Cell Biol.* **136**, 45–59.

Spiro, R. G. (2000). Glucose residues as key determinants in the biosynthesis and quality control of glycoproteins with N-linked oligosaccharides. *J. Biol. Chem.* **275**, 35657–35660.

Suzuki, T., Yan, Q., and Lennarz, W. J. (1998). Complex, two-way traffic of molecules across the membrane of the endoplasmic reticulum. *J. Biol. Chem.* **273**, 10083–10086.

Suzuki, T., Park, H., Hollingsworth, N., Sternglanz, R., and Lennarz, W. J. (2000). *PNG1*, a yeast gene encoding a highly conserved peptide:*N*-glycanse. *J. Cell Biol.* **149**, 1039–1052.

Suzuki, T., Park, H., and Lennarz, W. J. (2002). Cytoplasmic peptide: *N*-glycanase (PNGase) in eukaryotic cells: Occurrence, primary structure, and potential functions. *FASEB J.* **16**, 635–641.

Suzuki, T., Yano, K., Sugimoto, S., Kitajima, K., Lennarz, W. J., Inoue, S., Inoue, Y., and Emori, Y. (2002). Endo-β-*N*-acetylglucosaminidase, an enzyme involved in processing of free oligosaccharides in the cytosol. *Proc. Natl. Acad. Sci. U.S.A.* **99**, 9691–9696.

Biography

Tadashi Suzuki is Visiting Assistant Professor in the Department of Biochemistry, Graduate School of Medicine, Osaka University. His principal research interest is the biological functions of deglycosylating enzymes, including cytoplasmic peptide:*N*-glycanase (PNGase) and endo-β-*N*-acetylglucosaminidase (ENGase) in eukaryotes. He received a D.Sc. degree from the University of Tokyo and served as a Postdoctoral Fellow and Research Assistant Professor at the Department of Biochemistry and Cell Biology, State University of New York at Stony Brook.

Oncocytes

Bernard Tandler and Charles L. Hoppel
Louis Stokes VA Medical Center, Cleveland, Ohio, USA

Oncocytes, first described by H. Hamperl, are large cells possessing a granular, eosinophilic cytoplasm that are present in many glands and various epithelial linings, particularly in humans; they rarely are found in other mammalian species. In humans, they increase in number with age and may come to constitute a sizeable portion of particular organs; e.g., the oxyphil cells of the parathyroid gland are oncocytes. Oncocytes can occur in neoplastic tissues as well as in normal tissues. Oncocytes in normal tissues can themselves undergo neoplastic transformation and, because they are capable of division, result in a tumor composed wholly or partially of oncocytes, e.g., oncocytoma and Warthin's tumor. These generally are benign, but occasionally various oncocytic neoplasms can be malignant, e.g., Hürthle cell carcinoma and malignant oncocytoma. It is clear that oncocyte formation and neoplasia are independent processes that can occur in either sequence.

Structure of Oncocyte Mitochondria

The fundamental morphological nature of oncocytes was firmly established from the earliest examination of these cells by electron microscopy. They are filled with an abundance of mitochondria, which are responsible for the eosinophilic granularity of the cytoplasm as seen by optical microscopy. Other cytoplasmic organelles are inconspicuous, but sparse lysosomes can be revealed by cytochemistry. Special features normally found in specific precursor cell types, such as folded plasma membranes, microvilli, or secretory granules, are reduced or entirely absent. The mitochondria can be regular in form and are usually ovate, but occasionally are discoidal, rod-shaped, or pleomorphic. In some oncocytic cells, various mitochondrial forms co-exist side by side.

The ovate mitochondria frequently contain an unusual number of cristae, which often are arranged in a central stack where they are closely applied to one another (Figures 1 and 2). With transmission electron microscopy (TEM), the cristae appear to be merely simple infoldings of the boundary membrane, but scanning electron microscopy (SEM) reveals that at least some lamelliform cristae are connected to the boundary membrane by several short tubules, the so-called crista junctions. In certain oncocyte mitochondria in Hürthle cell carcinomas, individual cristae may have a lattice-like form. Despite their altered morphology, oncocyte mitochondria are capable of division by medial partition formation.

Those oncocyte mitochondria that are flattened disks often are aggregated like a stack of pancakes. In such organelles, the cristae occasionally are oriented in a longitudinal pile or may appear to be vesicular. Although conventional matrix granules have not been detected in oncocyte mitochondria, these organelles sometimes include in their inner compartment amorphous densities ranging from small to large. Certain mitochondria contain inclusions filled with either α- or β-glycogen; such inclusions are delimited by a single membrane, showing that they truly are intramitochondrial, rather than being cytosolic glycogen aggregates that merely have been engulfed by intact mitochondria. In oncocytes of the parotid gland in the vampire bat, adjacent mitochondria are linked by periodic cross-bridges measuring 10 nm, separated by a 12.5 nm interval. Such linked organelles have not been observed in human oncocytes.

Mitochondrial Biochemistry

The physiological capacity of oncocyte mitochondria is not well established. Histochemical studies of oncocytes and oncocytomas, irrespective of their site of occurrence, invariably show an increase in mitochondrial oxidative enzymatic activity. At the same time, biochemical studies show an increase in the amount of mitochondrial DNA per cell. Both of these phenomena can be accounted for by the increased number of mitochondria (up to 10-fold) in oncocytes. There are no gross alterations in the mitochondrial DNA. A biochemical study of mitochondria isolated from Warthin's tumor of the parotid gland found them to be partially uncoupled. Analysis of mitochondria from thyroid oncocytic tumors showed significant decrease in ATP synthesis, whereas in renal oncocytomas the

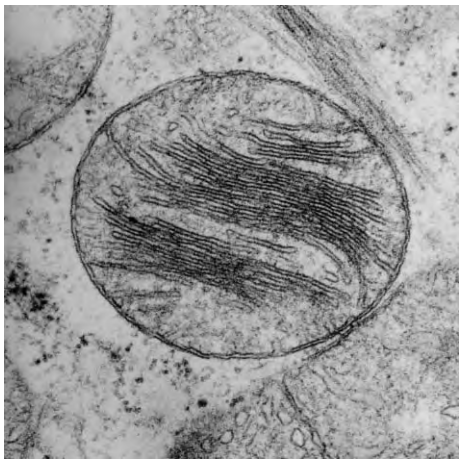

FIGURE 1 Transmission electron microscopy of a typical mitochondrion in an oncocytoma of human parotid gland origin. The abundant cristae are closely packed in a sheaf. Original magnification, ×34,000.

mitochondrial ATPase activity is normal. These data suggest site-specific differences in oncocytic metabolism. The nuclear factor responsible for the increase in mitochondrial number in oncocytes has not been identified. However, this factor does not change in response to decreased respiratory chain activity, decreased ATPase activity, or mitochondrial DNA abnormalities. Study of the biochemistry and genetics of oncocytes is hampered by the comparative rarity of metaplastic or neoplastic aggregates of such cells and by the fact that they occur mostly in humans.

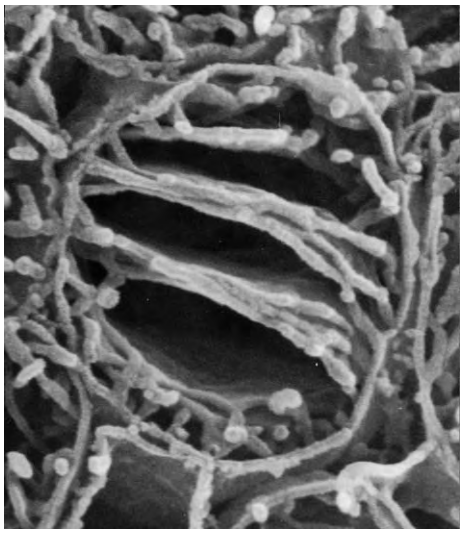

FIGURE 2 A scanning electron microscope micrograph of a mitochondrion from a human oncocyte of submandibular gland origin. All soluble material has been extracted from this specimen, leaving only membranes. A portion of the outer and boundary membranes has been removed from this organelle, allowing the internal sheaf of cristae to become apparent. Original magnification, ×25,000. Micrograph courtesy of Alessandro Riva.

See Also the Following Articles

Imaging Methods • Mitochondrial DNA • Mitochondrial Membranes, Structural Organization • Parathyroid Hormone/Parathyroid Hormone-Related Protein Receptor

Glossary

eosinophilic Stainable by eosin (tetrabromofluorescein), a red dye used to study cell structures.

lysosome A cytoplasmic structure in eukaryotic cells that contains various hydrolytic enzymes and is involved in intracellular digestion.

metaplastic Of or characterized by metaplasia, the transformation of cells from a normal to an abnormal form.

neoplastic Of or characterized by neoplasia, a new and abnormal growth or proliferation of cells.

Further Reading

Ambu, R., Riva, A., Lai, M. L., Loffredo, F., Testa Riva, F., and Tandler, B. (2000). Scanning electron microscopy of the interior of cells in Hürthle cell tumors. *Ultrastruct. Pathol.* **24**, 211–218.

Ebner, D., Rödel, G., Pavenstaedt, I., and Haferkamp, O. (1991). Functional and molecular analysis of mitochondria in thyroid carcinoma. *Virchows Arch. B Cell Pathol.* **60**, 139–144.

Hamperl, H. (1931). Onkocyten un Geschwulste der Speicheldrüsen. *Virchows Arch. Pathol. Anat.* **282**, 724–736.

Heddi, A., Faure-Vigny, H., Wallace, D. C., and Stepien, G. (1996). Coordinate expression of nuclear and mitochondrial genes involved in energy production in carcinoma and oncocytoma. *Biochim. Biophys. Acta* **1316**, 203–209.

Müller-Höcker, J. (1998). Defects of the respiratory chain in hepatic oncocytes. *Virchows Arch.* **432**, 349–356.

Riva, A., and Tandler, B. (2000). Three-dimensional structure of oncocyte mitochondria in human salivary glands. *Ultrastruct. Pathol.* **24**, 145–150.

Tandler, B., and Shipkey, F. H. (1964). Ultrastructure of Warthin's tumor. I. Mitochondria. *J. Ultrastruct. Res.* **11**, 292–305.

Tandler, B., Hutter, R. V. P., and Erlandson, R. A. (1970). Ultrastructure of oncocytoma of the parotid gland. *Lab. Invest.* **23**, 567–580.

Biography

Bernard Tandler was a long-time Professor of Oral Biology and of Anatomy at the Case Western Reserve University Schools of Dentistry and Medicine, where he currently is a Visiting Professor of Oral Diagnosis, as well as a Consultant at the VA Medical Center in Cleveland. He also served as Visiting Professor of Anatomy at Kyushu Dental College and of Biological Sciences at Texas Tech University. His major research interests concern the biogenesis, structure, and physiology of giant mitochondria, as well as the structure, function, and evolution of mammalian salivary glands and of secretory cells in general.

Charles L. Hoppel graduated from Gonzaga University and St. Louis University School of Medicine. He is Professor of Pharmacology, Medicine and Oncology at Case Western Reserve University, Co-Director of the Center for Inherited Disorders of Energy Metabolism at CWRU, and Associate Director, Research in the Geriatric Research, Education, and Clinical Center at the Louis Stokes VA Medical Center, Cleveland. His research interests are in mitochondrial structure and function, mitochondrial fatty acid oxidation, and regulation of carnitine palmitoyltransferase-I.

Opioid Receptors

P.Y. Law and Horace H. Loh
University of Minnesota, Minneapolis, Minnesota, USA

Opioid receptors are transmembrane proteins located at the synaptic membranes that serve as targets of an efficacious pain relief drug: morphine. The identification of these binding sites at neural membrane for plant alkaloids has led to the discovery of the first class of endogenous drug molecules, i.e., the enkephalins and endorphins. These opioid receptors belong to the superfamily of G protein-coupled receptor, and upon activation, the activities of multiple cellular effectors are modulated, leading to inactivation of the ascending and activation of the descending pain pathways. Eventually, pain perception is altered. Unfortunately, with the "good" therapeutic actions of morphine, there are also "bad" side effects of the drug, e.g., tolerance and addiction. Thus, the molecular mechanism in the cellular regulation of these opioid receptors, and the designs of specific agonists for these opioid receptors to be ideal analgesic agents are of great interest in pain medicine development.

Historical Perspectives

For centuries, extracts from the opium poppy, *Papaver somniferum*, have been prescribed for pain relief, to control cough, and to treat diarrhea. However, in addition to its medicinal uses, due to its psychological effects, man has abused opium since the time of the ancient Greeks. The isolation of the principal alkaloid by the German pharmacist, Friedrich W. Serturner in 1805, which he named morphine after the Greek god of dreams, Morpheus, has enabled pharmacologists to determine the relationships between structures and their analgesic activities. From the relatively low concentration of morphine needed to relieve pain in 70% of the patients (10 mg/70 kg body-weight), to the stereoselective requirement for analgesic action of the drug, it is apparent that morphine acts by high-affinity binding to proteins, or specific receptor, located in the central nervous system (CNS). The presence of specific morphine receptor was not demonstrated until 1973, when three research groups: Lars Terenius, Soloman Snyder, and Eric Simon, following the guideline established by Avram Goldstein, independently reported the presence of high affinity and stereoselective binding sites at the synaptic membrane preparations of rodent brain. The affinities of various opiate analgesics for these binding sites and the location of these sites correlated well respectively with the *in vivo* potencies and sites of action of the drug. Thus, the era of the opiate receptor is launched. Immediately, it is apparent that these mammalian CNS binding sites could not be evolved for plant alkaloids. This dichotomy was resolved by the isolation of the endogenous opioid peptide, enkephalin, by John Hughes and Han Kosterlitz in 1975 followed later by the identification of the proenkephalin A gene. The subsequent identification of two other gene products, β-endorphin deriving from the pro-opiomelanocortin gene, and dynorphin deriving from the *prodynorphin*or *proenkephalin B* gene suggests that the *in vivo* actions of morphine and its congeners must be a reflection of these endogenous opioid peptides actions. The presence of multiple endogenous opioid peptides genes also suggests the probable existence of multiple opioid receptors.

Discovery of Multiple Opioid Receptors

In 1976, Bill Martin and his colleagues hypothesized the presence of multiple opioid receptors. Concluding from the physiological responses such as blood pressure and respiration, Martin and co-workers coined the multiple opioid receptors terminology based on the prototypic ligands within each group, with morphine being the mu (μ) agonist, ketocyclazocine being the kappa (κ) agonist, and SKF10 047 being the sigma (σ) agonist. The existence of multiple opioid receptors was further demonstrated by measuring the amount of an opiate antagonist to reverse the agonist effect in two *in vitro* bioassay systems, the guinea pig (GP) ileum and the mouse vas deferens. These bioassays were responsible for the identification of the fourth type of opioid receptor, the delta (δ) with enkaplin being the prototypic agonist. Additional studies such as the cross-tolerance measurements also supported the existence of multiple opioid receptors. In the cross-tolerance studies, animals or the *in vitro* GP ileum were treated with an opioid

receptor-selective agonist. Chronic exposure to the agonist resulted in a loss in response, or tolerance development. However, activities of agonists that are selective for other opioid receptors remained unaltered, or no cross-tolerance was developed. These *in vivo* and *in vitro* experiments support the original hypothesis of multiple opioid receptors.

The implication of the existence of multiple opioid receptors by the animals' studies and bioassays was supported initially by the direct receptor-binding experiments reported by Law and Loh, K.J. Chang, Hans Kosterlitz, and their colleagues. The development of receptor-selective antagonists, such as naltrindole (δ) and nor-binaltorphimine (κ), and the development of ligands that would alkylate receptor selectively, such as β-funaltrexamine (μ), have enabled investigators to characterize the properties of these multiple opioid receptors biochemically further by generating membrane preparations that contain single-receptor type. Only after the molecular cloning of the δ-opioid receptor, concurrently by the groups of Chris Evans and Brigitte Kieffer in 1992, followed by the cloning of μ- and κ-opioid receptors in 1993 by others, is the hypothesis of multiple opioid receptors firmly established. These multiple opioid receptors are products of three separate receptor genes and with high amino acid sequence homology (>60%). Although subtypes of these opioid receptors have been postulated, various gene products that exhibit the reported ligand selectivity of the various opioid receptor subtypes have not been identified. Also, from additional pharmacological and the molecular cloning studies, the sigma (σ) receptor does not belong to the opioid receptor family. Hence, the μ-, κ-, and δ-opioid receptors are the sites that endogenous opioid peptides and exogenous opiate alkaloids exert their actions.

Distribution and Pharmacology of Multiple Opioid Receptors

Prior to the cloning of the opioid receptors, the distribution of the receptors within various brain regions or tissues, was determined with autoradiographic studies using radioactive ligands selective for a specific receptor. These autoradiographic results were later substantiated and extended with the *in situ* hybridization studies using the cloned receptor mRNA and with the histochemical or immunofluorescence studies using the receptor-specific antibodies. In general, these data indicate that the location of the multiple opioid receptors coincides with the pharmacological actions of the drugs. These opioid receptors are mainly localized in the limbic system that are involved in the control of emotion and reward behaviors, the ascending and descending pain pathways that include the different laminae layers of cortex, thalamus, periaqueductal gray, midbrain median raphae and the dorsal horn of the spinal cord, and specific brain regions that are known to control locomotion, emesis, cough, and temperature.

The distributions of the μ- and δ-opioid receptor are very similar but distinct. Although these receptors do not co-localize in the pre- or post-synaptic membrane of the same neuron, they are observed to be located in the same components of the limbic systems such as the nucleus accumbens and the amygdala. Their locations at the cortex, the 4th ventricle and at the substantia gelatinosa of the spinal cord are the reasons why both μ- and δ-opioid receptor selective drugs have strong spinal and supraspinal analgesic effects. Similarities in the distribution of these two opioid receptors suggest the μ- and δ-opioid receptors have similar pharmacological profile (Table I). There are reports using δ-opioid receptor selective antagonist or using mice that the δ-opioid receptor has been genetically deleted that implicate the role of δ-opioid receptor in modulating both the acute and chronic effects of the μ-opioid receptor selective agonist.

On the other hand, distribution of the κ-opioid receptor in the central nervous system is distinct from that of μ- and δ-opioid receptors. The most striking difference is the uniform pre-synaptic location of the κ-opioid receptor in the caudate putamen area. Such location could be the explanation for the observed κ-opioid agonist induced decrease in locomotion and the decrease of dopamine release in this brain area. The inhibition of dopamine release is the basis for the dysphoric effects of the κ-opioid agonists. The brainstem and spinal cord distribution of the κ-opioid receptor resemble that of μ-opioid receptor. Hence, κ-opioid agonists could produce spinal analgesia (Table I).

The multiple opioid receptors are not confined to the central nervous system. The presence of the receptors in the gastrointestinal tract accounts for the constipative

TABLE I

Pharmacological Effects Associated with the Multiple Opioid Receptor

	μ	δ	κ
Analgesia	Supraspinal Spinal	Supraspinal Spinal	 Spinal
Pupil constriction	++	++	–
Respiratory depression	+++	++	+
Diuresis	Antidiuresis	–	++
GI	Constipate	Constipate	–
Smooth muscle	Spasm	Spasm	–
Behavior/effect	Euphoria Sedation ++		Dysphoria Sedation +
Physical dependent	++	++	+

effect of μ- and δ-opioid agonists. The presence of the κ-opioid receptor in the cardiac myocytes could be the reason for the bradycardia effect observed with the κ-opioid agonists, though the bradycardia effect of the opioid agonists is mainly associated with the agonist actions at the brainstem medulla. Opioid receptors have been reported also to be present in the immune cells. The true identities of these receptors are yet to be identified, whether they are the μ-, δ-, or κ-opioid receptor types or the "non-classical" opioid receptors. Nevertheless, the pronounced effects that morphine has in the immune responses of animals, and the fact that intravenous drug users are one of the high risk groups for HIV have led to many studies, and the effects of various opioid agonists and antagonists on the functions of immune cells cannot be ignored.

Opioid Ligands Selectivity for the Multiple Opioid Receptors

With the cloning of the opioid receptors and the subsequent generation of mice in which the transcription of selective opioid receptor gene could be disrupted, it is possible now to delineate the opioid receptor types that various opioid ligands could activate. By expressing the three cloned receptors individually into cells that do not express opioid receptor endogenously, it is possible to generate models that could determine the affinities of the opioid ligands to a specific receptor type accurately. Likewise, by genetically eliminating the *in vivo* expression of an individual opioid receptor type, the loss or gain in functions of a specific opioid agonist can be evaluated *in vivo*. These data in combination with the receptor-selective antagonists studies have determined the selectivity of various opioid ligands and their functions, as summarized in Table II.

It is apparent that morphine and its congeners are agonists in the μ-opioid receptor. Although in the *in vitro* cell line models that express the δ-opioid receptor morphine has partial agonist activities, morphine does not exhibit measurable analgesic activities in mice that do not express the μ-opioid receptor. Since these animals have intact δ- and κ-opioid receptor systems, it is unequivocal that morphine pharmacological effects are mediated via the activation of μ-opioid receptor.

Other opiate alkaloids have been shown to exhibit nonselectivity toward these three opioid receptors. The oripavine derivatives (etorphine and diprenorphine) and the benzomorphans (ketocyclazocine and bremazocine) have been shown by many to have similar affinities for all three opioid receptors. This is surprising since ketocyclazocine was used by Bill Martin to define one of the multiple opioid receptors, the κ-opioid receptor. Such dichotomy may be resolved by the fact that some opiate alkaloids have different activities in different opioid receptor types. For example, nalorphine exhibits antagonistic properties in the μ-and δ-opioid receptors but possesses agonistic activities in the κ-opioid receptor. Another example is pentazocine that possesses both κ-agonistic and μ-antagonistic properties. The mixed agonist-antagonist properties of various alkaloids are being exploited in the clinic so as to minimize the side effects of the drug, most noticeably, the addictive liability of the opiate analgesics.

The endogenous ligands, noticeably the products of the three peptides genes – enkephalin, β-endorphin, and dynorphin do not appear to have specificity toward these multiple opioid receptors. Initially, enkephalin and β-endorphin have been considered to be the prototypic ligands for the δ- and μ-opioid receptors respectively. Dynorphin, with the positively charged amino acids arginine and lysine, has been shown to preferentially interact with the κ-opioid receptor. Since then, it has been shown that Met^5-enkephalin has equal affinity for the μ- and δ-opioid receptor, and that dynorphin has high affinity for the δ-opioid receptor. Only when the peptides are restricted in their rotation is receptor selectivity observed, e.g. the D-penicillamine derivatives of enkephalin, DPDPE. This peptide has been shown

TABLE II

Relative Receptor Selectivity of Various Opioid Ligands and their Functions in Respective Receptors

Opioid ligands	μ	δ	κ
Bemazocine	AG	AG	AG
Buprenorphine	PA		AN
Butrophanol	PA		AG
Diprenorphine	AN	PA	AN
Ethylketocyclazocine		AG	AG
Etorphine	AG	AG	AG
Fentenyl	AG		
β-Funaltrexamine	AN		AG
Levorphanol	AG	PA	
Methadone	AG		
Morphine	AG	PA	
Nalorphine	AN	AN	AG
Naloxone	AN	AN	AN
Naltrexone	AN	AN	AN
Naltrindole		AN	
Nor-Binaltorphimine			AN
NTB		AN	
Pentazocine	PA		AG
Spiradoline			AG
Sufentanyl	AG		
U50,488			AG
U69,593			AG

AG = agonist; PA = partial agonist; AN = antagonist.

in vitro to be selective for the δ-opioid receptor and with minimal activity in the μ-opioid receptor. Hence, the *in vivo* effect of DPDPE has been the hallmark for the δ-opioid receptor activation. However, recent *in vivo* studies using mice lacking the μ- or the δ-opioid receptor, clearly suggest that the DPDPE analgesic effect is mediated by activation of μ-opioid receptor. This conflicting *in vitro* and *in vivo* receptor selectivity of the endogenous peptides and their derivatives requires further detailed investigation.

Molecular Mechanism of Multiple Opioid Receptor Function

A general feature of the opioid agonist is the inhibition of neurotransmitter release. Although there are instances that opioid agonist could increase the neurotransmitter release, it is due to the location of the receptor and the disinhibition of the neurotransmitter release. An excellent example is the dopamine release within the nigrostriatal loop. κ-Opioid agonist inhibits dopamine release by acting directly at the presynaptic dopaminergic terminals, whereas μ- and δ-opioid agonists increase the release by inhibiting the GABAergic interneurons that inhibit the dopamine release. Thus, in either case, the activation of opioid receptor results in the direct inhibition of synaptic transmission.

From the cloning studies, it is unequivocal that the opioid receptors belong to the superfamily of proteins, the G protein-coupled receptors (GPCR) and the subfamily of rhodopsin-like receptors. One common feature of these receptors is that they contain hydrophobic regions that would span the membrane 7 times. Thus these receptors are commonly known as seven-transmembrane receptors. Another common feature is that their signals are mediated by promoting the dissociation of the nucleotide GDP from the α-subunits of the heterotrimeric proteins. The dissociation of GDP allows the association of GTP to the α-subunits resulting in the dissociation of the heterotrimeric proteins into α- and βγ subunits. These subunits will then control the activities of various intracellular or membrane bound proteins and enzymes. For the multiple opioid receptors, the GTP/GDP-binding proteins involved in their actions are the pertussis-toxin-sensitive Gi/Go proteins.

In order for opioid receptors to regulate the neurotransmitter release, two of the proteins that the receptors regulate are the voltage-dependent Ca^{2+} channels and the inward rectifying K^+ channels. By inhibiting the Ca^{2+} channels and thus reducing the influx of Ca^{2+}, opioid agonists could regulate the fusion of vesicles containing the neurotransmitters with the synaptic membrane. Also opioid agonists could activate the voltage-dependent inward rectifying K^+ channels and thus hyperpolarizing the synaptic membrane. By controlling these two ions channels, activation of the opioid receptors would reduce the excitability of the membrane and reduce the transmitter release.

Other prominent proteins and enzymes that are regulated by the multiple opioid receptors are the enzymes responsible for cAMP synthesis, adenylyl cyclase, and that which is involved in the long-term cellular adaptational events, the mitogen-activated protein kinase (MAP kinase). Opioid receptors inhibit the adenylyl cyclase activity, thereby reducing the intracellular cAMP content. This second messenger could control the activities of a protein kinase that, in turn, could regulate the activities of other proteins, such as the ion channels. The MAP kinase has been known to participate in the cellular proliferation and apoptotic events. Thus, it is probable that MAP kinase activation by the multiple opioid receptors could signify their involvement in long-termed potential and learning, two of the probable mechanisms for the basis of chronic drug actions.

Summary and Future Direction

The similarities in the sequence and the molecular action of these multiple opioid receptors are striking. Hence, it is unclear why nature would evolve three different genes coding for three different proteins from the same ancestral gene so as to carry out the same functions. To complicate the picture, there are three endogenous peptides that exhibit selectivity but not specificity among these multiple opioid receptors. It is still unresolved why an endogenous opioid peptide such as Met^5-enkephalin that exhibits *in vitro* agonistic properties in μ-opioid receptor would not produce analgesic effect *in vivo*. There is no debate that endogenous peptides and opiate alkaloids have different recognition motifs within these opioid receptors, and that the cellular regulations of the peptide- and alkaloid-receptor complexes are different. Whether such differences could contribute to the differences in the pharmacological responses of these drugs or simply the spatial distribution of the receptors, remains to be investigated.

In the past, the approach to eliminate the undesirable side effects of the opiate alkaloids was to design drugs that would have selectivity toward one specific opioid receptor. A classic example is the development of drugs that would have κ-opioid receptor selectivity, because the dysphoric effect of κ-opioid receptor activation would reduce the addictive liability of the drug. Unfortunately, drugs marketed thus far do not exhibit the ultimate property of opiate analgesic, i.e., efficacious pain relief with no side effects. The problem lies mainly with the presence of multiple opioid receptors and the selectivity of the drugs for these receptors. Hence new approaches should be taken in

the future for development of pain-management paradigms. With the advent of gene therapy, one could envision the use of receptor engineering in the treatment of pain. If an opioid-receptor mutant could be identified that exhibits distinct phenotype from that of the endogenous receptors, and that this receptor mutant could be delivered to the site of action, e.g., substantia gelatinosa of the spinal cord, then activation of such mutants by a drug that normally would not activate the endogenous receptors, e.g., an opiate antagonist, would result in pain relief. Such an approach would not only provide specificity, but also would eliminate the side effects of the opiate drugs; but this approach could only be accomplished when the molecular basis for the action of the multiple opioid receptors is fully elucidated.

See Also the Following Articles

DNA Damage: Alkylation • DNA Helicases: Dimeric Enzyme Action • DNA Helicases: Hexameric Enzyme Action • DNA Polymerase I, Bacterial • Zinc Fingers

Further Reading

Law, P. Y., Wong, Y. H., and Loh, H. H. (2000). Molecular mechanisms and regulation of opioid receptor signaling. *Annu. Rev. Pharmacol. Toxicol.* **40**, 389–430.

Minami, M., and Satoh, M. (1995). Molecular biology of the opioid receptors: Structures, functions and distributions. *Neurosci. Res.* **23**, 121–145.

Pasternak, G. W. (1988). Multiple morphine and enkephalin receptors and the relief of pain. *J. Amer. Med. Assoc.* **259**, 1362–1367.

Reisine, T., and Pasternak, G. (1996). Opioid analgesics and antagonists. In *The Pharmacological Basis of Therapeutics* (Joel G. Hardman, Lee E. Limbird, Perry B. Molinoff, Raymond W. Ruddon and Alfred G. Gilman, eds.) 9th edition, pp. 521–555. McGraw Hill, New York.

Simon, E. J., and Gioannini, T. L. (1993). Opioid receptor multiplicity: Isolation, purification and chemical characterization of binding sites. In *Opioid I, Handbook of Experimental Pharmacology* (A. Herz, ed.) Vol 104, pp. 3–36. Springer, Berlin.

Biography

P. Y. Law is a Professor in the Department of Pharmacology at the University of Minnesota in Minneapolis. His principal research interests are the cellular control of the opioid receptor signaling. He holds a Ph.D. from the University of Illinois and received his postdoctoral training at the University of California, San Francisco. He has authored numerous research and review articles on the molecular mechanism of opioid receptor actions.

Horace H. Loh is the F. and A. Stark Professor and Head of the Department of Pharmacology at University of Minnesota in Minneapolis. His principal research interests are the neurochemical basis for opiate tolerance and dependence. He holds a Ph.D. from the University of Iowa and received his postdoctoral training from the University of California, San Francisco. He has authored numerous research and review articles on opioid receptors, and has served as an editor on several scientific journals. He is a member of the Chinese National Academy of Sciences.

Ornithine Cycle

Malcolm Watford
Rutgers University, New Brunswick, New Jersey, USA

The ornithine cycle, also known as the urea cycle and the Krebs–Henseleit cycle, is the pathway in mammalian liver that allows the detoxification and excretion of excess nitrogen as urea. Flux through the cycle is driven by the demand to remove excess ammonia derived from the degradation of amino acids that arise either from the diet or from endogenous proteolysis. In a healthy individual, consuming a typical western diet, flux through the ornithine cycle produces some 30–35 g of urea per day but as much as 25% of this can be recycled via hydrolysis to ammonia and bicarbonate by colonic bacteria.

History

Three major systems have evolved for the elimination of excess nitrogen from the body, and animals may be classified according to their major nitrogenous excretion product. Thus most fish are ammoniatelic (ammonia excretion), reptiles and birds are uricotelic (uric acid excretion), and mammals are ureotelic (urea excretion). In addition, urea excretion is seen in some teleost fish, and urea synthesis is also present in elasmobranchs (sharks and rays) where urea functions primarily in an osmotic role, not in nitrogen excretion.

Urea was first described as "substance savoneuse," that yielded ammonia on hydrolysis, isolated from urine by Roulle in 1773 and was obtained in pure form by Proust in 1820. There is evidence that Davy synthesized urea from cabonyl chloride and ammonia in 1812 but he failed to recognize the product. Thus Wholer is credited for achieving the synthesis, in 1828, of urea from ammonia and lead cyanate in what is best remembered as the first synthesis of an organic compound from inorganic substrates. Over the next century many theories were developed to explain urea synthesis but the true pathway was not discovered until 1932. Working with liver slices in incubation Krebs and Henseleit found that the addition of small amounts of ornithine greatly accelerated the synthesis of urea from ammonia and furthermore, that the ornithine could be recovered at the end of the incubation. From this they formulated the idea that ornithine was acting as a "catalyst." They also identified citrulline as an intermediate and described the ornithine cycle as ammonia (together with bicarbonate) and ornithine combining to give citrulline that was then converted to arginine. The final step was hydrolysis of the arginine to urea and with the concomitant regeneration of ornithine. This was the first description of a cyclic biochemical pathway again illustrating the central role urea synthesis has had in the history of biology and chemistry.

Chemistry of the Cycle

Since Krebs and Henseleit's original discovery, the chemistry of the cycle has been completely described and although the ornithine cycle consists only of four enzymes, the need for carbamoyl phosphate means that carbamoyl phosphate synthetase 1 is usually considered an ornithine cycle enzyme.

The complete cycle (Figure 1) is only expressed in liver parenchymal cells with highest activity in those cells near the portal inlet (periportal cells). The substrates for the cycle are ammonia, bicarbonate, aspartate, and three ATP equivalents. In this text the term ammonia refers to the sum of NH_4^+ plus NH_3, and where a specific molecular species is important, it is shown in parentheses. Beginning in the mitochondria ammonia (NH_3) combines with bicarbonate to form carbamoyl phosphate involving 2 ATP and releasing 2 ADP plus inorganic phosphate, through the action of carbamoyl phosphate synthetase 1 (EC 6.3.4.16). The carbamoyl group is then transferred to ornithine via ornithine transcarbamoylase (EC 2.1.3.3) to yield citrulline that leaves the mitochondria in exchange for ornithine on the ORN 1 transporter. In the cytosol, citrulline condenses with aspartate in a reaction, requiring ATP and the formation of a citrulline-AMP intermediate, to give argininosuccinate, AMP, and pyrophosphate via the action of argininosuccinate synthetase (EC 6.3.4.5). The carbon skeleton of the aspartate is then cleaved from argininosuccinate by argininosuccinate lyase (EC 4.3.2.1) to yield fumarate and arginine. The final step is hydrolysis of arginine by arginase (EC 3.5.3.1) to give the end product urea with the regeneration of ornithine that can enter the mitochondria on the ORN 1 transporter and begin another round of the cycle.

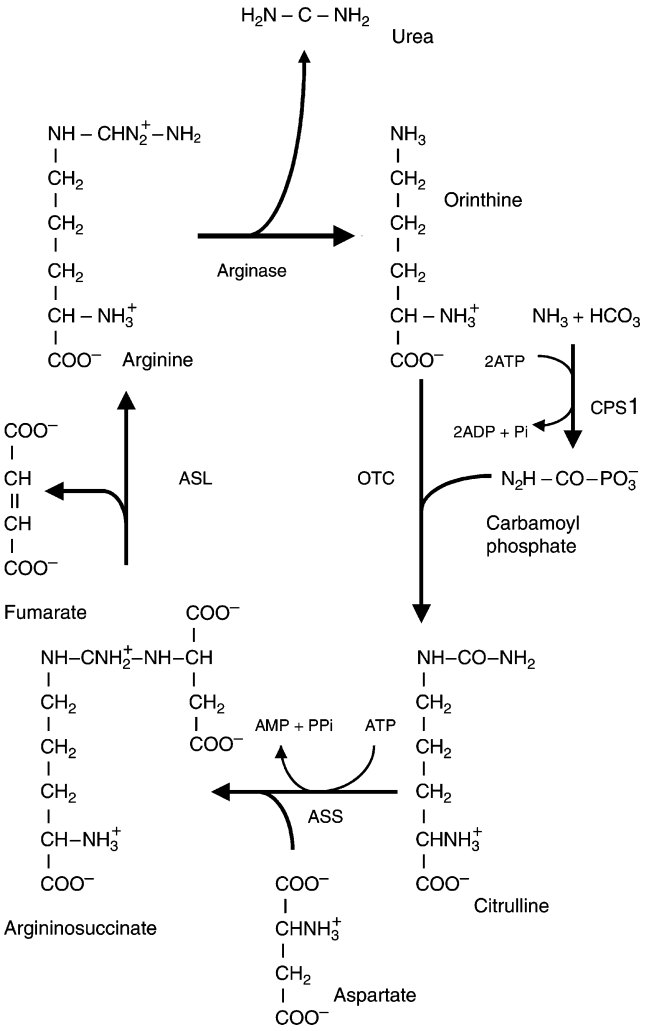

FIGURE 1 The chemistry of the ornithine cycle. CPS 1, carbamoyl phosphate synthetase 1, OTC, ornithine transcarbamoylase, ASS, argininosuccinate synthetase, ASL, argininosuccinate lyase.

Channeling in the Cycle

Although carbamoyl phosphate synthetase 1 and ornithine transcarbamoylase are mitochondrial matrix enzymes, they are localized in very close proximity to the cristae of the inner membrane. This would favor direct transfer of intermediates along the pathway and tracer experiments have shown that extra-mitochondrial ornithine is preferentially utilized for citrulline synthesis over ornithine generated within the mitochondria. Such findings indicate that the ORN 1 transporter, carbamoyl phosphate synthetase 1 and ornithine transcarbamoylase are working efficiently as a unit without free mixing of the intermediates within the mitochondria. In addition, there is evidence of similar channeling within the cytosolic section of the cycle. In permeabilized hepatocytes incubated with ^{14}C labeled bicarbonate, the formation of labeled urea is not significantly diluted by the addition of large amounts of cycle intermediates (arginine, argininosuccinate, or citrulline), again showing no mixing with exogenous intermediates. Therefore all intermediates of the cycle appear to be carefully channeled along the pathway which may be related to the need to ensure removal of the highly toxic substrate, ammonia.

Physiological Aspects of the Cycle

The function of the ornithine cycle is to detoxify excess ammonia in the mammalian body and as such the source of the ammonia must be considered whenever the cycle is discussed in more than simple chemical terms. There are two types of condition when the delivery of ammonia within the liver is high and thus require high rates of urea synthesis. The first is in response to dietary (exogenous) protein when excess amino acids are degraded and the second is in response to increased catabolism of endogenous amino acids, arising from proteolysis, during early starvation and in hypercatabolic states such as those that arise from sepsis and injury. A quantitative analysis of the fate of a typical daily load of dietary amino acids showed that, if those amino acids that must be catabolized within the liver were to undergo complete oxidation then, this would produce more ATP than the liver uses in a day. Since the liver oxidizes other fuels in addition to amino acids, it is evident that the carbon skeletons of the amino acids cannot undergo complete oxidation in the liver. In practice the amino acid carbon skeletons are conserved as either glycogen (indirect pathway of synthesis) or released into the circulation as free glucose. In the case of starvation and hypercatabolic states, the reason the amino acids are being degraded is to provide glucose for the body, and urea synthesis is simply coincidental. Thus the synthesis of urea from amino acids is always linked to the hepatic pathway of gluconeogenesis.

There is currently some debate about how much of the ammonia and aspartate for the cycle are taken up from the circulation directly and how much are synthesized within the liver from ammonia and/or other amino acids. Within the liver however, glutamate dehydrogenase and the major aminotransferases catalyze reactions close to equilibrium which allows the maintenance of a balanced substrate supply to the cycle (Figure 2).

By following the fate of a single amino acid, alanine, through hepatic metabolism, the integrative nature of the ornithine cycle with gluconeogenesis can be seen (Figure 3). Alanine undergoes transamination with α-ketoglutarate in the cytosol and both the pyruvate and glutamate formed enter the mitochondria where the pyruvate is carboxylated to oxaloacetate via the action of pyruvate carboxylase. The glutamate then transaminates with this oxaloacetate to give aspartate and α-ketoglutarate. The latter can then recycle via the

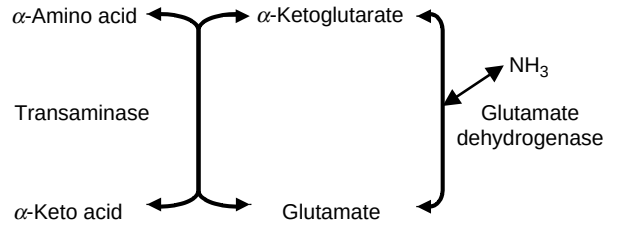

FIGURE 2 The equilibrium nature of glutamate dehydrogenase and the transaminases. Amino acids can transfer their amino group to α-ketoglutarate to produce glutamate via transamination. Glutamate can yield ammonia and α-ketoglutarate through glutamate dehydrogenase. Since glutamate dehydrogenase and the major transminases catalyze reactions close to equilibrium the entire system is freely reversible and thus ensures a balance of substrates, NH3 and aspartate (produced through aspartate aminotransferase) for the ornithine cycle.

cytosol to transaminate with another alanine. The aspartate leaves the mitochondria to be incorporated into the cycle by argininosuccinate synthetase in the cytosol. At the subsequent lyase step the carbon skeleton is released as fumarate. Since fumarate is unable to re-enter the mitochondria, it is metabolized to malate which is oxidized to oxaloacetate with the concomitant generation of NADH in the cytosol. The oxaloacetate is then converted to phosphoenolpyruvate, through the action of cytosolic phosphoenolypyruvate carboxykinase, and enters the gluconeogenic pathway with the utilization of the NADH at the glyceraldehyde 3-phosphate dehydrogenase step. Thus the transport of aspartate out of the mitochondria brings not only the nitrogen required for urea synthesis but also the carbon and the reducing power necessary for gluconeogenesis.

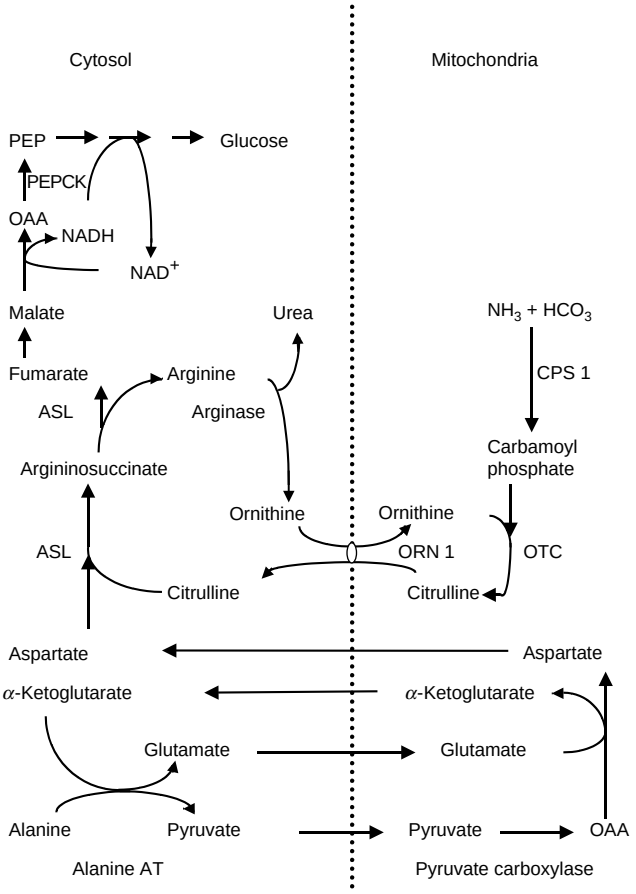

FIGURE 3 The ornithine cycle is linked to gluconeogenesis. CPS 1, carbamoyl phosphate synthetase 1, OTC, ornithine transcarbamoylase, ORN 1, orthine/citrulline transporter, ASL, argininosuccinate synthetase, ASL argininosuccinate lyase, Alanine AT, alanine aminotransferase, PEPCK, phosphoenolpyruvate carboxykinase.

Regulation

In 1905 Otto Folin, carrying out experiments on himself and others, described how urea excretion fluctuated with dietary protein, in particular, he showed how it reached a minimum within two days of consuming a zero protein diet. Thus it is clear that flux through the cycle is highly regulated and as with many biochemical pathways, this involves both short-term (changes in enzyme activity with no change in the amount of enzyme) and long-term (changes in the amount of enzyme) mechanisms. The need for the ornithine cycle is driven solely by the need to remove substrate (ammonia arising from amino acid catabolism), there is never a need for the end product (urea) and thus the cycle is not subject to product feedback regulation. Instead, flux through the cycle must increase rapidly whenever the substrate load increases.

Short-Term Regulation

Quantitative control analysis for the cycle has indicated that carbamoyl phosphate synthetase 1 plays a major regulatory role. In experiments *in vitro* however, where amino acid levels are held constant, the stimulation of carbamoyl phosphate synthetase 1 results in a fall in ammonia levels. This does not occur *in vivo* where the supply of amino acids varies, and at times of increased flux through the cycle, the concentration of ammonia shows little change or even a slight increase. Therefore the role of carbamoyl phosphate synthetase 1 is not to control flux through the cycle, rather it acts to maintain ammonia levels within a very limited range. The intrahepatic concentrations of the intermediates of the cycle are below the K_m for all of the enzymes which means that any increases in the concentration of intermediates, increase flux through the remainder of the cycle. From a teleological viewpoint a possible regulatory scheme would be the simple stimulation of carbamoyl phosphate synthetase 1 by increasing ammonia levels. Since carbamoyl phosphate synthetase 1 shows Michaelis–Menten kinetics towards ammonia

this would mean that a threefold increase in flux through the cycle would require a threefold increase in ammonia concentration. Ammonia levels however, must be held within a very narrow range. If intra-hepatic ammonia levels rise, some will escape from the liver and cause hyperammonemia and neurological toxicity. Conversely, if intra-hepatic ammonia levels decrease, this would disturb the equilibrium nature of the glutamate dehydrogenase and transaminase reactions with resultant dysregulation of non-essential amino acid levels.

Carbamoyl phosphate synthetase 1 has an absolute requirement for an allosteric effector, N-aceyl glutamate, which is made in the mitochondria from glutamate and acetyl CoA by N-acetyl glutamate synthetase (EC 2.3.1.1), and is degraded by an acylase in the cytosol. The synthesis of N-acetyl glutamate is stimulated by arginine and there is evidence that glucagon can increase N-acetyl glutamate levels through inhibition of transport out of the mitochondria thereby decreasing the rate of degradation. The major mechanism responsible for changing N-acetyl glutamate levels however, is substrate supply. Anytime there is an increase in amino acid catabolism this results in increased glutamate supply and a concomitant increase in N-acetyl glutamate levels. This allows carbamoyl phosphate synthetase 1 activity to increase and so prevent the ammonia levels from rising to toxic levels. Thus increased amino acid supply results in not only increased delivery of the direct substrates, ammonia and aspartate of the cycle, but also in the glutamate, and consequently the N-acetyl glutamate, required to allow flux through the cycle to increase and buffer intra-hepatic ammonia levels.

Long-Term Regulation

The urea cycle enzymes are not expressed in mammals until quite late in gestation since there is no need for the fetus to make urea, as the mother can dispose of any potentially toxic waste products. Such changes are also seen in other species, for example, as ammoniatelic tadpoles change to ureotelic frogs there is a dramatic increase in expression of the cycle. In non-carnivorous mammals the levels of all five enzymes can also change with diet and physiological/pathological conditions. Feeding high protein diets, early starvation, and hypercatabolic states are all accompanied by higher amounts of the enzymes, while low protein diets result in lower levels of the enzymes, and Schimke used the kinetics of these responses to develop the quantitative basis of protein turnover. Most of the changes are due to control at the level of gene transcription but the changes in arginase, seen during starvation, also involve changes in the rate of degradation of the arginase protein, and there is evidence that carbamoyl phosphate synthetase 1 expression is also regulated at the translational level. The agents responsible for the changes are predominantly glucagon (cAMP) and glucocorticoids acting to increase expression, with minor roles played by growth hormone, adrenergic hormones, and thyroid hormones. Insulin may act to downregulate expression but the importance *in vivo* is not clear. In addition, transcription of the gene encoding argininosuccinate synthase is suppressed by arginine, but this is likely to be of importance only in non-hepatic cells where the enzyme functions in arginine synthesis.

The half-lives of ornithine cycle enzyme proteins are relatively long, of the order of days, and thus any changes in the amount of protein would take some time to become significant. This means that the long-term changes do not play a role in the acute regulation of the cycle, rather they are adaptive in nature, preparing the body for long-term changes in substrate supply. This fits well with the time course of changes in amino acid catabolism within the body. Excess amino acid supply from a single meal can be readily detoxified through the cycle or temporarily buffered by synthesis of non-essential amino acids such as alanine. However, if the protein content of the diet has undergone a consistent increase then the capacity of the cycle increases to deal with it. Similarly, increased catabolism, of endogenous amino acids in starvation and hypercatabolic states, occurs over the course of days again allowing the cycle time to adapt. Conversely, at times of low protein feeding, expression of the cycle is decreased in order to conserve as much nitrogen as possible. This means that, in retrospect, the experiments of Folin (q.v.) involving the consumption of high protein diets after 14 days of a zero protein diet were potentially highly dangerous. The capacity of the cycle would have been very low and not able to deal with the sudden influx of ammonia. Thus it is important that subjects accustomed to very low protein diets be re-fed relatively small increments of dietary protein until the cycle has increased sufficiently in capacity to avoid hyperammonemia.

Long-term changes in the capacity of the ornithine cycle are always accompanied by similar changes in the expression of a number of genes encoding related hepatic enzymes and transporters. These include, the ORN 1 transporter, various plasma membrane amino acid transporters, tyrosine aminotransferase, glutaminase, and phosphoenolpyruvate carboxykinse. The last is a gluconeogenic enzyme, again illustraing the integrative nature of the entire process of amino acid catabolism.

Extra-Hepatic Expression of Ornithine Cycle Enzymes

The complete ornithine cycle is only found in the liver but some of the enzymes are expressed in other tissues where they function in arginine synthesis. Arginine is not an essential amino acid in non-carnivorous mammals

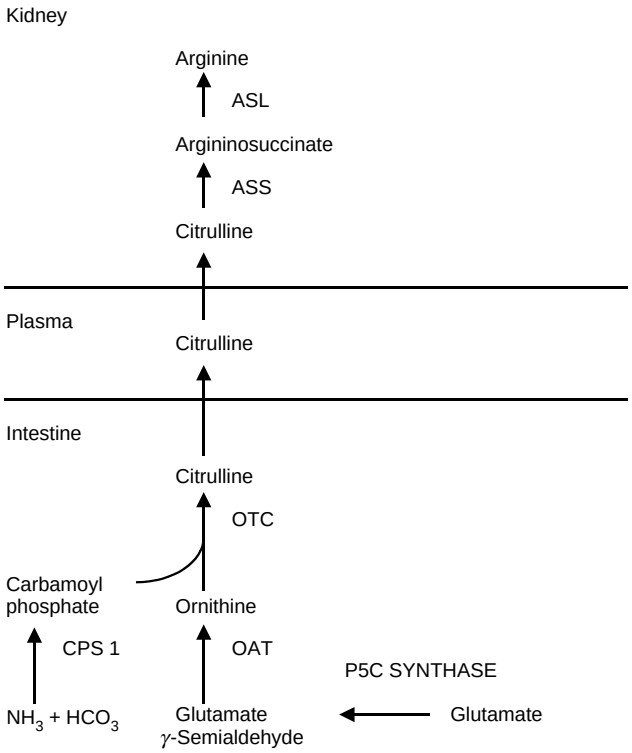

FIGURE 4 Extrahepatic arginine synthesis. ASL, argininosuccinate lyase, ASS, argininosuccinate synthetase, CPS 1, carbamoyl phosphate synthetase 1, OTC, ornithine transcarbomylase, OAT, ornithine aminotransferase, P5C, pyrroline 5-carboxylate.

but the very high arginase activity of the liver means that both dietary arginine and arginine synthesized within the liver are rapidly hydrolyzed and not available to the body. Thus the arginine required for the synthesis of protein, nitric oxide, polyamines, etc. is made in extra-hepatic tissues (Figure 4). The mucosa of the small intestine expresses both carbamoyl phosphate synthetase I and ornithine transcarbamoylase, and together with pyrroline 5-carboxylate synthase and ornithine aminotransferase, this allows the synthesis of citrulline from glutamate and ammonia. This citrulline is released into the circulation to be taken up by the kidney, which expresses both argininosuccinate synthase and argininosuccinate lyase, and used for arginine synthesis. Thus by restricting expression of four enzymes of the ornithine cycle to these two extra-hepatic tissues the body is able to obtain sufficient arginine. Strict carnivores, such as cats and ferrets, lack the intestinal part of this pathway and therefore arginine must be provided in the diet. This is not usually a problem but if, experimentally, they are fed an arginine-free diet, they are unable to generate sufficient ornithine in the liver to allow increased flux through the cycle. This results in hyperammonenia and is one of the very few known cases of acute toxicity arising from a nutritional deficiency.

Inborn Errors of the Ornithine Cycle

As detailed above, the ornithine cycle is not required in utero and thus the genes encoding the cycle enzymes are not expressed until very late in gestation. Therefore it is possible to develop to full term with a misfunctional ornithine cycle gene (inborn errors may arise from a complete lack of a protein, changes in V_{max} or K_M, or the ability to bind cofactors or regulators). Inborn errors for all five cycle enzymes, plus some of the ancillary proteins such as N-acetyl glutamate synthetase and the ORN 1 transporter, have been described. All are characterized by hyperammonemia that is usually accompanied by very high levels of the non-essential amino acids alanine and glutamine. Other intermediates of the cycle accumulate according to the specific enzyme defect. The severity is usually more pronounced with deficiencies of the first two enzymes, carbamoyl phosphate synthetase 1 and ornithine transcarbamoylase, especially if there is a complete lack of activity. The gene encoding ornithine transcarbamoylase is located on the X chromosome and thus boys are most severely affected, however due to Lyonization different alleles are expressed in different cells and some female carriers of a defective gene will present with very low ornithine transcarbamoylase activity. This was traditionally believed to be benign since these women often exhibit protein intolerance and simply self limit their protein intake. It is now recognized however, that times of increased endogenous proteolysis, such as occurs in hypercatabolic states or even pregnancy, can represent a risk for hyperammonemia in such individuals. In classic cases of ornithine transcarbamoylase deficiency, some of the excess carbamoyl phosphate in the mitochondria escapes to the cytosol where it enters the pyrimidine synthesis pathway. This causes production of relatively large amounts of orotic acid which is lost in the urine and the presence of significant orotate excretion is considered definitive evidence for ornithine transcarbamoylase deficiency.

A defect in argininosuccinate synthase results in citrullinemia and excretion of citrulline in the urine. To a limited extent, this lessens the need for urea synthesis and threrefore the ammonemia is not as severe as seen with defects in the first two enzymes. Similarly, with defects of argininosuccinate lyase and argininase, there is excretion of argininosuccinate and arginine, again lowering the need for urea synthesis and the severity of the condition.

The treatment for all inborn errors of the ornithine cycle begins with a limited protein diet to lower the need for urea synthesis. However, depending on the severity of the condition, patients will still encounter periods of hyperammonemia, and additional treatments have been developed. Most commonly, oral benzoic acid or

phenylacetate (or phenylbutyrate) are given since these are detoxified in the liver by conjugation with glycine or glutamine respectively. The amino acid conjugates are excreted which effectively removes nitrogen from the body, again lessening the need for urea synthesis. Recently a number of liver transplants have been carried out and gene therapy trials have been initiated. With inborn errors of the ornithine cycle, except arginase deficiency, arginine becomes an essential amino acid. In cases of argininosuccinate synthase and lyase deficiences, very large amounts of dietary arginine are required to replace the arginine equivalents lost as citrulline and argininosuccinate in the urine. Similarly, while liver transplantion or liver-specific gene therapy will correct the defect in urea synthesis, they do not change the defect in the extra-hepatic arginine synthesis pathway and thus, arginine remains an essential amino acid after such treatments.

See Also the Following Articles

Amino Acid Metabolism • Gluconeogenesis • Urea Cycle, Inborn Defects of

Glossary

ammonia In this context to the sum of NH_3 plus NH_4^+. In the cell, at physiological pH, >99% is present as NH_4^+.

equilibrium An enzyme-catalyzed reaction in which there is little change in Gibbs free energy between the substrates and products. In practice, this means that the reaction is freely reversible and both the direction and magnitude of net flux is determined by the rate of substrate supply and/or product removal.

gluconeogenesis The formation of glucose from non-carbohydrate prescursors such as lactate, glycerol, and amino acids.

hypercatabolic states Conditions in which the body is undergoing extensive catabolism (degradation) of tissues, particularly skeletal muscle, to provide amino acids for acute phase protein synthesis, gluconeogenesis, and tissue repair, after severe injury or infection.

transaminases Enzymes that catalyze the transfer of amino (NH_2) groups between α-amino acids and α-keto acids. Also known as aminotransferases usually glutamate and α-ketoglutarate act as the amino donor or acceptor respectively.

Further Reading

Grisolia, S., Baguena, R., and Mayor, F. (eds.) (1976). *The Urea Cycle*. Wiley-Interscience, New York.

Jungas, R. L., Halperin, M. L., and Brosnan, J. T. (1992). Quantitative analysis of amino acid oxidation and related gluconeogenesis in humans. *Physiol. Rev.* **72**, 419–448.

Krebs, H. A. (1982). The discovery of the ornithine cycle of urea synthesis. *Trends Biochem. Sci.* **7**, 76–78.

Lee, B., and Gross, J. (2001). Long term correction of urea cycle disorders. *J. Pediatr.* **138**, S62–S71.

Meijer, A. J. (1995). Urea synthesis in mammals. In *Nitrogen Metabolism and Excretion* (P. Walsh and P. Wright, eds.) pp. 193–204. CRC Press, Boca Raton, FL.

Morris, S. M. Jr (2002). Regulation of enzymes of the urea cycle and arginine metabolism. *Annu. Rev. Nutr.* **22**, 87–105.

Stipanuk, M. H., and Watford, M. (2000). Amino acid metabolism. In *Biochemical and Physiological Aspects of Human Nutrition* (M. H. Stipanuk, ed.) pp. 233–286, Saunders, Philadelphia, PA.

Watford, M. (1991). The urea cycle: A two-compartment system. *Essays Biochem.* **26**, 49–58.

Watford, M (2003). The urea cycle. *Biochem. Mole. Biol. Education* **31**, 289–297.

Wu, G., and Morris, S. M. Jr (1998). Arginine metabolism; nitric oxide and beyond. *Biochem. J.* **336**, 1–17.

Biography

Malcolm Watford obtained his D.Phil. from the Metabolic Research Laboratory, Oxford, and did postdoctoral work at the University of Montreal and Case Western Reserve University. He is currently on the faculty of the Department of Nutritional Sciences, Rutgers University where he teaches metabolic regulation and carries out research on glutamine metabolism and gluconeogenesis.

Oxygenases

Osamu Hayaishi
Osaka Bioscience Institute, Suita, Osaka, Japan

Oxygenases are a group of oxidative enzymes that catalyze the direct addition or fixation of molecular oxygen into various substrates. The terms "mono" and "di" oxygenases are generally assigned to the enzymes catalyzing the incorporation of either one or two atoms of oxygen per mole of substrate, respectively. Prior to the discovery of "oxygenases" in 1955, the essential characteristics of biological oxidation processes was believed to be the removal or transfer of electrons or hydrogen atoms from a substrate to an appropriate acceptor. These enzymes were termed "dehydrogenases" and when oxygen molecules serve as the immediate electron acceptor, the enzymes have been called "oxidases." Functionally, dehydrogenases and oxidases are mainly involved in energy metabolism whereas oxygenases play major roles in the anabolism and catabolism of biological materials as well as synthetic compounds.

Background

In 1932, Professor Heinrich Wieland, a German Nobel laureate, authored a book entitled "On the Mechanism of Oxidation," in which he proposed the famous "dehydrogenation theory." According to this theory, the principle of biological oxidation processes is the activation and transfer of hydrogen atoms, or their equivalent, from the substrate molecule to an appropriate acceptor such as coenzymes and various dyes. Oxygen molecules may, in some instances, serve as the immediate electron acceptor, and if so, then these enzymes are termed "oxidases." Thus, according to Professor Wieland, molecular oxygen accepts hydrogen atoms and is reduced to water or hydrogen peroxide. However, it is never incorporated into the substrate. When the overall reaction is envisaged as the addition of oxygen, the oxygen atoms are always derived from water molecule rather than from atmospheric oxygen. For example, when aldehydes are converted to acids, aldehydes are hydrated first and then dehydrogenation occurs so that the sum is the addition of oxygen to the substrate X to form XO, but this oxygen atom is derived from water rather than from molecular oxygen. Thus, the direct addition of molecular oxygen to a substrate was considered completely irrelevant to biological oxidation.

In 1955, a set of experiments was performed in which pyrocatechase from a pseudomonad was incubated with its substrate catechol and a heavy oxygen isotope, ^{18}O (oxygen-18), the latter being in its molecular form in air in one flask or in the form of water in the other. The product, muconic acid, was isolated and analyzed for its ^{18}O content by mass spectrometry. Contrary to the then generally held belief, the results clearly demonstrated that the oxygen atoms incorporated into the product molecules were derived exclusively from molecular oxygen and not from the oxygen of the water molecule. Concurrently and independently, the phenolase complex of the mushroom was shown to incorporate 1 atom of molecular oxygen into a substrate, 3, 4-dimethylphenol, to form 4, 5-dimethylcatechol; whereas the other atom of oxygen was reduced to water. These findings together with subsequent work by others established that "oxygen fixation" did occur in biological systems, and revealed a new biological role of molecular oxygen, thus, the new concept of "biological oxygenation" was introduced. These enzymes that catalyze the direct incorporation of molecular oxygen were then named "oxygenases." At first, these oxygenase reactions were generally thought to be rather unusual and were limited to only primitive living organisms such as soil bacteria or mushrooms. It took several years before the ubiquitous existence of oxygenases was confirmed in many laboratories; and during that time a large number of oxygenases were isolated from animals, plants, and microoganisms and were shown to play important roles in the metabolism of various nutrients, hormones, and neurotransmitters as well as synthetic compounds.

Nomenclature, Classification, and General Properties of Oxygenases

Dioxygenases

Dioxygenases are defined as enzymes catalyzing reactions in which both atoms of molecular oxygen are incorporated into substrates. In the many instances where one substrate can act as the oxygen acceptor, the term "intramolecular dioxygenase" may be used.

Pyrocatechase (catechol 1, 2-dioxygenase) (EC 1.13. 11.1) is a typical example. The dioxygenases acting upon two acceptor substrates may be referred to as "intermolecular dioxygenases." One of the two substrates for the latter type has so far been invariably 2-oxoglutarate. Hypoxia-inducible factor 1 (H1F1) is a global regulator of cellular and systemic O_2 homeostasis in animals. Prolyl hydroxylase, also known as procollagen-proline: α-ketoglutarate 4-dioxygenase (EC 1. 14. 11. 2), the enzyme that hydroxylates specific prolyl residues of the collagen chains during their translation and requires 2-oxoglutarate as a cosubstrate in addition to ascorbate and Fe^{2+}, serves as an oxygen sensor. More recent evidence indicates that asparaginyl hydroxylase that hydroxylates the asparagine residues by a similar mechanism also serves as a direct oxygen sensor. A third class of dioxygenases include various enzymes that require NADH or NADPH as an electron donor. Although it is quite possible that reactions of this class may involve a simple dioxygenation reaction followed by a reductive step, these two processes may be coupled in such a way as to justify a separate category. The formation of catechol from anthranilate is an example of this type of reaction.

Prostaglandin endoperoxide synthase (EC 1. 14. 99. 1) is a unique intramolecular dioxygenase catalyzing the sequential addition of two oxygen molecules to a substrate molecule arachidonic acid to produce prostaglandin G_2 followed by the peroxidase reaction to generate prostaglandin H_2. This enzyme is also called cyclooxygenase, abbreviated as COX, and is of great clinical significance as will be discussed.

Some dioxygenases, such as tryptophan 2, 3-dioxygenase, contain heme as the sole prosthetic group; whereas others, such as pyrocatechase, contain nonheme iron, or like quercetinase, contain copper as the prosthetic group.

Monooxygenases

Monooxygenases are defined as a group of enzymes that catalyze the incorporation of one atom of molecular oxygen into a substrate, with the other being reduced to water. Therefore, these enzymes are some times referred to as mixed function oxidases or mixed function oxygenases. The electron donors that serve as coenzymes for these enzymes include reduced forms of pyridine nucleotides, flavin nucleotides, cytochromes, ascorbic acid, and pteridine derivatives. In some cases, the substrate itself may serve as an electron donor.

Internal Monooxygenases

The simplest type of monooxygenase catalyzes the incorporation of a single atom of molecular oxygen concomitant with the reduction of the other oxygen atom by electrons derived from the substrate. Since the reducing agent is internally supplied, these enzymes may be referred to as internal monooxygenases. The first of these enzymes to be crystallized was the lactate oxidative decarboxylase from *Mycobacterium phlei*. This enzyme catalyzes the conversion of lactate to acetate with the incorporation of one atom of oxygen into acetate, the evolution of one mole of CO_2, and the reduction of one atom of oxygen to water.

External Monooxygenases

While the internal monooxygenases do not require external reducing agents, more common types of monooxygenases require various kinds of electron donors. The electron donor (DH_2) serves as a basis for the subclassification of external monooxygenases. Some examples are as follows:

1. Flavoprotein monooxygenases with reduced pyridine nucleotides as DH_2. Salicylate 1-monooxygenase, a flavoprotein, is an example of this type of enzyme and catalyzes the formation of catechol from salicylate.
2. Heme-containing monooxygenases. Aryl 4-monooxygenase (liver microsomal cytochrome p-450) catalyzes the hydroxylation of a variety of substrates with reduced flavin as DH_2.
3. Heme-containing monooxygenases with a reduced iron-sulfur protein as DH_2. Camphor 5-monooxygenase is a typical example of this type of enzyme.
4. Pteridine-linked monooxygenases. Phenylalanine-4-monooxygenase catalyzes the formation of tyrosine from phenylalanine. Nitric oxide (NO) is a ubiquitous bioactive substance and a unique messenger molecule. It is synthesized from L-arginine by NO synthase (NOS), (EC 1, 14, 13, 39) a unique monooxygenase that catalyzes two consecutive monooxygenase reactions and that requires NADPH, tetrahydrobiopterine (BH_4), heme and Ca^{2+}/calmodulin and contains FAD and FMN. The product of the reaction is L-citrulline.
5. External monooxygenases with ascorbate as DH_2. Dopamine β-monooxygenase is an example of this type of enzyme.
6. External monooxygenases with another "substrate" as DH_2. Monophenol monooxygenase is an example of this type. In this case, dopa may be considered as the electron donor in the reaction.

Chemistry of Oxygen Fixation Reactions

Molecular Oxygen as a Substrate

Oxygenases utilize two different species of substrate, namely, molecular oxygen and the oxygen acceptor,

which is called the substrate and may be either an organic or an inorganic compound. It has not yet been clarified whether gaseous oxygen or oxygen dissolved in water is utilized by these enzymes. It is generally believed that the latter type of oxygen is different from the former. In water, oxygen is considered to exist largely in a dimerized form, $O_2{-}O_2$ because of its biradical nature, and probably forms a charge transfer complex with a water molecule. Whatever form is taken by the oxygen dissolved in water, the type of oxygen that serves as a substrate for oxygenases is in rapid equilibrium with gaseous oxygen under normal experimental conditions and can be clearly distinguished through the use of $^{18}O_2$ from the oxygen in water molecules or other compounds in the reaction mixture.

Role of the Substrate that Acts as Oxygen Acceptor

As for the acceptor for molecular oxygen, a great variety of both organic and inorganic compounds can be oxygenated. In general, oxygen-rich and/or hydrophilic compounds such as carbohydrates are not favorable substrates for oxygenases since these usually have many reactive groups containing oxygen, such as the hydroxyl, carbonyl, or formyl, and their biochemical function does not require further oxygenation. On the other hand, hydrophobic compounds such as lipids and aromatic compounds are often metabolized by oxygenases. These oxygen-deficient compounds generally require oxygenation in order to become biologically active or more soluble in water. In contrast, purines and pyrimidines with their hydrophilic ring systems are usually hydroxylated by the addition of water, followed by dehydrogenation.

Reaction Mechanisms and the Nature of Active Oxygen

Evidence generated from a number of laboratories has indicated that the enzyme binds oxygen only in the presence of substrate to form the ternary complex, ESO_2, in which oxygen and substrate interact to form a product. Such a ternary complex was postulated in 1964 on the basis of binding experiments, but more direct experimental evidence was not available until 1967 when a ternary complex of tryptophan 2,3-dioxygenase · tryptophan · O_2 was demonstrated by spectrophotometric experiments. Since that time similar oxygenated intermediates have also been observed, such as those with protocatechuate 3,4-dioxygenase (an iron-sulfur protein dioxygenase), lysine monooxygenase (a flavoprotein), and cytochrome P-450. In each case, the enzyme must bind the organic substrate first, before it can be oxygenated, in contrast to oxygen-carrying pigments such as hemoglobin and hemoerythrin, which are freely and reversibly oxygenated in the absence of any effector or substrate. In fact, several lines of evidence indicate that the substrate tryptophan binds specifically to the heme coenzyme of tryptophan 2,3-dioxygenase; as a consequence, the state of the heme is altered in such a way that its reactivity toward ligands is increased by several orders of magnitude.

The nature of the so-called active form of oxygen in the above-mentioned ternary complexes has been one of the most difficult questions in this field. All oxygenase-catalyzed reactions are exothermic and are therefore irreversible. Nevertheless, molecular oxygen is a rather inert compound and at room temperature reacts slowly with the substrate compounds in the absence of enzymes. This low kinetic reactivity is usually explained on the basis that molecular oxygen is in a triplet ground state. The direct reaction of a triplet molecule with organic molecules in the singlet state is electronically spin forbidden, and therefore a substantial activation energy is required. For this reason singlet oxygen has been suggested as a likely intermediate in many oxygenase-catalyzed reactions; however, definitive evidence is so far unavailable. It has recently been discovered that during enzymic hydroxylation of aromatic substrates the substituent (deuterium, tritium, chlorine, bromine, etc.) displaced by the entering hydroxyl group migrates to an adjacent position in the aromatic ring. On the basis of extensive studies of this phenomenon, called the "NIH shift," the active oxygen species involved in certain monooxygenases was postulated to be oxenoid.

On the other hand, evidence has appeared indicating that $O_2^{\cdot-}$, i.e., the superoxide anion, may be the active form of oxygen in the case of indoleamine 2,3-dioxygenase, and also in the hydroxylation reactions catalyzed by hepatic cytochrome P-450. It is, however, uncertain whether or not the superoxide anion is the general form of active oxygen in all oxygenase-catalyzed reactions or whether these enzymes represent a new class of enzyme that utilizes the superoxide anion rather than molecular oxygen as an oxygenating agent.

Biological Function of Oxygenases

While oxidases and dehydrogenase are mainly involved in energy metabolism, namely, the generation of ATP, oxygenases play important roles in biosynthesis, transformation, and degradation of essential metabolites such as amino acids, lipids, sugars, porphyrins, vitamins, and hormones. They also play a crucial role in the metabolic disposal of foreign compounds such as drugs, insecticides, and carcinogens. Furthermore, they participate in the degradation of various natural and synthetic compounds by soil and airborne microorganisms in

nature and are therefore of great significance in environmental sciences. Therefore, the significance of biological oxygen fixation in medicine, agriculture, and microbiology, and also in food technology, cosmobiology, public health problems, and biochemistry in general, has now been well established.

For example, certain oxygenases fulfill exceptionally important biological functions as exemplified by prolyl and asparaginyl hydroxylases as oxygen sensor as well as NO synthase as already mentioned. Several other examples are being briefly described.

Ribilose 1,5-bisphosphate carboxylase/oxygenase (EC 4. 7. 1 39), also known as "rubisco," catalyzes the CO_2 fixation as well as dioxygenase reaction and is the most abundant naturally occurring catalyst in nature. The global fixation of O_2 by rubisco can be estimated to be $\sim 10^{11}$ metric ton (t) per year.

Tryptophan 2,3-dioxygenase (EC 1. 13. 11. 11), also known as tryptophan pyrrolase, catalyzes the pyrrole ring cleavage by the insertion of two atoms of oxygen to produce L-formylkynurenine. This enzyme is present in the liver and is highly specific for L-tryptophan.

On the other hand, indoleamine 2,3-dioxygenase (EC 1. 13. 11. 42), also known as IDO, shows broad substrate specificity including L- and D-tryptophan, L- and D-5-hydroxytryptophan, serotonin, and so forth and is widely distributed in almost all organs and tissues except in the liver. IDO is induced by interferon and has been implicated in the defence mechanism against infection by depleting tryptophan from the infected tissues and cells. More recently, allogenic fetal rejection was reportedly prevented by tryptophan catabolism by IDO.

The prostaglandin endoperoxide synthases I and II (COX-1 and COX-2) are the major targets of nonsteroidal anti-inflammatory drugs (NSAIDs) including aspirin, indomethacin, ibuprofen, and the new COX-2 inhibitors. These drugs reduce inflammation, pain, and fever and also fatal thrombotic events, colon cancer, and Alzheimer disease.

Another common dioxygenase involved in lipid metabolism and widely distributed in both animals and plants is lipoxygenase (EC 1. 13. 11. 12), which is also known as LOX, lipoxidase, lipoperoxidase, or carotene oxidase. It is a nonheme iron-containing dioxygenase and catalyzes the formation of hydroperoxy derivative of unsaturated fatty acids. Of particular interest is the 5-LOX that catalyzes the dioxygenation of arachidonic acid to produce corresponding cis, trans-diene hydroperoxide followed by the dehydration to generate leukotrien (LT) A_4, another biologically important lipid mediator.

Unspecific monooxygenase is a heme-thiolate enzyme commonly known as cytochrome P450, hepatic microsomal monooxygenase, xenobiotic monooxygenase or aryl-4-monooxygenase (EC 1. 14. 14. 1), and catalyzes hydroxylation of a wide variety of both aromatic and aliphatic compounds. Monooxygenases also catalyze a seemingly diverse group of reactions including epoxide formation, dealkylation, decarboxylation, deamination, and N- or S-oxide formation. Although the overall reactions catalyzed by various monooxygenases appear grossly unlike one another, the primary chemical event is identical, since these processes are all initiated by the incorporation of one atom of molecular oxygen into the substrate.

Oxygenases in Evolution

Primitive Earth is believed to have started with an oxygen-free anaerobic environment. Therefore, the minimum manifestation of life is capable of occurring in the absence of molecular oxygen, as exemplified by the strictly anaerobic microorganisms, which survive and grow solely in the absence of molecular oxygen. With the appearance of oxygen in the Earth's atmosphere, molecular oxygen became a more useful and efficient tool as the terminal electron acceptor. Oxygenases then appeared gradually with the subsequent development of extensive and complicated metabolic pathways for essential components of cell structures and of regulatory mechanisms of metabolism and growth. The appearance of aerobic form of life paved the way for oxygenase-catalyzed reactions by which complicated messengers and structural compounds such as sterols, prostaglandins, and neurotransmitters are efficiently synthesized, while cytochrome P450 plays an essential role in the metabolism of thousands of drugs, carcinogens, and other synthetic compounds and is probably the largest family of proteins that has been cloned and characterized to date. In an evolutionary sense, oxidases preceded oxygenases but the latter appears to be a more advanced oxygen-utilizing catalyst associated with the most advanced and highly specialized life processes.

See Also the Following Articles

Cytochrome P-450 • Dopamine Receptors

Glossary

dehydrogenase The enzyme that catalyzes electron transfer from a substrate to an acceptor.

E.C. numbers and trivial names Enzymes are classified and numbered by the international Enzyme Commission. In this list, the names of the enzymes are formal names whereas trivial names are more common names or informal names. For example, catechol 1, 2-dioxygenase is a formal name while pyrocatechase is a trivial name.

oxidase The dehydrogenase that utilizes molecular oxygen as an immediate electron acceptor.

oxygenase The enzyme that incorporates molecular oxygen into substrates.

Further Reading

Bruick, R. K., and McKnight, S. L. (2001). Oxygen sensing gets a second wind. *Science* **295**, 807–808.

Groves, J. T. (2003). The bioinorganic chemistry of iron in oxygenases and supramolecular assemblies. *Proc. Natl Acad. Sci. USA* **100**, 3569–3574.

Hayaishi, O., Katagiri, M., and Rothberg, S. (1955). Mechanism of the pyrocatechase reaction. *J. Am. Chem. Soc.* **77**, 5450–5451.

Hayaishi, O. (ed.) (1962). *Oxygenases*. Academic Press, New York and London.

Hayaishi, O. (ed.) (1974). *Molecular Mechanism of Oxygen Activation*. Academic Press, New York.

Ishimura, Y., Nozaki, M., Yamamoto, S., Shimizu, T., Narumiya, S., and Mitani, S. (eds.) (2002). *Oxygen and Life-Oxygenases, Oxidases and Lipid Mediators*. Elsevier, Amsterdam.

Mason, H. S., Fowlks, W. L., and Peterson, E. (1955). Oxygen transfer and electron transport of the phenolase complex. *J. Am. Chem. Soc.* **77**, 2914–2915.

Nozaki, M., Yamamoto, S., Ishimura, Y., Coon, M. J., Ernster, L., and Estabrook, R. W. (eds.) (1982). *Oxygenases and Oxygen Metabolism*. Academic Press, New York.

Purich, D. L., and Allison, R. D. (eds.) (2002). *The Enzyme Reference: A Comprehensive Guidebook to Enzyme Nomenclature, Reactions, and Methods*. Academic Press, San Diego, CA.

Solomon, E. I., Decker, A., and Lehnert, N. (2003). Non-heme iron enzymes: Contrasts to heme catalysis. *Proc. Natl. Acad. Sci. USA* **100**, 3589–3594.

Biography

Osamu Hayaishi is a Professor Emeritus of Kyoto University and Osaka Medical College and a Director Emeritus of Osaka Bioscience Institute. His principal research interests are oxygenases and molecular mechanisms of sleep and wakefulness. He is a member of the Japan Academy, the National Academy of Sciences USA, and several other academies and served as President of the International Union of Biochemistry from 1973 to 1976.

P2X Purinergic Receptors

Annmarie Surprenant
University of Sheffield, Sheffield, UK

Inside the cell, adenosine triphosphate (ATP) is the major source of energy for all cellular processes. Outside the cell, ATP has quite distinct actions as a neurotransmitter at nerve–smooth muscle and nerve–nerve synapses, as a chemical stimulant at primary afferent terminals, and as a pro-inflammatory stimulus at immune and endothelial cells. Extracellular ATP acts on two types of membrane receptors: G protein-coupled "metabotropic" P2Y purinergic receptors and "ionotropic" P2X purinergic receptors. They are termed purinergic because ATP is a purine nucleotide. Ionotropic P2X receptors are ion channels opened within ms by extracellular ATP. There are seven members of the P2X receptor family ($P2X_1$–$P2X_7$) which are not related to any other known protein. They show widespread tissue distribution; functional responses to activation of these receptors occur in neurons, glia, endothelia, epithelia, bone, smooth muscle, cardiac muscle, red blood cells, and cells of the immune system.

P2X Receptor Genes

There are seven genes encoding P2X receptor subunits (Figure 1A). In the human genome, $P2X_4$ and $P2X_7$ are adjacent to each other on chromosome 12, an occurrence that probably represents gene duplication. $P2X_1$ and $P2X_5$ receptor genes are also very closely associated on chromosome 13. The remaining genes are located on separate chromosomes. The genes have 11–13 exons and all share a common structure with conserved intron/exon boundaries. Many spliced forms of these receptors have been observed, most due to splicing out of one or more exons. Several non-mammalian homologues of P2X receptors have been identified but no homologous sequences from invertebrates have yet been identified.

P2X Receptor Proteins

P2X receptor proteins range from 384 amino acid residues ($P2X_4$) to 595 amino acids ($P2X_7$). Each subunit comprises a large extracellular domain, two transmembrane domains, and relatively short intracellular amino and carboxy terminal regions (Figure 1B). There are ten cysteines in the extracellular region of the P2X receptor subunit which are conserved through all members of the family. Amino acid residues in the second transmembrane region are involved in ion flux through the channel. The carboxy terminal regions show very little homology among individual P2X receptors, but the remaining amino acids show 40–55% identity with each other among the seven receptors (Figure 1A). There is no amino acid sequence homology between P2X receptors and any known ATP-binding protein, any other ion channel, or any known protein: this places the P2X receptors into their own unique gene/protein family. The receptors assemble in multimeric combinations of subunits, either as homomeric channels (all one subtype) or as heteromeric channels (two or more subtypes). $P2X_1$, $P2X_2$, $P2X_3$, $P2X_4$, and $P2X_7$ exist as homomeric channels but $P2X_2$ and $P2X_3$ also exist as a functionally important heteromeric channel ($P2X_{2/3}$). The current evidence suggests these channels are composed of three, or possibly six, subunits.

P2X Receptor Localization

While other ionotropic ion channels are found mainly on excitable cells (i.e., nerve and muscle), P2X receptor channels are unusual in showing a very widespread distribution in both excitable and nonexcitable cells. There is considerable overlap with multiple receptor subunits found in a single cell, particularly in neurons. However, it is possible and biologically useful to generalize the distribution of these receptors (Table I).

Physiology of P2X Receptors

Release of ATP onto P2X Receptors

Cells release ATP in various ways: ATP is coreleased with noradrenaline from sympathetic nerve endings, or with aceytlcholine from parasympathetic or brain cholinergic neurons. It is rapidly released from vascular endothelial cells during hypoxia which is likely to be present under conditions such as angina or myocardial infarction. ATP is released from red blood cells upon

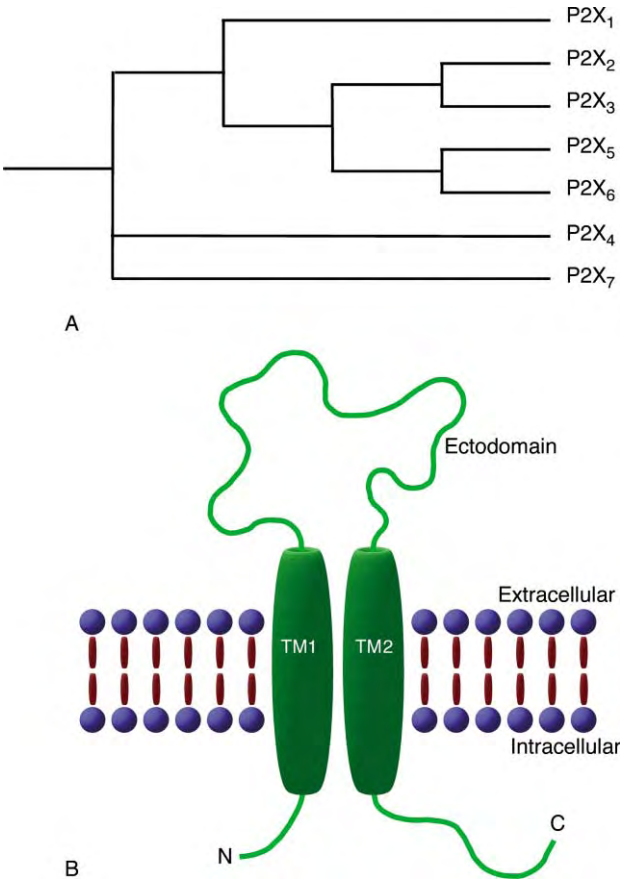

FIGURE 1 Molecular features of purinergic P2X receptor family. In (A) a dendrogram depicts the similarity in amino acid residues among the seven members of the P2X receptor family. $P2X_4$ and $P2X_7$ are the least similar while the pairs of $P2X_2/P2X_3$ and $P2X_5/P2X_6$ are most similar to each other. In (B) a cartoon representation of the likely membrane topology of a P2X receptor subunit shows the receptor protein crossing the lipid bilayer of the cell membrane at two regions (transmembrane TM1 and TM2). The large ectodomain contains the ATP-binding site and the TM2 region forms at least part of the ion channel structure. N and C refer to the intracellular amino (N) and carboxy (C) terminal amino acids.

mechanical distortion. Mechanical deformation of epithelial cells lining the bladder, lung, intestines, and ureter also causes rapid release of ATP. The mechanism by which ATP is released during mechanical displacement of these structures is unclear, but it may be transported from inside to outside by specific ATP transporter proteins or it may be released from storage vesicles by the process of exocytosis. Finally, high concentrations of ATP are released from damaged or dying cells at sites of inflammation and infection.

Activation of P2X Receptor Ion Channels ($P2X_1$ through $P2X_6$)

Although the molecular architecture of P2X receptors (see above) sets this family apart from all other ion channels, their functional properties are generally similar to the other two classes of "fast excitatory neurotransmitter receptors"—the nicotinic and the glutamate receptors. When extracellular ATP binds to specific amino acid residues in the ectodomain of the P2X receptor, a change in the conformation of the protein occurs within milliseconds and this structural alteration allows the influx of sodium ions from the outside concomitant with efflux of potassium ions from the inside. However, chloride or other anions are excluded; thus, the term cation-selective ion channel. This cation flux leads to plasma membrane depolarization and consequent excitation of nerve and muscle, or initiation of other signaling processes in nonexcitable cells. There is also appreciable influx of calcium ions with each P2X receptor allowing different levels of calcium to enter the cell; calcium entry through the $P2X_7$ receptor is several-fold higher than occurs at any other ionotropic (P2X, nicotinic or glutamate) receptor. When a continuous supply of ATP is presented to a cell expressing $P2X_1$ or $P2X_3$ receptors, the cation flux

TABLE I

Overview of Tissue Localization and Functional Role of Individual P2X Purinergic Receptors

Purinergic receptors	Tissue localization	Physiological role	Potential disease involvement
$P2X_1$	Vascular, visceral smooth muscle	Arteriolar vaso-constriction and genito urinary contractility	Male fertility
$P2X_2$	Autonomic neurons	Sympathetic drive	None implicated
$P2X_3$	Afferent neurons	Sensory perception	Neuropathic and visceral pain; bladder dysfunction
$P2X_4$	Epithelia and brain neurons	None identified	
$P2X_5$	Embryonic muscle spinal motor neurons	None identified	
$P2X_6$	Similar to $P2X_4$	None identified	
$P2X_7$	Immune cells	Release of IL-1β	Arthritis, irritable bowel syndrome

(or ionic current) fades away very rapidly (within a few hundred milliseconds) by a process termed desensitization. Desensitization does not occur, or is much slower at the other P2X receptors.

Activation of $P2X_7$ Ion Channels

The $P2X_7$ receptor is a most unusual ion channel in that it not only opens to allow bidirectional flux of cations in a manner similar to that described above for typical ionotropic receptors. However, it also dilates over several seconds to minutes to a size that allows the passage of molecules of either charge with size up to 900 Da. It is not known whether this is due to a true dilatation of the ion-passing pore region within the $P2X_7$ receptor protein itself, or whether the $P2X_7$ receptor couples to another protein which then transports the larger molecules. A further signaling event that is uniquely associated with $P2X_7$ receptor activation includes dramatic, rapid alterations in the cell cytoskeleton due to re-arrangement of the actin filaments within the cell. This causes dynamic membrane blebbing of the cell, visually appearing as though bubbles are continuously forming and retracting. The physiological significance of these membrane blebs are unknown but they have been associated with "programmed" cell death, or apoptosis. The intracellular carboxy-terminal amino acids of the $P2X_7$ receptor are required for the large pore formation and the membrane blebbing but not for its cation-selective ion channel function.

P2X Receptors and Sympathetic Neurotransmission ($P2X_1$ and $P2X_2$ Receptors)

$P2X_1$ receptors are highly expressed on vascular smooth muscle in the gastrointestinal (GI) tract and on visceral smooth muscle of the urogenital system, particularly the bladder, vas deferens, and ureter (Table I). $P2X_2$ receptors are equally highly expressed in the neurons that innervate these tissues, the sympathetic autonomic nerves. The functional role for $P2X_2$ receptors in autonomic neurotransmission is not understood, but $P2X_1$ receptors are now known to be

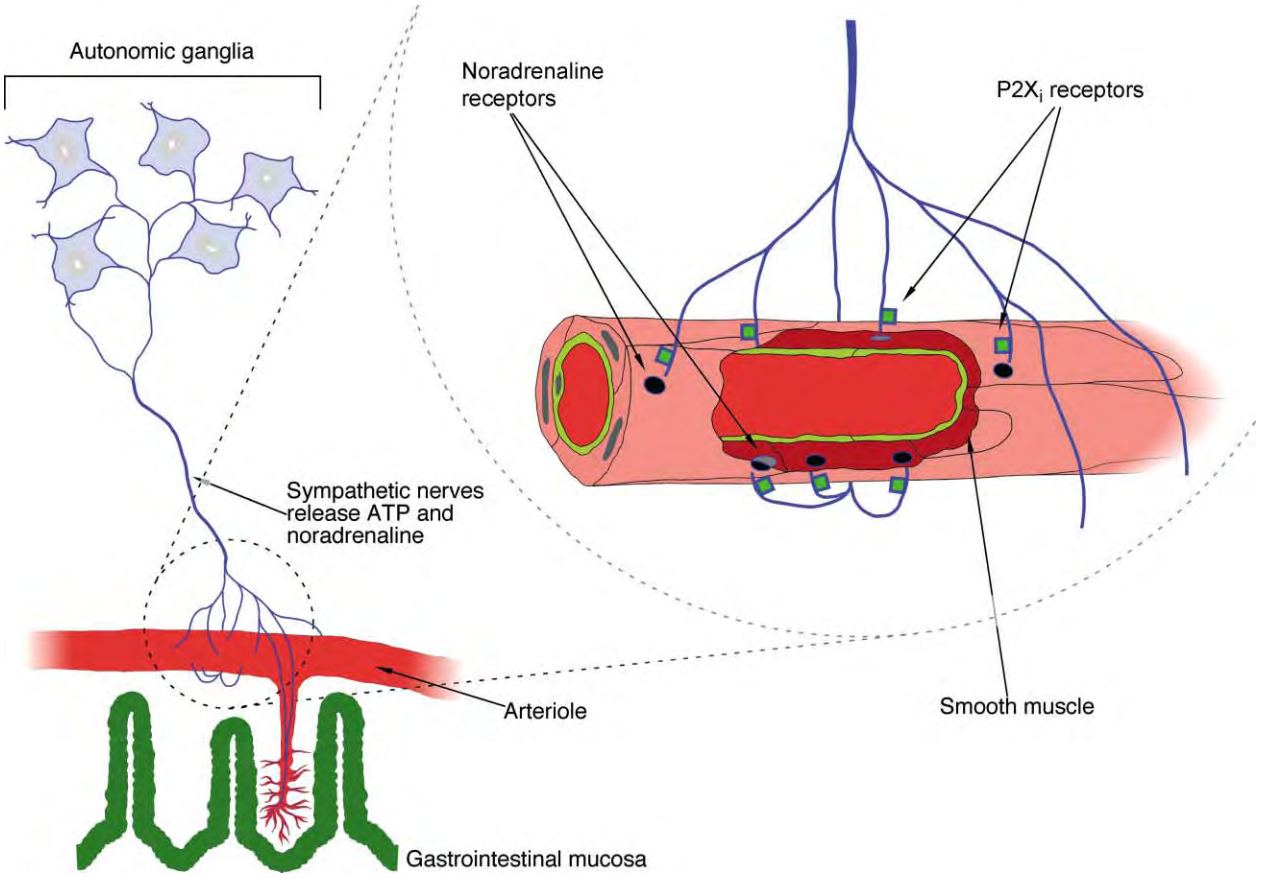

FIGURE 2 Sympathetic innervation to GI blood supply requires P2X receptors. Diagram illustrates the sympathetic nerves supplying the GI vasculature; the sympathetic nerves corelease noradrenaline and ATP. ATP activates postsynaptic $P2X_1$ receptors on the arteriolar smooth muscle to cause vasoconstriction. Noradrenaline released from these nerves acts only on presynaptic noradrenaline receptors which are present on the sympathetic nerve endings; the presynaptic action of noradrenaline alters the subsequent release of ATP.

the primarily, and in some cases, solely responsible for vasoconstriction or visceral smooth muscle contractions caused by sympathetic nerve activity. For example, male mice in which the $P2X_1$ receptor gene has been deleted are infertile, because the sympathetic nerve activity no longer causes smooth muscle of the vas deferens to contract. Thus, no sperm is released from the vas although all other aspects of ejaculation are unaltered. Similarly, in the GI vasculature, the vasoconstriction produced by sympathetic nerve activity is due to the release of ATP onto $P2X_1$ receptors on the vascular smooth muscle. In both of these cases, noradrenaline, which is the cotransmitter along with ATP, continues to be released and act effectively on its receptors. However, the noradrenaline released from these nerves acts on presynaptic noradrenaline receptors to alter the release of both noradrenaline and ATP, but it does not act on postsynaptic noradrenaline receptors present on the smooth muscle (Figure 2).

P2X Receptors and Sensory Pathways ($P2X_3$ and $P2X_{2/3}$)

Pain Pathways

ATP applied to sensory nerve terminals in the skin or tongue has long been known to elicit pain, specifically a tingling or burning sensation in humans. The molecular cloning and subsequent receptor localization studies revealed that the $P2X_3$ receptor subunit is preferentially localized to a specific subset of sensory afferent fibers which innervate skin and viscera. Most of these sensory fibers are nociceptors, i.e., they are activated by noxious stimuli. Both homomeric $P2X_3$ receptors and heteromeric $P2X_{2/3}$ receptors are found at presynaptic and postsynaptic sites in this pathway (Figure 3). When ATP is released as a result of tissue injury, gross visceral distention, or even excess sympathetic activation, it activates the $P2X_3$ and $P2X_{2/3}$ receptors on the nociceptor terminals and initiates excitatory flow to the dorsal horn neurons in the spinal cord. Here, P2X receptors play modulatory roles in further processing of painful stimuli. Presynaptic $P2X_2$ receptors are present on excitatory (glutamate) and inhibitory (glycine or γ-aminobutyrate, GABA) interneurons and can be activated by ATP released from the incoming primary afferents and also when it is coreleased with GABA from GABA interneurons. Activation of these presynaptic P2X receptors increases the further release of transmitters onto the doral horn neurons. There are also postsynaptic P2X receptors on the dorsal horn neurons which can be activated by the release of ATP from the GABA interneurons. These inhibitory and excitatory effects contribute to the "spinal" processing of pain information prior to transmission to central perception areas of the brain (Figure 3).

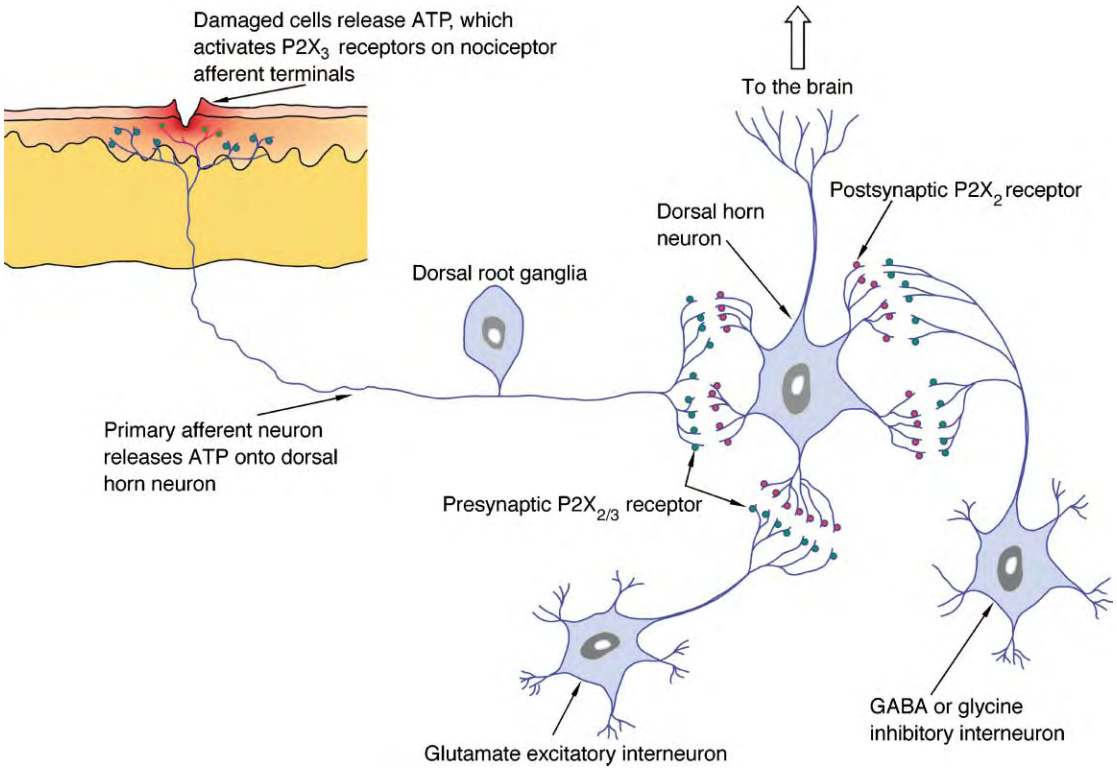

FIGURE 3 P2X receptors and pain pathways $P2X_2$, $P2X_3$, and $P2X_{2/3}$ receptors play a role in pain perception. See text for further description.

Afferent Reflex Pathways

P2X receptors are involved in the proper functioning of several visceral afferent reflexes; the micturation reflex is the best studied. The micturition reflex is initiated by bladder distention and subsequent contraction of the bladder and ureter smooth muscle. This distension releases ATP from the uroepithelium where it activates $P2X_3$ and/or $P2X_{2/3}$ receptors on the urothelial afferent nerve terminals to evoke neural discharge into spinal cord regions which, in turn, activate efferent parasympathetic nerves to bladder and ureter smooth muscle to complete the reflex loop.

P2X Receptors and Immune Cell Function ($P2X_7$)

$P2X_7$ receptors are most abundantly found on immune cells which become activated by tissue damage, inflammation, or infection, i.e., the so-called antigen-presenting cells of the immune system, primarily monocytes, and macrophage. Their synthesis and expression is increased in these cells when the immune response is triggered. Activation of $P2X_7$ receptors by ATP released from damaged cells at sites of inflammation or infection leads to the release of pro-inflammatory mediators (cytokines); the most important of these pro-inflammatory cytokines is interleukin-1β (IL-1β). IL-1β can produce fever, further inflammation, cell, and tissue death. Agents that may block its release are highly sought after with regard to treatment or prevention of diseases such as rheumatoid arthritis and inflammatory bowel disease, and intensive research efforts are currently underway to identify antagonists which selectively target $P2X_7$ receptors.

See Also the Following Articles

Cell Death by Apoptosis and Necrosis • Cytokines • Glutamate Receptors, Ionotropic • Glutamate Receptors, Metabotropic • Neurotransmitter Transporters • Nicotinic Acetylcholine Receptors • P2Y Purinergic Receptors

Glossary

cytokine A protein (usually interleukins or interferons) secreted by lymphoid cells that affects the activity of other cells and is important in controlling inflammatory responses.

dendrogram A diagram showing the relationships of items arranged like the branches of a tree.

exocytosis The release of a substance contained in a small sac (vesicle) within a cell by a process in which the membrane surrounding the vesicle fuses with the membrane forming the outer wall of the cell.

exon A discontinuous sequence of DNA that codes for protein synthesis and carries the genetic code for the final messenger RNA.

intron A length of DNA that is not expressed as an amino acid or messenger RNA.

ionotropic receptors Membrane receptors which are integral ion channels not requiring coupling via intracellular G proteins.

metabotropic receptors Membrane receptors which couple to heterotrimeric G proteins in order to produce an effect.

nociceptor A sensory nerve which subserves the perception of pain.

Further Reading

Burnstock, G. (2000). P2X receptors in sensory neurones. *British J. Anaesthesiol.* **84**, 476–488.

Le Novere, N., and Changeux, J. P. (2001). The ligand-gated ion channel database: An example of a sequence database in neuroscience. *Phil. Trans. Roy. Soc. London, B. Biolog. Sci.* **356**, 1121–1130.

North, R. A. (2002). Molecular physiology of P2X receptors. *Physiol. Rev.* **82**, 1013–1067.

Biography

Annmarie Surprenant is currently a Professor of Cellular Physiology at the University of Sheffield, United Kingdom. She has a long-standing history of research in the area of ion channel physiology. Her lab was the first to demonstrate that extracellular ATP is a synaptic transmitter in the nervous system and that ATP, not noradrenaline, was the neurotransmitter responsible for sympathetically mediated vasoconstriction in arterioles. These sets of findings led to her work over the past decade: the cloning and functional characterization of the ATP-gated P2X receptor-ion channels.

P2Y Purinergic Receptors

George R. Dubyak
Case Western Reserve University, Cleveland, Ohio, USA

P2Y receptors are intrinsic plasma membrane proteins that mediate functional responses of intact cells to extracellular nucleotides, including ATP, ADP, UTP, UDP, and UDP-glucose. P2Y receptors belong to the superfamily of G protein-coupled receptors (GPCR), an exceptionally large group of structurally and functionally related gene products that play critical roles in the transduction of signals between and among different types of cells. In response to the binding of extracellular nucleotides, P2Y receptors undergo conformational changes that facilitate their direct interaction with, and activation of, G proteins. In turn, the activated G proteins couple P2Y receptors to the regulation of enzymes and ion channels that facilitate generation of "second messengers" and intracellular signaling cascades used for the acute or chronic regulation of specific cellular functions. Appreciation of the physiological or pathological functions of P2Y receptors requires some understanding of the general mechanisms by which nucleotides are used as extracellular signaling molecules.

Extracellular Nucleotides as Signaling Molecules

In addition to their critical roles in intracellular energy metabolism and nucleic acid synthesis, nucleotides, such as ATP, and nucleosides, such as adenosine, play important roles as extracellular signaling molecules. Burnstock and his colleagues generated many of the initial hypotheses regarding the roles of purines in nonadrenergic, noncholinergic neurotransmission. They proposed that extracellular nucleotides and nucleosides are utilized for signal transduction at nerve endings in diverse tissues. Implicit in this concept of "purinergic" transmission or signaling was a requirement that ATP (or other nucleotides) be released and metabolized in a highly localized manner at sites of cell-to-cell communication. Given the emphasis on the role of purines in this neuronal signaling, initial characterization focussed on describing the release of nucleotide/nucleosides at neuron-to-neuron synapses, neuron-to-tissue varicosities, or the immediate locale of neuroendocrine cells. Such studies verified that neurons and neuroendocrine cells can release ATP via standard mechanisms involving exocytosis of nucleotides copackaged with biogenic amines or other neurotransmitters in specialized vesicles or granules.

However, subsequent research has resulted in the cloning and characterization of at least 15 distinct ATP/nucleotide receptor genes (including the P2Y receptors), four adenosine receptor genes, and a dozen different ectonucleotidase genes. Analysis of the expression of these genes revealed that most vertebrate cell types express one or more subtypes of nucleotide or nucleoside receptor along with one or more of the ectoenzymes used for metabolizing extracellular nucleotides. Because most cells lack direct proximity to nerve synapses or neuroendocrine cells, the identification of additional sources of extracellular nucleotides is a current area of investigation and speculation. Recent studies indicate that stressed or damaged cells in many tissues can locally release nucleotides via a variety of pathways ranging from irreversible cytolysis to nonlytic export through nucleotide-permeable channels. In turn, the released nucleotides activate autocrine or paracrine signaling cascades that permit those tissues to adapt to the particular stress or injury that precipitated release of the cellular nucleotides.

Regardless of the mechanisms by which ATP or other nucleotides are released from cells, their half-life within extracellular compartments is generally brief due to rapid catabolism by ectonucleotidases. Some of these ectoenzymes serially convert released nucleoside triphosphates (e.g., ATP) to their diphosphate (e.g., ADP) and monophosphate (AMP) forms. Other ectonucleotidases dephosphorylate the nucleoside monophosphates (e.g., AMP) to their corresponding nucleosides (e.g., adenosine). These nucleosides can be reaccumulated and reconverted to intracellular nucleotides via highly conserved nucleotide salvage pathways. In the case of adenosine, nucleosides can additionally function as agonists for G protein-coupled nucleoside receptors that are distinct from the P2Y nucleotide receptors. Thus, the local release of ATP may initially activate ATP-selective P2Y receptor subtypes. Although this hydrolysis of ATP to ADP by ecto-ATPases would act to terminate signaling by these particular P2Y subtypes,

this same extracellular metabolic reaction would result in activation of ADP-selective P2Y receptor subtypes. Further metabolism to adenosine might result to activation of G protein-adenosine receptors in same or adjacent cells. In these ways, ATP release in intact tissues can trigger the serial activation of multiple P2Y and adenosine receptor subtypes to generate complex patterns of positive or negative feedback among the various cell types that comprise the tissue. As a further complication, many cells export nucleoside diphosphokinases that catalyze transphosphorylation reactions between the various extracellular nucleoside tri- and diphosphates. Thus, released ATP may additionally drive the phosphorylation of ambient UDP to locally generate UTP that is a selective agonist for yet other P2Y receptor subtypes.

General Structure of the P2Y Receptors

As members of the GPCR superfamily, all P2Y receptors are intrinsic membrane proteins that consist of a single polypeptide chain with certain invariant structural domains. These include: (1) an extracellular amino terminal tail; (2) seven transmembrane-spanning segments (usually α-helices); (3) three short extracellular loops and three variably sized intracellular loops that connect transmembrane segments; and (4) an intracellular carboxyl terminal tail. The exact protein domains of P2Y receptors that facilitate selective recognition and binding of the extracellular nucleotide agonists have not been identified as yet. Significantly, no single P2Y domain contains amino acid sequences similar to the well-defined nucleotide-binding sites of the many intracellular proteins that interact with ATP (e.g., ATPases, protein kinases, nucleic acid polymerases).

Functional Classification of the P2Y Receptors

Genes encoding P2Y receptors have been identified in the genomes of all vertebrate species examined thus far. In contrast, no obvious P2Y receptor orthologues are apparent in the completely sequenced genomes of the insect, *Drosophila melanogaster*, or the nematode worm, *Caenorhabditis elegens*. At present, genes encoding eight distinct P2Y receptor subtypes have been characterized in a broad range of tissues and cell types from vertebrate organisms. These subtypes can be classified based either on their selective pharmacological recognition of different nucleotides or on their selective functional coupling to particular classes of heterotrimeric G proteins. Table I summarizes both the pharmacological and functional properties of the eight P2Y receptor subtypes.

Based on their functional coupling to G proteins, effector proteins, and second messenger cascades, P2Y receptors can be broadly subdivided into three major groups. The P2Y1, P2Y2, P2Y4, and P2Y6 receptor subtypes predominantly couple to G_q-family G proteins with consequent activation of phosphatidylinositol-specific phospholipase C effector (PI-PLC) enzymes resulting in accumulation of inositol trisphosphate, diacylglycerol, Ca^{2+} as second messengers. The P2Y12, P213, and P2Y14 subtypes activate G_i-family G proteins. As a result, stimulation of these latter receptors most often leads to inhibition of adenylyl cyclase effector enzymes and reduced intracellular levels of cyclic AMP. However, depending on cellular

TABLE I

Receptor subtype	G protein–effector cascade	Selectivity for physiological nucleotide agonists	Tissue/cellular expression
P2Y1	Gq → PI-PLC	ADP > ATP ≫ UDP, UTP	Platelets, Blood Vessels, Brain
P2Y2	Gq → PI-PLC	ATP = UTP ≫ ADP, UDP	Airways, Exocrine Glands, White Blood Cells, Blood Vessels, Brain
P2Y4	Gq → PI-PLC	UTP ≫ ATP, UDP, ADP (human) UTP = ATP ≫ UDP, ADP (rat, mouse)	Small Intestine, Inner Ear
P2Y6	Gq → PI-PLC	UDP > UTP > ADP ≫ ATP	Gallbladder, Airway
P2Y11	Gq → PI-PLC *and* Gs → AC	ADP > ATP ≫ UDP, UTP	Exocrine Glands, Kidney, White Blood Cells
P2Y12	Gi → AC/others	ADP > ATP ≫ UDP, UTP	Platelets, Brain Astrocytes
P2Y13	Gi → AC/others	ADP > ATP ≫ UDP, UTP	Brain Astrocytes
P2Y14	Gi → AC/others	UDP-glucose ≫ UTP, ATP, UDP, ADP	White Blood Cell Precursors, Stem Cells

background, these Gi-coupled P2Y receptor subtypes may also stimulate the activity of G protein-regulated K^+ channels and/or inhibit activity of N-type voltage-gated Ca^{2+} channels. Finally, the P2Y11 receptor represents a subtype that can couple to both G_q- and G_s-dependent signaling pathways; the activation of G_s allows P2Y11 receptors stimulate adenylyl cyclase effector enzymes and thereby induce accumulation of cyclic AMP. Thus, activation of the different P2Y receptor subtypes can variously trigger rapid changes in Ca^{2+}, cyclic AMP, lipid second messengers, and plasma membrane potential. In turn, these acute signals can be integrated within cell-specific transduction networks to regulate particular protein kinases, protein phosphatases, proteases, and transcription factors.

Pharmacological Classification of P2Y Receptors

P2Y receptors can also be categorized by their pharmacological selectivity for particular nucleotide agonists. The P2Y1, P2Y12, and P2Y13 receptors exhibit very high selectivity for ADP over ATP and are virtually insensitive to non-adenine nucleotides. The P2Y2, P2Y4, and P2Y6 subtypes can be effectively activated by uridine nucleotides albeit with subtype-selective preferences. P2Y2 receptors show high affinity for UTP and ATP, but not the corresponding diphosphates. P2Y4 receptors are most potently stimulated by UTP over ATP (but this is species-dependent), while P2Y6 receptors exhibit a preference for UDP. In general, P2Y11 receptors are activated by ADP or ATP, and less effectively by non-adenine nucleotides. The P2Y14 subtype, the most recently identified member of the P2Y family, exhibits a very high selectivity for sugar-conjugates of UDP, such as UDP-glucose. Given the complex and overlapping affinities of the P2Y subtypes for naturally occurring nucleotides, considerable effort is being directed toward generation of synthetic nucleotide agonists and non-nucleotide antagonists that selectively target particular P2Y subtypes. Such subtype-selective reagents may have high potential utility as therapeutic agents in diseases that involve hyperfunctional or hypofunctional P2Y receptors.

Important Physiological or Pathological Functions of P2Y Receptor Subtypes

Understanding of the most important physiological roles for P2Y receptors has been limited by: (1) the relatively recent identification of most P2Y receptor subtypes (post 1995); (2) the current paucity of subtype-selective drugs; and (3) the rather broad expression of P2Y receptors in most tissue types. However, gene-targeting approaches have been recently used to generate "knock-out" mice that lack the expression of P2Y1, P2Y2, P2Y4, or P2Y12 receptors. These mice (or tissues from the mice) exhibit significant deficits in several critical biological responses.

Mice lacking either the P2Y1 or P2Y12 receptor are characterized by abnormalities in the blood-clotting response (also known as hemostasis) that result in prolonged bleeding times. This reflects the synergistic roles of the P2Y1 and P2Y12 receptors in mediating the aggregation of platelets (the key blood cell type in the clotting reaction) in response to ATP/ADP released from damaged blood vessels. Because platelets also release large amounts of ATP/ADP during aggregation induced by other hemostatic factors (such as thrombin), P2Y1 and P2Y12 play additional roles in amplifying and extending the overall blood-clotting response. However, inappropriate platelet aggregation (thrombosis) can lead to interruption of normal blood flow (ischemia) to critical organs, such as the brain or heart, and thereby contribute to acutely life-threatening conditions including stroke and heart attack. For this reason, drugs that specifically block or antagonize P2Y1 and/or P2Y12 receptors are currently being tested for the treatment of thrombotic diseases in humans.

Analyses of other knockout mice strains have revealed important roles for the P2Y2 receptors that are highly expressed in airway cells and the P2Y4 receptors expressed in the jejunal section of the small intestine. Multiple P2Y receptor subtypes are expressed in the epithelial cells from organs such as the airways, lungs, kidneys, and intestines. The major function of epithelial cells and tissues is to act as both a barrier and selectively permeable interface between very different biological compartments. For example, airway epithelial cells comprise an interface between the inspired air compartment (which contains microbes, small particles, and volatile compounds from the outside environment) and the blood compartment. In addition to physically blocking the entry of these airborne particles, microbes, and compounds into the blood, airway epithelial cells secrete water, salt, mucus, and other protective proteins onto their extracellular surface that directly faces the inspired air compartment. While the secreted mucus solution acts to trap the microbes and particles, ciliated protrusions that extend from the epithelial cells beat in a synchronized manner to push the mucus solution – plus the entrapped microbes and particles – back to the nose and upper throat for eventual removal by sneezing or coughing. Activation, by ATP or UTP, of the P2Y2 receptors in different airway epithelial cells can coordinately regulate: (1) the secretion of the water, different salts, and mucus in sufficient amounts to generate

mucus solutions with appropriate viscosity, fluidity, and composition; and (2) the frequency and direction of the ciliary beating required for the appropriate retrograde flow of the mucus back to the upper airways. In airways from the P2Y2 receptor knockout mice, these important epithelial functions are not appropriately regulated. Analysis of small intestine function in P2Y4 receptor–receptor mice has indicated a similar role for this P2Y subtype in the regulation of salt and fluid secretion by intestinal epithelial cells.

Future studies of additional organ- and tissue-specific functions in mice lacking these and other P2Y receptor subtypes will undoubtedly reveal other important *in vivo* roles for these receptors. Insights from these animal studies, coupled with the development of subtype-selective antagonists, should facilitate delineation of how these receptors function in human physiology and pathology.

See Also the Following Articles

Adenylyl Cyclases • G Protein Signaling Regulators • Neurotransmitter Transporters • P2X Purinergic Receptors

Glossary

agonist A molecule that binds to a receptor resulting in functional activation of the receptor.

antagonist A molecule that binds to a receptor and keeps the receptor in a functionally inactive state.

effector protein An intracellular protein, such as an enzyme or ion channel, whose activity is regulated by interaction with G proteins. Effector proteins regulate the production of second messenger signals.

G protein An intracellular protein that becomes active when it binds GTP and becomes inactive when it hydrolyzes the bound GTP to GDP. G proteins act as signal transduction proteins that couple cell surface receptors to the regulation of intracellular effector proteins.

G protein-coupled receptor (GPCR) A cell surface receptor protein for an extracellular signaling molecule; GPCR reversibly interact with G proteins to activate intracellular signal transduction pathways. There are thousands of different GPCR that selectively bind a wide variety of extracellular signaling molecules including many hormones and neurotransmitters.

P2Y receptors A family of related G-protein coupled receptors that become active when bound to extracellular nucleotides such as ATP, ADP, or UTP.

second messenger A small intracellular molecule that is transiently formed in response to the activation of an effector protein by a cell surface receptors, such as a GPCR. Formation of the second messenger acts to relay the signal from the cell surface receptor to the interior of the cell.

Further Reading

Abbracchio, M. P., Boeynaems, J.-M., Barnard, E. A., Boyer, J. L., Kennedy, C., Miras-Portugal, M. T., King, B. F., Gachet, C., Jacobson, K. A., Weisman, G. A., and Burnstock, G. (2003). Characterization of the UDP-glucose receptor (re-named here the P2Y14 receptor) adds diversity to the P2Y receptor family. *Trends Pharmacol. Sci.* **24**, 52–55.

Bhatt, D. L., and Topol, E. J. (2003). Scientific and therapeutic advances in antiplatelet therapy. *Nat. Rev. – Drug Discovery* **2**, 15–28.

Dubyak, G. R. (2003). Knock-out mice reveal tissue-specific roles of P2Y receptor subtypes in different epithelia. *Mol. Pharmacol.* **63**, 773–776.

Lazarowski, E. R., Boucher, R. C., and Harden, T. K. (2003). Mechanisms of release of nucleotides and integration of their actions as P2X-and P2Y-receptor activating molecules. *Mol. Pharmacol.* **64**, 785–795.

Ralevic, V., and Burnstock, G. (1998). Receptors for purines and pyrimidines. *Pharmacol. Rev.* **50**, 413–492.

Von Kugelgen, I., and Wetter, A. (2000). Molecular pharmacology of P2Y receptors. *Naunyn-Schmiedeberg's Arch Pharmacol.* **362**, 310–323.

Zimmermann, H. (2000). Extracellular metabolism of ATP and other nucleotides. *Naunyn-Schmiedeberg's Arch Pharmacol.* **362**, 299–309.

Biography

George R. Dubyak is a Professor in the Department of Physiology and Biophysics at the Case School of Medicine of Case Western Reserve University, Cleveland. His broad research interest is in the field of signal transduction biology with particular focus on the roles of extracellular nucleotides in signal transduction during inflammation and regulation of cardiovascular function. He holds a Ph.D. in physiology from the University of Pennsylvania and received post-doctoral training in biophysics at that university.

p53 Protein

Jamie Hearnes and Jennifer Pietenpol
Vanderbilt University, Nashville, Tennessee, USA

p53 is a tumor suppressor gene that is mutated in over half of all human cancers. The tumor suppressive functions of p53 are dependent, in part, upon its activity as a transcription factor. This protein binds DNA in a sequence-specific manner to regulate the expression of select genes involved in a range of cellular processes including growth arrest, apoptosis, DNA repair, senescence (irreversible growth arrest), and angiogenesis (new blood vessel formation). The p53 protein is activated in response to various cellular stresses, and functions to suppress the transformation of a normal cell to a cancer cell. The p53 protein will continue to be a focus of cancer-based research as it plays a pivotal role in suppressing tumorigenesis.

p53 Functional Domains

The p53 protein was originally identified in 1979, and its name is derived from the apparent molecular weight of the protein (p53 = protein of 53 kDa). This protein consists of 393 amino acids and is divided into three functional domains (Figure 1).

Transcriptional Activation Domain

The transactivation domain is located at the amino terminus of the protein sequence (amino acids 1–73). Numerous proteins can bind to this region of the protein to regulate the function of p53. This region of the protein is constitutively and inducibly phosphorylated, which affects the protein's stability and activity.

DNA-Binding Domain

The central region of the p53 protein is the DNA-binding domain (amino acids 100–293). A majority of tumor-derived p53 mutations occur in the DNA-binding domain. The residues most commonly mutated in the DNA-binding domain either directly contact the DNA or are required for the structural integrity of the protein. Since p53 primarily functions as a transcription factor, these mutations result in a loss of function of the protein.

Oligomerization Domain

The carboxy terminus of the p53 protein (amino acids 293–393) contains an oligomerization domain, which is required for the formation of transcriptionally active dimers and tetramers. The oligomerization domain also contains nuclear localization and export sequences that are required for transport into and out of the nucleus, respectively. The carboxy terminus is also post-translationally modified in a regulatory manner.

p53-Mediated Signaling

p53 functions as a sequence-specific transcription factor regulating select genes (target genes) that are involved in numerous signaling pathways, including cell cycle progression, apoptosis, senescence (irreversible growth arrest), DNA repair, and angiogenesis (new blood vessel formation) (Figure 2). These are the same pathways that become deregulated during cancer progression. The p53 consensus DNA-binding site consists of 2 copies of the DNA sequence RRRCWWGYYY which are separated by a 0–13 base spacer region (R = A/G, W = A/T, Y = T/C). This binding site is present in a majority of p53 target gene regulatory regions. The degeneracy of the consensus DNA-binding site at 8 of the 10 bases is thought to contribute to the selectivity of p53 towards certain genes in response to various stresses. p53 can serve as a transcriptional activator or repressor, depending on the specific gene being regulated.

Growth Arrest and Apoptosis

Human cells are continuously exposed to external agents as well as internal agents that can induce cell damage. Eukaryotic cells have evolved a series of surveillance pathways termed cell-cycle checkpoints to ensure that cells copy and divide their genomes with high fidelity during each replication cycle. These checkpoint signaling pathways execute several tasks: rapid induction of cell-cycle delay, activation of DNA repair, maintenance of cell-cycle arrest until repair is complete, reinitiation of cell cycle progression after completed

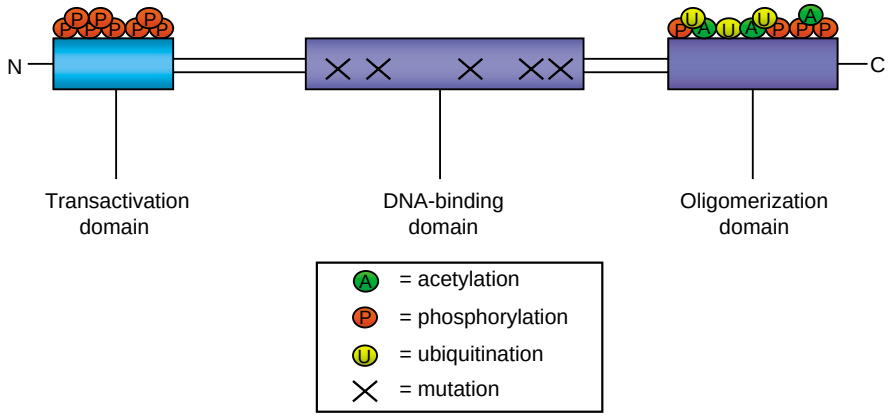

FIGURE 1 Functional domains of p53 are affected by post-translational modifications and mutations. The amino terminus contains the transactivation domain, which becomes phosphorylated in response to certain types of cell damage. The central region of the protein contains the DNA-binding domain that is very commonly mutated in human tumors. The oligomerization domain, which mediates the formation of p53 dimers and tetramers, is present at the carboxy terminus of the protein, and can be modified post-translationally by phosphorylation, acetylation, and ubiquitination.

repair or initiation of apoptosis if the damage is irreparable. These checkpoints provide a fail-safe mechanism by which cells are repaired or eliminated before the damaged DNA is transferred to the daughter cells. Loss of normal cell-cycle checkpoint signaling is a hallmark of tumor cells, and p53 is the most frequently altered cell-cycle checkpoint signaling molecule. One of the major functions of the p53 tumor suppressor protein is to modulate cellular responses to stress and induce cell-cycle arrest or death, as appropriate (Figure 2). Once a cell has been stressed or damaged, p53 initiates cell cycle arrest allowing time for the damage to be repaired or for the stress to dissipate. p53 halts cell growth by selectively activating certain target genes, including $p21^{Waf1/Cip1}$, a protein that inhibits molecules required for cell-cycle progression. If cell damage is extensive and cannot be repaired or the stress is prolonged, the cells may undergo p53-dependent apoptosis. p53 is responsible for both the activation of proapoptotic genes as well as the repression of antiapoptotic genes, and the array of p53-regulated genes involved in apoptosis is quite extensive. Although a given cell in the human body would not benefit from undergoing apoptosis, this process is sometimes necessary for the benefit of the whole organism, to prevent the development of cancer.

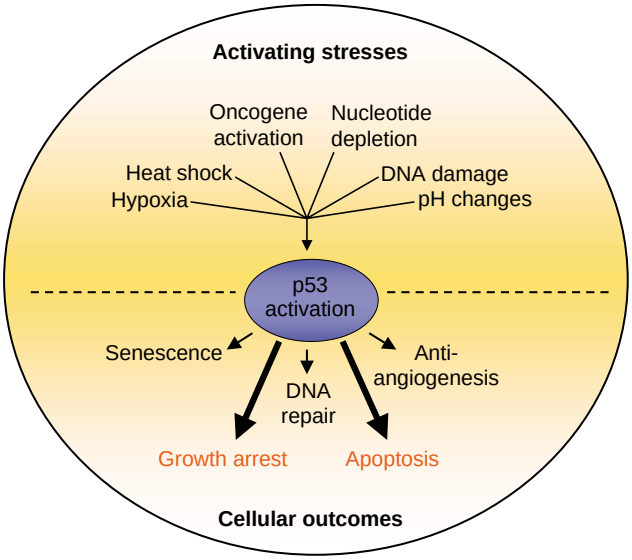

FIGURE 2 p53 signaling pathways. p53 is responsive to many cellular insults (activating stresses) that affect numerous pathways yielding various cellular outcomes. The two primary most well-characterized outcomes of p53 activation are growth arrest and/or apoptosis (thick arrows). However, p53-regulated genes also take part in numerous other signaling pathways (thin arrows).

Other Pathways Regulated by p53

p53 function is not limited to growth arrest and apoptosis. p53 also regulates genes involved in DNA repair, senescence, and angiogenesis (Figure 2). Although the relationships between p53 and these various pathways are not completely understood, future discoveries of novel p53 target genes and protein interactions will further elucidate the signaling networks in which p53 is involved.

p53 Regulation

p53 acts immediately after cell stress occurs, and thus, it is critical that the regulatory mechanism for this protein be fast acting. Following stress, the levels of many proteins in the cell are dictated by transcriptional regulation of the genes encoding the proteins; however, this is not the primary mechanism for p53. Instead, p53

regulation occurs predominantly at the protein level, which allows for rapid induction of p53 activity.

Activating Stresses

In a normal unstressed cell, the p53 protein is present at low levels due to the short half-life of the protein. However, p53 protein levels increase if the cell experiences a stress. There are numerous types of cellular stress and damage that can activate the p53 protein including lack of oxygen (hypoxia), elevated/lowered temperatures (heat/cold shock), DNA damage, metabolic changes, nucleotide depletion, pH changes, and oncogene activation (Figure 2). Cellular stresses trigger signaling pathways that converge on p53, resulting in stabilization and activation of the protein.

Post-translational Modifications

Post-translational modification events are dynamic processes that change protein stability and activity by altering protein–DNA and protein–protein interactions. Depending on the stress, p53 is post-translationally modified with various moieties resulting in diverse effects on the protein's stability, activity, and specificity of DNA binding (Figure 1).

Ubiquitination

Ubiquitination is the addition of ubiquitin molecules to lysine residues of a protein. Following ubiquitination, most proteins are targeted to the 26S proteosome for degradation. This is the mechanism used to rapidly turn over the p53 protein. The ubiquitination system involves numerous proteins, but the specificity of the system depends on the specific E3 ubiquitin ligase enzyme employed, which attaches an ubiquitin molecule to the correct substrate. The mouse double minute 2 (Mdm2) protein is the ligase used to ubiquitinate p53.

Phosphorylation

Phosphorylation of proteins at serine, threonine, and/or tyrosine residues is a common regulatory mechanism in the cell. p53 is phosphorylated at select serine and threonine amino acids in the amino- and carboxy-terminal regions of the protein in response to select cellular stresses. These stresses include exposure of cells to byproducts of cellular metabolism, ultra-violet (UV) radiation, and drugs used in cancer therapy. Numerous kinases have been identified that phosphorylate p53. The specific kinase activated is dependent upon the stress, and each kinase is responsible for phosphorylating a distinct residue(s) on the protein. Phosphorylation of the p53 protein can yield numerous outcomes including protein stabilization, increased transcriptional activity, and alterations in subcellular localization.

Acetylation

Acetylation is a modification that can occur on lysine residues of a protein. Acetylation of a transcription factor can affect the protein's transcriptional activity, either positively or negatively, depending on the specific factor. In response to DNA damage, known transcriptional coactivators acetylate p53 at certain carboxy-terminal lysines, however, the exact role of this modification on p53 activity is not well established.

Protein–Protein Interactions

There are numerous proteins that regulate p53 through a physical interaction. Many of these proteins are involved in post-translationally modifying the protein, but there are also other mechanisms of p53 protein regulation that involve protein–protein interactions. These interactions can both positively and negatively regulate p53.

Mdm2 is a protein that can bind to and ubiquitinate p53, as mentioned above. This p53–Mdm2 interaction results in two outcomes. The first is that Mdm2 inhibits the transcriptional activity of p53 by binding to the amino-terminal transactivation domain of the p53 protein, blocking other interactions that are necessary for p53 activity. The second outcome is p53 ubiquitination, export from the nucleus, and degradation. Mdm2 is responsible for maintaining p53 at low levels in a normal unstressed cell, as well as attenuating the p53 response after stress. Interestingly, Mdm2 is up-regulated by p53 in response to cellular insults, forming an autoregulatory negative feedback loop, which is the primary mechanism of negative regulation for p53.

Viral proteins can also interact with the p53 protein to affect its activity. For instance, the human papilloma virus (HPV) E6 proteins (type 16 and 18) negatively regulate p53 in a manner similar to Mdm2. The E6 protein binds to a protein complex containing p53, which leads to p53 ubiquitination and subsequent degradation.

In addition to protein interactions that negatively regulate p53 activity, there are interactions that have a positive impact on the protein as well. One example of this is the human $p14^{ARF}$ protein. This protein is a tumor suppressor activated in response to oncogenic stimuli. Once activated, $p14^{ARF}$ binds to the p53–Mdm2 complex, which disables Mdm2. This protects p53 from Mdm2-mediated degradation, resulting in p53 activation and subsequent growth suppression or apoptosis of cells that contain activated oncogenes.

p53 Family Members

p53 is a member of a newly identified family of related proteins that includes p73 and p63. p73 was discovered in 1997, with p63 quickly following in 1998. The three family members exhibit a high degree of sequence similarity and conserved functional domains. However, unlike p53 it appears that the functions of p73 and p63 are not restricted to tumor suppression. p73 is involved in neuronal signaling, immune cell apoptosis, and inflammation. p63 is involved in maintaining regenerative cells, and is essential for the normal development of numerous human tissues including the skin, breast, and prostate.

Cancer Therapeutics Involving p53

Since p53 is mutated in over 50% of all human tumors, many therapeutic strategies have been devised to target the p53 signaling pathway, including: (1) transfer of normal p53 genes into mutant p53-containing cancer cells, (2) introduction of small molecules that convert mutant p53 proteins to proteins that are structurally normal in function, (3) identification of small molecules that mimic the function of p53 target genes, and (4) disruption of protein–protein interactions that negatively regulate p53 activity. Due to its central role in preserving genetic stability, deciphering p53 function, regulation, and signaling pathways will continue to be a major focus of cancer-based research.

See Also the Following Articles

Cell Cycle: DNA Damage Checkpoints • Cell Death by Apoptosis and Necrosis • DNA Base Excision Repair • Transcription-Coupled DNA Repair, Overview

Glossary

apoptosis Programmed cell death; an active form of cell suicide.
cell cycle The ordered set of events by which a cell grows and divides.
cell-cycle checkpoint Point in the cell-division cycle where progression through the cycle can be halted until conditions are suitable for the cell to proceed to the next stage.
oncogene A gene whose product has the ability to transform a normal cell into a cancer cell.
tumor suppressor A gene that negatively regulates cell division and when lost allows the cell to progress through the cell cycle in an unrestricted manner.

Further Reading

Alberts, B., Bray, D., Lewis, J., Raff, M., Roberts, K., and Watson, J. D. (eds.) (1994). *Molecular Biology of the Cell*, 3rd edition. Garland Publishing, New York.
Appella, E., and Anderson, C. W. (2001). Post-translational modifications and activation of p53 by genotoxic stresses. *Eur. J. Biochem.* **268**, 2764–2772.
El-Deiry, W. S. (1998). Regulation of p53 downstream genes. *Semin. Cancer Biol.* **8**, 345–357.
Giaccia, A. J., and Kastan, M. B. (1998). The complexity of p53 modulation; emerging patterns from divergent signals. *Genes Dev.* **12**, 2973–2983.
Lane, P. L., and Lain, S. (2002). Therapeutic exploitation of the p53 pathway. *Trends Mol. Med.* **8**, S38–S42.
Lewin, G. (2000). *Genes VII*. Oxford University Press, New York.
May, P., and May, E. (1999). Twenty years of p53 research: Structural and functional aspects of the p53 protein. *Oncogene* **18**, 7621–7636.
Stewart, Z. A., and Pietenpol, J. A. (2001). p53 signaling and cell cycle checkpoints. *Chem. Res. Toxicol.* **14**, 243–263.
Yang, A., and McKeon, F. (2000). p63 and p73: p53 mimics, menaces, and more. *Nat. Rev. Mol. Cell Biol.* **1**, 199–207.

Biography

Jennifer A. Pietenpol, Ph.D., is a Professor of Biochemistry at Vanderbilt University and Associate Director for Basic Research Programs of the Vanderbilt-Ingram Cancer Center. Pietenpol received her Ph.D. in cell biology from Vanderbilt University and pursued postdoctoral studies at Johns Hopkins University. Pietenpol's research is focused on tumor suppressor signaling pathways, with particular focus on p53. A goal of her research is to define molecular changes in tumor cells that can be used as targets for therapeutic intervention.

Jamie Hearnes is a graduate student at Vanderbilt University and will receive her Ph.D. from the Department of Biochemistry. Her research in the Pietenpol Laboratory focuses on the identification of novel p53 target genes.

p70 S6 Kinase/mTOR

Christopher G. Proud
University of Dundee, Dundee, UK

p70 S6 kinase is a protein kinase that is activated by insulin and other stimuli, and which phosphorylates ribosomal protein S6, a component of the small (40S) ribosomal subunit in animal cells. Mammalian target of rapamycin (mTOR) is involved in regulating p70 S6 kinase, and other proteins, and serves to integrate hormonal and nutritional signals.

p70 S6 Kinase

This family of enzymes phosphorylates a series of seryl residues in the C-terminus of S6. It was identified in the 1980s following early work showing that insulin, and a range of other stimuli, led to increased phosphorylation of S6. The p70 S6 kinases were some of the earliest insulin- and mitogen-stimulated kinases to be studied in any detail, largely because the relatively high abundance of S6 means that it appears as a major insulin-stimulated phosphoprotein.

p70 S6 kinases are now believed to be the physiologically relevant S6 kinase. Confusion is possible here however, as a second type of kinase, $p90^{RSK}$, can also phosphorylate S6 *in vitro*. This gives rise to the abbreviation RSK (ribosomal protein S6 kinase) although it is generally thought that $p90^{RSK}$ is not a physiologically relevant S6 kinase. An important reason for favoring the p70 S6 kinases is that their activation and the phosphorylation of S6 are both blocked by rapamycin, while this drug has no effect on $p90^{RSK}$.

Different Isoforms of p70 S6 Kinase Exist in Mammals

In mammals, there are two genes encoding closely related kinases, both of which phosphorylate S6. Here, they are termed p70α S6 kinase (also called S6K1) and p70β S6 kinase (alternative name, S6K2). The overwhelming majority of studies have concerned the α-isoform, which was discovered much earlier than the β. However, the recent studies on S6K2 suggest that it is regulated in a way broadly similar to S6K1. Further diversity in this family is created by alternative splicing: in the cases of p70α and p70β S6 kinases, this gives rise to additional isoforms (p70α1 and p70β1) which are extended at the N-termini (see Figure 1: the shorter versions are termed p70α2 and p70β2). This extension contains a likely nuclear localization signal, which could mediate the transfer of the longer isoforms into the nucleus.

All four isoforms contain a catalytic domain near the N terminus and a regulatory domain towards the C terminus. Phosphorylation within the catalytic domain and at several sites in the C terminus leads to the activation of the S6 kinases (see Figure 1).

p70 S6 Kinase is Activated by a Variety of Stimuli

p70 S6 isoforms are activated by insulin, serum and mitogens, and also by a range of other stimuli including ones that work through G-protein-coupled receptors. A common feature of these stimuli is that they increase the cell's overall rate of protein synthesis. In all cases, activation of p70α S6 kinase involves increased phosphorylation of the protein (Figure 1), and is blocked by rapamycin, indicating a key role for mTOR in activation.

Less effort has so far been devoted to studying the more recently discovered p70β S6 kinase, but the available information suggests that it is also likely to be activated by a wide range of stimuli.

Roles of Nutrients and mTOR in Regulating p70 S6 Kinase

In a number of types of cells, p70α S6 kinase cannot be activated if the cells are deprived of amino acids. Amino acid starvation also results in a fall in the basal activity of the kinase. Readdition of amino acids results, within minutes, in increased basal activity and restoration of the ability of insulin, for example, to activate p70α S6 kinase. This suggests that amino acids provide an important input into the regulation of p70α S6 kinase, and this is discussed further below. The branched-chain amino acid leucine is the most effective amino acid in most cell types tested.

In some cell types, such as hepatoma cells and primary fat cells, the presence of external amino acids

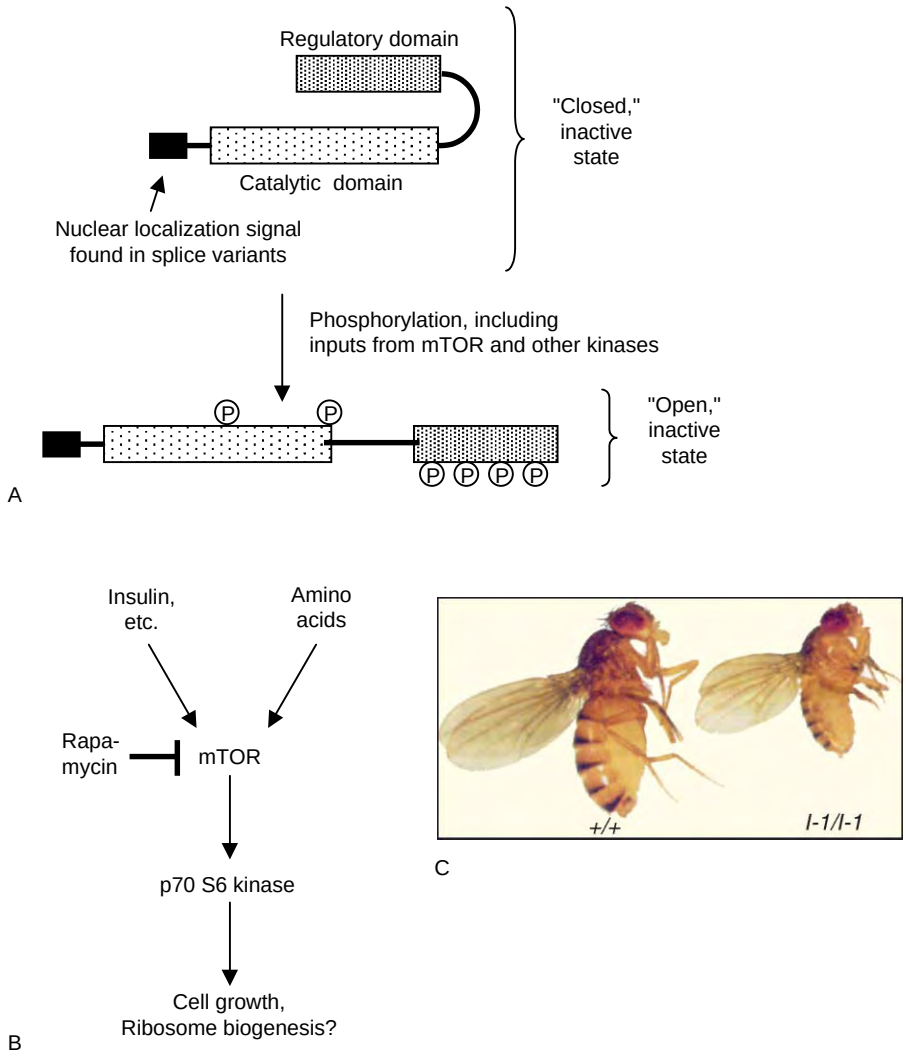

FIGURE 1 p70 S6 kinase. (A) This schematic figure indicates the arrangement of the enzyme into catalytic and regulatory domains. Phosphorylation of the regulatory domain allows the catalytic domain to be phosphorylated too, leading to activation of the enzyme. Phosphorylation involves several kinases and input from mTOR. For further details, see text. (B) Hormones, such as insulin (also growth factors), and amino acids positively regulate p70 S6 kinase via mTOR (its activation is therefore prevented by rapamycin). It has a clear role in regulating cell size, possibly through the control of ribosome biogenesis. (C) Genetic knockout of S6 kinase in *Drosophila melanogaster* dramatically decreases the size of the animals, with all body parts apparently affected to a similar degree: + /+ indicates a wild-type fly, while l-1/l-1 denotes one in which the S6K gene has been disrupted. Reproduced from Montagne, J., Stewart, M. J., Stockes, H., Hafer, E., Kozma, S. C., and Thomas, G. (1999). Drophila S6 kinase: a regulator of cell size. *Science* 285, 2126–2129. Copyright 1999 American Association for the Advancement of Science.

in the medium is not required for regulation of p70α S6 kinase. It is likely that this reflects the presence, within these cells, of sufficient amino acids to support regulation of this enzyme, rather than a fundamental difference in its control in these cells.

Mechanisms Involved in the Activation of p70 S6 Kinase

As noted above, the activation of S6 kinase involves its phosphorylation at several positions. One lies within the catalytic domain and most of the others lie in the C-terminal regulatory domain. It is possible that the C-terminal region blocks access to the catalytic domain, and that this block is alleviated by phosphorylation of the C-terminal sites. The kinases acting at these sites have not been conclusively identified. Since rapamycin blocks the phosphorylation of many sites in p70α S6 kinase, it is conceivable that the relevant kinases are regulated through mTOR, or that mTOR directly phosphorylates p70α S6 kinase, although other explanations are also possible. The proposed mechanism by which p70α S6 kinase is activated is illustrated in Figure 1.

p70 S6 Kinase Plays a Key Role in Growth Control

Genetic studies have revealed a key role for p70 S6 kinases in growth control. The fruit fly, *Drosophila melanogaster*, has just a single p70 S6 kinase gene. Disruption of this gene, to create flies lacking S6 kinase activity, has a dramatic effect on the growth of the flies. S6 kinase-deficient flies are markedly (~50%) smaller than wild-type flies (Figure 1C) and strikingly, this is due primarily to a defect in cell size rather than a reduction in cell number. The mutant flies contain the same number of cells as wild-type flies, but the sizes of these cells are decreased proportionately so that the mutant flies are morphologically very similar to the wild-type flies. This demonstrates a decoupling of cell size from cell proliferation, and implies a key role for S6 kinase in the poorly understood processes that determine cell size. This is discussed further below. A similar effect is observed in mice in which the p70α S6 kinase gene is disrupted, but the magnitude of the reduction in size is smaller, probably because the existence of the second mammalian gene (p70β S6 kinase) compensates to some extent.

Does p70 S6 Kinase Regulate Ribosomal Protein Synthesis?

It has been observed that insulin and serum increase the phosphorylation of ribosomal protein S6 that leads to the identification of the S6 kinases. What role, then, does S6 phosphorylation play? Since it is a ribosomal protein, one would suppose that its role lies in regulating some aspect of mRNA translation (protein synthesis).

In higher animals, the mRNAs encoding the ribosomal proteins all share an unusual feature, a run of pyrimidine nucleotides at the extreme 5′-end of the mRNA. This acts to suppress their translation under basal conditions (e.g., in cells starved of serum or of amino acids). In response to stimulation of cells with serum or amino acids, these mRNAs bind to ribosomes and undergo translation so that ribosomal protein synthesis is switched on. It clearly makes good sense for the production of ribosomes to be stepped up in response to agents that stimulate protein synthesis or cell proliferation, and in parallel with the availability of amino acids, important precursors for ribosome production and for general protein synthesis.

Initial studies showed that rapamycin blocked the activation of the translation of these mRNAs and pointed to a role for p70 S6 kinase in this. However, some more recent studies have questioned the links between p70 S6 kinase/S6 phosphorylation and the activation of the translation of this subset of mRNAs.

Regulation of Other Processes by p70 S6 Kinase

In addition to S6, p70α S6 kinase has also been shown to phosphorylate certain other proteins involved in regulating gene expression. These include a protein involved in the control of gene transcription (the cyclic AMP-response element (CRE) modulator, CREM) and a protein kinase that regulates the elongation stage of protein synthesis (elongation factor 2 kinase). The latter may allow insulin and amino acids to accelerate the rate at which proteins are synthesized. Further substrates for the p70 S6 kinases may, of course, also exist.

mTOR

mTOR is a protein that is implicated in the intracellular signaling events that control a variety of processes in eukaryotic cells. All eukaryotic organisms that have been studied so far contain proteins related to mTOR, and work on the yeast orthologues, TOR1 and TOR2, has been especially fruitful in helping understand TOR signaling.

mTOR Signaling is Inhibited by the Immunosuppressant Drug, Rapamycin

mTOR, and indeed orthologues in many (but perhaps not all) species, are inhibited by rapamycin. Rapamycin is produced by a soil microorganism, *Streptomyces hygroscopicus*, which originates from Easter Island (the indigenous name for this island is Rapa Nui, hence rapamycin). The finding that rapamycin blocks the activation of T-lymphocytes, and thus suppresses the immune response, led to a high level of interest in its mechanism of action. Screening of yeast mutants for strains that are insensitive to the growth-inhibiting effects of this drug led to the identification of TOR1 and TOR2, and to the subsequent identification of related proteins in other organisms, such as mTOR in mammals.

Rapamycin appears to be completely specific for mTOR and its orthologues. Rapamycin binds to mTOR as a complex with a small protein called FKBP12 (FK506-) and rapamycin-binding protein 12: FKBP12 has prolyl *cis/trans* isomerase activity which is inhibited by both rapamycin and FK506, an immunosuppressant (FK506 does not, however, inhibit mTOR). The fact that the binding of the FKBP12/rapamycin complex to mTOR involves contacts with both the drug and the protein probably explains the high specificity. The normal physiological role of FKBP12 is unknown.

mTOR Is a Multidomain Protein

mTOR is a very large protein (about 2500 residues, Figure 2A). Inspection of its sequence reveals a number of potential domains. Its N-terminal section contains multiple "HEAT" domains—such domains are known to be important in protein–protein interactions. Towards its C terminus lies a domain that resembles the catalytic domain of kinases that phosphorylate lipids such as the phosphoinositide (PI) 3-kinases.

The kinase domain of mTOR appears critical to its function since mutants designed to cripple the catalytic domain are not functional *in vivo*. The region with which the FKBP12/rapamycin complex binds and inhibits mTOR function is N-terminal to the kinase domain.

mTOR (and TOR) Regulate Multiple Processes in Eukaryotic Cells

Treatment of cells with rapamycin reveals roles for mTOR/TOR in many important cellular processes such as gene transcription, protein synthesis and degradation, RNA breakdown, nutrient transport, the cell cycle and the organization of the actin cytoskeleton. Recent work with yeast suggests that, in fact, rapamycin may not affect all the functions of yeast TOR2, so that it may have additional roles not revealed by studying the effects of rapamycin. In contrast, the data suggest that all the functions of the other TOR protein in yeast, TOR1, may be blocked by this drug. It was already known that TOR1 and TOR2 had similar, but distinct, functions in yeast.

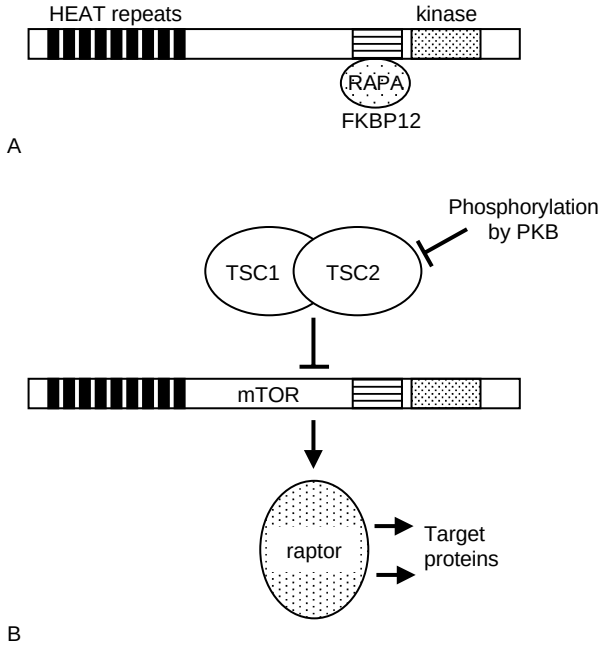

FIGURE 2 mTOR. (A) The figure depicts the principal domains found in mTOR. The complex of rapamycin with FKBP12 binds to and inhibits the function of mTOR. For other details, see text. (B) The complex of TSC1 and TSC2 binds to and inhibits mTOR: inhibition may be removed by phosphorylation of TSC2 by PKB. mTOR also binds a molecular scaffold, raptor, which appears to mediate the regulation of target proteins by mTOR.

The mechanisms by which mTOR/TOR regulates its downstream targets remain unclear. Since, where it has been studied, such regulation often involves changes in the phosphorylation of regulatory proteins, it is likely to be mediated by alterations in the activities of specific protein kinases and phosphatases, and there is evidence for both. In mammals, few of the target proteins that are controlled by mTOR have yet been identified. The best-understood ones are all involved in protein synthesis—they include the p70 S6 kinases, an elongation factor (eEF2) and a repressor of translation initiation, the initiation factor 4E-binding protein, 4E-BP1.

mTOR Interacts with Several Other Proteins

Very recent work has shed important new light on the ways in which mTOR may be regulated and how it signals to its target proteins. The key findings here were that mTOR (and the yeast TOR proteins) interact with other proteins. These interactions may involve the HEAT domains mentioned above. One type of interacting protein ("raptor") appears to be involved in the regulation of targets of mTOR signaling such as 4E-BP1 and the p70 S6 kinases. Others are probably involved in its upstream control.

Like mTOR, raptor is a large protein (1300 amino acids) that contains many motifs that may mediate protein–protein interactions. Related proteins are found in all eukaryotic species studied. Raptor binds to mTOR and also to its target 4E-BP1, and thus appears to act as a molecular scaffold (Figure 2B). The available evidence suggests that it is also required for the regulation of p70α S6 kinase by amino acids. Aspects of mTOR signaling such as raptor are currently a very active area of investigation and further important developments are likely.

Yeast TOR1 and TOR2 have been shown to bind the raptor orthologue in yeast and also to other proteins, although their roles are so far unknown.

mTOR Signaling Is Regulated by Hormones and Nutrients

Recent work has also identified proteins that bind to mTOR and act to regulate it, in response, for example, to insulin. TSC1 and TSC2 are components of the tuberous sclerosis complex, and appear to bind as a complex to mTOR, thereby inhibiting it (Figure 2B).

TSC1 and TSC2 were first identified as the genes that are mutated in tuberous sclerosis, an autosomal dominant disorder, that can lead to the occurrence of benign tumors characterized by excessively large cell size. This is accompanied by increased activity of p70α S6 kinase, consistent with the role described above for p70 S6 kinase in cell growth regulation. The effects of mutations appear to arise because they alleviate the normal inhibitory effect of the TSC1/2 complex on mTOR. The TSC1/2 complex is now also implicated in the normal regulation of mTOR: phosphorylation of TSC2 by a protein kinase B (PKB), which is activated by insulin, is thought to lead to the disruption of the TSC1/2 complex and activation of mTOR. The TSC1/2 complex acts to promote the hydrolysis of GTP on the small G-protein Rheb, which in its GTP-bound state promotes mTOR function. Much remains to be learned about how Rheb activates mTOR, and how other signaling inputs (such as amino acids) activate mTOR.

mTOR Displays Protein Kinase Activity

Although the kinase domain of mTOR resembles those of lipid kinases rather than of protein kinases, mTOR can phosphorylate certain proteins *in vitro*. These include p70α S6 kinase and the translational repressor protein 4E-BP1. However, the activity is weak and requires quite non-physiological conditions, so it is not clear whether this is really a physiological function of mTOR. It is quite conceivable that some of mTOR's partner proteins enhance its kinase activity *in vivo*.

Clinical Implications of mTOR Signaling

As noted above, rapamycin blocks the activation of cells of the immune system and thus acts as an immunosuppressant. As a consequence, rapamycin has found medical applications in combating graft rejection, particularly for recipients of kidney transplants. Very recent work also points to the potential for using rapamycin to treat certain types of cancer. These arise from mutations that inactivate the tumor suppressor protein PTEN and thus lead to unbridled activity of the PI 3-kinase signaling pathway that activates mTOR in response to insulin and many growth factors. Since the mTOR pathway clearly plays a central role in cell and animal growth, it will be of substantial importance for studies on clinical situations characterized by tissue atrophy or hypertrophy.

See Also the Following Articles

Phosphoinositide 3-Kinase • Protein Kinase B

Glossary

elongation/initiation factors Non-ribosomal proteins required for the initiation or elongation stages of protein synthesis.

mTOR The mammalian target of rapamycin, a multidomain protein that plays an important role in linking cellular responses to nutrients and other signals.

orthologue A term used for the distinct proteins found in different species that serve the same function (for example, yeast TOR and mammalian TOR).

ribosomal proteins The proteins that are found in the small and large subunits of the ribosome.

Further Reading

Abraham, R. T. (2002). Identification of TOR signaling complexes: More TORC for the cell growth engine. *Cell* **111**, 9–12.

Avruch, J., Belham, C., Weung, Q. P., Hara, K., and Yorezawa, K. (2001). The p70 S6 kinase integrates nutrient and growth signals to control translational capacity. *Prog. Mol. Subcell. Biol.* **26**, 115–154.

Dennis, P. B., Funagalli, S., and Thomas, G. (1999). Target of rapamycin (TOR): Balancing the opposing forces of protein synthesis and degradation. *Curr. Opin. Genet. Dev* **9**, 49–54.

Monniny, B. D., and Cantley, L. C. (2003). Rheb fills a GAP between TSC and TOR. *Trends Biochem. Sci.* **28**, 573–576.

Montagne, J., Stewart, M. J., Stockes, H., Hafer, E., Kozma, S. C., and Thomas, G. (1999). Drosophila S6 kinase: a regulator of cell size. *Science* **285**, 2126–2129.

Raught, B., Gingras, A. C., and Sorenberg, N. (2001). The target of rapamycin (TOR) proteins. *Proc. Natl Acad. Sci. USA* **98**, 7037–7044.

Rohde, J., Heitman, J., and Cardenas, M. E. (2001). The TOR kinases link nutrient sensing to cell growth. *J. Biol. Chem.* **276**, 9583–9586.

Biography

Christopher Proud is a Professor of Biochemical Physiology in the Faculty of Life Sciences at the University of Dundee. He holds a Ph.D. from the University of Dundee and did his postdoctoral training in Germany and England. His principal research interests are in the regulation of protein synthesis in mammalian cells by hormones and nutrients, and the roles of defects in protein synthesis and its control in the pathogenesis of human diseases.

Parathyroid Hormone/Parathyroid Hormone-Related Protein Receptor

Thomas J. Gardella
Massachusetts General Hospital and Harvard Medical School, Boston, Massachusetts, USA

The parathyroid hormone (PTH)/PTH-related protein (PTHrP) receptor (PPR) is a 593 amino acid, class 2 G protein-coupled receptor that mediates the actions of PTH, the major regulator of blood ionized calcium levels, and PTHrP, a key developmental protein. The PPR is abundantly expressed in bone osteoblasts and in renal tubule cells, the target cells of PTH, and in mesenchymal cells of developing tissues (e.g., skeleton, heart, teeth, and mammary glands), smooth muscle cells, and neurons, the target cells of PTHrP. The PPR binds PTH and PTHrP ligands via a bipartite mechanism involving binding interactions to the amino-terminal extracellular domain of the receptor and signaling interactions to the extracellular loops and seven transmembrane helices. The PPR couples strongly to the adenylyl cyclase (AC)/3′,5′-cyclic-adenosine monophosphate (cAMP)/protein kinase (PK)A signaling cascade, and can also activate the phospholipase (PL)C/inositol triphosphate (IP_3)/intracellular calcium (iCa^{2+})/PKC; PLD/phosphatidic acid/PKC; PLA_2/arachidonic acid/PKC; and MAP kinase pathways. Jansen's metaphyseal chondrodysplasia and Blomstrand's chondrodysplasia are rare diseases of skeletal development and calcium ion homeostasis that are caused by activating and inactivating mutations in the PPR gene, respectively. PTH(1–34) has anabolic effects on bone and is now used to treat osteoporosis.

Background and Physiology

Molecular Cloning of the PPR

The complementary (c)DNA encoding the parathyroid hormone (PTH)/PTH-related protein (PTHrP) receptor (PPR) was first isolated in 1991. This work revealed the classical seven transmembrane domain architecture of the G protein-coupled receptor (GPCR) superfamily (Figure 1). It also revealed that the PPR, along with the receptors for secretin, calcitonin, and several other peptide hormones, form a distinct subgroup – the class 2 GPCRs – which has been well-conserved, evolutionarily, with representatives present in *Drosophila* and *C. elegans*. The cloned PPR expressed in COS-7 cells binds PTH and PTHrP with equal affinities, and, in response to these ligands, activates both the AC/cAMP and PLC/IP_3/iCa^{2+} signaling pathways. It thus appears that the cloned receptor can account for all, or most, of the biological actions of two distinct ligands, PTH and PTHrP.

PTH

Discovery of PTH

Parathyroid hormone was identified as a key calcium-regulating hormone in the 1920s, when it was demonstrated that extracts of the parathyroid glands could modulate blood calcium levels and correct the tetany induced by parathyroid gland removal. The active hormone was purified from glands in 1959 and the complete 84 amino acid sequence of bovine PTH was determined in 1970. In 1971, the N-terminal PTH(1–34) fragment was synthesized and showed to be equipotent to native PTH in *in vitro* and *in vivo* assay systems. Physiological studies performed during this period established that PTH is the most important regulator of ionized calcium (Ca^{2+}) in the blood and extracellular fluids, and that it acts on bone, where it stimulates Ca^{2+} release from the mineralized matrix, and kidney, where it stimulates Ca^{2+} reabsorption from the glomerular filtrate. Related studies established that the secretion of PTH from the glands is regulated in a negative feedback fashion by the levels of extracellular Ca^{2+}; thus increases in blood Ca^{2+} result in decreased PTH secretion and decreases in blood Ca^{2+} result in increased secretion. This Ca^{2+}-mediated regulation of PTH secretion is determined by the actions of the calcium-sensing receptor expressed on the plasma membrane of parathyroid cells, and it is highly sensitive, such that blood Ca^{2+} levels are strictly maintained within the range of 1.1–1.3 mM. PTH is also a key regulator of blood phosphate, the principal Ca^{2+} counter ion, and suppresses the reabsorption of phosphate in the kidney.

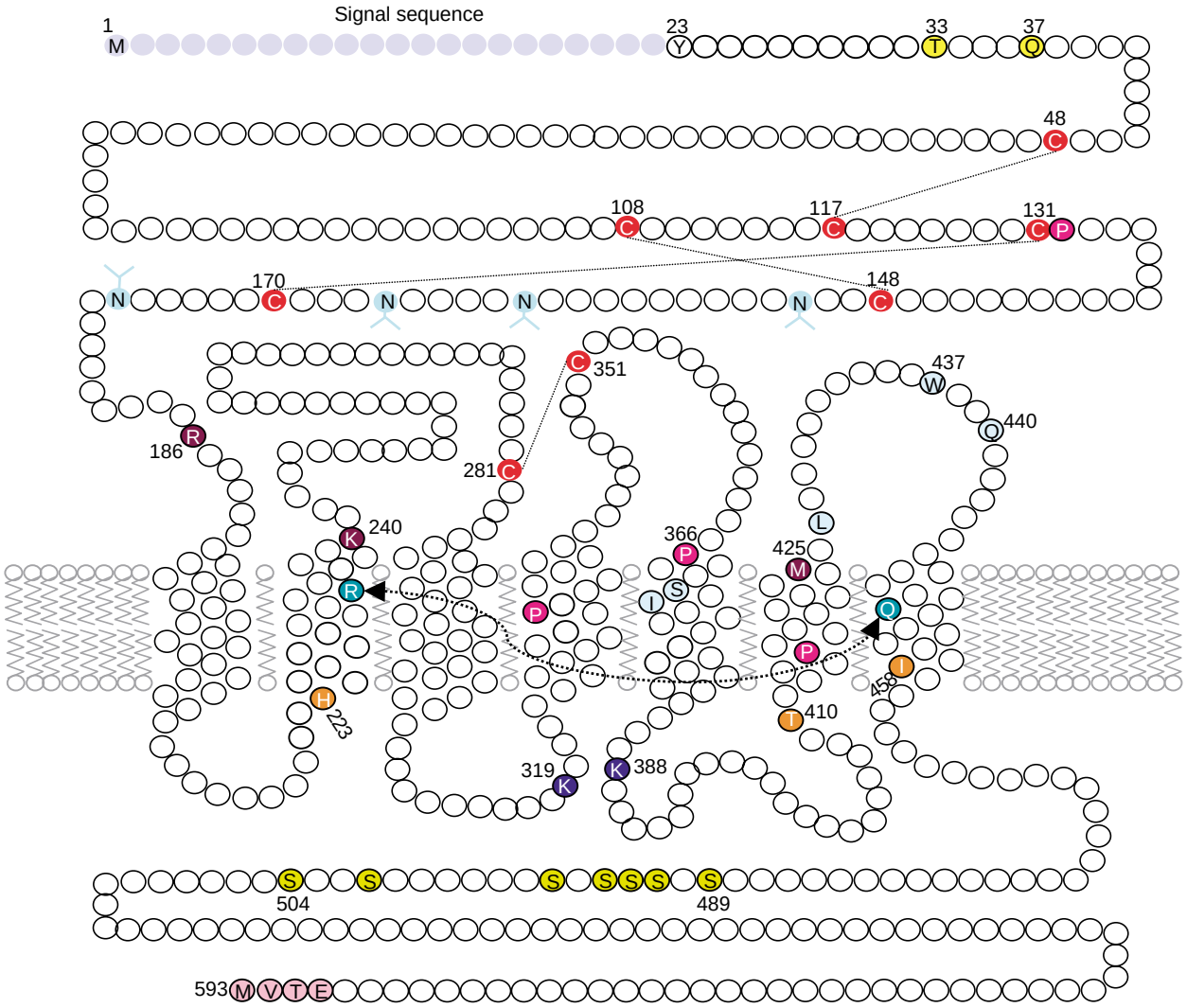

FIGURE 1 The human PTH/PTHrP receptor. Shown is a schematic of the PPR embedded in the lipid bilayer with selected features identified, including the conserved extracellular cysteines and their predicted disulfide linkages; the glycosylated asparagines (N); Thr33 and Gln37, which contribute to PTH(15–34) binding affinity; the probable cross-linking sites for ligand residues 13 (Arg186), 19 (Lys240) and 1 and 2 (Met425); conserved prolines (P), including Pro132, which is mutated to Leu in Blomstrand's chondrodysplasia; a putative inter-helical interaction between Arg233 and Gln451; Ser370, Ile371, Leu427, Trp437, and Gln440, at which mutations alter responsiveness to position 2-modified PTH(1–34) antagonist ligands (also includes Met425); His223, Thr410, and Ile458, which are mutated in Jansen's chondrodysplasia to result in constitutive signaling activity; Lys319 and Lys388, at which mutations impair G_q and G_s/G_q coupling, respectively; serines (S) that are phosphorylated upon agonist activation, and four C-terminal residues (Glu590–Met593) involved in NHERF binding.

PTH Effects in Bone

In bone, the PPR is expressed by osteoblast cells. These bone-forming cells display a variety of responses to PTH, including alterations in the rates of cell proliferation, apoptopsis, and changes in the expression patterns of a number of transcription factors, cytokines and bone-matrix factors. These effects can result in increased rates of bone formation. PTH however, also stimulates the bone-resorbing activity of osteoclastic cells, which are thought to be largely responsible for the calcium-releasing effects of PTH in bone. Osteoclasts, however, do not express the PPR but respond to the hormone via osteoclastogenic factors, such as RANK-ligand, that are expressed by PTH-stimulated osteoblasts. By modulating the activities of both osteoblasts (directly) and osteoclast (indirectly), PTH plays a major role in the continuous process of bone remodeling in the process of bone-remodeling. The mechanisms that control the balance between the anabolic and catabolic effects of PTH on bone are complex and not fully understood; however, it is well documented that intermittent exposure to PTH (once-daily injection) results in net bone formation, whereas continuous exposure (infusion) results in net bone resorption. Consistent with the anabolic effect of intermittent PTH on bone, a large clinical study

completed in 2001 showed that daily administration of PTH(1–34) significantly reduces the risk of bone fracture in patients with osteoporosis. As a result, the peptide is now used in the treatment of this common disease.

PTH Effects in the Kidney

In the kidney, the PPR is expressed by proximal and distal tubule cells. In the distal tubule, PTH stimulates the reabsorption of calcium from the urine, most likely by affecting calcium channel activity. In the proximal tubule, PTH stimulates the synthesis of 1,25-dihydroxy-vitamin D3, which in turn, promotes calcium absorption by the intestine and calcium release from bone. These calcium-regulating effects of vitamin D_3 occur on a longer time scale (days to weeks), than do those of PTH, which occur within seconds to minutes. Also in renal proximal tubule cells PTH suppresses the surface expression of the type II sodium-phosphate co-transporter and thereby decreases the re-uptake of phosphate from the urine.

PTHrP

Discovery of PTHrP

In the late 1980s, much effort was devoted to identifying the hypercalcemia-causing factor that is released by many tumors, and in 1987, the protein factor responsible, PTHrP, was purified from tumor extracts and partially sequenced. This sequence data, in turn, led to the cloning of the corresponding complementary(c) DNA, which revealed a protein of 141 amino acids that has clear N-terminal homology to PTH, as, 8 of the first 13 residues of the two proteins were found to be identical (Figure 2). PTHrP(1–34) peptides were shown to mimic the calciotropic actions of PTH on bone and kidney cells. It seemed clear, however, that PTHrP was not normally a calcium-regulating hormone, as its concentration in the normal circulation was too low (barely detectable). Furthermore, its mRNA was found in a wide variety of tissues (e.g. brain, lung, heart, adrenals, spleen, liver, bladder, skin, stomach, breast, placenta, ovaries, testes), in both adult and fetal life. These observations suggested that PTHrP acts in a paracrine manner, possibly in development.

```
                 1         10        20        30
hPTH(1-34)       SVSEIQLMHNLGKHLNSMERVEWLRKKLQDVHNF
hPTHrP(1-34)     AVSEHQLLHDKGKSIQDLRRFFLHHLIAEIHTA
```

FIGURE 2 PTH and PTHrP. Shown is an alignment of the bioactive (1–34) regions of human PTH and human PTHrP, with conserved residues in bold-faced type.

Genetic Manipulations of PTHrP in Mice

The above hypotheses regarding PTHrP action were largely confirmed in 1994 when mice having homozygous deletion of the *PTHrP* gene were generated and found to die at birth with defects in endochondral bone formation, namely, premature mineralization and short limbs. Subsequent genetic studies in mice determined that PTHrP also plays a role in the development of the mammary glands, hair follicles, and the heart. In 1996, mutant mice lacking the PPR gene were generated, and this established that the PPR mediates the developmental actions of PTHrP. Thus, PPR-deficient mice exhibit nearly the same perinatal lethality and developmental defects as those lacking the *PTHrP* gene.

PTHrP Actions in the Growth Plate

Extensive studies on the cartilaginous growth plates of the fetal tibia and femur in mice vividly demonstrated that PTHrP indeed acts in a paracrine fashion to control the program of events in tissue development. PTHrP is expressed by cells in the periarticular region of the growth plate and acts on prehypertrophic chondrocytes of the central zone to delay their terminal differentiation into hypertrophic chondrocytes. This action of PTHrP in the growth plate is further regulated by at least several other morphogenetic proteins, including Indian hedgehog (Ihh), which is produced by the prehypertrophic chondrocytes and stimulates chondrocyte proliferation. Ihh also induces, as part of a feedback regulatory network, the expression of PTHrP by the periarticular cells. Similar paracrine actions of PTHrP on PPR-expressing cells are also likely to operate in the mesenchyme of other developing tissues (e.g., heart, mammary glands, and hair follicles).

Structure–Activity Relationships in PTH and PTHrP

Functional Domains of PTH(1–34) and PTHrP(1–34)

Both PTH(1–34) and PTHrP(1–34) bind to and activate the PPR with affinities and potencies in the nanomolar range, and the two ligands interact with overlapping sites in the receptor. For both (1–34) ligands, the major determinants of PPR-signaling potency and binding affinity reside within the N-terminal and C-terminal portions, respectively. Based on this physical separation of functional domains, N-terminally truncated analogues, such as [Leu^{11},$DTrp^{12}$]PTHrP(7–34), have been developed as PTH receptor antagonists. The PTH(15–34) fragment represents the minimum-length binding fragment ($K_{dissociation} \sim 1\ \mu M$), and within this

domain, Trp-23, Leu-24, Leu-28, and Val-31 function as key determinants of binding affinity. These residues form the hydrophobic face of a predicted amphipathic α-helix that may contact the receptor. Within the N-terminal signaling domain of PTH, the highly conserved Val-2, plays a key role in PPR activation, as its deletion or replacement by bulky amino acids (e.g., Arg or Trp) confers antagonist behavior to PTH(1–34) analogues. Short amino-terminal fragments, such as PTH(1–14), exhibit little or no binding or signaling activity; however, recent studies have resulted in N-terminal fragment analogues with considerably enhanced binding and signaling capacities. For example, [Aib^{1,3},Gln^{10},Har^{11}, Ala^{12},Trp^{14}]PTH(1–14)NH_2 is ~100 000-fold more potent than native PTH(1–14) for stimulating cAMP formation (EC_{50}s = 2 nM versus 200 μM) and is thus as potent as PTH(1–34) in cell-based assay systems.

Structural Studies of PTH and PTHrP

Solution-phase NMR studies performed on PTH(1–34) analogues suggest that the peptide in solution adopts a bi-helical conformation in which a short N-terminal helix (residues ~3–10) is joined via a turn or flexible linker to a longer more stable C-terminal helix (residues ~17–31). In some studies a U-shaped structure has been proposed for the bi-helical peptide. In 2001, however, the X-ray crystal structure of PTH(1–34) was determined and this revealed a single, slightly bent α-helix that extended from Val-2 to His-32. What is needed now is a direct assessment, by physical methods, of the conformation of the ligand in the receptor-bound state; until this is accomplished, the true bioactive conformation of PTH will likely remain uncertain.

Structure Activity Relationships in the PPR

Molecular Architecture of the PPR

The Amino-Terminal Domain

The PPR contains an amino-terminal extracellular (N) domain of ~167 amino acids (excluding the 23 amino acid signal sequence) (Figure 1). This N domain is Asn-glycosylated at four sites and contains six cysteine residues. These six cysteine residues are very highly conserved among the class 2 GPCRs and they are predicted to form a network of three disulfide bonds that defines a tertiary fold common to the N domains of each of the class 2 receptors. At present, the three-dimensional structure of the N domain of any class 2 GPCR is unknown, but it is clear that for each receptor, the N domain contributes importantly to ligand-binding affinity. For the PPR, the isolated N domain protein, purified and refolded from an *E. coli* expression system, binds PTH(1–34) with micromolar affinity. Protease digestion and mass-spectrometry analysis of this protein reveled the probable disulfide bond arrangement for the PPR N domain (Figure 1), and the same disulfide bond pattern has also been determined for several other class 2 receptor N domain proteins.

The Juxtamembrane Domain

The juxtamembrane (J) region of the PPR is comprised of the heptahelical bundle and the interconnecting loops. The structure of this domain is likely to bear at least some similarity to the heptahelical core region of rhodopsin, the only GPCR for which an X-ray crystal structure is available. Computer models of the PPR J domain have been generated using the rhodopsin X-ray structure as a template, but because there is almost no amino acid sequence homology between rhodopsin, a class 1 GPCR, and the PPR, the accuracy of such models is uncertain. One structural feature that is predicted for the PPR J domain, and for nearly all GPCRs, is a disulfide bond between extracellular loop (ECL)-1 and ECL-2 (Figure 1). Within the transmembrane helices of the PPR there are residues that are well-conserved in the class 2 GPCR family and are likely to help define the topology and functionality of the J domain. These include the prolines in TMs 4, 5, and 6, expected to induce kinks in the helices, and polar residues, such as Arg233 in TM2 and Gln451 in TM7, that are likely to contribute to networks of inter- and intra-helical side-chain interactions. The connecting loops and carboxy-terminal tail (CT) of the PPR also contribute importantly to PPR function, but the structures of these domains are unknown.

The Ligand Interaction Mechanism in the PPR

The Two-Site Model

The ligand-binding mechanism for the PPR has been extensively analyzed by the complementary approaches of photochemical cross-linking and receptor mutagenesis, and the overall results suggest a two-site model. According to this model, the C-terminal binding domain of PTH(1–34) interacts with high affinity with the PPR N domain and this interaction enables the amino-terminal domain of the ligand to interact with lower affinity with the PPR J domain. Thus, the N domain interaction provides the major component of binding energy, while the J domain interaction provides the interactions that induce receptor activation and G protein coupling (Figure 3).

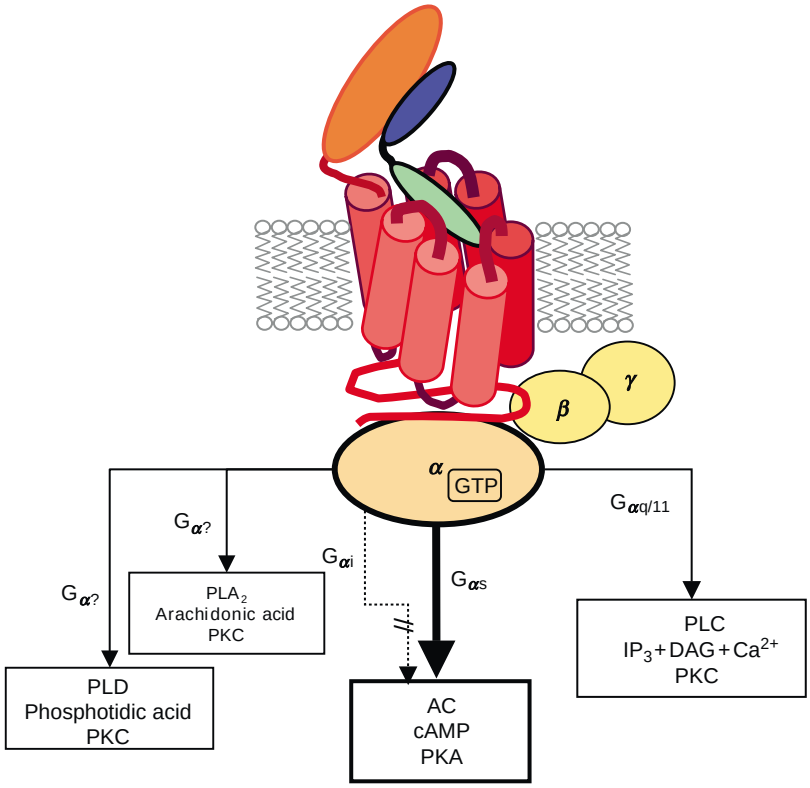

FIGURE 3 Ligand-binding and G protein-coupling mechanisms for the PTH/PTHrP receptor. The ligand, PTH(1–34) or PTHrP(1–34), is shown to interact with the PPR via a bipartite mechanism in which the ligand's C-terminal portion (blue) interacts with the receptor's amino-terminal extracellular domain (orange) to provide binding affinity, and the ligand's N-terminal portion (green) interacts with the receptor's extracellular loops and heptahelical portion (red) to induce receptor activation. The activated PPR can couple to multiple signaling pathways via several different heterotrimeric G proteins. It couples most strongly and in most cells to $G_{\alpha s}$ to stimulate the AC/cAMP/PKA pathway. It can also couple to $G_{\alpha q}$ to stimulate PLC/IP_3/Ca^{2+}/PKC signaling and to a pertussis toxin-sensitive G_i protein to inhibit AC/cAMP activity, but the magnitude of these response are generally less than that of the stimulatory AC/cAMP response. In some cells, the PPR can activate the PLD/phosphotidic acid/PKC and/or PLA_2/arachidonic acid/PKC pathways, but the G proteins involved are unknown.

N Domain Interactions

Cross-linking studies have identified proximities between specific sites in PTH and PTHrP ligands and the PPR. Thus, PTHrP(1–36) analogues modified with the photo-labile amino acid analogue, benzoylphenylalanine (Bpa), at positions 23, 27, 28, and 33 and cross-link to distinct segments of the PPR N domain: (33–40), (96–102), (64–95) and (151–172), respectively. The locations of the important functional contact sites within these N domain regions still need to be determined, but the large segment, residues (61–105), which corresponds precisely to exon E2 of the PPR gene, is not likely to contain such sites, as it can be deleted without affecting ligand-binding affinity. Two possible interaction residues in the N domain of the PPR include Thr33 and Gln37 (Figure 1), as mutation of these residues to alanine results in decreased affinity for PTH(15–34). These two residues are near the Bpa-23 contact site and thus could provide contacts for Trp-23 in the ligand.

J Domain Interactions

Other cross-linking studies identified Met425 at the extracellular end of TM6 as the probable contact site for PTH(1–34) or PTHrP(1–36) ligands modified with Bpa at position 1 or position 2. Interestingly, the Bpa-1-modified analogue (an agonist) and the Bpa-2-modified analogue (a partial antagonist/inverse agonist) cross-linked to overlapping, but not identical, sites at or near Met425, suggesting that the analogues could be used to distinguish between active and inactive receptor conformational states. In further studies, the mutation Met425 → Leu was shown to specifically increase the agonist efficacy (and reduce the inverse agonist efficacy) of [Bpa^2]PTHrP(1–36). These data, combined with earlier data showing that point mutations at the extracellular ends of TM5 (Ser370 → Ala, Ile371 → Val) and, TM6 (Leu427 → Thr) modulate the antagonist properties of [Arg_2]PTH(1–34), and that mutations in ECL-3 (Trp437 → Ala, Gln440 → Ala) impair binding of PTH(1–34) but not that of PTH(3–34), suggest

that residues in the TM5/TM6/ECL-3 region mediate interactions with Val-2 in the ligand that are involved in receptor activation.

Two other contact sites in the PPR J domain identified by cross-linking analyses include Arg186 at the N domain/TM 1 boundary, the probable contact site for ligand residue 13, and Lys240 at the extracellular of TM2, the probable contact site for ligand residue 19. The results of these cross-linking studies, combined with those above for the N-terminally modified ligand analogues, suggest that the portion of the ligand that interacts with the PPR J domain extends from residue 1 to residue 19. Consistent with this, the potencies of PTH(1–20) analogues on a PPR mutant construct (PPR-delNt) that lacks most (residues 23–181) of the N domain are the same as they are on the intact PPR. These studies using the PPR-delNt construct also suggest that the PPR N domain is not required for receptor activation. The PPR N domain is clearly required, however, for achieving full potency and affinity with PTH(1–34), as this ligand is 100-fold weaker on P1R-delNt, as it is on the intact PPR.

PPR Signaling and Regulation

Conformational Changes

As for all GPCRs, it is presumed that PPR activation involves movements in the TM helices and intracellular loops (ICLs), and that these movements result in increased accessibility of the receptor's cyctoplasmic surface to G proteins. The precise conformational changes involved are likely to be complex and are largely unknown. Inter-TM domain movements in the PPR have been analyzed using the Zn(II)-chelation strategy, and these studies have revealed that a movement of TM3 and TM6 away from each other, blocked by the addition of Zn(II), is required for Gs activation. In parallel experiments, a similar movement was also detected in the β2 adrenergic receptor, and has also been observed by this method of analysis in rhodopsin. The activation mechanisms used by the class 1 and class 2 GPCRs may, therefore, be similar. Using conventional mutational methods, specific residues in the IC loops of the PPR have been identified that modulate Gs and/or Gq coupling. These include Lys388 in ICL-3, at which mutations impair both AC/cAMP (G_s) and PLC/IP_3 (G_q) signaling and Lys319 in ICL2, at which mutations selectively impair PLC/IP_3 (G_q) signaling.

The Carboxyl-Terminal Tail

Classical pharmacological studies on PTH action in bone and kidney cells revealed that the PPR desensitizes and internalizes in response to hormone stimulation. More recent molecular studies have shown that the PPR carboxyl-terminal tail plays a major role in this regulation. Upon agonist activation, seven serines within the N-terminal-proximal portion of the tail (Figure 1) are rapidly phosphorylated, most likely by G protein-specific receptor kinase-2. This phosphorylation promotes the binding of β-arrestin and the internalization of the ligand–receptor complex, via clatherin-coated pits, to endosomal vesicles. At least some of the PPR recycles back to the cell membrane in a de-phosphorylated form, resulting in receptor resensitization. The PPR CT also mediates interaction with cytoskeletal scaffolding proteins, including members of the NHERF (Na^+/H^+ exchanger regulatory factor) family of proteins, which were identified in a yeast two-hybrid selection for proteins that bind the PPR CT. The C-terminal four amino acids (Glu-Thr-Val-Met) of the PPR mediate this interaction by binding to one of the PDZ domains of NHERF. The binding of NHERF to the PPR can alter the signaling pathways utilized, resulting in increased PLC signaling and diminished AC/cAMP signaling, and, as suggested by recent data, the internalization properties of the receptor, enabling the internalization of antagonist ligands.

The PPR in Human Disease

Jansen's Metaphyseal Chondrodysplasia

This rare autosomal dominant disease is characterized by short-limbed dwarfism (reflecting the role of PTHrP in the growth plates) and hypercalcemia (reflecting the role of PTH in bone and kidney). In 1995, a mutation in the *PPR* gene that changed His223 at the base of TM2 to Arg was identified in an affected individual. This mutation was then shown to confer high basal cAMP-signaling activity to the receptor expressed in COS-7 cells. Since this time, three other activating mutations in this disease have been identified, each of which alters a residue located near the intracellular termini of a TM helix: Thr410 → Pro and Thr410 → Arg in TM6 and Ile458 → Arg in TM7. In studies performed in transfected COS-7 cells, the antagonist [Leu^{11},$DTrp^{12}$]PTHrP(5–36) was shown to behave as an inverse agonist with the PPRs bearing either the His223Arg or Thr410Pro mutation, while the antagonist [Bpa^2]PTHrP(1–36) behaved as a selective inverse agonist, depressing cAMP signaling only with the His223Arg mutant. These findings with [Bpa^2]PTHrP(1–36) suggest that there may be variable conformational states of the active PPR.

Blomstrand's Chondrodysplasia

This rare perinatal lethal condition is characterized by a severely over-calcified fetal skeleton and short limbs.

Three different PPR-inactivating mutations have been identified in this recessive disorder: a messenger RNA splicing mutation that results in an eleven-amino acid deletion in TM5; a frameshift mutation in ECL-2, and a missense mutation (Pro132 → Leu) in the N domain. The phenotype seen in Blomstrand's chondrodysplasia mirrors that seen in mice having homozygous deletion of the *PPR* gene.

Conclusions

The PPR mediates the biological actions of two key proteins – PTH (calcium and phosphate homeostasis) and PTHrP (development). Disruptions of the PTH/PTHrP/PPR system result in a number of diseases of calcium ion homeostasis and tissue development (Figures 2 and 3). Further unraveling of the molecular mechanisms by which the PPR interacts with PTH and PTHrP is of fundamental biochemical interest and could lead to new therapies for diseases of bone and mineral metabolism.

See Also the Following Articles

Adenylyl Cyclases • Phospholipase C • Steroid/Thyroid Hormone Receptors • Thyroid-Stimulating Hormone/Luteinizing Hormone/Follicle-Stimulating Hormone Receptors • Vitamin D

Glossary

G (guanine nucleotide-binding) protein-coupled receptor (GPCR) An integral membrane protein characterized by seven membrane spanning helical domains and the capacity to activate heterotrimeric G proteins in response to agonist binding.

parathyroid hormone (PTH) An 84 amino acid secreted polypeptide that functions as the major regulator of calcium ion concentrations in blood and extracellular fluids; acts on bone and kidney cells.

PTH/PTHrP receptor (PPR, or PTH-1 receptor) A class 2 GPCR that mediates the actions of PTH and PTHrP. Highly expressed in osteoblasts, renal tubule cells, and a variety of tissues during development.

PTH-related protein (PTHrP) A 141 amino acid polypeptide that acts in a paracrine fashion to control development of the skeleton, heart, teeth, mammary glands, and other tissues. It is highly expressed in breast milk and is the most common mediator of hypercalcemia of malignancy.

Further Reading

Brown, E. M. (2000). Calcium receptor and regulation of parathyroid hormone secretion. *Rev. Endocr. Metab. Disord.* **1**, 307–315.

Gardella, T. J., and Jüppner, H. (2001). Molecular properties of the PTH/PTHrP receptor. *Trends Endocrinol. Metabol.* **12**, 210–217.

Hoare, S. R. J., and Usdin, T. B. (2001). Molecular mechanisms of ligand-recognition by parathyroid hormone 1 (PTH1) and PTH2 receptors. *Curr. Pharm. Design* **7**, 689–713.

Jüppner, H. W., Gardella, T. J., Kronenberg, H. M., and Potts, J. T., Jr. (2001). Parathyroid hormone and parathyroid hormone-related peptide in the regulation of calcium homeostasis and bone regulation. In *Endocrinology* (L. DeGroot and J. Jameson, eds.) Vol 2, pp. 969–1053. Endocrinology, W. B. Saunders, Philadelphia.

Strewler, G. J. (2000). The physiology of parathyroid hormone-related protein. *New England J. Med.* **342**, 177–185.

Biography

Thomas J. Gardella, Ph.D., is an Associate Professor in Medicine with appointments at the Massachusetts General Hospital and Harvard Medical School. He has been a member of the Endocrine Unit of the M.G.H. since 1988, and his research interests focus mainly on the structure–activity relationships of PTH and the PTH receptor. He received his Ph.D. degree in molecular genetics and microbiology from the University of Massachusetts Medical School, Worcester, Massachusetts and a B.S. degree in biochemistry from the University of Massachusetts, Amherst, Massachusetts.

PCR (Polymerase Chain Reaction)

Michael J. Brownstein
National Institute of Mental Health, National Institutes of Health, Bethesda, Maryland, USA

The polymerase chain reaction (PCR) is used to amplify DNA – i.e., to make millions of copies of a particular DNA segment. Invented by Kary Mullis in 1983, the process is simple, fast, and robust. It relies on synthetic oligonucleotide "primers," DNA polymerase(s), nucleotide bases, and a thermal cycler (a programmable instrument that varies and controls the temperature of the solution in which PCRs occur). The enzymes used, among them Taq, Pfu, and Vent polymerases are derived from *Thermus aquaticus*, *Pyrococcus furiosus*, and *Thermococcus litoralis*, respectively. These are bacteria that live in hot springs or undersea vents where the ambient temperature is high. Consequently, the enzymes they synthesize are thermostable. They differ in important ways, however. Taq polymerase, for example, is quite processive. That is, it copies DNA strands very efficiently, but it lacks 3′–5′ exonuclease activity, and is more error prone than Pfu and Vent polymerases, which have exonuclease activity and "proofread" their products. For this reason, enzyme mixtures are sometimes used to catalyze PCR reactions.

The Reaction Cycle

A polymerase chain reaction (PCR) cycle is illustrated in Figure 1. Step one is to melt or unzip the double-stranded DNA templates that will be copied. A thermocycler is used to increase the temperature of the reaction vessel to 90°C or more. At such temperatures most mammalian or bacterial enzymes would be inactivated, but they are well tolerated by the thermostable polymerases described above.

After the DNA strands have been separated, the temperature is dropped to permit short DNA primers to bind (anneal) to complementary sequences on the templates. The polymerases will not copy DNA in the absence of primers, and two are used – one for each of the two template strands that were liberated in step one.

Once they have found their specific target sequences, the polymerases can begin adding bases to the 3′ ends of the primers. Since this process is inefficient at the relatively low annealing temperature, the reaction temperature is increased to ~75°C. Now both of the DNA strands are quickly replicated, beginning at the priming site and ending, in theory, at the end of each template. As the figure shows, there are four DNA strands at the end of the first PCR cycle, instead of the original two. In subsequent cycles, products primed by the two oligonucleotides preferentially accumulate. The length of the "amplicons" is defined by the primers, which form their flanks. After about five PCR cycles have been completed, these amplicons predominate over longer species. It is important to note that at the beginning of a PCR, all of the reagents except for the template are present at high concentrations. Therefore, primer binding is favored over product renaturation, and the amplification is exponential. After many cycles have been completed, this may no longer be the case; product formation becomes linear and finally grinds to a halt. In practice, it is uncommon to use more than 30 reaction cycles.

Applications

PCR can be employed to amplify both DNA and RNA templates. In the latter case, reverse transcriptase (an RNA-directed DNA polymerase) is first used to make complementary DNA from the RNA of interest. DNA produced in this way can be substituted for the double-stranded DNA that served as the starting material in the scheme shown in Figure 1. This process is referred to as reverse transcriptase-PCR (RT-PCR). It allows much smaller amounts of RNA to be measured than can be detected with Northern blotting or RNase protection assays. In fact, real-time RT-PCR has become the method of choice for measuring changes in RNA when large numbers of samples have to be studied. This technique combines PCR with cycle-by-cycle detection of amplicons during the exponential phase of product buildup. Quantitation is based on the fact that many PCR cycles are needed to detect the products of rare targets, while few cycles are required to detect those of abundant ones. The dynamic range of the method spans 6–7 orders of magnitude. It is possible to amplify more than one product at a time with two or more primer pairs (multiplex PCR), and to detect the products with different dyes.

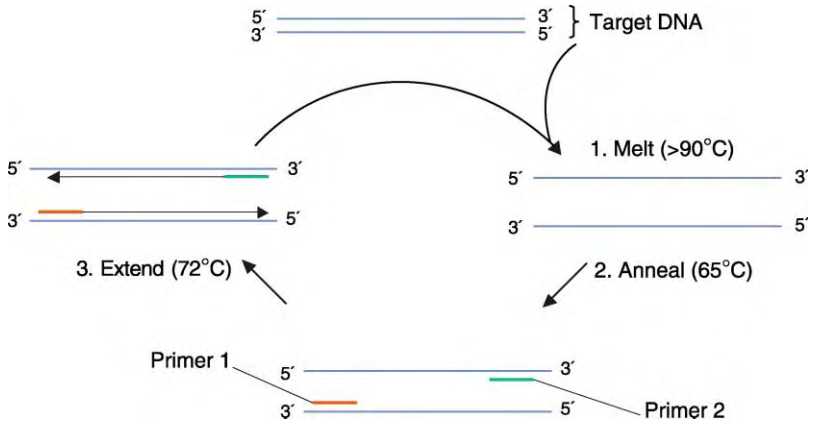

FIGURE 1 The PCR cycle.

It should already be clear that many PCR-based methods have been invented. Some are used for cloning, modifying, and/or sequencing amplicons; others are used for detection or measurement of RNA or DNA. To appreciate these methods, it is important to understand that many sorts of oligonucleotides can be used to prime PCR reactions. Thus, even though it is essential for the primers to be complementary to their targets on their 3′ ends, they can be quite different from the targets on their 5′ ends, where noncomplementary sequences, free amino groups, fluorescent dyes, or molecules like biotin can be added without adversely affecting the amplification process.

One of the earliest uses of PCR was in characterizing families of gene products, e.g., the rhodopsin-like G protein-coupled receptors. In humans there are more than 200 such proteins, exclusive of odorant receptors. After cDNA encoding the first few of these were cloned, it became clear that they were structurally similar, that they shared certain amino acid motifs. "Degenerate" PCR primer mixtures were designed on the basis of the conserved domains and used to amplify fragments of new family members from cDNA templates. Since these fragments lacked the 5′ and 3′ ends of the receptors' open reading frames, another PCR method called rapid amplification of cDNA ends (RACE) was used to identify and isolate the missing 5′ and 3′ termini. Once the sequences of the ends were determined, long-range PCR could be used to amplify the entire open reading frame, using primers with convenient restriction sites on the 5′ ends to facilitate "pasting" the inserts into vectors.

Some scientists were interested in studying the relationship between the structures of receptors (and other proteins) and their functions. To do this, they used PCR to introduce mutations into the receptors or to construct chimeric proteins – half one receptor, and half another, or tagged receptors, which could be used to study protein trafficking in cells. The constructs were sequenced before they were expressed in cells to be sure that no errors were made in producing them. The sequencing reactions were also PCR based. In fact, it is safe to say that the much-heralded sequencing of the human and mouse genomes could not have been accomplished without the method, and DNAs from living species are not the only templates that have been analyzed. PCR has allowed DNA from ancient samples (e.g., insects embedded in amber, tissue from mummies and extinct species like the Quagga) to be characterized.

The instruments used for DNA sequencing can be employed for genotyping as well. To do this, fluorescent PCR primers are used to amplify variable number tandem repeats or single nucleotide polymorphisms that serve as markers for inherited segments of chromosomes. The resulting data are used for linkage analysis, permitting scientists to determine the chromosomal location of disease-causing genes. Once these genes are known, robust screening methods – also based on PCR – can be developed to screen for carriers of deleterious mutations and even to look for mutations in pre-implantation embryos.

Genotyping has other potential uses too. It permits livestock and plants to be improved, and identity, paternity, or culpability of subjects to be determined by forensic scientists.

Finally, PCR is used to detect pathogens in clinical samples, food, and water, and to search for mutations in cancer-causing genes in tumors, or polymorphisms in drug metabolizing enzymes and transporters that affect efficacy/toxicity. It is not unlikely that it will play an important role in the development of personalized medicine in the future. In fact, its use may not be limited to assays of DNA and RNA. PCR-ELISA is an

exquisitely sensitive way to detect any molecule to which an antibody can be raised.

See Also the Following Article

DNA Sequence Recognition by Proteins

Glossary

DNA polymerase An enzyme that catalyzes DNA-directed synthesis of DNA from nucleotide triphosphates.

primer A single-stranded DNA molecule, typically 17–25 nucleotides in length that is required to initiate the synthesis of DNA by polymerase.

reverse transcriptase An enzyme that catalyzes RNA-directed synthesis of DNA from nucleotide triphosphates.

thermocycler A programmable instrument that heats and cools reaction tubes repeatedly allowing the user to move through melting, annealing, and extension steps in the PCR cycle.

Further Reading

McPherson, M. J., and Møller, S. G. (2000). *PCR*. BIOS Scientific, Oxfordshire, UK, http://www.pcrlinks.com/.

Mullis, K. B., and Faloona, F. A. (1987). Specific synthesis of DNA *in vitro* via a polymerase-catalyzed chain reaction. *Methods Enzymol.* **155**, 335–350.

Biography

Michael J. Brownstein is Chief of the Laboratory of Genetics, National Institute of Mental Health, NIH, Bethesda, MD. He received his Ph.D. and M.D. from the University of Chicago and did postdoctoral training with Julius Axelrod. His research has been in the areas of neurobiology, endocrinology, genetics, and genomics.

Pentose Phosphate (Hexose Mono Phosphate) Pathway

Bernard R. Landau
Case Western Reserve University, Cleveland, Ohio, USA

The pentose phosphate pathway is the major source of NADPH for reductive biosynthesis and is the source of ribose-5-P for nucleotide and nucleic acid synthesis. Its reactions are usually viewed in two segments. In the first, glucose-6-P is irreversibly oxidized, generating NADPH and pentose-5-P. In the second, the pentose-5-P is reversibly converted through a series of rearrangements to intermediates of the glycolytic pathway. The pathway is in the cytosol.

History

In 1931, Warburg demonstrated glucose-6-P's oxidation to 6-phosphogluconate with the formation of NADPH. In the following decade, Warburg, Lipmann, Dickens, and others found that the gluconate was decarboxylated to CO_2 and to a pentose phosphate that could then be reconverted to hexose-6-P. Details of the pathways were elucidated in the 1950s by Cohen, Racker, Horecker, and their associates. Figure 1 shows the pentose phosphate pathway.

Reactions

Oxidative Segment

Glucose-6-P oxidation is catalyzed by glucose-6-P dehydrogenase, yielding 6-phosphogluconolactone and NADPH (Figure 2). The spontaneous hydrolysis of the lactone, forms 6-phosphogluconate, catalyzed by a specific lactonase. The gluconate is oxidatively decarboxylated to yield another NADPH and ribulose-5-P. The overall reaction of this segment is then glucose-6-P $\rightarrow$ CO_2 + 2NADPH + ribulose-5-P.

Nonoxidative Segment

The ribulose-5-P is isomerized to ribose-5-P and also epimerized to xylulose-5-P (Figure 3). Transfer of the top 2 carbons as a unit from the xylulose-5-P to ribose-5-P, catalyzed by transketolase, yields seven carbon containing sedohepulose-7-P and glyceraldehyde-3-P. Transfer of the top 3 carbon unit as a unit from the sedohepulose-7-P to the glyceraldehyde-3-P, catalyzed by transaldolase, yields fructose-6-P and 4 carbon containing erythrose-4-P. Transfer of the top 2 carbons as a unit from another xylulose-5-P to the erythrose-4-P, again catalyzed by transketolase, yields fructose-6-P and glyceraldehyde-3-P. Thus, the overall reaction of this segment is 3 pentose-5-P $\leftrightarrow$ 2 fructose-6-P + glyceraldehyde-3-P.

Transketolase requires thiamine pyrophosphate as a cofactor. The 2 carbon unit is transferred via its addition to the thiamine ring of the vitamin. The mechanism is similar to that in the oxidative decarboxylation of pyruvate, catalyzed by the thiamine pyrophosphate containing E_1 subunit of the pyruvate dehydrogenase complex. In the transfer of the 3 carbons unit, catalyzed by transaldolase, a Schiff base is formed between the ketone group of the sedohepulose-7-P and a lysine residue at the active site of the enzyme. The mechanism is similar to that in fructose-1, 6-bisphosphatase aldolase catalysis.

Overall Balance and Carbon Fate

On balance, 3 glucose-6-P (18 carbons) are decarboxylated to yield 3 CO_2 and 3 pentose-5-P (15 carbons) (Figure 4). The rearrangements, catalyzed by transketolase and transaldolase produce 2 fructose-6-P (12 carbons) and glyceraldehyde-3-P (3 carbons). The CO_2 contains carbon 1 of the glucose-6-P (Figure 5). The origin of the top 3 carbons of the 2 fructose-6-P are carbons 2 and 3 of the glucose-6-P.

Mode of Operation

Shunt or Cycle

Since glucose-6-P is converted to fructose-6-P and glyceraldehyde-3-P, the pentose phosphate pathway has been viewed as an alternate route for the conversion

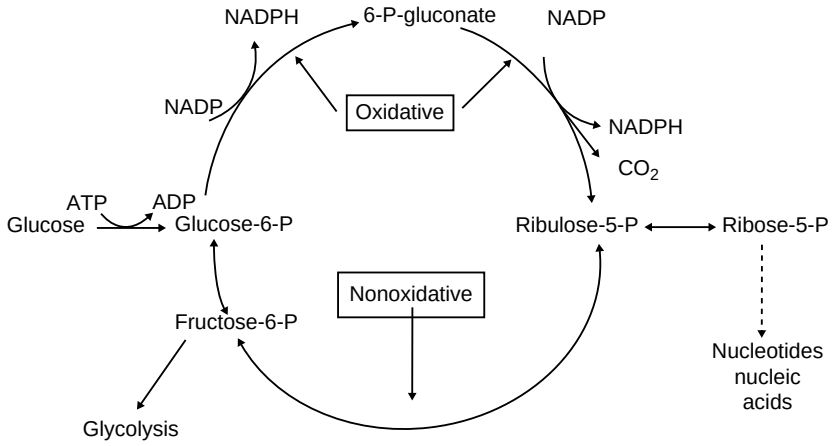

FIGURE 1 Depiction of the pentose phosphate pathway as a cycle composed of oxidative and nonoxidative segments.

of glucose-6-P to intermediates of the glycolytic pathway. Therefore, the pathway has also been called the hexose monophosphate shunt. Since the fructose-6-P can be isomerized to glucose-6-P that can re-enter the pentose phosphate pathway, the pathway has also been viewed as a cycle and called the pentose cycle.

Regulation

The dehydrogenation of glucose-6-P, the first step, is considered to be the rate-limiting step in the oxidative segment. Control is through the activity of glucose-6-P dehydrogenase regulated by the concentration of NADP. NADPH competes with the NADP for binding to the enzyme, thus tightly coupling NADPH production to utilization. When NADPH is utilized (e.g., in fatty acid synthesis), the NADPH is oxidized, increasing NADP and stimulating flux through the oxidative segment. Flux through the nonoxidative segment is determined by the concentration of pentose-5-P. The activity of the pathway is coordinated with that of the pathways utilizing its products. Recent studies identify xylulose-5-P in the pathway as mediating the effect of carbohydrate feeding on the glycolytic pathway and regulating the enzymes required for fatty acid and triglyceride synthesis.

Other Functions

The pentose phosphate pathway is the route by which pentose from food is metabolized. Erythrose-4-P in some organisms is used as an intermediate in the synthesis of the aromatic ring of the amino acids. D-xylulose formed in the glucuronic acid pathway, is further metabolized via the pentose phosphate pathway.

Quantitation

Methods

Estimates of the activity of the pathway rest on measurements of the activities of its enzymes, particularly of glucose-6-P dehydrogenase, and of concentrations of intermediates in the pathway, as well as yields

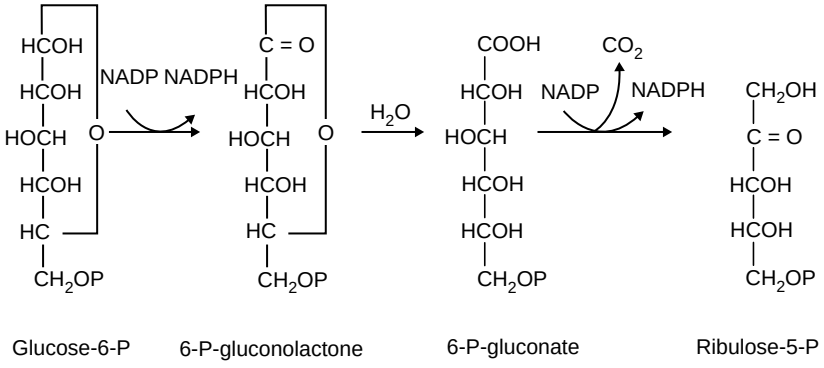

FIGURE 2 Reactions of the oxidative segment of the pentose phosphate pathway.

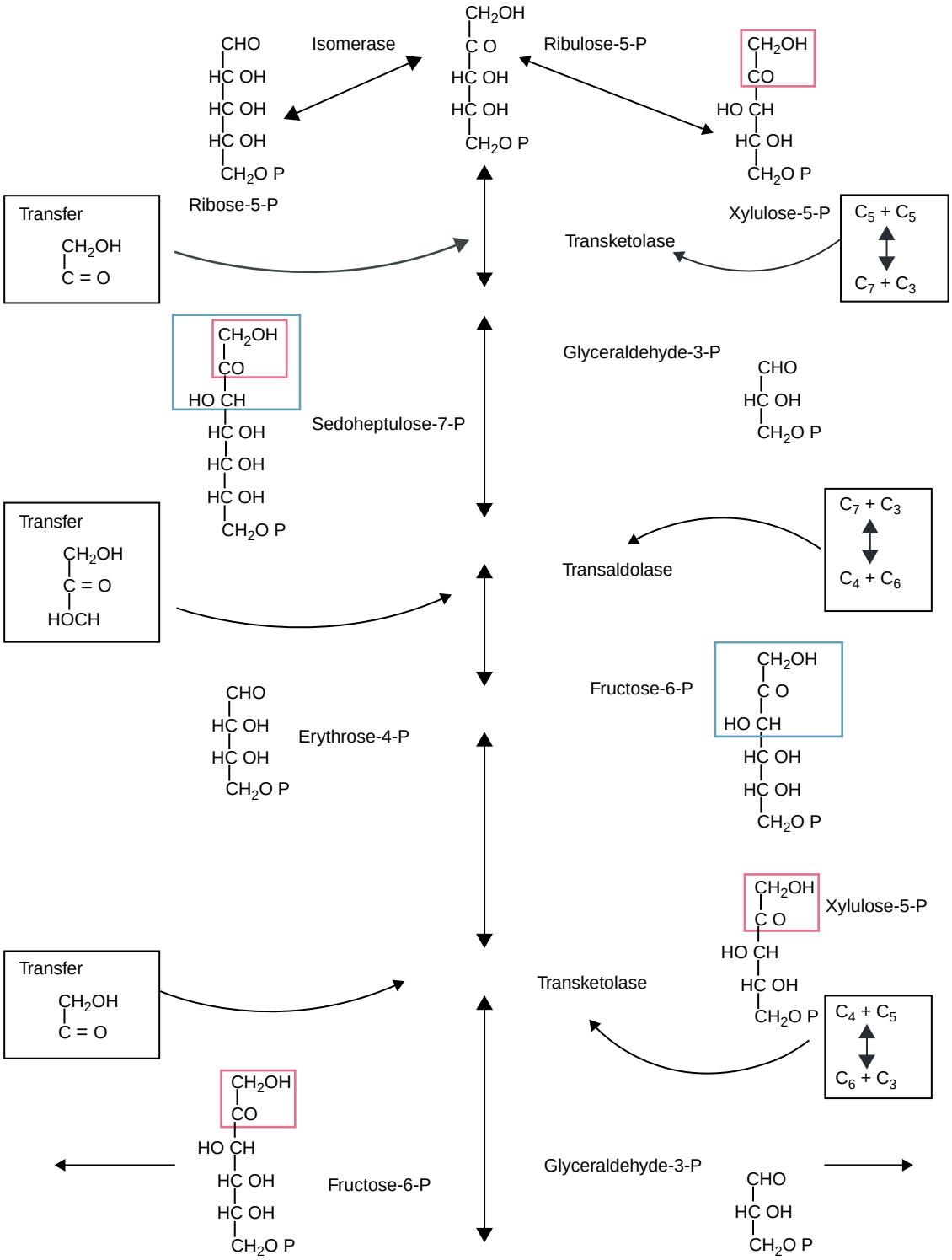

FIGURE 3 Reactions of the nonoxidative segment of the pentose phosphate pathway.

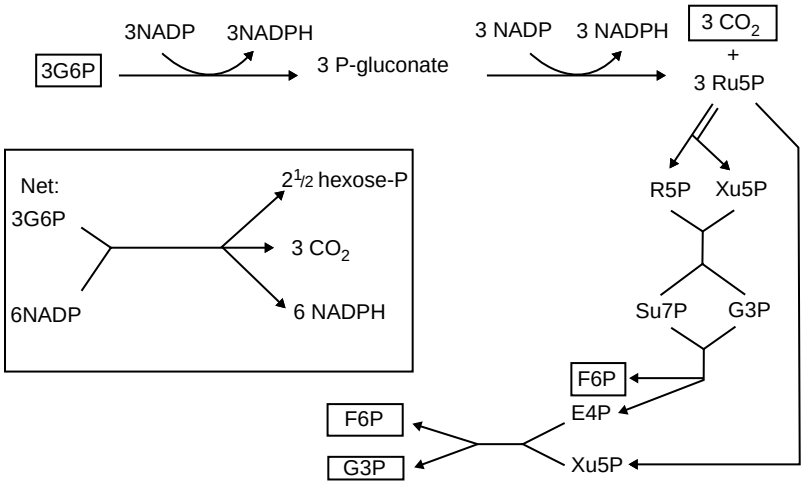

FIGURE 4 Chemical balance in the reactions of the pentose phosphate pathway.

of labeled products after administering labeled substrate and intermediates of the pathway. Specifically, carbon-labeled glucoses have been used to quantitate the amount of glucose utilized by the pathway relative to other pathways utilizing glucose. The quantitations depend on (1) the fact that carbon 1 of every molecule of glucose-6-P entering the pathway is oxidized to CO_2, while via glycolysis and the tricarboxylic acid cycle, carbons 1 and 6 are oxidized to CO_2 to essentially the same extent, or (2) the randomization of carbons 2 and 3 of glucose-6-P occurring in the nonoxidative segment (Figure 5).

The amounts of glucose oxidized and that utilized by the pathway are different. Thus, while the three molecules of glucose-6-P that enter the pathway (Figure 4) are oxidized, and 2 glucose-6-P equivalents are reformed, only a net of 1 glucose-6-P is utilized. It is converted to CO_2 and glyceraldehyde-3-P. If, as can occur in the liver, 2 glyceraldehyde-3-P that are formed are converted to 1 glucose-6-P, the balance becomes 6 glucose-6-P → 12 NADPH + 6 CO_2 + 5 glucose-6-P. Hence, 6 glucose-6-P are oxidized, but only 1 glucose-6-P is utilized (completely oxidized to CO_2).

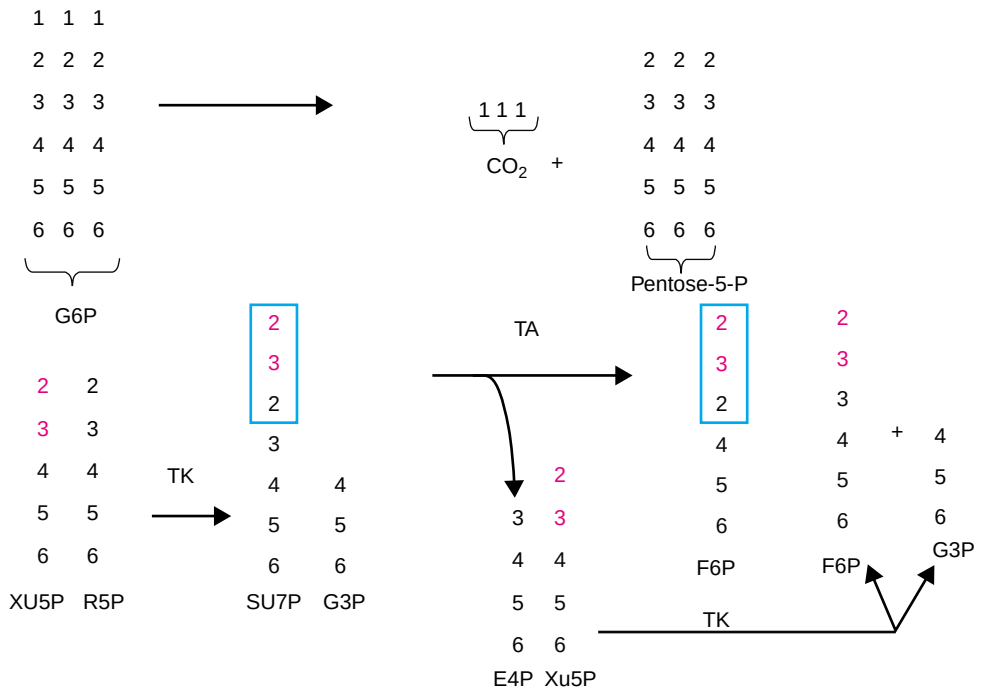

FIGURE 5 Fate of the carbons of the glucose-6-p (g6p) in its metabolism via the pentose phosphate pathway.

Estimates

The pathway is present in all cells. The highest activities are found in tissues where lipogenesis is prominent, e.g., liver, mammary gland, particularly during lactation, and adipose tissue. The pathway is also active in the reproductive glands, adrenal gland, and red blood cells. In those tissues 10–20% of glucose utilization may be via the pathway. The pathway has relatively high activity in growing tissue, e.g., in fetal and newborn tissues and tumors.

Clinical Importance

Maintaining the integrity of the red blood cells depends on having an adequate supply of reduced glutathione to protect the cells from toxic peroxides, as well as maintain hemoglobin in a reduced state. Several hundred million people, mainly in Africa, Asia, and the Mediterranean, have a genetic deficiency of glucose-6-P dehydrogenase. Drugs which increase the formation of peroxide, infections, and other causes of oxidative stress can induce acute hemolysis and hence anemia in those individuals.

The Wernicke–Korsakoff syndrome is a neuropsychiatric disorder occurring in individuals with a dietary deficiency of thiamine. Findings are eyeparalysis, abnormal gait, confabulation, and loss of memory. A genetic defect in transketolase has been suggested as the reason the syndrome is only observed in a small portion of those with thiamine deficiency. A genetic abnormality in transketolase has recently been found in a man with liver cirrhosis.

See Also the Following Articles

Pentose Phosphate Pathway, History of • Sugar Nucleotide Transporters

Glossary

NADPH Reduced form of nicotanamide adenine dinucleotide phosphate; the electron donor in reductive biosynthesis.

pentose phosphate pathway Pathway by which NADPH is generated for reductive biosynthesis and ribose-5-P for nucleotide and nucleic acid formation.

transaldolase Enzyme in the pentose phosphate pathway transferring 3 carbon units via the formation of a Schiff base.

transketolase Enzyme in the pentose phosphate pathway having thiamine as cofactor and transferring 2 carbon units.

Further Reading

Cabezas, H., Raposo, R. R., and Melendez-Hevia, E. (1999). Activity and metabolic roles of the pentose phosphate cycle in several rat tissues. *Mol. Cell. Biochem.* **201**, 57–63.

Horecker, B. L. (2002). The pentose phosphate pathway. *J. Biol. Chem.* **277**, 47965–47971.

Magnusson, I., Chandramouli, V., Schumann, W. C., Kumaran, K., Wahren, J., and Landau, B. R. (1988). Pentose pathway in human liver. *Proc. Natl. Acad. Sci.* **85**, 4682–4685.

Massillon, D., Chen, W., Barzilai, N., Prus-Wertheimer, D., Hawkins, M., Liu, R., Taub, R., and Rossetti, L. (1998). Carbon flux via the pentose pathway regulates the hepatic expression of the glucose-6-phosphatase and phosphoenolpyruvate carboxykinase genes in conscious rats. *J. Biol. Chem.* **273**, 228–234.

Mehta, A., Mason, P. J., and Vulliamy, T. J. (2000). Glucose-6-phosphate dehydrogenase deficiency. *Bailliere's Clin. Haematol.* **13**, 21–38.

Schenk, G., Duggleby, R. G., and Nixon, P. F. (1998). Properties and functions of the thiamin diphosphate dependent enzyme transketolase. *Int. J. Biochem. Cell. Biol.* **30**, 1297–1318.

Veech, R. L. (2003). A humble hexose monophosphate pathway metabolite regulates short- and long-term control of lipogenesis. *Proc. Nat. Acad. Sci.* **100**, 5878–5580.

Verhoeven, N. M., Huck, J. H., Roos, B., Struys, E. A., Salomons, G. S., Douwes, A. C., Van der Knaap, M. S., and Jakobs, C. (2001). Transaldolase deficiency: Liver cirrhosis associated with a new inborn error in the pentose phosphate pathway. *Am. J. Hum. Genet.* **68**, 1086–1092.

Wood, T. (1985). *The Pentose Phosphate Pathway.* Academic Press, Orlando.

Biography

Bernard R. Landau is a Professor of Medicine and Biochemistry at Case Western Reserve University and former Director of the Division of Endocrinology at University Hospitals of Cleveland. His research has focused on carbohydrate and lipid metabolism using radioactive and staple isotope tracer technology. He received a Ph.D. in chemistry from Harvard School of Arts and Sciences and an M.D. from Harvard Medical School.

Pentose Phosphate Pathway, History of

John F. Williams
Australian National University, Canberra, Australia

In this article the oxidative and non-oxidative segments of the pentose pathway (PP) of glucose metabolism are defined. The discovery in 1931–1935 by the German biochemist, Otto Warburg, of the oxidative division of the pathway and of the chemistry and role of a new pyridine nucleotide co-enzyme in its reactions is deliniated.

Background

The successful revelation of many of the reactants and enzymes of the non-oxidative PP was largely achieved by two American biochemists, Bernard L. Horecker and Ephraim Racker who, during 1950–1955, independently accomplished our current text-book knowledge of the classical reaction scheme of PP. A precise reaction order and metabolic map depiction of PP reactions was published by Horecker in 1955 from results of prediction labeling experiments that used variously labeled ^{14}C-ribose 5-phosphate dissimilation by liver and plant tissue extracts. Many PP reactions were also assigned roles in the path of carbon in photosynthesis that was unraveled by Calvin and colleagues during 1945–1954. The above accomplishments briefly terminated fundamental research on the nature of PP which was then replaced by an era (1958–1979) of metabolic pathway measurement.

Joseph Katz and Harland G. Wood were the pioneers who developed theory and methods for quantitative measurement of the contributions of pentose cycle (PC) and other pathways to total glucose metabolism. All of these methods depended on the metabolism of ^{14}C-labeled substrates. PC was measured to a significant level in many animal tissues but made its most notable contribution in adipose tissue, which resulted in the PP being renamed the (fat) F-type PP. Contrary to all expectation, many attempts to quantify PC in liver, the major tissue used by Horecker to establish the reaction scheme for the F-type PP, showed it measured a negligible and therefore puzzling contribution to glucose metabolism.

Based on these latter findings the reaction mechanism of PP was reinvestigated during 1965–1992 by Williams and colleagues in Australia. Liver featured in the investigations because it is a rich source of the enzymes and individual reactions of PP. New octulose and heptulose phosphate reactants and new enzyme activites were discovered. Using specifically ^{14}C-labeled substrates, a revised (liver) L-type PP was identified which quantitatively accounted for 25% of total glucose metabolism. These results aroused criticism and polemic by those defending F-type PC theory and measurement practice. This unsettling state was put to rest in 1993 when the Williams group, using ^{13}C-NMR spectrometry showed that the three group transferring enzymes of the PP, namely transketolase, transaldolase and aldolase catalyzed simultaneous mass transfer and group exchange reactions and in all cases the exchange rates exceeded the mass flux rate. As an example it was found that Transketolase exchange rates in normal and regenerating liver, four different neoplasms, spinach chloroplasts and adipocytes exceeded PP flux rates by 5–600 times. Since the groups being transferred by the above enzymes are ^{14}C-labeled in all of the unraveling investigations that involved F-type and L-type pathways, it is concluded that carbon isotope prediction labeling data are useless for the investigations of the reaction order and measurement of PP. Thus metabolic maps of PP in textbooks of biochemistry are erroneous. A concluding statement that best describes how the PP should now be viewed is given.

All or at least a substantial selection of the reactions of the pentose phosphate (PP) pathway of glucose metabolism occur in the cytoplasmic compartment of most cells. The reaction scheme is in two parts and consists of oxidative (Figure 1) and nonoxidative segments (Figure 2). The reactions of the oxidative segment are few and involve the decarboxylation of glucose-6-phosphate (Glc 6-P) to ribulose 5-phosphate (Ru 5-P) via 6-phosphogluconolactone and 6-phosphogluconate (6-Pg). There is concomitant production of two moles each of reduced nicotinamide-adenine dinucleotide phosphate (NADPH) and proton for each mole of Glc 6-P converted to Ru 5-P by oxidative decarboxylation. The non-oxidative reactions (Figure 2) are classically

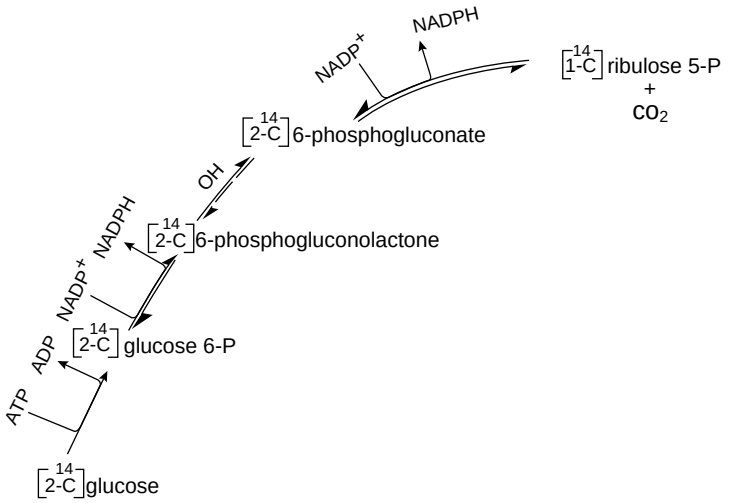

FIGURE 1 Reactions of the oxidative segment of the pentose pathway showing the conversion of [2-^{14}C]-glucose to CO_2 and [1-^{14}C]-ribulose 5-phosphate. Glucose is phosphorylated by hexokinase and oxidatively decarboxylated by the concerted actions of glucose 6-phosphate dehydrogenase, water at pH 7.4 or lactonase and 6-phosphogluconate dehydrogenase (see glossary for equation).

depicted as a diversity of reversible steps for the interconversion and linkage of other pentose phosphate products that arise from Ru 5-P, with triose and hexose phosphates that are also common intermediates in cytoplasm of the higher flux glycolytic pathway of glucose metabolism. The reactions of Figure 2 also show sugar phosphate intermediates (glycolyl units) with 3, 4, 5, 6, and 7 carbon atoms that are generated by the reversible reactions of the nonoxidative segment. There are thus three biosynthetic functions of PP reactions that relate to cellular energetics, growth, and repair: (1) the contribution by the oxidative segment to the provision and maintenance of a high NADPH/$NADP^+$ redox potential and thereby the supply of electrons for some reductive anabolic processes; (2) the formation of ribose 5-phosphate (Rib 5-P) for all nucleotide and nucleic acid biosynthesis; and (3) a storage pool of diverse phosphorylated glycolyl units that may be used in biosynthetic and energy-yielding reactions by other pathways. Finally, selected reactions of the nonoxidative segment are also part of the most extensive synthetic and life-sustaining event on the planet, namely, the photosynthetic reductive path of CO_2 assimilation in all C-3 plants.

Early Discoveries

A summary of the biochemistry of the reactions, enzymes, methods, distributions, and quantitation of the pathways of Figures 1 and 2 in tissues, together with all references cited in this article that relate to the history of the "unraveling" events of the pathway, are given in a comprehensive review of the PP by Williams J. F. *et al.* in 1987. Discoveries which led to the formulation of the classical depiction of the PP (Figures 1 and 2) commenced in 1931 with the discovery of glucose 6-phosphate dehydrogenase (Glc 6-P DH) by Otto Warburg, a German biochemist and a Nobel laureate of extraordinary distinction and influence. Warburg named the enzyme *Zwischenferment* (intermediate enzyme) in order to designate the branching of Glc 6-P away from the pathway of fermentation (glycolysis). In 1935 a second enzyme, 6-phosphogluconate dehydrogenase, was isolated together with a new pyridine nucleotide coenzyme (*Wasserstoffübertragendes*: hydrogen-carrying coferment), which is now called $NADP^+$. Warburg recognized that $NADP^+$ was chemically and functionally different from the NAD^+ coenzyme of glycolysis. With these discoveries Warburg had opened the way into an alternate path of glucose dissimilation. Warburg believed that the NADPH product of these reactions was the substrate of cellular respiration and was thus a prime chemical source of aerobic cellular energy. This view was strongly held and disseminated for the next 20 years, such that the PP was first called the "direct oxidative pathway" in order to distinguish it from the path of fermentation of glucose and lactic acid formation in muscle.

The proposition linking NADPH and respiration (eqns. [1]–[3]) was shared by Erwin Haas, who was a member of Warburg's Berlin-Dahlem laboratory. (Haas fled Germany in 1938 and proceeded to the University of Chicago, where he was joined by Bernard Horecker, a fresh Ph.D. graduate, who was already exhibiting a flair for enzymology.) Haas possessed much of Warburg's data, understood his methods very well, and had a plan of research to test the proposed role of NADPH in respiration. Haas and Horecker set out to isolate a putative NADPH-cytochrome *c* reductase (eqn. [1]) in order to demonstrate the existence and nature of an

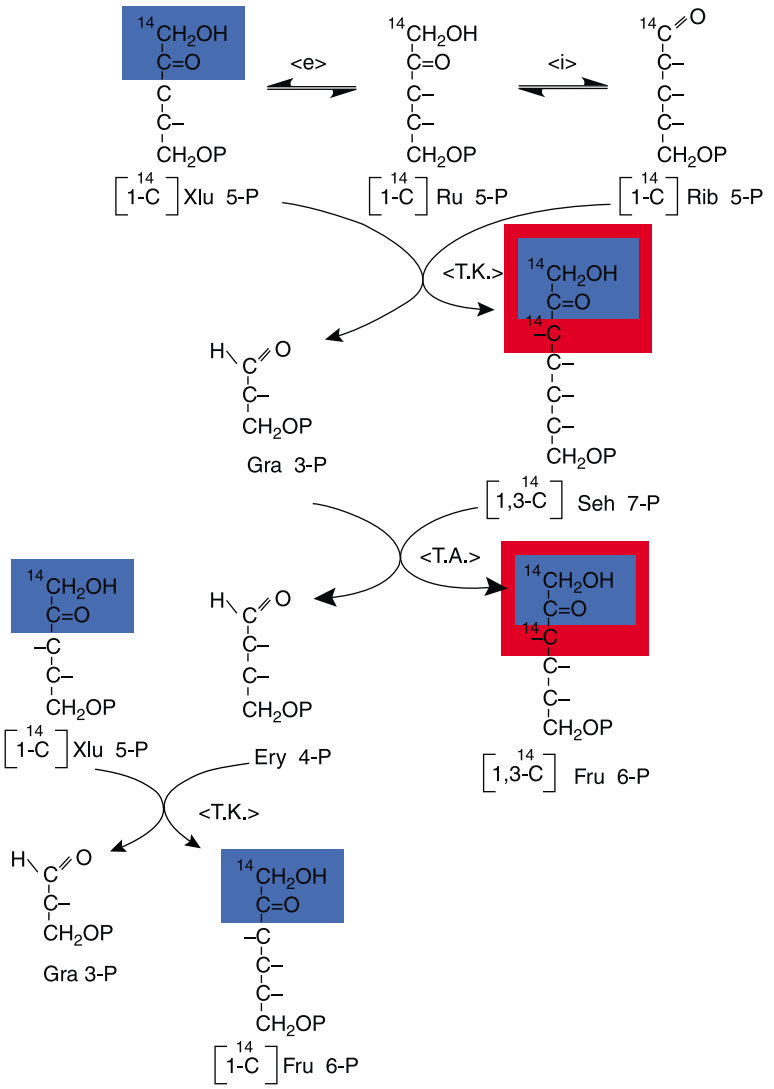

FIGURE 2 The proposed reaction sequence of the non-oxidative segment of the *classical* F-type pentose pathway *in vitro*. The [1-^{14}C]-ribulose 5-P substrate is the labeled product of the Figure 1 reaction scheme and the reactions display the theoretical distributions of ^{14}C-isotope from pentose 5-P into the carbon atoms of labeled intermediates and products. The enzymes catalyzing the reaction steps are: e, ribulose 5-phosphate 3-epimerase, i, ribose 5-phosphate isomerase; TK, transketolase; TA, transaldolase. The blue panels show the two-carbon active *glycolaldehyde* group that is conveyed by TK mass transfer and group exchange. The red panels show the three-carbon *dihydroxyacetone* group that is carried by TA mass transfer and exchange (see text and glossary for other detail).

enzyme that was hypothesized to be the "missing link" in a respiratory pathway between reduced pyridine nucleotide and oxygen via the cytochrome system (eqn. [3]):

$$\mathrm{NADPH + H^+ + Cyt\text{-}cFe^{3+} \xrightarrow{\text{NADPH cytochrome } c \text{ reductase}} NADP^+ + Cyt\text{-}cFe^{2+} + 2H} \quad [1]$$

$$\mathrm{2H + Cyt\text{-}cFe^{2+} + 0.5\ O_2 \xrightarrow{\text{Cytochrome oxidase}} H_2O + Cyt\text{-}cFe^{3+}} \quad [2]$$

Sum reaction:

$$\mathrm{NADPH + H^+ + 0.5\ O_2 \longrightarrow NADP^+ + H_2O.} \quad [3]$$

The search for an enzyme activity was successful and a reasonably pure flavoprotein, NADPH-cytochrome *c* reductase, was isolated from yeast in 1940. Research was interrupted and not taken up again until the end of the Second World War. By 1948, Horecker had returned to the project and soon extensively purified the enzyme from liver. However, by that time, there was growing evidence that the oxidation of NADPH was not the source of reducing equivalents for respiration and the entire proposal was abandoned in 1951, when Albert Lehninger showed that NADH was the "low-redox" respiratory chain substrate for oxidative phosphorylation in mitochondria.

The understandable disappointment with the realization that NADPH-cytochrome *c* reductase had no role in respiratory energy production (it is now known to be part of the cytochrome P-450 hydroxylation-detoxification scheme) directed Horecker's interest to a larger problem, namely, an inquiry into the nature, fate,

and metabolic role of the pentose product of 6-Pg decarboxylation (Figure 1). It is also noteworthy that the British biochemist Frank Dickens (Courtauld Institute, UK) had been making pioneering investigations on this topic since 1936. However, a solution of the problem was made in the USA, where metabolic biochemistry and enzymology were flourishing in the 1950s. The dominant contributions came from the laboratories of Bernard Horecker, Ephraim Racker, and Seymour Cohen. Moreover, a further stimulus was the spectacular investigation made in Melvin Calvin's laboratory at UC Berkeley, which led to a Nobel prize and an understanding of the path of carbon fixation in photosynthesis (PS). Calvin's progress was heavily dependent on success in research by the aforementioned biochemists to resolve the enzymology and chemical problems posed by the reactions of Figure 2.

By 1950 all investigators possessed strong clues which served as signposts for an ultimate elucidation of a PP reaction scheme. (1) There was clear evidence that an alternate path of Glc 6-P dissimilation existed in yeast, red cells, and other animal tissues. (2) Dickens had confirmed that 6-Pg was oxidatively decarboxylated at carbon 1, to yield pentose 5-phosphate and other sugar phosphate products including a putative tetrose-P. He also demonstrated that Rib 5-P was oxidized at 5 times the rates of arabinose 5-phosphate (Ara 5-P) and xylose 5-P (theoretical products of 6-Pg decarboxylation). (3) Finally, as early as 1938, Zacharias Dische, using red cell lysates, found that inosine and inorganic phosphate (P_i) were converted to triose and hexose phosphates. This last important finding of the possible end products of Rib 5-P dissimilation was confirmed in 1946 by Schlenk and Waldvogel, who showed Glc 6-P formation from Rib 5-P using rat liver extracts.

Post Second World War Discoveries of Reactions in the Nonoxidative Segment of the Pentose Pathway

With the above background, between 1950 and 1955, very significant discoveries of enzyme and substrate reactivities followed, which were incorporated into a reaction scheme (mechanism) for the "classical" nonoxidative PP (Figure 2). The diagram in the figure is also designated the F-type (for fat-cell) PP, because it was later shown to uniquely measure a quantitatively large contribution to metabolism when Glc was converted to fatty acid and triglyceride in insulin-stimulated adipocytes. The findings may be summarized in the following temporal conjunction. In 1951 Cohen's group showed that Rib 5-P and Ara 5-P were formed from 6-Pg oxidation. Horecker and his collaborators confirmed Rib 5-P formation and unequivocally established that Ru 5-P was the first pentose-P formed from 6-Pg decarboxylation. They also identified a new enzyme, ribose 5-phosphate isomerase, which catalyzed the interconversion of the two pentose phosphates (see Figure 2). In 1952, Horecker and Smyrniotis, using a liver enzyme preparation, reported the important observation that Rib 5-P was metabolized to sedoheptulose 7-phosphate (Seh 7-P). This seven-carbon ketosugar ester was also found by Andy Benson, in Calvin's laboratory, and was identified as an early product of PS carbon fixation. Seh 7-P was formed by the action of transketolase (TK) (see Figure 2). TK was discovered by Racker and his collaborators in 1951, and it was demonstrated that it catalyzed the transfer of a two-carbon fragment (an active glycolaldehyde group) from appropriately structured ketulose-sugar donors to a wide selection of aldo-sugar acceptors. Two of its donor transfer actions, using different aldo acceptors, are shown as blue rectangular panels in Figure 2. The enzyme requires Mg^{2+} and thiamine pyrophosphate to be active and the list of 15 of its glycolaldehyde acceptor substrates is tabulated. Horecker's group discovered another broad-specificity group transferring enzyme, namely, transaldolase (TA), which catalyzed the reversible transfer of a dihydroxyacetone-enzyme-bound moiety (shown as red panels in Figure 2) from Seh 7-P to glyceraldehyde 3-phosphate (Gra 3-P), thereby forming Fru 6-P and a tetrose phosphate, which was neither isolated nor identified. The availability of synthetic erythrose 4-phosphate (Ery 4-P) enabled Kornberg and Racker to demonstrate the reversal of the TA reaction (eqn. [4]), thus satisfying the reason for its specific inclusion as an intermediate in the reaction scheme of Figure 2. Ery 4-P probably only exists in exceedingly low concentrations in any tissue and to date there is no evidence that it has ever been correctly measured in, or isolated from, any preparation carrying out PP metabolism.

$$\text{Fru 6-P} + \text{Ery 4-P} \longleftrightarrow \text{Seh 7-P} + \text{Gra 3-P}. \quad [4]$$

Finally, in 1954, a third ketopentose ester, xlulose 5-phosphate (Xlu 5-P), was isolated as a product of Rib 5-P metabolism by Ashwell and Hickman. Racker showed that this new intermediate, rather than Ru 5-P, was a definitive substrate of TK. The ribulose 5-phosphate-3′-epimerase (see Figure 2) that catalyzed the formation of the ketosugar imparted the *trans*-configuration to the hydroxyl at C-3, which is the necessary stereochemical condition for substrate reactivity. The 3′-epimerase was simultaneously purified in 1956 by Stumpf and Horecker at NIH and by Dickens and Williamson in the UK (Williamson later became the lifelong collaborator of Hans

Krebs) in the UK. In summary, the above research had uncovered an array of substrates and enzymes that could possibly satisfy the minimum requirements for a new pathway that connected the product of 6-Pg decarboxylation with the formation of hexose and triose phosphates.

Finding a Reaction Sequence for the Nonoxidative Pentose Pathway

It is possible to draw various theoretical schemes that oblige the arithmetic conjunction of five carbon sugars with a summary outcome of sugar products that contain six and three carbon atoms, respectively. That variety is greatly enhanced if reactions by aldolase (Ald) are included. Aldolase occupies the same cellular compartment as the PP; it is a dihydroxyacetone 3-phosphate (DHAP) group transferring enzyme, with a catalytic capacity that is usually much greater than TK or TA (a notable exception is adipose tissue where Ald activity is low and only approximates the activity of TK and TA). Ald also has a broad substrate array of aldo-sugar phosphate acceptors, most of which are the same substrates as those involved in TK and TA reactions. (It has never been clear why the pioneering investigators of the nonoxidative PP assigned aldolase a role of catalytic "silence.")

The results of the two experiments that aimed to identify the reaction sequence (mechanism) of the PP were published by the Horecker group in 1954. Briefly, Horecker adopted a prediction-labeling technique using [1-^{14}C]- and [2,3-^{14}C]-Rib 5-P as substrates and enzyme preparations from rat liver, pea leaf, and pea root tissues to catalyze the formation of ^{14}C-labeled hexose 6-P. It was assumed that the position and degree of any ^{14}C- labeling in Glc 6-P formed from these variously labeled substrates would indicate the nature and order of the reactions involved in Fru 6-P formation (see Figure 2). The enzyme preparations were made from acetone-dried powders of the above tissues. They were therefore free of all nucleotides and thus confined the reactions to a hexose 6-P end point by preventing any possibility of its recycled return through the oxidative segment, with consequent further scrambling of a "predicting" isotope-labeling pattern. Mg^{2+} was also omitted from the reaction mixture in order to inhibit the activity of fructose bisphosphatase and thus the formation of a contaminating Fru 6-P resulting from aldolase manufactured Fru 1,6-P_2 using the triose-P products of TK-catalyzed reactions.

The experiments with liver enzyme preparation were of 17 h duration. Ribose 5-P was rapidly utilized during the initial 3 h and Seh 7-P also accumulated during this early period. Only with the slow decline in Seh 7-P at 6 h was there an increased linear production of Glc 6-P, which was harvested after 17 h and degraded carbon atom by carbon atom to produce the ^{14}C distribution pattern of the whole molecule. The results, using [1-^{14}C]-Rib 5-P as substrate showed that the Glc 6-P product was labeled with ^{14}C isotope in carbons 1 and 3 (see Figure 2) with a C-1/C-3 ratio of 3 (74% of the ^{14}C isotope in C-1 and 24% in C-3). Horecker "tentatively" proposed that the reaction scheme of Figure 2 was consistent with the above isotope distribution. Clearly the consistency is not there, because the pooled [1,3-^{14}C]-Fru 6-P formed in the TA and second TK-catalyzed reactions in Figure 2 impart a ^{14}C content in C-1 and C-3 with a ratio of 2 (twice as much in C-1 as C-3). The difference is serious and the isotope distributions cannot be reconciled with the Figure 2 reaction scheme, nor can the difference be attributed to the tedious analytical and degradative procedures, since the percentage errors in the determination of C-1 are only 2%; C-2, 2.7%; and C-3, 1% with a cumulative percentage error of 12% for the estimate of all carbons of the molecule. The results of the companion experiment conducted by Gibbs and Horecker in1954 used [2,3-^{14}C]-Rib 5-P as substrate and liver, pea root, and pea leaf enzyme preparations made from the acetone-dried powders of these tissues. The results deviated even more radically from the predictions imposed by the sequences of Figure 2 than the above data using [1-^{14}C]-Rib 5-P. It is emphasized that in the publications of these two studies, an ordered series of chemical equations for the nonoxidative PP was only "tentatively" proposed and a metabolic map was not shown. However, in 1955, Horecker authored two important and substantial reviews of carbohydrate metabolism and presented for the first time the diagram illustrating the new metabolic pathway (still with the "tentative" caveat). This illustration (Figure 2) is still the chart of the PP or pentose cycle (PC)—a pathway that has featured in textbooks of general biochemistry since 1956. It is astonishing that such a profound disagreement between practice and theory was so uncritically ignored by the general community of biochemists and glossed over by the very few who drew it to attention in the review literature. This indifference resulted in the prompt inclusion of the scheme of Figure 2 into the canon of metabolic biochemistry without further inquiry. It is also ironic that the participation of a large number of PP reactions into the path of carbon in PS added confidence and prestige to the status of the PP. However, there were two other comprehensive investigations of the mechanism of the PP, one by Joseph Katz and co-workers in 1955 using [1-^{14}C]-Rib metabolism in liver slices and the other by Howard Hiatt in 1957 using the same labeled substrate in mouse liver *in vivo*. These workers did not find ^{14}C distributions in the labeled glucose product with twice as much isotope in C-1 as C-3, but

instead found the carbons equally labeled. These independent early failures to confirm the predictions of Figure 2 were also ignored.

Other than valuable research by Patricia McLean and her collaborators at the Courtauld Institute (UK), who investigated the enzymology, endocrinology, and occurrence of PP reactions in many animal tissues, all fundamental research on the mechanism of the pathway essentially ceased in 1957 and was not taken up again for another decade. Instead the era of the quantitative measurement of pathways of carbohydrate metabolism had dawned and PP measurements featured hugely. This emphasis on quantitation is best summarized in the following statement by Harland G. Wood in 1955. "The determination of the relative role of different pathways in normal living cells is without doubt of the greatest fundamental importance to our understanding of life processes and will in the future require more attention in all fields of metabolism." Wood (Western Reserve University Medical School, Ohio) collaborated with Joseph Katz (Cedars of Lebanon Hospital, Los Angeles) over the next eight years in the development and elaborations of measurement theory for an entity denoted by H. G. Wood and later defined by Wood and Katz as the pentose cycle (PC).

The Quantitation of the Pentose Cycle: Theory and Practice

Between 1958 and 1979 a dozen elegant theoretical papers were published that provided the mathematical basis and formulas for measuring the F-type PC using ^{14}C-labeled substrates. All of these methods depended on a quantitative solution of the problem posed by the recycling of ^{14}C isotope distributions that emerge by the metabolism of the substrates [2-^{14}C]- or [3-^{14} C]-glucose in PC. Calculating the different distributions of labeled carbon to infinite cycles, for all percentage contributions of PC, is a difficult mathematical problem, which was solved by Joe Katz. Katz is not only a gifted biochemist but also an equally talented mathematician and innovative metabolic theorist. The acceptance of a PC definition imposed agreement that all ^{14}C-labeled Fru 6-P formed by the Figure 2 reaction sequence is converted to Glc 6-P and recycled again through the oxidative segment reactions. The quintessence of all measurement methods has involved the development of mathematical expressions describing the rhythmical and ordered redistributions of either carbon 2 or 3 from labeled substrate glucose, into positions 1, 2, and 3 of the hexose 6-P products for any percentage contribution of PC. Such a theoretical distribution is a unique property of the PC. Experimental data for the C-1/C-2 and C-3/C-2 ratios, that have definite limits and values imposed by Katz and Wood theory, measure the degree of redistribution of ^{14}C from the above labeled substrates into the top three carbons of the Glc 6-P product, which is isolated and analyzed for ^{14}C distribution following labeled substrate metabolism. The ratios, in their appropriate measurement equations, express the PC contribution relative to the total metabolism of glucose. The above statements cannot be qualified. They derive from the reaction sequence of Figure 2, which is the mechanistic basis for all the formulas of all the "measurement" papers. The precise values for C-1 and C-3 and the ratio of their isotopic labeling are the "identity" badge of the classically defined PC reaction sequence, which is the foundation of its theories of existence and quantitation. It was therefore intriguing to note, that notwithstanding the initial ambiguities in the establishment of the Figure 2 scheme and the failed efforts of the Katz and Hiatt experiments to support it, that no less than ten independent efforts, over nearly 30 years, have failed to find any significant level of PC in liver using the Katz and Wood method. Liver is a rich source of the enzymes of the PP and it can provide *inter alia* a ready display of the reactions of Figures 1 and 2. Thus, the failure by all measurement investigations to find an F-type PC in liver was mystifying.

The Search for a New Reaction Scheme for the Pentose Pathway

A solution to the mystery was sought in the author's laboratory, with investigations that began in 1965 at the University of New South Wales and later at the Australian National University. Work commenced with the propositions that the scheme of Figure 2 may be an erroneous interpretation of the PP and the coupling of Figures 1 and 2 reactions into a metabolic cycle (PC) was possibly ill-conceived. The following three sets of findings summarize selected aspects of progress in the unraveling of a new PP reaction sequence in liver that does significantly contribute (20–30%) to glucose metabolism.

First, the original experiment performed by Horecker in 1954 was repeated using [1-^{14}C]-Rib 5-P and exactly the same preparation of liver enzymes. However, reaction mixtures were sampled for the labeled Glc 6-P product at a series of much shorter time intervals and right up to the 17 h termination point described in the original work. The results showed a patterned assortment of label distributions in Glc 6-P, that drifted from 8 to 17 h towards the isotope composition in C-1 and C-3 that was originally reported by Horecker. Notably in this study, the C-1/C-3 ratio at 17 h, was the much-sought value of 2. Moreover, in the seven-time

samples, which commenced at 1 min, Glc 6-P was heavily labeled in C-2, C-4, and C-6, while C-1 and C-3 only began to accumulate ^{14}C-isotope after 3 h of reaction. Although this was a study *in vitro*, it is obvious that liver cells *in vivo* do not take between 3 and 17 h to elaborate a path of metabolism and that more enlightening events were being revealed by the isotope distributions in the samples analyzed between 1 and 30 min of reaction. A carbon balance analysis of all compounds in the various reaction mixtures showed that the intermediates of Figure 2 only accounted for 80% of the carbon in the Rib 5-P substrate. The compounds comprising the missing 20% were identified as sugar phosphates, mostly ketuloses (see Figure 3). They were isolated, identified, and shown to be radioactive. These keto-ester sugars were Seh 1,7-P_2, D-*manno*-Heptulose 7-P; D-*glycero*-D-*altro*-octulose 1,8-P_2(D-*g*-D-*a*-Oct); D-*glycero*-D-*ido*-octulose 1,8-P_2(D-*g*-D-*i*-Oct); and a small amount of Ara 5-P (see Figure 3). Octulose (Oct)-, mono- and bisphosphates, and Seh 1,7-P_2 were also isolated and measured in fresh liver. Figure 4 shows the structures and reactions of these sugar esters in a new and much modified reaction scheme for the PP in liver. The new intermediary compounds were easily isolated from all incubations from 30 min to 17 h. The scheme of Figure 4 shows the new PP with prediction ^{14}C-labeling patterns in the intermediates and products of the reactions. The reaction scheme for Figure 4 was initially formulated from the distributions of ^{14}C in the labeled Glc 6-P and D-*g*-D-*i*-Oct 1,8-P_2 formed from [1-^{14}C]-Rib 5-P during the early intervals of the repeat experiment performed by Horecker and co-workers in 1954. The new pathway, called L (liver)-type PP, is distinguished from depictions of the classical F-type PP by the inclusions of Seh-1,7-P_2 and octulose (Oct)-, mono-, and bisphosphates together with Ara 5-P as new intermediates. Aldolase, phosphotransferase (PT), and arabinosephosphate isomerase are new enzymes. Mass transfer catalysis by TA was omitted, but the effects of active TA-exchange reactions (TA_X), which accounted for the 4,6-^{14}C labeling of Glc 6-P, were encountered in all samples. The second TK reaction forming hexose 6-P products in the L-type PP (Figure 4) used D-*g*-D-*i*-Oct 8-P as a substrate and TK was also found to catalyze very active exchange reactions as does aldolase. A clear demonstration that aldolase is a mandatory catalyst in liver PP involved the immunochemical evidence of Bleakly and co-workers in 1984, who showed the cessation of all hexose 6-P formation when liver aldolase antibody titrated the removal of aldolase from the system where Rib 5-P was reacted with the rat liver enzyme preparation that was used to establish the scheme in Figure 2. Irrespective of the other contrary data, this evidence alone showed that there was another reaction mechanism involving Ald in liver PP. The claim that aldolase is an essential enzyme in the PP was also supported by data of Cori and Racker, who, in an *in vitro* "construction" of a PP preparation for the complete oxidation of Glc, noted the formation of Oct-P and the need to include aldolase and sedoheptulose 1,7-bisphosphatase for the construction system to work.

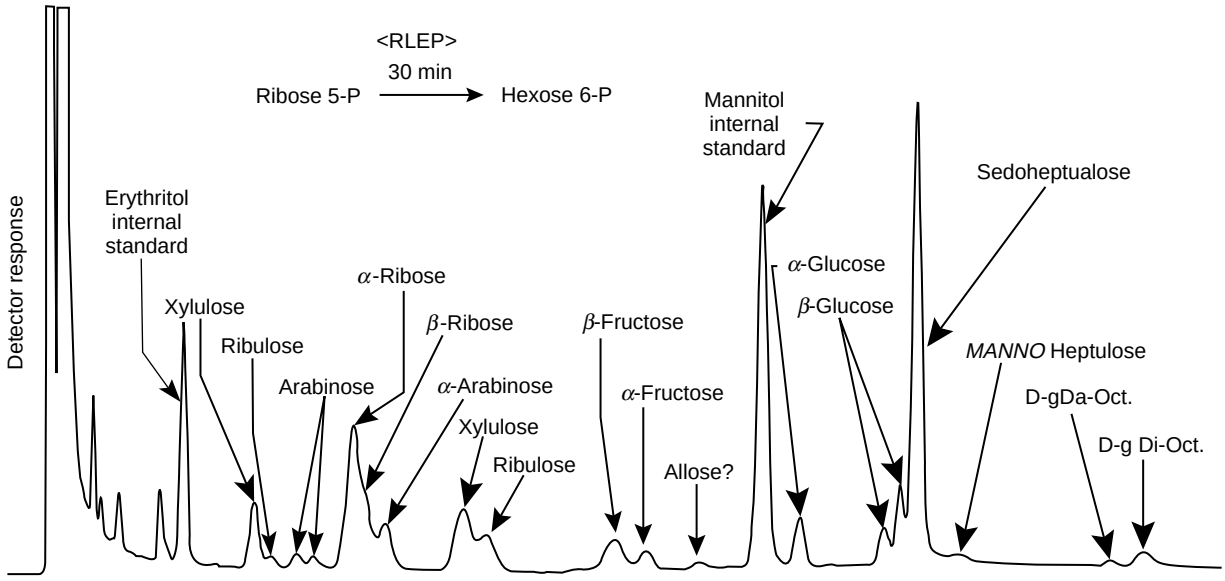

FIGURE 3 Gas liquid chromatogram (GLC) of the dephosphorylated derivatized sugars formed after 30 min reaction of rat liver enzyme preparation with ribose 5-phosphate. The procedures for sample processing and GLC are given in Williams, J. F., Clark, M. G., Arora, K. K., and Reichstein, I. C. (1984) Glucose 6-phosphate formation by L-type pentose pathway reactions of rat liver in vitro: Further evidence. *Seyler's Zeit. Physiol. Chem.* **365**, 1425–1434.

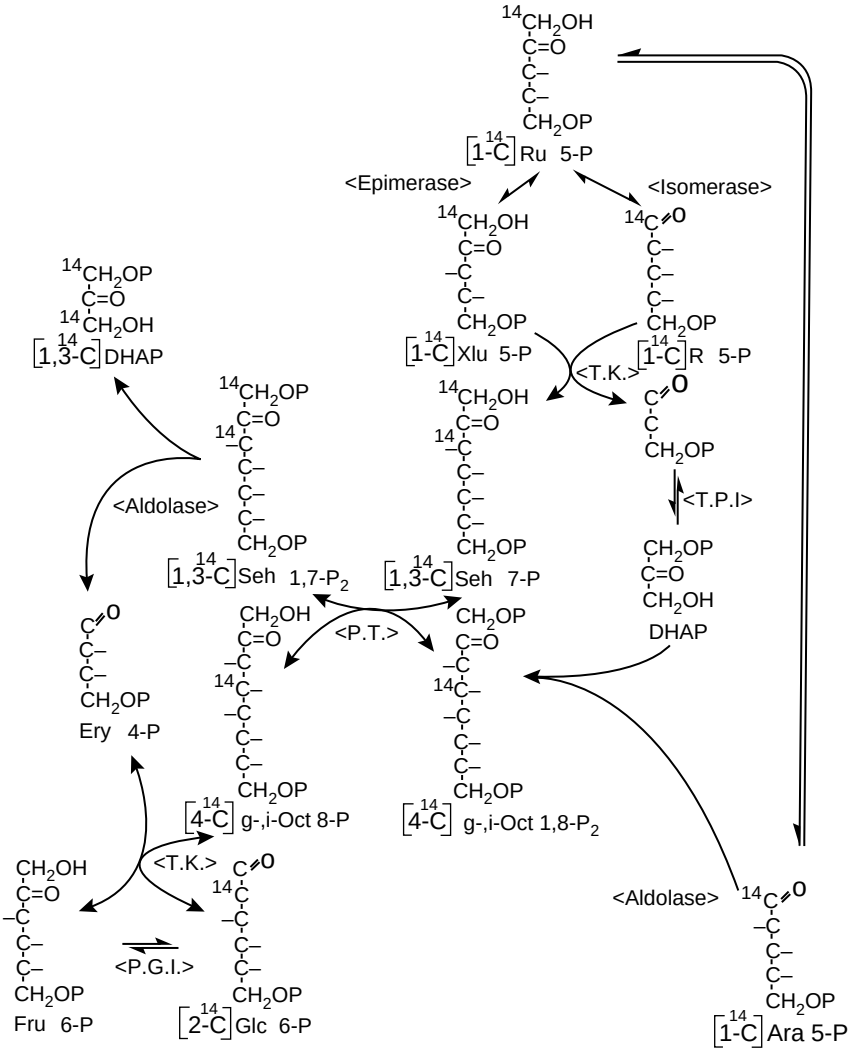

FIGURE 4 The proposed reaction sequence of the nonoxidative segment of the L-type pentose pathway. The [1-^{14}C]-ribulose 5-P substrate is the labeled product of the Figure 1 scheme and the reactions display the theoretical and the found distributions of ^{14}C-isotope from pentose 5-P substrate into labeled Glc, triose and Oct intermediates, and products. The epimerase, isomerase, and TK enzymes are the same catalysts that operate in the F-type pathway. New enzymes are arabinosephosphate isomerase that interconverts arabinose and ribulose 5-phosphates, aldolase, triosephosphate isomerase (EC 5.3.1.1), glucosephosphate isomerase and D-*glycero*-D-*ido*-octulose 1,8-bisphosphate: D-*altro*-Heptulose 7-phosphotransferase, called phosphotransferase (PT) (see Arora, K. K., Cortis, P. A., Bleakley, P. A., and Williams, J. F. (1985) Identification and measurement of D-glycero-D-ido-octulose 1,8-bisphosphate: D-altro heptulose 7-phosphotransferase enzyme in tissues with L-type pentose phosphate pathway activity. *Int. J. Biochem.* **17**, 1329–1337). Besides new enzymes and intermediates, the L-type pathway is distinguished from the F-type pathway by the formation of Glc 6-P labeled in the 2 position by flux and in positions 4 and 6 by group-transfer enzyme exchanges involving the [1,3 ^{14}C]-DHAP product. The triosephosphate formed by the F-type pathway is unlabeled.

Exposing the Problem of Assigning a Reaction Scheme to the Nonoxidative PP

The reactions and enzymes shown in Figure 4 occur in liver cytoplasm and probably in the soluble enzyme compartments of the tissues of most animals (exceptions are adipocytes and possibly lactating mammary gland), plants, and some microorganisms. The failure to uncover "uncontentious" evidence for both F- and L-pathways that permitted the placement of C-3 to C-8 glycolyl phosphates in a reaction order and with stoichiometry that satisfied flux demands of a metabolic pathway or cycle, is the crux of this 50-year-old enigma. Finding an answer to the problem proved to be quick, obvious, and simple. Uncovering irrefutable evidence and proof for the explanation was a more pressing task that was solved by Flanigan *et al.* in 1993. It was the universal use of ^{14}C isotopes in prediction-labeling experiments to both inquire into mechanism and predicate theories for quantifying the F- and L-type

pathways, which was the first fundamental error. The second misjudgment was lack of attention to the consequences of the glycolyl-group exchange reactions that are actively catalyzed by TK_x, TA_x, and Ald_x. The subscript x is used to distinguish exchange catalysis from the mass transfer activity of these enzymes. Moreover, there was an inchoate recognition and warning that both functions were simultaneously active during the unique catalytic roles of these enzymes in PP and PS. The qualitative and partial definition of TK_x and TA_x by Katz and Wood proved to be an insufficient and largely unheeded alarm to the PC measurers.

Flanigan and co-workers used ^{13}C-NMR spectroscopy for their investigations, thus bypassing any controversy concerning results that depended on "wet" chemical methods for the determination of ^{14}C labeling patterns. The maximum catalytic capacities for exchange by the three enzymes were all quantified in reaction mixtures at mass-transfer equilibrium, by measuring, for TA, the rate of exchange of the ^{13}C-TA dihydroxyacetone group with unlabeled Seh 7-P. TK_x was measured by the rate of incorporation of a (2-^{13}C)-TK glycolaldehyde group to unlabeled Fru 6-P and Ald_x by the exchange of an unlabeled DHAP-Ald group from D-*g*-D-*a*-Oct 1,8-P_2 to [1-^{13}C]-Rib 5-P and measurement of the rate of formation of [4-^{13}C]-D-*g*-D-*a*-Oct 1,8-P_2. A comparison of the exchange capacities of these enzymes with the maximum nonoxidative PP flux rates in three liver preparations showed that TK_x and Ald_x exceeded flux by 9–19 times in liver cytosol and acetone-powder enzyme preparations *in vitro* and by 5 in hepatocytes. TA_x was less effective in exchange, only exceeding the flux rate by 1.6 and 5 in liver cytosol and acetone-powder preparations. Values for the ratios of the rates of group exchange and pathway flux are important because of the feature roles of liver and of these preparations in the establishment and status of the schemes of Figures 2 and 4 in biochemistry. The prevalence of exchange activity was also investigated using the dominant TK_x rates relative to the max PP flux rates of normal and regenerating liver, Morris hepatoma, mammary carcinoma, melanoma, colonic epithelium, spinach chloroplasts, and epididymal adipocytes. TK_x rates in these preparations exceeded PP flux by 5–600 times.

Conclusion

It is the conclusion of this brief history that sufficient evidence is on record to show that predictions and calculations based on ^{14}C-distributions in PP products and intermediates are misleading. The isotope patterns cannot reveal the order of the reaction sequences, which can only be measured by an uncompromised net flow of carbon. Instead, the ^{14}C-distributions mainly reflect a composition of disorder, induced by random combinations of group exchanges that scramble, if not obliterate, flux influences. Thus, the description and metabolic map of PP is "in error" in biochemical texts.

How Should We Now View the PP—With or Without Conceptual Structures?

The reactions of Figure 1 are not in contention. The enzymes and intermediates of Figures 2 and 4 are probably present in most tissues, particularly where Ald activity is greater than that of TA. There is, however, no secure evidence that the individual reactions of either Figure 1 or 2 are so linked that they constitute a linear metabolic pathway with ordered reactant and end-product stoichiometry or fixed direction of operational flux. Nor is there uncontentious proof that the PP generally operates as a metabolic cycle. The reaction array is best perceived now as it was in 1958, when the late Prof. Merton Utter (Western Reserve University School of Medicine) so suggested limiting these reactions to an unstructured pool or reservoir of glycolyl phosphates, with as many accessible inputs and exits as there are intermediates in Figures 2 and 4. This includes hexose and triose phosphates that may react reversibly to form or be formed from pentose phosphates by mass action effects and in the process mix with all of the other glycolyl phosphates, which are not constrained by stoichiometric obligation to "connecting" reaction sequences, and which may be freely removed by the needs of other metabolism.

See Also the Following Articles

Pentose Phosphate (Hexose Mono Phosphate) Pathway • Sugar Nucleotide Transporters

Glossary

metabolic pathway A linear sequential order of consecutive enzymatic reactions that proceed from a flux-generating step. The pentose pathway (PP) consists of a set of freely diffusible soluble enzymes, coenzymes, and reactants.

non-oxidative PP (Figures 2 and 4) has the sum reaction of Eqn 1

$$3 \text{ Pentose 5-P} \longleftrightarrow 2 \text{ Fructose 6-P} + 1 \text{ Glyceraldehyde 3-P}. \quad [5]$$

oxidative segment of PP This segment is assigned the stoichiometry of eqn. [6] because of its link with the reactions of Figures 2 and 4.

$$3 \text{ Glc 6-P} + 6 \text{ NADP}^+ \longrightarrow 3 \text{ CO}_2 + 3 \text{ pentose 5-P} + 6 \text{ NADPH} + 6\text{H}^+. \quad [6]$$

pentose cycle (PC) This cycle is a theoretical construct, based on the reactions of Figure 2 for F-type PC and Figure 4 for L-type PC and

the reaction of eqn. [7]. The PC mechanisms permit mathematical treatment of theoretical ^{14}C distributions, generated by a conforming metabolism of labeled glucose, which leads to specific formulae for quantifying the two varieties of PC. The sum of eqns. [5], [6], and [7] is [8], which is the sum reaction of both F-type and L-type PC.

$$2\ \text{Fructose 6-P} \xleftrightarrow{\text{Glucosephosphate isomerase (EC 5.3.1.9)}} 2\ \text{Glucose 6-P}, \qquad [7]$$

$$\text{Glucose 6-P} + 6\ \text{NADP}^+ \longrightarrow 3\ \text{CO}_2 + \text{Gra 3-P} + 6\ \text{NADPH} + 6\ \text{H}^+. \qquad [8]$$

Further Reading

Arora, K. K., Cortis, P. A., Bleakley, P. A., and Williams, J. F. (1985). Identification and measurement of D-glycero-D-ido-octulose 1,8-bisphosphate: D-altro heptulose 7-phosphotransferase enzyme in tissues with L-type pentose phosphate pathway activity. *Int. J. Biochem.* **17**, 1329–1337.

Flanigan, I. L., Grant-Collins, J., Arora, K. K., MacLeod, J. K., and Williams, J. F. (1993). Exchange reactions catalyzed by group transferring enzymes oppose the quantitation and the unravelling of the identity of the pentose pathway. *European J. Biochem.* **213**, 477–485.

Florkin, M. (1979). The pentose phosphate cycle. In *Comprehensive Biochemistry* (M. Florkin and E. H. Stotz, eds.) Vol 33A, Part V, pp. 61–79. Elsevier/North-Holland Biomedical Press, Amsterdam.

Gumma, K. A., and McLean, P. (1971). Factors controlling the flux of glucose through the pentose phosphate pathway. *Post Grad. Med. J.* (June supplement), 403–406.

Horecker, B. L. (1961). Alternative pathways of carbohydrate metabolism in relation to evolutionary development. In *Proc. 5th Int. Congress of Biochemistry*, Vol 111, pp. 86–93. Moscow Pergamon Press, Oxford.

Horecker, B. L. (1982). Cytochrome reductase, the pentose phosphate pathway and Schiff base mechanisms. In *Oxygen, Fuels and Living Matter* (G. Smenza, ed.) Part 2, pp. 59–75. Wiley, Chichester.

Horecker, B. L. (2002). The pentose phosphate pathway. *J. Biol. Chem.* **277**, 47965–47971.

Katz, J. (1961). The use of glucose-^{14}C in the study of the pathways of glucose metabolism in mammalian tissues. In *Radioactive Isotopes in Physiology, Diagnostics and Therapy* (H. Schweigk and F. Turba, eds.) pp. 705–751. Springer, Berlin.

Longnecker, J. P., and Williams, J. F. (1980). Quantitative measurement of the L-type pentose phosphate cycle with [2-14C]-glucose and [5-14C]-glucose in isolated hepatocytes. *Biochem. J.* **188**, 859–865.

Novello, F., and McLean, P. (1968). The pentose phosphate pathway of glucose metabolism: Measurement of the non-oxidative reactions of the cycle. *Biochem. J.* **107**, 775–791.

Utter, M. F. (1958). Carbohydrate metabolism. *Ann. Rev. Biochem.* **27**, 245–284.

Williams, J. F., Clark, M. G., Arora, K. K., and Reichstein, I. C. (1984). Glucose 6-phosphate formation by L-type pentose pathway reactions of rat liver in vitro: Further evidence. *Seyler's Zeit. Physiol. Chem.* **365**, 1425–1434.

Williams, J. F., Arora, K. K., and Longnecker, J. P. (1987). The pentose pathway: a random harvest. Impediments which oppose acceptance of the classical (F-type) pentose cycle for liver, some neoplasms and photosynthetic tissue. The case for the L-type pentose pathway. *Int. J. Biochem.* **19**, 749–817.

Wood, T. (1985). *The Pentose Phosphate Pathway.* Academic Press, Orlando, FL.

Wood, H. G., and Katz, J. (1958). The distribution of 14C in the hexose phosphates and the effect of recycling in the pentose cycle. *J. Biol. Chem.* **233**, 1279–1282.

Biography

John F. Williams is Professor Emeritus and a former Professor and Head of Biochemistry in the faculties at the Australian National University, Canberra. He was a Research Fellow at Merton College, Oxford and is presently Visiting Fellow in The Research School of Chemistry at ANU. His principal research interests are in intermediary metabolism. He holds a Ph.D. from the University of New South Wales and D.Sc. from the ANU, and he received postdoctoral training at Western Reserve University School of Medicine.

Peptide Amidation

Mark J. Niciu, Richard E. Mains and Betty A. Eipper
The University of Connecticut Health Center, Farmington, Connecticut, USA

Generation of a C-terminal α-amide group on a peptide occurs by hydroxylation and cleavage of a C-terminal glycine residue and is a prevalent posttranslational modification essential for the production of many of the peptides that serve as hormones and neurotransmitters. Approximately half of all bioactive peptides are α-amidated, including gonadotropin-releasing hormone (GnRH), corticotropin-releasing hormone (CRH), thyrotropin-releasing hormone (TRH), oxytocin, vasopressin, calcitonin, gastrin, cholecystokinin (CCK), neuropeptide Y (NPY), substance P and pituitary adenylate cyclase-activating polypeptide (PACAP). The α-amide group prevents ionization of the C terminus, which may increase receptor binding, hydrophobicity and/or half-life. In vertebrates, C-terminal α-amidation is accomplished via the activity of peptidylglycine α-amidating monooxygenase (PAM), a bifunctional enzyme localized to large dense core vesicles in neuroendocrine tissues.

Biochemistry and Enzymology of PAM

PAM is composed of two protease-resistant catalytic cores targeted to the lumenal compartment of secretory granules, peptidylglycine α-hydroxylating monooxygenase (PHM; EC 1.14.17.3) and peptidyl-α-hydroxyglycine α-amidating lyase (PAL; EC 4.3.2.5). PHM catalyzes the stereospecific α-hydroxylation of all C-terminally glycine-extended peptide substrates. PAL then catalyzes cleavage of the N–C bond of the α-hydroxylglycine, generating the α-amidated peptide product and glyoxylate (Figure 1).

PAM Structure

Bifunctional PAM is a type I integral membrane protein whose structure is highly conserved in vertebrate phylogeny. From N to C terminus, it contains a signal sequence, proregion, PHM catalytic core, noncatalytic spacer region (exon A), PAL catalytic core, transmembrane domain and cytosolic domain. The hydrophobic signal sequence is cleaved cotranslationally in the endoplasmic reticulum; the prosequence is removed in a post*trans*-Golgi network compartment. Tissue-specific endoproteolytic cleavage at pairs of basic amino acids can remove the pro-region, separate the two catalytic domains, and release the catalytic domains from the transmembrane domain. Poorly conserved linker regions follow both catalytic domains and are susceptible to cleavage by exogenous proteases. Additionally, alternative splicing can generate soluble, monofunctional PHM or soluble, bifunctional PAM. Soluble PAM proteins are secreted with their amidated product peptides while integral membrane PAM proteins undergo endocytosis, guided by routing determinants and phosphorylation at multiple sites in the cytosolic domain (Figure 2).

PAM Substrates

Virtually any peptide with a C-terminal glycine residue can serve as a PAM substrate. PAM generates α-amides of all 20 amino acids. In addition, PAM catalyzes the amidation of nonpeptidergic substrates such as fatty acyl glycines, glutathione, the aspirin metabolite salicylurate, bile acid glycine conjugates and leukotriene C_4. In addition to stereospecific α-hydroxylation of glycine-extended precursors, purified PHM can also catalyze N-dealkylation, O-dealkylation, and sulfoxidation of nonpeptidergic substrates.

Peptidylglycine α-hydroxylating Monooxygenase – PHM

Essential Cofactors

PHM requires the presence of molecular oxygen, a single electron donor (generally ascorbic acid or vitamin C), and copper.

Ascorbic Acid (Vitamin C) Ascorbate is transported across the plasma membrane via a Na^+-dependent transporter enriched in neuroendocrine tissue, SVCT2. How cytosolic ascorbate reaches the lumen of the secretory pathway is currently unclear. Nevertheless, concentrations of ascorbate are five to tenfold higher in the lumen of the secretory pathway than in the cytosol. The mM concentrations of ascorbate in the

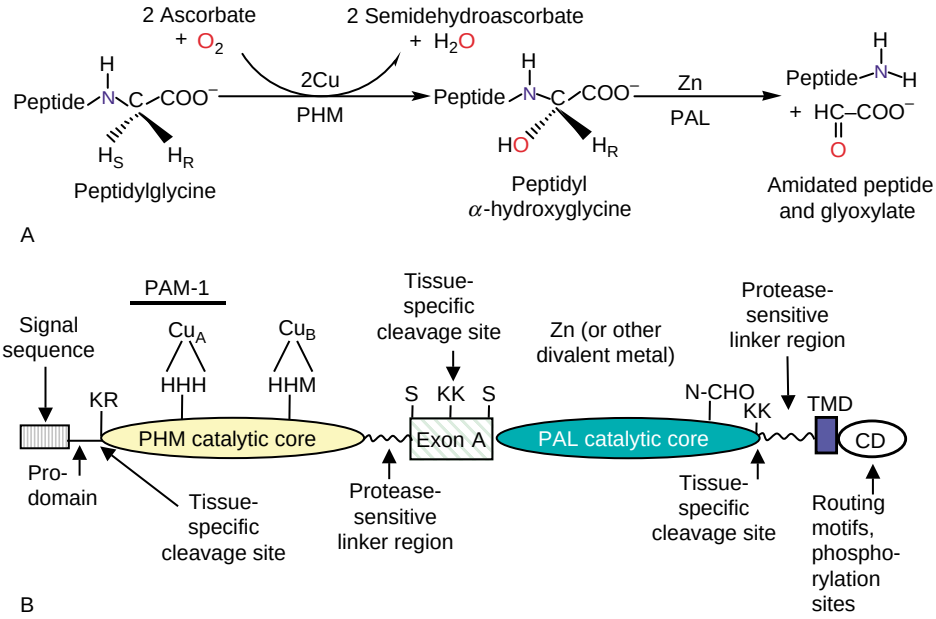

FIGURE 1 PAM reaction and structure. (A) Bifunctional PAM-catalyzed conversion of glycine-extended precursor into hydroxyglycine intermediate and amidated product plus glyoxylate. (B) Domains of integral membrane PAM-1 with salient features: KR and KK lysine-arginine and lysine-lysine dibasic cleavage sites; H, copper-binding histidine; M, copper-binding methionine; N-CHO, N-linked glycosylation site; TMD, transmembrane domain; CD, cytosolic domain; P, phosphorylation sites.

lumenal compartment ensure that lumenal copper is reduced, as required for the enzymatic cleavage of molecular oxygen by PHM. In this oxidation–reduction reaction, PHM converts 2 mol of ascorbate into 2 mol of semidehydroascorbate, which disproportionate to form dehydroascorbate and ascorbate. Other single-electron reductants can substitute for ascorbate to provide reducing equivalents for Cu^{2+}; consistent with this, no ascorbate-specific binding site has been identified on PHM.

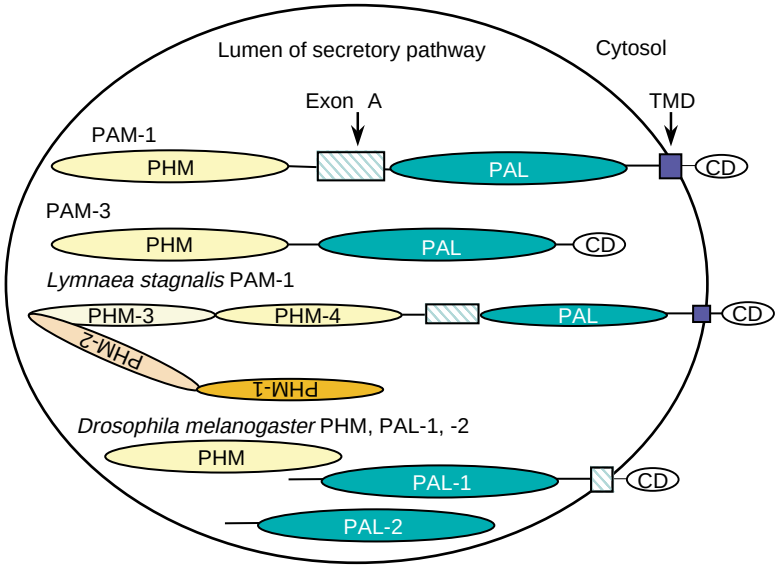

FIGURE 2 PAM in secretory granules. Soluble and membrane PAM isoforms from rat, pond snail and fruit fly in mature secretory granule. Alternative mRNA splicing at "hot spots" generates soluble PAM-3, which lacks exon A and the TMD; it is secreted with the amidated product. *Lymnaea stagnalis* membrane PAM contains four functional PHM domains and an exon A-like linker sequence. *Drosophila* PHM and PAL-1/-2 are encoded on separate genes. PAL-1 is a soluble protein and may be secreted with processed peptide. PAL-2 contains a transmembrane domain and may be recycled via endocytosis to post-Golgi complex compartments.

Copper Copper is required in trace amounts by a limited group of cuproenzymes. However, in excess, copper can support the Fenton reaction, generating reactive oxygen species, that attack cellular constituents with diffusion-limited kinetics. To avoid this problem, copper transporters and copper chaperones deliver this critical metal to these cuproenzymes while preventing toxic intracellular actions. The transport of Cu^{1+} across the plasma membrane requires Ctr1 in mammals. Atox1, a cytosolic copper chaperone, delivers Cu^{1+} to ATP7A and ATP7B, homologous P-type ATPases that pump Cu^{1+} into the lumen of the secretory pathway, where it can be loaded onto lumenal cuproproteins or excreted from the cell.

Structure and Reaction Mechanism

PHM binds two moles of copper, each of which plays a distinct role in the α-hydroxylation reaction. Composed almost entirely of β strands, the catalytic core of PHM consists of two structurally homologous domains (Figure 3). Mutagenesis and phylogenetic comparisons identify a limited number of conserved residues. The copper binding sites are conserved: 3 histidine residues in the N-terminal half of PHM bind Cu_A and two histidines plus one methionine residue in the C-terminal half bind Cu_B. Although reducing equivalents donated by both Cu_A and Cu_B are essential to the reaction, the two Cu ions are separated by a 10Å solvent filled cleft.

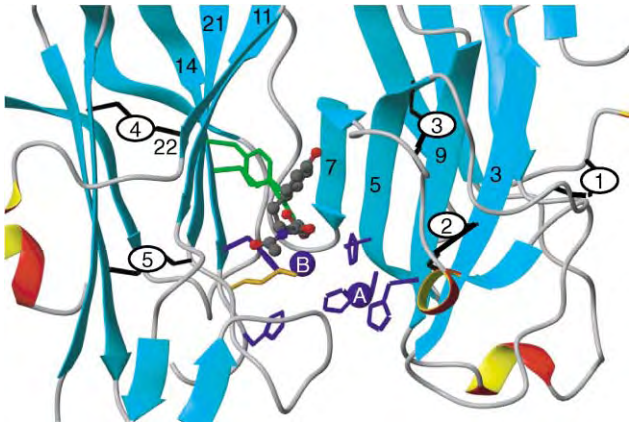

FIGURE 3 PHM active site. The structure determined by crystallization of oxidized PHMcc with its Ac-diiodo-Tyr-Gly substrate is shown to illustrate the structural role played by the disulfide bonds (Prigge, S. T., Mains, R. E., Eipper, B. A., and Amzel, L. M. (2000). New insights into copper monooxygenases and peptide amidation: Structure, mechanism and function. *Cell Mol. Life Sci.* 57, 1236–1259). Histidine ligands to Cu_A and Cu_B are blue; the methionine ligand to Cu_B is gold; substrate binding residues are green; the substrate is shown in ball and stick format. The disulfide bonds in PHM are numbered (except for bond 1, they are totally conserved): 1, Cys^{47}-Cys^{186}; 2, Cys^{81}-Cys^{126}, links β3 to the β5-β6 loop; 3, Cys^{114}-Cys^{131}, links β5 to the β6-β7 loop; 4, Cys^{227}-Cys^{334}, links β13 to β22; 5, Cys^{293}-Cys^{315}, links β19 to β21.

The glycine-extended peptide substrate binds in a conserved, hydrophobic substrate-binding pocket located near Cu_B, placing the α-carbon of the glycine adjacent to molecular oxygen bound to Cu_B with the C terminus of the glycine residue salt bridged to a conserved arginine residue. Several hydrophobic residues near the active site are conserved, along with proline and glycine residues that define the loop regions. The molecular oxygen consumed in the reaction binds only to the enzyme/peptidylglycine complex, and it is not yet clear how electron transfer is accomplished. The reaction is tightly coupled, with little generation of reactive oxygen species, and the two copper ions do not move much closer to each other during catalysis.

Pharmacological Inhibition

Disulfiram, used clinically in the treatment of chronic alcoholism, inhibits PHM activity *in vivo* via its ability to chelate copper. When assayed *in vitro*, after the addition of exogenous copper, the catalytic core of rat PHM displays paradoxically enhanced activity after *in vivo* disulfiram administration. A mechanism-based inhibitor of PHM, trans-styrylacetic acid (phenylbutenoic acid), has also been identified.

Peptidyl-α-Hydroxylglycine α-Amidating Lyase

Limited trypsin digestion and analysis of peptidyl-α-hydroxylglycine α-amidating lyase (PAL) truncation mutants revealed a stable catalytic core with no subdomains. The single N-linked glycosylation site near the COOH terminus of PAL is utilized, although glycosylation is without effect on the catalytic activity of PAL. When treated with divalent metal ion chelators, PAL activity was reduced and its thermal and protease resistance were decreased, suggesting both structural and catalytic roles for divalent metal ions. Approximately 0.7 mol of zinc is bound per mole of enzyme. The four cysteine residues in PAL form disulfide bonds, and conserved histidine, aspartate and glutamate residues are involved in binding zinc, playing both structural and catalytic roles. No reliable mechanism-based small molecule inhibitors of PAL have been characterized. The reaction catalyzed by PAL is most similar to the reaction catalyzed by ureidoglycolate lyase.

Evolutionary Relationships

The process of peptide amidation is highly conserved. In invertebrates like *Drosophila melanogaster* and *Caenorhabditis elegans*, PHM and PAL are encoded by separate genes; a single PHM gene may be accompanied by more than one PAL gene. PHM and PAL homologues

are not found in the genome of *Saccharomyces cerevisiae*. Intriguingly, *Lymnaea stagnalis*, a molluscan pond snail, expresses a huge membrane PAM with four independent, catalytically active PHM domains followed by a single PAL domain. *Schistosoma mansoni*, a nematode and potent human pathogen, expresses a heavily glycosylated, soluble PHM with atypical catalytic features. The copper binding ligands, substrate binding site, disulfide bonds, and selected glycine and proline residues of PHM are conserved across species.

The cofactor requirements of PHM suggest homology to another copper, ascorbate and dioxygen-requiring enzyme, dopamine-β-monooxygenase (DBM; EC 1.14.17.1). DBM converts dopamine to norephinephrine in selected neurons and adrenal chromaffin cells. The catalytic core of PHM is 32% identical to a 291 amino acid stretch in DBM. The Cu_A and Cu_B-binding motifs and disulfide-bonding patterns of PHM are conserved in DBM. *Cnidarians*, such as the sea anemone and *Hydra*, use amidated peptides, not catecholamines like norephinephrine for neural transmission, suggesting that PHM is the more ancestral enzyme. cDNA library screening of human senescent fibroblasts revealed the presence of a third sequence with significant homology to PHM, monooxygenase X (MOX; X13255). No substrates or hydroxylated products have yet been identified for this putative monooxygenase.

PAM Expression

PAM expression is most prevalent in heart atria, the pituitary gland, and peptide-producing neurons of the central and enteric nervous systems. Nevertheless, PAM expression is widespread, as transcripts can be detected in airway and olfactory epithelia, smooth muscle cells, endothelium, brain ependymal cells, astrocytes, and fibroblasts.

During development, PAM is first detected immunohistochemically at embryonic day 9 (E9) in the putative cardiogenic region and at E13 in peptide-producing neurons. PAM is also highly expressed in limb mesoderm and mesenchyme flanking the nasal, maxillary, palatal and dental epithelia during embryonic tissue fusion and remodeling. Most *Drosophila* PHM knockout flies die as young larvae, during the molting process, with malformation of the mouth hooks. A role for PAM in these areas during development is not yet clear.

PAM Molecular Genetics

The human *PAM* gene is located on chromosome 5q14-21 and the mouse *Pam* gene is on chromosome 1. The rat PAM gene contains at least twenty-eight exons encompassing >160 kB. At least two putative promoters upstream of the translational start site and proregion in exon two have been identified. PHM is encoded by exons three to fourteen (excluding exon thirteen). The alternately spliced non-catalytic region between PHM and PAL is encoded by exon sixteen, which is bordered by at least forty kB of intronic sequence. PAL is encoded by exons seventeen to twenty-four. Most of the intron/exon junctions in rat, which preferentially produce bifunctional PAM mRNA transcripts, and *D. melanogaster*, which contains separate PHM and PAL genes, are conserved. Interestingly, rat breeding stocks vary in their alternative splicing of PAM: Harlan Sprague-Dawley rats eliminate the exon A linker in their mRNA transcripts in pituitary, while Charles River Sprague-Dawley rats retain this domain.

Dysregulated Peptide Amidation

Due to the plethora of physiological functions regulated by amidated peptides, deficits in peptide amidation have very detrimental consequences for the organism.

Overexpression of Amidated Peptides

Many amidated peptides, e.g., PACAP, NPY, and gastrin-releasing peptide (GRP), serve as autocrine or paracrine growth factors. Numerous tumors of neuroendocrine origin secrete amidated peptides that serve this function, and PAM expression is concomitantly up-regulated. Amidated peptides secreted by neuroendocrine tumors disrupt normal physiological function. For example, small cell lung carcinomas often secrete GRP, while amidated isoforms of parathyroid hormone related protein (PTHrP) sustain bone growth and produce the hypercalcemia of malignancy. Gastrin-secreting tumors ("gastrinomas") are frequently encountered in Zollinger-Ellison syndrome, which presents clinically as peptic ulceration; vasoactive intestinal polypeptide-secreting tumors ("VIPomas") of pancreatic or duodenal origin present with voluminous watery diarrhea in Verner-Morrison syndrome. Hence, pharmacological inhibition of PAM activity may be a rational therapeutic strategy in the treatment of such amidated peptide-secreting tumors.

Impaired Peptide Amidation

Based on assays of amidated product peptides, peptide amidation is impaired in the context of dietary deficiencies of ascorbate or copper, genetic deficiencies of copper-translocating proteins or targeted gene disruption of the PAM gene.

Impaired Copper Delivery

A reduction in copper delivery to the secretory pathway results in a diminished ability to produce amidated peptides. This can be the result of nutritional deficiencies of copper or ascorbate or genetic malfunctioning of copper transporters. In mammals, ATP7A receives Cu^{+} from the cytosolic chaperone Atox1 and transports it into the lumen of the secretory pathway where the catalytic cores of cuproenzymes like PHM, DBM and tyrosinase reside. Mutations in ATP7A result in the X-linked copper-deficiency disorder, Menkes disease, which presents clinically with profound neurodegeneration. The mottled brindled (Mo^{Br}) mouse, which contains a six base pair in-frame deletion in ATP7A, serves as the mouse model of Menkes disease. Although PAM protein expression is unchanged, the concentrations of amidated neuropeptides, *e.g.*, joining peptide (JP), CCK, and PACAP, are reduced in the pituitary gland and central nervous system of afflicted males relative to age-matched wild type mice.

Targeted Gene Disruption

Insertion of a P-element containing transposon within the *D. melanogaster* PHM transcriptional unit eliminated PHM expression and resulted in early larval lethality with relatively few morphological defects. Recently, PAM null mice have been created. These mice do not survive past embryonic day 14.5, with the most noticeable defect being intractable edema. No PHM or PAL enzymatic activity is detectable in homogenates of null embryos, and heterozygotes display half the wild type level of PHM and PAL activity in age-matched wild type mice. Thus PAM is the only enzyme responsible for C-terminal peptide α-amidation *in vivo*.

See Also the Following Articles

Calcitonin Gene-Related Peptide and Adrenomedullin Receptors • Inorganic Biochemistry • Neuropeptide Y Receptors • P-Type Pumps: Copper Pump • Vasopressin/Oxytocin Receptor Family • Vitamin C

Glossary

large dense core vesicles/secretory granules Membrane-enclosed 300–500 nm diameter peptide-containing storage organelles formed from the *trans*-Golgi network in neuroendocrine cells.

P-type ATPase A family of pumps whose members use the energy of ATP to transport cations uphill across membranes, undergoing a cycle of phosphorylation and dephosphorylation.

type I integral membrane protein A protein that crosses a phosopholipid bilayer once, with its N-terminus projecting into the extracellular environment/lumen of the secretory pathway and a cytosolic C terminus.

Further Reading

Francisco, W. A., Blackburn, N. J., and Klinman, J. P. (2003). Oxygen and hydrogen isotope effects in an active site tyrosine to phenylalanine mutant of peptidylglycine alpha-hydroxylating monooxygenase: Mechanistic implications. *Biochemistry* **42**, 1813–1819.

Iwai, N., Martinez, A., Miller, M.-J., Vos, M., Mulshine, J. L., and Treston, A. M. (1999). Autocrine growth factor loops dependent on peptidyl alpha-amidating enzyme as targets for novel tumor cell growth inhibitors. *Lung Cancer* **23**, 209–222.

Jiang, N., Kolhekar, A. S., Jacobs, P. S., Mains, R. E., Eipper, B. A., and Taghert, P. H. (2000). PHM is required for normal developmental transitions and for biosynthesis of secretory peptides in *Drosophila*. *Develop. Biol.* **226**, 118–136.

Katopodis, A. G., and May, S. W. (1990). Novel substrates and inhibitors of peptidylglycine alpha-amidating monooxygenase. *Biochemistry* **29**, 4541–4548.

Kolhekar, A. S., Bell, J., Shiozaki, E. N., Jin, L., Keutmann, H. T., Hand, T. A., Mains, R. E., and Eipper, B. A. (2002). Essential features of the catalytic core of peptidyl-alpha-hydroxyglycine alpha-amidating lyase. *Biochemistry* **41**, 12384–12394.

Liang, W. J., Johnson, D., and Jarvis, S. M. (2001). Vitamin C transport systems of mammalian cells. *Mol. Membr. Biol.* **18**, 87–95.

Miller, L. A., Baumgart, L. E., Chew, G. H., deLong, M. A., Galloway, L. C., Jung, K. W., Merkler, K. A., Nagle, A. S., Poore, D. D., Yoon, C. H., and Merkler, D. J. (2003). Glutathione, S-substituted glutathiones, and leukotriene C_4 as substrates for peptidylglycine alpha-amidating monooxygenase. *Arch. Biochem. Biophys.* **412**, 3–12.

Prigge, S. T., Mains, R. E., Eipper, B. A., and Amzel, L. M. (2000). New insights into copper monooxygenases and peptide amidation: Structure, mechanism and function. *Cell Mol. Life Sci.* **57**, 1236–1259.

Puig, S., and Thiele, D. J. (2002). Molecular mechanisms of copper uptake and distribution. *Curr. Opin. Chem. Biol.* **6**, 171–180.

Rhames, F. C., Murthy, N. N., Karlin, K. D., and Blackburn, N. J. (2001). Isocyanide binding to the copper(I) centers of the catalytic core of peptidylglycine monooxygenase (PHMcc). *J. Biol. Inorg. Chem.* **6**, 567–577.

Steveson, T. C., Ciccotosto, G. C., Ma, X.-M., Mueller, G. P., Mains, R. E., and Eipper, B. A. (2003). Menkes protein contributes to the function of peptidylglycine alpha-amidating monooxygenase. *Endocrinology* **144**, 188–200.

Biography

Mark Niciu is an M.D.-Ph.D. student and Betty Eipper and Richard Mains are Professors in the Neuroscience Department at the University of Connecticut Health Center in Farmington, CT.

Drs. Eipper and Mains received their Ph.D. from Harvard University and were postdoctoral fellows with Dr. Ed Herbert at the University of Oregon. They developed an interest in peptide amidation when they observed that pituitary cells maintained in serum-free medium failed to amidate the products of proopiomelanocortin processing. Subsequent cloning and characterization of PAM identified ascorbate as the missing factor.

Periplasmic Electron Transport Systems in Bacteria

David J. Richardson
University of East Anglia, Norwich, UK

Gary Sawers
John Innes Centre, Norwich, UK

Rob J.M. Van Spanning
Free University of Amsterdam, The Netherlands

The periplasmic compartment lies between the inner (cytoplasmic) and outer membranes of Gram-negative bacteria. It is frequently termed the "periplasmic space," but this is a misnomer as the term "space" suggests a void and the periplasmic compartment is far from that. In fact, it is a highly metabolically active compartment where many important respiratory electron transfer proteins are located. In bacteria these periplasmic redox proteins result in a great respiratory diversity, as they can facilitate electron transfer between a range of electron donors (e.g., formate, hydrogen, reduced nitrogen species, and reduced sulfur species) and electron acceptors (e.g., nitrogen and sulfur oxyanions, dimethylsulfoxide, and trimethylamine N oxide). This underlies the success of bacteria in colonizing a wide range of the Earth's oxic and anoxic environments and the important contribution of bacteria to critical biogeochemical element cycles, such as the nitrogen, sulfur, and carbon cycles.

Respiratory Electron Transport Systems

In mammalian mitochondrial respiration, electrons flow from low-potential cytoplasmic electron donors (e.g., NADH or succinate) to the high-potential electron acceptor oxygen. The site of oxygen reduction is the aa_3-type cytochrome *c* oxidase that is located within the cytoplasmic membrane (Figure 1). The key postulate of P. Mitchell's chemiosmotic theory is that many energy-consuming reactions catalyzed by integral membrane proteins, such as the ATP synthase, are driven by the energy contained within a transmembrane-proton electrochemical gradient (proton-motive force (PMF)), which is generated by the electron transport system. Proton translocation is achieved via membrane-associated electron transfer proteins. Mitchell described a redox loop mechanism whereby two electrons are transferred from the positive (P, or bacterial periplasmic) side of the membrane to the negative (N, or bacterial cytoplasmic) side of the membrane. There they combine with two protons to reduce a quinone to quinol. The quinol then diffuses back across the membrane where it is reoxidized at the P face releasing protons (Figure 1B). This movement of negative charge from the P to the N side of the membrane, and counter movement of protons, produces a PMF. Structure–function studies of two key integral membrane enzymes of respiration (the structurally defined cytochrome bc_1 complex and the aa_3-type cytochrome *c* oxidase) illustrate yet another three different mechanisms that couple electron transfer to PMF generation. The cytochrome bc_1 complex utilizes a proton-motive Q-cycle mechanism that results in a q^+/e^- ratio of 1 (Figure 1A). The aa_3-type cytochrome *c* oxidase employs two different mechanisms to build up the PMF. Reduction of oxygen at the catalytic site involves proton transfer from the cytoplasm and electron transfer from a periplasmic donor. As a consequence, these charge movements from opposite sides of the membrane give rise to a net charge separation of 1 per electron transferred, $1q^+/e^-$. In addition, it utilizes a proton-pumping mechanism that results in one positive charge being moved across the membrane for each electron ($1\,q^+/e^-$). Therefore, the stoichiometry of charge movements in the oxidases adds up to $2\,q^+/e^-$ transferred from donor to oxygen. It is notable that neither the proton pump mechanism nor the Q-cycle mechanism of energy conservation was originally envisaged by Mitchell.

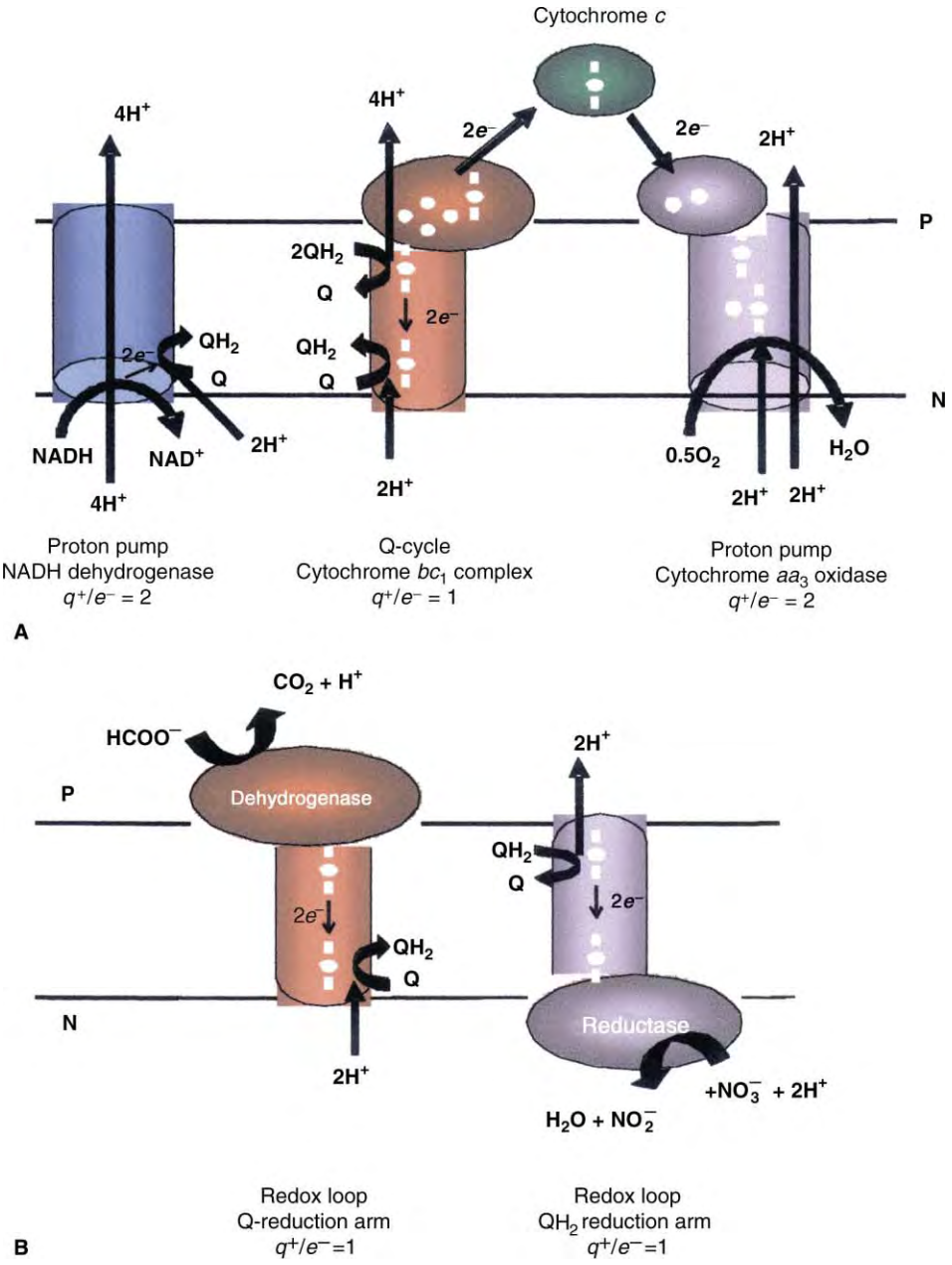

FIGURE 1 Mechanisms of energy conservation in respiration. (A) A basic mammalian mitochondrial electron transport chain illustrating proton pumps and Q-cycle mechanisms of energy conservation. (B) The organization of redox loops using periplasmic electron donors found in some cytochrome bc_1 complex-independent bacterial respiratory systems.

Bacterial Periplasmic Respiratory Electron Transport Systems that are Dependent on the Cytochrome bc_1 Complex

The mammalian mitochondrial-type of electron transport system is present in many aerobic and facultative anaerobic bacteria, for example, the well-studied soil-denitrifying bacterium *Paracoccus denitrificans*. However, many bacteria additionally have alternative electron transport systems that utilize periplasmic electron donors and acceptors. In some cases the periplasmic oxido-reductases will integrate easily into a mitochondrial-type of electron transport chain. For example, in *P. denitrificans* the periplasmic oxido-reductases for the reduction of nitrite or nitrous oxide, which are important reactions of denitrification in the biogeochemical nitrogen cycle, can accept electrons via the cytochrome bc_1 complex (Figure 2). Due to the Q-cycle mechanism of the latter enzyme, the overall

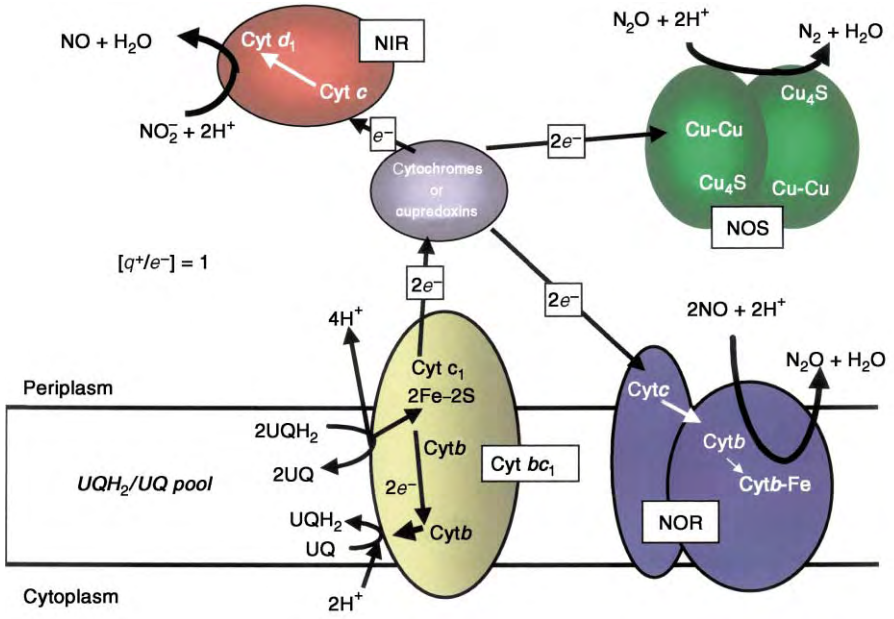

FIGURE 2 Cytochrome bc_1 complex-dependent periplasmic and membrane-bound oxido-reductases involved in denitrification in *Paracoccus* species. NIR, cytochrome cd_1 nitrite reductase dimer. NOR, nitric oxide reductase. NOS, nitrous oxide reductase.

electron transport pathway from quinol to nitrite and nitrous oxide is electrogenic, although the terminal nitrite and nitrous oxide reductases themselves are not. As a consequence, the electron transport from quinol to nitrite is less coupled ($q^+/e^- = 1$) (Figure 2) than electron transfer from quinol to oxygen ($q^+/e^- = 3$) (Figure 1A).

Periplasmic Electron Transport Systems that do not Depend on the Cytochrome bc_1 Complex

Many bacteria (e.g., *Escherichia coli*) do not have genes encoding a cytochrome bc_1 complex. Using periplasmic electron donors and acceptors independently of the cytochrome bc_1 complex can raise interesting questions about the bioenergetics of these systems, particularly with respect to the means by which the electron transfer process is coupled to the generation of a transmembrane electrochemical gradient. The molecular nature of some of these coupling mechanisms has been illuminated by recent structure–function studies on key anaerobic enzymes.

Some of these transmembrane enzymes possess two heme *b* groups at opposite sides of the membrane, which allows transmembrane electron transfer from a periplasmic to a cytoplasmic side. During oxidation of their substrate, two protons are released at the periplasmic side of the membrane while two electrons move inward via the hemes *b* to the cytoplasmic side of the membrane. There they are taken up by the acceptor along with two protons from the cytoplasm. This classical Mitchellian redox loop mechanism results in a net charge separation of one per electron transferred through the enzyme from donor to acceptor molecule ($1q^+/e^-$). Both dehydrogenases, which oxidize their substrate at the periplasmic side and reduce quinone at the cytoplasmic side, and terminal oxido-reductases, which oxidize quinol at the periplasmic site and reduce the acceptor at the cytoplasmic side, may have a redox-loop-type architecture. Examples of such electrogenic dehydrogenase are the HydABC-type hydrogenase and FdhN of *E. coli*, homologues of which are present in many bacteria and archae. An example of such an electrogenic terminal oxido-reductase is membrane-bound nitrate reductase (NarA). Periplasmic or membrane-bound enzymes that are not designed to contribute to the generation of a PMF will dissipate the redox free energy as heat. These enzymes receive their electrons and protons required for reduction of their allocated electron acceptor at the same side of the membrane, either the periplasm (trimethylamine N-oxide reductase (TOR), dimethylsulfoxide reductase (DMS), periplasmic nitrate reductase (Nap), the cytochrome *c* nitrite reductase (Nrf)), or the cytoplasm (succinate dehydrogenase, fumarate reductase). Electron transfer in pathways that are made up of a redox-loop-type dehydrogenase or oxido-reductase along with a non-electrogenic oxido-reductase or dehydrogenase, respectively, will yield a net proton movement of 1 from inside to outside during electron transfer from donor to terminal electron acceptor (q^+/e^- is 1) (Figure 3).

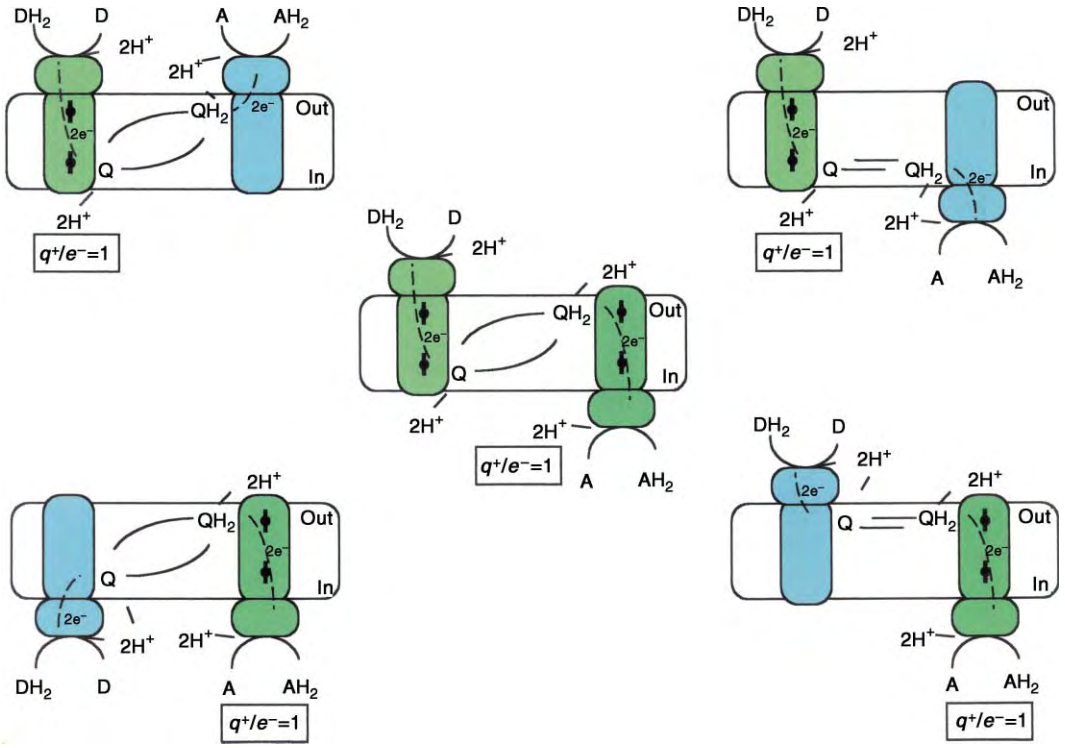

FIGURE 3 Examples of $q/e^- = 1$ and $q/e^- = 2$ redox loop mechanisms.

The most efficient free-energy transducing pathway of electron transfer from donor to acceptor requires the participation of a dehydrogenase and a terminal oxidoreductase, which both have a redox-loop-type architecture (Figure 3). The FdhN to NarA respiratory chain of *E. coli* and the Hyd to NarA (electron transfer from formate or hydrogen to nitrate, q/e^- is 2) are the classical systems used to illustrate such an efficient proton-motive redox loop.

Formate Dehydrogenase N

Formate is an important and widespread electron donor available to bacteria in anaerobic environments. During anaerobic growth with nitrate, *E. coli* can express a membrane-bound formate dehydrogenase (FdhN), which oxidizes formate in the periplasmic compartment and for which a high-resolution structure has been determined. The enzyme is a homo-trimer, with each monomeric unit being composed of an integral membrane di-heme cytochrome subunit (FdhI), a membrane-anchored periplasmic ferredoxin subunit (FdhH), binding four [4Fe–4S] clusters, and a periplasmic catalytic subunit (FdhG), which binds a [4Fe–4S] cluster and catalyzes formate oxidation at a Se-Mo-*bis*-guanine dinucleotide (Se-Mo-MGD) cofactor. Electrons extracted from formate at the periplasmic active site pass down a 90Å redox ladder to a menaquinone reductase site at the cytoplasmic face of the membrane. The redox ladder consists of eight redox centers, Se-Mo-*bis*-MGD, five iron–sulfur clusters, and two hemes. Each of these is within 12Å of its nearest neighbor, and this serves to ensure rapid electron transfer (Figure 4). In considering the whole electron transfer ladder from the Se-Mo-*bis*-MGD to the menaquinone, a notable feature is that the intermediary electron carriers usually function as one-electron transfer centers. However, formate oxidation and menaquinone reduction are two-electron reactions. Thus, the Se-Mo-*bis*-MGD plays a key role in gating electron transfer from formate into the redox ladder and the Q-reductase site is the key to gating the reduction of menaquinone.

Much of the FdhN redox ladder is periplasmic, being located in the extra-membranous periplasmic FdhGH subunits (Figure 4), but the two membrane-intrinsic hemes, bound within the four-helix bundle of FdhI, are critical to charge separation across the membrane. The midpoint redox potential at pH 7 of the formate/CO_2 couple is *c.* −420 mV and that of the MQH_2/MQ couple is *c.* −80 mV. This large, *c.* 340 mV, potential drop allows efficient electron transfer against a negative-inside membrane potential of *c.* 200 mV. The movement of one electron from the periplasmic (P) face to the cytoplasmic (C) face of the membrane and uptake of one proton at the C face gives a coupling stoichiometry of $q^+/e^- = 1$ (Figure 4).

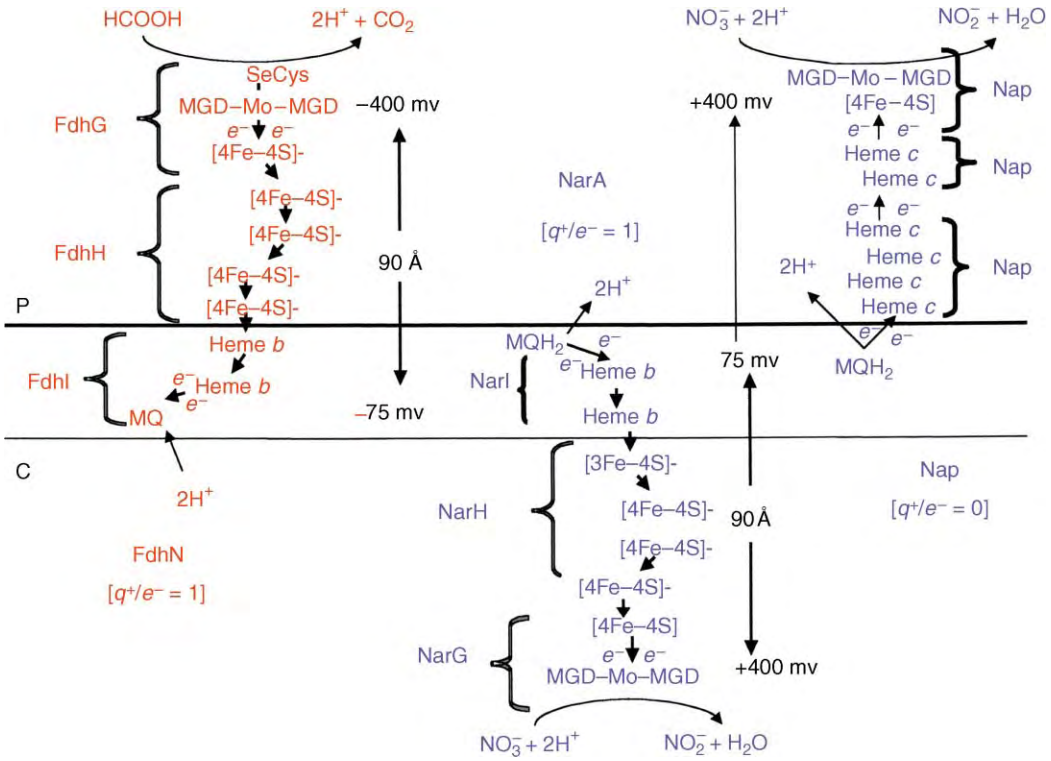

FIGURE 4 The organization of redox ladders involved in periplasmic formate-dependent nitrate reduction in *E. coli*. FdhN, formate dehydrogenase N. NarA, membrane-bound nitrate reductase A. Nap, periplasmic nitrate reductase.

Hydrogenase

Hydrogen is another important periplasmic electron donor for bacteria in anoxic environments. The Hya and Hyb enzymes of *E. coli* catalyze anaerobic hydrogen oxidation. There are no structures for these enzymes, but they are thought to be organized in a manner similar to FdhN. They are composed of three different subunits: an integral membrane di-heme subunit in which the hemes are stacked across the membrane; a periplasmic iron–sulfur protein (anchored by a single transmembrane helix); and a periplasmic catalytic subunit that binds a nickel–iron cofactor at the active side. The bioenergetics of periplasmic hydrogen oxidation are thus predicted to be very similar to that described for formate, with electrons extracted for hydrogen in the periplasm passing through a multi-cofactor redox ladder and combining with protons to reduce quinone at the cytoplasmic face, thus give $q^+/e^- = 1$.

Nitrate Reductase A

In *E. coli*, nitrate reductase A can serve as a second proton-motive arm in electron transfer from the periplasmic active site of FdhN or Hya (Figure 4). NarA is a three-subunit enzyme composed of NarGHI. NarG contains the *bis*-MGD molybdopterin cofactor at its catalytic site and a [4Fe–4S] cluster. NarH contains four additional iron–sulfur centers (one [3Fe–4S] and three [4Fe–4S]). NarGH are located in the cytoplasm and associate with NarI, an integral membrane protein of five transmembrane helices with the N-terminus and two inter-helix loops facing the periplasm. This subunit carries two hemes *b* stacked across the membrane. Oxidation of quinol occurs at the periplasmic side of NarI where the protons are released and the two electrons are moved from the outside low-potential heme *b* to the inside high-potential heme *b*. This charge separation makes the enzyme electrogenic, in that it contributes to the generation of a proton electrochemical gradient across the membrane (two charge separations during transfer of two electrons to nitrate; $q^+/e^- = 1$). Nar is organized in a manner very similar to FdhN, especially with respect to the equivalent FeS-containing NarH and FdhH subunits and Mo-*bis*-MGD NarG and FDHG catalytic subunits. However, the topology of the two systems is opposite (Figure 4), but the redox ladder arrangement of redox centers apparent in FdhN is also present in NarA. The midpoint redox potentials of individual cofactors in this ladder have been determined and suggest that both NarG and FdhN are part of a growing number of electron transfer complexes in bacteria that contain a mixture of endergonic and exergonic electron transfer steps. As in FdhN, the potential difference of *c*. 480 mV between the

MQH_2/MQ and nitrate/nitrite redox couples is sufficient to drive electron transfer across the membrane against the negative-inside PMF (Figure 4).

Non-Proton Motive Cytochrome bc_1 Complex-Independent Periplasmic Electron Transfer

In the FdhN–NarA electron transport system, both the quinone-reducing and quinol-oxidizing arms of the electron transport chain are proton-motive and, when operating together, they yield $q^+/e^- = 2$. However, in principle, only one arm needs to be proton-motive in order for a net PMF ($q^+/e^- = 1$) to be generated. Examples of this can be seen in a periplasmic formate–nitrate electron transport system in which nitrate is reduced by the periplasmic nitrate reductase (Nap) rather than NarA (Figure 3). Such a system operates under nitrate-limited growth conditions in *E. coli*.

The Periplasmic Nitrate Reductase (Nap)

Nap is widespread in many species of denitrifying and non-denitrifying proteobacteria, including both *P. denitrificans* and *E. coli*. Nap is normally found as part of a three-subunit electron transfer system composed of NapABC. NapA is a periplasmic catalytic subunit with a [4Fe–4S] cluster and a *bis*-MGD cofactor. The crystal structure of *Desulfovibrio desulfuricans* NapA reveals that the overall organization is similar to that of the catalytic subunits of the Mo-*bis*-MGD formate dehydrogenases. NapB is a periplasmic di-heme cytochrome *c*, with both hemes having bis-histidinyl ligation. NapC has a single N-terminal transmembrane helix that anchors a globular periplasmic domain with four *c*-type hemes to the periplasmic surface of the cytoplasmic membrane (Figure 4). All four hemes have relatively low midpoint redox potentials (in the region of 0 to −250 mV) and have *bis*-histidinyl axial ligation.

NapC may be made up of two subdomains, each containing a di-heme pair, and it belongs to a large family of bacterial tetra-heme and penta-heme cytochromes. These cytochromes have been proposed to participate in electron transfer between the quinol/quinone pool and periplasmic redox enzymes such as the trimethylamine N-oxide reductase, dimethylsulfoxide reductase, fumarate reductase, nitrite reductases, and hydroxylamine oxido-reductase. For an electron transport pathway from quinol to nitrate through Nap, the enzyme receives electrons from membrane-embedded quinols, which are donated to the tetra-heme periplasmic domain of NapC. From there they flow via the hemes in NapB and the [4Fe–4S] cluster in NapA to the bis-MGD-containing catalytic site of NapA where the two-electron reduction of nitrate to nitrite is catalyzed. As discussed above for NarA and FdhN, this electron transfer system also contains a mixture of endergonic and exergonic electron transfer steps but it is expected that none of the eight redox centers involved will be more than 14Å apart, thus ensuring rapid electron transfer. However, electron transfer from quinol to nitrate via Nap is non-electrogenic ($q^+/e^- = 0$) since both the electrons and the protons required for the reduction of nitrate to nitrite are taken up at the same side of the periplasmic face of the membrane.

Multi-Heme *c*-Type Cytochromes and Periplasmic Electron Transfer

Multi-Heme *c*-Type Cytochromes

In *E. coli* three other illustrative examples of non-electrogenic, quinol-oxidizing periplasmic electron transport systems that include extended redox ladders are illustrated in Figure 5. The cytochrome *c* nitrite reductase (Nrf) is a four-subunit electron transport system that involves 14 redox centers (10 *c*-type hemes and four [4Fe–4S] clusters). The trimethylamine N-oxide reductase (Tor) is a two-subunit system comprising of six redox centers (Mo-*bis*-MGD; and five *c*-type hemes). Finally, the dimethylsulfoxide reductase (Dms) is a three-subunit system containing an integral membrane subunit that is not involved in charge separation, and two periplasmic subunits that bind five redox centers (Mo-*bis*-MGD and four [4Fe–4S] clusters). Consideration of the Nap, Nrf, and Tor systems has revealed the participation of di-, tetra-, and penta-heme cytochromes in electron transfer. In mammalian mitochondria the P-facing cytochrome *c* involved in electron transfer is a small mono-heme protein. However, multi-heme cytochromes are a common feature of bacterial periplasmic electron transport. Other examples not mentioned so far include: (1) the octa-heme hydroxylamine oxido-reductase of nitrifying bacteria (e.g., *Nitrosomonas europeae*) and tetra-heme cytochrome *c554*, which, together with a tetra-heme NapC homologue CycB, mediate non-electrogenic electron transfer from hydroxylamine to quinone; (2) the tetra-heme fumarate reductase of *Shewanella* species that, together with the NapC homologue CymA, reduces fumarate to succinate using electrons drawn from the quinol pool. Structural analysis of these cytochromes and other multi-heme cytochromes such as the penta-heme NrfA reveals that the hemes are closely packed together to allow rapid electron transfer and are frequently arranged in pairs in which the porphyrin planes are nearly parallel or nearly perpendicular.

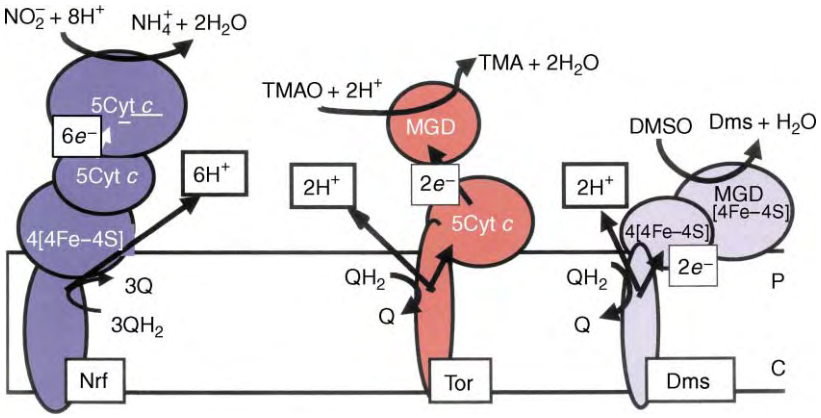

FIGURE 5 The organization of some non-electrogenic periplasmic electron transport systems in *E. coli*. Nrf, cytochrome *c* nitrite reductase, Tor, trimethylamine-N-oxide reductase; Dms, dimethylsulfoxide reductase.

Iron (III) Respiration and Inter-Membrane Periplasmic Electron Transport

Bacterial iron respiration is the process in which the Fe(III) acts as the terminal electron acceptor in an energy-conserving bacterial respiratory electron transport chain. It is an anaerobic process that provides a bacterium with a means of respiration when oxygen is absent and is distinct from the process of iron assimilation, in which iron is taken up into the cell by energy-consuming systems and incorporated into cell biomass. Although not a property of *E. coli*, the capacity for Fe(III) respiration is phylogenetically widespread and the ecological impact in microoxic and anoxic soils and sediments is considerable. A particular problem for gram-negative bacteria is that at neutral pH the speciation of Fe(III) is complex as the cation is present either as insoluble polynuclear oxo/hydroxo-bridged complexes or as soluble organic chelates. Thus, Fe(III) is frequently presented to bacteria in a range of insoluble forms. The best-characterized group of Fe(III)-respiring bacteria are species of the genus *Shewanella*, which are widespread facultative anaerobes of the gamma proteobacterium group. *Shewanella*, species can synthesize a number of periplasmic terminal respiratory reductases, including nitrate, nitrite, fumarate, and trimethylamine N-oxide reductases. During growth under iron-respiring conditions, *de novo* synthesis of a number of multi-heme *c*-type cytochromes that may a play a role in the Fe(III) respiration process occurs and a number of genetic loci that encode multi-heme cytochromes have been implicated as being important for Fe(III) respiration. Critically, these include an inner membrane tetra-heme cytochrome CymA (a NapC homologue), a small periplasmic 10 kDa tetra-heme cytochrome (STC); periplasmic deca-heme cytochromes (e.g., MtrA); and outer membrane cytochromes with deca-heme domains on the cell surface. The different cellular locations of these muti-heme cytochromes is critical to the transfer of electrons from the inner membrane across the periplasm to the outside of the outer-membrane where direct reduction of the insoluble extracellular substrate can occur. The multi-heme nature of the cytochromes may allow the proteins to form a multi-redox-centered electron wire that will be even longer than the redox ladders discussed for FdhN. Similar systems may also operate during the respiration of other insoluble respiratory substrates, such as manganese.

Synthesis of Periplasmic Electron Transport Systems

The periplasmic location of the cofactor-containing periplasmic electron transfer proteins raises the question as to how the organism assembles these proteins. This question is particularly relevant to a large protein complex with multiple redox centers, such as FdhN. In the case of periplasmic cytochromes *c* the protein is translocated in an unfolded state via the Sec pathway and heme is covalently attached using periplasmic or membrane-associated assembly proteins. However, many other classes of periplasmic redox protein possess a signal sequence, processed from the mature enzyme, that includes a twin arginine motif. This motif directs the protein to the twin arginine translocase (Tat), which transports pre-folded proteins with assembled redox cofactors. Some Tat substrates, including FdhGH are very large and consequently the pore of the Tat apparatus must be ~100Å in diameter to accommodate the largest substrates. The structure of the Tat complex is not yet known but there must be a gating mechanism, which maintains an ionic seal upon transport of these large substrates. The translocation process is also energy-driven, consuming PMF. This illustrates how

the overall consideration of the biochemistry and energetics of a periplasmic electron transfer system must take into account not only the operation of the system but also its biogenesis.

See Also the Following Articles

Cytochrome bc_1 Complex (Respiratory Chain Complex III) • Cytochrome *c* • Heme Proteins • Heme Synthesis • Iron–Sulfur Proteins • Photosystem I: F_X, F_A, and F_B Iron–Sulfur Clusters

Glossary

electrogenic Property of a transmembrane electron transport enzyme that generates a PMF.

heme A tetrapyrrole with a coordinated iron that can mediate electron transfer when bound to proteins. In *c*-type cytochromes the heme is covalently bound to the protein.

iron–sulfur cluster A protein cofactor that comprises of inorganic iron and sulfur, which together form a cluster that is often involved in electron transfer.

periplasm A subcellular compartment that lies between the inner (cytoplasmic) and outer membrane of Gram-negative bacteria.

proton-motive force A transmembrane gradient of protons (Δp) that has an electrical component ($\Delta\psi$) and a chemical component (ΔpH). Its magnitude is normally given in units of mV and can be calculated from $\Delta p = \Delta\psi - 60\Delta\text{pH}$.

Further Reading

Bertero, M. G., Rothery, R. A., Palak, M., Hou, C., Lim, D., Blasco, F., Weiner, J. H., Strynadka, N. C. (2003). Insights into the respiratory electron transfer pathway from the structure of nitrate reductase A. *Nat. Struct. Biol.* **10**, 681–687.

Einsle, O., Stach, P., Messerschmidt, A., Simon, J., Kroger, A., Huber, R., Kroneck, P. M. (2000). Cytochrome *c* nitrite reductase from *Wolinella succinogenes*. Structure at 1.6Å resolution, inhibitor binding, and heme-packing motifs. *J. Biol. Chem.* **275**, 39608–39616.

Ferguson, S. J. (2002). Keilin's cytochromes: How bacteria use them, vary them and make them. *Biochem. Soc. Trans.* **29**, 629–640.

Jormakka, M., Tornroth, S., Byrne, B., Iwata, S. (2002). Molecular basis of proton motive force generation: Structure of formate dehydrogenase-N. *Science* **295**, 1863–1868.

Page, C. C., Moser, C. C., Chen, X., Dutton, P. L. (1999). Natural engineering principles of electron tunnelling in biological oxidation–reduction. *Nature* **402**, 47–52.

Palmer, T., and Berks, B. C. (2003). Moving folded proteins across the bacterial cell membrane. *Microbiology* **149**, 547–556.

Potter, L., Angove, H., Richardson, D., Cole, J., (2001). Nitrate reduction in the periplasm of gram-negative bacteria. *Adv. Microb. Physiol.* **45**, 51–112.

Richardson, D. J. (2000). Bacterial respiration: A flexible process for a changing environment. *Microbiology* **146**, 551–571.

Richardson, D. J., and Sawers, G. (2001). PMF through the redox loop. *Science* **295**, 1842–1843.

Sawers, G. (1994). The hydrogenases and formate dehydrogenase of *Escherichia coli*. *Antonie van Leewenhoek* **66**, 57–88.

Simon, J. (2002). Enzymology and bioenergetics of respiratory nitrite ammonification. *FEMS Microbiol. Rev.* **26**, 285–309.

Van Spanning, R. J., Delgado, M. J., and Richardson, D. J. (2003). The nitrogen cycle: Denitrification and relationship to N_2 fixation, In *Nitrogen Fixation* (Newton, W., ed.), pp. 1888–2001. Kluver, Dordrecht, The Netherlands.

Biography

David Richardson is a Professor of Microbial Biochemistry and Director of the Centre for Metalloprotein Spectroscopy in the School of Biological Sciences at the University of East Anglia. He holds a Ph.D. in Biochemistry from the University of Birmingham. His principal research interests are in the field of bacterial respiration, where he studies the regulation, cellular organization, and biochemistry of a range of anaerobic electron transport systems. His contribution to this field was recognized by the Society for General Microbiology in 1999 when he was invited to give the Societies Fleming Lecture. He is on the editorial board of the *Journal of Biological Chemistry* and *Microbiology*.

Gary Sawers is a Project Leader in the Department of Molecular Microbiology at the John Innes Centre. He holds a Ph.D. in Biochemistry from the University of Dundee. His principal research interests include redox-dependent control of gene expression and metabolism in facultative anaerobes and *Streptomyces* and the biochemistry of metalloproteins. He is on the editorial board of *Microbiology*.

Rob van Spanning is an Assistant Professor in the Department of Molecular Cell Physiology at the Free University Amsterdam, The Netherlands. He holds a Ph.D. in Microbial Physiology and Molecular Microbiology from the Free University Amsterdam. His principal research interests are in understanding versatility and adaptive responses of bacterial respiration (from gene to function and back).

Peroxisome Proliferator-Activated Receptors

Mary C. Sugden, Edward A. Sugden and Mark J. Holness
Queen Mary, University of London, London, UK

PPARs (peroxisome proliferator-activated receptors) were originally identified by their ability to induce peroxisome proliferation, leading to the current nomenclaute. It has, however, emerged that PPARs do not induce peroxisome proliferation in man, but have an array of additional functions, most notably as master regulators of genes involved in metabolic control, particularly those involved in whole-body lipid homeostasis. PPARs are transcription factors, activated by binding key metabolic ligands, which exert their effects at the level of DNA to alter gene expression. Through this mechanism, PPARs, once activated, confer distinct properties of lipid handling to the tissues in which they are found, with an overall systemic lipid-lowering effect. There are three PPAR subtypes (α, γ, δ). PPAR subtypes are distributed non-uniformly in tissues. The individual PPARs act to reinforce each other's activities and also have complementary individual activities, all of wich are concerned with the removal of excess lipid from the blood. Acting as a team, the functions of the PPARs include regulation of fat breakdown by oxidation (PPARα and PPARδ), regulation of fat cell differentiation and lipid storage (PPARγ), together with others that include regulation of cholesterol fluxes into and out of cells (PPARγ and PPARδ). The physiological importance of the PPARs resides in lipid management, and the clinical importance of drugs acting via the PPARs lies in their ability to mimic nature's own messengers when harmful lipids accumulate. In this article, which of necessity cannot encompass all the actions of the PPARs, we will focus on how these receptors modulate lipid homeostasis in metabolically active tissues.

Lipids (triacylglycerol, cholesterol, phospholipids, fatty acids, and ketone bodies) are essential for many aspects of cellular processes, whilst also being linked to many pathological processes. Due to the varying demands of individual tissues for lipids, a highly regulated lipoprotein highway transports lipids to and from the periphery. The peroxisome proliferator-activated receptors (PPARs), α, γ, and δ, act as primary "metabolic" transcription factors, responding to fatty acids (FAs) and other metabolic signals to alter gene expression and thereby to confer distinct properties of lipid handling to the tissues in which they are found, with an overall systemic lipid-lowering effect. Thus, the PPARs act as a team with a common goal, but possess different attributes, including regulation of fat breakdown by oxidation (PPARα and PPARδ), regulation of adipocyte differentiation and fat storage (PPARγ), together with other functions that include regulation of cholesterol fluxes into and out of cells (PPARγ and PPARδ).

Lipids are essential for many aspects of cellular processes, including acting as substrates for energy production, steroid hormones and cellular structures. However, the availability and utilization of the various lipids must be carefully regulated since they are also linked to many pathological processes, including the development of obesity. The most familiar biological lipids are the triacylglycerols (TAG), which serve as principal energy stores, and cholesterol, both of which are present in the circulation at detectable levels. Because the hydrophobic lipids do not dissolve in water, moving them around the body requires transport mechanisms that are highly regulated. Due to the variable requirements for these compounds from a wide range of tissues, a lipoprotein highway exists that allows transport of the hydrophobic lipids with water soluble protein escorts enabling the movement of TAG and cholesterol to and from the periphery. TAG-enriched lipoproteins, chylomicrons (containing TAGs made from the re-esterification of newly absorbed FA and monoacylglycerol (MAG) in the gut) and very low density lipoproteins (VLDL) (containing TAG fabricated in the liver), deliver TAG to peripheral tissues for storage and energy production. The utilization by individual tissues of TAG in VLDL and chylomicron is carefully regulated through the expression of lipoprotein lipase (LPL), which is anchored to the outside of the cell in which it is expressed. LPL liberates FA and MAG in TAG for uptake by the tissue. Consequently, individual tissues can regulate their uptake of TAG-derived FA by altering the level of expression of LPL. At the same time, low-density lipoproteins (LDL) deliver cholesterol to tissues so that they can maintain membrane integrity and, in some instance, use it for the production of biologically important compounds, such as steroids.

Cholesterol uptake by cells is also regulated, in this case by the expression of the LDL receptor. In addition to the lipid highway from the liver/gut to peripheral tissues, a contraflow operates in the opposite direction, whereby high-density lipoproteins (HDL) transport surplus cholesterol from cells, such as those of the vessel wall, to the liver, where it can be redeployed to form bile. Gridlock in these lipid transfer and utilisation systems leading to the accumulation of VLDL and LDL in the circulation is integral to the development of metabolic diseases, including type 2 diabetes and cardiovascular disease.

PPARs: A Three-Pronged Attack

Peroxisome proliferator-activated receptors (PPARs) are transcription factors, activated by binding metabolic ligands, which exert their effects at the level of DNA to alter gene expression. There are three PPAR subtypes (α, γ, and δ). PPARs were originally identified by their ability to induce peroxisome proliferation, and this led to the current nomenclature. PPARα was first identified as the intracellular target for a particular class of rodent hepatocarcinogens, which include clofibrate. Clofibrate, a member of the fibrate amphipathic carboxylic acid family, was found to be a potent inducer of proliferation of peroxisomes, cell organelles found in high quantities in the liver, in addition to increasing FA oxidation and lowering lipid levels. Several other "peroxisome proliferating" agents were subsequently cloned. However, it has since emerged that the PPARs do not induce peroxisome proliferation in man, but have an array of additional functions, most notably as master regulators of genes involved in metabolic control, particularly those involved in whole-body lipid homeostasis. Inappropriately, the name PPAR has remained in common use! The PPAR subtypes are distributed non-uniformly in tissues. PPARα is expressed in a wide range of tissues and is highly expressed in liver, kidney, and heart. PPARγ has a more limited tissue distribution and is highly expressed in adipocytes and macrophages. PPARδ is widely expressed. After the PPARs are activated by binding specific ligands and/or by covalent modification (phosphorylation), they consort with another receptor, the 9-cis retinoic acid activated receptor (RXR), and, conjoined and active, recruit co-activators and together bind to peroxisome proliferator response elements (PPRE) to modify the expression of specific genes. This leads to an altered complement of enzymes in the cell, with a resultant alteration in cellular functional characteristics. Through this mechanism, each PPAR can, once activated, confer distinct properties of lipid handling to the tissues in which it is found, with an overall systemic lipid-lowering effect. The individual members of the PPAR gang act to reinforce each other's activities and also have complementary individual activities, all of which are concerned with the removal of excess lipid from the blood. Acting as a team with a common goal but differing attributes, the functions of the PPARs include regulation of fat breakdown by oxidation (PPARα and PPARδ), regulation of adipocyte differentiation and fat storage (PPARγ), together with others that include regulation of cholesterol fluxes in to and out of cells (PPARγ and PPARδ). The molecular messengers that bind to and activate the individual PPARs (the endogenous ligands) are not all identified. However, the close involvement of fat metabolism and lipid homeostasis with the PPAR family members arises, in part, because certain FAs and other lipid-derived molecules, including eicosanoids and arachidonic acid derivatives, can bind to and activate PPARs and are known to be primary natural ligands for these molecules. For example, PPARα is activated by polyunsaturated FAs, and PPARδ by long-chain FAs. Thereby, these lipid-signaling molecules can have power over their own fates by binding to PPARs and changing the expression of genes involved in modulating the patterns of tissue FA handling. The physiological importance of the PPARs thus resides in lipid management, and the clinical importance of drugs acting via the PPARs lies in their ability to mimic nature's own messengers when the task of lipid management becomes too onerous and harmful lipids accumulate. It is now established that the fibrates (e.g., clofibrate) and the anti-diabetic insulin-sensitizing thiazolidinediones (TZDs) both exert their systemic lipid-lowering effects via the PPARs. In this article, which of necessity cannot encompass all the actions of the PPARs, we will focus on how these receptors modulate lipid homeostasis in metabolically active tissues.

PPARα (NR1C1)

Too much FA, TAG or cholesterol circulating in the blood can be hazardous to health. High-fat diets, particularly those rich in very-long-chain FAs and polyunsaturated FAs induce FA oxidation via PPARα. Synthetic ligands for PPARα, in addition to the fibrate drugs, include phthalate ester plasticers, herbicides, and leukotriene D4 receptor antagonists. The fibrate PPARα agonists (clofibrate, gemfibrozil, fenofibrate, bezafibrate, and ciprofibrate) have been in clinical use for over 40 years for the treatment of dylipidemia.

The liver occupies a central position in whole-body lipid handling. In the case of FAs, the liver is capable of either oxidizing, or storing FAs depending on the prevailing requirements. FAs are stored after conversion to the TAG component of VLDL, and this function can be increased when FA delivery is higher than that

required to fuel hepatic ATP requirements via β oxidation. Incoming FAs, derived from the diet or endogenous stores, are re-esterified and stored in the fed state. During starvation, FAs, released from adipose tissue, are taken up by the liver and oxidized to create the water-soluble lipid-derived fuels, the ketone bodies (which are easily transported and oxidized by peripheral tissues), while TAG is incorporated into VLDL which is released into the circulation. These latter metabolic transformations of incoming FAs are enhanced by PPARα, the primary PPAR subtype expressed in liver. PPARα regulates specific genes that code for regulatory proteins involved in almost every stages of hepatic FA utilization, including FA uptake into the cell across the cell membrane, its retention within the cell, and its oxidation leading to ATP production and ketone body formation (Figure 1). PPARα therefore fulfills a critical role in the regulation of hepatic FA handling and, indeed, is essential for the up-regulation of the capacity of the liver for FA utilization in starvation or when lipid delivery is increased by a diet high in fat. This adaptive role is best illustrated by the inadequate response to high-fat feeding seen in PPARα-deficient mice, the Jack Sprats of lipid biochemistry. These animals exhibit an impaired ability to up-regulate hepatic FA oxidation in response to a high-fat diet, despite increases in FA supply, and the liver becomes engorged with lipid. Similarly, PPARα-deficient mice are unable to adapt to starvation, where delivery of FA from adipose tissue is increased. Secondary to impaired FA oxidation, compromised hepatic energy generation results in a low blood glucose concentration (hypoglycemia) when PPARα-deficient mice are fasted. Hypoglycemia arises by virtue of the necessity to continue to use glucose at high rates, rather than to be able to switch to FA or (in extrahepatic tissues) ketone bodies as alternative energy fuels, and because hepatic FA oxidation allows hepatic glucose synthesis (gluconeogenesis) through the generation of ATP and essential cofactors. The accumulation of large amounts of lipid in livers of PPARα-deficient mice, either on fasting or when they are maintained on a high-fat diet demonstrates the critical importance of PPARα-linked functions in matching hepatic FA delivery to FA clearance when the systemic delivery of lipid is increased. Hence, the TAG-lowering action of fibrates and related PPARα-targeted drugs in patients with hyperlipidemia is ascribed to increased FA clearance via oxidation, primarily but not exclusively in liver. Within the liver, PPARα also is heavily involved in the regulation of the synthesis and catabolism of lipoproteins, including some steps of the HDL synthetic pathway. Increased diversion of FA into oxidation decreases the availability of fatty acyl-CoA substrates for TAG synthesis, and thereby decreases VLDL

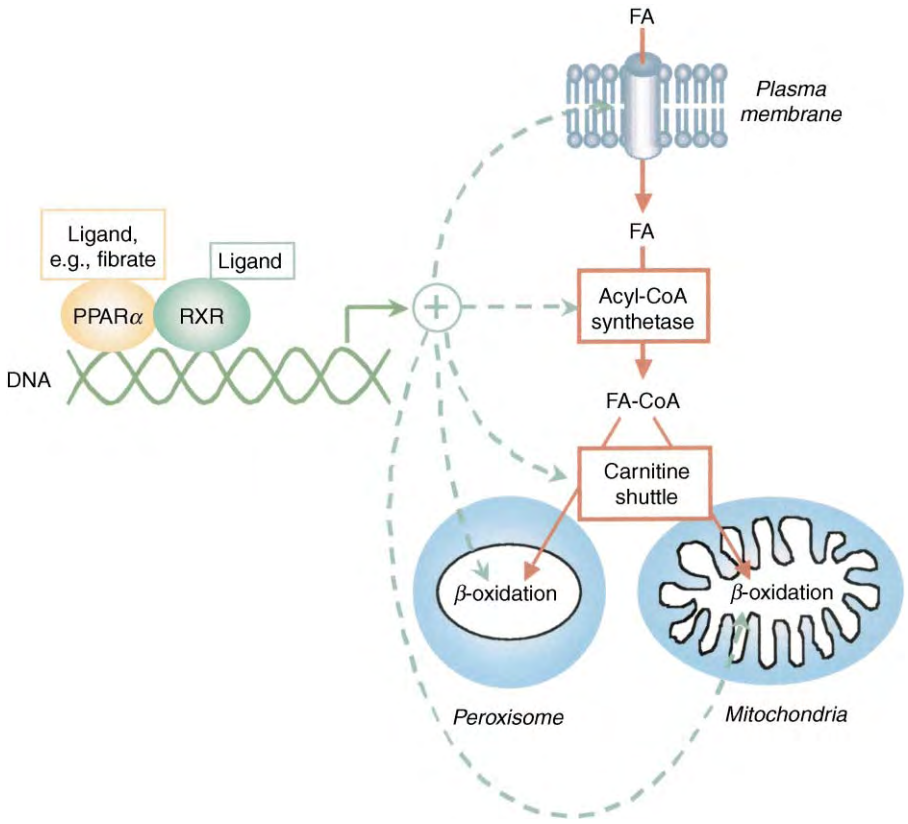

FIGURE 1 Mechanisms whereby activation of PPARα regulates fatty acid uptake, sequestration in the cell and oxidation.

secretion by the liver. In addition, PPARα inhibits expression of apolipoprotein (apo) C-III (a protein that may inhibit the TAG-hydrolysing action of LPL) and so enhances the hydrolysis of TAG contained in lipoproteins, and increases the hepatic uptake of TAG-enriched lipoprotein remnants. This decreases plasma TAG levels further and increases the transfer of other surface components of TAG-rich particles to HDL.

As well as in liver, PPARα is expressed abundantly in other tissues that are normally characterized by high rates of lipid oxidation. It is also present in the artery wall in monocytes/macrophages, vascular smooth muscle cells and endothelial cells. We focus here on the role of PPARα in kidney and heart, tissues which have a high energy demand related to their physiological functions. In these tissues, PPARα activation again enhances the expression of genes involved in FA uptake, activation, and oxidation. PPARα-deficient mice subjected to ischemia/reperfusion injury respond with greater renal cortical necrosis and worse kidney function compared with wild-type controls, indicating the vital role of PPARα in this tissue. PPARα is found predominantly in the renal cortex. Like liver, the renal cortex is a site of gluconeogenesis. Altered renal gluconeogenesis is increasingly recognized as contributing to fasting hyperglycemia in diabetes mellitus, and assumes increasing importance for maintenance of glycaemia after very prolonged food deprivation. Hence, as in liver, PPARα-facilitated gluconeogenesis driven by enhanced FA oxidation is likely.

Although functionally quite distinct from liver and kidney, there is ample evidence for an important role for PPARα in cardiac function in some circumstances. In adulthood, although the heart is a metabolic omnivore using most available fuels, lipids constitute the predominant energy substrate. However, during fetal and early life, in cardiac hypertrophy and in the failing heart, glucose utilization assumes greater importance, possibly as an adaptation to limited oxygen availability. Oxygen is essential for ATP production from FAs, but glucose oxidation needs less oxygen per mole than FA oxidation and glucose utilization can proceed, albeit less efficiently, in the absence of oxygen. The downside is that less ATP is generated per mole of glucose oxidized and when excess dietary lipid can be ingested, as in extrauterine life, the potential exists for myocardial lipid accumulation and lipotoxicity. Accordingly, the importance of PPARα in the adult heart appears relatively limited when the dietary lipid supply or endogenous lipid production is restricted, but PPARα assumes an important role in cardiac lipid management when lipid delivery to the heart is increased. PPARα-deficient mice provided with free access to a high-carbohydrate low-fat diet do not show any obvious cardiac abnormalities, but they accumulate myocardial lipid on starvation or if a high-fat diet is provided. This indicates a vital function for PPARα in allowing cardiac FA oxidation to occur at a rate sufficient to prevent the harmful accumulation of lipid within the heart itself.

Changes in the activity of the PPARα signaling pathway to gene expression characterize many common myocardial diseases. Whether changes in cardiac PPARα signaling are adaptive or causally related to myocardial pathology remains controversial, but there is no doubt that poor lipid management can cause a broken heart! Cardiac PPARα expression and activity are suppressed in the pathologically hypertrophied heart. The resultant decrease in the capacity for FA oxidation is associated with increased rates of glucose utilization and reversion to the fetal pattern of substrate use. Although causality between the reciprocal changes in lipid and glucose utilization has not been established, this metabolic switch may serve to preserve ventricular function within the context of pressure overload. The expression and activity of both PPARα and RXR are also suppressed in the hypoxic cardiac myocyte. To date, there are no reports of worsening of cardiac function in humans with cardiac hypertrophy through the use of the PPARα agonist fibrates. It is interesting that the heart is closely associated with adipose tissue in adult man, and epicardial and pericardial depots can represent a significant fraction of the total mass of the heart, suggesting a possible role as a local FA source. Both neutral lipid and FA adversely affect myofibrillar function. An intriguing possibility is that cardiac adipose tissue may act as a potential local sink for FA, mopping up FA when they are delivered in excess of the cardiac ATP requirement or when they cannot be cleared through oxidation, for example, during cardiac hypertrophy. The heart expresses LPL and, interestingly, LPL activity in cardiac myocytes is inhibited by PPARα activation. This effect may again help protect against a potentially toxic oversupply of FAs to the myocardium.

Epidemiological studies reveal that people with diabetes are at an extraordinary high risk for the development of cardiovascular disease. The heart in uncontrolled diabetes is constrained from switching to glucose oxidation and relies almost exclusively on lipid as an energy source. Cardiac-specific over-expression of PPARα, in the absence of alterations in lipid-fuel delivery, enhances the myocardial capacity for FA oxidation. This, however, is maladaptive, since many of the metabolic abnormalities of the diabetic heart, including decreased glucose utilization and ventricular dysfunction, are recapitulated. In this situation, the profile of myocardial TAG species is similar to the lipid species in the circulation, suggesting that the expanded lipid reservoir reflects increased uptake incompletely balanced by a corresponding increase in oxidation. When mice with cardiac-specific PPARα overexpression are made diabetic, they develop a more severe

cardiomyopathy than wild-type controls. In contrast, PPARα null mice are protected from cardiomyopathy.

PPARγ (NR1C3)

PPARγ, the predominant molecular target for the insulin-sensitizing TZDs and for specific prostanoids, such as 15-deoxy-$\Delta^{12,14}$ prostaglandin J2, is abundantly expressed in adipocytes, macrophages, the placenta and the fetal heart. The role of PPARγ as a critical regulator of adipose tissue development and metabolism is perhaps most well-established of the functions of the PPARs. Adipocytes expand as animals fatten, then shrink when the stored TAGs within them is mobilized because of food scarcity or, in the case of Mrs Sprat or the Atkins diet, lack of carbohydrate. A key feature of the fat cell is its ability to release the FA derived from TAG into the bloodstream: most other tissues are less altruistic and use FA derived from their endogenous TAG themselves. Detectable changes in gene expression in response to PPARγ activation in adipose tissue includes the induction of genes that allow adipose tissue to take up and accumulate lipid (Figure 2). Through this action, PPARγ contributes to lowering of circulating FA and TAG levels and, by sequestering lipid in the adipocyte, reduces the burden of excessive lipid delivery to tissues other than adipose tissue, including heart, skeletal muscle, kidney, and liver, where its accumulation could have deleterious effects. PPARγ can therefore enhance whole-body insulin action even though it is predominantly expressed in adipose tissue (which makes a relatively minor contribution to insulin-stimulated glucose disposal in lean individuals) by limiting the supply of lipid to other insulin-sensitive tissues and reducing the ability of FA to oppose insulin's actions in these tissues.

In addition to effects on genes involved in adipocyte lipid storage, TZDs increase adipocyte expression of the insulin-sensitive glucose transporter GLUT4, which allows increased use of circulating glucose for the synthesis of glycerol-phosphate which, in turn, allows FA esterification to form storage TAG (Figure 2). In addition, the TZDs may actually allow the fat cell to express enzymes that allow glycerol released from TAG breakdown (lipolysis) to be reclaimed or synthesized from circulating lactate, a process termed glyceroneogenesis (Figure 2). The presence of glycerol kinase allows glycerol released via the hydrolysis of stored triglyceride to be converted to glycerol phosphate which, in turn, allows reincorporation of released FA, or of FA derived from exogenous lipoproteins, into storage TAG, albeit at an energetic cost to the adipocyte. However, in obese people, as much as half of the body mass can be adipose tissue due to excessive enlargement of adipocytes and the presence of increased numbers of adipocytes.

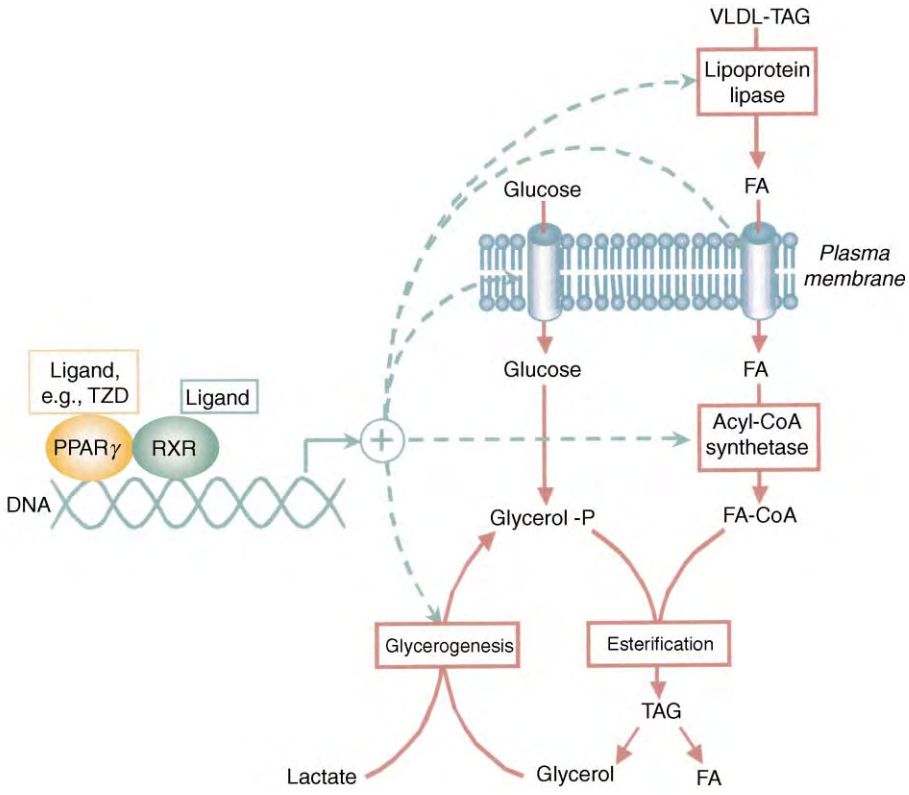

FIGURE 2 Mechanisms whereby activation of PPARγ regulates fatty acid uptake, sequestration and storage and glucose uptake and glycerogenesis in adipocytes.

Obese people invariably become glucose intolerant and insulin resistant, as well as developing other obesity-related complications which increase morbidity and mortality. "We fat all creatures else to fat us, and we fat ourselves for maggots" (Hamlet). It follows that the long-term use of TZDs could actually exacerbate obesity and insulin resistance, despite its more acute beneficial insulin-sensitizing action due to adipose-tissue lipid sequestration.

An additional action of PPARγ activation in adipose tissue is altered rates of secretion of biologically active adipokines (signaling molecules secreted by adipocytes), including leptin and TNFα, which can modulate insulin sensitivity in non-adipose tissue. Both leptin and TNFα have a role in obesity. Samples of adipocytes from obese people produce much more TNFα than those from lean people. Leptin is a molecule that informs the brain that adipose tissue is replete with lipid and signals a need to cease eating. PPARγ suppresses the production of both leptin and TNFα, thereby fooling the adipocyte that enough (lipid) is not enough, and allowing the adipocyte to continue to accumulate even more lipid.

Effects of the TZDs to ameliorate hyperglycemia and hyperlipidemia in fatless mice demonstrate that, although predominantly expressed in adipose tissue, PPARγ ligands may exert their effects via PPARγ in tissues in addition to adipose tissue. PPARγ agonists have been reported to be cardioprotective against ischaemic insult and to modify the cardiac hypertrophic growth response to pressure overload. However, most cardiac effects are likely to be indirect because of the low level of expression of PPARγ in cardiac myocytes themselves in adulthood, although the adipose tissue surrounding the heart itself may be targeted directly and act as a lipid buffer.

Most kinds of mammalian cells synthesize adequate cholesterol for their needs, but the human diet usually contains more than enough to supply our cells. Only the liver can degrade and eliminate cholesterol, so any excess has to be transported there from other tissues. LDL particles are rich in cholesterol. Some LDL leak through the thin lining of major vessels, where they become trapped under the endothelial cells, a process facilitated by hypertension (high blood pressure). Trapped LDL molecules attract macrophages, immune cells that can take up and degrade LDL. Some trapped LDL react with oxygen in the blood. Unfortunately, the oxidized LDL appear to be able to enter the macrophages in almost unlimited quantities, accumulating as pale, greasy particles that resemble the appearance of foam. Death of the lipid-bloated macrophages (foam cells) releases their lipid content forming fatty streaks in the arteries. The endothelial cells over the fatty streaks can become damaged and are replaced with fibrous plaques, narrowing the arteries. In the final stages of cardiovascular disease, the stiff narrow arteries ulcerate, increasing the risk of forming a blood clot, which will plug blood flow completely. The increased risk of cardiovascular disease in diabetic patients has prompted study of PPARγ function in lipid-laden macrophages. It has been reported that activation of PPARγ with the TZDs promotes cholesterol efflux from macrophages, improving the status of the atherosclerotic lesion, whereas macrophages lacking PPARγ are defective in cholesterol efflux and display accelerated lesion progression. Activation of PPARγ by components of oxidized LDL (9-hydroxyoctadecadienoic acid, 13-hydroxyoctadecadienoic acid) however, enhances macrophage lipid accumulation through induction of a scavenger receptor/transporter (FA translocase/CD36).

PPARδ (NR1C2)

Compared with PPARα and PPARγ, relatively little is known about PPARδ (also called PPARβ or FA-activated receptor, FAAR), except that it is relatively ubiquitously expressed. Nevertheless, its importance of PPARδ is established by the observation that most PPARδ-deficient mice die early in embryonic development due to a placental defect and those few that do survive have a reduced fat mass. PPARδ may also be involved in the cellular differentiation and inflammatory response of the epidermis. Importantly, PPARδ has been shown to mediate VLDL signaling to gene expression in the roving macrophages. Exposure of macrophages to VLDL results in enhanced expression of a lipid-droplet-coating protein that is implicated in lipid storage in these cells. Studies of PPARδ-deficient macrophages reveal that the TAG components of VLDL, released by LPL, serve as direct ligands for PPARδ to induce this protein, with accompanying lipid accumulation within the macrophage. These new data reveal a pathway whereby VLDL itself can directly regulate gene expression in atherosclerotic lesions.

Pharmacological activation of PPARδ lowers fasting TAG and LDL levels while increasing levels of HDL (the cardioprotective lipoprotein). It is unclear which tissue is targeted although skeletal muscle, in which PPARδ is highly expressed, is suspected. Slow-twitch oxidative skeletal muscle is a major site of FA catabolism, particularly during starvation and long-term exercise, when circulating lipid delivery increases. However, most evidence suggests that signaling via PPARα impacts predominantly on the regulation of lipid gene expression and fat burning in fast-twitch, not slow-twitch, skeletal muscle, even though fast-twitch muscle does not normally oxidize FA as avidly as slow oxidative muscle. Whereas PPARα ablation in the mouse results in abnormally high accumulation of neutral lipid in heart and liver in response to interventions increasing FA delivery, such as starvation, starvation of

PPARα-deficient mice leads to only minor abnormalities of skeletal-muscle FA metabolism. The lack of accumulation of neutral lipid has been attributed to the findings that PPARδ is the major type of PPAR found in mouse skeletal muscle. PPARδ may therefore assume greater importance in the modulation of lipid metabolism than PPARα in skeletal muscle, a conclusion supported by findings that PPARδ mRNA expression levels in muscle are dramatically increased on fasting, under conditions where FA oxidation by skeletal muscle is increased. Interestingly, PPARδ is also relatively abundant in the heart and exposure of cardiac myocytes to either PPARα- or PPARδ-specific agonists leads to significant induction of PPAR target genes involved in FA uptake and oxidation and both PPARs can be activated by FAs within this system.

Last Words

The question is raised as to why some non-adipose tissues express multiple PPARs, for example, PPARγ and PPARδ in macrophages, PPARα and PPARδ in muscle. Activation of all three PPARs appears to decrease systemic lipid availability and to decrease lipid (TAG and/or cholesterol) storage in non-adipose tissue. One possibility is that each individual PPAR activates overlapping but distinct downstream metabolic pathways. Perhaps more likely, it may be that the physiological ligands (presumably upstream lipid-based messengers) for activation of each of the PPARs are unique and that such ligand distinctness allows specificity of cellular downstream metabolic responses. PPARs are thus jacks of all trades, and masters of (at least) one! Although their individual specific physiological roles still require much further investigation, it is clear that, as ligand-activated transcription factors, the PPARs represent attractive targets for the development of selective therapeutic agents for pharmacological modulation of lipid metabolism.

See Also the Following Articles

Leptin • Lipases • Lipoproteins, HDL/LDL • Peroxisomes

Glossary

fibrates A group of compounds that act as agonists for PPARα.

peroxisome proliferator-activated receptors (PPARs) Are ligand-activated transcription factors, which alter gene expression to confer distinct properties of lipid handling to the tissues in which they are found, with an overall systemic lipid-lowering effect.

thiazolidinediones (TZDs) A group of compounds that act as agonists for PPARγ.

Further Reading

Finck, B. N., and Kelly, D. P. (2002). Peroxisome proliferator-activated receptor alpha (PPARalpha) signaling in the gene regulatory control of energy metabolism in the normal and diseased heart. *J. Molecul. Cell. Cardiology* **34**, 1249–1257.

Francis, G. A., Annicotte, J.-E., and Auwerx, J. (2003). PPAR alpha effects on the heart and other vascular tissues. *Amer. J. Physiol. Heart Circulatory Physiology* **285**, H1–H9.

Fruchart, J. C., Staels, B., and Duriez, P. (2001). PPARs, metabolic disease and atherosclerosis. *Pharmacol. Res.* **44**, 345–352.

Kersten, S., Desvergne, B., and Wahli, W. (2000). Roles of PPARs in health and disease. *Nature* **405**, 421–424.

Lee, C. H., Olson, P., and Evans, R. M. (2003). Lipid metabolism, metabolic diseases, and peroxisome proliferator-activated receptors. *Endocrinology* **144**, 2201–2207.

Biography

Mary C. Sugden is Professor in the Centre for Diabetes and Metabolic Medicine, ICMS at Bart's and the London School of Medicine and Dentistry in London, UK. Her principal research interests lie in the broad fields of insulin secretiion and action and in metabolic regulation, particularly with respect to fuel preference and the regulatory interactions between glucose and fats as energy sources. She holds M.A. and D.Phil. degrees from the University of Oxford and a D.Sc. from the University of London. Edward A. Sugden is associated with the group and assisted with analysis of the accessibility of the text to a lay audience.

Mark J. Holness a Senior Lecturer in the Centre for Diabetes and Metabolic Medicine, ICMS at Bart's and the London School of Medicine and Dentistry in London, UK. He holds B.Sc. and Ph.D. degress from the University of London. His principal research interests include the etiology of insulin resistance elicited by modification of dietary and hormonal status in early life and/or adulthood, the impact of lipid quantity and quality on pancreatic beta cell function and the role of PPARα in mediating changes in insulin sensitivity and secretion.

Peroxisomes

Suresh Subramani
University of California, San Diego, California, USA

Peroxisomes are among the simplest of the subcellular organelles that are characteristic of all eukaryotic cells. With ~60 known enzymes in the matrix and ~45 documented integral or peripheral membrane proteins, it is a reasonable guess that this organelle has only ~125 proteins, which makes it much less complex than other organelles. The peroxisome derives its name from the fact that many metabolic enzymes that generate hydrogen peroxide as a by-product are sequestered here because peroxides are toxic to cells. Within peroxisomes, hydrogen peroxide is degraded by the enzyme, catalase, to water and oxygen. Peroxisomes are surrounded by a single membrane and they range in diameter from 0.1 to 1 μm. They exist either in the form of a network of interconnected tubules (peroxisome reticulum), as in liver cells, or as individual microperoxisomes in other cells such as tissue culture fibroblasts.

Peroxisome-Like Organelles

Peroxisomes are related to specialized peroxisomes called glycosomes in parasites such as Trypanosomes, and to plant glyoxysomes, but are unrelated to hydrogenosomes, mitochondria, and chloroplasts. Collectively, peroxisomes, glyoxysomes, and glycosomes are also referred to as microbodies.

Peroxisome Distribution and Origin

Peroxisomes exist in all eukaryotes from single- and multicellular microorganisms, to plants and animals. Unlike mitochondria, nuclei, and chloroplasts, peroxisomes have no DNA. Consequently all their proteins are encoded by nuclear genes. They are proposed to have originated from endosymbionts that subsequently lost their DNA, but the evidence for an endosymbiont origin is much weaker than it is for mitochondria and chloroplasts.

Regulation of Peroxisome Number, Volume, and Contents

Peroxisomes can be induced to proliferate in many organisms in response to metabolic needs. Examples include the induction of proliferation of hepatic peroxisomes by fibrate drugs, phthalate plasticizers and xenobiotics, or the induction of peroxisomes in the methylotrophic yeast, *Pichia pastoris*, by methanol or oleate. The contents of the organelle are also responsive to the environment, as illustrated by the fact that peroxisomes of yeasts grown on oleate have induced levels of the fatty acid β-oxidation enzymes, whereas methylotrophic yeasts grown on methanol have elevated levels of alcohol oxidase and dihydroxyacetone synthase. Peroxisome volume can also be regulated by proteins such as Pex11p and Pex25p. Some mechanism must also exist for monitoring the need for peroxisomes and their function, because excess peroxisomes can be turned over by autophagic mechanisms involving the lysosome in mammals, or its yeast equivalent, the vacuole.

Functions of Peroxisomes

The principal function of peroxisomes is to house many metabolic pathways that are involved in various aspects of lipid metabolism. These include the following:

1. enzymes involved in the degradative oxidation (e.g., β-oxidation of very long chain fatty acids, 2-methyl-branched fatty acids, dicarboxylic acids, leukotrienes, bile acid intermediates and cholesterol side chains, and both α- and β-oxidation of 3-methyl-branched chain fatty acids);
2. the early steps in the synthesis of ether glycerolipids or plasmalogens;
3. the formation of bile acids, dolichol, and cholesterol; and
4. the catabolism of purines, polyamines, and amino acids, and the detoxification of reactive oxygen species such as hydrogen peroxide, superoxide anions, and epoxides. In methylotrophic yeasts, peroxisomes are also involved in the metabolism of methanol and methyl amines.

Glycosomes contain the glycolytic enzymes, in addition to enzymes common to most peroxisomes, whereas plant gloxysomes have some or all of the

glyoxylate pathway enzymes. Peroxisomes in the leaves of plants also participate in photorespiration.

Despite the fragility of the organelle during biochemical purification, the peroxisome membrane is impermeable to small molecules such as NAD(H), NADP(H), acetyl-CoA, and even protons *in vivo*. Consequently, it is not surprising that the peroxisomal membrane has a number of transporters for fatty acids, fatty-acyl-CoA esters, metabolites, and ATP.

Involvement in Human Disease

There are ~20 peroxisomal disorders, many of which are fatal. These diseases affect either a single metabolic enzyme, or the assembly of the organelle itself (Table I). Almost all of the genes involved in the human peroxisome biogenesis disorders (PBDs) are now known – they fall within the 25 *PEX* genes required for peroxisome biogenesis. Mouse models for human PBDs offer the promise of better insights into the symptoms of these diseases, their diagnoses, and eventually for therapeutic intervention.

Biogenesis of Peroxisomes

Because peroxisomes have no DNA, all their proteins must be imported from genes encoded in the nucleus. Most of proteins that reside in the peroxisome matrix and membrane are synthesized in the cytosol and then imported posttranslationally to the organelle. About 25 *PEX* genes, encoding proteins named peroxins, are necessary for the biogenesis of the organelle. Most of these genes are found in multiple organisms and 13 are conserved in humans (Table II). The general principles of biogenesis appear to be common to organisms across the evolutionary spectrum, but there are indeed organism-specific variations. More recently, additional *PEX* genes (*PEX23–PEX32*) have been defined and many of these are involved in the control of peroxisome division and number, rather than in protein import.

Peroxisomal Matrix Protein Import

Proteins destined for the peroxisome matrix have a few peroxisome targeting signals (PTSs). Most matrix polypeptides have a conserved, C-terminal, tripeptide PTS1 (-SKL in the one letter amino-acid code, or its conserved variants). Others have an N-terminal or internal sequence termed PTS2 [(R/K) (L/V/I))X_5(H/Q) (L/A)]. A few proteins, such *Saccharomyces cerevisiae* acyl-CoA oxidase, either have no canonical PTS1 sequence or have one that is dispensable, suggesting that they may possess other, as yet undefined, features that allow them to be targeted to the peroxisome lumen.

Matrix proteins synthesized in the cytosol are bound by cytosolic receptors – Pex5p in the case of PTS1, and

TABLE I

Human Peroxisomal Disorders Involving Metabolism and Biogenesis

Disease	*Peroxisomal enzyme affected*
Peroxisomal metabolic disorders	
Pseudoneonatal adrenoleukodystrophy	Acyl-CoA oxidase (Acox1)
Multifunctional protein 2 (MFP2) deficiency	MFP2 involved in β-oxidation of very long chain and 2-methylbranched fatty acids
Peroxisomal thiolase deficiency	3-ketoacyl-CoA-thiolase
X-linked adrenoleukodystrophy	ALDp (transporter)
Rhizomelic chondrodysplasia punctata Type 2	Dihydroxyacetonephosphate acyltransferase
Rhizomelic chondrodysplasia punctata Type 3	Alkyl-dihydroxyacetonephosphate synthase
Refsum's disease (classical)	Phytanoyl-CoA hydroxylase
Glutaric aciduria Type 3	Glutaryl-CoA oxidase
Hyperoxaluria Type I	Alanine:glyoxylate aminotransferase
Acatalasaemia	Catalase
Mevalonic aciduria	Mevalonate kinase
Di/trihydroxycholestanoic acidaemia	Trihydroxycholestanoyl-CoA oxidase (Acox2)
Mulibrey nanism	TRIM37
Adult-onset sensory motor neuropathy	2-methylacyl-CoA racemase
Disease	**Peroxin affected**
Peroxisome biogenesis disorders	
Zellweger syndrome	Pex1, Pex2, Pex3, Pex5, Pex6, Pex10, Pex12, Pex13, Pex16, Pex19
Neonatal adrenoleukodystrophy	Several peroxins (Pex1, Pex5, Pex6, Pex10, Pex12, Pex13)
Infantile Refsum's disease	Several peroxins (Pex1, Pex2, Pex5, Pex12)
Rhizomelic chondrodysplasia punctata Type I	Pex7

TABLE II

Proteins Involved in Peroxisome Biogenesis

Pex1	A 100–50 kDa ATPase (AAA family) in yeasts and humans. Interacts with Pex6 and other peroxins. Defects in Pex1 are the most common cause of the PBDs (CGI).
Pex2	A ~40 kDa integral PMP with a carboxy-terminal, cytoplasmically exposed, zinc-binding RING domain. Has been identified in yeasts and humans, interacts with Pex3, Pex10 and Pex12 and is defective in CG10 of the PBDs.
Pex3	A ~40 kDa integral PMP in yeast and humans that binds Pex19 and is defective in CG12 of the PBDs. Needed for assembly/stability of the RING–domain subcomplex comprised of Pex2, Pex10, Pex12 in yeast.
Pex4	A 20–24 kDa peroxisome-associated ubiquitin-conjugating enzyme that interacts with Pex22. Has been identified in several yeast species, but not in any metazoan.
Pex5	A ~70 kDa, predominantly cytoplasmic/partly peroxisomal protein that is found in yeasts, plants and humans. Contains a PTS1-binding, tetratricopeptide-repeat (TPR) domain in its carboxy-terminal half, interacts with several peroxins (Pex7, Pex8, Pex10, Pex12, Pex13 and Pex14) and is defective in CG2 of the PBDs.
Pex6	A ~100 kDa (AAA family) ATPase found in yeasts, plants and humans. Interacts with Pex1 and is defective in CG4 of the PBDs.
Pex7	A ~40 kDa, WD40-repeat-containing protein that binds the PTS2. Defective in CG11 of the PBDs.
Pex8	A variably sized (60–80 kDa), peripheral, but intraperoxisomal, PMP that interacts with Pex5 and the docking subcomplex, found only in yeast. It is an intraperoxisomal organizer of the peroxisomal import machinery in *S. cerevisiae*.
Pex9	A 44 kDa integral PMP found only in the yeast *Yarrowia lipolytica*.
Pex10	A ~35 kDa integral PMP with a carboxy-terminal, cytoplasmically-exposed, zinc binding RING domain. Has been identified in yeasts and humans, interacts with Pex2, Pex3, Pex5 and Pex12, and is defective in CG7 of the PBDs.
Pex11	A ~25 kDa integral PMP required for normal peroxisome abundance. Many species contain several Pex11 genes.
Pex12	A ~40 kDa integral PMP with a carboxy-terminal, cytoplasmically-exposed, zinc-binding RING domain. Has been identified in yeasts and humans, interacts with Pex2, Pex3, Pex5 and Pex10, and is defective in CG3 of the PBDs.
Pex13	A ~44 kDa integral PMP with a carboxy-terminal, cytoplasmically-exposed SH3 domain. Identified in yeasts and humans, interacts with Pex5 and Pex14, and is defective in CG13 of the PBDs.
Pex14	A ~40 kDa PMP of yeasts, plants and humans that interacts with Pex5, Pex8, Pex13 and Pex17.
Pex15	A 44 kDa integral PMP identified only in *Saccharomyces cerevisiae*. Interacts with Pex6 in yeast.
Pex16	In humans, Pex16 is a 36 kDa integral PMP that binds Pex19 and is defective in CG9 of the PBDs.
Pex17	A ~25 kDa integral PMP that interacts with Pex14. Has been identified only in *S. cerevisiae* and *P. pastoris*.
Pex18	A 31 kDa soluble protein involved only in PTS2-protein import. It is highly similar to Pex21, and might act as a Pex7 chaperone. Identified only in *S. cerevisiae*.
Pex19	A 33 kDa farnesylated protein of yeasts and humans. Predominantly cytoplasmic/partly peroxisomal, binds all known integral PMPs and recognizes some, but not all, mPTSs. It is defective in CG14 of the PBDs.
Pex20	A 46 kDa soluble protein involved only in PTS2-protein import. Identified only in *Y. lipolytica*. Substitutes functionally for Pex18/Pex21 in *S. cerevisiae*.
Pex21	A 31 kDa soluble protein involved only in PTS2-protein import, is highly similar to Pex18 and might act as a Pex7 chaperone. Identified only in *S. cerevisiae*.
Pex22	A 20 kDa integral PMP of yeasts that interacts with Pex4 and anchors it on the peroxisomal membrane.
Pex23	A 46 kDa integral PMP. Identified only in *Y. lipolytica*.
Pex24	A 61 kDa integral PMP found in yeasts required for the proper localization of some, but not all, PMPs and matrix proteins.
Pex25	A 45 kDa PMP found in *S. cerevisiae* that regulates peroxisome size and maintenance.

CG, complementation group; SH3, Src-Homology 3.

Pex7p in the case of PTS2 (see Figure 1). These receptor–cargo complexes then move to the peroxisome membrane where they dock with protein subcomplexes that are in or on the membrane. Two such complexes are a docking subcomplex, comprised minimally of peroxins Pex8p, Pex13p, Pex14p, and Pex17p, and a really interesting new gene (RING)–protein subcomplex, consisting of three RING–proteins Pex2p, Pex10p, and Pex12p (and other yeast peroxins, such as Pex3p and Pex8p). The RING–proteins have a characteristic zinc-binding domain and are members of a protein family whose first member was called RING. There is evidence that the protein subcomplexes are dynamic, e.g., the docking and RING–protein subcomplexes can come together as a larger complex during import. The PTS receptors, Pex5p and Pex7p, are believed to shuttle from the cytosol to the peroxisome membrane or lumen of the organelle, where they release their cargo, before they return back to the cytosol for another round of import. This is referred to as the extended shuttle model for matrix protein import. It is unclear at present whether the RING–protein subcomplex (also called the translocation complex in the literature) is involved directly in the translocation of proteins into peroxisomes, or in the shuttling of receptors (e.g., Pex5p) back to the cytosol. Many other peroxins and chaperones such as Djp1p, hsp70, and hsp40 are implicated in matrix protein import, but their precise roles are still under investigation.

The PTS2 pathway, which is dependent on the receptor, Pex7p, requires different additional proteins depending on the organism of its origin. In *S. cerevisiae*, the redundant proteins, Pex18p and Pex21p, fulfill this function, whereas in *Yarrowia lipolytica*, Pex20p is

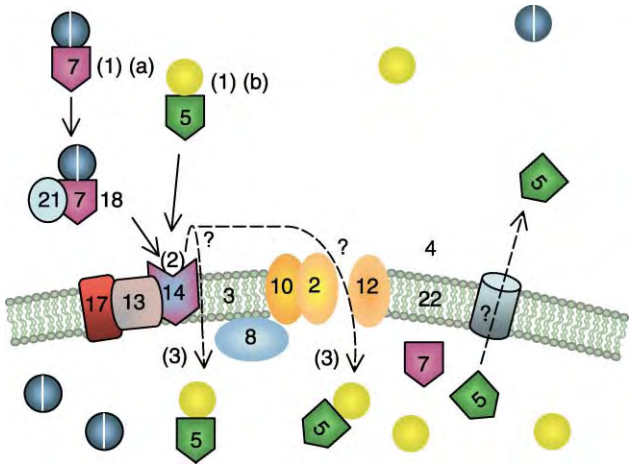

FIGURE 1 Model of peroxisomal matrix enzyme import. Numbers indicate the corresponding Pex protein. Three main steps are outlined: (1) Binding of PTS-containing proteins (yellow and blue circles depict PTS1- and multimeric PTS2-containing proteins, respectively) to the import receptors (Pex5p and Pex7p); (2) transport of receptor–cargo complexes to the peroxisome membrane and interactions with PMPs, such as Pex14p and, perhaps Pex13p, which are in a subcomplex with Pex17p and Pex8p; (3) receptor–cargo translocation through a proteinaceous pore formed either by the docking subcomplex (Pex14p, Pex13p, Pex17p, Pex8p) or the RING–peroxins subcomplex (Pex2p, Pex10p, Pex12p). PTS receptors may deliver cargo while inserted in the peroxisomal membrane or after entry into the lumen. Pex3p and Pex8p have been proposed to bridge proteins in the docking and RING–peroxins subcomplexes.

needed, and in mammals an alternatively spliced form of Pex5p (Pex5pL) is necessary for PTS2 import. However, the docking and RING–proteins are required in common for both PTS1 and PTS2 import pathways, leading to the current view that a common translocation machinery is involved for both these pathways.

Examples of organism-specific variations in the general scheme of biogenesis include the apparent lack of the entire PTS2 pathway (PTS2 proteins and Pex7p, the PTS2 receptor) in worms (*Caenorhabditis elegans*), and the dependence of the PTS2 import pathway on the PTS1 receptor, Pex5p, in mammals, but not in yeasts. However, even where such differences exist, the underlying molecular mechanism is similar. This is illustrated by the point that the proteins Pex18p and Pex21p from *S. cerevisiae*, Pex20p from *Y. lipolytica*, and Pex5pL in mammals all have a conserved motif that allows them to interact with Pex7p and/or PTS2 cargo to facilitate the PTS2 import pathway.

Unlike the transport of unfolded proteins into other organelles, such as the endoplasmic reticulum and mitochondria, folded and oligomeric proteins can be transported across the peroxisomal membrane. How such large multi-subunit complexes are transported across the membrane is unknown, because the translocon in the peroxisomal membrane has not been characterized.

Import of Peroxisomal Membrane Proteins

These proteins have one or more sequences (mPTSs) that direct them to the peroxisomal membrane with the correct topology. Although a dozen or so mPTSs have been defined in several yeast and mammalian peroxisomal membrane proteins (PMPs), they have no simple consensus sequence. The PMP receptor(s), the mechanism of insertion of PMPs into the peroxisomal membrane, and the rules that govern their topology are not completely known, although several peroxins that play a role in PMP biogenesis are defined. Most mutants affecting the import of either peroxisomal matrix or membrane proteins have organelle remnants, in some but perhaps not all, organisms.

Division and Proliferation of Peroxisomes

The division of peroxisomes is compatible with two models. One of these proposes that peroxisomes arise by budding and fission from pre-existing peroxisomes, and may be the one that is used in normal, mitotically dividing cells. The other model is that peroxisomes arise either *de novo* or from some other reservoir of membranes such as the endoplasmic reticulum. Mature peroxisomes are then generated from this membrane reservoir via a variety of biogenesis intermediates. This model may be more applicable to proliferating peroxisomes and to the regeneration of peroxisomes in *pex* mutants complemented by the affected gene.

Acknowledgments

This work was supported by grants NIH DK41737 and NIH DK59844. The author thanks Dr. Sebastien Leon for his help in assembling Table II and Figure 1. He regrets that the format of this article does not permit citation of the many original contributors to this field.

See Also the Following Articles

Fatty Acid Oxidation • Fatty Acid Receptors • Fatty Acid Synthesis and its Regulation • Flavins

Glossary

autophagy Degradation of cytosol and organelles by protein turnover involving the yeast vacuole or the lysosome in mammals.

biogenesis The process of assembly.

microbodies Another name for peroxisomes and similar organelles (glyoxysomes, glycosomes).

organelle A subcellular, membrane-enclosed compartment performing specialized functions.

peroxisomal matrix Lumen of the peroxisome.

peroxisome A subcellular organelle involved in many lipid metabolic pathways.

vacuole or lysosome Organelle in which protein turnover and recycling occurs. The organelle is called the vacuole in yeast and the lysosome in mammalian cells.

Further Reading

Baumgartner, M. R., and Saudubray, J. M. (2002). Peroxisomal disorders. *Semin. Neonatol.* **7**, 85–94.

Hettema, E. H., and Tabak, H. F. (2000). Transport of fatty acids and metabolites across the peroxisomal membrane. *Biochim. Biophys. Acta* **1486**, 18–27.

Purdue, P. E., and Lazarow, P. B. (2001). Peroxisome biogenesis. *Annu. Rev. Cell Develop. Biol.* **17**, 701–752.

Subramani, S., Koller, A., and Snyder, W. B. (2000). Import of peroxisomalmatrix and membrane proteins. *Annu. Rev. Biochem.* **69**, 399–418.

Titorenko, V. I., and Rachubinski, R. A. (1998). The endoplasmic reticulum plays an essential role in peroxisome biogenesis. *Trends Biochem. Sci.* **23**, 231–233.

Van den Bosch, H., Schutgens, R. B., Wanders, R. J., and Tager, J. M. (1992). Biochemistry of peroxisomes. *Annu. Rev. Biochem.* **61**, 157–197.

Biography

Suresh Subramani is a Professor in the Section of Molecular Biology, Division of Biological Sciences, University of California at San Diego. His current research interest is in organelle homeostasis. He holds a doctoral degree in biochemistry from the University of California, Berkeley, and did his postdoctoral work at Stanford University. He has been on the faculty at UCSD since 1982. He and his colleagues have made many important contributions to the field of peroxisome biogenesis and turnover.

Phage Display for Protein Binding

Henry B. Lowman
Genentech, Inc., San Francisco, California, USA

Phage display is a process in which large libraries of protein or peptide variants are prepared as fusion proteins with one of several coat proteins of bacteriophage. Because each phage-displayed variant is both displayed on the surface of the phage particle (virion) and encoded by the DNA packaged within that virion, phage display provides a useful means of purifying rare members of the library with specifically selected binding properties, amplifying the selected members over multiple rounds of selection, determining the sequence of the selected protein, and expressing the protein as a soluble product. Phage display has found many applications in the discovery, engineering, and analysis of peptides and proteins including 1) discovery of novel peptide mimotopes and human(ized) antibodies for binding to proteins and other targets, 2) affinity maturation and mutagenic scanning of antibodies and other proteins, and 3) identification of specific peptide substrates for proteases and other enzymes. Typically, filamentous phage such as Fd, M13 and related phages that infect *Escherichia coli* bacteria are used as vectors for phage display of peptide or protein diversity libraries.

Phage Display Vectors

Phage display is a rapid means for discovery of novel peptides and proteins from large libraries of genetically engineered variants. The process begins with construction of a phage or phagemid vector which encodes either an initial protein "scaffold" or a random peptide as a fusion protein with a phage coat protein. Typical constructs involve a promoter region driving expression of the fusion protein in which a secretion signal sequence (SS) is followed by the display gene and all or part of a phage coat protein, e.g., g3p or g8p (proteins encoded by gene-3 or gene-8 of bacteriophage M13). Alternatively, with appropriate modifications, the displayed protein may be fused at the C terminus of the coat protein. Filamentous phage(mids) are particularly useful vectors because their structure readily adapts to accommodate the size of DNA packaged into the virion.

Polyvalent and Monovalent Phage Display

When many copies of a fusion protein are displayed on each virion, each virion may simultaneously bind to several molecules of the target. In this format, called polyvalent display, even intrinsically weakly binding variants appear to bind tightly because of the avidity effect. As this effect can mask tighter binding (higher intrinsic affinity) interactions, constructs which limit the display of the fusion protein to yield virions that usually display no more than one copy were developed. This format, called monovalent display, facilitates stringent selections for very high-affinity interactions. Statistically, monovalent display vectors allow for display of multiple copies of the fusion protein by a small fraction of the virion population, but the difference between monovalent and polyvalent formats can be dramatic in terms of avidity effects. This difference has been exploited to: (1) identify novel, low-affinity binding peptides in a polyvalent system, followed by (2) "affinity maturation" of the low-affinity peptides through construction of secondary libraries and selection in a monovalent system.

Phage Vectors

Phage vectors consist of an essentially complete phage genome into which is inserted DNA encoding the protein or peptide of interest (Figure 1). Typically, the remainder of the phage genome is left unchanged and provides the other gene products needed for the phage life cycle. For facile growth and propagation of phage in *Escherichia coli*, the function of the fusion protein in the life cycle of the phage must be maintained and this places constraints on the types of fusions that are usually produced using phage vectors. For example, large proteins may be poorly displayed and/or may interfere with phage packaging or infection.

Phagemid Vectors

Phagemid vectors consist of a typical plasmid construct into which a phage origin of replication (ORI), including the phage-packaging region of DNA from the phage genome, and a gene for the displayed fusion protein have been inserted (Figure 1). In this case, the phagemid DNA can be replicated independently of phage production for mutagenesis and amplification. However, for phage

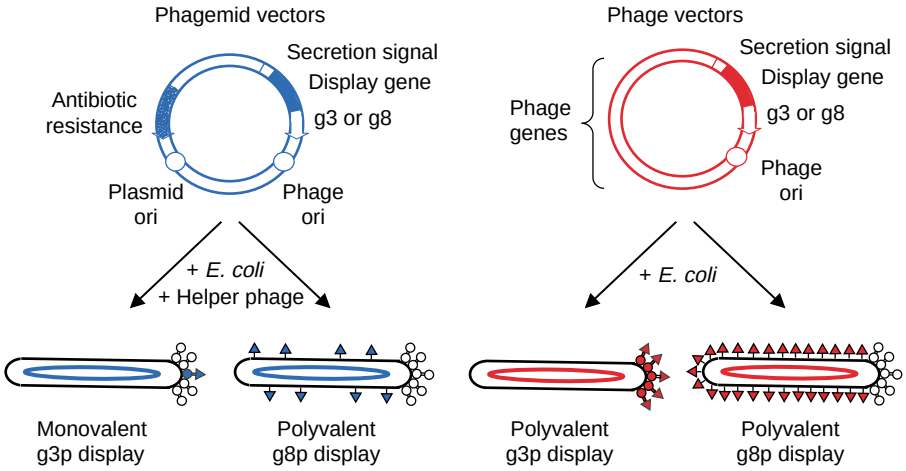

FIGURE 1 Construction of phagemid and phage vectors. Phagemid and phage DNA constructs are shown with appropriate origins of replication (ori), a gene for the protein of interest (shaded) fused the gene-3 or gene-8 encoded coat proteins of filamentous phage and preceded by a secretion-signal sequence, as well as a gene for antibiotic resistance. The remaining genes of the phage vector or helper phage encode other proteins. The DNA is packaged as a single strand in the virion (shown in cartoon form) with many copies of the g8 protein along the length of the particle, a few copies of the g3 protein (two-lobe structure) at one end, and other structural proteins (not shown). The g3p or g8p fusion proteins are shown as filled triangles attached to the corresponding coat protein. In monovalent phage display, expression of the fusion is statistically limited so that very few particles contain more than one copy of the fusion protein, while in polyvalent display, a range of fusion-protein densities is possible.

display, the remaining phage gene functions must be supplied by another construct, usually a "helper phage," which is packaged into virions with lower efficiency than the phagemid itself. When *E. coli* cells transfected with the phagemid, grown under selective pressure with an appropriate antibiotic, are infected with helper phage at an appropriate multiplicity of infection (MOI), both constructs undergo replication, but mature virions predominantly contain phagemid rather than helper-phage DNA. However, both types of particles can display the fusion protein; thus, antibiotic selection of cells containing the desired phagemid is needed. These examples indicate the most commonly used types of phage and phagemid vectors; however, other monovalent and polyvalent displaying phage and phagemid constructs have also been described.

Phage Libraries

A phage library may begin with a "wild-type" protein displayed on phage or with a phage(mid), into which DNA encoding completely novel peptides have been inserted.

Construction of Libraries

The generation of diversity in a phage-display library is usually accomplished by typical site-directed mutagenesis techniques, such as oligodirected single-stranded template mutagenesis, PCR mutagenesis, or cassette mutagenesis using restriction enzymes and DNA ligase to cut out a segment of DNA and replace it with a synthetic piece. Highly diverse DNA sequences can be generated using standard solid-phase deoxynucleotide synthesis techniques in which individual nucleotides are "randomized" by adding to the growing polynucleotide chain a mixture (which may be equimolar or of biased specified composition) of all four nucleotides, or a subset of A, G, C, or T, rather than a single nucleotide (Table I).

TABLE I
Nucleotide Abbreviations for Degenerate Codon Design

Abbreviation	Nucleotide
A	Adenosine
G	Guanosine
C	Cytidine
T	Thymidine
R	A, G
Y	C, T
B	C, G, T
D	A, G, T
H	A, C, T
K	G, T
M	A, C
V	A, C, G
W	A, T
N	A, G, C, T
S	G, C

TABLE II

Codon Degeneracy and the Generation of Diversity in Phage-Display Libraries. The 64 Possible Triplets are Shown, Along with the Corresponding Encoded Amino Acids in the First Two Columns. The Remaining Columns Show Examples of Degenerate Codons (see Table I) Encoding all Amino Acids with 32 Triplets (NNS), and other Selected Sets that Vary in Amino Acid Composition. Often a *sup* E Strain of *E. coli* is used for Phage Propagation, in which Case the Amber Stop Codon (*) is Translated as Gln (Q)

DNA codon	Amino acid	NNS	NYC	NHS	ARS
AAG	Lys (K)	X		X	X
AAC	Asn (N)	X		X	X
AGG	Arg (R)	X			X
AGC	Ser (S)	X			X
ACG	Thr (T)	X		X	
ACC	Thr (T)	X	X	X	
ATG	Met (M)	X		X	
ATC	Ile (I)	X	X	X	
GAG	Glu (E)	X		X	
GAC	Asp (D)	X		X	
GGG	Gly (G)	X			
GGC	Gly (G)	X			
GCG	Ala (A)	X		X	
GCC	Ala (A)	X	X	X	
GTG	Val (V)	X		X	
GTC	Val (V)	X	X	X	
CAG	Gln (Q)	X		X	
CAC	His (H)	X		X	
CGG	Arg (R)	X			
CGC	Arg (R)	X			
CCG	Pro (P)	X		X	
CCC	Pro (P)	X	X	X	
CTG	Leu (L)	X		X	
CTC	Leu (L)	X	X	X	
TAG	Stop*	X		X	
TAC	Tyr (Y)	X		X	
TGG	Trp (W)	X			
TGC	Cys (C)	X			
TCG	Ser (S)	X		X	
TCC	Ser (S)	X	X	X	
TTG	Leu (L)	X		X	
TTC	Phe (F)	X	X	X	
AAA	Lys (K)				
AAT	Asn (N)				
AGA	Arg (R)				
AGT	Ser (S)				
ACA	Thr (T)				
ACT	Thr (T)				
ATA	Ile (I)				
ATT	Ile (I)				
GAA	Glu (E)				
GAT	Asp (D)				
GGA	Gly (G)				
GGT	Gly (G)				
GCA	Ala (A)				
GCT	Ala (A)				
GTA	Val (V)				
GTT	Val (V)				
CAA	Gln (Q)				
CAT	His (H)				
CGA	Arg (R)				
CGT	Arg (R)				
CCA	Pro (P)				
CCT	Pro (P)				
CTA	Leu (L)				
CTT	Leu (L)				
TAA	Stop				
TAT	Tyr (Y)				
TGA	Stop				
TGT	Cys (C)				
TCA	Ser (S)				
TCT	Ser (S)				
TTA	Leu (L)				
TTT	Phe (F)				

(*continues*)

TABLE II

Continued

The degeneracy of the genetic code makes possible the generation of chemically related subsets of codons depending on the amino acids encoded (Table II). Once oligonucleotides with appropriate diversity have been designed and synthesized, mutagenesis is carried out with the phage or phagemid vector on an appropriate scale to yield a sufficient number of DNA molecules (moles of product) to represent the desired diversity as described below. The mutagenesis products are transformed into *E. coli* and propagated in culture (along with helper phage in the case of phagemid vectors) to yield a library of peptide- or protein-displaying phage particles.

Design of Diversity Libraries

The key consideration in the design of diversity libraries is the combinatorial complexity of the DNA and protein resulting from incorporation of random nucleotides at a given number of sites. For example, using NNS codon degeneracy (Table II), all 20 commonly used L-amino acids are encoded by 32 codons. With one NNS codon randomized in this way, the library has a theoretical diversity of 32 at the DNA level and 20 at the protein level. However, this complexity grows quickly as a larger number multiple sites, n, are simultaneously randomized. The experimentally obtained complexity

or diversity of the library is limited to the number of DNA molecules that can be produced at the synthesis and mutagenesis stage, and subsequently transformed into *E. coli* and packaged into a solution of phage(mid) particles. Therefore, the number of randomized codons or the diversity of the degenerate codons may be restricted in order to obtain libraries that completely represent the designed diversity. At the virion level, phage particles are only soluble to a level of $\sim 10^{14}$ particles/ml (10^{17}/l; or 170 nM), presenting an ultimate practical limitation for phage libraries to be produced and used at the laboratory scale. Additional limitations are imposed by the process of transformation of the phage or phagemid construct into *E. coli*, so that libraries are more commonly on the order of 10^9 or 10^{10} as measured by the total number of transformants obtained after mutagenesis and transformation using electroporation or other techniques.

Phage-Binding Selections

Phage libraries yield useful and interesting variants through a process of selection and amplification analogous to affinity-based protein purification (Figure 2).

Preparation of Packaged Virions

Once the products of random mutagenesis have been transformed into *E. coli*, phage amplification occurs through propagation of the infected culture, which in the case of phagemid libraries also includes a helper phage. Since filamentous phage particles are not lytic, large numbers of phage particles are produced during a few hours of culture growth. As the displayed protein is secreted, it is incorporated into the coat of the virion. Once a large number of phage have been produced, they are separated from the *E. coli* host by centrifugation, and often further purified using a series of precipitation and resuspension steps. The final phage stock is a solution of phage particles that are ready for appropriate binding selections.

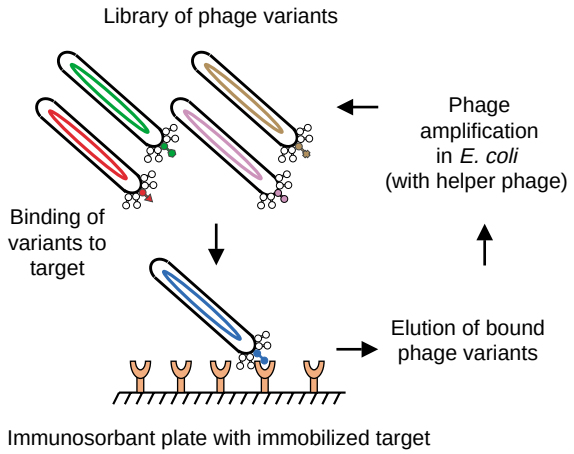

FIGURE 2 Affinity-selection process for binding to an immobilized target protein using a monovalent phagemid vector. One round of binding selection or "panning" is shown. A population of phage particles, each displaying a different peptide or protein variant, is allowed to bind to an immobilized target. After low-affinity variants are washed away, high-affinity variants are eluted and propagated to produce an enriched pool of high-affinity variants, which may be subjected to further rounds of selection.

Phage Binding and Elution

Early phage-binding selections used a simple process for separating variant protein phage that bind to a target molecule from those that do not bind. The target molecule was coated directly onto immunosorbent plastic plates or affixed to chemically activated resins. A variation on this technique involves binding of phage to a labeled target in solution, then capturing the bound phage through use of an affinity matrix that binds to the labeled target. Thereafter, the phage library is allowed to bind to the immobilized target, and then removed. Nonbinding and weakly binding phage variants are washed away, and the remaining tightly bound variants are eluted using affinity-selective reagents (e.g., a competing protein), mild to severe chaotropic agents, ranging from high/low pH buffers to urea, or site-specific proteases. Following elution, phage can be amplified by infecting fresh *E. coli* cells, and the resulting population again subjected to binding selection. This cycle is typically repeated for several rounds, followed by analysis of selectants through DNA sequencing, which may yield nonrandom occurrences of amino acids at p (particular) positions (i.e., a consensus sequence), or through direct binding analysis as described later. As in ELISA experiments, nonspecific binding leads to artifacts in phage display and can be reduced using proteins or detergents that block these typically low-affinity interactions. However, large diversity libraries sometimes contain peptides that can bind to the blocking agent itself. An enrichment ratio, representing the number of phage binding to the intended target versus the number binding to the matrix or blocking agent, is often used to monitor specificity during multiple rounds of binding selection.

Phage-Binding Analysis

The individual clones selected through phage display are often further analyzed in the form of the recombinant phage particles. Beyond the ability to select relatively rare protein variants with specific binding properties from diversity libraries of millions to tens-of-billions of combinatorial variants, phage display is also used to

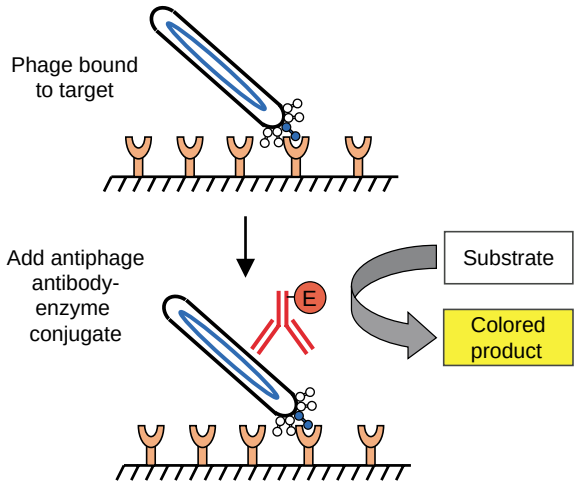

FIGURE 3 Binding assays using phage display. Binding of phage-displayed protein variants is analyzed as in a typical ELISA experiment, with binding of phage to an immobilized target followed by detection with an antiphage antibody conjugated to an appropriate enzyme such as horseradish peroxidase. Relative amounts of bound phage are measured by the amount of color produced when an appropriate substrate is added.

analyze protein–protein-binding interactions without the need to separately purify large numbers of protein variants. For example, to map the binding site on a phage displayed protein for a target protein, the target protein may be coated on an ELISA plate, and mutants or libraries of mutants constructed for phage display. In the case of point-mutation analysis, a phage stock of each mutant is prepared and titrated as in a typical protein-binding ELISA (Figure 3). Alternatively, using libraries of protein variants, the outcome of sequencing many selected variants may be analyzed to determine statistically which amino acids are preferred or disallowed at multiple positions. The utility of phage display has been demonstrated using many systems in which the results of phage selections and binding analysis have been translated into functional proteins whose properties correspond closely to their phage-displayed forms.

See Also the Following Articles

Amino Acid Metabolism • Protein Data Resources

Glossary

degenerate codon A three-nucleotide (triplet) sequence encoding more than one amino acid, realized by synthesis of a pool of triplets having more than one nucleotide at one or more positions. Degenerate codons may be represented in shorthand according to standard abbreviations, e.g., RNS, for (A or G) followed by (A, G, C, or T), followed by (G or C).

elution Process of dissociation which causes the dissociation of bound phage from an immobilized target molecule, for example, using low pH or chaotropic agents.

enrichment Process by which peptide or protein variants with specific binding properties are amplified from a diverse library. An enrichment ratio of the number of phage eluted from an immobilized target divided by the number eluted from a control is often used to measure enrichment.

enzyme-linked immunosorbent assay (ELISA) An assay for binding affinity, typically in which a target molecule is coated onto a plastic plate, a second molecule (the analyte) is added, and a third molecule is used to detect binding of the analyte.

helper phage A bacteriophage which supplies the necessary gene products for packaging of a phagemid construct and is usually deficient in packaging itself into virions.

panning Process of selecting phage for binding to a target protein, especially when the target is coated onto an immunosorbent plastic plate.

phagemid A DNA vector constructed from the combination of replication and other genetic elements from a plasmid with replication, packaging, and other genetic elements from the genome of a bacteriophage.

Further Reading

Barbas, C. F. III, Burton, D. R., Scott, J. K., and Silverman, G. J. (2001). *Phage Display: A Laboratory Manual*. Cold Spring Harbor Laboratory Press, Cold Spring Harbor, New York.

Clackson, T., and Lowman, H. B. (2003). *Phage Display: A Practical Approach*. Oxford University Press, Oxford, UK.

Dower, W. J., and Mattheakis, L. C. (2004). *In vitro* selection as a powerful tool for the applied evolution of proteins and peptides. *Curr. Opin. Chem. Biol.* **6**, 390–398.

Kay, B. K., Winter, J., and McCafferty, J. (1996). *Phage Display of Peptides and Proteins*. Academic Press, San Diego.

Messing, J. M. (1983). New M13 vectors for cloning. *Methods Enzymol.* **101**, 20–78.

Sidhu, S. S., Lowman, H. B., Cunningham, B. C., and Wells, J. A. (2000). Phage display for selection of novel binding peptides. *Methods Enzymol.* **328**, 333–363.

Smith, G. P. (1985). Filamentous fusion phage: Novel expression vectors that display cloned antigens on the virion surface. *Science* **228**, 1315–1317.

Biography

Henry Lowman is a Senior Scientist and Associate Director of Antibody Engineering, with joint appointments in the Departments of Protein Engineering and Immunology, at Genentech, Inc., South San Francisco, California. His research interests are in the structure–function analysis of proteins and the engineering of therapeutic peptides and proteins using structure-based and combinatorial techniques. He holds a Ph.D. from Purdue University and received postdoctoral training as an NIH Postdoctoral Fellow at Genentech, Inc.

Pheromone Receptors (Yeast)

James B. Konopka
State University of New York, Stony Brook, New York, USA

Jeremy W. Thorner
University of California, Berkeley, California, USA

Fungal cells secrete substances (pheromones) that stimulate the ability of haploid cells of different mating types to conjugate, thereby forming diploid cells. Compounds used by various fungal species include terpenes (e.g., *Allomyces* spp.), steroids (e.g., *Achlya* spp.), and peptides (many ascomycetes). The best-characterized fungal pheromone receptors are those for the peptide mating pheromones of the budding yeast, *Saccharomyces cerevisiae*. These receptors are integral membrane proteins that contain seven highly hydrophobic, and potentially α-helical, transmembrane segments. They bind their cognate pheromone at the cell surface, and then activate an intracellular heterotrimeric G protein that initiates a signaling pathway. This pathway induces physiological responses, including the expression of many genes needed to divert cells from the mitotic cell cycle required for vegetative proliferation into a developmental program that permits the fusion of the participating haploid cells. These yeast pheromone receptors are representatives of a very large superfamily that is conserved from yeast to humans.

Pheromone Receptors are Necessary for Conjugation

Pheromone signaling occurs only between cells of different mating type. In *Saccharomyces cerevisiae*, there are two mating types, which are defined by the combination of pheromone and receptor they produce (Figure 1). Haploid cells of the **a**-mating type secrete the **a**-factor pheromone, and express in their plasma membrane, the receptor (Ste2) for α-factor; conversely, haploids of the α-mating type produce α-factor pheromone and, express at their surface, the receptor (Ste3) for **a**-factor. The α-factor is an unmodified 13-residue peptide that is processed from a larger precursor and secreted from cells via the standard secretory pathway. By contrast, **a**-factor is a 12-residue lipopeptide that is modified by farnesylation of the side chain and methyl esterification of the carboxyl group of its C-terminal Cys residue and then exported from cells through the action of a dedicated ATP-driven transporter (Ste6). Cell-type identity is established by genes at the mating type locus (*MAT*) on chromosome III, which encode transcriptional regulators that control expression of the corresponding pheromones and receptors. The gene products required for signaling downstream of the receptors are identical and are expressed in both *MAT***a** and *MAT*α-cells. The genomes of other ascomycetes (i.e., those that pack their spores into an ascus), including the fission yeast, *Schizosaccharomyces pombe*, and the human pathogen, *Candida albicans*, encode homologues of both Ste2 and Ste3. However, in certain basidiomycetes, including the plant rust, *Ustilago maydis*, and the human pathogen, *Cryptococcus neoformans*, the pheromone receptors in the different mating types are all related to Ste3. Furthermore, other groups of fungi, such as many basidiomycetes (including mushrooms), have more than two and often many combinatorial possibilities for distinct mating types and, hence, correspondingly more complex regulation.

Binding of pheromone to a receptor triggers a signal-transduction pathway necessary for eliciting the physiological responses required to differentiate the cells and prepare them for mating. These responses include arrest of cell division in G1 to synchronize the cell cycles of the mating partners, and transcriptional induction of genes that specify proteins required for agglutination, specialized morphogenesis, cell fusion, and nuclear fusion. These proteins and the capacities they confer permit the cells to conjoin, fuse, and form a diploid zygote.

Pheromone Receptors Stimulate a Signal Transduction Pathway

The pheromone receptors induce mating by stimulating a G protein-initiated signaling pathway that has been extensively studied in *S. cerevisiae* and will be described briefly here. Upon binding of the cognate pheromone, an activated pheromone receptor stimulates exchange of GTP for GDP in the α-subunit (Gpa1) of the coupled heterotrimeric G protein. The ensuing conformational

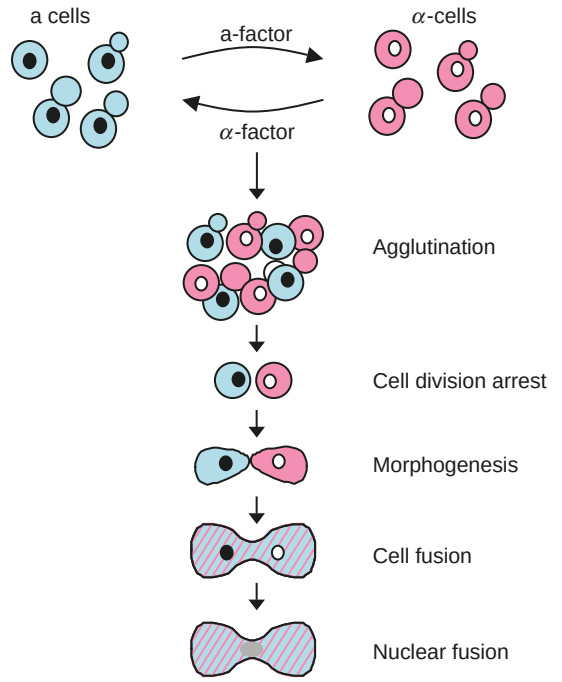

FIGURE 1 Landmark events during conjugation of *S. cerevisiae*. Intercellular communication between cells of mating type **a** and cells of mating type α induces the indicated stages of conjugation, as described in the text.

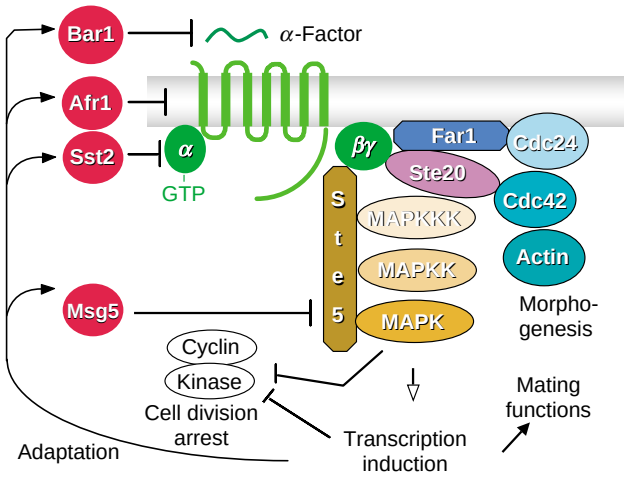

FIGURE 2 Schematic representation of the mating pheromone response pathway in *S. cerevisiae*. A diagram showing the main components involved in transmitting the pheromone signal in *MAT***a** cells. A similar pathway operates in *MAT*α-cells. Activated pheromone receptors stimulate the Gα-subunit to release the G$\beta\gamma$-subunits. The free G$\beta\gamma$-subunits then recruit a scaffold protein, Ste5, to the membrane. Ste5 carries the components of a MAP kinase cascade and places them in proximity to another protein kinase, Ste20. The free G$\beta\gamma$ complex also recruits another scaffold protein, Far1, which carries the activator (Cdc24) of the small GTPase, Cdc42, which is, in turn, the activator of Ste20. Ste20 is further concentrated at these sites because its C terminus also binds to free G$\beta\gamma$-subunits. Conjunction of these components achieved by the pheromone-dependent and receptor-initiated release of G$\beta\gamma$ results in activation of the protein kinase cascade, and ultimately stimulates the pheromone-responsive transcription factor, Ste12, in the nucleus. Activation of Cdc42 also promotes actin polymerization and other aspects of morphogenesis to promote highly polarized growth. Negative regulators of the pathway (shown in red on the left side) are also induced and constitute a negative feedback loop. Bar1 is a secreted protease that degrades α-factor in the medium. Afr1 negatively regulates receptor function. Sst2 is an RGS protein that promotes hydrolysis of the GTP bound to the Gα-subunit. Msg5 is a phosphatase that dephosphorylates and inactivates the terminal MAPK (Fus3).

change in GTP-bound Gpa1 dissociates its associated G$\beta\gamma$ complex (Ste4-Ste18). The free G$\beta\gamma$ complex, which is firmly anchored in the plasma membrane by both C-terminal farnesylation and carboxymethylation of the C-terminal Cys and palmitoylation of the penultimate Cys in Ste18, now exposes surfaces that are able to bind and recruit to the plasma membrane the proteins needed for subsequent events (Figure 2).

One protein that binds to G$\beta\gamma$ is Ste5, which acts as a scaffold by associating with the three protein kinases, Ste11 (MEKK or MAPKKK), Ste7 (MEK or MAPKK), and Fus3 (ERK or MAPK) of a mitogen-activated protein kinase (MAPK) cascade. The existence of such a cascade was first demonstrated unequivocally in *S. cerevisiae*. Phosphorylation and activation of Ste11 requires the action of yet another protein kinase, Ste20. Ste20 is recruited to the membrane in two ways. The activator of Ste20, the small GTPase, Cdc42 (a protein of about 21 kDa), is tethered to the membrane because it is geranylgeranylated and carboxymethylated on its C-terminal Cys, and, in its GTP-bound state, binds to the N-terminal regulatory domain of Ste20. Thus, Ste20 was the first member of the family of protein kinases known as PAKs (for p21-activated protein kinases) to be recognized. In addition, Ste20 is localized specifically near the rest of the pheromone response machinery at the plasma membrane because a motif near the C terminus of Ste20 binds to G$\beta\gamma$. The third component recruited to the plasma membrane by the released G$\beta\gamma$ complex is another scaffold protein (Far1) that carries the guanine nucleotide exchange factor (Cdc24) that stimulates conversion of Cdc42 from its GDP- to its GTP-bound state. Once activated via this phosphorylation cascade, Fus3 is released from Ste5, translocates to the nucleus, and relieves negative regulation of a transcription factor (Ste12) that is poised on the promoters of pheromone-responsive genes, thereby inducing the expression of those genes. Complete sequence analysis of the *S. cerevisiae* genome, accomplished in 1996, identified all of the genes that contain potential Ste12-binding sites in their promoter regions, subsequent chromatin immunoprecipitation demonstrated that many of these promoters are indeed occupied by Ste12 before induction, and now with the advent of DNA microarrays, all genes actually induced by pheromone have been identified. Not surprisingly,

this set of genes includes those needed for cell cycle arrest, agglutination, morphological changes, cell fusion, and nuclear fusion. Interestingly, many signaling components, including the pheromones and receptors, as well as additional gene products that function in adaptation (down-regulation) of the response are induced as part of the highly organized intercellular communication that occurs between mating cells. Collectively, these gene products control the spatial and temporal events of the mating process, as well as recovery from those changes if conjugation does not occur successfully (Figure 2).

Pheromone Receptors Sense Spatial Gradients

A key role played by pheromone receptors in conjugation is in sensing the position of the mating partner and providing proper spatial orientation for the subsequent morphogenesis that enables cells of opposite mating type to grow toward each other, thereby enhancing the probability of their encounter and subsequent fusion. The ability of a yeast cell to track a gradient of pheromone emanating from a cell of the opposite mating type requires dynamic interplay of signaling and adaptation, particularly at the level of the pheromones and receptors. For example, exposure of *MAT*α cells to **a**-factor increases transcription of the α-factor genes, whereas exposure of *MAT***a** cells to α-factor induces expression of an extracellular protease that degrades α-factor in the medium. Another aspect of this interplay involves removal of ligand-bound receptors by endocytosis and their replacement by newly synthesized receptors, which are deposited at the site on the surface immediately adjacent to the partner cell (because the oriented morphogenesis mentioned above directs secretory vesicles to their destination). This behavior sustains the highest degree of receptor activation in the region nearest to the site, on the surface that is exposed to the highest concentration of pheromone emanating from the closest potential partner. Such localized receptor signaling is thought to establish and then reinforce the spatial cues that stimulate properly oriented actin polymerization and other aspects of the directed morphogenesis necessary for conjugation.

Pheromone Receptors are Regulated at Several Levels

Control of pheromone receptor expression and function are key for proper intercellular communication and also for allowing cells to return to normal growth in the event that mating does not occur. These controls have been best studied for Ste2 (α-factor receptor). The C-terminal cytosolic domain of Ste2 is the target for several adaptation mechanisms (and similar mechanisms are known to regulate the **a**-factor receptor, Ste3). First, once ligand-bound, rapid phosphorylation of Ste2 within the C-terminal sequence appears to inhibit the ability of the receptor to continue to signal. It is most likely that the conformational change caused by pheromone binding makes the C-terminal segment of the receptor more accessible to certain protein kinases (casein kinase I family members) that are constitutive residents of the plasma membrane, once again due to the prenylation, carboxylmethylation, and palmitoylation of the C termini of these enzymes. Second, phosphorylation creates a determinant that leads to recognition by a ubiquitin ligase complex and the subsequent covalent addition of ubiquitin to Lys337 in the C terminus (Figure 3). This monoubiquitination triggers endocytosis and removal of the receptor from the cell surface. Third, receptors are also regulated by association with a protein (Afr1) that localizes to the neck of the growing projection in mating cells, prevents receptor-G protein coupling, and thereby restricts receptors that are competent to signal to the leading edge of the projection.

Other components of the pheromone signaling pathway also undergo pheromone-induced down-regulation. For example, induction of Sst2, the first regulator of G protein-signaling (RGS) protein to be recognized, promotes hydrolysis of the GTP bound to Gpa1, thereby deactivating Gα and promoting its reassociation with G$\beta\gamma$. Similarly, induction of Msg5, a dual-specificity MAPK-specific phosphatase, dephosphorylates and thereby inactivates Fus3 (Figure 2).

Pheromone Receptor Synthesis Requires the Secretory Pathway

In the description that follows, Ste2 will continue to be the model because it has been studied most extensively. Ste2 is inserted into the plasma membrane such that it spans the membrane seven times (Figure 3). Biogenesis of Ste2 commences with its import into the endoplasmic reticulum (ER) via a classical N-terminal signal peptide, with concomitant addition of two Asn-linked oligosaccharides, which are further modified and extended with mannose-rich outer chains during transport of Ste2 through the Golgi complex. Although this N-glycosylation does not seem to be critical for receptor function, it may direct or stabilize proper folding of Ste2. While still in the secretory pathway, Ste2 self-associates to form dimers. The interface is thought to include a region of the first transmembrane segment (TMD1) containing Gly56 and Gly60 (Figure 3), which form a GxxxG motif similar to one that mediates dimerization of the red

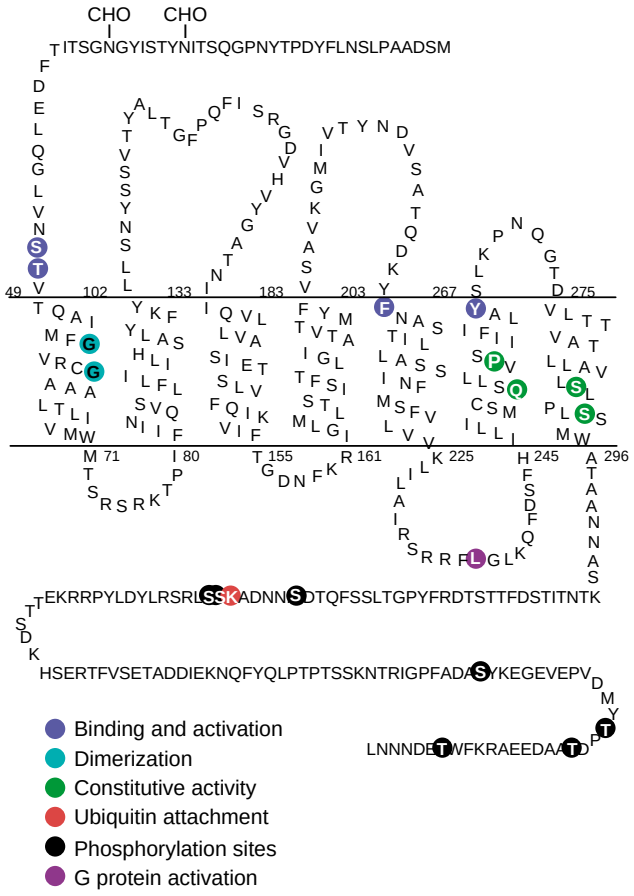

FIGURE 3 Primary structure of *S. cerevisiae* Ste2 (α-factor receptor). The amino acid sequence of Ste2, in the one-letter code, is arranged to represent the seven membrane-spanning elements in their presumed topology across the plasma membrane. Residues discussed in the text that have key functional properties in receptor signaling and adaptation are shaded according to their role in ligand recognition (blue), receptor dimerization (turquoise), conformational constraint (green), phosphorylation (black), and ubiquitination (red). Two sites in the extracellular amino terminus are modified by N-linked glycosylation (CHO). The consensus site for attachment of Asn-linked oligosaccharide (N-X-T or N-X-S) at residue 25 is used close to 100% of the time, whereas that at residue 32 is used only about 50% of the time, and that at residue 46 is not used at all, presumably because it is too close to the membrane for recognition by the eight-subunit oligosaccharyltransferase enzyme complex that transfers the mannose-rich core oligosaccharide from its membrane-bound dolichol carrier to N-X-T or N-X-S motifs in secreted and membrane-localized proteins. Certain naturally occurring neutral polymorphisms exist in the primary structure of Ste2, specifically: residue 269 is E in some *S. cerevisiae* strains, but K in others.

blood cell transmembrane protein, glycophorin A. Dimerization appears to be important for efficient trafficking of Ste2 to the plasma membrane and available evidence suggests that the native signaling-competent state of Ste2 is the dimer. Receptors that fold improperly in the ER are ultimately degraded by ER quality control-mechanisms; those misfolded receptors that make it to the Golgi are sorted to the vacuole (equivalent of the mammalian lysosome) for degradation. It is not clear where or when, properly folded and dimerized receptors first encounter and couple to the quiescent form of the G$\alpha\beta\gamma$ heterotrimer (Gpa1-Ste4-Ste18). However, receptors at the plasma membrane are associated with the heterotrimeric G protein in preactivation complexes primed for the arrival of their pheromone ligand.

Pheromone Receptors Bind Ligand via Contacts with the Extracellular Ends of the Transmembrane Segments

The ligand-binding site in the pheromone receptors (and in other seven-transmembrane segment, G protein-coupled receptors) are conceivably rather complex in that they have the potential to be composed of determinants that reside within the seven transmembrane segments, and/or the three extracellular loops, and/or the extracellular N-terminal extension (or combinations of these elements). The lipid modification of **a**-factor has prevented the application of standard methods for analyzing its binding to Ste3. Hence, the binding of α-factor to Ste2 has been examined in much greater detail. A combination of genetic and biochemical studies strongly implicates residues near the extracellular ends of the transmembrane segments (TMDs) as forming the α-factor-binding pocket. This conclusion suggests a model for receptor activation in which ligand binding to the ends of the TMDs could influence the overall packing or structure of part or all the seven-helix bundle. The resulting conformational change could then be relayed to the intracellular side, and thereby communicated to the associated G protein to promote its activation. Two residues in Ste2 that are necessary for pheromone-induced receptor activation are Phe204, situated near the end of TMD5, which is required for high-affinity α-factor binding, and Tyr266, located near the end of TMD6, which, although not important for binding affinity *per se*, is nonetheless needed for subsequent signaling. The extracellular ends of TMDs 5 and 6, are of course, directly connected to their intracellular ends, and the third intracellular loop of Ste2, which spans the intracellular ends of TMDs 5 and 6, has been implicated in G protein-activation. This situation provides a ready explanation for how conformational change upon pheromone binding could be directly coupled to the associated G protein. Residues (Ser47 and Thr48) near the end of TMD1 are also thought to contact α-factor and may constitute part of the ligand-binding pocket, but do not appear to play a significant role in activation.

Pheromone Receptor Activation may Involve Relief of Conformational Constraint

Current models for signaling by G protein-coupled receptors (GPCRs) suggest that, in the absence of ligand, the off-state is conformationally restricted and that conformational changes upon ligand binding are manifested as greater conformational flexibility. Insights about the conformational state of Ste2 that accompanies its activation have been provided by analysis of constitutively active mutants that signal in a ligand-independent manner. These mutations primarily alter residues within the TMDs, suggesting that constitutive activity can result from changes in the packing of the bundle of transmembrane α-helices. Genetic analysis of constitutive mutants suggests that one restraint may involve interaction between TMD6 and TMD7 mediated via H-bonding between Gln253 in TMD6 and both Ser288 and Ser292 in TMD7. Likewise, a high degree of constitutive receptor activity is caused by substitutions that alter Pro258 in TMD6. In an otherwise α-helical segment, Pro has the unique property of introducing a kink. Thus, substitution of Pro258 with other residues should affect the topology of TMD6. Moreover, TMD6 is the segment whose intracellular end is the most proximal to those residues in the third intracellular loop most strongly implicated in G protein-activation. Hence, the effect of substitution of Pro258 in TMD6 may reflect the conformational change induced within TMD6 that normally occurs only upon ligand binding. In this regard, it is noteworthy that the majority of mammalian receptors of this class also contain Pro at a similar position in TMD6. In those mammalian proteins where it has been examined, the Pro in TMD6 has been implicated in receptor activation, suggesting mechanistic similarities in the activation process from yeast to humans.

Pheromone Receptors Promote G-Protein Activation via the Third Intracellular Loop

The receptor residues on its cytoplasmic surface that contact the G protein and promote GDP–GTP exchange on the Gα-subunit have not been pinpointed precisely. Analysis of chimeras between Ste2 and Gpa1 indicate that merely bringing the receptor and G protein into close proximity is not sufficient to stimulate GDP–GTP exchange because ligand stimulation is still required for activation of downstream signaling by such receptor-Gα hybrids. As discussed above, current evidence suggests that pheromone binding promotes a conformational change at the extracellular ends of the transmembrane helical bundle in Ste2 that is propagated to the intracellular ends of the transmembrane segments, thereby probably exposing previously buried residues that promote G-protein activation. Mutagenesis indicates that, in Ste2, the third intracellular loop certainly plays a key role. Consistent with this view, biochemical studies have demonstrated conformational changes in the third intracellular loop that are induced upon ligand binding. Remarkably, functional ligand-dependent Ste2 can be reconstituted by co-expressing halves of the receptor that are split in the middle of the third intracellular loop. Thus, it is possible that the residues closest to where TMDs 5 and 6 exit, the plasma membrane boundaries are the most important for G protein activation, assuming that the residues closest to the cut ends of such split receptors are the least likely to remain in their native condition. However, substitution of Leu236 (with His) very near the "middle" (at least in terms of primary sequence) of the third loop, yields a Ste2 mutant that displays an essentially wild-type level of surface expression, an essentially wild-type ability to bind α-factor, and an essentially wild-type level of association with the G$\alpha\beta\gamma$ heterotrimer, yet is strongly defective in promoting signaling, suggesting it is specifically defective in activation of the associated G protein. Interestingly, Ste2(L236H) still undergoes ligand-stimulated endocytosis, indicating that the conformational changes and the determinants recognized by the endocytic machinery are distinct from those required for G-protein activation.

Further confounding understanding of the mechanism of G protein-activation is the fact that, although Ste2 and Ste3 both act through the same G protein (Gpa1-Ste4-Ste18), Ste2 and Ste3 do not share any recognizably significant tracts of sequence similarity, even at the intracellular ends of TMDs 5 and 6 or within the third intracellular loop. In this same regard, certain seven-transmembrane segment receptors from other organisms, including mammals, have been expressed in *S. cerevisiae* and in response to the appropriate agonist, are able to activate, albeit to different extents, the endogenous yeast G protein. Again, this cross-species functionality occurs even though the heterologous receptors do not share any obvious sequence identity with the yeast pheromone receptors. Although the ability of receptors from yeast to man to activate the same G protein suggests a common mechanism underlying receptor and G protein activation, the structural determinants of that common action are not readily apparent. Nevertheless, continued functional studies of the yeast pheromone receptors are likely to continue to shed light on how this important class of receptors operates.

See Also the Following Articles

Ubiquitin-Like Proteins • Ubiquitin System

Glossary

agonist A ligand that activates a receptor to transduce a signal.

ligand A substance, such as a mating pheromone, that binds to a receptor molecule.

mating projection A term used to describe the distinctive type of morphogenesis observed in yeast treated with mating pheromone. This structure is thought to form the conjugation bridge that connects mating cells. Commonly referred to as a shmoo.

transmembrane domain A region of a protein that spans a membrane bilayer. These domains are typically present in an ordered structure, such as an α-helix or β-sheet, which allows the polar carbonyl groups of polypeptide chains to be shielded from the hydrophobic membrane bilayer. In the case of the GPCRs the transmembrane domains are thought to form an α-helical structure.

Further Reading

Banuett, F. (1998). Signalling in the yeasts: An informational cascade with links to the filamentous fungi. *Microbiol. Mol. Biol. Rev.* **62**, 249–274.

Brown, A. J., and Casselton, L. A. (2001). Mating in mushrooms: Increasing the chances but prolonging the affair. *Trends Genet.* **17**, 393–400.

Dohlman, H. G., and Thorner, J. W. (2001). Regulation of G protein-initiated signal transduction in yeast: Paradigms and principles. *Annu. Rev. Biochem.* **70**, 703–754.

Elion, E. A. (2000). Pheromone response, mating and cell biology. *Curr. Opin. Microbiol.* **3**, 573–581.

Herskowitz, I. (1989). A regulatory hierarchy for cell specialization in yeast. *Nature* **342**, 749–757.

Kronstad, J. W., and Staben, C. (1997). Mating type in filamentous fungi. *Annu. Rev. Genet.* **31**, 245–276.

Leberer, E., Thomas, D. Y., and Whiteway, M. (1997). Pheromone signalling and polarized morphogenesis in yeast. *Curr. Opin. Genet. Dev.* **7**, 59–66.

Biography

James Konopka is a Professor in the Department of Molecular Genetics and Microbiology at the State University of New York, Stony Brook.

Jeremy Thorner is the William V. Power Professor of Biochemistry and Molecular Biology in the Department of Molecular and Cell Biology at the University of California, Berkeley. Konopka and Thorner's research laboratories are actively engaged in studying the molecular mechanisms that control yeast cell growth and development.

PHO Regulon

Bengt L. Persson
University of Kalmar, Kalmar, Sweden

The *PHO* (*pho*sphatase-encoding) regulon of the yeast *Saccharomyces cerevisiae* is a genetic regulatory circuit, involving structural and regulatory units, essential for controlled expression of phosphatase genes. The network consists of components encoded by ~30 genes which upon expression allow for a coordinated cellular response and adaptation to changes in availability of extracellular phosphate. When phosphate becomes limiting, the cells respond by an increase in the synthesis of high-affinity transporters and phosphatases in order to scavenge phosphate from the environment. Several of the *PHO* regulon components of *S. cerevisiae* are homologous to proteins that take part in the regulation of the eukaryotic cell cycle, including a cyclin-dependent kinase (CDK, Pho85), a cyclin, (Pho80) and a CDK inhibitor (Pho81). The regulator complex formed by these determines the transcription of executive genes encoding the phosphate transporters and phosphatases.

Background

Regulation of cellular activities in response to external nutrient levels is fundamental to all living cells. To achieve this, the cells make use of numerous and varied mechanisms by which changes in the extracellular conditions can be sensed.

Phosphate, an essential nutrient for all organisms, is required for the synthesis of many cellular components (nucleic acids, proteins, lipids, and sugars) as well as for metabolic needs (cellular metabolic pathways such as glycolysis and ATP production). In every cell, whether of prokaryotic or eukaryotic origin, phosphate acquisition plays a key role in maintaining cellular phosphate homeostasis. Therefore, these organisms have evolved regulatory mechanisms for acquisition, storage, and release of this molecule allowing them to respond and adapt to fluctuations in phosphate availability. Phosphate metabolism in the yeast *S. cerevisiae* has been extensively studied for many years and this unicellular organism has provided an excellent model system for understanding how a cell makes a coordinated response to environmental phosphate changes. This organism responds to a diverse array of signals, and many of the responses involve the regulation of gene expression. The transcriptional regulation results in a corresponding adjustment in signaling systems that are activated by a changed phosphate status. The signal transduction pathway involved in the regulation of phosphate-responsive genes is complex and involves at least 22 different genes. The regulation of cellular phosphate uptake activity as well as phosphate starvation responses are maintained by a phosphate signal transduction pathway, the so-called *PHO* regulon. The preferred phosphate source is inorganic phosphate (Pi). Carrier-mediated Pi transport across the plasma membrane, an essential step in the utilization of Pi by *S. cerevisiae*, is mediated by several specific plasma membrane transport systems allowing the cell to switch between a low-affinity and a high-affinity mode of phosphate acquisition. However, when Pi becomes limiting in the growth media, there is an increased production of a high-affinity transport system and of secreted phosphatases that scavenge Pi from a variety of organic compounds through the action of periplasmically located acid phosphatases and of alkaline phosphatases presumably involved in releasing Pi from intracellular substrates. The ability of yeast to utilize various Pi sources is thus highly regulated, and the expression of the genes required for the utilization has been a major topic of study for many years.

The *PHO* Genes and their Regulation

The expression of the *PHO* genes is under tight regulation of the *PHO* regulon. The status of the regulon is commonly genetically and biochemically monitored by use of the activity of a secreted acid phosphatase (the gene product of *PHO5*), which is transcriptionally induced in response to Pi starvation. Although secreted acid phosphatases are encoded by several genes, *PHO3*, *PHO5*, *PHO11*, and *PHO12*, the Pho5 protein is responsible for more than 90% of the acid phosphatase activity of the cells. Most of the information on *PHO5* regulation has been obtained by the isolation and characterization of *PHO* regulon mutants that are defective in Pi regulation of acid phosphatase synthesis.

Besides *PHO5* and its homologues, *PHO11* and *PHO12*, additional genes of the *PHO* regulon which are activated by a Pi-starvation signal include the vacuolar alkaline phosphatase gene, *PHO8*, the genes encoding high-affinity Pi transporters of the plasma membrane, *PHO84* and *PHO89*, the *PHO86* gene encoding an endoplasmatic reticulum (ER) resident protein required for the ER exit of the synthesized Pho84 protein, and the *PHO81* gene encoding an inhibitor (CKI) of a cyclin-dependent kinase (CDK).

At least five regulatory proteins of the *PHO* pathway are believed to be involved in the transcriptional regulation of the *PHO* genes: A complex of the Pho85 CDK and its cyclin Pho80, and the CKI Pho81, together with the transcription factors Pho4 and Pho2 constitute the core components of the regulation (Figure 1). By a yet unknown mechanism, Pi limitation initiates a signal transduction cascade that activates Pho81, the inhibitor of the phosphorylation activity of the cyclin–CDK, Pho80–Pho85.

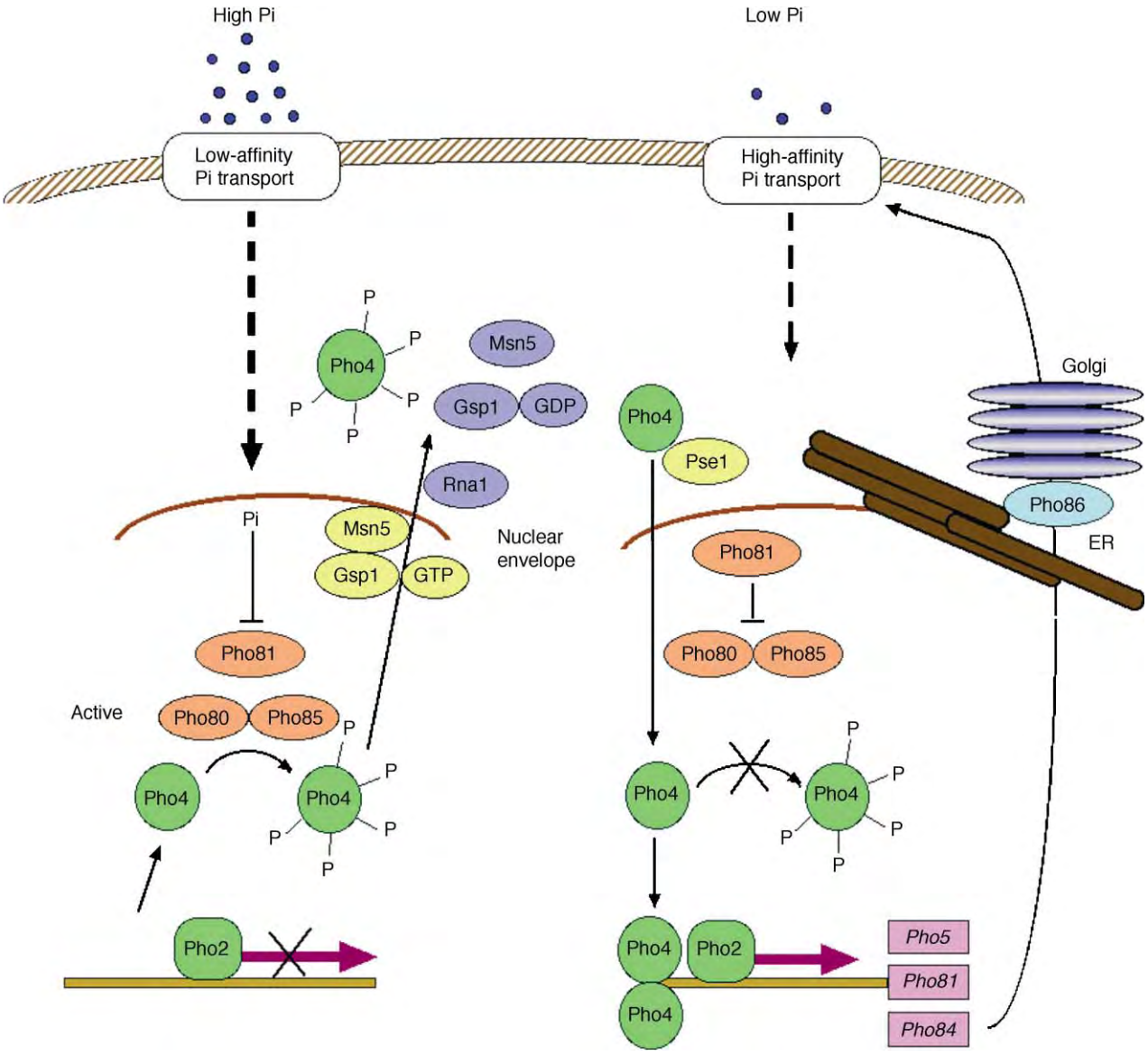

FIGURE 1 Transcriptional regulation of *PHO* genes through the *PHO* regulon at high (left) and low (right) external Pi concentrations. When Pi is abundant, the transcription factor Pho4 is phosphorylated by the Pho80–Pho85 cyclin–CDK complex, assembled with the Msn and Gsp1 proteins and exported to the cytoplasm resulting in a repressed transcription of the *PHO* genes. The CDK inhibitor, Pho81, is associated with the Pho80–Pho85 complex at both high and low Pi conditions, but exerts its inhibition on the complex under conditions of Pi limitations. Under these conditions, the Pho4 will be transported into the nucleus in unphosphorylated form via the Pse1 protein and together with Pho2 bind to the promoter regions and activate transcription of the *PHO* genes. Expression of *PHO*84, encoding a high-affinity Pi transporter results in synthesis and Pho86-mediated delivery of the Pho84 transporter via Golgi to the plasma membrane.

Pho2, Pho4, and Pho81 are positive regulators of *PHO5* and deletion of these genes confer an inability to induce *PHO5* expression upon Pi limitation. Deletion analysis of the *PHO5* promoter has revealed two distinct regulatory elements (upstream activator sequences, UAS), UAS1 and UAS2, to which the transcription factor Pho4 binds under Pi starvation, but not under high-Pi conditions. The binding sequences for Pho4, CACGTG or CACGTT, have been identified and the existence of at least one copy of these sequences has been shown in the immediate promoter region of all but one of the described *PHO* genes, suggesting that Pho4 is a transcriptional activator for all these genes. The structure of the DNA-binding domain of Pho4, resolved to 2.8Å, has revealed a folding of this domain into a C-terminal basic helix-loop-helix (bHLH) motif. A native cysteine residue in the bHLH motif is essential for Pho4 dimerization, binding of the homodimer to the UAS of *PHO5*, and for transcriptional activation of the *PHO* regulon. When localized to the nucleus, Pho4 binds to the two bHLH consensus sequences (CACGTG or CACGTT) in the *PHO* promoter sequences, and the transcriptional regulator Pho2, a homeobox DNA-binding protein, binds cooperatively with Pho4 to activate expression of target genes. As Pho2 binds to its consensus sequence (T/C)TAA(T/A)T(T/G)AAT with low affinity it interacts with several other proteins and participates in the regulation of a diverse array of genes. For its function in *PHO* regulation, Pho2 acts through multiple DNA-binding sites. At the *PHO5* promoter region, one of these sites significantly overlaps with the Pho4-binding site as UAS1, while another two sites flank the second Pho4-binding site, UAS2. As access of the transcriptional regulators Pho2 and Pho4 is aided or hindered by the chromatin structure, the nature of DNA packing is important for the regulation of gene expression. For a chromatin remodeling function in *PHO5* region, the participation of a nuclear-located inositol polyphosphate kinase, Arg82, has been proposed. Factors implicated in chromatin-packing arrangements are histone-DNA interactions in promoter regions of certain *PHO* genes, and acetylation, methylation, or phosphorylation of histones.

A central role in Pi regulation has been demonstrated for the Pho80 cyclin and the Pho85 cyclin-dependent kinase which upon complex formation allows for a differential hyperphosphorylation of the Pho4 transcription factor in the nucleus. Pho85 is one of five CDKs found in *S. cerevisiae*. Activation of CDKs requires binding of a cyclin. At least ten different cyclins involved in cell cycle and/or metabolic regulation are known to bind Pho85. In the Pi assimilation process, the kinase function of Pho85 is activated by interaction with Pho80 whereby the kinase activity of the Pho80–Pho85 cyclin–CDK complex phosphorylates Pho4. Protein phosphorylation has been found to play an important role in the control of diverse cellular processes, especially that of transcriptional factors in regulation of gene expression. The phosphorylated state of Pho4 is important for its localization in the cell and thus for its activity in transcriptional regulation of the *PHO* genes. The CKI Pho81 binds to the Pho80–Pho85 protein complex when cells are grown at both high and low Pi conditions but a pronounced inhibition of the kinase activity and hence an abolished hyperphosphorylation is seen only at Pi-limiting conditions. Under these conditions, the *PHO* genes, including *PHO81*, are activated. The unphosphorylated form of Pho4, which has a low affinity for the nuclear exportin receptor Msn5, is presumably transported into the nucleus through an import pathway that utilizes the importin Pse1. In contrast, the hyperphosphorylated form of Pho4, which is unable to bind to Pse1, is accessible for complex formation with Msn5 and Gsp1, a yeast Ran homologue, after which the complex is transported into the cytoplasm. Dissociation of the complex in the cytoplasm involves the participation of Rna1, a GTPase-activating protein responsible for the conversion of the GTP bound to Gsp1 in its complex active form to GDP. Thus, Pho4 is concentrated to the nucleus when yeast cells are starved for Pi and is predominantly cytoplasmic when yeast cells are grown at high, repressive Pi conditions. It has been proposed that also Pho2 can be phosphorylated by a kinase, possibly indicating a similar mechanism whereby the transcriptional activity of Pho2 may thus be regulated by a phosphate switch, not only enhancing the transcriptional activity but also facilitating the interaction between Pho2 and Pho4. Only when Pho2 is phosphorylated, the *PHO5* can be expressed under Pi limiting conditions. Transcription of *PHO* genes under Pi limitation would thus necessitate Pho4 dephosphorylation as well as Pho2 phosphorylation. Such a feedback Pi-controlled regulation of transcription ensures balanced levels of regulatory proteins and a swift response to changes in Pi concentrations.

The positive feedback-regulated inhibition of Pho85–Pho80 exerted by Pho81, makes Pho81 a key player in the *PHO* regulatory pathway. Pho81 harbors a tandem repeat of six ankyrin consensus regions, of which one is regarded to play an essential role in the CKI/CDK complex interaction. However, both the mechanisms by which the Pi limitation signal is transduced to Pho81 and where the signal originates are still unclear.

Due to a comprehensive identification and characterization of the *PHO*-regulated genes in the yeast genome, the late events in the *PHO* pathway are now well understood, an important step toward an understanding of the physiological regulation of Pi metabolism.

See Also the Following Articles

Diacylglycerol Kinases and Phosphatidic Acid Phosphatases • Mitochondrial Genes and their Expression: Yeast • Pentose Phosphate (Hexose Mono Phosphate) Pathway • Pentose Phosphate Pathway, History of

Glossary

ankyrin region Protein domains that contain 33-amino acid long sequences that often occur in tandem arrays and are involved in protein's molecular recognition.

CDK Cyclin-dependent kinases, a family of protein kinases that control cell cycle progression in all eukaryotes and require physical association with cyclins to achieve full enzymatic activity. CDK's are regulated by phosphoryation and dephosphorylation events.

CKI Cyclin-dependent kinase inhibitor, small protein that binds stoichiometrically to regulate the activity of CDKs.

cyclin Protein found in certain eukaryotic cells that helps regulate the cell cycle by causing cells to begin mitosis. Cyclins are regulatory subunits of the cyclin-dependent protein kinases.

homeobox genes Genes with a shared nucleotide segment that are involved in the formation of bodily segmentation during embryologic development.

***PHO* regulon** Genetic regulatory network of scattered genes involving structural and regulatory units active in phosphate signal transduction.

promoter A DNA sequence that enables a gene to be transcribed.

Further Reading

Carroll, A. S., and O'Shea, E. K. (2002). Pho85 and signaling environmental conditions. *Trends Biochem. Sci.* **27**, 87–93.

Lenburg, M. E., and O'Shea, E. K. (1996). Signaling phosphate starvation. *Trends Biochem. Sci.* **21**, 383–387.

Ogawa, N., DeRisi, J., and Brown, P. O. (2000). New components of a system for phosphate accumulation and polyphosphate metabolism in *Saccharomyces cerevisiae*. *Mol. Biol. Cell.* **11**, 4309–4321.

Oshima, Y. (1997). The phosphatase system in *Saccharomyces cerevisiae*. *Genes Genet. Syst.* **72**, 323–334.

Persson, B. L., Lagerstedt, J. O., Pratt, J. R., Pattison-Granberg, J., Lundh, K., Shokrollahzadeh, S., and Lundh, F. (2003). Regulation of phosphate acquisition in *Saccharomyces cerevisiae*. *Curr. Genet.* **43**, 225–244.

Torriani-Gorini, A., Silver, S., and Yagil, E. (1994). *Phosphate in Microorganisms: Cellular and Molecular Biology.* American Society for Microbiology, Washington DC.

Biography

Bengt L. Persson is a Professor in the Department of Chemistry and Biomedical Sciences at the University of Kalmar. His principal research interests are in molecular membrane biochemistry and cellular regulation of phosphate acquisition systems. He holds a Ph.D. from the University of Stockholm and received his postdoctoral training at the University of California, Los Angeles. He is presently conducting research on phosphate transport regulation at the Universities of Stockholm and Kalmar and has authored several papers on phosphate transporters of yeast.

Phosphatidylinositol Bisphosphate and Trisphosphate

Alex Toker
Harvard Medical School, Boston, Massachusetts, USA

Phosphatidylinositol (PtdIns) is a minor membrane phospholipid which is found in all eukaryotic cells. It is the precursor of a family of phosphorylated lipids which are collectively known as phosphoinositides, and rather than serving a structural role in cellular membranes, they act as functional second messengers to transduce biochemical signals in the cell. The article in detail discusses the synthesis, hydrolysis, and cellular functions of phosphotidylinosital bisphosphate and trisphosphate.

Phosphoinositides are composed of a water-soluble inositol ring which can be phosphorylated at each of three positions (D-3, D-4, and D-5), and a greasy fatty acid tail which is attached to a glycerol and linked to the inostol ring by a phosphodiester bond (Figure 1). The concerted actions of phosphoinositide kinases, phosphoinositide phosphatases, and phospholipases on phosphatidylinositol leads to the production of seven additional phosphoinositides which are known to exist in cells (Figure 2). Of these, phosphatidylinositol-4,5-bisphosphate (PtdIns-4,5-P_2) and phosphatidylinositol-3,4,5-trisphosphate (PtdIns-3,4,5-P_3) are the best understood and characterized. Both the synthesis and the degradation of PtdIns-4,5-P_2 and PtdIns-3,4,5-P_3 are tightly regulated, and this ensures efficient and coordinated signaling through these second messengers. Biochemical and genetic studies have implicated both PtdIns-4,5-P_2 and PtdIns-3,4,5-P_3 in numerous cellular responses, such as cell growth, cell survival, cell motility and modulation of the actin cytoskeleton, gene transcription and vesicle trafficking (Figure 3). The importance of these phosphoinositides in cell biology is exemplified by the fact that deregulation in the metabolism or mechanism of action of these lipids often results in human diseases such as cancer and type 2 diabetes.

Phosphatidylinositol-4,5-Bisphosphate

Synthesis

PtdIns-4,5-P_2 is often considered to be one of the most important functional lipids in eukaryotic cells, because it not only has a functional second messenger role *per se*, but can also serve as an intermediate for the production of additional lipid mediators. It can serve as a substrate for phosphoinositide 3-kinase (PI 3-K) to produce PtdIns-3,4,5-P_3, it can be hydrolyzed by phospholipases to produce diacylglycerol (DAG) and soluble inositol phosphates, and it can also be dephosphorylated by D-4 and D-5 lipid phosphatases (Figure 2). Although the bulk of PtdIns-4,5-P_2 is found at the plasma membrane, other distinct pools of PtdIns-4,5-P_2 have been reported. For example, there exists a nuclear phosphoinositide cycle where PtdIns-4,5-P_2 production has been detected. However, there are relatively modest, if any, changes in the total levels of PtdIns-4,5-P_2 upon cellular stimulation with agonists such as growth factors or hormones. This is difficult to reconcile with the second messenger hypothesis which dictates that a lipid mediator must rapidly accumulate to amplify downstream signaling. Therefore, it is likely that the constitutive levels of PtdIns-4,5-P_2 change locally at discrete intracellular sites, such that the accumulation of this lipid is regulated both spatially and temporally. In addition, there are two other isomers of phosphatidylinositol bisphosphate: PtdIns-3,4-P_2 and the recently discovered PtdIns-3,5-P_2. The function of these two phosphoinositides is not entirely clear, but they are likely to mediate certain responses downstream of PI 3-K.

The synthesis of PtdIns-4,5-P_2 is controlled by the sequential action of phosphoinositide 4-kinases, which use phosphotidylinositol (PtdIns) as substrate and produce PtdIns-4-P, and phosphoinositide phosphate kinases (PIPKs), which can use either PtdIns-4-P or PtdIns-5-P as substrates. In both cases, the product is PtdIns-4,5-P_2 (Figure 2). Much is known about the enzymes which produce PtdIns-4,5-P_2. There are two families of PIPKs, type I and type II. Type I kinases preferentially phosphorylate PtdIns-4-P at the D-5 position, and this appears to be the major route of PtdIns-4,5-P_2 synthesis. However, it was recently discovered that type II PIPKs can phosphorylate PtdIns-5-P at the D-4 position, and so it is likely that in some instances this represents an important pathway for the

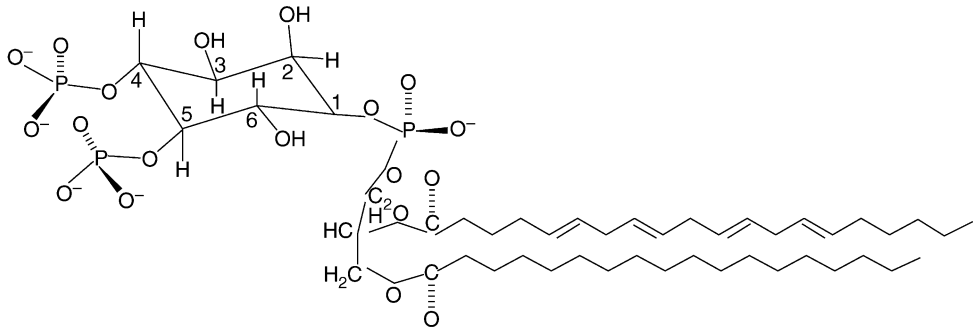

FIGURE 1 Structure of phosphatidylinositol-4,5-bisphosphate. The structure shows PtdIns-4,5-P_2\, which contains an inositol head group connected to a diacylglycerol via a phosphodiester linkage. The fatty acid moiety is typically stearoyl-arachidonyl. The inositol head group can be phosphorylated at one of three positions, D-3, D-4, and D-5. Shown are phosphate groups at the D-4 and D-5 position in PtdIns-4,5-P_2. Phosphoinositide 3-kinases phosphorylate the D-3 position of PtdIns-4,5-P_2 to produce PtdIns-3,4,5-P_3.

generation of PtdIns-4,5-P_2. Several forms of both type I and type II PIPKs exist in mammalian cells, and homologues are also found in lower eukaryotes such as yeasts, highlighting the importance of these enzymes in biology. The crystal structure of a type II enzyme has been solved, and has revealed an elongated, flat surface covered with highly basic, positively charged amino acids which are ideally positioned for interaction with the negatively charged phosphoinositides such as PtdIns-5-P. Finally, a separate route of synthesis for PtdIns-4,5-P_2 is the dephosphorylation of PtdIns-3,4,5-P_3 by D-3 phosphoinositide phosphatases, though it is not clear what fraction of the bulk PtdIns-4,5-P_2 pool is accounted for by this mechanism. Regardless, PIPKs represent the major pathway leading to the production of PtdIns-4,5-P_2, and as such their activities are tightly controlled.

Hydrolysis

PtdIns-4,5-P_2 is hydrolyzed by phosphoinositide-specific phospholipases. These enzymes, also known as type C phospholipases (PLC), hydrolyze PtdIns-4,5-P_2 into two important second messengers: the membrane-bound fatty acid moiety, also known as diacylglycerol (DAG), and the soluble portion which is an inositol trisphosphate (Ins-1,4,5-P_3, when PtdIns-4,5-P_2 is the PLC substrate). Each of these products has important roles

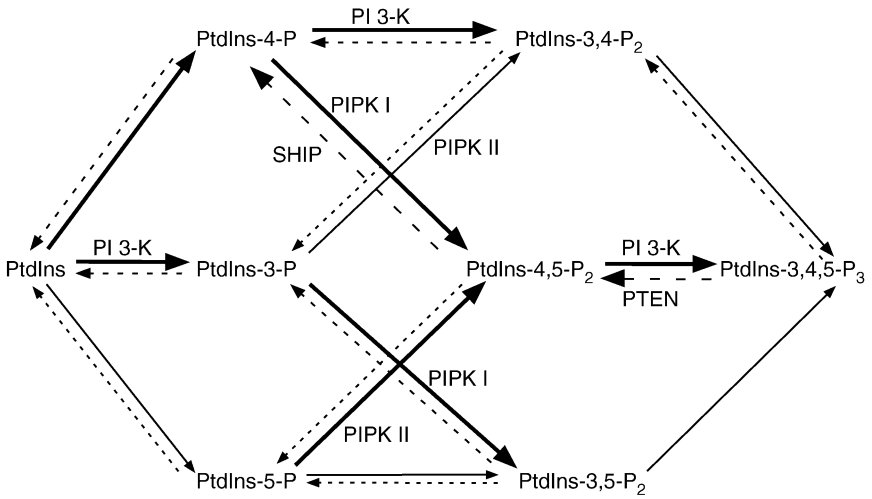

FIGURE 2 Phosphoinositide metabolism. The pathways responsible for the production of all known phosphoinositides are shown. The concerted actions of phosphoinositide kinases, such as PIPKs (type I and type II phosphoinositide 4-phophate and 5-phosphate kinases) and phosphoinositide 3-kinases (PI 3-K), as well as phosphatases (PTEN and SHIP) leads to the production of seven distinct phosphoinositides, from the precursor phosphatidylinositol (PtdIns). Although all of the forward (solid arrows, mediated by kinases) and reverse (broken arrows, mediated by phosphatases) reactions are possible, the pathways which are likely to predominate in cells are shown in bold arrows.

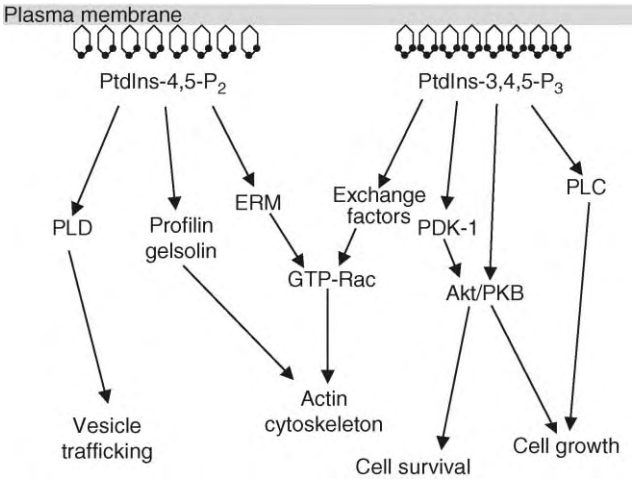

FIGURE 3 Targets of PtdIns-4,5-P_2 and PtdIns-3,4,5-P_3. A large number of proteins whose activities are directly regulated by either PtdIns-4,5-P_2 or PtdIns-3,4,5-P_3 exist. A few of these are depicted and serve to illustrate that the binding of the phosphoinositide to the protein can alter its cellular location as well as directly influencing catalytic activity when enzymes are the targets. These interactions are responsible for the activation of secondary signaling pathways, which ultimately lead to numerous physiological responses, as depicted. In many cases, PtdIns-4,5-P_2 and PtdIns-3,4,5-P_3 have overlapping functions, due to the activation of distinct effector molecules, such as the remodeling of the actin cytoskeleton which occurs as a consequence of both PtdIns-4,5-P_2- and PtdIns-3,4,5-P_3-dependent signaling.

in lipid signaling. DAG is the activator for members of the protein kinase C family of serine/threonine kinases, which are recruited to the membrane at the site of DAG production. Ins-1,4,5-P_3 plays an equally important role in lipid signaling as it is responsible for the release of Ca^{2+} from internal stores, such as the endoplasmic reticulum.

Although four distinct families of PLC exist in mammalian cells, they all share a similar catalytic mechanism employing calcium as a cofactor. All members of the PLC family use PtdIns-4-P and PtdIns-4,5-P_2 as substrates. PLCβ enzymes are regulated by binding to both $\beta\gamma$-as well as α-subunits of heterotrimeric GTP-binding proteins. PLCδ also appears to be regulated by G proteins, although the mechanism is unclear, and it is also reported that increases in Ca^{2+} alone are sufficient to activate PLCδ. Phospholipases belonging to the PLCγ family are activated by the binding of SH2 domains to phosphotyrosine-containing sequences in receptor tyrosine kinases, and as such participate in growth-factor-dependent responses such as cell growth. Tyrosine phosphorylation of PLCγ is also important in controlling catalytic activity. Very recently a new PLC subtype has been described, PLCε, and has shown to be a novel effector of the GTP bound form of the Ras GTPase. The diversity and complexity of the PLC family underscores the importance of PtdIns-4,5-P_2 hydrolysis and DAG/Ins-1,4,5-P_3 production in mediating cell proliferation, differentiation, and cell motility.

Cellular Function

In addition to serving as the substrate for additional lipid second messengers, PtdIns-4,5-P_2 is an important lipid mediator in its own right. Numerous studies have shown that PtdIns-4,5-P_2 can modulate the activity of proteins which regulate actin assembly, leading to rearrangements of the actin cytoskeleton (Figure 3). For example, PtdIns-4,5-P_2 has been shown to promote actin polymerization by directly interacting with actin-binding proteins such as profilin. Similarly, actin-capping proteins, such as CapZ, prevent spontaneous actin assembly by capping the free ends of actin filaments, and the binding to PtdIns-4,5-P_2 disrupts this capping event leading to filament assembly. The list of actin-binding proteins whose activities are also regulated by PtdIns-4,5-P_2 includes gelsolin, cofilin, filamin, and vinculin. The small GTPase Rac also plays an important role in the remodeling of the actin cytoskeleton, and in some instances this requires PtdIns-4,5-P_2. For example, the ERM family of proteins (*E*zrin, *R*adixin, and *M*oesin), a family of Rac effector molecules, are also PtdIns-4,5-P_2-binding proteins which regulate dynamic actin assembly, again linking PtdIns-4,5-P_2 function to the actin cytoskeleton. Rac, in the active GTP bound form, also interacts with PIP kinases, which are responsible for PtdIns-4,5-P_2 synthesis. Recent studies in cells have provided further evidence that PtdIns-4,5-P_2 is a critical regulator of the actin cytoskeleton. For example, expression of type I PIPK enzymes in cells leads to a dramatic reorganization of the actin cytoskeleton, and PIPK I appears to be targeted to focal adhesions, sites of cellular contact with the extracellular matrix. This targeting provides clear evidence for the localized accumulation of PtdIns-4,5-P_2 in the cell. Studies such as these, carried out in mammalian cells, have also been corroborated in yeasts, whereby genetic ablation of PIP kinases (such as Mss4p) leads to abnormalities in the actin cytoskeleton, which can be rescued by the introduction of human PIPK isoforms.

PtdIns-4,5-P_2 is also an important cofactor for the activity of a number of signaling enzymes. The best example is for *p*hospho*l*ipase *D* (PLD), an enzyme responsible for the production of *p*hosphotidic *a*cid (PA) in the cell. PLD requires PtdIns-4,5-P_2 for efficient catalytic function. Because certain PIP kinases also depend on PA for enzymatic activity, and PtdIns-4,5-P_2 stimulates PLD leading to PA production, the net result is a positive amplification loop which leads to amplification of PA and PtdIns-4,5-P_2 synthesis at specific intracellular compartment where these enzymes are located. Both PIPKs and PLD have been implicated in trafficking and secretion, and as such their products are

directly involved in controlling vesicle formation, as well as endocytosis (Figure 3).

Phosphatidylinositol-3,4,5-Trisphosphate

Synthesis

Unlike its substrate PtdIns-4,5-P_2, phosphotidylinositol-3,4-trisphosphate (PtdIns-3,4,5-P_3) is nominally absent in unstimulated cells and rapidly accumulates in response to virtually all known growth factors, hormones, cytokines, and other stimuli. In most cells, production of PtdIns-3,4,5-P_3 typically peaks within seconds to a few minutes after stimulation, and declines to near basal levels after 1–2 h. A second peak of PtdIns-3,4,5-P_3 has been observed in cells between 4 and 8 h after stimulation with mitogens such as platelet-derived growth factor (PDGF). This second peak of PtdIns-3,4,5-P_3 is responsible for efficient cell cycle progression in fibroblasts, specifically entry into the S phase where DNA synthesis occurs. Although the bulk of PtdIns-3,4,5-P_3 is produced at the plasma membrane, it is also known that there are discrete intracellular locations where this phosphoinositide is also found, particularly the nucleus. PI 3-Ks are responsible for the production of PtdIns-3,4,5-P_3 in higher eukaryotes. These enzymes phosphorylate the D-3 position of the inositol head ring, and depending on the substrate, four distinct products can result: PtdIns-3-P, PtdIns-3,5-P_2, PtdIns-3,4-P_2, and PtdIns-3,4,5-P_3 (Figure 1). Although different forms of PI 3-Ks exist, each with unique substrate selectivity, the class Ia enzymes are responsible for the production of PtdIns-3,4,5-P_3 in cells. These PI 3-Ks are composed of a p85 regulatory subunit and a p110 catalytic subunit. The regulatory subunit binds to specific phosphotyrosine-containing sequences in the cytosolic domains of activated receptor tyrosine kinases, via a tandem repeat of two Src-Homology 2 (SH2) domains. This interaction facilitates the activation of the catalytic subunit, whose activity is also increased by a direct interaction with the activated form of the small GTPase Ras. The newly activated PI 3-K converts PtdIns-4,5-P_2 to PtdIns-3,4,5-P_3. In addition, class Ib PI 3-Ks are also capable of producing PtdIns-3,4,5-P_3, and these kinases are typically activated downstream of heterotrimeric G protein-coupled receptors, such as the thrombin receptor in platelets. Class Ib enzymes are also composed of two subunits, a p120 catalytic subunit and a p101 regulatory subunit, which confers sensitivity to G$\beta\gamma$. Class Ib enzymes also require activated Ras for full catalytic function. Thus, the primary route of synthesis for PtdIns-3,4,5-P_3 in cells is through the activation of class I PI 3-Ks which use PtdIns-4,5-P_2 as substrate.

PtdIns-3,4,5-P_3 Phosphatases

Because the production of PtdIns-3,4,5-P_3 is critical for a number of physiological responses in cells, mechanisms exist which mediate the termination of PI 3-K and PtdIns-3,4,5-P_3 signaling. PI 3-K lipid products, including PtdIns-3,4,5-P_3, are not degraded by phospholipases, but instead are down-regulated by at least two different types of phosphoinositide phosphatases. SHIP1 and SHIP2 (*SH*2-containing *i*nositol 5′-*p*hosphatases) are lipid phosphatases which specifically remove the D-5 phosphate from both PtdIns-4,5-P_2 and PtdIns-3,4,5-P_3 (Figure 2). The action of SHIP1/2 on PtdIns-3,4,5-P_3 results in the production of PtdIns-3,4-P_2, and although this can impair signaling downstream of PI 3-K, PtdIns-3,4-P_2 is able to mediate certain responses which overlap with PtdIns-3,4,5-P_3. Despite this, loss of SHIP2 increases insulin sensitivity in responsive tissues such as muscle and fat. *P*hosphatase and *ten*sin (PTEN) homologue deleted on chromosome 1, is a D-3 phosphatase which dephosphorylates PtdIns-3,4,5-P_3 with PtdIns-4,5-P_2 as the product (Figure 2). PTEN is very effective at terminating PI 3-K and PtdIns-3,4,5-P_3 signaling, and this is evidenced by the fact that mutations in the PTEN gene have been detected in a large fraction of advanced human tumors. For this reason, PTEN is referred to as a tumor-suppressor gene. Thus, efficient termination of PtdIns-3,4,5-P_3 signaling is of critical importance for intracellular signaling, and deregulation of this signal can have adverse consequences for cellular responses, often leading to diseases such as diabetes and cancer.

PtdIns-3,4,5-P_3-Binding Proteins

The mechanism by which PI 3-K activates downstream secondary signaling pathway is by the recruitment of cytosolic proteins to the plasma membrane at the site of PtdIns-3,4,5-P_3 production. This recruitment can have a number of consequences; in addition to causing a change in the cellular location of the protein, it can induce a conformation change, and in the case of enzymes, it can increase (and sometimes decrease) enzymatic activity. Typically, a combination of these events results from the PtdIns-3,4,5-P_3-protein interaction. A number of protein domains have evolved which specifically recognize phosphoinositides, particularly PtdIns-3,4,5-P_3. The first described example is the *P*leckstrin *H*omology (PH) domain, a 100 amino acid sequence found in several signaling proteins which participate in PI 3-K responses. PH domains are found in both serine-threonine protein kinases (e.g., Akt/PKB and PDK-1), tyrosine kinases (e.g., Tec family kinases such as Btk), guanine nucleotide exchange factors of small GTP-binding proteins (e.g., SOS, Grp-1 and pREX), and GTPases themselves (e.g., dynamin). In some of these

cases, the PtdIns-3,4,5-P_3-protein interaction is well understood. For example, recruitment of Akt/PKB to the plasma membrane occurs in response to PtdIns-3,4,5-P_3 production. The PH domain of Akt/PKB directly binds to PtdIns-3,4,5-P_3 with high affinity and selectivity, and this leads to a conformational change in the protein kinase which leads to unfolding of the PH domain, revealing a sequence in the catalytic domain known as the activation loop. The PDK-1 kinase, which also has a PH domain and is recruited to the membrane simultaneously with Akt/PKB, can now phosphorylate Akt/PKB at a critical threonine residue in this loop. The phosphorylated Akt/PKB is now fully catalytically competent and can itself phosphorylate downstream protein substrates. This elegant mechanism is recapitulated in a large number of other protein kinases which are also regulated by PtdIns-3,4,5-P_3 or PDK-1, or both (e.g., protein kinase C and S6-kinases).

Recently, a distinct phosphoinositide-binding domain was described, and termed the *p*ho*x (PX)* domain. This 130 amino acid domain is also found in many important signaling proteins, and was originally described in the $p40^{phox}$ and $p47^{phox}$ subunit of the NADPH-oxidase superoxide-generating complex in phagocytic cells. Although PX domains do not appear to bind to PtdIns-3,4,5-P_3, they bind with high affinity to PtdIns-3-P and PtdIns-3,4-P_2, and thus are important in mediating signaling downstream of these PI 3-K lipids. Another domain which has been shown to bind PtdIns-3,4,5-P_3 is the SH2 domain. Although less well understood, binding of PtdIns-3,4,5-P_3 to the SH2 domain of the phospholipase PLCγ-1, for example, leads to an increase in its enzymatic activity. Thus, several domains have evolved in higher eukaryotic cells which have the ability to bind with distinct affinities and selectivity to PtdIns-3,4,5-P_3, and other phosphoinositides. This interaction has a profound effect on downstream signaling and cellular responses.

Cellular Function

Numerous biochemical, pharmacological, and genetic studies have demonstrated that PI 3-K, and its product PtdIns-3,4,5-P_3, regulates a multitude of cellular responses. These include cell growth, protection from cell death (apoptosis), remodeling of the actin cytoskeleton, cell migration and invasion, metabolism and insulin responses, cell cycle regulation, and gene transcription (Figure 3). It is beyond the scope of this article to discuss all of these in any detail, but some notable examples are given. Activation of the protein kinase Akt/PKB by the PI 3-K pathway regulates cellular survival mechanisms, as well as insulin-dependent metabolism. Most proteins which mediate Akt/PKB-dependent cellular survival are inhibited by the phosphorylation event. For example, phosphorylation of the Forkhead family of transcription factors (e.g., FKHR-L1) by Akt/PKB inhibits their translocation to the nucleus due to the creation of a binding site for 14-3-3, a family of molecular chaperones. This retention of FKHR-L1 in the cytoplasm inhibits the transactivation of genes intimately associated with cell death, and the net effect is an increase in survival. Similarly, Akt/PKB phosphorylation of the pro-apoptotic protein Bad also facilitates 14-3-3 binding, and this prevents Bad from binding to the anti-apoptotic proteins Bcl-2 and Bcl-X_L, effectively preventing apoptosis. Akt/PKB can also regulate both cell cycle progression and gluconeogenesis/glycolysis by phosphorylating *g*lycogen *s*ynthase *k*inase-*3* (GSK-3). This phosphorylation inhibits the elevated constitutive activity of GSK-3, which can no longer phosphorylate proteins such as Myc, the cell cycle regulator cyclin D, and glycogen synthase. Thus, Akt/PKB signaling results in the activation of several pathways which are normally inhibited by GSK-3.

Not all PI 3-K responses are mediated by Akt/PKB. In fact there are several other kinases which are activated by PtdIns-3,4,5-P_3 signaling, and which have important roles in cell physiology. For example, the S6-kinases, S6K-1 and S6K-2, regulate protein synthesis and insulin responses. The protein kinase C family of kinases can also be regulated by PtdIns-3,4,5-P_3-dependent mechanisms, and have been shown to mediate both cell growth and survival mechanisms, though these are not as well understood as the Akt/PKB pathway. The Tec family kinase *B*ruton's *t*yrosine *k*inase (Btk), which binds to PtdIns-3,4,5-P_3 via its PH domain, is important for B cell development, and importantly, genetic mutations within its PH domain have been shown to give rise to certain immunodeficiencies in humans.

Finally, regulation of the dynamics of the actin cytoskeleton is also achieved by PtdIns-3,4,5-P_3-dependent responses, and this leads to increased cell migration of many cell types (Figure 3). One important mechanism by which PtdIns-3,4,5-P_3 regulates such responses is by activating the small GTP-binding protein Rac, known to contribute to actin remodeling and directional migration in response to chemotactic stimuli. Small GTPases such as Rac are activated by binding to GTP, and this is stimulated by the activation of Rac-specific guanine nucleotide exchange factors, such as SOS, Vav and in particular, pREX. These exchange factors have PH domains which in some cases have been shown to bind to PtdIns-3,4,5-P_3, leading to an increase in exchange activity towards Rac. In summary, the diverse cellular responses attributed to PI 3-K signaling are explained by the fact that there exist numerous signaling proteins which interact with PtdIns-3,4,5-P_3. This binding has a profound

consequence on the function of the protein, leading to the activation of downstream pathways.

See Also the Following Articles

Diacylglycerol Kinases and Phosphatidic Acid Phosphatases • Inositol Lipid 3-Phosphatases • Inositol Phosphate Kinases and Phosphatases • Phosphatidylinositol-3-Phosphate • Phosphoinositide 3-Kinase • Phosphoinositide 4- and 5-Kinases and Phosphatases • Phosphoinositide-Dependent Protein Kinases • Phospholipase C • Phospholipase D

Glossary

phosphatidylinositol Membrane phospholipid which is a precursor to all known phosphoinositides and is composed of an inositol head ring and fatty acid tail.

phosphoinositide Phospholipid second messenger which is found in intracellular membranes and which can be phosphorylated on the inositol head ring at the D-3, D-4, and D-5 positions resulting in seven known phosphorylated species.

phosphoinositide kinase An enzyme which can use phosphoinositides as substrates, and can phosphorylate the inositol head ring at either the D-3, D-4, or D-5 positions.

phosphoinositide phosphatase An enzyme which can specifically remove the D-3, D-4, or D-5 phosphate from phosphorylated phosphoinositides.

phospholipase An enzyme which can hydrolyze the phosphodiester bond in phospholipids and produce soluble inositol lipids and membrane-bound diacylglycerol; type C phospholipases specifically use phosphoinositides as substrates.

PH domain A protein domain composed of approximately of 100 amino acids which can specifically bind to Ptdins-4,5-P_2 and Ptdins-3,4,5-P_3.

Further Reading

Anderson, R. A., Boronenkov, I. V., Doughman, S. D., Kunz, J., and Loijens, J. C. (1999). Phosphatidylinositol phosphate kinases, a multifaceted family of signaling enzymes. *J. Biol. Chem.* **274**, 9907–9910.

Cantley, L. C. (2002). The phosphoinositide 3-kinase pathway. *Science* **296**, 1655–1657.

Cullen, P. J., Cozier, G. E., Banting, G., and Mellor, H. (2001). Modular phosphoinositide-binding domains—their role in signalling and membrane trafficking. *Curr. Biol.* **11**, R882–R893.

Leslie, N. R., Biondi, R. M., and Alessi, D. R. (2001). Phosphoinositide-regulated kinases and phosphoinositide phosphatases. *Chem. Rev.* **101**, 2365–2380.

Rhee, S. G. (2001). Regulation of phosphoinositide-specific phospholipase C. *Annu. Rev. Biochem.* **70**, 281–312.

Toker, A. (2002). Phosphoinositides and signal transduction. *Cell Mol. Life Sci.* **59**, 761–779.

Vivanco, I., and Sawyers, C. L. (2002). The phosphatidylinositol 3-kinase AKT pathway in human cancer. *Nat. Rev. Cancer* **2**, 489–501.

Wishart, M. J., and Dixon, J. E. (2002). PTEN and myotubularin phosphatases: From 3-phosphoinositide dephosphorylation to disease. Phosphatase and tensin homolog deleted on chromosome ten. *Trends Cell Biol.* **12**, 579–585.

Biography

Alex Toker is an Associate Professor of Pathology at the Beth Israel Deaconess Medical Center, Harvard Medical School, Boston. His principal research interests are the role of lipid signaling pathways and protein kinases in regulating carcinoma cell growth, survival, and invasion. He holds a Ph.D. from the National Institute for Medical Research, London, and has done postdoctoral research first at Tufts University Medical School, then at Harvard Medical School, Boston. He joined the staff at the Boston Biomedical Research Institute, as a Staff Scientist in 1997, and in 2000 moved to the Department of Pathology, BIDMC.

Phosphatidylinositol-3-Phosphate

Joseph V. Virbasius and Michael P. Czech
University of Massachusetts Medical School, Worcester, Massachusetts, USA

Phosphatidylinositol is a polar phospholipid which comprises a small fraction of the total membrane lipids in cells. The hydroxyl moieties of the inositol head group may be reversibly modified by transfer of a phosphate group from ATP to one or more of three positions. This reaction is catalyzed by the class of enzymes referred to as phosphatidylinositol kinases (PI kinases). Specific PI kinases can produce three monophosphorylated phosphatidylinositols, PtdIns(3)P, PtdIns(4)P, and PtdIns(5)P in intact cells. These can be further phosphorylated by PI kinases to yield such polyphosphoinositides as PtdIns(4,5)P_2 and PtdIns(3,4,5)P_3, which function in regulating plasma membrane activities and cell signaling cascades, respectively. Although it is likely that PtdIns(4)P and PtdIns(5)P have important functions, molecular targets of these phosphoinositides have yet to be characterized. In contrast, through both genetic and biochemical studies our understanding of PtdIns(3)P functions and the PI 3-kinases which specifically produce PtdIns(3)P are well advanced. In recent years, a large number of proteins that interact with PtdIns(3)P have been discovered and their roles in various cellular processes including membrane trafficking and signaling have been elucidated.

Synthesis and Turnover of PtdIns(3)P

Although PtdIns(3)P synthesis is not known to be acutely activated by extracellular stimuli as is the case for certain other phosphoinositides, PtdIns(3)P content of membranes appears to be dynamically regulated and spatially restricted in intracellular compartments. Current data indicate that PtdIns(3)P is found primarily, and perhaps exclusively, in endosomal membranes (Figure 1). These membranes are vesicular structures which delimit compartments derived from endocytic internalization of patches of membrane from the cell surface. Mechanisms for generation of PtdIns(3)P must therefore be activated concurrently with or shortly after endocytosis, while turnover of PtdIns(3)P by hydrolysis or additional phosphorylation must occur during the progression of endosomes toward their cellular fates. These fates include recycling to the plasma membrane and fusion with lysosomes. Cellular proteins embedded in these membrane patches can likewise be targeted for recycling back to the plasma membrane where they may resume their functions, or for degradation in the lysosome. Recent discoveries indicate that PtdIns(3)P and its molecular targets play critical regulatory roles in such membrane trafficking pathways of endosomes, and thus help to determine the cellular distribution and fate of membrane proteins such as receptors for growth factors.

Synthesis of PtdIns(3)P by PI 3-Kinases

In the yeast genome, a single gene encoding a PtdIns 3-kinase has been identified. *VPS34* was originally identified in a screen for mutants that failed to properly direct a protein degradation enzyme to the vacuole, the organelle with functions similar to the lysosome of animal cells. The 100 kDa protein encoded by this gene, *Vps34p*, has a domain highly similar to mammalian PI 3-kinase and was subsequently shown to have PI 3-kinase activity. *Vps34p* exists in a complex with a 150 kDa serine/threonine kinase,Vps15p, which serves to target the Vps34p enzyme to membranes where its substrate phosphatidylinositol resides. Phosphorylation of Vps34p by the protein kinase activity of Vps15p is required for full activity of the Vps34p PI 3-kinase. A homologous PI 3-kinase complex exists in all eukaryotes studied. The mammalian Vps34 PI 3-kinase (also referred to as a class III PI 3-kinase) appears to be the predominant enzyme which produces PtdIns(3)P in cells. Although Class I and II PI 3-kinases are also capable of phosphorylating PI *in vitro*, their contribution to PtdIns(3)P production *in vivo* is not established. Additionally, other PtdIns(3)P-producing activities which differ from known enzymes in terms of inhibitor sensitivities have been reported to exist.

Dephosphorylation of PtdIns(3)P

PtdIns(3)P may be converted back to phosphatidylinositol by the action of a 3-phosphatase, an enzyme which catalyses the hydrolysis of the phosphate group on the 3′ position of the inositol ring. A number of

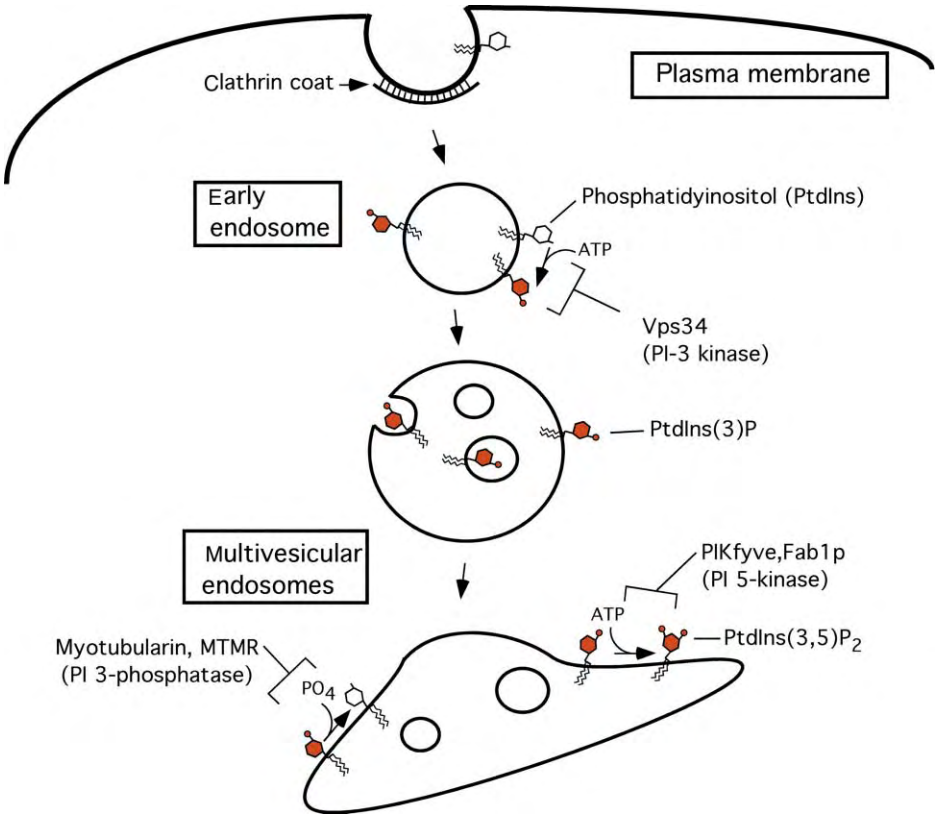

FIGURE 1 Production and turnover of PtdIns(3)P in endosomal membranes. In the process known as endocytosis patches of plasma membrane invaginate as the result of formation of clathrin coats. Subsequent scission from the plasma membrane and uncoating of these vesicles produce early endosomes where PtdIns(3)P is produced by the Vps34 PI 3-kinase. PtdIns(3)P also persists on the limiting membrane as well as intralumenal vesicles of the multivesicular endosome, a product of fusion of early endosomes. During subsequent maturation, the PtdIns(3)P may be hydrolyzed by the action of myotubularin family PI- phosphatases, or further phosphorylated by the PIKfyve/Fab1p PI 5-kinases to produce PtdIns(3,5)P2. These reactions may also take place in the intralumenal vesicles.

phosphoinositide phosphatases have been characterized in yeast and mammalian systems, but to date, activity against PtdIns(3)P has been attributed only to members of the myotubularin family. This family consists of at least 12 genes in humans with one putative homologue in yeast. Of the human proteins, eight have functional phosphatase domains, the others have similar protein sequences but apparently no catalytic activity. These proteins also have potential phosphoinositide-binding PH domains while two have FYVE domains likely to specifically target PtdIns(3)P. Details regarding the activity of myotubularin proteins in cells have yet to be reported. However, mutations in a number of human myotubularin genes have been linked to neuromuscular diseases pointing to significant roles in development or function of neural and muscle tissues.

Phosphorylation of PtdIns(3)P

In addition to hydrolysis of the 3-phosphate group by phosphatases, PtdIns(3)P levels may be modulated by additional phosphorylation. Recently, it was shown that significant levels of PtdIns(3,5)P_2 are present in yeast and mammalian cells. This phosphoinositide appears to be formed primarily by phosphorylation of PtdIns(3)P at the 5′ position of the inositol ring. The Fab1 protein of yeast and a mammalian homologue called PIKfyve possess this enzymatic activity. Both of these proteins are also able to bind specifically to PtdIns(3)P via a FYVE domain. Conversion of PtdIns(3)P to PtdIns(3,5)P_2 would serve to terminate PtdIns(3)P-dependent cellular functions, but may also contribute to cellular responses to osmotic stress or other signals as well as to maturation of endosomes. The relative contribution of phosphorylation versus hydrolysis to PtdIns(3)P turnover is as yet undetermined.

Molecular Targets and Cellular Functions of PtdIns(3)P

Protein Domains that Bind to PtdIns(3)P

Two structurally unrelated protein domains have been shown to bind to PtdIns(3)P. The first to be discovered

was the FYVE domain (named for the first four proteins in which it was recognized, Fab1p, YOTB, Vac1p, and EEA1). The domain is characterized by a RING finger structure which binds two Zn molecules. It is found in five yeast proteins and ~30 human proteins. Binding of FYVE domains to PtdIns(3)P-containing membranes relies on a combination of nonspecific membrane interactions and a groove which specifically accommodates the phosphate group of PtdIns(3)P while sterically excluding other phosphoinositide head groups. To date all FYVE domains studied bind exclusively to PtdIns(3)P.

The phox homology (PX) domain was first recognized in two components of the phagocyte NADPH oxidase (phox) complex (p40phox and p47phox). It is structurally unrelated to the FYVE domain except for a somewhat similar binding pocket which accommodates the inositol 3-phosphate head group. However, comparison of the crystal structures of the p40phox PX domain bound to dibutanoyl PtdIns(3)P and the FYVE domain of early endosome antigen-1(EEA1) bound to the head group inositol 1,3bisphosphate indicates that both proteins utilize basic residues to bind both phosphate and hydroxyl groups in the lipid head group. All 15 PX domains in yeast bind PtdIns(3)P with varying affinities. Of the mammalian proteins characterized, many bind PtdIns(3)P strongly, while several have lower affinity for other, and in some cases several, phosphoinositides.

PtdIns(3)P-Binding Proteins in Endosomal Membrane Trafficking

In accordance with the predominant localization of PtdIns(3)P to membranes of the endosomal system, several PtdIns(3)P binding proteins have been shown to function in various steps of endosome fusion, sorting, and maturation (Table I). In mammalian cells, a major function of these events is to direct membrane components to the lysosome whereas sorting of proteins to the vacuole is a major function in yeast.

Following internalization of plasma membrane patches to form small membrane vesicles denoted as early endosomes, a process of maturation is initiated which involves fusion of early endosomes into larger multivesicular bodies. These multivesicular bodies form specialized subdomains marked by the recruitment of different sets of proteins. Eventually these specialized domains and their cargo proteins form new compartments, which may then be returned to the plasma membrane or delivered to lysosomes or the trans-Golgi complex. This process is controlled in part by various members of the small GTPase Rab family. Rab5 in particular is required for fusion of early endosomes and it accomplishes this in part by stimulating the production of PtdIns(3)P via Vps34, with the resulting recruitment of PtdIns(3)P-binding proteins to the endosomes. Such proteins include EEA1 and rabenosyn-5, which both bind Rab5 itself as well as PtdIns(3)P via a FYVE domain. Once recruited to the endosome through these mechanisms, EEA1 and rabenosyn-5 appear to function in the tethering, docking, and ultimate fusion of early endosomes.

The sorting nexin (SNX) family containing up to 25 human proteins and the yeast homologues Mvp1p, Vps5p, Vps17p, and Grd19p all contain a PX domain. All of the yeast SNX proteins and some of the mammalian counterparts have been found to bind preferentially or specifically to PtdIns(3)P, and most characterized SNX proteins localize at least partially to endosomes. Consistent with the importance of PtdIns(3)P in vacuolar protein sorting in yeast, Vps5p and Vps17p have a role in the retrieval of the vacuolar protein sorting receptor Vps10p while Mvp1p and Grd19 participate in Golgi to vacuole trafficking. In mammalian cells, roles of the various SNX proteins are being assigned, and the emerging picture suggests that different sorting nexins may be required for regulating the distinct fates of endosomes, i.e., recycling to the cell surface, delivery to lysosomes, or delivery to the trans Golgi.

TABLE I

Cellular Functions of PtdIns(3)P and some Associated Proteins

Cellular function	Domain	PtdIns(3)P-binding proteins
Endosome fusion/maturation	FYVE	EEA1, rabenosyn-5, PIKfyve/Fab1p
Golgi-vacuole trafficking (yeast)	FYVE	Vps27p, Vac1p, Fab1p
	PX	Grd19p, Mvp1p, Vps5p, Vam7p
Receptor sorting/ targeting to lysosome	FYVE	Hrs
	PX	Sorting nexins
Signal transduction	FYVE	SARA
	PX	CISK
Phagosome function/maturation	FYVE	EEA1
	PX	$p40^{phox}$

PtdIns(3)P in Phagocytosis and Bacterial Invasion

Many of the PtdIns(3)P-binding proteins involved in the endocytic process are likely involved in the similar processes of phagocytosis and host cell invasion by bacteria and parasites. Phagosomes, like endosomes, form by invagination of patches of the plasma membrane followed by "pinching off" and sealing to form a

self-contained intracellular compartment. PtdIns(3)P appears transiently on phagosomes in a manner which parallels its appearance and disappearance in endosomes. Phagosomal PtdIns(3)P is apparently generated by the targeting and activation of the VPS34 PI 3-kinase. As in early endosomes, the PtdIns(3)P synthesized in phagosomes recruits FYVE- and PX-domain containing proteins including EEA1. Likewise, in the process of secretion-mediated invasion by *Salmonella*, the membrane vacuole which envelops the invading bacterial cells accumulates PtdIns(3)P. In certain cell types, recruitment of the NADPH oxidase to phagosomes may occur via PX domains in its p40 and p47 subunits. This mechanism may contribute to defense against pathogens since the NADPH oxidase produces reactive oxygen species toxic to invading bacterial cells. Disruption of this recruitment mechanism by pathogenic bacteria enhances their ability to escape host cell defenses.

PtdIns(3)P and Signaling from the Endosomal System

Recently it has become clear that the endosomal system is an essential component of signal transduction pathways regulating proliferation, survival, differentiation, and stress responses. Current evidence suggests that growth factor receptors, many of which are internalized into endosomes following binding of their ligands, can continue to generate signals to downstream effectors as they transit through the endosomal system. Furthermore, internalization and delivery of such receptors to lysosomes for degradation is an important mechanism for down-regulation of signaling in a variety of systems.

The FYVE-domain protein, SARA, localizes to early endosomes via its association with PtdIns(3)P. SARA also binds to Smad2, a downstream target of the transforming growth factor-β (TGFβ) receptor. Association of the SARA–Smad complex appears to be essential for efficient phosphorylation of Smad by the internalized receptor. Thus, PtdIns(3)P in endosomes can serve to assemble signaling complexes in which the local concentration of components is increased by association with specific intracellular membranes. The FYVE domain-containing protein homologue of the yeast protein Vps27p (Hrs) may function in a similar manner in the TGFβ signaling pathway. However, in other systems, Hrs may promote the internalization and ultimate degradation of growth factor receptors. Thus, there is precedent for the involvement of PtdIns(3)P-binding proteins in attenuation as well as enhancement of growth factor signals.

Endosomal localization via PtdIns(3)P binding may also serve to target or sequester components of signaling pathways several steps removed from the initial receptor signal. The PX domain-containing protein kinase CISK (also denoted SGK3) is localized to endosomes and may function in this way. Like its related family members Akt and SGK, CISK is activated by regulatory protein kinases in response to growth factor-mediated regulation of PI 3-kinases that produce PtdIns(3,4,5)P_3. Based on its endosomal disposition, it seems likely that the substrates of the CISK protein kinase are similarly localized. CISK may function to attenuate apoptosis or to promote other processes yet to be discovered based on this unique association with the endosomal compartment.

PtdIns(3)P may also serve as a component of the cellular stress response. In yeast and mammalian cells, PtdIns(3,5)P_2 is formed in response to osmotic stress by the FYVE-domain proteins Fab1p and PIKFYVE, respectively. Effectors of PtdIns(3,5)P specific for this function have not been identified.

See Also the Following Articles

Inositol Lipid 3-Phosphatases • Inositol Phosphate Kinases and Phosphatases • Phosphatidylinositol Bisphosphate and Trisphosphate • Phosphoinositide 4- and 5-Kinases and Phosphatases • Phosphoinositide-Dependent Protein Kinases

Glossary

endocytosis The process by which regions of plasma membrane and any embedded proteins are brought inside the cell by formation of a membrane-bound intracellular vesicle.

endosome The membrane-bound intracellular vesicle formed by the process of endocytosis.

phagocytosis Uptake of particles such as cell fragments or bacteria by engulfing and then internalizing them in a membrane vesicle.

phagosome The membrane-bound intracellular vesicle formed by the process of phagocytosis.

phosphatidylinositol (PtdIns) A membrane lipid consisting of a pair of membrane embedded fatty acid chains linked to a surface-exposed inositol head group. The hydroxyl groups of the inositol may be phosphorylated by PI kinases at the 3′, 4′, and 5′ positions.

Further Reading

Brumell, J. H., and Grinstein, S. (2003). Role of lipid-mediated signal transduction in bacterial internalization. *Cell. Microbiol.* **5**, 287–297.

Corvera, S. (2001). Phosphatidylinositol 3-kinase and the control of endosome dynamics: New players defined by structural motifs. *Traffic* **2**, 859–866.

Czech, M. P. (2003). Dynamics of phosphoinositides in membrane retrieval and insertion. *Annu. Rev. Physiol.* **65**, 791–815.

Ellson, C. D., Andrews, S., Stephens, L. R., and Hawkins, P. T. (2002). The PX domain: A new phosphoinositide-binding module. *J. Cell Sci.* **115**, 1099–1105.

Lemmon, M. A. (2003). Phosphoinositide recognition domains. *Traffic* **4**, 201–213.

Misra, S., Miller, G. J., and Hurley, J. H. (2001). Recognizing phosphatidylinositol 3-phosphate. *Cell* **107**, 559–562.

Raiborg, C., Rusten, T. E., and Stenmark, H. (2003). Protein sorting into multivesicular endosomes. *Curr. Opin. Cell Biol.* **15**, 446–455.

Stenmark, H., Aasland, R., and Driscoll, P. C. (2002). The phosphatidylinositol 3-phosphate-binding FYVE finger. *FEBS Lett.* **20**, 77–84.

Wishart, M. J., and Dixon, J. E. (2002). PTEN and myotubularin phosphatases: From 3-phosphoinositide dephosphorylation to disease. *Trends Cell Biol.* **12**, 579–585.

Worby, C. A., and Dixon, J. E. (2003). Sorting out the functions of sorting nexins. *Nat. Rev. Mol. Cell Biol.* **3**, 919–931.

Biography

Joseph Virbasius is an Assistant Professor and Dr. Michael Czech is a Professor and Chair of Molecular Medicine at the University of Massachusetts Medical School in Worcester. Their research interests include molecular mechanisms of insulin action and functions of PI 3-kinase and its downstream effectors in insulin-responsive cells. Dr. Virbasius holds a Ph.D. from Northwestern University and served as a postdoctoral fellow at the University of Massachusetts Medical School.

Michael Czech holds a Ph.D. from Brown University. He was a postdoctoral fellow in the Department of Biochemistry at Duke University Medical School from 1972 to 1974 and was a Professor of physiological chemistry at Brown University before coming to the University of Massachusetts Medical School as Chair of the Department of Biochemistry and Molecular Biology in 1981.

Phosphofructokinase-2/Fructose Bisphosphatase-2

Daniel M. Raben
The Johns Hopkins University School of Medicine, Baltimore, Maryland, USA

6-Phosphofructo-2-kinase/fructose-2,6-bisphosphatase (PFK-2/FBPase-2) is a bifunctional enzyme wherein a single polypeptide chain contains two enzymatic activities—PFK-2 and FBPase-2. PFK-2 catalyzes the transfer of phosphate from ATP to the second carbon (C-2) of fructose-6-phosphate (F6P), an intermediate in the glycolytic pathway, generating fructose-2, 6-bisphosphate (F2,6BP). Conversely, FBPase-2 catalyzes the dephosphorylation of F2,6BP resulting in the liberation of free inorganic phosphate and regeneration of F6P. In this manner, these two physically linked enzymes function to modulate the cellular concentration of F2,6BP. The importance of this regulation cannot be overstated as this sugar plays an essential signaling role in regulating glucose metabolism in a variety of tissues. Perhaps most importantly, it is largely responsible for regulating the balance between glycolysis and gluconeogenesis in the liver. This balance, critical for maintaining blood glucose levels within the normal range regardless of the nutritional state, principally results from the fact that F2,6BP activates a key regulatory glycolytic enzyme, PFK-1 (6-phosphofructo-1-kinase) and inhibits a regulatory enzyme in gluconeogenesis, FBPase-1 (fructose-1,6-bisphosphatase). Therefore, in the liver, when F2,6BP levels are high, glycolysis predominates and when F2,6BP levels are low, gluconeogenesis predominates. In other tissues, F2,6BP levels mainly serve to help regulate glycolytic flux. By regulating the level of this phosphorylated sugar, PFK-2/FBPase-2 activities play a central role in maintaining glucose homeostasis and utilization.

Discovery of PFK-2/FBPase-2

As with many discoveries, the identification of PFK-2/FBPase-2 was preceded by the discovery of its product F2,6BP. This sugar was first identified as the mediator responsible for stimulating hepatic gluconeogenesis. It had been known for some time that gluconeogenesis was induced in liver by elevated levels of glucagon. Emil van Shaftingen and Henri-Gery Hers demonstrated that rat liver lysates contained an acid-labile phosphoric acid ester that greatly stimulated PFK-1. The concentration of this compound in isolated hepatocytes was significantly increased by glucose and decreased by glucagon. They also showed that this molecule was F2,6BP. Following this discovery, Hers and Uyeda identified PFK-2/FBPase-2 in rat liver as the bifunctional enzyme responsible for the generation and degradation of F2,6BP.

General Structure of PFK-2/FBPase-2

In mammalian tissues, PFK-2/FBPase-2 is a single protein with the PFK-2 activity located at the N-terminal end and the FBPase-2 located at the C terminus. Structural analyses demonstrated that the catalytic domains are flanked by regulatory regions at both the N and C termini. The enzyme functions as a dimer with protein–protein contacts being made at the regulatory regions at the N terminus only. In contrast to this structure, the yeast PFK-2 and FBPase-2 enzymes are separate proteins, but most likely function as dimers.

Enzymology of PFK-2

While PFK-2 shares the same substrate as PFK-1, F6P, the reaction catalyzed by PFK-2 differs from that catalyzed by PFK-1 in four important aspects. First, PFK-1 catalyzes the transfer of the γ-phosphate of ATP to C-1 of F6P generating F1,6BP while PFK-2 catalyzes the transfer of this ATP phosphate to C-2 yielding F2,6BP. Second, PFK-1 is an α-anomer while PFK-2 prefers the β-anomer. Third, PFK-1 is strongly inhibited by ATP while PFK-2 is not sensitive to this nucleotide. Finally, PFK-2 is inhibited by both of its products, ADP and F2,6BP, which are activators of PFK-1.

The complete catalytic mechanism of PFK-2-mediated phosphorylation of F6P has not been elucidated. Important features of the reaction have, however, been identified. In general, PFK-2 activity is much

weaker than that of PFK-1. This may be due to the fact that specific residues involved in accelerating catalysis in PFK-1 are absent in PFK-2. The pH optimum of the enzyme-catalyzed reaction is between 8 and 9, requires magnesium, and prefers ATP as the phosphate donor, but will also use GTP. Inhibition studies indicate that the PFK-2-mediated transfer of phosphate from ATP to F6P occurs via a sequential-ordered mechanism with ATP binding prior to F6P binding. Binding sites for ATP and F6P have been identified as well as residues critical for catalysis.

Enzymology of FBPase-2

Much more is known about the reaction mechanism used for FBPase-2-mediated hydrolysis. The enzyme has a pH optimum between 5.5 and 6.5 and does not require divalent cations. FBPase-2 specifically hydrolyzes the phosphate on carbon 2 (C-2) of F2,6BP and will not hydrolyze C-6 of either F2,6BP, F1,6BP or glucose-1,6-bisphosphate. However, it is inhibited by both its substrate and product—F6P and F2,6BP. Interestingly, the FBPase-2 reaction mechanism involves an intermediate in which F6P is covalently bound to a histidine residue on the enzyme. This covalent intermediate has been useful in structural studies designed to elucidate the reaction mechanism, which appears to resemble, but is not identical to, the mechanism used by serine proteases. Both involve a "catalytic triad" in which three residues work together to form an intermediate in which the substrate is covalently bound to the enzyme followed by hydrolysis of this intermediate to release the product from the enzyme. In the case of serine proteases, a serine residue on the enzyme is covalently bound to the catalytic intermediate while in FBPase-2 a phosphohistidine is formed and F6P is released. The dissociation of the F6P product appears to be the rate-limiting step.

Isoforms of PFK-2/FBPase-2

Since the discovery of PFK-2/FBPase-2 mammalian tissues, a number of mammalian isoforms have been identified from four genes, which include alternatively spliced products. In all isoforms, the catalytic domains are highly conserved while the N and C termini are most divergent. Most tissues contain varying amounts of different isoforms, with one isoform predominating. For example, in liver ~10% of the total PFK-2/FBPase-2 is the skeletal muscle isoform. Even within the predominant liver isoform there are two different species, a 54–55 kDa species and a 58 kDa species with only the 58 kDa species being regulated by phosphorylation. In addition to these mammalian isoforms, yeast contain PFK-2 and FBPase-2 activities, but in this case the enzymes are monomeric although they likely work as dimers.

In addition to sequence differences, kinetic properties of the kinase and bisphosphatase activities also differ among the various isoforms. While the substrate affinities (measured as a K_m) and maximum velocities (V_{max}) vary between isoforms, there are some notable differences. Comparison of bovine brain, liver, and testes shows that these isoforms have similar kinetic properties for PFK-2 in terms of K_m for F6P, but the liver and muscle FBPase-2 enzymes have K_m values for F2,6BP that are approximately 100- to 1000-fold lower than the other isoforms. Based on V_{max}, the skeletal muscle also appears to have the lowest kinase activity and high-phosphatase activity, while the placental isoform has the highest kinase activity with very low-phosphatase activity.

Regulation and Physiological Roles of Specific Isoforms in Specific Tissues

PFK-2/FBPase-2 is exquisitely poised to regulate the levels of F2,6BP. F6P exerts a substrate level control over PFK-2 and is a product inhibitor of FBPase-2. The K_m of PFK-2 and K_i of FBPase-2 for F6P are within the physiological concentration ranges of this phosphorylated sugar in different tissues suggesting that small changes in the levels of F6P result in significant reciprocal alterations in these two enzymatic activities. Such alterations have different effects in different tissues, depending on the isoforms and relative level of the endogenous PFK-2/FBPase-2 activities.

Perhaps the best-studied form of PFK-2/FBPase-2 regulation involves the phosphorylation of the enzyme. Both the liver and heart isozymes are subject to regulation by phosphorylation. The brain isoform is phosphorylated, but this phosphorylation does not appear to affect enzymatic activities. Muscle and testis isoforms are not phosphorylated. A liver isoform (58 kDa) was the first one shown to be regulated by a PKA (protein kinase A)-mediated phosphorylation stimulated by the glucagon-induced second-messenger cyclic AMP (cAMP). Further studies showed that PFK-2/FBPase-2 is phosphorylated on a specific serine residue, serine-32, near the N terminus. This phosphorylation leads to inhibition of PKF-2 and activation of FBPase-2. For PFK-2 at physiological pH, this is primarily due to an increase in the K_m (i.e., lower affinity) for F6P, without affecting the K_m for ATP, and only slightly perturbing V_{max}. In contrast, this phosphorylation activates FBPase-2 by increasing the V_{max} of the enzyme without affecting the K_m for F2,6BP. It is believed that this effect is largely due to an increase in

the rate of F6P dissociation from FBPase-2, which enhances the rate at which the phosphohistidine intermediate is hydrolyzed. Consistent with the critical role of this enzyme in regulating liver carbohydrate metabolism, phosphorylation of the enzyme can be reversed by specific, regulated protein phosphatases (protein phosphatase 2A and 2C), which serves to activate PFK-2 while inhibiting FBPase-2. On the other hand, phosphorylation of the heart isoform modulates only the PFK-2 activity without affecting FBPase-2. Importantly, in stark contrast to the liver isoform, phosphorylation of the heart isoform activates PFK-2. In bovine and rat hearts, phosphorylation lowers the K_m (i.e., increases the affinity) for F6P. The bovine heart isoform may be phosphorylated by PKA, and the rat heart isoform can be phosphorylated and modulated by either PKA or the calcium/calmodulin-dependent protein kinase.

The fact that PKF-2 and FBPase-2 are located near the N and C termini respectively, on the same polypeptide begs the question as to how both activities of the liver enzyme are affected by a phosphorylation near the N terminus. While the exact mechanism underlying the reciprocal regulation of these two activities has not been resolved, a current view is that in the nonphosphorylated state, the N termini of two polypeptides interact and activate the kinase while the C-terminal regions are separated (Figure 1). This is consistent with the crystal structure of the rat testis PFK-2/FBPase-2. Phosphorylation is believed to induce a conformational change in the enzyme resulting in the separation of the N termini, which inactivates the kinase while activating the phosphatase.

The above regulation provides for short-term, acute regulation for rapid, transient responses. The enzyme is also subject to long-term regulation mediated by gene expression. Both insulin and dexamethazone stimulate an increase in the level of PFK-2/FBPase-2 gene expression. Consistent with this, levels of liver PFK-2/FBPase-2 are depressed during starvation or diabetes and increase upon re-feeding or administration of insulin, respectively. Additionally, levels of PFK-2/FBPase-2 decrease following partial hepatectomy and increase during liver regeneration.

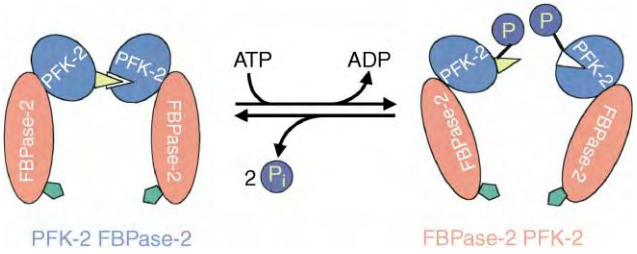

FIGURE 1 Reciprocal regulation of dimeric PFK-2/FBPase-2 in liver by phosphorylation. The blue indicates the N-terminal region containing PFK-2 activity and the red indicates the C terminus containing the FBPase-2 activity. The triangle at the N terminus and the pentagon at the C terminus represent regulatory regions.

The differences in isoforms and their regulation suggest different roles for each isoform. This is most dramatically seen when comparing the regulation of the liver isoform with that of the heart isoform. Liver not only consumes energy, it also stores energy mainly in the form of glycogen. It is also the only tissue, besides kidney to a small extent, which engages in gluconeogenesis to supply glucose to other glucose-dependent tissues in times of need. In that, as previously mentioned, the liver isoform is exquisitely poised to reciprocally regulate the level and activities of PFK-2/FBPase-2. This regulation is sensitive to glucose levels or hormones involved in regulating carbohydrate metabolism such as insulin, which stimulates glycolysis, and glucagons, which induces gluconeogenesis. On the other hand, heart muscle is a constant energy-consuming tissue, and, therefore, engages in glycolysis but not gluconeogenesis. Indeed, the heart does not respond to glucagon but does respond to another hormone that signals through PKA, epinephrine (adrenaline). Therefore, it is not surprising that the regulated heart isoform of PFK-2/FBPase-2 responds to phosphorylation by increasing PFK-2 activity, as this hormone would signal a need for increased glycolytic flux. The increased PFK-2 activity would lead to an increase in F2,6BP levels, thereby increasing glycolysis via activation of PFK-1. The regulation of liver and heart isoforms exemplifies how differential regulation of specific isoforms can serve different roles depending on the needs of various tissues in which they are expressed. This further illuminates the significant role PFK-2/FBPase-2 plays in appropriately regulating carbohydrate metabolism.

See Also the Following Articles

Enzyme Reaction Mechanisms: Stereochemistry • Glucagon Family of Peptides and their Receptors • Glycolysis, Overview • Pyruvate Carboxylation, Transamination and Gluconeogenesis

Glossary

anomer Stereoisomer (diastereoisomer) of sugars which differ with respect to their configuration about their anomeric carbon. The anomeric carbon is the carbon which forms a new stereocenter, when the sugar cyclizes on the former carbonyl carbon. The configuration may be α or β.

ATP Adenosine triphosphate, a molecule consisting of the nitrogenous base adenine linked to the sugar ribose, and containing three phosphate groups attached to the ribose. ATP, present in all living cells, serves as the principal energy source of energy for cells.

cAMP Cyclic adenosine monophosphate, a cyclic form of adenosine monophosphate where a single phosphate is attached to both

the third and fifth carbon of the ribose sugar linked to adenine. It is important in transmitting intracellular, as well as extracellular, signals induced by many agonists. cAMP binds to and activates the cAMP-dependent protein kinase, PKA.

gluconeogenesis The synthesis of glucose from noncarbohydrate sources occurring primarily in the liver and to a small extent in the kidney. It is stimulated during starvation or intense exercise.

glycolysis (glycolytic pathway) The anaerobic metabolism of glucose to pyruvate. This metabolism generates two molecules of ATP and one molecule of NADH per glucose molecule. The NADH may be used to generate energy in the form of ATP and the pyruvate may enter the tricarboxylic acid cycle to yield NADH for energy production under aerobic conditions.

GTP Guanosine triphosphate, a molecule consisting of the nitrogenous base, guanine, linked to the sugar ribose. The ribose contains three phosphate groups attached to the 5′ carbon. GTP is another source of metabolic energy and is involved in protein synthesis and a number of signal transduction cascades.

K_m A kinetic parameter that indicates the affinity of an enzyme for its substrate and often called the "Michaelis constant." It is defined as the concentration of substrate that results in half the maximal rate (V_{max}) of the enzyme-catalyzed reaction.

protein kinase A (PKA) An enzyme that catalyzes the phosphorylation of proteins on specific serine or theronine residues in response to cAMP.

V_{max} The maximal initial velocity of an enzyme-catalyzed reaction that occurs at saturating substrate concentrations.

Further Reading

Kurland, I. J., and Pilkis, S. J. (1995). Covalent control of 6-phosphofructo-2-kinase/fructose-2,6-bisphosphatase: Insights into autoregulation of a bifunctional enzyme. *Protein Sci.* **4**(6), 1023–1037.

Okar, D. A., Manzano, A., Navarro-Sabate, A., Riera, L., Bartrons, R., and Lange, A. J. (2001). PFK-2/FBPase-2: Maker and breaker of the essential biofactor fructose-2,6-bisphosphate. *TIBS* **26**(1), 30–35.

Pilkis, S. J., el-Maghrabi, M. R., and Claus, T. H. (1988). Hormonal regulation of hepatic gluconeogenesis and glycolysis. *Annu. Rev. Biochem.* **57**, 755–783.

Pilkis, S. J., Claus, T. H., Kurland, I. J., and Lange, A. J. (1995). 6-Phosphofructo-2-kinase/fructose-2,6-bisphosphatase: A metabolic signaling enzyme. *Annu. Rev. Biochem.* **64**, 799–835.

Biography

Daniel M. Raben is an Associate Professor in the Department of Biological Chemistry at the Johns Hopkins University School of Medicine. His principal research interests are in the broad fields of lipid biochemistry and chemistry, and signal transduction. He holds a Ph.D. from Washington University in St. Louis, Missouri and received his postdoctoral training at the University of California at Irvine. He is a well-published investigator, including several review articles on lipid-mediated signal transduction, and is on the editorial board of a number of biochemical journals.

Phosphoinositide 3-Kinase

Khatereh Ahmadi
PIramed Ltd., UK

Michael Waterfield
Ludwig Institute for Cancer Research, London, UK

The phosphoinositide 3-kinases (PI 3-kinases) are enzymes with intrinsic lipid kinase activity whose substrates are membrane phosphatidylinositol lipids. When activated by cell surface receptors, such as those that recognize growth factors, PI 3-kinases generate a PIP3 (phosphatidylinositol 3,4,5-triphosphate) second messenger lipid that binds and activates at the membrane, enzymes that control signal networks which control the life, death, and differentiated functions of cells. The loss of control of PI 3-kinase activity has been shown to be instrumental in causation or maintenance of major human diseases such as cancer, diabetes, and inflammation.

Identification of PI 3-Kinases as Signaling Molecules: A Historical Perspective

Signal transduction enables cells to communicate with each other and respond to their external environment through receptors on cell surfaces, which are activated by external ligands such as growth factors. Receptors send signals to the internal control systems of the cell and to internal organelles such as the mitochondria and the nucleus via a series of molecular cascades known as signaling pathways.

In the early 1990s, it was shown that ligand activation of receptors that have intrinsic tyrosine kinases (TK) causes autophosphorylation at specific sites on their kinase domains, initiating the formation of a signaling complex. Phosphoinositide (PI) 3-kinase activity was first found associated with the transforming complex of middle-T (mT) antigen and pp60c-src from polyoma virus-transformed cells and subsequently with the PDGF (platelet-derived growth factor) receptor, mediated by amino acid recognition sites around specific tyrosine residues. Since then it has become clear that PI 3-kinases are recruited to almost every receptor complex, including activated oncogenes and growth factor receptors, as well as heterotrimeric G proteins, a key effector of activated receptors.

PI 3-Kinases Phosphorylate Lipids

The discovery that the main product of these transforming protein-associated kinases was a PI that had a phosphate group on the D3 position of the inositol ring added a new second messenger to the armory of specific signal molecules used by cells. Three distinct signal molecules that are phosphorylated on the 3 position of the inositol ring can be generated by three classes of PI 3-kinase from specific phosphoinositol substrates. The signal molecules formed are phosphatidylinositol 3-phosphate or PI3P, PI(3,4)P2, and PI(3,4,5)P3 (see Figure 1).

A wide variety of receptor-mediated stimuli can lead to the rapid production of PI(3,4)P2 and PI(3,4,5)P3 in cells, whereas the intracellular levels of PI3P seem mostly unaffected by external cell stimulation. PI3P is used for internal cellular protein trafficking. The hydrolysis of these lipids occurs through the action of lipid phosphatases that remove the three phosphate groups from the inositol ring, thus regulating PI 3-kinase activity. The lipid signaling pathway initiated by PI 3-kinase is distinct from the classical pathway in which activation of phospholipase C causes to production of Ins(1,4,5)P3 and diacylglycerol, ultimately leading to mobilization of calcium and activation of protein kinase C.

Activation and Regulation of PI 3-Kinases

PI 3-kinase was first purified from bovine brain tissue as a lipid kinase activity and was shown, through a classical series of systematic biochemical analyses, followed by molecular cloning and expression of the recombinant proteins, to be a heterodimeric enzyme containing a

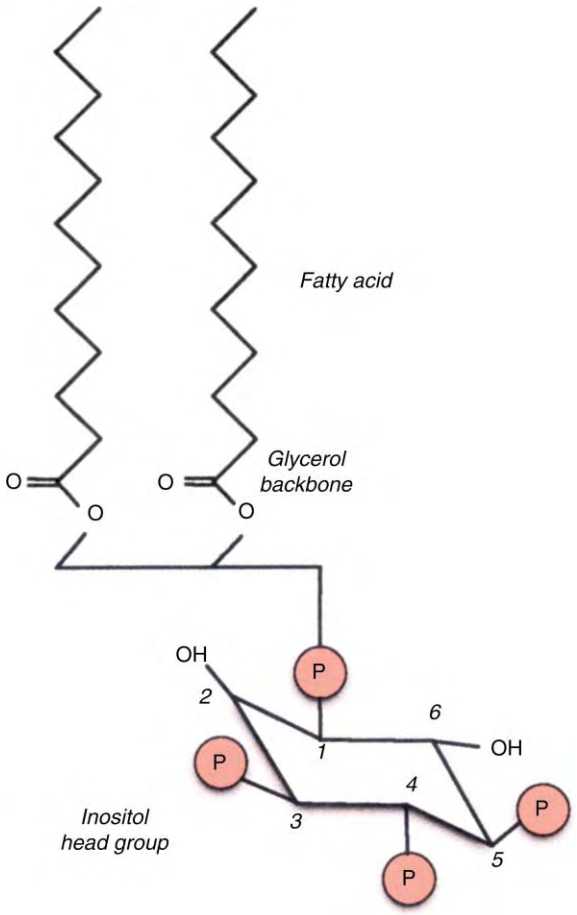

FIGURE 1 The signal molecule phosphatidylinositol 3-phosphate (PI 3-phosphate or PIP3).

110 kDa catalytic subunit (p110), and an 85 kDa adaptor subunit (p85). The primary structures of the p85 and p110 subunits were revealed through cDNA cloning using protein sequence data, thus shedding light on the mode of interaction between p85 and tyrosine phosphorylated proteins. The p85 subunit contains an N-terminal (src homology) SH3 domain, which binds to proline-rich sequences and two SH2 domains separated by an inter SH2 domain. SH2 domains have been found in many signaling proteins and bind phosphotyrosine residues within a specific polypeptide context, YXXM, where Y is a tyrosine, M is a methionine, and X can be any amino acid. The adaptor subunit also contains a breakpoint cluster region homology (BH) domain. These distinct functional domains make p85 an important interactive protein with a major regulatory role.

The p110 subunit was shown to contain an ATP-binding site, which is responsible for the catalytic activity of the enzyme. More recently the three-dimensional structure of a p110 (gamma) subunit revealed a modular structure comprising a Ras-binding domain (RBD), a C2 domain, a helical domain, and a catalytic domain. This structure has been invaluable in rationalizing the allosteric activation and regulation of PI 3-kinase, its ability to bind membranes, and its substrate specificity.

PI 3-kinases are recruited to activated receptors directly or to associated substrate scaffold molecules such as Grb3 or Shc through the binding of the SH2 domains of the p85 subunit to phosphorylated tyrosine residues. The current paradigm for the activation of PI 3-kinase is that interaction with the receptor brings the enzyme into close proximity to the membrane that contains the lipid substrates of PI 3-kinase. The p110 catalytic subunit is thus able to phosphorylate the lipids, which then act as second messengers, initiating a cellular signal that is carried to the cytoplasm, mitochondrion, or nucleus through a cascade of signaling molecules.

Down-Regulation of PI 3-Kinase Activity

The phosphatases SHIP (SH2 domain-containing inositol 5-phosphatase) and PTEN (phosphatase and tensin homologue deleted on chromosome 10) play a role in down-regulating PI 3-kinase activity by removing phosphate groups from the 3-phosphorylated lipid products of the enzyme. PTEN was identified as a tumor suppressor and tyrosine phosphatase. PTEN is now known to be the second most commonly mutated gene in all human cancers. SHIPs remove phosphate groups from the 5 position of the inositol ring and bind to diverse receptors and adaptor molecules.

PI 3-Kinases are a Family of Enzymes

Once the importance of PI 3-kinases in cell physiology was realized, several groups set out to purify and characterize PI-3 kinases from a variety of tissues. Eight PI 3-kinase isoforms are now known; they are divided into three classes based on their structure and *in vitro* substrate specificity.

Class I PI 3-Kinases

The class I molecules can use PI, PI(4)P, or PI(4,5)P2 as substrates *in vitro*. However, *in vivo*, they show a strong preference for PI(4,5)P2. The class I enzyme subtypes have been subdivided into class Ia and class Ib based on their mode of regulation (see Figure 2). The class Ia enzymes consist of three isoforms, p110α, p110β, and p110, which are encoded by three separate genes. The class Ia enzymes use p85 as their adaptor subunit, but this has at least seven adaptor variants, which are the alternative spliced products of three separate genes,

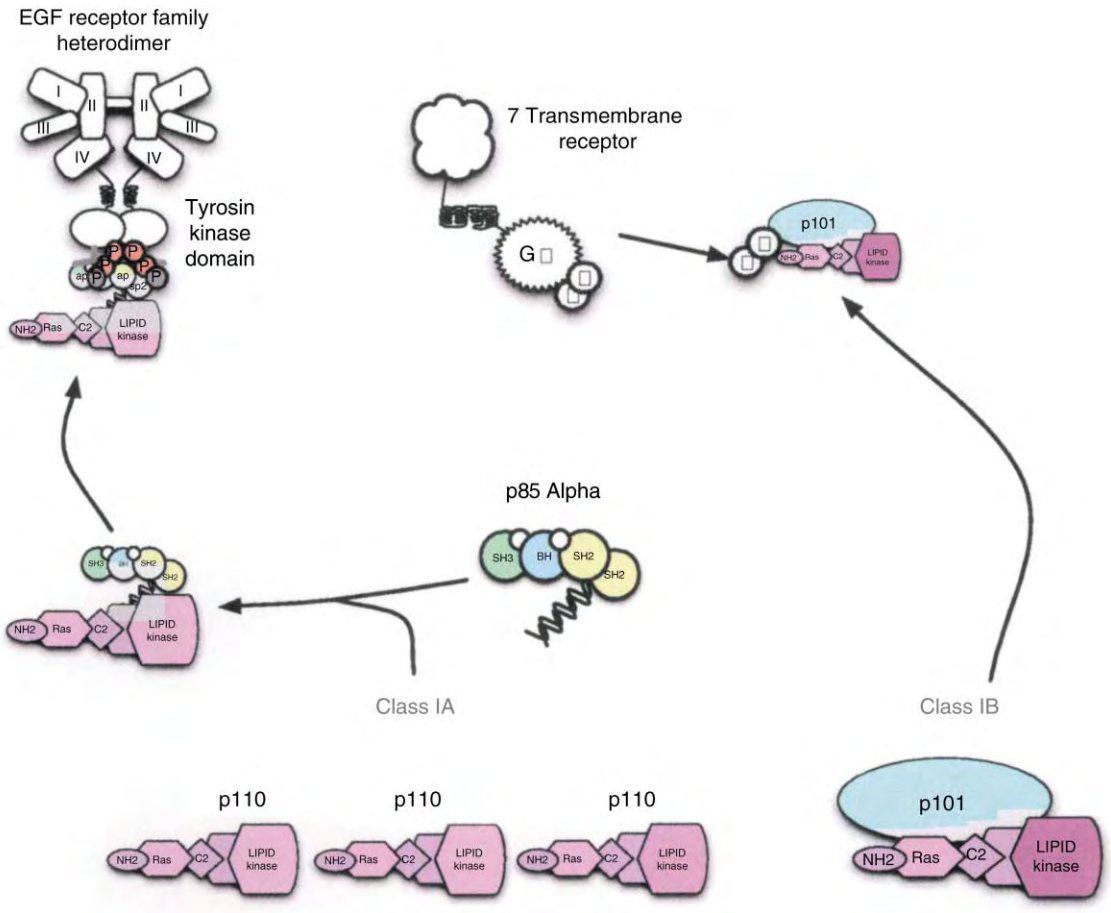

FIGURE 2 The class I PI 3-kinases are divided into groups Ia and Ib. Group 1a includes three catalytic subunits, p110α, β, and δ, which form heterodimers with their regulatory subunit p85. Class Ib includes the PI 3-kinase γ, which associates with the protein p101. The PI 3-kinases have amino-terminal (NH_2), Ras-binding, C2, and lipid kinase domains. The regulatory subunit p85 has an SH2 (src homology) region, which binds to phosphorylated sequences on growth factor receptors such as those of the EGF (epidermal growth factor) family, SH3, and BH domains. The PI 3-kinase γ is activated by G protein $\beta\gamma$ subunits that are released by signals from seven transmembrane receptors.

namely, p85α, p85β, and p55γ. The p110α and p110β subtypes are expressed ubiquitously, whereas p110δ has an expression pattern that is mainly restricted to hematopoietic cells. All mammalian cell types studied express at least one class Ia PI 3-kinase isoform class Ia PI 3-kinases are conserved in evolution and have been found and studied in *Drosophila melanogaster, Caenorhabditis elegans*, and *Dictyostelium discoideum*, as well as more recently in transgenic mice, with dramatic results.

Only one class Ib isoform exists, p110γ, which is activated by G protein-coupled receptors by binding to the G$\beta\gamma$ subunits of heterotrimeric G proteins. The p110γ catalytic subunit does not partner with the p85 adaptor subunits; instead, it forms a complex with a 101 kDa regulatory protein known as p101, which is not homologous to any known protein. The role of p101 is unresolved, although it may be involved in the interaction with G$\beta\gamma$. The p110γ/p101 complex has only been found in mammals and has a tissue distribution mainly restricted to hematopoietic cells. Some studies have shown that the class Ia isoform p110β can also bind to G$\beta\gamma$ and thus be activated by G protein-coupled receptors *in vitro*; however, the physiological significance of this interaction has not been established.

All class I subtypes bind to ras, a signaling molecule that is a key regulator of cell growth and transformation, which means that activated ras can turn on the PI 3-kinase pathway.

Transgenic mouse studies have helped to elucidate the functional specificity of the class I isoforms *in vivo*. For example, p110δ and p110γ clearly have a role in the regulation of the immune response, reflecting their restricted tissue distribution. P110γ knockout mice, in studies reported by three groups, had impaired neutrophil and macrophage chemotaxis and function and consequently were unable to mount an inflammatory response to bacterial infections. In another study, p110γ knockout mice were used to show that the enzyme acts as a negative regulator of heart muscle contractility.

The p110δ knockout mice have been described in studies by three groups, and the data have confirmed that p110δ functions primarily in B and T lymphocytes. The p110δ-deficient mice failed to raise an adequate immune response due to compromised B- and T-cell antigen receptor signaling. Deletion of the p110α gene gave an embryonic lethal phenotype, as did deletion of the p110β gene, which indicates that these isoforms play important roles in development.

Knockout studies of the adaptor subunits have shown that p85 is involved both in the cellular immune response and in the control of glucose metabolism Transgenic mice with deletions of all p85 isoforms resulted in perinatal lethality. Mice with were hypoglycemic, showed lower insulin levels, and had increased glucose tolerance. In addition, p85α knockout mice had diminished B-cell activity but functional T-cells, indicating that p85β but not p85α may be important in T-cell signaling.

Class II PI 3-Kinases

The class II enzymes have larger molecular weight catalytic subunits of 170 kDa, with a C-terminal C2 domain that can bind phospholipids *in vitro* in a Ca^{2+}-independent manner and possible amino-terminal protein interaction domains. The class II PI 3-kinases use mainly PI, and to a lesser extent PI(4)P and PI(4,5)P2, as substrates *in vitro*. However, the *in vivo* substrate specificity of class II PI 3-kinase is presently unknown. Three class II isoforms have been found in mammals, C2α, C2β, and C2γ. Only one isoform exists in *D. melanogaster*, and when it is mutated, developmental defects are induced. The function of PI 3-kinase class II in mammalian cells is far less characterized than that of the class I enzymes.

Class III PI 3-Kinases

The class III enzymes are homologues of the yeast enzyme vps34p; both enzymes use PI only as a substrate *in vitro*. Class III PI 3-kinases have a role in intracellular trafficking of proteins.

Signaling Downstream of PI 3-Kinases

The number of targets downstream of PI 3-kinase, which impinge on cellular functions as diverse as growth, apoptosis, glucose homeostasis, and heart muscle contractility, are ever expanding and comprise a vast area of research, a detailed account of which would be beyond the scope of this article.

The first direct target in downstream PI 3-kinase signaling is created by the interaction of their lipid products, the 3-phosphoinositides with proteins that have specific PI3P lipid-binding domains. Such proteins containing either a PH (pleckstrin homology) domain, such as AKT/PKB and PDK1, or a FYVE domain, named after the first four proteins shown to contain it, Fab1p, YOTB, Vac1p, and early endosome antigen 1 (EEA1). Both bind 3-phosphoinositides.

The protein AKT is a major player in PI 3-kinase signaling, lying directly downstream of PI 3-kinase in the pathway (see Figure 3). Both AKT and PDK contain PH domains and hence are brought to the membrane by binding to 3-phosphoinositides following PI 3-kinase activation. AKT activation is thought to occur via phosphorylation at two sites: Thr308 by PDK1 and S473 by a putative PDK2 molecule yet to be established. Once activated, AKT phosphorylates and regulates a diverse set of molecules. For example, AKT phosphorylates and inhibits the BCL-2 family member BAD and caspase 9, both of which promote apoptosis, and the forkhead transcription factors, which stimulate transcription of pro-apoptotic genes. These events have a combined antiapoptotic effect on the cell. AKT activation affects cell cycle activation by increasing cyclin D transcription and translation and by reducing levels of the cyclin-dependent kinase inhibitor p27kip1.

Studies of PI 3-kinase signaling in *D. melanogaster* have shown that overexpression of Dp110 in imaging disks increases cell growth and creates larger flies. The link between PI 3-kinase and cell growth is likely due to the fact the PI 3-kinase lies downstream of the insulin receptor and upstream of p70S6 kinase, which when activated phosphorylates the 40S ribosomal protein, S6. This process increases the translation of the 5′-TOP mRNAs, which encode ribosomal proteins and protein synthesis elongation factors. Another player in this pathway is mammalian target of rapamycin (mTOR), which lies downstream of PI 3-kinase and activates p70S6 kinase as well as the eukaryotic translation initiation factor (4E-BP1), promoting protein translation and ultimately cell growth.

The effects of PI 3-kinases on the regulation of the actin cytoskeleton occur not through AKT but via their interaction with guanosine nucleotide exchange factors (GEFs) and GTPase-activating proteins (GAPs) for small GTPases, such as Rac and members of the Arf family. These molecules are known to contain PH domains and thus are likely to be directly downstream of PI 3-kinases. The exact mechanism of the interaction of PI 3-kinase lipid products and GEFs has not been established, but it is clear that PI 3-kinase has at least a regulatory role in the organization of the cytoskeleton and thus cell motility.

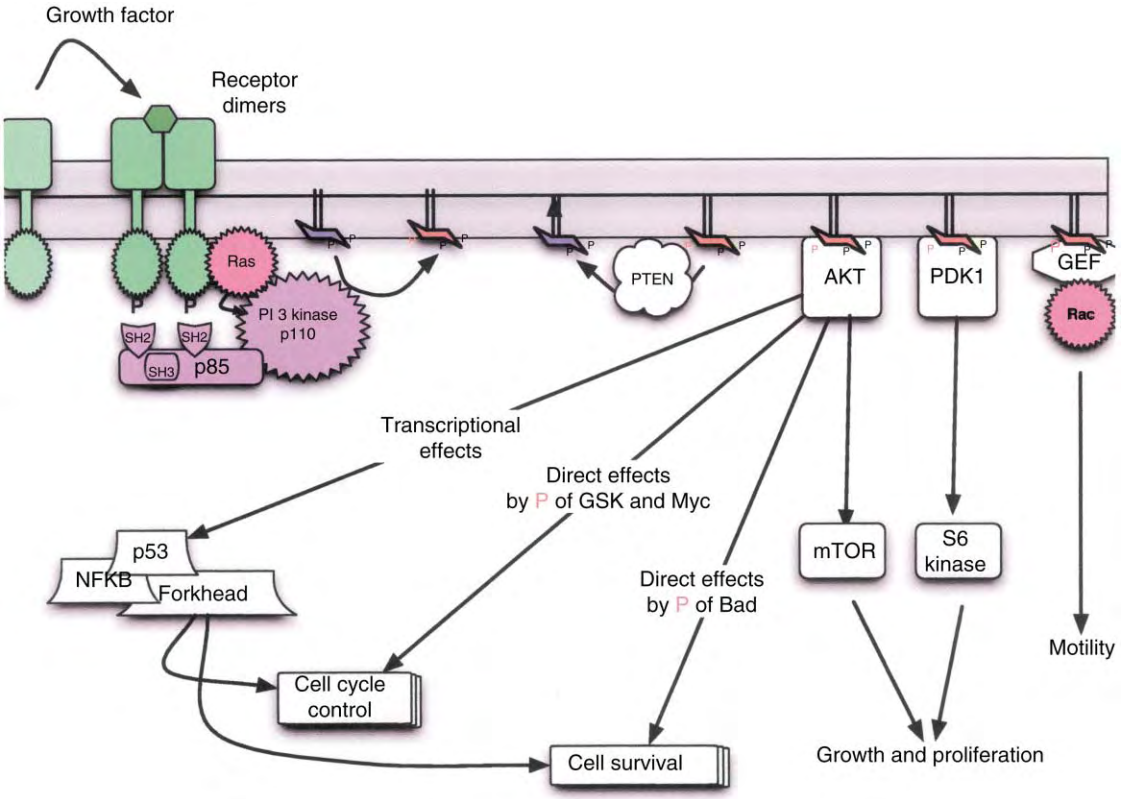

FIGURE 3 The PI 3-kinase signal pathways.

The Role of PI 3-Kinases in Human Disease

It is clear from the diverse role which PI 3-kinases plays in the cell that aberrations of the PI 3-kinase pathway are likely to perturb cellular homeostasis, leading to disease. Evidence has accumulated from transgenic manipulation studies of the PI 3-kinase genes in mice as well as from studies of disease models in nature. Interestingly, the transgenic studies in mice have revealed that the class I isoforms play important and distinct functions in cells of different tissue origin. Pharmaceutical companies have started to exploit the therapeutic potential of isoform selective PI 3-kinase inhibitors for various indications.

Cancer

The strongest link between PI 3-kinase and cancer is the tumor suppressor PTEN, which has been found to be the second most commonly mutated gene in cancer after p53 and a negative regulator of PI 3-kinase through its lipid phosphatase activity. Mutations that destroy function or the loss of PTEN are especially prevalent in prostate, brain (glioblastoma), and endometrial cancers. Increased PI 3-kinase activity associated either with lack of PTEN activity or mutation of the PI 3-kinase gene itself, as has been shown to occur in certain cancers, can promote the oncogenic action of this enzyme. Increased PI 3-kinase activity may lead to loss of the ability to regulate cell survival, loss of control of the cell cycle, and alterations in motility, which are some of the key events in cellular cancer progression. In addition, the enzyme PI 3-kinase lies downstream of the vascular endothelial growth factor (VEGF) receptor, a growth factor signal system that promotes angiogenesis in solid tumors, a key factor in supporting tumor growth. Therefore, inhibitors to PI 3-kinase would be suitable candidates for clinical evaluation in oncology.

Inflammatory Disease

Studies in transgenic mice either lacking or with mutated forms of the p110δ and p110γ isoforms have shown that these two enzymes have specific roles in regulating the immune response. Both isoforms have a tissue expression restricted mainly to hematopoietic cells. In addition, elegant studies in mice have allowed the differentiation of the role of these two isoforms. Thus p110γ has been shown to be involved in the innate immune response through regulation of macrophage and neutrophil function.

Knock-in mice with kinase-dead mutant versions of p110δ have been constructed, showing that this isoform regulated the development and function of B- and T-cell lymphocytes and thus the adaptive immune response. Several pharmaceutical companies have established programs to evaluate isoform-specific inhibitors to p110δ and p110γ in autoimmune and allergic disease.

Cardiovascular Disease

Tissue-specific knockout studies of PTEN have implicated the importance of PI 3-kinase enzymes in controlling both cardiac contractility and hypertrophy. Additional studies of these mice that involve the expression of dominant negative p110α and p110γ enzymes have given clues to the role of each isoform in the heart. The p110α isoform was found to be responsible for increases in the size of cardiomyocyte cells and p110γ to be associated with decreased heart contractility. Surprisingly, there were high levels of p110γ in total heart extracts of these mice, as this isoform was considered to be present primarily in leukocytes. Therefore, isoform selective inhibitors of PI 3-kinase may have therapeutic potential in treating heart failure.

See Also the Following Articles

Phosphatidylinositol Bisphosphate and Trisphosphate • Phosphatidylinositol-3-Phosphate • Phospholipase C • Protein Kinase C Family

Glossary

Akt A serine/threonine protein kinase that is activated by the lipid products of PI 3-kinase.

phosphatidylinositol 3,4,5-triphosphate (PIP3) A phosphatidylinositide that has three phosphate groups on the 3, 4, and 5 positions of the inositol ring that acts as a second messenger molecule in cells.

PI 3-kinase A family of enzymes that phosphorylate inositolphosphates on the 3 position of the inositol ring.

PTEN A lipid phosphatase that removes the phosphate from the 3 position of PIP3, thus down-regulating the growth and proliferation signal.

Further Reading

Leslie, N. R., and Downes, P. (2002). PTEN: The down side of PI 3-kinase signaling. *Cell. Signal.* **14**, 285–295.

Luo, J., Manning, B. D., and Cantley, L. (2003). Targeting the PI3K-Akt pathway in human cancer: Rationale and promise. *Cancer Cell* **4**, 257–262.

Vanhaesebroeck, B., Leevers, S. J., Ahmadi, K., Timms, J., Katso, R., Driscoll, P. C., Woscholski, R., Parker, P. J., and Waterfield, M. D. (2001). Synthesis and function of 3-phosphorylated inositol lipids. *Annu. Rev. Biochem.* **70**, 535–602.

Vivanco, I., and Sawyers, C. L. (2002). The phosphatidylinositol 3-kinase AKT pathway in human cancer. *Nat. Rev. Cancer* **7**, 489–501.

Walker, E. H., Pacold, M. E., Perisic, O., Stephens, L., Hawkins, P. T., Matthias, P., Wymann, T., and Williams, R. L. (2000). Structural determinants of phosphoinositide 3-kinase inhibition by wortmannin, LY294002, quercetin, myricetin, and staurosporine. *Mol. Cell* **6**, 909–919.

Wymann, M., Zvelebil, M., and Laffargue, M. (2003). Phosphoinositide 3-kinase signalling: Which way to target? *Trends Pharmacol. Sci.* **24**, 366–376.

Biography

Khatereh Ahmadi is Project Manager of the PI 3-kinase drug discovery program in oncology at Piramed, a start-up biotechnology company in the United Kingdom. She obtained a Ph.D. in immunology at Kings College London and was a postdoctoral Research Fellow at the Ludwig Institute for Cancer Research, working on PI 3-kinase biochemistry and molecular biology with Michael Waterfield. She managed the drug development program that led to the discovery of specific new inhibitors for these enzymes.

Michael Waterfield is Director of Research at the Ludwig Institute for Cancer Research at University College London where he is also Courtauld Professor of Biochemistry. With Peter Parker he first purified and characterized the PI 3-kinase enzymes and then co-developed specific inhibitors of these enzymes. Previously, he co-discovered the functional role of the sis oncogenes, and in studies of signal transduction with other colleagues, he purified and cloned the EGF receptor and found that when truncated it functioned as an oncogene. In 2003 he co-founded the Piramed company to develop PI 3-kinase inhibitors.

Phosphoinositide 4- and 5-Kinases and Phosphatases

Shawn F. Bairstow, Matthew W. Bunce and Richard A. Anderson
University of Wisconsin, Madison, Wisconsin, USA

Phosphoinositides are one of the many phospholipid families found within membrane bilayers of eukaryotic cells. Site-specific phosphorylation of phosphoinositides by lipid kinases results in the generation of multiple phosphatidylinositol phosphate isomers. These mono- or poly-phosphorylated isomers can be further modified by additional enzymes or can directly modulate numerous cellular functions. Because of the potential for phosphoinositides to alter a variety of cellular processes, their synthesis must be strictly regulated. A number of phosphoinositide kinases and phosphatases have been identified and characterized. By adding or removing phosphate groups at specific positions along the inositol ring, these kinases and phosphatases dictate the signaling capacity of phosphoinositides.

Phosphoinositides

Structure

The basic structure of phosphoinositides consists of a six-carbon inositol ring linked by a phosphodiester bond to diacylglycerol (DAG) (Figure 1). The two fatty acid tails of the DAG moiety anchor phosphoinositides into the various membrane structures throughout eukaryotic cells, such as the endoplasmic reticulum, Golgi apparatus, and plasma membrane. *In vivo*, phosphoinositides can be phosphorylated at the 3-, 4-, and 5-hydroxyl positions along the inositol ring in all possible combinations.

Nomenclature

Phosphatidylinositol (PI) is the initial substrate for a number of phosphoinositide kinases that phosphorylate the hydroxyl groups along the inositol ring. Mono- and polyphosphorylated phosphoinositides are named with respect to the positions of the inositol ring that are phosphorylated. Phosphorylation of PI at the 4-hydroxyl position generates phosphatidylinositol 4-phosphate (PI4P); a subsequent phosphorylation at the 5-hydroxyl position generates phosphatidylinositol 4,5-bisphosphate ($PI(4,5)P_2$). Phosphatidylinositol can be singly or severally phosphorylated at the 3-, 4-, and 5-hydroxyl positions to yield phosphatidylinositol mono-, bis-, or trisphosphate molecules.

Phosphatidylinositol 4-Kinases

Subfamilies

Phosphatidylinositol 4-kinases (PI 4-kinases) use PI as a substrate to generate PI4P. PI 4-kinases are classified as either type II or type III kinases based on their structural and kinetic properties. Two mammalian isoforms termed α and β have been identified for each PI 4-kinase subfamily. Type III PI 4-kinases are structurally and kinetically similar to PI 3-kinases. PI 3-kinases and type III PI 4-kinases have homologous catalytic domains, and type III PI 4-kinases are even inhibited by known PI 3-kinase inhibitors, such as wortmannin. Type II PI 4-kinases do not share these structural or catalytic similarities with PI 3-kinases.

Cellular Functions

The higher-order species such as $PI(4,5)P_2$ and $PI(3,4,5)P_3$ have received significant attention, whereas PI4P has typically been thought of simply as a metabolic intermediate in the synthesis of other phosphoinositides. However, a number of functional studies have demonstrated important roles for PI 4-kinases *in vivo*. Type II PI4-kinases have been linked to roles in both secretion and endocytosis. Type III PI4-kinases have been most thoroughly characterized in the budding yeast *Saccharomyces cerevisiae*. Stt4 and Pik1, the yeast homologues of mammalian type III α- and β-isoforms, respectively, are targeted to distinct subcellular locations and perform nonredundant functions. Pik1 is targeted to the nucleus and Golgi. The nuclear function of Pik1 is unknown, but several studies have indicated that Pik1 is required

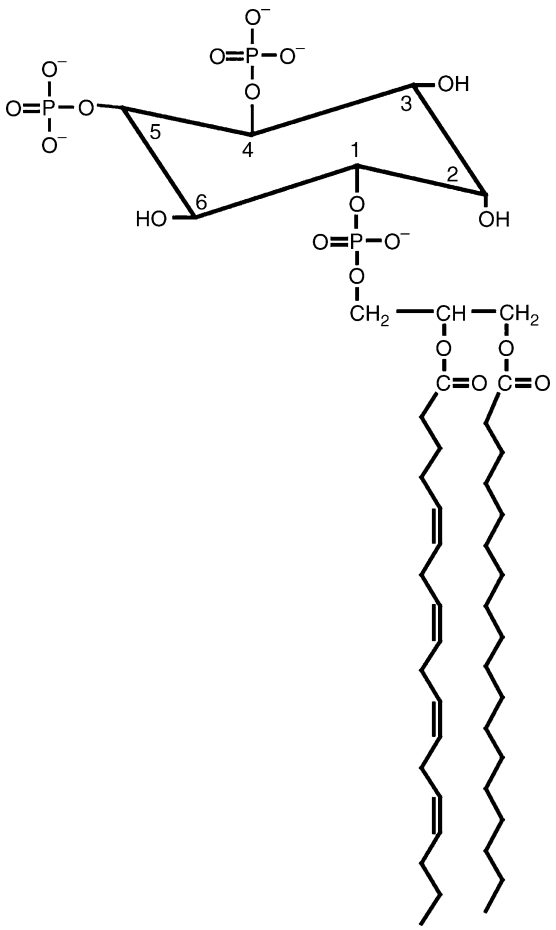

FIGURE 1 Phosphoinositide structure. Phosphoinositides are comprised of a six-carbon inositol ring linked by a phosphodiester bond to diacylglycerol. The inositol ring is numbered counterclockwise starting at the phosphodiester linkage. *In vivo*, phosphoinositides are phosphorylated at the 3, 4, and 5 positions of the inositol ring; phosphatidylinositol 4,5-bisphosphate ($PI(4,5)P_2$) is pictured.

for normal secretion from the Golgi. PI 4-kinase β, the mammalian homologue to Pik1, has also been implicated in Golgi function. Stt4 localizes primarily to the plasma membrane and ER and has been linked to actin cytoskeleton organization and cell wall stability. The PI4P generated specifically by Stt4 can be further phosphorylated by Mss4, the yeast homologue of type I phosphatidylinositol phosphate kinases, or dephosphorylated by the phosphoinositide phosphatase Sac1. The interplay between Stt4, Mss4, and Sac1 control actin dynamics in *S. cerevisiae*. As mentioned above, Pik1 and Stt4 are functionally nonredundant. A loss of activity in either PI 4-kinase causes a unique phenotype that cannot be rescued by increasing the activity of the other kinase. These observations suggest that Pik1 and Stt4 each generate discrete pools of PI4P at different subcellular locations, and that these pools of PI4P are utilized by unique sets of effectors.

Phosphatidylinositol Phosphate Kinases

Phosphatidylinositol phosphate kinases (PIP kinases) generate phosphatidylinositol bisphosphate (PIP_2) from phosphatidylinositol monophosphate isomers. PIP kinases are classified into type I, II or III subfamilies based on their structural and kinetic properties. Members of all three subfamilies have highly conserved kinase domains toward the C-terminus of the proteins, with more variable flanking sequences. Each PIP kinase subfamily has unique substrate specificity dictated by a region at the C-terminal end of the kinase domain named the activation loop. The activation loop is nearly identical for different isoforms within a subfamily but divergent between subfamilies (Figure 2).

Type I PIP Kinases

Type I PIP kinases are PI4P 5-kinases, i.e., they use PI4P as a substrate to generate $PI(4,5)P_2$. Three mammalian type I PIP kinase isoforms termed α, β, and γ have been identified. Type I PIP kinases modulate the organization of the actin cytoskeleton. $PI(4,5)P_2$ regulates the activity of many proteins that process actin at the plasma membrane. Mss4, the yeast homologue of mammalian type I PIP kinases, is required for proper actin cytoskeleton organization and cell wall integrity. Yeast lacking Mss4 activity can be rescued by expressing mammalian type I PIP kinase isoforms, illustrating that type I PIP kinases are functionally conserved in eukaryotes. Mammalian type I PIP kinases localize to sites of cortical actin dynamics, such as lamellipodia and focal adhesions, and modulate the assembly of these structures in a $PI(4,5)P_2$-dependent manner. The type Iγ isoform is targeted to focal adhesions by an association with the protein talin and is tyrosine phosphorylated in a focal-adhesion-kinase (FAK)-dependent manner. Kinase-dead PIP kinase Iγ mutants block focal adhesion assembly, reinforcing the requirement for $PI(4,5)P_2$ in focal adhesion signaling.

Type II PIP Kinases

Type II PIP kinases are PI5P 4-kinases, generating $PI(4,5)P_2$ from PI5P in a catalytically distinct reaction from type I PIP kinases. Like type I PIP kinases, the type II subfamily is comprised of α-, β-, and γ-isoforms. *In vivo* functions for type II PIP kinases have not been clearly defined. Although type I and type II PIP kinases both produce $PI(4,5)P_2$, the two subfamilies are functionally nonredundant. No homologues for mammalian type II PIP kinases have been identified in *S. cerevisiae*, so type II PIP kinases may have specialized functions in higher eukaryotes. One such function could be to modulate receptor-mediated signaling, as the type

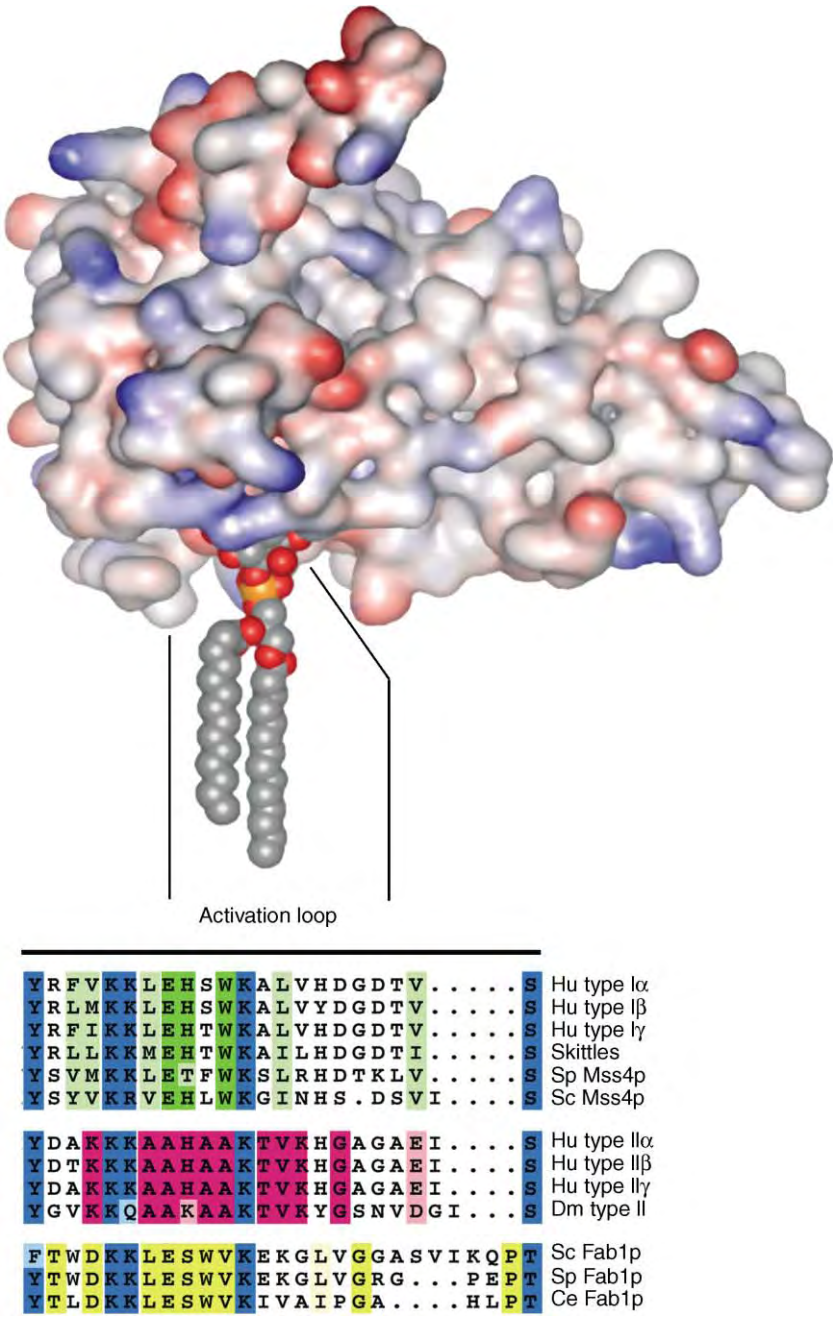

FIGURE 2 PIP kinase structure and the activation loop. The crystal structure for the human type IIβ PIP kinase isoform is shown above with PI5P modeled into the active site. Although the activation loop was not resolved in the crystal structure, its position relative to the active site is illustrated. A sequence alignment of type I, type II, and type III PIP kinase activation loops is shown below the crystal structure. The activation loop is highly conserved among members of each subfamily but divergent between subfamilies. Hu – human, Sp – *S. pombe*, Sc – *S. cerevisiae*, Dm – *D. melanogaster*, Ce – *C. elegans*.

IIβ-isoform has been identified in a complex with the p55 TNFα transmembrane receptor.

Type III PIP Kinases

Type III PIP kinases are PI3P 5-kinases, generating PI(3,5)P_2 from PI3P. The *S. cerevisiae* protein Fab1 was the first type III PIP kinase to be identified. In yeast, Fab1 and PI(3,5)P_2 are involved in vacuole morphology, membrane trafficking, and stress response. Type III PIP kinases were not initially identified in mammalian cells, and *in vitro* studies suggested that type I isoforms can generate PI(3,5)P_2 and thus may perform similar functions to those of Fab1 in yeast. More recently, however, proteins homologous to ScFab1 have been identified in mammalian cells. These mammalian enzymes have

similar *in vivo* substrate specificity to the *S. cerevisiae* Fab1 enzyme and appear to regulate membrane trafficking in a manner comparable to ScFab1.

Phosphatidylinositol Phosphatases

Phosphatidylinositol phosphatases are enzymes that can selectively dephosphorylate both lipid phosphoinositides and soluble inositol polyphosphates. As a family, they can be subdivided by their catalytic properties and substrate specificity.

Phosphoinositide 4-Phosphatases

The Phosphoinositide 4-Phosphatases (Inositol Polyphosphate 4-Phosphatases) are a family of enzymes that dephosphorylate the 4-position of the inositol ring in a magnesium-independent manner. The members of this family can utilize PI(3,4)P_2, Ins(3,4)P_2, and Ins(1,3,4)P_3 as substrates *in vitro*, generating PI3P, Ins3P, and Ins(1,3)P_2, respectively. Two genes have been identified in humans corresponding to type I and type II 4-phosphatases. These genes can be alternatively spliced, resulting in expression of several variant phosphatases. Both types share a 37% total sequence identity and a conserved CKSAKDRT consensus sequence. This C–X_5–R consensus sequence is consistent with other magnesium-independent phosphatases.

Cellular Functions of 4-Phosphatases

The PI-3 Kinase (PI3K) signaling pathway impacts cell growth, glucose metabolism, and apoptosis. Activation of the PI3K pathway results in the generation of PI(3,4,5)P_3 and PI(3,4)P_2, which stimulate downstream effectors such as protein kinase B/Akt and PI3K-dependent kinase 1. Phosphoinositide 4-phosphatases are thought to participate in regulation of the PI3K pathway by converting PI(3,4)P_2 to PI3P, thus attenuating the PI3K signal and subsequently deactivating PI3K effectors. An association identified between a PI 4-phosphatase and the PI3K p85 regulatory subunit supports this putative function for PI 4-phosphatases.

Phosphoinositide 5-Phosphatases

Phosphoinositide 5-phosphatases (inositol polyphosphate 5-phosphatases) dephosphorylate the 5-position of the inositol ring in a magnesium-dependent manner. This family collectively can utilize four substrates: PI(4,5)P_2, PI(3,4,5)P_3, Ins(1,4,5)P_3, and Ins(1,3,4,5)P_4. PI 5-Phosphatases contain a bipartite consensus sequence, (F/I)WXGDXN(F/Y)R, followed several amino acids downstream by (R/N)XP(S/A) (W/Y) (C/T)DR(I/V) (L/I). PI 5-phosphatases are classified into four groups based on their substrate specificity.

Group I 5-Phosphatases

Group I 5-phosphatases use Ins(1,4,5)P_3 and Ins(1,3,4,5)P_4 as substrates. Type I 5-phosphatase, one member of this group, is thought to play a role in the regulation of cellular calcium levels. Ins(1,4,5)P_3 (IP_3) is a pivotal regulator of cellular calcium levels and is generated by the cleavage of PIP_2 by phospholipase C. The resulting IP_3 binds to the IP_3 receptor, triggering a release of calcium ions from intercellular stores. Type I 5-phosphatase decreases this signal by dephosphorylating IP_3 into Ins(1,4)P_2.

Group II 5-Phosphatases

Members of group II 5-phosphatases can utilize all four of the substrates mentioned above. The synaptojanins, type II 5-phosphatase and the Oculocerebrorenal Syndrome of Lowe (OCRL) gene product, OCRL-1, are all members of this group. OCRL is an X-linked disorder resulting in mental retardation, renal dysfunction, and congenital cataracts. Although the pathogenesis for these symptoms is not currently known, OCRL-1 dysfunction results in an increase in PI(4,5)P_2 levels, as observed in cells cultured from individuals with this disorder. Interestingly, OCRL-1 shares 51% identity with type II 5-phosphatase. However, this enzyme cannot compensate for the lack of OCRL-1 activity, possibly due to a difference in substrate specificity or tissue localization. The synaptojanins have functions distinct from OCRL-1 and type II 5-phosphatase. Synaptojanin 1 has been shown to function in recycling of vesicles at neuronal synapses. Synaptojanin 2, on the other hand, is somewhat less characterized. This protein is alternatively spliced and some variants have been shown to have functions overlapping that of synaptojanin 1, while other variants have been localized to distinct cellular compartments, such as the outer mitochondrial membrane.

Group III 5-Phosphatases

Group III 5-phosphatases are active toward PI(3,4,5)P_3 and Ins(1,3,4,5)P_4, which have a 3-position phosphate group. Src homology domain containing inositol phosphatases (SHIPs), SHIP1 and SHIP2 are important members of this group. These proteins share 50% sequence identity and similar substrate specificity, but differ in their tissue expression levels. SHIP1 is primarily expressed in hematopoetic tissues while SHIP2 is expressed in nonhematopoetic tissues. Recent work has demonstrated an importance of SHIPs in signal

transduction. SHIP2 has been shown to associate with specific tyrosine kinase receptors, such as the EGF receptor. This places the phosphatase in an ideal location to attenuate the increased PI(3,4,5)P_3 and PI(3,4)P_2 levels generated by PI3K, which is also recruited to these receptors. SHIP2 mouse knockout experiments support SHIP2's role in PI3K signal termination and also suggest a link between SHIP2 activity and insulin resistance, a primary factor in type 2 diabetes.

Group IV 5-Phosphatases

Group IV phosphatases are the least-characterized of the four groups. One member, phosphoinositide 5-phosphatase type IV, has recently been identified. This phosphatase utilizes PI(3,4,5)P_3 as its primary substrate, but has also been shown to dephosphorylate PI(4,5)P_2 under certain conditions. Expression levels are highest in the brain for both humans and mice, with lower expression in other tissues. The cellular function of this phosphatase has yet to be determined.

See Also the Following Articles

Diabetes • Inositol Phosphate Kinases and Phosphatases • Phosphatidylinositol Bisphosphate and Trisphosphate • Phosphoinositide 3-Kinase • Phosphoinositide-Dependent Protein Kinases

Glossary

inositol A six carbon cyclic alcohol with hydroxyl residues present at each carbon.

kinase An enzyme that catalyzes the transfer of a phosphate group from adenosine triphosphate to a second substrate.

phosphatase An enzyme that hydrolyzes a phosphate group from a substrate.

phosphoinositide A phospholipid molecule composed of inositol and DAG.

Further Reading

Abel, K., Anderson, R. A., and Shears, S. B. (2001). Phosphatidylinositol and inositol phosphate metabolism. *J. Cell Sci.* **114**, 2207–2208.

Anderson, R., Boronenkov, I., Doughman, S., Kunz, J., and Loijens, J. (1999). Phosphatidylinositol phosphate kinases, a multifaceted family of signaling enzymes. *JBC* **274**, 9907–9910.

Cockcroft, S. (2000). *Biology of Phosphoinositides*. Oxford University Press, New York.

Majerus, P., Kisseleva, M., and Norris, F. (1999). The role of phosphatases in inositol signaling reactions. *JBC* **274**, 10669–10672.

Biography

Shawn F. Bairstow is a graduate student in the Department of Biomolecular Chemistry at the University of Wisconsin-Madison. His primary research focus is the spatial and temporal targeting of the type Iγ PIP kinase isoform and its involvement in focal adhesion assembly. He earned a B.S. in Biochemistry from the University of Illinois-Campaign/Urbana where he performed undergraduate research focusing on the catalytic mechanism of cytochrome P450.

Matthew W. Bunce earned a B.S. in Biochemistry at Virginia Tech and is currently a predoctoral graduate student in the lab of Dr. Richard Anderson at the University of Wisconsin-Madison. His research is focused on determining how PIP kinases interact with their substrates, and also on the identification and characterization of binding partners that direct PIP kinases to their unique subcellular compartments and modulate PIP kinase signaling.

Richard A. Anderson is Professor of Pharmacology and Director of Molecular and Cellular Pharmacology at the University of Wisconsin-Madison. His principal research interest is in cell signaling with an emphasis on phosphoinositide signal transduction mechanisms that modulate cancer development and metastasis. He holds a Ph.D. from the University of Minnesota and did his postdoctoral work at Yale University with Vincent T. Marchesi. He has authored numerous articles on the role of PIP kinases in signal transduction.

Phosphoinositide-Dependent Protein Kinases

Nick R. Leslie and C. Peter Downes
University of Dundee, Dundee, UK

The cells of multicellular organisms respond to external stimuli, such as growth factors, cytokines, neurotransmitters, and many hormones through regulated changes in the levels of cellular signaling molecules, termed second messengers. The inositol phospholipids (collectively known as phosphoinositides) are constituents of cell membranes that play important roles as second messengers in signal transduction and membrane trafficking. Many of the downstream effects of phosphoinositide signaling are mediated through reversible protein phosphorylation and in this article the principal focus will be upon protein kinases that function as downstream targets of the phosphoinositide 3-kinase (PI 3-kinase) lipid signaling pathway.

Phosphoinositide Signaling – An Overview

Phosphoinositides are a small family of differentially phosphorylated membrane-localized lipid second messengers. These lipids comprise the hydrophilic cyclic polyol, myo-inositol (Ins), linked via a diester phosphate in the 1-position to diacylglycerol, the hydrophobic membrane anchor. Several families of lipid kinases and phosphatases selectively insert and remove monoester phosphates in three of the remaining positions of the inositol ring, generating the eight currently known phosphoinositide species. This review focuses on some of the most intensively studied phosphoinositide signaling pathways initiated when growth factors, cytokines or insulin, and related hormones trigger the activation of one or more of the type I PI 3-kinases. These enzymes phosphorylate a small proportion of the cellular phosphatidylinositol 4,5 bisphosphate (PtdIns(4,5)P_2) to generate PtdIns(3,4,5)P_3 (often abbreviated to PIP_3). The latter is further metabolized by 5-phosphatases to PtdIns(3,4)P_2 or is returned to the PtdIns(4,5)P_2 pool by the tumor suppressor lipid phosphatase PTEN. PtdIns(3,4,5)P_3 activates downstream signaling through proteins which possess a phosphoinositide binding domain capable of distinguishing this target lipid within a membrane that contains at least 100-fold higher levels of the parent lipid PtdIns(4,5)P_2. Several modular protein domain families have now been identified that include members able to bind to specific phosphoinositides, such as pleckstrin homology (PH), Phox homology (PX), FYVE, and ENTH domains. Other domains, such as FERM, and PDZ domains may also function as phosphoinositide-binding motifs, although evidence for their selectivity between different phosphoinositides is currently lacking. In almost all cases presently identified, the PtdIns(3,4,5)P_3-specific-binding motifs mediating PI 3-kinase-dependent signaling are members of the PH domain family.

Protein Kinase B/Akt

Since the 1990s, it has become evident not only that PI 3-kinase signaling plays a pivotal role in regulating many diverse and significant cellular processes, including cellular proliferation, survival, size, and motility, but that many of the downstream effectors of PtdIns(3,4,5)P_3 are protein kinases. The best evidence for regulation by PtdIns(3,4,5)P_3 exists for three classes of kinase that carry PH domains able specifically to bind this lipid: the Ser/Thr kinases, PKB (or Akt), PDK1, and the Tec family Tyr kinases. Space limitations prevent us from addressing such enzymes as GSK3 or PAK, which can clearly be regulated by the PI 3-kinase pathway, though not by directly binding to PtdIns(3,4,5)P_3 and these enzymes can also be regulated by PI 3-kinase independent pathways. The PI 3-kinase signaling pathway has been dissected extensively using biochemical and genetic approaches. Significantly, the stimulated production of PtdIns(3,4,5)P_3 by PI 3-kinase enzymes is conserved in species from slime molds, through nematodes and flies to vertebrates. In species of all of these groups, genetic studies indicate that a principal (though not exclusive) cellular mediator of this signaling pathway is protein kinase B (PKB).

PKB, also known as Akt, has a C-terminal serine/threonine kinase domain and an N-terminal PH domain

that binds with high specificity to PtdIns(3,4,5)P_3 and PtdIns(3,4)P_2. The enzyme has been shown to be activated by phosphorylation of two key residues, threonine 308, in the activation loop (or T-loop) of the kinase domain, and serine 473 in the C-terminal tail. These phosphorylation events in turn are believed to alter the conformation of PKB greatly enhancing its activity, and although much of this work has focused on PKB, it now appears that a number of related kinases may be regulated by analogous mechanisms. Although PtdIns(3,4,5)P_3 and PI(3,4)P_2 do not directly enhance the activity of PKB *in vitro*, they play a critical role in the phosphorylation and activation of PKB, by recruiting PKB to the plasma membrane where it is activated, and by opening the conformation of the protein to allow phosphorylation. Thus it seems that in a normal cellular context the activity state of PKB is largely governed by cellular levels of PtdIns(3,4,5)P_3 and PI(3,4)P_2.

PDK1 and the Regulation of the AGC Kinases

3-Phosphoinositide dependent kinase 1 (PDK1) has been identified as the activating kinase that phosphorylates PKB in a PI 3-kinase dependent process at Thr 308 *in vitro* and *in vivo* (see Figure 1). This protein serine/threonine kinase also has a PH domain that specifically binds PtdIns(3,4,5)P_3 and PI(3,4)P_2 and is found both in the cytosol and on the plasma membrane. Significantly, after its initial identification as a PKB kinase, subsequent work has shown that it also phosphorylates and activates many other related kinases. A point of current controversy is whether the function of PDK1 itself is regulated through mechanisms such as phosphorylation or translocation to the plasma membrane. It has been proposed that PDK1 translocates to the plasma membrane in response to stimulated rises in cellular PtdIns(3,4,5)P_3 levels, as does PKB. However, this conclusion is not supported by other work, and as PDK1 has an affinity approximately tenfold greater for these lipids than does PKB, an alternative idea is that a pool of cellular PDK1 may be constitutively associated with the plasma membrane and that its activity is not normally regulated by changes in the levels of these lipids. It has also been proposed that PDK1 is activated in stimulated cells by tyrosine phosphorylation, possibly by a Src family kinase, although once more other work argues against this, and phosphorylation has not been observed in response to physiological stimuli, or in cells expressing physiological levels of the relevant kinases. Most of this work on the regulation of PDK1 function would suggest that if it is to be viewed as a phosphoinositide-regulated kinase, this regulation occurs through direct or indirect effects of PtdIns(3,4,5)P_3 on its substrates, rather than on PDK1 itself.

PKB exists as three isoforms in human cells (PKBα, β, and γ) but is itself a part of a diverse structurally-related

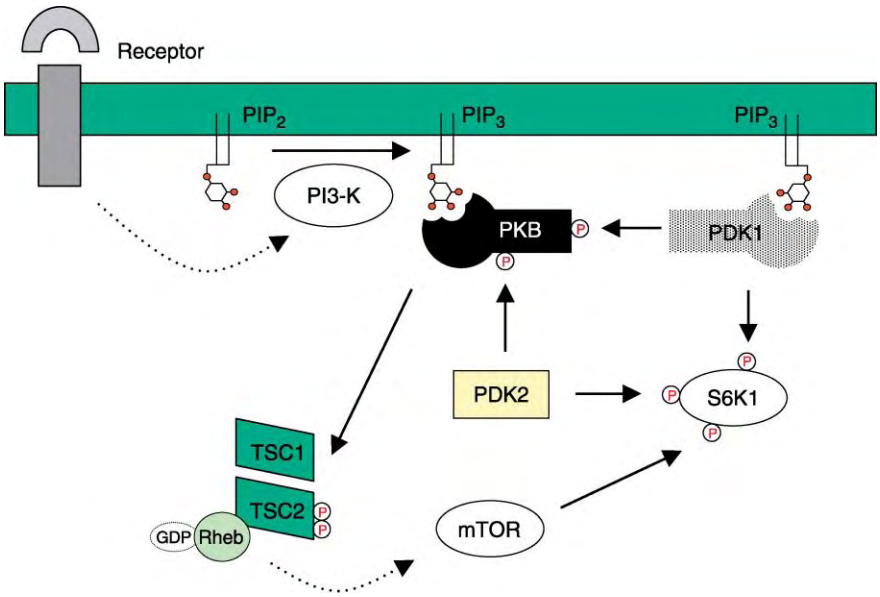

FIGURE 1 Mechanism of activation of PKB, mTOR, and S6K1 by PI 3-kinase. A model is shown for the activation of downstream kinases by a transmembrane receptor activating PI 3-kinase. Molecules are shown in the stimulated conformation. In unstimulated cells, PI3-kinase is less active, PIP_3 levels are low, PKB is cytosolic and along with TSC2 and S6K1, is unphosphorylated and inactive. Active TSC2 promotes the conversion of GTP to GDP by Rheb, although the mechanism by which this leads to the activation of mTOR signaling is unclear. Direct phosphorylation events are shown by bold arrows, indirect mechanisms of activation are represented by dotted arrows. Phosphates are represented by a circled letter P.

family of protein kinases, which are phosphorylated by PDK1 at a residue in the T-loop of each kinase. Although this PDK1-mediated phosphorylation plays a role in the activation of each of these kinases, in contrast to PKB, the phosphorylation of other family members is not directly responsive to cellular PtdIns(3,4,5)P_3 levels, and alternative signaling inputs seem to be required to activate these other kinases strongly. To allow efficient activation, most of these related kinases require the interaction of a hydrophobic motif, positioned C-terminal to their kinase domain, with a hydrophobic pocket on PDK1. In some cases, e.g., S6K1 and SGK, this hydrophobic motif contains a serine or threonine that must be phosphorylated to allow interaction with and activation by PDK1. In these cases, it appears that this phosphorylation is in turn mediated by an unknown PI 3-kinase-dependent kinase. In contrast, in place of this serine or threonine residue, PKCζ and PRK2 have an acidic residue which appears to mediate phosphorylation-independent interaction with, and activation by, PDK1. PKCζ, and probably the other atypical PKC kinases, PKCι and PKCλ, are also unusual in that there is some evidence for the direct activation of the kinase through interaction with PtdIns(3,4,5)P_3. However, these kinases lack a PH domain or other identified PtdIns(3,4,5)P_3-binding motif, and the mechanism and physiological relevance of this apparent activation is unclear.

PDK2 – The Unidentified Hydrophobic Motif Kinase

The term PDK2 was used originally to describe the unidentified kinase responsible for the phosphorylation of PKB at the hydrophobic motif serine 473. Since then, although several candidates have been proposed, such as ILK, MAPKAP-K2, NEK6, and both PKB and PDK1 themselves, the identity of PDK2 is still not clear. What is clear, however, is that most of the AGC family kinases become phosphorylated at a serine or threonine residue in a hydrophobic motif C-terminal to the kinase domain, and that this phosphorylation plays a critical role in the activation of each enzyme. It is quite possible that different PDK2s exist for different AGC family kinases, and it appears that a substantial component of the PI 3-kinase-dependent activation of kinases such as SGK and S6K1 may be mediated by an as yet unknown phosphoinositide-dependent hydrophobic motif kinase. As a consequence of the mechanisms of activation of this family of kinases, increases in cellular PtdIns(3,4,5)P_3 levels seem sufficient to activate PKB, since PtdIns(3,4,5)P_3 and PH domain-dependent colocalization of PKB and PDK1 appears to be the principal mechanism of regulation of this kinase. In contrast, most other PDK1-regulated kinases seem to require regulated docking with PDK1 through a protein–protein interaction to mediate activation in the cytosol, and it is this docking step that may be regulated by different upstream pathways, some of which may themselves involve phosphoinositide-dependent kinases.

Much of the interest in PKB stems from its role in mediating many of the effects of PI 3-kinase activation. Evidence now indicates that a substantial portion of the effects of elevated PtdIns(3,4,5)P_3 levels on cell-cycle progression, survival, growth, and insulin responses are mimicked by activation of PKB alone. In contrast, most PI 3-kinase-dependent cytoskeletal regulation appears to be PKB independent, but may rather result from the interaction of PtdIns(3,4,5)P_3 with the PH domains of guanine-nucleotide-exchange factors for Rho family GTPases. These findings go some way to explaining why isoforms of PKB have been found to be over-expressed in a range of human tumor types, and why activation of PKB activity appears to be an even more common feature of tumors.

Regulators of Cellular Growth – mTOR and S6K1

Work addressing the stimulation of cell growth by PtdIns(3,4,5)P_3 signaling implicates two protein kinases as key players in this process, the mammalian target of rapamycin (mTOR), and ribosomal protein S6 kinase 1 (S6K1, also known as p70S6K). While S6K1 seems to regulate translation through several mechanisms, mTOR has been proposed to play a central role in cellular growth control, as its activity is responsive to nutrients and ATP and is able to regulate a range of downstream processes related to cell growth, including transcription, tRNA and ribosome synthesis, autophagy, and nutrient transporter function. Although recent work has shed significant light on the regulation of both of these kinases, particularly the inputs from PtdIns(3,4,5)P_3 signaling, their regulation appears complex and many questions remain unanswered. mTOR activity now appears to be inhibited in nongrowing cells by the small GTPase Rheb, and a protein complex of two proteins, TSC1 and TSC2, the latter of which can function as a GTPase activating protein for Rheb. Upon activation of PI 3-kinase and PKB, TSC2 is phosphorylated by PKB, Rheb becomes inactive (in the GDP bound state) causing activation of mTOR. S6K1 is then believed to be stimulated through phosphorylation by activated mTOR (in addition to other activating

inputs such as PDK1). This model is represented in Figure 1.

The study of S6K1, and many other kinases that are affected by PtdIns(3,4,5)P_3 signaling, with the exception of PKB, highlights a possible role for the level of basal PtdIns(3,4,5)P_3 present in unstimulated growing cells in culture. For example, S6K1 can be potently activated by G protein-coupled receptors under conditions where PtdIns(3,4,5)P_3 levels do not increase. Thus, PtdIns(3,4,5)P_3 can play a permissive rather than stimulatory role in G protein-coupled receptor mediated S6K1 activation. Significantly, a similar role for basal PtdIns(3,4,5)P_3 has been proposed in the regulation of other molecules, such as Ras and PKCδ.

One important piece of evidence that cell growth responses stimulated by mTOR and S6K1 are downstream effectors specifically of PtdIns(3,4,5)P_3 is the sensitivity of PTEN null ES cells, MEFs, and tumors to the immunosuppressant rapamycin. Deletion of the PtdIns(3,4,5)P_3 specific phosphatase, PTEN, elevates PtdIns(3,4,5)P_3 levels and activates downstream PI 3-kinase dependent signaling without stimulating other pathways. Since these cells are unusually sensitive to growth inhibition by the mTOR (and thus S6K1) inhibitor rapamycin, this suggests that these pathways are significantly activated by increased PtdIns(3,4,5)P_3 levels, and that this is important for cell growth and tumor development.

Tec Family Kinases

The Tec family of tyrosine kinases has been implicated in signaling by lymphocyte antigen receptors. These kinases have an N-terminal PtdIns(3,4,5)P_3 binding PH domain and a C-terminal tyrosine kinase domain. They also contain a proline-rich region, and SH3 and SH2 domains in the central region of the proteins. It is believed that their activation requires recruitment to the plasma membrane by interaction of PtdIns(3,4,5)P_3 with the PH domain, and subsequent activation by members of the Src family of tyrosine kinases through phosphorylation of the kinase domain activation loop. These kinases are rather restricted in the range of tissues where they are expressed, most being hematopoietic specific, and appear to play a role most significantly in lymphocyte signaling. This picture has stemmed from the original identification of the first family member, Bruton's tyrosine kinase (Btk), as the gene mutated in a human immunodeficiency. The family is now known to include Btk, Tec, Itk, Bmx, and the slightly divergent Rlk. Interestingly, in Rlk, the PH domain has been replaced by an N-terminal palmitoylation and membrane targeting signal, leading to PI 3-kinase independent activation.

Perspectives

This article has focused largely upon well-studied kinases that are regulated through PtdIns(3,4,5)P_3 and PI(3,4)P_2 and the PI 3-kinase signaling pathway, and their roles in regulating cellular proliferation, survival, and growth. However, evidence for the regulation of kinases in these and other cellular signaling pathways by other phosphoinositides is emerging. For example, serum and glucocorticoid inducible protein kinase 3 (SGK3 or CISK) is localized to endosomes through a PX-domain-mediated interaction, probably via PtdIns(3)P. Although tethering to endosomes appears to be required for CISK to function, there is also evidence that its catalytic activity is controlled through stimulated type I PI 3-kinases and hence via a mechanism that also involves PtdIns(3,4,5)P_3. Since the human genome contains ~48 genes encoding proteins, many unstudied, with both a protein kinase domain, and a domain recognized as a potential phosphoinositide-binding domain (42 with PH domains and 6 with PX domains), it is quite possible that novel kinases exist that are regulated by any of the phosphoinositides and play a role in the regulation of quite distinct cellular processes.

See Also the Following Articles

Inositol Lipid 3-Phosphatases • Inositol Phosphate Kinases and Phosphatases • Phosphatidylinositol Bisphosphate and Trisphosphate • Phosphatidylinositol-3-Phosphate • Phosphoinositide 3-Kinase • Phosphoinositide 4- and 5-Kinases and Phosphatases • Protein Kinase B

Glossary

kinase An enzyme that catalyzes the transfer of a phosphate group from ATP onto another molecule.

phosphatase An enzyme that catalyzes the hydrolytic removal of phosphate from another molecule and its release as free phosphate.

phosphoinositide A phospholipid in which the polar head group is inositol or a phosphorylated derivative of inositol.

Further Reading

Biondi, R. M., and Nebreda, A. R. (2003). Signalling specificity of Ser/Thr protein kinases through docking-site-mediated interactions. *Biochem. J.* **372**, 1–13.

Kozma, S. C., and Thomas, G. (2002). Regulation of cell size in growth, development and human disease: PI3K, PKB and S6K. *Bioessays* **24**, 65–71.

Lawlor, M. A., and Alessi, D. R. (2001). PKB/Akt: A key mediator of cell proliferation, survival and insulin responses? *J. Cell Sci.* **114**, 2903–2910.

Leslie, N. R., and Downes, C. P. (2002). PTEN: The down side of PI 3-kinase signalling. *Cell Signal* **14**, 285–295.

Marygold, S. J., and Leevers, S. J. (2002). Growth signaling: TSC takes its place. *Curr. Biol.* **12**, R785–R787.

Vanhaesebroeck, B., and Alessi, D. R. (2000). The PI3K–PDK1 connection: More than just a road to PKB. *Biochem. J.* **346**, 561–576.

Vanhaesebroeck, B., Leevers, S. J., Ahmadi, K., Timms, J., Katso, R., Driscoll, P. C., Woscholski, R., Parker, P. J., and Waterfield, M. D. (2001). Synthesis and function of 3-phosphorylated inositol lipids. *Annu. Rev. Biochem.* **70**, 535–602.

Biography

Nick Leslie is a research fellow in the Division of Cell Signalling at the University of Dundee. He obtained his Ph.D. from Glasgow University (1995). Postdoctoral work at the Beatson Institute in Glasgow and the Division of Cell Signalling in Dundee University focused on mammalian signal transduction. His current projects involve phosphoinositide signaling and the tumor suppressor phosphatase PTEN.

Peter Downes is Director of the Inositol Lipid Signalling Laboratory in the Division of Cell Signalling, University of Dundee. He obtained his Ph.D. at the University of Birmingham, UK. After postdoctoral research in the MRC Neurochemical Pharmacology Unit in Cambridge, he worked for several years in the pharmaceutical industry before being appointed Professor of Biochemistry at the University of Dundee in 1989. He has been investigating the roles of inositol lipids in cell signalling for nearly 25 years.

Phospholipase A_2

Timothy R. Smith and Edward A. Dennis
University of California, San Diego, California, USA

Phospholipid membranes serve not only as structural components of the cell but are integral as a storage form for the precursors of numerous signaling molecules critically involved in a variety of inflammatory and immune responses including the production of the eicosanoids. Phospholipase A_2 (PLA_2) refers to a superfamily of enzymes that catalyze the hydrolysis of fatty acid esters from the *sn*-2 position of membrane phospholipids yielding a free fatty acid and a lysophospholipid. These enzymes have been shown to function both intra- and extracellularly and in some cases display molecular cross-talk between multiple family members. A classification system has been devised to subdivide the PLA_2 superfamily into 14 distinct groups based on sequence and structural homologies. Within these 14 groups, there are two distinct catalytic mechanisms employing either a catalytic serine or histidine, which the PLA_2 enzymes utilize to produce free fatty acids and lysophospholipids from membrane phospholipids. When the free fatty acid produced is an unsaturated one, such as arachidonic acid, it can be converted to the bioactive prostaglandins, leukotrienes and lipoxins by various downstream enzymes. Depending on the composition of the phospholipid precursor, the lysophospholipid can be converted to platelet activating factor (PAF), a potent inflammatory signaling molecule. While most PLA_2 enzymes function as signal initiators, the PAF acetyl hydrolases, which are actually PLA_2s, break down PAF and oxidized phospholipids to end the signaling process.

Phospholipase A_2 (PLA_2) Structures and Catalytic Mechanism

PLA_2 Enzymes Using a Catalytic Histidine ($sPLA_2$s)

The PLA_2 enzymes, initially described as small, secreted enzymes containing multiple disulfide bonds and a catalytic histidine, were first isolated and characterized from snake venoms and human pancreatic secretions. Based on their small size and the fact that they were secreted, these enzymes were referred to as $sPLA_2$s. The $sPLA_2$ enzymes are typically small, compact proteins held together by a network of integral disulfide bonds. These enzymes all contain an N-terminal signal peptide sequence that leads to them being secreted from cells and working extracellularly on membrane phospholipids. The only exception is that of the pancreatic group IB PLA_2 that is secreted with its propeptide intact and requires cleavage by trypsin in order to be catalytically active in the gut as a digestive enzyme. All of these enzymes share a requirement for millimolar levels of Ca^{2+}, which is necessary for catalysis. The catalytic core of the $sPLA_2$ enzymes is a His/Asp dyad made up of the catalytic histidine and a structurally adjacent aspartate residue. None of the $sPLA_2$ molecules show appreciable substrate specificity for saturated versus unsaturated fatty acids.

The structure and catalytic mechanism of *sn*-2 ester bond cleavage has been elucidated for the evolutionarily related Group I, II, V, and X PLA_2s. X-ray structures have been determined for the Group IA and IB, several of the Group II subfamily, the Group V and the Group X, and all of the members of these groups share a common protein fold and are 13–18 kDa in size. They all possess six common disulfide bond linkages. These disulfide bonds provide stabilization of the protein structure and allow the enzyme to remain functional in environmental extremes. There are up to two additional disulfide bonds that have been used to differentiate the groups from one another. Additionally they all share a common Ca^{2+} binding loop that includes the catalytically essential Asp. This residue acts to provide two coordinate interactions for the Ca^{2+} molecule that serves to stabilize the transition state of the PLA_2 reaction.

The first step in catalysis for any of the $sPLA_2$s is binding to the membrane interface. The Group I and II enzymes have been shown to preferentially bind to anionic vesicles that include phosphatidylserine or phosphatidylethanolamine while the group V and X PLA_2s are able to efficiently bind to zwitterionic vesicles, and are able to work on a phosphatidylcholine surface equally well. Once the enzyme is bound to the surface and Ca^{2+} is coordinated into the enzyme via the Asp, catalysis can occur. The catalysis is similar to

that observed with other lipase enzymes utilizing a histidine residue. The active site His recruits a water molecule and orients it for nucleophilic attack on the ester linkage of the *sn-2* fatty acid. The Ca^{2+} molecule is critical in positioning the catalytic water and the phosphate of the lipid. The result is the production of a free fatty acid and lysophospholipid coordinated to the Ca^{2+}. The catalytic mechanism for the other $sPLA_2$s (group III, IX, XI, XII, XIII, and XIV) is similar to that for the group I, II, V, and X, but with the exception of the group III enzyme, X-ray structures have not been reported to verify this.

PLA_2 Enzymes Utilizing a Catalytic Serine

In the mid-1980s, several laboratories discovered and characterized a cytosolic PLA_2 activity that utilized a catalytic serine as opposed to a histidine. Today, there are three classes of PLA_2 enzymes that utilize a catalytic serine, the $cPLA_2$s (group IV), the $iPLA_2$s (group VI), and the PAF-acetyl hydrolases (group VII and VIII).

$cPLA_2$

There are three PLA_2 enzymes classified as $cPLA_2$, group IVA, IVB, and IVC. The group IVA PLA_2 is the enzyme typically referred to as $cPLA_2$ and has been studied extensively. The group IVB and IVC enzymes have only recently been cloned and little is known about their structure, catalysis, or signaling roles.

The group IVA enzyme is an 85 kDa cytosolic enzyme initially cloned and purified from human neutrophils, platelets and monocytes. This enzyme contains two structurally distinct protein domains, a C2 domain and an α/β hydrolase PLA_2 catalytic domain. X-ray structure determination of the group IVA molecule by the Dessen and Somers group revealed that it possesses a novel fold unlike any other previously solved α/β hydrolase. The C2 domain controls the calcium-dependent enzyme translocation to the endoplasmic reticulum and nuclear envelope where the enzyme is catalytically active. The C2 domain and catalytic domain fold and can function independently, but the two domains together are required for biological activity. In addition to PLA_2 activity, the group IVA enzyme possesses both lysophospholipase and transacylase activity. There are several serine residues that are differentially phosphorylated on the group IVA enzyme; while none of these phosphorylation sites are critical for enzymatic activity, when modified they can increase the specific activity of the enzyme two to three fold. The group IVA enzyme utilizes micromolar levels of Ca^{2+} that binds to the C2 domain, but unlike the $sPLA_2$ enzymes the calcium functions in enzyme translocation and not for catalysis. Also unlike the $sPLA_2$s, the group IVA PLA2 shows a 10- to 20-fold specificity for arachidonic acid at the *sn-2* position over saturated or other unsaturated fatty acids.

The group IVA catalytic core is the Ser/Asp catalytic dyad with the serine in a Gly-Leu-Ser-Gly-Ser sequence similar to that of the classical lipase Gly-X-Ser-X-Gly motif found in other α/β hydrolases. The Ser/Asp dyad is unique among the α/β hydrolases and more closely resembles that of serine proteases, suggesting a novel catalytic mechanism. The proposed catalytic mechanism for the Group IVA PLA_2 enzyme is that once bound to the membrane bilayer, the side chain of an Arg stabilizes the phosphate head group of a membrane phospholipid in the active site. Once the enzyme-substrate complex is formed, the catalytic Asp activates the Ser side chain during nucleophilic attack of the *sn-2* acyl chain of the lipid. A serine acyl intermediate is formed, releasing a lysophospholipid, which then undergoes water mediated hydrolysis, releasing the free fatty acid chain. The oxyanion transition state is stabilized by the backbone amide protons of a Gly-Gly-Gly sequence.

$iPLA_2$

Like the group IV PLA_2 enzyme, the $iPLA_2$ enzyme has multiple group members, the group VIA PLA_2 and the group VIB PLA_2. These enzymes both localize in the cytosol and are unique from the group IV family of PLA_2s in that they are calcium-independent. The group VIA PLA_2 is most often referred to as $iPLA_2$ and was initially purified and characterized from the murine $P388D_1$ macrophage-like cell line. Of all of the $iPLA_2$ family members, the most is known about the enzymology and structural features of this enzyme. The group VIB enzyme has only recently been cloned and little is known about its enzymology or structure.

The group VIA enzyme is an 85–88 kDa cytosolic protein that is expressed as several distinct splice variants, only two of which are catalytically active (group VIA-1 and VIA-2). The enzyme contains a series of N-terminal ankyrin repeats, typically involved in the formation of protein–protein interactions, and the mouse group VIA-1 enzyme has been shown to function as a 340 kDa oligomeric complex. The group VIA-2 PLA2 has a 54 amino acid insertion in the eighth ankyrin repeat, likely a membrane-binding domain. The enzyme shows a consensus lipase motif, Gly-Thr-Ser-Thr-Gly. Other residues critical for catalysis have yet to be identified and the mechanism by which the $iPLA_2$ cleaves the *sn-2* linkage is still unclear, but it is likely to be an α/β hydrolase with a catalytic Ser/Asp dyad like the group IVA PLA_2. Like the group IVA enzyme, the group VIA PLA_2 exhibits both lysophospholipase and transacylase activities. Nucleotide di- and tri-phosphates have been shown to stabilize the purified enzyme and the nucleotides are not turned over during this process,

suggesting a structural role. Unfortunately at this time there is not a reported X-ray crystal structure of the group VIA PLA_2, so little is known about the overall fold or active site geometry.

PAF Acetyl-Hydrolase

The PAF acetyl-hydrolases are a family of enzymes first cloned in the mid-1990s that include members of both the group VII and group VIII PLA_2 enzymes. These enzymes are constitutively active, catalyzing the hydrolysis of short acyl chains at the *sn-2* position of 1-O-alkyl-2-acetyl phosphatidylcholine (PAF). They are unique among the PLA_2s in that they have little to no measurable activity on acyl chains longer than nine carbons.

The group VIIA PLA_2 is found in the blood plasma and is a 45 kDa monomeric enzyme of the α/β hydrolase family. This enzyme possesses a consensus lipase motif, Gly-His-Ser-Phe-Gly, with a catalytic serine residue. Unlike the group IV enzymes, the group VIIA proteins possess a classical hydrolase triad of Ser, Asp, and His, suggesting that its catalytic mechanism is similar to that of other α/β hydrolases. The group VIIA enzyme is the circulating form of the enzyme typically found associated with lipoproteins and binding to LDL causes an increase in PAF-AH activity through, as yet, an unknown mechanism. This enzyme has been reported to hydrolyze oxidized phospholipids in addition to PAF. The group VIIB enzyme is an intracellular monomeric 40 kDa protein closely related to the group VIIA enzyme with an identical active site lipase motif. Both of the group VII enzymes are able to hydrolyze PAF molecules with *sn-2* acyl chains as long as 5 carbons.

The group VIII enzyme is found most abundantly in brain tissues and is comprised of three subunits, α-1, α-2, and β, of which the α-1 and α-2 subunits both possess PAF-AH activity. The α-1 and α-2 subunits are 29 and 30 kDa respectively and share a 63% sequence identity between them. Both subunits contain a modified lipase motif of Gly-Asp-Ser-Met-Val and Gly-Asp-Ser-Leu-Val respectively. These enzymes both possess a classical Ser, Asp, His triad, again suggesting that their catalytic mechanisms is similar to that of other serine esterases. The β subunit does not possess any PLA_2 activity and is likely a structural or regulatory protein.

PLA_2 Cellular and Signaling Roles

The PLA_2 enzymes have been shown to be involved ubiquitously in almost all lipid signaling and metabolism functions within the cell. The group IVA and VIA enzymes have been shown to be linked to apoptosis. Additionally, the group VIA PLA_2 has been shown to be directly involved in cellular phospholipid remodeling. One of the most studied aspects of the mammalian PLA_2s, including the group II and V $sPLA_2$s and the group IVA $cPLA_2$, is their role in the production of arachidonic acid used in the production of the pro-inflammatory eicosanoids, including prostaglandins, leukotrienes, and lipoxins. These molecules play critical signaling roles in pathways as diverse as pain and inflammation, allergic responses, implantation and parturition, vasoconstriction and dilation, and renal function. Finally, the role of the group VII and VIII PLA_2 enzymes, the PAF acetyl hydrolases, is to break down the pro-inflammatory PAF molecule and terminate the signaling process. The group VIIA enzyme has also been shown to be associated with lipoproteins such as HDL and LDL and is thought to be critically involved in the breakdown of oxidized phospholipids.

See Also the Following Articles

Eicosanoid Receptors • Lysophospholipid Receptors • Phospholipid Metabolism in Mammals

Glossary

α/β hydrolase Superfamily of hydrolase enzymes containing a characteristic fold of 8 β-strands connected by α-helices commonly possessing a catalytic triad of Ser, Asp, and His.

eicosanoid Family of signaling molecules derived from the unsaturated fatty acid arachidonate that includes prostaglandins, leukotrienes, and lipoxins.

lysophospholipid Phospholipid in which either the *sn-1* or *sn-2* fatty acid has been removed.

PAF 1-O-alkyl-2-acetyl-*sn*-glycero-3-phosphocholine, a potent signaling molecule derived from 1-O-alkyl lysophospholipids involved in inflammation and allergic responses.

phospholipase A_2 Superfamily of enzymes which hydrolyze fatty acids from the *sn-2* position of membrane phospholipids.

phospholipid Major lipid component of biological membranes with an *sn*-glycerol-3-phosphate backbone, fatty acids on the *sn-1* and *sn-2* position, and a head group attached to the 3-phosphate.

Further Reading

Dessen, A., Tang, J., Schmidt, H., Stahl, M., Clark, J. D., Seehra, J., and Somers, W. S. (1999). Crystal structure of human cytosolic phospholipase A_2 reveals a novel topology and catalytic mechanism. *Cell* **97**, 349–360.

Nigam, S., Wilton, D. C., and Dennis, E. A (eds.) (2000). Molecular and cell biology of lipids phospholipase A_2 special issue. *Biochim. Biophys. Acta* **1488**, 1–2.

Singer, A. G., Ghomashchi, F., Le Calvez, C., Bollinger, J., Bezzine, S., Rouault, M., Sadilek, M., Nguyen, E., Lazdunski, M., Lambeau, G., and Gelb, M. H. (2002). Interfacial kinetic and binding properties of the complete set of human and mouse groups I, II, V, X, and XII secreted phospholipases A_2. *J. Biolog. Chem.* **277**, 48535–48549.

Biography

Edward A. Dennis is a Professor of Chemistry and Biochemistry at the University of California, San Diego. Since the 1970s, Dr. Dennis' laboratory has studied the structure and function of the phospholipase A_2 superfamily of enzymes, publishing over 250 articles on these topics. The Dennis laboratory was the first to purify and characterize the calcium independent PLA_2, has worked extensively on developing models for the action of PLA_2 enzymes at lipid interfaces, and explored the roles of individual PLA_2s in the eicosanoid cascade of macrophages.

Timothy Smith has been a Postdoctoral Associate in the Dennis laboratory since December 2000, working on the structural and biochemical characteristics of the calcium independent PLA_2 enzyme.

Phospholipase C

Fujio Sekiya, Yeun Ju Kim and Sue Goo Rhee
National Heart, Lung, and Blood Institute, Bethesda, Maryland, USA

Phospholipase C (PLC) is an enzyme that cleaves a glycerophospholipid at the phosphodiester bond between the glycerol backbone and the phosphate group. All known eukaryotic PLCs, including those implicated in calcium signaling in animal cells, utilize only phosphoinositides (phosphatidylinositol and its phosphorylated derivatives) as substrates, hence called phosphoinositide-specific PLC and frequently just referred to as PLC. The minor constituent of plasma membranes, phosphatidylinositol 4,5-bisphosphate (PIP2), appears to be the only physiological substrate of PLCs, though in test tubes other phosphoinositides can be hydrolyzed. PLC cleavage of PIP2 simultaneously generates two second messengers, inositol 1,4,5-trisphosphate (IP3) and 1,2-diacylglycerol (DAG). PLC is not a single entity but consists of members with various structures, and mechanisms to regulate PLC isozymes are also diverse. To date, 12 different mammalian PLCs have been identified, and they are grouped into 5 subfamilies based on their primary structures.

Biological Consequences of PLC Action

Early studies by Hokin and Hokin in the1950s revealed that stimulation of cells could induce rapid metabolism of inositol phospholipids, and in 1975 Robert Michell suggested the connection between phosphoinositide hydrolysis and calcium mobilization. Functions of IP3 and DAG as important second messengers were established in the mid-1980s by Michael Berridge and Yasutomi Nishizuka, respectively. It was these landmark discoveries that brought special attention to PLC as the key enzyme to generate the two second messengers.

The soluble part of PIP2 cleavage product, IP3, binds to its intracellular receptor present on the calcium storage site endoplasmic reticulum (ER), and the receptor constitutes a channel to gate calcium ions. IP3 ligation opens the channel, causing a transient increase in the cytoplasmic calcium concentration. The other cleavage product DAG stays in the plasma membrane and recruits protein kinase C (PKC) isozymes. Activation of certain PKC isozymes requires both binding to DAG and calcium ions. Activated PKC elicits a wide range of cellular responses through phosphorylation of many kinds of substrate proteins (Figure 1).

Increasing evidence indicates that PIP2 by itself participates in many cellular processes through binding to a number of proteins. First, the phospholipid is a focal point to bridge plasma membranes and networks of cytoskeletal proteins. It thus plays key roles in maintenance of cell morphology as well as in control of motility. Second, it can modify activities of various enzymes and channels; phospholipase D and capsaicin receptor (ion channel) are a few examples among many such PIP2 effectors. Third, it provides a platform to form functional signaling complexes, because many of those proteins participating in the complexes have lipid-binding modules, such as PH, FERM, and ENTH domains. Consistent with their physiological significance, cellular levels of PIP2 are maintained through strictly regulated production/destruction mechanisms involving many lipid kinases and phosphatases. Activation of PLC leads to a rapid reduction in cellular PIP2 level. Thus, both generation of IP3/DAG and destruction of PIP2 by PLC can dramatically affect the cell's physiology in many ways.

Given such diverse and profound consequences, PLC activation is one of central mechanisms of cellular signaling, and its activity is tightly controlled in cells. Indeed, a large number of hormones, growth factors, and neurotransmitters rely on PLC in transmitting their signals across plasma membranes.

Biochemistry of PLC

Structure of PLC

PLC has been found in yeasts, slime molds, plants, and animals, and is probably present in all taxa of eukaryotes. All eukaryotic PLCs appear to be evolved from a single archetype, and it is in the animal kingdom that PLC diversified. Eleven different genes encoding PLC isozymes have been identified in mammals, and they are grouped into four subfamilies, named as β, γ, δ, and ε. In addition, an isozyme named ζ, which has the simplest structure, has been found recently (Figure 2). Animals, from the nematode *Caenorhabditis elegans*

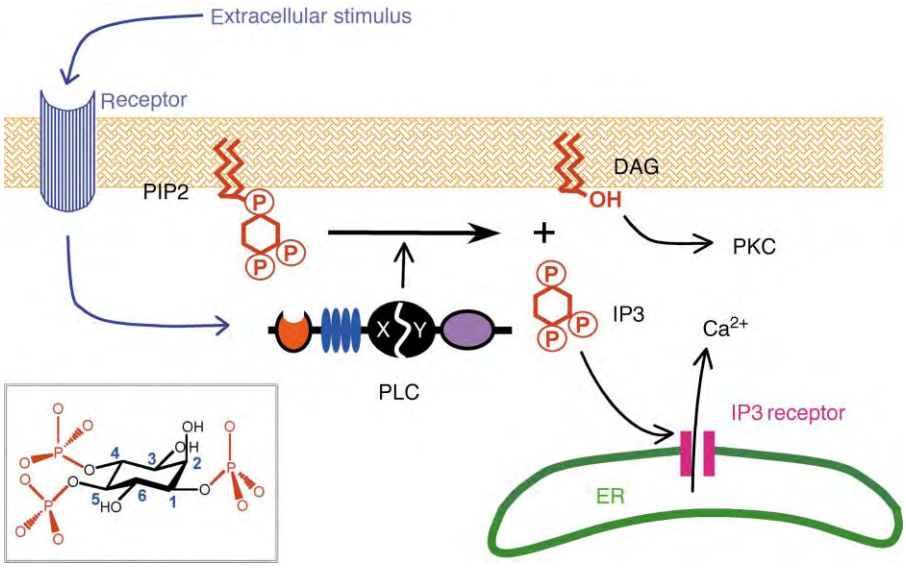

FIGURE 1 A scheme for the action of PLC in the cell. For abbreviations, see text. Inset shows chemical structure of IP3.

to the fly to the human, appear to have all subtypes, but only the primitive δ-like (or ζ-like) PLCs are found in other eukaryotes. The protein originally termed PLC-α was turned out to be a proteolytic fragment of PLC-δ1, and was thus eliminated from the nomenclature. Some isozymes have alternatively spliced variants at the mRNA level, and the total number of mammalian PLC polypeptides exceeds 20.

All PLC isozymes possess common structural features, indicating origination from a common ancestor. The δ-isozyme consists of an N-terminal PH (pleckstrin-homology) domain, four copies of EF-hands, regions called X and Y, followed by a C2 domain. Other three types of PLC isozymes are made up by additions (or replacements) of some regulatory domain structures to the δ-subtype (Figure 2). PH domains are ~120-residue units, which oftentimes function as membrane-binding sites through interaction with phosphoinositides. EF-hands are the calcium-binding motifs identified in calmodulin, but it is unclear whether PLC's EF-hands actually bind calcium ions. C2 domains (~120 residues) are the structures originally found in PKC that act as calcium-dependent lipid-binding modules. X and Y regions are unique to eukaryotic PLCs. Evidence shows that the two regions together form a discrete unit of catalyst, though they are separated by a linker in the primary structure.

Mechanism of Catalysis

Based on crystallographic structures of PLC-δ1 and biochemical data, the catalytic mechanism for PLC has been postulated. Calcium ion, which is required for all PLC isozymes, was seen in the catalytic center interacting with the IP3 moiety of PIP2; the cation activates the 2-hydroxy group of inositol ring that in turn attacks the 1-phosphate, cleaving off the head group to form a 1,2-cyclic phosphate intermediate and DAG. The cyclic derivatives are subsequently hydrolyzed to acyclic inositolphosphates. Several positive residues found in the active site pocket interact with the phosphate groups at the 4- and 5-positions of inositol ring, explaining the preference of enzyme for PIP2 over phosphatidylinositol or phosphatidylinositol 4-phosphate. The structure has also indicated that the pocket cannot accommodate phosphoinositides with phosphate at the 3-position (e.g., phosphatidylinositol 3,4,5-trisphosphate), explaining why 3-phosphorylated inositides are not substrates of PLC.

PLC Isozymes and their Regulation Mechanisms

PLC-β

Signals of many chemical and physical stimuli are received by cells via receptors that couple to heterotrimeric G proteins. A large portion of such stimulation induces PIP2 hydrolysis by activating PLC-β isozymes. Beta isozymes (β1 ~ β4; ~150 kDa) are unique in having long C-terminal extensions that are absent in other classes of isozymes (Figure 2).

Upon activation of receptor, the receptor-associated αβγ heterotrimer of G protein dissociates into α- and βγ-subunits. Both α-and βγ-subunits are able to transmit signals. The members of G_q family of α-subunits (αq, α11,

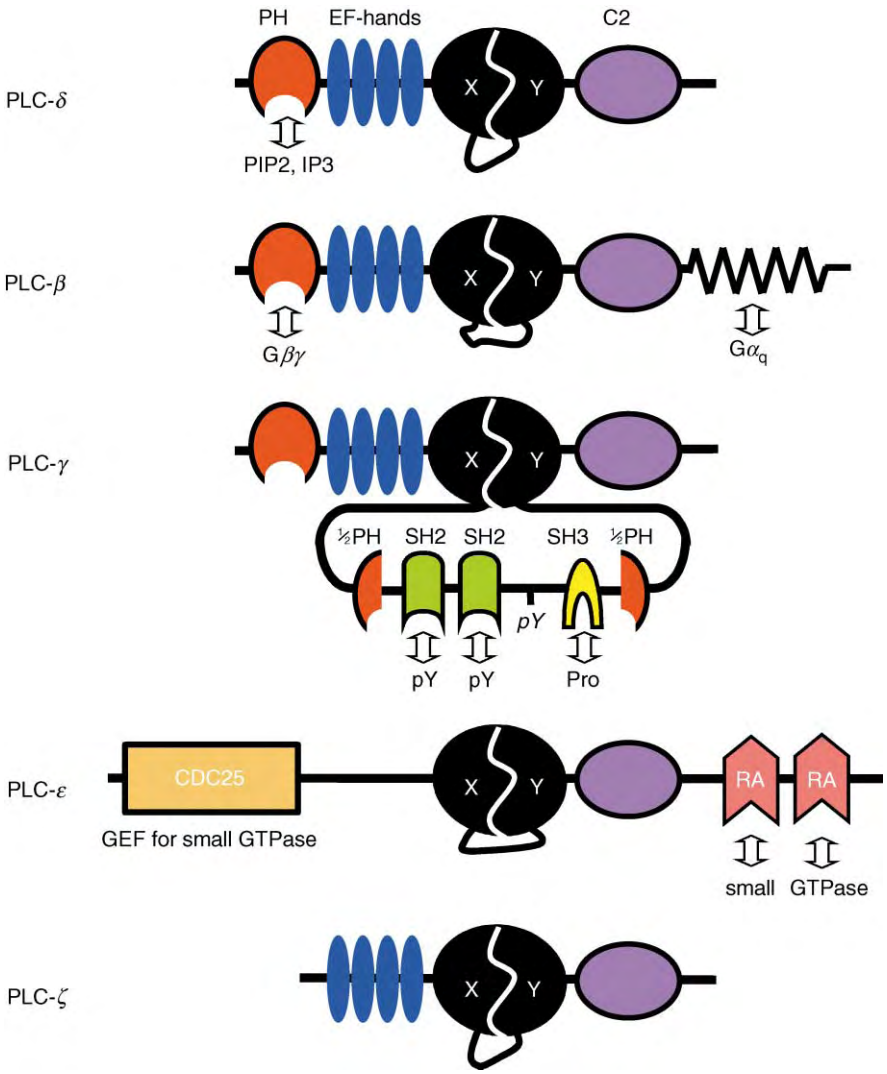

FIGURE 2 Structural organizations of PLC isozymes. Known ligands of domains of PLCs are shown. *p*Y, phosphotyrosine; Pro, proline-rich sequence.

α14, and α16) can activate PLC-β, but not PLC-δ and PLC-γ. In contrast, the α-subunits of other G protein subclasses (Gs, Gi, and G12/13) do not activate PLC-β. Also, $\beta\gamma$-complexes can specifically stimulate PLC-β. αq- and $\beta\gamma$-subunits appear to interact with different regions in the PLC-β molecule: αq is recognized by the C-terminal region unique to β-isozymes, whereas the $\beta\gamma$-subunit binds to the N-terminal PH domain. In most cells the Gi family of G protein is abundant compared to other classes. It is considered that only Gi-coupled receptors can provide significant amounts of $\beta\gamma$, and that agonists inducing activation of Gi are responsible for $\beta\gamma$-mediated activation of PLC-β.

Four isozymes of this subfamily appear to be expressed in different tissues and to have different sensitivities to the G protein subunits. PLC-β1 and β3 are widely expressed in various tissues and are more sensitive to the activation by αq compared to other isozymes. PLC-β2 expression is restricted to blood cells and is most sensitive to the activation by $\beta\gamma$ among the four PLC-βs. PLC-β4 expression is only seen in some parts of the brain and in the retina. Genes for all four β-isozymes have been disrupted in mice, and none of those single knockouts appeared to be fatal, probably because their functions overlap. Reported phenotypes of knockouts include: PLC-β1, epilepsy; PLC-β2, dysfunctions in neutrophils and platelets; PLC-β3, hyperresponse to opioid stimulation; and PLC-β4, ataxia and impairment in visual perception.

PLC-γ

Activation of PLC-γ is controlled by phosphorylation of its tyrosine residues, and the two isozymes of this subfamily (γ1 and γ2; $\sim$140 kDa) have a long linker sequence between the X and Y regions, which is indispensable for their regulation. The linker region consists of a half of a PH domain, two SH2

(Src-homology 2) domains, an SH3 (Src-homology 3) domain, and the remaining half of the split PH domain (Figure 2).

Binding of peptide growth factors (such as platelet-derived growth factor, epidermal growth factor, and nerve growth factor) to their cognate receptors results in activation of the intrinsic protein tyrosine kinase activity of the receptor and consequent autophosphrylation of their cytoplasmic tails, creating docking sites for phosphotyrosine-binding motifs. PLC-γ binds those phosphotyrosines using its SH2 domain and is then phosphorylated by the receptor protein tyrosine kinases. Tyrosine phosphorylation that occurs within the linker region leads to activation of PLC-γ by a mechanism not fully understood.

Immunoreceptors in blood cells, such as the T-cell receptor and the B-cell receptor for antigens, do not have intrinsic tyrosine kinase activity but are also able to activate PLC-γ. Ligand-induced clustering of immunoreceptors causes phosphorylation in the domain termed immunoreceptor tyrosine-based activation motif (ITAM) by receptor-associated Src-family tyrosine kinases (e.g., Lck, Lyn, and Fyn). Phosphorylated ITAMs recruit and activate Syk-family tyrosine kinases (Syk and ZAP-70), and the recruited Syk-kinases, in turn, phosphorylate many kinds of adaptor proteins, such as linker of activation of T cells (LATs) and B-cell linker protein (BLNK). PLC-γ then binds to and is phosphorylated by the resultant supermolecular complex consisting of aggregated immunoreceptors, Src kinases, Syk kinases, and adaptor proteins. Stimulation of blood cells, moreover, can activate another class of tyrosine kinase, Tec-family kinases (e.g., Btk), via a phosphoinositide 3-kinase-dependent mechanism. Tec-kinases are also implicated in PLC-γ activation.

PLC-γ1 is expressed ubiquitously and disruption of its gene is lethal at an early embryotic stage. PLC-γ2 is expressed in a set of hematopoietic lineages including B cells, platelets, neutrophils, and mast cells. Knockout of γ2 is not lethal but abolishes maturation of B cells, resulting in immunodeficiency, and causes dysfunctions of Fc-receptor-mediated signaling in platelets and mast cells.

PLC-δ

PLC-δ isozymes (δ1 ~ δ4; ~90 kDa) have simpler structures compared to other isozymes (Figure 2). They lack obvious regulatory domains that facilitate coupling to receptors. The exact nature of their activation mechanisms remains unclear, but probably they do not couple to hormone receptors directly. PLC-δ has greater calcium sensitivity compared to β- and γ-isozymes. It is proposed that PLC-δ can be secondarily activated when cytoplasmic calcium concentrations are elevated via PLC-β(or PLC-γ)/IP3-mediated mechanisms. The PH domain of PLC-δ binds to PIP2 and also recognizes IP3 with a higher affinity: this domain is thought to mediate tethering of PLC-δ to plasma membranes. When PIP2 hydrolysis occurs, generated IP3 causes dissociation of the enzyme from membranes, thus terminating the reaction. This mechanism constitutes a feedback negative regulation system for this isozyme.

Among four δ-isozymes known, gene targeting of δ1 and δ4 isozymes has been conducted. Both resulted non-fatal. PLC-δ1-deficient mice experienced progressive hair loss. The isozyme appears to be necessary for commitment of skin stem cells. Male homozygotes of PLC-δ4-deficient mice were infertile, and it was reasoned that the isozyme was required for the acrosome reaction of sperms.

PLC-ε

The ε-isozyme (>200 kDa) contains a CDC25-like domain in the N terminus, which has guanine nucleotide exchange factor (GEF) activity toward small GTPases, and two copies of Ras-binding motifs (RA domains) following the C2 domain, but neither a PH domain nor EF-hand is evident (Figure 2). It has been shown that (1) PLC-ε is capable of catalyzing PIP2 hydrolysis both *in vitro* and *in vivo*, (2) the CDC25-like domain can function as a GEF for Rap1A but not for Ras, and (3) the RA domains are able to bind to active forms of Ras and Rap1A. Because of the presence of domain structures that interact with small GTPase of Ras superfamily, it seems likely that PLCs-ε regulation utilizes these class of proteins. Whether they are regulators (upstream of PLC-ε) or effectors (downstream) or both is yet to be determined. Studies done so far are somewhat inconsistent with each other, and it is still premature to picture the exact mechanism by which this isozyme functions in the cell.

PLC-ζ

A novel type of PLC named PLC-ζ (~70 kDa) was recently identified as a sperm-specific isozyme. PLC-ζ has a very primitive structure. It even lacks the N-terminal PH domain (Figure 2) and rather resembles PLCs found in plants or yeasts. A phylogeny analysis revealed its least divergence from a hypothetical precursor among all mammalian PLCs. It has been shown that this sperm-specific isozyme is responsible to calcium oscillation in fertilizing eggs.

See Also the Following Articles

G_q Family • IP_3 Receptors • Phosphatidylinositol Bisphosphate and Trisphosphate • Phosphoinositide 3-Kinase • Protein kinase C Family

Glossary

diacylglycerol A product of PIP2 cleaved by PLC. It serves as a second messenger activating some members of PKCs, and is readily converted to phosphatidic acid in the cell by the action of diacylglycerol kinases.

IP3 The other product of PIP2 cleavage by PLC. IP3 is also a short-life second messenger due to inactivation either through dephosphorylation by specific phosphatases or through phosphorylation by the IP3 kinase.

pleckstrin homology (PH) domain A domain structure that occurs in a wide range of proteins involved in intracellular signaling or as constituents of the cytoskeleton. It was originally found in pleckstrin (platelet C-kinase substrate protein). It binds to phosphoinositides such as PIP2 and/or PIP3.

Src homology 2/3 (SH2/3) domain Domain structures that occur in various signaling proteins, initially identified in the protooncoprotein *src*. SH2 domain recognizes phosphorylated tyrosine residues in target peptides, whereas SH3 domain binds to peptide sequences rich in proline residues.

Further Reading

Carpenter, G., and Ji, Q.-S. (1999). Phospholipase C-γ as a signal-transducing element. *Exp. Cell Res.* **253**, 15–24.

Cockcroft, S. (1997). Phosphatidylinositol transfer proteins: Requirements in phospholipase C signaling and in regulated exocytosis. *FEBS Lett.* **410**, 44–48.

Fukami, K. (2002). Structure, regulation, and function of phospholipase C isozymes. *J. Biochem. (Tokyo)* **131**, 293–299.

Irvine, R. F. (2003). 20 years of Ins(1,4,5)P3, and 40 years before. *Nat. Rev. Mol. Cell Biol.* **4**, 586–590.

Rhee, S. G. (2001). Regulation of phosphoinositide-specific phospholipase C. *Annu. Rev. Biochem.* **70**, 281–312.

Williams, R. L., and Katan, M. (1996). Structural views of phosphoinositide-specific phospholipase C: Signaling the way ahead. *Structure* **4**, 21387–21394.

Biography

Fujio Sekiya is a Staff Scientist in the Laboratory of Cell Signaling at the National Heart, Lung, and Blood Institute (NHLBI), National Institutes of Health in Bethesda, Maryland. He received a Ph.D. from the Tokyo Institutes of Technology in 1991.

Yeun Ju Kim is a graduate student of the Ewha Womens University, Seoul, Korea, now staying at the Laboratory of Cell Signaling, NHLBI. She holds an M.Sc. degree from the Ewha Women's University.

Sue Goo Rhee is Chief of the Laboratory of Cell Signaling, NHLBI, NIH. He received a Ph.D. from the Catholic University of America in 1972.

Phospholipase D

Mary M. LaLonde and Michael A. Frohman
Stony Brook University, Stony Brook, New York, USA

The phospholipase D gene superfamily encodes a diverse array of enzymes that carry out phosphodiesterase actions on phospholipid and DNA substrates. All members share a structural domain known as the HKD catalytic motif. While bacterial PLD is constitutively active, eukaryotic PLDs are tightly regulated by signaling pathways. Mammalian PLD is synergistically regulated by PI4,5P_2, ARF, and Rho GTPases, and protein kinase C. Upon activation, eukaryotic PLDs, which are phsophatidylcholine-specific, cleave the substrate phosphatidylcholine to yield the pleiotropic lipid phosphatidic acid, which can serve as either a signal transducer, lipid anchor, signaling intermediate, or fusogenic lipid. *In vivo* roles for PLD consist of regulated membrane trafficking events including prospore membrane formation in yeast and regulated secretion in neuroendocrine cells, and cell shape dynamics.

Introduction

Phospholipase D (PLD) was the founding member of a superfamily that is now recognized to include phosphatidylserine synthase, a cardiolipin synthase, an atypical endonuclease, an enzyme that rescues covalently bound topoisomerase from DNA, a toxin from the black-death causative agent Yersinia pestis, a viral envelope protein required for pox virus (e.g., smallpox) pathogenesis, and many other gene products of unknown function. Despite the biologically diverse functional roles that these proteins undertake, they share a common catalytic mechanism that invariably targets a phosphodiester bond found in a varied set of substrates (see Figures 1 and 2). The phosphodiester-bond-containing substrates include several phospholipid species in which the phosphodiester bond forms a bridge between the lipid phosphate portion of the molecule and its headgroup; DNA, where the phosphodiester bond forms the link between individual nucleotides and a DNA-topoisomerase complex linked by the bond that occasionally inadvertently persists during DNA unwinding. Additional homologues that encode the PLD catalytic motif, but for which no function has been assigned, still await characterization. No doubt there are yet other interesting substrates and stories that will emerge from continued study of this superfamily.

PLDs found in yeast and animals catalyze hydrolysis of the phosphodiester bond found in the phospholipid phosphatidylcholine (PC). This generates soluble choline and the lipid phosphatidic acid (PA). Bacterial PLDs are promiscuous and will also use as substrate phospholipids with other headgroups, such as phosphatidylethanolamine or phosphatidylinositol. Although the hydrolysis of these phospholipids has been reported in mammals and yeast, the hydrolyzing proteins have not been identified and the eukaryotic PLDs have never been shown to perform these activities. Hence, additional genes of related function, if not sequence, may await discovery.

PLD Gene Families

The PLD gene families are relatively small in yeast (one member) and animals (generally one or two members). By contrast, plants encode up to a dozen PLDs, some of which are highly similar to the mammalian genes in structure. Two mammalian PLDs exist, PLD1 and PLD2, which are structurally similar and 55% identical on the amino acid level but are thought to be regulated somewhat differently and to carry out different cell biological roles. PLD1 has more commonly been shown to regulate vesicular trafficking events whereas PLD2 has been associated more often with regulation of cell shape. However, some overlap in function has also been described. Although many (but not all) cell types express both isozymes, the relative amounts of PLD1 and PLD2 expressed in individual tissues vary dramatically, suggesting that the enzymes carry out cell-type specific rather than universal constitutive roles.

PLD Structure

PLD superfamily members are defined by the presence of one or two copies of the consensus sequence, $HXK(X)_4D(X)_6GSXN$, denoted as the "HKD" domain, which encodes the key residues involved in catalysis (Figure 3). *Bona fide* PLD proteins also

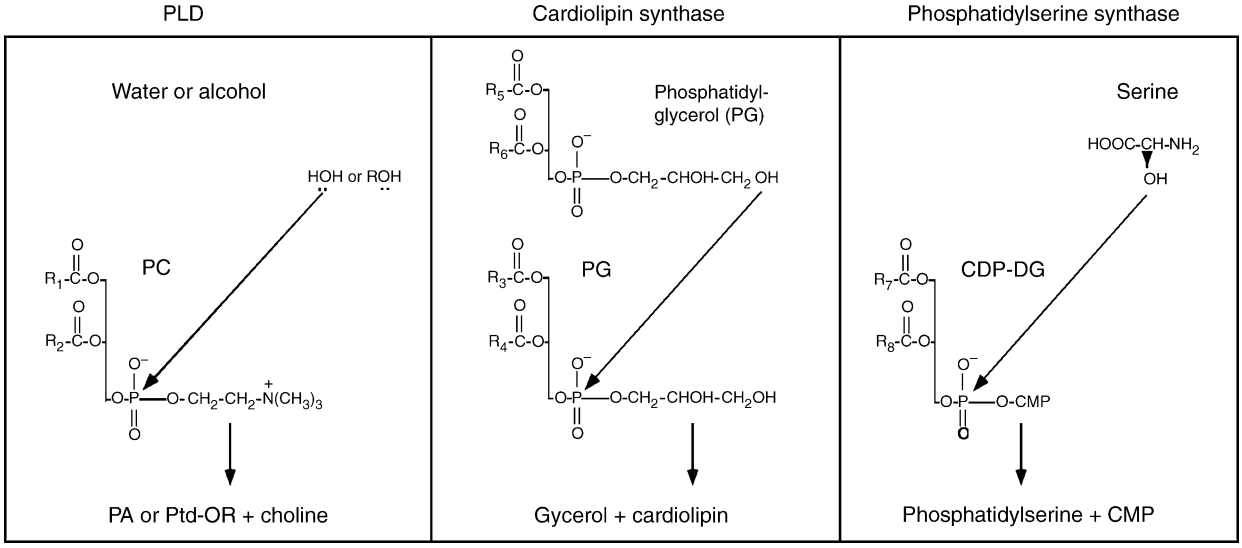

FIGURE 1 PLD, cardiolipin synthase, and phosphatidylserine synthase catalytic reactions. Each reaction involves nucleophile attack on a phosphate bond as shown. Two biochemical activities for PLD have been observed: phosphodiester bond hydrolysis and phospholipid transphosphatidylation. Using H_2O as an electron donor, PLD functions as a phospholipid hydrolysis enzyme, cleaving phosphatidylcholine (PC) to produce phosphatidic acid (PA) and choline. Through the same mechanism, but using alcohol instead of H_2O as the electron donor, PLD can generate phosphatidylalcohols. Nucleophiles that can be used by PLD include exogenously supplied butanol or endogenous diacylglycerol, yielding phosphatidylbutanol and bisphosphatidic acid, respectively. CLS and PSS only carry out synthetic reactions in which alcohols are used as the nucleophile, as shown. Reprinted from Sung, T. C., Roper, R., Zhang, Y., Rudge, S., Temel, R., Hammond, S., Morris, A., Moss, B., Engebrecht, J., and Frohman, M. (1997). Mutagenesis of phospholipase D defines a superfamily including a *trans*-Golgi viral protein required for poxvirus pathogenicity. *EMBO J.* **16**, 4519-4530, with permission of Oxford University Press.

invariably contain several additional conserved domains that assist in proper functioning of the catalytic site. The PLD catalytic core is comprised of two HKD motifs that juxtapose to create the active site, within which the histidine residues directly coordinate the transphosphatidylation reaction. This results in the formation of a covalent phosphatidyl-enzyme intermediate. Both HKD domains must be intact for PLD to be catalytically active. It has been suggested that protein modulators of mammalian PLD activity may influence activation by affecting the orientation of the HKD domains or their distance from the substrate. However, this remains hypothetical since only the mammalian isoforms are thusly regulated, and they have not yet been crystallized in a complex, with or even without their regulators.

Other domains universally found in animal and yeast PLD proteins include a PH domain, which is not essential for enzymatic activity but does regulate subcellular localization and translocation. A basic amino acid-rich phosphatidylinositol 4,5 bisphosphate ($PI4,5P_2$) binding site located near the center of the proteins is essential for catalysis, and plays an important but less conserved role in membrane association and subcellular localization. In addition to these domains, the proteins encode a Phox homology (PX) domain which also helps direct PLD subcellular localization. Finally, mammalian PLD1 is regulated not only by the phospholipid $PI4,5P_2$, but by at least three separate protein factors as well. These effectors (ARF GTPases, Rho GTPases, and PKC family members) act synergistically through binding at distinct sites in PLD1.

Regulation

Overview

Whereas bacterial PLD is constitutively active, eukaryotic PLD is generally activated during events associated with dynamic changes in cells. PLD in plants is activated by wounding and other external environmental cues. PLD in mammals has long been recognized to be activated in response to agonists that stimulate cells through G-protein-coupled or tyrosine kinase receptors. Examples of such agonists include neurotransmitters, serum-derived growth factors, hormones, and cytokines. Yeast PLD does not appear to be directly activated by receptor systems, but its transcription and its subcellular localization are tightly regulated by signaling pathways, which lead qualitatively to the same outcome.

Regulation of Mammalian Phospholipase D

Stimulation of mammalian PLD through G-protein-coupled or tyrosine kinase receptors is mediated principally by a phospholipid ($PI4,5P_2$) and three classes of proteins: ARF GTPases, Rho GTPases, and protein kinase C (PKC). The specific mechanism of

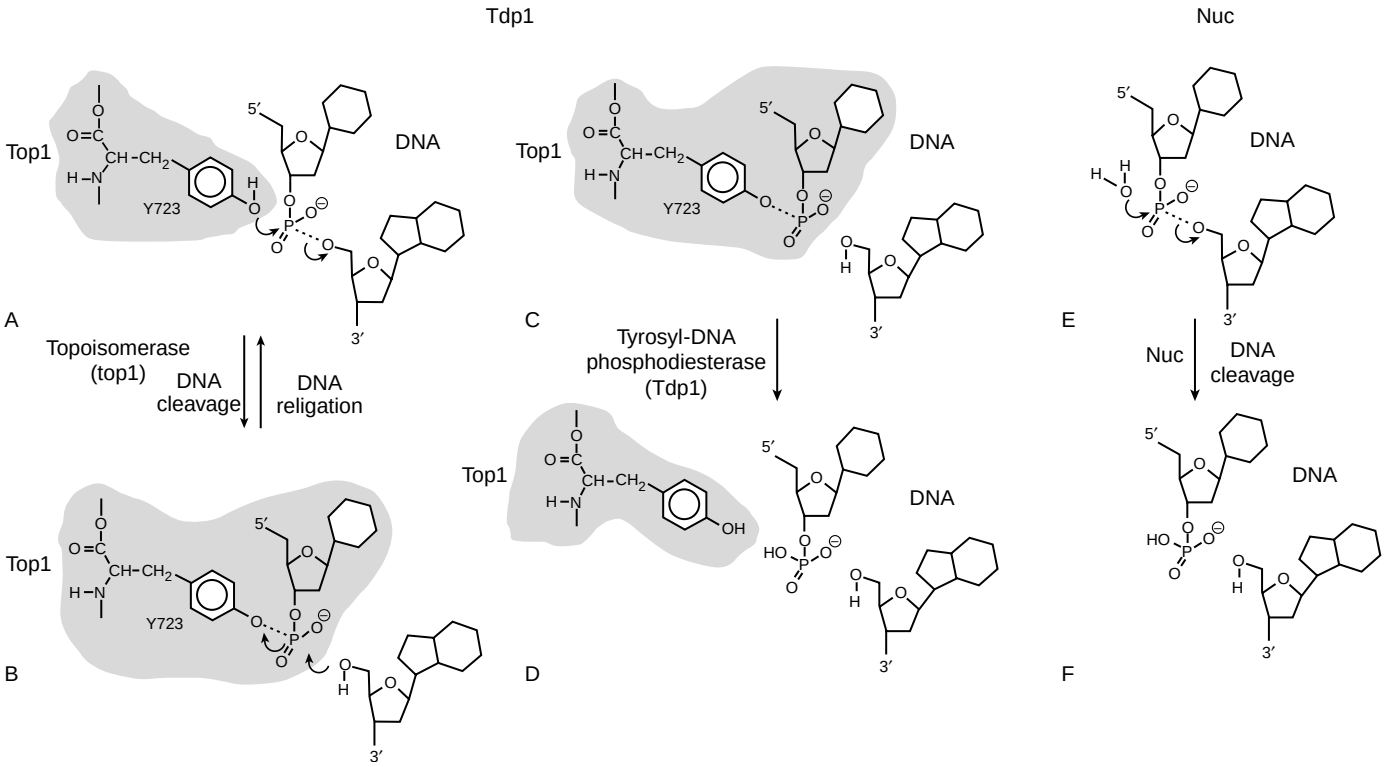

FIGURE 2 Schematic representation of mechanism of action of more divergent members of the PLD superfamily. (A) Topoisomerase I (top1) reversibly generates a cleavage complex by forming a covalent link between tyrosine 723 in top1 and the DNA backbone (B). (C, D) If top1 becomes stalled in the cleavage complex form, it is rescued by Tdp1 hydrolysis of the phosphotyrosyl (phosphodiester) bond (dotted line in (C)). (E,F) The bacterial endonuclease Nuc similarly uses water to attack the backbone phosphodiester bond in DNA to hydrolyze it. Cartoon adapted from Debethune *et al.* (2002).

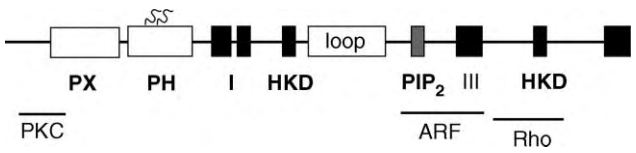

FIGURE 3 PLD structure. Mammalian PLD contains catalytic domains (HKD, I, III, and C-terminus), a $PI4,5P_2$ interacting motif (PIP_2), and PX and PH-membrane association domains. The PH domain is palmitoylated in PLD1. PLD1's activators Rho, ARF, and PKC interact with PLD1 within the regions depicted to activate it.

PLD activation varies with cell type and receptor system examined.

Phosphoinositides

A role for phosphoinositides in the regulation of PLD was first suggested by the finding that $PI4,5P_2$ was required for ARF stimulation of PLD in HL-60 cells and has since been confirmed using purified reagents in *in vitro* reconstitution systems. Activation of PLD1 by phosphoinositides is independent of the stimulatory effects of GTP-binding proteins and protein kinases. Phosphoinositides may function to anchor PLD to the phospholipid surface, thereby increasing the rate of catalysis by placing PLD in close proximity to its substrate.

Protein Kinase C

PKCα and PKCβ directly and indirectly mediate agonist-dependent activation of PLD. Overexpression of either PKC isoform potentiates PLD responses to agonists such as endothelin, thrombin, and PDGF. Down-regulation of PKC through long-term exposure to phorbol esters, antisense depletion of PKCα, or mutation of the site in PLD1 at which PKC interacts decreases agonist-stimulated PLD activity. PKC most commonly activates its targets through phosphorylation. Although PKC does phosphorylate PLD1, it has been shown convincingly that this is not the mechanism through which it activates the same. Activation by PKCα occurs in the absence of ATP (*in vitro*) and is not inhibited by staurosporine, a catalytic-site inhibitor. This non-kinase-dependent stimulatory activity resides within the regulatory domain of PKCα, and PKCα interacts directly with the amino terminus of PLD1. PKC also mediates activation of PLD through a kinase-dependent non-direct mechanism involving calcium influx into cells but which otherwise is not understood clearly. For both PLD isoforms, multiple kinase-dependent downstream consequences of PKC activation may also contribute to PLD activation. To give one such example, a major substrate for PKC subsequent to activation is the protein myristoylated alanine-rich C-Kinase substrate (MARCKS). Under basal conditions, MARCKS localizes to membrane surfaces through multiple low-affinity interactions with $PI4,5P_2$. Once phosphorylated by PKC, MARCKS relocates to the cytosol, making the previously sequestered $PI4,5P_2$ available for other interactions including PLD activation. Consistent with this idea, mutations to MARCKS that eliminate its phosphorylation decrease PKC-mediated PLD activation.

Rho Family of GTPases

The finding that a GTPγS-dependent factor required for PLD activity in neutrophils was removed by RhoGDI first suggested a role for Rho in PLD activation. Rho has since been shown to mediate agonist-dependent PLD activation downstream of numerous agonist-receptor combinations. Many studies on this topic have inhibited Rho using bacterial toxins such as C3 exotoxin from *C. botulinum* (inactivates Rho through ADP-ribosylation) or Toxin B from *C. difficile* (blocks Rho function through monoglucosylation). Dominant-negative Rho mutants have also been used and block phorbol ester-stimulated PLD activity in human adenocarcinoma A549 cells, suggesting that there is cross-talk between the Rho and PKC activation pathways. Direct activation of PLD1 by Rho through an interaction at the C-terminus has been demonstrated; this appears not to be the case, however, for PLD2. Indirect mechanisms of activation are also likely. Rho activates phosphatidylinositol 4-phosphate 5-kinase, which phosphorylates phosphatidylinositol-4-phosphate to generate $PI4,5P_2$, the cofactor required for PLD activity. Rho may also regulate PLD activity through activation of Rho kinase.

ADP-Ribosylation Factor Family of GTPases

ARF is the most potent activator of PLD activity *in vitro*. Activation of PLD by ARF is GTP-dependent, and appears to involve the N-terminus of ARF and the C-terminus of PLD. ARF proteins have been shown to mediate PLD activation by a number of agonists, including insulin, PDGF, angiotensin II, endothelin, N-FMLP, and glutamate. ARF-mediated activation of PLD is not believed to be specific to any particular ARF isoform. Overexpression of dominant-negative ARF1 and ARF6 mutants or BFA-mediated interference with ARF activation inhibits agonist-induced PLD activation in some settings.

Protein Phosphorylation

Both PLD isoforms appear to be phosphorylated by PKC. Recent studies indicate that PLD1 and PLD2 may be phosphorylated by serine/threonine kinases, including cyclic AMP-dependent protein kinase and calcium-calmodulin-dependent protein kinase, as well as by receptor and non-receptor tyrosine kinases. For example, mouse PLD2 associates with EGFR in a

ligand-independent manner and becomes tyrosine phosphorylated on Y11 in response to signaling by EGF. However, since mutation of Y11 to alanine does not affect PLD activation, and since this residue is not conserved in human PLD2, the physiological significance of the modification is not clear. Ultimately, the physiological relevance of phosphorylation on PLD activity and function has not yet been convincingly demonstrated.

Subcellular Localization of Mammalian Phospholipase D

Phospholipase D activity has been reported in almost every cellular compartment, including the plasma membrane, mitochondria, secretory granules, lysosomes, Golgi, endoplasmic reticulum membranes, and nuclear envelope. Immunolocalization of PLD protein presents a more restricted picture. PLD1 is found primarily on peri-nuclear vesicles in many cell types and on the plasma membrane in others; PLD2 is found primarily on the plasma membrane. However, the proteins may transit through multiple subcellular sites subsequent to cellular stimulation, leading to a record of PLD activity at a broader range of sites. The PLD1 PH domain is palmitoylated and this appears to play a role in targeting PLD1 to specific locations. Elimination of palmitoylation through mutation of key amino acids results in the redistribution of PLD1 from peri-nuclear vesicles to the plasma membrane. PLD2 contains one palmitoylation site. It is not known whether its subcellular localization is effected through lipid modification.

Function of PLD's Product

PA is a pleiotropic lipid. Four basic roles have been proposed for it.

Signal Transducer

PA has been shown to stimulate the activity of several different kinds of enzymes. One of these is phosphatidylinositol 4-phosphate 5-kinase, which phosphorylates the lipid phosphatidylinositol 4-phosphate (PI4P) to generate PI4,5P_2. PI4,5P_2 is well known for its roles in regulating trafficking of membrane vesicles in cells and for regulating cell shape and changes in morphology. PA also activates NADPH oxidase, which plays an important role as part of the neutrophil-mediated immunological response to infection. Another target has been identified recently as mTor, a key component in the regulation of protein translation and cell growth. Additional enzymes regulated by PA are likely to continue to emerge; current candidates include ARF GAPs, enzymes that deactivate ARF small G-proteins and thus are involved in regulating vesicular trafficking and cell shape.

Lipid Anchor

PA has also been reported to bind to and anchor a rapidly growing list of proteins involved in signaling, regulating vesicular trafficking and cell shape, or that have unknown functions. Although in some of these cases, PA may also be stimulating changes in the biochemical behaviors of the target proteins and thus act as a signal transducer, it seems likely that in many of the instances, it serves as a means to recruit effector molecules to a focused location in the cell. For example, at sites of budding from the Golgi or exocytosis at the plasma membrane. In another such example, Raf-1 kinase is activated by the oncogene Ras only at membrane surfaces, but Raf-1 is normally cytosolic and has been reported to become membrane associated only through interaction with PA, like the one which occurs subsequent to insulin receptor activation.

Signaling Intermediate

PA can also be dephosphorylated to yield diacylglycerol, a key lipid which activates protein kinase C (PKC), or monodeacylated to form lysoPA, a potent mitogen found in serum that mediates cell proliferation and shape change.

Biophysical Role

Space-filling models have suggested that with two acyl chains and a small headgroup, PA may act as a "hinge" lipid and promote membrane curvature towards the leaflet in which it is located. Conversely, lysoPA, which has the same headgroup but only one acyl chain, has been proposed to promote membrane curvature in the opposite direction. Since membrane vesicles undergoing budding from or fusion into planar membrane surfaces, pass through energetically unfavorable transition states as the membranes bend and fold at the neck of the vesicles, it is an attractive idea that conversion of PA into lysoPA, and vice versa, could make these events happen more efficiently (i.e., lower the activation energy). These models are supported by the observations that endophilin I, a protein that promotes endocytosis, is an enzyme that converts lysoPA into PA, and that adding PA to vesicles promotes accelerated rates of fusion in *in vitro* reconstitution assays.

Cell Biological Roles

Yeast

PLD function is best understood in yeast, where it was identified in a genetic screen for mutants unable to complete the late stages of meiosis. At the point in the meiotic process where PLD is required, duplication of the chromosomal DNA has been completed and individual sets of chromosomes are segregating to each pole of the four-lobed nucleus. The outer half of the spindle pole body found at each pole serves as a nucleating site for the formation of a new structure called the prospore membrane. The prospore membrane is built by aggregation and fusion of vesicles sent from the Golgi apparatus. These vesicles normally function in exocytosis and travel to the plasma membrane, but are redirected to the spindle pole body to build the prospore membrane during meiosis. As meiosis progresses, the prospore membranes grow in length and extend to cover each lobe of the nucleus (picture someone rolling socks onto their hands and feet), and eventually pinch off the nuclear lobes. This results in the "capture" of individual sets of chromosomes in their own nuclear envelopes. Each of these are immature spores, and the prospore membrane now surrounding them becomes the new plasma membrane. A cell wall eventually forms around each spore, making them ready for release from the original yeast cell.

When PLD is missing, the prospore membrane fails to form. PLD is distributed throughout the cell prior to meiosis but translocates to the spindle pole at the time when the prospore membrane needs to be built. PLD activity is not required for its translocation, indicating that it is not involved in the trafficking of membrane vesicles to the spindle pole body; however, the vesicles subsequently fail to aggregate and fuse when PLD is missing or catalytically inactive.

Although the precise mechanism mediated by PLD or its product PA in prospore membrane development remains unknown, this is the best-understood example of what is now recognized as a common theme for PLD function; regulation of vesicle production, trafficking, or fusion.

Mammals

Investigation of roles for PLD in mammals has been more challenging. Cells and animals lacking PLD have not yet been generated, and specific pharmacological PLD agonists and antagonists have not been identified. Nonetheless, an approach for probing PLD function exists that has been widely used, although interested readers need to keep in mind that it comes with significant caveats. This method involves exposing cells to moderately high levels of primary alcohols such as ethanol or 1-butanol. Short-chain primary alcohols can competitively substitute for water in the PLD hydrolysis reaction, leading to formation of phosphatidylalcohols at the expense of PA. Phosphatidylalcohols are believed to be relatively inert; that is, they do not activate the downstream pathways triggered by PA. Accordingly, diverting PA production to phosphatidylalcohol diminishes PLD-mediated activation of PA-dependent events. In addition, since phosphatidylalcohols are relatively metabolically inert, they serve as a history of PLD activation over the period during which the alcohols are present. Measuring accumulation of phosphatidylalcohols is very useful for quantitating PLD activity, since PA, in contrast, turns over rapidly once formed, and in fact can be generated through pathways other than PLD as well. Limitations of this approach include the facts that alcohols alter the fluidity of membranes, which affects many biological processes, and block activation of many tyrosine kinase receptors; for example, the insulin receptor. Moreover, at the concentrations of alcohol required to divert PA production effectively, levels of phosphatidylinositol lipids become significantly altered; for example, PIP levels decrease dramatically. Accordingly, although alcohol-mediated inhibition of PA production provides initial evidence for PA involvement in specific processes, it should not be considered definitive in the absence of other approaches. More recent approaches for manipulating PLD activity include overexpression or injection of wild-type PLD proteins to increase levels of activity or use of catalytically inactive PLD proteins to serve as dominant interfering mutants. Using such techniques, roles have been described for PLD in a number of settings.

Secretion

One of the better-characterized model systems involves regulated secretion from neuroendocrine cells, such as primary adrenal chromaffin cells. Exposure of these cells to the agonist nicotine stimulates receptors that activate PLD and triggers release of catecholamines through fusion of neurotransmitter-containing secretory granules with the plasma membrane. Analogous to the role of PLD in yeast meiosis, PLD in adrenal chromaffin cells is found on the acceptor membrane, in this case the plasma membrane. Increasing PLD activity through overexpression leads to increased regulated exocytosis and reducing PLD activity through any of the approaches described above leads to inhibition of catecholamine release. In this setting, PA appears to mediate the rate and efficacy of fusion of secretory granules into the plasma membrane as inhibition of PLD activity leads to individual granules fusing into the plasma membrane and disgorging their contents more slowly (Figure 4). Once again, the precise mechanism of PA function remains unknown, and could involve more than one of the possibilities described above. PLD activity has

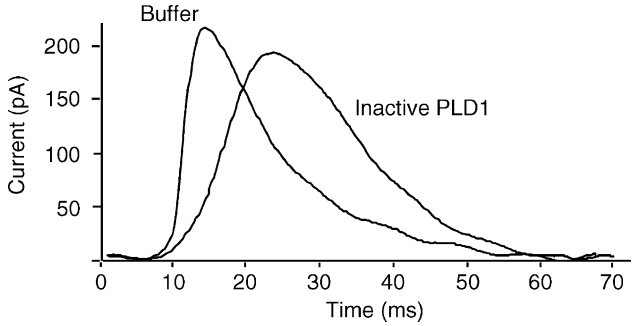

FIGURE 4 Catalytically inactive PLD1 inhibits nicotine-evoked catecholamine secretion from chromaffin cells, revealing a requirement for PA in the fusion of secretory granules into the plasma membrane. Chromaffin cells were microinjected with buffer or with catalytically inactive PLD1 protein which acts as a dominant negative mutant. Cells were stimulated 10–15 min later by a local application of nicotine for 5 s. Catecholamine secretion, which causes a change in local conductance due to its highly charged nature, was recorded using a carbon fiber electrode. Numerous spikes of current, representing fusion of individual granules of catecholamines with the plasma membrane are observed, but many fewer after injection of catalytically inactive PLD1 (not shown). Individual fusion events are shown above on the millisecond timescale. The fusion event observed for a normal (buffer-injected) cell occurs rapidly. The fusion event in the cell injected with catalytically inactive PLD1 protein occurs more slowly, indicated that the fusion pore formed between the secretory granule and the plasma membrane enlarges at a slower rate, causing the contents to be released more slowly as well. Reprinted from Vitale, N., Caumont, A. S., Chasserot-Golaz, S., Du, G., Wu, S., Sciorra, V. A., Morris, A. J., Frohman, M. A., and Bader, M. F. (2001). Phospholipase D1: a key factor for the exocytotic machinery in neuroendocrine cells. *EMBO J.* **20**, 2424–2434, with permission of Oxford University Press.

similarly been shown to promote or be required for fusion of histamine-containing secretory granules into the plasma membrane after IgE-triggered degranulation of mast cells, and for translocation of the Glut-4 glucose transporter from storage vesicles to the plasma membrane subsequent to insulin stimulation.

Finally, PLD activity has also been shown to promote the release of membrane vesicles from the trans-Golgi in endocrine cells. It may be that PLD promotes both budding and fusion of vesicles. Alternatively, the budding process could be facilitated by PLD-regulated fusion of vesicles into the trans-Golgi at an earlier step.

Morphology

The activators that stimulate mammalian PLD, i.e., ARF and Rho small G-protein family members and protein kinase C, are also well known for their roles in controlling changes in cell shape. Although, again, the precise role played by PA remains undefined, it is clear that inhibition of PLD activity blocks actin cytoskeleton-mediated cell shape changes in some settings (for example, formation of actin stress fibers in response to agonist stimulation) and that overexpression of PLD promotes them. At high levels of overexpression of the PLD2 isoform, cells undergo spontaneous changes in morphology, extending finger-like projections and undergoing continued ruffling. These sorts of responses indicate that PLD and PA play a role in regulating cell shape, although their role at normal levels of expression remains to be determined. Leading hypotheses include the possibilities that PLD activity increases levels of $PI4,5P_2$, a lipid known to be involved in reorganization of the actin cytoskeleton, or that it activates ARF GAPs, enzymes that deactivate ARF-stimulated pathways.

Other Roles

PLD-generated PA also promotes activation of Raf-1 kinase and mTor, key regulatory factors in cell growth, and NADPH-oxidase, a component of the respiratory burst response in inflammation and infection.

Summary

Phospholipase D, a lipid-modifying enzyme activated via complex regulation through G-protein and receptor tyrosine kinase signal transduction pathways, has roles in numerous cell biological settings including vesicular trafficking, cell shape modifications, and proliferation.

See Also the Following Articles

ARF Family • Phosphatidylinositol Bisphosphate and Trisphosphate • Phospholipid Metabolism in Mammals • Rho GTPases and Actin Cytoskeleton Dynamics

Glossary

phosphatidylalcohols Biologically inert, metabolically inactive compounds formed when primary alcohols are available to serve as the nucleophile instead of water in a PLD reaction.

phospholipases Enzymes that cleave phospholipids. Phospholipase A, C, and D each cleave distinct sites on phospholipids.

phospholipid A membrane lipid consisting of one or more fatty acid side chains linked to a glycerol phosphate backbone. The phosphate group frequently terminates in a "headgroup" such as choline or inositol via a phosphodiester bond that constitutes the target for PLD superfamily action.

Further Reading

Cockcroft, S. (2001). Signaling roles of mammalian phospholipase D1 and D2. *Cell Mol. Life Sci.* **58**, 1674–1687.

Exton, J. H. (2002). Phospholipase D-structure, regulation and function. *Rev. Physiol. Biochem. Pharmacol.* **144**, 1–94.

Frohman, M. A., Sung, T.-S., and Morris, A. J. (1999). Mammalian phospholipase D-structure and regulation. *Biochim. Biophys. Acta* **1439**, 175–186.

Jones, D., Morgan, C., and Cockcroft, S. (1999). Phospholipase D and membrane traffic: Potential roles in regulated exocytosis, membrane delivery and vesicle budding. *Biochim. Biophys. Acta* **1439**, 229–244.

Liscovitch, M., Czarny, M., Fiucci, G., and Tang, X. (2000). Phospholipase D: Molecular and cell biology of a novel gene family. *Biochem. J.* **345**, 401–415.

Rizzo, M., and Romero, G. (2002). Pharmacological importance of phospholipase D and phosphatidic acid in the regulation of the mitogen-activated protein kinase cascade. *Pharmacol. Therap.* **94**, 35–50.

Sung, T. C., Roper, R., Zhang, Y., Rudge, S., Temel, R., Hammond, S., Morris, A., Moss, B., Engebrecht, J., and Frohman, M. (1997). Mutagenesis of phospholipase D defines a superfamily including a *trans*-Golgi viral protein required for poxvirus pathogenicity. *EMBO J.* **16**, 4519–4530.

Biography

Mary LaLonde is a trainee in the Medical Scientist Training Program at Stony Brook who is exploring the role of Phospholipase D in Drosophila.

Michael A Frohman, M.D., Ph.D. is a Professor in the department of pharmacology and the Director of the Medical Scientist Training Program at Stony Brook. His group cloned the mammalian PLD genes and conducted many of the early molecular biological studies on them.

Phospholipid Metabolism in Mammals

Claudia Kent
University of Michigan, Ann Arbor, Michigan, USA

Phospholipids form the bilayer matrix of all natural biological membranes. In mammals, phospholipids take on additional importance as components of lipoproteins and as intermediates in signal transduction pathways. While the term "phospholipid" includes any lipid containing a phosphate moiety, in everyday usage the term has come to refer to glycerophospholipids, which are lipids containing glycerol phosphate as the "backbone," plus the phosphosphingolipid, sphingomyelin. These molecules are synthesized *de novo* in all mammalian cells, and actively degraded in those cells by multiple phospholipases. This article focuses on the metabolism of glycerophospholipids.

Biosynthesis of Phospholipids

Diacylglycerophospholipids

Major Glycerophospholipid Classes

The structures of the major classes of mammalian phospholipids are shown in Figure 1. Phosphatidate, or *sn*-1,2-diacylglycerol-3-phosphate, is a central intermediate in the biosynthesis of all phospholipids. In addition, this lipid has various functions in signal transduction pathways. Phosphatidylcholine is the major eukaryotic phospholipid, usually accounting for 40–50% of cellular phospholipids. Phosphatidylcholine plays a major structural role in biological membranes because of its excellent bilayer-forming properties. It is also found as a structural component of serum lipoproteins and pulmonary surfactant. In addition, phosphatidylcholine is a component of signal transduction pathways as a substrate for phospholipases that produce lipid mediators.

Phosphatidylethanolamine is also a major mammalian phospholipid, accounting for ~20–30% of cellular phospholipids. This lipid also plays a structural role in the bilayer, contributing to curvature stress because of its nonlamellar propensities, which in turn influences membrane–protein interactions. Phosphatidylserine represents roughly 10–15% of cellular phospholipids. This lipid plays a critical role in apoptosis, during which its exposure on the external leaflet of the plasma membrane is a recognition feature for engulfment by phagocytic cells.

Phosphatidylglycerol is found only in trace amounts in most mammalian cells, primarily in mitochondria. In lung, however, appreciable amounts of phosphatidylglycerol are found in type II alveolar cells and in their principal secretory product, pulmonary surfactant. The metabolic derivative of phosphatidylglycerol is diphosphatidylglycerol, commonly called cardiolipin; this lipid is found exclusively in mitochondria, where its role is to interact with proteins of the electron transport chain. Phosphatidylinositol is an important constituent of mammalian membranes, but is more widely appreciated as a substrate for kinases that convert it to multiply phosphorylated forms that participate in many signal transduction pathways.

Biosynthesis of the Central Intermediates

All mammalian glycerophospholipids, as well as triacylglycerols, are ultimately derived from phosphatidate. The main source of phosphatidate is the fatty acylation of *sn*-glycerol-3-phosphate (Figure 2), which in turn is formed by the reduction of dihydroxyacetone phosphate, a central intermediate of the glycolytic/gluconeogenic pathway. The first fatty acyl group is added by glycerol-3-phosphate acyltransferase, forming the product 1-acylglycerol-3-phosphate or lysophosphatidate. Two isoforms of glycerol-3-phosphate acyltransferase are found in mammals, one in the endoplasmic reticulum and the other in the mitochondrial outer membrane. The *sn*-2 position of lysophosphatidate is acylated by 1-acylglycerol-3-phosphate acyltransferase, a component of the endoplasmic reticulum. Fatty acyl-CoA serves as the donor for both acyltransferase reactions. Phosphatidate may also be formed by the action of phospholipase D, as is discussed in this article later, or by the action of diacylglycerol kinase; however, these last two enzymes do not participate in *de novo* phospholipid biosynthesis.

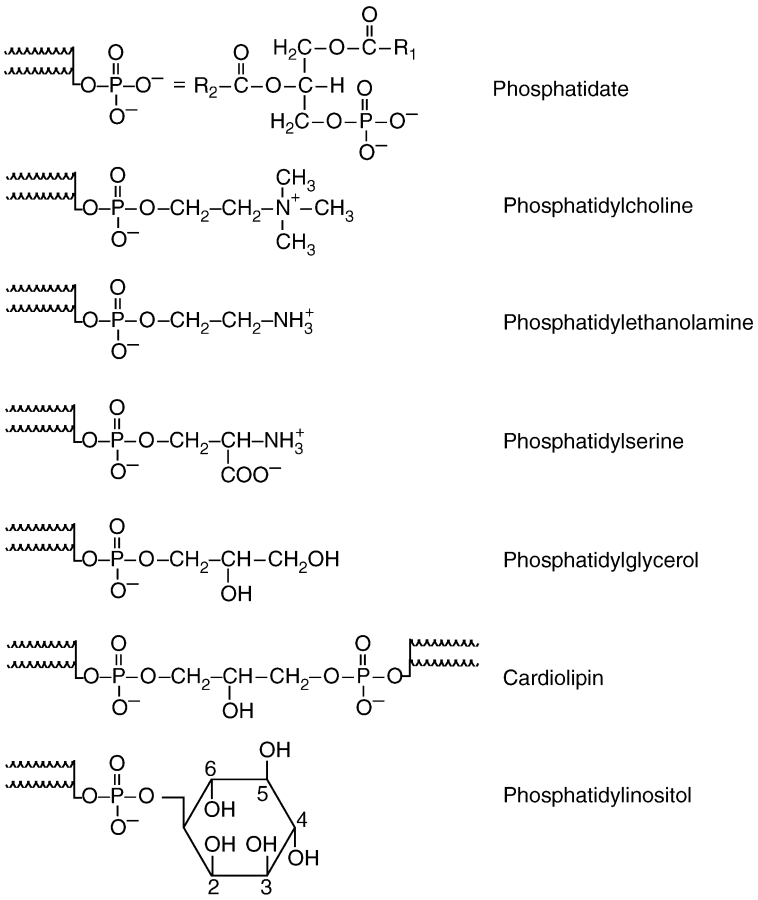

FIGURE 1 Structures of major glycerophospholipid classes. R_1 and R_2 refer to the different fatty acyl chains esterified to positions 1 and 2 of *sn*-glycerol-3-phosphate. The diacylglycerol moiety is represented by wavy horizontal lines connected to a vertical line.

Newly synthesized phosphatidate is channeled into two biosynthetic pathways, which are then used for the synthesis of different groups of phospholipids. In one pathway, phosphatidate phosphohydrolase converts its substrate to *sn*-1,2-diacylglycerol. Two isoforms of phosphatidate phosphohydrolase are found in mammalian cells; the one involved in glycerolipid biosynthesis appears to be both cytosolic and in the endoplasmic reticulum. The other isoform is plasma membrane-associated and functions primarily in signal transduction. The other pathway of phosphatidate utilization involves the formation of CDP-diacylglycerol, which takes place primarily in the endoplasmic reticulum.

The Diacylglycerol Pathway: Biosynthesis of Phosphatidylcholine, Phosphatidylethanolamine, and Phosphatidylserine

The biosynthetic pathways for all glycerophospholipids include at least one cytidylylated intermediate. The pathways for *de novo* biosynthesis of lipids that are derived from diacylglycerol involve the use of CDP-choline or CDP-ethanolamine (Figure 3). These nucleotide intermediates are made by the phosphorylation of choline and ethanolamine by choline/ethanolamine kinases, followed by transfer to the CMP moiety of CTP, catalyzed by phosphocholine and phosphoethanolamine cytidylyltransferases. The CDP-alcohols then react with diacylglycerol to form phosphatidylcholine and phosphatidylethanolamine.

The choline and ethanolamine kinases are soluble enzymes and are presumed to be cytosolic. Most of these enzymes can use either choline or ethanolamine as substrate but ethanolamine-specific kinases also exist. The cytidylyltransferases are specific for either phosphocholine or phosphoethanolamine and are regulatory for the CDP-choline and -ethanolamine pathways. There are nuclear and cytoplasmic isoforms of the phosphocholine cytidylyltransferase that are encoded by separate genes. These isoforms have an intriguing mode of regulation in which a membrane-binding segment of the enzyme "senses" the lipid composition and conveys a deficit of phosphatidylcholine to the active site of the enzyme, which is then activated in response to

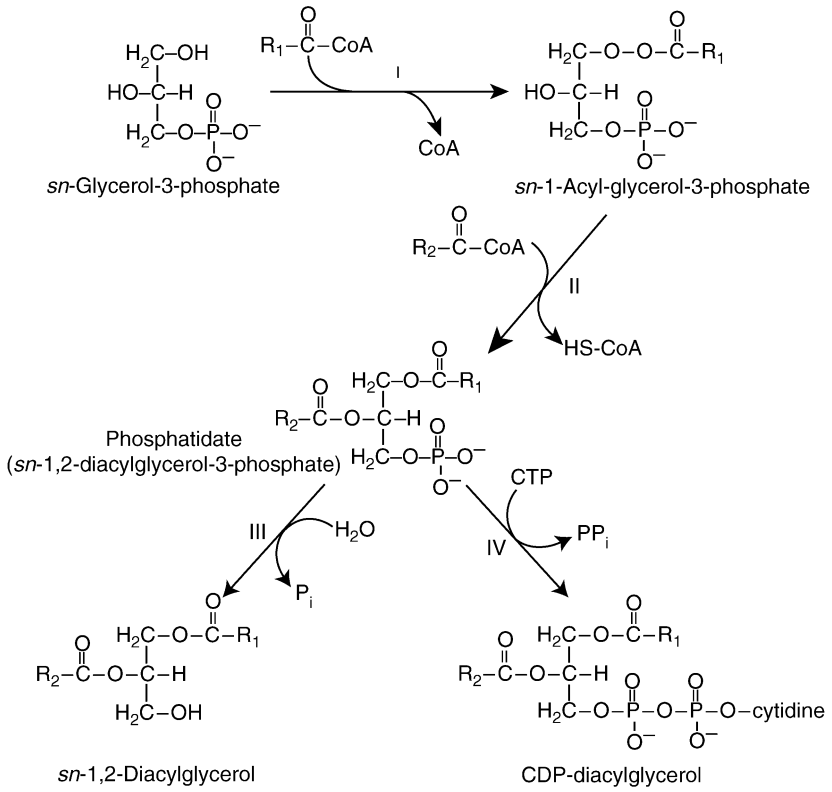

FIGURE 2 Biosynthesis of central intermediates of glycerophospholipid biosynthesis. Enzymes are I, glycerol-3-phosphate acyltransferase; II, 1-acylglycerol-3-phosphate acyltransferase; III, phosphatidate phosphohydrolase, and IV, CDP-diacylglycerol synthase.

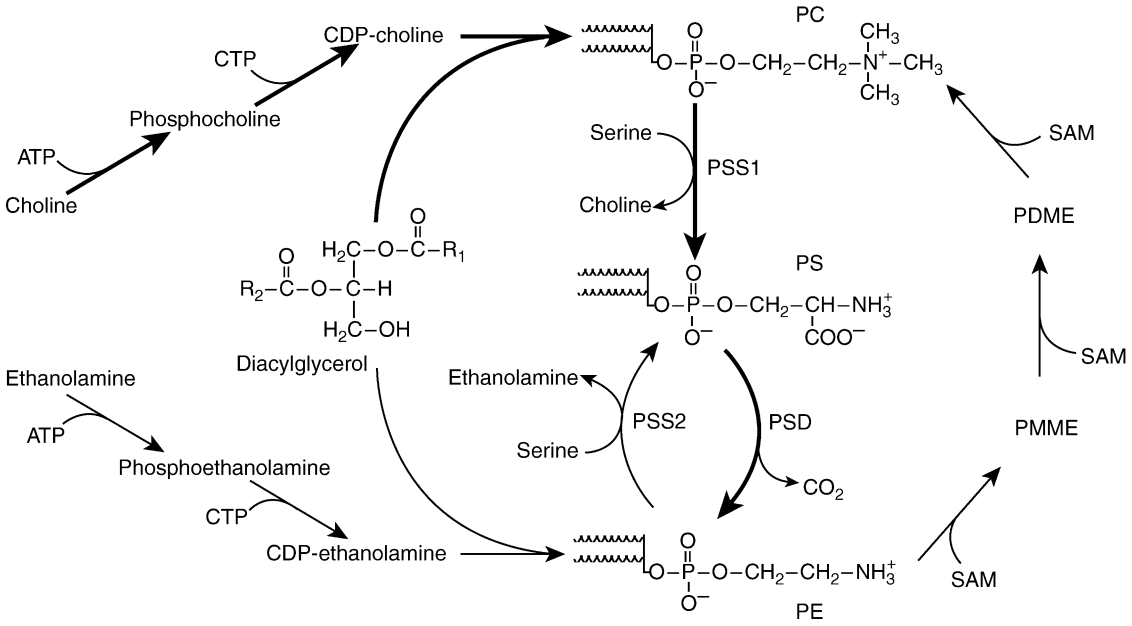

FIGURE 3 Synthesis of phospholipids derived from diacylglycerol. PC, phosphatidylcholine; PS, phosphatidylserine, PE, phosphatidylethanolamine; PMME, phosphatidylmonomethylethanolamine; PDME, phosphatidyldimethylethanolamine; SAM, S-adenosylmethionine. PSS1, phosphatidylserine synthase 1; PSS2, phosphatidylserine synthase 2; PSD, phosphatidylserine decarboxylase. Other enzymes are identified in the text. The thick arrows denote the major biosynthetic pathways.

the deficit. The phosphoethanolamine cytidylyltransferase is readily solubilized but appears to be associated with the endoplasmic reticulum. The alcohol phosphotransferases that catalyze the last steps, the formation of phosphatidylcholine and phosphatidylethanolamine, are embedded in the endoplasmic reticulum.

The CDP-choline pathway is the only mode for biosynthesis of phosphatidylcholine in most mammalian tissues. In liver, however, phosphatidylcholine is also made by the stepwise methylation of phosphatidylethanolamine, with S-adenosylmethionine as the methyl donor. In mammals, one phospholipid methyltransferase carries out all three steps; this methyltransferase activity is found in a specialized portion of the endoplasmic reticulum known as the mitochondria-associated membrane.

The CDP-ethanolamine pathway is important for the biosynthesis of ether lipids, but is a minor pathway for biosynthesis of diacyl ethanolamine phosphoglyceride. The predominant pathway for biosynthesis of the diacyl lipid is, rather, the decarboxylation of phosphatidylserine. The latter lipid in mammals is produced by exchange enzymes, in which serine exchanges with either the choline moiety of phosphatidylcholine, or ethanolamine of phosphatidylethanolamine, to form phosphatidylserine. The enzymes catalyzing these two exchanges are distinct; the choline exchange enzyme is responsible for bulk production of phosphatidylserine, which is then decarboxylated to form phosphatidylethanolamine. It is intriguing that the exchange enzymes are components of the endoplasmic reticulum, while the decarboxylase is mitochondrial. This dual location necessitates phospholipid transport systems that facilitate the transfer of phosphatidylserine and ethanolamine between these locations.

The CDP-Diacylglycerol Pathway: Synthesis of Phosphatidylglycerol, Cardiolipin, and Phosphatidylinositol

The nucleotide intermediate, CDP-diacylglycerol, is used for the biosynthesis of non-nitrogenous glycerophospholipids in mammals (Figure 4). In the pathway for the synthesis of the mitochondrial lipid, cardiolipin, CDP-diacylglycerol reacts with glycerol-3-phosphate to form phosphatidylglycerol-3-phosphate, which is then hydrolyzed to form phosphatidylglycerol. The usual fate of phosphatidylglycerol is to be converted to cardiolipin. In mammals that conversion involves reaction of phosphatidylglycerol with another molecule of CDP-diacylglycerol.

CDP-diacylglycerol is also used for the biosynthesis of phosphatidylinositol by reaction of the nucleotide lipid with free inositol. This reaction takes place predominantly in the endoplasmic reticulum. A number of phosphoinositide kinases have been identified that convert phosphatidylinositol to polyphosphoinositides.

Biosynthesis of Ether Glycerophospholipids

Ether phospholipids, in which the *sn*-1 acyl linkage is replaced by an ether bond, are major constituents of certain tissues, especially brain. They appear to play an

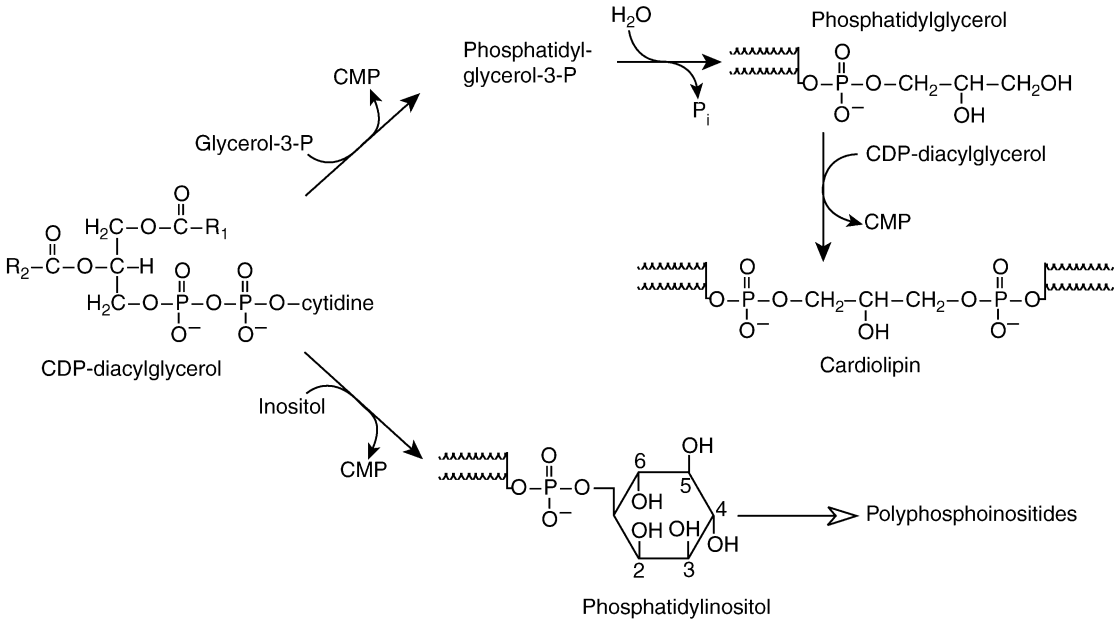

FIGURE 4 Synthesis of phospholipids derived from CDP-diacylglycerol. The open arrow in the lower right represents many phosphorylation steps leading to the polyphosphoinositides.

important role in mammalian physiology as judged by the severity of diseases resulting from abnormalities in their metabolism. These lipids are derived from dihydroxyacetone phosphate, which becomes fatty acylated at position 1 (Figure 5). The fatty acyl group is then replaced by a fatty alcohol to create the ether linkage. Reduction at C-2 followed by a second acylation produces 1-alkyl-2-acyl-glycerol-3-phosphate. This compound is then dephosphorylated, and the resultant free hydroxyl reacts with CDP-ethanolamine to produce 1-alkyl-2-acylglycerol-3-phosphoethanolamine, also known as plasmanylethanolamine. Introduction of a double bond at this stage into the fatty alcohol moiety results in the formation of the plasmalogen, plasmenylethanolamine. The mechanism of formation of plasmanyl/plasmenyl choline is not well established but may occur after hydrolysis of the ethanolamine ether lipids to 1-alkyl/alkenyl-2-acylglycerol, followed by reaction with CDP-choline. Ether lipid biosynthesis is unusual in that the first two enzymes are located in peroxisomes, the third step occurs in both peroxisomes and the endoplasmic reticulum, and the remaining steps occur in the endoplasmic reticulum.

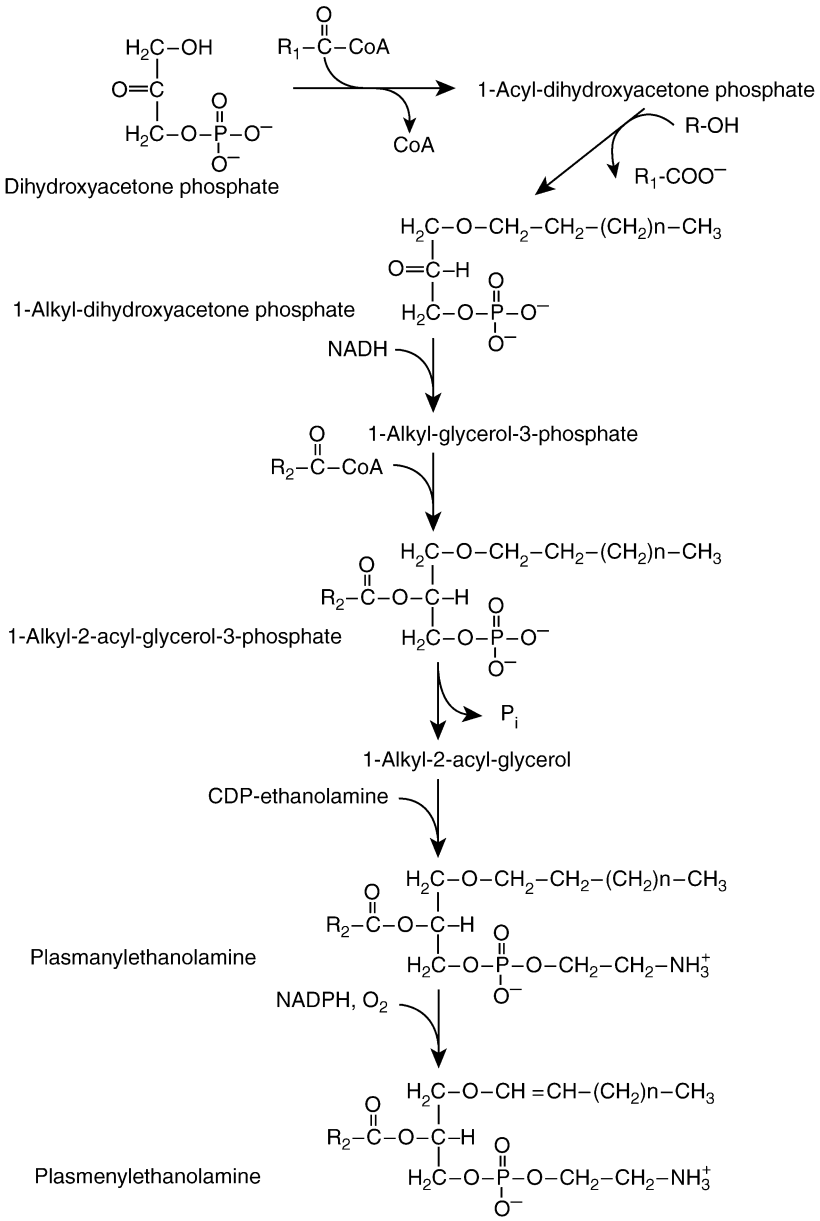

FIGURE 5 Biosynthesis of the ether lipids, plasmanylethanolamine, and plasmenylethanolamine. The ethanolamine ether lipids are precursors of choline ether lipids, but the conversion steps have not been firmly established.

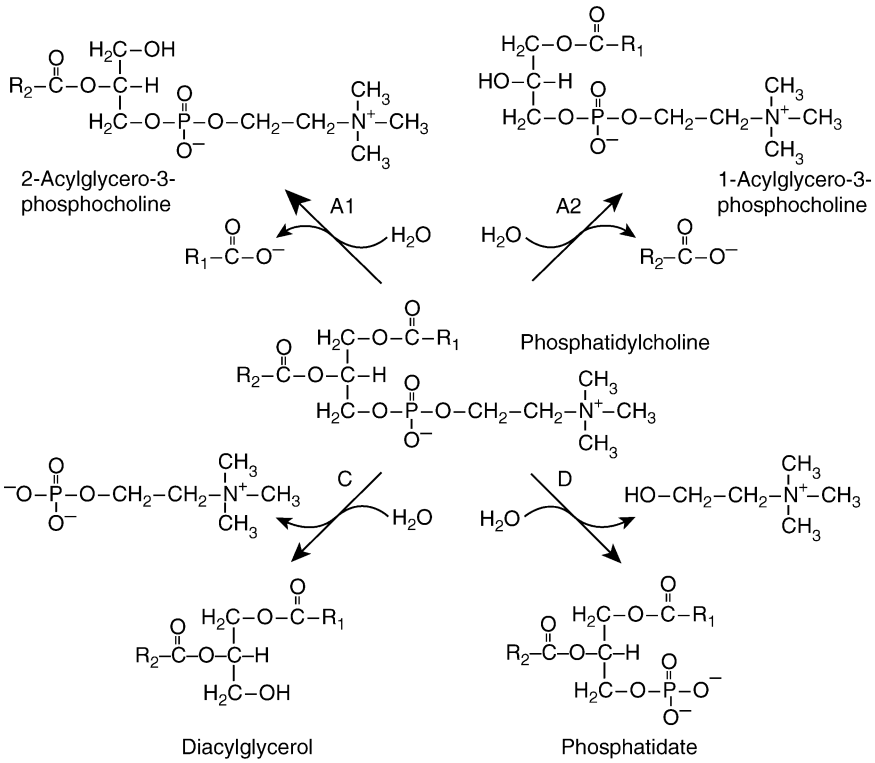

FIGURE 6 Specificity of phospholipases. A1, A2, C, and D refer to phospholipases of that specificity, as described in the text.

Catabolism of Phospholipids: Phospholipases

The degradation of phospholipids takes place during normal membrane turnover, as well as in response to the need for production of lipid mediators. The phospholipases that perform this degradation are divided into four general classes according to the reactions they catalyze (Figure 6). Hydrolysis of the fatty ester bond at C-1 is catalyzed by phospholipase A1. Multiple phospholipases A1 are found in mammals. Lysosomal phospholipase A1 functions in general phospholipid catabolism while phosphatidylserine-specific phospholipase A1 appears to generate the lipid-signaling molecule, 2-lysophosphatidylserine.

The best-studied phospholipases are phospholipases A2, which hydrolyze the ester bond at C-2. Mammalian phospholipases A2 function predominantly in the generation of free arachidonate, which is then converted by cyclooxygenases and lipoxygenases to a variety of eicosanoid-signaling molecules. Platelet-activating factor acetylhydrolase is a very specific phospholipase A2 that utilizes 1-alkyl-2-acetylphosphatidylcholine, also known as platelet activating factor, an important inflammatory lipid. Phospholipases A2 are also found in lysosomes where they play a more general catabolic role.

The phosphate ester bonds of phospholipids are hydrolyzed by phospholipases C, with the production of diacylglycerol, and D, with the production of phosphatidate. The best-studied phospholipases C are those involved in the hydrolysis of polyphosphoinositides, with the generation of diacylglycerol, which activates certain protein kinases, as well as inositol polyphosphates, which have many signaling functions. Phospholipases D mainly hydrolyze phosphatidylcholine and function both in signal transduction as well as in vesicular trafficking. Catabolism of sphingomyelin in mammals is carried out by neutral and acid sphingomyelinases that have a C-type specificity in that they generate ceramide and phosphocholine.

See Also the Following Articles

Phosphatidylinositol Bisphosphate and Trisphosphate • Phosphoinositide 3-Kinase • Phosphoinositide 4- and 5-Kinases and Phosphatases • Phosphoinositide-Dependent Protein Kinases • Phospholipase A_2 • Phospholipase D • Phospholipid Synthesis in Yeast • Sphingolipid Biosynthesis • Sphingolipid Catabolism

Glossary

ceramide The "backbone" of sphingolipids, consisting of sphingosine with an amide linkage to a fatty acid.

ether lipids Lipids containing a hydrocarbon chain in ether linkage to C-1 of the glycerol phosphate backbone.

glycerophospholipids Lipids composed of a backbone of *sn*-glycerol-3-phosphate, the first and second positions of which are fatty acylated.

phosphatidate *sn*-1,2-diacylglycerol-3-phosphate, also called phosphatidic acid.

phospholipase An enzyme catalyzing the hydrolysis of a phospholipid.

plasmalogen An ether lipid containing a *cis* double bond in the hydrocarbon chain, adjacent to the ether linkage.

polyphosphoinositide A phospholipid derived by phosphorylation of the inositol ring of phosphatidylinositol.

sphingomyelin A phospholipid consisting of ceramide linked to phosphocholine.

Further Reading

Nagan, N., and Zoeller, R. A. (2001). Plasmalogens: Biosynthesis and functions. *Prog. Lipid Res.* **40**, 199–299.

Vance, D. E. (2002). Phospholipid biosynthesis in eukaryotes. In *Biochemistry of Lipids, Lipoproteins, and Membranes* (D. E. Vance and J. E. Vance, eds.) 4th edition, pp. 205–232. Elsevier Science B.V., Amsterdam.

Voelker, D. R. (2000). Interorganelle transport of aminoglycerophospholipids. *Biochim. Biophys. Acta* **1486**, 97–107.

Biography

Claudia Kent is a Professor of Biological Chemistry at the University of Michigan. Her research interests have centered on phospholipid metabolism in eukaryotes and prokaryotes, with the principal focus being the enzymes that regulate phosphatidylcholine metabolism. She obtained a Ph.D. from Johns Hopkins University, and was a postdoctoral trainee at Washington University and a faculty member in biochemistry at Purdue University before moving to Michigan.

Phospholipid Synthesis in Yeast

Gil-Soo Han and George M. Carman
Rutgers University, New Brunswick, New Jersey, USA

Phospholipids are essential molecules that contribute to the structural definition of the cell. They also play a role as signaling molecules that participate in the regulation of cellular processes. The yeast *Saccharomyces cerevisiae* has been used as a model system to study phospholipid synthesis and its regulation in eukaryotes. Molecular, genetic, and biochemical studies have shown that phospholipid synthesis is regulated in a coordinated fashion. The mechanisms that govern this regulation mediate the mRNA and protein levels of the biosynthetic enzymes, as well as their activity and localization.

Phospholipid Composition

The major phospholipids found in the membranes of *S. cerevisiae* include phosphatidylcholine (PC), phosphatidylethanolamine (PE), phosphatidylinositol (PI), and phosphatidylserine (PS) (Figure 1). Mitochondrial membranes also contain phosphatidylglycerol (PG) and cardiolipin (CL). The composition of phospholipids in the cell can vary dramatically when culture conditions are altered. However, the average charge of the membrane phospholipids remains relatively constant. Genetic and biochemical regulation of the enzymes in the phospholipid biosynthetic pathways can compensate for changes in the levels of phospholipids of one charge by orchestrating parallel changes in the levels of phospholipids of the opposite charge.

Phospholipid Synthesis

Phospholipid synthesis is a complex process containing many branch points. A key molecule in this process is phosphatidate (PA). It plays a central role in phospholipid synthesis as the precursor of all phospholipids synthesized via the CDP–diacylglycerol (DAG), CDP–choline, and CDP–ethanolamine pathways (Figure 2). In the CDP–DAG pathway, PA is converted to CDP–DAG, which is then utilized for the synthesis of PS, PE, and PC. CDP–DAG is also utilized for the synthesis of PI and CL. In the CDP–choline and CDP–ethanolamine pathways, DAG is generated from the dephosphorylation of PA, and is utilized for the synthesis of PC or PE when cells are supplemented with choline or ethanolamine, respectively. The DAG derived from PA is also used for the synthesis of triacylglycerols. The nucleotide CTP is another important precursor in the synthesis of phospholipids. CTP, which is synthesized from UTP, is the direct precursor of the activated, energy-rich phospholipid pathway intermediates CDP–DAG, CDP–choline, and CDP–ethanolamine (Figure 2).

Synthesis of PA

PA is synthesized from glycerol 3-phosphate via two acylation reactions. The first acylation step, which results in the formation of lysoPA, is catalyzed by the *GAT1*- and *GAT2*-encoded glycerol 3-phosphate acyltransferases. Deletion of either gene does not affect cell viability, but deletion of both genes results in a lethal phenotype. Acylation of lysoPA, which is catalyzed by the *SLC1*-encoded lysoPA acyltransferase, generates PA. In addition to the *de novo* synthesis, PA can be produced from phospholipid turnover: (1) hydrolysis of PC by the *SPO14/PLD1*-encoded phospholipase D; (2) phosphorylation of DAG by CTP-dependent DAG kinase (whose structural gene is not yet known); and (3) dephosphorylation of diacylglycerol pyrophosphate (DGPP) by the *DPP1*- and *LPP1*-encoded lipid phosphate phosphatase enzymes.

CDP–DAG Pathway

PS, PE, and PC are synthesized via reactions in the CDP–DAG pathway. The committed step in this pathway is the synthesis of CDP–DAG from PA and CTP. This reaction is catalyzed by the essential enzyme CDP–DAG synthase, which is encoded by the *CDS1* gene. CDP–DAG is then converted to PS by the *PSS1/CHO1*-encoded PS synthase. This enzyme displaces the CMP moiety of CDP–DAG with serine. PS is then decarboxylated to PE by the *PSD1*- and *PSD2*-encoded PS decarboxylases. The *PSD1*-encoded PS decarboxylase is responsible for $>90\%$ of the cellular PS decarboxylase activity, while the *PSD2*-encoded enzyme is responsible for $\sim 10\%$ of the enzyme activity. Finally, PE is

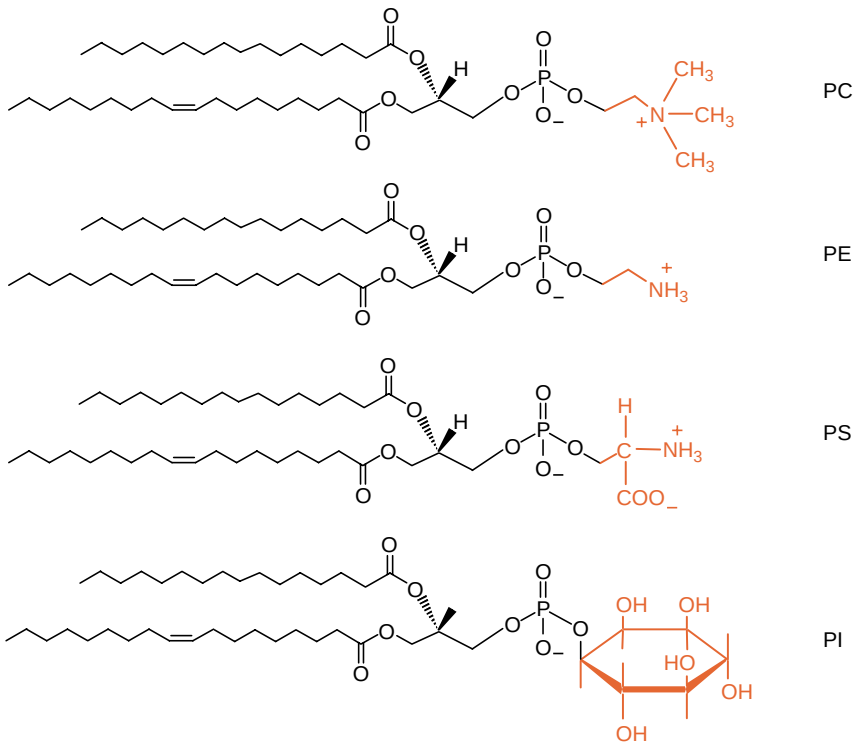

FIGURE 1 Major phospholipids in *S. cerevisiae*. The phospholipid headgroups (i.e., choline, ethanolamine, serine, and inositol) are shown in red.

converted to PC via three sequential methylation reactions. The first methylation reaction is catalyzed by the *PEM1/CHO2*-encoded PE methyltransferase, whereas the last two methylation reactions are catalyzed by the *PEM2/OPI3*-encoded phospholipid methyltransferase.

CDP–Choline and CDP–Ethanolamine (Kennedy) Pathways

When cells are supplemented with choline and ethanolamine, PC and PE are also synthesized via the CDP–choline and CDP–ethanolamine pathways, respectively. In the CDP–choline pathway, choline is phosphorylated with ATP to form phosphocholine by the *CKI1*-encoded choline kinase. Phosphocholine is then converted to CDP–choline by the reaction catalyzed by the *CCT1/PCT1*-encoded phosphocholine cytidylyltransferase. In the last step, PC is synthesized from CDP–choline and DAG by the *CPT1*-encoded choline phosphotransferase. The enzyme reactions in the CDP–ethanolamine pathway are similar to those in the CDP–choline pathway. The *EKI1*-encoded ethanolamine kinase catalyzes the phosphorylation of ethanolamine to phosphoethanolamine. Phosphoethanolamine is then converted to CDP–ethanolamine by the *ECT1*-encoded phosphoethanolamine cytidylyltransferase. In the last step, PE is synthesized from CDP–ethanolamine and DAG by the *EPT1*-encoded ethanolamine phosphotransferase. The Kennedy pathways become essential when the enzymes in the CDP–DAG pathway are defective or repressed. Mutants defective in the synthesis of PS, PE, or PC require choline for growth in order to synthesize PC via the CDP–choline pathway. Mutants defective in the synthesis of PS and PE can also synthesize PC if they are supplemented with ethanolamine. Ethanolamine is converted to PE via the CDP–ethanolamine pathway, and the PE is subsequently methylated to form PC via the CDP–DAG pathway. The CDP–choline pathway was once viewed as an auxiliary or salvage pathway used by cells when the CDP–DAG pathway was compromised. However, it is now known that the CDP–choline pathway contributes to PC synthesis even when wild-type cells are grown in the absence of exogenous choline. The PC synthesized via the CDP–DAG pathway is constantly hydrolyzed to form free choline and PA through the reaction catalyzed by the *SPO14/PLD1*-encoded phospholipase D. The free choline is incorporated back into PC via the CDP–choline pathway, and the PA is recycled into PC and other phospholipids via CDP–DAG and DAG.

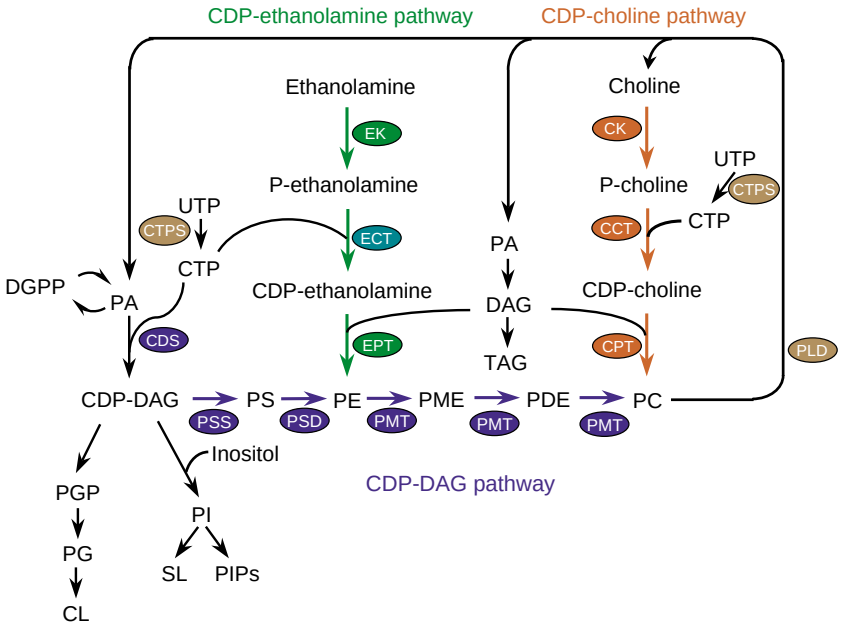

FIGURE 2 Pathways for the synthesis of the major phospholipids in *S. cerevisiae*. The pathways shown for synthesis of phospholipids include the relevant steps discussed in the text. The CDP–DAG, CDP–choline, and CDP–ethanolamine pathways are indicated. The enzymes CDP–DAG synthase (CDS), PS synthase (PSS), PS decarboxylase (PSD), and the PE methyltransferases (PMT) catalyze reactions that lead to the formation of PC by the CDP–DAG pathway (shown in blue). Choline kinase (CK), choline–P cytidylyltransferase (CCT), and choline phosphotransferase (CPT) catalyze reactions that lead to the formation of PC by the CDP–choline pathway (shown in red). Ethanolamine kinase (ET), ethanolamine-P cytidylyltransferase (ECT), and ethanolamine phosphotransferase (EPT) catalyze reactions that lead to the formation of PE by the CDP–ethanolamine pathway (shown in green). The reactions catalyzed by CTP synthetase (CTPS) and phospholipase D (PLD) are shown in brown. A more comprehensive description that includes the synthesis of PA and additional steps in these pathways may be found elsewhere. PA, phosphatidate; CDP–DAG, CDP–diacylglycerol; PS, phosphatidylserine; PE, phosphatidylethanolamine; PME, phosphatidylmonomethylethanolamine; PDE, phosphatidyldimethylethanolamine; PC, phosphatidylcholine; DAG, diacylglycerol; TAG, triacylglycerol; PGP, phosphatidylglycerophosphate; PG, phosphatidylglycerol; CL, cardiolipin; SL, sphingolipids; PIPs, polyphosphoinositides, DGPP, diacylglycerol pyrophosphate.

Other Pathways from CDP–DAG

The essential *PIS1*-encoded PI synthase enzyme catalyzes the displacement of the CMP moiety of CDP–DAG with inositol, resulting in the formation of PI. In this reaction, the water-soluble inositol is provided either by receptor-mediated transport from the growth medium or by *de novo* synthesis from glucose 6-phosphate. When cells are grown in the absence of inositol, glucose 6-phosphate is converted to inositol 1-phosphate, which is catalyzed by the *INO1*-encoded inositol 1-phosphate synthase. Inositol 1-phosphate is then dephosphorylated to form inositol by the *INM1*-encoded inositol monophosphatase. PI is itself a branch point in phospholipid biosynthesis: it is further converted to multiple phosphorylated forms (polyphosphoinositides) by PI kinases, or its phosphoinositol moiety is transferred to ceramide to form sphingolipids. In the CL pathway, CDP–DAG is converted to phosphatidylglycerolphosphate (PGP) by displacement of CMP from CDP–DAG with glycerol 3-phosphate. This reaction is catalyzed by the *PGS1/PEL1*-encoded PGP synthase. PGP is then converted to PG by PGP phosphatase whose structural gene has not yet been identified. In the last step, CL is synthesized from PG and CDP–DAG by *CLS1/CRD1*-encoded CL synthase.

Regulation of Phospholipid Synthesis

Phospholipid synthesis is regulated by a number of factors. These include water-soluble phospholipid precursors (e.g., inositol and choline), nucleotides (e.g., ATP and CTP), lipids (e.g., PA, CDP–DAG, and sphingolipids), growth phase, and phosphorylation. The regulation of phospholipid synthesis by these factors is complex and mediated not only by genetic mechanisms that control the synthesis of mRNA and protein, but also by biochemical mechanisms that modulate enzyme activity.

Genetic Regulation

The effect of inositol supplementation on phospholipid synthesis is a representative example of genetic regulation. When wild-type cells are grown in the presence of inositol, the levels of PS, PE, and PC decrease, while the level of PI increases. These changes in phospholipid composition result from the coordinated regulation of enzyme activities in phospholipid synthesis. Genetic regulation by inositol supplementation affects the enzyme activities by controlling protein content at the transcriptional level. Thus, inositol supplementation represses the transcription of *INO1* and other genes in the CDP–DAG and CDP–choline pathways, whereas inositol starvation stimulates the transcription of the coregulated genes. In many instances, the repressive effect of inositol is enhanced by the addition of choline or ethanolamine to the growth medium. All of the coordinately regulated genes contain a *cis*-acting element, UAS_{INO} (inositol-sensitive upstream activation sequence), in the promoter region. The UAS_{INO} element has the core consensus-binding site (CANNTG) for basic helix-loop-helix (bHLH) proteins. Ino2p and Ino4p are members of the bHLH family of DNA-binding proteins. They bind the UAS_{INO} element as a heterodimer and activate transcription. In addition, Ino2p (but not Ino4p) contains a transcriptional activation domain and is subject to autoregulatory control. Thus, levels of Ino2p appear to be limiting for the formation of the Ino2p/Ino4p heterodimer. In contrast, Opi1p represses the transcription of UAS_{INO}-containing genes. Opi1p contains a leucine zipper and two glutamine-rich domains that are required for Opi1p repressor activity. Opi1p mediates its negative regulatory activity through the UAS_{INO} element, but not by direct interaction. Instead, *in vitro* data indicate that Opi1p interacts with DNA-bound Ino2p within the leucine zipper domain of Opi1p. In addition, the global repressor Sin3p interacts with the N-terminal region of Opi1p. Studies using mutant alleles of *INO2*, *INO4*, *OPI1*, and *SIN3* support a model whereby these interactions play a role in the expression of UAS_{INO}-containing genes *in vivo*.

In addition to inositol, the transcription of the UAS_{INO}-containing genes is also regulated by growth phase. Cells entering stationary phase reveal the repression of the *INO1* gene expression even in the absence of inositol from the growth media. The stationary phase repression of *INO1* transcription is also controlled by Opi1p. Deletion of the *OPI1* gene results in the derepression of *INO1* transcription in stationary phase.

Some enzymes in phospholipid synthesis are regulated in an opposite fashion: they are up-regulated by inositol and derepressed in stationary phase. For example, inositol supplementation results in an increase in the level of DGPP phosphatase (encoded by *DPP1*) activity in both exponential and stationary phase cells. The activity is greater in stationary phase cells when compared with exponential phase cells, and the inositol- and growth phase-dependent regulation of DGPP phosphatase are additive. Analyses of DGPP phosphatase mRNA and protein levels indicate that transcriptional regulation is responsible for the control of the enzyme activity. This regulation is not mediated through a UAS_{INO} element, as the element does not exist in the *DPP1* promoter.

Biochemical Regulation

Alterations in phospholipid synthesis in response to environmental changes are also regulated by biochemical mechanisms. In addition to its role in regulating enzyme expression, inositol regulates the activity of phospholipid biosynthetic enzymes. Inositol inhibits PS synthase activity as a noncompetitive inhibitor, and regulates PI synthase activity through substrate availability. Since both enzymes share the common substrate CDP–DAG, inositol-mediated regulation of PS synthase activity contributes to the synthesis of PI at the expense of PS.

Phosphorylation is a mechanism by which an enzyme activity may be regulated, and indeed several phospholipid biosynthetic enzymes are phosphorylated. For example, the CTP synthetase, choline kinase, and PA phosphatase enzymes are phosphorylated and activated by protein kinase A, whereas the phosphorylation of PS synthase by protein kinase A results in the inhibition of activity. These phosphorylation reactions favor the synthesis of PC via the CDP–choline pathway.

Lipids regulate some phospholipid biosynthetic enzymes. For example, PS synthase activity is stimulated by PA and inhibited by CL and DAG. The PA phosphatase enzyme is stimulated by CL, CDP–DAG, PI, and DGPP. PS synthase and PA phosphatase are also inhibited by the sphingoid bases phytosphingosine and sphinganine.

Nucleotides regulate the activity of some phospholipid biosynthetic enzymes. For example, choline kinase is subject to allosteric regulation by its substrate ATP and its product ADP. ATP promotes the oligomerization of choline kinase, whereas ADP inhibits its activity by affecting the catalytic properties of the enzyme and the apparent affinity of the enzyme for substrates ATP and choline. CTP inhibits PS synthase activity by chelating its cofactor manganese ions. CTP synthetase is regulated by CTP product inhibition. The CTP-mediated inhibition of CTP synthetase activity increases the positive cooperativity of the enzyme for UTP. CTP synthetase with a mutation at Glu^{161} is less sensitive to CTP product inhibition, and cells carrying the mutant CTP synthetase accumulate elevated levels of CTP.

Because CTP inhibits PS synthase activity, the higher levels of CTP result in an increase in the utilization of the CDP–choline pathway at the expense of the CDP–DAG pathway.

In this article, we have only scratched the surface in discussing the complex mechanisms that govern the synthesis of membrane phospholipids. Moreover, once phospholipids are synthesized, they must be transported to the various organelles in the cell. These processes are complex, and in some cases, they regulate phospholipid synthesis. The availability of sequence information of the yeast genome continues to facilitate studies on the molecular genetic and biochemical mechanisms that regulate phospholipid synthesis.

See Also the Following Articles

Inositol Lipid 3-Phosphatases • Inositol Phosphate Kinases and Phosphatases • Lipid Bilayer Structure • Phosphatidylinositol Bisphosphate and Trisphosphate • Phosphatidylinositol-3-Phosphate • Phosphoinositide 3-Kinase • Phosphoinositide 4- and 5-Kinases and Phosphatases • Phosphoinositide-Dependent Protein Kinases • Phospholipase D

Glossary

biochemical regulation Process of controlling the activity of enzymes.

genetic regulation Process of controlling the expression of genes.

phospholipid A lipid molecule that contains two fatty acyl chains that are esterified to the *sn*-1 and *sn*-2 positions of a glycerol phosphate backbone. Different phospholipid molecules (e.g., PC, PE, etc.) are distinguished by the water-soluble head group (e.g., choline, ethanolamine, etc.) that is attached to the phosphate moiety of the molecule.

Saccharomyces cerevisiae A species of yeast that is commonly used in genetic and biochemical research. It serves as an excellent model eukaryotic organism because it is easily cultured and genetically manipulated.

Further Reading

Carman, G. M., and Henry, S. A. (1999). Phospholipid biosynthesis in the yeast *Saccharomyces cerevisiae* and interrelationship with other metabolic processes. *Prog. Lipid Res.* **38**, 361–399.

Daum, G., Lees, N. D., Bard, M., and Dickson, R. (1998). Biochemistry, cell biology and molecular biology of lipids of *Saccharomyces cerevisiae*. *Yeast* **14**, 1471–1510.

Greenberg, M. L., and Lopes, J. M. (1996). Genetic regulation of phospholipid biosynthesis in *Saccharomyces cerevisiae*. *Microbiol. Rev.* **60**, 1–20.

Henry, S. A., and Patton-Vogt, J. L. (1998). Genetic regulation of phospholipid metabolism: Yeast as a model eukaryote. *Prog. Nucleic Acid Res.* **61**, 133–179.

Wu, W.-I., and Voelker, D. R. (2002). Biochemistry and genetics of interorganelle aminoglycerophospholipid transport. *Semin. Cell Dev. Biol.* **13**, 185–195.

Biography

Gil-Soo Han is a Postdoctoral Associate in the Department of Food Science at Rutgers University. Dr. Han received B.S. and M.S. degrees from Sogang University in Korea, and a Ph.D. from Rutgers University. His research concerns the genetic and biochemical regulation of phospholipid biosynthetic enzymes in yeast.

George M. Carman is a Professor of Food Science at Rutgers University. He received a B.A. degree from William Paterson College, an M.S. degree from Seton Hall University, and a Ph.D. from the University of Massachusetts. His postdoctoral training was at the University of Texas Medical School in Houston. Dr. Carman's laboratory is recognized internationally for its work on the biochemical and molecular characterization of phospholipid metabolism in yeast. Dr. Carman is a Fellow of the American Academy of Microbiology.

Photoreceptors

King-Wai Yau
Johns Hopkins University School of Medicine, Baltimore, Maryland, USA

Photoreceptors are cells that can detect light by virtue of a light-absorbing pigment they contain. In most cases, photoreceptors are neurons in the nervous system, and they signal light to the organism for behavioral changes. In some cases, however, photoreceptors are simply modified epithelial cells, such as melanophores in lower animals that can change color by virtue of aggregation or dispersion of intracellular pigmented granules in response to illumination. In humans, all photoreceptors known to date are present in the retina of the eyes. In lower vertebrates such as birds and fish, photoreceptors are also present in the pineal gland and elsewhere in the brain (deep-brain photoreceptors). In some lizards and frogs, photoreceptors are present in the parietal eye (also called the third eye or the frontal organ). In invertebrates, photoreceptors are present in diverse locations either singly or in small or large clusters to form well- or ill-defined eyes. In this article, the discussion is confined to vertebrate photoreceptors in the nervous system.

Retinal Photoreceptors

The well-known retinal photoreceptors in all vertebrates are the rods and cones. Rods are extremely sensitive to light, being able to detect and signal the absorption of a single photon; they are responsible for dim-light vision. Cones are much less sensitive to light, and they also adapt to steady light much more effectively than rods; they are responsible for bright-light vision. In most animals, including humans, rods are predominant in the retina. In occasional diurnal species (such as ground squirrel), however, cones are very abundant.

Rods

In mammals, all rods in a retina are identical. Morphologically, they can be distinguished into the outer segment, the inner segment, the cell body, and the synaptic terminal (Figure 1).

Outer Segment

The outer segment is a modified cilium that has become a highly expanded structure, with hundreds of internalized membrane disks stacked on top of each other and oriented transverse to the longitudinal axis of the cell. The membrane disks are chock-full of the rod visual pigment, rhodopsin, a transmembrane protein. Rhodopsin consists of rod opsin, the apoprotein, covalently linked to the chromophore, 11-*cis*-retinaldehyde (a derivative of vitamin A). In the mammalian retina, there is a single class of rods, all with the same opsin. The wavelength of maximum absorption (λ_{max}) of rhodopsin is near 500 nm (blue-green monochromatic light).

Inner Segment

The inner segment contains much of the metabolic machinery of the cell, and gives rise to the outer segment. The part of the inner segment adjacent to the outer segment is packed with mitochondria, reflecting the heavy metabolic load on the cell.

Cell Body

The cell body contains primarily the nucleus of the cell.

Synaptic Terminal

The synaptic terminal contacts second-order retinal neurons, including the bipolar and horizontal cells. It releases glutamate as the neurotransmitter. The synapse has a ribbon structure that is typical of most sensory neurons.

Cones

In humans, there are three types of cones, each with a different cone opsin covalently linked to 11-*cis*-retinaldehyde. The three cone pigments have λ_{max} at ~430 nm (blue), 530 nm (green), and 560 nm (yellow), respectively. The functional interactions between the three cone types allow us to perceive colors. The morphology of cones is very similar to that of rods, except that the membrane disks in the outer segment are continuous with the plasma membrane.

Phototransduction

The process by which light triggers an electrical response (the signal that neurons use to communicate with each

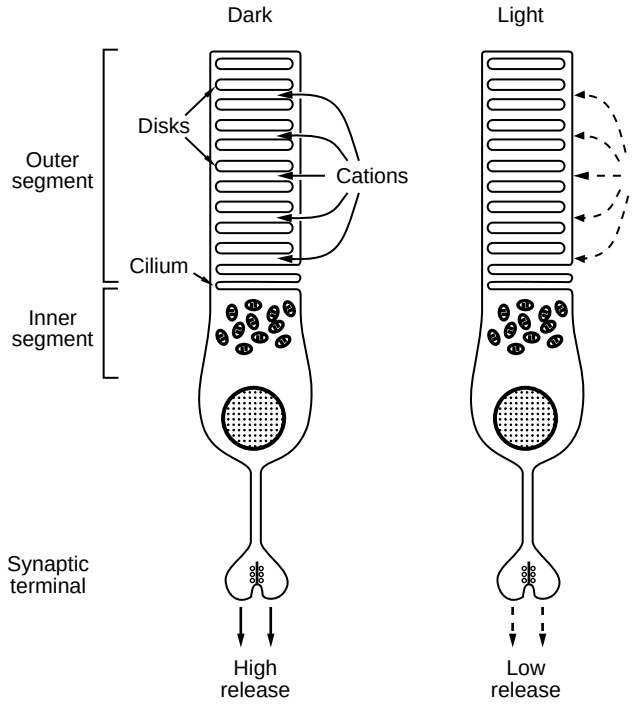

FIGURE 1 Diagram to show the overall morphology of a retinal rod photoreceptor and its response to light. See Figure 2 for the phototransduction mechanism underlying the response. Reproduced from Yau K.-W. (1994). Phototransduction mechanism in retinal rods and cones. The Friendenwald Lecture. *Invest. Ophthalmol. Vis. Sci.* **35**, 10–32, with permission through Copyright Clearance Center, Inc.

other) in rods and cones is called phototransduction. It is similar in both photoreceptor classes, and is now very well understood (Figure 2). There are nonselective cation channels on the plasma membrane of the outer segment that open (i.e., conduct ions) upon binding intracellular cGMP (cGMP-gated channels). In darkness, the free cGMP concentration in the outer segment is relatively high, thus keeping some of these cGMP-gated channels open. These open channels depolarize the cell and sustain a continuous release of glutamate from the synaptic terminal. Upon absorbing a photon, the 11-*cis*-retinaldehyde in a visual pigment molecule isomerizes to all-*trans*-retinaldehyde, as a result of which the opsin moiety undergoes several extremely rapid conformational changes, one of which (meta-II state) is catalytically active. It activates a G protein called transducin, which in turn stimulates a cGMP-phosphodiesterase to hydrolyze cGMP. As a result, the free cGMP concentration decreases, and the cGMP-gated channels close, producing a membrane hyperpolarization that reduces or completely stops neurotransmitter release from the synapse. This signal is picked up by the second-order retinal neurons. The inward, depolarizing membrane current through the open cGMP-gated channels in darkness in part involves Ca^{2+} (the rest is mostly Na^{+}), which is steadily pumped out of the cell by an antiporter involving exchange of external Na^{+} for internal Ca^{2+} and K^{+}. The dark Ca^{2+} influx decreases or stops in the light because the cGMP-gated channels close, but the Ca^{2+} efflux through the Na/Ca,K exchange continues, as a

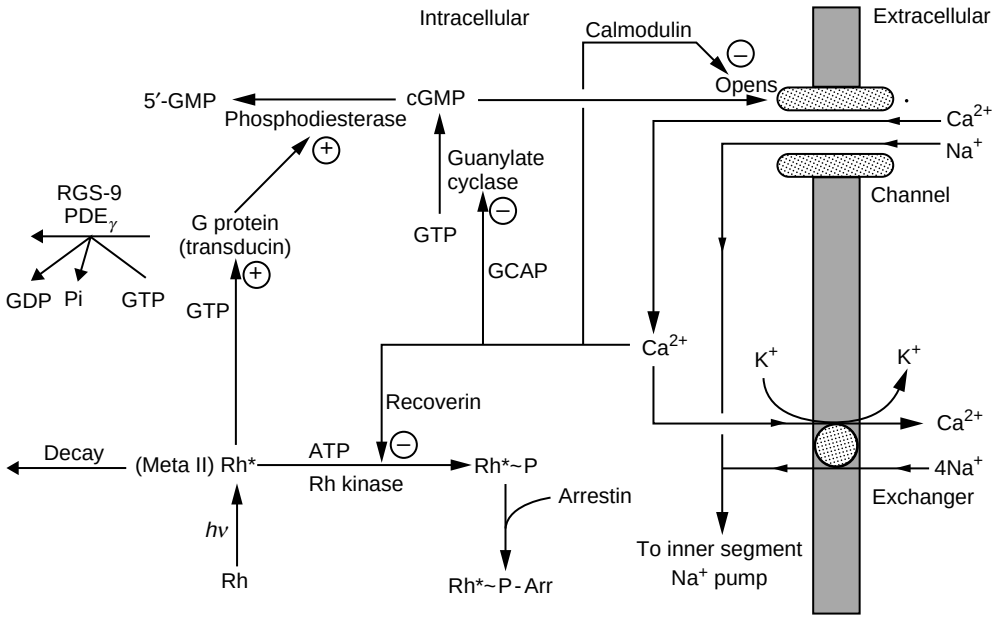

FIGURE 2 Phototransduction mechanism underlying the light response in rods. GCAP, guanylate-cyclase-activating protein; *hν*, photon; Rh, rhodopsin; Rh*, photoactivated rhodopsin; Rh* ~ P, phosphorylated form of rhodopsin; RGS-9, regulator of G protein-signaling isoform 9; PDE_{γ}, inhibitory (γ) subunit of the phosphodiesterase; +, stimulation or positive modulation; −, inhibition or negative modulation. Modified from Koutalos, Y., and Yau, K.-W. (1996). Regulation of light sensitivity in retinal rods. *Trends Neurosci.* **19**, 73–81, with permission from Elsevier.

result of which the free Ca^{2+} in the outer segment decreases. This Ca^{2+} decrease triggers negative feedback on multiple targets in the phototransduction machinery, leading to an attenuation of the initial cGMP decrease induced by light, and hence reopening of some of the cGMP-gated channels. This negative feedback constitutes the key mechanism for light adaptation by the photoreceptor, and is particularly important for cones because they function in bright light. The active, meta-II state of the pigment is deactivated by phosphorylation followed by binding of a protein called arrestin, which caps the pigment activity. After a delay, the meta-II decays into the inactive meta-III state and eventually splits into apo-opsin and all-*trans*-retinaldehyde (i.e, the pigment is bleached). The latter is reduced to all-*trans*-retinol (i.e., the corresponding alcohol), then leaves the photoreceptor to the neighboring retinal pigment epithelial cells, where all-*trans*-retinol is reisomerized/reoxidized to 11-*cis*-retinaldehyde. The 11-*cis*-retinaldehyde returns to the rod and cone outer segments, where it recombines with opsin to form a functional pigment molecule again.

Retinal Nonrod / Noncone Photoreceptors

Very recently, a different class of retinal photoreceptors has been discovered. These are a small subset of retinal ganglion cells, third-order retinal neurons that send light signals to the brain via their axons (optic-nerve fibers). The activity of the great majority of retinal ganglion cells is synaptically driven by the second-order retinal neurons, which in turn receive inputs from rods and cones. About 1% of the ganglion cells, however, are also intrinsically photosensitive. They express an opsin-like protein, melanopsin, which may or may not be the photopigment that makes these cells photosensitive (Figure 3). Light depolarizes these cells, leading to the firing of action potentials. The phototransduction mechanism underlying this depolarizing response is still unknown. While most retinal ganglion cells convey light information for image-forming vision, such as used in the detection and recognition of objects, the intrinsically photosensitive ganglion cells convey light information for nonimage-forming (accessory) visual functions, such as circadian photoentrainment and the pupillary light reflex. Accordingly, their axons project primarily to brain nuclei involved in these functions.

Parietal-Eye Photoreceptor

The parietal-eye photoreceptor bears remarkable morphological similarity to rods and cones (especially cones).

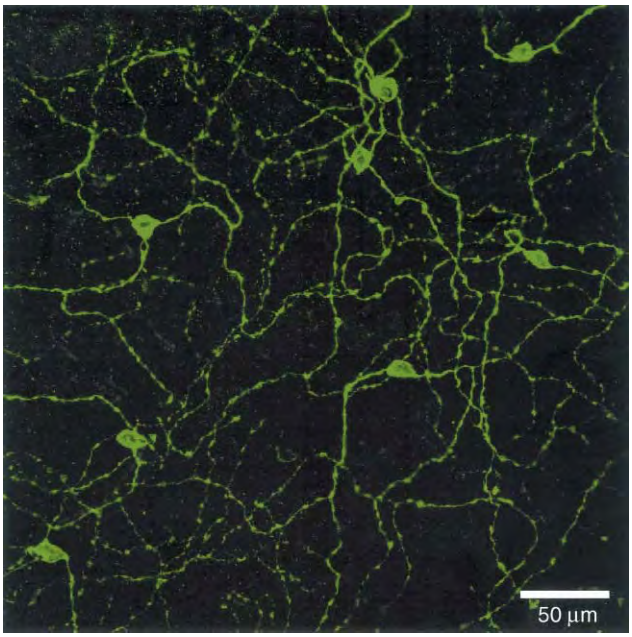

FIGURE 3 Immunofluorescent labeling of a flat-mounted rat retina with an antimelanopsin antibody. Green color shows the labeling. Stacked confocal images. (Reproduced from Hattar, S., Liao, H.-W., Takao, M., Berson, D. M., and Yau, K.-W. (2002). Melanopsin-containing retinal ganglion cells: Architecture, projections and intrinsic photosensitivity. *Science* **295**, 1065–1070, with permission.)

However, there are several interesting differences between them and rods and cones. First, even in isolation, the parietal-eye photoreceptor continues to respond to light after intense illumination, suggesting that there is a chromophore-recycling system within the cell that allows autonomous pigment regeneration. Second, there appear to be two pigments in the same cell, optimally responding to blue and green light, respectively. The green pigment when active depolarizes the cell, whereas the blue pigment when active hyperpolarizes the cell. The phototransduction mechanism is very similar to that in rods and cones, except that, although the blue pigment activates a cGMP-phosphodiesterase, the green pigment inhibits it. Thus, there is a chromatic antagonism in a given cell. Depending on the relative intensities of green and blue light, the cGMP level rises or falls, causing the cGMP-gated channels to open or close, hence a depolarization or hyperpolarization. The exact function of the parietal eye is unclear, but may also have to do with circadian photoentrainment.

Pineal Photoreceptors

In birds and fish, the pineal gland is photosensitive. Morphologically, the pineal photoreceptors roughly resemble rods and cones. Light elicits a hyperpolarizing response from these cells, with an underlying

transduction mechanism also similar to that in rods and cones.

Deep-Brain Photoreceptors

At least in birds, there is evidence that certain cells in the brain are intrinsically photosensitive. Also, immunocytochemistry and *in situ* hybridization studies suggest that opsin proteins are present in small populations/ clusters of neurons in the diencephalon. No other details are known at present.

See Also the Following Articles

G Protein-Coupled Receptor Kinases and Arrestins • The The Neuronal Calcium Signal in Activity-Dependent Transcription

Glossary

circadian photoentrainment The shifting of the (endogenous) circadian clock by light so that it is synchronized with the ambient light–dark cycle.

depolarization Phenomenon in which the electrical potential inside the cell relative to outside becomes more positive compared to the resting state.

hyperpolarization The electrical potential inside the cell relative to outside becomes more negative compared to the resting state.

nonselective-cation channel An ion channel that allows only cations (largely Na^+, K^+, and Ca^{2+}) to go through but does not discriminate much between them.

phototransduction The cellular mechanism that transduces light into an electrical signal in the photoreceptor.

Further Reading

Baylor, D. A. (1987). Photoreceptor signals and vision. The Proctor Lecture. *Invest. Ophthalmol. Vis. Sci.* **28**, 34–49.

Hattar, S., Liao, H.-W., Takao, M., Berson, D. M., and Yau, K.-W. (2002). Melanopsin-containing retinal ganglion cells: Architecture, projections and intrinsic photosensitivity. *Science* **295**, 1065–1070.

Koutalos, Y., and Yau, K.-W. (1996). Regulation of light sensitivity in retinal rods. *Trends Neurosci.* **19**, 73–81.

Vigh, B., Manzano, M. J., Zadori, A., Frank, C. L., Lukats, A., Rohlich, P., Szel, A., and David, C. (2002). Nonvisual photoreceptors of the deep brain, pineal organs and retina. *Histol. Histopathol.* **17**, 555–590.

Xiong, W. H., Solessio, E. C., and Yau, K.-W. (1998). An unusual cGMP pathway underlying depolarizing light response of the vertebrate parietal-eye photoreceptor. *Nat. Neurosci.* **1**, 359–365.

Yau, K.-W. (1994). Phototransduction mechanism in retinal rods and cones. The Friedenwald Lecture. *Invest. Ophthalmol. Vis. Sci.* **35**, 10–32.

Biography

King-Wai Yau is a Professor of Neuroscience Johns Hopkins University School of Medicine. His principal interest is in phototransduction in the retina and olfactory transduction in the nose. He received an A.B. (Physics) from Princeton and a Ph.D. (Neurobiology) from Harvard. He is a Fellow of the American Academy of Arts and Sciences.

Photosynthesis

Richard C. Leegood
University of Sheffield, Sheffield, UK

Photosynthesis involves the capture of the Sun's energy into biochemical energy that sustains all life on Earth. It is a massive process that has radically changed the composition of the atmosphere. Its scale can be judged from the fact that man's entire fossil fuel use from 1860 to 1988 was equivalent to only two years' global photosynthesis. Although photosynthesis occurs in a wide range of organisms (bacteria, cyanobacteria, algae, and plants), and about a third of it occurs in the oceans, the present discussion will concentrate on plants.

Photosynthetic Structures

Leaves contain many different types of cell, including stomata, which regulate gas exchange through the epidermis, and the photosynthetic palisade and mesophyll cells, which are thin-walled and have abundant air spaces for the diffusion of gases. Chloroplasts are the organelles which carry out photosynthesis within these cells. The chloroplast has a double-membrane envelope, which regulates transport of metabolites and proteins with the cytosol. It contains thylakoids, a system of membranes, which contain the components of photosynthetic light harvesting (including chlorophyll), electron transport, and ATP synthesis. The thylakoids form sacs with an internal lumen. Thylakoid sacs can occur singly or in stacks, called grana, which resemble a pile of coins. The soluble phase of the chloroplast is the stroma, which contains enzymes of a wide range of biosynthetic processes (Figure 1).

Harvesting Light

Light Harvesting

The first step in photosynthesis is light absorption by pigments. Besides various types of chlorophyll, these pigments include carotenoids, and open-chain tetrapyrrole bilin pigments found in, for example, cyanobacteria. Chlorophyll is a pigment based on a tetrapyrrole ring, rather like hemoglobin, except that it contains magnesium rather than iron. The ring is linked to a long side chain. Chlorophyll absorbs blue and red light, while it transmits the green, and hence appears green. In plants, two types of chlorophyll, *a* and *b*, increase the range of wavelengths absorbed. The light energy absorbed by chlorophyll molecules can either be lost as heat or fluorescence, or it can be transferred between adjacent chlorophyll molecules by resonance transfer. Chlorophyll and carotenoids associate with proteins in light-harvesting complexes. The light-harvesting complexes are doughnut shaped in bacteria, probably surrounding the reaction center. A light-harvesting complex acts like an antenna, similar to a satellite dish, feeding photons into the reaction centers, which contain a dimeric form of chlorophyll, where charge separation occurs. The concept of an antenna arose from the discovery in 1932, by Emerson and Arnold, that only one CO_2 molecule was produced from ~2500 chlorophyll molecules after a short flash of light.

At a higher level of organization, the leaf and its cells are also adapted to harvest light efficiently. In shade, the photosynthetic apparatus is spread out in large thin leaves, to increase the area of light capture and to allow light to penetrate adequately, and there is more light-harvesting chlorophyll per antenna. Within the leaf, epidermal cells can act to focus light, elongated palisade cells act as light guides, while mesophyll cells reflect light, acting like a "hall of mirrors" and increasing the distance that photons travel, thereby increasing the chance that they will hit an antenna complex.

Energy Capture

Reaction centers are multisubunit protein complexes situated in the photosynthetic membrane. These complexes contain the reaction center chlorophylls as well as other components involved in electron transfer. The reaction center is the core of the photosynthetic process, converting the energy of sunlight into a usable chemical form. Reaction centers carry out light-driven electron transfer reactions that result in charge separation across the photosynthetic membrane. Rapid electron transfer to secondary acceptors is necessary to prevent recombination of these separated charges. There are two classes of reaction center with different terminal electron acceptors: those with Fe_4S_4 clusters (type 1) and those

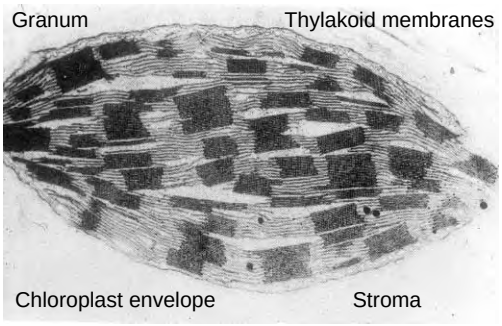

FIGURE 1 Electron micrograph of a chloroplast from maize.

with pheophytin/quinones (type 2). In plants, green algae and cyanobacteria, both reaction centers are present (in photosystems 1 and 2 respectively), while photosynthetic bacteria have only one type of reaction center (e.g., type 1 in green sulfur bacteria, type 2 in purple bacteria). In plants, photosystem 2 contains a chlorophyll dimer which, when in the excited state ($P680^*$), is an extremely strong reducing agent. An acceptor molecule, a quinone, Q, becomes reduced, leaving the positively charged chlorophyll dimer ($P680^+$). This is an extremely strong oxidant, so strong that it can extract electrons from water.

Water Oxidation

Water oxidation is a unique feature of photosystem 2. Water is the electron donor for photosynthetic electron transport. Each photon absorbed by P680 enables it to extract one electron from a manganese-containing enzyme, in an oxygen-evolving complex. Once four electrons have been extracted, this complex can, in turn, oxidize water, releasing O_2 to the atmosphere, as well as releasing $4H^+$ to the thylakoid lumen. Photosynthetic bacteria utilize other sources, such as H_2S or organic compounds, as electron donors.

Energy Dissipation and Repair

In addition to acting as accessory pigments in the antenna, carotenoids also have a photoprotective function. When there is an excess of light energy (e.g., when CO_2 uptake is limited by stomatal closure brought about by water stress), carotenoids can quench the excited triplet state of chlorophyll before it reacts with oxygen, forming destructive singlet state oxygen. Carotenoids can also regulate energy flow in the antenna by dissipating excitation of the chlorophylls as heat (nonphotochemical chlorophyll fluorescence quenching). Energy dissipation is associated with the accumulation of the carotenoid, zeaxanthin, which is interconverted with another carotenoid, violaxanthin, in the xanthophyll cycle. Physical changes, such as chloroplast movements within cells and heliotropic leaf movements, can also reduce or enhance light absorption, and photorespiration can dissipate excess photosynthetic energy. Photosystem 2 itself is very prone to photodamage, with one of its components, the D1 protein, undergoing constant turnover. The photosystem 2 complex is continuously disassembled and reassembled to insert repaired D1.

Electron Transport and ATP Synthesis

There are two photosystems, 1 and 2, involved in photosynthesis in plants, algae, and cyanobacteria. The structures of both have been determined. In 1960, Hill and Bendall published the "Z" scheme, which describes how the two photosystems and the electron carriers are organized with respect to their redox potentials (Figure 2). Electrons from photosystem 2 reduce a number of intermediate electron carriers, such as plastoquinone (PQ), the cytochrome *b/f* complex (including the Rieske iron-sulfur center) and plastocyanin (PC). The reaction center of photosystem 1 (P700) receives its electrons from photosystem II via these carriers and thus oxidizes Q. Photosystem 1 reduces an initial acceptor, A_o, then a series of Fe–S acceptors and ferredoxin (Fd, another iron–sulfur protein) and, finally, NADP is reduced to NADPH. Electrons may also cycle around photosystem 1, leading to ATP generation, as also occurs in some photosynthetic bacteria.

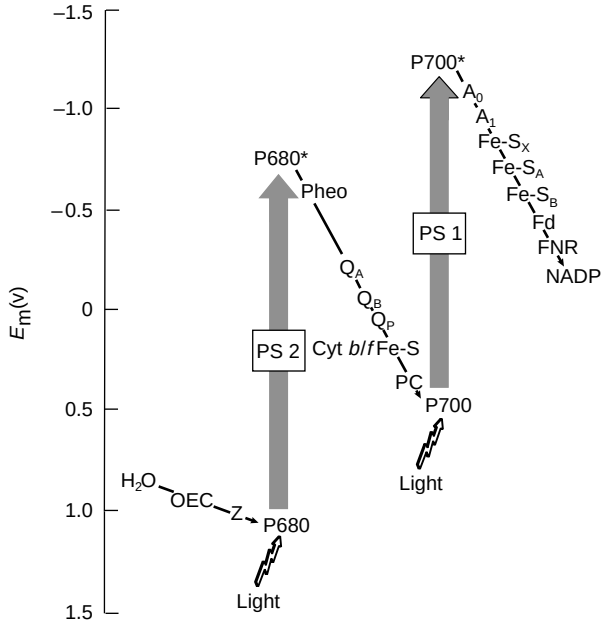

FIGURE 2 The Z-scheme of photosynthetic electron transport, showing the mid-point redox potentials of electron donors, acceptors, and carriers.

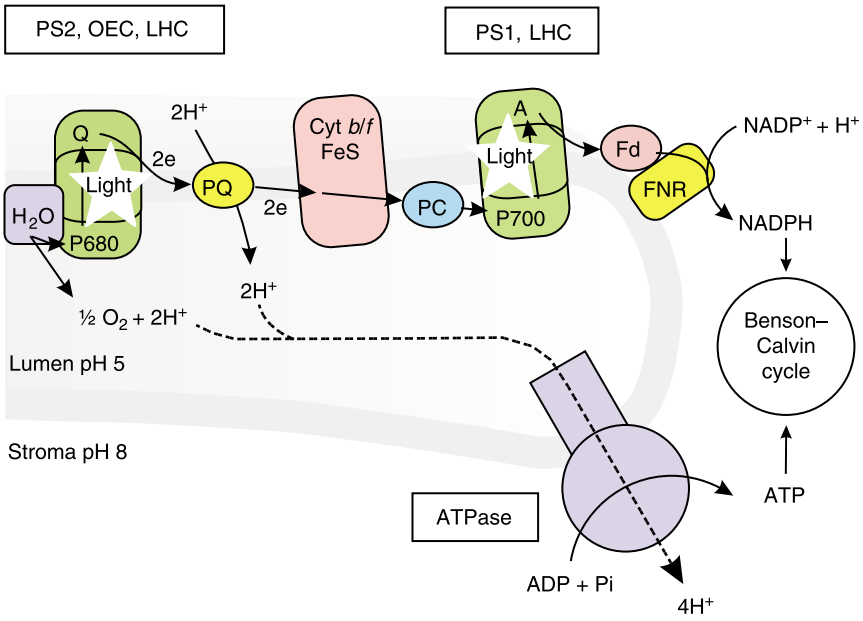

FIGURE 3 Organization of photosynthetic electron transport within the thylakoid membrane, showing how proton production and translocation generates a proton gradient between the thylakoid lumen and the stroma.

Electron transport components are organized within the thylakoid membrane so that, as electrons flow from water to NADP, protons are transferred from the stroma to the thylakoid lumen (Figure 3). This is possible because the key component linking the two photosystems is PQ which is a hydrogen carrier, carrying both an electron (e) and a proton (H^+). Electrons from photosystem II reducePQ, together with protons from the stroma, while oxidation of PQ releases electrons to the cytochome *b/f* complex and protons to the thylakoid lumen. This proton shuttle is driven by photosynthetic electron transport. Protons are also released to the thylakoid lumen when water is oxidized. These processes decrease the pH in the stroma (from pH 7 in the dark to pH 8 in the light) and acidifies the lumen (to ~pH 5). A pH gradient is therefore created which is used to drive ATP synthesis (chemiosmosis). For each molecule of ATP synthesized, $4H^+$ move from the lumen to the stroma. Movement of protons through the ATPase causes its central crankshaft-like core to rotate. This rotational movement causes conformational changes in the active sites of other subunits which result in the synthesis of ATP from ADP and Pi.

Carbon Fixation and Photorespiration

The chloroplast is one of the plant cell's most important factories. ATP and NADPH are utilized to drive biosynthetic processes in the chloroplasts, including the reduction of sulfate and nitrite and the synthesis of lipids and amino acids, in addition to CO_2 fixation.

Benson–Calvin Cycle

Although often termed the "dark reaction" of photosynthesis, CO_2 fixation can only proceed in the light, both because it requires photosynthetically-generated ATP and NADPH and because many of the enzymes which catalyze the process are themselves activated by light. The Benson–Calvin cycle (or Reductive Pentose Phosphate Pathway) is the only mechanism in plants and algae which can catalyze the net fixation of CO_2, although some bacteria have an alternative mechanism. The Benson–Calvin cycle (Figure 4) was discovered in the early 1950s by Melvin Calvin and co-workers, who supplied algae, such as *Chlorella*, with $^{14}CO_2$. The first product of photosynthesis, containing 100% of the radioactivity at zero time, was a three-carbon compound, glycerate 3-phosphate (hence the term C_3 plants). The primary acceptor was identified as ribulose 1,5-bisphosphate (RuBP). RuBP is a five-carbon sugar phosphate which is carboxylated to form two molecules of glycerate-3-P. The Benson–Calvin cycle comprises three phases: (1) carboxylation by ribulose 1,5-bisphosphate carboxylase-oxygenase (Rubisco); (2) reduction of glycerate-3-P to triose-P (which requires ATP and NADPH); and (3) regeneration of the acceptor, RuBP, from triose-P in a "sugar-phosphate shuffle," which requires ATP. Triose-P is a simple sugar phosphate produced by the Calvin cycle. Triose-P that is not

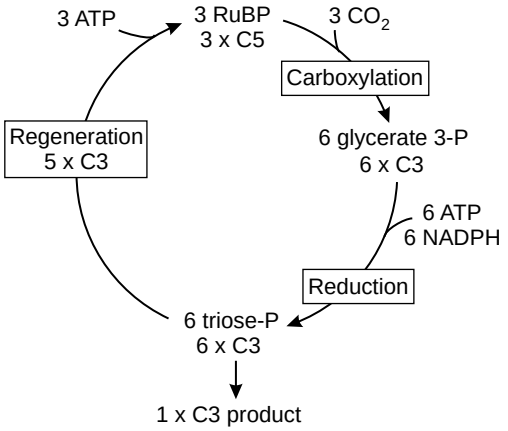

FIGURE 4 A simplified scheme for the Benson–Calvin cycle, showing the carboxylation of RuBP by Rubisco, reduction of glycerate 3-P to triose-P, and regeneration of the initial acceptor from triose-P.

needed for regeneration of RuBP can either be converted to starch in the chloroplast or it can be exported to the cytosol, via the phosphate translocator, to make sucrose.

Photorespiration

Rubisco is an inefficient enzyme. It has a slow catalytic turnover rate, and about half the soluble protein in leaves is Rubisco, making it the most abundant protein in nature.

$$\text{RuBP} + \text{O}_2 \xrightarrow{\text{RuBP oxygenase}} \text{glycerate-3-P} + \text{glycollate-2-P}$$

Rubisco also catalyzes a side-reaction with oxygen, an inevitable consequence of its reaction mechanism. Rubisco evolved in the photosynthetic bacteria in an atmosphere which was richer in CO_2 and depleted in O_2 by comparison with the present atmosphere. The ratio of oxygenation to carboxylation by Rubisco depends upon the relative concentrations of CO_2 and O_2 and oxygenation increases as the temperature increases. Photorespiration is the process by which two molecules of glycollate-2-P, which is not a metabolite of the Benson–Calvin cycle, are retrieved and converted into two molecules of an amino acid, glycine (C2), and then into one molecule of glycerate-3-P (C3). This involves shuttling of metabolites between the chloroplasts, cytosol, peroxisomes, and mitochondria. During this process, one quarter of the carbon in glycollate-2-P is lost as CO_2 and ammonia is liberated. Photorespiration is therefore a wasteful process because it both reduces carbon gain and dissipates photosynthetic energy (because CO_2 is fixed and released again). There is, therefore, a selection pressure on plants to reduce the rate of photorespiration by means of CO_2-concentrating mechanisms, so as to improve their carbon economy. This will be particularly strong when high rates of photorespiration are favored, as at high temperatures. However, a future doubling of ambient CO_2 will reduce photorespiration by ~50% and it would be completely eliminated by a 5-fold rise in atmospheric CO_2.

CO_2-Concentrating Mechanisms

C_4 Photosynthesis

C_4 plants include many tropical grasses and are among the world's most important crop species (maize, sugar cane). Although small in terms of total number of flowering plant species (3%), they constitute ~50% of the 10,000 grass species. Their productivity is high and C_4 grasses in savanna regions (15% of the Earth's vegetated surface) are responsible for ~20% of global photosynthesis. C_4 plants have a distinctive leaf anatomy (Kranz anatomy), with chlorophyll-containing mesophyll and bundle-sheath cells, which form a gas-tight cylinder surrounding the vascular bundle. A CO_2 pump (the C_4 cycle) takes CO_2 from the mesophyll and transfers it into the bundle-sheath, which contains Rubisco and the enzymes of the Benson–Calvin cycle (Figure 5). The process raises the concentration of CO_2 in the bundle-sheath, sufficient to saturate Rubisco with CO_2 and to eliminate photorespiration. Like all pumps, the C_4 cycle requires an input of energy in the form of ATP. Recently, two terrestrial plants have been shown to have single-celled C_4 photosynthesis.

The mechanism of photosynthesis in C_4 plants was elucidated in the 1960 s by Hatch and Slack in Australia. C_4 plants are so-called because the first product of CO_2

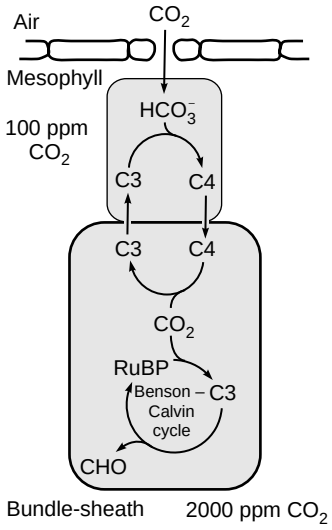

FIGURE 5 A simplified scheme for the mechanism of C_4 photosynthesis, showing how the C_4 cycle shuttles C_4 acids into to bundle-sheath, where they are decarboxylated to raise the CO_2 concentration in the vicinity of Rubisco and thereby suppress photorespiration.

fixation is a C4 organic acid, oxaloacetate, formed by the carboxylation of phosphoenolpyruvate (PEP) by PEP carboxylase. The oxaloacetate is converted to other C4 acids (malate or aspartate) and transferred to the bundle-sheath. Transport of metabolites between the mesophyll and bundle-sheath occurs by diffusion via plasmodesmata. In the bundle-sheath, the C4 acids are decarboxylated to generate CO_2, and a C3 compound returns to the mesophyll. The mechanism of decarboxylation differs, with NADP-malic enzyme in the chloroplast (maize), NAD-malic enzyme in the mitochondria (millet), or PEP carboxykinase in the cytosol (e.g., guinea grass).

C_4 plants are commonly found in warm-to-high temperature environments, such as tropical grasslands, where photorespiratory rates would be high in C_3 plants. C_4 plants have double the water-use efficiency of C_3 plants because photosynthesis can operate at low intercellular concentrations of CO_2, and hence lower stomatal conductances. Nitrogen-use efficiency is also improved because Rubisco is used more efficiently, due to the suppression of photorespiration.

Aquatic Photosynthesis

The aquatic environment poses serious problems for the acquisition of CO_2. First, the diffusion of CO_2 in water is 10 000 times slower than in air. Second, inorganic carbon is present in water as CO_2, HCO_3^- and CO_3^{2-}, the relative amounts of which depend upon the pH of the water. Most inorganic carbon in alkaline waters is therefore present as carbonate and bicarbonate. Photosynthesis by aquatic plants, algae, and phytoplankton may raise the local O_2 concentration and enhance photorespiration. Aquatic organisms (cyanobacteria, micro- and macro-algae, aquatic angiosperms) have developed means of taking up dissolved inorganic carbon (CO_2 and HCO_3^-) actively from their environment. They can concentrate it internally in Rubisco-containing structures, such as carboxysomes and pyrenoids, and thus suppress photorespiration.

Crassulacean Acid Metabolism

Leaves are faced with a difficult task. Leaf cells have thin walls and the intercellular spaces are saturated with water vapor. As leaves assimilate CO_2 (5 000 litres of air are needed to manufacture 1 g of sucrose), they need to restrict the amount of water lost from the leaf via the stomata. There is therefore a conflict between the requirements for CO_2 fixation and water conservation. Crassulacean acid metabolism (CAM) is a photosynthetic adaptation to periodic water supply, occurring in plants in arid regions (e.g., cacti) or in tropical epiphytes (e.g., orchids and bromeliads). CAM plants close their stomata during the day and take up CO_2 at night, when the air temperature is lower. Water loss can be lowered by an order of magnitude. CAM occurs in between 5% and 10% of plants and is always associated with succulence, at least at a cellular level.

Although the biochemistry is similar to that of C_4 plants, two carboxylations are now separated in time rather than in space. Malic acid is synthesized from carbohydrates, via PEP carboxylase, at night and is stored in the vacuole. During the day malate is decarboxylated, via PEP carboxykinase or NAD(P)-malic enzymes in the cytosol, CO_2 is refixed via the Benson–Clavin cycle, and carbohydrates are reformed. This process occurs behind closed stomata. The internal concentration of CO_2 is raised as high as 10 000 ppm, which also suppresses photorespiration. CAM plants show a high degree of metabolic flexibility. Seedlings and well-watered plants may show little or no CAM and perform C_3 photosynthesis, opening their stomata during the day. This allows increased carbon gain during periods of water availability or during seedling establishment. Water or salt stress can then induce CAM, switching on gene expression for synthesis of the component enzymes.

See Also the Following Articles

Chlorophylls and Carotenoids • Chloroplasts • Ferredoxin • Green Bacteria: The Light-Harvesting Chlorosome • Light-Harvesting Complex (LHC) I and II: Pigments and Proteins • Photosynthetic Carbon Dioxide Fixation • Photosystem I: F_X, F_A, and F_B Iron-Sulfur Clusters • Photosystem II Light Harvesting System: Dynamic Behavior • Photosystem II: Water Oxidation, Overview

Glossary

CO_2-concentrating mechanism A biochemical (in terrestrial plants) or biophysical pump (in many aquatic photosynthetic organisms), which concentrates CO_2 around Rubisco so as to reduce photorespiration.

photorespiration The wasteful process by which glycollate 2-phosphate, which results from the oxygenation reaction of Rubisco, is recycled to the Benson–Calvin cycle.

reaction center A multisubunit protein complex situated in the photosynthetic membrane. containing the reaction center chlorophylls as well as other components involved in electron transfer, which together convert the energy of sunlight into a usable chemical form.

Further Reading

Blankenship, R. E. (2002). *Molecular Mechanisms of Photosynthesis*. Blackwell Science, Oxford.

Capaldi, R. A., and Aggeler, R. (2002). Mechanism of the F_1F_0-type ATP synthase, a biological rotary motor. *Trends Biochem. Sci.* **27**, 154–160.

Chitnis, P. R. (2001). Photosystem I: Function and physiology. *Annu. Rev. Plant Physiol. Plant Mol. Biol.* **52**, 593–626.

Horton, P., Ruban, A. V., and Walters, R. G. (1996). Regulation of light-harvesting in green plants. *Annu. Rev. Plant Physiol. Plant Mol. Biol.* **47**, 655–684.

Kaplan, A., and Reinhold, L. (1999). CO_2 concentrating mechanisms in photosynthetic microrganisms. *Annu. Rev. Plant Physiol. Plant Mol. Biol.* **50**, 539–570.

Rutherford, A. W., and Faller, P. (2001). The heart of photosynthesis in glorious 3D. *Trends Biochem. Sci.* **26**, 341–344.

Sage, R. F., and Monson, R. K. (1999). *C_4 Plant Biology.* Academic Press, San Diego.

Spreitzer, R. J., and Salvucci, M. E. (2002). Rubisco: Structure, regulatory interactions, and possibilities for a better enzyme. *Annu. Rev. Plant Biol.* **53**, 469–475.

Walker, D. A. (1992). *Energy, Plants, and Man*. Oxygraphics, Brighton.

http://www.wkap.nl/prod/s/AIPH—All volumes in the series "Advances in Photosynthesis and Respiration" published by Kluwer Academic Publishers, Dordrecht.

Biography

Richard C. Leegood is a Professor of Plant Sciences in the Department of Animal and Plant Sciences and a member of the Robert Hill Institute for Photosynthesis Research at the University of Sheffield, U.K. His principal research interests are carbon and nitrogen metabolism and their regulation in plants. He holds a Ph.D. from the University of Cambridge. He has authored and edited several texts and many review articles in the field of photosynthesis and metabolism.

Photosynthetic Carbon Dioxide Fixation

Matthew J. Paul
Rothamsted Research, Harpenden, UK

Photosynthetic carbon dioxide fixation is the point of entry of carbon into organic molecules. Light provides the energy (ATP) and reducing power (NADPH) from electron flow in chloroplasts for CO_2 to be reduced to triose phosphate in reactions of the Calvin cycle. The cycle is the starting point for the synthesis of sugars, amino acids, and other plant products. Accompanying the provision of ATP and NADPH in light reactions of photosynthesis is the production of O_2. Thus, photosynthesis generates organic molecules that underpin all biology and agriculture and provides the necessary oxygen that also enables aerobic respiration to proceed for them to be metabolized in the growth and maintenance of all living things. In Earth's early history, photosynthesis enabled the evolution of complex multicellular life forms and continues till today to regulate the gas composition of the atmosphere and hence climate.

Light Provides Energy (ATP) and Reducing Power (NADPH) for CO_2 Fixation

Photons in the range 400–700 nm – except green light, which is reflected – drive photosynthesis through provision of ATP and NADPH. Light also regulates the Calvin cycle in other ways. Photons interact with electrons in chlorophylls of light-harvesting antenna in thylakoid membranes of chloroplasts. There are two light-absorbing photosystems that cooperate in the reduction of NADP by electrons derived from water. Energy is passed from these to reaction centers of photosystem II, where electrons are excited and passed to an acceptor and down an electron transport chain to photosystem I. Electrons and protons pass to NADP, yielding NADPH. The open reaction of photosystem II is filled with electrons from water, from which O_2 is evolved. A pH gradient across the thylakoid membrane from H^+ accumulation in the thylakoid lumen provides the impetus for ATP synthesis by ATP synthase (Figure 1).

The Path of Carbon in Photosynthesis

The sequence of reactions that fix CO_2 into triose phosphate using ATP and NADPH from these light reactions was determined using C14 radioisotopes by Melvin Calvin and colleagues, for which the Nobel prize for chemistry was awarded. This sequence of reactions is now known as the Calvin cycle, reductive pentose phosphate pathway, or photosynthetic carbon reduction cycle. It consists of three distinct phases. First, the fixation of CO_2 into 3-phosphoglyceric acid (3-PGA) (carboxylation). Second, the reduction of 3-PGA into the triose phosphate, glyceraldehyde-3-phosphate (GAP), which can be exported to the cytosol for sucrose synthesis or remain in the chloroplast for starch synthesis or the other biosynthetic reactions that occur there. Triose phosphate also has to remain in the cycle to allow regeneration of the CO_2 acceptor, ribulose 1,5-bisphosphate (RuBP), in the third, regenerative phase of the cycle (Figure 2).

Carboxylation Phase

Carboxylation is catalyzed by the Earth's most abundant protein, ribulose bisphosphate carboxylase/oxygenase (Rubisco), which can constitute up to 50% of the soluble protein in a leaf. The combination of CO_2 with RuBP, a five-carbon compound, yields two molecules of the three carbon compound 3-PGA. Many enzymes will bind molecules in addition to the ones they have primary affinity for, if they are present at high enough concentrations. Present-day atmospheric O_2 concentration is a thousand times higher than that of CO_2 and in ambient conditions oxygenation of RuBP also occurs. This produces phosphoglycolate which is metabolized in the glycolate pathway outside the chloroplast and returned to the Calvin cycle as 3-PGA in a process termed photorespiration because CO_2 is evolved in the process (Figure 1). Some plants have evolved a supplementary

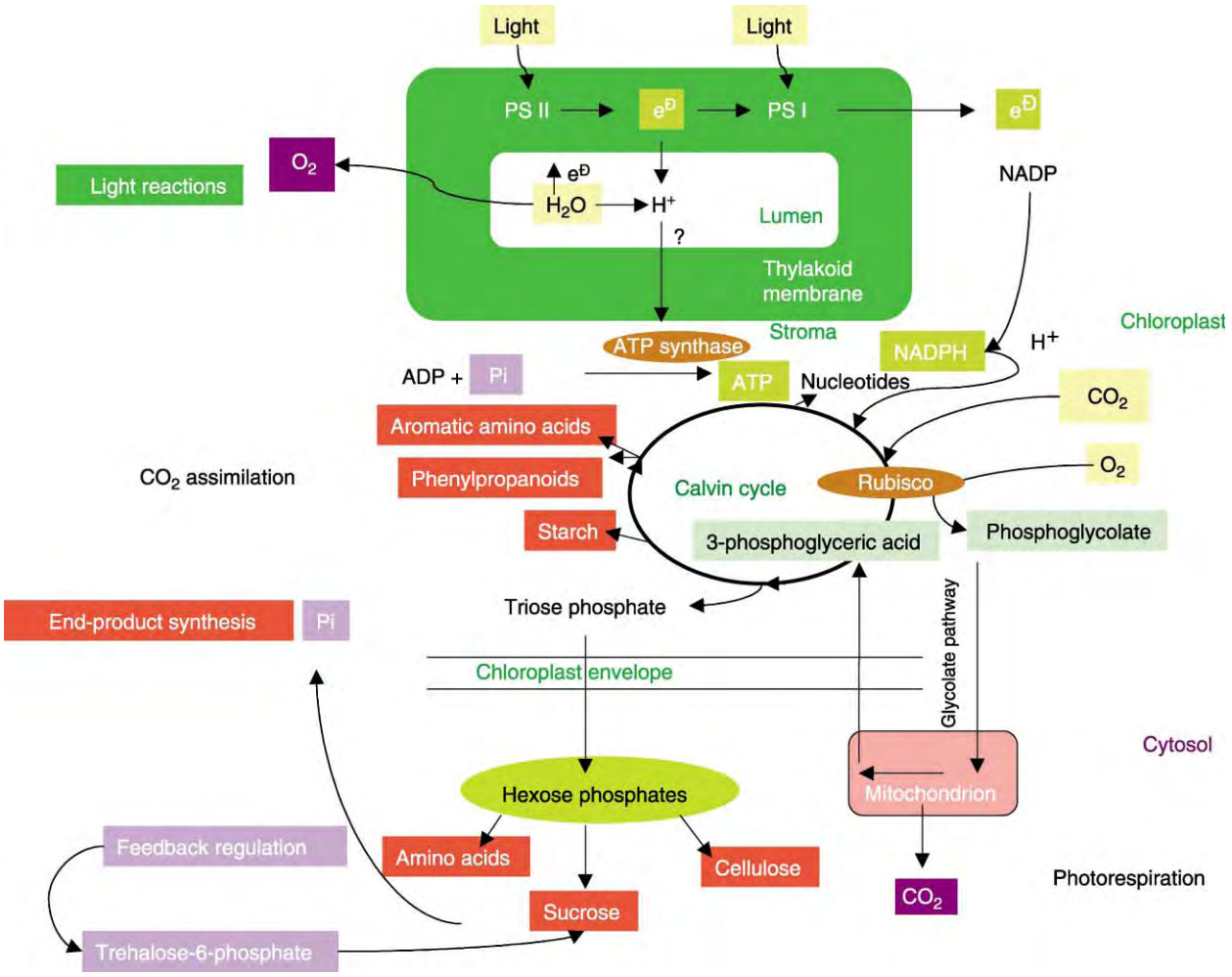

FIGURE 1 Schematic of photosynthetic metabolism summarizing the principal components of light reactions, CO_2 fixation into the Calvin cycle and the synthesis of end products.

carboxylation reaction catalyzed by phosphoenol pyruvate carboxylase where minimal oxygenation occurs. Such plants are known as C4 plants because the first products of CO_2 fixation are carboxylic acids containing four carbon atoms. A high concentration of CO_2 generated from the decarboxylation of these acids at the site of the Calvin cycle minimizes the oxygenation reaction of Rubisco and hence suppresses photorespiration. Other specialized plants known as Crassulacean acid metabolism (CAM) plants fix CO_2 into C4 acids at night. These metabolic adaptations of C4 and CAM ensure a high intercellular CO_2 concentration which maintains a small stomatal aperture, conserving water, an overriding selection force in some environments. In CAM plants stomata can be shut for much of the day and is observed in more extreme xerophytes such as cacti and succulents. C4 grasses are very common in Australia. More recent evolution has resulted in these adaptations rather than large modification of the properties of Rubisco to further favor carboxylation rather than oxygenation. Instead Rubisco has been the target of biotechnologists to improve photosynthesis. However, altering Rubisco properties more in favor of carboxylation has proved technically demanding and is being superseded by other strategies of enhancing photosynthesis.

Reduction Phase

The 3-PGA produced in the carboxylation phase (and returned from photorespiration) is reduced to triose phosphate, GAP, in two steps. The first, a phosphorylation step, requires ATP. The 1,3-bisphosphoglycerate formed is then reduced with NADPH to GAP. The high ATP and NADPH concentrations associated with photosynthesis shift these reactions in favor of triose phosphate.

Regeneration Phase

Triose phosphate is essentially the end product of photosynthesis as it is exported from the chloroplast.

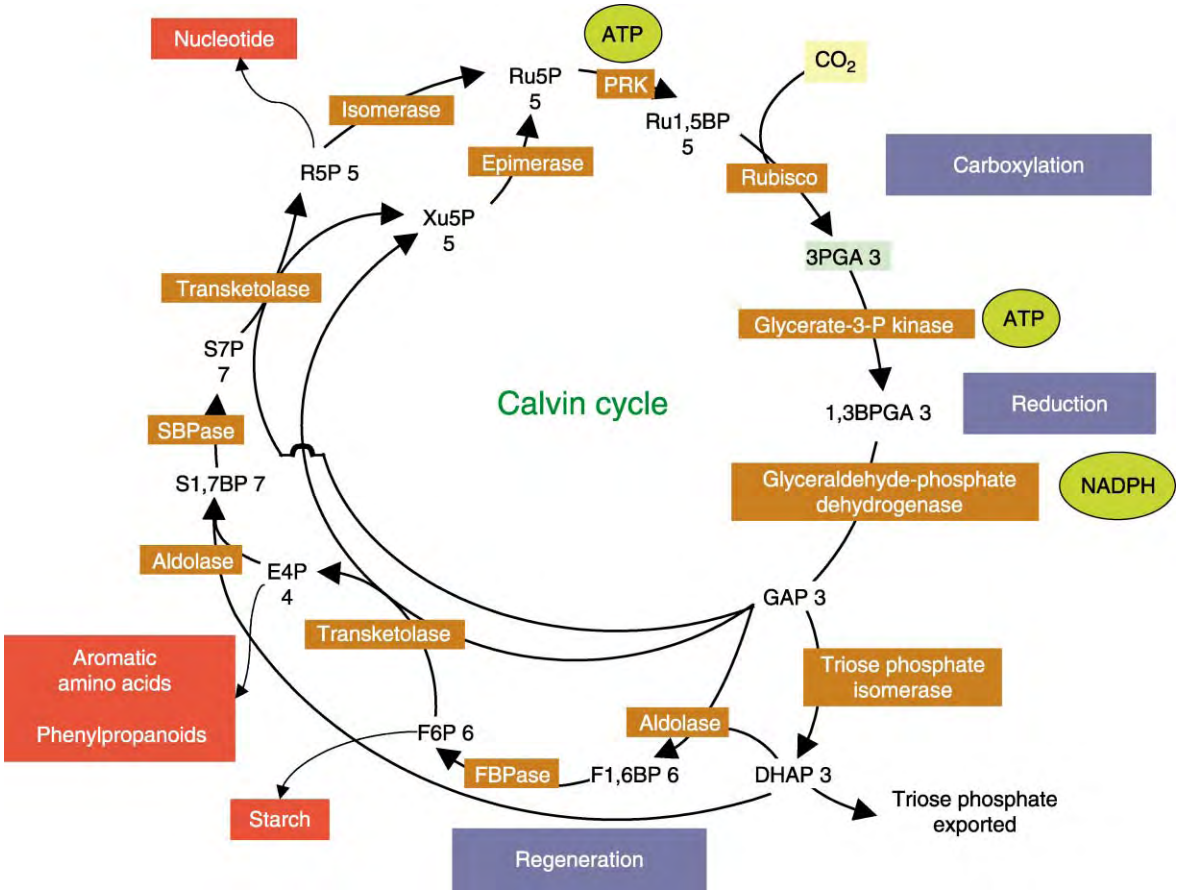

FIGURE 2 Calvin cycle of reactions that incorporate CO_2 into triose phosphate and which regenerate ribulose-1,5-bisphosphate (Ru1,5BP) for continued CO_2 fixation. Numbers after compounds indicate number of carbon atoms. 3-PGA, 3-phosphoglyceric acid; 1,3 BPGA, 1,3 bisphosphoglyceric acid; GAP, glyceraldehydes-3-phosphate; DHAP, dihydroacetone phosphate; F1,6BP, fructose-1,6-bisphosphate; F6P, fructose 6-phosphate; E4P, erythrose-4-phosphate; S1,7BP, sedoheptulose-1,7-bisphosphate; S7P, sedoheptulose-7-phosphate; R5P, ribose-5-phosphate; Ru5P, ribulose-5-phosphate; Xu5P, xylulose-5-phosphate. Enzymes are Rubisco, ribulose-1,5-bisphosphatase; FBPase, fructose-1,6-bisphosphatase; SBPase, sedoheptulose-1,7-bisphosphatase; PRK, phosphoribulokinase.

However, some must be retained in the cycle to resynthesize the acceptor molecule for CO_2 fixation, RuBP to keep the cycle going. In this series of reactions, five trioses are converted into three pentoses. The first part involves the conversion of GAP to fructose-6-phosphate (F6P). Then the carbon atoms in F6P, GAP, and dihydroxyacetone phosphate are rearranged into the pentose, ribulose-5-phosphate (Ru5P). In the final step Ru5P is converted to RuBP in an ATP-requiring step. Like the rest of the cycle this phase is highly regulated and can strongly affect the ultimate rate of CO_2 fixation. An important branch point in this segment of the cycle, catalyzed by transketolase links primary and secondary metabolism. The substrates and products of transketolase can supply carbon (erythrose-4-phosphate) for the synthesis of aromatic amino acids and phenylpropanoids (compounds important for flavor, texture, color), nucleotide synthesis (R5P), and starch (F6P) in addition to the regeneration of RuBP.

Regulation of the Calvin Cycle

Metabolic regulation enables the balance between substrate and product of enzyme-catalyzed reactions to be maintained so that ordered metabolic flow to sustain life can occur in response to developmental requirements and environmental constraints. The Calvin cycle is regulated by light which ensures its temporal separation and prevents competition with other reactions, such as the oxidative pentose phosphate pathway, also present in the chloroplast stroma. Light regulates the cycle through provision of ATP and NADPH, which regulate those steps dependent on them. Light also causes an increase in the pH of the chloroplast stroma to ~8, the pH optimum for Calvin cycle enzymes. Pumping of protons into the thylakoids is also coupled with flow of magnesium necessary for enzyme activity into the stroma. A further way that light regulates the cycle is through photosynthetic electron transport. Reducing equivalents from photosystem I via ferredoxin-thioredoxin reductase

reduce the thiol groups of GAP dehydrogenase (GAPDH), fructose-1,6-bisphosphatase (FBPase), sedoheptulose-1,7-bisphosphatase (SBPase) and phosphoribulokinase (PRK) increasing their activity. Rubisco is activated by CO_2 and magnesium in a process called carbamylation, a process promoted by an activating protein, Rubisco activase. Enzymes of the Calvin cycle are associated as enzyme complexes. For example GAPDH and PRK are linked by the protein CP12. The precise role of this association of such complexes is not yet known, but is likely to facilitate further regulation of metabolic flow.

Are Some Calvin Cycle Enzymes More Important in Regulating Carbon Flux than Others?

The equilibrium position of reactions catalyzed by Rubisco, SBPase, FBPase, and PRK as a consequence of their regulation lies very much in favor of the end-product. These enzymes are termed irreversible enzymes because of the large amount of energy that would be required to reverse the reaction. Such enzymes have traditionally been seen as key enzymes because of their importance in directing carbon flow. Since the early 1990s genetic modification has enabled individual enzymes to be targeted through use of antisense RNA to decrease the synthesis of target proteins. Lines of transgenic plants exhibiting progressive decreases in activity of an enzyme has enabled metabolic control analysis to be undertaken and flux control coefficients for individual enzymes assigned. For the Calvin cycle a change in enzyme activity can then be related to flux through the pathway by measuring CO_2 uptake by leaves using infra-red gas analysis. The flux control coefficient is given as $C = \delta J/J$, where J is original flux, and δJ is changed flux. This coefficient can also be written as $C = \delta E/E$, where E is original enzyme activity, and δE is changed enzyme activity.

So, if a 50% decrease in enzyme activity achieves a 25% decrease in CO_2 uptake then the flux control coefficient is 0.5 (25/50); essentially half the control of the pathway resides with that enzyme. If a 50% decrease achieves no change in flux then the flux control coefficient is zero and the enzyme is in excess under those conditions. Over the course of a day, and during the life cycle of a plant, an enzyme may exhibit a range of flux control coefficients. Variation during the course of a day will be caused largely by changes in illumination, whereas over the life cycle by nitrogen availability and changes in light environment. Both light and nitrogen affect the amount of enzyme synthesized and light affects enzyme activity to different extents for different enzymes, so relative contributions to flux control change. Other aspects of environment, for example temperature and phosphorus nutrition are also influential.

Calvin Cycle Enzymes that Most Limit Flux

The first enzyme for which detailed flux control analysis was conducted using transgenics was Rubisco. Quite surprisingly at the time, in view of the perceived importance of the enzyme, the first data showed that removing half of it with antisense resulted in little change in CO_2 fixation. However, when plants were grown at high light the flux control coefficient rose, and combined with low nitrogen, could reach 0.8. Rubisco is the enzyme that imposes the greatest potential limitation of Calvin cycle carbon fixation. SBPase is another enzyme with a potentially high flux control coefficient at high light. A major surprise was that nonregulated equilibrium enzymes, aldolase, and transketolase could have flux control coefficients around 0.3 under high light conditions. Other enzymes in the cycle when decreased up to 50% have showed no large impact on flux. The most extreme example of this is phosphoribulokinase, where a decrease up to 85% has no impact on CO_2 fixation.

The important message to come from this work is that both highly regulated and unregulated equilibrium enzymes could control flux. The work supported the von Caemmerer and Farquhar 1981 model, which proposed that photosynthesis was colimited between carboxylation (Rubisco activity) and the capacity to regenerate ribulose-1,5-bisphosphate. Control was seen as poised between carboxylation and regeneration, but under saturating light the balance would shift toward Rubisco and under low light toward regeneration. The research using antisense confirmed this assumption and gave useful indications as to which enzymes in the regeneration phase would be most likely to increase rates of CO_2 fixation if their activities could be increased. Thus, there would most likely be benefit if one or more of activities of SBPase, aldolase, or transketolase could be increased.

Genetic Modification of Photosynthesis to Improve Growth and Yield

Direct Targeting of Calvin Cycle

In support of the findings of flux control analysis, expression of a bifunctional SBPase/FBPase from a cyanobacterium resulted in increased photosynthesis and biomass production. This was the first report of an increase in activity of one or more Calvin cycle enzymes

benefiting photosynthesis and biomass production. There is also evidence that overexpressing the plant SBPase improves photosynthetic rates. Improved photosynthesis has also been achieved through expressing a cyanobacterial gene in plants involved in HCO_3^- accumulation which releases CO_2 within the leaf for CO_2 fixation and hence improves carboxylation. These former targets constitute direct targeting of the Calvin cycle. Another approach has been to target feedback mechanisms that regulate CO_2 fixation.

Feedback Regulation of the Calvin Cycle and its Targeting to Improve Photosynthesis

In addition to the sophisticated control mechanisms that relate CO_2 fixation to light availability (feedforward regulation), feedback mechanisms relate Calvin cycle activity to the demand for the end products of photosynthesis. Inorganic phosphate (Pi) is a component of phosphorylated intermediates in pathways and is liberated when end product, e.g., sucrose, is synthesized (sucrose contains no Pi). This recycling of Pi is necessary to ensure that metabolic flow can continue. Photophosphorylation and ATP synthesis are particularly sensitive to Pi supply. Slow recycling of Pi caused by low temperature, for example, can restrict the recycling of Pi and so limit photosynthesis.

Demand for end product is also determined by the genetic potential of the plant for growth and by other environmental factors, particularly nitrogen, which facilitates high growth rates. The assimilation of nitrogen into amino acids requires carbon skeletons derived from triose phosphates supplied by the Calvin cycle. An impairment of nitrogen supply slows growth, which can lead to a build of sugar in leaves, because photosynthates are no longer being used in growth and nitrogen assimilation. It was shown in 1990 that seven maize photosynthetic genes were repressed by glucose or sucrose in a maize protoplast system. Further evidence of control of photosynthetic gene expression by sugars has been obtained where sugars were made to accumulate in leaves due to genetic modification, environmental treatments (high CO_2 and low N, in particular), and through direct feeding of sugars to leaves. The exact mechanism through which this may operate is not clear, but it is likely to be part of a fundamental metabolic signaling process that links photosynthesis with requirement for sugar. Recently it has been shown that modification of such feedback mechanisms may be a way forward to improving photosynthesis. The trehalose pathway, once thought to have become largely extinct in plants, is now known to be ubiquitous with an indispensable role in regulating carbohydrate use. Modification of a key component of this regulation, trehalose 6-phosphate (T6P), has been shown to alter sugar metabolism in growth processes and alter photosynthesis. There is a close correlation between T6P, Rubisco content, and photosynthetic rate. Increasing amounts of T6P by genetic modification increased amounts of Rubisco and photosynthetic rate of leaves. It is thought that T6P links carbohydrate utilization to photosynthesis as part of a feedback loop that regulates photosynthesis in response to sugar use. Modification of this process provides a route toward increasing Rubisco activity and photosynthesis.

Photosynthetic CO_2 Fixation of Whole Plants

A central strategy of photosynthetic regulation of whole plants is to balance photosynthetic rate of leaves with the overall leaf area of the plant. Surveys of variations in photosynthesis per unit leaf area of many crops demonstrate a strong negative relationship with leaf area. Many environmental factors, particularly light, and the genetic make up of the plant determine this trade off. Growth rate and productivity are more closely related to leaf area than the photosynthetic rate of individual leaves. This is reflected in crop breeding for yield which has increased leaf area often at the expense of photosynthetic rate. Large leaf area combined with use of fertilizers and control of pests and diseases has maximized photosynthesis per unit of land for high crop yields. Improvements in yields in this way may be reaching a limit, so advances in improvement of photosynthetic rate combined with large leaf area may be the way forward to increasing photosynthesis and for future productivity gains. The complexity of photosynthetic regulation at the pathway and whole plant level show there are many things to consider in trying to genetically engineer photosynthesis and productivity. However, the nature of recent progress gives much room for optimism.

See Also the Following Articles

ATP Synthesis in Plant Mitochondria: Substrates, Inhibitors, Uncouplers • Chlorophylls and Carotenoids • Chloroplasts • Ferredoxin • Pentose Phosphate (Hexose Mono Phosphate) Pathway • Photosynthesis

Glossary

Calvin cycle, reductive pentose phosphate pathway or **photosynthetic carbon reduction cycle** Series of reactions that reduce CO_2 into triose phosphate in the chloroplast from which sugars, amino acids, and other plant products are synthesized.

chloroplast Organelle in which light reactions and Calvin cycle take place.

feedback regulation Regulates carbon flow through the Calvin cycle in response to the demand for photosynthate in end-product synthesis. It can operate at the level of recycling inorganic phosphate back to the Calvin cycle and at the level of gene expression of Calvin cycle enzymes by sugars and their metabolism.

feedforward regulation Enables the Calvin cycle to respond sensitively to light by affecting the synthesis of Calvin cycle enzymes and their activity.

light reactions They drive electron flow which leads to the reduction of NADP to NADPH and synthesis of ATP necessary for the operation of the Calvin cycle.

Further Reading

Calvin, M. (1961). The path of carbon in photosynthesis. In *Nobel Lectures, Chemistry 1942–1962*. Elsevier, Amsterdam.

Leegood, R. C., Sharkey, T. D., and von Caemmerer, S. (eds.) (2000). Advances in photosynthesis. In *Photosynthesis: Physiology and Metabolism*, Vol. 9, Kluwer Academic, Dordrecht.

Lieman-Hurwitz, J., Rachmileuitch, S., Mittler, R., Marcus, Y., and Kaplan, A. (2003). Enhanced photosynthesis and growth of transgenic plants that express ictB, a gene involved in HCO_3^- accumulation in cyanobacteria. *Plant Biotechnol.* **1**, 43–50.

Miyawaga, Y., Tamoi, M., and Shigeoka, S. (2001). Over expression of a cyanobacterial fructose-1,6-bisphosphatase/sedoheptulose-1,7 bisphosphatase in tobacco enhances photosynthesis and growth. *Nat. Biotechnol.* **19**, 965–969.

Pellny, T. K., Ghannoum, O., Conroy, J. P., Schluepmann, H., Smeekens, S., Andralojc, J., Krause, K.-P., Goddijn, O., and Paul, M. J. (2004). Genetic modification of photosynthesis with *E. coli* genes for trehalose synthesis. *Plant Biotechnol. J.* **2**, 71–82.

Raines, C. A. (2003). The Calvin cycle revisited. *Photosynthesis Res.* **75**, 1–10.

Von Caemmerer, S., and Farqhuar, G. D. (1981). Some relationships between the biochemistry of photosynthesis and the gas exchange of leaves. *Planta* **153**, 376–387.

Biography

Matthew Paul is a Research Leader at Rothamsted Research, grant aided by the Biological and Biotechnological Sciences Research Council of the United Kingdom. His principal research interests are the regulation of sugar metabolism and photosynthesis by metabolic signaling processes and in particular the role of the trehalose pathway in this regard. He holds a Ph.D. from the University of Leicester and worked as a Royal Society postdoctoral fellow at the University of Bayreuth, Germany.

Photosystem I, Structure and Function

Petra Fromme
Arizona State University, Tempe, Arizona, USA

Photosystem I (PS I) is a bio-solar energy converter that plays the key role in the first steps of oxygenic photosynthesis: the conversion of the light energy from the sun into chemical energy. It is a large membrane protein complex, consisting of 12 proteins, to which 127 cofactors (as chlorophylls, carotenoids, FeS clusters, and vitamin K1) are noncovalently bound. The function of PS I can be described as a bio-solar cell. It captures the light from the sun by a large antenna system (consisting of 90 chlorophylls and 22 carotenoids) and transfers the energy to the center of the complex, where the electron transfer chain is located. When the excitation energy reaches the center of the complex, charge separation takes place. An electron is ejected and transferred across the membrane to the terminal FeS cluster by a chain of six different electron carriers. In the next step of the reaction cycle, the electron is transferred from PS I to the soluble electron carrier protein ferredoxin leading finally to the reduction of $NADP^+$ to NADPH by the ferredoxin:NADP:reductase (FNR). The cycle is completed by the re-reduction of the donor site of PS I by either plastocyanin or cytochrome c_6.

Photosynthesis

Oxygenic photosynthesis is the main process on earth that converts the light energy from the sun into chemical energy. The process supplies all higher life on earth with food and produces all the oxygen in the atmosphere. Three different kinds of organisms are able to perform oxygen-evolving photosynthesis: plants, algae, and cyanobacteria. Whereas plants and algae are eukaryotic cells containing chloroplasts, cyanobacteria are prokaryotes. It was suggested that chloroplasts had been formed in early times of evolution by endosymbiosis. During this process an ancestor of the plant cell may have incorporated an early ancestor of cyanobacteria which subsequently lost its independent status and became a cell organelle in later stages of evolution. Whereas this process may have occurred billions of years ago, the primary steps of photosynthesis have been conserved and are still essentially the same in plants and cyanobacteria.

The initial steps of photosynthesis, the light reactions, occur on a membrane system, known as the thylakoids. Two large membrane protein complexes – the photosystems I and II (abbreviated as PS I and PS II, respectively) that are embedded in this membrane – catalyze the initial steps of photosynthesis, the light-induced charge separation. A pool of plastoquinones, the cytochrome b_6f complex, and plastocyanine or cytochrome c_6 functionally couple both photosystems. The thylakoid membrane is charged by this process (comparable to the charging of a battery) and a proton gradient develops across the membrane. Both the electrical gradient and the proton gradient (i.e., the electrochemical gradient) drive the synthesis of ATP. Reduced hydrogen for sugar formation is provided by reduction of $NADP^+$ and H^+ to NADPH. The reaction is driven by the electrons provided by PS I.

Function of PS I

PS I is a large membrane protein complex; in cyanobacteria it consists of 12 protein subunits to which 127 cofactors are noncovalently bound. It catalyzes the light-driven electron transfer from the soluble Cu-containing protein plastocyanine on the lumenal side (i.e., the inside of the thylakoids) to ferredoxin at the stromal side (outside) of the thylakoid membrane. Cyanobacteria can also use the hem containing soluble protein cytochrome c_6 as an alternate or unique electron donor to PS I. There is also some flexibility concerning the electron acceptor. In the case of iron deficiency, flavodoxin can act as the electron acceptor instead of ferredoxin.

In plants, the system contains at least four additional subunits whose functions are still under investigation. It is known that the main proteins, including all cofactor-binding sites, are well conserved between plants and cyanobacteria. However, detailed structural information is available only for the latter one from the X-ray structure of PS I from the thermophilic cyanobacterium *Synechococcus elongatus* at 2.5Å resolution. In cyanobacteria, PS I is a trimer with a molecular weight of more than 1000 kDa. Figure 1 shows the picture of the trimeric complex, pointing out the complex organization of this nano-bio-solar system. PS I is the largest and most complex membrane protein for which the structure has been determined.

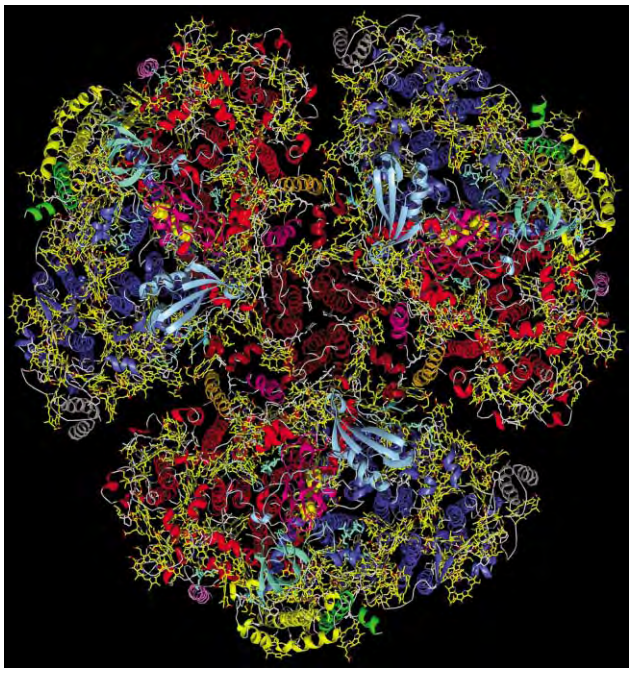

FIGURE 1 The trimeric structure of PS I from cyanobacteria; the view direction is from the stromal side onto the membrane plane. The 12 proteins are shown in a backbone representation (PsaA, blue; PsaB, red; PsaC, pink; PsaD, turquoise; PsaE, light blue; PsaF, yellow; PsaI, dark pink; PsaJ, green; PsaK, gray; PsaL, brown; PsaM, orange, and PsaX, light pink). The head groups of the chlorophylls are shown in yellow, their phytyl-tails have been omitted for clarity. The carotenoids are depicted in gray; the lipids, in dark turquoise.

Each monomeric unit contains 12 proteins, 96 chlorophylls (the pigments that give the plants the green color), 22 carotenoids (orange pigments, which become visible in autumn), 3 [4Fe–4S] clusters, 2 phylloquinone molecules, and 4 lipids.

The first step of the whole process is the light capturing, performed by the large antenna system, which consists of 90 antenna chlorophylls and 22 carotenoids. The energy is transferred to the center of the complex, where the electron transport chain is located. When the energy excites a special pair of two chlorophylls, located in the center of the complex, the "action" takes place and charge separation occurs. Due to its absorption maximum at 700 nm, this pair of chlorophylls was named P700. The electron is transferred from P700 across the membrane by a chain of electron carriers. These electron carriers were previously identified by spectroscopic investigations, and their historical names have been maintained. The electron transport chain consists of five steps. The electron is stepwise transferred from P700 to A (a chlorophyll *a* molecule), A0 (also a chlorophyll *a* molecule), A1 (a phylloquinone molecule) and from there to the three [4Fe–4S] clusters – FX, FA, and FB. After the docking of the soluble electron carrier ferredoxin, the electron is transferred from PS I to ferredoxin, which subsequently leaves the docking site responsible for bringing the electron to the ferredoxin-$NADP^+$-reductase, which then finally reduces $NADP^+$ to NADPH. After this process has occurred once, $P700^+$ has to be re-reduced to complete the reaction cycle. There is a docking site for soluble electron carrier proteins located at the lumenal site of the complex, just underneath P700. In plants reduced plastocyanine docks to this site and reduces $P700^+$, whereas cytochrome c_6 can substitute plastocyanine in cyanobacteria.

The Proteins

The structure and location of the proteins in PS I is shown in Figures 2A and 2B. Cyanobacterial PS I consists of 12 different protein subunits, which are named PsaA to PsaX, according to their genes. The two most important proteins are the large subunits PsaA and PsaB. They harbor most of the antenna system as well as most of the cofactors of the electron transport chain from P700 to the first FeS cluster, FX. The latter is a rare example of an inter-protein FeS cluster coordinated by four cysteines, two of them provided by PsaA and the other two cysteine ligands provided by PsaB. Each of the two large subunits consists of 11 transmembrane helices, connected by partially extended loops that also contain many secondary structural elements as α-helices and β-sheets. The docking site of plastocyanine/cytochrome c_6 is formed by two of these surface helices. The five C-terminal helices are located in the center of the PS I and surround the electron transfer chain, whereas the six N-terminal helices flank the inner core on both sites. They are arranged as a trimer of dimers and they coordinate a large part of the antenna pigments in PS I. The six smaller membrane-embedded proteins (PsaF, PsaI, PsaJ, PsaK, PsaL, and PsaX) surround the core formed by PsaA and PsaB. Their main function is the stabilization of the antenna complex. PsaL also has an important structural role, because it is involved in the formation of the trimer. A further function of the smaller subunits may be the interaction of PS I with external antenna complexes. Cyanobacteria contain large membrane-associated antenna complexes, called phycobillisomes, which are either connected to PS I or to PS II, depending on the light conditions. There is some indication from deletion mutants that PsaF may play an important role in the connection of PS I with the phycobillisomes. Under an environmental stress, such as iron deficiency, the phycobillisomes are degraded and PS I is supplied with additional energy by a ring of 18 subunits of a membrane integral antenna complex, which is named IsiA (for iron stress induced protein A). With a molecular weight of 43 kDa, this protein has homologies to the internal antenna protein of PS II (CP43) and is therefore also

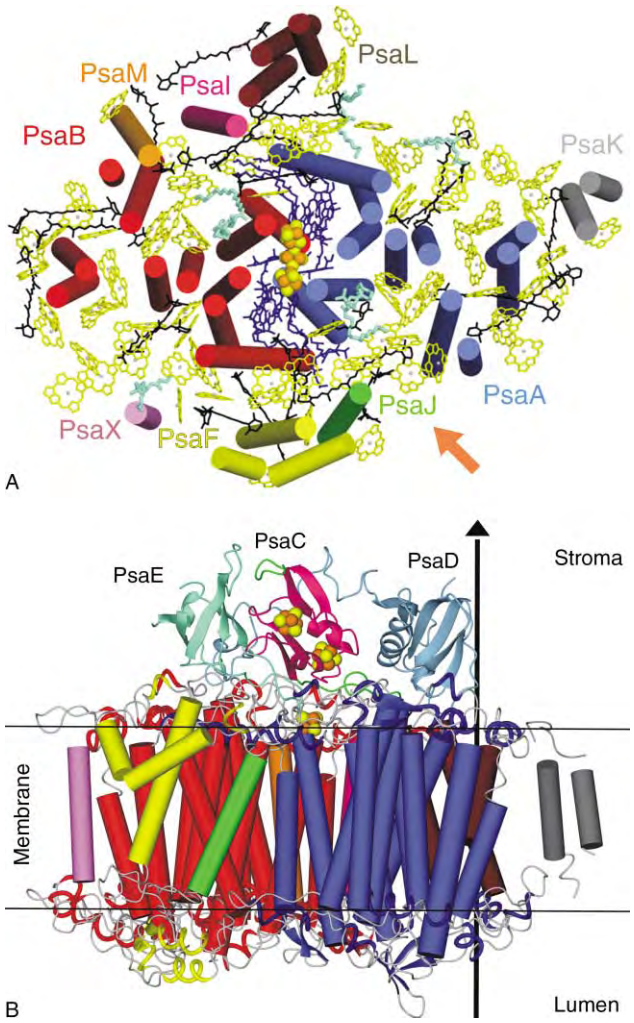

FIGURE 2 Arrangement of protein subunits and cofactors in one monomeric unit of PS I (A) view from the stromal side onto the membrane plane. The three stromal subunits have been omitted for clarity. Color coding of the membrane intrinsic subunits is as shown in Figure 1: PsaA, blue; PsaB, red; PsaF, yellow; PsaI, dark pink; PsaJ, green, PsaK, gray; PsaL, brown; PsaM, orange, and PsaX, light pink. Transmembrane α-helices of the membrane intrinsic subunits are represented as colored cylinders, the loops as well as the three stromal subunits PsaC, PsaD, and PsaE are omitted for clarity. (B) Side view of the monomer of the PS I complex. The view is parallel to the membrane plane. The orange arrow in (A) indicates the view direction in (B). All cofactors have been omitted except the three FeS clusters. For an explanation of the colors see legend to Figure 1. The three stromal subunits PsaE (light green), PsaC (violet), and PsaD (light blue) are located on top of the transmembrane α-helices.

called CP43′. The interaction with the IsiA ring may be performed by PsaF, PsaJ, PsaK, and PsaX.

Plant PS I is very homologous to its cyanobacterial sister, however the external antenna systems are quite different in plants and cyanobacteria. Plants do not have phycobillisomes, instead, the membrane intrinsic antenna proteins LHCI (light harvesting complex I) and LHCII (light harvesting complex II) can be connected to the monomeric core of PS I.

In addition, the plant system does not contain PsaM and PsaX but instead contains at least four additional proteins not found in cyanobacteria: PsaG, PsaH, PsaN, and PsaO. There is not any detailed structural information available on the plant PS I, but biochemical studies have shown that PsaH and PsaO may be located close to PsaL, and may interact with the LHC II complex, whereas the interaction with the LHC I complex is mediated by PsaF, PsaJ, and PsaK. PsaF is also involved in the docking of plastocyanine in plants by its lumenal N-terminal extension.

Both in plants and cyanobacteria, three extrinsic subunits, which do not contain any transmembrane helices, are located at the stromal site of the PS I complex. These three subunits (PsaC, PsaD, and PsaE) form a "stromal hump" that extends the membrane by 35Å and provides the docking site for the soluble electron carriers ferredoxin and flavodoxin. The central subunit PsaC thereby carries the terminal electron acceptors, the two [4Fe–4S] clusters named FA and FB.

The Electron Transport Chain

The electron transport chain is the heart of PS I. Figure 3 shows the structural organization of the cofactors of the electron transport chain. The organic cofactors of the electron transfer chain are arranged in two branches. They are named the A- and B-branches, because most – but not all – cofactors of the A-branch and B-branch are coordinated by PsaA and PsaB, respectively.

The pair of chlorophylls assigned to P700 is located close to the lumenal surface of PS I. It consists of two chemically different chlorophyll molecules. The chlorophyll on the B-branch is the common chlorophyll *a* molecule, chemically identical to all of the other 95 chlorophylls in PS I, whereas the chlorophyll at the A-branch is chlorophyll *a*′, the epimer at the C13 position of the chlorine ring system. The protein environment further enhances the asymmetry of the two chlorophylls: three hydrogen bonds are formed between the protein and the P700-chlorophyll *a*′ at the A-branch, whereas the P700 chlorophyll at the B-branch does not form any hydrogen bonds to the protein environment. The asymmetry could lead to significant differences in the redox potential of both chlorophylls, which may explain why more than 85% of the unpaired electron of $P700^+$ is located, on the B-branch chlorophyll. A possible function of the asymmetry may be a gating of electrons along the two branches but to date this suggestion has not been proven experimentally. From P700 the electron is transferred via one of the chlorophylls from the second pair chlorophylls, "A", to the first stable electron acceptor "A0," which may be located on one of the chlorophylls located in the middle of the membrane.

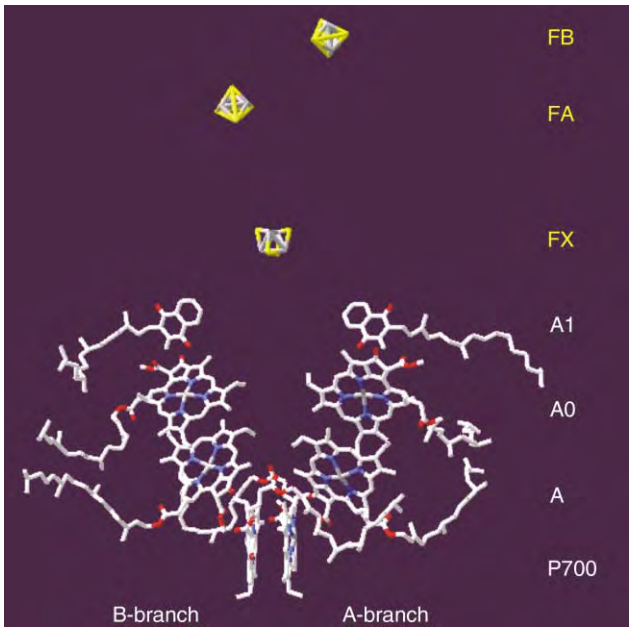

FIGURE 3 The electron transfer system of PS I. The view is parallel to the membrane plane. The organic cofactors of the electron transfer chain are arranged in two branches. The left branch is called the B-branch, whereas the right branch is the A-branch. The three [4Fe–4S] clusters FX, FA, and FB are located at the stromal side of the membrane (on top of the figure). At right margin the names of the cofactors are given as derived from spectroscopic investigations.

These first steps of electron transport occur in less than 3 ps (3/1000 000 000 parts of a second) so that the second pair of chlorophylls has not been detected by spectroscopy so far. The coordination of the chlorophylls of "A" and "A0" is very remarkable, because none of them is coordinated by histidine, the favorite side chain for providing the fifth ligand to the Mg^{2+} in a chlorophyll molecule. Instead, both chlorophylls of "A" are coordinated by a water molecule, which forms the second H-bond to two asparagine side chains of the opposite branch. That means that the first electron acceptor at the A-branch is coordinated by PsaB and *vice versa*. The coordination of the two chlorophylls of "A0" is even more remarkable. The sulfur atom of methionine in both cases provides the fifth ligand of the Mg^{2+}. This is very unusual, because there should be only a very weak interaction between sulfur as a weak acid and Mg^{2+} as a strong base. In can be suggested that the weak interaction hinders a strong base (like water) from entering the site, thereby leading to a chlorophyll which may behave as if it lacks a fifth ligand. There is not an example of a sulphur–Mg^{2+} ligandation in the whole realm of inorganic or organic chemistry. It may be responsible for the extreme negative redox potential of A0 of -1000 mV. The unusual ligandation is absolutely essential for the electron transport, because replacement of the Methionine by histidine, which provides a strong ligand to the chlorophyll, blocks electron transport at the level of A0. In the next step of the electron transfer chain; the electron is further transferred from A0 to one of the phylloquinones, which represent the electron acceptor "A1". The two phylloquinones, which may represent A1, are located at the stromal side of the membrane. The binding pockets are identical on both sites but differ significantly from all other quinone-binding pockets found in proteins so far. Both quinones are π-stacked with a tryptophane residue and both show asymmetric hydrogen bonding: only one of the two oxygen atoms forms an H-bond to an NH backbone group, whereas the other oxygen atom is not hydrogen bonded at all. This could lead to a protein-induced asymmetry in the distribution of the unpaired electron in the radical state $A1^{-\cdot}$, formed when one of the phylloquinones gets reduced. This may answer the question of why A1 has the most negative redox potential (-770 mV) of all quinones found in nature. The electron proceeds from A1 to the FeS cluster FX. This is the rate-limiting step of the electron transfer in PS I. Still, a lively scientific discussion is going on regarding the question of whether one or both branches are active.

There is now experimental evidence that this step can proceed on both branches, but with different rates. In the green algae *Chlamydomonas reinhardtii*, the electron transfer is about a factor of 50 slower on the A- than on the B-branch. This could be the result of a higher activation energy barrier on the A- compared to the B-branch. This finding raises the question of the reason for this difference. There is not a significant difference concerning the protein environment in both branches, but there are two lipid molecules located close to the pathway from A1 to FX that could be responsible for the asymmetry. A negatively charged phospholipid is located on the slower A-branch and the electron has to be transferred against this negative charge, whereas on the faster B-branch a neutral galactolipid has replaced the phospholipid. This is the most reasonable explanation for the higher activation energy barrier.

The Antenna System

The antenna system of PS I consists of 90 chlorophyll *a* molecules and 22 carotenes. The arrangement of the pigments is shown in Figure 4. The function of the antenna chlorophylls (shown in green) is to capture light and transfer the excitation energy to the center of the complex, where the electron transfer chain is located (pigments of the electron transfer chain are shown in blue). The efficiency of the energy transfer is very high. After excitation of any of the antenna chlorophylls the chance that the energy is successfully transferred to P700

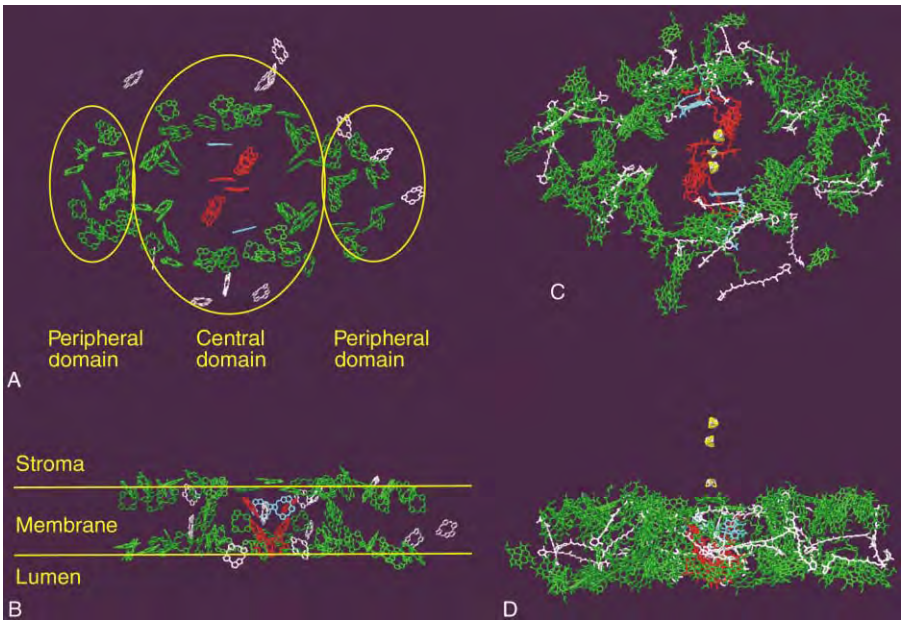

FIGURE 4 The antenna system of PS I (A) Organization of the chlorophylls. The view is from the stromal side onto the membrane plane. For clarity only the ring system of the chlorophylls is shown. The antenna chlorophylls that are coordinated by PsaA and PsaB are shown in green, the chlorophylls coordinated by the smaller membrane integral subunits are depicted in gray. The chlorophylls of the electron transport chain are highlighted in red and the two chlorophylls that may link the electron transport chain and the antenna system are depicted in turquoise. (B) Organization of the chlorophylls. Side view of the cofactors of PS I; the view direction is parallel to the membrane plane. The colors depicted are the same as shown in (A). (C) Complete depiction of the cofactors of the antenna system and the electron transfer chain. The view direction is as in (A). All antenna chlorophylls are shown in green, the carotenoids in white, the chlorophylls of the electron transfer chain in red and the FeS clusters in yellow/gray. (D) Complete depiction of the cofactors of the antenna system and the electron transfer chain. The view direction is as in (B) and the colors are identical to (C).

and subsequent charge separation occurs is 99.98% at room temperature.

The arrangement of the antenna system in PS I is unique. Instead of forming a symmetric ring surrounding the reaction center core, as it is in the light harvesting systems of purple bacteria, the chlorophylls form a clustered network. Each of the chlorophylls have several neighbors at a distance of less than 15Å, so energy can be efficiently transferred in multiple pathways to the center of the complex. The system can be, to some extent, compared to the nerve-network system in the brain where multiple connections are responsible for the high efficiency of information transfer. The antenna system in PS I is highly optimized for efficiency and robustness. The side view along the membrane plane shows that it can be divided into a central domain, which surrounds the electron transfer chain, and two peripheral domains, flanking the core on both sides. In the peripheral domains, the antenna chlorophylls are arranged in two layers, one close to the stromal surface of the membrane and the other close to the lumenal surface of the membrane. When a peripheral antenna chlorophyll is excited the energy will be first transferred from this "two-dimensional" layer to the central domain. In the central domain, chlorophylls are distributed over the full depths of the membrane, i.e., the excitation energy can be exchanged between the two layers. From the chlorophylls of the central domain the excitation energy is then transferred to the electron transfer chain. There are two chlorophylls that seem to structurally link the antenna system to the electron transfer chain (yellow in Figure 4), but the question as to whether they play a crucial role in energy transfer is still not solved.

The carotenoids fulfill three functions in PS I. They play a structural role, function as additional antenna pigments and prevent the system from damage by over-excitation caused by excess light (photoinhibition). The latter function is very critical for the whole system. Chlorophylls are in principle dangerous and reactive molecules. Over-excitation can lead to the formation of chlorophyll triplets (Chl^3), which can react with oxygen to form the highly toxic singlet oxygen, a very dangerous cell poison. Multiple interactions can be observed between the carotenoids and the chlorophylls of the antenna system. The carotenoids are distributed over the whole antenna system and prevent photo damage by the quenching of chlorophyll triplet states. The energy from the triplet chlorophylls is transferred to

the carotenoids that form the carotenoids' triplet state Car^3. The energy of the Car^3 is too low to react with O_2, this results in the carotenoids returning to the ground state by the dissipation of the energy just as heat, thereby preventing photodamage. The system works very efficiently, even under high-light conditions, as the Chl^3 triplet state cannot be detected in the intact PS I.

See Also the Following Articles

Chlorophylls and Carotenoids • Chloroplasts • Cytochrome *c* • Ferredoxin • Green Bacteria: Secondary Electron Donors (Cytochromes) • Photosynthesis • Photosystem I: F_X, F_A, and F_B Iron-Sulfur Clusters • Purple Bacteria: Electron Acceptors and Donors • Purple Bacteria: Photosynthetic Reaction Centers • The Cytochrome b_6f Complex

Glossary

chloroplast Organelle of the plant cell, where photosynthesis takes place.

electron donor/acceptor Molecules that donate or accept electrons in a redox reaction.

electron transfer chain Sequential arrangement of pigments within the PS I, which transports the electron across the membrane.

excitation energy transfer Transfer of the energy absorbed by the antenna pigments to the site of charge separation.

photosystem I and II Large membrane protein complexes that perform the first reaction of energy conversion, the light-induced charge separation.

thylakoid Membrane system, located inside the chloroplasts. The site where the proteins of the electron transfer chain are located and the primary processes of photosynthesis take place.

Further Reading

Bibby, T. S., Nield, J., and Barber, J. (2001). Iron deficiency induces the formation of an antenna ring around trimeric photosystem I in cyanobacteria. *Nature* **412**, 743–745.

Boekema, E. J., Hifney, A., Yakushevska, A. E., Piotrowski, M., Keegstra, W., Berry, S., Michel, K. P., Pistorius, E. K., and Kruip, J. (2001). A giant chlorophyll-protein complex induced by iron deficiency in cyanobacteria. *Nature* **412**, 745–748.

Brettel, K., and Leibl, W. (2001). Electron transfer in photosystem I. *Biochim. Biophys. Acta* **1507**, 100–114.

Fromme, P., Jordan, P., and Krauss, N. (2001). Structure of photosystem I. *Biochim. Biophys. Acta* **1507**, 5–31.

Gobets, B., and van Grondelle, R. (2001). Energy transfer and trapping in photosystem I. *Biochim. Biophys. Acta* **1507**, 80–99.

Jordan, P., Fromme, P., Witt, H. T., Klukas, O., Saenger, W., and Krauß, N. (2001). Three-dimensional structure of cyanobacterial photosystem I at 2.5Å resolution. *Nature* **411**, 909–917.

Scheller, H. V., Jensen, P. E., Haldrup, A., Lunde, C., and Knoetzel, J. (2001). Role of subunits in eukaryotic photosystem I. *Biochim. Biophys. Acta* **1507**, 41–60.

Biography

Petra Fromme is a Professor in the Department of Chemistry and Biochemistry at Arizona State University. Her principal research interest is in the broad field of the structure and function of membrane proteins, with a special focus on the proteins involved in the primary steps of photosynthesis. Her group and co-workers have determined the structures of both PS I and PS II. She holds a Ph.D. in chemistry from the Technical University Berlin and has authored several reviews and book chapters on the structure and function of PS I and PS II. She has received several awards, including the Hill Award from the Photosynthetic Society, the Lemberg Fellowship of the Australian National Academy of Science, and the Biology 2001 award of the Academy of Science of Goettingen. She is a fellow of the Biophysical Society and the Gesellschaft fuer Biologische Chemie.

Photosystem I: F_X, F_A, and F_B Iron–Sulfur Clusters

Mikhail L. Antonkine
Max-Planck Institut für Bioanorganische Chemie, Mülheim, Germany

John H. Golbeck
Pennsylvania State University, University Park, Pennsylvania, USA

Photosystem I is a membrane-bound pigment–protein complex found in photosynthetic organisms that converts the energy of light into chemical bond energy. It is classified as a type I reaction center because it uses iron–sulfur clusters as the terminal electron acceptors. Two variants of low-potential iron–sulfur clusters are employed in photosystem I. The membrane-spanning subunits PsaA and PsaB provide the binding site for F_X, which is a rare instance of an interpolypeptide [4Fe–4S] cluster ligated between the protein heterodimer. The stromal subunit PsaC provides the binding sites for F_A and F_B, which are [4Fe–4S] clusters located on a tightly bound, bacterial ferredoxin-like protein. F_X, F_A, and F_B serve as electron wires to vector the electron from the initial site of charge separation located deep in the membrane to soluble ferredoxin located on the stromal surface of the membrane. They provide good examples of how the physical and biochemical properties of iron–sulfur clusters can be adjusted to suit a specific function in electron transfer.

Photosynthesis

Photosynthesis is the process by which solar energy is converted into chemical bond energy by living organisms. This process can be conveniently divided into two parts, the light reactions and the dark reactions. The light reactions employ four major membrane-bound multisubunit complexes in the energy-conversion process: photosystem I, photosystem II, the cytochrome b_6f- Reiske iron–sulfur complex, and ATP synthase. NADPH is produced directly as a result of photosystem I, and molecular oxygen is produced directly as a result of photosystem II. A proton gradient is generated, in part, by the cytochrome b_6f- Reiske iron–sulfur complex and utilized by ATP synthase for the generation of ATP. During the dark reactions, carbon dioxide is enzymatically converted into carbohydrates at the expense of ATP and NADPH. The chemical bond energy of ATP and NADPH is also used by the organism for cellular processes such as metabolism, growth, and reproduction.

Types of Photosynthetic Reaction Centers

Two types of photosynthetic reaction centers have evolved that are capable of performing light-induced charge separation. Type I reaction centers utilize iron–sulfur clusters as terminal electron acceptors. This type is represented by the green-sulfur bacterial reaction center, the heliobacterial reaction center, and photosystem I in cyanobacteria, algae, and higher plants. Type II reaction centers utilize quinones as terminal electron acceptors. This type is represented by the purple bacterial reaction center, the green nonsulfur bacterial reaction center, and photosystem II in cyanobacteria, algae, and higher plants. Photosystem I is the best studied of the type I reaction centers and is considered the prototype for the entire class.

Photosystem I: The Best-Studied Type I Reaction Center

Photosystem I is a component of the photosynthetic electron transfer chain in all oxygen-evolving organisms. The X-ray crystal structure of cyanobacterial photosystem I has been solved at a resolution of 2.5Å. This large membrane-bound pigment–protein complex exists as a trimer in cyanobacteria; each monomer consists of 12 subunits, labeled PsaA through PsaF, PsaI through PsaM, and PsaX. Among the 127 cofactors are 96 chlorophylls, 2 phylloquinones, and 3 [4Fe–4S] clusters, referred to as F_X, F_A, and F_B. The majority of the electron transfer cofactors are bound to the two large, membrane-embedded subunits PsaA and PsaB. They form the heterodimeric core of photosystem I, and are related by a pseudo-C_2 symmetry axis that also includes the electron transfer cofactors (Figure 1A). The terminal

electron acceptors, iron–sulfur clusters F_A and F_B, are bound to the PsaC subunit on the stromal (cytoplasmic) side of the thylakoid membrane (Figure 1B). Light-induced charge separation occurs between the primary electron donor P700 ($E_m' \sim -1300$ mV), which is a chlorophyll a/a′ heterodimer located on the luminal (inner) side of the membrane, and the primary electron acceptor A_0 ($E_m' \sim -1000$ mV), which is a chlorophyll a monomer. The electron is quickly passed to A_1 ($E_m' \sim -800$ mV), which is a phylloquinone molecule, to F_X ($E_m' = -705$ mV), the interpolypeptide [4Fe–4S] cluster, and finally to F_A ($E_m' = -540$ mV) and F_B ($E_m' = -590$ mV), the [4Fe–4S] clusters bound to PsaC. The soluble protein ferredoxin accepts the electron from F_B on the stromal side of the membrane and interacts with NADP:ferredoxin oxidoreductase to generate NADPH. The initial charge-separated state between $P700^+$ and A_0^- is thus stabilized by the displacement of the electron through a series of acceptors arranged from the lumenal to the stromal side of the thylakoid membrane. The F_X, F_A, and F_B iron–sulfur clusters participate in this process by functioning as a molecular wire. This allows the charge-separated state to be separated in space and lengthened in time, thus permitting a high quantum yield. This strategy represents an excellent example of how Gibbs free energy, in the form of diminishing reductive power of every successive cofactor, is traded to gain time in the form of longer-lived charge-separated states.

Iron–Sulfur Clusters in Biology

Geometry and Oxidation States

Iron–sulfur clusters are one of the most common biological cofactors. They are employed in biological systems in many different roles. For example, iron–sulfur clusters can play a structural role (endonuclease III) as well as a functional role such as in catalysis (aconitase) and in the regulation of gene expression (SoxR). However, by far the most common function is in electron transfer. A few examples include relatively simple proteins such as plant and bacterial ferredoxins, and complex multisubunit proteins such as hydrogenase, complex I, and photosystem I. There are four basic prototypes of iron–sulfur clusters; each differs in the number of iron and sulfur atoms. These differences lead to a widespread variation in geometry, in reduction potential, and ultimately in biological function. (1) In a rubredoxin, a single iron is tetrahedrally coordinated by four cysteine ligands. (2) In a [2Fe–2S] cluster, the iron atoms are bridged by the sulfur atoms in a rhombic structure. Each of the iron atoms is ligated by two cysteines (although in the case of Rieske iron–sulfur proteins, one of the iron atoms is ligated by two histidines) that are positioned in a plane perpendicular to the bridging sulfur atoms. (3) In a [4Fe–4S] cluster, the iron and sulfur atoms alternate in corner positions of a cube (Figure 2). Each of the iron atoms is ligated by a cysteine (in rare instances by water or aspartate); the sulfur atoms form a tetrahedron around the cluster. (4) In a [3Fe–4S] cluster, one of the iron atoms is missing from the corner of the cube; hence, the overall geometry is nearly the same as that of a [4Fe–4S] cluster. Among these prototypes, the [4Fe–4S] clusters are unique because they can potentially exist in three different oxidation states 3+, 2+, and 1+. However, in any given protein, only one of the two different oxidation–reduction pairs is found: 3+/2+ or 2+/1+; the choice is determined by the surrounding protein matrix. In high potential iron–sulfur proteins (HiPIP), the 3+/2+ pair is used, and in low-potential iron–sulfur proteins, the 2+/1+ pair is used. Thus, the protein plays a crucial role in determining the oxidation–reduction pair employed by the cofactor, thereby determining the approximate range of its midpoint potential. The midpoint potential of a [4Fe–4S] cluster is further modulated by coulombic interaction with the protein, polarizability of the protein, and accessibility to solvent; these factors specify the biological function of the [4Fe–4S] cluster. In photosystem I, low-potential [4Fe–4S] clusters are found. In the reduced (+1) state there exist three Fe^{2+} ions and one Fe^{3+} ion, however, due to valence delocalization, only two pairs of iron atoms are observed. One is an equal-valence pair in which both iron atoms exist in a 2+ oxidation state, and the other is mixed-valance pair in which both iron atoms exist in a 2.5+ oxidation state. The position of both pairs, with respect to protein ligands, can change at room temperature, i.e., any iron atom can assume the 2+ or 2.5+ oxidation state at any time, and as a result, the mixed- and equal-valence pairs migrate around the cube. Since in proteins the [4Fe–4S] clusters are slightly distorted due to the interactions with a nonhomogeneous matrix, preferential positions for both pairs exist. The positions can be determined by studying temperature dependence of the NMR chemical shift of the αH and βCH_2 protons of the cysteines ligands of the [4Fe–4S] cluster in a biologically relevant temperature range. In the reduced (+1) state, low-potential [4Fe–4S] clusters are paramagnetic, i.e., the cluster as a whole has an unpaired electron. This property allows detection by electron paramagnetic resonance (EPR) spectroscopy, which is sensitive only to paramagnetic species. Thus, EPR spectroscopy focuses on the properties of the cofactor and not on the properties of the surrounding protein matrix, which is diamagnetic. However, the EPR spectrum is sensitive to changes in the environment of the cofactor caused by changes in surrounding protein. A combination of these properties makes EPR an indispensable tool in the investigation of protein

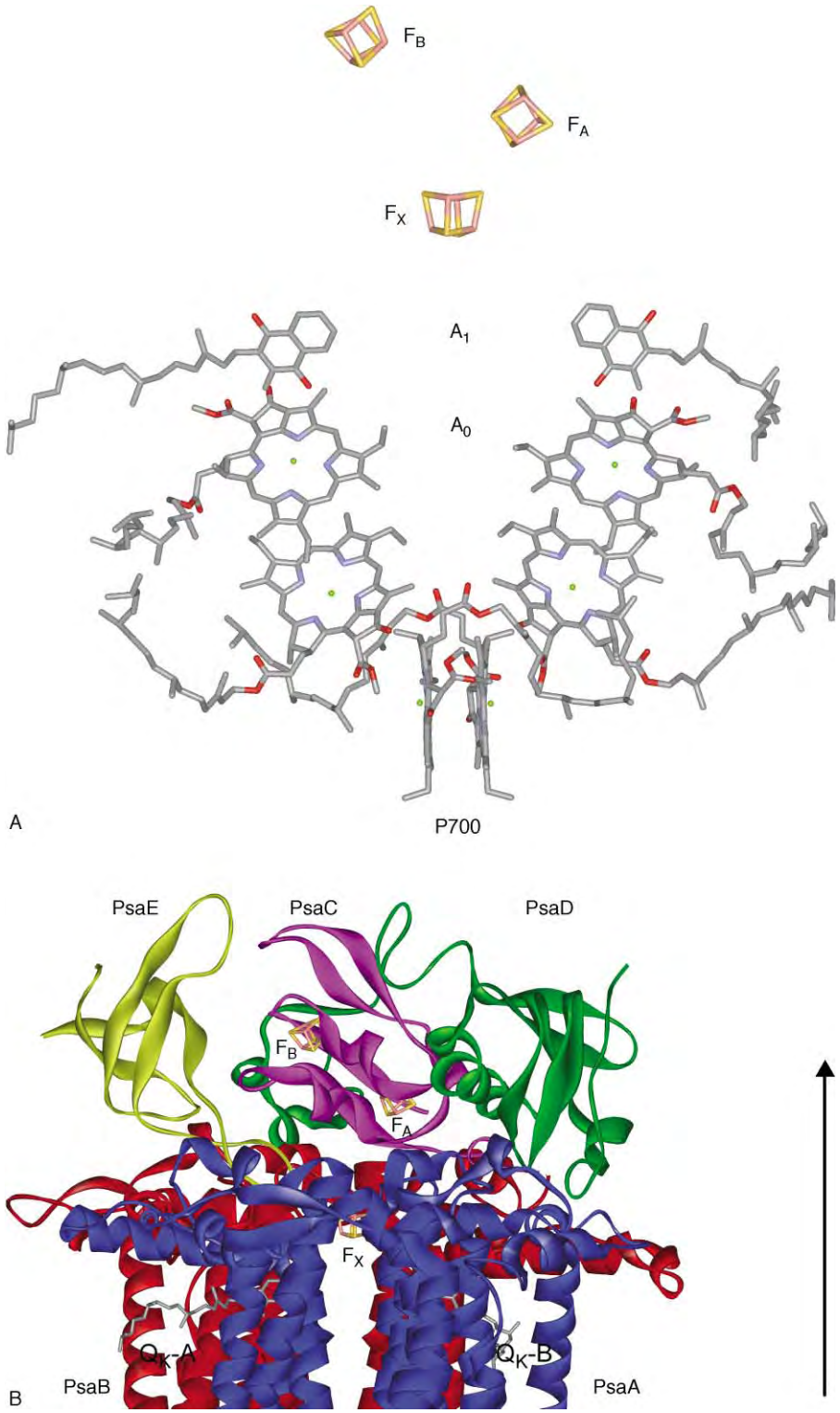

FIGURE 1 The X-ray structure of photosystem I at 2.5Å resolution (PDB entry 1JB0). Detail of the structural model of the photosystem I monomer. View parallel to the membrane plane. (A) Photosystem I cofactors involved in electron transfer. All cofactors are shown as "stick" models; the positions of the carbon, nitrogen, and oxygen atoms are indicated by light gray, blue, and red colors respectively. The positions of Mg^{2+} ions are indicted by green spheres. The [4Fe–4S] clusters F_X, F_A, and F_B are shown as cubes in which the yellow corners indicate the positions of sulfur atoms and the pink corners the position of iron atoms. Note the C_2-symmetric arrangement of cofactors P700, A_0, A_1, and F_X, all of which are bound by two core, membrane-spanning subunits PsaA and PsaB; as well as the symmetry-breaking arrangement of cofactors F_A and F_B, bound by stromal subunit PsaC. (B) The complete backbones of the stromal subunits PsaC, PsaD, and PsaE proteins, as well as their respective arrangement on the stromal surface of the PsaA/PsaB heterodimer. PsaA is shown in blue, PsaB in red, PsaC in magenta, PsaD in green, PsaE in olive; peripheral proteins are omitted for clarity; [4Fe–4S] iron–sulfur clusters F_X, F_A, and F_B are shown as cubes, in which the yellow corners indicate positions of

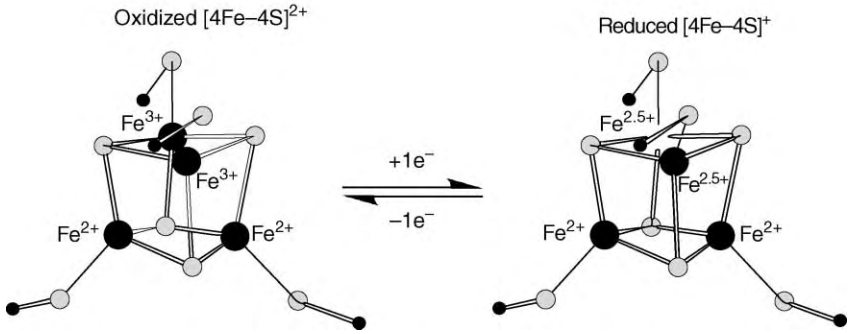

FIGURE 2 The structure of a [4Fe–4S] cluster. The presence of equal valence (Fe^{2+}) and mixed valence ($Fe^{2.5+}$) iron pairs in the reduced state is shown. The iron and sulfide atoms of the [4Fe–4S] clusters as well as sulfur and Cβ atoms of the cysteines ligating the [4Fe–4S] cluster are shown with iron atoms as large black spheres, sulfur atoms as light-gray spheres and Cβ as small black spheres. Reprinted from Vassiliev, I. R., Antonkine, M. L., and Golbeck, J. H. (2001). Iron–sulfur clusters in Type I reaction centers. *Biochim. Biophys. Acta* (special issue on Photosystem I), **1507**, 139–160, with permission from Elsevier.

cofactors in general, and iron–sulfur clusters in particular. This technique is especially advantageous for studying of cofactors in large protein complexes, in which it is difficult to apply other techniques due to the presence of interfering chromophores or to the size of the biomolecule.

Self-Assembly in Solution

Iron–sulfur clusters self-assemble in aqueous solutions under anaerobic (oxygen-free) conditions in presence of iron and sulfide ions along with a thiol-containing reductant. If an apoprotein with an iron–sulfur cluster-binding site is added to the solution, the clusters self-insert into the site via a thiol exchange mechanism. In the living cell the assembly of iron–sulfur clusters is tightly regulated and is performed by a set of special enzymes that act sequentially. However, iron–sulfur proteins with *in vitro* or *in vivo* inserted clusters have identical spectroscopic and biochemical properties. Thus, *in vitro* insertion of clusters is a useful preparative tool for investigation of iron–sulfur proteins.

The F_X, F_A, and F_B Clusters of Photosystem I

F_X, the Interpolypeptide [4Fe–4S] Cluster Bound by PsaA and PsaB

F_X in the interpolypeptide iron–sulfur cluster bound between the PsaA and PsaB subunits (Figure 1). EXAFS and Mössbauer spectroscopic studies unambiguously identified F_X as a [4Fe–4S] cluster. The midpoint potential of F_X was measured directly and was found to be -705 mV, making it one of the most reducing [4Fe–4S] clusters known in biology. The binding site of F_X was identified from amino acid sequences of the PsaA and PsaB polypeptides that comprise the membrane-bound core of photosystem I. The site consists of two identical amino acids sequences, FPCDGPGRGGTC, located in loops connecting helices *j* and *k* on PsaA and *j*′ and *k*′ on PsaB. Each of these sequences provides two conserved cysteine ligands to the cluster; thus, F_X represents a highly unusual instance of a [4Fe–4S] cluster bound between a protein heterodimer. The high-resolution crystal structure of cyanobacterial photosystem I shows that charged amino acids within the conserved F_X-binding sequences on PsaA and PsaB provide a set of ionic contacts for the binding of PsaC. The F_X-binding sequences on both PsaA and PsaB are parts of large, extramembrane loops that have a completely symmetric three-dimensional structure. In addition to providing ligands for F_X they serve several additional functions such as forming the ionic contacts with PsaC and shielding the F_X cluster from molecular oxygen. F_X is additionally shielded by α-helices that comprise the core of the PsaA/PsaB heterodimer. The iron protein of nitrogenase (e.g., protein data bank (PDB) entry 1CP2) and 2-hydroxyglutaryl-CoA dehydratase component A (PDB entry 1HUX) are the only other proteins that have both an interpolypeptide [4Fe–4S] cluster and a solved three-dimensional

sulfur atoms and light-brown corners the position of iron atoms; quinones Q_K-A and Q_K-B are shown as "stick" models, both represent the acceptor A_1 bound to PsaA and PsaB respectively. The position of the trimer C_3-symmetry axis is indicated by an arrow. Reprinted from Antonkine, M. L., Jordan, P., Fromme, P., Krauβ, N., Golbeck, J. H., and Stehlik, D. (2003). Assembly of protein subunits within the stromal ridge of Photosystem I. Structural changes between unbound and sequentially PS I-bound polypeptides and correlated changes of the magnetic properties of the terminal iron–sulfur clusters. *J. Mol. Biol.*, **327**, 671–697, with permission from Elsevier.

structure. However, the environments of these [4Fe–4S] clusters are significantly different in that each subunit of these homodimeric proteins has two fully conserved cysteines that are located far apart from each other in the amino acid sequence. Hence, in these proteins, there is no short consensus binding sequence for the [4Fe–4S] cluster as exists for F_X. It follows that properties of these interpolypeptide [4Fe–4S] clusters are also very different from F_X. They have midpoint potentials of -420 to -430 mV (i.e., 250–300 mV more oxidizing than F_X), which is more typical for low-potential [4Fe–4S] clusters in monocluster and dicluster bacterial ferredoxins. Moreover, the [4Fe–4S] clusters in nitrogenase and 2-hydroxyglutaryl-CoA dehydratase component A are highly oxygen sensitive, probably because the binding site of the interpolypeptide cluster is open and accessible. In contrast, F_X needs to be oxygen insensitive because it is probably assembled as an intermediate in the biogenesis of the photosystem I reaction center.

F_A AND F_B, THE [4Fe–4S] CLUSTERS BOUND BY PSAC

The Amino Acid Sequence of PsaC

F_A and F_B are iron–sulfur clusters bound to the PsaC subunit. A 9 kDa iron–sulfur protein, with an unusual EPR spectrum, was originally isolated by methanol/acetone extraction of spinach chloroplast membranes. Although at the time no function could be assigned, it was later shown to be identical to PsaC. When this protein was rebound to photosystem I cores, the characteristic EPR signals of F_A and F_B could be restored to that found in the wild type. The amino acid sequence of PsaC in a variety of organisms was deduced by direct amino acid sequencing of the protein and from the sequences of the *psaC* genes. The 80 amino acids are extremely well conserved both in cyanobacteria and in higher plants. PsaC has sequence similarity to bacterial ferredoxins, from which it is presumed to have evolved, in the regions surrounding the two [4Fe–4S] clusters (Figure 3). Similar to bacterial ferredoxins, PsaC contains two consensus [4Fe–4S] cluster-binding sites consisting of C(I)xxC(II)xxC(III)xxxC(IV)P, where C is cysteine, P is proline, and x is any other amino acid. Cysteines I, II, and III of the first binding site ligate the first [4Fe–4S] cluster, while cysteine IV ligates the second [4Fe–4S] cluster; cysteines I′, II′, and III′ of the second binding site ligate the second [4Fe–4S] cluster, while cysteine IV′ ligates the first [4Fe–4S] cluster. The distance between the two [4Fe–4S] clusters in the protein is predetermined by the distance between Cys(III) and Cys(IV) in the binding site because they always ligate different clusters. Through site-directed mutagenesis studies, it was shown that in PsaC cysteines 10, 13, 16, and 57 ligate F_B and cysteines 47, 50, 53, and 20 ligate F_A. F_B and F_A in PsaC are equivalent to cluster I and cluster II in bacterial ferredoxins, respectively. The similarity of PsaC to bacterial ferredoxins fostered the use of the three-dimensional structures of these proteins as models for PsaC. This is a valid approach, particularly if one is interested in the structure of the iron–sulfur core of the protein. However, there are several significant regions where their amino acid sequences differ. PsaC has a sequence insertion between the two consensus iron–sulfur binding sites and a sequence extension at the C-terminal end of the protein. Not surprisingly both of these sequences are involved in photosystem I-specific functions of PsaC. The sequence insertion, known as the Z-loop, participates in ferredoxin/flavodoxin binding and the C-terminal

```
                        10  13 16  20                          47 50 53  57
C. acidi urici  --AYVINEACISCGACEPECPVNAIS--------SGDDRYVIDADTCIDCGACAGVCPVD
C. pasteurianum --AYKIADSCVSCGACASECPVNAIS--------QGDSIFVIDADTCIDCGNCANVCPVG
P. aerogenes    --AYVINDSCIACGACKPECPVNIQ---------QG-SIYAIDADSCIDCGSCASVCPVG
Synechococcus   SHSVKIYDTCIGCTQCVRACPLDVLEMVPWDGCKAGQIASSPRTEDCVGCKRCETACPTD
                  .  * ..*. *  *   **.             *       .. *. *  *   **

C. acidi urici  APVQA---------------
C. pasteurianum APVQE---------------
P. aerogenes    APNPED-------------
Synechococcus   FLSIRVYLGAETTRSMGLAY
```

FIGURE 3 Sequence alignment of PsaC from *Synechococcus* sp. PCC 7002 and dicluster bacterial ferredoxins from *Clostridium pasteurianum*, *Clostridium acidi urici*, and *Peptococcus aerogenes*. The cysteines that coordinate the [4Fe–4S] clusters are indicated by bold underlined letters and their number in *Synechococcus* sp. PCC 7002 PsaC sequence is shown at the top. The sequences were aligned with CLUSTALW (1.60). Conserved amino acids are indicated by an asterisk, conservative substitutions by a dot. Reprinted from Antonkine, M.L., Bentrop, D., Bertini, I., Luchinat, C., Shen, G., Bryant, D. A., Stehlik, D., and Golbeck, J. H. (2000). Paramagnetic ^{1}H NMR spectroscopy of the reduced, unbound Photosystem I subunit PsaC: sequence-specific assignment of contact-shifted resonances and identification of mixed- and equal-valence Fe–Fe pairs in the [4Fe–4S] centers $F'_A$and F'_B. Reprinted from (2000). *J. Biol. Inorg. Chem.*, **5**, 381–392, with permission from Springer.

sequence extension is one of the key elements involved in binding to the photosystem I core. One of the interesting features of the amino acid sequence of PsaC that was not recognized immediately is the increased number of charged amino acids in the vicinity of the binding site of the F_A cluster, as compared both to the binding site of F_B and to the binding sites of clusters I and II in bacterial ferredoxins. The basic amino acids of the F_A site are now known to be responsible for binding PsaC; they form the majority of the contacts that anchor PsaC to the PsaA/PsaB heterodimer. This is achieved by formation of ionic bonds with acidic amino acids in the [4Fe–4S] cluster F_X-binding site.

The Three-Dimensional Structure PsaC

PsaC is tightly bound to the PsaA/PsaB stromal surface and is packed between the PsaD and PsaE subunits (Figure 1B). However, PsaC is also a highly soluble protein, a property that has allowed study of its structure in the unbound state. The biochemical and magnetic properties of the F_A and F_B iron–sulfur clusters are similar in unbound PsaC, while they are distinctly different in photosystem I-bound PsaC. Rebinding studies of PsaC, PsaD, and PsaE to the PsaA/PsaB core proteins have been aided by the availability of large amounts of recombinant PsaC, PsaD, and PsaE proteins from overexpression systems in *Escherichia coli*. The EPR properties of F_A and F_B change in three distinct steps during the assembly of photosystem I. The first is unbound PsaC in solution; the second is PsaC bound to photosystem I in the absence of PsaD; and the third is PsaC bound to photosystem I in the presence of PsaD. The presence or absence of PsaE has no effect on the EPR properties of F_A and F_B. Since EPR is highly sensitive to changing environment of the [4Fe–4S] clusters, these results were interpreted as a change in the conformation of PsaC in three distinct steps. PsaD does not bind any cofactors; rather, the binding of PsaD induces conformational changes in PsaC and locks it into its final state. The solution structure for unbound PsaC (PDB entry 1K0T) was solved by NMR. In the iron–sulfur core of PsaC, the [4Fe–4S] clusters F_A and F_B are connected by two short α-helices and assume a very similar geometry in both unbound and bound PsaC (Figure 4). As predicted from the amino acid sequence, this region shows structural features similar to those of bacterial ferredoxins. In particular, the position, distance and relative orientation of the two [4Fe–4S] clusters as well as the conformation of two-cluster consensus binding sites are similar in PsaC and bacterial ferredoxins. A comparison of the unbound PsaC structure with that in the X-ray structure of bound PsaC reveals significant differences that mainly concern the structure of the N, pre-C, and C termini. In unbound PsaC the C terminus assumes a disordered helical conformation, and is clearly different from the extended coil conformation in bound PsaC. Indeed, this is one of the structural elements required to anchor PsaC to the photosystem I core heterodimer. In solution, the N terminus of PsaC is in contact with the pre-C-terminal region (equivalent to the C terminus in bacterial ferredoxins). As compared to bound PsaC, the N terminus in unbound PsaC is bent and is located in between the pre-C-terminal region and the iron–sulfur core region of the protein. The same N- and pre-C-terminal regions are arranged as an antiparallel β-sheet and are much closer to F_A-binding site in bound PsaC. The antiparallel β-sheet arrangement of the N terminus and C terminus (equivalent to the pre-C terminus in PsaC) is typical for bacterial ferredoxins. Thus, PsaC assumes a ferredoxin-like conformation only in the photosystem I-bound form.

Assembly of the Stromal Subunits of Photosystem I

The changes in the structure of PsaC are caused by the sequential formation of multiple networks of ionic and hydrogen bond contacts with the PsaA/PsaB core proteins and with the other two proteins of the stromal side, PsaD, and PsaE. A comparison of the structure of unbound and bound PsaC, PsaD, and PsaE suggests a probable assembly scenario for the sequential binding of the stromal proteins. The assembly of F_X and the proper folding of the large loops that provide a binding site for F_X are preconditions for the binding of the stromal proteins. PsaC has a defined three-dimensional structure only after insertion of both [4Fe–4S] clusters. Therefore, the presence of the iron–sulfur clusters F_A and F_B is precondition for binding of the PsaC and the other stromal proteins. PsaC binds first. Its conformation changes after it binds to photosystem I; the binding of PsaD causes further conformational changes in PsaC, whereupon both assume their final structures. The biochemical and magnetic properties of [4Fe–4S] clusters F_A and F_B, typical for the photosystem I bound state of PsaC, are now established. PsaE probably binds last of the three stromal proteins, thereby completing the assembly process.

Resolution of the Sequence of Electron Transfer: $F_X > F_A > F_B$

Since the reduction potential of F_A (E_m' −540 mV) is higher than F_B (E_m' −590 mV), it was long assumed that F_A was the terminal electron acceptor in photosystem I. In this view, electron transfer in photosystem I is always thermodynamically favorable from $P700^*$ ($E_m' = -1300$ mV) to soluble ferredoxin ($E_m' = -420$ mV). However, EPR studies of PsaC

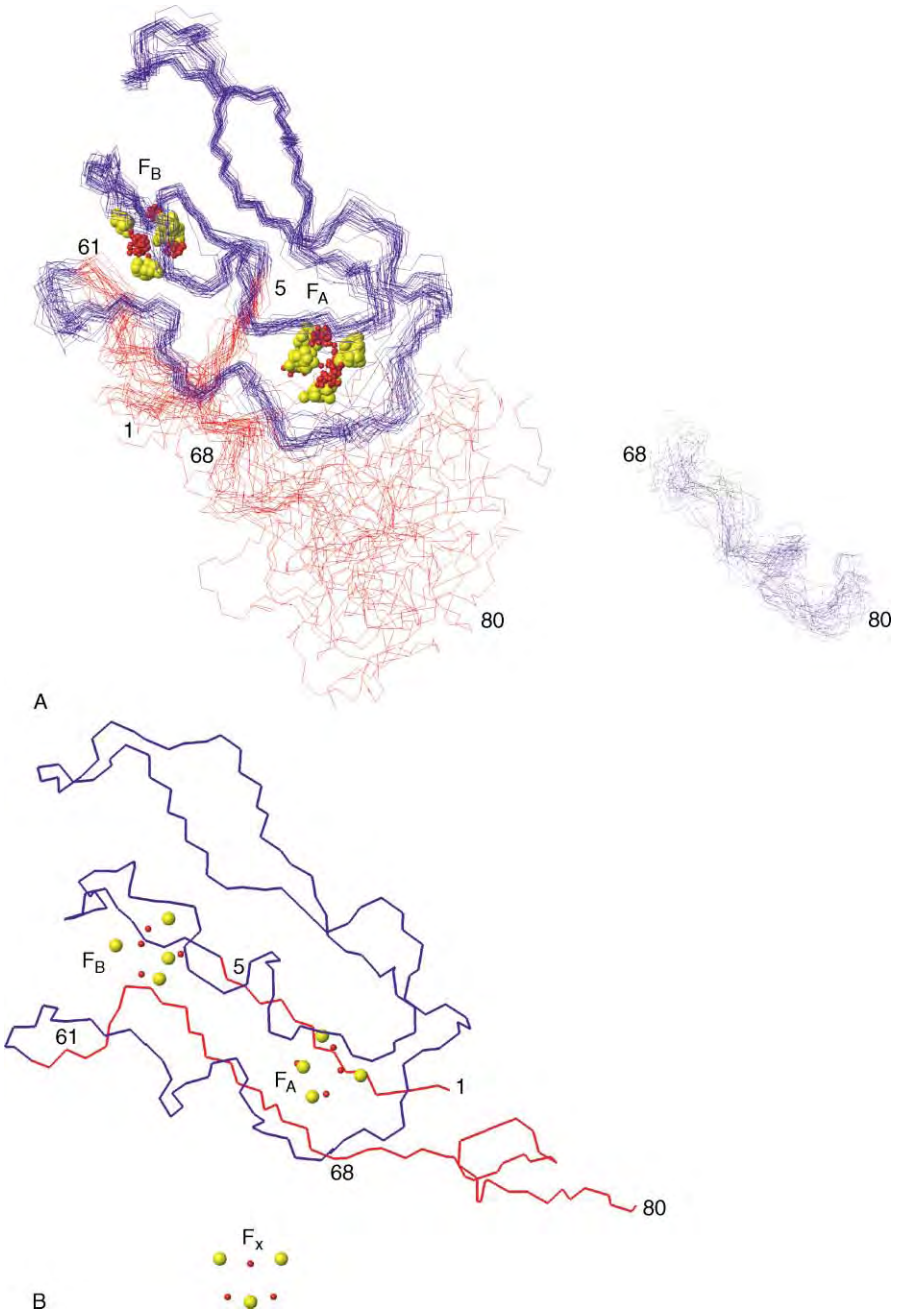

FIGURE 4 Comparison of the NMR solution structure of unbound PsaC (PDB entry 1K0T) with bound PsaC as part of the 2.5Å X-ray structure of Photosystem I (PDB entry 1JB0). The regions where the two structures show significant differences are identified by the red color. Iron atoms are represented by red circles, and sulfur atoms are represented by yellow circles. (A) Backbone drawing of the final family of 30 superimposed structures of unbound, oxidized PsaC from *Synechococcus* sp. PCC 7002 determined by solution NMR. Backbone of the family of 30 structures is shown in a superposition of residues 5–67. The iron and sulfur atoms of the [4Fe–4S] clusters of each of the 30 structures are shown. The view direction is equivalent to the membrane plane of the assembled photosystem I complex (see Figure 1). The inset shows the backbone of residues 68–80 in the same family of 30 PsaC structures. Superposition of solely the residues 68–80 reveals the helical secondary structure of the C-terminus. (B) Structure of photosystem I-bound PsaC taken from the PS I X-ray structure at 2.5Å X-ray resolution (PDB entry 1JB0). The polypeptide backbone and iron–sulfur clusters F_A and F_B are shown. F_X is included to indicate the position and the correct orientation of PsaC on PS I. This figure was prepared using MOLMOL. Reprinted from Antonkine, M. L., Jordan, P., Fromme, P., Krau*β*, N., Golbeck, J. H., and Stehlik, D. (2003). Assembly of protein subunits within the stromal ridge of Photosystem I. Structural changes between unbound and sequentially PS I-bound polypeptides and correlated changes of the magnetic properties of the terminal iron sulfur clusters. *J. Mol. Biol.*, **327**, 671–697, with permission from Elsevier.

mutants, in which cysteine II in the F_A or F_B consensus binding sequence was changed to glycine, alanine, serine, or aspartate, led to the assessment that F_B is the terminal electron acceptor in photosystem I. This was in agreement with EPR relaxation and optical spectroscopy data obtained, around the same time, on photosystem I samples with selectively destroyed F_B. The presence of this small, thermodynamically unfavorable electron transfer step has little consequence because overall, electron transfer remains highly thermodynamically favorable from the excited state of $P700^*$ to ferredoxin. Furthermore, each forward electron transfer step in photosystem I is sufficiently rapid such that charge recombination events are negligible, and this results in the extraordinary quantum yield of ~1.0.

See Also the Following Articles

Chlorophylls and Carotenoids • Ferredoxin • Iron–Sulfur Proteins • Photosynthesis • Photosystem I, Structure and Function • Quinones

Glossary

cofactor Organic or inorganic molecule bound (covalently or through non-covalent interactions) to the protein that is necessary for/or aiding its function. For example, chlorophylls, quinones, and iron–sulfur clusters are cofactors in photosystem I.

F_A A low potential [4Fe–4S] cluster bound by cysteines 20, 47, 50, and 53 of the PsaC subunit of photosystem I; it is equivalent to Cluster II in bacterial ferredoxins that contain two [4Fe–4S] clusters.

F_B A low potential [4Fe–4S] cluster bound by cysteines 10, 13, 16, and 57 of the PsaC subunit of photosystem I; it is equivalent to Cluster I in bacterial ferredoxins that contain two [4Fe–4S] clusters.

F_X A low potential interpolypeptide, [4Fe–4S] cluster bound by two consensus FPCDGPGRGGTC sequences on the PsaA and PsaB subunits of photosystem I.

high-potential iron–sulfur proteins (HiPIP) These contain [4Fe–4S] clusters that shuttle between oxidation states of 3+/2+ .

low-potential iron–sulfur proteins These contain [4Fe–4S] clusters that shuttle between oxidations states of 2+/1+ .

quantum yield The number of electrons transferred per photon absorbed.

type I Photosynthetic reaction centers that use a [4Fe–4S] cluster as the terminal electron acceptor.

type II Photosynthetic reaction centers that use a mobile quinone as the terminal electron acceptor.

Further Reading

Antonkine, M. L., Jordan, P., Fromme, P., Krauß, N., Golbeck, J. H., and Stehlik, D. (2003). Assembly of protein subunits within the stromal ridge of photosystem I. Structural changes between unbound and sequentially PS I-bound polypeptides and correlated changes of the magnetic properties of the terminal iron sulfur clusters. *J. Mol. Biol.* **327**, 671–697.

Antonkine, M. L., Liu, G., Bentrop, D., Bryant, D. A., Bertini, I., Luchinat, C., Golbeck, J. H., and Stehlik, D. (2002). Solution structue of the unbound, oxidized photosystem I subunit PsaC, containing [4Fe-4S] clusters F_A and F_B: a conformational change occurs upon binding to photosystem I. *J. Biol. Inorg. Chem.* **7**, 461–472.

Antonkine, M. L., Bentrop, D., Bertini, I., Luchinat, C., Shen, G., Bryant, D. A., Stehlik, D., and Golbeck, J. H. (2000). Paramagnetic ^{1}H NMR spectroscopy of the reduced, unbound photosystem I subunit PsaC: sequence-specific assignment of contact-shifted resonances and identification of mixed- and equal-valence Fe-Fe pairs in [4Fe-4S] centers F_A and F_B. *J. Biol. Inorg. Chem.* **5**, 381–392.

Bentrop, D., Capozzi, F., and Luchinat, C. (2001). Iron–sulfur proteins. In *Handbook on Metalloproteins* (Bertini, I., Sigel, A., and Sigel, H., Eds.) pp. 357–460, Marcel Dekker, New York.

Chamorovsky, S. K., and Cammack, R. (1982). Direct determination of the midpoint potential of the acceptor X in chloroplast photosystem I by electrochemical reduction and ESR spectroscopy. *Photobiochem. Photobiophys.* 4, 195–200.

Compendium of authors (2001). Type 1 photosynthetic reaction centers (P. Heathcote ed.), *Biochim. Biophys. Acta-Bioenerg.* 1507, 1–310.

Golbeck, J. H., Parrett, K. G., Mehari, T., Jones, K. L., and Brand, J. J. (1988). Isolation of the intact photosystem I reaction center core containing P700 and iron-sulfur center F_X. *FEBS Lett.* **228**, 268–272.

Golbeck, J. H. (1999). A comparative analysis of the spin state distribution of *in vivo* and *in vitro* mutants of PsaC. A biochemical argument for the sequence of electron transfer in Photosystem I as F_X -> F_A -> F_B -> ferredoxin/flavodoxin. *Photosynth. Res.* **61**, 107–149.

Golbeck, J. H. (1994). Photosystem I in cyanobacteria. In *The Molecular Biology of Cyanobacteria* (Bryant, D. A., Ed.) pp. 179–220. Kluwer Academic Publishers, The Netherlands.

Golbeck, J. H. (2003). The binding of cofactors to photosystem I analyzed by spectroscopic and mutagenic methods. *Annu. Rev. Biophys. Biomol. Struct.* **32**, 237–256.

Jordan, P., Fromme, P., Witt, H. T., Klukas, O., Saenger, W., and Krauß N. (2001). Three dimensional structure of cyanobacterial photosystem I at 2.5Å resolution. *Nature* **411**, 909–917.

Li, N., Zhao, J., Warren, P. V., Warden, J. T., Bryant, D. A., and Golbeck, J. H. (1991). PsaD is required for the stable binding of PsaC to the photosystem I core protein of *Synechococcus* sp. PCC 6301. *Biochemistry* **30**, 7863–7872.

Lippard, S. J., and Berg, J. M. (1994). *Principles of Bioinorganic Chemistry.* University Science Books, Mill Valley, California, USA.

Malkin, R., Aparicio, P. J., and Arnon, D. I. (1974). The isolation and characterization of new iron-sulfur protein from photosynthetic membranes. *Proc. Natl Acad. Sci. USA* **71**, 2362–2366.

Zhao, J., Li, N., Warren, P. V., Golbeck, J. H., Bryant, D. A. (1991). Site-directed conversion of a cysteine to aspartate leads to the assembly of a [3Fe-4S] cluster in PsaC of photosystem I – The photoreduction of F_A is independent of F_B. *Biochemistry* **31**, 5093–5099.

Biography

Mikhail L. Antonkine is Postdoctoral Fellow at Max-Planck Institut for Bioinoganic Chemistry. His principal research interests are the structure and function of iron–sulfur proteins including photosystem I. He holds a Ph.D. from the Pennsylvania State University and received postdoctoral training at The Free University of Berlin. He participated in determination of the solution structure of PsaC and in the

development of an assembly scenario for the stromal proteins of photosystem I.

John H. Golbeck is a Professor of Biochemistry and Biophysics at the Pennsylvania State University. His research interests are the structure, function, and organization of photosystem I and the biogenesis of iron–sulfur clusters. He holds a Ph.D. from Indiana University and received his postdoctoral training at Martin Marietta Laboratories. He developed methods to remove and reconstitute PsaC, PsaD, and PsaE in photosystem I, and he assigned the F_A and F_B clusters to the cysteine ligands on PsaC.

Photosystem II Light Harvesting System: Dynamic Behavior

Peter Horton and Alexander Ruban
University of Sheffield, Sheffield, UK

The light harvesting proteins of higher plants play a vital role in the regulation of photosynthesis. These proteins show striking structural and functional flexibility. This dynamic behavior provides a key physiological function to plants, which adapts them to continuously changing environmental conditions. In particular, dynamic properties of the light harvesting proteins of photosystem II promote the efficient collection of sunlight when the intensity is limiting photosynthesis and effective photoprotection when the intensity is excess.

Photosynthetic Light Harvesting

Photosystem II (PSII) is the multisubunit chloroplast membrane-associated pigment–protein complex that uses the energy of sunlight to drive the oxidation of water, evolving oxygen, donating electrons into the photosynthetic electron transfer chain, and depositing protons into the thylakoid lumen. Along with the photosystem I (PSI) it forms the electron–proton transfer chain, which drives the synthesis of ATP and NADPH (Figure 1). Vitally important components of both photosystems are the light-harvesting antennas, light-collecting units (mainly LHCI and LHCII for PSI and PSII, respectively) which ensure high rates of energy input into the photosynthetic reaction centers (RCI and RCII, respectively) by intercepting large numbers of light quanta of various energies/colors. The analogy of LHCs as funnels feeding the RCs with light energy is most appropriate.

Structure and Function of LHCII

The light-harvesting antenna of PSII consists of several proteins which together bind ~300 chlorophyll molecules. Associated tightly with the D1/D2 reaction center are the core antenna complexes CP47 and CP43. The remainder of the antenna consists of the Lhcb proteins, Lhcb1–6. These bind chlorophyll *a*, chlorophyll *b*, and xanthophylls to form several different complexes – LHCII, CP24, CP26, and CP29. LHCII is the main complex and contains ~40% of the PSII chlorophyll – it is the most abundant chlorophyll protein in nature.

Figure 2 depicts the current knowledge of LHCII structure on different levels of organization. The single monomeric unit is a relatively small protein, ~25–28 kDa, containing three transmembrane α-helical structures and binding 12 molecules of chlorophyll (seven chlorophyll *a* and five chlorophyll *b*). Three LHCII monomers are associated together into heterotrimers containing Lhcb1, Lhcb2, and Lhcb3. Additional pigments, carotenoids, are also present in LHCII. Two xanthophylls, luteins, are associated with the helices A and B. A third carotenoid, neoxanthin, is associated with the helix C and the trimer also binds peripherally the carotenoids violaxanthin or zeaxanthin. The xanthophylls play several important roles: (1) ensuring correct assembly of LHCII during biosynthesis; (2) protection of chlorophylls against photooxidation by quenching chlorophyll triplet states and scavenging oxygen radicals; (3) being structurally flexible molecules they allow dynamic behavior of LHCII leading to alteration in chlorophyll interaction and subsequent change in light collection efficiency; and (4) they modulate the interactions between LHCII trimers. Indeed, it was shown that extent of interaction between trimers depends on the type of peripherally bound carotenoid, violaxanthin, or zeaxanthin. *In vivo*, PSII unit is built on the stereo principle: two reaction center complexes build the dimeric PSII core complex, which binds four trimeric LHCII and six monomeric CP24, CP26, and CP29 (Figure 2C). In the photosynthetic membrane these PSII units are often seen as ordered arrays (Figure 2D). Here the LHCII antenna forms an entire network, or macrodomain, of monomeric and trimeric subunits, associated with each other and the reaction center complex. Associated with this macrostructure is the stacking of the complexes together in the characteristic grana membranes.

Three major parameters determine the efficiency of light harvesting: (1) cross-section or number of pigments and their ability to intercept light quanta with the broad

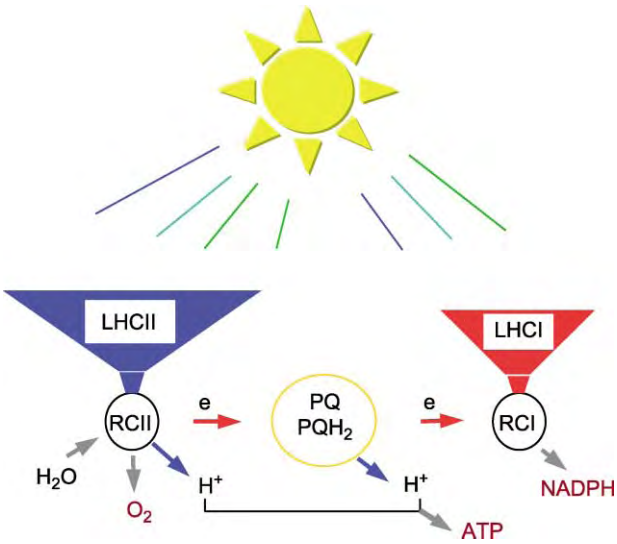

FIGURE 1 Photosynthetic electron transfer. LHCI and LHCII – light harvesting antenna of photosystem I and II, respectively; RCI and II – reaction centers; e – electrons; PQ and PQH_2 – intermediate electron carrier plastoquinone in oxidized and reduced form; H^+ – protons.

range of energy (color); (2) the time during which energy of light can be kept in antenna so it can be funneled into the reaction center; and (3) rate of the funneling. Thus, a large cross-section, long excitation energy lifetime, and high rate of energy transfer to the reaction center are the attributes of an efficient antenna and productive photosynthetic unit. Hence, the efficiency of light harvesting in PSII is determined by the number of LHCII subunits, the pigment order within them, the interaction between subunits and their closeness to the reaction center complex.

The Need for Control of the Light Reactions of Photosynthesis

The light and dark reactions of photosynthesis are tightly coupled, the ATP and NADPH provided by the electron-proton transfer system driving the fixation of CO_2 into carbohydrate. During a day, the light spectrum changes dramatically due to filtering by atmosphere, clouds and sometimes by other plants. Since LHCI and

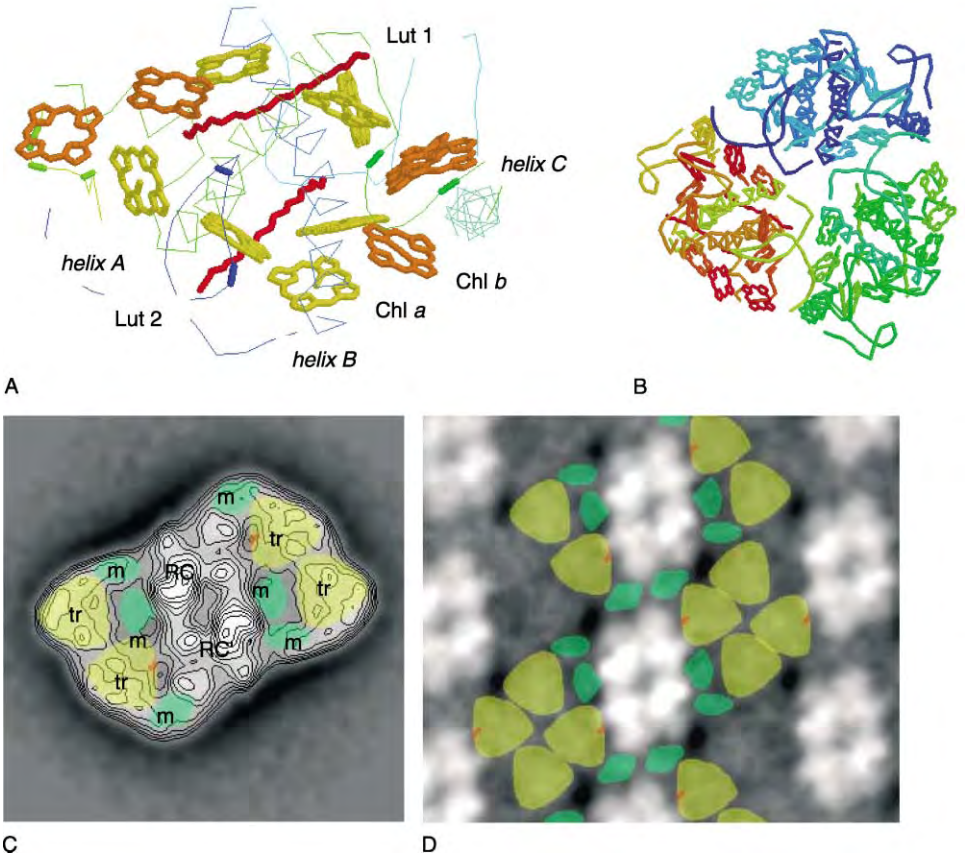

FIGURE 2 Structure of LHCII. (A) Atomic structure based on the electron diffraction analysis of 2D crystals of the isolated LHCII; Chl *a* and *b* – chlorophyll *a* and *b*; Lut 1 and 2 – luteins. (B) 3 monomeric LHCII forming the trimer. (C) Assembly of light harvesting complexes, monomers of CP26, CP29, and CP24 (m) and LHCII trimers (tr, highlighted light green) around two reaction center complexes (RC) in the photosystem II supercomplex. (D) Arrangement of ordered 2D arrays of photosystem II complexes in the photosynthetic membrane; highlighted structures: LHCII trimers – light green, monomers of CP24, CP26 and CP29 – dark green.

LHCII have different capacities to absorb light of different colors – the former preferring more red light than the latter – there will be a frequent imbalance in light energy input into reaction centers. This imbalance will decrease the electron transfer efficiency, hence the quantum yield of photosynthesis. The light intensity is also a very changeable parameter, sometimes varying 1000-fold. Whenever light input exceeds the capacity of electron transport and CO_2 assimilation, there is an excess of light, which may cause photoinhibition – the destabilization (by over-reduction and over-energization) and even damage (by photo-oxidation and generation of reactive oxygen species) to photosynthetic components, mainly in PSII. The effects of changes in light delivery can be amplified by alterations in photosynthetic capacity brought about by changes in other environmental factors, or by changes in metabolic demand, which result in variation in the rate of turnover and the stoichiometry of ATP and NADPH.

In order to achieve balance and stability of the photosynthetic process, regulatory mechanisms are necessary. The plant cell first has to assemble a chloroplast with the "correct" composition, and then various parts of the photosynthetic process need to be able to adjust their activities in response to internal and external information. Thus, the electron transport and carbon metabolism can be considered to be linked by a feedback and feed-forward control network. There is a compromise between maximizing the collection and utilization of light, and the avoidance of instability when light is in excess. The most appropriate way of looking at the regulatory mechanisms is, given a fixed composition and a fluctuating environment, that they extend the range of conditions over which photosynthesis can remain in balance – they provide homeostasis of excitation energy level, redox state, and ΔpH.

To optimize light harvesting function, two distinct regulatory strategies are required. The first aims to balance the input of light energy to PSI and PSII reaction centers in order to optimize electron transfer rate – this is called the state transitions. The second should regulate the amount of light energy directed to PSII – this is called nonphotochemical energy dissipation, or quenching (NPQ). As a result of evolution, both regulatory mechanisms have developed in the LHCII system and rely on its abilities to sense the "state" of the light energy balance and structurally respond, being capable of dynamic behavior.

State Transitions

The Lhcb1 and Lhcb2 polypeptides of LHCII are reversibly phosphorylated by a redox-regulated thylakoid-associated protein kinase. Phosphorylation at threonine residues near the N terminus of LHCII

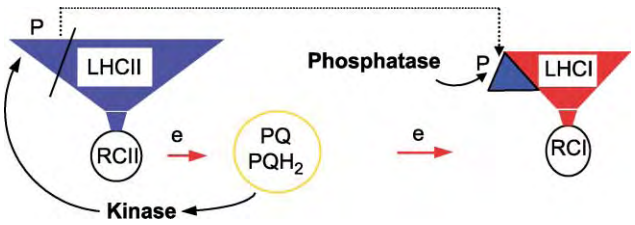

FIGURE 3 State transitions: the mechanism of compensation against imbalance of energy input into photosystems I and II. The redox controlled protein kinase phosphorylated LHCII when PQH_2 accumulates. A constitutive phosphatase activity dephosphorylates LHCII. This self-regulating system depends upon the different affinities of LHCII and phospho-LHCII for RCI and RCII.

weakens the association between PSII and LHCII, as a result of electrostatic and conformational changes. Phospho-LHCII partitions in favor of PSI, the association depending on the presence of the PSI-H subunit – in mutants without PSI-H phospho-LHCII remains associated with PSII. The kinase is activated when the plastoquinone pool is reduced, this being sensed by the quinone oxidation site on the cytochrome b_6f complex. The kinase therefore monitors the relative rates of delivery of excitation energy to PSII and PSI (Figure 3); overexcitation of PSII (state 1) activates the kinase, decreases delivery of excitation energy to PSII, and increases transfer to PSI (state 2). Levels of LHCII phosphorylation are lower at high light compared to low light, showing that the state transitions optimize photosynthesis in limiting light. This includes not only optimizing linear electron transport, but also the provision of optimal ΔpH and ATP/NADPH ratios by controlling the proportion of cyclic electron transfer around PSI.

Nonphotochemical Energy Dissipation

Energy-Dependent Quenching, qE

Dissipation, or quenching, of excess excitation energy absorbed by LHCII occurs by two processes, distinguished by the speeds with which they are induced upon exposure to illumination, their relaxation times in darkness and the light intensity threshholds. The major process under "normal" conditions is called qE, since it depends upon the energization of the thylakoid membrane as a result of ΔpH formation. Thus, the progressive increase in ΔpH that occurs as light saturation of photosynthesis is reached and is the trigger for energy dissipation. It can therefore be referred to as feedback de-excitation. The formation of qE occurs within seconds – minutes of exposure to excess light, and relaxes with a similar rate in darkness. In contrast, the sustained qI-type of quenching may take several

minutes or even hours to appear and relax, and under some conditions (such as low temperature) may be stable for days.

The Site of Quenching

Application of mathematical models for PSII energy transfer showed that quenching associated with qE occurred in the light harvesting antenna. Refinements of the analysis showed that qE is best explained by the transition between two states of the antenna, with different rate constants for energy dissipation. Subsequently, analysis of the chlorophyll fluorescence lifetimes provided direct support for this suggestion. Spectroscopic data and biochemical analysis confirmed that the PSII antenna was the site of quenching. A powerful way to determine which proteins are involved in qE is to investigate plants deficient in specific components. Experiments using plants deficient in all of the Lhcb proteins suggested that qE was not a property of the core antenna. However, plants in which Lhcb1 and 2, Lhcb4 and 5 have been separately reduced to less than 5% wild-type levels of protein by antisense technology show little or no change in qE, and in plants it has not proved possible to invoke a particular antenna complex as having an obligatory role. A major landmark in qE research was the identification of the *npq4* mutant, a mutant lacking qE and which is deficient in the Lhc-related protein PsbS. This four-helix protein is located in PSII, and contains protonatable amino acid residues which are thought to sense the thylakoid lumen pH.

The Xanthophyll Cycle

Under conditions of excess light, violaxanthin is de-epoxidized to zeaxanthin via the mono-epoxide antheraxanthin due to the activation of violaxanthin de-epoxidase, a thylakoid lumen enzyme. Another enzyme, zeaxanthin epoxidase, reverses the reaction in low light. A vast amount of data, from a wide variety of plant species under many different environments, showed correlations between the extent of qE and the de-epoxidation state of the xanthophyll cycle pool. Zeaxanthin is an activator of qE in that the apparent pK_a of the protonation reaction inducing qE shifts from near 4.5 to well over 5.0 in the presence of zeaxanthin. Since the ΔpH *in vivo* does not fall below 5.5, qE will depend completely on de-epoxidation of violaxanthin. Therefore, qE is an allosteric process, under the control of the interacting effects of protonation and zeaxanthin binding, similar to a regulated enzyme (Figure 4). This mode of regulation explained how the chloroplast could have a ΔpH high enough in limiting light to allow ATP synthesis without qE, yet in saturating light, how to have maximum electron transport rates and high qE simultaneously.

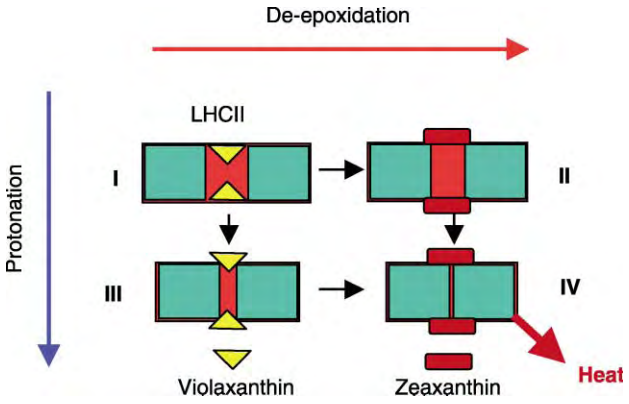

FIGURE 4 Model for the excess energy dissipation in the LHCII antenna. I – light-harvesting mode, a dark-adapted state; II – partially energy-dissipative, intermediate state; III – light "memory" mode, a dark-adapted mode after zeaxanthin was formed; IV – energy dissipative mode. The closeness of the boxes represents the extent of pigment interaction in LHCII and controls the level of quenching.

It has proved difficult to distinguish between the proposal that zeaxanthin was directly involved in quenching chlorophyll excited states by chlorophyll/zeaxanthin energy transfer, and the notion that zeaxanthin was working indirectly, modifying or inducing a quenching process intrinsic to the PSII antenna.

The Nature of the Quenched State of LHCII

Changes in the absorption spectra of chlorophyll and carotenoid occur upon formation of qE. A band with a maximum at 535 nm (ΔA_{535}) has attracted most attention, since its appearance is perfectly correlated to the amount of "quencher." Resonance Raman spectroscopy of leaves and chloroplasts has shown that ΔA_{535} is electronic in origin, and arises from a pool of one or two zeaxanthin molecules per PSII, which undergo a strong red shift in the presence of ΔpH. A similar red shift occurs when zeaxanthin binds to PsbS *in vitro*, and it is concluded that ΔA_{535} arises from this interaction.

Analysis of fluorescence lifetimes shows that the qE state of the PSII antenna has a lifetime of 0.4 ns, and the unquenched state 1.6 ns. Experiments with isolated light harvesting complexes have shown how such a change can arise. Detergent-solubilized LHCII has a lifetime of 4 ns, but reduction of the detergent concentration causes formation of oligomers with an average lifetime of 0.3 ns. This quenching has many features that are similar or identical to qE. The spectral changes in chlorophyll accompanying this *in vitro* quenching indicate that a particular LHCII domain is involved. The *in vitro* quenched state can also be investigated by reconstitution of light harvesting complexes with altered carotenoid content.

Substitution of lutein with zeaxanthin in LHCII causes partial chlorophyll fluorescence quenching.

In general, the ease with which LHCII *in vitro* can adopt a quenched state reflects the high density of pigment within it. Its design as a light harvesting complex means it maximizes the amount of chlorophyll per unit volume. Specific features of protein structure are needed to control the interactions between pigments, to promote energy transfer and to prevent formation of quenchers – dimers or excimers of chlorophylls and/or chlorophyll-xanthophyll associates. Therefore, only rather small changes in structure are needed to allow a quencher to form. Indeed, the activation energy for the formation of a quencher in LHCII is only 6 kcal mol^{-1}, indicative of the breakage of just a couple of H bonds. Thus, LHCII is uniquely poised to allow a switch between an unquenched state functioning in photosynthetic energy capture and a quenched state, dissipating excess energy as heat.

Biological Diversity of qE

The amount of qE in different plants is highly variable. High light grown plants may have 2–3 times more qE capacity and plant species adapted to growing in stressful environments have a much higher qE capacity than those inhabiting milder conditions. Genetic manipulation to increase the level of the PsbS protein results in an increase in qE, suggesting that the level of this protein is an important determinant of qE capacity.

Algae exhibit different qE properties as compared to higher plants. In *Chlamydomonas*, qE is smaller and forms more slowly, and mutation of an LHCII subunit decreases the capacity of qE, suggesting that here a less efficient process is controlled directly by the antenna and not by PsbS. In diatoms, which have light harvesting proteins of a different type, qE can be much larger than in higher plants, and its formation and relaxation totally depend upon the de-epoxidation of the violaxanthin analogue, diadinoxanthin. It seems that some features of the molecular mechanism for the regulation of light harvesting have diverged during evolution of classes of organisms.

Other Responses of LHCII to Excess Light

The sustained qI-type of quenching appears to also result, in part at least, from alteration in the antenna of PSII. At low temperature strong quenching is induced by light which has some features diagnostic of an increase in aggregation state of LHCII – formation of a red-shifted fluorescence emission band at 77 K. This state of LHCII seems to be semipermanent in some evergreen plants during winter. The mechanism by which such quenching is formed is currently unknown, although one possibility is that it arises from a direct effect of light on LHCII. Such an effect is well known for LHCII *in vitro*, and it appears to be triggered by a light-induced dissociation of trimers into monomers. At elevated temperature increased light-induced quenching arises from a different process – LHCII dissociates from PSII to be quenched by PSI, in a process that resembles the state transition, and in fact phosphorylation of LHCII and elevated temperature act synergistically.

When plants grown under low light are exposed to a sustained increase in light intensity, LHCII degradation is induced. Only monomers can be the substrates for proteolysis, and so this process must be preceded by a light-induced breakdown of trimers. Little is known about the biochemistry or regulation of this proteolytic process. Under extreme conditions, not only LHCII but complete photosystems are degraded as the plants seek to minimize oxidative damage.

The content of LHCII varies significantly depending on the light intensity under which the plants are grown. Typically, a low light grown plant may have 4–5 trimers per PSII core complex, whereas in high light this reduces to 1–2. The extra LHCII in low light plants appears to be present in membrane domains deficient in PSII core complexes. These LHCII domains can still be involved in efficient energy transfer, even transferring energy to pigments on opposite membranes in the grana.

The adjustment of the composition of photosystem II upon growth in high light compared to low light maintains the redox potential and ΔpH at the correct level, optimizing photosynthesis and avoiding oxidative stress. At higher growth irradiance, when LHCII cannot decrease any more, there are increases in the capacity for photoprotection (e.g., through an increase in xanthophyll cycle activity or PsbS content) and, eventually, decrease in the chlorophyll content of the leaf in order to lower light absorption. Even macroscopic events such as chloroplast movements or changes in leaf orientation can be similarly viewed as contributing to the optimization of light harvesting and counter-acting photodamage. Thus, plants do whatever they can, by a multitude of mechanisms, to limit the level of excitation energy in the PSII antenna, giving balance with the demands of photosynthesis, and optimising the redox state and ΔpH.

See Also the Following Articles

Chlorophylls and Carotenoids • Light-Harvesting Complex (LHC) I and II: Pigments and Proteins • Photosynthesis

Glossary

grana membrane The characteristic organization of the chloroplast thylakoids in which regions of membrane become tightly appressed together to form stacks of membranes, associated with the lateral segregation of the photosystems.

nonphotochemical quenching The quenching of chlorophyll fluorescence that arises because of an increase in thermal dissipation of excitation energy, contrasted to the photochemical quenching that arises because energy is used to drive photosynthetic electron transfer.

ΔpH The pH gradient, ~pH 7–8 outside and pH 5–6 inside, across the thylakoid membrane that results from light-induced proton uptake.

photoinhibition The inhibition of photosynthesis that arises during excess illumination, either from sustained quenching of antenna or reaction center complexes, or from accumulation of damaged photosystem II D1 proteins.

state transitions The reversible adaptation of the light harvesting system to differential excitation of PSI and PSII; in state 1, induced by overexcitation of PSI, energy transfer from LHCII to PSII is maximum, and in state 2, induced by overexcitation of PSII, energy transfer from LHCII to PSI is maximum.

xanthophyll cycle The reversible de-epoxidation of thylakoid bound violaxanthin to zeaxanthin, via the intermediate antheraxanthin.

Further Reading

Blankenship, R. E. (2001). *Molecular mechanisms of photosynthesis.* Blackwell Science, UK, p.328.

Demmig-Adams, B., and Adams, W. W. (2002). Antioxidants in photosynthesis and human nutrition. *Science* **298**, 2149–2153.

Green, B. R., and Dunford, D. G. (1996). The chlorophyll-carotenoid proteins of oxygenic photosynthesis. *Annu. Rev. Plant Physiol. Plant Molecul. Biol.* **47**, 685–714.

Haldrup, A., Jensen, P. E., Lunde, C., and Scheller, H. V. (2001). Balance of power: a view of the mechanism of photosynthetic state transitions. *Trends Plant Sci.* **6**, 301–305.

Hankamer, B., and Barber, J. (1997). Structure and membrane organization of photosystem II in green plants. *Annu. Rev. Plant Physiol. Plant Molecul. Biol.* **48**, 641–671.

Horton, P., Ruban, A. V., and Walters, R. G. (1996). Regulation of light harvesting in green plants. *Annu. Rev. Plant Physiol. Plant Molecul. Biol.* **47**, 655–684.

Horton, P., Ruban, A.V., Young, A.J (1999). Regulation of the structure and function of the light harvesting complexes of photosystem II by the xanthophyll cycle. In *The Photochemistry of Carotenoids: Applications in Biology* (H.A. Frank, A.J. Young and R.J. Cogdell, eds.) pp. 271-291, Dordrecht, The Netherlands, Kluwer Academic.

Horton, P., Murchie, E. H., Ruban, A. V., and Walters, R. G. (2001). Increasing rice photosynthesis by manipulation of the acclimation and adaptation to light. Rice biotechnology: improving yield, stress tolerance and grain quality. *Novartis Foundation Symposium,* **236**, 117–134.

Niyogi, K. K. (1999). Photoprotection revisited: genetic and molecular approaches. *Annu. Rev. Plant Physiol. Plant Molecul. Biol.* **50**, 333–359.

Muller, P., Li, X. P., and Niyogi, K. K. (2001). Non-photochemical quenching. A response to excess light energy. *Plant Physiol.* **125**, 1558–1566.

Biography

Peter Horton is a Professor of Plant Biochemistry in the department of Molecular Biology and Biotechnology at the University of Sheffield in the United Kingdom. His principal research interest is in photosynthesis and related aspects of plant biology. He holds a D.Phil. and D.Sc. from the University of York and received postdoctoral training at Purdue University. He has developed the concepts involved in the regulation of the light reactions of photosynthesis, establishing the role of LHCII phosphorylation in the state transitions, developing the methodology and framework of chlorophyll fluorescence analysis, and determining the basic mechanisms underlying nonphotochemical quenching.

Alexander Ruban is a Research Associate at the University of Sheffield where his principal research interest is in the biophysical aspects of photosynthesis. He holds a Ph.D. from the University of Kiev. Dr. Ruban has developed a number of spectroscopic approaches to investigate the dynamics of LHCII *in vitro* and *in vivo*.

Photosystem II: Assembly and Turnover of the D1 Protein

Eira Kanervo and Eva-Mari Aro
University of Turku, Turku, Finland

Photosystem II (PSII) is an integral membrane protein complex of ~25 subunits. It resides in the thylakoid membrane of organisms performing oxygenic photosynthesis, i.e., in chloroplasts of higher plants, mosses, ferns and algae, as well as in prokaryotic cyanobacteria. The synthesis and assembly of a new PSII complex in eukaryotic organisms require cooperation of both chloroplast and nuclear genomes. Besides structural protein subunits, PSII contains pigments and cofactors involved in the photochemistry of PSII. Most of the cofactors are ligated to the reaction center proteins D1 and D2. Such an arrangement together with the toxic nature of PSII photochemistry renders the reaction center prone to a photo-induced damage and accelerates the turnover rate of PSII subunits. The primary target of photodamage and the most rapidly turning-over subunit is the D1 protein. This protein has to be constantly replaced in order to maintain the PSII complex in an active state. This dynamic process, known as the PSII photoinhibition repair cycle, occurs in the thylakoid membrane at the rate depending on light intensity. The repair cycle is an absolute requirement for the maintenance of PSII complexes active in photosynthesis.

Biogenesis and Assembly of a New PSII Complex

Cooperation between Chloroplast and Nucleus

The PSII complex of eukaryotic organisms contains both nuclear and chloroplast-encoded gene products, as is the case with other photosynthetic protein complexes in the thylakoid membrane. This indicates that a tight cooperation exists between the organelle and nucleus in building up the PSII complex. From at least 25 genes encoding the PSII proteins, 15 genes reside in the chloroplast genome, rest of them locating in the nucleus.

Targeting the Chloroplast-Encoded PSII Proteins

The majority of the PSII core proteins are chloroplast encoded. These comprise the D1, D2, CP43, CP47, cyt $b559\alpha$, and cyt $b559\beta$ proteins encoded by the *psbA*, *psbD*, *psbC*, *psbB*, *psbE*, and *psbF* genes, respectively. In addition, the PSII core proteins include the *psbH*, *psbI*, *psbJ*, *psbK*, *psbL*, *psbM*, *psbN*, *psbTc*, and *psbZ* gene products of low molecular weight. Translation of the chloroplast-encoded PSII core proteins takes place on the surface of the thylakoid membrane. Initiation of translation of many chloroplast-encoded proteins is regulated by nuclear-encoded mRNA-binding proteins. To what extent these proteins are involved in targeting the ribosome–mRNA complexes to the thylakoid membrane is, however, unclear. Insertion of the chloroplast-encoded PSII proteins to the thylakoid membrane occurs both co- and posttranslationally, and several soluble and membrane proteins are involved in assisting these processes. Cotranslational membrane insertion is typical for the PSII core proteins with several transmembrane helices, such as the D1, D2, CP43, and CP47 proteins.

Targeting the Nuclear-Encoded PSII Proteins

The nuclear-encoded PSII core monomer proteins are three low-molecular-weight (LMW) subunits, namely the *psbW*, *psbX*, and *psbTn* gene products. In addition, proteins of the light-harvesting chlorophyll *a/b*-binding protein complex II (LHCII) and the oxygen-evolving complex (OEC) are nuclear encoded. All the nuclear-encoded proteins are synthesized as precursors on cytosolic ribosomes. These precursors are subsequently targeted to the chloroplast via an N-terminal transit peptide, which is proteolytically cleaved after import into the chloroplast. The nuclear-encoded precursor proteins targeted to the thylakoid lumen contain a bipartite N-terminal transit peptide, the last part of which is removed after the arrival of the transported protein into the lumen. The lumenal proteins, including those for the OEC, use both the Sec machinery and the ΔpH pathway in their insertion and translocation to the lumenal side of the thylakoid membrane. Integration of the LHCII proteins to the membrane is dependent on the presence of the thylakoid-located Alb3 protein.

Assembly of a New PSII Complex

General Features

Understanding of the assembly of the PSII complex is, so far, in its infancy. Besides purely biochemical approaches, the assembly of PSII has been studied using plant and cyanobacterial mutants. Such mutants have been deficient in a specific PSII subunit or they have carried a mutation in a nuclear gene that affects the expression or assembly of a structural PSII subunit. Also studies on plastid development from etioplast to chloroplast have contributed to the understanding of PSII assembly. Furthermore, research on the light-induced turnover of the PSII complex has produced information that can be applied also for the research on the assembly process of a new PSII center.

Sequence of the Assembly of PSII Core, OEC and LHCII Proteins

Light is required for maturation of etioplasts to chloroplasts and for synthesis and assembly of most of the PSII subunits. However, some of the PSII subunits do not need light for synthesis, since they exist already in etioplasts. This is the case particularly with cyt *b559* and the OEC proteins. In the assembly of the PSII core proteins, the two-subunit cyt *b559* functions as the first assembly partner for the D2 protein. All these together form an initial complex that functions as a receptor for the cotranslational assembly of the precursor-D1 protein. The assembly process then continues by association of the *psbI* gene product and the CP47 protein to the PSII subcomplex. Subsequently, the *psbH* gene product, the CP43 protein, and several LMW subunits attach to the growing PSII subcomplex. Assembly of the additional LMW subunits, namely the *psbJ* and *psbL* gene products, is essential for subsequent proper association of the OEC proteins to the lumenal side of the PSII core monomer. Finally, the rest of the LMW subunits, such as the *psbK*, *psbW*, and *psbZ* gene products, are required for the last events of the assembly process. These events include dimerization of the PSII core monomer and the attachment of LHCII to the PSII complex resulting in formation of a PSII supercomplex. An array of such PSII supercomplexes exists in the grana membranes of chloroplasts.

Regulation of the PSII Assembly

Light is required for an efficient translation elongation and accumulation of the D1 protein as well as for synthesis of the CP43 and CP47 core proteins. In addition to light, regulation of synthesis and assembly of the PSII complex involves the availability of a variety of factors, including the ligation of pigments and cofactors (chlorophyll *a*, pheophytin, β-carotene, Fe, Mn, plastoquinone) and the availability of the assembly partners.

The chloroplast-encoded core proteins D1, D2, CP43, and CP47 are cotranslationally inserted into the thylakoid membrane. Pigments are thought to bind to these proteins during their cotranslational membrane translocation and during the concomitant association of the protein with its assembly partner(s). Light is needed for the chlorophyll biosynthesis at the level of conversion of protochlorophyllide to chlorophyll *a*. Currently, we lack information on details of the pigment binding, even though the importance of this event as a regulative step in the PSII assembly has been known for a long time. It is clear, however, that the chlorophyll-binding proteins of PSII are stabilized by ligation of pigments. Most chlorophyll-binding proteins do not accumulate at all in a nonpigmented form.

Successful synthesis of the PSII core proteins requires the availability of assembly partners. Synthesis of the D2 protein is dependent on the presence of cyt *b559*. Furthermore, cyt *b559*/D2 subcomplex is indispensable for the synthesis of D1, and the cyt *b559*/D2/D1 subcomplex, in turn, functions as an assembly partner for CP47. From the PSII core proteins, CP43 seems to be synthesized quite independently.

Turnover of the D1 Protein of PSII

PSII Photoinactivation and the D1 Protein Damage

The PSII complex performs a remarkable task in splitting water molecules to oxygen and hydrogen (protons). Such oxidizing electron transfer reactions of PSII in an atmosphere containing oxygen readily lead to the formation of highly reactive radicals that are potentially harmful to the protein moiety. Conditions that lead to imbalance between the various steps during the linear electron transfer process can lead to photoinactivation of PSII. Thus PSII, when performing its normal function, is hazardous for itself.

Photoinactivation of PSII increases almost linearily with increasing light intensity. Under low light the rate of photoinactivation is also low. The rate of inactivation correlates with the amount of photons absorbed and mediated to the reaction center. Upon inactivation, the PSII complex becomes unable to transfer electrons and split water molecules. A constant repair of inactivated complexes is required to guarantee the maintenance of a sufficient level of active PSII complexes for photosynthesis. The efficiency of repair is affected negatively by environmental stress factors, such as high light and the extremes of temperature. If the repair process cannot keep up with the rate of photodamage, nonfunctional PSII complexes start to accumulate. This situation leads to the measurable decrease in the rate of total photosynthesis.

The primary target of the photo-induced PSII damage is the reaction center protein D1. This fact reflects the "grand design" of PSII: only one protein of the multi-subunit complex is primarily destroyed, the rest of the proteins being rescued for further use, i.e., reparation of the PSII complex. The primary photodamage is thought to include a conformational change and an oxidative damage to the D1 protein. These events, in turn, trigger the reaction center protein D1 to a substrate for proteolytic degradation. However, the actual nature of the primary photodamage is not yet properly understood.

PSII Photoinhibition Repair Cycle

Start of the Repair Process

Active PSII centers exist as dimers in the thylakoid membranes of grana stacks (Figure 1). After a light-induced damage to PSII, the LHCII antenna dissociates and monomerization of PSII occurs. PSII monomers then migrate from the grana to the stroma-exposed thylakoid membranes where a contact with the components acting in degradation and synthesis of the D1 protein is feasible. OEC dissociates from PSII and a partial disassembly of the PSII core proteins takes place. The stages from photodamage to degradation of the D1 protein are regulated by phosphorylation-dephosphorylation events of the PSII core proteins.

Degradation of the D1 Protein

Degradation of the light-damaged D1 protein is a proteolytic process that occurs in a well-coordinated manner on the stroma-exposed thylakoid membranes, leaving the closest partner, the D2 protein, most often

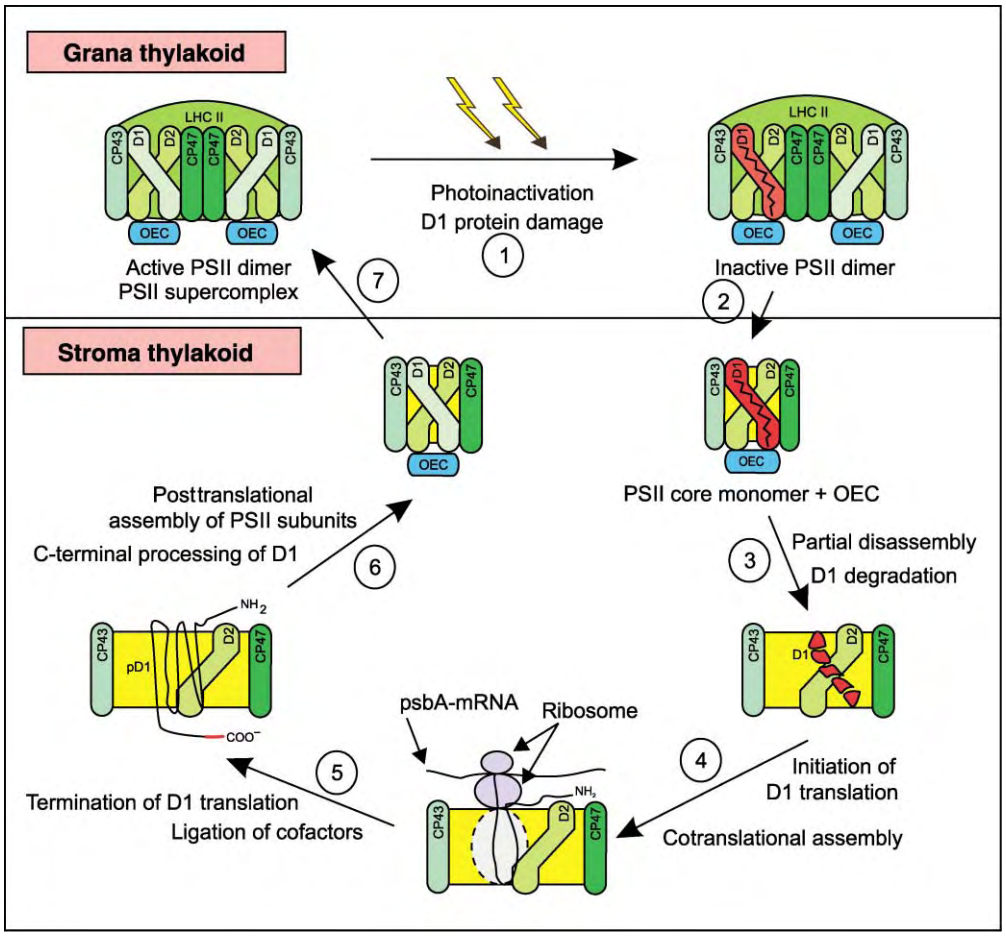

FIGURE 1 Model for the PSII photoinhibition repair cycle. 1) Photoinactivation of PSII and damage to the D1 protein. 2) Monomerization of the inactive PSII complex and its translocation from the grana thylakoids to the stroma-exposed thylakoids. 3) Partial disassembly of the PSII core proteins and proteolytic degradation of the D1 protein. 4) Initiation of D1 translation and cotranslational assembly of the nascent D1 chain into the D1-depleted PSII core monomer. 5) Ligation of cofactors during translation elongation and termination of D1 translation. 6) C-terminal processing of the pD1 protein; posttranslational assembly of the PSII core subunits and OEC. 7) Translocation of the repaired PSII monomer from the stroma-exposed thylakoids to the grana thylakoids; dimerization of PSII and the attachment of the LHCII antenna. D1, D2, CP43, CP47 = chlorophyll *a*-binding proteins of the PSII core; LHCII = light-harvesting chlorophyll *a*/*b* binding protein complex II; OEC = oxygen-evolving complex; pD1 = precursor-D1 protein.

intact. The D1 protein is an integral membrane protein with five transmembrane helices. Between helices there are loops both on the stromal and lumenal sides of the thylakoid membrane. The loops are the preferential sites of the primary cleavage of an integral membrane protein, in general, the stromal DE-loop being the most important one in the case of the D1 protein. The primary proteolysis of D1 produces fragments that are further degraded by the secondary proteolysis. Proteases from the DegP and FtsH families are known to act on the proteolysis of the D1 protein.

Synthesis of the D1 Protein

Synthesis of the D1 protein during the PSII repair cycle shares features with synthesis of the D1 protein in the assembly of a new PSII complex (see above). The D1 protein is encoded by the *psbA* gene residing in the chloroplast genome. The *psbA* mRNA-ribosome complex is targeted to the stroma-exposed thylakoid membrane, where elongation of the nascent D1 chain takes place. The nascent D1 chain is cotranslationally inserted into the thylakoid membrane, where the D2 protein and cyt *b559* act as the first association partners. Elongation is controlled by a variety of factors. Such factors include association of the nascent chain with a translocon, availability of the assembly partners, redox control of translation elongation and ligation of pigments. Resynthesis of the assembly partners is not needed, since they originate mainly from the existing PSII centers under repair.

When all the five transmembrane helices have been synthesized, the precursor D1 protein releases from the ribosome. The fifth transmembrane helix traverses the membrane, finally having its carboxy terminus in the thylakoid lumen.

Posttranslational Events of the D1 Synthesis and Reactivation of the PSII Complex

Posttranslational events of the D1 protein synthesis include several steps. First, during maturation of the D1 protein, the lumenal processing protease CtpA removes the extension of 9–16 amino acids from the carboxy terminus of the precursor D1 protein. This cleavage is necessary for ligation of the manganese cluster and reassociation of the OEC to the PSII complex. Before the OEC proteins can reassociate, the core proteins CP47, CP43 and most of the LMW subunits have to be reassembled to the PSII subcomplex. Finally, the properly assembled PSII monomer migrates back to the grana thylakoids, where PSII core dimerization and full reactivation of the PSII complex take place. The final reactivation stage also includes an association of the LHCII antenna proteins to the PSII dimer. These final stages in the grana thus accomplish the PSII photoinhibition repair cycle providing an active PSII dimer for photosynthesis.

See Also the Following Articles

Chloroplasts • Photosystem II Light Harvesting System: Dynamic Behavior • Photosystem II: Protein Components • Photosystem II: Water Oxidation, Overview

Glossary

D1 protein turnover Replacement of a nonfunctional D1 protein in the PSII complex.

photoinactivation Light-induced inactivation of the PSII electron transfer and water splitting.

PSII (photoinhibition) repair cycle Cycling of the PSII complexes between the grana- and stroma-exposed thylakoid membranes during the turnover of the D1 protein.

Further Reading

Andersson, B., and Aro, E.-M. (2001). Photodamage and D1 protein turnover in photosystem II. In *Regulation of Photosynthesis* (E.-M. Aro and B. Andersson, eds.) Vol. 11, pp. 377–393. Kluwer, Dordrecht, The Netherlands.

Baena-Gonzáles, E., and Aro, E.-M. (2002). Biogenesis, assembly and turnover of photosystem II units. *Phil. Trans. Roy. Soc. Lond. B* **357**, 1451–1460.

Herrmann, R. G., and Westhoff, P. (2001). Thylakoid biogenesis and dynamics: the result of a complex phylogenetic puzzle. In *Regulation of Photosynthesis* (E.-M. Aro and B. Andersson, eds.) Vol. 11, pp. 1–28. Kluwer, Dordrecht, The Netherlands.

Paulsen, H. (2001). Pigment assembly – Transport and ligation. In *Regulation of Photosynthesis* (E.-M. Aro and B. Andersson, eds.) Vol. 11, pp. 219–233. Kluwer, Dordrecht, The Netherlands.

Van Wijk, K. J. (2001). Proteins involved in biogenesis of the thylakoid membrane. In *Regulation of Photosynthesis* (E.-M. Aro and B. Andersson, eds.) Vol. 11, pp. 153–175. Kluwer, Dordrecht, The Netherlands.

Zerges, W. (2002). Does complexity constrain organelle evolution? *Trends Plant Sci.* **7**, 175–182.

Biography

Eva-Mari Aro is a Professor and Academy Professor in the Department of Biology at the University of Turku in Finland. Her principal interests are in the field of photosynthesis, including the photosystem II photoinhibition repair cycle, the assembly of PSII, and the redox regulation of thylakoid protein phosphorylation. Her scientific training abroad includes research visits to the University of California in Berkeley, USA, CEN Cadarache in France, the University of Stockholm in Sweden, and CSIRO in Canberra, Australia.

Eira Kanervo is a lecturer in the Department of Biology at the University of Turku in Finland. Her principal research interests include regulation of the D1 protein degradation and stress physiology of plants. She has been as a post-doc researcher at the National Institute for Basic Biology in Okazaki, Japan, and at the University of Linkoping, Sweden.

Photosystem II: Protein Components

James Barber
Imperial College, London, UK

Photosystem II (PSII) is a multisubunit protein complex embedded in the thylakoid membranes of oxygenic photosynthetic organisms: plants, algae, diatoms, and cyanobacteria. By using chlorophyll and several redox active cofactors, it captures and uses solar energy to split water into molecular oxygen and reducing equivalents.

$$2H_2O \xrightarrow[PSII]{4h\nu} O_2 + 4H^+ + 4e^-$$

To produce a dioxygen molecule, four photons ($h\nu$) are needed to provide the energy to split two water molecules The dioxygen released maintains our oxygenic atmosphere and provides an ozone layer which protects us from the damaging effects of UV radiation. The reducing equivalents which exit PSII as plastoquinol, are ultimately used, with the aid of additional light energy absorbed by photosystem I, to convert atmospheric carbon dioxide to the organic molecules that make up virtually all the biomass on our planet.

Morphology

Thylakoid Membrane

In chloroplasts of plants and green algae, the thylakoids are highly folded membranes having stacked (grana) and unstacked (stromal) lamellae regions. PSII is located mainly in the stacked regions. In cyanobacteria, diatoms, and other types of algae the thylakoids do not have a clear differentiation into stacked and unstacked regions and PSII is more evenly distributed along the plane of the membrane. In all cases the thylakoid membrane encloses an inner aqueous compartment known as the lumen while the outer compartment is either the stroma of the chloroplast or cytoplasm of cyanobacteria.

Reaction Center (RC)

RC is that part of a photosystem, like PSII, where light energy is converted to electrochemical potential energy. It is composed of protein-bound redox active cofactors that facilitate charge separation across the membrane.

Light-Harvesting Complexes

These pigment–protein complexes capture light energy and transfer it to the reaction center. They are often composed of several hundred pigment molecules, the exact number being dependent on growth conditions. Various pigments are used so as to fully utilize the solar spectrum and for PSII these are different types of chlorophyll, phycobilins, and carotenoids. Some light-harvesting complexes (LHCs) are contained within the thylakoid membrane (intrinsic) and some attach to the surface (extrinsic) of the membrane.

Redox Active Cofactors

P680

P680 is composed of a chlorophyll *a* molecule which, after excitation by the absorption of light to form $P680^*$, gives up an electron to an acceptor, converting it to $P680^{\cdot+}$. The redox potential of this radical cation is estimated to be 1.1 V or more, which is required to oxidize water. Its oxidation causes a bleach in its absorption spectrum centered at 680 nm. P680 is located on the lumenal side of the PSII RC. Recent work suggests that the excited state $P680^*$ is delocalized over four chlorophyll molecules and that upon oxidation the "hole" becomes localized on a single chlorophyll.

Pheophytin *A*

Pheophytin *a* (Pheo) is the primary electron acceptor of PSII located toward the stromal side of the RC. It receives an electron from $P680^*$ in a few picoseconds to form a radical pair $P680^{\cdot+}Pheo^{\cdot-}$. The reduction of Pheo can be detected as an optical absorption decrease at 422 nm and its reduction potential is ~ -600 mV.

Q_A

Q_A is a bound plastoquinone (PQ) molecule which undergoes a single reduction by $Pheo^{\cdot-}$ in $\sim$200 ps, forming the charge transport state $P680^{\cdot+}$ Pheo $Q_A^{\cdot-}$ where the redox potential of the semi-plastoquinone (Q_A^-) is ~ -150 mV.

Q_B

Q_B is also a plastoquinone (PQ) which can accept two electrons successively from $Q_A^{\cdot -}$ and together with two protons (H^+) from the stroma or cytoplasm to form plastoquinol (PQH_2). In this fully reduced form PQH_2 is released from the Q_B-binding site of the PSII RC and diffuses into the lipid matrix of the thylakoid membrane until it is oxidized by the cytochrome b_6f complex. The reducing equivalents are further "energized" by a second light reaction which occurs in photosystem I (PSI) so as to reach a redox potential sufficient to reduce carbon dioxide.

Y_Z

Y_Z is redox active tyrosine which reduces $P680^{\cdot +}$. In so doing, it loses an H^+ from its phenolic group and the resulting species is a neutral tyrosine radical $Y_Z^{\cdot}$.

$(Mn)_4$-Cluster

A cluster of four manganese atoms together with a Ca^{2+} atom, make the catalytic center (Mn_4Ca^{2+}-cluster), where the splitting of two substrate molecules occurs. The removal of 4e and $4H^+$ requires four successive oxidations of P680, and there is evidence that $Y_z^{\cdot}$ may act as an H^+ as well as an electron acceptor and therefore is directly involved in the water oxidation reaction.

Proteins

The RC core complex of PSII is composed of a large number of proteins encoded by Pcb genes (see Table I). The RC core is serviced by LHC proteins, the number and type of which varies between different types of organisms. Plants and green algae have their LHC proteins encoded by *cab* genes while red algae and cyanobacteria contain phycobiliproteins encoded by *apc* and *cpc* genes. Here we confine ourselves to PSII RC core proteins encoded by the *psb* genes (Figure 1).

PsbA-D1 Protein

After C-terminal posttranslational modification this protein has a molecular mass ~38 kDa and contains ~350 amino acids depending on species. It has five transmembrane α-helices (A–E), DE stromal surface α-helix, and CD lumenal surface α-helix. It binds the majority of the cofactors involved in PSII-mediated electron transport: Y_Z is Tyr161, $P680^{\cdot +}$ is chlorophyll *a* ligated by His198, Pheo is probably H-bounded by Tyr126 and Glu130, Q_B via interactions with His 215 and Ser 264. The Mn_4Ca^{2+}-cluster, is probably ligated by Asp170, Glu189, Ala344, His332, Glu 333, and His337. The D1 protein also binds a non-heme iron, which is normally redox inactive and positioned between Q_A and Q_B, and is ligated by His215 and His272.

Another important property of the D1 protein is that it turns over more rapidly than any other protein in the thylakoid membrane. This remarkable feature is linked to the fact that PSII is susceptible to photoinduced damage leading to photoinhibition and a lowering of photosynthetic efficiency. The degradation, synthesis, and reinsertion of this protein into the RC core complex represents a very important aspect of the dynamics of PSII.

PsbB-CP47

This highly conserved PSII RC protein consists of ~500 amino acids and has a molecular mass of ~56 kDa depending on species. It is often known as CP47 and has 6 transmembrane α-helices (I–VI) arranged in a ring consisting of 3 pairs with N and C termini exposed at the stromal surface. The lumenal loop joining transmembrane helices V and VI is large, consisting of 200 amino acids. It binds 16 chlorophyll *a* molecules and probably 3 β-carotenes. Most of the Chls are ligated to His residues located in the transmembrane helices and form an LHC system for the RC. The large lumenal loop functions indirectly in the water oxidation reaction by interacting with the D2 protein. Depletion of the *psb*B gene and a wide range of site-directed mutational studies have emphasized the absolute requirement of the PsbB protein in PSII assembly and function.

PsbC-CP43

After posttranslational processing the PsbC-CP43 protein, depending on species, contains ~470 amino acids and has a molecular mass of ~50 kDa. It is homologous with PsbB (CP47) in that it has 6 transmembrane α-helices arranged in the same way. It also contains a considerable number of histidine residues which are involved in ligating some of the 14 Chl*a* bound to this protein. Like CP47, CP43 probably binds 3 β-carotene molecules and has a large lumenal loop joining helices V and VI. However, this loop is slightly smaller, having ~150 amino acids. It also differs from CP47 in that in plants (but not in algae and cyanobacteria) the N-terminal threonine of CP43 can be reversibly phosphorylated. Moreover CP43 seems to be more weakly associated with PSII than with CP47, a feature which may be important when the D1 protein is degraded and replaced. Despite these differences, CP43, like CP47 acts as a LHC for PSII and its presence is also necessary for water splitting activity since it provides a ligand for the Mn_4Ca^{2+}-cluster.

TABLE I

Protein Subunits of PSII Core Reaction Center Complex

Gene	Subunit	Mass (kDa)	No. of transmembrane α-helices
*psb*A (c)	D1	38.021 (S)	5
*psb*B (c)	CP47	56.278 (S)	6
*psb*C (c)	CP43	50.066 (S)	6
*psb*D (c)	D2	39.418 (S)	5
*psb*E (c)	α-cyt b559	9.255 (S)	1
*psb*F (c)	β-cyt b559	4.409 (S)	1
*psb*H (c)	H protein	7.697 (S)	1
*psb*I (c)	I protein	4.195 (S)	1
*psb*J (c)	J protein	4.116 (P)	1
*psb*K (c)	K protein	4.283 (S)	1
*psb*L (c)	L protein	4.366 (S)	1
*psb*M (c)	M protein	3.755 (P)	1
*psb*N (c)	N protein	4.722 (T)	1
*psb*O (c)	33 kDa O protein	26.539 (S)	0
*psb*P (n)	23 kDa P protein	20.210 (S)	0
*psb*Q (n)	16 kDa Q protein	16.523 (S)	0
*psb*R (n)	R protein	10.236 (S)	0
*psb*S (n)	S protein	29.197 (S)	4
*psb*T (c)	T_C protein	3.849 (S)	1
*psb*T (n)	T_n protein	5.000 (A)	0
*psb*U	U protein	10.491 (Sy)	
*psb*V	V protein	15.121 (Sy)	0
*psb*W (n)	W protein	5.928 (S)	1
*psb*X (n)	X protein	4.225 (S)	1
*psb*Y (c)	Y protein	4202 (Sy)	1
*psb*Z (c)	Z protein	6.541 (S)	2

These proteins are products of the *psb*A to *psb*Z genes that occur in oxygenic organisms. In eukaryotic organisms the *psb* genes are located in either the chloroplast (c) or nuclear (n) genes. The molecular masses of the mature PsbA–PsbZ proteins are calculated from the protein sequences reported in the SwissProt database using the MacBioSpec program (Sciex Corp., Thornhill, ON, Canada) for spinach (S), pea (P), tobacco (T), *Arabidopsis* (A), and *Synechocystis* PCC6803 (Sy).

PsbD-D2 Protein

The PsbD-D2 protein is homologous to the D1 protein. Although it is slightly larger than the D1 protein, having in the region of 353 amino acids and a molecular mass of ~39.5 kDa, depending on species it has 5 transmembrane helical segments organized in the same way as the D1 protein. Compared with the D1 protein it is involved to a lesser extent in binding active cofactors. Another chlorophyll that forms a cluster constituting $P680^*$ is ligated to His197, while the binding of Q_A may involve at least His214, Phe261 and possibly Trp253 and Leu267. The D2 protein also provides ligands for the non-heme iron being His214 and His268. Normally the D2 protein does not turn over rapidly like the D1 protein but, under extreme conditions (e.g., irradiation with damaging UV light), it will be replaced by a repair process.

PsbE and PsbF

These are the α- and β-subunits respectively of cytochrome b559. After processing, the PsbE and PsbF contain 82 and 38 amino acids in most higher plants, and have molecular masses of ~9.3–4.4 kDa. Both subunits have a single transmembrane helix with their N termini exposed to the stromal surface.

The α-subunit is characterized by having a long C terminus of ~44 amino acid residues extending from the lumenal surface of the membrane while the β-subunit has essentially no lumenal domain. Of considerable importance is that each subunit contains a conserved

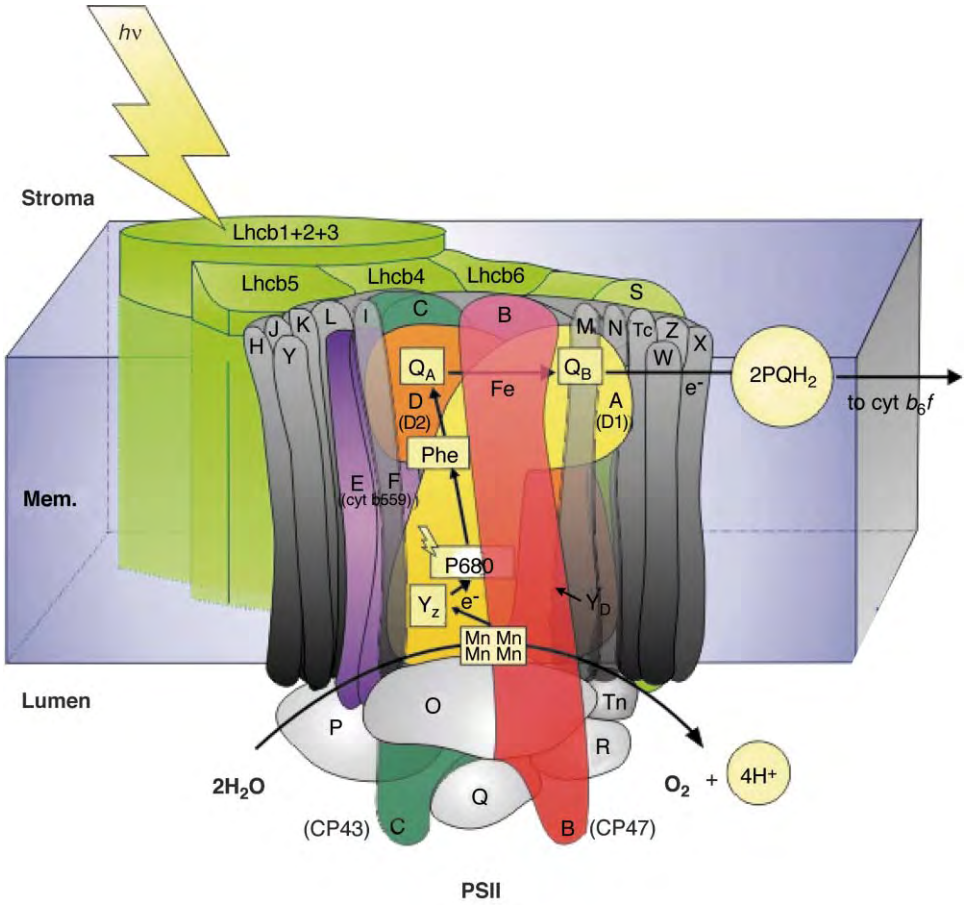

FIGURE 1 Cartoon showing the protein components of PSII of plants and algae, and the primary and secondary electron steps that occur in the reaction center D1 and D2 proteins. The RC core proteins are labeled according to their gene letter (e.g., *psb*A = A). Also shown are the Lhcb Chl*a*/Chl*b*-binding proteins encoded by *cab* genes that form the outer light-harvesting antenna system of higher plants and green algae.

histidine residue which is located within the membrane-spanning region towards the stromal surface. These two residues form axial ligands to the heme of the cytochrome. Although it had been argued by some that there are two cyt b559 per RC, there is strong evidence favoring a single copy of the cytochrome per RC. The deletion of the *psb*E gene results in a lack of assembly of PSII. On the other hand replacement of the His residue in the α-subunit can lead to an assembled and functionally active PSII complex even when no heme is ligated to the PsbE and PsbF proteins. Normally the heme has a high redox potential of $\sim$0.4 V but under some circumstances this potential is lowered to 0.15 V or less. The chemical basis of this redox shift and its significance, if any, is unclear. Under some circumstances, usually when the water splitting reactions are inhibited such as at low temperature, the heme of cyt b559 is oxidized by $P680^{+}$. According to recent structural models the heme is at least 40Å from P680, which is too far to account for the millisecond time constant for its oxidation. Accordingly it has been suggested that a β-carotene molecule bound within the D1/D2 heterodimer acts as a redox intermediate between the cyt b559 and $P680^{+}$. The reduction of the oxidized heme may involve Q_A^-, Q_B^-, or $Pheo^-$ but again there is a distance problem, with the required electron donation occurring over distances of 28Å or more, according to the recent X-ray structure. It seems likely that cyt b559 plays a protective role in minimizing photodamage of the RC.

PsbG

A chloroplast gene was initially called *psb*G but it was shown later that the product of this gene was not a PSII protein but rather a component of a chloroplast located NADPH/quinone oxidoreductase. This gene is now known as *ndh*K.

PsbH

In higher plants, the PsbH protein contains 72 amino acids and has a calculated mass of $\sim$7.7 kDa.

In cyanobacteria the protein is slightly smaller (~6.5 kDa) with a truncated N terminus and as such does not have the N-terminal threonine residue which is conserved in all higher plant and green algal sequences which is the site for reversible phosphorylation. The functional significance of the phosphorylation process is unclear. The higher plant protein is characterized by having a single transmembrane helix with a long N-terminal region consisting of ~41 amino acids at the stromal surface, which reduces to ~30 residues in the case of cyanobacteria. The *psb*H gene can be deleted from the cyanobacterium *Synechocystis* without impairing the assembly of PSII and photoautotrophic growth. The knockout mutant was, however, more sensitive to photoinhibition than the wild type. This sensitivity seemed to be due to the partial inhibition of the D1 protein repair process rather than to an increase in photochemical damage. In contrast, when the *psb*H gene was deleted in *Chlamydomonas reinhardtii*, PSII did not assemble.

PsbI

The PsbI protein has a molecular mass of ~4.2 kDa. In most eukaryotes this protein contains 35 amino acids and is predicted to have a single transmembrane helix with a short N-terminal region at its stromal end. It is located close to the D1/D2 heterodimer being adjacent to the B-helix of the D1 protein. Interestingly, the mature protein retains the initiating N-formyl group at its N-terminal methionine residue. The *psb*I gene has been deleted in the green alga *Chlamydomonas* and the cyanobacterium *Synechocystis*, without inhibiting PSII assembly and photoautotrophic growth. Thus, the function of the PsbI protein remains unknown.

PsbJ

In most organisms the *psb*J gene is located in a gene cluster also containing the *psb*E, *psb*F, and *psb*L genes. The PsbJ protein is highly conserved, consists of 39 amino acids and has a calculated molecular mass of 4.1 kDa. It is predicted to have one transmembrane helix. The *psb*J gene has been deleted in cyanobacteria to generate a knockout mutant which assembles PSII at a lower level than the wild type and consequently has a slower photoautotrophic growth rate.

PsbK

This ~43 kDa protein is highly conserved and has 37 amino acid residues. It is predicted to have a single transmembrane helix. Of particular note is that in higher plants, 24 amino acids are posttranslationally cleaved from the initial gene product. In cyanobacteria eight amino acids are removed after translation. These presequences probably bring about the insertion of the protein into the thylakoid membrane such that its N terminus is on the lumenal side. Deletion of the *psb*K gene in cyanobacteria has very little effect on photoautotrophic growth and PSII activity. In the case of green algae, however, the deletion of the gene destabilized the PSII complex and the transformant was unable to grow photoautotrophically.

PsbL

This highly conserved PSII protein contains 37 amino acids and has a calculated molecular mass of ~4.4 kDa. In most organisms its gene is located in the cluster together with *psb*E, *psb*F, and *psb*J. Hydropathy analysis suggests that it contains a single transmembrane helix. Inactivation of the *psb*L gene in cyanobacteria resulted in a loss of PSII-mediated oxygen evolution and the transformant was unable to grow photoautotrophically. It has also been reported that PsbL is required for normal functioning of the Q_A site based on studies with isolated PSII complexes. This conclusion was reinforced by the finding that PsbL is required for the oxidation of Y_Z by $P680^{+}$. As a consequence, the primary quinone acceptor is destabilized by the increased probability of rapid recombination between Q_A^- and $P680^{+}$.

PsbM

The PsbM protein is predicted to have one transmembrane helix with a very short N-terminal extension on the stromal side. It contains 33 amino acids and has a molecular mass of ~3.7 kDa. PsbM has been identified in PSII isolated from cyanobacteria and green algae. Together with PsbL and PsbTc this protein may function to stabilize PSII as a dimer.

PsbN

As in the case of PsbM, this protein is predicted to be in both cyanobacterial and plant PSII. However, it has not been detected directly in plant PSII although it has been identified in cyanobacteria. PsbN has a predicted single transmembrane helix. Deletion of both *psb*N and *psb*H genes from *Synechocystis* caused no effect other than those observed in the absence of *psb*H alone. Thus, the function and location of *psb*N are unknown.

PsbO

PsbO is a 33 kDa manganese stabilizing protein. Between higher plants and cyanobacteria this protein is

highly conserved containing, after processing, 241–247 residues. Although the mature PsbO protein is often referred to as the 33 kDa protein, its calculated molecular mass is ~26.5 kDa. It is an extrinsic protein with high β-sheet content and plays an important role in maintaining an optimal environment for water oxidation to occur. Various studies indicate that it does so by controlling Ca^{2+} and Cl^- levels at the catalytic site and by stabilizing the Mn_4-cluster, but it does not bind Mn directly. For this reason it is often called the "manganese stabilizing protein." Its deletion in cyanobacteria does not prevent water oxidation although the equivalent mutant in green alga does not assemble a functional PSII RC complex.

PsbP

PsbP is a 23 kDa extrinsic protein. After processing, this protein consists of ~186 amino acids with a calculated molecular mass of ~20 kDa. Although found in higher plants and green algae, it is not conserved in cyanobacteria. Like PsbO, its function seems to be to optimize the Ca^{2+} and Cl^- levels needed for the water oxidizing reaction and is located in the vicinity of the 33 kDa protein to which it binds.

PsbQ

The PsbQ mature protein contains ~49 amino acids and, like PsbP, is located close to the 33 kDa protein and the Mn_4-cluster. It is predicted to be an all α-protein and also seems to be involved in optimizing the ionic environment necessary for oxygen evolution. PsbQ, however, is not found in cyanobacterial PSII although a *psb*Q-like gene is present. Its binding to PSII requires the presence of PsbO and PsbP.

PsbR

The role of PsbR is unknown. It has a molecular mass of 10.2 kDa and consists of ~99 amino acids. It seems to be an extrinsic protein of plants, and is bound relatively tightly to the lumenal surface in the vicinity of the water splitting site. Whether it has a transmembrane helix is a matter for debate. It does not exist in cyanobacteria.

PsbS

The PsbS protein consists of ~205 amino acids and has an apparent molecular mass of 22 kDa although its calculated mass is ~29 kDa. It is predicted to have four transmembrane helices. Helices I and III, and II and IV, are homologous indicating that the protein is derived from internal gene duplication. Sequence homology studies suggest that PsbS is related to Chl*a*/Chl*b*-binding antenna Lhcb1–6 proteins (*cab* gene products) and is likely to be a chlorophyll-binding protein. A functional role for PsbS, therefore, could be to act as a pigment chaperonin which aids the incorporation of chlorophyll molecules into the various pigment-binding proteins of PSII. This protein has also been implicated in the protection of PSII against photoinduced damage (photoinhibition). It does not exist in cyanobacteria.

$PsbT_C$

The chloroplast-encoded $PsbT_C$ protein is also found in cyanobacteria. It contains 30–34 amino acids, has a molecular weight of ~3.9 kDa and retains the initiating N-formyl group on its N-terminal methionine residue. It is predicted to have a single transmembrane helix which is located in the N terminus of the protein. The *psb*T_C gene was formerly known as ycf8 and is located close to the *psb*B gene in the chloroplast genome. The first identification of this subunit was made by comparing wild type and a mutant of *Chlamydomonas* and lacked the *psb*T_C gene. This work also showed that the $PsbT_C$ is a PSII protein and is required for optimal activity under high-light conditions so as to prevent photoinhibition. It is located with PsbM and PsbL in the dimerization domain.

$PsbT_N$

A nuclear-encoded hydrophilic 5 kDa protein which copurifies with PsbO. Although its function is unknown, it seems to be an extrinsic protein located on the surface of PSII. The mature $PsbT_n$ protein consists of ~28 amino acids in higher plants and the presence of two cysteine residues suggests that it contains a disulfide bridge. It is not present in cyanobacteria.

PsbU

This is a cyanobacterial all α-protein reported to be extrinsically located on the lumenal surface of PSII close to the 33 kDa protein. It has an apparent molecular mass of ~11 kDa. It is also found in red algae but not in plants and green algae.

PsbV

PsbV is also known as cytochrome c550 and is found only in cyanobacteria and red algae. It has a molecular mass of 15 kDa and is an extrinsic protein found on the lumenal surface of PSII. It plays no direct role in water

oxidation although it does help to provide a Ca^{2+}/Cl^{-} environment at the catalytic site. It does not, however, bind directly to PsbO but indirectly via PsbU, which forms a bridge.

PsbW

The PsbW protein is found in higher plants and green algae. A cyanobacterial "PsbW-like" gene has also been documented which has a low homology with the eukaryotic equivalent, and therefore there is some uncertainty whether or not cyanobacteria contain the PsbW protein. In higher plants and green algae, it is nuclear-encoded and is processed to a mature protein having an apparent molecular mass of 6.1 kDa and consists of 54–56 amino acids. It is predicted to have one membrane-spanning region with its N terminus located on the lumenal side of the membrane. This orientation is consistent with the pre-sequence of the PsbW protein having characteristics of a target sequence typical for lumenal proteins. The function of PsbW is unknown.

PsbX

The PsbX protein is nuclear-encoded in higher plants and green algae, and consists of ~42 amino acids. In higher plants its synthesis is tightly regulated by light. The mature PsbX protein is reported to have a molecular mass of 4.1 kDa and predicted to have a single transmembrane helix. It has been detected in the oxygen-evolving PSII core complex of higher plants and cyanobacteria. The deletion of the *psb*X gene in cyanobacteria did not inhibit PSII assembly and photoautotrophic growth. However these studies suggest that PsbX may play a role in the function of Q_A and Q_B. It is located close to the B-helix of the D2 protein.

PsbY

This protein is located in PSII of plants, algae, and cyanobacteria. It has a molecular mass of ~4.2 kDa, consists of 36–39 amino acid residues, and has one transmembrane segment. The deletion of the *psb*Y gene in cyanobacteria did not impair the water oxidation process and is therefore likely to be located in a peripheral region of the PSII complex.

PsbZ

This 6.8 kDa protein contains 62 amino acids and forms two transmembrane helices. It is located at the peripheral edge of the PSII complex adjacent to PsbC (CP43) where, in plants and algae, it could be involved in binding the outer Chl*a*/Chl*b* light-harvesting systems.

Conclusion

Here 26 different Psb subunits have been described that are found in the PSII RC core. In a few cases, the subunits are either specific to plants and green algae or to red algae and cyanobacteria. In addition, there may be some other candidates which have yet to be characterized in detail. Recently X-ray structures of the cyanobacterial PSII RC core have been obtained and the resolution is now sufficient to unambiguously assign proteins to most electron densities. This has proved relatively easy for the D1, D2, CP43, CP47, PsbE, PsbF, and the extrinsic proteins. The most recent X-ray structure has identified the positions of 12 low-molecular-weight subunits in the cyanobacterial PSII complex.

See Also the Following Articles

Chlorophylls and Carotenoids • Chloroplasts • Light-Harvesting Complex (LHC) I and II: Pigments and Proteins • Photosystem II: Assembly and Turnover of the D1 Protein • Photosystem II Light Harvesting System: Dynamic Behavior • Photosystem II: Water Oxidation, Overview

Glossary

light-harvesting system Proteins that bind chlorophyll, carotenoids, and phycobilins which absorb light and transfer excitation energy to the reaction center.
oxidation The process of removing an electron to a chemical species.
photosystem Pigment–protein complex containing a light-harvesting system and a reaction center.
radical Reactive chemical species with an unpaired electron.
reaction center Protein subunits of the photosystem that bind redox active cofactors which use excitation energy to bring about charge transfer across the membrane.
reduction The process of donating an electron to a chemical species.

Further Reading

Barber, J. (2003). Photosystem: II. The engine of life. *Quart. Revs. Biophys.* **36**, 71–89.
Barber, J., Nield, J., Morris, E. P., Zheleva, D., and Hankamer, B. (1997). The structure, function and dynamics of photosystem two. *Physiol. Plant.* **100**, 817–827.
Blankenship, R. E. (2002). *Molecular Mechanisms of Photosynthesis*. Blackwell, Chichester, UK.
Ferreira, K., Iverson, T., Maghlaoui, K., Barber, J., and Iwata, S. (2004). Architecture of the photosynthetic oxygen-evolving centre. *Science* **303**, 1831–1838.
Hankamer, B., Morris, E. P., Nield, J., Carne, A., and Barber, J. (2001). Subunit positioning and transmembrane helix organisation in the core dimer of photosystem II. *FEBS Lett.* **504**, 142–151.

Kamiya, N., and Shen, J.-R. (2003). Crystal structure of oxygen-evolving photosystem II from *Thermosynechococcus vulcanus* at 3.7Å resolution. *Proc. Natl. Acad. Sci. USA* **100**, 98–103.

Ort, D. R., and Yocum, C. F. (1996). Oxygenic photosynthesis. In *The Light Reactions, Advances in Photosynthesis*, Vol 4, Kluwer, Dordrecht, The Netherlands.

Zouni, A., Witt, H. T., Kern, J., Fromme, P., Krauss, N., Saenger, W., and Orth, P. (2001). Crystal structure of photosystem II from *Synechococcus elongatus* at 3.8 Å resolution. *Nature* **409**, 739–742.

Biography

James Barber is the Ernst Chain Professor of Biochemistry and Former Dean of the Royal College of Science and Head of the Department of Biochemistry at Imperial College, London. His principal research interest is light absorption and utilization in photosynthesis, with special focus on photosystem II and the water oxidation process. He has published over 500 papers, edited many specialized books, and was elected to Academia Europaeae in 1989 and a Foreign Member of the Swedish Royal Academy of Sciences in 2003.

Photosystem II: Water Oxidation, Overview

Fabrice Rappaport and Pierre Joliot
Centre National de la Recherche Scientifique, Paris, France

The appearance of oxygen-producing organisms about three billions years ago is widely believed to be at the origin of the conversion of our atmosphere from anaerobic to its present oxygen rich composition. The switch from reduced carbon or sulfur compound oxidation to water oxidation and carbon dioxide reduction did not only result in a major change in the gas composition of the earth atmosphere, but also boosted the apparition of aerobic metabolism, which produces 18 times more energy per unit of substrate than anaerobic metabolism. Photosynthetic oxygen evolution, which accompanies the conversion of solar energy to biomass is thus rightly considered as the source of most of the energy available to life on Earth as well as a mandatory process to fuel the respiratory metabolism. Since the discovery by Priestley of the gas exchange (oxygen production and carbon dioxide assimilation), resulting from the photosynthetic process, till today, much insight into the mechanism of water splitting into dioxygen has been gained with an impressive acceleration in the last 30 years. The enzymatic machinery which drives water oxidation is identified, its three-dimensional structure has first been determined, by the groups of W. Saenger and H.T. Witt, with a resolution of 3.5Å, which has improved since then. Yet, the precise chemistry and energetics of water splitting remains to be clarified, if not understood.

Photosystem II and the Water Splitting Enzyme

The Photosystem II Complex

Water oxidation into dioxygen (O_2) follows the equation: $2H_2O \rightarrow O_2 + 4H^+ + 4e^-$, where H^+ and e^- stand for protons and electrons, respectively. Water is obviously a very stable compound and its oxidation requires the availability of strongly oxidizing species (at pH 7.0 the midpoint potential of the H_2O/O_2 couple is 810 mV). This oxidizing power is formed at the expense of light absorption and the conversion of light energy into electrochemical energy. The action spectrum of oxygen emission showed that it is sensitized by pigments associated with Photosystem II (PS II). Photosystem II is a large pigment protein complex located in the thylakoid membrane of the chloroplast, in green algae or higher plants or in the cytoplasmic membrane in cyanobacteria. As illustrated in Figure 1, the core of PS II is composed of two homologous polypeptides (D_1 and D_2, D for diffuse electrophoretic profile) each of which consists of five transmembrane helices. It bears various redox cofactors among which a chlorophyll dimer (P_AP_B), two chlorophyll monomers (B_A and B_B), two pheophytins (Ph_A and P_B), and two quinones Q_A and Q_B. Among the various photosynthetic reaction centers, PS II is unique since it bears a tetra manganese cluster which, coupled to a redox active tyrosine Y_Z, is responsible for water splitting into oxygen. The core of the reaction center is surrounded by pigment (chlorophyll and carotenoid)-binding proteins, which increase by a factor of ~200 its absorption cross-section. Thus, under normal solar radiance, one photon is absorbed by PSII every 10 ms or so. The absorption of a photon by one of the chlorophyll borne by the pigment-binding proteins results in the formation of an excited state of a chlorophyll, i.e., an electron jumps from the highest occupied molecular orbital to the lowest unoccupied orbital of higher energy. Provided other pigments are close enough, this excitation energy may hop from one pigment to another and then be funneled to the core of the reaction center and more precisely to the primary donor P (denoted P^* in the excited state). The singularity of P resides in the fact that in its close vicinity one finds an electron acceptor (Ph_A). The excitation energy, by weakening the binding energy of the electron by the energy of the transition between the two molecular orbital, allows the electron transfer reaction between P^* and this nearby acceptor to occur, yielding the "charge separated state" ($P^+Ph_A^-$). This state is then further stabilized by successive electron transfer step between the different redox compounds. At room temperature the first oxidized cofactor is essentially P_A. It is reduced in a few tens of nanoseconds by the redox active Y_Z (Y161 of the D_1 polypeptide), which is in turn reduced at the expense of the water

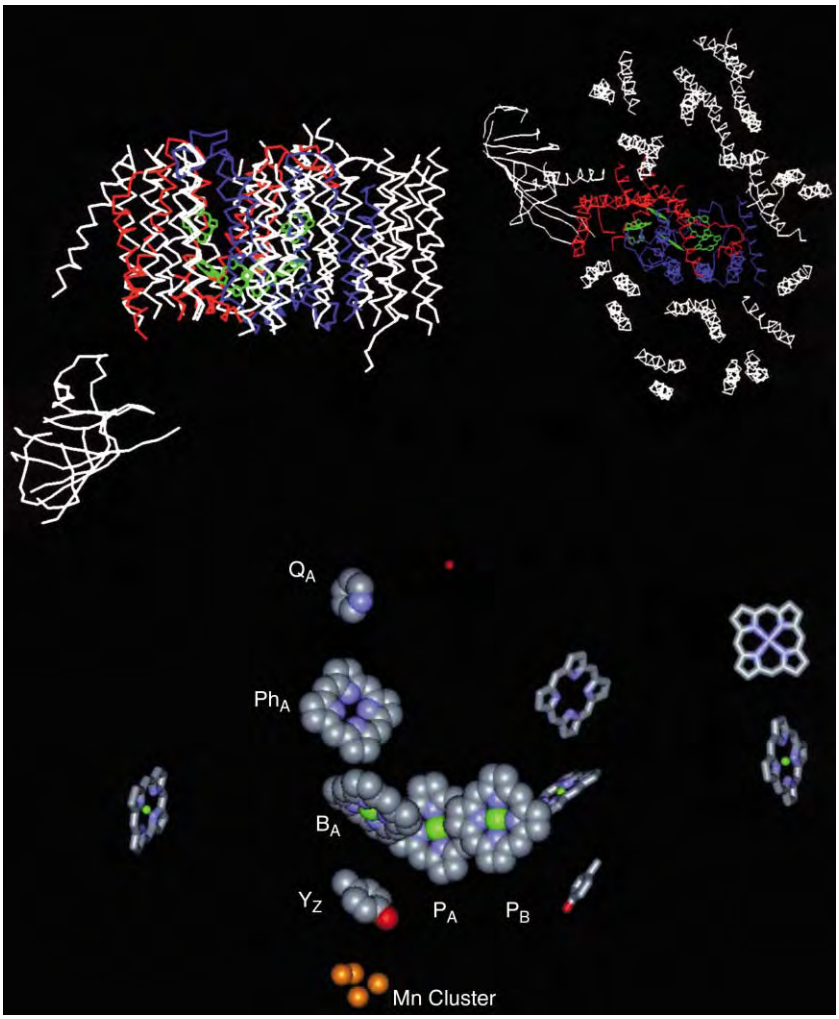

FIGURE 1 A structural model of Photosystem II based on X-ray diffraction studies by Zouni *et al.* (2001). *Nature* **409**, 739–743, with permission of Nature pdb: 1FE1. Top: parallel (left panel) and normal (right panel) views with respect to the membrane plane of the photosystem II complex. In red and blue are the D1 and D2 subunits which bear the main redox cofactors involved in water oxidation (shown in green). Bottom: The structural arrangement of the redox active components of photosystem II.

splitting enzyme. As shown in Figure 1, despite the arrangement of the various redox cofactors in two symmetrical branches with respect to a pseudo C_2 symmetry axis perpendicular to the membrane plane, electron transfer only proceeds down one of these two branches indicating that function does not strictly follow structure.

The Water Splitting Enzyme

As just described, conversion of light energy into electrochemical energy is a one-electron process. However, water oxidation into dioxygen is a four-electron process. Taking advantage of the possibility to trigger the light-induced electron-transfer reaction by short light flashes P. Joliot showed that the oxygen emission yield is maximum after the third, seventh, eleventh… flash of a series (Figure 2). This oscillating pattern with a periodicity of four was modeled by B. Kok who postulated, on this basis, the existence of a charge storing device allowing, in a single catalytic unit associated with PSII, the accumulation of the four oxidizing equivalent needed to split water into oxygen. In this model, illustrated in Figure 2, the catalytic center has five different oxidation states (S_0, S_1, S_2, S_3, and S_4). Four successive light-induced oxidation triggers the four successive transitions between the S_i and S_{i+1} states. Upon S_4 formation, oxygen is produced and released while S_0 is regenerated. The beauty of the Kok model resides in its ability to fully describe the function of the enzyme without any assumption neither on the chemical nature of the transient states it involves, nor on the precise mechanism underlaid by the successive transition between the S states. This accounts for its success as a working model ever since it was enounced. Simultaneously to the discovery of this charge-storing device,

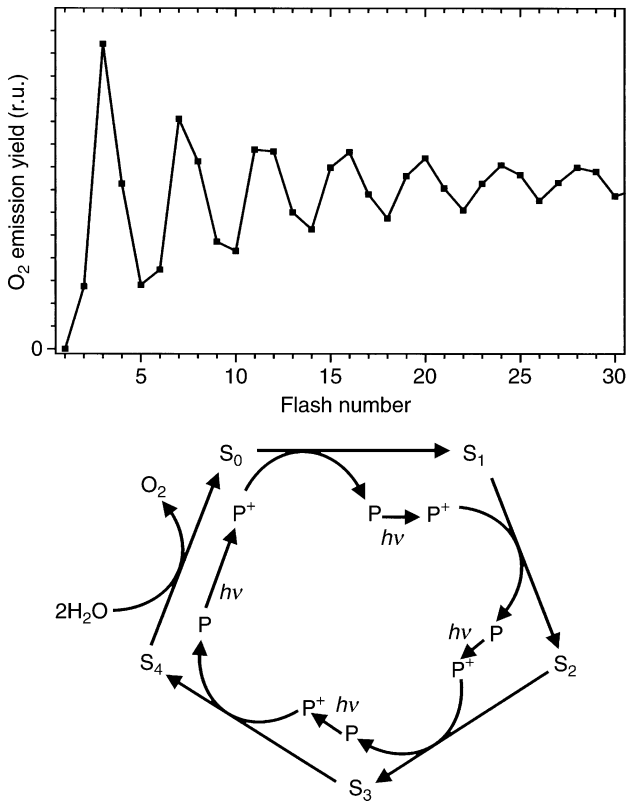

FIGURE 2 Top: The O_2 emission yield as a function of the flash number in a series. Note that this yield depends on the flash number with a periodicity of four. Bottom: The charge storing device allowing accumulation of the oxidizing power needed to split water as modeled by Kok.

Cheniae and co-workers evidenced the requirement for manganese atoms in water splitting. The determination of a stoichiometry of four Mn atoms per PSII complexes provided the chemical basis for the catalytic center where the accumulation of the oxidizing equivalent produced by light-induced charge separation occurs. Together with this manganese cluster, the catalytic center bears two ions, Ca^{2+} and Cl^-, which may be removed by various chemical treatments. In the absence of either one of these two ions, the lower S states (S_0 and S_1) may undergo oxidation but the advancement of the Kok cycle cannot be completed and water splitting is inhibited. The water splitting enzyme further comprises extrinsic polypeptides, which stabilizes the assembled tetranuclear cluster.

The Assembly of the Manganese Cluster

The ligands involved in the Mn cluster binding to the protein backbone are provided by the polypeptide D_1. They have not been all identified but amongst the good candidates are: three histidines, three carboxylic acids, and the C terminus alanine. The assembly of the Mn cluster requires Mn^{II}, in the $Mn(OH)^+$ or $Mn(OH)_2$ form, Ca^{2+}, Cl^- and light. The absorption of light by PSII produces the oxidant Y_Z^{ox},which oxidizes the Mn^{II} ions. The first oxidation of a Mn^{II} has a high quantum yield unlike the following steps which are needed for the oxidation-induced association of the stable tetra nuclear cluster.

The Thermodynamic and Kinetic Features of the Water Splitting Enzyme

Before attempting to address the mechanism of water oxidation one should question the thermodynamic and kinetic issues of this reaction. Obviously water is a very stable molecule under physiological condition, while its oxidation into molecular oxygen is likely to involve the transient formation of highly reactive species such as oxo-radicals, hydrogen peroxides, etc. The enzyme must meet the following requirements: accumulate enough oxidizing power to perform a very demanding reaction with respect to common biological redox potential but also prevent side reactions, which are thermodynamically made possible by the accumulation, in a single catalytic site, of such an oxidative power.

The Redox Potential of the Different S States

Until now, the redox potentials of the different S states have not been determined by direct redox titration. They could only be inferred from the redox potentials of other cofactors found in the PS II reaction centers combined with the free energy change associated with the electron transfer reaction between the S states and these cofactors. There are thus large error bars on the value, which can be found in the literature. The redox potential of the P^+/P couple, which drives the catalytic cycle, has been estimated to 1.1–1.3 V, making the P^+ species the strongest oxidant found in biology. With an estimated midpoint potential of $\sim$0.75 V, the S_1/S_0 couple lies $\sim$0.5 V below the P^+/P couple whereas the S_2/S_1, S_3/S_2, and S_4/S_3 midpoint potentials are estimated to $\sim$1 V. The overall free energy available to oxidize water is thus $\sim$3.75 V. This is sufficient to drive the reaction at neutral pH (the minimal driving force required to reversibly oxidize water at pH 7 is 0.81 V per electron) but becomes low when the reaction has to occur at a pH close to 5, a value often quoted when the photosynthetic chain is at work.

The Rates of Oxidation of the Various S States

The rates of the various electron transfer reactions between the oxidized tyrosine Y_Z^{ox} and the S-states S_i are in the tens or hundreds of microseconds for the three lower S states. The S_4 to S_0 transition is significantly slower, in the millisecond time range, and concomitant with O_2 production and release. Based on the distance between the electron acceptor Y_Z^{ox} and the Mn cluster (7Å) combined with the free energy changes associated with these reactions, these rates appear much too slow for the reaction to be kinetically limited by the electron transfer proper. This has been taken as an indication of either redox-induced structural changes or/and of a coupling with other processes than electron transfer such as proton transfer. Interestingly, a lag phase of a few tens of microseconds preceding the decay of S_4 into S_0, which is accompanied by O_2 release might evidence such events.

The Structure of the Catalytic Center and the Redox Events during the Reaction Cycle

Despite the tremendous amount of effort put into its elucidation, the structure as well as the valence of the Mn cluster are still matters of strong debate. Numerous sophisticated spectroscopic methods have been used to address this issue without completely succeeding to define a clear picture. Electron paramagnetic resonance (EPR) and X-ray absorption spectroscopy were by far the most productive methods and provided a set of possible structures. Recently, a low resolution crystallographic structure put additional constraints on the structures, which can be considered.

The Structure of the Manganese Cluster

The light-induced formation of the S_2 state results in a remarkable EPR signal which was first reported by Dismukes and Siderer. This signal shows very rich hyperfine structures (it is commonly referred to as the "multiline" signal), which have been taken as the spectroscopic signature of a mixed valence dinuclear Mn cluster. The multiline signal has provided experimental basis for modeling the structure and the valence state of the Mn cluster in the S_2 state. X-ray absorption spectroscopy (EXAFS), pioneered by M. Klein, has provided valuable data on the distances separating the heavy atoms such as Mn or Ca, which are found in the catalytic center. These data put severe constraints on the possible structures. From both the EPR and EXAFS data, a dimer of di-μ-oxo Mn dimers has long been favored. However, several other structures with oxo-bridged Mn atoms are compatible with the data. Although not settled yet, the debate seems to be converging to structures with three strongly coupled Mn and one weakly coupled Mn. Indeed the electron density map obtained by Zouni *et al*. can accommodate these structures but not the earlier favored dimers.

The Redox Events during the Catalytic Centers

As alluded to above, EPR and X-ray spectroscopies have also generously fed the debate on the valence state of the tetranuclear cluster during the catalytic cycle. Mn edge absorption spectroscopy has provided strong evidences for oxidation of an Mn atom during the S_0 to S_1 and S_1 to S_2 transitions. EPR and (less clearly) UV spectroscopies supported this view. Based on a kinetic analysis the S_4 is equivalent to the $[S_3Y_Z^{ox}]$ state. This seems to ground the accumulation of four oxidizing equivalents within the catalytic center (which would then include Y_Z as a partner), before water is oxidized. Yet, the assignment of the substrate of the oxidation associated with the S_2 to S_3 transition is still an open question. This ambiguity mainly comes from the fact that depending on the group involved in these studies, X-ray absorption spectroscopy shows either a shift in the absorption edge consistent with a Mn oxidation, or little, if any, shift in the absorption edges, ruling out this latter assignment and favoring the formation of a radical species. Unfortunately other spectroscopies such as EPR or UV absorption did not provide either unequivocal results. The disappearance upon S_3 formation of the EPR "multiline signal" arising from S_2 could be taken as a strong support for a Mn oxidation. However, this disappearance could be as well accounted for by a magnetic interaction between a radical species and the Mn cluster as argued by Styring, Rutherford, and Boussac.

The Mechanism of Water Oxidation

If indeed, the S_2 to S_3 transition involves the formation of a radical species, the possibility arises that a water molecule is oxidized during this step. If, on the contrary, the three successive steps leading to the formation of S_3 only involve Mn oxidation, an obvious conclusion is that water oxidation only takes place after the formation of S_4 (i.e., $S_3Y_Z^{ox}$). As just seen, this alternative could not be settled by spectroscopic approach. However, recent experiments on substrate binding tilt the scale toward

the latter and further constrain the inventiveness when attempting to draw possible mechanism for water splitting.

Substrate/Bulk Water Molecule Exchange

In a series of very elegant studies, Hillier and Wydrzynski have used isotopically labeled water ($H_2\ ^{18}O$) and measured the release of either O_2^{34} or O_2^{36} after a rapid mixing with PSII in the presence of unlabeled water. Most interestingly, they observed that substrate water may be exchanged with bulk water up to the S_3 state. This has been, until now, the strongest result in favor of a O–O bond-formation step occurring after S_3 is formed and thus during the S_4 to S_0 transition.

Proton Release during the Catalytic Cycle

The oxidation of two water molecules does not only release oxygen as a byproduct but also four protons. From the pioneering work of Fowler it is known that proton release accompanies the S_i to S_{i+1} transitions, which precedes the final S_4 to S_0 step during which O_2 is released. However, it is commonly agreed that these proton release events do not result from water chemistry. Indeed, proton transfers are often associated with redox changes either when the species which undergo the redox change is itself protonated or when the change in electrostatic potential resulting from the redox change shifts the affinity of a nearby acid group for proton. The two non-exclusive processes are likely to be at work, simultaneously or not, during the S_0 to S_1, S_1 to S_2, and S_2 to S_3 steps. The different groups which are deprotonated during these steps would be reprotonated by the protons produced during water oxidation. Although they most probably do not originate from water splitting, the proton release events occurring during the first three steps do play an important role in the overall water chemistry. They obviously compensate the charge accumulation which would otherwise result from three successive electron abstractions from a single catalytic unit. They control the thermodynamics of the enzyme by modulating the redox potential of the successive intermediate.

The Mechanisms for O_2 Formation

As discussed above, many issues regarding the catalytic cycle are still obscure. This may explain why there are almost as many mechanistic models for water splitting as groups studying this fascinating enzyme. It is beyond the scope of the present overview to present them all. As described Mn atoms are oxidized during some, if not all, transitions between S states. Obviously many models have incorporated these results and are based upon Mn-centered redox chemistry. There is a trend toward mechanisms in which only two among the four Mn atoms really participate in the water chemistry. The oxo or μ-oxo bridges which are thought to link the Mn atoms may also participate to the formation of the final O–O product. Last, the tyrosine Y_Z could play a crucial catalytic role. As discussed above, the S_4 state is equivalent to the $[S_3Y_Z^{ox}]$ state so that Y_Z may be considered as a full member of the catalytic center. The close proximity between Y_Z and the Mn cluster supports this view. Furthermore the phenolic oxygen of the tyrosine side chain is protonated when Y_Z is in the reduced state, whereas EPR spectra shows Y_Z^{ox} is deprotonated. Its reduction must thus be accompanied by its reprotonation. This led G. Babcock to propose that Y_Z could act as H atom abstractor undergoing a simultaneous reprotonation and reduction at the expense of water molecule. Although it seems to be agreed that this process does not occur on each step, as previously proposed, this model is largely resorted to for the higher S-states transitions.

Perspective

Obviously important questions such as when and how does water oxidation chemistry come into play are still unsettled. However, as illustrated by the recent release of new structural models by Shen or Iwata and Barber, the expected improvement in our knowledge of PSII at the atomic level should clarify if not solve some of the remaining ambiguities. Yet, it will not put an end to the sparkling development of models and concepts since identifying the different intermediate states during the overall reaction is a constantly renewed challenge, which is likely to be taken up by the field.

Glossary

chlorophyll excited state State that is formed after absorption by a chlorophyll molecule of a light quantum. At the molecular orbital level it corresponds to the hopping of an electron from the highest occupied molecular orbital to the lowest unoccupied molecular orbital.

oxidation De-electronation reaction or abstraction of an electron from a molecule.

reduction Electronation reaction. An electron transfer reaction occurs between an electron donor (which is oxidized) and an electron acceptor (which is reduced). In the case of photosynthetic water oxidation, two molecules of water (H_2O) are oxidized into molecular oxygen and serve as an electron source.

S_i states Successive states, as defined by B. Kok, formed during the accumulation in the catalytic center of the water-splitting enzyme of the oxidizing power required to split water into dioxygen. The transition from state S_i to state S_{i+1} reflects the abstraction of one electron from the catalytic center.

Further Reading

Cramer, W. A., and Soriano, G. M. (2000). Thermodynamics of energy transduction in biological membranes. Biophysics Textbook Online http://www.biophysics.org/btol/bioenerg.html#1.

Debus, R. J. (2000). The polypeptides of Photosystem II and their influence on mangano-tyrosyl-based oxygen evolution. In *Metal in Biological Systems* (H. Sigel and A. Sigel, eds.) Marcel Dekker, New York.

Diner, B. A., and Babcock, G. (1996). In *Oxygenic Photosynthesis: The Light Reactions* (D. R. Ort and C. F. Yocum, eds.), pp. 213–247. Kluwer Academic Publishers, Dordrecht, The Netherlands.

Goussias, C., Boussac, A., and Rutherford, A. W. (2002). Photosystem II and photosynthetic oxidation of water: An overview. *Philos. Trans. R. Soc. Lond. B Biol. Sci.* **357**, 1369–1381.

Hoganson, C. W., and Babcock, G. T. (1997). A metalloradical mechanism for the generation of oxygen from water in photosynthesis. *Science* **277**, 1953–1956.

Lavergne, J., and Junge, W. (1993). Proton release during the redox cycle of the water oxidase. *Photosynt. Res.* **38**, 279–296.

Lavergne, J., and Joliot, P. (2000). Thermodynamics of the excited states of photosynthesis. Biophysics Textbook Online http://www.biophysics.org/btol/bioenerg.html#2.

Nicholls, D. G., and Ferguson, S. J. (2002). *Bioenergetics 3*. Academic Press, London.

Nugent, J. (ed.) (2001). Photosynthetic water oxidation. *Biochim. Biophys. Acta* **1503**(1–2), 1–260.

Biography

Fabrice Rappaport joined Pierre Joliot's Lab in 1990 and holds a permanent position in the Centre National De La Recherche Scientifique. His principal interests are in proton and electron transfer in photosynthetic bioenergetic chain.

Pierre Joliot is a Professor Honoraire at the Collège De France And member of the French And United States Academies Of Science. He has developed tools to study the photosynthetic process *in vivo* and is mainly interested in the photosynthetic electron transfer chain with an emphasis on its supramolecular organization.

Plant Signaling: Peptides

Clarence A. Ryan and Gregory Pearce
Washington State University, Pullman, Washington, USA

Peptide hormones are extracellular signaling molecules that are found in animals, yeast, and plants. In animals, many physiological processes are regulated by peptide signals including, for example, metabolism, cell division, growth, pain, well-being, reproduction, and immunity. Before 1991, plants were thought to utilize small, non-peptide organic molecules called phytohormones, to regulate all physiological processes. Since then, over a dozen peptide hormones have been isolated from plants, or identified by genetic approaches, that regulate physiological processes, such as defense, cell division, growth and development, and reproduction.

Many similarities exist between some animal and plant peptide hormones, their receptors, and their signaling pathways, indicating that they may have evolved from common ancestral origins. Several plant peptide hormones and their precursor are shown in Figure 1. Plant peptide hormones and their receptors provide new approaches for improving crop yields and for the production of phytochemicals for industry and medicine.

Systemins

Tomato Systemin

The tomato systemin peptide $^{+}$AVQSKPPSKRD PPKMQTD^{-} is composed of 18 amino acids and is derived from a 200 amino acid precursor protein. The precursor, called, prosystemin, differs from animal peptide hormone precursors in that it lacks a signal sequence at its N terminus and is not synthesized through the secretory pathway. The potency of systemin is similar to animal peptide hormones, being active in the nanomolar range. The function of systemin as a primary signal for the activation of defense genes was confirmed by producing transgenic tomato plants that constitutively express an antisense prosystemin gene. The plants do not exhibit a systemic induction of proteinase inhibitors in response to *Manduca sexta* larval damage or to other mechanical wounding, and the larvae rapidly consume the plants in contrast to the less palatable wild-type plants.

Prosystemin genes are present in various solanaceous species, but not all, and its gene has not been identified in any other plant family. Why and how systemin evolved as a systemic wound signal only in some solanaceous species is not known. The mechanism for the release and transport of systemin through the plants is also not understood, but its long range signaling effects in response to wounds caused by attacking insects are thought to involve a mechanism for amplification of the signal. The presence of prosystemin in vascular bundle cells suggests that its localization there is important for long distance signaling. The proteolytic processing of prosystemin does not involve the typical dibasic sites usually found for processing of animal secretory prohormones. Processing enzymes that convert prosystemin to systemin have not been identified, nor have the initial cleavage sites.

Systemin exhibits only weak structural features in aqueous solutions, which reflect a poly(L-proline) II, 3_1 helix secondary structure that is due to the two proline doublets in the central region of the peptide. The resulting kinks in the peptide appear to be important for recognition by its receptor. The systemin receptor is a 160 kDa membrane-bound protein. It is a leucine-rich repeat (LRR) receptor kinase with a K_d of about 10^{-10} M, which is generally similar to many peptide-LRR receptor kinase interactions found in animals.

Systemin activates a complex signaling pathway that is analogous to the inflammatory response in animals. Early events following the systemin-receptor interaction include the activation of a MAP kinase and a phospholipase that cleaves linolenic acid from membranes, in much the same manner as arachidonic acid is released from animal membranes in response to cytokines. In plants, linolenic acid is converted to the oxylipin, jasmonic acid, a powerful inducer of defense genes, while in animals arachidonic acid is converted to the oxylipin prostaglandins, a mediator of inflammation.

Tomato and Tobacco Hydroxyproline-Rich Glycosylated Defense Signals

Other peptide signals have been associated with the activation of defense genes in response to herbivore attacks; two in tobacco leaves and three in tomato leaves. These peptides range from 15 amino acids to

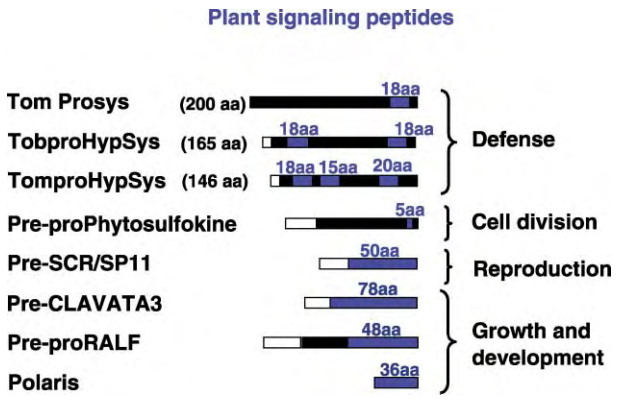

FIGURE 1 Box representations of plant peptide hormones and, where known, the precursor proteins from which they were derived. The locations of the peptides within the precursor are designated by the blue boxes.

20 amino acids in length and are structurally different from systemin in that they are hydroxyproline-rich and are glycosylated. This suggests that they are synthesized through the secretory pathway. The peptides activate proteinase inhibitor genes when supplied to plants at nMolar levels. Because of their sizes and their biological activites in signaling the activation of defense genes, they have been assigned to the systemin family, which is now a functionally defined family of peptide defense signals that are derived from plants.

The tobacco peptides are called Tobacco Hydroxyproline-rich Systemins, abbreviated to TobHypSys I and TobHypSys II. Wounding tobacco leaves results in a strong local response but a very weak systemic response, and these peptides are thought to be involved in signaling that is localized within the wounded leaves. The two tobacco systemins are derived from a single precursor protein of 165 amino acids that includes a signal sequence, with TobHypSys I sequence near the N terminus and TobHypSys II sequence near the C terminus.

The three tomato peptides, called TomHypSys I, II, and III, may also be localized signals, since prosystemin antisense tomato plants do not respond systemically to wounding but do generate a substantial localized wound response. As in tobacco, the localized defense response may result from the release of the TomHypSys peptides near the wound sites. The three TomHypSys peptides are derived from a single 146 amino acid precursor that has a leader peptide at its N terminus. Multiple peptide signals derived from a single precursor, as found with both TobHypSys and TomHypSys peptides is a scenario that is often found among precursors of peptide hormones in animals.

Standard protein–protein and nucleotide–nucleotide searches for cDNAs and pre-proproteins with homologies to the systemin precursor genes did not reveal homologues in other plant species, but short regions (less than 10 amino acids) in the N and C termini of the TomHypSys and TobHypSys precursors exhibit identity, suggesting that their genes may have evolved from a common ancestor.

Peptide Signals for Growth and Development

Phytosulfokine

A sulfated pentapeptide, called phytosulfokine (PSK), with the structure Tyr(SO_3H) -Ile-Tyr(SO_3H) -Thr-Gln, regulates plant cell proliferation. The peptide was initially found to cause low-density suspension cultured cells to proliferate rapidly. PSKs with identical structures are found in many plants, where they are derived from larger precursor pre-proproteins. The rice (*Orizae sativa) PSK* gene, for example, is a single-copy gene consisting of one large intron and two exons. The gene codes for a PSK pre-prohormone precursor of 89-amino acids including a leader peptide, suggesting that it is synthesized through the secretory pathway, where sulfation and processing occur. Sulfated tyrosines are often found in animal proteins, but to date PSK is the only example of a post-translational sulfated tyrosine in plants.

PSK is the ligand for a 150 kDa membrane-bound LRR receptor kinase with a K_d in the nMolar range. It plays *in vivo* functional roles in differentiation of cell cultures of zinnia into tracheary elements, in somatic embryogenesis in carrot, in the induction of adventitious root and bud formation in *Antirrhinum* callus, and in the formation of adventitious roots on cucumber hypocotyls. These effects of PSK require the presence of various levels of two small phytohormones, auxin, and cytokinin, indicating that PSK is part of a complex, but integrated, signaling network.

Clavata3

Clavata3 (CLV3) is an extracellular signaling polypeptide composed of 96 amino acids of which 18 residues comprise an N-terminal leader peptide. CLV3 and its receptor CLV1 have been studied extensively in *Arabidopsis thaliana*. CLV3 helps determine the fate of cells in shoot apical meristems (SAM). The identity and position of aerial organs in plants is initiated and established in the SAM, where a balance between the division of stem cells and differentiation is maintained as the plant grows. The stem cells divide slowly while the surrounding cells divide and differentiate.

No evidence is available to support any further processing of CLV3 after removal of the signal peptide, but dibasic or monobasic residues are present internally

that could be candidates for processing sites to produce smaller peptides that may have a role in signaling.

The CLV3 receptor, CLV1, is an 980 bp LRR receptor kinase that is associated with a 720-amino acid LRR receptor-like protein lacking a kinase domain. The CLV3-receptor complex results in autophosphorylation, leading to the binding of downstream signaling proteins as an early step in stem cell differentiation.

SCR/SP11: Signals for Self-Incompatibility

A family of intercellular signaling peptides of 47–60 amino acids in length play a central role in pollen self-incompatibility in the Brassicaceae family. The peptides are cumulatively called S-locus Cysteine Rich proteins (SCR) or S-locus Protein 11 (SP11), and are signals from the pollen that determine incompatibility when recognized by the appropriate receptor. During pollination, as pollen comes in contact with the papilli of the stigma, a self-recognition occurs that results in dehydration of the papilli and cessation of the pollenation process. SCR/SP11 peptides are found as a large gene family of 28 members that are derived from cysteine-rich pre-proteins of 74–83 amino acids in length that include leader peptides. In contrast to animal and plant leader peptides, the amino acid sequences of the SCR/SP11 leader peptides are highly conserved, while the mature SCR/SP11 peptides share only weak identities except at the eight cysteine positions that are conserved among most of the family members.

SCR/SP11 interacts with an S-locus Receptor Kinase (SRK). The receptor in Arabidopsis is composed of 858 amino acids including a 31 amino acid leader peptide. It is localized in membranes associated with the cell walls of stigma papillae. The SRK has a functional serine/threonine kinase at its C terminus with a transmembrane region in the middle and an extracellular cysteine-rich domain at its N-terminal region. An abundant soluble 60 kDa S-Locus Glycoprotein (SLG) appears to be associated with SRK and is often present in a 100-fold excess and appears to facilitate a functional SCR/SRK/SLG complex that results in signaling intracellular events leading to dehydration and incompatibility.

RALF, a Signal for Root Growth

The rapid alkalinization factor, called RALF, is a 49 amino acid peptide that is derived from the C terminus of a 115-amino acid precursor that contains a 25 amino acid leader peptide at its N terminus. RALF was named because of its ability to cause a rapid alkalinization of suspension cultures of tomato, tobacco, and alfalfa. Databases revealed the existence of RALF homologues in more than 15 plant species from nine families, present in a variety of tissues and organs. Two binding proteins of 120 and 25 kDa are thought to be part of a receptor complex that recognizes RALF to initiate a signaling pathway. The addition of micromolar solutions of tomato RALF to germinating tomato and Arabidopsis seedlings caused root growth to immediately cease. RALF inhibits both cell elongation and cell division. While its specific biochemical role in plants is not known, the ubiquity of the RALF peptides suggests that they have a fundamental physiological role in different organs and tissues of the plants. Nine RALF genes are present in Arabidopsis that contain highly conserved RALF sequences. The N-terminal amino acid sequences of each RALF precursor are much less conserved than the C-terminal sequences encoding the RALF peptide. The presence of two Arg residues just upstream from the putative N termini may be a recognition site for processing enzymes. The region just upstream of the dibasic site is rich in polar residues that are highly conserved among RALF precursors from different species and, as in animals, may be part of a recognition site for a RALF-processing proteinase.

Other Signaling Peptides

Several other peptides have been suggested to be hormone-like signaling molecules in plants with various roles related to growth, development, and differentiation. A small peptide of 36 amino acids lacking a signal peptide is translated from a 450 bp mRNA in Arabidopsis seedlings and root tips. This peptide, called POLARIS, is required for cytokinin and ethylene signaling during root growth, but its specific role in signaling is not known.

Several laboratories have looked for homologues of animal peptide hormone genes in plants, but none have been found.

Concluding Remarks

Since the discovery of insulin in 1922, hundreds of peptide hormones have been found in animals that regulate fundamental physiological processes. Over a dozen peptide hormones have now been identified in plants, establishing a new frontier for studies of plant growth, development, reproduction, defense, and responses to the environments. In many respects the properties of plant peptide hormones resemble those of animals, but several plant peptides have unique properties, indicating that the diversity of properties of peptide signals in plants may be the rule, rather than the exception. It is not clear whether all peptide signaling traces back to a common ancestral signaling system, or if

peptide signaling was reinvented many times by nature during the evolution of plants and animals. It is clear that peptide signaling has conferred a distinct advantage to the organisms, whether animal or plant. The recent discovery of peptide signals has laid to rest the long held hypothesis that all plant processes are regulated by small phytohormones.

To date, the receptors for peptide hormones appear to be either LRR receptor kinases or cysteine-rich receptor kinases (SRK). Although only a small number of plant peptide hormones and their receptors have been identified, peptide signaling in plants has become a focus of inquiry to gain a better understanding of plant signaling. Peptide signaling is a new area of research for the discovery of fundamental knowledge about plants. Such knowledge holds promise to reveal novel regulatory systems that can be used for biotechnological approaches to improve man's environment, to increase crop yields, and to provide nutraceuticals and medicines for human health.

See Also the Following Articles

G Protein-Coupled Receptor Kinases and Arrestins • Mitogen-Activated Protein Kinase Family• Glycoproteins, Plant

Glossary

Arabidopsis thaliana A small plant of the Cruciferae family with a very small genome that serves as a model for biochemical and genetic studies of plants.

leader peptides Short N-terminal amino acid sequences of nascent polypeptides that target the proteins to the Golgi for processing and secretion, and are removed by leader peptidases during transport across the Golgi membrane.

peptide hormones Intercellular signaling peptides.

phytohormones Small organic molecules that regulate numerous processes in plants. These hormones include auxins, gibberellins, cytokinins, ethylene, abscissic acid, and brassinolides.

shoot apical meristem The region of the growing tip of a plant shoot in which stem cells are produced and differentiate into plant organs as the plant grows.

systemins A functionally defined family of signaling peptides from plants that are released at sites of herbivore or pathogen attacks and activate defensive genes.

Further Reading

Bergey, D., Howe, G., and Ryan, C. A. (1996). Polypeptide signaling for plant defensive genes exhibits analogies to defense signaling in animals. *Proc. Natl Acad. Sci (USA)* **93**, 12053–12058.

Fletcher, J. C., Brand, U., Running, M. P., Simon, R., and Meyerowitz, E. M. (1999). Signaling of cell fate decisions by *CLAVATA3* in Arabidopsis shoot meristems. *Science* **283**, 1911–1914.

Kachroo, A., Nasrallah, M. E., and Nashallah, J. (2002). Self-incompatibility in the Brassicaceae: Receptor–ligand signaling and cell-to-cell communication. *Plant Cell* **14**, S227–S238.

Kende, H., and Zeevaart, J. A. D. (1997). The five "classical" plant hormones. *Plant Cell* **9**, 1197–1210.

Ryan, C. A., Pearce, G., Moura, D., and Scheer, J. (2002). Polypeptide hormones. *Plant Cell* **14**, S251–S264.

Suzuki, G., Kai, N., Hirose, T., Fukui, K., Nishio, T., Takayama, S., Isogai, A., Watanabe, B., and Hinata, K. (1999). Genomic organization of the S locus: Identification and characterization of genes in SLG/SRK region of S^9 haplotype of *Brassica campestris* (syn. rapa). *Genetics* **153**, 391–400.

Yang, H., Matsubayshi, Y., Hanai, H., and Sakagami, Y. (2000). Phytosulfokine-α, a peptide growth factor found in higher plants: Its structure, functions, precursor and receptors. *Plant Cell Physiol.* **41**, 825–830.

Biography

Clarence Ryan is a Professor of Biochemistry in the Institute of Biological Chemistry at Washington State University. He received a Ph.D. from Montana State University, Bozeman, MT, and was a postdoctoral fellow at Oregon State University, Corvallis, OR and at the USDA Pioneering Laboratory in Albany, CA.

Gregory Pearce is the Senior Laboratory Supervisor in the Ryan laboratory. He received his B.S. in Biochemistry and M.S. in Animal Nutrition at Washington State University.

Plasma-Membrane Calcium Pump: Structure and Function

Emanuel E. Strehler
Mayo Clinic College of Medicine, Rochester, Minnesota, USA

Plasma-membrane calcium pumps, also called plasma-membrane calcium ATPases (PMCAs), are integral membrane proteins responsible for the expulsion of ionized calcium (Ca^{2+}) from the cell interior to the extracellular milieu. They use adenosine triphosphate (ATP) as energy source to pump Ca^{2+} "uphill" against a large concentration gradient, thereby ensuring that the resting free intracellular Ca^{2+} concentrations remain low and that Ca^{2+} signaling can occur with fidelity and spatial precision.

Plasma-Membrane Calcium Pump Abundance and Isoforms

Plasma-membrane calcium pumps are ubiquitous in eukaryotic cells, although there are differences in expression during development in various tissues and even among different membrane domains within the same cell.

Isoforms

In mammals, multiple plasma-membrane calcium pumps are generated from multigene families and via alternative RNA splicing, giving rise to pump isoforms with distinct regulatory and functional properties. Humans, rats, mice, and other mammals express four distinct genes (human genome database nomenclature ATP2B1–ATP2B4) coding for PMCA isoforms 1–4. Alternative RNA splicing of the primary gene transcripts occurs at two major sites (called splice sites, A and C) and involves multiple exons that can either be spliced out or wholly or partially retained in the final mRNA (Figure 1). Combinatorial alternative splicing produces multiple splice variants of each PMCA isoform.

Expression

Development

Plasma-membrane calcium pumps are differentially expressed during mammalian development, though mouse embryonic stem cells express all four PMCA genes. In mice, PMCA1 is expressed from the earliest embryonic stage identified, and is ubiquitously present in all tissues. PMCA 2, 3, and 4 are first detected at ~12 days postcoitum and show a changing and restricted tissue distribution during embryonic development. PMCA2 is essentially confined to neuronal tissues, PMCA3 initially shows widespread expression but eventually becomes restricted to the nervous system and muscle, and PMCA4 is transiently expressed at high levels in the liver but then becomes less abundant and more evenly distributed in multiple tissues including the brain, heart, and intestine.

Tissues

In the adult, PMCA1 and PMCA4 are expressed in virtually all tissues, with PMCA1 normally being the most abundant isoform. PMCA2 is largely confined to nervous tissue as well as to epithelia of the breast and kidney, and PMCA3 is expressed at generally low levels and restricted to specific areas in the brain and to skeletal muscle.

Cells

Differential distribution of PMCA isoforms in different plasma membrane domains has been demonstrated in many cell types, notably in highly polarized cells such as retinal photoreceptors, auditory, and vestibular hair cells, cerebellar Purkinje cells, and epithelial cells. In cochlear hair cells, for example, PMCA2 is exclusively and highly expressed in the apical stereocilia, whereas PMCA1 may be concentrated along the basolateral membrane and close to synaptic terminals.

Plasma-Membrane Calcium Pump Structure

The overall structure of plasma-membrane calcium pumps resembles that of the calcium pump of the

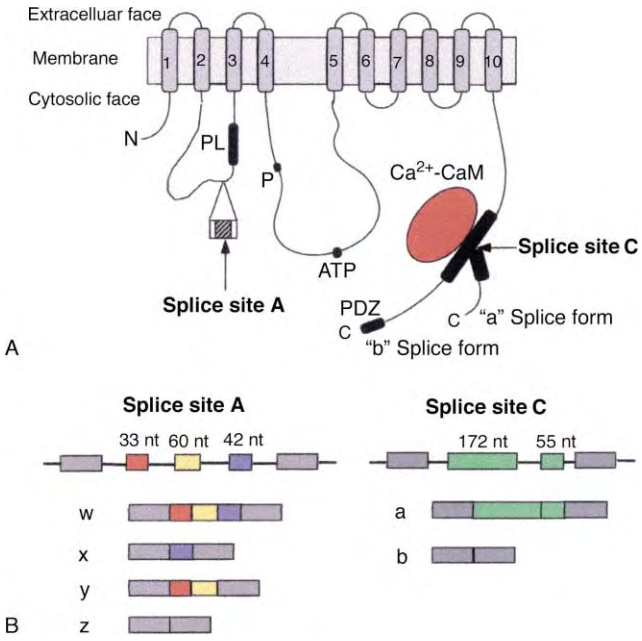

FIGURE 1 (A) Schematic model of the plasma membrane calcium pump, showing the major domain substructure. The ten transmembrane regions are numbered and indicated by shaded boxes. The cytosolic amino- (N) and carboxyl-terminal (C) ends are labeled, and a phospholipid-sensitive region (PL), the calmodulin-binding region and the C-terminal PDZ domain binding sequence of the "b" splice forms are shown as black boxes. P is the site (aspartate residue) of the obligatory aspartyl-phosphate formed during each Ca^{2+} transport cycle, and ATP denotes the specific residues involved in nucleotide (ATP) binding. The PMCA is shown in its active form, with Ca^{2+}-loaded calmodulin (Ca^{2+} -CaM, red oval) bound to the regulatory C-terminal tail. Arrows labeled "splice site A" and "splice site C" denote the regions affected by alternative splicing. At site A, the peptide segment encoded by alternatively spliced exon(s) is indicated by a hatched box, and at site C, the two major splice variants (a and b splice forms) created by alternative splicing are drawn as separate carboxyl-terminal tails. (B) Major alternative splicing options for the generation of PMCA splice variants. The example given is that of human PMCA2. At splice site A, three exons (shown as red, yellow, and blue boxes) can be all excluded or variably included to generate splice variants w, x, y, and z. At splice site C, two exons (green boxes) are either included or excluded to generate splice variants a or b, respectively. The sizes of the exons in human PMCA2 RNA are indicated in nucleotides (nt). Constitutively spliced exons are shown as dark gray boxes. Note that the combinatorial use of splicing options at sites A and C can generate a large number of different PMCA variants.

sarco/endoplasmic reticulum membrane. Major features include intracellular amino- and carboxyl-terminal ends, ten membrane-spanning domains, and three distinct intracellular domains involved, respectively, in ATP binding (N-domain), formation of an obligatory phosphorylated intermediate (P-domain), and actuating large conformational movements (A-domain) to complete the catalytic cycle that links ATP hydrolysis to transmembrane movement of Ca^{2+} (Figure 2).

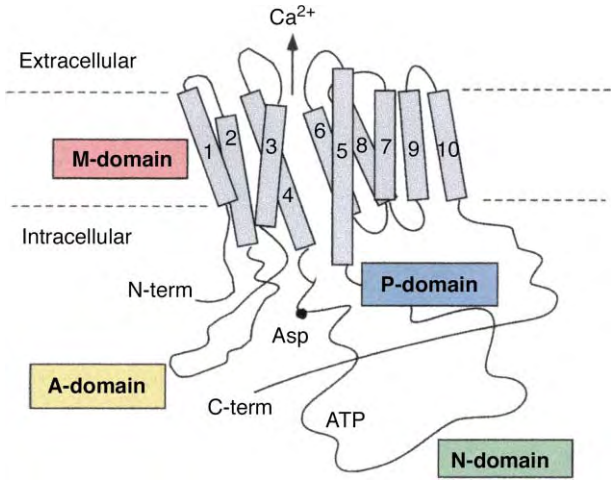

FIGURE 2 Folding and domain model of the PMCA based on structural homology to the sarco/endoplasmic reticulum calcium pump. The ten membrane-spanning regions are numbered and shown as gray cylinders forming the M-domain. The invariant aspartate residue (Asp) undergoing phosphorylation during the reaction cycle is indicated, as is the ATP-binding site (ATP). The three major cytosolic domains are labeled A (actuator), P (phosphorylation), and N (nucleotide-binding). The amino (N-term) and carboxyl ends (C-term) are indicated; the arrow shows the direction of Ca^{2+} pumping. The extended C-terminal tail is drawn to indicate its intramolecular interaction with other cytosolic domains as found in the autoinhibited state of the pump.

Mechanistic Aspects

The plasma-membrane calcium pumps belong to the superfamily of P-type ion-motive ATPases, where they are classified into the type II subfamily that also includes organellar Ca^{2+} ATPases, Na^+/K^+ ATPases, and H^+/K^+ ATPases. The salient feature of the P-type ATPases is the formation of a phosphorylated intermediate during the reaction cycle, whereby the γ-phosphate of ATP is transferred to an invariant aspartate residue in the central catalytic domain of the pump (see Figures 1 and 2). The basic reaction scheme for the stepwise cycling of the pump between conformational states which link ATP hydrolysis and ion translocation across the membrane is described by the E1–E2 model (Figure 3). In this scheme, the pump alternates between the E1 and E2 conformations, where the E1 state describes the pump with its ion (Ca^{2+}) sites facing the cytoplasmic side and the E2 state that of the pump having its ion sites facing the extracellular side. The energy of hydrolysis of one ATP molecule is required for each Ca^{2+} ion transported by the plasma membrane calcium pump. The Ca^{2+} transport cycle is accompanied by large conformational changes in the pump protein, whereby the reactions occurring at the cytoplasmic ATP binding and phosphorylation sites are coupled to the rearrangement of the membrane-spanning domains corresponding to the Ca^{2+} transport site. The positive charge

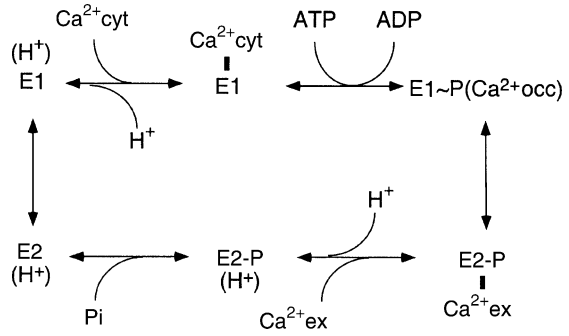

FIGURE 3 Reaction scheme of the plasma membrane calcium pump. The pump adopts two major states E1 and E2. The E1 state shows high affinity for Ca^{2+} on the cytosolic side of the membrane (Ca^{2+} cyt). Ca^{2+}-binding stimulates the ATPase activity of the pump, leading to the formation of the phosphorylated intermediate E1 ~ P and "occlusion" (occ) of the bound Ca^{2+} ion. Translocation of the Ca^{2+} ion across the membrane occurs concomitantly with the release of stored energy during the conformational transition from the E1 ~ P to the E2-P state. The Ca^{2+} affinity of the pump in the E2-P state is low and Ca^{2+} dissociates on the extracellular side of the membrane (Ca^{2+} ex). This is followed by hydrolysis of the phosphoenzyme and rearrangement of the E2 to the E1 state. The charge movement during Ca^{2+} transport is at least partially neutralized by countertransport of protons (H^+).

movement accompanying the transport of Ca^{2+} from the intracellular to the extracellular side of the membrane is at least partially compensated by countertransport of H^+ ions. When fully active, the turnover number of the PMCA is of the order of 50–100, i.e., a single PMCA molecule can pump about 50–100 Ca^{2+} ions per second across the membrane.

Domain Structure

The plasma-membrane calcium pumps can be divided into an N-terminal cytoplasmic domain followed by a first membrane-spanning hairpin loop, an intracellular loop making up most of the A-domain, a second membrane-spanning hairpin loop, the major cytosolic catalytic loop containing the nucleotide-binding and phosphorylation domains, three additional membrane-spanning hairpin loops and a final, cytosolic C-terminal domain containing multiple regulatory sequences (Figures 1 and 2). Based on structural homology to the sarco/endoplasmic reticulum calcium ATPase (SERCA) for which a high-resolution three-dimensional structure is available, the PMCAs consist of a compact membrane-embedded domain comprising the ten membrane-spanning regions, and of a large cytoplasmic domain that can be subdivided into the three well-separated A, N, and P domains (see Figure 2). The P (phosphorylation) domain of the PMCA assumes the structural-fold characteristic of haloacid dehalogenase. The three-dimensional structure of the C-terminal regulatory domain unique to the PMCAs is not yet known, but chemical cross-linking and proteolysis studies indicate that this domain is involved in extensive intramolecular interactions with the A and the N/P domains.

Plasma-Membrane Calcium Pump Regulation and Function

Plasma-membrane calcium pumps function to maintain and reset the low (~100 nM) intracellular Ca^{2+} concentrations required for effective Ca^{2+} signaling. Through multifaceted regulation, these pumps also participate in spatio-temporal Ca^{2+} signaling by restricting the spread of Ca^{2+} signals and reducing noise in local signal transduction.

Regulation

The calcium sensor protein calmodulin is a major regulator of the plasma-membrane calcium pumps. In general, the PMCAs are autoinhibited at very low cytosolic-free Ca^{2+} concentrations ($[Ca^{2+}]_i$ < 50–100 nM). Upon a rise in $[Ca^{2+}]_i$, Ca^{2+}-calmodulin activates the PMCAs by releasing the autoinhibition. Calmodulin binds to a specific binding site of varying length in the C-terminal tail of the PMCAs (Figure 1). Different PMCA isoforms and alternative splice variants show different affinities for Ca^{2+}-calmodulin, and hence are differently sensitive to rises in $[Ca^{2+}]_i$. The PMCAs are also regulated by phosphorylation. Protein kinases A and C phosphorylate specific residues in the C-terminal tail of various PMCAs downstream of and/or overlapping the calmodulin-binding domain. The effects of phosphorylation on PMCA activity are complex, involving both direct activation (by deinhibiting the pump) as well as interference with calmodulin regulation. Different PMCA isoforms and splice variants react differently to Ser/Thr phosphorylation in their C-terminal domains, depending on the specific sites of phosphorylation and the surrounding sequence context. Tyrosine phosphorylation also has been observed in some PMCAs and may lead to changes in the cellular distribution of the pumps. Additional regulatory mechanisms for the PMCAs involve activation by dimerization or oligomerization and stimulation by various acidic phospholipids (such as phosphatidic acid, phosphatidylinositol-phosphates). A phospholipid-sensitive region has been identified near the third membrane-spanning region in the A-domain (Figure 1). PMCA splice variants ending with the C-terminal amino acid sequence … GluThrSerVal or … GluThrSerLeu ("b" or CI splice variants, see Figure 1) bind directly to the PDZ (*PSD95/Dlg/ZO-1*) protein–protein interaction domain found in many scaffolding,

anchoring, and signaling proteins. These interactions may anchor the PMCAs to the submembraneous actin cytoskeleton and recruit them into multiprotein complexes with other membrane receptors, transporters, and signaling molecules.

Function: Resetting and Maintenance of Resting Calcium Levels

The primary function of the PMCAs has been traditionally linked to the maintenance of low resting levels of intracellular Ca^{2+}. In cell types such as human erythrocytes where the PMCA is the sole system for Ca^{2+} expulsion from the cytosol, the function of this pump is essential for Ca^{2+} homeostasis and normal cell physiology. Because of its low capacity (turnover number < 100) and low abundance in most membranes, the PMCA is not well suited to the mass evacuation of high Ca^{2+} loads that may occur after global Ca^{2+} influx (such as happens with every beat of a heart muscle). In these cases other, low-affinity but high-capacity systems such as the Na^+/Ca^{2+} exchangers are responsible for the bulk export of Ca^{2+} from the cell. However, with their high Ca^{2+} affinity in the fully activated state ($Kd_{Ca^{2+}} < 0.2\ \mu M$), the PMCAs are the only transport system of the plasma membrane capable of reducing cytosolic Ca^{2+} levels down to the required submicromolar and even nanomolar levels. The specific PMCA isoform and splice variant expression pattern enables each cell to fine-tune and maintain its $[Ca^{2+}]_i$, and to reset $[Ca^{2+}]_i$ to the resting level following transient increases generated by Ca^{2+} signals.

Function: Vectorial Calcium Transport And Local Calcium Signaling

In epithelia involved in transcellular Ca^{2+} transport, e.g., in the intestine and the distal kidney, the PMCAs are concentrated in the basolateral membrane of the cells where they play an important role in vectorial Ca^{2+} transport from the apical (intestinal lumen, kidney urinary lumen) to the basal (blood) side. In other tissues and cell types, e.g., in the choroid plexus and cochlear hair cells, specific PMCA isoforms are uniquely expressed in the apical plasma membrane where they are responsible for local Ca^{2+} transport into the cerebrospinal fluid and the endolymph, respectively. An important function of the PMCAs thus consists in their participation in localized Ca^{2+} transport to allow the selective enrichment of Ca^{2+} in a specific extracellular compartment. Besides their role in the maintenance of overall Ca^{2+} homeostasis, PMCAs also participate in Ca^{2+} signaling. Specific PMCA isoforms and splice variants are concentrated in multiprotein complexes localized in distinct membrane domains (e.g., in caveolae or at the neck of dendritic spines of hippocampal and cerebellar neurons). As part of "Ca^{2+} signalosomes," the PMCAs are involved in the spatial and temporal regulation of Ca^{2+} signaling. By preventing the spread of a local increase in Ca^{2+}, they contribute to the spatial resolution of Ca^{2+} signaling and suppress signaling "noise." By counteracting the local rise in Ca^{2+} following the temporary opening of influx channels, they also contribute to the termination of Ca^{2+} signaling and thus to its temporal regulation.

Diseases Linked to Plasma-Membrane Calcium Pumps

Specific human diseases linked to PMCA mutations or the lack of a particular PMCA isoform are not yet known. However, spontaneous mouse mutants called "deafwaddler" and "wriggle mouse Sagami" have been described in which mutations in the PMCA2 gene lead to a defective PMCA2 protein. Homozygous mutant mice are deaf and show an unsteady gait, underlining the importance of PMCA2 function in the auditory and vestibular hair cells. The same phenotype is observed in homozygous PMCA2 "knockout" mice, which are profoundly deaf and severely ataxic. By contrast, homozygous knockout mice lacking PMCA1 are embryonic lethal, as might be expected given the ubiquitous expression pattern of this PMCA. On the other hand, numerous disease conditions have been linked to abnormal expression of PMCAs. These include diabetes where a significant decrease in PMCA activity in erythrocytes has been described, and neurodegenerative disorders such as Alzheimer disease and stroke, where complex changes in PMCA isoform expression accompany or precede neuronal malfunction and death. Because of their large size (average > 100 kb), the human PMCA genes almost certainly suffer relatively frequent mutations. Many familial and "spontaneous" diseases with an incompletely understood etiology are therefore likely to be linked at least in part to abnormal PMCA expression and function.

See Also the Following Articles

ER/SR Calcium Pump: Function • ER/SR Calcium Pump: Structure

Glossary

alternative splicing Process in the cell nucleus whereby pieces of a primary gene transcript are optionally excised or included in the final messenger RNA. Translation of these differently spliced mRNAs normally leads to protein products that differ only in the region affected by the alternative splice.

apical membrane The part of the plasma membrane facing the lumen in polarized (asymmetric) epithelial cells separating two different extracellular compartments. The apical membrane is separated from the basolateral membrane by tight junctions formed between neighboring cells.

calcium signalosome Multiprotein complex of several functionally and physically linked proteins to allow the spatially defined generation and transmission of Ca^{2+} signals.

isoform A protein structurally and functionally similar to a given protein.

plasma membrane The lipid- and protein-rich structure defining the boundary between the extracellular space and the interior of a cell.

Further Reading

Andersen, J. P., and Vilsen, B. (1996). Primary ion pumps. In *Principles of Medical Biology* (E. E. Bittar and N. Bittar, eds.) Vol 4, pp. 1–66. Cell Chemistry and Physiology Part III, JAI Press, Greenwich, CT.

Axelsen, K. B., and Palmgren, M. G. (1998). Evolution of substrate specificities in the P-type ATPase superfamily. *J. Mol. Evol.* **46**, 84–101.

Carafoli, E. (1991). Calcium pump of the plasma membrane. *Physiol. Rev.* **71**, 129–153.

Dumont, R. A., Lins, U., Filoteo, A. G., Penniston, J. T., Kachar, B., and Gillespie, P. G. (2001). Plasma membrane Ca^{2+}-ATPase isoform 2a is the PMCA of hair bundles. *J. Neurosci.* **21**, 5066–5078.

Lehotsky, J., Kaplan, P., Murin, R., and Raeymaekers, L. (2001). The role of plasma membrane Ca^{2+} pumps (PMCAs) in pathologies of mammalian cells. *Front Biosci.* **7**, d53–d84.

Kozel, P. J., Friedman, R. A., Erway, L. C., Yamoah, E. N., Liu, L. H., Riddle, T., Duffy, J. J., Doeschman, T., Miller, M. L., Cardell, E. L., and Shull, G. E. (1998). Balance and hearing deficits in mice with a null mutation in the gene encoding plasma membrane Ca^{2+}-ATPase isoform 2. *J. Biol. Chem.* **273**, 18693–18696.

Moller, J. V., Juul, B., and leMaire, M. (1996). Structural organization, ion transport, and energy transduction of P-type ATPases. *Biochim. Biophys. Acta* **1286**, 1–51.

Pedersen, P. L., and Carafoli, E. (1987). Ion motive ATPase. I. Ubiquity, properties, and significance to cell function. *Trends Biochem. Sci.* **12**, 146–150.

Strehler, E. E., and Zacharias, D. A. (2001). Role of alternative splicing in generating isoform diversity among plasma membrane calcium pumps. *Physiol. Rev.* **81**, 21–50.

Street, V. A., McKee-Johnson, J. W., Fonseca, R. C., Temple, B. L., and Noben-Trauth, K. (1998). Mutations in a plasma membrane Ca^{2+}-ATPase gene cause deafness in deafwaddler mice. *Nature Genet.* **19**, 390–394.

Takahashi, K., and Kitamura, K. (1999). A point mutation in a plasma membrane Ca^{2+}-ATPase gene cause deafness in *Wriggle Mouse Sagami*. *Biochem. Biophys. Res. Commun.* **261**, 773–778.

Toyoshima, C., Nakasako, M., Nomura, H., and Ogawa H. (2000). Crystal structure of the calcium pump of sarcoplasmic reticulum at 2.6Å resolution. *Nature* **405**, 647–655.

Zacharias, D. A., and Kappen, C. (1999). Developmental expression of the four plasma membrane calcium ATPase (Pmca) genes in the mouse. *Biochim. Biophys. Acta* **1428**, 397–405.

Biography

Emanuel E. Strehler is a Professor in the Department of Biochemistry and Molecular Biology at the Mayo Clinic College of Medicine in Rochester, Minnesota. His principal research interest is in the molecular mechanisms of calcium regulation and calcium signaling, including calcium transport systems of the membrane and calcium sensor proteins. He holds a Ph.D. from the Swiss Federal Institute of Technology (ETH) in Zurich, Switzerland, and received his postdoctoral training at Harvard Medical School in Boston. He was involved in the first molecular cloning of a human plasma membrane calcium ATPase, and his laboratory has made seminal contributions to the characterization of the human plasma membrane calcium pump and calmodulin gene families.

Plastocyanin

Elizabeth L. Gross
Ohio State University, Columbus, Ohio, USA

The photosynthetic electron transport chain of higher plants, algae, and cyanobacteria consists of two light reactions (photosystem II (PSII) and photosystem I (PSI)) which act in series to produce molecular oxygen, reduce $NADP^+$ to NADPH, and synthesize ATP. The cytochrome b_6f complex is a large multi-subunit complex involved in the transfer of electrons from PSII to PSI. Plastocyanin is a ~10 kDa Cu-protein which acts as a mobile electron carrier, located in the lumen of the chloroplast thylakoid, which shuttles electron from cytochrome *f* (Cyt *f*) in the cytochrome b_6f complex to P700 in PSI. It can be replaced by an Fe-containing cytochrome (cytochrome c_6) in some green algae and cyanobacteria under conditions of copper deficiency.

Plastocyanin Structure

The Copper Center

Plastocyanin (PC) is a β-sheet protein (Figure 1) with a Cu atom that acts as the redox center. The Cu atom is coordinated to four amino acid residues (H87, H37, S84, and M92) in a distorted tetrahedral geometry. The distorted tetrahedral geometry of the Cu center together with the protein matrix promotes efficient electron transfer between Cyt *f* and P700. Electrons enter and leave PC via the H87 ligand to the copper which is located on the surface of the PC molecule (Figures 1 and 2A).

The Surface of the PC Molecule

Higher Plant and Green Algal PCs

Figure 2A depicts the surface of spinach PC which is a typical representative of higher plant and green algal PCs. There are two important features. The first is the patch of hydrophobic residues (green in Figures 2A and 2B) that surround the H87 ligand to the copper. These residues – including G10, L12, G34, F35, P36, L62, P86, G89, and A90 – are either conserved or replaced with similar residues in all PCs. They provide a hydrophobic binding surface for both Cyt *f* and PSI (see below). The second feature consists of two patches of negatively charged residues surrounding Y83 (yellow in Figures 2A and 2B). Negatively charged residues are shown in red and positively charged residues are shown in blue in Figure 2. The lower patch consists of anionic residues #42–44 and either #45 or #79. The upper patch consists of anionic residues #59–61 in most higher plant PCs. In a few higher plant species and in all green algae, one of the anionic residues in the upper patch is deleted and is replaced by a glutamate at position #85. Also, all higher plant and green algal PCs contain an additional anionic residue at either position #51 or #53. Thus, there are a total of eight anionic residues that contribute to large negatively charged electrostatic field surrounding Y83.

Cyanobacterial PCs

Cyanobacterial PCs are similar to those from higher plants and green algae in that a patch of hydrophobic residues surrounds the H87 ligand to the Cu (Figure 2B) (residues from cyanobacterial PCs are numbered so as to be consistent with those from higher plant PCs). However, the distribution of charged residues on their surface of cyanobacterial PCs is quite different than observed for higher plants and green algae. The only conserved anionic residue is D42. Instead, there are a series of positively charged residues on PC including R88, K44, and K51 that contribute to a positively charged electrostatic field surrounding Y83.

The Interaction of PC with Cyt *f*

The Structure of Cyt *f*

Cyt *f* is also a β-sheet protein with two domains. The heme is located on the large domain. The sixth ligand to the heme is the amino group of Y1 which may provide a pathway of electron transfer from the heme to H87 on PC. Y1 and the heme are surrounded by a patch of highly conserved hydrophobic residues. Cyt *f*s from higher plants and green algae have a highly conserved basic patch consisting of five residues (K58, K65, K66, K187, and R209 in turnip Cyt *f*). The negatively charged residues on higher plant and algal PCs are attracted to the positive patch on Cyt *f*. In contrast, Cyt *f* from

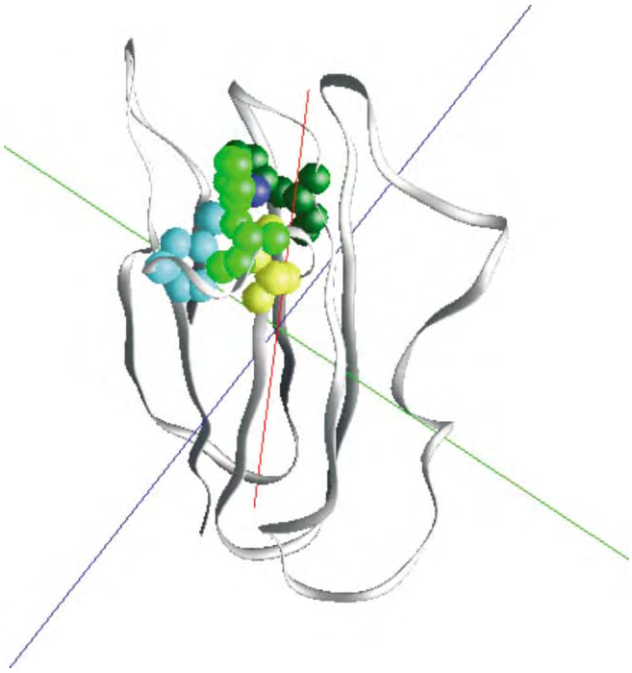

FIGURE 1 The structure of spinach plastocyanin: the copper center. The copper atom in PC (dark blue) is coordinated to two histidines (H87 – light green and H37 – dark green), C84 (yellow) and M92 (cyan). PC structures are taken from the Protein Data Bank from Berman H. M., Westboro, J., Feng, Z., Gilliland, G., Bhat, T. N., Weissig, H., Shindyalou, I. N. and Baume, P. E. (2000). The Protein Data Bank. *Nucleic Acids Res.* **28**, 235–242 and displayed using the Program GRASP (Nicholls, A., and Honig B. (1991). A rapid finite-difference algorithm, utilizing successive over-relaxation to solve the Possion-Boltzmann equation. *J. Comp. Chem.* 435–445).

the cyanobacterium *Phormidium lamanosum* has a large number of negatively charged residues on its surface that attract the positively charged residues on cyanobacterial PCs.

Complex Formation between PC and Cyt *f*

Figure 3 depicts a complex between spinach PC and turnip Cyt *f* determined by NMR. Two types of interactions are observed. First, there is an electrostatic attraction between cationic residues on Cyt *f* (blue) and the anionic residues surrounding Y83 on PC (red). These electrostatic interactions serve to bring the two molecules together and to orientate them properly. Evidence for electrostatic interactions come from cross-linking, chemical modification, and mutagenesis experiments. Second, hydrophobic residues surrounding the heme and Y1 on Cyt *f* interact with those surrounding the H87 ligand and the Cu on PC. These hydrophobic interactions anchor the two proteins in the proper orientation for efficient electron transfer from the heme and Y1 on Cyt *f* to H87 and the Cu on PC. Complexes formed between *Phormidium* Cyt *f* and *Phormidium* PC show a greater influence of hydrophobic as opposed to electrostatic interactions.

The Interaction of PC with PSI

The Structure of PSI

Recently, the structure of PSI from *Synechococcus elongatus* has been determined at a resolution of 2.5Å by X-ray crystallography. A simplified model of PSI is presented in Figure 4. Two regions of PSI have been implicated in PC binding. The first region includes the two largest subunits, PsaA and PsaB. These two subunits form a heterodimer containing P700 as well

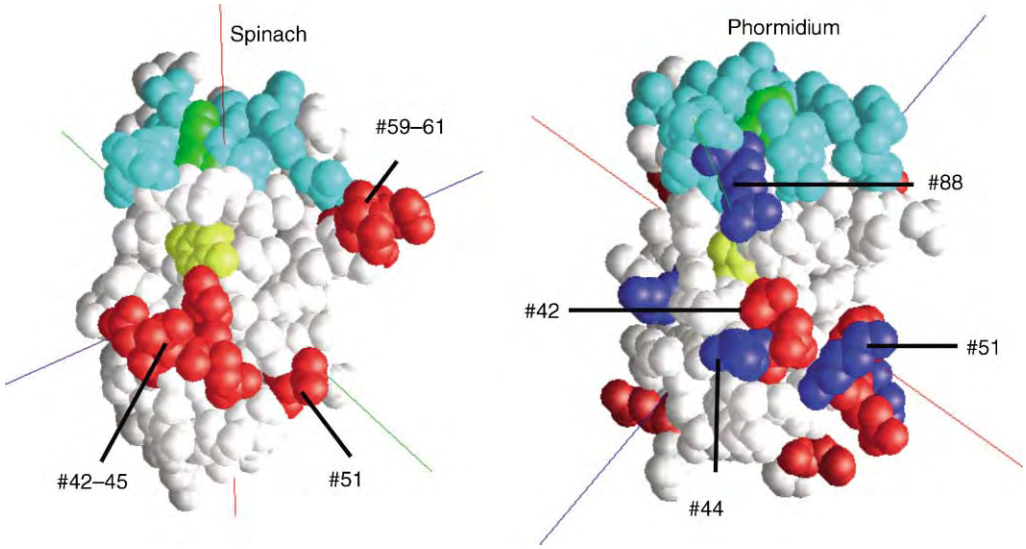

FIGURE 2 Surface residues on PC. H87, green; Y83, yellow; hydrophobic, cyan; cationic, blue; anionic, red: (A) spinach PC; (B) cyanobacterial PC from *P. lamanosum*. Other conditions were the same as for Figure 1.

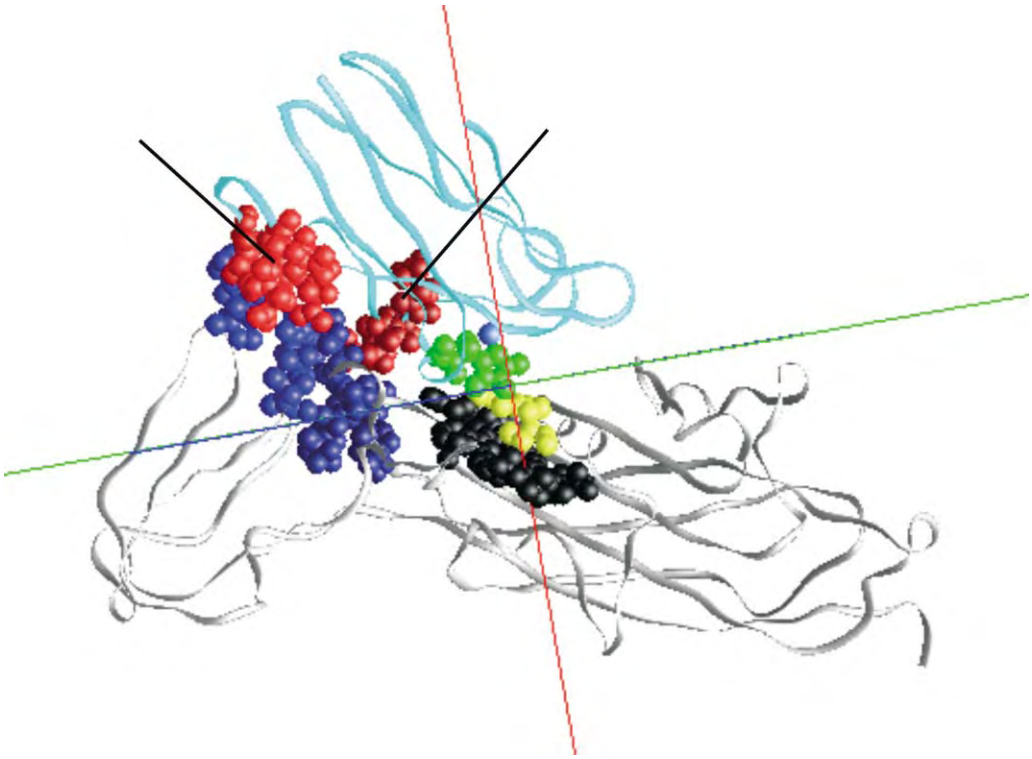

FIGURE 3 Complex formed between turnip Cyt *f* and spinach PC. Model 1 taken from Ubbink *et al.* (1988) *Structure* **6**, 323–335. Backbone of Cyt *f*, gray; backbone of PC, cyan. Other colors are the same as for Figure 2.

as the early electron acceptors A_0, A_1, and F_x. The second region includes the small subunit PsaF.

The Involvement of the PsaA and PsaB Subunits in Hydrophobic Interactions with PC

The PsaA–PsaB heterodimer has a 10Å depression which has been postulated to form a binding pocket for PC and cyt c_6 (Figure 4). Two surface-exposed hydrophobic helices line the binding pocket. One is part of PsaA and extends from residue #646 to residue #664; the second is located on PsaB and extends from residue #Y621 to residues #N639. Also, W655 on PsaA and W631 on PsaB are located in these helices and point toward the binding pocket. It has been postulated that these residues may be involved in the transfer of electrons from PC to P700. The observation that two mutants of residues located in the surface-exposed PsaB helix (W627F and E613N) caused significant inhibition of electron transport from PC to P700, support the hypothesis that these helices participate in the binding of PC to PSI.

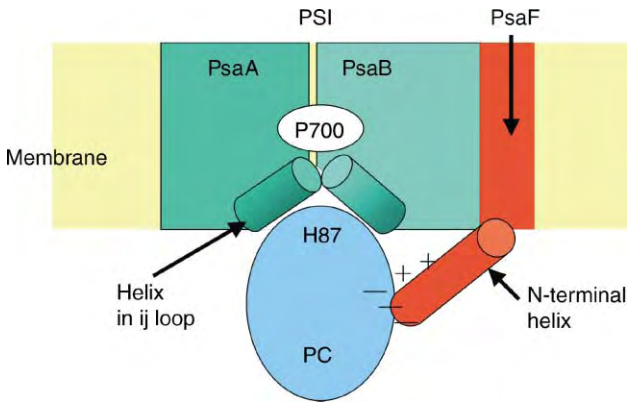

FIGURE 4 Model of the interaction of PC with PSI in higher plants and algae. The interactions of PC (blue) with: (1) the PsaA and PsaB subunits of PSI (green) and (2) the N-terminal positively charged helix of PsaF (red) are shown. The hydrophobic helices in the ij loops of PsaA and PsaB that have been postulated to be part of the binding pocket are also shown.

Involvement of the PsaF Subunit in Electrostatic Interaction between PC and PSI in Higher Plants and Green Algae

The PsaF subunit in green plants and algae has been implicated in PC binding to PSI (Figure 4). The evidence for this is as follows. First, removal of PsaF by either detergent treatment or mutagenesis inhibits the fast phase of electron transfer from PC to P700. This rapid phase has a half-time of ~11 ps and represents electron transfer from PC to P700 in preformed PC–PSI complexes. Second, mutagenesis of residues #42–45 in

the lower patch of PC inhibited the fast phase of electron transfer. In contrast, mutagenesis of the upper patch (residues #59–61) had very little effect. The N-terminal portion of PsaF consists of an amphipathic helix in which six lysine residues are lined up on one side of the helix. Third, mutagenesis of the lysine residues in this region of PsaF inhibited cross-linking and electron transfer from PC to P700; the greatest effect was observed for K23Q. Fourth, PC can be chemically cross-linked to PsaF. It was found that residues from the lower acidic patch of PC (#42–45) were cross-linked to residues #10–24 on PsaF, and residues from the upper acidic patch (#59–61) were cross-linked to residues #24–51 on PsaF.

The situation is different in cyanobacteria. Cyanobacteria show no rapid phase of electron transfer from PC to P700. In fact, the rate of electron transfer in cyanobacteria is approximately 2 orders of magnitude lower than that observed in green plants or algae. Also, removal of PsaF has no effect. An examination of PsaF in cyanobacteria shows that it lacks the N-terminal lysine-rich helix found in higher plant and green algae. However, when a chimeric PsaF, made up of the N-terminal sequence from *Chlamydomonas* PsaF and the C-terminal sequence from the cyanobacterium *Synechococcus*, was placed in *Synechococcus* cells, rapid electron transfer was observed between *Chlamydomonas* PC (and cyt c_6) and P700 which had the same characteristics as observed in *Chlamydomonas* cells. However, there is some evidence for electrostatic effects in cyanobacteria since removal of the negative charge of D42 on a cyanobacterial PC increased the rate of electron transfer to P700, whereas removal of the positive charge of R88 decreases it.

In conclusion, binding of PC to PSI in green plants and algae is similar to its binding to Cyt *f* in that electrostatic forces steer PC (and cyt c_6) to the hydrophobic binding sites on PSI (Figure 4) where electron transfer to P700 occurs in a rapid and efficient manner.

See Also the Following Articles

Cytochrome *c* • Photosystem I: F_X, F_A, and F_B Iron–Sulfur Clusters • Photosystem I, Structure and Function • Cytochrome b_6f Complex

Glossary

cytochrome b_6f complex Large multi-subunit complex located in the thylakoid membrane that mediates electron transport between plastoquinone and PC. Cyt *f*, a member of this complex, donates electrons directly to PC.

photosystem I Large multi-subunit complex located in the thylakoid membrane which accepts electrons from PC and donates them to ferredoxin. It contains the primary electron donor P700 and acceptors A_0, A_1, and Fx.

PsaA, PsaB, and PsaF Protein subunits of PSI.

P700 Chlorophyll dimer in the reaction center of PSI which is oxidized by light and reduced by PC.

thylakoid Portion of the inner membrane system of the chloroplast where the light reactions take place and where the cytochrome b_6f complex and PSI are located.

Further Reading

Berman H. M., Westboro, J., Feng, Z., Gilliland, G., Bhat, T. N., Weissig, H., Shindyalou, I. N. and Bourne, P. E. (2000). The Protein Data Bank. *Nucleic Acids Res.* **28**, 235–242.

Fromme, P., Jordan, P., and Krauss, N. (2001). Structure of photosystem I. *Biochim. Biophys. Acta* **1507**, 5–31.

Gross, E. L. (1996). Plastocyanin: structure, location, diffusion, and electron transfer mechanisms. In *Oxygenic Photosynthesis: The Light Reactions* (D. Ort and C. Yocum, eds.) pp. 413–429. Kluwer Academic Publishers, Dordrecht, The Netherlands.

Hippler, M., Reichert, J., Sutter, M., Zak, E., Altschmeid, L., Schroer, U., Herrmann, R. G., and Haehnel, W. (1996). The plastocyanin binding domain of photosystem I. *EMBO J.* **23**, 6376–6384.

Hippler, M., Drepper, F., Rochaix, J.-D., and Muhlenhoff, U. (1999). Insertion of the N-terminal part of PsaF from *Chlamydomonas reidhardtii* into photosystem I from *Synechococcus elongatus* enables efficient binding of algal plastocyanin and cytochrome c_6. *J. Biol. Chem.* **274**, 4180–4188.

Hope, A. B. (2000). Electron transfers amongst cytochrome *f*, plastocyanin and photosystem: I. Kinetics and mechanisms. *Biochim. Biophys. Acta* **1456**, 5–26.

Kannt, A., Young, S., and Bendall, D. S. (1996). The role of acidic residues of plastocyanin in its interaction with cytochrome *f*. *Biochim. Biophys. Acta* **1277**, 115–126.

Martinez, S. E., Huang, D., Szczepaniak, A., Cramer, W. A., and Smith, J. L. (1994). Crystal structure of the chloroplast cytochrome *f* reveals a novel cytochrome fold and unexpected heme ligation. *Structure* **2**, 95–105.

Nicholls, A., and Honig, B. (1991). A rapid finite-difference algorithm, utilizing successive over-relaxation to solve the Poisson-Boltzmann equation. *J. Comp. Chem.* **12**, 435–445.

Sigfridsson, K. (1998). Plastocyanin, an electron-transfer protein. *Photosynth. Res.* **57**, 1–28.

Ubbink, M., Ejdebäck, M., Karlsson, B. G., and Bendall, D. S. (1998). The structure of the complex of plastocyanin and cytochrome *f*, determined by paramagnetic NMR and restrained rigid-body molecular dynamics. *Structure* **6**, 323–335.

Biography

Dr. Elizabeth L. Gross is a Professor of Biochemistry and former Head of the Interdisciplinary Biophysics Graduate Program at the Ohio State University. Her research includes a study of chloroplast electron transport in general with an emphasis on plastocyanin using both experimental and computational methods. She has authored over 70 articles on the subject. She holds a Ph.D. in biophysics from the University of California, Berkeley and did postdoctoral work at the C. F. Kettering Research Laboratory in Yellow Springs, OH.

Platelet-Activating Factor Receptor

Katherine M. Howard and Merle S. Olson
University of Texas Health Science Center, San Antonio, Texas, USA

The platelet-activating factor (PAF) receptor is a member of the G protein-coupled seven transmembrane receptor superfamily. PAF receptor stimulation and the subsequent intracellular signaling events are involved in both physiological and pathophysiological processes but mainly participate in transcellular communication during inflammatory events. PAF receptor activation is instigated by the binding of PAF (1-*O*-alkyl-2-acetyl-sn-glycero-3-phosphocholine), a potent lipid mediator which produces biological responses at very low molar concentrations (10^{-10} M).

Platelet-Activating Factor

Although PAF was first identified in the 1970s as a soluble mediator responsible for platelet aggregation when IgE-sensitized basophils were challenged with antigen, researchers have since established that PAF has diverse and potent biological activities. In addition to platelet aggregation, PAF can activate monocytes/macrophages, induce hypotension and bronchoconstriction, stimulate glycogenolysis and participates in ovulation and ovoimplantation. In addition, PAF has a profound role in acute inflammation, allergic disorders, and endotoxic and anaphylactic shock. Unlike other cytokines and inflammatory mediators, PAF is not synthesized and stored in a preformed state; rather, it is rapidly synthesized in response to specific stimuli. Cells that participate in inflammatory reactions including monocytes/macrophages, polymorphonuclear neutrophils, eosinophils, basophils, and platelets all rapidly produce PAF upon stimulation. Most cells that produce PAF also express PAF receptors. Therefore, PAF can operate in an autocrine, paracrine, or juxtacrine fashion. For instance, stimulated monocyte/macrophages release a majority of the PAF synthesized into the fluid phase and this PAF can interact with PAF receptors on its own cell surface (autocrine) or can bind to PAF receptors on other inflammatory cells in the immediate vicinity (paracrine). In the case of endothelial cells and leukocytes, synthesized PAF remains partially cell associated. For endothelial cells, this PAF is presented on the cell surface for the juxtacrine activation of infiltrating leukocytes. The biological responses resulting from PAF receptor activation occur as a consequence of direct interactions of the mediator with receptors on target cells or through indirect secondary signaling effects.

In 1979, Hanahan and colleagues defined the chemical structure of this novel ether phospholipid and the chemical structure of the lipid is presented in Figure 1. The PAF molecule contains several specific structural features which are necessary for its potent biological activity. PAF contains an *O*-alkyl ether residue at the sn-1 position of the glycerol backbone. The ether-linked side chain can vary in chain length and degree of saturation but the 16:0 moiety is predominant. 18:0-, 17:0-, and 18:1-containing molecules also occur naturally but these molecules exhibit several orders of magnitude less biological activity. There is an acetyl moiety at the sn-2 position of PAF and removal of this acetate group by the enzyme PAF acetylhydrolase generates lyso-PAF which is biologically inactive. In addition to the strict structural requirements at the sn-1 and sn-2 positions, PAF requires a polar head group containing choline at the sn-3 position for specific PAF-binding and functional activation of the PAF receptor. Both PAF synthetic and degradative enzymes recognize these unique structural features of PAF.

There are two distinct synthetic routes for PAF production, a remodeling and a *de novo* pathway. The *de novo* pathway produces low levels of PAF and has been attributed to the formation of constitutive levels of PAF for normal physiological actions. The remodeling pathway is the predominant route of PAF production by cells and tissues in response to systemic or local injury and trauma. Such stimulants for PAF generation can be microbial agents like lipopolysaccharide (LPS) and zymosan or biological agents such as cytokines, chemotactic peptides, thrombin, and calcium ionophores.

Stimulating the remodeling pathway generates PAF in a two-step process. PAF synthesis begins with the activation of cytoplasmic phospholipase A_2 ($cPLA_2$). This enzyme preferentially cleaves membrane ether phospholipids with arachidonate at the sn-2 position. This reaction releases arachidonic acid during the formation of lyso-PAF. The arachidonic acid is converted

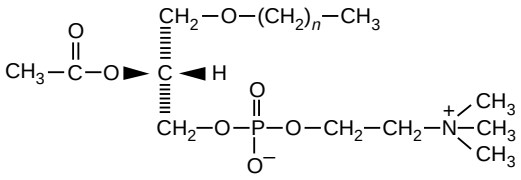

FIGURE 1 Chemical structure of PAF.

to eicosanoids via the lipoxygenase or cyclooxygenase pathways while the lyso-PAF is further converted to PAF by the actions of acetyl-CoA-lysoPAF acetyltransferase. Therefore, production of PAF occurs concomitant with the production of the eicosanoids which also contain far-reaching biological activities. The essential role of $cPLA_2$ in the synthesis of PAF has been confirmed from $cPLA_2$ knockout animals but little is known about the regulation of acetyl-CoA-lysoPAF acetyltransferase.

While the synthesis of PAF is tightly controlled, PAF-like species capable of binding and activating the PAF receptor can arise from the oxidation of unsaturated phosphatidylcholine. These ligands of the PAF receptor arising from oxidative damage of membrane phospholipids contribute to dysfunctional PAF receptor signaling and to the pathophysiological events associated with numerous disease entities.

Many of the biological and pathophysiological actions of PAF were initially investigated using specific PAF receptor antagonists. These PAF receptor antagonists include compounds with structural resemblance to PAF such as CV-3988 (phospholipid analogues) and nonstructural antagonists such as WEB 2086 and BN 50739. Classical ligand-binding experiments demonstrated specific PAF binding in numerous tissues and cells including platelets, neutrophils, macrophages, mononuclear leukocytes, eosinophils, Kupffer cells, epithelial cells, and endothelial cells.

The unique structural features of PAF, the existence of PAF receptor antagonists, and direct binding data utilizing radiolabeled PAF, as well as biochemical evidence for the diverse activation of second messenger signal cascades, all provided evidence for the existence of specific PAF receptors. Confirmation that PAF signaling occurs through receptor-mediated mechanisms was affirmed in 1991 with the molecular identification of the first receptor cloned for a lipid mediator by Shimizu and colleagues.

PAF Receptor Structure

Numerous attempts by investigators to isolate the PAF receptor proved unsuccessful. The eventual cloning of the PAF receptor was accomplished in an elegant strategy involving expression cloning of a guinea-pig lung cDNA library in *Xenopus laevis* oocytes. The initial cDNA library, constructed from size-fractionated poly (A) RNA, was converted *in vitro* into cRNA using the phage DNA as a template. Pools of cRNA were introduced into oocytes and a PAF-induced electrophysiological detection of G protein-coupled phosphatidylinositol (PI) turnover was assayed. A single PAF-receptor cDNA sequence isolated by the cloning strategy predicted a protein of 342 amino acids and a calculated molecular mass of ~39 kDa. However, immunological detection of the PAF receptor on Western blots revealed an apparent MW of 69 kDa suggesting the presence of posttranslational modifications of the receptor. In fact, two potential N-linked glycosylation sites were identified in the PAF receptor cDNA sequence. Hydropathy plot analyses of the deduced PAF receptor amino acid sequence predicted the presence of seven transmembrane-spanning domains within the PAF receptor. A schematic representation of the PAF receptor is presented in Figure 2. Through site-directed

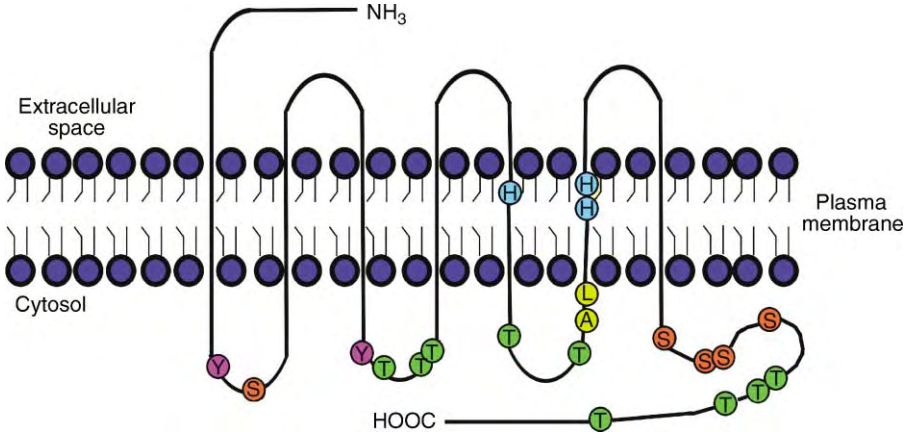

FIGURE 2 Schematic representation of the seven transmembrane spanning PAF receptor.

mutagenesis studies, several key features of the PAF receptor have been determined. Similar to other G protein coupled receptors, the ligand-binding site is defined in three dimensions by amino acids from several of the transmembrane-spanning regions. Mutations in membrane-spanning segments II (N58A, D63A), III (N100A, T101A, S104A), and VII (D289A) increased affinity of PAF binding while mutations in V (H188A), VI (H248A, H249A, Q289A), and VII (Q276A, T278A) lowered the affinity of PAF for the receptor. The third intracellular loop of the receptor is coupled to phosphatidylinositol turnover. The C-terminal cytoplasmic tail of the receptor containing a cluster of serine and threonine residues are candidate sites for phosphorylation by G protein receptor kinases, and are critical for agonist-induced desensitization.

Subsequent to the isolation of the guinea-pig cDNA, cDNA for numerous other species were isolated by cross hybridization. The PAF receptor maintains ~74% sequence identity between the various species identified to date. Because the PAF receptor mRNA is present in only subsets of cells, Northern blot hybridizations have limitations in detecting PAF receptor expression in some tissues. The relative tissue abundance among different species varies but in general lung, neutrophils, monocytes, macrophages, placenta, small intestine, heart, liver, kidney, brain, and spleen have detectable PAF receptor expression.

The isolation of human PAF receptor cDNAs identified two unique 5′-noncoding regions designated transcript 1 and transcript 2. The tissue- and cell-type distribution of these two transcripts are disparate. Transcript 1 can be found ubiquitously but is expressed abundantly in leukocytes, eosinophils, and monocytes/macrophages. Conversely, transcript 2 is found predominantly in heart, lung, spleen, kidney, and skin epithelial cells but not in leukocytes, eosinophils or monocyte/macrophages. Analysis of human genomic DNA sequence localized the PAF receptor to chromosome 1 and revealed other features of the PAF receptor gene. The PAF receptor gene contains no introns within the coding sequence of the gene (exon 3). Many G protein-coupled receptor genes also lack introns within their open reading frame. The first two exons of the PAF receptor gene are located entirely within 5′ -non-coding sequences and were identified by sequence comparisons to the human cDNAs. These two exons reside more than 20 kb upstream of exon 3 and each exon is spliced to the common exon encoding the PAF receptor protein thus creating PAF receptor transcript 1 and 2 (Figure 3). The two transcripts are controlled by distinct promoters immediately 5′ of the exons. Because transcript 1 was identified first, the exon further upstream was designated exon 2. Neither PAF receptor promoter region contains canonical TATA or CCAAT box regulatory sequences commonly found in the promoter regions of eukaryotic genes. Each PAF receptor promoter contains distinct regulatory features that reflect the requirement for PAF receptor expression in different target cells and tissues.

The promoter for transcript 1 contains three consensus transcription factor binding sites for nuclear factor-κB (NF-κB) and one for Sp1. The transcript 1 promoter also contains a pyrimidine-rich initiator sequence (Inr) which includes the transcriptional start site. Inr sequences aid in positioning the start site of transcription in many TATA-less genes. Functional analysis of the promoter region demonstrated that PAF and phorbol 12-myristate 13-acetate (PMA) increased PAF receptor transcript 1 levels through these three NF-κB sites. The NFκB transcription factor plays a crucial role in the regulation of many inflammatory response genes and is activated by various cytokines, PMA, and lipopolysaccharide (LPS).

The promoter for PAF receptor transcript 2 contains consensus sequences for AP-2 and Sp-1 that were demonstrated to control basal promoter activity. In addition to the basal promoter activity, a hormone responsive element (HRE) and a TGF-β inhibitory element function in regulating transcript 2 levels. Retinoic acid and thyroid hormone increase transcript 2 expression levels while TGF-β suppresses promoter activity. Thus, it is apparent that PAF receptor promoter 1 responds to inflammatory stimuli, whereas

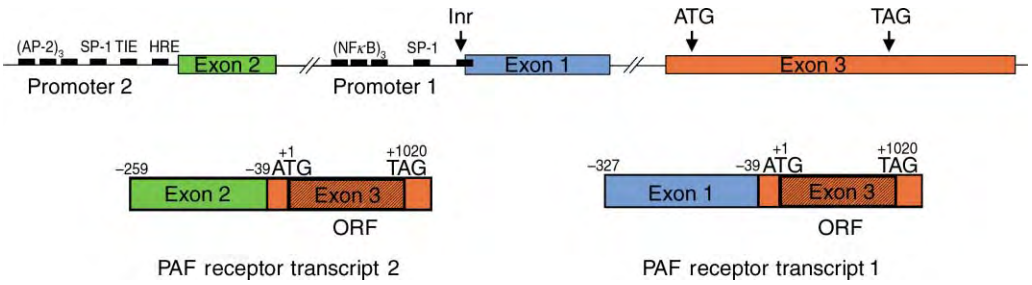

FIGURE 3 PAF receptor gene structure and transcript organization.

the PAF receptor transcript 2 expression is controlled by differentiation signals.

PAF Receptor Regulation

Because of the crucial role that PAF and PAF receptor activation plays in numerous physiological and pathophysiological events, PAF-instigated signaling is tightly controlled. The first manifestation of PAF receptor regulation is the expression in specific cells and tissues as already discussed. Another mechanism for tightly controlled regulation of PAF receptor signaling is controlling the availability of PAF. This mechanism includes regulation of both PAF synthesis and release, and the rapid inactivation of PAF by PAF acetylhydrolases. Other mechanisms of regulation of this signaling system are intrinsic to the PAF receptor and include homologous desensitization to repeated or sustained administration of PAF. Desensitization of the PAF receptor leads to decreased PAF-induced cellular responses in GTPase activity, IP_3 production, and calcium mobilization. The carboxy terminus of the PAF receptor is the target for phosphorylation required to desensitize the receptor. PAF receptor desensitization may occur by uncoupling of the receptor to G proteins and by ligand-induced internalization of the receptor.

As opposed to the fairly rapid process of controlling PAF availability and PAF receptor responsiveness, long-term regulation of the PAF receptor includes alterations in PAF receptor expression. Transient elevation of cyclic AMP (cAMP) reduces expression of the PAF receptor. This down-regulation is accompanied by a decreased responsiveness to a prolonged exposure of PAF. Conversely, priming of macrophages with low levels of LPS can induce a threefold increase in PAF receptor transcript levels thereby amplifying subsequent response to stimulation.

PAF Receptor Signal Transduction

The wide range of biological responses instigated by PAF receptor activation can be attributed to complicated intracellular signaling mechanisms. Calcium, cAMP, IP_3, and diacylglycerol (DAG) are all proven second messengers for PAF signaling. Figure 4 presents an overview of PAF receptor-mediated signaling pathways. Heterotrimeric G proteins are intricately involved in the signal transduction events generated by PAF receptor occupancy. G proteins bind guanine nucleotides, are activated by GTP and possess intrinsic GTPase activity. Binding of PAF activates the associated G protein by exchanging guanosine triphosphate for guanosine diphosphate. The PAF receptor is linked to more than one G protein because some processes are sensitive to pertussis toxin treatment while others are resistant. In fact, this G protein utilization also can differ in different cell types. The activated G proteins, in turn, activate polyphosphoinositide turnover mediated by phospholipase C (PLC). The subsequent generation of inositol 1,4,5-triphosphate (IP3) and diacylglcerol mobilizes intracellular Ca^{+2} and activates protein kinase C (PKC) respectively. PAF receptor associated G protein activation also leads to the activation of cytoplasmic phospholipase A_2 with the subsequent cleavage of arachidonic acid (AA) and the formation of leukotrienes (LT), prostaglandins (PG) and thromboxanes (TX). More recently, investigators demonstrated broader activation of kinases and phospholipases following PAF receptor activation. For instance, PAF receptor activation has been shown to activate mitogen-activated protein kinase (MAPK), phosphatidylinositol 3-kinases (PI3K), protein tyrosine kinases, and G protein receptor kinase.

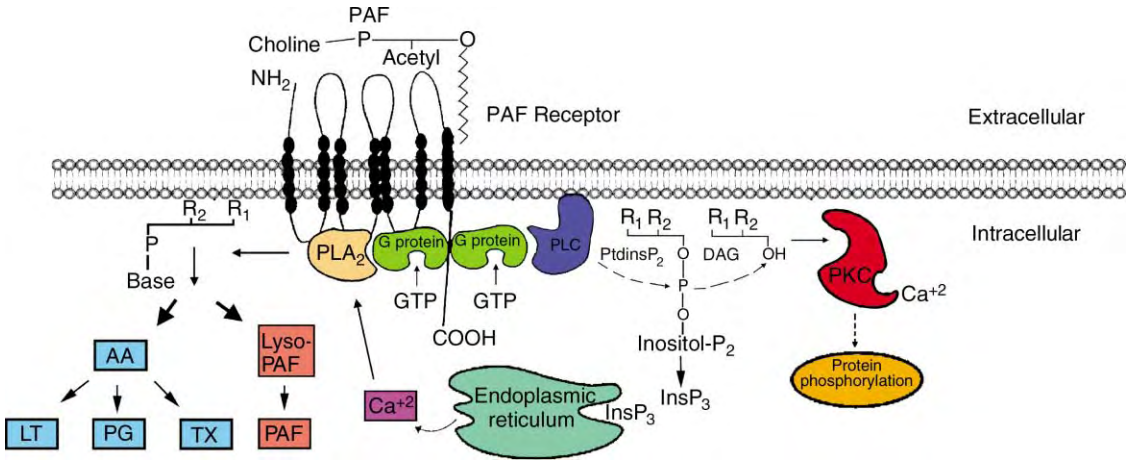

FIGURE 4 PAF receptor intracellular signaling pathways. See text for abbreviations.

Experiments in both PAF receptor knockout animals and transgenic animals overexpressing PAF receptors support the pathophysiological role attributed to PAF receptor signaling. Deletion of PAF receptors in mice drastically attenuates systemic anaphylactic responses after antigen challenge; whereas mice overexpressing PAF receptors exhibit hypersensitivity to bacterial endotoxin. It is not surprising then that PAF receptor activation is being investigated as a contributing factor in numerous disease entities including asthma, atherosclerosis, inflammatory bowel disease, ischemia-reperfusion injury, endotoxemia, and allergic disorders.

See Also the Following Articles

Eicosanoid Receptors • G Protein-Coupled Receptor Kinases and Arrestins • G_{12}/G_{13} Family • G_i Family of Heterotrimeric G Proteins • G_q Family • G_s Family of Heterotrimeric G Proteins

Glossary

autocoid Autopharmacologic substance that has potent local activity.

G protein-coupled receptor A class of receptors for a diverse set of ligands including hormones, lipid inflammatory mediators, and chemokines that use associated trimeric G proteins for intracellular signal transduction.

lipopolysaccharide A component of the cell wall of gram-negative bacteria containing both lipid and carbohydrate moieties that instigates many innate immune responses such as secretion of cytokines, activation of macrophages, and expression of leukocyte adhesion molecules. Synonymous with endotoxin.

platelet-activating factor (PAF) Lipid autocoid.

zymosan An insoluble protein–carbohydrate complex from the cell wall of yeast.

Further Reading

Chao, W., and Olson, M. S. (1993). Platelet-activating factor: Receptors and signal transduction. *Biochem. J.* **292**, 617–629.

Honda, Z., Nakamura, M., Miki, I., Minami, M., Watanabe, T., Seyama, Y., Okado, H., Toh, H., Ito, K., and Miyamoto, T. (1991). Cloning by functional expression of platelet-activating factor receptor from guinea-pig lung. *Nature* **349**, 342–346.

Ishii, S., and Shimizu, T. (2000). Platelet-activating factor (PAF) receptor and genetically engineered PAF receptor mutant mice. *Prog. Lipid Res.* **39**, 41–82.

Ishii, S., Kuwaki, T., Nagase, T., Maki, K., Tashiro, F., Sunaga, S., Cao, W. H., Kume, K., Fukuchi, Y., Ikuta, K., Miyazaki, J., Kumada, M., and Shimizu, T. (1998). Impaired anaphylactic responses with intact sensitivity to endotoxin in mice lacking a platelet-activating factor receptor. *J. Exp. Med.* **187**, 1779–1788.

Izumi, T., and Shimizu, T. (1995). Platelet-activating factor receptor: Gene expression and signal transduction. *Biochim. Biophys. Acta* **1259**, 317–333.

Nagase, T., Ishii, S., Katayama, H., Fukuchi, Y., Ouchi, Y., and Shimizu, T. (1997). Airway responsiveness in transgenic mice overexpressing platelet-activating factor receptor – Roles of thromboxanes and leukotrienes. *Am. J. Respir. Crit. Care Med.* **156**, 1621–1627.

Prescott, S. M., Zimmerman, G. A., Stafforini, D. M., and McIntyre, T. M. (2000). Platelet-activating factor and related lipid mediators. *Annu. Rev. Biochem.* **69**, 419–445.

Biography

Merle S. Olson is currently Dean of the Graduate School of Biomedical Science and former Chair of the Department of Biochemistry at the University of Texas Health Science Center, San Antonio. He received his Ph.D. from the University of Minnesota and has published over 200 articles in the field of PAF and hepatic mediators involved in intercellular communication.

Platelet-Derived Growth Factor Receptor Family

Marina Kovalenko and Andrius Kazlauskas
Harvard Medical School, Boston, Massachusetts, USA

Platelet-derived growth factor (PDGF) is a potent mitogen, chemoattractant, and survival factor for cells of mesenchymal origin (such as fibroblasts, smooth muscle cells (SMC), or glial cells). PDGF exists as a number of isoforms that initiate signaling via two closely related receptor tyrosine kinases (RTKs) named α- and β-receptors. PDGFs and their receptors (PDGFRs) are important for embryonic and postnatal development. Knockout mice lacking either PDGFs or receptors develop severe defects in various tissues and organs, and die before or shortly after birth. In adult organisms, PDGFs participate in wound healing, regulation of blood vessel tonus, and maintenance of the interstitial fluid pressure. PDGF signaling is also involved in the pathogenesis of various proliferative diseases (certain tumors, atherosclerosis and restenosis, fibrotic conditions). PDGFs and their receptors have been best characterized in mammals. However, there is evidence that PDGFR-like proteins are expressed in lower vertebrates, and PDGF-like growth factors have been found in molluscs, annelids, sea urchins (*Lytechinus pictus*), and *Drosophila*. Taken together, these findings indicate that PDGFs and their receptors play an important role in a variety of biological processes throughout eukaryotic species.

PDGF Isoforms

At present, four genes encoding different PDGF chains are known: A, B, C, and D. Biologically active PDGFs exist as disulfide-bonded homodimers designated AA, BB, CC, and DD. A and B chains form a heterodimeric PDGF AB (Figure 1). The history of the discovery of PDGFs dates back as early as 1974, when mitogenic activity of whole blood serum was linked to the presence of platelets. PDGF AB was the first to be purified and biochemically characterized a few years later, followed by PDGF BB and AA. Cloning of PDGF A and B cDNAs and determination of the structure of corresponding genes were completed in the 1980s.

New members of the PDGF family, PDGF C and PDGF D, were found only recently by searching the database of human-expressed sequences. PDGFs C and D have a 2-domain structure with N-terminal CUB domain and C-terminal PDGF/VEGF (core) domain, separated by a hinge region (Figure 1). No heterodimers involving C or D chains have been detected. The unique feature of these two new PDGFs is the requirement for proteolytic cleavage of the CUB domain upon secretion in order to achieve biological activity. Thus, latency may be the reason why these growth factors were not originally detected by functional assays.

PDGF Receptors

PDGFs exert their biological functions by binding to two isoforms of PDGF receptors, α and β, with different degrees of affinity. Both receptors are transmembrane tyrosine kinases, composed of extracellular, transmembrane, and intracellular parts. The extracellular part consists of five immunoglobulin-like domains that are involved in ligand binding (domains I–III) and receptor dimerization (domain IV). The intracellular kinase domain of the PDGF receptors is split into two by ~100-amino acid insert (Figure 1).

PDGF A chain binds specifically to α-receptor, and PDGF B can bind to both α and β. PDGF C was originally described as a ligand for PDGF α-, but not β-receptor, however, later it was shown to bind PDGF β-receptor in cells expressing both α- and β-isoforms. PDGF D has been reported to be a β-receptor ligand, but its ability to bind α-receptor in α/β-expressing cells remains controversial. Interactions of PDGFs with α- and β-receptors are summarized in Figure 1. A bivalent dimer, PDGF molecule binds to two receptor subunits causing them to dimerize. Upon dimerization, PDGF receptors become rapidly phosphorylated on multiple tyrosine residues. One of them ("regulatory tyrosine") is located in the second part of the kinase domain and is important for receptor kinase activity (Tyr857 in β-receptor and, by homology, Tyr849 in α-receptor). Most of other phosphorylation sites lie in noncatalytic parts of the receptor (Figure 2). The exact sequence of events during receptor activation and formation of signaling complex is unknown. By analogy to other RTKs, it is likely that

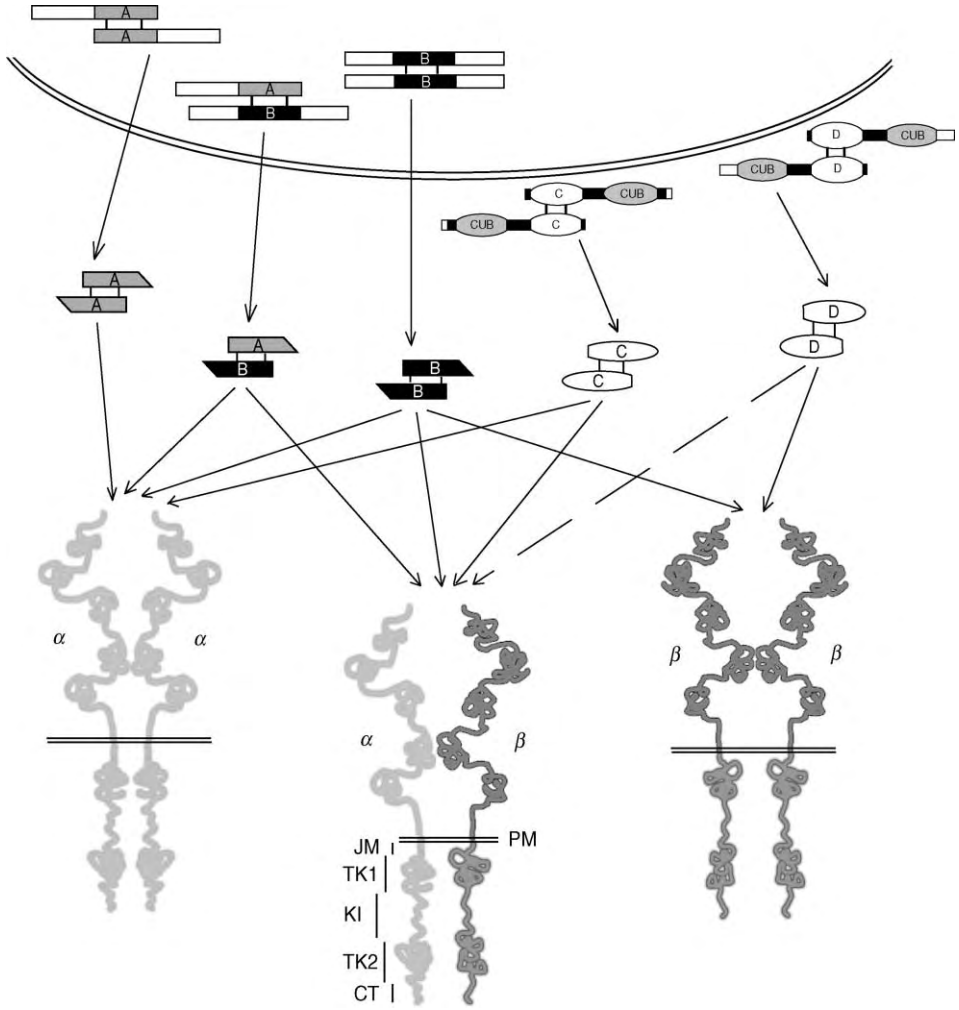

FIGURE 1 Platelet-derived growth factors and their receptors. PDGFs A and B are synthesized as precursors that are proteolytically processed before secretion. PDGFs C and D are secreted in latent form and activated by proteolytic cleavage of the CUB domain. All PDGF isoforms dimerize prior to the proteolytic cleavage. Specificity of binding of mature active PDGFs to their receptors is shown; dashed arrow indicates the lack of consensus regarding the ability of PDGF DD to cause the formation of a heterodimeric receptor. Domain structure of the PDGF receptor α-subunit (identical to that of β-subunit) is presented. The extracellular part of the receptor consists of 5 Ig-like domains. PM, plasma membrane; JM, juxtamembrane domain; TK1 and TK2, proximal and distal parts of tyrosine kinase domain; KI, kinase insert; and CT, carboxyl-terminal tail.

ligand binding and subsequent dimerization of the receptor induces a conformational change that facilitates transphosphorylation of regulatory tyrosine residues within the dimer. Importantly, the regulatory tyrosine lies within activation loop, the region that is conserved among receptor tyrosine kinases. As shown for the insulin receptor, the activation loop blocks the catalytic site in nonphosphorylated receptor, whereas upon ligand-induced phosphorylation it moves away providing access for substrate. It is possible that the PDGF receptor activation occurs via similar mechanism, although there is no direct evidence for this in the absence of crystal structure of the PDGF receptors.

Recently, ligand-bound dimerized PDGF β-receptor was found to be less susceptible to dephosphorylation by protein tyrosine phosphatases (PTPs) than the monomeric receptor. It is suggested that this "phosphatase protection" may contribute to maintenance of activated (phosphorylated) state of the receptor.

Proteins Associated with the PDGF Receptors and PDGF-Driven Signaling Pathways

A total of 13 tyrosine residues in β-receptor and 11 in α-receptor get phosphorylated upon PDGF stimulation. Phosphorylation of most of the tyrosines within PDGF receptors results in the creation of docking sites for a variety of proteins many of which in turn get phosphorylated upon association with the

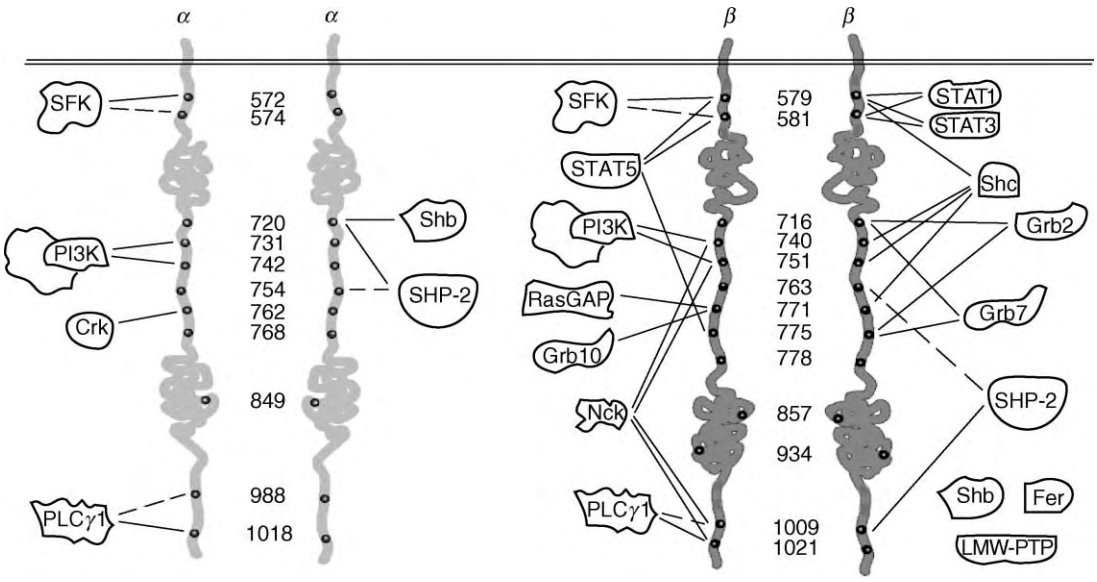

FIGURE 2 Intracellular domains of $\alpha\alpha$ and $\beta\beta$ homodimers of the PDGF receptor. Phosphorylated tyrosine residues are shown (dark circles). Numbers indicate their positions in the human PDGF receptor sequence. Association of signaling proteins with phosphorylation sites of the activated PDGF receptors is shown by solid lines (major binding sites) or dashed lines (additional sites). Proteins binding with high affinity (e.g., PI3-kinase, PLCγ1, RasGAP) bind to the receptor via one or two phosphotyrosine residues on the receptor, whereas low-affinity binding (e.g., Nck, Shc, or Shb binding to β-receptor) involves multiple sites. Shb was found to bind to most of the phosphorylated tyrosines on the PDGF β-receptor. Fer and LMW-PTP bind to as yet unidentified sites on the PDGF β-receptor.

receptors (Figure 2). These proteins include enzymes (phosphatidylinositol 3′-kinase (PI3-kinase), phospholipase C-γ1 (PLCγ1), SH2 domain-containing protein tyrosine phosphatase-2 (SHP-2), GTPase-activating protein of Ras (RasGAP), Src family kinases (SFKs), transcription factors (members of STAT family), or adaptor proteins, such as Grb2, Grb7, Shc, Shb, Nck, or Crk, linking the receptor to signaling proteins further downstream. Some proteins that are recruited to the PDGF receptors are both adaptors and enzymes, e.g., tyrosine phosphatase SHP-2 is able to recruit Grb2 via its phosphorylated C terminus. Association is mediated in most cases by SH2 (Src homology 2) domains of these proteins and is remarkably specific, each phosphorylation site having its own binding partner(s). This specificity is based on the ability of SH2 domains to differentially recognize amino acid sequence following the phosphorylated tyrosine. Many receptor-binding proteins also contain SH3 (Src homology 3), PTB (phosphotyrosine binding), or PH (pleckstrin homology) domains that may facilitate recruitment of other yet unidentified signaling molecules to the complex.

Cellular Responses Mediated by the PDGF Receptors

Assembly of the PDGF receptor complex initiates a number of signaling pathways leading to cellular responses (Figure 3): chemotaxis, proliferation, differentiation (in certain cell types), and protection from apoptosis. One pathway may lead to several different responses, whereas some of the pathways are redundant and converge on the same cellular effect.

Proliferation

Proliferation is the major and most well studied cellular effect induced by PDGFs. Virtually all signaling proteins binding to the receptors have been implicated in proliferation, but not all of them have to be present in the signaling complex at the same time to induce the response.

Ras-Dependent Pathway

The mitogenic pathway that involves Ras, a small GTPase, can be activated through multiple ways in response to PDGF. The complex of Grb2 (adaptor protein) and Sos1 (nucleotide exchange factor for Ras) can bind to the β-receptor either directly or via phosphorylated Shc or SHP-2. This association brings the complex to the plasma membrane where it activates Ras. Activated Ras GTPase interacts directly with Raf-1 serine/threonine kinase, in turn activating it. Raf-1 is the first kinase in MAP kinase cascade. Elevation of its activity is followed by sequential activation of MEK and MAP kinases Erk1 and 2, which are translocated to the nucleus and phosphorylate a number of transcription factors.

As for the PDGF α-receptor, Grb2 is able to bind to it via SHP-2, but there is no evidence of its involvement in

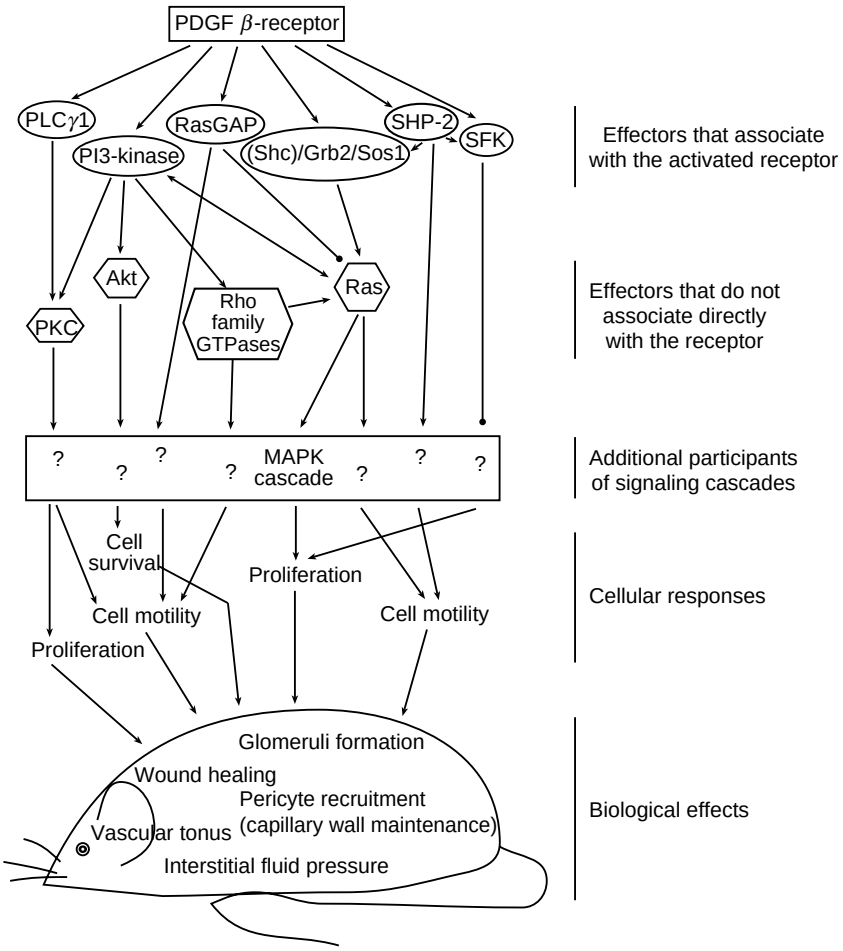

FIGURE 3 Major events initiated by the PDGF β-receptor and culminating in biological responses. Upon ligand binding, activated PDGF β-receptor recruits enzymes and adaptor proteins that start a number of distinct signaling pathways, some of which are shown on the figure. Note that not all of them are initiated by the same receptor dimer or in the same cell. Arrows represent either physical or functional interactions along the pathways. The least defined part of the signaling cascade is the one that bridges the receptor-proximal events with proteins that carry out cellular responses. PDGF is necessary but not sufficient to achieve biological effects. In a living organism, other growth factors and hormones, as well as cell–cell and cell–matrix interactions within tissues and organs make indispensable contributions.

Ras activation. Therefore, pathways other than the Ras-mediated one are likely to contribute to α-receptor-mediated proliferation.

The Ras pathway is believed to be counteracted by RasGAP that binds to the PDGF β-receptor (but not to α-receptor) and is able to enhance GTPase activity of Ras, thus converting it from active (GTP-bound) to inactive (GDP-bound) state. The extent to which this negative signaling affects proliferation may depend on many factors (cell type, environmental conditions).

Src

Src ($p60^{c\text{-}src}$) has been shown to be important for PDGF-driven mitogenesis. However, its association with the PDGF receptors and early PDGF-induced elevation of activity are dispensable for proliferative response and may have a different function. Yet, Src is required at multiple time points during PDGF-dependent cell-cycle progression. Thus, elevation of Src activity early in G1 leads to increase of *c-myc* expression, which is required for transition through G1. Importance of Src also has been confirmed for late G1 and for the exit from M-phase of the cell cycle.

PLCγ1

PLCγ1 binds to the PDGF receptors upon ligand stimulation and becomes phosphorylated and activated. Increasing the catalytic activity of PLCγ1 leads to production of inositol 1,4,5-trisphosphate (IP3) and diacylglycerol (DAG). IP3 is involved in regulation of cytoplasmic Ca^{2+} levels, which, together with direct action of DAG, can contribute to activation of certain members of the PKC family. In particular, DAG has been shown to activate protein kinase C-ζ (PKC-ζ) which then activates Raf-1 and, consequently,

the rest of MAP kinase cascade, leading to proliferation. PLCγ1 is involved in PDGF-stimulated proliferation mediated by β-receptor, whereas in the case of α-receptor, it is important mostly for the motility response.

PI3-Kinase

PDGF-dependent PI3-kinase activation is critical for mitogenesis in most cell types. Prolonged exposure to PDGF, needed to induce cell-cycle progression in quiescent cells, causes two distinct peaks of PI3-kinase activity, one within minutes and another following a delay of several hours. Only the second peak was found to be important for the cell-cycle progression, whereas the early increase of activity is required only for immediate responses to PDGF such as chemotaxis.

How this biphasic increase of PI3-kinase activity is linked to the cell-cycle machinery still remains an open question. Continuous treatment with PDGF can be substituted by two separate pulses of the growth factor, the first getting cells out of G0 to early G1 and the second pushing them through late G1 and into S phase. Early elevation of *c-myc* and sustained activation of the MAP kinase pathway can replace the first pulse of PDGF, but is not sufficient to drive the cell through late G1. To complete cell-cycle progression, a properly timed second peak of PI3-kinase activity (second pulse of PDGF or just the addition of PI3-kinase lipid products) is required. It is hypothesized that early *c-myc* and Erk activation trigger expression of new protein(s) whose interaction with the late PI3-kinase products is critical for S phase entry.

Chemotaxis

Most receptor-expressing cells exhibit chemotaxis upon exposure to PDGF. Migration of pericytes in response to SMC-released PDGF plays a critical role in capillary formation, which is particularly important during embryonic development. In the process of wound healing, PDGF causes chemotaxis of neutrophils and macrophages, as well as fibroblasts and SMC.

α- and β-PDGF receptors differ in their ability to mediate chemotaxis. PDGF β-receptor homodimer as well as α–β heterodimer potently stimulate it. However, the ability of α–α homodimer to drive chemotaxis remains controversial and may depend on the cell type. This difference may be explained by variations in composition of the signaling complex assembled by different receptor dimers, which may be cell-type specific.

PI3-Kinase and Ras Pathways

Chemotaxis involves dynamic remodeling of cytoskeleton, including rearrangement of actin filaments and microtubules, changes of focal adhesions, and formation of lamellipodia or filopodia. These processes are controlled, in part, by the Rho family of small GTPases (RhoA, Rac1 and Cdc42), that are activated by the PDGF receptors via different pathways. The PI3-kinase pathway is considered to be the major one. Activation of the Rho family of small GTPases is dependent on PI3-kinase lipid products. The Ras pathway that can be initiated by the PDGF receptor independently from PI3-kinase pathway, leads to chemotactic response via activation of Rac1, another small GTPase Ral, and in some cell types, MEK1 and stress-activated kinase p38. Interestingly, PI3-kinase is able to interact directly with Ras and activate it, whereas both Ras and Rho family GTPases can activate PI3-kinase, forming a positive feedback loop. Thus, reciprocal regulation of Ras and PI3-kinase provide an example of interaction between different PDGF-dependent pathways.

RasGAP, a negative regulator of Ras, has been shown to inhibit chemotaxis. However, in some cell types, RasGAP has also been shown to have a positive impact on motility that is most likely independent from Ras.

PLCγ1

PLCγ1 promotes chemotaxis in many cell types, but the knowledge about what happens downstream of PLCγ1 is only starting to emerge. Upon PDGF stimulation, PLCγ1 activates sphingosine kinase through IP3 formation and subsequent release of Ca^{2+} from intracellular stores. Sphingosine kinase product, sphingosine-1-phosphate (SPP), is a ligand for EDG-1, a G-protein coupled receptor (GPCR). Stimulation of EDG-1 by SPP leads to activation of Rho family GTPases, which, in turn, results in remodeling of actin cytoskeleton and cell–matrix adhesion sites. This is a new example of receptor crosstalk, where an RTK requires activation of a GPCR to achieve a cellular response.

PKC isoforms that are activated via both PI3-kinase and PLCγ1 pathways, are also involved in chemotactic signaling, as chemotaxis is reduced when PKCs are inhibited or downregulated.

SHP-2 and Low Molecular Weight Phosphatase (LMW-PTP)

Two other positive mediators of PDGF-induced chemotaxis are tyrosine phosphatases SHP-2 and LMW-PTP, both directly associated with the phosphorylated PDGF receptor and activated by PDGF-dependent phosphorylation. Involvement of SHP-2 in chemotactic signaling may occur via the Ras pathway, since SHP-2 can serve as

an adaptor protein for Ras binding. LMW-PTP is likely to act through dephosphorylating and inactivating one of its cellular targets, p190RhoGAP, a negative regulator of Rho GTPase, thus leading to increased activation of Rho and subsequent cytoskeletal rearrangements.

SFKs

The role of Src family kinases in PDGF-induced chemotaxis is not clear. A pathway leading to chemotaxis is initiated at SFK-binding sites in the juxtamembrane domain of the PDGF α-receptor, since mutating these tyrosines to phenylalanine residues results in chemotaxis inhibition. However, it is not yet clear whether it is Src family kinases or other signal transduction molecules binding to the same sites that are responsible for cell migration, since in triple SFK knockout cells PDGF-AA-dependent cell migration is intact.

It is necessary to note that $\alpha\alpha$- and $\beta\beta$-homodimers of the PDGF receptor cause different, although partially overlapping, cellular responses, due to the differences in their ability to bind signaling proteins (Figure 2). For instance, α-receptor homodimer has been found to send a less potent mitogenic signal than the β-receptor homodimer. Additionally, in some cell types (SMC, human foreskin fibroblasts), it fails to mediate a chemotactic response to PDGF AA and inhibits chemotaxis induced by other agents. PDGF β-receptor homodimer formation generally results in higher mitogenicity and chemotaxis. The heterodimeric $\alpha-\beta$ receptor is believed to have unique signaling properties, due to altered phosphorylation pattern of both α- and β-subunits, which results in recruitment of a different subset of signaling proteins. In particular, the heterodimer mediates a stronger mitogenic response than either $\alpha-\alpha$ or $\beta-\beta$ complexes. Distinct signaling properties of different PDGF receptor dimers are based not only on different intrinsic properties of receptor isoforms, but also on the type of cells where these receptors are expressed and on varying experimental conditions.

Negative Regulation of the PDGFR Signaling

Down-regulation mechanisms described for the PDGFR include internalization, ubiquitin-mediated proteolysis (degradation), and dephosphorylation by PTPs. Their relative contribution to the termination of signaling appears to be different.

Internalization and Degradation

Internalization of the PDGF receptors, mediated by clathrin-coated pits, occurs shortly after ligand stimulation and is dependent on the receptor kinase activity. Intracellular trafficking of the PDGF β-receptor involves PI3-kinase but is not entirely elucidated yet. Internalized receptors can be recycled and go back to the cell surface or can be directed to lysosomal degradation, which actually results in receptor down-regulation. However, before they are degraded, internalized receptors remain associated with downstream proteins and continue to signal. For this reason, internalization and subsequent trafficking can be considered a late signaling stage rather than the way of receptor inactivation only.

Additionally, PDGFRs can be targeted for cytoplasmic degradation in proteasomes via polyubiquitination. Ubiquitination of the receptors occurs upon ligand binding and is strictly dependent on receptor autophosphorylation. Generally, multi-ubiquitin chain is added to proteins by E3–E2 ubiquitin ligase system and after that ubiquitinated proteins are recognized by the 26S proteasome and degraded. c-Cbl, a E3 ubiquitin ligase, has been shown to be phosphorylated upon PDGF stimulation and is therefore likely to contribute to the PDGFR ubiquitination and subsequent proteolysis. Proteolytic degradation can be considered a true mechanism of receptor down-regulation that terminates signaling through decreasing the number of the PDGF receptor molecules.

Dephosphorylation by PTPs

PTP-dependent dephosphorylation of the PDGF receptors represents another level of regulation of PDGF-induced signaling. Thus, dephosphorylation of the regulatory site or non-specific removal of phosphate from all tyrosine residues would shut down all signaling, whereas site-specific dephosphorylation would selectively block corresponding signaling pathways. LMW-PTP, for instance, has been shown to act both ways. This PTP selectively interferes with two pathways initiated by the PDGF β-receptor: Src-dependent induction of *c-myc* and STAT1/3 mediated *c-fos* expression. It can also affect kinase activity of the PDGF β-receptor by dephosphorylating Tyr857, providing a general negative regulation of all downstream signals.

Unlike LMW-PTP that acts on membrane-bound PDGF β-receptor, PTP1B was found to dephosphorylate the receptor upon its internalization on the surface of the endoplasmic reticulum, shutting down signaling at a later time point, yet before the receptor gets degraded or recycled to the plasma membrane.

The ability of SHP-2 to act as both positive and negative regulator of PDGFR signaling puts it apart from other receptor-directed PTPs. It is able to dephosphorylate selectively, tyrosines 771 and 751 on the β-receptor, potentially turning off RasGAP and PI3-kinase pathways. On the other hand, SHP-2 can

serve as an adaptor for Grb2 binding, therefore initiating Ras-mediated signaling. Additionally, SHP-2 has been implicated as a positive regulator in the stimulatory effect of integrins on PDGF receptor signaling.

An increase of intracellular reactive oxygen species (ROS) is an early PDGF-dependent event mediated by PI3-kinase and Rac1, and it was shown to be important for mitogenic signaling. Since ROS reversibly inhibit PTPs, it is likely that this event helps to prevent the negative effect of PTPs on early stages of PDGF signaling.

Developmental Role of the PDGF Receptors

At very early stages of embryonic development (before gastrulation), both PDGF α-receptors and PDGF A chain are expressed throughout the embryo, suggesting that PDGF AA may be acting in autocrine manner to stimulate cell proliferation. At later stages, PDGF β-receptor and PDGF B chain appear, and both receptors and growth factor chains start to show distinct expression pattern. The expression of PDGF C largely overlaps with that of PDGF A, and information about PDGF D expression in embryo is still incomplete. PDGF receptors are found mainly in cells of mesodermal origin, with some exceptions (e.g., central nervous system), whereas PDGFs are present in adjacent ecto- and endodermal derivatives. This distribution indicates that, during morphogenesis, PDGFs act in a paracrine manner to induce migration of receptor-expressing mesenchymal cells.

As shown by genetic analysis in mice, interruption of PDGF signaling leads to morphogenic defects and embryonic or perinatal lethality. PDGFR α-null mice die before birth, many (but not all) at a very early stage. Those available for analysis have myotomal abnormalities, rib fusions, defects in neural crest derivatives, and incomplete cephalic closure. PDGF A knockouts demonstrate an emphysema-like lung condition characterized by the absence of mature alveoli. This defect originates due to a lack of migration of PDGF α-receptor expressing alveolar SMC progenitors in the walls of alveolar sacs. Both PDGF A and PDGFR α-null mice also display hypoplasia of skin mesenchyme and abnormal intestinal villi formation. The most pronounced phenotypic features of the PDGF B and PDGF β-receptor knockout mice are defects in kidney glomeruli and capillary microaneurisms. Both result from failure of capillary branching and dilation of capillary walls in the absence of PDGF-dependent recruitment of pericytes and kidney mesangial cells. Other abnormalities include dilation of heart and large arteries, thrombocytopenia, and anemia.

See Also the Following Articles

Chemotactic Peptide/Complement Receptors • Phospholipase C • Ras Family • Rho GTPases and Actin Cytoskeleton Dynamics • Src Family of Protein Tyrosine Kinases

Glossary

adaptor A protein linking together proteins that are otherwise unable to interact.

autocrine signaling Type of signaling in which the cell responds to a stimulus (e.g., growth factor) that is produced by the same cell.

cell cycle Tightly regulated sequence of events exhibited by dividing cells. Consists of the following phases: Gap 0 (G0; temporary or permanent quiescence), Gap 1 (G1; growth and preparation of the chromosomes for replication), S (synthesis of DNA), Gap 2 (G2; growth and preparation for mitosis) and M (mitosis).

chemotaxis The ability of cells to migrate toward a gradient of chemoattractant.

growth factor A substance that needs to be present in the environment of responsive cells in order for them to divide.

ligand A molecule (or ion) that can interact with a receptor.

mitogen A substance (e.g., growth factor) that can initiate cell division.

paracrine signaling Type of signaling in which the cell responds to a stimulus (e.g., growth factor) that is produced by a nearby cell.

pericytes Pluripotential cells surrounding blood vessels.

receptor A molecule (mostly of protein nature) able to detect the presence of a specific stimulus (ligand) and give rise to signaling events leading to physiological response(s).

transphosphorylation A phosphorylation event in which two protein kinases phosphorylate each other (e.g., within the dimer).

Further Reading

Betsholtz, C., Karlsson, L., and Lindahl, P. (2001). Developmental roles of platelet-derived growth factor. *BioEssays* **23**, 494–507.

Heldin, C.-H., Östman, A., and Rönnstrand, L. (1998). Signal transduction via platelet-derived growth factor receptors. *Biochim. Biophys. Acta* **1378**, F79–F113.

Östman, A., and Heldin, C.-H. (2001). Involvement of platelet-derived growth factor in disease: Development of specific antagonists. *Adv. Cancer Res.* **80**, 1–38.

Pietras, K., Östman, A., Sjöquist, M., Buchdunger, E., Reed, R. K., Heldin, C.-H., and Rubin, K. (2001). Inhibition of platelet-derived growth factor receptors reduces interstitial hypertension and increases transcapillary transport in tumors. *Cancer Res.* **61**, 2929–2934.

Rosenkranz, S., and Kazlauskas, A. (1999). Evidence for distinct signaling properties and biological responses induced by the PDGF receptor α and β subtypes. *Growth Factors* **16**, 201–216.

Smits, A., and Funa, K. (1998). Platelet-derived growth factor in primary brain tumours of neuroglial origin. *Histol. Histopathol.* **13**, 511–520.

Takehara, K. (2000). Growth regulation of skin fibroblasts. *J. Dermatol. Sci.* **24**(Suppl. 1), S70–S77.

Biography

Andrius Kazlauskas is currently a Senior Scientist at the Schepens Eye Research Institute, and Associate Professor at Harvard Medical School. He studies signal transduction pathways used by receptor tyrosine kinases to drive cell proliferation. He graduated from Cleveland State University with a Ph.D. in Chemistry in 1986, and

then studied signaling by tyrosine kinases as a postdoctoral fellow at the Fred Hutchinson Cancer Research Center from 1986 to 1990. He has held an independent research position from 1991.

Marina Kovalenko is a postdoctoral fellow in the lab of Andrius Kazlauskas. After graduating from Moscow State University, she earned her Ph.D. in Biochemistry from Friedrich Schiller University in Jena, Germany, in 1996. Then, she studied PDGF receptor-directed tyrosine phosphatases as a postdoctoral fellow at the Ludwig Institute for Cancer Research in Uppsala, Sweden. Both her thesis work and postdoctoral research were devoted to antagonists of the PDGF receptor tyrosine kinase.

Polysialic Acid in Molecular Medicine

Frederic A. Troy II
University of California School of Medicine, Davis, California, USA

Molecular medicine is an emerging new science that seeks to understand the complex interaction between genes (genomics), proteins (proteomics), carbohydrates (glycomics), and lipids (lipomics) in health and disease. Studies in this field are directed at elucidating the structure, synthesis, and function of these major classes of molecules in both normal and abnormal processes, including disorders in all organ systems of the human body. A major impact of molecular medicine is in the field of cancer metastasis, which is discussed in this article, with focus on the polysialic acid (polySia) molecule.

The cell surface of normal and cancer cells is decorated with a remarkable array of information-rich sugar molecules, usually attached to proteins (glycoproteins) and lipids (glycolipids). Surface expression of many of these complex sugars changes dramatically during the developmental life of a cell and with the onset of cancer. Importantly, these sugars carry specific information that determines the cell behavior at different stages in their life cycle, for example, when to detach and move to different locations and when to stop dividing and become adherent. A specific example of one class of these surface carbohydrates is "polysialic acid" (polySia), the focus molecule of this article.

The emerging importance of polySia in molecular medicine has given rise to a new sub-discipline of glycobiology, termed sialobiology. When polySia chains are attached to surface proteins designated neural cell adhesion molecules (N-CAMs), they help direct in a controlled way this "stop–go" signaling during development. During neural development, for instance, polySia is normally expressed on N-CAM during the embryonic stage, when cells need to avoid sticking together and must migrate to where their "zip code" has programmed them to go. When cells have reached their correct address and need to adhere, other molecular events signal the removal of the embryonic or polysialylated form of N-CAM (polySia-N-CAM) from the cell surface, thus facilitating N-CAM-mediated cell–cell adhesion. In this sense, polySia is an "anti-adhesive glycotope" that forbids cell adhesion and allows cell movement. But polySia is also an oncodevelopmental or oncofetal, tumor-associated antigen, which means that it can be re-expressed on the surface of adult cancer cells. When this re-expression occurs, polySia becomes a metastatic factor that promotes tumor cell detachment, invasion, and colonization at distant sites. Indeed, many human cancers that express polySia have a predilection for metastasis to the brain. How this re-expression occurs is not well understood, but the hereditary information or genes containing the "blueprint" for building the protein catalysts or enzymes required for synthesizing polySia (the polysialyltransferases (polySTs)) are reactivated in cancer cells, having been silenced at the end of embryonic development. The up-regulated polyST genes now allow the adult cancer cell to again synthesize the embryonic form of polySia-N-CAM, thus facilitating cell detachment and migration. This fundamental event may be key in allowing a number of polysialylated human cancer cells to detach from their original site and to spread or metastasize throughout the body. It is this metastatic property of cancer cells that is so feared and deadly, and that is the hallmark of malignancy.

In humans, the pathogenic neuroinvasive bacteria *Escherichia coli* (*E. coli*) K1 and *Neisseria meningitidis* (*N. meningitidis*) that cause meningitis express a surface capsule of polySia acid that is structurally identical to the polySia chains expressed on N-CAM. In this case, the capsule coats the entire surface of the bacterium and as such is a neurovirulent determinant that allows for the invasion and colonization of the brains (meninges) of neonates. Accordingly, the polySTs in both pathogenic bacteria and human cancer cells have become important targets for chemotherapeutic agents directed at treating meningitis and in slowing or stopping cancer cells from metastasizing. This article summarizes information related to the structure,

occurrence, function, synthesis, and glycopathology of polysialic acid in mammalian cells.

The Importance of Molecular Medicine in Health and Disease

The field of molecular medicine is important in human biology and medicine because of the new information it is providing towards the discovery, diagnosis, and treatment of known and emerging diseases. The discipline uses contemporary methodologies of biochemistry (molecular genetics, and molecular cell developmental and structural biology), to identify and analyze new information on the "molecule signature" and interaction of molecules, which are key molecular players in all aspects of health and disease. The outcome of studies in molecular medicine is already leading to a new generation of synthetic and biotechnology-based approaches for the diagnosis and treatment of a variety of health-related diseases.

Natural Occurrence and Structure of Oligo-Polysialic Acids

As shown in Figure 1, the polySia are linear sugar chains usually composed of one of the two most common sialic acid residues, N-acetylneuraminic acid (Neu5Ac) or N-glycolylneuraminic acid (Neu5Gc). Shorter chains of KDN (2-keto-3-deoxy-D-*glycero*-D-*galacto*-nonoic acid), the newest member of the class of sialic acids, occurs in some fish egg sialoglycoproteins and bacterial capsule polysaccharides. The sialic acids are unusual 9-carbon sugar acids that are joined internally by α2,8-, α2,9-, or alternating α2,8/α2,9-ketosidic linkages. The α2,8-linked chains are the most common, and are the principal polySia synthesized by mammalian cells. Their chain length, or degree of polymerization (DP) exceeds 200 Sia residues in *E. coli* K1 and 100 residues in some mammalian tissues. A striking feature of these chains is the bewildering degree of structural diversity and wide range of expression on the surface of both prokaryotic and eukaryotic cells. The operative paradigm is that this diversity in both structure and DP is related to the myriad of cellular functions regulated by polySia, including cell–cell adhesion, cell migration, neuronal development and regeneration, synaptic plasticity, neurotropism, and the possible activation of cell proliferation by initiating second messenger-related signaling pathways. A review of the structural and functional features of oligo-polySia has appeared in *Biology of the Sialic Acids*.

Polysialylated Neural Cell Adhesion Molecules

Embryonic and Adult Forms of N-CAM

N-CAMs are morphoregulatory glycoproteins that are members of the immunoglobulin gene superfamily. They represent a class of high-molecular-weight cell surface sialoglycoproteins that affect a number of cell adhesive and cell migration processes, including neurite fasciculation and neuromuscular interactions. N-CAMs are the most prevalent carrier proteins of polySia chains in mammalian cells and, as such, are the most thoroughly characterized. There are four different isoforms of N-CAM, which arise by alternative mRNA splicing. These include polypeptides with molecular masses of 180, 140, 120, and 110 kDa. The 180- and 140-kDa isoforms are linked to the plasma membrane via a transmembrane spanning domain, and each has a cytoplasmic domain. In contrast, the 120-kDa protein is attached to the membrane via a glycosylphosphatidylinositol anchor and thus lacks a cytoplasmic domain. The 110-kDa N-CAM is a secreted isoform. The 180-kDa isoform is expressed primarily on neurons but not on muscle cells, while the 140-kDa protein is expressed on both neural and muscle cells. A unique structural feature of N-CAM is the presence of α-(2,8)-linked polySia (polyNeu5AC) chains that posttranslationally modify the protein during embryonic development. These chains are attached to both N- and O-linked oligosaccharides that are located on the extracellular domain of N-CAM. No α2,9-ketosidic linkages, which characterize the polySia capsule in neuroinvasive

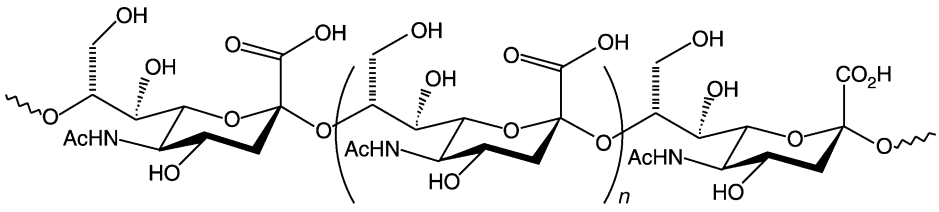

FIGURE 1 Structure of α2,8-polysialic acid.

N. meningitidis Gp. C, nor Neu5Gc or KDN residues have been reported as constituents of N-CAM. The covalent attachment of polySia chains to N-CAM, which characterizes the embryonic form of the molecule, decreases N-CAM-dependent cell adhesion in a variety of tissues, thereby acting as a negative regulator of cell–cell interactions. In contrast, cells expressing relatively low levels of polysialylated N-CAM, which characterizes the adult form, aggregate much more readily than those with high levels of polySia. Thus, polysialylation of N-CAM is an essential reaction that mediates cell recognition events that modulates cell migration and cell adhesion. As such, polysialylation plays a central role in regulating mammalian developmental processes, including neural cell differentiation, migration, and synaptic plasticity.

Temporal Expression of Polysialic Acid during Embryonic Neural Development

Maximal expression of the polysialylated form of N-CAM usually occurs in embryonic neural tissue, when cells are migratory, and is greatly reduced in adult tissue, where little cell migration occurs. The embryonic form of N-CAM has a high Sia content that undergoes a postnatal conversion to the adult form with a low Sia content. During development, the presence of polySia is closely correlated with axon pathfinding, synaptogenesis, and neuron–muscle formation. As the embryo develops, most of the N-CAM changes from the embryonic, or high-polySia form, to the adult, or low-polySia form. The adult form is postulated to help stabilize mature tissues. In this way, N-CAM plays a role in both facilitating two adjacent cells to form regions of contact and in inhibiting such contacts. If neighboring cells express the adult form of N-CAM, strong cell adhesion is promoted. In contrast, if cells express the polysialylated forms of N-CAM, cell adhesion is reduced. Thus, the polySia moiety on N-CAM is an anti-adhesive glycotope that has a regulatory effect on adhesion between living cells. The amount of this carbohydrate is important for normal development, and while the DP of polySia chains on N-CAM changes during embryonic chick brain development, the significance of this change is unknown.

Expression of Polysialic Acid in Adult Human Brain

Although polySia expression is most abundant during early stages of embryonic development in both neural and non-neural tissues, polysialylated N-CAM is also expressed in restricted parts of the adult brain that exhibit synaptic plasticity, and may be required for the rearrangement of neural cells or their interconnections. In rat brain and spinal cord, polysialylated N-CAMs are expressed in discrete regions of the hypothalamic and thalamic nuclei, the hippocampal dentate gyrus, mesencephalic central gray matter, the supraotic nucleus, and the olfactory bulb. It is also expressed on neurohypophysial astrocytes and on mesencephalic dopaminergic cells in the brain that persist throughout development. Functional studies on the role of polySia in adult brain suggest that its primary role is to promote plasticity in cell interactions, thus facilitating changes in the structure and function of the nervous system. PolySia therefore represents one of the few defined carbohydrate structures with an identifiable role in a morphogenic pathway.

Expression and Function of Polysialic Acid on Extraneural Cells

Roth and colleagues first showed that expression of the embryonic form of N-CAM was developmentally regulated in rat and human kidney, a mesodermally derived tissue. The polySia chains in kidney are maximally expressed early in development and, like brain, may regulate cell–cell adhesive interactions during kidney differentiation and development. The polySia chains are re-expressed in Wilms tumor, a highly malignant tumor of the kidney. Polysialylated N-CAM is also expressed on newborn heart and muscle tissue. In human, rat and chicken embryos polySia-N-CAM is expressed on cells derived from mesoderm (mesenchymal cells) and endoderm (pancreas, lung epithelium), and on neuroectoderm cells (neural or lung endocrine cells). In the thyroid gland, calcitonin-producing cells, which are endocrine derivatives of the neural crest, also express the embryonic form of polysialylated N-CAM. During the early stages of rat heart development, polySia-N-CAM is expressed on myocardial, endocardial, and some atrioventricular cells in the epicardium. Later during development, its appearance in the epicardium decreases. In the adult heart, the only significant expression of polysialylated N-CAM is during innervation. Polysialylated N-CAM is transiently expressed in developing chicken osteoblasts during osteogenesis and on dermal and smooth muscle cells in the chick during feather development. In *Drosophila melanogaster*, expression of α2,8-linked polySia chains is developmentally regulated, and occurs only during the early stages of development. The possible function of the polySia glycotope in prokaryotic and eukaryotic cells is summarized in Table I.

TABLE I

Possible Functions of the Polysialic Acid Glycotope

Bacterial polysialic acid capsules
- In neuroinvasive *E. coli* K1 and *N. meningitidis*, functions as a neurotropic determinant; facilitates invasion of the blood–brain barrier and colonization of the meninges of neonatal brains
- Polyanionic shield that masks the somatic O-antigen chains of lipopolysaccharide and renders cell resistant to immune detection and phagocytosis
- Receptor for binding K1-specific bacteriophages

Fish egg polysialoglycoproteins
- Implicated in regulating cell–cell interactions and cell migration during oogenesis
- May function as recognition markers for mediating egg–sperm interaction
- May protect the embryo from osmotic lysis, artificial activation, mechanical destruction, and bacterial infection by retaining Ca^{2+} around the embryo (KDN-gp has affinity for Ca^{2+} ions)
- *O*-Acetylation and KDN cosylation render polySia chains resistant to depolymerization by sialidases; consequence unknown (protective?)
- Expression of an $\alpha 2 \rightarrow 8$-polysialyltransferase is developmentally regulated

Polysialic acid-containing glycoproteins in the jelly coat of sea urchin eggs
- May mediate cell–cell interactions during gastrulation when endodermal cells interact with ectodermal cells
- May be involved in inducing the acrosome reaction in sperm
- Expression of an $\alpha 2,8$-polysialyltransferase is developmentally regulated

Polysialylated neural cell adhesion molecules (N-CAMs)
- Implicated in embryonic neural development and neuronal plasticity; mediates cell adhesive interactions including neurite fasciculation, neuromuscular interactions, and cell migration. Expression of polySia usually decreases N-CAM-mediated cell adhesion
- The amount of polySia on N-CAM is critical for normal morphogenesis and neural development
- Influences cell–cell apposition and regulates contact-dependent cell interactions. PolySia "shield" may simply increase the intercellular space between cells
- Participates in the establishment of neuronal connections and in modulating neurite outgrowth. May activate a second messenger pathway in primary neurons
- May influence the formation of new neural circuits in the dentate gyrus, and in reorganization of the piriform cortex in the adult rat
- Proposed to regulate intramuscular nerve branching during embryogenesis
- Implicated in the normal separation of secondary myotobes from primary myotobes during muscle development
- Influences the interaction of cells of the preimplantation mammalian embryo
- May couple the morphogenic effects of adhesion and synaptic activity-dependent processes
- In bone formation, may mediate the interaction of osteoblasts and regulate skeletogenesis
- May mediate the formation of fiber cell gap junctions and adherence junction during lens cell differentiation
- May control the migration and maturation of dopaminergic cells of the developing mesencephalon
- Participates in the internalization of the Antennapedia homeobox peptide involved in late expression of some homeogenes in the CNS

Expression on tumors
- In developing human kidney, brain (neuroblastomas), and plasma cells, polysialylated N-CAM is an oncodevelopmental antigen
- On some human cancers, e.g., natural killer-like and T-cell malignant lymphomas, acute myeloid leukemia, multiple myeloma, and some head and neck tumors, polySia expression may enhance neuroinvasive potential and metastases
- May protect malignant cells from immune surveillance

Sodium channel glycoproteins
- Function unknown. By analogy with bacterial polySia capsules, the polyanionic surface charge over the channel may maintain a solute reservoir and shield channel from toxins

Expression and Function of Polysialic Acid in Cancer

Prokaryotic-Derived Reagents for the Detection and Analysis of PolySia

α-(2,8)-Polysialylated N-CAM expression on a number of human cancers was revealed using anti-polySia and anti-N-CAM antibodies in combination with Endo-N-acylneuraminidase (Endo-N), a diagnostic enzyme specific for catalyzing the depolymerization $\alpha 2,8$-linked polySia chains. The ease with which these reagents can be used to discover and confirm the presence of polySia chains in mammalian cells and human cancers provides a way to study polysialylation that had not been previously possible. Using these specific molecular probes, α-(2,8)-polysialylated N-CAM expression was identified on a variety of human cancers, including high-grade tumors, e.g., medulloblastomas, neuroblastomas, pheochromocytomas, medullary thyroid carcinomas, small cell lung carcinomas, pituitary adenomas, and congenital

TABLE II

Human Tumors Expressing the $\alpha 2 \rightarrow 8$-Linked Polysialic Acid Glycotope

Neuroblastomas
Nephroblastomas (Wilms' tumor)
Medulloblastomas
Pheochromocytomas
Medullary thyroid carcinomas
Small-cell lung cancers
Lung carcinoid tumors
Pituitary adenomas
Congenital mesoblastic nephroma
Multiple myelomas
T-cell malignant lymphomas
Leukemias (AML)
Head and neck tumors (principally squamous cell carcinomas)
Malignant melanomas
Human tumor expression $(\rightarrow 9Neu5Ac\alpha 2 \rightarrow)_2$
Ovarian teratocarcinoma (PA1 embryonal carcinoma cells)

mesoblastic nephromas. Table II summarizes human cancers that have been shown to express the polySia glycotope. The human breast cancer cell line, MCF-7 and rat basophilic leukemia (RBL-1) cells are unique in that the $\alpha 2$,8-linked polySia chains are attached to O-linked oligosaccharides, suggesting that polysialylation of glycoproteins on tumor cells may be more prevalent than heretofore recognized. While few studies have been carried out to determine the length of polySia chains on cancer cells, polySia chains containing >55 Sia residues are expressed on human neuroblastoma cells. Because of methodological limitations, accurate DP values are difficult to obtain. Reported values thus represent minimum estimates, as some pre-hydrolysis of the polySia chains occurs during isolation and purification and/or derivitization procedures that are required for most chromatographic separation and detection methods.

Polysialic Acid as an Oncodevelopmental Antigen and its Relationship to Tumor Metastasis

Extended chains of polySia were first shown to be expressed on human neuroblastomas, some of which were metastatic to bone and brain. Concurrent studies showed that polySia was temporally expressed in human embryonic kidney, but not in adult kidney, and was re-expressed in malignant Wilms' tumors. These findings led to the important conclusion that polySia was an oncodevelopmental (oncofetal) antigen in human kidney and brain because the long-chain forms of polySia, which characterized the embryonic form of N-CAM, were infrequently expressed in adult brain. An exception to this paradigm, as noted above, is the hypothalamo-neurohypophysial system in the adult brain, where polySia-N-CAM is postulated to function in plasticity.

Evidence for the Role of Polysialic Acid in Cancer Metastasis

Several independent *in vivo* studies reveal a specific role for polySia in tumor metastasis. First, mice injected subcutaneously with polysialylated mouse leukemia cells develop tumors that are metastatic to the spleen. All of the metastatic tumors express polySia. Second, a significant correlation between the level of polySia-N-CAM expression and growth rate, invasion, hormone secretion, and metastasis occurs in rat pituitary tumors. Tumors showing the highest level of polySia-N-CAM expression show the highest level of metastasis. Third, human rhabdomyosarcoma cells expressing polysialylated N-CAM are able to form lung metastases in nude mice. Metastasis is decreased in mice receiving injections of Endo-N, the endo-sialidase that specifically removes polySia from the surface of the cancer cells.

Role of PolySia in Lung Cancer (Small-Cell Lung Carcinoma (SCLC) and Non-SCLC)

There is a positive correlation between polysialylated N-CAM expression and malignant behavior in SCLC and non-SCLC. This finding suggests that polySia functions to reduce cell–cell adhesion and cell–matrix interactions leading to tumor cell detachment, aggressive behavior, and a higher incidence of metastases. The overall survival of SCLC patients with polySia-negative cancers is higher than in patients with polySia-positive tumors. Thus, the polysialylated state of N-CAM may be a prognostic indicator in SCLC patients, corroborating earlier studies in which polySia-N-CAM is associated with poor differentiation and aggressive clinical behavior in patients with SCLC and other neuroendocrine lung tumors. The role of polySia in SCLC was confirmed by an analysis of surgically resected SCLC tumors. Patients with polySia-N-CAM-positive tumors have a significantly lower probability of survival than patients with polySia-negative tumors, again showing the prognostic value of polySia-N-CAM in SCLC. PolySia expression is also an important clinical marker in non-SCLC carcinomas, as patients with polySia-positive tumors have a poorer prognosis for survival. In non-SCLC patients, polySia expression shows a positive correlation with nodal and distant metastasis.

Biosynthesis of Polysialic Acid

The Polysialyltransferases

Molecular insight into the problem of how polySia is synthesized and how surface expression of oligo/polySia-containing glycoconjugates is controlled is currently an active area of investigation. These studies use a combination of biochemical, molecular genetic, and biophysical techniques. Two closely related polyST genes have been cloned, sequenced, and their encoded proteins shown to catalyze the biosynthesis of polySia chains. They are the CMP-Sia:α2,8-polySTs designated STX (ST8SiaII) and PST (ST8SiaIV). Both polySTs catalyze the transfer of sialic acid from the activated sugar nucleotide precursor, CMP-sialic acid, to endogenous or exogenous acceptor substrates. In mammalian cells, N-CAM is the most common endogenous acceptor. The catalytic domains of STX and PST are located in the lumen of the Golgi complex. The amino acid sequence of the human PST is 97% homologous with the hamster and mouse, and is encoded by a single gene (2.0 kb) that codes for a protein with a predicted molecular mass of 41.2 kDa. PST and STX show $\sim$60% homology at the protein level. The genomic structures and promoter activities of the mouse PST and STX genes have been reported, although there is little information about how transcription and translation of these genes are regulated. While the overall structure and genomic organization of STX and PST genes are similar, the 5′-flanking regions of PST and STX are distinctly different. The STX gene is about 80 kb long and consists of six exons, whereas the PST gene is $\sim$60 kb long and contains five exons. PST and STX can independently polysialylate N-CAM in transfected cell lines, where there are reports that the two enzymes may act cooperatively.

Autopolysialylation of the Polysialyltransferases

Soluble constructs of STX and PST both undergo "autopolysialylation" in cell lines transiently transfected with V5 epitope-tagged PST and STX cDNAs. The question of whether autopolysialylation is required for N-CAM polysialylation remains a point of some controversy, although it does not appear to be an obligatory requirement. STX is not autopolysialylated during neuronal development in embryonic chick brain, and it may not be so in cell lines that express no or low levels of N-CAM. It is possible that soluble constructs do not have the same catalytic properties as their membrane-bound counterparts, particularly in the presence of N-CAM. Soluble constructs of polySTs show reduced activity compared with the activity of the membrane-bound form, indicating that N-CAM may modulate polyST activity, and hence the extent and DP of N-CAM polysialylation.

How many Sialyltransferases does it take to Polysialylate?

Results from transfection experiments have been interpreted to support the hypothesis that only one enzyme is required for polySia chain synthesis, since individual cDNAs encoding for polySTs induce polySia expression in cell lines previously shown to be polySia negative. However, some transfected cell lines have pre-existing disialyl (Siaα2,8-Siaα2,3-) terminal residues that can serve as initiating sites for polySia chain polymerization. The presence of diSia in an acceptor substrate would obviate the need for an α2,8-monoST, or "initiase." Thus, while the transfection studies support the necessity of a PST or STX for polySia chain synthesis, they do not exclude the possibility that more than one enzyme may be involved. An alternative theory to the single-enzyme hypothesis is that more than one sialyltransferase is required to catalyze both chain initiation and polymerization. This hypothesis is based on structural studies of the cognate di-, oligo-, and polySia chains that are expressed at different stages of development in the rainbow trout. These studies show that at least two α2,8 sialyltransferases are required. The first, an "initiase," transfers the first α2,8-Sia residue to Siaα2,6/3Gal-acceptors forming the disialyl derivative, Siaα2,8Sia-. A separate polyST or "polymerase" is required to complete polySia chain elongation, based on the later appearance in the development of polysialylated glycoproteins.

Rationale for Chemotherapeutic Inhibition of PolySia Biosynthesis

The studies described above show that surface expression of polySia is positively correlated with increased metastasis in a number of human tumors. Accordingly, the design and synthesis of compounds that selectively inhibit the synthesis of polySia is an important area of research with direct impact on cancer metastasis and treatment of meningitis. The rationale for this idea is that if the oncofetal expression of polySia on the surface of human cancers can be inhibited, then the detachment and anti-adhesive properties of these cells may be diminished, and tumor metastasis may be slowed or stopped. The same rationale holds for treating neuroinvasive meningitis caused by the polysialylated *E. coli* K1 and *N. meningitidis* pathogens.

Selectivity of the PolySTs as Chemotherapeutic Targets

The specificity of chemotherapeutics to selectively inhibit the polySTs and not the monoST, which could have an effect on other tissues, is based on the fact that the two classes of enzymes are structurally and functionally distinct. They differ in the following key properties:

1. The polySTs, in contrast to the monoSTs, are oncodevelopmental enzymes that are selectively re-expressed in cancer. An exception, as noted above, is expression of polySia in the hypothalmo–neurohypophysial region of adult brain, the function/consequence of which is not known.
2. At the protein level, the two classes of enzymes are distinct and have different kinetic properties (K_m and V_{max} values). This is a key feature that favors the design of inhibitors to selectively target the polySTs.
3. The polySTs and monoSTs show limited structural homology and exhibit different structural properties. The polySTs, but not the monoSTs, contain a uniquely extended basic amino acid domain of 31 residues upstream of sialylmotif S. This cationic domain is essential for polysialylation, and thus provides a selective target for the polySTs.
4. The two classes of enzymes show differences in response to thiol reagents, thiol-directed alkylating reagents, and metal ion requirements. The polySTs contain a cystinyl residue required for polysialylation, while the monoSTs do not, and;
5. The polySTs catalyze a processive mechanism of synthesis while the monoSTs catalyze a distributive mechanism of synthesis.

The significance of these differences is two-fold. First, they provide new insight into the enzymatic basis of polysialylation. Second, they reveal for the first time structural features unique to the polySTs that are essential in the design of chemotherapeutic inhibitors to selectively target this class of glycosyltransferases. To our knowledge, no other family of mammalian glycosyltransferases exhibit such marked differences. As such, to use this new information to selectively target the polySTs represents a paradigm shift from the more conventional approaches and targets currently underway in the "glyco-drug" discovery field.

See Also the Following Articles

Glycoproteins, N-Linked • Glycoprotein-Mediated Cell Interactions, O-Linked • Oligosaccharide Chains: Free, *N*-Linked, *O*-Linked

Glossary

endo-N-acylneuraminidase (Endo-N) An endosialidase that catalyzes the depolymerization of polysialic acid chains and is a diagnostic enzyme for identifying **α**2,8-linked polysialic acid.

malignant Describing or referring to a tumor or cancer cell that is invasive and undergoes metastasis.

metastasis The process whereby malignant cancer cells spread from one location in the body to another.

monosialyltransferases (monoSTs) A family of sialyltransferases distinct from the polySTs that catalyze the addition of a single sialic acid residue to acceptor substrates.

neural cell adhesion molecules (N-CAMs) Cell surface glycoproteins that control cell adhesion and cell migration and are the major protein carriers of polysialic acid in mammalian cells.

oncodevelopmental/oncofetal antigens Glycoproteins or glycolipids that are most often expressed during embryonic development and are usually undetected in the differentiated adult. Many are then re-expressed in malignant cancer cells.

polysialic acid (polySia) Complex sugar molecules containing sialic acid that decorate the cell surface of neuroinvasive bacteria causing meningitis and some non-mammalian and mammalian cells. They are oncodevelopmental, tumor-associated antigens that regulate cell–cell interactions and allow some cancer cells to metastasize.

polysialyltransferases (polyST) A family of glycosyltransferases (enzymes) that catalyze the polymerization of multiple sialic acid residues forming polysialic acid.

sialobiology A sub-discipline of the field of glycobiology that focuses on the chemistry and biology of sialic acids in the molecular life sciences.

Further Reading

Close, B. E., Wilkinson, J. M., Bohrer, T. J., Goodwin, C. P., Broom, L. J., and Colley, K. J. (2001). The polysialyltransferase ST8Sia II/STX: Posttranslational processing and role of autopolysialylation in the polysialylation of neural cell adhesion molecule. *Glycobiology* **11**, 997–1008.

Fukuda, M. (1996). Possible roles of tumor-associated carbohydrate antigens. *Cancer Res.* **56**, 2237–2244.

Gluer, S., Schelp, C., von Schwenitz, D., and Gerardy-Schahn, R. (1998). Polysialylated neural cell adhesion molecule in childhood rhabdomyosarcoma. *Pediatric Res.* **43**, 145–147.

Inoue, Y., Lee, Y. C., and Troy, F. A., III (eds.) (1999). *Sialobiology and other novel forms of glycosylation.* Gakushin Pub. Co., Osaka, Japan, 307 pp.

Roth, J., Taatjes, D. J., Bitter-Suermann, D., and Finne, J. (1987). Polysialic acid units are spatially and temporally expressed in developing postnatal rat kidney. *Proc. Natl Acad. Sci. USA* **84**, 1969–1973.

Scheidegger, E. P., Lackie, P. M., Papay, J., and Roth, J. (1994). *In vitro* and *in vivo* growth of clonal sublines of human small cell lung carcinoma is modulated by polysialic acid of the neural cell adhesion molecule. *Lab. Investigation* **70**, 95–106.

Sevigny, M. B., Ye, J., Kitazame-Kawaguchi, S., and Troy, F. A., 2nd. (1998). Developmental expression and characterization of the α2, 8-polysialyltransferase activity in embryonic chick brain. *Glycobiology* **8**, 857–867.

Troy, F. A., II (1995). Sialobiology and the polysialic acid glycotope: Occurrence, structure, function, synthesis and glycopathology. In *Biology of the Sialic Acids* (A. Rosenberg, ed.) pp. 95–144. Plenum Press, New York.

Vimr, E. R., McCoy, R. D., Vollger, H. F., Wilkison, N. C., and Troy, F. A. (1984). Use of prokaryotic-derived probes to identify

poly (sialic acid) in neonatal membranes. *Proc. Natl Acad. Sci. USA* **81**, 1971–1975.

Biography

Frederic A. Troy II is professor and past chairman of the Department of Biochemistry and Molecular Medicine, University of California School of Medicine, Davis, California and a member of the UC Davis Cancer Center. His major area of research is glycoscience, cancer biology, and membrane chemistry. He received his Ph.D. in biological chemistry from Purdue University and carried out postdoctoral studies at Johns Hopkins University School of Medicine. He was a visiting professor in tumor biology at Karolinska Institute and has coedited two major texts in the field of Sialobiology.

Porphyrin Metabolism

Mark Shepherd and Harry A. Dailey
University of Georgia, Athens, Georgia, USA

Porphyrins are cyclic tetrapyrroles that perform critical roles in a variety of biological systems. Examples of important tetrapyrroles include heme and siroheme (both with chelated iron), chlorophyll (with chelated magnesium), coenzyme B_{12} (with chelated cobalt), and factor F_{430} (with chelated nickel). All of these are derived from a common precursor, δ-aminolevulinic acid (ALA). Heme, as a prosthetic group to various hemoproteins, is necessary for oxygen transport and storage as part of hemoglobin and myoglobin. It is essential for electron transport as part of various cytochromes and is also required by mixed function oxidases as a part of cytochrome P450. Additionally, heme is needed for the decomposition and production of hydrogen peroxide as a cofactor of catalase and peroxidase, respectively. Siroheme is the cofactor in both nitrite and sulfite reductases, and hence is not synthesized by mammals.

Several types of chlorophyll exist which differ with respect to the substituents on the tetrapyrrole ring. Chlorophylls are employed by photosynthetic organisms to absorb energy for photosynthesis. This process harnesses the vast majority of energy consumed by living organisms, and only chemolithotrophic bacteria are independent of this energy source. Chlorophylls are required in the first stage of photosynthesis, whereby visible radiation excites an electron in the porphyrin that, upon returning to a lower energy state, provides the energy needed for the synthesis of ATP and NAD(P)H.

Coenzyme B_{12} consists of cobalamin (vitamin B_{12}), a corrin ring, which is linked to dimethylbenzimidazole and 5′ deoxyadenosine via its central cobalt atom. The bond between the cobalt and the latter substituent is a weak cobalt–carbon bond, the only example known in biology, which catalyzes intramolecular rearrangements by cleaving homolytically to generate a free radical. Examples include methylations in methionine synthesis and the reduction of ribonucleotides to deoxyribonucleotides. Finally, there is a nickel (II) tetrapyrrole, factor F_{430}, which is found in methanogenic bacteria and is involved in methane metabolism.

Biosynthesis of Porphyrins

Figure 1 illustrates the first three steps of tetrapyrrole biosynthesis, which is common to all the tetrapyrroles mentioned above. All these molecules have a core structure of four pyrrole rings, designated A–D, as shown on the structure of heme in Figure 1. The carbon atoms are numbered 1–20 starting in ring A and ascending in a clockwise direction around the perimeter of the porphyrin ring.

Formation of δ-Aminolevulinic Acid

The first common intermediate in tetrapyrrole biosynthesis is δ-ALA. Two pathways for its synthesis are found in nature: the C_4 pathway in animals and some bacteria including *Rhodobacter sphaeroides*, and the C_5 pathway in plants, algae, and other bacteria including cyanobacteria. In the C_4, or Shemin pathway, ALA is formed by the condensation of glycine and succinyl coenzyme A in a reaction catalyzed by the enzyme ALA synthase. In the C_5 pathway an NADPH-dependent glutamyl-tRNA reductase produces glutamate 1-semialdehyde (GSA) from glutamyl-tRNA, which is subsequently converted to ALA by the replacement of the aldehyde moiety with an amide group. The C_5 pathway is thought to be ancestral to the Shemin pathway as bacteria with the former lack the α-ketoglutarate–dehydrogenase complex to make succinyl CoA. This group includes cyanobacteria such as *Synechocystis*, which may explain why plants today retain the C_5 pathway.

δ-Aminolevulinic Acid to Uroporphyrinogen III

In all organisms studied to date, the conversion of δ-aminolevulinic acid to uroporphyrinogen III proceeds via exactly the same steps. This process is summarized in Figure 1. The first step involves the condensation of two ALA molecules to form porphobilinogen with the release of two molecules of H_2O. This reaction is catalyzed by porphobilinogen synthase, also known as ALA dehydratase. Hydroxymethylbilane synthase, also known as porphobilinogen deaminase, catalyzes the condensation of four molecules of porphobilinogen in the order A, B, C, D

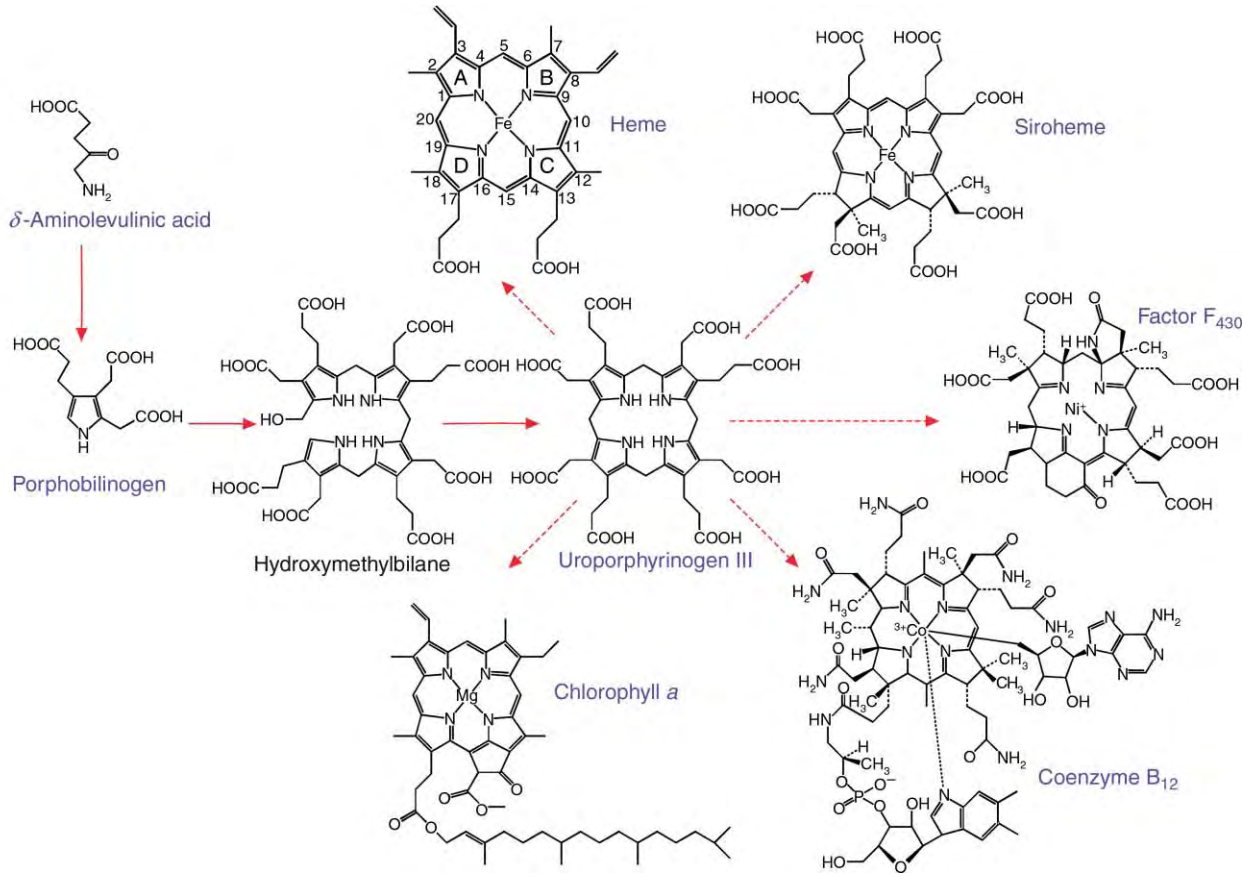

FIGURE 1 The porphyrins. The first three steps common to all porphyrin biosynthesis and the ultimate products of this branched metabolic pathway.

(the letters representing the rings of the ultimate tetrapyrrole product). This condensation gives rise to the first tetrapyrrole, hydroxymethylbilane, also known as preuroporphyrinogen, which is unstable and can close spontaneously, forming the biologically inactive isomer uroporphyrinogen I.

Several enzyme–substrate intermediates exist that are linked via a dipyrromethane cofactor (a modified dipyrrole). The dipyrromethane cofactor is posttranslationally attached to a cysteine residue of the enzyme. The first porphobilinogen molecule condenses with the cofactor and further porphobilinogen molecules are subsequently added to form hydroxymethylbilane. The enzymatic formation of the first macrocyclic tetrapyrrole, uroporphyrinogen III, is catalyzed by the enzyme uroporphyrinogen III synthase. During this reaction, the D pyrrole ring of hydroxymethylbilane undergoes an inversion, via a *spiro* intermediate. As free hydroxymethylbilane spontaneously reacts to form the biologically inactive isomer, uroporphyrinogen I, the enzyme must be present during or immediately after the release of hydroxymethylbilane from hydroxymethylbilane synthase to ensure that the correct isomer is formed.

Heme and Chlorophyll Biosynthesis

The biosynthesis of heme and chlorophyll proceeds along a common pathway until a branchpoint is reached at protoporphyrin IX (Figure 2). This pathway is conserved for almost all organisms studied, except *Desulfobrio vulgaris*, in which coproporphyrinogen III is formed from uroporphyrinogen III indirectly via precorrin-2. The formation of protoporphyrin IX from uroporphyrinogen III is achieved via a series of decarboxylation and oxidation steps. Uroporphyrinogen decarboxylase catalyzes the removal of a carboxyl group from each pyrrole ring to form coproporphyrinogen III. This is converted to protoporphyrin IX via the action of two enzymes, coproporphyrinogen oxidase and protoporphyrinogen oxidase. During aerobic growth both enzymes use oxygen as the terminal electron acceptor. However, anaerobic organisms have been shown to possess oxygen-independent isozymes and some facultative anaerobes encode both types of coproporphyrinogen oxidase.

The next step involves the insertion of a divalent cation into the porphyrin ring. Ferrochelatase catalyzes

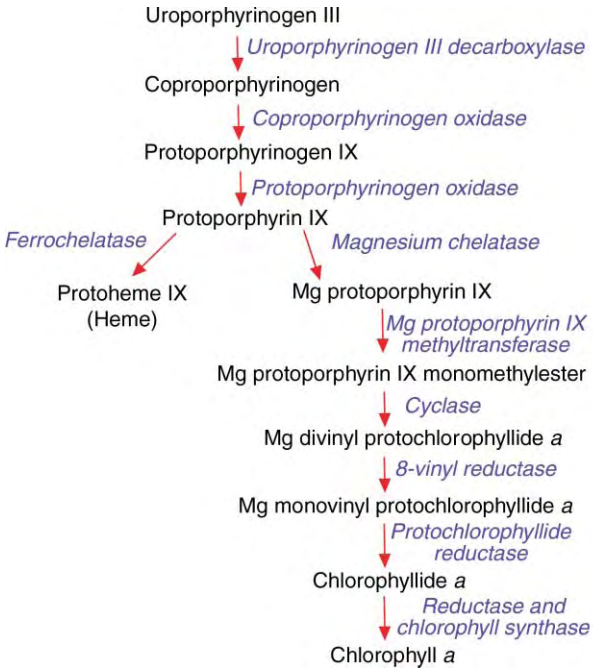

FIGURE 2 Heme and chlorophyll biosynthesis. The branching of the heme and chlorophyll biosynthetic pathways. The enzymes that catalyze the individual steps are shown in blue.

the insertion of an iron (II) ion whilst magnesium chelatase, as its name suggests, catalyzes the insertion of a magnesium (II) ion. It is thought that ferrochelatase distorts the porphyrin ring in such a way that allows the spontaneous insertion of iron (II). The insertion of magnesium requires the presence of MgATP and the participation of all three subunits of the heterotrimeric magnesium chelatase.

Subsequent steps of the chlorophyll biosynthetic pathway involve methylation and cyclization of the propionate group on ring C. After the reduction of the vinyl group on ring C, a light-dependent reaction takes place. This is catalyzed by protochlorophyllide reductase (POR) and is one of only two reactions known to be light dependent, the other being DNA photolyase. This reaction can also proceed via a light-independent reaction, catalyzed by dark protochlorophyllide reductase (DPOR). The formation of chlorophylls requires the addition of a hydrophobic tail to the propionate group on ring D via an esterification reaction. In the cases of chlorophyll and bacteriochlorophyll, these long chain alcohols are phytol and geranylgeraniol, respectively.

Coenzyme B_{12} and Factor F_{430} Biosynthesis

Figure 3 summarizes the synthesis of coenzyme B_{12} and factor F_{430} from uroporphyrinogen III. The first step

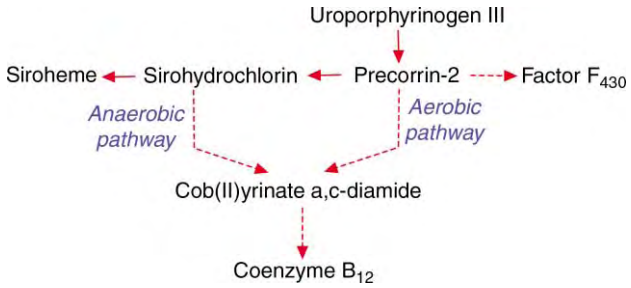

FIGURE 3 Coenzyme B_{12} and factor F_{430} biosynthesis. The branching of the coenzyme B_{12} and factor F_{430} biosynthetic pathways. The enzymes that catalyze the individual steps are shown in blue.

involves the methylation of uroporphyrinogen on rings A and B to form precorrin-2. Reduction to form sirohydrochlorin and subsequent ferrochelation yields siroheme, the prosthetic group for both nitrite and sulfite reductases. Factor F_{430} synthesis requires the cyclization of substituents on rings B and D and the chelation of nickel (II), which is bound to the pyrrole nitrogen on ring C. This final step is thought to be catalyzed by an ATP-dependent nickel chelatase.

The formation of coenzyme B_{12} involves a branched pathway consisting of several reactions. Figure 3 shows that the synthesis of cob(II)yrinate a,c-diamide can occur by either an anaerobic or an aerobic pathway. Both pathways involve the methylation, reduction, and isomerization of precorrin-2, along with the insertion of a central cobalt atom. The anaerobic chelatase has been compared to ferrochelatase as it is encoded by a single gene and does not require MgATP. The aerobic cobalt chelatase is similar to the magnesium chelatase involved in chlorophyll biosynthesis, as it is heterotrimeric and requires MgATP for catalysis. Coenzyme B_{12} is then formed via various alkylations, phosphorylation, an internal rearrangement, and the coordination of an adenosyl group to the central cobalt atom.

Regulation

As δ-ALA is the universal precursor for porphyrin synthesis, the supply of this metabolic intermediate ultimately governs whether or not porphyrin synthesis may take place. However, there are several examples where other key points in the pathway are subject to regulation. Heme plays a key role as a cofactor for many redox reactions in several different cell types and requires iron as a cofactor. From this it is clear that the regulation of heme biosynthesis must be dealt with on a global scale amongst different cell types and subcellular compartments. The model of negative feedback regulation mediated by a single regulator (heme) at a single site (ALA synthase) remained dogma for many years. Only after compelling evidence was generated to

support regulation at other sites, was it accepted that heme biosynthesis is subject to more complex control.

The biosynthesis of cofactor B_{12} or Factor F_{430} is more poorly understood. As mammals do not synthesize these cofactors, little work has been performed on the regulation of these pathways.

Regulation of Heme Biosynthesis

Role of ALA Synthase

In animal cells two ALA synthase (ALAS) genes exist that are classified by their histological localization. ALAS-E (or ALAS-2) is induced during erythroid differentiation and ALAS-1 encodes ALA synthase in other tissues. ALAS-1 is also referred to as ALAS-H (housekeeping) or ALAS-N (non-erythroid). The primary sequence of both ALAS proteins is highly conserved. However, significant differences exist between the regulatory regions of the genes and the untranslated regions of their respective mRNAs, which are manifested by the tissue-specific expression of the two enzymes.

Regulation at Sites Other than ALAS

Although it is accepted that ALAS is the major site of regulation, several examples of pathway control exist at the level of gene expression. In mammals, all the genes that encode heme biosynthetic enzymes possess both housekeeping and erythroid-specific promoter elements, although only ALAS is represented by two distinct genes.

A good example of regulation in response to an external stimulus is exhibited by the coproporphyrinogen oxidase of the nitrogen fixing bacterium *Azorhizobium caulinodans*. The enzyme responsible for nitrogen fixation, nitrogenase, requires the absence of oxygen to convert dinitrogen into ammonia. This organism is thought to possess both aerobic and anaerobic coproporphyrinogen oxidases and switches to the anaerobic isozyme in response to falling oxygen levels. Furthermore, the respiratory electron transport chain has been shown to act as the electron acceptor for protoporphyrinogen oxidase in anaerobically grown *E. coli*. This reaction is thought to be catalyzed by an enzyme distinct from the oxygen-dependent protoporphyrinogen oxidase.

Deficiencies in Porphyrin Synthesis

Porphyria

Porphyria is a mammalian disease caused by point mutations or deletions in the genes encoding heme biosynthetic enzymes. Individuals with this disorder are usually able to synthesize normal amounts of heme, but accumulate pathway intermediates that cause the clinical symptoms of porphyria. The disease can be divided into three groups: (1) cutaneous porphyrias, characterized by photosensitization; (2) acute porphyrias, where individuals experience abdominal pain, psychiatric disorders, constipation, vomiting, and paralysis; and (3) mixed porphyrias, which manifest themselves as a combination of both. Figure 4 illustrates the porphyrias that result from deficiencies in specific parts of the pathway.

Herbicides

The porphyrin biosynthetic pathway has been targeted for inhibition by certain herbicides to curtail the production of chlorophyll. Diphenyl ether-type herbicides, acifluorfen in particular, have been shown to act as potent inhibitors of protoporphyrinogen oxidase, the last enzyme before the branchpoint of heme and chlorophyll biosynthesis. These molecules compete for the tetrapyrrole-binding site on the enzyme, which impedes the binding of protoporphyrinogen. Hence, protoporphyrinogen production is inhibited, leading to reduced levels of heme and chlorophyll. As a result, plants treated with such herbicides appear chlorotic (yellow colored) due to their ability to produce

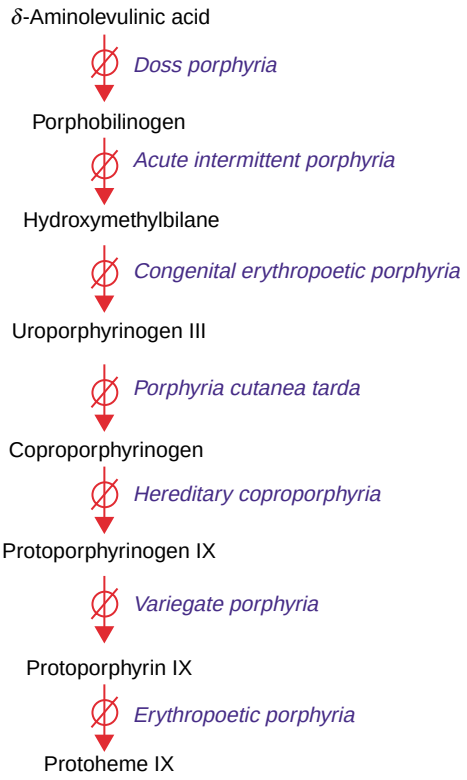

FIGURE 4 The porphyrias. The porphyric disorders that characterize deficiencies in specific parts of the heme biosynthetic pathway are shown in blue.

carotenoids but not chlorophylls. The action of these herbicides is characterized by the accumulation of protoporphyrinogen IX. This diffuses out of the plastids/mitochondria and is oxidized to protoporphyrin IX, either via non-enzymatic means or catalyzed by peroxidase. This mislocation of protoporphyrin IX leads to phototoxicity through the evolution of singlet oxygen species.

See Also the Following Articles

Chlorophylls and Carotenoids • Cytochrome P-450 • Heme Proteins • Heme Synthesis • Vitamin B_{12} and B_{12}-Proteins

Glossary

chelation The removal of free metal ions from solution by an organic chemical.

herbicide Chemical agent used to curtail plant growth.

plastid Generic name for chloroplasts and chloroplast precursors.

singlet oxygen A reactive oxygen radical with a single unpaired electron.

Further Reading

Beale, S. I. (1999). Enzymes of chlorophyll biosynthesis. *Photosyn. Res.* **60**, 43–73.

Bottomly, S. S., and Muller-Eberhard, U. (1988). Pathophysiology of heme synthesis. *Semin. Hematol.* **25**, 282–302.

Dailey, H. A. (1997). Enzymes of heme biosynthesis. *J. Biol. Inorg. Chem.* **2**, 411–417.

Falk, J. E. (1964). *Porphyrins and Metalloporphyrins: Their General, Physical and Coordination Chemistry, and Laboratory Methods*. Elsevier, Amsterdam.

Kadish, K. M., Smith, K., and Guilard, R. (2003a). The iron and cobalt pigments: Biosynthesis, structure, and degradation. In *The Porphyrin Handbook*, Vol 12. Academic Press, San Diego.

Kadish, K. M., Smith, K., and Guilard, R. (2003b). Chlorophylls and bilins: Biosynthesis, structure, and degradation. In *The Porphyrin Handbook*, Vol 13. Academic Press, San Diego.

Warren, M. J., and Scott, A. I. (1990). Tetrapyrrole assembly and modification into the ligands of biologically functional cofactors. *Trends Biochem. Sci.* **15**, 486–491.

Warren, M. J., Jay, M., Hunt, D. M., Elder, G. H., and Röhl, J. C. G. (1996). The maddening business of King George III and porphyria. *Trends Biochem. Sci.* **21**, 224–231.

Biography

Harry A. Dailey received a B.A. (bacteriology) in 1972 and a Ph.D. (microbiology) in 1976 from UCLA. He joined the Department of Microbiology at the University of Georgia in 1980 as an Assistant Professor following postdoctoral studies at the University of Connecticut Health Center. He served as Head, Department of Microbiology at UGA (1987–1996) and was appointed Director of the Biomedical and Health Sciences Institute in 2001. His research interests involve heme biosynthesis and the genetic diseases named porphyrias.

Mark Shepherd received a B.Sc. (1999) (Biochemistry) and a Ph.D. (2003) from the University of Sheffield. He then moved to the University of Georgia to perform postdoctoral research in the laboratory of Harry A. Dailey. His research interests involve the enzymology of heme and chlorophyll biosynthesis.

Pre-tRNA and Pre-rRNA Processing in Bacteria

Sidney R. Kushner
University of Georgia, Athens, Georgia, USA

In bacteria, tRNAs and rRNAs represent the large majority of RNA molecules found inside cells. rRNAs along with a variety of ribosomal proteins are the structural components of the ribosomes, the macromolecular complexes that carry out protein synthesis. In an exponentially growing bacterium such as *Escherichia coli*, there are 30 000–45 000 ribosomes per cell. tRNAs are also required for protein synthesis, being the molecules that bring individual amino acids to the ribosome for the process of peptide bond synthesis. Both of these types of RNA molecules are very stable and are essential for cell viability.

Interestingly, tRNAs and rRNAs are synthesized as parts of larger precursor molecules that must be processed to generate the mature forms that are either incorporated into ribosomes or that can be charged with amino acids. The processing of these RNA molecules is carried out by a series of ribonucleases that have very specific functions. These processing reactions, as described, have been studied extensively in *E. coli*, but may be significantly different in other bacteria.

tRNAs

Mature tRNAs are relatively small molecules that can range in length from 73 to 94 nucleotides (Figure 1). In order for them to be functional, they must contain the trinucleotide CCA at their 3′ termini (Figure 1) to which specific amino acids can be covalently attached. In some bacteria such as *E. coli* the CCA is encoded in the DNA. In others, the CCA has to be added posttranscriptionally to some of the tRNAs transcripts. In addition, there can be multiple tRNAs that can be charged with the same amino acid. For example, in *E. coli* there are 86 tRNA genes even though there are only 21 amino acids. Each tRNA folds into a characteristic cloverleaf structure (Figure 1), most likely during or even prior to the various processing events.

Primary Structure of tRNA Genes

Although there are large numbers of tRNA genes in each bacterium, they are not clustered in one specific region of the genome. Rather, they may exist as independent genes (Figure 2A), in a group of tRNA genes that are all transcribed from a single promoter (Figure 2B), in a group of genes that also include mRNAs or embedded in an operon that contains rRNA genes (Figure 2C). In all cases, the tRNA transcripts contain extra nucleotides (Figure 2, black lines) that must be removed to generate the mature, functional tRNAs that can be recognized by their respective aminoacyl transferases, the enzymes that specifically charge each of the tRNAs with the appropriate amino acid.

Enzymatic Processing of tRNA Precursors

Some features of tRNA processing have been universally conserved, while others may be specific to certain classes of bacteria. For example, the mature 5′ terminus of every tRNA is generated by an endoribonuclease called RNase P. This enzyme is composed of a catalytic RNA and a protein subunit, and is found in both prokaryotes and eukaryotes. However, at least in *E. coli*, RNase P cleavage requires prior processing at the 3′ terminus. Thus, in the initial processing step for most, if not all, *E. coli* tRNAs, RNase E cleaves endonucleolytically near the mature CCA sequence (1–3 nucleotides downstream, Figure 3, blue arrows). Cleavage by this enzyme is required whether the tRNA is a monocistronic transcript (Figure 3A) or exists as part of a polycistronic operon (Figure 3B).

Following RNase E processing, RNase P cuts at the 5′ end (Figure 3, red arrows), generating the mature terminus. Subsequently, the few extra nucleotides found at the 3′ terminus are removed exonucleolytically by a combination of RNase T, RNase D, RNase BN, RNase II, RNase PH, and possibly polynucleotide phosphorylase (Figure 3, dashed orange arrows). Based on the substrate preferences of these various 3′ → 5′ exonucleases, RNase T appears to be the most important of the various enzymes. In the case of organisms where the 3′ CCA nucleotides are not encoded in the DNA, an enzyme called tRNA nucleotidyltransferase is capable of

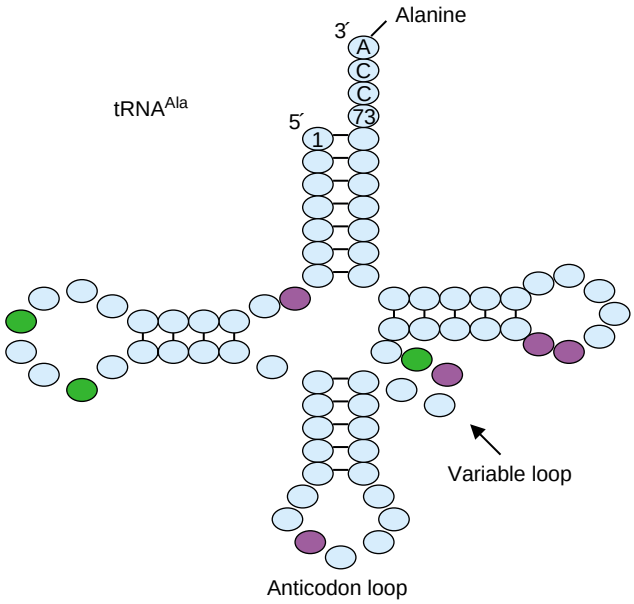

FIGURE 1 Schematic drawing of *Escherichia coli* alanine tRNA. This particular tRNA contains 76 nucleotides. The green ovals indicate positions at which one nucleotide may be deleted yielding tRNAs between 73–75 long or additional nucleotides can be added, yielding species up to 94 nucleotides in length. The magenta ovals indicate the locations of bases that are modified posttranscriptionally in this tRNA. Each tRNA has a unique pattern of base modification. The anticodon loop, used for reading the messenger RNA, as well as the CCA at the 3′terminus are indicated. The short black lines indicate positions of Watson–Crick base pairing.

adding the two Cs and one A, using CTP and ATP as substrates, to generate the mature 3′ terminus. Most bacteria contain this enzyme, which can also be used to repair 3′ termini that have been partially degraded during the exonucleolytic processing reactions (Figure 3A).

Modification of Individual Bases in tRNAs

Although tRNAs are synthesized using the standard nucleoside triphosphates containing either adenine, uracil, guanine or cytosine, each tRNA contains a number of modified bases that are generated posttranscriptionally (Figure 1). For example, a common modification involves the replacement of an oxygen atom at the 3 position of uracil with a nitrogen atom, generating a new base called pseudouracil. Additional alterations arise by the addition of methyl groups at specific locations. Some modifications occur through a single enzymatic step (methylation), while others require a series of biosynthetic steps (1-methylinosinic acid). Research has shown that only some of the modified bases are required for normal tRNA function. Many of the modifications are found not only in bacteria but in eukaryotic organisms as well.

rRNAs

rRNAs provide the structural core to which ribosomal proteins bind to form both the 30S and 50S bacterial ribosomal subunits. The 16S rRNA is found in the 30S subunit while the 23S and 5S species are located in the 50S ribosomal subunit. Numerous ribosomal proteins are associated with each subunit but recent crystallographic data suggest that it is the RNA component of the 50S subunit that catalyzes peptide bond formation. In bacteria all three rRNA species are transcribed as part of a single polycistronic transcript (30S) in the order of 16S, 23S, and 5S (Figure 2C). In addition, the rRNA genes are duplicated in most bacteria (seven copies in *E. coli*) and generally contain one or more tRNAs (Figure 2C).

Primary Processing

The primary 30S rRNA transcript is cleaved during its synthesis by the endoribonuclease RNase III. This enzyme recognizes specific stem-loop structures that are generated by inverted repeats within the RNA transcript. In bacteria, the 16S and 23S rRNAs form two adjacent stem-loop structures (Figure 4). RNase III

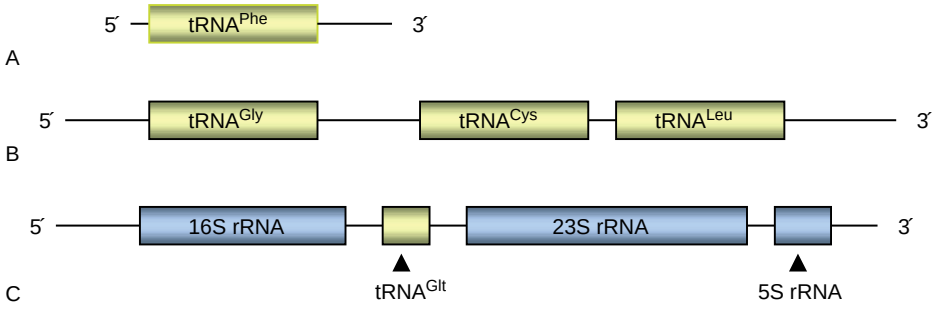

FIGURE 2 Organization of tRNA and rRNA genes. (A) The monocistronic phenylalanine tRNA gene from *E. coli*. (B) The polycistronic operon from *E. coli* containing glycine, cysteine, and leucine tRNA genes. (C) One of seven *E. coli* rRNA operons (*rrnB*) containing the sequences for 16S, 23S, and 5S rRNAs, as well as a glutamine tRNA. Colored boxes (yellow for tRNAs and blue for rRNAs) represent what will become the mature sequences. Black lines indicate sequences that will be removed by nucleolytic processing reactions.

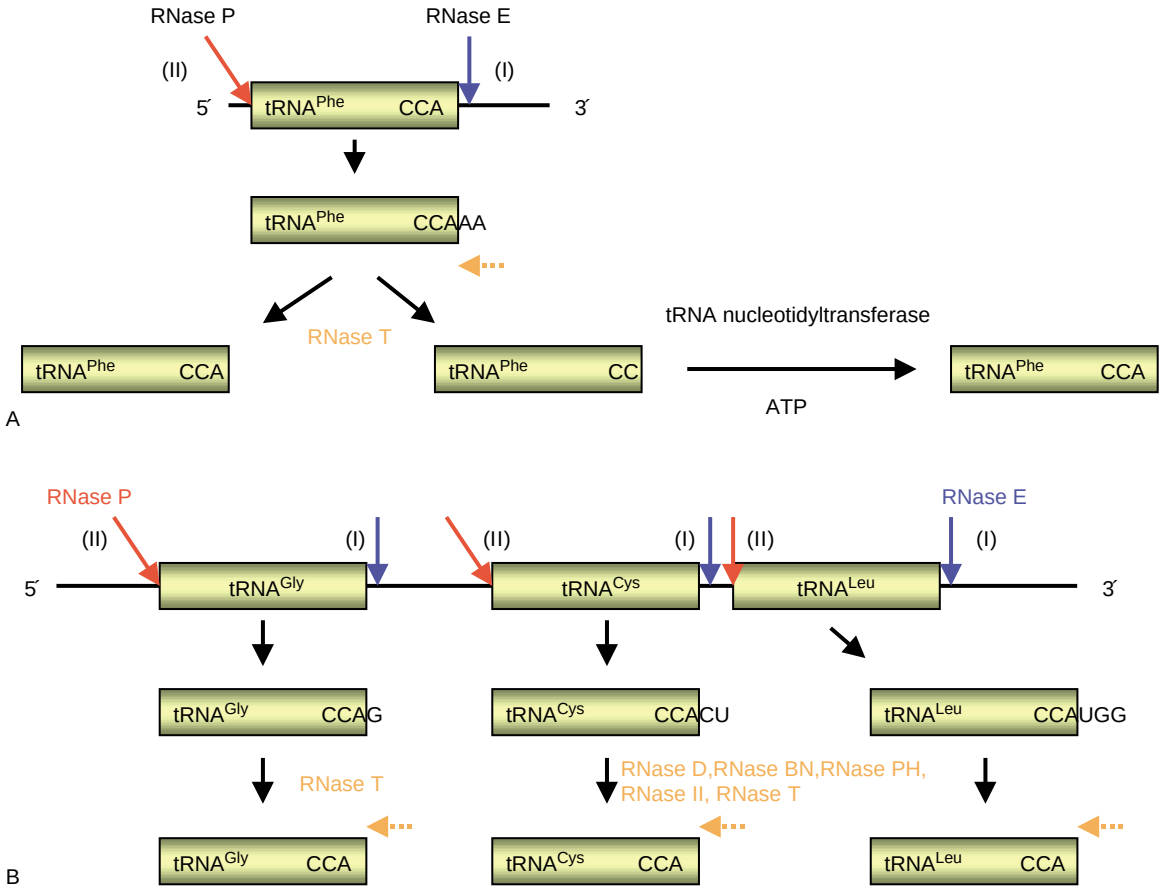

FIGURE 3 Processing of tRNAs in *E. coli*. (A) With a monocistronic operon, the initial cleavage (I) at the 3′ end is catalyzed by RNase E (blue arrow), followed by RNase P processing (red arrow) at the 5′ end (II). While RNase P cleavage generates the mature 5′ terminus, RNase E cleavage leaves a small number of extra nucleotides at the 3′ end. Based on extensive analysis of the various 3′ → 5′ exonucleases found in *E. coli*, it appears that RNase T (dashed orange arrow) is primarily responsible for processing the phenylalanine tRNA. If, however, RNase T removes one too many nucleotides, the A residue can be restored by the action of tRNA nucleotidyltransferase. (B) In the case of a polycistronic operon, the first series of cleavage reactions is again carried out by RNase E (blue arrows) (I). Subsequently, RNase P cuts (red arrows) at the 5′ end (II). Final processing normal involves RNase T (dashed orange arrow). In some cases, additional riboexonucleases, as indicated, are also required.

cleaves on both sides of each stem (Figure 4, magenta arrows). In one case, a 17S precursor of what will become the mature 16S rRNA is released. This molecule contains an extra 115 nucleotides at its 5′ terminus and 33 nucleotides at the 3′ terminus. In the case of the 23S rRNA, RNase III cleavage leaves an extra 3 or 7 nucleotides at the 5′ terminus and 7–9 nucleotides at the 3′ terminus. The RNase III cleavages release the 5S rRNA as part of a 9S precursor.

Generation of Mature rRNAs

16S rRNA

Recent studies have shown that the mature 5′ terminus of 16S rRNA is generated as a two-step process in which RNase E initially cuts endonucleolytically to remove 49 nucleotides from the immature 5′ end (Figure 4, blue arrow). Following this step RNase G cleaves to generate the mature 5′ end (Figure 4, green arrow). Removal of the extra 33 nucleotides at the 3′ end is thought to also occur endonucleolytically, even though the actual enzyme responsible for this processing event has not yet been identified (Figure 4, brown arrow).

23S rRNA

For the 3′ end of the immature 23S rRNA, experiments have indicated that a combination of polyadenylation and the activity of several exoribonucleases serve to generate the mature terminus (Figure 4, dashed orange arrows). In particular, RNase T appears to be the primary exonuclease involved in this process, but additional RNases such as RNase PH, RNase BN, RNase D and RNase II probably also participate. It is not known at this time how the extra nucleotides are removed from the 5′ end (Figure 4, brown arrow).

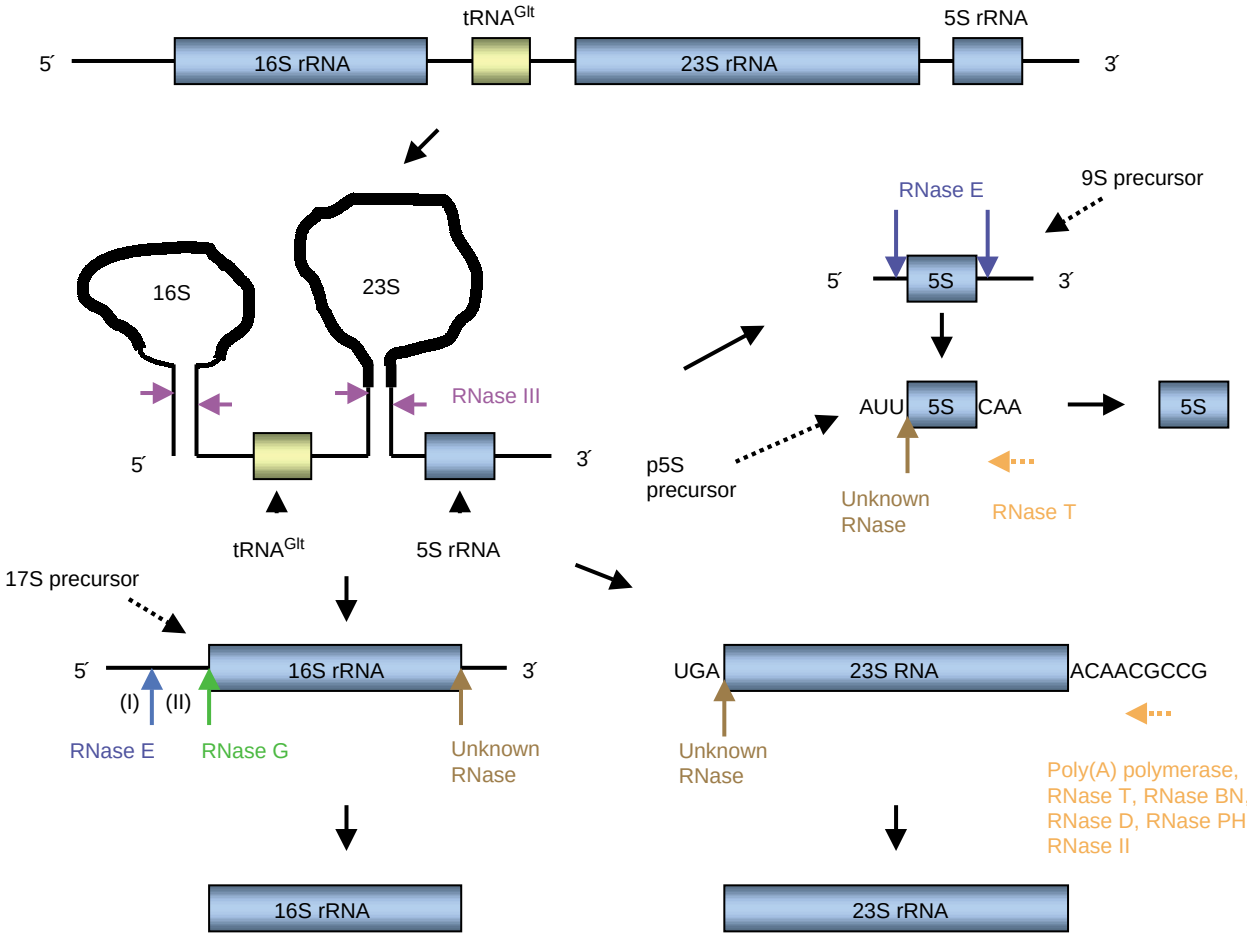

FIGURE 4 Processing of rRNA in *E. coli*. The polycistronic rRNA operon is shown initially in a linear form. Because of the presence of inverted repeats two double-stranded stems form, which loop out both the 16S and 23S rRNA sequences (thick lines). These stem-loop structures are recognized by RNase III (magenta arrows), which cuts on both sides of each stem to release pre16S (17S), 23S, and 9S species. The 17S species contains 115 extra nucleotides at the 5′end and 33 nucleotides at the 3′end. Processing at the 5′end involves a sequential series of reactions involving RNase E (blue arrow) first (I) followed by RNase G (green arrow) (II) to generate the mature 5′ end. An unknown endoribonuclease (brown arrow) is thought to generate the mature 3′ terminus. With the 23S rRNA, there are a few extra nucleotides at the 5′ end that are removed by an unidentified as yet RNase (brown arrow). At the 3′ end the extra 7–9 nucleotides are removed by a combination of polyadenylation and 3′ → 5′ exonucleases (dashed orange arrow). To generate 5S rRNA, RNase E (blue arrows) cuts the 9S precursor at both the 5′ and 3′ ends to release a p5S form that has three extra nucleotides at either end. RNase T (dashed orange arrow) processes the 3′ end, while the 5′ end is matured by an unknown ribonuclease (brown arrow). Processing of the glutamine tRNA is as described in Figure 3B.

However, since no 5′ → 3′ riboexonucleases have been identified in *E. coli*, it is presumed that this processing is carried out by an endoribonuclease.

5S rRNA

The 9S precursor, formed by RNase III cleavage of the 30S transcript, is cut twice by RNase E to release a p5S molecule (Figure 4, blue arrows). The p5S form contains three additional nucleotides at either end. In *E. coli*, RNase T has been shown to be essential for the removal of the extra nucleotides at the 3′ end (Figure 4, dashed orange arrow). It is not known how the 5′ end is processed (Figure 4, brown arrow).

Processing Differences among Various Bacterial Species

While the general genomic organization of the rRNA operons and tRNAs is conserved among bacterial species, it is not clear whether the processing reactions are identical in all organisms. For example, while certain enzymes such as RNase III and RNase P are highly conserved in large numbers of prokaryotes, others such as RNase G, RNase E, and RNase T, are found only in a limited number of bacteria. For example, RNase T homologues have been identified in gram-negative bacteria but have not been found in gram-positives. In addition, neither RNase E, RNase

G, nor RNase II exists in the Gram-positive organism *Bacillus subtilis*. Thus, while some aspects of processing are highly conserved in bacteria (RNase III cleavage of the 30S rRNA precursor and 5′ end processing of tRNAs by RNase P), there is probably considerable variation in the other aspects of processing.

What Happens when Processing is Defective?

Since mutations in either RNase E or RNase P lead to cell death, tRNA processing is essential for cell viability. This is not overly surprising because an immature 3′ terminus of a tRNA cannot be charged with the appropriate amino acid. Without charged amino acids, protein synthesis will not take place. This presumably is the reason for the presence of redundant enzymes (RNase T, RNase PH, RNase BN, RNase D, and RNase II) capable of removing the few remaining nucleotides at the 3′ terminus following RNase E cleavage. Loss of any one of these exoribonucleases does not compromise cell viability, as long as the others remain active. In addition, if processing happens to remove the 3′ terminal A, tRNA nucleotidyltransferase functions to restore a functional 3′ terminus (Figure 3A).

In contrast, the requirements for rRNA maturation are not as strict. Immature forms of 16S rRNA, 23S rRNA, and 5S rRNA can be incorporated into ribosomes that are biologically active. In addition, there are probably backup processing pathways for rRNA. For example, in RNase III mutants of *E. coli*, full-length 30S rRNA precursors are observed, but the cell is still viable. Under these circumstances, it is quite likely that alternative processing is carried out by either RNase G or RNase E. In *B. subtilis*, which lacks both these enzymes, RNase III is essential for cell viability.

See Also the Following Articles

Ribosome Assembly • Ribosome Structure

Glossary

polarity RNA molecules have 5′ and 3′ ends (termini) which are named for the orientation of the 5′ and 3′ carbon atoms of the ribose rings in the sugar/phosphate backbone.

riboendonuclease An enzyme that degrades a RNA molecule at internal locations.

riboexonuclease An enzyme that degrades an RNA molecule, one nucleotide at a time. If the enzyme initiates the degradation from the 3′ terminus it is called a 3′ → 5′ riboexonuclease.

sedimentation coefficient (*S*) Named after the Swedish scientist Svedberg, the *S* value is an indication of the size of a large macromolecule. It is based on the mobility of large molecules in a centrifugal field. Thus, the higher the number the larger the molecule.

Further Reading

Deutscher, M. P., and Li, Z. (2001). Exoribonucleases and their multiple roles in RNA metabolism. *Prog. Nucl. Acid Res. Mol. Biol.* **66**, 67–105.

Gopalan, V., Vioque, A., and Altman, S. (2002). RNase P: Variations and uses. *J. Biol. Chem.* **277**, 6759–6762.

Li, Z., and Deutscher, M. P. (1995). The tRNA processing enzyme RNase T is essential for maturation of 5S RNA. *Proc. Natl Acad. Sci. USA* **92**, 6883–6886.

Li, Z., Pandit, S., and Deutscher, M. P. (1999). Maturation of 23S ribosomal RNA requires the exoribonuclease RNase T. *RNA* **5**, 139–146.

Li, Z., Pandit, S., and Deutscher, M. P. (1999). RNase G (CafA protein) and RNase E are both required for the 5′ maturation of 16S ribosomal RNA. *EMBO J.* **18**, 2878–2885.

Ow, M. C., and Kushner, S. R. (2002). Initiation of tRNA maturation by RNase E is essential for cell viability in *Escherichia coli*. *Genes Develop.* **16**, 1102–1115.

Zuo, Y., and Deutscher, M. P. (2002). The physiological role of RNAse I can be explained by its unusual substrate specificity. *J. Biol. Chem.* **277**, 29654–29661.

Biography

Sidney Kushner is a Professor and former Head of the Department of Genetics at the University of Georgia. His research focuses on understanding the molecular mechanisms of RNA processing and decay, as well as polyadenylation in bacteria. He holds a Ph.D. from Brandeis University and was a Postdoctoral Fellow at the University of California, Berkeley and Stanford University. He is a Fellow of the American Association for the Advancement of Science and the American Academy of Microbiology.

Pre-tRNA and Pre-rRNA Processing in Eukaryotes

Hendrik A. Raué
Vrije Universiteit, Amsterdam, The Netherlands

The two most abundant stable RNA species in eukaryotic cells, tRNA and rRNA, are synthesized in the form of precursor molecules containing extra sequences not present in the mature molecules. By processing the ordered removal of these extra sequences by exo- and/or endonucleases is meant and, in the case of tRNA, covalent linkage of the fragments arising from removal of an internal region (splicing). In a wider sense, processing also encompasses various types of modification of particular nucleotides, as well as addition of nucleotides that are not encoded in the DNA (editing). This article describes the present knowledge of the mechanisms responsible for pre-tRNA and pre-rRNA processing. The emphasis is on the yeast *Saccharomyces cerevisiae*, where this processing has been studied in greatest detail. However, the general principles, and even many of the details, apply to most other eukaryotes as well.

Pre-tRNA Processing

Eukaryotic tRNAs are generally synthesized as individual precursor molecules that contain extra sequences at both the 5′- and 3′-end, called leader and trailer, respectively. Some, though not all, pre-tRNAs also contain an intron, which is always located directly downstream (i.e., 3′) from the anticodon. Consequently, the conformation of the mature domain of the tRNA is largely conserved in its precursor and structural features of this mature domain are in fact the major recognition elements for the various processing enzymes (Figure 1A).

Processing of eukaryotic pre-tRNA takes place in the nucleus and only fully processed tRNAs are recognized by the export machinery that transfers them to the cytoplasm (Figure 1B). However, there does not seem to be an obligatory order of the different steps leading from the pre-tRNA to the mature molecule.

Removal of Precursor-Specific Sequences

5′-End Processing

Removal of the 5′-leader region is normally the first event in eukaryotic pre-tRNA processing. It is carried out by the nuclear endonuclease RNase P, a ribonucleoprotein complex that has orthologues in eubacteria and archaebacteria, as well as in mitochondria and chloroplasts. RNase P contains a single, small RNA molecule the conformation of which, though not the sequence, has been strongly conserved from bacteria to man. This RNA molecule is associated with a variable number of proteins, depending on the organism, that show a lesser degree of conservation.

The substrate for RNase P is a complex of pre-tRNA and the La protein which binds to the 3′-end of the precursor immediately after termination of transcription. Substrate recognition is mainly based upon the consensus tertiary structure of the mature domain of the pre-tRNA, but the 3′-trailer region also contributes to efficient cleavage by RNase P.

In yeast 5′-end maturation of pre-tRNAs takes place mostly in the nucleolus, a specialized region of the nucleus not bound by a membrane that is also involved in the first stages of pre-rRNA processing (Figure 1B). However, 5′-end maturation can also occur in the nucleoplasm, though it is as yet unclear whether this applies to a small portion of all pre-tRNAs or only to a few specific pre-tRNA species. All subsequent steps in yeast pre-tRNA maturation occur in the nucleoplasm. In mammalian cells, the situation seems to be reversed with most 5′-end processing occurring in the nucleoplasm.

3′-End Processing

Removal of the 3′-trailer sequence follows cleavage by RNase P and is performed by, as yet, an unidentified endonuclease that acts upon the precursor/La-protein complex. In the absence of bound La-protein both the timing and the mechanism of 3′-end processing are altered. The naked pre-tRNA is first attacked by 3′ → 5′ exonucleases that remove the portion of the 3′-trailer not base-paired to the leader. Removal of the latter by RNase P, then exposes the remainder of the trailer to further exonucleolytic digestion.

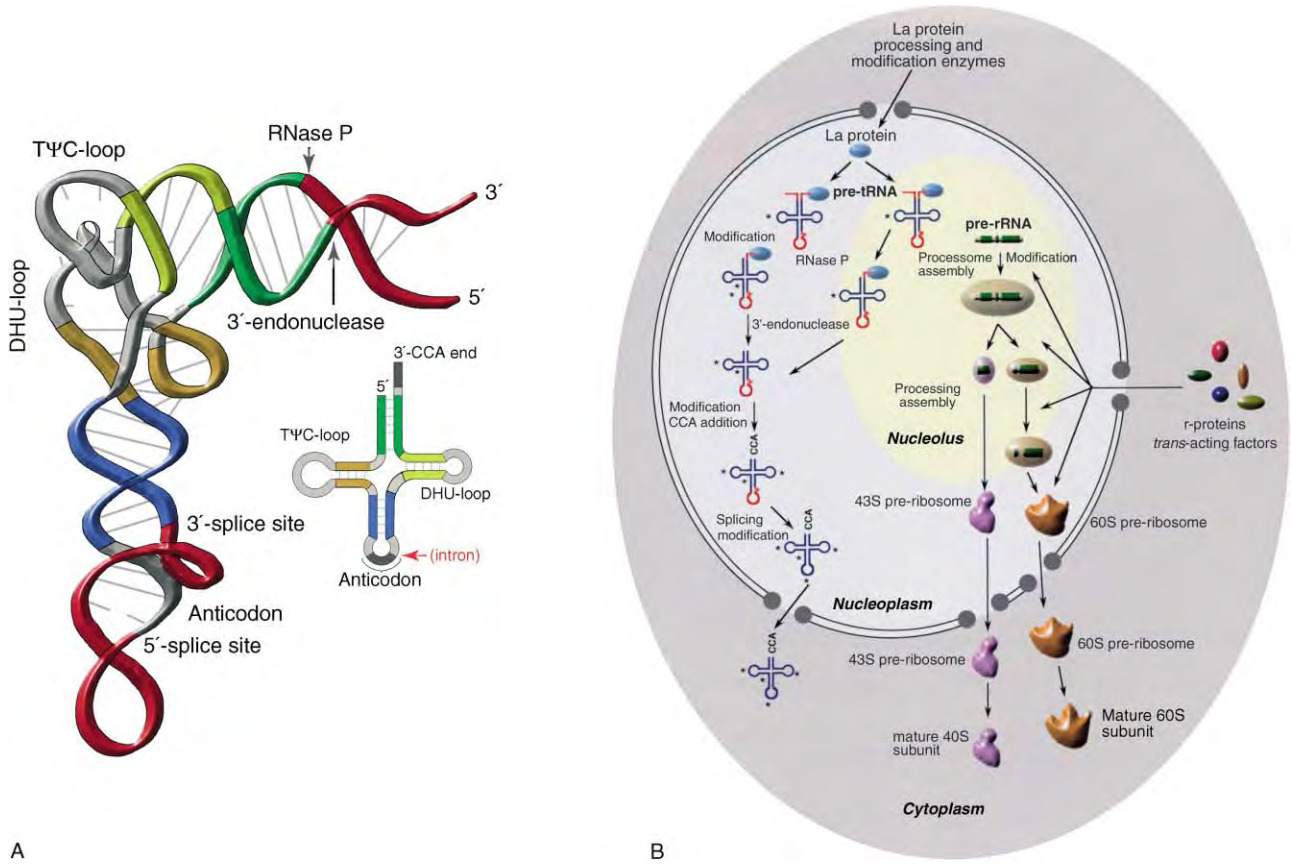

FIGURE 1 Overview of pre-tRNA processing and pre-rRNA processing/assembly in eukaryotic cells. (A) Conformation of pre-tRNA. The various regions are color-coded in the same manner as in the 2D model. Leader, trailer, and intron are in red. The mature domain of the precursor has essentially the same conformation before and after processing. (B) Subcellular localization. As discussed in the text pre-tRNA processing takes place in both the nucleolus and the nucleoplasm. Note that nucleotide modifications (indicated by asterisks) occur – in a specific order – at various stages. Pre-rRNA processing and its assembly with ribosomal proteins starts in the nucleolus with later stages taking place in the nucleoplasm. The finishing steps in formation of functional ribosomal subunits occur in the cytoplasm. In yeast this includes the final processing of 20S pre-rRNA into mature18S rRNA. In other eukaryotes the latter also occurs in the nucleoplasm. Export of tRNA and each of the two types of ribosomal subunits to the cytoplasm occurs by different pathways, which, however, do share some components. Note the nuclear pores are not selective for either the type of macromolecule to be transported or the direction of transport.

Removal of the Intron (Splicing)

Splicing is normally a late step in pre-tRNA processing, although under particular conditions it can occur prior to end maturation. Splicing involves the consecutive action of three enzymes. First, a splicing endonuclease cleaves the phosphodiester bonds at both ends of the intron. The yeast enzyme is a multi-subunit, integral membrane protein that may be located in the inner nuclear envelope. It contains two distinct active sites, one for each of the two splice sites. The enzyme selects the splice sites primarily by measuring their distance from specific structural features in the mature domain, using different features for each site. The intron, however, also contributes to this specific recognition.

The two, base-paired tRNA fragments left by the endonuclease are converted into a contiguous molecule by tRNA ligase in a complex three-step reaction that leaves a 2′-phosphate at the junction. This phosphate is removed by the third enzyme, an unusual NAD-dependent phosphotransferase.

Changes in Nucleotide Sequence of the Mature Domain

Addition of the 3′-CCA End

In contrast to their eubacterial counterparts, eukaryotic tRNA genes do not encode the 3′-CCA-end essential for tRNA function. These three nucleotides are added to the 3′-end formed after removal of the trailer by ATP[CTP]:tRNA nucleotidyltransferase. A cytoplasmic version of this enzyme is probably involved in repair of damaged CCA-ends.

Modification

tRNAs contain ~80 different types of modified nucleotide. All modifications are carried out by specialized

proteinaceous enzymes, that, depending upon their nature act on the primary precursor transcript, on one of the processing intermediates or possibly even on the cytoplasmic tRNA. Since in yeast most of the tRNA modifications studied are nonessential the presence of modified nucleotides probably serves to fine-tune tRNA function.

Pre-rRNA Processing

Each eukaryotic, cytoplasmic ribosome contains single copies of four different rRNA species. The18S rRNA (1500–2300 nucleotides, or nt) is part of the small (40S) subunit, while the large (60S) subunit contains 5S (~120 nt), 5.8S (~150 nt), and 25/28S rRNA (3400–5000 nt). The 18S, 5.8S, and 25/28S rRNAs are encoded by one or more sets of tandemly repeated rDNA units, each of which is transcribed by RNA polymerase I into a single long pre-rRNA molecule (35–45S), containing external transcribed spacers (ETS) at both ends (5′- and 3′-ETS) as well as two internal transcribed spacers (ITS1 and ITS2) that separate the coding regions (Figure 2). In *S. cerevisiae*, a single 5S rRNA gene is embedded in the DNA that separates two consecutive rDNA units, whereas in higher eukaryotes the 5S rRNA genes are scattered throughout the genome, often in clusters. All 5S rRNA genes are transcribed individually by RNA Polymerase III into a precursor carrying a short 3′-ETS.

Removal of the transcribed spacer sequences from the primary precursor transcript occurs in an ordered series of endo- and exonucleolytic steps, which, in the case of the 35–45S precursor, is preceded by modification.

Pre-rRNA transcription, a large portion of its maturation, i.e., modification and processing, as well as ordered association of the intermediate precursor species with most of the ribosomal proteins (r-proteins), takes place in the nucleolus. Later stages occur in the nucleoplasm and formation of functional ribosomal subunits is completed in the cytoplasm (Figures 1 and 3).

Modification of Pre-rRNA

Modification of pre-rRNA is limited to the mature 18S and 25/28S rRNA sequences and consists mostly of two types: conversion of U residues into Ψ (pseudouridylation) and 2′-*O*-methylation of the ribose moiety of nucleotides. A few nucleotides are base-methylated. The number of modified nucleotides increases with increasing complexity of the organism but most of the modifications found in lower eukaryotic cells (e.g., yeast) are conserved in higher eukaryotes, including man. 2′-*O*-Methylation and pseudouridylation take place on the primary pre-rRNA transcript and are carried out by two classes of small nucleolar ribonucleoprotein particles (snoRNPs). A collection of box C/D snoRNPs is responsible for methylation, whereas a similar collection of box H/ACA snoRNPs perform the U → Ψ conversions. The names refer to common primary and secondary structural features present in the RNA component of each member of that class. Each box C/D or box H/ACA snoRNA also contains at least one, and sometimes two, specific "guide" sequence(s) that are complementary to the rRNA region(s) containing the modification site. The specific rRNA/snoRNA base-pairing guides the modifying enzyme, which is an integral part of the snoRNP, to its target nucleotide. Base-methylation, occurs at later stages of ribosome formation and is carried out by conventional proteinaceous enzymes.

Experiments with yeast cells indicate that rRNA modification is not essential for ribosome formation or function but does strongly enhance functional efficiency of the ribosome.

Removal of the Spacer Regions

The Processing Pathway

In *S. cerevisiae*, the first detectable precursor of 18S, 5.8S, and 25S rRNA is called 35S pre-rRNA. This precursor has already lost most of the 3′-ETS due to endonucleolytic cleavage that occurs before its transcription has been terminated. The pathway by which the 35S precursor is subsequently converted into the mature rRNAs is depicted in Figure 2A.

Maturation of 35S pre-rRNA starts with the removal of the 5′-ETS by two successive cleavages, which produce first the short-lived 33S and then the 32S species. The latter is cleaved within ITS1 separating the small subunit 20S pre-rRNA from the 27SA2 large subunit intermediate. Processing of 20S pre-rRNA is completed in the cytoplasm by endonucleolytic cleavage at the mature 3′-end of 18S rRNA. So far none of the nucleases involved in these processing steps have been identified.

Processing of yeast 27SA2 pre-rRNA is more complicated and occurs via two separate pathways that produce the same 25S rRNA, but two distinct species of 5.8S rRNA whose 5′-ends differ by 6 nucleotides, in ratio of about 10:1 (Figure 2A). The physiological relevance of this phenomenon remains unclear.

As would be expected for such a vital process pre-rRNA processing shows considerable plasticity, which is revealed in cells in which a particular processing step is disturbed by a mutation in either the pre-rRNA or in an accessory factor. The 5′-ETS can be removed in a single step by cleavage at the 5′-end of the 18S rRNA sequence. Initial cleavage within ITS1 can occur at A3 instead of A2 giving rise to an aberrant 21S small subunit pre-rRNA that is still efficiently converted into 18S rRNA. When cleavage at A3 is prevented almost all of the 27SA2 pre-rRNA is processed via the "long" pathway

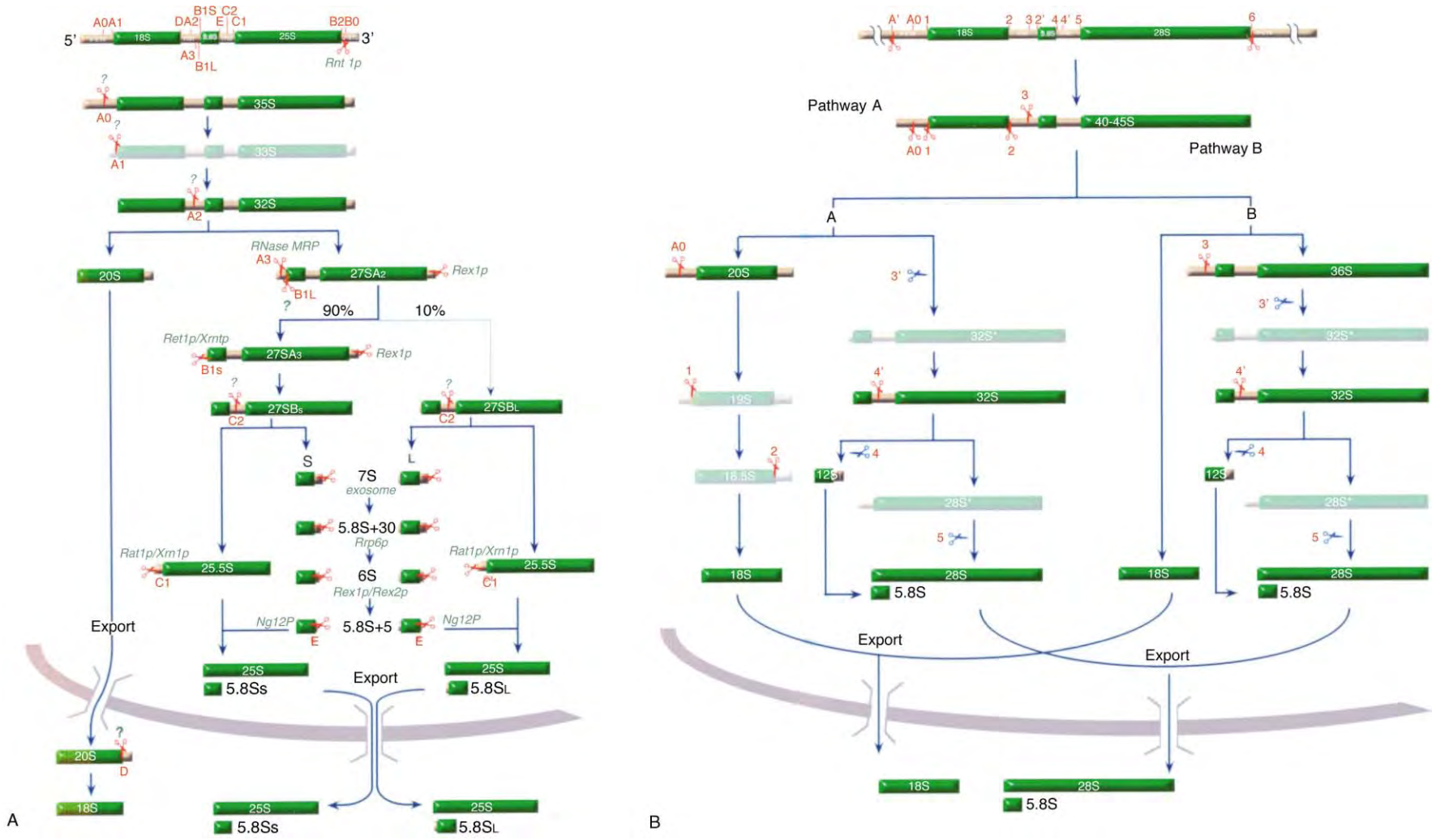

FIGURE 2 Pre-rRNA processing pathways in lower (panel A; *S. cerevisiae*) and higher (panel B) eukaryotic cells. The structure of the primary transcript including the processing sites is depicted at the top with the processing intermediates below. Regions encoding the mature rRNAs are in green, spacer regions are in brown. Light-colored intermediates are short-lived and not detectable under normal conditions. Vertical and horizontal scissors indicate endonucleolytic cleavages and exonucleolytic trimming, respectively. Blue scissors in panel B indicate that the nature of the processing step is unknown but, by analogy with yeast is likely to be exonucleolytic. Where known the enzyme(s) involved in a particular processing step is (are) identified. A question mark indicates that the enzyme is still unknown.

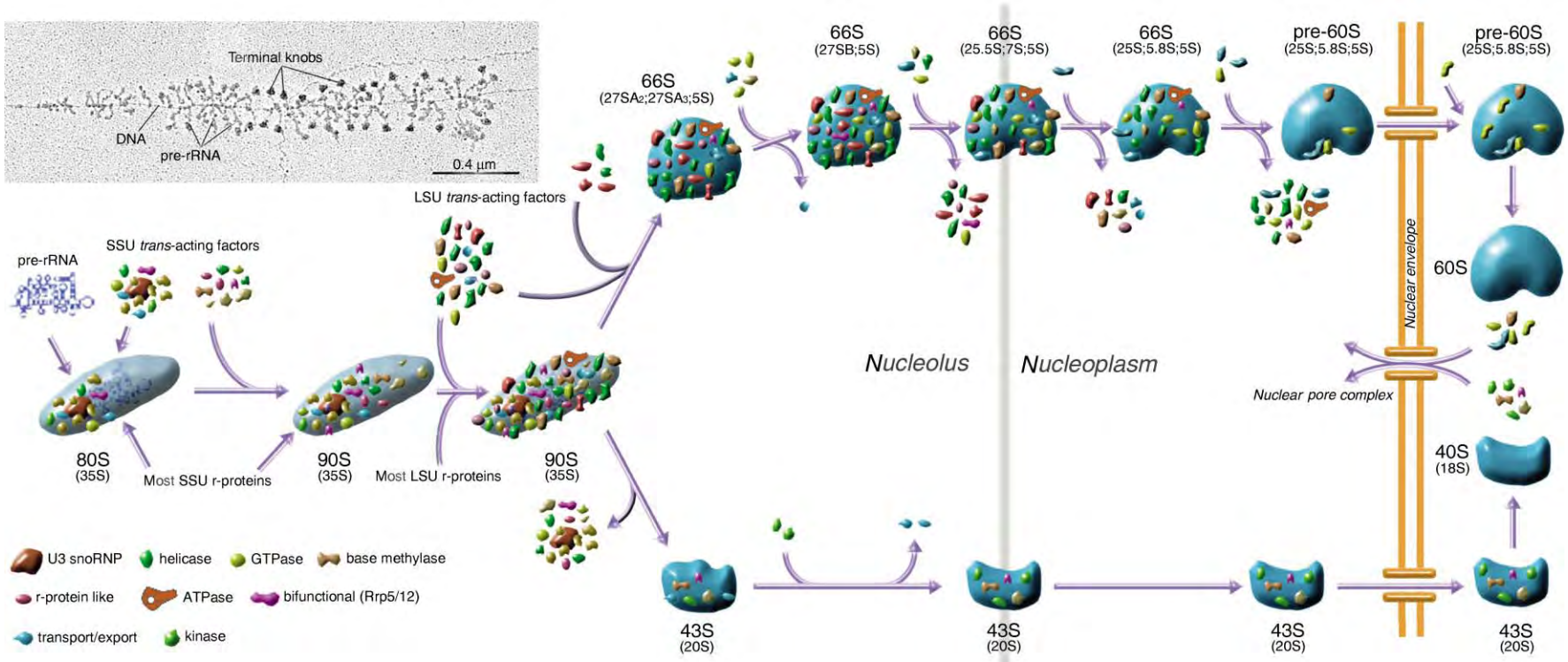

FIGURE 3 The pre-rRNA processing/assembly machinery in *S. cerevisiae*. The different intermediate pre-ribosomal particles so far identified are shown with their S value and, in parentheses, their pre-rRNA constituents. Note that the number of intermediates is tentative as is the nature of the components that associate or dissociate at the various stages. The inset shows an EM picture of the 'terminal balls' thought to correspond to the early stage in assembly of the 80S particle (photograph by Dr. Yvonne Osheim, University of Virginia).

producing 5.8S_L rRNA with little or no adverse effects on cell growth or maintenance.

Cleavage at site C2 is essential to initiate removal of ITS2 from either 27SB precursor but there is considerable redundancy among the exonucleases that remove the spacer nucleotides from the resulting 7S and 25.5S precursors.

Studies on pre-rRNA processing in other eukaryotes are limited mostly to *Drosophila*, *Xenopus laevis*, mouse and human and have not reached the same level of detail as those performed in *S. cerevisiae*. As shown in Figure 2B two pathways have emerged, of which the one labeled B is very similar, though not identical, to that of yeast. This pathway operates in *Xenopus* somatic cells, mouse and *Drosophila*. In *Xenopus* oocytes pre-rRNA processing can follow either pathway, even in the same cell, whereas pathway A occurs in human cells. In this pathway, cleavage at sites A0, 1, and 2 follows, rather than precedes processing at site 3.

Cis-Acting Elements

Correct and efficient processing of eukaryotic pre-rRNA is critically dependent upon structural features of the pre-rRNA (*cis*-acting elements). Such elements have been identified by *in vivo* mutational analysis, in particular in yeast, in both the mature and the spacer regions of the pre-rRNA. Some consist of short sequence elements, whereas for others their conformation, rather than their sequence, appears to be important. In only a few cases, the precise role of the element is known, e.g., the sequence spanning site A3, which constitutes the recognition element for RNase MRP.

Trans-Acting Factors

A large body of biochemical and molecular genetic studies, carried out mostly in yeast, have demonstrated that eukaryotic pre-rRNA processing and its assembly into functional ribosomes, apart from the ribosomal proteins, also requires a multitude of non-ribosomal factors. These *trans*-acting factors, whose number presently stands at ~200, include the modifying snoRNPs discussed before, a small number of additional snoRNPs (5 in yeast, including RNase MRP) and a large variety of proteins. Most have orthologues in other eukaryotes ranging from *C. elegans* to human, which underscores the strong evolutionary conservation of eukaryotic ribosome biogenesis.

Recent advances in the purification of large (ribonucleo) protein complexes by affinity chromatography (tandem-affinity-purification or TAP) and the identification of their constituents have clearly established that the *trans*-acting factors are the parts of two, essentially independent processing/assembly machineries (processomes) that govern formation of the small and large subunit, respectively. Both machineries are dynamic in nature, i.e., they lose particular components and acquire others in an ordered manner as subunit biogenesis progresses (Figure 3). Only two proteins have been found that are constituents of both the small and large subunit machinery.

Assembly of the small subunit (SSU) processome and the association of many of the SSU r-proteins on the pre-rRNA starts well before its transcription has been completed. The U3 box C/D snoRNP (which has no modification activity) plays a central role in the formation of the resulting 80S/90S pre-ribosome, the initial stages of which can be visualized as "terminal knobs" at the ends of the nascent transcripts by electron microscopy of an actively transcribed rDNA unit (inset in Figure 3). Actual processing is deferred, however, until the transcript has been released. Assembly of the large subunit (LSU) machinery starts a little later, immediately before cleavage at site A2 separates the 90S pre-ribosome into a 43S and a 66S particle, and many of the components of the LSU machinery may join only after this separation. Current, but definitely still incomplete, data indicate that the yeast 43S particle goes through at least two more stages before being exported to the cytoplasm, where cleavage at site D converts the 20S pre-rRNA into mature 18S rRNA. This final step requires several *trans*-acting factors that are coexported with the 43S particle and, after their release, are re-imported. The 66S pre-ribosome goes through at least five stages before an export-competent particle emerges that does contain the fully mature rRNA species but still has to undergo some structural rearrangement in the cytoplasm to acquire functionality. Again, some *trans*-acting factors needed for these finishing touches are already added in the nucleus and move back after having completed their task. Others may associate in the cytoplasm.

Studies on the specific function of the various *trans*-acting factors are still in their infancy. Comparative analysis, however, has identified several functional classes, whose role can at least be inferred (Figure 3). Nucleases constitute the most obvious, but also the most elusive, of these classes (Figure 2A). Remarkably, only one of the known processing nucleases (the $5' \rightarrow 3'$ exonuclease Xrn1p) has so far been detected in pre-ribosomes. A second class (19 members in yeast) is formed by proteins containing the signature motifs of RNA helicases. These proteins, therefore, could be involved in structural rearrangements of the pre-rRNA necessary for processing and assembly. Additional structural rearrangements may be carried out by a third class of proteins that show similarity to known GTPases or ATPases. A fourth class consists of proteins that may assist the association of particular r-proteins with the pre-ribosome. Circumstantial evidence points to the existence of at least two such assembly

chaperones for both the small and large subunit. Biochemical experiments have also identified several proteins involved in translocation of either the 43S or 66S pre-ribosome from the nucleolus to the nucleoplasm, while a considerable number has been implicated in export of either subunit to the cytoplasm. The latter include components of the generic nuclear export machinery as well as subunit-specific export factors. Four *trans*-acting factors have a structure strongly resembling that of a particular r-protein. It has been suggested that these rp-like proteins may play a role in timing the order of processing/assembly events by associating first and later giving way to their r-protein counterpart. A recent addition to this inventory are several protein kinases required for the final cytoplasmic step in 40S subunit formation.

This necessarily brief article leaves out the large majority of *trans*-acting factors for which little or no functional information is yet available. Obtaining this information and integrating it into a working model for the course of events in pre-rRNA processing/assembly is one of the major tasks for the future investigations into eukaryotic ribosome biogenesis.

See Also the Following Articles

Nucleolus, Overview • Ribosome Assembly • RNA Editing

Glossary

eukaryote Organism consisting of one or more cells containing a nucleus.

molecular genetics Changing the genetic make-up of an organism—often in a predetermined manner—by application of recombinant DNA technology.

nucleolus A distinct region within the nucleus where transcription of pre-rRNA and most of its processing and assembly with ribosomal proteins, as well as part of pre-tRNA maturation, takes place.

nucleoplasm The region of the nucleus not occupied by the nucleolus.

oocyte Unripe, unfertilized amphibian egg cell.

ribonucleoprotein A complex consisting of one or more RNA molecules associated with a number of proteins.

snoRNP Small nucleolar ribonucleoprotein particle.

somatic Of the body (somatic cell: differentiated body cell).

Further Reading

Abelson, J., Trotta, C. R., and Li, H. (1998). tRNA splicing. *J. Biol. Chem.* **273**, 12685–12688.

Fatica, A., and Tollervey, D. (2002). Making ribosomes. *Curr. Op. Cell Biol.* **14**, 313–318.

Kiss, T. (2002). Small nucleolar RNAs: An abundant group of noncoding RNAs with diverse cellular functions. *Cell* **109**, 145–148.

Kressler, D., Linder, P., and DeLaCruz, J. (1999). Protein *trans*-acting factors involved in ribosome biogenesis in *Saccharomyces cerevisiae*. *Mol. Cell. Biol.* **19**, 7897–7912.

Raué, H. A. (2003). Pre-ribosomal RNA processing and assembly in *Saccharomyces cerevisiae*. The machine that makes the machine. In *The Nucleolus* (M. O. J. Olson, ed.) Kluwer Academic/Plenum Publishers, New York, http://www.eurekah.com/chapter.php?chapid = 1223&bookid = 88&catid = 54.

Wolin, S. J., and Matera, A. G. (1999). The trials and travels of tRNA. *Genes Develop.* **13**, 1–10.

Biography

Hendrik A. Raué is a Professor of Biochemistry in the Faculty of Sciences at the Vrije Universiteit in Amsterdam, The Netherlands. He obtained his Ph.D. in Biochemistry at Groningen University, The Netherlands, and received his postdoctoral training at the National Institute of Child Health and Human Development in Bethesda, Maryland. His primary research interest is in eukaryotic ribosome biogenesis, using the yeast *S. cerevisiae* as a model organism.

Prions and Epigenetic Inheritance

Reed B. Wickner
National Institutes of Health, Bethesda, Maryland, USA

Just as nucleic acids can carry out enzyme reactions, it has now been found that proteins can be genes. The nonchromosomal genes [URE3], [PSI], and [PIN] of *Saccharomyces cerevisiae* and [Het-s] of the filamentous fungus *Podospora anserina* are self-propagating amyloid forms of normal cellular proteins Ure2p, Sup35p, Rnq1p, and HET-s, respectively. The phenotypes produced are due to the absence of the soluble forms in the [URE3] and [PSI] cases, but due to the presence of the amyloid forms in [PIN] and [Het-s]. The portions of the Ure2p, Sup35p, and Rnq1p molecules primarily responsible for prion formation and propagation (prion domains) are very rich in asparagine and glutamine residues, unlike the HET-s prion domain or the PrP molecule that plays a central role in the mammalian transmissible spongiform encephalopathies. The [Het-s] prion is of particular interest because it carries out a normal function for *Podospora*, namely, heterokaryon incompatibility. Chaperones play a critical role in prion propagation, by generating seeds for formation of the amyloid filaments.

Yeast and Fungal Prions: Genetic Criteria

The word "prion" means an infectious protein, by whatever mechanism. This idea arose from studies of the transmissible spongiform encephalopathies (TSEs) of mammals, believed to be due to an infectious form of a protein called PrP. Two nonchromosomal genes of *Saccharomyces cerevisiae*, called [URE3] and [PSI^+], were identified as prions because their unusual genetic properties were inconsistent with their being nucleic acid replicons, but were just what one would expect for a prion (Figure 1). First, each could be efficiently eliminated (cured) from cells, but from the cured cells could again arise at low-frequency cells carrying the nonchromosomal gene. Second, overproduction of the normal form of the protein was shown to increase the frequency with which the prion form arose *de novo*. And it was the protein whose overproduction induced the appearance of the nonchromosomal gene, not the RNA or the gene in high copy number. Finally, the chromosomal gene encoding the protein was of course necessary for the propagation of the prion, but the phenotype of mutants in the chromosomal gene was the same as that of the presence of the prion.

Known Prions of Yeasts and Fungi

[URE3] has each of these properties as a prion of the Ure2 protein, a regulator of nitrogen catabolism in yeast. Similarly, [PSI] has the properties expected of a prion of the Sup35 protein, a subunit of the translation termination factor. A prion of *Podospora anserina*, called [Het-s], is unique in performing a function for this fungus, being required for an antiviral defense mechanism called heterokaryon incompatibility. A third *S. cerevisiae* prion, called [PIN^+], was discovered by its ability to promote the *de novo* development of the [PSI^+] prion and is an altered form of Rnq1p. While [URE3] and [PSI^+] make their presence known by the absence of the normal form of Ure2p and Sup35p, respectively, both [Het-s] and [PIN^+] produce a phenotype by the presence of the abnormal forms of HET-sp and Rnq1p, respectively, similar to the case with the mammalian TSEs.

Prion Domains and Functional Domains

In Ure2p and Sup35p prion proteins, the C-terminal part of the protein carries out the normal function of the protein and the N-terminal segment is responsible for the prion properties (Figure 2). The prion domain can propagate the prion completely independent of the functional domain, and can even confer prion properties to a suitable unrelated reporter protein. The HET-s protein and Rnq1p also have special domains responsible for their prion properties. The Ure2p, Sup35p, and Rnq1p prion domains are all rich in asparagine or glutamine residues, and these runs of N or Q are important for the prion properties of the proteins. However, neither the HET-s protein nor mammalian PrP have regions rich in N or Q (Figure 2). The N-, Q-rich prion domains of Ure2p, Sup35p, and

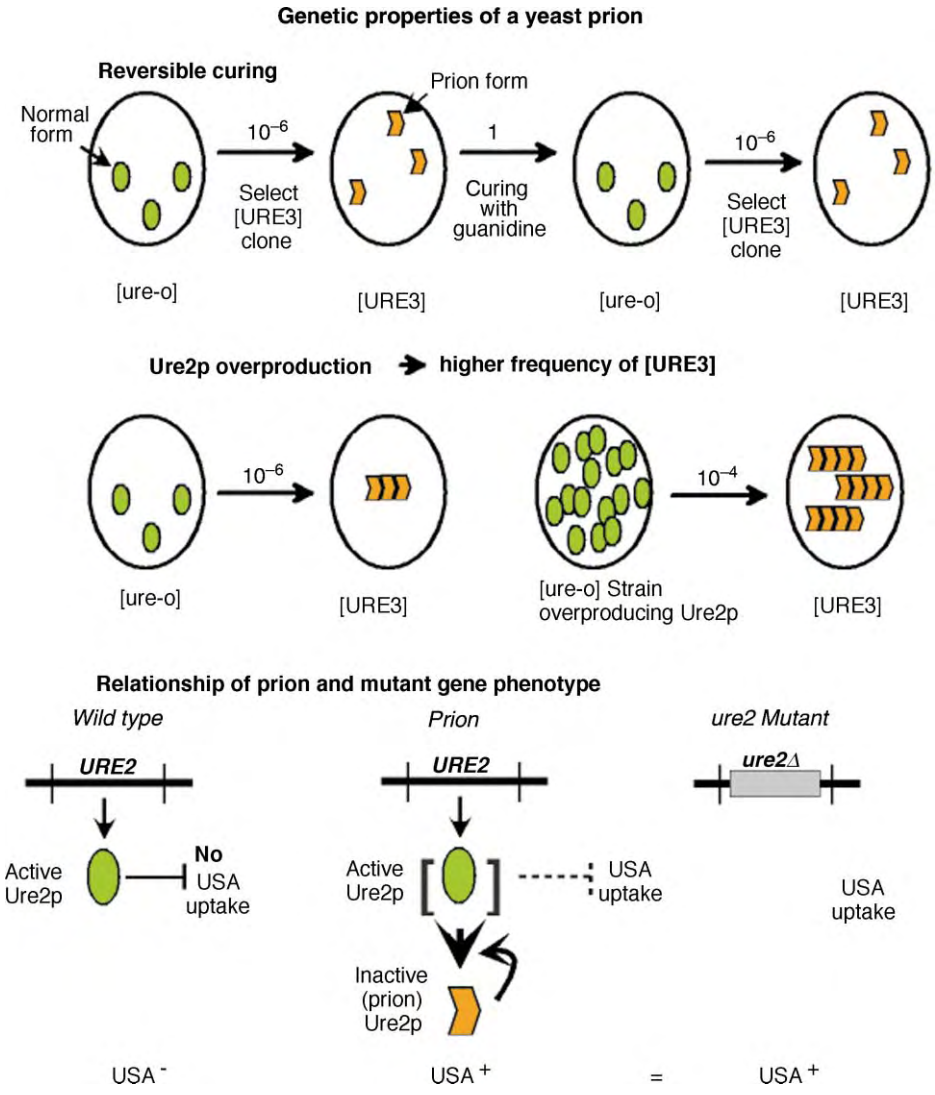

FIGURE 1 Genetic properties identify prions.

Rnq1 resemble the polyQ of Huntingtin whose amyloid formation is the central event in Huntington's disease.

In Ure2p, Sup35p, and HET-sp, the prion domain is stabilized by the rest of the molecule and largely prevented from converting into the prion form. This suggests that there is an interaction between the prion domains and the remainder of the molecule. In Ure2p, the prion domain helps with the nitrogen regulation function of Ure2p, although it is not essential for this activity.

Yeast, Fungal Prions [PSI$^+$], [URE3], and [Het-s] are Self-Propagating Amyloidoses

Amyloid is a special form of protein structure that is characteristic of a number of human diseases. Amyloid is a filamentous structure which is high in β-sheet structure, and which displays a characteristic yellow–green birefringence on staining with the aromatic dye Congo red. Amyloid filaments are partially resistant to protease digestion, probably reflecting their very stable β-sheet structure. Demonstration of aggregation is always simpler than that of amyloid structure, but it is evident that not all aggregates are amyloid. Amyloid formation by the Aβ peptide is the central event in Alzheimer's disease, while amyloid of amylin is a prominent feature of late-onset diabetes. Parkinson's disease features intracellular amyloid formation by α-synuclein, and amyloid of serum amyloid A protein is a complication of many long-term infectious and inflammatory processes.

Sup35p, Ure2p, and HET-sp each form amyloid *in vitro*. Moreover, the characteristics of the amyloid formed and the requirements for its formation closely reflect the corresponding properties and conditions of

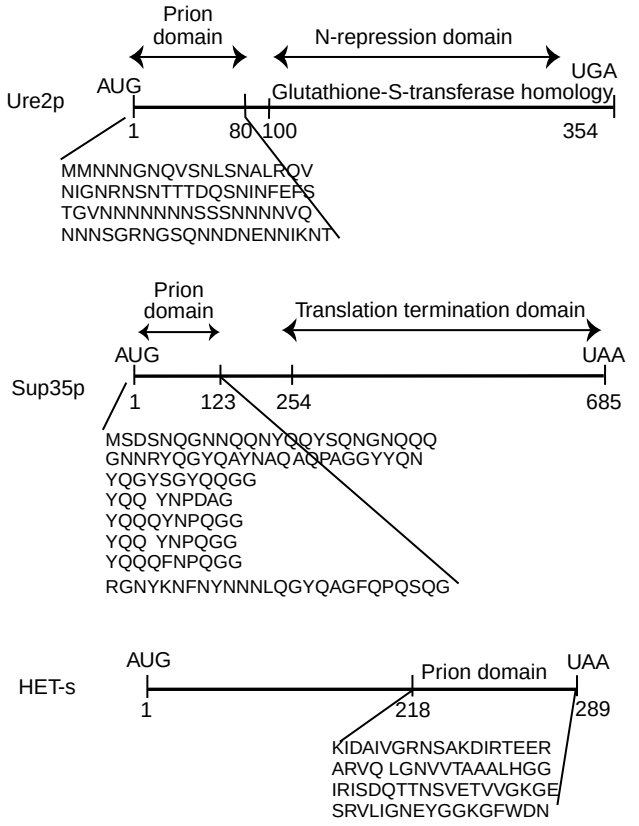

FIGURE 2 Prion domains of Ure2p, Sup35p, and HET-s. While the prion domains of Ure2p and Sup35p are rich in N and Q, that of HET-s is rich in neither.

prion formation *in vivo*. For example, extracts of [PSI$^+$] cells can prime the formation of amyloid by Sup35p much better than can extracts of normal cells. The prion domain of Ure2p induces amyloid formation by the full-length native Ure2p *in vitro* just as the prion domain produced *in vivo* induces *de novo* generation of the [URE3] prion (Figure 3). Indeed, filaments of the Ure2 protein have actually been visualized specifically in [URE3] cells.

Recombinant HET-s protein converted into amyloid *in vitro* efficiently transmits the [Het-s] trait to *Podospora* colonies when introduced by the "gene gun." The same protein, aggregated by heat denaturation or acid, or in its soluble form, has little or no such effect. This is a dramatic demonstration of the prion nature of [Het-s] which has not yet been accomplished in any of the yeast or mammalian systems.

The mechanism by which amyloid formation inactivates Ure2p is apparently not by a conformational change of the functional domain of the molecule. Fusion of the Ure2p prion domain to any of several enzymes shows no loss of their activity, but suggests that being in the amyloid filament sterically blocks access to binding Gln3p (the target of Ure2p action) or imposes a diffusion limitation.

The [HET-s] Prion Carries Out a Normal Function

Amyloidoses of humans are all associated with disease states, and the TSEs, in particular, are uniformly fatal. The [URE3] prion is associated with slow growth under most culture conditions. [PSI$^+$] and [PIN$^+$] do not confer any consistent phenotype on otherwise normal cells, although [PSI$^+$] is lethal in cells carrying a strong tRNA suppressor mutation. Searches by two groups for [PSI$^+$] in wild strains have failed to find it, supporting the notion that it is a disease, like the mammalian counterparts.

A colony of a filamentous fungus is not a pile of cells (as in yeast), but rather a syncytium – cells connected by cytoplasmic bridges. When two compatible colonies of *Podospora* or other filamentous fungi grow together, they fuse cellular processes (hyphae) thereby joining the two colonies into one, called a heterokaryon. This allows the colonies to share nutrients, but has the danger that a virus infecting one will spread by cytoplasmic mixing throughout the other. To minimize this risk, filamentous fungi have a system, called "heterokaryon incompatibility" which tests for identity between the partners at about a dozen polymorphic chromosomal loci. Nonidentity of alleles at a single locus is sufficient to abort the fusion process and a barrier to further fusion is formed. Most of these *het* loci are genetically unremarkable. The *het-s* locus of *Podospora* can have either of two alleles, *het-s* or *het-S*. A colony with the *het-s* allele is only incompatible with a *het-S* colony if the HET-s protein is in an amyloid form. This amyloid form is infectious and is the [Het-s] prion. The HET-S, which differs by only 14 amino acid residues from the HET-s protein, does not form amyloid, and residue 33 is critical in this difference.

Thus, the [Het-s] prion is the (so far) unique case of a prion that is necessary for a normal function, heterokaryon incompatibility. Consistent with this view is the fact that most wild strains of *P. anserina* with the *het-s* allele carry the [Het-s] prion.

Prion Generation

[PIN$^+$] was discovered as a nonchromosomal gene whose presence was necessary for the efficient induction of the *de novo* appearance of [PSI$^+$] by overexpression of Sup35p. [PIN$^+$] was found to be a prion of the Rnq1 protein, which had already been shown capable of a self-propagating aggregation *in vivo*. In fact, [URE3] was also capable of [PIN$^+$]-like activity. This showed that one prion could promote the generation of another. This may be because all of these prions ([PSI$^+$], [PIN$^+$], and [URE3]) are based on amyloid of asparagine-glutamine

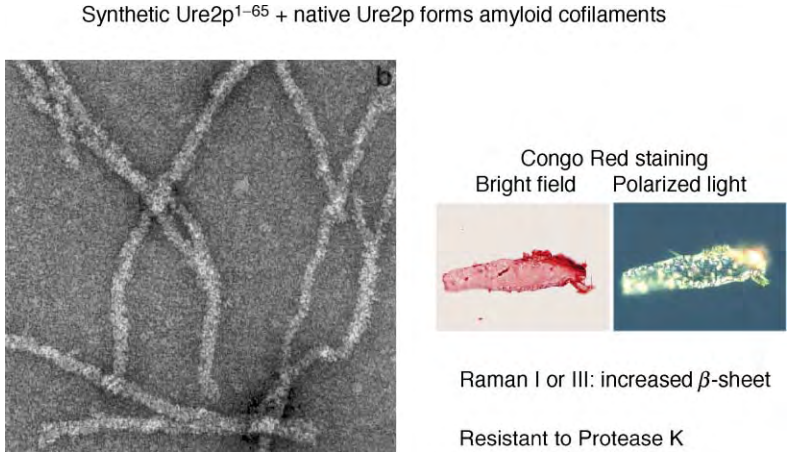

FIGURE 3 Amyloid and prions. The prion domain of Ure2p (for example) can form amyloid and can induce amyloid formation by the full-length native protein *in vitro*, just as overexpression of the prion domain *in vivo* induces prion formation by Ure2p.

rich segments. Although cross-priming of polymerization is not as efficient as self-priming (the usual propagation reaction), it is far more efficient than the truly spontaneous development of a prion. A similar, though weaker, effect of [PIN$^+$] on [URE3] generation has also been observed.

[URE3] has a very strong requirement for the Mks1 protein for *de novo* generation. Increasing or decreasing Mks1p levels dramatically increase or decrease the frequency of [URE3] arising. Although *mks1*Δ cells are nearly incapable of generating a new [URE3] prion, propagation of [URE3] is normal in such cells. Mks1p was discovered as a protein whose strong overproduction slows cell growth, but is inhibited in this activity by the Ras-cAMP pathway. Indeed, activation of Ras, like deletion of *MKS1*, dramatically diminishes [URE3] generation. Mks1p is also a regulator of glutamate biosynthesis, but the effects on [URE3] generation appear not to be mediated via glutamate levels. The detailed mechanisms of these effects remain to be elucidated.

Chaperones and Prion Propagation

Chaperones play a central role in the propagation of yeast prions (Table I). Hsp104 is a disaggregating chaperone critical in the cellular reaction to heat shock, and either increasing or decreasing its level adversely affects propagation of [PSI$^+$]. Overexpression of Hsp104 probably blocks propagation by completely disaggregating the Sup35p aggregates allowing return of the protein to its normal form. Elimination of Hsp104 interferes with seed formation. Amyloid aggregates are clumpy and may all remain in one of the daughter cells if they form a single lump in the mother cell. Modest levels of Hsp104 carry out the partial fragmentation of these filaments insuring that both daughter cells receive one or more seeds. [URE3] likewise requires Hsp104 for propagation, but unlike [PSI$^+$] is not cured by Hsp104 overproduction. Guanidine cures all the yeast prions and it has recently been shown that guanidine works by inhibiting Hsp104.

Different Hsp70s and Hsp40s have positive and negative functions with different prions as summarized in Table I. For example, overexpression of the Hsp40 protein, Ydj1, can cure [URE3]. Clearly, the detailed interactions of each prion with chaperones will be different, and this remains an important area to investigate. There is circumstantial evidence for a role of chaperones in the mammalian TSEs, but direct evidence has so far been limited to the yeast systems.

The importance of the discovery of the role of chaperones in yeast prions goes far beyond these systems and even the mammalian prion diseases. Amyloidoses are common (almost universal) diseases of old age, and one suspects that one of the primary roles of the heat-shock proteins is to defend against amyloid formation. It will be critical to learn how these systems can be marshaled to contend with the otherwise largely intractable human amyloidoses.

TABLE I

Chaperones and Prions

Chaperone	[PSI$^+$]	[URE3]	[PIN$^+$]
Hsp104	↑ → lost	↑ → OK	↑ → OK
	↓ → lost	↓ → lost	↓ → lost
Ssa1p (Hsp70)	↑ → OK	↑ → lost	
	↓ → lost		
Ssa2p	↑ → OK	↑ → OK	
Ydj1p (Hsp40)	↑ → OK	↑ → lost	
Sis1p (Hsp40)			↓ → lost

Conclusions

The ability of proteins to bear hereditary information recalls the earlier discovery by Sonneborn of cortical inheritance in *Paramecium*, in which the surgically altered arrangement of cilia on the surface of the cell was shown to be faithfully inherited by the progeny of the original cell. Self-propagating protein structures in the former case are closely analogous to self-propagating organellar structures in the latter. Efforts to find other self-propagating organellar structures have not yet met with any clear successes, and the mechanisms operating in the cortical inheritance phenomenon have not yet been elucidated.

All of the prions discussed here appear to be based on self-propagating amyloid of the corresponding protein. Of course, most amyloidoses are not prions, although nearly all have been shown to be self-seeding *in vitro*. Prion propagation requires both expansion of amyloid within one individual cell or compartment, but also a mode of transmission. There are indications that mature amyloid fibers may not be the infectious form of prions, and it is evident that the shorter the fiber, the higher the ratio of growing ends to mass of material. However, the *Podospora* studies show that amyloid itself can serve as the infectious material, and most infectivity assays with scrapie material show that the infectious material is relatively rapidly sedimenting.

The direct parallels between these yeast, fungal, and mammalian prions and amyloidoses have opened new areas for investigation of these very difficult human diseases.

A new prion (infectious protein) based on an enzyme whose active form is necessary *in trans* for activation of its inactive precursor has been described. This is the vacuolar protease B of *S. cerevisiae*. It is not news that a protease can activate its inactive precursor, but it is remarkable that such a protease can be a gene. Moreover, this suggests that other protein-modifying enzymes may prove to be prions under some circumstances.

See Also the Following Articles

Amyloid • Chaperones, Molecular • Prions, Overview

Glossary

amyloid A filamentous form that many proteins can assume characterized by high β-sheet content, protease-resistance and yellow-green birefringence on staining with Congo red.

chaperone A protein that aids the folding (or refolding or renaturation) of another protein.

prion A protein that transmits a trait or disease without the need for an accompanying nucleic acid.

prion domain Part of a protein that determines the prion properties of the full protein.

Further Reading

Chernoff, Y. O., Lindquist, S. L., Ono, B.-I., Inge-Vechtomov, S. G., and Liebman, S. W. (1995). Role of the chaperone protein Hsp104 in propagation of the yeast prion-like factor [psi+]. *Science* **268**, 880–884.

Kushnirov, V. V., and Ter-Avanesyan, M. D. (1998). Structure and replication of yeast prions. *Cell* **94**, 13–16.

Liebman, S. W., and Derkatch, I. L. (1999). The yeast [*PSI*+] prion: making sense out of nonsense. *J. Biol. Chem.* **274**, 1181–1184.

Masison, D. C., and Wickner, R. B. (1995). Prion-inducing domain of yeast Ure2p and protease resistance of Ure2p in prion-containing cells. *Science* **270**, 93–95.

Roberts, B. T., and Wickner, R. B. (2003). Heritable activity: a prior that propagates by covalent autoactivation. *Genes and Dev.* **17**, 2083–2087.

Saupe, S. J. (2000). Molecular genetics of heterokaryon incompatibility in filamentous ascomycetes. *Microbiol. Mol. Biol. Revs.* **64**, 489–502.

Serio, T. R., and Lindquist, S. L. (2001). [PSI+], SUP35, and chaperones. *Adv. Protein Chem.* **57**, 335–366.

Wickner, R. B. (1994). Evidence for a prion analog in *S. cerevisiae*: The [URE3] non-Mendelian genetic element as an altered *URE2* protein. *Science* **264**, 566–569.

Wickner, R. B., Edskes, H. K., Roberts, B. T., Pierce, M., and Baxa, U. (2002). Prions of yeast as epigenetic phenomena: High protein "copy number" inducing protein "silencing". *Adv. Genet.* **46**, 485–525.

Wickner, R. B., Liebman, S. W., and Saupe, S. J. (2004). Prions of yeast and filamentous fungi: [URE3], [PSI^+], [PIN^+] and [Het-s]. In *Prion Biology and Diseases* (S. B. Prusiner, ed.) Cold Spring Harbor Laboratory Press, pp. 305–372.

Biography

Reed B. Wickner, M.D. is Chief of the Laboratory of Biochemistry and Genetics in the National Institute of Diabetes Digestive and Kidney Diseases of the National Institutes of Health in Bethesda. He is interested in nonchromosomal inheritance, and has long studied yeast RNA viruses. He discovered yeast prions based on their unusual genetic properties and has studied the mechanisms of generation, propagation, and curing of the [URE3] prion, and the structure of the Ure2p amyloid that forms its basis.

Prions, Overview

Cedric Govaerts and Fred E. Cohen
University of California, San Francisco, California, USA

Prions are transmissible pathogens responsible for a series of fatal neurodegenerative diseases including, in humans, Creutzfeld–Jacob disease (CJD), Gerstmann–Straussler–Scheinker disease (GSS), fatal familial insomnia (FFI), and kuru. Other mammals succumb to prion diseases including sheep scrapie, bovine spongiform encephalopathy (BSE, also known as mad-cow disease), chronic wasting disease (CWD) in mule, deer, and elk, feline spongiform encephalopathy (FSE), and transmissible mink encephalopathy (TME). In each case the emergence of a misfolded form of the prion protein, PrP^{Sc}, is pathognomonic for the disease.

Misfolding Diseases

More than 20 human pathologies, including Alzheimer's, Parkinson's, Huntington's, and prion diseases, are associated with the "misfolding" of specific proteins or protein fragments. Under normal conditions, some newly synthesized proteins are folded and post-translationally modified in specific cellular compartments, called endoplasmic reticulum (ER), in an effort to deliver the protein to the appropriate cellular location in its native (physiologically relevant) conformation. However, occasionally, proteins can adopt an aberrant conformation either during the initial folding process or through a "conformational transition" from the native state. A misfolded protein, if not cleared by cellular or extracellular machinery, can cause disease. Two mechanisms of disease must be considered: loss of function and gain of function/dominant-negative effect. With loss of function, the misfolded protein cannot serve the biological function normally achieved by the native protein. Cystic fibrosis is a useful example where the quality control machinery prevents the misfolded mutant CFTR protein from reaching the cell surface. Conversely, pathology can arise from gain of function, when the aberrant conformation leads to a new and potentially harmful function of the protein. The prion diseases follow this paradigm. Invariably, misfolded forms of proteins have a strong propensity to aggregate into insoluble material. In several diseases, these aggregates adopt a fibrillar structure called "amyloid" and can form large deposits or plaques which are found in the affected tissue. Following proteolytic fragmentation, prions can form amyloid fibers and plaques. As with other amyloid-forming diseases, it remains unclear whether oligomers of the misfolded protein or much larger polymeric aggregates (or fibrils) injure cells and cause neurodegeneration.

Prion Protein and Diseases

PrP^{C} and PrP^{Sc}

The prion protein, or PrP, is a membrane anchored protein, expressed predominantly in neurons and lymphocytes. The biological function of the normally folded prion protein (cellular PrP, PrP^{C}) has yet to be identified, but PrP^{C} is known to bind copper and could be involved in its homeostasis. Prion diseases are associated with the emergence of a misfolded form of PrP^{C} called PrP^{Sc} (for scrapie form, the oldest known prion disease). A wealth of data suggest that PrP^{Sc} is the etiologic agent in the disease. While PrP^{C} and PrP^{Sc} have the same amino acid sequence, they differ in their structural characteristics, PrP^{C} is rich in α-helical structure while PrP^{Sc} has substantially more β-sheet structure. While PrP^{C} is monomeric and protease sensitive, PrP^{Sc} is resistant to degradation by protease and is multimeric.

Replication Cycle

The global mechanism of PrP^{Sc} production is fairly well understood. It involves the presence of an initial PrP^{Sc} multimer which can either be exogenous (infectious forms of the diseases) or endogenous (inherited or sporadic forms). This first prion will initiate PrP^{Sc} accumulation by sequentially converting PrP^{C} molecules, following a "replication cycle" (see Figure 1). As illustrated, PrP^{C} is thought to exist in equilibrium with a transient intermediate, PrP^{*}, which is normally in low abundance compared to PrP^{C}. Binding of a PrP^{Sc} molecule to PrP^{*} may lead to its conversion into a new PrP^{Sc} molecule, through structural templating. This newly formed PrP^{Sc} molecule can in turn convert neighboring PrP^{*} molecules and therefore amplify the replication cycle. Importantly, PrP^{C}, PrP^{*}, and PrP^{Sc} are

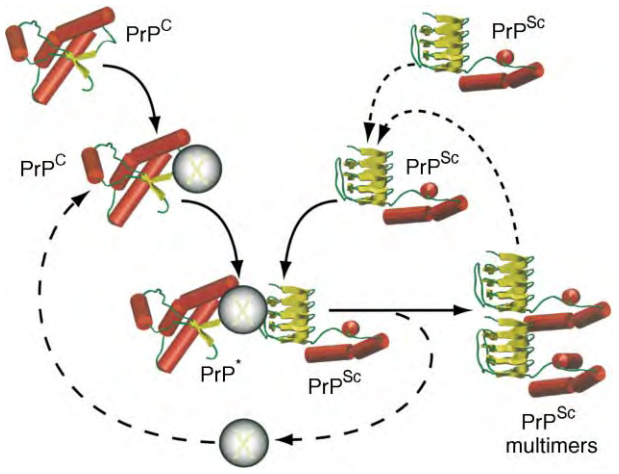

FIGURE 1 Exogenous or endogenous PrP^{Sc} initiates PrP^{Sc} synthesis by binding to a $PrP^{C/*}$/X complex. Facilitated by protein X and directed by the PrP^{Sc} template, PrP^{*} changes conformation and forms PrP^{Sc}. When PrP^{Sc} forms, the heteromultimeric complex dissociates, yielding recycled protein X and endogenous PrP^{Sc}. The newly generated PrP^{Sc} can then facilitate two replication cycles leading to an exponential rise in PrP^{Sc} formation.

not the only molecules involved in prion replication, as it has been demonstrated that at least one other protein is required for $PrP^{C} \rightarrow PrP^{Sc}$ conversion. This auxiliary protein remains to be identified and has been termed "protein X" (see Figure 1). Such additional complexity is probably responsible for the difficulties investigators have faced in building *in vitro* conversion protocols, leaving cell-based assays and animal systems (such as transgenic mice) as the only suitable experimental systems for the study of prion disease.

Transmission and Inheritance

Prion diseases are rare neurodegenerative disorders which affect approximately one person per million. Sporadic disease is the most common mechanism in humans and represents 85% of all cases. Individuals present in the sixth or seventh decade of life with a variety of cognitive defects. A rapidly progressive course leads to death in less than a year. Familial prion diseases (like GSS or FFI) represent 15% of all cases and are caused by mutations in the PrP gene. These mutations appear to favor the transition from the cellular form to the pathological form of PrP. PrP^{Sc} accumulates and neurodegeneration results.

In humans, infectious diseases are rare but have been a source of great concern, given the nature of the transmissible agent and its resistance to typical disinfection strategies. In the laboratory, disease can be readily transmitted to mice or hamster by intracranial injection of brain homogenate taken from prion-infected animals. Propagation of kuru disease in New Guinea Highlanders was due to ritualistic cannibalism involving ingestion of contaminated brain. Recently, it has been discovered that BSE had been transmitted to humans in Europe after consumption of infected beef, producing a variant of the CJD called vCJD (variant CJD). This constitutes a rare violation of the "species barrier," a term coined after observing that infectious material from one species inefficiently transmits to another species (this has presumably protected the human population from infection by scrapie-infected sheep).

Prion Strains

The various prion diseases are characterized by different incubation times and neuropathologic profiles, although in all cases the same misfolded protein (PrP^{Sc}) is responsible. This phenomenon has been attributed to the existence of various "prion strains." Although PrP^{Sc} molecules from different strains are chemically identical, they differ in their exact conformations. The structural characteristics of individual prion strains are propagated via the replication cycle. These characteristics appear to direct the precise tissue targeting, incubation time, and pathogenesis of the strain. For example, it has been established that consumption of BSE-infected meat has led to prion disease in over 100 people. Affected individuals suffer from a new form of CJD called vCJD, are drawn from a younger cohort and exhibit distinct clinical characteristics from CJD patients. The PrP^{Sc} molecules found in patients with vCJD can be conformationally distinguished from those of classical CJD, and have been shown to resemble PrP^{Sc} molecules from BSE-infected cattle. Therefore, vCJD is a different strain of prion from CJD, and is probably the human form of the bovine prion strain from BSE.

Physiopathology of Prion Diseases

Prions are neurodegenerative diseases, that induce neuronal dysfunction accompanied by neuronal loss with no inflammatory response. In most cases, the pathogenic process is characterized by vacuolar degeneration of the gray matter, which correlates with abundance of PrP^{Sc}. This vacuolation process creates spongiform change in the cerebral tissue. Prion diseases are therefore often referred to as transmissible spongiform encephalopathies (TSE). The precise location of tissue damage (e.g., cerebral cortex versus cerebellar cortex) may vary between the different prion diseases, but always correlates with the presence of PrP^{Sc}. In some forms, such as GSS, the disease is also characterized by the presence of amyloid plaques composed of PrP^{Sc} molecules. Although technological advances in medical imaging provide promising tools for the near

future, the definitive diagnostic for prion disease is currently achieved postmortem by histological analysis of brain tissue.

Structural Studies

As for any misfolding disease, the pathological form of the prion protein differs from the cellular one in its conformation. While no chemical difference is observed, biophysical and immunological measurements reveal important structural differences between the two isoforms. Notably, only a fraction of the specific antibodies targeted against PrP^{C} molecules are able to recognize the PrP^{Sc} isoforms. This suggests that the molecular structures of the two isoforms are significantly different.

The PrP^{C} molecule is soluble and its three-dimensional structure can be solved by classical techniques such as solution nuclear magnetic resonance (NMR). These experiments reveal that PrP^{C} fold is dominated by α-helices, tight helical structures found in a vast number of proteins with very little β-sheet, extended structures also commonly found (see Figure 2). While the structure of PrP^{Sc} cannot be probed by NMR due to its insolubility, biophysical measurements such as Fourier transform infrared spectroscopy (FT-IR) have deciphered important structural properties of PrP^{Sc}. These techniques have shown that the fold of PrP^{Sc} is composed of both β-sheet structures (40%), and α-helices (30%). Enrichment in β-sheet structure is commonly observed in proteins associated with misfolding diseases. This has led many to speculate that there are mechanistic similarities in the misfolding diseases. For a variety of technical reasons, resolving the atomic structure of PrP^{Sc} is extremely challenging. Recent advances include the discovery of two-dimensional crystals of PrP^{Sc} suitable for electron microscopic analysis. These data have led to the development of new models of the structure of PrP^{Sc}.

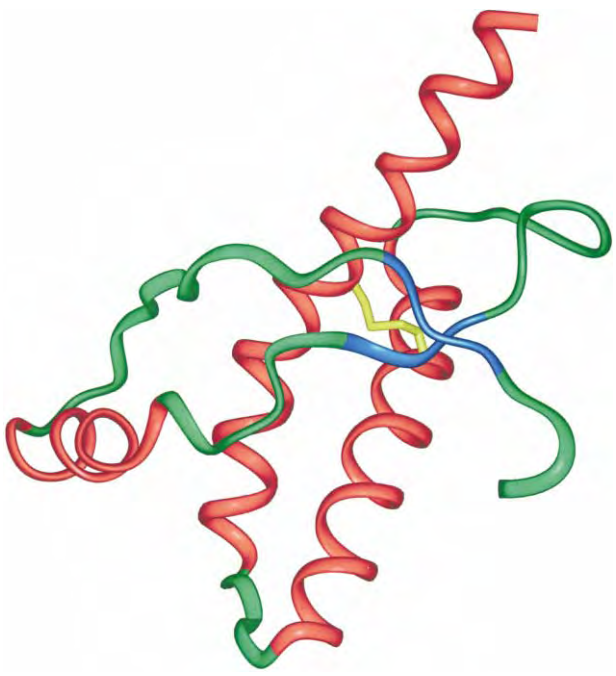

FIGURE 2 NMR structure of PrP^{C}. Ribbon representation of the globular structure of human PrP resolved by NMR, comprising residues 125–228. The three α-helices are colored in red and the small β-sheet is in blue.

Therapeutic Strategies

Currently, prion diseases are uniformly fatal illnesses. Diverse approaches are being taken to develop therapeutics for prion diseases. Compounds can be designed to specifically disrupt the replication cycle (illustrated in Figure 1), either by stabilizing the PrP^{C} conformation versus PrP^{*}, or by blocking interaction with the auxiliary partner protein X. Design of such compounds has proven successful in cell-based models of prion diseases but must now be extended to animal models and human clinical trials. Screenings of existing drugs that are known to penetrate the blood–brain barrier (and therefore potentially reach prion-infected tissues) have identified the drug quinacrine as being effective against PrP^{Sc} replication in cells. Quinacrine is currently approved for the treatment of giardiasis and has been used historically to treat malaria. Clinical trials are underway to determine its therapeutic utility in CJD patients. Similar approaches have identified a number of other potentially interesting compounds, but more efforts will be required to assess their therapeutic utility. Hopefully, one of these efforts will lead to potent antiprion drugs in the foreseeable future.

See Also the Following Articles

Amyloid • Glycosylation in Cystic Fibrosis • Prions and Epigenetic Inheritance • Protein Folding and Assembly

Glossary

amyloid fibers Fibrillar structures of misfolded protein aggregates, observed in human diseases such as prion diseases or Alzheimer's disease.

conformational transition Process during which the protein undergoes major structural change.

misfolding Process leading to an aberrant conformation of a protein, often linked to pathogenesis.

prion strains The subclassification of prions following their fine structural characteristics which appear to define their pathological profile.

PrP^{C} Cellular (normal) isoform of the PrP protein.

PrP^{Sc} Misfolded (pathological) isoform of the PrP protein.

replication cycle Mechanism by which PrP^{C} molecules are converted into PrP^{Sc} isoform with the help of pre-existing PrP^{Sc} molecules.

species barrier Apparent inability of prion from one species to infect organism from another species. Violations of the barrier have been observed.

Further Reading

Cohen, F. E., and Prusiner, S. B. (1998). Pathologic conformations of prion proteins. *Annu. Rev. Biochem.* **67**, 793–819.

DeArmond, S. J., and Bouzamondo, E. (2002). Fundamentals of prion biology and diseases. *Toxicology* **181–182**, 9–16.

Dobson, C. M. (1999). Protein misfolding, evolution and disease. *Trends Biochem. Sci.* **24**, 329–332.

Dobson, C. M. (2003). Protein folding and disease: A view from the first horizon symposium. *Nat. Rev. Drug Discov.* **2**, 154–160.

Prusiner, S. B. (ed.) (2004). *Prion Biology and Diseases*, 2nd edn. Cold Spring Harbor Laboratory Press, Cold Spring Harbor.

Prusiner, S. B., Scott, M. R., DeArmond, S. J., and Cohen, F. E. (1998). Prion protein biology. *Cell* **93**, 337–348.

Sacchettini, J. C., and Kelly, J. W. (2002). Therapeutic strategies for human amyloid diseases. *Nat. Rev. Drug Discov.* **1**, 267–275.

Biography

Fred E. Cohen is a Professor in the Departments of Cellular and Molecular Pharmacology and Biochemistry and Biophysics at the University of California, San Francisco. He holds a B.S. from Yale University, a D.Phil. from Oxford University and an M.D. from Stanford University. His fields of investigation include protein structure, protein folding, prion diseases, drug design against prions disease and parasitic diseases, and various aspects of computational biology.

Cedric Govaerts holds a B.S. and a Ph.D. from the Free University of Brussels. He is currently a postdoctoral fellow in the group of Fred Cohen and works on structural studies of prions.

Processivity Clamps in DNA Replication: Clamp Loading

Megan J. Davey and Mike O'Donnell
The Rockefeller University, New York, USA

DNA processivity clamps are ring-shaped proteins that encircle and slide freely along the DNA. These clamps tether replicative DNA polymerases to the DNA ensuring that they remain attached to the template for the many thousands of base pairs necessary to copy genomes. The stable toroidal structure of processivity clamps necessitates specialized machinery, termed a clamp loader, to open the clamp and place it onto DNA. Clamp loaders are hetero-oligomeric protein complexes that use the energy of ATP binding and hydrolysis for their function.

DNA Processivity Clamps

Chromosomal replicases are multi-subunit machines that use ATP to maintain a tight grip on DNA and thus are highly processive. Study of the T4 bacteriophage, *Escherichia coli*, and eukaryotic replisomes has demonstrated that these replicases consist of a polymerase and two accessory factors. Work on the *E. coli* system has identified the two accessory factors as a clamp and a clamp loader (Figure 1).

The first clue that one accessory protein acted alone as a ring-shaped sliding clamp was provided in the *E. coli* system. Biochemical experiments have shown that the *E. coli* DNA processivity clamp, β, binds tightly to circular DNA, yet slides freely along the duplex. Linearizing the DNA results in β sliding off the ends. This behavior led to the prediction that the clamp forms a topological link with DNA, independent of sequence and that it is shaped like a ring and encircles the duplex like a donut. This prediction was fulfilled by the crystal structure, which confirmed that β is ring shaped (Figure 2). Since that first structure, ring-shaped DNA processivity clamps have also been demonstrated in archaea, bacteriophage, and eukaryotes (Figures 1B and 2). These clamps share a common chain-fold; however, they employ slightly different strategies to achieve this structure. The *E. coli* β-clamp is composed of two crescent-shaped molecules that form a head-to-tail dimer. Each of the subunits is composed of three globular domains that lack sequence similarity yet have the same chain-folding pattern and are nearly superimposable. Thus, each β-clamp is composed of six globular domains arranged in a circle around a central channel (Figure 1A). The diameter of the central channel is $\sim$35 Å and is large enough to fit double strand DNA. The outside diameter of β is $\sim$80 Å. The structure contains 12 α-helices that are all positioned on the inside of the ring, lining the central channel. Although β has an overall negative charge, the helices carry a positive charge and are thought to contact the DNA phosphate backbone through nonspecific, water-mediated interactions, allowing the clamp to slide along DNA.

In eukaryotic cells the clamp is proliferating cell nuclear antigen (PCNA). PCNA shares very little sequence similarity with the β-clamp, yet the overall structure of PCNA is very similar to that of β (Figures 2A and 2C). The two structures have similar inner and outer diameters, and the domains have the same chain-folding pattern, making the molecules nearly superimposable. However, there is one major difference between the two clamps: PCNA is a trimer rather than a dimer. PCNA has two rather than three domains per monomer and trimerizes to form a six-domain ring. Eukaryotic PCNA is homologous to PCNA in archaea and, as expected, they share similar structures (Figure 2D). The replicase of bacteriophage T4 and the related phage RB69 also utilize a clamp and clamp loader. The T4 gene protein (gp) 45 has no sequence similarity with PCNA or β, but is a trimer, like PCNA, and the overall structure is quite similar to all the other clamps (Figure 2B).

Processivity Clamp Loaders

β and PCNA appear to be tightly closed rings. On circular DNA, β and PCNA remain associated with a half-life of 0.5–1 h at 37 °C, demonstrating that the interfaces between the protomers remain tightly associated. This tight association, while important for processivity, necessitates the use of a clamp loader to rapidly open and close the clamp.

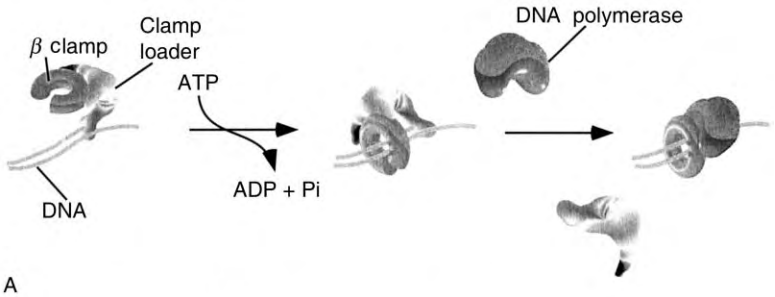

A

Organism	Clamp	Clamp loader
E. coli	Clamp (β_2)	γ-Complex ($\gamma_3^{\delta\delta'}\chi\psi$)
T4 bacteriophage	gp45 (trimer)	gp44/62 Complex
Eukaryotes	PCNA (trimer)	RFC *S. cerevisiae* Rfc 1-5 Human, p140, p37, p36, p40, p38
Archaea	PCNA (trimer)	RFC RFCS/RFCL

B

FIGURE 1 Components of a replicase. (A) Cellular replicases are composed of a ring-shaped clamp that is placed on DNA by a clamp loader. The clamp is utilized by DNA polymerase to remain tightly linked to DNA for highly processive replication. (B) Table of clamps and clamp loaders from different organisms.

Clamp loaders, both prokaryotic and eukaryotic, are hetero-oligomeric protein complexes, usually hetero-pentamers, that use the energy of ATP binding and hydrolysis to drive the loading of processivity clamps onto primed DNA. The loading process includes opening of the clamp, bringing the clamp to the DNA, and closing of the clamp around double-strand DNA. The different subunits within clamp loaders share sequence and/or structural homology. In addition, most of the clamp loader subunits from bacteria, T4 phage, eukaryotes, and archaea share sequence homology with each other, particularly within the sequences necessary for ATP binding and hydrolysis. Because of these similarities, clamp loaders from different systems are thought to function similarly. The clamp-loading mechanism has been most extensively studied in *E. coli*.

E. Coli Clamp Loader, γ-Complex

The clamp loader in *E. coli* is composed of five different subunits, γ, δ, δ', χ, and ψ. A complex composed of γ, δ, and δ' is sufficient for clamp loading and replication *in vitro*; χ and ψ are not absolutely required for clamp loading and their role will be discussed later in this entry.

The δ Subunit Opens the β Clamp

δ is the clamp loader subunit that binds β the tightest and is also capable of opening β on its own. Neither β nor δ can bind ATP, δ must open the clamp using the energy of protein–protein interaction. Only one δ subunit binds to one β dimer, suggesting that only one interface of β_2 is opened by δ. Furthermore, β_2 that has been cross-linked at one interface is capable of being loaded by γ complex, and therefore only one interface needs to be opened during the clamp-loading operation. Maintaining the integrity of one dimer interface ensures that β is easily reclosed.

Structure of the β_1–δ Complex Biochemical studies have shown that δ binds tightly to a mutant $\beta(\beta_1)$ that is rendered monomeric by mutating two hydrophobic residues at the dimer interface. This stable complex

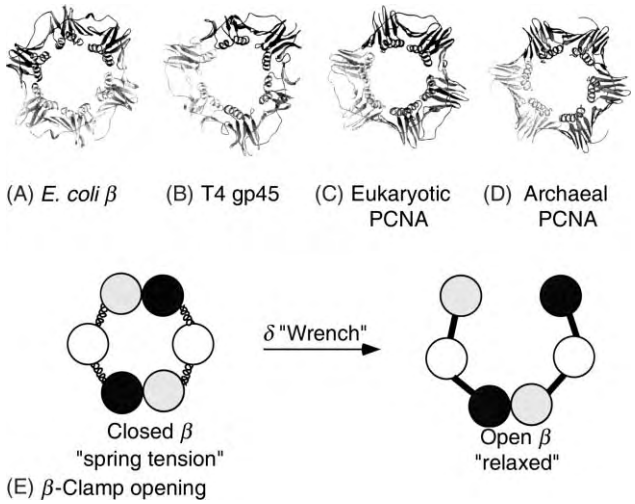

FIGURE 2 Similarity of clamp structures: The structures of (A) *E. coli* β-clamp, (B) T4 bacteriophage gp45, (C) *S. cerevisiae* PCNA, and (D) *P. furiousus* PCNA are shown. Each protomer in the ring is a different shade. Shown in (E) is a schematic of how β opens once it is cracked open by δ. Closed β is under spring tension, which is relieved when β is cracked, driving further opening of the ring.

enables the formation of a $\beta_1-\delta$ co-crystal. The crystal structure of $\beta_1-\delta$ suggests how δ may open β. δ contacts β in two different places. One contact is within a hydrophobic pocket between the middle and C-terminal domains of β and is thought to provide most of the binding energy. A second site of contact is between an α-helix in δ and a loop in β. This loop in β is near the dimer interface and is connected to an α-helix that contains hydrophobic core residues involved in formation of the β-dimer. In the $\beta_1-\delta$ structure the hydrophobic core residues are rotated out of the dimer interface. Perhaps, δ-binding to β forcibly disrupts the hydrophobic core of the dimer interface. Alternatively, there is a rapid exchange between open and closed forms of β, and δ simply stabilizes β in the open conformation. The stability of β on circular DNA suggests that the former case is more likely; however, the exact mechanism remains to be determined.

The β-Dimer is Under Spring Tension The distortion of the β_2-interface by δ may crack the ring, but does not explain how the edges of the crack open wide enough for passage of DNA. A striking difference in the shape of β_1 (with δ) and β_2 provides a strong clue as to how the ring opens up. The β-protomers within the β_2-structure have a higher degree of curvature than β_1. The change in curvature seems to result from rigid body motions between the three domains of the β-monomer. The largest of these changes occurs farthest away from the area of δ contact, suggesting that these rigid body motions are not a direct result of δ-binding β but are instead powered intrinsically within β itself. The increased curvature of β within β_2 suggests that β_2 is strained. Presumably, the two protomers come together and inward to form a ring due to the strength of the interaction. In other words, the free energy of forming the dimer interface is greater than the energy needed to bend the domains and form a closed ring. When the interface is disrupted by δ, the tension between the domains is allowed to relax and the ring opens (Figure 2E). This idea of a "spring-loaded" β-dimer is supported by molecular dynamics simulations that demonstrate that a protomer of β in the dimeric, strained conformation rapidly assumes the relaxed, monomeric conformation. When β_1 is modeled as a dimer, a gap at one interface is produced (as illustrated in Figure 2E).

Clamp Opening by γ Complex

Although δ is able to open the β-clamp in the absence of ATP, γ-complex requires ATP to open the β-clamp. γ is the only subunit that utilizes ATP and thus may be thought of as the motor that drives clamp loading. In the absence of ATP, γ-complex can no longer bind β, suggesting that other subunits occlude δ from binding β. In the presence of ATP, γ re-establishes a tight interaction between δ and β, suggesting that ATP binding (ATP hydrolysis is not necessary) powers a conformational change that exposes δ for interaction with β. Study of γ and δ' suggests that they interfere with $\delta-\beta$ interaction, implying that within the γ complex, δ' and γ may prevent $\delta-\beta$ contact in the absence of ATP.

$\gamma_3\delta\delta'$ Form a Heteropentameric Ring

The structure of the minimal $\gamma_3\delta\delta'$-clamp loader reveals that the subunits are arranged in a circle in which δ and δ' bracket three γ-subunits (Figure 3B). Each of the subunits shares a similar three-domain structure (Figure 3A). In fact, they share the exact same-chain-folding topology from head to tail. This similar structure was expected for γ and δ' since they are homologous to one another. However, this observation is somewhat surprising for δ since it shares no sequence similarity with δ' and γ. Most of the subunit contacts within $\gamma_3\delta\delta'$ are within the carboxy-terminal domains, which form a closed pentameric circle. However, when viewed from the amino-terminal face of the assembly, there is a gap between the amino-terminal domains of δ and δ'.

One of the striking features of this structure is the position of nucleotide-binding sites; they are located at the interfaces between subunits. There are three ATP-binding sites, one in each γ subunit, at the $\delta'-\gamma_1$, $\gamma_1-\gamma_2$, and $\gamma_2-\gamma_3$ interfaces. Each nucleotide-binding site seems to rely on residues from two different subunits for function. For example, the $\delta'-\gamma_1$ site is comprised of a canonical nucleotide-binding site in γ_1 and an arginine residue from δ'. The arginine residue is encoded by an SRC motif that is conserved in clamp loader residues from bacteria, phage, archaea, and eukaryotes.

Active and Inactive States of γ Complex The β-binding element in δ is located on the amino-terminal domain of δ, and is positioned in the gap between δ and δ'. This was somewhat surprising since the crystal structure was determined in the absence of ATP and thus should not be able to bind β. However, when β is modeled onto the $\gamma_3\delta\delta'$ assembly, using the $\beta_1-\delta$ structure as a guide, there is a severe clash between β and the clamp loader subunits. Thus, the complex would appear to be in an inactive state, unable to bind β.

What changes in the γ-complex structure occur, dependent on ATP binding, to accommodate interaction between δ and β? To dock β onto δ without clashing with other subunits, the N-terminal domain (domain I) of δ must be rotated outwards by at least 20–30° with respect to the C-terminal domain (domain III). Presumably, the binding of ATP to the γ subunits powers this change.

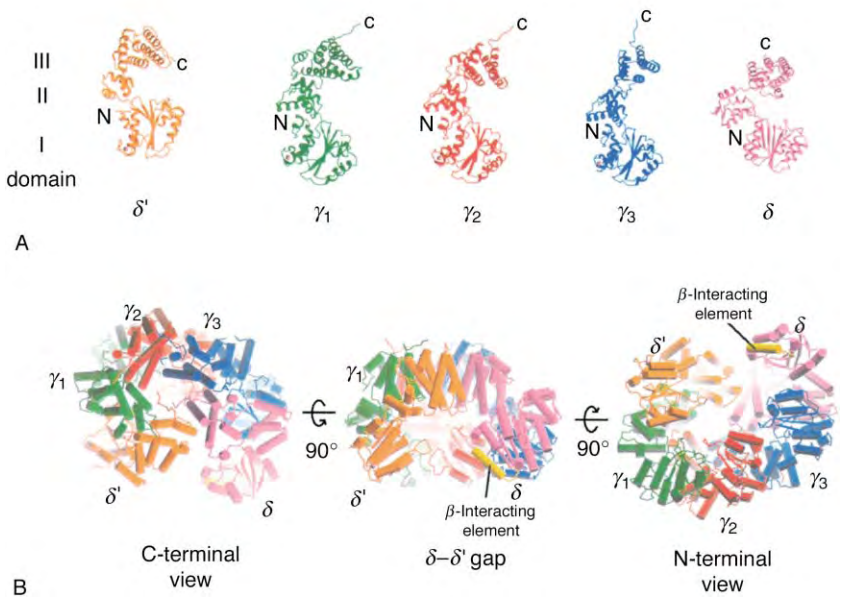

FIGURE 3 The structure of $\gamma_3\delta\delta'$ and individual subunits. Each of the clamp loader subunits is shown in (A). The three domains are indicated as well as the amino (N) and carboxy (C) terminal of each protein. In (B), the $\gamma_3\delta\delta'$-assembly is shown from three different views.

δ′ as a Stator All three subunits are present in different conformations, mainly due to the rigid body motion between domain III and domains I/II. Likewise, δ has a similar conformational difference upon comparing δ in $\beta_1-\delta$ and $\gamma_3\delta\delta'$-complexes. These observations suggest a flexibility between domain III and domains I/II in these protomers. However, the crystal structure of δ' alone is very similar to the structure of δ' in the $\gamma_3\delta\delta'$-assembly, implying that δ' is a more rigid protein than γ or δ. Examination of the structure of δ' reveals extra packing interactions between domains II and III, which may account for the apparent rigidity. Because of this seeming rigidity, δ' has been termed the stator (the stationary part of a motor against which other parts move). δ' can also be thought of as a backboard against which the ATP-dependent motions of the other subunits are braced.

Release of β and Closing of the Clamp

Once the γ-complex has bound to β and opened the clamp, it brings β to the primed site. The clamp loader-clamp complex binds tightly to primed DNA, which is, in fact, the best effector of ATP hydrolysis by γ-complex. When the clamp loader–clamp complex interacts with the primed site, the clamp loader hydrolyzes ATP and dissociates from β, leaving it on the primed site (Figure 4). It is proposed that the clamp loader is brought back to the inactive state upon hydrolysis of ATP (Figure 4). This presumably brings δ back into close proximity to γ and δ', pushing β off the δ wrench thereby releasing and allowing it to close around DNA.

The Role of χ and ψ

Neither χ nor ψ are required for clamp loading *in vitro*. However, when χ and ψ are missing from the clamp loader, both clamp loading and elongation become

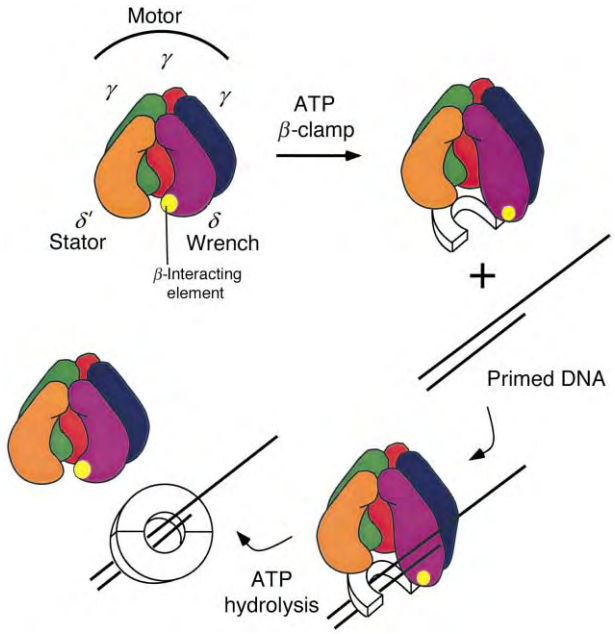

FIGURE 4 Clamp loading cycle by γ-complex. First, γ-complex binds ATP, which renders it capable of binding to and opening β. The clamp loader–clamp complex interacts with primed DNA which triggers ATP hydrolysis by γ-complex. ATP hydrolysis may cause γ-complex to release the clamp, allowing it to close around DNA.

sensitive to increased salt concentrations. This sensitivity is thought to arise from an interaction between χ and single strand DNA-binding protein, SSB. The contact between χ and SSB is important for the exchange of primase for both clamp loader and polymerase at the primed site. The role of ψ is somewhat less clear. It interacts with χ in a 1:1 complex. ψ also binds γ and forms a link between χ and the γ complex.

τ-Subunit and Interaction with DNA Polymerase III

The *dnaX* gene that encodes γ (47 kDa) also produces another protein, τ (71 kDa). A translational frameshift results in a stop codon to produce γ, whereas τ is the full-length protein. Therefore, τ is composed of γ plus 24 kDa of extra carboxy-terminal sequence. τ can fully substitute for γ in the clamp loader. Furthermore, while cells can survive in the absence of γ, they lack viability in the absence of τ. Thus, the carboxy-terminal residues unique to τ are essential. The carboxy-terminal sequences of τ interact with the DNA polymerase III core and with the replicative helicase, DnaB, providing a link between the clamp loader and the replisome. In the replicase, the clamp loader is thought to contain two τ subunits and one γ subunit, enabling this single clamp loader to cross-link two core polymerases for simultaneous synthesis of leading and lagging strands of the chromosome.

T4 Bacteriophage Clamp Loader

Although most viruses and bacteriophage do not employ a clamp and clamp loader machinery, T4 phage produces a clamp (gp45) and clamp loader for its chromosomal replicase (gp43). The clamp loader is composed of two different subunits, gp44 and gp62. Each clamp loader contains four copies of gp44 and one copy of gp62. Thus, the T4 phage clamp loader is a heteropentamer, like γ-complex. The gp44 subunit is homologous to γ and δ', and thus probably provides the motor function of the clamp loader. Gp62 has no known homologues.

In T4 bacteriophage, as in several eukaryotic DNA viruses, replication is tightly coordinated with late gene transcription (i.e., the early to late gene switch). Several elegant studies have revealed that the gp45 clamp slides along DNA and binds directly to RNA polymerase, specifically activating it at late gene promoters.

Archaeal RFC

Like the T4 bacteriophage clamp loader, archaeal cells contain only two different clamp loader subunits. These subunits are referred to as RFCL (L for large subunit) and RFCS (S for small subunit). Together these proteins form a complex that is capable of loading its cognate clamp onto DNA and stimulating the replicative DNA polymerase in several species of archaea. Initial characterization of the composition of these RFC complexes suggests a pentamer, with one or two copies of RFCL and three or four copies of RFCS, depending on the species. A structure of the small subunit from *Pyrococcus furiousus* has been solved. RFCS forms a dimer of trimers, and the trimer unit shares similar structure to the γ-trimer in γ-complex. In fact, RFCS has the same chain-fold and three-domain structure as γ, δ, and δ'.

Eukaryotic Clamp Loader

The eukaryotic clamp loader, termed replication factor C (RFC), is composed of five different subunits known as Rfc1-5 in *S. cerevisiae* and p140, p37, p36, p40, and p38 in human cells. All five subunits share sequence homology to each other and to the γ and δ' subunits of γ complex. Analogous to γ complex, the C termini of the RFC subunits are needed to form the pentamer. There is no crystal structure information on eukaryotic RFC; however, atomic force and electron microscope studies of RFC indicate a similarity to *E. coli* γ-complex. Atomic force microscope images of RFC indicate that the subunits are arranged in a circle similar to the C-terminal view of γ-complex. Electron microscope images of RFC in the presence of ATP show a gap in the circle similar to the amino-terminal face of γ-complex.

The results of biochemical experiments suggest that RFC may also function similarly to γ-complex. However, there are some important differences between γ-complex and RFC. For example, RFC has four rather than three ATP sites. This observation and the observation of five different subunits in RFC may reflect the greater complexity of eukaryotic cells compared to bacteria. It has been shown that PCNA interacts with numerous other proteins besides DNA polymerases. In addition, there are modified RFC assemblies in which one of the subunits has been substituted with a different protein. Hence, RFC (and modified RFCs) are thought to be involved in many different cellular processes such as DNA repair, cell cycle control/checkpoint, and chromosome segregation. PCNA can therefore be thought of as a "bull's eye," targeting proteins to DNA for specific events.

See Also the Following Articles

DNA Polymerase III, Bacterial • DNA Replication Fork, Bacterial • Eicosanoid Receptors • Sliding Clamps in DNA Replication: *E. coli* β-Clamp and PCNA Structure

Glossary

processivity The ability of an enzyme to catalyze more than one turnover before releasing the product or the substrate.

replicase Protein machinery that copies a strand of DNA. Chromosomal replicases typically contain a core polymerase, a processivity clamp, and a clamp loader.

replisome Protein machinery that copies DNA (both strands of DNA). Replisomes include the replicase (polymerase, clamp and clamp loader) as well as a helicase to unwind DNA. A priming activity is required for one strand.

Further Reading

Benkovic, S. J., Valentine, A. M., and Salinas, F. (2001). Replisome-mediated DNA replication. *Annu. Rev. Biochem* **70**, 181–208.

Jeruzalmi, D., Yurieva, O., Zhao, Y., Young, M., Stewart, J., Hingorani, M., O'Donnell, M., and Kuriyan, J. (2001). Mechanism of processivity clamp opening by the delta subunit wrench of the clamp loader complex of *E. coli* DNA polymerase III. *Cell* **106**, 417–428.

Lehninger, A. L., Nelson, D. L., and Cox, M. M. (2000). *Principles of Biochemistry.* Worth Publishing, New York.

O'Donnell, M., Jeruzalmi, D., and Kuriyan, J. (2001). Clamp loader structure predicts the architecture of DNA polymerase III holoenzyme and RFC. *Curr. Biol.* **11**, R935–R946.

Biography

Megan J. Davey is a Research Associate with Mike O'Donnell at The Rockefeller University, where she has pursued her interest in the assembly of replication–initiation complexes in bacterial and eukaryotic systems. Previously, Megan earned her Ph.D. studying plasmid segregation with Barbara Funnell at the University of Toronto.

Mike O'Donnell works in the area of DNA-replication mechanisms in several systems. He initially discovered the circular sliding clamp and the clamp–loader complex in the *E. coli* DNA-replication system in 1991. He obtained his Ph.D. from the Biological Chemistry Department at the University of Michigan, and then did postdoctoral training with Arthur Kornberg and Robert Lehman at Stanford University. He is now an Investigator at Howard Hughes Medical Institute (HHMI) and Professor at Rockefeller University in Manhattan, New York.

Propionyl CoA–Succinyl CoA Pathway

Wayne A. Fenton
Howard Hughes Medical Institute and Yale School of Medicine, New Haven, Connecticut, USA

The importance of the short metabolic pathway from propionyl CoA to succinyl CoA in humans was recognized in the 1960s with the description of newborns with severe, often fatal, metabolic acidosis accompanied by massive excretion of propionic or methylmalonic acid. It was established that these conditions resulted from deficiencies in the activity of propionyl CoA carboxylase or methylmalonyl CoA mutase, respectively, two of the enzymes in the pathway. These enzymes themselves were found to be defective in many cases. Because each requires a vitamin-derived coenzyme for activity, however, other cases resulted from defects in the transport or metabolism of the vitamins (biotin and vitamin B_{12}, respectively). Many of the proteins and enzymes involved in these steps have subsequently been described.

The Propionyl CoA–Succinyl CoA Pathway

The pathway involved is shown in eqn. [1]. Propionyl CoA is carboxylated by propionyl CoA carboxylase (EC 6.4.1.3), a biotin-containing enzyme, to form D-methylmalonyl CoA. This product is racemized by methylmalonyl CoA racemase (epimerase) (EC 5.1.99.1) to D,L-methylmalonyl CoA. The L-isomer is the substrate for methylmalonyl CoA mutase (EC 5.4.99.2), which carries out an adenosylcobalamin (coenzyme B_{12})-dependent rearrangement of the carbon backbone to form succinyl CoA. This product then enters the tricarboxylic acid cycle.

Propionyl CoA arises from a number of metabolic pathways, predominantly the catabolism of certain amino acids (isoleucine, methionine, threonine, and valine) and the β-oxidation of odd-chain fatty acids, with minor contributions from the degradation of thymine, uracil, and the side chain of cholesterol. Methylmalonyl CoA is produced essentially only from propionyl CoA. Gut bacteria produce a significant amount of propionic acid (and lesser amounts of methylmalonic acid); thus, propionyl CoA can also arise from this source by the action of cellular acyl CoA synthases.

The Enzymes

Propionyl CoA Carboxylase

Propionyl CoA carboxylase (PCC) is a large enzyme (~770 kDa) composed of two dissimilar subunits, α (72 kDa) and β (56 kDa), arranged in an $(\alpha\beta)_6$ quaternary structure. It is ubiquitously expressed and is localized to the mitochondrial matrix. The individual subunits are synthesized in the cytosol as larger precursors, which are proteolytically processed to their mature sizes and assembled after translocation into the mitochondrion. The α-subunit bears the lysine to which biotin is covalently bound via an isopeptide linkage to the ε-amino group and carries out the half-reaction in which carbon dioxide is activated to react with biotin, forming an enzyme-bound carboxyl-biotin intermediate. The β-subunit completes the reaction by transferring the carboxyl moiety to propionyl CoA to form methylmalonyl CoA.

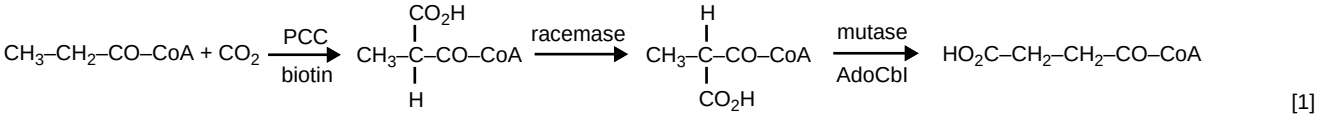

[1]

propionyl CoA | D-methylmalonyl CoA | L-methylmalonyl CoA | succinyl CoA

Methylmalonyl CoA Racemase

It is a dimer of identical subunits (~16 kDa) and is likely to be mitochondrially localized, but its expression pattern has not been established. The reaction mechanism appears to involve a simple abstraction/replacement of the labile proton on the α-carbon. In fact, racemization of methylmalonyl CoA occurs spontaneously in solution at a significant rate under physiologic conditions by exchange of this proton.

Methylmalonyl CoA Mutase

It is a dimer of identical subunits (78.5 kDa) and is expressed in all tissues examined. Its subunits are synthesized as larger precursors in the cytosol, translocated into mitochondria, and processed and assembled in the mitochondrial matrix. The coenzyme, adenosylcobalamin (AdoCbl), is very tightly bound to mutase; X-ray crystallography of the homologous enzyme from *P. shermanii* indicates that AdoCbl is buried in the interior of the enzyme. The reaction mechanism, while typical of AdoCbl-dependent enzymes, is unique in mammalian metabolism. In the presence of substrate, the carbon–cobalt bond of AdoCbl cleaves homolytically to form a free radical pair, Cbl^{II} and a deoxyadenosyl radical. The deoxyadenosyl radical abstracts hydrogen from the substrate to form a substrate radical that undergoes a rearrangement to form the product radical. This species recovers the hydrogen from deoxyadenosine to generate the final product and the original radical pair, which reverts to AdoCbl as the product leaves. Because these radical species are very labile to quenching by solvent, they appear to be highly protected in a buried active site. Crystal structures of the *P. shermanii* enzyme complexed with substrate analogues have been interpreted to suggest that the active site cleft opens to permit substrate entry, then closes until the reaction is completed, at which time it opens again to release the product.

The Cofactors

Biotin

Biotin is an abundant vitamin, available from a variety of plant and animal sources. It is used directly as a cofactor by four carboxylases in humans: acetyl CoA carboxylase, pyruvate carboxylase, β-methylcrotonyl CoA carboxylase, and PCC. Its metabolism is relatively uncomplicated, involving only two enzymes of note. One is biotinidase, a serum enzyme in man and other mammals, which specifically cleaves the isopeptide bond in biocytin (-biotinyl-lysine), the end product of proteolysis of biotin-containing enzymes, to release biotin for reuse. The other is holo-carboxylase synthase, the enzyme that forms the isopeptide bond between cellular biotin and the ε-amino group of the active site lysine in the apocarboxylases. Genetically determined defects in each of these have been described in humans, leading to a general deficiency of all of the carboxylases (multiple carboxylase deficiency) and pleiotropic metabolic effects, including propionic acidemia/aciduria (PA).

Vitamin B_{12} (Cobalamin)

In contrast to biotin, cobalamin is a rare vitamin that is available only from animal sources, which largely derive it in turn from gut bacteria. Plants, including yeast, do not synthesize the vitamin or use its cofactor forms. Although the daily requirement for vitamin B_{12} in humans is low (the current recommended dietary allowance, RDA, is 2.4 μg), an elaborate system of digestive enzymes and specific, high-affinity binding and transport proteins exists to ensure its efficient capture from dietary sources and delivery to cells throughout the body. Two distinct cofactor forms of the vitamin, methylcobalamin (MeCbl) and AdoCbl, are produced by a series of intracellular metabolic steps (eight have been recognized genetically) and are used by only two enzymes, methionine synthase and methylmalonyl CoA mutase, respectively. Deficiencies of many of these enzymes and proteins have been described. The most common are acquired defects in the activities of the digestive and gut transport proteins resulting from diseases of the digestive tract or surgical resection of these organs. These lead to a general vitamin B_{12} deficiency and the condition known as pernicious anemia. Genetic defects in these same proteins have been described, but are much rarer; they also lead to a form of pernicious anemia, generally at a much earlier age. Pernicious anemia is usually accompanied by methylmalonic acidemia/aciduria, although the hematologic defects are clinically more significant. Defects in cellular cobalamin metabolism lead to a variety of conditions, including methylmalonic acidemia/aciduria.

The Diseases

Propionic Acidemia/Aciduria (PA)

PA occurs in the setting of reduced activity of PCC (Figure 1). This can be due to biotin deficiency (very rare), biotin transport and activation defects (biotinidase or holocarboxylase synthase deficiency; sites 3 and 2, respectively), or defects in PCC itself (site 1). The first two of these lead to multiple carboxylase deficiency, in which all four biotin-dependent carboxylases are affected. This condition is characterized by neurologic symptoms, hypotonia, and failure to thrive, sometimes accompanied by skin rashes and allopecia. In genetically

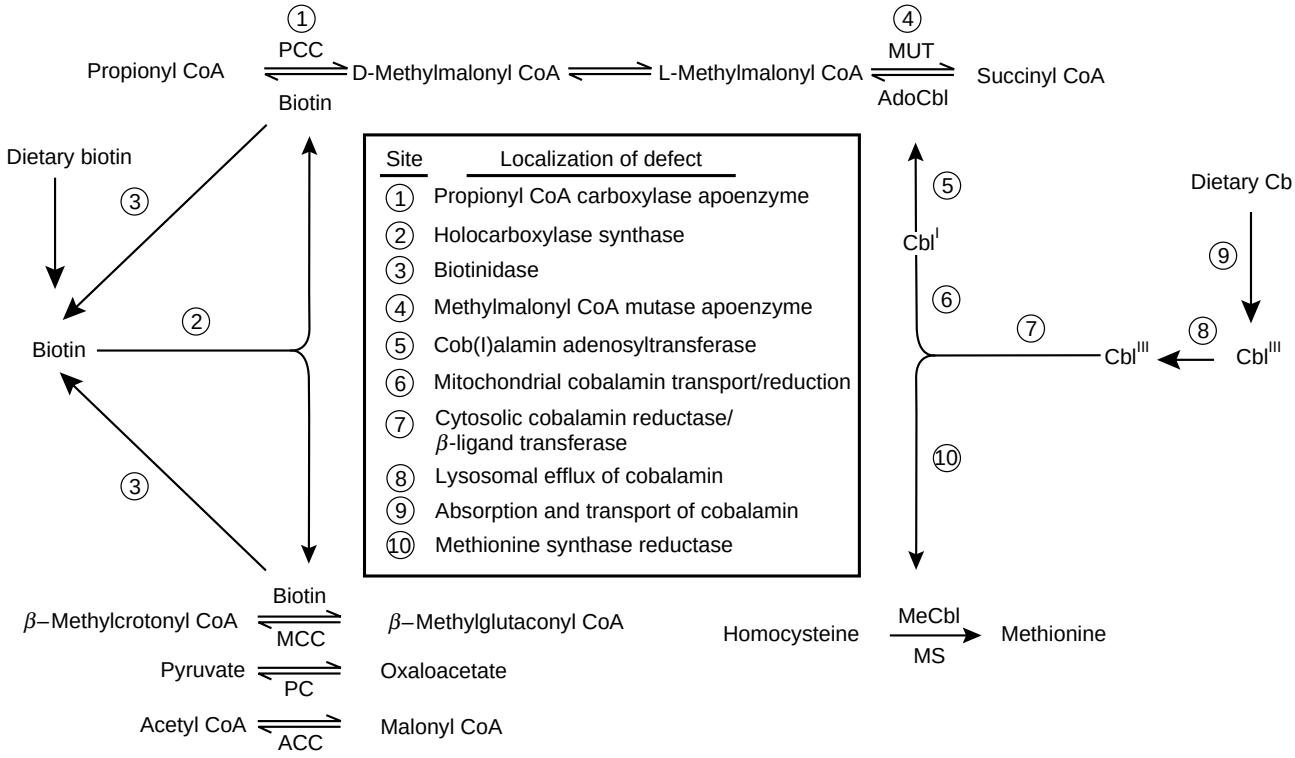

FIGURE 1 Sites of defects affecting the propionyl CoA–succinyl CoA pathway. A schematic of the biotin and cobalamin metabolism pathways is shown, along with their intersections with the propionyl CoA pathway. In several instances, the indicated sites encompass more than one enzyme or gene product. Genetic analysis suggests two gene products are involved at site 6; only one, of undefined activity, has been identified. Likewise, two gene products affect site 7 and the indicated metabolic activity. Defects in multiple gene products can contribute at site 9, including those in intrinsic factor, intrinsic factor receptor (megalin), and transcobalamin II, the serum cobalamin-carrying protein. Note that defects at site 10 and in methionine synthase (MS) affect a separate branch of cobalamin metabolism that has no impact on the propionyl CoA pathway. ACC, MCC, PCC, PC, acetyl CoA, β-methylcrotonyl CoA, propionyl CoA, and pyruvate carboxylase, respectively; MS, methionine synthase; MUT, methylmalonyl CoA mutase; Cbl, Cbl^{I}, Cbl^{III}, cobalamin and its 1+ and 3+ oxidation states, respectively; AdoCbl, MeCbl, adenosylcobalamin and methylcobalamin, respectively.

determined cases, onset of symptoms is often neonatal (synthase deficiency) or infantile (biotinidase deficiency), but may be delayed beyond the second decade. Biochemically, multiple carboxylase deficiency is marked by specific excretion of both propionic acid and methylcrotonic acid, their secondary metabolites (such as β-hydroxy propionic acid and tiglic acid), and glycine conjugates of these acids. Activities of the affected enzymes are low in serum (biotinidase) or cultured cells from patients, as are the activities of the carboxylases. At the genetic level, multiple carboxylase deficiency is an autosomal recessive trait, and mutations have been found in the genes for each of these enzymes. Treatment with high doses of biotin is usually effective in ameliorating these conditions.

PA arising from genetic defects in PCC itself is both more specific and often more severe. Neonatal onset is common, with vomiting, hypotonia, and neurologic symptoms resulting from an overwhelming metabolic acidosis. Massive excretion of propionic acid and its metabolites and conjugates is often accompanied by severe hyperammonemia. PCC activity is low or absent in cultured cells, but the other carboxylases are unaffected. PCC deficiency is inherited as an autosomal recessive trait, and causative mutations have been found in the genes for both the α- and β-subunits. Initially, treatment is supportive, seeking to reverse the profound metabolic acidemia and equally life-threatening hyperammonemia. Long-term therapy includes protein restriction using synthetic diets formulated to have reduced amounts of the metabolic precursors of propionate, such as branched-chain amino acids and odd-chain fatty acids, and antibiotic treatment to reduce the contribution of gut bacteria to the total metabolic load of propionate. Only a few patients with isolated PCC deficiency have responded to biotin supplementation. The long-term outcome for most patients has been poor, with many succumbing to acute metabolic decompensation triggered by infectious illnesses. However, a few have survived to adulthood and there are also a number of patients who have not been diagnosed until late into their second or even third decade. Although it has been suggested that genetic factors, such as the severity of the effects of a mutation on PCC activity, may

play a role in determining long-term survival, no clear genotype/phenotype correlation has been uncovered.

Methylmalonic Acidemia/Aciduria (MMA)

MMA arises from deficiencies in the activity of mutase. Although racemase deficiency would also be expected to produce MMA, no patients with this defect have been described. Environmental cobalamin deficiency, acquired and genetically determined cobalamin transport deficiencies, and cellular cobalamin activation defects, as well as defects in mutase itself, all of these contribute to the occurrence of this condition. Although environmental cobalamin deficiency is rare, it does occur in strict vegans and particularly in their breast-fed children. Much more common is acquired cobalamin deficiency resulting from disease processes affecting the stomach, including ulcers, alcoholism-induced destruction of the gastric mucosa, and surgical intervention including gastric bypass. All of these reduce the ability of the gastric parietal cells to produce intrinsic factor, a cobalamin transport protein that is essential for delivering ingested cobalamin to cells of the intestinal mucosa, where it is taken up and transported into the blood stream. The multi-step intestinal transport system for cobalamin (site 9) is also subject to genetic defects, although these are relatively rare. Clinically, the resulting cobalamin deficiency in all of these cases produces pernicious anemia, a characteristic megalobastic anemia. Biochemically, MMA can be demonstrated in these patients, although it is often mild, depending on the degree of cobalamin deficiency, and cellular mutase activity may be reduced. Therapeutically, the pernicious anemia and MMA resulting from cobalamin deficiency, whatever the underlying cause, can be treated effectively by injections of vitamin B_{12}.

Much more profound MMA occurs in patients with genetically determined defects in cellular cobalamin metabolism or in mutase itself. In these cases, severe neonatal metabolic acidosis is accompanied by massive excretion of methylmalonic acid, as well as lesser amounts of propionic acid and their metabolites. Because at least three of the eight cellular metabolic steps are common to AdoCbl and MeCbl production (sites 7 and 8), patients with defects in these steps also excrete homocystine, the oxidized form of homocysteine, the substrate of methionine synthase. Mutase activity is reduced or absent in cultured cells from patients with these disorders and from those with defects in the three metabolic steps that affect only AdoCbl metabolism (sites 5 and 6), although it can be restored in extracts of cells from patients by the addition of exogenous AdoCbl. Extracts from cells of patients with defects in mutase itself (site 4) generally do not show activity even with AdoCbl supplementation, except in rare cases where massive amounts of the coenzyme produce activity from a defective mutase enzyme with an abnormally high binding constant for AdoCbl. Genetically, all of these conditions appear to be inherited as autosomal recessive traits. In most cases, causative mutations in the individual genes for the affected enzymes have been found. Treatment of patients with defects in cellular cobalamin metabolism and in mutase has included symptomatic treatment of the severe metabolic acidosis, followed by protein restriction, synthetic diet, and antibiotic therapy, as with PA. Similarly, the long-term prognosis of these patients is poor, with one group of exceptions. In contrast to the lack of biotin-responsiveness in isolated PA, the clinical state of some MMA patients respond dramatically to supplementation with massive amounts of coenzyme in the form of injected hydroxocobalamin, with almost complete resolution of their clinical condition. Most of these patients have defects in one particular cobalamin metabolic enzyme (at site 6). The long-term prognosis of patients in this group seems very promising, although the effect of chronic MMA, which these patients still exhibit, remains unclear.

See Also the Following Articles

Biotin • Vitamin B_{12} and B_{12}-Proteins

Glossary

coenzyme/cofactor A small bio-organic compound, usually derived from a vitamin, that plays an essential role in assisting a specific enzyme to carry out its reaction.

hyperammonemia The condition of a high concentration of ammonium ion (ammonia) in the blood; ammonium ion is a common metabolic product and is normally found in significant amounts in the blood, but moderate elevations can damage the central nervous system if untreated.

metabolic acidosis A condition of reduced blood pH and bicarbonate ion concentration in response to the overproduction or decreased excretion of acidic metabolites.

pernicious anemia A distinctive blood disorder characterized by macrocytes in circulation and megaloblasts in bone marrow, generally due to a deficiency of either vitamin B_{12} (cobalamin) or folic acid.

propionic/methylmalonic acidemia The condition of excessive amounts of these metabolites in blood, where they are normally present in very small amounts.

propionic/methylmalonic aciduria The condition of excretion of very large amounts of these metabolites in the urine.

Further Reading

Banerjee, R. (ed.) (1999). *Chemistry and Biochemistry of B_{12}*. Wiley, New York.

Fenton, W. A., Gravel, R. A., and Rosenblatt, D. S. (2001). Disorders of propionate and methylmalonate metabolism. In *The Metabolic and Molecular Bases of Inherited Disease* (C. R. Scriver, A. L. Beaudet, W. S. Sly and D. Valle, eds.) 8th edition, pp. 2165–2193. McGraw-Hill, New York.

Rosenblatt, D. S., and Fenton, W. A. (2001). Inherited disorders of folate and cobalamin transport and metabolism. In *The Metabolic*

and Molecular Bases of Inherited Disease (C. R. Scriver, A. L. Beaudet, W. S. Sly and D. Valle, eds.) 8th edition, pp. 3897–3933. McGraw-Hill, New York.

Wolf, B. (2001). Disorders of biotin metabolism. In *The Metabolic and Molecular Bases of Inherited Disease* (C. R. Scriver, A. L. Beaudet, W. S. Sly and D. Valle, eds.) 8th edition, pp. 3935–3962. McGraw-Hill, New York.

Biography

Wayne A. Fenton is a Research Scientist in Genetics at Yale University School of Medicine. His general interests are in cobalamin metabolism and the mechanisms of protein folding and unfolding. He received a Ph.D. from Brandeis University and carried out postdoctoral work at Yale University.

Prostaglandins and Leukotrienes

William L. Smith
University of Michigan Medical School, Anna Arbor Michigan, USA

Robert C. Murphy
University of Colorado Medical School, Colorado, Denver, USA

Prostaglandins and leukotrienes are different types of eicosanoids – oxygenated, 20 carbon fatty acids synthesized from arachidonic acid (AA) (all *cis* 5,8,11,14-eicosatetraenoic acid). AA is a member of the n-6 family of fatty acids that are essential for mammals. There are three major groups of eicosanoids formed via three distinct pathways – the cyclooxygenase, lipoxygenase, and epoxygenase pathways. These pathways occur in higher eukaryotes that contain highly unsaturated fatty acids. Prostanoids, which include the prostaglandins (PGs) and thromboxanes (TXs), are formed through the cyclooxygenase pathway, leukotrienes and related hydroxy fatty acids come from the lipoxygenase pathway, and epoxy and dihydroxy acids are formed via epoxygenase (P450) pathways. Prostanoids and leukotrienes function through G protein-linked receptors, and there are one or more receptors for each prostanoid and leukotriene. These compounds act locally near their sites of synthesis without entering the circulation. They coordinate intercellular communication between the same (autocrine) and different (paracrine) cell types. Prostanoids promote inflammation and thrombosis and leukotrienes are involved in asthma. Nonsteroidal anti-inflammatory drugs such as aspirin, ibuprofen, and COX-2 inhibitors function by attenuating prostanoid synthesis while inhibitors of leukotriene synthesis and action such as zileuton and montelukast, respectively, are used to treat asthma.

Prostanoid Structures

Figure 1 shows the biosynthetic relationships among the prostanoids formed from arachidonic acid (AA). The letters following the abbreviation prostaglandins (PGs) indicate the nature and location of the oxygen-containing substituents present in the cyclopentane ring; the subscript indicates the number of carbon–carbon double bonds in the side chains. Greek subscripts denote the orientation of ring hydroxyl groups (e.g., $PGF_{2\alpha}$). Prostanoids known as isoprostanes are formed from AA by nonenzymatic autooxidation and consequently contain many stereoisomers. Interestingly, the amounts of isoprostane metabolites in urine are greater than prostanoids formed enzymatically.

Prostanoid Biosynthesis

Eicosanoids are not stored in cells but are formed on demand in response to extracellular hormonal stimuli (e.g., bradykinin, angiotensin, thrombin) that increase cell Ca^{2+} concentrations. Prostanoid formation requires three enzymatic steps: (1) mobilization of AA (or 2-arachidonylglycerol (2-AG)) from membrane phospholipids, (2) conversion of arachidonate (or 2-AG) to PGH_2 (or 2-PGH_2-glycerol), and (3) isomerization of PGH_2 (or 2-PGH_2-glycerol) to one of the major prostanoids by a terminal synthase. Mobilization of AA involves cytosolic phospholipase A_2 ($cPLA_2$) which translocates to the endoplasmic reticulum (ER) and nuclear membrane (NM) when intracellular Ca^{2+} concentrations rise and cleaves AA from a phospholipid on the cytosolic surface of the membrane. Newly released AA moves, methyl end first, to the luminal half of the bilayer where it enters the active site of a prostaglandin endoperoxide H synthase (PGHS) and is oxygenated to PGG_2 and its 15-hydroperoxyl group is then reduced to form PGH_2; PGHSs are also called cyclooxygenases (COX) and there are two isoforms (PGHS-1 and -2; COX-1 and -2). Once formed, PGH_2 is isomerized by a synthase located in the ER (e.g., TXA synthase, PGE synthase). Recently, 2-AG has been found to be converted to 2-PGH_2-glycerol by PGHS-2. This latter intermediate can be converted to the 2-prostanyl-glycerol derivatives but not 2-thromboxane-glycerol. 2-AG itself is probably formed from phosphatidylcholine by phospholipase C and monoacylglycerol lipase.

PGHS Catalysis and Inhibition

Figure 2 is a model of the cyclooxygenase and peroxidase active sites of ovine PGHS-1. To initiate oxygenation of AA at the cyclooxygenase site, the heme group at the peroxidase site must first be oxidized by a hydroperoxide. This causes formation of an oxidized

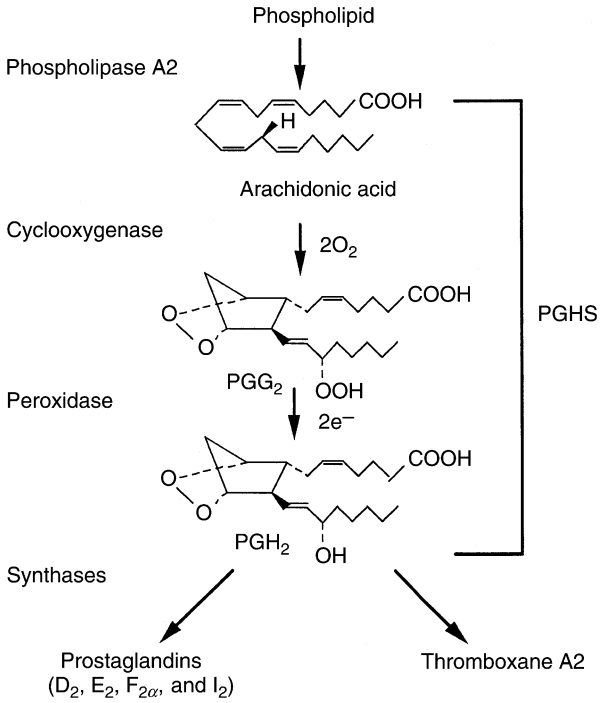

FIGURE 1 Biosynthesis of common prostanoids from AA.

heme intermediate that is reduced by an electron from Tyr385 thereby generating a Tyr385 radical. This radical abstracts a hydrogen from AA so that it can react with oxygen (Figure 1). The guanidino group of Arg120 binds to the carboxylate group of AA.

PGHS-1 is a constitutive enzyme purified in 1975 and its cDNA cloning has been reported in 1988. PGHS-2 is an inducible enzyme discovered in 1991 as an immediate early gene product in phorbol ester-activated murine 3T3 cells and in *v-src*-transformed chicken fibroblasts. PGHS-2 contains a unique 18 amino acid insert of as yet unknown function near its carboxyl terminus. The reason for the existence of the two PGHS isoforms is not known. Each protein functions as a homodimer with a monomer mass of 72 kDa. PGHSs are integral membrane proteins which instead of having transmembrane helices have a cluster of four amphipathic helices that interact with only one face of the lipid bilayer.

PGHSs are inhibited by nonsteroidal anti-inflammatory drugs (e.g., aspirin, ibuprofen, naproxen), which compete with AA for binding to the cyclooxygenase site of PGHSs. Prostaglandin synthesis mediated by PGHS-2 can be inhibited by anti-inflammatory steroids, which block the synthesis of PGHS-2 protein. Drugs called COX-2 inhibitors (e.g., rofecoxib and celecoxib) target PGHS-2 specifically and are used as anti-inflammatory and analgesic agents. Aspirin, acetylsalicylic acid, binds the cyclooxygenase site of PGHSs and acetylates Ser530 causing irreversible inhibition of PGHSs (Figure 2). Low doses of aspirin are used prophylactically to reduce coronary thrombosis; at low doses, aspirin inhibits PGHS-1 in platelets blocking thromboxane formation. PGHS inhibitors appear to reduce mortality from colon cancer.

PGHS-1 and PGHS-2 Gene Expression

There are separate genes for PGHS-1 and PGHS-2 located on different chromosomes. They have similar intron/exon structures but the PGHS-2 gene is 8 kb and the PGHS-1 gene is 22 kb. Little is known about the regulation of PGHS-1 gene expression. PGHS-2 gene transcription can be induced by cytokines and growth factors that function through multiple response elements in the PGHS-2 gene promoter. There is much interest in

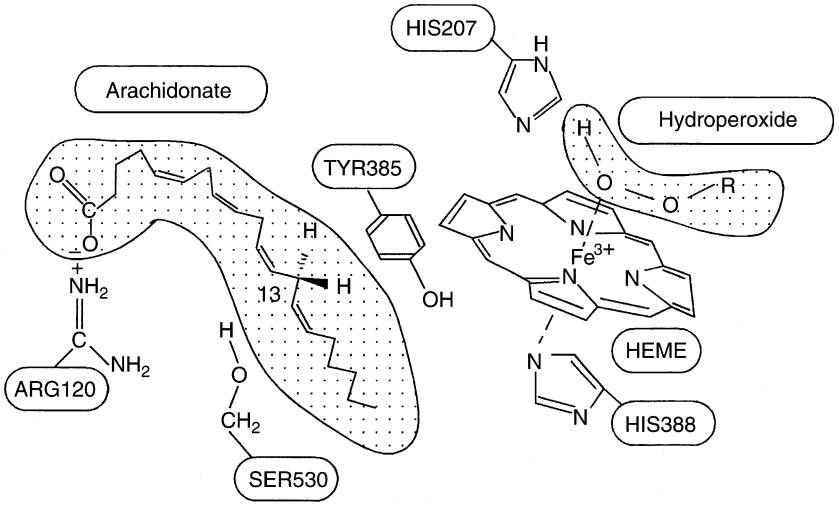

FIGURE 2 Model of the cyclooxygenase and peroxidase active sites of the ovine PGHS-1.

this because of the potential role of altered PGHS-2 expression in carcinogenesis.

PGH_2 Metabolism

Different cells form different prostanoids. PGE_2, PGD_2, PGF_2, PGI_2, and TXA_2 synthesis from PGH_2 is catalyzed by PGE synthase, PGD synthase, PGF synthase, PGI synthase, and TXA synthase, respectively; all of these enzymes catalyze isomerization reactions. PGF_2 formation involves a two-electron reduction of PGH_2. PGI synthase and TXA synthase are cytochrome P-450s. PGE synthase is a member of the MAPEG family of transmembrane ER proteins and requires reduced glutathione for activity. There are two PGD synthases; one is glutathione dependent and has been isolated from spleen and another is glutathione independent and occurs in brain.

Prostanoid Catabolism

The initial step in the inactivation of PGE_2 is oxidation of the 15-hydroxyl group to a 15-keto group catalyzed by 15-hydroxyprostaglandin dehydrogenase. Further catabolism involves reduction of the double bond between C-13 and C-14, β-oxidation, and ω-oxidation.

Prostanoid Actions

There are pharmacologically distinct receptors for each of the known prostanoids. In the case of PGE_2, four different prostaglandin E (EP) receptors have been identified and designated as EP1, EP2, EP3, and EP4 receptors. EP1 is coupled through G_q to the activation of phospholipase C, EP2 and EP4 are coupled via G_s to the stimulation of adenylate cyclase and EP3 receptors are coupled via G_i to inhibition of adenylate cyclase (16).

EP3 receptors are involved in the development of fever, EP2 and EP4 function in bone resorption and EP1 receptors are involved in chemically induced colon cancer. Prostanoids can activate some isoforms of peroxisomal proliferator activated receptors (PPARs). PGI_2 can be involved in PPARδ-mediated responses such as decidualization and apoptosis.

Leukotrienes and Lipoxygenase Products

Leukotrienes were discovered in 1979 during the search for the chemical structure of the "slow reacting substance of anaphylaxis." Leukotrienes are produced by the action of 5-lipoxygenase (5-LO) (Figure 3) which catalyzes both an oxygen insertion to form 5-HpETE and a dehydration reaction to form leukotriene A_4 (LTA_4). LTA_4 is converted to the biologically active leukotrienes LTB_4 and LTC_4 by LTA_4 hydrolase and LTC_4 synthase, respectively. LTB_4 is a potent chemotactic and chemokinetic agent for human polymorphonuclear leukocytes whereas LTC_4 constricts specific smooth muscle (e.g., bronchial smooth muscle) and mediates leakage of vascular fluid in the process of edema. The formation of LTC_4 versus LTB_4 is controlled by the expression of LTA_4 hydrolase or LTC_4 synthase by specific cell types. For example, the human neutrophil expresses LTA_4 hydrolase and produces LTB_4 while mast cells and eosinophils express LTC_4 synthase and produce LTC_4.

5-Lipoxygenase

Human 5-lipoxygenase (5-LO) (E.C.1.13.11.34) is a nonheme iron containing protein of 673 amino acids. It catalyzes the abstraction of a hydrogen atom from C-7 of AA and insertion of O_2 at C-5 to generate 5(S)-HpETE (Figure 3). The LTA_4 synthase activity of 5-LO then catalyzes removal of 10 pro-R hydrogen atoms from 5(S)-HpETE through a second redox cycle and an internal rearrangement of double bonds to form LTA_4. LTA_4, has a half-life of less than 10s at pH 7.4. Purified 5-LO requires Ca^{2+}, ATP, fatty acid hydroperoxide, and phosphatidylcholine in addition to the AA and O_2 substrates. Ca^{2+} facilitates the association of 5-LO with internal membranes. The need for an increase in intracellular Ca^{2+} concentrations differentiates 5-LO from other lipoxygenases. 5-LO oxygenates AA at the interface between membrane and cytosol. When Ca^{2+} concentrations increase in neutrophils and mast cells, 5-LO and cytosolic PLA_2 become associated with the nuclear membrane (NM) where another protein required for LTA_4 synthesis – 5-lipoxygenase activating protein (FLAP) – is found. In other cells 5-LO is constitutively associated with the NM while in alveolar macrophages 5-LO is present in the nucleus. The drug zileuton inhibits 5-LO.

The 5-LO gene is large (ca. 80 kb) and has 14 exons. It is on human chromosome 10. The human 5-LO gene promoter contains Sp1 and EGR-1 binding sites at -88 to -212 bp upstream of the translation start site. Genetic polymorphisms in humans are found in Sp1 binding sites.

5-Lipoxygenase Activating Protein (FLAP)

FLAP was discovered as a novel protein essential for leukotriene synthesis which was the target of an

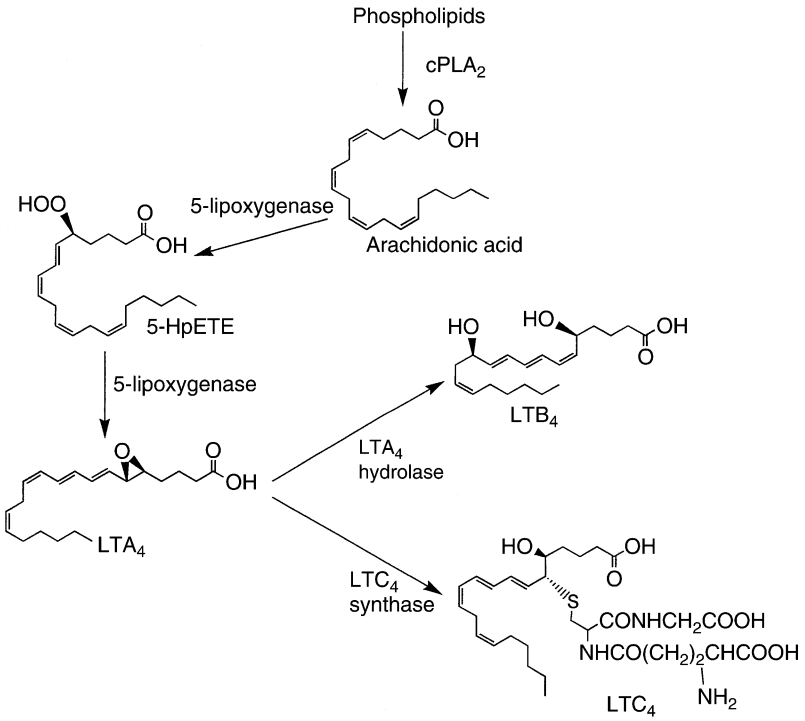

FIGURE 3 Biochemical pathway of the conversion of AA into the biologically active leukotrienes. AA released from phospholipid by $cPLA_2$ is metabolized by 5-LO to 5-hydroperoxyeicosatetraenoic acid (5-HpETE) and leukotriene A_4 (LTA_4) which is then converted to LTB_4 by LTB_4 hydrolase or conjugated to glutathione to form LTC_4 by LTC_4 synthase.

investigational drug from Merck (MK886). FLAP is an integral membrane protein of the NM containing 161-amino acids. The function of FLAP is unclear but it does bind AA analogues suggesting that it may transfer AA to 5-LO. LTC_4 synthase has 31% amino acid identity to FLAP with a highly conserved region putatively involved in AA binding.

LTA_4 Hydrolase and LTC_4 Synthase

LTA_4 hydrolase catalyzes the stereochemical addition of water to C-12 of LTA_4 to form the neutrophil chemotactic factor LTB_4. LTA_4 hydrolase contains 610 amino acids and one essential zinc atom. The enzyme is structurally related to zinc metalloproteases and exhibits protease activity; bestatin and captopril inhibit the enzyme. LTA_4 hydrolase is found in many cells including those which do not contain 5-LO, and it is felt that such cells function in transcellular LTB_4 synthesis. LTA_4 hydrolase is localized in the cytosol. To metabolize the unstable LTA_4, LTA_4 hydrolase must either come in contact with the NM during LTA_4 formation or a carrier protein must transfer LTA_4 to LTA_4 hydrolase. The crystal structure of LTA_4 hydrolase has been determined.

LTC_4 synthase (E.C.2.5.1.37) conjugates reduced glutathione (γ-glutamyl-cysteinyl glycine) to LTA_4. LTC_4 synthase is located on the NM. The enzyme has significant sequence homology to microsomal glutathione-S-transferases and FLAP. LTC_4 synthase is found predominantly in mast cells, macrophages, eosinophils, and monocytes. MK-886, which interacts with FLAP, also inhibits LTC_4 synthase. The gene for LTC_4 synthase is located on human chromosome 5.

Leukotriene Metabolism

LTB_4 can be oxygenated to 20-hydroxy-LTB_4 by specific cytochrome P-450s of the CYP4F family. 20-hydroxy-LTB_4 can be further metabolized to 20-carboxy-LTB_4 by CYP4F3 or to 20-oxo-LTB_4 by alcohol dehydrogenase then to 20-carboxy-LTB_4 by fatty aldehyde dehydrogenase. An alternative pathway involves an initial oxidation of the 12-hydroxy group to a 12-oxo moiety followed by reduction of the conjugated dienone and the 10,11 double bond. A secondary catabolic pathway, β-oxidation can occur from the C-1 carboxyl moiety of LTB_4 resulting in the loss of the C-5 hydroxyl group and from the 20-carboxy terminus of 20-carboxy-LTB_4. Individuals with genetic deficiencies in peroxisomal metabolism (Zellweger disease) that reduce β-oxidation or in aldehyde dehydrogenase (Sjogren–Larsson

syndrome) excrete intact LTB_4 and 20-hydroxy-LTB_4. LTC_4 catabolism involves peptide cleavage reactions involving glutamyl transpeptidase and various dipeptidases to yield LTD_4 and LTE_4, both of which have biological activity. The sulfur atom of sulfidopeptide leukotrienes can be oxidized by reactive oxygen species. More specific metabolic processing of the sulfidopeptide leukotrienes includes ω-oxidation by cytochrome P-450 followed by β-oxidation from the I terminus.

Leukotriene Biology and Leukotriene Receptors

LTB_4 functions in inflammatory processes through its chemotactic and chemokinetic affects human polymorphonuclear leukocytes. LTB_4 induces the adherence of neutrophils to vascular endothelial cells and enhances the migration of neutrophils (diapedesis) into extravascular tissues. The biological activity of LTB_4 is mediated through two specific G-protein coupled receptors termed BLT_1 and BLT_2. LTC_4 and its peptide cleavage products LTD_4 and LTE_4 mediate bronchial smooth muscle contraction in asthma and cause edema. There are two G protein-linked receptors for cysteinyl leukotrienes called $CysLT_1$ and $CysLT_2$. $CysLT_1$ is found in bronchial and intestinal smooth muscle; LTD_4 and LTC_4 activate $CysLT_1$. Montelukast, pranlukast, and zafirlukast inhibit the $CysLT_1$ receptor in humans. $CysLT_2$ receptors are abundant in the heart and in vascular endothelial cells.

See Also the Following Articles

Cytochrome P-450 • Eicosanoid Receptors • Phospholipase A_2 • Phospholipase C

Glossary

aspirin A nonsteroidal anti-inflammatory drug that inhibits cyclooxygenase by acetylating an active site serine residue and blocking productive binding of arachidonic acid.

cyclooxygenase Common name of the oxygenase enzyme that converts arachidonic acid and related 20 carbon essential fatty acids to prostanoids.

FLAP 5-lipoxygenase activating protein, an accessory protein that is required for 5-lipoxygenase functioning in intact cells.

leukotriene Those oxygenated derivatives of 20 carbon essential fatty acids formed through the action of 5-lipoxygenase and containing a conjugated triene system of double bonds.

5-lipoxygenase The oxygenase that converts arachidonic acid and related 20 carbon essential fatty acids to leukotrienes.

montelukast A drug used in the treatment of asthma that inhibits the binding of peptidoleukotrienes to the $CysLT_1$ receptor.

prostanoid Those oxygenated derivatives of 20 carbon essential fatty acids formed through the action of prostaglandin endoperoxide H synthase.

Further Reading

Kozak, K., Prusakiewicz, J., Rowlinson, S., Prudhomme, D., and Marnett, L. (2003). Amino acid determinants in cyclooxygenase-2 oxygenation of the endocannabinoid anandamide. *Biochemistry* **42**(30), 9041–9049.

Lam, B. K., and Frank Austen, K. (2000). Leukotriene C4 synthase. A pivotal enzyme in the biosynthesis of the cysteinyl leukotrienes. *Am. J. Respir. Crit. Care Med.* **161**(2 Pt 2), S16–S19.

Murphy, R. C., and Wheelan, P. (1998). Pathways of leukotriene metabolism in isolated cell models and human subjects. In *Five-Lipoxygenase Products in Asthma* (J. M. Drazen, ed.) pp. 87–123. Marcel-Dekker, New York.

Peters Golden, M., and Brock, T. G. (2000). Intracellular compartmentalization of leukotriene biosynthesis. *Am. J. Respir. Crit. Care Med.* **161**(2 Pt 2), S36–S40.

Smith, W. L., and Murphy, R. C. (2002). The eicosanoids: Cyclooxygenase, lipoxygenase and epoxygenase pathways. In *Biochemistry of Lipids, Lipoproteins and Membranes* (D. E. Vance and J. E. Vance, eds.) 4th edition., pp. 341–372. Elsevier Science B.V, Amsterdam.

Smith, W. L., DeWitt, D. L., and Garavito, R. M. (2000). Cyclooxygenases: Structural, cellular and molecular biology. *Annu. Rev. Biochem.* **69**, 149–182.

von der Donk, W., Tsai, A., and Kulmacz, R. (2002). The cyclooxygenase reaction mechanism. *Biochemistry* **41**(52), 15451–15458.

Biography

William L. Smith is a Professor of Biological Chemistry at the University of Michigan Medical School. His research interests are in the area of lipid mediators, particularly the enzymes involved in the biosynthesis of prostanoids. He has contributed to understanding the molecular basis for the actions of nonsteroidal anti-inflammatory drugs such as aspirin.

Robert C. Murphy is a Professor of Pharmacology at the University of Colorado Health Sciences Center in Denver. His research interests are in the area of lipids and lipid mediators particularly the metabolism of leukotrienes and related lipoxygenase products. Dr. Murphy determined the structures of the peptidoleukotrienes and has developed tools (mass spectrometry) for characterizing and quantifying lipids and lipid mediators.

Proteases in Blood Clotting

John D. Kulman and Earl W. Davie
University of Washington, Seattle, Washington, USA

Proteases are enzymes that hydrolyze peptide bonds within protein substrates. In vertebrates, proteases play an essential role in preventing the loss of blood by promoting hemostasis, a process that culminates in the formation of a platelet plug and the deposition of a polymerized fibrin network at sites of vascular injury. The mechanism of this process was first studied in the mid-1800s by a Scottish surgeon Andrew Buchanan, who proposed the existence of a clot-promoting factor that he called thrombin. This article discusses the coagulation cascade, and the structure and function of the blood clotting proteases.

The biochemical pathways leading to thrombin formation are now well understood, as are the mechanisms by which thrombin promotes and modulates hemostasis. In response to vascular damage, thrombin is generated from an inactive precursor by a series of biochemical reactions collectively known as the coagulation cascade (Figure 1). Thrombin subsequently catalyzes a series of reactions that lead to platelet aggregation, fibrin polymerization, and ultimately, feedback down-regulation of the coagulation cascade itself (Figure 2). The enzymes involved in these pathways are structurally and functionally related to trypsin, the prototypical serine protease of the digestive system. However, in contrast to trypsin, the coagulation proteases are characterized by a complex modular architecture that facilitates interactions with one another, with other protein substrates, as well as with protein cofactors. These interactions serve to restrict the proteolytic reactions of the blood coagulation cascade to coagulation-promoting surfaces at sites of vessel injury.

The Coagulation Cascade

The Extrinsic Pathway

Almost since the 1960s, the coagulation cascade has been envisaged as a series of stepwise reactions in which inactive forms of serine proteases are converted to active forms by limited proteolysis in a process known as zymogen activation. The coagulation cascade is initiated when tissue factor, an integral membrane protein located in the tissue adventitia, is exposed to circulating blood following a vascular injury (Figure 1). The binding of tissue factor to factor VII or to the active serine protease factor VIIa (trace amounts of which circulate in the blood) initiates the extrinsic pathway of coagulation. The tissue factor–factor VIIa complex converts factors IX and X to their active forms (IXa and Xa). Feedback amplification is achieved when inactive factor VII bound to tissue factor is converted to its active form (VIIa) by factors VIIa, IXa, and Xa, resulting in enhanced generation of factor Xa. The factor Xa thus produced generates thrombin from its inactive form (prothrombin) in the presence of calcium, the nonenzymatic cofactor factor Va, and anionic phospholipid (primarily phosphatidylserine (PS)) exposed on the surface of activated platelets or other cells. Thrombin generated in the extrinsic pathway initiates an additional feedback amplification loop by generating factors Va and VIIIa by limited proteolysis. These surface-bound protein cofactors serve as scaffolds for the assembly of complexes that facilitate the production of factors Xa and thrombin (the Xase and prothrombinase complexes, respectively).

The Intrinsic Pathway

Thrombin enhances flux through the coagulation cascade by activating the intrinsic pathway of coagulation. In this arm of the cascade, thrombin generates factor XIa from its zymogen form (XI) by limited proteolysis. Factor XIa then generates factor IXa by a similar mechanism. The precise physiological role of the intrinsic pathway has been the subject of considerable debate, particularly since defects or deficiencies of factor XI are mild, and are associated with a form of hemophilia that is quite distinct from classical hemophilia. Bleeding due to factor XI deficiency is typically associated only with major surgery or trauma, whereas deficiencies of factor VIII (hemophilia A) or factor IX (hemophilia B) give rise to spontaneous soft tissue and joint bleeding. Thus, whereas the extrinsic pathway is required in most cases of vessel injury, the intrinsic pathway appears to be necessary for sustained thrombin generation in response to severe hemostatic challenges.

The Role of Thrombin

Thrombin is a multifunctional enzyme that employs limited proteolysis to effect a variety of biochemical

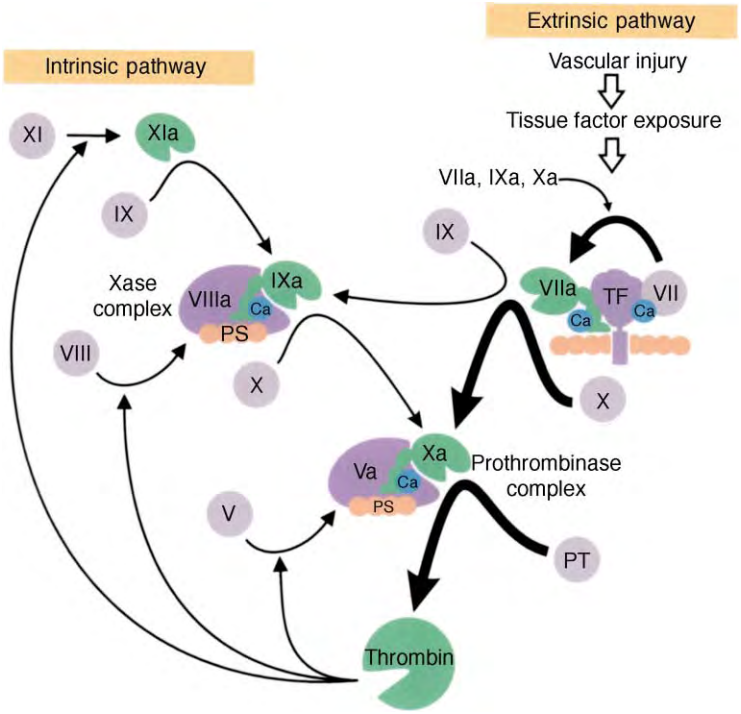

FIGURE 1 The blood coagulation cascade. Inactive cofactors and inactive (zymogen) forms of serine proteases are represented by gray circles. Active proteases are shown in green. Active protein cofactors are shown in purple. Phospholipid membranes are shown in orange. Proteolytic reactions are indicated by solid arrows. Ca, divalent calcium ions; PS, membrane surface-exposed phosphatidylserine; TF, tissue factor; PT, prothrombin.

reactions at the site of vascular injury (Figure 2). Thrombin has many physiological roles, such as promoting the formation of a cross-linked fibrin clot, the activation and aggregation of platelets, and ultimately, the attenuation of the clotting cascade.

Fibrin Polymerization

Fibrinogen is one of the more abundant proteins in the blood, circulating at a concentration of ~ 3 mg ml^{-1}. The fibrinogen molecule consists of six individual polypeptide chains arranged roughly in a dumbbell shape, with the amino termini localized to a central core and the carboxy termini located at each of the two ends. The carboxy terminal end comprises binding pockets that are unoccupied in the circulating fibrinogen molecule. Thrombin converts fibrinogen to fibrin by selectively cleaving short peptides (fibrinopeptides) from the central core region, thereby exposing new amino termini that interact with the carboxy terminal binding pockets on adjacent fibrin molecules (Figure 2, arrow A). In this way, fibrin monomers associate to form thin fibrils that thicken to form an insoluble fibrin clot.

Fibrin Cross-Linking by Factor XIIIa

When fibrin is formed, it accelerates the conversion of factor XIII to XIIIa in a reaction catalyzed by thrombin in the presence of calcium ions (Figure 2, arrow B). Factor XIIIa is unique among the coagulation enzymes in that it is not a serine protease. Rather, it is a transglutaminase that covalently links the side chains of lysine and glutamine residues present in the carboxy terminal regions of adjacent fibrin molecules. This cross-linking imparts structural integrity and rigidity to the clot.

Platelet Activation

Thrombin activates platelets by limited proteolysis of proteins called protease-activated receptors (PARs). PARs constitute a small subset of a much larger family of G protein-coupled receptors (GPCRs). GPCRs are seven-pass transmembrane proteins that transduce extracellular signals via intracellular activation of heterotrimeric G protein signaling pathways. The PARs are unique among the GPCRs in that they utilize a "tethered ligand" mechanism in which limited proteolysis within the extracellular region of the receptor unmasks a protein sequence that auto-activates the receptor itself (Figure 2, arrow C). In platelets, the proteolysis of PARs 1 and 4 by thrombin results in the expression of the hallmarks of platelet activation, namely, morphological change, degranulation, the expression of surface proteins required for aggregation, and the translocation of PS from the inner to the outer leaflet of the platelet membrane.

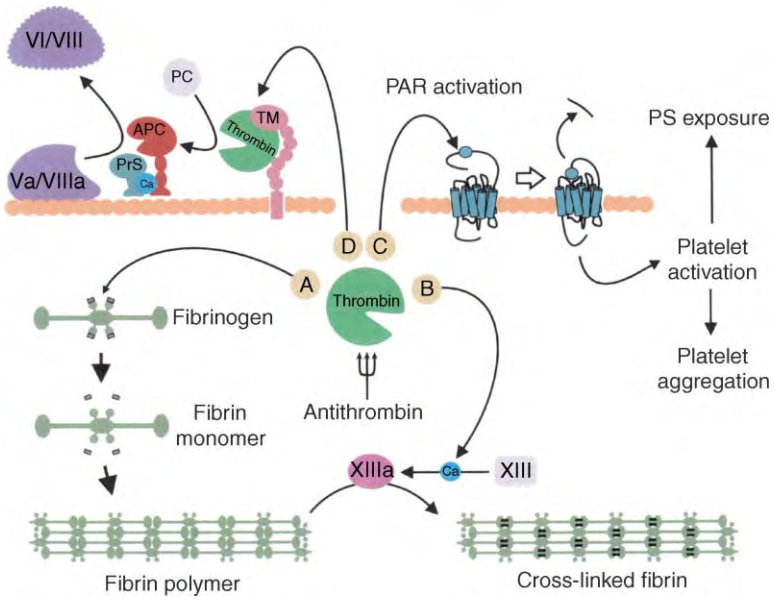

FIGURE 2 Effects of thrombin. Arrow A: Thrombin cleaves short fibrinopeptides from the central region of fibrinogen. The newly exposed termini spontaneously associate with the terminal domains of adjacent molecules allowing formation of polymeric fibrin. Arrow B: Proteolytic cleavage of factor XIII converts it into an active transglutaminase (XIIIa) that chemically cross-links adjacent fibrin molecules, providing structural integrity to the clot. Arrow C: Thrombin cleaves the extracellular region of protease-activated receptors (PARs) on the platelet surface. This modification exposes a tethered ligand that auto-activates the PAR, leading to platelet activation. Activated platelets aggregate to form a hemostatic plug and expose phosphatidylserine (PS), providing a pro-coagulant surface for the coagulation cascade. Arrow D: Feedback down-regulation of the coagulation cascade. Thrombin binds to thrombomodulin on the surface of endothelial cells. This association alters the substrate specificity of thrombin such that it cleaves protein C (PC) to form activated protein C (APC). In the presence of calcium and the cofactor protein S (PrS), APC promotes anticoagulation by proteolytically converting factors Va and VIIIa to their inactive forms (Vi and VIIIi).

The exposure of PS has dramatic consequences for amplification of the coagulation cascade. Under normal cellular homeostasis, PS is tightly restricted to the inner leaflet of the plasma membrane and, as such, is not exposed to the general circulation. However, the exposure of PS (whether through translocation on the platelet surface or by mechanical disruption of cells lining the vasculature) provides a surface for the recruitment of the components of the coagulation cascade, including the serine proteases and factors V and VIII. Viewed in this light, platelet activation and subsequent PS exposure provide yet another positive feedback loop for the generation of thrombin.

Attenuation of the Coagulation Cascade

The unregulated activation of the coagulation cascade would have serious consequences for an organism, including the occlusion of blood vessels and the formation of clots at locations other than the site of injury. Numerous serine protease inhibitors are present in the blood, and serve to restrict coagulation to sites of vessel injury. The most abundant among these is antithrombin, which is present at a concentration ~3 times that of prothrombin. Antithrombin rapidly and irreversibly inactivates thrombin, particularly in the presence of heparan sulfate, a proteoglycan present in the blood vessel wall. Antithrombin has also been shown to inhibit factors IXa, Xa, and XIa.

In an alternative mechanism for attenuating the coagulation cascade, thrombin initiates a pathway that leads to the destruction of factors Va and VIIIa. In this pathway, thrombin binds to thrombomodulin, an integral membrane protein located on the vascular endothelium (Figure 2, arrow D). As the name implies, thrombomodulin modulates the specificity of thrombin such that it generates activated protein C (APC), by limited proteolysis of protein C. APC then inactivates both factors Va and VIIIa by minor proteolysis in a reaction that requires calcium ions, anionic phospholipid, and the protein cofactor, protein S.

Structure and Function of the Blood-Clotting Proteases

Similarity to Trypsin

The proteases involved in blood coagulation are functionally and structurally related to trypsin, the

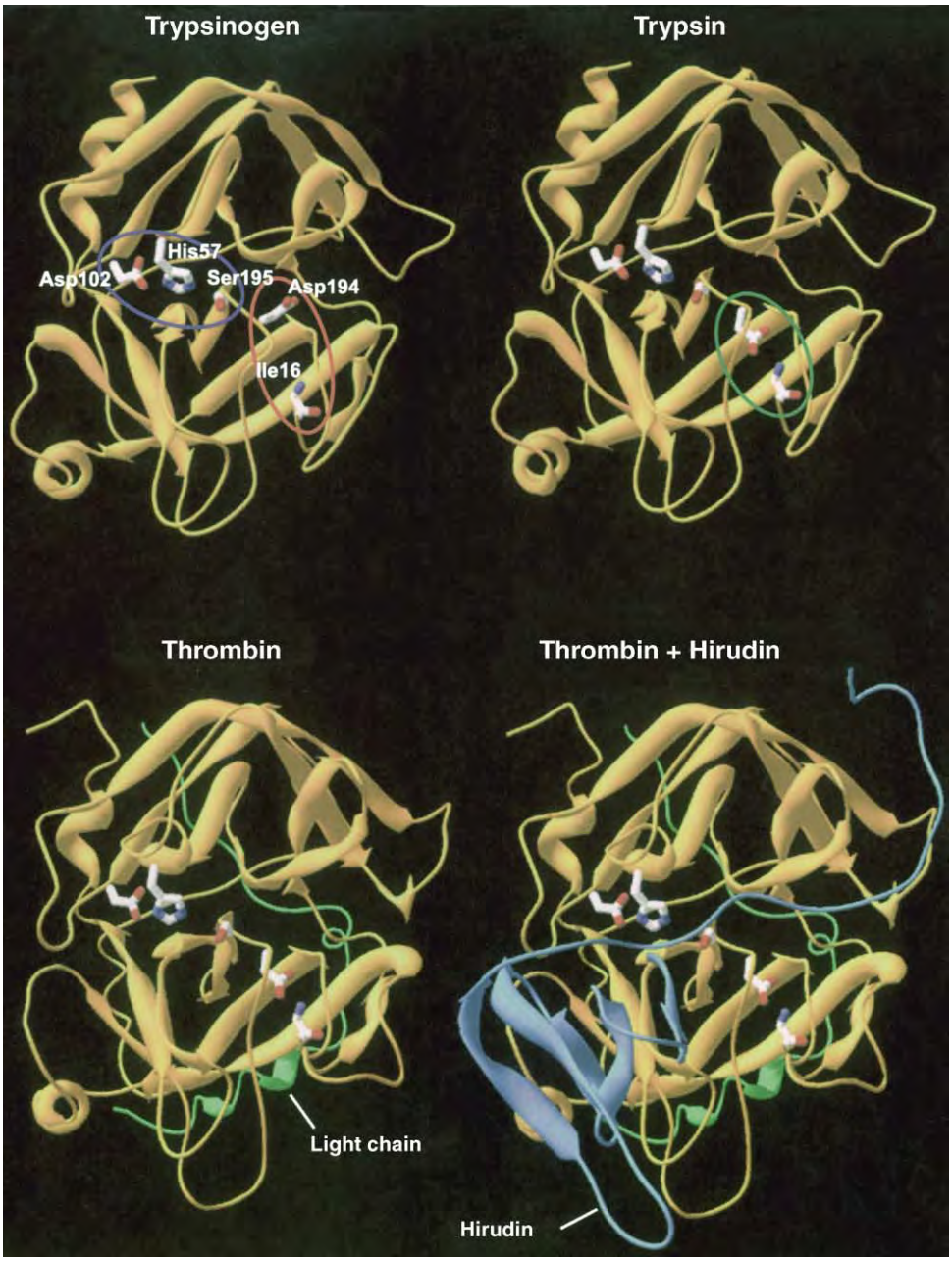

FIGURE 3 Related structures of trypsinogen, trypsin and thrombin. The structure of trypsinogen (upper left panel) reveals clamshell topology with a cleft harboring the active site. Residues His57, Asp102, and Ser195 constitute the catalytic triad (blue oval). In the inactive (zymogen) form of the enzyme the sidechain of Asp 194 does not contact the amide nitrogen (blue atom) of Ile16 (bounded by red oval). The preceding 15 residues have been omitted from the structure to provide ease of interpretation. The structure of trypsin (upper right panel) illustrates the structural change upon zymogen activation. Here the newly formed amino terminus at Ile16 forms a salt bridge with the side chain of Asp194. The structure of thrombin (lower left panel) illustrates its overall topological similarity with that of trypsin. The light chain of thrombin is shown in green. The structure of thrombin bound to the leech anticoagulant protein hirudin (lower right panel) demonstrates the molecular basis for hirudin's anticoagulant effect. Hirudin (depicted as a blue ribbon) blocks the active site of thrombin and extends an arm around thrombin to block its fibrinogen-binding exosite.

prototypical serine protease of the digestive system. Like trypsin, the proteases involved in blood coagulation (thrombin, APC and factors VIIa, IXa, Xa, and XIa) constitute a class of serine proteases that cleave their target proteins after basic (arginine and lysine) amino acid residues. However, trypsin cleaves nonspecifically after basic residues, whereas proteases of the coagulation cascade recognize and cleave only after basic residues surrounded by specific sequences within their targets. As is the case with the clotting proteases,

trypsin exists in a zymogen form (trypsinogen) that is activated by limited proteolysis. Thus, while trypsin does not possess the high degree of substrate specificity of the coagulation proteases, it shares the same general mode of zymogen activation and mechanism of catalysis.

The three-dimensional representation of trypsinogen solved by X-ray crystallography reveals a two-lobed structure resembling a clamshell with a cleft running between the two individual halves (Figure 3). The primary catalytic machinery of trypsin, the so-called "catalytic triad" consisting of histidine, aspartic acid, and serine residues, resides within this cleft. (It is the catalytic serine residue from which the serine proteases derive their name.) Trypsinogen is catalytically inactive until it is cleaved just prior to an isoleucine residue located near the amino terminus of the molecule. This proteolytic event triggers a subtle rearrangement of the molecule, driven by the generation of an electrostatic interaction between the positively charged amino group at the new amino terminus and a negatively charged aspartic acid residue adjacent to the catalytic serine residue. The formation of this salt bridge alters the structure of trypsin and renders it catalytically active.

The structure of thrombin is remarkably similar to that of trypsin (Figure 3), as are those of the other coagulation proteases. Thrombin shares with trypsin its overall clamshell structure, its catalytic triad, and its mode of zymogen activation upon limited proteolysis. However, in addition to the trypsin-like catalytic domain (heavy chain), thrombin possesses an additional polypeptide (the light chain)—a property shared by the other clotting proteases. In addition, thrombin possesses a secondary binding site on its surface that confers specificity for both fibrinogen and PAR1. The position of this so-called "fibrinogen-binding exosite" is illustrated in the structure of thrombin complexed with the leech

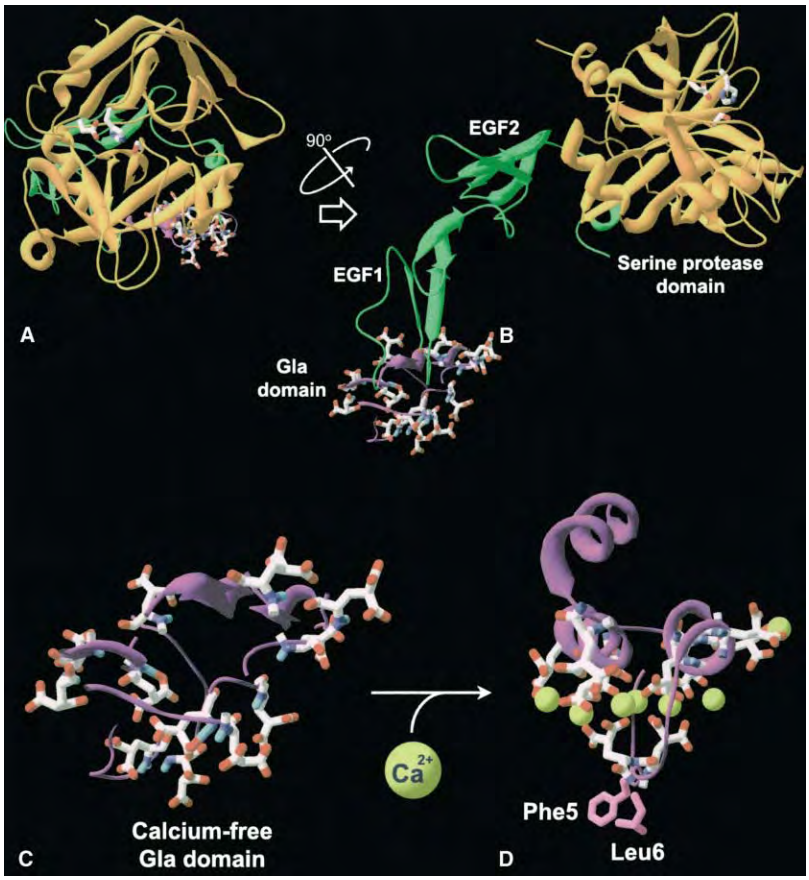

FIGURE 4 The role of Gla domains in the blood-clotting proteases. Panel A: Structure of factor IXa showing the serine protease domain with amino acid residues of the catalytic triad highlighted. In this view the light chain, consisting of a Gla domain and two tandem EGF domains is obscured. The factor IXa structure depicted was determined in the absence of calcium ions. Panel B: Rotation of the structure reveals the amino terminal Gla domain as well as the EGF domains. Panel C: Close-up of the Gla domain of calcium-free factor IXa. In the absence of calcium, the Gla domain is relatively disordered with the Gla residues projecting outward into solution. Panel D: The calcium-bound form of a Gla domain. The coordination of calcium ions by Gla residues within the core of the domain drives the exposure of a hydrophobic "thumb" consisting of a phenylalanine and a leucine residue. This region of the domain contacts the hydrophobic region of membranes. The nearly planar arrangement of positively charged calcium ions may provide specificity for negatively charged phospholipids such as PS.

salivary protein hirudin, which exerts its anticoagulant effect by simultaneously blocking access to the active site and occupying the fibrinogen-binding exosite with a long "arm" (Figure 3).

Gla Domains

The presence of both a catalytic heavy chain and a light chain is a common feature of the activated coagulation proteases. However, in contrast to thrombin, which has a relatively short light chain, the light chains of factors VIIa, IXa, Xa, and APC are longer and are characterized by the presence of multiple modular protein domains. (The crystal structure of factor IXa illustrates this arrangement—Figure 4, panel A.) When viewed in the same orientation as previously depicted structures of trypsinogen, trypsin and thrombin, the serine protease domain with its characteristic catalytic triad is clearly visible. However, this orientation obscures the light chain, which consists of an amino terminal Gla domain followed by two tandem modules that bear structural and sequence similarity to epidermal growth factor (EGF1 and EGF2). The modular structure of the factor IXa light chain is visible when the protein is rotated (Figure 4, panel B).

The Gla domain derives its name from a modification of glutamate residues that occur during the biosynthesis of factors VII, IX, and X, prothrombin, and protein C. The amino terminal 45 residues of these proteins contain between 9 and 13 glutamate (Glu) residues that are converted to γ-carboxyglutamate (Gla) residues in a reaction that requires vitamin K as a cofactor. Gla residues are capable of binding divalent ions, particularly calcium. The three-dimensional structure of factor IXa, determined in the absence of calcium, reveals an amino terminal Gla domain that is relatively disordered, with Gla residues projecting into solution. However, at physiological calcium levels found in the blood, the Gla residues coordinate with calcium and drive the Gla domain into its native conformation (Figure 4, panel C). In this form, the Gla domain is organized around a nearly planar array of calcium ions and projects a hydrophobic 'thumb' into solution. It is believed that the hydrophobic thumb associates with the hydrophobic regions of membranes, while the positively charged calcium ions associate electrostatically with the negatively charged head groups of PS exposed on coagulation-promoting surfaces such as the surface of activated platelets.

Gla domains are essential for localizing factors VIIa, IXa, and Xa, and APC, as well as their zymogen forms, to PS on the surface of activated platelets located at sites of vascular injury. (Thrombin is unique in that its Gla domain is removed from the light chain during the proteolytic activation of prothrombin.) The essential role of Gla domains and the Gla residues that they bear in directing the components of the coagulation cascade to PS-containing surfaces is underscored by the anticoagulant effect of warfarin, a potent vitamin K antagonist. Warfarin inhibits the conversion of Glu residues to Gla residues, rendering the clotting factors incapable of binding to the platelet surface. Originally employed at high doses as a rodent poison, warfarin is currently one of the most widely prescribed drugs for depressing the coagulation cascade in patients who are at risk of heart attack or stroke.

See Also the Following Articles

Platelet-Activating Factor Receptor • Vitamin K: Blood Coagulation and Use in Therapy

Glossary

Gla The amino acid gamma-carboxyglutamic acid.

hemophilia Any of several hereditary blood coagulation disorders in which the blood fails to clot normally.

hemostasis The stoppage of blood flow characterized by vasoconstriction and the formation of a platelet plug and polymerized fibrin.

platelet A small, non-nucleated, cell body found in the blood that functions to promote blood clotting.

protease Any of various enzymes that catalyze the hydrolytic breakdown of proteins into peptides or amino acids.

proteolysis The hydrolytic breakdown of proteins into smaller proteins, peptides, or individual amino acids.

transglutaminase Any of various enzymes that catalyze the covalent linkage of protein-bound glutamine and lysine amino acid side-chains.

vitamin K A fat-soluble vitamin that promotes blood coagulation and prevents hemorrhage.

warfarin A synthetic organic compound, derived from the natural product "coumarin," that antagonizes the effect of vitamin K.

zymogen The inactive precursor of an enzyme, converted into an active enzyme by proteolysis.

Further Reading

Brandstetter, H., Bauer, M., Huber, R., Lollar, P., and Bode, W. (1995). X-ray structure of clotting factor IXa: Active site and module structure related to Xase activity and hemophilia B. *Proc. Natl Acad. Sci. USA* **92**, 9796–9800.

Davie, E., Fujikawa, K., and Kisiel, W. (1991). The coagulation cascade: Initiation, maintenance, and regulation. *Biochemistry* **30**, 10364–10370.

Esmon, C. (2000). Regulation of blood coagulation. *Biochim. Biophys. Acta* **1477**, 349–360.

Fehlhammer, H., Bode, W., and Huber, R. (1977). Crystal structure of bovine trypsinogen at 1.8 angstrom resolution: II. Crystallographic refinement, refined crystal structure and comparison with bovine trypsin. *J. Mol. Biol.* **111**, 415–438.

High, K., and Roberts, H. (eds.) (1995). *Molecular Basis of Thrombosis and Hemostasis*. Marcel Dekker, New York.

Macfarlane, S., Seatter, M., Kanke, T., Hunter, G., and Plevein, R. (2001). Proteinase-activated receptors. *Pharmacol. Rev.* **53**, 245–282.

Scarborough, R., Naughton, M., Teng, W., Hung, D., Rose, J., Vu, T., Wheaton, V., Turck, C., and Coughlin, S. (1992). Tethered ligand agonist peptides. Structural requirements for thrombin receptor

activation reveal mechanism of proteolytic unmasking of agonist function. *J. Biol. Chem.* **267**, 13146–13149.

Soriano-Garcia, M., Padmanabhan, K., de Vos, A., and Tulinsky, A. (1992). The Ca^{2+} ion and membrane binding structure of the Gla domain of Ca-prothrombin fragment 1. *Biochemistry* **31**, 2554–2566.

Vitali, J., Martin, P., Malkowski, M., Robertson, W., Lazar, J., Winant, R., Johnson, P., and Edwards, B. (1992). The structure of a complex of bovine alpha-thrombin and recombinant hirudin at 2.8 angstrom resolution. *J. Biol. Chem.* **267**, 17670–17678.

Biography

John Kulman is a postdoctoral fellow in the Department of Biochemistry at the University of Washington. He earned an M.Phil. from the University of Cambridge where he studied biotin-dependent enzymes while in residence at Churchill College. He holds a Ph.D. from the University of Washington where he completed his doctoral research in the laboratory of Professor Earl W. Davie in the Department of Biochemistry. His principal research interests are in elucidating novel physiological roles of vitamin K and investigating the interplay between vitamin K-dependent proteins and cellular ubiquitination pathways.

Earl W. Davie received his Ph.D. from the Department of Biochemistry at the University of Washington, and then did postdoctoral studies with Professor Fritz Lipmann at Harvard University. After six years on the faculty at Case Western Reserve University, he joined the Department of Biochemistry at the University of Washington where he is a Professor. His research interests have focused mainly on the coagulation cascade and the proteins involved in fibrin formation.

26S Proteasome, Structure and Function

Peter Zwickl and Wolfgang Baumeister
Max Planck Institute of Biochemistry, Martinsried, Germany

The ubiquitin–proteasome pathway is the major route used by eukaryotic cells for disposing of misfolded or damaged proteins and for controlling the lifespan of regulatory proteins. The 26S proteasome is a huge molecular machine of ~2.5 MDa, which degrades protein substrates by an energy-dependent mechanism. It comprises two subcomplexes, the 20S-core particle and one or two regulatory complexes, the 19S caps. The 20S complex allows confining the proteolytic action to a nanocompartment, in which sequestered from the cellular environment substrates undergo degradation. The 19S regulatory complex recruits substrates targeted for degradation and prepares them for translocation into the 20S-core complex. The sequence of events encountered by a substrate until it is finally degraded is reflected by a linear arrangement of functional modules within the 45 nm long supramolecular assembly (Figure 1).

The 20S Proteasome

20S proteasomes are found in all domains of extant organisms in archaea, bacteria, and eukaryotes and share a highly conserved quaternary structure. Although their complexity in terms of subunit composition is surprisingly different, 20S proteasomes are generally built from two types of subunits, α and β, which segregate into seven-membered rings and collectively form a barrel-shaped complex with a network of internal cavities. These cavities or "nanocompartments" harbor the active sites and thus allow segregating the proteolytic action from the surrounding cytoplasm. This regulatory principle, referred to as "self-compartmentalization," is for prokaryotes, which lack membrane-bordered compartments, the only means of spatial confinement.

In addition to self-compartmentalization, proteasomes rely on another mechanism to prevent the uncontrolled breakdown of proteins that is not uncommon amongst proteases. The β-type subunits of 20S proteasomes, which bear the active site residues, are synthesized in an inactive precursor form; for the formation of the active sites, the propeptides must be removed posttranslationally. This process is tied in with the assembly of the 20S proteasome in such a manner that activation is delayed until assembly is complete and the active sites are sequestered from the cellular environment. In mature 20S proteasomes access to the inner proteolytic compartment is through narrow gates at the polar ends of the complex and thus restricted to small peptides and unfolded proteins. Therefore, the proteasome behaves, with respect to folded proteins, as a "latent" protease, which is dependent on regulatory complexes to assume its function. At the heart of the regulatory complexes, or "activators," are members of the AAA family of ATPases. In prokaryotes, members of this family form homohexameric complexes; in eukaryotes, six paralogs form heterohexameric complexes, which are integrated into the larger and multifunctional 19S regulatory complexes.

Subunit Composition

20S proteasomes from all three domains of life have a common overall architecture. They are built of 28 subunits arranged in a stack of four seven-membered rings. All subunits are members of the same superfamily of proteins, which group into two families, designated α and β. The two polar rings of the proteasome are formed by α-type subunits; the two equatorial rings are formed by β-type subunits (Figure 2A). Both families comprise a number of subfamilies. The sequence similarity between members of a subfamily, even from evolutionary distant species, is considerably higher than similarity between the members of different subfamilies from one species. While human and yeast proteins of the same subfamily have at least 50% similarity, there is only ~30% similarity between the seven subfamilies, and even less among the two families, α and β.

The main difference between eukaryotic and prokaryotic 20S proteasomes is one of complexity. Prokaryotic proteasomes are mostly composed of identical copies of 14 α-subunits and 14 β-subunits, eukaryotic proteasomes recruit α- and β-subunits out of 14 different subfamilies. Thus, the multiple axes of

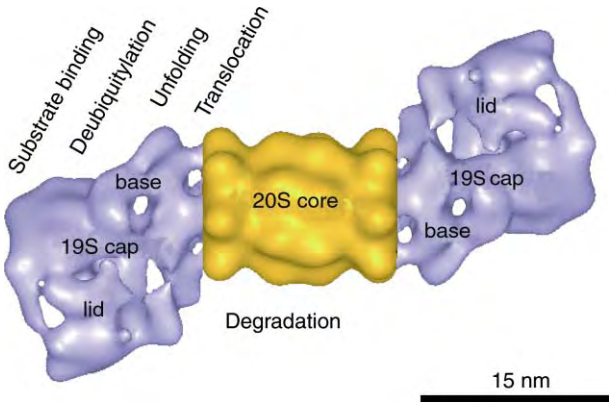

FIGURE 1 Composite model of the three-dimensional (3D) structure of the 26S proteasome combining a 3D reconstitution from electron micrographs of *Drosophila* 26S complexes and the crystal structure of the *Thermoplasma* 20S proteasome.

symmetry of the *Thermoplasma* proteasome are reduced to C2 symmetry in the eukaryotic proteasome; each of the 14 different subunits is found twice within the complex and occupies well-defined positions. According to their location within the α and β rings, yeast subunits are sequentially numbered $\alpha 1/\beta 1$ through $\alpha 7/\beta 7$, and those related by C2 symmetry are distinguished by the prime symbol ($\alpha 1'/\beta 1'$ through $\alpha 7'/\beta 7'$). The subunit topology in higher eukaryotes corresponds to that in yeast, i.e., members of the same subfamily occupy the same positions. Hence, that systematic nomenclature is generally applicable. While lower eukaryotes assume a stoichiometry of $(\alpha_1-\alpha_7)$ $(\beta_1-\beta_7)$ $(\beta_1-\beta_7)$ $(\alpha_1-\alpha_7)$, vertebrates have achieved an even higher degree of complexity. In addition to the 14 constitutive subunits, they contain 3 γ-interferon-inducible β-type subunits, which can replace their constitutive counterparts ($\beta 1$, $\beta 2$, and $\beta 5$) to form "immunoproteasomes."

Structure

On electron micrographs, 20S proteasomes from prokaryotes and eukaryotes are virtually indistinguishable, and also the crystal structures of *Thermoplasma* and yeast proteasomes are very similar. Proteasomes are barrel-shaped particles, with overall dimensions of 15 nm in length and 11 nm in diameter. A channel traverses the particle from end to end and widens into three internal cavities, each ~5 nm in diameter (Figure 2B). The two outer cavities are formed jointly by one α- and one β-ring; the central cavity is formed by the two adjacent β-rings. At a glance there appears to be one major difference between the crystal structures of the *Thermoplasma* and the yeast proteasome: In the archaeal proteasome 1.3 nm wide openings are visible at the center of the α rings, while in the yeast proteasome this channel appears to be closed. However, one has to keep in mind that in the crystal structure of the *Thermoplasma* proteasome the 12 N-terminal residues of the α-subunits remained invisible because of disorder; in yeast the corresponding residues plug the channel and act as a gate.

As expected from their sequence similarity, proteasome α- and β-subunits have the same fold (Figure 2C): a four-layer structure with two five-stranded antiparallel β-sheets (S1–S10) flanked on either side by α-helices, two on the one (H1 and H2), three on the other side (H3, H4, and H5). The β-sheet package is unusual in that one sheet is rotated relative to the other through a positive dihedral angle of +30°, in contrast to the value of the typical β-sheet twist, which is −30°. In the β-type subunits, the β-sheet sandwich is open at one end to form the active site cleft, and closed at the other end by four hairpin loops. In α-type subunits, however, an additional helix (H0) crosses the top of the β-sheet sandwich and fills the cleft. The fold of proteasome subunits was initially considered to be unique, but as it turned out, it is prototypical of a new family of proteins referred to as Ntn (N-terminal nucleophile) hydrolases.

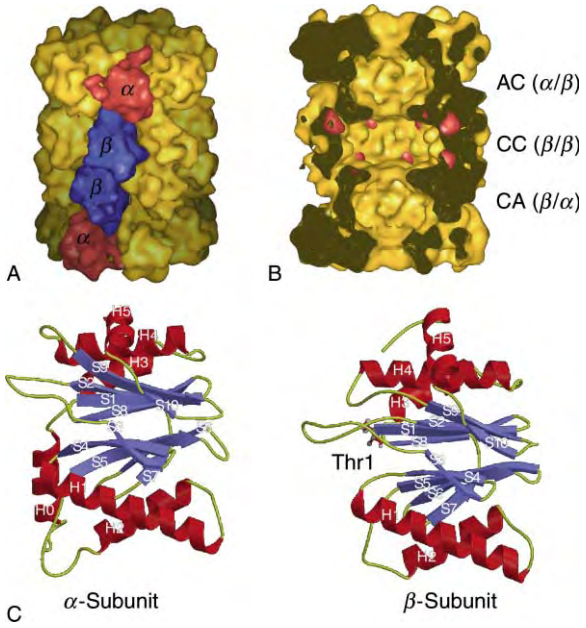

FIGURE 2 Structure of the 20S proteasome. (A) Low-resolution model (1 nm) of the 20S proteasome from the crystal structure of the *Thermoplasma* 20S proteasome. (B) The same structure as in (A) cut open along the sevenfold axis to display the two antechambers (AC and CA) and the central chamber (CC) with the 14 active sites (marked in red). The channel openings at the two ends of the cylinder are 1.3 nm in diameter. (C) Folds of the α and β-subunit from *Thermoplasma* 20S proteasomes. Helices are numbered H0 to H5 in the α-subunit, and H1 to H5 in the β-subunit; strands are numbered S to S10. H0 in the α-subunit occupies the cleft leading to the active site in the β-subunit. The active site threonine (Thr1) in the β-subunit is shown in ball-and-stick representation.

Currently known members of this family, whose primary structures have diverged beyond recognizable similarity, are aspartylglucosaminidase (AGA), glutamine phosphoribosyl pyrophosphate amidotransferase (GAT), penicillin acylase (PA), and L-aminopeptidase D-Ala-esterase/amidase (DmpA). Beyond the common fold, these enzymes share the mechanism of the nucleophilic attack and autocatalytic processing, but none of them has a quaternary structure similar to the proteasome.

The Active Site

A characteristic feature of Ntn hydrolases is a "single-residue" active site; both the nucleophile and the primary proton acceptor are provided by the same N-terminal residue of the proteins. The nucleophilic attack is initiated when the free N terminus, the primary proton acceptor, strips the proton off the catalytic side chain, the nucleophile; for steric reasons, a water molecule is supposed to mediate the proton shuttle, at least in the proteasome and in penicillin acylase. Different N-terminal residues are used as nucleophiles in Ntn hydrolases; serine in PA and DmpA, cysteine in GAT, and threonine in AGA and in the proteasome. In agreement with a catalytic mechanism that relies on a single residue, there is no consensus of residues in the vicinity of the active site. Nevertheless, several other residues are critical for activity of proteasomes, as consistently shown by site directed mutagenesis with archaeal, bacterial, yeast, and mammalian proteasomes. The exact roles of these residues, all highly conserved and in close proximity to Thr1, remain to be clarified. Lys33, which forms a salt bridge to Glu17, may lower the pK_a of the N terminus by electrostatic effects or may be part of the charge relay system in delocalization of the proton from the Thr1 hydroxyl group. Asp166 may be required for the structural integrity of the active site or directly be involved in catalysis.

Although all proteasome subunits have the Ntn-hydrolase fold, not all are actively involved in substrate cleavage. As mentioned above, in α-subunits, the active site cleft is occupied by an additional N-terminal α-helix, H0 (Figure 2C). Of the different eukaryotic β-type subunits, only three (β1, β2, and β5 and their interferon inducible counterparts) display proteolytic activity, whereas subunits β3, β4, β6, and β7 lack one or more of the critical residues and are inactive. This assignment, initially derived from the conservation pattern of the active site residues, has been confirmed by the crystal structure of yeast 20S proteasomes soaked in N-acetyl-Leu-Leu-norleucinal; only three subunits, β1/Pre3, β2/Pup1, and β5/Doa3, contain the inhibitor bound to Thr1. Since the backbone geometry is well conserved between all subunits, active or inactive, one would expect that introducing all residues regarded as critical would render inactive subunits active. However, this is not the case; the yeast subunits β3/Pup3, β6/Pre7, and β7/Pre4 remained unprocessed and consequently inactive, when the respective mutations were made.

The 26S Proteasome

Cellular Functions

In eukaryotic cells, the 20S proteasome assembles with one or two 19S regulatory complexes (RC) in an ATP-dependent manner to form the 26S proteasome. The 26S holoenzyme is the most downstream element of the ubiquitin–proteasome pathway. It is an abundant complex, both in the nucleus and in the cytoplasm, and studies with proteasome inhibitors indicate that the bulk of cellular proteins, 80–90%, are degraded via this pathway. It is not only used as a disposal machinery for misfolded proteins (termed DRiPs, for defective ribosomal products) and for proteins damaged by stress or aging, but also the lifespan of many short-lived regulatory proteins is controlled via this pathway. Interestingly, the 26S proteasome does not only degrade proteins completely, but also activates certain transcription factors by limited proteolytic processing of precursors, e.g., human NFκB and NFκB2, *Drosophila* Ci or yeast Spt23 and Mga2. In addition to its function in ubiquitin-dependent proteolysis, the 26S proteasome was also found to mediate ubiquitin-independent degradation of several proteins, e.g., ODC, c-Jun, IκBα, and $p21^{Cip1}$. Moreover, not yet fully understood nonproteolytic roles of proteasomes in nucleotide excision repair and transcriptional regulation have been described.

The 19S Regulator and its Subcomplexes

Slightly differing sets of RC subunits have been reported for different organisms and the abundance of factors that have been described to associate to the RC in a tissue- and development-specific manner and with variable affinities, makes it difficult to draw the line between interacting factors, transiently bound subunits or integral components of the RC. However, as the mass of the *Drosophila* RC, ~890 kDa, determined by scanning-transmission electron microscopy (STEM) measurements is in good agreement with the summed masses of the 18 individual subunits (932 kDa) identified on 2D gels, it seems likely that the catalogue of integral subunits is now complete. The catalogues of the *Drosophila* and yeast 19S subunits are identical, except for a single subunit (p37A), which seems to be absent from yeast 26S proteasomes.

The 19S regulator of the yeast proteasome can be dissociated into two subcomplexes, the "base" and the "lid," which are located proximally and distally with respect to the 20S core (Figure 1). The complex formed by the base and the 20S proteasome is sufficient for the ATP-dependent degradation of nonubiquitylated protein substrates, but does not mediate degradation of ubiquitylated substrate proteins. From the location of the base in the 26S complex, it had been inferred to have a role in substrate unfolding, acting as a "reverse chaperone," and in controlling the gate in the coaxial opposed α-rings of the 20S particle. A chaperone-like activity was demonstrated for the base, and likewise for the ancestral PAN complex. Both have the ability to recognize proteins destined for degradation, to unfold and to translocate them into the proteolytic-core complex in an ATP-dependent manner. The degradation signals remain to be defined, possibly some local unfolding and an exposure of hydrophobic segments is sufficient for targeting substrates. In one case, specific recognition of an ubiquitylated substrate by the Rpt5 ATPase subunit of the base was shown.

As only the 26S holoenzyme, but not the 20S-base complex degrades ubiquitylated proteins, it is likely that recognition, and binding of ubiquitin-tagged substrates is mainly mediated by the eight subunits of the lid subcomplex. Very little is known about the molecular mechanisms of substrate shuttling from the E3 ubiquitin–ligase complexes, where the final step of ubiquitylation takes place, to the lid subcomplex of the 26S proteasome. Free diffusion of ubiquitylated substrates to the 26S proteasomes would be consistent with the rather high-binding constants observed *in vitro*. On the other hand, subcomplexes or subunits of the RC, such as the lid or S5a/Rpn10, could serve as substrate carriers. Indeed, free-lid complexes exist and can be isolated from human erythrocytes as stable particles. Recently, it has been reported that E2 ubiquitin-conjugating enzymes, E3 ubiquitin-ligases, such as Ubr1 and Ufd4, and E3 ubiquitin-ligase complexes, such as SCF and APC, interact directly with subunits of the RC. In addition, adapter proteins such as Rad23 and Dsk2 proteins were shown to bind ubiquitylated proteins via their UBA (ubiquitin-pathway-associated) domain and to the S1 or S2 subunit of the base via their ubiquitin-like (UBL) domain. The latter findings imply that certain substrates may be first recognized and bound by uncomplexed adapter proteins, before the latter bind to the 19S regulator and transfer the substrate for degradation. Moreover, there is evidence that molecular chaperones were also involved in protein degradation by the 26S proteasome. It was found recently that the Hsp70 cochaperone CHIP has E3 ubiquitin-ligase activity and mediates degradation of certain substrate proteins by the 26S proteasome. Bag-1, another Hsp70-interacting protein, was also shown to stimulate substrate ubiquitylation and to bind directly to the 26S proteasome via its UBL domain. Thus, two distinct molecular machineries, the molecular chaperones and the 26S proteasome, seem to interact physically and cooperate in cellular protein quality control.

The molecular understanding of the steps involved in transferring ubiquitylated substrates from the lid to the base and eventually into the 20S core is crucial. One prerequisite for substrates to enter the proteolytic center is the removal of the multi-ubiquitin chain. In yeast, the deubiquitylating enzyme Doa4 was shown to interact physically and functionally with the proteasome supporting the model that Doa4 removes ubiquitin from proteolytic substrates en route to the 20S complex. Mammalian and *Drosophila* RCs were shown to contain a deubiquitylating subunit with a molecular mass of ~37 kDa. However, so far, this activity has only been reported to decrease substrate degradation rates, suggesting that it may have an editing function, rescuing incompletely ubiquitylated substrates. Very recently, Rpn11, a constituent subunit of the lid, was found to be essential for deubiquitylation and subsequent degradation of substrates. This suggests that coupling between deubiquitylation and degradation exists, which assures that a recognized substrate is irreversibly committed to destruction.

See Also the Following Articles

Chaperones, Molecular • Proteasomes, Overview • Ubiquitin-Like Proteins • Ubiquitin System

Glossary

AAA ATPases ATPases associated with a variety of cellular activities, comprising a Walker-type ATPase domain and a so-called second region of homology, as characteristic features.

base Subcomplex of the 19S regulator, which in the 26S proteasome is located proximal to the 20S proteasome and comprises the AAA ATPase subunits.

lid Subcomplex of the 19S regulator, which in the 26S proteasome is located distal to the 20S proteasome.

Ntn hydrolases N-terminal nucleophile hydrolases, enzymes with a similar fold and a single-residue N-terminal catalytic residue, threonine, serine, or cysteine, which mediates the nucleophilic attack on the substrate.

self-compartmentalizing A regulatory principle in which the quaternary structure creates inner compartments with limited access where degradation takes place.

UBA Ubiquitin-pathway-associated domain, responsible for ubiquitin binding.

ubiquitin A highly conserved eukaryotic protein of 76 amino acids, which is linked via its C-terminal carboxyl group to the ε amino group of a lysine residue in a protein destined for degradations.

UBL Ubiquitin-like domain similar in structure to ubiquitin, and which is mediating binding to the 26S proteasome.

Further Reading

Baumeister, W., Walz, J., Zühl, F., and Seemüller, E. (1998). The proteasome: Paradigm of a self-compartmentalizing protease. *Cell* **92**, 367–380.

Hershko, A., and Ciechanover, A. (1998). The ubiquitin system. *Annu. Rev. Biochem.* **67**, 425–479.

Rechsteiner, M., Realini, C., and Ustrell, V. (2000). The proteasome activator 11 S REG (PA28) and Class I antigen presentation. *Biochem. J.* **345**, 1–15.

Rock, K. L., York, I. A., Saric, T., and Goldberg, A. L. (2002). Protein degradation and the generation of MHC class I-presented peptides. *Adv. Immunol.* **80**, 1–70.

Varshavsky, A., Turner, G., Du, F. Y., and Xie, Y. M. (2000). The ubiquitin system and the N-end rule pathway. *Biolog. Chem.* **381**, 779–789.

Voges, D., Zwickl, P., and Baumeister, W. (1999). The 26S proteasome: A molecular machine designed for controlled proteolysis. *Annu. Rev. Biochem.* **68**, 1015–1068.

Biography

Peter Zwickl is a Research Group Leader in the Department of Structural Biology at the Max Planck Institute of Biochemistry. His principal research interest is the functional and structural characterization of ATP-dependent proteases. He holds a doctorate from the Technical University of Munich and received his postdoctoral training at Harvard Medical School, Boston.

Wolfgang Baumeister is Director at the Max Planck Institute of Biochemistry and Head of the Department of Structural Biology. His principal research interests are in the field of intracellular protein degradation and in the development of new techniques for structural studies, in particular electron tomography. He is an Honorary Professor of physics at the Technical University, Munich, and a member of several academies, including the German Academy of Sciences, Leopoldina and the American Academy of Arts and Sciences (Foreign Honorary Fellow). He has received several awards, most recently the Louis-Jeantet Prize for Medicine (2003).

Proteasomes, Overview

Martin Rechsteiner
University of Utah, Salt Lake City, Utah, USA

Proteasomes are cylindrical, multisubunit proteases found in eukaryotes, eubacteria, and archaebacteria. Eukaryotic proteasomes come in two sizes, the 20S proteasome and the considerably larger, ATP-dependent 26S proteasome formed when the 20S proteasome binds a regulatory complex. The 26S proteasome is the central protease in the ubiquitin (Ub)-mediated proteolytic pathway and is essential for a vast array of cellular processes including cell cycle traverse, transcription control, regulation of enzyme levels, and antigen presentation. Both 20S and 26S proteasomes can associate with protein complexes that activate peptide hydrolysis and may serve to localize the enzymes within cells.

The 20S Proteasome

Structure

The 20S proteasome is a cylindrical particle consisting of 28 subunits arranged as four rings of heptamers stacked upon one another (see Figure 1). The simpler archaebacterial enzyme is composed of just one kind of α-subunit and one β-subunit which form the end rings and the two central rings, respectively. Proteolysis is the province of the β-subunits, and their active sites face a central chamber within the cylinder. The α-subunit rings seal off the proteolytic chamber from the external solvent making the 20S proteasome a perfect protease to have among the critical proteins that comprise nucleus and cytoplasm. Unless a native protein is forced into the proteasome interior, it will be impervious to the enzyme. Moreover, proteasome β-subunits are not catalytically active unless they are present in the holoenzyme.

Eukaryotic proteasomes maintain the overall structure of the archaebacterial enzyme, but they exhibit a more complicated subunit composition. There are seven different α-subunits and at least seven distinct β-subunits. Although current evidence indicates that only three of its seven β-subunits are catalytically active, the eukaryotic proteasome cleaves a wider range of peptide bonds. The archaebacterial enzyme, with its 14 identical β-subunits, preferentially hydrolyzes peptide bonds following hydrophobic amino acids and is therefore said to have chymotrypsin-like activity. By contrast, the eukaryotic proteasome contains two copies each of trypsin-like, chymotrypsin-like, and post-glutamyl-hydrolyzing subunits. For this reason it is capable of cleaving almost any peptide bond having difficulty only with Pro-X, Gly-X, and to a lesser extent with Gln-X bonds. There is a further complication in higher eukaryotes. In immune tissues or after exposure to interferon γ, the three catalytically active β-subunits found in the proteasomes of most organs are replaced by β-subunits with differing substrate specificities. Thus, in higher vertebrates there are constitutive and immunoproteasomes. The latter are thought to play an important role in class I antigen presentation.

Enzyme Mechanism and Proteasome Inhibitors

Whereas most proteases use serine, cysteine, or metals to cleave peptide bonds, the proteasome employs N-terminal threonines in an unusual catalytic mechanism. The N-terminal threonines, generated by self-removal of short peptide extensions from the active β-subunits during assembly of the 20S particle, act as nucleophiles during peptide hydrolysis. There are highly specific inhibitors of the proteasome. The fungal metabolite lactacystin and the bacterial product epoxomicin covalently modify the active site threonines and inhibit the enzyme. Both compounds are commercially available; other inhibitors include vinylsulfones and various peptide aldehydes that are generally less specific.

The 26S Proteasome

Whereas bacteria may possess as many as five ATP-dependent proteases, the 26S proteasome is the only ATP-dependent protease discovered so far in the nuclear and cytosolic compartments of eukaryotic cells. As the 20S proteasome's internal cavities are inaccessible to intact proteins, openings must be generated in the enzyme's outer surface for proteins to be degraded. A number of protein complexes have been found to bind the proteasome and stimulate peptide hydrolysis. The most important of the proteasome-associated

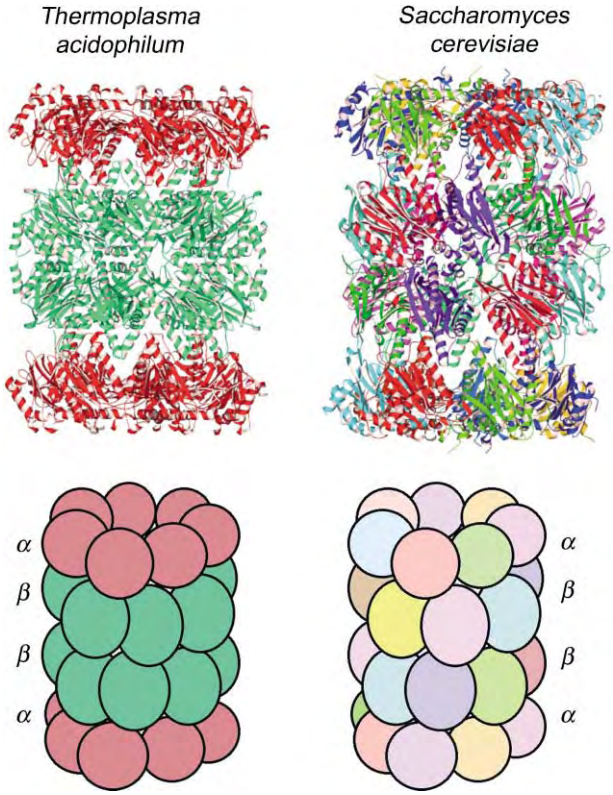

FIGURE 1 20S Proteasomes. At the top are ribbon diagrams of an archaebacterial proteasome (left) and a eukaryotic proteasome (right) as revealed by X-ray crystallography. Schematic representation of their subunit arrangements are shown below each crystal structure. Note that the archaebacterial proteasome is assembled from 14 copies of a single α-subunit and 14 copies of the same β-subunit. By contrast, the yeast 20S proteasome consists of two copies each of seven different α- and seven different β-subunits.

components is the 19S regulatory complex (RC) for it is a major part of the 26S ATP-dependent enzyme that degrades ubiquitylated proteins in eukaryotic cells (see Figure 2). As its name suggests, this 19S particle is roughly the same size as the 20S proteasome except that it is a more complex protein assemblage containing 18 different subunits. Among the RC subunits are six ATPases, an isopeptidase, a subunit that recognizes polyubiquitin chains, and a number of subunits whose functions are yet to be determined. RC subunits are arranged in two large subcomplexes, called the base and the lid. The ATPases and two other subunits comprise the base that sits directly on the end rings of the 20S proteasome; the lid is separated from the base by what appears to be a cavity. Overall the regulatory complex looks much like a Chinese dragon-head in negatively stained EM images.

Presumed Mechanism

The six ATPases in the 19S RC are members of the large family of AAA nucleotidases, whose members share the common property of altering the conformation or association state of proteins. In the case of the 19S RC ATPases, they are thought to act as "unfoldases" and translocases. Presumably ubiquitylated proteins are captured by the RC after which the ATPases unfold the bound substrate protein and thread it through the α ring of the 20S proteasome for its subsequent degradation in the central proteolytic chamber (see Figure 3). Most of the resulting peptide fragments are 5–10 residues in length, but fragments as long as 35 amino acids can be present. Furthermore, in some cases the 26S proteasome only partially degrades the substrate protein, releasing instead functionally processed domains.

How the 26S proteasome recognizes ubiquitylated proteins has not been firmly established. Ub chains containing four or more monomers are preferred substrates, and one RC subunit, called S5a, has been shown to bind polyUb. However, deletion of the gene encoding this subunit in budding yeast has only minor impact on intracellular proteolysis. Hence there must be other subunits or additional mechanisms by which the 26S enzyme recognizes polyUb-substrates. In this regard, there are recent reports that the 26S proteasome interacts directly with ubiquitin ligases or ligase-associated proteins that are ubiquitylated but not degraded. It should be noted that some non-ubiquitylated proteins are also degraded by the 26S proteasome.

Tissue and Subcellular Distribution of Proteasomes

Proteasomes are found in all organs of higher eukaryotes, but the degree to which the composition of proteasomes and its activators varies among tissues is largely unexplored territory. At the subcellular level 26S proteasomes are present in cytosol and nucleus where they appear to be freely diffusible. They are not found in the nucleolus or within membrane-bound organelles other than the nucleus. When large amounts of misfolded proteins are synthesized by a cell, they often accumulate around the centrosome in what are called "aggresomes". Under these conditions 26S proteasomes, chaperones, and proteasome activators also redistribute to the aggresomes presumably to refold and/or degrade the misfolded polypeptides.

Physiological Importance

Deletion of yeast genes encoding 20S proteasome and 19S RC subunits is usually lethal indicating that the 26S proteasome is required for eukaryotic cell viability. Known substrates of the 26S proteasome include transcription factors, cell cycle regulators, protein

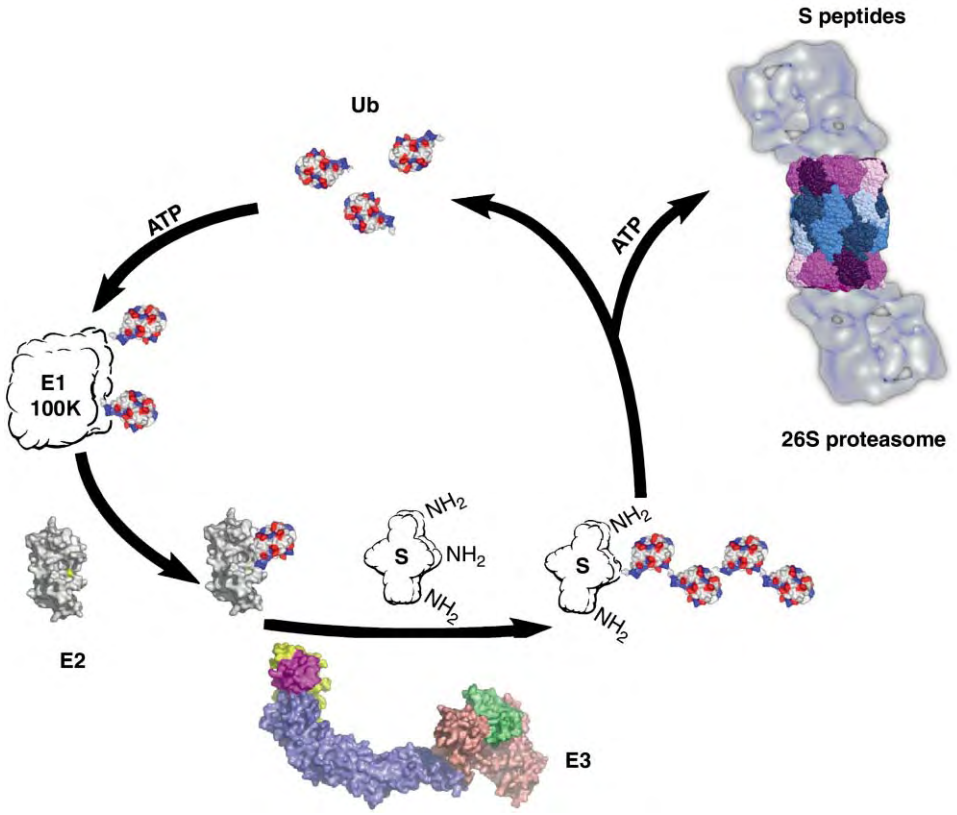

FIGURE 2 Schematic representation of ubiquitin activation and ATP-dependent proteolysis of conjugated substrates. Ubiquitin molecules are activated by an E1 enzyme in an ATP-dependent reaction, transferred to a cysteine residue (yellow) on an E2 or Ub carrier protein and subsequently attached to a substrate protein (S) by an E3 or ubiquitin ligase. Note that chains of Ub are generated on the substrate and these are recognized by the 26S proteasome depicted in the upper right at 1/20th scale.

kinases, etc., – essentially most of the cell's important regulatory proteins. Surprisingly even proteins secreted into the endoplasmic reticulum are returned to the cytosol for degradation by the 26S proteasome. Given the scope of its substrates, it is hardly surprising that in higher eukaryotes the ubiquitin-proteasome system affects a vast array of physiological processes ranging from cell cycle traverse to circadian rhythms to learning. The ubiquitin-proteasome system impacts a number of human neurological diseases that include Parkinson's, Huntington's, and Alzheimer's. Mutations in components of the ubiquitin-proteasome pathway also cause various other diseases.

Proteasome Activators

In addition to the RC there are two protein complexes, REG$\alpha\beta$ and REGγ, and a single polypeptide chain, PA200, that bind and stimulate peptide but not protein degradation by the proteasome (see Figure 4). A fourth protein, called ecm29 in yeast, associates with the proteasome. Like the RC, proteasome activators bind the ends of the 20S proteasome, and importantly, they can form mixed or hybrid 26S proteasomes in which one end of the 20S proteasome is associated with a 19S RC, and the other is bound to a proteasome activator. This latter property raises the possibility that proteasome activators serve to localize the 26S proteasome within eukaryotic cells. At present, we do not know whether activation, or targeting or something else is the primary function of proteasome activators.

REGs or PA28s

There are three distinct subunits of the 11S regulator (REG) called α, β, and γ. REGsα and β form hetero-heptamers found principally in the cytoplasm, whereas REGγ forms a homo-heptamer located in the nucleus. REGα and β are abundantly expressed in immune tissues while REGγ is highest in brain. In addition to their different locations the REGs differ in their activation properties. REG$\alpha\beta$ activates all three proteasome active sites; REGγ only activates the trypsin-like subunit. There is reasonably solid evidence that REG$\alpha\beta$ plays a role in class I antigen presentation, but we have no idea what REGγ does especially since REGγ knockout mice have almost no phenotype.

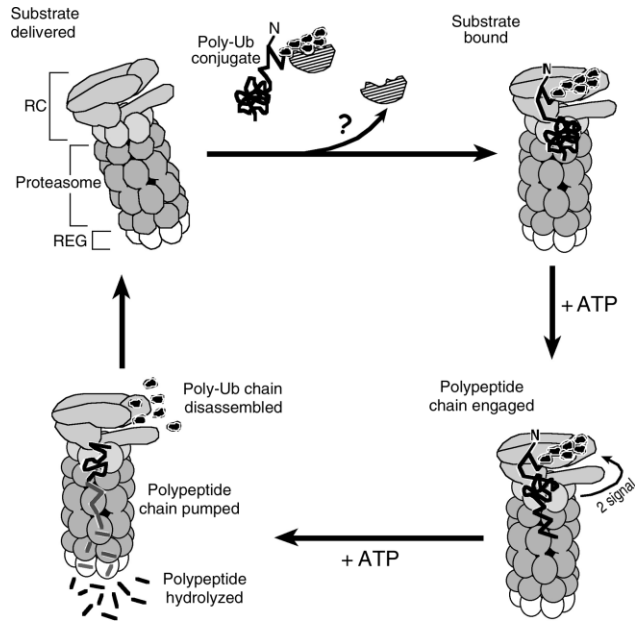

FIGURE 3 Hypothetical Reaction Cycle for the 26S Proteasome A polyubiquitylated substrate is delivered to the 26S proteasome possibly by chaperones (step 1). Substrate is bound by polyubiquitin recognition components of the regulatory complex (RC) until the end of the polypeptide chain is engaged by the ATPases (step 2). As the polypeptide chain is unfolded and pumped down the central pore of the proteasome, a signal is conveyed to the metallo-isopeptidase to remove the polyUb chain (step 3). The unfolded polypeptide is eventually degraded within the inner chamber of the proteasome (step 4) and peptide fragments exit the enzyme.

The crystal structure of REGα reveals seven subunits that form a donut-shaped structure with a central aqueous channel, and the structure of an REG–proteasome complex provides important insight into the mechanism by which REGα activates the proteasome. The carboxyl tail on each REG subunit fits into a corresponding cavity on the α-ring of the proteasome and loops on the REG subunits cause N-terminal strands on several proteasome α-subunits to reorient upward into the aqueous channel of the REG heptamer. These movements open a continuous channel from the exterior solvent to the proteasome central chamber.

PA200

A new proteasome activator, called PA200, was recently purified from bovine testis. Human PA200 is a nuclear protein of 1843 amino acids that activates all three catalytic subunits with some preference for the PGPH active site. Homologues of PA200 are present in budding yeast, worms, and plants. A single chain of PA200 can bind each end of the proteasome, and when bound, PA200 molecules look like volcanoes in negatively stained EM images. Mutation of yeast PA200 results in sensitivity to the DNA-damaging agent bleomycin, and evidence from both yeast and mammals indicates that PA200 is involved in DNA repair.

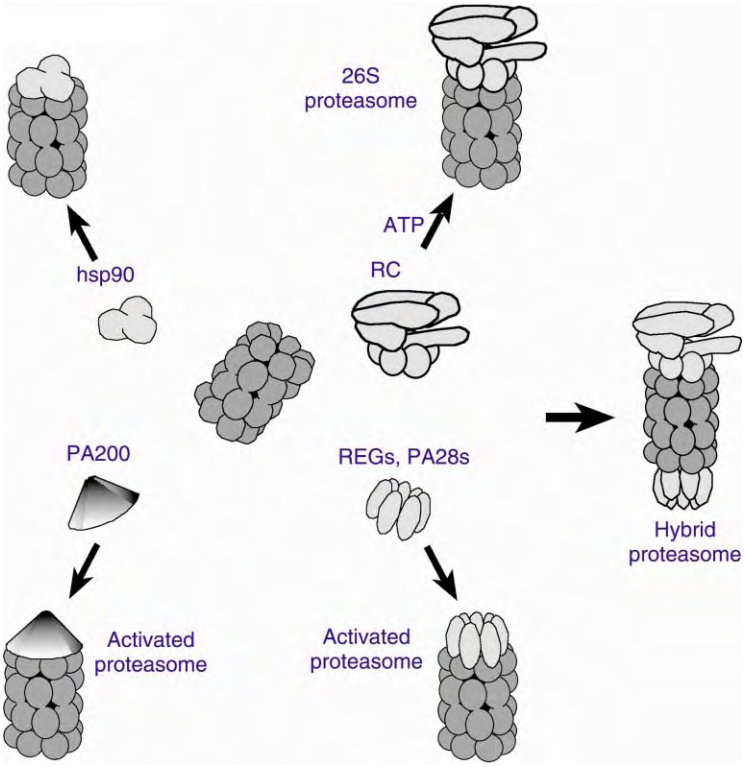

FIGURE 4 Schematic representation of the 20S proteasome assembling with various activator proteins (RC, REGs, PA200) and with the chaperone hsp90, a protein that inhibits the enzyme.

Ecm29

Another proteasome-associated protein, called ecm29p, has been identified in several recent proteomic screens. It has been reported that ecm29p serves to stabilize the yeast 26S proteasome, but the human homologue of ecm29p is found predominately associated with secretory and endocytic membranes, as per an unpublished observation by Gorbea and his associates, a location suggesting a role in secretion rather than 26S proteasome stability. Ecm29p clearly associates with the 26S proteasomes; whether it activates proteasomal peptide hydrolysis is unknown.

Protein Inhibitors of the Proteasome

Two proteins have been found to suppress proteolysis by the proteasome. One of these is PI31; the other is the abundant cytosolic chaperone, Hsp90. Both may affect how the proteasome functions in Class I antigen presentation. PI31 is a 30 kDa proline-rich protein that inhibits peptide hydrolysis by the 20S proteasome and can block activation by both RC and REG$\alpha\beta$. Although surveys of various cell lines show PI31 to be considerably less abundant than RC or REG$\alpha\beta$, when overexpressed, PI31 is reported to inhibit Class I antigen presentation by interfering with the assembly of immuno-proteasomes. A number of studies have shown that Hsp90 can bind the 20S proteasome and inhibit its chymotrypsin-like and PGPH activities. Interestingly inhibition by Hsp90 is observed with constitutive but not with immuno-proteasomes, a finding consistent with proposals that Hsp90 shuttles immuno-proteasome-generated peptides to the endoplasmic reticulum for Class I presentation.

Summary

The 20S proteasome was discovered in 1980 and its 26S version six years later. Since the 1980s, a great deal of knowledge has been gained about these two enzymes and their central importance in eukaryotic cell physiology. Still, there is much more to discover, e.g., the crystal structure of the 19S RC and the mechanism by which the 26S proteasome degrades its substrates; how the 26S proteasome is itself regulated; and the extent to which proteasomal components vary among tissues in higher eukaryotes.

See Also the Following Articles

26S Proteasome, Structure and Function • Chaperones, Molecular • Ubiquitin System • Ubiquitin-Like Proteins

Glossary

hybrid proteasome A 20S proteasome with an RC at one end and a proteasome activator at the other, essentially a 26S proteasome bound to a proteasome activator.

immuno-proteasome A 20S proteasome in which each of the three active β-subunits are replaced by interferon-γ inducible catalytic subunits.

proteasome activators Single polypeptide chains or small protein complexes that bind 20S proteasomes and stimulate peptide hydrolysis.

regulatory complex A particle containing 6 ATPases and 12 other subunits that binds the 20S proteasome to form the 26S proteasome, the eukaryotic cell's major ATP-dependent protease.

ubiquitin A small highly conserved protein that can be covalently attached to other proteins and to itself. Chains of ubiquitin target proteins for destruction by the 26S proteasome.

Further Reading

Bochtler, M., Ditzel, L., Groll, M., Hartmann, C., and Huber, R. (1999). The proteasome. *Annu. Rev. Biophys. Biomol. Struct.* **28**, 295–317.

Hampton, R. Y. (2002). ER-associated degradation in protein quality control and cellular regulation. *Curr. Opin. Cell Biol.* **14**, 476–482.

Hartmann-Petersen, R., Seeger, M., and Gordon, C. (2003). Transferring substrates to the 26S proteasome. *Trends Biochem. Sci.* **28**, 26–31.

Hershko, A., and Ciechanover, A. (1998). The ubiquitin system. *Annu. Rev. Biochem.* **67**, 425–479.

Hill, C. P., Masters, E. I., and Whitby, F. G. (2002). The 11S regulators of 20S proteasome activity. *Curr. Top Microbiol. Immunol.* **268**, 73–89.

Taylor, J. P., Hardy, J., and Fischbeck, K. H. (2002). Toxic proteins in neurodegenerative disease. *Science* **296**, 1991–1995.

Voges, D., Zwickl, P., and Baumeister, W. (1999). The 26S proteasome: A molecular machine designed for controlled proteolysis. *Annu. Rev. Biochem.* **68**, 1015–1068.

Yewdell, J. W., and Bennink, J. R. (2001). Cut and trim: Generating MHC class I peptide ligands. *Curr. Opin. Immunol.* **13**, 13–18.

Biography

Martin Rechsteiner is a Professor of Biochemistry at the University of Utah. Intracellular proteolysis has been his principal scientific interest since the 1980s. During this period, the laboratory discovered and functionally characterized the 26S proteasome as well as several proteasome activators, and also proposed that PEST sequences, regions rich in proline (P), glutamic acid (E), serine (S), and threonine (T), target proteins for rapid degradation.

Protein Carboxyl Esterification

Shilpa G. Lalchandani and Jeffry B. Stock
Princeton University, Princeton, New Jersey, USA

Carboxyl methylation is a reversible protein modification that regulates cellular responses to environmental stimuli. The present article describes this process in bacterial chemotaxis and eukaryotic signal transduction proteins.

Introduction

The methylation and demethylation reactions are catalyzed by two types of enzymes; methyltransferase (Mtase) and methylesterase (MEase). The Mtase transfers methyl groups from the universal methyl donor S-adenosylmethionine (SAM), to a carboxyl group in a target protein. This converts a negatively-charged carboxylate anion on the protein surface into a neutral methyl ester with concomitant formation of S-adenosylhomocysteine (SAH). The methyl group is subsequently removed by a MEase, that catalyzes the hydrolysis of the methyl ester to restore the carboxylate anion on the target protein with the concomitant production of methanol.

$$\text{MTase}: \text{SAM} + \text{Protein} \rightarrow \text{SAH} + \text{Methylated Protein}$$

$$\text{MEase}: \text{Methylated Protein} + H_2O \rightarrow \text{Methanol} + \text{Protein}$$

The central role of carboxyl methylation in sensory receptor function was first evidenced by the discovery, that membrane receptors proteins are methylated and demethylated during bacterial chemotaxis. The involvement of methylation in sensory regulation was extended to vertebrate systems by the finding that RAS related and heterotrimeric G proteins were subject to carboxyl methylation and demethylation. Finally, an exhaustive search for additional systems of carboxyl methylation revealed a second major regulatory locus in eukaryotic cells that involves methylation and demethylation of phosphoprotein phosphatase 2A (PP2A), the major phosphoprotein phosphatase in brain.

To understand how carboxyl methylation works to regulate cellular responses to extracellular signals, it is informative to consider the role of another type of protein modification chemistry, the phosphorylation, and dephosphorylation of protein side chains. As with carboxyl methylation, protein phosphorylation is controlled by two types of converter enzymes. A kinase catalyzes the transfer of a phosphoryl group from the universal phosphodonor, ATP, to an acceptor residue at the surface of a target protein with concomitant formation of ADP, and a phosphoprotein phosphatase catalyzes the hydrolysis of the protein phosphoester with concomitant production of inorganic phosphate. Phosphorylation generally acts as a switch to control the activity of a target protein. The first example of this regulatory mechanism was obtained through studies of the regulation of hormonal control of glucose metabolism in muscle and liver. There it is shown that the release of glucose from glycogen in response to epinephrine involves the activation of a specific kinase that turns on glycogen phosphorylase by transferring a phosphoryl group from ATP to a serine hydroxyl side chain in the enzyme. This modification is later reversed by a phosphoprotein phosphatase to turn off glycogen phosphorylase under resting conditions when glucose needs to be stored. Subsequent research has shown that regulation by phosphorylation and dephosphorylation is a ubiquitous mechanism. A typical vertebrate genome encodes upward of a thousand different protein kinases whose activities are controlled by different regulatory signals, and it has been estimated that a quarter of the proteins in a typical vertebrate cell are subject to regulation by phosphorylation and dephosphorylation.

One might suppose that carboxyl methylation and demethylation would provide the same type of switching mechanism as phosphorylation and dephosphorylation, however this is not the case. Whereas phosphorylation is quite common, carboxyl methylation is rare and present at only 2% of the level of phosphorylation. There appear to be only three MTase enzymes in living systems: one in prokaryotes that methylates chemotaxis receptors, and two in eukaryotes, the G protein and PP2A MTases. Moreover, in these instances carboxyl methylation does not function as an on/off switch, but serves instead to modulate the output of a regulatory network of kinase/phosphatase switches to optimize the response to a given stimulatory input. The global regulatory role of carboxyl methylation is best understood within the context of bacterial chemotaxis.

Carboxyl Methylation in Bacterial Chemotaxis

Virtually all motile prokaryotes use the same basic mechanism to control their motor activities in response to attractant and repellent stimuli. Generally, each cell has a signal transduction apparatus composed of a cluster of thousands of α-helical hair-like fibers that traverse the cytoplasmic membrane (Figure 1). The portion of each fiber located at the outside surface of the membrane acts as a sensory receptor, interacting with specific-attractant and -repellent stimuli in the extracellular medium. The portion of the fibrous array inside the cell controls the activity of an associated protein kinase that catalyzes the transfer of a phosphoryl group from ATP to a small protein in the cytoplasm, that subsequently interacts with the motor apparatus affecting a chemotaxis response. While the cytoplasmic domains of receptor fibers and their associated kinase/phosphatase signaling enzymes are highly conserved, the extracellular sensing domains are variable depending on the particular stimuli with which they interact. The number of different sensory receptor fibers encoded in a given genome ranges from just a few, e.g., five in the case of *Escherichia coli*, to a several dozen, e.g., 46 in *Vibrio cholera*.

Stimulus-response coupling through this phosphorelay signaling apparatus is modulated by carboxyl methylation. Sequences within the cytoplasmic portions of each fiber between the membrane spanning domain and the kinase regulatory domain contain a series of at least four glutamate residues that are subject to methylation and demethylation by specific MTase and MEase enzymes. The degree of methylation of the glutamyl carboxylate side chains control the link between stimulus binding to the extracellular sensory portions of the fibrous array and the intracellular kinase. In most bacteria lower levels of methylation act to increase the cell's sensitivity to attractant stimulation. The level of methylation is controlled by several parameters including the availability of SAM and feedback from the kinase, as well as by conformational changes in the fibers induced by stimulus interactions with the extracellular sensory receptor domains. Since changes in methylation occur at a much slower rate than changes in kinase activity, methylation provides an adaptive mechanism, whereby the sensory apparatus adjusts the phosphorylation response, to fit a given background stimulus intensity. The result is analogous to light–dark adaptation in vertebrate visual systems where sensitivity is shifted in response to background light intensity.

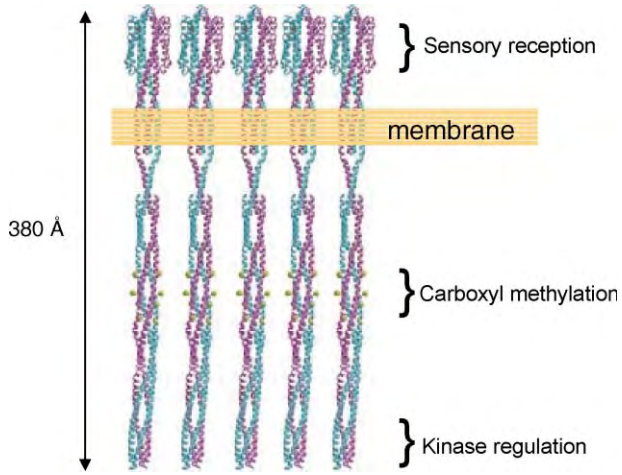

FIGURE 1 Model of the chemotaxis receptor fibers. Transmembrane methylatable receptors are employed as sensors in bacterial chemotaxis.

Carboxyl Methylation of Eukaryotic Signal Transduction Proteins

Responses of eukaryotic cells to extracellular signals is generally mediated by sensory receptor proteins that traverse the cytoplasmic membrane. Portions of these proteins at the cell surface interact with hormones and other stimuli. These interactions cause structural changes in portions of the proteins that extend into the cytoplasm, and these changes act in turn to cause associated G proteins to exchange bound GDP for GTP. The G proteins in their GTP-bound state are activated to produce second messengers such as cAMP that activate protein kinases that regulate key enzymatic activities by phosphorylating serine and threonine side chains. The phosphoryl groups are subsequently removed through the action of phosphoprotein phosphatases such as PP2A. These types of signal transduction pathways are modulated by carboxyl methylation and demethylation of alpha carboxyl groups at the C terminus of the G proteins and PP2A. Thus, although the chemistry is somewhat different, carboxyl methylation modulates receptor-mediated responses in eukaryotes just as it does in bacterial cells.

Ras-Related and Heterotrimeric G Protein

The majority of carboxyl methylated proteins in eukaryotic cells are Ras-related and heterotrimeric G proteins. These signal transduction proteins are targeted to membranes where they relay information from sensory receptors. Membrane targeting depends on a series of posttranslational modifications at the C terminus that includes prenylation, proteolytic cleavage and carboxyl methylation (Figure 2). The initial event, prenylation,

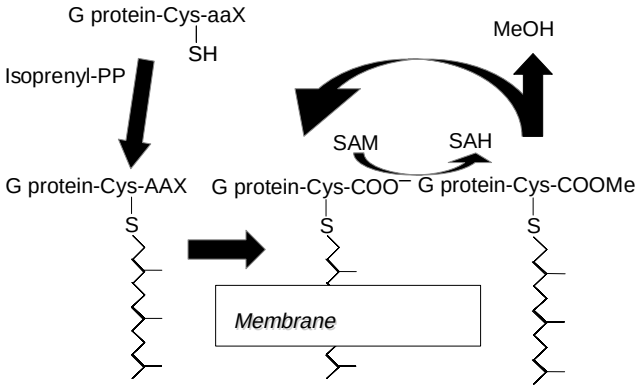

FIGURE 2 Sequence of processing events involved in isoprenylcysteine carboxyl methylation. The methylated molecules are soluble GTPases in the cytosol which are targeted to the membranes by a series of posttranslational modifications at the C-terminal that includes a prenylation, C-terminal proteolytic cleavage, and carboxyl methylation reactions.

depends on a characteristic C-terminal tetrapeptide, termed a CaaX motif, consisting of a cysteine, C, followed by two aliphatic amino acids, aa; and a final amino acid that is variable, X. The prenyl group is either a C-15, farnesyl, or C-20, geranylgeranyl, polyisoprenoid depending primarily on the nature of the C-terminal, X, residue. In either case, prenylation causes the G protein to become associated with Endoplasmic Reticulum (ER) membranes where a membrane-associated protease catalyzes the cleavage of the aaX sequence leaving a prenylcysteine alpha carboxyl group at the C terminus. This is the site of methylation by a specific MTase and demethylation by one or more MEase activities.

G protein methylation is catalyzed by an integral membrane protein that is localized in the ER. This MTase appears to have a broad specificity for prenylcysteine alpha carboxyl groups. It even catalyzes the methylation of amino acids such as N-acetyl-S-farnesylcysteine or N-acetyl-S-geranylgeranylcysteine. The rate of methylation is controlled at several levels. Whereas G protein activation leads to increases in methylation, elevated levels of SAH, feed back to inhibit MTase activity. Methylation is not required for receptor-mediated G protein signaling per se, but rather acts to modulate the stimulus response coupling. Mutant mice with MTase deletions die during early development.

Protein Phosphatase 2A

Protein phosphotase 2A (PP2A) is generally isolated as a trimeric complex consisting of three nonidentical subunits A, B, and C. The 65 kDa, A-subunit serves as a scaffold for the association of the 36 kDa catalytic C-subunit, and of regulatory B subunits. Although, AC dimers are abundant in tissue, ABC trimers of PP2A enzyme are prevalent *in vivo* and account for the main biological activities of the phosphatase. While only two isoforms of the A and C subunits have been reported so far in humans, there is a wide array of B-subunits and these B-subunits are reported to be in part responsible for the specificity of PP2A toward its numerous phosphoprotein substrates. It has been estimated that PP2A is responsible for roughly half of the total phosphoprotein phosphatase activity in vertebrate tissues. It is one of the most abundant enzymes in brain where it plays a critical role in the regulation of axonal microtubule assembly.

The PP2A catalytic subunit has a highly conserved C-terminal extension. The last six residues, TPDYFL being identical in all PP2As. The alpha carboxyl group of the C-terminal leucine residue is the site of methylation and demethylation (Figure 3). Methylation is essential for the assembly of PP2A holoenzymes. The discovery of the PP2A methylation system led to the purification and characterization of specific enzymes responsible for PP2A methylation and PP2A demethylation.

The PP2A MTase was initially purified from bovine brain as a soluble 38 kDa monomer. The enzyme appears to be completely specific for the methylation of PP2A AC dimers. PP2A methyl esters are hydrolyzed by the action of a specific MEase with similar specificity. The PP2A MEase has been purified from bovine brain as a soluble 46 kDa monomer. The MTase and MEase are highly conserved in species ranging from yeast to human.

Methylation has been demonstrated to function as a molecular switch that controls the assembly of the PP2A subunits. PP2A holoenzyme assembly could alter dephosphorylation of proteins due to changes in substrate targeting. Differential methylation of PP2A has been observed during cell cycle progression, suggesting that methylation might be altering the subcellular localization

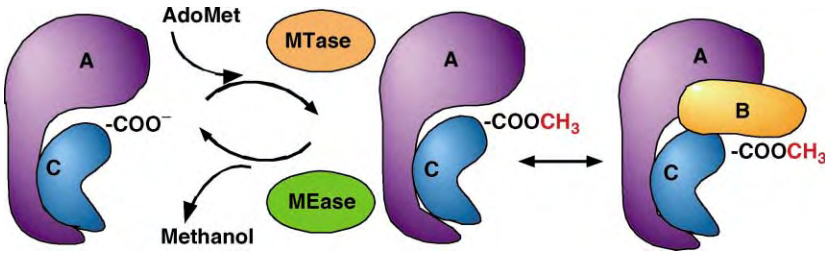

FIGURE 3 Carboxyl methylation regulates PP2A by controlling the association of regulatory B-subunits.

of PP2A. Selective microtubule-associated PP2A is differentially regulated during the cell cycle, implying that PP2A is regulated by methylation. The level of PP2A methylation is stimulated by cAMP and inhibited by SAH.

PP2A methylation seems to play an important role in growth control. Mutant yeasts that completely lack PP2A MTase activity are resistant to rapamycin and sensitive to antibiotics such as nacotazol that inhibit microtubule function. It has recently been proposed that in humans, inhibition of PP2A by SAH in brain may help explain why elevated homocysteine levels are a risk factor for Alzheimer's disease since homocysteine can condense with adenosine to generate SAH.

See Also the Following Articles

G Protein Signaling Regulators • G_{12}/G_{13} Family • G_q Family • G_s Family of Heterotrimeric G Proteins • Ras Family

Glossary

methylesterase Enzyme responsible for demethylating the target protein by hydrolysis of the methyl ester.

methyltransferase Enzyme that transfers a methyl group from the universal methyl donor S-adenosylmethionine, SAM, to a carboxyl group in a target protein.

Further Reading

Djordjevic, S., Stock, A. M., Chen, Y., and Stock, J. B. (1999). Protein methyltransferases in signal transduction. In *S-Adenosylmethionine-Dependent Methyltransferases: Structure and Functions* (X. Cheng and R. M. Blumenthal, eds.) pp. 149–183. World Scientific Publishing, Singapore.

Biography

Shilpa Lalchandani is a Postdoctoral Research Associate with Dr. Stock.

Jeffry B. Stock is Professor of Molecular Biology and Chemistry at Princeton University. His principal research interest is concerned with the biochemistry and biophysics of signal transduction with an emphasis on reversible methylation. He holds a Ph.D. in Biochemistry from Johns Hopkins University. Dr. Stock served as a postdoctoral research associate with Dr. D.E. Koshland, Jr., at the University of California, Berkeley. He is also on the editorial board of the *Journal of Biological Sciences* and serves as a member of Molecular Biophysics, Neuroscience and Materials Science Programs at Princeton University. He has authored and edited several books in his field and has over 150 peer-reviewed publications.

Protein Data Resources

Philip E. Bourne
University of California, San Diego, California, USA

Protein resources are defined here as Internet accessible data sources containing both primary data and interpretations of these data. Asking a bioinformatician to write about such resources is like asking a molecular biologist to write about cell signaling. Both are very broad and dynamic topics to which data and knowledge are constantly being added. To avoid providing a superficial view of protein resources, or a view that is going to be outdated before it is published, this article provides a description that will likely not change regardless of what new knowledge is acquired. Hence, this overview will focus on well-established resources of interest to the molecular and possibly cellular biologist. In short, the article addresses content associated with the sequence–structure–function triad, but does not address the significant amount of informatics and computational science research that goes into such resources. The number of protein resources addressing this triad is large and volatile – resources come and go. Emerging are resources that address proteins in the larger biological context through their role in biochemical pathways and in the functioning of a complete model organism. Examples of such resources are introduced to illustrate what can be expected in the future.

Primary and Secondary Resources

What are well-established resources? Well established implies the resource will likely be accessible in five years. That is, they are valuable enough to a broad community to warrant continuous financial support. Broadly speaking, established resources are of two types, primary and secondary. Primary resources are those which directly receive scientific input from the community in the form of protein sequences (usually translated from the DNA sequence), protein structures, expression data, NMR data, mass spectrometry data, measured binding constants, and so on. These data are usually annotated and curated either by humans, by machine, or by a combination of both. They form a backbone from which the study of the life sciences can proceed in an orderly way. Examples of primary resources are Genbank (primary sequences) and the protein data bank (PDB; macromolecular structure).

Secondary resources are derived using data from the primary resources and add value to this primary information either through expert opinion, computation or both. Examples of secondary resources include Swiss-Prot annotated protein sequences taken from TrEMBL and SCOP (Structure Classification of Proteins), which classifies structures from the PDB according to fold, family, and superfamily. Consider the process by which data enters and is processed by a primary and secondary resource so that the quality of these resources can be evaluated. Quality can be broadly judged by four criteria: amount, accuracy, completeness, and usability. This brief discussion does not consider usability.

The Process of Data Acquisition and Processing

We consider the PDB as an example of a primary data resource and Swiss-Prot as an example of a secondary data source.

Primary Data Acquisition – the PDB

The PDB is the single worldwide repository for data on the structure of biological macromolecules derived primarily by X-ray crystallography and NMR spectroscopy. Structural biologists submit depositions to the PDB almost exclusively through a web interface to one of three sites worldwide (Rutgers University, USA; the European Bioinformatics Institute, UK; and Osaka University, Japan). This submission comprises the final output of a program describing the atomic coordinates and any annotation provided by the depositor. The depositor immediately receives a PDB identifier which is the unique and immutable reference to that structure. The incentive to deposit comes from most journals not accepting a structure-based paper unless it includes a PDB identifier. Once received an annotator takes responsibility for processing this entry. A series of checks are performed to validate the integrity of this entry, these include the use of correct atom, residue and ligand naming, stereochemical correctness, and association of the structure with the nearest protein sequence derived

from the sequence databases. A completely annotated and validated entry is returned to the depositor usually within 1–2 working days for their approval. Either the depositor approves or a further round of refinement of the entry will ensue. Once finalized, the entry is released immediately, held until the primary paper associated with the structure is published and then released (the most common situation) or held for a maximum of 1 year. Every effort is made to make entries as complete, consistent, and accurate as possible based on the knowledge of the field at the time. The PDB in no way polices the data – the depositor always has the final say about what is released.

Secondary Data Acquisition – Swiss-Prot and TrEMBL

Swiss-Prot connects amino acid sequences with an annotated description of that protein. Each protein entry provides an interdisciplinary overview of relevant information, bringing together experimental results, computed features and sometimes even contradictory conclusions. Swiss-Prot provides annotated entries for all species, but concentrates on the annotation of entries from human and other model organisms. As a complement, TrEMBL strives to comprise all protein sequences that are not yet represented in Swiss-Prot, by incorporating a perpetually increasing level of mostly automated annotation. Consider the annotation steps associated with a Swiss-Prot entry, the source of which is TrEMBL. Much of this description is available from the Swiss-Prot web site.

The annotation steps are different depending on the source of the sequence. Sometimes scientists' isolate and then biochemically characterize the protein encoded by the gene they have sequenced. Other times they infer this information through similarity to other proteins within the same, conserved family. If it does not belong to a particular family they infer through purely sequence similarity. Finally there are the genome sequence data that often does not have an accompanying citation reporting any such classification. As a first step the sequence is aligned, using FastA or Blast, against all existing Swiss-Prot and TrEMBL entries. This determines whether the sequence can be related to existing families in Swiss-Prot. The next step is to read the article(s), assess the information given, and add relevant comments and features to the entry.

Often from reading the abstract of the paper and analyzing the FastA results the protein can be seen to belong to a particular family. In these cases, care is taken to look at other members of the family and to become familiar with the annotation that already exists. Any standard annotation that is common to the family, for example, the description line(s) and the keywords, can be added to the new entry. Other comments and features, specific to the family, can be added in conjunction with reading the paper. Any additional information from the paper, for example posttranslational modifications, is then added to the entry.

In the majority of articles reporting gene sequencing, the gene is translated to give the protein sequence but the *in vivo* protein is rarely isolated and characterized. Often a probe from a similar organism is used to pinpoint the gene and then the authors infer biochemical characteristics. In these cases, curators assess what the authors imply with the results of the alignments against Swiss-Prot and TrEMBL. When the sequence "hits" against a particular family the description line(s), the similarity comments, and keywords specific to the family, can be added to the new entry. More care is taken when looking at function, subunit, and sequence features. The annotation is then characterized as "probable," "potential," and "by similarity."

Genome sequencing has caused a massive influx of data into the nucleotide sequence databases and this has led to the same influx into TrEMBL giving thousands of entries waiting to go into Swiss-Prot. This sequence data is submitted to the nucleotide sequence databases and is reported in publications that show the entire genome sequence as well as genes that are predicted by a number of methods. Apart from these gene designations the papers rarely include experimental information about any of the predicted proteins from these analyses. By making use of what is reported coupled to the assessment of results from sequence alignments, that hit against both characterized and part-characterized protein sequences, Swiss-Prot makes an effort to add relevant biochemical information to these translated protein sequences.

In summary, established protein resources are generally staffed by knowledgeable scientists dedicated to the task of providing a worldwide community with accurate and timely information.

Data Dissemination

Currently the majority of access to protein resources is via the web, and the following sections provide details of access to a variety of resources. However, access via a web browser is by no means the only forms of access. Some resources provide bulk downloads either via ftp sites or through distribution of hard media, notably CDROM. For example, see http://www.rcsb.org/pdb/cdrom.html for receiving CDROMs of the PDB or contact datalib@ebi.ac.uk by email to receive copies of Swiss-Prot on CDROM. Users can also link to different resources from their own web pages and download data on demand, see for example, http://www.rcsb.org/pdb/

linking.html for linking to the PDB. The National Center for Biotechnology Information (NCBI) has an interesting service called Cubby to use with their Entrez integrated service. Cubby allows you to customize and store searches for future use. It is likely that in the future more protein resources will become more journal-like in that updates to the contents of the database will be provided by email in the same way the table or contents are provided by journals today. The sheer volume of data will require some prefiltering. One can imagine subscribing to a service that returns results of a user request such as "once per month send me a list of all serine/threonine kinase structures solved by X-ray crystallography to better than 2.5Å."

A Roadmap to Protein Data Resources

To anyone who has searched for protein data using a web browser it is immediately apparent there is an endless source of information, some good, some bad. Peer review is clearly needed and fortunately has been undertaken by the journal *Nucleic Acids Research* (NAR; http://nar.oupjournals.org/). NAR publishes both an annual database issue in January each year and a web server issue in July of each year. Resource developers strive to be included in these issues and reviewers carefully check the capabilities of the resource in the same way a scientific paper is considered for publication. The ever expanding list of quality resources are catalogued on-line at http://nar.oupjournals.org/cgi/content/full/31/1/1/DC1. This article considers a subset of those resources, which are considered most widely useful.

Primary Resources

As stated above, primary resources (Table I) are defined here as those that accept primary biological data through direct deposition from the author(s). These data may be supplemented by annotators adding data from the published literature and with some form of validation and cross checking. The vast majority of protein sequence data are derived from translation of DNA sequences. Sequence data ranges from data submitted on complete genomes via high throughput sequencing technologies to individual sequences submitted as part of a biochemical study to expressed sequence tags. A more complete list of resources can be found at the National Center for Biotechnological Information (NCBI; http://www.ncbi.nlm.nih.gov/Sitemap/index.html), perhaps the major keeper of biological information worldwide.

Structure data found in the PDB are derived both from high throughput structural genomics projects and more functionally driven conventional structural biology. The sequences of structures under consideration by the structural genomics projects can be found at http://targetdb.rcsb.org. The sequences of some structures awaiting release by the PDB can be found at http://www.rcsb.org/pdb/status.html.

TABLE I

Major Sources of Primary Data

Name	Description
Genbank	Primary source of DNA sequence information and coordinated with EMBL and DDBJ – http://www.ncbi.nlm.nih.gov/Genbank/index.html
PDB	Primary source of the 3D structures of biological macromolecules determined by X-ray crystallography and NMR – http://www.pdb.org
Entrez-Genome	Over 1000 genomes from bacteria, archea, and eukaryota – http://www.ncbi.nlm.nih.gov/entrez/query.fcgi?db = Genome
dbEST	Sequence data and other information on "single-pass" cDNA sequences, or Expressed Sequence Tags, from a number of organisms – http://www.ncbi.nlm.nih.gov/dbEST/

Secondary Sources

Secondary resources (Table II) in some way add value to data available through the primary resources. This occurs through processes such as provision of additional experimental data and/or additional annotation, validation, and checking, reductionism, computation of derived features, and provision of alternative views on the data. For example, for protein sequences, Swiss-Prot specializes in annotation, Pfam, SMART, and ProDOM are examples of resources that provide annotation at the level of the domain, whereas Prosite, Blocks and Prints use different methodologies to provide details at the level of short (usually functional) motifs.

For structure, PDBSum, MSD, and PDBj provide alternative views and mode of access to PDB primary data. A variety of structure classification tools exist as shown in Table II. SCOP is the most popular and classifies protein structures by fold, family (close sequence-structure-function relationship), and superfamily (structural and suggested evolutionary relationship).

Since proteins sequences outnumber structures by several orders of magnitude, yet structure provides an important linkage between sequence and function, there is a very significant effort to predict three-dimensional structure from sequence. Progress in this field is

TABLE II

Major Sources of Secondary Data

Sequence	
Swiss-Prot	Annotated protein sequence database – http://us.expasy.org/sprot/
TrEMBL	A computer-annotated supplement of Swiss-Prot that contains all the translations of EMBL nucleotide sequence entries not yet integrated in Swiss-Prot http://us.expasy.org/sprot/
Uniprot	The Universal Protein Knowledgebase is a central database of protein sequence and function by joining the forces of the Swiss-Prot, TrEMBL and PIR protein database activities – http://www.pir.uniprot.org/
Sequence – domains	
Pfam	Multiple sequence alignments and hidden Markov models covering many common protein domains and families – http://www.sanger.ac.uk/Software/Pfam/
SMART	A Simple Modular Architecture Research Tool which allows the identification and annotation of genetically mobile domains and the analysis of domain architectures – http://smart.embl-heidelberg.de/
ProDOM	A comprehensive set of protein domain families automatically generated from the SWISS-PROT and TrEMBL sequence databases – http://prodes.toulouse.inra.fr/prodom/current/html/home.php
Sequence – short sequence motifs	
Prosite	Protein families and domains with assigned functional motifs – http://us/expasy.org/prosite/
Blocks+	Blocks are multiply aligned ungapped segments corresponding to the most highly conserved regions of proteins – http://www.blocks.fhcrc.org/
Prints	A compendium of protein fingerprints – http://bioinf.man.ac.uk/dbbrowser/PRINTS/
Genomic sequence	
Ensembl	Genome browser for a number of model organisms – http://www.ensembl.org/
Structure	
PDBSum	Summaries for all protein structures including validation checks – http://www.biochem.ucl.ac.uk/bsm/pdbsum/
MSD	Database and tools for access and manipulation of PDB data – http://www.ebi.ac.uk/msd/
PDBj	Database and tools for access and manipulation of PDB data – http://pdbj.protein.osaka-u.ac.jp
Structure classification	
SCOP	The Structure Classification of Proteins – http://scop.mrc-lmb.cam.ac.uk/scop/
CATH	Class (C), Architecture (A), Topology(T), and Homologous superfamily (H) – http://www.biochem.ucl.ac.uk/bsm/cath_new/index.html
DALI	DALI Domain Dictionary – http://www.embl-ebi.ac.uk/dali/domain/
VAST	Vector Alignment Search Tool – http://www.ncbi.nlm.nih.gov/Structure/VAST/vast.shtml
CE	Polypeptide chain comparison – http://cl.sdsc.edu/ce.html
3Dee	Protein Domain Definitions – http://jura.ebi.ac.uk:8080/3Dee/help/help_intro.html
Structure prediction	
Eva	Evaluate of protein prediction servers – http://cubic.bioc.columbia.edu/eva/
LiveBench	Benchmarking of structure prediction servers – http://bioinfo.pl/LiveBench/
Protein–protein interactions	
DIP	Database of Interacting Proteins – http://dip.doe-mbi.ucla.edu/
BIND	The Biomolecular Interaction Network Database – http://www.bind.ca/

measured by the bi-annual Critical Assessment of Structure Prediction (CASP) meeting. CASP provides a blind test of how researchers worldwide are improving the ability to predict structure using comparative (homology) modeling, fold recognition (threading), and other more *ab initio* techniques. Progress in CASP is documented in a special issue of *Proteins, Structure, Function and Genetics*. A promising approach to the problem is the use of metaservers that provide a consensus view of prediction over a number of individual resources and approaches. Livebench and Eva are the most popular in this regard (Table II).

Data Reduction

The current wealth of proteomic data is both a blessing and a curse. It depends on what a user is trying to determine. If the results of a sequence search for

TABLE III
Reduced Data Subsets

Resource	Description
RefSeq	Curated, nonredundant set including genomic DNA contigs, mRNAs and proteins for known genes, mRNAs and proteins for gene models, and entire chromosomes – http://www.ncbi.nlm.nih.gov/RefSeq/
Astral	Nonredundant structure subsets at different levels of sequence identity – http://astral.stanford.edu/

homology returns hundreds of near identical sequences it may confuse the result rather than lead to a meaningful solution. Nonredundancy can assist in this regard by providing a filtered set of data. The issues then become the level of redundancy retained, the type of redundancy and the choice of a representative. Table III outlines the two common sources of reduced sequence and structure data. It should be noted that protein sequence redundancy is different than protein structure redundancy. Two protein sequences sharing a sequence identity of over 30% will likely share the same fold. However, structures with the same fold could have a sequence identity of less than 10% – the evolutionary drift of sequences is greater than that of structure. A key issue is then redundancy with respect to what. Table III describes two resources dealing with sequence redundancy, RefSeq provides a set of reference sequences and Astral a set of reference structures filtered by sequence identity and with an effort to select the most accurate structure as a representative. Some of the resources under structure classification in Table II provide a nonredundant set of structures with respect to the three-dimensional structure, not the sequence.

Consistent Annotation

Comparison of data, either within a given resource or certainly across resources, requires consistent annotation. This presents a very significant problem across molecular biology and thus with protein data. For example, there are issues of multiple common versus systematic names for proteins, lack of a singular systematic description at the time the protein was discovered and lack of the use of systematic nomenclature even when it exists. The use of International Union of Pure and Applied Chemistry (IUPAC; http://www.iupac.org) descriptors for chemical descriptions helps, as does the use of Enzyme Commission (EC; http://us.expasy.org/enzyme/) numbers for describing enzymes. Most recently, thanks to the work of database developers in recognizing the need for standardization, the Genome Ontology (GO) has been developed by the GO Consortium (http://www.geneontology.org/). GO provides consistent descriptions for biochemical process, molecular function, and cellular location in the form of a directed acyclic graph. That is, a node can have multiple parents, for example, a given protein can have multiple functions. Many of the resources described in Table I and II now assign GO annotation to their entries.

TABLE IV
Integrated Resources

Resource	Description
InterPro	InterPro is a database of protein families, domains and functional sites – http://www.ebi.ac.uk/interpro/
Entrez	Integrated scientific data and literature – http://www3.ncbi.nlm.nih.gov/Entrez/
Kegg	Kyoto Encyclopedia of Genes and Genomes – http://www.genome.ad.jp/kegg/kegg2.html
AfCS	The Alliance for Cell Signaling – http://www.afcs.org/
SRS	Sequence Retrieval System – http://srs.ebi.ac.uk
EcoCyc	Integrated description of *E. coli* – http://www.ecocyc.org

Integrated Resources

A number of cross-referenced resources which include primary and secondary protein data have been developed. Table IV provides a flavor of the wide variety of resources available. Usually this integration is achieved by sequence comparison between resources and subsequent cross checking of information like GO terms. Such cross checking also reveals errors in these databases. InterPro combines data from PROSITE, PRINTS, Pfam, SMART, TIGRFAMs, PIR SuperFamily, and SUPERFAMILY (sequence-motif methods) and ProDom (a sequence cluster method). Entrez combines a variety of sequence and structure data with the literature described mostly as abstracts in PubMed. SRS links a large variety of biological databases (over 200) and is a good place to start to explore resources in general, since the majority of major resources are cross referenced here.

The Future

A compendium of protein sequences or structures is not how a biologist thinks about a problem. Rather they often see a protein as part of a network of interactions with one or more roles that can be measured by a biochemical or phenotypic response, where the data associated with that response can be downloaded and further analyzed. Resources that place proteins as part of a pathway or more specifically in the correct biological

context are likely to be more common in the future. Several exist today (Table IV) and offer a window into what will become commonplace in the next five years. Ecocyc provides literature-based curation of the entire genome of *Escherichia coli* K12 MG1655 including transcriptional regulation, transporters, and metabolic pathways. The Alliance for Cell Signaling is modeling signaling pathways in several organisms and Kegg offers an integrated view of pathways and genomic data.

Clearly the challenge of the future is not having appropriate data, rather how to make the best use of the wealth of data in a way that it can be interpreted by those scientists who can gain most from it. At the same time traditional publishing models are changing through the use of the Internet and Open Access models. One can imagine a future in which the traditional journal article is merely one type of user interface to the data. Interesting times indeed!

See Also the Following Articles

Genome-Wide Analysis of Gene Expression • X-Ray Determination of 3-D Structure in Proteins

Glossary

curation The process of validating and annotating experimental or derived data.

data reduction The process of representing multiple data by a single representative data set based on some criteria of similarity.

integrated resource Single access point to data from multiple primary and secondary resources.

ontology Quantitative description of a field of study of defined scope.

primary resource Protein resource that accepts experimental data from the community.

protein resource Internet accessible information on protein sequence, structure, and function.

secondary resource Protein resource that post-processes experimental data to add derived data.

Further Reading

Ashburner, M., Ball, C. A., Blake, J. A., Botstein, D., Butler, H., Cherry, J. M., Davis, A. P., Dolinski, K., Dwight, S. S., Eppig, J. T., Harris, M. A., Hill, D. P., Issel-Tarver, L., Kasarskis, A., Lewis, S., Matese, J. C., Richardson, J. E., Ringwald, M., Rubin, G. M., and Sherlock, G. (2000). Gene ontology: Tool for the unification of biology. The gene ontology consortium. *Nat. Genet.* **25**, 25–29.

Baxevanis, A. D. (2003). The molecular biology database collection: 2003 update. *Nucleic Acids Res.* **31**, 1–12.

Benson, D. A., Karsch-Mizrachi, I., Lipman, D. J., Ostell, J., and Wheeler, D. L. (2003). GenBank. *Nucleic Acids Res.* **31**, 23–27.

Berman, H. M., Westbrook, J., Feng, Z., Gilliland, G., Bhat, T. N., Weissig, H., Shindyalov, I. N., and Bourne, P. E. (2000). The protein data bank. *Nucleic Acids Res.* **28**, 235–242.

Boeckmann, B., Bairoch, A., Apweiler, R., Blatter, M. C., Estreicher, A., Gasteiger, E., Martin, M. J., Michoud, K., O'Donovan, C., Phan, I., Pilbout, S., and Schneider, M. (2003). The SWISS-PROT protein knowledgebase and its supplement TrEMBL in 2003. *Nucleic Acids Res.* **31**, 365–370.

Gilman, A. G., Simon, M. I., Bourne, H. R., Harris, B. A., Long, R., Ross, E. M., Stull, J. T., Taussig, R., Arkin, A. P., Cobb, M. H., Cyster, J. G., Devreotes, P. N., Ferrell, J. E., Fruman, D., Gold, M., Weiss, A., Berridge, M. J., Cantley, L. C., Catterall, W. A., Coughlin, S. R., Olson, E. N., Smith, T. F., Brugge, J. S., Botstein, D., Dixon, J. E., Hunter, T., Lefkowitz, R. J., Pawson, A. J., Sternberg, P. W., Varmus, H., Subramaniam, S., Sinkovits, R. S., Li, J., Mock, D., Ning, Y., Saunders, B., Sternweis, P. C., Hilgemann, D., Scheuermann, R. H., DeCamp, D., Hsueh, R., Lin, K. M., Ni, Y., Seaman, W. E., Simpson, P. C., O'Connell, T. D., Roach, T., Choi, S., Eversole-Cire, P., Fraser, I., Mumby, M. C., Zhao, Y., Brekken, D., Shu, H., Meyer, T., Chandy, G., Heo, W. D., Liou, J., O'Rourke, N., Verghese, M., Mumby, S. M., Han, H., Brown, H. A., Forrester, J. S., Ivanova, P., Milne, S. B., Casey, P. J., Harden, T. K., Doyle, J., Gray, M. L., Michnick, S., Schmidt, M. A., Toner, M., Tsien, R. Y., Natarajan, M., Ranganathan, R., and Sambrano, G. R. (2002). Overview of the alliance for cellular signaling. *Nature* **420**, 703–706.

Kanehisa, M., Goto, S., Kawashima, S., and Nakaya, A. (2002). The KEGG databases at GenomeNet. *Nucleic Acids Res.* **30**, 42–46.

Karp, P. D., Riley, M., Saier, M., Paulsen, I. T., Collado-Vides, J., Paley, S. M., Pellegrini-Toole, A., Bonavides, C., and Gama-Castro, S. (2002). The EcoCyc database. *Nucleic Acids Res.* **30**, 56–58.

Mulder, N. J., Apweiler, R., Attwood, T. K., Bairoch, A., Barrell, D., Bateman, A., Binns, D., Biswas, M., Bradley, P., Bork, P., Bucher, P., Copley, R. R., Courcelle, E., Das, U., Durbin, R., Falquet, L., Fleischmann, W., Griffiths-Jones, S., Haft, D., Harte, N., Hulo, N., Kahn, D., Kanapin, A., Krestyaninova, M., Lopez, R., Letunic, I., Lonsdale, D., Silventoinen, V., Orchard, S. E., Pagni, M., Peyruc, D., Ponting, C. P., Selengut, J. D., Servant, F., Sigrist, C. J., Vaughan, R., and Zdobnov, E. M. (2003). The InterPro Database, 2003 brings increased coverage and new features. *Nucleic Acids Res.* **31**, 315–318.

Venclovas, C., Zemla, A., Fidelis, K., and Moult, J. (2003). Assessment of progress over the CASP experiments. *Proteins* **53**(Suppl. 6), 585–595.

Biography

Philip E. Bourne is a Professor in the Department of Pharmacology, University of California, San Diego and Co-Director of the Protein Data Bank. He is a former President of the International Society for Computational Biology and a Fellow of the American Medical Informatics Association. He received his Ph.D. from the Flinders University of South Australia. His research interests are broadly in the area of structural bioinformatics and the application of high performance computing technology to problems in the life sciences.

Protein Degradation

Tomo Šarić
Institute of Neurophysiology, University of Cologne, Cologne, Germany

Alfred L. Goldberg
Harvard Medical School, Boston, Massachusetts, USA

Nearly all proteins within cells and most in the extracellular space are in a state of continuous turnover, being synthesized from amino acids and, after varying life spans, broken down back to amino acids. The term "protein degradation" refers to several intracellular processes by which proteins are broken down to their basic constituents. Protein degradation occurs in all living species, from bacteria to humans, and is mediated by the sequential action of several endo- and exopeptidases.

Essential Biological Functions of Protein Degradation

Because cells use significant amount of energy for new protein synthesis, the continual destruction of proteins might appear highly wasteful. However, this process serves multiple important biological functions that are essential for life. The degradation of intracellular proteins is a highly selective and tightly regulated process that is required for removal of many regulatory proteins (transcription factors and signal transducers) and many key rate-limiting enzymes, whose rapid degradation is essential for maintaining cellular homeostasis.

Unlike most regulatory mechanisms (e.g., phosphorylation, ubiquitylation), peptide bond cleavage is an irreversible process, and proteases therefore act as unidirectional biological switches. The only way that cells can reduce the steady-state level of a particular protein is by proteolytic degradation, and removal of certain proteins permits cells to adapt to changes in cellular environment and new physiologic conditions. This kind of adaptation occurs in mammals, for example, in the liver during fasting when enzymes for glycogen production are removed and enzymes required for gluconeogenesis are up-regulated.

Under fasting conditions, protein breakdown also serves as a source of essential amino acids, especially in skeletal muscle, where it provides essential precursors for gluconeogenesis, protein biosynthesis, or energy production. Protein breakdown functions also as a quality control mechanism that selectively removes abnormal proteins resulting from mutation, chemical damage (e.g., oxidation), biosynthetic errors (e.g., premature termination of translation), or failure of normal folding or assembly (which may be a common event in cytosol and endoplasmic reticulum).

Most extracellular proteins (such as plasma proteins) also continuously turn over, mainly by uptake and degradation inside the cells. In higher vertebrates, protein degradation is critical for the function of the immune system. Proper defense against intracellular pathogens (e.g., viruses) or pathogens in the extracellular space (e.g., bacteria) is dependent on continual production of peptide antigens by intracellular proteolytic pathways. In eukaryotic cells, there are two principal pathways for complete degradation of proteins: endocytic–lysosomal and the ATP-dependent ubiquitin–proteasome pathway. The former occurs within the membrane-enclosed vesicles and the latter operates in the cytosol and nucleus. These pathways involve very different enzymes and serve different functions in the cell. Proteolytic systems are also present in some organelles (e.g., mitochondria). Bacteria and archaea do not have lysosomes or ubiquitin but, nevertheless, possess soluble or membrane-bound proteases, many of which are evolutionary precursors of more sophisticated eukaryotic enzymes. One critical feature of all these intracellular degradative systems is that they require metabolic energy, unlike the typical proteases functioning in the extracellular space. As explained in this article, energy-dependent processes help insure exquisite selectivity and allow regulation of the proteolytic enzymes.

Endocytic–Lysosomal Pathway

This pathway is responsible for degradation of extracellular proteins, most membrane proteins, some organelles, and some intracellular proteins. It is composed of heterogeneous groups of vesicles that differ in

morphology, function, and biochemical and biophysical properties. The principal component of this pathway where most protein degradation takes place is the lysosome (or the vacuole in yeast).

Lysosomes

Lysosomes are single membrane-bound spherical organelles in the cytoplasm. They were discovered by Christian de Duve and co-workers in the mid 1950s and are found in all mammalian cells except red blood cells. Lysosomes are not found in higher plants, but the plant cell vacuole performs some of their degradative functions. Lysosomes play an important role in innate immunity, adaptation to stress or starvation, recycling of cytoplasmic organelles, development, cell differentiation, and some forms of programmed cell death.

Uptake of Substrates

Lysosomes receive substrates for degradation by fusing with other intracellular vesicles that are formed by endocytosis (endosomes, pinosomes, phagosomes) or autophagy (autophagosomes). Endocytosis refers to the process of uptake of extracellular material or membrane proteins by invagination of the cell membrane, followed by formation of vesicles inside the cell. Before these vesicles reach the lysosomes (pH 4.5–5.0), ingested material moves from the less acidic early endosomes (pH 6.0–6.5) to the more acidic late endosomes (pH 5.0–6.0). There are three major forms of endocytosis: (1) receptor-mediated endocytosis (uptake of membrane proteins, such as cell surface receptors and their ligands), (2) pinocytosis (ingestion of extracellular liquid with its solute molecules), and (3) phagocytosis (engulfing of large particles such as bacteria or apoptotic bodies by specialized cells such as neutrophils, macrophages, or amoeba) (Figure 1). Pinocytosis and phagocytosis are nonselective bulk processes, but receptor-mediated endocytosis is a specific, regulated cellular process that is used, for example, by most cells to take up extracellular products (e.g., lipoproteins, transferin) or to reduce the levels of surface receptors (down-regulation) after receptors are occupied by ligands, or by some cells, such as B lymphocytes, to internalize antigens using antibodies on the cell surface as receptors. Autophagy is regulated, but nonselective, digestion of intracellular material (Figure 1). It serves an adaptive role in response to nutritional deprivation and stress and is responsible for digestion of some cytosolic proteins and redundant or damaged intracellular organelles, such as mitochondria and peroxisomes. In addition, some cytosolic proteins that contain specific amino acid motifs (e.g., KFERQ) are transported into lysosomes selectively through a specific energy-, chaperone-, and receptor-mediated process that is activated by nutrient deprivation (Figure 1).

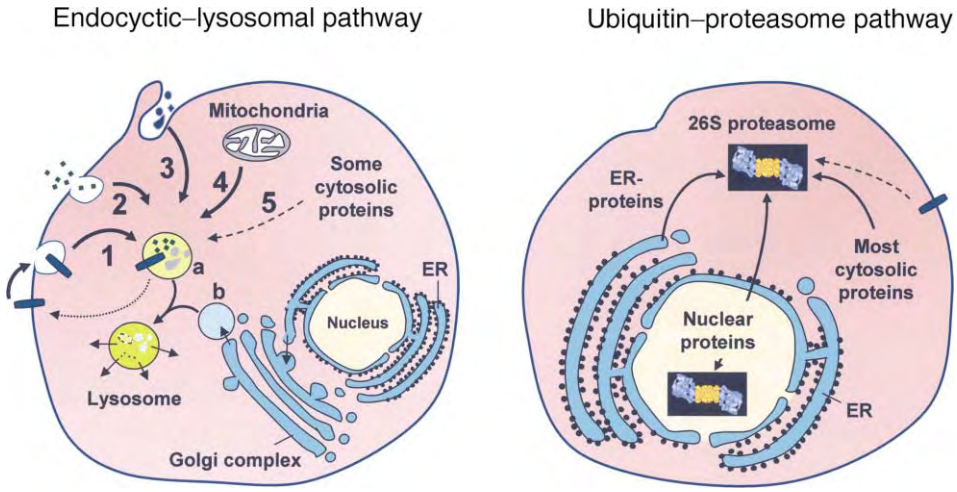

FIGURE 1 Pathways of protein breakdown in mammalian cells. Most intracellular proteins in the cytosol, nucleus, and endoplasmic reticulum (ER) are degraded by the ubiquitin–proteasome pathway (right panel). Extracellular and autophagocytized proteins and most membrane proteins are broken down within the endocytic–lysosomal compartment (left panel). Substrates are delivered to this pathway by receptor-mediated endocytosis (1), pinocytosis (2), phagocytosis (3), autophagy (4), and a selective process for some cytosolic proteins containing specific amino acid motifs (5). Some internalized membrane proteins are recycled back to the plasma membrane (dotted arrows). After the internalized material is enclosed in vesicles (a), the vesicle fuses with primary lysosomes (b), derived from the Golgi complex and ER, to form secondary lysosomes where final degradation takes place. Degradation products are transported across the lysosomal membrane into the cytosol. Some plasma membrane proteins are broken down by the ubiquitin–proteasome pathway, and some cytosolic proteins are degraded in lysosomes (dashed arrows). Although worn out mitochondria are cleared by autophagy, mitochondrial proteins are selectively broken down by their own ATP-dependent proteases.

Lysosomal Enzymes

Lysosomes contain at least 50 different hydrolytic enzymes, which catalyze the breakdown of proteins, nucleic acids, carbohydrates, and lipids into their components. Lysosomal hydrolases normally cannot escape into the cytoplasm and their isolation in this vesicular compartment is essential for protecting from nonspecific degradation of key cell constituents. However, during necrotic cell death, lysosomes release their content, which helps destroy the cell. Release of lysosomal enzymes outside of cells causes severe inflammation and contributes to the symptoms of some diseases (e.g., gout). Most lysosomal enzymes are optimally active at an acidic pH of 4–6, which is maintained by a cell membrane hydrogen ion ATPase. Many lysosomal proteases are traditionally called cathepsins, and most belong to the mechanistic family of cystein proteases. The most abundant proteases are cathepsins D and L (endopeptidases) and cathepsins B and H (exopeptidases). The acidic milieu in lysosomes not only keeps lysosomal enzymes at their most active state, but it also helps denature protein substrates, which enhances their susceptibility to proteolytic digestion. Once the protein substrates are degraded, the products of their digestion are transported across the membrane into the cytosol, where they are further metabolized.

Additional Roles of the Endocytic Pathway

The endocytic–lysosomal pathway plays an important role in maintaining the structural integrity of plasma membrane by continuously recycling internalized membranes and some membrane receptors back to the cell surface. In addition, in specialized antigen-presenting cells (macrophages, dendritic cells, and B cells), some peptides derived from breakdown of extracellular proteins escape complete destruction and are bound in late endosomes by specialized membrane receptors, called major histocompatibility (MHC) class II molecules. These complexes are transported to the cell surface for presentation to a subpopulation of T lymphocytes responsible for generation of humoral immune responses against non-native proteins, e.g., ones from pathogens.

Ubiquitin–Proteasome Pathway

Most cytosolic and nuclear proteins are degraded by the ubiquitin–proteasome pathway (Figure 2). This system catalyzes the breakdown of most normal long-lived proteins, which comprise the bulk of proteins in cells, and many short-lived proteins that regulate a wide variety of essential cellular processes, ranging from cell cycle progression to signal transduction and gene transcription. In addition, it catalyzes the selective and rapid elimination of damaged, misfolded, or mutated proteins, which are continuously produced due to imperfections of biosynthetic and folding machineries in the cell. The discovery of the ubiquitin–proteasome pathway resulted from the finding that the breakdown of intracellular proteins was ATP-dependent, which was surprising because the peptide bond cleavage *per se* does not require energy. Biochemical dissection of this pathway in the early 1980s revealed that it consists of two ATP-dependent processes: the conjugation of a small protein ubiquitin to proteins that marks them for degradation, and the hydrolysis of ubiquitylated proteins by the very large proteolytic machine, the 26S proteasome (Figure 2), (S refers to Svedberg – the unit of time used to measure velocity at which the protein sediments in a centrifuge).

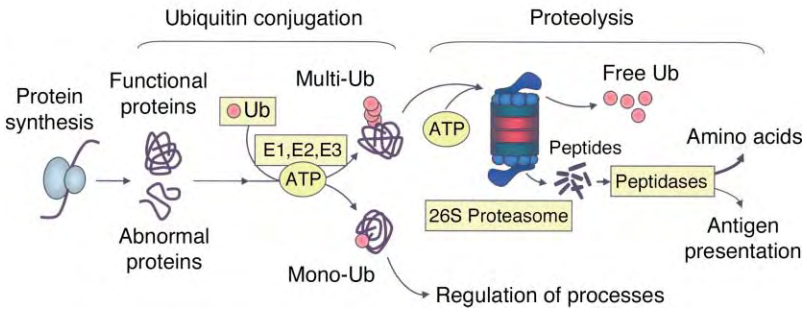

FIGURE 2 Ubiquitin–proteasome pathway for degradation of intracellular proteins. In eukaryotic cells, the site for degradation of most intracellular proteins is a large proteolytic particle, termed the 26S proteasome. Protein substrates destined for degradation by the 26S proteasome are first polyubiquitylated in ATP-dependent manner in a series of reactions involving at least three groups of enzymes (see text for details). Polyubiquitylated substrates are rapidly hydrolyzed by the 26S proteasome and monomeric ubiquitin is recycled by the action of deubiquitinating enzymes. The energy of ATP is required for ubiquitin conjugation, binding, and unfolding of a substrate and its translocation into the inner cavities of the proteasome. Most peptides produced by proteasomes are further degraded to amino acids by endo- and exopeptidases in the cytosol and nucleus, but a small fraction of peptides escapes complete hydrolysis and are utilized for MHC class I antigen presentation. Some proteins are conjugated to only a single ubiquitin molecule. This modification does not mark proteins for degradation by proteasomes but is utilized for regulation of cellular processes, such as endocytosis and transcription.

Ubiquitin Conjugation

Formation of Polyubiquitin Chains

In order to be degraded by 26S proteasomes, most intracellular proteins must be first conjugated to a chain of ubiquitin molecules. This process ensures that only selected substrates are degraded in a regulated manner and prevents the uncontrolled degradation of other cellular proteins. Ubiquitin is a 76-residue globular protein, which is present only in eukaryotic cells, and not in bacteria and archaea, where highly selective protein degradation is achieved through ATP-dependent proteolysis independent of ubiquitin. Ubiquitin conjugation to other proteins and the formation of polyubiquitin chains is mediated by the sequential action of three types of enzymes, called E1 (ubiquitin-activating enzyme), E2s (ubiquitin-conjugating enzymes or ubiquitin-carrier proteins) and E3s (ubiquitin-protein ligases). In this process, the single E1 enzyme activates ubiquitin in an ATP-dependent reaction by forming a highly reactive thiolester linkage between the C terminus of ubiquitin and the thiol group in the active site of the E1. The activated ubiquitin is then passed from the E1 to a sulfhydryl group on one of the cell's $\sim$30 E2s. Next, the activated ubiquitin molecules are linked to a lysine side chain or, in some cases, to the N-terminal amino group in the substrate protein, directly from the E2 (or in some cases after transfer of ubiquitin from the E2 to the E3). A single E2 may function with multiple E3s to provide specificity in a combinatorial fashion. Cells contain hundreds of distinct E3s. These enzymes are the main determinants of substrate specificity and are capable of recognizing a few or multiple substrates through specific degradation signals. E3s are soluble or membrane-bound proteins; some are monomeric enzymes containing distinct domains for binding a substrate and a specific E2 enzyme, while others are very complex oligomeric structures in which different subunits subserve different functions required for highly specific and efficient substrate recognition and ubiquitylation. A polyubiquitin chain is synthesized by linking new ubiquitin molecules to previously conjugated ubiquitin through its lysine residues. In most cases, proteasomal degradation requires formation of ubiquitin chain where ubiquitin molecules are linked to lysine 48, but other types of ubiquitin chains exist in cells and serve other regulatory roles distinct from proteolysis. Once conjugated to chains of four or more ubiquitins, proteins are degraded by 26S proteasomes. Ubiquitylation of certain cell surface receptors (e.g., growth factor receptors) results in their internalization and degradation in lysosomes, but not in proteasomes.

Mechanisms of Substrate Recognition

Ubiquitylation of proteins is triggered by various features of the substrates that act as signals (the so-called "degrons") that are recognized by the E3 and thus decrease the stability of the protein in the cell. These structural features can be constitutive elements in the substrate itself (e.g., a specific N-terminal amino acid residue or a short internal sequence of amino acids in a target protein) or can be acquired covalent modifications. Phosphorylation of substrates is one of the frequently employed acquired signals that regulate protein ubiquitylation. In many instances, this modification leads to direct recognition of a substrate by the specific E3, but, in some cases, phosphorylation of a substrate can inhibit ubiquitylation. Phosphorylation-dependent ubiquitylation is responsible for degradation of IκB during inflammatory response and of the various cyclins that control progression through the cell cycle. Other types of posttranslational protein modifications can either prevent or stimulate ubiquitylation, including acetylation, glycosylation, or attachment of small ubiquitin-like proteins, SUMO-1 or Nedd8. An interesting posttranslational modification that induces ubiquitylation of a substrate is hydroxylation of proline residues in the transcription factor HIF1-α, which plays an important role in transcriptional adaptation to hypoxia. Under normoxic conditions, two prolines in HIF1-α are readily hydroxylated, leading to its recognition and ubiquitylation by the specific E3. In yet another scenario for substrate recognition, association of the substrate with an adapter protein is required for its recognition and ubiquitylation by the specific E3 enzyme. This strategy is particularly exploited by some viruses. The best example is the E6/E6-AP-mediated ubiquitylation of p53. The selective degradation of unfolded proteins involves their initial recognition and binding by specific molecular chaperones and a chaperone-dependent E3, termed CHIP. For most substrates, degradation signals have not yet been defined. For example, it is unclear how cells recognize and selectively degrade abnormal proteins or normal myofibrilar proteins in skeletal muscle during muscle atrophy.

Deubiquitination

Ubiquitin conjugation to cellular proteins is a reversible process and is mediated by deubiquitinating enzymes, which are all cystein proteases. They catalyze the continuous disassembly of ubiquitin conjugates during degradation of ubiquitin-conjugated proteins by the 26S proteasome. They must play important roles in recycling monomeric ubiquitin for use in new conjugation reactions, and in preventing the accumulation of free polyubiquitin chains that could act as competitive inhibitors of the binding of ubiquitylated substrates to

the proteasome. These enzymes also probably serve as a proofreading system, which insures that no erroneous ubiquitylation of substrates takes place. Mutations in deubiquitinating enzymes can cause neuronal degeneration and may contribute to the occurrence of cancer.

Protein Degradation

The 26S Proteasome

Proteasomes are abundant evolutionarily highly conserved multimeric structures localized in the cytosol and nucleus of all eukaryotic cells. The proteasome complex responsible for degradation of ubiquitylated proteins is termed the 26S proteasome, which consists of the 20S core particle and one or two regulatory 19S particles (Figure 3).

The 20S Core Particle In eukaryotes, the 20S proteasome is a hollow cylinder and consists of four stacked rings, each containing seven homologous subunits. There are two identical outer α-rings and two identical inner β-rings (Figure 3). Three of the subunits in each inner β-ring contain the proteolytic active sites. The outer α-rings surround the narrow openings into the 20S particle at either end, through which substrates can enter into the inner proteolytic chamber. These openings are tightly regulated and protein access is enabled through the association of α-rings with different regulatory particles. This closed architecture with isolated active centers evolved to prevent the uncontrolled destruction of needed cell proteins. The proteasomal active sites in β-rings are confined to the interior of the cylinder where proteins are degraded. Each of the three active subunits has a different catalytic activity: one cleaves preferentially after basic amino acids in a protein substrate, one after large hydrophobic residues, and one after acidic residues. The active site nucleophile of the proteasome is the hydroxyl group of the threonine at the amino terminus of the β-subunit, and proteasomes thus belong to a novel mechanistic class of threonine proteases. The existence of this new type of proteolytic mechanism, not utilized by other known proteases, has enabled the synthesis of highly specific proteasome inhibitors. They are now an irreplaceable research tool and are very promising in clinical trials to treat myeloma and other cancers, and in animals have dramatic effect against diseases such as arthritis and stroke.

19S Regulatory Particle The 19S particle consists of at least 18 different subunits and associates with α-rings on one or both ends of the 20S proteasome. Two functionally different substructures of this complex have been distinguished: the base and the lid (Figure 3). The base, which touches the α-rings of the 20S core

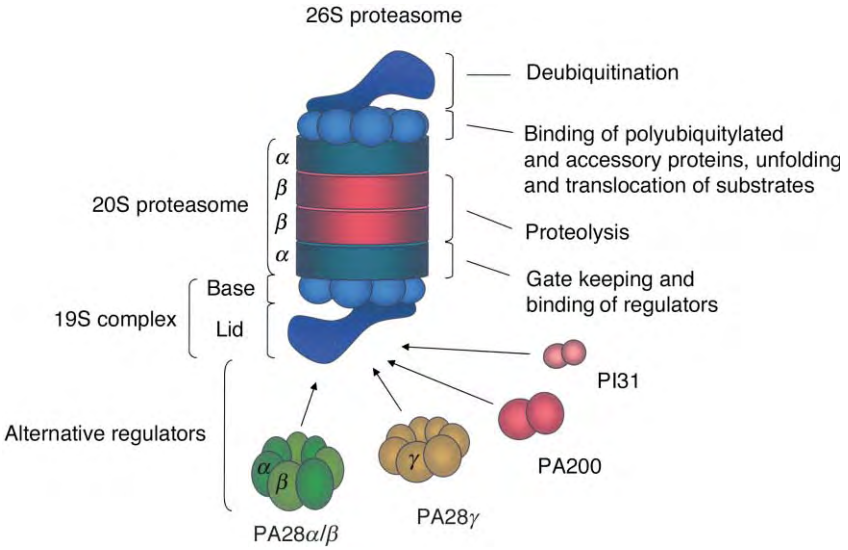

FIGURE 3 The 26S proteasome and its regulatory components. The 26S proteasome consists of the 20S core particle and one or two regulatory 19S particles. Different structures comprising the 26S proteasome carry out distinct functions (as detailed in the illustration). In addition to 19S regulators, eukaryotic 20S proteasomes can also associate with other ring-forming complexes, such as PA28α/β or PA28γ, or simpler proteins (PA200 or PI31). PA28α/β is a heptameric ring composed of α- and β-subunits. It promotes opening the channel enclosed by α-rings of 20S proteasomes. PA28γ is related to α- and β-subunits of PA28α/β and forms a homoheptameric complex that binds to 20S proteasomes and activates mainly the cleavages after charged residues in peptide substrates. It is predominantly found in the nucleus and, in some cells, is down-regulated by interferon γ. Its biological function is still not well understood. PA200 is a recently discovered 20S proteasome-interacting protein of 200 kDa that is localized in the nucleus. The mechanism of its association with proteasomes is not well understood, but like PA28, it activates only peptide hydrolysis by proteasomes. It appears to play a role in DNA repair by recruiting proteasomes to damaged DNA. PI31 is a homodimeric protein that was discovered by its ability to inhibit peptide hydrolysis by 20S proteasomes *in vitro*. Recent *in vivo* data suggest that this protein does not affect proteasome-mediated proteolysis but rather interferes with MHC class I antigen presentation by slowing maturation of immunoproteasomes.

particle, contains eight polypeptides including six ATPases that form a ring. These ATPases bind substrates and use the energy of the ATP to unfold protein substrates, open the gate in α-rings, and promote rapid translocation of substrates into the 20S core particle for degradation. The base of the 19S particle also contains surfaces responsible for transient binding of: (1) polyubiquitin chains, (2) deubiquitinating enzymes, and (3) ubiquitin-like domains of various adaptor proteins that may function in bringing ubiquitylated substrates to close proximity of proteasomes. The lid contains eight non-ATPase subunits of unknown function. This structure is required for proteolysis of ubiquitylated proteins, probably through interaction with the polyubiquitin chain.

Immunoproteasome and Hybrid Proteasome

In higher vertebrates that have an immune system, a small fraction of peptides generated by proteasomes is not completely degraded to free amino acids but instead transported into the ER, where they associate with specific membrane-bound MHC class I molecules and are subsequently transported to the cell surface. The immune system is continually surveying the surface of all cells for non-native peptides originating from viral or mutated proteins. If cells carrying such non-native peptides are encountered, they are rapidly destroyed by cytotoxic T-lymphocytes. Proteasomes found in most of the tissues (the so-called constitutive proteasomes) contribute to the generation of basal levels of antigenic peptides in the absence of infection. However, during inflammation, two additional types of proteasomes appear to play a major role in enhancing MHC class I antigen presentation and are termed immunoproteasomes and hybrid proteasomes. They are normally found in lymphoid tissues (e.g., spleen and thymus), but are induced in other tissues during infection in response to the cytokine interferon γ. Immunoproteasomes are formed by replacement of all three catalytic β-type subunits in constitutive proteasomes with alternative proteolytically active β-subunits. The alternative immunosubunits possess qualitatively different cleavage specificities than constitutive β-subunits and appear to play a major role in increasing the supply of appropriate peptides for MHC class I antigen presentation. Hybrid proteasomes are formed when 20S immunoproteasomes are capped on one side with the 19S particle and on the other side with an alternative protein complex, called PA28α/β (Figure 3). Most probably, in these hybrid particles, ubiquitylated substrates initially bind to the 19S regulator and peptide products are released at the opposite side through the PA28α/β that apparently promotes opening the channel enclosed by α-rings and allows generation of peptide fragments particularly suitable for MHC class I antigen presentation during inflammation.

Mechanism of Protein Degradation

Although the exact sequence of events in which proteins are degraded by 26S proteasomes is not fully understood, a rough outline of steps can be provided. Upon binding of the polyubiquitylated substrate by the proteasome, the substrate is first unfolded in an energy-dependent manner by the action of ATPases localized in the base of the 19S particle. Recent data suggest that proteins are unfolded prior to their translocation into the proteasome's inner cavity. Conformational changes induced by hydrolysis of ATP promote opening the gate in α-rings followed by translocation of the unfolded substrate into the inner chambers of the proteasome. Successful translocation of the substrate must follow disassembly of polyubiquitin chain by deubiquitinating enzymes attached to the 19S particle. Translocation can occur from its free amino or carboxyl terminus, depending on the substrate, or even internally by the process in which a polypeptide loop enters the axial channel to permit initial endoproteolytic cleavage. In some cases, proteasomes degrade substrates only partially, yielding biologically active protein fragments, like in the generation of the p50 subunit of the transcription factor NFκB from the larger precursor and in the processing and activation of some membrane-bound transcription factors. Once in the central chamber of the 20S particle, the substrate is cleaved by six catalytic subunits into small peptides ranging from 3 to 25 residues in length. Unlike traditional proteases, the proteasome does not simply cleave a protein and release the partially digested fragments; on the contrary, a protein substrate, once bound by the proteasome, is cut until small peptides are generated. This behavior ensures that partially digested proteins do not accumulate within cells. The product release may be facilitated in some cells by PA28α/β, as well as by hydrophobic products themselves which can trigger gate opening in α-rings. In eukaryotic cells, the products generated by proteasomes appear to be hydrolyzed into amino acids by the sequential actions of endopeptidases and aminopeptidases. The whole process of degradation of one molecule of the protein substrate requires several hundred molecules of ATP and is completed in a matter of seconds or minutes, depending on the size of a substrate. Generally, subtrates must be first ubiquitylated in order to be degraded by proteasomes. However, 26S proteasomes can degrade certain substrates *in vivo* (e.g., ornithin decarboxylase associated with cofactor antizyme) and many polypeptides *in vitro* (e.g., denatured casein, aged calmodulin) in ubiquitin-independent manner. It still remains uncertain whether *in vivo*

TABLE I

Disturbances of Ubiquitin-Dependent Proteolysis in Human Disease

Protein substrate	Disease	Mechanism
Increased proteolysis		
p53	Cervical carcinoma	E6/E6-AP-mediated degradation of p53
$p27^{Kip1}$	Colorectal/breast Ca.	Enhanced degradation of a cell cycle inhibitor
IκB	Inflammation	Activation of NFκB transcription factor
CFTR	Cystic fibrosis	Point mutation in CFTR, misfolding and degradation through ERAD
MHC class I heavy chain	Cytomegalovirus infection	Down-regulation of MHC class I by viral proteins
Most muscle proteins	Muscle atrophy, cachexia	Up-regulation of an SCF E3, Atrogin-1, and the RING finger E3, MurF-1
Decreased proteolysis		
HIF1-α	von Hippel–Lindau disease	Mutation in SCF E3, VHL
ENaC	Liddle syndrome	Mutation in HECT E3, NEDD4
Receptor tyrosine kinases	Cancer	Mutation in RING finger E3, c-Cbl
α-synuclein, unknown	Parkinson disease	Mutation in RING finger E3, Parkin
Unknown	Angelman syndrome	Mutation in HECT E3, E6-AP
α1-antitrypsin	Liver disease in some α1-antitrypsin deficient patients	Decreased degradation of mutated α1-antitrypsin by ERAD pathway
Epstein–Barr virus nuclear antigen 1 (EBNA1)	Epstein–Barr virus-associated malignancies	Immune evasion due to lack of EBNA1 degradation

there are more proteins that are degraded in ubiquitin-independent manner.

Endoplasmic Reticulum-Associated Degradation (ERAD)

Many newly synthesized proteins are translocated into the lumen of the ER or are inserted into the ER-membrane. They may remain in the ER or be exported into other organelles, or the cell surface membrane or be secreted into the extracellular space. The ER contains an abundant set of chaperones and enzymes that assist newly synthesized proteins in attaining their correct conformation and activity, but sometimes, this maturation process fails and misfolded proteins are generated. Such abnormal proteins are effectively removed so as not to aggregate and form potentially toxic inclusions and the process of their disposal is often called ER-associated degradation (ERAD). In this process, misfolded proteins are retrotranslocated from the ER back into the cytosol, where they are ubiquitylated and degraded by 26S proteasomes. This export is necessary because the ER does not contain proteolytic enzymes necessary for protein degradation. ERAD is used by some viruses to down-regulate MHC class I molecules in the ER (e.g., cytomegalovirus) as a means of viral evasion of the immune system. In addition, disturbances in ERAD pathway can cause serious human disease, such as cystic fibrosis or a form of α1-antitrypsin deficiency (Table I).

Proteolysis in Mitochondria

As in the cytosol and nucleus, proteins in mitochondria also have different half-lives and mitochondria can selectively degrade abnormal proteins. Although mitochondria as a whole can be degraded in lysosomes by autophagy, this process is nonselective and cannot account for different turnover rates of regulatory mitochondrial proteins. Since the matrix and the inner membrane of mitochondria are not accessible to cytosolic proteases, these sites harbor their own autonomous proteolytic system, which consists of several evolutionarily conserved ATP-dependent proteases. This system has dual functions; it mediates complete degradation of nonassembled or misfolded proteins, and it enables selective proteolysis of specific normal regulatory proteins that are important for the maintenance of mitochondrial functions. The matrix of mammalian mitochondria contains two kinds of soluble proteases that are homologous to eubacterial Lon and ClpXP proteases and responsible for degradation of matrix proteins. The mitochondrial inner membrane of all eukaryotic cells has two proteases that belong to the AAA superfamily of ATPases, termed *i*-AAA

(*i*, intermembrane) and *m*-AAA (*m*, matrix). These enzymes are complex structures with a native molecular mass of ~1 MDa composed of smaller subunits of 70–80 kDa. They expose their catalytic sites toward either the matrix or intermembrane space and have chaperone-like activity that is required for protein unfolding and subsequent degradation at proteolytic sites. Substrates of these proteases are proteins located in the inner membrane, and their degradation is essential for the maintenance of oxidative phosphorylation. Impaired function of these proteases causes neurodegeneration in humans and severe growth defects in yeast.

Proteolysis in Bacteria and Archaea

Roles of Proteolysis in Bacteria

Although bacteria and archaea do not have lysosomes, ubiquitin, or 26S proteasomes, they carry out very selective and highly regulated degradation of intracellular proteins. These prokaryotes contain several distinct ATP-dependent proteases that mediate initial steps in degradation of proteins in their cytoplasm. These enzymes serve functions similar to those in eukaryotic cells. Bacteria selectively destroy abnormal proteins, including those arising from mutations, gene fusions, misfolding, chemical damage, or genetic engineering. In fact, successful expression of many recombinant proteins in *Escherichia coli* (*E. coli*) has been hampered by the action of these enzymes, and several bacterial strains defective in some of these proteases have been developed to increase the stability of cloned foreign proteins. Exposure to harsh environmental conditions, such as high temperature (heat shock), induces the genes which encode several molecular chaperones and ATP-dependent proteases to refold or degrade unfolded proteins that may be generated and protect against the buildup of these potentially toxic polypeptides. During normal exponential growth, most normal bacterial proteins are quite stable entities. However, even during normal growth, certain polypeptides with major regulatory functions are degraded very rapidly. For example, the specific component of bacterial RNA polymerase, so-called sigma factor σ^{32}, has a half-life of 1–2 min in *E. coli* under normal conditions, but it becomes transiently stabilized during heat shock, when it mediates the heat shock response. A general enhancement of protein breakdown occurs in nongrowing cells deprived of nutrients in order to provide the starving organism with a source of amino acids for new protein synthesis or energy production. In many gram-positive bacteria, prolonged starvation triggers sporulation, which is also accompanied by the marked degradation of most normal cellular proteins to provide amino acids for the expression of spore-specific genes.

Bacterial ATP-Dependent Proteases

Many eubacterial and archaeal ATP-dependent proteases are ancestors of more complex eukaryotic enzymes. Archaea, for example, contain proteasomes that have similar architecture as eukaryotic 20S proteasomes, but are built only from single α- and β-subunits and function in protein breakdown in association with the ATPase PAN. This hexameric-ring structure is homologous to the six ATPases found in the 19S base of the eukaryotic proteasome and has the capacity to unfold globular proteins and promote their entry into the 20S particle. The major ATP-dependent proteases in eubacteria are the cytoplasmic serine proteases La/Lon, "caseinolytic serine proteases" ClpAP and ClpXP, the cytoplasmic threonine protease HslUV, and the inner membrane zinc-metalloprotease FtsH. The proteases La/Lon and caseinolytic proteases have their homologues in eukaryotic mitochondria. Bacterial ATP-dependent proteases are multimeric enzymes (400–700 kDa) that have distinct substrate specificities and subunit composition. They are composed of proteolytic domains and regulatory ATPase domains, which actually determine substrate specificities. The simpler proteases, La/Lon and FtsH, contain these two domains in a single polypeptide chain. Lon consists of four or eight identical 87 kDa protein subunits and was the first ATP-dependent protease described. Other proteases that are structurally related to the eukaryotic 20S proteasomes (such as HslUV and ClpAP) contain these domains in two separate structures. For example, the HslUV contains a central proteolytic chamber (HslV) composed of two hexameric rings with the active sites facing inward. Two ring-forming HslU complexes have ATPase activity and associate with proteolytic HslV cylinders on both ends to form a four-ring 20S proteasome-like particle capable of binding, unfolding, and degrading bacterial proteins. Besides proteases, the degradation of many proteins *in vivo* also requires chaperones of the Hsp70 and chaperonin (GroEL) families as cofactors that act in the recognition of unfolded substrates. ATP-dependent proteases generate short peptides of 10–40 amino acids, and they are degraded to amino acids by energy-independent peptidases.

Selection of Substrates

Bacteria lack ubiquitin and any homologous mechanism for covalent modification of substrates destined for proteolysis. The ATPase-ring components (e.g., HslU, ClpA or ClpX) of bacterial proteases determine the substrate specificity. With some exceptions, the exact recognition motifs on bacterial proteins are not well defined. However, special sequences on the N and C

termini of cell proteins have been identified that lead to recognition by ClpXP and may become particularly important in conditions when overall protein degradation is accelerated. All bacteria selectively degrade prematurely terminated proteins. A specific tRNA incorporates the tagging peptide SsrA (11-residue stretch of amino acids) into nascent polypeptide chain if ribosomes are stalled. The presence of an SsrA tag at the C terminus of a protein leads to its rapid hydrolysis by ClpXP and FtsH proteases. In addition to this recognition motif, in the case of multiprotein complexes, some proteins become substrates if present in cells without their natural binding partners because the motifs that are recognized may be more accessible. Finally, chaperones may also provide some assistance in increasing susceptibility of substrates to bacterial proteases.

Targeting Proteolysis for Drug Development

Although a number of lysosomal diseases are known, the major ones are not due to defects in lysosomal proteases but rather to failure to degrade polysaccharides or lipids due to lack of a specific lysosomal hydrolase. Commonly, these diseases are called lysosomal storage diseases because undegraded material progressively accumulates in lysosomes. One component of the endocytic–lysosomal pathway, the autophagy, has been reported to be disturbed in some malignancies, neurodegenerative, and cardiovascular disease; however, it is unknown if the impaired breakdown of a specific protein(s) is part of the underlying pathophysiological mechanism, or a secondary consequence. However, a number of major malignant, neurological, metabolic, and viral diseases are caused by the gain or loss of function of the ubiquitin–proteasome proteolytic system (Table I). Since the disturbances in the ubiquitin–proteasome system underlie the pathogenesis of many human diseases, drugs that target this system are being developed. The proteasome inhibitors are the first so far to be tested in animal models and are now in clinical trials for treatment of neoplastic disease. However, proteasome inhibition is not a very specific strategy to modulate stability of a specific protein and more selective approaches should prove to be more effective and have fewer side effects. A typical approach would be to develop small molecule inhibitors to target events upstream of proteasomes (e.g., ubiquitin ligation and substrate recognition).

See Also the Following Articles

Autophagy in Fungi and Mammals • Chaperones, Molecular • Endocytosis • Endoplasmic Reticulum-Associated Protein Degradation • N-End Rule • Proteasomes, Overview • 26S Proteasome, Structure and Function • Ubiquitin System • Ubiquitin-Like Proteins • Unfolded Protein Responses

Glossary

AAA ATPase (ATPases Associated with diverse cellular Activities) A distinct family of ATPases characterized by the presence of highly conserved domains in their primary sequence, hexameric structure, and protein unfolding activity.

ATPase Type of enzyme that hydrolyzes ATP and uses the energy released to drive biological processes such as pumping ions, unfolding proteins, and moving molecules.

folding A process in which newly synthesized polypeptides attain their native three-dimensional structures.

molecular chaperones Specialized proteins, many being ATPases, that prevent protein aggregation and may function to facilitate proteins attaining their native conformations; some can promote protein unfolding and solubilization of aggregated proteins.

Further Reading

Bryant, P. W., Lennon-Dumenil, A. M., Fiebiger, E., Lagaudriere-Gesbert, C., and Ploegh, H. L. (2002). Proteolysis and antigen presentation by MHC class II molecules. *Adv. Immunol.* **80**, 71–114.

Cuervo, A. M., and Dice, J. F. (1998). Lysosomes, a meeting point of proteins, chaperones, and proteases. *J. Molecul. Med.* **76**, 6–12.

Glickman, M. H., and Ciechanover, A. (2002). The ubiquitin–proteasome proteolytic pathway: Destruction for the sake of construction. *Physiol. Rev.* **82**, 373–428.

Goldberg, A. L., Cascio, P., Saric, T., and Rock, K. (2002). The importance of the proteasome and subsequent proteolytic steps in the generation of antigenic peptides. *Molecul. Immunol.* **39**, 147–164.

Gottesman, S. (1996). Proteases and their targets in *Escherichia coli*. *Annu. Rev. Genet.* **30**, 465–506.

Käser, M., and Langer, T. (2000). Protein degradation in mitochondria. *Semin. Cell Develop. Biol.* **11**, 181–190.

Kisselev, A. F., and Goldberg, A. L. (2001). Proteasome inhibitors: From research tools to drug candidates. *Chem. Biol.* **8**, 739–758.

Ogura, T., and Wilkinson, A. J. (2001). AAA + superfamily ATPases: Common structure–diverse function. *Genes Cells* **6**, 575–597.

Turk, V., Turk, B., and Turk, D. (2001). Lysosomal cysteine proteases: Facts and opportunities. *EMBO J.* **20**, 4629–4633.

Biography

Tomo Šarić is currently a Senior Scientist at the Institute for Neurophysiology, University of Cologne, Germany. His principal research interest is in intracellular proteolysis, especially in proteases acting downstream of proteasomes and their role in regulating immune responses. He holds an M.D. and a Ph.D. from the University of Zagreb in Croatia and received his postdoctoral training at the University of Texas and Harvard Medical School.

Alfred L. Goldberg is Professor of Cell Biology at Harvard Medical School in Boston. His principal research interests are in the field of protein degradation. His laboratory has contributed to many major discoveries in this field, such as the discovery of the ATP requirement for degradation of most intracellular proteins, discovery of the first ATP-dependent proteases in bacteria and proteasomes in eukaryotic cells, introduction of proteasome inhibitors and the role of the proteasome in antigen presentation, and muscle atrophy.

Protein Folding and Assembly

David P. Goldenberg
University of Utah, Salt Lake City, Utah, USA

In order to carry out their biological functions, most polypeptide chains must fold into stable three-dimensional (3D) structures, for it is the precise spatial distribution of chemical groups within a protein that gives the molecule its ability to interact specifically with other molecules and, in the case of an enzyme, catalyze a chemical reaction. In many cases, individual polypeptide chains must also assemble into larger structures containing additional proteins or nucleic acids. The folding of many proteins is reversible, so that the native structure can be disrupted by a change in temperature or addition of a chemical denaturant, and the unfolded protein can then be induced to refold and assemble by returning it to physiological conditions. Experiments of this type demonstrate that the information specifying the native structure of a protein resides in its amino acid sequence, and *in vitro* studies have provided important insights about the energetic factors that drive folding and assembly and the kinetic mechanisms of these processes. Folding *in vivo* is often facilitated by transient interactions with other proteins, molecular chaperones. Folding may also compete with the formation of aberrant aggregates *in vivo*, sometimes leading to pathological conditions such as amyloid diseases.

Thermodynamics of Protein Folding

The thermodynamic stability of a protein is defined by the equilibrium between the native folded form and the highly disordered unfolded state that is induced by elevated temperatures or chemical denaturants, such as urea or guanidinium chloride (GuHCl). Relatively small monomeric proteins, composed of 50–150 amino acid residues, typically unfold and refold efficiently and cooperatively, so that the process can be described as a simple equilibrium:

$$N \rightleftharpoons U$$

where N and U represent the native and unfolded states (Figure 1). While the native state usually has a well-defined 3D structure, the unfolded state is best thought of as a broad distribution of rapidly interconverting conformations.

Under physiological conditions, the change in free energy for unfolding (ΔG_u) for a small monomeric protein typically lies in the range of 5–15 kcal mol^{-1}. This relatively small preference for the native protein reflects a delicate balance between three major factors: (1) A large loss of entropy as the chain is converted from a highly disordered state to an ordered state, (2) the transfer of nonpolar groups from an aqueous environment to a nonpolar environment in the protein interior, and (3) the formation of stabilizing interactions within the protein, including hydrogen bonds, salt bridges, and van der Waals interactions.

During the 1980s and 1990s, a great deal of effort was devoted to measuring the stabilities of genetically modified proteins in which single amino acid residues were replaced so as to delete one or a few stabilizing interactions. Taken together, these studies revealed that proteins are surprisingly tolerant of amino acid replacements, so that most mutations destabilize the native state by only a few kcal mol^{-1}, and substitutions that completely prevent folding are quite rare. Substitutions that remove hydrogen bonds or nonpolar interactions cause, on an average, roughly similar degrees of destabilization (usually of the order of 1–3 kcal mol^{-1}), implying that both types of interactions play important roles in stabilizing native proteins.

Folding Kinetics and Mechanisms

Levinthal's Paradox

Much of the work on folding mechanisms, both experimental and theoretical, has been motivated by the realization that the number of possible conformations accessible to a polypeptide chain is so immense that random sampling to find the structure with minimum free energy would take a ridiculously long time. For instance, if a chain is composed of 100 residues, and each residue can take on ten possible conformations, then the total number of conformations is 10^{100}. If the various conformations are randomly sampled at a rate of 10^{13} s^{-1} (approximately the rate of rotation for a covalent bond), then the total time

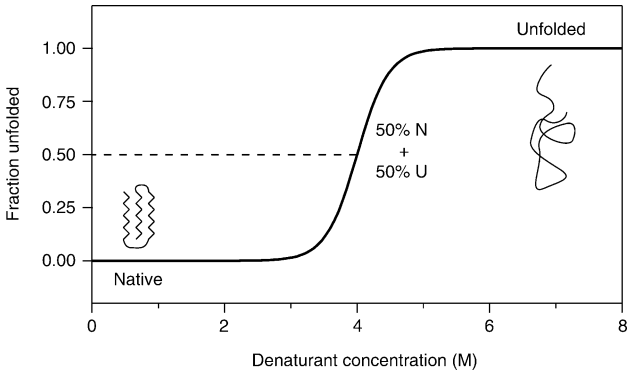

FIGURE 1 A cooperative protein unfolding–refolding transition. In a typical experiment, the native protein is incubated in solutions with increasing concentrations of denaturant such as urea or guanidinium chloride, and the fraction of unfolded molecules is determined by monitoring a spectroscopic signal, such as UV absorbance, fluorescence, or circular dichroism. For small monomeric proteins, the transition is usually highly cooperative, so that only the fully folded and unfolded forms are significantly populated and the fraction unfolded represents the relative concentrations of the two forms.

required to sample all of the conformations would be $\sim 10^{80}$ years!

The calculation outlined above is frequently identified as the "Levinthal Paradox," in recognition of an insightful 1969 paper by Cyrus Levinthal. Although this argument undoubtedly represents a great oversimplification, since many of the conformations assumed to be accessible to the chain will, in fact, be excluded by steric clashes among atoms in different residues, the calculation suggests that there must be some mechanism by which the search for the native conformation is limited.

Folding and Unfolding Rates

The rates at which different proteins fold and unfold vary tremendously. Even considering only relatively small proteins composed of a single domain, experimentally determined folding rate constants cover at least the range from 0.1 to $10^5\ s^{-1}$. While it might be expected that smaller and thermodynamically more stable proteins would fold the fastest, folding rates for unrelated proteins are poorly correlated with size or stability. Instead, a major determinant of folding rate appears to be the topological complexity of the native structure. While true topological knots are rarely found in folded proteins, different structures vary with respect to the relative prevalence of interactions formed between closely and distantly spaced residues, and faster folding in often associated with topologies in which short-range interactions are more prominent. The physical basis for this correlation is not yet fully understood, but it strongly suggests that the rate-determining step in folding is associated with formation of the correct topology, as opposed, for instance, to formation of a local structure that then nucleates rapid folding of the rest of the chain.

Unfolding rates also vary greatly among different proteins and under different solution conditions. For some proteins, unfolding may be a surprisingly common event, even under physiological conditions. For instance, if the stability of a protein, ΔG_u, is 5 kcal mol^{-1} at 25°C, and the folding rate is $10^3\ s^{-1}$, the unfolding rate is predicted to be about $0.5\ s^{-1}$, so that 99% of the molecules in a population will undergo an unfolding event over a period of 10 s. Since unfolded proteins are typically much more sensitive to proteolysis than folded proteins, spontaneous unfolding may be an important factor in determining the rate of protein turnover *in vivo*. Transient unfolding may also contribute to formation of aberrant structures, such as the amyloid fibers described below.

Folding Intermediates

Following the tradition of biochemists who have successfully dissected other processes by identifying and characterizing discrete intermediates, many investigators have studied kinetic intermediates that accumulate transiently before protein-folding reactions reach equilibrium. While there is considerable diversity in the intermediates observed in the folding of different proteins, there appear to be common features among many of them.

Generally, the most easily detected intermediates form very rapidly (on the ms timescale or faster) after the unfolded protein is transferred to conditions that favor the native state. Often, the intermediate appears to contain ordered secondary structure, especially α-helices, but there is little evidence of well-defined interactions between the side chains from different segments of the chain. The average dimensions of the chain in these intermediates typically lie between those of the native protein and the fully unfolded state in denaturants. Kinetic intermediates of this type also resemble partially unfolded states that can sometimes be generated under special solution conditions, including low pH for some proteins, or when a ligand (such as a metal ion or heme group) is removed from a native protein. These states, typically characterized by the presence of regular secondary structure but the absence of stable tertiary interactions, are described as "molten globules."

Because the most frequently observed partially folded states often interconvert rapidly with the fully unfolded protein, establishing whether or not these species are actually productive intermediates in folding, as opposed to products of side reactions, is quite difficult. As a consequence, there is presently a great deal of uncertainty and disagreement about the significance of these states for understanding folding mechanisms. Some authors believe that the formation of intermediates

is important for limiting the search for the native conformation, while others argue that they are simply compact forms of the denatured state and do not play any special role in directing the chain towards the native state.

Transition States

It might seem surprising that the concept of a transition state, derived from studies of simple chemical reactions, could be usefully applied to a process as complex as protein folding. However, the folding kinetics of many proteins can be well-described by a simple model in which the rate is determined by an equilibrium between the unfolded state and a higher energy state that is rapidly converted to the native conformation (Figure 2). The transition state can be envisioned as an ensemble of partially ordered conformations that collectively have an equal probability of being converted to either the native or fully unfolded states.

By their very nature, transition states cannot be characterized directly by spectroscopic or other physical methods. Instead, their properties must be inferred from the results of experiments in which the kinetics of folding and unfolding are compared after perturbing either the structure of the protein or its environment. For instance, replacing an amino acid residue that contributes to the stability of the transition state is expected to increase the free energy barrier for folding and, thereby, decrease the folding rate. On the other hand, a substitution that weakens an interaction that is present in the native protein but not the transition state is expected to increase the unfolding rate, without affecting the folding kinetics.

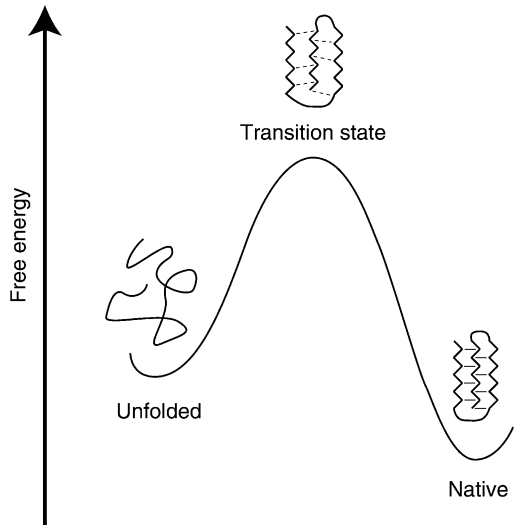

FIGURE 2 Hypothetical energy profile for a protein folding reaction. Currently available data, especially from mutational analyses of folding kinetics, suggest that the transition state for folding and unfolding is an ensemble of conformations that possess much of the topology of the native protein, but in which many of the native interactions are missing or weakened. The transition state ensemble is poised to fold completely or unfold rapidly.

Detailed mutational analyses of transition states have now been carried out for several proteins. In general, it has been found that substitutions that destabilize the native protein most often increase the unfolding rate more than they decrease the folding rate, suggesting that most interactions that are present in the native protein are significantly weakened in the transition state. Also, the relatively few residues that appear to play specific roles in stabilizing the transition state are often separated in the amino acid sequence but lie relatively close together in the native protein. These patterns suggest that the transition state ensemble may have a topology similar to that of the native protein, but not the network of cooperative interactions found in the fully folded structure (Figure 2). Poised with the correct topology, the molecules in the transition state can rapidly form these interactions, but can also unfold rapidly.

Collectively, studies of folding intermediates and transition states over the past decade generally support a view of folding in which there is considerable breadth in the distribution of conformations representing different stages of the process, a view that has also emerged from computational simulations of folding. The conformational heterogeneity of these states makes detailed structural analysis very difficult, and there is much about folding mechanisms that still remains hidden from experimental view. More detailed descriptions of folding can in principle be derived from computational simulations, and the rapidly increasing power of computers and the development of new algorithms is now making it possible to carry out detailed molecular dynamics simulations of folding reactions. The past several years have seen much more extensive collaborations between experimentalists and computational scientists working on protein folding, and this development is already leading to important new insights into both the details of specific folding reactions and the general principles of the process.

More Complex Folding Reactions

Although the great majority of protein-folding experiments and simulations have been carried out with small monomeric proteins, most proteins found in nature are larger and more complex structures. Most polypeptides form multiple domains when they fold, and many assemble into structures composed of multiple subunits. In addition, some proteins are stabilized by disulfide bonds, which are formed during the folding process, and others contain tightly bound ligands such as metal ions, heme groups, or cofactors required for enzyme activity.

Proteins with Multiple Domains

Early in the study of protein structure, it was recognized that most proteins composed of more than 100–200 amino acid residues are typically organized into domains in which segments of 50–150 residues are folded into compact structures that are relatively independent of one another. Although a precise definition of a domain is somewhat elusive, the organization of a protein into substructures is often quite apparent from inspection of the 3D structure or by computer analysis (Figure 3). Experimentally, domains can often be defined by limited treatment with a protease, since the polypeptide segments separating domains are usually much more sensitive to digestion than the regions within domains. The functions of larger proteins are often divided among their substituent domains, with different domains typically interacting with different molecules. It is clear from comparisons of protein structures and sequences that the same domains have frequently been exchanged among different proteins by genetic recombination, and the domain architecture of a protein can often be deduced by comparison of its sequence with those of known domains.

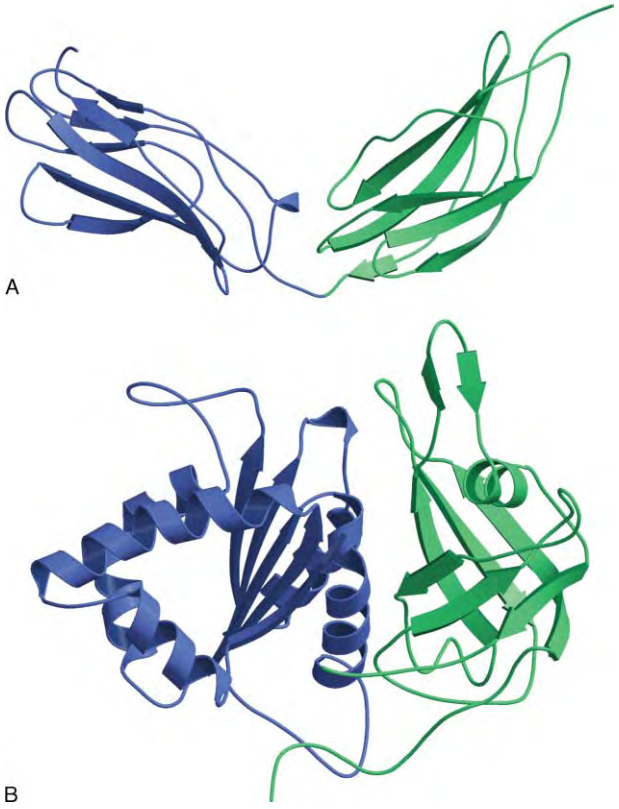

FIGURE 3 Domain structures of two proteins. In each drawing, the domains are distinguished by color. (A) Two domains of a cellular adhesion molecule, neuroglian from *Drosophila melanogaster*. The intact protein contains nine other domains, three of which are similar to the two shown here, which are members of the fibronectin III domain family. Drawn from the atomic coordinates of entry 1CFB in the Protein Data Bank (Huber, A. H., Wang, Y. M., Bieber, A. J., and Bjorkman, P. J. (1994). Crystal structure of tandem type III fibronectin domains from *Drosophila* neuroglian at 2.0Å. *Neuron* **12**, 717–731). (B) Ferrodoxin reductase from spinach chloroplasts. In this structure, the two domains do not resemble one another and interact much more extensively than the two fibronectin domains shown in (A). Drawn from the atomic coordinates of entry 1FNB in the Protein Data Bank (Bruns, C. M., and Karplus, P. A. (1995). Refined crystal structure of spinach ferredoxin reductase at 1.7Å resolution: Oxidized, reduced and 2′-phospho-5′-AMP bound states. *J. Mol. Biol.* 247, 125–145). The drawings in Figures 3 and 4 were made with the computer programs MOLSCRIPT and Raster3d.

When isolated from the rest of the protein, individual domains typically retain their native conformations and undergo cooperative unfolding transitions similar to those observed with smaller proteins. Furthermore, when the intact protein unfolds, the resulting spectroscopic signals often resemble a simple superposition of those for the isolated domains. In these cases, the domains appear to be truly independent, and studying their folding individually probably provides a good description of the folding mechanism for the intact protein. In other cases, however, the domains may interact more intimately, so that the entire structure unfolds cooperatively. The folding mechanism may also involve interactions among the domains before their individual structures are fully defined.

Disulfide-Coupled Folding

Many proteins, especially among those that function extracellularly, are stabilized by disulfide bonds, covalent bonds between the sulfur atoms of cysteine (Cys) residues that are formed by oxidation of the Cys thiol groups. *In vivo*, disulfide bonds are formed after the polypeptide is synthesized and translocated to either the endoplasmic reticulum in eukaryotes, or the periplasmic space in bacteria. In both types of cells, disulfides in the newly synthesized proteins are formed by exchange with disulfides present in special proteins that act as catalysts of the process.

In a landmark series of experiments in the early 1960s, C. B. Anfinsen and his colleagues demonstrated that the four disulfide bonds of bovine ribonuclease A could be induced to reform spontaneously *in vitro* after the protein had been fully reduced and unfolded in urea. The regeneration of active enzyme, even after the covalent constraints on the polypeptide chain had been broken, provided a vivid demonstration that the 3D structure was encoded by the amino acid sequence.

When refolding of a reduced protein is initiated, disulfides typically form quite randomly, leading to a distribution of molecules with different disulfide bonds that can rapidly interconvert. The formation of an initial disulfide, however, can often favor conformations that then bring other Cys residues together to form a second disulfide. These conformations can also be stabilized by

noncovalent interactions, leading to a high degree of cooperativity among the various interactions.

As more of the 3D structure forms and is stabilized by additional disulfides, the ability of the molecule to undergo additional disulfide formation and rearrangement steps can become severely constrained, leading to the accumulation of species that contain most or all of the native structure but lack one or more disulfides. *In vivo*, disulfide isomerase enzymes can catalyze the slow rearrangements necessary to convert the trapped molecules to the native form, or may promote alternative pathways that avoid the kinetic traps.

Ligand Binding

Yet another way in which folding can be influenced is through the binding of ligands such as metal ions or prosthetic groups. In most cases, ligands have little tendency to interact with unfolded proteins, so that the molecule must be at least partially folded before the interaction takes place. A thermodynamic consequence of this is that the stability of the folded protein is enhanced by the presence of ligand and depends on both the affinity of the interaction and the concentration of free ligand in solution. If the binding site is formed only when the protein is fully folded, binding may not greatly alter the folding process either *in vitro* or *in vivo*. On the other hand, interactions of ligands with partially folded species could favor some pathways over others and might prevent aberrant interactions with other molecules.

Proteins that require the binding of reactive metal ions such as those of iron, copper, or nickel present a particularly interesting problem during folding *in vivo*. Because these ions are highly toxic, their free concentrations are maintained at very low levels by transport and storage proteins that bind tightly to them. The ions must then be transferred to other proteins for which they are required for activity, such as catalysis. Although the details are not yet well-understood, it appears that quite elaborate systems involving multiple transfer proteins have evolved to facilitate the safe transfer of ions to their proper sites.

Some prosthetic groups, such as the heme group of cytochrome *c*, are covalently bonded to the polypeptide chain. For these proteins, the covalent modifications, and the enzymes that catalyze them, are likely to be intimately involved in the folding process.

Molecular Chaperones

While many proteins refold spontaneously and efficiently *in vitro*, it is now known that folding *in vivo* is often facilitated by molecular chaperones, proteins that interact transiently with the polypeptide chain and either promote folding or decrease the likelihood of nonproductive interactions. The best-characterized molecular chaperones include members of the GroEL/-GroES and HSP70 families. Members of both groups utilize the energy of ATP hydrolysis to couple conformational changes in the chaperone to a cycle of substrate protein binding and release, during which the substrate folds to its native conformation. Other examples of molecular chaperones include the catalysts of disulfide formation and exchange and the metal chaperones mentioned above. Although the chaperones can increase the efficiency of folding, it does not appear that they influence the final structure. Their discovery, therefore, has not required a revision of the fundamental idea that the folded structure of a protein is determined by the amino acid sequence. But, we now have a much greater appreciation of protein folding as a biological process that is intimately coupled to numerous other intracellular events.

Assembly of Oligomeric Proteins

Only a minority, perhaps 20%, of proteins contain a single polypeptide chain, the remainder being assemblies of multiple subunits. Dimeric and tetrameric complexes are the most common, but assemblies of 20–50 subunits are also known. The assembly of subunits into larger complexes can offer a variety of functional advantages, including mechanisms for regulating the activities of enzymes, the creation of novel binding sites at subunit interfaces and the coordination of multiple related functions in a single complex.

Multimeric proteins can be assembled from a single type of subunit, resulting in a homo-oligomer, or they can be hetero-oligomers composed of two or more different kinds of chains. Quite often, these structures are highly symmetrical. Dimers of identical polypeptide chains are especially common, and dimers are often the basic units of higher order structures, such as tetramers, hexamers, etc.

The types of interactions that hold the subunits of oligomers together are essentially the same as those found within monomeric proteins or the individual subunits themselves, including hydrogen bonds, ionic and van der Waals interactions. However, surveys of the distribution of different interaction types in various protein environments have revealed some differences between those found between and within subunits, with ionic interactions being more common in the interfaces between subunits.

Many oligomeric proteins have been successfully refolded and assembled *in vitro* after being unfolded in denaturants, though the reactions are often slower and less efficient than the folding of small monomeric proteins. In some cases, the rate of refolding is dependent on protein concentration, indicating that the rate is determined by intermolecular association

reactions. In other cases, the reaction kinetics are limited by intramolecular rearrangements that occur either before or after subunit association.

These differences in kinetic behavior suggest that oligomeric structures may form by a variety of mechanisms. In order to assure specificity, the initial interactions between two subunits presumably requires that one or both of them first takes on at least a partially folded conformation. In some cases, the interaction may only occur after the subunits are fully folded, so that folding and assembly are distinct processes. This mechanism requires that the individual subunits have compact self-contained structures similar to those of monomeric proteins, as epitomized by the four subunits of hemoglobin (Figure 4A). For some oligomers, however, the subunits form extensive interactions with one another along extensive interfaces that make it unlikely that the individual subunits could fold completely before assembling. In extreme cases, the subunits are actually wrapped around one another, as observed in the structure of the tailspike protein of bacteriophage P22 (Figure 4B). These more complex arrangements of subunits likely lend the structures a great deal of kinetic stability, but possibly at the cost of more complex folding mechanisms involving unstable intermediates that may be prone to aberrant misfolding or aggregation reactions.

Protein subunits can also form complexes with either RNA or DNA, as in ribosomes or the nucleosomes of eukaryotic chromatin. These interactions are often mediated by electrostatic interactions between Arg or Lys residues of the proteins and the negatively charged phosphate groups of the nucleic acids, but nonpolar interactions can also play a role. Just as protein subunits can associate with one another either before or after being fully folded, the formation of protein–nucleic acid complexes may involve folding processes that take place after association as well as before.

Protein Folding Pathologies

Over the past decade, defects in protein folding or assembly have become recognized as important factors leading to a variety of diseases. These include cystic fibrosis, some forms of emphysema and a large number of conditions associated with the formation of long fibrillar protein structures, the amyloid diseases. Mutations that destabilize the native protein may lead to premature degradation or the formation of aberrant assemblies, which, in turn, may lead to a deficiency for an important activity or the formation of structures that are actually toxic. At present, the amyloid diseases appear to be the most important category of folding pathologies. Diseases associated with amyloid formation include neurodegenerative conditions such as Alzheimer's and Parkinson's diseases and amyotrophic lateral sclerosis, as well as several systemic amyloid diseases. In an intriguing minority of diseases, particles of amyloid fibers from one individual can promote fibril

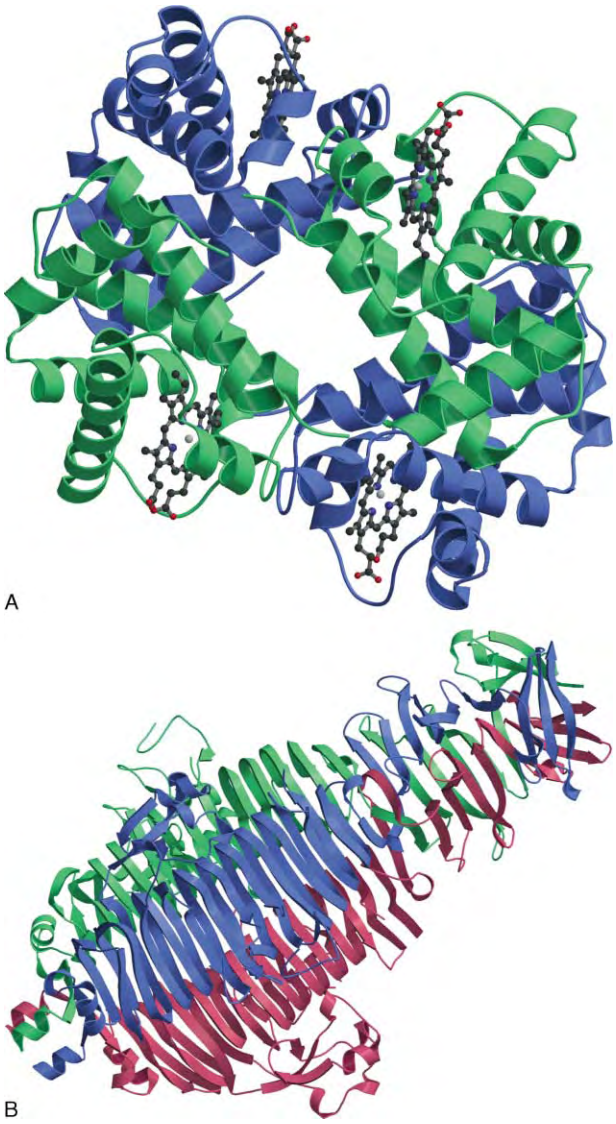

FIGURE 4 Subunit structures of two proteins. (A) Human hemoglobin, a tetramer formed of two types of subunits, colored green and blue in the drawing. Each of the subunits is a compact and self-contained structure. The heme groups associated with each of the four chains are also shown in a ball-and-stick representation. Drawn from entry 2HHB in the Protein Data Bank (Fermi, G., Perutz, M. F., Shaanan, B., and Fourme, R. (1984). The crystal structure of human deoxyhaemoglobin at 1.74Å resolution. *J. Mol. Biol.* 175, 159–174). (B) A fragment of the trimeric tailspike protein of bacteriophage P22. The intact protein includes an additional domain at the amino-terminus of the chain (at the lower left corner of the drawing), by which the tailspike binds the rest of the virus particle. In this structure, the individual subunits interact extensively with one another and are intertwined, requiring an assembly mechanism in which the chains do not fold completely until after they have associated. Drawn from entry 1TSP of the Protein Data Bank (Steinbacher, S., Seckler, R., Miller, S., Steipe, B., Huber, R., and Reinemer, P. (1994). Crystal structure of P22 tailspike protein: Interdigitated subnits in a thermostable trimer. *Science* **265**, 383–386).

formation in another, providing a mechanism of infectivity that does not involve either bacteria or viruses. These infectious agents have been named "prions" and the diseases they are associated with include scrapie (in sheep) and bovine spongiform encephalopathy (BSE or "mad cow disease"), as well as the human disease Kuru and a variant of Creutzfeld–Jacob disease that is believed to be derived from BSE. The transmission of an altered physiological state by a protein amyloid is not at all restricted to mammals, however, as a very similar process has been found in the unicellular yeast, *Saccharomyces cerevisiae*, and this discovery has provided an important experimental system for analyzing the prion phenomenon. A surprisingly large number of proteins are now known to form amyloid-like fibers under at least some *in vitro* conditions, and it may be that the ability to form these structures is a nearly universal property of polypeptide chains. Remarkably, there is a great deal of similarity among the structures of fibers formed from proteins with quite different native structures. The fibers are generally about 50–100Å in diameter and a fraction at least of the polypeptide chain has a β-strand conformation, with the strands oriented so that their backbones are approximately perpendicular to the fiber axis.

Fibril formation *in vitro* is typically favored by conditions that destabilize the normal folded conformation but do not fully unfold and solubilize the polypeptide. *In vivo*, conversion to the amyloid state may be promoted by inherited mutations, environmental stress or, as noted above, "seeding" by an existing fibril fragment. At present, it is difficult to establish a clear mechanistic link between fibril formation and the physiological changes associated with amyloid diseases. In some cases, the amounts of protein deposited in fibrils are so large, as much as several kg in some patients, that these structures are clearly able to interfere with normal organ function. Smaller fibrils may similarly be toxic at the cellular level. In other cases, it may be that diversion of essential proteins into fibrils leads to functional deficiencies.

Because amyloid fibril formation usually competes with normal folding, investigators are actively pursuing the possibility that these diseases might be prevented or treated by agents that favor productive folding or disfavor unfolding, for instance by binding to the native structure. These developments provide a vivid link between the basic science of protein folding and important medical problems.

See Also the Following Articles

Amyloid • Chaperones, Molecular • Disulfide Bond Formation • Glycoprotein Folding and Processing Reactions • Prions and Epigenetic Inheritance • Prions, Overview • Unfolded Protein Responses

Glossary

amyloid A polymeric and fibrous form of a protein, usually formed by polypeptides that have undergone unfolding or misfolding.

domain A compact structure composed of 50–150 amino acid residues that can fold independently of other parts of a protein.

folding intermediate A partially folded conformational state that may form transiently during the conversion of an unfolded protein to the native state.

molten globule A partially folded state that is characterized by the presence of regular secondary structure (usually α-helices), but lacking well-defined interactions between side-chains distant in the sequence.

native state The well-defined folded structure of a protein usually associated with biological activity.

unfolded state An ensemble of rapidly interconverting conformations with little or no stable structure, usually generated by incubating a native protein with a denaturant or at elevated temperature. *In vivo*, polypeptides that have not yet folded into their native conformations may resemble artificially unfolded proteins.

Further Reading

Bruns, C. M., and Karplus, P. A. (1995). Refined crystal structure of spinach ferredoxin reductase at 1.7Å resolution: Oxidized, reduced and 2′-phospho-5′-AMP bound states. *J. Mol. Biol.* **247**, 125–145.

Daggett, V., and Fersht, A. (2003). The present view of the mechanism of protein folding. *Nat. Rev. Mol. Cell Biol.* **4**, 497–502.

Dobson, C. M. (1999). Protein misfolding, evolution and disease. *Trends Biochem. Sci.* **24**, 329–332.

Englander, S. W. (2001). An amino acid code for protein folding. *Proc. Natl Acad. Sci. USA* **98**, 105–112.

Fermi, G., Perutz, M. F., Shaanan, B., and Fourme, R. (1984). The crystal structure of human deoxyhaemoglobin at 1.74Å resolution. *J. Mol. Biol.* **175**, 159–174.

Horwich, A. L. (ed.) (2002). Protein Folding in the Cell. In *Advances in Protein Chemistry*, Vol 59. Academic Press, New York.

Huber, A. H., Wang, Y. M., Bieber, A. J., and Bjorkman, P. J. (1994). Crystal structure of tandem type III fibronectin domains from *Drosophila* neuroglian at 2.0Å. *Neuron* **12**, 717–731.

Levinthal, C. (1969). How to fold graciously. In *Mossbauer Spectroscopy in Biological Systems* (J. T. B. DeBrunner and E. Munck, eds.) University of Illinois Press, Urbana, IL.

Matthews, C. R. (ed.) (2000). Protein Folding Mechanisms. In *Advances in Protein Chemistry*, Vol 53. Academic Press, New York.

Pain, R. (ed.) (2000). *Mechanisms of Protein Folding*, 2nd edition. Oxford University Press, Oxford, UK.

Steinbacher, S., Seckler, R., Miller, S., Steipe, B., Huber, R., and Reinemer, P. (1994). Crystal structure of P22 tailspike protein: Interdigitated subunits in a thermostable trimer. *Science* **265**, 383–386.

Biography

Dr. David Goldenberg is a Professor of biology at the University of Utah. He received his Ph.D. at the Massachusetts Institute of Technology and carried out postdoctoral research at the Medical Research Council Laboratory of Molecular Biology in Cambridge, UK. His research interests are in the areas of protein folding and dynamics, and he has worked extensively on the folding of disulfide-bonded proteins and the effects of mutations on folding energetics.

Protein Glycosylation Inhibitors

Alan D. Elbein
University of Arkansas for Medical Sciences, Little Rock, Arkansas, USA

Many proteins that are synthesized in eukaryotic cells undergo chemical modifications other than addition of amino acids, either while the protein is being synthesized, or after protein synthesis is finished. One of the major types of modifications that occur on many proteins is glycosylation, i.e., the covalent attachment of sugars to these proteins, to form glycoproteins. Proteins may be glycosylated either with O-linked sugars (sugars attached via hydroxyl groups of serine or threonine), or with N-linked-sugars (oligosaccharides attached to protein via the amide nitrogen of asparagine), or some proteins have both types of oligosaccharides. This article discusses the use of glycosylation inhibitors that either prevent the formation of N-linked oligosaccharides, or that modify the structure of the N-linked oligosaccharide chain after it is transferred to protein. The specific N-linked sugar structure on a particular protein may play an important role in protein folding, protein targeting, chemical recognition, and/or various disease processes. For this reason, inhibitors that alter the structure of the oligosaccharide can be valuable as tools to help decipher how specific carbohydrate structures are recognized by proteins that mediate these processes. In addition, this information can be utilized to prevent some of these processes, or to enhance those that are useful, and such a situation may be important in various therapies.

Mechanism of Action of Glycosylation Inhibitors

There are a number of glycosylation inhibitors that work on enzymes in the first series of reactions, i.e., the lipid-linked saccharide pathway that involves the participation of dolichyl-phosphate (see Figure 1). One of the most widely used and useful of these inhibitors is the antibiotic tunicamycin (Tun), a reversible tight-binding inhibitor of the GlcNAc-1-P transferase. This glycosyltransferase catalyzes the initial reaction in the assembly of N-linked oligosaccharides, i.e., the transfer of GlcNAc-1-P to dolichol-P to form GlcNAc-PP-dolichol. Since this inhibitor prevents this initial reaction, it essentially blocks the assembly of all N-linked oligosaccharide chains, and those proteins that normally have this type of glycosylation are synthesized in the unglycosylated form. As a result, many of these unglycosylated proteins do not fold properly in the ER, and are therefore degraded by the ubiquitin protein degrading system. In some cases, especially with hydrophobic membrane proteins, absence of the hydrophilic carbohydrate structure renders these proteins insoluble and causes them to aggregate into insoluble complexes. In most systems where N-linked glycoproteins are involved in recognition and binding interactions, Tun has dramatic effects. For example, this drug inhibits cell adhesion and spreading in various animal cell systems, and causes defects in the transport of glucose, uridine, and amino acids in chick fibroblasts. Treatment of mouse 3T13 fibroblasts with Tun inhibits their *in vitro* differentiation into adipose-like cells. This antibiotic also inhibited the fusion of myoblasts to form myotubes during muscle development. The difficulty with using tunicamycin in animal systems, or in chemotherapy against cancer or other diseases, is that it prevents glycosylation of all N-linked glycoproteins and therefore is quite toxic to most cells.

Amphomycin (Ampho) is a lipopeptide antibiotic that inhibits the formation of lipid-linked sugars in membrane fractions, but is not effective in whole cells, probably because it cannot cross the plasma membrane and get into the cells. This inhibitor blocked the formation of dolichyl-P-mannose (also refered to as mannosyl-P-dolichol), the donor of the last four mannose residues of the $Man_9GlcNAc_2$-PP-dolichol, resulting in the accumulation of $Man_5GlcNAc_2$-PP-dolichol in cell-free membrane preparations. Ampho has been a useful tool to demonstrate that the last four mannoses are donated by dolichyl-P-mannose, rather than by GDP-mannose.

Various sugar analogues, such as 2-deoxy-D-glucose (2-DG) and 2-deoxy-2-fluoro-D-glucose, also inhibit N-linked glycosylation and viral replication, as well as other processes that involve N-linked glycoproteins. This inhibition is probably due to the fact that these sugar analogues are incorporated by intact cells into various biosynthetic intermediates in place of the normal mannose residues, but these intermediates cannot be further elongated by addition of other sugars. These various inhibitors and others not reported here have been used in a variety of living systems to prevent

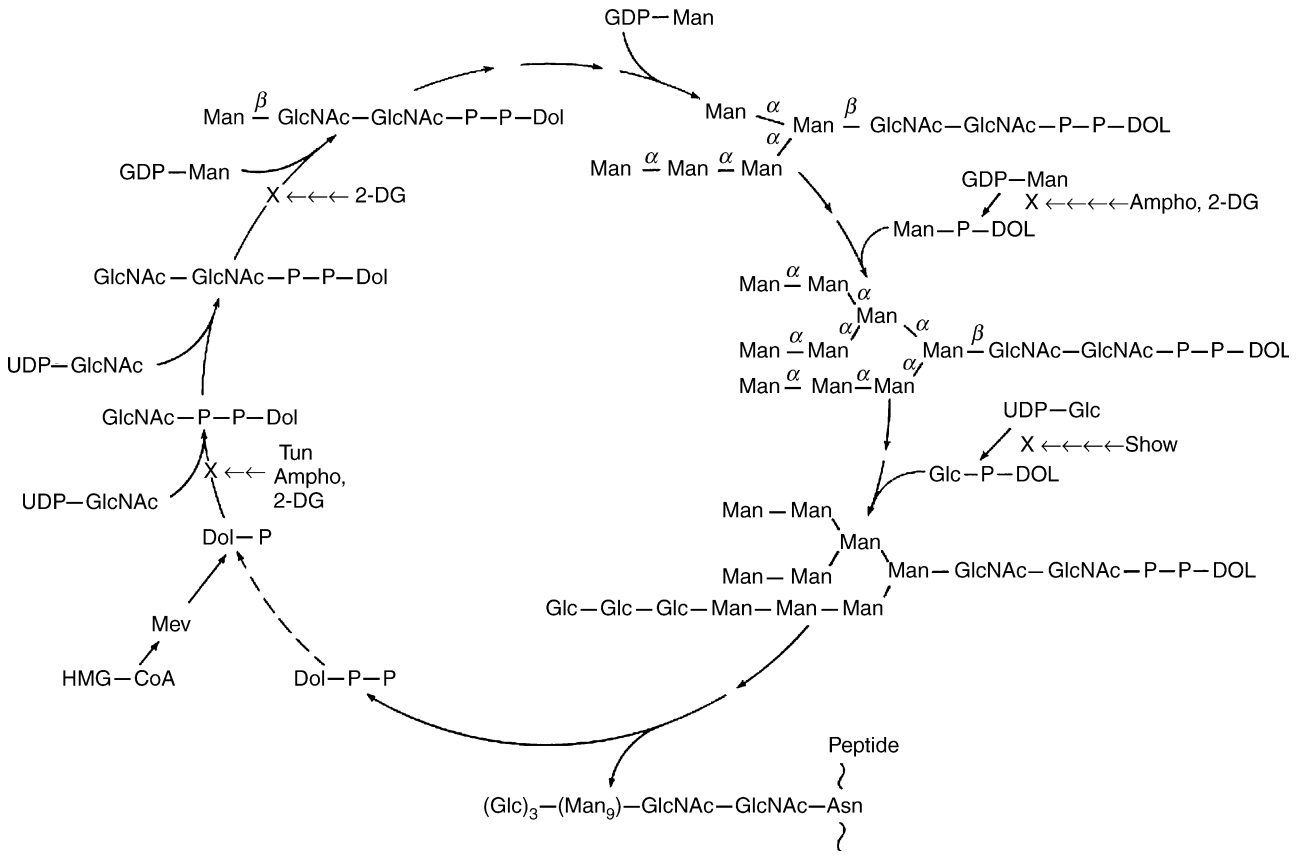

FIGURE 1 Inhibitors of N-linked oligosaccharide assembly. The biosynthesis of the N-linked oligosaccharides occurs on a dolichol carrier lipid in the endoplasmic reticulum. The individual sugars, N-acetylglucosamine (GlcNAc), mannose and glucose are sequentially added to the lipid from their activated form (i.e., UDP-GlcNAc, GDP-mannose or mannosyl-P-dolichol, UDP-glucose or glucosyl-P-dolichol) to form the 14 sugar oligosaccharide attached by a pyrophosphoryl bridge to the dolichol. Various compounds have been found to inhibit at specific sites in the pathway and these inhibitors have been useful tools to decipher and interrupt the biosynthetic pathway. Thus, tunicamycin (Tun), amphomycin (Ampho) and 2-deoxyglucose (2-DG) inhibit the first step in the assembly, i.e., the transfer of GlcNAc-1-P to dolichyl-P. Amphomycin and 2-deoxyglucose also inhibit the addition of the last four mannose residues by inhibiting the formation of mannosyl-P-dolichol (man-P-dol), while showdomycin (Show) inhibits formation of glucosyl-P-dolichol, the glucosyl donor for the three glucose units in the initial N-linked oligosaccharide.

glycosylation, and to show the necessary role of the N-linked oligosaccharides in key biological processes such as growth, cell–cell interactions, differentiation, development, and so on.

Mechanism of Action and Effect of Glycoprotein Processing Inhibitors

A number of plant alkaloids have a structure similar to that of the sugars glucose and mannose, but differ in having a nitrogen rather than an oxygen in the pyranose ring. These types of alkaloids have been found to be potent inhibitors of various glycosidases including those that are involved in the initial processing reactions that lead to the formation of complex N-linked oligosaccharides. The structures of several of these alkaloids and their sites of action in the processing pathway are shown in Figure 2. Castanospermine resembles glucose and inhibits both glucosidase I and glucosidase II, the ER glucosidases that remove all three glucose residues from the initial N-linked oligosaccharide. Castanospermine has been used in many cell culture systems, and in some whole animal studies to block the removal of glucose and prevent the formation of complex types of oligosaccharides. This has provided useful information on the function of specific glycoproteins. For example, in HepG2 cells, blocking the removal of glucoses from the N-linked oligosaccharides greatly reduced the rate of secretion of the serum protein, α_1-antitrypsin. Castanospermine also reduced the number of insulin receptors at the cell surface in IM-9 lymphocytes treated with this drug, and caused a significant decrease in the formation of new HIV viral particles, and in syncytium formation in cell culture. All of these effects were demonstrated to be attributable to the absence of glucose removal, leading to improper

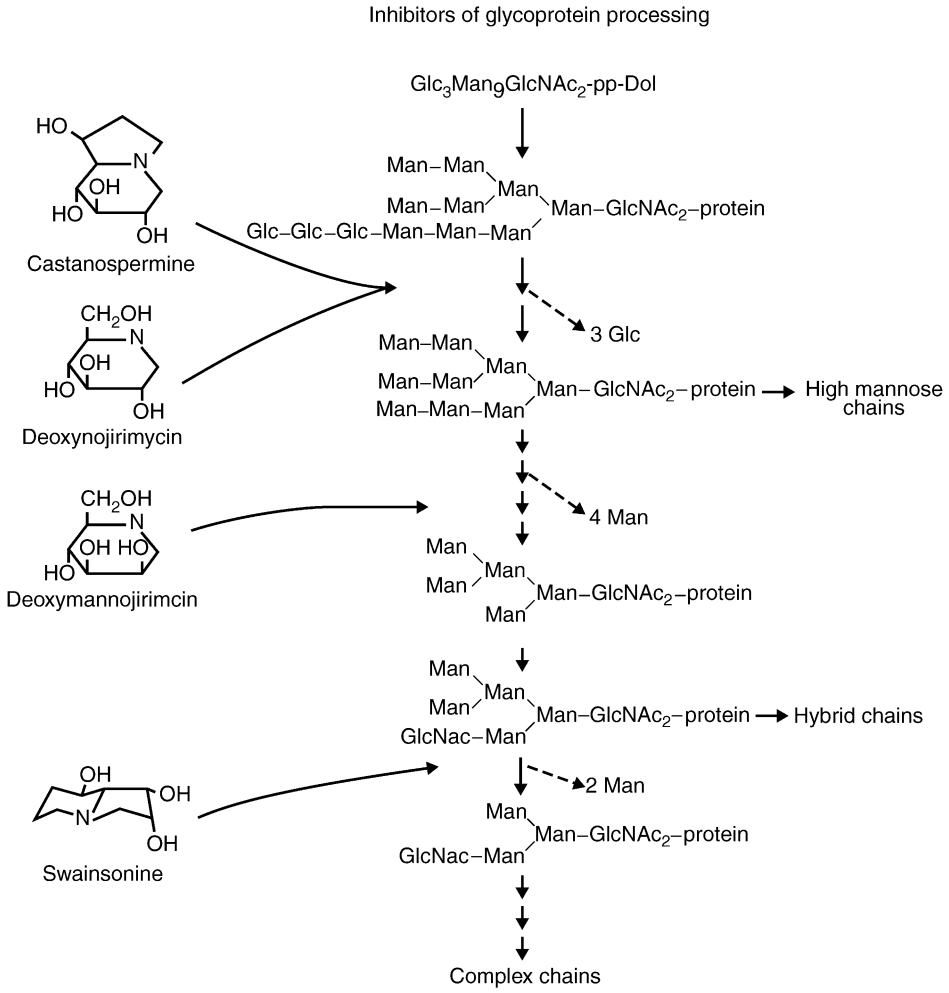

FIGURE 2 Inhibitors of glycoprotein processing. The processing of the oligosaccharide can be blocked at the very first step by the plant alkaloid, castanospermine, which inhibits α-glucosidases such as glucosidase I and glucosidase II. The trimming can also be stopped after the glucoses are removed by the α-mannosidase inhibitors, deoxymannojirimycin or kifunensine to cause accumulation of high mannose oligosaccharides. Finally the plant alkaloid swainsonine inhibits mannosidase II and causes the formation of hybrid structures.

protein folding and degradation of these proteins in the ER. Other glucosidase inhibitors have the same effect.

A second site of processing inhibition is at the stage of removal of the mannose residues. Deoxymannojirimycin (DMJ) is a chemically synthesized compound that resembles the structure of mannose, while kifunensine (KF) is a natural product that also resembles the mannose structure. Both of these compounds inhibit the Golgi α-mannosidase that releases four α1,2-linked-mannoses from the high mannose oligosaccharide. This is an essential step in the formation of complex chains, i.e., the addition of the first N-acetylglucosamine of the complex chains (structure 5 from top) requires a specific $Man_5GlcNAc_2$ structure. As far as formation or secretion of N-linked glycoproteins, these mannosidase inhibitors had essentially no effect on these processes. They also did not affect the formation in tissue culture cells of the influenza viral hemagglutinin, an N-linked glycoprotein coat protein that normally has 3 or 4 complex chains, nor the production of infectious influenza viral particles. These results suggest that the complex chain structures on this viral glycoprotein are not necessary for virus recognition or penetration in tissue culture cells.

DMJ has proven to be a useful tool to demonstrate that the initial removal of mannose residues from the high-mannose oligosaccharides in some cells occurs in the endoplasmic reticulum, and that there is also a mannosidase in the ER that removes a single mannose residue. That ER mannosidase is not susceptible to DMJ or KF. However, the next three mannoses are removed in the cis-Golgi compartment by another mannosidase which is inhibited by these two processing inhibitors. DMJ did inhibit the addition of L-fucose and sulfate into the N-linked oligosaccharides indicating that fucose and sulfate were added after the mannosidase I processing step. It is not clear whether DMJ and KF would affect the function of cell surface glycoproteins that are

involved in specific chemical recognition reactions, but one would expect that they should, since the specific carbohydrate structure should be involved.

A third site of inhibition is another mannosidase called mannosidase II that removes two mannoses from GlcNAc-Man_5-$GlcNAc_2$ to give a GlcNAc-Man_3-$GlcNAc_2$ structure, but this enzyme requires that the GlcNAc be added before it can release the two mannoses. Mannosidase II is not susceptible to DMJ or KF but is inhibited by swainsonine (SW), another plant alkaloid that has a structure related to mannose. Inhibition of mannosidase II by SW gives rise to hybrid structures like those found in humans with HEMPAS disease. In many systems, SW had little effect on functional aspects of the proteins in question, although it did cause the oligosaccharide structures to be of the hybrid type. However, SW did inhibit the attachment of osteoblasts to bone, and it also inhibited the interaction of the parasite *Trypanosoma cruzi* with macrophages when either the parasite or the macrophages were treated with this drug. This alkaloid also caused a dramatic decline in the ability of B16 melanoma cells to colonize the lungs of experimental animals. As a result of these studies, SW has been undergoing various tests to determine whether it will be useful as an anticancer drug.

See Also the Following Articles

Carbohydrate Chains: Enzymatic and Chemical Synthesis • GlcNAc Biosynthesis and Function, O-Linked • Glycosylation, Congenital Disorders of • Glycosylation in Cystic Fibrosis • Glycosylphosphatidylinositol (GPI) Anchors • Lectins • *N*-Linked Glycan Processing Glucosidases and Mannosidases • Oligosaccharide Chains: Free, *N*-Linked, *O*-Linked • Protein Glycosylation, Overview

Glossary

chemical recognition The chemical process by which molecules recognize other molecules and interact with or bind to them; in many cases of chemical recognition in living cells, a protein (called a lectin) on one cell recognizes a specific carbohydrate structure on another cell.

glycosidases Enzymes that cleave glycosidic bonds and release the monosaccharide from the nonreducing end of an oligosaccharide chain; these enzymes are specific for the sugar released and for the anomeric configuration.

glycosylation The process of addition of sugars to another molecule; in the context of this treatise it refers to the addition of sugars to proteins.

glycosylation inhibitors In the broadest context, this terminology refers to compounds that inhibit the formation of glycosidic bonds; in this treatise it refers to compounds that either prevent glycosylation of proteins or cause modifications in the oligosaccharide structure.

glycosyltransferases Enzymes that transfer sugars from their activated state to other sugars or to other molecules with the formation of a glycosidic linkage.

lectins Proteins that recognize specific carbohydrate structures and bind to these carbohydrates; they are frequently involved in recognition.

***N*-linked glycoproteins** Those proteins that have sugars (i.e., oligosaccharides) attached to the protein via an N-glycosidic linkage, which is to the amide nitrogen of asparagines.

Further Reading

Elbein, A. D. (1987). Inhibitors of the biosynthesis and processing of N-linked oligosaccharide chains. *Annu. Rev. Biochem.* **56**, 497–534.

Elbein, A. D. (1991). Glycosidase inhibitors: Inhibitors of N-linked oligosaccharide processing. *FASEB J.* **5**, 3055–3063.

Varki, A., Cummings, R., Esko, J., Freeze, H., Hart, G., and Marth, J. (1999). *Essentials of Glycobiology.* Cold Spring Harbor Laboratory Press.

Biography

Alan Elbein is Professor and Chairman of the Department of Biochemistry and Molecular Biology at the University of Arkansas for Medical Sciences in Little Rock. He received his Ph.D. in microbial biochemistry from Purdue University and did postdoctoral research at the University of Michigan and the University of California at Berkeley. He joined the faculty as an Assistant Professor of Biology at Rice University and then moved to the Department of Biochemistry at the University of Texas Health Science Center at San Antonio as Professor. His research focuses on the role of complex carbohydrates in glycoprotein function, and on novel carbohydrate target sites in chemotherapy of microbiol diseases.

Protein Glycosylation, Overview

Natasha E. Zachara and Gerald W. Hart
The Johns Hopkins University School of Medicine, Baltimore, Maryland, USA

Protein glycosylation is the enzymatically catalyzed attachment of glycans (carbohydrates) through a covalent bond to the polypeptide backbone of proteins. Protein glycosylation is a common co and/or posttranslational modification of eukaryotic proteins, and has now been found on a subset of proteins in both eubacteria and archaebacteria. Glycosylated proteins, termed glycoproteins, are distributed widely throughout the eukaryotic cell, being found in the extracellular space, on integral and peripheral membrane proteins, in the cytoplasm and nucleus, and in other subcellular organelles. Glycoproteins of prokaryotes (eubacteria and archaebacteria) are predominantly extracellular.

Basic Nomenclature

For small molecules, carbohydrates are complex! Carbohydrates gather their name from early studies which showed they had the chemical composition $(C(H_2O))_x$, or hydrated carbon. The carbons can be arranged in either an open conformation (less common) or one of two ring forms – the furanose (*f*) form (5 membered) or the pyranose (*p*) form (6 membered). Like amino acids, there is a dextrorotatory (D) and a levorotatory (L) enantiomer. The anomeric carbon, the carbon which forms the cyclic hemiacetal, is defined as carbon 1 (See Figure 1) and then the carbons are labeled two through six sequentially around the ring. Moreover, bonds formed by the hydroxyl group of the anomeric carbon can be in either of two conformations, leading to the α-sugar (axial bond), or β-sugar (equatorial bond). A nomenclature has evolved to describe all of these features accurately. For example, glucose or D-Glucopyranose, is abbreviated to D-Glc*p*. When defining the anomericity of the carbohydrate, the abbreviation (α,β) is included preceding the name of the sugar, for example the α-anomer of D-Glc*p* becomes D-αGlc*p*.

Carbohydrates can form covalent linkages through all of their hydroxyl groups to proteins, other carbohydrates or small molecules such as sulfate and phosphate. When sugars are linked together and then to a protein the structure is written from the nonreducing to reducing end (carbohydrate attached to the protein backbone). The position of the linkage is designated by the carbon residue to which the hydroxyl group forming the bond is linked. Thus, when the anomeric carbon of D-βGal*p* (galactose) is linked to the number 3 hydroxyl of D-αGalNAc*p* (*N*-acetylgalactosamine), which is then linked to protein, the resulting disaccharide is written D-βGal*p*1–3 D-αGalNAc*p*1-. Sometimes this is written as D-Gal*p*β1–3 D-GalNAc*p*α1-.

The Protein Carbohydrate Linkage

In the 1930s, Albert Neuberger and co-workers were able to demonstrate the first nonmucin protein carbohydrate linkage. These and subsequent studies showed that there was an amide bond between an asparagine (Asn) residue in chicken egg albumin (ovalbumin) and *N*-acetylglucosamine (GlcNAc). It is now known that of the 20 common amino acids, eight are involved in one of five chemically distinct covalent linkages to one of 13 different classes of carbohydrates. Variations in the covalent linkage, configuration of the linkage (α or β), the amino acid and the carbohydrate result in at least 41 different carbohydrate-protein linkages (Table I).

The five common covalent linkages between carbohydrates and proteins are:

1. *N-linked glycosylation*. This glycosylation typically refers to the amide bond formed between GlcNAc and Asn in the β-conformation. Less common amide bonds have been found between Asn and Glc, GalNAc and Rhamnose (Rham), and more recently between arginine (Arg) and Glc (Table I).
2. *O-linked glycosylation*. This glycosylation describes carbohydrates bound to the protein backbone through hydroxyl residues, such as those in serine (Ser), threonine (Thr), tyrosine (Tyr), hydroxylysine (Hly), and hydroxyproline (Hpr). O-linked sugars involve the greatest number of amino acids, sugars, and anomeric linkages (Table I), although in mammals the best characterized-O-linkage is to αGalNAc. As it was first characterized on mucins, it is often referred to as mucin-like glycosylation.

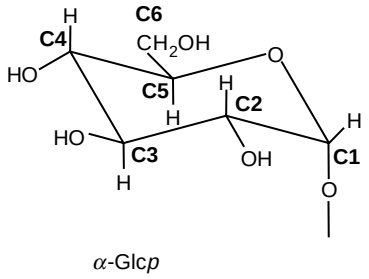

FIGURE 1 The hemiacetyl form of glucopyranose. Carbons are labeled from the anomeric carbon, C1.

3. *Glycosylphosphatidyl inositol (GPI)-anchors*. This is sometimes referred to as glypiation. GPI-anchors link the terminal residue of a protein through phosphoethanolamine to a core structure, which contains mannose (Man), glucosamine (GlcN), and inositol, to a lipid moiety, which anchors the protein in the lipid bilayer.

4. *C-mannosylation*. This is the attachment of an α-Man to carbon-2 of the indole ring of tryptophan (Trp). This form of protein glycosylation has been identified in eukaryotes on proteins such as RNAse2, interleukin-12 and properdin.

5. *Phosphoglycosylation*. This is the linkage of a carbohydrate through a phosphodiester bond to amino acids, such as Thr and Ser.

There are some posttranslational modifications of proteins that contain sugar, such as ADP-ribosylation that will not be discussed in this article. In addition, nonenzymatic glycation, the chemical reaction of reducing sugars with proteins, common in tissues and cells exposed to high levels of reducing saccharides, is not a form of protein glycosylation as (1) this reaction is not catalyzed by glycosyltransfereases; and (2) the Schiff base addition and subsequent Amadori rearrangement of the reducing sugar results in advanced glycation end products which can no longer be classified as carbohydrates.

Glycoprotein Synthesis

The extension of the first carbohydrate linked to the amino acid, sometimes referred to as the reducing terminal sugar, to form longer structures is typically performed in a stepwise manner. The exceptions are N-linked glycosylation and glypiation, where a core structure is added *en bloc* to the polypeptide chain and then remodeled.

Glycosyltransferases

The enzymatic addition of a carbohydrate to the protein backbone and the further modification of this carbohydrate is catalyzed by glycosyltransferases. These enzymes are typically type 2 membrane proteins that are situated in either the membrane of the endoplasmic reticulum (ER) or Golgi apparatus (Golgi), typically orientated toward the lumen of each organelle. Each different carbohydrate linkage is catalyzed by at least one glycosyltransferase.

Activated sugar nucleotide precursors, such as uridine diphosphate (UDP)- and guanosine diphosphate (GDP)-sugars, are necessary for the formation of all enzymatically synthesized glycosidic bonds. However, in some types of glycosylation, the sugar is transferred to a different intermediate donor, such as a lipid carrier, for example polyisoprenol monophosphate:dolichol phosphate (Dol-P), before transfer to the protein.

N-Linked Glycosylation

In eukaryotes, the initiation of N-linked glycosylation involves the synthesis of the core N-linked oligosaccharide, dolichol-diphosphate-$GlcNAc_2Man_9Glc_3$, on the cytosolic side of the ER membrane. After translocation to the lumen of the ER, the core structure is transferred *en bloc* to an Asn residue in the amino acid motif Asn-Xaa-Ser/Thr (Xaa $\neq$ Pro). Recently, it has been shown that when Cys is substituted for Ser/Thr, glycosylation may still occur in some cases. After transfer of the polypeptide to the Golgi, the core structure undergoes remodeling, resulting in three classes of N-linked glycosylation: high-mannose, hybrid, and complex (Figure 2).

High mannose structures contain more than the three mannose residues found in the core structure, and typically no other carbohydrate residues; while in complex structures both the terminal mannose residues in the core structure are typically modified by lactosamine (Gal1-4βGlcNAc) which can subsequently be modified further. Hybrid structures contain more than the three mannose residues in the core structure, as well as one or more lactosamine units.

O-Linked Glycosylation

Mammalian ER /Golgi Glycosylation

Unlike N-linked glycosylation, there is no single glycosylation motif that predicts the addition of O-linked carbohydrates to hydroxyl residues. O-glycosylation of cell-surface and secreted proteins in mammals appears to be initiated in the Golgi with the transfer of a monosaccharide residue from an activated sugar nucleotide to a hydroxyl residue. The reducing terminal sugar is further modified by stepwise addition of sugars from activated sugar nucleotides in the Golgi.

TABLE I

Different Types of Enzymatic Protein Glycosylation

Type	Reducing terminal linkage	Amino acid	Occurrence
N-linked	βGalNAc	Asn	Archaebacteria
	βGlc	Asn	Laminin only (Animals), Archaebacteria
	βGlcNAc	Asn	Common
	Rham	Asn	Eubacteria
	βGlc	Arg	Plants
O-linked	α Ara*f*	Hpr	Plants
	βAra	Hpr	Plants
	α Fuc	Ser, Thr	Animals
	αGal	Hpr	Plants, Eubacteria
	αGal	Ser, Thr	Plants, Eubacteria
	αGal	Hyp	Plants
	βGal	Hly	Collagen only (Animals)
	βGal	Tyr	Eubacteria
	αGalNAc	Ser, Thr	Common
	βGalNAc	Ser, Thr	Eubacteria
	αGlc	Tyr	Glycogen only (Animals)
	βGlc	Tyr	*C. thermohydrosulfuricum*
	βGlc	Ser, Thr	Eubacteria, Animals
	αGlcNAc	Ser, Thr	Protozoan
	βGlcNAc	Ser, Thr	Animals (cytoplasmic/nuclear)
	GlcNAc	Hyp	*D. discoideum*
	αMan	Ser, Thr	Animals, Fungi
	β FucNAc	Ser	*P. aeruginosa*
	β Xyl	Ser	Proteoglycans
	Diactrideoxyhexose	Ser, Thr	*N. meningitidis*
	αpseudaminic acid	Ser, Thr	*C. jejuni*
Phosphoglycosylation	β Fuc	Ser	*D. discoideum*
	αGlcNAc	Ser	*D. discoideum*
	αMan	Ser	*Leishmania mexicana*
	Xy1	Ser, Thr	*Trypanosoma cruzi*
C-mannosylation	αMan	Trp	Mammals
GPI-anchor	Conserved Core	C-terminal	Eukaryotic

Nonmammalian ER /Golgi Glycosylation

O-glycosylation of the protein backbone in fungi appears to be through lipid-P-donors. In yeast, addition of O-linked glycans is restricted to Dol-P-Man, although other fungi are capable of modifying the protein backbone with Glc and Gal. The study of prokaryotic glycosylation is an emerging field, and little information about the biosynthesis of prokaryotic glycosylation is available.

Cytosolic Glycosylation in Eukaryotes

Many nuclear and cytoplasmic proteins are glycoproteins, these proteins are modified with the simplest of the carbohydrate modifications, O-linked β-GlcNAc (*O*-GlcNAc). Unlike other forms of protein glycosylation, this modification is usually not further extended and occurs exclusively on cytoplasmic and nuclear proteins of metazoans. Consequently, the enzyme, which catalyzes the addition of *O*-GlcNAc, UDP-GlcNAc:polypeptide *O*-*N*-acetylglucosaminyl transferase, is not a type 2 membrane protein. Unlike other glycosyltransferases, this protein has tetratricopeptide repeat domains, which are protein–protein interaction domains and which have been shown to play a role in substrate recognition. Another form of intracellular protein glycosylation, involves the addition of GlcNAc to hydroxyproline of the ubiquitin ligase, Skp1, of the slime mold *Dictyostelium discoideum*. The enzyme has

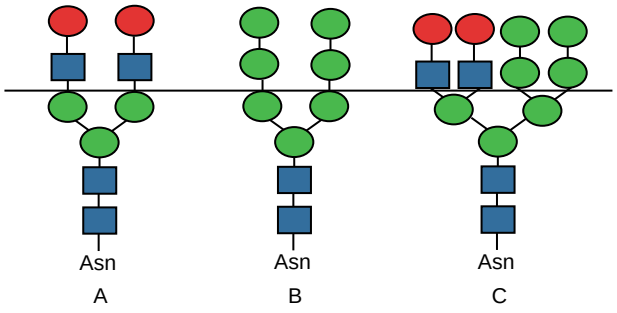

FIGURE 2 Different subgroups of N-linked oligosaccharides. (A) A complex-type oligosaccharide; (B) high-mannose-type oligosaccharide; (C) hybrid-type oligosaccharide. Structures below the solid line are common, while the structures above the line can vary. Further modification of the common structure with GlcNAc and Fuc is known. Different carbohydrates are represented by blue boxes (GlcNAc), green circles (Man), and red circles (Gal).

recently been cloned and appears unrelated to the metazoan GlcNAc transferase.

GPI-Anchors

There are several parallels between the biosynthetic pathways of GPI-anchors and N-linked oligosaccharides. Like the synthesis of N-linked glycosylation, a donor molecule is assembled on the cytosolic side of the ER membrane. Here, UDP-GlcNAc is first added to a phosphatidyl inositol ring, before the acetyl group is removed. Subsequent addition to the GlcN is via Dol-P-Man. Once complete, the structure is translocated through the ER membrane into the lumen, where it is attached to the completed polypeptide after a GPI-anchor consensus motif (C-terminal peptide) is cleaved off. During transit to the cell-surface the lipid component can be remodeled and the carbohydrate core structure can be further processed to give a range of glycoforms. While the core structure of all GPI-anchors appears to be identical, variations in structure appear to involve the nature of the lipid anchor and modification of the core carbohydrate structure with ethanolamine or other carbohydrate chains, the nature of which appear to be species and genera specific.

C-Mannosylation

C-mannosylation represents a linkage in which αMan is attached through a C-glycosidic linkage to the indole ring of Trp. Recently, it has been shown that this modification is added to the first Trp in the motif Trp-Xaa-Xaa-Trp, from a Dol-P-Man donor. This activity has been isolated in crude membrane preparations, suggesting ER/Golgi localization of this enzyme.

Phosphoglycosylation

First identified in *D. discoideum* in 1980 on the endopeptidase proteinase I, this modification, which involves the attachment of carbohydrate through a phosphodiester linkage to the protein backbone, has now been identified on a number of other proteins and in a number of different organisms, although the carbohydrate component differs. Recently, the *N*-acetylglucosamine-α-1-phosphate transferase from *D. discoideum* was partially purified from microsomal preparations and characterized.

Glycoforms of Glycoproteins

The carbohydrate components of proteins are by nature heterogeneous! Variations can occur in terms of the occupancy of potential sites of glycosylation (macroheterogeneity) or in the structures at sites of glycosylation (microheterogeneity), resulting in a variety of protein populations or glycoforms. One example of microheterogeneity is ovalbumin, which has one site of N-linked glycosylation, at which 22 different polysaccharides have been characterized.

Unlike proteins, the sequence of carbohydrates are not directly encoded for by the genome. The modification of proteins is dependent on the expression and regulation of different glycosyltransferases, sugar nucleotide levels, folding and transport of the polypeptide, and a myriad of other factors. Thus, different organisms, tissues and proteins are modified differently depending on the cellular environment, that is, the state of differentiation, development, disease, and cell cycle.

Glycosylation and Function

Deletion or mutation of glycosyltransferases results in predominantly severe to lethal phenotypes, underlying the importance of carbohydrates in the development and maintenance of organisms. While the inherent heterogeneity of carbohydrates has made defining the exact function of carbohydrate structures challenging, several clear roles have emerged from functional studies (Table II). Some examples are discussed below:

Protective

The epithelial surfaces of many organisms are coated with a mucous layer, one component of which are mucins. These high molecular weight glycoproteins are heavily glycosylated, and the carbohydrate component of these proteins are multifunctional. The negatively

TABLE II

Known Functions of the Carbohydrate Component of Glycoconjugates

Function
Stabilization of structure, protective
Modulation of biological activity
Antigenic determinants and modifiers of immune response
Cell-recognition and adhesion
Signal transduction
Protein folding
Protein trafficking and turnover
Hormonal actions

charged sugars in the oligosaccharides bind water tightly, preventing evaporation from the cell. In addition, the resulting gel protects cells from mechanical damage and bacterial attack, while providing specific binding sites for lectins.

Structural

Heavily glycosylated domains, that are reminiscent of mucins, are sometimes referred to as mucin-like domains. Here, hydration of the sugar residues appears to stiffen the protein backbone projecting different domains of proteins from each other and/or the plasma membrane.

Regulatory

The modification of nuclear and cytoplasmic proteins of metazoans with monosaccharides of O-Linked β-*N*-acetylglucosamine (*O*-GlcNAc) has been implicated in cellular control, playing an analogous role to protein phosphorylation. Like many forms of protein glycosylation, deletion of the *O*-GlcNAc transferase is lethal. While all of the functions of *O*-GlcNAc have not been elucidated, it is now clear that this modification alters protein–protein interactions, turnover rate of proteins and the phosphorylation state of proteins by competing with kinases for hydroxyl residues. Recently, perturbations in the regulation of *O*-GlcNAc have been implicated in the etiology of Type 2 diabetes.

Proteolysis and Stability

Carbohydrate modifications of proteins can affect the stability of proteins by several mechanisms. Carbohydrate modifications can reduce the availability of the protein backbone to proteolytic attack by steric hindrance, one example of this is seen on tissue plasminogen activator. Carbohydrates can stabilize protein structure by forming bonds, such as hydrogen bonds, with the protein backbone. Examples of this have been found in proteins such as CD2 and PMP-c protease inhibitor.

Intermolecular Interactions

Protein–protein interactions can be mediated by proteins through carbohydrate-binding domains. Proteins with such domains and which do not modify the carbohydrate are called lectins. There are several well-characterized families of lectins which are both intracellular and extracellular. Lectins mediate many important interactions within and between cells, possibly the best-characterized example are those of the selectins. Selectins mediate the interactions/movement between leukocytes and the endothelial surfaces of blood vessels.

Another key example of lectin–carbohydrate interactions are those that occur within the endoplasmic reticulum, between N-linked carbohydrates and the lectins, calnexin and calreticulin. If a protein folds properly, processing of N-linked glycosylation progresses, and calnexin and calreticulin fail to bind; improperly folded proteins are not processed, are bound by the lectins and presented to proteins such as Erp57, a protein disulphide isomerase, for refolding. Lectins are also involved in the export and degradation of misfolded proteins, as well and the transport of proteins from the ER to the Golgi.

See Also the Following Articles

Carbohydrate Chains: Enzymatic and Chemical Synthesis • GlcNAc Biosynthesis and Function, O-Linked • Glycosylation, Congenital Disorders of • Glycosylation in Cystic Fibrosis • Glycosylphosphatidylinositol (GPI) Anchors • Oligosaccharide Chains: Free, *N*-Linked, *O*-Linked • Protein Glycosylation Inhibitors

Glossary

glycoprotein A glycosylated protein.

glycosyltransferase An enzyme which transfers a sugar from a high energy donor to a protein, carbohydrate, or lipid.

reducing terminal sugar The carbohydrate linked directly to the protein backbone is often referred to as the reducing terminal saccharide or carbohydrate. This term is derived from early colorometric assay where the free hemiacetal form of sugars reduced ferric iron to ferrous iron.

saccharides Saccharide is derived from the Latin word for sugar, *saccharum*. A single sugar unit is referred to as a monosaccharide, two units as a disaccharide, three as a trisaccharides and several (2–10) as oligosaccharides and many (>10) as polysaccharides.

Further Reading

Fukuda, M., and Hindsgaul, O. (eds.) (2000). *Molecular and Cellular Glycobiology.* Oxford University Press, New York.

Furmanek, A., and Hofsteenge, J. (2000). Protein C-mannosylation: Facts and questions. *Acta Biochim. Pol.* **47**, 781–789.

Haynes, P. A. (1998). Phosphoglycosylation: A new structural class of glycosylation? *Glycobiology* **8**, 1–5.

Schaffer, C., Graninger, M., and Messner, P. (2001). Prokaryotic glycosylation. *Proteomics* **1**, 248–261.

Spiro, R. G. (2002). Protein glycosylation: Nature, distribution, enzymatic formation, and disease implications of glycopeptide bonds. *Glycobiology* **12**, 43R–56R.

Taylor, M. E., and Drickamer, K. (eds.) (2003). *Introduction to Glycobiology.* Oxford University Press, New York.

Varki, A. (1993). Biological roles of oligosaccharides: All of the theories are correct. *Glycobiology* **3**, 97–130.

Varki, A., Cummings, R., Esko, J., Freeze, H., Hart, G., and Marth, J. (eds.) (1999). *Essentials of Glycobiology.* Cold Spring Harbor Press, New York.

Zachara, N. E., and Hart, G. W. (2002). The emerging significance of O-GlcNAc in cellular regulation. *Chem. Rev.* **102**, 431–438.

Biography

Natasha E. Zachara received Bachelor of Technology (Biotechnology), Honours, from the School of Chemistry at Macquarie University (Sydney, Australia), in 1994. She completed her thesis entitled "Sequencing Proteins, Sequencing Sugars: A Unified Approach" at the Macquarie University Center for Analytical Biotechnology (Sydney, Australia), in 1998. She is currently working in the laboratory of Prof. G. W. Hart (Johns Hopkins University School of Medicine).

Gerald W. Hart is Director and DeLamar Professor of Biological Chemistry at the Johns Hopkins University School of Medicine. He received his Ph.D. in developmental biology at Kansas State University (USA) in 1977 and did his postdoctoral work with William J. Lennarz at Johns Hopkins, before joining the faculty in the Department of Biological Chemistry (1979). He was the founding editor-in-chief of *Glycobiology.*

Protein Import into Mitochondria

Johannes M. Herrmann and Walter Neupert
University of Munich, Munich, Germany

Mitochondria are essential organelles of eukaryotic cells that accommodate some 10–20% of the cellular proteome. They are made up by two membrane systems that divide the organelle into two aqueous subcompartments: the intermembrane space between the outer and the inner membrane, and the matrix which is enclosed by the inner membrane. The vast majority of mitochondrial proteins are encoded by the nuclear genome and synthesized on cytosolic ribosomes as precursors (also called preproteins). These proteins contain targeting information for specific sorting of each polypeptide to its respective mitochondrial subcompartment. Protein import into mitochondria is achieved by the concerted action of translocation complexes located in both membranes of the organelle.

Mitochondrial Targeting Signals

Targeting signals direct mitochondrial precursor proteins to their particular destination in the organelle. In addition, these sequences can prevent folding of precursor proteins in the cytosol and thereby maintain them in a transport-competent conformation. Proteins of the mitochondrial matrix and many inner membrane proteins are made with N-terminal extensions which are proteolytically removed by proteases following translocation into the mitochondrial matrix. These matrix targeting signals (MTSs) are referred to as presequences. Most mitochondrial proteins carry such N-terminal presequences. In addition, less defined internal signals are used for mitochondrial targeting, typically by proteins of the outer membrane, the intermembrane space, and by some inner membrane proteins.

Presequences

Presequences typically comprise 15–80 amino acid residues that have the potential to form amphipathic α-helices with one hydrophobic and one positively charged face. These signals are both necessary and sufficient for mitochondrial targeting. The addition of presequences to unrelated proteins typically leads to a targeting of the fusion proteins to mitochondria. The MTSs direct the extended polypeptide in an N-to-C-direction across both mitochondrial membranes. Examples were reported in which MTSs are located not at the N terminus, but at the C terminus or in the interior of a preprotein. In the latter case, the internal signal forms an amphipathic hairpin loop which precedes import of the N- and C-terminal parts of the preprotein. Typical N-terminal presequences can be detected by computer algorithms which predict the intracellular location of proteins.

Internal Targeting Signals

Many mitochondrial proteins contain less defined targeting signals which are a part of the mature polypeptide. These are referred to as internal signals. For example, proteins of the solute carrier family of the inner membrane are made up by modules of pairs of transmembrane domains which are imported as loop-like structures. The regions flanking these transmembrane domains are critical for the uptake of these proteins by the mitochondria. The nature of these signals and how they are deciphered is, however, not well understood.

Proteins of the outer membrane are often anchored in the lipid bilayer by terminal transmembrane domains. A moderate degree of hydrophobicity and flanking positive charges specify these proteins for mitochondria and differentiate them from other tail-anchored proteins of the cell.

Little is known about the targeting information that directs proteins into the intermembrane space of mitochondria. Many of these proteins are very small and bind cofactors such as metal ions or heme. The best-characterized example of the latter group of proteins is cytochrome *c*. Although many cytochrome *c* mutants were isolated that fail to be imported into mitochondria, a targeting signal of this protein was not identified so far.

Transport to and Across the Outer Membrane

A number of cytosolic factors were identified that bind to mitochondrial preproteins following their synthesis. Among these factors are members of the general chaperone system, such as Hsp70 and Hsp90,

and components that appear to play a more specific role in the targeting of mitochondrial proteins. These factors keep preproteins in an import-competent conformation and accompany them to the surface of mitochondria.

The TOM Translocase

The outer membrane harbors surface receptors that expose binding sites for MTSs to the cytosol (see Table I). These receptors are part of a multimeric protein translocase, called the *t*ranslocase of the *o*uter *m*embrane (TOM) complex. In fungi, the TOM complex comprises the receptor subunits Tom70, Tom22, and Tom20. These surface receptors direct preproteins to the so-called "general insertion pore" of the outer membrane, the main constituent of which is Tom40. Tom40 is thought to be present in a β-barrel structure in the outer membrane, similar to bacterial porin proteins, and

TABLE I

Components of the Mitochondrial Import Machinery

Components		
Fungi	**Mammals**	**Function**
Outer membrane, TOM complex		
Tom70, Tom71	Tom70	Surface receptor
Tom40	Tom40	Pore formation
	Tom34	Surface receptor, Tom70 homologue
Tom22	Tom22	Surface receptor
Tom20	Tom20	Surface receptor
Tom7	Tom7	Structural or regulatory component
Tom6		Structural component
Tom5		Receptor function
Intermembrane space		
Tim13	Tim13	Receptor and/or chaperone function
Tim12		Receptor and/or chaperone function
Tim10	Tim10 a, b	Receptor and/or chaperone function
Tim9	Tim9	Receptor and/or chaperone function
Tim8	DDP1, DDP2	Receptor and/or chaperone function
Inner membrane		
TIM23 complex		
Tim50	Tim50	Potentially receptor subunit
Tim44	Tim44	mtHsp70-binding
Tim23	Tim23	Receptor and channel activity
Tim17	Tim17	Function unclear
TIM22 complex		
Tim54		Function unclear
Tim22	Tim22	Channel activity
Tim18		Function unclear
Oxa1	Oxa1	Protein insertion from the matrix
Mba1		Protein insertion from the matrix
Imp1, Imp2	Imp1, Imp2	Sorting signal peptidases
Matrix		
Ssc1, Ecm10	mtHsp70	Chaperone, ATP-dependent precursor binding
Mge1	mtGrpE	Nucleotide exchange factor for mtHsp70
MPP	MPP	Processing of presequences
MIP	MIP	Processing of presequences
Mdj1	hTid (mtDnaJ)	Folding of imported proteins
Hsp60	Cpn60	Folding of imported proteins
Hsp10	Cpn10	Folding of imported proteins

by oligomerization forms protein-conducting channels. Three small additional subunits, Tom5, Tom6, and Tom7, appear to play a role as structural components and might be involved in regulating the interaction of the receptors with Tom40. In mammals, the TOM complex consists essentially of a similar set of homologous components. High-resolution electron microscopy of isolated TOM complexes revealed two membrane-traversing cavities of 2.2 nm, which most likely represent the preprotein-conducting channels in the outer membrane. Following translocation of preproteins through the general insertion pore, preproteins associate with the *trans* site of the TOM complex. This *trans*-binding site is formed by the intermembrane space domains of Tom40 and perhaps Tom22. An increasing binding affinity from *cis* to *trans* sites on the TOM complex was suggested to drive translocation of preproteins across the outer membrane into the intermembrane space.

Insertion into the Outer Membrane

In addition to its translocation function, the TOM complex facilitates the insertion of proteins into the lipid bilayer of the outer membrane (Figure 1, pathway 1). Although the molecular mechanism of this process is poorly understood, a critical role of the TOM complex was shown for membrane integration and assembly of TOM subunits, as well as for the insertion of other outer membrane proteins. The most abundant protein of the outer membrane, porin, and several tail-anchored proteins, like the apoptosis regulator bcl-2, require cytosolic receptor domains of TOM subunits for mitochondrial targeting. But, whereas integration of porin requires the general insertion pore in the TOM complex, bcl-2 was reported not to use the TOM channel.

Translocation into the IMS

The intermembrane space is a compartment of very small volume since the outer and inner membrane are ~ 8 nm apart which is about the diameter of a membrane. Only a rather small number of components of the intermembrane space are known most of which are required for mitochondrial biogenesis or have a function in respiration. A prominent example is cytochrome *c*, which plays a role in apoptosis apart from its function in shuttling electrons between complexes III and IV. Apocytochrome *c* is imported by the TOM complex and associates in the intermembrane space with the protein cytochrome *c* heme lyase (CCHL). CCHL represents a docking site for apocytochrome *c* and converts it to holocytochrome *c* by incorporation of a heme group. Holocytochrome *c* is not able to traverse the TOM channel and, thus, remains in the intermembrane space. Like cytochrome *c*, many intermembrane space proteins bind cofactors and may be imported by a similar mechanism (Figure 1, pathway 2).

A second group of intermembrane space proteins is synthesized with N-terminal presequences followed by sorting signals. These signals are proteolytically removed by the Imp1/Imp2 protease of the inner membrane and the mature parts of the precursors are released into the intermembrane space. These sorting signals can be transplanted to unrelated sequences and direct these into the intermembrane space. Examples for this type of proteins are cytochrome b_2 or cytochrome b_5 reductase.

Translocation into the Matrix

The mitochondrial matrix contains a large number of proteins, many of which fulfill important functions in metabolic processes, energy production or the replication and expression of the mitochondrial genome. These proteins typically contain N-terminal presequences and are imported on a common import route (Figure 1, pathway 4).

The TIM23 Complex

The TIM23 complex consists of the integral membrane proteins Tim50, Tim23, and Tim17, and the peripherally associated matrix protein Tim44. Tim23 and Tim17 are homologous to each other and form the translocation pore in the inner membrane. In yeast, the N terminus of Tim23 protrudes into the outer membrane and thereby may mediate close contact of the TOM and the TIM23 translocase. Tim50 exposes a large domain to the intermembrane space and might play a role in guiding preproteins from the TOM to the TIM23 complex. Binding of the presequence to the TIM23 complex leads to a membrane-potential-dependent gating of the channel, which allows the presequence to traverse the inner membrane. This translocation reaction is driven by the membrane potential which probably supports the movement of the positively charged presequences to the negatively charged matrix face of the inner membrane. In the matrix, the presequences are bound by the chaperone mtHsp70, which prevents backsliding of the translocation intermediate. MtHsp70 is recruited to the TIM23 translocase by the Tim44 subunit of the complex which warrants a high concentration of mtHsp70 at the exit of the TIM23 channel and, thus, the efficient trapping of the incoming polypeptide. The ATP-dependent interaction of mtHsp70 with the preprotein is regulated by a nucleotide exchange factor, mtGrpE/Mge1, and is responsible for the ATP dependence of the mitochondrial import process. Binding of the preprotein to mtHsp70 leads to the

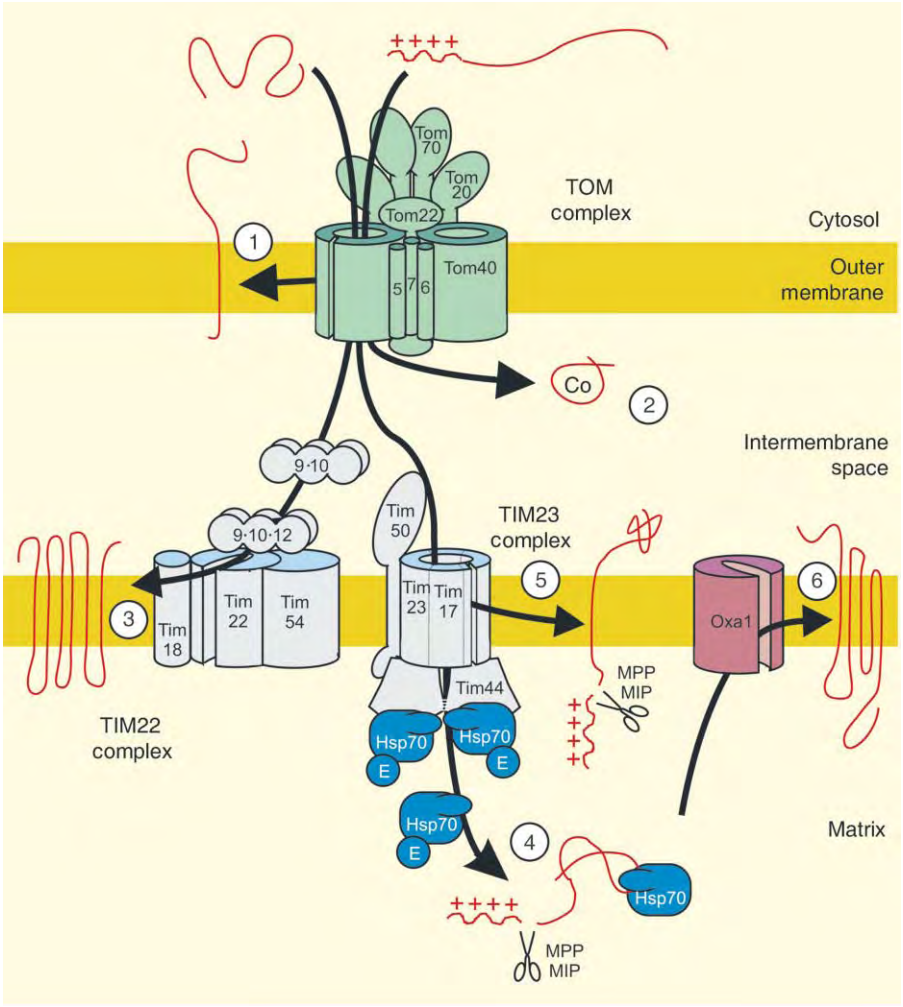

FIGURE 1 Protein import pathways in mitochondria. (1) Most outer membrane proteins bind to the receptor subunits of the TOM complex before they integrate into the membrane. The role of the general insertion pore in this process is not fully understood. (2) Proteins of the intermembrane space are often of small size and bind cofactors. These proteins are translocated through the general insertion pore of the TOM complex formed by Tom40. In the case of cytochrome c, the acquisition of the cofactor heme (Co) is required for efficient translocation of the protein. (3) Members of the solute carrier family and some Tim subunits traverse the outer membrane forming loop-like structures. They are escorted to the TIM22 translocase in the inner membrane by complexes of small Tim proteins in the intermembrane space. (4) Matrix proteins contain presequences that mediate translocation through the TOM channel and interact with the TIM23 complex in the inner membrane. The presequences are transported across the inner membrane in a membrane potential- and ATP-dependent manner, and removed by processing peptidases. After complete translocation across the inner membrane, matrix proteins fold under assistance of molecular chaperones. (5) Monotopic inner membrane proteins can be arrested at the TIM23 translocase and laterally integrated into the lipid bilayer of the inner membrane. (6) Conservatively sorted proteins are first transported into the matrix and form sorting intermediates bound by mtHsp70. Subsequently, these proteins are inserted into the inner membrane in a membrane potential-dependent reaction. The inner membrane protein Oxa1 is required for membrane integration of several of these proteins.

release of mtHsp70 from Tim44, and allows further translocation of the preprotein into the matrix driven by the Brownian movement of the polypeptide. Repeated binding cycles of mtHsp70 then lead to the vectorial import reaction. This mechanism is referred to as Brownian ratchet model as mtHsp70 would prevent backsliding of the preprotein. It was suggested that in addition to its trapping function, mtHsp70 undergoes an intramolecular conformational change and thereby mechanically pulls the bound preprotein into the matrix. The validity and significance of this motor model is still under debate.

Protein Folding and Assembly

In the matrix the presequences are typically removed by processing peptidases. The mitochondrial processing peptidase (MPP) consists of two conserved subunits which convert most matrix proteins into their mature form. In addition, some preproteins are further

processed by the mitochondrial intermediate peptidase, which removes another eight N-terminal amino acid residues. The mature proteins are then allowed to fold into their native structure. This process is facilitated by mtHsp70 which cooperates in this process with the DnaJ homologue Mdj1/hTid. Folding of some matrix proteins depends on the chaperonin complex formed by Hsp60 and Hsp10, which is homologous to the GroEL/GroES complex of the bacterial cytosol.

Protein Insertion into the Inner Membrane

The inner membrane contains a large number and diversity of proteins and belongs to the protein-richest membranes of eukaryotic cells. Inner membrane proteins reach their destination on several different insertion routes.

Insertion via the TIM23 Translocase

A number of monotopic inner membrane proteins are integrated into the inner membrane following translocation arrest at the level of the TIM23 complex (Figure 1, pathway 5). This sorting route was named the "stop-transfer" pathway. Most of these proteins are of $N_{in}-C_{out}$ topology, but some examples were reported which are oriented in a $N_{out}-C_{in}$ topology by internal loop-forming presequences.

Insertion from the Matrix

Alternatively, proteins can be inserted into the inner membrane following complete translocation into the matrix (Figure 1, pathway 6). This transport scheme was called conservative sorting, since the process employs a bacterial-like insertion reaction from the matrix. Examples for this sorting path are both mono- and polytopic inner membrane proteins of prokaryotic origin. Not only the direction of the membrane integration reaction resembles that in prokaryotes, but also the topogenic signals and the components that catalyze the insertion process. Conservatively sorted proteins adhere to the positive-inside rule according to which negative charges flanking the transmembrane segments are preferentially translocated across a membrane. A central player in the insertion process of these proteins is the inner membrane protein Oxa1 which forms the only translocation complex known to be conserved from bacteria to mitochondria. Besides its role in membrane integration of conservatively sorted proteins, the Oxa1 translocase mediates the insertion of mitochondrial translation products into the inner membrane.

Insertion via the TIM22 Translocase

The third group of inner membrane proteins is inserted by an alternative TIM complex, the TIM22 translocase (Figure 1, pathway 3). This pathway is used by members of the solute carrier family and by some TIM subunits. These proteins do not contain presequences but internal signals. Upon translocation through the TOM complex these proteins associate with the hexameric Tim9·Tim10 and Tim8·Tim13 complexes of the intermembrane space which belong to the family of "small Tim proteins." These complexes escort the hydrophobic precursor proteins from the TOM complex through the intermembrane space to the TIM22 complex. The TIM22 complex comprises the membrane-embedded subunits Tim54, Tim22, and Tim18 to which a Tim9·Tim10·Tim12 hexamer is associated. Tim22 is related to Tim17 and Tim23, and forms the translocation pore of the complex. Mutations in the human Tim8 homologue, DDP1, lead to the deafness dystonia (Mohr-Tranebjaerg) syndrome, a progressive, neurodegenerative human disorder.

See Also the Following Articles

Cytochrome *c* • Lipid Bilayer Structure • Membrane Fusion • Mitochondrial Membranes, Structural Organization • Mitochondrial Outer Membrane and the VDAC Channel • Protein Folding and Assembly

Glossary

Oxa1 translocase Protein complex of the inner membrane of mitochondria that facilitates membrane insertion of both nuclear and mitochondrially encoded proteins.

preprotein Precursor form of a mitochondrial protein; preproteins often contain presequences that have to be removed by mitochondrial processing peptidases.

presequence Typically N-terminal extension on a protein that serves as mitochondrial targeting signal (MTS).

TIM translocases Oligomeric translocation complexes of the inner membrane of mitochondria.

TOM translocase Multisubunit translocation complex of the outer membrane of mitochondria consisting of receptor subunits and a protein-translocating channel.

Further Reading

Herrmann, J. M. (2003). Converting bacteria to organelles: Evolution of mitochondrial protein sorting. *Trends Microbiol.* **11**, 74–79.

Hoogenraad, N. J., Ward, L. A., and Ryan, M. T. (2002). Import and assembly of proteins into mitochondria of mammalian cells. *Biochim. Biophys. Acta* **1592**, 97–105.

Koehler, C. M. (2000). Protein translocation pathways of the mitochondrion. *FEBS Lett.* **467**, 27–31.

Neupert, W. (1997). Protein import into mitochondria. *Annu. Rev. Biochem.* **66**, 863–917.

Neupert, W., and Brunner, M. (2002). The protein import motor of mitochondria. *Nat. Rev. Mol. Cell Biol.* **3**, 555–565.

Pfanner, N., and Geissler, A. (2001). Versatility of the mitochondrial protein import machinery. *Nat. Rev. Mol. Cell Biol.* **2**, 339–349.

Stuart, R. A. (2002). Insertion of proteins into the inner membrane of mitochondria: the role of the Oxa1 complex. *Biochem. Biophys. Acta* **1592**, 79–87.

Biography

Johannes Herrmann is a Group Leader in the Department of Physiological Chemistry of the University of Munich, Germany. He holds a Ph.D. from the University of Munich.

Walter Neupert is Chair of the Department of Physiological Chemistry in Munich. He holds a Ph.D. and an M.D. from the University of Munich.

Their principal research interest is the biogenesis of mitochondria, and especially the sorting and assembly of mitochondrial proteins.

Protein Kinase B

Bettina A. Dummler and Brian A. Hemmings
Friedrich Miescher Institute for Biomedical Research, Basel, Switzerland

Protein kinase B (PKB, also known as AKT) is an important mediator in intracellular signaling. Activation of PKB occurs in response to several cellular stimulants that act through receptor tyrosine kinases or G protein-coupled receptors. As a protein kinase, PKB catalyzes phosphorylation of proteins (the covalent linking of a phosphate group) on serine and threonine residues within a specific recognition sequence. Phosphorylation is a common mechanism in signal transduction to reversibly alter protein function, such as intrinsic activity, subcellular localization, half-life, or interaction of proteins with binding partners. Multiple PKB substrates have been identified and regulation of these molecules by phosphorylation plays an important role in the elaboration of physiological changes in a cell in response to extracellular signal molecules. Depending on cell type and stimulus, widely divergent cellular processes are regulated by PKB, including apoptosis, proliferation, differentiation, and metabolism.

Structure of PKB and Activation Mechanism

The AGC Family of Protein Kinases

Protein kinase B (PKB) is a member of a family of protein kinases that originally contained protein kinase *A*, cGMP-dependent protein kinase, and protein kinase *C*, termed the AGC family. Other members of the AGC family include p70 S6 kinase, protein kinase C-related kinase 2 (PRK2), and serum- and glucocorticoid-inducible kinase (SGK). The protein kinases of the AGC family show similarities in many structural and regulatory features. Highly similar in all AGC kinases is a flexible peptide loop (activation loop) proximal to the catalytic pocket of the kinase domain, and phosphorylation of this loop is required for the activation of virtually all AGC kinases.

Isoforms of PKB

There are three mammalian isoforms of PKB, PKBα (AKT1), PKBβ (AKT2), and PKBγ (AKT3). They are products of distinct genes but highly related, exhibiting greater than 80% sequence identity and sharing the same structural organization (see Figure 1A). The three genes are expressed differentially, with PKBα and PKBβ displaying fairly broad and PKBγ more restricted tissue distribution.

Structure of PKB

Each isoform possesses an amino-terminal pleckstrin homology (PH) domain that binds to 3-phosphoinositides, a central catalytic domain, and a carboxy-terminal regulatory domain (Figure 1A). Furthermore, all three isoforms possess two conserved phosphorylation sites, and phosphorylation of both sites is required for full activation of the kinase. The first one (Thr308 in PKBα) lies within the activation loop of the kinase domain and its phosphorylation induces a catalytically active conformation of the kinase. The second one lies within the regulatory domain in a six-amino-acid-long sequence termed the hydrophobic motif (FPQFS^{473}Y). Phosphorylation at Ser473 enables the hydrophobic motif to bind into a pocket within the small lobe (N-lobe) of the kinase domain and thereby it stabilizes the active conformation of PKB (Figure 1B). All PKB isoforms are assumed to have identical or similar substrate specificity. The minimal consensus sequence of preferred PKB *in vitro* phosphorylation sites has been defined as ArgXArgXXSer/Thr-Hyd, where X is any amino acid and Hyd is a bulky hydrophobic residue. Multiple PKB substrates have now been identified (Table 1).

The PI3K/PKB Signaling Pathway

Activation of receptor tyrosine kinases by ligands such as epidermal growth factor (EGF) and platelet-derived growth factor (PDGF) leads to autophosphorylation of specific tyrosine residues on the intracellular portion of the receptor (Figure 2). Recruitment of phosphoinositol 3-kinase (PI3K) then occurs, via binding of the Src homology 2 (SH2) domains of the regulatory subunit (p85) to specified phosphotyrosine residues on the receptor (in the case of insulin receptor this recruitment

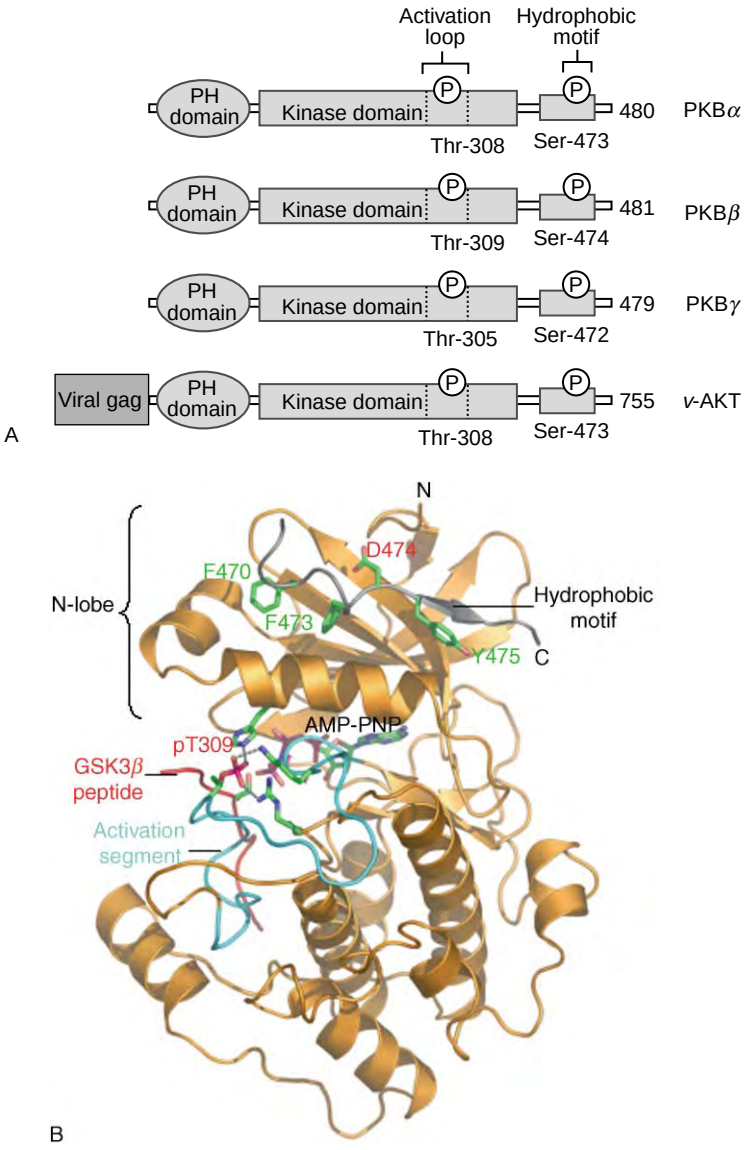

FIGURE 1 (A) Domain structure and regulatory phosphorylation sites of PKB. All isoforms contain a pleckstrin homology (PH) domain, a catalytic domain and a C-terminal regulatory domain. Phosphorylation of the activation loop and the hydrophobic motif (Thr308 and Ser473 in PKBα) are critical for kinase activation. v-Akt is the viral form of PKB and is a fusion between the viral Gag protein and mouse PKBα. (B) Structure of activated PKB. The ribbon diagram shows an activated PKBβ ternary complex with GSK3-peptide (red) bound in the substrate-binding site and AMP-PNP (a hydrolysis-resistant ATP analogue) bound in the ATP-binding site. To obtain an activated conformation, the hydrophobic motif of PKB was replaced with that of another AGC kinase, PRK2, and T309 in the activation segment (blue) was phosphorylated by PDK1. The hydrophobic motif of PRK2 contains an acidic residue (D474) in place of a phosphorylatable serine and binds constitutively to the N-lobe without needing phosphorylation. (Reproduced from Yang, J., Cron, P., Good, V. M., Thompson, V., Hemmings, B. A., and Barford, D. (2002). Crystal structure of an activated Akt/protein kinase B fernary complex with GSK3-peptide and AMP-PNP. *Nat. Struct. Biol.* **9**(12), 940–944, with permission.)

is largely mediated by the insulin receptor substrate (IRS) adapter proteins). This leads to a conformational change in PI3K and consequently to activation of the catalytic subunit (p110). Activated PI3K phosphorylates inositol-containing membrane lipids at the 3′-OH position of the inositol ring, generating phosphatidyl-inositol 3,4,5-trisphosphate (PI(3,4,5)P3). Subsequently, inactive PKB is recruited from the cytosol to the membrane via binding of its PH domain to PI(3,4,5)P3. Membrane recruitment brings PKB in close proximity to 3-phosphoinositide-dependent kinase (PDK1). PDK1 possesses a PH domain in its carboxy terminus, which binds PI(3,4,5)P3 and localizes PDK1 at the membrane. Co-localization of the two proteins and the conformational change induced in PKB upon lipid binding then enable PDK1 to phosphorylate PKB on Thr308 in the activation loop. For full kinase activation, PKB requires phosphorylation of an additional site,

TABLE I

PKB Substrates[a,b]

Protein	Biological effect
BAD	Phosphorylated BAD binds to 14-3-3 and is sequestered in the cytoplasm
BRCA1	Interferes with nuclear localization of BRCA1?
CREB	Increases association with CBP and p130
eNOS	Activates eNOS and leads to NO production
Forkhead family members (FKHR, FKHRL1, AFX)	Inhibits transcriptional activities of Forkhead family members
GSK3α/β	Inactivates GSK3 activity
IKKα	Activates transcriptional activity of NFκB
IRS-1	Positive regulation of IRS-1 function
Mdm2	Nuclear translocation of Mdm2, decreases p53 levels
Nur77	Inhibits transcriptional activity of Nur77
PFK-2	Activates PFK-2
Procaspase-9	Suppression of caspase-9-induced cell death
p21/Cip1	Cell cycle progression
p27/Kip1	Relieves inhibitory effect of p27/Kip1 on Cdk2
Raf1	Inhibition of Raf1 signaling
TSC2	Destabilizes TSC2 and disrupts its interaction with TSC1, leading to p70S6K activation

[a] Abbreviations: BAD, Bcl-2 pro-apoptotic family member; CBP, cAMP binding protein; Cdk2, cyclin-dependent kinase 2; CREB, cAMP responsive element binding protein; eNOS, endothelial nitric oxide synthase; GSK3, glycogen synthase kinase-3; IKKα, I-kB kinase α; IRS-1, insulin receptor substrate-1; NFκB, nuclear factor κB; NO, nitric oxide; PFK-2, phosphofructokinase-2; TSC2, tuberous sclerosis complex 2.

[b] Data supporting the *bona fide* nature of these substrates differs between proteins. Note also that because of space restrictions, not all published PKB substrates are included in the table.

Ser473, by an as yet unidentified Ser473 kinase. Following activation, PKB is detached from the plasma membrane and translocates to the cytosol and the nucleus to phosphorylate its substrates.

Negative Regulation of PKB Activity

Just as important as activation is the negative regulation of PKB activity, to avoid sustained signaling in absence of an appropriate extracellular signal. The key pThr308 and pSer473 residues in PKB have a relatively short half-life and become dephosphorylated by the action of phosphatases, such as PP2A, which returns PKB to its inactive conformation in the cytosol (see Figure 2). Another negative regulator of PKB activity is PTEN, a 3-phosphoinositide-specific phosphatase that dephosphorylates PI(3,4,5)P3, and thus antagonizes PI3K activity and recruitment of PKB to the membrane. Recently, a PKB-binding protein has been identified, carboxy-terminal modulator protein (CTMP), which appears to negatively regulate PKB by inhibiting its phosphorylation at Ser473 and thus maintaining the kinase in an inactive state.

Physiological Functions and Cellular Processes Regulated by PKB

Apoptosis and Cell Survival

The ability of a diverse array of physiological stimuli to promote cell survival can be attributed, at least in part, to the activation of the PI3K/PKB signaling pathway. Direct targets that PKB phosphorylates to protect cells from apoptosis include BAD, the Forkhead family of transcription factors, Mdm2, and the NFκB regulator IκB kinase (IKK) (Figure 3A). Each of these plays a critical role in cell death and by phosphorylation through PKB their pro-apoptotic function is inhibited and anti-apoptotic function promoted, respectively.

PKB Controls Subcellular Localization of BAD

The Bcl-2 protein family is a large family of structurally related proteins, of which some promote cell death and others survival. BAD is a pro-apoptotic member of this family that in its dephosphorylated form directly interacts with pro-survival Bcl-2 family

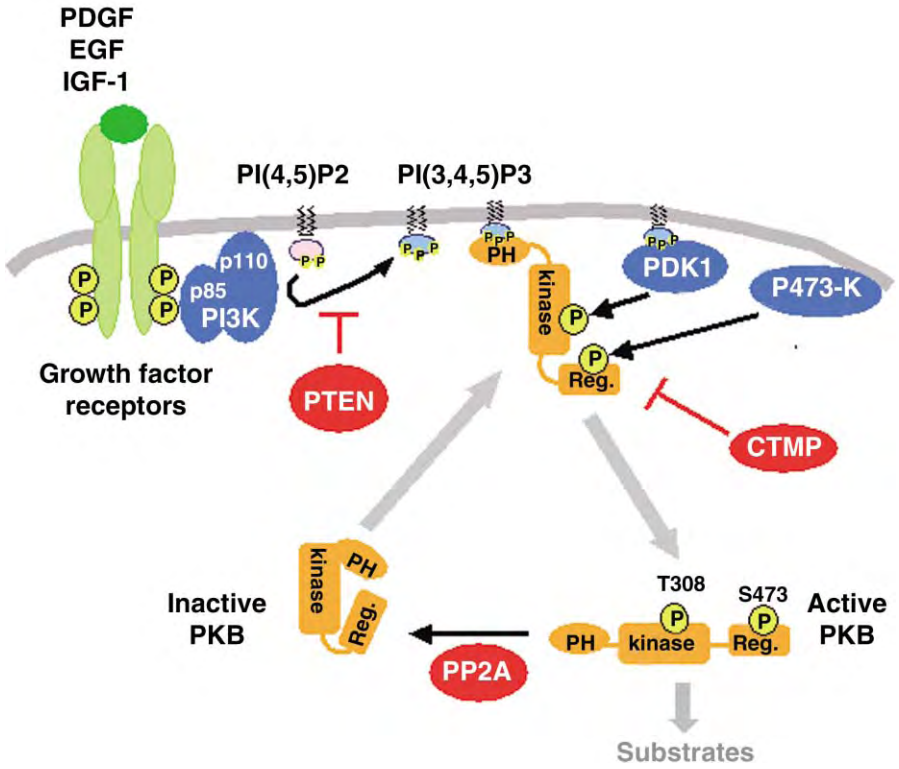

FIGURE 2 Current model for PKB regulation by receptor tyrosine kinases. Growth factor-mediated activation of PI3K leads to generation of PI(3,4,5)P3, which recruits inactive PKB to the plasma membrane. Residues Thr308 in the catalytic site and Ser473 in the hydrophobic motif are subsequently phosphorylated by PDK1 and by an as yet unidentified Ser473 kinase, respectively. Activated PKB can then phosphorylate substrates at the plasma membrane, in the cytosol, and in the nucleus. Activation of PKB is inhibited by the action of PTEN and presumably also by CTMP, which inhibits phosphorylation of PKB at Ser473. The kinase is deactivated by phosphatases such as PP2A.

members, such as Bcl-X_L. This interaction blocks pro-survival function of Bcl-X_L. Phosphorylation of BAD by activated PKB results in dissociation from Bcl-X_L and instead preferential association with cytoplasmic 14-3-3 proteins. The ability of BAD to bind to and inactivate Bcl-X_L is thereby disrupted and cell survival promoted.

PKB Controls Transcriptional Activity of Forkhead Transcription Factors

Many apoptotic stimuli also induce *de novo* gene expression of critical death genes and the Forkhead family of transcription factors mediates transcription of a defined subset of these genes. PKB-mediated phosphorylation of these transcription factors regulates their subcellular localization. In an unphosphorylated state, Forkhead family proteins translocate into the nucleus and activate transcription of their target (death) genes. But under conditions during which PKB is activated, these transcription factors are phosphorylated and are retained in the cytoplasm, potentially by interaction with 14-3-3 proteins, and are thus unable to mediate transcription.

PKB Controls p53 Levels in Cells via Mdm2 Phosphorylation

The p53 tumor suppressor protein is a short-lived protein, which is stabilized in response to cellular stress and promotes apoptosis. The ubiquitination and degradation of p53 are largely controlled by Mdm2, an E3 ubiquitin ligase. PKB can influence degradation of p53 through phosphorylation of Mdm2. Phosphorylation mediates translocation of Mdm2 to the nucleus, where it can bind to and modify nuclear p53, resulting in enhanced p53 degradation.

PKB Controls Transcriptional Activity of NFκB

Cell death is not only prevented by inhibition of apoptosis-promoting proteins on posttranslational and transcriptional level, but also through upregulation of survival-promoting genes. PKB is a signaling intermediate upstream of survival gene expression, which is dependent on the transcription factor NFκB (nuclear factor-κB). This transcription factor is retained in the cytoplasm by proteins of the IκB family. Phosphorylation of IκB by a specific IκB kinase (IKK) targets it for ubiquitination and proteosome-mediated degradation.

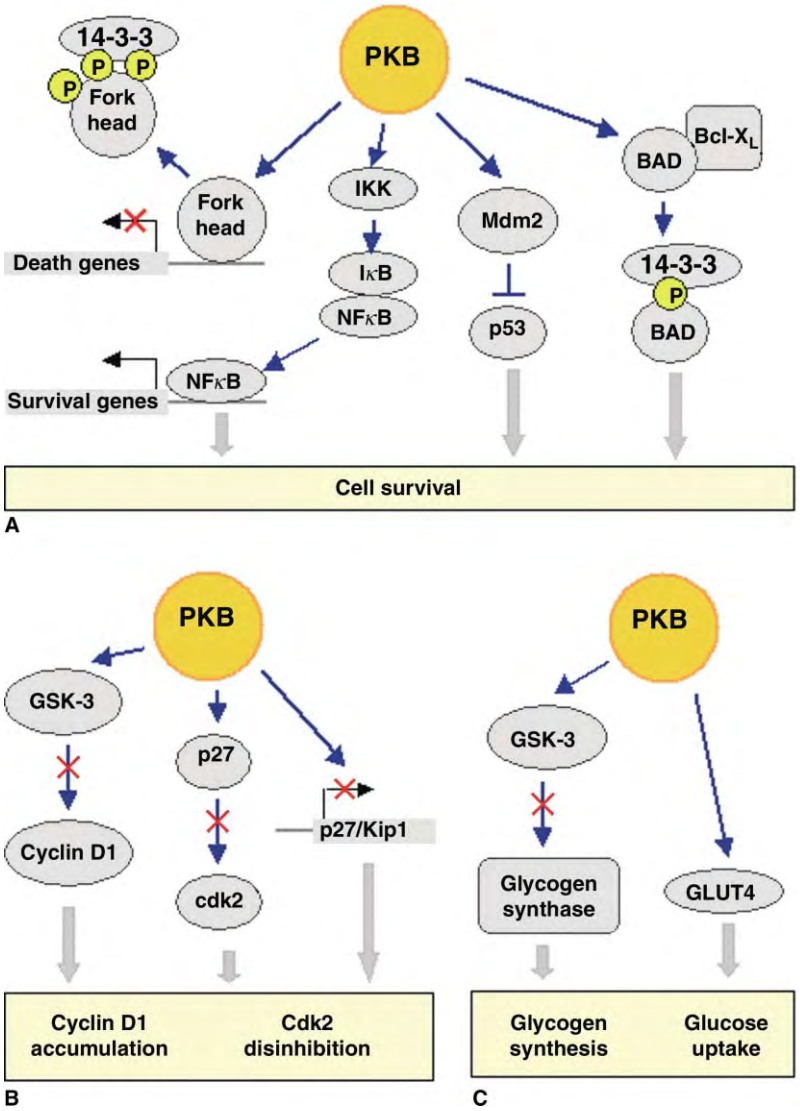

FIGURE 3 Physiological functions of PKB. PKB regulates (A) cell survival and apoptosis, (B) proliferation, and (C) glucose metabolism through phosphorylation of multiple substrates.

PKB regulates NFκB transcriptional activity through regulation of IKK activity. Activation of IKK leads to degradation of IκB and releases NFκB, allowing its nuclear translocation and subsequent activation of target genes.

Regulation of Proliferation

PKB may not be required for cell cycle progression *per se* but several downstream targets of PKB have an impact on the cell cycle machinery (Figure 3B). p27/Kip1 is a protein that blocks cell cycle. Anti-proliferative signals mobilize stored p27 and enable it to bind to and inhibit its nuclear target, cyclin-dependent kinase 2 (Cdk2), an important kinase for the initiation of DNA synthesis in the cell cycle. Phosphorylation of p27 on Thr157 by activated PKB relieves the inhibition on Cdk2. Thr157 lies within a nuclear localization signal and its phosphorylation impairs nuclear import of p27. Thus sequestered in the cytoplasm, p27 can no longer interact with Cdk2 and the kinase is allowed to remain active. In addition, PKB has been reported to downregulate transcription of p27. Another mechanism, by which PKB promotes cell proliferation, is the indirect regulation of cyclin D1 protein stability. The levels of cyclin D1 are important in G1/S phase transition in the cell cycle, and phosphorylation of cyclin D1 by glycogen synthase kinase-3 (GSK3) targets it for degradation by the proteosome. Active PKB can negatively regulate GSK3 activity by phosphorylation and thereby prevent cyclin D1 degradation. Subsequent accumulation of cyclin D1 promotes cell cycle progression.

Regulation of Glucose Metabolism

In skeletal muscle and adipocytes, PKB regulates insulin-stimulated glucose uptake and glycogen synthesis (Figure 3C). In both tissues PKBβ is the predominant isoform and becomes rapidly activated by insulin in a PI3K-dependent fashion. In unstimulated cells, glycogen synthase, the enzyme mediating incorporation of glucose from uridine diphosphoglucose into glycogen, is kept in an inactive state via phosphorylation through GSK3. Activated PKB phosphorylates and thereby inactivates GSK3, thus promoting dephosphorylation of glycogen synthase and increased glycogen synthesis. Another important PKB-dependent metabolic response to insulin is the translocation of GLUT4 from its intracellular storage pool to the plasma membrane. GLUT4 is an insulin-regulated glucose transporter in skeletal muscle and adipocytes, which in resting cells is present in intracellular endosome-like vesicles. Insulin-activated PKB triggers recruitment of these GLUT4-containing vesicles to the plasma membrane, which leads to a marked increase in the rate of glucose uptake.

Kinase-Independent Functions of PKB

In addition to acting as a kinase toward many substrates, PKB forms complexes with other proteins that are not substrates. Such proteins may serve to anchor PKB in different cellular compartments, to protect it from degradation and dephosphorylation, to regulate PKB kinase activity, or to recruit PKB substrates and/or upstream kinases. As an example, heat shock protein 90 (Hsp90) has been found to interact with PKB, possibly indirectly via the co-chaperone Cdc37, and this complex may stabilize active PKB, protecting it from dephosphorylation and degradation. Furthermore, Hsp90 might function as a scaffold protein that recruits the PKB substrate endothelial nitric oxide synthase (eNOS), an enzyme important in cardiovascular homeostasis and angiogenesis.

PKB and Cancer

PKB is the cellular homologue of the transforming oncogene v-Akt, which was found in a retrovirus termed AKT8. This retrovirus was originally isolated from mice with a high incidence of spontaneous lymphoma. v-Akt encodes a fusion protein between the viral protein Gag and full-length cellular PKBα (see Figure 1A). The viral gag domain in v-Akt possesses a myristoylation signal that mediates targeting to the plasma membrane and it thereby confers to v-Akt increased ligand-independent kinase activity as compared to cellular PKB. Deregulation of normal PKB signaling has been documented as a frequent occurrence in several human cancers. In a large number of cancers PTEN, which normally limits PKB activation, is mutated or deleted, resulting in elevated $PI(3,4,5)P_3$ levels and increased PKB activity. Furthermore, PKB gene amplification, mRNA upregulation or protein overexpression have also been reported. Aberrant elevated levels of PKB activity cause transformation of cells predominantly due to the anti-apoptotic function of PKB. Cells that have damaged DNA or are behaving in a discoordinated fashion will survive in this context instead of undergoing apoptosis, and can thus accumulate further mutations. Additionally, implication of PKB in angiogenesis and cell cycle control may contribute to cancer induction.

See Also the Following Articles

Cell Death by Apoptosis and Necrosis • Nuclear Factor kappaB • Phosphatidylinositol Bisphosphate and Trisphosphate • Protein Kinase C Family

Glossary

activation loop A short peptide loop present in protein kinases. Its conformation is altered by phosphorylation to increase or decrease catalytic activity.

apoptosis Programmed cell death, induced in cells when they are damaged (e.g., DNA damage), unnecessary, or harmful to the body.

extracellular signaling molecules Specific substances that are synthesized and released by signaling cells and produce a specific response in target cells, which have receptors for these molecules. Extracellular signaling molecules include hormones, growth factors, and neurotransmitters.

oncogene A gene whose product is involved in inducing cancer. Most oncogenes are mutant forms of normal genes involved in the control of cell cycle progression.

pleckstrin homology domain A sequence of about 100 amino acids that is present in many signaling molecules and has affinity for certain phospholipids.

Further Reading

Brazil, D. P., and Hemmings, B. A. (2001). Ten years of protein kinase B signalling: A hard Akt to follow. *Trends Biochem. Sci.* **26**, 657–664.

Brazil, D. P., Park, J., and Hemmings, B. A. (2002). PKB binding proteins: Getting in on the Akt. *Cell* **111**, 293–303.

Datta, S. R., Brunet, A., and Greenberg, M. E. (1999). Cellular survival: A play in three Akts. *Genes Develop.* **13**, 2905–2927.

Galetic, I., Andjelkovic, M., Meier, R., Brodbeck, D., Park, J., and Hemmings, B. A. (1999). Mechanism of protein kinase B activation by insulin/insulin-like growth factor-1 revealed by specific inhibitors of phosphoinositide 3-kinase–significance for diabetes and cancer. *Pharmacol. Ther.* **82**, 409–425.

Mayo, L., and Donner, D. (2002). The PTEN Mdm2, p53 tumor suppressor-oncoprotein network. *Trends Biochem. Sci.* **27**, 462–467.

Vivanco, I., and Sawyers, C. L. (2002). The phosphatidylinositol 3-kinase-Akt pathway in human cancer. *Nat. Rev. Cancer* **2**, 489–501.

Yang, J., Cron, P., Good, V. M., Thompson, V., Hemmings, B. A., and Barford, D. (2002). Crystal structure of an activated Akt/protein Kinase B Fernary complex with GSK3-peptide and AMP-PNP. *Nat. Struct. Biol.* 9(12), 940–944.

Biography

Brian Hemmings is Senior Group Leader at the Friedrich Miescher Institute. He has devoted a major part of his career to delineating the regulatory mechanisms utilized by protein kinases in signal transduction cascades.

Bettina Dummler is currently working on a Ph.D. thesis in Brian Hemmings' group at the Friedrich Miescher Institute.

Protein Kinase C Family

Alexandra C. Newton
University of California, San Diego, California, USA

Protein kinase C is a family of enzymes that has a central role in transducing information from external stimuli to cellular responses. Members of this family of serine/threonine kinases respond to signals that cause lipid hydrolysis. Protein kinase C isozymes phosphorylate an abundance of substrates, leading to both short-term cellular responses such as regulation of membrane transport and long-term responses such as memory and learning.

Historical Perspective

Protein kinase C was discovered in the late 1970s by Yasutomi Nishizuka and colleagues at Kobe University, Japan. Their initial discovery was of a constitutively active enzyme that required only Mg^{2+} for activity (and hence was named protein kinase M, PKM). Further studies revealed that PKM was a proteolytic product of a full-length enzyme; this enzyme was named protein kinase C because its enzymatic activity could be released by a Ca^{2+}-dependent protease. The subsequent discovery that protein kinase C is activated by the phospholipid hydrolysis product, diacylglycerol, was a major finding in biology: it provided the molecular mechanism for how lipid hydrolysis, discovered 25 years earlier to be triggered by stimuli such as acetylcholine, couples to cellular signaling pathways.

But the discovery that catapulted research on protein kinase C to the forefront of cellular signaling was the finding that it is the receptor for the potent tumor-promoting phorbol esters. Phorbol esters are present in the milky sap exuded from plants of the Euphorbiaceae family; the oil from the seeds of one member of this family, in particular croton tiglium, has particularly strong irritant properties and, as such, has been used over the millennia for purposes as varied as poison for hunting arrows to medicinal purposes. In the 1960s, the active ingredient in the oil was found to be a family of diesters of the tetracyclic diterpene phorbol. Phorbol esters were shown to be extremely potent tumor promoters, and classic studies revealed that painting phorbol esters on the skin of mice allowed otherwise subthreshold amounts of carcinogens to promote tumors. The finding that protein kinase C is the direct molecular target of phorbol esters placed this enzyme at the center of signaling pathways that control normal cell function and carcinogenesis.

Protein Kinase C Family Members

There are ten mammalian isozymes of protein kinase C that share in common a carboxyl-terminal kinase domain linked to an amino-terminal regulatory moiety (Figure 1). The regulatory moiety, in turn, contains a number of functional modules and it is the composition of these functional modules that further defines the three subfamilies of the protein kinase C isozymes. These modules are an autoinhibitory-pseudosubstrate sequence that maintains the enzyme in an inactive conformation, and one or two membrane-targeting modules that direct protein kinase C to the membrane following generation of the appropriate second messengers. Specifically, the C1 domain binds diacylglycerol and phorbol esters and the C2 domain binds Ca^{2+}; each event promotes the binding of the respective domain to membranes.

Conventional protein kinase C isozymes (α, βI, βII, and γ), have a C1 and a C2 domain and respond to both diacylglycerol and Ca^{2+}. Novel protein kinase C isozymes (δ, ε, η, and θ/L) have a C1 domain that binds diacylglycerol, but an impaired C2 domain that does not bind Ca^{2+}. These isozymes respond to cellular increases in diacylglycerol but not Ca^{2+}. Atypical protein kinase C isozymes (ζ and ι/λ) have an impaired C1 domain and no C2 domain and bind neither diacylglycerol nor Ca^{2+}. Thus, stimuli that elevate intracellular diacylglycerol activate conventional and novel protein kinase C family members, with conventional isozymes being additionally regulated by Ca^{2+}.

Protein Kinase C Phosphorylation

Before protein kinase C is competent to signal, it must first be processed by a series of ordered phosphorylations. The first is mediated by an upstream kinase, the phosphoinositide-dependent kinase, PDK-1.

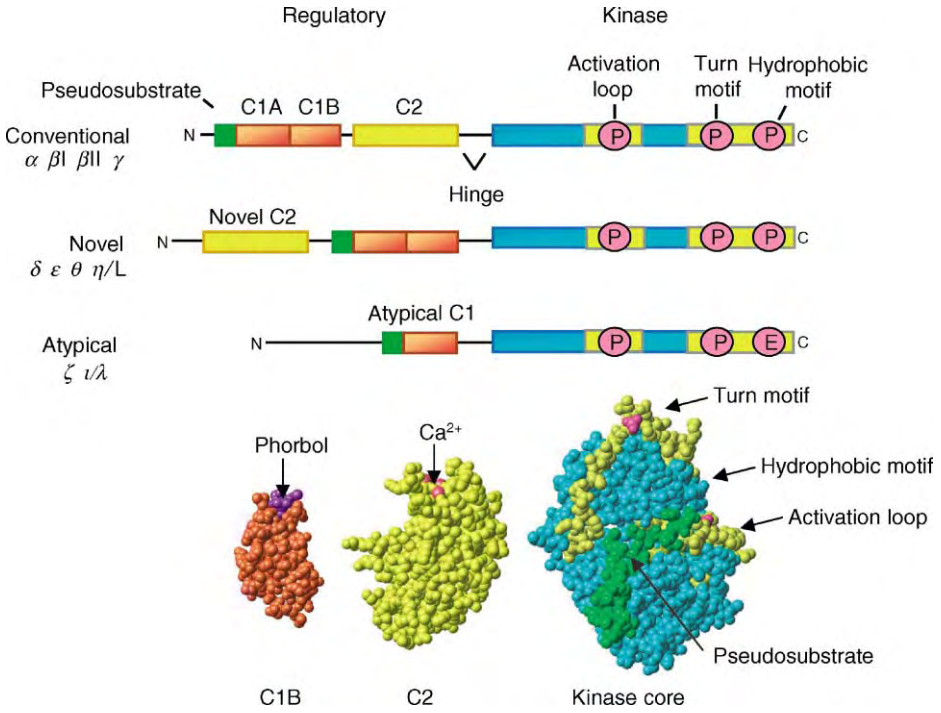

FIGURE 1 Primary structure and domain composition of protein kinase C family members. The amino terminal regulatory moiety contains the autoinhibitory pseudosubstrate sequence (green), the C1 domain, which binds diacylglycerol/phorbol esters (orange; present as a tandem repeat in conventional and novel protein kinase C isozymes), and the C2 domain, which binds Ca^{2+} (yellow). The C2 domain in novel protein kinase Cs and the C1 domain in atypical protein kinases are nonligand-binding variants. The carboxyl terminal catalytic moiety contains the kinase core which has two phosphorylation segments, the activation loop segment and the carboxyl-terminal segment (yellow), with a total of three phosphorylation sites (pink circles; the negatively charged amino acid glutamate (E) occupies the position of the phospho-acceptor position of the hydrophobic motif in atypical protein kinase Cs). The 3D structures of the domains are shown below the primary structure. Reproduced from Newton, A. C. (2003). Regulation of the ABC kinases by phosphorylation: Protein kinase C as a paradigm. *Biochem. J.* **370**, 361–371, by permission of the Biochemical Society.

This kinase has a pivotal position in cell signaling because it provides the activating phosphorylation to many other protein kinases, including the prosurvival kinase, Akt/protein kinase B. PDK-1 phosphorylates a conserved segment near the entrance to the active site referred to as the activation loop (Figure 1), an event that structures the active site for substrate binding and catalysis. The phosphorylation of the activation loop by PDK-1 triggers two intramolecular autophosphorylation reactions at two conserved positions in the carboxyl terminus, the turn motif, and hydrophobic motif (Figure 1). These phosphorylations lock protein kinase C in its mature and catalytically competent conformation. It is this species of protein kinase C that is activated by lipid hydrolysis and transduces signals.

Protein Kinase C Translocation

Mature (i.e., phosphorylated) protein kinase C is typically localized to the cytosol where it bounces on and off the membrane by diffusion-controlled mechanisms. It is maintained in an inactive conformation because the pseudosubstrate sequence occupies the substrate-binding cavity. For conventional protein kinase C isozymes, generation of Ca^{2+} and diacylglycerol target protein kinase C to the membrane by binding the C2 and C1 domains and thus tethering the enzyme to membranes. The membrane-bound species adopts an active conformation by removal of the pseudosubstrate from the substrate-binding cavity, allowing substrate binding, phosphorylation, and downstream signaling. Finding a membrane-embedded ligand (diacylglycerol) by diffusion from the cytosol is a low-probability event, and, in the case of conventional protein kinase Cs, nature has chosen a clever mechanism to increase the efficiency of this. Binding of Ca^{2+} to the C2 domain essentially pretargets protein kinase C to the membrane, where it can now initiate a much more effective search for its membrane-embedded ligand, diacylglycerol. As a consequence, conventional protein kinase Cs translocate to membranes ~1 order of magnitude faster than novel protein kinase C isozymes, which do not have the advantage of pretargeting by a Ca^{2+}-responsive C2 domain.

The advent of fluorescent methodologies has allowed imaging of protein kinase C translocation, and, most recently, activity in real time in living cells (Figure 2).

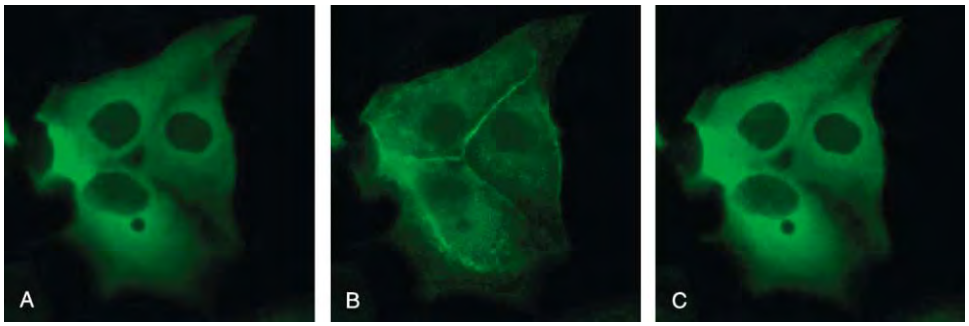

FIGURE 2 Protein kinase C was visualized in cells by expression of a construct of protein kinase C fused to a naturally fluorescent protein from the jellyfish *Aequorea victoria*, the green fluorescent protein (GFP). Panel A shows that protein kinase C is localized to the cytosol in unstimulated MDCK cells (diffuse fluorescence throughout the cell); panel B shows that protein kinase C translocates to the membrane (strong fluorescence intensity at cell peripheri) following 1 min of treatment with the agonist UTP, which induces phospholipid hydrolysis and generation of the two second messengers for protein kinase C:Ca^{2+} and diacyglycerol. Panel C shows that protein kinase C has redistributed back to the cytosol 5 min after UTP treatment; second messenger levels have returned to resting levels. Images courtesy of Jon Violin.

In general, protein kinase C translocation and activity mirrors the generation of its second messengers. For example, histamine stimulation of HeLa cells results in oscillations in protein kinase C substrate phosphorylation that are phase-locked with Ca^{2+} oscillations.

Protein Kinase C Scaffolds

Correct subcellular location is essential for normal signaling by protein kinase C. An abundance of scaffold proteins that tether protein kinase C near its substrates, activators, and regulatory proteins, such as phosphatases, has been described. The importance of correct subcellular location is perhaps best illustrated in the *Drosophila* visual cascade, where mutants lacking the protein kinase C-binding scaffold, InaD, are defective in visual transduction because components of the signaling cascade are mislocalized.

Protein Kinase C Downregulation

Prolonged activation of protein kinase C by treatment of cells with phorbol esters results in degradation of protein kinase C, a phenomenon referred to as down-regulation. In fact, prolonged treatment of cells with phorbol esters is a commonly used approach to deplete cells of all except atypical protein kinase Cs (these are resistant to phorbol ester-dependent down-regulation because they do not bind phorbol esters). The molecular mechanism of this down-regulation involves dephosphorylation of activated protein kinase C, followed most likely by ubiquitination and proteolysis. The molecular chaperone HSP70 has recently been shown to protect protein kinase C from down-regulation by allowing rephosphorylation of the enzyme and sustaining its signaling lifetime.

Protein Kinase C Signaling

Protein kinase C phosphorylates an abundance of substrates, including membrane proteins, cytoskeletal proteins, cytosolic proteins, and nuclear proteins. Yet identifying the precise cellular role and cellular targets of protein kinase C remains elusive. Genetic deletion of specific isozymes results in subtle phenotypic differences, suggesting functional redundancy of the isozymes. Nonetheless, sifting through the abundant studies on protein kinase C function reveals a few defined themes in addition to the general involvement in cell growth and proliferation. Notably, animals deficient in protein kinase C isozymes are deficient in adaptive responses. For example, mice lacking protein kinase C ε have reduced anxiety and have reduced tolerance to alcohol. Mice lacking protein kinase C γ have reduced pain perception, and mice lacking protein kinase C β II have reduced learning abilities and an impaired immune response. This theme carries over to the molecular level where many of the substrates of protein kinase C are receptors which become desensitized following phosphorylation by protein kinase C.

Isozyme-specific functions have been most clearly delineated for novel and atypical protein kinase C isozymes. For example, protein kinase C δ activation has been shown to play a role in apoptosis. Protein kinase C θ plays a key role in immune responses, and mice deficient in this isozyme have impaired T cell signaling and interleukin 2 production. Defined functions have also been established for protein kinase C ζ: this isozyme is required for maintenance of cell polarity and, in addition, regulates cell growth, DNA synthesis, and activation of the transcription factor, NFκB. Much less is known about defined physiological substrates and functions of conventional protein kinase C isozymes. Defining the precise raison d'etre for this

multi-membered class of kinases is one of the pressing issues in biological chemistry.

See Also the Following Articles

Calcium/Calmodulin-Dependent Protein Kinases • Glycine Receptors • Natriuretic Peptides and their Receptors • Neurotransmitter Transporters • Nicotinic Acetylcholine Receptors • Phosphoinositide 3-Kinase • Phospholipase C • Phospholipase D

Glossary

diacylglycerol The membrane-retained lipid backbone released from phospholipids following activation of appropriate phospholipases, enzymes that hydrolyze phospholipids. Diacylglycerol is considered a second messenger because it transfers information from stimuli such as hormones to protein kinase C, which transduces the signal by phosphorylating protein substrates.

kinase The class of enzymes that covalently transfer phosphate from ATP to hydroxyl groups of proteins.

phosphorylation The covalent attachment of phosphate from the cellular energy currency, ATP to hydroxyl residues of proteins, a modification that changes the properties of the protein.

Further Reading

Blumberg, P. M., Acs, G., Areces, L. B., Kazanietz, M. G., Lewin, N. E., and Szallasi, Z. (1994). Protein kinase C in signal transduction and carcinogenesis. *Prog. Clin. Biol. Res.* **387**, 3–19.

Kazanietz, M. G. (2002). Novel "nonkinase" phorbol ester receptors: The C1 domain connection. *Mol. Pharmacol.* **61**, 759–767.

Newton, A. C. (2000). Protein kinase C. In *Molecular Recognition* (P. M. Conn and A. R. Means, eds.) pp. 205–218. Humana Press, Totowa, NJ.

Newton, A. C. (2003). Regulation of the ABC kinases by phosphorylation: Protein kinase C as a paradigm. *Biochem. J.* **370**, 361–371.

Parker, P. J., and Parkinson, S. J. (2001). AGC protein kinase phosphorylation and protein kinase C. *Biochem. Soc. Trans.* **29**, 860–863.

Biography

Alexandra Newton is a Professor in the Department of Pharmacology at the University of California, San Diego, where her research team investigates the biology and chemistry of signaling by protein kinases, with particular focus on the molecular mechanisms of protein kinase C. She holds a Ph.D. in chemistry from Stanford University and received her postdoctoral training with Daniel E. Koshland, Jr., at the University of California, Berkeley.

Protein N-Myristoylation

Erica Dutil Sonnenburg and Jeffrey I. Gordon
Washington University School of Medicine, St. Louis, Missouri, USA

Protein N-myristoylation refers to the covalent attachment of myristic acid, a 14-carbon saturated fatty acid (C14:0), to the N-terminal glycine of proteins. Linkage occurs via an amide bond and takes place as proteins are being synthesized. N-myristoylproteins have varied intracellular destinations, and are involved in myriad cellular functions ranging from signal transduction to protein and vesicular trafficking. N-myristoylproteins are encountered in members of all Kingdoms of the eukaryotic domain (Protist, Fungi, Plant, and Animal) but are not produced by members of Bacteria or Archaea. MyristoylCoA:protein N-myristoyltransferase (Nmt), E.C. 2.3.1.97, a member of the GCN5 acetyltransferase (GNAT) superfamily, is responsible for catalyzing the transfer of myristate from myristoylCoA to proteins. While the acylCoA substrate specificity of Nmt has been highly conserved during evolution, its peptide substrate specificities have diverged among eukaryotes.

Protein N-myristoylation has relevance to a number of diseases. Genetic and pharmacologic studies have shown that Nmt activity is essential for the survival of a number of fungi that cause systemic infections in immunocompromised humans. These organisms include *Candida albicans* and *Cryptococcus neoformans*. Protein N-myristoylation is also critical to the life cycle of viruses, such as human immunodeficiency virus-1. Nmt levels are elevated in human gastrointestinal tract malignancies. Other pathogens, including *Plasmodium falciparum*, the parasite that causes malaria, have Nmts. Therefore, understanding the contributions of myristate to protein function, elucidating the structural basis for the divergent protein substrate specificities of orthologous Nmts, characterizing the myristoyl transfer reaction, and identifying biologically active, species-selective Nmt inhibitors may provide new therapeutic strategies and agents.

N-Myristoylproteins

Function of N-Myristoylation

Myristate exposed on the surface of a protein increases its lipophilicity, allowing transient, low-affinity interactions with cellular membranes or other proteins. This feature makes N-myristoylation an attractive choice for molecules involved in a variety of signaling cascades, such as protein kinases, kinase substrates, and protein phosphatases.

Myristate is not sufficiently hydrophobic to allow stable anchorage to cellular membranes. Therefore, most N-myristoylproteins utilize an additional mode of attachment. One supplementary membrane tether is provided by the reversible posttranslational covalent attachment of palmitate, a 16-carbon saturated fatty acid (C16:0), to cysteine (S-palmitoylation). Alpha subunits of heterotrimeric G proteins provide examples of this type of dual acylation. Other N-myristoylproteins, such as the protein tyrosine kinase Src, uses positively charged exposed residues to interact electrostatically with negatively charged groups in membrane lipids. Some N-myristoylproteins regulate their association with membranes through reversible exposure of their myristoyl moiety. Recoverin, a retinal photoreceptor protein involved in light adaptation, illustrates this "myristoyl-conformational switch": its myristoyl group is unfurled when the protein binds calcium; in the absence of calcium, the acyl chain is encased in a hydrophobic pocket.

Heterogeneous acylation is another device used by N-myristoylproteins to achieve regulated membrane association. Heterogenous acylation refers to Nmt-catalyzed linkage of tetradecanoate (C14:0), tetradecenoate (C14:1$^{\Delta 5}$), tetradecadienoate (C14:2$^{\Delta 5,8}$), or laurate (C12:0) to a substrate protein. At present, this phenomenon has only been described in retinal photoreceptor cells. Augmented production of these acyl-CoAs, and/or increased access of Nmt to these species, are among the mechanisms that have been invoked to account for the observed cell lineage-specificity of heterogenous acylation.

Examples of heterogeneously acylated proteins include recoverin, the α-subunit of the G protein transducin (Gtα), guanylyl cyclase activating protein, and the catalytic subunit of cAMP-dependent protein kinase. Lauric acid, and C14 fatty acids containing a *cis* double bond between C5–C6 (C14:1$^{\Delta 5}$) or C5–C6 and C8–C9 (C14:2$^{\Delta 5,8}$), have reduced hydrophobicity compared to C14:0. A less hydrophobic acyl chain may be required for these proteins to properly operate in photoreceptor cells,

either because of their extraordinarily high concentrations of membranes, and/or because the proteins require short-lived anchorage to membranes to rapidly transduce responses in visual signaling pathways.

Substrate Selection

Most proteins targeted for cotranslational N-myristoylation have an N-terminal consensus sequence of Met-Gly-X-X-X-Ser/Thr. The initiator methionine must first be removed from the nascent protein by another enzyme, methionylaminopeptidase, to expose the acceptor glycine. However, this consensus sequence is too general to allow definitive identification of Nmt substrates. Furthermore, in at least one case involving the pro-apoptotic protein BID, an internal myristoylation site is exposed after posttranslational proteolytic cleavage. Figure 1 provides a more detailed recognition consensus sequence that has been developed from an analysis of known N-myristoylproteins, as well as currently available X-ray crystal structures of Nmt.

There are a number of ways to establish that a protein is N-myristoylated, including metabolic labeling with tritiated or iodinated myristate, mass spectrometric analysis of the purified protein, or *in vitro* Nmt assays that contain the purified acyltransferase, myristoylCoA, and a peptide encompassing the N-terminal 8–15 residues of the candidate protein substrate. A current listing of experimentally confirmed as well as candidate N-myristoylproteins can be found at http://mendel.imp.univie.ac.at/myristate.

Escherichia coli containing a dual plasmid expression system has also been used widely to determine whether a protein is an Nmt substrate, and to study the functional significance of its myristoyl group. The system takes advantage of the fact that this bacterium is able to generate myristoylCoA but does not have any endogenous Nmt activity. The eukaryotic protein modification is recapitulated in this prokaryote by using one plasmid with an inducible promoter to direct expression of an Nmt, and another plasmid, containing a different inducible promoter, to express a candidate Nmt substrate. Production of Nmt is initiated first. Synthesis of the protein substrate is then turned on to allow for its cotranslational acylation. Incorporation of myristate can be verified by metabolic labeling or by mass spectrometry. The properties of the N-myristoylated protein can be compared and contrasted to that of the nonmyristoylated isoform produced in *E. coli* lacking the Nmt expression vector.

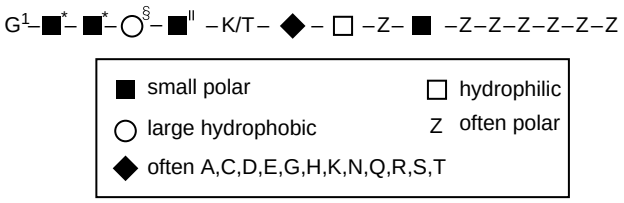

FIGURE 1 Consensus sequence for recognition of protein substrates by Nmt (*side chain volume compensation allowed; fungal Nmts allow hydrophobic residues; § some fungal Nmts prefer small residues; and ‖ often S or T). Figure based on Maurer-Strohl, S., Eisenhaber, B., and Eisenhaber, F. (2002). *J. Mol. Biol.* **317**, 523–540; 541–557.

N-Myristoyltransferase

Thus far, a total of 68 known and postulated Nmts have been identified from 63 species. Four mammalian genomes (*Homo sapiens*, *Mus musculus*, *Rattus norvegicus*, and *Bos Taurus*), plus a plant genome (the mustard weed *Arabidopsis thaliana*), contain two Nmt genes (designated type I and type II). Type I Nmts show a high degree of conservation among one another, as do the type II acyltransferases. Type I and II enzymes diverge most prominently at their N termini. These N-terminal domains are not required for catalytic activity *in vitro* but may help direct the acyltransferase to different intracellular sites. For example, the N terminus of type I human Nmt appears to be involved in its targeting to the ribosome.

Reaction Mechanism

The N-myristoyltransferase reaction mechanism has been characterized using the *Saccharomyces cerevisiae* enzyme as a model. *S. cerevisiae* Nmt contains 455 amino acids, is monomeric, and has no known cofactor requirements. Steady-state kinetics, isothermal titration calorimetrics, and X-ray crystallographic studies indicate that the enzyme has an ordered Bi–Bi reaction mechanism. The apo-Nmt first binds myristoylCoA to form a Nmt:myristoylCoA binary complex. MyristoylCoA binding allows subsequent binding of a nascent protein substrate to generate a Nmt:myristoylCoA:peptide ternary complex. Following the chemical transformation step (conversion of the enzyme:substrate complex to the enzyme:product complex), CoA and then myristoylpeptide are released. Pre-steady-state kinetic studies indicate that the rate determining step occurs after the chemical transformation, most likely involving release of myristoylpeptide.

Catalysis occurs through a classic nucleophilic addition–elimination reaction where the nucleophilic N-terminal Gly amine of the peptide substrate attacks the polarized thioester carbonyl of myristoylCoA. Several elements in the enzyme's active site facilitate this reaction. An oxyanion hole, formed by the backbone amides of two conserved residues, Phe170

and Leu171, polarizes the reactive carbonyl of myristoylCoA. The C-terminal carboxylate (Leu455 in the yeast enzyme) functions as a catalytic base to deprotonate the Gly1 ammonium to a nucleophilic amine. The amine rotates 180Å along Ψ to reduce its distance from the thioester carbonyl of myristoylCoA. H-bonding interactions between the Gly1 amine, Asn169, and Thr205 help direct the reaction trajectory, and facilitate nucleophilic attack of the polarized carbonyl. The oxyanion hole, together with the H-bonding network formed by Asn169 and Thr205, stabilizes the developing tetrahedral intermediate. With subsequent collapse of the intermediate, CoA is extruded. The Gly1 amine is deprotonated, while the thiolate leaving group of CoA is reprotonated (see www.jbc.org/cgi/content/full/276/43/39501/DC1 for an animated schematic of the reaction mechanism).

Three-Dimensional Structure of NMT: Insights about Substrate Recognition/Acquisition and Release

Presently, three X-ray crystal structures of *S. cerevisiae* Nmt have been reported: a binary complex containing bound myristoylCoA (Protein Data Bank (PDF) (www.rcsb.org/pdb/) accession 1IIC), plus two ternary complexes – one with a peptide substrate and S-(2-oxo)pentadecylCoA (a nonhydrolyzable myristoylCoA analogue containing a methylene interposed between the sulfur of CoA and the carbonyl of myristate; PDF 1IID), the other with S-(2-oxo)pentadecylCoA and a dipeptide inhibitor (PDB, 2NMT). In addition, three structures of *C. albicans* Nmt are available: the apo-enzyme (PDB, 1NMT), the enzyme with bound myristoylCoA and peptidic inhibitor (PDB, 1IYK), and the enzyme with a bound benzofuran inhibitor (PDB, 1IYL).

The Nmt fold consists of a large saddle-shaped β-sheet with several α-helices located on either side (Figure 2). There is pseudo-twofold symmetry. The N-terminal half forms the myristoylCoA binding site while the C-terminal half contributes to peptide recognition. The N terminus is disordered.

Binding of myristoylCoA induces two important conformational changes. A 3_{10} helix (A′ in Figure 2) is formed from part of the disordered N terminus, to complete the myristoylCoA binding site. There is also a change in the conformation of a loop connecting helix A and strand b (Ab loop), thereby opening a "lid" overlying the peptide binding site. The pantetheine group of CoA forms a key component of the peptide recognition site. Together, these observations indicate why myristoylCoA binding is a prerequisite for subsequent acquisition of a nascent protein substrate.

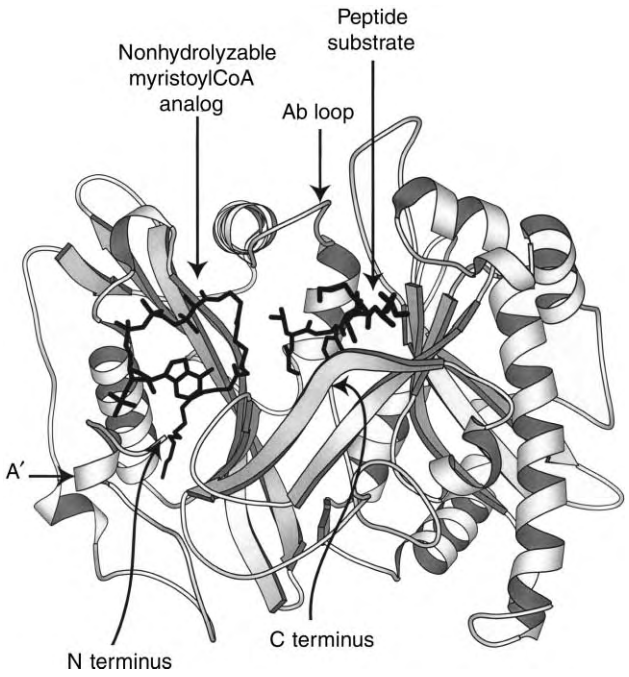

FIGURE 2 Ribbon diagram of *S. cerevisiae* Nmt. The enzyme is shown with a S-(2-oxo)pentadecylCoA, a non-hydrolyzable myristoylCoA analog and competitive inhibitor, and an octapeptide substrate (GlyLeuTyrAlaSerLysLeuAla) derived from the N terminus of ADP ribosylation factor 2 (Arf2). Binding of the myristoylCoA induces ordering of a 3_{10} helix (A′), a change in the conformation of the Ab loop, and completion of the peptide binding site. The C-terminal carboxylate (Leu455) functions as a catalytic base to deprotonate the Gly1 ammonium to a nucleophilic amine.

MyristoylCoA is bound to Nmt in a conformation that resembles a question mark (Figure 2). Nmt uses residues that produce bends at C1 and C6 of the bound myristoyl chain, as well as the floor of its acylCoA binding pocket, to measure and properly position myristoylCoA. Available X-ray structures indicate that the two additional methylenes present in palmitoylCoA cannot be accommodated by the enzyme without adversely affecting positioning of its thioester carbonyl within the oxyanion hole.

The X-ray structures suggest that the extent of ordering of the Ab loop may correlate with the overall catalytic efficiency of different Nmt peptide substrates, and that the rate limiting step in the Nmt reaction is an isomerization involving reversal of the conformational changes that take place when myristoylCoA is bound. In other words, disordering of the 3_{10} A′ helix and opening the lid formed by the Ab loop.

Therapeutics

Alignments of known Nmts disclose that their N-terminal halves are more conserved than

their C-terminal halves. This finding is consistent with their shared specificity for myristoylCoA, and with the divergent nature of their protein substrate specificities. Exploiting the differences in peptide recognition among Nmts may be key to developing species-specific inhibitors. This divergence, and the fact that genetic experiments have established that pathogenic fungi such as *C. albicans* and *C. neoformans* require Nmt for their survival, make N-myristoyltransferase an attractive target for developing new classes of fungicidal agents. The need for such agents is great given the limited number of existing drugs that effectively kill these organisms, and the increasing resistance being encountered to these available compounds.

Several classes of Nmt-targeted anti-fungal agents have been identified to date. Peptidomimetic inhibitors have been produced starting from an octapeptide substrate representing the N terminus of *S. cerevisiae* ADP ribosylation factor 2 (Arf2) (involved in vesicular trafficking). Benzofuran inhibitors have emerged from high throughput screens of chemical libraries. These benzofurans have several advantages over the Arf-derived compounds – smaller size, increased bio-availability, and resistance to degradation. Crystallographic studies of *C. albicans* Nmt revealed that one of the lead benzofurans was positioned in a hydrophobic pocket located within the enzyme's peptide substrate binding site. Using this structural information, a more biologically active derivative, substituted with difluorophenoxy- and pyridyl-terminated side chains, was created that inhibits fungal growth in a rat model of systemic Candidiasis. Further screens for compounds that display specificity for fungal compared to human Nmts are likely to yield additional classes of fungicidal compounds in the future.

See Also the Following Articles

Lipid Modification of Proteins: Targeting to Membranes • Src Family of Protein Tyrosine Kinases

Glossary

heterogeneous acylation Nmt-catalyzed attachment of the following acyl chains having somewhat lower hydrophobicity than C14:0: tetradecenoate (C14:1$^{\Delta 5}$), tetradecadienoate (C14:2$^{\Delta 5,8}$) or laurate (C12:0). At present, this modification is only known to occur in retinal photoreceptor cells.

N-myristoylproteins This diverse group of covalently modified proteins use their acyl chain to promote a variety of readily reversible interactions with various cellular membranes or with other proteins. The stability of their interactions can be regulated by other modifications, including conformational changes that affect the presentation of the myristoyl moiety, post-translational acylation at other sites with other lipids, or charge–charge interactions mediated by protein side chain atoms.

N-myristoyltransferase (Nmt) An enzyme that catalyzes the linkage of myristate, via an amide bond, to the N-terminal glycine amine of cellular proteins. Catalysis occurs through the nucleophilic addition–elimination reaction. The acyl chain length specificity of the enzyme has been highly conserved during evolution while its peptide substrate specificity has diverged among species. Nmt is a target for the development of drugs against fungal and other human pathogens.

protein N-myristoylation The covalent attachment of myristate, a 14-carbon saturated fatty acid (C14:0), to the N-terminal glycine residue of eukaryotic proteins.

Further Reading

Ames, J. B., Ishima, R., Tanaka, T., Gordon, J. I., Stryer, L., and Ikura, M. (1997). Molecular mechanics of calcium-myristoyl switches. *Nature* **389**, 198–202.

Devadas, B., Freeman, S. K., McWherter, C. A., Kishore, N. S., Lodge, J. K., Jackson-Machelski, E., Gordon, J. I., and Sikorski, J. A. (1998). Novel biologically active nonpeptidic inhibitors of myristoylCoA: Protein N-myristoyltransferase. *J. Med. Chem.* **41**, 996–1000.

Ebiike, H., Masubuchi, M., Liu, P., Kawasaki, K., Morikami, K., Sogabe, S., Hayase, M., Fujii, T., Sakata, K., Shindoh, H., Shiratori, Y., Aoki, Y., Ohtsuka, T., and Shimmma, N. (2002). Design and synthesis of novel benzofurans as a new class of antifungal agents targeting fungal N-myristoyltransferase. *Bioorg. Med. Chem. Lett.* **12**, 607–610.

Farazi, T. A., Manchester, J. K., Waksman, G., and Gordon, J. I. (2001). Pre-steady state kinetic studies of *Saccharomyces cerevisiae* myristoylCoA: Protein N-myristoyltransferase reveal that a step after chemical transformation is rate limiting. *Biochemistry* **40**, 9177–9186.

Georgopapadakou, N. H. (2002). Antifungals targeted to protein modification: Focus on protein N-myristoyltransferase. *Expert Opin. Invest. Drugs* **11**, 1117–1125.

Johnson, R. S., Ohguro, H., Palczewski, K., Hurley, J. B., Walsh, K. A., and Neubert, T. A. (1994). Heterogeneous N-acylation is a tissue- and species-specific post-translational modification. *J. Biol. Chem.* **269**, 21067–21071.

Lodge, J. K., Jackson-Machelski, E., Toffaletti, D. L., Perfect, J. R., and Gordon, J. I. (1994). Targeted gene replacement demonstrates that myristoylCoA: Protein N-myristoyltransferase is essential for the viability of *Cryptococcus neoformans*. *Proc. Natl. Acad. Sci. USA* **91**, 12008–12012.

Maurer-Strohl, S., Eisenhaber, B., and Eisenhaber, F. (2002). N-terminal N-myristoylation of proteins: prediction of substrate proteins from amino acid sequence. *J. Mol. Biol.* **317**(4): 541–547. N-terminal N-myristoylation of proteins: refinement of the sequence motif and its taxon-specific differences. *J. Mol. Biol.* **317**(4): 523–540.

Weinberg, R. A., McWherter, C. A., Freeman, S. K., Wood, D. C., Gordon, J. I., and Lee, S. C. (1995). Genetic studies reveal that myristoylCoA: protein N-myristoyltransferase is an essential enzyme in *Candida albicans*. *Mol. Microbiol.* **16**, 241–250.

Weston, S. A., Camble, R., Colls, J., Rosenbrock, G., Taylor, I., Egerton, M., Tucker, A. D., Tunnicliffe, A., Mistry, A., Mancia, F., de la Fortelle, E., Irwin, J., Bricogne, G., and Pauptit, R. A. (1998). Crystal structure of the antifungal target N-myristoyltransferase. *Nat. Struct. Biol.* **5**, 213–221.

Biography

Erica Dutil Sonnenburg is an Instructor in the Department of Molecular Biology and Pharmacology at Washington University School of Medicine in St. Louis. She holds a Ph.D. from the University

of California, San Diego in biomedical sciences and received her postdoctoral training at the Salk Institute for Biological Study in structural biology.

Jeffrey Gordon is the Dr. Robert J. Glaser Distinguished University Professor and Head of the Department of Molecular Biology and Pharmacology. He received his M.D. from the University of Chicago. In addition to characterizing the enzymology and biological significance of protein N-myristoylation, his laboratory uses mouse models to study gut development and the contributions of its indigenous microbial communities to health.

Protein Palmitoylation

Robert J. Deschenes
University of Iowa, Iowa City, Iowa, USA

Palmitoylation is the covalent modification of proteins with 16 carbon acyl chains related to palmitic acid. Protein palmitoylation was first described in the 1970s and is now recognized as a major form of posttranslational modification in all eukaryotes, with a few examples in prokaryotes as well. In many cases palmitoylation is a reversible modification, suggesting that the cell uses it to regulate protein function. This article will focus on the enzymology and functional significance of protein palmitoylation.

Covalent Modification of Proteins with Palmitoyl Groups

Palmitoylation refers to a family of protein modifications involving palmitic acid (Figure 1). The most common forms of palmitoylation are S-palmitoylation and N-palmitoylation. S-palmitoylation occurs on cysteine residues and involves a thioester linkage. In the cases where it has been investigated, S-palmitoylation is a reversible modification. Examples include receptors, signaling proteins, and scaffold proteins. N-palmitoylation reactions occur on the amino terminus or on the epsilon amino group of lysine. Reports of esterification of palmitate with serine and threonine residues (O-palmitoylation) have appeared for myelin proteolipids, however, other studies conclude that myelin proteolipids are S-palmitoylated. Protein palmitoylation is generally detected by labeling cells or cell extracts with [^{3}H]-palmitate. Identification of the covalently linked lipid is done by chemical or enzymatic cleavage followed by HPLC analysis. In most cases, palmitate is found, but in some cases unsaturated forms of palmitate are also detected. An estimate of the total extent of protein palmitoylation in the cell is difficult to obtain because of the rapid reversibility of palmitoylation and the chemical lability of thioesters. Proteomic methods that account for posttranslational modifications have begun, but application to lipid modifications needs further development. However, based on the growing list of palmitoylated proteins reported it is clear that palmitoylation is a significant posttranslational modification.

Palmitoyltransferases

There has been a debate concerning whether palmitoylation is spontaneous or enzyme mediated. The thiol of cysteine is capable of serving as a nucleophile in a spontaneous S-acylation reaction using palmitoyl-CoA as the acyl donor. However, it is difficult to know whether spontaneous palmitoylation occurs *in vivo*. It is more likely that protein acyltransferase(s) (PAT) are responsible for palmitoylation under physiological conditions. In fact, PAT activities have been reported that cofractionate with the plasma membrane and endomembranes suggesting that either there is ubiquitous expression of a single PAT or multiple PATs with distinct subcellular distributions. The recent discovery of protein PATs in model organisms has begun to shed light on this question.

Plasma membrane localization of Ras requires palmitoylation of a conserved cysteine located close to the C terminus. Palmitoylation is associated with the translocation of Ras from the endoplasmic reticulum (ER) to the plasma membrane where it functions in signaling. A genetic screen was carried out in yeast to identify mutants affecting Ras palmitoylation. Mutations in two genes, *ERF2* and *ERF4*, were identified. Lobo and co-workers found Erf2p and Erf4p form a complex that together carries out the enzymatic palmitoylation of Ras. The new enzyme is called Ras PAT. Erf2p has a conserved domain referred to as a DHHC–CRD motif (Pfam designation zfDHHC). Another yeast DHHC–CRD protein, Akr1p, has been shown to be the PAT for yeast casein kinase, Yck2p. Thus, Erf2p/Erf4p and Akr1p are founding members of a new class of S-PATs. The DHHC–CRD motif is found in six other yeast proteins, ~23 human proteins, and all other organisms examined.

Not all palmitoylated proteins are intracellular. The *Drosophila* secretes signaling molecules Hedgehog and Wnt, which are also palmitoylated. Again, genetic screens led to a candidate PAT. The gene goes by the names *skinny hedgehog* (*ski*), *sightless* (*sit*), *or rasp* depending on the group that isolated the mutation. A clue to the function came from a short region of sequence similarity with O-acyltransferases. Members

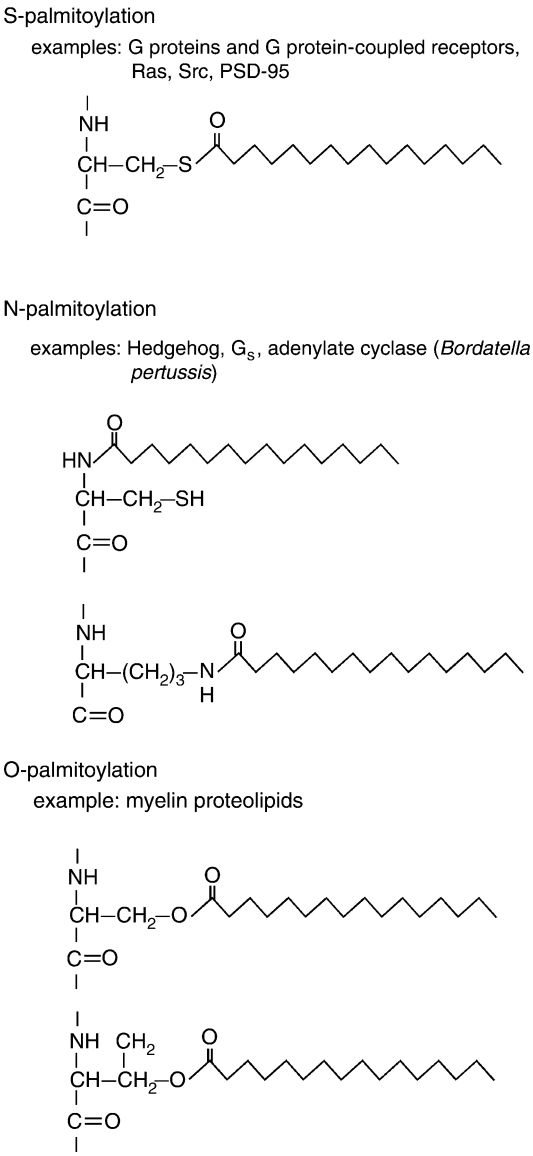

FIGURE 1 The three major classes of covalent attachment of palmitate in proteins. Representative examples of each type are listed.

of this family transfer fatty acids onto hydroxyl groups of nonproteinaceous targets. Mutation of residues in the conserved domain of *ski*/*sit*/*rasp* results in loss of Hedgehog palmitoylation and signaling. Biochemical studies are still needed to confirm that *ski*/*sit*/*rasp* is a PAT and to elucidate the mechanism.

The Wnt proteins are cysteine-rich secreted glycoproteins that have recently been shown to be palmitoylated on conserved cysteine. The modification could be removed by an acylprotein thioesterase (APT1) consistent with it being a thioester. Sequence alignment of Wnt family members reveals that this is the first cysteine residue in the sequence that is conserved in all family members. Thus, palmitoylation is likely to be found on all Wnt signaling proteins. Enzymatic depalmitoylation of purified Wnt3a protein results in the loss of its ability to stabilize β-catenin in mouse L cells, a measure of the Wnt signaling pathway. *porcupine* (*por*) is a segment polarity gene in *Drosophila* that is required for processing and secretion of Wingless (Wg). In *por* mutants, Wg is confined to cells where it is synthesized. Like *skinny hedgehog* (*ski*)/*sightless* (*sit*)/*rasp*, porcupine shares sequence homology with O-acyltransferases making it an excellent candidate for the Wnt PAT.

Palmitoylthioesterases

Given the reversible nature of protein palmitoylation, thioesterases are predicted to play an important regulatory role. However, the first protein thioesterases identified, PPT1 and PPT2, are apparently involved in protein turnover. PPT1 is found in lysosomes and mutations that reduce or eliminate its expression causes a severe neurodegenerative disorder, infantile neuronal ceroid lipofuscinosis (INCL). INCL is formally classified as a lysosomal-storage disorder. The neurological phenotype arising from a deficiency of PPT thioesterases is likely to be caused by the accumulation of palmitoyl peptides or palmitoylcysteine.

A cytosolic palmitoyl protein thioesterase, APT1, was discovered in rat liver extracts. APT1 was originally described as a lysophospholipase, but Duncan and Gilman showed that APT1 cleaves thioesters in acyl-CoAs and acylproteins, as well as oxyesters in lysolipids. In fact, APT1 exhibits a strong substrate preference for acylproteins over lipid substrates consistent with a role for APT1 as a regulator of protein thioacylation and not as a regulator of lipid metabolism. A number of substrates have been proposed for APT1 including G_α-subunits, Ras, and eNOS. APT1 orthologues have been identified in a large number of species, ranging from yeast to humans.

Palmitoylation and Protein Function

The functional significance of reversible palmitoylation depends on the protein under consideration. For peripheral membrane/cytosolic proteins lipid addition can be the primary determinant of membrane recruitment. It can also specify a particular membrane or microdomain of a membrane. A theme that has emerged from many studies is that palmitoylation operates along with other lipid modifications or membrane association sequences. Ras proteins are a case in point. Farnesylation of the C-terminal C*aaX* box targets H-Ras and N-Ras to the cytosolic surface of the ER membrane where it is further processed by a C*aaX* box protease

and methyltransferase. Plasma membrane localization of H-Ras requires palmitoylation by the Erf2p/Erf4p Ras PAT. Once at the plasma membrane, H-Ras reversibly associates with microdomains believed to be involved in signaling. There is intense interest in defining the nature of this microdomain and the role of palmitoylation in Ras signaling.

Reversible palmitoylation also influences the subcellular trafficking of integral membrane proteins. For example, receptor endocytosis and recycling is often controlled by palmitoylation status. In viral infected cells, palmitoylation directs Env proteins to lipid rafts where viral assembly occurs. In addition to surface expression and stability, palmitoylation has been proposed to play a role in signaling of some receptors. Palmitoylation can effect signaling by altering effector binding. For example, mutations in the palmitoylation site on the cytoplasmic tail of the β-adrenergic receptor leads to uncoupling of the receptor, its cognate G protein.

Palmitoylation also plays a role in vesicle trafficking and membrane fusion. Palmitoyl-CoA is required for efficient vesicle fusion in cell free assays. It is generally believed that palmitoylation of a specific protein or proteins accounts for this requirement. A possible candidate has emerged from the study of vacuole inheritance in yeast. Vac8p is a myristoylated and palmitoylated peripheral membrane protein that is required for vacuole inheritance. Palmitoylation, but not myristoylation, is required for Vac8p function. Palmitoylation of Vac8p may be involved in the interaction of Vac8p with vacuole specific SNARE complexes.

Not all palmitoylation is involved with membrane-mediated processes. Mitochondrial methylmalonyl semialdehyde dehydrogenase is covalently modified by palmitate on an active site cysteine residue. Insertion of [^{125}I]-labeled analogue of myristoyl-CoA at this site results in enzyme inhibition. This observation, together with other results that palmitoyl-CoA inhibits the activity of several mitochondrial enzymes suggests a regulatory role of S-acylation in metabolism.

Palmitoylation Inhibitors

The role of palmitoylation in cellular processes has been investigated using inhibitors such as 2-bromo or 2-fluoropalmitate, cerulenin, and tunicamycin. Each inhibits protein palmitoylation, but their mechanisms of action may differ. Cerulenin inhibits fatty acid synthase, but analogues with selectivity toward PATs are being developed and tested. Tunicamycin is a fatty acyl-CoA analogue and has been found to reduce protein palmitoylation without significantly affecting palmitoyl-CoA levels. In some cases 2-flouropalmitate has been shown to decrease uptake of [^{3}H]palmitate and thereby lower the levels of labeled palmitoyl-CoA levels and apparent protein palmitoylation. The recent identification of palmitoyltransferases should allow a more detailed characterization of these inhibitors and the development of new inhibitors with specificity toward the different classes of palmitoylated proteins.

Concluding Remarks

Protein palmitoylation has emerged as an important posttranslational modification used by cells to organize the subcellular distribution of proteins on membranes. The study of protein palmitoylation has entered a new phase with the identification of PATs in yeast and *Drosophila*. As the tools develop, the role of protein palmitoylation, in the cellular physiology, should come into better focus. PATs may be excellent targets for the design of drugs that alter the subcellular distribution of receptors and signaling molecules.

See Also the Following Articles

Fatty Acid Oxidation • Fatty Acid Receptors • Fatty Acid Synthesis and its Regulation • Lysophospholipid Receptors • Protein N-Myristoylation • Ras Family

Glossary

DHHC–CRD motif A protein sequence motif that is associated with the class of palmitoyltransferase that carries out the S-palmitoylation of proteins.

palmitoylation The process by which proteins become covalently modified by long-chain fatty acids related to palmitic acid.

palmitoylthioesterase An enzyme that cleaves palmitate from S-palmitoylated proteins.

protein acyltransferarse (PAT) An enzyme that carries out the palmitoylation of proteins.

Further Reading

Bijlmakers, M. J., and Marsh, M. (2003). The on–off story of protein palmitoylation. *Trends Cell Biol.* **13**, 32–42.

Chamoun, Z., Mann, R. K., Nellen, D., von Kessler, D. P., Bellotto, M., Beachy, P. A., and Basler, K. (2001). Skinny hedgehog, an acyltransferase required for palmitoylation and activity of the hedgehog signal. *Science* **293**, 2080–2084.

El-Husseini Ael, D., and Bredt, D. S. (2002). Protein palmitoylation: A regulator of neuronal development and function. *Nat. Rev. Neurosci.* **3**, 791–802.

Duncan, J. A., and Gilman, A. G. (1998). A cytoplasmic acyl-protein thioesterase that removes palmitate from G protein alpha subunits and p21 (RAS). *J. Biol. Chem.* **273**, 15830–15837.

Hancock, J. F. (2003). Ras proteins: Different signals from different locations. *Nat. Rev. Mol. Cell Biol.* **4**, 373–384.

Lee, J. D., and Treisman, J. E. (2001). Sightless has homology to transmembrane acyltransferases and is required to generate active Hedgehog protein. *Curr. Biol.* **11**, 1147–1152.

Linder, M. E. (2001). Reversible modification of proteins with thioester-linked fatty acids. In *The Enzymes: Protein Lipidation*, (F. Tamanoi and D. S. Sigman, eds.) Vol XXI, pp. 215–240. Academic Press, San Diego.

Linder, M. E., and Deschenes, R. J. (2003). New insights into the mechanisms of protein palmitoylation. *Biochemistry* **42**, 4311–4320.

Lobo, S., Greentree, W. K., Linder, M. E., and Deschenes, R. J. (2002). Identification of Ras palmitoyltransferase in *Saccharomyces cerevisiae*. *J. Biol. Chem.* **277**, 41268–41273.

Micchelli, C. A., The, I., Selva, E., Mogila, V., and Perrimon, N. (2002). Rasp, a putative transmembrane acyltransferase, is required for Hedgehog signaling. *Development* **129**, 843–851.

Nusse, R. (2003). Wnts and Hedgehogs: Lipid-modified proteins and similarities in signaling mechanisms at the cell surface. *Development* **130**, 5297–5305.

Resh, M. D. (1999). Fatty acylation of proteins: New insights into membrane targeting of myristoylated and palmitoylated proteins. *Biochim. Biophys. Acta* **1451**, 1–16.

Roth A. F., Feng, Y., Chen, L., and Davis, N. G. (2002). The yeast DHHC cysteine-rich domain protein Akrlp is a palmitoyl transferase. *J. Cell Biol.* **159**, 23-28.

Thompson, Jr. G. A., and Okuyama, H. (2000). Lipid-linked proteins of plants. *Prog. Lipid Res.* **39**, 19–39.

Biography

Robert Deschenes is a Professor in the Department of Biochemistry at the Carver College of Medicine, University of Iowa, Iowa City, Iowa. His research interests focus on signal transduction pathways that regulate eukaryotic cell growth, with an emphasis on the Ras oncogene. He holds a Ph.D. in biochemistry from Purdue University and was an Anna Fuller Cancer Fund Postdoctoral Fellow in the Molecular Biology Department of Princeton University. He is a member of the American Society of Biochemistry and Molecular Biology.

Protein Tyrosine Phosphatases

David J. Pagliarini, Fred L. Robinson and Jack E. Dixon
University of California, San Diego, California, USA

The process of reversible phosphorylation is perhaps the cell's most prevalent means of regulation at the molecular level. It has been estimated that up to 30% of all cellular proteins are phosphorylated, and phosphorylation has been shown to play a crucial regulatory role in such diverse cellular events as metabolism, growth and differentiation, vesicular transport, and gene transcription. Phosphorylation and dephosphorylation are carried out by kinases and phosphatases, respectively. There are currently predicted to be 518 kinases and ~125 phosphatases encoded in the human genome, further underscoring the overall importance of phosphorylation in molecular regulation. Phosphatases are generally divided into two main families based on their catalytic mechanism and substrate specificity: the protein phosphatases (PPs), which exclusively desphosphorylate serine and threonine residues, and the protein tyrosine phosphatases (PTPs), which can dephosphorylate tyrosine residues, and are the focus of this article. PTPs can be further classified into subfamilies based on (1) subcellular location (receptor versus intracellular), (2) substrate preference, and (3) three-dimensional topology. In this article, we describe the different subfamilies of PTPs and their conserved catalytic mechanism. In addition, human diseases that result from disrupted PTP signaling, and the pursuit of PTPs as drug targets are discussed.

Catalytic Mechanism of PTPs

PTPs, regardless of subfamily, are predicted to use similar mechanisms for catalyzing the removal of a phosphate group. All PTPs possess a catalytic domain that contains the active site signature motif cysteine-X_5-arginine (CX_5R; X = any amino acid), which constitutes the phosphate-binding pocket, or "P-loop". The dephosphorylation reaction is initiated when the thiol nucleophile of the active site cysteine attacks the phosphate group on the substrate molecule, forming a cysteinyl-phosphate intermediate (Figure 1). A conserved aspartic acid, usually residing outside of the P-loop, then acts as a general acid to aid in the ejection of the substrate molecule. In the second step of the reaction, the phosphoenzyme intermediate is hydrolyzed by a water molecule that has been activated by the aspartate, thereby releasing free phosphate and regenerating the active enzyme.

Classification of Protein Tyrosine Phosphatases

Intracellular PTPs

PTPs

PTPs can be classified as receptor-like (RPTPs) or intracellular based on their location within a cell. Whereas all RPTPs to date exhibit specificity towards phosphotyrosine substrates (referred to as "classic" PTPs), intracellular PTPs can be classic or dual-specific (DS-PTPs), having the ability to dephosphorylate serine/threonine, RNA, or inositol lipids in addition to pTyr (Figure 2). The major distinguishing factor between classic and dual-specific PTPs appears to be the depth of the substrate-binding pocket, with DS-PTPs having a shallower landscape less conducive to the binding of the long side chain of tyrosine. A series of structural studies over the past decade have revealed that all PTPs possess one of three distinct topologies (Figure 3). This first and largest topological family, referred to simply as PTPs, includes all of the RPTPs, such classic PTPs as PTP1B and the *Yersinia* PTP, and DS-PTPs such as VHR and PTEN, among others (Figure 2).

CDC25 family

The CDC25 family is a set of DS-PTPs involved in the regulation of the cell cycle. Each enzyme of this family is highly specific for a particular serine or threonine residue on a cyclin-dependent kinase/cyclin complex. Although presence of the signature CX_5R motif suggests a common catalytic mechanism, the PTP domains of these enzymes share little sequence homology with other PTPs (Figure 3).

LMW-PTPs

The third family of topologically distinct CX_5R phosphatases is the low-molecular-weight phosphatases

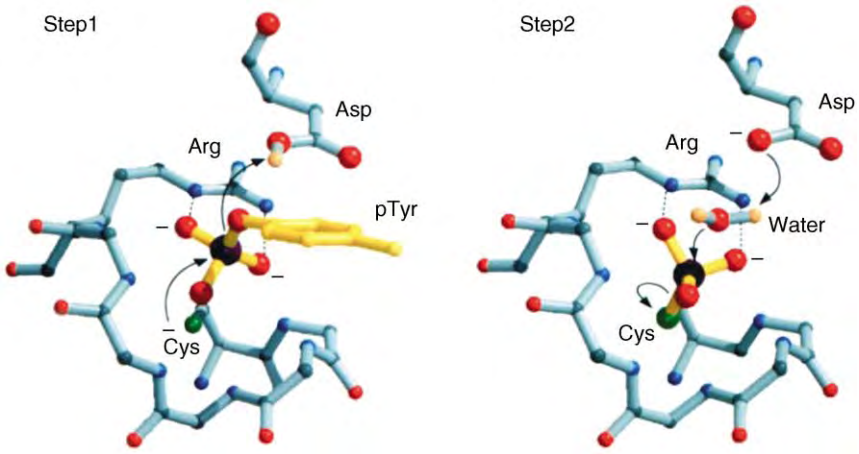

FIGURE 1 Catalytic mechanism of protein tyrosine phosphatases. Step 1: A thiolate anion of the active site cysteine performs a nucleophilic attack on the phosphate of phosphoryl-tyrosyl substrates, resulting in the formation a phospho-enzyme intermediate. An aspartic acid, acting as a general acid, donates a proton to the phosphate group, ejecting the tyrosine side chain. Hydrogen bonds between phosphate oxygen atoms and nitrogen atoms of the arginine guanido group promote phosphate binding and stabilize the transition state. Step 2: Acting as a general base, aspartate activates a water molecule for a nucleophilic attack on the phosphorous atom. The phosphorous–sulfur bond is hydrolyzed, thus regenerating the native enzyme. (Reproduced from Denu, J. M., Stuckey, J. A., Saper, M. A., and Dixon, J. E. (1996). Form and function in protein dephosphorylation. *Cell* **87**, 361–364.)

(LMW-PTPs). Conservation of the catalytic cysteine, arginine, and aspartic acid residues strongly suggests that these enzymes also utilize a similar catalytic mechanism. As with the CDC25 family, however, LMW-PTPs show no homology with other PTPs, and a lack of any other domains outside of their small (~150 amino acids) PTP domain provides few clues to their *in vivo* function. All LMW-PTPs examined to date have been specific for tyrosine-phosphorylated substrates.

Receptor-Like Tyrosine Phosphatases

Receptor-like tyrosine phosphatases (RPTPs) possess an extracellular receptor-like domain, a single transmembrane domain, and one or two intracellular classic tyrosine-specific PTP domains. Where two PTP domains exist, the membrane proximal domain accounts for the majority of catalytic activity. Based on their active site homology and common features of their extracellular domains, RPTPs can be further subdivided into eight subtypes: R1/R6, R2A, R2B, R3, R4, R5, R7, and R8 (Figure 2). The CD45 family (R1/R6) are expressed on nucleated hematopoietic cells and are thought to be involved in the positive regulation of antigen receptor signaling via dephosphorylation of the Src family kinases. RPTPs ρ, μ, κ, and λ (R2A) are marked by an extracellular MAM and an intracellular Cahedrin-like domains. They also possess extracellular fibronectin type III-like repeats and an immunoglobulin-like domain on their extracellular region that are involved in cell adhesion. The LAR-like PTPs (R2B) are primarily expressed in neuronal cells where they are thought to play an important role in neuronal development. They are marked by tandem repeats of immunoglobulin-like and fibronectin type III-like domains resembling neuronal adhesion molecules. Members of the R3 subfamily, e.g., the mammalian OST-PTP, possess multiple fibronectin type III repeats resembling cell adhesion molecules such as collagen type VII, fibronectin, and tenascin. PTP α and PTP ε (members of R4) are marked by their relatively small, highly glycosylated extracellular domains. PTP γ and PTP ζ represent the R5 subfamily, which have a carbonic anhydrase-like domain. RPTPs possessing a meprin domain in addition to immunoglobulin-like and fibronectin type III-like repeats comprise R6. Members of the R7 subfamily possess no additional extra- or intracellular domains, and the more evolutionarily distant R8 family members are predicted to be catalytically inactive.

PTPs and Human Disease

Involvement of PTPs in Mammalian Biology and Disease

At least 18 human protein tyrosine kinases (PTKs) have been shown to behave as oncoproteins when inappropriately activated by mutation. Given this, it was expected that PTPs, which can terminate tyrosine kinase signaling, might be found as genes frequently mutated in cancers. This has generally not proven to be the case. However, links between specific PTPs and human genetic diseases have been, and are continuing to be, established. In addition, numerous studies involving

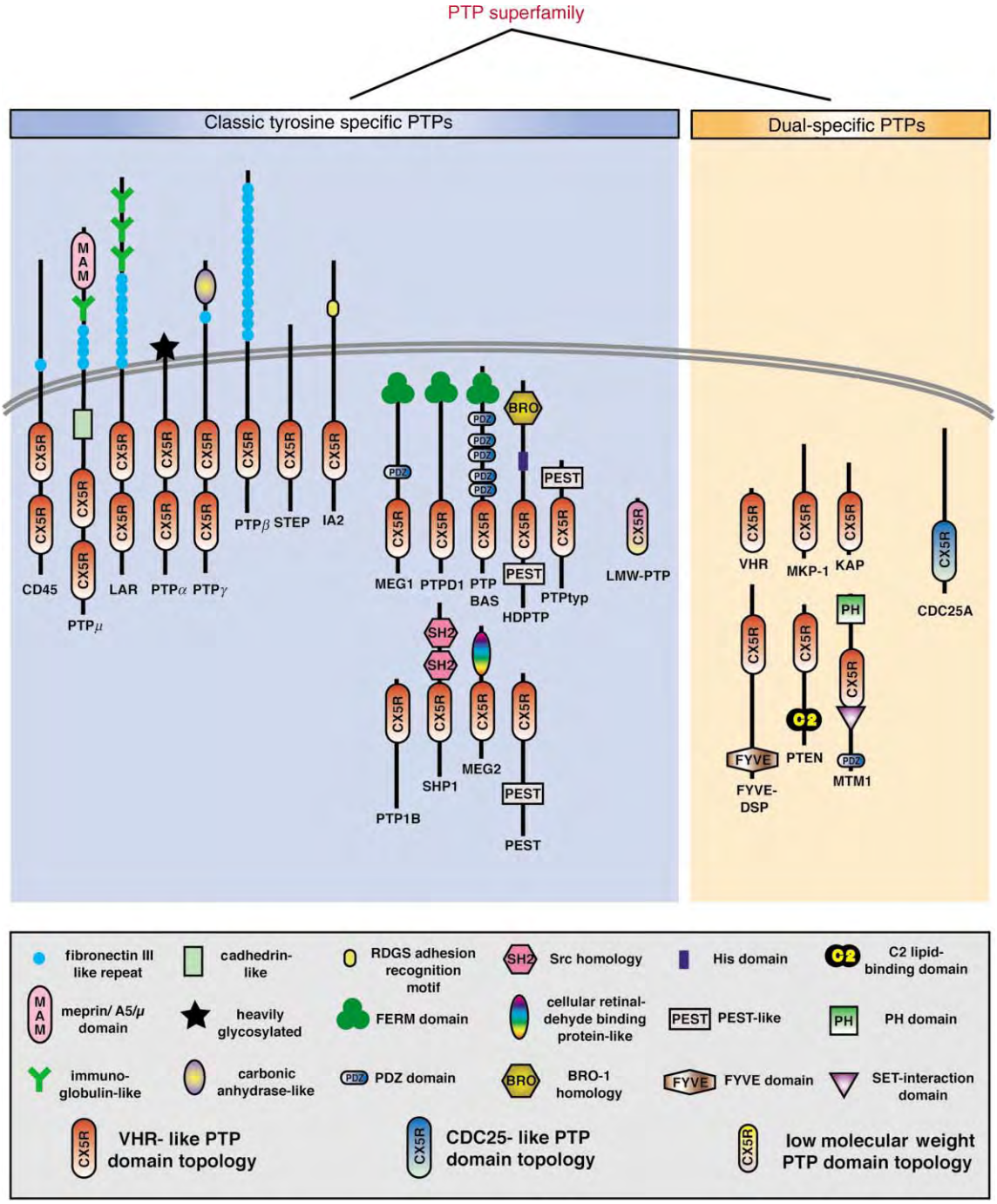

FIGURE 2 Schematic illustration of representative members of the PTP superfamily.

mice with targeted disruptions of individual PTP genes have provided *in vivo* evidence for the involvement of individual PTPs in specific biological processes. Abnormal PTP function has been implicated in a wide array of pathological conditions including diabetes, obesity, cancer, immune disease, neurodegeneration, and vascular disease. In this section, links between PTPs and human disease are briefly discussed. Studies of three PTPs that play essential roles in mammalian physiology are offered in examples. In addition, a summary of the results of PTP gene disruption experiments in mice is provided (Table I). Finally, the development of PTP inhibitors for use as therapeutics and research tools is discussed.

PTP-1B

A number of studies since the late 1990s have indicated that PTP-1B plays a specific role in down-regulating both insulin and leptin receptor signaling in mice.

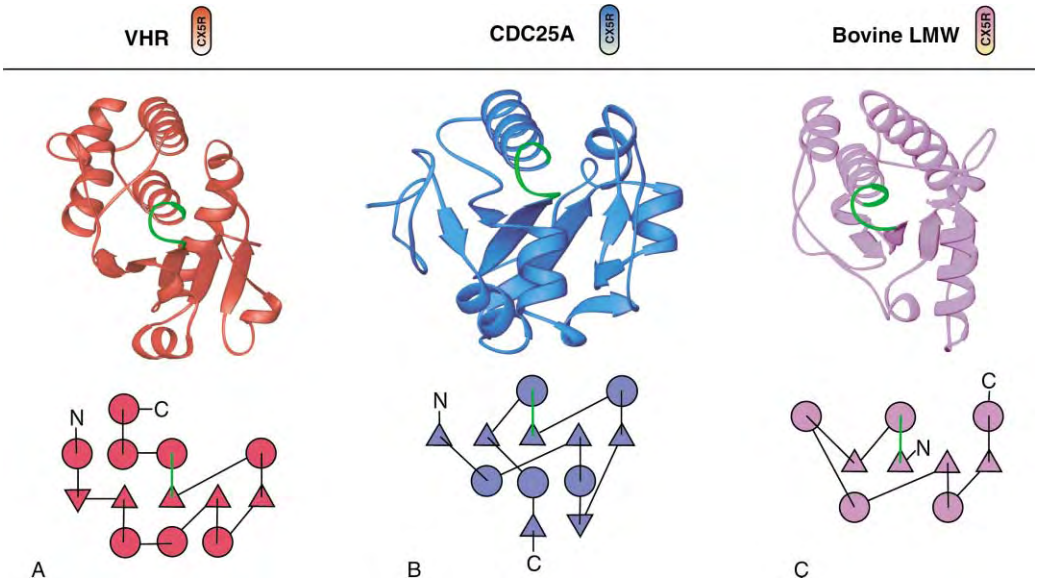

FIGURE 3 Crystal structures and topologies of representative members of each of the three topologically distinct PTP subfamilies. The amino (N) and carboxyl (C) termini of the proteins are indicated. Circles represent α-helixes; triangles represent β-strands. The location of the P-loop possessing the signature CX_5R motif is highlighted in green.

Studies from the laboratories of both Kennedy and Kahn have demonstrated that mice lacking PTP-1B are resistant to diabetes and diet-induced obesity, while displaying no other apparent physiological defects. Enhanced insulin sensitivity in PTP-1B-deficient mice likely results from hyperphosphorylation of the insulin receptor, as these mice display enhanced auto-phosphorylation of this protein in liver and muscle tissues. PTP-1B has been shown to associate with the insulin receptor PTK *in vivo* and both the insulin receptor and insulin receptor substrate 1 (IRS1) have been implicated as substrates for PTP-1B. Taken together, these data indicate a critical role for PTP-1B in turning off insulin signaling in sensitive mammalian tissues. The apparent *in vivo* specificity of PTP-1B function came as a surprise given the many other cellular processes in which this enzyme was thought to be involved. A number of pharmaceutical companies are attempting to generate specific inhibitors of PTP-1B for use as drugs to treat diabetes and obesity.

CD45

CD45 is an RPTP highly expressed in all nucleated hematopoietic cells. The extracellular portion CD45 contains fibronectin-like repeat sequences (Figure 2), is heavily glycosylated and is involved in the homodimerization of the molecule. Ligands for the extracellular domain of CD45 have not been identified, but this segment of the protein is important for the regulation of phosphatase activity. The cytoplasmic portion of CD45 contains two PTP domains; however, only the membrane proximal PTP domain is catalytically active and required for CD45 function. Homodimerization of CD45 is believed to maintain the phosphatase domain in a low activity state. CD45 mutations in either humans or mice result in a severe-combined immune deficient (SCID) phenotype, in which both B and T cells are affected (Table I). Consistent with the SCID phenotype, studies in CD45-deficient mice have indicated a role for this PTP as a critical positive regulator of immuno-receptor signaling in both B and T cells. In T cells, binding of an antigen to the extracellular portion of the T-cell receptor (TCR) results in the assembly of a cytoplasmic complex of TCR-associated signaling proteins. The PTKs Lck and Fyn phosphorylate a number of components of the assembled TCR signaling complex, leading to the recruitment and activation of the ZAP-70 PTK. Activated ZAP-70 participates in the transmission of stimulatory signals to downstream pathway components, ultimately leading to T-cell activation. The kinase activities of Lck and Fyn are negatively regulated by tyrosine phosphorylation on specific residues. By dephosphorylating these key inhibitory tyrosines, CD45 acts to prime Lck and Fyn for full activation, which is achieved through further phosphorylation. In this manner, CD45 is thought to function by setting an important threshold for T-cell activation.

Laforin

Mutations in the human gene for Laforin, a predicted DS-PTP, have been shown to cause Lafora disease, a progressive form of monoclonus epilepsy. The hallmark of Lafora disease is the accumulation of polyglucosan inclusions ("Lafora bodies") in the cytoplasm of cells of

TABLE I

Summary of PTP Gene Disruption Experiments in Mice

PTP	Mouse gene disruption phenotype and references
CD45	Severe-combined immunodeficiency (*1–3*)
CD148	Embryonic lethal (day 11.5); extensive vascular defects (*4*)
Cdc25b	Female sterility due to permanent meiotic arrest of oocytes (*5*)
Cdc25c	No phenotypic defects identified (*6*)
HePTP	Enhanced ERK activation in lymphocytes, but no physiological defects identified (*7*)
Laforin	Neurodegeneration and Lafora body accumulation; ataxia, epilepsy, and impaired behavioral responses (*8*)
LAR	Decreased basal forebrain cholinergic neuron size and hippocampal cholinergic innervation; delayed regenerative neurite outgrowth following nerve injury; impaired mammary gland development; abnormal glucose homeostasis (*9–14*)
PTP-1B	Enhanced sensitivity to insulin, leptin and growth hormone; obesity resistance (*15–19*)
PTPα	No gross phenotypic defects; reduced activation of Src and Fyn kinases; altered integrin signaling and cell migration (*20–23*)
PTPβ	No phenotypic defects identified (*24*)
PTPδ	Impaired learning; altered hippocampal long-term potentiation (*25*)
PTPε	No gross phenotypic defects; abnormal macrophage responsiveness; hypomyelination of sciatic nerve neurons; abnormal voltage-gated potassium channel function (*26*, *27*)
PTPσ	Neonatal or early lethality; developmental defects in neuronal and neuroendocrine cell lineages (*28–33*)
SHP-1	Early lethality ($<$12 weeks); severe hematopoetic dysregulation and autoimmunity (*34–37*)
SHP-2	Embryonic lethality (day 10.5) with gastrulation defects; enhanced MAP kinase activation (*38*, *39*)
TC-PTP	Early lethality ($<$*5* weeks); defective bone marrow function; impaired B and T cell function (*40–43*)

(1) Byth *et al.* (1996); (2) Mee *et al.* (1999); (3) Kishihara *et al.* (1993); (4) Takahashi *et al.* (2003); (5) Lincoln *et al.* (2002); (6) Chen *et al.* (2001); (7) Gronda *et al.* (2001); (8) Ganesh *et al.* (2002); (9) Van der Zee *et al.* (2003); (10) Xie *et al.* (2001); (11) Yeo *et al.* (1997); (12) Ren *et al.* (1998); (13) Schaapveld *et al.* (1997); (14) Van Lieshout *et al.* (2000); (15) Elchebly *et al.* (1999); (16) Klaman *et al.* (2000); (17) Cheng *et al.* (2002); (18) Zabolotny *et al.* (2002); (19) Gu *et al.* (2003); (20) Ponniah *et al.* (1999); (21) Su *et al.* (1999); (22) Zeng *et al.* (2003); (23) Zheng, D. Shalloway (2001); (24) Harroch *et al.* (2000); (25) Uetani *et al.* (2000); (26) Peretz *et al.* (2000); (27) Sully *et al.* (2000); (28) Batt, *et al.* (2003); (29) Meathre (2002); (30) McLean *et al.* (2002); (31) Batt *et al.* (2002); (32) J. Wallace *et al.* (1999); (33) Elchebly *et al.* (1999); (34) Kozlowski *et al.* (1993); (35) W. Tsui *et al.* (1993); (36) D. Shultz *et al.* (1993); (37) Kamata *et al.* (2003); (38) Saxton *et al.* (1997); (39) Arrandale *et al.* (1996); (40) Ibarra-Sanchez *et al.* (2001); (41) Dupuis (2003); (42) Galic *et al.* (2003); (43) You-Ten *et al.* (1997).

the brain, liver, kidney, skeletal and cardiac muscle, and skin. This human disease phenotype has recently been replicated in Laforin-deficient mice, through the work of Yamakawa and colleagues. In addition to its DS-PTP domain, Laforin possesses a carbohydrate-binding domain, which is required for its association with glycogen particles, and responsible for targeting the phosphatase to the same subcellular location as glycogen synthase. The cellular substrate(s) of Laforin have yet to be identified, but are actively being pursued.

PTPs as Drug Targets

Given the potential involvement of PTPs in many aspects of human biology and disease, there is considerable interest in the development of small molecule inhibitors of PTPs for use as therapeutics. In addition to their potential medical value, highly selective and potent PTP inhibitors would be powerful research tools for determining the functions of individual PTPs in mammalian cells. However, the development of specific PTP inhibitors has proved challenging. Like protein kinases, PTPs comprise a large family of enzymes that utilize a common chemical mechanism for catalysis. Accordingly, structure-based drug design is likely to be critical for the development of highly specific PTP inhibitors.

Structural studies have suggested a strategy by which inhibitor specificity for individual PTPs might be achieved. Investigations with PTPs have indicated that residues adjacent to the pTyr-binding site play essential roles in achieving substrate specificity and catalytic efficiency. Contemporary work has taken advantage of unique properties of the PTP-1B molecule to develop inhibitors with high selectivity. PTP-1B possesses a second phosphate-binding site on the protein surface, adjacent to its active site. Zhang and colleagues have designed small nonpeptide molecules containing two nonhydrolyzable phosphate moieties. Such molecules inhibit PTP-1B at nanomolar concentrations and are highly selective for this enzyme. High affinity and specificity are achieved by the combined action of the two phosphate moieties, with one binding in the active site and the other at the adjacent site. Such "bidentate" inhibitor compounds may serve as a model for the development of additional, highly specific PTP

inhibitors, as they target both the active site, which is highly conserved among PTPs, and adjacent portions of the structure, which are less highly conserved.

See Also the Following Articles

B-Cell Antigen Receptor • Serine/Threonine Phosphatases

Glossary

"classic" PTP (protein tyrosine phosphatase) These enzymes are specific for phosphotyrosine substrates.

DS-PTPs ("dual-specific" PTPs) In addition to having the ability to dephosphorylate phosphotyrosine substrates *in vitro*, DS-PTPs have been shown to utilize phosphoserine/threonine, RNA, or inositol lipids as their physiological substrate.

kinase Enzymes that work opposite of phosphatases by catalyzing the addition of phosphate group to a target substrate.

phosphatases Catalyze the removal of a phosphate group from a target substrate.

RPTP PTPs possessing a transmembrane domain and one or two classic, phosphotyrosine specific PTP domains.

Further Reading

Andersen, J. N., Mortensen, O. H., Peters, G. H., Drake, P. G., Iversen, L. F., Olsen, O. H., Jansen, P. G., Andersen, H. S., Tonks, N. K., and Moller, N. P. (2001). Structural and evolutionary relationships among protein tyrosine phosphatase domains. *Mol. Cell. Biol.* **21**, 7117–7136.

Arrandale, J. M., Gore-Willse, A., Rocks, S., Ren, J. M., Zhu, J., Davis, A., Livingston, J. N., and Rabin, D. U. (1996). Insulin signaling in mice expressing reduced levels of Syp. *J. Biol. Chem.* **271**, 21353–21358.

Batt, J., Asa, S., Fladd, C., and Rotin, D. (2002). Pituitary, pancreatic and gut neuroendocrine defects in protein tyrosine phosphatase-sigma-deficient mice. *Mol. Endocrinol.* **16**, 155–169.

Batt, J., Cutz, E., Fladd, C., and Rotin, D. (2003). Apparent normal lung architecture in protein tyrosine phosphatase-sigma-deficient mice. *Am. J. Physiol. Lung Cell. Mol. Physiol.* **284**, L214–L223.

Blume-Jensen, P., and Hunter, T. (2001). Oncogenic kinase signalling. *Nature* **411**, 355–365.

Byth, K. F., Conroy, L. A., Howlett, S., Smith, A. J., May, J., Alexander, D. R., and Holmes, N. (1996). CD45-null transgenic mice reveal a positive regulatory role for CD45 in early thymocyte development, in the selection of CD4 + CD8 + thymocytes, and B cell maturation. *J. Exp. Med.* **183**, 1707–1718.

Chen, M. S., Hurov, J., White, L. S., Woodford-Thomas, T., and Piwnica-Worms, H. (2001). Absence of apparent phenotype in mice lacking Cdc25C protein phosphatase. *Mol. Cell. Biol.* **21**, 3853–3861.

Cheng, A., Uetani, N., Simoncic, P. D., Chaubey, V. P., Lee-Loy, A., McGlade, C. J., Kennedy, B. P., and Tremblay, M. L. (2002). Attenuation of leptin action and regulation of obesity by protein tyrosine phosphatase 1B. *Dev. Cell* **2**, 497–503.

Denu, J. M., and Dixon, J. E. (1998). Protein tyrosine phosphatases: Mechanisms of catalysis and regulation. *Curr. Opin. Chem. Biol.* **2**, 633–641.

Denu, J. M., Stuckey, J. A., Saper, M. A., and Dixon, J. E. (1996). Form and function in protein dephosphorylation. *Cell* **87**, 361–364.

Dupuis, M., De Jesus lbarra-Sanchez, M., Tremblay, M. L., and Duplay, P. (2003). Gr-I + myeloid cells lacking T cell protein tyrosine phosphatase inhibit lymphocyte proliferation by an IFN-gamma- and nitric oxide-dependent mechanism. *J. lmmunol.* **171**, 726–732.

Elchebly, M., Payette, P., Michaliszyn, E., Cromliih, W., Collins, S., Loy, A. L., Normandin, D., Cheng, A., Himms-Hagen, J., Chan, C. C., *et al.* (1999a). Increased insulin sensitivity and obesity resistance in mice lacking the protein tyrosine phosphatase-1B gene. *Science* **283**, 1544–1548.

Elchebly, M., Wagner, J., Kennedy, T. E., Lanctot, C., Michaliszyn, E., Itie, A., Drouin, J., and Tremblay, M. L. (1999b). Neuroendocrine dysplasia in mice lacking protein tyrosine phosphatase sigma. *Nat. Genet.* **21**, 330–333.

Galic, S., Klingler-Hoffmann, M., Fodero-Tavoletti, M. T., Puryer, M. A., Meng, T. C., Tonks, N. K., and Tiganis, T. (2003). Regulation of insulin receptor signaling by the protein tyrosine phosphatase TCPTP. *Mol. Cell. Biol.* **23**, 2096–2108.

Ganesh, S., Delgado-Escueta, A. V., Sakamoto, T., Avila, M. R., Machado-Salas, J., Hoshii, Y., Akagi, T., Gomi, H., Suzuki, T., Amano, K., Agarwala, K. L., Hasegawa, Y., Bai, D. S., Ishihara, T., Hashikawa, T., Itohara, S., Cornford, E. M., Niki, H., and Yamakawa, K. (2002). Targeted disruption of the Epm2a gene causes formation of Lafora inclusion bodies, neurodegeneration, ataxia, myoclonus epilepsy and impaired behavioral response in mice. *Hum. Mol. Genet.* **11**, 1251–1262.

Gronda, M., Arab, S., Iafrate, B., Suzuki, H., and Zanke, B. W. (2001). Hematopoietic protein tyrosine phosphatase suppresses extracellular stimulus-regulated kinase activation. *Mol. Cell. Biol.* **21**, 6851–6858.

Gu, F., Dube, N., Kim, J. W., Cheng, A., Ibarra-Sanchez Mde, J., Tremblay, M. L., and Boisclair, Y. R. (2003). Protein tyrosine phosphatase 1B attenuates growth hormone-mediated JAK2-STAT signaling. *Mol. Cell. Biol.* **23**, 3753–3762.

Harroch, S., Palmeri, M., Rosenbluth, J., Custer, A., Okigaki, M., Shrager, P., Blum, M., Buxbaum, J. D., and Schlessinger, J. (2000). No obvious abnormality in mice deficient in receptor protein tyrosine phosphatase beta. *Mol. Cell. Biol.* **20**, 7706–7715.

Ibarra-Sanchez, M. J., Wagner, J., Ong, M. T., Lampron, C., and Tremblay, M. L. (2001). Murine embryonic fibroblasts lacking TC-PTP display delayed G1 phase through defective NF-kappaB activation. *Oncogene* **20**, 4728–4739.

Jackson, M. D., and Denu, J. M. (2001). Molecular reactions of protein phosphatases – insights from structure and chemistry. *Chem. Rev.* **101**, 2313–2340.

Kamata, T., Yamashita, M., Kimura, M., Murata, K., Inami, M., Shimizu, C., Sugaya, K., Wang, C. R., Taniguchi, M., and Nakayama, T. (2003). src homology 2 domain-containing tyrosine phosphatase SHP-1 controls the development of allergic airway inflammation. *J. Clin. Invest.* **111**, 109–119.

Kishihara, K., Penninger, J., Wallace, V. A., Kundig, T. M., Kawai, K., Wakeham, A., Timms, E., Pfeffer, K., Ohashi, P. S., Thomas, M. L. *et al.* (1993). Normal B lymphocyte development but impaired T cell maturation in CD45-exon6 protein tyrosine phosphatase-deficient mice. *Cell* **74**, 143–156.

Klaman, L. D., Boss, O., Peroni, O. D., Kim, J. K., Martino, J. L., Zabolotny, J. M., Moghal, N., Lubkin, M., Kim, Y. B, Sharpe, A. H., Stricker-Krongrad, A., Shulman, G. I., Neel, B. G., and Kahn, B. B. (2000). Increased energy expenditure, decreased adiposity, and tissue-specific insulin sensitivity in protein-tyrosine phosphatase 1B-deficient mice. *Mol. Cell. Biol.* **20**, 5479–5489.

Kozlowski, M., Mlinaric-Rascan, I., Feng, G. S., Shen, R., Pawson, T., and Siminovitch, K. A. (1993). Expression and catalytic activity of the tyrosine phosphatase PTP1C is severely impaired in motheaten and viable motheaten mice. *J. Exp. Med.* **178**, 2157–2163.

Li, L., and Dixon, J. E. (2000). Form, function, and regulation of protein tyrosine phosphatases and their involvement in human diseases. *Semin. Immunol.* **12**, 75–84.

Lincoln, A. J., Wickramasinghe, D., Stein, P., Schultz, R. M., Palko, M. E., De Miguel, M. P., Tessarollo, L., and Donovan, P. J. (2002). Cdc25b phosphatase is required for resumption of meiosis during oocyte maturation. *Nat. Genet.* **30**, 446–449.

McLean, J., Batt, J., Doering, L. C., Rotin, D., and Bain, J. R. (2002). Enhanced rate of nerve regeneration and directional errors after sciatic nerve injury in receptor protein tyrosine phosphatase sigma knock-out mice. *J. Neurosci.* **22**, 5481–5491.

Meathrel, K., Adamek, T., Batt, J., Rotin, D., and Doering, L. C. (2002). Protein tyrosine phosphatase sigma-deficient mice show aberrant cytoarchitecture and structural abnormalities in the central nervous system. *J. Neurosci. Res.* **70**, 24–35.

Mee, P. J., Turner, M., Basson, M. A., Costello, P. S., Zamoyska, R., and Tybulewicz, V. L. (1999). Greatly reduced efficiency of both positive and negative selection of thymocytes in CD45 tyrosine phosphatase-deficient mice. *Eur. J. Immunol.* **29**, 2923–2933.

Peretz, A., Gil-Henn, H., Sobko, A., Shinder, V., Attali, B., and Elson, A. (2000). Hypomyelination and increased activity of voltage-gated K(+) channels in mice lacking protein tyrosine phosphatase epsilon. *EMBO J.* **19**, 4036–4045.

Ponniah, S., Wang, D. Z., Lim, K. L., and Pallen, C. J. (1999). Targeted disruption of the tyrosine phosphatase PTPalpha leads to constitutive downregulation of the kinases Src and Fyn. *Curr. Biol.* **9**, 535–538.

Puius, Y. A., Zhao, Y., Sullivan, M., Lawrence, D. S., Almo, S. C., and Zhang, Z. Y. (1997). Identification of a second aryl phosphate-binding site in protein-tyrosine phosphatase 1B: A paradigm for inhibitor design. *Proc. Natl. Acad. Sci. USA* **94**, 13420–13425.

Ren, J. M., Li, P. M., Zhang, W. R., Sweet, L. J., Cline, G., Shulman, G. I., Livingston, J. N., and Goldstein, B. J. (1998). Transgenic mice deficient in the LAR protein-tyrosine phosphatase exhibit profound defects in glucose homeostasis. *Diabetes* **47**, 493–497.

Saxton, T. M., Henkemeyer, M., Gasca, S., Shen, R., Rossi, D. J., Shalaby, F., Feng, G. S., and Pawson, T. (1997). Abnormal mesoderm patterning in mouse embryos mutant for the SH2 tyrosine phosphatase Shp-2. *EMBO J.* **16**, 2352–2364.

Schaapveld, R. Q., Schepens, J. T., Robinson, G. W., Attema, J., Oerlemans, F. T., Fransen, J. A., Streuli, M., Wieringa, B., Hennighausen, L., and Hendriks, W. J. (1997). Impaired mammary gland development and function in mice lacking LAR receptor-like tyrosine phosphatase activity. *Dev. Biol.* **188**, 134–146.

Shen, K., Keng, Y. F., Wu, L., Guo, X. L., Lawrence, D. S., and Zhang, Z. Y. (2001). Acquisition of a specific and potent PTP1B inhibitor from a novel combinatorial library and screening procedure. *J. Biol. Chem.* **276**, 47311–47319.

Shultz, L. D., Schweitzer, P. A., Rajan, T. V., Yi, T., Ihle, J. N., Matthews, R. J., Thomas, M. L., and Beier, D. R. (1993). Mutations at the murine motheaten locus are within the hematopoietic cell protein-tyrosine phosphatase (Hcph) gene. *Cell* **73**, 1445–1454.

Su, J., Muranjan, M., and Sap, J. (1999). Receptor protein tyrosine phosphatase alpha activates Src-family kinases and controls integrin-mediated responses in fibroblasts. *Curr. Biol.* **9**, 505–511.

Sully, V., Pownall, S., Vincan, E., Bassal, S., Borowski, A. H., Hart, P. H., Rockman, S. P., and Phillips, W. A. (2001). Functional abnormalities in protein tyrosine phosphatase epsilon-deficient macrophages. *Biochem. Biophys. Res. Commun.* **288**, 184–188.

Takahashi, T., Takahashi, K., St John, P. L., Fleming, P. A., Tomemori, T., Watanabe, T., Abrahamson, D. R., Drake, C. J., Shirasawa, T., and Daniel, T. O. (2003). A mutant receptor tyrosine phosphatase, CD148, causes defects in vascular development. *Mol. Cell. Biol.* **23**, 1817–1831.

Tsui, H. W., Siminovitch, K. A., de Souza, L., and Tsui, F. W. (1993). Motheaten and viable motheaten mice have mutations in the haematopoietic cell phosphatase gene. *Nat. Genet.* **4**, 124–129.

Uetani, N., Kato, K., Ogura, H., Mizuno, K., Kawano, K., Mikoshiba, K., Yakura, H., Asano, M., and Iwakura, Y. (2000). Impaired learning with enhanced hippocampal long-term potentiation in PTPdelta-deficient mice. *EMBO J.* **19**, 2775–2785.

Van der Zee, C. E., Man, T. Y., Van Lieshout, E. M., Van der Heijden, I., Van Bree, M., and Hendriks, W. J. (2003). Delayed peripheral nerve regeneration and central nervous system collateral sprouting in leucocyte common antigen-related protein tyrosine phosphatase-deficient mice. *Eur. J. Neurosci.* **17**, 991–1005.

Van Lieshout, E. M., Van der Heijden, I., Hendriks, W. J., and Van der Zee, C. E. (2001). A decrease in size and number of basal forebrain cholinergic neurons is paralleled by diminished hippocampal cholinergic innervation in mice lacking leukocyte common antigen-related protein tyrosine phosphatase activity. *Neuroscience* **102**, 833–841.

Wallace, M. J., Batt, J., Fladd, C. A., Henderson, J. T., Skarnes, W., and Rotin, D. (1999). Neuronal defects and posterior pituitary hypoplasia in mice lacking the receptor tyrosine phosphatase PTPsigma. *Nat. Genet.* **21**, 334–338.

Xie, Y., Yeo, T. T., Zhang, C., Yang, T., Tisi, M. A., Massa, S. M., and Longo, F. M. (2001). The leukocyte common antigen-related protein tyrosine phosphatase receptor regulates regenerative neurite outgrowth in vivo. *J. Neurosci.* **21**, 5130–5138.

Yeo, T. T., Yang, T., Massa, S. M., Zhang, J. S., Honkaniemi, J., Butcher, L. L., and Longo, F. M. (1997). Deficient LAR expression decreases basal forebrain cholinergic neuronal size and hippocampal cholinergic innervation. *J. Neurosci. Res.* **47**, 348–360.

You-Ten, K. E., Muise, E. S., Itie, A., Michaliszyn, E., Wagner, J., Jothy, S., Lapp, W. S., and Tremblay, M. L. (1997). Impaired bone marrow microenvironment and immune function in T cell protein tyrosine phosphatase-deficient mice. *J. Exp. Med.* **186**, 683–693.

Zabolotny, J. M., Bence-Hanulec, K. K., Stricker-Krongrad, A., Haj, F., Wang, Y., Minokoshi, Y., Kim, Y. B., Elmquist, J. K., Tartaglia, L. A., Kahn, B. B., and Neel, B. G. (2002). PTP1B regulates leptin signal transduction in vivo. *Dev. Cell* **2**, 489–495.

Zeng, L., Si, X., Yu, W. P., Le, H. T., Ng, K. P., Teng, R. M., Ryan, K., Wang, D. Z., Ponniah, S., and Pallen, C. J. (2003). PTP alpha regulates integrin-stimulated FAK autophosphorylation and cytoskeletal rearrangement in cell spreading and migration. *J. Cell Biol.* **160**, 137–146.

Zheng, X. M., and Shalloway, D. (2001). Two mechanisms activate PTPalpha during mitosis. *EMBO J.* **20**, 6037–6049.

Zhang, Z. Y. (2002). Protein tyrosine phosphatases: Structure and function, substrate specificity, and inhibitor development. *Annu. Rev. Pharmacol. Toxicol.* **42**, 209–234.

BIOGRAPHY

Dave Pagliarini graduated with honors from the University of Notre Dame in 1999 with a B.S. in biochemistry, and is currently a doctoral candidate in Jack Dixon's lab at the University of California, San Diego. His thesis work deals with the novel mitochondrial phosphatase, PLIP.

Fred L. Robinson is a Postdoctoral Research Fellow in the laboratory of Jack E. Dixon at the University of California San Diego. He holds a Ph.D. from the University of Texas Southwestern Medical Center in Dallas. His primary research interests are protein tyrosine and lipid phosphatases.

Jack E. Dixon is a Professor of Pharmacology, Cellular and Molecular Medicine, and Chemistry and Biochemistry, as well as Dean for Scientific Affairs, at the University of California, San Diego. His principal research interests are protein tyrosine phosphatase signaling and molecular mechanisms of bacterial pathogenesis. He holds a Ph.D. from the University of California, Santa Barbara and was a postdoctoral fellow at the University of California, San Diego. He is a member of the American Academy of Arts and Sciences and the National Academy of Science.

Proteinase-Activated Receptors

Kristina K. Hansen and Morley D. Hollenberg
University of Calgary, Calgary, Alberta, Canada

Proteinase-activated receptors (PARs) are members of a recently discovered receptor family, belonging to the seven-transmembrane superfamily of cell-surface G-protein-coupled receptors. They are found in various organs across several species and have a number of physiological roles. To date, four members of this family have been cloned (PAR_1, PAR_2, PAR_3, and PAR_4). Their unique mechanism of activation involves enzymatic cleavage of the N-terminal domain. This cleavage then allows the newly unmasked N-terminal domain of the receptor to bind to another site of the receptor to start the signaling process. This process is an example of a tethered-ligand mechanism. Additionally, synthetic receptor-activating peptides (PAR-APs) of 5–6 amino acids can also bind to the receptor. Once the tethered ligand or PAR-AP binds to the receptor, a conformational change of the receptor leads to G-protein activation, which triggers the signal transduction cascade. This cascade is responsible for transcription, mitogenesis, growth, and differentiation.

Structure

Proteinase-activating receptors are composed of ~400 amino acids (Table I). All four PARs possess a number of potential N-linked glycosylation sequences on their extracellular domains. The sequence homology between all of the PARs is ~30%. The tethered ligand is revealed upon enzymatic cleavage at an arginine or lysine residue present in all of the PARs (Table I). Much evidence has supported the key role for extracellular loop 2 of PAR_1 and PAR_2 in the activation of PARs by PAR-APs. In PAR_1, a sequence of ~10 amino acids in the N-terminal extracellular domain (residues 83-93 in human PAR_1) is also involved in signaling by either the tethered ligand or by the PAR-AP. For activation by proteinases, however, the importance of extracellular loop 2 is less clearly understood. The human genes encoding PAR_1, PAR_2, and PAR_3 are all located on chromosome 5q13, while PAR_4 is located on chromosome 19p12. All of the PAR genes have similar overall structures.

Activating Proteinases

Thrombin was the first proteinase that was shown to activate PARs (Figure 1A). In fact, the original name for PAR_1 was thrombin receptor. It is now known that PAR_1, PAR_3, and PAR_4 are all targeted by thrombin. Thrombin is a key serine proteinase that regulates the blood coagulation cascade. Thrombin, however, does not activate PAR_2. The most common activator of PAR_2 is trypsin. Other serine proteinases that have been shown to target PARs include: cathepsin G, plasmin, granzyme A, factors VIIa/X/Xa/TF, mast cell tryptase, and the dust mite proteinases, Der p3 and Der p9. As already mentioned, the cleavage site that leads to activation for all of the PARs is adjacent to either an arginine or lysine residue ~40 amino acids from the N terminus (see Table I).

Inactivation

Once activated, the individual PAR receptor is no longer capable of producing another signal because it is rapidly desensitized and internalized by phosphorylation-dependent mechanisms, similar to other G-protein-coupled receptors. Another means of inactivation of PAR receptors is by cleavage of the receptor downstream (towards the C terminus) of the activation cleavage site (Figure 1D). For example, the neutrophil enzymes elastase, proteinase 3, and cathepsin G cleave PAR_1 on platelets and endothelial cells downstream of the thrombin cleavage site. The actions of these proteinases effectively inhibit thrombin from activating PAR_1.

Agonist Peptides

Specific agonist peptides (PAR-APs) modeled on the sequence of the tethered ligands can be used in place of proteinases to determine whether or not a certain PAR may be present and responsive in cells or tissues (Figure 1B). These receptor-selective peptide agonists can be used to help understand the physiological role of a particular PAR. Unlike thrombin and trypsin, which can act on various PARs, PAR-APs selective for PAR_1, PAR_2, and PAR_4 have been developed. The sequences of the selective PAR-APs for these three receptors, as designated by the one-letter codes for each amino acid are: TFLLR-NH_2 (PAR_1), SLIGRL-NH_2 (PAR_2), and

TABLE I

Summary of Human Protease-Activated Receptors

	PAR_1	PAR_2	PAR_3	PAR_4
Amino acid composition	425	397	374	385
Cleavage site for receptors	LDPR[41] ↓ SFLLRN	SKGR[36] ↓ SLIGKV	LPIK[38] ↓ TFRGAP	PAPR[47] ↓ GYPGQV
Proteinase activators	Thrombin	Trypsin, tryptase	Thrombin	Thrombin
Selective peptide agonists	TFLLR-NH_2	SLIGRL-NH_2	None known	AYPGKF-NH_2

AYPGKF-NH_2 (PAR_4), respectively (Table I). The peptide SFLLRN-NH_2, which matches exactly the tethered-ligand sequence of human PAR_1, activates both PAR_1 and PAR_2. Although SLIGRL is the tethered-ligand sequence of PAR_2 in both the rat and mouse but not the human, the peptide SLIGRL-NH_2 is a more potent agonist for human PAR_2 than SLIGKV-NH_2. Similarly, AYPGKF-NH_2 is 10 times as potent as a human PAR_4 agonist than the sequences GYPGQV-NH_2 or GYPGKF-NH_2, which represent the tethered ligands of the human and mouse receptors, respectively. The reasons for the improved selectivity and potency of the synthetic sequences versus the naturally occurring sequences have yet to be explained. At present, there is not a selective PAR_3 agonist peptide known.

Activation of PARs by Neighboring PARs

In addition to the ability of proteinases and agonist peptides to activate an individual PAR directly, one PAR can be activated via a neighboring PAR in the cell membrane. For example, it has been demonstrated that the proteolytically revealed tethered ligand of PAR_1 can in turn activate PAR_2 (Figure 1C). Thus, theoretically, PAR_2 can generate a response to thrombin without being directly activated by the enzyme. Further, by acting as a "docking site" for thrombin, PAR_1 and PAR_3 can potentially facilitate thrombin's ability to activate PAR_4. In this manner, the PARs are acting as coreceptors, the one for the other. To date, although able to act as a coreceptor for PAR_4, PAR_3 has not been found to generate an intracellular signal on its own.

Antagonists

To understand the physiological effects of the PARs fully, selective antagonists that inhibit activation of PARs by both activating proteinases and peptides will be of great use. Activation of PAR_1, by either thrombin or a PAR_1-AP, is inhibited by compounds 1 and 2 (Figure 2). Similarly, PAR_4 activation is inhibited by compound 3 (Figure 2). As yet, there are no known synthetic antagonists of PAR_2 or PAR_3.

Distribution

PARs have been detected in a variety of tissues by northern blot analysis. The brain, lung, heart, stomach, colon, kidney, small intestine, liver, pancreas, testes, prostate, uterus, placenta, trachea, thymus, lymph node, skeletal muscle, and adrenal gland have all been shown to have at least one of the PARs. Table II summarizes the tissues and cells in which each PAR is found. It is important to note, however, that cellular expression is not necessarily conserved across species. For example, human platelets express PAR_1 and PAR_4 while mouse platelets express PAR_3 and PAR_4.

Detection Methods

Reverse Transcriptase-Polymerase Chain Reaction (RT-PCR)

To see if known PARs are present in a given cell type or tissue, reverse transcriptase-polymerase chain reaction (RT-PCR) analysis, using the primers specific for each of the individual PARs, may be performed with the total RNA isolated from the cells or tissues. After complementary DNA purification by agarose gel electrophoresis and DNA sequence analysis, it can be concluded whether or not certain PARs are expressed in the sample tested. This method, however, does not guarantee that the PARs are present in their active states.

Northern Blot Analysis

In order to detect if any of the PARs are present in a tissue sample, northern blot analysis can also be performed. The total RNA is isolated from the tissue, separated by agarose gel electrophoresis, and transferred to a blotting membrane (i.e., nitrocellulose paper) via an electric field. The RNA of interest is identified by treatment of the blotting membrane with a complementary RNA or DNA probe that is labeled with ^{32}P or

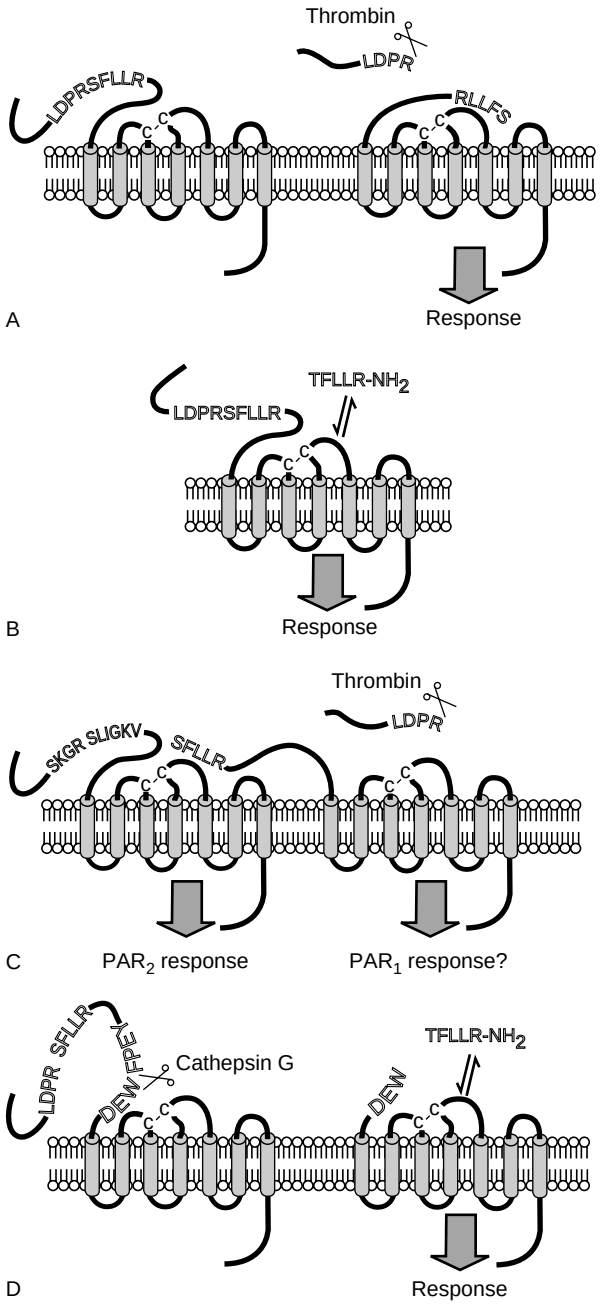

FIGURE 1 Mechanisms of activation and inactivation of PARs. (A) The functional PARs cloned to date contain within their receptor N terminus a serine protease cleavage/activation site that once cleaved by a serine protease, results in the unmasking of a cryptic tethered-ligand sequence. The revealed tethered-ligand sequence is believed to bind to and subsequently activate the receptor. The example provided (A) is for human PAR_1 activation by thrombin. (B) PARs may be activated independently of proteolytic unmasking of the tethered-ligand sequence by small synthetic peptides (PAR-APs) corresponding to the first five or six amino acids of the tethered-ligand sequence. Activation by the receptor-selective PAR_1AP, TFLLR-NH_2, is shown. (C) Intermolecular activation of PAR_1 or PAR_2 may occur following PAR_1 activation, whereby the unmasked tethered ligand of a PAR_1 receptor activates an uncleaved neighboring PAR_2 or PAR_1 receptor. (D) Inactivation of PARs may occur by proteases cleaving the receptor C-terminally of the tethered-ligand sequence, thus amputating the tethered ligand from the receptor body. These amputated receptors can no longer be activated by proteinases but are still responsive to exogenously applied PAR-APs. Note: a putative cysteine palmitoylation site in the C-terminal tail (present in all PARs except human PAR_4) may result in a fourth intracellular loop (not shown) that could play a role in receptor signaling. Reproduced with permission from Hollenberg, M. D., and Compton, S. J. (2002). International Union of Pharmacology XXVIII. Proteinase-activated receptors. *Pharmacol. Rev.* **54**, 203–217.

a fluorescent marker, followed by detection with the appropriate camera. One of the advantages of northern blot analysis is that the sequence of the probe does not need to be an exact match (e.g., from the same species).

Flow Cytometry

Flow cytometry is a technique for identifying and sorting cells that contain a component of interest by staining with a fluorescent dye and detecting the fluorescence by laser beam illumination. Cell-surface expression of PARs in a particular cell line can be identified by treatment of the cells first with anti-PAR antiserum (antibody) followed by the binding of fluorescein isothiocyanate-labeled goat antirabbit IgG that binds to the PAR antibody. Cell-surface expression of the PAR of interest can be quantified by fluorescence-activated cell sorting (FACS) analysis.

Immunocytochemistry/ Immunohistochemistry/ Immunofluorescence

These techniques take advantage of the strong interactions between antigens and their antibodies. The cells are immobilized by centrifugation onto slides using a cytospin machine or are grown directly on the slides, while tissues are embedded in paraffin, cut, and mounted on slides. The cell or tissue preparation is treated with anti-PAR antiserum (antibody) followed by a secondary antibody, which allows for detection. Antirabbit fluorescein isothiocyanate- or rhodamine-conjugated antibodies are examples of secondary antibodies used for fluorescence detection. An example of a visible detection approach is a sandwich streptavidin-conjugated peroxidase method using 3,3′diaminobenzidine as a substrate. These techniques detect the receptor directly.

In Situ Hybridization to Detect Receptor mRNA

In situ hybridization uses a complementary oligonucleotide, DNA, or RNA probe to detect a specific complementary mRNA sequence in intact tissue sections or cell preparations. This technique to locate PARs uses

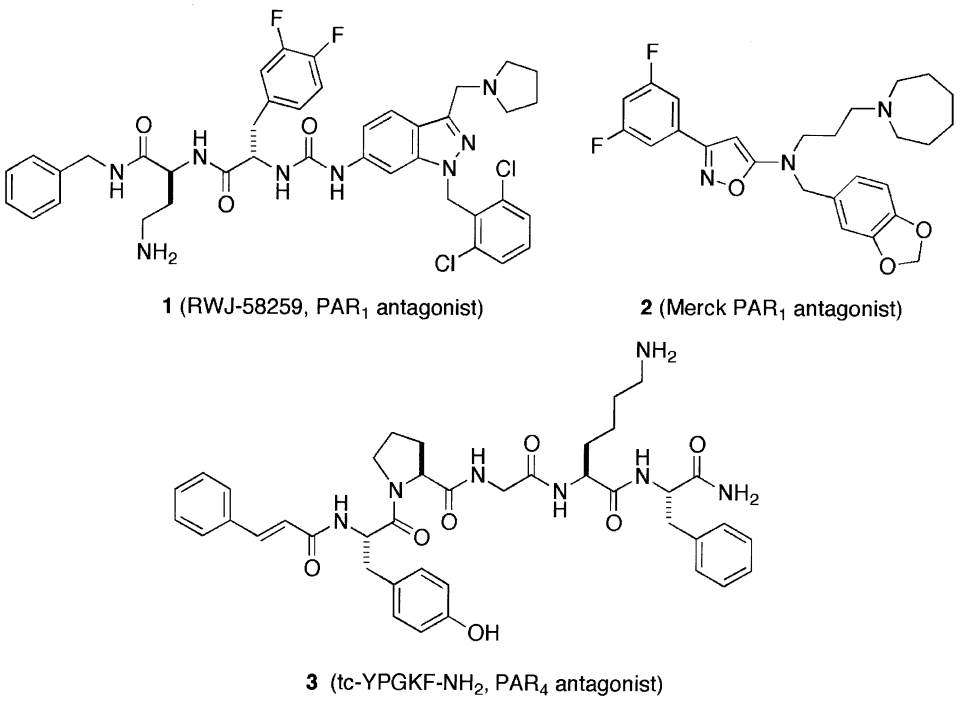

FIGURE 2 PAR antagonists.

the same principles used in northern blot analysis, except that the exact location of the mRNA can be identified. Immunohistochemistry techniques similar to those described above are used to detect the mRNA, instead of the receptor, to show where the receptor is being synthesized.

Bioassays

Measurement of Calcium Signaling Using Fluorescence Emission in Cultured Cells

As PARs are G protein-coupled receptors, once PARs are activated, the G protein undergoes a conformational change that activates phospholipase C (PLC), which then converts phosphatidyl inositol 4,5-bisphosphate (PIP_2) to inositol 1,4,5-trisphosphate (IP_3) and diacylglycerol (DAG). The IP_3 causes calcium to be released from the endoplasmic reticulum, thus increasing the intracellular calcium levels. This increase in intracellular calcium concentration can be measured in cells preincubated with a fluorescent calcium-sensitive dye (fluo-3 or fura-2) which is taken up into the cytoplasm. The fluorescence properties of the dye differ whether or not calcium is bound. For a calcium signaling assay, a fluorescence spectrophotometer measures the change in fluorescence at a defined wavelength versus time of a suspension or monolayer of cells preincubated with a fluorescent dye. When a specific PAR agonist is added to PAR expressing cells, a fluorescence peak is observed that reflects increased intracellular calcium. To confirm whether or not an unknown agonist or proteinase activates a certain PAR, cross-desensitization experiments can be performed. For example, PAR_1 and PAR_2 expressing HEK293 cells can be treated first with the PAR_1-specific agonist TFLLR-NH_2 (maximum dose) two times to desensitize PAR_1. This pretreatment is then followed by addition of the unknown agonist. If there is still a response, it can be concluded that the unknown agonist does not activate PAR_1. Likewise, to test for activation of PAR_2 by the same unknown agonist, the experiment can be repeated by exposing the cells first to the PAR_2-specific agonist SLIGRL-NH_2 to desensitize PAR_2. Alternatively, TFLLR-NH_2 may be added after two doses of the unknown agonist (maximum dose). If there is no response to TFLLR-NH_2, it can be concluded that the unknown agonist must have desensitized PAR_1 either by activation or another process.

Tissue Bioassays (Contraction or Relaxation)

To understand better how the activation of PARs leads to a biological response, blood vessels and smooth muscle strips may be treated with PAR-APs. The relaxation of rat aorta via the endothelium-dependent nitric oxide-mediated pathway can be measured. Similarly, contraction of the rat gastric longitudinal muscle can be assessed. For the bioassay experiment, a tissue is

TABLE II

Localization and Potential Roles of Human Proteinase-Activated Receptors

	PAR_1	PAR_2	PAR_3	PAR_4
Tissue distribution[a] (Northern blot analysis)	Brain, lung, heart, stomach, colon, kidney, testis	Prostate, small intestine, colon, liver, kidney, pancreas, trachea	Heart, kidney, pancreas, thymus, small intestine, stomach, lymph node, trachea	Lung, pancreas, thyroid, testis, small intestine, placenta, skeletal muscle, lymph node, adrenal gland, prostate, uterus, colon
Cellular expression	Platelets, endothelium, vascular smooth muscle, leukocytes, GI tract epithelium, fibroblasts, neurons, mast cells	Endothelium, leukocytes, GI tract epithelium and lung, airway and vascular smooth muscle, neurons, mast cells, keratinocytes, lung fibroblasts, renal tubular cells	Airway smooth muscle, platelets	Platelets, megakaryocytes
Known physiological role	Platelet activation			Platelet activation
Potential physiological roles	Pro-inflammatory, embryonic development, regulation of vascular tone	Pro-inflammatory, mediator of nocioception, airway protection, regulation of vascular tone	Cofactor for PAR_4	Platelet activation

[a] Information for PAR_2, PAR_3, and PAR_4 is provided for human tissues; for PAR_1, distribution is recorded in rat tissues, for which more extensive data are available than in human tissues.

GI, gastrointestinal.

Reproduced from Hollenberg, M. D., and Compton, S. J. (2002). International Union of Pharmacology XXVIII. Proteinase-activated receptors. *Pharmacol. Rev.* **54**, 203–217, with permission.

mounted under a resting tension in an organ bath. Changes in tension are detected using a force displacement transducer coupled to an amplifier and a data acquisition system. Known compounds that give a response are added to the organ bath to serve as a control. For example, acetylcholine is known to relax preconstricted aortic rings via an endothelium-dependent process, and potassium chloride is known to cause a large contractile response by acting directly on the smooth muscle present in the gastric or vascular preparation. PAR-APs are then added to the organ bath and the response is compared to the standards. As in the calcium signaling assay, cross-desensitization experiments can be performed to assess the potential contribution of each PAR to the biological response.

Platelet Aggregation

Platelets are known to express PARs. Activation of PARs on platelets causes aggregation. Using a light-transmission aggregometer, platelet aggregation can be monitored by measuring the turbidity of a suspension of platelets. Simply by adding agonists to a suspension of platelets, aggregation can be quantified either as a percentage increase in light transmission relative to that of the initial platelet suspension, or as a percentage of the maximal aggregation, versus time. This assay is commonly used to determine whether or not a compound is an agonist or an antagonist of PAR_1 and PAR_4. For example, if an antagonist is added before a specific PAR-AP, the aggregation of the platelets will be diminished.

Physiological Roles of PARs

PAR_1 plays an aggregatory and secretory role in human platelets and a role as a regulator of endothelial cell function. PAR_1 has also been shown to have an important role in the process of narrowing the arteries after vascular injury. PAR_2 has been suggested to be involved in the cardiovascular, pulmonary, and gastrointestinal systems, as well as having an important role in the settings of inflammation and pain sensation. Since the only role of PAR_3 shown to date is that it functions as a cofactor for thrombin-mediated activation of PAR_4, its physiological role is the same as for PAR_4. PAR_4, like PAR_1, has been shown to be responsible for the activation of platelets. There are many other physiological roles of PARs that have yet to be discovered.

See Also the Following Articles

PCR (Polymerase Chain Reaction) • Two-Dimensional Gel Electrophoresis

Glossary

agonist Compound that stimulates a cellular receptor to give a biological response.

antagonist Compound that binds to a cellular receptor which prevents a biological response from occurring.

antibody Protein produced by specialized B cells after stimulation by an antigen (foreign substance). Acts specifically against an antigen in an immune response.

glycosylation sequence Three amino acid sequence where the first amino acid is asparagine, the second is any amino acid except proline, and the third is serine or threonine.

proteinase Enzyme which selectively catalyzes the hydrolysis of peptide bonds.

PAR Acronym for proteinase-activated receptor. A G-protein-coupled receptor that is activated upon cleavage of the N-terminal domain by a proteinase.

PAR-AP Synthetic peptide that causes activation of a PAR.

Further Reading

Coughlin, S. R. (2000). Thrombin signalling and protease-activated receptors. *Nature* **407**, 258–264.

Déry, O., Corvera, C. U., Steinhoff, M., and Bunnett, N. W. (1998). Proteinase-activated receptors: Novel mechanisms of signaling by serine proteases. *Am. J. Physiol.* **274**, C1429–C1452.

Hollenberg, M. D., and Compton, S. J. (2002). International Union of Pharmacology XXVIII. Proteinase-activated receptors. *Pharmacol. Rev.* **54**, 203–217.

MacFarlane, S. R., Seatter, M. J., Kanke, T., Hunter, G. D., and Plevin, R. (2001). Proteinase-activated receptors. *Pharmacol. Rev.* **53**, 245–282.

O'Brien, P. J., Molino, M., Kahn, M., and Brass, L. F. (2001). Protease activated receptors: Theme and variations. *Oncogene* **20**, 1570–1581.

Biography

Kristina K. Hansen is a postdoctoral Fellow in the laboratory of Dr. Morley D. Hollenberg at the University of Calgary. In 2002, she received her Ph.D. in Organic Chemistry from the University of California, Berkeley.

Morley D. Hollenberg is a Professor in the Department of Pharmacology and Therapeutics and the Department of Medicine at the University of Calgary, Faculty of Medicine. His principal research interests focus on membrane receptors and signal transduction. He holds an M.D. from The Johns Hopkins University School of Medicine, Baltimore, Maryland and a D.Phil. From Oxford University, Oxford, UK.

Proteoglycans

Sara K. Olson and Jeffrey D. Esko
University of California, San Diego, La Jolla, California, USA

Proteoglycans (PGs) are glycoconjugates that contain glycosaminoglycans (GAGs) covalently attached to a protein core. They differ from glycoproteins by the unbranched, negatively charged GAG chains, which enables them to interact with numerous ligands, including growth factors, chemokines, cell adhesion proteins, protease inhibitors, and enzymes. This diverse group of molecules turns out to be essential for biological processes ranging from embryonic development to hemostasis and infection.

Proteoglycan Structure

Glycosaminoglycans

Proteoglycans (PGs) consist of two main structural components – the glycosaminoglycan (GAG) chains and the protein cores.

Three classes of GAG chains are covalently attached to PG core proteins: chondroitin sulfate (CS) /dermatan sulfate (DS), heparan sulfate (HS)/heparin, and keratan sulfate (KS) (Figure 1). Their structure, site of assembly, and pattern of sulfation and epimerization distinguish each of these types of GAGs. In addition, vertebrates contain a fourth class of GAGs called hyaluronan (hyaluronic acid, HA), but unlike the other GAGs, HA is not covalently bound to a protein core.

Building Blocks

Sugars used in GAG formation include xylose (Xyl), galactose (Gal), glucuronic acid (GlcA), N-acetylglucosamine (GlcNAc), and N-acetylgalactosamine (GalNAc). All of these sugars are hexoses (6-carbon sugars) except xylose, which contains five carbons. In order to build the chains, individual sugars are added in a stepwise manner. The enzymes that catalyze these reactions use activated sugar nucleotide donors, such as UDP-GlcNAc and UDP-GlcA for HA; UDP-GlcNAc or UDP-GalNAc, UDP-GlcA, UDP-Xyl, UDP-Gal and an activated form of sulfate called phosphoadenosine-5′phosphosulfate (PAPS) for HS/heparin and CS/DS; and UDP-Gal, UDP-GlcNAc, UDP-GalNAc, PAPS, and two additional sugar nucleotides for making keratan sulfate (GDP-Man and CMP-sialic acid). With the exception of UDP-xylose, which is derived from UDP-GlcA in the endoplasmic reticulum, all of the other sugar nucleotides assemble in the cytosol, and sugar nucleotide transporters shuttle them into the Golgi apparatus where they are used. The sugar and sulfate residues add to the growing chain, releasing UDP, PAP, GMP, or CMP for subsequent recycling in the cytoplasm.

Hyaluronan

Hyaluronan or HA is structurally the simplest GAG. It consists of repeating disaccharide units of GlcNAcβ1-4GlcAβ1-3, and does not undergo any further modification. HA is unique among the GAGs in that it does not assemble on a protein core and it is made at the plasma membrane instead of the Golgi apparatus. This orientation facilitates its extrusion from the cell into the surrounding extracellular matrix (ECM). The ECM is the network of polysaccharides and fibrous proteins that give strength, support, and structure to the cells embedded within it. HA chains are especially long, typically reaching 10^4 disaccharides. Due to their length they can intertwine to form a mesh-like material with interesting chemical properties, such as water retention and high viscosity. The turgor properties of the vitreous of the eye, the umbilical cord, and rooster combs reflect the high concentration of HA in these tissues. Several proteins, known as hyalectins, contain motifs that allow specific interactions with HA. HA helps to organize the extracellular matrix, and can bind to signaling and adhesion receptors on the cell surface, affecting growth and migration.

Chondroitin Sulfate/Dermatan Sulfate

Unlike HA, CS/DS (as well as HS/heparin) is synthesized while attached to a core protein. The chains initiate at Serine (Ser) residues of protein cores through the addition of Xyl from UDP-Xyl, followed by addition of two Gal residues, and finally GlcA from their corresponding sugar nucleotides. This linkage tetrasaccharide can undergo additional modifications, including sulfation of the Gal residues and phosphorylation of xylose, which may play a regulatory role in the assembly

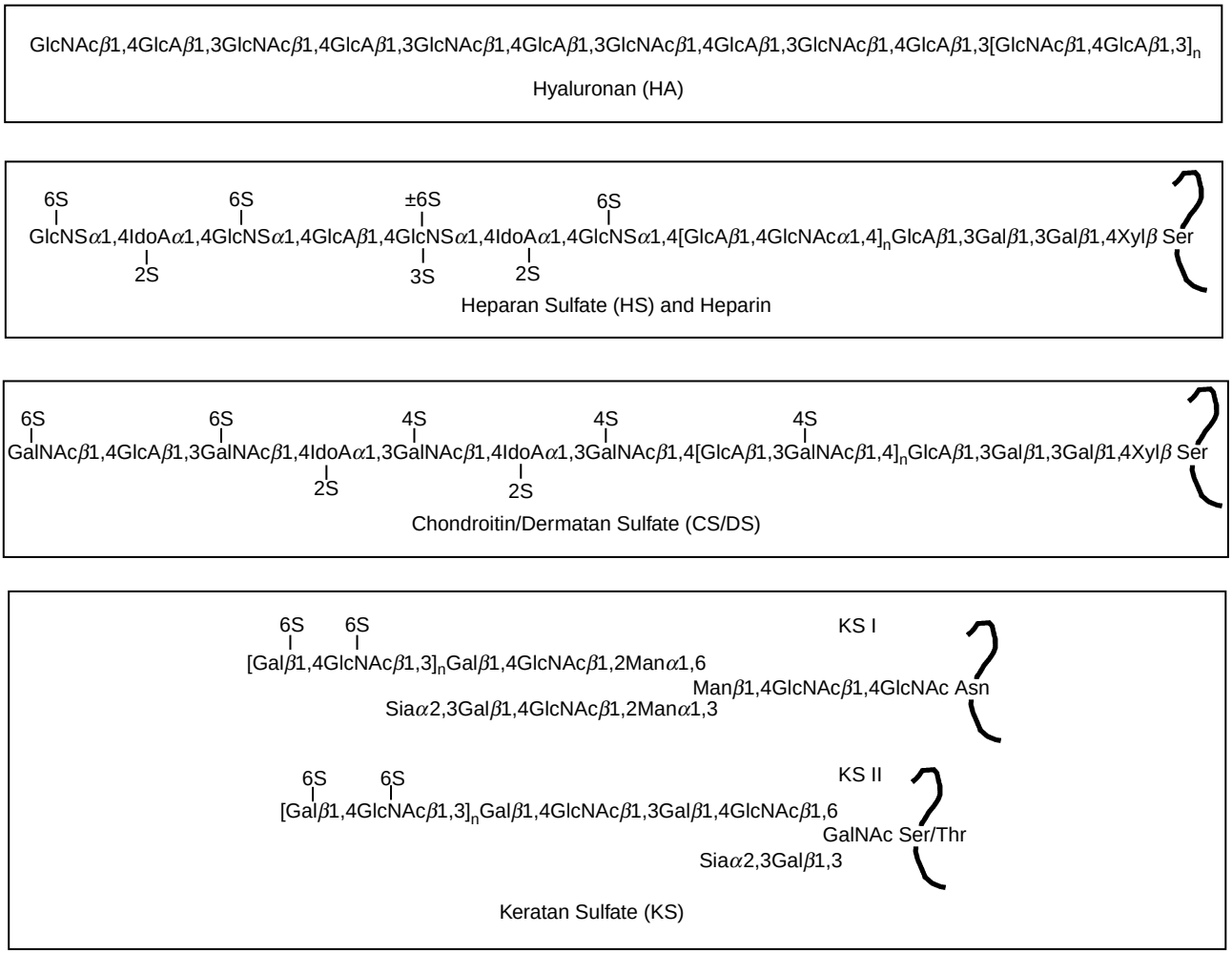

FIGURE 1 Classes of glycosaminoglycans. Hyaluronan (HA) is made up of repeating units of GlcNAc and GlcA. Heparan sulfate (HS) and chondroitin sulfate (CS) arise from a common linkage tetrasaccharide precursor linked to a protein core at serine (Ser) residues. HS consists of repeating GlcNAc and GlcA, while CS is composed of GalNAc and GlcA. Keratan sulfate (KS) is generated by the step-wise addition of GlcNAc and Gal residues. KS I is linked to the protein core via asparagine (Asn), whereas KS II is attached at Ser or threonine (Thr) residues.

process. Separate enzymes catalyze each step of the assembly of the linkage tetrasaccharide.

The growing chain is committed to become chondroitin by the addition of GalNAcβ1-4, and the chain then elongates by the assembly of the repeating units GalNAcβ1-4GlcAβ1-3, by the chondroitin synthase enzyme family. An average chain consists of $\sim$40 disaccharides, but the size varies in different tissues. The chondroitin backbone can be modified by sulfation of GalNAc units at the C-4 and/or C-6 positions, which tends to occur across the entire chain. In DS, a subset of D-GlcA units undergoes epimerization to L-IdoA, which can then be sulfated at C-2. Epimerization of GlcA to IdoA occurs by stereochemical inversion at C-5 (the proton is axial in D-GlcA but planar in L-IdoA).

CS/DS PGs are generally secreted into the extracellular matrix where they perform a variety of structural and developmental roles. The model organism *C. elegans* requires a nonsulfated form of chondroitin for the first embryonic cell division and the process of epithelial cell invagination in the vulva. In vertebrates, chondroitin sulfate plays numerous structural roles in cartilage, tendon, and other organized extracellular matrices. In the nervous system, it appears to affect axonal outgrowth and guidance. Very few binding proteins have been described, suggesting that some of chondroitin's properties may be related to its biophysical properties (hydrostatic and electrostatic effects). DS binds with growth factors and protease inhibitors involved in hemostasis.

Heparan Sulfate/Heparin

HS and heparin synthesis initiates in a manner similar to CS/DS by the assembly of the linkage tetrasaccharide.

The nascent chain becomes heparan upon addition of a GlcNAcα1-4 residue. Polymerization of the chain then ensues by the stepwise addition of GlcAβ1-4 and GlcNAcα1-4. As the chain elongates, it undergoes a number of modifications. Subsets of GlcNAc residues can be N-deacetylated, N-sulfated, and O-sulfated at the C-3 and C-6 positions. As in the case of CS/DS, epimerization of GlcA to IdoA can occur at residues neighboring GlcNS. Additionally, the uronic acids can be sulfated at C-2. HS chains are generally modified in sections, with highly sulfated blocks interspersed between nonmodified regions. Variable deacetylation, epimerization, and sulfation patterns give rise to specific binding sites for a large number of ligands, including growth factors (FGFs, Wnts, BMPs), anticoagulant proteins (antithrombin III, heparin cofactor II, which also binds DS, and thrombin), and matrix components (e.g., laminin, fibronectin, and some collagens). HS plays a vital role in numerous biological processes involved in cell growth, migration, and differentiation. A human disease called hereditary multiple exostosis (HME), characterized by bony outgrowths on the long bones, is caused by mutation of the enzymes responsible for polymerizing the HS chain (EXT-1 and EXT-2).

Heparin is a form of HS that has potent anticoagulant activity due to its ability to bind and activate antithrombin, a protease inhibitor, by way of a unique pentasaccharide sequence. In general, heparin is much more extensively modified compared to HS, containing as much as 85% GlcNS units and 75% IdoA, whereas HS contains 40–50% GlcNS and 25–40% IdoA. However, sections of HS chains can be extensively modified by sulfation and epimerization like heparin. Heparan sulfate is made by virtually all cells, whereas heparin is made selectively by connective tissue-type mast cells and stored in secretory granules. Therapeutic heparin derives from porcine and equine tissue digests. Commercial heparin Sepharose is often used to aid in the purification of proteins.

Keratan Sulfate

KS is classified as a glycoprotein as well as a PG. The chain consists of repeating Galβ1-4GlcNAcβ1-3 units (N-acetyllactosamine), containing sulfate groups in the C-6 positions of Gal and GlcNAc residues. Two forms of KS PGs vary by their linkage to core proteins. In KSI, the linkage of the polylactosamine is identical to conventional Asn-linked glycoproteins, whereas in KSII, the linkage is identical to that found in mucins (Figure 1). Like HS, the disaccharide units of KS can be unsulfated, monosulfated, or disulfated. KS is expressed in cartilage and a number of epithelial and neural tissues, playing a role in events as diverse as collagen fiber assembly, wound healing, and embryogenesis. They are also present in neurosecretory vesicles, suggesting unique roles in vesicle formation and neuronal activity.

Protein Cores

With the exception of HA, all GAGs are synthesized while attached to a protein core. Some PG cores serve functional roles by binding to other matrix molecules and bridging the extracellular matrix to the cytoskeleton. The number of GAG chains carried by individual PGs depends on the number of attachment sites, ranging from a single chain (decorin) up to 100 chains (aggrecan) (Table I). Most PGs contain multiple glycosylation sites, any or all of which may be used. A loose consensus sequence has been identified for HS and CS glycosylation sites on the protein core. Xylose is added to Ser residues that are followed by glycine (Gly), typically flanked by two or more acidic amino acids (Asp or Glu). The factors that regulate the efficiency of initiation are unknown. Evidence also exists that the presence of hydrophobic residues near the attachment sites, the density of attachment sites, as well as inhibitory sequences in the protein cores determine the selection of sites for the assembly of HS/heparin or CS/DS.

Proteoglycan Families

More than 25 PGs have thus far been identified in mammalian systems (Table I), and many fall into gene families based on sequence homologies. Some PGs carry a single type of GAG, whereas others can be hybrid molecules carrying HS and CS or CS and KS. Many PGs also carry other types of O-linked and N-linked glycans. Some PGs are large globular molecules reaching masses of 400 kDa, while others have small masses around 10 kDa. While structurally diverse, they can be classified into the following families based on location and homology.

Secreted and Matrix Proteoglycans

PGs secreted into the ECM can carry CS or DS chains. This group includes the small interstitial PGs, the aggrecan family, the basement membrane PG bamacan, and secretory granule PGs, such as serglycin. Perlecan and agrin are the only known HSPGs specifically secreted into the ECM. However, some membrane HSPGs can be shed from the cell surface and the ectodomains can become part of the ECM or accumulate in extracellular fluids.

TABLE I

Proteoglycan Families

Class	Family	Proteoglycan	Core mass (kDa)	Chain #	Chain type	Tissue
Matrix/secreted	Small interstitial	Decorin	36	1	CS	Connective tissue cells
		Biglycan	38	1–2	CS	Connective tissue cells
		Endocan	20	1	CS	Endothelial cells
		Epiphycan	35	2–3	CS	Cartilage
		Fibromodulin	42	2–3	KS	Broad
		Lumican	38	3–4	KS	Broad
		Keratocan	38	3–5	KS	Broad
		Mimecan/osteoglycin	25–35	2–3	KS	Broad, sulfated in cornea
		Osteoadherin	49	2–3	KS	Bone
	Aggrecan	Aggrecan	208–220	~100	CS/KS	Cartilage
		Versican	265	12–15	CS	Fibroblasts
		Neurocan	145	1–2	CS	Brain
		Brevican	96	0–4	CS	Brain
	Basement membrane	Bamacan	138	1–3	CS	Basement membranes
		Perlecan	400	1–3	HS	Basement membranes
		Agrin	212	2–3	HS	Basement membranes
	Intracellular storage	Serglycin	10–19	10–15	Heparin/CS	Mast cells
		SV2	80	1–3	KS	Synaptic vesicles
	Miscellaneous	Collagen α2 type IX	68	1	CS	Cartilage, vitreous humor
		Collagen type XVIII	150	1–3	HS	Epithelial cells, basement membranes
		Phosphacan	176		CS/KS	Brain
		Testicans 1–3	50	1–3	HS/CS	Testes, brain endothelium
Membrane bound	Syndecans	Syndecans 1–4	31–45	1–3	HS/CS	Epithelial cells, fibroblasts
	Glypicans	Glypicans 1–6	~60	1–3	HS	Epithelial cells, fibroblasts
	Miscellaneous	Betaglycan	110	1–2	HS/CS	Fibroblasts
		Thrombomodulin	58	1	CS	Endothelial cells
		CD44	37	1–4	CS	Lymphocytes
		NG2	251	2–3	CS	Neural cells
		Invariant chain	31	1	CS	Antigen-processing cells

Small Interstitial Proteoglycans (Small Leucine-Rich Proteoglycans)

This class of PGs includes proteins with leucine-rich repeats flanked by cysteines in their central domain. The family has over nine members, and all carry either CS/DS or KS GAG chains. Members include decorin and biglycan, which interact with collagen in the matrix. Much work to date has concentrated on understanding the role of these PGs in stabilizing and organizing collagen fibers. In decorin, this activity appears to be dictated by the PG core since removal of the GAG chains fails to disrupt fibrillogenesis. Mice lacking the decorin PG live to adulthood but show a fragile skin defect. Decorin mutants exhibit great variation in fibril diameter and spacing. In the cornea, KSPGs maintain the register of collagen fibers, which is required for transparency. Decorin is also able to bind TGF-β, serving as a sink to keep the growth factor sequestered.

Aggrecan Family

The Aggrecan family of PGs includes aggrecan, versican, brevican, and neurocan. All four members share these common features: the N-terminal domain is able to bind HA, the central region contains GAG attachment sites, and the C-terminal domain contains a C-type lectin domain (lectins are nonimmunoglobulin, nonenzymatic proteins that bind sugar chains). Aggrecan is the most well-known member of this family, since it is the

major PG present in cartilage. It contains by far the largest number of GAG chains, as many as 100 CS and KS chains per protein. It complexes with HA in the ECM and draws water into cartilage, thereby providing the ability to resist compressive forces. Versican is the largest member of the aggrecan family with a mass of 265 kDa, but it also undergoes alternative splicing events that generate smaller proteins. Roles in neural crest cell and axonal migration have been suggested. Neurocan and brevican are both localized to the brain. Neurocan is expressed in the late embryonic central nervous system (CNS) and acts to inhibit neurite outgrowth. Brevican is expressed in the terminally differentiated CNS, particularly in the perineuronal nets.

Basement Membrane Proteoglycans

The basement membrane is an organized layer of ECM that lies flush against epithelial cells and consists of laminin, collagen, nidogen, and PGs. Basement membranes contain three types of large PGs, each containing 1–3 GAG chains. Bamacan is the most recently cloned member of this family and has not yet been studied in detail. It carries predominantly CS chains. Perlecan and agrin, on the other hand, are HSPGs (though perlecan has been shown to carry CS on occasion). Perlecan is the largest known PG with a mass of 400 kDa and is a modular protein with multiple domains that serve numerous functions. It appears to play a role in embryogenesis and tissue morphogenesis. It is present in the pre-implantation blastocyst and endothelial cells. Agrin is a well-characterized PG that acts in the nervous system by aggregating acetylcholine receptors at the neuromuscular junction, and is additionally expressed in the renal tubules where it plays an important role in determining the filtration properties of the kidney. Homologues of the basement membrane PGs exists in flies and worms.

Secretory Granule Proteoglycans

Serglycin is the main PG localized to intracellular cytoplasmic secretory granules. It is synthesized by endothelial, endocrine, and hematopoietic cells, and it can carry CS, DS or heparin chains. Serglycin is stored in secretory granules until the host cell becomes activated, resulting in secretion of granular contents into the surrounding environment. Serglycin may play a role in packaging granular contents, maintaining proteases in an inactive state, and regulating activities after secretion, such as coagulation, host defense, and wound repair. Heparin, the highly sulfated form of HS, is made exclusively on serglycin present in mucosal mast cells.

Membrane-Bound Proteoglycans

Many PGs reside in cell membranes as type I transmembrane proteins (e.g. syndecan family) or glycosylphosphatidylinositol (GPI)-linked proteins (e.g. glypican family).

Syndecans

In syndecans, a short hydrophobic domain spans the membrane, linking the larger extracellular domain containing the GAG attachment sites to a smaller intracellular cytoplasmic domain. There are four members in mammalian systems, whereas lower organisms such as flies and worms contain only one homologue. They can carry HS and/or CS chains, which bind a wide range of extracellular ligands such as growth factors and matrix molecules. These interactions likely account for the requirement of syndecans at numerous stages of embryonic development and in the adult animal. Syndecans can additionally coordinate signals from the extracellular environment to the intracellular cytoskeleton via their cytoplasmic tails. For example, binding of a ligand to a GAG chain can induce oligomerization of syndecans at the cell surface. This leads to recruitment of factors at the cytoplasmic tail of syndecan, such as kinases (e.g. c-Src), PDZ-domain proteins, or cytoskeletal proteins. The recruitment of cytosolic proteins in turn triggers a signal that leads to actin filament assembly. Proteolytic cleavage of the syndecans occurs, resulting in release of the ectodomains bearing the GAG chains. These ectodomains can have potent biological activity.

Glypicans

The glypican family of cell-surface PGs is involved in numerous aspects of animal development. The C terminus is embedded in the membrane by a hydrophobic GPI-linked anchor, and thus the glypicans do not have a cytoplasmic tail like the syndecans. The N-terminal portion of the protein is globular and has been shown to carry only HS chains *in vivo*. The glypicans bind a wide array of factors that are essential for development and morphogenesis. Their roles in growth factor signaling potentially include both positive and negative regulation. HS chains are able to positively promote signaling by bringing a ligand and its receptor into close proximity. On the other hand, HS chains could negatively regulate signaling by binding a particular ligand and preventing its diffusion or interaction with a receptor.

Six glypican family members exist in mammals, two in flies and one in worms. Glypican-3 (GPC3) is the best-studied member of the family. Human patients lacking functional GPC3 exhibit Simpson–Golabi–Behmel Syndrome, which is characterized as an overgrowth

disorder. The overgrowth phenotype suggests that GPC3 normally functions to inhibit cell proliferation, likely mediated at the level of growth factor signaling at the cell surface.

Miscellaneous Membrane Proteoglycans

A number of membrane PGs do not show homology to syndecans or glypicans, but are expressed on the surface of many different cell types. The CSPG NG2 is a surface marker expressed on stem cell populations that are able to divide throughout an organism's life, including cartilage chondroblasts, myoblasts, endothelial cells of the brain, and glial progenitors. It has been shown to play a role in angiogenesis and inhibits neurite outgrowth. CD44 is a transmembrane cell surface receptor that plays a role in processes as diverse as immune function, axon guidance, and organ development. CD44 is considered a PG since it can carry GAG chains in certain cell types, such as lymphocytes. It is also an HA binding protein. The GAG chains allow CD44 to interact with ECM proteins and growth factors.

Processing

PGs are born in the endoplasmic reticulum (ER) and Golgi, but important steps of the PG life cycle also occur at the cell surface and other intracellular compartments.

Cell Surface Desulfation

The majority of sulfation reactions occur in the Golgi apparatus as the chains assemble prior to secretion. However, a family of cell surface sulfatases has been identified that removes sulfate groups from the C-6 position of glucosamine residues in HS. This sulfatase, called QSulf1 (first identified in quail), can promote Wnt growth factor signaling through HS in a finely tuned manner by desulfating HS at the appropriate time and place.

Turnover and Degradation

PGs are turned over on a continual basis (Figure 2). The syndecans undergo proteolytic cleavage and shedding at the cell surface, mediated by one of the matrix metalloproteases (MMP7). Additionally, some if not all membrane PGs are internalized by endocytosis. Enzymes called heparanases cleave the HS chains into fragments of a defined size, which then become localized to lysosomal compartments. Cells also endocytose HA, CS/DS, and KS proteoglycans, and sulfatases and exoglycosidases degrade the chains completely, while proteases degrade the core proteins. The liberated sugars (GlcNAc, GalNAc, Gal, and Man) and amino acids can then be recycled for the formation of new GAG chains and PGs, whereas the uronic acids and xylose are thought to undergo oxidative catabolism since no salvage pathway has been identified. The function of continuous turnover of the GAG chains and PGs is unclear. However, disruption of this pathway leads to lysosomal storage disorders with devastating health consequences.

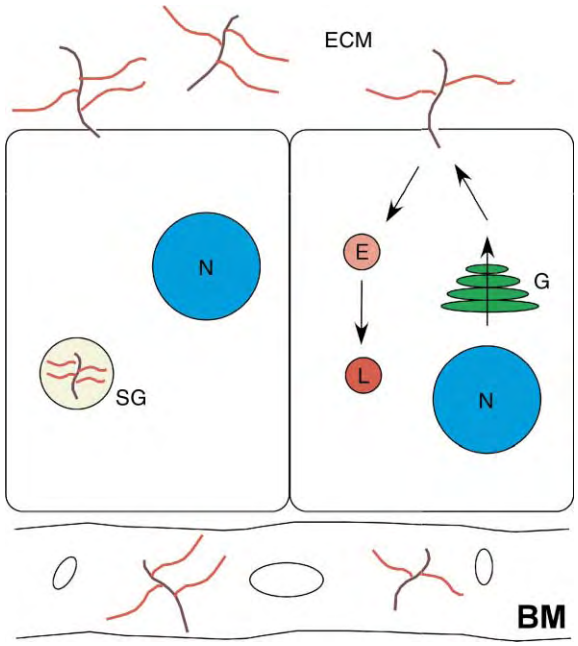

FIGURE 2 Life cycle of a proteoglycan. Proteoglycans are predominantly synthesized in the Golgi apparatus (G). A mature proteoglycan can be embedded in the plasma membrane, stored in secretory granules (SG), or secreted into the extracellular matrix (ECM) or basement membrane (BM). Degradation of proteoglycans begins with endocytic internalization, followed by cleavage of the GAG chains and protein core by glycosidases and proteases, respectively, in endosomes (E) and lysosomes (L). Nucleus (N).

See Also the Following Articles

Endoplasmic Reticulum-Associated Protein Degradation • Glycosylation, Congenital Disorders of • Glycosylation in Cystic Fibrosis • *N*-Linked Glycan Processing Glucosidases and Mannosidases • Protein Glycosylation, Overview • Protein Glycosylation Inhibitors

Glossary

chondroitin sulfate A type of glycosaminoglycan defined by the disaccharide unit (GalNAcβ1,4GlcAβ1,3)$_n$, modified with ester-linked sulfate at certain positions and typically found covalently linked to a PG core protein.

dermatan sulfate A modified form of chondroitin sulfate in which a portion of the β-glucuronic acid residues are epimerized to α-iduronic acid.

glycan Generic term for a sugar or assembly of sugars, existing either in free form or attached to another molecule.

glycosaminoglycan Polysaccharide side chains of PGs or free complex polysaccharides composed of linear disaccharide repeating units, each composed of a hexosamine and a hexose or a hexuronic acid.

glycosyltransferase An enzyme that forms a glycosidic linkage between a sugar and an acceptor.

heparan sulfate A glycosaminoglycan defined by the disaccharide unit $(GlcNAc\alpha1,4GlcA\beta1,4/IdoA\alpha1,4)_n$, containing N- and O-sulfate esters at various positions, and typically found covalently linked to a PG core protein.

heparin A type of heparan sulfate made by mast cells that has the highest amount of iduronic acid and of N- and O-sulfate residues.

hyaluronan A glycosaminoglycan defined by the disaccharide unit $(GlcNAc\beta1,4GlcA\beta1,3)_n$ that is neither sulfated nor covalently linked to protein, referred to in older literature as hyaluronic acid.

keratan sulfate A polylactosamine $(Gal\beta1,4GlcNAc\beta1,3)_n$ with sulfate esters at C-6 of GlcNAc and galactose residues found as a side chain of a keratan sulfate PG.

lectin A protein (excluding an antibody) able to bind glycans without causing modification of the glycan structure.

proteoglycan A protein with one or more covalently attached glycosaminoglycan chains.

sugar nucleotide Activated forms of monosaccharides, such as UDP-Xyl, UDP-Gal, UDP-GlcA, and UDP-GlcNAc, UDP-GalNAc, typically used as donor substrates by glycosyltransferases.

Further Reading

Bernfield, M., Gotte, M., Park, P. W., Reizes, O., Fitzgerald, M. L., Lincecum, J., and Zako, M. (1999). Functions of cell surface heparan sulfate proteoglycans. *Annu. Rev. Biochem.* **68**, 729–777.

Esko, J. D., and Selleck, S. B. (2002). Order out of chaos: Assembly of ligand binding sites in heparan sulfate. *Annu. Rev. Biochem.* **71**, 435–471.

Iozzo, R. (1998). Matrix proteoglycans: From molecular design to cellular function. *Annu. Rev. Biochem.* **67**, 609–652.

Song, H., and Filmus, J. (2002). The role of glypicans in mammalian development. *Biochim. Et. Biophys. Acta* **1573**, 241–246.

Varki, A., Cummings, R., Esko, J., Freeze, H., Hart, G., and Marth, J. (eds.) (1999). *Essentials of Glycobiology.* Cold Spring Harbor Laboratory Press, Cold Spring Harbor, New York.

Yoneda, A., and Couchman, J. (2003). Regulation of cytoskeletal organization by syndecan transmembrane proteoglycans. *Matrix Biol.* **22**, 25–33.

Biography

Sara Olson is a graduate student in the Biomedical Sciences Graduate Program in the School of Medicine at the University of California, San Diego (UCSD). She received her undergraduate education at Lawrence University where she developed an interest in developmental biology. She helped discover that vulval invagination in *C. elegans* depends on chondroitin biosynthesis.

Jeffrey D. Esko is a Professor of Cellular and Molecular Medicine and Co-director of the Glycobiology Research and Training Center at UCSD. He received his Ph.D. from the University of Wisconsin at Madison and was a Fellow of the Molecular Biology Institute at the University of California, Los Angeles. His principal research interests are in proteoglycan assembly and function using genetically altered cell lines and conditional mouse knockouts.

Pteridines

S. Colette Daubner and Paul F. Fitzpatrick
Texas A&M University, College Station, Texas, USA

The pteridines are a group of heterocyclic compounds containing a wide variety of substitutions on the basic compound pterin. Pterin itself is composed of a pyrazine ring and a pyrimidine ring; the pyrimidine ring has a carbonyl oxygen and an amino group. The biosynthesis of pterins begins with the molecule GTP; the enzyme which controls the conversion of GTP to pterin, GTP cyclohydrolase, is found in both prokaryotes and eukaryotes. Pterins were first discovered in the pigments of butterfly wings and perform many roles in coloration in the biological world. Pterins also function as cofactors in enzymatic catalysis. Folates, "conjugated" pterins which contain p-amino benzoic acid and glutamates in addition to the pterin ring system, are critical compounds in methyl transfer biochemistry. Tetrahydrobiopterin, the major unconjugated pterin in vertebrates, is involved in the hydroxylation of aromatic compounds and synthesis of nitric oxide. Molybdopterin, which contains pterin, a third heterocyclic ring containing an ether oxygen and two thiol substitutes, and molybdenum, is involved in biological hydroxylations, reduction of nitrate, and respiratory oxidation.

The name pteridine refers to the heterocyclic aromatic compound shown in Figure 1, composed of a pyrimidine ring fused to a pyrazine ring. However, the word pteridines has come to stand for an entire group of naturally occurring compounds. Their structures are based upon pteridine, but they have substituents on the pyrimidine ring: an amino group or a carbonyl at position 2 and a carbonyl group at position 4 (position numbers as shown in Figure 1). Pterin contains the amino substituent at position 2; all pterins are derivatives of this molecule. Most naturally occurring pteridines are pterins. The first pterins to be studied, leucopterin and xanthopterin, were pigments isolated from butterfly wings by Sir Frederich Gowland Hopkins at Cambridge University in the late nineteenth century. Their names are derived from the Greek words for wing, *pteron*, white, *leukos*, and yellow, *xanthos*.

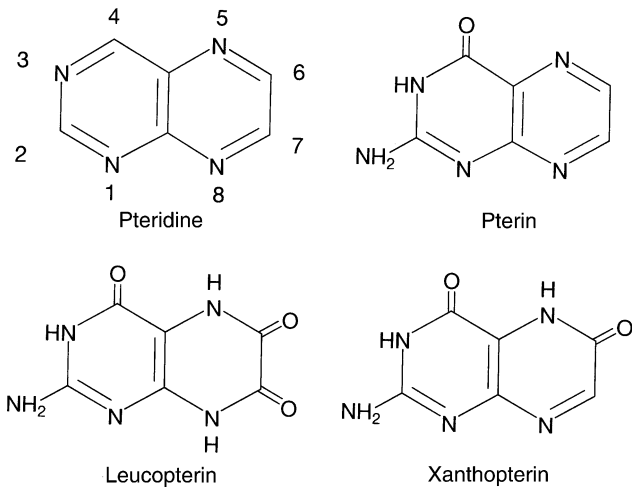

FIGURE 1 Structures of pteridine and three pteridines.

Pterins are referred to as being conjugated or unconjugated. The conjugated pterins are folates, derivatives of folic acid. They contain a *p*-aminobenzoate substituent at the 6-position and one or more glutamate residues. The folates are covered in a separate article in this series. As a general but not fast rule, folates are involved in one-carbon transfers in metabolism and pterins are involved in oxygenation reactions or in pigmentation.

Distribution of Pterins in Nature

Pterins are found in all living organisms, from bacteria, blue-green algae, and trypanosomes, to mammals; they have also been detected in the chloroplasts of spinach leaves and the cotyledons of pea sprouts. A wide variety of pterins exist in bacteria, such as the various pterins with three-carbon side chains of *Escherichia coli*, the glucuronidated pterins of *Bacillus subtilis*, the three ribityl pteridines of the marine bioluminescent bacterium *Photobacterium phosphoreum*, the molybdopterins of photosynthetic bacteria, and the tetrahydromethanopterin of methanogenic bacteria.

As pigments, pterins are not only found in butterfly wings, but also in moth heads, silkworm skin, grasshopper bodies, and honeybee larvae. A list of examples demonstrates the very wide use nature has made of pterins in coloration; diversity is found in species distribution, chemical structures, and hue. Unusual dimeric pterins are found in the eyes of the fruit fly, *Drosophila*. A blue pigment in the roundworm

Ascaris lumbricoides contains biopterin. Pterins are common in the skins of amphibians and fish, and photolabile pterins are found in some amphibians' eyes. The red color of some salmon, the Siamese fighting fish, and the red lizard *Anolis* is due to pterins, as is the green color of some snakes.

Clearly pterins serve widely in coloration, but they are also critical compounds in metabolic pathways. In the vertebrates the major pterin is tetrahydrobiopterin, which serves as a redox cofactor in enzymatic reactions utilizing molecular oxygen.

Biosynthesis of Neopterin and Biopterin

The synthesis of all pterins begins with the ring opening and reclosing of the nucleotide guanosine triphosphate (GTP) by the enzyme GTP cyclohydrolase (GTPCH). GTPCH has been isolated and sequenced from many sources. It is a decamer, each active site containing a zinc atom. As the rate-limiting enzyme of pterin biosynthesis, it is carefully regulated, both by transcriptional and posttranslational mechanisms. The catalytic domains of the *E. coli* and human enzyme are 37% identical in amino acid sequence, testifying to the ancient status of pterins in the living world.

The reaction catalyzed by GTPCH is shown in Figure 2. The purine ring system of guanine supplies all but two of the carbons in the ring system of pterin. The ribose moiety of GTP supplies the two new carbons for the pyrazine ring and the carbons of the erythrose side chain; one carbon from the guanine ring is released as formate. The pterin product is dihydroneopterin triphosphate. In eukaryotes, dihydroneopterin triphosphate is converted to dihydrobiopterin (Figure 3). In contrast, dihydrobiopterin is not formed in most bacteria.

The structures of biopterin and its reduced forms are shown in Figure 3. Reduction of the 7,8 double bond yields 7,8-dihydrobiopterin (a tautomer of 7,8-dihydropterin is quinonoid dihydropterin). Further reduction at the 5,6 double bond gives tetrahydrobiopterin.

Pterins in Metabolism

The Aromatic Amino Acid Hydroxylases (AAHs)

One of the most-studied processes involving biopterin is the hydroxylation of the aromatic amino acids. This is catalyzed by a small family of enzymes containing phenylalanine (PheH), tyrosine (TyrH), and tryptophan (TrpH) hydroxylase. They contain an iron atom and utilize tetrahydrobiopterin and molecular oxygen to hydroxylate a fairly unreactive entity, an aromatic ring. The AAHs are only active in the Fe^{II} state; one role of the tetrahydrobiopterin may be to keep the iron reduced. The major role of tetrahydrobiopterin is to activate the oxygen for eventual transfer to the aromatic amino acid

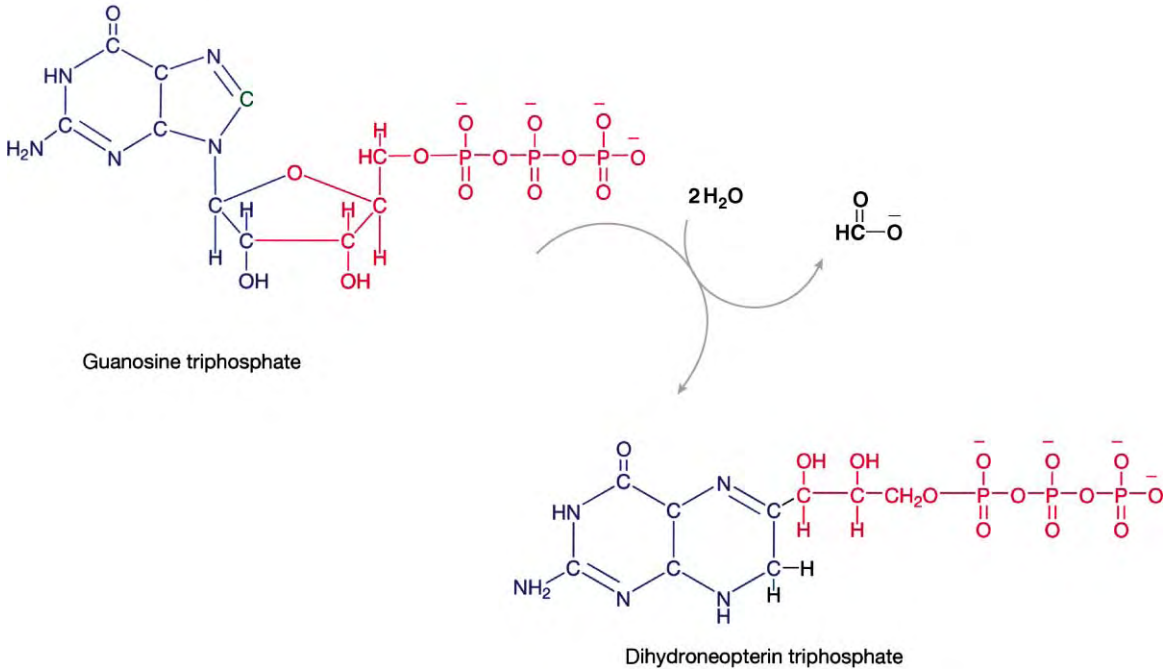

FIGURE 2 The first step in the synthesis of pterins from guanosine triphosphate. The atoms of GTP are color-coded to show their positions in the resulting neopterin molecule. Note that one carbon of GTP, colored green, is lost as formate.

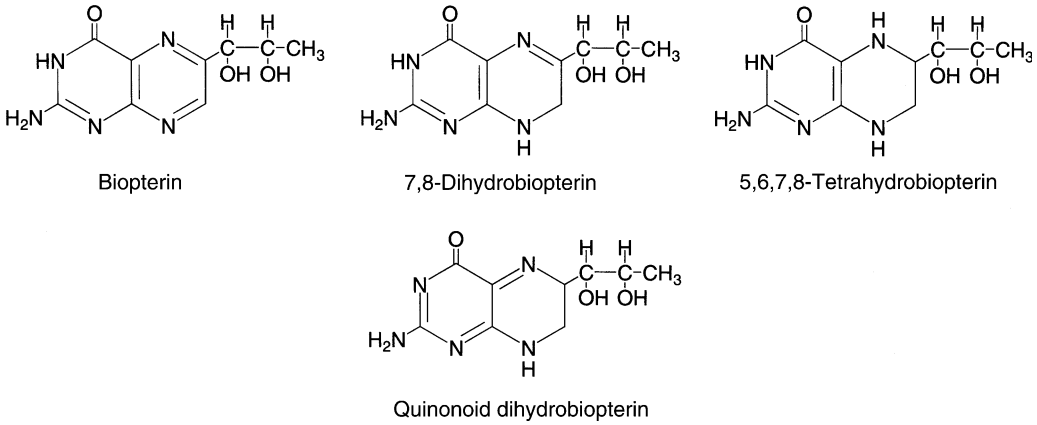

FIGURE 3 Structures of biopterin and its reduced forms.

substrate, probably through formation of a C4a-peroxy pterin intermediate (Figure 4).

Each of the AAHs catalyzes the rate-limiting step in its metabolic pathway: PheH in phenylalanine catabolism, TyrH in synthesis of the catecholamine neurotransmitters, and TrpH in serotonin synthesis. The three enzymes are homologous to a great extent in their catalytic domains (between any two there is 60% identity and 75% similarity). These enzymes as a rule are not found in bacteria, consistent with the general absence of biopterin from prokaryotes. However, PheH has been isolated from several prokaryotes, and from one, *Chromobacterium violaceum*, the sequence is 30% identical to the catalytic domain of human PheH. Two amino acid residues which bind tetrahydrobiopterin (in TyrH, F300 and E332) are conserved in all the aromatic amino acid hydroxylases studied, suggesting a central role for biopterin in the evolution of neurotransmitters and higher nervous systems.

The pterin product of the AAHs is C4a-carbinolamine dihydrobiopterin (Figure 4). It is released from the enzyme and is returned to the state needed for amino acid hydroxylation by the action of two more enzymes, C4a-carbinolamine dehydratase and dihydropterin reductase.

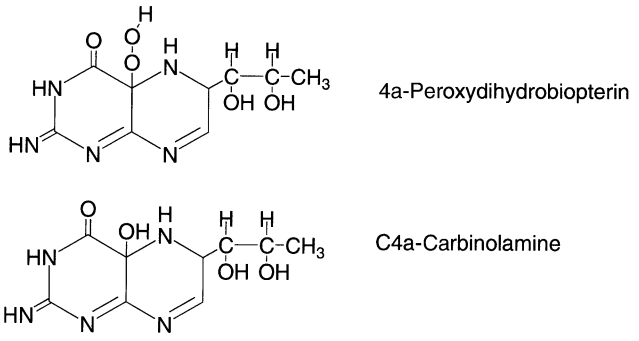

FIGURE 4 Peroxypterin and carbinolamine intermediates in the hydroxylation of aromatic amino acids.

Nitric Oxide Synthase

Nitric oxide synthase (NOS) is responsible for the synthesis of nitric oxide, NO. NOS utilizes tetrahydrobiopterin, NADPH, and molecular oxygen to convert L-arginine to L-citrulline and NO (Figure 5). Nitric oxide is a gas and a highly toxic compound. Because of its toxicity, its short half-life (1–5 s), and its diffusibility, NO serves the mammalian immune system as a killer of foreign intruders and cancer cells. It is also a cellular signal through its stimulation of cGMP synthesis.

NOSs are dimers of identical subunits. NOS contains flavin mononucleotide (FMN), flavin adenine dinucleotide (FAD), heme, and tetrahydrobiopterin. The tetrahydrobiopterin binding site is positioned close to the heme to facilitate electronic interaction between them. The tetrahydrobiopterin binding site is formed by residues in both subunits at the interface where the subunits associate; the pterin ring is sandwiched between a tryptophan residue from one subunit and a phenylalanine from the other. In contrast to the two-electron loss in AAHs, the tetrahydrobiopterin of NOS loses only one electron generating a biopterin radical. Biopterin remains bound to NOS before and after catalysis, another difference between NOS and the AAHs.

Molybdopterin-Containing Enzymes

A very large group of enzymes contain molybdenum (or in a few cases tungsten) in conjunction with a unique pterin, molybdopterin. These enzymes function in general to transfer oxygen to or from a physiological molecule. They can be assigned to two

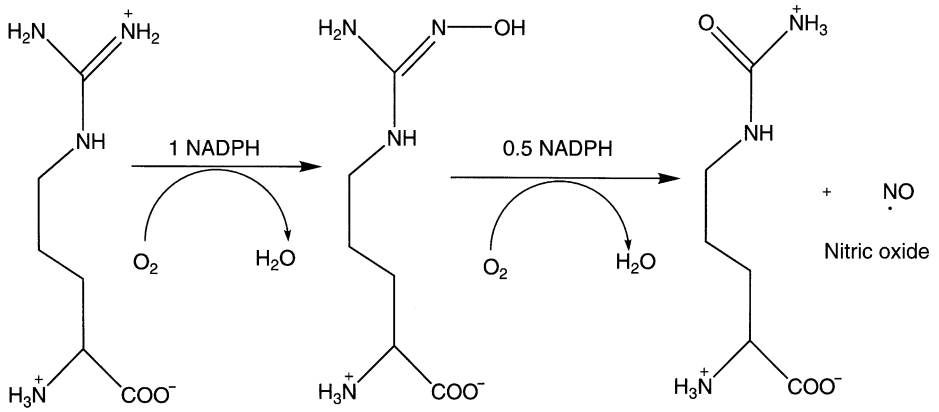

FIGURE 5 Reaction catalyzed by NOS.

categories based on the reaction catalyzed. The first group, the true hydroxylases, performs hydroxylation of aldehydes or aromatic rings; some of the enzymes in this category are milk xanthine oxidase, liver aldehyde oxidase, and bacterial enzymes such as formate dehydrogenase and nicotine dehydrogenase. The second category can be subdivided into: (1) sulfite oxidases and enzymes which reduce nitrate to enable a cell to utilize ammonia and (2) bacterial enzymes which function as terminal respiratory oxidases.

The structures of molybdopterin and the molybdenum cofactor are shown in Figure 6. The R group in prokaryotic systems can be guanine, cytosine, adenine, or hypoxanthine; in eukaryotes it is a hydrogen. The mode of binding the molybdenum cofactor to the protein differs from protein to protein in accord with the classification described above. The enzymes of the xanthine oxidase group contain one single molybdenum center per enzyme subunit, the sulfite oxidase family members are likely to have one molybdenum cofactor bound to a cysteine of the protein, and the final group can contain two molydopterins coordinated to one molybdenum, which can be coordinated to a selenium, sulfur, or cysteine. The biosynthetic pathways of these pterins have not been solved as yet.

The molybdenum enzymes are a vast enough group that a discussion of their properties is inappropriate here. In general, they contain other redox centers in addition to their pterin cofactor, such as heme, iron–sulfur clusters, and flavin. The role of the pterin is postulated to include mediation of electron transfer to the other redox active centers and modulation of the reduction potential of the molybdenum. The pterin is not thought to be itself oxidized and reduced during catalysis, a distinct difference between these enzymes and the NOSs and AHHs.

Tetrahydrobiopterin and Human Disease

Tetrahydrobiopterin deficiency is associated with a rare variant of hyperphenylalaninemia, which cannot be treated by the low phenylalanine diet successful for typical phenylketonuria (PKU) patients. It is characterized by a deficit of catecholamine neurotransmitters and serotonin as well (the products of the AAHs), affecting the nervous system as well as the liver. It can be caused by mutations in GTPCH or in the enzymes which recycle dihydrobiopterin. Decreased levels of tetrahydrobiopterin in cerebrospinal fluid have also

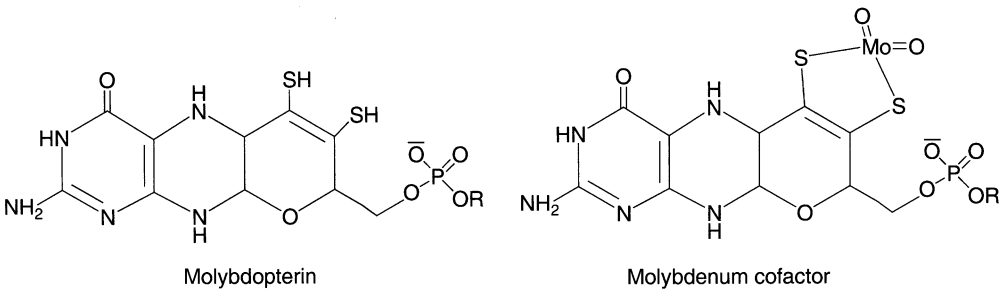

FIGURE 6 The structures of molybdopterin and the molybdenum cofactor.

been noted in such diseases as Parkinson's, autism, depression, and Alzheimer's.

See Also the Following Articles

Amino Acid Metabolism • Calcium Signaling: NO Synthase • Flavins • Heme Proteins

Glossary

aromatic amino acid Aromatic compounds are cyclic compounds containing double bonds so that their three-dimensional structure is planar. Amino acids are small molecules which consist of a central carbon atom, tetrahedrally bonded to a carboxylic acid group, an amino group, a hydrogen, and a fourth group, often called an R group; in the aromatic amino acids it is this R group which is aromatic.

heme A large planar heterocyclic compound consisting of four bridged pyrrole rings which binds Fe in biological systems for the transport or reactivity of oxygen.

heterocycle A ring-shaped compound made up of more than one kind of atom.

pyrimidine and pyrazine Organic heterocyclic compounds consisting of a six-membered ring with two nitrogen atoms separated by one carbon in pyrimidine and two carbons in pyrazine.

radical An atom or group of atoms possessing an odd (unpaired) electron.

Further Reading

Brown, G. M. (1985). Biosynthesis of pterins. In *Folates and Pterins, Chemistry and Biochemistry of Pterins* (R. L. Blakley and S. J. Benkovic, eds.) Vol 2, pp. 115–154. Wiley, New York.

Fitzpatrick, P. F. (2000). The aromatic amino acid hydroxylases. *Adv. Enzymol. Relat. Areas Mol. Biol.* **74**, 235–294.

Hille, R. (1996). The mononuclear molybdenum enzymes. *Chem. Rev.* **96**, 2757–2816.

Nixon, Jon C. (1985). Naturally occurring pterins. In *Folates and Pterins, Chemistry and Biochemistry of Pterins* (R. L. Blakley and S. J. Benkovic, eds.) Vol 2, pp. 1–42. Wiley, New York.

Rebel, J., Auerbach, G., Bader, G., Bracher, A., Nar, H., Hosl, C., Schramek, N., Kaiser, J., Bacher, A., Huber, R., and Fischer, M. (2003). Biosynthesis of pteridines. Reaction mechanism of GTP cyclohydrolase I. *J. Mol. Biol.* **326**, 503–516.

Thony, B., Auerbach, G., and Blau, N. (2000). Tetrahydrobiopterin biosynthesis, regeneration and functions. *Biochem. J.* **347**, 1–16.

Wei, C.-C., Crane, B. R., and Stuehr, D. J. (2003). Tetrahydrobiopterin radical enzymology. *Chem. Rev.* **103**, 2365–2383.

Biography

Colette Daubner and Paul Fitzpatrick have been working on the structure and function of the aromatic amino acid hydroxylases in the Department of Biochemistry and Biophysics at Texas A&M University since 1986. Dr. Daubner is a Research Scientist.

Paul Fitzpatrick is a Professor with joint appointment in Departments of Biochemistry and Biophysics and Chemistry. They received their Ph.D. at the University of Michigan and did postdoctoral research at The Pennsylvania State University.

P-Type Pumps: Copper Pump

Ilia Voskoboinik and James Camakaris
The University of Melbourne, Melbourne, Victoria, Australia

Copper pumps are copper-translocating P-type adenosinetriphosphatases (ATPases). Copper P-type ATPases, alongside other heavy-metal pumps, including silver, cadmium, lead, and zinc transporters, constitute group IB of the P-type ATPase family. Copper pumps are indispensable for maintaining copper homeostasis, including the delivery of copper to essential cuproenzymes and efflux of excess copper from the cell. P-type ATPases are the family of enzymes, which translocate a substrate across the lipid bilayer using the energy of ATP hydrolysis and which involve formation of an acyl-phosphate intermediate. P-type ATPases are ubiquitous proteins identified in most organisms, from bacteria to humans. These enzymes have evolved substrate specificity and regulatory mechanisms, which are essential for homeostasis of respective physiological or toxic substrates, amongst which are calcium, magnesium, sodium, potassium, protons, copper, and toxic heavy metals.

P-Type ATPases

Molecular and crystal structures of P-type ATPases have been revealed only in the last few years, despite massive efforts beginning in the early 1970s, to characterize the mechanisms of these enzymes. The best-studied molecules, at this stage, are calcium P-type ATPases, particularly the sarcoplasmic reticulum calcium pump. The catalytic mechanism, based on site-directed mutagenesis studies and the elegant studies by Toyoshima, who recently identified the crystal structure of sarcoplasmic reticulum calcium ATPase, consists of several fundamental steps (Figure 1): (1) Cation binding to high-affinity binding sites in the cation channel, which is formed by several transmembrane domains, leads to (2) conformational changes in the cytosolic ATP-binding domain, which acquire a conformation with high affinity for ATP. Subsequently, the terminal γ-phosphate is transferred to the invariant aspartate residue within the -DKTG- motif and forms a transient acyl-phosphate (aspartyl-phosphate) bond. The residual adenosine diphosphate dissociates from the cytosolic domain. These changes cause such significant conformational alterations within the transmembrane cation channel that its affinity for the cation is reduced and (3) the cation translocates across the membrane in a vectorial fashion. Subsequently, (4) the acyl-phosphate bond is hydrolyzed and (5) the enzyme returns to its original high-affinity cation-binding state. This model is generally accepted as a paradigm for P-type ATPases, including the copper pumps.

Copper

Copper is an essential trace element, whose redox properties (Cu^{2+}/Cu^{+}) are utilized by a number of enzymes catalyzing redox reactions. Cuproenzymes are found in various intracellular compartments, in the cytosol (e.g., Cu,Zn-superoxide dismutase), in the mitochondria (e.g., cytochrome *c* oxidase) and in the Golgi membranes (e.g., lysyl amine oxidase). At the same time, when present in excess, copper may exert its toxicity through the same redox properties. Thus, in the reduced intracellular environment copper undergoes redox cycling, which results in the generation of reactive oxygen species leading to oxidative stress, which, if not counterbalanced by antioxidant systems, may lead to cellular toxicity. In addition, copper, particularly copper(I), binds nonspecifically with high affinity to cellular proteins and can affect their physiological function. Biological systems accommodated both, the beneficial and potentially toxic roles of copper, through the evolution of the finely tuned machinery of copper homeostasis.

General Structure of Group IB P-Type ATPases

The first heavy-metal P-type ATPase was identified in 1989 through studies on cadmium-resistant bacteria. The predicted amino acid sequence analysis revealed little general similarity with other P-type ATPases, apart from some essential catalytic motifs. Since then, dozens of heavy-metal pumps, including copper, zinc, and cadmium transporters, as well as putative heavy-metal ATPases of unknown cation specificity, have either been identified through the predicted open reading frame

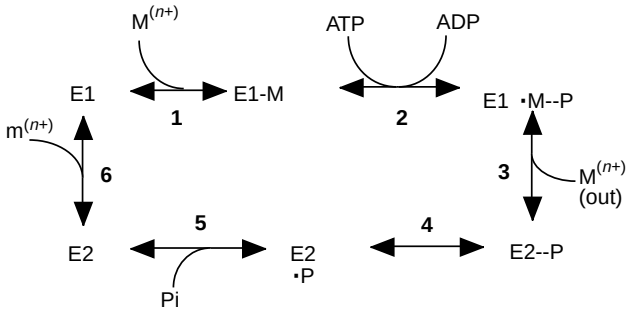

FIGURE 1 General concept of catalytic cycle of P-type ATPases, including copper transporters. $M^{(n+)}$ – cation to be translocated; $m^{(n+)}$ – counterion; P – terminal phosphate group of ATP forming an acyl-phosphate bond with invariant aspartate residue in the -DKTG- motif. (1) High-affinity cation binding; (2) high-affinity ATP binding and the transfer of the terminal γ-phosphate from ATP to the invariant aspartate residue, the formation of acyl-phosphate bond; (3) conformational change from the E1 to E2 state, translocation of the cation to the lumen; (4) transition to the low-energy acyl-phosphate bond; (5) dissociation of inorganic phosphate from the invariant aspartate residue; and (6) potential counterion translocation, transition from the E1 to E2 conformation. Reprinted from Voskoboinik, I., Camakaris, J., and Mercer, J. F. (2002). Understanding the mechanism and function of copper P-type ATPases. *Advances in Protein Chemistry* **60**, 123–150.

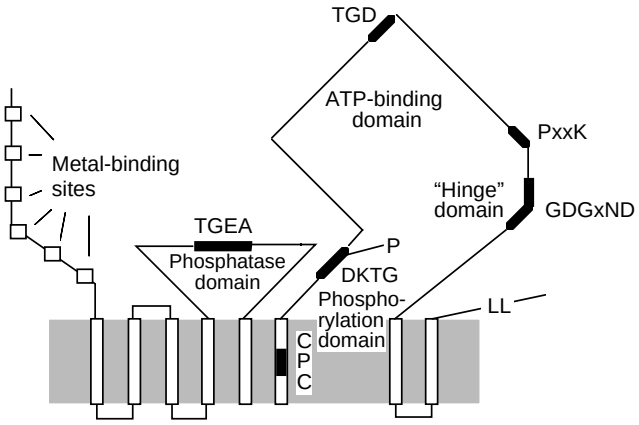

FIGURE 2 General structure of a heavy-metal P-type ATPase. "Metal-binding sites" are putative copper-binding motifs -GMxCxxC-; "phosphatase domain" – a cytosolic loop with conserved region(s), e.g., -TGEA-, essential for de-phosphorylation of the transient acyl-phosphate; P-DKTG is the phosphorylation domain, where P – indicates transient aspartyl-phosphate; "ATP-binding domain" and "hinge domain" – a large cytosolic loop with several conserved regions (e.g., -TGD-, -PxxK-, GDGxND) essential for ATP binding and the transfer of the terminal γ-phosphate of ATP to the invariant aspartate residue of the phosphorylation domain; the -CPC- motif is believed to constitute a part of the cation channel in heavy-metal P-type ATPases; -LL- motif is the internalization signal in ATP7A (position 1487/1488) and ATP7B (position 1454/1455). (Reprinted from Voskoboinik, I., Camakaris, J., and Mercer, J. F. (2002). Understanding the mechanism and function of copper P-type ATPases. *Advances in Protein Chemistry* **60**, 123–150.)

(ORF) analysis or characterized functionally in prokaryotes and eukaryotes. Heavy-metal transporters have eight predicted transmembrane domains (nonheavy-metal transporters contain ten) with an essentially invariant -CPC- motif in transmembrane domain 6 (Figure 2). The N terminus of these pumps generally contains up to six putative heavy-metal binding sites, with a common sequence GMxCxxC. Heavy metals have been shown to bind within this region with various affinities. The cytosolic ATP-binding loop contains the invariant acyl-phosphorylation motif -DKTG-, putative nucleotide and magnesium binding motifs -TGD- and -MVGDGIND-, yet lacks other conserved, among nonheavy-metal ATPases, regions. Furthermore, the phosphatase domain contains only one, TGE motif, out of three conserved regions (Figure 2). While additional functional motifs ought to be present in heavy-metal ATPases, they are yet to be identified and characterized.

Copper P-Type ATPases

Physiological Roles

Copper P-type ATPases have been identified in a variety of organisms, from bacteria to humans, which indicates their crucial importance for copper homeostasis. This has been proven experimentally in various experimental systems. Thus, the disruption of copper pumps in bacteria decreased their copper resistance, presumably through inability to efflux excess copper from the cell. In yeast, the plasma membrane copper pump, PcaI, also appears to be important for copper efflux. In contrast, the Golgi membrane copper P-type ATPase, Ccc2, has no direct role in copper resistance, but has been shown to be indispensable as a high-affinity copper transporter to the cuproenzyme, Fet3, which is required for high-affinity iron uptake. Similarly, in plants the Golgi membrane copper transporter, RAN1, has a crucial role in ethylene biosynthesis. Interestingly, plants appear to encode far more putative heavy-metal transporters than other organisms. However, their cation specificity and intracellular roles are yet to be identified. The analysis of the *Drosophila melanogaster* genome indicated the presence of a single copper P-type ATPase homologous to its human counterparts. However, the physiological role of this transporter has not been identified. In humans, two copper-translocating P-type ATPases have been identified and characterized: the ubiquitous (except the liver) Menkes protein (ATP7A), and the predominantly hepatic Wilson protein (ATP7B) which has ~65% homology with ATP7A. Unlike in unicellular organisms and in plants, these two transporters evolved a dual role in copper homeostasis, namely, the delivery of copper to cuproenzymes and the efflux of physiological or excess copper from the cell.

The latter function is essential for absorption of alimentary copper from the gastrointestinal tract and the reabsorption of copper in the kidney. The clinical symptoms of inherited genetic diseases, the X-linked recessive Menkes disease, and the autosomal-recessive Wilson disease, which are caused by detrimental mutations in the respective genes, demonstrate the essentiality of both proteins in copper homeostasis. Furthermore, the clinical features of Menkes and Wilson disease represent, respectively, the ultimate effects of systemic copper deficiency due to malabsorption, and toxicity due to copper hyperaccumulation.

Catalysis

Copper P-type ATPases vary in size from ~700 amino acids in bacteria to 1500 amino acids in humans. Nevertheless, they share significant structural similarity within regions, which have been postulated to be important for the catalysis of copper translocation. General elements of the catalytic cycle appear to be similar to those reported for calcium P-type ATPases (Figure 1). Thus, copper binding, presumably within the transmembrane cation channel, precedes the binding of ATP within the high-affinity cytosolic ATP-binding domain. This is followed by acyl-phosphorylation of the invariant, among all P-type ATPases, aspartate residue in the -DKTG- motif and subsequent copper translocation from the cytosolic to the lumenal side of the membrane. To complete the catalytic cycle the acyl-phosphate bond is hydrolyzed and the protein returns to its high-affinity copper-binding state. While copper pumps can be inhibited by orthovanadate, a classical inhibitor of P-type ATPases, the concentration required for such inhibition is considerably higher than the one observed for nonheavy-metal ATPases. Biochemical evidence suggests that copper ATPases can transport only reduced copper (Cu^+), which is the major form of copper in the reduced intracellular environment. The specificity of copper pumps for monovalent copper explains their silver (Ag^+) transporting activity and the lack of cross-specificity with divalent cations of heavy metals, e.g., cadmium, zinc, and lead. Copper ATPases investigated so far appear to be less catalytically active, with respect to cation translocation, than their non-heavy-metal transporting counterparts, as measured by the amount of ATPase-specific cation transported per minute. At the same time, the affinity of copper pumps for ATP is similar to the one determined for other P-type ATPases, consistent with conservation of essential ATP and magnesium-binding motifs in the ATP-binding cytosolic loop. The unique feature of copper P-type ATPases (as well as other heavy-metal pumps) is the presence of cytosolic N-terminal putative copper-binding sites with the sequence -GMxCxxC-. These conserved motifs bind copper(I) with higher affinity compared to copper(II) and other divalent heavy-metal cations. Furthermore, copper binding results in these motifs acquiring a conformation, which protects copper from being removed from these sites by nonspecific ligands, such as glutathione. The exact role of the N-terminal metal-binding sites is yet to be fully clarified, but they do not appear to play an essential role in cation translocation by copper ATPases. Yet these motifs have been shown to regulate the affinity of copper pumps for copper and may be particularly important in allowing its acquisition or delivery to a specific target under basal or copper-limited conditions. Similar findings were reported for the putative metal-binding sites of other heavy-metal P-type ATPases.

Regulation

The mechanisms of regulation of copper pumps vary considerably between prokaryotes and multicellular differentiated eukaryotic systems.

Prokaryotes

In prokaryotes, genes encoding copper ATPases are organized in an operon, which is regulated through a *trans*-acting repressor/activator system. Thus, in *Enterococcus hirae* under physiological or copper deficient conditions copper binds to a copper operon repressor, CopY, whose binding to the promoter region of the operon results in the suppression of copper ATPase synthesis. Conversely, in the presence of elevated copper concentrations, copper binding to a copper activator, CopZ, results in its overcompeting CopY–copper complex at the promoter region. This leads to overexpression of copper pumps, which, through efflux of excess copper, restores copper homeostasis. A member of the MerR family of DNA-binding metal-responsive transcriptional regulators, CueR, has been identified as a regulator of the copper export pump, CopA, in *Escherichia coli*. CueR binds in the promoter region of CopA and responds to elevated copper(I) or silver(I) concentrations by overexpression of CopA. The disruption of CueR causes the loss of CopA expression in bacteria.

Eukaryotes

Copper ATPases in yeast are represented by two pumps, which are localized at the cellular membrane, PcaI, and at the Golgi membrane, Ccc2. These transporters have defined functions: PcaI is presumed to function in copper efflux from the cell, while Ccc2 delivers copper to the multicopper ferroxidase, Fet3, and has no direct copper resistance function. Importantly, Ccc2 is a high-affinity transporter, which, under limited copper concentrations, receives copper from a low-molecular-weight copper chaperone, AtxI. This protein binds copper(I) within the high-affinity copper-binding site, GMxCxxC, and delivers it to the analogous site at the N terminus of Ccc2.

Copper does not appear to directly regulate the expression levels of PcaI or Ccc2. These protein–protein interactions between the copper chaperone Atx1 and the P-type ATPase permit copper transport under conditions where essentially no free ionic copper is available.

Mammals have evolved a novel system for regulating copper homeostasis via the Menkes (MNK; ATP7A) and Wilson (WND; ATP7B) P-type ATPases. These transporters exert a dual role in copper homeostasis by catalyzing efflux of copper from the cell at the plasma membrane and supplying copper to cuproenzymes of the secretory pathway in the Golgi compartment. These functions are achieved through copper-regulated vesicular trafficking of the transporters. Thus, under physiological copper concentrations both pumps are localized at the trans-Golgi network, where they supply copper to cuproenzymes. In the presence of elevated copper concentrations the proteins relocalize to the plasma membrane, they efflux excess copper from the cell. Once copper concentrations subside to physiological levels, the proteins relocate to the trans-Golgi network. Several signaling motifs have been shown to be responsible for regulation of the subcellular localization of ATP7A and ATP7B. These include the N-terminal putative copper-binding sites (important for exocytosis), and the C-terminal dileucine endocytic motifs (important for endocytosis). Importantly, under physiological concentrations copper is delivered to the copper-binding sites of ATP7A and ATP7B by a copper chaperone, ATOX1. The essentiality of such an interaction has been shown by using ATOX1 knock out mice. These transgenic animals have exhibited severe systemic copper deficiency, which has been associated with malabsorption of alimentary copper.

Two inherited diseases associated with mutations in copper P-type ATPases have been identified in humans and analogous disorders are found in other mammals. The systemic copper deficiency disorder, the X-linked Menkes disease, has been associated with detrimental mutations in the *ATP7A* gene, while the copper hepatotoxicity and neurotoxicity disorder, the autosomal-recessive Wilson disease, has been linked to mutations in the *ATP7B* gene. Importantly, the mutations which affect either the catalytic or the trafficking function of the pump can result in the disease phenotype. The nature and severity of the disease phenotype in Menkes and Wilson diseases can be explained for a number of mutations, based on predicted faulty localization/trafficking and magnitude of reduction in catalytic activity.

See Also the Following Articles

Chaperones for Metalloproteins • Chaperones, Molecular • Cytochrome *c* • Cytochrome Oxidases, Bacterial • Inorganic Biochemistry

Glossary

copper chaperone A small protein that binds, transports, and delivers copper to copper-requiring enzymes/proteins.

cuproenzyme An enzyme in which copper constitutes a core part of the active site; these enzymes usually utilize redox properties of copper to catalyze reactions of oxidation or reduction.

operon A cluster of genes that is coordinately regulated.

ORF (open reading frame) DNA sequence that contains features required for encoding a protein.

protein trafficking Relocalization of proteins from one part of the cell to another, normally via vesicles.

redox Chemical reaction involving oxidation and reduction.

Further Reading

Huffman, D. L., and O'Halloran, T. V. (2001). Function, structure, and mechanism of intracellular copper trafficking proteins. *Annu. Rev. Biochem.* **70**, 677–701.

Silver, S., and Phung, L. T. (1996). Bacterial heavy metal resistance: New surprises. *Annu. Rev. Microbiol.* **60**, 753–789.

Toyoshima, C., Nakasako, M., Nomura, H., and Ogawa, H. (2000). Crystal structure of the calcium pump of sarcoplasmic reticulum at 2.6 Å resolution. *Nature* **405**, 647–655.

Tumer, Z., Moller, L. B., and Horn, N. (1999). Mutation spectrum of ATP7A, the gene defective in Menkes disease. *Adv. Exp. Med. Biol.* **448**, 83–95.

Voskoboinik, I., Camakaris, J., and Mercer, J. F. (2002). Understanding the mechanism and function of copper P-type ATPases. *Adv. Protein Chem.* **60**, 123–150.

Biography

James Camakaris is an Associate Professor and Reader in Genetics and is also Head of the Department of Genetics, The University of Melbourne, and a research associate of the Murdoch Children's Research Institute. His primary research interest is in understanding the genes, proteins, and mechanisms of copper homeostasis with a current focus on structure–function aspects of the Menkes copper-translocating P-type ATPase.

Ilia Voskoboinik is a Postdoctoral Research Fellow in the Department of Genetics, The University of Melbourne. His primary research interest is in understanding structure–function of mammalian copper-translocating P-type ATPases, the Menkes, and the Wilson protein.

P-Type Pumps: H^+/K^+ Pump

Jai Moo Shin and George Sachs
University of California at Los Angeles and VA Greater Los Angeles Healthcare System, California, USA

The gastric H^+/K^+ pump is a member of the P_2-type ion-motive ATPase family and is responsible for the elaboration of HCl by the parietal cell of the gastric mucosa. The gastric H^+, K^+-ATPase catalyzes H^+ for K^+ exchange by an electroneutral exchange of cytoplasmic protons for extracytoplasmic potassium, while the protein undergoes phosphorylation and dephosphorylation related to ion binding and release. The gastric H^+, K^+-ATPase is composed of two subunits, the catalytic or α-subunit having ten transmembrane segments and the β-subunit having one transmembrane segment. The gastric H^+, K^+-ATPase α-subunit is a 100 kDa protein consisting of ~1034 amino acids and β-subunit is a glycoprotein with ~290 amino acids.

Structure of the Gastric H^+, K^+-ATPase

The α-Subunit of Gastric H^+, K^+-ATPase

The primary sequences of the α-subunits deduced from cDNA have been identified from pig, rat, and rabbit. The hog gastric H^+, K^+-ATPase α-subunit sequence deduced from its cDNA consists of 1034 amino acids with an M_r of 114 285 Da. The rat gastric H, K ATPase consists of 1033 amino acids with an M_r of 114 012 Da, and the rabbit gastric H, K ATPase consists of 1035 amino acids, showing an M_r of 114 201 Da. The degree of conservation among the α-subunits is extremely high (over 97% identity) among species. The gene sequence for human and the 5′ part of the rat H^+, K^+-ATPase α-subunits have been determined showing that the human gastric H^+, K^+-ATPase gene has 22 exons and encodes a protein of 1035 residues including the initiator methionine residue ($M_r = 114\,047$ Da). These H^+, K^+-ATPase α-subunits show high homology (~60% identity) with the Na^+, K^+-ATPase catalytic α-subunit. The putative distal colon H^+, K^+-ATPase α-subunit has also been sequenced and shares 75% homology with both the H^+, K^+- and Na^+, K^+-ATPases.

The gastric H^+, K^+-ATPase α-subunit has conserved consensus sequences along with the other P type ATPases, the sarcoplamic reticulum Ca^{2+}-ATPase and the Na^+, K^+-ATPase, for the ATP-binding site, the phosphorylation site, the pyridoxal 5′-phosphate-binding site and the fluorescein isothiocyanate-binding site. These sites are thought to be within the ATP-binding domain in the large cytoplasmic loop between transmembrane segments 4 and 5. Structurally, this enzyme can be divided into three domains, viz., cytoplasmic, membrane, and extracytoplasmic domains. The cytoplasmic domain contains four sub-domains, a stalk domain, N-domain, P-domain, and A-domain. The N-domain or nucleotide-binding domain is a large cytoplasmic domain between M4 and M5 where ATP binds. The P-domain or phosphorylation domain is a cytoplasmic domain near M4 where there is phosphorylation and dephosphorylation. The A-domain or activation domain is a cytoplasmic domain between M2 and M3, which moves depending on conformational changes. The stalk domain contains the extension of the transmembrane segments into the cytoplasmic region and forms a link for the passage of ions into the membranes and for transmission of conformational changes from the cytoplasm. The gastric α-subunit structure that is based on the 3D crystal of the SR Ca-ATPase structure is shown in Figure 1. Although this model is probably true in general, it is almost certainly incorrect in its detail.

There is much biochemical evidence showing the applicability of the ten transmembrane segment model to this ATPase. The C terminal amino acids of the α-subunit, tyr–tyr, are present in the cytoplasmic region, which was shown by a method of iodination with peroxidase-H_2O_2–^{125}I followed digestion with carboxypeptidase Y. Four transmembrane pairs connected by their luminal loop were detected in a tryptic digest of the hog gastric H^+, K^+-ATPase. A peptide fragment beginning at gln^{104} represents the H1/loop/H2 sector. The H3/loop/H4 sector was found at a single peptide peak beginning at thr^{291}, and the H5/loop/H6 sector at a peptide beginning at leu^{776}. The H7/loop/H8 region was found in a single peptide fragment of 11 kDa, beginning at leu^{853}. Surprisingly no peptide representing H9 and H10 was found in any enzyme digest procedure.

Antibody 95 inhibits ATP hydrolysis in the intact vesicles, and appears to be K^+ competitive. The sequence

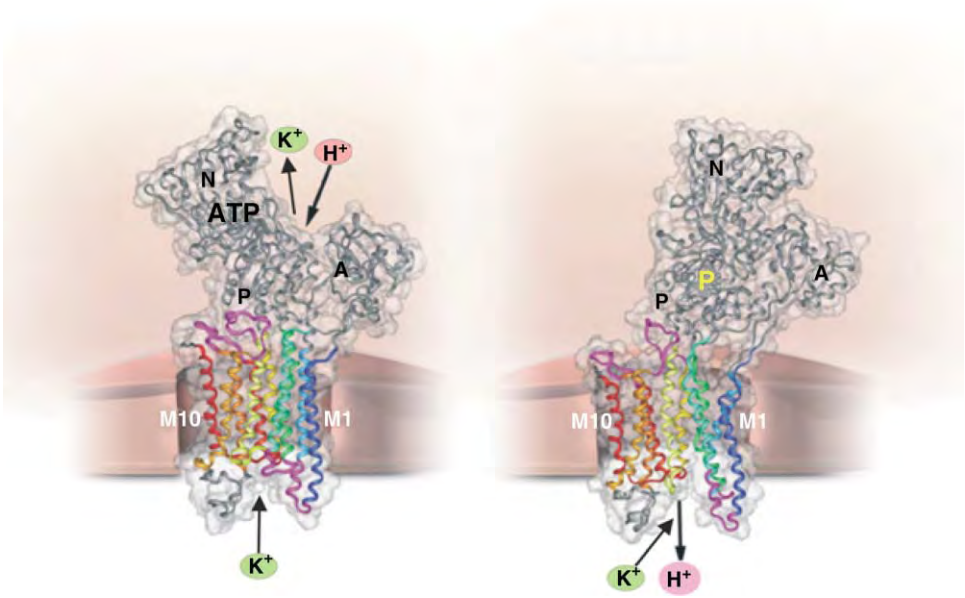

FIGURE 1 Proposed structure of the gastric H^+,K^+-ATPase α-subunit in E_1 (left) and E_2 (right) conformations. There are three lobes in the cytoplasmic domain: N (ATP binding), P (phosphorylation), and A (activation) regions. With binding of H^+ and MgATP to the E_1 form there is transient association of the N and P lobes with phosphorylation of asp386 and a conformational change to E_2P so that the A domain associates with the P domain. This change is transmitted to the membrane domain in the region of TM6 (dark yellow) and H^+ binding to the cation binding domain in the middle of the membrane domain is followed by release of H^+ and binding of K^+ from the luminal surface. There is then dephosphorylation and reformation of the E_1 conformation with release of K^+ to the cytoplasm.

recognized by this antibody was between amino acid positions 529 and 561. Since it inhibits the enzyme in intact cytoplasmic side out vesicles this epitope must be cytoplasmic and it is close to the region known to bind the cytoplasmic reagent, fluorescein isothiocyantate, FITC, a lysine reagent, namely in the loop between H4 and H5. Antibody 1218 was shown to have its major epitope between amino acid positions 665 and 689 in the same N domain. A second epitope for mAb 1218 was also identified to be between amino acid positions 853 and 907. Monoclonal antibody 146 epitope was defined to be between positions 873 and 877 of the hog α-subunit. This is on or close to the extra-cytoplasmic face of H7. The presence of H9 and H10 was shown by *in vitro* transcription/translation of cDNAs encoding these sequences. This technique also showed the presence of H1 through H4 but was unable to detect H5 or H6.

The β-Subunit of Gastric H^+, K^+-ATPase

The primary sequences of the β-subunits have been reported for rabbit, hog, rat, mouse, and human. The β-subunit with ~290 amino acids is a glycoprotein having one transmembrane segment located at the region between amino acid sequence positions 38 and 63 near the N terminus and six or seven N-linked glycosylation sites in the extracytoplasmic region. Using lectin affinity chromatography, the H^+, K^+-ATPase α-subunit was co-purified with the β-subunit, showing that the α-subunit interacts with the β-subunit. By cross-linking with low concentrations of glutaraldehyde, the β-subunit was shown to be closely associated with the α-subunit. In the extracytoplasmic domain, there are six cysteines which are linked through disulfide bonds. Reduction of the disulfides of the β-subunit inhibits the activity of the H^+, K^+-ATPase. In the case of the Na^+, K^+-ATPase, the effect of reducing agents on the ability of the enzyme to hydrolyze ATP and bind ouabain was quantitatively correlated with the reduction of disulfide bonds in the β-subunit. Seven putative N-glycosylated sites (AsnXaaSer and AsnXaaThr) are shown in rabbit H^+, K^+-ATPase β-subunit, which are conserved in rats and humans. Six putative N-glycosylation sites are found in the hog gastric β-subunit. The N-linked oligosaccharides of the β-subunit of rabbit gastric H^+, K^+-ATPase was identified. All N-linked AsnX(Ser/Thr) sequences at positions 99, 103, 130, 146, 193, and 222 were fully glycosylated. Asn 99 was modified exclusively with oligomannosidic-type structures, $Man_6GlcNAc_2$–$Man_8GlcNAc_2$, and Asn193 has $Man_5GlcNAc_2$–$Man_8GlcNAc_2$ and lactosamine-type structures. Asn 103, 146, 161, and 222 contain lactosamine-type structures. All the branches of the lactosamine-type structure

were terminated with Galα-Galβ-GlcNAc extensions. The role of the carbohydrate chains was studied using HEK-293 cells. The enzyme activity was not affected by removal of any one of seven carbohydrates of the β-subunit; however, removal of all carbohydrate chains resulted in the complete loss of activity. Except for the second glycosylation site, each site was essential for trafficking from Golgi to plasma membrane, but not for ER to Golgi movement.

The function of the β-subunit is not clearly known, but this subunit appears to be required for proper assembly and targeting of the catalytic subunit. Perhaps the β-subunit has a function in maintaining the structure of the α-subunit to enable effective binding of K^+ ion to the outside face of the α-subunit. The H^+, K^+-ATPase β-subunit has the sequence Phe-Arg-His-Tyr in its cytoplasmic domain. This tyrosine has been shown to be important for the retrieval of the H^+, K^+-ATPase from the apical membrane of the parietal cells and to ensure its return to the tubulo-vesicular compartment in order to terminate the process of acid secretion. The participation of a tyrosine-based signal in the retrieval of the H^+, K^+-ATPase suggests that this process involves interactions with adaptins and is mediated by clathrin-coated pit formation. In knockout mice deficient in the H^+, K^+-ATPase β-subunit, cells that express the H^+, K^+-ATPase α-subunit had abnormal canaliculi and were devoid of typical tubulo-vesicular membranes.

Regions of Association in the Oligomeric Structure

There has been much suggestive evidence that the $\alpha-\beta$ heterodimeric H^+, K^+-ATPase exists as an oligomer. Such evidence includes target size by irradiation and unit cell size of the enzyme in two-dimensional crystals. Using Blue native gel separation and cross-linking with Cu^{2+}-phenanthroline, it was shown that the enzyme did indeed exist as an $(\alpha\beta)_2$ heterodimeric dimer. Membrane-bound H^+, K^+-ATPase reacted with Cu-phenanthroline to provide an $\alpha-\alpha$ dimer. The site of Cu^{2+}-oxidative cross-linking was either at cys^{565} or cys^{616}. Hence, this region of the α-subunit is in close contact with its neighboring α-subunit. No evidence was obtained for $\beta-\beta$ dimerization. ATP prevents this Cu-phenanthroline-induced $\alpha-\alpha$ dimerization. The M7/loop/M8 sector of the α-subunit is tightly associated with the β-subunit. An antibody mAb 146-14 recognizes the region of the α-subunit at the extra-cytoplasmic face of the M7 segment as well as the β-subunit, a finding consistent with the association found by column chromatography. Using a yeast two-hybrid analysis, a fragment Leu855 to Arg922 of the α-subunit was identified to bind the β-subunit. This is at the entrance of the TM8 into the membrane domain.

Kinetics and Conformational Changes of the Gastric H^+, K^+-ATPase

The gastric H^+, K^+-ATPase exchanges intracellular hydrogen ions for extracellular potassium ions by consuming ATP. The H^+ for K^+ stoichiometry of the H^+, K^+-ATPase is not clear. There are reports of two different stoichiometries, one or two H^+ per ATP hydrolyzed. In ion-tight vesicles studied at pH 6.1, the stoichiometry is $2H^+$:1ATP but at full pH gradient where the pH reaches 1.0, this has to fall to 1:1. Probably protonation of a carboxylic acid at the lower luminal pH is then maintained.

There are several steps in the reaction scheme of the H^+, K^+-ATPase. The enzyme is phosphorylated by ATP at asp^{386}. The rate of formation of the phosphoenzyme (EP) and the K^+-dependent rate of phosphoenzyme breakdown are sufficiently fast to allow the phosphoenzyme to be an intermediate in the overall ATPase reaction. The initial step is the reversible binding of ATP to the enzyme in the absence of added K^+ ion, followed by an Mg^{2+} (and proton) dependent transfer of the terminal (gamma) phosphate of ATP to asp^{386} of the catalytic subunit (E_1-P·H^+). The Mg^{2+} remains occluded until dephosphorylation. The addition of K^+ to the enzyme-bound acyl phosphate results in a two-step dephosphorylation. The faster initial step is dependent on the concentration of K^+, whereas the slower step is not affected by K^+ concentration. The second phase of EP breakdown is accelerated in the presence of K^+ but, at K^+ concentration exceeding 500 μM, the ratio becomes independent of K^+ concentration. This shows that two forms of EP exist. The first form E_2P is K^+ sensitive and converts spontaneously in the rate-limiting step to E_1P, the K^+ insensitive form. ATP binding to the H^+, K^+-ATPase occurs in both the E_1 and the E_2 state, but with a lower affinity in E_2 state (2 000 times lower compared to E_1). The effects of H^+ and K^+ on formation and breakdown of phosphoenzyme were determined using transient kinetics. Increasing hydrogen ion concentrations on the ATP-binding face of the vesicles accelerate phosphorylation, whereas increasing potassium ion concentrations inhibit phosphorylation. Increasing hydrogen ion concentration reduces this K^+ inhibition of the phosphorylation rate. Decreasing hydrogen ion concentration accelerates dephosphorylation in the absence of K^+, and K^+ on the luminal surface accelerates dephosphorylation. Increasing K^+ concentrations at constant ATP decreases the rate of phosphorylation and increasing ATP concentrations at

constant K^+ concentration accelerates ATPase activity and increases the steady state phosphoenzyme level. Therefore, inhibition by cations is due to cation stabilization of a dephospho form at a cytosolically accessible cation-binding site. The reaction mechanism is similar to that of the Na^+, K^+-ATPase.

The ions transported from the cytoplasmic side are H^+ at high pH. Since Na^+ is transported as a surrogate for H^+, it is likely that the hydronium ion, rather than the proton per se is the species transported. The ions transported inwards from the outside face of the pump are Tl^+, K^+, Rb^+, or NH_4^+. Presumably the change in conformation changes a relatively small ion-binding domain in the outward direction into a larger ion-binding domain in the inward direction.

The E_1 conformation of the H^+, K^+-ATPase binds the hydronium ion from the cytoplasmic side at high affinity. With phosphorylation, the conformation changes from $E_1P{\cdot}H_3O^+$ to $E_2P{\cdot}H_30^+$ form, which has high affinity for K^+ and low affinity for H_3O^+ allowing release of H_3O^+ and binding of K^+ on the extra-cytoplasmic surface of the enzyme. The rapid breakdown of the E_2P form requires K^+ or its congeners on the outside face of the enzyme. With dephosphorylation, the E_1K^+ conformation is produced with a low affinity for K^+, releasing K^+ to the cytoplasmic side, allowing rebinding of H_3O^+.

Fluorescein isothiocyanate (FITC) binds to the H^+, K^+-ATPase, inhibiting ATPase activity but not pNPPase activity. Fluorescence of the FITC-labeled enzyme, representing the E_1 conformation, was quenched by K^+, Rb^+, and Tl^+. The quenching of the fluorescence by KCl reflects the formation of E_2K^+. FITC binds at lys^{516} in the hog enzyme sequence. This FITC-binding site apparently becomes less hydrophobic when KCl binds to form the $E_2{\cdot}K$ conformation. In the E_1 form, the FITC region is relatively closer to the membrane and the extra-cytoplasmic loop relatively hydrophilic. With the formation of the $E_2{\cdot}K^+$ form, the FITC region is more distant from the membrane. These postulated conformational changes are therefore reciprocal in the two major conformers of the enzyme. When the gastric H^+, K^+-ATPase was cleaved by Fe^{2+}-catalyzed oxidation under various ligand, cleavage patterns were different between the different conformations. There are two Fe^{2+} cleavage sites. In Fe^{2+} site1, the parallel appearance of the fragments at ^{230}ESE, near ^{624}MVTGD, and at ^{728} VNDS upon transition from E_1 to E_2(Rb) conformations were observed. Meanwhile, in Fe^{2+} site2, the fragment near ^{299} HFIH was cleaved independent of conformational changes. These cleavage patterns were the same as those of the Na^+, K^+-ATPase. The cleavage data showed that the structural organization and changes in the cytoplasmic domains, association with E_1/E_2 transitions, are essentially the same for the H^+, K^+-ATPase, the Na^+, K^+-ATPase, and sr Ca-ATPase. N-domain where ATP binds inclines nearly 90° with respect to the membrane and the A-domain rotates by about 110° horizontally during the E1 to E2 conformation.

Functional Residues of the H^+, K^+-ATPase

When the gastric H^+, K^+-ATPase was digested by trypsin in the presence of high concentration of KCl, the tryptic membrane digest showed the presence of Rb^+ occlusion, i.e., stable binding of Rb^+ in the membrane domain of the catalytic subunit as does the Na^+, K^+-ATPase. Some regions near the membrane such as the region between gly^{93} and glu^{104} near the M1 segment, the region between asn^{753} and leu^{776} near the cytoplasmic side of the M5 segment, and the region after the M8 segment, especially the region between ile^{945} and ile^{963} containing five arginines and one lysine, were K^+ protected against digestion. Furthermore, when K^+ was removed from this membrane digest, the M5/M6 hairpin was released from the membrane, showing that M5M6 membrane hairpin is stabilized by K^+ ions. Proton pump inhibitors such as omeprazole, pantoprazole, lansoprazole, and rabeprazole all bind to Cys813 of M5M6, giving inhibition of activity.

Using site-directed mutagenesis of the gastric H^+, K^+-ATPase transfected in HEK293 cells, M5M6 luminal loop was studied in terms of K^+ access to the ion-binding domain. Mutations of M5, M5–M6, and M6 regions such as P798C, Y802L, P810A, C813A or S, F818C, T823V, and mutations of M7–M8 and M8 such as E914Q, F917Y, G918E, T929L, F932L, reduced the affinity for SCH28080, a reversible proton pump inhibitor, up to tenfold without affecting the nature of the kinetics. The L809F substitution in the loop between M5 and M6 resulted in about 100-fold decrease in inhibitor affinity. C813T mutant showed ninefold loss of SCH28080 affinity. All these data suggest that the binding domain for SCH28080 contains the surface between L809 and C813, where M5–M6 loop and the luminal end of M6 locate. Mutations of C813 and I816 in M6 and M334 in M4 also showed that the inhibitor binds close to the luminal surface of the enzyme. Mutations of the negatively charged amino acid residue in the α-subunit showed that the carboxyl group of the membrane-spanning domain is important for cation binding. Mutation of E820Q showed decreased K^+ sensitivity and the dephosphorylation was not stimulated by either K^+ or ADP, indicating that E820 might be involved in K^+ binding and transition to the E_2 form of the H^+, K^+-ATPase. Mutation of E795 showed a decrease of the phosphorylation rate and the apparent ATP affinity, indicating that E795 is involved in both K^+ and H^+

binding. Mutation of E795 and E820 in M5 and M6 resulted in a K^+-independent, SCH28080-sensitive ATPase activity, caused by a high spontaneous dephosphorylation rate. Thus the sixth transmembrane (M6) segment of the catalytic subunit plays an important role in the ion recognition and transport in the type II P-type ATPase families. When all amino acid residues in the M6 segment of gastric H^+, K^+-ATPase α-subunit were singly mutated with alanine, four mutants, L819A, D826A, I827A, and L833A, completely lost K^+-ATPase activity. Mutant L819A was phosphorylated but barely dephosphorylated in the presence of K^+, whereas mutants D826A, I827A, and L833A were not phosphorylated from ATP. Amino acids involved in the phosphorylation are located exclusively in the cytoplasmic half of the M6 segment and those involved in the K^+-dependent dephosphorylation are in the luminal half. Several mutants such as I821A, L823A, T825A, and P829A partly retained the K^+-ATPase activity accompanying the decrease in the rate of phosphorylation. Substituting three residues in the Na^+, K^+-ATPase sequence with their H^+, K^+-ATPase counterparts (L319F, N326Y, T340S) and replacing the TM3–TM4 ectodomain sequence with that of the H^+, K^+-ATPase result in a pump that gives 50% of ATPase activity in the absence of Na^+ at pH 6. The cation selectivity of the Na^+, K^+- and H^+, K^+-ATPase would be generated through a cooperative effort between residues of the transmembrane segments and the flanking loops that connect these transmembrane domains. A model that results from these studies and the 3D structure of the SR Ca-ATPase suggests that ion transport occurs between TM4, 5, 6 and perhaps TM8 and that the vestibule around cys813 is the binding domain of both compounds such as omeprazole and SCH28080.

Acid Secretion and the Gastric H^+, K^+-ATPase

The H^+, K^+-ATPase is present only in the gastric parietal cell and the intercalated cell of the distal renal tubule. In the resting parietal cell, it is present in smooth surfaced cytoplasmic membrane tubules. Upon stimulation of acid secretion, the pump is translocated to the microvilli of the secretory canaliculus of the parietal cell. This morphological change results in a several fold expansion of the canaliculus. There are actin filaments within the microvilli and the subapical cytoplasm. In the cytoskeleton system, there is abundance of microtubules among the tubulovesicles. Some microtubules appeared to be associating with tubulovesicles. A large number of electron-dense coated pits and vesicles were observed around the apical membrane vacuoles in cimetidine-treated resting parietal cells, consistent with an active membrane uptake in the resting state. Cultured parietal cells also undergo morphological transformation under histamine stimulation, resulting in great expansion of apical membrane vacuoles. Immunogold labeling of H^+, K^+-ATPase was present not only on the microvilli of expanded apical plasma membrane vacuoles but also in the electron-dense coated pits.

There is activation of a K^+ and Cl^- conductance in the pump membrane which allows K^+ to access the extra-cytoplasmic face of the pump. This allows H^+ for K^+ exchange to be catalyzed by the ATPase.

The covalent inhibitors of the H^+, K^+-ATPase that have been developed for the treatment of ulcer disease and esophagitis depend on the presence of acid secreted by the pump. They are also acid activated prodrugs that accumulate in the acid space of the parietal cell. Hence their initial site of binding is only in the secretory canaliculus of the functioning parietal cell. These data show also that the pump present in the cytoplasmic tubules does not generate HCl.

The upstream DNA sequence of the α-subunit contains both Ca and cAMP responsive elements in the case of the rat H^+, K^+-ATPase. There are gastric nuclear proteins present that bind selectively to a nucleotide sequence, GATACC, in this region of the gene. These proteins have not been detected in other tissues. Stimulation of acid secretion by histamine increases the level of mRNA for the α-subunit of the pump. Elevation of serum gastrin, which secondarily stimulates histamine release from the enterochromaffin-like cell in the vicinity of the parietal cell, also stimulates the mRNA levels in the parietal cell. H_2 receptor antagonists block the effect of serum gastrin elevation on mRNA levels. It seems therefore that activity of the H_2 receptor on the parietal cell determines in part the gene expression of the ATPase. It might be expected therefore that chronic stimulation of this receptor would up-regulate pump levels whereas inhibition of the receptor would down-regulate levels of the ATPase.

However, chronic administration of these H2 receptor antagonists, such as famotidine, results in an increase in pump protein, whereas chronic administration of omeprazole (which must stimulate histamine release) reduces the level of pump protein in the rabbit. Regulation of pump protein turnover downstream of gene expression must account for these observations.

See Also the Following Articles

Actin Assembly/Disassembly • Actin-Capping and -Severing Proteins • Actin-Related Proteins • Amino Acid Metabolism • Membrane Transport, General Concepts

Glossary

gastric H^+, K^+-ATPase An enzyme, which is one of the P_2-type ionmotive ATPases, that allows an electroneutral exchange of cytoplasmic protons for extracytoplasmic potassium.

α-subunit of gastric H^+, K^+-ATPase Functional subunit consisting of 1034 amino acids with an M_r of 114 KDa, which has ten transmembrane segments.

β-subunit of gastric H^+, K^+-ATPase A glycoprotein consisting of ~290 amino acids having one transmembrane segment and six or seven N-linked glycosylation sites in the extracytoplasmic region.

Further Reading

Melle-Milovanovic, D., Lambrecht, N., Sachs, G., and Shin, J. M. (1998). Structural aspects of the gastric H,K ATPase: The M5/M6 domain and alpha beta association. *J. Physiol. Scand.* **163**(suppl. 643), 147–162.

Munson, K., Lambrecht, N., Shin, J. M., and Sachs, G. (2000). Analysis of the membrane domain of the gastric H^+, K^+-ATPase. *J. Exp. Biol.* **203**(Pt 1), 161–170.

Munson, K., Vagin, O., Sachs, G., and Karlish, S. (2003). Molecular modeling of SCH28080 binding to the gastric H,K-Atpase and MgATP interactions with SERCA- and Na,K-ATPases. *Ann. New York Acad. Sci.* **986**, 106–110.

Shin, J. M., Bayle, D., Bamberg, K., and Sachs, G. (1998). The gastric H,K-ATPase. In *Advances in Molecular and Cell Biology*, Vol 23A, pp. 101–142. JAI Press, Connecticut.

Vagin, O., Munson, K., Denevich, S., and Sachs, G. (2003). Inhibition kinetics of the gastric H,K-ATPase by K-competitive inhibitor SCH28080 as a tool for investigating the luminal ion pathway. *Ann. New York Acad. Sci.* **986**, 111–115.

Biography

George Sachs is a Professor in the Department of Medicine and Physiology at The University of California, Los Angeles and Wilshire Chair in Medicine, University of California, Los Angeles, and Co-Director, Center for Ulcer Research and Education, University of California, Los Angeles, and VA Greater Los Angeles Healthcare System.

Jai Moo Shin is an Associate Researcher in the Department of Physiology at The University of California, Los Angeles.

P-Type Pumps: Na^+/K^+ Pump

Peter L. Jorgensen
University of Copenhagen, Copenhagen, Denmark

The Na^+/K^+ pump transforms the chemical energy in ATP to electric or osmotic work and maintains electrochemical Na^+ and K^+ gradients across cell membranes. At rest, the pump converts 20–30% of the current ATP production in mammals to active Na^+/K^+-transport in kidney, intestine, muscle, heart, central nervous system, and other cells of the body where Na^+/K^+ gradients are required for maintaining membrane potential and cell volume. The Na^+/K^+ pump is the largest protein complex in the family of P-type cation pumps. The minimum functional unit is an $\alpha\beta$-heterodimer of the calytic α-subunit containing the Na^+/K^+, ATP, and phosphate binding sites, and the glycosylated β-subunit required for the correct folding of the complex in the endoplasmic reticulum. The $\alpha\beta$-unit can also be coexpressed with small ion transport regulators of the FXYD family. Individual genes of four α-isoforms and at least three β-isoforms of the Na^+/K^+ pump are expressed in a tissue- and cell-specific manner to cover the demands for the specific physiological functions in epithelia, skeletal and heart muscles, nerves, and the reproductive system.

The Na^+/K^+ Pump Reaction Cycle

The Na^+/K^+ pump is a molecular machine which binds ATP in the cytoplasmic protrusion and couples the scalar processes of phosphorylation and dephosphorylation to the vectorial extrusion of $3Na^+$ ions and uptake of $2K^+$ ions. The reaction is specifically inhibited by high-affinity binding of cardiac glycosides like digoxin or ouabain. The driving force of the reaction is the free energy of ATP hydrolysis, which depends on the cytoplasmic concentrations of ATP, ADP, and Pi. In normal cells containing mitochondria, the free energy of ATP hydrolysis is close to $-60\,kJ\,mol^{-1}$ and the electrical driving force of the Na^+/K^+ pump is close to -600 mV ($-\Delta G/F$; where F is Faradays constant ($96\,485\,C\,mol^{-1}$)). Most of the electrochemical work (~ 390 mV) is used for the outward translocation of three Na^+ ions per cycle against the inside negative membrane potential and the tenfold-steep chemical gradient for Na^+ ions. Less energy (~ 40 mV) is used for the inward transport of two K^+ ions per cycle since potassium in most cells is close to electrochemical equilibrium.

In the first step of the reaction cycle of the Na^+/K^+ pump in Figure 1, ATP acting with low affinity accelerates inward transport of $2K^+$ ions coupled to the E_2 [2K] $\leftrightarrow$ E_1ATP transition. After dissociation of $2K^+$ ions, binding of $3Na^+$ ions at sites oriented towards the cytoplasm promotes phosphorylation of Asp-369 from ATP and occlusion of $3Na^+$ ions in the E_1-P[3Na] form. Outward transport of $3Na^+$ ions is coupled to the E_1-P $\leftrightarrow$ E_2-P conformational transition. Binding of $2K^+$ ions at extracellularly oriented sites of the E_2P form activates dephosphorylation and $2K^+$ ions are stably occluded in the E_2 [2K] form.

In normal cells, the extracellular $[K^+]_e$ activities (4–5 mM) exceed those required for full activation, since the $K_{1/2}$ value is 1 mM. At cytoplasmic ATP concentrations of 2–3 mM, the rate of turnover depends on the $[Na^+]/[K^+]$ activity ratios. In most cells the $[Na^+]/[K^+]$ activity ratios in the cytoplasm are in the range of 10/140–30/120 mM and below the $K_{1/2}$ value for activation of the pump at 37/113 mM. For the renal $\alpha 1\beta 1\gamma$-Na^+/K^+ pump, the rate at 10 mM $[Na^+]_i$ and 140 mM $[K^+]_i$ in the cytoplasm is less than 5% of the maximum velocity ($V_{max} = 7500\,ATP\,min^{-1}$). Due to the cooperativity of Na^+ activation, the rate raises steeply with the $[Na^+]_i$ activity in the cytoplasm to 10% at 16 mM $[Na^+]_i$ and 134 mM $[K^+]_i$ or 20% of V_{max} at 22 mM $[Na^+]_i$ and 128 mM $[K^+]_i$ in the cytoplasm. This autoregulatory mechanism is very important since regulatory processes, in particular coexpression with FXYD proteins, can alter the affinity for Na^+ ions and thus become very efficient regulators of Na^+/K pump rate.

E_1- and E_2-Conformations of the Na^+/K^+ Pump

The E_1- and E_2-conformations differ with respect to orientation and specificity of intramembrane cation sites for Na^+ and K^+. In the E_2 [2K] form there is a 3000-fold preference for binding of K^+ over Na^+ at the extracellular surface and this requires that K^+ binding

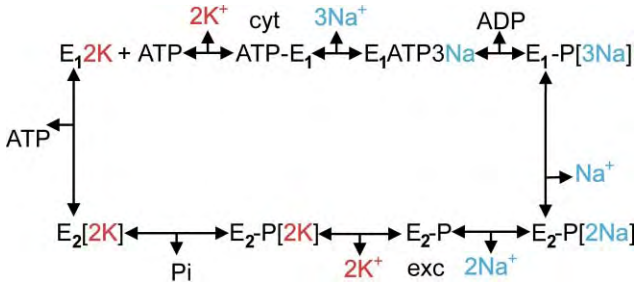

FIGURE 1 E_1–E_2 reaction cycle of the Na^+/K^+ pump with ping-pong sequential cation translocation. $[Na^+]$ or $[K^+]$ ions within brackets are occluded or tightly bound and prevented from exchanging with medium cations.

is 18 kJ mol^{-1} more stable than binding of Na^+. In the E_1ATP form, the affinity for Na^+ ions at the cytoplasmic surface is 16-fold higher than that for K^+ ions and this requires that binding of Na^+ is 6 kJ mol^{-1} more stable than binding of K^+. These adjustments of the cation sites are accompanied by changes of both the number of coordinating groups and their distances from the bound cations. The protein structure of the intramembrane domain of the Na^+/K^+ pump has not yet been solved at atomic resolution, but homology models based on the high-resolution structure of the Ca^{2+} pump of sarcoplasmic reticulum are efficient tools in interpretation of structure–function relationships of both the E_1- and E_2-conformations of the Na^+/K^+ pump, Figure 2. Modeling of the intramembrane domain shows that the structural changes accompanying the adjustments from an E_2-form with specificity for K^+ to an E_1-form with specificity for Na^+ can be achieved by twisting or tilting of the intramembrane helices to adapt the distances between the oxygen atoms of the coordinating groups of cation sites I and II in the intramembrane domain, Figure 2.

The overall structure of the α-subunit of the Na^+/K^+ pump is that the cation sites and transport path is made up of a bundle of transmembrane helices connected to a cytoplasmic protrusion consisting of three domains: the actuator or anchor (A), the phosphorylation (P) and the nucleotide-binding (N) domains. The N-domain is inserted between two Rossmann folds ($\alpha\beta\alpha\beta\alpha$) of the P-domain, which is directly connected to the extensions of the M4 and M5 transmembrane domains. The A-domain consists of the N-terminal portion of the α-subunit peptide chain and an insertion between M2 and M3. As seen from Figure 2, the $E_1P \rightarrow E_2P$ transitions are accompanied by large movements of the cytoplasmic A-, N-, and P-domains. The P-domain is rotated with reorientation of the catalytic site, including the important phosphorylated residue, Asp369, and the Mg^{2+} coordinating residue, Asp710. Movement of the N-domain is due mainly to the rotation of the P-domain. To stabilize the E_2P form, the A-domain rotates ~90°

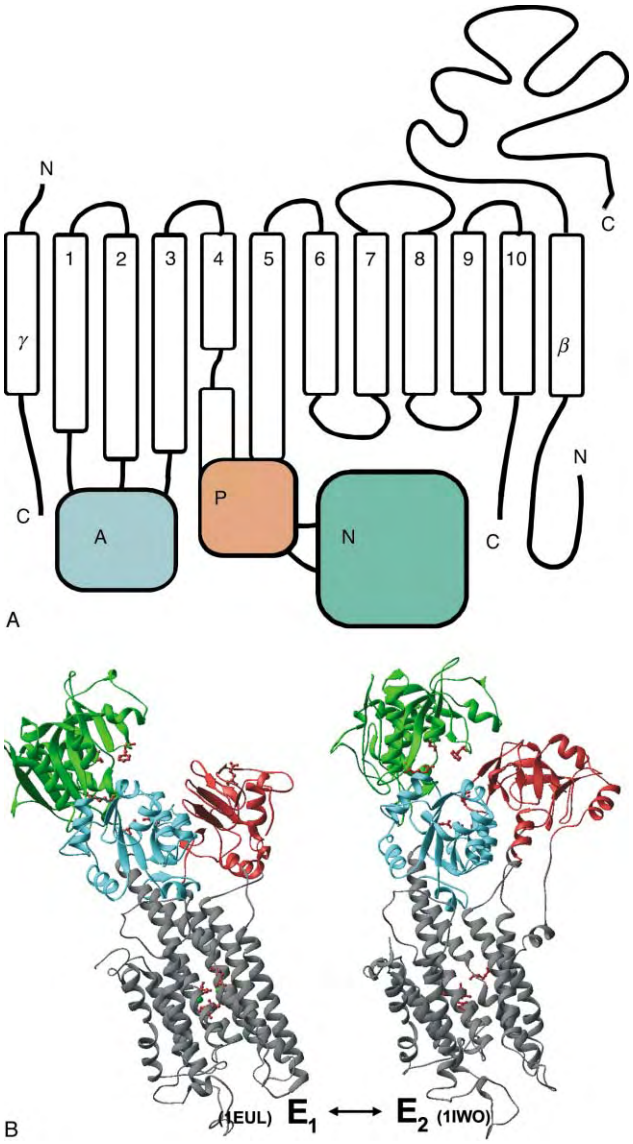

FIGURE 2 (A) Topology of the $\alpha\beta\gamma$-Na^+/K^+ pump. The β- and γ-subunits are single-pass membrane proteins. The α-subunit has ten transmembrane segments and the cytoplasmic protrusion is split in three domains: A, the anchor or attenuator domain; P, the phosphorylation domain, and N, the nucleotide binding site domain. (B) Models of E_1- and E_2-forms of the α-subunit of the Na^+/K^+ pump based on the high-resolution structure of Ca-ATPase in the E_1[2Ca] form (1EUL) and in the E_2-form (1IWO) stabilized by thapsigargin and Mg^{2+}. Side chains in ball and stick are shown for Phe475, Lys501, and Arg544 in the N-domain, for D369 and D710 in the P-domain, and for Glu327, Glu770, Asp804, and Asp808 in the cation binding domain. The position of the N-domain has been adjusted to allow spanning of an ATP molecule over the N- and P-domains.

about a vertical axis, thus docking the segment around Glu183 onto the P domain. These movements of the cytoplasmic domains are transmitted to tilting and twisting of the intramembrane helices and adjustment of the cation sites from a specificity for Na^+ in the E_1-form to a specificity for K^+ in the E_2-form.

Regulation of the E_1-E_2 Conformational Equilibrium

Physiological short-term regulation of the complex reaction cycle of the Na^+/K^+ pump is often directed towards rate limiting steps of the catalytic reaction, the long-range E_1-E_2 conformational changes which are linking the catalytic reactions to cation movements.

In the Na^+/K^+ pump, the conformational equilibria of both the phosphoforms (E_1P-E_2P) and dephosphoforms are poised heavily in direction of the E_2-forms. Thus in presence of K^+, the equilibrium constant (K_c) for the ratio E_2K/E_1K approaches a value of 1000. Changes of the conformational equilibrium may therefore have a strong influence on the turnover rate of the enzyme. Deletion of the N-terminal 30 residues by tryptic cleavage at 30Leu-Lys (T2) causes a 3–4-fold shift of the conformational equilibrium towards the E_1-form with reduction of Na^+/K^+ pump turnover to 45–50% of V_{max} values and the affinities for Na^+ or ATP are increased, while the apparent affinity for extracellular K^+ is reduced without interference with the capacity of the binding sites. Similar changes are seen after PKC mediated phosphorylation in the positively charged segment of the N terminus of the α1-subunit. The most pronounced structural variability between α-subunit isoforms occur at the N terminus. Comparison of the properties of α-isoforms shows that the maximum turnover rate is lower for the $\alpha2\beta1$-Na^+/K^+ pump ($4600\ min^{-1}$) than for the $\alpha1\beta1$-Na^+/K^+ pump ($7600\ min^{-1}$). The apparent affinities for Na^+ and ATP are two- and fourfold higher for α2- than for α1-isoforms, whereas the apparent affinity for K^+ is twofold lower for α2- than for α1-isoforms. These data are consistent with a shift of the E_1-E_2 conformational equilibrium toward E_1 in the α2-isoform. The properties of the α2-isoform are similar to those seen for the α1-isoform after deletion of 30 amino acid residues from the N terminus and they can be regarded as E_1-E_2 conformational isoforms. The rate of $\alpha3$-Na^+/K^+ pumps is about twofold lower than that of isoforms containing the α2-subunit.

Na^+/K^+ Pumps in Epithelial Cells of Kidney, Intestine, Lung, and Glands

The $\alpha1\beta1$-Na^+/K^+ pump is constitutively expressed in most cells and it maintains the Na^+ gradients driving the active transcellular transport in kidney, intestine, lung, and various glands. There is a close relationship between the capacity for reabsorption of Na^+ in these tissues and the abundance of $\alpha1\beta1$-Na^+/K^+ pumps in the basolateral membranes of the epithelial cells. The Na^+/K^+ pumps in human kidneys hydrolyze over 2 kg of ATP per day and over 600 g sodium is reabsorbed per day. Accordingly, ouabain binding data reveal 40–50 million Na^+/K^+ pumps per cell in thick ascending limbs of Henle (TALH) or distal convoluted tubules (DCT) as compared to a few hundred in red cells or a few thousand pumps in other nonpolarized cells. In all tubular cells the Na^+/K^+ pump maintains electrochemical gradients for sodium ($\Delta\mu Na^+$), the driving force for secondary active transport of other solutes and ions, such as H^+, Ca^{2+}, and Cl^-. In the TALH, the Na^+/K^+ pump functions in concert with the Na, K, $2Cl^-$ cotransporter and channels for K^+ or Cl^- to bring about transcellular NaCl transport, Figure 3. NaCl is reabsorbed at very high rates, while lumenal and cytoplasmic [Na^+] activities remain relatively high, 20–40 mM in the lumen of TALH.

The γ-subunit belongs to the FXYD family of small ion transport regulators. They are small single pass membrane proteins which share a 35 amino acid

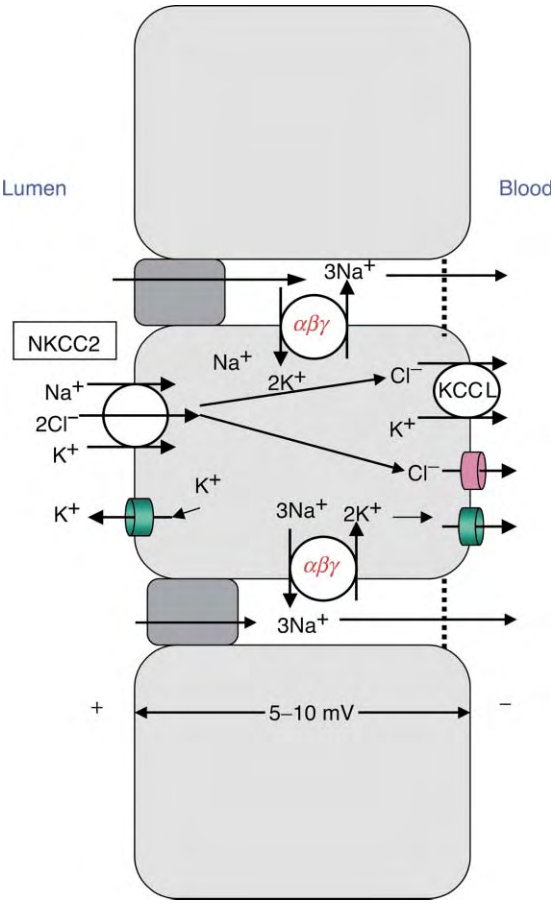

FIGURE 3 Mechanism of transcellular NaCl transport in thick ascending limb of Henle (TALH). The functions of the $\alpha1\beta1\gamma$-Na^+/K^+ pump are integrated with those of NKKCC2, the Na,K,Cl-cotransporter, KCCL, the K,Cl-cotransporter, and channels for K^+ and Cl^-.

TABLE I

Human Genes of Na^+/K^+ Pump Proteins: Isoforms of α and β Subunits are Expressed from Individual Genes[a]

Isoform	Gene	Human chromosome	Amino acid residues	Cell or tissue specific expression
$\alpha 1$	ATP1A1	1p13.1	1023	Constitutive, ubiquitous, dominant in epithelia of kidney, glands, and intestine
$\alpha 2$	ATP1A2	1q23.2	1020	Brain, muscle, heart
$\alpha 3$	ATP1A3	19q13.2	1013	CNS, brain
$\alpha 4$	ATP1A4	1q21–q23	1029	Testis, spermatozoa
$\beta 1$	ATP1B1	1q24.2	303	Ubiquitous, like the $\alpha 1$-subunit
$\beta 2$	ATP1B2	17p13.1	290	Brain, adhesion molecule (AMOG), liver
$\beta 3$	ATP1B3	3q23	279	Mostly in neural tissue, heart, kidney, lung

[a]Data from the genome database of National Center for Biotechnology Information.

signature sequence domain, beginning with the sequence FXYD and containing seven invariant and six highly conserved amino acids. The approved human gene nomenclature for the family is listed in Table I. Coexpression of the γ-subunit (FXYD2) with the $\alpha 1\beta 1$-Na^+/K^+ pump modifies the enzymatic properties with respect to the affinity for cytoplasmic $[Na^+]$. The $\alpha 1\beta 1\gamma$-Na^+/K^+ pump complex has a relatively low affinity for $[Na^+]_{cyt}$ and it is expressed at very high densities in the basolateral membranes of the TALH.

In the IMCD, the inner medullary collecting duct, Na^+/K^+ pump functions are integrated with those of the sodium channel, ENAC, and K^+-channels to drive reabsorption of Na^+ under the regulation of aldosterone. In the IMCD, the expression of FXYD4 or CHIF is stimulated by aldosterone and the CHIF-$\alpha 1\beta 1$-Na^+/K^+ pump complex has a relatively high affinity for $[Na^+]_{cyt}$, thus enabling the pump to reduce the activity of $[Na^+]$ to 2–5 mM in the tubular lumen and in the cytoplasm of the principal cells of the IMCD.

Aldosterone also regulates Na^+ reabsorption driven by the $\alpha 1\beta 1$-Na^+/K^+ pumps in epithelia of lung, glands, and colon, thus providing a major force in the regulation of Na^+ metabolism and extracellular fluid volume.

Na^+/K^+ Pump Isoform Expression and Regulation in Muscle and Central Nervous System

Extensive analyses have been performed to clarify the tissue specific gene expression and the molecular mechanisms of the regulation of the α- and β-subunit genes, Tables I and II. Experiments on animal models allow reverse genetic strategy to analyze the function of transport proteins. Targeted disruption of the $\alpha 1$- and $\alpha 2$-subunit isoforms in mice confirm that the Na^+/K^+ pump is essential for life of all mammalian cells. Egg cells lacking both copies of the ubiquitous $\alpha 1$-isoform do not pass the blastocyst stage. Homozygote knockouts of the $\alpha 2$-isoform results in death few minutes after birth of the mice apparently due to malformation of neural connections in the medulla oblongata. Knockout of one of

TABLE II

Human Genes of Na^+/K^+ Pump Proteins: Small Ion Transport Regulators of the FXYD Family

Isoform	Gene	Human chromosome	Amino acid residues	Cell or tissue specific coexpression with $\alpha\beta$-unit of Na,K-pump
FXYD1	PLM	19q13.1	92	Phospholemman coexpression with $\alpha 1\beta 1$ or $\alpha 2\beta$ suppress Na^+ affinity of Na,K-pump in muscle
FXYD2	ATP1G	11q23	66	Two splice variants, gamma(a) and gamma(b). Coexpression with $\alpha 1\beta 1$ reduces the Na^+ affinity of the Na,K-pump
FXYD3	MAT-8	19q13.11	87	
FXYD4	CHIF	10p11	89	In kidney and colon coexpression with $\alpha 1\beta 1$ increases the Na^+ affinity of the Na,K-pump
FXYD5	RIC	19q12–q13.1	178	
FXYD6	PHL	11q23.3	95	Phosphohippolin in brain and kidney
FXYD7		19q13.13	80	In brain, reduces K^+ affinity of Na,K-pump

the genes shows that α1- and α2-isoforms have different physiological functions. An increased force of contraction of the heart is seen in animals lacking one copy of the α2-isoform, whereas the force of contraction is reduced after elimination of one copy of the α1-isoform. There is a correlation between the expression of the α2-Na^+/K^+ pump and the Na^+/Ca^{2+} exchanger in plasma membrane domains overlaying the endoplasmic reticulum. Elevation of local activities of $[Na^+]_{cyt}$ may therefore increase the $[Ca^{2+}]_{cyt}$ activity in the space of the cytosol near the endoplasmic reticulum and thus amplify the force of contraction. This may explain the specific role of the α2-isoform as a regulator of calcium and the force of contraction in the heart.

In skeletal muscle, long-term regulation involves thyroid hormone-mediated changes of the expression level of Na^+/K^+ pumps. Short-term regulation of the Na^+/K^+ pump is mediated either by changes in intracellular Na^+ activity or by hormone-mediated protein kinase reactions leading to changes of the Na^+/K^+ pump transport properties or in its cell surface expression. Insulin causes translocation of α2-Na^+/K^+ pumps to the cell surface and the α2-Na^+/K^+ pumps in skeletal muscle are involved in specific regulation in response to hypokalemia. Exercise stimulates exocytosis of α1- and α2-Na^+/K^+ pumps to the plasma membranes of muscle cells and this response is important for recovery of K^+ after repetitive muscle contractions. Phospholemman (FXYD1) interacts with α1- and α2-isoform Na^+/K^+ pumps and modulates their properties to cause a decrease in the affinity to Na^+. The presence of Na^+/K^+ pumps with low affinity can also be important for the recovery process after muscle contractions. Skeletal muscles are the main intracellular store of K^+, and the Na^+/K^+ pumps in the sarcolemma are important for maintaining plasma K^+ along with H^+/K^+ pumps in kidney and colon.

All three α1-, α2-, and α3-isoforms are expressed in the central nervous system. During embryogenesis, the α2-Na^+/K^+ pumps are expressed in most regions of the brain and they are important in the modulation of neuronal activity in the neonate. In the adult, α2-Na^+/K^+ pumps are expressed primarily in astrocytes, where glutamate is transported in a sodium- and potassium-dependent fashion. FXYD7 has been identified as an isoform-specific regulator of the Na^+/K^+ pump in brain. The properties of α3-Na^+/K^+ pumps may allow reuptake of K^+ at low extracellular activities in the brain.

The α4-isoform is exclusively expressed in spermatozoa in the testis. In the mid-piece containing the flagellar motor, the α4-Na^+/K^+ pumps are tightly coupled to Na^+/H^+ exchange of primary importance for generation of ATP and thus for the mobility of spermatozoa.

See Also the Following Articles

Membrane Transport, General Concepts • Membrane Transporters: Na^+/Ca^{2+} Exchangers • Plasma-Membrane Calcium Pump: Structure and Function

Glossary

digoxin Cardiac glycoside, also known as digitalis. It is derived from the leaves of the foxglove plant (*Digitalis purpurea*) and is a classic drug which increases the force of contraction of the incompensated heart, probably by increasing the $[Ca^{2+}]$ activity in the cytoplasm of heart muscle cells.

E_1P The phosphorylated intermediate that is formed by Na^+-stimulated transfer of the γ-phosphate from ATP to form an acyl bond with the carboxylate group of Asp369 of the α-subunit. $E_1P[3Na]$ occludes $3Na^+$ ions and it is a high-energy intermediate as it can transfer its phosphate to ADP and form ATP.

E_2P It is formed in the conformational transition $E_1P \leftrightarrow E_2P$. The E_2P conformation has two cation sites with preference for K^+ over Na^+. The $E_2P[2Na]$ form may react with Na^+ and ADP to form ATP. In the forward reaction, K^+ will replace Na^+ and stimulate hydrolysis and release of inorganic phosphate. The $E_2P[2K]$ form is insensitive to ADP and can only react with water to release inorganic phosphate.

Na, K-ATPase The enzymatic equivalent of the Na^+/K^+ pump is the *in vitro* $Na^+ + K^+$ stimulated ATPase activity which is inhibited by ouabain.

ouabain Strophanthin G, a plant alkaloid from *Strophantus gratus*, a fast acting cardiac glycoside that binds with high affinity to the α-subunit of the Na^+/K^+ pump.

Further Reading

Blanco, G., and Mercer, R. W. (1998). Isozymes of the Na-K-ATPase: Heterogeneity in structure, diversity in function. *Am. J. Physiol.* **275**, F633–F650.

Feraille, E., and Doucet, A. (2001). Sodium-potassium-denosinetriphosphatase-dependent sodium transport in the kidney: Hormonal control. *Physiol. Rev.* **81**, 345–418.

Jorgensen, P. L., Hakansson, K. O., and Karlish, S. J. (2003). Structure and mechanism of Na,K-ATPase: Functional sites and their interactions. *Annu. Rev. Physiol.* **65**, 817–849.

Jorgensen, P. L., Karlish, S. J. D., and Maunsbach, A. B. (eds.) (2003) Na,K-ATPase and related cation pumps: structure, function and regulatory mechanisms. *Annu. New York Acad. Sci.* **896**.

Läuger, P. (1991). *Electrogenic Ion Pumps*. Sinauer Associates, Sunderland Massachusetts, USA.

Ogawa, H., and Toyoshima, C. (2002). Homology modeling of the cation binding sites of Na^+K^+-ATPase. *Proc. Natl Acad. Sci. USA* **99**, 15977–15982.

Toyoshima, C., and Nomura, H. (2002). Structural changes in the calcium pump accompanying the dissociation of calcium. *Nature* **418**, 605–611.

Toyoshima, C., Nakasako, M., Nomura, H., and Ogawa, H. (2000). Crystal structure of the calcium pump of sarcoplasmic reticulum at 2.6Å resolution. *Nature* **405**, 645–655.

Woo, A. L., James, P. F., and Lingrel, J. B. (2000). Sperm motility is dependent on a unique isoform of the Na, K-ATPase. *J. Biol. Chem.* **275**, 20693–20699.

Biography

Peter L. Jorgensen is a Professor of Molecular Physiology at the August Krogh Institute of the University of Copenhagen, Denmark. He holds a degree as medical doctor and a doctorate of medical sciences from the University of Aarhus, Denmark. He determined the physiological functions of the Na^+/K^+ pump in kidney and developed procedures for purification of the Na^+/K^+ pump from mammalian kidney and crystallization of the protein in the membrane plane. This led to detection of the distinct proteolytic cleavage patterns of the E_1- and E_2-conformations of the Na^+/K^+ pump and Ca^{2+} pump proteins. Recently, he contributed to solving the structure–function relationships of the binding sites for Na^+, K^+, Mg^{2+}, and ATP in the Na^+/K^+ pump protein.

P-Type Pumps: Plasma-Membrane H^+ Pump

A. Brett Mason and Carolyn W. Slayman
Yale University, New Haven, Connecticut, USA

Plasma-membrane H^+ pumps (also known as H^+-ATPases) are widely distributed throughout the fungal and plant kingdoms. They use the energy from ATP hydrolysis to generate a sizeable electrochemical gradient across the surface membrane, which in turn drives nutrient uptake into the cell via a series of H^+-coupled cotransporters (Figure 1A). The proton-pumping activity of the ATPase also contributes to the regulation of intracellular pH. Representative pumps have been cloned from budding (*Saccharomyces cerevisiae*) and fission (*Schizosaccharomyces pombe*) yeast, *Neurospora crassa*, several pathogenic fungi, and numerous plant species including *Arabidopsis thaliana*, *Nicotiana plumbaginifolia* (tobacco), and *Lycopersicon esculentum* (tomato).

Introduction

The fungal and plant plasma-membrane H^+-ATPases belong to a ubiquitous family of cation pumps known as P-type ATPases, so named because they hydrolyze ATP via a covalent aspartyl–phosphate reaction intermediate. When the P-ATPases are classified based on sequence alignments, membrane topology, and the nature of the transported cation(s), H^+-ATPases fall into a category designated as P_2 or type III.

Since 1986, when the *PMA1* genes of *S. cerevisiae* and *N. crassa* were cloned and sequenced, these two H^+-ATPases have served as prototypes for the group as a whole. Yeast in particular has proven to be an extremely useful model system. By virtue of the ease with which site-directed mutants can be made and analyzed, a large collection of *pma1* mutants has been generated which are providing molecular details as to the structure and function of the H^+-ATPase. The abundance of the ATPase in the yeast plasma membrane, where it may constitute up to 25% of total protein, is another feature of considerable value in the molecular characterization of the enzyme. Finally, the use of yeast as a vehicle for heterologous expression of other ATPases such as the individual isoforms of plant H^+-ATPase is providing information as to specific features of these enzymes that cannot be analyzed in their natural setting.

In addition to its utility in a comparative sense, the fungal ATPase has emerged as a potentially valuable target for the development of antifungal drugs. Most of the antifungals commonly used in the treatment of systemic fungal infections are either fungistatic compounds that inhibit the biosynthesis of ergosterol (the principal sterol in fungal membranes), or fungicidal compounds that interact with ergosterol directly, leading to disruption of the plasma membrane. Many pathogenic fungi are either innately resistant to existing antifungals, or are able to acquire resistance by developing mechanisms based on limitation of drug uptake, active drug efflux, or target resistance. In this regard, the H^+-ATPase has several properties that render it a promising new antifungal target: (1) it is an essential cell component, which favors the chances of fungicidal rather than fungistatic effect and simultaneously decreases the chances of resistance; (2) its cell surface location allows for targeting by drugs which do not enter the cell, thus avoiding multi-drug resistance (MDR) pumps and reducing the likelihood of toxic effects on host cells; and (3) it is structurally and functionally conserved across a wide range of fungal genera, promising broad-spectrum antifungal activity.

Structure

At the structural level, the fungal and plant plasma-membrane H^+-ATPases are composed of a 100 kDa polypeptide that is deeply embedded in the lipid bilayer, requiring detergents for solubilization. The predicted transmembrane topology of the 100 kDa polypeptide is shown in Figure 1B. As in other P_2-type ATPases, four hydrophobic segments at the N-terminal end of the polypeptide (M1–M4) and six hydrophobic segments at the C-terminal end (M5–M10) serve to anchor the ATPase in the membrane, while a large (340 amino acid) cytoplasmic loop in the center of the polypeptide

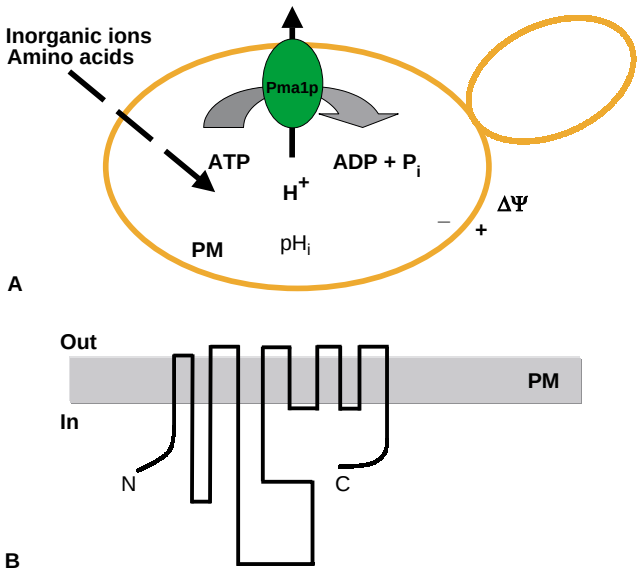

FIGURE 1 (A) The plasma membrane H^+-ATPase plays an essential role in yeast cell physiology. The pumping of protons (H^+) across the membrane at the expense of ATP hydrolysis establishes the membrane potential ($\Delta\Psi$) required for nutrient import and helps to regulate intracellular pH (pH_i). PM, plasma membrane. (B) Transmembrane topology of the fungal and plant H^+-ATPases. The ATPase has 10 transmembrane α-helices. Both N and C termini as well as the large catalytic domain of the enzyme are located in the cytoplasm. PM, plasma membrane.

contains the critical catalytic sites that bind ATP and form the aspartyl–phosphate intermediate.

The first three-dimensional glimpse of H^+-ATPase structure came from cryoelectron microscopic maps of the *Neurospora* enzyme at 8Å resolution. Ten transmembrane segments could be discerned clearly, connected by a narrow stalk to the multi-lobed, cytoplasmic headpiece of the enzyme. This low-resolution view has recently been confirmed and extended by comparison with X-ray crystallographic structures of the related mammalian sarcoplasmic reticulum Ca^{2+}-ATPase in two different conformations. In the first structure, with two Ca^{2+} ions bound, the headpiece of the Ca^{2+}-ATPase displayed a relatively open structure consisting of three well-separated domains: N (nucleotide-binding), P (phosphorylation), and A (actuator). In the second structure, obtained in the presence of a specific inhibitor known as thapsigargin, the three cytoplasmic domains had shifted towards one another to produce a relatively closed structure. Kühlbrandt and colleagues have demonstrated that the amino acid sequence of the *Neurospora* H^+-ATPase can be overlaid upon the Ca^{2+}-ATPase template to give a three-dimensional structure that agrees well with the earlier cryoelectron microscopic maps. Thus, structural information is now in hand that will serve as a valuable framework for mechanistic studies.

Reaction Mechanism

Like the intensively studied mammalian Na^+-, K^+-, and Ca^{2+}-ATPases, the fungal and plant plasma-membrane H^+-ATPases are considered to alternate between two major conformational states (E_1 and E_2) during their reaction cycle (Figure 2A). In E_1, the enzyme binds and hydrolyzes ATP to form a phosphorylated intermediate (E_1P), accompanied by protonation of the membrane-embedded transport site. It then undergoes a conformational change from E_1P to E_2P, during which the proton is extruded into the extracellular medium. After the release of inorganic phosphate, the E_2 conformation shifts back to E_1 to complete the cycle. The physical scale of these molecular movements can be appreciated by comparing the two crystal structures of Ca^{2+}-ATPase, where the top of the N-domain moves more than 50 Å and the A-domain rotates 90° to interact with the P-domain. A simple representation of this E_1 to E_2 conformational shift for a general P_2-type ATPase is depicted in Figure 2B. A stretch of 13 consecutive residues in stalk segment 4 of the yeast H^+-ATPase has

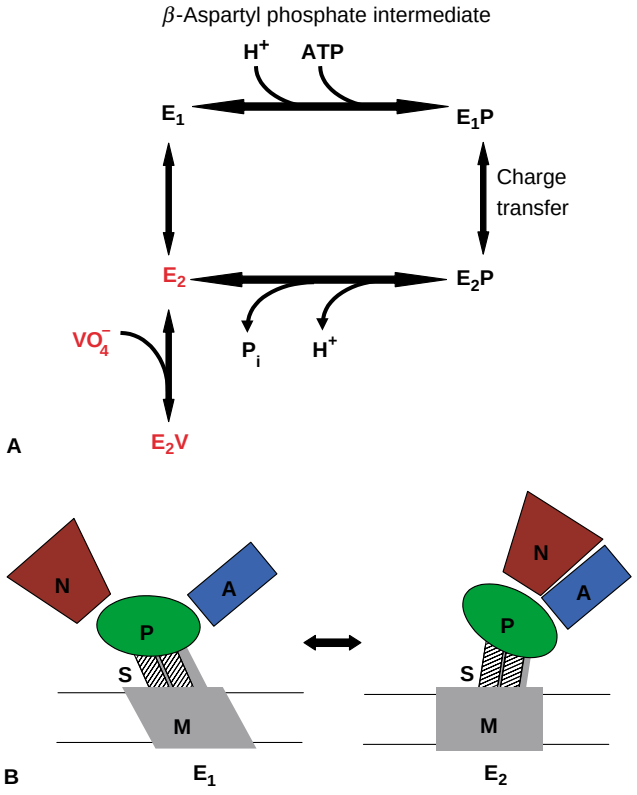

FIGURE 2 (A) The H^+-ATPase reaction cycle. See text for explanation. VO_4^-, vanadate, a potent P-type ATPase inhibitor. (B) Major domain movements that occur during conversion of the ATPase from the E_1 (cation-bound) to the E_2 (cation-free) conformation. N, nucleotide-binding domain; P, phosphorylation domain; A, actuator domain; S, stalk region; M, membrane sector formed by 10 transmembrane helices.

recently been shown to play a key role in the E_1-E_2 conformational change.

Given the similar arrangement of membrane-spanning α-helices (M1–M10) in the Ca^{2+}- and H^+-ATPase crystal structures, the cation pathway through the H^+-ATPase is probably formed by M4, M5, M6, and M8 as it is in the Ca^{2+}-ATPase. Consistent with this idea, site-directed mutations in three of these segments (M5, M6, and M8) have been shown to alter the stoichiometry of proton transport. These studies were carried out with inside-out secretory vesicles, using the fluorescence quenching of acridine orange to measure H^+ transport into the vesicle. When such measurements were made over a range of MgATP concentrations, and the initial rate of quenching was plotted as a function of the initial rate of ATP hydrolysis, wild-type ATPase and most mutant forms of the enzyme displayed a linear relationship, with a slope corresponding to a stoichiometry of $1H^+$ translocated per ATP hydrolyzed. By contrast, several mutants in M5, M6, and M8 exhibited a decreased slope indicating partial uncoupling, and two mutants in M8 exhibited an increased slope reflecting an apparent increase in transport stoichiometry.

Considerable efforts are currently being made to obtain higher-resolution crystal structures of the H^+-ATPase. Information from these studies, in combination with further site-directed mutagenesis experiments, will soon provide more insight into the proton's path across the membrane bilayer.

Biogenesis

Biogenesis of the H^+-ATPase begins with its synthesis in the rough endoplasmic reticulum (ER), from which it travels to the plasma membrane via the secretory pathway (Figure 3). Because of its abundance in the membrane, together with the ease of making site-directed mutants, the yeast H^+-ATPase has served as a valuable model for studying this process.

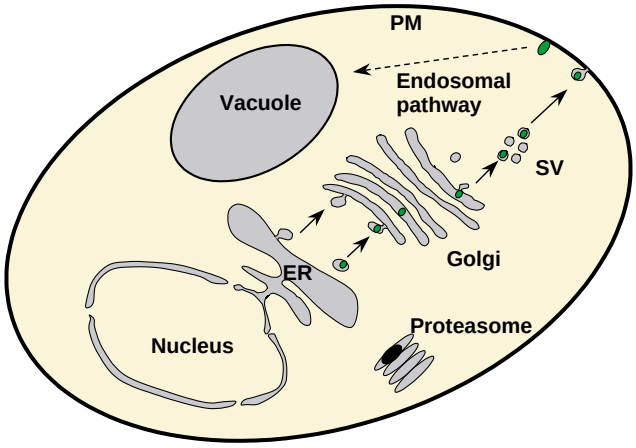

FIGURE 3 The yeast secretory pathway. ER, endoplasmic reticulum; SV, secretory vesicles; PM, plasma membrane.

While still in the ER, the ATPase adopts a fully folded structure that has the protease-resistant characteristics of the mature enzyme at the plasma membrane. The folded molecule is then incorporated into coat protein complex II (COPII) vesicles and shuttled to the *cis*-Golgi. Of considerable interest, a subpopulation of COPII vesicles has recently been identified that preferentially recruits and packages the H^+-ATPase by virtue of a specific coat protein, Lst1p. At least in principle, this mechanism provides a way to regulate biogenesis, underscoring the significance of the ATPase to the functioning of the cell as a whole.

Recent research has begun to shed light on the form of the ATPase as it exits the ER. Oligomeric forms of the *Neurospora* H^+-ATPase have been known for many years, and were originally thought to be by-products of detergent treatment. In the past several years, however, oligomers of the yeast H^+-ATPase have been detected early in biogenesis by three different methods: blue native gel electrophoresis, sucrose gradient centrifugation, and cross-linking of epitope-tagged polypeptides. In addition, oligomer formation provides a logical explanation for the existence of dominant negative *pma1* mutants, which cause coexpressed wild-type H^+-ATPase to be retained in the ER. The functional significance of the oligomers is not yet clear, given an earlier demonstration that the *Neurospora* H^+-ATPase is fully active when solubilized and reconstituted as a monomer. There has been speculation that the oligomers may play a special role in biogenesis and/or as a storage form of the ATPase, but further work will be required to test these ideas.

Parallel studies have been carried out recently to explore the association of the yeast H^+-ATPase with lipid rafts, sterol-, and sphingolipid-rich structures that are believed to segregate certain plasma-membrane proteins en route to the cell surface. Based on its insolubility in 1% Triton X-100 at 0°C, wild-type ATPase becomes associated with rafts prior to exiting the ER. Preventing the association by means of a mutation in sphingolipid biosynthesis does not block export, however, indicating that rafts do not play an obligatory role in this process.

Many mutations in the *PMA1* gene that lead to misfolding of the H^+-ATPase result in arrest of the polypeptide in the ER and massive accumulation of internal membranes. This represents the first level of quality control in biogenesis and, in most instances, is followed by redirection of the offending ATPase via the ER-associated degradation (ERAD) pathway for digestion in the proteasome. Quality

control screening is maintained, however, as the H^+-ATPase progresses through the secretory pathway. There are now several examples of mutant ATPases that escape the ER quality control mechanism only to be recognized as aberrant and differentially processed at later stages of the secretory pathway by vacuolar proteases.

Regulation

In addition to the major H^+-ATPase gene (*PMA*1), *S. cerevisiae* and *S. pombe* each have a second gene, *PMA2*, that encodes a nearly identical protein. The expression level of *PMA2* is so poor that it is unable to support growth, however, and the physiological function of the second ATPase remains unclear.

By contrast, plants possess multiple H^+-ATPase genes. In *A. thaliana*, for example, whole-genome sequencing has identified a family of 11 such genes, most or all of which are expressed in a tissue-specific way. Where tested, the corresponding H^+-ATPase isoforms differ detectably in their catalytic behaviors, suggesting that enzyme characteristics may be matched to the physiological requirements of individual tissues.

A diversity of environmental conditions and stress factors influence the biosynthesis and the activity of fungal and plant plasma-membrane H^+-ATPases (Figure 4). In yeast, two mechanisms have been identified, both resulting in up-regulation of the H^+-ATPase by glucose. At the transcriptional level, addition of glucose to the growth medium leads to a rapid increase in mRNA for the H^+-ATPase, and analysis of the promoter region of the *PMA1* gene has revealed active binding sites for several recognized transcription factors including Tuf1/Rap1/Grf1 and Gcr1. It is almost certainly significant that the same factors promote transcription of genes encoding glycolytic enzymes, pointing to a coordinated set of mechanisms that enable rapid, efficient growth on glucose.

Because the yeast H^+-ATPase has an unusually long half-life at the plasma-membrane (~11 h), posttranslational mechanisms are required to modulate its activity rapidly. Indeed, within minutes of glucose addition, the yeast ATPase displays an increased V_{max}, a lowered K_m, and a more alkaline pH optimum. There is growing evidence that this ensemble of changes results from posttranslational phosphorylation near the C terminus of the 100 kDa polypeptide. Truncation of the C terminus leads to constitutive activation, suggesting that the domain normally behaves in an autoinhibitory fashion. Detailed mutational analyses have linked the glucose-induced change in V_{max} with amino acids Arg^{909} and Thr^{912} and the change in K_m with Ser^{899} and Glu^{901}. Both pairs of residues constitute potential phosphorylation sites, and two novel phosphopeptides have been observed (though not yet sequenced) in proteolytic digests of H^+-ATPase from glucose-metabolizing yeast cells. Studies using site-directed mutagenesis of the yeast H^+-ATPase, coupled with suppressor analysis, suggest that the C terminus interacts with the stalk region near the cytoplasmic surface of the membrane and also with the ATP-binding (N) domain.

In plants, a variety of physiological conditions can affect the expression of specific ATPase isoforms, but

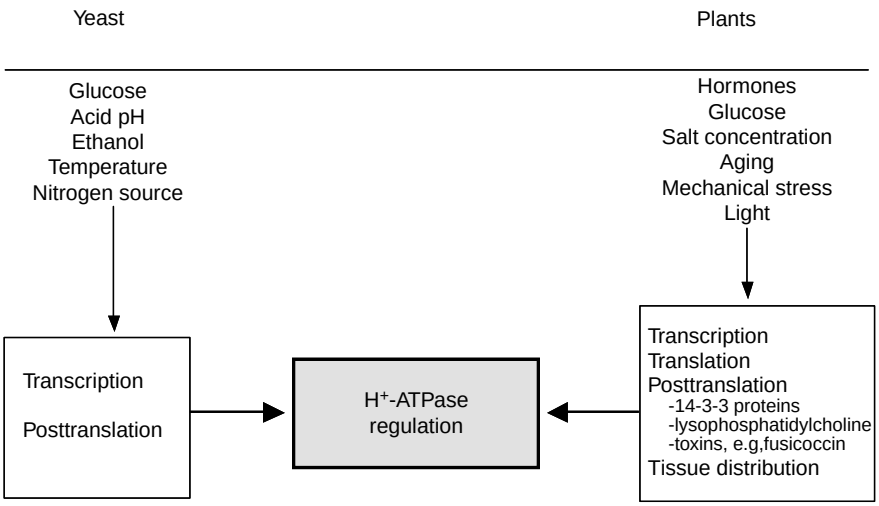

FIGURE 4 A comparison of the major environmental factors and mechanisms that regulate yeast and plant plasma membrane H^+-ATPase activity.

precise transcriptional mechanisms have not yet been elucidated. Translational mechanisms may also exist, possibly involving an untranslated leader sequence on the mRNA transcript that contains a short open reading frame (ORF). As in yeast, however, the primary modulator of plant H^+-ATPase activity is the C terminus of the enzyme, again acting in an autoinhibitory fashion. Growing evidence indicates that regulation is mediated by the binding of 14–3–3 proteins, a highly conserved family of acidic proteins expressed ubiquitously in eukaryotic cells. 14–3–3 proteins interact with many phosphoproteins, probably acting as dimers. A recent study of the Aha2p isoform of *Arabidopsis* H^+-ATPase expressed in yeast suggests that phosphorylation of Thr^{947} leads to the binding of 14–3–3 proteins, activating the enzyme. In the same study, the removal of two inhibitory sequences from the carboxyl terminus was also able to activate the Aha2p ATPase.

Regulation of H^+-ATPase activity is achieved through the coordinated action of multiple pathways. Our appreciation of the significance and complexity of this network will increase as our ability to explore cell physiology on a genome-, transcriptome-, and proteome-wide basis improves.

Summary

Research into the structure, function, biogenesis, and regulation of fungal and plant plasma-membrane H^+ pumps continues to provide a wealth of scientific information about the physiology of their host cells. Moreover, these pumps are invaluable as protein models not only for P_2-type ATPases but for complex integral membrane proteins in general.

And finally, with the continued increases in the incidence and variety of life-threatening fungal infections, particularly in immunocompromised patients, the fungal H^+-ATPase has assumed added significance as a viable target for the development of antifungal drugs.

See Also the Following Articles

Membrane Transport, General Concepts • Proteasomes, Overview

Glossary

fusicoccin A compound toxic to plants that is produced by the fungus *Fusicoccum amygdali*.

Gcr1 *G*ly*c*olysis *r*egulation 1. A yeast transcription factor that acts together with Rap1 to increase expression of some glycolytic enzymes.

lysophosphatidylcholine A phospholipid that activates plant plasma-membrane H^+-ATPases.

proteasome A large cytosolic protease complex that is responsible for intracellular protein degradation.

Tuf1/Rap1/Grf1 *T*ranslation *u*pstream *f*actor 1/*R*epressor *a*ctivator *p*rotein 1/*G*eneral *r*egulatory *f*actor 1. A yeast transcription factor involved in a variety of cellular processes including telomere regulation, chromatin silencing, glycolysis.

Further Reading

Ferreira, T., Mason, A. B., and Slayman, C. W. (2001). The yeast Pma1 proton pump: A model for understanding the biogenesis of plasma membrane proteins. *J. Biol. Chem.* **276**, 29613–29616.

Kühlbrandt, W., Zeelen, J., and Dietrich, J. (2002). Structure, mechanism, and regulation of the *Neurospora* plasma membrane H^+-ATPase. *Science* **297**, 1692–1696.

Morsomme, P., Slayman, C. W., and Goffeau, A. (2000). Mutagenic study of the structure, function and biogenesis of the yeast plasma membrane H^+-ATPase. *Biochim. Biophys. Acta* **1469**, 133–157.

Portillo, F. (2000). Regulation of plasma membrane H^+-ATPase in fungi and plants. *Biochim. Biophys. Acta* **1469**, 31–42.

Schekman, R. (2002). SEC mutants and the secretory apparatus. *Nat. Med.* **8**, 1055–1058.

Shimoni, Y., and Schekman, R. (2002). Vesicle budding from endoplasmic reticulum. *Meth. Enzymol.* **351**, 258–278.

Biography

Carolyn W. Slayman, Sterling Professor of Genetics and Cellular and Molecular Physiology at Yale University School of Medicine, has studied the plasma membrane H^+-ATPases of yeast and Neurospora for many years, focusing on the structure–function relationships that underlie proton transport.

A. Brett Mason, Associate Research Scientist in the Department of Genetics at Yale, began research on the yeast H^+-ATPase 10 years ago in New Zealand and joined the Slayman laboratory in 2000 to investigate the mechanism of ATPase biogenesis.

Purple Bacteria: Electron Acceptors and Donors

Evaldas Katilius and Neal W. Woodbury
Arizona State University, Tempe, Arizona, USA

Cyclic electron transport in the purple photosynthetic bacteria is facilitated by several soluble and integral membrane proteins. These proteins contain redox active cofactors serving as electron acceptors or donors. The cofactors are bacteriochlorophyll, bacteriopheophytin, quinone, or heme molecules. The electrochemical properties of these molecules are strongly affected by their protein environment allowing their midpoint potentials to be tuned to different values appropriate for their role in the cyclic electron transfer process.

General Description of the Cyclic Electron Transfer Chain

Generation of an electrochemical membrane gradient in purple nonsulfur bacteria involves light-driven electron transfer across the intracytoplasmic membrane followed by cotransport of electrons and protons in the opposite directions. The cycle starts with light-induced charge separation in the reaction center protein, where the electron transfer results in double reduction of a quinone molecule to quinol (see Figure 1) accompanied by proton uptake. Quinol then leaves the reaction center protein and is oxidized in the ubiquinol–cytochrome *c* oxidoreductase (also called cytochrome bc_1 complex). The quinol oxidation involves electron transfer both to a soluble cytochrome c_2 and to heme cofactors in the cytochrome bc_1 complex. This heme-mediated electron transfer in the cytochrome bc_1 complex results in the reduction of one quinone molecule bound in the Q_i site for every two quinol molecules oxidized in the Q_0 site (see Figure 1). The protons taken up from the cytoplasm during quinone reduction to quinol in the reaction center and cytochrome bc_1 are released to the periplasm during oxidation. Cytochrome c_2 in turn reduces the oxidized initial electron donor in the reaction center. The cyclic electron transfer results in the translocation of four protons from the cytoplasm to the periplasm for every two photons of light absorbed by the initial electron donor in the reaction center (Figure 1).

Reaction Center

The reaction center is an integral membrane protein, consisting of 3–4 protein subunits. In all species of purple bacteria, the reaction center contains two membrane-spanning protein subunits, called L (light) and M (medium), and the third subunit, called H (heavy), which is positioned on the cytoplasmic side of the membrane. Many species also contain a fourth subunit, a permanently associated cytochrome. The two membrane-spanning subunits bind the redox-active cofactors: four bacteriochlorophyll, two bacteriopheophytin, and two quinone molecules (see Figure 2). The protein also contains a redox inactive, nonheme iron atom and carotenoid molecule. Depending on the species, reaction centers contain either bacteriochlorophyll *a* or *b*, bacteriopheophytin *a* or *b*, and ubiquinone or menaquinone cofactors. The bacteriochlorophylls, bacteriopheophytins, and quinones are arranged in two nearly C_2 symmetric branches (see Figure 2). However, only one of these branches (usually called the A-branch), made up from cofactors mostly associated with the L protein subunit, is photochemically active *in vivo* (Figure 2). Upon the excitation with light, the initial electron donor P (a pair of bacteriochlorophyll molecules on the periplasmic side of the protein) donates an electron to a monomer bacteriochlorophyll, B_A, in ~3 picoseconds (ps), forming the charge-separated state $P^+B_A^-$, and then in ~1 ps the electron is further transferred to the bacteriopheophytin, H_A, forming the state $P^+H_A^-$. Electron transfer then proceeds to a primary quinone acceptor, Q_A, in ~200 ps, creating the charge-separated state $P^+Q_A^-$. From Q_A, the electron is transferred to a secondary quinone acceptor, Q_B, in 10–100 microseconds (μs). The semiquinone form of Q_B remains tightly bound to the reaction center. It is reduced to the quinol form after a second electron transfer event, which is coupled to proton uptake. The second electron transfer cycle is initiated when oxidized P^+ is reduced by cytochrome c_2, allowing light-induced charge separation to occur from P for a second

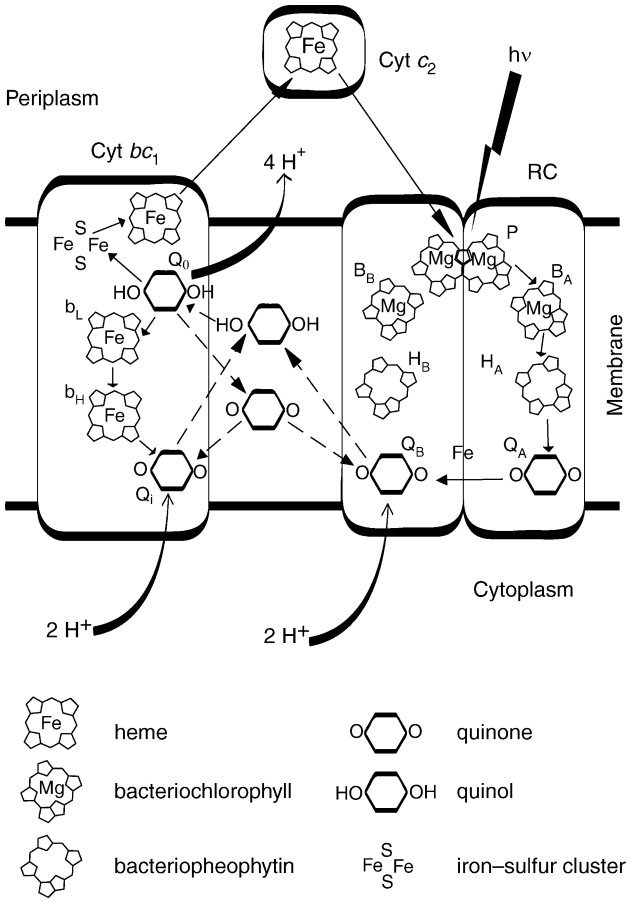

FIGURE 1 Cartoon diagram of the cyclic electron transfer reactions in photosynthetic purple bacteria. The main proteins involved in the reactions and their cofactors are shown schematically. RC stands for reaction center, Cyt c_2 – cytochrome c_2, Cyt bc_1 – cytochrome bc_1 complex. Q_0 and Q_i label two different quinone-binding sites in the cytochrome bc_1 complex. P, B_A, B_B, H_A, H_B, Q_A, Q_B label different cofactors in the reaction center (see Figure 2 for detailed explanation). Movement of the electrons is shown by solid arrows, dashed arrows depict movement of quinone and quinol cofactors.

time. The proton-coupled reduction of Q_B to a quinol occurs in ~1 millisecond (ms). The doubly reduced Q_B, Q_BH_2, then leaves the reaction center and enters the quinone pool (later binding to the cytochrome *bc*1 complex).

Properties of Reaction Center Cofactors

The initial electron donor, P, in purple bacteria consists of an excitonically coupled pair of bacteriochlorophyll molecules. The cation of P is a rather strong oxidant, with a P/P^+ midpoint potential of 0.50 V. On the other hand, the excited state of P, P^*, is a strong reductant with an estimated P^*/P^+ midpoint potential of ~ − 0.9 V, as the P to P^* transition energy is ~1.4 eV. The standard free energy of the first charge-separated state $P^+B_A^-$ is ~0.05 eV below P^* and the standard free energy of the state $P^+H_A^-$ is in the range of 0.15–0.25 eV below P^* (see Figure 2C). Further electron transfer from H_A to the quinone Q_A is driven by a larger free energy gap; $P^+Q_A^-$ is ~0.85 eV below P^*. The reduction potential of Q_A is ~ − 0.05 V, and therefore the free energy captured in the state $P^+Q_A^-$ is ~0.55 eV, or ~40% of the P to P^* transition energy (Figure 2C). The last charge-separated state $P^+Q_B^-$ is only slightly lower in free energy than $P^+Q_A^-$, given that the reduction of Q_B to the semiquinone has a midpoint potential ($E_m(Q_B/Q_B^-)$) of 0.02 V, while the reduction potential of semiquinone forming the quinol has an $E_m(Q_B^-/Q_BH_2)$ of ~0.1 V.

The fact that the reaction center has a symmetric arrangement of cofactors, yet an asymmetric electron transfer pathway, has intrigued researchers ever since the crystal structure was determined. Experimental results answering the question of what determines the electron transfer directionality have been presented over

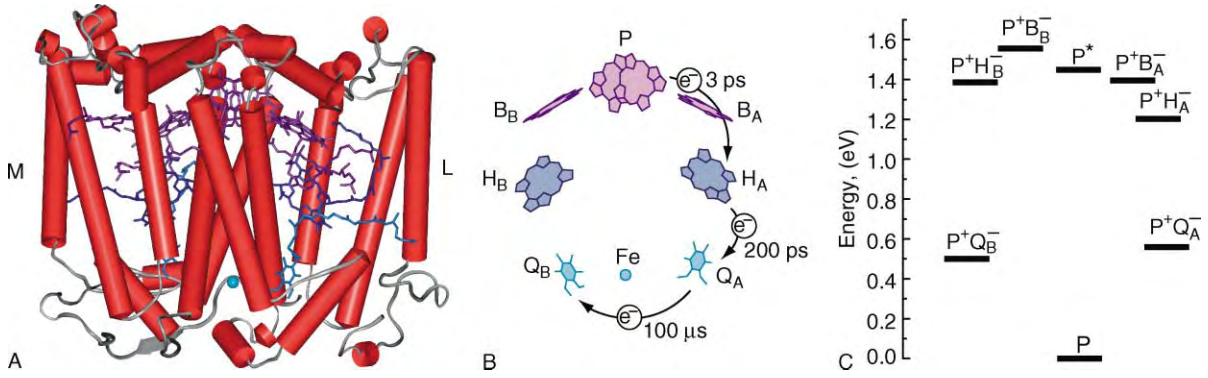

FIGURE 2 (A) Structure of the core subunits of the purple bacterial reaction center. The α-helices of the two subunits, L and M, are shown as red barrels. Bacteriochlorophyll, bacteriopheophytin, and quinone cofactors are shown inside the protein. This figure was created using the 1PCR entry from the Protein Data Bank. (B) Schematic arrangement of the symmetric branches of the bacteriochlorophyll (P and B), bacteriopheophytin (H), and quinone (Q) cofactors. The two branches, usually called A and B, are depicted as the subscripts. The asymmetric electron transfer reactions and their lifetimes are also shown. (C) The energetics of the charge-separated states in the reaction centers of purple bacteria. The free energies of the states are presented relative to the ground state of P, which was set at 0 eV.

the last few years. From site-directed mutagenesis studies, it has been deduced that the main factor limiting the electron transfer along the inactive B branch is the lower midpoint potential of the monomer bacteriochlorophyll cofactor B_B, which makes the standard free energy of the state $P^+B_B^-$ above the state P^* by ~ 0.1 eV (see Figure 2C). This high energetic barrier essentially blocks the electron transfer along the inactive branch, even though the standard free energy of the other charge-separated state, $P^+H_B^-$, is apparently slightly below P^*. The ability of the normally inactive branch (the B-side) to take part in charge separation has been demonstrated in various mutants of the reaction center in which the free energies of the charge-separated states involved were adjusted such that B-side electron transfer could effectively compete with A-side transfer.

Cytochromes

Light-induced charge separation in the reaction center generates both a reduced and an oxidized cofactor. While the doubly reduced quinone, Q_BH_2, has the ability to leave the reaction center to join the quinone pool, oxidized P (the cation free-radical P^+) has to be re-reduced to the neutral state by an external electron donor. This is accomplished by a *c*-type cytochrome. Purple bacteria can be categorized into two groups based on the type of the cytochrome *c* donor used and how it is associated with the reaction center.

The first and major group of bacteria has reaction centers that have permanently associated *c*-type heme-containing cytochrome subunits. These permanent RC-cytochrome complexes are best characterized in the purple bacteria *Blastochloris (Bl.) viridis* (previously named *Rhodopseudomonas viridis*), as this is the strain of bacteria from which the first crystal structure of reaction centers was determined. The cytochrome subunit, which is attached to the periplasmic side of the reaction center, is ~ 40 kDa and contains four heme cofactors. A separate water-soluble cytochome c_2 provides the electrons for the "fixed" cytochrome and mediates the cyclic electron flow between the reaction center and cytochrome bc_1 complex.

Another group of purple bacteria have simpler reaction centers with no permanently attached cytochrome subunit. Instead, a water-soluble cytochrome c_2 acts directly as the donor to oxidized P^+ as well as the acceptor of electrons from the cytochrome bc_1 complex. This group of bacteria includes such strains as *Rhodobacter (Rb.) sphaeroides* and *Rb. capsulatus*. Cytochrome oxidation and P^+ reduction in these strains occur through transient complexes that are formed between the reaction center and cytochrome c_2. The association of the two proteins is mediated mostly by electrostatic interactions, involving negatively charged residues on the periplasmic surface of the reaction center and positively charged residues on the surface of cytochrome c_2.

Properties of the Redox Active Centers in the Cytochromes

Cytochrome c_2 is a small protein containing only one covalently attached heme group. The redox potential of the heme cofactor ranges from 280 to 360 mV in various strains of purple bacteria. Electron transfer between cytochrome c_2 and P occurs with biphasic kinetics, with the major reaction phase having a reaction time constant of 1–4 μs and a slower phase with a 100–400 μs time constant. The first phase reflects the fast electron transfer from the cytochromes that are already associated with the reaction centers, while the slower phase represents the diffusion-limited second-order reaction.

Reduction of P^+ in the other group of the purple bacteria is performed by the permanently attached cytochrome. This cytochrome subunit contains two high and two low midpoint potential heme cofactors. As the best-studied example, the cytochrome from *Bl. viridis* has two hemes with low midpoint potentials of -60 and 20 mV and two high potential hemes, with midpoint potentials of 320 and 380 mV, respectively. The heme arrangement in the cytochrome is such that the heme with the highest midpoint potential is closest to the primary electron donor in the reaction center; the order (from proximal to distal) is: 380 mV → 20 mV → 320 mV → -60 mV. The reduction of P^+ in this cytochrome–reaction center complex is much faster than electron transfer between the soluble cytochrome c_2 and the reaction center. P^+ is reduced by the highest midpoint potential heme; the actual reaction rate depends on the redox state of the other hemes in the subunit and its time constant is on the order of a few hundred nanoseconds. Upon electron donation to P^+, the oxidation of heme 1 is followed by its reduction by heme 3 (with the midpoint potential of 320 mV) in several microseconds. The re-reduction of the oxidized hemes in the reaction center-associated cytochrome is again mediated by soluble cytochrome c_2; this reaction occurs in several hundred microseconds.

Ubiquinol–Cytochrome *c* Oxidoreductase (Cytochrome bc_1 Complex)

Ubiquinol–cytochrome *c* oxidoreductase (or the cytochrome bc_1 complex) is an integral membrane protein

involved in cyclic light-driven electron transfer as well as dark respiration. This complex both oxidizes and reduces quinones and reduces oxidized cytochrome c_2. The simplest of the cytochrome bc_1 complexes are found in the purple bacteria. In most species, this complex consists of only three subunits – cytochrome b, cytochrome c_1, and the "Rieske" iron–sulfur protein. Cytochrome b binds two redox-active heme molecules, called b_L and b_H, with the subscripts referring to the relatively low (~ -100 mV) and high (50 mV) redox midpoint potentials of the two hemes. Cytochrome c_1 binds only one heme molecule, which has a much higher midpoint potential of 290 mV. The "Rieske" iron–sulfur protein contains a $[Fe_2S_2]$ cluster with a relatively high midpoint potential of $\sim$280 mV.

The cytochrome bc_1 complex completes the electron transfer cycle in purple bacteria by re-reducing the cytochrome c_2 that was oxidized by the reaction center and performing the net oxidation of the quinol molecules released by the reaction center. First, the high potential iron–sulfur cluster is oxidized by cytochrome c_2 in $\sim$150–200 μs. Then, quinol binds to the Q_0 site at the interface of cytochrome c_1 and the "Rieske" protein on the complex and re-reduces the iron–sulfur cluster in a one-electron transfer. The second electron from the quinol is used to reduce the b_L cofactor and subsequently is transferred to b_H in $\sim$700 μs. The resulting oxidation of quinol in the Q_0 site results in release of two protons to the periplasmic side of the photosynthetic membrane. Heme b_H then reduces a quinone molecule bound in the second quinone-binding site Q_i, followed by proton uptake to form a semiquinone. This cycle repeats resulting in reduction of a second cytochrome c_2 and oxidation of a second quinol molecule in the Q_0 site, accompanied by release of two more protons on the periplasmic side of the membrane. The semiquinone molecule bound in the Q_i site is then reduced to quinol and released into the quinone pool. The reduction of the quinone molecule to quinol in the Q_i site results in uptake of two protons from the cytoplasmic side of the membrane. Thus, in total four protons are transferred from the cytoplasm to the periplasm, but the net number of quinol molecules oxidized in the cytochrome bc_1 complex is only one. This proton pumping creates the electrochemical gradient needed to drive ATPsynthase.

See Also the Following Articles

Chlorophylls and Carotenoids • Cytochrome bc_1 Complex (Respiratory Chain Complex III) • Cytochrome c • Purple Bacteria: Photosynthetic Reaction Centers • Quinones

Glossary

intracytoplasmic membrane A specially modified portion of the inner cell membrane made up of membrane invaginations which form tubes, vesicles, or flat lamellar membranes.

quinol (also dihydroquinone) Doubly reduced form of the ubiquinone.

quinone (also ubiquinone or coenzyme Q) Any member of a class of cyclic organic compounds containing two carbonyl groups, C = O, in a six-membered unsaturated ring. Widely distributed in plants, animals, and microorganisms, quinones function in oxidation–reduction processes.

semiquinone A stable anion free radical of the ubiquinone.

Further Reading

Berry, E. A., Guergova-Kurras, M., Huang, L., and Crofts, A. R. (2000). Structure and function of cytochrome *bc* complexes. *Annu. Rev. Biochem.* 69, 1005–1075.

Blankenship, R. E. (2002). *Molecular Mechanisms of Photosynthesis*. Blackwell Science, UK.

Hoff, A. J., and Deisenhofer, J. (1997). Photophysics of photosynthesis. Structure and spectroscopy of reaction centers of purple bacteria. *Phys. Rep.* 287, 1–247.

Scott, R. A., and Mauk, A. G. (eds.) (1996). *Cytochrome c: A Multidisciplinary Approach*. University Science Books, Sausalito, CA.

van Brederode, M. E., and Jones, M. R. (2000). Reaction centres of purple bacteria. In *Subcellular Biochemistry* (N.S. Scrutton and A. Holzenburg, eds.), Vol. 35: Enzyme-Catalysed Electron and Radical Transfer, pp. 621–676. Kluwer Academic/Plenum Publishers, New York.

Biography

Evaldas Katilius is a Faculty Research Associate in the Department of Chemistry and Biochemistry at Arizona State University in Tempe, Arizona. He holds a Ph.D. in chemistry from Arizona State University and M.S. in biophysics from Vilnius University, Lithuania.

Neal W. Woodbury is a Professor of Chemistry and Biochemistry at Arizona State University in Tempe, Arizona. He is the Director of the Center for BioOptical Nanotechnology in the AZBiodesign Institute and has a variety of interests in photochemistry and photobiology including energy and electron transfer in photosynthesis, single molecule spectroscopy of DNA/protein interactions, and optically directed molecular evolution. He holds a Ph.D. in biochemistry from the University of Washington, Seattle and performed postdoctoral study at the Carnegie Institution of Washington and Stanford University.

Purple Bacteria: Photosynthetic Reaction Centers

C. Roy D. Lancaster
Max Planck Institute of Biophysics, Frankfurt am Main, Germany

Located within photosynthetic membranes, reaction centers (RCs) are defined as the minimal functional units that can catalyze light-induced electron transfer reactions, thus stabilizing the separation of charged species across the membrane. The RC essentially functions as a ferrocytochrome c_2:quinone photo-oxidoreductase. The absorption of two photons of light leads to two one-electron oxidations of cytochrome c_2 in the periplasm and to the two-electron reduction of a quinone, which is coupled to the uptake of two protons from the cytoplasm. The resulting quinol then leaves its binding site, diffuses in the photosynthetic membrane and is reoxidized by a second membrane protein complex, the cytochrome bc_1 complex, which results in proton release to the periplasm. The electrons are transferred to re-reduce the cytochrome c_2 in the periplasm. This net proton transport produces a transmembrane electrochemical proton potential that can drive ATP synthesis through a third membrane-spanning complex, the ATP synthase.

Photosynthetic Reaction Centers

Virtually all life on Earth ultimately depends on the ability of photosynthetic organisms to convert solar energy into biochemically amenable energy. Photosynthesis is performed by higher plants, algae, and photosynthetic bacteria. Photosynthetic organisms absorb photons for the generation and storage of energy and for the production of biomass. A large proportion of photosynthetically active organisms consists of anoxygenic photosynthetic bacteria. In contrast to the higher plants, algae, and cyanobacteria of oxygenic photosynthesis, which contain the two membrane-bound photosystems I and II, each of the anoxygenic photosynthetic bacteria has only one type of reaction center. While the iron–sulfur type RCs of heliobacteria and anaerobic green sulfur bacteria resemble that of photosystem I, the pheophytin-quinone type RCs of purple bacteria are more similar to the RC of photosystem II.

Purple bacteria find their ecological niche in deeper layers of stagnant bodies of water. In all purple bacteria, the photosynthetic pigments and the photosynthetic apparatus are located within a more or less extended system of invaginated intracytoplasmic membranes. Unlike photosystem II, however, the purple bacterial RC is incapable of extracting electrons from water. Instead it must oxidize inorganic or organic molecules available in the environment. According to their electron donor requirements, sulfur and nonsulfur purple bacteria have traditionally been distinguished. In contrast to sulfur purple bacteria (*Chromatiaceae*, *Ectothiorhodospira*), nonsulfur purple bacteria (*Rhodospirillaceae*) do not require inorganic sulfur compounds, such as hydrogen sulfide, but instead use organic electron donors such as malate or succinate as electron donors. Most of what is known today about purple bacterial RCs results from studies on RCs from nonsulfur purple bacteria. These are currently the best-characterized membrane protein complexes.

Subunit Composition and Molecular Characterization

Most purple bacterial reaction centers contain four protein subunits (Figure 1), referred to as H, M, L, and C (a tetraheme cytochrome *c*). Some, however, such as the RCs of *Rhodobacter* (*Rb.*) *sphaeroides*, *Rb. capsulatus*, and *Rhodospirillum* (*Rs.*) *rubrum*, contain only the H, M, and L subunits. The related RC of the green aerobic thermophilic bacterium *Chloroflexus* (*Cf.*) *aurantiacus* lacks the H subunit.

Generally, RCs from purple bacteria have been isolated and characterized from *Rhodopseudomonas* (*Rp.*) *viridis* (suggested by Hiraishi in 1997 to be to referred to as *Blastochloris viridis*), *Rb. sphaeroides*, *Rb. capsulatus* and a number of other purple bacteria. Variant RCs have been created by site-directed mutagenesis as well as classical herbicide-resistance selection procedures and have been isolated and characterized from *Rb. capsulatus*, *Rb. sphaeroides*, and *Rp. viridis*.

RC preparations have a nonheme iron and four magnesium-containing bacteriochlorophyll cofactors

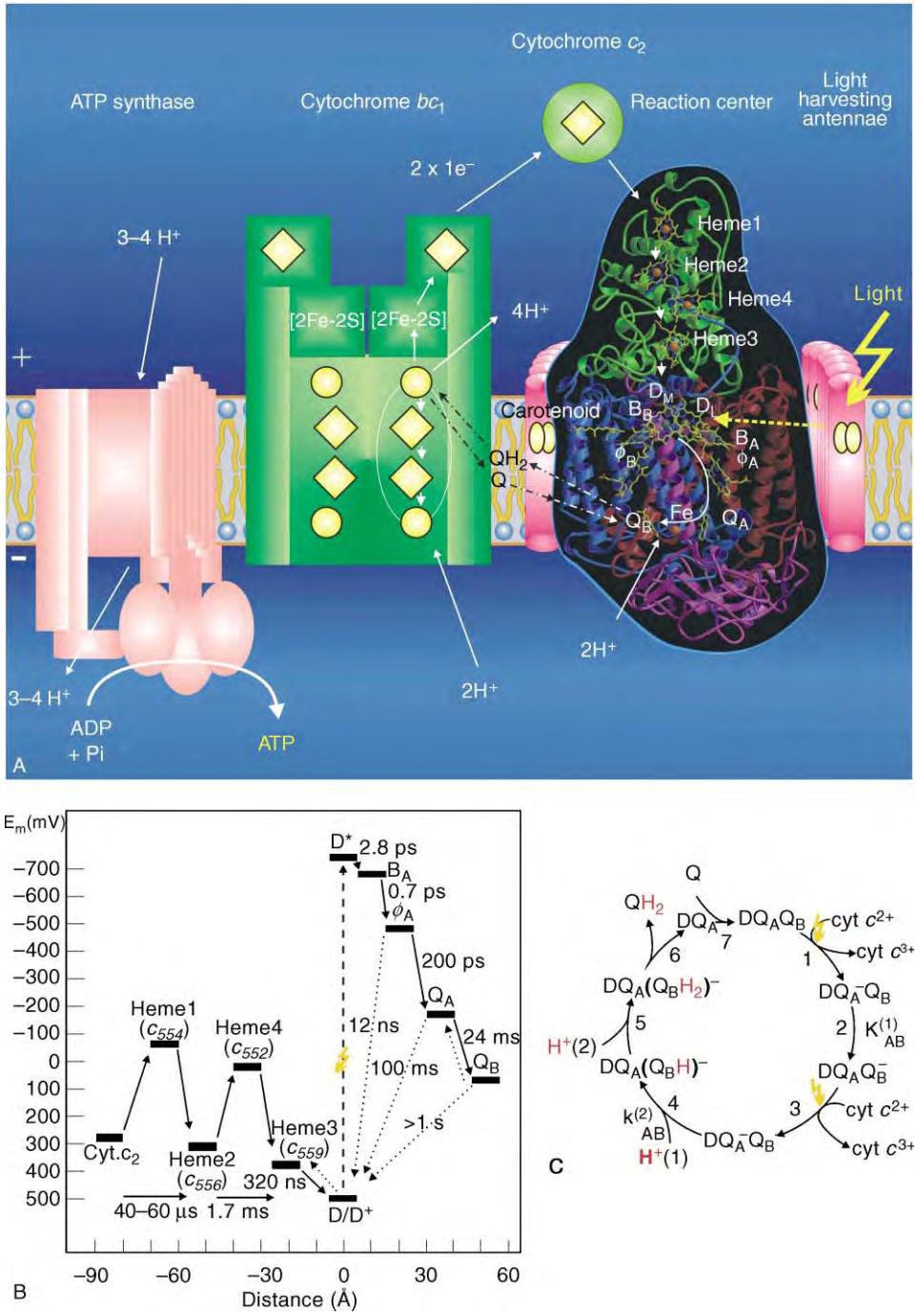

FIGURE 1 Structure and function of the photosynthetic RC. (A) Light-induced cyclic electron flow and the generation and utilization of a transmembrane electrochemical potential in the purple bacterium *Rp. viridis*. The structure of the *Rp. viridis* RC is represented schematically showing the heterotetramer of C, L, M, and H subunits as Cα traces in green, brown, blue, and purple, respectively, plus the fourteen cofactors, which have been projected on to the molecule for better visibility. Also for the sake of clarity, the quinone tails are truncated after the first isoprenoid unit and the phytyl side chains of the bacteriochlorophyll and bacteriopheophytin molecules have been omitted, as have those atoms of the carotenoid molecule, which were not observed in the electron density and assigned zero occupancy in the PDB entry 2PRC. Carbon, nitrogen, and oxygen atoms are drawn in yellow, blue, and red, respectively. (B) Equilibrium oxidation–reduction potentials of the *Rp. viridis* RC cofactors (as compiled by Lancaster, C. R. D., and Michel, H. (2001). Photosynthetic reaction centers. In *Handbook of Metalloproteins* (A. Messerschmidt, R. Huber, T. Poulos and K. Wieghardt, eds.) Vol 1, pp. 119–135. Wiley, Chichester, UK and references therein) as a function of inter-cofactor distance. The soluble electron donor protein cytochrome c_2 has been included as suggested in Figure 4A. Reaction halftimes indicated are taken from the references cited by Lancaster, C. R. D., and Michel, H. (2001). Photosynthetic reaction centers. In *Handbook of Metalloproteins* (A. Messerschmidt, R. Huber, T. Poulos and K. Wieghardt, eds.) Vol 1, pp. 119–135. Wiley, Chichester, UK. The photochemical excitation is indicated by a dashed arrow and unphysiological charge recombination reactions are shown as dotted arrows. (C) Quinone reduction cycle. Steps 2, 4, 5, and 6 are reversible. See text for details.

per RC, as measured by atomic absorption spectroscopy. In *Rb. sphaeroides* and *Rp. viridis*, these are bacteriochlorophyll *a* and bacteriochlorophyll *b*, respectively (Figures 1A and 2A). Those preparations with a tightly bound C subunit have four iron-containing heme groups, which are covalently bound to the protein via thioether bonds formed with the Cys residues of the heme attachment site sequences Cys-X-Y-Cys-His and the His is the fifth ligand to the heme iron. In the *Rp. viridis* RC, the sixth ligands to heme1, heme2, and heme3 are Met residues (His-Met-ligated hemes), whereas the sixth ligand to heme4 is a second His (*bis*-His ligation). Apart from these four hemes, all other cofactors are noncovalently bound by the L and M subunits. The six-coordinated nonheme ferrous iron is coordinated by the Nε atoms of four His residues and the two Oε atoms of a Glu residue. The fifth ligands to the five-coordinated bacteriochlorophyll-magnesium ions are provided by the Nε atoms of His side chains. In addition to these metal-containing cofactors, there are two bacteriopheophytin groups, a carotenoid, and two quinones bound by the RC. In *Rb. sphaeroides*, these are bacteriopheophytin *a*, spheroidene, and ubiquinone-10, respectively, whereas *Rp. viridis* contains bacteriopheophytin *b*, 1,2-dihydroneurosporene, menaquinone-9, and ubiquinone-9 (Figures 1A and 2A–2C).

Apart from the availability of high resolution crystal structures discussed, one major reason why, despite its complexity, the purple bacterial RC has become the "hydrogen atom of protein electron transfer" (W.W. Parson), is the richness of its characterization by optical absorption, electron paramagnetic resonance

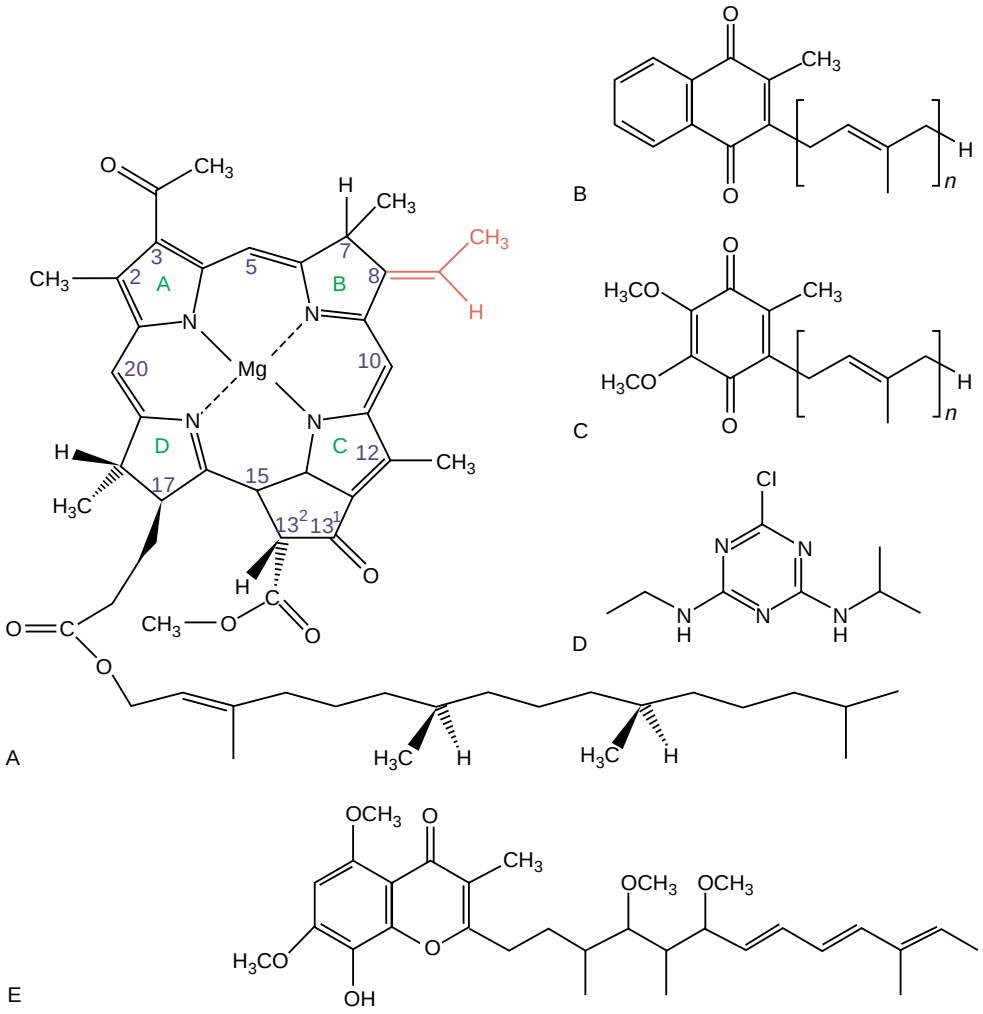

FIGURE 2 Chemical structures of RC cofactors (A–C) and inhibitors at the Q_B site (D–E). (A) Bacteriochlorophyll *b*, as bound in the *Rp. viridis* RC. The bacteriochlorophyll *a* bound in the *Rb. sphaeroides* RC differs by the presence of a C8 ethyl group instead of the C8 ethylidene group indicated in red. Bacteriopheophytins (*a* or *b*) are the metal-free variants of the bacteriochlorophylls (*a* or *b*) with two protons bonded to the nitrogens of the unsaturated pyrrole rings "A" and "C." (B) Menaquinone-n. The native Q_A in the *Rp. viridis* RC is menaquinone-9. (C) Ubiquinone-n. The native Q_A in the *Rp. viridis* RC is ubiquinone-9. In the *Rb. sphaeroides* RC, both Q_A and Q_B are ubiquinone-10. (D) Atrazine (2-chloro-4-ethylamino-6-isopropylamino-*s*-triazine). (E) Stigmatellin A.

(EPR), electron-nuclear double resonance (ENDOR), Fourier transform infrared (FTIR), Resonance Raman (RR), fluorescence, Stark effect, and other types of spectroscopy.

X-Ray Crystal Structures of RCs from Purple Bacteria

The photosynthetic RC from *Rp. viridis* was the first membrane protein complex for which an atomic structural model could be determined by X-ray crystallography (Protein Data Bank (PDB) entry 1PRC). The structure of the four-subunit *Rp. viridis* RC is shown schematically in Figure 1A. The structure of the RC from *Rb. sphaeroides* (not shown) would appear almost identical except for the C subunit at the top, which would be missing. The recently determined structure of the RC from the sulfur purple bacterium *Thermochromatium tepidum* (PDB entry 1EYS) is very similar in overall architecture to that of *Rp. viridis*.

The *Rp. viridis* RC has an overall length of 130Å in the direction perpendicular to the membrane. Parallel to the membrane, the maximum width is ~70Å. The central core of the RC is formed by the L subunit and the M subunit, which possess five membrane-spanning segments each. Both subunits are closely associated and noncovalently bind ten cofactors as detailed above and shown in Figure 1A. Large parts of the L and M subunits and their associated cofactors are related by a two-fold axis of symmetry perpendicular to the plane of the membrane. The H subunit is anchored to the membrane by a single membrane-spanning helix and is attached to the LM core on the cytoplasmic side. On the periplasmic side, the C subunit with its four covalently bound heme groups is attached. The N-terminal diacylglycerol moiety which, in addition to the interaction with the LM core, anchors the C subunit in the membrane is not visible in the electron density map.

The pigments form two symmetry-related branches, also shown in Figure 1A, each consisting of two bacteriochlorophylls, one bacteriopheophytin and one quinone, which both cross the membrane starting from the "special pair" D of two closely associated bacteriochlorophylls (D_M and D_L) near the periplasmic side, followed by the "accessory" bacteriochlorophyll, B, one bacteriopheophytin, ϕ, and a quinone, Q. As shown in Figure 1A, only the branch more closely associated with L subunit is used in the light-driven electron transfer. It is called the A-branch, the inactive one the B-branch. The active branch ends with the primary quinone Q_A, the inactive one with the secondary quinone Q_B. Halfway between both quinones, the nonheme iron is located. The carotenoid is in van der Waals contact with B_B and disrupts the twofold symmetry. In both species, the crystallographic temperature factors, which are a measure for the rigidity of the structure, are considerably higher along the B-branch than along the A-branch.

Functional Aspects

Oxidation–Reduction Potentials

The oxidation–reduction midpoint potentials, E_M, of the four heme groups follow the order low, high, high, low in the sequence or low, high, low, high if the hemes are ordered with decreasing distance (see Figure 1B) from the primary electron donor D. Theoretical analysis by the application of continuum electrostatics to the crystal structure of the C subunit has provided quantitative estimations of the factors contributing to the equilibrium E_M values of the four hemes. Specific residues and the propionic side chains on the hemes are calculated to strongly modulate the E_M values. The correct division into low and high potential hemes can be obtained by taking only the protein into account. Consideration of heme–heme interactions is required to reproduce the experimental data quantitatively.

The redox potentials of the other *Rp. viridis* RC cofactors are also included in Figure 1B. The potential of the excited state D^* is derived from the free energy difference between the lowest vibrational levels of D and D^*. Estimated from the wavelength of the absorption maximum, the dimer of bacterichlorophyll *b* in *Rp. viridis* provides an energy of 1240 meV between D and D^*, that of the bacteriochlorophyll *a* dimer in *Rb. sphaeroides* one of 1380 meV. The redox potential of *Rb. sphaeroides* D has been increased from 505 to 765 mV by the introduction of three additional hydrogen bonds to the special pair bacteriochlorophylls by site-directed mutagenesis, thus destabilizing the oxidized state of the donor, D^+.

The redox potential of Q_A is higher in the *Rb. sphaeroides* RC than in the *Rp. viridis* RC because of the different chemical nature of the quinones (ubiquinone versus menaquinone). However, it is still 67 mV lower than that of *Rb. sphaeroides* Q_B, even though both cofactors are chemically identical, thus requiring a role of the protein in tuning the *in situ* redox potentials of the quinones.

Kinetics

Figures 1A and 1B show schemes of the electron transfer steps that occur in the purple bacterial reaction center. Light absorption leads to an excited primary donor D^*, from which an electron is transferred via the monomeric bacteriochlorophyll B_A (reaction halftime: 2.8 ps) and the bacteriopheophytin ϕ_A (700 fs) to Q_A in 200 ps, leading to the formation of $D^+Q_A^-Q_B$. Re-reduction of

D^+ by cytochrome c_{559} (heme 3) occurs in 320 ns. These processes are much faster than the subsequent proton uptake and inter-quinone electron transfer reactions. Therefore, the first step of quinone reduction in the RC can be viewed as a "photochemical cytochrome oxidation," giving rise to the radical state $DQ_A^-Q_B$ (Figure 1C). Re-reduction of cytochrome c_{559}^+ by cytochrome c_{556} (heme 2) occurs in 1.7 μs. The second step of quinone reduction involves the transfer of the first electron to Q_B in 17–25 μs, resulting in the state $DQ_AQ_B^-$. The one-electron reduction of Q_B is not associated with direct protonation and the semiquinone species is anionic. However, the $Q_A^-Q_B \rightleftarrows Q_AQ_B^-$ equilibrium constant is pH-dependent, as electron transfer is accompanied by substoichiometric proton uptake due to the protonation of amino acid residues. Cytochrome c_{556}^+ is re-reduced by cytochrome c_2 in 40–60 μs. In species that lack the C subunit, e.g., *Rb. sphaeroides*, the photoxidized special pair is directly re-reduced by cytochrome c_2 in a biphasic reaction. The fast phase of ~1 μs is attributed to intermolecular electron transfer, the slow phase of 100 μs is limited by docking and reorientation of the cytochrome c_2-RC complex. After a second "photochemical cytochrome oxidation," the diradical state $DQ_A^-Q_B^-$ is formed at rates similar to those for the first electron transfer. Coupled transfer of the first proton and the second electron to Q_B^- leads to the monoprotonated, doubly reduced state $DQ_A(Q_BH)^-$. Transfer of the second proton for the formation of Q_BH_2 is kinetically indistinguishable from the first proton transfer in the wild-type RC and can only be resolved in the case of mutants with significantly retarded second proton transfer rates.

Functional Derivatives

Substrate Analogue and Inhibitor Complexes

In the original *Rp. viridis* RC structure (PDB entry 1PRC), the Q_B site was poorly defined because it was only partially occupied with the native ubiquinone-9 in the standard RC crystals. However, ubiquinone-2-reconstitution experiments have yielded crystals with full quinone occupancy of the Q_B site. Subsequent X-ray diffraction analysis and refinement has led to a well-defined Q_B-site model (2PRC), with the quinone bound in the "proximal" position, i.e., close to the nonheme iron (hydrogen-bonded to its ligand His L190, see Figure 3A). In the RC structure with a Q_B-depleted Q_B site (3PRC, Figure 3B), refined at 2.4Å, apparently five, possibly six, water molecules are bound instead of the ubiquinone head group, and a detergent molecule binds in the region of the isoprenoid tail. Using the structures 2PRC and 3PRC as references, the original data set 1PRC was re-examined. A more quantitative analysis of the original data resulted in 20% of the Q_B sites being occupied with quinone in the proximal site, 30% having quinone bound in a more distal site, not hydrogen-bonded to His L190 and further away from the nonheme iron (see Figure 3A), and half of the Q_B sites being empty or having the quinone unaccounted for. A further structure, the RC complex with the inhibitor stigmatellin (see Figure 2E), refined at 2.4Å, indicates that additional hydrogen bonds stabilize the binding of stigmatellin over that of ubiquinone-2 (4PRC, see Figure 3C). The binding pattern observed for the stigmatellin complex can be viewed as a model for the stabilization of a monoprotonated reduced intermediate (Q_BH or Q_BH^-). This indicates that the Q_B site is not optimized for Q_B binding, but for Q_B reduction to the quinol. In combination with the results of electrostatic calculations, these crystal structures can provide models for intermediates in the reaction cycle of ubiquinone reduction to ubiquinol, as discussed next.

The Q_B site is also a well-established site of herbicide action. Over half of the commercially available herbicides function by inhibition of higher plants at the QB site of the D1 polypeptide of the photosystem II RC. A commercially very important class of herbicides are the triazines, which were introduced by J.R. Geigy S.A. in the 1950s. A prominent example is atrazine (Figure 2D), first reported in 1957. According to statistics from 1995, atrazine was used on ~67% of all US corn acreage, 65% of sorghum acreage, and 90% of sugarcane acreage. Another well-known triazine is terbutryn (2-*t*-butylamino-4-ethylamino-6-methylthio-*s*-triazine). X-ray crystal structures of complexes of the RC with atrazine (PDB entry 5PRC) and terbutryn (PDB entry 1DXR) have been determined at 2.35Å and 2.00Å resolution, respectively. In both cases, three hydrogen bonds bind the distal side of the inhibitors to the protein, and four additional hydrogen bonds, mediated by two tightly-bound water molecules are apparent on the proximal side, as shown for atrazine in Figure 3D. In contrast to the proximal binding of stigmatellin (Figure 3C), the triazine inhibitor partially overlaps with both the distal- and the proximal ubiquinone-binding sites (Figure 3D).

Mutants

Work on site-directed mutagenesis of photosynthetic reaction centers started with the RC from *Rb. capsulatus*. This species is genetically very well characterized and able to grow non-photosynthetically under aerobic conditions, as well as under anaerobic conditions using e.g., dimethylsulfoxide as an electron acceptor. Most importantly, under these latter conditions, the photosynthetic apparatus is fully induced. Unfortunately, the RC from *Rb. capsulatus* could not be crystallized, thus thwarting proper inspection for structural changes.

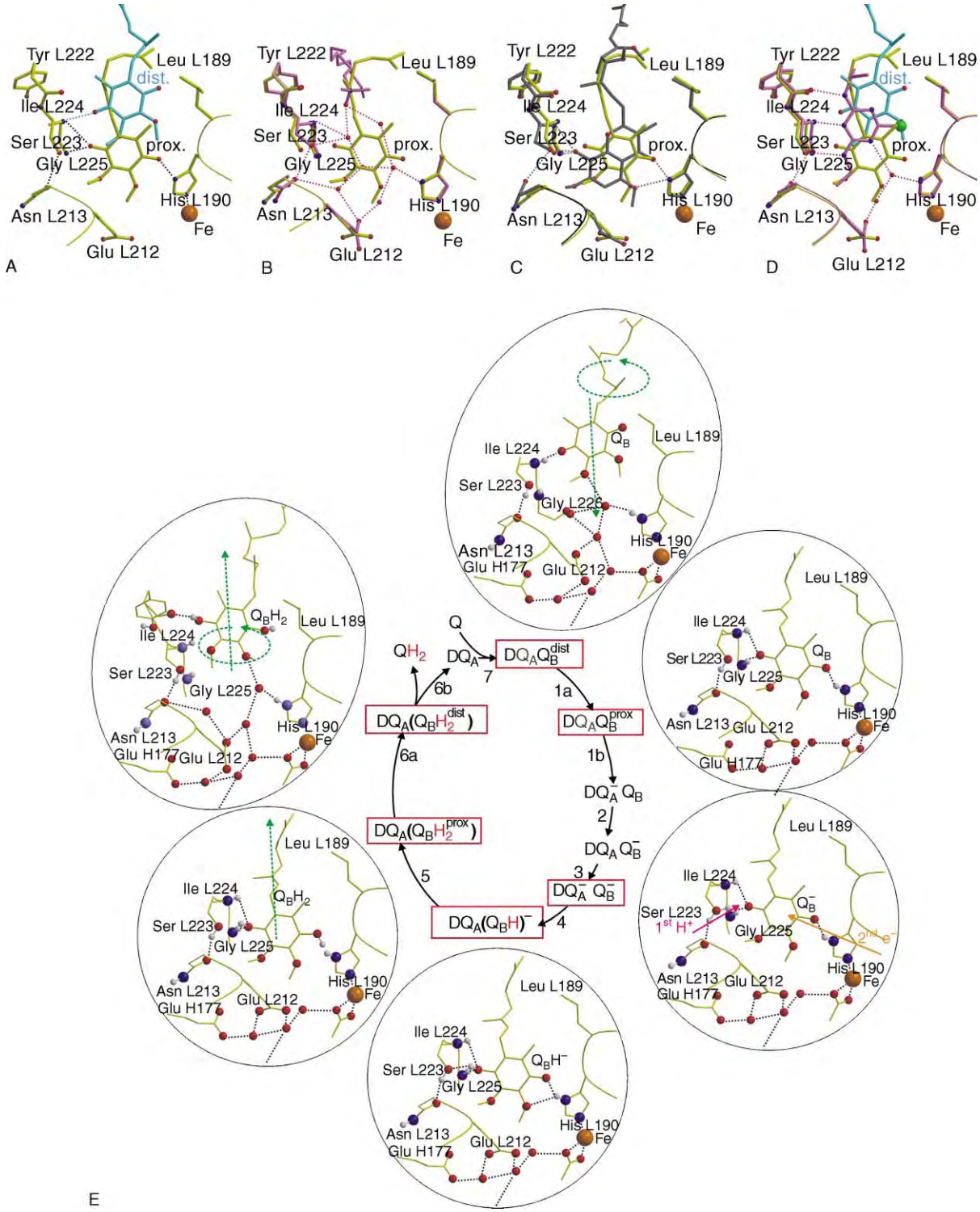

FIGURE 3 Derivatives at the Q_B site of the *Rp. viridis* RC. (A) Comparison of distal ($1PRC_{new}$, cyan) and proximal (2PRC, yellow) ubiquinone-binding sites. (B) Comparison of Q_B-depleted (3PRC, pink) and ubiquinone-2-occupied (2PRC, yellow) Q_B sites. (C) Comparison of stigmatellin binding (4PRC, gray) and ubiquinone-2 binding (2PRC, yellow). (D) Atrazine binding (5PRC, pink) compared to distal ($1PRC_{new}$, cyan) and proximal (2PRC, yellow) ubiquinone-binding sites. (E) Mechanistic implications of the structures 2PRC, 3PRC, 4PRC, and the revised model $1PRC_{new}$ for the events at the Q_B site within the reduction cycle of quinone to quinol. The numbering of the steps is analogous to that in Figure 1C. Hydrogen atoms are drawn as small light gray spheres. Dashed green arrows symbolize quinone movements.

The closely related *Rb. sphaeroides* can be grown under similar non-photosynthetic conditions, so that site-directed mutagenesis is also straightforward. As mentioned above, this RC is amenable to inspection by X-ray crystallography for structural changes. Many amino acids which were considered to be of importance for pigment binding, electron transfer or proton transfer were changed in *Rb. sphaeroides* RCs. In addition to mutagenesis, quinone or bacteriochlorin cofactors may be removed or replaced chemically with a wide range of similar compounds.

Site-directed mutagenesis of the RC from *Rp. viridis* is possible but more difficult. *Rp. viridis* can grow only under photosynthetic and, very slowly, under microaerophilic conditions. However, under microaerophilic conditions, the photosynthetic apparatus is hardly induced and photosynthetic growth conditions exert a selection pressure for revertants and suppressor mutants if the RCs are functionally impaired. On the other hand, very interesting herbicide-resistant mutants were obtained by classical selection procedures, with mutations some of which would not have been made by site-directed mutagenesis.

Some of these herbicide resistant mutants of the *Rp. viridis* RC have also been analyzed by X-ray crystallography. For instance, the mutation Tyr L222 → Phe unexpectedly leads to resistance against the herbicide terbutryn. In the wild type, Tyr L222 forms a hydrogen bond with the peptide carbonyl oxygen of Asp M43. Since this hydrogen bond is now missing, a stretch of the M subunit (M25–50) moves into a new position. The side chain of Phe L222 rotates by 90° into the herbicide binding site, thereby preventing the binding of terbutryn by steric hindrance, but at the same time introducing sensitivity to two other classes of photosystem II inhibitors normally inactive in bacterial RCs, the ureas and phenolics.

Using site-directed mutagenesis, the highly conserved Tyr L162, positioned halfway between D and the proximal heme3 (cytochrome c_{559}) in the *Rp. viridis* RC (see Figure 4A, below), was exchanged against a number of amino acids. All mutants grew photosynthetically. The redox potentials of D and c_{559} were changed by the mutations. The structures of two variant RCs (Tyr L162 → Phe and Tyr L162 → Thr) were determined and found not to differ significantly from the wild-type structure. Analysis of the kinetics of electron transfer led to the conclusion that the tyrosine residue at position L162 is not required for fast electron transfer from c_{559} to D^+.

Mutation of Arg C264 → Lys decreases the midpoint potential of heme3 (cytochrome c_{559}) from +380 mV to +270 mV, i.e., below that of heme2 (+320 mV, see Figure 1B). In the structure of the variant RC at 2.46Å resolution, no remarkable differences were found apart from the mutated residue itself. The halftime of electron transfer between heme2 and heme3 was the same as in the wild-type, indicating that the observed reaction rate is limited by the very uphill electron transfer from heme2 to heme4 (see Figure 1B).

Inter- and Intramolecular Electron and Proton Transfer and Catalytic Mechanism

Intramolecular Electron Transfer

The kinetics of light-induced electron transfer via Q_A to Q_B and of the re-reduction of the special pair have been detailed earlier. The reasons for the unidirectionality of electron transfer along the active A branch and not along the inactive B branch, despite the twofold pseudosymmetry of the LM core of the RC, have been the subject of numerous theoretical and experimental investigations. Slight differences in geometry, differences in rigidity, and differences in the amino acid composition of the L and M subunits have been suggested to contribute to unidirectionality. The latter aspect was specified by the theoretical identification of a large electrostatic field favoring charge separation along the A branch. A major contributor to the potential gradient is Arg L103, whose positive charge is stabilized by different sections of the polypeptide backbone. This dipolar stabilization leads to a much longer-range effect of the positive charge than if it were stabilized by a counter ion.

An experimental observation consistent with this electrostatic analysis is the finding that a site-directed double mutant in *Rb. capsulatus* RCs (Leu L212 → His; Gly L201 → Asp) appears to show significant electron transfer to ϕ_B. The first mutation leads to the incorporation of the β bacteriochlorophyll in the ϕ_A position and the second mutation introduces a negative charge close to B_A, thus making electron transfer down the A branch less favorable.

Quinone Reduction and Protonation

Both Q_A and Q_B sites are deeply buried within the photosynthetic reaction center complex, ~15Å from the cytoplasmic surface. Proton transfer to the reduced quinone within the Q_B site could occur by protons moving along a chain of proton donors and acceptors by a "proton wire," or hydrogen-bonded chain mechanism. Possible proton donors and acceptors are protonatable amino acid residues and water molecules. A number of the protonatable residues between the Q_B site and the cytoplasmic surface have been shown to be functionally relevant to the proton transfer process by analysis of site-directed mutations and second site revertants.

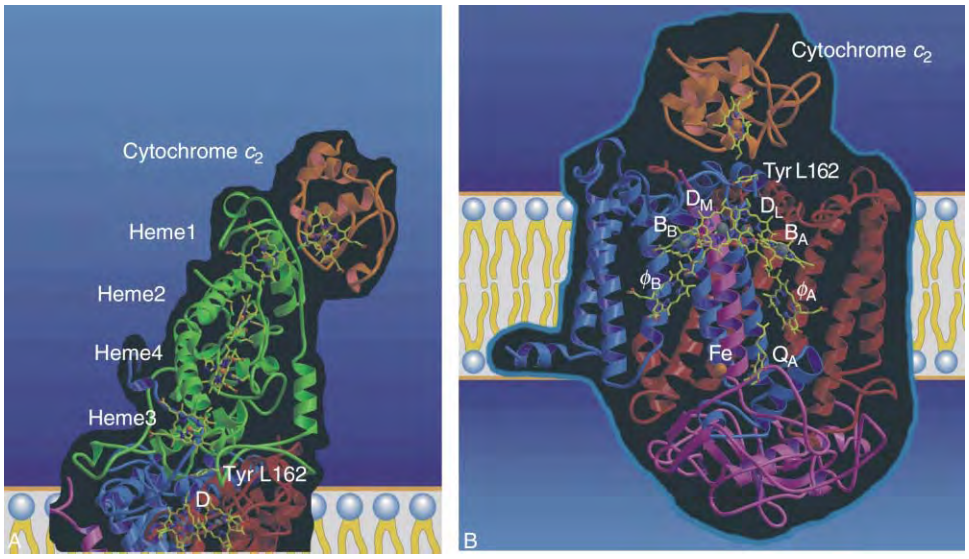

FIGURE 4 Cytochrome c_2 oxidation by the photosynthetic RCs of *Rp. viridis* and *Rb. sphaeroides*. (A) Reduction of the photo-oxidized tetraheme C subunit of the *Rp. viridis* RC (color-coding as in Figure 1A) by *Rp. viridis* cytochrome c_2 (orange). Theoretical docking as suggested from mutagenesis experiments. (B) Reduction of the special pair D in the *Rb. sphaeroides* RC (color coding of the L, M, and H subunits analogous to Figure 1A) by *Rb. sphaeroides* cytochrome c_2 (orange) as determined by X-ray crystal structure analysis (PDB entry 1L9B).

The observed effects can be due to the modification of the kinetics and thermodynamics of electron or proton transfer. Electrostatic calculations based on the X-ray structure coordinates of the RCs from *Rb. sphaeroids* and *Rp. viridis* led to the identification of residues that can contribute to the changes in equilibrium distributions of protons in the different redox states of the protein, thus helping to determine the role of the functionally important residues.

In combination with the results of electrostatic calculations, the crystal structures 3PRC, $1PRC_{new}$, 2PRC, and 4PRC already discussed (cf. Figures 3A–3D) can provide models for intermediates in the reaction cycle of ubiquinone reduction to ubiquinol (see Figure 3E). The binding of the incoming Q_B to the distal site displaces some of the water molecules present in the "empty" pocket. The quinone ring is flipped around the isoprenoid tail and further water molecules are displaced for the Q_B to occupy the proximal position (step 1a in Figure 3E). This is the position in which neutral Q_B accepts an electron from Q_A^-. The hydrogen bonds donated to the quinone will automatically lead to a tighter binding of the negatively charged semiquinone Q_B^- compared to the neutral Q_B (step 2). Additionally, the side chain of Ser L223 can reorient by rotation of its χ_2 (Cα–Cβ–Oγ–Hγ) torsional angle, thus establishing an additional hydrogen bond to Q_B^-. Coupled to the transfer of the second electron, the first proton is transferred, possibly via a transiently protonated Ser L223-OH_2^+, thus forming the monoprotonated, doubly reduced intermediate Q_BH^- (steps 3 and 4). After transfer of the second proton (step 5), movement of the quinol from the proximal to the distal position (step 6a) may be facilitated by increased stacking interactions of the aromatic ring systems with the Phe L216 ring and the diffusion of water molecules back into the pocket. The structures of these intermediates provide explanations for their relative binding affinities, as required for proper enzymatic function of the Q_B site. A rearrangement of hydrogen bonds, most prominently the reorientation of the Ser L223 side chain for Q_B reduction, as suggested by the scenario in Figure 3E, has also been calculated by Alexov and Gunner to be necessary to make Q_B reduction more favorable than Q_A reduction. These local rearrangements may constitute the conformational changes deduced to be required for function by a variety of experiments.

Cytochrome c_2 Oxidation

All four hemes of the *Rp. viridis* RC tetraheme C subunit are located close enough to the surface of the protein to accept electrons from soluble cytochrome c_2. Site-directed mutagenesis in another non-sulfur purple bacterium, *Rubrivivax gelatinosus*, has led to the identification of a patch of acidic residues immediately surrounding the distal low-potential heme1 of the tetraheme C subunit that apparently forms an electrostatically favorable binding site for soluble cytochromes. Thus all four hemes in the C subunit appear to be directly involved in the electron transfer toward the photo-oxidized special pair. Based on these findings, a model was proposed for the transient cytochrome c_2-RC complex for *Rp. viridis* (see Figure 4A).

In the case of the *Rb. sphaeroides* RC, which lacks the C subunit, the photo-oxidized special pair D^+ is directly re-reduced by cytochrome c_2. The structure of the co-complex of the *Rb. sphaeroides* RC and cytochrome c_2 has been determined by X-ray crystallography at 2.4Å resolution (cf. Figure 4B). In these crystals, D^+ is reduced by cytochrome c_2 at the same rate as measured in solution, indicating that the structure of the complex in the region of electron transfer is the same in the crystal and in solution. The binding interface can be divided into two domains. The first domain contributes to the strength and specificity of cytochrome c_2 binding and is a short-range interaction domain that includes Tyr L162 (cf. Figure 4B), and groups exhibiting non-polar interactions, hydrogen bonding, and a cation-π interaction. The second is a long-range, electrostatic interaction domain that contains complementary charges on the RC and cytochrome c_2. In addition to contributing to the binding, this domain may help steer the unbound proteins into the right orientation.

Relevance to Photosystem II

Based on the determined structure of the purple bacterial RC, very specific sequence homologies, and azidoatrazine labeling, the RC core of higher plant photosystem (PS) II was proposed to be similar to the LM core of the bacterial RC, with the D1 and D2 proteins corresponding to the L- and M subunits, respectively. This proposal could be verified experimentally. Recently, suitably designed, modified bacterial RCs have been shown to mimic tyrosine oxidation in PS II. In the absence of a high-resolution structure of the photosystem II RC, the purple bacterial RC still serves as the basis for models of PS II.

See Also the Following Articles

Cytochrome bc_1 Complex (Respiratory Chain Complex III) • Cytochrome *c* • Green Sulfur Bacteria: Reaction Center and Electron Transport • Heme Proteins • Heme Synthesis • Light-Harvesting Complex (LHC) I and II: Pigments and Proteins • Photosystem II: Protein Components • Purple Bacteria: Electron Acceptors and Donors • Quinones

Glossary

cytochrome c_2 A heme-containing hydrophilic protein that functions as an electron carrier in both photosynthesis and respiration.

photosynthetic reaction center A membrane-intrinsic protein complex that carries out the primary photochemical event, the charge separation process.

purple bacteria Prokaryotes that catalyze photosynthetic electron transfer. Divided into *Rhodospirillaceae* (nonsulfur) and *Chromatiaceae* (sulfur).

ubiquinone (formerly called coenzyme Q) A quinone derivative with a variable length side chain of isoprene units (mostly 8–10). It occurs in the lipid core of the eukaryotic inner mitochondrial membranes and of bacterial cytoplasmic membranes and functions as a mobile, lipophilic carrier of electrons (and protons).

Further Reading

Blankenship, R. E., Madigan, M. T., and Bauer, C. E. (eds.) (1995). *Anoxygenic Photosynthetic Bacteria*. Kluwer Academic Publishers, Dordrecht, NL.

Deisenhofer, J., and Michel, H. (1989). The photosynthetic reaction center from the purple bacterium *Rhodopseudomonas viridis* (Nobel Lecture). *EMBO J.* **8**, 2149–2170.

Hoff, A. J., and Deisenhofer, J. (1997). Photophysics of photosynthesis – structure and spectroscopy of reaction centers of purple bacteria. *Phys. Rep. Rev. Sect. Phys. Lett.* **287**, 1–247.

Lancaster, C. R. D. (1999). Quinone-binding sites in membrane proteins: What can we learn from the *Rhodopseudomonas viridis* reaction centre? *Biochem. Soc. Trans.* **27**, 591–596.

Lancaster, C. R. D., and Michel, H. (2001). Photosynthetic reaction centers. In *Handbook of Metalloproteins* (A. Messerschmidt, R. Huber, T. Poulos and K. Wieghardt, eds.) Vol 1, pp. 119–135. Wiley, Chichester, UK.

Michel-Beyerle, M. E. (ed.) (1996). *The Reaction Center of Photosynthetic Bacteria – Structure and Dynamics*. Springer-Verlag, Berlin.

Moser, C. C., Page, C. C., Cogdell, R. J., Barber, J., Wraight, C. A., and Dutton, P. L. (2003). Length, time, and energy scales of photosystems. *Adv. Prot. Chem.* **63**, 71–109.

Paddock, M. L., Feher, G., and Okamura, M. Y. (2003). Proton transfer pathways and mechanism in bacterial reaction centers. *FEBS Lett.* **555**, 45–50.

Parson, W. W. (2003). Electron donors and acceptors in the initial steps of photosynthesis in purple bacteria: A personal account. *Photosynth. Res.* **76**, 81–92.

Wraight, C. A. (2004). Proton and electron transfer in the acceptor quinone complex of photosynthetic reaction centers from *Rhodobacter sphaeroides*. *Front. Biosci.* **9**, 309–337. http://www.bioscience.org

Biography

C. Roy D. Lancaster is a Group Leader in the Department of Molecular Membrane Biology at the Max Planck Institute of Biophysics in Frankfurt am Main, Germany. He holds an M.Sc. from McMaster University, Hamilton, Ontario, Canada, and a Dr. phil. nat. degree from J. W. Goethe University, Frankfurt am Main. He teaches Biochemistry and Biophysical Chemistry at J. W. Goethe University. His principal research interests are in the structure and mechanism of action of selected membrane protein complexes, including photosynthetic reaction centers.

Pyridoxal Phosphate

David E. Metzler
Iowa State University, Ames, Iowa, USA

Pyridoxal phosphate (PLP) is one of several small organic molecules known as coenzymes, compounds that are essential to all forms of life. PLP, together with over 60 different enzymatic proteins, acts to catalyze a variety of specific chemical reactions, many of which are steps in chemical pathways of synthesis or degradation of amino acids or of other nitrogen-containing compounds. PLP is the phosphoric acid ester of pyridoxal, a form of vitamin B_6. This vitamin is synthesized by plants and by many microorganisms, but humans must obtain it from dietary sources. The major form of vitamin B_6 in plants (and in vitamin pills) is the alcohol pyridoxol (pyridoxine). In tissues of our bodies (as well as of other organisms) this is converted to pyridoxol 5′-phosphate, which can be dehydrogenated (oxidized) to the aldehyde PLP (Figure 1). Some enzymes can convert PLP reversibly to pyridoxamine phosphate (PMP) by a process known as transamination (Figure 2). All organisms contain PLP and PMP, much of which is bound to enzyme proteins. Excess PLP is rapidly dephosphorylated to pyridoxal and oxidized to the corresponding carboxylic acid, pyridoxic acid.

Transamination

Transamination is a biologically important process by which living cells exchange the oxygen atoms of α-oxoacids with amino groups (and associated hydrogen atoms) of amino acids such as glutamic acid (Figures 1 and 2). The process occurs via two half-reactions. In the first the amino group is transferred from the amino acid to PLP to form PMP. In the second the PMP that is formed transfers the amino group to the carbon skeleton of the original oxoacid (Figure 2). During the reactions the PLP or PMP is held tightly in the active sites of the enzymes where it reacts rapidly and reversibly to form intermediates known as aldimines (Figure 3) or ketimines (Figure 4). The coenzymes function many times before the less tightly bound PMP loses its hold on the active site or the coenzyme is inactivated by a side reaction.

In the human body transaminases (aminotransferases) catalyze numerous steps in biosynthesis or breakdown of amino acids. For example, glutamic acid from the diet can donate nitrogen to oxoacids to form such amino acids as alanine and aspartic acid. In plants and other autotrophic organisms glutamic acid also donates nitrogen to additional oxoacids to synthesize amino acids that cannot be made in the human body.

The Variety of PLP-Dependent Reactions

Transamination is only one of many reactions of amino acids and other amines that are catalyzed by PLP-dependent enzymes. Some of these are listed in Table I. Groups *a*, *b*, and *c* in this table are defined by the cleavage of one of three possible chemical bonds, *a*, *b*, or *c*, in an amino acid substrate (see Figure 3). The enzymes in group *a*, which includes transaminases, initiate the reaction by removing the α-hydrogen as H^+. In this way each enzyme creates an intermediate chemical species, the quinonoid-carbanionic form (Figure 3). For transaminases and several other enzymes this intermediate has been identified by spectroscopic studies and X-ray crystallography. The quinonoid-carbanionic form reacts in different ways that depend upon the individual enzymes. Transaminases catalyze addition of an H^+ ion at a new position to create a ketimine form as illustrated in Figure 4. Subsequent hydrolysis yields PMP and the oxoacid product of the transamination.

Racemases, after removal of the α-hydrogen of the aldimine as H^+, add an H^+ ion back to the same carbon atom but from the opposite side of the planar quinonoid-carbanionic structure (Figure 3). The effect is to catalyze the interconversion of the two stereoisomers known as the L- and D-forms of the amino acid. Many bacteria form D-alanine from the predominate "natural" L-alanine using a PLP-dependent racemase. Bacteria utilize the D-alanine, as well as D-glutamic acid, formed by a special aminotransferase, in construction of their cell walls. The D-amino acids help provide protection from enzymes that act on L-amino acids. In a similar way small amounts of D-serine, which functions in the brain, are formed from L-serine by a racemase. A third type of reaction of a quinonoid-carbanionic species (Figure 3) is formation of the cyclic

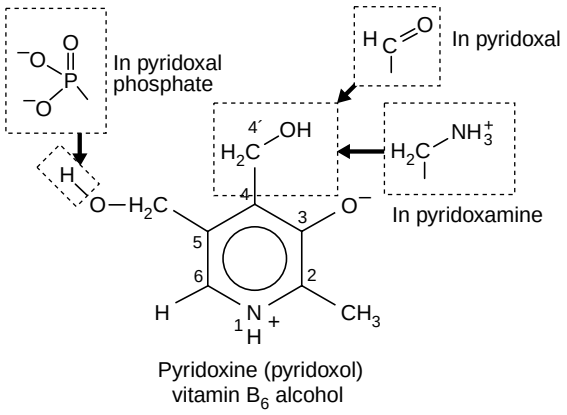

FIGURE 1 The vitamin B_6 (pyridoxine) family: pyridoxol, pyridoxal, pyridoxamine, and the coenzyme forms pyridoxal and pyridoxamine phosphates.

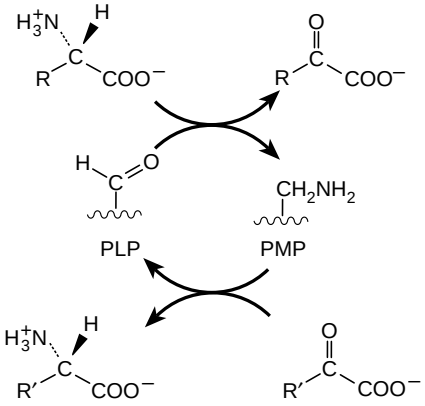

FIGURE 2 The transamination reaction by which amino groups are transferred from one carbon skeleton (in the form of an α-oxoacid) to another to form or to degrade an amino acid.

amino acid aminocyclopropane carboxylic acid, a precursor to the plant hormone ethylene. A large group of enzymes catalyze a fourth type of reaction, which involves elimination of a chemical group such as –OH, or –SH (designated – Y in Figure 3). This may be followed by a decomposition with liberation of NH_3 and other products or replacement of the eliminated group by a new group. These reactions play many roles in

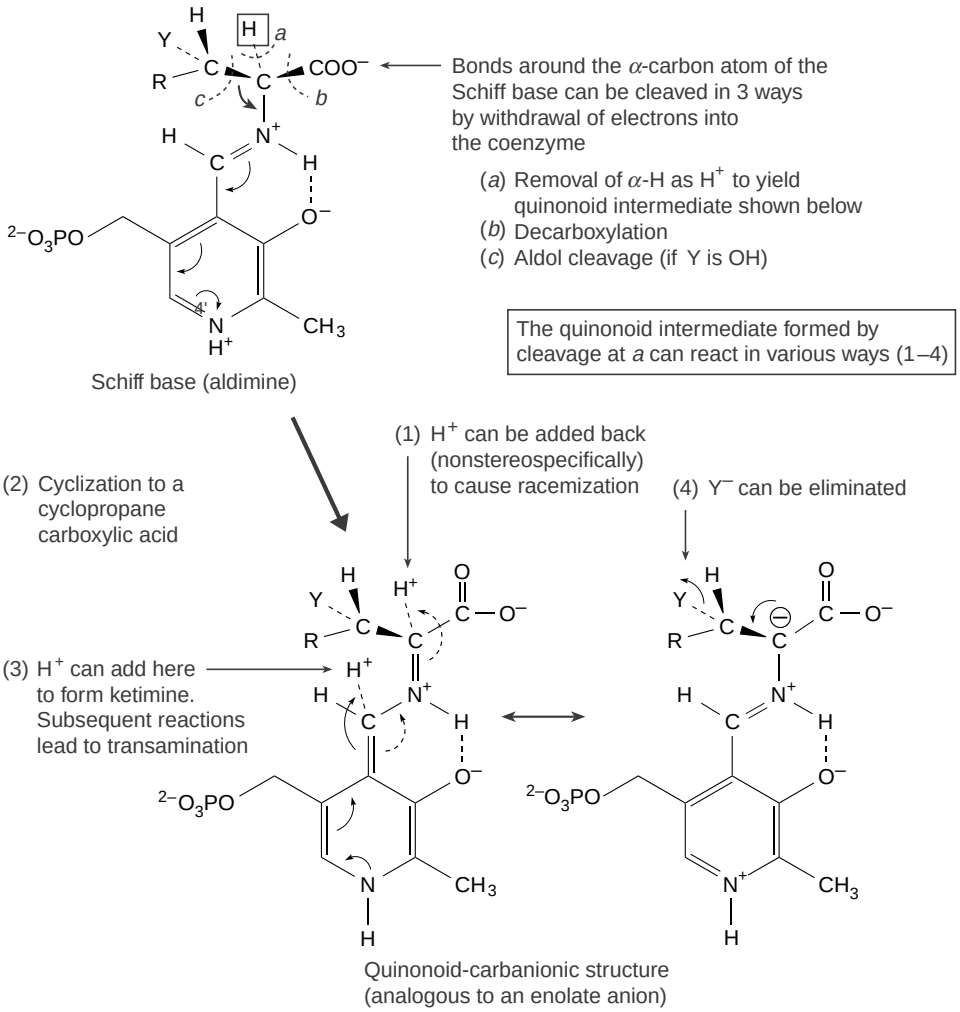

FIGURE 3 The action of pyridoxal phosphate in initiating catalysis of numerous reactions of α-amino acids. Completion of the various reactions requires a large variety of different enzyme proteins.

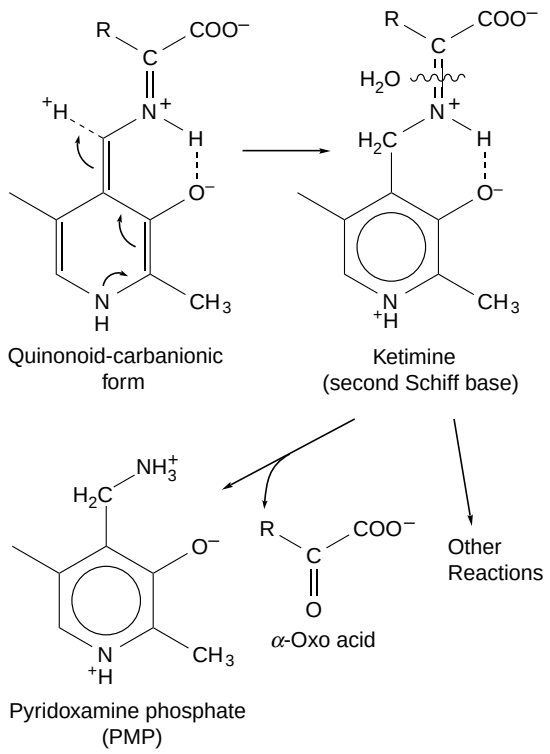

FIGURE 4 Conversion of the quinonoid-carbanionic intermediate into a ketimine which may give rise to PMP in a half-transamination reaction or may undergo alterations in the side chain (R–) to give other products.

TABLE I

Some Enzymes that Require Pyridoxal Phosphate as a Coenzyme

(a) Removing alpha hydrogen as H^+
- (1) Racemization
  - Alanine racemase
  - Serine racemase
- (2) Cyclization
  - Aminocyclopropane carboxylate synthase
- (3) Amino group transfer
  - Aspartate aminotransferase
  - Alanine aminotransferase
  - D-Amino acid aminotransferase
  - Branched chain aminotransferase
  - γ-aminobutyrate aminotransferase
  - ω-Amino acid:pyruvate aminotransferase
- (4) Beta elimination or replacement
  - D- and L-Serine dehydratases (deaminases)
  - Tryptophan indole-lyase (tryptophanase)
  - Alliinase
  - O-Acetylserine sulfhydrylase (cysteine synthase)
  - Tryptophan synthase

(b) Removal of alpha carboxylate as CO_2
- Diaminopimelate decarboxylase
- Glycine decarboxylase (requires lipoyl group)
- Glutamate decarboxylase
- Histidine decarboxylase
- Dopa decarboxylase
- Tyrosine decarboxylase

(c) Removal or replacement of side chain (or —H) by aldol cleavage or condensation
- Serine hydroxymethyltransferase
- δ-aminolevulinate synthase
- Serine palmitoyltransferase

(d) reactions of ketimine intermediates
- Aspartate γ-decarboxylase
- Selenocysteine lyase
- *Nif S* protein of nitrogen-fixing bacteria
- Gamma elimination and replacement
  - Cystathionine γ-synthase
  - Cystathionine γ-lyase
  - Threonine synthase

metabolism, both decomposing amino acids and forming new amino acids. A familiar example of such a decomposition reaction initiates the release of compounds giving the characteristic odor to crushed garlic.

A second major group of PLP-dependent enzymes (*b* in Figure 3 and Table I), the decarboxylases, remove a CO_2 molecule from a substrate. These enzymes also function in both catabolic and biosynthetic pathways. In each case the loss of CO_2 helps to drive the pathway in the needed direction. The most familiar decarboxylases participate in the formation of neurotransmitters such as γ-aminobutyrate, dopamine, adrenaline, and serotonin. A third major group of PLP-dependent enzymes (*c* in Figure 3 and Table I) catalyze cleavage or formation of carbon–carbon bonds in amino acids. These reactions resemble aldol-type reactions of organic chemistry. An example is formation of serine from glycine and formaldehyde. The latter, being a toxic compound, is carried as a derivative of another coenzyme tetrahydrofolic acid. The enzyme serine hydroxymethyltransferase (Table I), which catalyzes this reaction, allows bacteria and plants to form serine from glycine and also allows our bodies to form glycine from serine.

A fourth large group of enzymes (d in Table I) have more complex mechanisms that involve initial formation of ketimines followed by additional steps. One of these is a bacterial enzyme that converts the selenium-containing selenocysteine into L-alanine and elemental selenium (Se^0). Related enzymes in all organisms transfer sulfur, as S^0, into important metal–sulfur clusters such as Fe_4S_4 or the $MoFe_7S_9$ cluster, which participates in conversion of N_2 to HN_3 by nitrogen-fixing bacteria.

Chemical Mechanisms

Some details of mechanism have been indicated in Figures 3 and 4. However, many individual chemical steps performed in sequence are required of each enzyme. For several enzymes details have been established by use of spectroscopic techniques and by determination of

structures at atomic resolution by X-ray crystallography. In the first step of a reaction the enzymes must "recognize" a substrate molecule that repeatedly bumps against it as a result of the random movements of the molecules in the liquid environment in which it acts. Each protein, which is much larger than its substrate, contains a specifically constructed cavity that permits close contacts with the substrate molecule in the "active site." Close contact allows van der Waals attractive forces and electrostatic forces between oppositely charged ionic groups to hold the substrate if the latter has the appropriate structure. The PLP, which is also held by the protein, forms part of the binding cavity. In the free enzyme the PLP has a structure similar to that in Figure 3. However, the Schiff base linkage is not to the substrate, as in Figure 3, but to the $-NH_2$ group of a side chain of a lysine unit in the protein structure. This "internal aldimine" is the "resting form" of the PLP in the active site. Notice the positive charges provided by H^+ ions bound to the PLP at top and bottom and the negative charge provided by the oxygen atom attached to the ring (Figure 3). These charges provide electrostatic interactions that function both in the binding of substrates and in subsequent reactions. The reaction steps must occur rapidly, each step setting the stage for the next and permitting the whole sequence to be completed in a millisecond or less in some enzymes.

Recognition of a substrate often induces some movement in the protein. In some proteins a chemical group moves into a new position or a flap of protein folds over to partially cover the substrate. At some point in the sequence an H^+ ion must be removed from the $-NH_3^+$ group of the substrate. The resulting $-NH_2$ group, sometimes aided by a tilting of the bound PLP, moves toward the 4′-carbon atom of PLP and reacts via a chemical addition to form a transient geminal diamine (not shown here). Additional rapid steps release the lysine $-NH_2$ group and form the "external aldimine" shown at the top of Figure 3. The released lysine $-NH_2$ then serves as a "catalytic base" able to remove the α-H to form lysine $-NH_3^+$. In a transaminase the resulting lysine $-NH_3^+$ can place the H^+ that it carries onto the 4′ position of the PLP to form a ketimine (Reaction 3 of Figures 3 and 4). A water molecule then reacts to release the α-oxoacid product (Figure 3) and to leave PMP bound weakly to the protein. This represents the first of the two half reactions (Figure 2) occurring in transamination. The same sequence in reverse, using a different oxoacid, completes the transamination. This also illustrates the fact that every step catalyzed by transaminases is reversible, the overall reaction being driven by differences in concentration of reactants and products. The individual structures, chemical groups involved, and individual steps vary from one enzyme and one reaction type to another. Most do not form PMP as an intermediate. However, virtually all PLP-dependent enzymes use an active site lysine and multiple H^+ transfers.

The fundamental importance of the ring nitrogen at the bottom of the structure in Figure 3 lies in its action as an electron-attracting center. This is indicated by the curved arrows in the figure. The flow of electrons in this manner is thought to be coordinated with the major bond-breaking reactions catalyzed by these enzymes. In many of the enzymes a negatively charged carboxylate ($-COO^-$) side chain of the protein forms a hydrogen bond to the N^+-H at the bottom of the PLP ring. This carboxylate helps keep the H^+ on the ring and may also modulate the electron flow. At the same time the $-O^-$ group on the 3-position of the ring opposes the electron withdrawal from the substrate, perhaps assisting in other steps in the reaction. The $-O^-$ also helps to hold a proton onto the Schiff base nitrogen as shown in Figure 3. Each specific enzyme must hold its substrate in such a way that one of the bonds to the α-carbon atom (*a*, *b*, or *c* in Figure 3) is perpendicular to the plane of the pyridoxal phosphate ring. This is the bond that will be broken in the key step of the reaction sequence.

See Also the Following Articles

Amino Acid Metabolism • B_{12}-Containing Enzymes

Glossary

aldol-type reaction Biochemical reactions related in their chemical mechanisms to the classical aldol condensation and cleavage reactions of organic chemistry.

coenzymes Small organic molecules that function together with enzymes to catalyze specific types of chemical reactions.

lysine unit A lysine residue, a molecule of the amino acid lysine incorporated into a protein molecule.

substrate The substance which undergoes the reaction catalyzed by an enzyme.

tetrahydrofolic acid A coenzyme formed by reduction of the vitamin folic acid.

Further Reading

Anthony, C., John, R. A., and Wilmot, C (eds.) (2003). 3rd international symposium on vitamin B6, PQQ, carbonyl catalysis and quinoproteins. *Biochim. Biophys. Acta.* **1647**, 1–408.

Bender, D. A. (1999). Non-nutritional uses of vitamin B_6. *British J. Nutr.* **81**, 7–20.

Christen, P., and Metzler, D. E. (1985). *Transaminases*. Wiley, New York.

Cooper, A. J. L., and Meister, A. (1989). An appreciation of Professor Alexander E. Braunstein. The discovery and scope of enzymatic transamination. *Biochimie* **71**, 387–404.

Dolphin, D., Poulson, R., and Arramovic, O. (1986). Vitamin B_6 Pyridoxal Phosphate Chemical, Biochemical, and Molecular Aspects, 2 Vols. Wiley, New York.

Jansonius, H. (1998). Structure, evolution, and action of vitamin B_6-dependent enzymes. *Curr. Opin. Struct. Biol.* **8**, 759–769.

Mehta, P. K., and Christen, P. (1998). The molecular evolution of pyridoxal-5′-phosphate-dependent enzymes. *Adv. Enzymol. Relat. Areas Mol. Biol.* **74**, 129–184.

Metzler, D. E. (2001, 2003). *Biochemistry. The Chemical Reactions of Living Cells*. Academic Press, San Diego.

Snell, E. E. (1958). Chemical structure in relation to biological activities of vitamin B_6. *Vit. Horm.* **16**, 77–125.

Biography

David E. Metzler is Professor Emeritus in the Department of Biochemistry, Biophysics, and Molecular Biology at Iowa State University, Ames, Iowa. He holds a Ph.D. from the University of Wisconsin. His research area is the chemistry of coenzymes, mechanism of their reactions, and the chemistry and structures of transaminases.

Pyrimidine Biosynthesis

Monika Löffler and Elke Zameitat
Philipps-University, Marburg, Germany

Pyrimidines are structural components in many natural compounds, such as nucleotides, nucleic acids, vitamins, pterins, and antibiotics. In all organisms pyrimidine nucleotides serve essential functions in cell metabolism as well as in nucleic acids such as the activation of sugars for polysaccharide and phospholipid synthesis, and glycosylation of proteins and lipids. In mammals pyrimidines are crucial to detoxification reactions in the liver. They are regarded as modulators of blood flow and have functions in the peripheral and central nervous system. The size of the pyrimidine nucleotide pools in cells is determined by the relative contributions of *de novo* synthesis and the interconversion reactions, together with salvage and presence or absence of enzymes of catabolic degradation. Some inherited disorders of pyrimidine biosynthesis and degradation have been diagnosed. Synthetic pyrimidine analogs act as antimetabolites and by selective interference in metabolic pathways, RNA and DNA synthesis, these and synthetic or natural enzyme inhibitors can combat infection, virus, tumor, and autoimmune diseases.

De novo Synthesis

Formation of UMP

Chemically, pyrimidines are heterocyclic six-membered ring structures containing two nitrogen atoms. The pyrimidine bases of nucleic acids possess an amino or hydroxyl group at position 4, and always an oxygen function at position 2. Thymine, in addition, has a methyl group at position 5. This gives rise to tautomeric structures for the bases uracil, cytosine, and thymine. The first pyrimidine nucleotide in cells, uridine monophosphate (UMP), is synthesized from CO_2, the glutamine amide group, aspartate, and phosphoribosyl-1-pyrophosphate (PRPP) (Figures 1 and 2). In contrast to the biosynthesis of purine nucleotides, the pyrimidine ring is assembled first and then linked to ribose phosphate to form a pyrimidine nucleotide. In higher eukaryotes, the cytosolic enzyme catalyzing formation of carbamoyl phosphate, carbamoylphosphate synthetase II (CPSase, Figure 1, no. 1), is distinctly different from carbamoylphosphate synthetase I, which is found in mitochondria as the first reaction of arginine biosynthesis and urea cycle in mammalian liver, and thus CPSase II is the first step committed to pyrimidine metabolism in higher animals (Figure 2). The formation of N-carbamoylaspartate (ATCase, no. 2) is the committed step for pyrimidine synthesis in prokaryotes, but is unregulated in eukaryotes. Next, the pyrimidine ring is cyclized by dihydroorotase (DHOase, no. 3). In higher animals the first three enzymes together with glutaminase (which provides the amino group from the side-chain amide group of glutamine) have been fused together (exon shuffling) during evolution to form a single polypeptide, CAD. This protein is located mainly in the cytosol and to some extent in the nucleus. Plants, such as prokaryotes, possess these enzymes individually encoded and located in chloroplasts. Formation of orotate from dihydroorotate is catalyzed by the mitochondrial flavoenzyme dihydroorotate dehydrogenase (DHODH, no. 4) transferring the reducing equivalents to the proximal acceptor ubiquinone and final acceptor molecular oxygen in the respiratory chain. Thus, the energy of dihydroorotate oxidation can be stored in ATP. Orotate phosphoribosyltransferase (OPRTase, no. 5) and orotidine decarboxylase (ODCase, no. 6) are fused on one bifunctional polypeptide, UMP synthase, operating in the cytosol of higher eukaryotes except in plants. Thus, only three genes (chromosomal location in Man: 2p21(CAD), 16q22 (DHODH), and 3q13 (UMP synthase)) code for the enzymes catalyzing the reaction of *de novo* UMP synthesis.

Regulation

Pyrimidine *de novo* synthesis is a demonstration that compartmentation within different parts of the cell – cytosol, mitochondria, chloroplasts – enhances the mode of regulation and flexibility of a metabolic pathway. Because of gene duplication, eukaryotes now have the potential to compartmentalize the synthesis of carbamoylphosphate for either pyrimidines (cytosol), or arginine and urea (mitochondria). In humans, urea synthesis takes place in liver only. The location of DHODH (Figure 2) in the inner mitochondrial membrane and its connection to the functional respiratory chain ensures the most efficient oxidation of

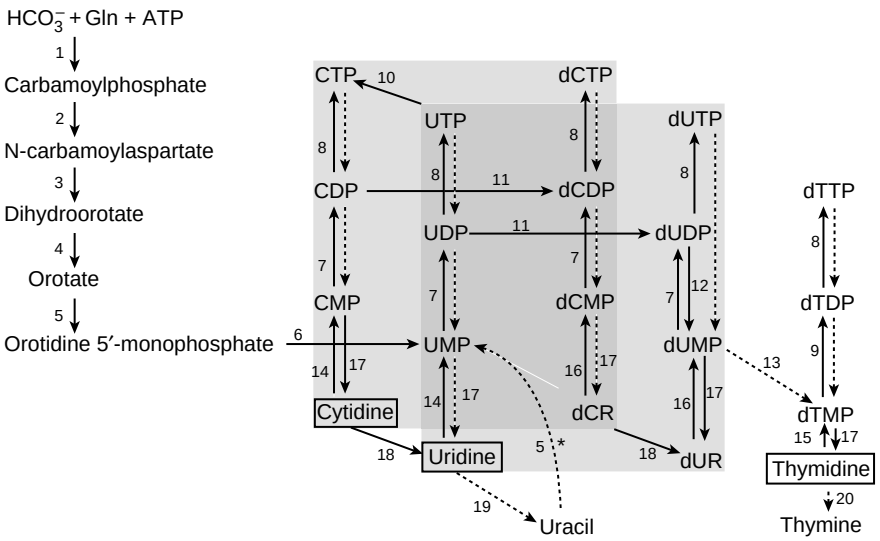

FIGURE 1 Biosynthesis and interconversion of pyrimidine nucleotides. The enzymes (given by numbers in the scheme) perform the *de novo* synthesis (1–6), interconversion of UMP to other ribonucleotides and deoxyribonucleotides (7–13), the salvage of preformed metabolites from dietary products or catabolism of nucleic acids (14–18), and the first steps of catabolism (19–20): 1, carbamoyl phosphate synthetase; 2, aspartate transcarbamoylase; 3, dihydroorotase; 4, dihydroorotate dehydrogenase; 5, orotate phosphoribosyltransferase; 6, orotidine 5′-monophosphate decarboxylase; 7, uridine(pyrimidine) monophosphate kinase; 8, pyrimidine diphosphate kinases; 9, thymidine monophosphate kinase; 10, cytidine triphosphate synthetase; 11, ribonucleoside diphosphate reductase; 12, dUDP phosphohydrolase; 13, thymidylate synthase; 14, uridine/cytidine kinase; 15, thymidine kinase; 16, deoxycytidine/uridine kinase; 17, 5′-nucleotidase; 18, (deoxy)cytidine deaminase; 19, uridine phosphorylase; and 20, thymidine phosphorylase. → (Pyro)Phosphohydrolases, not specified here. 5 * Uptake of 5′-fluoruracil by OPRTase.

dihydroorotate in aerobes. In turn, pyrimidine biosynthesis becomes a pacemaker for cell growth and proliferation under limited oxygen tension. Patients with acquired or inherited defects in mitochondria energetics, however, may suffer from a concomitant pyrimidine nucleotide starvation or imbalance. The two multienzyme polypeptides (CAD and UMP synthase) achieve a micro-compartmentation of pyrimidine *de novo* synthesis. Encoding five activities on two polypeptides simplifies the coordination and regulation of gene expression and activity. In addition, the direct transfer of a product from one active site to the next enzyme (channelling) considerably increases the efficiency of pyrimidine biosynthesis in higher eukaryotes. The first evidence for the location of CAD and UMP synthase close to the mitochondria surface has been obtained in a recent electron microscopic study. A metabolonlike complex facilitating the movement of substrate and product between cytosol and mitochondrion would allow a rapid increase in *de novo* synthesis when needed. The molecular regulation of pyrimidine *de novo* synthesis occurs at step 1 of CAD. The CPSase specific activity is low relative to that of the subsequent enzymes. It is allosterically activated by PRPP and feedback inhibited by UTP. The CAD activity is tuned by phosphorylation at two sites: MAP kinase action reduces the efficacy of UTP and increases that of PRPP, and phosphoylation by protein kinase A abolishes UTP inhibition but also makes PRPP less effective. Hence, by loosing feedback inhibition, carbamoyl phosphate synthesis is activated rapidly and sensitively in response to external growth-promoting signals. A modulation of ATCase activity is assured by a cooperative binding of carbamoyl phosphate and aspartate. An overflow into pyrimidine biosynthesis can occur from overabundant carbamoyl phosphate production in the case of urea cycle defects in liver: the carbamoyl phosphate leaves the mitochondria and is used by the ATCase of CAD. Under these conditions UMP synthase is the limiting enzyme, presumably because of an insufficient supply of PRPP for OMP synthesis, causing orotate to accumulate and to be excreted (secondary orotic aciduria).

Deficiency and Interference

The only hereditary but rare defect of pyrimidine *de novo* synthesis diagnosed so far in living humans is that of one or both activities in UMP synthase (OPRT domain or ODC domain) with different clinical manifestations, such as anemia or megaloblastic changes in bone marrow, immunodeficiency and gross orotate excretion in type 1 deficiency or orotidine plus orotic acid excretion, neurological deficits, and intellectual impairment, but no megaloblastic anemia in type 2 deficiency. There are

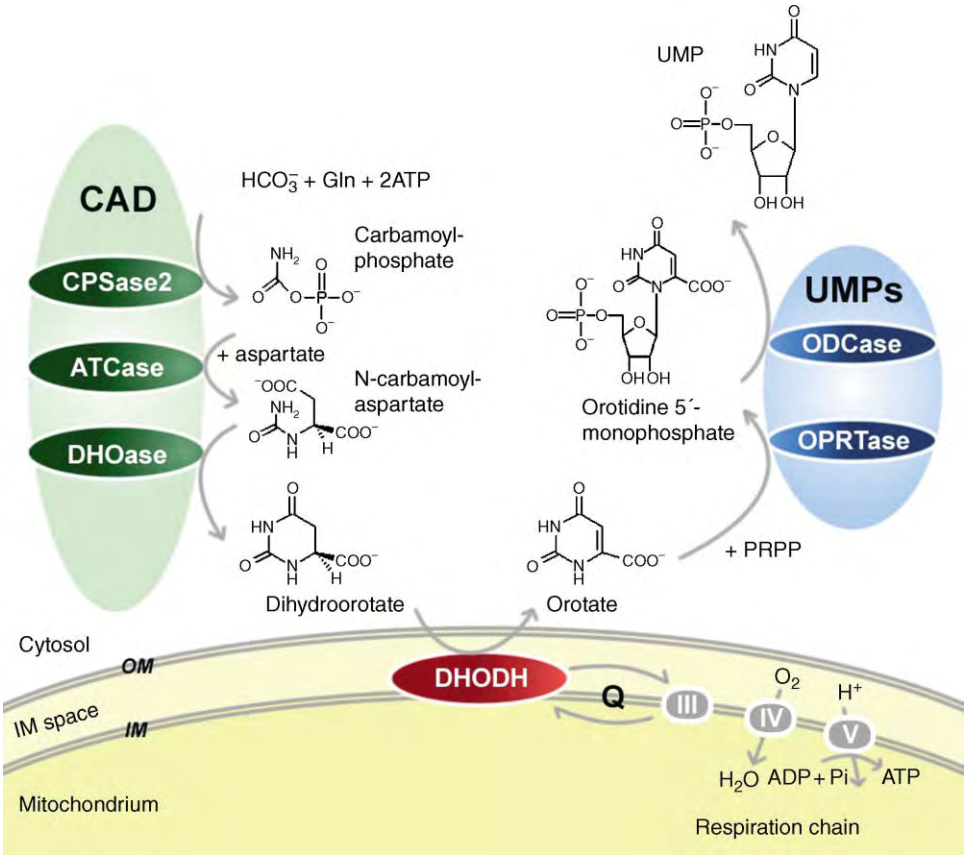

FIGURE 2 Compartmentation of pyrimidine *de novo* synthesis. In higher eukaryotes the multifunctional enzyme CAD (CPSase II + ATCase + DHOase, no. 1 + 2 + 3) and UMP synthase (OPRTase + ODCase, no. 5 + 6) are cytosolic, the monofunctional DHODH (no. 4) is in mitochondria and connected via ubiquinone (Q) to the functional respiratory chain at the stage of complex III (III). Electrons are transferred to oxygen via cytochrome oxidase (IV). ATP synthetase (V). Note that in plants no. 1,2,3 and no. 5 + 6 are in chloroplasts. In Gram-negative bacteria the quinone-dependent DHODH is attached to the plasma membrane. In Gram-positive bacteria and anaerobic yeasts all enzymes are cytosolic.

no specific inhibitors of CPSase of chemotherapeutic interest. N-phosphonoacetyl-L-aspartate (PALA), a model inhibitor of ATCase in prokaryotes, was clinically disappointing because gene amplification leading to overproduction of CAD caused resistance of human cancer cells. Current drug design for DHOase focuses on its Zn^{+2} center. Natural and chemical ubiquinone analogs, potent inhibitors against DHODH, failed to get clinical approval as anticancer drugs. The naphthoquinone atovaquone, a competitor for ubiquinone-dependent reactions, has been applied for treatment of opportunistic infections and malaria. The inhibition of DHODH by the isoxazol leflunomide, which was licenced recently, is central to the efficacy of this drug in treating rheumatoid arthritis and other autoimmune diseases. Antimetabolites of UMP synthase with anticancer activity but limited by toxicity at high dosage to patients (e.g., 6-azauracil, pyrazofurin) have been shown to suppress reproduction of *Toxoplasma gondii* and *Plasmodium falciparum*, because *de novo* pyrimidine synthesis is obligatory for these organisms to grow. Some widely used drugs, e.g., the calcium channel blockers nifedipine and nimodipine, were shown to suppress murine OMP decarboxylase and uridine kinase; barbiturates and aspirin interfered in the DHODH reaction. This emphasizes that the direct inhibition of pyrimidine biosynthesis is a potential side effect of drugs.

Interconversions in Pyrimidine Biosynthesis

Formation of Cytidine and Thymidine Nucleotides

Pyrimidine nucleotide di- and triphosphates are produced by ATP-dependent kinases (Figure 1, no. 7–9). CTP synthase (no. 10) catalyzes the formation of CTP from UTP using the amide group of glutamine – a GTP-dependent reaction (Figure 3A). Only at the time of DNA replication, do deoxynucleotide pools increase noticeably. Nucleoside 5′-diphosphate reductase

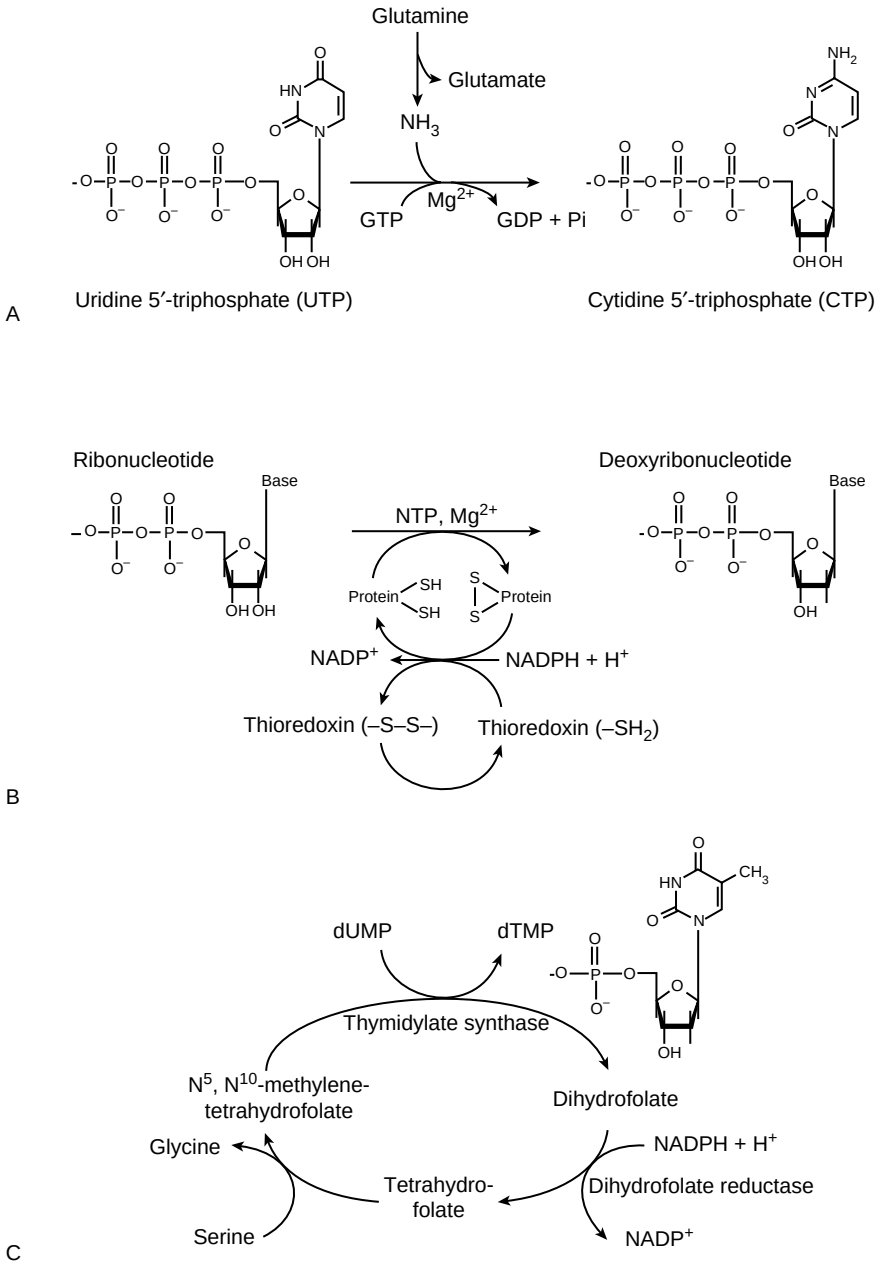

FIGURE 3 Formation of cytidine and thymidine nucleotides. (A) The synthesis of CTP from UTP by CTP synthase. (B) Conversion of UMP to dUMP by ribonucleotide reductase, schematic presentation of the enzyme. (C) The thymidylate synthase catalyzed reaction and regeneration of methylenetetrahydrofolic acid (THF) by means of dihydrofolate reductase.

(ribonucleotide reductase, no. 11) catalyzes the formation of deoxyribose (exchange of H for OH at C2′) of pyrimidine as well as purine ribonucleotides using NADPH and thioredoxin or glutaredoxin (Figure 3B). The product dUDP is dephosphorylated to dUMP (no. 12). In case of dUTP formation, this can effectively be reconverted to dUMP by the deoxyuridine triphosphate nucleotidohydrolase (pyrophosphohydrolase, Figure 1) in order to prevent its incorporation into DNA. dUMP is used by thymidylate synthase (no. 13) to form dTMP by means of (N^5, N^{10}-) methylenetetrahydrofolic acid (THF) as a one-carbon donor and reducing agent (Figure 3C).

Regulation

The enzymes of this part of pyrimidine synthesis are cytosolic. Their activity is strictly controlled by availability of substrates or by their products and other ribonucleotides and deoxyribonucleotides, respectively. This is a well-understood mechanism to ensure well-balanced pools of pyrimidine and purine

(deoxy)ribonucleotides in cells. For example, CTP is a negative effector of CTP synthase. This enzyme and CAD are connected with the cytoskeleton, hence are able to move around according to change in cell shape. Ribonucleotide reductase (no. 11) consists of two nonidentical protein subunits, one containing different effector binding sites, the other a nonheme iron and a tyrosyl radical generated by oxygen, giving the second control point for nucleic acid synthesis by O_2 in aerobes. This enzyme is subject to a sophisticated control mechanism, in which an excess of one deoxyribonucleotide inhibits reduction of all other ribonucleotides. Effective inhibition by dATP, dGTP, or dTTP explains the intrinsic toxicity of deoxyadenosine, deoxyguanosine, and thymidine to many organisms and the immunodeficiency in adenosine deaminase and purine nucleoside phosphorylase deficiency. dCTP and dTTP are major positive or negative effectors for the interconversion and salvage of deoxyribonucleosides. The key regulatory mechanism for thymidylate synthase is the delivery of THF by dihydrofolate reductase (Figure 3C). In plants and parasitic protozoa only, this enzyme is fused as a bifunctional polypeptide with thymidylate synthase.

Deficiency and Interference

Effective inhibitors of ribonucleotide reductase (e.g., hydroxyurea, HU) are potent inhibitors of DNA synthesis and hence of replication. HU also exerts a synergistic effect with nucleoside analogs used in the treatment of HIV-1. This is attributed to reduction in intracellular deoxyribonucleotides coupled with interference in antigen-dependent T-lymphocyte activation. However, the clinical application is disputed. It is noteworthy that healthy human lymphocytes do not pick up exogenous orotic acid, nor do they convert UTP to CTP. However, both these pathways are up-regulated in malignancy. Most of the CTP synthase inhibitors that have been developed and tested with experimental tumors are synthetic pyrimidine analogs (e.g., deazauridine and cyclopentenyl cytosine). Thymidylate synthase and dihydrofolate reductase are well-established target enzymes in cancer therapy using 5-F-UMP (from 5-fluoruracil which can be activated by OPRTase) and folate analogs (e.g., methotrexate) preventing THF regeneration.

Salvage

Phosphorylation and Dephosphorylation

The fact that hereditary orotic aciduria does respond to life-long supply with uridine but not to uracil indicated that pyrimidine nucleoside salvage can compensate for the lack of *de novo* synthesis in Man, if the dosage as food additive is in grams per day and increasing from child to adulthood. This is in direct contrast to purines where the gut mucosa contains a complement of enzymes which degrades all dietary purines to the end-product uric acid. Prominent salvage capacity is expressed in lymphoid cells, polymorphonuclear cells, and the central nervous system. Uridine, (deoxy)cytidine, and thymidine originating from daily nutrients or intracellular breakdown from nucleic acids are rescued from circulation by cytosolic (deoxy)ribonucleoside kinases that show a high level of specificity with respect to the base and sugar moieties, with ATP as the major phosphate donor (no. 14–16). In contrast to purines the salvage of free pyrimidine bases at the expense of PRPP does not occur in any mammalian tissue. Orotate as a natural component of dairy food is taken up and converted to UMP only by liver and erythrocytes. It can also stem from food additives such as zinc orotate and magnesium orotate, which are used for metal ion substitution therapy. Salvage of deoxycytidine is important in DNA repair. Deoxycytidine kinase is also responsible for activating some nucleoside analogs as well as natural deoxyribonucleosides – such as deoxyadenosine in adenosine deaminase deficiency. Pyrimidine and purine deoxyribonucleoside kinases seem to have evolved from a common progenitor multisubstrate kinase. Multisubstrate deoxyribonucleoside kinases were found in several insect species and shown to phosphorylate pyrimidines as well as purine (deoxy)nucleosides with high efficiency. The dephosphorylation of pyrimidine(deoxy)ribonucleoside monophosphates is catalyzed by 5′-nucleotidases (no. 17) which are found to occur as specific isoforms in different tissues. This reaction is a prerequisite for transport and delivery of pyrimidines by the circulation. In cells uridine and deoxyuridine can be formed from cytidine and deoxycytidine by cytidine deaminase (no. 18). The cleavage of uridine and thymidine by phosphorylases (no. 19–20) to the appropriate bases and ribose-1-phosphate would initiate the catabolic pathway.

Regulation

The balance between excretion and uptake is set by intracellular substrate cycles involving 5′-nucleotidases, kinases, and nucleoside transport through the plasma membrane of cells. Uridine is taken up effectively by a carrier-mediated concentrated transport process or by cotransport, by all human cells except erythrocytes.

Deficiency and Interference

Different mutants of the pyrimidine-5′nucleotidase are known causing enzyme deficiency. This is inherited as an

autosomal recessive trait. The symptoms include nonspherocytic hemolytic anemia, splenomegaly, and hepatomegaly; gross elevation in erythrocyte UTP/CTP are characteristic findings. A different deficiency of 5′-nucleotidase associated with hemolytic anemia has been described in patients with lead poisoning or thalassemia. Deficiency of the mitochondrial form of thymidine phosphorylase has major effects on many systems in humans. Patients with mutations in the mitochondria-specific thymidine kinase-2 develop myopathy and depletion of muscular mitochondrial DNA. Pyrimidine(deoxy)ribonucleoside kinases are critical constituents for interference by pharmacological agents: they are of key importance for the channelling of nucleoside analogs (such as arabinosyl cytosine, azidothymidine, 2′3′-dideoxycytidine) in cell metabolism of human and pathogens; mutants of thymidine kinases from virus and other organisms are proposed as "suicide agents" for gene therapy of cancers. On the other hand, strategies for inhibition of pyrimidine biosynthesis by drugs can be anticipated in cells with high activities in the salvage reactions. This aspect underlies current research on structure and function of pyrimidine (deoxy)ribonucleoside transporters in plasma and mitochondria membranes and their connection with salvage and biosynthesis of pyrimidines.

See Also the Following Articles

Membrane Transport, General Concepts • Urea Cycle, Inborn Defects of

Glossary

antipyrimidine A structural analog that is taken up by cells and interferes with normal metabolism.

flavoenzyme Enzyme containing a flavin group as redox cofactor.

metabolon Physically associated enzymes of a metabolic pathway to facilitate substrate channelling.

nucleoside Consists of [1 base + 1 (deoxy)ribose] such as uridine.

nucleotide Consists of [1 base + 1 (deoxy)ribose + 1–3 phosphate groups] such as dTTP or NTP (N, base not specified).

salvage Recycling of preformed nucleosides by cells.

Further Reading

Davidson, J. N., Carrey, E. A., Neuhard, J., and Franklin, C. (eds.) (1993–1999). *Path to Pyrimidines. An International Newsletter*, Vols 1–7, Chandler Medical Center, University of Kentucky, Lexington, USA.

Webster, D., Becroft, D. M. O., Van Gennip, A. H., and Van Kuilenburg, A. B. P. (2001). Hereditary orotic aciduria and other disorders of pyrimidine metabolism. In *The Metabolic and Molecular Bases of Inherited Disease* (C. R. Scriver, *et al.*, eds.) 8th edition, Vol II, pp. 2663–2702. McGraw-Hill, New York.

Biography

Monika Löffler is a Professor for Biochemistry at Philipps-University, Marburg, Germany. Her present research interest is enzymology of pyrimidine biosynthesis, its crosstalk to functional mitochondria. Further work of the group, metabolomics of pyrimidine metabolism in Man, is devoted to improve diagnosing and treating inherited and acquired disorders.

Elke Zameitat, having secured a diploma and degree in human biology, and presently a Ph.D. student, is involved in cloning, expression, and characterization of recombinant dihydroorotate dehydrogenase from different organisms, also for structure–activity relationship studies with inhibitors.

Pyruvate Carboxylation, Transamination, and Gluconeogenesis

Sarawut Jitrapakdee
Mahidol University, Bangkok, Thailand

John C. Wallace
University of Adelaide, Adelaide, Australia

The processes of transamination and pyruvate carboxylation combine to provide the pathway of gluconeogenesis with one of its principal substrates. For example, in transamination, a single amino acid (e.g., alanine) transfers its amine group to a ketoacid (typically α-ketoglutarate or oxaloacetate) to form their corresponding amino acids (i.e., glutamate and aspartate) while it is converted to its corresponding ketoacid (viz., pyruvate). Pyruvate carboxylation yields oxaloacetate, essential for gluconeogenesis in liver and kidney, for glyceroneogenesis in adipose tissue, and for the continuing operation of the Krebs tricarboxylic acid cycle. Gluconeogenesis is essential in maintaining normal blood glucose concentration during the postabsorptive state and especially in starvation, enabling brain, blood cells, and renal medulla to continue functioning properly.

Gluconeogenesis

Overview

Glucose occupies a central role in metabolism, both as a fuel for certain tissues and as a precursor of essential structural and other biomolecules in most tissues. The maintenance of a supply of glucose is essential for brain, renal medulla, and both red and white blood cells. These tissues rely exclusively on glucose as their energy source under normal circumstances, yet unlike liver and muscle do not store glucose as glycogen. When carbohydrate is not available from dietary sources in adequate amounts the blood glucose level is maintained within relatively narrow limits by a combination of glycogenolysis and gluconeogenesis. Liver glycogen can be broken down to release glucose into the blood circulation to other tissues, but it is usually depleted within 18–72 h after meals, depending on the species. Liver and kidney cortex cells circumvent this situation, especially during prolonged starvation, by having the pathway to synthesize glucose from substrates such as lactate derived from glycolytic tissues like skeletal muscle and red blood cells, glycerol from the breakdown of triglycerides stored in adipose tissue, and certain amino acids derived from the breakdown of muscle and other tissue proteins. The conversion of these precursor molecules to glucose is known as "gluconeogenesis." Gluconeogenesis, in part a reversal of glycolysis occurs exclusively in liver and kidney cortex utilizing most of the glycolytic enzymes except for three steps: (1) the conversion of pyruvate to phosphoenolpyruvate (PEP) via oxaloacetate, (2) fructose 1,6-bisphosphate to fructose-6-phosphate, and (3) glucose-6-phosphate to glucose. These reactions cannot be simply reversed by pyruvate kinase, phosphofructokinase and hexokinase, respectively, due to the large negative free energy changes in the direction of glycolysis. However, liver and kidney cortex cells overcome this situation by having another four enzymes including pyruvate carboxylase (PC) working in tandem with phosphoenolpyruvate carboxykinase (PEPCK) to form PEP, along with fructose-1,6-bisphosphatase and glucose-6-phosphatase which bypass the energy barriers as shown in Figure 1.

Control of Gluconeogenesis

As these three steps (often known as three "substrate cycles") are catalyzed by four separate enzymes, they are the targets to be controlled by short- and long-term mechanisms. Short-term regulation (seconds to minutes) of hepatic gluconeogenesis can be achieved through hormonal changes which in turn alter the enzymatic activities of the bifunctional enzyme 6-phosphofructo-2-kinase/fructose-2,6-bisphosphatase (PFK-2/F2,6BPase), and also of 6-phosphofructo-1-kinase (PFK-1), fructose-1,6-bisphosphatase (F1,6BPase) and pyruvate kinase (PK). Plasma glucagon and catecholamines, elevated during fasting, trigger an increase in cAMP levels leading to a rise in protein kinase A activity that results in the phosphorylation of pyruvate kinase and thus a

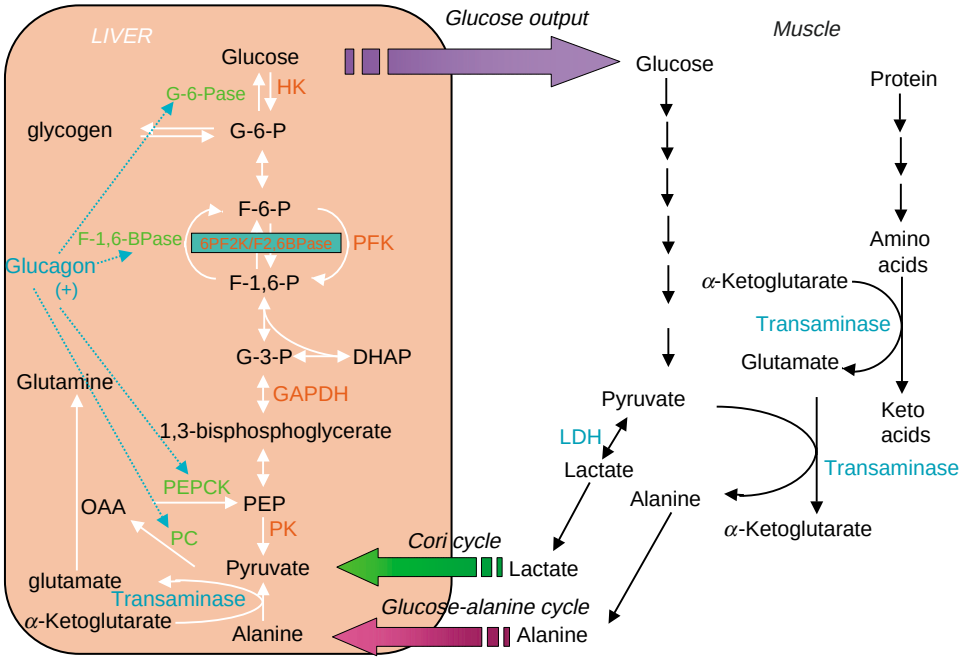

FIGURE 1 Glycolytic and gluconeogenic pathways. Also shown are the Cori cycle and glucose–alanine cycle. In glycolysis, glucose is oxidized by various enzymes to produce pyruvate, while in gluconeogenesis pyruvate is reconverted to glucose using most of the glycolytic enzymes plus four different enzymes, i.e., PC, PEPCK, fructose-1,6-bisphosphatase (F-1,6-BPase), and glucose-6-phosphatase (G-6-Pase). Lactate produced by anaerobic glycolysis in muscle can be converted to pyruvate by lactate dehydrogenase (LDH) in liver as part of the Cori cycle, while alanine produced by the breakdown of muscle protein can also be converted to pyruvate by transaminase in liver as part of glucose-alanine cycle. DHAP, dihydroxyacetone phosphate; HK, hexokinase; PFK, phosphofructokinase; GAPDH, glyceraldehyde-3-phosphate dehydrogenase; PC, pyruvate carboxylase; PEPCK, phosphoenolpyruvate carboxykinase.

decrease in its activity. Glucagon also exerts its effects on 6-phosphofructo-2-kinase/fructose-2,6-bisphosphatase through the same mechanism as for pyruvate kinase, resulting in the phosphorylation of this bifunctional enzyme. This leads to an increase in its F2,6BPase activity and a concomitant loss of its PFK-2 activity. The resulting reduction in the level of fructose-2,6-bisphosphate derepresses fructose-1,6-bisphosphatase activity while also reducing the activities of both phosphofructokinase and pyruvate kinase. These events therefore represent a major force in driving glucose metabolism in a gluconeogenic direction.

Long-term regulation (minutes to hours) of glucose metabolism can also be effected via hormonal changes. These occur when the dietary intake is low in carbohydrate, during starvation or prolonged exercise – all conditions which lead to low levels of insulin and high levels of plasma glucagon, catecholamines, and glucocorticoids. Glucagon and catecholamines act via cAMP to exert their effects by stimulating the transcription of genes encoding gluconeogenic enzymes. Therefore, it is not surprising to see the presence of cAMP-responsive elements in the promoters of the genes encoding PEPCK, fructose-1,6-bisphosphatase, and glucose-6-phosphatase. Glucocorticoids, acting via the glucocorticoid receptor, bind to the responsive element on promoters of PEPCK and glucose-6-phosphatase, and up-regulate transcription of both genes. These changes also drive glucose metabolism in the direction of gluconeogenesis. However, the opposite effect occurs when animals are fed a carbohydrate-rich diet that causes an increase in plasma insulin levels. The insulin signaling cascade results in the inhibition of transcription of genes encoding gluconeogenic enzymes. The very fine control of these enzymes' genes via hormones is a hallmark of long-term regulation in gluconeogenic tissues.

It is noteworthy that gluconeogenesis does not begin in the liver of rodents until immediately after birth as the maternal circulation provides glucose for the developing fetus. Of the four gluconeogenic enzymes present in liver, pyruvate carboxylase, PEPCK, and glucose-6-phosphatase are present in the liver at negligible levels before birth but appear rapidly after birth consistent with the onset of gluconeogenesis. The hormonal mechanism which mediates the increase in these three enzymes in liver at birth is not clearly defined. At least one of the following events that occur within a few hours after birth is likely to regulate gluconeogenesis: (1) a rapid and marked fall in the concentration of blood glucose which was hitherto supplied to the fetus from the maternal circulation via the placenta, and a low portal glucose concentration caused by a low

carbohydrate diet. This results in an increase in the cAMP level via elevated levels of glucagon and epinephrine and a low level of insulin. (2) An increased supply of plasma fatty acids to the liver caused by the hydrolysis of triglycerides in dietary milk.

Pyruvate Carboxylation

The carboxylation of pyruvate is a very important anaplerotic reaction to provide oxaloacetate for the Krebs cycle to operate continuously, as oxaloacetate and other intermediates are withdrawn from the cycle for a number of biosynthetic pathways including gluconeogenesis in liver and kidney, production of neurotransmitter substances in the glial cells of the brain, glyceroneogenesis in adipocytes, and fatty acid synthesis in liver, adipocytes and lactating mammary glands (see Figure 2). Therefore, oxaloacetate must be replenished at all times by the activity of PC (EC 6.4.1.1) that catalyzes the carboxylation of pyruvate to oxaloacetate as described in the following equation:

$$\text{Pyruvate} + HCO_3^- + \text{ATP} \overset{Mg^{2+},\text{acetyl-CoA}}{\rightleftharpoons} \text{oxaloacetate} + \text{ADP} + \text{Pi}.$$

PC contains covalently bound biotin as a prosthetic group that acts as a swinging arm to convey CO_2 between the two catalytic domains, i.e., the biotin carboxylation domain and the transcarboxylation domain. In mammals, PC is located in the mitochondrial matrix where its anaplerotic activity can be directly applied to the Krebs cycle. The control of pyruvate carboxylation can be achieved by three different ways: (1) control of substrate supply, (2) control by the enzyme's allosteric regulator(s), and (3) transcriptional/posttranscriptional control (see Table I).

Control by Substrate Supply

The first step to regulate pyruvate carboxylation is to control the availability of substrates to be converted to pyruvate and enter the mitochondria. These substrates are lactate, and gluconeogenic amino acids, principally alanine but also serine and several others indirectly. Due to a limiting O_2 supply to the muscle cells during intense exercise, skeletal muscle glycogen is metabolized anaerobically by the glycolytic pathway for ATP production. The pyruvate derived from glycolysis is reduced to lactate with the concomitant oxidation of NADH by the action of lactate dehydrogenase. This lactate is exported from muscle cells to the liver via the blood circulation. Lactate once taken up by liver cells is converted back to pyruvate and subsequently carboxylated to oxaloacetate for gluconeogenesis. In what is known as the Cori cycle, glucose produced from liver cells is then circulated to muscle to replenish its glycogen after the exercise. Therefore intense exercise enhances gluconeogenesis via pyruvate carboxylation. Breakdown of muscle protein during starvation yields gluconeogenic amino acids that also contribute to the supply of pyruvate. Glycerol derived from the hydrolysis of triglyceride in adipose tissue during prolonged fasting and in

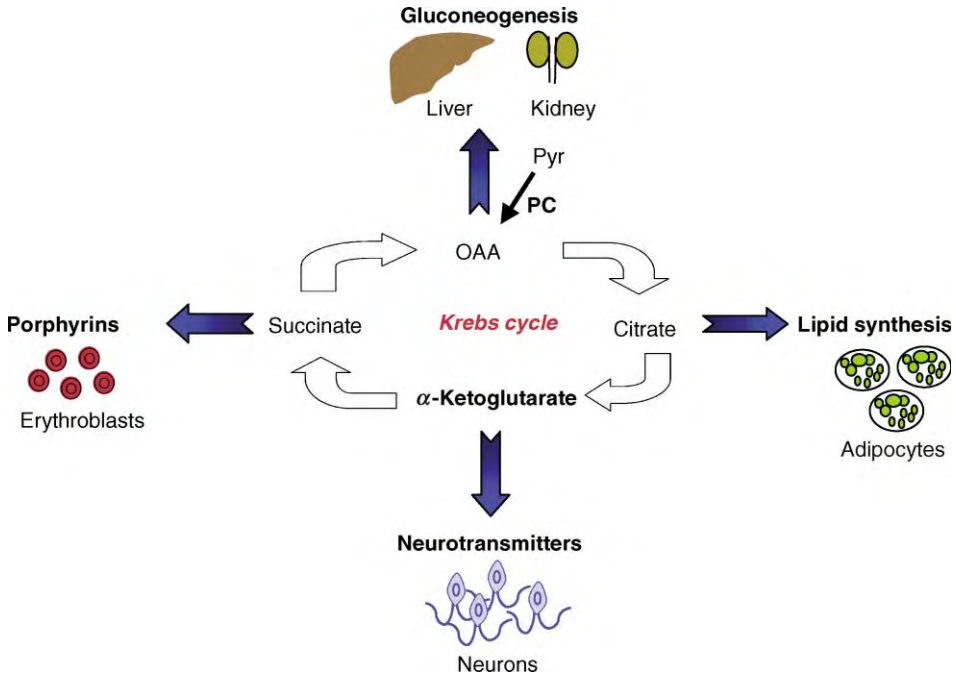

FIGURE 2 The anaplerotic function of PC in mammalian tissues in which oxaloacetate is withdrawn from the Krebs tricarboxylic acid cycle for various biosynthetic pathways. OAA, oxaloacetate; Pyr, pyruvate.

TABLE I

Factors Affecting Pyruvate Carboxylation

Factor	Mechanism of action
Insulin	Inhibits PC gene expression; inhibits protein breakdown and hence restricts substrate supply
Thyroid hormone	Stimulates PC synthesis
Glucocorticoids	Increases substrate supply
Glucagon	Increases ATP/ADP ratio
Acetyl-CoA	Allosteric activation

diabetes is another substrate that is converted to glucose. It has been estimated that ~15% of hepatic glucose production are derived from the Cori cycle while ~12% are derived from the glucose–alanine cycle. Glycerol accounts to only 2% of hepatic glucose production in the postabsorptive state but can become more significant (~10–15%) in prolonged fasting or in diabetes.

Control by Allosteric Regulator

Short-term regulation of pyruvate carboxylation is principally controlled by its allosteric activator, acetyl-CoA. The β-oxidation of free fatty acids during fasting results in an elevated level of acetyl-CoA in the mitochondria, and the binding of acetyl-CoA by PC results in its allosteric activation thereby enhancing pyruvate carboxylation.

Control by Transcriptional/ Posttranscriptional Mechanisms

Long-term regulation of pyruvate carboxylation is a slow response process taking several hours or days and involves alteration of transcriptional and posttranscriptional mechanisms. In rat, two tissue-specific promoters of the PC gene are activated differentially to mediate the production of mRNA transcripts bearing different 5′-noncoding regions with distinct translational efficiencies. Pathophysiological conditions including diabetes, hyperthyroidism, and obesity are known to affect pyruvate carboxylase activity in the long term.

Link between Pyruvate Carboxylation and Insulin Secretion

It is known that pancreatic islets contain high concentrations of PC mRNA and protein, and that the latter's specific activity is equivalent to that in liver and kidney. However, the islets lack PEPCK activity and its mRNA. This provides us with a clue that here PC does not serve the purpose of gluconeogenesis. It has been shown that there are two alternative routes for using oxaloacetate produced by PC, i.e., the pyruvate/malate and the pyruvate/citrate shuttles operating across the mitochondrial membrane. These routes are essential for glucose-induced insulin secretion as specific inhibition of PC activity also reduces the secretion of insulin in response to glucose, further suggesting a role for PC in insulin secretion.

Transamination

Breakdown of Amino Acids in Liver

Dietary proteins are digested by enzymes in the stomach and small intestine to yield various amino acids. This process provides both nitrogen and carbon sources for various biosynthetic pathways. Once transported to liver, these amino acids are subjected to a variety of enzymatic reactions, some are anabolic while others are catabolic. Of the latter the first is called "transamination." This process removes the NH_2 group from each amino acid to produce an α-keto acid. The α-amino group is most frequently transferred to α-ketoglutarate to form glutamate. This reaction is catalyzed by enzymes called a "transaminase" or an "aminotransferase." For example, alanine aminotransferase or aspartate aminotransferase transfers the α-amino group from alanine or aspartate to α-ketoglutarate:

$$\text{Alanine} + \alpha\text{-ketoglutarate} \leftrightarrow \text{pyruvate} + \text{glutamate}.$$

$$\text{Alanine} + \alpha\text{-ketoglutarate} \leftrightarrow \text{oxaloacetate} + \text{glutamate}.$$

Transaminases or aminotransferases are known to require pyridoxal phosphate (a derivative form of vitamin B6) as a cofactor of the reaction. Glutamate is then converted back to α-ketoglutarate by glutamate dehydrogenase in liver. This reaction yields NH_3, which enters the urea cycle.

Breakdown of Amino Acids in Muscle and the "Glucose–Alanine Cycle"

At rest, muscle can utilize fatty acids, ketone bodies, or blood glucose as carbon sources, depending on their availability, while during intense exercise muscle utilizes glycogen as an energy source via anaerobic glycolysis to produce lactate. However, vigorously contracting muscle or prolonged starvation triggers protein breakdown thereby producing amino acids which either can be oxidized or in some cases used as gluconeogenic substrates. As mentioned above, transamination of most amino acids prior to the oxidation of their ketoacid derivative produces

glutamate as the end product. The α-amino group of glutamate can be transferred to pyruvate, the readily available product of glycolysis in muscle, to form alanine. The alanine is then transported through the blood circulation to the liver where alanine is converted back to pyruvate by alanine aminotransferase. This reaction is exceptionally important in liver as it provides pyruvate to be used for gluconeogenesis. Glucose produced in liver is then circulated back to the muscle where it is utilized for glycogen synthesis or as an energy source during rest periods. The transfer of an amino group from glutamate to pyruvate to form alanine in muscle and the conversion of alanine back to glucose via pyruvate is known as "glucose–alanine cycle"(see Figure 1). The operations of the glucose–alanine cycle and the Cori cycle in liver provide an economic means to produce glucose from the end products of muscle metabolism.

See Also the Following Articles

Anaplerosis • Biotin • Biotinylation of Proteins • Branched-Chain α-Ketoacids • Fatty Acid Synthesis and Its Regulation • Gluconeogenesis • Phosphofructokinase-2/Fructose Bisphosphatase-2

Glossary

allosteric regulation Process by which enzyme activity is modulated by noncovalent binding of a specific chemical at a site other than the active site.

anabolic Promoting biosynthesis (opposite of catabolic).

anaplerotic Replenishing what has been removed (e.g., Krebs tricarboxylic acid cycle intermediates).

catecholamines Group of hormones including epinephrine and norepinephrine.

phosphorylation Process of adding a phosphate group from ATP to protein.

responsive element DNA sequence upstream of transcription initiation where a regulatory protein is bound and stimulates or represses transcription.

Further Reading

Brooks, G. A. (2002). Lactate shuttles in nature. *Biochem. Soc. Trans.* **30**, 258–264.

Corssmit, E. P. M., Romijn, J. A., and Sauerwein, H. P. (2002). Regulation of glucose production with special attention to non-classical regulatory mechanisms: A review. *Metabolism* **50**, 742–755.

Jitrapakdee, S., and Wallace, J. C. (1999). Structure, function and regulation of pyruvate carboxylase. *Biochem. J.* **340**, 1–16.

Magnuson, M. A., She, P., and Shiota, M. (2003). Gene-altered mice and metabolic flux control. *J. Biol. Chem.* **278**, 32485–32488.

Owen, O. E., Kalhan, S. C., and Hanson, R. W. (2002). The key role of anaplerosis and cataplerosis for citric acid cycle function. *J. Biol. Chem.* **277**, 30409–30412.

Roden, M., and Bernroider, E. (2003). Hepatic glucose metabolism in humans – its role in health and disease. *Best Practice Res. Clin. Endocrinol. Metabolism* **17**, 365–383.

Yang, D., and Brunengaber, H. (2000). Glutamate, a window on liver intermediary metabolism. *J. Nutr.* **130**, 991S–994S.

Biography

Sarawut Jitrapakdee has studied the regulation of pyruvate carboxylase in liver and pancreatic islets with particular reference to glucose-induced insulin secretion by β-cells and the relevance of this to obesity and type 2 diabetes. He has been awarded several distinguished prizes for his graduate studies at the University of Adelaide and subsequently since taking up a Faculty position at Mahidol University, Bangkok.

John C. Wallace undertook postdoctoral studies on gluconeogenesis with Sir Hans Krebs (Oxford), and with the codiscoverers of pyruvate carboxylase, Professor Merton Utter (Cleveland) and Dr. Bruce Keech (Adelaide). He has published 70 papers on structure/function studies of pyruvate carboxylase, and has been awarded the LKB Medal and the Lemberg Medal by the Australian Society for Biochemistry and Molecular Biology. His other research interests include the insulin-like growth factor system with 69 publications and several international patents in this area.

Pyruvate Dehydrogenase

Sam A. Johnson
Salk Institute, La Jolla, California, USA

James G. McCormack
OSI Pharmaceuticals Ltd., Oxford, UK

The Pyruvate dehydrogenase (PDH) complex (EC 1.2.4.1 + 2.3.1.12 + 1.8.1.4) is a multi-enzyme complex, which in eukaryotes is located within the mitochondrial matrix associated with the inner mitochondrial membrane. PDH catalyzes the oxidative decarboxylation of pyruvate with the concomitant formation of carbon dioxide, acetyl CoA, and NADH (reaction [1]), and thus forms the link between the glycolytic and Kreb's citric acid cycle (TCA) pathways.

$$\text{Pyruvate} + \text{CoA} + \text{NAD}^+ \rightarrow \text{Acetyl-CoA} + \text{NADH} + \text{H}^+ + \text{CO}_2 \quad [1]$$

This reaction is essentially irreversible ($\Delta G^{o'} = -39$ kJ) and, as it represents the "point-of-no-return" for carbohydrate utilization in mammals, it is highly regulated. This is primarily achieved by regulation of the amount of PDH in the active state by reversible phosphorylation by multiple dedicated kinases and phosphatases, and also by end-product inhibition.

Components and Structure of PDH

The known components of the PDH complex and its associated regulatory enzymes are listed in Table I. PDH complex isolated from mammalian tissues has an overall molecular weight of 7–10 MDa (i.e., ~2 times that of a eukaryotic ribosome) and can be visualized using an electron microscope.

The structure of the mammalian PDH complex is based around a core 60-mer of 6 E3-BP and 54 E2-subunits arranged as a pentagonal dodecahedron (E3-BP has previously been called component (or protein) X). The inner domains of the E2 and E3-BP-subunits interact to produce the core frame of the complex. The lipoyl domains protruding from the core contain flexible linkers allowing the outer domains some mobility with respect to the core. Both E2 and E3-BP have subunit-binding domains that bind other proteins in the complex and anchor them to the core 60-mer (see Figure 1). The lipoyl groups (covalently attached to E2 lysines) participate in catalysis and their flexibility relative to the core is essential for this function. The E3 component is also present in two similar complexes, the 2-oxo-acid dehydrogenase and the branched chain oxo-acid dehydrogenase complexes, as well as in the glycine-cleavage system, all of which are also located within the mitochondrial matrix.

It is thought that the six E3-BPs are located at the faces of the pentagons where they each bind an E3 homodimer. The $\alpha_2\beta_2$ heterotetramers of E1 (20–30 per complex) are thought to be localized to the edges of the pentagons. The regulatory kinases and phosphatases associate with the E2-subunits and act on serine residues in the E1α-subunits. The precise stoichiometry of the regulatory proteins in the complex is unknown but there are estimated to be approximately three molecules of kinase per complex. This is obviously fewer than the number of E1-subunits and it is thought the kinase moves over the surface of the core by utilizing the mobility of the lipoyl groups.

The structure of the bacterial form of PDH has been studied more extensively than the mammalian form; it is based on a 24-mer core of E2 with 24 E1 and 12 E3-subunits attached. No E3BP is present and the complex is not regulated by phosphorylation. The yeast *Saccharomyces cerevisiae* form of the complex is based on a 60-mer core, possibly with the E3-subunits located inside of the hollow E2 core at the 12 holes. The yeast complex, although more like the mammalian form in structure, is not regulated by reversible phosphorylation, a fact supported by the lack of homologues of PDK or PDP in the complete yeast genome sequence.

There are a number of inherited metabolic defects which have been described where various components of the PDH system, or their expression, have been shown to be defective, and interestingly, the auto-immune response which is thought to be the basis of primary biliary cirrhosis appears to be directed primarily against the E3BP and E2 components of the PDH complex.

TABLE I

Components of the PDH Complex and its Regulatory Enzymes

Components	EC reference	Full name	Subunit M_R (kDa)	Cofactors	Stoichiometry in mammalian complex
E1	1.2.4.1	Pyruvate dehydrogenase	α 42 β 36	TPP, Mg^{2+}	20–30 α_2 β_2 heterotetramers
E2	2.3.1.12	Dihydrolipoamide acetyltransferase	52	Lipoate	54
E3	1.8.1.4	Lipoamide dehydrogenase	55	FAD	6 homodimers
E3BP	None	E3 binding protein	51	Lipoate	6
PDK	2.7.1.99	Pyruvate dehydrogenase kinase	45–48 (4 isoforms)	Mg^{2+}	?Few
PDP	3.1.4.33	Pyruvate dehydrogenase phosphatase	cat 50	Mg^{2+}	?Few
			r 90	FAD?	

Mechanism of the Reaction Catalyzed by PDH

The multi-step reaction catalyzed by the PDH complex involves sequential reactions with the intermediates being relayed between the subunits via the flexible lipoyl domains.

E1 catalyzes the decarboxylation of pyruvate forming 2-(1-hydroxyethyldiene)-TPP bound to E1 (TPP is thiamin pyrophosphate). E1 also catalyzes the transfer of the intermediate as an acetyl group to the lipoyl moiety of E2. Each E2-subunit contains two flexible lipoyl groups. The acetyl group is shuttled between them to achieve the transfer between reaction centers that are too distant to be connected by one lipoyl group. E2 catalyzes the transfer of the acetyl group from the attached lipoyl group to CoA forming acetyl-CoA, leaving the lipoate group in the reduced form. E3 (and possibly E3-BP) catalyzes the transfer of electrons from the reduced lipoyl group attached to E2 to NAD^+ generating NADH and an oxidized lipoyl group. Thus, the overall reaction has been catalyzed and the PDH complex is returned to its original state.

Role of PDH in Metabolism

The reaction catalyzed by the PDH complex is central within metabolic pathways, most importantly linking glycolysis to the TCA cycle. Pyruvate has multiple sources and the acetyl-CoA produced has multiple

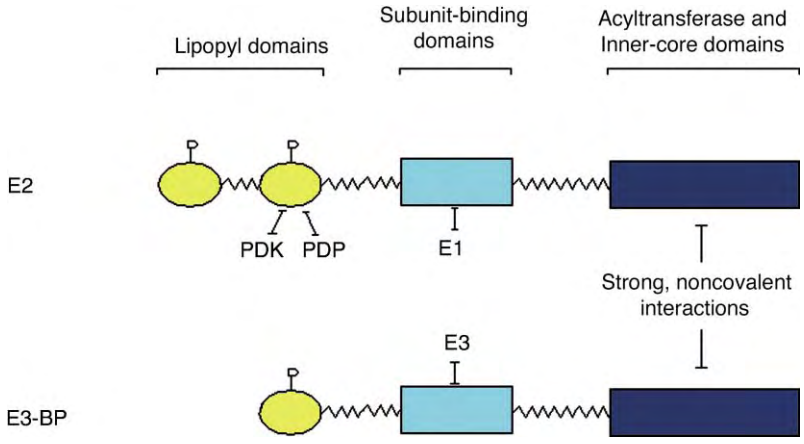

FIGURE 1 Schematic structures of the E2- and E3BP-subunits of the PDH complex. The acetyltransferase domains of the E2-subunits and the inner-core domains of the E3-BP-subunits interact to produce the dodecahedral core of the PDH complex. The subunit-binding domains and lipoyl domains (the majority of the proteins) are exterior to the core. The other major subunits (E1 and E3) are bound to the relevant subunit-binding domains. The regulatory proteins associate with the lipoyl domains of E2 and act to regulate the phosphorylation status of E1. Domains are linked by flexible linker regions composed of sequences rich in alanine and proline.

destinations, both catabolic and anabolic. The correct rate of flux through PDH is essential for the homeostasis of the cell. Coupled with the fact that the reaction catalyzed by PDH is irreversible in mammals and thus represents the point of commitment of carbohydrate metabolism, this means that the regulation of PDH is extremely important.

Regulation of PDH

Regulation of Activity by Phosphorylation

The major regulation of PDH is based on phosphorylation. The activity of the complex is modulated by phosphorylation of the E1α-subunits on three serine residues. The complex is inactive in the phosphorylated state (PDH-P) and active in the non-phosphorylated state (PDHa). The three phosphorylation sites (site 1 (S264), site 2 (S271), and site 3 (S203)) do not have equal importance in causing inactivation of the complex. Site 1 is the main inhibitory site and has been shown to account for at least 98% of the inhibition in rat heart mitochondria. Sites 2 and 3 are thought to reinforce the inactivating action of phosphorylation at site 1 and to make dephosphorylation more prolonged.

The phosphorylation status of PDH is regulated by dedicated kinases and phosphatases (Figure 2). The only other known phosphorylated protein within the mitochondrial matrix of mammalian cells is the related branched chain oxo-acid dehydrogenase complex which appears to have its own dedicated set of regulatory enzymes that are sequentially related to those for PDH.

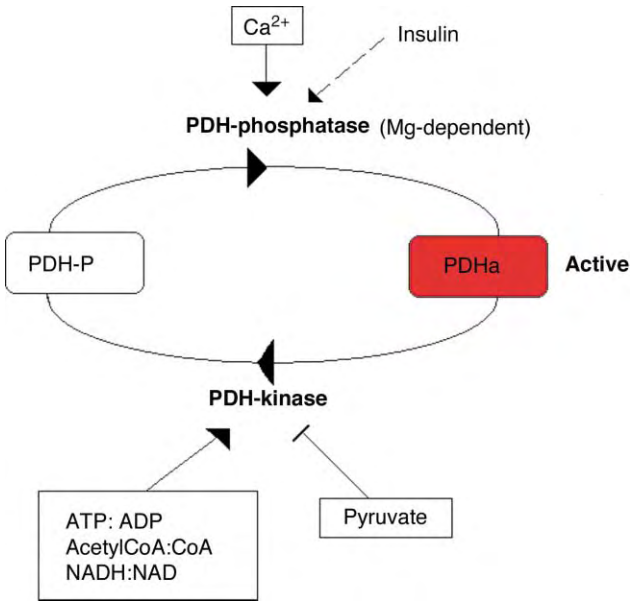

FIGURE 2 Regulation of PDH activity by phosphorylation-dephosphorylation. PDH is inactive in the phosphorylated form and active in the dephosphorylated form. Both intrinsic and extrinsic regulation is based on interconversion of the two forms by dedicated kinases and phosphatases.

Pyruvate Dehydrogenase Kinase

Currently, four isoforms of pyruvate dehydrogenase kinase (PDK) have been cloned from mammalian sources and studied (a fifth member of the family is present in the human genome sequence). These are expressed in a tissue-specific manner and differ substantially in their kinetics and allosteric modulation. Their expression is also altered differentially by hormones and nutritional status. The differences between the properties of the isoforms are substantial. For example, PDK3 has the highest specific activity and is virtually insensitive to NADH and acetyl-CoA inhibition, whereas PDK2 and PDK4 (which appears to be preferentially up-regulated in starvation and diabetes) have lower specific activities and are much more sensitive to NADH and acetyl-CoA. There is also evidence that different PDK isoforms have different activities towards the different phosphorylation sites in PDH E1α.

The kinases are strongly associated with the inner lipoyl domains of the E2-subunit of the PDH complex. The kinases act on the three serine residues on the E1α-subunit previously described. Their association with the E2-subunit increases the efficiency of phosphorylation of E1α.

The primary sequences of the PDKs are more like bacterial histidine kinases than eukaryotic serine/threonine kinases and evidence exists for the similarity of mechanism between PDK and a bacterial histidine kinase. However, the sites phosphorylated by the PDH kinases are situated in consensus sequences typical of eukaryotic serine/threonine phosphorylation sites. It is interesting to speculate that this situation arose by evolution from the endosymbiotic status of mitochondria in eukaryotic cells.

Pyruvate Dehydrogenase Phosphatase

Pyruvate dehydrogenase phosphatase (PDP) is a member of the PPM-family of phosphatases. PDP dephosphorylates the E1α-subunit and so causes the activation of PDH complex. PDP appears to act exclusively on PDH: no other substrates of PDP are known. PDP is also the only known phosphatase to act on PDH *in vivo*.

PDP has been cloned from a number of species. The phosphatase was originally cloned from bovine tissues, where the phosphatase is heterodimeric consisting of a catalytic (PDP_{cat}) and regulatory (PDPr) subunit. In rat, two isoforms of the catalytic subunit have been cloned, but as yet no regulatory subunit has been cloned.

The bovine phosphatase is the most extensively studied. It is Ca^{2+}-activated with Ca^{2+} causing a reduction in the $K_{0.5}$ for Mg^{2+}. Ca^{2+} also causes a reversible E2-PDP association and resultantly a 20-fold reduction in the $K_{0.5}$ of PDP for phosphorylated E1.

The two cloned rat isoforms of the phosphatase appear to differ in their regulation. PDP1 (orthologue of PDP_{cat}) is activated by Ca^{2+} but not by spermine. PDP2 has a much higher $K_{0.5}$ for Mg^{2+} (17.4 ± 2.7 mM versus 1.5 ± 0.5 mM for PDP1 in the absence of Ca^{2+}) and is not activated by Ca^{2+} but is activated by spermine. PDP1 appears to be the more strongly expressed form in skeletal muscle whereas PDP2 is the more strongly expressed in 3T3-L1 adipocytes and liver.

The role of the regulatory subunit of PDP is unclear. Studies in which recombinant PDP_{cat} and highly purified PDP are compared suggest several potential properties of PDPr. Firstly, it causes an increase in the $K_{0.5}$ of PDP_{cat} for Mg^{2+}. Secondly, the presence of PDPr confers spermine sensitivity to the phosphatase. Thirdly, differences in affinity of PDP to E2 were found with and without PDPr, so that it is likely that PDPr contributes to the binding and/or orientation with the core PDH complex via E2. PDPr was not found to have any native phosphatase activity and, despite the homology of PDPr to the enzyme dimethylglycine dehydrogenase, no enzymatic activity towards dimethylglycine or related molecules was found. Intriguingly, PDPr is a flavoprotein that binds a dissociable FAD, but it is not clear if this is involved in the function of the protein.

Intrinsic Regulation of PDH

Intrinsic regulation is predominantly based on the reversible phosphorylation mechanism of E1α-subunits as described above, and on end-product inhibition. Intrinsic regulation ensures that the rate of flux through PDH is appropriate for the metabolism of the cell. As illustrated in Figure 2, the kinase is activated by increased ratios of [ATP]/[ADP], [acetyl-CoA]/[CoA] and [NADH]/[NAD^+]. Thus, in the states where the ratios of [products]/[reactants] are high, the kinases are activated and so PDH is inactivated. This is reinforced by increased ratios of [acetyl-CoA]/[CoA] and [NADH]/[NAD^+] also causing end-product inhibition of the catalytic activity of PDH itself. This is also the principal regulatory mechanism by which the so-called glucose-fatty acid (or Randle) cycle operates, and ensures that carbohydrate is preserved when fatty acids are being oxidized (which will lead to increases in intramitochondrial NADH and acetyl-CoA levels). Conversely, high concentrations of pyruvate inhibit the kinase and so favor the active state of PDH where pyruvate will be metabolized. NADH also has an inhibitory effect on PDP, thus making the regulation more efficient by coordinate action on the activities of the kinase and phosphatase.

Extrinsic Regulation of PDH

Extrinsic (i.e., hormonal) regulation of PDH is also predominantly based on the modulation of complex activity by reversible phosphorylation. The localization of PDH exclusively within the mitochondrial matrix presents a problem to the cell in transmitting an extracellular signal to the PDH system: not only must the signal cross the plasma membrane, but also cross the largely impermeable mitochondrial inner membrane.

Calcium Regulation of PDH

Calcium has a physiological role in activating mitochondrial metabolism. For example, in muscle cells, increased cytosolic Ca^{2+} concentration stimulates contraction and so increases ATP usage. The increased cytosolic Ca^{2+} concentration is relayed into the mitochondrial matrix by a specific Ca^{2+}-uniporter in the inner membrane (where there are also specific Ca^{2+} export mechanisms). The increases in mitochondrial Ca^{2+} concentration cause activation of PDP and so an increase in PDHa as well as activation of two other intramitochondrial dehydrogenases that are sensitive to calcium (NAD^+-isocitrate dehydrogenase and 2-oxoglutarate dehydrogenase which are activated by Ca^{2+} causing decreases in their K_m values for isocitrate and 2-oxoglutarate respectively). The overall result is increased production of NADH for ATP generation by oxidative phosphorylation. This mechanism can thus override the intrinsic mechanisms described above and thereby increase metabolic flux whilst maintaining or even increasing key metabolite ratios such as [ATP]/[ADP] and [NADH]/[NAD^+]. Increases in cytosolic and mitochondrial Ca^{2+} can be brought about by several different hormones acting on several different tissues.

Insulin Regulation of PDH

Insulin causes an acute increase in the activity of PDH, so increasing the production of acetyl-CoA and the rate of lipogenesis in certain tissues. Insulin is not thought to cause an acute response in the PDKs, but long-term insulin stimulation down-regulates the transcription of these enzymes. Acutely, insulin acts via an increase in the activity of PDP. Insulin causes a reduction of the $K_{0.5}$ for Mg^{2+} and so an activation of PDP, and hence an activation of PDH. The precise mechanism by which insulin transduces a signal into the mitochondria to cause this effect is unknown.

See Also the Following Articles

Calcium Transport in Mitochondria • Glycolysis, Overview • Insulin Receptor Family • Tricarboxylic Acid Cycle

Glossary

extrinsic regulation Regulation of a component of a cell by an extrinisic factor, commonly a hormone (e.g., insulin activation of PDH).

intrinsic regulation Regulation of a component of a cell by factors within the cell to ensure homeostasis (e.g., the rate of flux through PDH is regulated by end-product feedback to ensure that the supply of acetyl-CoA is sufficient for the needs of the cell).

$K_{0.5}$ or K_m value Concentration of effector at which 50% of the observed effect occurs.

Further Reading

Harris, R. A., Bowker-Kinley, M. M., Huang, B., and Wu, P. (2002). Regulation of the activity of the pyruvate dehydrogenase complex. *Adv. Enzyme Regul.* **42**, 249–259.

Patel, M. S., and Harris, R. A. (1995). Mammalian alpha-keto acid dehydrogenase complexes: Gene regulation and genetic defects. *FASEB J.* **9**, 1164–1172.

Patel, M. S., and Korotchkina, L. G. (2001). Regulation of mammalian pyruvate dehydrogenase complex by phosphorylation: Complexity of multiple phosphorylation sites and kinases. *Exp. Mol. Med.* **33**, 191–197.

Popov, K. M., Hawes, J. W., and Harris, R. A. (1997). Mitochondrial alpha-ketoacid dehydrogenase kinases: A new family of protein kinases. *Adv. Second Messenger. Phosphoprotein Res.* **31**, 105–111.

Randle, P. J. (1998). Regulatory interactions between lipids and carbohydrates: the glucose fatty acid cycle after 35 years. *Diabetes Metab. Rev.* **14**, 263–283.

Robinson, B. H., MacKay, N., Chun, K., and Ling, M. (1996). Disorders of pyruvate carboxylase and the pyruvate dehydrogenase complex. *J. Inherit. Metab. Dis.* **19**, 452–462.

Roche, T. E., and Patel, M. S. (eds.) (1989). Alpha-keto acid dehydrogenase complexes: organization, regulation, and biomedical ramifications. *Ann. NY Acad. Sci.* **573**, 474.

Roche, T. E., Baker, J. C., Yan, X., Hiromasa, Y., Gong, X., Peng, T., Dong, J., Turkan, A., and Kasten, S. A. (2001). Distinct regulatory properties of pyruvate dehydrogenase kinase and phosphatase isoforms. *Prog. Nucl. Acids Res. Mol. Biol.* **70**, 33–75.

Yeaman, S. J., Kirby, J. A., and Jones, D. E. (2000). Autoreactive responses to pyruvate dehydrogenase complex in the pathogenesis of primary biliary cirrhosis. *Immunol. Rev.* **174**, 238–249.

Biography

Sam Johnson received his doctoral training in the laboratory of Professor Richard Denton at the University of Bristol, United Kingdom. He is currently undertaking postdoctoral work at the Salk Institute, La Jolla, California.

Jim McCormack also obtained his Ph.D. through Dick Denton's lab in Bristol, and later a D.Sc. from the same University. He is currently Vice President of UK Discovery for OSI Pharmaceuticals in Oxford, and was previously vice president for Scientific Affairs and for Target Cell Biology at Novo Nordisk in Denmark. Previously he was Director of Diabetes Discovery at Novo Nordisk, head of Biochemical Pharmacology at Syntex Research in Edinburgh, and a tenured lecturer in Biochemistry at Leeds University, where he was also a research fellow of the Lister Institute of Preventive Medicine.

Together, Sam and Jim estimate that the number of assays of PDH and its associated enzymes which they have carried out is well into six figures.

Pyruvate Kinase

Kosaku Uyeda
University of Texas Southwestern Medical School, Dallas, Texas, USA

Pyruvate kinase catalyzes the last step of glycolysis which is important for generating ATP. Mammals express four major pyruvate kinase isozymes, muscle (M1), liver (L), erythrocyte (R) and the ubiquitous M2 types. All but the M1 isozyme exhibit positive cooperative kinetic behaviors upon binding the allosteric activator fructose-1,6-diphosphate and in the presence of increasing phosphoenolpyruvate concentrations. All four isozymes are inhibited by phenylalanine. The L-pyruvate kinase isozyme activity also is inhibited by phosphorylation in response to glucagon. Consistent with its important role in regulating glucose metabolism and fat synthesis in liver, L-pyruvate kinase also is extensively regulated at the level of transcription. L-pyruvate kinase transcription increases in response to glucose and insulin and decreases in response to glucagon and high fat diets.

Pyruvate Kinase Reaction

Pyruvate kinase (PK) (EC 2.7.1.40) catalyzes the final step of glycolysis,

$$\text{P-enolpyruvate} + \text{ADP-Mg}^{2+} \rightarrow \text{Pyruvate} + \text{ATP-Mg}^{2+} + \text{H}^{+}$$

The enzyme requires two equivalents of divalent cation and K^+ for a full activity. One divalent cation complexes with ATP or ADP and the other cation binds to the protein and functional groups of pyruvate. The γ-phosphate of ATP bridges the two divalent cations.

Structure

All PKs from a variety of sources are tetramers (Mr = 240 kDa). Mammals express four isozymes designated as M1 and M2 for muscle type, L for liver, and R for erythrocytes. M1 muscle isozyme is the only PK exhibiting hyperbolic kinetics for phosphoenolpyruvate (PEP). However, in the presence of the allosteric ligand such as phenylalanine, it shows cooperative saturation for PEP. All other isozymes exhibit cooperativity with respect to PEP and are activated by fructose 1,6-diphosphate (Fru1,6-P_2) by lowering K_{PEP}.

PK has been isolated and characterized from a number of prokaryotes and from eukaryote tissues. Each consists of ~500 amino acid residues. Crystal structures of the enzymes from cat and rabbit muscle, yeast, *Escherichia coli* and *Leishmania mexicana* have been reported (1 and reviewed in 2). They all exhibit a very similar 3D structure (Figure 1A). Each subunit contains three domains: the A domain with the classic $(\alpha/\beta)_8$ structure; the B domain with an irregular fold; and the C domain with an α- and β-organization (Figure 1B). The eukaryotic enzymes contain additional short N-terminal peptides. The active site is situated on the C-terminal side of the A domain, facing the cleft between the A and B domains. The Fru 1,6-P_2 complex of yeast PK has revealed that the Fru 1,6-P_2-binding site is located in the C (regulatory) domain, which is 40Å away from the catalytic center.

Regulation of LPK *in vitro*

Effect of pH

In alkaline pH, LPK exhibits a sigmoidal saturation curve with PEP, but at lower pH the enzyme shows Michaelis–Menten kinetics. The transition between these two enzyme conformational states occurs at a narrow pH range between 6.8 and 7.3.

Allosteric Effectors

Fru 1,6-P_2 reduces the cooperative effects of PEP and converts the enzyme to a form exhibiting Michaelis–Menten kinetics with a higher affinity for the substrate. ATP and alanine are inhibitors of liver PK (LPK), and these ligands raise the apparent K_{PEP} to higher values. The inhibitory effect of ATP and alanine is counteracted by PEP and Fru 1,6-P_2. Pig LPK is inhibited by phenylalanine more strongly than alanine.

Phosphorylation/ Dephosporylation

LPK was first shown to be regulated by phosphorylation catalyzed by cAMP-dependent protein kinase (PKA), resulting in loss of the enzyme activity. The phosphate

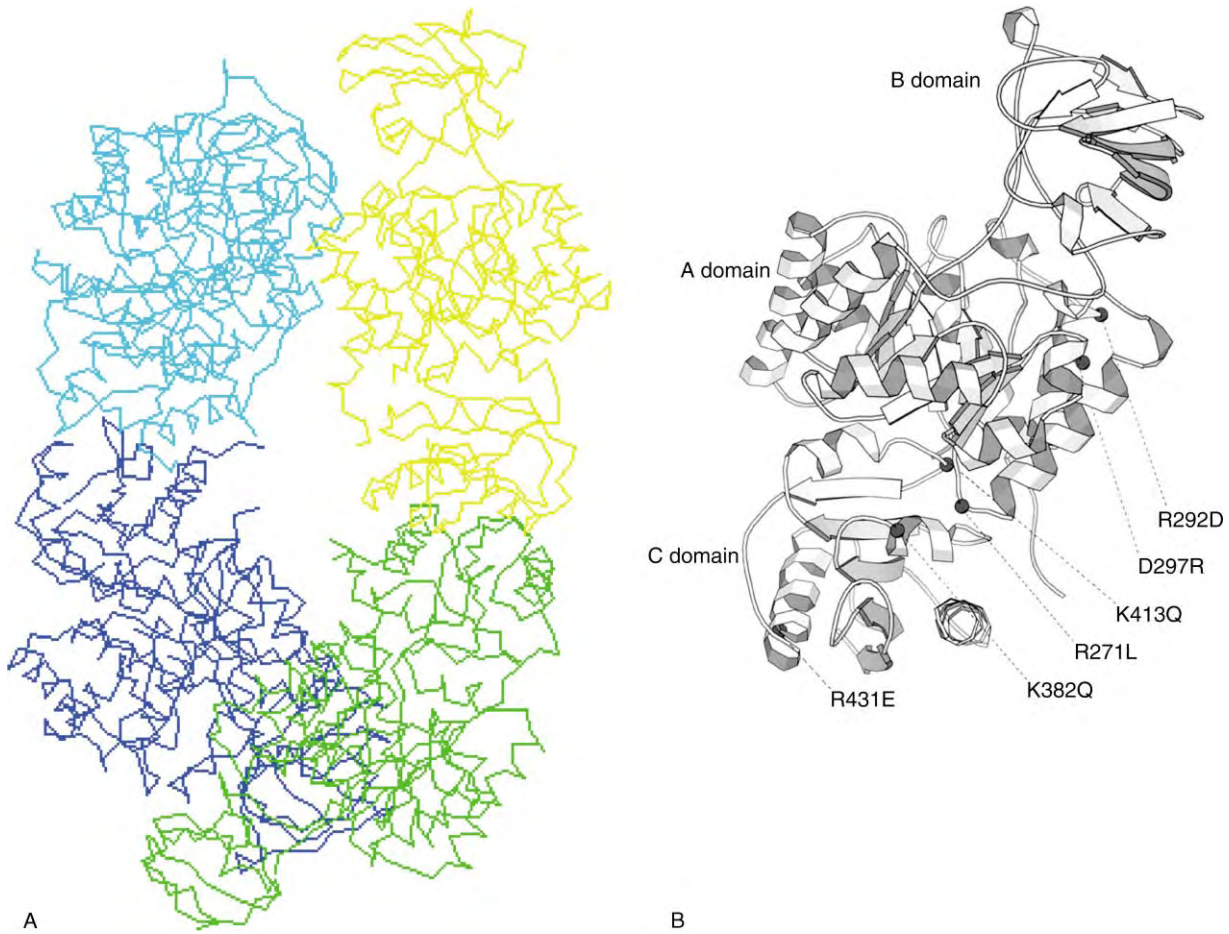

FIGURE 1 (A) Tetrameric *E. coli* PK in inactive T state. (B) *E. coli* PK subunit. The orientation is same as in A. (Reproduced from Valentini, G. *et al.* (2000). The allosteric regulation of pyruvate kinase. *J. Biol. Chem.* **275**, 18145–18152.)

incorporation is one mole phosphate per mole enzyme subunit on the N-terminal Ser within the consensus PKA target sequence (ArgArgAlaSerPVal). When the phosphorylated LPK was dephosphorylated by histone phosphatase, the enzyme recovered full activity.

The major effect of phosphorylation is to raise the apparent K_{PEP} approximately threefold (from 0.3 to 0.8 mM). It also increases the Hill coefficient from 1.1 to 1.5. V_{max} remains the same for both enzyme forms. This inhibitory effect of phosphorylation is counteracted by Fru 1,6-P_2 and H^+. Phosphorylation does not inhibit the rat LPK in the presence of 5 μM Fru 1,6-P_2 at pH 7.3, and the enzyme follows Michaelis–Menten kinetics with K_{PEP} of 0.04 mM. Phosphorylated LPK is more sensitive to inhibition by ATP and alanine than is the dephospho form.

Crystallographic Studies

Crystallographic and mutagenesis studies provided the mechanistic features for the allosteric transition in PK at the molecular level. The enzyme displays significant conformational changes involving all three domains of each subunit in the tetrameric enzyme in moving from the T- to R-state (Figure 2). This model is based on the X-ray structure determination of the allosteric *E. coli* PK in the inactive T-state and the M1 isozyme, which is an active R-conformation. In general, the allosteric transition involves two kinds of movements, (1) the rotation of the B and C domains (17° and 15°) within each subunit and, (2) a 16° rotation of each subunit within the tetramer. Thus, the allosteric activation of PK appears to involve rotation of both domain and subunit. This model is further supported by the observation that the 3D structure of each domain is not altered by their movement, suggesting that they rotate as rigid bodies connected by flexible hinges. The transition from R- to T-state also causes significant changes in the active site including distortion of the PEP-binding site, suggesting the poor substrate affinity of the T-state. It also shrinks the cleft between the A and C domains preventing effector binding.

These kinetic changes induced by various ligands and by phosphorylation are the acute regulation of PK activity by hormonal and nutritional states. Experiments performed on intact animals confirm the regulation of

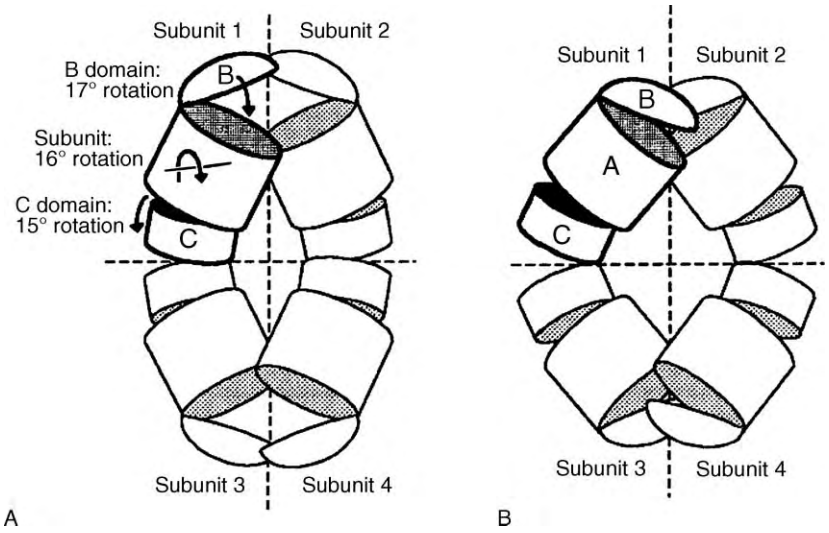

FIGURE 2 Schematic representation of the domain and subunit rotations in the T- and R-state transitions of PK.

PK *in vivo*. Intravenous administration of glucagon causes rapid inactivation of PK in liver. The effect of glucagon also raises cAMP concentration. Insulin causes rapid activation of PK.

Regulation of LPK Concentration by Gene Expression

Effect of Insulin, Glucagon, and Carbohydrate in Liver

In long-term regulation, LPK gene expression is controlled also by hormones and nutrients. Feeding mammals a diet rich in carbohydrate and low in fat leads to an increase in insulin levels and a fall in glucagon. Insulin and glucagon can activate and repress, respectively, the LPK transcription. These hormonal effects are mediated by direct response to the hormonal signals acting via membrane receptors.

In addition to increased insulin secretion, the excess glucose leads to activation of LPK gene transcription. This activation of gene expression is mediated by glucose, independent of insulin, and requires metabolism of glucose. Thus, glucose is not only a source of energy but also is able to stimulate glycolytic, and lipogenic enzyme genes.

Carbohydrate Response Element of LPK Promoter

The LPK gene promoter contains the glucose response element (−168 to −145 nucleotides upstream of open reading frame) and several other nuclear factor binding sites including nuclear factor (NF) and HNF4. The transcription factor binding to the glucose response element was identified recently and termed carbohydrate response element binding protein (ChREBP). In addition, it contains multiple phosphorylation sites, subject to regulation by protein kinase/phosphatase.

Carbohydrate Response Element Binding Protein

ChREBP is a large protein (Mr = 94.6 kDa) containing 846 amino acids. It consists of several functional domains including nuclear localization signaling (NLS) site, basic/helix-loop-helix/Zip region, polyproline, and Zip-like regions (Figure 3). ChREBP belongs to the MyoD family of transcription factors and binds to two consensus sequences (5′-CANNTG-3′) that are separated by five bases.

Regulation of ChREBP in Response to Glucose and cAMP

Inhibition by cAMP-Dependent Protein Kinase, PKA

ChREBP contains multiple phosphorylation sites including three sites for PKA, located at Ser196 (near NLS site), Ser626, and Thr666. ChREBP is controlled at two levels, nuclear entry and DNA binding. PKA-catalyzed

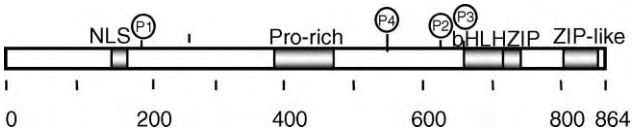

FIGURE 3 The domain structure of ChREBP. The locations of NLS, proline-rich stretch, bHLH/Leucine zipper, and Zip like domains are indicated. The locations of four phosphorylation sites of PKA are designated as P1, P2, and P3. The AMPK site is indicated as P4.

phosphorylation of Ser196 results in inhibition of nuclear import of ChREBP, while that of Thr666 leads to complete inhibition of the DNA binding. In low glucose, ChREBP is localized in the cytoplasm as the phosphorylated form, but in high glucose, it migrates to the nucleus as a dephosphorylated form.

Inhibition by AMP-Activated Protein Kinase, AMPK

Incubation of hepatocytes in fatty acids results in inhibition of glucose activated LPK transcription. This inhibition is mediated by phosphorylation of another site (Ser568) by AMPK. AMPK is activated by increased AMP generated by fatty acylCoA synthetase.

Activation by Glucose

Excess glucose activates the LPK gene expression by increased metabolism of glucose which activates ChREBP by dephosphorylation catalyzed by a specific protein phosphatase (PPase). A specific PP2A activated by Xu5P catalyzes the dephosphorylation and activation of phosphorylated/inactive ChREBP in liver in response to high carbohydrate. Xu5P is a metabolite in the pentose shunt pathway which increases with increased glucose metabolism, and serves as a glucose signaling compound. Thus, these results outline how glucagon/cAMP and high-fat diet repress ChREBP activity by phosphorylation. Glucose, however, activates the ChREBP activity and this activation of ChREBP leads to increased transcription of the LPK gene (and probably others), increasing glucose metabolism.

See Also the Following Articles

Gluconeogenesis • Glycolysis, Overview • Insulin- and Glucagon-Secreting Cells of the Pancreas • Insulin Receptor Family

Glossary

carbohydrate response element A DNA sequence within the promoter of a gene to which a specific transcription factor binds in response to excess carbohydrate.

gene promoter A region of a gene that responds to glucose, hormones, and other stimuli and binds a number of transcription factors that affect transcription.

liver pyruvate kinase An isoenzyme of pyruvate kinase that occurs mainly in liver.

transcription Synthesis of mRNA transcribed from a specific sequence of DNA of a gene.

Further Reading

Girard, J., Ferre, P., and Foufelle, F. (1997). Mechanism by which carbohydrates regulate expression of genes for glycolytic and lipogenic enzymes. *Annu. Rev. Nutr.* **17**, 325–352.

Mattevi, A., Bolognesi, M., and Valentini, G. (1996). The allosteric regulation of pyruvate kinase. *FEBS Lett.* **389**, 15–19.

Uyeda, K., Yamashita, H., and Kawaguchi, T. (2002). Carbohydrate responsive element – binding protein (ChREBP): A key regulator of glucose metabolism and fat storage. *Biochem. Pharmacol.* **63**, 2075–2080.

Valentini, G. *et al.* (2000). The allosteric regulation of pyruvate kinase. *J. Biol. Chem.* **275**, 18145–18152.

Wool, J. O., Friesen, R. H. E., White, M. A., Watowich, S. J., Fox, R. O., Lee, J. C., and Czerwinski, E. W. (2001). Structural and functional linkages between subunit interfaces in mammalian pyruvate kinase. *J. Mol. Biol.* **312**, 525–540.

Biography

Kosaku Uyeda is a Professor in the Biochemistry Department of University of Texas Southwestern Medical School in Dallas. His principal research interests are in mechanism of regulation of carbohydrate metabolism and lipogenesis. He holds a Ph.D. from the University of California, Berkeley. His laboratory codiscovered an important allosteric activator of glucose metabolism (fructose 2,6-P_2). In addition, they isolated and identified a new transcription factor (ChREBP) which stimulates glucose metabolism and conversion to fat in liver in response to excess carbohydrate.

Quinones

Giorgio Lenaz and Maria Luisa Genova
University of Bologna, Bologna, Italy

Chemistry of Quinones

Quinones are diketones derived by oxidation of dihydroxyarenes; the simplest quinones are those derived by benzenediols (1,2- and 1,4-dihydroxybenzene:

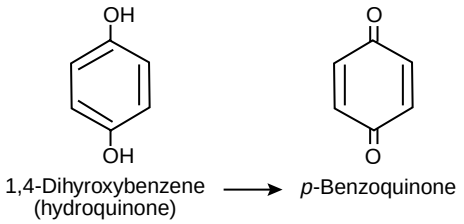

Also condensed arenes give quinones, e.g., the naphthoquinones:

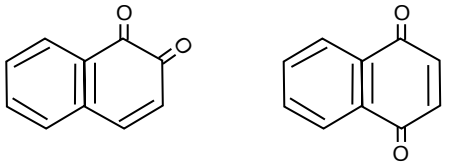

The reversible oxidation of dihydroxyarenes to the respective quinones is a two-electron process with the intermediate formation of the radical form of semiquinones, e.g.,

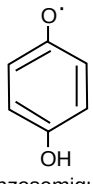

The redox systems quinone/diphenol (or quinol) are widely present in nature. Also known is the charge transfer complex quinhydrone, where quinone is the electron acceptor while diphenol is the electron donor:

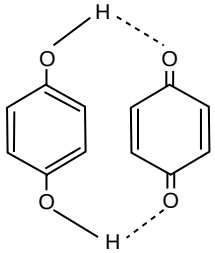

Biological Benzoquinones: Coenzyme Q and Plastoquinone

Chemistry and Distribution

Coenzyme Q was discovered in 1957 by F. L. Crane in Wisconsin as a yellow oily substance, extracted from bovine heart mitochondria, and having redox properties. It is also called ubiquinone, initially from the European nomenclature. The bovine compound is 2,3-dimethoxy-5-methyl-6-decaprenyl-1,4-benzoquinone (Coenzyme Q_{10}), but other homologues exist having polyprenyl chains of different lengths in the 6-position (Table 1). Also some analogues with different substitutions in the benzene ring have been found in nature or synthetized.

Coenzyme Q homologues were initially found in the inner membrane of mitochondria of eukaryotic cells and in the plasma membranes of aerobic and photosynthetic bacteria and they were discovered to be essential components of respiratory and photosynthetic chains. A different analogue, plastoquinone-9 (2,3-dimethyl-5-nonaprenyl-1,4-benzoquinone), was found in chloroplasts of higher plants and algae and in cyanobacteria and proven as an essential component of the photosynthetic apparatus (see structure below).

TABLE 1

Naturally Occurring Homologues and Analogues of Coenzyme Q

Homologue or analogue	Molecular weight	Occurrence
Coenzyme Q_6	590	*Saccharomyces cerevisiae* and other yeasts
Coenzyme Q_7	659	Minor component of some yeasts
Coenzyme Q_8	728	Some yeasts, *Escherichia coli*, and many other bacteria
Coenzyme Q_9	794	Rat, mouse, shark, some insects, protozoa, molds, yeasts, basidiomycetes, *Pseudomonas fluorescens*, and other bacteria
Coenzyme Q_{10}	862	Most mammals including man, birds, amphibia, most invertebrates, most photosynthetic bacteria, and some other bacteria
Rhodoquinone-10	847	*Rhodospirillum rubrum*
Ubichromenol-10	862	Accompanies Q_{10} in minor amounts as a cyclization product
Plastoquinone-9	747	Chloroplasts of higher plants and algae

See text for chemical structures.
Rhodoquinone-10 is 2-methoxy-3-amino-5-methyl-6-decaprenyl-1,4-benzoquinone.

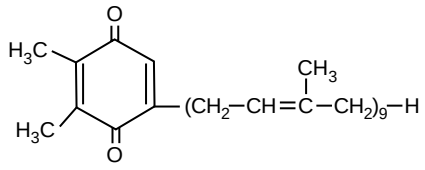

Plastoquinone-9

Soon after its discovery, Coenzyme Q was also found to be present in other cellular membranes of eukaryotic cells, including Golgi apparatus, lysosomes, and plasma membrane.

The major redox forms of Coenzyme Q, with their prevalent protonation states, are the following:

unit of the side chain forming the respective ubichromenols:

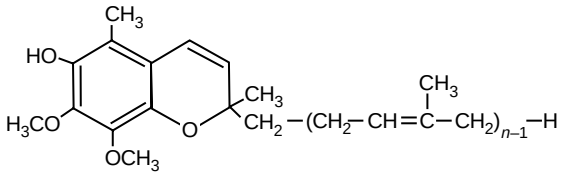

Ubichromenols

Coenzyme Q homologues 1–12 are soluble in most organic solvents but not in water due to their isoprenoid sidechains. Only homologues 6–12 are obtained in crystalline form at room temperature.

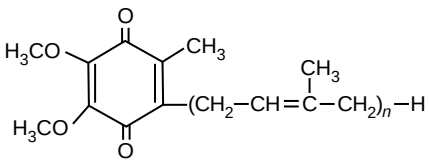

ubiquinone (Q)

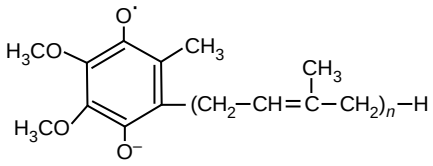

ubisemiquinone anion (Q·)

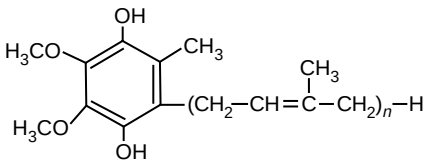

ubiquinol (QH_2)

The standard redox potential of the ubiquinone/ubiquinol couple at pH 7 is $\sim +100$ mV. The semiquinone radical is intermediate in most redox reactions of Coenzyme Q; however, it is very unstable and is rapidly dismutated to the quinone and quinol forms:

$$2Q\cdot + 2H^+ \longleftrightarrow Q + QH_2$$

Under some conditions, ubiquinones undergo cyclization between the ring and the first isoprenoid

In water, Coenzyme Q homologues form micelles or aggregates. They are soluble in lipids and disperse in monomeric form in phospholipid bilayers as well as in biological membranes.

Coenzyme Q absorbs light in the UV with a maximum at 275 nm in ethanol and at 270 nm in hydrocarbons when in oxidized form (extinction coefficient 15 $mM^{-1}\,cm^{-1}$), and with a maximum at 290 nm in all organic solvents when in reduced form (extinction coefficient 4 $mM^{-1}\,cm^{-1}$). The ubisemiquinone anion

has a maximum at 318 nm (extinction coefficient 10.7 mM^{-1} cm^{-1}) and minor peaks also in the visible spectrum. The semiquinones are best detected by electron spin resonance techniques.

The lateral mobility of Coenzyme Q in phospholipid bilayers is very high: using the method of collisional fluorescence quenching with membrane-bound fluorescent molecules, a lateral diffusion coefficient was calculated $\sim 10^{-7}$ cm^2 s^{-1}. Such mobility seems essential for the function of the quinone in electron transfer chains in energy-transducing membranes.

Functions of Coenzyme Q

Electron Transfer Chains of Mitochondria and Bacteria

The best known function of Coenzyme Q is as a redox component of the mitochondrial respiratory chain, localized in the inner membrane. A standard scheme of the respiratory chain is depicted in Figure 1.

Coenzyme Q was first described as a mobile diffusible component localized between Complex I (NADH Coenzyme Q reductase) or Complex II (succinate Coenzyme Q reductase) and Complex III (ubiquinol cytochrome *c* reductase); in these systems, Coenzyme Q is reduced by Complex I or II and reoxidized by Complex III; it was then found that Coenzyme Q is also reduced by other mitochondrial enzymes, such as glycerol-1-phosphate dehydrogenase, electron transfer flavoprotein (ETF) dehydrogenase (an enzyme involved in fatty acyl CoA oxidation), and dihydro-orotate dehydrogenase.

Due to its extremely hydrophobic nature, Coenzyme Q is localized in the hydrocarbon interior of the lipid bilayer of the inner mitochondrial membrane, where its diffusion rate may be very high. In such way it behaves as a common pool of molecules, so that any molecule would be randomly reduced by any Complex I or II and reoxidized by any Complex III.

Besides the Coenzyme Q pool dissolved in the lipid bilayer, Coenzyme Q molecules bound to the individual complexes have also been described. These bound quinones may be important for the mechanism of outward proton translocation, required in the chemiosmotic mechanism of oxidative phosphorylation. The best-known mechanism is the Q-cycle, first proposed by the Nobel laureate Peter Mitchell (Figure 2).

Tight Coenzyme Q binding to proteins (Q-binding proteins) in the respiratory complexes is required to stabilize the semiquinone form that is an essential intermediate in the mechanism of proton translocation.

Moreover, a well-known example of bound quinones is represented by the reaction center of photosynthetic bacteria that has been crystallized and resolved by X-ray diffraction together with its bound prosthetic groups (Figure 3). In bacteria, besides ubiquinone, also menaquinone (a naphthoquinone) may participate in electron transfer.

In chloroplasts of photosynthetic algae and higher plants, the function of ubiquinone is exploited by plastoquinone, present in bound form in photosystem II and free as a pool in the lipid bilayer.

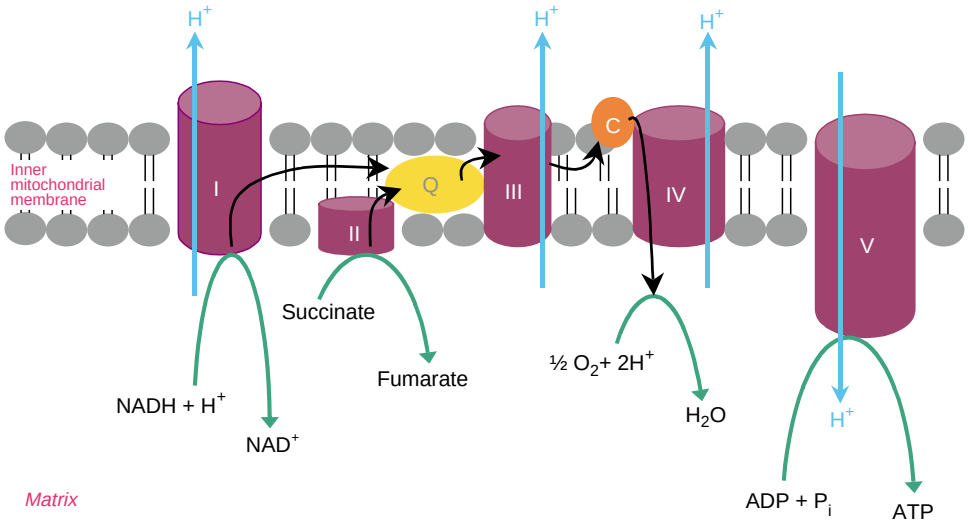

FIGURE 1 Schematic view of the mitochondrial oxidative phosphorylation system, showing the role of Coenzyme Q as a shuttle of electrons between Complex I or Complex II and Complex III. Other dehydrogenases using Coenzyme Q as acceptor are not shown for simplicity. Roman numbers refer to the respective enzyme complexes. Black arrows indicate the flux of electrons, green arrows indicate chemical reactions, and blue arrows indicate proton translocation. During redox reactions catalyzed by Complex I, III, and IV, protons are extruded forming a transmembrane gradient that is used by Complex V (ATP synthase) for synthesizing ATP.

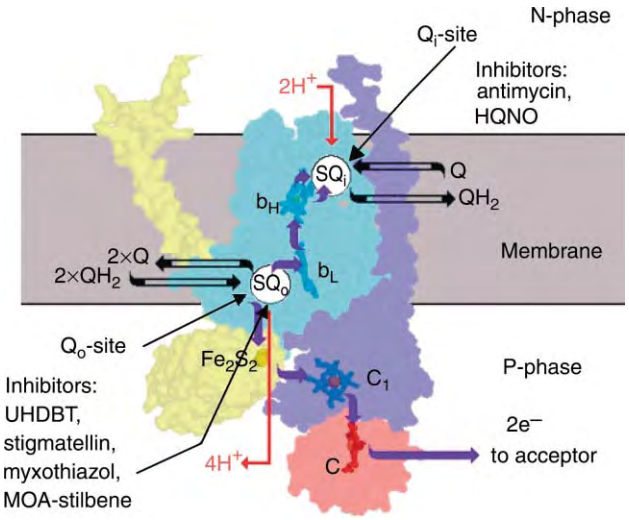

FIGURE 2 The Q-cycle as a mechanism of proton translocation in complex III of the mitochondrial respiratory chain. The scheme shows the Q-cycle in the context of the enzyme structure where the catalytic subunits are shown by their surfaces and made transparent so as to show the redox centers (cyan: cytochrome *b*; yellow: iron-sulfur protein; blue: cytochrome c_1). Quinol (QH_2) is oxidized in a bifurcated reaction at the Q_o-site of the complex located at the outer positive side of the membrane (P-phase): one electron is transferred to the high-potential chain, consisting of the Fe_2S_2 center and cytochrome c_1, and then to cytochrome *c* (red) that carries the electron to Complex IV. Since the semiquinone formed (SQ_o) is unstable, another electron is transferred through the low-potential chain of cytochrome hemes (b_L and b_H) to the Q_i-site where a quinone molecule is fully reduced to quinol. In order to provide the two electrons required at the Q_i-site, located at the inner negative side of the membrane (N-phase), the Q_o-site oxidizes two equivalents of quinol ($2 \times QH_2$) in successive turnovers. Information about inhibitor specificity of the above-mentioned reactions is shown in the figure. The integration of the redox reactions with the release or uptake of protons in the aqueous phases (red arrows) allow the complex to pump protons across the membrane. With permission of Dr. A. R. Crofts, University of Illinois at Urbana-Champaign, IL, USA.

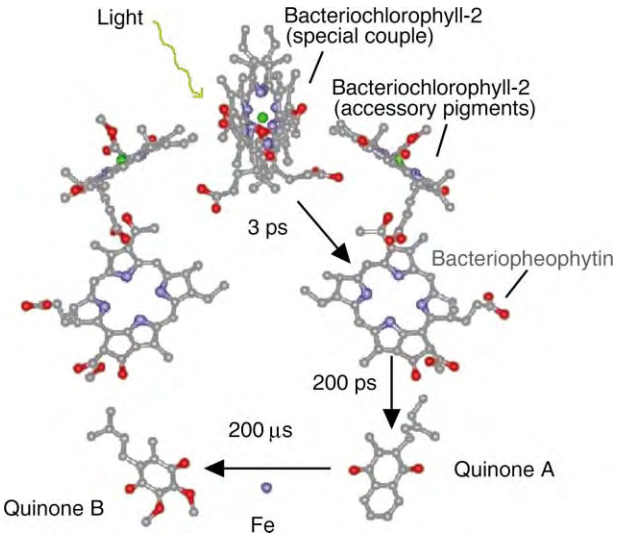

FIGURE 3 Bound quinones in the photosynthetic reaction center of Rhodopseudomonas viridis. Following excitation, the special pair of bacteriochlorophyll molecules donates an electron to a nearby bacteriopheophytin pigment (time constant: 3 ps). Subsequent transfer to the primary quinone (QA, a bound menaquinone) occurs with a half-time of 200 ps. Further electron transfer occurs from QA to the quinone acceptor QB, a bound ubiquinone occupying an active site near the cytoplasmic surface of the protein. QB accepts two electrons and two protons, then it undergoes exchange with the mobile pool of quinones in the lipid bilayer. With permission of Dr. R. Baxter, University of Chicago, IL, USA.

Other Electron Transfer Chains

Coenzyme Q of eukaryotic cells is present in most intracellular membranes and in the plasma membrane as well. Its function in these systems is better known in the plasma membrane oxidoreductase (PMOR) where the quinone appears to participate in transmembrane electron transfer between intracellular NADH or NADPH and extracellular acceptors including the ascorbic acid free radical, derived from the partial oxidation of ascorbic acid. This system may be involved in the antioxidant defenses of the cell since it regenerates ascorbic acid, an antioxidant.

Coenzyme Q as an Antioxidant

Coenzyme Q and other quinones are powerful antioxidants in their reduced form. The ubiquinol reacts with peroxide radicals, such as the lipid peroxide radical LOO·:

$$QH_2 + LOO\cdot \longrightarrow QH\cdot + LOOH$$

where LOOH is a lipid hydroperoxide.

In addition, it may be used to regenerate the reduced antioxidant form of vitamin E (α-tocopherol, T-OH) from the tocopheroxyl radical TO·:

$$T\text{–}OH + LOO\cdot \longrightarrow T\text{–}O\cdot + LOOH$$

$$T\text{–}O\cdot + QH_2 \longrightarrow T\text{–}OH + QH\cdot$$

The semiquinone form of Coenzyme Q, originated from its antioxidant action, is readily converted to the oxidized form by another radical:

$$QH\cdot + X\cdot \longrightarrow Q + XH$$

The cell contains several enzymatic systems to reduce oxidized Coenzyme Q (Q) back to its antioxidant form (QH_2). Among these are the cytosolic enzyme DT-diaphorase (NAD(P)H dehydrogenase (quinone) E.C.1.6.99.2), also found bound to the plasma membrane, a cytosolic NADPH quinone reductase, and microsomal NADH cytochrome b_5 reductase.

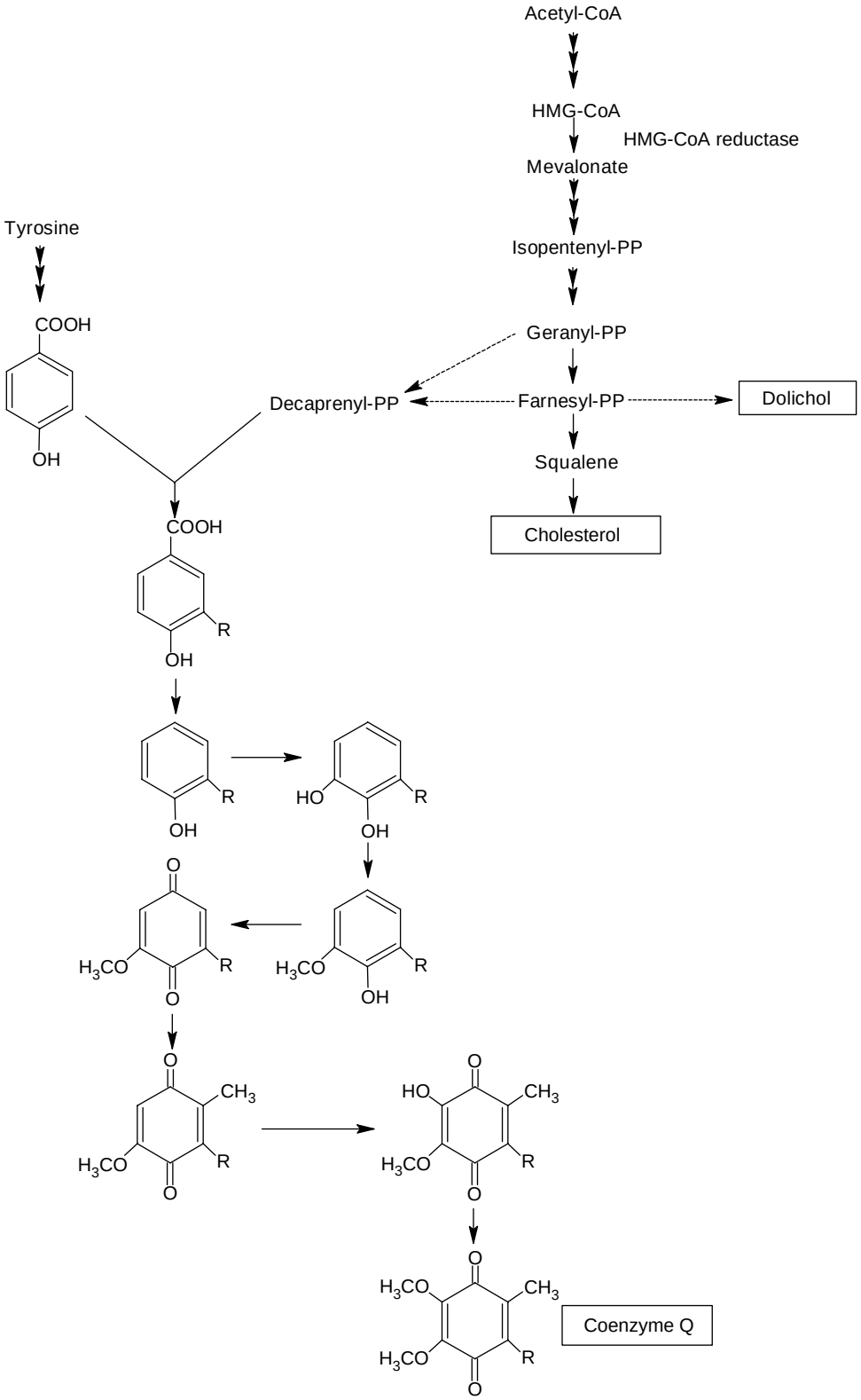

FIGURE 4 Simplified scheme of the biosynthesis of Coenzyme Q. R = isoprenoid side chain; HMG-CoA = 3-hydroxy-3-methyl-glutaryl Coenzyme A.

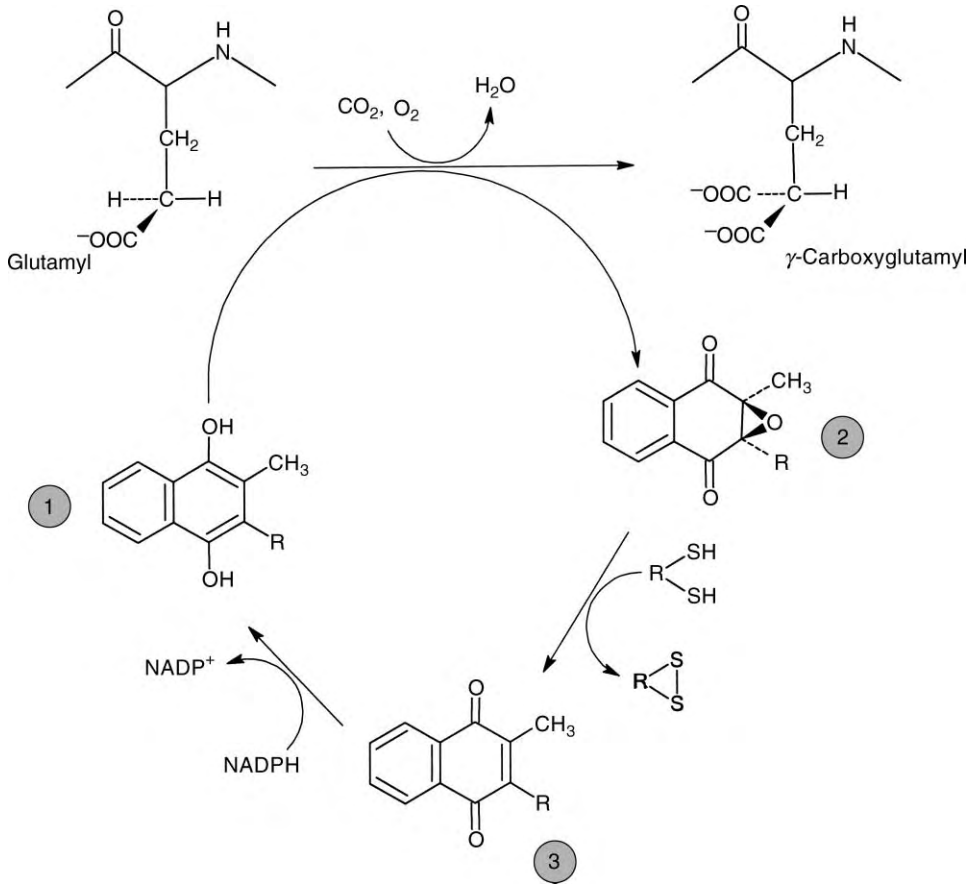

FIGURE 5 Mechanism of action of vitamin K in protein carboxylation. The γ-carboxylation reaction of protein-bound glutamate requires molecular oxygen and the reduced form of vitamin K (1); the hydroquinone is converted to the vitamin K epoxide (2) during the reaction. The vitamin K epoxide must be reconverted to the hydroquinone; this happens in two steps: in the first step the epoxide is converted to the quinone form (3) using the coenzyme thioredoxin [$R(SH)_2$]; the quinone is then reduced to the hydroquinone in an NADPH-dependent reaction.

Biosynthesis of Coenzyme Q

Coenzyme Q is synthetized by animals starting from the amino acid tyrosine which is converted to *p*-hydroxybenzoate; after insertion of the isoprenoid side chain in the 6-position, the ring is completed by a complex series of reactions involving hydroxylations and O-methylations. The isoprenoid side chain is synthesized starting from acetyl CoA through the mevalonate pathway and isopentenyl pyrophosphate, which is common to the synthesis of cholesterol, dolichol, and other polyprenyl compounds (Figure 4). It was found that cholesterol-lowering agents acting on the enzyme 3-hydroxy-3-methyl-glutaryl CoA reductase, which converts 3-hydroxy-3-methyl-glutaryl CoA to mevalonate, besides lowering plasma cholesterol, also lower Coenzyme Q levels, suggesting caution in the use of these agents.

The biosynthesis of Coenzyme Q requires several vitamin-derived coenzymes and appears to be easily limiting on the normal levels of the quinone in the body. For this reason dietary intake of Coenzyme Q, as a vitamin-like supplement, has been recommended by many authors.

Biological Naphthoquinones: Menaquinone and Vitamin K

Menaquinone is the quinone used for electron transfer by many bacteria, either alone or together with ubiquinone (Figure 3).

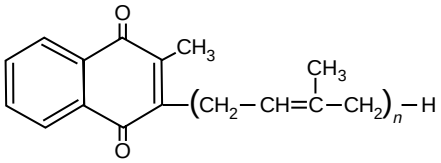

Menaquinones ($n = 7–9$)

Vitamin K exists in two natural forms, phylloquinone (K1) and menaquinone (K2), with 4 and 6 isoprenoid units, respectively. In phylloquinone, three isoprenoid units are hydrogenated. Menadione (K3), without an

isoprenoid chain, is a synthetic derivative.

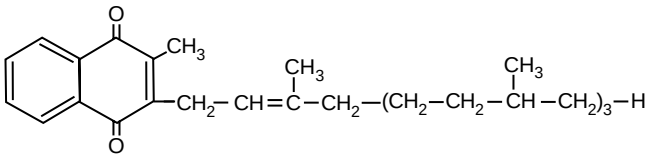

Vitamin K1

Vitamin K is involved in the process of blood coagulation, being required for the synthesis of prothrombin and factors VII, IX, and X. Vitamin K is involved in posttranslational modifications of these proteins consisting in the γ-carboxylation of glutamate residues. Vitamin K is the coenzyme of the carboxylase enzyme and acts in its reduced hydroquinone form. The mechanism of action is shown in Figure 5.

See Also the Following Articles

Purple Bacteria: Electron Acceptors and Donors • Respiratory Chain Complex II and Succinate: Quinone Oxidoreductases • The Cytochrome b_6f Complex • Vitamin K: Biochemistry, Metabolism, and Nutritional Aspects • Vitamin K: Blood Coagulation and Use in Therapy

Glossary

antioxidants Molecules capable of preventing the propagation of free radicals and hence protecting cellular and extracellular biomolecules from free-radical-induced damage, such as lipid peroxidation and genetic mutations in DNA. There are water-soluble antioxidants, such as ascorbic acid (vitamin C), and lipid-soluble antioxidants such as α-tocopherol (vitamin E). Ubiquinol belongs to this latter category.

chloroplasts Organelles present in photosynthetic higher plants and in eukaryotic algae that carry out the process of oxygen-evolving photosynthesis by extracting electrons from water, in a complex electron transfer chain containing plastoquinone among other components, and reducing CO_2, thus yielding carbohydrates by a complex synthetic process (Calvin cycle).

coenzyme A nonprotein compound required for the catalytic action of an enzyme that can be strongly bound to the enzyme itself as a prosthetic group or participate as a substrate to the enzyme-catalyzed reaction. Several coenzymes cannot be synthetized *de novo* and derive from nutritionally supplied vitamins.

free radical An atom or molecule having one or more unpaired electrons. For this reason free radicals are usually very reactive, in the attempt to donate or receive an electron, and may damage biological molecules by establishing a chain reaction of propagation followed by permanent chemical modification of the attacked molecules. Among free radicals are some of the so-called reactive oxygen species, derived by partial reduction of molecular oxygen during mitochondrial respiration and other biological processes.

mitochondria Organelles present in most eukaryotic cells carrying out the process of oxidative phosphorylation and several other metabolic pathways. Mitochondria consist of two membranes, the inner membrane being the site of the respiratory chain, delimiting two aqueous compartments (called the intermembrane space and the matrix).

vitamin A biological molecule, acting in small amounts (therefore not a structural component), that cannot be synthetized by the body and therefore requires dietary supplementation. Many vitamins are part of coenzymes. Vitamins are classified as water soluble and lipid soluble.

Further Reading

Ebadi, M., Marwath, J., and Chopra, R. (eds.) (2001). *Mitochondrial Ubquinone (Coenzyme Q_{10}): Biochemical, Functional, Medical, and Therapeutic Aspects in Human Health and Diseases*, **2 vols.** Prominent Press, Scottsdale, AZ.

Kagan, V. E., and Quinn, P. J. (eds.) (2001). *Coenzyme Q: Molecular Mechanisms in Health and Disease*. CRC Press, Boca Raton, FL.

Lenaz, G. (ed.) (1985). *Coenzyme Q: Biochemistry, Bioenergetics and Clinical Applications of Ubiquinone*. Wiley, London.

Many authors (1999). *BioFactors* 9. Special Issue dedicated to the First Conference of the International Coenzyme Q_{10} Association.

Many authors (2002). *Free Radical Research* 36(4). Special Issue dedicated to the Second Conference of the International Coenzyme Q_{10} Association.

Website of the International Coenzyme Q_{10} Association – http://www.csi.unian.it/coenzymeQ.

Biography

Giorgio Lenaz is a Professor of biochemistry at the Medical School of the University of Bologna, Italy. After his medical degree at the University of Bologna he was a postdoctoral fellow at the University of Wisconsin. His main research interest is mitochondrial bioenergetics in health and pathology, in particular mitochondrial encephalomyopathies and aging. He is an expert in Coenzyme Q and related compounds and has published many experimental papers and reviews in leading journals on the subject. He is a member of the executive committee of the International Coenzyme Q_{10} Association.

Maria Luisa Genova is a postdoctoral fellow in biochemistry at the University of Bologna. She holds a Ph.D. in biochemistry, and was trained at Rice University in Houston, Texas; she has published several papers on the subject of Coenzyme Q and mitochondrial bioenergetics.

Rab Family

Mary W. McCaffrey and Andrew J. Lindsay
University College, Cork, Republic of Ireland

Rab proteins are monomeric small GTPases that function as key regulators of eukaryotic membrane trafficking. Specifically, they have been implicated in the budding, transport, docking, and fusion of lipid bilayer vesicles. The Rabs form the largest and most diverse branch of the Ras protein superfamily. They are evolutionarily conserved and are present in all eukaryotes investigated, localizing to specific organelles of the secretory and endocytic pathway. The human genome project has demonstrated the existence of at least 60 members in the human Rab family, which can be divided into 10 subfamilies. Members of each subfamily have similar subcellular localization and some functional overlap. Most Rab proteins are ubiquitously expressed; however, a number such as Rab3A, which is expressed neurons, and Rab27, expressed in melanocytes and platelets, are cell-type specific. Rab proteins are characterized by their functional cycle. As their name suggests they bind GTP, which results in their activation. The GTP can then be hydrolyzed to GDP resulting in the Rab adopting an inactive (GDP-bound) conformation and leading to its subsequent membrane dissociation. Several Rab-interacting proteins have been identified, which regulate either the Rab nucleotide-bound state, its localization, or act as "effectors" of Rab function.

Discovery

The first Rab GTPases were discovered in the late 1980s, through the pioneering work of the Tavitian group, in Paris, which set out to identify homologues of the Ras oncogenes. They screened a brain cDNA library with degenerate oligonucleotides designed against the most conserved regions of G proteins (the G boxes). Besides known G proteins, new ras-related genes were identified in this screen. These were sufficiently different from Ras and Rho to be placed in a new family of the Ras superfamily and were named the Rabs–*Ra*s homologue from *b*rain.

Sequencing revealed that these new Rab genes bore greatest similarity to two previously described yeast secretory mutant genes, *sec4* and *ypt1*. The fact that these two yeast orthologues had previously been implicated in membrane trafficking provided the first clues that the members of the Rab GTPase family function in membrane trafficking in higher eukaryotes. In the years that followed, several research groups (notably the Zerial group) extended the family to 11 then to between 30 and 40 distinct members. With the aid of information from the human genome project, 60 distinct human Rab GTPases have now been identified.

Primary Structure and Evolution

The Rab family members are the most divergent and extensive branch of the ras superfamily. They contain ~200 amino acids with a molecular mass between 20 and 25 kDa, and are hydrophilic in nature (see Figure 2 for a schematic representation of Rab functional domains). Like all G proteins, they contain well-conserved guanine nucleotide binding domains (G-boxes) but otherwise are quite divergent – particularly in their carboxy-terminal region. This region is known to be critical for specifying membrane localization.

Their extreme carboxy termini also possess a characteristic conserved CC or CXC motif (C = cysteine, X = any amino acid). This motif is post-translationaly modified, in a process known as isoprenylation, by the addition of geranyl groups. The addition of a hydrophobic moiety on the cysteine results in a protein that is chemically competent for insertion into the lipid bilayer (further details on post-translational modifications are discussed later in this article).

By analogy with the Ras proteins, a further domain has been identified in the Rabs – the "effector" domain. This domain of ~10 amino acids was found to be critical for transmission of the Ras signal to its downstream machinery. Mutation of this effector domain abolishes growth signaling, independent of Ras GTP binding. Thus, this region was named the effector domain of ras. The equivalent region in the Rabs, also termed the effector domain, is frequently mutated in studies that investigate Rab function.

By analogy with the oncogenic Ras mutants, a number of Rab mutations have been generated. The most frequently utilized activating mutant for the

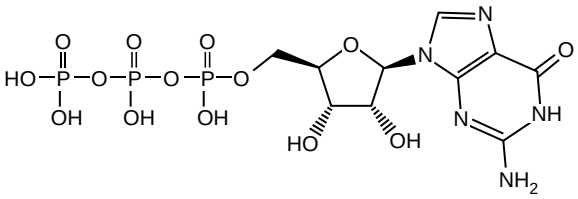

FIGURE 1 The structure of GTP.

Rabs is at amino acid position ~70 and is generated by the conversion of a glutamine (Q) to a leucine (L) at this position. Such Rab mutants are deficient in GTPase activity and thus remain in the 'activated' GTP-associated state (see Figure 1 for GTP structure). A serine (S) to asparagine (N) mutation, near amino acid 20, generates a dominant negative Rab mutant, that is constitutively GDP-bound and therefore inactive. Expression of these mutants in mammalian cells has revealed important Rab functional data.

In a study of the evolution and complexity of the core protein machinery involved in intracellular trafficking (coat complexes, Rab GTPases, SNAREs, and Sec1s) by the Scheller group, 60 distinct Rab genes were identified in humans. It was noted that there was a significant expansion of the Rab family from yeast to worms, and a further expansion from worms to mammals. A phylogenetic tree of the human Rab family is reproduced from Bock *et al.* (see Figure 3). Of the four core membrane-trafficking families compared, the Rabs were the only family that underwent such a significant expansion. It is likely that the higher degree of complexity in multicellular organisms is reflected by the greater requirement for Rabs, not only for more intricate regulation of intracellular trafficking but also for tissue specialization of membrane-trafficking functions.

The Rab family can be divided into ~10 subfamilies. Representative members of these subfamilies are Rab1, Rab3, Rab4, Rab5, Rab6, Rab8, Rab11, Rab22, Rab27, and Rab40.

Post-translational Modifications

Rab proteins are hydrophilic, thus, in order for membrane binding they must possess one, or two, C20 geranyl–geranyl lipid groups at their carboxy terminus. The process by which they gain these lipid moieties is known as isoprenylation. Newly synthesized, unprenylated, Rab GTPases are bound by Rab escort protein (REP) and delivered to Geranylgeranyl Transferase (GGTase). GGTase catalyzes the attachment of the lipid groups to two carboxy-terminal cysteine residues present on all Rab GTPases. REP appears to be a specialized Rab GDI that can deliver newly synthesized, GDP-bound, Rab proteins to GGTase for isoprenylation, and then transport the modified protein to its target membrane. It is thought that Rab-GDP binds its host membrane via a protein receptor, which 'senses' the Rab carboxy-terminal domain, however, very little evidence currently exists in the literature regarding the identity of such Rab receptors. Thus, while the amino acid sequence in the C-terminal region confers membrane specificity to a given Rab, the isoprenoid group confers chemical compatibility with the membrane, anchoring the otherwise hydrophilic protein in the hydrophobic lipid bilayer.

Cellular Localization

Rab proteins have now become standard markers for organelles of the secretory and endocytic pathways. Not all 60 human Rab GTPases have yet been sufficiently characterized such that the entire Rab localization pattern is known. However, for those that have been characterized, it is clear that they localize to distinct membrane organelles. For example, Rab1 localizes to the ER/*cis*-Golgi and Rab3 localizes to synaptic vesicles/chromaffin granules of the neuroendocrine system, while Rab5, Rab4, and Rab11 localize to distinct early endosomal membranes, Rab6 is located

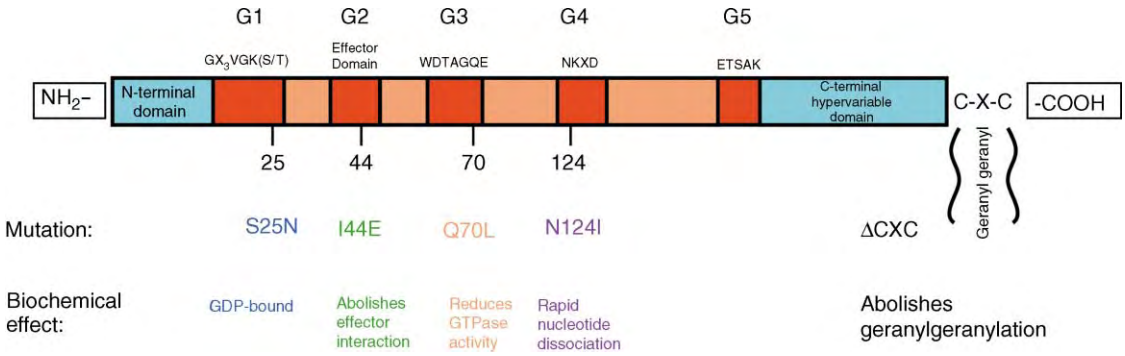

FIGURE 2 Schematic diagram of the general domain structure of Rab GTPases. Indicated are the commonly used Rab11 mutations and their biochemical consequences.

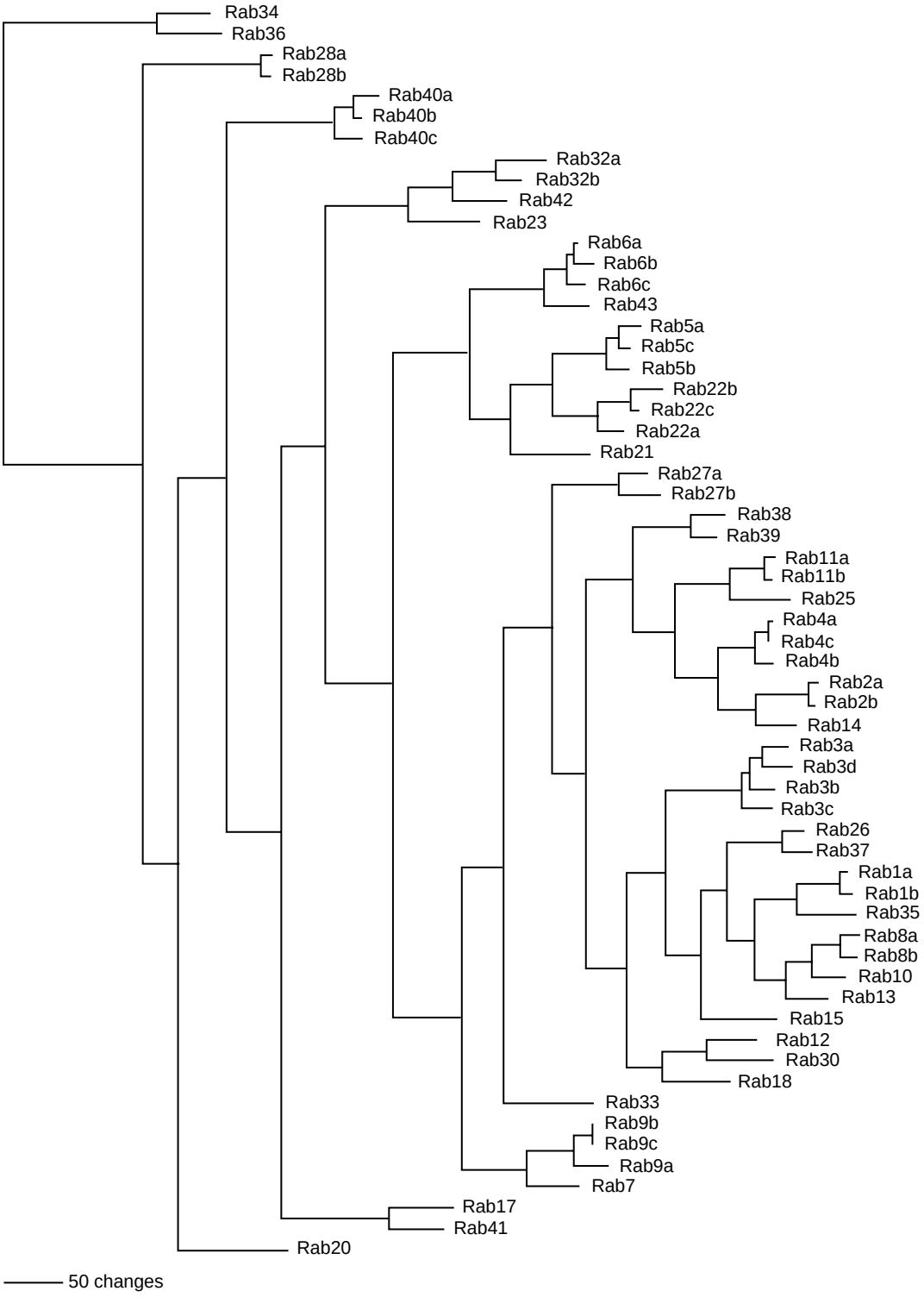

FIGURE 3 Phylogenetic tree of the human Rab GTPases. (Reprinted from Bock, J. B., Matern, H. T., Peden, A. A., and Scheller, R. H. (2001). A genomic perspective on membrane compartment organization. *Nature* **409**, 839– 841, by permission of Nature.)

on the Golgi apparatus, Rab7 is on late endosomes, Rab22 localizes to endosomes and the Golgi and Rab27 to melanosomes and lytic granules. Figure 4 and Table I indicate the known localization and trafficking steps controlled by Rabs characterized to date.

Functional Cycle

The functional cycle of Rab5 has been extensively characterized and is used here as a paradigm of all Rabs (see Figure 5 for generalized Rab GTPase cycle).

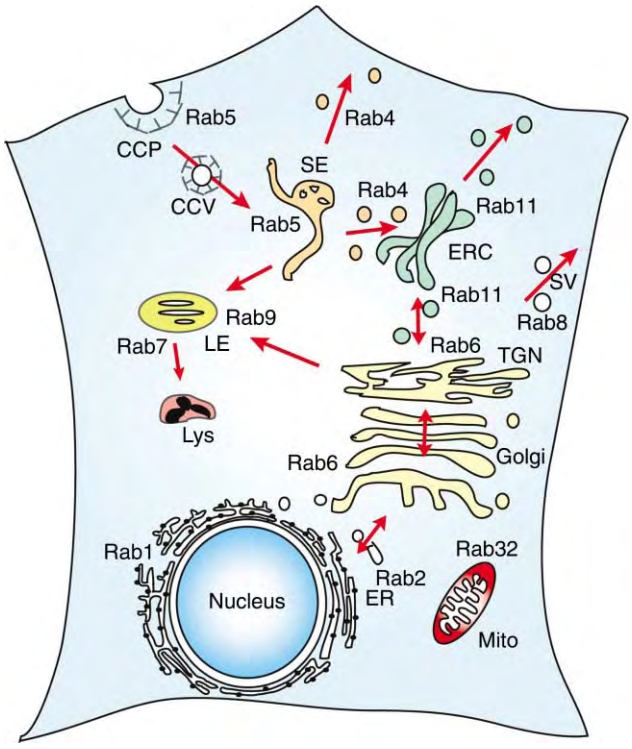

FIGURE 4 Localization of selected Rab GTPases and the membrane-trafficking pathways they regulate. The endocytic pathway involves internalization of cargo in clathrin-coated vesicles (CCV) and delivery to the early/sorting endosome (SE). Cargo is then either sorted for transport along the degradative pathway to the late endosomes (LE) and lysosomes (Lys), or directly recycled back to the plasma membrane from the SE, or indirectly, via the endocytic recycling compartment (ERC). The biosynthetic pathway transports proteins from the endoplasmic reticulum (ER) through the Golgi complex from where they are delivered to the cell surface in secretory vesicles (SV). The endocytic and secretory pathways communicate through the *trans*-Golgi network (TGN).

GDP-bound Rab5 is delivered to its target membrane by Rab guanine nucleotide dissociation inhibitor (Rab GDI). Rab guanine nucleotide exchange factor (Rab GEF) then catalyzes the exchange of the GDP for GTP, allowing Rab5 to adopt its active conformation. The GTP-bound Rab is now resistant to extraction by Rab GDI. Once membrane associated and in its active conformation the Rab protein is now competent to exert a controlling function on membrane trafficking. Rab5 mediates its function by recruiting a repertoire of specific effector proteins necessary for fusion of early endosomes. Upon completion of Rab function the GTP is hydrolyzed by the Rab GTPase enzymatic activity, releasing inorganic phosphate and resulting in an inactive Rab bound to GDP. This GTPase activity is stimulated by Rab GTPase *a*ctivating *p*rotein (Rab GAP).

Rabs have been variously implicated in vesicle budding from the donor membrane, transport along the cytoskeleton, docking to, and fusion with, the acceptor membrane. Though there is evidence for various Rabs of their involvement in these distinct events in membrane trafficking, it is not clear whether some Rabs function in vesicle budding exclusively, while others function in vesicle transport or docking, or whether a given Rab, in association with one specific set of effector proteins, functions in budding and in combination with other sets of effector proteins functions in transport, docking, or fusion.

Effectors

Several putative Rab effectors have been identified – primarily by two-hybrid library screening with GTPase deficient (dominant-positive) Rab mutants. While a survey of all of the Rab effectors reported in the literature is beyond the scope of this review, it is clear that there are likely to be many more Rab effectors than Rab GTPases. The GTP-bound form of Rab5 has been shown to interact specifically with at least 20 different proteins. Several Rab effectors have coiled-coil and/or phospholipid-binding domains (such as FYVE or C2 domains), while some are enzymes, or cytoskeletal (actin or tubulin) motor proteins. Identification of Rab effectors, and regulatory proteins, is a very important approach towards understanding the function of Rab GTPases and is likely to be an area of continued research for several years to come.

Rabs and Diseases

Sequencing of the human genome has revealed that a substantial number of disease-causing genes are involved in membrane trafficking. A proportion of these genetic diseases are the result of mutations in Rab GTPases, or their interacting proteins. Griscelli syndrome is an autosomal recessive disorder that results in pigmentation defects. There are two variants of this disease, one that results in immunological defects, and the other is associated with neurological dysfunction. The former is caused by missense mutations in the Rab27a gene, and the latter is the result of mutations in its putative effector, myosin Va. Both are located side-by-side on chromosome 15. Rab27a functions to regulate the transport of melanosomes to the periphery of melanocytes, also regulating the secretion of lytic granules in cytotoxic T lymphocytes. Hence, the lack of functional Rab27a results in the loss of pigmentation and in the uncontrolled activation of T lymphocytes. Mutation of myosin Va causes pigmentation defects, but since it is not involved in lytic granule movement, it does not cause immunological defects. Choroideremia is an X-linked disease that results in the degeneration of the pigment epithelium of the eye. It is caused by a defect in the REP-1 gene. REP-1 is one of the two

TABLE I

Localization, Tissue Distribution, and Function of the Human Rab GTPases

Rab GTPase	Localization	Tissue expression	Function
Rab34	Golgi	Ubiquitous	Lysosome positioning
Rab36	Golgi	Unknown	Unknown
Rab28	Unknown	Unknown	Unknown
Rab40	Unknown	Unknown	Unknown
Rab32	Mitochondria	Ubiquitous	A-kinase anchoring protein
Rab42	Unknown	Unknown	Unknown
Rab23	Unknown	Brain	Negative regulator of Sonic hedgehog pathway in mouse
Rab6	Golgi	Ubiquitous	Retrograde Golgi transport
Rab43	Unknown	Unknown	Unknown
Rab5	Plasma membrane, CCVs, and early endosomes (EE)	Ubiquitous	Transport from the plasma membrane to EE
Rab22	EE, LE, Golgi	Ubiquitous	Communication between biosynthetic and endocytic pathways
Rab21	Apical vesicles	Ubiquitous	Unknown
Rab27	Melanosomes and granules	Melanocytes, platelets, and lymphocytes	Transport of melanosomes and lytic granules
Rab38	Melanosomes	Melanocytes	Melanosome sorting
Rab39	Golgi-associated organelles	Ubiquitous	Endocytosis
Rab11/Rab25	Recycling compartment (RC) and TGN	Ubiquitous	Endocytic recycling and transport to TGN
Rab4	EE	Ubiquitous	Endocytic recycling and degradation
Rab2	Golgi	Ubiquitous	Golgi to ER transport
Rab14	ER/Golgi/Endosomes	Ubiquitous	Transport between Golgi endosomes
Rab3	Synaptic vesicles (SV)	Neurons	Regulation of neuro-transmitter release
Rab26	Secretory granules	Parotid gland	Regulated secretory pathway
Rab37	Secretory granules	Mast cells	Mast cell degranulation
Rab1	ER/*cis*-Golgi	Ubiquitous	ER to Golgi transport
Rab35	Unknown	Unknown	Unknown
Rab8	Transport vesicles	Ubiquitous	Regulates polarized membrane transport
Rab10	Golgi	Ubiquitous	Unknown
Rab13	Junctional complexes	Epithelial cells	Regulation of structure and function of tight junctions
Rab15	EE and RC	Ubiquitous	Inhibitor of endocytic recycling
Rab12	Granules/Golgi	Ubiquitous	Unknown
Rab30	Golgi	Unknown	Unknown
Rab18	Apical dense tubules	Epithelial cells	Unknown
Rab33	Unknown	Unknown	Unknown
Rab9	LE	Ubiquitous	LE to TGN transport
Rab7	Late endosomes (LE)	Ubiquitous	Transport from LE to lysosomes
Rab17	Epithelial cells	Apical RC	Transport through apical RC
Rab41	Unknown	Unknown	Unknown
Rab20	Apical dense tubules in kidney tubule epithelial cells	Epithelial cells	Unknown

isoforms of GGTase that prenylate Rab GTPases. It is essential for the prenylation of Rab27a in the retinal pigment epithelium. REP-2 appears to be sufficient for the efficient geranyl-geranylation of all other Rab GTPases. Thus, the lack of functional REP-1 results in nonfunctional Rab27a and the onset of the disease. The pathology of this disease may be caused by the degeneration of the retinal epithelium due to deficient melanosome transport, and hence lack of protection during light exposure.

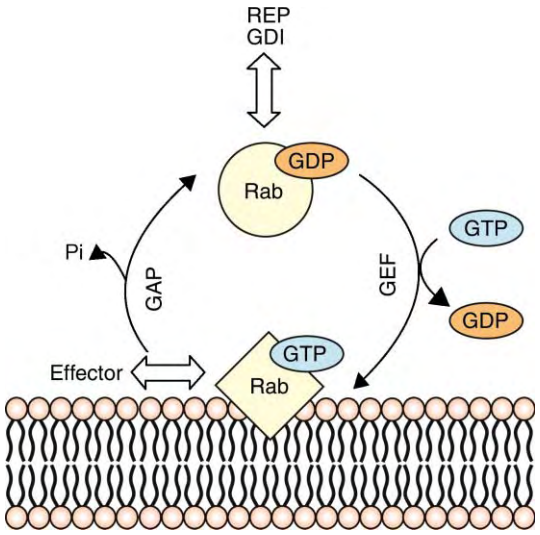

FIGURE 5 The Rab GTPase cycle. Rab GTPases cycle between GTP- and GDP- bound forms, allowing the Rab to adopt active and inactive conformations. The cycle is mediated by various accessory factors. A guanine-nucleotide exchange factor (GEF) exchanges the GDP for GTP. Conversion from the GTP- to the GDP-bound form is mediated by a GTPase-activating protein (GAP) which stimulates the Rab to hydrolyze bound GTP. The active GTP-bound form mediates its function through specific effector molecules. Newly synthesized cytosolic, GDP-bound Rab, interacts with Rab escort protein (REP) for membrane delivery. Subsequently, after each functional round, the GDP-bound Rab is extracted by the GDP dissociation inhibitor (GDI) from its host membrane and delivered to a new membrane location for another functional round.

Tuberin is a tumor suppressor protein that interacts with Rabaptin-5 and negatively regulates endocytosis by acting as a Rab5-GAP. Its inactivation causes tuberous sclerosis, a disease that results in malformations and tumors of the central nervous system. Finally, mutations in the GDI1 gene, which encodes GDI-α have been found in a subgroup of patients with X-linked nonspecific mental retardation. GDI-α is particularly abundant in brain tissue, thus defective membrane recycling of one or more Rab GTPases in brain synapses is likely to be the cause of this condition.

See Also the Following Articles

Ras Family • Rho GTPases and Actin Cytoskeleton Dynamics • Small GTPases

Glossary

effectors Proteins that are necessary to effect small GTPase function. Many (putative) effectors of the Ras superfamily have been described in the past decade.

GTPases Proteins capable of hydrolyzing GTP by cleavage of its terminal phosphate. This reaction results in the protein being switched to the inactive state, i.e., associated with GDP.

Ras Monomeric GTPases, first identified as oncogenes/oncoproteins, which function as central players in mitogenic signalling pathways.

Rho The first ras homologue to be identified, Rho proteins control actin cytoskeleton organization and structure.

Further Reading

Aridor, M., and Hannan, L. A. (2002). Traffic jams II: An update of diseases of intracellular transport. *Traffic* **3**, 781–790.

Bock, J. B., Matern, H. T., Peden, A. A., and Scheller, R. H. (2001). A genomic perspective on membrane compartment organization. *Nature (London)* **409**, 839–841.

Stenmark, H., and Gillooly, D. J. (2001). Intracellular trafficking and turnover of phosphatidylinositol 3-phosphate. *Semin. Cell Dev. Biol.* **12**, 193–199.

Woodman, P. (1998). Vesicle transport: More work for the Rabs? *Curr. Biol.* **8**, R199–R201.

Zerial, M., and McBride, H. (2001). Rab proteins as membrane organisers. *Nat. Rev. Mol. Cell Biol.* **2**, 107–119.

Biography

Mary W. McCaffrey is a Lecturer in Biochemistry and Science Foundation Ireland (SFI) Investigator in the National University of Ireland, Cork. Her principal research focus involves the functional characterization of Rab proteins in mammalian endosomal trafficking. She holds a Ph.D. from the University of London, England and received postdoctoral training in the Pasteur Institute, Paris, France. Her group is a world leader in the identification and characterization of the Rab11 effector machinery.

Ran GTPase

Mary Shannon Moore
Baylor College of Medicine, Houston, Texas, USA

Ran (Ras related nuclear protein) is a 25 kDa member of the Ras superfamily of small GTPases. To date, a Ran homologue has been found in every nucleated cell of every eukaryotic organism on Earth, and Ran is essential for the viability of all those cells. During interphase, Ran plays an essential role in driving and regulating the active transport of cargo between the nucleus and cytoplasm. Ran also has critical functions during mitosis when Ran is essential for mitotic spindle assembly and placement as well as re-assembly of the nuclear envelope.

Small GTP-Binding Proteins as "Molecular Switches"

Ran is called a GTPase because it binds and hydrolyzes GTP. All small GTPases of the Ras superfamily cycle between GTP- and GDP-bound states, and undergo a marked conformational change upon conversion from one state to the other. Thus, GTPases in the GTP-bound form can bind proteins that the GDP-bound form cannot, and vice versa. This key property confers on small GTPases the ability to function as "molecular switches" that cycle between active and inactive states, the GTP-bound form generally being the active form.

Ran represents its own family of small GTP-binding proteins in the Ras superfamily, of which it is the only member. The other families include the Ras, Rab, Arf, Rac, and Rho families that regulate signal transduction, vesicular transport, cytoskeletal organization, and cell proliferation. Ran's role is to act as a "switch" to regulate nuclear transport during interphase and spindle, and nuclear envelope assembly during mitosis.

Nucleocytoplasmic Transport

A basic necessity of the eukaryotic cell is the ability to transport macromolecules bidirectionally between the nucleus and cytoplasm. The traffic between these two compartments is both heavy and complex with multiple classes of cargo being actively transported in both directions (Figure 1). Nuclear proteins such as transcription factors and histones are, like all proteins, made in the cytoplasm and must cross the nuclear envelope into the nuclear interior to carry out their function. Conversely, ribosomal subunits, tRNAs, and mRNAs produced inside the nucleus must cross the nuclear envelope in the opposite direction into the cytoplasm in order to be used for protein translation.

Nucleocytoplasmic traffic is restricted to nuclear pore complexes (NPCs), which are large proteinaceous structures that bridge the double membrane of the nuclear envelope to form aqueous channels linking the cytoplasm and nucleoplasm. The vertebrate NPC is composed of ~30 different proteins and a HeLa cell contains ~3000 NPCs. At present, all NPCs appear to be functionally identical with the same NPC capable of carrying out both import and export virtually simultaneously. While molecules up to ~50 kDa can diffuse through the NPC, the majority of nuclear proteins (both larger and smaller than 50 kDa) as well as the other classes of transport cargo appear to undergo signal-mediated active transport rather than diffusion.

There are two types of nuclear transport signals, NLSs (nuclear localization sequences) that mediate nuclear import and NESs (nuclear export sequences) that mediate nuclear export. There are multiple types of NLSs and NESs found on different types of cargo, and, in general, each type of signal is recognized by a different nuclear receptor/carrier. Most nuclear carriers are members of the karyopherin-β superfamily and there are over twenty members of this family in human cells. During nuclear import, a soluble carrier binds the NLS-containing cargo in the cytoplasm, then moves the cargo through the NPC and releases it in the nuclear interior. Nuclear export works essentially the same way in reverse, with an NES-containing cargo being recognized by its specific carrier inside the nucleus, movement of the export complex through the NPC, and disassembly of the complex and release of the cargo upon reaching the cytoplasm.

The Ran GTPase

The Cellular Gradient of RanGTP

A key player in the majority of the known nuclear transport pathways is the small GTPase Ran and, not

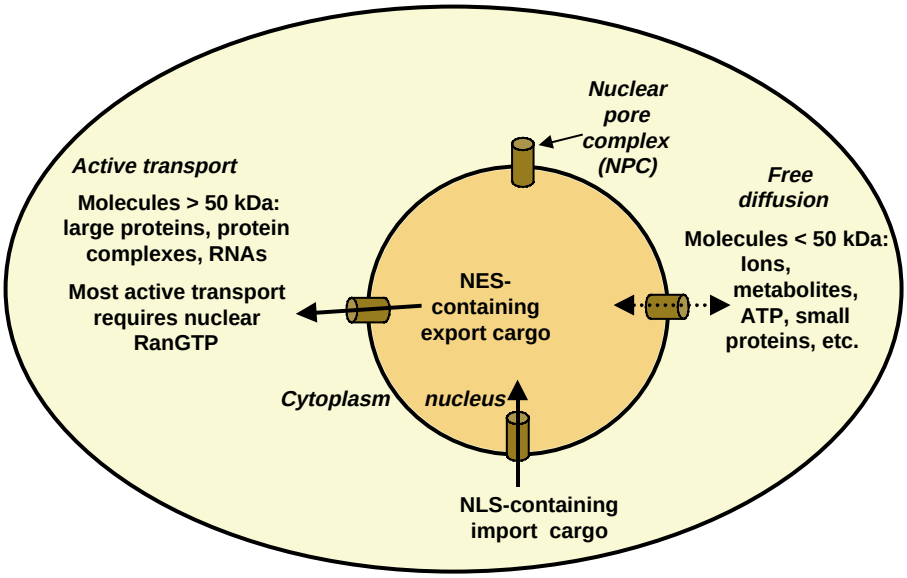

Some NLS-containing import cargo:	Some NES-containing export cargo:
Nuclear proteins	Shuttling proteins
Shuttling proteins	Newly formed ribosomal subunits
	tRNAs
	mRNAs

FIGURE 1 Overview of nucleocytoplasmic transport. Most nuclear transport requires nuclear RanGTP, however mRNA export does not. Carriers of the NTF2 family mediate mRNA export, and this transport pathway is Ran-independent. Active transport of the rest of the cargo listed does require nuclear RanGTP.

incidentally, the main region of homology between all the karyopherin-β nuclear carriers is a RanGTP-binding domain. Inside the cell, Ran is primarily nuclear in spite of the fact it does not appear to contain an NLS in its sequence. This is because Ran is actively imported into the nucleus by a small protein called p10/NTF2, which is a member of a second class of nuclear carriers, the NTF2 family.

Importantly, whether Ran is in the cytoplasm or nucleus determines whether it is RanGTP or RanGDP (Figure 2). Inside the nucleus, Ran is converted to the GTP-bound form by the RanGEF (guanine nucleotide exchange factor), which stimulates RanGDP to release GDP and bind GTP. In contrast, the RanGAP (GTPase-stimulating protein) is located in the cytoplasm. The RanGAP rapidly converts any RanGTP entering the cytoplasm to RanGDP by stimulating Ran to hydrolyze its bound GTP.

The resulting concentration gradient of low RanGTP in the cytoplasm to high RanGTP in the nucleus is vitally important for controlling the directionality of nuclear transport by regulating the assembly and disassembly of karyopherin-β containing transport complexes. Also, because the RanGEF is bound to chromatin, the concentration of RanGTP is highest near the chromatin where it is produced (Figure 2C). This location becomes important during mitosis, when chromatin-localized RanGTP stimulates mitotic spindle and nuclear envelope assembly in the correct location around chromatin.

Cellular Functions of Ran

Nuclear Transport

The increasing RanGTP concentration from the cytoplasm to the nuclear interior is the primary factor that triggers the disassembly of transport complexes at their correct final destination. Members of the karyopherin-β family preferentially bind RanGTP with a much lower affinity for RanGDP, and upon binding RanGTP, the karyopherin-β carrier undergoes a conformational change that alters its cargo-binding domain. NLS receptors of the karyopherin-β family can only bind their cargo when they do not have bound RanGTP, which is their probable state in the cytoplasm. After movement across the NPC into the nuclear interior where the import complex encounters RanGTP,

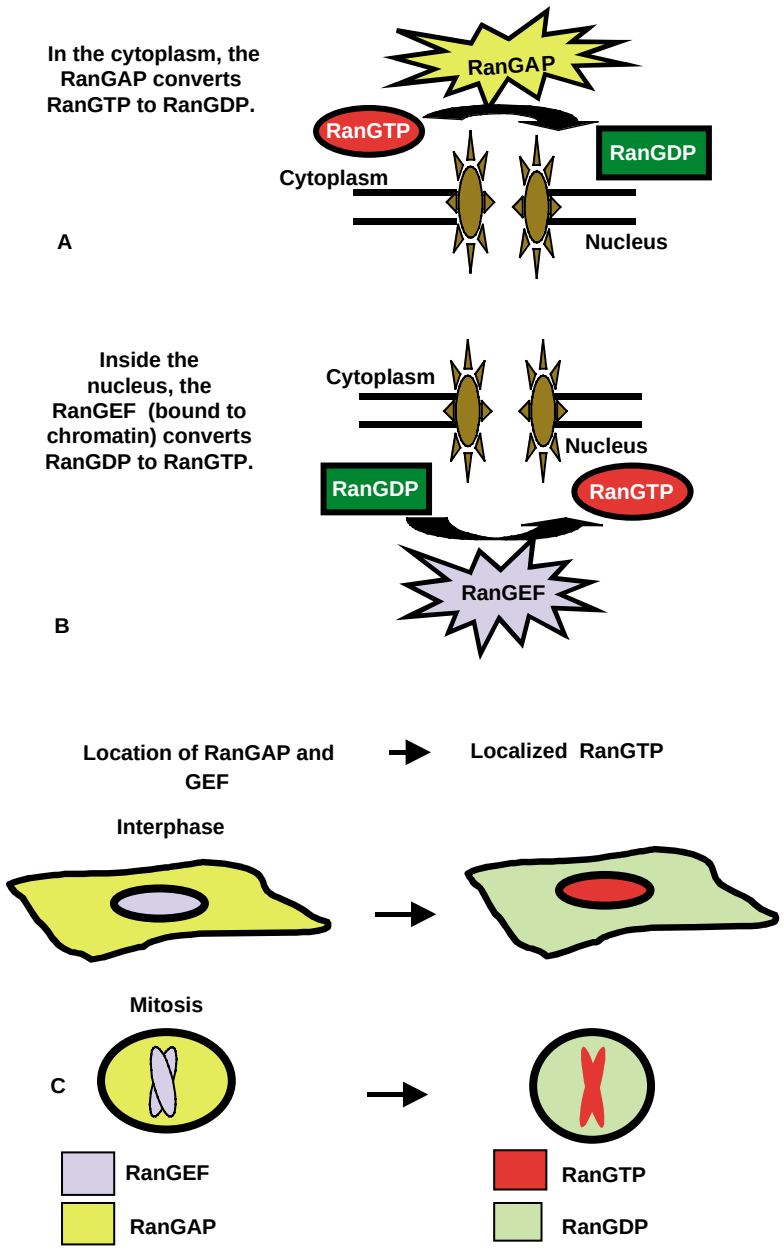

FIGURE 2 Establishment of the RanGTP gradient between the cytoplasm and nucleoplasm. (A) The RanGAP, which stimulates Ran to hydrolyze its bound GTP, is restricted to the cytoplasm. (B) The RanGEF, which stimulates Ran to release bound GDP and take up GTP, is found inside the nucleus bound to chromatin. (C) Restricting the RanGAP and the RanGEF to different compartments results in high levels of RanGTP inside the nucleus and low levels of RanGTP in the cytoplasm during interphase (top). The resulting gradient of RanGTP concentration between the cytoplasm and nucleoplasm is the key regulatory mechanism controlling the assembly and disassembly of nuclear import and export complexes in the correct cellular location (see Figure 3). Also, the RanGEF remains bound to chromatin throughout the cell cycle, and production of RanGTP at the chromatin surface in mitotic cells is required for proper placement of the mitotic spindle and re-assembly of the nuclear envelope around chromatin at the end of mitosis (bottom).

the carrier binds RanGTP, and as a result, releases its cargo into the nuclear interior (Figure 3A).

Export carriers of the karyopherin-β family behave just the opposite. These export carriers, in order to simultaneously bind their export cargo, must first bind RanGTP. After movement through the NPC, the cargo:export carrier:RanGTP complex encounters the RanGAP in the cytoplasm. Ran is stimulated to hydrolyze its bound GTP, and after hydrolysis, becomes RanGDP. The export carriers have a low affinity for RanGDP and, as a result, both RanGDP and an export cargo dissociate from the export carrier in the cytoplasm.

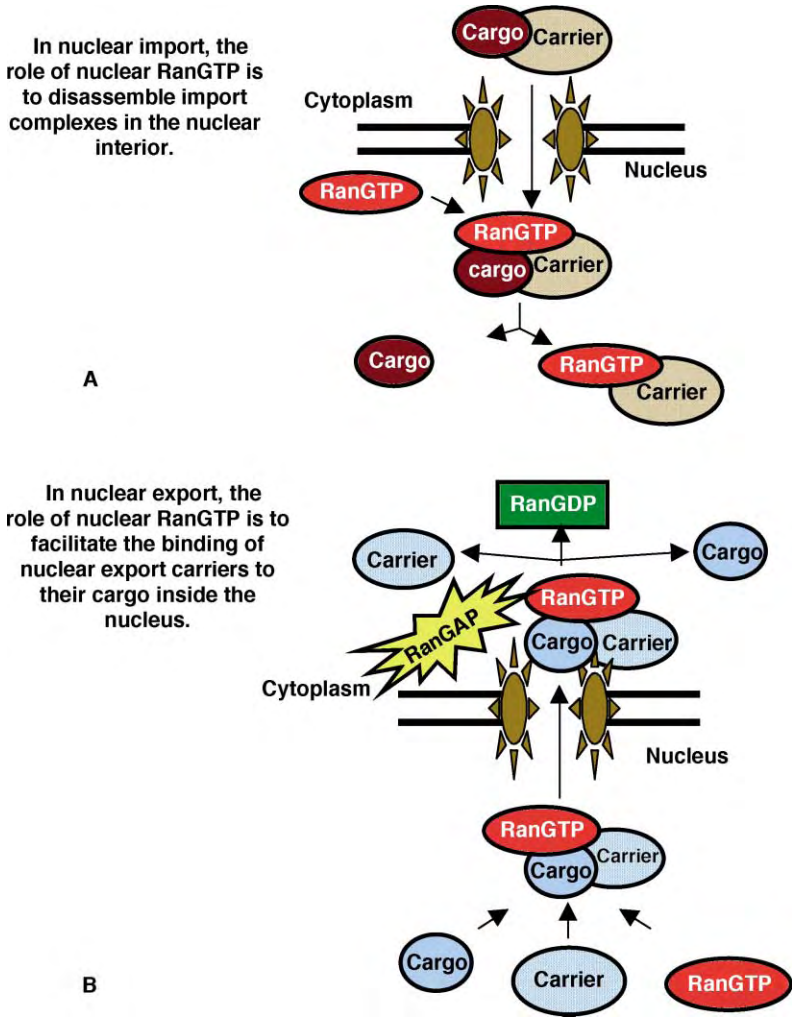

FIGURE 3 The RanGTP gradient across the NPC controls the assembly and disassembly of nuclear transport complexes. (A) Nuclear import carriers cannot bind import cargo and RanGTP simultaneously. After import of the import carrier:cargo complex through the nuclear pore complex (NPC), the carrier binds nuclear RanGTP. As a result of binding RanGTP, the import carrier releases the import cargo in the nuclear interior. (B) In contrast to nuclear import carriers, nuclear export carriers require bound RanGTP in order to bind their export cargo with high affinity. After export through the NPC, the export complex (RanGTP:export carrier:cargo) encounters the RanGAP in the cytoplasm that stimulates Ran to hydrolyze its bound GTP. Conversion of RanGTP to RanGDP results in the release of RanGDP and export cargo from the export carrier into the cytoplasm.

Regulation of Spindle and Nuclear Envelope Assembly at Mitosis

The nuclear envelope vesiculates and breaks apart during mitosis in vertebrate cells, and then reforms after the daughter cells are divided. Accordingly, no nuclear transport occurs during this time because there is no nuclear envelope and the cytoplasmic and nuclear contents are mixed. Ran however has additional functions critical to this period. Nuclear proteins containing an NLS are once again exposed to the NLS receptors and can be re-bound by them. However, as during nuclear import, RanGTP can break this complex apart, releasing the proteins.

Many of the proteins responsible for assembly of the mitotic spindle at mitosis are nuclear during interphase and contain an NLS. To be active for spindle assembly, RanGTP must first release these spindle assembly factors from NLS receptors. Because the concentration of RanGTP is highest, close to the chromatin due to the RanGEF located there; active spindle assembly factors (as opposed to inactive factors complexed with NLS receptors) are also most concentrated there. RanGTP is thus essential for spindle formation; both to release spindle assembly factors from NLS-binding carriers and for correct orientation of the spindle around chromatin.

As stated above, when a human cell enters mitosis at the beginning of cell division, the nuclear envelope fragments into vesicles. At the end of mitosis, after the two daughter cells have separated, these membrane vesicles bind to the decondensing chromatin and then

fuse together laterally to re-form an intact nuclear envelope. RanGTP is essential for this fusion step, as is one particular nuclear carrier of the karyopherin-β family (importin-β), however the exact mechanism is not yet known.

Other Roles of Ran

In addition to the cellular roles for Ran discussed above, Ran has also very recently been implicated in prevention of re-replication of chromatin during S phase and in regulation of kinetochore function throughout the cell cycle. It should be noted that in all of the multiple pathways in which Ran has been implicated, the general nature of the biochemical reaction carried out by Ran remain constant. Switching between RanGDP and RanGTP controls Ran's association with different proteins, and Ran's association with assorted proteins has different downstream effects depending on the protein involved, the cellular location where the interaction occurs, and the stage of the cell cycle when the interaction occurs. In summary, the Ran GTPase plays a powerful and irreplaceable role in the eukaryotic cell, both for constitutive viability and for cell division.

See Also the Following Articles

ARF Family • Mitosis • Nuclear Pores and Nuclear Import/Export • Ras Family

Glossary

GDP Guanosine 5′-diphosphate, a nucleotide analogous to ADP that is composed of guanine linked to ribose and two phosphates.

GTP Guanosine 5′-triphosphate, an energy-rich nucleotide analogous to ATP that is composed of guanine linked to ribose and three phosphates.

GTPase A protein that can bind and hydrolyze GTP.

interphase A period or stage between two successive mitotic divisions of a cell nucleus.

mitosis The sequential differentiation and segregation of replicated chromosomes in a cell nucleus that precedes complete cell division.

nuclear pore complex (NPC) Large organelles of the nuclear envelope through which passage of proteins and RNAs between the cytoplasm and nuclear interior occurs.

Further Reading

Arnaoutov, A., and Dasso, M. (2003). The Ran GTPase regulates kinetochore function. *Dev. Cell* **5**, 99–111.

Dasso, M. (2002). The Ran GTPase: theme and variations. *Curr. Biol.* **12**, R502–R508.

Kunzler, M., and Hurt, E. (2001). Targeting of Ran: Variation on a common theme? *J. Cell Sci.* **114**, 3233–3241.

Steggerda, S. M., and Paschal, B. M. (2002). Regulation of nuclear import and export by the GTPase Ran. *Int. Rev. Cytol.* **217**, 41–91.

Talcott, B., and Moore, M. S. (1999). Getting across the nuclear pore complex. *Trends Cell Biol.* **9**, 312–318.

Weis, K. (2003). Regulating access to the genome: nucleocytoplasmic transport throughout the cell cycle. *Cell* **112**, 441–451.

Yamaguchi, R., and Newport, J. (2003). A role for Ran-GTP and Crm1 in blocking re-replication. *Cell* **113**, 115–125.

Biography

Mary Shannon Moore is an Assistant Professor in the Department of Molecular and Cellular Biology at Baylor College of Medicine, Houston. Her principal research interests are nuclear structure and function and nucleocytoplasmic transport. She received her Ph.D. from UT Southwestern Medical Center at Dallas, and did her postdoctoral work in Dr. Günter Blobel's laboratory at Rockefeller University in New York. In 1993, Drs. Moore and Blobel published the first paper showing a role for Ran in nucleocytoplasmic transport.

Ras Family

Lawrence A. Quilliam
Indiana University School of Medicine, Bloomington, Indiana, USA

Since the discovery of Ras activity in a cancer-causing retrovirus in 1964, it has become the prototype of a superfamily of over 100 GTP-binding proteins that regulate a myriad of biological functions in eukaryotic cells. This superfamily can be subdivided based on primary sequence or biological function into five major subfamilies; Ras, Rho, Rab, Ran, and ARF. This article will focus on the Ras subfamily of proteins that are primarily responsible for regulating cell proliferation and differentiation. These proteins function as molecular switches that alternate between active GTP and inactive GDP-bound conformations. Acquisition of the active GTP bound state and its hydrolysis to GDP are tightly regulated by guanine-nucleotide-exchange factors (GEFs) and GTPase activating proteins (GAPs) that in turn receive direction from the signal transduction pathways that are elicited by hormone and growth factor binding to cell surface receptors. Upon activation, Ras proteins bind specific downstream effector proteins, promoting their subcellular relocalization or conformational changes that result in their activation and transmission of a signal to induce events that include gene expression and cytoskeletal rearrangement. Mutations that prevent GTP hydrolysis result in constitutive signaling to downstream effectors and promote uncontrolled cell growth. These mutations are found in several common human cancers and can be used by researchers to understand their mechanism of action.

Physical Properties

Ras family proteins are often referred to as small or low-molecular weight GTPases. This is due to their 20–25 kDa size being smaller than the 38–52 kDa α-subunits of the heterotrimeric G proteins, another class of cell signaling molecules that bind and hydrolyze GTP. Ras proteins consist of a core GTP-binding/GTPase domain that encompasses ~160 amino acids, followed by a hypervariable domain that is thought to act as a flexible linker, and a C-terminal CAAX (cysteine-aliphatic-aliphatic-other amino acid) motif that is the signal for posttranslational lipid modification, see Figure 1. Addition of a 15 carbon farnesyl or 20 carbon geranylgeranyl isoprene group to the Cys, cleavage of the three C-terminal (AAX) residues, and methylation of the C-terminal COO- group help promote the membrane targeting of most Ras subfamily GTPases. Additional palmitylation of nearby cysteine(s) or presence of many basic (arginine, lysine) residues in the hypervariable region help maintain tight membrane association. Membrane association is essential for Ras protein function and mutation of the CAAX cysteine, preventing the series of posttranslational modifications, disables Ras function. Most of the Ras superfamily proteins are modified by a geranylgeranyl transferase that adds the 20 carbon lipid. However, H-, K-, and N-Ras are modified by a farnesyl transferase that recognizes a different CAAX sequence that adds a 15 carbon farnesyl lipid instead. Because of this specificity, drugs that mimic the C terminus of Ras and/or the farnesyl lipid can block posttranslational modification and clinical trials are being performed to evaluate their use in cancer chemotherapy.

The GDP/GTP Cycle and Ras Mutations

Ras binds GTP and GDP, but not GMP, with very high affinity. The intrinsic rates of nucleotide exchange and GTP hydrolysis by Ras *in vitro* are very slow (on the order of minutes to hours) and not practical for a signaling molecule that needs to rapidly respond to stimuli. However, this is by design. Each Ras protein is tightly regulated by one or more guanine-nucleotide-exchange factors (GEFs) that help turn it on and GTPase activating proteins (GAPs) that subsequently help to inactivate it, see Figure 2.

Ras GEFs contain a CDC25 homology domain that shares similarity with the yeast RAS1/2 GEF, CDC25. There are over 30 CDC25 homologues in the human genome. Some are highly specific for one Ras protein while others catalyze nucleotide exchange and multiple family members. GEFs promote the release of GDP, then stabilize the nucleotide-free protein until GTP can bind and displace them. This occurs very rapidly *in vivo* due to the high affinity of Ras for GTP. Also because GTP is in a 10–20-fold excess over GDP, the GEF is predominantly

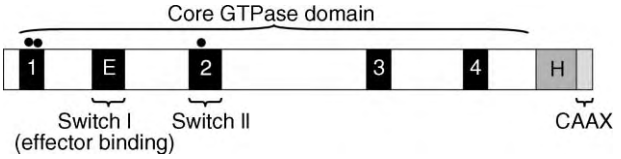

FIGURE 1 Linear diagram of Ras protein highlighting key sequences. Black areas are highly conserved across the entire Ras superfamily and form the guanine-nucleotide-binding pocket. Closed circles indicate sites of activating mutations found in human cancers. Switch I and II domains change conformation upon GDP versus GTP binding. E = effector binding loop that associated with downstream effectors. H = hypervariable domain, a 10–20 amino acid linker that also contributes to membrane binding. CAAX represents the terminal four residues that signal for posttranslational lipid modification of the cysteine residue. The identity of residue X dictates whether the G protein receives a 15 or 20 carbon lipid tail.

displaced by GTP. Because of the ability of nucleotide-free Ras to bind tightly to GEFs, dominant inhibitory mutants have been designed that have low affinity for nucleotide. These bind tightly to GEFs and prevent them from activating the endogenous wild type Ras, so blocking signaling pathways. These are useful tools for implicating Ras proteins or Ras pathways in the control of cellular events.

Although Ras is a GTPase, it has a poorly designed catalytic site. However, GAPs help stabilize the catalytic site and contribute a critical arginine residue that greatly accelerated nucleophilic attack of the GTP. One reason the α-subunits of heterotrimeric G proteins are bigger than Ras proteins is that they have an extra domain that contributes an "arginine finger" resulting in their typically having a higher intrinsic GTPase activity than Ras. Mutations that block intrinsic and GAP-stimulated GTP hydrolysis result in Ras proteins being locked in their active GTP-bound state. Such mutations at residues 12, 13, and 61 are found in H-, K-, or N-Ras in various human tumors. To date only ~10 Ras subfamily GAPs have been characterized. These fall into two structurally distinct families; those that regulate Rap/Rheb and those that regulate Ras and other GTPases. One of the Ras GAPs, neurofibromin, is the product of the NF1 tumor suppressor and, upon its loss, Ras GTP levels become elevated contributing to increase signaling that results in cancer and other proliferative diseases. Information on the better-characterized Ras subfamily members is discussed next.

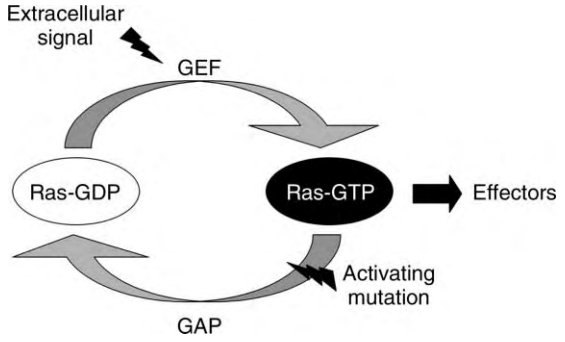

FIGURE 2 GDP/GTP cycle activity of Ras family GTPases. Ligand binding induce receptor-mediated activation or membrane-recruitment of guanine-nucleotide-exchange factors (GEFs) which promote the release of GDP from Ras and acquisition of GTP from the cytosol. GTP binding promotes a conformational change permitting Ras to associate with downstream effector proteins to elicit a biological response. GTPase activating proteins (GAPs) also recognize Ras-GTP and their binding promotes rapid acceleration of Ras' intrinsic GTPase activity. This converts Ras back to its inactive GDP-bound state from which the cycle can begin again. Mutations that block the intrinsic and GAP-stimulated GTPase activity lock Ras in its active, GTP-bound state.

H-, K-, and N-Ras

H-, K-, and N-Ras represent the original and best-studied/understood Ras proteins. Mutations of each of these proteins are found in human tumors with those in K-Ras being the most prevalent. K-Ras can have alternate splicing of its fourth exon with the 4B version being the most predominant.

It was long known that Ras was involved in growth control downstream of growth factor receptors and in 1993 an entire pathway from cell-surface receptor to the nucleus was delineated. The binding of growth factors to their protein tyrosine kinase receptors leads to phosphorylation of the receptors on tyrosine residues. This enables the binding of various adapter proteins that contain modular Src homology 2 or SH2 domains that recognize specific primary sequences that contain phospho-tyrosine. One such molecule is Grb2 that also has two SH3 domains that bind to proline-rich sequences like those found in the Ras GEF, Sos. Binding of a preformed Grb2-Sos complex to receptor tyrosine kinase results in recruitment of Sos to the plasma membrane where it promotes GTP-loading of Ras. In its active GTP-bound state, Ras now adopts a conformation that enables it to bind to the serine/threonine protein kinase, Raf. This in turn recruits Raf to the membrane, promotes a conformational change, and enables Raf to be phosphorylated by nearby kinase(s). Raf then phosphorylates MEK, which phosphorylates extracellular signal-regulated kinases (ERKs) 1 and 2. Phospho-ERKs dimerize and translocate into the nucleus where they phosphorylate transcription factors such as Elk1, leading to increased gene expression. It is now known that a number of additional signals activate Ras. For example, Ras GEFs (such as GRF1 in brain and GRP1 in T cells) and GAPs (Capri, Rasal) can be activated by Ca^{2+} elevation and/or diacylglycerol. Additionally, G protein-coupled receptors can trigger tyrosine phosphorylation to regulate the Grb2/Sos complex.

Ligand receptors reside on the plasma membrane and Ras also localizes there. However, recent studies indicate that Ras is also found on the Golgi membrane and that many of the events mediated by Ras occur at this intracellular site. One mechanism whereby activation of cell-surface receptors might signal to Ras at a remote intracellular membrane is via Ca^{2+} elevation, resulting in the activation of a $Ca2^{+}$-regulated exchange factor. This has been reported in T cells.

Binding of GTP triggers a conformational change in Ras in two regions called switch I and II. Switch I, which encompasses residues ~32–40 is the main determinant for effector binding. Conformation of this and switch II dictate which targets various Ras subfamily members associate with. A number of putative Ras effectors have been described however three have been best characterized. These include the protein kinase Raf, phosphatidylinositol 3 kinase, and RalGDS, an exchange factor for the Ras-related GTPase, Ral. There are several isoforms of each of these effectors that have different tissue distribution and affinities for various Ras family members. Each of these effectors has a related ~60 residue Ras association (RA) or Ras-binding domain (RBD). Since RA domains bind specifically to Ras-GTP, the isolated domains (typically fused to glutathione S-transferase and immobilized on glutathione-conjugated beads) can be used to precipitate Ras-GTP from cell lysates to gauge intracellular Ras activity. The Raf RBD is typically used to detect H-, K-, or N-Ras activity. While most Ras activity is associated with increasing cell growth and transformation, several recently characterized Ras targets that include RASSF1 appear to have tumor-suppressing properties.

Ral

As indicated above, a family of four Ral GEFs (RalGDS, Rgl, Rgl2/Rlf, Rgl3/RPM) possess Ras-binding domains and are downstream effectors of Ras. The primary function of Ras here is in recruiting Ral-GEFs to the membrane where they can activate Ral. In addition to being regulated by Ras/RalGDS, Ral is activated by Ca^{2+}, possibly due to its ability to bind calmodulin and by a second class of GEFs (the RalGPS or RalGEF2 family) that lack an RA domain.

Due to its regulation by Ras, initial studies focussed on its ability to regulate transformation. Recently RalGDS was found to be an important mediator of Ras-induced transformation in human epithelial cells. However, the downstream target(s) responsible for this effect remain to be identified. Ral or its GEFs have been reported to regulate various transcription factors including c-Fos, c-Jun, STAT3, and AFX (a member of the forkhead family). Interestingly, Ral-GEFs are often more potent at inducing biological effects than activated (GTPase-defective) Ral mutants. This may be because GTP/GDP cycling is required for Ral function or that binding of Ral-GEFs to additional proteins such as the serine/threonine kinase PDK1 or the scaffold protein, β-arrestin contributes to their biological activity.

Studies on Ral-binding proteins revealed the involvement of this GTPase in additional cellular functions that include vesicle sorting. This is not surprising since much of the Ral protein localizes to intracellular vesicles in both endocytic and exocytic compartments. Ral binds to and may assist in the formation of the exocyst, a complex of at least eight proteins, which directs vectorial targeting of vesicles from the Golgi to the basolateral but not apical membrane of epithelial cells. Ral is essential for this process in higher eukaryotes but, puzzlingly, Ral is not present in yeast where the exocyst was first identified. Ral also regulates receptor-mediated endocytosis but this is achieved via a distinct effector, RalBP1/RLIP76. RalBP1 binds to proteins associated with endocytosis but also contains a GAP-like domain for the Rho family GTPase, CDC42. It is via this activity that it may also regulate cell morphology. Given these myriad functions it is not surprising that Ral can contribute to cell proliferation and cancer.

R-Ras 1, 2, and 3

R-Ras, TC21 (R-Ras2), and M-Ras (R-Ras3) are closely related to Ras (Figure 3) and have overlapping signaling and biological function. However, although some activating mutations have been found in cultured cell lines, these GTPases appear to seldomly if ever be mutated in human cancers despite the transforming activity of laboratory-engineered mutants. R-Ras activates PI3K but does not regulate the Raf/ERK or RalGDS pathway. Distinct from H-Ras, it has been implicated in "inside-out" signaling, increasing the ability of integrin to bind extracellular matrix. This results in increased cell attachment and spreading. One study has implicated Rap1 as a mediator of R-Ras action, another example of a Ras protein cascade. The binding of R-Ras to focal adhesion kinase has also recently been reported, providing another avenue for it to regulate integrins and/or cell adhesion. Like R-Ras, TC21 and M-Ras also effectively activate PI3K. M-Ras preferentially activates B-Raf over the more common Raf-1 isoform. While M-Ras is most abundant in brain, the exact function of either M-Ras or TC21 is unclear.

Rap1 and 2

There are five members of the Rap cluster: Rap1A and 1B and Rap2A, 2B, and 2C. Rap1A/Krev-1 was isolated in 1988 due to sequence homology with Ras

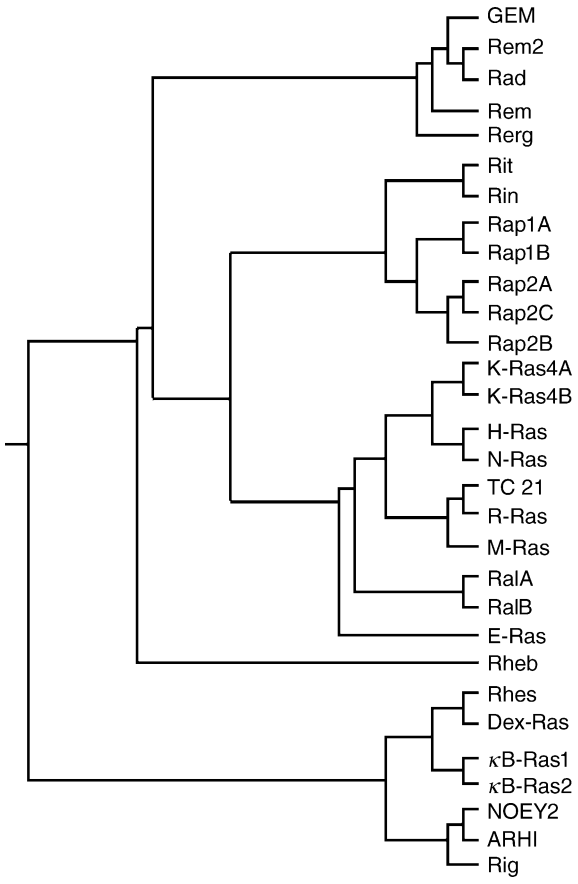

FIGURE 3 Dendrogram showing the relatedness of mammalian Ras subfamily GTPases.

(Ras proximate) and also due to its ability to revert the transforming activity of K-Ras. The revertant activity was believed due to Rap1A binding to Ras effectors and acting as a competitive antagonist of Ras. This indeed may be the true function of Rap in, e.g., T cells where Rap needs to be turned off by a costimulatory receptor such as CD28 in order for T cell receptor-induced activation of Ras to have its desired effect. However, the main role of Rap1 appears to be in the inside-out regulation of integrins. A Rap1 effector RAPL has recently been described in leukocytes that is responsible for promoting integrin clustering but how Rap regulated adhesion of cells in solid tissues has yet to be determined. While early studies described Rap1 and 2 localization to endocytic and Golgi membranes, recent studies have found Rap1 on epithelial cell junctions. It is likely that Rap1 and 2 plays multiple cell type-specific roles.

Rap1 and 2 are regulated by the same GEFs and GAPs. Strikingly, at least ten of the CDC25 family as well as the unrelated Smg GDS and DOCK4 proteins act as Rap GEFs suggesting that Raps play fundamental roles in cell biology that are triggered by a broad spectrum of extracellular stimuli. Signals from Ca^{2+}, diacylglycerol, receptor and nonreceptor protein tyrosine kinases, and cyclic AMP can all activate Rap. Indeed the protein kinase A-independent effects of cyclic AMP are due to activation of two Rap GEFs, Epac1 and 2 that contain cyclic nucleotide-binding domains. Several Rap GEFs contain RA domains, suggesting that they are recruited to membranes as downstream effector of other GTPases. This suggests that Rap activation may be a requisite for other Ras family members to execute their biological functions.

Rheb

Despite its name (Ras homologue expressed in brain), Rheb is found in many tissues. However it was discovered in 1995 as a protein whose expression was induced by synaptic stimulation. Although no Rheb GEFs have been found to date, Rheb's GTPase activity is regulated by TSC2, a tumor suppressor whose C terminus resembles Rap GAPs. Following loss of TSC2 or mutation of its GAP domain, the loss of GAP activity results in the accumulation of Rheb GTP. This activates a kinase cascade involving mTOR and ribosomal S6 kinase that promotes protein synthesis. Interestingly, Rheb is posttranslationally farnesylated similarly to H, K-, and N-Ras. It is therefore possible that Rheb represents an additional target of farnesyl transferase inhibitors designed to block Ras action and that these drugs might have use in the treatment of the proliferative disorders associated with tuberous sclerosis (TSC).

Other Ras Family Members

A number of additional GTPases exist (Figure 3) that are less well characterized but help exemplify the diversity of GTPase functions. These include ARHI/NOEY, Rig, and Rerg that have each been shown to play inhibitory roles. Critical conserved residues within their GTP-binding pockets diverge from those of most other Ras family members suggesting that these G proteins are constitutively GTP bound. The expression of these proteins can be induced by various agonists suggesting that they are regulated at the level of gene expression rather than by GEFs and GAPs. Further, it is their loss rather than mutation that contributes to cellular proliferation/transformation. Regulation at the level of transcription is not limited to these proteins; for example Dex-Ras expression is induced by corticosteroids, Rhes by thyroid hormone and as noted above Rheb by synaptic stimulation. Expression of many Ras family GTPases is also regulated by growth factors. Another branch of the Ras subfamily regulates transcription: κB-Ras binds to the IκB/NFκB complex and helps mask a nuclear localization sequence so that this transcription factor complex cannot translocate to the

nucleus and induce gene expression. The function of the Rad/Gem branch of the Ras family has until recently eluded investigators. However, they were recently shown to be negative regulators of the Rho–Rho kinase pathway, helping to explain their ability to modulate the actin cytoskeleton. Finally, several of the Ras family proteins lack the characteristic C-terminal CAAX box required for their posttranslational lipid modification. These include the closely related Rit and Rin proteins as well as Rerg and κB-Ras. While the former two proteins have been reported to regulate PC12, pheochromocytoma, cell differentiation, an event regulated by several Ras proteins via Raf and/or PI3K, Rit, and Rin appear to act via some alternative pathway(s). Interestingly, although Rit lacks any known recognition signal for C-terminal lipidation, Rit-transformed cell growth and survival in low serum is dependent on a farnesylated protein. Since most prenylated proteins are G proteins this suggests, once again, the existence of crosstalk between members of this subfamily of GTPases.

See Also the Following Articles

Rab Family • RAN GTPase • Small GTPases

Glossary

effector Proteins (typically enzymes) that GTP-bound Ras proteins bind to elicit a biological response.

GTPase Describes the intrinsic GTP hydrolyzing enzymatic activity of Ras. Binds GDP or GTP with high affinity and catalyzes the hydrolysis of GTP to GDP and phosphate.

GTPase activating proteins (GAPs) Negative regulators of Ras that bind the GTPase and accelerate its ability to hydrolyze bound GTP.

Guanine-nucleotide-exchange factors Upstream positive regulators of Ras proteins that promote increased nucleotide exchange so that Ras can bind to GTP.

isoprenylation Process of irreversible post-translational covalent modification of the C terminus of proteins by 15 carbon farnesyl or 20 carbon geranylgeranyl isoprene-derived lipids.

Ras A high-affinity guanine nucleotide-binding protein with intrinsic GTPase activity that acts as a molecular switch or bio-timer by cycling between inactive GDP- and active GTP-bound states.

Further Reading

Berg, J. M., Tymoczko, J. L., and Stryer, L. (2002). *Biochemistry*, 5th edition. W. H. Freeman, New York.

Bos, J. L., de Rooij, J., and Reedquist, K. A. (2001). Rap1 signalling: Adhering to new models. *Nat. Rev. Mol. Cell Biol.* **2**, 369–377.

Caron, E. (2003). Cellular functions of the Rap1 GTP-binding protein: A pattern emerges. *J. Cell Sci.* **116**, 435–440.

Feig, L. A. (2003). Ral-GTPases: Approaching their 15 minutes of fame. *Trends Cell Biol.* **13**, 419–425.

Hancock, J. F. (2003). Ras proteins: Different signals from different locations. *Nat. Rev. Mol. Cell Biol.* **4**, 373–384.

Quilliam, L. A., Rebhun, J. F., and Castro, A. F. (2002). A growing number of guanine nucleotide exchange factors is responsible for activation of ras family GTPases. *Prog. Nucl. Acid Res. Mol. Biol.* **71**, 391–444.

Takai, Y., Sasaki, T., and Matozaki, T. (2001). Small GTP-binding proteins. *Physiol. Rev.* **81**, 153–208.

Biography

Lawrence Quilliam received his Ph.D. from the University of Sheffield, England and obtained postdoctoral training at the Scripps Research Institute, La Jolla, CA. He is currently an Associate Professor of biochemistry and molecular biology at Indiana University School of Medicine and a member of the Walther Oncology Center. His research focuses on the delineation of cellular signaling pathways involved in cancer with particular emphasis on Ras family proteins and their guanine nucleotide exchange factors.

Recombination: Heteroduplex and Mismatch Repair *in vitro*

Leroy Worth Jr.
National Institute of Environmental Health Sciences, Research Triangle Park, North Carolina, USA

The methyl-directed repair pathway of *Escherichia coli* ensures genome stability by testing for the occurrence of mismatched base pairs. In addition to rectifying biosynthetic errors that occur through misincorporation during DNA biosynthesis, this pathway also controls the level of recombination between closely related sequences.

Mismatch Repair in Genetic Exchange

Early indications of the role of mismatch repair in genetic exchange were initially provided by the observation that null mutations in *mutS*, *mutL*, *mutH*, or *uvrD* genes result in a hyper-rec phenotype. Thus, in addition to replication error, DNA mismatches that arise during recombination are subject to the action of these activities. Specifically, the formation of hybrid or heteroduplex DNA during genetic exchange results in mispaired bases, which are formed at regions of sequence divergence between two homologous chromosomes. However, unlike mismatches produced during DNA replication, these mispairs are not necessarily promutagenic, but rather substrates for repair.

Homeologous recombination is defined as the genetic exchange between DNA sequences that are nearly identical. During this type of exchange, newly formed heteroduplex that failed to escape mismatch repair results in non-reciprocal exchange (gene conversion; non-Mendelian segregation), as one allele is replaced by the other.

Several studies have shown that as the level of divergence between DNAs decreases, so does the frequency with which they will recombine. Mismatch repair provides an efficient homology-sensing tool that assists in maintaining an energetic barrier to exchange between closely related sequences. Conversely, the low level of mismatches that happen to escape repair does not appear to be detrimental, but rather favors the appearance of newly formed recombinants, which may or may not be beneficial. Certainly, during meiotic recombination, a process required for proper chromosome segregation, a possible intolerable outcome of genetic exchange is imprecise chromosome disjunction.

The barrier to recombination caused by sequence divergence is most likely manifested at two distinct stages of recombination: the formation of heteroduplex joints and subsequent action of mismatch repair. The molecular steps of genetic recombination have been studied extensively in *Escherichia coli* and *Saccharomyces cerevisiae* and to a lesser extent in other systems. In *E. coli*, initial processing of the donor DNA is necessary to produce free single-stranded tails. The RecBCD enzyme unwinds and digests double-stranded DNA until a characteristic chi (χ) sequence (octanucleotide: 5′-GTCGGTGG-3′) is encountered. Once bound to chi, a cascade of events ensues, resulting in a free single-stranded 3′-end that is the substrate for RecA strand transfer. This free end is invasive and is able to displace one of the recipient strands in a RecA-dependent fashion.

In fact, no homologue of the RecD protein, which is necessary for DNA cleavage, is observed in *Bacillus*. All subsequent recombination functions are dependent on the function of RecA. The recombinant joint is subject to strand extension, branch migration mediated by the RuvAB (branch migration activity) complex, and editing. In *E. coli*, the editing process involves the methyl-directed mismatch repair system, controlled by the MutS and MutL proteins. In *Streptococcus pneumoniae*, the editing function is carried out by the homologous, nick-directed HexAB repair system. If mismatches are detected, the repair system may reject the entire donor strand and abort the recombination process.

RecA Strand Transfer

The level of homeologous recombination depends upon the degree of sequence divergence between the recombining sequences. It is known that independent of sequence identity, the degree of exchange is at least an order of magnitude lower than that between completely

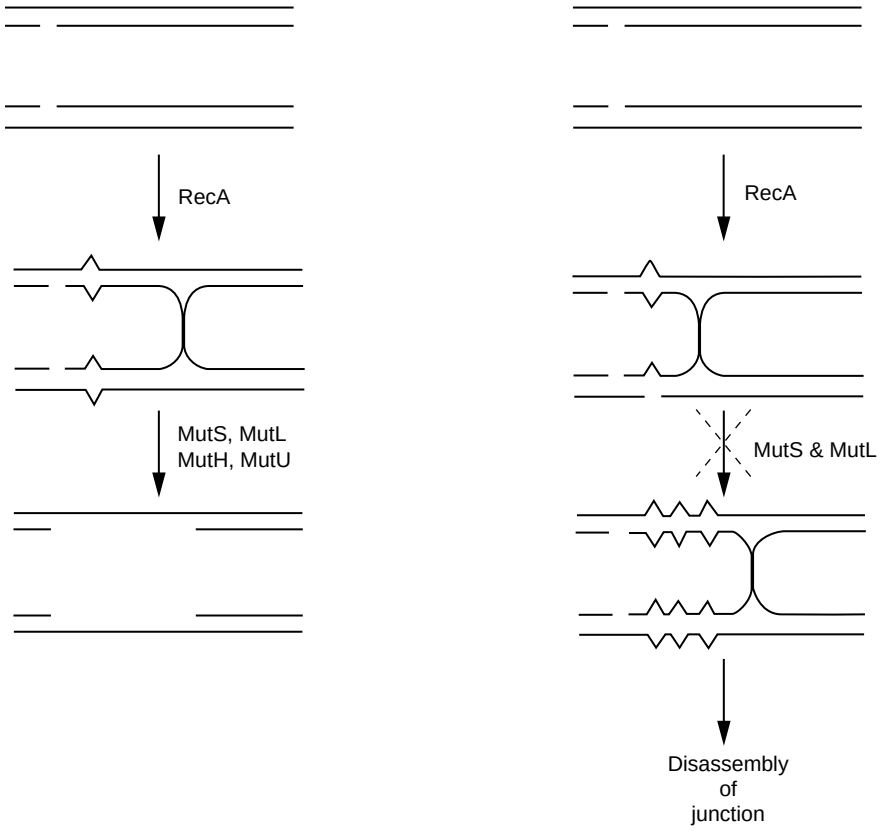

FIGURE 1 Potential mechanisms of DNA mismatch repair in modulating heteroduplex formation between divergent DNAs.

identical DNAs. This effect is remarkably independent of mismatch correction and can only be alleviated by the overproduction of proteins involved in recombination, specifically RecA protein.

The process of heteroduplex formation by RecA is associated with the initiation step of recombination and involves the formation of branched joints that proceed in a polarity-dependent fashion (Figure 1, top). These branched intermediates are stable and possess the ability to move through regions of lower sequence identity, thus the introduction of DNA mismatches. That near-perfect sequence identity is required for initiation is probably due to RecA-mediated homology search and the subsequent stability of the recombinant joint within the filament.

Mismatch Repair Mediates Heteroduplex Formation

DNA mismatch repair is able to recognize incorrect base pairs in DNA, but it is less known mechanistically as to how this pathway controls recombination between nearly identical DNAs. In terms of possible modes that could be envisioned, one might imagine that, as in replication fidelity, activities such as MutS and MutL could be involved in recognizing mismatches that are generated in newly formed heteroduplex. Indeed, these activities could act as a "mismatch sensing" and recognize regions of sequence divergence once they are encountered during the strand exchange process (Figure 1). Biochemical evidence for such a possibility was first demonstrated by studies of Worth *et al.* using purified *E. coli* repair activities. Both MutS and MutL proteins were shown to block RecA-mediated strand transfer between DNAs that shared more than 96% sequence identity. Specifically, using filamentous bacteriophage DNAs M13 and fd, whose DNAs share approximately 97% sequence identity, and the model three-strand *in vitro* transfer reaction, this study was able to show that RecA catalyzes the complete transfer of the complement strand, beginning with the 3′-end originating from a linear duplex molecule. The transfer of the complement results in a displaced linear single-strand that is formed from the 5′-end of the opposite strand, which in this case is identical in nature to the recipient DNA and the formation of full-length heteroduplex (Figure 1). This reaction requires the presence of single-stranded binding protein (SSB) and ATP. SSB acts to remove any secondary structure that might form and to aid in strand transfer by binding the growing displaced single-stranded DNA. Strand exchange between these DNAs (M13–fd) is not as efficient as those reactions carried out between identical DNAs

(e.g., M13–M13). This reduction in full-length heteroduplex suggests that the formation of mismatches, an indication of sequence divergence, acts as an energetic barrier to recombination.

MutS Inhibits Strand Exchange

Further data demonstrating the role of MutS in this process were provided by titration studies, which showed that increasing concentrations of this activity completely abolished heteroduplex formation between M13–fd DNAs. This process was shown to be dependent upon the formation of mismatches, as MutS had no effect on exchange reactions between identical DNAs. Because MutS is a known ATPase, and ADP is known to cause RecA to dissociate from DNA, it was thought that this inhibition could be due to an equilibrium shift in nucleotide, as more hydrolysis would occur for heteroduplex formation and therefore higher ADP pools. This possibility was shown not to be the case, however, as an ATP-regenerating system alleviated the potential to build up ADP and thus caused RecA to dissociate. Indeed, subsequent studies showed that mismatch recognition alone could act to block the heterologous reaction and thus partly explain the role of these activities in recombination.

MutL Enhances Inhibition

To test other components in the pathway, an additional *in vitro* study evaluated the role of MutL, if any, in this block. Studies involving equimolar MutS and MutL revealed an attenuated block of strand transfer between M13–fd DNAs beyond that exhibited by MutS alone. Although high concentrations of MutL alone failed to block strand transfer between these phage DNAs, it stimulated the inhibition afforded by MutS, as lower concentrations of this activity were required in eliminating full-length heteroduplex formation. This level of inhibition by mismatch repair was afforded when these individual activities were present in a 1:1 stoichiometry. Again, these activities did not inhibit DNA exchange as catalyzed by RecA when the donor and recipient DNAs were identical. This inhibition of the heterologous reaction thus demonstrates an act of synergy between these activities in sensing for the occurrence of DNA mismatches. Similar to replication fidelity, these components appear to act in concert to impose their anti-recombinogenic activity.

Recent studies have evaluated the role of mismatch repair in mediating downstream components of recombination, specifically RuvAB complex. These activities are involved in branch migration and are more efficient than RecA in extending newly recombinant DNA. Recent studies have shown that MutS and MutL also act to mediate branch migration as a consequence of the activities, which are not subject to the polarity restrictions associated with RecA. This observation suggests that mismatch repair might have a role in the resolution of DNA joints that are in the vicinity of DNA sequence divergence.

Alternative Role of Repair in Recombination

A second possibility to explain mismatch repair anti-recombination activity, which should not be viewed as mutually exclusive, is the removal of the invading strand through the recruitment of downstream components of the repair pathway (Figure 1). Indeed, similar to the proposed role of the *E. coli* system, these activities could react to the recombination intermediates by a mechanism similar to that for replication fidelity. The excision system could eradicate the newly formed intermediates by mismatch-dependent loading on the invading strand. In this case, mismatch detection along with a 3′-end would suffice as normal repair signals and thereby act to abort the recombining event through removal of the invading strand and full recovery of the recipient DNA through DNA synthesis. This process would require the unwinding activity of helicase II, which drives orientation-specific loading of the proper excision machinery.

The role of DNA repair in modulating heteroduplex formation is ongoing, and continued studies will seek to define how these activities regulate the frequency of genetic exchange as a function of sequence divergence.

See Also the Following Articles

DNA Mismatch Repair: *E. coli* Vsr and Eukaryotic G–T Systems • DNA Mismatch Repair in Bacteria • Recombination: Strand Transferases

Glossary

filamentous bacteriophage Viral non-lytic ssDNA encapsulated in coat protein (capsid).

full-length heteroduplex A process involving the complete transfer of an invading (donor) single-strand DNA to the recipient complement.

heteroduplex The joining or annealing of two single strands originating from differing origins.

homeologous Similar but non-identical in nature.

homoduplex The joining or annealing of two single strands originating from identical origins.

recombination A combining of nucleotide sequences or genes different from what they were in the parents.

transformation The heritable conversion in properties of a competent bacterium by DNA from another bacterial strain.

Further Reading

Au, K. G., Welsh, K., and Modrich, P. (1992). Initiation of methyl-directed mismatch repair. *J. Biol. Chem.* **267**, 12142–12148.

Abdulkarim, F., and Hughes, D. (1996). Homologous recombination between the tuf genes of *Salmonella typhimurium*. *J. Mol. Biol.* **260**, 506–522.

Burdett, V., Baitinger, C., Viswanathan, M., Lovett, S. T., and Modrich, P. (2001). *In vivo* requirement for RecJ, ExoVII, ExoI, and ExoX in methyl-directed mismatch repair. *Proc. Natl. Acad. Sci. USA* **98**, 6765–6770.

Datta, A., Adjiri, A., New, L., Crouse, G. F., and Jinks Robertson, S. (1996). Mitotic crossovers between diverged sequences are regulated by mismatch repair proteins in *Saccaromyces cerevisiae*. *Mol. Cell. Biol.* **16**, 1085–1093.

Fabisiewicz, A., and Worth, L., Jr. (2001). *Escherichia coli* MutS,L modulate RuvAB-dependent branch migration between diverged DNA. *J. Biol. Chem.* **276**, 9413–9420.

Humbert, O., Prudhomme, M., Hakenbeck, R., Dowson, C. G., and Claverys, J. P. (1995). Homeologous recombination and mismatch repair during transformation in *Streptococcus pneumoniae*: Saturation of the Hex mismatch repair system. *Proc. Natl. Acad. Sci. USA* **92**, 9052–9056.

Modrich, P., and Lahue, R. (1996). Mismatch repair in replication fidelity, genetic recombination, and cancer biology. *Annu. Rev. Biochem.* **65**, 101–133.

Petit, M. A., Dimpfl, J., Radman, M., and Echols, H. (1991). Control of large chromosomal duplications in *Escherichia coli* by the mismatch repair system. *Genetics* **129**, 327–332.

Selva, E. M., New, L., Crouse, G. F., and Lahue, R. S., (1995). Mismatch correction acts as a barrier to homeologous recombination in *Saccharomyces cerevisiae*. *Genetics* **139**, 1175–1188.

Stambuk, S., and Radman, M. (1998). Mechanism and control of interspecies recombination in *Escherichia coli*. I. Mismatch repair, methylation, recombination and replication functions. *Genetics* **150**, 533–542.

Worth, L. J. Jr, Clark, S., Radman, M., and Modrich, P. (1994). Mismatch repair proteins MutS and MutL inhibit RecA-catalyzed strand transfer between diverged DNAs. *Proc. Natl. Acad. Sci. USA* **91**, 3238–3241.

Worth, L., Jr., Bader, T., Yang, J., and Clark, S. (1998). Role of MutS ATPase activity in MutS,L-dependent block of in vitro strand transfer. *J. Biol. Chem.* **273**, 23176–23182.

Zahrt, T. C., and Maloy, S. (1997). Barriers to recombination between closely related bacteria: MutS and RecBCD inhibit recombination between *Salmonella typhimurium* and *Salmonella typhi*. *Proc. Natl. Acad. Sci. USA* **94**, 9786–9791.

Biography

Leroy Worth, Jr., is a Scientific Review Administrator at the National Institute of Environmental Health Sciences (NIEHS), in the Division of Extramural Research Training. He was previously a researcher in the NIEHS Laboratory of Molecular Genetics. Dr. Worth holds a B.S. in chemistry from the University of North Carolina and a Ph.D. in biochemistry from the University of Maryland. He did post-doctoral training with Dr. Paul Modrich at Duke University. Dr. Worth's major research interest is in DNA replication/repair mechanisms and oxidative stress.

Recombination: Strand Transferases

Floyd R. Bryant
The Johns Hopkins University, Baltimore, Maryland, USA

The recombination of homologous DNA molecules plays a central role both in gene rearrangement reactions and in the repair of damaged DNA. Genetic and biochemical studies have established that homologous recombination proceeds via the formation of intermediate structures in which the two recombining DNA molecules are joined together by single-stranded crossover connections. A continuing strand exchange between the two polynucleotide chains can then occur, leading to the generation of heteroduplex DNA. The formation of the recombinational intermediates is carried out by a class of proteins known as recombination strand transferases or DNA recombinases.

DNA Recombinases

The most well-studied members of this class of proteins are the bacterial RecA proteins and the eukaryotic Rad51 proteins. Other members of this class include the archaeal RadA proteins and the bacteriophage T4 UvsX protein.

Bacterial RecA Proteins

The prototypical DNA recombinase is the RecA protein of *Escherichia coli* (*E. coli*). Genetic studies have shown that the RecA protein is involved in virtually all aspects of homologous recombination in *E. coli*. Moreover, *E. coli recA* mutants are highly susceptible to DNA damaging agents (e.g., ultraviolet light or chemical mutagens), and in recent years the central role played by the RecA protein in recombinational DNA repair has been more clearly defined.

The *E. coli* RecA protein is composed of 352 amino acids (37 842 Da). The purified RecA protein binds to DNA, is a DNA-dependent ATPase, and promotes a variety of ATP-dependent DNA strand transfer reactions that are presumed to reflect *in vivo* recombination functions. In addition to its strand transfer activities, the RecA protein also promotes the autocatalytic cleavage of several proteins that are involved in the bacterial response to DNA damage. Although the *E. coli* RecA protein is the best characterized of the bacterial RecA proteins, RecA-like genes have been identified in all bacterial species that have been examined and RecA protein homologues have been analyzed from several other bacterial species, including *Bacillus subtilis* and *Streptococcus pneumoniae*.

Eucaryotic Rad51 Proteins

Eucaryotic homologues of the RecA protein, the Rad51 proteins, have been isolated and characterized from yeast and from human cells. The Rad51 proteins have been shown to play an essential role in DNA recombination and repair in eucaryotic cells.

The human and yeast Rad51 proteins are composed of 339 amino acids (36 966 Da) and 400 amino acids (42 961 Da), respectively. Although not as extensively investigated as the *E. coli* RecA protein, the human and yeast Rad51 proteins have been shown to promote ATP-dependent strand exchange reactions that are generally similar to those of the *E. coli* RecA protein.

A second group of eucaryotic RecA homologues which function specifically during meiosis, the Dmc1 proteins, has been isolated and characterized from yeast and human cells. However, the DNA strand exchange properties of the Dmc1 proteins have not yet been fully evaluated.

Other RecA Homologues

RecA-like proteins, known as the RadA proteins, have also been isolated and characterized from various archaeal cells, including *Sulfolobus solfataricus* and *Archaeoglobus fulgidus*. In addition, a RecA-like protein, the UvsX protein, is encoded by *E. coli* bacteriophage T4. The universal presence of RecA-like proteins suggests that functionally related homologous recombination and recombinational DNA repair systems are operative in all organisms.

Structure

The RecA and Rad51 proteins have been analyzed by a variety of structural methods. X-ray crystallography and electron microscopy have been especially useful in identifying the functional form of these proteins.

X-Ray Crystallography

The three-dimensional structure of the *E. coli* RecA protein has been determined by X-ray crystallography. The RecA protein consists of a central core domain (amino acids 34–240) which contains the ATP-binding site and possibly the DNA-binding site(s), and a smaller amino-terminal domain (amino acids 1–33) and carboxy-terminal domain (amino acids 241–352). Sequence comparisons indicate that a structurally similar central core domain is present in the Rad51 proteins. The Rad51 proteins, however, lack the carboxy-terminal domain found in the RecA protein, and have an extended amino-terminal domain that is not present in the RecA protein.

Electron Microscopy

Electron microscopy studies have shown that RecA protein monomers assemble on single-stranded DNA (ssDNA) in the 5′ to 3′ direction to form a right-handed helical nucleoprotein filament with one RecA monomer per three nucleotides of ssDNA, and approximately six RecA monomers per helical turn of the filament (Figure 1). The RecA protein forms a structurally similar filament on double-stranded DNA (dsDNA), with one RecA monomer per three base pairs of dsDNA.

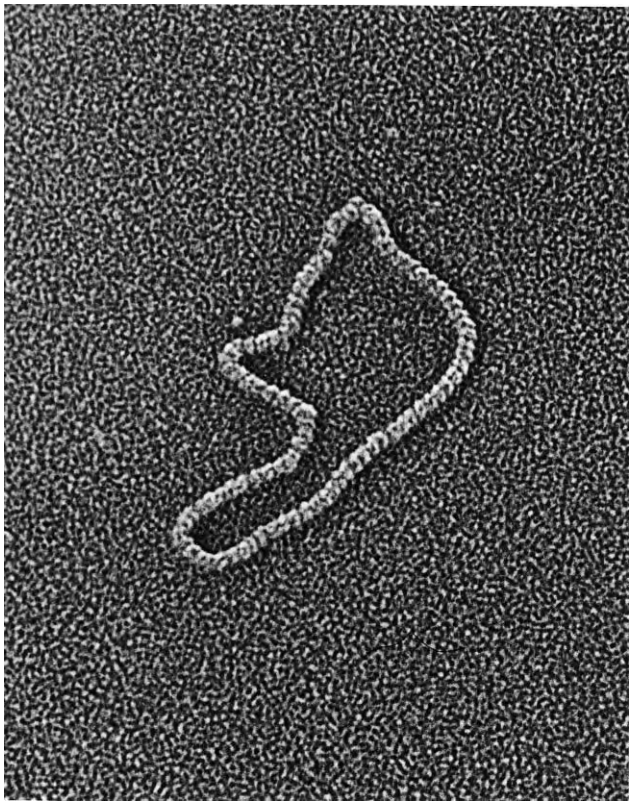

FIGURE 1 Circular ssDNA molecule covered by a helical filament of *E. coli* RecA protein (electron micrograph by Dr. Jack Griffith).

However, the binding to dsDNA is much slower than to ssDNA, and occurs only in the presence of ATP, whereas the binding to ssDNA occurs in either the presence or absence of ATP.

The conformation of the nucleoprotein RecA-DNA filament changes in response to the binding of nucleotide cofactors. In the absence of nucleotide cofactor, or in the presence of ADP, the filament adopts a compressed conformation with a helical pitch of ~70–85Å (seen on ssDNA only). In the presence of ATP, however, the filament assumes a more extended conformation with a helical pitch of 95Å (seen on ssDNA or dsDNA). In the ATP-activated state, the DNA inside the filament is stretched to 5.1Å per base/base pair (compared to 3.4Å per base pair in free dsDNA), and untwisted to 18.6 bases/base pairs per turn (compared to 10.5 base pairs per turn in free dsDNA).

The Rad51 proteins form filaments on DNA that are structurally similar to those formed by the RecA protein. This indicates that the altered conformation that is imposed on DNA in the ATP-activated state of the nucleoprotein filament is integral to the mechanism of action of the RecA and Rad51 proteins.

Model Reactions

The RecA and Rad51 proteins promote a variety of ATP-dependent DNA strand transfer reactions with defined DNA substrates. These reactions include D-loop formation and the three-strand exchange reaction.

D-Loop Formation

The RecA and Rad51 proteins can promote the pairing of a ssDNA with the complementary strand of a homologous covalently closed circular dsDNA to form a three-stranded structure known as a D-loop. However, because the dsDNA substrate lacks a free end, the invading ssDNA and the complementary strand from the dsDNA are unable to fully interwind, and the amount of strand transfer that can occur in this reaction is limited.

Three-Strand Exchange Reaction

The most extensively studied DNA strand transfer reaction is the three-strand exchange reaction, in which a circular ssDNA and a homologous linear dsDNA (typically from bacteriophage ϕX174 or M13 DNA; 5000–10 000 bases/base pairs in length) are recombined to yield a nicked circular dsDNA molecule and a linear ssDNA molecule. This reaction is a convenient model reaction for mechanistic studies because the substrates and products can be easily separated by agarose gel electrophoresis. Most of our understanding of the mechanism of action of the RecA

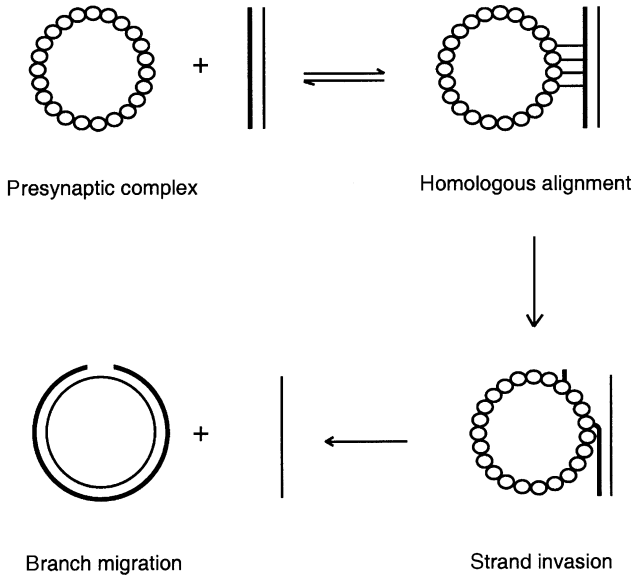

FIGURE 2 Schematic representation of the three-strand exchange reaction. A presynaptic complex (consisting of a circular ssDNA covered with a filament of RecA or Rad51 protein) interacts with a homologous linear dsDNA to produce a nicked circular dsDNA and a linear ssDNA. See text for details.

and Rad51 proteins has been derived from the study of this model reaction.

The three-strand exchange reaction proceeds in three distinct phases (Figure 2). In the first phase, stoichiometric amounts of RecA or Rad51 protein assemble onto the circular ssDNA substrate, forming a nucleoprotein filament known as the *presynaptic complex*. In the second phase, the presynaptic complex interacts with the linear dsDNA substrate, the homologous regions of the ssDNA and dsDNA are brought into register (*homologous alignment*), and new base-pairing interactions are formed between the circular ssDNA and the complementary strand of the linear dsDNA (*strand invasion*). In the third phase, strand exchange continues in a unidirectional manner, leading to the complete transfer of the complementary strand from the linear dsDNA to the circular ssDNA (*branch migration*).

ATP Hydrolysis

The RecA and Rad51 protein-promoted three-strand exchange reactions are absolutely dependent on ATP (or dATP) as a nucleotide cofactor. Curiously, however, the rate of ATP hydrolysis by the Rad51 protein ($0.1–1\ min^{-1}$) is much lower than that by the RecA protein ($20–30\ min^{-1}$). The mechanistic role of ATP hydrolysis in DNA strand exchange reactions is still poorly understood, and the functional significance of the difference between the RecA and Rad51 proteins is not clear. However, studies with nonhydrolyzable ATP analogues, and with mutant RecA proteins which bind but do not hydrolyze ATP, suggest that the homologous alignment and strand invasion reactions require ATP binding but not ATP hydrolysis, whereas the subsequent branch migration reaction may be coupled to the hydrolysis of ATP. These and other findings have led to the suggestion that the RecA protein may use the energy of ATP hydrolysis to actively drive branch migration. The Rad51 protein, in contrast, may stabilize the heteroduplex DNA formed by spontaneous branch migration in a process that is largely independent of ATP hydrolysis. Consistent with this view, it has been shown that RecA protein-promoted strand exchange proceeds uniquely in a 5′ to 3′ direction relative to the invading ssDNA (as expected for a coupled process), whereas the Rad51 protein-promoted reaction can proceed in either the 5′ to 3′ or 3′ to 5′ direction (as expected for a spontaneous process).

Accessory Proteins

The strand exchange activities of the RecA and Rad51 proteins are influenced by a host of recombination accessory proteins. These accessory proteins include the ssDNA-binding proteins and specialized recombination mediator proteins.

Single-Stranded DNA-Binding Proteins

The three-strand exchange activity of the RecA protein is stimulated by the *E. coli* SSB protein, a homotetrameric, non-sequence-specific, ssDNA-binding protein that is involved in many aspects of DNA biochemistry. SSB protein stimulates the strand exchange reaction both presynaptically (by removing secondary structure in the ssDNA substrate which otherwise impedes RecA binding) and postsynaptically (by binding to the displaced strand that is generated when the ssDNA substrate invades the homologous dsDNA). The strand exchange activity of the Rad51 protein is similarly stimulated by the heterotrimeric eucaryotic ssDNA-binding protein, replication protein A(RPA).

Mediator Proteins

The activities of the RecA and Rad51 proteins are also regulated by recombination mediator proteins. In bacterial systems, these mediator proteins include the RecO, RecR, and RecF proteins. The RecO and RecR proteins facilitate the binding of RecA protein to SSB protein-covered ssDNA and stabilize the resulting RecA-ssDNA filament, whereas the RecF and RecR proteins limit the extension of the RecA filament from an ssDNA gap or tail into an adjacent region of dsDNA. The best characterized

mediator of Rad51 protein activity is the Rad52 protein. The Rad52 protein, which may be a functional analogue of the bacterial RecO protein, stimulates Rad51 filament formation by facilitating the displacement of RPA protein from ssDNA.

Biological Reactions

The characterization of the biochemical activities of the RecA and Rad51 proteins has served to identify the mechanistic pathways that may occur in the cell during homologous recombination and recombinational DNA repair. The likely biological roles of the RecA and Rad51 proteins can be illustrated using the double-strand break repair model, which has emerged as a favored model for both the recombinational repair of fragmented DNA molecules and for programmed gene rearrangement reactions (Figure 3).

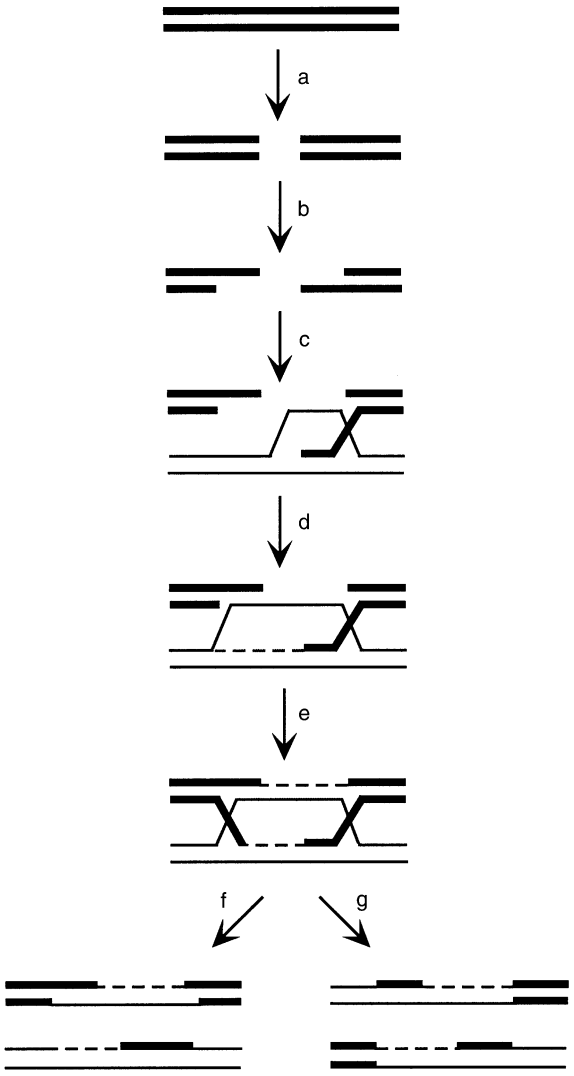

FIGURE 3 Schematic representation of the double-strand break repair model. The bold lines indicate a dsDNA undergoing a double-strand break, the thin lines indicate an intact homologous dsDNA, and the dashed lines indicate newly synthesized DNA. See text for details.

In this model, a double-strand break is introduced into a dsDNA molecule, either by a DNA-damaging agent or by a recombination-specific nuclease (*step a*). The ends of the two dsDNA fragments are then processed by specific nucleases so as to produce 3′-single-stranded "tails" (*step b*). RecA or Rad51 protein then assembles onto each of the single-stranded tails (with the assistance of various accessory proteins) to form active presynaptic nucleoprotein filaments. The single-stranded tail from one DNA fragment then pairs with an intact homologous dsDNA molecule (*step c*), forming a D-loop structure. The ssDNA tail from the second DNA fragment then pairs with the resulting displaced strand (*step d*). This sequence of strand transfer steps links the DNA molecules together by two single-stranded crossover connections, known as "Holliday junctions." A continuing strand exchange reaction, together with the synthesis of new DNA, results in the formation of regions of heteroduplex DNA in the linked DNA molecules (*step e*). Finally, cleavage of the crossover connections by a DNA junction-specific nuclease results in the separation or resolution of the two DNA molecules. Depending on direction of cleavage, the resolution step can produce either two DNA molecules that have been rejoined in the original linkages (*step f*), or two DNA molecules in new recombinant linkages (*step g*).

See Also the Following Articles

Cell Cycle: DNA Damage Checkpoints • DNA Mismatch Repair and Homologous Recombination • DNA Mismatch Repair and the DNA Damage Response • Homologous Recombination in Meiosis • Recombination: Heteroduplex and Mismatch Repair *in vitro* • X-Ray Determination of 3-D Structure in Proteins

Glossary

adenosine triphosphate (ATP) A nucleoside triphosphate whose hydrolysis to adenosine diphosphate (ADP) and phosphate can be coupled to various energy-requiring processes in the cell.

ATPase An enzyme that catalyzes the hydrolysis of ATP to produce ADP and phosphate.

heteroduplex DNA Double-stranded DNA formed from complementary single strands derived from two different DNA molecules.

homologous recombination Recombination between two DNA molecules with similar sequences.

nuclease An enzyme that catalyzes the hydrolysis of phosphodiester bonds in DNA or RNA.

Further Reading

Bianco, P. R., Tracy, R. B., and Kowalczykowski, S. C. (1998). DNA strand exchange proteins: A biochemical and physical comparison. *Front. Biosci.* **3**, d570–d603.

Cox, M. M. (2001). Historical overview: Searching for replication help in all of the rec places. *Proc. Natl Acad. Sci. USA* **98**, 8173–8180.

Egelman, E. H. (2003). A tail of two polymers: New insights into helical filaments. *Nat. Rev. Mol. Cell. Biol.* **4**, 621–630.

Lusetti, S. L., and Cox, M. M. (2002). The bacterial RecA protein and the recombinational DNA repair of stalled replication forks. *Annu. Rev. Biochem.* **71**, 71–100.

West, S. C. (2003). Molecular views of recombination proteins and their control. *Nat. Rev. Mol. Cell. Biol.* **4**, 1–11.

Biography

Floyd Bryant is a Professor in the Department of Biochemistry and Molecular Biology at the Johns Hopkins University, Bloomberg School of Public Health. He holds a Ph.D. from the Pennsylvania State University and received his postdoctoral training at Stanford University. His principal research interests are in the mechanistic analysis of bacterial RecA proteins and in the role of DNA recombination in the development of antibiotic resistance in pathogenic bacteria.

Recombination-Dependent DNA Replication

Kenneth N. Kreuzer
Duke University Medical Center, Durham, North Carolina, USA

Over the last several decades, the processes of homologous genetic recombination and DNA replication have largely been studied in isolation from one another. However, beginning with a few studies of bacteriophages in the 1960s and 1970s, the possibility emerged that extensive DNA replication can sometimes be triggered by homologous genetic recombination. Over the last several years, scientists working with diverse organisms have shown that recombination-dependent DNA replication (RDR) is very common and that this process provides an important back-up mechanism for completing DNA replication when replication forks fail. Mutational inactivation of certain proteins that are involved in RDR or related processes can lead to genome instability and a predisposition to cancer in higher organisms.

Early Models of Homologous Recombination Invoke RDR

One of the early molecular models for homologous recombination, called break-and-copy, invoked *r*ecombination-*d*ependent DNA *r*eplication (RDR). One simple version of this model invoked a break in one molecule, with a resulting 3′ broken end being used as primer for DNA replication. Another DNA molecule, of different parentage, is used as the template, resulting in a genetic crossover in the resulting DNA molecule.

As the field progressed, evidence accumulated in a number of systems for break-and-rejoin models, without extensive DNA replication, and break-and-copy models fell into disrepute. We now understand that there are indeed many pathways of homologous recombination that do not involve extensive DNA replication, but also some very important recombination pathways that trigger extensive replication, as in the original break-and-copy models.

Modern versions of the break-and-rejoin model, such as the Meselson–Radding and double-strand-break repair (DSBR) models, invoke limited DNA replication events (e.g., gap filling) to fill in missing information. Such limited replication will not be considered here as RDR. Rather, the definition of RDR will be restricted to those events that are dependent on homologous recombination proteins and capable of replicating large portions of a chromosome.

RDR Pathways in Bacteriophage

Most of the early data arguing for the existence of RDR came from studies of bacterial viruses. For example, recombination-deficient mutants of well-known bacteriophages such as T4, T7, and lambda were found to be partially defective in DNA replication. The interpretation of that replication defect has not been straightforward, because recombination reactions can play indirect roles in viral DNA replication. For example, if recombination links multiple bacteriophage genomes together into a linear concatamer, a single initiation event from a conventional replication origin can result in much more DNA replication than if the genomes are not linked. Furthermore, recombination proteins might play a role in converting a theta-form replication intermediate into a rolling circle, resulting in numerous replication products rather than just two.

Studies with bacteriophage T4, however, demonstrated that the involvement of homologous recombination proteins in DNA replication is very direct. At early times of infection, T4 DNA replication initiates at replication origins by a mechanism that involves a persistent RNA–DNA hybrid (R-loop), but this origin-dependent replication is turned off after several minutes. For the remainder of the infection cycle, all DNA replication initiates by an RDR mechanism in which a fully functional replication complex is assembled on a displacement loop (D-loop; Figure 1). The D-loop is formed when the 3′ single-stranded end of one phage DNA molecule invades a homologous region of another phage DNA molecule, or the other end of the same molecule (since T4 DNA is terminally redundant).

Most or all D-loop formation depends on the phage-encoded UvsX and UvsY proteins, acting in concert with the T4 single-stranded DNA binding protein gene

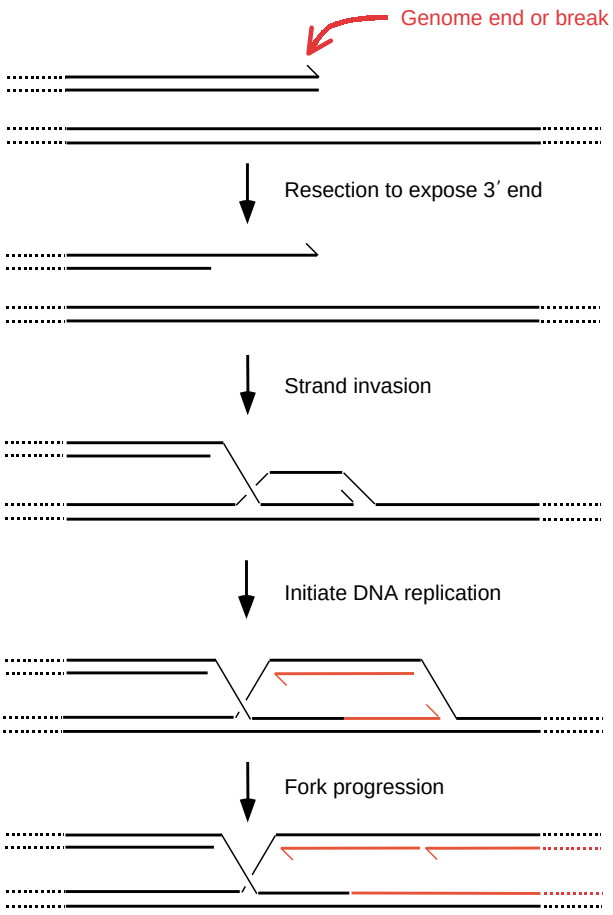

FIGURE 1 Model for bacteriophage T4 RDR. A single-stranded 3′ end is generated from a genomic end or break in the first step, either by exonuclease resection or by prior DNA replication up to the end (not shown in the figure). The strand invasion step creates a D-loop, upon which replication is initiated after assembly of the replication complex. The dotted lines indicate extended regions of the phage chromosome, and all newly replicated DNA is in red.

*p*roduct 32 (gp32). UvsX is a strand invasion protein, homologous to bacterial RecA and eukaryotic Rad51 protein, while UvsY plays the key role of loading UvsX onto gp32-coated single-stranded DNA (i.e., the 3′ end).

Once a D-loop is formed, the phage protein gp59 is the critical component that directs the replication machinery to the D-loop. The gp59 protein preferentially binds branched DNA and also gp32-coated DNA, and one or both of these preferences are thought to explain D-loop recognition. Gp59 has been first identified based on its ability to stimulate the loading of the replicative helicase (gp41) onto DNA during *in vitro* replication reactions. Once the replicative helicase is loaded, more extensive template unwinding, loading of additional replication proteins, and extensive DNA replication becomes possible. Proteins that allow the loading of replicative helicases onto recombination intermediates are central to the process of RDR, and the corresponding bacterial proteins will be discussed below.

There is now quite convincing experimental evidence for the T4 RDR pathway. A variety of physical and genetic experiments support the proposal that genome ends trigger DNA replication after a strand-invasion reaction. Furthermore, artificially introduced double-strand breaks (DSBs) dramatically stimulate the replication of homologous DNA *in vivo*. Finally, a robust *in vitro* system of RDR has been established using the T4 system, and recapitulates the major features of *in vivo* RDR.

Demonstration of RDR in *Escherichia coli* and Yeast

An apparent cellular RDR pathway, called inducible stable DNA replication (iSDR), was first uncovered by the late Tokio Kogoma and colleagues. They found that *E. coli* cells deficient in normal origin-directed replication can nonetheless replicate if their SOS system for DNA damage response is activated. This DNA replication required the strand invasion protein RecA, and a variety of results led to the proposal that iSDR also required chromosomal DNA breaks induced by some component of the SOS system. The simplest model is that the induced DNA breaks lead to invasive 3′ ends, and that resulting D-loops become the sites of assembly of new replication complexes (much like in Figure 1). More recent experiments have demonstrated that artificially induced DSBs can indeed trigger DNA replication in *E. coli*, providing strong support for a cellular pathway of RDR.

A key protein for *E. coli* RDR is PriA, which like T4 gp59, allows the loading of the replicative helicase (DnaB in this case) onto D-loop structures. Several other *E. coli* proteins, including DnaC, PriB, and PriC, can also participate in this reaction. The importance of PriA in the survival of *E. coli* will be discussed later, when we consider the role of RDR in completing genome replication. It is interesting to note at this point, however, that mutational inactivation of PriA dramatically reduces phage P1-mediated generalized transduction and also conjugal recombination. Therefore, these seemingly well-studied genetic pathways, which had been thought for decades to occur by a break-and-rejoin-like mechanism, may actually occur by a mechanism similar to RDR.

RDR is apparently not limited to prokaryotic systems such as T4 and *E. coli*. Indeed, genetic experiments have provided very strong evidence that RDR is a legitimate pathway of DNA break repair in the yeast *Saccharomyces cerevisiae*. Several different genetic approaches have revealed RDR in yeast. One approach used a diploid cell with a site that can be cleaved to create a DSB on one of the two copies of a particular chromosome (Figure 2). The arms of the two

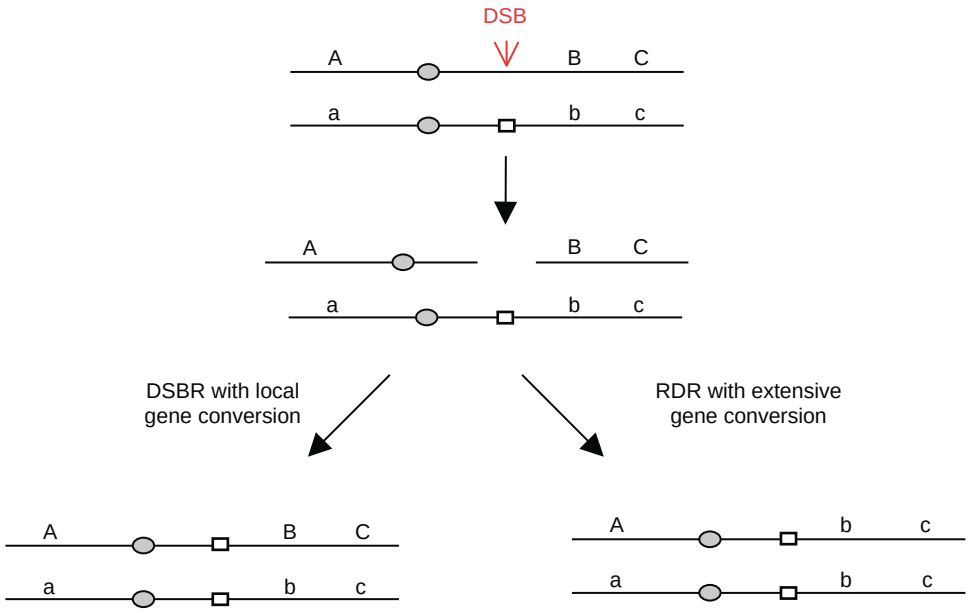

FIGURE 2 Two pathways for repair of a chromosomal DSB in yeast. Repair of a DSB occurs by a localized DSBR pathway on the left side; this pathway involves the reattachment of the two broken arms and a small region of DNA replication to replace any missing DNA near the break site. In the pathway on the right side, the smaller chromosomal fragment (containing alleles B and C) is lost. However, an intact chromosome is regenerated by an RDR reaction in which the broken end of the larger chromosomal fragment invades the intact homologous chromosome, and then triggers a DNA replication fork that travels to the end of the intact chromosome. This duplicates the chromosomal arm that contains alleles b and c, and with Holliday junction resolution, provides the cell with two complete and intact chromosomes to fulfill the diploid state. In this figure, each solid line is a DNA double helix, and gray ovals indicate centromeres. The downward pointing arrow indicates the site for the DSB, while the empty box indicates the DNA sequence at the corresponding site on the noncleavable chromosome (the sequences in this region of the two chromosomes are different from each other). Based on Malkova *et al.* (1996). *Proc. Natl Acad. Sci. USA* **93**, 7131–7136.

chromosomes were marked with a series of heteroalleles (indicated by the letters A/a, B/b and C/c in Figure 2). In wild-type cells, when the DSB is induced on the top chromosome, the diploid that resulted from DSB repair usually maintained each of the three pairs of heteroalleles, indicating a local DSBR event that caused gene conversion at the site of the DSB and that reattached the broken distal arm of the chromosome (Figure 2; left). At a low frequency, however, the resulting diploid cell experienced an extensive gene conversion event in which all alleles in the arm distal to the DSB had been converted to the form that was originally located on the unbroken (homologous) chromosome (Figure 2; right). Apparently, the distal chromosomal fragment with the "B" and "C" alleles had been lost, and replaced with a newly replicated copy of the distal arm from the unbroken chromosome.

While these RDR products were normally quite rare in wild-type cells, they became predominant when the cells had a mutation that inactivated the Rad51 protein (strand invasion protein, homologous to RecA/UvsX). Also, when the experimental setup was altered so that the distal fragment of the broken chromosome had no homology to the intact chromosome, wild-type cells efficiently utilized this RDR pathway to regenerate an intact chromosome. The only general mechanism to explain this extensive gene conversion of a large portion of a chromosome is that the centromere-proximal chromosomal end undergoes a strand-invasion reaction with the homologous chromosome, and the resulting D-loop triggers a new replication fork just as in the RDR pathways.

RDR as a Backup Mechanism to Complete DNA Replication

Nearly 30 years ago, Ann-Marie Skalka proposed that recombination could provide a mechanism for creating new replication forks after a previous fork encountered a template nick. Her proposal dealt with the complexities of phage lambda DNA replication, and has not been ascribed any broader significance for some time. However, many years later, scientists realized that a similar mechanism provides a means of restarting a replication fork that has been destroyed by a template nick. As diagrammed in Figure 3, when a replication fork encounters a template nick, one of the two arms can be broken off and replication thereby terminated. The broken end can be reconfigured into a replication fork by first forming a D-loop using a strand-invasion

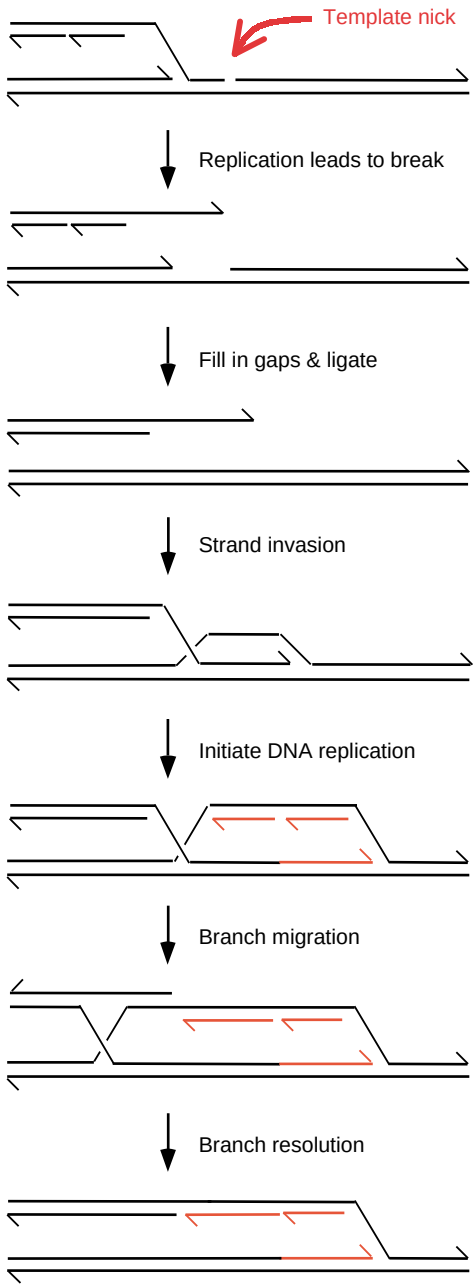

FIGURE 3 Replication fork breakage at a nick and restart by recombination. A template nick leads to a broken fork, which is then restarted by RDR. Note that one DNA strand has been flipped to the top in the molecule immediately after the arrow indicating branch migration (because DNA is a double helix but the drawing depicts only parallel lines, this flipping is just a convenience to make the drawing simpler).

reaction, and then assembling a replication complex onto the D-loop. Subsequent branch migration and junction resolution can thereby regenerate a simple replication fork and allow the completion of replication and normal segregation of the products at the next cell division (Figure 3).

We now believe that this pathway explains why many recombination-deficient mutants of bacteria and yeast grow poorly – they have great difficulty completing DNA replication due to problems at the fork. Notably, PriA-deficient mutants of *E. coli*, whose primary defect is in replication fork restart, are nearly inviable and quickly accumulate suppressor mutations that improve their viability.

In vivo experiments have demonstrated that replication forks are indeed broken when they encounter a template nick. It is not clear how often replication forks encounter template nicks, but broken replication forks also arise by another pathway that could be even more common. In bacterial and phage systems, it has been demonstrated that certain stalled or blocked replication forks are prone to breakage. This breakage depends on the branched-DNA-specific nucleases that normally resolve Holliday junctions (i.e., *E. coli* RuvC and T4 endonuclease VII). Results in eukaryotic systems also suggest that some blocked forks are broken, although the identity of the cleaving nuclease is uncertain.

It may seem strange that blocked replication forks would be actively cleaved by recombination nucleases, and this is indeed a dangerous reaction. However, this cleavage is apparently under strict control, and may only be used as a "last resort" when a stalled or blocked replication fork cannot be restarted by other mechanisms. By coupling fork cleavage with an RDR reaction, the replication fork can potentially be restarted and the cell saved from the dire consequences that result from trying to segregate a partially replicated DNA molecule in the next cell division.

With this new view that recombination provides a back-up mechanism to restart broken replication forks, it is worth reconsidering an interesting question from evolutionary biology—how and why did homologous recombination evolve? It is now clear that homologous recombination can play an important role at the level of single cell survival, namely the completion of DNA replication. Furthermore, it seems likely that DNA replication was even more prone to failure early in the evolution of cells, before very sophisticated replication machineries and repair pathways have been fully developed. Therefore, many scientists in the field now believe that homologous recombination first evolved as a means to complete cellular DNA replication, and that all the other wonderful benefits of recombination came later.

Replication Fork Failure and Direct Restart Pathways

The above description of replication fork restart is incomplete, focusing only on the restart of forks that end up being broken. As might be expected, other pathways

are able to directly restart stalled or blocked replication forks without the dangerous step of breaking the fork. Indeed, bacterial cells have multiple pathways for directly restarting forks. Although these pathways need not involve any recombination of the DNA molecules, some of the proteins that are involved in direct restart pathways are nonetheless recombination proteins that play roles in recombinational restart or other homologous recombination pathways.

One of the important unanswered questions is the fate of the various components of the replication machinery when forks are blocked or stall. It is clear that replication fork restart pathways require proteins that can load the replicative helicase, and so by inference, the replicative helicase seems to be lost when forks stop prematurely. We don't know which other components of the replication machinery are lost upon fork failure. Because the replicative helicase is thought to encircle the lagging-strand template, it is presumably lost whenever that strand is broken. In other cases (e.g., breakage of the leading strand and fork arrest without breakage), it remains to be determined how exactly the helicase is lost, and for that matter, whether the helicase is lost in only a subset of replication fork failures.

There are many possible reasons why a replication fork might stop prematurely. For example, a particular nucleotide might be temporarily limiting, a noncovalently bound protein might be encountered on the template duplex, or one of the key proteins of the replication machinery might become damaged or displaced from the replication fork. Sidestepping the question of how and why the replicative helicase and other proteins might be lost from such a fork, it is easy to see how direct restart pathways can solve the immediate problem and allow a completion of DNA replication.

However, the true complexities and benefits of replication fork restart pathways only become obvious when we consider other problems that a replication fork can encounter, particularly the many different forms of template DNA damage. The most obvious problem is when the replication machinery encounters a damaged base on the leading-strand template. In this case, one can easily see the advantage of disassembling the normal replication machinery—namely that an appropriate DNA repair complex can be recruited to fix the template damage or, if that fails, a translesion DNA polymerase can be recruited to incorporate something opposite the damaged base (Figure 4; left). After the repair or translesion synthesis event, the normal replication machinery would need to be assembled to resume replication, hence the need for a direct restart pathway (or an RDR event if the fork has become broken). This description of the behavior of the replication fork at sites of template DNA damage is very superficial and incomplete, in part because there are many forms of damage and multiple pathways of repair. The more serious limitation at this time, however, is that the field is just beginning to investigate what promises to be a very rich area, this interface where DNA replication, repair and recombination all intersect at troubled replication forks.

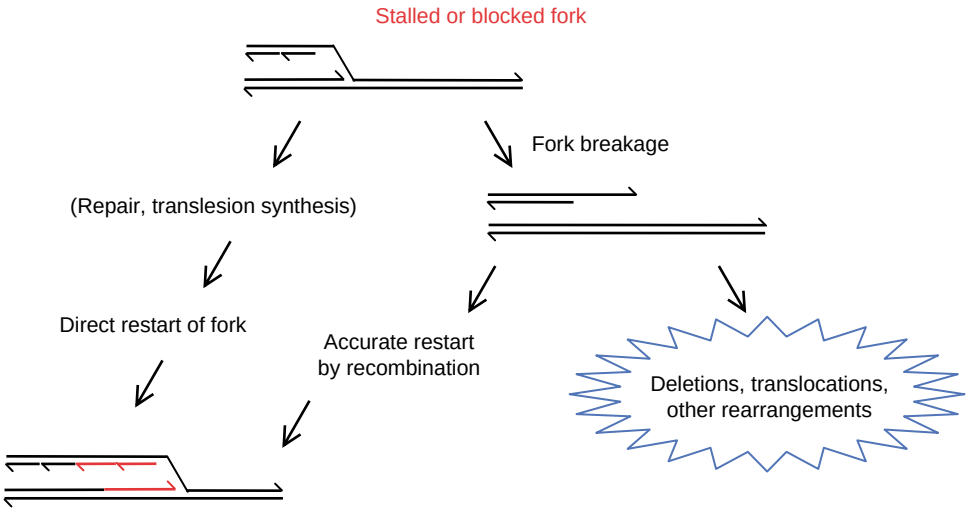

FIGURE 4 Pathways for restarting replication forks. Replication forks may stall due to the absence of nucleotides or problems with the replication machinery, or may be blocked due to template damage or bound proteins ahead of the fork. If the fork is blocked by template damage, repair of the damage or translesion synthesis may precede direct fork restart. If the fork is simply stalled, direct fork restart can occur without repair. In either case, some or all of the replication proteins need to be reassembled on the fork to reinitiate replication. In the pathway on the right, the stalled or blocked fork is broken, for example, by a recombination nuclease. Accurate restart of the fork by RDR (as in Figure 3) can lead to a normal cell without any genetic damage, but failure of this accurate pathway can lead to chromosomal rearrangements.

Disturbances in Fork Processing Lead to Genome Instability and Cancer Predisposition

DNA breaks are inherently dangerous. A broken fragment of a chromosome that lacks the centromere may be lost during mitosis to generate a terminal chromosomal deletion (assuming that the centromere-containing fragment acquires a new telomere). A broken end might engage in a non-homologous end joining reaction, or if the end is located within a repeat region, might undergo homeologous recombination with another copy of the repeat. In both cases, chromosomal deletions, inversions, and translocations can result.

With an understanding that DNA replication can lead to DNA breaks, it is therefore not surprising to find a strong association between disturbances in replication fork processing and genome instability. For example, studies in *S. cerevisiae* have shown that mutational inactivation of genes involved in the recombinational restart of replication forks (RDR) leads to genome instability. Apparently, when the normal pathway of restarting broken forks is disturbed, the broken DNA can result in chromosomal rearrangements (Figure 4).

Cells from individuals who suffer from certain human cancer predisposition syndromes (Werner's, Bloom's, and Rothmund–Thomson syndrome) show increased genome instability. Genetic analysis has traced these defects to genes that encode proteins that are suspected to be involved in replication fork integrity, recombinational restart of broken forks, and/or direct restart pathways. All three of these proteins belong to the RecQ family of DNA helicases (named after the founding member, bacterial RecQ). The precise role of any of these proteins is presently unclear, but it is easy to imagine that genome instability could result from a defect in recombinational restart of broken forks, or from a higher incidence of replication fork breakage. Increased fork breakage could potentially arise from a defect in a protein that is involved in direct restart pathways, or from any mutation that leads to more frequent fork arrest.

In summary, the period since the early 1990s has seen a remarkable merger of studies of DNA replication, recombination, and repair. These three processes apparently participate in an intricate choreography that is necessary for the accurate and complete replication of the genome, which in turn is important for genome stability and for the prevention of cancer in humans.

See Also the Following Articles

DNA Replication Fork, Bacterial • DNA Replication Fork, Eukaryotic • Phosphoinositide 3-Kinase • Protein Kinase B

Glossary

direct restart pathways Pathways that restart replication forks that are intact but have become stalled or blocked.

gene conversion Nonreciprocal recombination event in which one allele is converted into the form of the second allele.

homeologous recombination Recombination between two nearly identical sequences that are not allelic (i.e., not at the same corresponding position on the chromosome).

recombination-dependent replication (RDR) Extensive replication of a chromosome that is dependent on homologous genetic recombination and recombination proteins.

recombinational restart The restart of replication forks by an RDR reaction.

Further Reading

Cox, M. M., Goodman, M. F., Kreuzer, K. N., Sherratt, D. J., Sandler, S. J., and Marians, K. J. (2000). The importance of repairing stalled replication forks. *Nature* **404**, 37–41.

Haber, J. E. (1999). DNA recombination: The replication connection. *Trends Biochem. Sci.* **24**, 271–275.

Hickson, I. (2003). RecQ helicases: Caretakers of the genome. *Nat. Rev. Cancer* **3**, 169–178.

Kogoma, T. (1997). Stable DNA replication: Interplay between DNA replication, homologous recombination, and transcription. *Microbiol. Mol. Biol. Rev.* **61**, 212–238.

Kowalczykowski, S. C., and von Hippel, P. H. (2000). Special issue: The DNA replication—recombination interface. *Trends Biochem. Sci.* **25**, 155–206.

Malkova, A., Ivanov, E. L., and Habes, J. E. (1996). Double-strand break repair in the absence of RAD51 in yeast: a possible role for break induced DNA replication. *Proc. Natl Acad. Sci. USA* **93**, 7131–7136.

McGlynn, P., and Lloyd, R. G. (2002). Genome stability and the processing of damaged replication forks by RecG. *Trends Genet.* **18**, 413–419.

Radding, C. (2001). Links between recombination and replication: Vital roles of recombination. *Proc. Natl Acad. Sci. USA* **98**, 8172. (This is the introductory article for a special colloquium issue, and is followed by numerous articles on the same topic.)

Skalka, A.-M. (1974). A replicator's view of recombination (and repair). In *Mechanisms in Recombination* (R. F. Grell, ed.), Plenum Press, New York, pp. 421–432.

Biography

Kenneth N. Kreuzer is a Professor of Biochemistry and Microbiology at Duke University Medical Center in Durham, North Carolina. He was trained as an undergraduate at MIT, earned his Ph.D. from the University of Chicago, and received his postdoctoral training at the University of California, San Francisco. The research interests in his laboratory include mechanisms of DNA replication, recombination and repair, and the mechanism of action of antitumor agents that target DNA topoisomerases.

recQ DNA Helicase Family in Genetic Stability

Mary A. Risinger and Joanna Groden
University of Cincinnati College of Medicine, Cincinnati, Ohio, USA

Helicases are enzymes that use nucleoside triphosphate (usually ATP) hydrolysis to unwind nucleic acid duplexes (DNA–DNA, RNA–RNA, or DNA–RNA). Most helicases exclusively unwind either DNA or RNA duplexes, although some can unwind DNA duplexes and RNA duplexes as well as DNA–RNA hybrids. Because virtually all forms of DNA metabolism (including transcription, replication, recombination, and repair) require the unwinding of double stranded DNA (to allow access to the bases which encode the genetic information), DNA helicases are essential to the function and maintenance of the genome. This article deals with one family of DNA helicases, the recQ family, named for the similarity of family members to the prototype *Escherichia coli* recQ helicase, which participates in the recF genetic recombination pathway. Loss of recQ helicase function results in a loss of genomic stability that can be manifested in various ways. In humans, loss of function of certain recQ helicases results in cancer predisposition and variable degrees of premature aging. The study of these ubiquitous and highly conserved proteins promises to yield important information concerning tumorigenesis and the aging process.

Classification of Helicases

By primary structure comparisons helicases are divided into five superfamilies. The recQ family belongs to superfamily II (Sf2), one of the largest of the superfamilies. All Sf2 helicases contain seven conserved helicase motifs designated I, Ia, II, III, IV, V, and VI. Motifs I and II are the Walker A and B sequences characteristic of ATPases. Motif II of recQ helicases contains the DEXH motif (single-letter amino-acid code) that is a major characteristic of this family and is essential for ATP hydrolysis and, consequently, for helicase activity.

In *E. coli*, recQ is the sole member of its family. Most lower eukaryotic organisms also have a single recQ helicase. Examples are sgs1 from the budding yeast, *Saccharomyces cerevisiae*, and rqh1 from the fission yeast, *Schizosaccharomyces pombe*. However, higher organisms generally have multiple recQ helicases, presumably needed to maintain more complex genomes. Humans have at least five recQ helicases encoded by the *BLM*, *RECQ1* (also referred to as *RECQL*), *RECQ4*, *RECQ5*, and *WRN* genes.

Human Genetic Disorders Resulting from Defects in recQ Helicases

Defects in three of the five human recQ helicases result in defined clinical disorders known as chromosome breakage syndromes (autosomal recessive human disorders characterized by spontaneous genomic instability). Bloom syndrome, Rothmund–Thomson syndrome, and Werner syndrome are caused by germ-line defects in the *recQ* genes *BLM*, *RECQ4*, and *WRN*, respectively. Hallmarks of these rare diseases are genomic instability (apparent at the cellular level), cancer predisposition, and variable characteristics of premature aging.

Bloom Syndrome

Bloom syndrome (BS) persons (who lack the BLM protein due to various mutations in the *BLM* gene) are proportional dwarfs with sun-sensitive facial erythema (redness), impaired fertility, immune deficiency, and a high incidence of almost all forms of cancer with a very early age of onset (average 24 years). This makes BS a particularly interesting model for the study of tumorigenesis since most other hereditary cancer predisposition disorders result in the development of site-specific cancers. Cells cultured from BS persons demonstrate genomic instability in the form of a higher rate of the same types of chromosomal aberrations detected in cells cultured from normal individuals. Chromosomal breaks and rearrangements that are a result of increased homologous recombination are frequently observed. The classic feature of BS cells, which is considered diagnostic of the disease, is a several-fold increase in the frequency of sister chromatid exchanges (SCEs; reciprocal exchanges of DNA between sister

chromatids by homologous recombination). BS cells also demonstrate an abnormal profile of DNA replication intermediates.

Rothmund–Thomson Syndrome

Rothmund–Thomson syndrome (RTS) persons have progressive poikiloderma (a variegated hyperpigmentation and telangiectasia of the skin, followed by atrophy) that is apparent in early childhood. Common characteristics include numerous skeletal abnormalities, thin hair, cataracts, hypogonadism, and short stature. RTS persons are primarily susceptible to a single type of cancer, osteosarcoma (median age of onset 12 years), but skin malignancies and other forms of cancer have also been reported. Cells isolated from RTS persons reveal genomic instability in the form of chromosome translocations, rearrangements, and deletions.

Werner Syndrome

Werner syndrome (WS) is a hallmark premature aging disease. It is generally not detected until adolescence when WS persons fail to undergo the usual growth spurt and begin to display symptoms of premature aging including graying and thinning of the hair, wrinkling of the skin, cataracts, type II diabetes mellitus, osteoporosis, and atherosclerosis. WS persons are short in stature due to lack of the adolescent growth spurt and often have reduced fertility. They demonstrate a high incidence of malignancies, particularly sarcomas. The major causes of death are malignancy and vascular disease (average lifespan 47 years). Cells isolated from WS persons have a reduced replicative lifespan (they divide fewer times before becoming senescent) and are marked by increased genomic instability in the form of chromosomal alterations including chromosome translocations, rearrangements, and large deletions.

Structural Characteristics of recQ Helicases

In recQ family members, the helicase domain containing seven helicase motifs (I, Ia, III–VI) is generally centrally located (Figure 1). Most recQ helicases also have an recQ family C terminal (RQC) domain located just C terminal to the helicase domain. Since mutations of conserved residues in this region severely decrease ATPase activity, helicase activity, and single stranded DNA binding, it has been suggested that this domain may be involved in coupling DNA binding to ATP hydrolysis. More distal to the helicase domain is another conserved C-terminal domain designated as the helicase RNase D C-terminal (HRDC) domain. The HRDC domain is thought to be an auxiliary DNA binding domain. Unlike the RQC domain that is characteristic of recQ helicases, the HRDC domain is also found in other types of DNA-binding proteins (including other helicases, recombinases, and polymerases). With the exception of a nuclear localization signal identified in some recQ helicases, there is little additional C-terminal homology among recQ helicases. N-terminal domains vary greatly in length among recQ family members and there is generally little homology in this region. Several family members have N-terminal acidic regions and some have C-terminal acidic regions, which may be involved in protein–protein interactions.

Functional Characteristics of recQ Helicases

All recQ helicases studied to date are ATP- and Mg^{2+}-dependent 3–5′ helicases, i.e., they translocate along the DNA strand to which they bind in the 3–5′ direction as they unwind duplex DNA. Human *WRN* helicase and frog *FFA-1* helicase are unique in that they also have a 3–5′ exonuclease activity. It has been difficult to define the functions of recQ helicases at the molecular level *in vivo*. Since higher organisms have multiple recQ helicases and the loss of function of a single recQ helicase is compatible with survival, it is likely that recQ helicases have some overlapping functions where the remaining helicases can partially compensate for the loss. (RecQ helicases must also have some independent functions since diseases associated with the loss of a particular helicase have distinct characteristics.) The processes in which recQ helicases are likely involved (replication, recombination, and repair) are also closely intertwined. Clues to the *in vivo* functions of recQ helicases are provided by associated clinical syndromes (described above), *in vitro* studies, and *in vivo* localizations and associations.

Functional Clues Provided by *in vitro* Studies

RecQ helicases are unusual among helicases in their DNA substrate preferences. Although they are generally unable to unwind blunt-ended duplex DNA (unless a bubble is present), they efficiently unwind such non-Watson–Crick DNA structures as G-quadruplexes (extremely stable DNA secondary structures that can form in guanine-rich regions of DNA) and Holliday junctions (four-way crossover structures formed by DNA strand exchange during homologous recombination). They also unwind displacement loops (D-loops; intermediates formed during the strand invasion step of recombination).

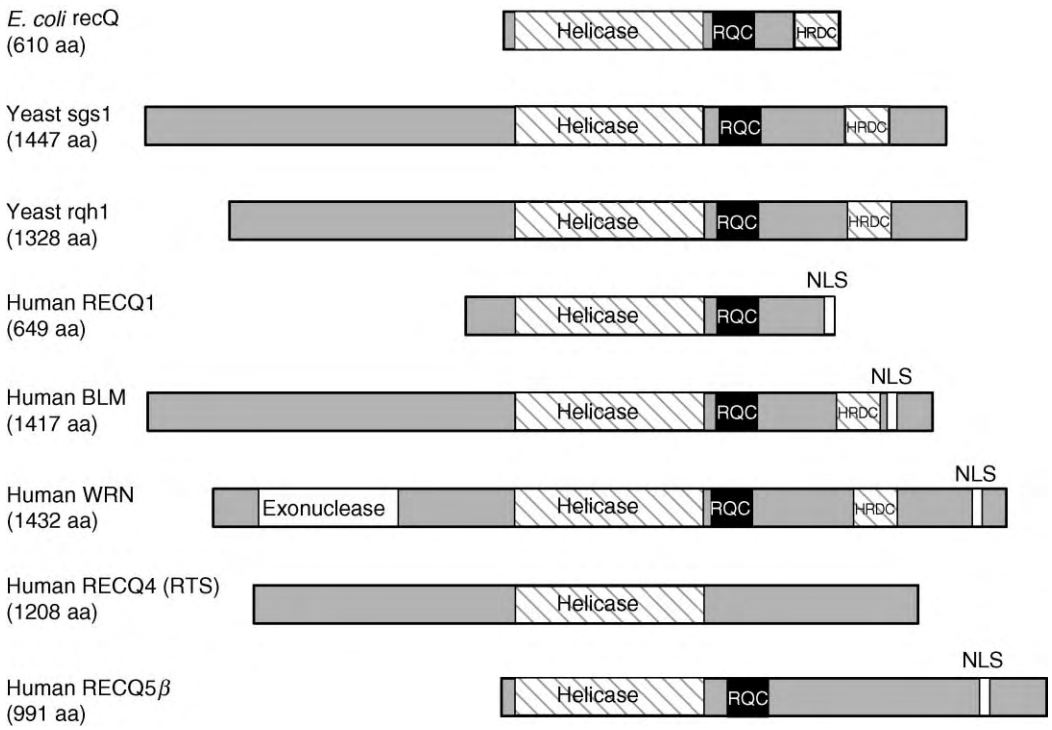

FIGURE 1 Schematic representation of domain structure of several recQ helicases. The names and sizes (numbers of amino acids) of the helicases are listed on the left. The positions of the conserved helicase, RQC (RecQ family C terminal), and HRDC (Helicase RNase D C terminal) domains are indicated on each diagram. The locations of the known nuclear localization signals (NLS) and the exonuclease domain of human WRN are also indicated.

Functional Clues Provided by Localizations and Associations

RecQ helicases undergo subnuclear relocalizations under various conditions. For instance, BLM generally has a punctate distribution within the nucleus that is at least partially associated with PML bodies (named for the presence of promyelocytic leukemia tumor suppressor protein). After treatment of cells with DNA damaging agents or inhibitors of DNA replication, BLM becomes associated with sites of DNA repair (defined by the presence of RAD51, required for the initial DNA strand pairing and invasion of homologous recombination). BLM directly binds to RAD51. BLM also associates with other proteins involved in DNA repair including ATM (ataxia telangiectasia mutated; serine/threonine kinase which phosphorylates BLM and other proteins involved in DNA damage repair), RPA (Replication Protein A; single stranded DNA binding protein involved in replication, recombination, and repair), BRCA1 (breast cancer susceptibility gene product), and MLH1 (mismatch repair protein). BLM (and most recQ helicases from lower organisms) binds topoisomerase III (relaxes negatively supercoiled DNA) and stimulates its activity. The tumor suppressor p53 binds to BLM and regulates its helicase activity.

WRN is generally associated with the nucleolus and/or is nucleoplasmic but undergoes translocation to DNA replication foci when DNA synthesis in inhibited. Potential roles for WRN in DNA replication, recombination, and repair are suggested by its association with a number of proteins involved in these processes including: RPA, FEN 1 (flap endonuclease 1; 5–3′ DNA structure-specific nuclease implicated in replication, recombination, and repair), EXO-1 (exonuclease 1; member of the RAD2 family of nucleases implicated in replication, recombination, and repair), pol-δ (DNA polymerase-δ; major DNA polymerase involved in replication), PCNA (Proliferating Cell Nuclear Antigen; pol-δ accessory factor), pol-β (DNA polymerase-β; major DNA polymerase involved in both short and long patch base excision repair), RAD52 (mediator of homologous recombination), the DNA-PK holoenzyme (DNA-PK_{CS} plus Ku70/80; serine/threonine kinase which phosphorylates WRN and other DNA repair proteins) and p53.

Potential Functions for recQ Helicases in Replication-Associated DNA Repair

Although loss of recQ helicase function leads to a number of phenotypic cellular changes, two consistent features are abnormal DNA replication and an increased occurrence of recombination. Distinctive characteristics of recQ helicases include their unusual substrate preferences

(G-quadruplexes, structures which resemble Holliday junction recombination intermediates, and D-loops) and their associations with other proteins implicated in replication, recombination, and repair. They also associate with what are presumed to be stalled replication forks after replication has been interrupted or DNA damage has occurred. These data suggest that the major function of recQ helicases is to maintain genomic stability by restarting stalled replication forks, although more than one mechanism could be responsible for this function. RecQ helicases may resolve DNA secondary structures such as G-quadruplexes ahead of the replication fork to allow the replication fork to proceed unimpeded. Indeed, WRN and *E. coli* recQ enable DNA polymerase-δ to traverse DNA tetraplex and hairpin structures *in vitro*.

RecQ helicases also may reset replication forks when they stall after encountering an area of DNA damage. One model that explains how this might occur is the "chickenfoot" model (Figure 2). In this case, leading strand synthesis is blocked by a lesion in the template while lagging strand synthesis continues for a short distance (Figure 2B). When replication stops, positive supercoiling surrounding the replication fork favors the formation of a four-way junction, the so-called chickenfoot that is analogous to a Holliday junction (Figure 2C). The shorter leading strand can now be extended to the end of the longer lagging strand with which it is now paired, past the lesion in the template (Figure 2D). RecQ helicases might then unwind these structures to restart the replication fork past the area of damage (Figure 2E). In the absence of a recQ helicase, the chickenfoot could be resolved by homologous recombination to re-establish the replication fork. RecQ helicases also may have a role in DNA repair by homologous recombination as suggested by their ability to unwind D-loops *in vitro* (disrupting less productive or inappropriate recombination intermediates). This could partially explain the observation of increased homologous recombination in cells lacking the BLM recQ-like helicase.

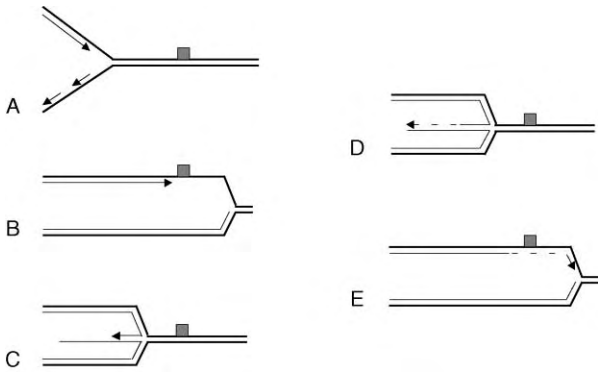

FIGURE 2 Chickenfoot model for the role of recQ helicases in restarting replication forks stalled by DNA damage. A replication fork is shown with the leading strand on top and the lagging strand on bottom (A). The long arrow represents leading strand synthesis, while the short arrows indicate lagging strand synthesis. When the fork encounters a lesion in the template on the leading strand (gray square), leading strand synthesis is halted but lagging strand synthesis can proceed for a short distance (B). When replication stops, positive supercoiling surrounding the replication fork favors the formation of a four-way junction, the chickenfoot (C). The shorter leading strand can now be extended to the end of the longer lagging strand with which it is now paired, past the lesion in the template (D). RecQ helicases would then unwind these structures to restart the replication fork past the area of damage (E).

Potential Function for recQ Helicases in Telomere Maintenance

Telomeres are structures composed largely of G,C-rich DNA repeat sequences that cap the ends of eukaryotic chromosomes and are required for chromosome stability. Telomeres become shorter each time a cell replicates its chromosomes. Stem cells and most immortal tumor cells overcome telomeric shortening using telomerase (a reverse transcriptase) to extend telomere ends. A relatively small proportion of human cancers use a telomerase-independent mechanism called alternative lengthening of telomeres (ALT) to extend telomeres and allow for continued cell division. Through recombination, long stretches of telomeric-repeat DNA are added to telomeres. Budding yeast strains that lack telomerase use a telomere maintenance pathway that resembles ALT and requires the recQ helicase sgs1. The human recQ helicases BLM and WRN have been localized to telomeres in ALT cells; both helicases bind to the telomere-associated protein TRF2 (Telomeric Repeat Factor 2). These data suggest that recQ helicases might have a role in telomere maintenance, at least in ALT cells. Since telomeres are G,C-rich structures in which G-quadruplexes are likely to form, recQ helicases might unwind these structures prior to replication of telomeric DNA. Additionally (or alternatively), recQ helicases might have a more direct role in the recombination process used for telomere lengthening.

See Also the Following Articles

DNA Helicases: Dimeric Enzyme Action • DNA Helicases: Hexameric Enzyme Action • DNA Polymerases: Kinetics and Mechanism • Exonucleases, Bacterial • Telomeres: Maintenance and Replication

Glossary

chromosome breakage syndromes Autosomal recessive human disorders characterized by spontaneous genomic instability and including Bloom, Rothmund–Thomson, and Werner syndromes.

D-loops Displacement loops; intermediates formed during the strand invasion step of recombination.

G-quadruplexes Extremely stable DNA secondary structures that can form in guanine-rich regions of DNA.

helicases Enzymes that use nucleoside triphosphate (usually ATP) hydrolysis to unwind nucleic acid duplexes (DNA–DNA, DNA–RNA, or RNA–RNA).

Holliday junctions Four-way crossover structures formed by DNA strand exchange during homologous recombination.

sister chromatid exchanges Reciprocal exchanges of DNA between sister chromatids by homologous recombination.

Further Reading

Cox, M. M. (2001a). Historical overview: Searching for replication help in all of the rec places. *Proc. Natl. Acad. Sci.* **98**, 8173–8180.

Cox, M. M. (2001b). Recombinational DNA repair of damaged replication forks in *Escherichia coli*: Questions. *Annu. Rev. Genet.* **35**, 53–82.

Gorbalenya, and Koonin (1993). Helicases: amino acid sequence comparisons and structure–function relatinship. *Curr. Opin. Struct. Biol.* **3**, 419–429.

Haber, J. E. (1999). DNA recombination: The replication connection. *Trends Biochem. Sci.* **24**, 271–275.

Hickson, I. D. (2003). RecQ helicases: Caretakers of the genome. *Nat. Rev. Cancer* **3**, 169–178.

Higgins, N. P., Kato, K., and Strauss, B. (1976). A model for replication repair in mammalian cells. *J. Mol. Biol.* **101**, 417–425.

Moheghegh, P., and Hickson, I. D. (2002). Premature aging in RecQ helicase-deficient human syndromes. *Int. J. Biochem. Cell Biol.* **34**, 1496–1501.

Nakayama, H. (2002). RecQ family helicases: Roles as tumor suppressor proteins. *Oncogene* **21**, 9008–9021.

Oakley, T. J., and Hickson, I. D. (2002). Defending genome integrity during S-phase: Putative roles for RecQ helicases and topoisomerase III. *DNA Repair* **1**, 175–207.

Singleton, M. R., and Wigley, D. B. (2002). Modularity and specialization in Superfamily 1 and 2 helicases. *J. Bacteriol.* **184**, 1819–1826.

Soultanas, P., and Wigley, D. B. (2001). Unwinding the "Gordian knot" of helicase action. *Trends Biochem. Sci.* **26**, 47–54.

Umezu, K., Nakayama, K., and Nakayama, H. (1990). *Escherichia coli* RecQ protein is a DNA helicase. *Proc. Natl. Acad. Sci.* **87**, 5363–5367.

Biography

Joanna Groden is a Professor in the Department of Molecular Genetics, Biochemistry, and Microbiology at the University of Cincinnati College of Medicine, and an Assistant Investigator of the Howard Hughes Medical Institute. Her principal research interest is inherited susceptibility to cancer. She holds a Ph.D. from Cornell University and received her postdoctoral training at the University of Utah. Her work resulted in the cloning and characterization of two human disease genes that determine cancer susceptibility, the *APC* tumor suppressor and the *BLM* helicase.

Regulated Intramembrane Proteolysis (Rip)

Jin Ye, Michael S. Brown and Joseph L. Goldstein
University of Texas Southwestern Medical Center, Dallas, Texas, USA

Regulated intramembrane proteolysis (Rip) is a newly recognized mechanism for signal transduction that involves the generation of regulatory molecules from membrane proteins. Such cleavage liberates cytoplasmic or lumenal/extracellular fragments from transmembrane precursor proteins, allowing the cleaved fragments to function at a new location. Rip influences processes as diverse as cellular differentiation, lipid metabolism, and the response to unfolded proteins, as originally addressed in a review article by Brown *et al.*. In addition to its occurrence in animal cells, Rip has been observed in bacteria, and, remarkably, the bacterial proteases are related evolutionarily to the ones used in animal cells. Proteins that are known to undergo Rip, span all the membrane bilayer at least once. In nearly all cases, the intramembrane cleavage does not take place until the bulk of the protein on the extracytoplasmic (lumenal or extracellular) face has been removed by a primary cleavage. This primary cleavage shortens the extracytoplasmic segment to less than 30 amino acids, which is a prerequisite for the secondary intramembrane cleavage. At least ten membrane proteins are currently known to undergo Rip, and their intramembrane cleavage is mediated by four different families of membrane-bound proteases (Figure 1).

Rip Mediated by Site-2 Protease (S2P) Family

S2P is a polytopic membrane protein with the characteristics of a membrane-embedded zinc metalloprotease (Figure 2). Genes similar to the one encoding mammalian S2P have been identified in DNA sequences from multiple species, including archaea, bacteria, plants, and animals. The encoded proteins share a similar hydrophobicity profile that predicts a highly hydrophobic structure with multiple membrane-spanning regions (Figure 2). The NH_2-terminal portion of all of these proteins contains a sequence conforming to the HE*xx*H consensus that is found in a large subfamily of zinc metalloproteases (where *x* is typically a noncharged amino acid). In these proteins, the two histidines of the HE*xx*H motif coordinate with a zinc atom, and the glutamate activates a water molecule, allowing it to make a nucleophilic attack on the peptide bond. Unlike its location in hydrophilic domains of classic zinc metalloproteases, the HE*xx*H sequence of S2P is embedded in a highly hydrophobic segment (Figure 2).

In addition to the HE*xx*H motif, classic zinc metalloproteases contain a remote residue (tyrosine or aspartate) that provides an additional coordination bound for the zinc. In the S2P-like proteins, this function is believed to be filled by the aspartate of the sequence LDG, which resides in a hydrophobic segment that shows a characteristic double peak in hydrophobicity plots and is located near the COOH terminus (Figure 2). The hydrophobic nature of S2P is consistent with its postulated role in cleaving a peptide bond that is located within a membrane bilayer.

Five membrane proteins, two in animals and three in bacteria, are known to be cleaved by the S2P family (Figure 2). In animal cells, both S2P substrates (SREBP and ATF6) contain one conserved asparagine and one conserved proline residue in the middle of the transmembrane domain, located about ten residues COOH-terminal to the cleavage site. Single amino acid substitution of either the asparagine or proline reduces cleavage only slightly, but substitution of both residues abolishes cleavage. The asparagine–proline sequence may serve as an NH_2-terminal cap that allows a portion of the transmembrane α-helix to unwind partially to expose the peptide bond for cleavage by S2P.

Sterol Regulatory Element-Binding Proteins (SREBPs)

SREBPs are membrane-bound transcription factors that regulate the synthesis of cholesterol, a major component of membranes in mammalian cells. As shown in Figure 1, SREBP is inserted in membranes of the endoplasmic reticulum (ER) in a helical hairpin fashion. The cytosolic NH_2-terminal domain is a transcription factor of the basic-helix-loop-helix-leucine zipper family. The COOH-terminal domain, also cytosolic, forms a

Membrane protein	Organism	Primary cleavage enzyme	Enzyme mediating Rip	Regulator of cleavage	Sites of cleavage	Function or consequence of cleaved protein
					Extracytosolic / Membrane / Cytosolic	
Rip by S2P family of proteases						
SREBP	Mammals/ *Drosophila*	S1P	S2P	Sterols/ phospholipids		Activates genes for lipid metabolism
ATF6	Mammals	S1P	S2P	Unfolded proteins		Activates genes for ER chaperones
RseA	*E.coli*	DegS	YaeL	Unfolded proteins		Releases σ^E, which activates stress induced genes
cAD1	*E. faecalis*	Signal peptidase	Eep	?		Stimulates mating
pro-σ^k	*B. subtilis*	None	SpoIVFB	SpoIVB		Activates genes for sporylation
Rip by γ-Secretase (Presenilin)						
APP	Mammals	β-Secretase	γ-Secretase	?		Generates Aβ peptide
Notch	Mammals/ *Drosophila*	TACE	γ-Secretase	Delta		Activates genes for differentiation
ErbB-4	Mammals	TACE	γ-Secretase	Heregulin		Phosphorylates nuclear proteins that inhibit cellular growth
Rip by Other Proteases						
MHC, class I	Mammals	Signal peptidase	Signal-peptide peptidase	?		Generates peptide for antigen presentation by HLA-E
Spitz	*Drosophila*	None	Rhomboid	Star		Generates ligand for EGF receptor

FIGURE 1 Membrane proteins that undergo regulated intramembrane proteolysis (Rip) categorized according to the Rip protease. The cleaved protein fragments are highlighted in red. For simplicity, proteins are not drawn to scale, and we do not show the alternate pathway for APP processing, which involves cleavage by TACE. For Notch, we show only the transmembrane subunit.

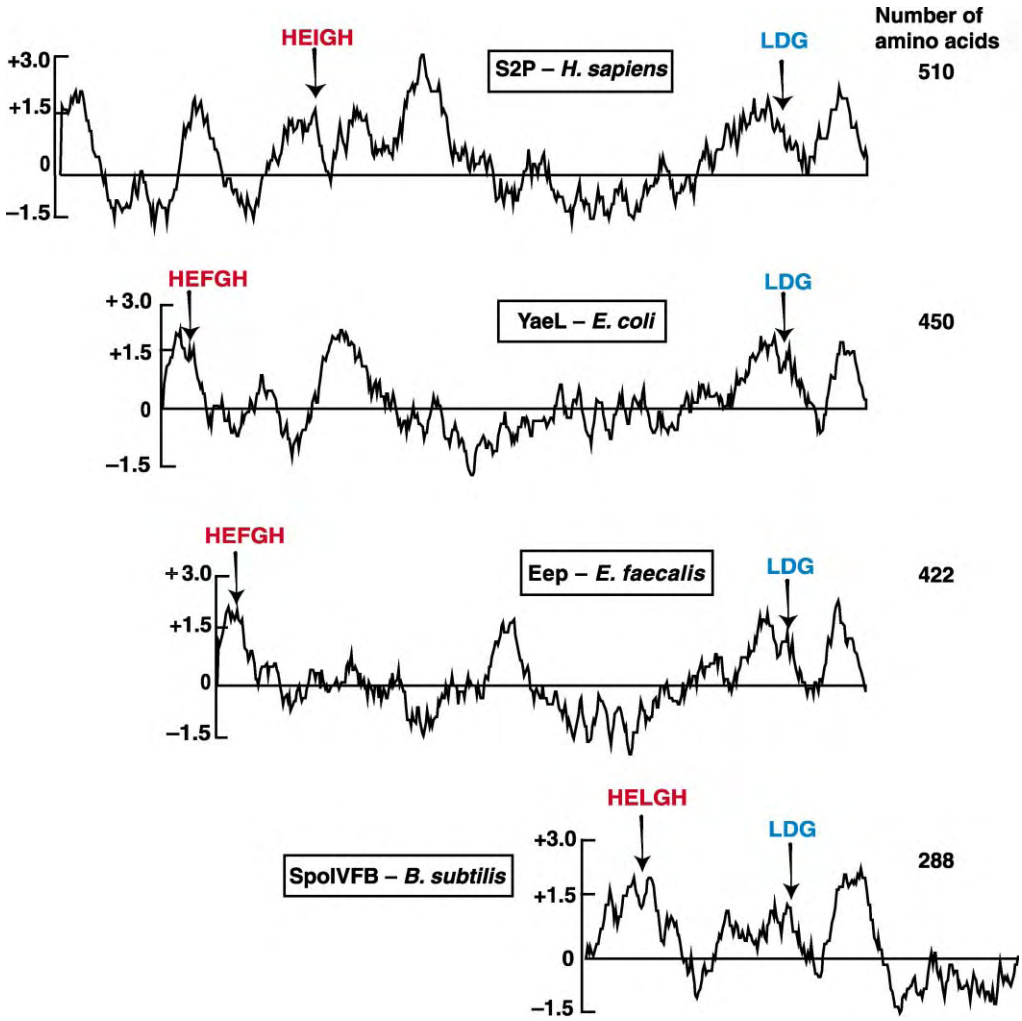

FIGURE 2 Hydropathy plots of human S2P and its bacterial family members. The HE*xx*H and LDG motifs (discussed in the text) are highlighted in red and blue, respectively. Each plot is drawn on the same scale and aligned by the position of the LDG motif. GenBank Accession numbers for the amino acid sequences are as follows: S2P, AAC51937; YaeL, AAC73287; Eep, AAD47948; and SpoIVFB, p26937.

complex with a polytopic membrane protein called SCAP. Upon deprivation of sterols, SCAP transports SREBP from ER to Golgi, where cleavage occurs. When cells are overloaded with sterols, the SCAP/SREBP complex is trapped in the ER and cleavage cannot occur. Inasmuch as SREBPs activate genes encoding enzymes of cholesterol synthesis, this sterol-mediated block in transport allows cholesterol to inhibit its own synthesis in a classic feedback fashion.

The first cleavage of SREBP is catalyzed by site-1 protease (S1P), a membrane-bound serine protease that is oriented with its active site in the lumen of the Golgi complex. Cleavage by S1P separates the two transmembrane helices of SREBP, but the NH_2-terminal fragment remains membrane-bound until it is cleaved by S2P at a site that is three residues within the transmembrane segment (Figure 1). Even though the activity of S2P is not regulated directly by sterols, S2P does not act until the two transmembrane segments have been separated by S1P, which effectively brings this reaction under cholesterol control.

In *Drosophila*, orthologues of SREBP, SCAP, S1P, and S2P are all expressed even though *Drosophila* cells do not produce sterols. *Drosophila* SREBP is processed by S1P and S2P in a reaction that requires SCAP and presumably requires ER to Golgi transport. The major SREBP targets in *Drosophila* S2 cells are enzymes required for synthesis of saturated fatty acids, which are incorporated into the major phospholipid, phosphatidyl ethanolamine (PE). PE, rather than sterols, is the feedback regulator of SREBP cleavage in these cells.

ATF6 AND RSEA

ATF6 is a type 2 membrane protein with a single transmembrane domain (Figure 1). Its NH_2-terminal

cytosolic domain is a transcription factor of the bZIP family. When mammalian cells produce unfolded endoplasmic reticulum (ER) proteins, ATF6 translocates from ER to Golgi, where it is cleaved sequentially by S1P and S2P, the same proteases that process SREBP. The intramembrane proteolysis carried out by S2P liberates the NH_2-terminal domain of ATF6 from the membrane, allowing it to activate transcription of *BiP/GRP78* and other genes whose products assist the folding of ER proteins. This regulatory pathway, called the unfolded protein response, helps cells to survive conditions of ER stress.

In *E.coli*, σ^E is the transcription factor that regulates extracytoplasmic stress response. Under nonstress conditions, σ^E is negatively regulated by RseA, an inner membrane protein with one transmembrane domain (Figure 1). The NH_2-terminal cytosolic domain of RseA binds to σ^E and is sufficient to inhibit σ^E activity. When unfolded proteins accumulate in the periplasmic space (similar to ER lumen in eukaryotic cells), RseA is first cleaved by DegS, a membrane-bound serine protease with its active site projecting into the periplasmic space. Cleavage by DegS removes the majority of the COOH-terminal periplasmic domain of RseA. YaeL, an orthologue of S2P, then cleaves the remaining part of RseA, after which RseA is rapidly degraded. This frees σ^E to associate with RNA polymerase and direct transcription of its target genes.

The similarity between mammalian and bacteria unfolded-protein response suggests that S2P-mediated Rip has been selected to cope with extracytoplasmic stress during evolution, although individual organisms use the mechanism in different ways: in mammalian cells Rip directly releases the active transcription factor from its substrate, whereas in bacteria Rip leads to degradation of a membrane-bound inhibitor of the responsible transcription factor.

Other Bacterial Proteins

Enterococcus faecalis, a Gram-positive bacterium, secretes an 8-amino acid peptide pheromone called cAD1, which induces a mating response in other enterococci that harbor a plasmid called pAD1 (Figure 1). Genomic sequencing revealed that the octapeptide pheromone is derived from a 143-amino acid precursor that contains a signal peptide at the NH_2-terminus and is inserted into the plasma membrane with a type 2 orientation. The pheromone corresponds to the COOH-terminal 8 amino acids of the signal peptide (Figure 1). The octapeptide is generated by cleavage of the precursor at two sites, at the extracellular side of the membrane in a reaction carried out by signal peptidase and at a site in the middle of the transmembrane signal peptide by Eep, an S2P orthologue. This system differs from the others in that the active fragment is released by S2P into the extracellular space rather than the cytosol.

Another prokaryotic relative of S2P is a *B. subtilis* protein called spoIVFB. This protein contains an HE*xx*H motif in a hydrophobic segment near the NH_2 terminus and an LDG motif in a double-peaked hydrophobic segment toward the COOH terminus (Figure 2). The overall hydrophobicity profile of SpoIVFB differs from those of the other family members. SpoIVFB is a much smaller protein, and it contains a hydrophilic extension on the COOH-terminal side of the hydrophobic LDG segment. SpoIVFB is the protease that removes a membrane-embedded NH_2-terminal hydrophobic peptide from a transcription factor, pro-σ^K, thereby releasing the factor into the cytosol and allowing it to activate gene transcription. This process is necessary for completion of spore formation in response to nutrient deprivation. The membrane orientation of pro-σ^K is opposite to the type 2 orientation of other known S2P substrates, and it is the only S2P substrate that does not require a primary cleavage (Figure 1). These differences in catalytic requirements may account for the differences in structure between SpoIVFB and the other members of the S2P family.

Rip Mediated by γ-Secretase

γ-Secretase is a membrane-bound complex consisting of several proteins, including presenilin and nicastrin. Presenilin contains two conserved aspartate residues that are located in 2 of its 8 transmembrane helices at positions that are predicted to place them at the same depth in the membrane. This property is reminiscent of soluble aspartyl proteases, which contain two closely apposed aspartates that are required for activity. Experiments with active-site-modifying agents specific for aspartyl proteases provide evidence that presenilin contains the active proteolytic site. The second component of γ-secretase, also required for catalytic activity, is a membrane protein called nicastrin. Nicastrin is believed to present substrates to presenilin, regulate its stability, and deliver it to the cell surface.

Several membrane proteins are believed to be cleaved by γ-secretase, but only three have been well characterized, as discussed here.

Amyloid Precursor Protein (APP)

APP is a type 1 membrane protein with an NH_2-terminal extracellular domain and a COOH-terminal cytosolic tail (Figure 1). Processing of APP generates a toxic amyloid β peptide that is responsible for Alzheimer's disease. APP is first cleaved at a site that is 28 amino acids from the transmembrane helix by β-secretase, a membrane-bound aspartyl protease with an extracytoplasmic active

site. This cleavage shears off the bulk of the extracellular domain of APP, which then allows the protein to be cleaved within the membrane by γ-secretase. Intramembrane cleavage can occur at either of the two sites separated by two amino acids, leading to two different amyloid β peptides, designated $A\beta_{1-40}$ and $A\beta_{1-42}$, which accumulate extracellularly. After the intramembrane γ-secretase cleavage, the cytosolic tail of APP enters the nucleus where it may affect transcription of genes that are not yet identified.

In addition to cleavage by β-secretase, APP can be cleaved by TNFα converting enzyme (TACE), a membrane-bound metalloprotease whose active site faces the extracellular surface. TACE cuts the extracytosolic domain of APP even closer to the membrane, leaving only 12 amino acids on the external surface. Like the β-secretase cleavage, TACE cleavage is followed by γ-secretase cleavage. In this case, the liberated fragment is too short to form an amyloid deposit, and thus cleavage by TACE does not lead to Alzheimer's disease.

Notch

The cell surface receptor Notch is synthesized as a type 1 membrane protein (Figure 1) that is processed constitutively by a furin-like enzyme in the secretory pathway. The enzyme cleaves the precursor to generate two subunits: an extracellular subunit and a transmembrane subunit, which remain associated as a noncovalent heterodimer. The heterodimer travels to the cell surface and remains intact until it binds its ligand Delta, a membrane protein that resides on the surface of an adjacent cell. Binding leads to cleavage of the transmembrane subunit of Notch by TACE, the same enzyme that cleaves APP. TACE cleavage releases most of the extracellular portion of the transmembrane subunit of Notch along with the attached extracellular subunit. The shortened transmembrane subunit is then cleaved by γ-secretase within the membrane-spanning helix, liberating a cytosolic fragment. The cytosolic fragment translocates to the nucleus where it activates several genes whose products influence the fate of cells during development.

ErbB-4

ErbB-4 is a transmembrane receptor tyrosine kinase that regulates cell proliferation and differentiation. It adopts a type 1 orientation with an NH_2-terminal extracellular ligand-binding domain and a COOH-terminal cytosolic tyrosine kinase domain (Figure 1). Upon binding to its ligand, heregulin, the ErbB-4 ectodomain is cleaved by TACE, followed by intramembrane proteolysis carried out by γ-secretase. The intramembrane cleavage results in the release of the cytosolic fragment, which travels to the nucleus where it phosphorylates substrates that regulate cell growth.

Rip Mediated by Signal-Peptide Peptidase (SPP)

SPP, a resident ER protein with 7 transmembrane domains, contains two conserved aspartate residues, each within adjacent transmembrane helices. As discussed above, such motifs are characteristic of the presenilin-type of aspartic protease. Similar to S2P, cleavage by SPP requires helix-breaking residues within the transmembrane domain of its signal peptide substrates.

The best-studied example of Rip mediated by SPP is the proteolytic processing of signal peptides from MHC class I molecules such as HLA-A, -B, -C, and -G. These molecules are expressed with a typical signal sequence for targeting to the secretory pathway. During their translocation through the ER membrane, the signal sequences are cleaved off from the pre-protein by signal peptidase. The cleaved signal peptides, which remain membrane-bound with a type 2 orientation, are then cleaved by SPP in the middle of the membrane to liberate the NH_2-terminal half of the signal peptides into the cytosol (Figure 1). These cytosolic fragments are then transported into the ER lumen where they bind to HLA-E, a nonclassical MHC class I molecule. The HLA-E/peptide complexes travel to the cell surface where they bind to CD94/NKG2A receptors on natural killer (NK) cells and inhibit NK cell-mediated lysis. This pathway protects cells expressing normal MHC class I molecules from killing by NK cells.

Rip Mediated by Rhomboid

Rhomboid, a Golgi membrane protein with 7 transmembrane domains, is a serine protease whose catalytic triad is buried within the membrane bilayer. Rhomboid belongs to a large gene family that is conserved throughout archaea, bacteria, yeast, plants, and animals, including humans. To date, rhomboid has only been characterized in *Drosophila* where it initiates epidermal growth factor receptor (EGFR) signaling.

Spitz is the main ligand for *Drosophila* EGFR. It is synthesized as a transmembrane precursor with an NH_2-terminal extracellular EGF-like domain and a short COOH-terminus cytosolic tail (Figure 1). Spitz is confined to the ER and is inert until it binds to another protein named star. Star escorts spitz from ER to Golgi where spitz is cleaved by rhomboid. The intramembrane cleavage liberates the extracellular

EGF-like domain from the membrane, allowing it to be secreted out of the cell.

Unlike Rip mediated by other proteases, a primary cleavage that sheds the extracytoplasmic domain of spitz is not required for the action of rhomboid, as rhomboid itself is directly responsible for the release of the extracellular domain of spitz (Figure 1). It remains unclear why spitz is subjected to Rip rather than being cleaved by an extracellular protease such as TACE.

See Also the Following Articles

Amyloid • Cholesterol Synthesis • Secretases

Glossary

regulated intramembrane proteolysis (Rip) A process of signal transduction in which a membrane-bound protease cleaves its substrate within the lipid bilayer, thus allowing the cleaved protein fragment to function at a new location.

rhomboid An intramembrane serine-protease involved in the Rip of Spitz.

γ-secretase A protein complex containing an intramembrane aspartyl-protease catalytic subunit involved in the Rip of APP, Notch, and ErbB-4.

S2P An intramembrane metalloprotease involved in the Rip of SREBPs and ATF6.

SPP An intramembrane aspartyl-protease involved in the Rip of signal peptides released from certain MHC class I molecules.

Further Reading

Alba, B. M., Leeds, J. A., Onufryk, C., Lu, C. Z., and Gross, C. A. (2002). DegS and YaeL participate sequentially in the cleavage of RseA to activate the σ^E-dependent extracytoplasmic stress response. *Genes Develop.* **16**, 2156–2168.

Brown, M. S., Ye, J., Rawson, R. B., and Goldstein, J. L. (2000). Regulated intramembrane proteolysis: A control mechanism conserved from bacteria to humans. *Cell* **100**, 391–398.

Haze, K., Yoshida, H., Yanagi, H., Yura, T., and Mori, K. (1999). Mammalian transcription factor ATF6 is synthesized as a transmembrane protein and activated by proteolysis in response to endoplasmic reticulum stress. *Molecul. Biol. Cell* **10**, 3787–3799.

Lee, J. R., Urban, S., Garvey, C. F., and Freeman, M. (2001). Regulated intracellular ligand transport and proteolysis control EGF signal activation in *Drosophila*. *Cell* **107**, 161–171.

Lemberg, M. K., and Martoglio, B. (2002). Requirements for signal peptide peptidase-catalyzed intramembrane proteolysis. *Molecul. Cell* **10**, 735–744.

Ni, C.-Y., Murphy, M. P., Golde, T. E., and Carpenter, G. (2001). γ-Secretase cleavage and nuclear localization of ErbB-4 receptor tyrosine kinase. *Science* **294**, 2179–2181.

Rawson, R. B., Zelenski, N. G., Nijhawan, D., Ye, J., Sakai, J., Hasan, M. T., Chang, T-Y., Brown, M. S., and Goldstein, J. L. (1997). Complementation cloning of *S2P*, a gene encoding a putative metalloprotease required for intramembrane cleavage of SREBPs. *Molecul. Cell* **1**, 47–57.

Rudner, D. Z., Fawcett, P., and Losick, R. (1999). A family of membrane-embedded metalloproteases involved in regulated proteolysis of membrane-associated transcription factors. *Proc. Natl Acad. Sci. USA* **96**, 14765–14770.

Selkoe, D. J., and Podlisny, M. B. (2002). Deciphering the genetic basis of Alzheimer's disease. *Annu. Rev. Genomics Hum. Genet.* **3**, 67–99.

Ye, J., Rawson, R. B., Komuro, R., Chen, X., Dave, U. P., Prywes, R., Brown, M. S., and Goldstein, J. L. (2000). ER stress induces cleavage of membrane-bound ATF6 by the same proteases that process SREBPs. *Molecul. Cell* **6**, 1355–1364.

Biography

The authors are members of the Department of Molecular Genetics at the University of Texas Southwestern Medical Center in Dallas. Dr. Ye is a postdoctoral fellow in the Department of Molecular Genetics at the University of Texas Southwestern Medical Center in Dallas. He delineated the role of S2P in cleaving membrane-bound SREBPs and ATF6 and advanced a provocative hypothesis to explain the mechanism by which intramembrane proteases cleave transmembrane proteins.

Brown and Dr. Goldstein are Professors in the Department of Molecular Genetics at the University of Texas Southwestern Medical Center in Dallas. They have worked together for 30 years on the genetics and regulation of cholesterol metabolism. They received the Nobel Prize in Physiology or Medicine in 1985 and the Albany Medical Center Prize in Medicine and Biomedical Research in 2003.

Respiratory Chain and ATP Synthase

David G. Whitehouse and Anthony L. Moore
University of Sussex, Brighton, UK

The respiratory chain and ATP synthase are, in eukaryotic cells, located in the inner membrane of mitochondria. Mitochondria are oval-shaped organelles, typically 1–2 μm long and 0.5 μm in diameter, whose principal cellular functions are to generate energy, in the form of ATP and carbon skeletons for biosynthetic purposes. The shape and appearance of mitochondria vary considerably and these organelles appear to be most numerous in mammalian tissues with a high-energy demand (heart, liver, muscle, and brain and in rapidly dividing plants cells). The respiratory chain functions to oxidize NADH ($+H^+$) and $FADH_2$ and reduce molecular oxygen to water. These functions are electron transfer (electronmotive) processes and result in a substantial release of energy, which generates a protonmotive force, that is used to drive the ATP synthase in the forward direction thereby synthesizing ATP for use in cellular reactions.

Components of the Respiratory Chain

The conversion of the electronmotive force (NADH and FADH oxidation) into a protonmotive force is carried out by three electron-driven proton-pumping respiratory chain complexes. These large transmembrane complexes contain numerous reduction–oxidation (redox) components that include flavins, iron–sulfur proteins, cytochromes, ubiquinone, and metal ions.

Flavins

Flavin mononucleotide (FMN) and flavin dinucleotide (FAD) are tightly bound (to their enzymes) cofactors that can accept (or donate) two electrons and two protons (to become fully reduced) or a single electron and proton to form the semiquinone intermediate.

Iron–Sulfur Proteins

Iron–sulfur (or nonheme iron proteins) contain iron atoms covalently bound to the apo-protein by cysteine sulfurs and to other iron atoms via acid labile sulfur bridges. In general, there are three types of Iron–sulfur proteins namely a single iron atom coordinated to the sulphydryl groups of four cysteine residues of the protein, a protein containing two irons and two inorganic sulfides (2Fe–2S) and four irons and four inorganic sulfides (4Fe–4S). Similar to the single iron cluster, both are coordinated by four cysteine residues. All three types of Iron–sulfur proteins can act as single electron carriers.

Cytochromes

Cytochromes are proteins containing a prosthetic group called a heme. The basis of the heme is a porphyrin, which consists of four pyrrole rings linked in a cyclic manner by methene bridges with a central coordinated iron atom that acts as a single electron carrier. There are at least four classes of cytochromes (cytochrome A–D) differentiated from each other by the ability to absorb light at different wavelengths (due to differences in the side chains on the porphyrin).

Ubiquinone

Ubiquinone or coenzyme Q is a hydrophobic quinone derivative that in mammalian mitochondria has a side chain of ten 5-carbon isoprene units (Q_{10}). Ubiquinone can be fully reduced to the quinol form by the acceptance of $2H^+$ and $2e^-$ (or the semiquinone derivative can be formed through the acceptance of a single proton and electron).

Respiratory Chain Complexes

The following respiratory chain complexes (I, III, and IV) are associated with proton translocation across the inner mitochondrial membrane.

Complex I (NADH-Ubiquinone Oxidoreductase)

NADH-ubiquinone oxidoreductase is the largest (750 kDa) and most complicated of the respiratory

chain complexes, having ~43 subunits. Although it is well established that complex I contains FMN and numerous Iron–sulfur proteins as redox centers, the exact route of electron transfer is uncertain. What is certain, however, is that the enzyme transfers two protons and two electrons from NADH ($+H^+$) to ubiquinone, and electron transfer is accompanied by the translocation of protons across the membrane with a stoichiometry of $4H^+/2e^-$. Enzyme activity is potently inhibited by rotenone and piercidin A. Electron microscopic studies suggest that complex I has an L-shape with the majority (if not all) of the redox centers being located within the peripheral part of the enzyme. The exact mechanism whereby protons are translocated across the membrane is uncertain.

Complex III (Ubiquinone–Cytochrome *c* Oxidoreductase or the bc_1 Complex)

Complex III is a large (250 kDa) multicomponent complex that catalyzes the oxidation of ubiquinol and the reduction of cytochrome c_1 and results in the vectorial transport of protons across the inner mitochondrial membrane. Redox centers include a 2Fe-2S protein (the Rieske center), two *b* cytochromes (cytochrome b_L and b_H) and cytochrome c_1. X-ray crystallography studies reveal that the enzyme is dimeric, with each of the two monomers being composed of at least 11 subunits (8 of which appear to have no catalytic role). Crystallography has also revealed that the monomers do not function independently but cooperate during electron transfer. Structural studies have also shown that the Rieske center shuttles between the quinone-binding site (of one of the monomers) in its oxidized state and cytochrome c_1 (of the second monomer) in its reduced state. Although the pathway of electron flow through complex III (known as the Q-cycle) is complicated, the net equation is:

$$QH_2 + 2\text{cyt}c_{1(\text{oxidized})} + 2H^+_N = Q + 2\text{cyt}c_{1(\text{reduced})} + 4H^+_P$$

where N and P refer to the negative and positive sides of the membrane (Figure 1).

The Q-cycle accommodates the fact that there is a mixture of two and one electron carriers and hence there must be a switch between ubiquinol (a two electron carrier), the cytochromes, and Rieske center (all of which are single electron carriers). It also explains the well-documented observation that the H^+/e^- stoichiometry for the bc_1 complex is 4. Complex III is inhibited by antimycin A, myxothiazol, and stigmatellin.

Complex IV (Ferrocytochrome *c* – Oxygen Oxidoreductase or Cytochrome *c* Oxidase)

Complex IV is a third large transmembrane enzyme (204 kDa) that catalyzes the oxidation of reduced cytochrome *c* and the reduction of molecular oxygen to water. It is also associated with the translocation of protons across the membrane and has at least 13 subunits of which only subunits I and II appear to play

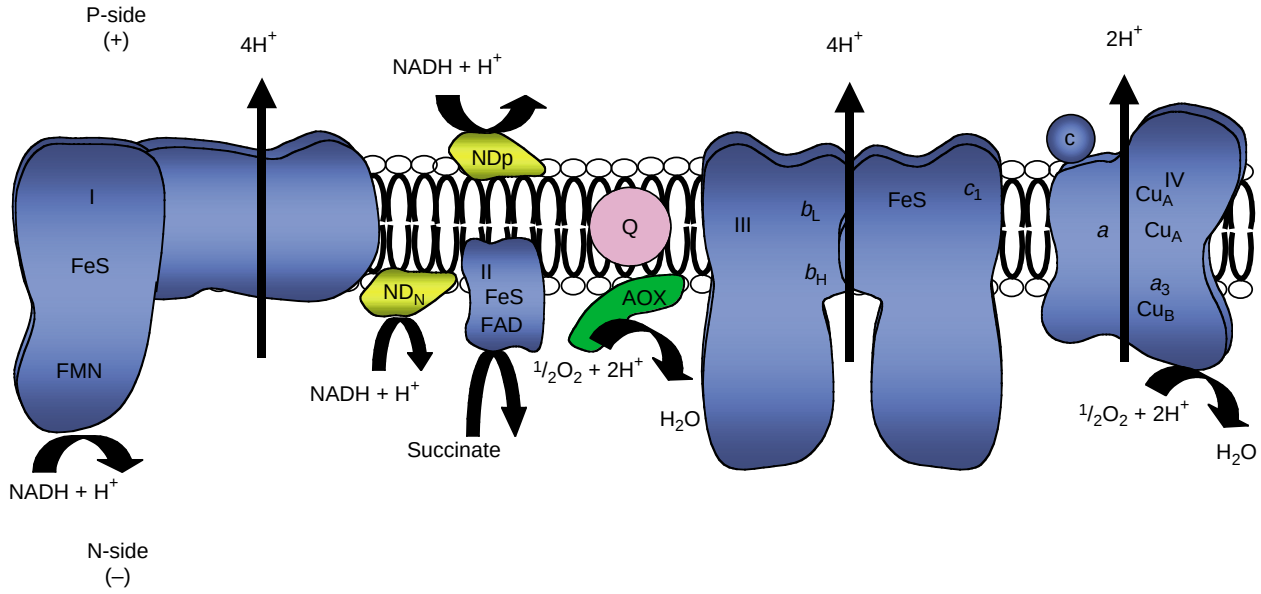

FIGURE 1 A schematic representation of the respiratory chain. The P- and N-sides of the membrane refer to the intermembrane space (positive) and matrix (negative), respectively. ND_P and ND_N refer to NADH dehydrogenases (such as the ETF, glycerol-3-phosphate and externally located NADH dehydrogenases) located on the P- and N-sides, respectively. AOX is the alternative oxidase.

a role in catalysis. The complex contains three Cu atoms and two heme *a* (cytochrome *a* and cytochrome a_3). High-resolution structural studies reveal that subunit II contains two of the Cu atoms complexed with sulfur atoms to form a binuclear center (known as Cu_A center). Subunit I contains the two cytochromes and the third Cu atom (Cu_B), which is closely associated with cytochrome a_3 forming a second binuclear center. Electron transfer through complex IV is from cytochrome *c* to the Cu_A center (which acts as a single electron receptor), then to heme *a* (which is slightly closer to the Cu_A center than heme a_3) onto the heme a_3–Cu_B center and finally onto oxygen bound to heme a_3. For every four electrons passing through the complex, one molecule of oxygen is reduced to two molecules of water, four protons are consumed from the matrix, and four protons are translocated across the membrane. It should be noted that the four electron reduction of molecular oxygen occurs as four single electron events and hence it is important that the potentially dangerous partially reduced intermediates such as superoxide anion are not released but remain tightly bound until completely reduced to water. Cytochrome *c* oxidase is potently inhibited by cyanide, azide, and carbon monoxide, which bind at the oxygen-binding site. Nitric oxide is also a reversible inhibitor of this complex.

Other Ubiquinone-Reducing Enzymes

Animal, plant, and a number of protest mitochondria also contain a number of membrane-bound enzymes that can reduce ubiquinone. These enzymes do not transfer charge across the membrane, i.e., protons are not vectorially transported across the inner mitochondrial membrane and are detailed in the following section.

Succinate Dehydrogenase

Succinate dehydrogenase is the only membrane-bound enzyme of the citric acid cycle that interacts directly with the respiratory chain. Succinate dehydrogenase is much smaller than complex I (140 kDa) being composed of four subunits. The two larger of these subunits are peripheral proteins that contain covalently bound FAD (on subunit I) and three Iron–sulfur centers (on subunit II). These two large subunits are anchored to the inner surface of the inner membrane by two integral membrane polypeptides (subunits III and IV) in which a single heme *b* is located. Although the exact route of electron transfer from succinate to ubiquinone is uncertain, it is known that the reduction of ubiquinone by succinate is not associated with any charge movement.

Electron-Transferring Flavoprotein (ETF)-Ubiquinone Reductase

The ETF-ubiquinone oxidoreductase is a globular protein located on the inner surface of the inner membrane and contains FAD, an Fe–S center and a ubiquinone-binding site. The enzyme can accept reducing equivalents from a variety of dehydrogenases including those involved in fatty acid oxidation or amino acid and choline catabolism.

Glycerol-3-phosphate Dehydrogenase

Glycerol-3-phopshate dehydrogenase is located on the outer surface of the inner membrane and catalyzes the oxidation of glycerol-3-phosphate to dihydroxyacetone phosphate and the reduction of ubiquinone. Although little is known about the structure or the route of electron transfer to ubiquinone, redox centers include FAD and probably an Iron–sulfur center.

External NADH Dehydrogenase

There are a number of rotenone-insensitive NADH dehydrogenases located on the outer and inner surface of the inner mitochondrial membrane in plant and yeast mitochondria. Again there is little structural information apart from the presence of FAD and possibly an Iron–sulfur center. Electron transfer is probably similar to that described for the ETF-ubiquinone oxidoreductase since the enzyme catalyzes the oxidation of NADH and the reduction of ubiquinone. In plants, the external NADH dehydrogenase (on the outer surface of the inner membrane) is regulated by cytosolic Ca^{2+}. These enzymes are not associated with proton pumping across the mitochondrial membrane.

Other Ubiquinol Oxidizing Enzymes (The Alternative Oxidase)

Although mammalian mitochondria do not possess any other ubiquinol-oxidizing enzymes apart from cytochrome oxidase (complex IV), most plants, some yeasts, fungi, and trypanosomes possess a cyanide- and antimycin-insensitive alternative oxidase that catalyzes the oxidation of ubiquinol and reduces molecular oxygen to water. Unlike cytochrome *c* oxidase, electron transfer does not result in proton translocation and redox energy is released as heat. Although no structural information is available, the enzyme is believed to contain two nonheme iron atoms linked by an oxygen atom as its only redox carrier (di-iron protein) and is probably globular with two of its amphiphilic helices lying parallel to the membrane plane. Enzyme activity is insensitive to all complex IV inhibitors but can be potently inhibited by salicylhydroxamic acid and the alkyl gallates.

Organization of the Respiratory Chain

The respiratory chain complexes in mammalian and plant mitochondria are generally considered to be free to diffuse laterally and independently of each other within the plane of the membrane. They are connected electronically to each other by ubiquinone and cytochrome *c* with electron transfer occurring by diffusion-based collisions between these components. There is also evidence to suggest that the numbers of complexes within the membrane are unequal with the following ratio: complexes I:II:III:IV: cytochrome *c*: ubiquinone = 1:2:3:7:14:63. Both cytochrome *c* and ubiquinone are considered to function as common pools and hence act as mobile carriers mediating electron transfer between freely diffusible large respiratory complexes.

For every $2e^-$ passing from NADH ($+H^+$) to oxygen to produce one molecule of water a total of ten protons are released at the P-side of the membrane. Since four protons are required to synthesize and export one ATP, then the amount of ATP formed by the oxidation of NADH is 2.5 (1.5 for succinate).

The ATP Synthase

The ATP synthase (or F_1F_0 ATPase and also referred to as complex V) uses the free energy of an electrochemical gradient of protons (or sodium ions) generated by the respiratory chain to synthesize ATP. The ATP synthases comprise a very large group of highly conserved enzymes that are found in the bacterial cytoplasmic membranes, the thylakoid membranes of chloroplasts, and the inner membranes of mitochondria. Most members of the group use H^+ as the coupling ion (the *Propionigenium modestum* enzyme is an example of the few ATP synthases that can use Na^+ as the physiological coupling ion).

Structure of the ATP Synthase

The ATP synthase is a miniature rotating motor and the simplest or prototype enzyme is that isolated from *E. coli*. The enzyme has a bipartite structure composed of a membrane-bound (hydrophobic) F_0 component crossing the inner mitochondrial membrane and a water-soluble (hydrophilic) F_1 component that protrudes into the mitochondrial matrix.

The F_0 Component

The F_0 entity is composed of three subunits (*a*, *b*, and *c*) with a stoichiometry of: *a*:2*b*:9–12*c* and it functions as a proton channel. The proton channel is a ring of 9–12 *c* subunits (the number of subunits may depend on the carbon source used for growth) positioned in the membrane and tightly bound to one *a*-subunit plus two *b*-subunits of F_0 and also bound to the γ, δ, and ε subunits of the F_1 component of the synthase.

The F_1 Component

The F_1 component has five types of subunits (α, β, γ, δ, and ε) with a stoichiometry of $3\alpha{:}3\beta{:}\gamma{:}\delta{:}\varepsilon$. The $\alpha_3\beta_3$ subunits are arranged as a hexamer of alternating α- and β-subunits with the γ-subunit projecting into the central cavity of this hexamer. The β-subunits contain the catalytic site for ATP synthesis/hydrolysis and bind the adenylates and inorganic phosphate.

ATP synthases from other sources all have very similar structures to the *E. coli* synthase except the mitochondrial enzyme. It contains an inhibitor protein and a mitochondrial oligomycin-sensitivity-conferring protein (OSCP factor). The mitochondrial δ-subunit is related to the ε-subunit of the *E. coli* synthase (Figure 2).

Mechanism of ATP Synthesis

ATP synthesis is driven by the rotation of the single γ-subunit, which extends into the center of the α_3/β_3 hexamer that contains the catalytic sites. As the single γ-subunit rotates so it alternately alters the conformation (and hence binding characteristics) of the catalytic sites. Changes in nucleotide affinity occur in the three β-subunits and arise from their interactions with the γ-subunit. This results in the sequential binding of ADP and Pi, followed by ATP synthesis and ATP release. This concept recognizes that the β-subunit can exist in three conformations: open, tight, or loose forms. These forms correspond to the binding, synthesis, and release of ATP and are driven by the rotation of the γ-subunit. The hydrolysis of ATP will drive the rotation of the γ-subunit in the opposite direction to that of synthesis.

Subunits c_{9-12}, γ, and ε constitute the rotor (rotating unit) and subunits α_3, β_3, δ, *a*, and b_2 constitute the stator (stationary unit). The protonmotive force drives rotation of the oligomeric ring of the *c*-subunits and of the γ-subunit in F_0 (since the γ-subunit is attached to the *c*-oligomer). Thus, protons moving from the P-side to the N-side of the inner membrane (i.e., down the electrochemical gradient are converted into rotational torque of γ, which alters nucleotide binding at the β-catalytic site and results in the synthesis/hydrolysis of ATP. It is not the synthesis of ATP but its release from the synthase that is driven by the protonmotive force. Subunits γ and ε rotate relative to the $\alpha_3\beta_3$ hexamer to alter the nucleotide affinities (and hence binding) in the β-catalytic sites. Probably subunit γ of F_1 and two copies of subunit *b* in F_0 stabilize the synthase complex.

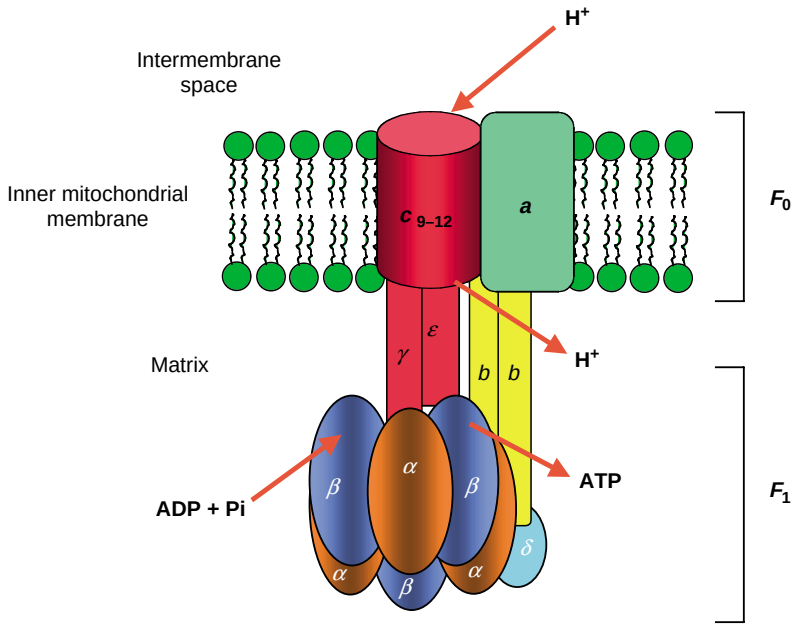

FIGURE 2 Diagram of the ATP synthase. Note that during ATP synthesis, subunits *c*, γ, and ε rotate as a complete unit with respect to the other (fixed) subunits.

A simplified mechanism suggests that it is the flow of protons through *c* via *a* channel (or two half channels) that protonates an aspartate residue and the proton is released through the channel (or second half channel). Conformational changes during this cycle of protonation–deprotonation provide the basis to explain rotation. This protonated *c* subunit then rotates through 360° during ATP synthesis/hydrolysis and both the subunits γ and ε rotate by 120° for each ATP synthesized (or hydrolyzed) with the rotation being coupled to the protonation-deprotonation of three–four *c* subunits.

See Also the Following Articles

ATP Synthesis in Plant Mitochondria: Substrates, Inhibitors, Uncouplers • Cytochrome bc_1 Complex (Respiratory Chain Complex III) • Cytochrome *c* • Flavins • Iron–Sulfur Proteins

Glossary

binuclear center A binuclear center comprises two redox-active components in close proximity, e.g., copper and cytochrome *a* or two iron atoms linked by an oxygen atom that function as a single entity to mediate electron transfer.

proton pump A transmembrane protein which mediates the active transport of protons across the inner mitochondrial membrane/thylakoid membrane.

protonmotive force The energy contained in an electrochemical gradient of protons across the inner mitochondrial membrane/thylakoid membrane and composed of two components, the membrane potential and pH gradient. It is the driving force for the transport of substrates across the membrane and for the synthesis of ATP.

respiratory chain An assemblage of electron carriers normally arranged as a multicomponent complex and located in the inner mitochondrial membrane.

Further Reading

Abrahams, J. P., Leslie, A. G., Lutter, R., and Walker, J. E. (1994). The structure of F_1-ATPase from bovine heart mitochondria determined at 2.8 Å resolution. *Nature (London)* **370**, 621–628.

Boyer, P. D. (1997). The ATP synthase: A splendid molecular machine. *Annu. Rev. Biochem.* **66**, 717–749.

Mitchell, P. (1979). Keilin's respiratory chain concept and its chemiosmotic consequences. *Science* **206**, 1148–1159.

Nelson, D. L., Cox, M. M., and Lehninger, A. L. (2000). In *Principles of Biochemistry*, 3rd Edition. Worth Publishers, New York.

Nicholls, D. G., and Ferguson, S. J. (2002). In *Bioenergetics 3*. Academic Press, London.

Biography

Anthony L. Moore is a professor in the Department of Biochemistry at the University of Sussex, United Kingdom. His principal research interests are in the structure and function of plant mitochondrial respiratory chain proteins. He holds a Ph.D. from the University of Aberdeen and received his postdoctoral training at the University of Pennsylvania. He developed a procedure for measuring the steady-state redox poise of the ubiquinone pool in isolated mitochondria, which his laboratory has used to investigate the regulation of the alternative oxidase.

David G. Whitehouse is a research fellow in the Department of Biochemistry at the University of Sussex, United Kingdom. His principal research interests are in the structures and functions of both the plant mitochondrial and the chloroplast electron transport chains. He holds a Ph.D. from the University of London and received his postdoctoral training at Imperial College, London. He has published a number of research articles and chapters on the regulation of mitochondrial electron transport.

Respiratory Chain Complex I

Ulrich Brandt
Johann Wolfgang Goethe-University, Frankfurt, Germany

Complex I (EC 1.6.5.3) is a multi-subunit respiratory chain NADH:ubiquinone oxidoreductase that is found in the inner mitochondrial membrane of almost all eukaryotes and in the plasma membrane of many bacteria. It contains one molecule of flavine mononucleotide (FMN) and eight to nine iron–sulfur clusters as redox prosthetic groups.

Mammalian complex I couples the transfer of two electrons to the pumping of four protons across the mitochondrial inner membrane and thereby provides up to 40% of the driving force for ATP generation by oxidative phosphorylation (OXPHOS). Complex I is the target of numerous pathological human mutations in both the mitochondrial and the nuclear genomes. Since single electron transfer is part of its catalytic cycle and semiquinone radicals are natural intermediates, complex I is also considered a major source for reactive oxygen species that have been implicated in the etiology of neurodegenerative disorders and in aging.

Complex I Structure

Overall Shape and Subcomplexes

Till date there is no detailed structural information available for complex I. Electron microscopic analysis using single particles and 2D crystals have demonstrated that the enzymes from bovine heart mitochondria, the eubacterium *Escherichia coli*, and the fungi *Neurospora crassa* and *Yarrowia lipolytica* are L-shaped with a hydrophobic membrane integral arm and a hydrophilic peripheral arm that protrudes into the mitochondrial matrix (Figure 1).

When *N. crassa* is grown in the presence of the mitochondrial protein synthesis inhibitor chloramphenicol, a small form of complex I is made which consists of hydrophilic proteins only. Chaotropic agents such as NaBr or detergents can separate the two arms of complex I and also dissociate them further. Subcomplexes have been studied extensively for bovine heart, *N. crassa*, and *E. coli* complex I (Table I).

Central Subunits and Redox Clusters

A minimal form of complex I, consisting of 14 subunits, is found in bacteria such as *E. coli*. Seven of these make up the peripheral arm and contain all the known redox prosthetic groups, namely, one molecule of FMN and eight to nine iron–sulfur clusters. The remaining seven are hydrophobic proteins located in the membrane arm. All these 14 central subunits are also present in eukaryotic complex I. In most eukaryotes, the seven central subunits of the membrane arm (ND1-6, ND4L) are encoded by the mitochondrial genome (Figure 1).

Accessory Subunits

Eukaryotic complex I also contains a large number of additional subunits, resulting in a total number of more than 35 subunits in fungi and at least 45 subunits in mammals. While some may simply serve as a scaffold to increase the stability of the enzyme, there are indications that others may confer additional features specific to eukaryotic complex I. One such example is the acyl carrier protein (ACP) that carries a phosphopantheteine prosthetic group and may function in mitochondrial lipid biosynthesis. The AQDQ subunit seems to be involved in regulation. Phosphorylation at a cAMP-dependent protein kinase consensus site (RVS) was found to stimulate complex I activity. The B16.6 kDa subunit is identical with the programmed cell death regulatory GRIM19 protein and may link complex I function to apoptosis. The MWFE subunit of the membrane arm seems to be involved in complex I assembly. Overall very little is known about the function of the accessory subunits.

A nomenclature established for the bovine enzyme by John Walker and co-workers has been generally accepted for the subunits of complex I. Apart from some of the nuclear-coded subunits that were originally named by their molecular masses, the first four amino acids of the mature protein are used (see Table I). If the mature protein is N-terminally blocked, a number indicating the molecular mass preceded by the letter B identifies the subunit.

Assembly Factors

Two proteins, named CIA30 and CIA84 (for complex I associated), were found to be associated with peripheral

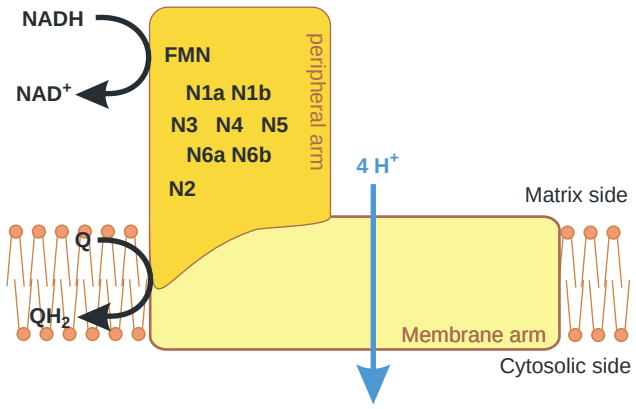

FIGURE 1 Schematic representation of mitochondrial complex I. The peripheral arm contains the seven nuclear-encoded central subunits and harbors all known redox prosthetic groups. The membrane arm contains the seven mitochondrially encoded subunits which are all highly hydrophobic. Eukaryotic complex I contains a number of additional "accessory" subunits distributed over both arms. The mechanism by which the transfer of electrons from NADH to ubiquinone is linked to proton translocation is essentially unknown. Q, ubiquinone; QH_2, ubiquinol.

arm subcomplexes in complex I mutants of *N. crassa*, but are not present in the fully assembled enzyme. Deletion of CIA30 or CIA84 led to complex I assembly defects in *N. crassa*. A CIA30 homologue is also present in mammalian genomes.

Complex I Evolution

Complex I was assembled from at least three pre-existing structural and functional modules during evolution. The homology to [NiFe] hydrogenases from various archae- and eubacterial sources has been especially useful for the understanding of complex I.

The Hydrogenase Module

Water-soluble hydrogenases from *Desulfovibrio* species consist of a large subunit which carries the [NiFe] site and is homologous to the 49 kDa subunit of complex I, and a small subunit which carries three iron–sulfur clusters and is homologous to the PSST subunit of complex I. In membrane-bound [NiFe] hydrogenases, exemplified by the enzyme encoded by the *ech* operon in *Methanosarcina barkeri*, the PSST homologue has suffered a C-terminal deletion abolishing two iron–sulfur clusters. Instead, an additional subunit carrying two iron–sulfur clusters in a ferredoxin-like fold has been acquired in this type of hydrogenase that is homologous to the TYKY subunit of complex I. It has been proposed that the hydrogenase structural fold has been conserved and shaped the catalytic core of complex I. According to this hypothesis, a significant part of the ubiquinone binding site of complex I has been derived

TABLE I

The Fourteen Central Subunits of Complex I and their Evolutionary Relationship to [NiFe] Hydrogenase Subunits; Eucaryotic Complex I Contains a Large Number (31 in Heart) of Additional "Accessory" Subunits

Subunit symbol			Location in[a]			Homologous subunit in [NiFe] hydrogenases	
Bovine	*Y. lipolytica*	*E. coli*	*Bovine*	*E. coli*	Redox prosthetic groups[b]	Water-soluble, e.g., *D. fructosovorans*	Membrane-bound, e.g., *M. barkeri*
75 kDa	NUAM	NuoG	Iλ	PA-DF	N1b N5 N4		
51 kDa	NUBM	NuoF	Iλ	PA-DF	FMN, N3		
49 kDa	NUCM	NuoD[c]	Iλ	PA-CF		Large subunit	EchE
30 kDa	NUGM	NuoC[c]	Iλ	PA-CF			EchD
24 kDa	NUHM	NuoE	Iλ	PA-DF	N1a		
TYKY	NUIM	NuoI	Iλ	PA-CF	N6a, N6b		EchF
PSST	NUKM	NuoB	Iλ	PA-CF	N2	Small subunit	EchC
ND1	ND1	NuoH	Iγ	MA			EchB
ND2[d]	ND2[d]	NuoN	Iγ	MA			EchA
ND3	ND3	NuoA	Iγ	MA			
ND4[d]	ND4[d]	NuoM	Iβ	MA			EchA
ND4L	ND4L	NuoK	Iγ	MA			
Nd5[d]	Nd5[d]	NuoL	Iβ	MA			EchA
ND6	ND6	NuoJ	?	MA			

[a] In *bovine* and *E. coli* complex I. Iλ, Iβ, Iγ, different subcomplexes of bovine heart complex I; PA-DF, peripheral arm, dehydrogenase fragment; PA-CF, peripheral arm, connecting fragment; MA, membrane arm.

[b] Compiled from EPR studies of the bovine heart (N1–N5) and the *N. crassa* enzymes (N6a, N6b). N1a and N1b are binuclear clusters, N2, N3, N4 and N5 are tetranuclear clusters. N6a and N6b are EPR-silent tetranuclear clusters in a ferredoxin-like arrangement.

[c] NuoC and NuoD are fused to a single polypeptide in *E. coli*.

[d] These subunits are similar to each other and to a family of Na^+/H^+ or K^+/H^+ antiporters.

from the [NiFe] site in the large subunit, while cluster N2 corresponds to the proximal iron–sulfur cluster in the small subunit of water-soluble hydrogenases. Based on known X-ray structures of water-soluble [NiFe] hydrogenases, a structural model for the catalytic core of complex I was deduced by Brandt and co-workers and validated by site-directed mutagenesis in the yeast *Y. lipolytica*.

The Na^+/H^+ Transporter Module

One of the two transmembrane subunits of the Ech hydrogenase is homologous to the complex I subunit ND1, while the other exhibits similarities to the three complex I subunits ND2, ND4, and ND5. These three subunits are in turn related to a particular type of Na^+/H^+ or K^+/H^+ antiporter, exemplified by the MrpA and MrpD proteins of *Bacillus subtilis*. Recruitement of this transmembrane module by the water-soluble [NiFe] hydrogenases clearly was an important step toward development of complex I as it provided a component most likely critical for the development of a proton translocation machinery.

The NADH Dehydrogenase Module

The "electron input device" of complex I is related to the NAD^+-reducing [NiFe] hydrogenase from *Ralstonia eutropha*, encoded by the *hox* operon. The 24 and 51 kDa subunits are homologous to HoxF and the first 200 residues of the 75 kDa subunit are homologous to HoxU. The C-terminal half of the 75 kDa subunit shows sequence similarity to a formate dehydrogenase from *Methanobacterium formicicum*.

Variants of Complex I

Interestingly, several complex I variants are known that lack the 75, 51, and 24 kDa subunits of the NADH dehydrogenase module. Two archaebacterial proton pumping enzymes, $F_{420}H_2$:methanophenazine oxidoreductase from *Methanosarcina mazei* and $F_{420}H_2$:menaquinone oxidoreductase from *Archaeoglobus fulgidus*, accept electrons from coenzyme F_{420}, which is specific for methanogenic archaebacteria. The metabolic function of complex I from cyanobacteria and the chloroplasts of higher plants is not known. It may catalyze electron transfer from either NADH, NADPH, or ferredoxin to plastoquinone.

Complex I from the bacteria *Helicobacter pylori* and *Campylobacter jejuni* lack the 51 and 24 kDa subunits and contain a modified version of the 75 kDa subunit. Therefore, it is likely that the electron donor to these enzymes is also not NADH.

Complex I Function

The overall reaction of respiratory chain complex I is the transfer of electrons from NADH to ubiquinone or menaquinone in some bacteria and the concomitant buildup of chemiosmotic membrane potential that in mammalian mitochondria contributes ~40% to the total proton-motive force generated during oxidative phosphorylation.

Electron Transfer and Redox Centers

The physiological reaction of complex I involves electron transfer from NADH via FMN onto a series of iron–sulfur clusters with E_{m7} values between −370 and −250 mV. The tetranuclear iron–sulfur cluster N2 (E_{m7} −150 mV) is generally regarded as the last redox center in this electron transfer chain and there is evidence that it is the immediate electron donor for ubiquinone. Electron transfer from NADH to artificial acceptors such as ferricyanide or hexaammineruthenium(III) chloride does not involve the quinone binding site and can also be observed with a three-subunit subcomplex (flavoprotein, FP) of bovine heart complex I which consists of the peripheral arm subunits 51, 24, and 10 kDa.

Proton Pumping

Experimental data with intact mitochondria and submitochondrial particles indicate that complex I pumps protons with a stoichiometry of 4 $H^+/2\,e^-$. The mechanism how proton translocation is coupled to redox chemistry is still unknown. A large number of concepts and more or less detailed hypothetical mechanisms have been proposed over the last decades, but even the fundamental issue, whether there is just one integrated pumping device or two pumps transporting 2 $H^+/2e^-$ each are operational in complex I, remains unsolved. While FMN could be ruled out as a component of the proton pump, most researches in the field consider iron–sulfur cluster N2 as probable candidate to be directly involved in ubiquinone reduction and proton translocation. This view is supported by experimental evidence for the most part obtained by Tomoko Ohnishi and co-workers demonstrating for this redox center a pH-dependent midpoint potential and magnetic coupling to ubisemiquinone species. However, all known redox centers of complex I reside in the peripheral arm and it remains obscure how electron transfer drives proton translocation across the membrane part. In recent years, different directly linked mechanisms essentially inverting the proton-motive ubiquinone cycle of the cytochrome bc_1 complex have been put forward, but emerging

evidence seems to favor a more indirect mechanism based on conformational coupling.

Na^+ Pumping by Bacterial Complexes I

In some bacteria, complex I pumps sodium ions in addition or instead of protons across the plasma membrane generating a sodium motive force rather than a proton motive force. For the purified and reconstituted complex I of *Klebsiella pneumonia*, a pump stoichiometry of 1 Na^+/e^- was determined.

Inhibitors of Complex I

A plethora of structurally diverse hydrophobic compounds have been reported to inhibit complex I and are considered to interfere with ubiquinone binding. Among these inhibitors are naturally occurring antibiotics as well as synthetic insecticides and acaricides. Also a number of drugs such as amytal and meperidine, neurotoxins related to 1-methy-4-phenylmeperidinium, and even detergents such as Triton X-100 and Thesit inhibit complex I. Kinetic studies suggested that these inhibitors can be grouped into three different classes that are represented by the well known and widely used inhibitors DQA (2-decyl-4-quinazolinyl amine) and piericidin A (class I/A-type), rotenone (class II/B-type), and capsaicin (C-type). Except for capsaicin, all these inhibitors exert their inhibitory potential at I_{50} values in the nanomolar range. Competition experiments demonstrated that these inhibitors share one common binding domain with partially overlapping sites. In agreement with this observation, cross-resistance between DQA/piericidin A and rotenone is observed in inhibitor resistant mutants.

Complex I in Disease

Genetic defects in complex I typically result in multisystem disorders with a wide spectrum of severities ranging from adult onset exercise intolerance to fatal infantile lactic acidosis. Disease is often progressive.

Mitochondrial Mutations

Deletions within the mitochondrial genome or point mutations in mitochondrial tRNA genes affect the function of several respiratory chain complexes simultaneously. Skeletal muscle biopsies from such patients typically show ragged red fibers caused by mitochondrial hypertrophy. The typical clinical phenotype of mitochondrial point mutations in the ND genes is Leber's Hereditary Optic Neuropathy (LHON), characterized by optic nerve atrophy or LDYT (LHON plus dystonia), characterized by additional lesions in the caudate and putamen. Ragged red fibers are not commonly observed in patients with isolated complex I defects.

Nuclear Mutations

Due to the large number of potential target genes, mutations affecting nuclear-coded subunits of complex I have been described only recently. The typical clinical picture is Leigh syndrome, a severe, early onset neuromuscular disorder, associated with lactic acidosis, ataxia, hypotonia, spasticity, developmental delay, optic atrophy, and, in the terminal stage, degeneration of the basal ganglia. Sometimes, this is accompanied by hypertrophic cardiomyopathy. Such mutations were found in the 75 kDa, 51 kDa, 49 kDa, PSST, TYKY, and AQDQ homologues.

Mechanisms of Complex I Pathology

Complex I dysfunction has several biochemical consequences which may be relevant for producing disease symptoms. (1) Feedback inhibition of the NADH-producing citric acid cycle and pyruvate dehydrogenase complex results in elevated blood lactate levels. (2) Lowered OXPHOS efficiency will reduce ATP production. OXPHOS defects often show a remarkable degree of tissue- and organ specificity. This has been explained by assuming different energetic thresholds, in descending order for optic nerve, neuronal cells, heart muscle, skeletal muscle, and liver. (3) Increased generation of reactive oxygen species. Oxidative stress is evident from the induction of MnSOD mRNA in complex I patients. ROS damage of complex I and the ND genes in the mitochondrial genome may result in a vicious cycle of mitochondrial damage. (4) Reduced mitochondrial energy production and elevated oxidative stress may lead to the opening of the mitochondria permeability transition pore, release of pro-apoptotic factors, and apoptotic cell death.

Poisoning of Complex I

The neurotoxin 1-methyl-4-phenyl 1,2,3,6 tetrahydropyridine (MPTP), a synthetic meperidine analogue, is able to rapidly and persistently induce symptoms of acute Parkinsonism in humans and other primates. MPTP is metabolized to 1-methyl-4-phenylpyridinium (MPP^+) by the action of glial cell monoamine oxidase B. Since MPP^+ is a substrate for the dopaminergic re-uptake pathway, it accumulates in the nigrostriatal dopaminergic neurons, where it causes a specific reversible inhibition of complex I. Strikingly, highly selective neurodegeneration of the nigrostriatal dopaminergic system was also observed

following chronic exposure of rats to the common complex I inhibitor rotenone. These results support the view that complex I deficiency may also be involved in the etiology of idiopathic Parkinsonism.

See Also the Following Articles

Cytochrome bc_1 Complex (Respiratory Chain Complex III) • Mitochondrial DNA • Mitochondrial Genome, Overview • Photosystem I: F_X, F_A, and F_B Iron–Sulfur Clusters • Respiratory Chain Complex II and Succinate: Quinone Oxidoreductases • Respiratory Chain Complex IV

Glossary

iron–sulfur clusters Nonheme iron prosthetic groups found in a wide range of redox enzymes. The reduced forms of binuclear and tetranuclear iron–sulfur clusters are paramagnetic and can be studied by electron-paramagnetic-resonance (EPR) spectroscopy.

mitochondrial DNA Small genome that codes for 13 subunits of the respiratory chain complexes and ATP synthase. A typical mammalian cell contains several hundreds of mitochondria and several thousands of mitochondrial genomes that are inherited exclusively through the oocyte cytoplasm.

oxidative phosphorylation (OXPHOS) "Fuel cell" of aerobic metabolism. Process by which redox energy derived from NADH or $FADH_2$ is converted into the phosphorylation potential of ATP. Electron transport and ATP synthesis are energetically coupled through an electrochemical proton potential across the inner mitochondrial membrane.

reactive oxygen species (ROS) Superoxide ($O_2^{\cdot-}$), hydrogen peroxide (H_2O_2), and hydroxyl radical ($OH^{\cdot}$) that may cause severe damage to lipids, proteins, and DNA. In mitochondria ROS are generated by side reactions of the respiratory chain complexes.

Further Reading

Brandt, U. (1997). Proton-translocation by membrane-bound NADH:ubiquinone-oxidoreductase (complex I) through redox-gated ligand conduction. *BBA-Bioenergetics* **1318**, 79–91.

Brandt, U., Kerscher, S., Dröse, S., Zwicker, K., and Zickermann, V. (2003). Proton pumping by NADH:ubiquinone oxidoreductase. A redox driven conformational change machanism? *FEBS Lett.* **545**, 9–17.

Complex I website: http://www.scripps.edu/mem/biochem//CI/MITOMAP: A Human Mitochondrial Genome Database: http://www.mitomap.org.

Degli Esposti, M. (1998). Inhibitors of NADH-ubiquinone reductase: An overview. *BBA-Bioenergetics* **1364**, 222–231.

Friedrich, T., and Scheide, D. (2000). The respiratory complex I of bacteria, archaea and eukarya and its module common with membrane-bound multisubunit hydrogenases. *FEBS Lett.* **479**, 1–5.

Hirst, J., Carroll, J., Fearnley, I. M., Shannon, R. J., and Walker, J. E. (2003). The nuclear encoded subunits of complex I from bovine heart mitochondria. *Biochim. Biophys. Acta* **1604**, 135–150.

Ohnishi, T. (1998). Iron–sulphur clusters/semiquinones in complex I. *BBA–Bioenergetics* **1364**, 186–206.

Schulte, U., and Weiss, H. (1995). Generation and characterization of NADH:ubiquinone oxidoreductase mutants in *Neurospora crassa*. *Methods Enzymol.* **260**, 1–14.

Smeitink, J., Sengers, R., Trijbels, F., and van der Heuvel, L. (2001). Human NADH:ubiquinone oxidoreductase. *J. Bioenerg. Biomembr.* **33**, 259–266.

Steuber, J. (2001). Na^+ translocation by bacterial NADH:quinone oxidoreductases: An extension to the complex-I family of primary redox pumps. *BBA-Bioenergetics* **1505**, 45–56.

Yagi, T., Yano, T., Di Bernardo, S., and Matsuno-Yagi, A. (1998). Procaryotic complex I (NDH-1), an overview. *Biochim. Biophys. Acta* **1364**, 125–133.

Biography

Ulrich Brandt is Professor at the Gustav-Embden Center for Biological Chemistry of the Johann Wolfgang Goethe-University in Frankfurt am Main, Germany. His principal research interest is the structure and function of respiratory chain complexes and the molecular causes of mitochondrial disorders. He holds a Ph.D. from the University of Munich and received his postdoctoral training at the Dartmouth Medical School, New Hampshire and the Glynn Research Institute, Cornwall, United Kingdom. He has studied the mechanism by which mitochondrial cytochrome bc_1 complex is inhibited by strobilurins, a family of compounds now widely used as potent fungizides in agriculture. He serves as the General Secretary of the German Society for Biochemistry and Molecular Biology.

Respiratory Chain Complex II and Succinate: Quinone Oxidoreductases

C. Roy D. Lancaster
Max Planck Institute of Biophysics, Frankfurt am Main, Germany

Succinate:quinone oxidoreductases (SQORs) are enzymes that couple the two-electron oxidation of succinate to fumarate [Eq. (1)] to the two-electron reduction of quinone to quinol [Eq. (2)]:

$$\text{succinate} \leftrightarrows \text{fumarate} + 2H^+ + 2e^- \quad (1)$$

$$\text{quinone} + 2H^+ + 2e^- \leftrightarrows \text{quinol} \quad (2)$$

They can also catalyze the opposite reaction, the coupling of quinol oxidation to the reduction of fumarate. Depending on the direction of the reaction catalysed *in vivo*, the members of the superfamily of SQORs can be classified as either succinate:quinone reductases (SQR) or quinol:fumarate reductases (QFR). SQR and QFR complexes are anchored in the cytoplasmic membranes of archaebacteria, eubacteria, and the inner mitochondrial membrane of eukaryotes with the hydrophilic domain generally extending into the cytoplasm and the mitochondrial matrix, respectively. SQR (respiratory complex II) is involved in aerobic metabolism as part of the citric acid cycle (Krebs cycle) and of the aerobic respiratory chain (Figure 1A). QFR participates in anaerobic respiration with fumarate as the terminal electron acceptor (Figure 1B) and is part of the electron transport chain catalyzing the oxidation of various donor substrates (e.g., H_2 or formate) by fumarate. These reactions are coupled via an electrochemical proton potential (Δp) to ADP phosphorylation with inorganic phosphate by ATP synthase.

Succinate:Quinone Oxidoreductases Classification

Functional Classification

Succinate:quinone oxidoreductases (SQORs) can be divided into three functional classes based on the quinone substrate and the *in vivo* function of the enzyme. Subclass 1 contains those enzymes that oxidize succinate (with an oxidation–reduction potential at pH 7, $E_{M7,}$ of +25 mV) and reduce a high-potential quinone, e.g., ubiquinone ($E_{M7} = +90$ mV) or caldariella quinone ($E_{M6.5} = +103$ mV). The succinate:quinone reductases (SQRs) from mammalian mitochondria (respiratory complex II) and many prokaryotes belong to this group. Subclass 2 comprises those enzymes that catalyze the oxidation of a low-potential quinol, e.g., menaquinol ($E_{M7} = -74$ mV) or rhodoquinol ($E_{M7} = -63$ mV), and the reduction of fumarate. All quinol:fumarate reductases (QFRs) studied so far belong to this subclass. Subclass 3 includes those enzymes that catalyze the oxidation of succinate and the reduction of a low-potential quinone, e.g. menaquinone or thermoplasmaquinone. These subclass 3 enzymes are found in gram-positive bacteria (e.g., *Bacillus subtilis*, *Paenibacillus macerans*, *Bacillus licheniformis*) and archaebacteria (e.g., *Thermoplasma acidophilum*).

Structural Classification

SQORs generally contain four protein subunits, referred to as A, B, C, and D. Subunits A and B are hydrophilic, whereas subunits C and D are integral membrane proteins. Among species, subunits A and B have high sequence homology, while that for the hydrophobic subunits is much lower. Most of the SQR enzymes of gram-positive bacteria and the QFR enzymes from ε-proteobacteria contain only one larger hydrophobic polypeptide (C), which is thought to have evolved from a fusion of the genes for the two smaller subunits C and D. While subunit A harbors the site of fumarate reduction and succinate oxidation, the hydrophobic subunit(s) contain the site of quinol oxidation and quinone reduction.

Based on their hydrophobic domain and heme *b* content, SQORs are divided into five types (Figure 2A). Type A enzymes contain two hydrophobic subunits and two heme groups, e.g., SQR from the archaea *Archaeoglobus fulgidus*, *Natronomonas pharaonis*, and *T. acidophilum*. Type B enzymes contain one hydrophobic subunit and two heme groups, as is the case for SQR from the gram-positive bacteria *B. subtilis* and *P. macerans* and for QFR from the ε-proteobacteria *Campylobacter jejuni*, *Helicobacter pylori*, and

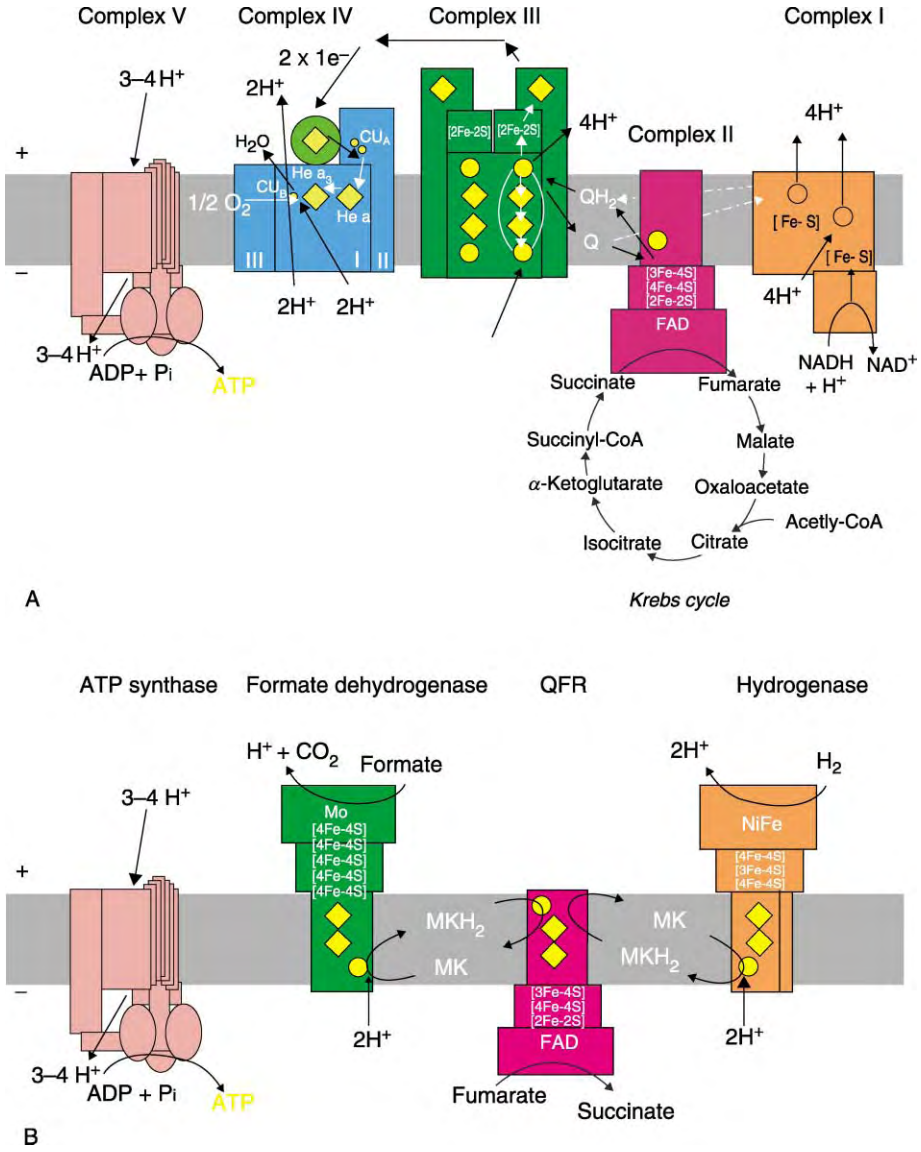

FIGURE 1 Electron flow and the generation and utilization of a transmembrane electrochemical potential in aerobic respiration (A) and anaerobic respiration (B). Modified from Lancaster, C. R. D. (2003). The role of electrostatics in proton-conducting membrane protein complexes. *Adv. Protein Chem.* **63**, 131–149. *FEBS Lett.* **545**, 52–60.

Wolinella succinogenes. Examples for type C enzymes, which possess two hydrophobic subunits and one heme group, are SQR from mammalian mitochondria and from the proteobacteria *Paracoccus denitrificans* and *Escherichia coli*, and QFR from the nematode *Ascaris suum*. The QFR of *E. coli* is an example of a type D enzyme, which contains two hydrophobic subunits and no heme group. Finally, type E enzymes, such as SQRs from the archaea *Acidianus ambivalens* and *Sulfolobus acidocaldarius*, but also from the proteobacterium *C. jejuni* and the cyanobacterium *Synechocystis*, also contain no heme, but have two hydrophobic subunits very different from the other four types and more similar to those of heterodisulfide reductase from methanogenic archaea.

SQOR Structure and Function

Overall Description of the Structure

The currently available crystal structures of SQORs (Figure 2B–2D) are those of two prokaryotic QFRs, both from 1999, and one prokaryotic SQR, from 2003. The *E. coli* QFR (Figure 2D), determined at 3.3Å resolution, belongs to the type D enzymes, and the QFR of *W. succinogenes* (Figure 2B), refined at 2.2Å resolution, is of type B. The structure of the SQR from *E. coli* (Figure 2B) was reported at 2.6Å resolution. Interestingly, *E. coli* QFR appears to be a monomeric complex of one copy each of the A, B, C, and D subunits, whereas

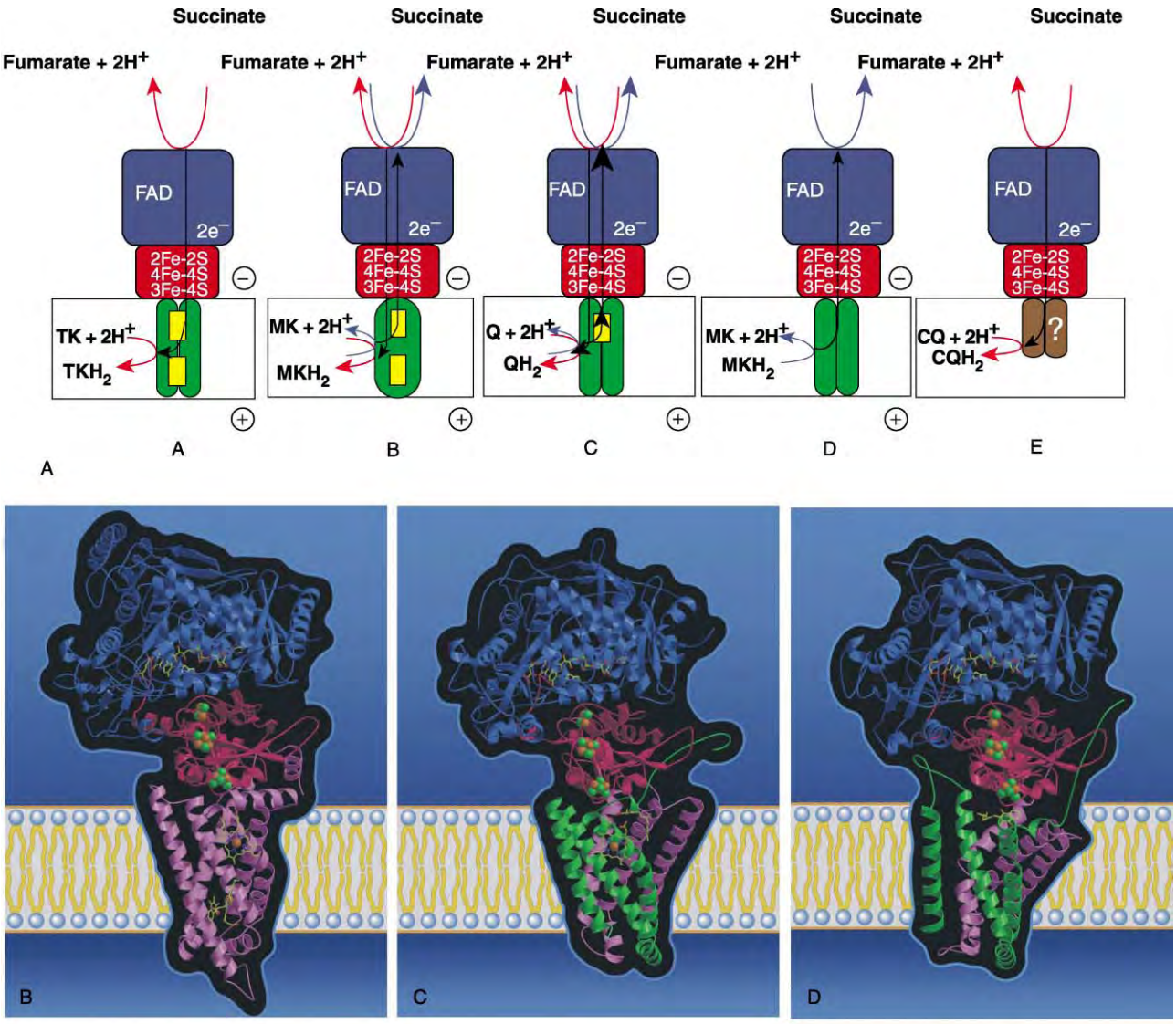

FIGURE 2 (A) Classification (A to E) of succinate:quinone oxidoreductases based on their hydrophobic domain and heme content. The hydrophilic subunits A and B are drawn schematically in blue and red, respectively; the hydrophobic subunits C and D in green. Heme groups are symbolized by small yellow rectangles. The directions of the reactions catalyzed by SQR and QFR are indicated by red and blue arrows, respectively. White rectangles symbolize the respective cytoplasmic or inner mitochondrial membrane bilayer. The positive (+) and negative (−) sides of the membrane are indicated. In bacteria, the negative side is the cytoplasm ("inside"), the positive side the periplasm ("outside"). For mitochondrial systems, these are the mitochondrial matrix and the intermembrane space, respectively. The type of quinone transformed in vivo is not necessarily unique for each type of enzyme. The examples given are thermoplasma-quinone (TK), menaquinone (MK), ubiquinone (Q), and caldariella quinone (CQ).(-B-D) Three-dimensional structures of *W. succinogenes* QFR, a B-type SQOR (B) (determined by Lancaster, C.R., Kroger, A., Auer, M., and Michel, H. (1999). Structure of fumarate reductase from *Wolinella succinogenes* at 2.2Å resolution. *Nature* **402**, 377–385), *E. coli* SQR, a C-type SQOR (C) (determined by Yankovskaya, V., Horsefield, R., Tornroth, S., Luna-Chavez, C., Miyoshi, H., Leger, C., Byrne, B., Cecchini, G., and Iwata, S. (2003). Architecture of succinate dehydrogenase and reactive oxygen species generation. *Science* **299**, 700–704), and *E. coli* QFR, a D-type SQOR (D) (determined by Iverson, T. M., Luna-Chavez, C., Cecchini, G., and Rees, D. C. (1999). Structure of the *Escherichia coli* fumarate reductase respiratory complex. *Science* **284**, 1961–1966). The Cα traces of the A subunits are shown in blue, those of the B subunits in red, those of the C subunits in pink, and those of the D subunits in green. The atomic structures of the prosthetic groups are superimposed for better visibility. From top to bottom, these are the covalently bound FAD, the [2Fe–2S], the [4Fe–4S], and the [3Fe–4S] iron–sulfur clusters, and (where present) the proximal and the distal heme *b* groups. Atomic color coding is as follows: C, N, O, P, S, and Fe are displayed in yellow, blue, red, light green, green, and orange, respectively. Figures with atomic models were prepared with a version of Molscript (Kraulis, P. J. (1991). MOLSCRIPT: a program to produce both detailed and schematic plots of protein structures. *J. Appl. Crystallogr.* **24**, 946–950) modified for color ramping (Kraulis, P. J. (1997). Esnouf Rm. An extensively modified version of MolScript that includes greatly enhanced coloring capabilities. *J. Mol. Graphics Mod.* **15**, 132–134) and rendered with the program Raster3D (Merrit, E. A. and Bacon, D. J. (1997). Raster 3D: Photorealistic molcecular graphics. *Meth. Enzymol.* **277**, 505–524).

W. succinogenes QFR is apparently a homodimer of two sets of A, B, and C subunits, and *E. coli* SQR is a homotrimer of three sets of A, B, C, and D subunits. For the *Wolinella* enzyme, analytical gel filtration experiments have shown that the homodimer is apparently also present in the detergent-solubilized state of the enzyme, implying that it is unlikely to be an artifact of crystallization. However, functionally all three enzymes appear to act as monomers, which is why only the monomeric complexes are shown in Figure 2B–2D.

The Relative Orientations of Soluble and Membrane-Embedded SQOR Subunits

The structures of all three enzymes shown in Figure 2B–2D can be superimposed on the basis of the Cα positions of the conserved hydrophilic subunits A and B. In this superimposition, large parts of the membrane-embedded subunits can be aligned in the case of *W. succinogenes* QFR and *E. coli* SQR, but not for *E. coli* QFR. However, as demonstrated by Lancaster and coauthors, in an alternate orientation the transmembrane subunits of *E. coli* QFR and of *W. succinogenes* QFR can be overlaid in spite of the respective absence and presence of the two heme groups. Consequently, the relative orientations of the hydrophilic subunits and the transmembrane subunits is similar in *W. succinogenes* QFR and *E. coli* SQR and different in *E. coli* QFR.

Subunit A and the Site of Succinate Oxidation/Fumarate Reduction

The flavoprotein or A subunit (64–73 kDa) of all described membrane-bound SQOR complexes contains a flavin adenine dinucleotide (FAD) prosthetic group covalently bound to a conserved His residue as an 8α-[Nε-histidyl]-FAD. The two most important domains of subunit A are the bipartite FAD-binding domain and the "capping" domain, which is inserted between the two parts of the FAD-binding domain. The capping domain contributes to burying the otherwise solvent-exposed FAD isoalloxazine ring from the protein surface.

The binding site of succinate/fumarate is located between the FAD-binding domain and the capping domain next to the plane of the FAD isoalloxazine ring. The structures and results from site-directed mutagenesis suggest that the *trans*-dehydrogenation of succinate to fumarate occurs via the combination of a hydride ion transfer from one succinate methylene group to the N5 position of the FAD and a proton transfer from the other succinate methylene group to the side chain of a conserved Arg residue of the capping domain (Figure 3). All residues implicated in substrate binding and catalysis are conserved throughout the superfamily

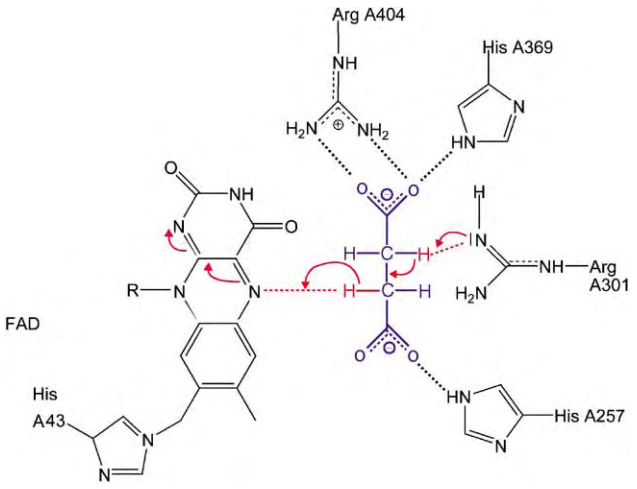

FIGURE 3 Possible mechanism of succinate oxidation. Modified from Lancaster C. R. D. (2001). *Eur. J. Biochem.* **268**, 1820–1827.

of SQORs, so that this reversible mechanism is considered generally relevant for all SQORs. Release of the product could be facilitated by movement of the capping domain away from the dicarboxylate site.

Subunit B: The Iron–Sulfur Protein

Generally, SQORs contain three iron–sulfur clusters, which are exclusively bound by the B subunit of 26–30 kDa. Enzyme types A–D contain one [2Fe–2S]$^{2+,1+}$, one [4Fe–4S]$^{2+,1+}$, and one [3Fe–4S]$^{1+,0}$ cluster, whereas an additional [4Fe–4S]$^{2+,1+}$ cluster apparently replaces the [3Fe–4S]$^{1+,0}$ in the type E enzyme. This subunit consists of two domains, an N-terminal plant ferredoxin domain, in contact with subunit A and binding the [2Fe–2S] cluster, and a C-terminal bacterial ferredoxin domain, in contact with the hydrophobic subunit(s) and binding the [4Fe–4S] and the [3Fe–4S] clusters. In general, these iron–sulfur clusters are coordinated by conserved Cys residues, although one of the ligands to the [2Fe–2S] cluster in *E. coli* SQR is an Asp. At the position corresponding to the fourth Cys of the [4Fe–4S] cluster, the [3Fe–4S] cluster contains a Leu (*W. succinogenes* QFR), Ile (*E. coli* SQR), Val (*E. coli* QFR), or Ser (*B. subtilis* SQR). Whereas the introduction of a Cys into *E. coli* QFR could replace the native [3Fe–4S] by a [4Fe–4S] cluster, this was not the case for *B. subtilis* SQR.

The Integral Membrane Subunit(s) C (and D) and the Sites of Quinol Oxidation/Quinone Reduction

Type A, C, and D SQOR enzymes contain two hydrophobic polypeptides with three membrane-spanning

helices each (numbered I, II, and III and IV, V, and VI, respectively). According to an evolutionary model proposed by C. Hägerhäll and L. Hederstedt, the large single hydrophobic polypeptides of type B SQOR enzymes with five membrane-spanning helices are thought to have evolved from the fusion of the genes for the two small hydrophobic polypeptides with concomitant loss of transmembrane helix III. This view is supported by the structural superpositions previously discussed. To a varying degree, all transmembrane segments are tilted with respect to the membrane normal.

The planes of both heme molecules bound by *W. succinogenes* QFR are approximately perpendicular to the membrane surface, and their interplanar angle is 95°. The His axial ligands to the proximal heme b_P, located toward the cytoplasmic surface of the membrane, and thus toward the [3Fe–4S] cluster, are located on transmembrane helices II and V. Residues of the two other transmembrane helices I and IV interact with the propionate groups of heme b_P via hydrogen bonds and salt bridges; this underscores the structural importance of the bound heme. The axial ligands to the distal heme b_D are located on helices I and IV. The binding of the two heme *b* molecules by an integral membrane protein four-helix bundle described here is very different from that described for other diheme-binding membrane protein complexes, such as the cytochrome bc_1 complex, where only two transmembrane segments provide two axial heme *b* ligands each, and also the membrane-bound hydrogenases and formate dehydrogenases, where one transmembrane helix provides two axial His ligands and two others provide one His ligand each. One consequence of this difference is that the distance between the two heme iron centers is distinctly shorter in *W. succinogenes* QFR (15.6Å) than it is in the mitochondrial cytochrome bc_1 complex (21Å) and in *E. coli* formate dehydrogenase-N (20.5Å). The mode of heme binding for the single (proximal) heme of *E. coli* SQR is analogous to that described for heme b_P of *W. succinogenes* QFR.

The sites of quinol oxidation/quinone reduction have been localized in all three enzymes of known three-dimensional structure by a combination of X-ray crystallography, site-directed mutagenesis, functional characterization of resulting variant enzymes, and/or inhibitor-binding studies, respectively. In *E. coli* QFR, the menaquinol oxidation site is located proximally, close to the [3Fe–4S] cluster. In *E. coli* SQR, this position is occupied by the heme *b* group, but the ubiquinone reduction site is also located proximally, close to the [3Fe–4S] cluster, at an alternate position. In *W. succinogenes* QFR, the menaquinol oxidation site is located distally, close to heme b_D.

Electron and Proton Transfer

Electron Transfer

For the function of QFR, electrons have to be transferred from the quinol-oxidizing site in the membrane to the fumarate-reducing site, protruding into the cytoplasm. Conversely, for the function of SQR, electrons have to be transferred from the succinate oxidation site in subunit A to the quinone reduction site in the membrane. The linear arrangement of the prosthetic groups in the complexes shown in Figure 2B–2D therefore provides one straightforward pathway by which electrons could be transferred efficiently between the two sites of catalysis. It has been shown for other electron transfer proteins that physiological electron transfer between prosthetic groups occurs if the edge-to-edge distances relevant for electron transfer are shorter than 14Å, but does not occur if they are longer than 14Å. In all three cases, this indicates that physiological electron transfer can occur between the prosthetic groups of one heterotrimeric or heterotetrameric complex, but not between the two (*W. succinogenes* QFR) or three (*E. coli* SQR) complexes in the respective homodimer or homotrimer.

Prior to the determination of the three-dimensional structures, because of its very low midpoint potential ($E_m < -250$ mV), it had been suggested that the [4Fe–4S] cluster does not participate in electron transfer. However, the determined low potential may be an artifact due to anti-cooperative electrostatic interactions between the redox centers. The position of the [4Fe–4S] cluster as revealed in the structures is highly suggestive of its direct role in electron transfer between the [3Fe–4S] cluster and the [2Fe–2S] cluster. Despite this major thermodynamically unfavorable step, the calculated rate of electron transfer is on a microsecond scale, demonstrating that this barrier can easily be overcome by thermal activation as long as the electron transfer chain components are sufficiently close to promote intrinsically rapid electron tunneling.

The positioning of the heme in *E. coli* SQR is puzzling because it does not seem to be required for electron transfer between the catalytic sites. A possible explanation for this also explains why SQR is favored over QFR in *E. coli* when oxygen is present. Under aerobic conditions, reduced *E. coli* QFR produces large amounts of reactive oxygen species (ROS), including superoxide radical (O_2^-) and hydrogen peroxide (H_2O_2), which has been suggested to be caused by electron accumulation around the FAD. In sharp contrast, *E. coli* SQR reacts poorly with molecular oxygen, producing modest amounts of O_2^- and no H_2O_2. On the basis of their crystal structure, Yankovskaya *et al.* (2003) argued that the heme group

in SQR provides an electron sink when the quinone site is not occupied, thus preventing buildup of electrons around the FAD and subsequent ROS generation. However, this electron-sink mechanism is predicted to be less effective for mitochondrial SQRs because heme *b* has a lower redox potential than in *E. coli* SQR.

Electron-Coupled Proton Transfer

In addition to the transfer of electrons, two protons are bound at the site of reduction and two protons are liberated at the site of oxidation [see Eqs. (1) and (2)]. An overview of the current status of discussion of electron and proton transfer in succinate:quinone oxidoreductases is shown in Figure 4A–4D. In mitochondrial complex II and other C-type enzymes such as SQR from *P. denitrificans* and *E. coli*, electron transfer from succinate to ubiquinone does not lead to the generation of a transmembrane electrochemical potential, Δp, since the protons released by succinate oxidation are on the same side of the membrane as those consumed by quinone reduction (Figure 4A). Similarly, in *E. coli* QFR, the protons released by proximal quinol oxidation are balanced by the protons consumed by fumarate reduction (Figure 4B). Succinate oxidation by menaquinone, an endergonic reaction under standard conditions, is catalyzed by a B-type SQOR in gram-positive bacteria, e.g., *B. subtilis*. There is experimental evidence indicating that the menaquinone reduction site in *B. subtilis* SQR is close to the heme b_D in a position analogous to the menaquinol oxidation site of *W. succinogenes* QFR. This arrangement of the catalytic sites of succinate oxidation and menaquinone reduction would allow succinate oxidation by menaquinone in *B. subtilis* to be driven by the electrochemical proton potential (Figure 4C), and there is indeed experimental evidence that this is the case. This reaction is analogous to that suggested by the arrangement of the catalytic sites for *W. succinogenes* QFR, but in the opposite direction. Experimental results do indicate that *B. subtilis* SQR generates a proton potential when functioning as a QFR. However, the experimental results on intact bacteria, with inverted vesicles or liposomes containing *W. succinogenes* QFR, indicate that the oxidation of menaquinol by fumarate as catalyzed by *W. succinogenes* QFR is an electroneutral process. In order to reconcile these experimental findings with the arrangement of the catalytic sites in the structure, it has been proposed that transmembrane electron transfer in dihemic QFRs is tightly coupled to the compensatory, parallel transfer of protons across the membrane, thus balancing the protons released to the periplasm upon menaquinol oxidation and the protons bound from the cytoplasm upon fumarate reduction (Figure 4D). A key residue in this proposed proton transfer pathway is a Glu residue located in the middle of the membrane that is conserved only in dihemic menaquinol:fumarate reductases, but not in dihemic succinate:menaquinone reductases. The first experimental results supporting this E-pathway hypothesis have recently been obtained.

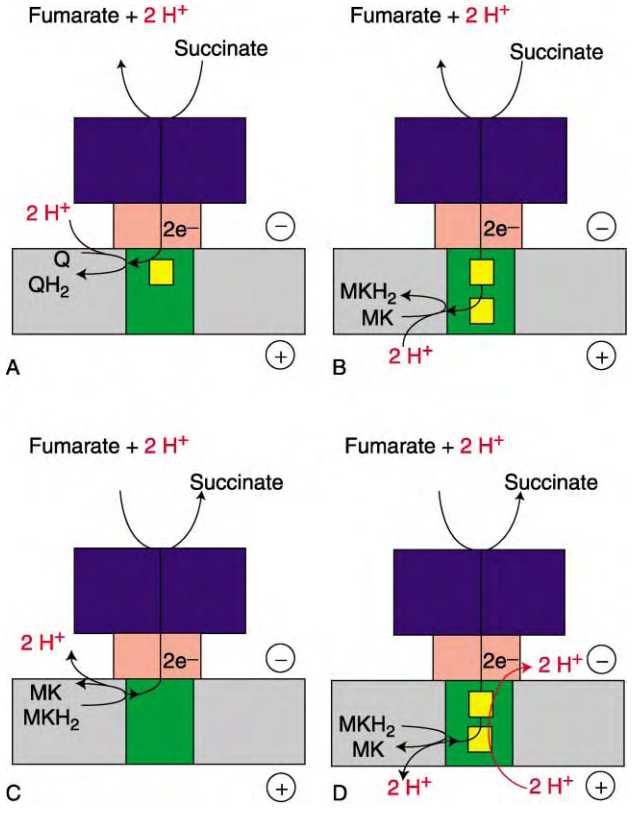

FIGURE 4 The coupling of electron and proton flow in succinate: quinone oxidoreductases in aerobic (A, B) and anaerobic respiration (A, C), respectively. Positive and negative sides of the membrane are as described for Figure 2 (A and B). Electroneutral reactions as catalyzed by C-type SQR enzymes (A) and D-type *E. coli* QFR (C). (B) Utilization of a transmembrane electrochemical potential Δp as possibly catalyzed by A-type and B-type enzymes. (D) Electroneutral fumarate reduction by B-type QFR enzymes with a proposed compensatory E-pathway.

See Also the Following Articles

Ferredoxin • Ferredoxin-NADP$^+$ Reductase • Flavins • Iron–Sulfur Proteins • Photosystem I: F_X, F_A, and F_B Iron–Sulfur Clusters

Glossary

flavin adenine dinucleotide (FAD) A riboflavin-containing hydrogen acceptor molecule in the Krebs cycle and a coenzyme of some oxidation–reduction enzymes.

fumarate A dicarboxylate anion ($^{-}OOC-CH{=}CH-COO^{-}$) that occurs as an intermediate compound in metabolic processes, most importantly in the citric acid cycle (Krebs cycle).

heme group A complex organic red iron-containing pigment used by proteins to bind oxygen and/or electrons.

His ligand A histidine residue that participates in forming a complex around a central atom or ion, e.g., the central iron of a heme group.

succinate A dicarboxylate anion ($^{-}OOC-CH_2-CH_2-COO^{-}$) that occurs as an intermediate compound in metabolic processes, most importantly in the citric acid cycle (Krebs cycle).

Further Reading

Ackrell, B. A. C., Johnson, M. K., Gunsalus, R. P., and Cecchini, G. (1992). Structure and function of succinate dehydrogenase and fumarate reductase. In *Chemistry and Biochemistry of Flavoenzymes* (F. Mueller, ed.) Vol 3 pp. 229–297. CRC Press, Boca Raton, FL.

Cecchini, G. (2003). Function and structure of complex II of the respiratory chain. *Annu. Rev. Biochem.* **72**, 77–109.

Hägerhäll, C. (1997). Succinate:quinone oxidoreductases: Variations on a conserved theme. *Biochim. Biophys. Acta Bioenerg.* **1320**, 107–141.

Hederstedt, L. (1999). Respiration without O_2. *Science* **284**, 1941–1942.

Hederstedt, L. (2003). Complex II is complex too. *Science* **299**, 671–672.

Lancaster, C. R. D. (2001). Succinate:quinone oxidoreductases. In *Handbook of Metalloproteins* (A. Messerschmidt, R. Huber, T. Poulos and K. Wieghardt, eds.) Vol 1, pp. 379–401. John Wiley & Sons, Chichester, UK.

Lancaster, C.R.D (ed.) (2002). Special issue on fumarate reductases and succinate dehydrogenases. *Biochim. Biophys. Acta* **1553**, 1–176.

Lancaster, C. R. D. (2003). The structure of *Wolinella succinogenes* quinol:fumarate reductase and its relevance to the superfamily of succinate:quinone oxidoreductases. *Adv. Protein Chem.* **63**, 131–149.

Ohnishi, T., Moser, C. C., Page, C. C., Dutton, P. L., and Yano, T. (2000). Simple redox-linked proton-transfer design: New insights from structures of quinol-fumarate reductase. *Structure* **8**, R23–R32.

Biography

C. Roy D. Lancaster is a Group Leader in the Department of Molecular Membrane Biology at the Max Planck Institute of Biophysics. He teaches biochemistry and biophysical chemistry at J.W. Goethe University, Frankfurt am Main. His principle research interests are in the structure and mechanism of action of membrane protein complexes. He holds an M.Sc. degree from McMaster University and a Dr. phil. nat. degree from J.W. Goethe University. His postdoctoral training was at the Max Planck Institute of Biophysics. He has determined the highest resolution structure to date of a succinate:quinone oxidoreductase and has authored and edited key texts in the field.

Respiratory Chain Complex IV

Hartmut Michel
Max Planck Institute of Biophysics, Frankfurt, Germany

Located within the inner membranes of mitochondria, or within the cytoplasmic membranes of aerobic bacteria, complex IV is the terminal enzyme of aerobic respiratory chains. It belongs to the superfamily of heme/copper containing terminal oxidases and catalyzes the reduction of oxygen to water. Typical representatives of this enzyme superfamily, as those found in mitochondria, use reduced cytochrome *c* as electron donor and are therefore also called cytochrome *c* oxidases. Cytochrome *c* provides its electrons from the outer side of the membrane, whereas the protons required for water formation access the active site from the inner ("matrix") side of mitochondria or from the cytoplasm of bacteria. As a result of the different spatial origin of the electrons and protons consumed in the reaction, four elementary charges per oxygen molecule reduced are translocated across the inner mitochondrial (or bacterial) membrane. In addition, four protons are transported ("pumped") from the mitochondrial matrix (or bacterial cytoplasm, respectively) to the outside of mitochondria or bacteria. Therefore the reaction can be written as

$$4e^- + O_2 + 8H_i^+ \rightarrow 2H_2O + 4H_o^+,$$

where H_i^+ stands for protons originating from the matrix (cytoplasmic) space and H_o^+ for protons released at the external side.

The proton transport produces a transmembrane electrochemical proton potential that drives the synthesis of adenosine-5′-triphosphate ("ATP") from adenosine-5′-diphosphate ("ADP") and inorganic phosphate through another membrane-spanning complex, the ATP synthase, which is also called complex V of the respiratory chain.

Background

Aerobic, oxygen-consuming respiration is the major means of producing energy in animals, fungi, many yeasts and bacteria. Oxygen itself is a side product of the oxygenic photosynthesis occuring in plants, algae, and cyanobacteria. These organisms produce reduced coenzymes (NADPH, quinols) and ATP in the course of the photosynthetic light reaction. NADPH is used to fix carbon dioxide and to synthesize carbohydrates and other organic compounds during the photosynthetic dark reactions. This organic matter is consumed by heterotrophic organisms. NADH and quinols are formed during the degradation of foodstuff and oxidized in the respiratory chain. In the typical mitochondrial respiratory chain (Figure 1) NADH is oxidized by complex I (NADH dehydrogenase). The electrons are transferred onto ubiquinone, the ubiquinol formed is oxidized by complex III (cytochrome bc_1 complex, also called ubiquinol-cytochrome *c* oxidoreductase) which reduces cytochrome *c*. This electron carrier is oxidized again by complex IV (cytochrome *c* oxidase). The latter uses the electrons to reduce oxygen and to form water, thus closing the cycle. Complex II (succinate dehydrogenase) constitutes a parallel entry into the respiratory chain and is also part of the citric acid cycle.

The respiratory chains from aerobic bacteria contain many more membrane-protein complexes and are often branched. They may contain up to four different terminal oxidases reacting with molecular oxygen. The electron donating substrates for the individual terminal oxidases may be cytochromes of the *c* type, various quinols, or even high-potential iron sulfur proteins. Most of them belong to the family of heme/copper containing terminal oxidases. The exception is cytochrome *bd*, which is a ubiquinol oxidase and not related to the heme/copper containing terminal oxidases. Cytochromes *bd* do not pump protons, however, electrons and protons, as in the heme/copper containing oxidases, enter the active site of this enzyme from opposite sides of the membrane leading to a net translocation of four charges per oxygen molecule consumed.

Astonishingly, the superfamily of the heme/copper containing terminal oxidases appears to be rather old. Family members are found in bacteria, as well as in archaea. The splitting into these lineages during evolution predates the conversion of the atmosphere from a reducing one to an oxidizing one, which dates back to ~2 billion years, when cyanobacteria developed the water-splitting, oxygen-releasing photosystem II. It turned out that the nitric oxide reductase (nitrogen monoxide reductase, NO reductase) is closely related to the heme/copper containing terminal oxidases. An iron atom in the NO reductases replaces a copper atom

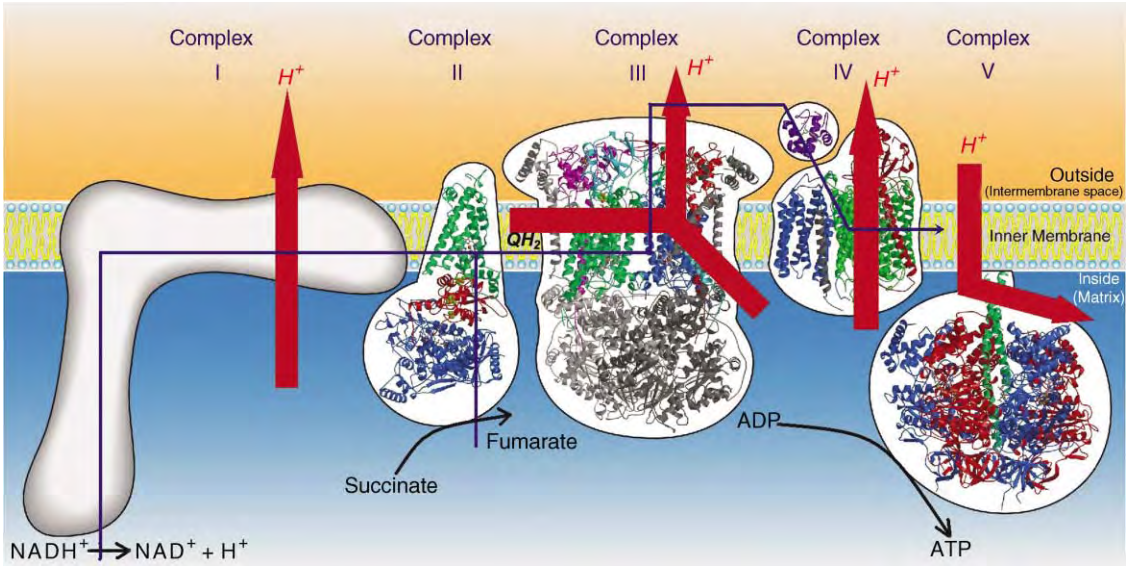

FIGURE 1 The mitochondrial respiratory chain. The five complexes of the respiratory chain are presented with their known structures in a functional context. The atomic structure of complex I or NADH dehydrogenase (left) is not known, but its shape has been determined by electron microscopy. It reduces ubiquinone to ubiquinol and pumps protons. Complex II (succinate dehydrogenase) is represented by a chain model. It also produces ubiquinol (QH_2). Ubiquinol is oxidized by complex III (cytochrome bc_1 complex). The cytochrome bc_1 complex releases protons at the outside and uses a quinone cycle to translocate additional protons across the membrane. The cytochrome bc_1 complex from yeast is shown. It reduces cytochrome *c*, which is oxidized by cytochrome *c* oxidase. The bacterial cytochrome *c* oxidase from *Paracoccus denitrificans* is shown. Cytochrome *c* oxidase pumps protons. The pumped protons flow back via the membrane part of complex V (ATP synthase). The backflow leads to a rotation of a subunit in the extramembraneous part of the ATP synthase, which is coupled to the synthesis of ATP. Proton flows are indicated by the red arrows. Figure drawn by P. Lastrico and E. Olkhova.

which is a part of the active site in the heme/copper containing terminal oxidases. NO reductases appear to be unable to pump protons. The original task of both the heme/copper containing terminal oxidases (which are OO reductases) and the NO reductases might have been detoxification. Molecular oxygen, being toxic for the organisms living under the reducing atmosphere, might have been created by photolysis of water by ultraviolet light and had to be destroyed.

Prosthetic Groups

The heme/copper containing terminal oxidases minimally contain two heme groups and one copper atom as prosthetic groups. One of the heme groups is a high-spin heme. A copper atom, called Cu_B, is found in ~5Å distance. Cu_B and the high-spin heme form the so-called binuclear center. During turnover, molecular oxygen is bound to the central iron atom of the high-spin heme between the heme and Cu_B and reduced there during the catalytic cycle of the enzyme. The second heme is a low-spin heme and acts as an intermediate electron carrier.

The optical absorbance spectra have been the signature for the cytochrome *c* oxidases. In the mitochondrial cytochrome *c* oxidases both hemes are of the A type (see Figure 2), which give rise to characteristic absorbance maxima at around 600 nm. The high-spin heme of the active site is called heme a_3, the low spin one heme *a*. The term cytochrome aa_3 was used for the terminal oxidase of mitochondria. In many bacteria, the low-spin heme is a heme B, giving rise to a terminal oxidase of the ba_3 type. One ubiquinol oxidase of *Escherichia coli* contains heme O as the high-spin heme, therefore it is also called cytochrome *bo* or bo_3.

Cytochrome *c* oxidases contain another copper center, which is called Cu_A. It is actually formed by two copper atoms, which share one electron upon reduction. During turnover of the enzyme, Cu_A receives the electron from cytochrome *c* and transfers it to the low-spin heme. Ubiquinol oxidases do not possess this Cu_A center. Several terminal oxidases also contain a covalently bound cytochrome *c*. Depending on the nature of the other hemes these enzymes are called caa_3, or *cbo*, or cbb_3 oxidases. The terminal oxidases of the cbb_3-type operate at rather low-oxygen concentrations and, for example, are required for the nitrogen fixation in *Rhizobia* in order to keep the oxygen levels very low.

Cytochrome *c* oxidases also contain a magnesium or manganese atom close to the periplasmic (intermembrane) face of the enzyme. It is missing in the ubiquinol

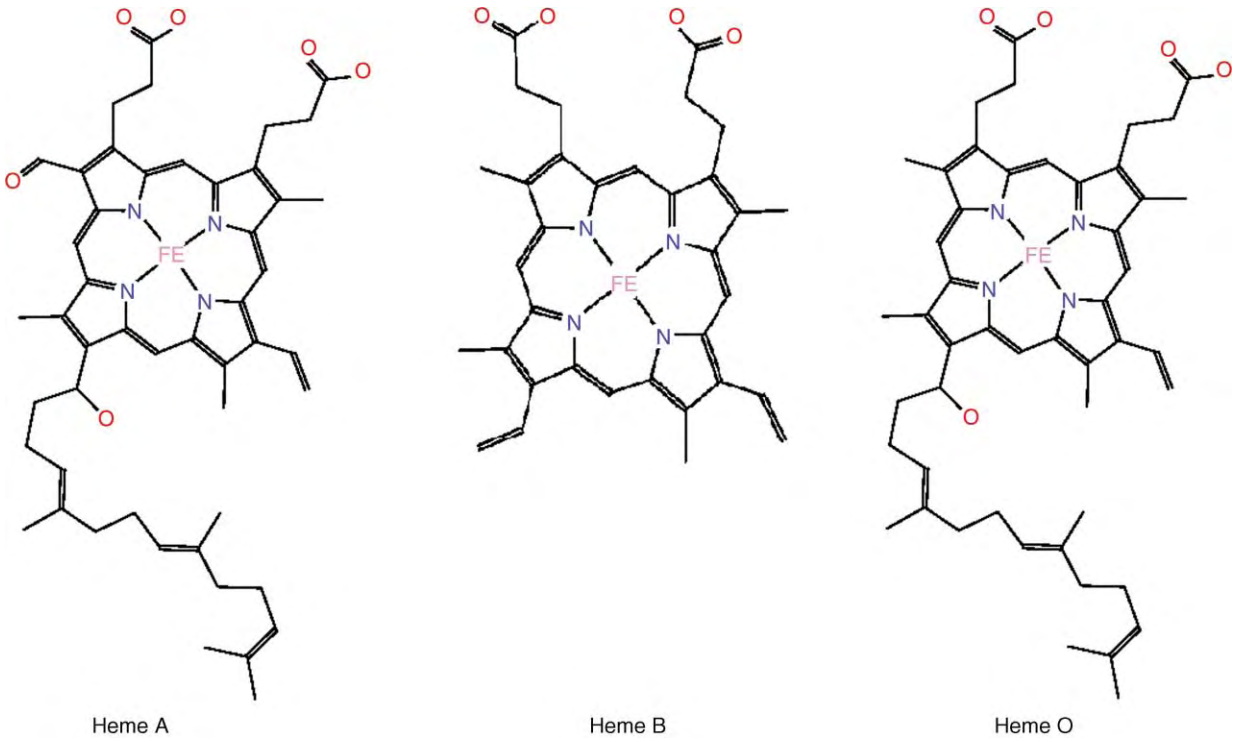

FIGURE 2 Chemical structures of the noncovalently bound hemes found in terminal oxidases. The structures of heme A, heme B, and heme O (from left to right) are shown.

oxidases and does not appear to be involved in electron transfer.

Protein Composition

The mitochondrial cytochrome *c* oxidases possess a core consisting of three protein subunits. These subunits are encoded by the mitochondrial genome. Subunit I is the largest subunit and possesses between 500 and 600 amino acid residues. It binds heme *a* as well as the heme a_3-Cu_B binuclear center and is the major catalytic subunit. Subunit II provides the binding site for the Cu_A-center and is anchored to the membrane by two N-terminal membrane-spanning helices. Subunit III possesses seven membrane-spanning helices but no prosthetic groups. Its function is unknown; it is not required for the catalytic activity. If its gene is deleted in bacteria, an active two-subunit enzyme is still found, albeit at a reduced level. If subunit III is removed the enzyme becomes rather unstable under turnover conditions.

The mitochondrial cytochrome *c* oxidases contain up to eight additional smaller subunits, which are encoded by the nuclear genome. For some of the subunits, organ specific subtypes exist; for example, there are liver and heart types of the so-called subunit VIa in the mammalian cytochrome *c* oxidase. It has been suggested that the presence of the liver or heart type determines the efficiency of proton pumping, and that only two protons per oxygen molecule are pumped by cytochrome *c* oxidase in liver, but four in heart. Subunit VIa also seems to be responsible for the dimer formation of cytochrome *c* oxidase from bovine heart mitochondria.

The bacterial cytochrome *c* oxidases of known structure contain one additional small protein subunit, called subunit IV. It has no counterpart in the mitochondrial enzyme and its function is not known.

X-Ray Crystal Structures of Cytochrome *c* Oxidases and Other Terminal Oxidases

Protein Structure

Until now atomic structures, determined by X-ray crystallography, have been presented for the cytochrome *c* oxidases from the soil bacterium *Paracoccus denitrificans*, from the purple photosynthetic bacterium *Rhodobacter sphaeroides* and from bovine heart mitochondria. These are rather typical closely related enzymes. Both *Paracoccus* and *Rhodobacter* are grouped within the α-proteobacteria, and the symbiotic ancestor of the mitochondria belonged to this group. In addition, the structure of the aberrant ba_3 type cytochrome *c* oxidase (e.g., it does not possess a

homologue of subunit III) from the bacterium *Thermus thermophilus*, and that of the ubiquinol oxidase (cytochrome bo_3) from *E. coli* have been determined.

In the cytochrome *c* oxidases the subunits I, II, and III form the core, which, viewed parallel to the membrane, has a trapezoidal shape, when seen from above it looks oval. The length of the trapezoid is about 90Å, its height 55Å. It comprises 21 membrane-spanning helical segments. The globular polar domain of subunit II is attached to the narrow, periplasmic (intermembrane, respectively) side of the trapezoid (see Figures 1 and 3). Subunit I contains twelve membrane-spanning helices which are arranged in a threefold symmetric manner. In this kind of arrangement three "pores" are formed. One contains the heme *a* with two histidine residues as axial iron ligands, another heme a_3 with one axial histidine ligand and Cu_B, and the third one is blocked by aromatic residues. Subunit II contains two N-terminal membrane-anchoring transmembrane helices. The globular domain contains a ten-stranded β-barrel similar to the copper proteins plastocyanin and azurin. The copper-binding site is in the same position, but to subunit II two copper atoms instead of one are bound. Subunit III possesses seven transmembrane helices. They form two bundles, one of five, the other of two transmembrane helices. Between them a V-shaped cleft exists, which is partially filled by lipid molecules. In the cleft at the center of the membrane, an entrance to a hydrophobic channel can be seen which leads to the active site. It has been proposed that this channel is a diffusion channel for oxygen because it leads to the active site, and because the solubility of oxygen in the hydrophobic center of the membrane is considerably higher than in the aqueous phase. Subunit III of the ubiquinol oxidase (cytochrome bo_3) from *E. coli* consists of five transmembrane helices only. The loss is compensated by the addition of two transmembrane helices to the twelve of subunit I.

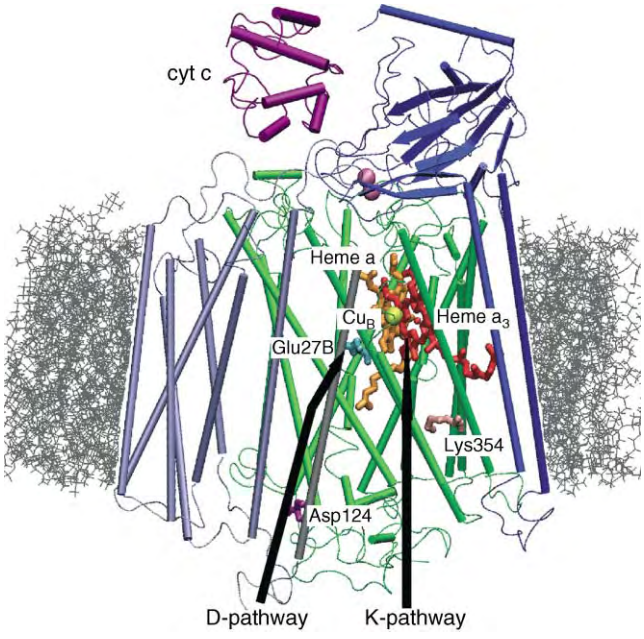

FIGURE 3 Cytochrome *c* oxidase in a bilayer membrane. The four subunits containing cytochrome *c* oxidase from *Paracoccus denitrificans* is shown together with its substrate cytochrome *c* (purple, top). Helices are represented as columns, β-strands as ribbons with arrows. Green: subunit I; dark blue: subunit II; iceblue: subunit III; gray: subunit IV; heme *a* is shown in orange, heme a_3 in red, Cu_B in yellow, and Cu_A in mauve. The lipid bilayer is represented in gray as atomic model. Figure prepared by E. Olkhova using the program vmd.

Arrangement of the Prosthetic Groups

Cu_A receives an electron from cytochrome *c* at the periplasmic (intermembrane) surface of the membrane. Tryptophan 121 (*Paracoccus* numbering) appears to play an important role in the electron transfer. From Cu_A the electron is transferred to heme *a*, the distance of the lower Cu-atom to the iron atom of heme *a* is ~20Å. Heme a_3 lies in the membrane in the same height, so that electron transfer from heme *a* to heme a_3 occurs parallel to the membrane. The center-to-center distance of both hemes is 13–14Å. The propionate side chains of both heme groups are oriented towards the external (periplasmic or intermembrane) side. Their charges are partially compensated by the formation of ion pairs with two arginine residues.

Cu_B is ~5Å away from the heme a_3 iron, so that a very rapid electron transfer between heme a_3 and Cu_B has to be expected. It is a general problem in cytochrome *c* oxidase research that Cu_B is silent and there is no spectroscopic technique available which allows determining the redox state of Cu_B. Cu_B possesses three histidine ligands. One of them is covalently linked to a nearby tyrosine. The existence of a covalent histidine-tyrosine cross-link was unknown prior to the X-ray crystallographic structure determinations.

Proton Transfer Pathways

The structural knowledge combined with the results of previous site-directed mutagenesis experiments lead to the identification of two proton transfer pathways. One, called the K-pathway because of the existence of an essential lysine residue as a component of this pathway, leads straight from the cytoplasmic (matrix) surface into the binuclear site. The cross-linked tyrosine is a part of it. Mutation of the essential lysine residue to other residues prevents the initial reductions of the binuclear site during the catalytic cycle.

A second proton transfer pathway has been called the D-pathway because an aspartic residue at the protein surface is a part of it. A change of this aspartate residue to an asparagine still allows a (reduced) turnover of the enzyme, but proton pumping is abolished. The D-pathway is wider than the K-pathway, and many water molecules are involved. It leads straight up first, then changes direction at a water filled cavity, which leads to a glutamate residue (E278 in *Paracoccus* numbering). The further pathway is unclear. There must be a possibility for proton transfer to the active site, because the reaction cycle can be started from an artificially fully reduced enzyme in K-pathway mutants, proceeds quite normally and water is formed in the active site. Proton transfer using a temporarily established chain of water molecules is a possibility. Alternatively, pumped protons can be transferred to the heme propionates and stored there in some parts of the catalytic cycle.

The existence of a third pathway, called H-pathway, has been suggested for the bovine heart mitochondrial cytochrome *c* oxidase. However, there is no evidence for it on the basis of mutagenesis experiments in bacterial enzymes and the proposal has met with a lot of skepticism.

The Catalytic Cycle and Proton Pumping

The catalytic cycle starts with a fully oxidized enzyme (O-state). All four prosthetic groups (Cu_A, heme *a*, heme a_3 and Cu_B) are oxidized. In cytochrome *c* oxidases an electron is first transferred from cytochrome *c* to Cu_A, and then to heme *a* with a time constant of 20–50 μs. The published values for the electron transfer to heme a_3 from heme *a*, vary greatly and most likely this electron transfer requires proton uptake via the K-pathway first. Most likely in this E-state, the single electron equilibrates over all prosthetic groups. A second electron has to be provided by cytochrome *c*. When the binuclear site is doubly reduced, an oxygen molecule can be bound to the iron atom of heme a_3, thus the oxygenated form, called compound A, corresponding, for example, to oxygenated myoglobin, is formed. This reacts to an intermediate state called P, which is characterized by an absorption maximum at 607 nm. P stands for peroxy because the original (incorrect) belief was that this form contains a peroxide dianion. After the input of a third electron into the enzyme a state absorbing visible light at 580 nm is formed. This was believed to be the oxoferryl state and called F. After the fourth reduction step the iron-bound oxygen atom was thought to be converted to a second water molecule under consumption of two protons and the O-state is formed again. Such a simple catalytic cycle is presented in Figure 4A.

In recent years much of the accepted knowledge had to be revised. First, it is clear now that there are two P- and F-states each, one each in the two-electron reduced enzyme, and one each in the three-electron reduced enzyme. It cannot be excluded that all of them are part of the catalytic cycle (Figure 4). Second, it has been convincingly demonstrated by resonance Raman spectroscopy and chemical experiments that in the P-state the O=O double bond is already broken and that an oxoferryl state already exists. This finding causes the problem that four electrons are required to split the O=O double bond, but only three (two from the Fe^{II} to Fe^{IV} transition upon formation of the oxoferryl state, and one from Cu_B) are available from the prosthetic group. Although definite proof could not be presented yet, it is the general belief that the fourth electron (and a proton) is provided by the cross-linked tyrosine, which becomes a neutral tyrosine radical. The existence of the cross-link which most likely is a side product formed by a tyrosine radical in one of the first turnovers, has to be considered as a hint for the occurrence of a tyrosine radical. Also most likely, a hydroxide as a Cu_B-ligand is generated, and may cause the difference of the optical absorbance spectra between the P- and the F-states. The F-state in the three-electron reduced enzyme is most likely to contain water instead of the hydroxide, and the tyrosine radical has become a neutral tyrosine.

The question, which of the electron transfer steps are coupled to proton pumping, is currently a matter of intense debate. The already generally accepted proposal that only the P to F-, and F to O-transitions are linked to proton pumping with two protons pumped each, could not be maintained. There is good evidence that one proton is pumped upon the input of the second electron into the oxidized enzyme in the absence of oxygen, and it has also been proposed that under turnover conditions already the first reduction step is connected to proton pumping. For a final answer, further experiments are required. It is a general problem in cytochrome *c* oxidase research that many kinetic experiments are started from a fully reduced enzyme (all four prosthetic groups are artificially reduced). However, this state is not part of the catalytic cycle and the value of the conclusions drawn is limited.

As long as it is unknown, when proton pumping occurs in the catalytic cycle, it is very difficult to find out the mechanism of proton pumping. A rather general mechanism of proton pumping, that has found many supporters, is based on the charge-compensation principle. This principle states that each electron transfer into the membrane to heme *a* is

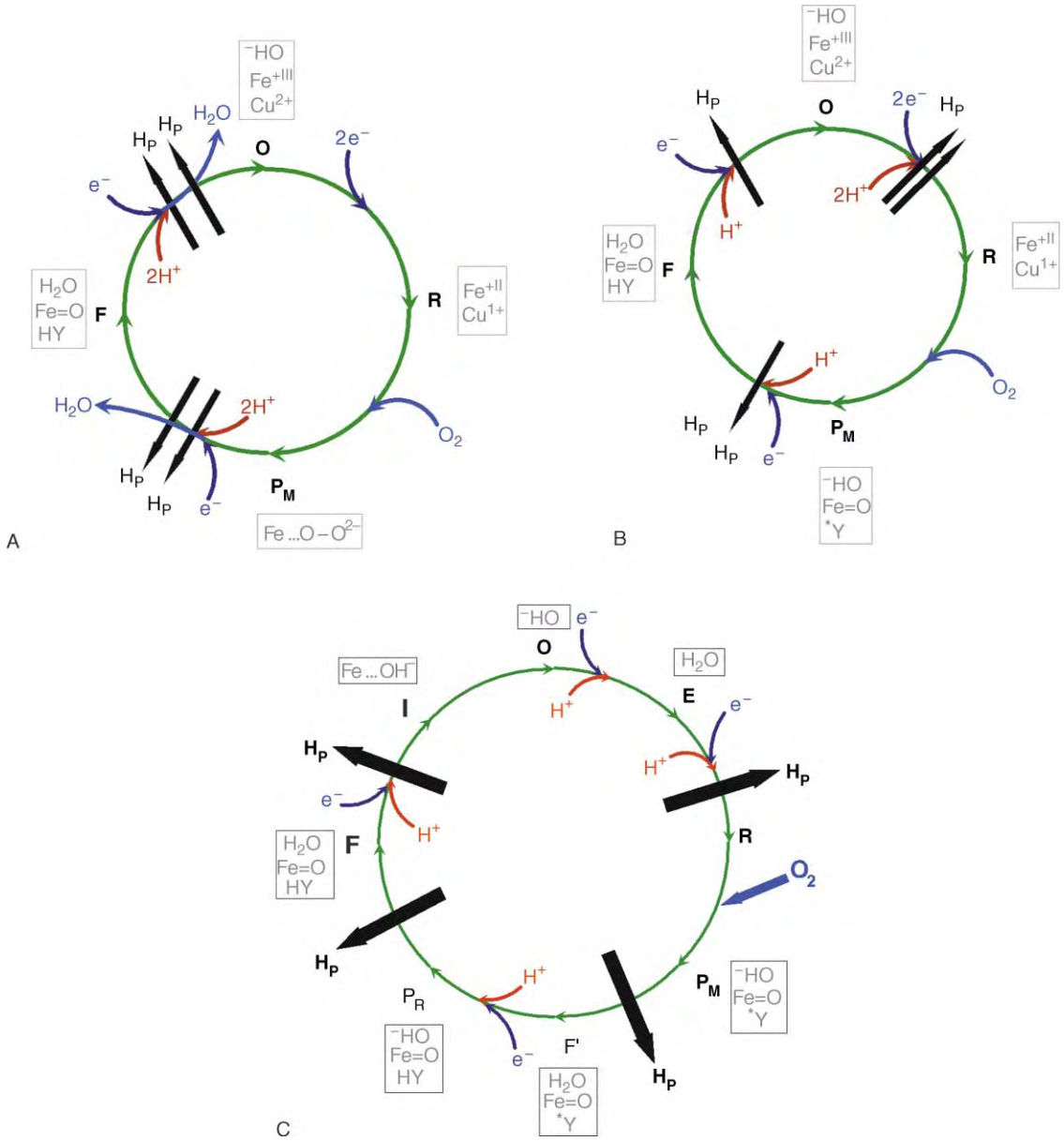

FIGURE 4 Catalytic cycles of cytochrome *c* oxidase. Classical, now obsolete cycle with only four states. The P-state erroneously has a peroxide anion bound to the heme a_3-iron; two protons are pumped during the P to F-, and during the F to O transitions under consumption of two protons each. It is clear now, that only one proton is consumed during each transition. (A) Adaptation of the classical cycle to recent findings. Two protons are taken up already during the initial two-electron reduction of the enzyme, and two protons are pumped in this phase (under turnover conditions). The P_M-state contains a oxoferryl-iron, a tyrosine radical and a hydroxide in the binuclear center, only one proton is pumped during the P to F-, and during the F to O transitions. (B) A recent cycle with two P and two F-states. The protonations of the hydroxides in the binuclear sites of the P-states leads to proton pumping, each electron uptake is accompanied by a charge compensating proton uptake. Tyrosine radicals are present in the two-electron reduced states, tyrosines in the three-electron reduced states. One proton is pumped during the second reduction step, which could now be experimentally demonstrated. One electron is pumped during the F to O-transition as a result of the protonation of the oxo-group at the heme a_3 iron. (C)

charge-compensated by uptake of one proton from the opposite side of the membrane and not consumed in water formation. This proton is supposed to be electrostatically repelled and thus pumped by those protons, which are later taken up and consumed in water formation. The mechanism requires storage of the charge-compensating protons in a way that they cannot be used for water formation.

It is evident that still many experiments are required before the mechanism of proton pumping by cytochrome *c* oxidases can be considered to be known.

See Also the Following Articles

Cytochrome bc_1 Complex (Respiratory Chain Complex III) • Cytochrome *c* • Heme Proteins • Heme Synthesis

Glossary

α-proteobacteria A group of eubacteria containing many well characterized.

bacterial species The evolutionary ancestor of mitochondria is most likely a close relative of the *Rickettsiaceae* which belong to the this group of bacteria.

cyanobacteria Prokaryotes that perform oxygenic photosynthesis. They developed the water-splitting system converting the atmosphere to an oxidizing one. They are considered to be the evolutionary ancestor of chloroplasts.

cytochrome *c* A heme-containing hydrophilic protein that functions as an electron carrier in respiration.

ubiquinol A hydrophobic coenzyme which carries hydrogen atoms in membranes. It can release protons and electrons separately. It forms ubiquinone upon oxidation.

Further Reading

Ferguson-Miller, S., and Babcock, G. T. (1996). Heme/copper terminal oxidases. *Chem. Rev.* **96**, 2889–2907.

Jünemann, S. (1997). Cytochrome *bd* terminal oxidase. *Biochim. Biophys. Acta* **1321**, 107–127.

Michel, H. (1999). Cytochrome *c* oxidase: Catalytic cycle and mechanism of proton pumping – a discussion. *Biochemistry* **38**, 15129–15140.

Michel, H., Behr, J., Harrenga, A., and Kannt, A. (1998). Cytochrome c oxidase: Structure and spectroscopy. *Annu. Rev. Biophys. Biomol. Struct.* **27**, 329–356.

Ostermeier, C., Harrenga, A., Ermler, U., and Michel, H. (1997). Structure at 2.7 angstrom resolution of the Paracoccus denitrificans two-subunit cytochrome c oxidase complexed with an antibody F-V fragment. *Proc. Natl. Acad. Sci. USA* **94**, 10547–10553.

Pereira, M. M., Santana, M., and Teixeira, M. (2001). A novel scenario for the evolution of haem-copper oxygen reductases. *Biochim. Biophys. Acta* **1505**, 185–208.

Ruitenberg, M., Kannt, A., Bamberg, E., Fendler, K., and Michel, H. (2002). Reduction of cytochrome *c* oxidase by a second electron leads to proton translocation. *Nature* **417**, 99–102.

Saraste, M. (1999). Oxidative phosphorylation at the fin de siecle. *Science* **283**, 1488–1493.

Saraste, M., and Castresana, J. (1994). Cytochrome-oxidase evolved by tinkering with denitrification enzymes. *FEBS Lett.* **341**, 1–4.

Yoshikawa, S., Shinzawa-Itoh, K., Nakashima, R., Yaono, R., Yamashita, E., Inoue, N., Yao, M., Fei, M. J., Peters Liebeu, C., Mizushima, T., Yamaguchi, H., Tomizaki, T., and Tsukihara, T. (1998). Redox-coupled structural changes in bovine heart cytochrome *c* oxidase. *Science* **280**, 1723–1729.

Biography

Hartmut Michel is a Director at the Max Planck Institute of Biophysics and Head of the Department of Molecular Membrane Biology in Frankfurt am Main, Germany. He received a Diploma (equivalent to M.Sc.) in Biochemistry at the University of Tübingen and a Dr. rer. nat degree from the University of Würzburg. His principal research interest is to understand the mechanism of action of selected membrane–protein complexes based on accurately known structures. The focus of his current research lies on the complexes of the respiratory chain and on G protein-coupled receptors. Dr. Michel received the Nobel prize in chemistry in 1988 "for the determination of the three-dimensional structure of a photosynthetic reaction center." This was the first structure determination of a membrane protein or of a membrane–protein complex.

Respiratory Processes in Anoxygenic and Oxygenic Phototrophs

Roberto Borghese and Davide Zannoni
University of Bologna, Bologna, Italy

Phototrophic microrganisms include "*anoxygenic phototrophs,*" which are bacteria capable of growing photosynthetically with no oxygen generation, and *Cyanobacteria* which are "*oxygenic phototrophs*" because their photosynthetic apparatus generates oxygen. Several genera of anoxygenic phototrophs are capable of obtaining energy also from *aerobic* and *anaerobic respiration* in darkness; conversely, only a few filamentous cyanobacteria can grow in the dark on glucose or other sugars using the organic material as both carbon and energy source. The latter observation suggests that besides the bioenergetic aspect, respiration in cyanobacteria plays other roles such as to control the redox balance or to act as a scavenger for O_2 during nitrogen fixation. Facultative phototrophs (capable of both respiration and photosynthesis) contain a photosynthetic apparatus whose synthesis is repressed by oxygen; an exception to this rule is the group of aerobic-anoxygenic phototrophs, mainly marine microorganisms, requiring the presence of oxygen to synthesize their photosynthetic apparatus.

Anoxygenic Phototrophs

On a phylogenetic basis (16S rRNA analyses) phototrophic bacteria and their relatives are grouped in a class, the Proteobacteria, which is formed by several subclasses, named α, β, γ, δ, and ε. Facultative photosynthetic bacteria belong to α and β subclasses, e.g., genera *Rhodobacter*, *Rhodospirillum*, *Rhodocyclus*, *Rubrivivax*, and *Erytrobacter.*

Metabolic Aspects of Facultative Anoxygenic Bacteria

Facultative phototrophs are probably the most metabolically flexible organisms of the microbial world. Species such as *Rhodobacter* (*Rba.*) *capsulatus* and *Rba. sphaeroides* can grow by aerobic respiration and photosynthesis using either organic or inorganic substrates but also by anaerobic respiration with trimethylamine-N-oxide (TMAO) or dimethyl sulfoxide (DMSO) as electron acceptors. Further, some strains of the species *Rhodopseudomonas* (*Rps.*) *palustris*, *Roseobacter* (*Rsb.*) *denitrificans* and *Rba. sphaeroides* can reduce nitrate (NO_3^-) into dinitrogen (N_2) via nitrite (NO_2^-), and, in some cases, also nitric oxide (NO) and nitrous oxide (N_2O). These energy generating processes are catalyzed by oxido-reduction protein complexes forming composite electron transport chains. Apparently not all the above summarized metabolic options are activated or can be available simultaneously in a single species; however, cells of *Rba. capsulatus* or *Rba. sphaeroides* grown photosynthetically in the presence of low oxygen tension ($<1\%$) contain both photosynthetic and respiratory apparatuses.

Electron Transport Chains

Respiration in facultative phototrophs involves numerous redox carriers, namely: (1) transmembrane protein complexes such as NADH- and succinate-quinone oxidoreductases (NQR and SQR, respectively), cytochrome (cyt) bc_1 or hydroquinone-cytochrome *c* oxidoreductase (QCR), quinol oxidase(s) (QOX), and cyt cbb_3 and/or aa_3 oxidases (COX); (2) electron and/or proton carriers such as ubiquinones (UQ), cyt c_2, HiPIP, and cyt c_y; (3) enzymes of the periplasmic space such as NO_3^-, NO_2^-, N_2O, and DMSO reductases. With O_2 as final electron acceptor, the NQR, QCR, and COX enzymes constitute three main coupling sites where the potential energy between the initial donor and the final acceptor molecules is released in small steps, that are controlled by the differences between the redox midpoint potentials (E_m) of the redox couples involved, and efficiently coupled to the generation of an electrochemical proton gradient ($\Delta\mu_{H+}$). Photosynthesis converts the radiant energy into chemical energy at the level of the photochemical reaction center (RC). This transmembrane protein complex generates a charge separation that is followed by a cyclic electron transfer involving quinone molecules (UQ-10), cyt bc_1 complex, and soluble cyt c_2 in addition to the membrane-bound cyt c_y, in the case of *Rba. capsulatus*. Under dark aerobic

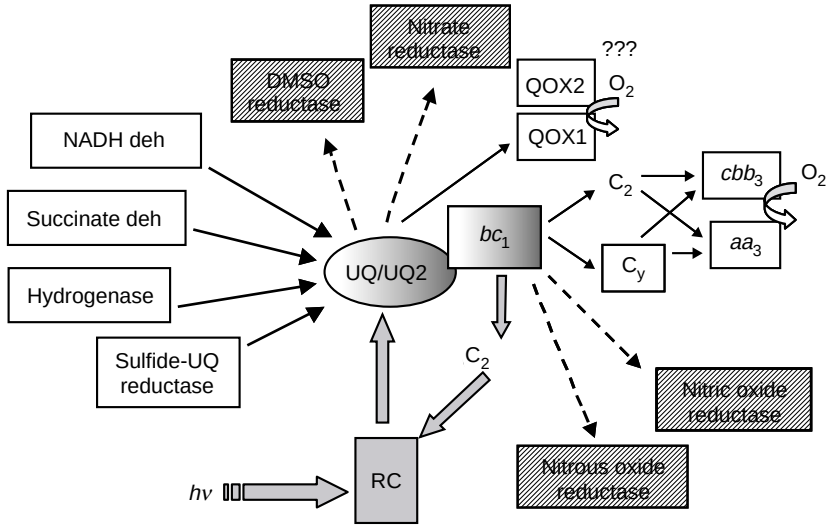

FIGURE 1 Block scheme illustrating the complex network of electron transport chains in *Rba. sphaeroides*. Black arrows indicate the influx of reducing equivalents and the efflux of electrons leading to the membrane-bound oxidases. Dashed black arrows indicate output of electrons involved in anaerobic respiration. Gray-colored redox components and arrows are those specifically involved in photocyclic electron transfer while those shaded off are shared by photosynthesis and respiration. RC, photochemical reaction center; *hν*, radiant energy; C_2, soluble cyt c_2; C_y, membrane-attached cyt c_y; QOX1, functional ubiquinol oxidase (*qxtAB* operon); QOX2, not functional ubiquinol oxidase (*qoxBA* operon).

conditions, facultative phototrophs use a respiratory chain, closely related to that present in mitochondria. The last step of O_2 reduction into H_2O is catalyzed by two oxidases (not always present in a single species): a cyt *c* oxidase (of cbb_3 and/or aa_3 type), inhibited by μM cyanide, and a quinol oxidase (of *bo* type), inhibited by mM cyanide, branching the electron flow at the level of the UQ-10 pool. Figure 1 shows a block scheme of the different electron transport pathways operating in *Rhodobacter sphaeroides*.

Interaction between the Diverse Electron Transport Chains

The interaction between the different bioenergetic chains of photosynthetic bacteria occurs by two nonexclusive mechanisms, namely: (1) an indirect mechanism, exerted by the proton motive force (PMF) as a "back pressure" on the rate of electron transport catalyzed by redox complexes, and (2) a direct mechanism of interaction between electron carriers, e.g., UQ-10 or cyt c_2, that are engaged in multiple bioenergetic processes. In this way, the activity of a given bioenergetic chain would affect the redox state of the components in common and, consequently, the functioning of the other chains.

Respiratory and photosynthetic apparatuses are localized in different parts of the internal bacterial membrane (CM); this implies the diffusion of some electron carriers such as UQ, in the lipid phase, or cyt c_2, in the periplasmic space. However, the diffusion of these elements does not occur on the entire internal membrane; thus, the different redox chains are not necessarily in thermodynamic equilibrium. For example, two functional pools of soluble cyt c_2 exist in *Rba. sphaeroides* and *Rba. capsulatus*. Further, the membrane-bound cyt c_y is a direct electron donor to the cbb_3-type oxidase of *Rba. capsulatus* or to the cbb_3/aa_3 type oxidases of *Rba. sphaeroides*. Consequently, the redox chain containing cyt c_y must be organized in *supramolecular* complexes and operate independently of the redox state of the other respiratory pathways.

Genetic Regulation of Respiration and Photosynthesis in Facultative Phototrophs

Oxygen is the key factor in the coordinated regulation of respiratory and photosynthetic activities since it participates, directly or indirectly, in determining the levels of expression of all components involved in these processes (Figure 2). The main regulatory element in *Rba. capsulatus* is the RegA/RegB couple (PrrA/PrrB in *Rba. sphaeroides*), which is able to sense the change in O_2 partial pressure in the environment, and to transform this information into a regulatory response. Within this couple, RegA is the effector component while RegB is the sensor partner. This sensor-effector couple functions according to a widespread regulatory model in which the sensor protein (RegB) detects changes in the environment, in this case variations in O_2 tension, and modifies the effector protein (RegA) by phosphorylating it. Depending on its phosphorylated or dephosphorylated status, the effector can regulate the expression of

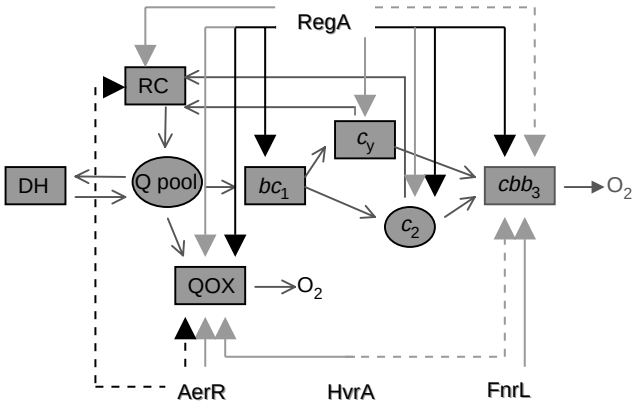

FIGURE 2 Genetic regulatory network of respiratory and photosynthetic activity in *Rhodobacter capsulatus*. Black and gray arrows indicate regulation under aerobic and anaerobic conditions, respectively. Straight lines are for positive regulation (induction), dotted lines are for negative regulation (repression). Genetic regulators are written in black while respiratory/photosynthetic components, connected by thin arrows, symbolising electron flow, are in dark gray. DH, NADH dehydrogenase; RC, photosynthetic reaction center; Q pool, ubiquinone-10 pool; bc_1, transmembrane cyt bc_1 complex; c_y, membrane-anchored cyt c_y; c_2, periplasmic (soluble) cyt c_2; cbb_3, membrane-bound cyt *c* oxidase; QOX, membrane-bound quinol oxidase. See text for further details.

a number of genes. RegA/RegB is a general aerobic/anaerobic regulatory couple that influences the expression of many processes in addition to respiration and photosynthesis: N_2 fixation, CO_2 fixation, and H_2-ase activity. The electron transport chain (ETC) genes that have been shown to be regulated by RegA/RegB are the ones coding for COX and QOX, which are specific for the respiratory chain, and those coding for the *bc*1 complex, cyt c_2 and cyt c_y which participate in both respiration and photosynthesis (Figure 2). RegA/RegB also regulate the level of the RC. Other regulatory elements that participate in the regulation of respiratory ETC components are AerR, that operates in the presence, as well as in the absence, of O_2; HvrA and FnrL are anaerobic regulators only (Figure 2). Although the interaction of all the aforementioned regulatory elements is quite complex, it allows the fine tuning and controlled interplay of respiratory and photosynthetic activities.

Oxygenic Phototrophs

Cyanobacteria are capable of oxygenic photosynthesis, differing in that from anoxygenic phototrophs. Cyanobacteria form one of the major phila of *Bacteria* and they were most likely the first oxygen-evolving organisms on Earth changing the atmosphere from anoxic to oxic. Oxygenic phototrophs are grouped into several morphological groups; however, most of the available biochemical and genetic data concern mainly unicellular genera such as *Synechococcus* and *Synechocystis*.

Respiration is by definition a membrane-bound process; in this respect, cyanobacteria contain three different types of membranes: (1) the outer membrane, typical of Gram negatives, which has no specific role in respiration; (2) the cytoplasmic membrane (CM); and (3) the intracytoplasmic membranes (ICMs) or thylakoids. Both CM and ICM contain respiratory redox complexes; electron microscopy also indicates that CM and ICM might be connected, at least in *Synechococcus* sp. strain PCC 6301, although a correct picture of the membrane arrangement *in vivo* is lacking at present.

Electron Transport Pathways in Oxygenic Phototrophs

Respiratory and photosynthetic electron transports are intimately connected in two distinct bioenergetically active membranes, ICM and CM. All photosynthetic electron transport is located in the ICM, where photosynthesis and respiration share components (Figure 3). In addition, ample experimental evidences indicate the presence of respiratory chain(s) in the CM. Cyanobacterial respiratory terminal oxidases (RTOs) have no direct function in photosynthesis and therefore can be considered the key enzymes of respiration. All cyanobacteria (investigated so far) contain several respiratory branches ending in different RTOs but their actual location in the membrane cell (ICM, CM, or both) is far from being assessed. The best-characterized species is *Synechocystis* sp. strain PC 6803, for which the complete genomic sequence is available. Three sets of genes for RTOs were found, the well-characterized aa_3-type cyt *c* oxidase (COX, encoded by *coxBAC*), a related set of genes also belonging to the heme-copper oxidase superfamily, termed alternate RTO (ARTO; encoded by *ctaCII-ctaDIIEII*), and two genes (*cydAB*) encoding a putative cyt *bd*-type quinol oxidase (Cyd).

The CM forms the inner boundary of the periplasmic space and is known to contain proteins typically associated with respiratory electron transport, such as NAD(P)H dehydrogenase, cyt b_6/f (homologous of the bc_1 complex), and terminal oxidases (presumably, ARTO). Two types of NAD(P)H dehydrogenase have been found. One is a NADPH-type I dehydrogenase (NDH-1), that is encoded by *ndh* genes, which consists of about 12 subunits and contributes to a proton gradient ($\Delta\mu_{H+}$) across the membrane. The second type of dehydrogenase is a NADH-type II dehydrogenase (NDH-2) consisting of a single subunit and probably not contributing to energy transduction.

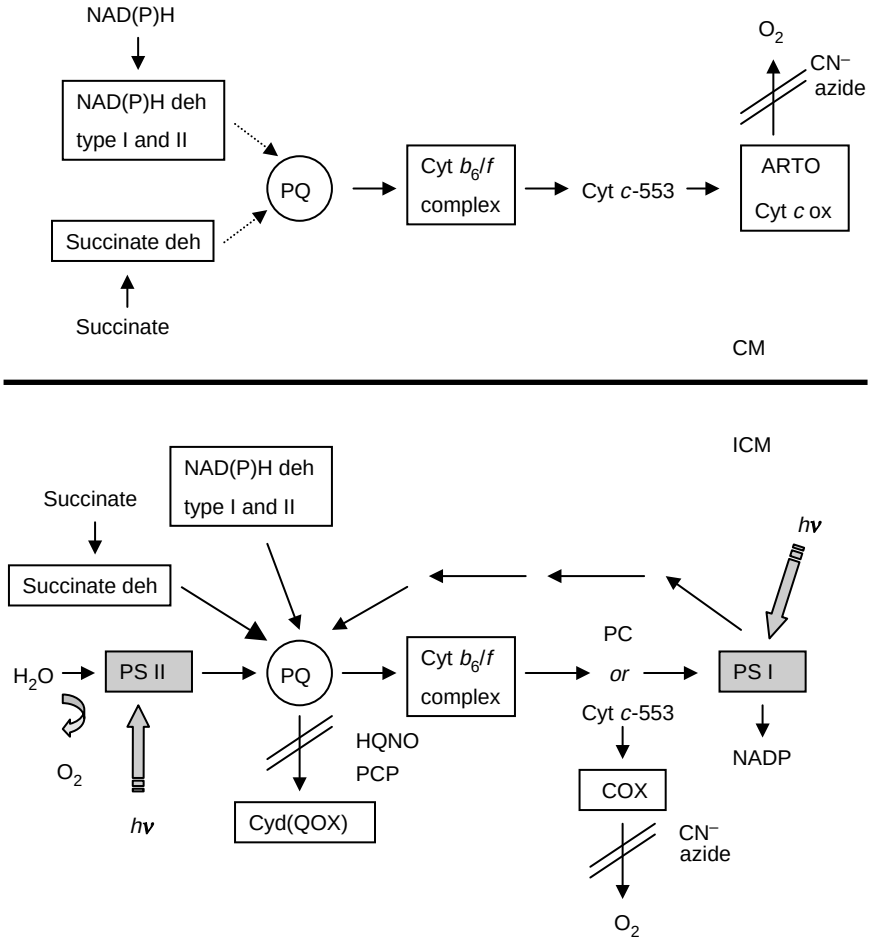

FIGURE 3 Working model of photosynthetic and respiratory electron transport chains in *Synechocystis* sp. strain PCC 6803 in CM and ICM. Membrane-bound redox complexes are indicated as rectangular boxes. Dotted arrows (CM redox chain) symbolize the lack of evidence for electron flow while the thickness of arrows (ICM redox chain) symbolize their relative activities. HQNO, 2-heptyl-4-hydroxy-quinoline-N-oxide; PCP, pentachlorophenol; CN^-, cyanide anion; PC, plastocyanin; PQ, plastoquinone pool; *hν*, radiant energy; see text for further details.

In *Synechocystis* sp. strain PCC 6803, three genes coding for NDH-2 (*ndbA,B,C*) are found.

Three intermingling pathways are dominant in *Synechocystis* sp. strain PCC 6803 thylakoids (ICM), namely: (1) a linear electron transport from H_2O to NADPH, catalyzed by photosystems I and II (PSI/PSII), (2) a respiratory transport from NAD(P)H and succinate to both COX and QOX, and (3) a cyclic electron flow around PSI, i.e. electrons at the acceptor side of PSI returning to the PQ pool (Figure 3). However, as generally seen in facultative anoxygenic phototrophs, electrons can move from one pathway to another at the level of the PQ pool, b_6/f complex, and/or soluble carriers such as plastocyanin (PC) or cyt *c*-553 (Figure 3). For example, in the absence of PSI, reducing equivalents generated by PSII are fed into COX, while in darkness, respiratory electrons are used to reduce the acceptor side of PSII if terminal oxidases are blocked. Results with mutants of *Synechocystis* sp. strain PCC 683 impaired in several combinations of respiratory and photosynthetic redox complexes indicate that succinate dehydrogenase (SDH) is the main electron transfer pathway into the PQ pool and that type I and II NAD(P)H dehydrogenases might simply operate as regulators of NADP and NAD reduction levels. This indicates that respiration in cyanobacteria plays an important role in the control of the intracellular redox balance.

In general, the genes for components of the respiratory chain(s) are present in only one copy per chromosome even in those species having two respiratory chains (Figure 3). How one gene directs its gene product into two different membranes (CM and ICM) is an intriguing yet unanswered question. Further, the amounts of several components of the respiratory chain(s) are regulated by external factors such as the concentration of Cu^{2+} for synthesis of cyt *c*-553 and plastocyanin or the ionic strength for cyt aa_3-type oxidase synthesis. Unfortunately, the mechanisms of gene regulation are largely unknown at present and they will be important topics for future studies in respiration of oxygenic phototrophs.

See Also the Following Articles

Cytochrome bc_1 Complex (Respiratory Chain Complex III) • Photosynthesis • Respiratory Chain Complex II and Succinate:Quinone Oxidoreductases

Glossary

cytochromes Redox proteins with an iron-containing porphyrin ring (heme).

electrochemical proton gradient It defines the membrane energized state in terms of electrical units.

genetic regulatory element A molecule that regulates gene expression by interacting with DNA.

phototroph An organism that converts radiant energy into chemical energy.

proton motive force An energized state of the membrane resulting from the separation of charges across the membrane.

respiration The process in which a compound is biologically oxidized by an electron acceptor (O_2 or an O_2 substitute) linked to generation of a proton motive force.

Further Reading

Schmetterer, G. (1995). Cyanobacterial respiration. In *The Molecular Biology of Cyanobacteria* (D. A. Bryant, ed.) Vol. 1, pp. 409–435. Kluwer, Dordrecht.

Vermeglio, A., Borghese, R., and Zannoni, D. (2004). Interaction between photosynthesis and respiration in facultative phototrophs. In *Respiration in Archaea and Bacteria* (D. Zannoni, ed.) Kluwer, Dordrecht, Vol. 16.

Zannoni, D. (1995). Aerobic and anaerobic electron transport chains in anoxygenic phototrophic bacteria. In *Anoxygenic Photosynthetic Bacteria* (R. E. Blankenship, M. T. Madigan and C. E. Bauer, eds.) Vol. 2, pp. 949–971. Kluwer, Dordrecht.

Biography

Davide Zannoni is Professor of General Microbiology in the Department of Biology at the University of Bologna, Italy. His main research interests are in the broad field of microbial physiology and biochemistry of facultative phototrophic and aerobic bacteria. He holds a degree in biology from the University of Bologna and received postdoctoral training at the St. Louis University School of Medicine. He carried out pioneering studies on bioenergetics of bacterial respiration and interaction between photosynthetic and respiratory redox complexes in facultative phototrophs.

Roberto Borghese is Research Associate and Lecturer of General Microbiology in the Department of Biology at the University of Bologna, Italy. He holds a degree in biology from the University of Bologna and a Ph.D. from the University of Missouri – Columbia. His main research interest is in genetics of anoxygenic photosynthetic bacteria.

Retinoblastoma Protein (pRB)

Nicholas Dyson and Maxim Frolov
Massachusetts General Hospital Cancer Center, Boston, Massachusetts, USA

The retinoblastoma protein (pRB) is the product of the retinoblastoma tumor susceptibility gene (*RB1*). The gene takes its name from the discovery that mutation of both copies of *RB1* is the critical rate-limiting event in the development of retinoblastoma, a rare form of cancer that affects very young children. Mutation of *RB1* is also found in a variety of cancers and pRB is thought to be functionally inactivated in most tumor cells. pRB is a nuclear protein, present in most cell types, that functions as a general negative regulator of cell proliferation. It is a member of a family of proteins (the pRB family) that have overlapping functions and are regulated by cyclin-dependent kinases. pRB is generally thought to function by controlling gene expression, and its best known target is the E2F transcription factor.

The pRB Family of Proteins

pRB-related proteins are conserved in plants and animals. Mammalian cells contain three pRB-family members (pRB, p107, and p130) that share a similar domain structure and a low, but significant, degree of primary sequence homology. All three proteins contain a conserved pocket domain that provides binding sites for E2F proteins, and complexes that repress transcription. In addition pRB, p107, and p130 contain many sites for phosphorylation by cyclin-dependent kinases (cdks). p130 is most highly expressed in differentiated cells, whereas p107 is highly expressed in populations of proliferating cells.

Although pRB, p107, and p130 are currently studied for their roles in the control of cell proliferation, they were first discovered as proteins that associate with the viral oncoprotein Adenovirus E1A. The binding sites for pRB, p107, and p130 map to the regions of E1A that are needed for its oncogenic properties. Similar sequences are also present in the E7 proteins of human papilloma viruses and large T antigens of several polyoma viruses. In each case, genetic studies show that the ability of the viral proteins to bind to pRB/p107/130 allows them to interfere with control of cell proliferation. The viruses are thought to use these interactions to create a cellular environment that is favorable for viral replication.

The RB Tumor Suppressor

The *RB1* gene was the first tumor suppressor gene to be identified and it is often described as a prototype for this class of cancer-related genes. Unlike oncogenes, whose activation promotes tumorigenesis, it is the inactivation of tumor suppressor genes that is linked to the development of cancer.

Individuals inheriting a mutant allele of *RB1* are very highly predisposed to develop retinoblastoma within the first two years of life. Patients, successfully treated for the eye cancer, often develop osteosarcoma in later life. Inactivation of *RB1* appears to be essential for the development of both familial and sporadic retinoblastoma, and also occurs in many osteosarcomas. *RB1* mutation is common in small cell lung cancers and has also been found in other tumors including bladder, prostate, and breast carcinomas. Although *RB1* is mutated in only a subset of tumors, it is thought that pRB is functionally compromised in most tumor cells. pRB is broadly expressed and thought to control the proliferation of most cell types. Precisely why people who inherit a mutant allele of *RB1* are only predisposed to certain types of cancer is still largely unclear. Studies with mice suggest that variations in the extent of functional overlap between pRB and other pRB family members may be important. Animals carrying a mutant allele of the murine *Rb* gene do not develop retinoblastoma but develop pituitary and thyroid tumors instead. However, the combined mutation of *Rb* and the related *p107* gene allows tumors to develop in the retina. This suggests that p107 is able to compensate for the absence of pRB in the developing mouse retina, and it may do so in other cell types.

In addition to its role in E2F regulation, which occurs in many diverse cell types, pRB also interacts with cell-type specific factors. These additional functions may explain why the inactivation of pRB has a greater effect on some cell types than others. For example, pRB interacts with the osteoblast transcription factor CBFA1 to promote the expression of bone specific genes. This role, particularly when combined with its functions in E2F regulation, may explain why pRB is important for suppression of osteosarcoma.

The Cellular Function of pRB

pRB function is often viewed through the prism of the cellular changes that occur when pRB is removed. pRB-deficient cells are smaller than wild-type cells and have defective cell cycle control. In tissue culture assays *Rb-/-* cells are generally less responsive to signals that cause wild-type cells to stop proliferating, and they are more readily driven from quiescence into the cell cycle. *Rb-/-* cells fail to arrest in G1, or S-phase, in response to DNA damage, and they show a reduced sensitivity to $p16^{INK4}$-induced cell cycle arrest and ras-induced senescence. Studies in primary cultures of mouse embryonic fibroblasts show that *Rb-/-* cells are genetically unstable and prone to polyploidy and aneuploidy.

Rb-deficient mice die fairly early in development (day 13–15 of embryogenesis) and display elevated levels of apoptosis, inappropriate cell proliferation, and developmental defects in several tissues. Studies of the murine pRB-family have revealed an extensive degree of redundancy and compensation between family members. Each of the pRB family members has been inactivated in the mouse by homologous recombination. Animals lacking two pRB family members are more severely affected than the single knockouts, and the inactivation of all three family members renders cells unresponsive to most types of G1 control. Triple knockout cells differentiate poorly, are readily immortalized, and easily transformed.

Remarkably and unexpectedly, the early lethality of *Rb-/-* animals has recently been shown to be an indirect consequence of a placental defect. When pRB is expressed specifically in the placenta, the rescue of placental function allows *Rb*-mutant embryos to survive close to birth. Although these mutant animals have defects in cell cycle control, and in skeletal muscle development, the development of these animals is surprisingly normal. Experiments in tissue culture using cells derived from the knockout animals have shown that the sudden removal of pRB causes more severe cell cycle control defects than those seen in cells derived from *Rb-/-* animals. This difference is due, at least in part, to an up-regulation of p107 that occurs in the sustained absence of pRB and appears to allow p107 to compensate for the loss of pRB function.

Regulation of pRB Activity

pRB is a long-lived protein (half-life > 16 h) and its activity is controlled by phosphorylation. When normal cells proliferate, pRB is inactivated by cdks, the kinases that drive progression through the phases of the cell division cycle. When cells cease to proliferate, the loss of cdk activity allows pRB to accumulate in its active form. Inactivation of pRB is not achieved by the phosphorylation of a single site but by the accumulation of phosphorylated residues at multiple sites that are scattered throughout the protein. A cluster of phosphorylation sites is found in the C-terminal fragments of pRB, p107, and p130 and the accumulation of negative charge in this domain is believed to drive a large conformation shift.

As quiescent cells enter the cell cycle pRB is sequentially phosphorylated by a series of cyclin-dependent kinases. Cyclin D/cdk4 is believed to be the first kinase to act on pRB with cyclin E/cdk2, and perhaps cyclin A-dependent kinases completing the process. Phosphorylation of pRB causes it to migrate slowly on SDS-PAGE gels. This mobility shift is often used as an indicator of pRB activity, but it is an unreliable measure; pRB inactivation appears to involve the cumulative effects of multiple phosphorylation events, and some modifications have no effects on the migration of the protein, whereas changes at others sites have a major effect.

Microinjection experiments on cultures of synchronized cells revealed that the ability of pRB to prevent cells from entering S-phase is restricted to a window within G1 phase of the cell cycle. Once cells progressed beyond a point in G1, ~ 2–4 h prior to S-phase, the introduction of pRB had no effect. The loss of a pRB-induced arrest correlates with the accumulation of cdk activity, and corresponds approximately to the "restriction point," a point in G1 where cells become irreversibly committed to progress through a complete cell cycle.

pRB that has been phosphorylated by cdks *in vitro* is unable to arrest cells in G1. *In vivo*, pRB is abruptly dephosphorylated at metaphase of mitosis and, presumably, reactivated. Phosphorylation is not the only type of posttranslational modification of pRB. Recent studies have shown that pRB is also acetylated on lysine residues but the functional significance of pRB aceylation is not well established at present.

The Rb Pathway

It has been proposed that pRB is a component of a critical regulatory pathway that is functionally inactivated in most tumor cells. This pathway comprises pRB, cyclin D/cdk4 (the kinase that phosphorylates pRB in G1), and $p16^{INK4}$ (a cdk inhibitor that antagonizes cyclin D/cdk4 activity and is induced in response to certain cellular stresses). Molecular studies have shown that the overexpression of cyclinD/cdk4 phosphorylates pRB and prevents it from arresting the cell cycle. In addition, cells lacking pRB are largely insensitive to $p16^{INK4}$-induced cell cycle arrest.

The $p16^{INK4}$/cyclin D/cdk4/pRB pathway is disrupted in a variety of ways in tumor cells. Retinoblastoma cells, for example, contain mutations in *RB1*. Many cervical cancers, on the other hand, express HPV E7 proteins that bind and inactivate all three of the pRB family members. Other cells contain lesions that elevate the activity of the cyclin D/cdk4 kinase (overexpression of cyclin D1, loss of the $p16^{INK4}$ cdk inhibitor, or mutations of cdk4 that are resistant to $p16^{INK4}$). Although most tumor cells contain one of these changes, these lesions primarily occur in a mutually exclusive manner. This may mean that there is no further selection for changes in this group of genes once the $p16^{INK4}$/cyclin D/cdk4/pRB pathway is disrupted. However, it is also true that several types of tumors are associated with specific types of mutations (e.g., pRB mutations are the only types of lesions in this pathway found in retinoblastoma, while most breast cancers contain elevated levels of cyclin D1), hence the relative importance of individual components of the pathway varies greatly between cell types.

Molecular Functions of pRB

Over 120 proteins have been reported to associate with pRB and many of these have been proposed to contribute to its tumor-suppressing properties. Most of these pRB-associated proteins are transcription factors and, although the list is diverse, in general pRB has been proposed to inhibit the activity of factors that are needed for cell proliferation, but to augment the activity of factors that promote cell differentiation.

The best-characterized property of pRB is its ability to repress E2F-dependent transcription. The E2F transcription factor allows the periodic expression of many proliferation-related genes to be tightly coupled with cell cycle position. E2F controls the expression of an extensive network of genes that includes essential components of the DNA synthesis machinery, and proteins needed for cell cycle progression, Mitosis, checkpoint responses, as well as regulators of apoptosis. pRB blocks cell proliferation, at least in part, by blocking the expression of E2F-regulated genes.

E2F complexes act as strong repressors of transcription in quiescent cells and during G1 phase of the cell cycle. As cells progress towards S-phase, these repressor complexes are disrupted and replaced by E2F activator complexes in a cdk-regulated process. All three pRB-family members associate with E2F proteins. In wild type cells, p107 and p130 associate primarily with E2F4 and E2F5 and are components of E2F repressor complexes. In these complexes the pRB-family members act as adapter proteins: binding to E2F with one surface, and to chromatin remodeling proteins through a second binding site (the LXCXE-binding cleft). In doing so, they allow a variety of enzymatic activities to be recruited to E2F regulated promoters. In a similar way, pRB also interacts with E2F4 and has the potential to recruit repressor complexes to DNA. In addition, pRB has the important ability to regulate E2F1, E2F2, and E2F3, the activator forms of E2F. pRB binds to an element that is buried within the transcriptional activation domain of the E2Fs, preventing them from activating transcription. Biochemical studies have also shown that pRB that is recruited to DNA by its association with E2F is also able to prevent adjacent DNA-bound transcription factors from interacting with the basal transcription machinery.

Chromatin immuno-precipitation experiments have given a detailed picture of the sequential binding of E2F and pRB-family members to E2F-regulated promoters during cell cycle progression. Surprisingly, p107 and p130 are the pRB-family members that are most easily detected at most E2F targets in proliferating cells. While some studies have found pRB at E2F-regulated promoters in cultures of proliferating cells, others have shown that pRB is most clearly recruited to E2F targets in response to specific signals, such as p16-induced cell cycle arrest, or ras-induced senescence. Under these circumstances pRB is thought to recruit histone deacetylase and/or histone methylase activities to DNA. These complexes repress transcription through modification of histone tails, changing the local chromatin structure to a form that is non-conducive to gene expression.

Genetic interactions between *Rb* and *E2F* genes have been demonstrated in multiple experimental systems and in species as diverse as mice and fruit flies. However, precisely how much of pRB's functions in development and tumor suppression are mediated through its interaction with E2F is uncertain. In addition to the many transcription factors that can bind to pRB, pRB has also been reported to relocalize to origins of replication following DNA damage and to interact with a diverse collection of chromatin-associated complexes. Further studies are needed to demonstrate the functional significance of almost all of pRB's proposed binding partners.

See Also the Following Articles

Cell Cycle Controls in G_1 and G_0 • Cell Death by Apoptosis and Necrosis • Chromatin Remodeling • Chromatin: Physical Organization

Glossary

apoptosis Programmed cell death.

cell cycle The complete sequence of events needed for the production of a new daughter cell. A mitotic cell cycle has two major landmarks, S-phase and Mitosis, which are separated by two gap phases, G1 (the period before DNA synthesis) and G2 (the period between the S and M-phases).

cell proliferation The overall increase in cell number that occurs when the rate of cell division is greater than the rate of cell death.

compensation A change in function that allows one type of gene product to perform a function that is normally carried out by another type of gene product.

redundancy The situation that occurs when two or more genes have a similar function and either gene is sufficient for a biological process.

Further Reading

Dyson, N (1998). The regulation of E2F by pRB-family proteins. *Genes Dev.* **12**, 2245–2262.

Goodrich, D. W., Wang, N. P., Qian, Y. W., Lee, E. Y., and Lee, W. H (1991). The retinoblastoma gene product regulates progression through the G1 phase of the cell cycle. *Cell* **67**, 293–302.

Harbour, J. W., and Dean, D. C. (2000). The Rb/E2F pathway: Expanding roles and emerging paradigms. *Genes Dev.* **14**, 2393–2409.

Robanus-Maandag, E., Dekker, M., van der Valk, M., Carrozza, M. L., Jeanny, J. C., Dannenberg, J. H., Berns, A., and te Riele, H. (1998). p107 is a suppressor of retinoblastoma development in pRb-deficient mice. *Genes Dev.* **12**, 1599–1609.

Sage, J., Mulligan, G. J., Attardi, L. D., Miller, A., Chen, S., Williams, B., Theodorou, E., and Jacks, T. (2000). Targeted disruption of the three Rb-related genes leads to loss of G(1) control and immortalization. *Genes Dev.* **14**, 3037–3050.

Sage, J., Miller, A. L., Perez-Mancera, P. A., Wysocki, J. M., and Jacks, T. (2003). Acute mutation of retinoblastoma gene function is sufficient for cell cycle re-entry. *Nature* **424**, 223–228.

Sherr, C. J. (1996). Cancer cell cycles. *Science* **274**, 1672–1677.

Thomas, D. M., Carty, S. A., Piscopo, D. M., Lee, J. S., Wang, W. F., Forrester, W. C., and Hinds, P. W. (2001). The retinoblastoma protein acts as a transcriptional coactivator required for osteogenic differentiation. *Mol Cell.* **8**, 303–316.

Weinberg, R. A. (1995). The retinoblastoma protein and cell cycle control. *Cell* **81**, 323–330.

Wu, L., de Bruin, A., Saavedra, H. I., Starovic, M., Trimboli, A., Yang, Y., Opavska, J., Wilson, P., Thompson, J. C., Ostrowski, M. C., Rosol, T. J., Woollett, L. A., Weinstein, M., Cross, J. C., Robinson, M. L., and Leone, G. (2003). Extra-embryonic function of Rb is essential for embryonic development and viability. *Nature* **421**, 942–947.

Biography

Nicholas Dyson and Maxim Frolov are members of the Massachusetts General Hospital Cancer Center. Their research interests are focused on the control of cell proliferation by RB and E2F family members. Dr. Dyson is a Professor of Medicine at Harvard Medical School.

Retinoic Acid Receptors

Martin Petkovich
Queen's University, Kingston, Ontario, Canada

Retinoic acid receptors (RARs) are nuclear transcription factors that, once activated by retinoic acid (RA), regulate the expression of RA target genes, leading to changes in cell differentiation, cell proliferation, and apoptosis. The discovery of the first RAR in 1987 defined for the first time the mechanism of action of vitamin A outside of the visual cycle. Three RAR subtypes have been identified in the vertebrate genome and have been named RARα, RARβ, and RARγ.

RA and RA Signaling

Retinoic acid (RA) is a signaling molecule derived from vitamin A (retinol) that is essential for normal embryonic development and health in the adult. RA is produced in a two-step enzymatic process involving the alcohol dehydrogenase-mediated conversion of retinol to retinaldehyde and, in a subsequent retinaldehyde dehydrogenase-catalyzed step, to RA. RA signaling is mediated by retinoic acid receptors (RARs).

RARs belong to the superfamily of nuclear receptors and bear conserved structural similarities to other members of this family, including estrogen and androgen receptors, glucocorticoid receptor, thyroid hormone receptor, and vitamin D receptor. In general, members of this family can be distinguished by the linear arrangement of six more or less conserved functional domains labeled A through F. Key functional domains of RARs include the RA-binding domain, the DNA-binding domain, and two separate transcription activation domains (see Figure 1). While the DNA- and RA-binding domains of the RARs are similar between subtypes, the transcription activation domains vary considerably, possibly reflecting target gene-specific interactions. Several regions within RAR domains mediate specific interactions with retinoid-x-receptor subtypes (RXRα, RXRβ, or RXRγ), forming an obligatory heterodimeric partnership required for activation of RA target genes. RAR/RXR heterodimers bind to specific DNA elements called retinoic acid response elements (RAREs) usually found in the promoters of such genes. The unique expression patterns of each RAR subtype in the embryo and the adult also support the specific functional role that each of the RARs fulfills. Murine knockout studies have revealed that although there is functional redundancy between RARs, each receptor is essential for normal physiology.

RAR Structure and Function

RARs share structural similarities with other members of the nuclear receptor family. The key functional domains of RARs include the RA-binding domain, the DNA-binding domain, transcriptional activation domains, and amino acid sequence motifs that are necessary for interactions between RARs and other transcription factors, including RXRs. RARs form heterodimeric complexes with RXRs in order to regulate gene expression.

DNA-Binding Domain

The hallmark of all nuclear receptors is the DNA-binding domain (domain C), which comprises a highly conserved, 66–68 amino acid stretch encoding two zinc-binding fingers labeled C1 and C2. The RARs' DNA-binding domain is 66 amino acids in length, and its structure has been determined by X-ray crystallographic studies. The two zinc fingers fold into a globular domain such that residues of the first zinc-binding finger (C1) make specific contacts with DNA through interactions between three conserved amino acid residues (P-box) with specific base residues in the major groove of the DNA double helix. The second zinc finger (C2) is more basic in nature, making contacts with the negatively charged phosphate backbone of DNA. This helps to stabilize the interaction between RARs and the DNA motifs to which they bind, RAREs. RARs do not bind to RAREs independently but rather as a heterodimeric complex formed between an RAR and an RXR. Residues in C2 are critical for heterodimer formation.

Retinoic Acid-Binding Domain

The retinoic acid-binding domain (domain E) fulfills several important functions, including, of course, retinoic acid binding, transcription activation, and nuclear localization. The RA-binding domain binds

FIGURE 1 Domain structure of RARs. All RARs and RXRs have domain structures similar to other members of the nuclear receptor family. Domains A–F are shown. DNA-binding domain (C) and ligand-binding domain (E) are highly conserved. Transcription activation functions are found in E (AF-2) and A (AF-1) domains.

both *all-trans* and 9-*cis* isomers of RA with high affinity. In contrast, the ligand-binding domain of RXRs bind only the 9-*cis* RA isomer. These ligand-binding domains possess a series of 12 α-helical structures (H1–H12) that fold together to form the ligand-binding pocket. H12 contains the transcription activation domain AF-2. From X-ray crystallographic studies, it has been proposed that conformational changes occurring with the binding of RA alter the position of H12 and thus the ability of the AF-2 to interact with transcription factors that repress or activate gene transcription. In the "mouse-trap" model of ligand activation, H12 is extended into the solvent in the absence of RA but snaps shut once ligand enters the RA-binding pocket. These dynamic conformational reconfigurations result in differential interactions with cofactors that functionally link the receptor complex with the transcription initiation complex.

Other Functional Regions of RARs

The N terminus of RARs, comprising domains A and B, contains another region important for transcriptional activation. Interestingly, differential splicing/alternate promoter usage can give rise to multiple A domains for each subtype. This multiplicity of RAR isoforms and their potential to form partnerships with RXR subtypes creates, at least conceptually, a remarkable number of combinatorial possibilities that may each have subtly different yet important contributions to RA target gene regulation. Domain D, or the hinge region, has been described as a tether that connects DNA and ligand-binding functions. This domain also appears to posses a nuclear localization motif required to sequester receptors in the nucleus. Unlike steroid hormone receptors, which reside in the cell cytoplasm bound to heat-shock proteins that are released to the nucleus upon ligand binding, RARs and RXRs are complexed with DNA in their unliganded state. The role of the F-domain located at the extreme C terminus of RAR is not known.

Retinoic Acid Response Elements

RAREs are DNA motifs to which RAR/RXR heterodimers can bind with high affinity. In most cases, these motifs comprise a direct repeat of the half-site consensus, PuGGTCA, separated by five base pairs; however, other configurations are also possible. These elements can be found in variations of number and orientation from within a few base pairs of transcription initiation sites to several thousand base pairs (usually upstream). These elements concentrate RAR/RXR heterodimers, which are normally in very low abundance, near transcription complexes.

RA Transcriptional Activation

RARs act as biosensors to detect RA in the local environment. The binding affinity of these receptors for RA is on the order of 10–30 nM. Once RAR-expressing cells are exposed to RA, changes in the pattern of gene transcription will occur. The role of transcription activators is to increase the efficiency of RNA polymerase II binding to the promoter and engage the successful transcription of a gene – and in the case of RARs, to do so only in the presence of RA. In unliganded form, the RAR/RXR heterodimer, when bound to an RARE on a target gene, can act to repress transcription (Figure 2). This complex recruits a specific type of transcription factor called a corepressor. The first such nuclear receptor corepressor found to interact with unliganded RAR was N-CoR/SMRT. The presence of RA causes allosteric modulation of the ligand-binding domain, shifting the cofactor binding preference from corepressor to coactivator. Thus, release of N-CoR/SMRT by RA results in the complex having increased affinity for coactivators such as p140 and p160. Many coregulators that interact with RAR/RXRs and that also have other chromatin-remodeling functions, such as histone-deacetylase activity, kinase activity, or methylase activity, have been isolated. In addition to chromatin-remodeling functions, some of these cofactors correspond to factors critical for establishing a stable transcription initiation complex. The net effect of these interactions is increased or decreased transcription of target genes, depending on the promoter sequence, the local concentrations of factors binding to the promoter, and whether other signaling pathways are regulating the activities of any of these factors. In this way, RA signal is processed in a manner that integrates the activities of many pathways of a given cell type.

Retinoic Acid Receptor Function

Each of the murine RAR and RXR subtypes has been knocked out by homologous recombination in order to determine their functions during embryonic development and in the adult. Although there are multiple receptor isoforms, there are distinct roles for each defined by spatiotemporal distribution and

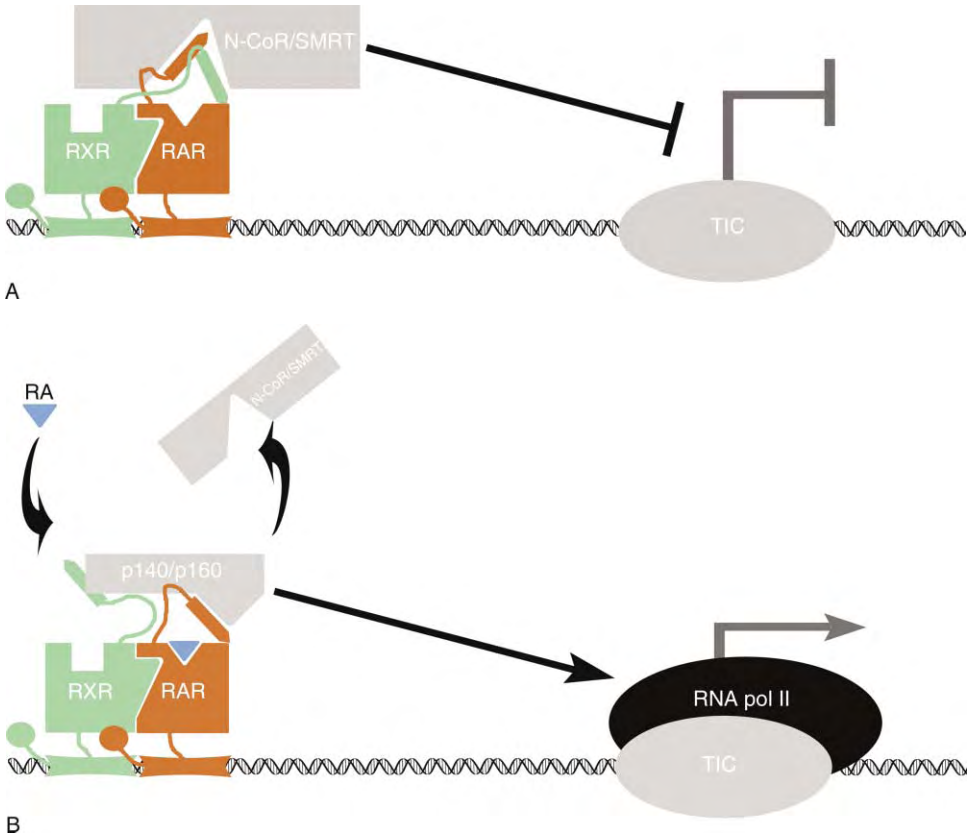

FIGURE 2 The RAR/RXR complex regulates transcription. (A) Transcriptional repression occurs when unliganded RAR/RXR heterodimer binds to an RARE in the promoter region upstream of the transcription start site of an RA-responsive gene. Unliganded receptors bind to corepressor factors such as N-CoR/SMRT that act to limit the function of the transcription initiation complex (TIC) through reorganization of chromatin structure. (B) Binding of RA ligand to the RXR/RAR complex induces a conformational change in the ligand-binding domain of RAR, causing the release of N-CoR/SMRT and allowing the recruitment of transcriptional coactivators such as the p160 complex. This coactivator complex promotes the binding of transcription accessory factors essential for the efficient engagement of RNA pol II activity.

promoter-specific activities. Throughout the murine life cycle, RARα is ubiquitously expressed and may play a role in some general housekeeping functions. In contrast, RARβ transcript distribution indicates that this receptor may be involved in ontogenesis of the central nervous system during development and differentiation of epithelia in the adult. Similarly, the expression patterns of RARγ are spatiotemporally regulated, suggesting that this receptor is involved in embryonic tail bud development, craniofacial morphogenesis, chondrogenesis, and maintenance of squamous epithelia. Among RXRs, RXRα is ubiquitously expressed, whereas RXRβ and RXRγ are more restricted during embryogenesis.

Gene knockout studies confirmed distinct roles for each RAR and RXR subtype and also revealed a high level of functional redundancy. Whereas the RARα- and RARβ-null mutants display some of the postnatal defects observed in vitamin A-deficient (VAD) mice (poor viability, growth deficiency, and male sterility), most of the RAR- or RXR-null single mutants exhibit only subtle or, in some cases, undetectable developmental abnormalities. In contrast, RAR double mutants exhibit reduced viability and recapitulate most symptoms of VAD.

RXR$\beta^{-/-}$RXR$\gamma^{-/-}$RXR$\alpha^{+/-}$ triple-mutant mice exhibit marked growth deficiency but, surprisingly, display no obvious congenital or postnatal abnormalities. However, mutation of both RXRα alleles is lethal. Therefore, RXRα may carry out most of the vital developmental and postnatal functions of the RXRs.

See Also the Following Articles

RNA Polymerase II and Basal Transcription Factors in Eukaryotes • RNA Polymerase II Elongation Control in Eukaryotes • RNA Polymerase II Structure in Eukaryotes • Zinc Fingers

Glossary

retinoic acid The derivative of the fat-soluble vitamin A that is active in the regulation of gene expression by activating nuclear retinoic acid receptors.

transcription The process by which RNA polymerase II is recruited to the promoter of a gene and enzymatically copies the base sequence of a gene into an RNA transcript.

transcription factor A protein or collection of proteins that are involved in altering the efficiency of RNA polymerase II activity in transcribing a gene.

Further Reading

Chambon, P. (1996). A decade of molecular biology of retinoic acid receptors. *FASEB J.* **10**, 940–954.

Clagett-Dame, M., and DeLuca, H. F. (2002). The role of vitamin A in mammalian reproduction and embryonic development. *Annu. Rev. Nutr.* **22**, 347–381.

Rosenfeld, M. G., and Glass, C. K. (2001). Coregulator codes of transcriptional regulation by nuclear receptors. *J. Biol. Chem.* **276**, 36865–36868.

Ross, S. A., McCaffery, P. J., *et al.* (2000). Retinoids in embryonal development. *Physiol. Rev.* **80**, 1021–1054.

Biography

Martin Petkovich is a Professor of Biochemistry and Pathology in the Cancer Research Institute at Queen's University in Kingston, Ontario. His research interests include molecular genetics of retinoid signaling and metabolism in embryonic development and pattern formation. He discovered the first nuclear receptor for retinoic acid and has also identified key enzymes involved in regulating RA levels in tissue.

Reverse Transcriptase and Retroviral Replication

Laura Tarrago-Litvak, Marie-Line Andréola and Simon Litvak
Réplication et Expression des Génomes Eucaryotes et Rétroviraux (REGER), Bordeaux, France

Since its discovery, reverse transcriptase (RT) has been associated with retroviruses. In the following years this RNA-dependent DNA polymerase was found in eukaryotes, prokaryotes, retrotransposons, hepadnaviruses, retrons, and even humans. The role of RT in all retroviruses is to synthesize double-stranded DNA copying the retrovirus single-stranded RNA genome. This DNA is then integrated into the host cell's chromosomes as a provirus. Transcription then leads to copies of the viral RNA genome, from which the virus's own proteins and enzymes are formed. New viral particles then bud from the membrane of the cell. Thus, reverse transcriptase is essential for viral replication.

RT performs a remarkable feat, reversing the normal flow of genetic information. The polymerases synthesizing DNA and RNA in cells are very accurate and make very few mistakes. This is essential because they are the caretakers of our genetic information, and mistakes may be passed on to the offspring. RT, on the contrary, makes mistakes very often by incorporating a non-complementary nucleotide. One might think that this would cause severe problems to the virus. But, in fact, this high error rate turns out to be an advantage for the virus. The errors allow the retrovirus to mutate rapidly in order to fit new conditions and escape, for instance, the immunological response of the host or the effect of therapeutic agents.

Discovery of Reverse Transcriptase

The publication of the presence of reverse transcriptase (RT) in retroviruses in 1970 by the groups of Howard Temin and David Baltimore in the same issue of *Nature* must be considered as a landmark in the story of biological sciences in the second half of the twentieth century. The presence of a DNA polymerase able to copy RNA into DNA (contrary to all the enzymes of this family described before which copy a DNA template into DNA), violated the so-called central dogma of molecular biology which stated that genetic information always flowed from DNA to RNA to protein. It is of interest to point out that while the laboratory of Baltimore came to this conclusion by searching for the mechanisms used by polymerases, involved in the replication of different viruses, the findings of Temin's group came as a strong support of his earlier experiments, which showed that the replication of retroviruses was sensitive to inhibitors of DNA-dependent polymerases. Since the early 1960s Temin had proposed the idea, widely rejected at that time, that the replication of RNA oncoviruses, as they were called, had to go via a DNA intermediate that may be integrated in the host genome. Years later, after the discovery of RT, the finding in 1983 that the cause of AIDS was a retrovirus, the human immunodeficiency virus type 1 (HIV-1), and the consequent emotion provoked by the AIDS pandemics led to an explosive burst of research on this virus. It can be considered that very few organisms have provided so much information on their structure and function in such limited time as in the case of HIV-1. Most of the information on retroviral replication since the early 1980s has come from the work on this human retrovirus.

Retrovirus Genome

All retroviral genomes consist of two identical molecules of RNA, which are single-stranded, (+) sense and have a 5′-end cap and a 3′-end pol (A) as in the case of eukaryotic messenger RNAs (mRNAs). Retroviral genomes vary in size from 8 to 11 kb. Some distinctive features of the retrovirus genomes concern the fact that they are the only RNA viruses which are not only truly diploid but also whose genome is produced by the cellular transcriptional machinery, without the involvement of a viral-encoded polymerase (Figure 1). Moreover, they are the only (+) sense RNA viruses whose genome does not serve directly as mRNA immediately after infection. The two RNA genomic molecules are physically linked as a dimer by hydrogen bonds. In addition, another nucleic acid is present in all viral particles, a specific transfer RNA (tRNA) required for the initiation of replication. Most, if not all, DNA polymerases require a primer carrying

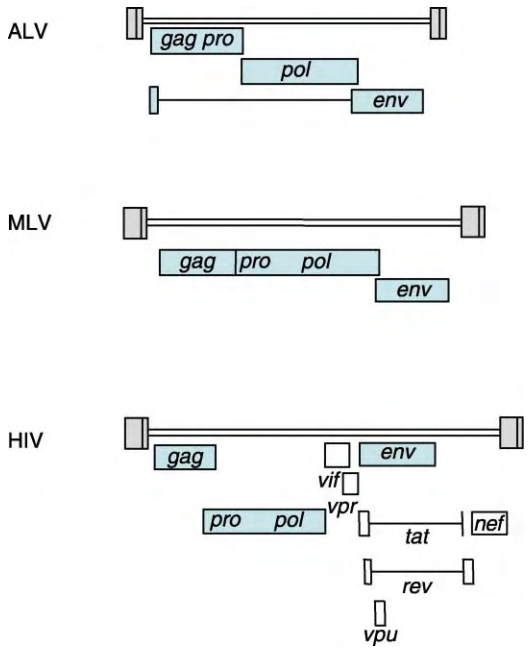

FIGURE 1 Genetic organization of prototypic retroviruses. An open rectangle indicates the open reading frame for the gene marked. Gag, pol, and env, common to all retroviruses, are shown in blue. *Gag*: encodes a polyprotein (Gag), whose cleavage products are the major structural proteins (matrix [MA], capsid [CA], and nucleocapsid [NC]) of the virus core; *pro*: encodes part of a polyprotein (Gag-Pro, or Gag-Pro-Pol), whose cleavage products include protease (PR); *pol*: encodes part of a polyprotein (Gag-Pro-Pol), whose cleavage products include reverse transcriptase (RT) and integrase (IN); *env*: encodes a polyprotein (Env), whose cleavage products SU (surface) and TM (transmembrane) are the structural proteins of the viral envelope; *tat*: an accessory gene encoding for a low-molecular-weight protein (trans activator) that activates transcription by binding to TAR; *rev*: an accessory gene encoding a protein that regulates splicing and RNA transport; *nef*: an accessory gene encoding a protein that reduces the level of CD4 on the cell surface, and also stimulates some infected cells to divide; *vpu*: an accessory gene encoding a protein (viral protein u) that triggers CD4 degradation. Enhances virion release; *vif*: an accessory gene encoding a protein (virion infectivity factor) that affects infectivity of viral particles; *vpr*: an accessory gene encoding a protein (viral protein r) that causes infected cells to arrest in G_2 and may also promote transport of the preintegration complex into the nucleus after reverse transcription. Horizontal lines indicate that this segment is spliced out. ALV: avian leukemia virus; MLV: murine leukemia virus; HIV: human immunodeficiency virus.

a free 3′-end OH from where DNA synthesis is initiated. In the case of retroviruses, this primer is a cellular tRNA, which is able to anneal partially to a region near the 5′-end of the RNA viral genome, the "primer-binding site" (PBS). Examination of the sequences of several retroviruses has shown that the PBS is complementary to the 3′-end of a given tRNA: $tRNA^{Trp}$ in avian retroviruses, $tRNA^{Pro}$ in murine viruses and $tRNA^{Lys3}$ in HIV-1. The mechanism involved in the selection of a specific tRNA is not fully understood. While the role of the viral genome has been ruled out, early results with avian retroviruses suggested that RT was involved in tRNA packaging. Very recent work seems to indicate that in the case of HIV-1, the lysine aminoacyl-tRNA synthetase may encapsidate the cognate tRNA primer in the retroviral particle. The small basic nucleocapsid (NC) protein encoded in the C-terminal region of the *gag* gene seems to play an important role in the annealing of primer tRNA to the PBS region, thus allowing the initiation of retroviral replication. The gene order in all retroviruses is invariant: 5′-gag-pol-env-3′. However, some complex retrovirus, like HIV-1, encode several other small regulatory proteins.

Activities Associated with the Reverse Transcriptase

With the exception of some murine retroviral polymerases, most RTs are heterodimeric enzymes. The retroviral-encoded protease cleaves a polyprotein precursor leading to an RT subunit that is further cleaved by the same protease (Figure 2). Thus, RTs are formed by two subunits where the smallest one carries the same sequence as the largest. Retroviral DNA synthesis is

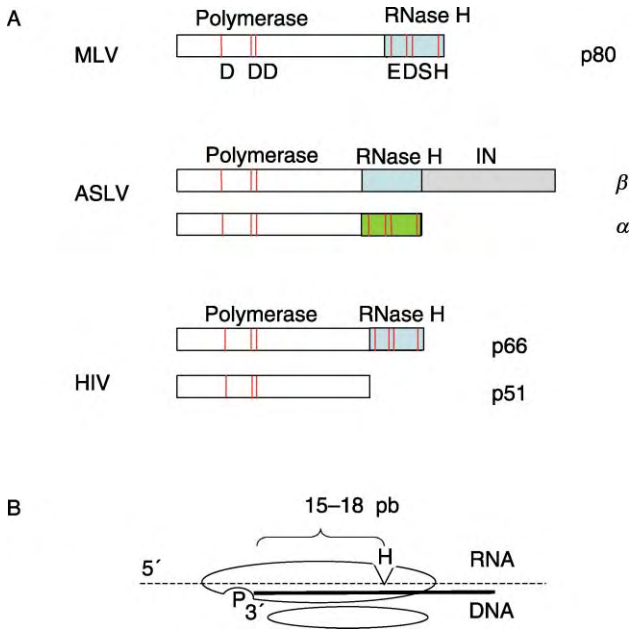

FIGURE 2 (A). Subunit structure of various retroviral RT. The MLV RT is a monomer. The ASLV RT is a heterodimer, the cleavage at the RT-IN boundary is incomplete. In HIV, the IN is produced as a separate protein. Vertical lanes show the positions of the active site residues in the polymerase and RNase H domains. (B). Mode of HIV-1 RT positioning for synthesis and RNase H cleavage. The 3′-end of the DNA directs RT positioning for optimal RNase H cleavage.

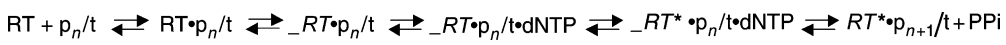

FIGURE 3 Model for the kinetic mechanism of the polymerase reaction. Asterisks distinguish structural states of the system. p_n: primer containing n nucleotides; p_{n+1}: primer containing $n + 1$ nucleotides; t: template; PPi: pyrophosphate.

absolutely dependent on the two enzymatic activities associated with RT: a DNA polymerase that can use either RNA or DNA as a template, and a nuclease, named ribonuclease H (RNase H), that is specific for the RNA strand of RNA·DNA hybrids. All of the enzymatic functions required to complete the series of steps involved in the generation of a retroviral DNA can be attributed to either the DNA polymerase or the RNase H of RT as described below. However, it cannot be ruled out that certain viral proteins, such as the nucleocapsid protein, may increase the efficiency of reverse transcription.

Reverse transcription of the retroviral genome depends on the coordination of the polymerase and RNase H activities of RT. The spatial arrangement between the two active sites of the enzyme (corresponding to ~15–18 bases in the template) contributes to the coordination of these two activities. While the 3′-OH of the primer strand is positioned close to the RT amino acid residues important in the DNA polymerase active site, the template strand is positioned close to RT residues important for RNase H activity.

Biochemistry of Reverse Transcriptase

Mechanism of Action

The study of the mechanism of the RNA- and DNA-dependent DNA polymerase activity has led to a model involving a two-step binding mechanism. DNA polymerization catalyzed by RT is a multistep reaction, requiring the binding of the primer·template duplex and a deoxynucleoside triphosphate (dNTP) to RT prior to deoxy-nucleoside-5′-monophosphate addition to the 3′ end of the primer. Kinetic experiments have established the order of binding of the substrates. The primer·template duplex binds prior to binding of the deoxynucleoside triphosphate substrate to form the catalytically competent ternary complex. The rate-limiting step for nucleotide incorporation prior to dissociation of the enzyme is a conformational change. Following pyrophosphate liberation, the elongated product is released. Small changes in the rates and equilibrium constants have been observed for RNA- versus DNA-dependent DNA synthesis. All these mechanisms have been derived from pre-steady-state or steady-state kinetic assays using short primer·templates and do not always reflect the true nature of reverse transcription, although they are necessary in determining the kinetics and affinity of substrate binding to RT (Figure 3).

Processivity

The elongation phase of DNA synthesis by DNA polymerases may be processive or distributive. A processive DNA polymerase is able to synthesize long DNA stretches without dissociation of the enzyme from the primer·template duplex, while a distributive polymerase dissociates easily after incorporation of few nucleotides. Reverse transcriptase is considered to be poorly processive as compared with replicative DNA polymerases. However, a higher processivity of RT may be observed when copying specific regions of the viral genome or in the presence of some viral proteins.

Fidelity

All RTs show poor fidelity when compared to host DNA polymerases in *in vitro* systems. The lack of a proofreading function as well as the enzyme ability to extend mismatched primer termini probably explains much of this high error rate. The tendency of RT to switch templates, paired with its ability to extend mismatches by incorporating "wrong" nucleotides may be a significant source of replication errors. The error rates of various RTs estimated in different types of assays can be significantly affected by altering the parameters of the reaction. The error rate is quite dependent on sequence context and "hot spots," where errors occur frequently, and may differ according to the particular RT used in the assay. In addition, error rates may be different on RNA and DNA templates. As a consequence, it is not possible to define the error rate as a single number. These studies, taken together, do suggest that the overall error rate is high: about one per genome in a reverse transcription cycle. Cellular factors may alter error rates and some studies suggest that somewhat lower error rates occur *in vivo*. However, the *in vitro* data lead to the generally accepted impression that the average retroviral DNA genome differs from its parent by at least one mutation, and have provided the evidence for the existence of retroviral "quasi-species."

Replication Errors *in Vivo* and the Emergence of Antiviral Resistance

The rates at which mutations accumulate in retroviral and host genomes are very different since the viral genomes are found to evolve at rates perhaps a million-fold higher than the genomes of their hosts. The lack of RT fidelity and the accumulation of nonlethal mutations are closely related to the emergence of resistance towards antiviral therapeutic agents. This effect is especially dramatic in the case of HIV-1, the causal agent of AIDS. After short spans of treatment, viral quasi-species appear with mutations in the viral target proteins (the most used targets against HIV-1 are RT and protease). The introduction of the so-called combination therapy against AIDS has greatly improved the possibility to keep the seropositive patients for several years with a low or undetectable viral charge. The combination of several anti-proteases and anti-RTs makes it possible that if a given mutation leads to the apparition of resistance against a specific drug, the other antivirals are still effective, giving time to replace the one to which the target enzyme has become resistant.

Inhibitors of Reverse Transcriptase

Emphasis in the search of RT inhibitors has been obviously focused on the HIV-1 enzyme but some of the inhibitors developed against this agent may be useful in arresting retroviruses involved in other pathologies. Inhibitors of HIV-1 RT were the first therapeutic agents described against AIDS. The protease inhibitors appeared later, and currently inactivating agents against several viral targets (viral entry, integrase, etc.) are actively being studied. As mentioned elsewhere in this article the combined use of anti-proteases and anti-RTs has led to a great improvement in the control of HIV-1 proliferation in AIDS patients. Two main families of HIV-1 RT inhibitors are used against AIDS, the nucleoside analogue inhibitors of RT (NRTI) and the non-nucleoside inhibitors of RT (NNRTI). The first one is recognized and incorporated by RT in the newly synthesized DNA but as they lack or have a modified group in the 3′ position of the ribose they cannot be linked to the following dNTP precursor and thus they act as chain terminators. To be active *in vivo* the putative NRTI, which are active against all retroviral RTs, must be triphosphorylated by cellular kinases. The first NRTI described was azidothymidine or zidovudine but currently more than a dozen of these inhibitors have been approved by the US FDA and are used in clinics. The second family, the NNRTIs, is specific of the HIV-1 RT since they inhibit the viral polymerase after binding to a hydrophobic region of this enzyme. They do not have a typical nucleoside structure but belong to a variety of different chemical families of compounds and in contrast to NRTIs they do not need to be metabolized inside the cell to display their antiviral effect.

Recombination

Since retroviruses ordinarily carry two identical or nearly identical RNAs, the genetic consequences of using only one RNA versus portions of both of the RNAs to template DNA synthesis are usually the same. However, under certain conditions, two genetically distinct RNAs can be encapsidated. Portions of each template can be used to generate a single DNA, producing a recombinant. Recombination does occur in virions produced by a single cell that has been co-infected by two different viruses demonstrating that recombination requires co-packaging of two viral genomes into the same particle. During reverse transcription in such heterozygous virion particles, the DNA product can be generated containing portions of each of the two genomic sequences in one molecule.

The Role of RT in Reverse Transcription

Reverse transcription catalyzed by RT begins when the viral particle enters the cytoplasm of a target cell. DNA synthesis using the RNA retroviral genome as template takes place in the cytoplasm leading to a linear double-stranded DNA (dsDNA), co-linear with the viral RNA template, the proviral DNA. However, proviral DNA contains terminal duplications known as the long terminal repeats (LTRs) that are not present in viral RNA (Figure 4).

The following scheme is widely accepted to reflect the process of retroviral DNA synthesis catalyzed by RT:

1. Minus-strand DNA synthesis starts from the 3′ end of a tRNA partially annealed to the primer-binding site (PBS) in genomic RNA. Minus-strand DNA synthesis proceeds until the 5′-end of genomic RNA is reached, generating a short DNA intermediate termed minus-strand strong-stop DNA (−sssDNA). Since the PBS is near the 5′end of viral RNA, the length of this strong-stop DNA is ~100–150 nucleotides.
2. Following RNase H-mediated degradation of the RNA strand of the RNA·(−sssDNA) duplex, the first strand transfer involves the annealing of the −sssDNA to the 3′-end of a viral genomic RNA. This transfer is allowed by the presence of identical sequences known as the repeated (R) sequences, present at the 5′- and 3′-ends of the RNA genome. The 3′-end of (−sssDNA) is copied from the R sequences at the 5′-end of the viral genome and therefore contains sequences

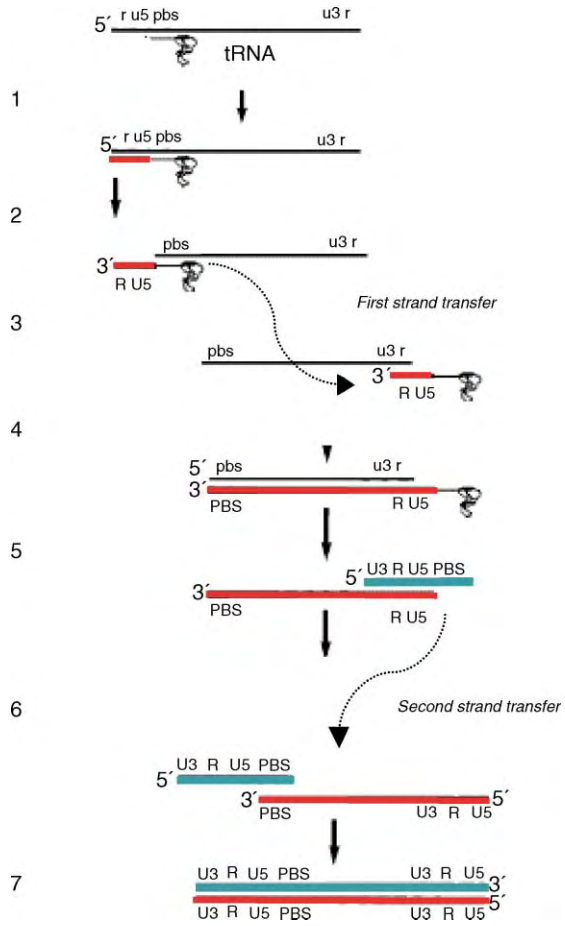

FIGURE 4 Process of reverse transcription. Thick lane, DNA; thin lane, RNA.

complementary to R. After the RNA template has been removed, the (− sssDNA) can anneal to the R sequences at the 3′-end of the RNA genome. The annealing reaction related to the first strand transfer, appears to be facilitated by the NC protein.

3. Once the (− sssDNA) has been transferred to the 3′ R region on viral RNA, minus-strand DNA synthesis may start again, followed by RNase H digestion of the template strand.

4. RNase H degradation is not complete since some hybrid regions seem to be more resistant to the nuclease. The RNA genome contains a short polypurine tract (PPT) that is relatively resistant to RNase H degradation. A defined RNA segment derived from the PPT primes plus-strand DNA synthesis. Plus-strand synthesis is halted after a portion of the primer tRNA is reverse-transcribed, leading to a DNA called plus-strand strong-stop DNA (+sssDNA). Some retroviruses generate more than one plus-strand primers from the RNA genome.

5. RNase H removes the primer tRNA, exposing sequences in (+sssDNA) that are complementary to sequences at or near the 3′ end of plus-strand DNA.

6. Annealing of the complementary PBS segments in (+sssDNA) and minus-strand DNA constitutes the second strand transfer.

7. Plus- and minus-strand syntheses are then completed, with the plus and minus strands of DNA each serving as a template for the other strand.

Integration and Retroviral Replication

As proposed by Temin since the early 1960s, retrovirus replication is performed via a DNA intermediate, the proviral DNA is synthesized by the RT in the cytoplasm. Integrase (IN), the third retroviral encoded enzyme in addition to RT and protease, is involved in the integration of the proviral DNA in the nuclear DNA of the infected cell. Integration is a crucial step in viral replication since retroviral DNA molecules are not ordinarily able to replicate autonomously and they depend on integration for stable maintenance in dividing cells. Once integrated the proviral DNA is recognized by the host-cell enzymatic machinery for efficient transcription of viral DNA into new copies of the viral genome and mRNAs that encode viral proteins. Moreover, integration also stabilizes the viral DNA against degradation and allows its genetic transfer as an integral element of the host genome.

Role of Reverse Transcriptase in Modern Biology

It is now well known that RT is present not only in animal retroviruses but also plays a crucial role in DNA replication of prokaryotic and eukaryotic cells, in the replication of some plant and animal DNA viruses, as well as in the function of several classes of transposable elements. As mentioned in the remarkable book *Retroviruses* "it should be remembered that RT has had a critical role in the development of modern biology. The ability to convert RNA into DNA has been as important to molecular biologists as it has been to retrovirologists. It is worth taking a moment to reflect on how much more difficult it would have been to solve the puzzles posed by the organization and expression of genes in higher eukaryotes if RT did not exist."

See Also the Following Articles

HIV-1 Reverse Transcriptase Structure • Non-Homologous Recombination: Retro-Transposons

Glossary

cap The structure at the 5′-end of eukaryotic mRNA introduced after transcription. It results from adding a methylated G to the terminal base of the mRNA.

DNA polymerase An enzyme that systhesizes a daughter strand of DNA under direction from a DNA or an RNA template.

hot spot A site at which the frequency of mutation (or recombination) is increased significantly.

LTR An abbreviation for long-terminal repeat, a sequence directly repeated at both ends of a retroviral DNA.

primer A short sequence (often of RNA) that provides a free 3′-OH end at which a DNA polymerase starts synthesis of a deoxyribonucleotide chain.

retrovirus An RNA virus that propagates *via* conversion into duplex DNA.

template A polynucleotide which furnishes the instructions for the sequence of nucleotides to be added to the primer strand during DNA polymerization.

Further Reading

Arts, E. J., and Le Grice, S. F. (1998). Interaction of retroviral reverse transcriptase with template-primer duplexes during replication. *Prog. Nucleic Acid Res. Mol. Biol.* **58**, 339–393.

Baltimore, D. (1970). RNA-dependent DNA polymerase in virions of RNA tumor viruses. *Nature* **226**, 1209–1211.

Coffin, J. M., Hughes, S. H., and Varmus, H. E. (eds.) (1997). *Retroviruses*. Cold Spring Harbor Laboratory Press, New York.

Darlix, J. L., Lapadat-Tapolsky, M., de Rocquigny, H., and Roques, B. P. (1995). First glimpses at structure–function relationships of the nucleocapsid protein of retroviruses. *J. Mol. Biol.* **254**, 523–537.

De Clercq, E. D. A. (ed.) (2001). *Antiretroviral Therapy*. ASM Press, Washington, DC.

Skalka, A. M., and Goff, S. P. (eds.) (1993). *Reverse Transcriptase*. Cold Spring Harbor Laboratory Press, New York.

Tarrago-Litvak, L., Andreola, M. L., Nevinsky, G. A., Sarih-Cottin, L., and Litvak, S. (1994). The RT of HIV-1: From enzymology to therapeutic intervention. *FASEB J.* **8**, 497–503.

Temin, H. M. (1993). Retrovirus variation and reverse transcription: Abnormal strand transfers result in retrovirus genetic variation. *Proc. Natl Acad. Sci. USA* **90**, 6900–6903.

Temin, H. M., and Mizutani, S. (1970). RNA-dependent DNA polymerase in virions of Rous sarcoma virus. *Nature* **226**, 1211–1213.

Verma, I. M. (1997). The reverse transcriptase. *Biochim. Biophys. Acta.* **473**, 1–38.

Waters, L. C., and Mullin, B. C. (1997). Transfer RNA into RNA tumor viruses. *Prog. Nucleic Acid Res. Mol. Biol.* **20**, 131–160.

Biography

Laura Tarrago-Litvak was born in Santiago, Chile. She did her university undergraduate studies at the University of Chile and obtained her Ph.D. at the University of Bordeaux, France. Her current research interest is in the field of retroviruses, mainly in two retroviral enzymes, reverse transcriptase and integrase.

Marie-Line Andréola was born in Sainte-Foy-la-Grande, France. She did her university undergraduate studies and obtained her Ph.D. at the University of Bordeaux, France. Her current research interest is in the field of retroviruses, focused on the mechanism of action and search of inhibitors of two retroviral enzymes, reverse transcriptase (RNase H activity) and integrase.

Simon Litvak was born in Valparaiso, Chile. He did his university undergraduate studies at the University of Chile at Santiago and obtained his Ph.D. at the University of Paris, France. He is affiliated to the CNRS as Principal Investigator and is currently the Director of the REGER Laboratory (UMR-5097. CNRS – University of Bordeaux 2) and former Director of the Institut Federatif des Recherches "Pathologies Infectieuses et cancers," Bordeaux, France. His current research interest is in the field of retroviruses. Research in his group is focused on the mechanism of action of two key HIV-1 enzymes: reverse transcriptase and integrase. He has also contributed in the search for specific inhibitors of HIV-1 RT and IN (small ligands and oligonucleotides).

Rho GTPases and Actin Cytoskeleton Dynamics

Priam Villalonga and Anne J. Ridley
Ludwig Institute for Cancer Research and University College London, UK

The dynamic regulation of the actin cytoskeleton plays a crucial role in the control of cell shape and movement, and therefore has a profound impact on the biology of multicellular organisms. Accordingly, actin cytoskeleton regulators modulate a broad array of cellular processes such as cell migration, tissue morphogenesis, inflammation, vesicular trafficking, secretion, and cancer cell invasion and metastasis, just to name a few of them. Members of the Rho family of small GTPases have emerged as major regulators of the actin cytoskeleton in all eukaryotic cells. Like other small GTPases, these proteins are molecular switches that are exquisitely regulated by several positive and negative regulators that can either "switch" them on or off. Once activated, they bind to and activate a number of downstream effectors, most of them directly implicated in the regulation of actin-related biochemical events (e.g., actin polymerization). This enables Rho GTPases to act as key players in processes that require the dynamic regulation of the actin cytoskeleton.

Rho GTPase Family: Overview and Regulation

Rho GTPases constitute a separate family within the larger Ras superfamily of small GTPases. In mammalian cells, the prototypical Rho family members are RhoA, Rac1, and Cdc42, which have been the most extensively characterized. However, there are many other members in this family including Rho, Rac, and Cdc42 isoforms and several other proteins that are more or less related to these three in terms of sequence homology, thereby defining subfamilies within the Rho family (Figure 1). Some Rho family members show a tissue-specific pattern of expression, although most of them are expressed in the vast majority of mammalian cells, localizing to different cellular membranes as a consequence of lipid modifications at their carboxy termini. Like other GTPases, Rho proteins bind to guanine nucleotides and, except for members of the Rnd subfamily, cycle between an active GTP-bound state and an inactive GDP-bound state. Three different types of regulators can modulate the activation levels of these GTPases: guanine-nucleotide-exchange factors (GEFs), GTPase-activating proteins (GAPs), and guanine-nucleotide-dissociation inhibitors (GDIs), as illustrated in Figure 2.

Guanine-Nucleotide-Exchange Factors

GEFs promote the release and exchange of bound nucleotides on the GTPase, effectively leading to an increase in the number of GTP-bound molecules due to the higher intracellular concentration of GTP. GEFs are, therefore, positive regulators of Rho GTPases that promote their activation. In mammalian cells, a large number of GEFs have been described, all sharing a highly conserved exchange factor domain termed Dbl-homology (DH), named after the first GEF identified, Dbl. They also have other conserved domains such as the phospholipid-binding domain PH (Pleckstrin homology), involved in the localization of GEFs in the vicinity of the GTPases on membranes, providing a mechanism for GEF regulation. In addition to their regulation by phospholipid binding, GEFs can be regulated by binding to other proteins or by phosphorylation. Rho GEFs exhibit different degrees of specificity *in vitro* towards Rho GTPases, but it still has not been clearly established which GEFs regulate each of the Rho GTPase members *in vivo*.

GTPase-Activating Proteins

GAPs act by binding to the GTPase and enhancing hydrolysis of GTP, an otherwise slow and inefficient process, and by promoting the conversion of GTP to GDP they are negative regulators of Rho GTPases. Rho GAPs share in common a 140 amino acid domain, termed the RhoGAP domain, that confers GAP activity. However, they are usually large

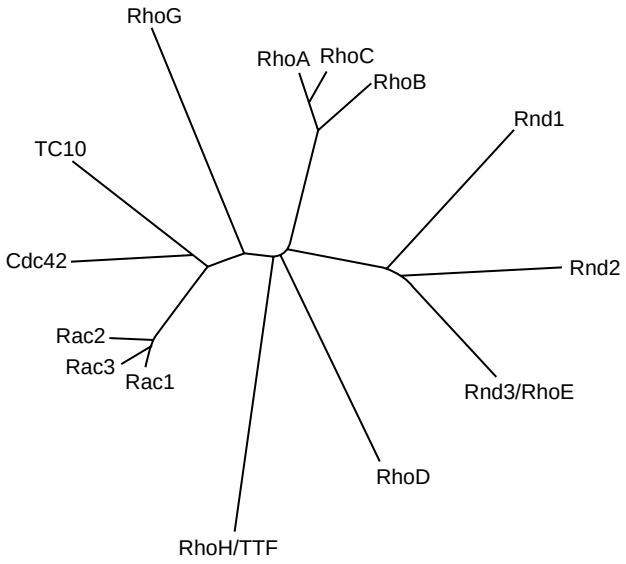

FIGURE 1 Phylogenetic tree of the Rho GTPase family. Rho GTPase family members can be grouped into subfamilies according to their sequence similarity.

proteins containing other domains involved in signaling and lipid and protein binding. Although these domains are thought to influence GAP function in cells, very little is known concerning how these proteins are regulated *in vivo*, although it has been reported that some of them can be regulated by tyrosine phosphorylation.

Guanine-Nucleotide-Dissociation Inhibitors

GDIs bind to Rho GTPases in the cytosol and prevent their interaction with the membranes, and with both GEFs and GAPs. For these reasons they are considered to be negative regulators of Rho GTPases that sequester them in an inactive form in the cytoplasm. Signals that activate Rho GTPases will disrupt the GTPase/GDI complex and localize the GTPase to membranes. It has been reported that GDIs can be phosphorylated by protein kinase C, leading to their dissociation from GTPases and consequently to GTPase activation. There are three RhoGDIs in mammalian cells that show differences in their pattern of expression, activity, and specificity.

Rho GTPase Family Activity: Downstream Targets

Rho GTPases exert their function by binding to and modulating the activity of an array of downstream effectors. Here the manner in which Rho GTPases activate some of their most relevant targets in terms of actin cytoskeleton control will be described (Table 1).

Rho Effectors

The archetypical responses elicited by Rho activation in cells are the assembly of bundles of filamentous actin

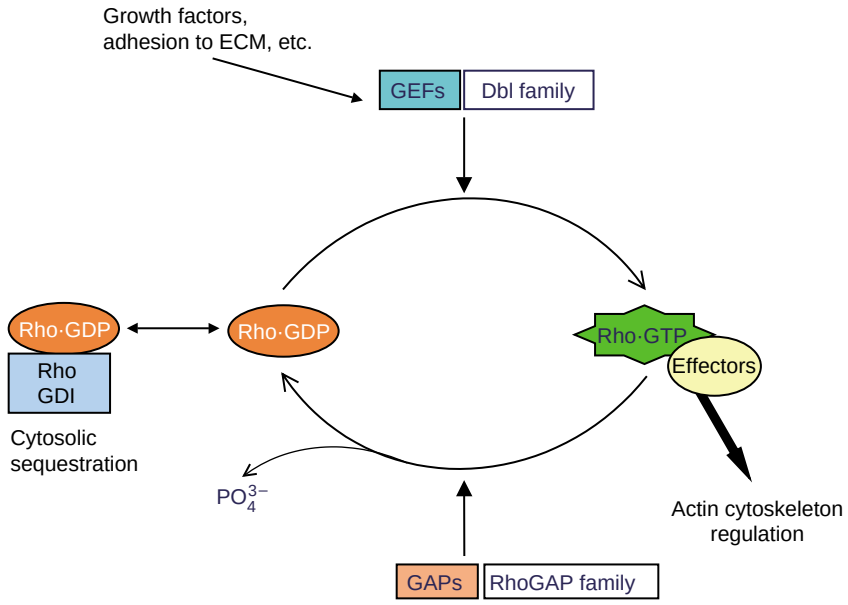

FIGURE 2 Rho GTPase regulation. Rho GTPases cycle between a GDP-bound, inactive state, and a GTP-bound active state. When GDP-bound, Rho GTPases can bind to RhoGDIs and remain sequestered in the cytoplasm. Extracellular signals induce the exchange of GDP for GTP, which is regulated by GEFs, thereby activating Rho GTPases and localizing them on membranes. In their GTP-bound form, Rho GTPases interact with their downstream effectors and regulate the actin cytoskeleton. Inactivation is achieved through GTP hydrolysis, which is often promoted by GAP binding to Rho GTPases.

TABLE 1

Rho GTPase, Downstream Effectors, and their Functions

Rho GTPase	Downstream effectors	Function in cell biology
RhoA, B, C	ROCK I, II	Actomyosin contractility: Stress fiber and focal adhesion formation. Tail retraction and new focal adhesion formation in cell migration
	mDia	Actin filament formation
Rac1, 2, 3	IRSp53	Actin polymerization, through WAVE activation, and Lamellipodia formation. Driving force in cell migration
	PAK1, 2, 3	Actin polymerization through LIMK-induced cofilin inhibition
Cdc42	WASP/N-WASP	Actin polymerization and filopodia formation. Sensor role in cell migration
Rnd1, 2, 3/RhoE	Unknown (RhoE binds to ROCK I)	Antagonizing RhoA effects: Disassembly of actin stress fibers and focal adhesions
RhoH/TTF	Unknown	Antagonizes some aspects of RhoA signaling in lymphocytes
TC10	WASP	Actin polymerization, filopodia formation

and myosin, termed stress fibers, and the formation of multimolecular complexes at the end of those fibers at sites of integrin-mediated cell adhesion, termed focal adhesions. Both effects can be largely attributed to one Rho effector, the serine/threonine kinase, Rho-kinase (ROCK). Rho-GTP binding to ROCK unfolds and relieves its kinase domain from an otherwise closed, autoinhibited, conformation. The two isoforms of ROCK phosphorylate a number of proteins involved in regulating the actin cytoskeleton, including the myosin-binding subunit of myosin light-chain phosphatase, thereby inhibiting its phosphatase activity and enhancing myosin light-chain phosphorylation and actomyosin-based contractility. Other Rho effectors contribute to Rho-mediated actin cytoskeleton regulation, such as mDia, which binds to the actin-binding protein profilin and stimulates actin filament formation.

Cdc42 Effectors

Activation of Cdc42 in most cells promotes the formation of filopodia, spike-like membrane protrusions induced by actin polymerization in parallel bundles. As with Rac-induced lamellipodia, these structures are associated with the leading edge of migrating cells. A clear model has emerged in which a Cdc42 effector, WASP (Wiskott Aldrich syndrome protein), directly controls actin polymerization to extend filopodia in response to extracellular signals. The hematopoietic-specific WASP or its widely expressed isoform, N-WASP, induce *de novo* actin polymerization through their binding to the Arp2/3 (actin-related protein) complex. Binding of active Cdc42 to WASP changes its conformation, relieving it from an autoinhibited state and exposing a previously masked domain, the VCA domain (verprolin-homology, cofilin-homology and acidic region). Once exposed, this domain binds to G-actin through the V-domain and to the Arp2/3 complex through the CA-domain, strongly activating Arp2/3 complex-induced actin nucleation and polymerization. WASP also binds to the actin-binding protein profilin, which further enhances WASP-mediated actin filament formation through its ATP/ADP exchange activity towards actin. Activation of WASP family proteins by Rho GTPases, such as WASP activation by Cdc42, is a typical example of downstream effector activation by binding to active GTPases (Figure 3).

Rac Effectors

In most mammalian cells, activation of Rac induces lamellipodia and membrane ruffles, both being plasma membrane protrusions that extend over the substratum or upwards, respectively. These protrusions are driven by a branching network of actively polymerizing actin filaments, and are usually found at the leading edge of migrating cells. The Rac effector pathway that leads most directly to actin polymerization involves WAVE proteins (wasp/verprolin homologous protein). WAVEs are members of the WASP family that are crucial mediators of actin polymerization mediated by the Arp2/3 complex. WAVE1 and WAVE2 have been shown to be activated downstream of Rac, although Rac does not bind directly WAVEs and the mechanism of activation is different to Cdc42 stimulation of WASP, but with similar consequences: activation of Arp2/3 complex-mediated actin polymerization (see Figure 3). Other Rac effectors also contribute to actin polymerization and to extension of lamellipodia and membrane ruffles. For example, PAKs (p21-activated

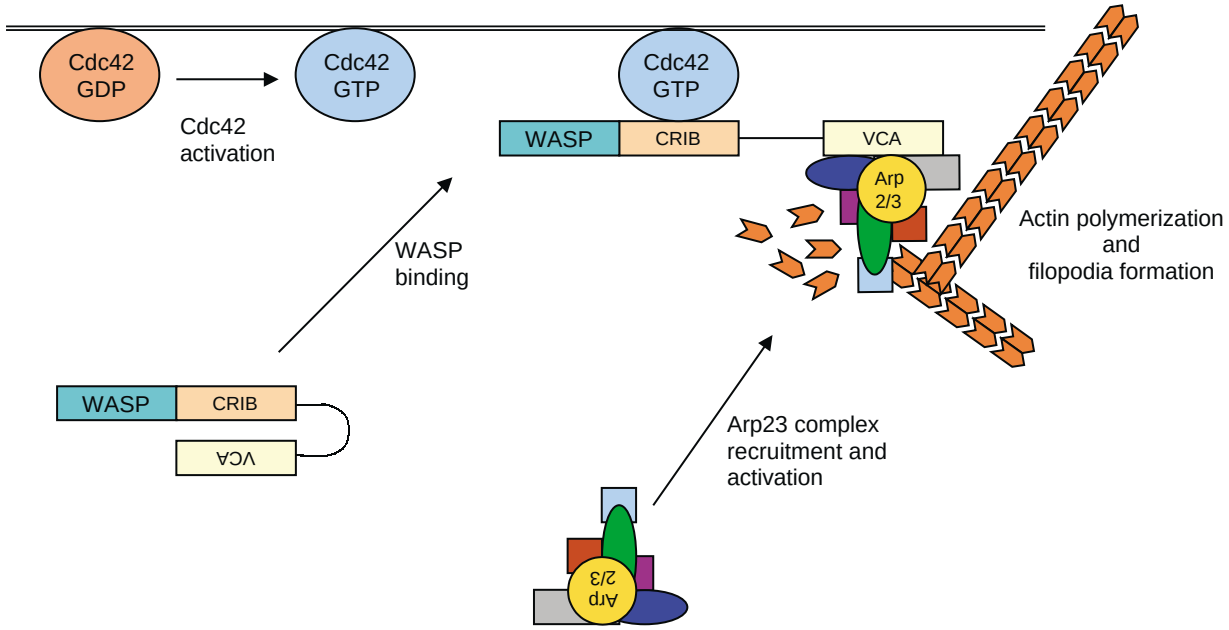

FIGURE 3 Model of effector activation by Rho GTPases: Cdc42-induced WASP activation promotes filopodia. When Cdc42 is inactive, WASP is in an auto-inhibited conformation. Upon Cdc42 activation, inactive WASP binds to Cdc42-GTP through its CRIB domain, relieving its inhibitory conformation and exposing its VCA domain. The VCA domain is now available to recruit and activate the Arp2/3 complex, stimulating actin polymerization and formation of filopodia.

kinases) are a family of kinases that can be activated by Rac and Cdc42 and contribute to actin reorganization, for instance through phosphorylation of LIM kinase, which phosphorylates and inhibits the actin-depolymerizing protein cofilin, and thus promotes actin polymerization.

Other Members

Although RhoA, Rac1, and Cdc42 are the most-extensively studied members of the Rho family, evidence is now accumulating that they are not alone in their regulatory roles on the actin cytoskeleton. First of all, it is not yet clear what the specific roles are of closely related isoforms of these proteins such as RhoB or Rac2, and other less-characterized members of the family are only starting to be investigated. The Rnd proteins are an exciting new subfamily that have been shown to be unusual examples of GTP-binding proteins as they do not cycle between an active GTP-bound state and an inactive GDP-bound state. Among these proteins, Rnd1 and Rnd3/RhoE have been shown to antagonize RhoA in its effects on the actin cytoskeleton, promoting stress fiber and focal adhesion disassembly in several different types of mammalian cells. Similarly to Rnd proteins, RhoH/TTF seems to antagonize some of the RhoA GTPase functions, but it is only expressed in hematopoietic cells. Other members have more similar effects to those of the prototypical Rho GTPases: RhoG signals in parallel to Rac and Cdc42, whereas TC10 is more related to Cdc42 and induces filopodia.

Rho GTPase Family: Functions in Cell Biology

The ability to regulate the actin cytoskeleton dynamically enables Rho GTPases to be involved in many cellular processes, the most obvious of them being cell migration. However, there are many other processes that require Rho GTPases, such as secretion, endocytosis, and cell proliferation.

Cell Migration

Cell movement requires an orchestrated spatio-temporal regulation of the actin cytoskeleton, which involves coordinated activation of several members of the Rho GTPase family. Rac isoforms are important to induce actin polymerization in the leading edge of the cell, in the form of lamellipodia and membrane ruffles, pushing forward the plasma membrane and generating the driving force for cell motility. Cdc42 has shown to be essential for directionality, for instance in macrophage chemotaxis, through the formation of filopodia that are believed to sense the extracellular environment. Rho, in turn, contributes to cell motility by providing actomyosin-based contractility necessary for cell body contraction and tail retraction. Rac activity is also crucial to form adhesions as cells move forward and interact with new extracellular matrix. In addition, Rho GTPases affect microtubule dynamics, which is also important for cell migration. Although the principal

roles of Rho GTPases in cell migration have been already established, there are important differences in the role that these proteins have in different cell types, such as epithelial cells versus macrophages. Furthermore, it is not yet fully understood how these proteins and their effectors are spatially and temporally regulated, and how such an exquisite level of coordination in their functions is achieved in cell migration.

Secretion and Endocytosis

Vesicle trafficking requires both the actin cytoskeleton and the microtubule network, and Rho GTPases have been shown to affect different aspects of vesicle trafficking. Activation of Rho, Rac, and Cdc42 enhance secretion in mast cells, and conversely, their inhibition reduces secretion induced by different agents in these cells. Although it has been established that secretion is accompanied by Rho GTPase-dependent actin reorganization, it is not clear how each Rho GTPase specifically contributes to this process. Rho GTPases have also been shown to modulate endocytosis, and interestingly, two less-studied Rho family members, RhoB and RhoD, have been found to localize to endosomes, and RhoD has been shown to modulate endosome dynamics, fuelling the concept that these proteins may play an important role in endocytosis.

Proliferation and Transformation

Both Rho and Rac isoforms have been shown to be necessary for cell proliferation. Although Rho effectors are important for the actin ring contraction that drives cytokinesis, it is in the G_1 phase of the cell cycle where Rho GTPase function seems to be essential in cell cycle progression. Activation of both Rho and Rac have been linked to the activation of cyclin-dependent kinases through the expression of D-type cyclins and the inhibition of the expression of cyclin-dependent kinase inhibitors, such as $p21^{cip1}$ and $p27^{kip1}$. However, the downstream effectors that lie between Rho GTPases and cell cycle regulators remain completely unknown. Interestingly, Rho GTPases also contribute to cell transformation. Active mutants of Rho, Rac, and Cdc42 all have positive effects on cell transformation and anchorage-independent growth, although they are not considered to be true oncogenes when compared to mutant forms of Ras or Src, for example. However, their biological effects on cell proliferation and actin cytoskeleton place them as potentially important mediators of neoplastic transformation. For instance, their crucial role in cell motility has been shown to influence the loss of epithelial polarity and invasiveness of cancer cells.

See Also the Following Articles

Actin Assembly/Disassembly • Actin-Capping and -Severing Proteins • Actin-Related Proteins • Cell–Matrix Interactions • Endocytosis • Small GTPases

Glossary

cell transformation A complex alteration of cellular behavior that is characteristic of cancer cells. It involves a reduction in the dependence on soluble mitogens and anchorage to the extracellular matrix in order for the cells to proliferate, together with loss of the ability to respond to growth-inhibitory signals both from the extracellular environment or arising from intracellular checkpoint controls.

cytoskeleton Filaments consisting of protein polymers that are responsible for giving the cell mechanical strength, controlling its shape and driving cell movement. Three types of filaments are found in animal cells: actin filaments, microtubules, and intermediate filaments.

leading edge The front of an actively migrating cell, which generally displays a fan-shaped meshwork of actin filaments that push forward the plasma membrane as they polymerize and grow.

small GTPases Monomeric GTP-binding proteins, as opposed to the transmembrane receptor-coupled family of heterotrimeric G proteins, that bind guanine nucleotides and have different conformations when bound to GTP or GDP. This enables them to act as molecular switches and transiently activate several effector proteins.

Further Reading

Bishop, A. L., and Hall, A. (2000). Rho GTPases and their effector proteins. *Biochem. J.* **348**, 241–255.

Etienne-Manneville, S., and Hall, A. (2002). Rho GTPases in cell biology. *Nature* **420**, 629–635.

Peck, J., Douglas, G. I. V., Wu, C. H., and Burbelo, P. D. (2002). Human RhoGAP domain-containing proteins: Structure, function and evolutionary relationships. *FEBS Lett.* **25**(528), 27–34.

Ridley, A. J., and Hall, A. (1992). The small GTP-binding protein rho regulates the assembly of focal adhesions and actin stress fibers in response to growth factors. *Cell* **70**, 389–399.

Sahai, E., and Marshall, C. J. (2002). Rho-GTPases and cancer. *Nat. Rev. Cancer* **2**, 133–142.

Zheng, Y. (2001). Dbl family guanine nucleotide exchange factors. *Trends Biochem. Sci.* **26**, 724–732.

Biography

Priam Villalonga completed his M.Sc. in Pharmacy (Biochemistry) in the University of Barcelona, and then obtained his Ph.D. working on Ras signaling and cell cycle in the School of Medicine in Barcelona. He is now a postdoctoral fellow working on RhoE and its role in cell proliferation and transformation in Anne Ridley's laboratory in the Ludwig Institute for Cancer Research in London.

Anne Ridley studied biochemistry in Cambridge, then carried out her Ph.D. research in London, studying the role of Ras in cell transformation. She worked as a postdoctoral fellow in Cambridge, Massachusetts and then in London, investigating the functions of Rho and Rac proteins. She is now a Laboratory Leader at the Ludwig Institute for Cancer Research, studying the molecular basis for eukaryotic cell migration, concentrating on intracellular signaling processes involving the Rho family of GTPases.

Ribosome Assembly

John L. Woolford
Carnegie Mellon University, Pittsburgh, Pennsylvania, USA

The assembly of ribosomal proteins with rRNAs to form ribosomes is a major metabolic pathway in cells. Because ribosomes are central to the growth and proliferation of cells, many cellular functions have evolved to ensure a steady and regulated supply of ribosomes. Ribosomes consist of two ribonucleoprotein particles that catalyze protein synthesis through translation of the genetic code in mRNA. This is an essential step in the expression of genes in all organisms. The smaller (30S to 40S) subunit of the ribosome serves as a platform to bring together messenger RNA, aminoacylated transfer RNAs, and translation factors. The larger (50S to 60S) ribosomal subunit provides peptidyl transferase activity to catalyze peptide bond formation in nascent polypeptides.

Introduction

The 30S ribosomal subunit of prokaryotes and archaea contains ~20 different proteins (depending on the species), and a 16S ribosomal RNA (rRNA), while the 50S ribosomal subunit contains 30–40 proteins, a 5S rRNA, and a 23S rRNA. Eukaryote ribosomes are more complex. The 40S subunit contains ~32 proteins and the 18S rRNA, while the 60S subunit contains ~47 proteins and the 5S, 5.8S, and 25S (or 28S in metazoans) rRNAs. The structure and function of these ancient multimolecular machines have been explored in great detail. Each ribosomal subunit contains an intricate structural core of RNA decorated on its surface with the ribosomal proteins. A significant fraction of the nucleotides in the RNA contact ribosomal proteins or base pair with other sequences in the RNA.

How these multiple, dynamic protein–RNA, RNA–RNA, and protein–protein interactions are established and rearranged during the assembly of ribosomes is a central question in ribosome biology. In eukaryotes, ribosome assembly occurs primarily in the nucleolus, a subcompartment of the nucleus where the rDNA genes are actively transcribed. There are several major steps in ribosome assembly: synthesis, modification, and nucleolytic processing of the pre-rRNAs, ordered assembly of ribosomal proteins with the pre-rRNAs, and in eukaryotes, release of the nascent ribonucleoprotein particles from the nucleolus to the nucleoplasm, and subsequent export to the cytoplasm, where the mature ribosomes catalyze protein synthesis.

Model Systems

Much has been learned about ribosome biogenesis from studies of bacterial ribosome assembly *in vitro* and from analysis of yeast ribosome synthesis *in vivo*. Analysis of the nucleotide sequence of genomes from prokaryotic and eukaryotic model organisms demonstrates that ribosomes and the RNAs, and proteins necessary for their production are highly conserved. Thus, the principles and mechanisms of ribosome assembly learned from bacteria and yeast will be applicable to other organisms.

Assembly of Bacterial Ribosomes *in vitro*

Functional bacterial 30S and 50S ribosomal subunits can be reconstituted *in vitro* from rRNA plus each of the ribosomal proteins. These studies provide useful paradigms to understand the mechanism of assembly of ribosomes *in vivo*. For example, reconstitution studies defined an "assembly map" for the order of association of each ribosomal protein with rRNA (Figure 1). Ribosomal proteins can be divided into three obligatory binding classes. Primary binding proteins associate directly with the rRNA, often requiring or inducing changes in the conformation of the RNA. Secondary binding ribosomal proteins bind only after a primary protein has assembled and create a binding site for the next protein. Tertiary proteins assemble upon association of the primary and secondary proteins, to complete the pathway of assembly. Despite its hierarchical, interdependent nature, ribosome assembly is not completely cooperative. Three nucleation sites assemble independently to form three structurally separate domains of the 30S subunit: the body, platform, and head. The body assembles around the 5′ structural domain of 16S rRNA, the platform with the central domain, and the head around the 3′ major domain of

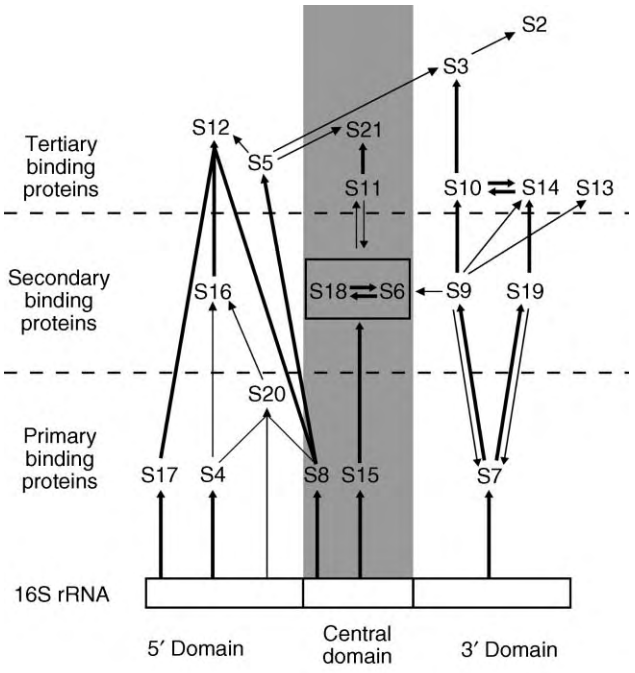

FIGURE 1 Assembly map for reconstitution of *E. coli* 30S ribosomal subunits from 16S rRNA and 20 ribosomal proteins. Each of the three structural domains of the 16S rRNA independently assembles with a subset of ribosomal proteins in a defined order. Primary ribosomal proteins bind first, then secondary proteins, and finally tertiary proteins. The thick or thin arrows represent the relative strength of binding or the relative facilitating effect on binding of one protein to another protein or to RNA.

16S rRNA (Figure 1). Each domain can be independently reconstituted *in vitro*. Formation of the central platform nicely illustrates details of assembly. First, the primary protein S15 binds to a particular conformer of the junction of rRNA helices 20, 21, and 22. Binding is stabilized by additional contacts between S15 and a tetraloop at the end of helix 23a, and by an interhelical RNA–RNA base pairing. The latter is required for binding of secondary proteins S6 and S18, which first form a heterodimer. Their association with the growing platform may establish a conformation of helix 23b, required for assembly of the tertiary binding protein S11. Bound S11 is further stabilized through interactions with S18.

Self-assembly of 30S ribosomal subunits *in vitro* suggests that extrinsic factors are not required to build a ribosome. However, several other results indicate otherwise. First, *in vitro* assembly is temperature dependent. At low temperatures, 16S rRNA binds to a subset of ribosomal proteins to form a 21S–26S assembly intermediate. Subsequent heating is required for conformational rearrangements to create an activated intermediate that can bind the remaining ribosomal proteins. The requirement for this heat-sensitive step can be circumvented by addition of the DnaK, DnaJ, and GrpE proteins plus ATP. This molecular chaperone system may recognize exposed hydrophobic surfaces of incompletely folded proteins or RNA in the assembling ribosome and either prevents misfolding and aggregation into nonproductive intermediates or promotes productive conformational changes. Second, a number of bacterial mutants have been identified that are deficient in production of ribosomes. Such mutants, including a *DnaK* mutant of *E. coli*, may be defective in assembly due to loss of function of a *trans*-acting assembly factor. As described below, a large number of *bona fide trans*-acting factors involved in ribosome biogenesis have been identified in eukaryotes.

Eukaryotic Ribosome Biogenesis *in vivo*

Synthesis, Modification, and Processing of rRNA

The 18S, 5.8S, and 25S/28S eukaryotic rRNAs are derived from a single 35S (47S in metazoans) transcript synthesized by RNA polymerase I (Figure 2). The 5S rRNA is transcribed from separate genes by RNA polymerase III. The genes for rRNA are tandemly repeated (100 to 10,000 copies – depending on the organism) at one or a few chromosomal loci. In yeast and a few other eukaryotes, the 5S and 35S genes are interspersed, comprising one repeat unit, although in most organisms the two classes of genes (5S and 35S/47S) are unlinked. The high copy number of these genes enables cells to produce large quantities of ribosomes when necessary, e.g., ~40 ribosomes per second in rapidly dividing yeast cells.

Immediately following transcription, the 35S pre-rRNA is covalently modified. In yeast cells, rRNA undergoes 2′-O-ribose methylation at 55 positions, pseudouridylation (rotation of a uridine) at 45 positions, and methylation of 12 bases. The sites of modification are located within conserved, functionally important domains of the mature rRNA. Although base methylations are catalyzed by individual proteins, most of the modification sites are identified and modified by a large collection of small nucleolar RNAs (snoRNAs). Each snoRNA contains sequences complementary to one of the modified rRNA sequences and thus functions as a "modification guide" to identify a potential target. The snoRNAs are associated with a small set of proteins, in small nucleolar ribonucleoprotein particles (snoRNPs). One class of snoRNP proteins is associated with the "C + D" class of snoRNAs responsible for methylation, and a different set of snoRNP proteins is present in the "H + ACA" snoRNPs catalyzing pseudouridylation.

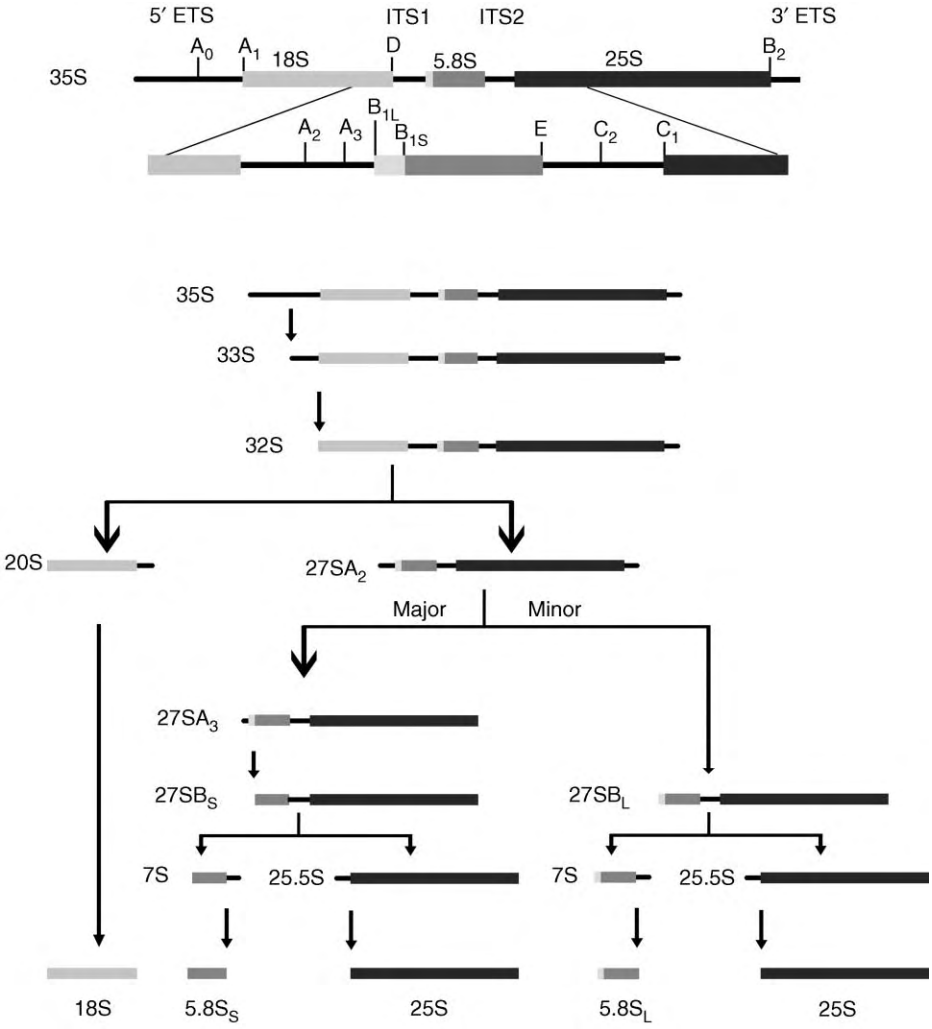

FIGURE 2 (A) Structure of the 35S pre-rRNA primary transcript. The external and internal transcribed spacers are indicated by thin lines, and the mature rRNA sequences by thick lines. Locations of the known processing sites are indicated. (B) Pathway of processing of 35S pre-rRNA to produce the mature 18S, 5.8S, and 25S rRNAs. Each pre-rRNA processing intermediate in the pathway is shown. The ordered set of processing steps is indicated.

Among these snoRNP proteins are the potential rRNA 2′-O-methyl transferase Nop1p and the putative pseudouridine synthase Cbf5p. Although snoRNPs associate with nascent rRNA, modification does not occur until transcription is completed. It is not clear what triggers these modifications, or how the snoRNPs are released from the assembly complex. Also, the function of the modifications is not known.

Eukaryotic rRNA precursors contain two internal transcribed spacers, ITS1 and ITS2 separating the 18S, 5.8S, and 25S/28S rRNA sequences, respectively. Additionally, there are 5′ and 3′ external transcribed spacers, 5′ETS and 3′ETS flanking the mature rRNA sequences (Figure 2). The predicted secondary structures of the mature rRNAs are highly conserved, although their lengths vary slightly among species. However, these features are somewhat less conserved for the transcribed spacer RNAs. The spacers are removed from the 35S–47S primary transcript to produce the three mature rRNAs by a series of conserved endonucleolytic and exonucleolytic processing steps (Figure 2). The secondary structures of the excised spacers are important for their removal. The pathways of rRNA processing appear to be quite similar among the best-studied eukaryotes – yeast, *Drosophila*, Xenopus, mouse, rat, and humans. However, certain ambiguities still exist concerning the precise locations of processing sites and whether sites are generated exo- or endonucleolytically (or by a combination).

In yeast, the first detectable precursor is the 35S pre-rRNA, which has already undergone cleavage by the Rnt1p endonuclease near the 5′ end of the 3′ ETS. The 5′ ETS of 35S pre-rRNA is then removed by rapid sequential endonucleolytic cleavages at the A_0 and A_1

sites to generate the 33S and 32S intermediates. The biosynthetic pathway then bifurcates upon cleavage at the A_2 site to generate the 20S and $27SA_2$ pre-rRNAs. The remainder of ITS1 is removed from the 20S pre-rRNA by processing at site D to generate the mature 18S rRNA. The $27SA_2$ pre-rRNA undergoes a more complex series of processing reactions to produce mature 5.8S and 25S rRNAs. The majority of $27SA_2$ is cleaved at site A_3 by the endonuclease activity of the MRP RNP, immediately followed by $5' \rightarrow 3'$ exonucleolytic trimming of $27SA_3$ to the B_{1S} site by Rat1p or Xrn1p exonucleases to generate $27SB_{1S}$. Alternatively, a small fraction of $27SA_2$ is processed to $27SB_{1L}$, by a mechanism yet to be determined. The two 27SB pre-rRNAs are endonucleolytically cleaved at the C_2 and perhaps C_2' sites, to create the 7S and 25.5S pre-rRNAs. The $3'$ end of 7S is removed by the exosome complex of $3' \rightarrow 5'$ exonucleases to generate the $5.8S_L$ and $5.8S_S$ rRNAs. The $5'$ end of the 25.5S pre-rRNA undergoes rapid $5' \rightarrow 3'$ trimming to the C_1 site by the Rat1p or Xrn1p exonucleases, generating mature 25S rRNA.

Endonucleolytic cleavage at the A_0, A_1, and A_2 sites requires the U3, U14, snR10, and snR30 snoRNPs as well as several individual proteins. Cleavage at A_0 requires base pairing between the U3 snoRNA and sequences in the $5'$ ETS ~140 nucleotides, $5'$ of the A_0 site. Likewise, base pairing between U14 snoRNA and rRNA is necessary for U14 function. The exact roles of these molecules are not known; no endonucleases have been identified that cleave the A_0, A_1, and A_2 sites. The interdependence observed for these three processing reactions may reflect a complex series of rearrangements of the architecture of the processing rRNA, mediated by the snoRNPs and protein factors.

Ribosome Assembly

Initial studies revealed a crude outline of the assembly pathway. 35S pre-rRNA is present in a 90S rRNP that is converted to 43S and 66S rRNP assembly intermediates. These precursor particles are then converted to the mature 40S and 60S ribosomal subunits, respectively (Figure 3). The 43S assembly intermediate contains the 20S pre-rRNA. There are at least six 66S assembly intermediates containing the $27SA_2$, $27SA_3$, $27SB_{1L}$, $27SB_{1S}$, 25.5S + 7S, and 25S + 5.8S rRNAs, respectively. Each of these rRNPs contains a subset of the ribosomal proteins found in mature subunits, plus a number of nonribosomal proteins not present in mature functioning ribosomes. More than 150 such *trans*-acting factors required for assembly of ribosomes have been identified in yeast, using genetic screens or selections to identify mutants defective in ribosome biogenesis or using proteomic approaches to purify and characterize assembly intermediates. Recently, metazoan counterparts of most of these proteins have been identified by mass spectrometry of proteins from purified nucleoli.

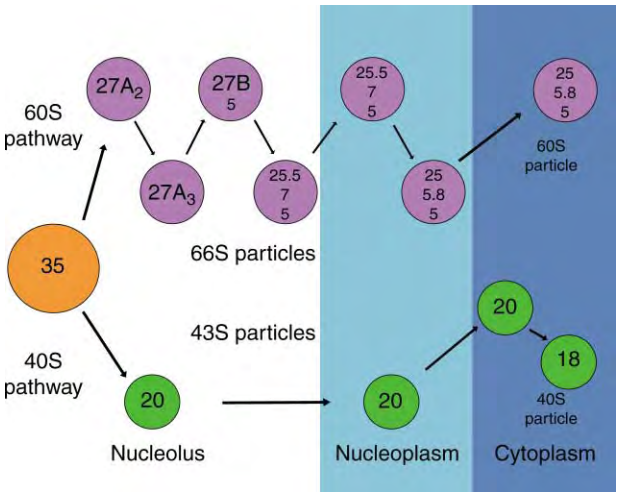

FIGURE 3 Pathway of ribosome assembly. The earliest ribosome precursor particle is the 90S rRNP, which is converted to 43S and 66S rRNP assembly intermediates. Each 66S rRNP intermediate contains a unique successive pre-rRNA processing intermediate. Most steps in assembly occur in the nucleolus. However, the 43S rRNP undergoes final maturation in the cytoplasm, and the 66S rRNP undergoes late maturation steps in the nucleoplasm and the cytoplasm. The pre-rRNA intermediates present within each rRNP are indicated.

The earliest defined step in ribosome assembly is association of the U3 snoRNP with the $5'$ ETS of the nascent 35S pre-rRNA. Electron microscopy of chromatin spreads reveals "terminal knobs" present near the $5'$ ends of nascent rRNA, which contain the U3 snoRNP. During or immediately after completion of transcription, 20–30 nonribosomal proteins plus the U14, snR10, and snR30 snoRNPs also associate with the 35S pre-rRNA. At the same time, a large number of ribosomal proteins destined for the 40S subunit, as well as a few destined for the 60S subunit, assemble into the nascent rRNP. Thus, upon termination of its transcription, the 35S rRNA is packaged into a rapidly changing, short-lived, and heterogeneous collection of RNPs ~90S in size. Cleavage at the A_0, A_1, and A_2 sites occurs within these rRNPs.

The 43S and 66S rRNPs are generated from the 90S rRNP by cleavage of the A_2 site. All but seven of the nonribosomal molecules present in the 90S rRNP are absent from the 43S rRNP or 66S rRNPs. The 43S pre-rRNP travels rapidly from the nucleolus through the nucleoplasm to the cytoplasm, where it undergoes final steps in maturation, including cleavage of 20S pre-rRNA at site D, to form the functional 40S subunit. Several of the ribosomal and nonribosomal proteins present in the 43S rRNP are required for this step, which is likely to involve the reconfiguration of the 20S pre-rRNA and the 43S rRNP into conformations favoring cleavage.

Late assembling ribosomal proteins associate with the 43S rRNP in the nucleoplasm and in the cytoplasm.

While most of the nonribosomal proteins necessary for production of 40S ribosomal subunits assemble with the 35S pre-rRNA in 90S rRNPs, only a few factors involved in 60S subunit biogenesis have been found in association with 35S pre-rRNA. The mechanism of transition from the 90S rRNPs to 66S rRNPs is less clear than that for the 43S rRNP. The first defined 66S rRNP contains $27SA_3$ pre-rRNA and several dozen nonribosomal proteins necessary for 60S subunit production. It is not clear whether these 60S assembly factors associate weakly with the 90S rRNP and therefore cannot be detected in the purified particle, or else assemble into early 66S complexes during or immediately after processing at the A_2 site.

What functions must occur to produce mature ribosomal subunits from the precursor particles and what kinds of molecules carry out these functions? Clues come not only from the paradigms of bacterial ribosome assembly *in vitro*, but also from functions suggested by the amino acid sequence motifs within the nonribosomal proteins implicated in assembly. For example, a number of nonribosomal proteins necessary for ribosome assembly contain RNA-binding motifs. Such proteins may function as RNA chaperones to help fold the pre-rRNA or to prevent misfolding. In addition to nucleases that catalyze rRNA processing, ribosome biogenesis requires cofactors necessary to remodel the rRNA and rRNPs into configurations necessary for the processing. Dynamic rearrangement of the nascent RNPs most likely also creates binding sites for the many ribosomal proteins (and nonribosomal proteins) added to the growing subunit. Such rearrangements must also enable dissociation of processing or assembly factors. Seventeen putative RNA-dependent helicases/ATPases, six potential GTPases, and an AAA-type ATPase are involved in production of ribosomal subunits. These RNA helicases are thought to catalyze winding or unwinding of RNA helices as well as rearrangement of protein conformations in the rRNP. As observed for the prototype GTPase translation factor G, the nucleotidases may also reconfigure the RNP. In addition, they have been hypothesized to serve as checkpoint or quality control factors, for successfully monitoring assembly of functional ribosomal precursors. The assembly factors Rlp7, Rlp24, and Mrt4p are ribosome-like proteins, close relatives of the ribosomal proteins, Rpl7, Rpl24, and RpP0, respectively. They may function as "stunt-doubles" to form or maintain a potential ribosomal protein assembly site. Alternatively, the exchange of such an Rlp protein with the corresponding ribosomal protein may provide another "structural proofreading" function in the assembly pathway. A number of potential scaffolding proteins are present in assembly intermediates; they may function as platforms for assembly of multimolecule-subassembly complexes. Several proteins associated with 90S, 66S, and 43S rRNPs are implicated in triggering release of 43S and 66S rRNPs from the nucleolus to the nucleoplasm. It is not known whether these proteins help make subunits competent for nucleolar exit by (1) serving as receptors or tags to "mark" subunits for exit, (2) reconfiguring the nascent subunits to expose such a tag, or (3) helping overcome mechanisms of retention in the nucleolus or nucleoplasm. Nuclear export of pre-60S RNPs involves binding of ribosomal protein rpL10 to the adaptor protein Nmd3p. Nmd3p binds to the export receptor Xpo1p/Crm1p which links ribosomes to Ran GTP and nuclear pore proteins. Likewise, 43S rRNPs require Ran GTP for export to the cytoplasm.

Integration of Ribosome Biogenesis with Cell Growth and Proliferation

Regulation of the biogenesis and function of ribosomes appears to play a critical role in mechanisms that couple cell growth and cell proliferation. However, few details are clear for how this occurs. A number of proteins necessary for ribosome assembly are also involved in cell growth and proliferation. These include not only nonribosomal proteins, but also ribosomal proteins. For example, several of the ribosome assembly factors interact with the origin recognition complex (ORC) and are required for DNA replication. Some are required for exit from Go and entry into the cell cycle, or for progression through other steps of the cell cycle. A recent screen for yeast mutants with abnormally small or large cell volumes identified 15 proteins, previously implicated in ribosome biogenesis. It will be of great interest to learn whether and how these molecules help couple growth and proliferation.

Another important question remaining to be explored is how ribosome synthesis is coupled with cell cycle progression. Cyclin-dependent kinases are thought to govern formation and maintenance of the nucleolus during the cell cycle. A number of protein phosphatases and protein kinases are localized to the nucleolus or copurify with ribosome assembly factors, but their functions in ribosome biogenesis remain to be explored.

See Also the Following Articles

Nucleolus, Overview • Ribosome Structure • RNA Polymerase I and RNA Polymerase III in Eukaryotes • RNA Polymerase II and Basal Transcription Factors in Eukaryotes

Glossary

nucleolus Nuclear subcompartment of eukaryotic cells defined by the location of actively transcribing rDNA genes. Most, but not all steps of ribosome assembly occur in the nucleolus.

pre-rRNA rRNA primary transcript or processing intermediate; precursor to mature rRNA.

ribosomal protein Protein stably associated with mature, functional ribosomes.

rRNA RNA molecule present in mature, functional ribosomes.

rRNP Ribosomal ribonucleoprotein particle; ribosome assembly intermediate containing pre-rRNAs, ribosomal proteins, and nonribosomal proteins involved in assembly.

Further Reading

Balakin, A. G., Smith, L., and Fournier, M. J. (1996). The RNA world of the nucleolus: Two major families of small RNAs defined by different box elements with related functions. *Cell* **86**, 823–834.

Eichler, D. C., and Craig, N. (1994). Processing of eukaryotic ribosomal RNA. *Prog. Nucl. Acid Res. Molecul. Biol.* **49**, 197–239.

Fatica, A., and Tollervey, D. (2002). Making ribosomes. *Curr. Opin. Cell Biol.* **14**, 313–318.

Nomura, M. (1989). History of ribosome research: A personal account. In *The Ribosome: Structure, Function and Evolution* (W. E. Hill, A. Dahlberg, R. A. Garrett, P. B. Moore, D. Schlessinger and J. R. Warner, eds.) pp. 3–55. American Society for Microbiology, Washington, DC.

Recht, M. I., and Williamson, J. R. (2001). Thermodynamics and kinetics of central domain assembly. In *The Ribosome*, Cold Spring Harbor Symposia on Quantitative Biology LXVI, pp. 591–598. Cold Spring Harbor Laboratory Press, Woodbury, NY.

Traub, P., and Nomura, M. (1968). Structure and function of *E. coli* ribosomes, V. Reconstitution of functionally active 30S ribosomal particles from RNA and proteins. *Proc. Natl. Acad. Sci. USA* **59**, 777–784.

Warner, J. R. (2001). Nascent ribosomes. *Cell* **107**, 133–136.

Biography

John Woolford is a Professor of Biological Sciences at Carnegie Mellon University in Pittsburgh, Pennsylvania. His principal research interests are in the regulation of expression of ribosomal protein genes and the mechanism of ribosome assembly. He holds a Ph.D. in biochemistry from Duke University and was a postdoctoral fellow at Brandeis University. His laboratory has made several important contributions towards the understanding of coordinate expression of ribosomal protein genes, and was one of the first groups to purify and characterize intermediates in the assembly of eukaryotic ribosomes.

Ribosome Structure

Brian T. Wimberly
Rib-X Pharmaceuticals, Inc., New Haven, Connecticut, USA

The ribosome is the large and complex polymerase responsible for translation, the synthesis of protein according to genetic instructions encoded in a mRNA template. Ribosomes make proteins by joining amino acids delivered by its substrates, the aminoacyl tRNAs. The most important activities of the ribosome are accurate substrate selection, catalysis of peptide bond formation, and movement of the substrate–template complex through the ribosome. Understanding and exploiting these activities will require determination of three-dimensional structures of this universal and uniquely complex macromolecular machine in its many different functional states.

Ribosome Function

Overview

In all organisms, template-directed protein synthesis is performed by the ribosome. The ribosome translates genetic information contained within its template, messenger RNA (mRNA), by joining amino acids carried by its substrate, transfer RNA (tRNA). The mRNA template is a linear sequence of non-overlapping three-nucleotide codons, each of which codes for a single amino acid to be added to the protein chain. There are 20 different tRNA substrates, one for each kind of amino acid. Each is a fairly large, L-shaped macromolecule with functionally important ends. One end, the 3′ CCA terminus, is the site of covalent attachment of the amino acid, while the other end features a three-nucleotide anticodon that forms base-pairing interactions with a complementary mRNA codon while in the ribosome. As the base-paired tRNA–mRNA complex passes through the ribosome, each tRNA adds its amino acid to the growing peptide chain. After passing through the ribosome, tRNAs dissociate from the mRNA template, since their triplet base-pairing interaction is only marginally stable.

The chemistry of peptide bond formation originally suggested that the ribosome should contain binding sites for mRNA and two tRNAs. In fact, the ribosome contains three distinct binding sites for substrate tRNAs, as well as a path for mRNA (Figure 1A). The three tRNA-binding sites are named after the distinguishing amino acid or peptide group attached to their resident tRNAs. The A site binds an incoming aminoacyl tRNA, which carries a single amino acid, the next to be added to the growing peptide chain. The P site contains the peptidyl tRNA, to which the nascent peptide chain is covalently attached. The E site contains an "empty" or exiting tRNA, which has already donated its amino acid to the growing chain and is therefore deacylated (not esterified by an amino acid or peptide). As translation proceeds, the tRNA–mRNA complex moves in concert through the ribosome, from right to left, while the growing peptide chain exits the ribosome through a separate tunnel.

Fundamental Activities of the Ribosome

All of the most important ribosomal functions are exemplified during the elongation cycle of translation. At the beginning of the cycle, a candidate aminoacyl tRNA binds to the A site. The ribosome then determines whether the candidate tRNA is a correct (or cognate) tRNA, or one of the more numerous incorrect (noncognate) tRNAs. This gate-keeping function, known as decoding, is crucial for maintaining the accuracy of translation. Decoding is a multistep process that requires testing the fit of the aminoacyl tRNA in the A site. Although not all of the details are known, it is clear that decoding depends on the ribosome's ability to monitor both the geometry and the affinity of the three base-pairing interactions between the aminoacyl tRNA anticodon and the A-site mRNA codon.

Once an incoming aminoacyl tRNA has been accepted in the A site, its amino acid must be added to the peptide chain attached to the P-site tRNA. Catalysis of the formation of the new peptide bond, known as peptidyl transfer, is the second fundamental ribosomal activity. The reaction occurs when the α-amino group of the A site amino acid attacks the C-terminal carbonyl of the growing peptide (Figure 1B). This results in the transient attachment of the now slightly longer peptide chain to the tRNA in the A site and the transient presence of a deacylated tRNA in the P site. Subsequent movement of the tRNA–mRNA complex relative to the

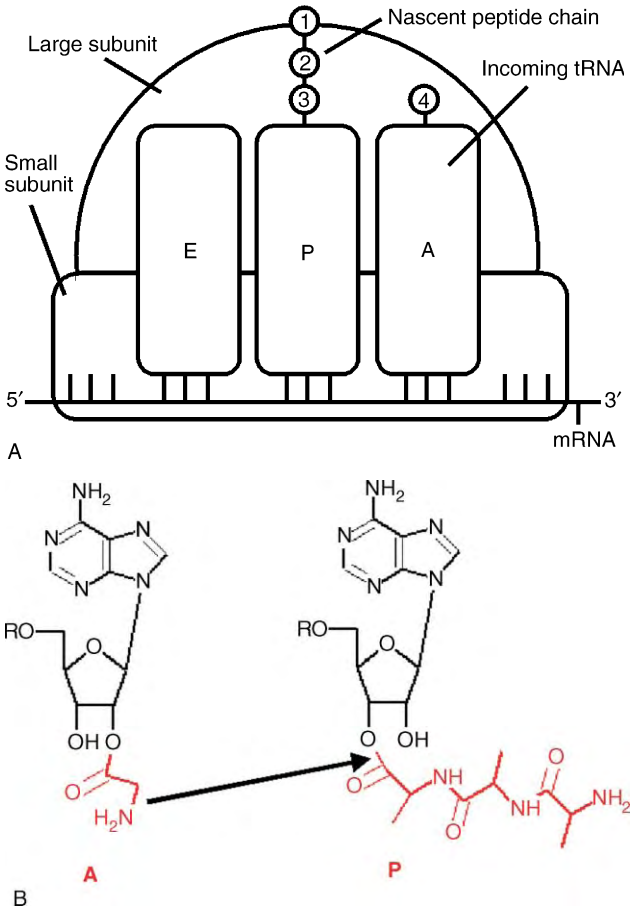

FIGURE 1 (A) Schematic view of a translating ribosome. Three amino acids (circles numbered 1–3) have already been joined to form the nascent peptide chain, whose C-terminal end is covalently attached to the tRNA (center rectangle) in the P site. The N-terminal end of the peptide is traversing a tunnel in the large ribosomal subunit. The next amino acid to be added (circle 4) is attached to an aminoacyl tRNA (right rectangle), which has just bound the ribosomal A site. A deacylated tRNA (left rectangle) is in the E site and will soon exit the ribosome. Vertical triplet bars represent codons in the mRNA, which base-pair to complementary anticodons in the tRNAs. The tRNA–mRNA complex moves through the ribosome from right to left, with each tRNA donating its covalently attached amino acid to the growing peptide chain as it passes through the peptidyltransferase site. See text for further details. (B) The chemistry of peptide bond formation. The 3′-terminal aminoacylated adenosine of an incoming aminoacyl tRNA in the A site (left) and the 3′-terminal peptidyl adenosine of the P-site tRNA (right) are shown at the moment of peptide bond formation. The peptidyl and aminoacyl moieties are highlighted in red. The N terminus of the A-site amino acid attacks the esterified C-terminal end of the peptidyl moiety. This reaction results in addition of a new amino acid to the peptide chain and transient attachment of the chain to the tRNA in the A site.

ribosome (from right to left in Figure 1A) restores a peptidyl tRNA in the P site and places a deacylated tRNA in the E site. This movement, known as translocation, is a third crucial ribosomal activity. The mechanism of translocation is still not well understood. It is thought to proceed in at least two steps, with movement of the tRNA CCA ends preceding movement of the anticodon ends. Because the tRNA substrates are so large, translocation requires large tRNA displacements of tens of Angstroms. Thus the ribosome is not only an enzyme; it is also a molecular machine.

The need for translocation also highlights an additional requirement seemingly at odds with the need for ligand movement. During translocation, the ribosome must prevent slippage of the tRNA substrates relative to the mRNA template. In other words, the reading frame must be maintained. Such a slippage, known as a frameshift event, results in the synthesis of an incorrect and usually prematurely terminated protein, which is usually detrimental to the organism. Because translocation must involve releasing and reforming of ribosome–ligand contacts, whereas maintaining the reading frame requires keeping such contacts, the structural basis of translocation is of particular interest.

This simplified summary of elongation neglects the important contributions of the nonribosomal protein elongation factors, which vastly accelerate translation rates and are essential for translation *in vivo*. Moreover, like other polymerization processes, translation also has distinct initiation and termination phases, each of which normally requires nonribosomal initiation and termination factors. Nevertheless, the fundamental ribosomal functions – decoding, peptidyltransferase, translocation, and maintenance of the reading frame – have been shown to be intrinsic to the ribosome itself.

Ribosome Structure

Distinguishing Structural Features of the Ribosome

Ribosomes have functions more complex than virtually any other enzyme, so it is not surprising that ribosomes have a unique and complex structure. The ribosome's most striking and distinguishing structural feature is its great size. The simplest ribosomes from bacteria have a mass of some 2.5 million Da, which is many times larger than a typical monomeric enzyme that catalyzes a reaction between small-molecule substrates. However, because the ribosomal substrates are themselves macromolecules – tRNAs have a mass of 25 kDa and measure some 75Å end to end – the size of the ribosome is, in fact, in normal proportion to the size of its substrates. When one considers that the ribosome must accommodate not one but three substrate tRNAs, as well as the mRNA template and large-scale movements of all of these ligands, the ribosome begins to look like a marvel of structural efficiency.

A second distinguishing feature of the ribosome is its unusual and complex composition. All ribosomes

consist of an RNA core and a large number of small proteins. Bacterial ribosomes, for example, are about two-thirds RNA by mass and contain approximately 50 different proteins, while ribosomes from eukaryotic organisms contain relatively more protein. It does not appear to be an accident that the ribosome is an RNA-based enzyme, whereas most other enzymes are made entirely of protein. After all, if proteins were made by a hypothetical ribosome composed entirely of protein, then it would be hard to imagine how this protein-only ribosome could have evolved. An RNA-based ribosome solves this "chicken-and-egg" problem, and jibes well with speculations about an "RNA world" preceding the existence of large proteins and DNA.

Subunit Organization and Nomenclature

All ribosomes consist of two loosely associated subunits of unequal size. In the well-studied bacterial ribosome, the larger subunit is denoted 50S, the smaller subunit 30S, and the entire ribosome 70S, according to their rates of sedimentation during ultracentrifugation. The bacterial small subunit RNA is the 16S RNA of approximately 1500 nucleotides, while the large subunit contains two RNAs, the 23S RNA (about 2900 residues) and the 5S RNA (about 120 residues). All eukaryotic cells contain both cytoplasmic and mitochondrial ribosomes; plants also have chloroplast ribosomes. The mitochondrial and chloroplast ribosomes are very similar to the bacterial ribosome, although the mitochondrial ribosome has a much smaller RNA component and an expanded number of proteins. The eukaryotic cytosolic ribosome is denoted 80S, with a 60S large subunit and a 40S small subunit. The RNA of the 40S subunit is the 18S RNA, and the large subunit RNAs are denoted 5S, 28S, and 5.8S (the last two of which are homologous to the bacterial 23S RNA). In all ribosomes, the large subunit interacts with the CCA end of the tRNAs and contains the active site that catalyzes peptide bond formation (the peptidyltransferase center). The small subunit binds the anticodon end of the tRNAs, both monitoring (during decoding) and maintaining (during translocation) the tRNA–mRNA base-pairing interactions. The ribosomal proteins are numbered and assigned to a subunit using a prefix of S (small) or L (large), so that individual proteins are denoted S1, S2, …, S21, L1, L2, and so forth.

Struggling with Ribosome Structure

The great size and complex composition of ribosomes have been enormous barriers to efforts to determine the structural basis of ribosome function. The ribosome is of an inconvenient size for structural biology: it has been until very recently too large for X-ray crystallography, but also rather too small for traditional electron microscopy (EM) methods. EM played a crucial role in the discovery and early structural characterization of ribosomes. However, negatively stained EM images were of very low resolution, allowing identification of only the largest structural features. During the 1970s and 1980s, many ingenious new genetic, biochemical, and biophysical methods were developed to probe ribosome structure, and an enormous amount of data was obtained. Combination of these data with EM-derived structures allowed the low-resolution assignment of a variety of functional sites. A complementary "divide and conquer" strategy to determine high-resolution structures of ribosomal fragments began to bear fruit in the 1980s and early 1990s, when a number of X-ray and NMR-derived structures of individual ribosomal proteins and ribosomal RNA fragments began to appear. Such data provided valuable insights into ribosome function and were useful guides for the design of new experiments, but it was not clear how such methods could ever result in a complete structure of a subunit, let alone the entire ribosome, at a resolution that would reveal the chemical basis of protein synthesis. However, in the mid-1990s, new techniques combining EM with single particle reconstruction revealed higher resolution images, including the first direct visualization of tRNAs and elongation factors bound between the ribosomal subunits. Ultimately, however, these new EM methods did not win the race to the long-sought goal of high resolution. In 2000, the first near-atomic resolution structures of ribosomal subunits were determined by X-ray crystallography methods, and in 2001 a medium-resolution crystal structure of the bacterial 70S ribosome was determined.

Why do we need to know the structure of the ribosome at high resolution? One motivation is the desire to determine the fundamental physical mechanisms of translation. Understanding exactly how ribosomes work will enrich and advance understanding of other aspects of biology in ways that are difficult to predict. Because the ribosome has many distinct functional states, a complete understanding of translational mechanisms will require many different structures – in other words, a "movie" of translation. Moreover, these structures must be of atomic or near-atomic resolution in order to identify the substrate–ribosome interactions that suggest mechanisms, and to direct additional experiments (for example, site-directed mutagenesis) to test these mechanistic hypotheses. The other reason to determine high-resolution ribosome structures is the more practical need to exploit fundamental knowledge

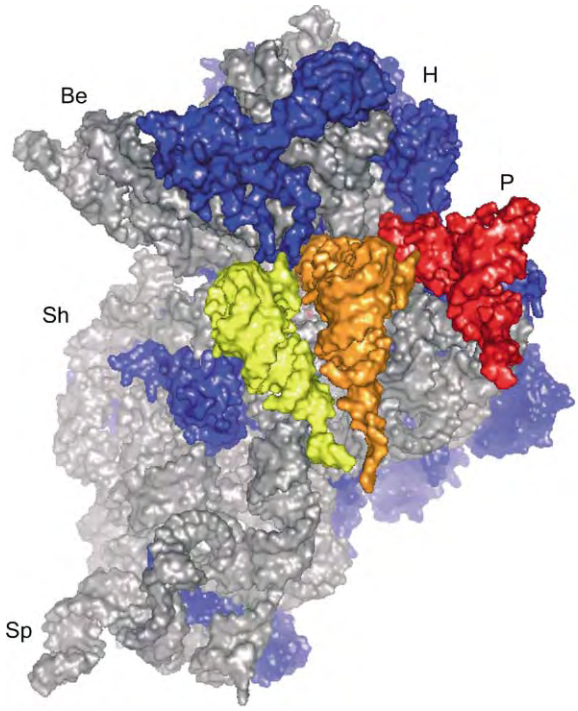

FIGURE 2 The high-resolution structure of the bacterial small ribosomal subunit, as determined by X-ray crystallography. The view is from the large subunit. Ribosomal RNA is gray, and ribosomal proteins are blue. Landmark features previously known from lower resolution methods are labeled: H (the head domain), Be (the beak), P (the platform), Sh (the shoulder), and Sp (the spur). The A-site (yellow), P-site (orange), and E-site (red) substrate tRNAs are also shown, in positions determined from the crystal structure of the entire bacterial 70S ribosome. The mRNA template (not visible in this view) is buried in the neck region, a crevice between the head, shoulder, and platform. Note the proximity of the CCA ends of the A- and P-site tRNA substrates (foreground), as required for peptide bond formation.

of biological mechanisms. Because the ribosome is the target of many clinically useful antibiotics, high-resolution ribosome structures will have a very practical use: structure-based design of improved new antibiotics that overcome the increasingly serious problem of antibiotic resistance mutations. It is also possible that a detailed structural understanding of human translation could be used to treat diseases caused by defects in normal human translation.

General Features of Ribosomal Architecture Revealed from the Subunit Structures

After more than 40 years of only low-resolution ribosome structures, the crystal structures of the large and small subunits, reported within a few months of each other in 2000, suddenly revealed almost all of the details of ribosomal architecture, as well as many fundamental new insights into the structural basis for translation mechanisms. Both its overall architecture and the composition of its functional centers reveal the ribosome to be essentially an RNA-based machine. The overall shape of both subunits is determined by the RNA component: only one of the landmark features visible at low resolution (the L7/L12 stalk) is composed only of protein (Figures 2 and 3). Moreover, the overall distribution of the proteins is not uniform: the proteins are concentrated on the back and sides of the subunits, away from the most functionally important regions at the subunit interface. The protein component is also concentrated on the surface, rather than buried in the middle of the subunits; the ribosome thus literally has an RNA core. Many of the proteins contain both a globular component on the periphery of the subunits, and one or more narrow extended peptide "tails" that penetrate deeply into crevices of the RNA core. Many of the proteins are found to interact with RNA multistem junctions and tight bends in the RNA, which suggests particular functional roles in subunit assembly. In the case of the 30S subunit, there are extensive biochemical data on the mechanisms of assembly, and an analysis of the crystal structure is in good overall agreement with these data. The subunit crystal structures have provided an enormous boost to the understanding of RNA–protein interactions, since relatively few

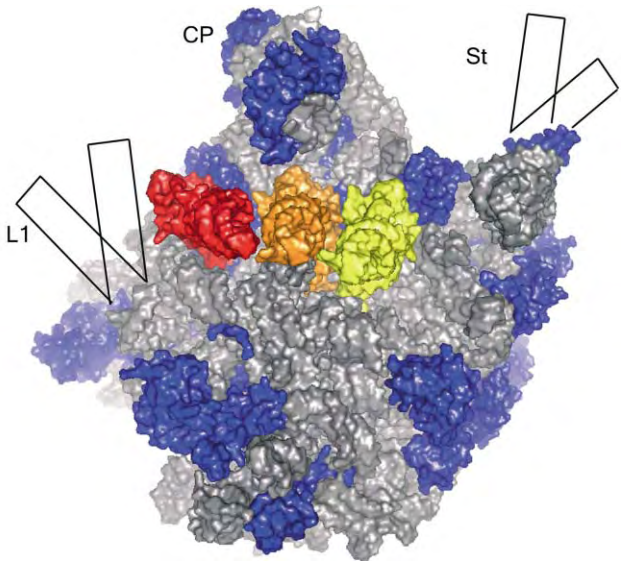

FIGURE 3 The high-resolution structure of the large ribosomal subunit from *Haloarcula marismortui*, as determined by X-ray crystallography. The view is from the small subunit, and the color scheme is as in Figure 2. The central protuberance (CP), a landmark feature previously known from lower resolution methods, is labeled. Two additional landmark features (the L1 arm and the L7/L12 stalk) are partially disordered in the crystal structure; their approximate locations and range of motions are schematically indicated. Substrate tRNAs are also shown, in positions determined from the crystal structure of the entire bacterial ribosome.

structures of RNA–protein complexes were available prior to 2000. Even less was known about RNA tertiary structure, and the subunit structures have revealed several new principles of RNA higher order structure. A common strategy for packing RNA helices makes use of patches of adenine residues, whose bases and 2′ OH moieties pack favorably against the minor groove of another RNA helix. Four different classes of this A-minor motif were defined, some of which had been previously observed in other structures. Another common RNA structural motif is the kink-turn, a tight bend that is often stabilized, although in various ways, by a bound protein. There is also a special role for G-U pairs in mediating some helix–helix packings. Analysis of the structures is continuing, and may lead to improvements in the prediction of RNA tertiary structure. The resolution of the *Haloarcula marismortui* 50S structure – at 2.4Å, significantly higher than any of the other subunit structures, and much higher than that of the 70S structures – allows reliable identification of metal ions and water molecules, which play important roles in stabilizing RNA structure. The relatively high resolution also allows the finer details of the conformation of RNA and protein to be determined. The *H. marismortui* 50S structure therefore serves as the "gold standard" for ongoing efforts to mine the recently vastly expanded RNA structure database.

There is one difference between the large-scale architectures of the 30S and 50S subunits that is probably functionally important. Whereas the secondary structure domains of the 23S rRNA interact closely to form a single, nearly hemispherical mass, the 16S rRNA secondary structure domains are for the most part independent globular entities – i.e., true three-dimensional domains – that have relatively few interactions with each other. One domain of the 16S rRNA constitutes the head, another the platform, and another the bulk of the body (Figure 2). This architecture suggests that independent movement of one or more of the domains (e.g., the head or platform domains, as has been observed in cryo-EM work) may be functionally important. For example, several groups had previously suggested that rotation of the head may accompany translocation; this hypothesis now seems probable.

High-Resolution Structure of the Small Subunit

The crystal structure of the 30S subunit from the thermophilic bacterium *Thermus thermophilus* has been determined at 3Å resolution (Figure 2). The refined structure includes virtually all of the 16S rRNA and almost all of the small subunit proteins, except for protein S1, which can be considered an initiation factor. The structure was determined in the absence of any explicitly added tRNA or mRNA ligands. However, the relatively high affinity of the 30S subunit for an RNA stem-loop in its P site resulted in a crystal packing arrangement that provides a high-resolution model for how the P-site tRNA and mRNA interact with the P site of 30S subunit. Helix 6, which constitutes the spur feature, was found to pack into the P site of a neighboring 30S subunit in a manner that mimics how the P-site tRNA anticodon stem-loop would bind. In addition, the hairpin loop of this helix was found to base-pair with a segment of single-stranded RNA – a mimic of the P-site mRNA. For several reasons, this model is only approximate, but it is nevertheless in good agreement with the lower resolution view of tRNA/mRNA–30S interactions seen in the 70S crystal structures from Noller and co-workers (see later discussion).

The 30S subunit plays a crucial role in decoding, by directly monitoring base-pairing interactions between the tRNA anticodon and the mRNA codon in the A site. The role of 30S in decoding has been investigated by determining several crystal structures with a cognate, near-cognate, or noncognate tRNA oligonucleotide analogues bound to the 30S subunit. In the presence of a cognate A-site tRNA anticodon stem-loop, several conformational changes occur in the 16S rRNA. First, Gua-530 and Ade-1492/Ade-1493 (*Escherichia coli* numbering) swing out and dock into the minor groove of the A-site codon-anticodon minihelix. Together with other conserved elements of the head (helix 34) and body (the 530 loop) previously implicated in decoding, these mobile 16S rRNA residues directly sense the "correctness" of the codon–anticodon interaction. Second, in the presence of a cognate tRNA substrate there is a more global conformational change, movement of the head and shoulder elements, resulting in a tightened grip on the A-site tRNA–mRNA helix. This larger scale conformational change from an open to a closed form has been proposed to be the signal for GTP hydrolysis by EF-Tu, the elongation factor that delivers the incoming candidate tRNAs to the A site.

Interestingly, binding of error-inducing antibiotics of the aminoglycoside family induces some of these conformational changes, such as the swinging out of A1492-3. These aminoglycosides were thus proposed to induce miscoding by stabilizing a conformation very similar to the "closed" form adopted during normal translation. Structures of the *Thermus thermophilus* 30S subunit bound to many other antibiotics (streptomycin, spectinomycin, tetracycline, hygromycin B, pactamycin, edeine) and two different initiation factors (IF-1 and IF-3) have also been reported.

High-Resolution Structures of the 50S Subunit

The structure of the 50S subunit from the halophilic archaeon *H. marismortui* was determined by Moore, Steitz, and co-workers. Despite the presence of many RNA insertions and an expanded protein repertoire, this archaeal 50S subunit is sufficiently similar to the *E. coli* subunit to allow exploitation of the vast literature describing the bacterial subunit. The 50S subunit features several protuberances, two of which are particularly disordered in the crystal structure (Figure 3). Both features are known to be functionally important. The L1 arm is thought to play a role in release of the E-site tRNA from the ribosome, while the L7/L12 stalk plays an important but poorly understood role in stimulating the GTPase activity of the elongation factors. A better understanding of how the 50S subunit interacts with these factors will come from studies on whole ribosomes. The 50S structure is more useful in understanding the nature of the peptidyl transferase activity. There is no protein at all within 18Å of the peptidyl transferase site, which was localized crystallographically by soaking in a transition-state analogue: definitive proof at last that the ribosome is an RNA enzyme, or ribozyme. This structural work and supporting biochemical data were also used to propose a mechanism for peptidyltransferase activity, with a catalytic role for nucleotide Ade-2486 (Ade-2451 in the *E. coli* numbering). However, subsequent genetic and biochemical experiments cast doubt on the proposed role of Ade-2486 as a general acid or base. More work is needed to nail down the details of the peptidyl transferase mechanism.

In 2001, a structure of the 50S subunit from the bacterium *Deinococcus radiodurans* was reported by Yonath, Franceschi, and co-workers at lower resolution. Most of the structural results are in good agreement with the *H. marismortui* structure. Interestingly, however, there are significant differences in the positioning of the L1 arm and in the conformation of RNA residues surrounding the peptidyltransferase center. The *D. radiodurans* 50S subunit structure has also been solved in the presence of five different antibiotics, four macrolides and chloramphenicol, at reported resolutions of 3.1–3.5Å. Structures of the *H. marismortui* 50S subunit bound to a variety of different antibiotics have also been reported. Such high-resolution structures of 50S–antibiotic complexes will be of great utility in the rational design of improved antibacterial drugs.

Medium-Resolution Structure of the 70S Ribosome

Structures of the *T. thermophilus* 70S ribosome with tRNA and mRNA ligands were reported by Noller, Cate, Yusupov, and colleagues in 2001, at resolutions as high as 5.5Å. This apparently rather modest resolution is in fact a phenomenal achievement, given the even greater biochemical and crystallographic difficulties of the 70S system. At this resolution, it is possible to trace RNA (but not protein) chains, albeit with errors in registry, if there are additional data to constrain the chain tracing. Once available, the high-resolution 30S structures were used to correct errors in the registry of the 16S rRNA trace and as a source for the structures of the small subunit proteins. Similarly, the high-resolution *H. marismortui* 50S structure was also invaluable for interpretation of the electron density for the large subunit in the 70S maps, although the many differences between the archaeal and eubacterial 50S subunits limited the extent to which the *T. thermophilus* 50S proteins could be built. The 70S crystal structures are largely complementary to the higher resolution subunit structures described previously. The 70S system is clearly more relevant for an understanding of the structure of the entire ribosome; thus, the 70S structures can be used to confirm the relevance of certain aspects of the higher resolution subunit structures. On the other hand, the 70S structures suffer from a lack of resolution. Thus, the high-resolution structures are of crucial importance in maximizing the utility of the 70S structures.

Comparison of the high-resolution subunit crystal structures with their structures in the context of the 70S particle reveals many small but significant differences, many of which can be ascribed to the effects of crystal packing in the "naked" high-resolution subunit structures. Some of the functionally important protein and RNA features that protrude from the 50S subunit, and that were partly disordered in one or both of the 50S structures, are found to be well ordered in the 70S structure by virtue of their interactions with the 30S subunit or tRNA ligands. Indeed, the most exciting aspects of the 70S structure are the identification of the 30S–50S contacts and the ribosome–tRNA contacts. The core of the 30S–50S contact region consists of RNA–RNA contacts, with a more peripheral ring of RNA–protein and protein–protein contacts. As with the overall architecture of each subunit, this RNA-based manner of subunit association once again emphasizes the overriding functional importance of the RNA component. Analysis of the tRNA–ribosome interactions is equally fascinating. The three tRNA substrates are intimately cradled by intersubunit bridges in the intersubunit space (Figure 4), in such a way that relative movement of the subunits, as seen in cryo-EM experiments, could effect translocation of the tRNAs.

Clearly, a more complete understanding of translational mechanisms will require more, and higher resolution, structures of distinct functional states of the

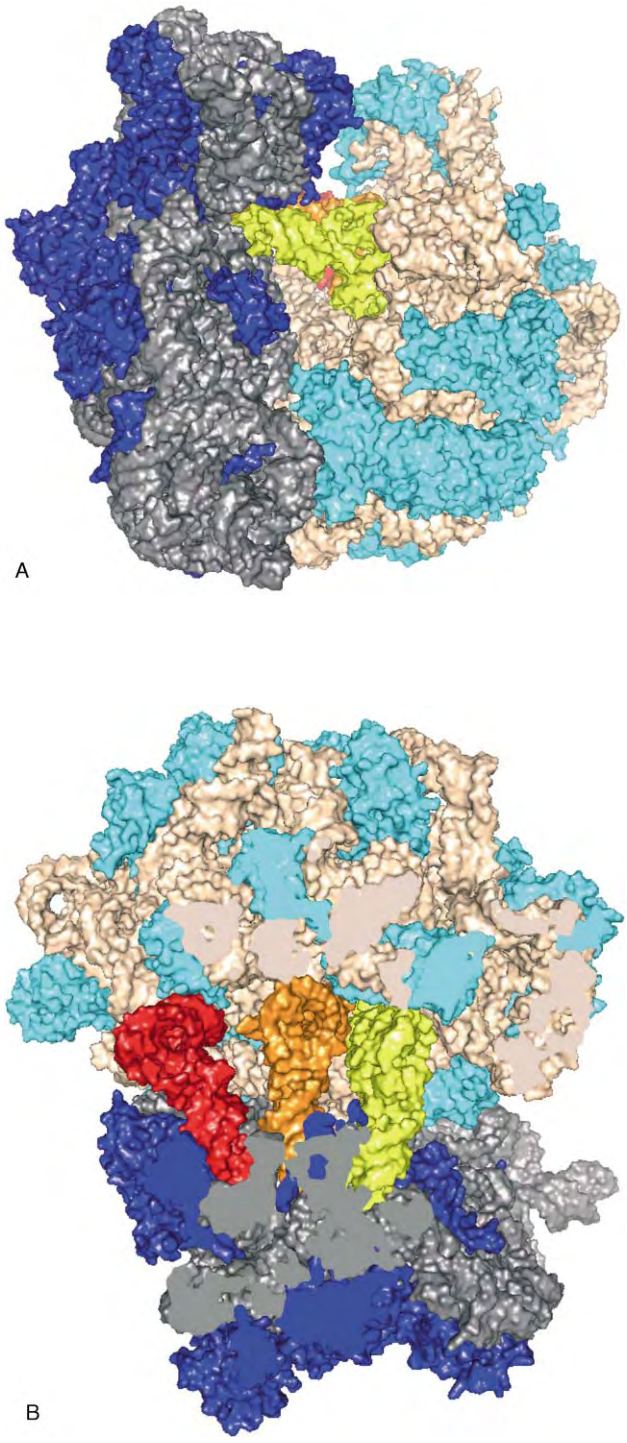

FIGURE 4 (A) The medium-resolution structure of the entire ribosome, as determined by X-ray crystallography. The view is from the A-site side, with the small subunit on the left and the large subunit on the right. For clarity, the small subunit RNA is gray, the small subunit proteins are blue, the large subunit RNA is salmon, and the large subunit proteins are light blue. The tRNAs (colored as in Figure 2) bind between the 50S and 30S subunits, with the tRNA anticodons base-paired with mRNA (not visible here), and the aminoacyl ends of the A- and P-site tRNAs are located in the peptidyltransferase site on the 50S subunit. (B) Cutaway view of the substrate tRNAs in the ribosome, with the color scheme as in A.

ribosome. Both X-ray crystallography and cryoelectron microscopy will be used toward these ends. Equally importantly, the structures now available are being used to design new genetic, biochemical, and kinetic experiments. Thus, this burst of structural information is by no means the end of the story; it is instead a new beginning.

See Also the Following Articles

Multiple Sequence Alignment and Phylogenetic Trees • Nucleolus, Overview • Ribosome Assembly • Translation Elongation in Bacteria • Translation Initiation in Bacteria: Factors and Mechanisms • Translation Termination and Ribosome Recycling

Glossary

A site The ribosomal binding site for the incoming aminoacyl tRNA, whose covalently bound amino acid will be the next addition to the growing peptide chain.

decoding The multistep process in which the ribosome decides whether an incoming tRNA carrying the next amino acid to be added is correct or incorrect. If incorrect, the tRNA is rejected.

E site The ribosomal binding site for the exiting tRNA, which has already donated its amino acid to the peptide chain.

messenger RNA (mRNA) A transient RNA copy of the DNA instructions coding for the protein to be synthesized, hence the genetic template for protein synthesis on the ribosome.

peptidyltransfer The chemical reaction between the free amino group of an amino acid and the esterified carboxy terminus of a peptide, which results in the formation of a new peptide bond. The RNA-based ribosomal activity that catalyzes this reaction is referred to as peptidyltransferase.

P site The ribosomal binding site for the peptidyl tRNA, which is covalently attached to the growing peptide.

ribosome The macromolecular complex of several large RNAs and about 50 small proteins that performs translation.

translation The synthesis of protein, as determined by a messenger RNA template; it is catalyzed by ribosomes and ribosome-associated proteins, such as the initiation, elongation, and termination factors.

transfer RNA (tRNA) The substrate for the ribosome. One end of the L-shaped tRNA base pairs with mRNA, which allows ribosomal decoding, while the other end bears a covalently attached amino acid, which is added to the growing protein in the ribosome.

translocation The movement of tRNAs and associated mRNA through the ribosome, from A site to P site, and from P site to E site.

Further Reading

Frank, J. (2003). Toward an understanding of the structural basis of translation. *Gen. Biol.* **4**, 237.

Jenni, S., and Ban, N. (2003). The chemistry of protein synthesis and voyage through the ribosomal tunnel. *Curr. Opin. Struct. Biol.* **13**, 212–219.

Moore, P. B., and Steitz, T. A. (2003). The structural basis of large ribosomal subunit function. *Ann. Rev. Biochem.* **72**, 813–850.

Ogle, J. M., Carter, A. P., and Ramakrishnan, V. (2003). Insights into the decoding mechanism from recent ribosome structures. *Trends Biochem. Sci.* **28**, 259–266.

Ramakrishnan, V., and Moore, P. B. (2001). Atomic structures at last: The ribosome in 2000. *Curr. Opin. Struct. Biol.* **11**, 144–154.

Ramakrishnan, V. (2002). Ribosome structure and the mechanism of translation. *Cell* **108**, 557–572.

Steitz, T. A., and Moore, P. B. (2003). RNA, the first macromolecular catalyst: The ribosome is a ribozyme. *Trends Biochem. Sci.* **28**, 411–418.

Van Heel, M. (2000). Unveiling ribosomal structures: The final phases. *Curr. Opin. Struct. Biol.* **10**, 259–264.

Wilson, D. N., and Nierhaus, K. (2003). The ribosome through the looking glass. *Angew. Chem. Int. Ed.* **42**, 3464–3486.

Yonath, A. (2002). The search and its outcome: High-resolution structures of ribosomal particles from mesophilic, thermophilic, and halophilic bacteria at various functional states. *Ann. Rev. Biophys. Biomol. Struct.* **31**, 257–273.

BIOGRAPHY

Brian T. Wimberly is Associate Director of Structure-Based Drug Design at Rib-X Pharmaceuticals, where he leads the X-ray crystallography part of the effort to discover new antibiotics active against bacterial ribosomes. He holds a Ph.D. from the University of California at Berkeley. During his postdoctoral training with Venki Ramakrishnan, he played a leading role in the determination of the high-resolution crystal structure of the bacterial 30S ribosomal subunit.

Ribozyme Mechanisms

John Hsieh and Carol A. Fierke
University of Michigan, Ann Arbor, Michigan, USA

RNA-catalyzed reactions are ubiquitous and important in many processes. RNA enzymes, or ribozymes, enhance chemical reaction rates using a variety of catalytic strategies, similar to those used by protein enzymes, to stabilize the transition state of the reaction. RNA and protein enzymes both use acid–base groups and metal ions to activate nucleophiles and to stabilize developing charge in the leaving group. Although limited by the ranges of functional groups and naturally occurring structure motifs, RNA enzymes can function as well as protein enzymes. The catalytic mechanisms of several well-characterized RNA enzymes, including ribonuclease P, *Tetrahymena* group I self-splicing intron and hammerhead ribozyme are discussed in detail.

Introduction

A class of naturally occurring RNA molecules, called ribozymes, enhance the speed and specificity of biologically important phosphodiester bond cleavage and peptide bond synthesis reactions, with rates that are increased by many orders of magnitude. Ribozymes have been discovered in all types of organisms from viruses to humans. Additionally, many new ribozymes that catalyze a broad range of chemical reactions have been identified in laboratory experiments called *in vitro* selection experiments. These observations have given credibility to the hypothesis of an ancient RNA World, where RNA initially served both as the genetic material and the principal cellular catalyst. During evolution, the catalytic functions of many RNA molecules were taken over by proteins. The remaining ribozymes catalyze essential biological reactions and often form complexes with proteins.

Today, many important biological processes in organisms from bacteria to humans are still carried out by RNA–protein (ribonucleoprotein, or RNP) complexes (Table I). These complexes vary greatly in size and function. For example, more than 40 protein and several RNA components are present in the ribosome, the protein synthesis machinery. Recently, the RNA components in the ribosome have been proposed to be the site responsible for catalytic activity. The spliceosome, which catalyzes the removal of noncoding sequences (introns) from pre-messenger RNA (pre-mRNA), consists of 30–100 proteins and several RNA species. Additionally, in most eukaryotes, the ends of chromosomes (the telomeres) are replicated by an enzyme called telomerase, in which an RNA subunit acts as a template, and a protein subunit catalyzes the synthesis of telomeric DNA. These examples demonstrate the importance of RNA catalysts in biology.

To understand the chemical repertoire and limitations of RNA-catalyzed reactions, this review will focus on several topics: the chemical structure of RNA, the folding of RNA molecules, and examples of the mechanism of specific ribozyme-catalyzed reactions.

Chemical Structure of RNA

Similar to DNA, RNA is made of repeating units of ribonucleotides. Each ribonucleotide consists of a five-carbon sugar in ring form (the ribose), a phosphate group, and a nitrogenous base (a pyrimidine or a purine). The same two purines, adenine (A) and guanine (G), are found in RNA and DNA. The two pyrimidines found in RNA are cytosine (C) and uracil (U); in DNA, thymine is incorporated instead of uracil. The polymer is formed by linking the monomer units via a phosphodiester bond between the 3′-hydroxyl group on one ribose unit and the 5′-phosphate group on its neighbor. Hence, the RNA polymer exhibits 5′ to 3′ directionality. The 2′-hydroxyl group on the ribose moiety of the ribonucleotide can react with the adjacent 3′-phosphodiester group to cleave the RNA polymer. This reaction is accelerated by the interaction of metal ions with the 2′-hydroxyl. The reactivity of the 2′-hydroxyl group is important for the activity of many catalytic RNAs but this moiety also makes RNA less stable in solution than DNA, which lacks a 2′-hydroxyl group.

Similar to DNA, the nucleotide bases of RNA can interact with complementary bases by hydrogen bonds. However, base pairing in RNA does not strictly obey the Watson–Crick base-pairing scheme observed in DNA, where A/T and G/C pairing occurs through hydrogen

TABLE I

Naturally Occurring Ribozymes

Ribozyme	Catalytic function	Biological function
Ribosome	Peptide bond formation	Protein synthesis
Ribonuclease P	Phosphodiester bond hydrolysis	Maturation of transfer RNA
Spliceosome Self-splicing group I and group II introns	Phosphodiester bond hydrolysis and ligation	Remove introns from precursor messenger RNA
Hairpin ribozyme Hammerhead HDV *Neurospora* Varkud Satellite	Phosphodiester bond hydrolysis	RNA virus replication pathway

bonding. In addition, since single-stranded RNA is more flexible than DNA, complementary RNA strands or different regions of the same strand can base-pair to form complex secondary and tertiary structures. This process is called RNA folding, and the stable compact structure of an RNA polymer is often referred to as its native structure. Because of the high density of negative charges when the RNA strands are brought into proximity with each other, the folding of RNA is accompanied by the binding of positively charged cations to prevent charge repulsion between the backbone phosphate ions. Therefore, RNA folding can be stimulated by the presence of cations (monovalent or divalent) as well as interactions with basic proteins. In many cases, divalent cations such as magnesium are strictly required for RNA to fold into a functional conformation; in a few cases, monovalent cations, such as potassium and ammonium ions, may make important contributions.

Catalytic Requirements of RNA and Protein Enzymes

In many aspects, protein and RNA enzymes face the same main challenge in catalysis: stabilizing the most unstable species formed during the chemical reaction, called the transition state. Like protein enzymes, RNA catalysis requires the formation of a specific tertiary structure and is sensitive to mutations in the RNA. Under optimized conditions, ribozymes can be as efficient as protein enzymes. For example, the hepatitis delta virus (HDV) ribozyme carries out phosphodiester bond cleavage ($10^2 - 10^4\ s^{-1}$) as fast as the protein enzyme RNase A ($1.4 \times 10^3\ s^{-1}$) at room temperature. However, catalysis by RNA enzymes differs from protein enzymes in several ways. First, since RNA contains only four unique nucleotide bases while proteins are composed of 20 different amino acids, RNA lacks the diverse functional groups characteristic of protein enzymes. This fact potentially limits the range of mechanisms that can be catalyzed by RNA. Nonetheless, small RNAs that can catalyze diverse chemical reactions have been selected in the laboratory from large pools of RNA molecules, in experiments termed *in vitro* selection. Second, the amino acid side chains are mainly located on the outside of protein secondary structures (α-helices or β-sheets) where they can form tertiary and quaternary contacts, while the chemical groups of the RNA bases are largely on the interior of base-paired duplexes. The third way that RNA and protein enzymes differ is that the proteins fold around a central hydrophobic core, whereas RNA usually folds by the packing of domains around a central conserved region. The high density of negative charges and the flexibility of the phosphate backbone of RNA could prevent RNA from forming stable active-site pockets. These differences affect how RNA and protein enzymes function.

The lack of diverse functional groups in RNA molecules and the propensity for RNA to bind metal ions led to the early hypotheses that all ribozymes require bound divalent metal ions to catalyze chemical reactions. However, small ribozymes, such as the hairpin and hammerhead ribozymes, can both fold and catalyze phosphodiester bond cleavage in the presence of monovalent ions (i.e., Na^+, Li^+, and NH_4^+) without any divalent cations. These small enzymes perform site-specific strand scission reactions using base-pairing and other interactions to align the cleavage site to the ribozyme active site. Current data indicate that cleavage reactions catalyzed by RNA enzymes use diverse mechanisms.

The examples of RNA enzymes described below are those whose catalytic mechanisms are among the best characterized. There are still many RNA reactions in which the catalytic mechanisms have not yet been elucidated.

Metalloribozymes

Ribonuclease P

Ribonuclease P (RNase P) catalyzes site-specific hydrolysis of precursor tRNA substrates to produce 5′-phosphate and 3′-hydroxyl end groups. This reaction is essential for the formation of mature tRNA required for protein translation. In bacteria, RNase P consists of one catalytically active RNA and one protein subunit. RNase P enzymes in eukaryotes contain multiple protein subunits. The bacterial RNA component alone is capable of catalyzing the cleavage of multiple substrate tRNAs in the presence of high salt. The protein

component is required for cleavage by RNase P *in vivo* and increases the catalytic efficiency *in vitro*. Evidence that RNase P is a metalloenzyme comes from several experimental observations. First, catalytic activity is observed only in the presence of divalent cations such as Mg^{2+} or Mn^{2+}, even though the RNA component forms a native-like structure in the absence of divalent cations. Second, the substitution of phosphate oxygen atoms with sulfur atoms at the phosphodiester bond that is cleaved in precursor tRNA leads to a significant decrease in catalytic activity in the presence of Mg^{2+}, which prefers to coordinate oxygen atoms. The decrease in the catalytic activity is less in the presence of Mn^{2+} or Cd^{2+} which can more readily coordinate the sulfur atom, suggesting that a metal ion may directly coordinate to the phosphate oxygen to enhance catalysis. These observations have led to a model for the RNase P catalyzed cleavage reaction (Figure 1A). In this model, a hydroxide ion, or metal-coordinated hydroxide, attacks the phosphate atom at the same time as the phosphate–oxygen bond begins to break. In the transition state, the phosphate atom has trigonal-bipyramidal geometry. This model is very similar to the catalytic mechanism of phosphoryl transfer reactions catalyzed by many protein enzymes. The essential metal ion(s) have been proposed to play multiple roles, including activation of the water nucleophile and stabilization of the developing negative charge in the transition state. The exact position and function of the catalytic metal ions in this reaction have not been completely elucidated.

Self-Splicing Introns

Introns are small segments of noncoding RNA that are interspersed among the regions of mRNA that code for protein. Prior to translation, these segments must be removed to form a mature mRNA. Certain intron sequences contain a common secondary structure core and use a common mechanism to catalyze excision of the RNA, termed self-splicing. This self-splicing reaction is a two-step transesterification reaction. In group I introns, self-splicing is initiated by nucleophilic attack of an exogenous molecule of guanosine. In a second type of reaction used by group II introns, the 2′-hydroxyl group of a specific adenosine within the intron acts as the nucleophile. Metal ions, Mg^{2+} and/or Mn^{2+}, are essential for the self-splicing reaction catalyzed by group I and II introns. A recent model for the transition state of the group I intron from *Tetrahymena*, based on kinetic assays of metal-dependent activity in introns containing single sulfur atom substitutions, suggests that up to three metal ions are catalytically important. In addition to promoting the formation of the correct active site structure, the catalytically important metal ions are proposed to correctly position the substrates with respect to the catalytic groups, activate the nucleophilic attack by deprotonating the 2′ hydroxyl group of the guanosine, and stabilize the developing negative charge in the transition state (Figure 1C).

Small Ribozymes that do not Require Divalent Metals

A number of small, virally encoded ribozymes have been identified, including the hammerhead, the hairpin, the HDV, and the *Neurospora* Varkud satellite (VS) ribozymes. These ribozymes are distinguished from each other by different secondary and tertiary structures. However, they all catalyze the nucleophilic attack of a 2′-hydroxyl on the neighboring 3′ phosphate to form a 2′–3′ cyclic phosphate (Figure 1B). Since this is not an irreversible reaction, these ribozymes are also observed to catalyze religation. This class of ribozymes retains significant catalytic activity with high concentrations of monovalent cations and no divalent cations, suggesting a mechanism that is different than that used by RNase P and self-splicing introns. In these ribozymes, the phosphoryl transfer reaction is proposed to be catalyzed by a general acid–base mechanism, similar to reactions catalyzed by protein RNases. The 2′-hydroxyl adjacent to the scissile phosphate is activated for nucleophilic attack by abstraction of a proton by a basic group. Concurrently, a proton is donated to stabilize the developing negative charge on the leaving group oxygen (Figure 1B).

Acid–base chemistry was not initially considered for RNA-catalyzed reactions, since there are no functional groups in ribonucleotides that can be protonated near neutral pH. In RNA, the pK_a values of the ring nitrogens of adenine and cytosine are between 3.5 and 4.1. However, in the folded RNA, the environment around the ionizing group can significantly alter the pK_a of a group. The first evidence of acid–base catalysis was observed in the HDV ribozyme when the catalytic activity of a mutant ribozyme could be partially rescued by the addition of exogenous imidazole, proposed to function as a general acid–base catalyst. A similar function has been proposed for a conserved and catalytically important guanosine of the hairpin ribozyme based on its proximity to the 2′ hydroxyl group near the scissile phosphodiester bond in the active site, as observed in the X-ray crystallographic studies. Therefore, general acid–base catalysis may be a common mechanism for RNA-mediated reactions. However, it is difficult to test this mechanism unambiguously since chemical modification or mutations of the nucleotides may perturb both chemical interactions and the structure of the RNA.

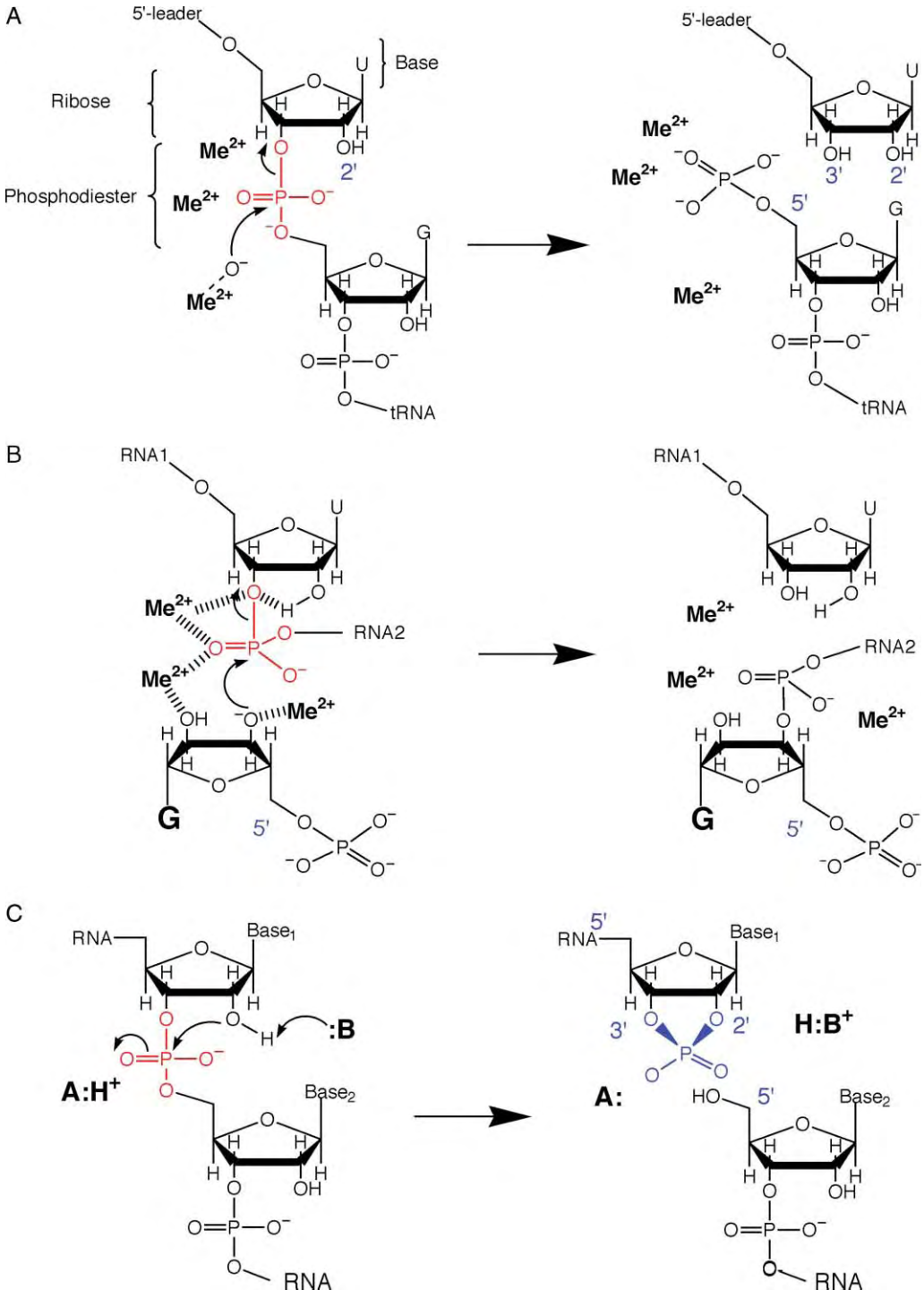

FIGURE 1 Models for ribozyme-catalyzed reactions. The phosphodiester bond is colored red. (A) Metal-mediated reaction catalyzed by RNase P. As many as four metal ions (Me) are proposed to enhance this reaction. One of the products has a 3′ hydroxyl group and the mature tRNA product contains a 5′ phosphate group. (B) General acid–base mechanism proposed for the reaction catalyzed by hammerhead or HDV ribozyme. The 2′-hydroxyl adjacent to the scissile phosphodiester is activated by a base (:B) for nucleophilic attack. Concurrently, a proton is donated to stabilize the developing negative charge on the leaving group oxygen. Note that one of the products is a 2′–3′ cyclic phosphate (in blue), and the other, a 5′ hydroxyl group. (C) Proposed metal-catalyzed mechanism for RNA cleavage catalyzed by the *Tetrahymena* group I intron.

Summary

RNA-catalyzed reactions are ubiquitous and important in many processes. Due to the limited range of functional groups and naturally occurring structure motifs, it is surprising that RNA enzymes can function as well as protein enzymes. The general catalytic strategies used by both biological catalysts appear to be similar; RNA and protein enzymes both use acid-base groups and metal ions to activate nucleophiles and to stabilize developing charge on the leaving group. Both types of enzymes use a variety of strategies to stabilize the transition state and thereby enhance the reaction rate.

See Also the Following Articles

Ribosome Assembly • Ribosome Structure • Ribozyme Structural Elements: Group I Introns • Ribozyme Structural Elements: Hairpin Ribozyme • Ribozymes and Evolution • RNA Editing • RNA Polymerase I and RNA Polymerase III in Eukaryotes • RNA Polymerase II and Basal Transcription Factors in Eukaryotes • RNA Polymerase II Elongation Control in Eukaryotes • RNA Polymerase II Structure in Eukaryotes • RNA Polymerase Reaction in Bacteria • RNA Polymerase Structure, Bacterial • T7 RNA Polymerase • Translation Termination and Ribosome Recycling

Glossary

catalysis Process by which the speed of a chemical reaction is enhanced by stabilization of unstable species formed during the reaction.

introns Regions in the precursor messenger RNA that do not code protein sequences.

***in vitro* selection** Process in which a large pool of different RNA molecules is prepared and RNAs with specific properties (such as catalytic activity) are selected based on these properties.

phosphodiester A functional group containing two alcohols attached to an oxygen atom in a single phosphate group. A phosphodiester bond links adjacent nucleotides in both DNA and RNA.

ribonuclease P A ribonucleoprotein complex that catalyzes cleavage of the 5′ end of the precursor transfer RNA to form mature tRNA.

ribonucleoprotein (RNP) Cellular particles consisting of both RNA and protein components. Known RNP's include the ribosome, ribonuclease P, and the spliceosome.

ribosome A cellular complex made up of ribosomal RNA and proteins that carries out protein synthesis using messenger RNA sequences as templates.

ribozyme An RNA molecule that catalyzes biological reactions.

RNA folding The process by which an RNA molecule forms a compact, tertiary structure through formation of specific interactions, including hydrogen-bond interaction between bases.

RNA World A hypothetical time in the early evolution of life when RNA functioned both as the sole genetic material, and as catalyst for biological reactions.

spliceosome Complexes made up of small nuclear RNA and protein that remove noncoding regions from precursor messenger RNA.

telomere A noncoding, repetitive DNA sequence located at the terminus of a chromosome.

transition state The highest energy species formed during the chemical transformation of a substrate into a product.

Further Reading

Cech, T. R. (2002). Ribozymes, the first 20 years. *Biochem. Soc. Trans.* **30**, 1162–1166.

DeRose, V. J. (2002). Two decades of RNA catalysis. *Chem. Biol.* **9**, 961–969.

Doudna, J. A., and Cech, T. R. (2002). The chemical repertoire of natural ribozymes. *Nature* **418**, 222–228.

Fedor, M. J. (2002). The role of metal ions in RNA catalysis. *Curr. Opin. Struct. Biol.* **12**, 289–295.

Orgel, L. F. (1994). The origin of life on earth. *Sci. Am.* **October**, 77–83.

Steitz, T. A., and Moore, P. B. (2003). RNA, the first macromolecular catalyst: The ribosome is a ribozyme. *Trends Biochem. Sci.* **28**, 411–418.

Biography

John (Chang-tai) Hsieh holds a Ph.D. from Washington University in Saint Louis, and is a postdoctoral research fellow at the University of Michigan. His research interests have been in the catalytic properties of enzymes in nucleic acid metabolisms. With Dr. Fierke, his research focuses on the elucidation of the kinetic properties of the ribonuclease P.

Carol Ann Fierke received her Ph.D. from Brandeis University and was an NIH postdoctoral fellow at the Pennsylvania State University. She was appointed as an Assistant Professor of Biochemistry at Duke University Medical Center and was promoted to associate professor. She then moved to the University of Michigan, where she is appointed as the Jerome and Isabella Karle Collegiate Professor of Chemistry and Professor of Biological Chemistry. Her research focuses on mechanisms of biological catalysis in metalloenzymes and ribozymes.

Ribozyme Structural Elements: Group I Introns

Barbara L. Golden
Purdue University, West Lafayette, Indiana, USA

Many eukaryotic genes are interrupted by segments of DNA called intervening sequences or introns. These introns are transcribed into RNA along with the coding segments of gene, called exons. In most cases, the introns are removed from the RNA by a cellular apparatus called the spliceosome. In the presence of biologically relevant concentrations of magnesium and guanosine nucleoside, some introns, called group I introns, are capable of self-splicing: excising themselves from the flanking RNA, and religating the RNA exons to form a functional RNA. Group I introns are the relics of selfish genetic elements that carried with them genes encoding enzymes capable of integrating the entire genetic element into cellular DNA. The self-splicing activity of the RNA transcript allowed the element to have minimal impact upon the host gene. Group I introns are found within a diverse variety of genes including those encoding the energy transducing machinery in mitochondria, ribosomal RNAs, tRNAs, and phage genes. By appropriate engineering, a group I intron can be converted into a multiple turnover RNA enzyme, or ribozyme, capable of cleaving single-stranded RNA substrates. The catalytic activity of these molecules depends on accurate folding into a three-dimensional structure that precisely positions both functional groups on the RNA and divalent metal ions to catalyze a specific phosphotransesterification reaction.

The Self-Splicing Reaction

The self-splicing reaction of group I introns is accomplished by two sequential phosphotransesterification reactions (Figure 1A). In the first step of splicing, a guanosine nucleoside substrate (guanosine, GMP, GDP, or GTP) is bound by the intron and positioned for nucleophilic attack at the 5′ splice site. The 3′-OH of the guanosine attacks at the phosphorus of the 5′ splice site and displaces the 3′-OH of the 5′ exon. This reaction results in release of the 5′ exon, and covalent attachment of the guanosine molecule to the intron. In the second step of splicing (Figure 1A), a conserved guanosine at the 3′ end of the intron (called ωG) is positioned by the intron in a manner similar to binding of the exogenous guanosine substrate in the first step of splicing. In a reaction chemically analogous to the reverse of the first step of splicing, the 3′-OH of the 5′ exon displaces the 3′-OH of ωG from the phosphate at the 3′ splice site. Ligation of the 5′- and 3′ exons, and release of the intron results.

Secondary Structure

Structured RNAs, such as tRNAs, ribosomal RNAs, and ribozymes do not have extended linear structures; they are folded. While not completely double-stranded-like genomic DNA, they have short base-paired regions formed from self-complementary sequences within the primary structure of the RNA. Group I introns have a conserved secondary structure consisting of a series of double-stranded regions labeled P1–P9 (Figure 2). These helical regions are linked by "single-stranded," or joining, stretches of RNA labeled for the two helices that they connect (e.g., J8/7) and are capped by loops designated with an "L." While most joining and loop regions are not involved in forming Watson–Crick base pairs, they usually form well-defined structures, including base pairs. These helices, loops, and joining nucleotides are organized into three domains designated P1–P2, P3–P9, and P4–P6 (Figure 2).

The P1–P2 domain, or substrate domain, spans the 5′ end of the molecule and contains the 5′ splice site, which is located within the short helix P1. The final nucleotide in the 5′ exon is a uridine, which is base-paired to guanosine on the complementary RNA strand of the intron, forming a G·U wobble base pair. The P3–P9 domain immediately follows the P1–P2 domain in the primary structure of the intron. This domain contains the helix P7 that binds to an exogenous guanosine substrate in the first step of splicing, and to ωG in the second step of splicing. The P3–P9 domain also contains a single-stranded stretch of 5–6 nucleotides called J8/7 that is involved in binding and positioning the P1 helix, and thereby the 5′ splice site. The P3–P9 domain is interrupted by the P4–P6 domain. The P4–P6 domain folds together with the P3–P9 domain, to comprise most, if not all, of the catalytic core of the intron.

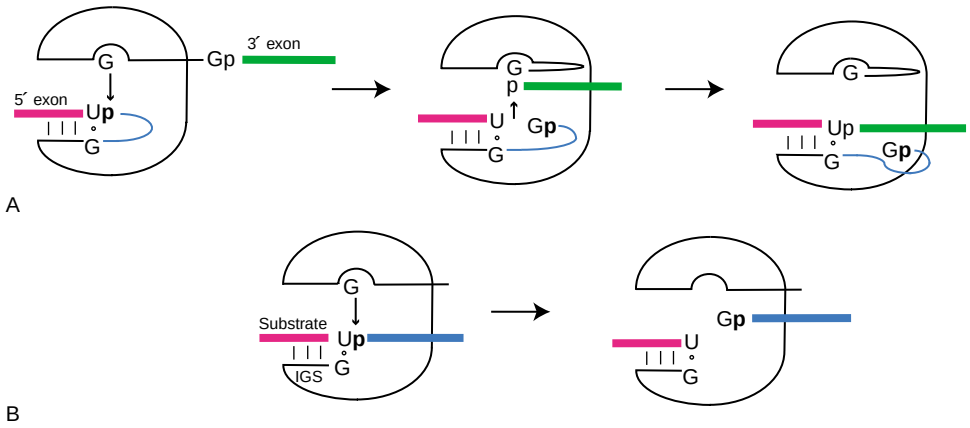

FIGURE 1 Reactions of group I intron RNAs. A. The self-spicing reaction is initiated by binding of a guanosine nucleoside. The 3′-OH of the nucleoside is activated for attack at the 5′ exon–intron junction. In the first step of splicing the guanosine becomes covalently attached to the intron, and the 5′ exon (pink) is cleaved from the intron (blue). In the second step of splicing, the 3′-OH of the 5′ exon attacks at the junction of the intron and the 3′ exon (green). This reaction links the 5′ and 3′ exons and releases the intron. B. The intron can be converted into a ribozyme capable of cleaving an RNA substrate using a guanosine nucleoside. The substrate RNA, like the 5′ exon in the self-splicing molecule, can base-pair to the 5′ end of the ribozyme that is called the IGS (G = guanosine, GMP, GDP, or GTP).

This domain also participates in splice-site recognition by binding the guanosine within the G·U wobble base pair at the 5′ splice site.

Tertiary Structure

The secondary structures in the intron fold in a magnesium-dependent manner to form a compact tertiary structure much like a globular protein enzyme (Figure 3). Formation of the folded structure is absolutely dependent on divalent metal ions, usually Mg (II), which serve to stabilize the structure by neutralizing the negative charges of the phosphate groups on the RNA backbone and by organizing the RNA into specific structures required for proper folding. In crystal structures of group I intron domains, magnesium ions are seen bound within the major groove, mediating the close approach of RNA helices, and stabilizing unusual conformations that allow the formation of intramolecular RNA–RNA contacts. Folding of the RNA creates binding sites for the P1 helix and the guanosine nucleotide cofactor described below.

The tertiary structure of group I introns has been investigated from two opposite directions. Fragments of group I introns have been crystallized to generate models of the three-dimensional structure. These studies have provided high-resolution structural information for one of the domains, medium-resolution structural information for a second domain, and no structural information for the third domain. Complementary work has been performed to elucidate contacts between individual atoms within the ribozyme as it approaches the transition state. These data can be put together to help elucidate the structural basis for group I intron catalysis.

The crystal structure of the P4–P6 domain of a group I intron reveals many of the strategies used by RNAs to form tertiary structures. Perfectly double-stranded helical RNAs do not tend to form stable tertiary structures. The structural information encoded by the RNA sequence is sequestered within the base pairs of a perfect helix, and the exposed, accessible surface is limited to the backbone and the shallow minor groove.

To facilitate tertiary structure formation, "flaws" in the helices are often present, containing base pairs other than the standard Watson–Crick A–U and G–C base pairs. These can readily form in between helices and, when present, they distort the major and minor grooves of the double-stranded helix to create distinct shapes and to expose hydrogen-bonding groups on the bases. This forms complementary surfaces that allow RNA domains to pack together. Loops, particularly four nucleotide sequences called tetraloops, which cap helices can also form distinct structures that mediate long-range tertiary interactions. These interactions are further stabilized by hydrogen bonds that can form between the 2′-OH groups of the ribose backbone. These tertiary structures are termed "ribose zippers."

Substrate Recognition

Group I introns have binding sites for two substrates: a guanosine nucleophile and a short duplex containing a G·U wobble base pair.

The Guanosine-Binding Site

The guanosine cofactor (in the ribozyme reaction and in the first step of splicing) and ωG (in the second step of

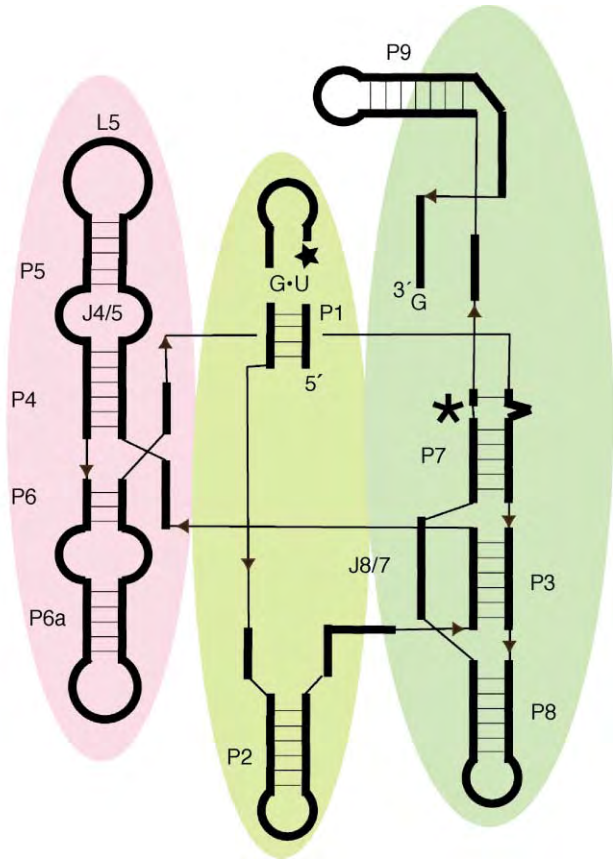

FIGURE 2 Secondary structure of a group I intron. The sequence of a group I intron folds into a secondary structure containing a series of base-paired regions called P1–P9. These short duplexes are linked by "single-stranded" nucleotides designated "J" and capped with loop sequences designated "L." These secondary structural elements are organized into three domains termed P1–P2, P3–P9, and P4–P6 that are shaded yellow, green, and pink, respectively. The P1 helix is formed by base pairing between the 5′ end of the ribozyme and the 5′ intron. Folding of the ribozyme brings the 5′ splice site (★) and the guanosine substrate binding site (∗) into proximity.

splicing) are recognized by a single guanosine-binding site located in the major groove of helix P7, a distorted double helix with a narrowed major groove. A G–C base pair near the "top" of the P7 helix provides significant specificity for the guanosine base. Recognition of the guanosine base can largely be described as a base triple. Additional orientation of the ribose group of the guanosine comes from magnesium ions bound at the intron's active site (Figure 4).

Helix P1 and 5′ Splice-Site Recognition

The 5′ splice site is recognized in the context of a short double-stranded region called P1. In self-splicing introns, helix P1 is formed by intramolecular base pairing between the 5′ exon and a complementary sequence near the 5′ end of the intron, creating a stem-loop structure (Figure 2). The helix is 3–6 bp in length, depending on the specific intron, and the final base pair is a G·U wobble pair composed of the last nucleotide in the 5′ exon, and a guanosine near the 5′ end of the intron. G·U wobble pairs, like A–U base pairs, contain two hydrogen bonds between the two bases (Figure 4), but the geometry of the pair is slightly altered compared to a Watson–Crick base pair: the guanosine base is pushed slightly into the minor groove and the uridine base is pushed slightly into the major groove. This base pair can be readily incorporated into an RNA double helix and is about as stable as an A–U base pair.

The intron may be converted into a ribozyme by splitting the P1 helix into two molecules (Figure 1). The first strand is formed from the very 5′ end of the ribozyme and is called an internal guide sequence (labeled IGS in Figure 1). The second strand serves as

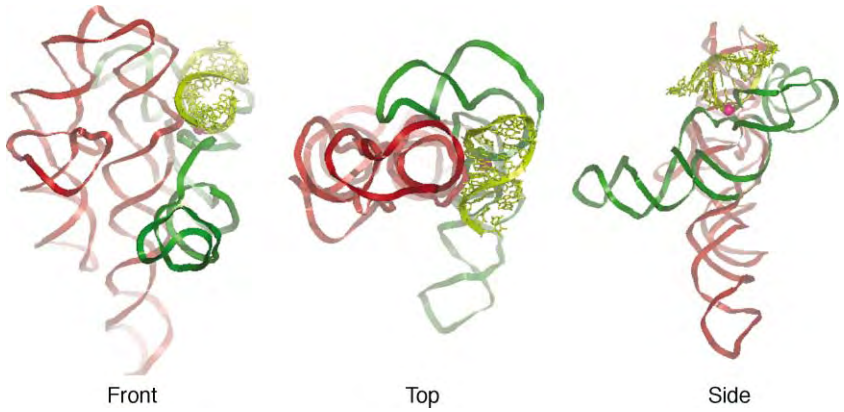

FIGURE 3 The three domains of a group I intron packed closely together to create an active site made of RNA. The model consists of the crystal structure an RNA spanning the P4–P6 (red) and P3–P9 (green) domains of a group I intron from *Tetrahymena* ribosomal RNA. Docked into the active site is a model of helix P1 that contains the 5′ splice site helix (yellow). The phosphorus atom at the 5′ splice site is drawn as a magenta sphere. The P1 helix is bound and positioned by cooperative action of the P4–P6 and P3–P9 domains.

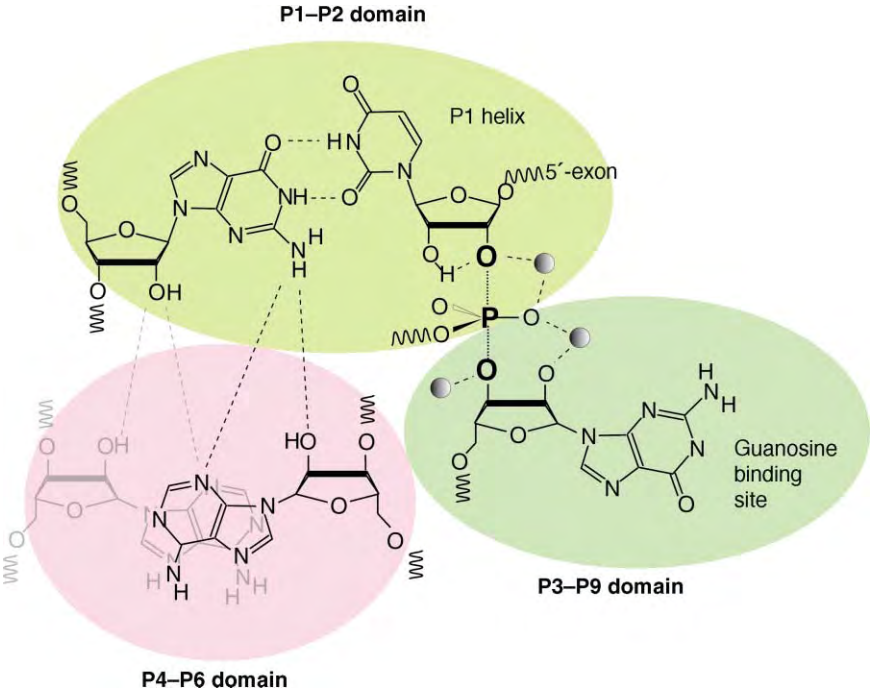

FIGURE 4 Interactions between the three domains in the transition state. Near the transition state for the ribozyme reaction, the bond between the 5′ exon and the intron is partially broken and the bond between the guanosine substrate and the intron is partially formed. Three magnesium ions help orient the substrates and stabilize the transition state, facilitating catalysis. The G·U wobble at the 5′ splice site is shaded yellow. The guanosine bound in the guanosine-binding site is shaded green. Adenosines within the P4–P6 domain involved in positioning the G·U wobble are shaded pink. Magnesium ions that participate in catalysis are drawn as spheres. Hydrogen bonds and metal interactions are indicated by dashed lines, and partial bonds are indicated by dotted lines.

a substrate for the ribozyme. It is complementary to the first strand, maintains the G·U wobble base pair, and extends for at least one nucleotide beyond the cleavage or splice site.

P1, whether composed of a hairpin in the self-splicing intron or composed of an intermolecular duplex in a ribozyme form, docks into the active site of the ribozyme. Docking is stabilized by interactions between the single-stranded region J8/7 and the minor groove of P1. These contacts are primarily hydrogen bonds to the ribose backbone and, therefore, are sequence independent. Except for the G·U wobble base pair, identity of base pairs within the P1 helix is not critical for recognition. Thus, by appropriate variation of the nucleotides in the IGS, almost any RNA substrate containing a uridine can be recognized and cleaved by a group I ribozyme.

The guanosine of the G·U wobble base pair is recognized by the J4/5 region of the P4–P6 domain. The J4/5 region contains tandem A·A non-Watson–Crick base pairs that interact with the exocyclic amine and the 2′-OH of the guanosine in the wobble pair (Figure 4). With the ribozyme "pinched" down upon the guanosine in the wobble pair, the phosphate that follows the uridine is placed in an optimal position to interact with the guanosine nucleophile and the intron's active site. The requirement for a G·U instead of a G–C Watson–Crick base pair at this position can be attributed to two characteristics of this special base pair. First, the exocyclic amine of the guanosine is displaced into the minor groove, allowing it to hydrogen bond to the J4/5 region. The exocyclic amine of a guanosine within a G–C base pair is involved in hydrogen bonding to the cytosine and is, therefore, sterically occluded from this interaction. Second, if the guanosine base in a G·U base pair is superposed on the guanosine G–C base pair, the position of the pyrimidine (U or C), and therefore the phosphate at the 3′ position, is quite different in the two structures. Displacement of the uridine towards the major groove as occurs in a wobble base pair is required to place the phosphate at the 5′ splice site into the active site of the intron.

In summary, group I introns may be thought of as RNA restriction endonucleases, capable of recognizing double-stranded RNA and specific for cleavage at G·U wobble base pairs. The catalytic activity of group I introns is dependent on proper folding of the RNA into a stable three-dimensional structure containing three domains. The three domains act cooperatively to position the 3′-OH of the guanosine nucleophile, the 5′ splice-site phosphate, and at least three magnesium

ions bound in the heart of the ribozyme (Figure 4), and thereby promote catalysis.

See Also the Following Articles

Ribozyme Mechanisms • Ribozymes and Evolution • Spliceosome

Glossary

exons Segments within a gene that encode a functional cellular protein or RNA.

introns Noncoding DNA sequences that interrupt functional genes and are removed by splicing once the gene has been transcribed into RNA.

RNA splicing Process by which intervening sequences are removed from a transcribed RNA and the flanking exons are joined to make a functional cellular RNA.

Further Reading

Cate, J. H., Gooding, A. R., Podell, E. R., Zhou, K., Golden, B. L., Kundrot, C. E., Cech, T. R., and Doudna, J. A. (1996). Crystal structure of a group I ribozyme domain: Principles of RNA packing. *Science* **273**, 1678–1685.

Golden, B. L., and Cech, T. R. (1999). Building a catalytic active site using only RNA. In *The RNA World* (R. F. Gesteland, T. R. Cech and J. F. Atkins, eds.) 2nd edition, pp. 321–349. Cold Spring Harbor Laboratory Press, Cold Spring Harbor, NY.

Golden, B. L., Gooding, A. R., Podell, E. R., and Cech, T. R. (1998). A preorganized active site in the crystal structure of the *Tetrahymena* ribozyme. *Science* **282**, 259–264.

Shan, S.-O., Kravchuk, A. V., Piccirilli, J. A., and Herschlag, D. (2001). Defining the catalytic metal ion interactions in the *Tetrahymena* ribozyme reaction. *Biochemistry* **40**, 5161–5171.

Strobel, S. A., and Doudna, J. A. (1997). RNA seeing double: Close-packing of helices in RNA tertiary structure. *TIBS* **22**, 262–266.

Biography

Barbara Golden is an Associate Professor in the Department of Biochemistry at Purdue University. Her research interests include the structural biology of catalytic RNAs and RNA-binding proteins. She holds a Ph.D. from Duke University and received postdoctoral training at the University of Colorado.

Ribozyme Structural Elements: Hairpin Ribozyme

Adrian R. Ferré-D'Amaré
Fred Hutchinson Cancer Research Center, Seattle, Washington, USA

The hairpin ribozyme is an RNA that catalyzes sequence-specific cleavage and ligation of the phosphate backbone of its RNA substrate. Two short irregular double helices, stems A and B, dock to form the active RNA. The scissile phosphate is in stem A. The reaction catalyzed by this RNA requires that the reactive groups adopt an in-line conformation. Prior to docking, the conformation of stem A is such that the reaction cannot take place. Docking of stems A and B results in a dramatic rearrangement that produces a reactive, in-line substrate conformation. Comparison of structures of the hairpin ribozyme in complex with a noncleavable substrate mimic, a transition-state mimic, and the cleavage products shows that the ribozyme has an active site with a rigid arrangement of purine bases that make more hydrogen bonds to the transition state than to the precursor or products, thus lowering the activation energy of the reaction. Because RNAs have less chemical diversity than proteins, catalytic strategies such as precise reactive group orientation and transition state stabilization are important for ribozyme function.

Biological Context

Four RNAs that catalyze RNA cleavage and ligation through transesterification have been identified from natural sources: the hammerhead, hairpin, hepatitis delta virus (HDV), and Varkud satellite (VS) ribozymes. In nature, all four function in the life cycle of satellite RNAs of viruses, or a replication intermediate of a plasmid (VS). In all cases, the ribozyme domain is part of a larger circular RNA that is replicated through a rolling-circle mechanism by host RNA polymerases. The linear concatamers produced by rolling-circle replication self-cleave into unit-length RNA molecules. These can then be ligated (either by the RNA itself or by a different catalyst) into circles. These circles, which are complementary in sequence to the infecting circular RNA, undergo an equivalent replication/self-cleavage/ligation cycle to produce copies of the original RNA.

The domain responsible for cleavage and ligation of the minus strand of the satellite of tobacco ringspot virus (-sTRSV) was mapped by deletion analysis. When synthesized *in vitro*, this RNA domain can act as a multiple turnover catalyst. This is the hairpin ribozyme. Because of its small size (constructs less than 60 nucleotides in length are active *in vitro*) the hairpin ribozyme has been amenable to extensive genetic, biochemical, and structural analysis, and constitutes one of the paradigms of catalytic RNA.

Primary and Secondary Structures

The minimal sequence elements required for hairpin ribozyme activity *in vitro* are contained in two helical segments, stems A and B (Figure 1). Each stem comprises a central portion of conserved nucleotides that engage in nonstandard base pairing or are unpaired (these are referred to as loops A and B in the older literature), flanked on both sides by canonical Watson-Crick base-paired duplexes. As long as base pairing is maintained, the sequences of these flanking duplexes can be varied arbitrarily.

One of the strands of stem A is the substrate RNA. As indicated in Figure 1, the cleavage site can be preceded by any nucleotide (position − 1), but must be followed (position + 1) by a G residue. Three other residues on the substrate strand are conserved at positions − 2, +2, and + 3. As long as these four nucleotides are present in the correct order in a substrate, a hairpin ribozyme can be engineered to cleave it by making the sequence of the Watson–Crick segments of the other strand of stem A complementary to the sequence of the target RNA.

Tertiary Structure

Stems A and B can be synthesized as separate molecules, and mixed to reconstitute activity in the test tube. The two stems associate with modest affinity to form the active species. In the biological RNA, stems A and B are connected to each other as part of a four-helix junction. The four-helix junction increases the

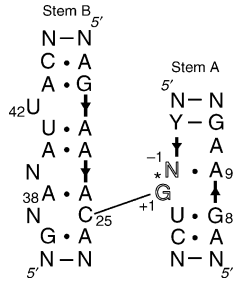

FIGURE 1 Schematic secondary structure of the core of the hairpin ribozyme. Two irregular double helices, stems A and B, dock to form the active ribozyme. One of the strands of stem A is the substrate, and carries the scissile phosphate (* , flanked by the two nucleotides shown in outline letters). Nucleotides whose identity is essential to function are identified in single letter code (A, C, G, U), those that can be varied freely without compromising activity, as N. Y denotes either pyrimidine. Thin lines denote Watson–Crick pairs, black circles, noncanonical pairs. Numbering is according to convention. Note the interhelical Watson–Crick base pair between G + 1 (in the substrate strand of stem A) and C25 (stem B).

local concentration of stems A and B and places the two stems in the optimal orientation relative to each other. Constructs that incorporate the junction are much more active *in vitro* than the two isolated stems, or even the two stems connected by a flexible linker. Four-helix junction constructs of the hairpin ribozyme bind two equivalents of divalent metal ions with high affinity and, upon metal ion binding, undergo a conformation rearrangement at the junction that brings the conserved, noncanonical segments of stems A and B into close spatial proximity.

The three-dimensional structure of a four-helix junction form of the hairpin ribozyme was determined by X-ray crystallography. Stems A and B were revealed to be highly irregular (with stem B particularly overwound), and to associate through their minor groove faces (Figure 2). The interhelical interface buries $\sim 1600 Å^2$ of solvent accessible surface area, implying that considerable binding energy is available from docking of the stems. The scissile phosphate lies at the interface of the two stems, surrounded by the purine bases of residues 8, 9, 10, and 38. These four nucleotides are all highly conserved (Figure 1) and have been shown by mutagenesis experiments to be essential for catalysis.

The structures of the isolated stems A and B were determined by nuclear magnetic resonance spectroscopy. Comparison of their free and docked structures shows that both stems undergo dramatic conformation rearrangements upon association. Only two out of nine noncanonical base pairs that constitute the core of the docked ribozyme are present in the free stems. Of particular importance is the extrusion of the base of G + 1 from the stem-A helical stack upon assembly of the ribozyme. As can be seen in Figure 2B, this base forms part of an interhelical pair in the docked

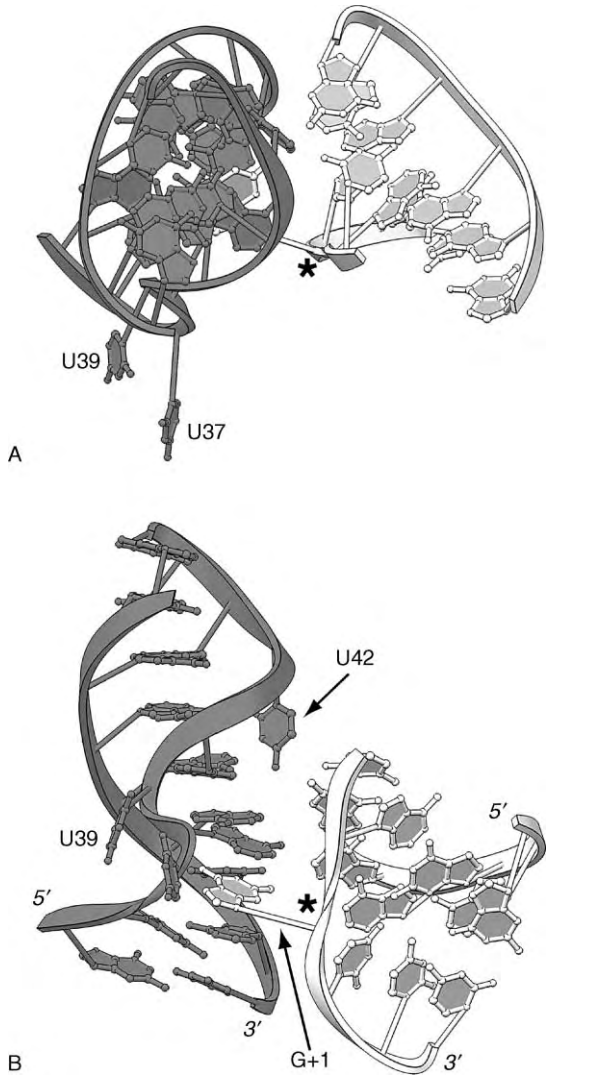

FIGURE 2 Simplified representation of the three-dimensional structure of the hairpin ribozyme. The RNA backbone is depicted as a ribbon; nucleotide bases are shown in ball-and-stick representation. Stem A is in white; stem B in dark gray. The position of the scissile phosphate is indicated byasterisk. Panel A is a view orthogonal to panel B. The scissile phosphate is buried in the interface of the two irregular helices.

ribozyme. G + 1 forms a Watson–Crick pair with C25 (from stem B; see also Figure 1).

The S_N2 (bimolecular nucleophilic substitution) reaction catalyzed by the hairpin ribozyme requires that the 2′-OH nucleophile and the 5′-oxo leaving groups be aligned with the phosphorus of the scissile phosphate. Prior to docking, the conformation of stem A is such that the reaction cannot take place. Extrusion of G + 1 from stem A concomitant with docking results in a reactive, in-line substrate conformation. The ribozyme uses the energy resulting from formation of the interhelical interface to properly orient its substrate.

Catalytic Mechanism

Although divalent metal ions are essential for activity of the hairpin ribozyme, biochemical and structural studies have shown that these ions play a structural role, rather than acting as cofactors in the active site. The hairpin ribozyme is active in a variety of divalent cations. The ribozyme is also active when the divalent cations are replaced by the complex ion cobalt (III) hexammine. The amine ligands that coordinate the cobalt in this complex do not exchange with solvent ions. While cobalt hexammine mimics hydrated magnesium ion (with its six water ligands), it is incapable of making direct metal to RNA interactions (inner sphere coordination), or to bind water and activate it to act as a base. Full activity of the hairpin ribozyme in cobalt hexammine implies that the RNA does not need to make direct coordination with its bound metal ions, nor does it use the cations as cofactors for generating hydroxyl ions. The crystal structure of the docked hairpin ribozyme shows the locations of several bound metal ions. These are in the narrow major groove of stem B, not in the wide minor groove where the active site lies.

Crystal structures have been determined of the hairpin ribozyme in complex with a noncleavable substrate mimic, a transition-state mimic (Figure 3), and the cleavage products. Comparison of these structures shows that the ribozyme has an active site with a rigid arrangement of purine bases that make more hydrogen bonds to the transition state than to the precursor or products, thus lowering the activation energy of the reaction. Although this has not been demonstrated directly, it appears that the pK_a of one of the active site adenosines (A38, Figure 3) is shifted towards neutral pH, resulting in protonation of its N1 imino nitrogen. The positive charge thus acquired by this active-site adenosine may also aid in catalysis.

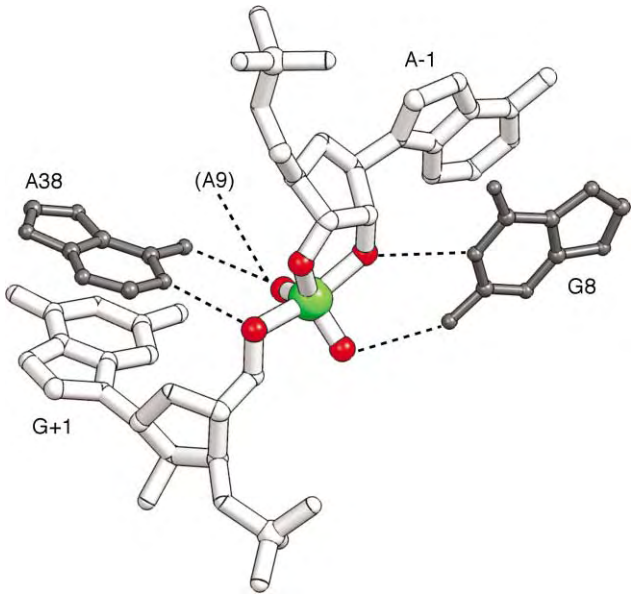

FIGURE 3 Structure of the active site of a transition-state mimic complex of the hairpin ribozyme. Vanadate (vanadium coordinated to five oxygens, three of which are provided by the RNA) mimics the trigonal bipyramidal coordination geometry of the scissile phosphate, which is pentavalent in the transition state. The vanadium atom is colored green, and the five oxygen atoms to which it coordinates are red.

Comparison with Other Ribozymes

Whereas protein enzymes can use 20 chemically varied amino acids to construct their active sites, ribozymes are limited to four nucleotides with limited functional group diversity. Studies on the group I intron, the first catalytic RNA discovered, demonstrated that this ribozyme overcomes the chemical limitations of RNA by recruiting multiple divalent cations into its active site. The group I intron uses these to orient reactive moieties, to activate water (to generate basic hydroxyl ions), and as sources of positive charge to stabilize negatively charged transition states. Early work on ribozymes assumed that RNA catalysts would always use cations as active-site cofactors.

We now know that ribozyme mechanisms can be more varied. Although isolated nucleotides do not have functional groups with near-physiologic pK_a, intricately folded RNA structures are capable of perturbing the acidities of purine and pyrimidine bases. For instance, the HDV ribozyme uses a cytosine whose pK_a is shifted from 4.2 to ~7 as a general acid catalyst (analogous to His119 in RNase A, a protein enzyme that catalyzes the same transesterification reaction as the hairpin ribozyme; see Figure 4). The hairpin ribozyme demonstrates

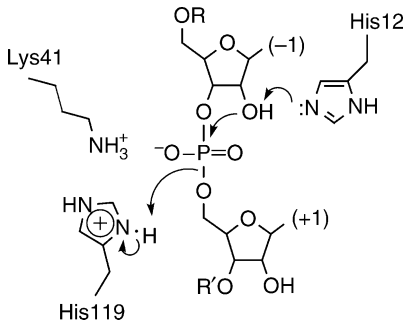

FIGURE 4 Catalytic mechanism of ribonuclease A. Histidine is particularly well suited to act as a general acid–base catalyst because its p*Ka* is close to physiologic pH. In RNase A, histidines 12 and 119 act as general base and acid, deprotonating the nucleophile and protonating the leaving group of the transesterification, respectively. Deprotonation of the 2′-OH makes it a better nucleophile, and protonation of the 5′-oxo leaving group lowers the energy of the product state. Lysine 41 (which has a positively charged side chain at physiologic pH) counteracts the increased negative charge at the scissile phosphate during the transition state, and thus helps lower the activation energy of the reaction.

another way in which a catalytic RNA can achieve catalysis: selective hydrogen bonding to one state of the reaction. Nucleotide bases are well suited for hydrogen bonding, and the ribozyme provides a rigid structure to orient them precisely. It appears that the ribosome also achieves catalyses (protein synthesis in this case) by precise orientation of functional groups, rather than general acid-base catalysis.

See Also the Following Articles

Ribozymes and Evolution • Ribozyme Mechanisms • Ribozyme Structural Elements: Group I Introns

Glossary

acid dissociation constant (pK_a) pH at which half the acid exists in the protonated form and the other half in the deprotonated, or conjugate-base, form.

four-helix junction Nucleic acid structure in which four double helices abut, and are connected by sharing of the strands between adjacent helices.

general acid–base catalysis Mode of chemical catalysis in which a functional group that is not water accelerates a chemical reaction by facilitating proton transfer.

minus strand The anti-sense strand of a single-stranded circular RNA. For infectious RNAs, the infecting strand is the plus strand. This gets copied into its complement (minus strand), which in turn is copied to regenerate the original species.

ribozyme Ribonucleic acid that acts as a catalyst, accelerating the rate of a chemical transformation without itself undergoing a permanent chemical change.

specific acid–base catalysis Chemical catalysis in which water functions as a base (in the form of the hydroxyl ion) or an acid (as a hydronium ion) to increase the rate of a reaction.

Further Reading

Fedor, M. (2002). The role of metal ions in RNA catalysis. *Curr. Opin. Struct. Biol.* **12**, 289–295.

Klostermeier, D., and Millar, D. P. (2002). Energetics of hydrogen bond networks in RNA: Hydrogen bonds surrounding G + 1 and U42 are the major determinants for the tertiary structure stability of the hairpin ribozyme. *Biochemistry* **41**, 14095–14102.

Murchie, A. I., Thomson, J. B., Walter, F., and Lilley, D. M. J. (1998). Folding of the hairpin ribozyme in its natural conformation achieves close physical proximity of the loops. *Molecul. Cell* **1**, 873–881.

Raines, R. T. (1998). Ribonuclease A. *Chem. Rev.* **98**, 1045–1065.

Rupert, P. B., and Ferré-D'Amaré, A. R. (2001). Crystal structure of a hairpin ribozyme–inhibitor complex with implications for catalysis. *Nature* **410**, 780–786.

Rupert, P. B., Massey, A. P., Sigurdsson, S. Th., and Ferré-D'Amaré, A. R. (2002). Transition state stabilization by a catalytic RNA. *Science* **298**, 1421–1424.

Ryder, S. P., and Strobel, S. A. (2002). Comparative analysis of hairpin ribozyme structures and interference data. *Nucleic Acids Res.* **30**, 1287–1291.

Biography

Adrian R. Ferré-D'Amaré is a Faculty Member in the Division of Basic Sciences of the Fred Hutchinson Cancer Research Center in Seattle. His principal research interests are in RNA catalysis and RNA–protein interactions. He received his Ph.D. from the Rockefeller University, and was a postdoctoral fellow at Yale University. He has developed procedures that facilitate the crystallization of RNA, and his laboratory was the first to obtain crystallographic "snapshots" of a catalytic RNA as it carries out its reaction.

Ribozymes and Evolution

Niles Lehman
Portland State University, Portland, Oregon, USA

Ribozymes, also known as ribonucleic acid (RNA) enzymes, have been known since the early 1980s when it was first discovered that RNA could catalyze chemical reactions. Previously it had been thought that all enzymes were proteins, but it is now clear that RNA-directed catalysis plays many important cellular functions, and that numerous ribozymes can be found in organisms spanning the tree of life. Notably, for example, we now realize that the catalytic core of the ribosome itself, the cellular machinery for protein synthesis, consists of RNA such that peptide-bond formation is catalyzed by ribosomal RNA. These findings suggest strongly that RNA, or some RNA-like molecule, was an integral piece of the earliest biochemical processes to evolve on the Earth. In 1986 Walter Gilbert coined the phrase "RNA World" to invoke a time during the coalescence of life when RNA was responsible for most if not all of the genetic transformations of the planet's first organisms. Ribozymes have thus played an important role in biological evolution and have recently been used to perform evolution experiments in the laboratory.

RNA

RNA is a polymer of ribonucleotides. RNA differs from DNA in three basic respects. First, RNA employs uracil as a nitrogenous base, in place of the thymine used in DNA. Second, RNA nucleotides possess a hydroxyl group at the 2′ position, while DNA is deoxygenated at that position to a proton. And third, RNA is more often found single stranded than DNA, which is typically completely base paired into a double helix. All three of these features help engender RNA with catalytic capabilities, although they also tend to make RNA chains less chemically stable than DNA. From an informational point of view, both DNA and RNA have the capability to store and transmit biological information through complementary base paring: C with G, and T(U) with A.

Catalytic RNA

RNA as an Enzyme

Enzymes are molecules that can catalyze a chemical reaction by lowering the activation energy needed to transit from reactants to products. Proteins, built up from amino acids of twenty or more varieties, are well known to perform catalysis in biological systems. RNA is built up from only four nucleotide varieties but still can perform catalysis. Similar to protein-directed catalysis, the basis for this is the acquisition of a three-dimensional structure that contains a catalytic pocket. Many ribozymes can speed up the rate of reaction 10^3- to 10^{11}-fold over the corresponding uncatalyzed rate, and can behave as true enzymes by "turning over," catalyzing more than one reaction event.

Chemistry

In the catalytic pocket, RNA usually relies on metal-ion coordination and one or more chemical strategies to accomplish catalysis. In some cases, the 2-hydroxy group itself can serve as a nucleophile to attack a chemical bond in the substrate molecule. In other cases, the chemical moieties on the nitrogenous bases (adenine, guanine, uracil, or cytosine) can act as acids or bases to stimulate a reaction. For example, it is now thought that peptide-bond formation in the heart of the ribosome is promoted by some type of interaction between amino acids and a phylogenetically invariant adenosine residue in the ribosomal RNA. In most cases, RNA must bind divalent metals such as magnesium to help properly position the substrate molecules in order to stabilize the transition state.

Classes of Natural Ribozymes

Since 1982, several types of naturally occurring ribozymes have been discovered (Figure 1). With the notable exception of the ribosome, these ribozymes are generally limited in their capacity to making and/or breaking phosphoester bonds that hold nucleic acids together. In addition to the list below, RNA plays an important role in the catalytic events promoted by ribonucleoproteins such as telomerases, spliceosomes, and editosomes. Other natural ribozyme will undoubtedly be discovered in the near future.

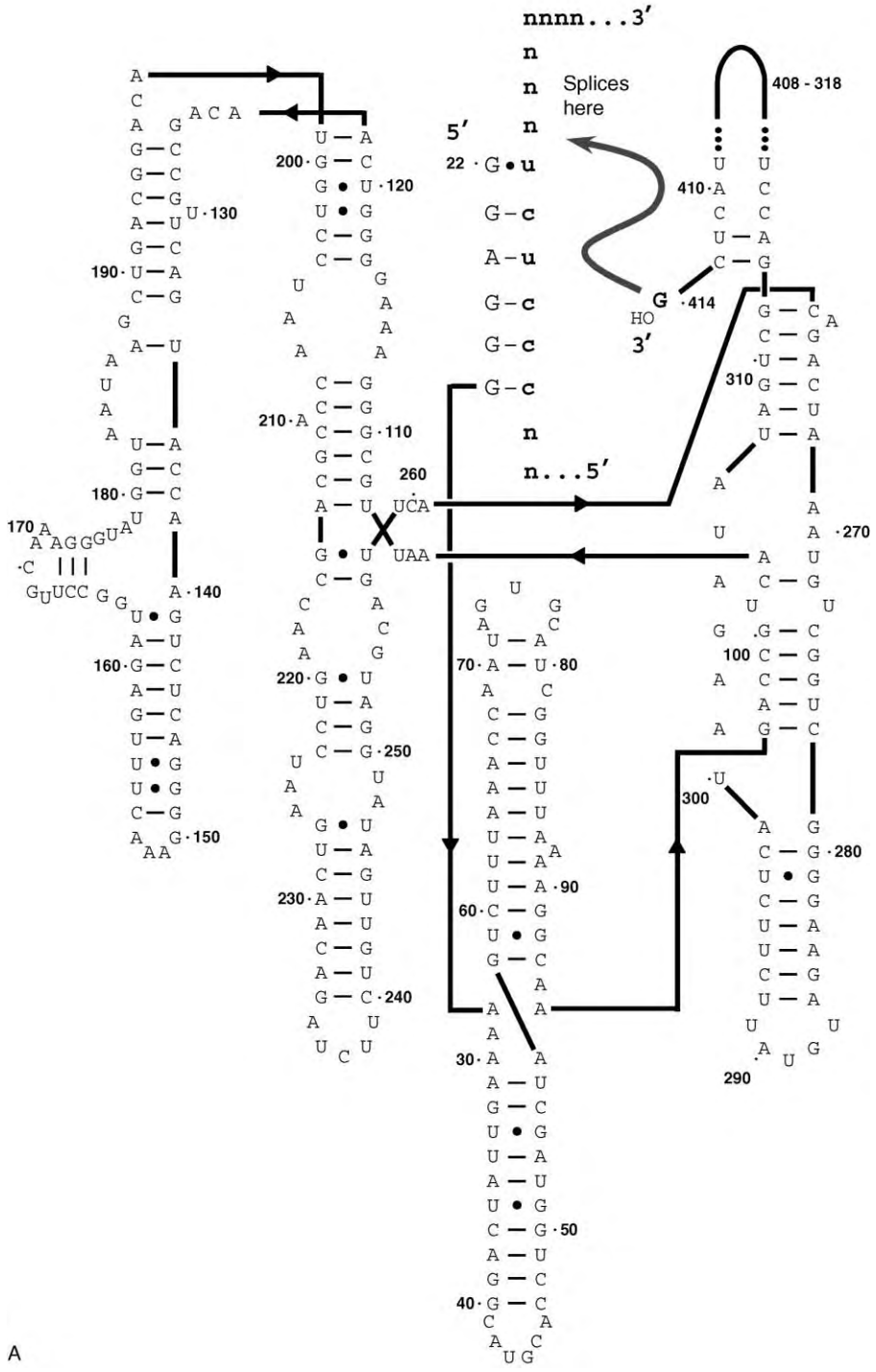

FIGURE 1 Some known ribozymes. (A) The group I intron from the ciliate *Tetrahymena thermophila*. Shown is the shortened version of the natural rRNA intron; this 414 nucleotide ribozyme binds a complementary RNA substrate (lower case letters) via complementary base pairing and catalyzes phosphoester bond cleavage and ligation reactions at the site indicated by the arrow. (B) One possible hammerhead ribozyme. This ribozyme self-cleaves at the site indicated by the arrow.

Group I and Group II Introns

These are large (>200 nucleotides) self-splicing introns: rRNA or tRNA introns that excise themselves from nascent RNA transcripts via ribozyme activity.

RNase P

RNase P is a large ribozyme that allows maturation of nascent tRNA transcripts and a few other small RNAs by removing the 5′-leader portion of those transcripts.

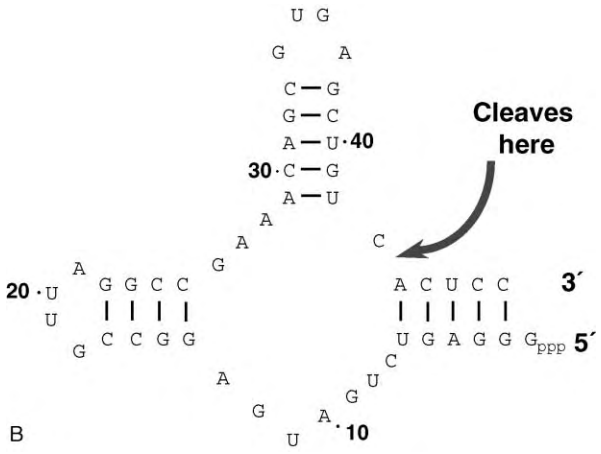

FIGURE 1 (*continued*)

Hammerhead

These small ribozymes, of which there are many throughout nature, possess three base-paired stems and catalyze self cleavage of a RNA phosphodiester bond.

Hairpin

Like the hammerheads, hairpin ribozymes, originally found in a tobacco RNA virus, self-cleave an RNA bond, but unlike the hammerheads, consist of four stems in two general domains.

Hepatitis Delta Virus

The HDV ribozyme is another viral-derived small ribozyme that catalyzes RNA bond cleavage, but it is slightly more complex, having a "pseudoknot" folded structure.

VS

The VS motif is another small self-cleaving ribozyme, found first in a satellite plasmid of *Neurospora* mitochondria. This ribozyme, as is the case for all RNA enzymes, can also catalyze the reverse reaction, which here would be ligation of two RNA strands.

Unnatural Ribozymes

Using the techniques of SELEX, *in vitro* selection, and *in vitro* evolution, many novel catalytic RNA sequences have been discovered (Figure 2), many of which promote chemistries not yet seen in natural ribozymes. The existence of these ribozymes demonstrates not only that RNA has a wide repertoire of catalytic capabilities, but that evolutionary forces are quite adept at molding RNA-based catalysis.

Ligase Ribozymes

Isolated from random pools of RNA sequences, the ligase ribozymes were one of the first type of unnatural ribozymes to be fashioned. These RNAs catalyze phosphoester-bond formation between themselves and an exogenous oligoribonucleotide. Several classes of ligase ribozymes exist, with differing RNA folds. Ligases catalyze bond formation by a chemistry that is distinct from that of known natural ribozymes, but which is remarkably similar to the chemistry used by the protein enzyme RNA polymerase. In fact some ligases can be engineered to behave as rudimentary RNA polymerases.

Diels-Alderase Ribozymes

To move from phosphoester chemistry to carbon–carbon bond chemistry, it was necessary to derivatize one of the four bases, uridine, with a pyridyl moiety. This allowed the selection *in vitro* of a Cu^{2+}-dependent ribozyme that could catalyze a Diels-Alder cycloaddition reaction.

Three- and Two-Base Ribozymes

Recently ribozymes have been selected that use only three (i.e., A, G, and U) nucleotides to perform catalysis. Also, if only U and 2,6-diaminopurine are available, a 2-base ligase ribozyme can be constructed through *in vitro* evolution.

Other Unnatural Ribozymes

Many other unnatural ribozymes exist and more are being constructed. These ribozymes can catalyze amide bond formation, N-alkylation, porphyrin metallation, thioester bond formation, and a host of other chemical reactions.

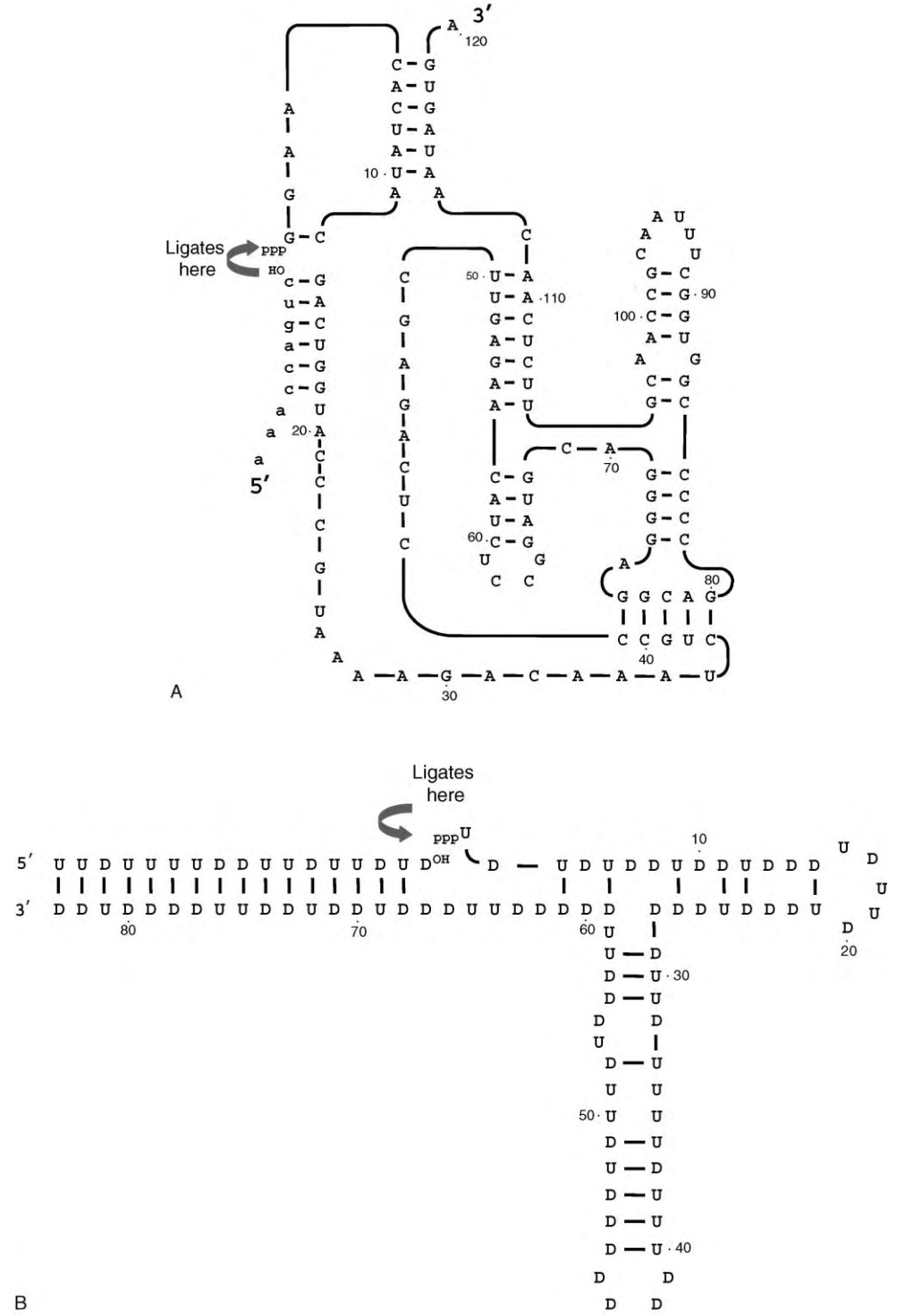

FIGURE 2 Some known unnatural ribozymes. (A) The b1-207 ligase ribozyme selected *in vitro* from a random pool of RNA sequences. This ribozyme binds a complementary RNA substrate (lower case letters) via complementary base pairing and catalyzes a ligation to form a new phosphoester bond. (B) A ligase ribozyme evolved *in vitro* to function with only two nucleotides: D = 2,6-diaminopurine and U = uridine.

Phylogenetic Distribution of Ribozymes

Judging from the phylogenetic distribution of natural ribozymes (Figure 3) and from the central nature of the reactions that they catalyze, it is clear that catalytic RNA was likely present in the last common universal ancestor (LUCA) of contemporary life. Group I ribozymes for example, are present in eukaryotes (e.g., the ciliated protozoan *Tetrahymena*) and in eubacteria, including some bacteria thought to occupy basal lineages in the tree of life (e.g., the hyperthermophilic bacterium *Thermatoga*). Ribozymes are wide spread in RNA viruses, group II introns have been recently isolated from deep-sea hydrothermal vent bacteria, and small ribozymes have been isolated from genomes in organelles such as mitochondria and chloroplasts. Also, the RNase P ribozyme is present in a variety of archaeal species.

RNA and the Origins of Life

In addition to the inference that ribozymes were a feature in the LUCA, there is much evidence and corresponding speculation that RNA, in particular catalytic RNA, was critical in the earliest life forms on the Earth. RNA, or an RNA-like molecule, could even have been the basis for the origins of life itself. Initially this postulate was based on the observation that RNA was the only known polymer to possess simultaneously a genotype and a phenotype. Subsequently, more direct evidence of the antiquity of RNA has come to light. These data include the realization that, the ribosome is a ribozyme, RNA can catalyze a diverse array of reactions, a ligase-derived RNA can catalyze rudimentary RNA polymerization, RNA can catalyze recombination, and, importantly, populations of RNA can evolve in a test tube and respond to environmental pressures in manners quite analogous to natural populations of organisms. Moreover, much is now known about plausible abiotic synthetic routes to RNA precursors such as purines, pyrimidines, carbohydrates, and phosphorylated compounds. For example, cationic clays such as montmorillonite can promote the polymerization of RNA-like monomers into RNA chains of 50 or more nucleotides in length.

In vitro Evolution of RNA

SELEX

Systematic evolution of ligands by exponential enrichment (SELEX) is a powerful method to isolate RNA sequences that bind to particular substrates without necessarily reacting with them. Random pools of RNA, typically 40–100 nucleotides in length, are created such that billions of possible sequences are represented. These pools are challenged to bind a target substrate, such as a

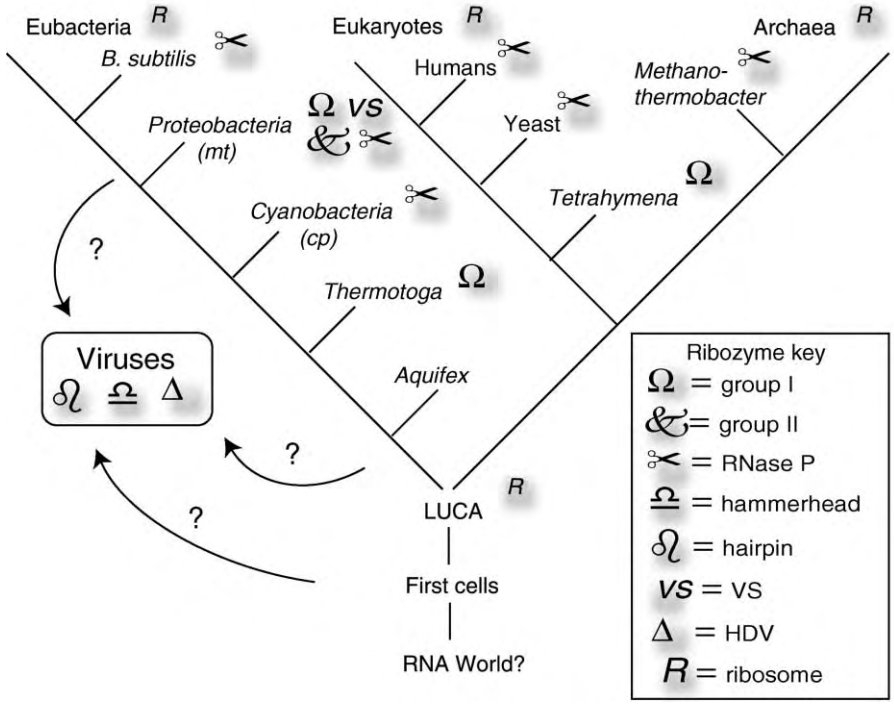

FIGURE 3 Distribution of ribozymes in the tree of life. The examples shown here are not exhaustive; branch lengths are not indicative of extinction events or amount of evolutionary change. Mitochondria (mt) and chloroplasts (cp) are included with their bacterial precursors.

particular protein or small molecule such as an amino acid, and the successful binders are separated from the failures and amplified. Repetition of this process 5–10 times often generates a small subset of RNA sequences, called aptamers that have a high-binding affinity toward the substrate.

Selection *in vitro*

Selection *in vitro* (in a test tube) follows the same basic strategy as SELEX, only RNAs are isolated that catalyze a target chemical reaction (Figure 4). These RNAs must bind one or more substrates and then promote a reaction in such a way that the RNA is modified or "tagged" for amplification. In this technique, the initial pool can either be a set of random RNA sequences, or a set of mutants based on a particular known wild-type sequence.

Evolution *in vitro*

Evolution *in vitro* follows the strategy of selection *in vitro* except that in each round, mutations are deliberately introduced into the RNA population to provide additional variation on which natural selection can operate (Figure 4). The mutation can come from error-prone protein polymerase enzymes, from mutagenic PCR, or from sexual PCR. Evolution *in vitro* can in principle be carried out for an indefinite number of rounds, but in principle convergence on a particular catalytic solution, if one exists, typically occurs after 10–20 rounds and will occur in general accordance to the principles of population genetics.

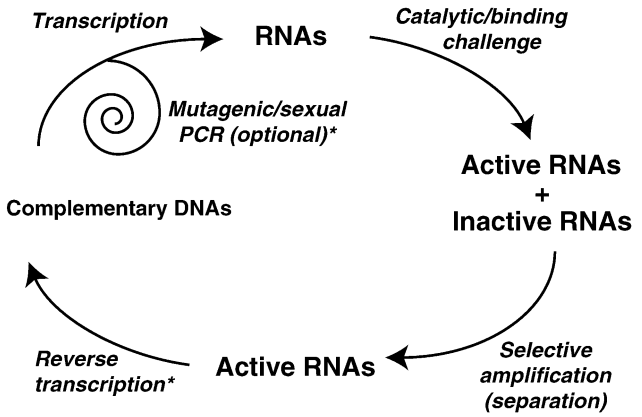

FIGURE 4 *In vitro* selection/evolution. A pool of RNA molecules, partially or completely randomized in nucleotide sequence, is challenged to perform a novel binding and/or catalytic event. As a result of successfully performing that event, RNA molecules become physically tagged in such a manner that they can be separated from unsuccessful RNA molecules. The successful RNAs then get converted to a corresponding DNA sequence through reverse transcription and back into RNA by forward transcription. A complete cycle is called a round, or a generation, and may or may not include mutagenic steps (indicated by asterisks) to introduce an evolutionary element into the process.

Continuous Evolution *in vitro*

The most recent modification of these RNA evolution techniques is to mimic a prebiological milieu in which all the components of evolution – the RNA, the nucleotides, the salts, the oligonucleotides, and the protein enzymes, if any – are simultaneously present in a single test tube. In this fashion several rounds of evolution occur autonomously before equilibrium is reached. Serial dilution and fresh additions of reagents can result in the extremely rapid evolution of RNA populations.

See Also the Following Articles

Ribozyme Mechanisms • Ribozyme Structural Elements: Group I Introns • Ribozyme Structural Elements: Hairpin Ribozyme • Spliceosome

Glossary

abiotic Formed in the absence of life.
nucleotide A chemical subunit of nucleic acids (A = adenosine, C = cytidine, G = guanosine, U = uridine).
phylogeny A tree-like representation of the ancestral–descendant relationships among species.
polypeptide A polymer of amino acids that forms a protein.
ribozyme An enzyme made of RNA.
RNA Ribonucleic acid, a polymer of nucleotide subunits.

Further Reading

Bartel, D. P., and Unrau, P. J. (1999). Constructing an RNA world. *Trends Cell Biol.* **9**, M9–M13.
Bittker, J. A., Phillips, K. J., and Liu, D. R. (2002). Recent advances in the *in vitro* evolution of nucleic acids. *Curr. Opin. Chem. Biol.* **6**, 367–374.
Breaker, R. R., and Joyce, G. F. (1994). Inventing and improving ribozyme function: Rational design versus iterative selection methods. *Trends Biotech.* **12**, 268–275.
Gilbert, W., and de Souza, S. J. (1999). Introns and the RNA world. In *The RNA World* (R. F. Gesteland, T. R. Cech and J. F. Atkins, eds.) 2nd edition, pp. 221–231. Cold Spring Harbor Press, Cold Spring Harbor, NY.
Joyce, G. F. (1992). Directed molecular evolution. *Sci. Am.* **267**, 90–97.
Lilley, D. M. (2003). The origins of RNA catalysis in ribozymes. *Trends Biochem. Sci.* **28**, 495–501.
Wilson, D. S., and Szostak, J. W. (1999). In vitro selection of functional nucleic acids. *Ann. Rev. Biochem.* **68**, 611–647.

Biography

Niles Lehman is an Associate Professor in the Department of Chemistry at Portland State University in Portland, Oregon. His principal research interests are in molecular evolution and the origins of life on the Earth. He holds a Ph.D. from the University of California, Los Angeles and received postdoctoral training at The Scripps Research Institute and the University of Oregon. He is an associate editor of the *Journal of Molecular Evolution*, and his laboratory has pioneered the studies on RNA-directed recombination of RNA.

RNA Editing

Charles E. Samuel
University of California, Santa Barbara, California, USA

RNA editing is the posttranscriptional modification of an RNA nucleotide sequence at one or more positions. There are two general types of RNA editing, viz., substitution editing and insertion/deletion editing. RNA editing of either type leads to the formation of transcripts whose sequence differs from that found in the genome. Such RNA sequence differences between mature transcript and encoding genome represent a form of genetic recoding. The sequence changes generated by RNA editing are different from those arising from 5′-capping, 3′-polyadenylation, and splicing, processing events that also may occur as part of mRNA biogenesis. RNA editing is widely observed in eukaryotic organisms and their viruses. Editing, like splicing, represents a form of processing that has the capacity to amplify genetic diversity and product function by altering the information transfer process at the posttranscriptional level of gene expression.

Discovery of RNA Editing

RNA editing was discovered in a unicellular protozoan. The frameshifted cytochrome oxidase *coxII* transcript of trypanosome mitochondria was found to contain four inserted uridines that were not encoded by the genomic DNA. Then editing by nucleotide substitution was found in two mammalian RNAs. The apolipoprotein B (apoB) mRNA in mouse intestine had a translation stop codon at a position in the mature mRNA, where the genomic DNA specified the amino acid glutamine, and the glutamate-gated ion channel (GluR-B) mRNA in mouse brain had the amino acid arginine in place of the genome-encoded glutamine at the same position. Several biochemical mechanisms account for the RNA editing identified in mRNA transcripts. These include A-to-I substitution editing; C-to-U substitution editing; U insertion/deletion editing; C insertion editing; and G insertion editing. In addition, 2′-O-methyl ribose nucleotide modification and uridine to pseudouridine conversion represent editing events mediated by complexes of small nucleolar RNA (snoRNA) cofactor guides and associated proteins that modify ribosomal RNAs and other RNAs. This article will focus on A-to-I and C-to-U RNA editing that occur by selective RNA-specific deamination reactions that lead to nucleotide substitutions. Genetic recoding by such substitution editing can create gene products with altered sequence and hence altered function.

Adenosine-to-Inosine Substitution RNA Editing

RNA Substrates that Undergo A-to-I Editing

RNA editing by adenosine (A) to inosine (I) substitution is catalyzed by C6-adenosine deaminases that act on double-stranded RNA substrates (Figure 1A). A-to-I editing occurs in several eukaryotes including *Caenorhabditis* (nematode worm), *Drosophila* (fruit fly), and *Xenopus* (frog) in addition to mammals and their viruses. Among mammalian RNAs, transcripts encoding glutamate-receptor (GluR) channels of the α-amino-3-hydroxy-5-methyl-isoxaole-4-propionate (AMPA) and kainate GluR receptor subtypes represent one of the best-understood cases of A-to-I editing. This is illustrated by the AMPA receptor subunit B (GluR-B), one of four GluR subunits. Exon 11 possesses a genome-encoded glutamine (Q) codon (CAG) in unedited GluR-B transcripts. This exon codes for a hydrophobic domain (TM2) that loops into the cytoplasmic membrane. The edited GluR-B mRNA possesses an arginine (R) codon (C*I*G) at the same codon position, because I is recognized as G by decoding ribosomes during the translational process. Editing at this site, known as the Q/R site, occurs almost completely in the brain of adult rodents. Q/R editing of GluR-B affects channel subunit assembly in a manner that results in reduced permeability to Ca^{++} ions. A second A-to-I editing site in GluR RNA, termed the R/G site, involves the conversion of a genome-encoded arginine (R) codon (*A*GA) to a glycine (G) codon (*I*GA) in exon 13 of edited GluR-B, -C, and -D subunit transcripts. Editing at the R/G site controls the kinetic properties of AMPA receptor channels and leads to faster recovery rates from receptor desensitization.

Editing of GluR-B occurs at the pre-mRNA level within the nucleus, prior to splicing. RNA elements

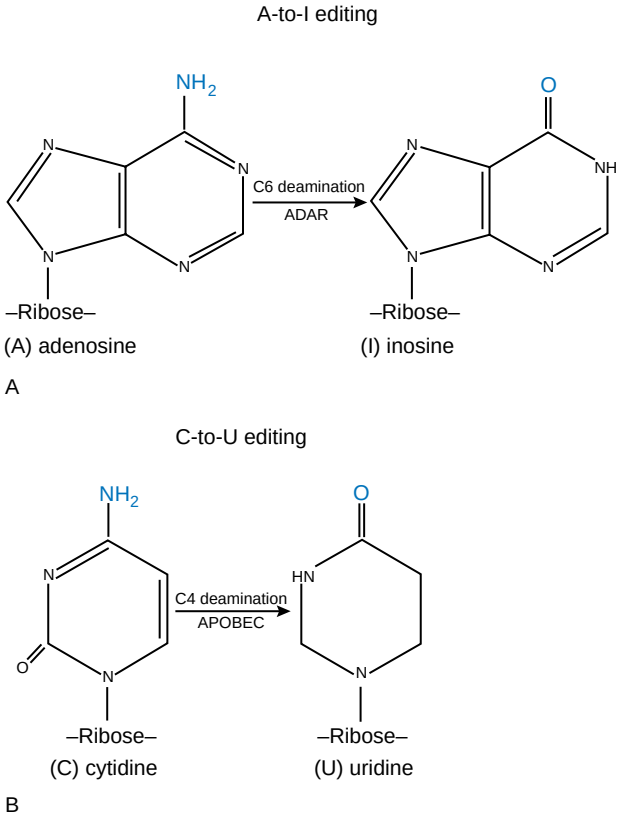

FIGURE 1 Substitution RNA editing by hydrolytic deamination. (A) A-to-I RNA editing involves the C6 deamination of adenosine to generate inosine catalyzed by ADAR enzymes. (B) C-to-U RNA editing involves the C4 deamination of cytidine to generate uridine catalyzed by APOBEC enzymes.

dictate the specificity of editing at the Q/R and R/G sites. The elements consist of unique *cis*-acting complementary inverted repeat sequences that are present in the intron adjacent to the exon possessing the edited adenosine. For the Q/R site in exon 11, the inverted repeat in intron 11 is predicted to form an imperfect duplex structure spanning the edited "A" at the Q/R site. A similar duplex RNA structure also exists within exon 13 containing the R/G site and the proximal portion of the adjacent intron 13. These exon–intron double-stranded RNA structures are absolutely essential for efficient editing at the Q/R and R/G sites of GluR-B.

The serotonin (5-hydroxytryptamine)-2C receptor (5-HT_{2c}R) provides another example of a neurotransmitter receptor whereby A-to-I editing of the pre-mRNA prior to splicing leads to amino acid substitutions in the encoded protein that alter activity. In the case of rat 5-HT_{2c}R pre-mRNA, four selective A-to-I editing sites denoted A, B, C, and D have been identified in exon 3 that specify three amino acid substitutions. The 5-HT_{2c}R genomic sequence specifies the sequence …AUA CGU AAU CCU AUU… that encodes …*ile*-arg-*asn*-pro-*ile*… in the unedited RNA. Editing of the four sites leads to the sequence …IUI CGU AIU CCU IUU… in fully edited RNA that encodes …*val*-arg-*ser*-pro-*val*… The three amino acid substitutions created by A-to-I editing of 5-HT_{2c}R transcripts occur in the putative intracellular loop II of the receptor and they cause an ~tenfold reduction in G protein-mediated signaling. Here again, the selective editing of 5-HT_{2c}R pre-mRNAs is dictated by imperfect inverted repeat sequence that forms an RNA duplex between the 3′-end of exon 3 spanning the four editing sites and the 5′-end of the adjacent intron-3.

One of the challenges of A-to-I editing is to identify additional substrates. The GluR-B and 5-HT_{2c}R substrates in rodents and humans were identified serendipitously. In *Drosophila*, a comparative genomics approach has identified 16 new targets for A-to-I editing; all were voltage-gated ion channels, ligand-gated ion channels, or part of the synaptic release machinery.

Adenosine Deaminases that Act on RNA

A-to-I editing events of substrates such as GluR-B and 5-HT_{2c}R are catalyzed by a multigene family of enzymes known as ADARs, *a*denosine *dea*minases that act on *R*NA. Two mammalian genes are known to encode catalytically active deaminases, *ADAR1* and *ADAR2*, that efficiently deaminate both synthetic and naturally occurring double-stranded RNA substrates (Figure 2). The ADAR1 and ADAR2 enzymes show different activities for the different sites in the GluR-B and 5-HT_{2c}R transcript RNAs. The ADAR2 deaminase efficiently edits the Q/R site of GluR-B, but the ADAR1 enzyme possesses little editing activity at Q/R. Both ADAR1 and ADAR2, however, are capable of editing the R/G site of GluR-B. For 5-HT_{2c}R, ADAR1 very efficiently edits the A site but is inactive for the D site, whereas ADAR2 efficiently edits the D site. ADAR1 and ADAR2 possess multiple copies of a canonical double-stranded RNA-binding motif (R, dsRBM) that are located in the central region of the protein. The interferon inducible form of ADAR1 possesses, in addition to the R motifs, two copies of a Z-DNA-binding motif (Zα and Zβ) in the N-terminal region of the protein. The dsRNA- and Z-DNA-binding motifs of ADAR1 are distinct from the deaminase catalytic domain located in C-terminal region of the ADAR proteins (Figure 2). The dsRNA-binding motifs are presumed to play a role in the binding of substrate RNAs, but it is also possible that they too play a role in regulation of enzymatic activity. For example, adenovirus VA_I RNA, a small and highly structured viral gene product transcribed by cellular RNA polIII, efficiently antagonizes ADAR deaminase activity.

The expression of ADAR enzymes in cells is a complex process. For example, in the case of the

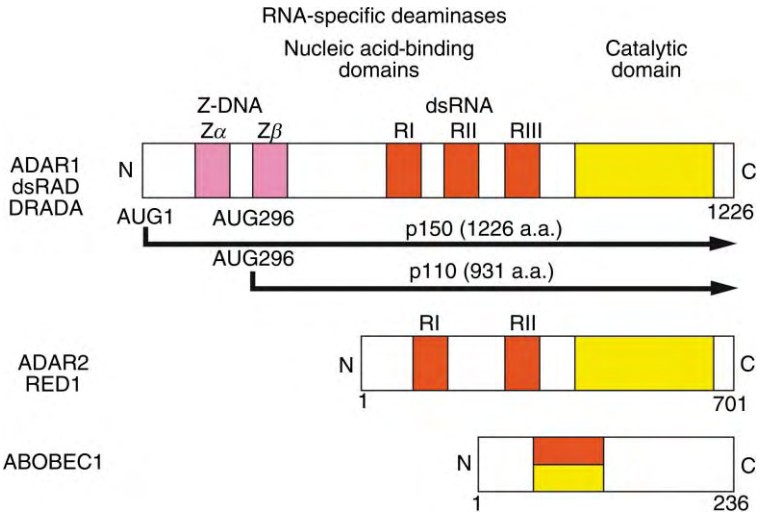

FIGURE 2 Schematic structure of mammalian RNA-specific deaminases. ADAR1 and ADAR2 possess double-stranded RNA-binding (R) motifs (red) and Z-DNA-binding motifs (pink). The RNA-binding motif of APOBEC1 overlaps with the catalytic domain. The catalytic domains of ADAR and APOBEC are shown in yellow. Two size forms of ADAR1 are expressed, the larger p150 interferon inducible form and the smaller constitutive p110 form. ADAR2 and APOBEC1 are not known to be regulated by cytokines or growth factors.

human *ADAR1* gene, alternative promoters including one inducible by interferons together with alternative exon 1 splicing give rise to two differently sized enzyme isoforms, p150 and p110 (Figure 2). The interferon inducible form of ADAR1, p150, is found in both the cytoplasm and nucleus of cells. The constitutive p110 form, which lacks the N-terminal 295 amino acids that includes the Zα-binding motif, is found predominantly if not exclusively in the nucleus. Additional ADAR protein multiplicity is achieved by alternative splicing involving downstream exons, both in the case of ADAR1 and ADAR2. The physiological significance of the splice variants of ADAR is not known; one possibility may relate to the substrate selectivity of the enzymes.

Cytidine-to-Uridine Substitution RNA Editing

RNA Substrates that Undergo C-to-U Editing

Cytidine (C) to uridine (U) substitutional RNA editing is catalyzed by C4-cytidine deaminases that act on single-stranded RNA substrates (Figure 1B). C-to-U editing has been characterized in both plants and mammals. One of the best-understood examples is the mammalian mRNA transcript that encodes apolipoprotein B (apoB) that functions in lipid metabolism. There are two forms of apoB. The larger form (apoB100) is synthesized in the liver and assembled into lipoprotein particles that are secreted into the bloodstream. The carboxyl terminal region of apoB100 interacts with the low-density lipoprotein receptor to remove LDL from circulation. Editing of apoB mRNA by deamination of a single cytidine changes a genome-encoded glutamine codon (*CAA*) to a translation termination codon (*UAA*). This C-to-U editing happens in the small intestine but not the liver. ApoB RNA editing causes the synthesis of a truncated intestinal lipoprotein known as apoB48 that lacks the C-terminal region of apoB100, but otherwise is identical to the N-terminal 48% of apoB100. While apoB100 is associated with LDL protein particles, apoB48 is associated with chylomicron and lacks receptor-binding activity.

Editosome Complex

C-to-U editing of apoB mRNA occurs in the nucleus and is selective for spliced transcripts rather than pre-mRNAs. Deamination is mediated by a multiprotein complex as illustrated by the schematic diagram shown as Figure 3. This complex, called an editosome, includes a protein that possesses catalytic activity (*Apo*lipoprotein *B E*diting Catalytic subunit 1, APOBEC-1) together with one or more associated proteins that include an *a*pobec-1 *c*ompetence *f*actor (ACF), which possesses RNA-binding activity. Unlike the ADARs, APOBEC does not possess a separate canonical RNA-binding motif, but rather RNA-binding activity overlaps with the catalytic domain residues (Figure 2). A tripartite RNA motif that includes efficiency elements, spacer, and a mooring sequence surrounds the edited nucleotide C6666 of apoB mRNA and appears sufficient to confer the required specificity in the C-to-U editing reaction. ACF protein binds apoB RNA selectively at the region of the editing site and interacts with APOBEC-1 deaminase to mediate C-to-U editing activity. Multiple

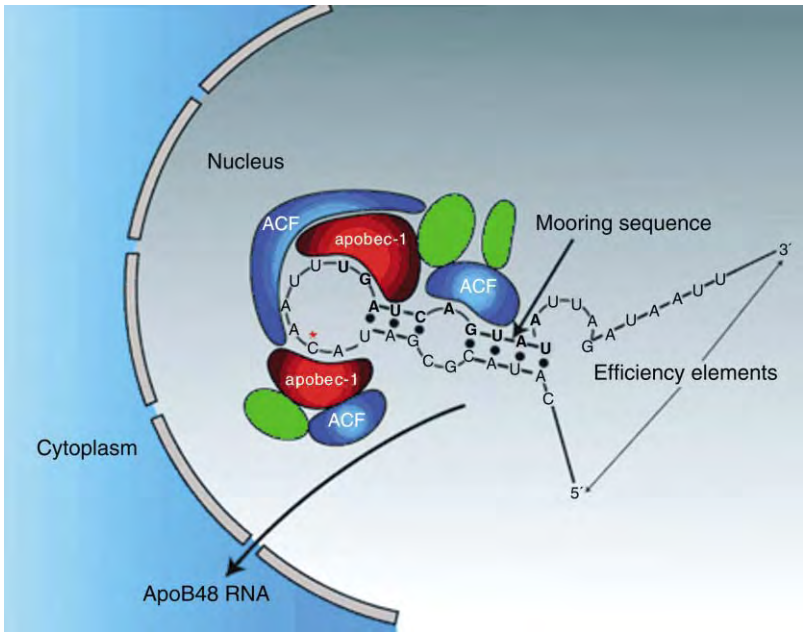

FIGURE 3 Model for C-to-U editing of apolipoprotein B mRNA. The schematic representation shows the APOBEC-1 enzyme (red) and ACF competence factor (blue) binding to the apoB RNA both 5′ and 3′ to the edited C. Additional proteins (green) may modulate assembly of the editosome complex. The mooring sequence is shown in bold font. (Reprinted from Blanc, V., and Davidson, N. O. (2003). C-to-U RNA editing: Mechanisms leading to genetic diversity. *J. Biol. Chem.* **278**, 1395–1398, with permission of the American Society for Biochemistry & Molecular Biology.)

splice variants of the ACF protein are found in different human tissues, but their functional significance remains unknown. Likewise, several homologues of the APOBEC-1 catalytic deaminase have been identified including ARCD1/APOBEC-2, AID, and phorbolin/ARCD2-7/APOBEC-3A to G. The target substrates and physiologic roles of the many APOBEC homologue proteins in RNA editing are not yet well defined.

The existence of multiple APOBEC-1 homologues and ACF variants points to the existence of primary substrates beyond apoB mRNA that may undergo C-to-U editing. One candidate for site-specific cytidine deamination is the cellular mRNA for the neurofibromatosis type 1 (NF1) protein encoded by NF1 tumor suppressor gene. This protein, neurofibromin, functions as a Ras-GTPase-activating protein (GAP). Site-specific deamination of a cytidine (nucleotide C3916) in NF1 mRNA converts a genome coded arginine codon (*C*GA) to a translation termination codon (*U*GA). The shortened NF1 open reading frame that results from this C-to-U editing has been observed in neuronal tissue from NF1 patients and is predicted to give rise to a truncated neurofibromin protein product deficient in GAP activity.

Substitution Editing of Viral RNAs

RNA editing may play a significant role in viral pathogenesis and affect the host response to viral infection. A number of viral RNAs, including those of avian leukosis virus (ALV), hepatitis delta virus (HDV), measles virus, parainfluenza virus 3, polyoma virus, respiratory syncytial virus, and vesicular stomatitis virus, all show codon changes under certain infection conditions that are consistent with A-to-I editing. The best-characterized viral RNA substrate is that of HDV. Both ADAR1 and ADAR2 convert an amber translation stop codon (UAG) to a tryptophan codon (UIG) in HDV antigenomic RNA. This editing allows for the synthesis of two delta virus antigen forms, a short form used in viral replication and a long form necessary for assembly of viral particles. A viral RNA candidate for A-to-I editing is that of measles virus (MV), where viral RNAs isolated from brains of persistently infected subacute sclerosing panencephalitis (SSPE) patients, possess multiple sequence differences from the viral RNA genome that correspond to A-to-G and U-to-C substitution mutations. Because MV, a negative-strand RNA virus, replicates in the cytoplasm, it is presumed that ADAR1 is the responsible enzyme. The DNA virus vaccinia that also replicates in the cytoplasm of cells encodes a protein product (E3L) that efficiently antagonizes ADAR1 deaminase activity, and mutations in E3L are known to affect viral pathogenesis in the mouse model.

Finally, C-to-U RNA editing like A-to-I editing may play a role in the interactions between viral pathogens and their hosts. Among the homologues of APOBEC-1, the APOBEC-3G gene product has been shown to possess broad anti-retroviral activity. The antiviral effects of APOBEC-3G appear to result from the generation of biased G to A hypermutations that impair

virus replication in a manner that, in the case of human immunodeficiency virus, is modulated by an accessory protein of the virus known as Vif.

Editing by Nucleotide Insertion/Deletion

A second general type of RNA editing, in addition to base substitution editing, is nucleotide insertion/deletion editing. Among the best-characterized examples of insertion/deletion editing is that of U-insertion and U-deletion. Uridine insertion/deletion editing occurs by an enzymatic cleavage-ligation mechanism. The specificity of U-insertion/deletion editing is determined by RNA–RNA base pairing between a complementary guide RNA (gRNA) and the target RNA (mRNA) substrate. The base-paired RNA complex serves to position the enzymatic machinery at the site of U insertion or deletion, thereby "guiding" the modification process. Much has been learned from the trypanosome mitochondrial system about the features and requirements of the complimentary gRNAs that act in trans to target enzyme complexes to the mRNA site of uridine insertion/deletion editing. The enzymatic cleavage-ligation mechanism of U insertion/deletion editing involves hybridization of gRNA to mRNA to form a gRNA:mRNA anchor duplex, after which the mRNA is specifically cleaved by a gRNA-dependent ribonuclease at the site of the gRNA:mRNA mismatch. For U-insertion editing, a 3′-terminal uridylyl transferase (TUTase) then adds U's to the 3′-end of the 5′-fragment guided by base pairing with the gRNA, followed by ligation of the two fragments by an RNA ligase. For U-deletion editing, a U-specific 3′-5′ exonuclease removes the bulged U residues, followed by ligation of the two RNA fragments. Finally, in addition to U-insertion editing as exemplified by the cytochrome oxidase mRNA in trypanosome mitochondria, C-insertion editing and G-insertion editing also are known to occur as illustrated by Physarum mitochondria and by negative-strand RNA viruses, respectively. In the case of paramyxoviruses such as Sendai virus, G-nucleotide insertion occurs during the RNA transcription process to generate edited P/C mRNA that includes nontemplated Gs.

Roles of RNA Editing

Altering the information transfer process at the post-transcriptional level of gene expression by RNA editing represents an important strategy for amplifying genetic diversity and modifying the functions of products encoded by an organism's genome. Some of the mechanistic roles that substitution editing through A-to-I and C-to-U deamination play, or are anticipated to play, in biological processes are summarized in Figure 4. These biochemical mechanisms include effects of editing on mRNA translation, pre-mRNA splicing, RNA degradation, RNA replication, and RNA structure that result from nucleotide substitution via deamination or nucleotide insertions. Site-specific editing may change the coding potential of mRNA transcripts, leading to proteins with altered function due to amino acid substitutions following A-to-I editing. This is exemplified

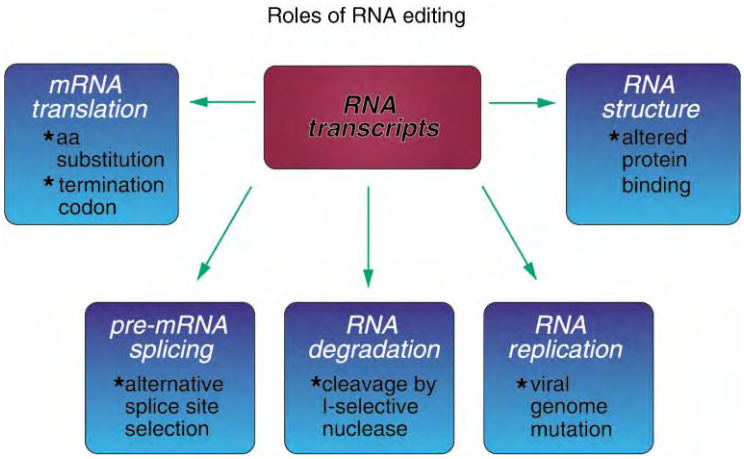

FIGURE 4 Established and potential roles of RNA editing by deamination. Edited RNA transcripts (A-to-I; C-to-U) possess different sequences than their unedited transcript counterparts, and hence may display different functional activities than that shown by the unedited transcripts. Editing may alter processes including mRNA translation, by changing codons and hence coding potential; editing may alter pre-mRNA splicing patterns by changing splice site-recognition sequences; editing may affect RNA degradation by modifying RNA sequences involved in nuclease recognition; editing may affect viral RNA genome stability by changing template and hence product sequences during RNA replication; and, editing potentially may affect RNA structure-dependent activities that entail binding of RNA by proteins. (Reprinted from Samuel, C. E. (2003). RNA editing minireview prologue. *J. Biol. Chem.* **278**, 1389–1390, with permission of the American Society for Biochemistry & Molecular Biology.)

by the GluR-B and serotonin-2c receptor proteins. Introduction or removal of translation termination codons may also occur, as exemplified by apoB and NF1 mRNAs where C-to-U editing generates UAA and UGA translation termination codons respectively, and HDV RNA where A-to-I editing converts an amber UAG stop to a tryptophan codon. ADAR2 edits its own transcript, to create an alternative splice acceptor site; and, a novel ribonuclease selective for inosine-containing RNAs has been described, consistent with the notion that A-to-I edited transcripts may be degraded preferentially relative to the unedited transcripts. For viral RNAs, deaminations in either the plus- or minus-strand RNA could lead to mutations in the encapsidated viral genome sequence. Finally, sequence changes resulting from editing may subsequently affect RNA structure and function, including protein–RNA interactions (Figure 4).

See Also the Following Articles

Nuclear Pores and Nuclear Import/Export • Pre-tRNA and Pre-rRNA Processing in Eukaryotes • Ribozyme Mechanisms • tRNA Synthetases

Glossary

adenosine-to-inosine (A-to-I) editing The deamination of adenosine (A) to yield inosine (I), which is recognized as G rather than A, and hence represents a kind of base substitution RNA editing.

cytidine-to-uridine (C-to-U) editing The deamination of cytidine (C) to yield uridine (U), which is a kind of base substitution RNA editing.

deamination editing The replacement of the amino group of adenosine (A) with oxygen from water to generate inosine (I), or in the case of cytidine (C) to generate uridine (U).

edited RNA RNA transcript in which the RNA nucleotide sequence differs from that of the encoding genome sequence at one or more sites, either by base substitution or by nucleotide insertion/deletion.

RNA editing The posttranscriptional modification of an RNA nucleotide sequence by base substitution or by nucleotide insertion/deletion.

unedited RNA RNA transcript in which the nucleotide sequence corresponds to that encoded by the genome.

Further Reading

Bass, B. L. (2002). RNA editing by adenosine deaminases that act on RNA. *Annu. Rev. Biochem.* **71**, 817–846.

Blanc, V., and Davidson, N. O. (2003). C-to-U RNA editing: Mechanisms leading to genetic diversity. *J. Biol. Chem.* **278**, 1395–1398.

Decatur, W. A., and Fournier, M. J. (2003). RNA-guided nucleotide modification of ribosomal and other RNAs. *J. Biol. Chem.* **278**, 695–698.

Gott, J. M., and Emeson, R. B. (2000). Functions and mechanisms of RNA editing. *Annu. Rev. Genet.* **34**, 499–531.

Maas, S., Rich, A., and Nishikura, K. (2003). A-to-I RNA editing: Recent news and residual mysteries. *J. Biol. Chem.* **278**, 1391–1394.

Reenan, R. (2001). The RNA world meets behavior: A to I pre-mRNA editing in animals. *Trends Genet.* **17**, 53–56.

Samuel, C. E. (2001). Antiviral actions of interferons. *Clin. Microbiol. Rev.* **14**, 778–809.

Samuel, C. E. (2003). RNA editing minireview prologue. *J. Biol. Chem.* **278**, 1389–1390.

Seeburg, P. H., and Hartner, J. (2003). Regulation of ion channel/neurotransmitter receptor function by RNA editing. *Curr. Opin. Neurobiol.* **13**, 279–283.

Simpson, L., Sbicego, S., and Aphasizhev, R. (2003). Uridine insertion/deletion RNA editing in trypanosome mitochondria: A complex business. *RNA* **9**, 265–276.

Biography

Charles Samuel is the C. A. Storke II Professor and Chair of the Department of Molecular, Cellular, and Developmental Biology at the University of California, Santa Barbara. His research concerns the mechanisms of interferon action, including the modification of RNA by editing. He holds a Ph.D. in biochemistry from the University of California, Berkeley, was a Damon Runyon Scholar at Duke University Medical School, and has authored more than 150 research publications in the fields of virology and biochemistry.

RNA Polymerase I and RNA Polymerase III in Eukaryotes

Robert J. White
University of Glasgow, Glasgow, UK

RNA polymerases are the enzymes responsible for synthesizing RNA, in a process called transcription. They use DNA as a template, and the RNA they produce carries a faithful copy of the genetic information contained in the template. Whereas bacteria use a single RNA polymerase to transcribe all their genes, the nuclei of eukaryotes contain three. Each is responsible for transcribing a unique set of essential genes. RNA polymerase I synthesizes most of the rRNA, RNA polymerase II synthesizes the protein-encoding mRNA and most snRNA, while RNA polymerase III synthesizes a variety of small untranslated RNAs, including tRNA and 5S rRNA. An additional RNA polymerase is present in mitochondria, which carry a small DNA molecule of their own. This division of labor could have become necessary as genomic complexity increased during evolution. In actively growing cells, RNA polymerase I can be responsible for ~70% of all nuclear transcription, whereas RNA polymerases II and III contribute ~20% and 10%, respectively.

Genes Transcribed by RNA Polymerases I and III

Despite its very high activity, RNA polymerase I only transcribes a single type of gene, which encodes the large rRNA precursor molecule. This precursor is then processed into the mature 5.8S, 18S, and 28S rRNA components of ribosomes. A single molecule of each of these rRNAs, along with a 5S rRNA molecule and ~85 proteins, is incorporated into each ribosome. The pre-rRNA is encoded by multiple gene copies, the number of which varies between different organisms; mammals have ~150–200 copies arranged in tandem head-to-tail arrays.

The genes transcribed by RNA polymerase III are invariably very short, rarely exceeding 300 bp in length. Many of their products have essential functions, such as the 5S rRNA and tRNAs (required for protein synthesis), 7SL RNA (involved in intracellular trafficking of proteins as part of the signal recognition particle), and the U6, MRP, and H1 RNAs (involved in the processing of mRNA, rRNA, and tRNA, respectively). Mammalian genomes also contain large numbers of short interspersed repeats (SINEs) that are transcribed by RNA polymerase III, such as the Alu family in man. In addition, certain viruses carry genes that are transcribed by RNA polymerase III, such as the VA genes of adenovirus and the EBER genes of Epstein–Barr Virus. The products of these viral genes can subvert the translational machinery of an infected cell, diverting it towards the more effective production of viral proteins.

Nucleoli

Within the nucleus, the most obvious landmarks under a light microscope are nucleoli, because of their high density. These form around the actively transcribed rRNA gene repeats and contain closely packed molecules of transcribing RNA polymerase I, each with a nascent pre-rRNA attached. Furthermore, ribosomal proteins assemble on the nascent transcript whilst it is being made. Although nucleoli have the appearance of organelles, they are in fact dynamic structures without membranes that disappear when transcription stops (e.g., during the general suppression of gene expression that accompanies mitosis). Transferring rRNA genes to a novel chromosomal location can result in the appearance of an ectopic nucleolus. When cells become very old, their nucleoli fragment; it has been suggested that nucleolar degeneration may be an important aspect of cellular aging.

The RNA Polymerase Molecules

RNA polymerases I, II, and III are large and complex proteins, consisting of 14, 12, and 17 subunits, respectively. Five of these subunits are shared, and a further two are found in RNA polymerases I and III, but not in RNA polymerase II. The two largest subunits of each enzyme are unique, but share substantial homology with each other and also with bacterial RNA polymerases;

they fold together to provide the catalytic site of the enzyme. Besides these, RNA polymerases I, II, and III each have an additional set of unique subunits. Although most of the subunits are required for cell viability, their precise roles remain poorly characterized.

The RNA Polymerase I and III Transcription Apparatus

Despite their complexity, the nuclear RNA polymerases require considerable assistance to locate their genetic templates. Sets of transcription factor proteins assemble at promoter DNA sequences near the initiation sites of genes and then serve as molecular beacons which recruit the appropriate RNA polymerase.

For the large rRNA genes, promoter recognition is achieved by the homodimeric factor UBF that binds across the promoter region upstream of the transcription start site. UBF bends the DNA and wraps it around itself to create a three-dimensional nucleoprotein structure that is recognized by SL1, the factor responsible for polymerase recruitment. RNA polymerase I is pre-assembled with a polypeptide called Rrn3 that serves as an essential bridge between the polymerase and SL1 (Figure 1A). Several additional transcription factors are also associated with RNA polymerase I and are recruited with it in a concerted manner. Although these principles apply to mammals and frogs, the machinery required for rRNA synthesis is rather different in yeast. Indeed, the RNA polymerase I transcription apparatus is much less well conserved through evolution than those of RNA polymerases II or III; whereas human proteins can transcribe a yeast tRNA gene, they will not even recognize the large rRNA genes from mouse.

In the case of RNA polymerase III, two key transcription factors, TFIIIB and TFIIIC, play central roles in both yeast and man (Figure 1B). The former is responsible for recruiting RNA polymerase III and positioning it over the transcription initiation site; it also helps separate the two strands of the DNA helix, thereby facilitating the start of RNA synthesis. However, TFIIIB is unable to recognize the DNA sequences of most RNA polymerase III promoters, but must be brought into position through protein-protein interactions with DNA-bound TFIIIC. An unusual feature of this system is that the promoter sequences recognized by TFIIIC are located downstream of the transcription start site, within the transcribed region. Although in most cases TFIIIC binds directly to DNA, this is not possible for the 5S rRNA genes which have a distinct promoter arrangement. In these cases, an additional polypeptide, TFIIIA, binds along the DNA and provides a protein scaffold to which TFIIIC binds (Figure 1C). TFIIIA contains nine tandem copies of the zinc finger DNA-binding domain. Indeed, it was the

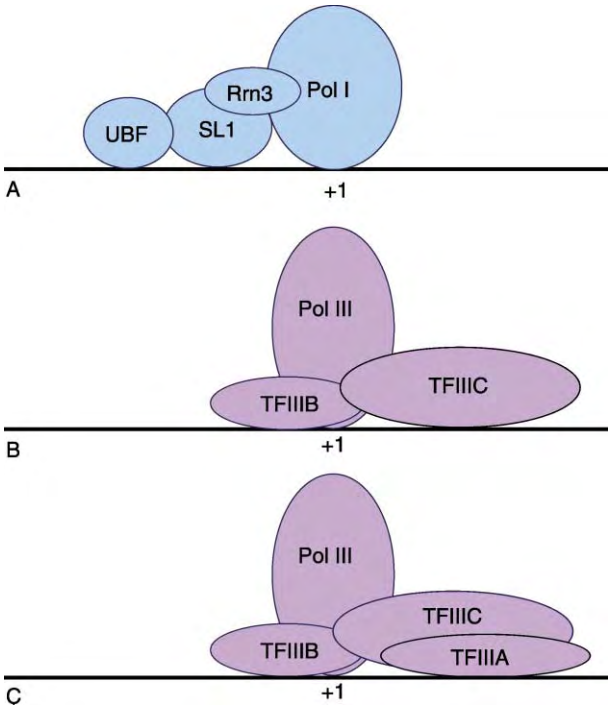

FIGURE 1 Simplified model of the transcription complexes used by RNA polymerases I and III. (A) UBF and SL1 assemble at the promoters of large rRNA genes and then recruit a preassembled complex containing Rrn3 and RNA polymerase I (Pol I), as well as additional factors not shown. (B) TFIIIC binds directly to the promoters of most genes transcribed by RNA polymerase III, e.g., tRNA genes. TFIIIB is recruited by protein/protein interactions with TFIIIC and then serves to bring RNA polymerase III (Pol III) to the transcriptional start site. (C) Similar events occur at 5S rRNA genes, but these are initiated by TFIIIA, which binds promoter DNA and provides a scaffold for TFIIIC assembly. + 1 denotes where transcription initiates.

founder member of the zinc finger family, the largest group of transcription factors in organisms ranging from yeast to man (~900 members in humans).

Alu Genes and Retrotransposition

The human genome carries over a million copies of the Alu gene, which provides ~10% of our total DNA. Despite their abundance, only small numbers of Alu genes are actually transcribed, the remainder being silenced through epigenetic mechanisms, including methylation and incorporation into repressive chromatin. SINEs propagate by retrotransposition, in which their RNA transcripts are copied into DNA and then inserted into novel genomic sites. These insertions occur preferentially into areas of active transcription, perhaps because of their more open and accessible chromatin structure. This increases the danger that integrating SINEs will disrupt genes at the recipient loci, thereby having a mutagenic effect. Indeed, cases of haemophilia,

neurofibromatosis, and breast cancer are believed to have arisen in this way. It is estimated that Alu insertions account for ~0.1% of all human genetic disorders. In contrast, retrotransposition is much more active in mice, where it may contribute ~10% of mutations.

RNA Polymerases I and III and Tumor Suppression

The RNA polymerase I and III transcription systems are both targeted directly by two key tumor suppressor products, p53 and RB. Both these proteins bind to TFIIIB and block its interactions with TFIIIC and RNA polymerase III, thereby repressing transcription. RB also binds to UBF to inhibit synthesis of large rRNA, whereas p53 inactivates SL1. The ability of RB and p53 to suppress the output of RNA polymerases I and III may contribute to their capacity to restrain cell growth. RB has been described as a gatekeeper that only allows cells to grow and proliferate when conditions are propitious. Inherited mutations in RB can cause the paediatric eye cancer retinoblastoma. Indeed, it is widely believed that RB function must be compromised in some way before any tumor can develop. The most commonly mutated gene in human cancer is p53, which is famous as "the guardian of the genome." If a cell's DNA gets damaged, for example, through exposure of skin to excessive doses of UV light, p53 gets activated and triggers a protective response; this can involve halting growth and cell cycle progression until the damage has been mended or, under extreme circumstances, apoptotic death. These responses ensure that DNA carrying potentially harmful mutations are not passed on to further generations of cells.

Links between Human Disease and RNA Polymerases I and III

RNA polymerases I and III together may contribute ~80% of nuclear transcription and provide ~95% of the total RNA in cells. This very high level of production is necessary to make the several million new ribosomes that are needed per generation to maintain protein synthetic capability. Because they are such major determinants of biosynthetic capacity, the activities of RNA polymerases I and III are closely linked to the rate of cellular growth. In hyperproliferative diseases such as cancer, there is generally an elevated rate of transcription by these polymerases. Indeed, pathologists use enlarged nucleoli (a sign of accelerated rRNA synthesis) as a diagnostic indicator of tumor formation. To a large degree, the elevated activity of RNA polymerases I and III in cancer cells is likely to reflect the inactivation of p53 and/or RB; since these tumor suppressors play a major role in restraining transcription by RNA polymerases I and III in healthy cells, their inactivation during cancer development will remove a major restraining influence and allow deregulated gene expression. These effects must be extremely widespread, since p53 is mutated in ~50% of human tumors and RB function may be compromised in all forms of malignancy. In addition to their release from these transcriptional repressors, the output of RNA polymerases I and III is also increased in some cancers through the action of certain oncogenic proteins. An example is c-Myc, which is deregulated in many tumor types and is believed to contribute to one in seven US cancer deaths. TFIIIB is bound and activated by c-Myc, leading to elevated rates of RNA polymerase III transcription. Certain types of cancer also produce abnormally high levels of the transcription factors used by RNA polymerases I and III. For example, UBF is frequently overexpressed in hepatocellular carcinomas, whereas TFIIIC is unusually abundant in ovarian tumors.

Epstein–Barr Virus is associated with gastric and nasopharyngeal carcinomas, Burkitt's lymphoma, Hodgkin's disease, and AIDS-associated lymphoma. Its most highly expressed gene products are the EBER RNAs, which are synthesized by RNA polymerase III. The presence of these transcripts is used diagnostically as a test for Epstein–Barr Virus. Indeed, very few other viral genes are expressed in Burkitt's lymphomas. Recent studies have shown that the EBER1 transcript can be sufficient for oncogenic transformation, a remarkable fact since it is only 167 nucleotides long. This provides the first reported example of an untranslated RNA that can transform cells.

An inherited-developmental disorder has been shown to result from mutations in the MRP gene that is transcribed by RNA polymerase III to produce a short RNA that is required for mitochondrial replication and for the processing of large rRNA. Families afflicted with this condition suffer from cartilage–hair-hypoplasia, a complex syndrome involving short stature (adult heights of 104-149 cm), abnormal cartilage, and hypoplastic hair, sometimes with a compromised immune system. This disorder is especially common amongst the Old Order Amish of Pennsylvania.

See Also the Following Articles

Nucleolus, Overview • RNA Polymerase II and Basal Transcription Factors in Eukaryotes

Glossary

chromatin The DNA wrapped up with proteins, as found in chromosomes.

promoter A stretch of DNA located near the transcription start site that influences the efficiency of transcription.

RNA polymerase The enzyme responsible for synthesizing RNA.

transcription The process using DNA as template to synthesize a complementary RNA.

transcription factor Protein that influences the ability of RNA polymerase to carry out transcription.

Further Reading

Batzer, M. A., and Deininger, P. L. (2002). Alu repeats and human genomic diversity. *Nat. Rev. Genet.* **3**, 370–380.

Carmo-Fonseca, M., Mendes-Soares, L., and Campos, I. (2000). To be or not to be in the nucleolus. *Nat. Cell Biol.* **2**, E107–E112.

Felton-Edkins, Z. A., Kenneth, N. S., Brown, T. R. P., Daly, N. L., Gomez-Roman, N., Grandori, C., Eisenman, R. N., and White, R. J. (2003). Direct regulation of RNA polymerase III transcription by RB, p53 and c-Myc. *Cell Cycle* **2**, 181–184.

Geiduschek, E. P., and Kassavetis, G. A. (2001). The RNA polymerases II transcription apparatus. *J. Molecul. Biol.* **310**, 1–26.

Moss, T., and Stefanovsky, V. Y. (2002). At the center of eukaryotic life. *Cell* **109**, 545–548.

Paule, M. R. (1998). *Transcription of Ribosomal Genes by Eukaryotic RNA Polymerase I*. Landes Biosciences, Austin.

Paule, M. R., and White, R. J. (2000). Transcription by RNA polymerases I and III. *Nucleic Acids Res.* **28**, 1283–1298.

Schramm, L., and Hernandez, N. (2002). Recruitment of RNA polymerase III to its target promoters. *Genes Develop.* **16**, 2593–2620.

White, R. J. (2001). *Gene Transcription: Mechanisms and Control*. Blackwell Science, Oxford.

White, R. J. (2002). *RNA Polymerase III Transcription*. Landes Biosciences, Austin, http://www.eurekah.com.

Biography

Robert J. White is Professor of Gene Transcription at the Institute of Biomedical and Life Sciences at the University of Glasgow, UK. His principal research interests concern transcription by RNA polymerases I and III, and how this is regulated in health and disease. Most noted for his work on RNA polymerase III and cancer, he was chosen by the European Association for Cancer Research as the Young Cancer Researcher of 2003.

RNA Polymerase II and Basal Transcription Factors in Eukaryotes

Joan Weliky Conaway and Ronald C. Conaway
Stowers Institute for Medical Research, Kansas City, Missouri, USA

In eukaryotes from yeast to man, synthesis of messenger RNA is catalyzed by the 12 subunit enzyme RNA polymerase II, with the assistance of a set of five basal transcription factors designated TFIIB, TFIID, TFIIE, TFIIF, and TFIIH. The basal transcription factors function together to promote proper binding of RNA polymerase II to the promoter-regulatory regions of genes and synthesis of the first few phosphodiester bonds of new transcripts.

Structure and Catalytic Activity of RNA Polymerase II

RNA polymerase II (pol II) is a DNA-dependent RNA polymerase that is responsible for transcription of protein-coding genes in the nucleus of eukaryotic cells. Pol II transcription results in synthesis of an RNA copy of the protein-coding DNA strand of genes. This primary RNA transcript is referred to as pre-mRNA and is subsequently spliced and polyadenylated to form mature mRNA, which can then be exported to the cytoplasm to direct translation of its protein products by the ribosomes. Pol II is capable of initiating transcription in a promoter-independent fashion on single-stranded DNA templates and of elongating transcripts on single- or double-stranded DNA templates without assistance from auxillary transcription factors. To initiate transcription from the promoters of protein-coding genes, however, pol II requires the assistance of a set of auxillary transcription factors referred to as the "basal" factors.

Pol II carries out initiation and synthesis of pre-mRNA by catalyzing DNA template-directed addition of single nucleotides to the 3′-end of growing transcripts. Pol II accomplishes this by catalyzing formation of phosphodiester bonds between the 3′-nucleotide of the transcript and incoming ribonucleoside triphosphates specified by the DNA. Phosphodiester bonds are formed by nucleophilic attack of the 3′-hydroxyl of the transcript on the α-phosphorus of the incoming ribonucleoside triphosphate, with the release of pyrophosphate. A remarkable feature of transcribing pol II is the enormous stability of the pol II–DNA–RNA ternary elongation complex, which can synthesize transcripts as long as the two-million-nucleotide *dystrophin* pre-mRNA without dissociating from the DNA.

Pol II is a multisubunit enzyme composed of ~12 subunits designated Rpb1–Rpb12, with sizes ranging from ~220 to ~10 kDa, respectively. Pol II is highly evolutionarily conserved from yeast to man. High-resolution X-ray crystal structures of free and transcribing *Saccharomyces cerevisiae* pol II have revealed that the two largest pol II Rpb1 and Rpb2 subunits associate with one another to form the core of the enzyme, with the remaining pol II subunits positioned on the outer surface of the Rpb1–Rpb2 core. The pol II catalytic site is contained within a positively charged cleft formed at the Rpb1–Rpb2 interface. The cleft extends from the enzyme's outer surface to the catalytic Mg^{2+} ion buried deep in the enzyme. The cleft is of sufficient size to accommodate as many as 20 bp of DNA. The catalytic Mg^{2+} ion participates directly in formation of phosphodiester bonds, most likely by coordinating the phosphates of the incoming ribonucleoside triphosphate in preparation for nucleophilic attack by the oxygen of the 3′-hydroxyl of the nascent transcript.

The X-ray crystal structure of the transcribing pol II–DNA–RNA ternary complex has revealed features of the complex that provide insights into the mechanism of pol II transcription. Approximately nine nucleotides of RNA at the 3′-end of the nascent pre-mRNA transcript are base-paired to the DNA in a DNA–RNA hybrid that holds the transcript's 3′-hydroxyl properly positioned with respect to the catalytic Mg^{2+} ion. Approximately 4 bp of DNA ahead of the 3′-end of the nascent transcript are unwound, providing the incoming ribonucleoside triphosphates with access to the single-stranded DNA template to ensure proper base-pairing with the template. The pre-mRNA is physically separated from the DNA–RNA hybrid ~10 nucleotides upstream of the transcript's 3′-end and exits the pol II catalytic site through a discrete RNA-binding groove in the enzyme. Finally, a large ~50 kDa clamp comprising portions

of the Rpb1, Rpb2, and Rpb3 subunits closes tightly around the DNA–RNA hybrid, providing a molecular explanation for the great stability and high processivity of the pol II–DNA–RNA ternary elongation complex.

Mechanism of Transcription Initiation by RNA Polymerase II

Synthesis of eukaryotic pre-mRNA by pol II requires that the enzyme finds and binds selectively to promoters located upstream of the protein-coding genes they control and, in most cases, buried amid thousands of base pairs of DNA separating adjacent genes on the chromosomes. Unlike most bacterial RNA polymerases, which are capable of recognizing and binding their promoters and initiating transcription pol II requires a minimum set of five basal transcription factors designated as TFIIB, TFIID, TFIIE, TFIIF, and TFIIH, which are necessary to direct selective binding of the enzyme to its promoters and to support transcription initiation. Like pol II, the basal factors exhibit a high degree of evolutionary conservation from yeast to man. The basal factors assemble with pol II at promoters into a stable preinitiation complex that can initiate transcription when provided with an ATP or dATP cofactor and the ribonucleoside triphosphates needed for RNA synthesis.

Pol II Promoters

Pol II promoters vary considerably from gene to gene and can include as little as a few hundred to many thousands of base pairs of DNA located upstream and even within or downstream of the genes they control. All pol II promoters include a "core" element, which surrounds the transcriptional start site and is sufficient to direct synthesis of accurately initiated transcripts. Core promoters include some combination of three types of promoter element: (1) an ~7 bp, degenerate motif called the TATA box, which is found from ~24 to ~30 bp upstream of the transcriptional start site and has the consensus sequence TATAAAA, (2) an initiator element (Inr), which surrounds the transcriptional start site and has the consensus sequence Y_{4-5}CANTY_{4-5} (where Y is a pyrimidine, and N can be any of the four bases A, C, G, or T), and (3) a 5 bp downstream promoter element or DPE, which is positioned at residues 28–32 bp downstream of the conserved A residue within the Inr. The consensus sequence for the *Drosophila melanogaster* DPE, which has been most thoroughly studied, is (A/G)G(A/T)Y(G/A/C).

In metazoans, a recognizable TATA element is found in a little less than half of the promoters examined, while Inr elements are included in ~70% of promoters. Some promoters have both a TATA element and an Inr, and others have only one or the other of these elements. DPEs are most commonly found in promoters that lack TATA boxes. Unlike the TATA or Inr elements, DPEs cannot function independently of other core promoter elements, but must be precisely positioned downstream of an Inr.

In addition to a core promoter, pol II promoters include additional DNA sequence motifs that serve as binding sites for one or more of the large number of DNA-binding transcriptional regulatory proteins that control the frequency of pol II transcription initiation from the core promoter. Among these DNA motifs are upstream promoter elements (UPEs), enhancers, and silencers. UPEs are typically clustered a few hundred base pairs upstream of the core promoter. Enhancers and silencers can be located thousands of base pairs upstream or downstream of the core promoter. Estimates suggest that as many as 10 000 human genes encode UPE, enhancer, and silencer DNA-binding proteins that function alone and in combination to fine tune the levels of pol II transcription of eukaryotic protein-coding genes.

Roles of the Basal Factors in Transcription Initiation by Pol II

Transcription initiation by pol II is a multistep process that begins with assembly of the enzyme with the basal factors at the core promoter to form a stable preinitiation complex and culminates with ATP (dATP)-dependent unwinding of core promoter DNA at the transcriptional start site, synthesis of the first few phosphodiester bonds of the nascent transcript, and escape of polymerase from the promoter. In the first step, the basal factor TFIID binds to the core promoter to form the nucleoprotein recognition site for pol II on the DNA. TFIID is a multisubunit protein composed of the TATA-box binding protein (TBP) and as many as 13 additional proteins designated TBP-associated factors (TAFs). The TBP subunit of TFIID binds directly to the TATA box and is capable of recognizing and binding stably to TATA boxes not only with the consensus TATAAA sequence, but also with a large number of divergent TATA-box sequences. The TFIID subunit TAF2 can bind in a sequence-specific manner to the Inr element surrounding the transcriptional start site. Although it is not yet clear how the DPE is recognized, some evidence suggests that the TFIID subunits TAF6 and TAF9 are located close to the DPE and may make sequence-specific contacts with it.

Once TFIID has bound the core promoter, the basal factor TFIIB recruits pol II to the TFIID–core promoter complex through specific protein–protein interactions with both the TBP subunit of TFIID and pol II. TFIIB is a small, modular protein of ~30 kDa with distinct

protein–protein interaction domains capable of interacting independently with TBP and pol II. Once pol II and TFIIB have bound to the TFIID–core promoter complex, TFIIF can enter the preinitiation complex. TFIIF is a two-subunit protein that strongly stabilizes binding of pol II to the core promoter. TFIIF is also required for stepwise entry of TFIIE and TFIIH into the pol II complex to form the fully assembled preinitiation complex. TFIIE is a two-subunit protein, and TFIIH is a nine-subunit protein possessing both DNA helicase and protein kinase activities. As a component of the preinitiation complex, the TFIIH DNA helicase catalyzes ATP(dATP)-dependent unwinding of core promoter DNA at the transcriptional start site to provide pol II access to a short stretch of single-stranded DNA to allow initiation of pre-mRNA synthesis.

See Also the Following Articles

DNA Helicases: Dimeric Enzyme Action • DNA Helicases: Hexameric Enzyme Action • RNA Polymerase I and RNA Polymerase III in Eukaryotes • RNA Polymerase II Elongation Control in Eukaryotes • RNA Polymerase II Structure in Eukaryotes

Glossary

basal transcription factors Minimal set of auxillary transcription factors required to support promoter-specific transcription initiation by pol II.

DNA helicase Enzyme that uses the energy of ATP(dATP) hydrolysis to unwind the two strands of DNA.

DNA template DNA that is transcribed by RNA polymerases.

promoter DNA sequences that direct RNA polymerases to transcribe genes.

RNA polymerase Enzyme that catalyzes synthesis of RNA.

Further Reading

Conaway, J. W., and Conaway, R. C. (1997). General transcription factors for RNA polymerase II. *Prog. Nucleic Acid Res. Mol. Biol.* **56**, 327–346.

Coulombe, B., and Burton, Z. F. (1999). DNA bending and wrapping around RNA polymerase: A "revolutionary" model describing transcriptional mechanisms. *Microbiol. Mol. Biol. Rev.* **63**, 457–478.

Cramer, P., Bushnell, D. A., and Kornberg, R. D. (2001). Structural basis of transcription: RNA polymerase II at 2.8 Angstrom resolution. *Science* **292**, 1863–1876.

Dvir, A., Conaway, J. W., and Conaway, R. C. (2001). Mechanism of transcription initiation and promoter escape by RNA polymerase II. *Curr. Opin. Genet. Develop.* **11**, 209–214.

Gnatt, A. L., Cramer, P., Fu, J., Bushnell, D. A., and Kornberg, R. D. (2001). Structural basis of transcription: An RNA polymerase II elongation complex at 3.3 Angstrom resolution. *Science* **292**, 1876–1882.

Smale, S. T., and Kadonaga, J. T. (2003). The RNA polymerase II core promoter. *Annu. Rev. Biochem.* **72**, 449–479.

Biography

Joan Weliky Conaway and Ronald C. Conaway are investigators at the Stowers Institute for Medical Research in Kansas City, Missouri. Research in their laboratory is aimed at contributing to an understanding of the molecular mechanisms that control the synthesis of eukaryotic messenger RNA. They hold Ph.D.s from the Stanford University School of Medicine.

RNA Polymerase II Elongation Control in Eukaryotes

David H. Price
University of Iowa, Iowa City, Iowa, USA

During the 1990s, it became clear that the elongation properties of RNA polymerase II are regulated and the factors responsible play a critical role in controlling gene expression in eukaryotic cells. One set of factors helps RNA polymerase II to negotiate pause and arrest sequences in the template and to maintain an elongation rate of 1000–1500 nucleotides per minute. The initiation factor TFIIF reduces RNA polymerase II pause times and stimulates the rate of elongation. The elongation factor S-II or (TFIIS) rescues polymerase molecules that are blocked from further elongation at arrest sites. Another set of factors is responsible for an elongation control process that regulates the fraction of initiated polymerases that enter productive elongation to generate mRNAs. Negative transcription elongation factors (N-TEFs), such as DSIF and NELF, slow the rate of elongation and restrict the polymerase to promoter proximal sequences. The positive transcription elongation factor, P-TEFb, overcomes the effect of the negative factors and allows the production of full length transcripts. The function of P-TEFb is regulated through interactions with many other transcription factors and the amount of active P-TEFb in the cell is precisely regulated through a reversible inhibition by the small cellular RNA, 7SK.

Historical Perspective

It has been clear for some time that much of the regulation of prokaryotic gene expression is accomplished by controlling the elongation potential of RNA polymerase, but only recently has it become apparent that eukaryotic gene expression is similarly regulated. Early work in John Lis's lab showed that there was an RNA polymerase II molecule engaged in transcription of the major *Drosophila* heat shock gene, HSP70, under conditions where no full length mRNAs were being produced. Only after heat shock were the polymerases allowed to continue elongation and produce mRNAs. Similarly, regulated premature termination of transcription was seen on a number of viral genes, most notably from HIV, as well as on cellular genes, including oncogenes such as c-myc and c-fos. In the early 1990s *in vitro* systems were beginning to reproduce the elongation control process and ultimately these systems allowed the identification and purification of some of the specific factors involved. The current model of RNA polymerase II elongation control has the look and feel of models of prokaryotic antitermination, but there are important differences in mechanistic details.

Positive and Negative Elongation Factors

Elongation Maintenance Factors

During transcription, RNA polymerase II is aided by specific factors as it encounters numerous blocks to elongation inherent in a template sequence. During normal transcription *in vivo*, each nucleotide addition to an RNA chain requires ~50 ms on average. However, *in vitro* RNA polymerase II may pause for seconds or minutes at specific sites in the absence of any accessory factors. TFIIF, a factor required for RNA polymerase II initiation, can also decrease the time that the polymerase spends at pause sites. This has the effect of increasing the overall elongation rate because, for the most part, the elongation rate is determined by how long the polymerase stops at the strongest pause sites. It has been hypothesized that the mechanism utilized by TFIIF involves an interaction-induced change in the polymerase from the paused conformation to the elongation competent form. Other factors that belong in this same class are ELL and elongin, but TFIIF has the most dramatic elongation stimulatory activity. The elongation factor S-II functions by a completely different mechanism. At some sites a fraction of RNA polymerase II molecules fall into an arrested conformation from which they cannot escape unaided. At these sites the 3′ end of the nascent transcript is removed from the active site of the polymerase as the polymerase "backslides" along the template while maintaining an RNA:DNA hybrid. When this happens, the polymerase may remain engaged for hours or days without extending the transcript. S-II stimulates an intrinsic ribonuclease activity of the

polymerase that removes the unpaired 3′ end of the transcript and puts the new 3′ end in register with the active site of the polymerase. This reactivates elongation and the polymerase has a second chance to pass the arrest site. Eventually, all polymerases can pass the arrest site although many may require several rounds of S-II-mediated transcript cleavage. Through the combined function of both classes of factors, the elongation rate of RNA polymerase II is maintained between 1000 and 1500 nucleotides per minute.

Elongation Control

In addition to the factors that maintain efficient elongation, there is another set of factors responsible for regulating the efficiency of initiated polymerases to reach the 3′ end of genes. This process has been termed RNA polymerase II elongation control and is best viewed as an obligatory event mediated by the default action of negative factors, N-TEFs, and the regulated action of a positive factor, P-TEFb (Figure 1). The process was demonstrated *in vitro* by first showing that the transcription inhibitor 5,6-dichlororibofuranosyl benzamidizole (DRB) could block the production of long, but not short transcripts. Elongation control was further characterized by the separation of N-TEFs, which direct polymerases to generate only short promoter proximal transcripts, from a positive factor, ultimately identified as P-TEFb, which reverses the action of the N-TEFs. A combination of the action of the N-TEFs and the activity of transcription termination factor 2 (TTF2) results in a process called abortive elongation characterized by the premature termination of transcripts before the mature 3′ end of the gene is reached. P-TEFb plays a key role in that it is responsible for the transition into productive elongation. Stated in another way, the ability to produce mRNAs is directly linked to the activity of P-TEFb. Elongation control machinery exists in all eukaryotic species that have been examined and the current evidence suggests that P-TEFb is required for transcription of most genes.

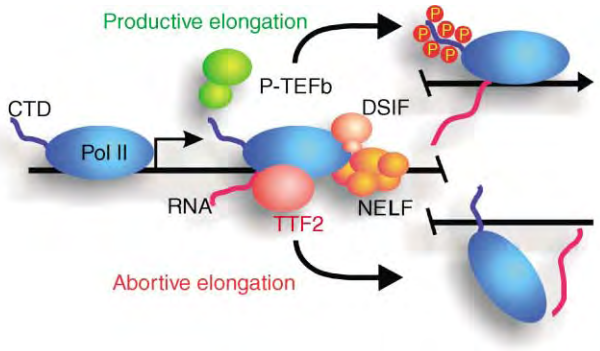

FIGURE 1 RNA polymerase II elongation control. After initiation pol II enters abortive elongation by default because of the action of N-TEFs, such as DSIF and NELF. Phosphorylation of the CTD of the large subunit of RNA polymerase II by P-TEFb causes the transition into productive elongation. If P-TEFb does not act, transcription is prematurely terminated by TTF2.

N-TEFs and Termination Factors

The evidence gathered so far points to the existence of two factors (DSIF and NELF) that play a negative role in elongation control. DSIF, the DRB sensitivity-inducing factor, was discovered as a protein required for DRB sensitive transcription *in vitro*. It is comprised of two subunits with strong sequence similarity to the yeast proteins SPT4 and SPT5. DSIF has almost no function on RNA polymerase II alone. The negative elongation factor (NELF) also has no effect on RNA polymerase II alone, but the combination of NELF and DSIF is able to slow the elongation rate and cause the polymerase to reside longer at pause sites. In this way, NELF and DSIF act in exactly the opposite way as TFIIF, which reduces pause time. NELF is comprised of four subunits, including a putative RNA-binding protein called RD. A defined elongation control system comprised of isolated RNA polymerase II elongation complexes (NELF, DSIF, and P-TEFb) displays many of the properties of elongation control seen when transcription is carried out in nuclear extract. DSIF is involved in controlling transcription from the HSP70 locus in *Drosophila*, but the generality of its function has not been demonstrated. Although removal of DSIF in *C. elegans* using RNAi techniques relieved most of the requirements of P-TEFb at a heat shock locus, similar results were not found in expression of several other genes. These facts along with the fact that homologues of NELF subunits have not been identified in many organisms suggest that other negative factors, which operate at a wide variety of genes, remain to be discovered.

So far only one transcription termination factor, TTF2 (formerly and uninformatively called factor 2), has been identified. It is a member of the SWI2/SNF2 family of proteins that are generally involved in disrupting protein nucleic acid interactions. It binds to both single- and double-strand DNA and has a strong dsDNA-dependent ATPase activity that is required for termination activity. The termination activity of TTF2 is inhibited by TFIIF, and while the mechanism of this inhibition is unknown, it provides a possible method to control the activity of TTF2 during transcription. The role of TTF2 seems to operate outside of the elongation control process in that its negative effect is not directly reversed by P-TEFb. However, a role for the factor in abortive elongation (premature termination) or in normal termination associated with mature 3′ end formation has not been ruled out.

P-TEFb

Subunits and Activity

P-TEFb is a cyclin-dependent kinase comprised of Cdk9 and one of several cyclin subunits. Three genes in humans – T1, T2, and K – encode cyclin subunits that can associate with and activate Cdk9. Two cyclin T genes have been found in *C. elegans*, but only one in *Drosophila*. Supporting a broad role in gene expression, knockout of Cdk9 in *C. elegans* causes loss of gene expression and death at the same early stage as knockout of one of the subunits of RNA polymerase II. The same lethal phenotype is observed when both cyclin T's are knocked out. The carboxyl terminal domain (CTD) of the large subunit of RNA polymerase II is phosphorylated by P-TEFb and this domain has been shown to be required for the function of P-TEFb in the transition into productive elongation. The CTD is comprised of multiple repeats of the heptapeptide YSPTSPS, and P-TEFb predominately phosphorylates the second serine. P-TEFb had been shown to have broad substrate specificity *in vitro* and will phosphorylate the large subunit of both DSIF and TFIIF. Although the CTD is phosphorylated by P-TEFb and is required for the function of P-TEFb in transcription, there may be other important functional phosphorylation targets. The effect of DRB on transcription is explained by the fact that it inhibits the kinase activity of P-TEFb. All P-TEFb inhibitors reduce the production of mRNAs *in vivo* and are lethal at high concentrations. Flavopiridol, the most potent P-TEFb inhibitor found, is in clinical trials against cancer.

Recruitment of P-TEFb

P-TEFb interacts in a functional way with a number of important transcription factors. Cyclin T1 interacts with the HIV transactivator Tat, and P-TEFb containing cyclin T1 can be recruited to elongation complexes on the HIV template through the interaction of Tat and cyclin T1 with a stem loop structure that forms in the nascent HIV transcript called TAR. This recruitment of P-TEFb activates transcription of the HIV genome. A cellular factor, CIITA, which is involved in activating transcription of the MHC class II genes, has also been shown to function through interaction with P-TEFb. That interaction is blocked in the presence of Tat suggesting that the binding site is similar for the viral and cellular protein and providing a mechanism for inhibition of MHC class II gene expression during HIV infection. Other transcription factors and enhancer binding proteins – including NFκB, c-myc, MCEF, and the androgen receptor – have been demonstrated to various degrees to have functional interactions with P-TEFb.

Recruitment of P-TEFb through artificial targeting to promoter DNA or to nascent RNA has revealed several important aspects of its function. First, when a protein is expressed in which Cdk9 or cyclin T1 or T2 is tethered to the DNA-binding domain of a yeast protein (Gal4) and the binding sites for that protein are placed close to a human promoter, transcription is stimulated from that promoter. Besides the core promoter elements, SP1 binding sites are also required to see an effect of the recruited P-TEFb in this system. This is consistent with the model for P-TEFb function because P-TEFb only affects polymerases that have already initiated and SP1 increases the initiation efficiency. Expression of Cdk9, cyclin T1, T2, or K tethered to an RNA-binding domain (e.g., HIV rev) activates transcription of a gene containing the appropriate RNA element. In both tethering experiments, the untethered component of P-TEFb is also recruited due to the inherent interaction between P-TEFb subunits. Cyclin K does not work when tethered to DNA elements because it lacks a CTD present on both cyclin T1 and T2 that plays another role by interacting with the CTD of the large subunit of RNA polymerase II.

Control of P-TEFb by 7SK

Very recently, the laboratories of Olivier Bensaude and Qiang Zhou simultaneously discovered the small cellular RNA, 7SK, in association with a fraction of P-TEFb in cells. The large complex containing P-TEFb and 7SK was relatively inactive compared to the free P-TEFb (Figure 2). Addition of small amounts of compounds that inhibit elongation by RNA polymerase II causes a reduction in the large form of P-TEFb *in vivo* and a concomitant increase in the small active form. Evidently, a cell will try to compensate for reduced production of mRNAs by activating more P-TEFb. The change in large to small form of P-TEFb can occur within minutes and is reversible. The significance of the large form of P-TEFb was demonstrated using a mouse model of cardiac hypertrophy. Heart cells that were stimulated to grow in size had an increase in P-TEFb activity, but no increase in the amount of P-TEFb. It was shown that all hypertrophic signals tested caused a release of 7SK. The signal transduction pathways involved in hypertrophy of cardiac cells at least partially routes through the elongation control pathway.

Integration of Elongation Control and Gene Expression

Elongation control may play a very significant role in controlling eukaryotic gene expression. Most RNA polymerase II molecules found transcribing human genes require the prior function of P-TEFb. Recruitment

FIGURE 2 Control of P-TEFb by 7SK. The amount of P-TEFb activity in the cell can be quickly adjusted by the reversible association of 7SK RNA. The large form with 7SK bound is inactive.

of P-TEFb by transcription factors allows specific genes to be targeted, and both the targeted and the untargeted functions of P-TEFb may allow global regulation of mRNA production. Regulating the conversion of the large to small P-TEFb form by signal transduction pathways is another global means to regulate mRNA levels. Overall, the combined action of negative and then positive factors results in a kinetic delay of the progression of polymerases down the gene. This may provide a window of opportunity for RNA processing machinery to function or associate with the elongating polymerase, ensuring a truly productive elongation event resulting in a complete, functional mRNA. The human capping enzyme is functionally coupled to transcription and guanylates the nascent transcript before P-TEFb acts. However, some components of the polyadenylation and splicing machinery have been shown to associate with the phosphorylated CTD. Perhaps the processing machinery is functionally coupled to transcription through interactions provided by elongation control and scans the nascent transcript for processing sites as it is being made. Many mechanistic details of how RNA polymerase II elongation control is accomplished and the ramifications of the process on subsequent events remain to be determined.

See Also the Following Articles

RNA Polymerase II and Basal Transcription Factors in Eukaryotes • RNA Polymerase II Structure in Eukaryotes

Glossary

DRB The P-TEFb inhibitor 5,6-dichlororibofuranosyl benzamidizole.

DSIF DRB sensitivity inducing factor, an N-TEF.

NELF Negative elongation factor, an N-TEF.

N-TEFs Negative transcription elongation factors.

P-TEFb Positive transcription elongation factor b composed of Cdk9 and a cyclin partner.

Further Reading

Marshall, N. F., and Price, D. H. (1992). Control of formation of two distinct classes of RNA polymerase II elongation complexes. *Mol. Cell Biol.* **12**, 2078–2090.

Nguyen, V. T., Kiss, T., Michels, A. A., and Bensaude, O. (2001). 7SK small nuclear RNA binds to and inhibits the activity of CDK9/cyclin T complexes. *Nature* **414**, 322–325.

Price, D. H. (2000). P-TEFb, a cyclin-dependent kinase controlling elongation by RNA polymerase II. *Mol. Cell Biol.* **20**, 2629–2634.

Sano, M., Abdellatif, M., Oh, H., Xie, M., Bagella, L., Giordano, A., Michael, L. H., DeMayo, F. J., and Schneider, M. D. (2002). Activation and function of cyclin T-Cdk9 (positive transcription elongation factor-b) in cardiac muscle-cell hypertrophy. *Nat. Med.* **8**, 1310–1317.

Shim, E. Y., Walker, A. K., Shi, Y., and Blackwell, T. K. (2002). CDK-9/cyclin T (P-TEFb) is required in two postinitiation pathways for transcription in the *C. elegans* embryo. *Genes Dev.* **16**, 2135–2146.

Zhu, Y., Pe'ery, T., Peng, J., Ramanathan, Y., Marshall, N., Marshall, T., Amendt, B., Mathews, M. B., and Price, D. H. (1997). Transcription elongation factor P-TEFb is required for HIV-1 tat transactivation in vitro. *Genes Dev.* **11**, 2622–2632.

Biography

David Price, Ph.D., is a Professor of Biochemistry at the University of Iowa. His interest is in understanding the basic mechanisms controlling eukaryotic gene expression. His laboratory focuses on postinitiation activities of RNA polymerase II, including elongation and termination, and how RNA processing and transcription are functionally coupled. The discovery of P-TEFb and its involvement in HIV in his laboratory is currently being extended by mechanistic studies concerning how HIV controls P-TEFb during infection.

RNA Polymerase II Structure in Eukaryotes

Patrick Cramer
University of Munich, Munich, Germany

RNA polymerase II (pol II) carries out transcription of protein-coding genes by catalyzing DNA-directed synthesis of messenger RNA. Detailed three-dimensional structures are now available for yeast pol II in free form, in form of a minimal elongation complex with bound nucleic acids, in an inhibited form with the bound toxin α-amanitin, and in complex with two additional subunits, Rpb4 and Rpb7. Together with functional data, these structures provide many insights into the mechanism of mRNA transcription.

Architecture

A ten-polypeptide pol II core enzyme is sufficient to elongate the RNA transcript. For transcription initiation, an additional two-subunit Rpb4/7 complex, and several general transcription factors are required. In the crystal structures of the pol II core, the two large subunits, Rpb1 and Rpb2 (Table I), form the central mass of the enzyme, and opposite sides of a positively charged "cleft" that contains the active center (Figure 1). The two large subunits are bridged on one side by a module of subunits Rpb3, Rpb10, Rpb11, and Rpb12. Around the periphery of the enzyme, Rpb5, Rpb6, and Rpb8 bind to Rpb1, and Rpb9 binds to both Rpb1 and Rpb2. The structures lack subunits Rpb4 and Rpb7, which form a stable heterodimer that can dissociate from the yeast pol II core. The structure of an archaeal Rpb4/7 counterpart revealed that Rpb7 spans the elongated heterodimer and is organized in two domains. The Rpb4 homologue forms a conserved hydrophobic interface with the Rpb7 homologue at the connection between the two Rpb7 domains. Recent structures revealed that the Rpb4/7 complex binds to the pol II core via subunit Rpb7 and that it protrudes from the pol II core surface near subunit Rpb6.

Structural Elements

The Rpb1 side of the pol II cleft is formed by a mobile clamp, whereas the Rpb2 side consists of the lobe and protrusion domains. The entrance to the cleft is formed between the upper and the lower jaw, which include subunits Rpb9 and Rpb5, respectively. The end of the cleft is blocked by a protein wall. The active center is at the floor of the cleft, between the protrusion, the wall, and the clamp. Before the active center and opposite of the wall, a long bridge helix spans the cleft. The bridge partially lines a pore in the active center, which widens toward the other side of the enzyme, creating an inverted funnel. The rim of the pore includes the highly conserved aspartate loop of Rpb1 that binds a catalytic Mg^{2+} ion, termed metal A. A second metal ion, metal B, is weakly bound next to metal A further in the pore. Both metal ions are accessible from one side.

The clamp is trapped in two different open states in the free core structures, but is rotated and closed in the structure of the pol II transcription–elongation complex that comprises template DNA and the RNA transcript. In this structure, the clamp binds the DNA template strand with three out of five switch regions. The switch regions form the base of the clamp, connecting to the remainder of pol II. Upon clamp closure, the switches change conformation or undergo folding transitions. The closed conformation of the clamp is also observed in the complete pol II that contains the Rpb4/7 complex. The Rpb4/7 complex appears to form a wedge between the clamp and subunit Rpb6, thus preventing clamp opening.

The Rpb1 polypeptide chain protrudes below the Rpb4/7 complex on the outside of pol II, and gets disordered after a few residues. These residues of Rpb1 constitute the beginning of a flexible linker that connects to the mobile C-terminal repeat domain (CTD). The CTD, a unique feature of pol II, consists of repeats of a heptapeptide with the consensus sequence Tyr-Ser-Pro-Thr-Ser-Pro-Ser. A total of 26 and 52 CTD repeats are found in yeast and human Rpb1, respectively.

Mechanism

Transcription Cycle

The transcription cycle is divided into three phases: initiation, elongation, and termination. Steps during

TABLE I

Polypeptide Composition of Cellular RNA Polymerases

Pol I	Pol II	Pol III	Archaea	Bacteria	Class[a]
A190	Rpb1	C160	$A' + A''$	β'	Core
A135	Rpb2	C128	B ($B' + B''$)	β	Core
AC40	Rpb3	AC40	D	α	Core
AC19	Rpb11	AC19	L	α	Core
Rpb6	Rpb6	Rpb6	K	ω	Core, common
Rpb5	Rpb5	Rpb5	H		Common
Rpb8	Rpb8	Rpb8			Common
Rpb10	Rpb10	Rpb10	N		Common
Rpb12	Rpb12	Rpb12	P		Common
A14	Rpb4	C17	F		Rpb4/7
A43	Rpb7	C25	E		Rpb4/7
A12.2	Rpb9	C11	X		Specific
A34.5					Specific
A49					Specific
		C82			Specific
		C34			Specific
		C31			Specific

[a] Core, sequence partially homologous in all RNA polymerases; common, shared by all eukaryotic RNA polymerases; Rpb4/7, Rpb4/7 heterodimer and its structural counterparts.

initiation include promoter binding, DNA melting, and synthesis of short RNA transcripts. The transition from initiation to elongation is referred to as promoter escape, and results in a stable elongation complex that is characterized by an open DNA region, the transcription bubble. The bubble contains the DNA–RNA hybrid, a heteroduplex of eight or nine base pairs. The growing RNA 3′-end is located at the end of the hybrid that is engaged with the pol II active site. Pol II alone can maintain an open transcription bubble, translocate along the DNA template, synthesize RNA, and detect errors in the nascent RNA. For all other steps, however, pol II requires the help of additional proteins.

Several steps of the transcription cycle are accompanied by phosphorylation or dephosphorylation of the pol II CTD. During initiation, the CTD gets phosphorylated, and the CTD phosphorylation pattern changes during elongation. CTD phosphorylation patterns govern specific interaction with RNA processing factors, thereby coupling transcription to RNA processing. The CTD is flexibly linked to a region beyond the saddle, from which RNA exits, consistent with its role in coupling transcription to mRNA processing. Several kinases and at least one phosphatase control the phosphorylation state of the pol II CTD.

Initiation

To bind and melt promoter DNA, pol II assembles on DNA with the general transcription factors TFIIB,

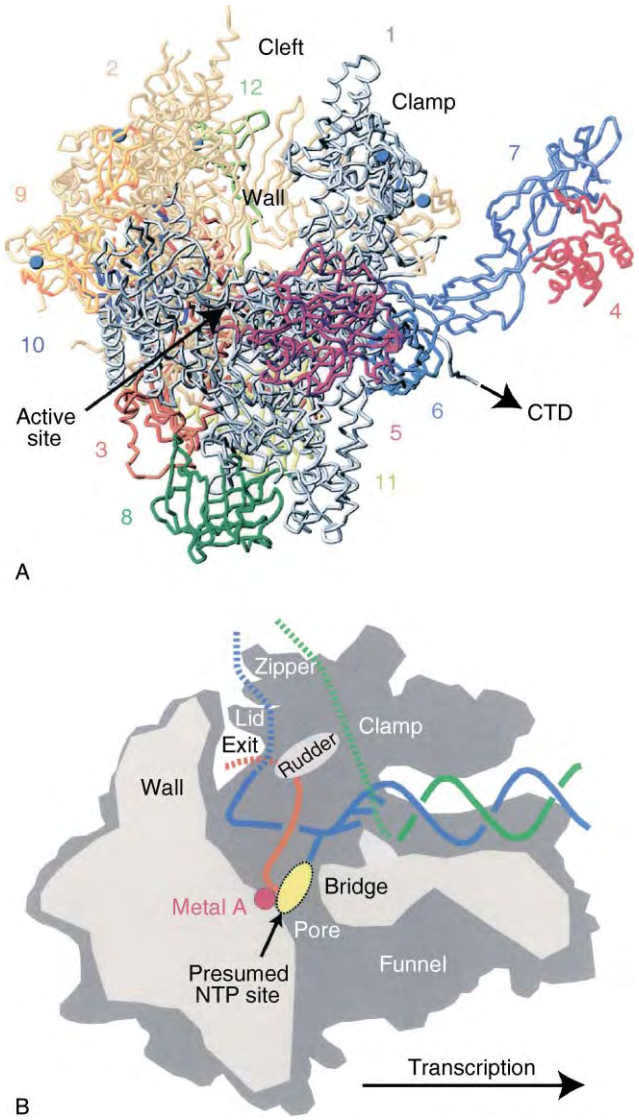

FIGURE 1 RNA polymerase II structures. (A) Ribbon model of yeast RNA polymerase II. The 12 subunits are shown in different colors. The active site metal ion A is depicted as a pink sphere. Zinc ions are shown as cyan spheres. (B) Schematic cut-away view of the pol II core elongation complex. The view is related to the one in (A) by a 90° rotation around a vertical axis. The DNA template and nontemplate strands are in blue and green, respectively, and the RNA is in red. Four of the bases in the DNA template strand are indicated as sticks protruding from the backbone. The yellow oval depicts the presumed binding site for the incoming nucleoside triphosphate substrate.

-D, -E, -F, and -H. The general factors are involved in sequence-specific promoter recognition (TFIIB, TFIID), prevention of nonspecific DNA binding (TFIIF), and DNA melting and CTD phosphorylation (TFIIE, TFIIH). RNA synthesis initiates within the bubble. The early transcribing complex is functionally unstable. Short RNAs are frequently released and pol II has to restart transcription (abortive cycling). There is a decline in abortive transcription when the RNA reaches a length of about four nucleotides, a transition

termed "escape commitment." RNA that has grown to a length of at least four nucleotides is generally not contacted by pol II anymore and is held in the elongation complex by base pairing with the DNA template strand. A second barrier in the transition from initiation to elongation has to be overcome when the RNA reaches a length of about ten nucleotides. At this length, the 5′-end of the RNA is detached from the DNA template strand, and is redirected to the pol II "saddle" and an exit tunnel. A third transition of the early elongation complex is reflected in the continued requirement for ATP and TFIIH until the RNA is about 15 nucleotides long. This transition may reflect successful positioning of all bubble-maintaining structural elements of pol II with respect to the bubble, and detachment of RNA from the pol II surface. Two possible RNA exit grooves have been suggested beyond the saddle, and binding of RNA to the saddle and to one of the exit grooves could account for an additional gain in stability of the elongation complex. Successful passage of early pol II elongation complexes through all three transitions has been referred to as "promoter clearance."

Elongation

During elongation, downstream DNA enters pol II at two mobile "jaws," and extends through the cleft toward the active site. Beyond the active site, a nine base pair DNA–RNA hybrid extends upward, toward the wall. The axes of the downstream DNA duplex and the DNA–RNA hybrid heteroduplex enclose an angle of ~90°. The growing RNA 3′-end is located above the pore, which allows entry of nucleoside triphosphate substrates from below. In the crystal structure of the pol II elongation complex, the incoming DNA duplex is mobile and badly ordered. However, three nucleotides before the active site, the DNA template strand becomes well-ordered by binding to the bridge helix and to two "switch" regions at the base of the clamp. A 90° twist between subsequent nucleotides orients a DNA base toward the active site for base pairing with an incoming nucleotide.

The property of the polymerase to stay attached to the template, even during transcription of long genes, is often referred to as processivity. The major cause of processivity is the high stability of the pol II elongation complex, caused by tight binding of the DNA–RNA hybrid. This stability can be accounted for by the highly complementary hybrid-binding site on pol II, which is partially created upon clamp closure and folding of the switches. Several pol II structural elements are predicted to maintain the hybrid and the transcription bubble during elongation, including the fork loops, the top of the wall, and three loops protruding from the edge of the clamp, called rudder, lid, and zipper.

The nucleotide addition cycle during RNA chain elongation begins with entry of the nucleoside triphosphate (NTP) substrate, maybe together with metal B, and its binding between the bridge helix and the end of the hybrid, to form a base pair with the coding DNA base. Correct orientation of the substrates and metal ions would lead to synthesis of a new phosphodiester bond and to the release of pyrophosphate, maybe together with metal B. The resulting complex adopts the pre-translocation state, which was apparently trapped in the pol II elongation complex structure, with the RNA 3′-terminal nucleotide occupying the NTP-binding site. Subsequent translocation of nucleic acids would align the new RNA 3′ end with metal A, and would free the NTP-binding site, preparing pol II for another cycle of nucleotide addition.

Specificity for synthesizing RNA rather than DNA is achieved by at least three mechanisms. First, the discriminating 2′-OH group of the incoming NTP may be hydrogen-bonded by a conserved pol II residue. Second, 2′-OH groups of the last few nucleotides that were incorporated into the growing RNA are directly hydrogen-bonded by pol II residues. Finally, the active center of pol II is complementary to the resulting DNA–RNA hybrid duplex that adopts a conformation intermediary between canonical A- and B-forms.

It is a mystery of the transcription mechanism how rapid translocation of nucleic acids can be achieved while nucleic acids are bound tightly by pol II. Hints for understanding translocation are, however, provided by the pol II structures. First, nucleic acids are only contacted via their backbones; base interactions that would impede translocation are not observed. Second, long-range electrostatic attraction of the nucleic acid backbones by positively charged protein groups in a "second shell" may enable tight binding of nucleic acids without restricting their movement. Finally, translocation may be accompanied by conformational changes in pol II that could maintain some of the protein–nucleic acid contacts during translocation. Structural comparisons suggest that one such conformational change may be bending of the bridge helix.

Pol II elongation is inhibited by the cyclic octapeptide α-amanitin, the toxin of the "death cap" mushroom. α-Amanitin does not greatly influence NTP binding, and a phosphodiester bond can still be formed when the toxin is added to an elongation complex. However, the rate of transcription is dramatically reduced. Only several nucleotides are incorporated per minute. In the structure of a pol II core–α-amanitin complex, α-amanitin binds to the bridge helix, and could restrain a possible movement of this helix, thereby blocking conformational changes that are important for translocation. However, the exact mechanism of pol II inhibition by α-amanitin is not understood.

Pol II does not move along the DNA template in a unidirectional manner, it rather oscillates between movements forward and backward ("backtracking"). During backtracking, RNA is extruded through the pol II pore into the funnel. Backtracking can lead to transcriptional pausing and arrest. Pausing is defined as a temporary block to elongation, from which pol II can escape by itself. In contrast, pol II cannot escape from arrest without the help of the transcript cleavage factor TFIIS, which stimulates a weak intrinsic nuclease activity of pol II, which cleaves RNA. Access of TFIIS to the pol II active site is apparently provided via the funnel and pore. Backtracking and TFIIS action may also underlie "proofreading" of the nascent transcript. During proofreading, a misincorporated nucleotide results in a mismatch base pair within the DNA–RNA hybrid. The induced distortion of the hybrid destabilizes the elongation complex and can lead to immediate cleavage of a mononucleotide, or it can trigger in backtracking, which results in threading of a short stretch of RNA (comprising the misincorporated nucleotide) into the pore and cleavage with the help of TFIIS. Any proofreading reaction creates a new RNA 3′-end at the active site, from which transcription can resume.

Termination

Transcription termination occurs in a reaction coupled to RNA 3′-end processing. Most eukaryotic mRNA precursors are cleaved in a site-specific manner in the 3′-untranslated region, followed by polyadenylation of the upstream cleavage product. A large number of proteins is involved in these reactions. The exact mechanism of coupling between 3′-end processing and transcription termination remains unclear. Termination is accompanied by dephosphorylation of the pol II CTD, but the precise timing of pol II dephosphorylation is also unclear. Dephosphorylation is required for the reinitiation of transcription, since pol II can only join an initiation complex in its unphosphorylated form. The CTD phosphatase Fcp1 plays a key role in pol II dephosphorylation and recycling. Fcp1 binds to pol II via Rpb4. Rpb4 apparently recruits Fcp1 to the vicinity of the CTD since the Rpb4/7 complex binds near the linker that connects the pol II core to the CTD.

Conservation

Pol II belongs to the family of cellular RNA polymerases, which also includes the two other eukaryotic RNA polymerases, pol I and pol III, and the bacterial and archaeal RNA polymerases. All three eukaryotic RNA polymerases share five common subunits (Table I). Four core subunits of pol II, Rpb1, Rpb2, Rpb3, and Rpb11, as well as subunit Rpb9, all have close homologues in pol I and pol III. Recent studies show that the Rpb4/7 complex of pol II also has structural and functional counterparts in pol I and pol III, and in the archaeal RNA polymerase. Since the 12 subunits of pol II are either identical or homologous in all three eukaryotic enzymes, the pol II structure is a good model for all eukaryotic RNA polymerases. Comparison of pol II with a bacterial RNA polymerase structure revealed that five core subunits underlie a general RNA polymerase architecture with an active center cleft. Twenty-two regions of sequence homology cluster around the active site and generally adopt the same structure in all cellular RNA polymerases. The structurally conserved core includes the functional elements of the active center, indicating that all cellular RNA polymerases share common mechanistic features. Homologues for all pol II subunits (except Rpb8) are found in archaeal RNA polymerases. Thus the overall structure of archaeal RNA polymerases is very similar to that of pol II except several external domains.

The pol II structure is strikingly different from structures of the many single subunit DNA and RNA polymerases. However, in functional complexes of these diverse enzymes, nucleic acids take a similar course through the active center. The entering DNA duplex encloses an angle of $\sim 90°$ with the exiting template–product duplex. At the location of the bend, subsequent DNA template bases are twisted. This twist aligns the coding base with the binding site for the incoming nucleoside triphosphate substrate. The nucleoside triphosphate enters through an opening that is found in all polymerases, and generally binds between an α-helix and two catalytic metal ions. The exiting template–product duplex is bound from the minor groove side in all polymerases. Conformational changes upon nucleic acid binding have been detected for several different polymerases, but the nature of this "induced fit" differs.

See Also the Following Articles

Recombination: Heteroduplex and Mismatch Repair *in vitro* • RNA Polymerase I and RNA Polymerase III in Eukaryotes • RNA Polymerase II and Basal Transcription Factors in Eukaryotes • RNA Polymerase II Elongation Control in Eukaryotes

Glossary

backtracking Reverse movement of pol II along DNA and RNA.
DNA–RNA hybrid 8–9 base pair double-stranded heteroduplex formed between the DNA template strand and the RNA transcript within the transcription bubble.
downstream DNA DNA that is going to be transcribed.
Rpb1–Rpb12 RNA polymerase B (II) polypeptide subunits 1–12.

transcription bubble Open DNA region in the active center of pol II.
translocation Movement of pol II by a step of one base pair along the DNA template.
upstream DNA DNA that has been transcribed.

Further Reading

Armache, K.-J., Kettenberger, H., and Cramer, P. (2003). Architecture of the initiation-competent 12-subunit RNA polymerase II. *Proc. Natl. Acad. Sci. USA* **100**, 6964–6968.

Bushnell, D. A., and Kornberg, R. (2003). Complete 12-subunit RNA polymerase II at 4.1Å resolution: Implications for the initiation of transcription. *Proc. Natl. Acad. Sci. USA* **100**, 6969–6973.

Cramer, P. (2002). Multisubunit RNA polymerases. *Curr. Opin. Struct. Biol.* **12**, 89–97.

Cramer, P., Bushnell, D. A., Fu, J., Gnatt, A. L., Maies-Davis, B., Thompson, N. E., Burgess, R. R., Edwards, A. M., David, P. R., and Komberg, R. D. (2000). Architecture of RNA polymerase II and implications for the transcription mechanism. *Science* **288**, 640–649.

Cramer, P., Bushnell, D. A., and Kornberg, R. D. (2001). Structural basis of transcription: RNA polymerase II at 2.8 angstrom resolution. *Science* **292**, 1863–1876.

Gnatt, A. L., Cramer, P., Fu, J., Bushnell, D. A., and Kornberg, R. D. (2001). Structural basis of transcription: An RNA polymerase II elongation complex at 3.3Å resolution. *Science* **292**, 1876–1882.

Woychik, N. A., and Hampsey, M. (2002). The RNA polymerase II machinery: Structure illuminates function. *Cell* **108**, 453–463.

Biography

Patrick Cramer is Assistant Professor of Biochemistry at the Institute of Biochemistry and Gene Center of the University of Munich. His research interest is in the structural biology of the eukaryotic mRNA transcription machinery. He obtained a Ph.D. from Heidelberg University and the European Molecular Biology Laboratory, and carried out postdoctoral research at Stanford University. For his work on the structure determination of RNA polymerase II, he was elected EMBO Young Investigator in 2000 and received the GlaxoSmithKline Science Award in 2002.

RNA Polymerase Reaction in Bacteria

Arkady A. Mustaev and Alexander D. Goldfarb
Public Health Research Institute, Newark, New Jersey, USA

The expression of genetic information encoded in DNA requires the production of an RNA molecule (known as transcription) using DNA as a template. The resulting RNA (the transcript) represents an exact copy of the transcribed DNA segment, or the gene. Information in RNA is encoded using a four-letter alphabet of nitrous bases, the same as in DNA, with the difference that uracil (U) is used in RNA instead of thymine (T). In addition to the copying of the DNA sequence into RNA, the transcription process involves the selection of the beginning (promoter) and the end (terminator) of each gene.

Transcription: Basic Mechanism

RNA synthesis requires base-pairing interactions between the single-stranded DNA template and ribonucleoside-5′-triphosphate (NTP) substrates. Thus, transcription involves unwinding of a small section (10–13 nucleotide residues) of the DNA double helix at which point one of the two DNA strands acts as a template for RNA synthesis. The unwound portion of DNA is called the transcription bubble; it contains a DNA–RNA hybrid of 8–9 base pairs. Each elementary step of transcription constitutes the incorporation of an NTP at the 3′ terminus of the growing RNA chain, so that the bubble propagates stepwise along the template accompanied by unwinding of the DNA duplex ahead, peeling of the transcript from the hybrid, and closing of the DNA duplex behind.

The nucleotide addition is accomplished through the formation of a phosphodiester bond and the release of pyrophosphate (PPi). It is a highly energetically favorable reaction ($\Delta G \cong 7$ kcal/mol), which is practically irreversible under physiological conditions but may be reversed *in vitro* by excess of PPi. As the result, a linear RNA polymer is built in the 5′ to 3′ direction. Selection of the substrates is achieved through hydrogen bonding between complementary bases, adenine to thymine (or uracil), and guanine to cytosine.

The enzyme that performs transcription of cellular DNA is called DNA-dependent RNA polymerases (RNAPs). The best characterized RNAP is that from the bacterium *Escherichia coli*. RNAP's catalytic core enzyme contains five subunits (α_2, β, β', and ω) and has an M_r of 390 kDa. The sixth interchangeable subunit, σ, is derived from a group of related polypeptides of different size. The σ-subunit is a specificity factor, which transiently associates with the core enzyme to form the holoenzyme that is capable of recognition of and specific binding to the promoter. The most common σ-factor in the bacterial cell is σ70. In contrast to DNA polymerase, the RNAP holoenzyme is able to initiate RNA synthesis starting from NTP and does not require a primer. Transcription is completely processive, i.e., RNAP is associated with the transcription bubble at all times in a ternary complex in which the nucleic acid scaffold slides through the protein as the bubble propagates. At the termination site, the ternary complex dissociates, the bubble collapses, and single-stranded RNA product is released.

Thus, synthesis of a particular transcript can be divided into three distinct steps: initiation, elongation, and termination, which jointly constitute the transcription cycle (Figure 1). Each step of the transcription cycle is subject to regulation either by factors external to the transcriptional apparatus or by signals encoded in the DNA sequence.

Transcription Initiation

The search for a promoter occurs through occasional collision and sliding of RNAP along DNA. Sliding greatly accelerates the search, which is concluded by establishment of specific contacts between RNAP and a promoter in a relatively unstable closed complex. In bacteria, the RNAP holoenzyme binds to the promoter region from -70 to -40 to $+30$ nucleotides relative to the transcription start site. Within the promoter, RNAP usually recognizes two relatively short sites centered around the positions -35 and -10 (Figure 2A), which are contacted by the σ-subunit. Some of the promoters contain an additional recognized sequence, the so-called UP element, which spawns the register -60 to -40 and interacts with the α-subunit of RNAP.

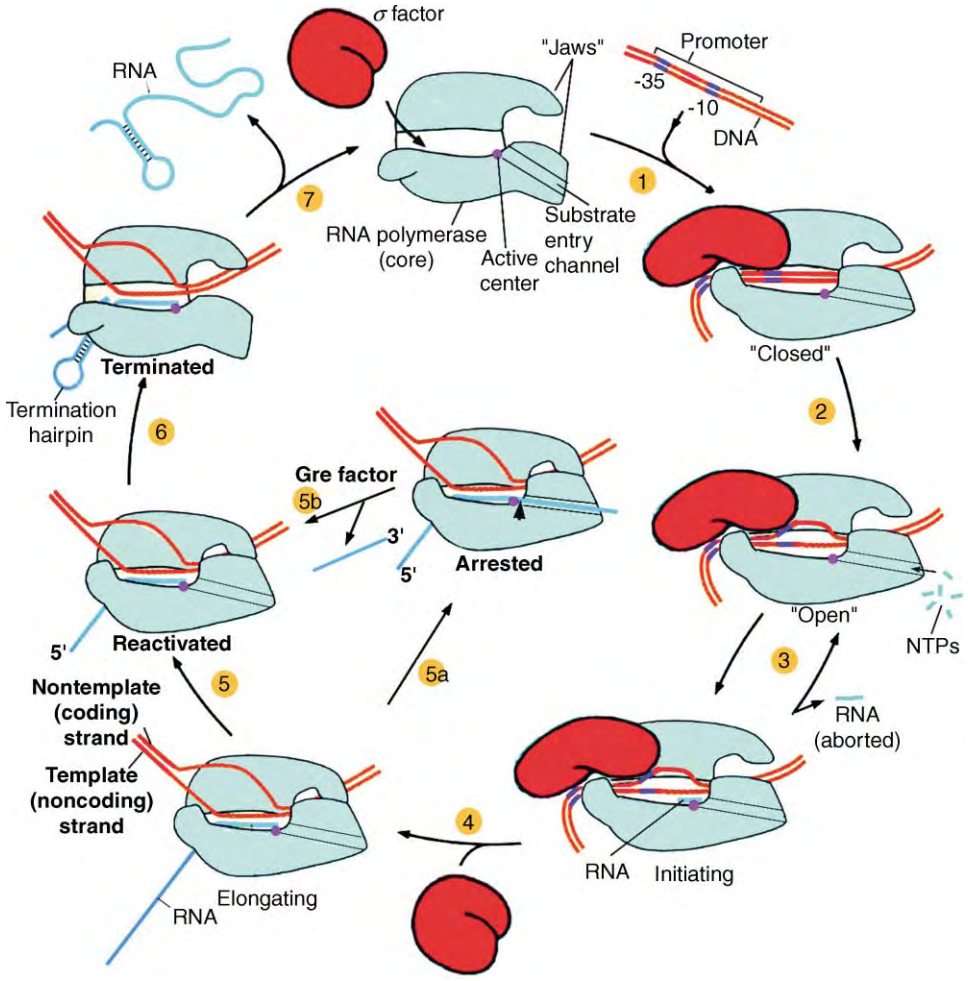

FIGURE 1 The transcription cycle. The RNAP core enzyme associates with the σ-factor and recognizes a promoter (step 1). RNAP locally melts the DNA duplex and starts RNA synthesis on the template strand of DNA (steps 2 and 3). The enzyme is still anchored to the promoter due to specific contacts with the recognition sequence, which impede the promoter escape, causing premature dissociation of short RNA products and their resynthesis in the cyclic reaction of abortive initiation. Occasionally, some RNA products that have reached a critical size (approximately 8–10 nucleotides) enter the RNA exit channel and displace the σ-factor. This leads to the stabilization of the transcription complex and relinquishing of the contacts between the σ-subunit and the promoter (step 4). The ternary elongating complex is highly processive. At certain sequences, RNAP occasionally backtracks, losing its grip on the growing RNA end, which extrudes beyond the active center, rendering the complex inactive (step 5a). The transcription factor GreB assists with cleavage of the extruded RNA, reactivating the enzyme (step 5b). Eventually, the elongating complex encounters a terminator, which causes the enzyme to stop and release the transcript due to a conformational change induced by the RNA hairpin. The RNAP core enzyme can rebind σ-factor and perform another cycle of transcription.

Even though the sequence of promoters is not strictly conserved (which accounts for variations in their efficiency), there are certain nucleotides that are found with high frequency at each position of a consensus sequence. The consensus sequences for the -35 and -10 positions are TTGACA and TATAAT, respectively. Some promoters have an extended -10 recognition region with the invariant dinucleotide TG just one nucleotide upstream of the main consensus sequence. The typical length of the nonspecific spacers between the -35 and -10 regions and from the -10 region to the first transcribed nucleotide are 17 and 7 nucleotides, respectively, with slight variations (Figure 2B).

Much of the regulation of gene expression occurs at the level of promoter recognition. Promoters can be subdivided into two groups, constitutive promoters, whose activity always remains constant, and regulated promoters, in which RNAP has to be recruited by an auxiliary protein factor or the promoter is blocked by bound repressor. For example, cAMP receptor protein activates promoters for the production of enzymes involved in the metabolism of some sugars, whereas Lac repressor blocks transcription of the genes for utilization of lactose.

After promoter recognition, the DNA double helix unwinds locally, resulting in the formation of the open

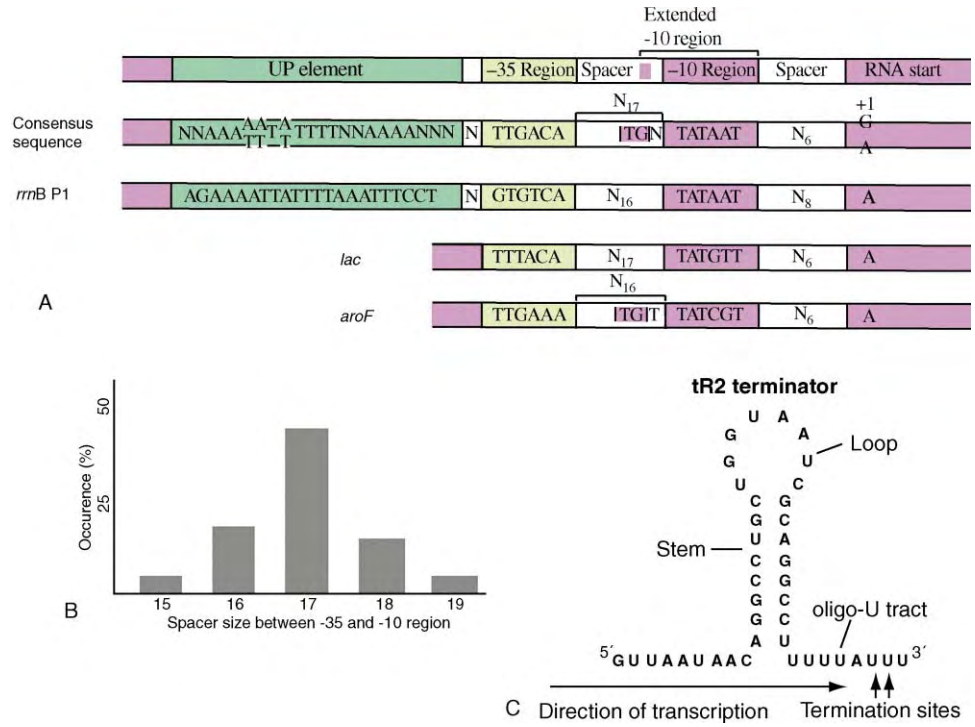

FIGURE 2 Bacterial promoters and terminators. (A) Typical promoters recognized by the RNAP holoenzyme containing σ70. Sequences of the nontemplate strand at the recognition sites are shown in the direction from 5′ to 3′. The structure of the promoters is variable, which is consistent with the wide range of their efficiency. The recognition sequences are highlighted. (B) Variation in the spacer size between the −10 and −35 regions in natural promoters. (C) The structure of a typical ρ-independent terminator. The tR2 terminator shown contains two self-complementary G-C reach regions followed by oligo-U tracts. The termination site is usually located 7–8 nucleotides downstream from the stem of the RNA hairpin.

complex (Figure 1, step 2). At this point, the active center of the RNAP enzyme can initiate synthesis. The initial short RNA molecules are poorly retained at the active center and dissociate into solution in a phenomenon called abortive synthesis (Figure 1, step 3). After each abortion cycle, the enzyme remains promoter bound, and it reinitiates and releases RNA again until it eventually escapes the promoter. This escape to the elongation phase occurs after the size of the transcript reaches 7–11 nucleotides. Transition from initiation to elongation (promoter clearance) (Figure 1, step 4) is accompanied by the relinquishing of the sequence-specific interactions between DNA and the σ-subunit complex and often by dissociation of σ. In some cases, however, the subunit remains associated with RNAP.

Transcription Elongation

Even though the ternary elongation complex (TEC) is exceptionally stable to dissociation, it is maintained only by topological contacts between protein, DNA, and RNA, which allow free sliding of the enzyme along the template. During elongation, TEC acts as a powerful motor, generating a force (25 pN) greatly exceeding that for conventional cellular motors such as kinesin and myosine. The relative force generated by RNAP is about 10^6 times greater than that generated by the space shuttle carrier.

The principal nucleic acid–protein interactions in TEC occur at three crucial operationally defined sites (Figure 3): the DNA-binding site that holds on to the downstream DNA duplex and acts as a sliding clamp, and the front and rear zip-locks at the ends of the RNA–DNA hybrid-binding site that accommodates the RNA–DNA heteroduplex (Figure 3B). The rear zip-lock ensures displacement of RNA product from the template during elongation. The front zip-lock coincides with the RNAP active center and also enables peeling of RNA from DNA upon TEC's occasional backtracking, a process in which the bubble propagates backward while extruding the 3′ terminus of RNA (Figure 1, step 5a).

In the X-ray crystal structure of TEC (Figure 3A), the DNA-binding site is seen as a deep trough formed by the β'-subunit, which is topped by a "roof" formed by a domain of the β-subunit. The RNA–DNA hybrid is enclosed in the main channel formed by the β- and β'-subunits of the enzyme, between the active center at its downstream end and the rudder loop of the β'-subunit at its upstream end, corresponding to the front and rear zip-locks, respectively. The active center, which contains

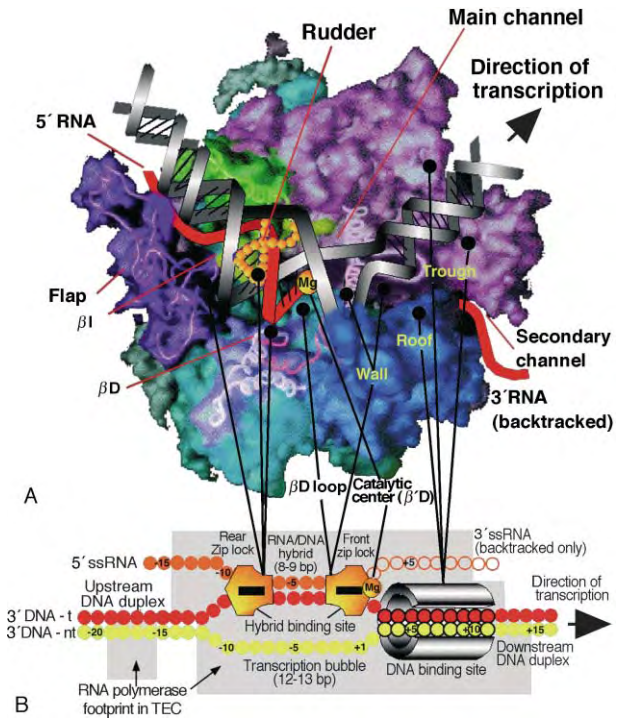

FIGURE 3 A structure–function model of the ternary elongating complex (TEC). (A) A model of TEC based on the X-ray crystal structure of RNAP. White lines show the correspondence between the operationally defined functional elements and the structural features of TEC. (B) The nucleic acid scaffold and its interactions with RNAP protein in TEC. The five elements are the upstream and downstream DNA duplexes, the 8–9 bp RNA–DNA hybrid, the single-stranded region of DNA in the transcription bubble, and the nascent single-stranded RNA upstream of the hybrid. In the "backtracked" complex, an additional segment of RNA appears downstream of the bubble. Filled circles represent the DNA (red, template strand; yellow, nontemplate strand); the DNA-binding site is represented by the sliding clamp that encloses 9 bp of the downstream DNA duplex. The hybrid-binding site that accommodates the RNA–DNA heteroduplex is flanked by the two zip-locks that hold on to the edges of heteroduplex and either zip or unzip the hybrid, maintaining its constant size during lateral movement of RNAP. The gray area shows the RNAP footprint on DNA.

the stably bound catalytic Mg^{2+} ion, marks the beginning of the secondary channel, which is used for the supply of NTP substrates and which accommodates the 3′-terminal end of single-stranded RNA upon RNAP backtracking. The secondary channel is branched from the main channel by the wall. The 5′ segment of the nascent transcript exits through the channel underneath the flap, which is a long flexible loop of the β-subunit.

The rate of RNA synthesis in elongation is sequence dependent, usually about 10 to 50 nucleotides per second, but can slow down to a full stop at points called pausing sites. One of the reasons for pausing is the energetics of base-pairing in the DNA–RNA scaffold of TEC. The energy of base-pairing is not equal for different nucleotides (ranging from 0.9 to 3.2 kcal/mol), so that TEC translocation is strongly suppressed at certain sites. In extreme cases, this causes reversible backtracking or even irreversible transcriptional arrest. The GreB protein rescues the arrested complex by stimulating RNA cleavage activity intrinsic to the RNAP active center, releasing the extruded 3′ RNA segment, and allowing RNA synthesis to continue (Figure 1, step 5b). A homologous GreA protein facilitates RNA cleavage in slightly backtracked TECs (by 1 or 2 nucleotides), thus preventing the arrest pathway.

Pausing, backtracking, and excision regulate elongation rate and serve to correct errors of elongation, which occur at a rate of one per every 10^4–10^5 nucleotides (compare with the fidelity of replication—one misincorporation per 10^7 nucleotides).

The RNA synthesis in bacteria is sensitive to inhibitors. The most important are rifampicin, streptolydigin, and microcin J-25. Rifampicin plugs the RNA exit channel in TEC, streptolydigin inhibits RNAP translocation, and microcin J-25 most likely blocks the NTP entry into the active center.

The Unified Catalytic Mechanism of RNA Synthesis and Degradation

The principal enzymatic activity of RNAP is the transfer of nucleotidyl moiety from the NTP substrate to the 3′ hydroxyl of the RNA terminus. Thus, the RNAP active center (Figure 4) *a priori* includes the binding site for the RNA terminus (i site) and the site for the NTP donor of the nucleotidyl residue (i + 1 site). The formation of the phosphodiester bond is followed by translocation of the newly formed RNA terminus from the i + 1 to the i site. The reaction and the movement are reversible: excess of PPi stimulates processive degradation of RNA (pyrophosphorolysis) with the release of 3′-terminal RNA residues in the form of NTPs. The RNAP active center can also perform hydrolysis of RNA in backtracked and arrested complexes. Central to these reactions is a symmetrical pair of Mg^{2+} ions that switch their roles in synthesis and degradation (Figure 4). One ion is retained in RNAP permanently (I) while the other is recruited for each act of catalysis (II). In polymerization reactions, it is recruited by incoming NTP (Figure 4A), whereas in cleavage reactions it is recruited by carboxylate residues of the Gre factors (Figure 4B).

Transcription Termination

Termination signals are encoded in the DNA sequence. There are two classes of termination signals in bacteria: one in which termination is assisted by a protein factor ρ, and another in which termination is ρ independent. The ρ-independent terminators (Figure 2C) contain

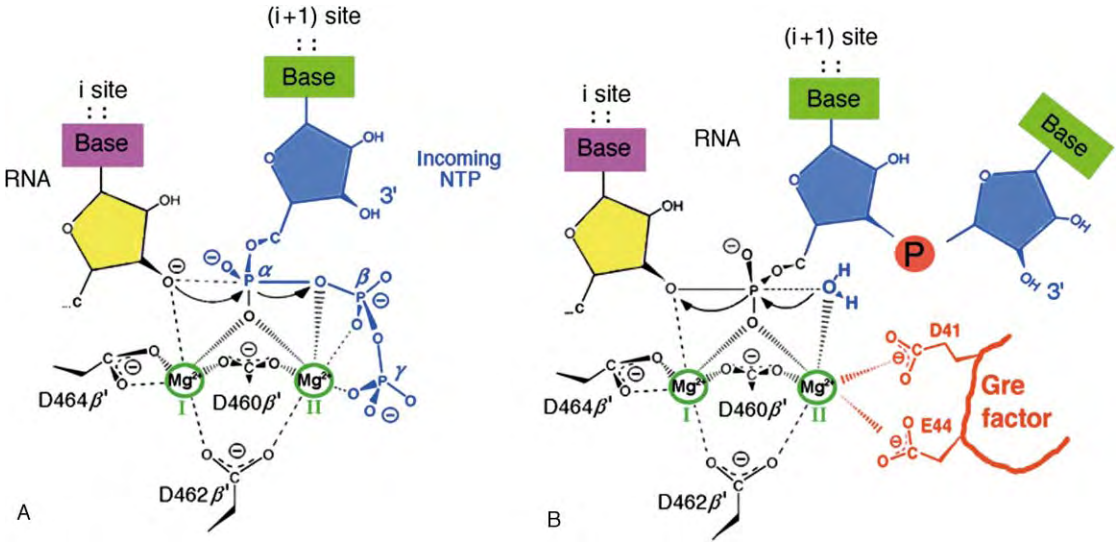

FIGURE 4 Catalytic mechanism of in RNA synthesis and degradation by RNAP. (A) The nucleotidyl transfer reaction. Two Mg^{2+} ions coordinated by three aspartate residues of the active center are enclosed in green circles. The tightly bound Mg-I activates the 3′ hydroxyl of the terminal RNA residue, promoting its attack on the α-phosphorus of the incoming NTP, and stabilizes the penta-coordinated transition state, while Mg-II facilitates the release of PPi during the phosphodiester bond formation. (B) The transcript cleavage reaction, assisted by the Gre factor. The Gre protein recruits the weakly bound Mg-II by providing residues for additional coordination. Mg-II orients and activates the attacking water molecule for hydrolytic cleavage of the phosphodiester bond. Mg-I coordinates the 3′ hydroxyl group of the RNA residue occupying the i site of the active center, making it a better leaving group. The disengaged 3′ RNA terminus is tilted to reflect the loss of base-pairing with DNA through backtracking.

short self-complementary GC-rich sequences followed by an oligo-A tract. Transcription of such sequences is accompanied by pausing of RNAP due to backtracking, which ensures the formation of a hairpin-like RNA structure (Figure 1, step 6). The RNA hairpin destroys the nucleic acid contacts in the rear zip-lock, forcing the rudder and the flap to open, which leads to collapse of the transcription bubble and disintegration of the transcription complex (Figure 1, step 7).

The ρ-dependent termination also requires pausing, but entails sequences without oligo-A tracts. The ρ protein loads onto RNA at some distance behind TEC and moves along the transcript toward RNAP, using the energy of ATP hydrolysis. Eventually, the factor bumps into the enzyme and pulls out RNA from the complex, causing the release of the transcript and dissociation of RNAP from DNA.

See Also the Following Articles

DNA Polymerase I, Bacterial • DNA Polymerase II, Bacterial • DNA Polymerase III, Bacterial • T7 RNA Polymerase • Transcription Termination

Glossary

operator A short segment of DNA in a bacterial chromosome that controls the transcription of an adjacent gene.

operon In the bacterial chromosome, a group of adjacent genes that are transcribed to a single mRNA molecule.

transcription factor Any protein required to initiate or regulate transcription.

Further Reading

Borukhov, S., and Nudler, E. (2003). RNA polymerase holoenzyme: Structure, function and biological implications. *Curr. Opin. Microbiol.* **6**, 93–100.

Darst, S. A. (2001). Bacterial RNA polymerase. *Curr. Opin. Struct. Biol.* **11**, 155–162.

Gnatt, A. L., Cramer, P., Fu, J., Bushnell, D. A., and Kornberg, R. D. (2001). Structural basis of transcription: An RNA polymerase II elongation complex at 3.3 A resolution. *Science* **292**, 1876–1882.

Korzheva, N., Mustaev, A., Nudler, E., Nikiforov, V., and Goldfarb, A. (1998). Mechanistic model of the elongation complex of *Escherichia coli* RNA polymerase. *Cold Spring Harbor Symp. Quant. Biol.* **63**, 337–345.

Korzheva, N., Mustaev, A., Kozlov, M., Malhotra, A., Nikiforov, V., Goldfarb, A., and Darst, S. A. (2000). Structural model of transcription elongation. *Science* **289**, 619–625.

Korzheva, N., and Mustaev, A. (2001). Transcription elongation complex: Structure and function. *Curr. Opin. Microbiol.* **4**, 119–125.

Losick, R., and Chamberlin, M. (eds.) (1976). *RNA Polymerase*. Cold Spring Harbor, New York.

Murakami, K. S., and Darst, S. A. (2003). Bacterial RNA polymerases: The wholo story. *Curr. Opin. Struct. Biol.* **13**, 31–39.

Sosunov, V., Sosunova, E., Mustaev, A., Bass, I., Nikiforov, V., and Goldfarb, A. (2003). Unified two-metal mechanism of RNA synthesis and degradation by RNA polymerase. *EMBO J.* **22**, 2234–2244.

Biography

Arkady A. Mustaev is a Research Associate at the Public Health Research Institute in Newark, New Jersey. He holds a Ph.D. from the Novosibirsk Institute of Bioorganic Chemistry (Russia). His principal research interest is studies of the catalytic mechanism of RNA polymerase. He developed superselective affinity labeling and fast mapping of the cross-linking sites in proteins, use of which allowed the design of a high-resolution model of the transcription elongation complex.

Alex Goldfarb is a Professor at the Public Health Research Institute. He holds a Ph.D. from the Weizmann Institute of Science in Israel. His principal research interest is the molecular mechanisms of transcription.

RNA Polymerase Structure, Bacterial

Michael Anikin, Dmitri Temiakov and William T. McAllister
State University of New York, Downstate Medical Center, Brooklyn, New York, USA

The first step in gene expression, transcription of genetic information in the DNA into messenger RNA, is carried out by DNA-dependent RNA polymerase (RNAP). Understanding how this enzyme carries out RNA synthesis and responds to regulatory signals is of fundamental importance to the comprehension of gene regulation. Extensive studies over the past decade (i.e., since 1990s) have probed the nature of the machinery that carries out this process. These approaches have involved genetics (identification and characterization of the genes that encode the protein subunits of the RNAP and the transcription factors that interact with the RNAP) and biochemical approaches (such as cross-linking experiments to characterize the trajectory of the nucleic acid components within the transcription complex). More recently, structural studies using methods such as NMR, X-ray crystallography, and fluorescence resonance energy transfer (FRET) have been brought to bear in an attempt to characterize the transcription complex in greater detail. The past few years have seen unprecedented breakthroughs in our understanding of the organization and function of the transcription complex, resulting in high resolution structures that may be interpreted in light of the abundant genetic and biochemical data. An overview of our understanding of the organization of bacterial RNAPs, and the relationship of structure to the mechanism of polymerase action is provided in this article.

Organization of the Transcription Complex

In a bacterium such as *E. coli* (the paradigm for studies of bacterial RNAPs), the minimal configuration needed for transcript elongation is a "core" complex that consists of five subunits, ($\alpha_2\beta\beta'\omega$) having an aggregate molecular weight of ~400 kDa and an additional factor, σ, is required for recognition of the promoter during initiation, and other factors may regulate the ability of the polymerase to clear the promoter, enhance processivity, or modulate termination. RNAPs from eukaryotic cells also have multiple subunits, and many of these subunits are homologous to the core subunits found in the bacterial RNAP. Thus, much of the information that comes from the study of bacterial RNAPs has direct relevance to studies of RNAPs from higher organisms.

Unlike DNA polymerases (DNAPs), which extend a primer and leave the polynucleotide product in association with the template, RNAPs must displace the RNA product from the template and restore the DNA to duplex form after the passage of the enzyme. To accomplish this, the polymerase establishes a locally unwound transcription bubble of ~12–14 bp which encloses an RNA:DNA hybrid that extends ~8 bp upstream from the growing end of the RNA chain. As the polymerase moves downstream, the two DNA strands are separated at the leading edge of the bubble and reannealed at the trailing edge, where the RNA is displaced (see Figure 1).

Extensive biochemical and genetic experimentation anticipated the essential elements that are required for RNA synthesis, and a general understanding of the organization of the complex (Figure 1). A central cavity encloses the active site and the short RNA:DNA hybrid where the nascent transcript is found before its displacement from the template (T) strand of the DNA. Leading into this cavity are pores and channels for the entrance and exit of the duplex DNA, an exit channel for the RNA product, and a substrate entrance pore. Another channel is required to accommodate the locally displaced nontemplate (NT) strand of the DNA in the transcription bubble.

Structure of the Core Enzyme

For a number of reasons, RNAPs from thermophilic organisms such as *Thermus aquaticus* (*Taq*) have proven more amenable for crystallographic analysis than the *E. coli* enzyme. A high resolution structure of the *Taq* core RNAP is shown in Figure 2. The overall organization of the enzyme resembles that of a crab claw which surrounds an open cleft in which the DNA is bound. The active site (which involves coordination of two Mg^{++} ions that are essential for the phosphoryl transferase reaction) is located at the back of this cleft. Many of the features that are important for the catalytic steps and processivity described above may be visualized

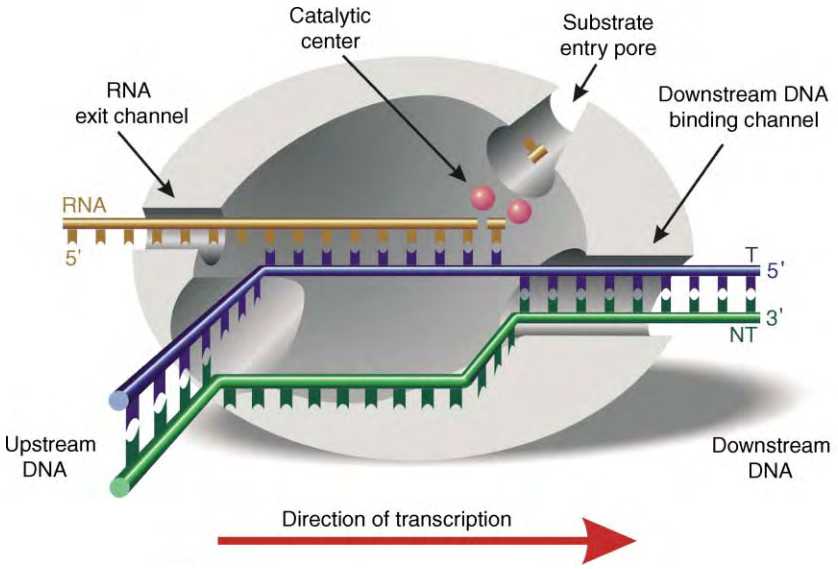

FIGURE 1 Organization of the transcription complex. The elongating RNA is found in the interior of the protein as an 8 bp RNA:DNA hybrid (RNA yellow, DNA blue). The nontemplate strand of the DNA (green) is displaced from the template strand at the leading edge of the transcription bubble and reannealed at the trailing edge. Channels that lead to the interior cavity allow for entry and exit of the duplex DNA, exit of the RNA product, and entrance of substrate. Elongation of the RNA chain occurs at the active site (catalytic center) where the phosphoryl transferase reaction is catalyzed by a pair of magnesium ions (purple spheres).

in this structure. Although the structure of an elongation complex of the bacterial RNAP in association with all of the nucleic acid components has not yet been determined, the structure of a yeast RNAP elongation complex has been solved. The organization of the eukaryotic complex is remarkably similar to that of the bacterial enzyme.

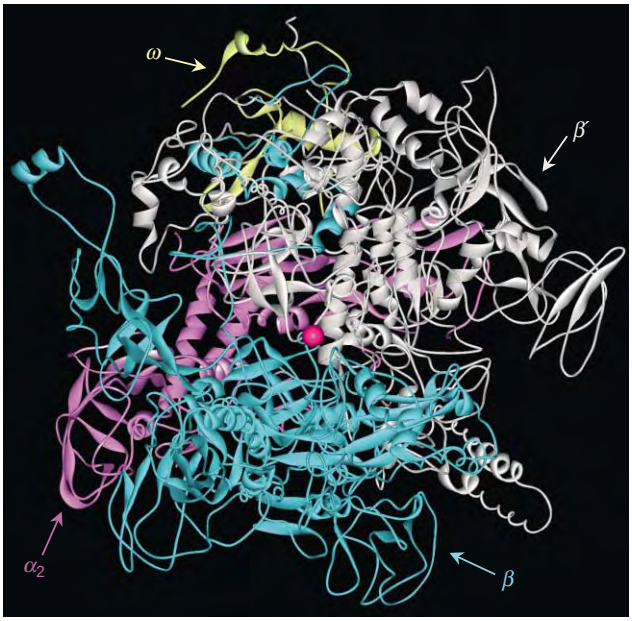

FIGURE 2 Structure of the *Taq* core enzyme. The core subunits are color coded as indicated. A magnesium ion in the active site is indicated by a purple sphere.

The bacterial RNAP structure is supported, and is made interpretable, by the results of previous biochemical and genetic experiments that identified important functional regions of the various subunits, and the nature of their interactions with nucleic acid components. In addition to the general features described in Figure 1, more details concerning the mechanism of transcription are revealed by the structure. These include upstream and downstream "zippers" for unwinding and rewinding the duplex DNA and displacing the product, and the organization of the active site. Nevertheless, more information will be required to understand other aspects of transcription, such as the mechanism of substrate selection and discrimination (ribo- versus deoxyribonucleotides), and how the movement of the RNAP along the template (translocation) is controlled.

Structure of the Holoenzyme

One of the key events during the transcription process is the transition from an unstable initiation complex to a processive elongation complex, which is accompanied by release of the promoter contacts and movement of the RNAP away from the promoter. The σ factor is intimately involved in promoter recognition and in the early stages of transcription. Association of σ with the core enzyme results in the formation of the "holoenzyme", which carries out the early stages of transcription. The structure of the holoenzyme from *Thermus thermophilus* (*Tth*) is shown in Figure 3.

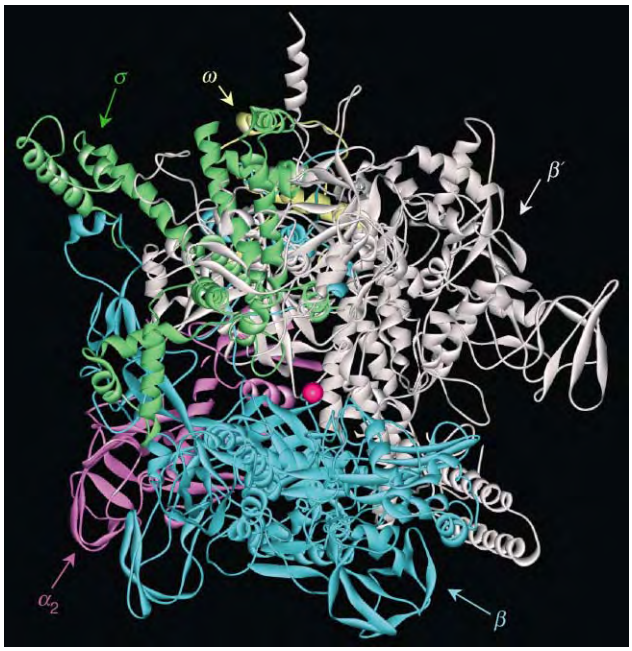

FIGURE 3 Structure of the *Tth* holoenzyme. The subunits of the core enzyme are colored as in Figure 2; (σ factor is green). The surface-exposed components are available for binding to the promoter DNA in a specific manner; a portion of σ is embedded in the hybrid binding cleft, and must be displaced during initiation.

In this structure, the regions of σ that are known to be involved in promoter recognition are displayed on the surface of the enzyme, where they would be able to interact with the upstream regions of the promoter. However, a flexible loop segment of σ is buried within the core enzyme, and occupies part of the RNA exit channel and the RNA:DNA hybrid binding cavity. This portion of σ would need to be displaced during initiation, perhaps precipitating the loss of σ that occurs during the transition to the elongation phase.

Structure of a Single Subunit Phage RNAP

Although the multisubunit RNAP described above is responsible for transcription of cellular DNA under normal growth conditions, there are occasions in which other RNAPs may also be operative within the bacterial cell. For example, certain viruses that infect bacteria encode a new RNAP that is responsible for transcription of the viral genome. The paradigm of this is the RNAP encoded by bacteriophage T7, which consists of a single subunit of ~100 kDa. Although this enzyme does not exhibit any amino acid sequence conservation with the bacterial enzymes, it is related to mitochondrial polymerases and with many organellar RNAPs from higher cells and plants (e.g., chloroplasts). It thus appears to be an evolutionarily conserved RNAP that arose at a different time from the multisubunit RNAPs. Interestingly, the phage RNAPs are also related to bacterial DNAPs and to reverse transcriptases. They are therefore members of a superfamily of nucleotide polymerases that is distinct from the multisubunit RNAPs.

Despite the differences in the sequence and detailed structure of the phage RNAP versus the bacterial RNAP, the phage RNAP nevertheless carries out all of the steps in the transcription cycle in an identical manner to the multisubunit RNAPs, including promoter recognition, elongation, and termination.

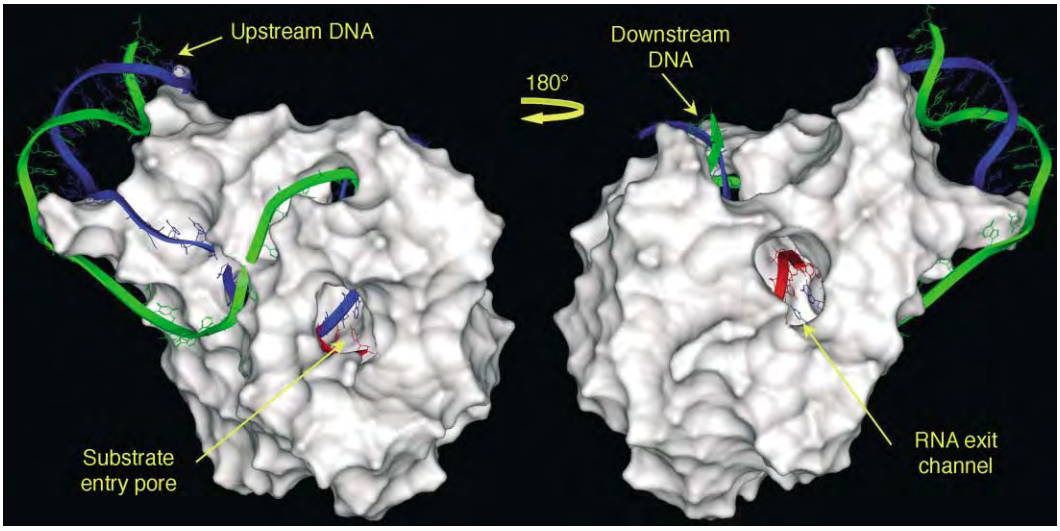

FIGURE 4 Model of a T7 RNA polymerase elongation complex just prior to promoter release. The RNAP maintains contacts with the upstream region of the promoter until it enters a fully processive elongation mode; potential interactions of the promoter with the RNAP at this stage of initiation are shown (DNA template strand, blue; nontemplate strand, green; RNA, red). The substrate entry and RNA exit channels are indicated.

Characterization of phage RNAP structures is more comprehensive than that of the bacterial RNAPs. Structures have now been solved for the free enzyme, the enzyme in association with its promoter, an early initiation complex, and elongation complexes in the presence and absence of substrate. Thus, many of the events in the overall transcription cycle have been captured in atomic detail for the phage RNAP.

The transition from an initiation complex to an elongation complex by T7 RNAP is accompanied by a massive reorganization of the amino terminal one-third of the enzyme (Figure 4). Remarkably, after the transition to an elongation complex, the overall organization of T7 RNAP resembles the organization of the bacterial RNAP, having an RNA:DNA hybrid of ~8 bps, pores for substrate entry and exit, a channel for the displaced NT strand, and regions for binding of upstream and downstream DNA. More detailed examination of the phage RNAP reveals elements that are involved in displacing the RNA product and for reannealling the T and NT strands at the upstream edge of the bubble, as well as mechanisms for substrate selection and translocation control. Due to the conservation in the overall mechanism of transcription, many of the findings from the phage RNAPs are likely to inform experimental approaches in the multisubunit RNAPs.

Future Prospects

Until the past few years, characterization of transcription complexes had relied largely upon biochemical and genetic approaches. The merger of structural methods with biochemical and genetic methods now affords the opportunity to determine the organization of the complexes at each stage of the transcription cycle with atomic resolution, and to correlate this structure with mutational and biochemical analyses.

See Also the Following Articles

RNA Polymerase II and Basal Transcription Factors in Eukaryotes • RNA Polymerase II Structure in Eukaryotes • RNA Polymerase Reaction in Bacteria • Sigma Factors • T7 RNA Polymerase

Glossary

initiation The first step in transcription, in which the RNAP forms an unstable initiation complex before clearing the promoter and entering into the elongation phase.

processive elongation RNAP continuously extends the RNA chain without dissociating from the template.

promoter Specific sequence in the DNA that directs RNAP to bind to the template and to begin transcription.

termination RNAP recognizes a specific signal in the template that causes it to release the RNA and to dissociate from the template.

Further Reading

Borukhov, S., and Nudler, E. (2003). RNA polymerase holoenzyme: Structure, function and biological implications. *Curr. Opin. Microbiol.* **6**, 93–100.

Cheetham, G. M., and Steitz, T. A. (2000). Insights into transcription: Structure and function of single-subunit DNA-dependent RNA polymerases. *Curr. Opin. Struct. Biol.* **10**, 117–123.

Darst, S. A. (1988). Two-dimensional crystals of Escherichia coli RNA polymerase holoenzyme on positively charged lipid layers. *J. Mol. Biol.* **203**, 269–273.

Murakami, K. S., and Darst, S. A. (2003). Bacterial RNA polymerases: The whole story. *Curr. Opin. Struct. Biol.* **13**, 31–39.

Murakami, K. S., Musada, S., and Darst, S. A. (2002). Structural basis of transcription initiation: RNA polymerase holoenzyme at 4Å resolution. *Science* **296**, 1280–1284.

Murakami, K. S., Musada, S., Campbell, E. A., Muzzin, O., and Darst, S. A. (2002). Structural basis of transcription initiation: An RNA polymerase holoenzyme-DNA complex. *Science* **296**, 1285–1290.

Tahirov, T. H., Temiakov, D., Anikin, M., Patlan, V., McAllister, W. T., Vassylyev, D. G., and Yokoyama, S. (2002). Structure of a T7 RNA polymerase elongation complex at 2.9Å resolution. *Nature* **420**, 43–50.

Vassylyev, D. G., Sekine, S.-I., Laptenko, O., Lee, J., Vassyleva, N., Borukhov, S., and Yokoyama, S. (2002). Crystal structure of a bacterial RNA polymerase holoenzyme at 2.6Å resolution. *Nature* **417**, 712–719.

Yin, Y. W., and Steitz, T. A. (2002). Structural basis for the transition from initiation to elongation transcription in T7 RNA polymerase. *Science* **298**, 1387–1395.

Zhang, G., Campbell, E. A., Minakhin, L., Richter, C., Severinov, K., and Darst, S. A. (1999). Crystal structure of *Thermus aquaticus* core RNA polymerase at 3.3Å resolution. *Cell* **98**, 811–824.

Biography

Michael Anikin received his Ph.D. in Bioorganic Chemistry from the Moscow Institute of Fine Chemical Technology.

Dmitri Temiakov received his Ph.D. in Molecular Biology from the Institute for Genetics and Selection of Microorganisms, Moscow.

William McAllister, Professor and Chair, received his Ph.D. from the University of New Hampshire, and postdoctoral training at the University of Heidelberg.

The authors are in the Morse Institute for Molecular Genetics, Department of Microbiology and Immunology, SUNY Downstate Medical Center, Brooklyn, NY. The research interests of the laboratory focus upon the structure and function of the single subunit bacteriophage T7 RNA polymerase.

Editors-in-Chief

William J. Lennarz

State University of New York at Stony Brook, Stony Brook, New York, USA

Section: Lipids, Carbohydrates, Membranes and Membrane Proteins

WILLIAM J. LENNARZ received his B.S. in Chemistry from Pennsylvania State University and a Ph.D. in Organic Chemistry from the University of Illinois. Subsequently he carried out postdoctoral work at Harvard with Konrad Bloch on fatty acid biosynthesis. In 1962 he was appointed Assistant Professor at Johns Hopkins in the Department of Physiological Chemistry. After promotion to Associate Professor in 1967, and full Professor in 1971, he remained at Hopkins until 1983. At that time, he was appointed Robert A. Welch Professor and Chair of the Department of Biochemistry and Molecular Biology at the University of Texas Cancer Center, M.D. Anderson Hospital. In 1989 he became a Leading Professor and Chair of the Department of Biochemistry and Cell Biology at SUNY at Stony Brook. In 1990 he founded and became Director of the Institute for Cell and Developmental Biology at Stony Brook.

Dr. Lennarz has served on many national and international committees. He has served as President of the Biochemistry Chairman's Organization, President of the American Society for Biochemistry and Molecular Biology and President of the Society for Glycobiology. He was a member of the Executive Committee of the International Union of Biochemistry and Molecular Biology for almost a decade.

He has presented special lectures at the University of Notre Dame, the NIH, the University of West Virginia, Johns Hopkins University, Florida State University, the University of California at San Diego, the University of Arkansas, Indiana University and the Medical College of Virginia.

He is a member of the National Academy of Sciences. The focus of his early work was on lipids and bacterial cell surfaces. More recent efforts have been in the structure, biosynthesis and function of cell surface glycoproteins. The biosynthesis studies initially were carried out in liver and oviduct, but these efforts now are focused in yeast. The functional studies have concentrated on the role of cell surface glycoproteins in fertilization and early development in the sea urchin and, more recently, the frog. For over 30 years Dr. Lennarz' research has been supported by federal sources, primarily the National Institutes of Health. Recently he was appointed Distinguished Professor and Chair of his department.

M. Daniel Lane

The Johns Hopkins University, School of Medicine, Baltimore, Maryland, USA

Section: Metabolism, Vitamins and Hormones

M. DANIEL LANE received B.S. and M.S. degrees in 1951 and 1953 from Iowa State University and a Ph.D. in 1956 from the University of Illinois. He was a Senior Postdoctoral Fellow with Professor Feodor Lynen at the Max-Planck Institute Fur Zellchemie in Munich. Following faculty positions at Virginia Polytechnic Institute and New York University School of Medicine, he joined the faculty at the Johns Hopkins University School of Medicine in 1969 and served as DeLamar Professor and Director of the Department of Biological Chemistry from 1978 to 1997. He is presently Distinguished Service Professor at Johns Hopkins. In 2002 he received an honorary degree, Doctor of Humane Letters, from Iowa State University.

Dr. Lane was elected to membership in the National Academy of Sciences (in 1987) and was elected as a Fellow of the American Academy of Arts and Sciences (in 1982) and of the American Society of Nutritional Sciences (in 1996). He received the Mead Johnson Award from the American Society for Nutritional Sciences in 1966 for his research on biotin-dependent enzymes and in 1981, the William C. Rose Award from the American Society for Biochemistry and Molecular Biology for his work on the insulin receptor. In 1990–1991 Lane served as President of the American Society of Biochemistry and Molecular Biology. He has presented many named lectureships (including the

Feodor Lynen Lecture in Germany in 1999) and served on numerous editorial boards including the Journal of Biological Chemistry and the Annual Reviews of Biochemistry. Currently he is Associate Editor for Biochemical and Biophysical Research Communications.

Dr. Lane has published 280 research papers in major scientific journals. His early work focused on various enzymatic CO_2 fixation reactions, notably the mechanisms by which the B-vitamin, biotin, functions in enzymes to catalyze carboxylation. Dr. Lane's work on the regulation of acetyl-CoA carboxylase, the key regulatory enzyme of fatty acid synthesis, led him to his present interests which are to understand the basic mechanisms of lipogenesis, adipogenesis and the consequence of aberrations in these processes, most notably obesity. Research currently underway in his laboratory focuses on: (1) the genes that signal stem cell "commitment" to the adipocyte lineage and subsequent differentiation into adipocytes, and (2) the mechanisms by which the region of the brain, known as the hypothalamus, monitors and controls the drive to eat.

Associate Editors

Ernesto Carafoli

Università degli Studi di Padova, Padova, Italy
Section: Bioenergetics

ERNESTO CARAFOLI earned his M.D. degree at the University of Modena in Italy in 1957. After postdoctoral studies in the Laboratory of Albert L. Lehninger at Johns Hopkins University in the mid 1960s he returned to his home institution in Italy where he worked until 1973, when he was appointed Professor of Biochemistry at the Swiss Federal Institute of Technology (ETH) in Zurich. He returned to Italy in 1998 as a Professor of Biochemistry at the University of Padova, where he now also directs the newly founded Venetian Institute of Molecular Medicine (VIMM).

Dr. Carafoli became interested in calcium as a signaling agent during his post-doctoral days at Johns Hopkins. When he arrived there his main interests were in mitochondrial bioenergetics and it was thus natural for him to expand them to the newly discovered area of mitochondrial calcium transport. He was involved in most of the early discoveries in the field, and he continued to work on mitochondria and calcium after his return to Italy and until he moved to the ETH. There his interests still remained focused on calcium, but the emphasis shifted to the proteins that transport it across membranes and to those that process its signal. His favorite object of study became the calcium pumps, especially that of the plasma membrane, an enzyme which is essential to the regulation of calcium homeostasis and thus to the well being of cells. His contributions on the enzyme, especially after he purified it in 1979, have helped establishing most of its properties and have clarified important problems of mechanism, regulation and structure.

Dr. Carafoli has authored or co-authored about 450 peer-reviewed articles and reviews, and has edited or co-edited about 20 books. He has served on the Editorial or Advisory Boards of several periodicals and has organized about 30 International Workshops and Symposia. He has been featured as a plenary or honorary lecturer at numerous events ranging from specialized Workshops to International Symposia and Congresses. Dr. Carafoli's honors and awards include several international prizes and medals, memberships in several Academies, and three honorary degrees.

Don W. Cleveland

University of California, San Diego, La Jolla, CA, USA
Section: Cell Architecture and Function

DON W. CLEVELAND has been a longstanding contributor to the elucidation of regulation of assembly of mitotic spindles and chromosome movement and how errors in these contribute to the chromosome loss characteristic of human tumors. He discovered the tubulin gene families encoding the major subunits of microtubules and the first mammalian example of control of gene expression through regulated RNA instability. He identified components required for microtubule nucleation and anchoring during spindle assembly. He identified the first human centromeric protein (CENP-B). He then discovered CENP-E, the centromere-associated, microtubule-motor that he showed to be essential for chromosome attachment and for activation and silencing of the mitotic checkpoint, the cell cycle control mechanism that prevents errors of chromosome segregation in mitosis.

Dr. Cleveland has also been a leading force in dissecting the disease mechanism for major human neurodegenerative disorders. He initially purified and characterized tau, the microtubule-associated protein that assembles aberrantly in human dementias including Alzheimer's disease and Pick's disease. He established that the extreme asymmetry of neurons acquired during development is achieved with a deformable array of interlinked neurofilaments, microtubules and actin. He showed that disorganization of neurofilament arrays caused selective death of motor neurons in mice and humans. He also demonstrated that neuronal death could also arise by a toxicity of mutant superoxide dismutase unrelated to its normal activity, thereby uncovering the mechanism underlying the major genetic form of amyotrophic lateral sclerosis. He showed that this toxicity could be

sharply ameliorated by lowering the content of neurofilaments.

Dr. Cleveland is currently Head, Laboratory for Cell Biology in the Ludwig Institute for Cancer Research and Professor of Medicine, Neurosciences and Cellular and Molecular Medicine at the University of California at San Diego. He is also the Editor of the Journal of Cell Biology and Current Opinion in Cell Biology.

Jack E. Dixon

University of California, San Diego School of Medicine,
La Jolla, CA, USA
Section: Protein/Enzyme Structure, Function, and Degradation

JACK E. DIXON earned his Ph.D. in Chemistry at the University of California, Santa Barbara in 1971 and did his postdoctoral training in Biochemistry at the University of California, San Diego.

Dr. Dixon is a pioneer and leader in the structure and function of the protein tyrosine phosphatases (PTPases). He demonstrated that the unique catalytic mechanism of the PTPases proceeds via a novel cysteine-phosphate intermediate. He discovered the first dual-specificity phosphatase, which led to the identification of the cell cycle protein, $p80^{cdc25}$, as a phosphatase. He also showed that the bacteria responsible for the plague or "black death" harbor the most active PTPase ever described. He and his colleagues went on to demonstrate that this PTPase gene product is essential for the pathogenesis of the bacteria. Dr. Dixon and his colleagues determined X-ray structures for both tyrosine and dual specificity phosphatases. Dr. Dixon also found that sequences outside of the PTPase catalytic domain could function to direct the subcellular localization of the PTPases and to restrict their substrate specificity. This is now a widely acknowledged regulatory paradigm for the PTPases. Recently, his laboratory demonstrated that the tumor suppressor gene, PTEN, which shares sequence identity with the PTPases, catalyzes the dephosphorylation of a lipid second messenger, phosphatidylinositol 3,4,5-trisphosphate (PIP3). This represents the first example of a PTPase dephosphorylating a lipid second messenger. PIP3 activates the protein kinase, AKT, which plays a critical role in controlling the balance between apoptosis and cell survival. The loss of the PTEN gene elevates PIP3 levels leading to constitutive activation by AKT and oncogenesis. Recently, Dr. Dixon in collaboration with Nikola Pavletich determined the X-ray structure of PTEN. Their structure–function studies explain the PIP3 substrate specificity of PTEN and also provide a rationale for many of the mutations seen in human cancers. Earlier in his career, Dr. Dixon adopted the tools of molecular biology as they became available in the 1970s, and his laboratory was among the first to use synthetic oligonucleotides to isolate and extensively characterize cDNAs encoding peptide hormones.

Dr. Dixon is Professor of Pharmacology, Cellular and Molecular Medicine and Chemistry and Biochemistry and Dean of Scientific Affairs at the University of California, San Diego. He is a member of the National Academy of Sciences, the Institute of Medicine and the American Academy of Arts and Sciences. Dr. Dixon was the recipient of the 2003 William C. Rose Award from the American Society for Biochemistry and Molecular Biology.

John H. Exton

Howard Hughes Medical Institute, Vanderbilt University School of Medicine, Nashvillie, TN, USA
Section: Signaling

JOHN H. EXTON was born and educated in New Zealand where he received his medical training and a Ph.D. in Biochemistry from the University of Otago in 1963. He did postdoctoral work at Vanderbilt University under Charles R. Park and Earl W. Sutherland, and became an Investigator of the Howard Hughes Medical Institute in 1968 and Professor of Physiology in 1970. He is presently Professor of Molecular Physiology and Biophysics, Professor of Pharmacology and a Hughes Investigator at Vanderbilt.

Dr. Exton's research initially focused on the changes in carbohydrate metabolism in liver during diabetes and treatment with various hormones using the perfused rat liver as the experimental system. His work concentrated on gluconeogenesis and identified the enzymatic reactions that were under control by insulin, epinephrine (adrenaline), glucagon and glucocorticoids, and demonstrated the importance of cyclic AMP in the regulation of these reactions. The role played by the supply of substrates, especially of alanine, was also shown.

Dr. Exton then turned his attention to the action of epinephrine (adrenaline) and demonstrated that many of its actions were not mediated by cyclic AMP but by calcium ions. This led to study of the breakdown of inositol phospholipids by phospholipase C that underlay the increase in calcium. Later this resulted in the discovery of G_q, a novel G protein that activated phospholipase C. Further studies demonstrated that agonists caused the breakdown of another phospholipid (phosphatidylcholine) by another phospholipase (phospholipase D). Current work is focused on the physiological role of phospholipase D.

Dr. Exton has authored over 350 scientific articles and is presently an Associate Editor of the Journal of Biological Chemistry. He has served on many scientific review groups and as a reviewer for many journals. He has won numerous awards, most notably the Lilly

Award of the American Diabetes Association, Fellow of the American Association for the Advancement of Science and election to membership in the National Academy of Sciences.

Paul Modrich

Duke University Medical Center, Durham, NC, USA
Section: Molecular Biology

PAUL MODRICH is an Investigator of the Howard Hughes Medical Institute and James B. Duke Professor of Biochemistry at Duke University Medical Center. He received his undergraduate degree from M.I.T. and his Ph.D. in Biochemistry from Stanford University. His current research addresses the mechanisms of DNA repair. He has served on the editorial boards of the Journal of Biological Chemistry, Biochemistry, Proceedings of the National Academy of Sciences, and DNA Repair. His honors include election to National Academy of Sciences and the Institute of Medicine, the Pfizer Award in Enzyme Chemistry, the General Motors Mott Prize in Cancer Research, and the Pasarow Foundation Award in Cancer Research.

Preface

Biological Chemistry is defined as the chemistry of the compounds and processes that constitute living organisms. The ultimate goal, of course, is to understand and define biology at a mechanistic level. This was aptly stated in an historical treatise on the founding of the *Journal of Biological Chemistry*, where John Edsall quoted a statement in a letter from J. L. Loeb (in Berkeley), "The future of biology lies with those who attack its problems from a chemical point of view." What was an emerging field in 1900 with its origins in physiology, nutrition and chemistry has broadened and expanded to include numerous other fields including mechanistic enzymology, molecular biology, structural biology, cell biology, genomics, proteomics, bioinformatics, metabolomics and others, that were not defined as discrete fields at that time.

Modern biochemistry (biological chemistry) began with the accidental discovery by Eduard Buchner in 1897 that a cell-free yeast extract could carry out fermentation of glucose to alcohol and CO_2 *in the absence of intact cells*. He named the dissolved substance responsible for this process zymase, the substance(s) we now refer to as enzymes. Importantly, Buchner recognized the significance of his discovery. This ended the dogma of the time, perpetuated by Pasteur, the concept of *vitalism*; i.e., that fermentation (and presumably other complex biological phenomena) required the action of intact cells. Thus, serendipity and a prepared mind ushered in a new era of discovery. Now it became possible to dissect complex physiological processes and to study them with preparations free of the constraints of intact cells. Once a metabolic pathway/process was established, it became possible to purify the enzymes, cofactors and substrates involved, to reconstitute the process with purified components and to characterize the components chemically. What followed was an information explosion in the field of biochemistry and progression through a series of trends, each "in vogue" in its time. The identification of the dietary essentials, the hunt for the vitamins/cofactors, the hormones, identification of metabolic pathways and the enzymes involved, oxidative phosphorylation, protein synthesis, molecular biology—each developed as a primary focus.

The need to associate chemistry with function came early and was evident in the naming of departments and journals. Over time names changed from Agricultural Chemistry to Physiological Chemistry to Biochemistry to Biological Chemistry. An example is the Department of Biochemistry at the University of Wisconsin, which began in 1883 as the Department of Agricultural Chemistry.

Where are we headed? We have reached the point where the borders of these areas have become blurred. What constitutes cell biology, molecular biology/genetics, developmental biology, physiology, immunology—ultimately reduces to chemistry. To understand these processes we must know what the molecules are and understand how they interact, i.e. the basic chemistry. That is what this encyclopedia is about.

The breadth of content of this encyclopedia aims to cover major topics of modern biochemistry, each authored by an expert in the area. We feel that the coverage is broad and we have been inclusive in choice of topics. The encyclopedia is a reference work encompassing four volumes containing over 500 articles with more than 750 authors or coauthors. Each article/topic covers an important area of the field which reflects the point of view of the authors. Together the articles cover virtually every aspect of biology for which we have "mechanistic" information. For those who wish to probe more deeply into a topic, references to further readings are included at the end of each article. The editorial board that made decisions on coverage consists of seven members, each an expert representing a major area in the field of biochemistry. A dedicated effort was made to provide coverage that is as complete as possible. The content is presented at a level that we hope will be interpretable to interested individuals with some background in chemistry and biology. It is intended for such individuals rather than specialists with extensive scientific backgrounds in specific areas. It is aimed at the generalist as opposed to the specialist.

Finally, we would like to single out Gail Rice and Dr. Noelle Gracy for their enormous contribution in putting this encyclopedia together. They, in fact, were a driving force that brought this major work to completion.

Notes on the Subject Index

Abbreviations used in subentries without explanation:

CoA	coenzyme A
DAG	diacylglycerol
ELISA	enzyme-linked immunosorbent assay
ERK	extracellular-signal regulated kinase
GlcNAC	N-Acetylglucosamine
HPLC	high-pressure liquid chromatography
IP_3	inositol 1,4,5-triphosphate
MAP	mitogen-activated protein
MMP	matrix metalloproteinase
mtDNA	mitochondrial DNA
NADPH	nicotinamide-adenine dinucleotide phosphate
PFK-2/ FBPase-2	6-phosphofructo-2-kinase/fructose-2,6-bisphosphatase
PI3K	phosphatidylinositol 3-kinase
PIP_2	phosphatidylinositol 4,5-bisphosphate
PIP_3	phosphatidylinositol-3,4,5-triphosphate
PPAR	peroxisome proliferator-activated receptor
RPLC	reversed-phase high-performance liquid chromatography

Volume 1

ABC Transporters, Pages 1-5, Andre Goffeau, Benoit De Hertogh and Philippe V. Baret

Abscisic Acid (ABA), Pages 6-11, Ramanjulu Sunkar and Jian-Kang Zhu

Actin Assembly/Disassembly, Pages 12-18, Henry N. Higgs

Actin-Capping and -Severing Proteins, Pages 19-26, Sankar Maiti and James R. Bamburg

Actin-Related Proteins, Pages 27-33, R. Dyche Mullins

Adenosine Receptors, Pages 34-39, Lauren J. Murphree and Joel Linden

Adenylyl Cyclases, Pages 40-45, Ronald Taussig

Adrenergic Receptors, Pages 46-50, David B. Bylund

Affinity Chromatography, Pages 51-56, Pedro Cuatrecasas and Meir Wilchek

Affinity Tags for Protein Purification, Pages 57-63, Joseph J. Falke and John A. Corbin

A-Kinase Anchoring Proteins, Pages 64-67, Lorene K. Langeberg and John D. Scott

Allosteric Regulation, Pages 68-73, Barry S. Cooperman

Alternative Splicing: Regulation of Fibroblast Growth Factor Receptor (FGFR), Pages 74-77, Mariano A. Garcia-Blanco

Alternative Splicing: Regulation of Sex Determination in Drosophila melanogaster, Pages 78-84, Jill K. M. Penn, Patricia Graham and Paul Schedl

Amine Oxidases, Pages 85-89, Giovanni Floris and Alessandro Finazzi Agro

Amino Acid Metabolism, Pages 90-95, Luc Cynober

Aminopeptidases, Pages 96-98, Ralph A. Bradshaw

Amyloid, Pages 99-104, Ronald Wetzel

Anaplerosis, Pages 105-110, Raymond R. Russell, III and Heinrich Taegtmeyer

Angiotensin Receptors, Pages 111-115, Tadashi Inagami

ara Operon, Pages 116-119, Robert F. Schleif

ARF Family, Pages 120-122, Gustavo Pacheco-Rodriguez, Joel Moss and Martha Vaughan

Aspartic Proteases, Pages 123-127, Ben M. Dunn

ATP Synthesis in Plant Mitochondria: Substrates, Inhibitors, Uncouplers, Pages 128-132, Kathleen L. Soole and R. Ian Menz

ATP Synthesis: Mitochondrial Cyanide-Resistant Terminal Oxidases, Pages 133-137, James N. Siedow

Autophagy in Fungi and Mammals, Pages 138-143, Daniel J. Klionsky and Ju Guan

B12-Containing Enzymes, Pages 145-151, Vahe Bandarian and Rowena G. Matthews

Bax and Bcl2 Cell Death Enhancers and Inhibitors, Pages 152-154, David L. Vaux

B-Cell Antigen Receptor, Pages 155-158, Thomas M. Yankee and Edward A. Clark

Bile Salts and their Metabolism, Pages 159-163, Ulrich Beuers and Thomas Pusl

Biliary Cirrhosis, Primary, Pages 164-169, Marshall M. Kaplan

Bioenergetics: General Definition of Principles, Pages 170-173, David G. Nicholls

Biotin, Pages 174-178, Steven W. Polyak and Anne Chapman-Smith

Biotinylation of Proteins, Pages 179-181, Ronald A. Kohanski

Bradykinin Receptors, Pages 182-185, Ronald M. Burch

Branched-Chain -Ketoacids, Pages 186-191, David T. Chuang

Brassinosteroids, Pages 192-197, Steven D. Clouse

Cadherin Signaling, Pages 199-204, David B. Sacks and Jonathan M. G. Higgins

Cadherin-Mediated Cell-Cell Adhesion, Pages 205-211, Frauke Drees and W. James Nelson

Calcitonin Gene-Related Peptide and Adrenomedullin Receptors, Pages 212-216, Debbie L. Hay, Alex C. Conner and David R. Poyner

Calcitonin Receptor, Pages 217-220, Samia I. Girgis, Niloufar Moradi-Bidhendi, Lucia Mancini and Iain MacIntyre

Calcium Buffering Proteins: Calbindin, Pages 221-225, Willi Hunziker and Igor Bendik

Calcium Buffering Proteins: ER Luminal Proteins, Pages 226-230, Jody Groenendyk and Marek Michalak

Calcium Oscillations, Pages 231-234, Marisa Brini

Calcium Sensing Receptor, Pages 235-240, Jacob Tfelt-Hansen and Edward M. Brown

Calcium Signaling: Calmodulin-Dependent Phosphatase, Pages 241-245, Claude Klee, Hao Ren and Shipeng Li

Calcium Signaling: Cell Cycle, Pages 246-249, Luigia Santella

Calcium Signaling: Motility (Actomyosin-Troponin System), Pages 250-255, Takeyuki Wakabayashi and Setsuro Ebashi

Calcium Signaling: NO Synthase, Pages 256-260, Zhi-Qiang Wang and Dennis J. Stuehr

Calcium Transport in Mitochondria, Pages 261-266, Rosario Rizzuto and Marisa Brini

Calcium Waves, Pages 267-269, Lionel F. Jaffe

Calcium, Biological Fitness of, Pages 270-273, Robert J. P. Williams

Calcium/Calmodulin-Dependent Protein Kinase II, Pages 274-280, Andy Hudmon and Howard Schulman

Calcium/Calmodulin-Dependent Protein Kinases, Pages 281-286, J. Robison and Roger J. Colbran

Calcium-Binding Proteins: Cytosolic (Annexins, Gelsolins, C2-Domain Proteins) , Pages 287-293, Joachim Krebs

Calcium-Modulated Proteins (EF-Hand), Pages 294-299, Robert H. Kretsinger

Calpain, Pages 300-306, Hiroyuki Sorimachi and Yasuko Ono

Carbohydrate Chains: Enzymatic and Chemical Synthesis, Pages 307-313, Thomas J. Tolbert and Chi-Huey Wong

Carnitine and -Oxidation, Pages 314-318, Janos Kerner and Charles L. Hoppel

Caspases and Cell Death, Pages 319-327, Don W. Nicholson, Pierluigi Nicotera and Gerry Melino

Cell Cycle Controls in G1 and G0, Pages 328-331, WengeShi and Steven F. Dowdy

Cell Cycle: Control of Entry and Progression Through S Phase, Pages 332-337, Susan L. Forsburg

Cell Cycle: DNA Damage Checkpoints, Pages 338-344, Jean Y. J. Wang

Cell Cycle: Mitotic Checkpoint, Pages 345-351, Tim J. Yen

Cell Death by Apoptosis and Necrosis, Pages 352-355, Pierluigi Nicotera

Cell Migration, Pages 356-361, J. Victor Small and Emmanuel Vignal

Cell-Matrix Interactions, Pages 362-366, Janet A. Askari and Martin J. Humphries

Centromeres, Pages 367-371, Beth A. Sullivan

Centrosomes and Microtubule Nucleation, Pages 372-376, Reiko Nakajima, Ming-Ying Tsai and Yixian Zheng

c-fes Proto-Oncogene, Pages 377-382, Thomas E. Smithgall and Robert I. Glazer

Chaperones for Metalloproteins, Pages 383-386, Valeria C. Culotta and Edward Luk

Chaperones, Molecular, Pages 387-392, Sue Wickner and Joel R. Hoskins

Chaperonins, Pages 393-398, Arthur L. Horwich, Wayne A. Fenton and George W. Farr

Chemiluminescence and Bioluminescence, Pages 399-404, Thomas O. Baldwin

Chemiosmotic Theory, Pages 405-412, Keith D. Garlid

Chemokine Receptors, Pages 413-418, Ann Richmond and Guo-Huang Fan

Chemolithotrophy, Pages 419-424, Alan B. Hooper

Chemotactic Peptide/Complement Receptors, Pages 425-429, Eric R. Prossnitz and Larry A. Sklar

Chlorophylls and Carotenoids, Pages 430-437, Hugo Scheer

Chloroplast Redox Poise and Signaling, Pages 438-445, John F. Allen

Chloroplasts, Pages 446-450, Nicoletta Rascio

Cholesterol Synthesis, Pages 451-455, Peter A. Edwards

Chromatin Remodeling, Pages 456-463, Eric Kallin and Yi Zhang

Chromatin: Physical Organization, Pages 464-468, Christopher L. Woodcock

Chromosome Organization and Structure, Overview, Pages 469-474, Elena Gracheva and Sarah C. R. Elgin

Coenzyme A, Pages 475-477, M. Daniel Lane

Collagenases, Pages 478-481, Kenn Holmbeck and Henning Birkedal-Hansen

Collagens, Pages 482-487, Darwin J. Prockop

Cyclic AMP Receptors of Dictyostelium, Pages 488-493, Dale Hereld and Peter N. Devreotes

Cyclic GMP Phosphodiesterases, Pages 494-500, Sharron H. Francis and Jackie D. Corbin

Cyclic Nucleotide Phosphodiesterases, Pages 501-505, Vincent C. Manganiello and Eva Degerman

Cyclic Nucleotide-Dependent Protein Kinases, Pages 506-511, Sharron H. Francis and Jackie D. Corbin

Cyclic Nucleotide-Regulated Cation Channels, Pages 512-515, Martin Biel and Franz Hofmann

Cysteine Proteases, Pages 516-520, David J. Buttle and John S. Mort

Cytochrome b6f Complex, Pages 521-527, Gunter A. Hauska and Thomas Schodl

Cytochrome bc1 Complex (Respiratory Chain Complex III), Pages 528-534, Bernard L. Trumpower

Cytochrome c, Pages 535-538, Hans Tuppy and Gunther Kreil

Cytochrome Oxidases, Bacterial, Pages 539-543, Peter Brzezinski and Pia Adelroth

Cytochrome P-450, Pages 544-549, Rita Bernhardt

Cytokines, Pages 550-555, Andrea L. Wurster and Michael J. Grusby

Cytokinesis, Pages 556-561, Masanori Mishima and Michael Glotzer

Cytokinin, Pages 562-567, Thomas Schmulling

Desmosomes and Hemidesmosomes, Pages 569-576, Rachel L. Dusek, Jonathan C. R. Jones and Kathleen J. Green

Detergent Properties, Pages 577-581, Darrell R. McCaslin

Diabetes, Pages 582-592, David W. Cooke

Diacylglycerol Kinases and Phosphatidic Acid Phosphatases, Pages 593-597, Stephen M. Prescott and Matthew K. Topham

Disulfide Bond Formation, Pages 598-602, Hiram F. Gilbert

DNA Base Excision Repair, Pages 603-608, Hilde Nilsen and Tomas Lindahl

DNA Damage: Alkylation, Pages 609-613, Anton B. Guliaev and B. Singer

DNA Glycosylases: Mechanisms, Pages 614-617, Daniel J. Krosky and James T. Stivers

DNA Helicases: Dimeric Enzyme Action, Pages 618-623, Timothy M. Lohman

DNA Helicases: HexamericEnzyme Action, Pages 624-631, Smita S. Patel

DNA Ligases: Mechanism and Functions, Pages 632-636, Alan E. Tomkinson and John B. Leppard

DNA Ligases: Structures, Pages 637-643, C. Kiong Ho, Mark Odell and Dimitar B. Nikolov

DNA Methyltransferases, Bacterial, Pages 644-651, Albert Jeltsch and Richard I. Gumport

DNA Methyltransferases, Structural Themes, Pages 652-659, Sanjay Kumar

DNA Methyltransferases: Eubacterial GATC, Pages 660-664, Martin G. Marinus

DNA Mismatch Repair and Homologous Recombination, Pages 665-670, Ivan Matic and Miroslav Radman

DNA Mismatch Repair and the DNA Damage Response, Pages 671-674, Guo-Min Li and Steven R. Presnell

DNA Mismatch Repair Defects and Cancer, Pages 675-681, Richard D. Kolodner

DNA Mismatch Repair in Bacteria, Pages 682-686, A-Lien Lu

DNA Mismatch Repair in Mammals, Pages 687-690, James T. Drummond

DNA Mismatch Repair: E. coli Vsr and Eukaryotic G-T Systems, Pages 691-693, Margaret Lieb

DNA Oxidation, Pages 694-697, Arthur P. Grollman and Dmitry O. Zharkov

DNA Photolyase, Pages 698-702, Carrie L. Partch and Aziz Sancar

DNA Polymerase, Eukaryotic α, Pages 703-707, Teresa S. -F. Wang

DNA Polymerase, Eukaryotic β, Pages 708-712, William A. Beard and Samuel H. Wilson

DNA Polymerase, Eukaryotic δ, Pages 713-715, Antero G. So and Kathleen M. Downey

DNA Polymerase, Eukaryotic ε, Pages 716-719, Yasuo Kawasaki and Akio Sugino

DNA Polymerase I, Bacterial, Pages 720-725, Catherine M. Joyce

DNA Polymerase II, Bacterial, Pages 726-728, Judith L. Campbell

DNA Polymerase III, Bacterial, Pages 729-733, Hisaji Maki

DNA Polymerases: Kinetics and Mechanism, Pages 734-739, Kenneth A. Johnson

DNA Replication Fork, Bacterial, Pages 740-744, Nancy G. Nossal

DNA Replication Fork, Eukaryotic, Pages 745-748, Lori M. Kelman, Jerard Hurwitz and Zvi Kelman

DNA Replication, Mitochondrial, Pages 749-752, David A. Clayton

DNA Replication: Eukaryotic Origins and the Origin Recognition Complex, Pages 753-760, Melvin L. DePamphilis and Cong-jun Li

DNA Replication: Initiation in Bacteria, Pages 761-766, Jon M. Kaguni

DNA Restriction and Modification: Type I Enzymes, Pages 767-771, David T. F. Dryden

DNA Restriction and Modification: Type II Enzymes, Pages 772-777, Darren M. Gowers and Stephen E. Halford

DNA Restriction and Modification: Type III Enzymes, Pages 778-781, Desirazu N. Rao and S. Srivani

DNA Secondary Structure, Pages 782-787, Albino Bacolla and Robert D. Wells

DNA Sequence Recognition by Proteins, Pages 788-793, Arabela A. Grigorescu and John M. Rosenberg

DNA Supercoiling, Pages 794-797, Tao-shih Hsieh

DNA Topoisomerases: Type I, Pages 798-805, James J. Champoux

DNA Topoisomerases: Type II, Pages 806-811, Renier Velez-Cruz and Neil Osheroff

DNA Topoisomerases: Type III-RecQ Helicase Systems, Pages 812-816, Rodney Rothstein and Erika Shor

Dopamine Receptors, Pages 817-822, Kim A. Neve

Dynactin, Pages 823-826, Trina A. Schroer

Dynein, Pages 827-831, K. Kevin Pfister

Volume 2

EF-G and EF-Tu Structures and Translation Elongation in Bacteria, Pages 1-5, Poul Nissen and Jens Nyborg

Eicosanoid Receptors, Pages 6-9, Richard M. Breyer and Matthew D. Breyer

Elastin, Pages 10-12, Judith Ann Foster

Endocannabinoids, Pages 13-15, Daniele Piomelli

Endocytosis, Pages 16-19, Julie G. Donaldson

Endoplasmic Reticulum-Associated Protein Degradation, Pages 20-23, Maurizio Molinari

Energy Transduction in Anaerobic Prokaryotes, Pages 24-30, Gottfried Unden

Enzyme Inhibitors, Pages 31-37, Vern L. Schramm

Enzyme Kinetics, Pages 38-44, Irwin H. Segel

Enzyme Reaction Mechanisms: Stereochemistry, Pages 45-50, Ming-Daw Tsai, Li Zhao and Brandon J. Lamarche

Epidermal Growth Factor Receptor Family, Pages 51-55, Denis Tvorogov and Graham Carpenter

ER/SR Calcium Pump: Function, Pages 56-60, Giuseppe Inesi

ER/SR Calcium Pump: Structure, Pages 61-65, Chikashi Toyoshima and Yuji Sugita

Exonucleases, Bacterial, Pages 66-72, Susan T. Lovett

F1-F0 ATP Synthase, Pages 73-79, Donata Branca

FAK Family, Pages 80-84, Steven K. Hanks

Fat Mobilization: Perilipin and Hormone-Sensitive Lipase, Pages 85-89, Constantine Londos and Alan R. Kimmel

Fatty Acid Oxidation, Pages 90-94, Horst Schulz

Fatty Acid Receptors, Pages 95-98, Christer Owman and Bjorn Olde

Fatty Acid Synthesis and its Regulation, Pages 99-103, Steven D. Clarke and Manabu T. Nakamura

Ferredoxin, Pages 104-106, Giuliana Zanetti and Vittorio Pandini

Ferredoxin-NADP+ Reductase, Pages 107-111, Giuliana Zanetti and Alessandro Aliverti

Fibroblast Growth Factor Receptors and Cancer-Associated Perturbations, Pages 112-117, Marko Kornmann and Murray Korc

Flavins, Pages 118-122, Barrie Entsch and David P. Ballou

Flippases, Pages 123-127, Charles J. Waechter

Focal Adhesions, Pages 128-133, Eli Zamir and Benjamin Geiger

Free Radicals, Sources and Targets of: Mitochondria, Pages 134-142, Alberto Boveris and Enrique Cadenas

Friedreich's Ataxia, Pages 143-145, Paul E. Hart and Anthony H. V. Schapira

G Protein Signaling Regulators, Pages 147-151, John H. Exton

G Protein-Coupled Receptor Kinases and Arrestins, Pages 152-157, Jeffrey L. Benovic

G12/G13 Family, Pages 158-161, Stefan Offermanns

GABAA Receptor, Pages 162-166, Richard W. Olsen and Gregory W. Sawyer

GABAB Receptor, Pages 167-170, S. J. Enna

Galectins, Pages 171-174, R. Colin Hughes

Genome-Wide Analysis of Gene Expression, Pages 175-180, Karine G. Le Roch and Elizabeth A. Winzeler

Gi Family of Heterotrimeric G Proteins, Pages 181-185, Maurine E. Linder

Giant Mitochondria (Megamitochondria), Pages 186-188, Bernard Tandler and Charles L. Hoppel

GlcNAc Biosynthesis and Function, O-Linked, Pages 189-192, Kaoru Sakabe and Gerald W. Hart

Glucagon Family of Peptides and their Receptors, Pages 193-196, Laurie L. Baggio and Daniel J. Drucker

Gluconeogenesis, Pages 197-203, Richard W. Hanson and Oliver E. Owen

Glucose/Sugar Transport in Bacteria, Pages 204-207, Lan Guan and H. Ronald Kaback

Glucose/Sugar Transport in Mammals, Pages 208-212, Silvia Mora and Jeffrey Pessin

Glutamate Receptors, Ionotropic, Pages 213-219, Derek B. Scott and Michael D. Ehlers

Glutamate Receptors, Metabotropic, Pages 220-223, P. Jeffrey Conn

Glutathione Peroxidases, Pages 224-228, Fulvio Ursini and Matilde Maiorino

Glycation, Pages 229-236, Suzanne R. Thorpe and John W. Baynes

Glycine Receptors, Pages 237-243, Bodo Laube and Heinrich Betz

Glycogen Metabolism, Pages 244-248, Peter J. Roach

Glycogen Storage Diseases, Pages 249-254, George H. Sack, Jr.

Glycogen Synthase Kinase-3, Pages 255-260, James R. Woodgett

Glycolipid-Dependent Adhesion Processes, Pages 261-265, Senitiroh Hakomori

Glycolysis, Overview, Pages 266-271, Robert A. Harris

Glycoprotein Folding and Processing Reactions, Pages 272-276, Armando J. Parodi

Glycoprotein-Mediated Cell Interactions, O-Linked, Pages 277-282, Robert S. Haltiwanger

Glycoproteins, N-Linked, Pages 283-292, Mark A. Lehrman

Glycoproteins, Plant, Pages 293-296, Carolyn J. Schultz

Glycosylation in Cystic Fibrosis, Pages 297-301, Andrew D. Rhim, Thomas F. Scanlin and Mary Catherine Glick

Glycosylation, Congenital Disorders of, Pages 302-307, Hudson H. Freeze

Glycosylphosphatidylinositol (GPI) Anchors, Pages 308-311, Anant K. Menon

Golgi Complex, Pages 312-315, Mark Stamnes

Gq Family, Pages 316-320, Wanling Yang and John D. Hildebrandt

Green Bacteria: Secondary Electron Donor (Cytochromes), Pages 321-324, Hirozo Oh-oka and Robert E. Blankenship

Green Bacteria: The Light-Harvesting Chlorosome, Pages 325-330, John M. Olson

Green Sulfur Bacteria: Reaction Center and Electron Transport, Pages 331-336, Gunter A. Hauska and Thomas Schodl

Gs Family of Heterotrimeric G Proteins, Pages 337-341, Susanne M. Mumby

Heat/Stress Responses, Pages 343-347, Davis T. W. Ng

Hematopoietin Receptors, Pages 348-353, Barbara A. Miller and Joseph Y. Cheung

Heme Proteins, Pages 354-361, Johannes Everse

Heme Synthesis, Pages 362-366, Gloria C. Ferreira

Hepatocyte Growth Factor/Scatter Factor Receptor, Pages 367-371, Selma Pennacchietti and Paolo M. Comoglio

Hexokinases/Glucokinases, Pages 372-377, Emile Van Schaftingen

Histamine Receptors, Pages 378-383, Stephen J. Hill and Jillian G. Baker

HIV Protease, Pages 384-387, Ben M. Dunn

HIV-1 Reverse Transcriptase Structure, Pages 388-392, Kalyan Das, Stefan G. Sarafianos, Eddy Arnold and Stephen H. Hughes

Homologous Recombination in Meiosis, Pages 393-397, Nancy M. Hollingsworth

HPLC Separation of Peptides, Pages 398-403, James D. Pearson

Imaging Methods, Pages 405-410, Gyorgy Szabadkai and Rosario Rizzuto

Immunoglobulin (Fc) Receptors, Pages 411-416, Mark Hogarth

Inorganic Biochemistry, Pages 417-420, Robert J. P. Williams

Inositol Lipid 3-Phosphatases, Pages 421-426, Gregory S. Taylor and Jack E. Dixon

Inositol Phosphate Kinases and Phosphatases, Pages 427-429, Stephen B. Shears

Insulin- and Glucagon-Secreting Cells of the Pancreas, Pages 430-435, Franz M. Matschinsky

Insulin Receptor Family, Pages 436-440, Paul F. Pilch and Jongsoon Lee

Integrin Signaling, Pages 441-445, Lawrence E. Goldfinger and Mark H. Ginsberg

Interferon Receptors, Pages 446-451, Christopher P. Elco and Ganes C. Sen

Intermediate Filament Linker Proteins: Plectin and BPAG1, Pages 452-457, Peter Fuchs and Gerhard Wiche

Intermediate Filaments, Pages 458-464, Kelsie M. Bernot and Pierre A. Coulombe

Intracellular Calcium Channels: cADPR-Modulated (Ryanodine Receptors), Pages 465-468, Antony Galione

Intracellular Calcium Channels: NAADP+-Modulated, Pages 469-472, Armando A. Genazzani and Marcella Debidda

Ion Channel Protein Superfamily, Pages 473-477, William A. Catterall

IP3 Receptors, Pages 478-481, Colin W. TaylorEdward Morris and Paula da Fonseca

Iron-Sulfur Proteins, Pages 482-489, Helmut Beinert

JAK-STAT Signaling Paradigm, Pages 491-496, Edward Cha and Christian Schindler

Keratins and the Skin, Pages 497-504, Pierre A. Coulombe and Kelsie M. Bernot

Ketogenesis, Pages 505-507, Janos Kerner and Charles L. Hoppel

Kinesin Superfamily Proteins, Pages 508-516, Nobutaka Hirokawa and Reiko Takemura

Kinesins as Microtubule Disassembly Enzymes, Pages 517-521, Susan L. Kline-Smith and Arshad Desai

Kinetic Isotope Effects, Pages 522-527, Justine P. Roth and Judith P. Klinman

lac Operon, Pages 529-534, Liskin Swint-Kruse and Kathleen S. Matthews

Lectins, Pages 535-540, Nathan Sharon and Halina Lis

Leptin, Pages 541-545, Thomas W. Gettys

LexA Regulatory System, Pages 546-550, Veronica G. Godoy, Penny J. Beuning and Graham C. Walker

Ligand-Operated Membrane Channels: Calcium (Glutamate), Pages 551-561, Elias K. Michaelis

Ligand-Operated Membrane Channels: GABA, Pages 562-566, F. Minier and Erwin Sigel

Light-Harvesting Complex (LHC) I and II: Pigments and Proteins, Pages 567-570, Stefan Jansson

Lipases, Pages 571-575, Howard L. Brockman

Lipid Bilayer Structure, Pages 576-579, Erwin London

Lipid Modification of Proteins: Targeting to Membranes, Pages 580-583, Marilyn D. Resh

Lipid Rafts, Pages 584-587, Deborah A. Brown

Lipoproteins, HDL/LDL, Pages 588-593, Fayanne E. Thorngate and David L. Williams

Low Barrier Hydrogen Bonds, Pages 594-598, Perry A. Frey

Luft's Disease, Pages 599-601, Salvatore DiMauro

Lysophospholipid Receptors, Pages 602-604, Gabor J. Tigyi

MDR Membrane Proteins, Pages 605-609, Nathan C. Rockwell

Meiosis, Pages 610-616, Neil Hunter

Melanocortin System, Pages 617-620, Roger D. Cone

Membrane Fusion, Pages 621-626, Joshua Zimmerberg and Leonid V. Chernomordik

Membrane Transport, General Concepts, Pages 627-630, Stanley G. Schultz

Membrane Transporters:Na+/Ca2+ Exchangers, Pages 631-636, Jonathan Lytton

Membrane-Associated Energy Transduction in Bacteria and Archaea, Pages 637-645, Gunter Schafer

Metabolite Channeling: Creatine Kinase Microcompartments, Pages 646-651, Uwe Schlattner and Theo Wallimann

Metalloproteases, Pages 652-656, David S. Auld

Metalloproteinases, Matrix, Pages 657-665, Hideaki Nagase and Gillian Murphy

Metaphase Chromosome, Pages 666-671, Sharron Vass and Margarete M. S. Heck

Methyl-CpG-Binding Proteins, Pages 672-675, David G. Skalnik

Microtubule-Associated Proteins, Pages 676-682, Nobutaka Hirokawa and Reiko Takemura

Mitochondrial Auto-Antibodies, Pages 683-688, Harold Baum

Mitochondrial Channels, Pages 689-692, M. Catia Sorgato and Alessandro Bertoli

Mitochondrial DNA, Pages 693-696, Gottfried Schatz

Mitochondrial Genes and their Expression: Yeast, Pages 697-702, Piotr P. Slonimski and Giovanna Carignani

Mitochondrial Genome, Evolution, Pages 703-708, B. Franz Lang, Dennis V. Lavrov and Gertraud Burger

Mitochondrial Genome, Overview, Pages 709-715, Douglas C. Wallace

Mitochondrial Inheritance, Pages 716-719, Eric A. Shoubridge

Mitochondrial Membranes, Structural Organization, Pages 720-724, Carmen A. Mannella

Mitochondrial Metabolite Transporter Family, Pages 725-732, Ferdinando Palmieri and Martin Klingenberg

Mitochondrial Outer Membrane and the VDAC Channel, Pages 733-736, Marco Colombini

Mitogen-Activated Protein Kinase Family, Pages 737-742, Hidemi Teramoto and J. Silvio Gutkind

Mitosis, Pages 743-747, Patricia Wadsworth and Nasser M. Rusan

mRNA Polyadenylation in Eukaryotes, Pages 748-752, Mary Edmonds

mRNA Processing and Degradation in Bacteria, Pages 753-757, Deborah A. Steege

Mucin Family of Glycoproteins, Pages 758-764, Juan Perez-Vilar and Robert L. Hill

Mucins in Embryo Implantation, Pages 765-769, Daniel D. Carson

Multiple Sequence Alignment and Phylogenetic Trees, Pages 770-774, Russell F. Doolittle

Muscarinic Acetylcholine Receptors, Pages 775-777, Neil M. Nathanson

Myosin Motors, Pages 778-781, Roy E. Larson

Volume 3

Natriuretic Peptides and their Receptors, Pages 1-5, Lincoln R. Potter

N-End Rule, Pages 6-10, Alexander Varshavsky

Neoglycoproteins, Pages 11-15, Y. C. Lee and Reiko T. Lee

Neuronal Calcium Signal, Pages 16-20, Hilmar Bading

Neuronal Intermediate Filaments, Pages 21-25, Ronald K. H. Liem

Neuropeptide Y Receptors, Pages 26-31, Eric M. Parker

Neurotensin Receptors, Pages 32-36, William Rostene, Patrick Kitabgi and Didier Pelaprat

Neurotransmitter Transporters, Pages 37-40, Aurelio Galli, Randy D. Blakely and Louis J. DeFelice

Neurotrophin Receptor Signaling, Pages 41-45, Jennifer J. Gentry and Bruce D. Carter

Nicotinamide Nucleotide Transhydrogenase, Pages 50-56, Jan Rydstrom

Nicotinic Acetylcholine Receptors, Pages 57-61, Nivalda O. Rodrigues-Pinguet and Henry A. Lester

Nitric Oxide Signaling, Pages 62-65, Michael A. Marletta

N-Linked Glycan Processing Glucosidases and Mannosidases, Pages 46-49, Linda O. Tremblay and Annette Herscovics

Non-Homologous End Joining, Pages 66-70, Penny A. Jeggo

Nonhomologous Recombination: Bacterial Transposons, Pages 71-79, Bao Ton Hoang and Michael G. Chandler

Nonhomologous Recombination: Retrotransposons, Pages 80-86, Siew Loon Ooi and Jef D. Boeke

Nuclear Compartmentalization, Pages 87-91, Kelly P. Smith and Jeanne B. Lawrence

Nuclear Envelope and Lamins, Pages 92-95, Bryce M. Paschal

Nuclear Factor kappaB, Pages 96-99, Thomas D. Gilmore

Nuclear Genes in Mitochondrial Function and Biogenesis, Pages 100-104, Alexander Tzagoloff and Carol L. Dieckmann

Nuclear Organization, Chromatin Structure, and Gene Silencing , Pages 105-108, Lori L. Wallrath, John R. Danzer, Oya Yazgan and Pamela K. Geyer

Nuclear Pores and Nuclear Import/Export, Pages 109-114, Anita H. Corbett

Nucleoid Organization of Bacterial Chromosomes, Pages 115-118, Charles J. Dorman

Nucleolus, Overview, Pages 119-122, Thoru Pederson

Nucleotide Excision Repair and Human Disease, Pages 123-129, James E. Cleaver

Nucleotide Excision Repair in Eukaryotes, Pages 130-133, Laura A. Lindsey-Boltz and Aziz Sancar

Nucleotide Excision Repair, Bacterial: The UvrABCD System, Pages 134-142, Bennett Van Houten and Lawrence Grossman

Nucleotide Excision Repair: Biology, Pages 143-147, Errol C. Friedberg

Olfactory Receptors, Pages 149-154, Sigrun I. Korsching

Oligosaccharide Analysis by Mass Spectrometry, Pages 155-160, Andrew J. Hanneman and Vernon N. Reinhold

Oligosaccharide Chains: Free, N-Linked, O-Linked, Pages 161-164, Tadashi Suzuki

Oncocytes, Pages 165-166, Bernard Tandler and Charles L. Hoppel

Opioid Receptors, Pages 167-171, P. Y. Law and Horace H. Loh

Ornithine Cycle, Pages 172-177, Malcolm Watford

Oxygenases, Pages 178-182, Osamu Hayaishi

P2X Purinergic Receptors, Pages 183-187, Annmarie Surprenant

P2Y Purinergic Receptors, Pages 188-191, George R. Dubyak

p53 Protein, Pages 192-195, Jamie Hearnes and Jennifer Pietenpol

p70 S6 Kinase/mTOR, Pages 196-200, Christopher G. Proud

Parathyroid Hormone/Parathyroid Hormone-Related Protein Receptor, Pages 201-207, Thomas J. Gardella

PCR (Polymerase Chain Reaction), Pages 208-210, Michael J. Brownstein

Pentose Phosphate (Hexose Mono Phosphate) Pathway, Pages 211-215, Bernard R. Landau

Pentose Phosphate Pathway, History of, Pages 216-225, John F. Williams

Peptide Amidation, Pages 226-230, Mark J. Niciu, Richard E. Mains and Betty A. Eipper

Periplasmic Electron Transport Systems in Bacteria, Pages 231-238, David J. Richardson, Gary Sawers and Rob J. M. Van Spanning

Peroxisome Proliferator-Activated Receptors, Pages 239-245, Mary C. Sugden, Edward A. Sugden and Mark J. Holness

Peroxisomes, Pages 246-250, Suresh Subramani

Phage Display for Protein Binding, Pages 251-255, Henry B. Lowman

Pheromone Receptors (Yeast), Pages 256-261, James B. Konopka and Jeremy W. Thorner

PHO Regulon, Pages 262-265, Bengt L. Persson

Phosphatidylinositol Bisphosphate and Trisphosphate, Pages 266-271, Alex Toker

Phosphatidylinositol-3-Phosphate, Pages 272-276, Joseph V. Virbasius and Michael P. Czech

Phosphofructokinase-2/Fructose Bisphosphatase-2, Pages 277-280, Daniel M. Raben

Phosphoinositide 3-Kinase, Pages 281-286, Khatereh Ahmadi and Michael Waterfield

Phosphoinositide 4- and 5-Kinases and Phosphatases, Pages 287-291, Shawn F. Bairstow, Matthew W. Bunce and Richard A. Anderson

Phosphoinositide-Dependent Protein Kinases, Pages 292-296, Nick R. Leslie and C. Peter Downes

Phospholipase A2, Pages 297-300, Timothy R. Smith and Edward A. Dennis

Phospholipase C, Pages 301-305, Fujio Sekiya, Yeun Ju Kim and Sue Goo Rhee

Phospholipase D, Pages 306-313, Mary M. LaLonde and Michael A. Frohman

Phospholipid Metabolism in Mammals, Pages 314-320, Claudia Kent

Phospholipid Synthesis in Yeast, Pages 321-325, Gil-Soo Han and George M. Carman

Photoreceptors, Pages 326-329, King-Wai Yau

Photosynthesis, Pages 330-335, Richard C. Leegood

Photosynthetic Carbon Dioxide Fixation, Pages 336-341, Matthew J. Paul

Photosystem I, Structure and Function, Pages 342-347, Petra Fromme

Photosystem I: FX, FA, and FB Iron-Sulfur Clusters, Pages 348-356, Mikhail L. Antonkine and John H. Golbeck

Photosystem II Light Harvesting System: Dynamic Behavior, Pages 357-362, Peter Horton and Alexander Ruban

Photosystem II: Assembly and Turnover of the D1 Protein, Pages 363-366, Eira Kanervo and Eva-Mari Aro

Photosystem II: Protein Components, Pages 367-374, James Barber

Photosystem II: Water Oxidation, Overview, Pages 375-380, Fabrice Rappaport and Pierre Joliot

Plant Signaling: Peptides, Pages 381-384, Clarence A. Ryan and Gregory Pearce

Plasma-Membrane Calcium Pump: Structure and Function, Pages 385-389, Emanuel E. Strehler

Plastocyanin, Pages 390-393, Elizabeth L. Gross

Platelet-Activating Factor Receptor, Pages 394-398, Katherine M. Howard and Merle S. Olson

Platelet-Derived Growth Factor Receptor Family, Pages 399-406, Marina Kovalenko and Andrius Kazlauskas

Polysialic Acid inMolecular Medicine, Pages 407-414, Frederic A. Troy, II

Porphyrin Metabolism, Pages 415-419, Mark Shepherd and Harry A. Dailey

Pre-tRNA and Pre-rRNA Processing in Bacteria, Pages 420-424, Sidney R. Kushner

Pre-tRNA and Pre-rRNA Processing in Eukaryotes, Pages 425-431, Hendrik A. Raue

Prions and Epigenetic Inheritance, Pages 432-436, Reed B. Wickner

Prions, Overview, Pages 437-440, Cedric Govaerts and Fred E. Cohen

Processivity Clamps in DNA Replication: Clamp Loading, Pages 441-446, Megan J. Davey and Mike O'Donnell

Propionyl CoA-Succinyl CoA Pathway, Pages 447-451, Wayne A. Fenton

Prostaglandins and Leukotrienes, Pages 452-456, William L. Smith and Robert C. Murphy

Proteases in Blood Clotting, Pages 457-463, John D. Kulman and Earl W. Davie

Proteasomes, Overview, Pages 464-468, Martin Rechsteiner

26S Proteasome, Structure and Function, Pages 469-473, Peter Zwickl and Wolfgang Baumeister

Protein Carboxyl Esterification, Pages 474-477, Shilpa G. Lalchandani and Jeffry B. Stock

Protein Data Resources, Pages 478-483, Philip E. Bourne

Protein Degradation, Pages 484-492, Tomo ari and Alfred L. Goldberg

Protein Folding and Assembly, Pages 493-499, David P. Goldenberg

Protein Glycosylation Inhibitors, Pages 500-503, Alan D. Elbein

Protein Glycosylation, Overview, Pages 504-509, Natasha E. Zachara and Gerald W. Hart

Protein Import into Mitochondria, Pages 510-515, Johannes M. Herrmann and Walter Neupert

Protein Kinase B, Pages 516-522, Bettina A. Dummler and Brian A. Hemmings

Protein Kinase C Family, Pages 523-526, Alexandra C. Newton

Protein N-Myristoylation, Pages 527-531, Erica Dutil Sonnenburg and Jeffrey I. Gordon

Protein Palmitoylation, Pages 532-535, Robert J. Deschenes

Protein Tyrosine Phosphatases, Pages 536-542, David J. Pagliarini, Fred L. Robinson and Jack E. Dixon

Proteinase-Activated Receptors, Pages 543-548, Kristina K. Hansen and Morley D. Hollenberg

Proteoglycans, Pages 549-555, Sara K. Olson and Jeffrey D. Esko

Pteridines, Pages 556-560, S. Colette Daubner and Paul F. Fitzpatrick

P-Type Pumps: Copper Pump, Pages 561-564, Ilia Voskoboinik and James Camakaris

P-Type Pumps: H+/K+ Pump, Pages 565-570, Jai Moo Shin and George Sachs

P-Type Pumps: Na+/K+ Pump, Pages 571-576, Peter L. Jorgensen

P-Type Pumps: Plasma-Membrane H+ Pump, Pages 577-581, A. Brett Mason and Carolyn W. Slayman

Purple Bacteria: Electron Acceptors and Donors, Pages 582-585, Evaldas Katilius and Neal W. Woodbury

Purple Bacteria: Photosynthetic Reaction Centers, Pages 586-594, C. Roy D. Lancaster

Pyridoxal Phosphate, Pages 595-599, David E. Metzler

Pyrimidine Biosynthesis, Pages 600-605, Monika Loffler and Elke Zameitat

Pyruvate Carboxylation, Transamination, and Gluconeogenesis, Pages 606-610, Sarawut Jitrapakdee and John C. Wallace

Pyruvate Dehydrogenase, Pages 611-615, Sam A. Johnson and James G. McCormack

Pyruvate Kinase, Pages 616-619, Kosaku Uyeda

Quinones, Pages 621-627, Giorgio Lenaz and Maria Luisa Genova

Rab Family, Pages 629-634, Mary W. McCaffrey and Andrew J. Lindsay

Ran GTPase, Pages 635-639, Mary Shannon Moore

Ras Family, Pages 640-644, Lawrence A. Quilliam

Recombination: Heteroduplexand Mismatch Repair in vitro, Pages 645-648, Leroy Worth

Recombination: Strand Transferases, Pages 649-653, Floyd R. Bryant

Recombination-Dependent DNA Replication, Pages 654-659, Kenneth N. Kreuzer

recQ DNA Helicase Family in Genetic Stability, Pages 660-664, Mary A. Risinger and Joanna Groden

Regulated Intramembrane Proteolysis (Rip), Pages 665-670, Jin Ye, Michael S. Brown and Joseph L. Goldstein

Respiratory Chain and ATP Synthase, Pages 671-675, David G. Whitehouse and Anthony L. Moore

Respiratory Chain Complex I, Pages 676-680, Ulrich Brandt

Respiratory Chain Complex II and Succinate: Quinone Oxidoreductases, Pages 681-687, C. Roy D. Lancaster

Respiratory Chain Complex IV, Pages 688-694, Hartmut Michel

Respiratory Processes in Anoxygenic and Oxygenic Phototrophs, Pages 695-699, Roberto Borghese and Davide Zannoni

Retinoblastoma Protein (pRB), Pages 700-703, Nicholas Dyson and Maxim Frolov

Retinoic Acid Receptors, Pages 704-707, Martin Petkovich

Reverse Transcriptase and Retroviral Replication, Pages 708-713, Laura Tarrago-Litvak, Marie-Line Andreola and Simon Litvak

Rho GTPases and Actin Cytoskeleton Dynamics, Pages 714-718, Priam Villalonga and Anne J. Ridley

Ribosome Assembly, Pages 719-724, John L. Woolford

Ribosome Structure, Pages 725-732, Brian T. Wimberly

Ribozyme Mechanisms, Pages 733-737, John Hsieh and Carol A. Fierke

Ribozyme Structural Elements: Group I Introns, Pages 738-742, Barbara L. Golden

Ribozyme Structural Elements: Hairpin Ribozyme, Pages 743-746, Adrian R. Ferre-D'Amare

Ribozymes and Evolution, Pages 747-752, Niles Lehman

RNA Editing, Pages 753-758, Charles E. Samuel

RNA Polymerase I and RNA Polymerase III in Eukaryotes, Pages 759-762, Robert J. White

RNA Polymerase II and Basal Transcription Factors in Eukaryotes, Pages 763-765, Joan Weliky Conaway and Ronald C. Conaway

RNA Polymerase II Elongation Control in Eukaryotes, Pages 766-769, David H. Price

RNA Polymerase II Structure in Eukaryotes, Pages 770-774, Patrick Cramer

RNA Polymerase Reaction in Bacteria, Pages 775-780, Arkady A. Mustaev and Alexander D. Goldfarb

RNA Polymerase Structure, Bacterial, Pages 781-784, Michael Anikin, Dmitri Temiakov and William T. McAllister

Volume 4

Secondary Structure in Protein Analysis, Pages 1-6, George D. Rose

Secretases, Pages 7-10, Robert L. Heinrikson

Secretory Pathway, Pages 11-16, Karen J. Colley

Selenoprotein Synthesis, Pages 17-21, August Bock

Septins and Cytokinesis, Pages 22-26, Makoto Kinoshita and Christine M. Field

Serine/Threonine Phosphatases, Pages 27-32, Thomas S. Ingebritsen

Serotonin Receptor Signaling, Pages 33-37, Paul J. Gresch and Elaine Sanders-Bush

Siglecs, Pages 38-40, Ajit Varki

Sigma Factors, Pages 41-44, John D. Helmann

Sliding Clamps in DNA Replication: E. coli -Clamp and PCNA Structure, Pages 45-47, Eric R. Goedken and John Kuriyan

Small GTPases, Pages 48-54, Adam Shutes and Channing J. Der

Somatostatin Receptors, Pages 55-60, Agnes Schonbrunn

Spastic Paraplegia, Pages 61-66, Elena Irene Rugarli and Andrea Ballabio

Spectrophotometric Assays, Pages 67-75, Britton Chance

Sphingolipid Biosynthesis, Pages 76-81, Martina Leipelt and Alfred H. Merrill

Sphingolipid Catabolism, Pages 82-87, Akira Abe and James A. Shayman

Spliceosome, Pages 88-92, Timothy W. Nilsen

Src Family of Protein Tyrosine Kinases, Pages 93-98, Jonathan A. Cooper

Starvation, Pages 99-110, Oliver E. Owen and Richard W. Hanson

Steroid/Thyroid Hormone Receptors, Pages 111-116, Ramesh Narayanan and Nancy L. Weigel

Store-Operated Membrane Channels: Calcium, Pages 117-122, Indu S. Ambudkar

Substrate Binding, Catalysis, and Product Release , Pages 123-126, W. Wallace Cleland

Sugar Nucleotide Transporters, Pages 127-129, Carlos B. Hirschberg

SUMO Modification, Pages 130-134, Frauke Melchior and Andrea Pichler

Superoxide Dismutase, Pages 135-138, Irwin Fridovich

Syk Family of Protein Tyrosine Kinases, Pages 139-145, Andrew C. Chan

T7 RNA Polymerase, Pages 147-151, Rui Sousa

Tachykinin/Substance P Receptors, Pages 152-157, Mark D. Richardson and Madan M. Kwatra

Taste Receptors, Pages 158-161, John D. Boughter, Jr. and Steven D. Munger

T-Cell Antigen Receptor, Pages 162-168, Andrea L. Szymczak and Dario A. A. Vignali

Tec/Btk Family Tyrosine Kinases, Pages 169-173, Shuling Guo and Owen N. Witte

Telomeres: Maintenance and Replication, Pages 174-179, Alessandro Bianchi and David Shore

Thyroid-Stimulating Hormone/Luteinizing Hormone/Follicle-Stimulating Hormone Receptors, Pages 180-186, Deborah L. Segaloff, Dario Mizrachi and Mario Ascoli

Tight Junctions, Pages 187-189, Shoichiro Tsukita

Title, Pages, Authors

Toll-Like Receptors, Pages 190-194, Himanshu Kumar, Kiyoshi Takeda and Shizuo Akira

Transcription Termination, Pages 195-199, Thomas J. Santangelo and Jeffrey W. Roberts

Transcriptional Silencing, Pages 200-203, Ann Sutton and Rolf Sternglanz

Transcription-Coupled DNA Repair, Overview, Pages 204-208, Isabel Mellon

Transforming Growth Factor-β Receptor Superfamily, Pages 209-213, Mark de Caestecker

Translation Elongation in Bacteria, Pages 214-223, Oliver Vesper and Knud H. Nierhaus

Translation Elongation in Eukaryotes, Pages 224-229, William C. Merrick and Anton A. Komar

Translation Initiation in Bacteria: Factors and Mechanisms, Pages 230-236, Cynthia L. Pon and Claudio O. Gualerzi

Translation Initiation in Eukaryotes: Factors and Mechanisms, Pages 237-241, Tatyana V. Pestova and Christopher U. T. Hellen

Translation Termination and Ribosome Recycling, Pages 242-246, Nadja Koloteva-Levin and Mick F. Tuite

Translesion DNA Polymerases, Eukaryotic, Pages 247-250, Alexandra Vaisman and Roger Woodgate

Trehalose Metabolism, Pages 251-255, Alan D. Elbein

Tricarboxylic Acid Cycle, Pages 256-262, Richard L. Veech

tRNA Synthetases, Pages 263-266, Karla L. Ewalt and Paul Schimmel

trp Operon and Attenuation, Pages 267-271, Paul Gollnick

Tubulin and its Isoforms, Pages 272-276, Eva Nogales

Tumor Necrosis Factor Receptors, Pages 277-283, Karen G. Potter and Carl F. Ware

Two-Dimensional Gel Electrophoresis, Pages 284-289, Gerhard Schmid, Denis Hochstrasser and Jean-Charles Sanchez

Two-Hybrid Protein-Protein Interactions, Pages 290-293, Ilya Serebriiskii and Erica A. Golemis

Tyrosine Sulfation, Pages 294-297, Denis Corbeil and Wieland B. Huttner

Ubiquitin System, Pages 299-303, Aaron Ciechanover and Michael H. Glickman

Ubiquitin-Like Proteins, Pages 304-307, Edward T. H. Yeh

UmuC, D Lesion Bypass DNA Polymerase V, Pages 308-312, Zvi Livneh

Uncoupling Proteins, Pages 313-318, Daniel Ricquier and Frederic Bouillaud

Unfolded Protein Responses, Pages 319-325, David Ron

Urea Cycle, Inborn Defects of, Pages 326-330, Marsha K. Fearing and Vivian E. Shih

Vacuoles, Pages 331-336, Christopher J. Stefan and Scott D. Emr

Vascular Endothelial Growth Factor Receptors, Pages 337-342, Kenneth A. Thomas

Vasopressin/Oxytocin Receptor Family, Pages 343-348, Michael J. Brownstein

V-ATPases, Pages 349-353, Michael Forgac

Vitamin A (Retinoids), Pages 354-359, Joseph L. Napoli

Vitamin B12 and B12-Proteins, Pages 360-366, Bernhard Krautler

Vitamin C, Pages 367-371, Robert B. Rucker and Francene Steinberg

Vitamin D, Pages 372-377, Hector F. DeLuca and Margaret Clagett-Dame

Vitamin D Receptor, Pages 378-383, Diane R. Dowd and Paul N. MacDonald

Vitamin E, Pages 384-388, Ute C. Obermuller-Jevic and Lester Packer

Vitamin K: Biochemistry, Metabolism, and Nutritional Aspects, Pages 389-393, J. W. Suttie

Vitamin K: Blood Coagulation and Use in Therapy, Pages 394-398, Matthew D. Stone and Gary L. Nelsestuen

Voltage-Dependent K+ Channels, Pages 399-404, Ramon Latorre and Francisco J. Morera

Voltage-Sensitive Ca2+ Channels, Pages 405-408, Harald Reuter

Voltage-Sensitive Na+ Channels, Pages 409-415, William J. Brammar

Von Hippel-Lindau (VHL) Protein, Pages 416-418, Ronald C. Conaway and Joan Weliky Conaway

XPV DNA Polymerase and Ultraviolet Damage Bypass, Pages 419-421, Alan R. Lehmann

X-Ray Determination of 3-D Structure in Proteins, Pages 422-428, Martha L. Ludwig

Yeast GAL1-GAL10 System, Pages 429-433, Dennis Lohr and Ralph Bash

Zinc Fingers, Pages 435-439, Mark Isalan

Lipids, Carbohydrates, Membranes and Membrane Proteins

Carbohydrate Chains: Enzymatic and Chemical Synthesis; Vol.1 - Pages 307-313, Thomas J. Tolbert and Chi-Huey Wong

Cell–Matrix Interactions; Vol.1 - Pages 362-366, Janet A. Askari and Martin J. Humphries

Detergent Properties; Vol.1 - Pages 577-581, Darrell R. McCaslin

Endocytosis; Vol.2 - Pages 16-19, Julie G. Donaldson

Flippases; Vol.2 - Pages 123-127, Charles J. Waechter

Galectins; Vol.2 - Pages 171-174, R. Colin Hughes

GlcNAc Biosynthesis and Function, O-Linked; Vol.2 - Pages 189-192, Kaoru Sakabe and Gerald W. Hart

Glycation; Vol.2 - Pages 229-236, Suzanne R. Thorpe and John W. Baynes

Glycolipid-Dependent Adhesion Processes; Vol.2 - Pages 261-265, Senitiroh Hakomori

Glycoprotein Folding and Processing Reactions; Vol.2 - Pages 272-276, Armando J. Parodi

Glycoprotein-Mediated Cell Interactions, O-Linked; Vol.2 - Pages 277-282, Robert S. Haltiwanger

Glycoproteins, N-Linked; Vol.2 - Pages 283-292, Mark A. Lehrman

Glycoproteins, Plant; Vol.2 - Pages 293-296, Carolyn J. Schultz

Glycosylation in Cystic Fibrosis; Vol.2 - Pages 297-301, Andrew D. Rhim, Thomas F. Scanlin and Mary Catherine Glick

Glycosylation, Congenital Disorders of; Vol.2 - Pages 302-307, Hudson H. Freeze

Glycosylphosphatidylinositol (GPI) Anchors; Vol.2 - Pages 308-311, Anant K. Menon

Ion Channel Protein Superfamily; Vol.2 - Pages 473-477, William A. Catterall

Lectins; Vol.2 - Pages 535-540, Nathan Sharon and Halina Lis

Lipases; Vol.2 - Pages 571-575, Howard L. Brockman

Lipid Bilayer Structure; Vol.2 - Pages 576-579, Erwin London

Lipid Rafts; Vol.2 - Pages 584-587, Deborah A. Brown

Lipoproteins, HDL/LDL; Vol.2 - Pages 588-593, Fayanne E. Thorngate and David L. Williams

MDR Membrane Proteins; Vol.2 - Pages 605-609, Nathan C. Rockwell

Membrane Fusion; Vol.2 - Pages 621-626, Joshua Zimmerberg and Leonid V. Chernomordik

Mucin Family of Glycoproteins; Vol.2 - Pages 758-764, Juan Perez-Vilar and Robert L. Hill

Mucins in Embryo Implantation; Vol.2 - Pages 765-769, Daniel D. Carson

Neoglycoproteins; Vol.3 - Pages 11-15, Y. C. Lee and Reiko T. Lee

N-Linked Glycan Processing Glucosidases and Mannosidases; Vol.3 - Pages 46-49, Linda O. Tremblay and Annette Herscovics

Oligosaccharide Chains: Free, N-Linked, O-Linked; Vol.3 - Pages 161-164, Tadashi Suzuki

Phospholipid Metabolism in Mammals; Vol.3 - Pages 314-320, Claudia Kent

Phospholipid Synthesis in Yeast; Vol.3 - Pages 321-325, Gil-Soo Han and George M. Carman

Prostaglandins and Leukotrienes; Vol.3 - Pages 452-456, William L. Smith and Robert C. Murphy

Protein Glycosylation Inhibitors; Vol.3 - Pages 500-503, Alan D. Elbein

Proteoglycans; Vol.3 - Pages 549-555, Sara K. Olson and Jeffrey D. Esko

Secretory Pathway; Vol.4 - Pages 11-16, Karen J. Colley

Siglecs; Vol.4 - Pages 38-40, Ajit Varki

Sphingolipid Biosynthesis; Vol.4 - Pages 76-81, Martina Leipelt and Alfred H. Merrill, Jr.

Sphingolipid Catabolism; Vol.4 - Pages 82-87, Akira Abe and James A. Shayman

Sugar Nucleotide Transporters; Vol.4 - Pages 127-129, Carlos B. Hirschberg

Trehalose Metabolism; Vol.4 - Pages 251-255, Alan D. Elbein

Metabolism, Vitamins and Hormones

Amino Acid Metabolism; Vol.1 - Pages 90-95, Luc Cynober

Anaplerosis; Vol.1 - Pages 105-110, Raymond R. Russell, III and Heinrich Taegtmeyer

Bile Salts and their Metabolism; Vol.1 - Pages 159-163, Ulrich Beuers and Thomas Pusl

Biliary Cirrhosis, Primary; Vol.1 - Pages 164-169, Marshall M. Kaplan

Branched-Chain -Ketoacids; Vol.1 - Pages 186-191, David T. Chuang

Carnitine and -Oxidation; Vol.1 - Pages 314-318, Janos Kerner and Charles L. Hoppel

Cholesterol Synthesis; Vol.1 - Pages 451-455, Peter A. Edwards

Diabetes; Vol.1 - Pages 582-592, David W. Cooke

Fat Mobilization: Perilipin and Hormone-Sensitive Lipase; Vol.2 - Pages 85-89, Constantine Londos and Alan R. Kimmel

Fatty Acid Oxidation; Vol.2 - Pages 90-94, Horst Schulz

Fatty Acid Synthesis and its Regulation; Vol.2 - Pages 99-103, Steven D. Clarke and Manabu T. Nakamura

Gluconeogenesis; Vol.2 - Pages 197-203, Richard W. Hanson and Oliver E. Owen

Glucose/Sugar Transport in Bacteria; Vol.2 - Pages 204-207, Lan Guan and H. Ronald Kaback

Glucose/Sugar Transport in Mammals; Vol.2 - Pages 208-212, Silvia Mora and Jeffrey Pessin

Glycogen Metabolism; Vol.2 - Pages 244-248, Peter J. Roach

Glycogen Storage Diseases; Vol.2 - Pages 249-254, George H. Sack, Jr.

Glycolysis, Overview; Vol.2 - Pages 266-271, Robert A. Harris

Hexokinases/Glucokinases; Vol.2 - Pages 372-377, Emile Van Schaftingen

Insulin- and Glucagon-Secreting Cells of the Pancreas; Vol.2 - Pages 430-435, Franz M. Matschinsky

Ketogenesis; Vol.2 - Pages 505-507, Janos Kerner and Charles L. Hoppel

Ornithine Cycle; Vol.3 - Pages 172-177, Malcolm Watford

Pentose Phosphate (Hexose Mono Phosphate) Pathway; Vol.3 - Pages 211-215, Bernard R. Landau

Pentose Phosphate Pathway, History of; Vol.3 - Pages 216-225, John F. Williams

Phosphofructokinase-2/Fructose Bisphosphatase-2; Vol.3 - Pages 277-280, Daniel M. Raben

Photosynthesis; Vol.3 - Pages 330-335, Richard C. Leegood

Photosynthetic Carbon Dioxide Fixation; Vol.3 - Pages 336-341, Matthew J. Paul

Porphyrin Metabolism; Vol.3 - Pages 415-419, Mark Shepherd and Harry A. Dailey

Propionyl CoA–Succinyl CoA Pathway; Vol.3 - Pages 447-451, Wayne A. Fenton

Pyruvate Carboxylation, Transamination, and Gluconeogenesis; Vol.3 - Pages 606-610, Sarawut Jitrapakdee and John C. Wallace

Pyruvate Dehydrogenase; Vol.3 - Pages 611-615, Sam A. Johnson and James G. McCormack

Pyruvate Kinase; Vol.3 - Pages 616-619, Kosaku Uyeda

Starvation; Vol.4 - Pages 99-110, Oliver E. Owen and Richard W. Hanson

Tricarboxylic Acid Cycle; Vol.4 - Pages 256-262, Richard L. Veech

Urea Cycle, Inborn Defects of; Vol.4 - Pages 326-330, Marsha K. Fearing and Vivian E. Shih

Vitamin A (Retinoids); Vol.4 - Pages 354-359, Joseph L. Napoli

Vitamin B12 and B12-Proteins; Vol.4 - Pages 360-366, Bernhard Krautler

Vitamin C; Vol.4 - Pages 367-371, Robert B. Rucker and Francene Steinberg

Vitamin D; Vol.4 - Pages 372-377, Hector F. DeLuca and Margaret Clagett-Dame

Vitamin E; Vol.4 - Pages 384-388, Ute C. Obermuller-Jevic and Lester Packer

Vitamin K: Biochemistry, Metabolism, and Nutritional Aspects; Vol.4 - Pages 389-393, J. W. Suttie

Vitamin K: Blood Coagulation and Use in Therapy; Vol.4 - Pages 394-398, Matthew D. Stone and Gary L. Nelsestuen

Cell Architecture and Function

Actin Assembly/Disassembly; Vol.1 - Pages 12-18, Henry N. Higgs

Actin-Capping and -Severing Proteins; Vol.1 - Pages 19-26, Sankar Maiti and James R. Bamburg

Actin-Related Proteins; Vol.1 - Pages 27-33, R. Dyche Mullins

Autophagy in Fungi and Mammals; Vol.1 - Pages 138-143, Daniel J. Klionsky and Ju Guan

Bax and Bcl2 Cell Death Enhancers and Inhibitors; Vol.1 - Pages 152-154, David L. Vaux

Cadherin-Mediated Cell–Cell Adhesion; Vol.1 - Pages 205-211, Frauke Drees and W. James Nelson

Caspases and Cell Death; Vol.1 - Pages 319-327, Don W. Nicholson, Pierluigi Nicotera and Gerry Melino

Cell Cycle Controls in G1 and G0; Vol.1 - Pages 328-331, WengeShi and Steven F. Dowdy

Cell Cycle: Control of Entry and Progression Through S Phase; Vol.1 - Pages 332-337, Susan L. Forsburg

Cell Cycle: DNA Damage Checkpoints; Vol.1 - Pages 338-344, Jean Y. J. Wang

Cell Cycle: Mitotic Checkpoint; Vol.1 - Pages 345-351, Tim J. Yen

Cell Migration; Vol.1 - Pages 356-361, J. Victor Small and Emmanuel Vignal

Centromeres; Vol.1 - Pages 367-371, Beth A. Sullivan

Centrosomes and Microtubule Nucleation; Vol.1 - Pages 372-376, Reiko Nakajima, Ming-Ying Tsai and Yixian Zheng

Chaperones for Metalloproteins; Vol.1 - Pages 383-386, Valeria C. Culotta and Edward Luk

Chaperones, Molecular; Vol.1 - Pages 387-392, Sue Wickner and Joel R. Hoskins

Chaperonins; Vol.1 - Pages 393-398, Arthur L. Horwich, Wayne A. Fenton and George W. Farr

Chromosome Organization and Structure, Overview; Vol.1 - Pages 469-474, Elena Gracheva and Sarah C. R. Elgin

Cytokinesis; Vol.1 - Pages 556-561, Masanori Mishima and Michael Glotzer

Desmosomes and Hemidesmosomes; Vol.1 - Pages 569-576, Rachel L. Dusek, Jonathan C. R. Jones and Kathleen J. Green

Dynactin; Vol.1 - Pages 823-826, Trina A. Schroer

Dynein; Vol.1 - Pages 827-831, K. Kevin Pfister

Endoplasmic Reticulum-Associated Protein Degradation; Vol.2 - Pages 20-23, Maurizio Molinari

Focal Adhesions; Vol.2 - Pages 128-133, Eli Zamir and Benjamin Geiger

Golgi Complex; Vol.2 - Pages 312-315, Mark Stamnes

Heat/Stress Responses; Vol.2 - Pages 343-347, Davis T. W. Ng

Inositol Lipid 3-Phosphatases; Vol.2 - Pages 421-426, Gregory S. Taylor and Jack E. Dixon

Intermediate Filament Linker Proteins: Plectin and BPAG1; Vol.2 - Pages 452-457, Peter Fuchs and Gerhard Wiche

Intermediate Filaments; Vol.2 - Pages 458-464, Kelsie M. Bernot and Pierre A. Coulombe

Keratins and the Skin; Vol.2 - Pages 497-504, Pierre A. Coulombe and Kelsie M. Bernot

Kinesin Superfamily Proteins; Vol.2 - Pages 508-516, Nobutaka Hirokawa and Reiko Takemura

Kinesins as Microtubule Disassembly Enzymes; Vol.2 - Pages 517-521, Susan L. Kline-Smith and Arshad Desai

Meiosis; Vol.2 - Pages 610-616, Neil Hunter

Metalloproteinases, Matrix; Vol.2 - Pages 657-665, Hideaki Nagase and Gillian Murphy

Microtubule-Associated Proteins; Vol.2 - Pages 676-682, Nobutaka Hirokawa and Reiko Takemura

Mitosis; Vol.2 - Pages 743-747, Patricia Wadsworth and Nasser M. Rusan

Myosin Motors; Vol.2 - Pages 778-781, Roy E. Larson

N-End Rule; Vol.3 - Pages 6-10, Alexander Varshavsky

Neuronal Intermediate Filaments; Vol.3 - Pages 21-25, Ronald K. H. Liem

Nuclear Compartmentalization; Vol.3 - Pages 87-91, Kelly P. Smith and Jeanne B. Lawrence

Nuclear Envelope and Lamins; Vol.3 - Pages 92-95, Bryce M. Paschal

Nuclear Pores and Nuclear Import/Export; Vol.3 - Pages 109-114, Anita H. Corbett

Peroxisomes; Vol.3 - Pages 246-250, Suresh Subramani

26S Proteasome, Structure and Function; Vol.3 - Pages 469-473, Peter Zwickl and Wolfgang Baumeister

Protein Glycosylation, Overview; Vol.3 - Pages 504-509, Natasha E. Zachara and Gerald W. Hart

Rho GTPases and Actin Cytoskeleton Dynamics; Vol.3 - Pages 714-718, Priam Villalonga and Anne J. Ridley

Septins and Cytokinesis; Vol.4 - Pages 22-26, Makoto Kinoshita and Christine M. Field

SUMO Modification; Vol.4 - Pages 130-134, Frauke Melchior and Andrea Pichler

Tight Junctions; Vol.4 - Pages 187-189, Shoichiro Tsukita

Transcriptional Silencing; Vol.4 - Pages 200-203, Ann Sutton and Rolf Sternglanz

Tubulin and its Isoforms; Vol.4 - Pages 272-276, Eva Nogales

Unfolded Protein Responses; Vol.4 - Pages 319-325, David Ron

Vacuoles; Vol.4 - Pages 331-336, Christopher J. Stefan and Scott D. Emr

Protein/Enzyme Structure Function and Degradation

Allosteric Regulation; Vol.1 - Pages 68-73, Barry S. Cooperman

Aminopeptidases; Vol.1 - Pages 96-98, Ralph A. Bradshaw

Amyloid; Vol.1 - Pages 99-104, Ronald Wetzel

Aspartic Proteases; Vol.1 - Pages 123-127, Ben M. Dunn

B12-Containing Enzymes; Vol.1 - Pages 145-151, Vahe Bandarian and Rowena G. Matthews

Biotin; Vol.1 - Pages 174-178, Steven W. Polyak and Anne Chapman-Smith

Biotinylation of Proteins; Vol.1 - Pages 179-181, Ronald A. Kohanski

Calpain; Vol.1 - Pages 300-306, Hiroyuki Sorimachi and Yasuko Ono

Chemiluminescence and Bioluminescence; Vol.1 - Pages 399-404, Thomas O. Baldwin

Coenzyme A; Vol.1 - Pages 475-477, M. Daniel Lane

Collagenases; Vol.1 - Pages 478-481, Kenn Holmbeck and Henning Birkedal-Hansen

Collagens; Vol.1 - Pages 482-487, Darwin J. Prockop

Cysteine Proteases; Vol.1 - Pages 516-520, David J. Buttle and John S. Mort

Disulfide Bond Formation; Vol.1 - Pages 598-602, Hiram F. Gilbert

Elastin; Vol.2 - Pages 10-12, Judith Ann Foster

Enzyme Inhibitors; Vol.2 - Pages 31-37, Vern L. Schramm

Enzyme Kinetics; Vol.2 - Pages 38-44, Irwin H. Segel

Enzyme Reaction Mechanisms: Stereochemistry; Vol.2 - Pages 45-50, Ming-Daw Tsai, Li Zhao and Brandon J. Lamarche

Flavins; Vol.2 - Pages 118-122, Barrie Entsch and David P. Ballou

Heme Proteins; Vol.2 - Pages 354-361, Johannes Everse

HIV Protease; Vol.2 - Pages 384-387, Ben M. Dunn

Kinetic Isotope Effects; Vol.2 - Pages 522-527, Justine P. Roth and Judith P. Klinman

Lipid Modification of Proteins: Targeting to Membranes; Vol.2 - Pages 580-583, Marilyn D. Resh

Low Barrier Hydrogen Bonds; Vol.2 - Pages 594-598, Perry A. Frey

Metalloproteases; Vol.2 - Pages 652-656, David S. Auld

Peptide Amidation; Vol.3 - Pages 226-230, Mark J. Niciu, Richard E. Mains and Betty A. Eipper

Phage Display for Protein Binding; Vol.3 - Pages 251-255, Henry B. Lowman

Prions, Overview; Vol.3 - Pages 437-440, Cedric Govaerts and Fred E. Cohen

Proteases in Blood Clotting; Vol.3 - Pages 457-463, John D. Kulman and Earl W. Davie

Proteasomes, Overview; Vol.3 - Pages 464-468, Martin Rechsteiner

Protein Carboxyl Esterification; Vol.3 - Pages 474-477, Shilpa G. Lalchandani and Jeffry B. Stock

Protein Degradation; Vol.3 - Pages 484-492, Tomo ari and Alfred L. Goldberg

Protein Folding and Assembly; Vol.3 - Pages 493-499, David P. Goldenberg

Protein N-Myristoylation; Vol.3 - Pages 527-531, Erica Dutil Sonnenburg and Jeffrey I. Gordon

Protein Palmitoylation; Vol.3 - Pages 532-535, Robert J. Deschenes

Pteridines; Vol.3 - Pages 556-560, S. Colette Daubner and Paul F. Fitzpatrick

Pyridoxal Phosphate; Vol.3 - Pages 595-599, David E. Metzler

Regulated Intramembrane Proteolysis (Rip); Vol.3 - Pages 665-670, Jin Ye, Michael S. Brown and Joseph L. Goldstein

Secretases; Vol.4 - Pages 7-10, Robert L. Heinrikson

Selenoprotein Synthesis; Vol.4 - Pages 17-21, August Bock

Substrate Binding, Catalysis, and Product Release; Vol.4 - Pages 123-126, W. Wallace Cleland

Two-Hybrid Protein–Protein Interactions; Vol.4 - Pages 290-293, Ilya Serebriiskii and Erica A. Golemis

Tyrosine Sulfation; Vol.4 - Pages 294-297, Denis Corbeil and Wieland B. Huttner

Ubiquitin System; Vol.4 - Pages 299-303, Aaron Ciechanover and Michael H. Glickman

Ubiquitin-Like Proteins; Vol.4 - Pages 304-307, Edward T. H. Yeh

Zinc Fingers; Vol.4 - Pages 435-439, Mark Isalan

Bioenergetics

ABC Transporters; Vol.1 - Pages 1-5, Andre Goffeau, Benoit De Hertogh and Philippe V. Baret

Amine Oxidases; Vol.1 - Pages 85-89, Giovanni Floris and Alessandro Finazzi Agro

ATP Synthesis in Plant Mitochondria: Substrates, Inhibitors, Uncouplers; Vol.1 - Pages 128-132, Kathleen L. Soole and R. Ian Menz

ATP Synthesis: Mitochondrial Cyanide-Resistant Terminal Oxidases; Vol.1 - Pages 133-137, James N. Siedow

Bioenergetics: General Definition of Principles; Vol.1 - Pages 170-173, David G. Nicholls

Calcium Buffering Proteins: Calbindin; Vol.1 - Pages 221-225, Willi Hunziker and Igor Bendik

Calcium Buffering Proteins: ER Luminal Proteins; Vol.1 - Pages 226-230, Jody Groenendyk and Marek Michalak

Calcium Oscillations; Vol.1 - Pages 231-234, Marisa Brini

Calcium Sensing Receptor; Vol.1 - Pages 235-240, Jacob Tfelt-Hansen and Edward M. Brown

Calcium Signaling: Calmodulin-Dependent Phosphatase; Vol.1 - Pages 241-245, Claude Klee, Hao Ren and Shipeng Li

Calcium Signaling: Cell Cycle; Vol.1 - Pages 246-249, Luigia Santella

Calcium Signaling: Motility (Actomyosin–Troponin System); Vol.1 - Pages 250-255, Takeyuki Wakabayashi and Setsuro Ebashi

Calcium Signaling: NO Synthase; Vol.1 - Pages 256-260, Zhi-Qiang Wang and Dennis J. Stuehr

Calcium Transport in Mitochondria; Vol.1 - Pages 261-266, Rosario Rizzuto and Marisa Brini

Calcium Waves; Vol.1 - Pages 267-269, Lionel F. Jaffe

Calcium, Biological Fitness of; Vol.1 - Pages 270-273, Robert J. P. Williams

Calcium/Calmodulin-Dependent Protein Kinase II; Vol.1 - Pages 274-280, Andy Hudmon and Howard Schulman

Calcium-Binding Proteins: Cytosolic (Annexins, Gelsolins, C2-Domain Proteins); Vol.1 - Pages 287-293, Joachim Krebs

Calcium-Modulated Proteins (EF-Hand); Vol.1 - Pages 294-299, Robert H. Kretsinger

Cell Death by Apoptosis and Necrosis; Vol.1 - Pages 352-355, Pierluigi Nicotera

Chemiosmotic Theory; Vol.1 - Pages 405-412, Keith D. Garlid

Chemolithotrophy; Vol.1 - Pages 419-424, Alan B. Hooper

Chlorophylls and Carotenoids; Vol.1 - Pages 430-437, Hugo Scheer

Chloroplast Redox Poise and Signaling; Vol.1 - Pages 438-445, John F. Allen

Chloroplasts; Vol.1 - Pages 446-450, Nicoletta Rascio

Cytochrome b6f Complex; Vol.1 - Pages 521-527, Gunter A. Hauska and Thomas Schodl

Cytochrome bc1 Complex (Respiratory Chain Complex III); Vol.1 - Pages 528-534, Bernard L. Trumpower

Cytochrome c; Vol.1 - Pages 535-538, Hans Tuppy and Gunther Kreil

Cytochrome Oxidases, Bacterial; Vol.1 - Pages 539-543, Peter Brzezinski and Pia Adelroth

Cytochrome P-450; Vol.1 - Pages 544-549, Rita Bernhardt

Energy Transduction in Anaerobic Prokaryotes; Vol.2 - Pages 24-30, Gottfried Unden

ER/SR Calcium Pump: Function; Vol.2 - Pages 56-60, Giuseppe Inesi

ER/SR Calcium Pump: Structure; Vol.2 - Pages 61-65, Chikashi Toyoshima and Yuji Sugita

F1–F0 ATP Synthase; Vol.2 - Pages 73-79, Donata Branca

Ferredoxin; Vol.2 - Pages 104-106, Giuliana Zanetti and Vittorio Pandini

Ferredoxin-NADP+ Reductase; Vol.2 - Pages 107-111, Giuliana Zanetti and Alessandro Aliverti

Free Radicals, Sources and Targets of: Mitochondria; Vol.2 - Pages 134-142, Alberto Boveris and Enrique Cadenas

Friedreich's Ataxia; Vol.2 - Pages 143-145, Paul E. Hart and Anthony H. V. Schapira

Giant Mitochondria (Megamitochondria); Vol.2 - Pages 186-188, Bernard Tandler and Charles L. Hoppel

Glutathione Peroxidases; Vol.2 - Pages 224-228, Fulvio Ursini and Matilde Maiorino

Green Bacteria: Secondary Electron Donor (Cytochromes); Vol.2 - Pages 321-324, Hirozo Oh-oka and Robert E. Blankenship

Green Bacteria: The Light-Harvesting Chlorosome; Vol.2 - Pages 325-330, John M. Olson

Green Sulfur Bacteria: Reaction Center and Electron Transport; Vol.2 - Pages 331-336, Gunter A. Hauska and Thomas Schodl

Heme Synthesis; Vol.2 - Pages 362-366, Gloria C. Ferreira

Intracellular Calcium Channels: cADPR-Modulated (Ryanodine Receptors); Vol.2 - Pages 465-468, Antony Galione

Intracellular Calcium Channels: NAADP+-Modulated; Vol.2 - Pages 469-472, Armando A. Genazzani and Marcella Debidda

IP3 Receptors; Vol.2 - Pages 478-481, Colin W. TaylorEdward Morris and Paula da Fonseca

Iron–Sulfur Proteins; Vol.2 - Pages 482-489, Helmut Beinert, Jacques Meyer and Roland Lill

Ligand-Operated Membrane Channels: Calcium (Glutamate); Vol.2 - Pages 551-561, Elias K. Michaelis

Ligand-Operated Membrane Channels: GABA; Vol.2 - Pages 562-566, F. Minier and Erwin Sigel

Light-Harvesting Complex (LHC) I and II: Pigments and Proteins; Vol.2 - Pages 567-570, Stefan Jansson

Luft's Disease; Vol.2 - Pages 599-601, Salvatore DiMauro

Membrane Transport, General Concepts; Vol.2 - Pages 627-630, Stanley G. Schultz

Membrane Transporters:Na+/Ca2+ Exchangers; Vol.2 - Pages 631-636, Jonathan Lytton

Membrane-Associated Energy Transduction in Bacteria and Archaea; Vol.2 - Pages 637-645, Gunter Schafer

Metabolite Channeling: Creatine Kinase Microcompartments; Vol.2 - Pages 646-651, Uwe Schlattner and Theo Wallimann

Mitochondrial Auto-Antibodies; Vol.2 - Pages 683-688, Harold Baum

Mitochondrial Channels; Vol.2 - Pages 689-692, M. Catia Sorgato and Alessandro Bertoli

Mitochondrial DNA; Vol.2 - Pages 693-696, Gottfried Schatz

Mitochondrial Genes and their Expression: Yeast; Vol.2 - Pages 697-702, Piotr P. Slonimski and Giovanna Carignani

Mitochondrial Genome, Evolution; Vol.2 - Pages 703-708, B. Franz Lang, Dennis V. Lavrov and Gertraud Burger

Mitochondrial Genome, Overview; Vol.2 - Pages 709-715, Douglas C. Wallace

Mitochondrial Inheritance; Vol.2 - Pages 716-719, Eric A. Shoubridge

Mitochondrial Membranes, Structural Organization; Vol.2 - Pages 720-724, Carmen A. Mannella

Mitochondrial Metabolite Transporter Family; Vol.2 - Pages 725-732, Ferdinando Palmieri and Martin Klingenberg

Mitochondrial Outer Membrane and the VDAC Channel; Vol.2 - Pages 733-736, Marco Colombini

Neuronal Calcium Signal; Vol.3 - Pages 16-20, Hilmar Bading

Nicotinamide Nucleotide Transhydrogenase; Vol.3 - Pages 50-56, Jan Rydstrom

Nuclear Genes in Mitochondrial Function and Biogenesis; Vol.3 - Pages 100-104, Alexander Tzagoloff and Carol L. Dieckmann

Oncocytes; Vol.3 - Pages 165-166, Bernard Tandler and Charles L. Hoppel

Oxygenases; Vol.3 - Pages 178-182, Osamu Hayaishi

Periplasmic Electron Transport Systems in Bacteria; Vol.3 - Pages 231-238, David J. Richardson, Gary Sawers and Rob J. M. Van Spanning

Phosphatidylinositol-3-Phosphate; Vol.3 - Pages 272-276, Joseph V. Virbasius and Michael P. Czech

Photosystem I, Structure and Function; Vol.3 - Pages 342-347, Petra Fromme

Photosystem I: FX, FA, and FB Iron–Sulfur Clusters; Vol.3 - Pages 348-356, Mikhail L. Antonkine and John H. Golbeck

Photosystem II Light Harvesting System: Dynamic Behavior; Vol.3 - Pages 357-362, Peter Horton and Alexander Ruban

Photosystem II: Assembly and Turnover of the D1 Protein; Vol.3 - Pages 363-366, Eira Kanervo and Eva-Mari Aro

Photosystem II: Protein Components; Vol.3 - Pages 367-374, James Barber

Photosystem II: Water Oxidation, Overview; Vol.3 - Pages 375-380, Fabrice Rappaport and Pierre Joliot

Plasma-Membrane Calcium Pump: Structure and Function; Vol.3 - Pages 385-389, Emanuel E. Strehler

Plastocyanin; Vol.3 - Pages 390-393, Elizabeth L. Gross

Protein Import into Mitochondria; Vol.3 - Pages 510-515, Johannes M. Herrmann and Walter Neupert

P-Type Pumps: Copper Pump; Vol.3 - Pages 561-564, Ilia Voskoboinik and James Camakaris

P-Type Pumps: H+/K+ Pump; Vol.3 - Pages 565-570, Jai Moo Shin and George Sachs

P-Type Pumps: Na+/K+ Pump; Vol.3 - Pages 571-576, Peter L. Jorgensen

P-Type Pumps: Plasma-Membrane H+ Pump; Vol.3 - Pages 577-581, A. Brett Mason and Carolyn W. Slayman

Purple Bacteria: Electron Acceptors and Donors; Vol.3 - Pages 582-585, Evaldas Katilius and Neal W. Woodbury

Purple Bacteria: Photosynthetic Reaction Centers; Vol.3 - Pages 586-594, C. Roy D. Lancaster

Pyrimidine Biosynthesis; Vol.3 - Pages 600-605, Monika Loffler and Elke Zameitat

Quinones; Vol.3 - Pages 621-627, Giorgio Lenaz and Maria Luisa Genova

Respiratory Chain and ATP Synthase; Vol.3 - Pages 671-675, David G. Whitehouse and Anthony L. Moore

Respiratory Chain Complex I; Vol.3 - Pages 676-680, Ulrich Brandt

Respiratory Chain Complex II and Succinate: Quinone Oxidoreductases; Vol.3 - Pages 681-687, C. Roy D. Lancaster

Respiratory Chain Complex IV; Vol.3 - Pages 688-694, Hartmut Michel

Respiratory Processes in Anoxygenic and Oxygenic Phototrophs; Vol.3 - Pages 695-699, Roberto Borghese and Davide Zannoni

Spastic Paraplegia; Vol.4 - Pages 61-66, Elena Irene Rugarli and Andrea Ballabio

Store-Operated Membrane Channels: Calcium; Vol.4 - Pages 117-122, Indu S. Ambudkar

Superoxide Dismutase; Vol.4 - Pages 135-138, Irwin Fridovich

Uncoupling Proteins; Vol.4 - Pages 313-318, Daniel Ricquier and Frederic Bouillaud

V-ATPases; Vol.4 - Pages 349-353, Michael Forgac

Voltage-Dependent K+ Channels; Vol.4 - Pages 399-404, Ramon Latorre and Francisco J. Morera

Voltage-Sensitive Ca2+ Channels; Vol.4 - Pages 405-408, Harald Reuter

Voltage-Sensitive Na+ Channels; Vol.4 - Pages 409-415, William J. Brammar

Molecular Biology

Alternative Splicing: Regulation of Fibroblast Growth Factor Receptor (FGFR); Vol.1 - Pages 74-77, Mariano A. Garcia-Blanco

Alternative Splicing: Regulation of Sex Determination in Drosophila melanogaster; Vol.1 - Pages 78-84, Jill K. M. Penn, Patricia Graham and Paul Schedl

ara Operon; Vol.1 - Pages 116-119, Robert F. Schleif

Chromatin Remodeling; Vol.1 - Pages 456-463, Eric Kallin and Yi Zhang

Chromatin: Physical Organization; Vol.1 - Pages 464-468, Christopher L. Woodcock

DNA Base Excision Repair; Vol.1 - Pages 603-608, Hilde Nilsen and Tomas Lindahl

DNA Damage: Alkylation; Vol.1 - Pages 609-613, Anton B. Guliaev and B. Singer

DNA Glycosylases: Mechanisms; Vol.1 - Pages 614-617, Daniel J. Krosky and James T. Stivers

DNA Helicases: Dimeric Enzyme Action; Vol.1 - Pages 618-623, Timothy M. Lohman

DNA Helicases: HexamericEnzyme Action; Vol.1 - Pages 624-631, Smita S. Patel

DNA Ligases: Mechanism and Functions; Vol.1 - Pages 632-636, Alan E. Tomkinson and John B. Leppard

DNA Ligases: Structures; Vol.1 - Pages 637-643, C. Kiong Ho, Mark Odell and Dimitar B. Nikolov

DNA Methyltransferases, Bacterial; Vol.1 - Pages 644-651, Albert Jeltsch and Richard I. Gumport

DNA Methyltransferases, Structural Themes; Vol.1 - Pages 652-659, Sanjay Kumar

DNA Methyltransferases: Eubacterial GATC; Vol.1 - Pages 660-664, Martin G. Marinus

DNA Mismatch Repair and Homologous Recombination; Vol.1 - Pages 665-670, Ivan Matic and Miroslav Radman

DNA Mismatch Repair and the DNA Damage Response; Vol.1 - Pages 671-674, Guo-Min Li and Steven R. Presnell

DNA Mismatch Repair Defects and Cancer; Vol.1 - Pages 675-681, Richard D. Kolodner

DNA Mismatch Repair in Bacteria; Vol.1 - Pages 682-686, A-Lien Lu

DNA Mismatch Repair in Mammals; Vol.1 - Pages 687-690, James T. Drummond

DNA Mismatch Repair: E. coli Vsr and Eukaryotic G–T Systems; Vol.1 - Pages 691-693, Margaret Lieb

DNA Oxidation; Vol.1 - Pages 694-697, Arthur P. Grollman and Dmitry O. Zharkov

DNA Photolyase; Vol.1 - Pages 698-702, Carrie L. Partch and Aziz Sancar

DNA Polymerase α, Eukaryotic; Vol.1 - Pages 703-707, Teresa S. -F. Wang

DNA Polymerase β, Eukaryotic; Vol.1 - Pages 708-712, William A. Beard and Samuel H. Wilson

DNA Polymerase δ, Eukaryotic; Vol.1 - Pages 713-715, Antero G. So and Kathleen M. Downey

DNA Polymerase ε, Eukaryotic; Vol.1 - Pages 716-719, Yasuo Kawasaki and Akio Sugino

DNA Polymerase I, Bacterial; Vol.1 - Pages 720-725, Catherine M. Joyce

DNA Polymerase II, Bacterial; Vol.1 - Pages 726-728, Judith L. Campbell

DNA Polymerase III, Bacterial; Vol.1 - Pages 729-733, Hisaji Maki

DNA Polymerases: Kinetics and Mechanism; Vol.1 - Pages 734-739, Kenneth A. Johnson

DNA Replication Fork, Bacterial; Vol.1 - Pages 740-744, Nancy G. Nossal

DNA Replication Fork, Eukaryotic; Vol.1 - Pages 745-748, Lori M. Kelman, Jerard Hurwitz and Zvi Kelman

DNA Replication, Mitochondrial; Vol.1 - Pages 749-752, David A. Clayton

DNA Replication: Eukaryotic Origins and the Origin Recognition Complex; Vol.1 - Pages 753-760, Melvin L. DePamphilis and Cong-jun Li

DNA Replication: Initiation in Bacteria; Vol.1 - Pages 761-766, Jon M. Kaguni

DNA Restriction and Modification: Type I Enzymes; Vol.1 - Pages 767-771, David T. F. Dryden

DNA Restriction and Modification: Type II Enzymes; Vol.1 - Pages 772-777, Darren M. Gowers and Stephen E. Halford

DNA Restriction and Modification: Type III Enzymes; Vol.1 - Pages 778-781, Desirazu N. Rao and S. Srivani

DNA Secondary Structure; Vol.1 - Pages 782-787, Albino Bacolla and Robert D. Wells

DNA Sequence Recognition by Proteins; Vol.1 - Pages 788-793, Arabela A. Grigorescu and John M. Rosenberg

DNA Supercoiling; Vol.1 - Pages 794-797, Tao-shih Hsieh

DNA Topoisomerases: Type I; Vol.1 - Pages 798-805, James J. Champoux

DNA Topoisomerases: Type II; Vol.1 - Pages 806-811, Renier Velez-Cruz and Neil Osheroff

DNA Topoisomerases: Type III–RecQ Helicase Systems; Vol.1 - Pages 812-816, Rodney Rothstein and Erika Shor

EF-G and EF-Tu Structures and Translation Elongation in Bacteria; Vol.2 - Pages 1-5, Poul Nissen and Jens Nyborg

Exonucleases, Bacterial; Vol.2 - Pages 66-72, Susan T. Lovett

HIV-1 Reverse Transcriptase Structure; Vol.2 - Pages 388-392, Kalyan Das, Stefan G. Sarafianos, Eddy Arnold and Stephen H. Hughes

Homologous Recombination in Meiosis; Vol.2 - Pages 393-397, Nancy M. Hollingsworth

lac Operon; Vol.2 - Pages 529-534, Liskin Swint-Kruse and Kathleen S. Matthews

LexA Regulatory System; Vol.2 - Pages 546-550, Veronica G. Godoy, Penny J. Beuning and Graham C. Walker

Metaphase Chromosome; Vol.2 - Pages 666-671, Sharron Vass and Margarete M. S. Heck

Methyl-CpG-Binding Proteins; Vol.2 - Pages 672-675, David G. Skalnik

mRNA Polyadenylation in Eukaryotes; Vol.2 - Pages 748-752, Mary Edmonds

mRNA Processing and Degradation in Bacteria; Vol.2 - Pages 753-757, Deborah A. Steege

Non-Homologous End Joining; Vol.3 - Pages 66-70, Penny A. Jeggo

Nonhomologous Recombination: Bacterial Transposons; Vol.3 - Pages 71-79, Bao Ton Hoang and Michael G. Chandler

Nonhomologous Recombination: Retrotransposons; Vol.3 - Pages 80-86, Siew Loon Ooi and Jef D. Boeke

Nuclear Organization, Chromatin Structure, and Gene Silencing; Vol.3 - Pages 105-108, Lori L. Wallrath, John R. Danzer, Oya Yazgan and Pamela K. Geyer

Nucleoid Organization of Bacterial Chromosomes; Vol.3 - Pages 115-118, Charles J. Dorman

Nucleolus, Overview; Vol.3 - Pages 119-122, Thoru Pederson

Nucleotide Excision Repair and Human Disease; Vol.3 - Pages 123-129, James E. Cleaver

Nucleotide Excision Repair in Eukaryotes; Vol.3 - Pages 130-133, Laura A. Lindsey-Boltz and Aziz Sancar

Nucleotide Excision Repair, Bacterial: The UvrABCD System; Vol.3 - Pages 134-142, Bennett Van Houten and Lawrence Grossman

Nucleotide Excision Repair: Biology; Vol.3 - Pages 143-147, Errol C. Friedberg

PHO Regulon; Vol.3 - Pages 262-265, Bengt L. Persson

Pre-tRNA and Pre-rRNA Processing in Bacteria; Vol.3 - Pages 420-424, Sidney R. Kushner

Pre-tRNA and Pre-rRNA Processing in Eukaryotes; Vol.3 - Pages 425-431, Hendrik A. Raue

Prions and Epigenetic Inheritance; Vol.3 - Pages 432-436, Reed B. Wickner

Processivity Clamps in DNA Replication: Clamp Loading; Vol.3 - Pages 441-446, Megan J. Davey and Mike O'Donnell

Recombination: Heteroduplexand Mismatch Repair in vitro; Vol.3 - Pages 645-648, Leroy Worth, Jr.

Recombination: Strand Transferases; Vol.3 - Pages 649-653, Floyd R. Bryant

Recombination-Dependent DNA Replication; Vol.3 - Pages 654-659, Kenneth N. Kreuzer

recQ DNA Helicase Family in Genetic Stability; Vol.3 - Pages 660-664, Mary A. Risinger and Joanna Groden

Reverse Transcriptase and Retroviral Replication; Vol.3 - Pages 708-713, Laura Tarrago-Litvak, Marie-Line Andreola and Simon Litvak

Ribosome Assembly; Vol.3 - Pages 719-724, John L. Woolford

Ribosome Structure; Vol.3 - Pages 725-732, Brian T. Wimberly

Ribozyme Mechanisms; Vol.3 - Pages 733-737, John Hsieh and Carol A. Fierke

Ribozyme Structural Elements: Group I Introns; Vol.3 - Pages 738-742, Barbara L. Golden

Ribozyme Structural Elements: Hairpin Ribozyme; Vol.3 - Pages 743-746, Adrian R. Ferre-D'Amare

Ribozymes and Evolution; Vol.3 - Pages 747-752, Niles Lehman

RNA Editing; Vol.3 - Pages 753-758, Charles E. Samuel

RNA Polymerase I and RNA Polymerase III in Eukaryotes; Vol.3 - Pages 759-762, Robert J. White

RNA Polymerase II and Basal Transcription Factors in Eukaryotes; Vol.3 - Pages 763-765, Joan Weliky Conaway and Ronald C. Conaway

RNA Polymerase II Elongation Control in Eukaryotes; Vol.3 - Pages 766-769, David H. Price

RNA Polymerase II Structure in Eukaryotes; Vol.3 - Pages 770-774, Patrick Cramer

RNA Polymerase Reaction in Bacteria; Vol.3 - Pages 775-780, Arkady A. Mustaev and Alexander D. Goldfarb

RNA Polymerase Structure, Bacterial; Vol.3 - Pages 781-784, Michael Anikin, Dmitri Temiakov and William T. McAllister

Sigma Factors; Vol.4 - Pages 41-44, John D. Helmann

Sliding Clamps in DNA Replication: E. coli -Clamp and PCNA Structure; Vol.4 - Pages 45-47, Eric R. Goedken and John Kuriyan

Spliceosome; Vol.4 - Pages 88-92, Timothy W. Nilsen

T7 RNA Polymerase; Vol.4 - Pages 147-151, Rui Sousa

Telomeres: Maintenance and Replication; Vol.4 - Pages 174-179, Alessandro Bianchi and David Shore

Transcription Termination; Vol.4 - Pages 195-199, Thomas J. Santangelo and Jeffrey W. Roberts

Transcription-Coupled DNA Repair, Overview; Vol.4 - Pages 204-208, Isabel Mellon

Translation Elongation in Bacteria; Vol.4 - Pages 214-223, Oliver Vesper and Knud H. Nierhaus

Translation Elongation in Eukaryotes; Vol.4 - Pages 224-229, William C. Merrick and Anton A. Komar

Translation Initiation in Bacteria: Factors and Mechanisms; Vol.4 - Pages 230-236, Cynthia L. Pon and Claudio O. Gualerzi

Translation Initiation in Eukaryotes: Factors and Mechanisms; Vol.4 - Pages 237-241, Tatyana V. Pestova and Christopher U. T. Hellen

Translation Termination and Ribosome Recycling; Vol.4 - Pages 242-246, Nadja Koloteva-Levin and Mick F. Tuite

Translesion DNA Polymerases, Eukaryotic; Vol.4 - Pages 247-250, Alexandra Vaisman and Roger Woodgate

tRNA Synthetases; Vol.4 - Pages 263-266, Karla L. Ewalt and Paul Schimmel

trp Operon and Attenuation; Vol.4 - Pages 267-271, Paul Gollnick

UmuC, D Lesion Bypass DNA Polymerase V; Vol.4 - Pages 308-312, Zvi Livneh

XPV DNA Polymerase and Ultraviolet Damage Bypass; Vol.4 - Pages 419-421, Alan R. Lehmann

Yeast GAL1–GAL10 System; Vol.4 - Pages 429-433, Dennis Lohr and Ralph Bash

Signaling

Abscisic Acid (ABA); Vol.1 - Pages 6-11, Ramanjulu Sunkar and Jian-Kang Zhu

Adenosine Receptors; Vol.1 - Pages 34-39, Lauren J. Murphree and Joel Linden

Adenylyl Cyclases; Vol.1 - Pages 40-45, Ronald Taussig

Adrenergic Receptors; Vol.1 - Pages 46-50, David B. Bylund

A-Kinase Anchoring Proteins; Vol.1 - Pages 64-67, Lorene K. Langeberg and John D. Scott

Angiotensin Receptors; Vol.1 - Pages 111-115, Tadashi Inagami

ARF Family; Vol.1 - Pages 120-122, Gustavo Pacheco-Rodriguez, Joel Moss and Martha Vaughan

B-Cell Antigen Receptor; Vol.1 - Pages 155-158, Thomas M. Yankee and Edward A. Clark

Bradykinin Receptors; Vol.1 - Pages 182-185, Ronald M. Burch

Brassinosteroids; Vol.1 - Pages 192-197, Steven D. Clouse

Cadherin Signaling; Vol.1 - Pages 199-204, David B. Sacks and Jonathan M. G. Higgins

Calcitonin Gene-Related Peptide and Adrenomedullin Receptors; Vol.1 - Pages 212-216, Debbie L. Hay, Alex C. Conner and David R. Poyner

Calcitonin Receptor; Vol.1 - Pages 217-220, Samia I. Girgis, Niloufar Moradi-Bidhendi, Lucia Mancini and Iain MacIntyre

Calcium/Calmodulin-Dependent Protein Kinases; Vol.1 - Pages 281-286, J. Robison and Roger J. Colbran

c-fes Proto-Oncogene; Vol.1 - Pages 377-382, Thomas E. Smithgall and Robert I. Glazer

Chemokine Receptors; Vol.1 - Pages 413-418, Ann Richmond and Guo-Huang Fan

Chemotactic Peptide/Complement Receptors; Vol.1 - Pages 425-429, Eric R. Prossnitz and Larry A. Sklar

Cyclic AMP Receptors of Dictyostelium; Vol.1 - Pages 488-493, Dale Hereld and Peter N. Devreotes

Cyclic GMP Phosphodiesterases; Vol.1 - Pages 494-500, Sharron H. Francis and Jackie D. Corbin

Cyclic Nucleotide Phosphodiesterases; Vol.1 - Pages 501-505, Vincent C. Manganiello and Eva Degerman

Cyclic Nucleotide-Dependent Protein Kinases; Vol.1 - Pages 506-511, Sharron H. Francis and Jackie D. Corbin

Cyclic Nucleotide-Regulated Cation Channels; Vol.1 - Pages 512-515, Martin Biel and Franz Hofmann

Cytokines; Vol.1 - Pages 550-555, Andrea L. Wurster and Michael J. Grusby

Cytokinin; Vol.1 - Pages 562-567, Thomas Schmulling

Diacylglycerol Kinases and Phosphatidic Acid Phosphatases; Vol.1 - Pages 593-597, Stephen M. Prescott and Matthew K. Topham

Dopamine Receptors; Vol.1 - Pages 817-822, Kim A. Neve

Eicosanoid Receptors; Vol.2 - Pages 6-9, Richard M. Breyer and Matthew D. Breyer

Endocannabinoids; Vol.2 - Pages 13-15, Daniele Piomelli

Epidermal Growth Factor Receptor Family; Vol.2 - Pages 51-55, Denis Tvorogov and Graham Carpenter

FAK Family; Vol.2 - Pages 80-84, Steven K. Hanks

Fatty Acid Receptors; Vol.2 - Pages 95-98, Christer Owman and Bjorn Olde

Fibroblast Growth Factor Receptors and Cancer-Associated Perturbations; Vol.2 - Pages 112-117, Marko Kornmann and Murray Korc

G Protein Signaling Regulators; Vol.2 - Pages 147-151, John H. Exton

G Protein-Coupled Receptor Kinases and Arrestins; Vol.2 - Pages 152-157, Jeffrey L. Benovic

G12/G13 Family; Vol.2 - Pages 158-161, Stefan Offermanns

GABAA Receptor; Vol.2 - Pages 162-166, Richard W. Olsen and Gregory W. Sawyer

GABAB Receptor; Vol.2 - Pages 167-170, S. J. Enna

Gi Family of Heterotrimeric G Proteins; Vol.2 - Pages 181-185, Maurine E. Linder

Glucagon Family of Peptides and their Receptors; Vol.2 - Pages 193-196, Laurie L. Baggio and Daniel J. Drucker

Glutamate Receptors, Ionotropic; Vol.2 - Pages 213-219, Derek B. Scott and Michael D. Ehlers

Glutamate Receptors, Metabotropic; Vol.2 - Pages 220-223, P. Jeffrey Conn

Glycine Receptors; Vol.2 - Pages 237-243, Bodo Laube and Heinrich Betz

Glycogen Synthase Kinase-3; Vol.2 - Pages 255-260, James R. Woodgett

Gq Family; Vol.2 - Pages 316-320, Wanling Yang and John D. Hildebrandt

Gs Family of Heterotrimeric G Proteins; Vol.2 - Pages 337-341, Susanne M. Mumby

Hematopoietin Receptors; Vol.2 - Pages 348-353, Barbara A. Miller and Joseph Y. Cheung

Hepatocyte Growth Factor/Scatter Factor Receptor; Vol.2 - Pages 367-371, Selma Pennacchietti and Paolo M. Comoglio

Histamine Receptors; Vol.2 - Pages 378-383, Stephen J. Hill and Jillian G. Baker

Immunoglobulin (Fc) Receptors; Vol.2 - Pages 411-416, Mark Hogarth

Inositol Phosphate Kinases and Phosphatases; Vol.2 - Pages 427-429, Stephen B. Shears

Insulin Receptor Family; Vol.2 - Pages 436-440, Paul F. Pilch and Jongsoon Lee

Integrin Signaling; Vol.2 - Pages 441-445, Lawrence E. Goldfinger and Mark H. Ginsberg

Interferon Receptors; Vol.2 - Pages 446-451, Christopher P. Elco and Ganes C. Sen

JAK-STAT Signaling Paradigm; Vol.2 - Pages 491-496, Edward Cha and Christian Schindler

Leptin; Vol.2 - Pages 541-545, Thomas W. Gettys

Lysophospholipid Receptors; Vol.2 - Pages 602-604, Gabor J. Tigyi

Melanocortin System; Vol.2 - Pages 617-620, Roger D. Cone

Mitogen-Activated Protein Kinase Family; Vol.2 - Pages 737-742, Hidemi Teramoto and J. Silvio Gutkind

Muscarinic Acetylcholine Receptors; Vol.2 - Pages 775-777, Neil M. Nathanson

Natriuretic Peptides and their Receptors; Vol.3 - Pages 1-5, Lincoln R. Potter

Neuropeptide Y Receptors; Vol.3 - Pages 26-31, Eric M. Parker

Neurotensin Receptors; Vol.3 - Pages 32-36, William Rostene, Patrick Kitabgi and Didier Pelaprat

Neurotransmitter Transporters; Vol.3 - Pages 37-40, Aurelio Galli, Randy D. Blakely and Louis J. DeFelice

Neurotrophin Receptor Signaling; Vol.3 - Pages 41-45, Jennifer J. Gentry and Bruce D. Carter

Nicotinic Acetylcholine Receptors; Vol.3 - Pages 57-61, Nivalda O. Rodrigues-Pinguet and Henry A. Lester

Nitric Oxide Signaling; Vol.3 - Pages 62-65, Michael A. Marletta

Nuclear Factor kappaB; Vol.3 - Pages 96-99, Thomas D. Gilmore

Olfactory Receptors; Vol.3 - Pages 149-154, Sigrun I. Korsching

Opioid Receptors; Vol.3 - Pages 167-171, P. Y. Law and Horace H. Loh

P2X Purinergic Receptors; Vol.3 - Pages 183-187, Annmarie Surprenant

P2Y Purinergic Receptors; Vol.3 - Pages 188-191, George R. Dubyak

p53 Protein; Vol.3 - Pages 192-195, Jamie Hearnes and Jennifer Pietenpol

p70 S6 Kinase/mTOR; Vol.3 - Pages 196-200, Christopher G. Proud

Parathyroid Hormone/Parathyroid Hormone-Related Protein Receptor; Vol.3 - Pages 201-207, Thomas J. Gardella

Peroxisome Proliferator-Activated Receptors; Vol.3 - Pages 239-245, Mary C. Sugden, Edward A. Sugden and Mark J. Holness

Pheromone Receptors (Yeast); Vol.3 - Pages 256-261, James B. Konopka and Jeremy W. Thorner

Phosphatidylinositol Bisphosphate and Trisphosphate; Vol.3 - Pages 266-271, Alex Toker

Phosphoinositide 3-Kinase; Vol.3 - Pages 281-286, Khatereh Ahmadi and Michael Waterfield

Phosphoinositide 4- and 5-Kinases and Phosphatases; Vol.3 - Pages 287-291, Shawn F. Bairstow, Matthew W. Bunce and Richard A. Anderson

Phosphoinositide-Dependent Protein Kinases; Vol.3 - Pages 292-296, Nick R. Leslie and C. Peter Downes

Phospholipase A2; Vol.3 - Pages 297-300, Timothy R. Smith and Edward A. Dennis

Phospholipase C; Vol.3 - Pages 301-305, Fujio Sekiya, Yeun Ju Kim and Sue Goo Rhee

Phospholipase D; Vol.3 - Pages 306-313, Mary M. LaLonde and Michael A. Frohman

Photoreceptors; Vol.3 - Pages 326-329, King-Wai Yau

Plant Signaling: Peptides; Vol.3 - Pages 381-384, Clarence A. Ryan and Gregory Pearce

Platelet-Activating Factor Receptor; Vol.3 - Pages 394-398, Katherine M. Howard and Merle S. Olson

Platelet-Derived Growth Factor Receptor Family; Vol.3 - Pages 399-406, Marina Kovalenko and Andrius Kazlauskas

Protein Kinase B; Vol.3 - Pages 516-522, Bettina A. Dummler and Brian A. Hemmings

Protein Kinase C Family; Vol.3 - Pages 523-526, Alexandra C. Newton

Protein Tyrosine Phosphatases; Vol.3 - Pages 536-542, David J. Pagliarini, Fred L. Robinson and Jack E. Dixon

Proteinase-Activated Receptors; Vol.3 - Pages 543-548, Kristina K. Hansen and Morley D. Hollenberg

Rab Family; Vol.3 - Pages 629-634, Mary W. McCaffrey and Andrew J. Lindsay

Ran GTPase; Vol.3 - Pages 635-639, Mary Shannon Moore

Ras Family; Vol.3 - Pages 640-644, Lawrence A. Quilliam

Retinoblastoma Protein (pRB); Vol.3 - Pages 700-703, Nicholas Dyson and Maxim Frolov

Retinoic Acid Receptors; Vol.3 - Pages 704-707, Martin Petkovich

Serine/Threonine Phosphatases; Vol.4 - Pages 27-32, Thomas S. Ingebritsen

Serotonin Receptor Signaling; Vol.4 - Pages 33-37, Paul J. Gresch and Elaine Sanders-Bush

Small GTPases; Vol.4 - Pages 48-54, Adam Shutes and Channing J. Der

Somatostatin Receptors; Vol.4 - Pages 55-60, Agnes Schonbrunn

Src Family of Protein Tyrosine Kinases; Vol.4 - Pages 93-98, Jonathan A. Cooper

Steroid/Thyroid Hormone Receptors; Vol.4 - Pages 111-116, Ramesh Narayanan and Nancy L. Weigel

Syk Family of Protein Tyrosine Kinases; Vol.4 - Pages 139-145, Andrew C. Chan

Tachykinin/Substance P Receptors; Vol.4 - Pages 152-157, Mark D. Richardson and Madan M. Kwatra

Taste Receptors; Vol.4 - Pages 158-161, John D. Boughter, Jr. and Steven D. Munger

T-Cell Antigen Receptor; Vol.4 - Pages 162-168, Andrea L. Szymczak and Dario A. A. Vignali

Tec/Btk Family Tyrosine Kinases; Vol.4 - Pages 169-173, Shuling Guo and Owen N. Witte

Thyroid-Stimulating Hormone/Luteinizing Hormone/Follicle-Stimulating Hormone Receptors; Vol.4 - Pages 180-186, Deborah L. Segaloff, Dario Mizrachi and Mario Ascoli

Toll-Like Receptors; Vol.4 - Pages 190-194, Himanshu Kumar, Kiyoshi Takeda and Shizuo Akira

Transforming Growth Factor-β Receptor Superfamily; Vol.4 - Pages 209-213, Mark de Caestecker

Tumor Necrosis Factor Receptors; Vol.4 - Pages 277-283, Karen G. Potter and Carl F. Ware

Vascular Endothelial Growth Factor Receptors; Vol.4 - Pages 337-342, Kenneth A. Thomas

Vasopressin/Oxytocin Receptor Family; Vol.4 - Pages 343-348, Michael J. Brownstein

Vitamin D Receptor; Vol.4 - Pages 378-383, Diane R. Dowd and Paul N. MacDonald

Von Hippel-Lindau (VHL) Protein; Vol.4 - Pages 416-418, Ronald C. Conaway and Joan Weliky Conaway

Techniques and Methodology

Affinity Chromatography; Vol.1 - Pages 51-56, Pedro Cuatrecasas and Meir Wilchek

Affinity Tags for Protein Purification; Vol.1 - Pages 57-63, Joseph J. Falke and John A. Corbin

Genome-Wide Analysis of Gene Expression; Vol.2 - Pages 175-180, Karine G. Le Roch and Elizabeth A. Winzeler

HPLC Separation of Peptides; Vol.2 - Pages 398-403, James D. Pearson

Imaging Methods; Vol.2 - Pages 405-410, Gyorgy Szabadkai and Rosario Rizzuto

Inorganic Biochemistry; Vol.2 - Pages 417-420, Robert J. P. Williams

Multiple Sequence Alignment and Phylogenetic Trees; Vol.2 - Pages 770-774, Russell F. Doolittle

Oligosaccharide Analysis by Mass Spectrometry; Vol.3 - Pages 155-160, Andrew J. Hanneman and Vernon N. Reinhold

PCR (Polymerase Chain Reaction); Vol.3 - Pages 208-210, Michael J. Brownstein

Polysialic Acid inMolecular Medicine; Vol.3 - Pages 407-414, Frederic A. Troy, II

Protein Data Resources; Vol.3 - Pages 478-483, Philip E. Bourne

Secondary Structure in Protein Analysis; Vol.4 - Pages 1-6, George D. Rose

Spectrophotometric Assays; Vol.4 - Pages 67-75, Britton Chance

Two-Dimensional Gel Electrophoresis; Vol.4 - Pages 284-289, Gerhard Schmid, Denis Hochstrasser and Jean-Charles Sanchez

X-Ray Determination of 3-D Structure in Proteins; Vol.4 - Pages 422-428, Martha L. Ludwig

ENCYCLOPEDIA OF
Biological Chemistry

Editors
William J. Lennarz
M. Daniel Lane

Secondary Structure in Protein Analysis

George D. Rose
The Johns Hopkins University, Baltimore, Maryland, USA

Proteins are linear, unbranched polymers of the 20 naturally occurring amino acid residues. Under physiological conditions, most proteins self-assemble into a unique, biologically relevant structure: the native fold. This structure can be dissected into chemically recognizable, topologically simple elements of secondary structure: α-helix, 3_{10}-helix, β-strand, polyproline II helix, turns, and Ω-loops. Together, these six familiar motifs account for ~95% of the total protein structure, and they are utilized repeatedly in mix-and-match patterns, giving rise to the repertoire of known folds. In principle, a protein's three-dimensional structure is predictable from its amino acid sequence, but this problem remains unsolved. A related, but ostensibly simpler, problem is to predict a protein's secondary structure elements from its sequence.

Protein Architecture

A protein is a polymerized chain of amino acid residues, each joined to the next via a peptide bond. The backbone of this polymer describes a complex path through three-dimensional space called the "native fold" or "protein fold."

Covalent Structure

Amino acids have both backbone and side chain atoms. Backbone atoms are common to all amino acids, while side chain atoms differ among the 20 types. Chemically, an amino acid consists of a central, tetrahedral carbon atom, (–$\overset{|}{\underset{|}{C}}$–), linked covalently to (1) an amino group (–NH_2), (2) a carboxyl group (–COOH), (3) a hydrogen atom (–H) and (4) the side chain (–R). Upon polymerization, the amino group loses an –H and the carboxy group loses an –OH; the remaining chemical moiety is called an "amino acid residue" or, simply, a "residue." Residues in this polymer are linked via peptide bonds, as shown in Figure 1.

Degrees of Freedom in the Backbone

The six backbone atoms in the peptide unit [C$\alpha(i)$–CO–NH–C$\alpha(i+1)$] are approximately coplanar, leaving only two primary degrees of freedom for each residue. By convention, these two dihedral angles are called ϕ and ψ (Figure 2). The protein's backbone conformation is described by the ϕ,ψ-specification for each residue.

Classification of Structure

Protein structure is usually classified into primary, secondary, and tertiary structure. "Primary structure" corresponds to the covalently connected sequence of amino acid residues. "Secondary structure" corresponds to the backbone structure, with particular emphasis on hydrogen bonds. And "tertiary structure" corresponds to the complete atomic positions for the protein.

Secondary Structure

Protein secondary structure can be subdivided into repetitive and nonrepetitive, depending upon whether the backbone dihedral angles assume repeating values. There are three major elements (α-helix, β-strand, and polyproline II helix) and one minor element (3_{10}-helix) of repetitive secondary structure (Figure 3). There are two major elements of nonrepetitive secondary structure (turns and Ω-loops).

Repetitive Secondary Structure: the α-Helix

When backbone dihedral angles are assigned repeating ϕ,ψ-values near ($-60°$, $-40°$), the chain twists into a right-handed helix, with 3.6 residues per helical turn. First proposed as a model by Pauling, Corey, and Branson in 1951, the existence of this famous structure was experimentally confirmed almost immediately by

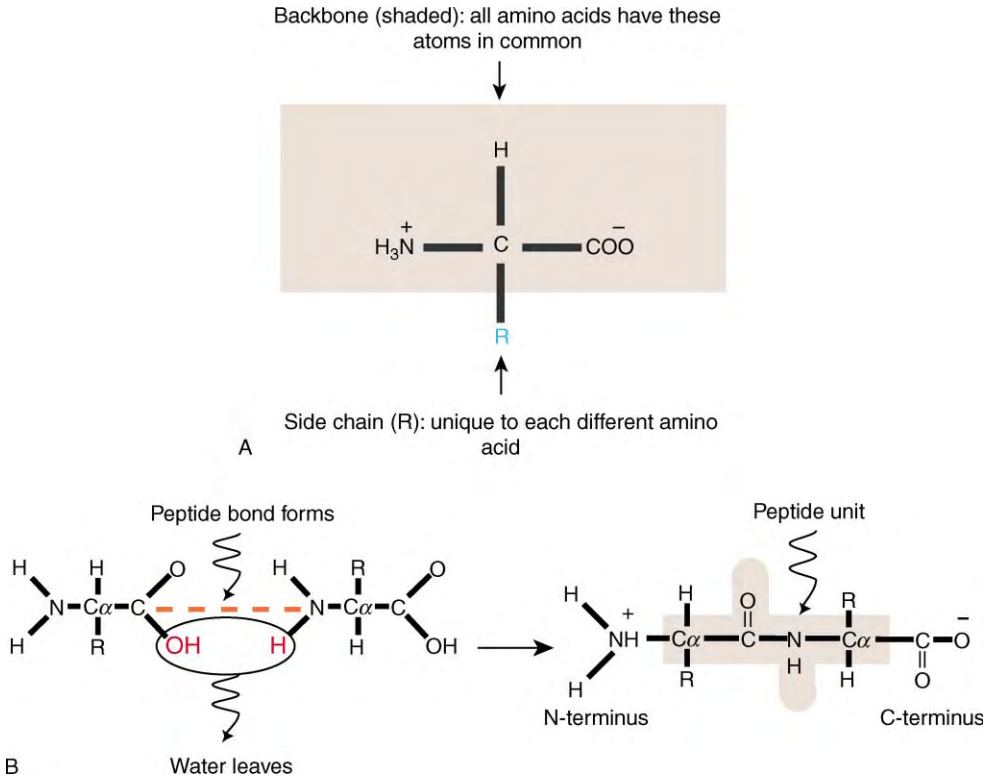

FIGURE 1 (A) A generic amino acid. Each of the 20 naturally occurring amino acids has both backbone atoms (within the shaded rectangle) and side chain atoms (designated R). Backbone atoms are common to all amino acids, while side chain atoms differ among the 20 types. Chemically, an amino acid consists of a tetrahedral carbon atom (–C–), linked covalently to (1) an amino group ($-NH_2$), (2) a carboxyl group (–COOH), (3) a hydrogen atom (–H), and (4) the side chain (–R). (B) Amino acid polymerization. The α-amino group of one amino acid condenses with the α-carboxylate of another, releasing a water molecule. The newly formed amide bond is called a *peptide bond* and the repeating unit is a *residue*. The two chain ends have a free α-amino group and a free α-carboxylate group and are designated the amino-terminal (or N-terminal) and the carboxy-terminal (or C-terminal) ends, respectively. The *peptide unit* consists of the six shaded atoms (Cα–CO–NH–Cα), three on either side of the peptide bond.

Perutz in ongoing crystallographic studies, well before elucidation of the first protein structure.

In an α-helix, each backbone N–H forms a hydrogen bond with the backbone carbonyl oxygen situated four residues away in the linear sequence chain (toward the N-terminus): N–H(i)$\cdots$O=C(i − 4). The two sequentially distant hydrogen-bonded groups are brought into spatial proximity by conferring a helical twist upon the chain. This results in a rod-like structure, with the hydrogen bonds oriented approximately parallel to the long axis of the helix.

In globular proteins, the average length of an α-helix is 12 residues. Typically, helices are found on the outside of the protein, with a hydrophilic face oriented toward the surrounding aqueous solvent and a hydrophobic face oriented toward the protein interior.

Inescapably, end effects deprive the first four amide hydrogens and last four carbonyl oxygens of Pauling-type, intra-helical hydrogen bond partners. The special hydrogen-bonding motifs that can provide partners for these otherwise unsatisfied groups are known as "helix caps."

In globular proteins, helices account for ~25% of the structure on average, but this number varies. Some proteins, like myoglobin, are predominantly helical, while others, like plastocyanin, lack helices altogether.

Repetitive Secondary Structure: the 3_{10}-Helix

When backbone dihedral angles are assigned repeating ϕ,ψ-values near (−50°, −30°), the chain twists into a right-handed helix. By convention, this helix is named using formal nomenclature: 3_{10} designates three residues per helical turn and 10 atoms in the hydrogen bonded ring between each N–H donor and its C=O acceptor. (In this nomenclature, the α-helix would be called a 3.6_{13} helix.)

Single turns of 3_{10} helix are common and closely resemble a type of β-turn (see below). Often, α-helices terminate in a turn of 3_{10} helix. Longer 3_{10} helices are sterically strained and much less common.

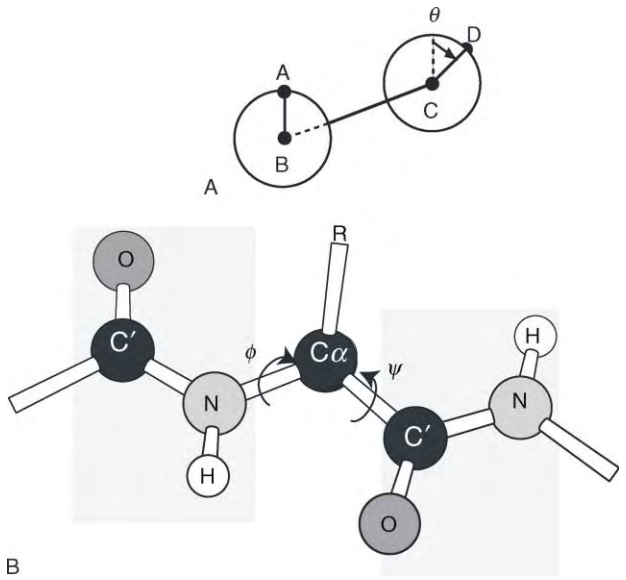

FIGURE 2 (A) Definition of a dihedral angle. In the diagram, the dihedral angle, θ, measures the rotation of line segment CD with respect to line segment AB, where A, B, C, and D correspond to the x,y,z-positions of four atoms. (θ is calculated as the scalar angle between the two normals to planes A–B–C and B–C–D.) By convention, clockwise rotation is positive and $\theta = 0°$ when A and D are eclipsed. (B) Degrees of freedom in the protein backbone. The peptide bond (C′–N) has partial double bond character, so that the six atoms, Ca(i)–CO–Ca($i+1$), are approximately co-planar. Consequently, only two primary degrees of freedom are available for each residue. By convention, these two dihedral angles are called ϕ and ψ. ϕ is specified by the four atoms C′(i)–N–Cα–C′($i+1$) and ψ by the four atoms N(i)–Cα–C′–N($i+1$). When the chain is fully extended, as depicted here, $\phi = \psi = 180°$.

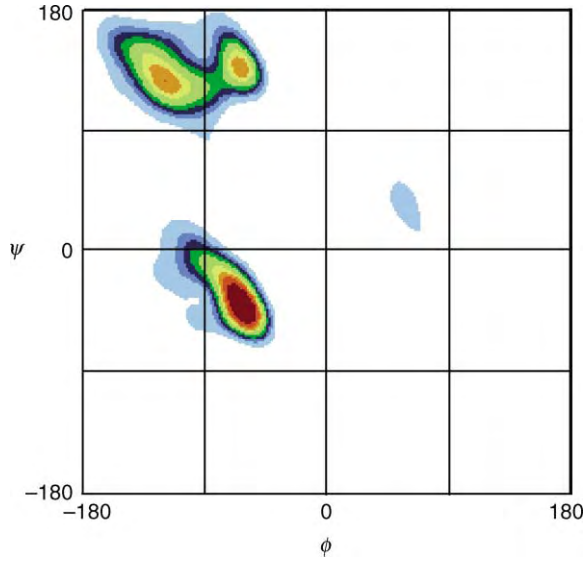

FIGURE 3 A contoured Ramachandran (ϕ, ψ) plot. Backbone ϕ,ψ-angles were extracted from 1042 protein subunits of known structure. Only nonglycine residues are shown. Contours were drawn in population intervals of 10% and are indicated by the ten colors (in rainbow order). The most densely populated regions are colored red. Three heavily populated regions are apparent, each near one of the major elements of repetitive secondary structure: α-helix ($\sim -60°$, $-40°$), β-strand ($\sim -120°$, $120°$), P_{II} helix ($\sim -70°$, $140°$). Adapted from Hovmöller, S., Zhou, T., and Ohlson, T. (2002). Conformation of amino acids in proteins. *Acta Cryst.* **D58**, 768–776, with permission of IUCr.

Repetitive Secondary Structure: the β-Strand

When backbone dihedral angles are assigned repeating ϕ,ψ-values near $(-120°, -120°)$, the chain adopts an extended conformation called a β-strand. Two or more β-strands, aligned so as to form inter-strand hydrogen bonds, are called a β-sheet. A β-sheet of just two hydrogen-bonded β-strands interconnected by a tight turn is called a β-hairpin. The average length of a single β-strand is seven residues.

The classical definition of secondary structure found in most textbooks is limited to hydrogen-bonded backbone structure and, strictly speaking, would not include a β-strand, only a β-sheet. However, the β-sheet is tertiary structure, not secondary structure; the intervening chain joining two hydrogen-bonded β-strands can range from a tight turn to a long, structurally complex stretch of polypeptide chain. Further, approximately half the β-strands found in proteins are singletons and do not form inter-strand hydrogen bonds with another β-strand. Textbooks tend to blur this issue.

Typically, β-sheet is found in the interior of the protein, although the outermost parts of edge-strands usually reside at the protein's water-accessible surface.

Two β-strands in a β-sheet are classified as either parallel or anti-parallel, depending upon whether their mutual N- to C-terminal orientation is the same or opposite, respectively.

In globular proteins, β-sheet accounts for about 15% of the structure on an average, but, like helices, this number varies considerably. Some proteins are predominantly sheet while others lack sheet altogether.

Repetitive Secondary Structure: the Polyproline II Helix (P_{II})

When backbone dihedral angles are assigned repeating ϕ,ψ-values near $(-70°, +140°)$, the chain twists into a left-handed helix with 3.0 residues per helical turn. The name of this helix is derived from a poly-proline homopolymer, in which the structure is forced by its stereochemistry. However, a polypeptide chain can adopt a P_{II} helical conformation whether or not it contains proline residues.

Unlike the better known α-helix, a P_{II} helix has no intrasegment hydrogen bonds, and it is not included in the classical definition of secondary structure for this reason. This extension of the definition is also needed in the case of an isolated β-strand. Recent studies have shown that the unfolded state of proteins is rich in P_{II} structure.

Nonrepetitive Secondary Structure: the Turn

Turns are sites at which the polypeptide chain changes its overall direction, and their frequent occurrence is the reason why globular proteins are, in fact, globular.

Turns can be subdivided into β-turns, γ-turns, and tight turns. β-turns involve four consecutive residues, with a hydrogen bond between the amide hydrogen of the 4th residue and the carbonyl oxygen of the 1st residue: N–H(i)$\cdots$O=C($i-3$). β-turns are further subdivided into subtypes (e.g., Type I, I′, II, II′, III,…) depending upon their detailed stereochemistry. γ-turns involve only three consecutive, hydrogen-bonded residues, N–H(i)$\cdots$O=C($i-2$), which are further divided into subtypes.

More gradual turns, known as "reverse turns" or "tight turns," are also abundant in protein structures. Reverse turns lack intra-turn hydrogen bonds but nonetheless, are involved in changes in overall chain direction.

Turns are usually, but not invariably, found on the water-accessible surface of proteins. Together, β,γ- and reverse turns account for about one-third of the structure in globular proteins, on an average.

Nonrepetitive Secondary Structure: the Ω-Loop

Ω-loops are sites at which the polypeptide loops back on itself, with a morphology that resembles the Greek letter "Ω" although often with considerable distortion. They range in length from 6–16 residues, and, lacking any specific pattern of backbone-hydrogen bonding, can exhibit significant structural heterogeneity.

Like turns, Ω-loops are typically found on the outside of proteins. On an average, there are about four such structures in a globular protein.

Identification of Secondary Structure from Coordinates

Typically, one becomes familiar with a given protein structure by visualizing a model – usually a computer model – that is generated from experimentally determined coordinates. Some secondary structure types are well defined on visual inspection, but others are not. For example, the central residues of a well-formed helix are visually unambiguous, but the helix termini are subject to interpretation. In general, visual parsing of the protein into its elements of secondary structure can be a highly subjective enterprise. Objective criteria have been developed to resolve such ambiguity. These criteria have been implemented in computer programs that accept a protein's three-dimensional coordinates as input and provide its secondary structure components as output.

Inherent Ambiguity in Structural Identification

It should be realized that objective criteria for structural identification can provide a welcome self-consistency, but there is no single "right" answer. For example, turns have been defined in the literature as chains sites at which the distance between two α-carbon atoms, separated in sequence by four residues, is not more than 7Å, provided the residues are not in an α-helix: distance[C$\alpha(i)$–C$\alpha(i+3)$] $\leq$ 7Å and C$\alpha(i)$–C$\alpha(i+3)$ not α-helix. Indeed, turns identified using this definition agree quite well with one's visual intuition. However, the 7Å threshold is somewhat arbitrary. Had 7.1Å been used instead, additional, intuitively plausible turns would have been found.

Programs to Identify Structure from Coordinates

Many workers have devised algorithms to parse the three-dimensional structure into its secondary structure components. Unavoidably, these procedures include investigator-defined thresholds. Two such programs are mentioned here.

The *D*atabase of *S*econdary *S*tructure Assignments in *P*roteins

This is the most widely used secondary structure identification method available today. Developed by Kabsch and Sander, it is accessible on the internet, both from the original authors and in numerous implementations from other investigators as well.

The *d*atabase of *s*econdary *s*tructure assignments in *p*roteins (DSSP) identifies an extensive set of secondary structure categories, based on a combination of backbone dihedral angles and hydrogen bonds. In turn, hydrogen bonds are identified based on geometric criteria involving both the distance and orientation between a donor–acceptor pair. The program has criteria for recognizing α-helix, 3_{10}-helix, π helix, β-sheet (both parallel and anti-parallel), hydrogen-bonded turns and reverse turns. (Note: the π-helix is rare and has been omitted from the secondary structure categories.)

*Pro*tein *S*econdary *S*tructure Assignments

In contrast to DSSP, protein secondary structure assignments (PROSS) identification is based solely on backbone dihedral angles, without resorting to hydrogen

bonds. Developed by Srinivasan and Rose, it is accessible on the *internet*.

PROSS identifies only α-helix, β-strand, and turns, using standard ϕ,ψ definitions for these categories. Because hydrogen bonds are not among the identification criteria, PROSS does not distinguish between isolated β-strands and those in a β-sheet.

Prediction of Protein Secondary Structure from Amino Acid Sequence

Efforts to predict secondary structure from amino acid sequence dates back to the 1960s to the works of Guzzo, Prothero and, slightly later, Chou and Fasman. The problem is complicated by the fact that protein secondary structure is only marginally stable, at best. Proteins fold cooperatively, with secondary and tertiary structure emerging more or less concomitantly. Typical peptide fragments excised from the host protein, and measured in isolation, exhibit only a weak tendency to adopt their native secondary structure conformation.

Predictions Based on Empirically Determined Preferences

Motivated by early work of Chou and Fasman, this approach uses a database of known structures to discover the empirical likelihood, f, of finding each of the twenty amino acids in helix, sheet, turn, *etc*. These likelihoods are equated to the residue's normalized frequency of occurrence in a given secondary structure type, obtained by counting. Using alanine in helices as an example

$$\text{fraction Ala in helix} = \frac{\text{occurrences of Ala in helices}}{\text{occurrences of Ala in database}}$$

This fraction is then normalized against the corresponding fraction of helices in the database:

$$f_{\text{Ala}}^{\text{helix}} = \frac{\text{fraction Ala in helix}}{\text{fraction helices in database}} = \frac{\dfrac{\text{occurrences of Ala in helices}}{\text{occurrences of Ala in database}}}{\dfrac{\text{number of residues in helices}}{\text{number of residues in database}}}$$

A normalized frequency of unity indicates no preference – i.e., the frequency of occurrence of the given residue in that particular position is the same as its frequency at large. Normalized frequencies greater than/less than unity indicate selection for/against the given residue in a particular position.

These residue likelihoods are then used in combination to make a prediction. When only a small number of proteins had been solved, these data-dependent f-values fluctuated significantly as new structures were added to the database. At this point there are more than 22 000 structures in the Protein Data Bank (www.rcsb.org), and the f-values have reached a plateau.

Database-Independent Predictions: the Hydrophobicity Profile

Hydrophobicity profiles have been used to predict the location of turns in proteins. A hydrophobicity profile is a plot of the residue number versus residue hydrophobicity, averaged over a running window. The only variables are the size of the window used for averaging and the choice of hydrophobicity scale (of which there are many). No empirical data from the database is required. Peaks in the profile correspond to local maxima in hydrophobicity, and valleys to local minima. Prediction is based on the idea that apolar sites along the chain (i.e., peaks in the profile) will be disposed preferentially to the molecular interior, forming a hydrophobic core, whereas polar sites (i.e., valleys in the profile) will be disposed to the exterior and correspond to chain turns.

Neural Networks

More recently, neural network approaches to secondary structure prediction have come to dominate the field. These approaches are based on pattern-recognition methods developed in artificial intelligence. When used in conjunction with the protein database, these are the most successful programs available today.

A neural network is a computer program that associates an input (e.g., a residue sequence) with an output (e.g., secondary structure prediction) through a complex network of interconnected nodes. The path taken from the input through the network to the output depends upon past experience. Thus, the network is said to be "trained" on a dataset.

The method is based on the observation that amino acid substitutions follow a pattern within a family of homologous proteins. Therefore, if the sequence of interest has homologues within the database of known structures, this information can be used to improve predictive success, provided the homologues are recognizable. In fact, a homologue can be recognized quite successfully when the sequence of interest and a putative homologue have an aligned sequence identity of 25% or more.

Neural nets provide an information-rich approach to secondary structure prediction that has become increasingly successful as the protein databank has grown.

Physical Basis of Secondary Structure

An impressive number of secondary structure prediction methods can be found in the literature and on the web. Surprisingly, almost all are based on empirical likelihoods or neural nets; few are based on physicochemical theory.

In one such theory, secondary structure propensities are predominantly a consequence of two competing local effects – one favoring hydrogen bond formation in helices and turns, and the other opposing the attendant reduction in sidechain conformational entropy upon helix and turn formation. These sequence-specific biases are densely dispersed throughout the unfolded polypeptide chain, where they serve to pre-organize the folding process and largely, but imperfectly, anticipate the native secondary structure.

Why Aren't Secondary Structure Predictions Better?

Currently, the best methods for predicting helix and sheet are correct about three-quarters of the time. Can greater success be achieved?

Several measures to assess predictive accuracy are in common use, of which the Q3 score is the most widespread. The Q3 score gives the percentage of correctly predicted residues in three categories: helix, strand, and coil (i.e., everything else):

$$\mathrm{Q3} = \frac{\text{number of correctly predicted residues}}{\text{total number of residues}} \times 100$$

where the "correct" answer is given by a program to identify secondary structure from coordinates, e.g., DSSP. At this writing, (Position-Specific PREDiction algorithm) PSIPRED has an overall Q3 score of 78%.

Is greater prediction accuracy possible? It has been argued that prediction methods fail to achieve a higher rate of success because some amino acid sequences are inherently ambiguous. That is, these "conformational chameleons" will adopt a helical conformation in one protein, but the identical sequence will adopt a strand conformation in another protein. Only time will tell whether current efforts have encountered an inherent limit.

See Also the Following Articles

Amino Acid Metabolism • Multiple Sequence Alignment and Phylogenetic Trees • Protein Data Resources • X-Ray Determination of 3-D Structure in Proteins

Glossary

α-helix The best-known element of secondary structure in which the polypeptide chain adopts a right-handed helical twist with 3.6 residues per turn and an $i \rightarrow i - 4$ hydrogen bond between successive amide hydrogens and carbonyl oxygens.

β-strand An element of secondary structure in which the chain adopts an extended conformation. A β-sheet results when two or more aligned β-strands form inter-strand hydrogen bonds.

Chou–Fasman Among the earliest attempts to predict protein secondary structure from the amino acid sequence. The method, which uses a database of known structures, is based on the empirically observed likelihood of finding the 20 different amino acids in helix, sheet or turns.

DSSP The most widely used method to parse x, y, z-coordinates for a protein structure into elements of secondary structure.

hydrophobicity A measure of the degree to which solutes, like amino acids, partition spontaneously between a polar environment (like the outside of a protein) and an organic environment (like the inside of a protein).

hydrophobicity profile A method to predict the location of peptide chain turns from the amino acid sequence by plotting averaged hydrophobicity against residue number. The method does not require a database of known structure.

neural network A pattern recognition method – adapted from artificial intelligence – that has been highly successful in predicting protein secondary structure when used in conjunction with an extensive database of known structures.

peptide chain turn A site at which the protein changes its overall direction. The frequent occurrence of turns is responsible for the globular morphology of globular (i.e., sphere-like) proteins.

secondary structure The backbone structure of the protein, with particular emphasis on hydrogen bonded motifs.

tertiary structure The three-dimensional structure of the protein.

Further Reading

Berg, J. M., Tymoczko, J. L., and Stryer, L. (2002). *Biochemistry*, 5th edition. W.H. Freeman and Company, New York.

Holm, L., and Sander, C. (1996). Mapping the protein universe. *Science* **273**, 595–603.

Hovmöller, S., Zhou, T., and Ohlson, T. (2002). Conformation of amino acids in proteins. *Acta Cryst.* **D58**, 768–776.

Jones, D. T. (1999). Protein secondary structure based on position-specific scoring matrices. *J. Mol. Biol.* **292**, 195–202.

Mathews, C., van Holde, K. E., and Ahern, K. G. (2000). *Biochemistry*, 3rd edition. Pearson Benjamin Cummings, Menlo Park, CA.

Richardson, J. S. (1981). The anatomy and taxonomy of protein structure. *Adv. Prot. Chem.* **34**, 168–340.

Rose, G. D., Gierasch, L. M., and Smith, J. A. (1985). Turns in peptides and proteins. *Adv. Prot. Chem.* **37**, 1–109.

Voet, D., and Voet, J. G. (1996). *Biochemistry*, 2nd edition. Wiley, New York.

Biography

George Rose is Professor of Biophysics and Director of the Institute for Biophysical Research at Johns Hopkins University. He holds a Ph.D. from Oregon State University. His principal research interest is in protein folding, and he has written many articles on this topic. He serves as the consulting editor of *Proteins: Structure, Function and Genetics* and as a member of the editorial advisory board of *Protein Science*. Recently, he was a Fellow of the John Simon Guggenheim Memorial Foundation.

Secretases

Robert L. Heinrikson
The Pharmacia Corporation, Kalamazoo, Michigan, USA

Secretases are proteolytic enzymes involved in the processing of an integral membrane protein known as Amyloid precursor protein, or APP. β-Amyloid (Aβ) is a neurotoxic and highly aggregative peptide that is excised from APP by secretase action, and that accumulates in the neuritic plaque found in the brains of Alzheimer's disease (AD) patients. The amyloid hypothesis holds that the neuronal dysfunction and clinical manifestation of AD is a consequence of the long-term deposition and accumulation of Aβ, and that this peptide of 40–42 amino acids is a causative agent of AD. Accordingly, the secretases involved in the liberation, or destruction of Aβ are of enormous interest as therapeutic intervention points toward treatment of this dreaded disease.

Background

Proteolytic enzymes play crucial roles in a wide variety of normal and pathological processes in which they display a high order of selectivity for their substrate(s) and the specific peptide bonds hydrolyzed therein. This article concerns secretases, membrane-associated proteinases that produce, or prevent formation of, a highly aggregative and toxic peptide called β-amyloid (Aβ). This Aβ peptide is removed from a widely distributed and little understood Type I integral membrane protein called amyloid precursor protein (APP). The apparent causal relationship between Aβ and AD has fueled an intense interest in the secretases responsible for its production. Herein will be discussed the current understanding of three of the most-studied secretases, α-, β-, and γ-secretases. A schematic representation of the Aβ region of APP showing the amino acid sequence of Aβ and the major sites of cleavage for these three secretases is given in Figure 1. Aβ is produced by the action of β- and γ-secretases, and there is an intense search underway for inhibitors of these enzymes that might serve as drugs in treatment of Alzheimer's disease (AD). The α-secretase cleaves at a site near the middle of Aβ, and gives rise to fragments of Aβ that lack the potential for aggregation; therefore, amplification of α-secretase activity might be seen as another approach to AD therapy.

α-Secretase

The activity responsible for cleavage of the Lys^{16}-Leu^{17} bond within the Aβ region (Figure 1) is ascribed to α-secretase. This action prevents formation of the 40–42 amino acid residue Aβ and leads to release of soluble APPα and the membrane-bound C83-terminal fragment. α-Secretase competes with β-secretase for the APP substrate, but the α-secretase product, soluble APPα (pathway A, Figure 1) is generated at a level about 20 times that of the sAPPβ released by β-secretase (pathway B). Because α-secretase action prevents formation of the toxic Aβ peptide, augmentation of this activity could represent a useful strategy in AD treatment, and this has been done experimentally by activators of protein kinase C (PKC) such as phorbol esters and by muscarinic agonists. The specificity of the α-secretase for the Lys^{16}-↓-Leu^{17} cleavage site (Figure 1) appears to be governed by spatial and structural requirements that this bond exist in a local α-helical conformation and be within 12 or 13 amino acids distance from the membrane. α-Secretase has not been identified as any single proteinase, but two members of the ADAM (a disintegrin and metalloprotease) family, ADAM-10 and ADAM-17 are candidate α-secretases. ADAM-17 is known as TACE (tumor necrosis factor-α-converting enzyme) and TACE cleaves peptides modeled after the α-secretase site at the Lys^{16}-↓-Leu position. This was also shown to be the case for ADAM-10; overexpression of this enzyme in a human cell line led to several-fold increase in both basal and PKC-inducible α-secretase activity. As of now, it remains to be proven whether α-secretase activity derives from either or both of these ADAM family metalloproteinases, or whether another as yet unidentified proteinase carries out this processing of APP.

β-Secretase

The enzyme responsible for cleaving at the amino-terminus of Aβ is β-secretase (Figure 1). In the mid-1980s, when Aβ was recognized as a principal component of AD neuritic plaque, an intense search was begun to identify the β-secretase. Finally, in 1999, several independent

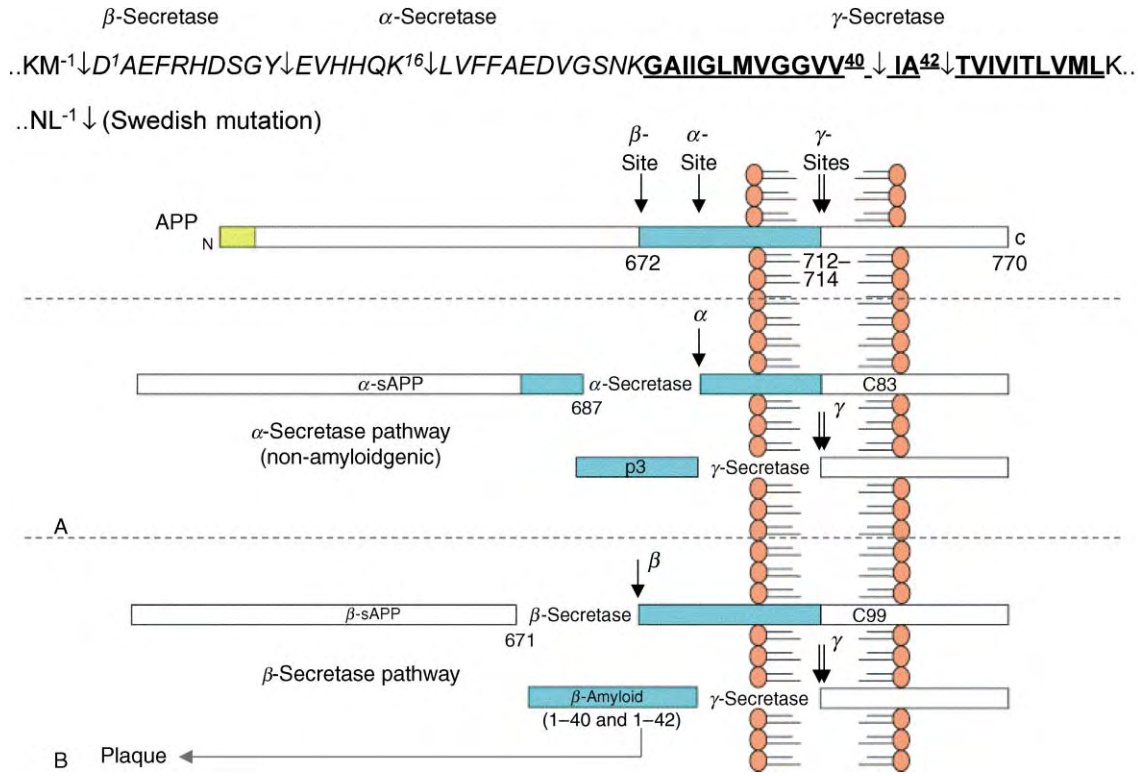

FIGURE 1 A schematic overview of APP processing by the α-, β-, and γ-secretases. The top panel shows the amino acid sequence of APP upstream of the transmembrane segment (underlined, bold), and encompassing the sequences of $A\beta_{1-40}$ and $A\beta_{1-42}$ (D^1–V^{40}, and D^1–A^{42}, respectively). The β-secretase cleaves at D^1 and Y^{10}; the α-secretase at Lys^{16}, and the γ-secretase at Val^{40} and/or Ala^{42}. Below the sequence is a representation of APP emphasizing its membrane localization and the residue numbers of interest in β- and γ-secretase processing. Panel A represents the non-amyloidogenic α-secretase pathway in which sAPPα and C83 are generated. Subsequent hydrolysis by the γ-secretase produces a p3 peptide that does not form amyloid deposits. Panel B represents the amyloidogenic pathway in which cleavage of APP by the β-secretase to liberate sAPPβ and C99 is followed by γ-secretase processing to release β-amyloid peptides ($A\beta_{1-40}$ and $A\beta_{1-42}$) found in plaque deposits.

laboratories published evidence demonstrating that β-secretase is a unique member of the pepsin family of aspartyl proteinases. This structural relationship to a well-characterized and mechanistically defined class of proteases gave enormous impetus to research on β-secretase. The preproenzyme consists of 501 amino acids, with a 21-residue signal peptide, a prosegment of about 39 residues, the catalytic bilobal unit with active site aspartyl residues at positions 93 and 289, a 27-residue transmembrane region, and a 21-residue C-terminal domain. The membrane localization of β-secretase makes it unique among mammalian aspartyl proteases described to date. Another interesting feature of the enzyme is that, unlike pepsin, renin, cathepsin D, and other prototypic members of the aspartyl proteases, it does not appear to require removal of the prosegment as a means of activation. A furin-like activity is responsible for cleavage in the sequence Arg-Leu-Pro-Arg-↓-Glu^{25} of the proenzyme, but this does not lead to any remarkable enhancement of activity, at least as is seen in recombinant constructs of pro-β-secretase. β-Secretase has been referred to by a number of designations in the literature, but the term BACE (β-site APP cleaving enzyme) has become most widely adopted. With the discovery of the β-secretase, it was recognized that there was another human homologue of BACE with a transmembrane segment and this has now come to be called BACE2. This may well be a misnomer, since the function of BACE2 has yet to be established, and it is not clear that APP is a normal substrate of this enzyme. At present, BACE2 is not considered to be a secretase.

There is considerable experimental support for the assertion that BACE is, in fact, the β-secretase involved in APP processing. The enzyme is highly expressed in brain, but is also found in other tissues, thus explaining the fact that many cell types can process Aβ. Use of antisense oligonucleotides to block expression of BACE greatly diminishes production of Aβ and, conversely, overexpression of BACE in a number of cell lines leads to enhanced Aβ production. BACE knockout mice show no adverse phenotype, but have dramatically reduced levels of Aβ. This not only demonstrates that BACE is the true β-site APP processor, but also that its elimination does not pose serious consequences for the animal, a factor of great importance in targeting BACE for inhibition in AD therapy.

Much of the evidence in support of the amyloid hypothesis comes from the observation of mutations near the β- and γ-cleavage sites in APP that influence production of Aβ and correlate directly with the onset of AD. One such mutation in APP, that invariably leads to AD in later life, occurs at the β-cleavage site where Lys-Met^{-1} is changed to Asn-Leu^{-1} (Figure 1). This so-called Swedish mutation greatly enhances production of Aβ, and as would be expected, β-secretase hydrolyzes the mutated Leu-Asp^{1} bond in model peptides $\sim$50 times faster than the wild-type Met-Asp^{1} bond. It is important to recognize that BACE cleavage is required for subsequent processing by the γ-secretase; in this sense, a BACE inhibitor will also block γ-secretase. Another BACE cleavage point is indicated in Figure 1 by the arrow at Y$^{10}\downarrow$E^{11}; the A$\beta_{11-40\text{ or }42}$ subsequently liberated by γ-secretase action also forms amyloid deposits and is found in neuritic plaque.

In all respects, therefore, BACE fits the picture expected of β-secretase, and because of its detailed level of characterization and its primary role in Aβ production, it has become a major target for development of inhibitors as drugs to treat AD. Great strides in this direction have become possible because of the availability of three-dimensional (3-D) structural information on BACE. The crystal structure of BACE complexed with an inhibitor is represented schematically in Figure 2. Homology with the pepsin-like aspartyl proteases is reflected in the similar folding pattern of BACE, with extensive β-sheet organization, and the proximal location of the two aspartyl residues that comprise the catalytic machine for peptide bond cleavage. The C-terminal lobe of the molecule is larger than is customarily seen in the aspartyl proteases, and contains extra elements of structure with as yet unexplained impact on function. In fact, before the crystal structure was solved, it was thought that this larger C-terminal region might contribute a spacer to distance the catalytic unit from the membrane and to provide mobility. This appears not to be the case. As denoted by the arrow in Figure 2, there is a critical disulfide bridge linking the C-terminal region just upstream of the transmembrane segment to the body of the molecule. Therefore, the globular BACE molecule is proximal to the membrane surface and is not attached via a mobile stalk that would permit much motion. This steric localization would be expected to limit the repertoire of protein substrates that are accessible to BACE as it resides in the Golgi region. Crystal structures of BACE/inhibitor complexes have revealed much about the nature of protein-ligand interactions, and information regarding the nature of binding sites obtained by this approach will be of critical importance in the design and development of inhibitors that will be effective drugs in treatment of AD.

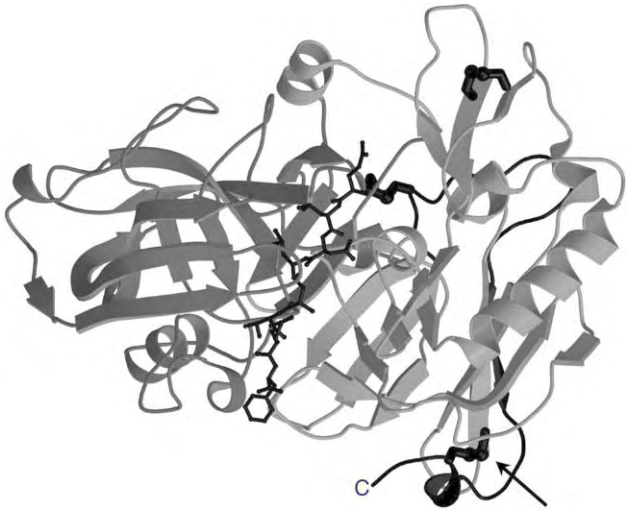

FIGURE 2 Schematic representation of the 3-D structure of the BACE (β-secretase) catalytic unit as determined by x-ray crystallography. Arrows and ribbons designate β-strands and α-helices, respectively. An inhibitor is shown bound in the cleft defined by the amino- (left) and carboxyl- (right) terminal halves of the molecule. The C-terminus of the catalytic unit is marked C to indicate the amino acid residue immediately preceding the transmembrane and cytoplasmic domains of BACE. These latter domains were omitted from the construct that was solved crystallographically. The arrow marks a disulfide bridge, which maintains the C-terminus in close structural association with the body of the catalytic unit. The catalytic entity as depicted sits directly on the membrane surface, thereby restricting its motion relative to protein substrates. (Courtesy of Dr. Lin Hong, Oklahoma Medical Research Foundation, Oklahoma City, OK.)

γ-Secretase

γ-Secretase activity is produced in a complex of proteins and is yet to be understood in terms of the actual catalytic entity and mechanism of proteolysis. This secretase cleaves bonds in the middle of the APP segment that traverses the membrane (underlined and boldface in Figure 1), and its activity is exhibited subsequent to cleavages at the α- or β-sites. In Figure 1, the γ-secretase cleavage sites are indicated by two arrows. Cleavage at the Val^{40}-Ile^{41} bond liberates the more abundant 40-amino acid residue Aβ (Aβ_{1-40}). Cleavage at Ala^{42}-Thr^{43} produces a minor Aβ species, Aβ_{1-42}, but one that appears to be much more hydrophobic and aggregative, and it is the 42-residue Aβ that is believed to be of most significance in AD pathology. As was the case for APP β-site mutations, there are human APP mutants showing alterations in the vicinity of the γ-site, and these changes, powerfully associated with onset of AD, lead to higher ratios of Aβ_{1-42}.

Central to the notion of the γ-secretase is the presence of presenilins, intregral membrane proteins with mass $\sim$50 kDa. There are a host of presenilin mutations in familial AD (FAD) that are associated with early onset disease and an increased production of the toxic Aβ_{1-42}. This correlation provides strong

support for the involvement of presenilin in AD, and its presence in γ-secretase preparations implies that it is either a proteolytic enzyme in its own right, or can contribute to that function in the presence of other proteins. In fact, much remains to be learned about the presenilins; it has been difficult to obtain precise molecular and functional characterization because of their close association with membranes and other proteins in a complex. Modeling studies have predicted a variable number of transmembrane segments (6–8), but presenilin function is predicated upon processing by an unknown protease to yield a 30 kDa N-terminal fragment (NTF) and a 20 kDa C-terminal fragment (CTF). These accumulate *in vivo* in a 1:1 stoichiometry within high molecular weight complexes with a variety of ancillary proteins. Some of the cohort proteins identified in the multimeric presenilin complexes displaying γ-secretase activity include catenins, armadillo-repeat proteins that appear not to be essential for γ-secretase function, and nicastrin. Nicastrin is a Type I integral membrane protein with homologues in a variety of organisms, but its function is unknown. It shows intracellular colocalization with presenilin, and is able to bind the NTF and CTF of presenilin as well as the C83 and C99 C-terminal APP substrates of γ-secretase. Interestingly, down-regulation of the nicastrin homologue in *Caenorhabditis elegans* gave a phenotype similar to that seen in worms deficient in presenilin and notch. Evidence that nicastrin is essential for γ-secretase cleavage of APP and notch adds to the belief that nicastrin is an important element in presenilin, and γ-secretase function. Efforts to delineate other protein components of γ-secretase complexes and to understand their individual roles in the enzyme function represent a large current research effort. Recently, two additional proteins associated with the complex have been identified through genetic screening of flies and worms. The *aph-1* gene encodes a protein with 7 transmembrane domains, and the *pen-2* gene codes for a small protein passing twice through the membrane. Both of these putative members of the γ-secretase complex are new proteins whose functions, either with respect to secretase activity or in other potential systems, remain to be elucidated.

At present, it is still unclear as to how γ-secretase exerts its function. What is known, however, is that γ-secretase is able to cleave at other peptide bonds in APP near the γ-site in addition to those indicated in Figure 1, and is involved with processing of intra-membrane peptide bonds in a variety of additional protein substrates, including notch. This lack of specificity is a major concern in developing drugs for AD targeted to γ-secretase that do not show side effects due to inhibition of processing of these additional, functionally diverse protein substrates.

See Also the Following Articles

Amyloid • Metalloproteinases, Matrix

Glossary

Aβ The peptide produced from APP by the action of β- and γ-secretases. Aβ shows neurotoxic activity and aggregates to form insoluble deposits seen in the brains of Alzheimer's disease patients. The α-secretase hydrolyzes a bond within the Aβ region and releases fragments which do not aggregate.

Alzheimer's disease (AD) A disease first described by Alois Alzheimer in 1906 characterized by progressive loss of memory and cognition. AD afflicts a major proportion of our aging population and is one of the most serious diseases facing our society today, especially in light of increasing human longevity. The secretases represent important potential therapeutic intervention points in AD treatment.

proteinases Enzymes that hydrolyze, or split peptide bonds in protein substrates; also referred to as proteolytic enzymes.

secretase A proteinase identified with respect to its hydrolysis of peptide bonds within a region of a Type I integral membrane protein called APP. These cleavages are responsible for liberation, or destruction of an amyloidogenic peptide of about 40 amino acid residues in length called Aβ.

Further Reading

Esler, W. P., and Wolfe, M. S. (2001). A portrait of Alzheimer secretases – New features and familiar faces. *Science* **293**, 1449–1454.

Fortini, M. E. (2002). γ-Secretase-mediated proteolysis in cell-surface-receptor signaling. *Nat. Rev.* **3**, 673–684.

Glenner, G. G., and Wong, C. W. (1984). Alzheimer's disease: Initial report of the purification and characterization of a novel cerbrovascular amyloid protein. *Biophys. Res. Commun.* **120**, 885–890.

Hendriksen, Z. J. V. R. B., Nottet, H. S. L. M., and Smits, H. A. (2002). Secretases as targets for drug design in Alzheimer's disease. *Eur. J. Clin. Invest.* **32**, 60–68.

Sisodia, S. S., and St. George-Hyslop, P. H. (2002). γ-Secretase, notch, Aβ and Alzheimer's disease: Where do the presenilins fit in? *Nat. Rev.* **3**, 281–290.

Biography

Robert L. Heinrikson is a Distinguished Fellow at the Pharmacia Corporation in Kalamazoo, MI. Prior to his industrial post, Dr. Heinrikson was Full Professor of Biochemistry at the University of Chicago. His principal area of research is protein chemistry, with an emphasis on proteolytic enzymes as drug targets. Dr. Heinrikson is on the editorial board of four journals, including the *Journal of Biological Chemistry*. He is a member of the American Society of Biochemistry and Molecular Biology and Phi Beta Kappa.

Secretory Pathway

Karen J. Colley
University of Illinois at Chicago, Chicago, Illinois, USA

The eukaryotic cell is separated into several functionally distinct, membrane-enclosed compartments (Figure 1). Each compartment contains proteins required to accomplish specific functions. Consequently, each protein must be sorted to its proper location to ensure cell viability. Proteins possess specific signals, either encoded in their amino acid sequences or added as posttranslational modifications, which target them for the various compartments of the cell. The pioneering work of Dr. George Palade provided scientists with their first picture of the functional organization of the mammalian secretory pathway. Later work showed that the secretory pathway acts as a folding, modification, and quality control system for proteins that function in the endoplasmic reticulum (ER) and Golgi apparatus, and for those that are targeted to the lysosome, plasma membrane, and extracellular space. This article will focus on protein targeting to and within the compartments of the secretory pathway, and how proteins within this pathway function to ensure that correctly folded and modified proteins are delivered to the cell surface and secreted from cells.

Targeting of New Proteins to the Secretory Pathway

What Kinds of Proteins are Targeted to the Secretory Pathway?

The proteins that are targeted to the secretory pathway can be separated into two groups – those that function in the ER and Golgi to ensure proper protein folding and modification (i.e., resident proteins), and those that are processed in the ER and Golgi, and are transported to later compartments like the lysosome, plasma membrane, and extracellular space (Figure 1). Each of these proteins not only possesses a signal to enter the secretory pathway, but also may have a secondary signal to localize it to a particular organelle within the pathway.

Signals and Mechanisms of Secretory Pathway Entry

The 1999 Nobel Prize in physiology or medicine was awarded to Dr. Günter Blobel for his contributions to our understanding of the mechanism of secretory pathway entry. Dr. Blobel and his colleagues found that in order to enter the secretory pathway, proteins are synthesized with an amino terminal signal peptide that allows them to cross the membrane of the endoplasmic reticulum (ER). The signal peptide is recognized by a complex of proteins and ribonucleic acid called the signal recognition particle (SRP) (Figure 2). As the signal peptide emerges from the ribosome during translation, SRP binds to it and halts translation, and then targets the new protein–ribosome complex to the cytoplasmic face of the ER membrane where it binds to the SRP receptor. Subsequently, the new protein–ribosome complex is released from SRP and its receptor, and transferred to an aqueous membrane channel known as the "translocon." Translation resumes and the new protein is co-translationally transferred through the translocon into the lumen of the ER, where in many cases the signal peptide is cleaved by a specific signal peptidase (Figure 2).

Soluble and Integral Membrane Proteins

Soluble proteins are completely translocated across the ER membrane into the lumen (Figure 2). These proteins will either remain in the ER, be targeted to another organelle, or be secreted from the cell. Integral membrane proteins that possess one or more hydrophobic membrane-spanning regions will use these sequences to insert into the membrane of the ER and either stay as ER-resident transmembrane proteins, or be targeted to another cellular membrane. A type-I membrane protein has a cleavable signal peptide and a separate hydrophobic stretch of amino acids that acts as a membrane-spanning region. This type of protein has its amino terminus in the lumen of an organelle or the outside of the cell (which are topologically equivalent), and its carboxy terminus in the cytoplasm (Figure 2). In contrast, a type-II membrane protein has an uncleavable signal peptide, or signal anchor that is not at the protein's amino terminus and serves a dual function as both signal peptide and a membrane-spanning region. Type-II membrane proteins employ a more elaborate insertion mechanism than do type-I membrane proteins.

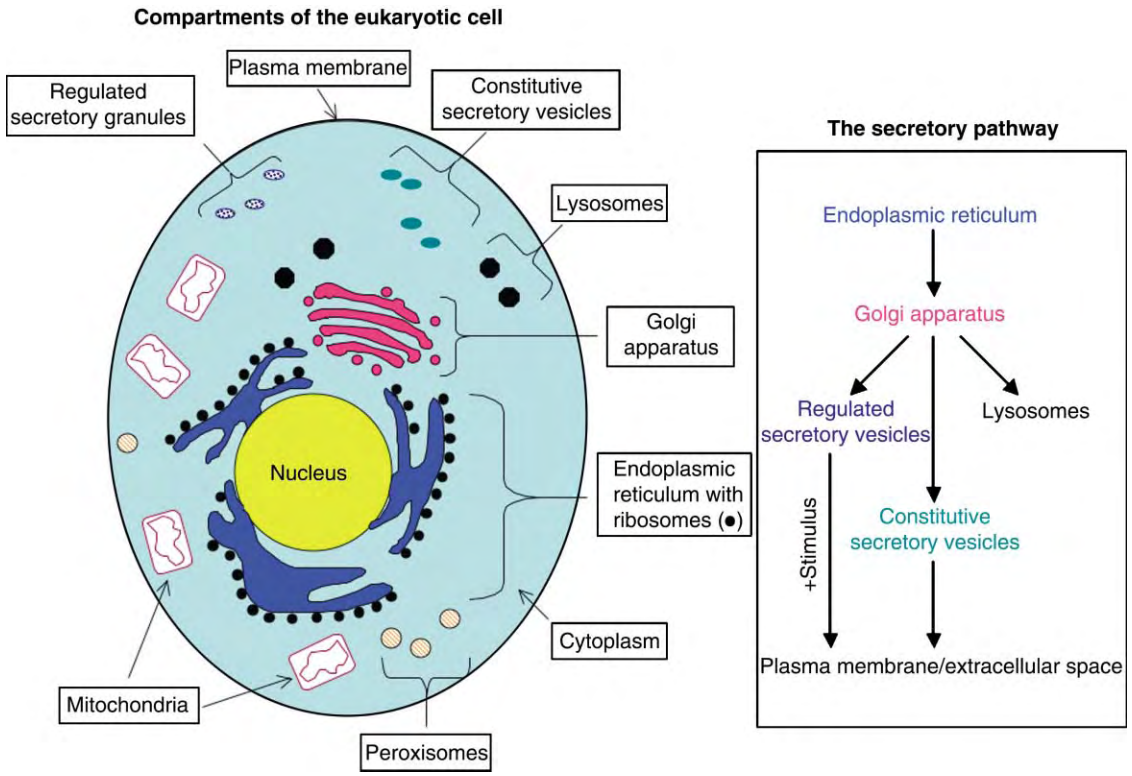

FIGURE 1 Compartments of eukaryotic cells and the organization of the secretory pathway. Diagrammatic representation of the compartments of the eukaryotic cell is shown. The anterograde flow of membrane and protein traffic in the secretory pathway is shown in the box. Anterograde flow is indicated by arrows. Retrograde flow between the ER and Golgi, endosome/lysosome system and Golgi, and plasma membrane and Golgi does occur, but is not shown.

For this reason, a type-II membrane protein will have its carboxy terminus in the lumen of an organelle or outside the cell, and its amino terminus in the cytoplasm (Figure 2). Other proteins span the membrane several times and are called type-III membrane proteins. They can start with either cleavable signal peptides or uncleavable signal anchors and possess variable numbers of hydrophobic membrane-spanning segments.

Protein Folding and Modification in the ER

The Initiation of Protein N-Linked Glycosylation in the ER

As proteins enter the ER lumen, they fold and assemble with the help of chaperone proteins. Many proteins are also co-translationally modified by the addition of carbohydrates to asparagine residues in the process of N-linked glycosylation (Figure 2). A preformed oligosaccharide, consisting of three glucoses, nine mannoses, and two N-acetylglucosamine residues ($Glc_3Man_9GlcNAc_2$) is transferred to accessible asparagine residues in the tripeptide sequence asparagine-X-serine or threonine (X cannot be proline) by the oligosaccharide protein transferase complex. Subsequent modification by glycosidases (enzymes that remove monosaccharides) and glycosyltransferases (enzymes that add monosaccharides) in the ER and Golgi lead to the remodeling of the N-linked oligosaccharides. These N-linked carbohydrates help proteins fold, protect them from proteolytic degradation and, in some cases, are critical for modulating and mediating protein and cell interactions at the cell surface and in the extracellular space.

Chaperones and the ER Quality Control System

An important function of the ER is to serve as a site of protein folding and quality control. Protein folding in the ER includes the formation of intra-molecular disulfide bonds, prolyl isomerization, and the sequestration of hydrophobic amino acids into the interior of the protein. Protein disulfide bonds are formed as the protein exits the translocon and may at first form incorrectly between cysteine residues close together in the protein's linear amino acid sequence. Thiol-oxidoreductases, such as protein disulfide isomerase (PDI), help to form and reorganize proteins' disulfide bonds into the most energetically favorable configuration. Different types of chaperones monitor a protein's

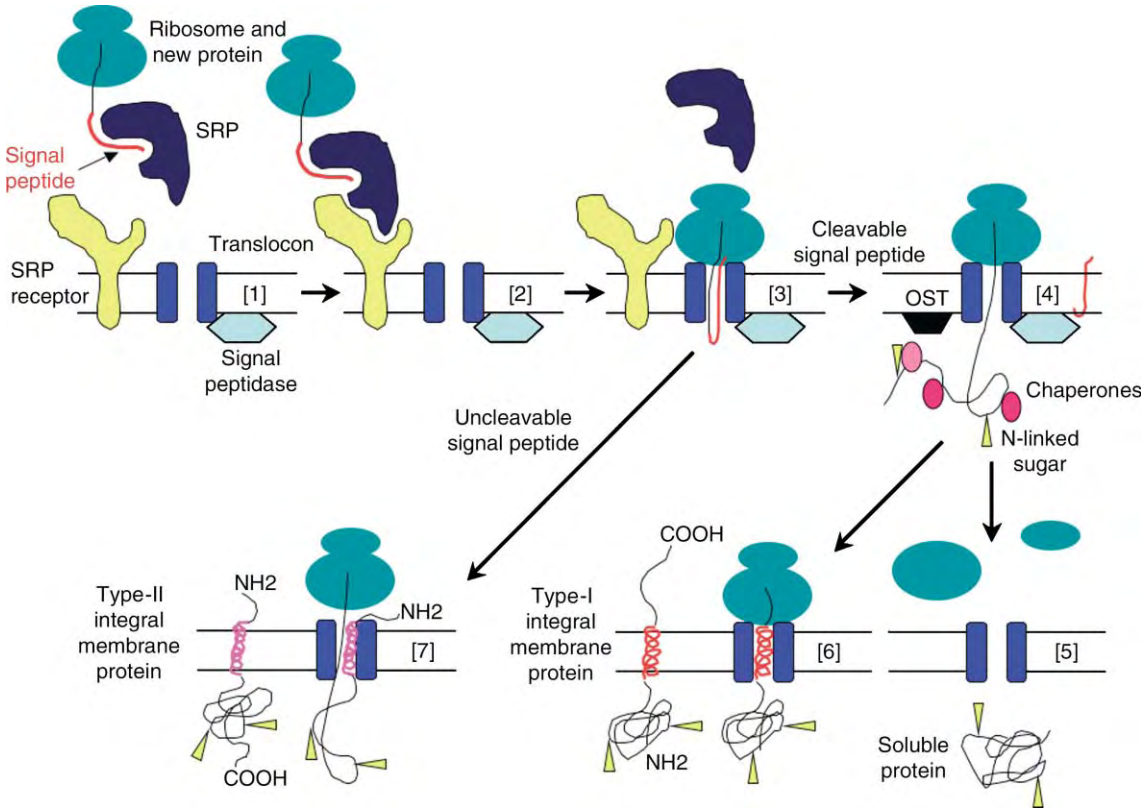

FIGURE 2 Entry into the secretory pathway. Many proteins are targeted for the secretory pathway by an amino terminal hydrophobic signal peptide that allows their co-translational translocation across the ER membrane. [1] Signal recognition particle (SRP) recognizes the new protein's signal peptide. [2] The ribosome–new protein–SRP complex interacts with the SRP receptor on the cytoplasmic face of the ER membrane. [3] The ribosome–new protein complex is transferred to the translocon channel, protein synthesis continues and the protein moves through the aqueous channel. [4] As the new protein enters the lumen of the ER, its signal peptide is cleaved by the signal peptidase, chaperone proteins bind to aid in folding and oligosaccharide protein transferase complex (OST) transfers oligosaccharides (arrowheads) to asparagine residues in the process of N-linked glycosylation. [5] Soluble proteins lack additional hydrophobic sequences and are translocated through the translocon to complete their folding and modification in the ER lumen. [6] Type-I integral membrane proteins have a second hydrophobic sequence that partitions into the lipid bilayer and acts as a membrane-spanning segment. These proteins have their amino termini in the lumen of an organelle or outstide the cell and their carboxy-termini in the cell cytoplasm. [7] Unlike proteins with cleavable amino-terminal signal peptides, type-II integral membrane proteins have an uncleavable signal anchor that target the protein to the secretory pathway and then partitions into the lipid bilayer to act as a membrane-spanning segment. These proteins have their amino termini in the cell cytoplasm and their carboxy-termini in the lumen of an organelle or outside the cell. Soluble and integral membrane proteins that enter at the level of the ER need not stay there, and can be transported out of the ER to other locations in the pathway (see Figure 1, Secretory Pathway box).

folding and prevent exit of unfolded and unassembled proteins from the ER. The chaperone BiP, originally identified as an immunoglobulin heavy-chain-binding protein, interacts with the exposed hydrophobic sequences of folding intermediates of many proteins and prevents their aggregation. Two chaperones called calnexin and calreticulin recognize a monoglucosylated carbohydrate structure ($Glc_1Man_9GlcNAc_2$) that is formed by a special glucosyltransferase that recognizes unfolded or misfolded proteins and adds a single glucose to the $Man_9GlcNAc_2$ structure. Proteins that are not folded properly or are not assembled into oligomers with partner subunits, are prevented from exiting the ER by chaperone interactions, and can be targeted back across the ER membrane through the translocon into the cytoplasm where they are degraded by the proteosome complex in a process called ER associated degradation (ERAD).

Protein Transport through and Localization in the Secretory Pathway

Vesicular Transport between the ER and Golgi

Proteins move between the ER and Golgi in vesicular carriers. These vesicles are coated with specific sets of cytoplasmic proteins that form the COP-I and COP-II coats. COP-II-coated vesicles move from the ER to the

intermediate compartment (IC)/*cis* Golgi, while COP-I-coated vesicles move from the Golgi back to the ER and may also mediate transport between Golgi cisternae in both the anterograde (toward the plasma membrane) and retrograde (toward the ER) directions (Figure 3). The process of vesicular transport can be separated into three stages—cargo selection and budding, targeting, and fusion. In the first stage, the COP coats serve to select cargo for exit from a compartment and help to deform the membrane for vesicle budding. They assemble on the membrane with the help of small GTPases called ARF (specific for COP I) and Sar1p (specific for COP II). After vesicle budding, the hydrolysis of GTP by ARF and Sar1p leads to the uncoating of the vesicle. This uncoating reveals other vesicle proteins that are essential for vesicle targeting and fusion. In the second and third stages, tethering proteins on the transport vesicle and target membrane interact weakly bringing the membranes together. This allows vesicle-associated SNARE proteins and target membrane-associated SNARE proteins to form complexes. Subsequent conformational changes in the SNARE protein complex bring the membranes together for fusion. Another group of small GTPases (Rabs) control the process of vesicular transport at several levels by recruiting and activating various proteins in the pathway.

Protein Localization in the ER

Proteins involved in protein folding, modification, and quality control must remain in the ER, while proteins destined for the Golgi, lysosome, cell surface or those that are secreted from the cell must exit. Exit from the ER is a selective process that involves cargo receptors that interact with COP-II coat components (Figure 3). It is likely that most resident ER proteins are not selected to exit the ER. It is clear, however, that some resident proteins escape from the ER and are retrieved from the Golgi and intermediate compartment by COP-I vesicles (Figure 3). These proteins have specific amino acid signals that allow their incorporation into COP-I vesicles either by direct interaction with COP-I components or indirectly by interaction with cargo

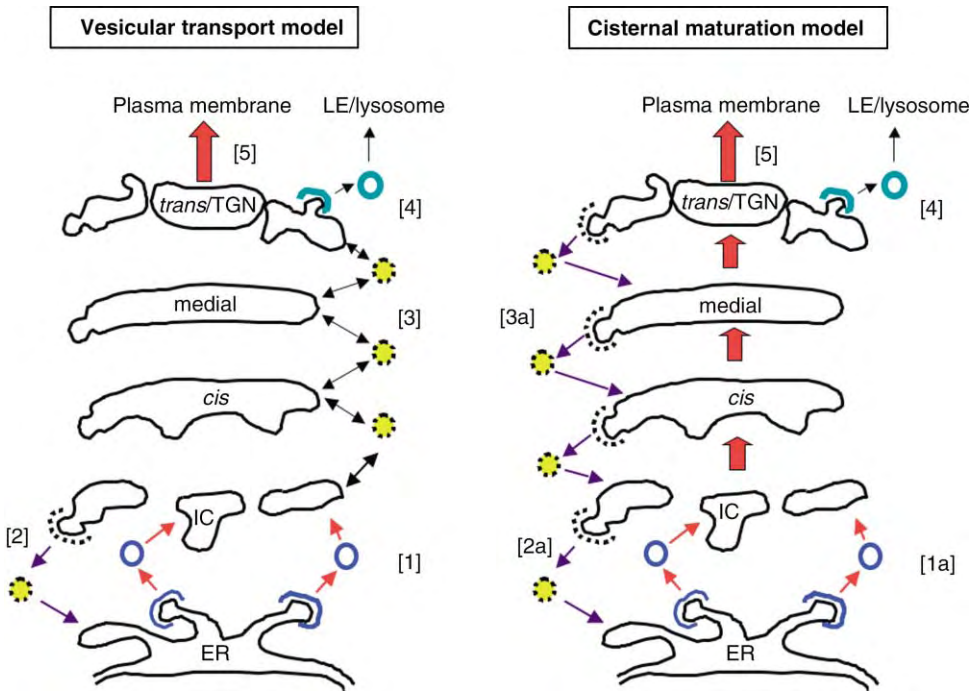

FIGURE 3 Comparison of two models of protein transport through the Golgi apparatus. In the vesicular transport model cargo proteins move between the cisternae in vesicles, while Golgi enzymes are retained in their resident cisternae. [1] COP-II-coated vesicles transport new proteins from the ER to the intermediate compartment (IC). [2] Resident ER proteins that escape the ER can be retrieved from the IC in COP-I-coated vesicles. [3] COP-I-coated vesicles also transport anterograde cargo proteins between the Golgi cisternae in both a retrograde and anterograde fashion ("percolating vesicles"). In the cisternal maturation model, cargo proteins enter a new cisterna at the cis face of the stack, and are modified (matured) by "resident" Golgi enzymes that are continuously transported in a retrograde fashion into the sequentially maturing cisternae. [1a] COP-II-coated vesicles transport new proteins from the ER to the IC where a new *cis* cisterna forms. [2a] Resident ER proteins that escape the ER can be retrieved from the IC in COP-I-coated vesicles. [3a] Golgi enzymes are transported in a retrograde fashion in COP-I-coated vesicles to modify the cargo proteins in earlier cisternae. Mechanisms of protein exit from the TGN are common to both models: [4] clathrin-coated vesicles mediate late endosome (LE)-lysosome transport, while [5] other proteins are secreted in either a regulated or constitutive fashion to the plasma membrane or extracellular space.

receptors. For example, mammalian BiP is a soluble ER protein that has the carboxy-terminal four amino acid sequence lysine–aspartate–glutamate–leucine (KDEL). This KDEL sequence is recognized by the KDEL receptor that mediates their incorporation into COP I vesicles moving from the intermediate compartment (IC) back to the ER.

Protein Modification in the Golgi

The Golgi apparatus consists stacks of flattened cisternae that contain enzymes and other proteins involved in the further modification and processing of newly made proteins. It is separated into cis, medial, and trans cisternae, followed by a meshwork of tubules and vesicles called the trans Golgi network (TGN). The process of N-linked glycosylation is completed through the action of glycosidases and glycosyltransferases localized in specific cisternae. Likewise, the glycosylation of serine and threonine residues (O-linked glycosylation) is accomplished by other glycosyltransferases. Additional modifications also occur in the Golgi. For example, proteins and carbohydrate are sulfated by sulfotransferases and some proteins are phosphorylated on serine and threonine residues by Golgi kinases. In addition, proteins like digestive enzymes (trypsin, carboxypeptidase) and hormones (insulin) are made as inactive precursors that must be proteolytically processed to their active forms in the late Golgi or post-Golgi compartments.

Transport of Proteins through the Golgi

Currently there are two different models to explain protein transport through the Golgi (Figure 3). The vesicular transport model proposes that proteins move sequentially between the Golgi cisterna in COP-I-coated vesicles, while the cisternae themselves are stationary. Proteins not retained in the *cis* Golgi, for example, would be incorporated into coated vesicles and be transported to the *medial* Golgi, and then to the *trans* Golgi. Proteins destined for post-Golgi compartments move through successive Golgi cisternae in this fashion, being modified by the resident enzymes in each compartment (Figure 3). In the cisternal maturation model a new cisterna is formed on *cis* face of the Golgi stack from ER-derived membrane. This requires both the anterograde transport of newly synthesized proteins from the ER in COP-II-coated vesicles and the retrograde transport of *cis* Golgi enzymes from the pre-existing *cis* cisterna in COP I-coated vesicles. The new *cis* cisterna and its contents progressively mature through the stack as resident Golgi enzymes are successively introduced by COP-I coated vesicles (Figure 3). In the vesicular transport model, the resident Golgi enzymes are retained in the cisternae while the cargo moves in vesicles between the different cisternae. In contrast, in the cisternal maturation model, the "resident" enzymes are continuously moving in a retrograde fashion, while the anterograde cargo remains in the cisternae. Evidence for both mechanisms is compelling, suggesting that both mechanisms may work in parallel.

Localization of Resident Golgi Enzymes

In the context of the vesicular transport model, Golgi enzymes are retained in specific cisternae. Two mechanisms have been suggested for Golgi protein retention. The "bilayer thickness" mechanism suggests that the relatively short transmembrane regions of Golgi proteins prevent their incorporation into the wider, cholesterol-rich lipid bilayers of the transport vesicles destined for post-Golgi compartments (such as the plasma membrane), and as a result, these proteins are retained in the relatively cholesterol-poor Golgi. The "oligomerization" mechanism predicts that once an enzyme has reached its resident cisterna it forms homo- or hetero-oligomers that prevent its incorporation into transport vesicles moving to the next compartment. In the context of the cisternal maturation model, resident Golgi enzymes are actively incorporated into COP-I vesicles for retrograde transport to a new cisterna, and one might predict that the cytoplasmic tails of these proteins would interact with COP-I-coat components to allow vesicle incorporation. Interestingly, there are only a few examples where the cytoplasmic tail of a Golgi enzyme plays a primary role in its localization, whereas the membrane-spanning regions of these proteins seem to be more critical. Again, it is possible that some or all of these mechanisms work together to maintain the steady-state localization of the resident Golgi proteins.

Protein Exit from the Golgi and Targeting to Post-Golgi Locations

Protein Exit from the Golgi

Once proteins reach the TGN they are sorted to post-Golgi compartments that include the lysosome, the plasma membrane, and the extracellular space (Figure 3). Trafficking to the lysosome–endosome system involves clathrin-coated vesicles similar to those that function in the uptake of proteins in endocytosis. In contrast, transport to the plasma membrane, or exocytosis, can occur either constitutively in secretory vesicles/tubules or in a regulated fashion from secretory granules found in specific cell types.

Protein Targeting to the Lysosome

The lysosome is a degradative compartment that contains numerous acid hydrolases that function to digest proteins, lipids, and carbohydrates. The trafficking of the majority of lysosomal enzymes to the lysosome requires mannose 6-phosphate residues on these enzymes' N-linked sugars. The mannose 6-phosphate residues are recognized by receptors in the TGN that mediate the incorporation of the new lysosomal enzymes into clathrin-coated vesicles destined for the late endosome compartment (Figure 3). These clathrin-coated vesicles move from the TGN and fuse with the late endosome, where a decrease in lumenal pH causes the lysosomal enzymes to dissociate from the mannose 6-phosphate receptors. The enzymes are then transported to the lysosome, while the receptors recycle to the TGN. Some lysosomal membrane proteins are also trafficked in clathrin-coated vesicles to the lysosome like the soluble enzymes but without the use of a mannose 6-phosphate marker, while others are transported to the cell surface, incorporated into a different set of clathrin-coated vesicles used in the process of endocytosis, and then trafficked to the lysosome via the late endosome.

Constitutive and Regulated Secretion

In many cell types, membrane-associated and soluble proteins move to the plasma membrane constitutively without a requirement for specific signals. Constitutively secreted proteins include receptors, channel proteins, cell adhesion molecules, and soluble extracellular matrix and serum proteins. Other proteins like hormones and neurotransmitters are targeted to secretory granules that are involved in regulated secretion from endocrine and exocrine cells, some types of immune cells, and neurons. These granules remain in a secretion-ready state until extracellular signals that lead to an increase in intracellular calcium levels trigger the exocytosis of their contents.

See Also the Following Articles

Chaperones, Molecular • Endoplasmic Reticulum-Associated Protein Degradation • Glycoproteins, N-linked • Golgi Complex • Protein Folding and Assembly • Protein Glycosylation, Overview

Glossary

chaperone A protein that aids in the folding and assembly of other proteins, frequently by preventing the aggregation of folding intermediates.

cisternal maturation/progression One model of protein transport through the Golgi apparatus that suggests that secretory cargo enters a new cisternae that forms at the *cis* face of the Golgi stack, and that this cisternae and its cargo progresses or matures through the stack by the sequential introduction of Golgi modification enzymes.

glycosylation The modification of lipids and proteins with carbohydrates in the endoplasmic reticulum and Golgi apparatus of the secretory pathway.

secretory pathway An intracellular pathway consisting of the endoplasmic reticulum, Golgi apparatus, and associated vesicles that is responsible for the folding, modification, and transport of proteins to the lysosome, plasma membrane, and extracellular space.

vesicular transport One model of protein transport through the Golgi apparatus, which suggests that secretory cargo moves sequentially between stationary Golgi cisternae in transport vesicles and is modified by resident Golgi enzymes in the process.

Further Reading

Ellgaard, L., Molinari, M., and Helenius, A. (1999). Setting the standards: Quality control in the secretory pathway. *Science* **286**, 1882–1888.

Farquhar, M. G., and Palade, G. E. 1998. The Golgi apparatus: 100 years of progress and controversy. *Trends Cell Biol.* **8**, 2–10.

Intracellular compartments and protein sorting (chapter 12) and intracellular vesicular traffic (chapter 13). In *The Molecular Biology of the Cell* (B. Alberts, A. Johnson, J. Lewis, M. Raff, K. Roberts, and P. Walter, eds.), 4th edition, pp. 659–766. Garland Science, New York.

Kornfeld, S., and Mellman, I. (1989). The biogenesis of lysosomes. *Annu. Rev. Cell Biol.* **5**, 483–525.

Palade, G. (1975). Intracellular aspects of the process of protein synthesis. *Science* **189**, 347–358.

Rapoport, T. A., Jungnickel, B., and Kutay, U. (1996). Protein transport across the eukaryotic endoplasmic reticulum and bacterial inner membranes. *Annu. Rev. Biochem.* **65**, 271–303.

Rockefeller University web site describing Dr. Günter Blobel's Nobel Prize research (http://www.rockefeller.edu).

Biography

Karen J. Colley is a Professor in the Department of Biochemistry and Molecular Genetics at the University of Illinois College of Medicine in Chicago. She holds a Ph.D. from Washington University in St. Louis, and received her postdoctoral training at the University of California, Los Angeles. Her principal research interests are in protein trafficking and glycosylation. Her recent studies focus on the elucidation of the signals and mechanisms of Golgi glycosyltransferase localization.

Selenoprotein Synthesis

August Böck
University of Munich, Munich, Germany

Selenoproteins contain one or more residues of the nonstandard amino acid selenocysteine, which is an analogue of cysteine in which a selenol group replaces a thiol. The majority of these proteins catalyze some oxidation/reduction function in which the selenol of the selenocysteine that is present in the active site of the respective enzyme takes part in the reaction. The advantage of having a selenol instead of a thiol lies in the fact that it confers to these enzymes a higher kinetic efficiency. In some biological systems, selenoproteins may also fulfill a structural role because of their capacity to oligomerize proteins via the formation of diselenide or mixed disulfide–selenide bridges. The biosynthesis of selenoproteins is unique since the incorporation of selenocysteine occurs co-translationally by the ribosome and not posttranslationally. Selenocysteine insertion is DNA encoded, requires the function of a cognate tRNA and of a specific translation elongation factor different from elongation factor Tu. Selenocysteine, therefore, has been designated as the 21st amino acid.

Bacterial Selenoprotein Synthesis

The structure and the function of the components involved in selenocysteine biosynthesis have been characterized to a considerable extent in the case of the bacterial system. The process can be divided into three functional steps, namely the biosynthesis of selenocysteine in the tRNA-bound state, the formation of a complex between elongation factor SelB, GTP, selenocysteyl-tRNA^{Sec} and the mRNA, and the decoding event at the ribosome. As far as it is known, though there are some major differences, similarities also exist between bacterial selenoprotein synthesis and the process characteristic of eukarya and archaea.

Selenocysteine Biosynthesis

Figure 1 summarizes the process of selenocysteine biosynthesis as it has been worked out for *Escherichia coli*. It requires the activities of three enzymes, namely seryl-tRNA synthetase (SerS), selenophosphate synthetase (SelD), and selenocysteine synthase (SelA) plus the specific tRNA (tRNA^{Sec}). Seryl-tRNA synthetase charges tRNA^{Sec} with L-serine, selenocysteine synthase converts the seryl-tRNA^{Sec} into selenocysteyl-tRNA^{Sec} using selenophosphate as a source for activated selenium. Selenophosphate is provided by selenophosphate synthetase from selenide in an ATP-dependent reaction. The genes for these components had been identified with the aid of *E. coli* mutants isolated by Mandrand–Berthelot as being pleiotropically deficient in formate dehydrogenase activities.

tRNA^{Sec}

tRNA^{Sec} (Figure 2) is the key molecule of selenoprotein synthesis since it serves both as the adaptor for selenocysteine biosynthesis and for incorporation of the amino acid at the ribosome. It deviates in size, secondary structure, and in normally conserved sequence positions from canonical elongator tRNA species. Because of the elongated extra arm and the one base-pair-extended aminoacyl acceptor arm, tRNA^{Sec} species are the largest members of the elongator tRNA family. All tRNA^{Sec} species identified thus far possess a UCA anticodon which enables them to pair with UGA stop codons (but only if these are in a special mRNA sequence context). Moreover, tRNA^{Sec} species deviate from canonical elongator tRNA species in sequence positions which are usually invariant and which are involved in the establishment of novel tertiary interactions within the molecule.

On the basis of its serine identity elements, tRNA^{Sec} is charged by the cellular seryl-tRNA synthetase which also aminoacylates serine inserting isoacceptors. However, both the affinity and the rate of aminacylation are diminished in comparison to the charging of tRNA^{Ser}, resulting in an overall 100-fold reduced efficiency.

Selenocysteine Synthase

The overall reaction catalyzed by selenocysteine synthase consists in the exchange of the hydroxylgroup of the serine moiety of seryl-tRNA^{Sec} by a selenol group (Figure 1). The reaction occurs in two steps; first, the amino group of serine forms a Schiff base with the carbonyl of the pyridoxal 5′-phosphate cofactor of selenocysteine synthase leads to the 2,3-elimination of a water molecule and the formation of dehydroalanyl-tRNA^{Sec} and second, nucleophilic addition of reduced

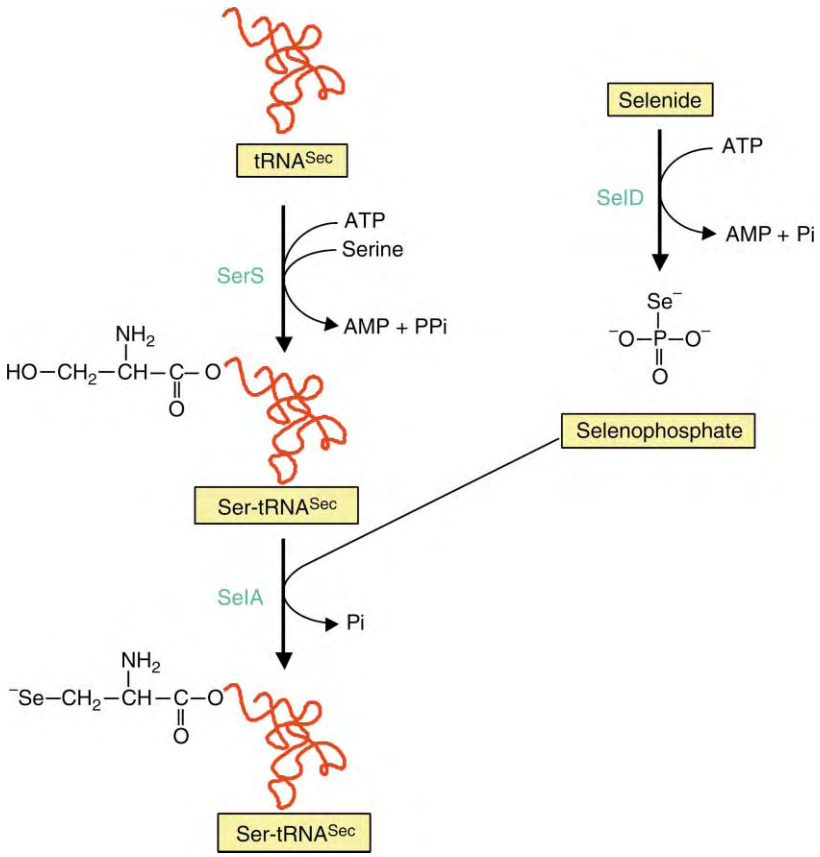

FIGURE 1 Path of selenocysteine biosynthesis. For explanation see text.

selenium to the double bond of dehydroalanyl-tRNA^{Sec} from selenophosphate as a donor yields selenocysteyl-tRNA^{Sec}.

Selenocysteine synthase from *E. coli* is a homodecameric enzyme and low resolution electron microscopy revealed that it is made up of two pentameric rings stacked on top of each other. Two subunits each are able to bind one molecule of seryl-tRNA^{Sec}, so the fully loaded enzyme can complex five charged tRNA molecules. As serine isoacceptor tRNAs are not recognized, the tRNA must have determinants for the specific recognition of seryl-tRNA^{Sec} by selenocysteine synthase and antideterminants for the rejection of seryl-tRNA^{Ser} species. The specificity for discrimination of the selenium donor is not as strict since the purified enzyme accepts thiophosphate instead of selenophosphate as a substrate. This results in the formation of cysteyl-tRNA^{Sec}. So the discrimination between sulfur and selenium must take place at some other step of selenocysteine biosynthesis.

Selenophosphate Synthetase

Purified selenocysteine synthase does not exhibit an absolute requirement for selenophosphate, as a substrate to convert seryl-tRNA^{Sec} into selenocysteyl-tRNA^{Sec}, since the reaction also occurs in the presence of high concentrations of selenide. Even sulfide is accepted although at a very low efficiency. So, the necessity for selenophosphate as a substrate may reside in one or more of the following three aspects, i.e., (1) to discriminate sulfide from selenide, (2) to efficiently use low concentrations of selenium compounds, and (3) to accelerate the reaction rate effected by the activation of the trace element. Indeed, selenophosphate synthetase efficiently discriminates between sulfide and selenide, and thus excludes sulfur from intrusion into the selenium pathway. Selenophosphate synthetase from *E. coli* is a monomeric enzyme with a unique reaction mechanism since formally it transfers the γ-phosphate of ATP to selenide with the intermediate formation of enzyme-bound ADP which is subsequently hydrolysed into AMP and inorganic phosphate.

Formation of the SelB × GTP × Selenocysteyl-tRNA × SECIS Complex

Elongation factor Tu, which forms a complex with all 20 standard aminoacyl-tRNAs and donates them to the ribosomal A-site, displays only minimal binding affinity

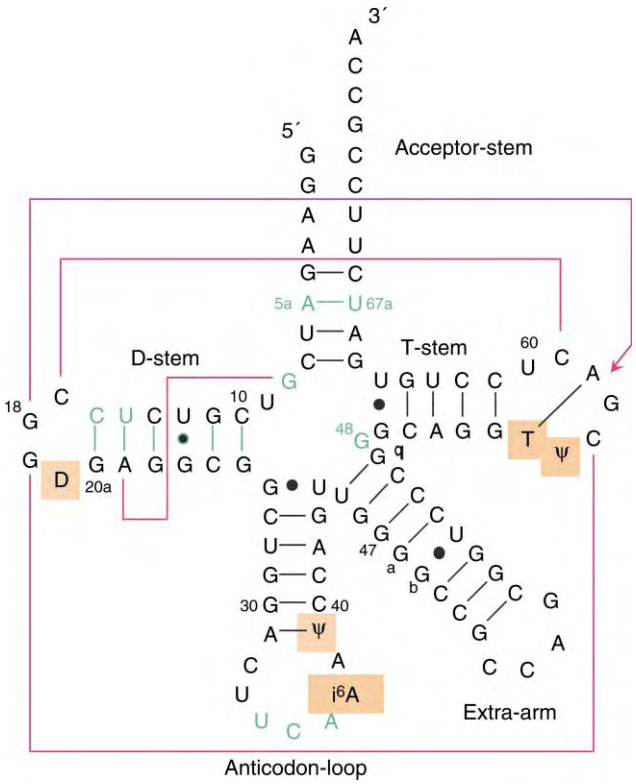

FIGURE 2 Cloverleaf presentation of the structure of $tRNA^{Sec}$ from *E. coli*. Modified bases are shaded. Tertiary interactions via base pairing are indicated by connecting red lines, and those involving intercalation are denoted by arrows. Bases and base pairings deviating from the consensus are indicated in green.

for selenocysteyl-$tRNA^{Sec}$. Consequently, insertion of selenocysteine requires the function of an alternate elongation factor which is SelB. SelB from *E. coli* is a 70 kDa protein which contains the sequence elements of elongation factor Tu in the N-terminal two-third of the molecule (designated domains I, II, and III) plus a domain IV of about 25 kDa which can be subdivided into domains IVa and IVb. Domains I, II and III share their functions with those of elongation factor Tu, namely the binding of guanosine nucleotides and of charged tRNA. An important difference, however, is that they can discriminate between the serylated and the selenocysteylated forms of $tRNA^{Sec}$. In this way, the insertion of serine instead of selenocysteine, which would lead to an inactive enzyme, is prevented. The structural basis for this discrimination ability has not yet been resolved. A second difference is that the overall affinity for GTP is about 10-fold higher than that for GDP which obviates the need for the function of a guanosine nucleotide release factor since GDP is chemically replaced by GTP. In accordance, the structure of SelB lacks those subdomains which in elongation factor Tu are responsible for interaction with the GDP release factor EF-Ts. The 25 kDa C-terminal extension of SelB (domain IV) is required for the function in selenoprotein synthesis since its truncation inactivates the molecule. The reason is that subdomain IVb binds to a secondary structure of the mRNA (the SECIS element) coding for selenoprotein synthesis. SelB, thus, is able to form a quaternary complex with GTP and two RNA ligands, namely selenocysteyl-tRNA and the SECIS element (Figure 3). The isolated domains IV or IVb retain the binding capacity for the SECIS element. Formation of the quaternary complex follows random order kinetics. An important feature also is that the stability of the complex is increased when both RNA ligands are bound.

The SECIS element itself is a hairpin structure formed within a section of 39 bases of the selenoprotein mRNA which follows the codon specifying selenocysteine insertion at the 3′-side. Binding of SelB takes place to its apical stem loop minihelix of 17 nucleotides. Genetic and structural analysis showed that bases in the loop region plus a bulged-out U in the helix are required for the interaction with SelB. This apical part of the SECIS element is separated by a short unpaired region from a helix at the base of the hairpin. Pairing within this second helix is not essential but it increases the efficiency of selenocysteine insertion. An absolute requirement,

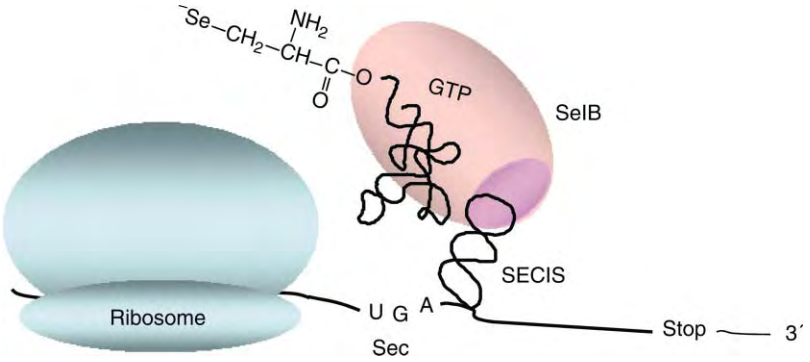

FIGURE 3 Translation of prokaryotic selenoprotein mRNA. Note that the SECIS element is within the mRNA reading frame and is complexed to domain IVb of SelB carrying selenocysteyl-$tRNA^{Sec}$ and GTP.

however, is that the codon determining selenocysteine insertion lies within a critical distance relative to the binding site of SelB.

Bacterial SECIS elements lie within the reading frame of their selenoprotein mRNAs; they are thus subject to stringent sequence constraints in order to deliver a functional gene product. However, they do not need to be translated since they also function when placed in the 3′-untranslated region at the correct distance to the selenocysteine codon within an upstream reading frame. The sequence constraint (which depends on the protein to be formed) and the requirement for binding of SelB restricts the number of selenoprotein mRNAs to be expressed in a single organism and explains why the vast majority of selenoprotein genes cannot be heterologously expressed unless the cognate SelB gene is coexpressed. Thus, SelB and their SECIS elements are subject to coevolution.

Decoding Event at the Ribosome

In all biological systems analyzed thus far, selenocysteine insertion is directed by the opal stop codon UGA but only if it is followed by an SECIS element at the correct distance. This violates the dogma that no codon can have more than one meaning within a single cell. The questions to be answered therefore are: (1) what prevents the UGA to be used as a termination signal, and (2) which mechanism interferes with insertion of selenocysteine at ordinary UGA stop codons?

Counteraction of Stop at the UGA?

A convincing answer to the question why the selenocysteine-specific UGA codon does not function as an efficient termination signal must await structural information on the decoding complex. It is, however, clear that termination always competes with selenocysteine insertion, especially under conditions when the capacity for decoding the UGA with selenocysteine is a limiting factor. This can be, for example, a surplus of selenoprotein mRNA in relation to the amount of SelB quaternary complex which forces the ribosome to stall at the UGA. One fact identified to be involved in the suppression of termination is that the base following the UGA at the 3′-side in selenoprotein mRNAs is prodominately an A or C, which renders the UGA a weak termination signal. Also, the two amino acids preceding selenocysteine in the nascent polypeptide chain are predominantly hydrophobic which counteracts the dissociation of the nascent polypeptide from the ribosome, when translation pauses at a "hungry" codon present in the A site. Additional mechanisms, however, must exist which contribute to the suppression of termination.

Selenocysteine Specificity of UGA Codons

From the colinearity between the mRNA nucleotide sequence and the amino acid sequence of the translation product, it is clear that UGA determines the *position* where selenocysteine is to be inserted during translation. The *specificity* of the UGA, however, is determined by the codon context, i.e., by the existence of a SECIS element at the 3′ side. The results of extensive biochemical and biophysical analysis suggest the following scenario for the decoding process: (1) SelB forms the quaternary complex at the mRNA in which the two RNA ligands display cooperativity in their interaction with the protein; (2) in this quaternary complex SelB attains a conformation compatible for interaction with the ribosome which then results in stimulation of GTP hydrolysis by SelB which in turn causes the release of the charged tRNA in the vicinity of the ribosomal A-site; (3) loss of the tRNA ligand causes the SelB protein to return to a conformation with about tenfold lower affinity for the SECIS element. As a consequence, the mRNA is released from the protein and freed for the translation of codons downstream of the UGA. The consequence of the complex cascade of reactions is that the efficiency of the decoding of UGA with selenocysteine is lower than that of any of the standard sense codons. It is also reflected by a considerable pause taking place when the ribosome encounters the quaternary complex at the mRNA. In the absence of selenocysteyl-tRNA, binding of SelB alone to the mRNA does not retard the rate of translation.

Archaeal and Eukaryal Selenoprotein Synthesis

$tRNA^{Sec}$ species from archaea and eukarya share several structural similarities with the bacterial counterparts but they are more related to each other than either one is to bacterial $tRNA^{Sec}$. There is also considerable sequence similarity between selenophosphate synthetases from all three lines of descent rendering their annotation in genome projects easy. On the other hand, homologues for the bacterial selenocysteine synthase have not been identified yet in any of the genomic sequences from organisms known to synthesize selenoproteins.

Whereas UGA directs selenocysteine insertion also in archaea and eukarya, a fundamental difference is that the SECIS element is not positioned within the reading frame but in the 3′-nontranslated region of the mRNA. SECIS elements from organisms of the three lines of descent are different by sequence and by secondary structure. They may be positioned at different distances from the actual termination codon and/or the selenocysteine inserting UGA codon but a critical distance must not be underpassed. It is thought that the selective value for having the SECIS element in the nontranslated

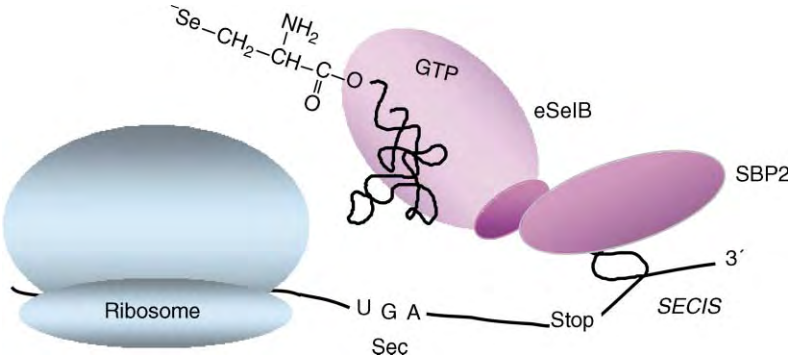

FIGURE 4 Translation of eukaryal selenoprotein mRNA. Note that the SECIS element is in the 3′-nontranslated region and serves as the binding site for SBP2 which in turn interacts with eukaryal SelB protein.

region consists in liberating it from the sequence constraint, and thus, allowing the translation of mRNAs with more than one UGA codon specifying selenocysteine insertion. Indeed, proteins with up to 17 selenocysteine residues are formed in some eukaryotes and in one instance a polypeptide with two such amino acids is synthesized in an archaeon.

Parallel to this deviation in both sequence, structure and position of the SECIS element, there is an alteration of the structure of the archaeal and eukaryal SelB-like translation factors. Domains I, II, and III closely resemble the three homologous domains from the bacterial SelB. However, the C-terminal extension is only short, less than 10 kDa, and accordingly and not unexpectedly, the archaeal and eukaryal SelB homologues do not bind to their cognate SECIS structures. In eukarya a second protein is fulfilling this task, namely SBP2 (SECIS binding protein 2) (Figure 4). There is evidence that SBP2 interacts with the SelB protein by direct contact in the decoding process. This interaction is stabilized in the presence of selenocysteyl-tRNA^{Sec}. However, the precise function of SBP2 has not yet been resolved.

See Also the Following Articles

EF-G and EF-Tu Structures and Translation Elongation in Bacteria • Ribozyme Structural Elements: Hairpin Ribozyme • Translation Termination and Ribosome Recycling

Glossary

elongation factor Helper protein assisting the ribosome in the polypeptide elongation process.

nonstandard amino acid Amino acid whose insertion is achieved by an expansion of the classical genetic code.

SECIS Selenocysteine insertion sequence of the mRNA which redefines a UGA stop codon, in a sense, codon for the insertion of selenocysteine.

selenoprotein Protein with one or more selenocysteine residues.

stop codon A codon signaling chain termination in protein synthesis in the classical genetic code UGA, UAA or UAG.

tRNA RNA molecule carrying an amino acid at its 3′-end and functioning as an adaptor to incorporate the amino acid into the growing polypeptide chain according to the triplet sequence of the mRNA.

Further Reading

Atkins, J. F., Böck, A., Matsufuji, S., and Gesteland, R. F. (1999). Dynamics of the genetic code. In *The RNA World* (R. F. Gesteland, T. R. Cech and J. F. Atkins, eds.) 2nd edition, pp. 637–673. Cold Spring Harbor Laboratory Press, Cold Spring Harbor, New York.

Copeland, P. R., Fletcher, J. E., Carlson, B. A., Hatfield, D. I., and Driscoll, D. M. (2000). A novel RNA binding protein, SBP2, is required for the translation of mammalian selenoprotein mRNAs. *EMBO J.* **19**, 306–314.

Flohe, L., Andreesen, J. R., Brigelius-Flohe, B., Maiorino, M., and Ursini, F. (2000). Selenium, the element of the moon, in life on earth. *Life* **49**, 411–420.

Hatfield, D. I. (ed.) (2001). *Selenium: Its Molecular Biology and Role in Human Health*. Kluwer, Academic Publishers, New York.

Krol, A. (2002). Evolutionary different RNA motifs and RNA–protein complexes to achieve selenoprotein synthesis. *Biochimie* **84**, 765–774.

Rother, M., Resch, A., Wilting, R., and Böck, A. (2001). Selenoprotein synthesis in archaea. *BioFactors* **14**, 75–83.

Stadtman, T. C. (1996). Selenocysteine. *Annu. Rev. Biochem.* **65**, 83–100.

Biography

August Böck is Professor Emeritus and former holder of the chair in Microbiology at the University of Regensburg from 1971 to 1978 and at the University of Munich from 1978 to 2002. He pursued his education at the University of Munich and his postdoctoral training at Purdue University. His main research interests are in microbial physiology with special emphasis on selenium biochemistry, bacterial metabolism and its regulation, and prokaryotic protein synthesis.

Septins and Cytokinesis

Makoto Kinoshita and Christine M. Field
Harvard Medical School, Boston, Massachusetts, USA

Septins are a family of conserved GTPases that has been identified in most animals from yeast to mammals. Each organism has multiple family members. Biochemical and genetic evidence indicate that multiple septin polypeptides form large, discrete complexes that further multimerize into filaments and higher order assemblies. Septins have been implicated in a variety of cellular processes including cytokinesis, vesicle trafficking, and axon migration. In yeast, they are involved in bud-site selection, cell polarity, and cytokinesis. Their name derives from their requirement during the final separation of the daughter cells in yeast, a process termed septation. While the precise molecular functions of septins are not known, a unifying hypothesis considers septin assemblies as scaffolds that localize, and perhaps regulate, diverse proteins involved in cortical dynamics. The septin scaffold may also have a fence-like function, limiting diffusion of proteins in the plane of the plasma membrane.

Cytokinesis

Cytokinesis is the process that physically separates the two daughter cells at the end of each division cycle. It must be temporally and spatially coupled to chromosome segregation to ensure that each daughter cell receives the correct number of chromosomes. The initiation of cytokinesis is controlled by cell-cycle-regulatory proteins, with the first step, the positioning of the cleavage plane (the site of division) beginning in late anaphase. In metazoa, the division site is determined by microtubules derived from the mitotic spindle. Next, a contractile ring made of actin, myosin-II, and other associated proteins, including septins, assembles at the plasma membrane at the specified position. The cleavage furrow ingresses by a combination of ring contraction driven by myosin-II, and targeted insertion of vesicles near the furrow to supply new plasma membrane. Finally, cytokinesis is completed in a complex process that involves the disassembly of the cleavage furrow and underlying microtubule structures, plasma membrane sealing and abscission (the actual separation) of the daughter cells. Targeted exocytosis and protein degradation are implicated in this completion phase (see Figure 1).

Septins localize to the cleavage furrow in all organisms that have been studied. Deletion, mutation,or inhibition of septins typically results in incomplete or abortive cytokinesis, though the severity of the defect varies between organisms. This suggests a conserved function of septins in cytokinesis that is not required for cleavage plane specification, but is required for normal furrow ingression, and/or completion.

Biochemical and Structural Properties of the Septins

Septins Bind Guanine Nucleotide and Form Complexes and Filaments

Sequence analysis shows that all septins have a central globular domain containing conserved motifs found in small GTPases, and most septins have a C-terminal predicted coiled-coil region of variable length. On purification, septins are found in large complexes containing multiple septin polypeptides. The septin complex purified from *Drosophila* embryos is composed of three septin polypeptides with a stoichiometry of 2:2:2. Yeast complexes contain a fourth septin polypeptide, and complexes from mammalian brain are heterogeneous, and may be built from at least six different septin proteins. When viewed by negative-stain electron microscopy (EM) a typical septin preparation appears as filaments 7–9 nm thick and of variable lengths. The shortest filament represents the complex itself and is the building block from which the longer filaments are formed (see Figure 2A and 2B) which show a purified yeast complex.

Purified septin complexes contain tightly bound guanine nucleotide at a level of one molecule per septin polypeptide. The GDP:GTP ratio is ~2:1 for both *Drosophila* embryos and yeast complexes. The role of bound nucleotide in septin biochemistry is still under investigation, and appears to be distinctly different from small GTPases whose function employs

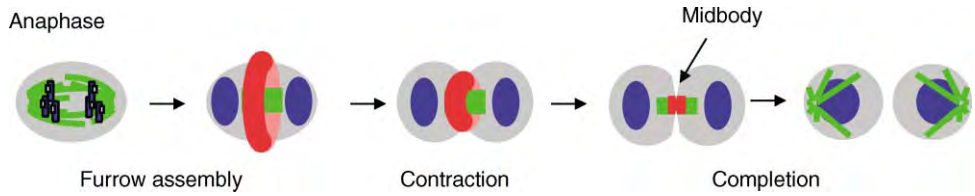

FIGURE 1 Schematic illustration of the different subprocesses of cytokinesis. DNA is shown in blue, microtubules (MT) in green, and the cleavage furrow/contractile ring (CR) in red. When the cleavage furrow assembles and contracts, microtubules become bundled and compacted into the midbody. Cytokinesis is completed by disassembly of the CR and MT structures and fusion of the membrane to create two daughter cells.

rapid exchange and hydrolysis. Isolated septin complexes exchange bound nucleotide very slowly, and in yeast, the majority of bound nucleotide does not turn over. These data suggest that GTP is bound during septin folding or complex assembly, and thereafter is not exchanged, at least on the majority of septins. Thus bound GTP may play a structural role, analogous to GTP bound to α-tubulin, and not a regulatory role, analogous to nucleotide in β-tubulin or small GTPases. However it is possible that GTP exchange and hydrolysis plays a more dynamic regulatory role for a subset of septins.

Septin Filaments Can Form Higher-Order Assemblies

Unit septin complexes are able to assemble into several different higher-order structures *in vitro*. Septin complexes from all organisms studied tend to polymerize end-to-end to form long filaments of the same thickness as the unit complexes. With yeast septins, these filaments tend to associate side by side in pairs a fixed distance apart, suggesting they may be cross-bridged by one of the septin polypeptides (see Figure 2C).

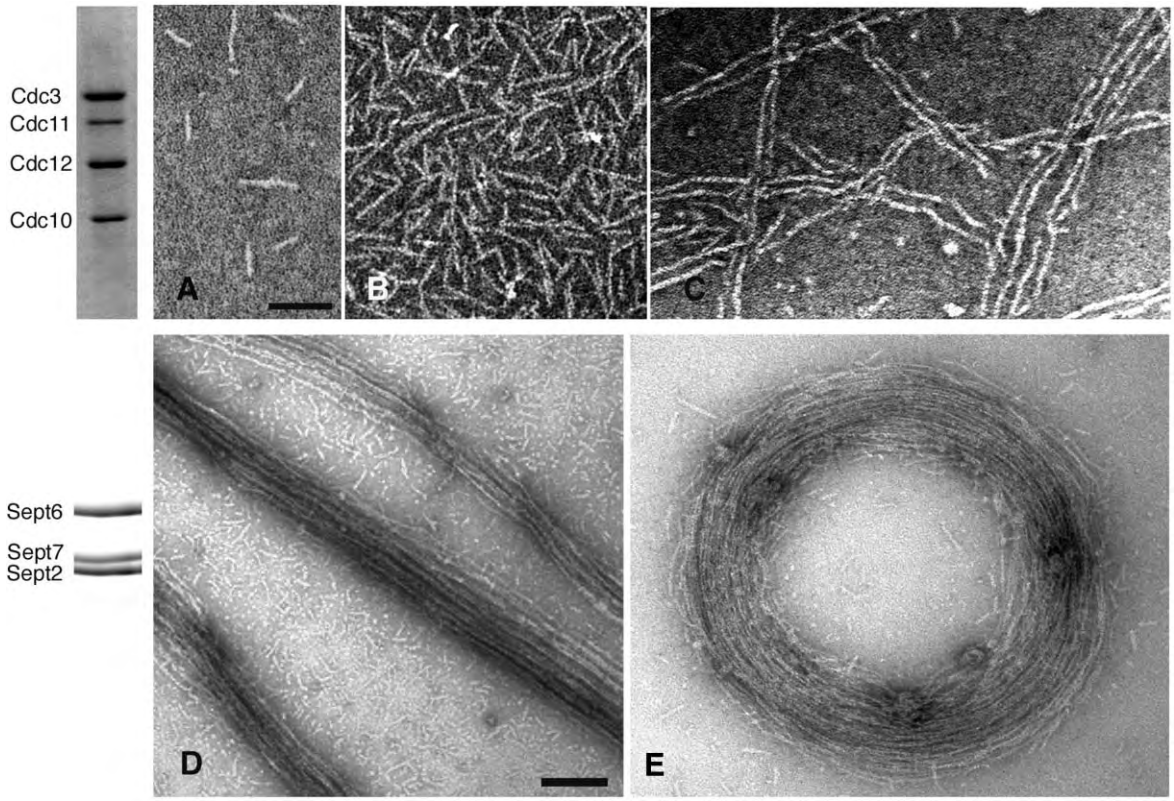

FIGURE 2 Negative stain electron micrographs of septin structures. (A–C) Examples of filamentous structures formed by a four polypeptide septin complex purified from *S. cerevisiae*. (A) Monomers and dimers. (Modified from Byers, B., and Goetsch, L. (1976). A highly ordered ring of membrane-associated filaments in budding yeast. *J. Cell Biol.* **69**, 717–721.) (B) Filaments of variable lengths. (C) Long paired filaments. (Courtesy of J. Frazier.) (D) and (E) are higher order structures formed by a three polypeptide recombinant mammalian septin complex. Complexes polymerize into long filaments that bundle (D) and curl up to form rings (E). Coomassie stained polyacrylamide gel analysis of complexes are on the left. Scale bars are 100 nm. (E is reproduced from Kinoshita, *et al.* (2002). *Develop. Cell.* **3**, 791–802, with permission from Elsevier.)

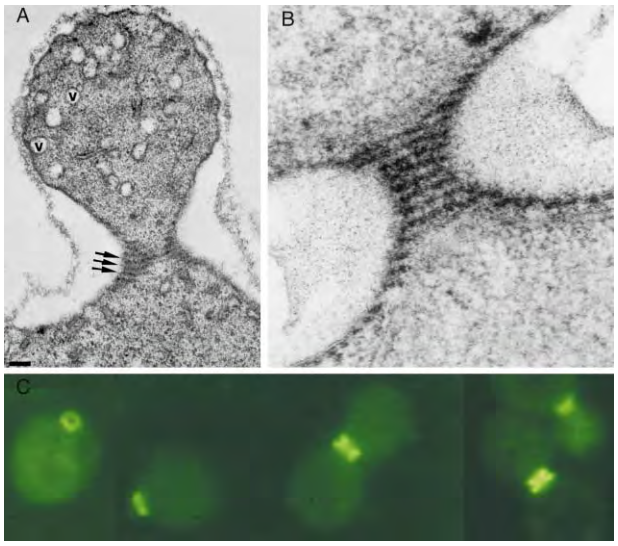

FIGURE 3 Septin structures/localization in *S. cerevisiae*. (A) and (B) are electron micrographs showing grazing sections through an early bud (A) and the neck of a large-budded cell (B) showing the 10 nm neck filaments (arrows in A) Figure 3A reproduced with permission of The Rockefeller University Press from Byers, B., and Goetsch, L. (1976). A highly ordered ring of membrane-associated filaments in budding yeast. *J. Cell Biol.* **69**, 717–721. (B) Reproduced from Strathern, J. N., Jones, E. W. and Broach, J. R. (Eds) (1981) The Molecular Biology of the Yeast Saccharomcyes : Life Cycle and Inheritance, pp. 59–96, with permission of Cold Spring Harbor Laboratory Press. (C) Shows yeast at various stages of the cell cycle stained with an antibody against Cdc3p. (Courtesy of J. Pringle.)

Purified mammalian septin filaments tend to assemble into bundles, that under some conditions curl up into rings and coils of ~0.7 μm diameter (see Figures 2D and 2E). Mammalian septins also tend to assemble into rings in cells. This tendency to curve is apparently intrinsic to the septin complex, and may play a role in deforming the plasma membrane in cells. The rings are comparable in size and shape to several septin assemblies in cells, including the yeast bud neck (Figure 3) and septin rings formed in cells under stress (Figure 4C).

Mammalian septin filaments can be recruited to actin bundles by another cytokinesis furrow protein, anillin. Anillin was originally identified as an actin-bundling protein in *Drosophila*. Septins and anillin are abundant in intracellular bridges between daughter cells in conventional cytokinesis and also stable bridges formed as the result of incomplete cytokinesis in *Drosophila* embryos. It is possible that these two proteins have a structural role in supporting a narrow neck in the plasma membrane after the contractile apparatus that formed the neck disassembles at the end of cytokinesis.

Septins Interact with Inositol Phospholipids

A number of studies have suggested that septins can bind directly to lipid bilayers containing inositol lipids, an activity which may be important in septin targeting or in regulating exocytosis. The question of exactly how septins target to plasma membranes, and how these proteins are involved in vesicular trafficking, are important topics for future study.

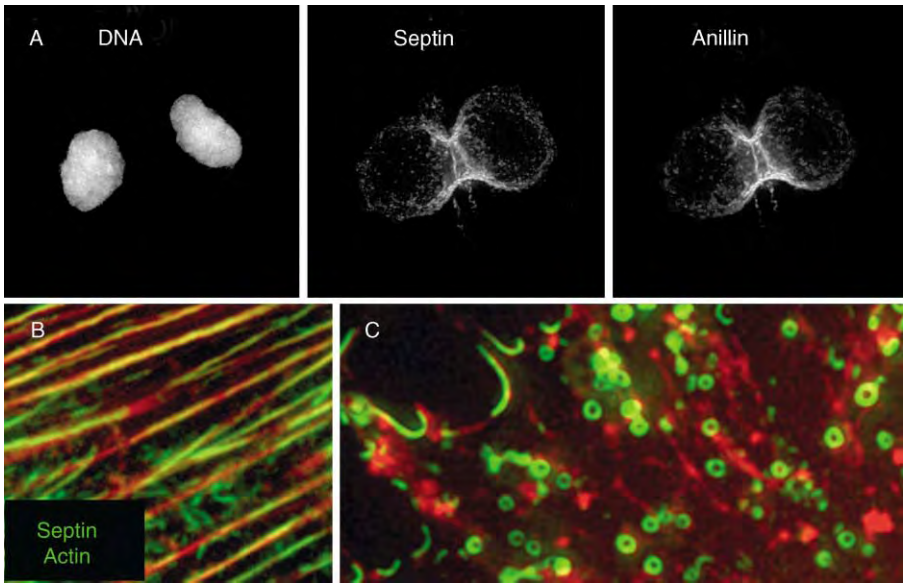

FIGURE 4 Septin structures/localization in mammalian cells. (A) A vertebrate cell in telophase showing sept7 and anillin colocalizing in the cleavage furrow. (Courtesy of Karen Oegema.) (B) and 4C Interphase cells costained for sept2 and actin. (B) Sept2 localizing along actin bundles. (C) A vertebrate cell treated with a drug that depolymerizes actin filaments. Removal of actin causes Sept2 to form rings of similar dimensions to those see by EM *in vitro* (Figure 2E). (4B and 4C are reproduced from Kinoshita, *et al.* (2002). *Develop. Cell* **3**, 791–802, with permission from Elsevier.)

Septin Behavior and Function in Cytokinesis

Budding Yeast

Septin proteins were originally identified in budding yeast (*Saccharomyces cerevisiae*) as the protein products of four genes *CDC3*, *CDC10*, *CDC11*, and *CDC12*. Temperature sensitive mutations of these genes exhibited hyperpolarized growth and defects in cell wall deposition and cytokinesis. These septin polypeptides localize to the mother/bud neck late in the G1 phase of the *S. cerevisiae* cell cycle, before the localization of other cleavage furrow components. Septin localization and assembly is controlled at least in part by the GTPase Cdc42, the master regulator of yeast cell polarity, and is independent of other cytoskeleton proteins including actin filaments. By EM, septins appear as 10 nm diameter filaments, termed neck filaments that appear to coil around the bud neck (Figure 3A and 3B). By immunofluorescence they appear as an hourglass-shaped assembly coating the inside of the bud neck. In projection, this hourglass can resemble two rings (Figure 3C). Photobleaching of GFP-tagged septins reveals that septins are quite dynamic before bud emergence, but once they assemble into neck filaments, their turnover rate is slowed considerably, and they can be considered static. This datum correlates well with their GTP exchange properties.

In budding yeast, septin localization at the bud neck is required for the sequential recruitment of all of the cytokinetic machinery including a type II myosin heavy chain (Myo1p), its associated light chain (Mlc1p), a formin homology (FH) protein Bni1p, probably responsible for nucleating contractile ring actin, a PCH protein (Hof1p/Cyk2p), and an IQGAP protein (Iqg1p/Cyk1p). All of these proteins have conserved roles in cytokinesis in other organisms, but it is not clear if their recruitment to the furrow depends on septins in metazoans. Neck filaments are also thought to anchor a chitin synthase complex (Chs3p/4p + Bni4p) responsible for cell-wall deposition during cytokinesis.

In budding yeast, septins are required for localization of many different proteins to the bud neck in addition to the basic cytokinesis machinery. A recent genome wide screen identified 98 proteins that localize to bud necks, and many of these depend on septins for their localization. Well-characterized examples include; the checkpoint kinases, Hsl1p, Gin4p, and Kcc4p, a component of the mitotic exit network (MEN), Dbf2/Mob1, and several proteins involved in bud site selection including Bud4.

Septins also act to restrict diffusion of proteins in the plane of the plasma membrane. The neck filaments form a fence that restricts membrane proteins to the bud, and presumably plays an important role in polarizing the yeast cell. This function may be direct as opposed to being mediated by other proteins dependent on septins for their localization.

Overall, septins play a central role in the cell biology of budding yeast. This role reflects the importance of the bud neck in cell polarity and cell division, and the function of septins as a scaffold for localizing other proteins to this site, and restricting diffusion through it. In organisms that do not grow by polarized budding, septins may be important, but perhaps their role is not as central to the overall biology of the cell.

Fission Yeast

In fission yeast, *Schizosaccharomyces pombe*, disruption of the septin genes result in a delay in septation (cell–cell separation), but not severe cytokinetic defects as seen in budding yeast. Septins assemble into a single ring structure in late cytokinesis, and are not required to recruit actin, myosin, or other contractile ring components. Stability of the septin ring requires the protein mid2p, that is related to metazoan anillin, suggesting this interaction is conserved. Interestingly, mutations in components of the exocyst, a large complex involved in exocytosis, have a similar septation defect. Thus, in *S. pombe*, the septin scaffold is involved only in the completion stage of cytokinesis, perhaps to target exocytotic vesicles required for membrane fusion or enzymes required for final digestion of the septum.

Metazoa

In animal cells, septin polypeptides are recruited in late anaphase to the equatorial cortex and assemble into the contractile ring at the same time as actin and myosin-II. Perturbation of septins by gene disruption, RNA interference, or microinjection of anti-septin antibodies blocks normal cytokinesis in mammalian cells and fly embryos. However, septins are dispensable in some cases. For instance, nematode eggs can complete cytokinesis without septins at early developmental stages, although, cytokinesis defects manifest in some cell lineages at postembryonic stages. This difference in requirement for septins indicates a divergence in cytokinesis mechanism that we do not understand.

While the concept of septins as a scaffold for recruiting other factors is probably relevant, the exact function of septins during cytokinesis is even less clear in metazoans than it is in yeast. Septins tend to colocalize with actin filaments in interphase cells, and they tightly colocalize with anillin during cytokinesis (Figure 4). Combined with biochemical data reconstituting an actin–septin–anillin interaction *in vitro*, these data suggest a cytokinesis function involving actin filaments. However, disruption of septins does not block positioning or initial contraction of the actomyosin ring, so

septin function is not as central as it is in *S. cerevisiae*. Most likely, septins and anillin function together late in cytokinesis, perhaps during the complex process of completion.

How might septins function in completion? Physical and functional interactions have been shown between mammalian septins and syntaxins (SNARE proteins involved in membrane fusion during secretion) and the exocyst complex (a complex of proteins required for exocytosis). As previously mentioned exocyst mutants in *S. pombe* have a similar phenotype to septin mutants. Thus, it is reasonable to speculate that septins play a role in regulating or targeting vesicle insertion associated with furrow ingression and completion. This role has not yet been explored in budding yeast. Additionally, septins and anillin may assemble into a structure that stabilizes the fully ingressed membrane after the contractile ring has disassembled, but before cytokinesis is completed. These roles might explain why septins are more important during cytokinesis in some cells than others: (1) the amount of new membrane required for cytokinesis may vary according to cell type and (2) the time delay between completing ingression and actually separating the daughter cells is quite variable between species and cell type.

See Also the Following Articles

Cytokinesis • Cytokinin • Mitosis

Glossary

cell cortex A specialized layer of cytoplasm beneath the plasma membrane. In animal cells it contains actin and actin-binding proteins.

cell cycle The sequence of events by which a cell duplicates its contents and divides in two. There is a network of regulatory proteins that govern the progression through the key events such as DNA replication, formation of the mitotic spindle, and segregation of the chromosome. The cell cycle ends with cytokinesis.

exocyst complex Complex of conserved proteins that are an essential part of the exocytotic apparatus.

FH proteins Conserved proteins required to assemble some types of actin structures such as actin cables (in yeast), stress fibers, and the contractile ring.

guanosine di-/tri-phosphate (GDP/GTP) Plays an important role in tubulin stability and microtubule assembly and in signal transduction pathways via small GTPases.

inositol phospholipids Membrane lipids containing inositol and phosphate(s) that are important in various cell-signaling pathways.

midbody The thin intercellular bridge of cytoplasm connecting two daughter cells in late cytokinesis. It contains a tightly packed antiparallel array of microtubules and an electron dense matrix at its center.

photobleach The exposure of a fluorescent probe to light such that it is rendered nonfluorescent or "bleached." Examining the recovery of fluorescence after photobleaching a tagged protein gives an indication of how dynamic it is.

septation In yeast, the formation of a new cell wall or septum to separate two daughter cells. Septation is separable from cytokinesis.

small GTPase GTP-binding and -hydrolyzing switch proteins. They alternate between an active/on state when they are GTP bound and an inactive GDP bound state.

Further Reading

Field, C. M., Li, R., and Oegema, K. G. (1999). Cytokinesis in eukaryotes: A mechanistic comparison. *Curr. Opin. Cell Biol.* **11**, 68–80.

Longtine, M. S., and Bi, E. (2003). Regulation of septin organization and function in yeast. *Trends Cell Biol.* **8**, 403–409.

Longtine, M. S., Demarini, D. J., Valencik, M. L., Al-Awar, O. S., Fares, H., De Virgilio, C., and Pringle, J. R. (1996). The septins, roles in cytokinesis and other processes. *Curr. Opin. Cell Biol.* **8**, 106–119.

Mitchison, T. J., and Field, C. M. (2002). Cytoskeleton: What does GDP do for septins? *Curr. Biol.* **12**, R788–R790.

Moffat, J., and Andrews, B. (2003). Ac'septin' a signal: Kinase regulation by septins. *Dev. Cell* **5**, 528–530.

Rajagopalan, S., Wachtler, V., and Balasubramanian (2003). Cytokinesis in fission yeast: A story of rings, rafts and walls. *Trends Genetics* **19**, 403–408.

Tolliday, N., Bouquin, N., and Li, R. (2001). Assembly and regulation of the cytokinetic apparatus in budding yeast. *Curr. Opin. Microbiol.* **4**, 690–695.

Trimble, W. S. (1999). Septins: A highly conserved family of membrane associated GTPases with functions in cell division and beyond. *J. Membr. Biol.* **169**, 75–81.

Biography

Makoto Kinoshita was a Postdoctoral Research Fellow at Department of Cell Biology, Harvard Medical School and currently is an Assistant Professor at Kyoto University Graduate School of Medicine. His principal research interest is in biochemistry, cell biology, and pathology of mammalian septins.

Christine M. Field is a Research Fellow and a graduate student at Department of Systems Biology, Harvard Medical School. Her principal research interest is in dissecting molecular mechanism of cytokinesis by biochemistry and genetics using *Drosophila* and other organisms.

Serine/Threonine Phosphatases

Thomas S. Ingebritsen
Iowa State University, Ames, Iowa, USA

Phosphorylation of proteins on serine, threonine, and tyrosine residues is a major mechanism for regulating the activity of cell proteins and it plays a central role in virtually all signal transduction pathways in eukaryotes. The steady-state level of phosphorylation of a protein at a particular site depends on the balance of the activities of the protein kinase(s) and protein phosphatase(s) acting on that site. Both protein kinases and protein phosphatases are important targets of cell regulation. This article will focus on the structure, regulation, and function of the two families of protein Ser/Thr phosphatases (PPP and PPM). Members of each family are present in all three domains of life (archae, bacteria, and eukarotes).

Protein Ser/Thr Phosphatase Catalytic Subunit Families

PPP Family

Members of this family possess a common catalytic core (280 residues) and can be further divided into four subfamilies termed PPP1, PPP2A, PPP2B, and PPP5. Three prokaryotic phosphatases: diadenosine tetraphosphatase, Φ80 phosphatase, λ phosphatase exhibit weaker similarity to the PPP family.

PPM Family

Members include PP2C, *Arabidopsis* ABI1 and ABI2, *Arabidopsis* KAPP, *Bacillus subtilis* SpoIIE phosphatase and pyruvate dehydrogenase phosphatase. The core PPM catalytic domains occur in diverse contexts. For example the catalytic domain of *Arabidopsis* ABI1 is fused to an EF-hand domain, the *Arabidopsis* kinase associated protein phosphatase (KAPP) catalytic domain is fused to a kinase-interaction domain. The kinase interaction domain of KAPP associates with a phosphorylated receptor-like protein. The N terminus of *Bacillus subtilis* SpoIIE phosphatase is fused to a domain with ten membrane-spanning segments.

Biochemical Characterization of Signature Protein Ser/Thr Phosphatases

PP1, PP2A, and PP2B are signature members of the PPP1, PPP2A, and PPP2B subfamilies while PP2C is the signature member of the PPM family. These four enzymes account for the majority of protein Ser/Thr phosphatase activity in cell extracts. The activities of these enzymes can be distinguished in cell extracts based on divalent cation requirements and the effects of physiological and pharmacological inhibitors (Table I). PP1, PP2A, and PP2C have broad and overlapping substrate specificities whereas the substrate specificity of PP2B is more restricted.

Three-Dimensional Structures and Catalytic Mechanism

Three-dimensional structures have been determined for two members of the PPP family (PP1 and PP2B) and for one member of the PPM family. A surprising finding was that the PPP and PPM families have similar three-dimensional architectures even though the primary structures of the two families are unrelated. The three-dimensional structure of the two families is quite distinct from that of the PTP family of protein Tyr phosphatases.

Three-Dimensional Structures

For both the PPM and PPP families, the core structure consists of a pair of mixed β-sheets that form a β-sandwich structure. The catalytic sites possess a binuclear metal ion center which has some similarity to the binuclear metal ion center of purple acid phosphatase (Figure 1). For the PPM family, the two metal ions are Mn^{2+}. In the case of the PPP family, the two metal ions are probably Fe^{2+} and Zn^{2+}, although there is some controversy about whether the second metal ion is Zn^{2+} or Mn^{2+} and also about whether the

TABLE I

Biochemical Characterization of Signature Protein Phosphatases

Type	Protein phosphatase	Substrate specificity	Divalent cation requirement	I_1 and I_2 inhibition	Okadaic acid inhibition (IC_{50})
1	PP1	Broad	None	Yes	20 nM
2	PP2A	Broad	None	No	0.2 nM
2	PP2B	Narrow	Ca^{2+}	No	5 μM
2	PP2C	Broad	Mg^{2+}	No	No effect

PP2B requires μM Ca^{2+} for activity whereas PP2C requires mM Mg^{2+}. Inhibitor-1 (I_1) and inibitor-2 (I_2) are PP1 modulator proteins. Okadaic acid is a pharmacological inhibitor of PPP family members. It is a polyether carboxylic acid that is a diarrhetic shell fish poison and a powerful tumor promoter. There are a number of other pharmacological inhibitors of the PPP family (e.g., microcystin, calyculin A, cantharidin). Okadaic acid, microcystin, and calyculin A inhibit by binding to the phosphatase active site.

Fe is in the 2+ or 3+ oxidation state. In both cases, metal ions are coordinated with water molecules.

Catalytic Mechanism

For both the PPP and PPM family hydrolysis of serine or threonine phosphate esters occurs through a single-step mechanism in which a metal-bound water acts as a nucleophile to attack the phosphorus atom of the substrate phosphate group (Figure 1). The metal ion acts as a Lewis acid to enhance the nucleophilicity of metal-bound water and it also enhances the electrophilicity of the phosphorus atom by coordinating the two oxyanions of the phosphate group. An active site His sidechain donates a proton to the leaving oxygen of Ser or Thr. This catalytic mechanism is quite different from that used by the PTP family which involves formation of a phospho-enzyme intermediate.

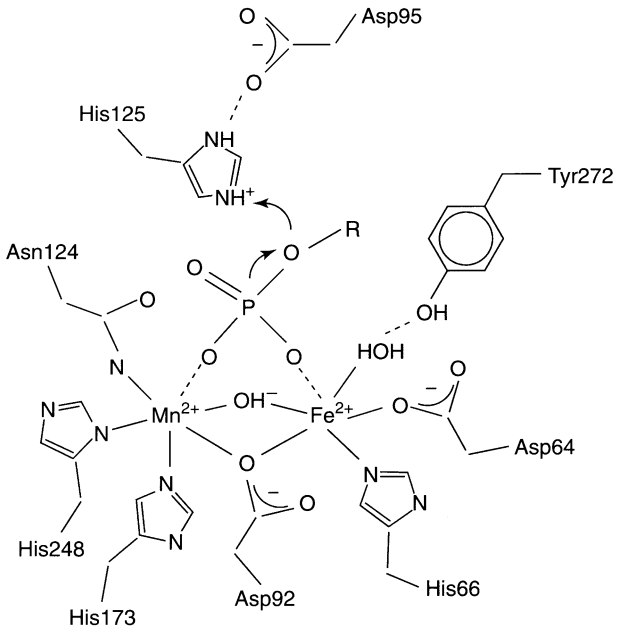

FIGURE 1 Active site structure and catalytic mechanism of PP1 catalytic subunit. (Reprinted from Barford, D. (1996). Molecular mechanisms of the protein serine/threonine phosphatases. *TIBS* **21**, 407–412.)

Subunit Structure of PPP Family Members

Members of the PPP family interact with diverse sets of regulatory subunits, which direct the catalytic subunits to specific subcellular locations, alter substrate specificity and/or confer regulatory properties.

Interaction of PP1 with Diverse Regulatory Subunits

The catalytic subunit of PP1 (PP1c) interacts with >50 regulatory subunits, which fall into two classes: targeting subunits and modulator proteins. Targeting subunits direct PP1c to a wide variety of subcellular locations including: glycogen particle, myosin/actin, spliceosomes/RNA, endoplasmic reticulum, proteasomes, nuclear membranes, plasma membranes/cytoskeleton, centrosomes, microtubules, and mitochondria. Targeting subunits also modulate substrate specificities and may regulate phosphatase activity.

Modulators are generally low-molecular-weight, heat-stable proteins that alter PP1 activity or substrate specificity. The activity of some of the modulators (e.g., inhibitor-1, DARPP-32, CPI-17, and G subunit) is regulated through reversible phosphorylation.

Strong binding of many of the regulatory proteins to PP1c is mediated through a short motif termed RVxF. This motif is found in two-thirds of the targeting subunits and one-half of the modulator proteins. The consensus sequence of the motif is: (K/R)x_1(V/I)x_2(F/W) where x_1 and x_2 may be any residue except a large hydrophobic residue. In some motifs x_1 is absent.

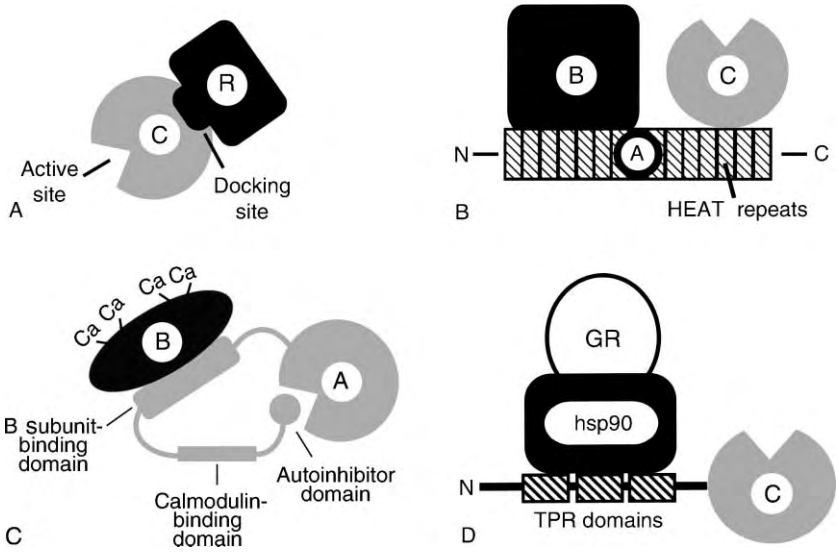

FIGURE 2 Subunit structure of PPP family members. (A) PP1. C and R designate catalytic and regulatory subunits, respectively. The docking site on the C subunit interacts with the RVxF motif of the regulatory subunit. (B) PP2A. The labels C, B, and A designate the catalytic, regulatory, and adaptor subunits, respectively. The three-dimensional structure of the A subunit has been determined. Tandem arrays of HEAT (*h*untingtin-*e*longation factor-*A* subunit-*T*OR) motifs are present in a variety of other proteins. The labels N and C designate the amino and carboxyl termini of the A subunit. (C) PP2B. The labels A and B designate the catalytic and regulatory subunits, respectively. The B subunit has four Ca^{2+}-binding sites. The B subunit-binding, calmodulin-binding and autoinhibitor domains are on a carboxyl-terminal extension of the A subunit. The region from the end of the B subunit-binding domain to the beginning of the autoinhibitor domain is disordered in the absence of calmodulin and thus not visible in the crystal structure. (D) PP5. C and GR designate the catalytic subunit and the glucocorticoid receptor, respectively. TPR domains are characterized by a degenerate 34 amino acid sequence. The label N designates the amino terminus of the C subunit. The three-dimensional structure of the amino terminal extension of C has been determined in the absence of the core catalytic domain.

The RVxF motif binds to a docking site that is remote from the active site (Figure 2A). The docking site consists of a hydrophobic groove which binds the two large hydrophobic residues of the RVxF motif and a cluster of negatively charged residues which interact with basic residues at the N-terminal end of the motif.

Additional interactions between the PP1c and the targeting and modulator proteins are thought to strengthen binding and mediate effects on PP1 activity. For example residues 7–11 of DARPP-32 (KKIQF) bind to the PP1c docking site whereas thr 34 which is phosphorylated by PKA binds to the active site of the phosphatase.

Interaction of PP2A with a Diverse Set of Regulatory Subunits

PP2A diversity is also generated by the interaction of a common catalytic (C) subunit with a diverse set of regulatory (B) subunits. However in this case, the regulatory subunits interact with the C subunit indirectly through an adapter subunit (A), thus forming a heterotrimeric phosphatase complex (Figure 2B).

Over 15 different B subunits are expressed in a tissue- and developmental-specific manner from four families of genes, termed PR55/B, PR61/B′, PR72/B′, and B′. Additional gene products are generated through alternate splicing. Functions of the B subunits include regulation of PP2A activity, subcellular targeting, and alteration of substrate specificity.

The A subunit is made up of 15 HEAT repeats which form an extended and curved structure reminiscent of a hook or the letter C. The catalytic subunit interacts with the C-terminal HEAT repeats (11–15) whereas the B subunits interact with N-terminal repeats (1–10).

Subunit Structure of PP2B

The catalytic (A) subunit of PP2B interacts with two EF-hand-type Ca^{2+}-binding proteins, an integral B subunit which binds in the absence of calcium, and calmodulin which requires calcium for binding. The A subunit has a regulatory C-terminal extension which has binding sites for the two Ca^{2+}-binding proteins as well as an autoinhibitor site (Figure 2C). Binding of Ca^{2+} to the B subunit is absolutely required for phosphatase activity. PP2B activity is further stimulated by Ca^{2+}-calmodulin.

PP5

The catalytic subunit of PP5 has an amino-terminal extension with three TPR domains. These domains are found in a variety of proteins and act as a scaffold that mediates protein–protein interaction. The TPR domains of PP5 mediate interaction of the phosphatase with the heat shock protein, hsp90, and the glucocorticoid

receptor (Figure 2D). TPR domains also suppress the catalytic activity of PP5 25-fold.

Examples of Functions and Regulation of Protein Ser/Thr Phosphatases

PPM Family

PPM family members are involved in stress responses in animals, plants, fungi, and prokaryotes. PP2C antagonizes stress response pathways involving two types of protein kinase cascades: mitogen-activated protein kinase (MAPK) and AMP-activated protein kinase (AMPK). Two other PPM family members (ABI1 and ABI2) play an essential role in the abscisic acid-mediated stress response of plants to water deprivation and in prokaryotes SpoIIE is involved in controlling sporulation.

PPM family members also have other cell functions. For example, the PDH phosphatase is involved in controlling the types of metabolic fuels used in body tissues through a dephosphorylation reaction that activates pyruvate dehydrogenase in mitochondria.

PPP Family

Regulation of PP1 Involving Targeting Subunits

There are four modes of regulation of PP1c involving targeting subunits: inducible expression of targeting subunits, allosteric regulation through targeting subunits, phosphorylation near the RVxF docking motif, and phosphorylation at sites remote from the docking motif.

The expression of two glycogen-targeting subunits in rat liver, G_L and R5, is decreased by diabetes and starvation and is restored by insulin treatment and refeeding, respectively.

G_L-PP1c is subject to allosteric regulation by glycogen phosphorylase *a* (phosphorylated, active form) which binds to a short segment at the C terminus of G_L with nanomolar affinity. Phosphorylase *a* binding inhibits the glycogen synthase phosphatase activity of G_L-PP1c but has no effect on phosphorylase phosphatase activity of the complex. This helps to coordinate the regulation of glycogen breakdown and synthesis in response to glucagon and perhaps to insulin.

G_M (muscle-specific glycogen targeting), NIPP1 (nuclear targeting), and Neurabin I (actin targeting) are phosphorylated by protein kinase A at sites near the RVxF docking motif leading to dissociation of PP1c. In the case of G_M-PP1c this results in decreased activity towards glycogen-bound substrates (glycogen synthase, phosphorylase *a*, and phosphorylase kinase).

The myosin-targeting protein M110 is phosphorylated on sites (Thr 697 and Ser 435) that are distant from the docking motif. The complex of PP1c with M110 is involved in regulating muscle contraction in smooth muscle and nonmuscle cells. Phosphorylation of Ser 435 occurs during mitosis and leads to activation of PP1c and enhanced binding to myosin II.

PP2A

One of the best-documented roles of PP2A is in the regulation of animal growth and development. A role in cell growth was first suggested by the potent inhibition of PP2A by the tumor promoter okadaic acid. Additionally the β-isoform of the A subunit of PP2A has been identified as a candidate tumor-suppressor gene and the myeloid-leukemia-associated protein SET is a potent inhibitor of PP2A.

PP2A dephosphorylates and inactivates protein kinases involved in growth-regulatory signal transduction pathways (e.g., ERK and Mek MAP kinases, protein kinase C, and protein kinase B). Additionally, PP2A is an important cellular target of the SV40 and polyoma DNA tumor viruses. Viral proteins associate with the AC dimer and displace B subunits. This leads to stimulation of growth-related (ERK/Mek) MAP kinase pathways and cell growth.

Genetic approaches in budding and fission yeast as well as in *Drosophila* demonstrate that PP2A has an essential role in regulating the cell cycle. Additionally, PP2A interacts with components of the Wnt signaling cascade, which controls the epithelial–mesenchymal transition during vertebrate development.

Central Role of PP2B in T Cell Activation

Stimulation of the T cell receptor leads to the activation of dual signal transduction pathways involving Ca^{2+} and Ras (Figure 3, left). Elevation of intracellular Ca^{2+} results in activation of PP2B which dephosphorylates NFAT. This leads to activation of NFAT as a transcription factor and translocation of the NFAT from the cytoplasm to the nucleus. The Ras pathway activates a nuclear transcription factor (AP-1) through a protein kinase cascade. NFAT and AP-1 bind cooperatively to DNA regulatory sites resulting in enhanced transcription of cytokine, cell surface receptor, and transcription factor genes.

PP2B is the site of action for the immune-suppressant drugs, Cyclosporin A and FK506, used to prevent rejection in organ transplant procedures. The use of these drugs has revolutionized organ transplant therapy. The two drugs interact with separate intracellular-binding proteins (cyclophin and FK506-binding protein) and the resulting complexes bind to and inhibit the activity of PP2B. This in turn inhibits T cell activation by

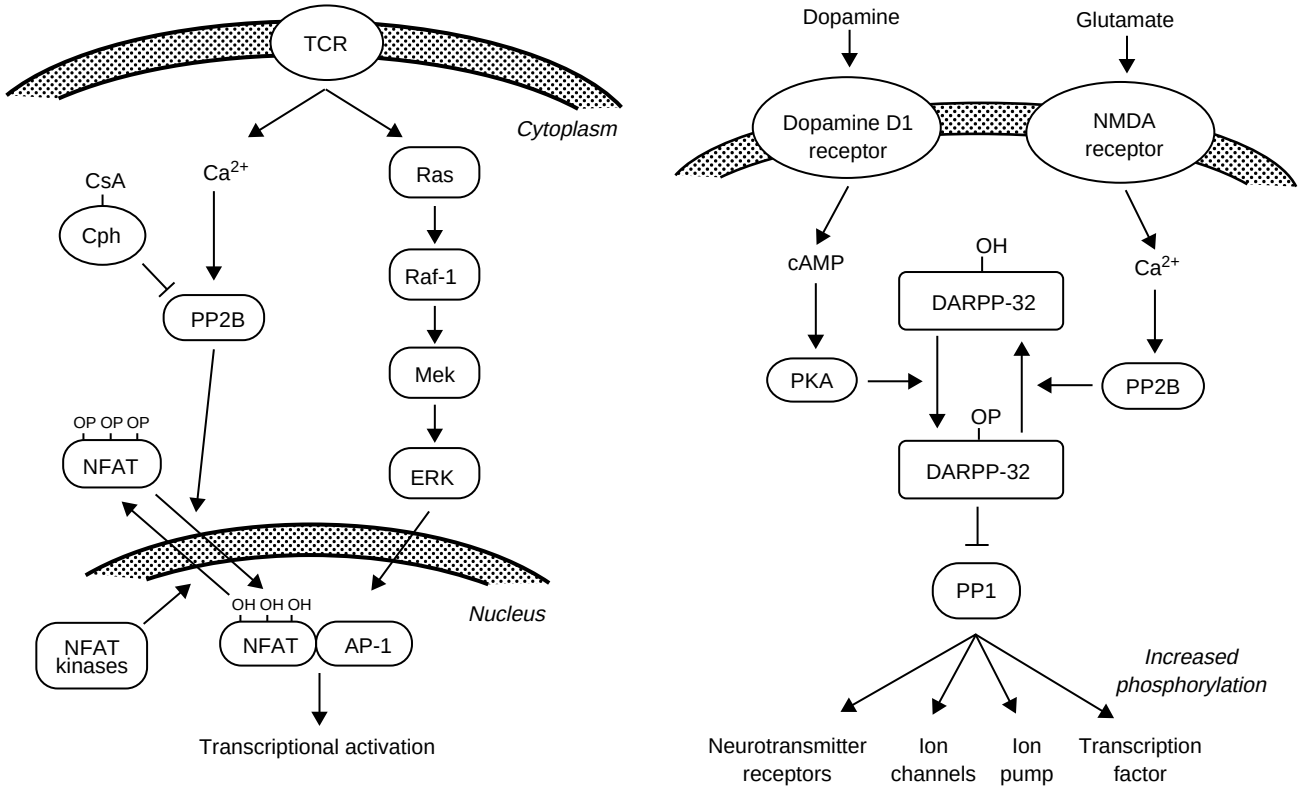

FIGURE 3 (Left) Role of PP2B in T cell activation. Raf-1, Mek, and ERK are protein kinases in the Ras signaling pathway. NFAT and AP-1 are transcription factors. NFAT are a family of transcription factors that exist in an inactive, phosphorylated state in the cytoplasm of resting T cells. These proteins are phosphorylated on multiple serine residues in a regulatory region in the amino-terminal half of the molecule. CsA and Cph designate cyclosporin and cyclophilin, respectively. (Right) Central role of DARPP-32 in the regulation of dopaminoceptive neurons. Inhibition of PP1 is associated with increased activity of NMDA and AMPA glutamate receptors, of L, N, and P type Ca^{2+} ion channels and CREB and with decreased activity of $GABA_A$ receptor, Na^+ channels, and Na^+/K^+ ATPase. There are a variety of other neurotransmitter receptors (opiate, adenosine, VIP) which elevate cAMP in medium spiny neurons. Glutamate acting through AMPA receptors and GABA acting through $GABA_A$ receptors also elevate Ca^{2+} in these neurons.

suppressing transcriptional activation through the NFAT:AP-1 complex.

Similar dual pathways involving PP2B and NFAT family members have been implicated in angiotensin-II-induced cardiac hypertrophy and in the morphogenesis of heart valves.

DARPP-32

DARPP-32 (dopamine and cyclic adenosine 3′,5′-monophosphate-regulated phosphoprotein, 32 kDa) is a specific inhibitor of PP1. It is expressed at high concentrations in medium spiny neurons of the neostriatum where it plays a central role in integrating responses to dopamine (acting via the cAMP) and glutamate (acting via Ca^{2+}) in dopaminoceptive neurons (Figure 3, right). Diseases associated with defects in dopaminergic neurotransmission include Parkinson's disease, Huntington's disease, ADHD, and schizophrenia.

Activation of the cAMP pathway in dopaminoceptive neurons leads to increased phosphorylation of DARPP-32 on Thr 34 and inhibition of PP1. This results in increased phosphorylation of neurotransmitter receptors, voltage-gated ion channels, an electrogenic ion pump (Na^+/K^+ ATPase), and a transcription factor (CREB).

In contrast, glutamate acting through NMDA receptors promotes dephosphorylation of brain proteins through activation of a protein phosphatase cascade involving PP2B and PP1. Activation of NMDA receptors elevates Ca^{2+} which activates PP2B. This leads to DARPP-32 dephosphorylation by PP2B and activation of PP1 through relief of inhibition by DARPP-32.

See Also the Following Articles

Allosteric Regulation • Angiotensin Receptors • Dopamine Receptors • Protein Kinase B • Protein Kinase C Family • Protein Tyrosine Phosphatases • Pyruvate Dehydrogenase

Glossary

modulator protein Generally a low-molecular-weight, heat-stable protein that alters protein phosphatase activity or substrate specificity.

protein kinase cascade A series of protein kinases arranged in a linear fashion in a signal transduction pathway such that an upstream protein kinase phosphorylates and activates the immediate downstream kinase.

protein phosphatase An enzyme whose physiological function is to remove phosphate groups from serine, threonine, or tyrosine residues of proteins.

targeting subunit A protein that directs a phosphatase to a specific subcellular location or a specific substrate and may also modulate substrate specificity and regulate phosphatase activity.

transcription factor A protein that binds to a regulatory site on a gene leading to enhanced transcription of the gene.

Further Reading

Barford, D. (1996). Molecular mechanisms of the protein serine/threonine phosphatases. *TIBS* **21**, 407–412.

Ceulemans, H., Stalmans, W., and Bollen, M. (2002). Regulatory-driven functional diversification of protein phosphatase-1 in eukaryotic evolution. *BioEssays* **24**, 371–381.

Cohen, P. (2002). Protein phosphatase 1 – targeted in many directions. *J. Cell Sci.* **115**, 241–256.

Greengard, P., Allen, P., and Nairn, A. (1999). Beyond the dopamine receptor: The DARPP-32/protein phosphatase-1 cascade. *Neuron* **23**, 435–447.

Ingebritsen, T., and Cohen, P. (1983). Protein phosphatases: Properties and role in cellular regulation. *Science* **221**, 331–338.

Janssens, V., and Goris, J. (2001). Protein phosphatase 2A: A highly regulated family of serine/threonine phosphatases implicated in cell growth and signalling. *Biochem. J.* **353**, 417–439.

Rao, A., Luo, C., and Hogan, P. (1997). Transcription factors of the NFAT family: Regulation and function. *Annu. Rev. Immunol.* **15**, 707–747.

Rodriquez, P. (1998). Protein phosphatase 2C (PP2C) function in higher plants. *Plant Mol. Biol.* **38**, 919–927.

Biography

Thomas S. Ingebritsen is an Associate Professor in the Department of Genetics, Development and Cell Biology at Iowa State University. His research interest is the structure, regulation, and function of protein phosphatases. He holds a Ph.D. in Biochemistry from Indiana University and received his postdoctoral training at the University of Dundee, Scotland. Together with Philip Cohen, he developed the scheme for classification of protein serine/threonine phosphatases and he has published extensively in the area of protein phosphorylation and protein phosphatases.

Serotonin Receptor Signaling

Paul J. Gresch and Elaine Sanders-Bush
Vanderbilt University, Nashville, Tennessee, USA

Serotonin (5-hydroxytryptamine; 5-HT) receptors are a family of G-protein-coupled receptors (GPCRs) and one ligand-gated ion channel that transduce an extracellular signal by the neurotransmitter serotonin to an intracellular response. 5-HT receptors are involved in multiple physiological functions such as cognition, sleep, mood, eating, sexual behavior, neuroendocrine function, and gastrointestinal (GI) motility. Since many physiological processes are influenced by 5-HT receptors, it is not surprising that dysfunction and regulation of 5-HT receptors are implicated in numerous disorders and disease states including migraine, depression, anxiety, schizophrenia, obesity, and irritable bowel syndrome. Therefore, understanding 5-HT receptor second messenger systems, their effector linkage, the multiplicity of coupling pathways, and how these pathways are regulated is critical to disease etiology and therapeutic discovery.

Serotonin Synthesis and Metabolism

The neurotransmitter serotonin (5-hydroxytryptamine; 5-HT) is found in the central nervous system, enterochromaffin cells, gastrointestinal tract, and platelets. 5-HT is synthesized from the essential amino acid tryptophan by the rate-limiting enzyme tryptophan hydroxylase and a ubiquitous l-aromatic amino acid decarboxylase. 5-HT is released into the synaptic cleft by exocytosis of vesicles in a TTX-sensitive and Ca^{2+}-dependent manner. Inactivation of 5-HT is mediated by reuptake into the presynaptic terminal through an Na^{+}-dependent 5-HT transporter. 5-HT is metabolized into the inactive form, 5-hydroxyindole acetic acid, by the enzymes monoamine oxidase and aldehyde dehydrogenase. Levels of synaptic 5-HT can be regulated. For instance, restriction of dietary tryptophan or chemical inhibitors of tryptophan hydroxylase reduce brain levels of 5-HT, while selective 5-HT reuptake inhibitors such as fluoxetine (Prozac) increase the amount of synaptic 5-HT. Released serotonin acts on multiple 5-HT receptors found throughout the body in various tissues including brain, spinal cord, heart, blood, and gut.

Serotonin Receptor Structure and Function

5-HT receptors are classified and characterized by their gene organization, amino acid sequences, pharmacological properties, and second messenger coupling pathways. With the exception of the 5-HT_3 receptor, the 5-HT receptor family consists of G- protein-coupled receptors (GPCRs). The basic protein structure is predicted to contain seven transmembrane regions, three intracellular loops, and three extracellular loops, with the amino terminus being extracellular and carboxy terminus, intracellular (Figure 1A). These receptors are linked to their signal transduction pathways through guanine nucleotide triphosphate (GTP)-binding proteins (G protein). The sequence of events involves the activation of the cell surface receptor by 5-HT or drugs, binding of receptor and G protein, which promotes the exchange of bound GDP for GTP on the G protein. The G protein is comprised of α-, β-, γ-subunits; the $\beta\gamma$ dimer dissociates when receptor binds and both Gα and G$\beta\gamma$ have the ability to interact with effector enzymes. The subunit interactions promote activation or inhibition of adenylate cyclase or activation of phospholipase C. In turn, the effector enzymes generate second messengers that regulate cellular processes such as Ca^{2+} release, and protein kinases and phosphatases. This multistep enzymatic process amplifies receptor signal, and provides the possibility of regulation and crosstalk at multiple levels. The numerous 5-HT receptors are grouped in Table 1 by their traditional (primary) G protein second messenger linkage. The multiple levels of diversity generated by RNA splicing, RNA editing, and promiscuity of receptor G-protein activation are discussed later.

Serotonin Receptors that Inhibit Adenylyl Cyclase

The five members of the 5-HT_1 receptor family (5-HT_{1A}, 5-HT_{1B}, 5-HT_{1D}, 5-HT_{1E}, and 5-HT_{1F}) and the 5-HT_5

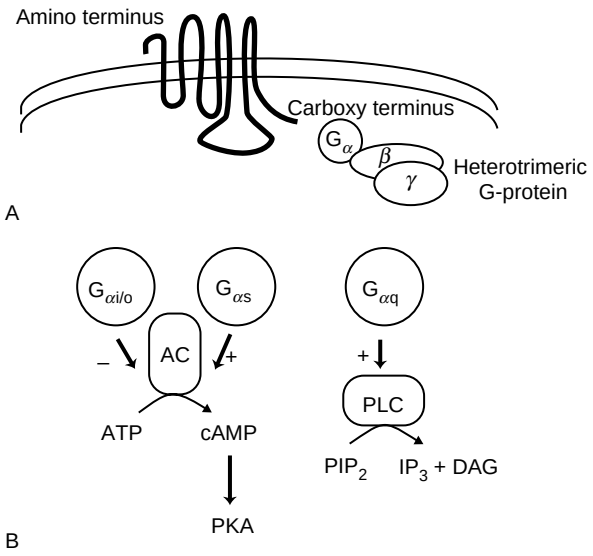

FIGURE 1 A. Schematic drawing of the basic components of a G-protein coupled receptor illustrating the extracellular amino terminus, seven transmembrane domains, three intracellular loops, three extracellular loops, intracellular carboxy terminus, and heterotrimeric G protein. B. The primary signaling pathways of the G-protein coupled receptors. Activation of $G_{\alpha i}$ protein inhibit AC resulting in the decrease of cAMP production. Receptors that stimulate AC through $G_{\alpha s}$ results in increased production of cAMP, with subsequent activation of PKA. Stimulation of PLCβ through $G_{\alpha q}$ results in the cleavage of PIP_2 into IP_3 and DAG.

receptor (5-HT_{5A}, 5-HT_{5B} subtype) couple primarily through $G_{i/o}$ proteins to inhibit the membrane-bound enzyme, adenylyl cyclase (AC). This inhibition of AC leads to a decrease of 3′5′-adenosine monophosphate (cAMP) molecules (Figure 1B). The 5-HT_1 receptors are the best characterized of this family. High densities of 5-HT_{1A} receptors are found on the cell bodies of 5-HT neurons in the brainstem nuclei, especially the dorsal raphe. In the dorsal raphe, the 5-HT_{1A} receptor functions as an autoreceptor that reduces cell firing when activated. The receptor elicits neuronal membrane hyperpolarization by activating G protein-linked K^+ channels. In addition, 5-HT_{1A} receptors are located on postsynaptic sites in the hippocampus and other limbic brain regions where they also produce hyperpolarization by opening K^+ channels. 5-HT_{1A} receptors are targets of a class of antianxiety drugs. Of the other 5-HT_1 receptors, much more is known about the 5-HT_{1B} and 5-HT_{1D} subtypes. These receptors are found in basal ganglia and frontal cortex, and function as terminal autoreceptors or heteroreceptors that modulate neurotransmitter release. 5-$HT_{1B/1D}$ heteroreceptors have been proposed to regulate the release of acetylcholine, glutamate, dopamine, norepinephrine, and γ-aminobutyric acid (GABA). Pharmacological and genomic (knock out/deletions) studies suggest that 5-HT_{1B} receptors are involved in aggressive behavior. 5-HT_{1D} receptors have a role in migraine headaches and many antimigraine drugs target this receptor. Less is known about 5-HT_{1F}, 5-HT_{1E}, and 5-HT_5 receptors.

TABLE 1

The Primary Signal Transduction Pathway for the Serotonin Receptor Family

G protein	5-HT receptor subtype	Effector linkage
G_i/G_o	1A	Inhibition of adenylate cyclase
	1B	
	1D	
	1E	
	1F	
	5	
G_s	4	Activation of adenylate cyclase
	6	
	7	
G_q/G_{11}	2A	Activation of phospholipase C
	2B	
	2C	
No G protein	3	Ligand-gated ion channel

Serotonin Receptors Linked to Activation of Adenylate Cyclase

5-HT_4, 5-HT_6, and 5-HT_7 receptors are all coupled to activation of AC. These receptors are linked via the G protein G_s to AC producing an increase cAMP production (Figure 1B). Historically, the first signal-transduction pathway to be linked to a 5-HT receptor was stimulation of AC, characterized in mouse collicular neurons. This receptor now known as the 5-HT_4 receptor is also found in hippocampus and peripheral tissues. In the periphery, it releases acetylcholine in the ileum, contracts the esophagus and colon, promotes ion transport in the gut, and elicits cardiac contraction. In the brain, the receptor has been linked to modulation of release of acetylcholine, dopamine, 5-HT, and GABA. Little is known about the 5-HT_6 receptor. It is found in the striatum, amygdala, nucleus accumbens, hippocampus, and cortex. 5-HT_7 receptors are widely expressed in the brain, with highest expression levels in the thalamus and the hippocampus. The 5-HT_7 receptor may have role in circadian rhythms and thermoregulation. Both the 5-HT_6 and 5-HT_7 receptor have high affinity for many of the atypical antipsychotics leading to speculation of a role for this receptor in schizophrenia.

Serotonin Receptors Coupled to the Activation of Phospholipase C

The 5-HT_2 class of receptor (subtype 2A, 2B, 2C) activates the membrane-bound enzyme phospholipase C (PLC) which catalyzes the degradation of the inositol lipid, phosphotidylinositol 4,5 bisphosphate (PIP_2) with the production of inositol 1,4,5 triphosphate (IP_3) and diacylglycerol (DAG) (Figure 1B). IP_3 mobilizes Ca^{2+} from intracellular storage sites; Ca^{2+} then induces multiple responses in the cell including activation of calcium/calmodulin-dependent protein kinase enzymes that phosphorylate protein substrates in the cell. DAG activates another kinase, protein kinase C. The 5-HT_2 receptors are coupled via the G protein G_q or G_{11} to activation of PLC.

The 5-HT_{2A} receptor is involved in smooth muscle contraction and platelet aggregation. In the brain, 5-HT_{2A} receptors are found in cerebral cortex, claustrum, and basal ganglia. It is thought that hallucinogenic drugs exert their psychotrophic action by activating 5-HT_{2A} receptors. The 5-HT_{2B} receptor was first described from the stomach fundus and later was identified in the gut, heart, kidney, and lung. Its presence in the brain is less certain. The 5-HT_{2C} receptor is found in choroid plexus, where it regulates cerebral spinal fluid production and ion exchange between the cerebral spinal fluid and brain. The 5-HT_{2C} receptor is also found in various brain regions such as frontal cortex and amygdala. Activation of brain 5-HT_{2C} receptors can lead to hypoactivity and hypophagia. Moreover, atypical antipsychotic drugs block the activation of 5-HT_{2A} and 5-HT_{2C} receptors, indicating that these receptors may be involved in the pathophysiology of schizophrenia.

The Serotonin-3 Receptor is a Ligand-Gated Ion Channel

The 5-HT_3 receptor is different from the other 5-HT receptors in that it forms an ion channel that regulates the flux of ions. The structure of receptor is a pentamer, similar to the nicotinic acetylcholine receptor. The receptors are found on neurons in the hippocampus, nucleus tractus solitarius, and area postrema, as well as in the periphery. They are located on pre and postganglionic autonomic neurons and alter GI tract motility and intestinal secretion. When activated by 5-HT, the receptor triggers rapid depolarization due to an inward current by opening a nonselective cation channel (Na^+, Ca^{2+} influx and K^+ efflux). The receptor is possibly involved in nausea, vomiting, and irritable bowel syndrome.

Alternative Splice Variants of Serotonin Receptors

Functional diversity of proteins can be produced by alternative splicing events. Many of the 5-HT receptor genes contain introns that are subject to alternative splicing with the generation of multiple-receptor mRNAs encoding slightly different proteins, referred to as isoforms. Seven carboxy-terminal splice variants of the 5-HT_4 receptor have been described. The most interesting feature of these splice variants is the level of constitutive activity of the receptor, which is markedly increased. Constitutive activity is the ability of a receptor to activate second-messenger pathways spontaneously without the binding of an external ligand. Four carboxy-terminal splice variants of the 5-HT_7 receptor have been identified. The functional consequence of these variants is uncertain. An alternatively spliced variant of the 5-HT_{2C} receptor has been described, which encodes a truncated, nonfunctional protein. More work needs to be done to determine the physiological relevance of these RNA splicing events; nonetheless, is it clear that this process leads to additional diversity in 5-HT receptor signaling.

RNA Editing Produces Multiple Functional 5-HT_{2C} Receptor Isoforms

The 5-HT_{2C} receptor undergoes a unique process termed RNA editing to yield multiple-receptor variants. RNA editing is an enzymatic reaction that alters nucleotide sequences of RNA transcripts. For the 5-HT_{2C} receptor, five encoded adenosine residues are converted to inosines by double-stranded RNA adenosine deaminases. In the human 5-HT_{2C} receptor, the adenosines within the predicted intracellular second loop can be converted to inosine at the RNA level resulting in multiple mRNA species with the potential to encode 24 different protein variants (Figure 2). The extensively edited isoforms have different abundances in brain tissue, and the translated proteins exhibit different binding properties, and differential activation of second-messenger systems. For example, 5-HT exhibits a decreased potency when activating the fully edited, VGV, isoform of the human receptor compared with the unedited, INI, form and there is a rightward shift in the dose-response curve for phosphoinositide hydrolysis. In addition, editing can alter the ability of 5-HT_{2C} receptors to couple to multiple G-proteins. For example, the non-edited 5-HT_{2C} receptor functionally couples to G_q and G_{13}, whereas the edited 5-HT_{2C} receptors has less coupling to G_{13}. RNA editing may have clinical

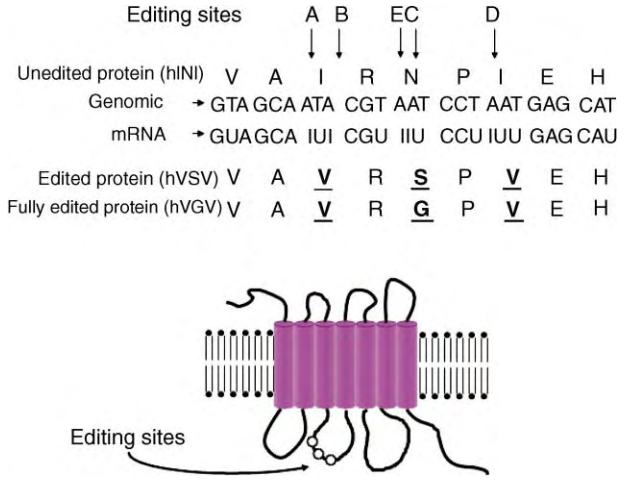

FIGURE 2 The positions of the editing sites within human 5-HT_{2C} receptors RNA and amino acid sequences are shown for hINI, hVSV, and hVGV edited isoforms of the 5-HT_{2C} receptor. These editing sites are located in the putative second intracellular loop.

significance; recent studies have indicated that alterations in the editing profile of the 5-HT_{2C} receptor are associated with the incidence of suicide and schizophrenia.

Single Nucleotide Polymorphisms Occur in the Serotonin Receptor Family

Normal genetic variations (single-nucleotide polymorphism, SNP) have been identified in almost all 5-HT receptors. Polymorphisms in the coding region of the gene have the potential to alter the receptor's ability to bind ligand, to activate signal-transduction pathways, or to adapt to environmental influences. For example, a polymorphism in the amino terminus of the human 5-HT_{1A} receptor attenuates the down-regulation and desensitization produced by the agonist 8-OH-DPAT. A polymorphic variant in the 5-HT_{1B} receptor in the putative third transmembrane domain alters the binding of the antimigraine drug, sumatriptan. In addition, a polymorphism in the carboxy terminus of 5-HT_{2A} receptor reduces the receptor's ability to mobilize internal Ca^{2+}. Currently, efforts are being made to link the occurrence of 5-HT receptor polymorphisms with various pathological disorders. Future progress in pharmacogenomics (using genetic information to predict drug response) may potentially lead to better design of serotonergic drugs to reduce side effects and target subpopulations of patients with specific therapies dependent on their genetic profile.

Promiscuous Coupling and Crosstalk between 5-HT Receptor Signal-Transduction Pathways

Promiscuous coupling is the ability of a receptor to couple to more than one signal transduction pathway. For example, the 5-HT_{1A} receptor can both inhibit and activate AC. As mentioned above, the primary coupling of this receptor is $G_{\alpha i/o}$ with subsequent inhibition of AC; this has been demonstrated both *in vivo* and in cultured cell systems. However, this receptor has been shown to activate AC, mediated by $\beta\gamma$ subunits released from $G_{\alpha i/o}$, rather than $G_{\alpha s}$ protein. This activation seems to require high receptor occupancy and high expression levels in cell expression systems. In addition, depending on cell type and experimental conditions, the 5-HT_{1A} receptor can activate or inhibit PLC. Many studies suggest that the G-protein $\beta\gamma$-subunits play a role in such crosstalk between signaling pathways. The 5-HT_{2C} receptor (as well as the 5-HT_{2A} receptor) is another promiscuous receptor that may activate multiple signal transduction pathways. The primary coupling of 5-HT_{2C} receptors is to activate PLC activity via G_q/G_{11} proteins to produce IP_3 and DAG. However, this receptor can activate other phospholipases, for example, phospholipase D through G_{13} proteins and free $\beta\gamma$-subunits. Phospholipase D can influence many neuronal functions including endocytosis, exocytosis, vesicle trafficking, and cytoskeletal dynamics. In addition, 5-HT_{2A} and 5-HT_{2C} receptors can activate phospholipase A-2 activity, which leads to the release of arachidonic acid and potential formation of bioactive eicosanoids such as the prostaglandins. There is evidence that 5-HT_{2A} and 5-HT_{2C} receptors differentially activate PLC compared to PLA2, dependent on the specific agonists employed. Moreover, there may be differences in the desensitization of these two pathways after repeated agonist treatment. The release of arachidonic acid can result in the activation of K^+ channels, regulation of neurotransmitter release, and can be a retrograde messenger. It is becoming apparent that specific 5-HT receptors interact with many G proteins, thereby regulating multiple signal-transduction pathways. This diversity may be a target for future therapeutics and interventions.

Summary: Potential Role of Receptor Diversity

There has been much speculation on the origin and significance of the 5-HT receptor diversity. One possible explanation for the numerous subtypes and variants is that the 5-HT neurotransmitter system emerged early

during evolution. Thus, there has been ample time for genetic variation and divergence to occur in the genetic encoding for the receptor proteins. Whatever the process of receptor diversity, the multiple receptor signaling has considerable biological significance. For example, inputs to the dorsal raphe nucleus are integrated into global 5-HT release, via both synaptic and volume transmission, that in turn can modulate multiple and diverse neuronal functions based on receptor subtype. Thus, one transmitter (5-HT) with multiple receptors/multiple pathways can introduce levels of complexity, yet specific physiological responses, that are localized to a given brain region or neural system. These responses can be cell-type specific or even cell-compartment specific. Furthermore, a level of fidelity is introduced based on the receptor's relative affinity for 5-HT. The exact nature of this diversity is at present unclear however the physiological implications are quite apparent, when considering the diverse role of these receptors in many physiological functions and disease states.

See Also the Following Articles

Adenylyl Cyclases • Neurotransmitter Transporters • Phospholipase C • RNA Editing

Glossary

autoreceptor A receptor on the neuronal cell body or presynaptic terminal can regulate its own cell firing and/or neurotransmitter release and synthesis.

constitutive activity Ability of a receptor to activate second-messenger pathways without the binding of an external ligand.

heteroreceptor A presynaptic receptor that regulates the release of neurotransmitter other than its own natural ligand.

promiscuous coupling The ability of a receptor to couple to more than one signal cascade.

RNA editing A process whereby the nucleotide sequence of RNA transcripts is chemically altered.

Further Reading

Aghajanian, G. K., and Sanders-Bush, E. (2002). Serotonin. In *Psychopharmacology: The Fifth Generation of Progress* (K. L. Davis, D. Charney, J. T. Coyle and C. Nemeroff, eds.) Lippincott, Williams, and Wilkins, Philadelphia.

Barnes, N. M., and Sharp, T. (1999). A review of central 5-HT receptors and their function. *Neuropharmacology* **38**, 1083–1152.

Hoyer, D., Clarke, D. E., Fozard, J. R., Hartig, P. R., Martin, G. R., Mylecharane, E. J., Saxena, P. R., and Humphrey, P. P. A. (1994). VII. International Union of Pharmacology classification of receptors for 5-hydroxytrytamine (serotonin). *Pharmacol. Rev.* **46**, 157–203.

Meltzer, H. Y. (1999). The role of serotonin in antipsychotic drug action. *Neuropsychopharmacology* **21**, 106S–115S.

Raymond, J. R., Mukhin, Y. V., Gelasco, A., Turner, J., Collinsworth, G., Gettys, T. W., Grewal, J. S., and Garnovskaya, M. N. (2001). Multiplicity of mechanisms of serotonin receptor signal transduction. *Pharmacol. Ther.* **92**, 179–212.

Biography

Elaine Sanders-Bush is a Professor of Pharmacology and Psychiatry at Vanderbilt University School of Medicine, Nashville, Tennessee. She earned a Ph.D. in pharmacology at Vanderbilt in 1967. Her research focuses on serotonin receptors, applying a multidisciplinary approach to define the role of signal transduction molecules and posttranscriptional and posttranslational modifications that alter receptor function. Dr. Sanders-Bush received a Merit Award from the National Institute of Mental Health in recognition of her research accomplishments.

Paul Gresch is a Postdoctoral Fellow in Dr. Sanders-Bush's laboratory. He earned a Ph.D. in cellular and clinical neurobiology from Wayne State University in Detroit, Michigan in 1999.

Siglecs

Ajit Varki
University of California, San Diego, Calfornia, USA

Sialic acid recognizing Ig-superfamily Lectins (Siglecs) are a major subset of the "I-type lectins." The latter are defined as animal proteins other than antibodies that can mediate carbohydrate (glycan) recognition via immunoglobulin(Ig)-like domains. Siglecs share characteristic amino-terminal structural features that are involved in their sialic acid-binding properties, and can be broadly divided into two groups: an evolutionarily conserved subgroup (Siglecs-1, -2, and -4) and a CD33/Siglec 3-related subgroup (Siglecs -3 and -5 to -11). While the precise functions of Siglecs are unknown, they seem to send inhibitory signals to the cells that express them, in response to recognition events on cell surfaces.

Historical Background and Definition

Sialic acids (Sias) are a family of nine-carbon acidic sugars that typically occupy a terminal position on glycan chains attached to the cell surface of "higher" animals. The immunoglobulin superfamily (IgSf) is an evolutionarily ancient group of proteins whose appearance predated the emergence of the immunoglobulins themselves. Until the 1990s, it was assumed that IgSf members (other than some antibodies) did not mediate carbohydrate recognition. Independent work on CD22 (eventually Siglec-2, a protein on mature resting B cells) and on sialoadhesin (Sn, eventually Siglec-1, a protein on certain macrophage subsets) revealed that their first Ig V-set-like domains could mediate Sia recognition. Homologous features of this V-set Ig-like domain and the adjacent C2-set domain then led to the discovery that two other previously cloned molecules—CD33 (eventually Siglec-3) and Myelin-associated Glycoprotein (MAG, eventually Siglec-4)—also had Sia-binding properties. Following consultation among all researchers working on these proteins, the common name "Siglec" and a numbering system were agreed upon. Criteria for inclusion of IgSf-related proteins as Siglecs are: (1) the ability to recognize sialylated glycans; and (2) significant sequence similarity within the N-terminal V-set and adjoining C2-set domains. Evaluation of the human and mouse genomes eventually defined 11 human and 8 mouse molecules that fulfill these criteria. Since humans have more Siglecs than mice and cloning of the mouse molecules initially lagged behind, the primary numbering system is based on the human molecules.

Two Broad Subgroups of Siglecs

While Siglecs -1, -2, and -4 appear to be evolutionarily rather conserved, the CD33/Siglec-3-related subgroup (Human Siglecs -3 and -5 to -11) appear to be rapidly evolving. Some CD33/Siglec-3-related Siglecs appear to have evolved as hybrids of pre-existing genes and/or by gene conversion. For these reasons, sequence comparisons alone do not allow the conclusive designation of the orthologue status of all mouse genes, and additional features such as gene position and exon structure must be taken into account. Until such issues are resolved, some mouse Siglecs have been assigned a temporary alphabetical designation.

Common Structural Features

All are single-pass Type 1 integral membrane proteins with extra-cellular domains consisting of uniquely similar N-terminal V-set Ig domains, followed by variable numbers of C2-set Ig domains, ranging from 16 in Sn/Siglec-1 to 1 in CD33/Siglec-3. Crystal structures for mouse Siglec-1 and human Siglec-7 indicate that the V-set immunoglobulin-like fold has several unusual features, including an intra-beta sheet disulphide and a splitting of the standard beta strand G into two shorter strands. These features along with certain key amino acid residues appear to be requirements for Sia recognition. In particular, a conserved arginine residue is involved in a salt bridge with the carboxylate of Sia in all instances studied to date.

Cell-Type Specific Expression

With the exception of MAG/Siglec-4 and Siglec-6, expression appears to be confined to the hematopoeitic

and immune systems. Within these systems each Siglec is expressed in a cell-type specific fashion, suggesting that each may be involved in discrete functions. However, systematic studies of Siglec expression outside the hematopoeitic system and during development have not yet been done.

Genomic Organization and Phylogeny

Based on probing for the canonical functional amino acids in the V-set domain of the typical Siglec, there is no evidence for Siglec-like molecules in prokaryotes, fungi or plants, nor in animals of the Protostome lineage, including organisms for which the complete genome is available. In contrast, it is relatively easy to find Siglec-like V-set domains in many vertebrate taxa (Sia recognition by fish and reptile Siglec candidates has not been formally shown as yet). While the relatively conserved Siglecs (-1, -2, and -4) have clear-cut single orthologues that are easy to identify in various species, the remaining "CD33/Siglec-3 related" Siglecs appear to have been evolving rapidly. Most of the latter genes are clustered together in a ~500 kb region on human chromosome 19q13.3–13.4.

Siglec Recognition of Sialic Acids and Their Linkages

The first two Siglecs discovered (Sn/Siglec-1 and CD22/Siglec-2) had strikingly different binding properties for sialosides—with Sn preferring alpha2–3 linked targets and CD22 being highly specific for alpha2–6 linkages. In the latter case, the binding affinity was in the low micromolar range. MAG/Siglec-4 also has an extended binding site that is even highly specific for the underlying sugar chain. There is also variable preference for certain types of sialic acids, with Sn and MAG not tolerating the common N-glycolyl modification of Sias. However the CD33/Siglec-3-related Siglecs are more promiscuous in their preferences for different types and linkages of Sias. Of course, many of the less common linkages and types of sialic acids have not been studied for Siglec recognition. The Golgi enzymes that are potential regulators of Siglec functions are primarily the sialyltransferases, and to some extent the enzymes which modify sialic acids. Some Siglecs show preferences for certain macromolecular ligands e.g., CD45 for CD22/Siglec-2, the mucins CD43, and Muc-1 for Sn/Siglec-1, and certain brain glycolipids for MAG/Siglec-4.

Potential Effects of Neu5Gc Loss on Human Siglec Biology

The most common Sias of mammalian cells are N-acetylneuraminic acid (Neu5Ac) and N-glycolylneuraminic acid (Neu5Gc). Humans are an exception, because of a mutation in CMP-sialic acid hydroxylase, which occurred after the time (~5–7 Ma) when we shared a common ancestor with great apes. The resulting loss of Neu5Gc and increase in Neu5Ac in humans could have potentially altered the biology of the Siglecs. For example, human cells have a higher density of Sn/Siglec-1 ligands than great apes, the distribution of Sn-positive macrophages in humans is different, and a much larger fraction of human macrophages is positive. Other emerging evidence suggests that there are further human-specific changes in Siglec biology that may be related to the loss of Neu5Gc.

Masking and Unmasking of Siglecs Binding Sites on Cell Surfaces

The initial assumption was that Siglecs were involved in intercellular adhesion. However, in most instances, their binding sites appear to be masked by Sias on the same cell surfaces on which they are expressed. Of course, external ligands with very high affinity/avidity may still compete for the endogenous masking ligands. There is also some evidence that unmasking can occur under certain conditions, but it is not known if this is biologically relevant. Overall, the significance of Siglec masking is unclear at this time.

Signaling Motifs in Cytosolic Tails

The CD33-related Siglecs have conserved tyrosine residues in the cytosolic tails, one of which corresponds to a canonical immunoreceptor tyrosine-based inhibition motif (ITIM). Various *in vitro* manipulations of these receptors indicate that these tyrosines are indeed targets for phosphorylation, and that they can modulate signaling events by recruiting certain tyrosine phosphatases. However, the true *in vivo* biological functions of these signaling motifs remain obscure. Another major unresolved question is: what is the connection between extra-cellular sialic acid recognition and signaling via the cytosolic motifs?

Known and Putative Functions of the Siglecs

Various lines of evidence indicate that MAG/Siglec-4 is involved in the maintenance of myelin organization

and in the inhibition of neurite outgrowth during regeneration after injury. It is also reasonably clear that CD22/Siglec-2 functions as an inhibitory component of the antigen receptor complex of B Cells, and is thus involved in regulating the humoral immune response. While Sn/Siglec-1 appears to mediate various macrophage adhesion events *in vitro* and *in vivo*, it is as yet unclear what the functions of these interactions are. Little is known about the functions of CD33-related Siglecs. It has been suggested that these molecules are involved in innate immunity. One hypothesis currently being tested is that Siglecs may be sensors for pathogens that have sialylated cell surfaces and/or express extra cellular sialidases.

See Also the Following Articles

Immunoglobulin (Fc) Receptors • Lectins • Polysialic Acid in Molecular Medicine

Glossary

immunoglobulin superfamily (IgSf) Proteins that have modules homologous to those of antibodies (immunoglobulins). This is an evolutionarily ancient group of proteins whose appearance actually predated the emergence of the immunoglobulins themselves.

I-type lectins Proteins (other than antibodies) in which immunoglobulin-like modules mediate binding to glycans (sugar chains).

sialic acids These acids are a diverse family of nine-carbon acidic sugars that typically occupy a terminal position on glycan chains attached to the cell surface of "higher" animals of the deuterostome lineage.

siglecs A major subset of the I-type lectins. Name is based on their defining properties, as sialic acid recognizing IgSf lectins.

Further Reading

Angata, T., and Brinkman-Van der Linden, E. (2002). I-type lectins. *Biochim. Biophys. Acta* **1572**, 294.

Angata, T., and Varki, A. (2002). Chemical diversity in the sialic acids and related alpha-keto acids: An evolutionary perspective. *Chem. Rev.* **102**, 439–470.

Crocker, P. R., and Varki, A. (2001). Siglecs, sialic acids and innate immunity. *Trends Immunol.* **22**, 337–342.

Crocker, P. R., Mucklow, S., Bouckson, V., McWilliam, A., Willis, A. C., Gordon, S., Milon, G., Kelm, S., and Bradfield, P. (1994). Sialoadhesin, a macrophage sialic acid binding receptor for haemopoietic cells with 17 immunoglobulin-like domains. *EMBO J.* **13**, 4490–4503.

Crocker, P. R., Clark, E. A., Filbin, M., Gordon, S., Jones, Y., Kehrl, J. H., Kelm, S., Le, D. N., Powell, L., Roder, J., Schnaar, R. L., Sgroi, D. C., Stamenkovic, K., Schauer, R., Schachner, M., Van den Berg, T. K., Van der Merwe, P. A., Watt, M., and Varki, A. (1998). Siglecs: A family of sialic-acid binding lectins [letter]. *Glycobiology* **8**(v2).

Kelm, S., Pelz, A., Schauer, R., Filbin, M. T., Tang, S., De, B. M.-E., Schnaar, R. L., Mahoney, J. A., Hartnell, A., Bradfield, P., and Crocker, P. R. (1994). Sialoadhesin, myelin-associated glycoprotein and CD22 define a new family of sialic acid-dependent adhesion molecules of the immunoglobulin superfamily. *Curr. Biol.* **4**, 965–972.

Powell, L. D., and Varki, A. (1995). I-type lectins. *J. Biol. Chem.* **270**, 14243–14246.

Powell, L. D., Sgroi, D., Sjoberg, E. R., Stamenkovic, I., and Varki, A. (1993). Natural ligands of the B cell adhesion molecule CD22beta carry N-linked oligosaccharides with alpha-2, 6-linked sialic acids that are required for recognition. *J. Biol. Chem.* **268**, 7019–7027.

Biography

Ajit Varki is Professor of Medicine and Cellular and Molecular Medicine, Director of the Glycobiology Research and Training Center, and Coordinator of the project for Explaining the Origin of Humans, at the University of California, San Diego. Dr. Varki's laboratory explores the biology and evolution of sialic acids in health and disease.

Sigma Factors

John D. Helmann
Cornell University, Ithaca, New York, USA

The sigma(σ)-subunit of bacterial RNA polymerase is essential for the process of promoter selection. Interactions between σ and promoter region DNA allow RNAP to recognize and physically open the start sites for transcription initiation. The majority of transcription under most conditions requires a single, essential σ-factor (primary σ). However, in most bacteria there are a number of alternative σ-factors that can activate specific sets of target genes, as defined by their distinct promoter sequences, in response to changing environmental conditions. The activation of groups of coregulated genes (regulons) by alternative σ-factors complements the more familiar gene-regulation mechanisms that rely upon transcription repressors and activators.

Introduction

DNA serves as a storehouse for the genetic information of each organism, but is itself a silent repository. Only upon copying of DNA segments into RNA (transcription), and translation into protein, is the genetic potential of each organism (and each cell type in multicellular organisms) able to be realized. For example, our skin, blood, hair, liver, and lung cells all contain the same DNA, yet they have differentiated into functionally distinct cell types based largely on the selective expression of a small subset of the genes contained within each cell. Similarly, comparative genomics has led to the realization that the evolutionary processes that have led to the divergence of humans and mice, for example, have more to do with changes in "how" genes are regulated than with "which" genes are actually present in each organism. These examples highlight the importance of gene regulation: those mechanisms that selectively activate and repress different genes depending on cell type and local environment.

Gene Regulation in Bacteria

Most of the principles of gene regulation were first developed from studies of bacterial cells and, in particular, *Escherichia coli*. The first step in gene expression is the transcription of the genetic code from DNA into an RNA copy that usually serves to direct protein synthesis (translation). RNA polymerase (RNAP) is the enzyme that copies (transcribes) DNA into RNA.

In bacterial cells, most gene regulation occurs at the level of transcription. Genes that are expressed are actively transcribed and translated into their corresponding protein products. Conversely, genes that are silent are not copied into RNA. Thus, factors that act to control the activity of RNAP are central to many processes of gene regulation. These regulators include activator proteins, repressor proteins, and σ-factors. In order to appreciate how these factors can control gene expression, the biochemical properties of RNAP and the overall features of the transcription cycle are discussed first, followed by σ-factors.

Bacterial RNA Polymerase and the Transcription Cycle

In bacteria, RNAP is a multisubunit protein complex and contains both a catalytic core enzyme and a specificity subunit known as σ. The core enzyme (containing the β, β', two α, and the ω polypeptide chains) is able to catalyze the synthesis of RNA directed by a DNA template. Core enzyme associates reversibly with another polypeptide chain, σ, to form the holoenzyme.

RNAP copies particular DNA segments into RNA chains by first initiating RNA synthesis at a promoter site, elongating the RNA chain, and finally terminating transcription (the transcription cycle). In bacteria, many protein-coding genes are organized into cotranscribed groups called operons. In these cases, each mRNA product can direct the synthesis of multiple protein products.

The first step in the transcription cycle is promoter site localization and requires the presence of the σ-subunit: only holoenzyme can recognize promoter sites. Promoter sites are typically characterized by defined DNA sequences located just upstream of the site where RNA synthesis begins (designated the +1 site). For example, sequences centered ~10 bp upstream often have a sequence, designated the "−10 region", similar to 5′TATAAT3′. A different conserved sequence

(TTGACA) is usually located between 16 and 18 bp further upstream and is designated the "−35 region." Together, the −35 and −10 sequences provide the necessary information to allow RNAP to identify a promoter. Specific interactions between the σ-subunit of holoenzyme and the −35 and −10 elements allow RNAP to tightly engage the promoter region. Once bound, RNAP interacts with an extended region of DNA, ultimately contacting the DNA over a region of 60 or more base pairs (from −40 to +20).

Once bound at a promoter site RNAP melts the DNA over approximately one turn of the helix (from about −10 to +2) to expose the template strand of the DNA. The process of converting the double-stranded promoter region DNA into a locally melted structure (called the open complex) requires the action of σ-factor to initiate the melting process and is then driven by the association of the template strand of the DNA with the RNAP active site (comprised largely of the β- and β'-subunits). The open complex is then poised to initiate synthesis of an RNA chain. The region of DNA strand-separation is often referred to as the transcription bubble, to distinguish it from the otherwise double-stranded DNA in the surrounding regions of the genome.

The process of transcription elongation involves the assembly of ribonucleoside triphosphate precursors into an RNA chain containing the sequence complementary to the template DNA. During transcription elongation the DNA template is threaded through the active site of RNAP and, as a result, the transcription bubble is propagated down the DNA with melting of the DNA occurring as the DNA enters the active site and reannealing of the template occurring as the DNA exits the RNAP. The complex containing the DNA template, RNAP, and the growing RNA chain is often referred to as the ternary complex. As the growing RNA chain emerges from RNAP, it is thought to displace the σ-subunit, and the process of transcription elongation is continued by the core RNAP subunits. Elongating RNAP sometimes associates with additional protein factors known as elongation factors which can modulate its properties. In general, elongation is highly processive: the RNAP that begins an RNA chain continues synthesis until the chain is terminated.

The process of transcription termination, like that of initiation, is critical for the controlled expression of genetic information. At the end of many transcription units the DNA sequence encodes a G:C-rich stem loop structure in the RNA chain followed by a short region rich in uridine. This structure functions as a transcription terminator and interacts with the core RNAP leading to dissociation of the ternary complex and release of the terminated RNA chain. In other cases, protein factors such as the rho protein can bind to unstructured regions of RNA and trigger transcription termination. Once released by the termination reaction, the core RNAP must rebind to a σ-subunit to reform holoenzyme and thereby complete the transcription cycle.

Since bacteria lack a nuclear membrane, the processes of transcription and translation can be coupled: ribosomes can bind to the mRNA chain as it emerges from RNAP and immediately initiate protein synthesis. Indeed, along actively transcribed genes several RNAP molecules may be simultaneously engaged in RNA chain elongation with each RNA chain in turn bound by one or more ribosomes engaged in protein synthesis.

Biochemical Properties

As expected for a critical component of the transcription apparatus, σ-factors have been highly conserved through evolution. Indeed, σ-factors from one bacterium can function, at least in some cases, with the core RNAP from distantly related species. In general, all σ-factors share certain defining properties. They all bind to the core RNAP, apparently at a common binding site, to form a holoenzyme. The presence of σ-factor determines the sequence of the promoters that can be bound by the corresponding holoenzyme. The σ-subunit, in those cases that have been studied, also plays a role in the initiation of the DNA-melting step that is an obligatory prelude to transcription initiation. Often, although perhaps not always, σ is released from the ternary complex during the process of RNA chain elongation.

Bacterial σ-factors can be divided, based in part on their protein sequences, into two families: the σ^{70} and the σ^{54} families. All bacteria contain at least one member of the σ^{70} family that is required for the transcription of those genes essential for growth under virtually all conditions (so-called "housekeeping" functions). This is referred to as the primary (or class 1) σ-factor. In addition, most bacteria contain at least one (and as many as 50 or more) alternative σ-factors (Table I). These factors typically control genes needed for specialized functions that may only be expressed under particular growth conditions. Examples include genes needed for stress responses, motility, sporulation, uptake or transport of specific nutrients, or antibiotic production.

Most alternative σ-factors are structurally related to the primary (class 1) σ-factors and are therefore considered to be members of the σ^{70} family. Some alternative σ-factors (class 2) are very similar to the primary σ-factors but are, however, dispensable for growth. One example is the *E. coli* σ^{S} (RpoS) protein that becomes active in stationary phase cells. A much larger class of alternative σ-factors are those more distantly related in sequence to the primary σ-factor, and often lacking one or more the conserved regions characteristic of the class 1 and 2 proteins. These alternative σ-factors (classes 3, 4, and 5) control a wide-range of physiological processes and are often only

TABLE I

σ Factors in *E. coli* and *B. subtilis*

Organism	σ	Gene	Function
E. coli	σ^{70}	*rpoD*	Housekeeping genes
	σ^{H}	*rpoH*	Heat shock
	σ^{E}	*rpoE*	Extreme heat shock, periplasmic stress (ECF[a])
	σ^{F}	*fliA*	Flagellar-based motility
	σ^{S}	*rpoS*	Stationary phase adaptations
	σ^{N}	*rpoN, glnF*	Nitrogen-regulated genes (σ^{54} family)
	σ^{fecI}	*fecI*	Ferric citrate uptake (ECF)
B. subtilis	σ^{A}	*sigA*	Housekeeping genes
	σ^{B}	*sigB*	General stress response
	σ^{D}	*sigD*	Flagellar-based motility, autolysins
	σ^{E}	*sigE*	Sporulation, early mother cell
	σ^{F}	*sigF*	Sporulation, early forespore
	σ^{G}	*sigG*	Sporulation, late forespore
	σ^{H}	*sigH*	Competence and early sporulation
	σ^{K}	*sigK*	Sporulation, late mother cell
	σ^{L}	*sigL*	Degradative enzymes (σ^{54} family)
	σ^{I}	*ykoZ*	Unknown
	σ^{Xpf}	*xpf*	PBSX regulation
	σ^{X}	*sigX*	Cell envelope modifications (ECF)
	σ^{W}	*sigW*	Antibiotic stress responses (ECF)
	σ^{M}	*sigM*	Cell wall stresses (ECF)
	σ^{V}	*sigV*	Unknown (ECF)
	σ^{Y}	*sigY*	Unknown (ECF)
	σ^{Z}	*sigZ*	Unknown (ECF)
	σ^{ylaC}	*ylaC*	Unknown (ECF)

[a] ECF indicates a factor that is a member of the large extracytoplasmic function family of alternative σ factors.

active under very specific growth conditions. Prominent among these alternative σ-factors are the numerically abundant extracytoplasmic function (ECF) σ-factors (class 4 proteins) that appear, in general, to control functions related to the cell surface. Finally, many bacteria have alternative σ-factors with a distinctly different protein sequence and define the σ^{54} family. Unlike members of the σ^{70} family, the σ^{54}-factors form holoenzymes that almost always require ATP-dependent activator proteins to activate their target promoters. The prototype of the σ^{54}-family is the *E. coli* σ^{54} (RpoN) protein that is important for nitrogen regulation of gene expression (Table I). Similar proteins in other bacteria control a variety of other functions.

The division of σ^{70}-family members into different structural classes is based in large part on the comparison of their protein sequences. All primary (class 1) σ-factors (and the closely related class 2 factors) have four conserved regions. Region 1 contains an autoinhibitory domain that prevents the free σ-factor from interacting with DNA. This inhibition is relieved when σ associates with core RNAP. Region 2 contains the key determinants for recognition of the −10 promoter element and for initiation of DNA-melting. Region 3 functions as a spacer domain between regions 2 and 4. Region 4 contains the elements that recognize the −35 promoter element and also serves as a site of contact for some transcription activator proteins. Recent advances in the determination of three-dimensional structures for both σ-factors and holoenzyme have made it clear that these protein sequence regions correspond to folded domains in the σ-structure. The two domains that are required for recognition of promoters, domains 2 and 4, are common to all σ^{70}-family members. In contrast, much of domains 1 and 3 is often deleted in alternative σ-factors.

Roles of σ in Gene Regulation

Just as DNA-binding transcriptional repressors and activators can control the activity of RNAP at promoter sites, alternative σ-factors provide a powerful avenue for the activation of specific sets of genes (the σ-factor regulon) during cell differentiation or in response to various stress conditions. The activity of alternative σ-factors can, in turn, be controlled in numerous ways. In some cases, the σ-factor is only synthesized under very specific conditions. In other cases, the σ-factor is synthesized but is maintained in an inactive state by binding to an inhibitory protein (called an anti-σ-factor) or it is synthesized as an inactive precursor protein that only becomes active when an inhibitory peptide is cleaved by proteolysis. Anti-σ-factors are, in many cases, associated with the cell membrane and thereby able to perceive signals from the external environment. In any event, once the active σ-factor is synthesized or released it can compete with other σ-factors for binding to core RNAP and thereby redirect some of the RNAP to its cognate target promoters.

Roles for alternative σ-factors in bacterial gene regulation are legion. For example, alternative σ-factors play key roles in the expression of heat shock genes, iron uptake systems, the developmental program of sporulation (in gram-positive bacteria), synthesis of flagella and chemotaxis machinery, and various stress responses. A summary of the roles of σ-factors in the two best-studied bacterial systems is presented in Table I.

Phylogenetic Distribution

σ-factors are always found associated with bacterial RNAP but have been functionally replaced by other proteins in the more complex RNAP characteristic of eukaryotes and Archaea. However, σ-like factors

are found in the chloroplasts of photosynthetic eukaryotes which are descended from a cyanobacterium. In contrast to chloroplasts, the transcription apparatus in present day mitochondria is most similar to certain bacteriophage-encoded, single-subunit RNAPs and is unlike the multisubunit RNAP of either bacteria or eukarya.

See Also the Following Articles

DNA Polymerase I, Bacterial • DNA Polymerase II, Bacterial • DNA Polymerase III, Bacterial • RNA Polymerase Reaction in Bacteria • RNA Polymerase Structure, Bacterial • T7 RNA Polymerase

Glossary

alternative σ A σ-factor that can replace the primary σ-factor in response to a particular stress or signal to activate the expression of a defined target regulon.

promoter DNA sequences necessary for the accurate initiation of transcription by RNA polymerase.

regulon The set of genes and operons that are regulated by a common factor.

RNA polymerase Enzyme that copies DNA sequences into the complementary RNA sequence.

Further Reading

Borukhov, S., and Nudler, E. (2003). RNA polymerase holoenzyme: Structure, function and biological implications. *Curr. Opin. Microbiol.* **6**, 93–100.

Borukhov, S., and Severinov, K. (2002). Role of the RNA polymerase sigma subunit in transcription initiation. *Res. Microbiol.* **153**, 557–562.

Buck, M., Gallegos, M. T., Studholme, D. J., Guo, Y., and Gralla, J. D. (2000). The bacterial enhancer-dependent sigma(54) (sigma(N)) transcription factor. *J. Bacteriol.* **182**, 4129–4136.

Gruber, T. M., and Gross, C. A. (2003). Multiple sigma subunits and the partitioning of bacterial transcription space. *Ann. Rev. Microbiol.* **57**, 441–466.

Helmann, J. D. (2002). The extracytoplasmic function (ECF) sigma factors. *Adv. Microb. Physiol.* **46**, 47–110.

Paget, M. S., and Helmann, J. D. (2003). The sigma70 family of sigma factors. *Genome Biol.* **4**, 203.

Wosten, M. M. (1998). Eubacterial sigma-factors. *FEMS Microbiol. Rev.* **22**, 127–150.

Biography

John D. Helmann is a Professor in the Department of Microbiology at Cornell University in Ithaca, New York. His principal research interest is the mechanisms of gene regulation in the gram-positive bacterium *Bacillus subtilis*. Major research directions include the characterization of alternative σ-subunits and regulators that respond to metal ions and oxidative stress. He received a Ph.D. in biochemistry from the University of California, Berkeley and did postdoctoral research at Harvard Medical School.

Sliding Clamps in DNA Replication: *E. coli* β-Clamp and PCNA Structure

Eric R. Goedken and John Kuriyan
University of California, Berkeley, California, USA

In the absence of additional protein factors, the DNA polymerases responsible for replicating entire genomes have a strong tendency to release from the DNA template after synthesizing short segments of DNA. Such enzymes are described as having low "processivity," meaning that polymerase adds only a small number of nucleotides to the growing chain before coming off the DNA template. Rapid replication of the millions of base pairs that constitute the genetic material of cells requires DNA polymerases with extremely high processivity. This is achieved by the utilization of proteins known as "sliding DNA clamps" that convert the poorly processive core polymerase enzymes (capable of synthesizing only tens of nucleotides without dissociation) to highly processive enzymes (capable of synthesizing several thousand nucleotides without dissociation).

Sliding clamps are dimeric or trimeric proteins that form a circular collar through which DNA is threaded. The polymerase enzyme is loosely tethered to the sliding clamp, thereby maintaining proximity to the DNA even when it does let go of the template. The detailed molecular architecture of these clamps is highly conserved from bacteria to eukaryotes, reflecting the fundamentally important role played by these proteins in DNA replication in all organisms.

Clamp Structure and Function

In the well-studied *Escherichia coli* system, the processivity clamp is called the β-subunit or β-clamp, and the polymerase responsible for replicating the genome is DNA polymerase III. The β-clamp is placed at primer/template junctions in an ATP-dependent manner by a complex of protein subunits known as the clamp loader (γ/τ) complex. In eukaryotes, the homologous sliding clamp is called proliferating cell nuclear antigen (PCNA), and the polymerase chiefly responsible for DNA replication is polymerase δ and its clamp loader is the replication factor C(RFC) complex.

Interestingly, clamps from bacteria and eukaryotes differ in the number of subunits that make up the clamp. Prokaryotic clamps such as β, are dimers, whereas eukaryotic PCNA is a trimer. Despite this difference in subunit stoichiometry, the crystal structures of the clamps from both *E. coli* and the yeast PCNA (as well as a number of others) reveal a very similar overall architecture (Figure 1). Each monomer in β consists of three similar domains containing two helices and two four-stranded β sheets, whereas in PCNA there are two of these conserved domains per monomer. Each assembled clamp complex then contains six of these domains despite the difference in subunit number. The conservation of this overall structure of the clamps throughout evolution is demonstrated by the presence of similarly shaped sliding clamps in archaebacteria and in certain bacteriophages such as T4 and RB69.

Both PCNA and β are highly negatively charged proteins. The distribution of charge has a marked asymmetry with positive charge concentrated around the interior hole through which negatively charged DNA can pass (Figure 1). In both proteins the α-helices of DNA, that line this central hole are oriented roughly perpendicular to the direction of the phosphate backbone of DNA as modeled inside the clamp. The orientation of the helices as well as their separation from DNA suggests that the electrostatic interaction between the protein and DNA is non-specific, thereby facilitating the sliding of the protein ring along the nucleic acid strands.

Biochemical results have indicated that the clamp is not broken into separate monomers prior to loading onto DNA and that only one of the two interfaces of the *E. coli* β-clamp dimer is opened before loading. Molecular dynamics simulations of β suggest that each monomer has an energetic preference for a state that is less "curved" than required to close both interfaces in the circular dimeric ring. This may provide a "spring-loaded" tension that makes it easier for the clamp loader to open the clamp.

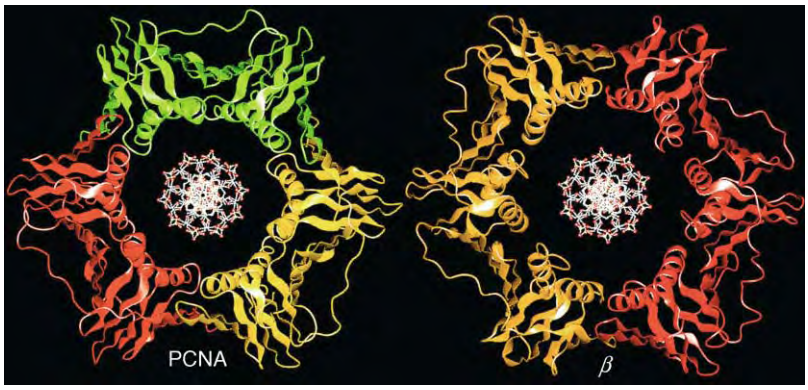

FIGURE 1 Ribbon diagrams of the structures of processivity clamps. DNA is shown as modeled in the interior of each clamp. Left, yeast PCNA; right, *E. coli* β-clamp.

Interaction with Other Proteins

Extended and flexible C-terminal segments of DNA polymerases are responsible for their interaction with the sliding clamps. A crystal structure of a trimeric bacteriophage clamp bounds to a peptide corresponding to the C-terminal region of the cognate DNA polymerase has been determined, showing the region of the clamp that interacts with the polymerase. This binding region turns out to be similar to the one seen earlier for the interaction between an inhibitory peptide (a segment of the cell-cycle protein p21/waf1-cip1) bound to PCNA. The peptide binds in a hydrophobic interface between the two domains that make up the clamp subunit. A recent crystal structure has revealed that the interaction between the clamp loader and the clamp has elements that resemble the polymerase-clamp interaction. A specific helix in the N-terminal domain of the δ-subunit of the *E. coli* clamp loader complex plugs into hydrophobic region of the clamp between the second and third domain of β. This suggests that the site of interaction for both the clamp loader and polymerase is located on the same region of the clamp and is likely conserved throughout the diversity of sliding clamps utilized in nature.

Clamp Loader Structure

The clamp loader in *E. coli* (γ complex) consists of five polypeptide chains: three γ-subunits, a δ-subunit and a δ′-subunit. The δ-subunit mentioned above is the "wrench" that opens the β-clamp. The wrench subunit is controlled by the coordinated actions of three γ "motor" subunits that hydrolyze ATP and an inert, δ′ "stator" subunit. A similar pentameric complex having sequence homology exists in eukaryotes (the RFC complex), and this loads the eukaryotic clamp (PCNA) onto DNA.

Structural studies have shown that each of the subunits of the *E. coli* clamp loader has a similar three-domain fold, with the first two domains being structurally related to the subunits of AAA+ATPases. Similar results have been obtained for the small subunit of the archaebacterial clamp loader complex. A flexible linker region tethers these nucleotide-binding domains to a helical C-terminal domain that clusters the five subunits into a pentameric assembly (Figure 2). ATP binding is required for the activation of the clamp loader, and nucleotide is potentially bound in each of the three γ-subunits. Once ATP is bound, the γ complex can bind to β and open one of its dimeric interfaces.

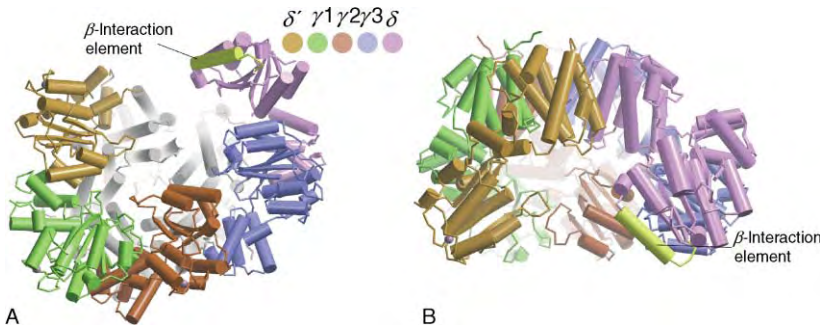

FIGURE 2 Two ribbon diagram of the structure of the *E. coli* clamp loader.

Upon interaction with DNA, the γ complex hydrolyzes these bound nucleotides and releases the β-clamp around the nucleic acid, where it is ready to tether the polymerase.

The mechanism by which ATP binding activates the clamp loader for binding to the clamp remains poorly understood, as is mechanism for coupling ATP hydrolysis to release the clamp around DNA at the proper sites.

See Also the Following Articles

DNA Polymerase δ, Eukaryotic • Processivity Clamps in DNA Replication: Clamp Loading

Glossary

clamp loader A multisubunit protein assembly that places sliding clamps around DNA at primer-template junctions in an ATP-dependent manner; examples include the γ complex in *E. coli* and the RFC complex in eukaryotes.

processivity The property of an enzyme that allows it to catalyze the addition of repeated rounds of reaction without releasing a substrate.

sliding clamp A circular multisubunit protein (either dimeric or trimeric) that slides along DNA to increase the processivity of DNA polymerase.

Further Reading

Gulbis, J. M., Kelman, Z., Hurwitz, J., O'Donnell, M., and Kuriyan, J. (1996). Structure of the C-terminal region of p21(WAF1/CIP1) complexed with human PCNA. *Cell* **87**, 297–306.

Huang, C. C., Hearst, J. E., and Alberts, B. M. (1981). Two types of replication proteins increase the rate at which T4 DNA polymerase traverses the helical regions in a single-stranded DNA template. *J. Biol. Chem.* **256**, 4087–4094.

Jeruzalmi, D., O'Donnell, M., and Kuriyan, J. (2001). Crystal structure of the processivity clamp loader γ complex of *E. coli* DNA polymerase III. *Cell* **106**, 429–441.

Jeruzalmi, D., Yurieva, O., Zhao, Y., Young, M., Stewart, J., Hingorani, M., O'Donnell, M., and Kuriyan, J. (2001). Mechanism of processivity clamp opening by the δ subunit wrench of the clamp loader complex of *E. coli* DNA polymerase III. *Cell* **106**, 417–428.

Kelman, Z., and O'Donnell, M. (1995). DNA polymerase III holoenzyme: Structure and function of a chromosomal replicating machine. *Annu. Rev. Biochem.* **64**, 171–200.

Kong, X. P., Onrust, R., O'Donnell, M., and Kuriyan, J. (1992). Three-dimensional structure of the beta subunit of *E. coli* DNA polymerase III holoenzyme: A sliding DNA clamp. *Cell* **69**, 425–437.

Krishna, T. S. R., Kong, X.-P., Gary, S., Burgers, P., and Kuriyan, J. (1994). Crystal structure of the eukaryotic DNA polymerase processivity factor PCNA. *Cell* **9**, 1233–1243.

Oyama, T., Ishino, Y., Cann, I. K., Ishino, S., and Morikawa, K. (2001). Atomic structure of the clamp loader small subunit from Pyrococcus furiosus. *Mol. Cell.* **8**, 8455–8463.

Shamoo, Y., and Steitz, T. A. (1999). Building a replisome from interacting pieces: Sliding clamp complexed to a peptide from DNA polymerase and a polymerase editing complex. *Cell* **99**, 155–166.

Biography

John Kuriyan is Chancellor's Professor in the Department of Molecular and Cell Biology and Department of Chemistry at the University of California at Berkeley and is an investigator in the Howard Hughes Medical Institute. His principal fields of interest are DNA replication and signal transduction. These areas are under study in his research group through structural techniques like X-ray crystallography, but also through molecular dynamics simulations and biophysics. He holds a Ph.D. from the Massachusetts Institute of Technology and received postdoctoral training at Harvard University.

Eric R. Goedken is an American Cancer Society postdoctoral fellow at the University of California, Berkeley, where he studies the mechanism of DNA polymerase clamp loaders.

Small GTPases

Adam Shutes and Channing J. Der
University of North Carolina, Chapel Hill, North Carolina, USA

Small GTPases (20–25 kDa) are a class of guanine nucleotide-binding proteins involved in the regulation of numerous signaling pathways and cellular processes in eukaryotic cells. The small GTPases are monomeric, distinguishing them from the heterotrimeric GTPases which are comprised of three separate subunits, α, β, and γ. Similar to the G α-subunits, the small GTPases bind GDP and GTP with high affinity and catalyze the hydrolysis of the covalent bond between the two terminal phosphate groups of bound GTP producing protein-bound GDP and a solvent-free phosphate group. The cleavage of this bond releases energy that changes the conformation of small GTPase from a GTP-bound one to an inactive GDP-bound conformation. An intrinsic GDP/GTP exchange activity allows the formation of the active GTP-bound conformation, which then interacts with one or more effector targets to promote a specific cellular response. This two-state structural change is fundamental for small GTPase biological function as a regulated binary switch.

Identification and Classification of Small GTPases

The first and prototypical small GTPases were identified as the proteins encoded by the retrovirus oncogenes of the Harvey and Kirsten rat sarcoma (Ras) viruses (Figure 1). Since its initial discovery, over 150 mammalian proteins have been identified which show varying degrees of both amino acid sequence and structural similarity with Ras proteins. Small GTPases were identified by a variety of approaches, some fortuitously (e.g., Rho), in yeast genetic studies (e.g., Rabs), and others by nucleic acid sequence homology (e.g., Ral, Rap). These 'Ras superfamily' proteins are further divided into families (e.g., the Rho and Rab families) by sequence identity and cellular function. The major branches are the Ras, Rho, and Rab families, with smaller branches including Arf, Sar, Rad/Gem, and Ran proteins (Figure 2). Small GTPases are well conserved in evolution, with structural and functional homologues of many of the mammalian proteins found in yeast, flies, worms, and plants.

In addition to the GTPase activity, a feature of many small GTPases is their modification by lipids. Members of the Ras, Rho, and Rab families are modified by either the C15 farnesyl or C20 geranylgeranyl isoprenoid lipid (Figure 3). Protein prenylation is signaled by carboxyl-terminal sequences. For Ras and Rho small GTPases, this lipid modification occurs at a particular motif, the CAAX tetrapeptide motif, consisting of a cysteine followed by any two hydrophobic amino acids, and a terminal X residue that determines whether the protein will be modified by farnesyltransferase (X = S, M) or geranylgeranyl transferase I (X = L, F). Rab proteins possess cysteine-containing carboxyl-terminal motifs (CC, CXC, CCX, CCXXX) that signal geranylgeranyl isoprenoid post-translational modification by a third prenyltransferase, geranylgeranyltransferase. Arf proteins are cotranslationally modified by the C14 myristate fatty acid at the amino-termini. Lipid modification is typically critical for protein function and facilitates the association of small GTPases with specific membrane compartments. Ran is unusual among the small GTPases and does not undergo any lipid modification.

GDP/GTP Regulation and Structure

The Small GTPase Cycle and its Regulation

The "on" and "off" switching nature of small GTPases can be best described as a GDP/GTP cycle (Figure 1). The processes of nucleotide exchange and GTP hydrolysis are able to occur at basal intrinsic rates that are characteristic to each small GTPase. However, there are two classes of regulatory proteins which act to increase the rate of these processes by several orders of magnitude: guanine nucleotide exchange factors (GEFs) increase the rate of nucleotide exchange, and GTPase-activating proteins (GAPs) increase the rate of the GTP hydrolysis. The Rho and Rab families of small GTPases have further regulatory proteins called guanine nucleotide dissociation inhibitors (GDIs).

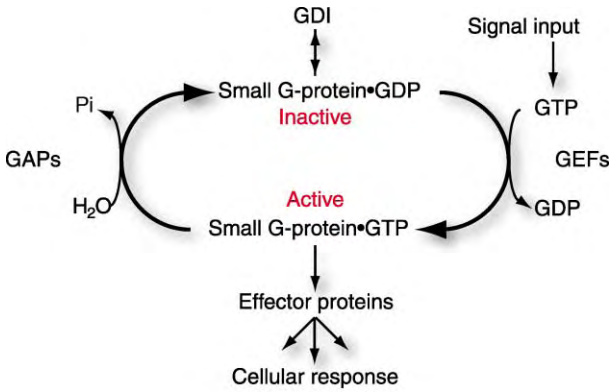

FIGURE 1 Small GTPases function as GDP/GTP-regulated molecular switches. The intrinsic GDP/GTP exchange activity is accelerated by guanine nucleotide-exchange factors (GEFs) to promote formation of the active, GTP-bound protein, whereas GTPase-activating proteins (GAPs) stimulate the intrinsic GTP hydrolysis activity to stimulate formation of the inactive, GDP-bound protein and the release of free phosphate (P_i). Guanine nucleotide dissociation inhibitors (GDIs) prevent nucleotide exchange as well as GAP stimulation. Small GTPase activation is most commonly mediated by a signal input that activates GEF function. The GTP-bound GTPase displays higher affinity for downstream effector targets, leading to stimulation of various cellular responses.

Guanine Nucleotide Exchange Factors

GEFs provide an important mechanism for regulated activation of small GTPases, and therefore their downstream effects. They are responsible for exchanging free cytosolic GTP for bound GDP. Exchange is not an active process; rather GEFs act to facilitate exchange of one nucleotide for another nucleotide, and it is the large excess of cytosolic GTP that favors the GTP exchange rather than GDP exchange. Furthermore, the binding of GTP to a small GTPase·GEF complex weakens the affinity of the GEF for the small GTPase causing their dissociation. The binding of GDP does not cause dissociation of the complex.

GEFs have been identified for many small GTPases. They are related by sequence within, but not between, the GEFs for specific small GTPase families. For example, there are currently two structurally distinct families of GEFs, which act upon either the Ras family (CDC25 homology domain-containing proteins) or the Rho family (Dbl homology domain-containing proteins) small GTPases. These two families act on the different Ras/Rho proteins since their catalytic domains are different, although their overall mechanism appears to be the same.

Different GEFs are Activated by Different Signaling Cascades Specific members of the Ras and Rho GTPases can be activated by multiple GEFs; for example, there are at least 30 characterized Ras family GEFs, and over 150 Rho family GEFs. GEFs often contain a large number of different signaling protein domains which allow them to respond to a wide variety of signals and thus allow divergent signals to converge on a common small GTPase (Figure 4). In contrast, only a handful of GEFs have been identified for Rab family proteins, the largest family of small GTPases.

A common mechanism for activation of GEFs is through their recruitment to the membrane. The classical model of small GTPase activation is that of Ras and its GEF, son of sevenless (Sos). Upon activation of a receptor protein tyrosine kinase (e.g., EGFR) and its autophosphorylation of specific tyrosine residues, an adaptor protein, Grb2, is recruited to the plasma membrane via its Src homology 2 (SH2) domain (Figure 4). Grb2 interacts

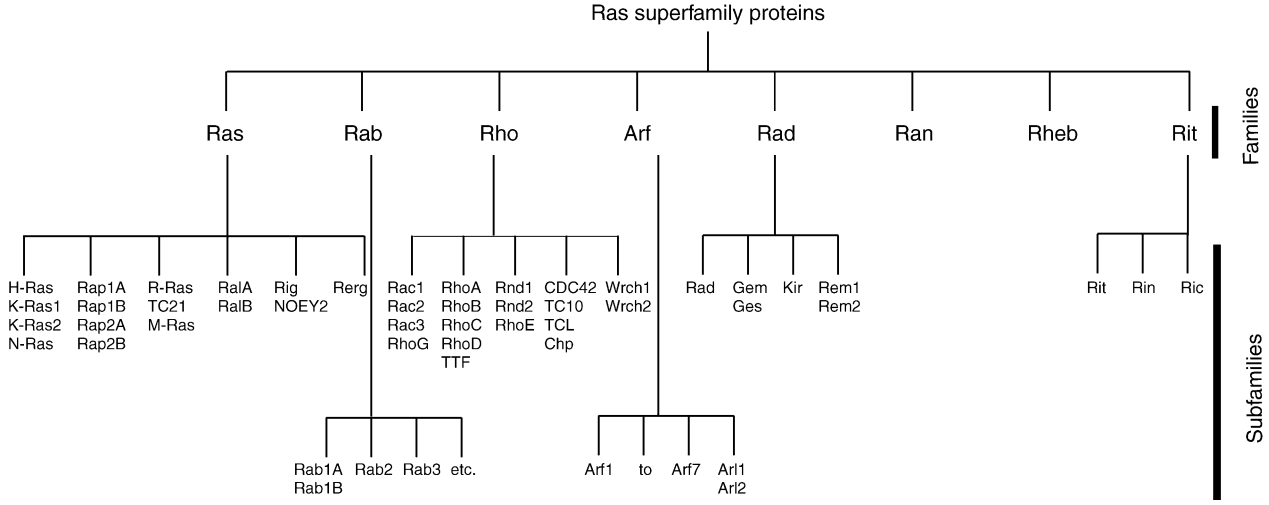

FIGURE 2 Small GTPase family.

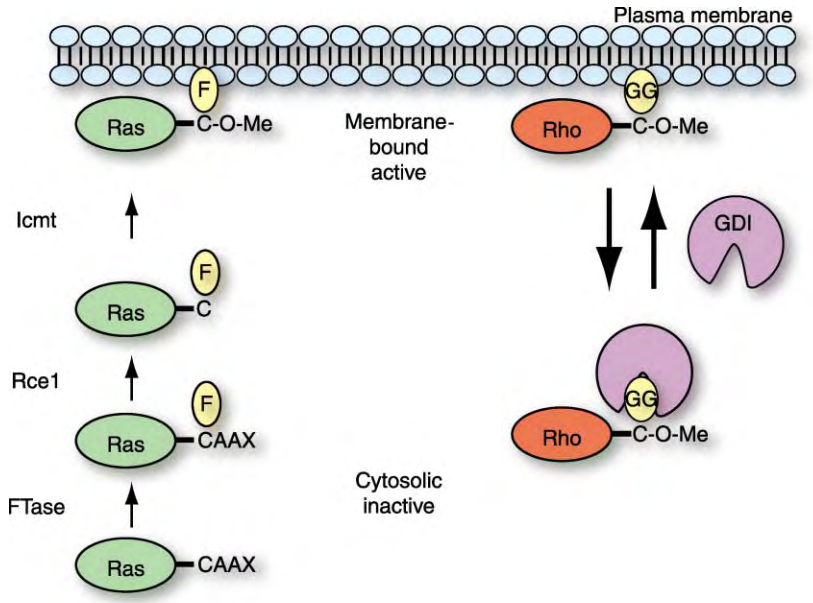

FIGURE 3 Post-translational modification by prenylation is important for the function of some small GTPases. Members of the Ras and Rho family of small GTPases terminate with CAAX tetrapeptide sequences that signal a series of post-translational modifications that promote association with membranes that is critical for function. For example, Ras proteins are synthesized initially as inactive, cytosolic proteins. Ras proteins are first modified by farnesyltransferase (FTase) which catalyzes the covalent addition of a C15 farnesyl isoprenoid (F) lipid to the cysteine residue of the CAAX motif. This is followed by Rce1-mediated proteolytic removal of the AAX peptide and Icmt-catalyzed carboxylmethylation (O-Me) of the now terminal farnesylated cysteine residue. Rho GTPases undergo the same series of modifications, with the first step catalyzed by geranylgeranyltransferase I (GGTaseI) and addition of the geranylgeranyl isoprenoid (GG). Rho GDIs recognize the prenylated form of Rho GTPases and prevent its association with membranes, thus leading to Rho GTPase inactivation.

via Src homology 3 (SH3) domain interaction with specific sequences on Sos, and recruits Sos to the membrane. The plasma membrane-bound Ras family proteins are now activated. Regulation of the production of membrane-bound lipids, such as diacylglycerol (DAG) or phosphatidylinositol 3,4,5-trisphosphate (PIP_3), are other mechanisms that regulate GEF membrane association and activation (Figure 4).

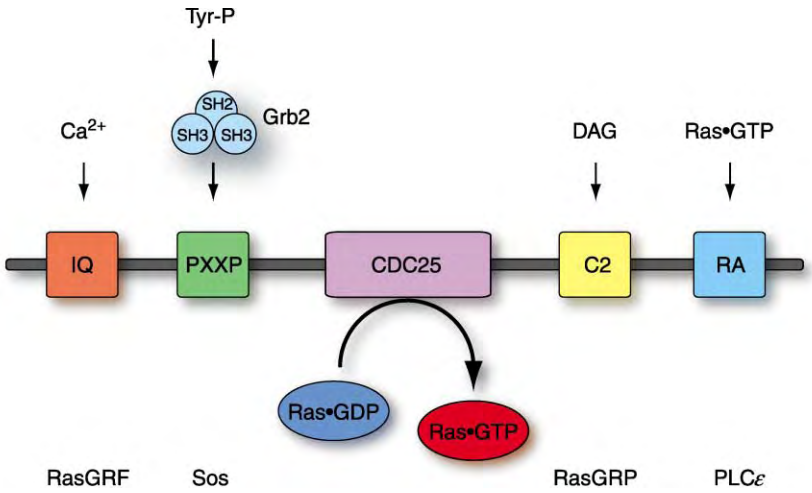

FIGURE 4 Ras guanine nucleotide exchange factors are activated by diverse upstream signals. Diverse extracellular signals promote Ras activation by stimulating the activity of different Ras GEFs. All Ras GEFs share a common CDC25 homology domain that catalyzes nucleotide exchange. The different Ras GEFs can be activated by calcium (RasGRF) through an IQ GAP homology domain, by tyrosine phosphorylation and interaction with the Grb2 adaptor protein and proline-rich sequences (PXXP) in Sos, by diacylglycerol (DAG) association with a C2 domain (RasGRP) or by association of Ras Association domains (RA) with other activated Ras family members.

GTPase Activating Proteins

The intrinsic hydrolysis rate of the majority of small GTPases is surprisingly slow, and sufficiently slow to be of little consequence in signaling cascades. Signals would not only be transduced too slowly, but the "on" state would persist for an excessive period of time. GEFs act to accelerate small GTPase activation, whereas GAPs act to accelerate the small GTPase hydrolysis and therefore make the signaling more transient (Figure 1).

In comparison to the vast number of Ras and Rho GEFs, the number of GAPs which act upon small GTPases is significantly smaller, fewer than ten for all the Ras family GAPs. There are structurally distinct GAPs for Ras and Rho family GTPases. Similar to the GEFs, these GAPs also typically contain additional sequences beyond the GAP catalytic domain. These sequences are involved in regulation, although much less is known about GAP regulation. Additionally, GAPs may possess functions, such as the effector function described for some Ras GAPs. Finally, the mutated Ras proteins found in human cancers contain single amino acid substitutions at glycine 12 (G12) or glutamine 61 (Q61), which render these mutants insensitive to GAP stimulation (Figure 5). These GTPase-deficient mutants are persistently GTP-bound in the absence of upstream stimulation and consequently cause deregulated effector activation. The experimental introduction of analogous mutations at residues corresponding to G12 and Q61 also renders other small GTPases GAP-insensitive and constitutively activated. Some wild-type small GTPases, however, possess naturally occurring sequence variation at these two residues, and are persistently GTP-bound proteins (e.g., RhoE/Rnd3). Thus, while GDP/GTP regulation is the major mode of small GTPase regulation, for some GTPases, regulation by other mechanisms (e.g., gene transcription, membrane association) is also important.

Other Small GTPase Regulatory Mechanisms

Guanine Nucleotide Dissociation Inhibitors (GDIs) GDIs have been identified for Rho and Rab proteins. Two distinct negative regulatory functions have been ascribed to GDIs. First, they bind to and mask the isoprenoid lipid modification in the carboxyl terminus of the small GTPase, thus preventing the association of the small GTPase with membranes (Figure 4). Second, their binding perturbs GAP and GEF regulation, preventing small GTPase activation. Three Rho GDIs and one Rab GDI have been described and can recognize multiple family members. The mechanisms of regulation of GDI activity are unclear, but may involve phosphorylation.

Small GTPase Structure

Small GTPases and Conserved Structural Elements

The structure of many forms of Ras proteins has been determined and has established the general rules and requirements for all small GTPases. H-Ras was the first small GTPase to have its structure solved, and

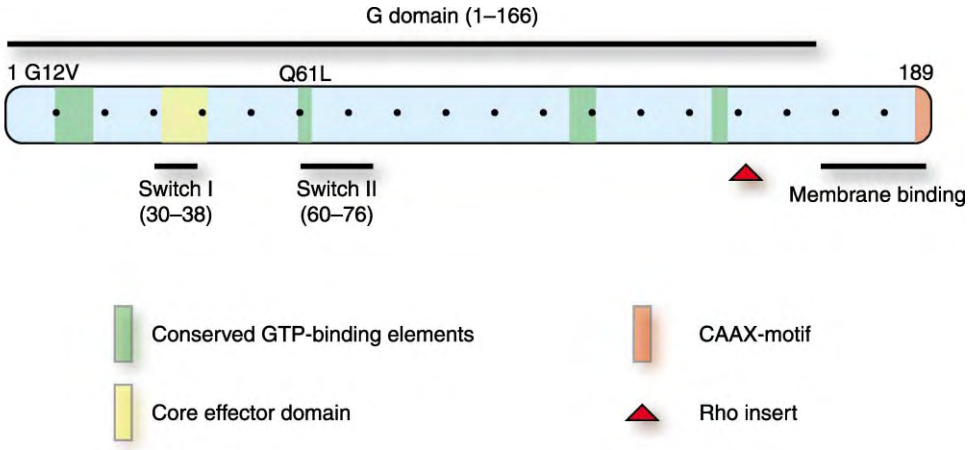

FIGURE 5 Small GTPase functional domains. Members of the small GTPase family share sequence similarities that define distinct functional domains. The residue numbers corresponding to H-Ras are shown. The G domain is comprised of a set of four conserved sequence elements involved in GTP-binding it alone is sufficient for the guanine nucleotide binding and GTPase activity, and is structurally similar among small GTPases. Mutated forms of Ras proteins are found in human cancers and possess single amino acid substitutions (e.g., G12V or Q61L) that render the protein insensitive to GAP stimulation and result in constitutively activated proteins. Similar mutations in other GTPases also result in constitutively activated proteins. Ras and Rho membrane association is facilitated by COOH-terminal sequences that include the CAAX motif as well as sequences upstream of this sequence. Effector binding involves the core effector domain (residues 32–40) and residues that change in conformation in the GDP- and GTP-bound states (switches I and II). Rho GTPases possess additional sequences (Rho insert) not found in other small GTPases. Some small GTPases contain additional NH_2- or COOH-terminal sequence extensions.

subsequent structures of related proteins have demonstrated a conserved overall canonical structural fold (designated the G domain) shared with all GTPases, but with variations in features for different small GTPase-family members (Figure 6).

All small GTPases possess a set of conserved sequence elements shared with other GTPases which represent the GDP/GTP nucleotide-binding pocket and GTP hydrolytic machinery (some, however, are GTPase deficient due to key residue changes), since the binding and hydrolysis of guanine nucleotides is the uniting element throughout small GTPases. A significant observation from Ras structural studies was the discovery of structural differences between the GDP- and GTP-bound forms, which are localized in two regions, termed switch I (residues 32–38) and switch II (residues 59–67). Similar switch-I and switch-II conformation changes have also been identified for the GDP- and GTP-bound states of other small GTPases.

Switch I and switch II show sequence divergence between families, although their loop-like structures are conserved. In addition to reflecting the nucleotide-bound state of the small GTPase, the switch regions are also involved in the interaction of small GTPases with effectors as well as GAPs and GEFs. The divergent sequence composition of these two regions contributes to the specificity of different small GTPases for these different binding partners.

Members of the Rho-family small GTPases possess a unique structural feature absent on all other small GTPases. The Rho family contains an insertion of 13 amino acids, called the insert region, positioned between Ras residues 122 and 123, which forms a surface-exposed loop (Figure 5). The primary sequence and secondary conformation of this insert region varies within the Rho family. Although the conformation of the insert region is not influenced by nucleotide binding, there is evidence that it is involved in effector interaction and activation.

Finally, other small GTPases possess additional amino- or carboxyl-terminal extensions important for function. For example, Arf and Sar1 proteins contain an amino-terminal extension necessary for insertion into and interaction with the membrane, whereas Ran has an elongated carboxyl-terminus that is crucial for its function in nuclear transport.

Diverse Biology and Function of Small GTPase

Despite their strong structural and biochemical similarities, small GTPases facilitate a remarkably divergent spectrum of cellular functions. This diversity is accomplished by the input signals that regulate the distinct GAPs and GEFs to modulate GDP/GTP cycling, and by the unique set of effectors that are recognized by the GTP-bound forms of small GTPases within and between families, resulting in many different cellular responses.

Ras Proteins as Signaling Nodes and Regulators of Cell Proliferation

The frequent mutation of Ras proteins in human cancers has made these small GTPases the most intensely studied

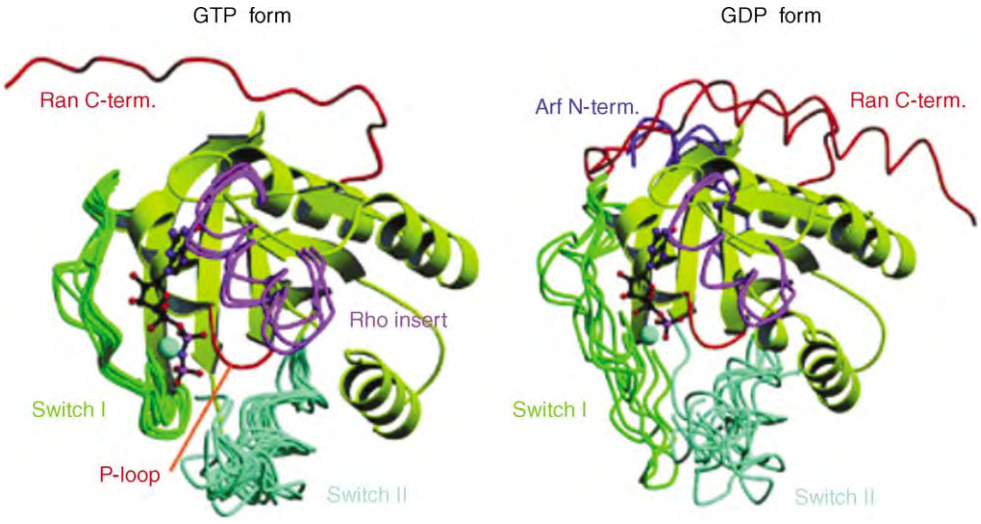

FIGURE 6 Canonical GTP conformation of small GTPases. Superimposition of a selection of Ras superfamily proteins on the G domain show the similar conformation changes in the switch-I and switch-II regions in the GDP- and GTP-bound forms. Rho GTPases possess additional sequences (Rho insert) not present in any other Ras superfamily proteins. Some small GTPases possess additional NH_2- and COOH-terminal sequences: the COOH-terminus of Ran is in red, the Rho insert in magenta and the Arf NH_2-terminal helix in blue.

and best characterized. Ras proteins serve as signaling nodes, where a wide diversity of extracellular signals such as growth factors (epidermal growth factor, platelet-derived growth factor), hormones (insulin), cytokines (interleukin-1), and the extracellular matrix proteins (via integrins) converge on and cause activation of Ras. Activated Ras in turn interacts with and regulates the activities of downstream effectors with highly divergent biochemical functions. Recent reviews have provided detailed discussions of Ras effector utilization. Therefore, we have highlighted various themes.

The Raf serine/threonine kinases are important effectors of Ras and facilitate activation of the ERK mitogen-activated protein kinase cascade (Figure 7). Ras promotes Raf activation by promoting the association of the normally cytosolic Raf with the plasma membrane, where a complex set of events, which includes protein phosphorylation, activates Raf kinase function. Activated Raf then phosphorylates and activates the MEK1 and MEK2 dual specificity protein kinases, which phosphorylate and activate ERK1 and ERK2. Activated ERK translocates to the nucleus and phosphorylates a variety of targets that include Ets family transcription factors. The Raf/MEK/ERK kinase cascade contributes significantly to the growth-regulatory functions of Ras.

The second best-characterized class of Ras effectors is the phosphatidylinositol 3-kinases (PI3K), a family of lipid kinases (Figure 7). A major activity of PI3K is the conversion of membrane-associated phosphatidylinositol 4,5-bisphosphate (PIP_2) to phosphatidylinositol 3,4,5-trisphosphate (PIP_3). PIP_3 in turn can regulate the activity of a diverse range of targets, including activation of the Akt serine/threonine kinase and Rac GEFs, via PIP_3 interaction with pleckstrin homology domains present in these proteins.

One significant theme that has emerged is that a number of Ras effectors are GEFs that link Ras with other small GTPases (Figure 7). First, there is a family of Ral GEFs that binds activated Ras and promotes activation of RalA and RalB, members of the Ras family of small GTPases. Second, Rin1 functions as a GEF for Rab5, thus linking Ras activity with regulation of vesicular trafficking. Third, Ras binds and activates Tiam1, which functions as a GEF for Rac. Fourth, Ras binds phospholipase C epsilon, which also contains a CDC25 homology domain that may activate the R-Ras small GTPase.

While Ras GTPases function as positive regulators of cell proliferation, some small GTPases appear to possess opposing functions and may function as tumor suppressors rather than oncogene proteins. This includes Rerg, NOEY2/ARH1, Rig, and DBC2. Thus, while these proteins share significant sequence and biochemical functions with Ras, clearly their effector functions are quite distinct. Additionally, whereas mutational activation of Ras proteins is associated with oncogenesis, it is the loss of gene expression of these proteins that accounts for their loss of function in tumor cells.

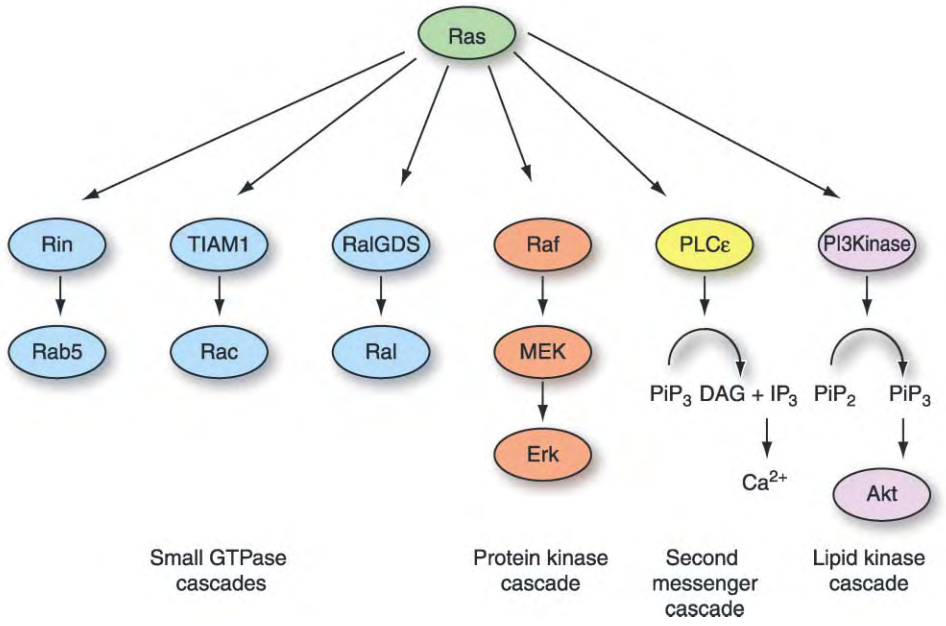

FIGURE 7 Ras effectors mediate diverse signaling outcomes. Activated, GTP-bound Ras can bind and regulate functionally diverse downstream effector targets. These include activation of a protein kinase cascade (Raf), activation of the PI3K lipid kinase, and activation of PLCE and the production of second messengers (DAG and calcium). Several Ras effectors are GEFs that activate other members of the Ras superfamily, including Rab5 (Rin1), Ral (RalGEFs), and Rac (Tiam1). Thus, Ras functions as a signaling node, where diverse signals converge and cause its activation (Figure 4), and once activated, results in activating of diverse downstream signaling pathways.

Rho-Family Proteins and Actin Cytoskeletal Organization, Cell Morphology, and Cell Movement

Similar to Ras proteins, Rho-family small GTPases also function as signaling nodes activated by diverse extracellular signals. Perhaps the best-characterized cellular function of these proteins is their regulation of actin cytoskeletal organization, which in turn influences cell morphology, cell–matrix and cell–cell interactions, and cell movement. For example, RhoA causes actin stress fiber formation, Rac causes actin accumulation at the leading edge of a motile cell and lamellipodia formation, whereas Cdc42 promotes actin microspikes and filopodia formation. These changes in actin organization can influence cell shape, cell motility, and cell–cell interactions.

Small GTPases and Membrane Trafficking

Rab proteins constitute the largest subfamily of small GTPases, with more than 60 mammalian members. Rab proteins are involved in the modulation of specific steps in eukaryotic membrane trafficking in the secretory and endocytic pathways. Arf and Sar small GTPases are also involved in the regulation of cytoplasmic vesicular trafficking. By contrast, Ran is a regulator of nucleocytoplasmic transport. The regulation of the GDP/GTP cycle is also critical for the functions of these small GTPases in their distinct transport function.

See Also the Following Articles

ARF Family • G_{12}/G_{13} Family • Phosphatidylinositol Bisphosphate and Trisphosphate • Rab Family • Ran GTPase • Ras Family • Rho GTPases and Actin Cytoskeleton Dynamics

Glossary

cytoskeleton A dynamic network of filaments, microfilaments, microtubules, and intermediate filaments.

effector proteins Proteins that bind preferentially to the GTP-bound form of small GTPases and facilitate the biological response of small GTPases.

GTPase High-affinity GDP-, GTP-binding, and GTP-hydrolyzing proteins that act as molecular switches and timers that cycle between inactive GDP-bound and active GTP-bound states.

GTPase activating protein Negative regulatory protein that accelerates the intrinsic GTP hydrolysis activity of small GTPases.

guanine nucleotide exchange factors Regulatory protein that accelerates the intrinsic GDP/GTP exchange activity of small GTPases.

guanine nucleotides Amine nucleotide bases composed of a guanine moiety attached to one (guanosine monophosphate, GMP), two (guanosine diphosphate, GDP), or three (guanosine triphosphate, GTP) phosphate groups.

isoprenylation Post-translational, covalent modification of proteins at carboxyl-terminal cysteine residues, by either C15 farnesyl or C20 geranylgeranyl isoprenoid lipids.

kinase An enzyme with phosphorylating activity on either proteins or lipids.

superfamily, family, and subfamily Small GTPases are classified into hierarchical phylogenies on the basis of structural, sequence, and functional similarity between members. Members of the Ras family share ~50% amino acid identity with the four Ras proteins whereas members of the Rho, Rab, and other Ras superfamily GTPases share ~25–30% amino acid identity with Ras proteins.

Further Reading

Der, C. J. (2002). Rho family proteins. In *Encyclopedic Reference of Cancer* (M. Schwab, ed.) pp. 799–804. Springer, Heidelberg, Germany.

Hall, A. (ed.) (2000). *GTPases*. Oxford University Press, New York.

Pruitt, W. M., and Der, C. J. (2002). Ras proteins. In *Encyclopedia of Cancer* (J. R. Bertino, ed.) 2nd edition, Vol 4, pp. 41–48. Academic Press, Orlando, FL.

Seabra, M. C., Mules, E. H., and Hume, A. N. (2002). Rab GTPases, intracellular traffic and disease. *Trends Mol. Med.* **8**, 23–30.

Vetter, I. R., and Wittinghofer, A. (2001). The guanine nucleotide-binding switch in three dimensions. *Science* **294**, 1299–1304.

Biography

Adam Shutes graduated from Oxford University before receiving his Ph.D. from University College London in 2001. He is currently a postdoctoral Fellow at the Lineberger Comprehensive Cancer Center, UNC, where his interests lie in small GTPases and their regulation.

Channing Der is a Professor of Pharmacology at the University of North Carolina at Chapel Hill, where his research is focused on Ras-related proteins and their roles in cancer. He graduated from University of California, Los Angeles, before receiving his Ph.D. from University of California, Irvine, in 1981.

Somatostatin Receptors

Agnes Schonbrunn
The University of Texas Health Science Center, Houston, Texas, USA

Somatostatin receptors (sst receptors) comprise a family of five distinct plasma membrane receptors that bind the neuroendocrine peptides somatostatin and cortistatin. These receptors exhibit the seven-transmembrane domain structure typical of G protein-coupled receptors (GPCRs) and signal primarily through pertussis toxin-sensitive G proteins. The different sst receptor subtypes are found in specific endocrine and exocrine tissues, including the pituitary and the pancreas, in addition to being widely distributed in the central and peripheral nervous systems and the gastrointestinal tract. They have important physiological roles in inhibiting hormone secretion, particularly the secretion of growth hormone, insulin, glucagon, and gastrin, inhibiting exocrine secretion by the pancreas and stomach, and modulating neuronal excitability and smooth muscle contraction. Additionally, many neuroendocrine tumors express high levels of somatostatin receptors, and, because of their ability to inhibit tumor cell secretion as well as proliferation, somatostatin analogues are now used to target these receptors for both cancer therapy and diagnosis.

Physiological Somatostatin Receptor Ligands

Somatostatin (SS), originally called somatotropin-release inhibiting factor or SRIF, was discovered accidentally over 30 years ago while investigators were hunting for the brain peptide responsible for stimulating the release of growth hormone, or somatotropin. Surprisingly, they found that extracts of the hypothalamus, a specialized brain region that regulates pituitary hormone secretion, inhibited rather than stimulated the secretion of growth hormone. Using this inhibition as an assay, R. Guillemin, A. Schally, and their co-workers purified the active factor from hypothalamic extracts and identified the 14-amino-acid form of somatostatin, a discovery that contributed to their receiving the Nobel Prize in 1977 for studies of hormone production in the brain.

SS is now known to exist in two biologically active isoforms, 14 (SS14) and 28 (SS28) amino acids in length, which are produced by alternate proteolytic processing from a common precursor of 116 amino acids. These cyclic peptides are synthesized by specific endocrine, gastrointestinal, immune, and neuronal cells, as well as some tumors, and act either locally as paracrine, autocrine, or neuronal modulators or through the bloodstream as hormones.

The cDNA for the related peptide cortistatin was discovered much later, in 1996, in the process of characterizing region-specific rat brain mRNAs. Cortistatin was named for its predominant expression in the brain cortex and its ability to depress cortical neuronal activity. Cortistatin is also synthesized as a precursor and is proteolytically processed into two biologically active products: a short (rat CST-14 and human CST-17) and an amino-terminally extended (CST-29) form. Although cortistatin is produced from a different gene than somatostatin, the two peptides have 10 of their 14 carboxy-terminal amino acids in common (Figure 1). Cortistatins are produced primarily by central nervous system neurons but have also been found in immune cells, lymphoid tissues, bone marrow, and the pancreas.

Because all forms of somatostatin and cortistatin bind to the different somatostatin receptor subtypes (sst's) with similar high affinities, it is not surprising that the peptides share many functional properties. However, they also produce some distinct biological effects. For example, intracerebroventricular injection of cortistatin in rats increases slow-wave sleep but not REM sleep, whereas somatostatin injection increases REM sleep. Thus, the identification of a human cortistatin selective G protein-coupled receptor (MrgX2, or Mas-related gene X2) fulfills prior predictions for the existence of distinct cortistatin-specific receptors. However, the rodent orthologue of this receptor has not been identified, and the relative roles of somatostatin receptors and cortistatin receptors in mediating the physiological actions of these peptides remain to be determined.

Biochemical and Molecular Characterization of Somatostatin Receptors

Somatostatin Receptor Subtypes

Five somatostatin receptor genes, located on different chromosomes, have been identified and named *sst1* to

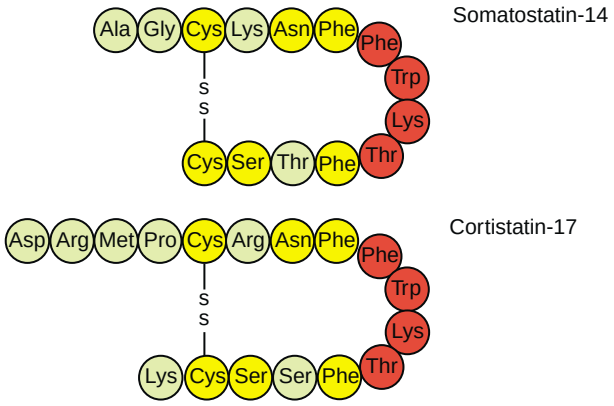

FIGURE 1 Structure of mammalian somatostatin-14 and human cortistatin-17. The amino acids in the red circles are required for high-affinity binding to somatostatin receptors. The amino acid differences between the two peptides are shown by the green circles.

sst5 in the order of their discovery (Table I). The coding regions of sst1, sst3, sst4, and sst5 all occur within a single exon. However, at least in some mouse and rat tissues, the mRNA for sst2 undergoes alternative splicing at the 3′ end, producing two protein products. The sst2A variant is the product of the unspliced mRNA, whereas the sst2B variant contains an alternative exon that encodes a different and somewhat shorter receptor carboxy terminus. Only the sst2A variant has been detected in normal human tissues.

Somatostatin receptors belong to the G protein-coupled receptor (GPCR) family and are predicted to contain seven α-helical transmembrane domains. Receptors for somatostatin have been cloned from a variety of mammals as well as from several nonmammalian species, including a number of fish. The human sst receptors exhibit between 40 and 57% amino acid identity with each other, and sequence identity among the rat, mouse, and human orthologues of each receptor subtype is even higher. The greatest sequence similarity between sst receptor subtypes occurs within the transmembrane domains; these domains, therefore, are thought to be involved in ligand binding. Sequence differences in the intra- and extracellular domains are presumably responsible for the unique signaling and trafficking properties of individual sst receptor subtypes.

Based on sequence similarity, sst receptors have been subdivided into two groups: sst1 and sst4 receptors form the SRIF2 subgroup, and sst2, sst3, and sst5 constitute the SRIF1 subgroup. In addition to a closer phylogenetic relationship (Figure 2), members of each group share several functional properties, such as their affinity for short synthetic somatostatin analogues, including octreotide and lanreotide, and sensitivity to agonist-induced receptor internalization (Table I).

The GPCRs most closely related to the sst receptor family are GPR7 and GPR8, which encode receptors for two paralogous brain peptides, neuropeptide B (NPB) and neuropeptide W (NPW) (Figure 2). The next most closely related family is the opioid receptor family, which also shares substantial sequence identity with the cortistatin receptor MrgX2 (Figure 2).

Somatostatin Receptor Structure

Somatostatin receptors contain many of the structural features characteristic of GPCRs, including consensus sites for Asn-linked glycosylation within the amino terminus and multiple Ser and Thr phosphorylation sites in the intracellular loops and carboxy-terminal tail (Table I). All sst receptor subtypes except sst3 also contain a conserved Cys residue in the carboxy-terminal region, which provides a site for receptor palmitoylation. Lipid modification has yet to be demonstrated biochemically for any of the sst subtypes. However, sst1, sst2, sst3, and sst5 are known to be glycosylated from

TABLE I

Properties of Human Somatostatin Receptor Subtypes

Property	sst1	sst2A/B	sst3	sst4	sst5
Chromosomal localization	14q13	17q24	22q13.2	20p11.2	16p13.3
Reference sequence[a]	NM 001049	NM 001050	NM 001051	NM 001052	NM 001053
Amino acids	391	369/356	418	388	364
Asn glycosylation sites	3	4	2	1	3
Receptor glycosylation	+	+	+	−	+
Cys palmitoylation site	+	+	−	+	+
Receptor phosphorylation	+	+	+	−	nd[b]
Octreotide/lanreotide binding affinity	Low	High	Moderate	Low	Moderate
SS-stimulated receptor internalization	Slow	Fast	Fast	Slow	Fast

[a] Accessible at http://www.ncbi.nlm.nih.gov/.
[b] nd, not determined.

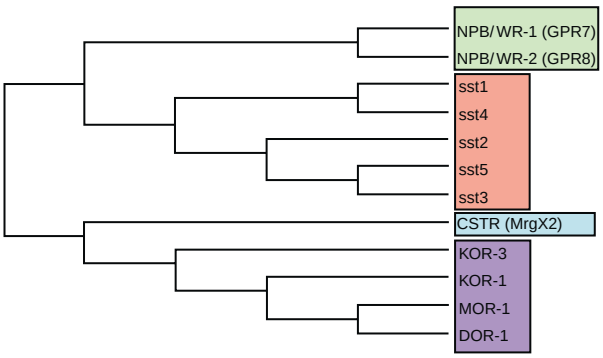

FIGURE 2 Sequence relationships between somatostatin receptors and closely related peptide receptors. The dendrogram was generated with the Clustal W program using MacVector's default parameters to align the peptide sequences. Human sequences were used in all cases and were obtained either from SwissProt or RefSeq. Somatostatin receptors: hsst1, P30872; hsst2A, P30874; hsst3, P32745; hsst4, P31391; hsst5, P35346. Cortistatin receptor: MrgX2, NP_473371. Opioid receptors: KOR-1, P41145; MOR-1, P35372; DOR-1, P41143; and KOR-3, P41146. Neuropeptide B/W receptors: NPBWR-1 or GPR7, P48145; and NPBWR-2 or GPR8, P48146. The plot shows that hsst1 and hsst4 form one subgroup and hsst2, hsst3, and hsst5 form a second subgroup within the somatostatin receptor family and that the cortistatin receptor is not a member of the sst receptor family.

the observation that treatment of these receptors with peptide-N-glycosidase F (PNGaseF), an enzyme that catalyzes the cleavage of N-glycosidically linked carbohydrate chains from Asn, causes a large decrease in their apparent molecular weights. Such a shift in molecular weight was not observed for sst4, either because it is not glycosylated or because glycosylation at its single consensus site does not significantly affect its apparent molecular weight.

Receptor phosphorylation, a covalent modification known to be important for GPCR regulation and signaling, has been examined biochemically for some but not all sst receptor subtypes. Somatostatin stimulates the incorporation of $^{32}PO_4$ into sst1, sst2A, and sst3 receptors, and protein kinase C activation also increases phosphorylation of sst1 and sst2A. However, phosphorylation of sst4 was not detected following agonist stimulation, and sst5 phosphorylation has not been investigated biochemically.

Pharmacology of Somatostatin Receptor Subtypes

The native somatostatin peptides exhibit little selectivity among the different receptor subtypes and have a very short lifetime in plasma (half-life < 3 min). Thus, analogues with increased metabolic stability and greater receptor specificity have been developed for therapy.

The earliest pharmaceuticals to target somatostatin receptors were short peptides, 6 to 8 amino acids in length, containing amino acids 7 to 10 of SS14, the region required for receptor binding (Figure 1). These agonists, including octreotide (SMS201-995), lanreotide (BIM 23014), and seglitide (MK-678), also contain D-amino acid substitutions and carboxy- or amino-terminal modifications to increase metabolic stability. These truncated peptides bind selectively to the SRIF1 group of receptors, exhibiting subnanomolar affinity for sst2 and nanomolar affinities for sst3 and sst5 (Table I). Further, octreotide does not bind to the MrgX2 cortistatin receptor. Both octreotide and lanreotide are used clinically to treat hormone-secreting pituitary adenomas and gastroenteropancreatic (GEP) tumors and comprise the only FDA-approved pharmaceuticals targeting sst receptors for therapy.

In an effort to generate receptor subtype specific analogues that are resistant to proteolytic degradation, S. Rohrer and co-workers at Merck screened combinatorial libraries to successfully identify the first highly selective, high-affinity, nonpeptide agonists for all sst subtypes. Such reagents offer the possibility of oral bioavailability, although they are not presently approved for clinical use. Nonetheless, they supply valuable tools for identifying the physiological roles of individual sst receptor subtypes.

The recognition that many tumors express several different sst receptors concomitantly has stimulated a search for stable somatostatin analogues that can bind to multiple somatostatin receptors. The hexapeptide analogue SOM230 shows high affinity for four of the five somatostatin receptor subtypes (sst1, sst2, sst3, and sst5), whereas the nonapeptide analogue KE108 appears to be truly universal since it binds to all five sst subtypes with nanomolar affinity. Because of their excellent metabolic stability, these broad-spectrum agonists have significant therapeutic potential.

The first somatostatin receptor antagonist, CYN-154806, described in 1996, showed high selectivity for the sst2 receptor. Since then, antagonists have been identified for all five somatostatin receptor subtypes, although none are used clinically.

In addition to their therapeutic applications, analogues of somatostatin have been developed to localize and stage sst receptor-positive tumors *in situ*. The radiolabeled derivatives used for tumor diagnosis contain a chelating group covalently attached to a stabilized somatostatin peptide, such that its receptor-binding properties are not compromised. The chelating group is then bound to a short-lived radioisotope, such as the gamma emitter ^{111}In, and injected into patients. After 24 h, accumulation of the radiolabel can be visualized in tumors expressing high levels of sst receptors by gamma camera scintigraphy, thus permitting localization of the tumors and their metastases. The analogue in current

clinical use is an indium-labeled octreotide derivative, [^{111}In-DTPA-D-Phe^1, Tyr^2]octreotide (OctreoScan), and hence is selective for the SRIF1 group of sst receptors, showing the most sensitive detection of sst2-expressing tumors. Unfortunately, this method cannot be used to localize tumors expressing sst1 or sst4 receptors, as appropriate somatostatin analogues are not yet available.

Somatostatin Receptor Signaling

Somatostatin receptors regulate a number of diverse signaling effectors, including adenylyl cyclase, phospholipases C and A2, calcium and potassium channels, protein and lipid kinases, and tyrosine and serine/threonine phosphatases. All sst receptors inhibit adenylyl cyclase via pertussis toxin-sensitive G proteins and thus decrease intracellular cyclic adenosine monophosphate (cAMP). However, other signal transduction pathways modulated by somatostatin receptors vary both with the receptor subtype and with the target cell.

The mechanism by which somatostatin receptors inhibit secretion in endocrine cells and neurons is understood in some detail. In addition to reducing intracellular cAMP levels, several sst receptors have been shown to reduce intracellular calcium levels in excitatory cells, also via pertussis toxin-sensitive G proteins. The reduction in cytosolic calcium can result either from a stimulation of various potassium channels, which hyperpolarize the cell membrane and thereby decrease influx through voltage-dependent calcium channels, or from direct calcium channel inhibition. The decrease in intracellular cAMP and calcium concentrations together contribute to the inhibitory action of somatostatin on secretion: when either signaling pathway is blocked, the magnitude of somatostatin's inhibitory effect is reduced.

Somatostatin stimulates contraction of intestinal smooth muscle cells by inhibiting adenylyl cyclase and activating phospholipase C-β3 via the α- and $\beta\gamma$-subunits, respectively, of pertussis toxin-sensitive G proteins. The activated phospholipase catalyzes the hydrolysis of the membrane lipid phosphatidylinositol 4,5-bisphosphate to form the second messengers inositol trisphosphate (IP_3) and diacylglycerol (DG). The binding of IP_3 to receptors on the sarcoplasmic reticulum results in the release of calcium from intracellular stores, producing a rise in cytosolic calcium concentrations. The released calcium forms a complex with the protein calmodulin, and this complex then activates myosin light-chain kinase (MLCK) to phosphorylate the light chain of myosin, leading to smooth muscle contraction. Because protein kinase A (PKA) decreases the sensitivity of MLCK to calcium, somatostatin inhibition of cAMP formation facilitates the calcium effect by reducing the activity of PKA. These pathways are also activated by somatostatin in aortic vascular smooth muscle cells. Interestingly, somatostatin does not activate phospholipase C-β3 in pituitary cells, even though the level of this enzyme in the pituitary appears to be similar to that in smooth muscle cells. The explanation for the signaling differences in these tissues remains to be elucidated, but could be due to differences either in the sst subtypes or in the signaling machinery present.

In endothelial cells, somatostatin inhibits cell migration, stress fiber assembly, and cytoskeletal reorganization produced by thrombin and other stimulators. In humans, these effects are mediated by the sst1 receptor and have been implicated in somatostatin's antiangiogenic actions. Although the molecular steps involved have not yet been identified, the mechanism includes an unusual pertussis toxin-independent inhibition of Rho, a low molecular mass GTPase that plays a central role in regulating cytoskeletal organization.

The mechanisms by which somatostatin inhibits cell proliferation and stimulates apoptosis are also poorly understood and appear to vary in the different cell types in which they have been examined. In most (though not all) cells, somatostatin activates the mitogen-activated protein kinase (MAPK) pathway and increases extracellular signal-related kinase (ERK)1/2 phosphorylation by a pertussis toxin-sensitive mechanism. However, this activation is often observed whether somatostatin inhibits or stimulates cell proliferation. Thus, it is likely that some of the other effectors activated by the sst receptors contribute to the final biological response. For example, in pancreatic acinar cells, which express sst2 receptors endogenously, somatostatin-induced growth arrest involves enhanced expression of the cyclin-dependent kinase inhibitor p27Kip and results from inhibition of the phosphatidylinositol-3-kinase (PI3K) pathway. In contrast, in sst2 transfected CHO cells, somatostatin induction of p27Kip appears to be dependent on stimulation rather than inhibition of PI3K, in that PI3K inhibitors block the effect of somatostatin analogues on ERK2 phosphorylation, which in turn is required for p27Kip up-regulation. These and other potential signaling pathways are under intense investigation in order to elucidate the clinically important actions of somatostatin to inhibit cell proliferation and stimulate apoptosis.

In summary, most but not all signaling by sst receptors involves the pertussis toxin-sensitive G_i/G_o family. However, depending on the sst receptor subtype and the cellular environment, a spectrum of nonoverlapping signaling pathways can be activated. The link between the different effectors regulated by sst

receptors and particular biological responses is understood for some but by no means all of somatostatin's actions.

Somatostatin Receptor Regulation

Alterations in sst receptor responsiveness during somatostatin exposure vary dramatically between tissues, depending both on the response being measured and on the nature of the target cell. In some instances, desensitization occurs within minutes following initiation of somatostatin treatment, whereas in others no desensitization is detected even after years of somatostatin analogue exposure. For example, in chick sympathetic neurons, somatostatin inhibition of N-type Ca currents desensitizes with a half-life of 3 min. In contrast, desensitization to pharmacologic doses of the somatostatin analogue octreotide does not occur in months or years of therapy for pituitary tumors. The molecular basis for such dramatic differences in somatostatin receptor regulation remains poorly understood.

Studies of the different sst receptor subtypes in transfected cells indicate receptor-specific differences in their regulation. As has been shown for many GPCRs, hormone treatment leads to the rapid phosphorylation of several sst receptor subtypes (Table I). Interestingly, however, this phosphorylation appears to have different consequences for the different sst receptors. For example, in CHO cells, although both sst1 and sst2 receptors are phosphorylated and desensitized within minutes following somatostatin exposure, only the sst2 receptor is rapidly internalized.

The cellular environment also plays an important role in the observed differences in the regulation of somatostatin responsiveness. Interestingly, the sst2 receptor, which desensitizes within minutes of somatostatin exposure in cultured cells but is resistant to desensitization in human tumors, was recently shown to be phosphorylated *in situ* in a human tumor. Hence, at least this first step in the desensitization process appears to be intact in human tumor tissue. As the other molecular components of sst receptor desensitization are characterized, it will be interesting to determine whether their functions are altered in the desensitization-resistant tumors.

Summary

The five known somatostatin receptors play important physiological roles in the regulation of the endocrine, neuronal, gastrointestinal, and immune systems. In addition, they are recognized to be important targets in the diagnosis and therapy of a number of neuroendocrine tumors.

Although a great deal remains to be learned about many of somatostatin's functions, studies with sst1, sst2, and sst5 knockout mouse models, all of which are viable, have begun to delineate the biological importance of the individual receptor subtypes. Future focus on these receptors in their normal cellular environments can take advantage of the many new receptor-specific agonists and antagonists that have become available and will undoubtedly provide much-needed insight into the function of this physiologically and therapeutically important G protein-coupled receptor family.

See Also the Following Articles

Adenylyl Cyclases • Mitogen-Activated Protein Kinase Family • Phospholipase A_2 • Phospholipase C • Rho GTPases and Actin Cytoskeleton Dynamics • Voltage-Sensitive Na^+ Channels

Glossary

acromegaly A condition caused by the excess secretion of pituitary growth hormone after maturity, usually by a pituitary tumor. The disease is characterized by enlargement of the extremities, including the nose, jaws, fingers, and toes, as well as certain internal organs.

cortistatins The short (rat CST-14 and human CST-17) and long (CST-29) biologically active products produced by proteolytic processing of the precursor peptide encoded by the cortistatin gene.

G protein One of a family of related heterotrimeric proteins that bind GTP and GDP. The heterotrimeric forms, which are inactive, become activated at the plasma membrane by agonist occupied G protein-coupled receptors (GPCRs) that stimulate the binding of GTP to the G protein α-subunit and cause dissociation of the α-subunit from the $\beta\gamma$-subunit complex. When activated, the G protein subunits regulate downstream effectors, such as ion channels and enzymes that generate second messengers. G proteins become inactivated by hydrolyzing GTP to GDP, which then permits the reassociation of the α-subunit with the $\beta\gamma$-subunit complex.

somatostatins (SSs) The 14-amino-acid (SS-14) and 28-amino-acid (SS-28) peptides produced by alternative proteolytic processing from a single 92-amino-acid precursor called prosomatostatin.

Further Reading

Alliance for Cellular Signaling (2004). The Signaling Gateway. http://www.signaling-gateway.org/. ID numbers: A002204 for sst1, A002205 for sst2, A002206 for sst3, A002207 for sst4, and A000075 for sst5. Accessed May 2004.

Hofland, L. J., and Lamberts, S. W. (2003). The pathophysiological consequences of somatostatin receptor internalization and resistance. *Endocr. Rev.* **24**, 28–47.

Kreienkamp, H. J. (1999). Molecular biology of the receptors for somatostatin and cortistatin. *Results Probl. Cell. Differ.* **26**, 215–237.

Patel, Y. C. (1999). Somatostatin and its receptor family. *Front. Neuroendocrinol.* **20**, 157–198.

Reubi, J. C. (2003). Peptide receptors as molecular targets for cancer diagnosis and therapy. *Endocr. Rev.* **24**, 389–427.

Schonbrunn, A. (1999). Somatostatin receptors: present knowledge and future directions. *Ann. Oncol.* **10**, S17–S21.

Schonbrunn, A. (2001). Somatostatin. In *Endocrinology* (L. J. Degroot and J. L. Jameson, eds.) 4th edition, pp. 427–437. Saunders, New York.

Selmer, I., Schindler, M., Allen, J. P., Humphrey, P. P., and Emson, P. C. (2000). Advances in understanding neuronal somatostatin receptors. *Regul. Pept.* **90**, 1–18.

Slooter, G. D., Mearadji, A., Breeman, W. A., *et al.* (2001). Somatostatin receptor imaging, therapy and new strategies in patients with neuroendocrine tumours. *Br. J. Surg.* **88**, 31–40.

Spier, A. D., and de Lecea, L. (2000). Cortistatin: A member of the somatostatin neuropeptide family with distinct physiological functions. *Brain Res. Brain Res. Rev.* **33**, 228–241.

Weckbecker, G., Lewis, I., Albert, R., Schmid, H. A., Hoyer, D., and Bruns, C. (2003). Opportunities in somatostatin research: Biological, chemical and therapeutic aspects. *Nat. Rev. Drug Discov.* **2**, 999–1017.

BIOGRAPHY

Agnes Schonbrunn is a Professor in the Department of Integrative Biology and Pharmacology at the University of Texas–Houston, School of Medicine. She holds a Ph.D. in Biochemistry from Brandeis University and received her postdoctoral training at Harvard Medical School. Her principal research interests include the signaling and regulation of somatostatin receptors and the functional role that these receptors play in neuroendocrine cancers.

Spastic Paraplegia

Elena Irene Rugarli
Telethon Institute of Genetics and Medicine, Naples, Italy

Andrea Ballabio
University of Naples, Federico II, Naples, Italy

Hereditary spastic paraplegia (HSP) is a group of neurodegenerative diseases characterized by weakness and spasticity of the lower limbs, loss of the vibratory sense, and urinary urgency. In 1983, Harding classified HSP in "pure" forms, when the symptoms are restricted to lower limbs weakness and spasticity, and in "complicated" forms, when the clinical picture is associated to a variety of neurological symptoms. These may include cerebral and cerebellar atrophy, optic atrophy, peripheral neuropathy, dementia, retinitis pigmentosa, amyotrophy. Age of onset is extremely variable, with a few forms arising in childhood, and most cases between 20 and 40 years of age. Usually the later the onset of the disease, the faster is the progression of its course. Although HSP is an invalidating disease, it never causes shortening of the life-span of patients.

Neuropathology

Hereditary spastic paraplegia (HSP) is characterized by the retrograde degeneration of the longest axons of the central nervous system: those of the crossed corticospinal tracts and of the fasciculus gracilis. In about half of the autoptic cases examined, the spinocerebellar tracts were also involved.

Axons of the corticospinal tracts arise from pyramidal neurons in layer V of the motor cortex and project through the internal capsule to reach the ventral surface of the medulla where they form two elongated swellings, the pyramids. These axons cross the midline at the junction between the bulb and the spinal cord and descend in the contralateral funiculus of the spinal cord. The crossed corticospinal tract conveys voluntary motor impulses to the secondary motor neurons located in the ventral horns of the spinal cord. The fasciculus gracilis is composed of the central branches of axons of pseudounipolar neurons located in dorsal root ganglia and ascend in the most medial part of the dorsal funiculus. These axons transmit deep sensory information from the lower extremities to secondary sensory neurons in the nucleus gracilis.

Characteristically, axonal degeneration in HSP involves preferentially the distal region of the axons. Degeneration of the corticospinal tracts is marked at lumbar levels, and less pronounced at cervical levels. In most cases the neuronal cell bodies are preserved. This pattern of axonal degeneration, also referred to as dying-back, is slowly progressive and occurs in several other conditions following a toxic, metabolic or genetic insult.

Genetics

It has become clear in the last decade that HSP is extremely heterogeneous from a genetic point of view. So far, 21 different loci have been mapped and it is expected that more will be identified. HSP can be transmitted as an X-linked (SPG1, SPG2, SPG16), autosomal dominant (SPG3A, SPG4, SPG6, SPG8, SPG9, SPG10, SPG12, SPG17, SPG19) or autosomal recessive trait (SPG5A, SPG7, SPG11, SPG14, SPG15, SPG20, SPG21). The molecular bases of the disease are also being unraveled with a quick pace. Eleven *HSP* genes have been identified, thus providing clues on the cellular pathways underlying the disease. Table I summarizes the current knowledge on the genetic bases of HSP. The following paragraphs describe the known *HSP* genes and classify them based on the existing functional information.

The Mitochondrial Forms

Two of the known HSP genes, SPG7 and SPG13, encode proteins that are involved in mitochondrial protein quality control. Their identification strongly indicates that at least a subgroup of HSPs should be regarded as mitochondrial diseases.

SPG7/Paraplegin

SPG7 was cloned in 1998 by Casari and colleagues, as the first autosomal recessive gene responsible for both pure and complicated forms of HSP. SPG7 encodes paraplegin, a 795 amino acid protein highly homologous to two yeast metalloproteases of the AAA family,

TABLE I

Genetic Bases of HSP

Acronym	MIM	Inheritance	Chromosomal location	Phenotype	Gene product	Proposed function
SPG1	312900	X-linked R	Xq28	Complicated	L1CAM	Development and guidance of the corticospinal tract
SPG2	312920	X-linked R	Xq21–22	Complicated	PLP	Axonal–glial interactions
SPG3A	182600	AD	14q11–q21	Pure	Atlastin	Guanilate-protein binding 1 homolog
SPG4	182601	AD	2p24-21	Pure	Spastin	Microtubule dynamics/nuclear role
SPG5A	270800	AR	8p21–q13	Pure		
SPG6	600363	AD	15q11.1	Pure	NIPA1	Transmembrane protein
SPG7	600146	AR	16q24.3	Pure/complicated	Paraplegin	Chaperone-like mitochondrial ATPase
SPG8	603563	AD	8q23–24	Pure		
SPG9	601162	AD	10q23–24	Complicated		
SPG10	604187	AD	12q13	Pure	KIF5A	Anterograde motor protein
SPG11	604360	AR	15q13	Pure		
SPG12	604805	AD	19q13	Pure		
SPG13	605280	AD	2q24	Pure	Hsp60	Mitochondrial chaperone
SPG14	605229	AR	3q27–28	Complicated		
SPG15	270700	AR	14q22–q24	Complicated		
SPG16	300266	X-linked R	Xq11.2	Complicated		
SPG17	270685	AD	11q12–q14	Complicated	Serpin	Endoplasmic reticulum protein, unknown function
SPG19	607152	AD	9q33–q34	Pure		
SPG20	275900	AR	13q12.3	Complicated	Spartin	
SPG21	248900	AR	15q22.31	Complicated	Maspardin	

Note: the loci SPG3B, SPG5B, and SPG18 are listed as "reserved" in the Hugo Gene Nomenclature Committee Database.

Yta10p (Afg3p), and Yta12p (Rca1p). Like its yeast homologues, paraplegin has an N-terminal mitochondrial leader sequence and two transmembrane domains that anchor the protein to the inner mitochondrial membrane. Paraplegin is composed of two functional domains: an ATPase domain typical of proteins of the AAA family (*A*TPases *a*ssociated with diverse cellular *a*ctivities) and a proteolytic domain with a consensus metal-binding site.

The yeast Yta10p and Yta12p assemble to form a high molecular weight complex of about 1 MDa, the *m*-AAA protease, which is embedded in the inner mitochondrial membrane but exposes proteolytic sites to the mitochondrial matrix (hence the prefix "*m*" in the name). The *m*-AAA protease ensures protein quality control system for inner membrane proteins, by guaranteeing the removal of non-assembled or misfolded proteins, and by performing crucial steps in mitochondrial biogenesis. Yeast cells lacking the *m*-AAA protease exhibit deficiencies in the expression of mitochondrially-encoded polypeptides and in the posttranslational assembly of respiratory chain complexes. These defects can be reproduced in yeast cells harbouring proteolytically inactive subunits, indicating that the phenotype is largely due to the loss of proteolytic activity. A recent study by Atorino *et al.* has shown that paraplegin co-assembles with the highly homologous AFG3L2 protein in human mitochondria to form a high-molecular-weight complex very similar to the one described in yeast. This complex complements the respiratory deficiency of yeast lacking the *m*-AAA protease, indicating functional conservation of the *m*-AAA protease across species and assigning proteolytic activity to the paraplegin/AFG3L2 complex.

Advancement in the understanding of the pathogenic basis of this form of HSP comes from the development by Ferreirinha *et al.* of a mouse model in which the *Spg7* gene has been knocked-out. Paraplegin-deficient mice recapitulate the human disease, being affected by a late-onset progressive distal axonopathy, characterized by axonal swelling and degeneration, and involving the longest axons in the central and peripheral nervous systems. Axons swell because of accumulation of membranous organelles and neurofilaments, suggesting that axonal transport is impaired. Neurotracer studies in the peripheral nervous system of symptomatic Spg7 $-/-$ mice indicated that retrograde axonal transport is delayed, suggesting that impairment of axonal trafficking processes may play a crucial role in the pathogenic process.

However, the first ultrastructural pathological sign that can be observed in paraplegin-deficient mice occurs several months before any evidence of axonal swelling and degeneration, and consists in the appearance of

abnormal mitochondria, first in synaptic terminals and then in the distal regions of the long spinal axons, that will later on undergo degeneration. Abnormal mitochondria include hypertrophic mitochondria, gigantic mitochondria, and mitochondria with disrupted or abnormal organization of cristae. This mitochondrial phenotype correlates with the onset of a measurable neurological impairment of the paraplegin-deficient mice on the rotarod apparatus, and is therefore the primary trigger of the pathological process. Since nothing is known so far about the substrates of paraplegin, the question of how lack of paraplegin is affecting mitochondrial morphology still awaits an answer. It is possible that abnormal mitochondria result from the accumulation of misfolded polypeptides that are not correctly cleared away by the paraplegin–AFG3L2 complex. Alternatively, this phenotype could underlie the abnormal processing of a regulatory molecule involved in some aspect of mitochondrial morphology.

Recent studies by Atorino *et al.* on fibroblast cell lines obtained from HSP patients with SPG7 mutations found a reduction of complex I activity and an increased sensitivity to oxidative stress, suggesting a potential mechanism for mitochondrial damage. This could be especially important in mitochondria located in nerve terminals where high energetic demands and increased concentration of free radicals are present.

SPG13/HSP60

Further support to the role of mitochondria in the pathogenesis of HSP came from the identification by Hansen *et al.* in 2002 of a missense mutation in the mitochondrial chaperonin heat shock protein 60 (HSP60) in one French family with an autosomal dominant form of pure HSP, mapping to chromosome 2q24–34. Hsp60 proteins belong to a conserved subgroup of chaperone proteins, termed chaperonins, which promote protein folding in the mitochondrial matrix, often in cooperation with the cochaperonin Hsp10. The mutation identified in the HSP family results in the V72I substitution. An elegant complementation assay performed in *E. coli* showed that only wild-type Hsp60, but not Hsp60–V72I, together with the cochaperonin Hsp10, can support the growth of bacteria in which the homologous chromosomal *groESgroEL* chaperonin genes have been deleted, indicating that the V72I mutant is functionally inactive. It is unclear whether this mutant leads to haploinsufficiency through the formation of functionally inactive mixed chaperonin rings made up by both normal and mutated subunits, or may exert a genuine dominant-negative effect.

Mitochondrial Protein Quality Control and Axonal Degeneration: A Pathogenic Hypothesis

The reason why the loss of ubiquitous mitochondrial proteins such as paraplegin and HSP60 causes the specific degeneration of a subset of axons, such as the corticospinal axons, is still to be unraveled. The most accepted hypothesis states that primary motor neurons would be particularly susceptible to any impairment of mitochondrial function due to their peculiar cellular homeostasis. These neurons have extremely long axons that can reach the length of more than 1 m in humans and depend for their life on efficient transport of organelles, molecular cargoes, and synaptic vesicles from the cell body to the distal tip of the axon, and back to the cell body. This process requires energy and is supported through the coordinated movement of mitochondria themselves along axons. Mitochondria located very distal to the cell body could be required to endure for longer period of time, and could be much less efficient in adapting to inefficient protein quality control mechanisms.

Genes Involved in Cellular Trafficking Events

A second group of genes involved in HSP appears to play a more or less direct role in cellular trafficking. Their identification supports the notion that axonal transport represents a key event for axonal homeostasis, and that any derangement from normal trafficking processes may lead with time to axonal degeneration. The long axons composing the corticospinal tracts and the fasciculus gracilis would be a privileged pathological target.

SPG10/KIF5A

The best example of the pathogenic role of impaired axonal transport in HSP comes from the identification by Reid *et al.* of a mutation in the gene encoding a specific neuronal kinesin heavy chain, KIF5A, in a family with an autosomal-dominant pure form of HSP. Kinesins are multisubunit complexes that work as motors for anterograde transport (from the cell body to the distal end of the axons) of membranous organelles and other macromolecular cargoes along microtubules. KIF5A is abundantly expressed in neurons, which is found in cell bodies, dendrites, and axons. The gene for the heavy chain of KIF5A is located within a large interval of chromosome 12 in which the SPG13 locus was mapped by cross-overs defined in a single large family affected by an autosomal-dominant pure form of HSP. A N256S missense mutation in KIF5A was identified in the

original family, and found to segregate with the disease. This mutation occurs at an invariant asparigine residue within the motor domain of the protein. Intriguingly, mutations at the corresponding residue in both the yeast Kar3 protein, a motor of the mitotic spindle, and the *Drosophila* Ncd kinesin motor, were found to block the microtubule-dependent stimulation of motor ATPase activity, thus acting with a dominant-negative mechanism. So far, the N256S mutation is the only one identified in HSP families.

SPG4/Spastin

Hazan *et al.* identified in 1999 the most frequent form of autosomal-dominant spastic paraplegia. SPG4 maps to chromosome 2p21-p22 and encodes a 616-amino-acid-protein, named spastin. Similarly to paraplegin, spastin belongs to the AAA (*A*TPases *A*ssociated with various cellular *A*ctivities) family, which is characterized by a conserved domain of 230 amino acids with ATPase activity. Based on sequence homology and phylogenetic analysis, spastin belongs to the subfamily-7 of AAA proteins, whose members are implicated in completely divergent cellular processes, such as microtubule severing and endosomal morphology and trafficking. The N-terminal part of the protein contains a newly recognized domain, the EPS or MIT domain, which is present in molecules involved in endosome trafficking, such as Vps4 and SNX15 (sortin nexin 15), and in spartin, another protein involved in HSP.

Mutations in SPG4 account for at least 40% of all autosomal-dominant HSP families. Missense, nonsense, and splice-site mutations as well as deletions or insertions have all been observed in the spastin gene. Notably, all the missense mutations fall into the AAA domain, with the exception of the S44L substitution that appears to be disease-causing only in the homozygous state, underlying the functional significance of this domain. The other mutations are scattered along the coding region of the gene and lead to premature termination codons, and mRNA instability, suggesting that haplo-insufficiency is the molecular cause of the disease.

The functional data available on spastin point to a complex cellular role. Recently, Charvin *et al.* found endogenous spastin to be localized in the nucleus, by using polyclonal antibodies raised against synthetic peptides. However, transient transfection experiments by Errico *et al.* suggested that the onset of spastin expression may be in the microtubule-organizing center and that, upon longer periods of expression, spastin may accumulate in cytoplasmic aggregates. The reason for the discrepancy between endogenous and exogenously expressed spastin is still to be determined.

Experimental evidence obtained in overexpression system suggests that spastin may interact dynamically with the microtubule cytoskeleton. In fact a stable association with a subset of microtubules and the formation of thick perinuclear bundles of microtubules are achieved when spastin mutants in the AAA domain are expressed in eukaryotic cells. A microtubule-binding domain was mapped to the N-terminal region of spastin. To explain these results, a hypothesis has been put forward that binding of spastin to microtubules may be transient *in vivo* and regulated through ATPase cycles. Mutations in the AAA domain would alter the ability of spastin to bind or hydrolyse ATP, and therefore entrap the protein in a microtubule-bound state.

To reinforce the idea that spastin is involved in microtubule dynamics, overexpression of wild-type spastin was found to promote microtubule disassembly in transfected cells. Although these data suggest that the degeneration of corticospinal axons, in HSP patients, could be due to impairment of fine regulation of the microtubule cytoskeleton, more studies are needed to demonstrate an interaction of endogenous spastin with the neuronal cytoskeleton, and to unravel its function in the nucleus.

SPG3A/Atlastin

The second most common gene involved in autosomal-dominant pure HSP with juvenile onset (~10% of the cases) has been linked to the SPG3A locus and found to encode a novel protein, atlastin, by Zhao *et al.* Four different missense mutations have been identified so far in SPG3A, all clustering in exons 7 and 8. Their mechanism of action is still to be determined. Although very little is known about the function of atlastin, this molecule shares very interesting homologies with members of the dynamin family of large GTPases, particularly with guanilate-binding protein-1. Dynamins are involved in important trafficking events in axons, including recycling of synaptic vesicles and mainteinance and distribution of mitochondria, again suggesting that abnormal axonal transport may be at the basis of this form of HSP.

SPG20/Spartin

SPG20 is the gene involved in Troyer syndrome, an autosomal recessive form of HSP complicated by disarthria, distal amyotrophy, mild developmental delay, and short stature, that occurs with high frequency in the Amish population. The cloning of this gene by Ciccarelli *et al.* in 2002 has revealed that its protein product, spartin, shares homology in the N-terminal region with spastin within the ESP/MIT domain. This has led to the hypothesis that spartin may be somehow involved in ensodome trafficking. This theory still awaits experimental confirmation.

SPG21/Maspardin

Mast syndrome is mutated in an autosomal recessive complicated form of HSP associated with dementia present at high frequency in the Old Order Amish population. Simpson *et al.*, in 2003, have mapped this condition to chromosome 15q22.31 and identified the causative gene, SPG21. SPG21 encodes an acid-cluster protein of 33 kDa (ACP33), renamed maspardin, previously shown to localize in the endosomal/trans-Golgi network. This data again emphasize the causative role of proteins involved in cellular sorting and trafficking in the pathogenesis of HSP.

Developmental Genes

HSP may result from mutations in genes involved in the development of the corticospinal tracts. This is the case of SPG1, which has been linked to mutations in the cell adhesion molecule L1CAM. Consistently, the available data from neuropathological studies found absent or severely reduced pyramids. In this form of HSP, spastic paraplegia begins in the first two decades of life, with delayed acquisition of motor milestones and slow progression of symptoms. Although this form may manifest as pure HSP, it is more often observed in association with a complex disorder, referred to either as MASA syndrome (*m*ental retardation, *a*dducted thumbs, *s*pasticity, and *a*phasia) or CRASH syndrome (*c*orpus callosum hypoplasia, mental *r*etardation, *a*dducted thumbs, *s*pastic paraplegia, and *h*ydrocephalus). L1CAM is a transmembrane glycoprotein, which is expressed during development on the surface of long axons and growth cones, including those of the corticospinal tracts. L1 mediates cell adhesion, neurite outgrowth, axon pathfinding, and fasciculation through homophilic and heterophilic binding with a variety of extracellular and transmembrane molecules, and plays an important role in mediating guidance of corticospinal axons through the pyramidal decussation.

Myelin-Associated Genes

Disruption of intimate glia to axon interactions underlies the axonal degeneration observed in SPG2 patients. SPG2 maps to Xq22 and results from mutations in the

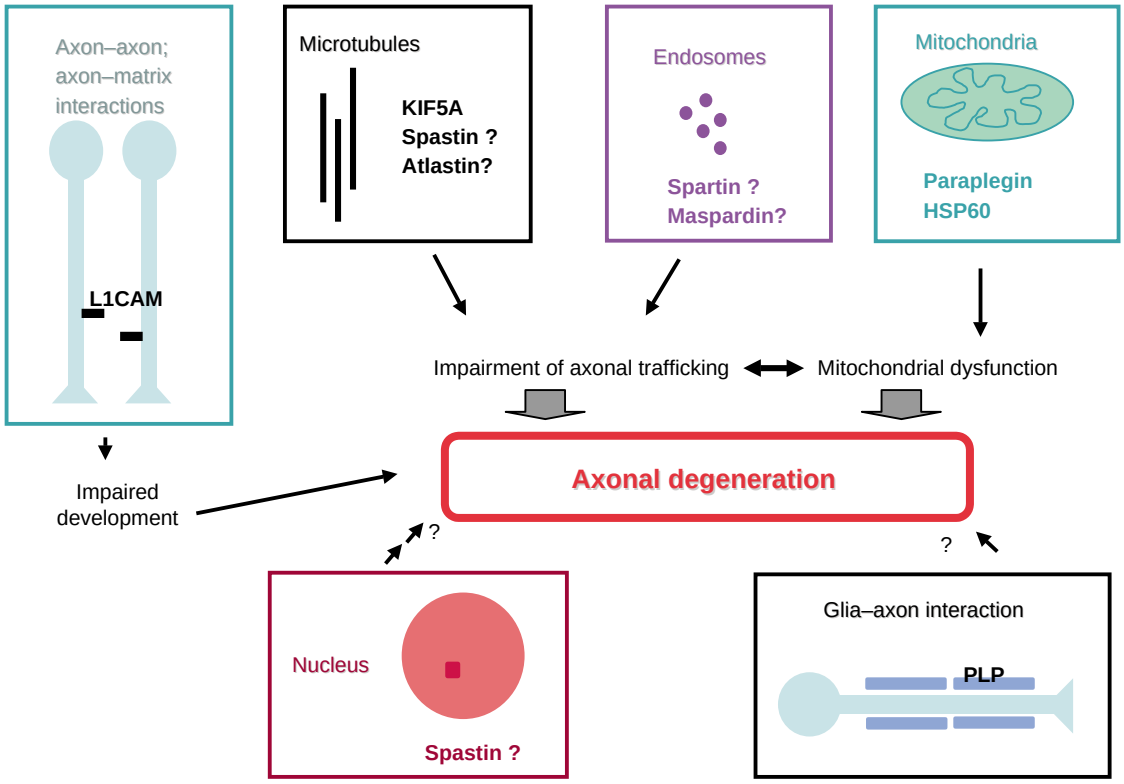

FIGURE 1 Proposed pathogenic mechanisms underlying axonal degeneration in HSP. Known proteins involved in HSP belong to different cellular compartments. Several of them, however, are believed to cause axonal degeneration either through mitochondrial dysfunction (paraplegin and Hsp60) or impairment of axonal transport (KIF5A, spastin, atlastin, spartin, and maspardin). Since mitochondria travel along axons, and play a major role in providing the energy necessary for axonal transport, the two pathways are likely to communicate. HSP can also be the result of defective development of the corticospinal tracts, as in the case of mutations in L1CAM, or of aberrant communications between glial cells and axons due to mutations in PLP1 protein. The role of spastin in the nucleus is still to be elucidated.

proteolipid protein (PLP), one of the major protein components of myelin in the central nervous system (CNS). PLP is a four-helix-spanning membrane protein that stabilizes the structure of the CNS myelin, by forming the intraperiod line. SPG2 comprises both pure and complicated forms of HSP, and is allelic to the severe hypomyelinating Pelizaeus–Merzbacher disease (PMD). A genotype-phenotype correlation between the nature of PLP mutation and the severity of the clinical picture has been described. In general, the milder phenotypes, such a pure spastic paraplegia, are observed when the gene mutations lead to the formation of protein products that are still able to traverse the secretory pathway and reach the cell surface. Surprisingly, knockout mice with complete absence of PLP, assemble compact myelin sheaths, but subsequently develop widespread axonal swelling and degeneration, most likely secondary to impaired axonal transport. It is still a mystery how the correct expression of PLP in olygodendrocytes provides support for myelinated axons. The future identification of putative signaling molecules would probably lead to a better understanding of this pathological cascade.

SPG6/NIPA1

In 2003, Rainier *et al.* reported mutations in the NIPA1 gene in a family with autosomal-dominant HSP linked to chromosome 15q11–q13 (SPG6). NIPA1 encodes for a predicted transmembrane protein, highly expressed in the brain. The function of NIPA1 is still unknown.

A Common Pathogenic Mechanism for HSP

The recent identification of several genes involved in HSP is beginning to shed light on the pathogenesis of this disorder. Although the known genes all belong to different families and have distinct subcellular localization (Figure 1), two common pathogenic themes have begun to emerge: (1) impairment of mitochondrial protein quality control and (2) defective axonal trafficking. These two routes likely intersect, since mitochondria themselves need to be transported along axons, and ATP is required to support transport of endosomes, cytoskeletal elements, synaptic vesicles, and other organelles. Future functional studies of the known HSP proteins, together with the identification of new genes, will provide new exciting insights in this chapter of neuro-degenerative diseases.

See Also the Following Articles

Chaperonins • DNA Oxidation • Kinesin Superfamily Proteins • Kinesins as Microtubule Disassembly Enzymes • Mitochondrial Genes and their Expression: Yeast

Glossary

haplo-insufficiency A locus shows haplo-insufficiency when the amount of the gene product produced by a single allele is not sufficient to achieve a normal phenotype.

paraplegia Paralysis of both lower limbs.

spasticity Muscular weakness associated with increased stiffness and overactive reflexes.

Further Reading

Casari, G., and Rugarli, E. (2001). Molecular basis of inherited spastic paraplegias. *Curr. Opin. Genet. Dev.* **11**, 336–342.

Crosby, A. H., and Proukakis, C. (2002). Is the transportation highway the right road for hereditary spastic paraplegia? *Am. J. Hum. Genet.* **71**, 1009–1016.

Harding, A. E. (1983). Classification of the hereditary ataxias and paraplegias. *The Lancet* **21**, 1151–1154.

Langer, T., Kaser, M., Klanner, C., and Leonhard, K. (2001). AAA proteases of mitochondria: Quality control of membrane proteins and regulatory functions during mitochondrial biogenesis. *Biochem. Soc. Trans.* **29**, 431–436.

Reid, E. (2003). Science in motion: Common molecular pathological themes emerge in the hereditary spastic paraplegias. *J. Med. Genet.* **40**, 81–86.

Biography

Elena Irene Rugarli is a Group Leader at the Telethon Institute of Genetics and Medicine (TIGEM) in Naples, Italy. Her principal research interest is in the field of neuro-degeneration, in particular, the pathogenic mechanisms of hereditary spastic paraplegia. She holds an M.D. from the University of Milan, Italy, and received her postdoctoral training at Baylor College of Medicine in Houston, TX.

Andrea Ballabio is Director of the Telethon Institute of Genetics and Medicine (TIGEM) and Professor of Medical Genetics of the Federico II University in Naples, Italy. He holds an M.D. and is board-certified in Pediatrics. His main scientific interests comprise the identification of the molecular basis and pathogenetic mechanisms of genetic diseases as well as the use of functional genomics in medicine.

Spectrophotometric Assays

Britton Chance
University of Pennsylvania School of Medicine, Philadelphia, Pennsylvania, USA

This brief history describes the impact of technical developments upon the progress of biophysics and biochemistry and focuses upon the contributions of optical spectroscopy. The optical method (now termed spectroscopy) served Otto Warburg well, and in the mid-1930s he developed a unique spectrophotometer. The device was so complicated that it was likely never used. However, it had some nice features; particularly, instead of balancing with slits and neutral density filters, it balanced intensities in the two beams by means of rotating sector discs. Furthermore, it had a high-quality monochromator that allowed Warburg to identify the important absorption bands of NADH (nicotinamide adenine dinucleotide; called DPNH at the time) and furthermore to identify the fluorescence of the reduced state. The optical determination of NADH was one of the great triumphs of analytical biochemistry, as evidenced by the large number of assays through which it was developed, primarily in Germany, where it eventually becomes the basis of the Boehringer company, and providing Olle Lowry, Janet Passoneau, and collaborators with a unique handle on micro-enzymatic assays. This quantitative method far surpassed the visual spectroscopic studies of David Keilin. Indeed, even the keen eyes of Keilin failed to confirm the absorption bands of flavoprotein and NADH as respiratory carriers. Surely flavoprotein was detectable, but because both flavoprotein and NADH were considered "Warburg's territory," it is not surprising that Keilin did not concentrate on flavin.

Manual Spectrometers

The rightfully famous physicist R. W. Wood made a high-quality plastic replica grating and incorporated a pair of them in the Coleman spectrophotometer to make a double-grating instrument that was valid from 400 to 700 nm, had a very good *f* number, and had a resolution independent of wavelength (~20 nm). This was an essential element of the kinetic and spectroscopic study of the enzyme–substrate compounds of catalases and peroxidase, as carried out in the laboratory of Hugo Theorell. While it was an excellent commercial instrument for laboratory work in a visible region, Cary's quartz monochromator, however, together with Beckman's unreferenced exploitation of DuBridge's ingenious electrometer (of the pH meter as well), made the Beckman DU instrument superior. However, if Charles Chaplin were to make a film of the biochemist similar to "City Lights," this instrument would serve the purpose. Dark current adjustment, slit-adjustment, cuvette holder shifting, and balancing to a null by hand were the earmarks of the instrument that most biochemists used from the 1940s to the early 1960s. Not that there were no alternatives. C. C. Yang invented what was called the "Yang machine," a very simple and robust instrument used by many in the Johnson Foundation laboratory, which used a vibrating mirror system to send light through a reference cuvette and a measure cuvette, together with dynode feedback, and gave a logarithmic output. Concurrently, Lenart Åckerman in the laboratory of Bo, Thorell in Stockholm invented the same machine that also provided spectral scans but that was held off the market for about a decade so the DU could have an orderly and prosperous senescence.

Dual-Wavelength Technology

The development of dual-wavelength systems began with Glen Millikan, who ingeniously scribed a barrier in the Weston photovoltaic cell and used green and red filters to measure myoglobin spectral changes in the visible region. However, he connected the output to a mirror galvanometer so that the system was intrinsically quite slow and thus unsuitable for the rapid measurements required for the flow apparatus. The dual-wavelength principle was continued in the Millikan ear oximeter used so effectively during World War II.

Rapid spectrophotometry required phototubes. The significant experience Britton Chance had acquired with them by inventing an automatic steering device while still in his teens led him to use cesium oxide on silver and then antimony as photocathodes. These were combined with the technology of high-gain DC amplification from the electrophysiologists Adrian, Gasser, Erlanger, and the Schmitt brothers, who all had to develop an entire field of electronic amplification for studying nerve action potentials. The three-wavelength system used to measure the kinetics of

enzyme–substrate compound formation in the Soret region, together with the overall formation of leucomalachite green to malachite green, provided measurements of enzyme–substrate compounds that required a mechanical differential analyzer for the transient solution of the Michaelis–Menten/Briggs–Haldane equations for enzyme kinetics (Figure 1). Indeed, the rapid flow apparatus led the field of fast spectrophotometric determinations, not only of the enzyme–substrate compounds of peroxidase but also, in the hands of Quentin Gibson, for measuring hemoglobin kinetics.

The introduction of the chopper-stabilized amplifiers in systems exploited during World War II by the Group 63 of Chance and colleagues (Precision Circuits Group at MIT RadLabs) led to a whole new generation of low-level amplifiers and was the basis for many commercial instruments. Furthermore, the basis for the integrated circuit was afforded by the subminiature triodes developed for the proximity fuse, for which the rejection rate was so high that thousands of these diodes suitable for peacetime applications became available and were made in the first step of integrated circuits, precursors of the integrated chips that were soon to come in the post-war era.

Photochemical Action Spectra

One historic experiment, which now seems almost to have been forgotten, was performed by the Schmitt brothers in order to validate the Warburg hypothesis, namely, to obtain the photochemical action spectrum for the propagation of action potentials in nerves. The results did, in fact, coincide with Warburg's hypothesis and provided the much-needed link between prokaryote and eukaryote. The Schmidt brothers received very

Michaelis-Menten Theory

These reactions are represented by Briggs and Haldane as the bimolecular combination of the enzyme, E, and substrate, S, to form an intermediate compound, ES, followed by a monomolecular decomposition into free enzyme and activated or altered substrate, Q, representative of the products of the "over-all" enzyme action.

$$E + S \underset{k_2}{\overset{k_1}{\rightleftharpoons}} ES \xrightarrow{k_3} E + Q \tag{4}$$

If e is the total molar enzyme concentration, x the molar substrate concentration, p the molar concentration of ES, k_1 the second order rate constant, and k_2 and k_3 the first order rate constants, then

$$\frac{dp}{dt} = k_1 x(e - p) - (k_2 + k_3)p \tag{5}$$

$$\frac{dx}{dt} = -k_1 x(e - p) + k_2 p \tag{6}$$

These two equations represent the rate of formation of the intermediate compound and the rate of disappearance of the substrate.

The solution of these equations has been already obtained by Briggs and Haldane for the special conditions of the steady state, when

$$p = p_{\max.}, \qquad \frac{dp}{dt} = 0, \qquad \text{and} \qquad \frac{p_{\max.}}{e} = \frac{x}{x - Km} \tag{7}$$

where

$$Km = \frac{k_2 + k_3}{k_1} = x\,\frac{(e - p_{\max.})}{p_{\max.}} \tag{8}$$

A further solution valid during the steady state is obtained by adding Equations 5 and 6,

$$\frac{dx}{dt} = -k_3 p_{\max.} \tag{9}$$

where dx/dt is the rate of disappearance of substrate.

FIGURE 1 Michaelis–Menten theory.

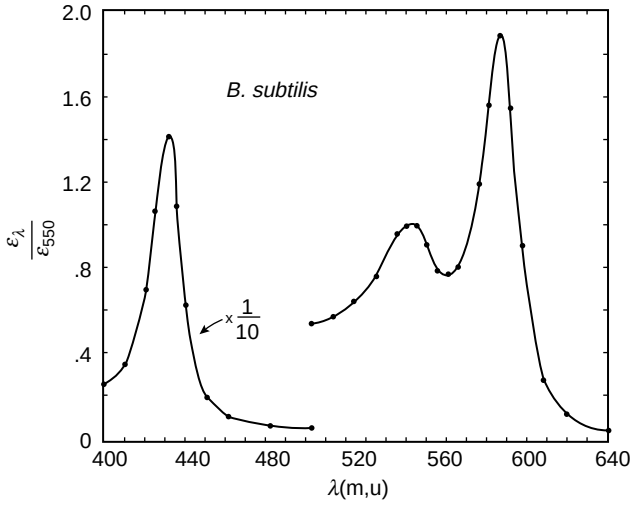

FIGURE 2 Photochemical action spectrum of cytochrome oxidase as obtained by the LeRoy Castor using the oxygen electrode to measure light activated respiration. It is seen that this spectrum is much better defined than Warburg's classic spectrum of yeast where mainly the lines of the mercury arc were employed. Here a continuous monochromated light would be used and the σ bands were clearly delineated as are the Soret bands.

little credit for their work, without which Warburg's and Keilin's work, based on yeast cells only, would have been less acceptable (Figure 2). At the time, there was no reason to believe that the eukaryotic yeast cell was a model for tissue studies. LaRoy Castor quickly improved the action spectral method and also discovered a heme prosthetic group oxidase (cytochrome *o*).

Tissue Spectroscopy

Glen Millikan was a pioneer in shining light through tissue and recording myoglobin deoxygenation in functional activity. During the same time, there were many microspectroscopic studies by Arvanitaki and Chalazonitis, and also, notably, by the laboratory of Casperson with his colleague Bo Thorell. Lundegårth was a pioneer in applying the spectroscopic technique to bundles of plant roots, but was unable to correct for the large changes of scattering due to the osmotic activity of the roots. However, Lou Duysens developed a sensitive single-beam method that he applied with diligence and effectiveness to cytochrome components of green leaves.

A time multiplex dual-wavelength system made possible by simply mounting on top of the "Brown" converter, or vibrating a small mirror at 60 Hz, allowed time sharing of two wavelengths through suspensions of highly scattered material derived from heart muscle or from liver as intact mitochondria. This dual-wavelength machine was the precursor of the time multiplex systems that have been used for exploiting near infrared spectroscopy.

The Scattered Light Problem

It was recognized early on that the scattered light would confound spectrophotometric measurements of pigments of tissue. Yet, in 1949, Chance recognized that the scattered light effect would be greatly diminished if the solid angle of the detector system were large instead of small, as in commercial spectrophotometers (for long cuvettes). Thus, instead of a 10-cm-long sample compartment, as used in most of the Beckman/Cary devices, Chance and colleagues placed a large area detector and an "end-on" photomultiplier almost in contact with the sample, particularly using the time-shared dual-wavelength system, from which very flat baselines were obtained for spectroscopic differences as long as the wavelength difference was not too great. The difference spectrum obtained from guinea pig liver mitochondria is shown in Figure 3 as an example of the data that were obtained with the dual-wavelength spectrophotometer, where the baseline was set at the suspected isosbestic points of 540 and 630 nm. The action spectrum for reduction of the oxidized form of the electron carriers was measured. This spectrum, although validating Keilin's microspectroscopy, clearly showed some anomalies. Cytochrome c_1 was a separate component. A trough due to the disappearance of oxidized flavin and peaks due to appearance of reduced NADH were not identified by Keilin's keen eye, which proved to be the most useful components of the respiratory chain because they were highly fluorescent. But most importantly, they were inhabitants of the mitochondrial matrix space where most of the citric acid cycle reactions were carried out. The instrument was surely very worthwhile. It had not only identified three components of the respiratory chain that had been previously underestimated or remained completely unobserved, but also, for example, the difference spectrum obtained by Lucille Smith and Aristid Lindenmeyer showed the P450 compound of carbon monoxide, an observation confirmed by G.R. Williams and used by P450 enthusiasts today.

Control of Respiration

No other phenomenon was as important to physiologists as the control of respiration. The topic had received very little attention until Lardy and Wellman's historic paper, which showed that isolated prepared mitochondria very nearly completely ceased respiration in the absence of ADP and phosphate but restarted respiration upon addition of ADP and phosphate. This led Chance and

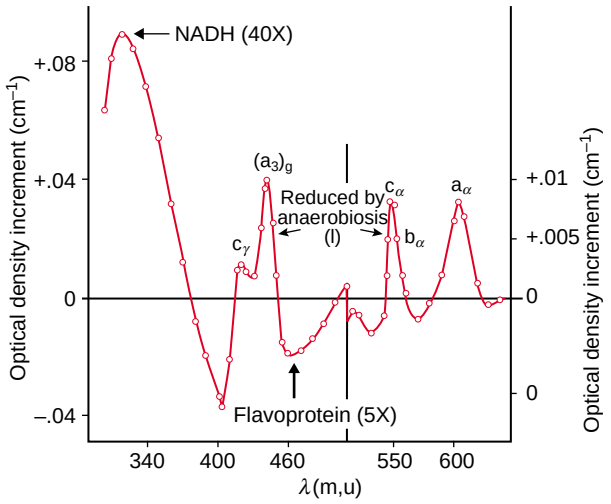

FIGURE 3 The difference spectrum of intact phosphorylating mitochondria. This was the first difference spectrum for oxidized minus reduced guinea pig liver mitochondria obtained with the dual wavelength method employing reference wavelengths of 540 nm for the alpha bands and 450 nm for the Soret band. The incremental absorption with respect to that reference is indicated giving the ratio of the Soret to the alpha bands to be 4 and the NADH peak to be 40 times that of the alpha peaks. The flavoprotein trough, i.e., oxidized flavoproprotein is the absorber, is shown at 460 nm. While the Soret peak of cytochrome oxidase was visible at 444 nm by Keilin's microspectroscope, the flavin trough and the NADH peak (the latter being responsible for the intense autofluorescence of cells) was not available to Keilin in Hartree's heart muscle preparation in which the absorbance of these two components was greatly diminished by the elimination of cytric acid cycle enzymes.

Williams to explore the nature of activation of the electron carrier in the respiratory chain. They found that that all spectroscopically identifiable components changed their steady-state values when ADP was added to the suspension of resting mitochondria. This phenomenon now provides the basis for all of the metabolic activations studied by magnetic resonance imaging (MRI) as the bulb effect, and for using the saturation of oxyhemoglobin *in vivo* as a measure of metabolic activity.

At the same time, Lehninger, Chance, and others studied the uptake of calcium into the mitochondrial matrix, and Chance and Williams found that calcium activated the suspensions of mitochondria to the same extent and with the same speed as did ADP suggesting, as recently discussed by Carafoli, the presence of a calcium carrier in the mitochondrial membrane.

Low-Temperature Technology

Perhaps the most secure instrumental data were those obtained at low temperature in liquid nitrogen, where the spectra were more intense. The delineation of the absorption bands, particularly in the bc_1 region, turned out to be essential in showing the two kinds of cytochromes *b*.

Lubbers' Rapid Scan

Tissue absorption and scattering occupied the minds of a number of workers, particularly those of Lubber and Thews, who not only did much theoretical work on scattering but also perfected a galvanometer-driven wavelength scanning device, whose speed far exceeded that of anything else available at the time and which has only been perfected recently by the work of Desr and his colleagues.

Photoactivation Studies

Perhaps the greatest advantage of the technique for observing tissue properties was the fact that it was possible to photoactivate the system under spectroscopic examination and observe the photoinduced absorption spectrum, a specialty of the Laboratory of Lou Duysems. This, of course, required a measure of common mode rejection, at which the dual-wavelength system excelled because the light flashes shared a single detector with an AC coupling, allowing the system to reject leakage of not only the photolysis light but also other disturbances that affected the common mode. Furthermore, illumination at subzero temperatures of the solid phase allowed the study of many photoactivated systems containing derivatives of chlorophyll or those rendered photoactivatable by combining with a ligand such as carbon monoxide. Thus, optical measurements in the region of the Soret band and illumination in the region of the alpha band allowed a measure of protection of the dual-wavelength detector system from very strong photolysis light, for example, that provided by intense sources such as the carbon arc. These studies bridged the gap between Otto Warburg's unbridgeable action spectrum experiment on yeast and Keilin and Hartree's microspectroscopical observations of cytochrome oxidase in yeast and in a pigeon heart muscle preparation.

Not only the cytochrome oxidase–CO complex CO, but also the splitting and recombination of myoglobin CO compounds were studied in detail, with optical spectroscopy as well as structural methods such as EXAFS (X-ray absorption spectroscopy), with results that make headlines even today for the subject of ligand docking concomitant with structural changes, confirming the X-ray structural studies in which the E7 histidine was altered by a ligation of myoglobin with CO.

The Ruby Laser and Electron Tunneling

Lacking powerful light sources of short duration, Chance and colleagues relied mainly upon xenon flash

lamps, particularly those of Edgerton and colleagues. However, construction of the first ruby laser used in biological studies by Bunkenberg and DeVault opened up a whole new time domain, not only because of the monochromaticity of the laser (which greatly simplified the filter leakages) but also because of the duration of the light pulse (in the microsecond region), which for the time was extraordinarily short. From this study came the totally unexpected observation that the photochemical oxidation of cytochrome *c* by photoactivated chlorophyll of *Chromatium* was temperature independent, not only from room temperature to liquid nitrogen temperature, but eventually at liquid helium temperatures, extending the time range of the spectroscopic method to one of the primary or near primary results and/or reactions of photosynthesis (Figure 4), and also introducing the concept of electron tunneling in biochemical reactions, a concept pursued by Les Dutton and Harry Gray.

The history of spectroscopy is checkered with unexpected results and meaningful interpretations on the nature of electron transfer reactions. In fact, the study of reactions obtained from photolysis activation of CO compounds in the presence of O_2 caused ligand exchange to occur, especially in the case of CO. Together with Carlo Saronio, Chance discovered a number of intermediate steps involving higher oxidation states of iron mirroring those obtained with peroxidase and H_2O_2, but much faster and more complex. This was because copper oxidation was involved in the active site of CO, enabling donation of four electrons sequentially for the reduction of oxygen to water without significant amounts of free radical intermediates. This contrasted with the photoactivation of porphyrins in the absence of electron donors, resulting in the creation of singlet oxygen, a process used extensively in photodynamic therapies.

Fluorochromes of Tissues

Spectroscopy of biological fluorochromes, such as NADH and flavoprotein compounds that exhibit strong fluorescence in mitochondria, led Chance and co-workers to study them extensively *in vivo* by a simple method in which excitation was obtained by the very strong 366 and 436 lines of the mercury arc. This yielded emission spectra characteristic of the chromophores in a variety of functional states, characterizing electron transfer through the citric acid cycle as reductant and the cytochrome chain as oxidants, giving essential features of the redox state of the mitochondrial matrix. Interpretations of the importance of metabolic control and thermodynamic principles of the system were derived from these, particularly by R. L. Veech.

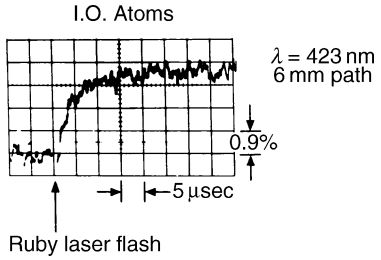

FIGURE 4 Typical recording of the oxidation of cytochrome c of photosynthetic bacteria at low temperatures as activated by a light flash of the ruby laser. Remarkably this reaction rate was affected very little by the transition from room temperature to liquid nitrogen temperature due to electron tunneling.

Hemoglobin and Cytochrome

It is perhaps ironic that the cell biologists and etymologists of the Molteno Institute focused on the cytochromes of hemoglobin-free cells and tissues and that the "real" physiology of oxygen delivery to tissues by hemoglobin and its utilization by CO had to wait for more sophisticated methods. Even now, the observation of cytochrome oxidase absorption bands in the presence of physiological concentrations of oxy and deoxy-hemoglobin is fraught with controversy, to the point that no reliable spectroscopic distinction of the copper component of cytochrome oxidase and the overlapping spectra of oxy-hemoglobin has been obtained. In fact, nearly all studies find that the so-called cytochrome oxidase Cu changes track those of HbO_2 due to the similarity of their spectroscopic absorption bands in the near infrared (NIR) region, and the great predominance of hemoglobin absorption over that of cytochrome oxidase.

NADH as an Oximeter

It has been shown that the fluorescence of NADH and flavoprotein, when used in a ratiometric manner, can exhibit a reasonable immunity to changes of hemoglobin concentration, and has afforded standards for the independent changes of hemoglobin and NADH in transient hypoxia and re-oxidation. Such independence of the measures of cytochrome and hemoglobin has never been clearly demonstrated for the copper component of cytochrome oxidase, due to the overlapping spectra of oxyhemoglobin.

An alternate approach was based upon the fluorescence of the newly discovered NADH and flavoprotein components of the mitochondrial respiratory chain, particularly by using the ratio of these two fluorochromes. Fortunately, NADH fluoresced in the reduced state while flavoprotein fluoresced in the oxidized state, so their ratio was a measure of the redox state of mitochondria, a signal that was found to be only marginally affected by changes in the oxygenation of hemoglobin in model systems. Using this criterion on the

very strong signal of NADH only, it was possible to show that the fluorescence of NADH was unchanged until the oxy/deoxy transition of hemoglobin was almost complete in a system in which functional activity was measured by the photoaction potential of an animal model, removing any doubt about the higher oxygen affinity of cytochrome *in vivo* as compared to hemoglobin (~20 Torr). This was a very important milestone for physiologists, who know that the deoxygenation of hemoglobin is very high and the critical pO_2 of mitochondrial function is compromised. Thus, the calibration of tissue oximeters in the region of intravenous saturation of hemoglobin (i.e., 20–30%) must be precisely measured to indicate critical tissue hypoxia *in vivo*. This indeed was subsequently validated by measurements of tissue energetics through phosphorus nuclear magnetic resonance (^{31}P NMR), particularly by measurements of the phosphocreatine:phosphate ratio.

NIR Spectroscopy

Jobsis used Kramer's technique to measure in the infrared, and developed a technology for the measurement of absorption of the copper component of cytochrome oxidase in the region of 830 nm based upon studies of the cat model and the heads of neonates, which he termed "transcranial spectroscopy." He further developed algorithms based upon fluorocarbon-perfused cat brain to give optical pathlengths that were believed to be transferable to the neonate brain and allow a deconvolution of blood volume and saturation changes from those of cytochrome oxidase signals using the full-length light algorithm. Delpy and co-workers avidly followed the lead of Jobsis and developed a close correlation between the decreased concentration of oxyhemoglobin and the so-called copper signal in a number of models, suggesting that the mitochondria in tissues contained a low-affinity cytochrome oxidase and responded to pO_2 (in a slice) in a way similar to that of hemoglobin. However, isolation of rat brain mitochondria failed to support this contention. Furthermore, the freeze-trapped hypoxic brain failed to show the absorption band of reduced cytochrome *c* in mild hypoxic stress that caused deoxygenated hemoglobin. In fact, the absorption band of reduced cytochrome *c* was not observed until the band of oxyhemoglobin was no longer detectable, according to the work of Bashford.

While attempts were made to detect the copper absorption band of hemoglobin in the NIR region, animal studies showed that the fluorescence of NADH and the flavoprotein could be used to detect anoxia in the presence of hemoglobin, particularly when the ratio of the fluorescent oxidized flavoprotein and the fluorescent reduced NADH were employed; this value was relatively insensitive to the hemoglobin concentration. In fact, further demonstrations showed that the fluorescence of NADH was unaffected by the deoxygenation of hemoglobin in animal model brain. The NADH fluorescence increased in hypoxia only when the hemoglobin was already almost completely deoxygenated. This observation suggests that measurements of the critical pO_2 in hypoxia require accurate measurement of extreme values of hemoglobin desaturation, at the critical pO_2 for mitochondrial function.

NIR Spectroscopy of Brain and the BOLD Effect Measured by MRI

Much interest in the NIR method is based upon Ogawa's finding that changes in deoxyhemoglobin concentration (changes of the paramagnetic species of deoxyhemoglobin) enhanced water relaxation in the brain. This opened up the field of study of the activation phenomenon in the human brain, in which changes in deoxyhemoglobin levels are measured by NMR and by NIR tissue spectroscopy. The MRI changes are precisely imaged, while the NIR images, although crude, are measures of the rapidity of the changes. But in addition to incremental changes of deoxyhemoglobin, NIR could measure the saturation value of hemoglobin, which, for reasons involving Beer's law, originates mainly from the arteriolar/capillary/venolar bed. This feature, namely, the value of local oxygen extraction due to incremental changes of mitochondrial functional activity (i.e., localized activation), is not measured by MRI. The two techniques are now widely accepted as indicative of localized brain activation and have afforded the basis for in-depth studies of visual and sensory motor function. But, most importantly, NIR gives an excellent rendition of prefrontal cortex (PFC) signals without the difficulty of the large water content of the ocular system encountered with NMR (Figure 5). The use of activation images is appropriate to the NIR system, where baseline values may be somewhat variable and difficult to calibrate. The incremental changes of blood volume measured as changes of total hemoglobin, together with the aforementioned oxygen extraction measure, i.e., desaturation of hemoglobin, can be directly related to local metabolic activity, opening up a new field of NIR study of the semi-quantitative nature of the hemoglobin signals.

NIR Imaging

While the above-mentioned studies used dual-wavelength technology stemming from that of Glenn Millikan, a completely new concept was introduced by the discovery that photon migration through tissues can

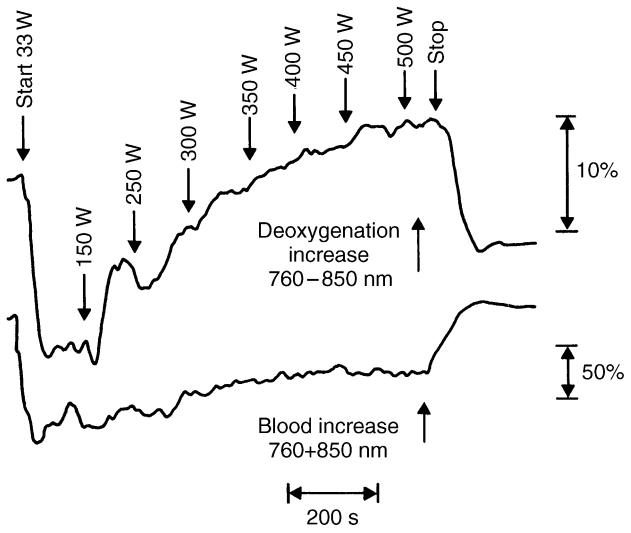

FIGURE 5 Evidence of activation of metabolism measured in the NIR (near infrared) by the dual wavelength method of 760–850 nm (equibestic wavelengths) which show progressive deoxygenation of the quadriceps muscle of a trained athlete during bicycle exercise up to the remarkable level 500 watts, at which nearly complete deoxygenation of hemoglobin can occur. As measured separately by the sum of signals at these two wavelengths. With appropriate coefficient, the increase of blood flow in the muscle also occurs giving a larger absorbance signal. At this level of exercise, it is probable that myoglobin is not deoxygenated as indicated by separate experiments with animal models.

be modeled by the diffusion equation. Multiple sources and detectors give very reasonable two- and three-dimensional imaging, and the propagation of light through tissue can be quantified by pulse time and phase and amplitude measurements, much as has been the case with measurement of fluorescence.

Photon Migration in Tissues

The discovery that photons migrating through tissue followed the diffusion equation and that the tracks could be simulated by Monte Carlo methods, together with the adaptation of time-correlated single photon counting (TCSCP) to the task of measuring propagation times in tissues, opened up an entire field of NIR spectroscopy and imaging. This grew to be a field of medical science in a manner similar to NMR, but differing in the fact that the necessary equipment is not nearly as expensive, so the proliferation of the technique in research laboratories could be much more rapid. Because the profit margins did not match those of NMR, commercial production of NIR imagers has been restricted to two or three companies.

Tissue Optical Properties

Three techniques are outstanding in the measurement of tissue optical properties. The first, and still the foremost, is the pulse time method, in which photon delay is caused by scattering and photon attenuation is caused by absorbers such as hemoglobin, water, and lipid. Because TRS (time-resolved spectroscopy) immediately deconvolutes scattering and absorption by time domain analysis, it is a preferred method. Similarly variable frequency modulated light will unravel by Fourier transformation exactly the same quantities as those obtained by TRS. However, the difficulty of stabilizing the phase shifts of electronic systems of variable frequency, together with the limitations of detection response to high-frequency radio waves, has limited this system to approximately 400 MHz. Nevertheless, many instruments have been made in the frequency range of 50 to 200 MHz that are used for quantifying absorption and scattering in multi-wavelength systems and that are capable of measuring hemoglobin saturation with significant precision. Such systems have adopted some cell phone components and are therefore compact and cheap. The most reliable and most used system modulates the light at very low frequencies in either, or time shares the light sources in a multiplex system, and appears to be the preferred system for many applications. The deconvolution of scattering and absorption can be obtained if sufficient data are taken at various source detector separations and optical wavelengths to include the scattering variations.

Cancer Detection

In cancer detection, scanning the breast for example, an activation signal based upon angiogenesis and hypermetabolism is given, causing more blood volume and more deoxygenated hemoglobin to be present. While this criterion may not be applicable to all cancers, it has given remarkably good scores in one breast cancer study.

Muscle Studies

A series of studies has been based upon activation measurements in which (e.g., in both muscle and brain), functional activation causes hemodynamic changes due to mobilization of blood flow and saturation changes due to varying metabolic activity (Figure 5). This has been used in muscle not only to evaluate exercise capability but also to quantify disability due to occlusive disease in the limbs.

Brain Functional Activation

In brain studies, whereas NMR and the optical method both measure hemodynamic activation due to functional activity, the NIR method is unique in that it measures changes of hemoglobin saturation caused by varying degrees of oxygen extraction from the capillary blood vessels of the brain. Thus, the convenience and economy of the optical method lends itself to studies of minimally

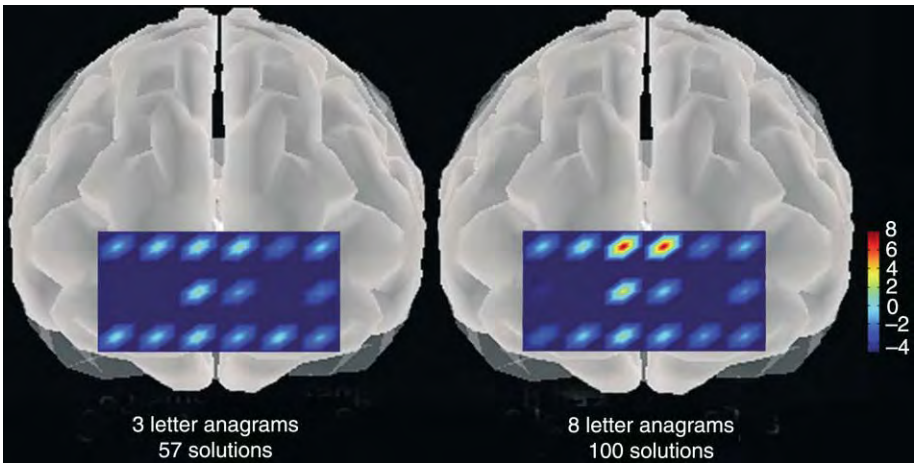

FIGURE 6 Illustrating the use of the NIR CW (continuous wave) dual wavelength system in localizing the particular voxels in the human forebrain at which brain functional activity is indicated to be increased by the oxygenation changes with respect to the baseline level of 3 letter anagrams. Each colored symbol represents the average of over 100 tests of a particular individual giving an average value of 8 μM oxygenation under this condition of maximal stress. The region observed is the Broadman's 9 and 10 or ear to ear and hairline to eyebrow region of the projection of the prefrontal cortex. This separation was 4 cm in order to ensure signaling from the prefrontal cortex to accentuate the absorbance changes due to the prefrontal cortex and minimize those which might be associated with tissue layers at smaller depths.

perturbed human subjects, be they adults or neonates (Figure 6).

Brain Studies: The Neuronal Signal

The early studies of David Hill, Tasaki, and Richard Keynes on transparency changes of axons upon stimulation suggest that a functional optical signal could be obtained in animal and human brain. While the studies of Salzberg did indeed verify the scattering changes in isolated preparations, studies using NIR to seek similar changes in the human brain suggest that only very small and somewhat irreproducible signals can be obtained. For example, the early experiments of Gabriele Gratton have not been duplicated either by himself or by others working in the field (Villringer and Franceschini, and Wolf), in part due to instrumental difficulties, and in part due to the very small size of the signal. The rise time of the signals appears to be in the range of 100 ms and the amplitude as small as one part in 10^4 or even smaller. However, the relatively robust signals obtained from the hemodynamic and metabolic activations discussed previously show the feasibility of measurements of functional activity in the human brain, particularly in the prefrontal region, and open up a reliable and economical method for human brain studies that predict a vibrant future of the optical methods in human studies.

Summary

The story of the development of optics in biochemistry and biophysics does not end here. In fact, some might say this is just the beginning of the transferability of optical tomography and optical biopsy to small animals on the one hand and human beings on the other. Perhaps spurred by the interest in online methods for evaluating the growth and recession of cancers under the influence of appropriate drugs in small animals, transferability of these principles to human subjects is becoming important. The optical method is taking its place along with MRI, PET, ultrasound, CT, and X-ray mammography as methods for studying pathologies in the human body.

See Also the Following Articles

Cytochrome bc_1 Complex (Respiratory Chain Complex III) • Cytochrome *c*

Glossary

Brown converter An electrical chopper developed by the Leeds and Northrup Company that had very little contact potential variation.

cytochrome oxidase The terminal enzyme of most oxygen-using systems.

dual-wavelength spectrophotometer A spectrophotometer with time shared to adjacent wavelengths in order to minimize the effect of scattering changes upon absorbance changes, because scattering varies very slowly with wavelength, while cytochrome absorption varies sensitivity with wavelength.

DuBridge electrometer (DU) A remarkable use of the suppressor grid of the pentode to control electron flow with very high input impedance, affording the basis of the Beckman pH meter and spectrophotometer.

electron tunneling The transfer of electrons between two proteins at a distance without collision of their active sites.

EXAFS X-ray absorption spectroscopy used to obtain high resolution structures of Fe and Cu enzymes.

flavoprotein A widely spread pigment, but in this article the prosthetic group of ketoglutarate and pyruvate dehydrogenase.

mercury arc A very useful light source for biological studies, which gives light at exactly the correct wavelength for hemoglobin and in some cases cytochrome studies.

Molteno Institute A famous institute directed by David Keilin through the 30s, 40s and 50s. It became a Mecca for those working with cell respiration.

near infrared (NIR) imaging The use of the wavelengths in the red region just at the verge of invisibility between 700 and 900 nm to better penetrate tissue.

photochemical action spectrum The effect of light upon a biological system often used to activate a carbon monoxide inhibited cytochrome.

photomultiplier A highly sensitive light detector used in many spectrophotometers.

photon migration The phenomenon of photon diffusion through tissues used in great detail recently to image subsurface objects.

ruby laser One of the early forms of the laser, emitting in the red region.

scattered light Light that does not proceed directly through tissue.

spectrophotometer A device that measures the absorbance of materials as a function of wavelength or, in some cases, energy.

time resolve spectroscopy (TRS) Spectroscopy using sharp pulses of light to distinguish the scattering from the absorption of tissues.

X-ray absorption spectroscopy (EXAFS) Spectroscopy used to obtain high-resolution structures of Fe and Cu enzyme.

Further Reading

Carafoli, E. (2003). Historical review: Mitochrondria and calcium: Ups and downs of an unusual relationship. *Trends Biochem. Sci.* **28**, 175–181.

Chance, B. (ed.) (1989). *Photon Migration in Tissues*. Plenum Press, New York, NY.

Chance, B. (1991). The optical method. *Ann. Rev. Biophys. Biophys. Chem.* **20**, 1–18.

Keilin, D. (1966). *The History of Cell Respiration and Cytochrome*. Cambridge University Press, Cambridge, UK.

Slater, E. (ed.) (1966). *Flavins and Flavoproteins*. Elsevier, Amsterdam.

Biography

Britton Chance is Eldridge Reeves Johnson University Professor Emeritus of Biochemistry and Biophysics and Physical Chemistry and Radiologic Physics at the University of Pennsylvania School of Medicine. His current research interests focus on optical spectroscopic methods for the study of brain cognition, breast cancer detection, and physiological function. He has received numerous honors and awards and honorary Ph.D. and M.D. and is noted for his contributions in basic science research and technological development.

Sphingolipid Biosynthesis

Martina Leipelt and Alfred H. Merrill, Jr.
Georgia Institute of Technology, Atlanta, Georgia, USA

Sphingolipids are a complex family of compounds that perform diverse structural and regulatory functions for eukaryotes and some prokaryotes and viruses. They share a common structural feature, a sphingoid base backbone that is synthesized *de novo* from serine and a fatty acyl-coenzyme A, then converted into ceramides, phosphosphingolipids, glycosphingolipids, and other species, including protein adducts. Several diseases result from disruption of *de novo* sphingolipid biosynthesis by environmental factors or hereditary defects, but modulation of sphingolipid biosynthesis is also being explored as a means to control other diseases, including sphingolipid storage diseases and cancer.

Structures and Nomenclature

Sphingolipids can be divided into several major categories: the sphingoid bases and their simple derivatives, ceramides, and more complex sphingolipids (Figure 1). The International Union of Pure and Applied Chemists (IUPAC) has recommended a systematic nomenclature for sphingolipids. The root name "sphingosin," in reference to the sphinx, was given by J. L. W. Thudichum in 1884 "in commemoration of the many enigmas which it presented to the inquirer."

Sphingoid Bases

The structure of sphingosine, the major sphingoid base of mammals, is (2S, 3R, 4E)-2-aminooctadec-4-ene-1, 3-diol (it is also called D-*erythro*-sphingosine and E-sphing-4-enine) (Figure 1). This is only one of many sphingoid bases found in nature, which vary in alkyl chain length and branching, the number and positions of double bonds, the presence of additional hydroxyl groups, and other features. The structural variation has functional significance; for example, sphingoid bases in skin have additional hydroxyls at position 4 and/or 6 that can interact with neighboring molecules, thereby strengthening the permeability barrier of skin.

Sphingoid bases function as intra- and extracellular signals and second messengers in the form of free sphingoid bases, sphingoid base 1-phosphates (Figure 1), and possibly other species. Nonetheless, sphingoid bases are present in cells primarily as the backbones of more complex sphingolipids.

Ceramides

Ceramides are fatty acid derivatives of sphingoid bases (Figure 1). The fatty acids are typically saturated or mono-unsaturated with chain lengths from 14 to 26 carbon atoms (or even longer in the special case of skin), and sometimes have a hydroxyl group on the α- or ω-carbon atom. These structural features favor the segregation of ceramides and some complex sphingolipids into specialized regions of the membrane (called "rafts" and "caveolae") that participate in cell signaling, nutrient transport, and other functions.

Ceramides also serve as second messengers that regulate cell growth, senescence, and programmed cell death (apoptosis). Their biologic activity depends on the type of sphingoid base and fatty acid; for example, dihydroceramides (i.e., without the 4,5-double bond of the sphingosine backbone) (Figure 1) are less potent than ceramides as inducers of apoptosis, whereas phytoceramides (i.e., with 4-hydroxysphinganine or "phytosphingosine" as the backbone) are more potent.

More Complex Phospho- and Glyco-Sphingolipids

The major phosphosphingolipids of mammals are sphingomyelins (ceramide phosphocholines) (Figure 1), whereas insects contain mainly ceramide phosphoethanolamines and fungi have phytoceramidephosphoinositols and inositol phosphates. Some aquatic organisms also contain sphingolipids in which the phosphate has been replaced by a phosphono- or arsenate group.

Glycosphingolipids are classified on the basis of carbohydrate composition: (1) neutral glycosphingolipids contain one or more uncharged sugars such as glucose (abbreviated Glc, hence, glucosylceramide is GlcCer), galactose (Gal), N-acetylglucosamine (GlcNAc), N-acetylgalactosamine (GalNAc), and fucose (Fuc); and (2) acidic glycosphingolipids contain ionized functional groups (phosphate or sulfate) attached to neutral sugars, or charged sugar residues such as sialic acid (N-acetylneuraminic acid). The latter are called gangliosides, and the number of sialic acid residues is usually denoted with a subscript letter (i.e., mono-, di- or tri-) plus a number reflecting the subspecies within that

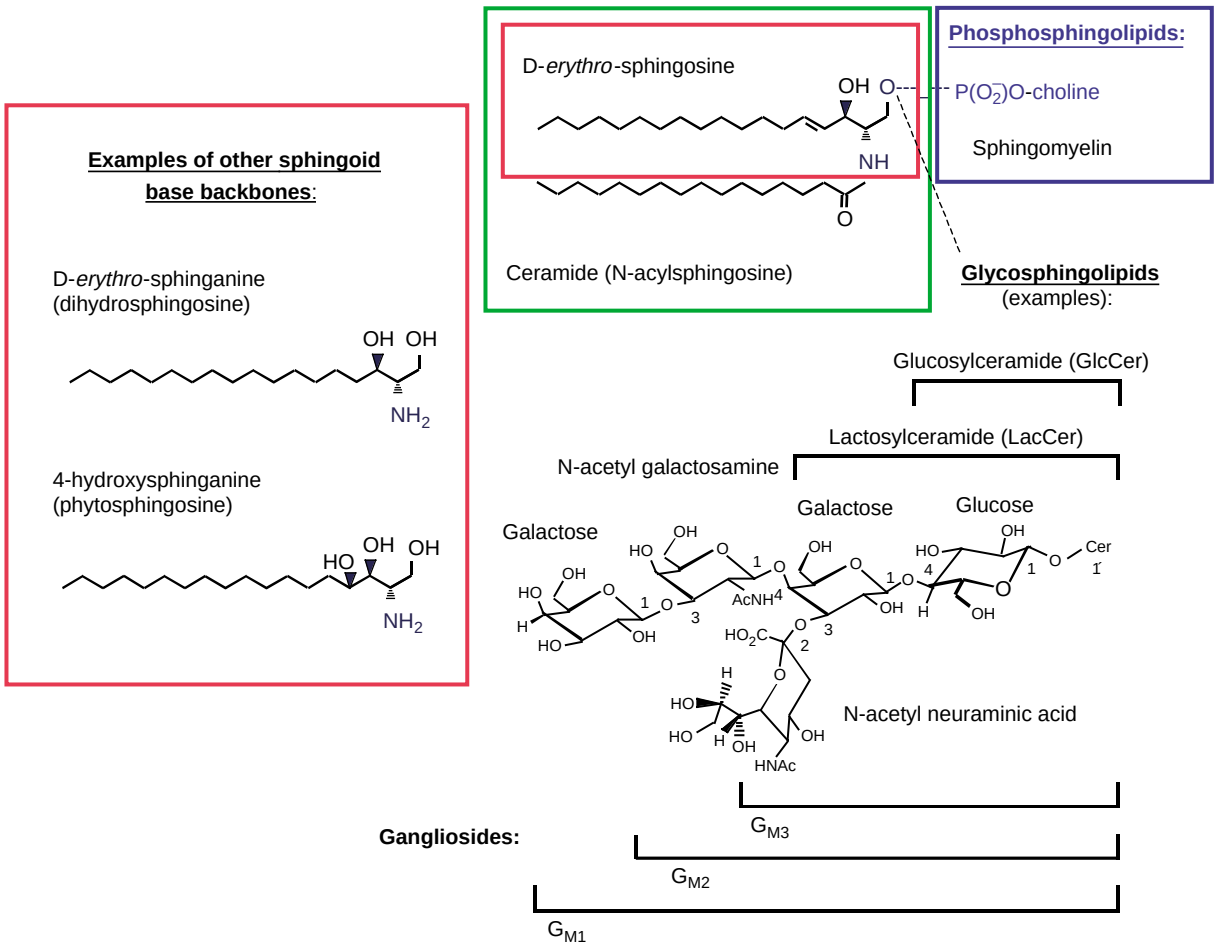

FIGURE 1 Structures of representative sphingolipids. Shown are several examples of sphingoid bases (sphingosine, sphinganine and 4-hydroxysphinganine, boxed in red), ceramide (in green), sphingomyelin (blue), and neutral (GlcCer and LacCer) and acidic (gangliosides G_{M1}, G_{M2}, and G_{M3}) glycosphingolipids.

category (see examples in Figure 1). For a few glycosphingolipids, historically assigned names as antigens and blood group structures are still in common usage (e.g., Lexis x and sialyl Lewis x).

Protein Adducts

Some sphingolipids are covalently attached to protein, e.g., *ω*-hydroxy-ceramides and -GlcCers are attached to surface proteins of skin and inositolphosphoceramides are used as membrane anchors for some fungal proteins, in a manner somewhat analogous to the glycosylphosphatidylinositol (GPI) anchors that are attached to proteins in other eukaryotes.

De novo Synthesis of the Ceramide Backbone

Sphingolipid biosynthesis is widespread among eukaryotic cells, and it appears that new synthesis (i.e., *de novo*) is relied upon more than reutilization of sphingolipids from exogenous sources, such as food. The biosynthetic pathway for such a diverse family of compounds (conservatively estimated to be in the tens of thousands) is obviously complex; however, its fundamental features can be summarized in Figures 2 and 3.

Serine Palmitoyltransferase

Serine palmitoyltransferase (SPT) catalyzes the initial step of the pathway which, for many organisms, is the condensation of serine and palmitoyl-CoA to form 3-ketosphinganine (Figure 2). However, for organisms that produce sphingoid bases with other alkyl chain lengths (such as the C14 species of insects), the first enzyme of the pathway utilizes a different cosubstrate (dodecanoyl-CoA, in this example) and could be renamed "serine dodecanoyltransferase."

SPT is a pyridoxal 5′ phosphate-dependent enzyme comprised of two gene products (termed SPTLC1 and SPTLC2 for humans, and LCB1 and LCB2 for yeast); a third has also been identified in yeast, but does not appear to have a homologue in mammals. In most organisms, SPT is associated mainly with the

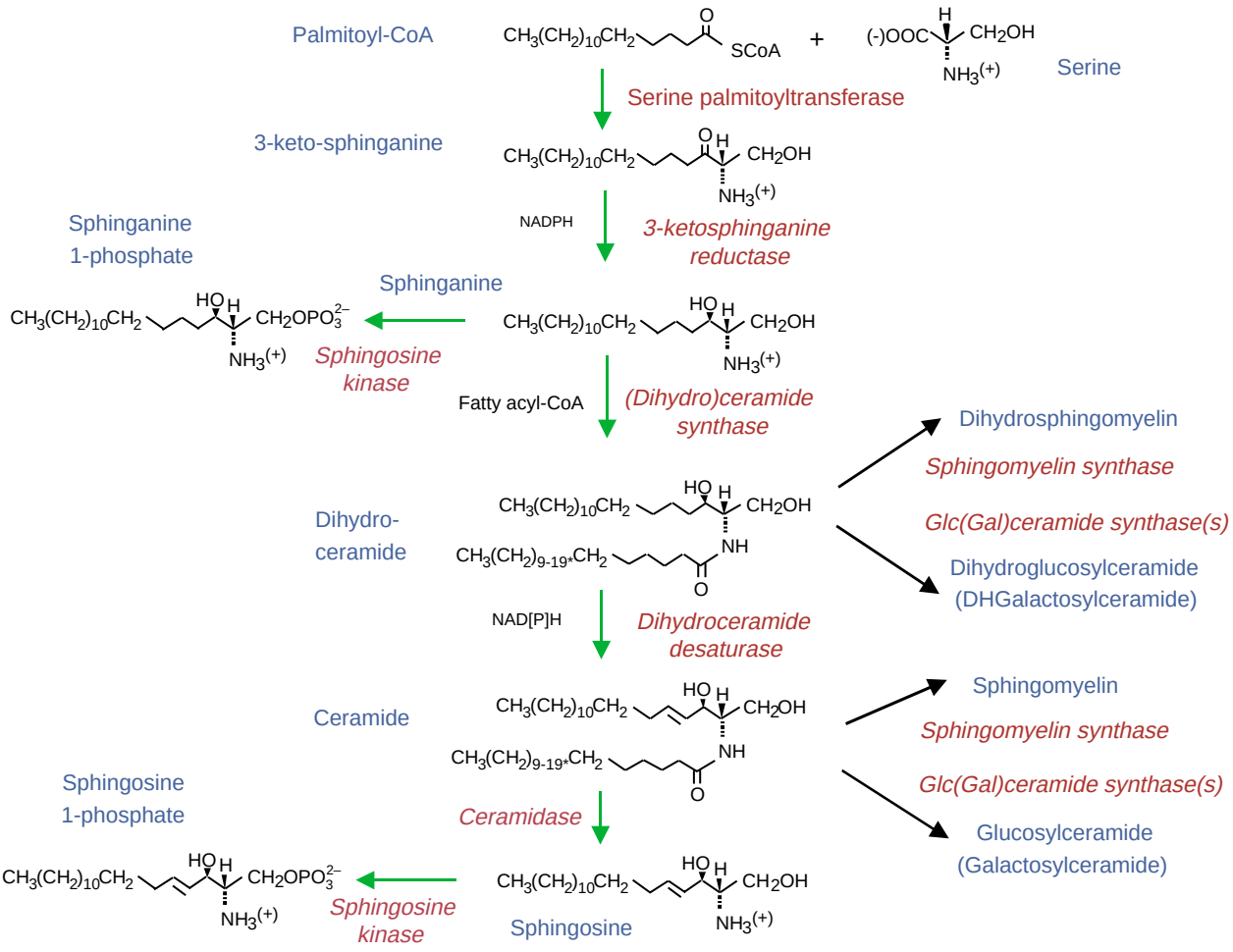

FIGURE 2 The *de novo* biosynthetic pathway for sphingoid bases, ceramide, (dihydro)sphingomyelins and (dihydro)glucosylceramides. The color coding distinguishes the enzyme names (in red) and the metabolites (in blue).

endoplasmic reticulum, as are the other enzymes of ceramide biosynthesis. SPT activity is affected by a wide range of factors: sphingosine 1-phosphate, endotoxin and cytokines, heat shock, UVB irradiation, cytotoxic drugs (including many cancer chemotherapeutic drugs), retinoic acid, and a number of small molecule inhibitors produced by microorganisms (one of which, ISP1 or myriocin, is often used to block *de novo* sphingolipid synthesis by cells in culture). The mechanisms of SPT regulation are not fully understood, but include (for example) both acute modulation by heat shock and increased expression of SPT mRNA by cytokines. Mutations in human SPTLC1 cause hereditary sensory neuropathy type I (HSN1), which is the most common hereditary disorder of peripheral sensory neurons.

Ceramide Synthase

3-Ketosphinganine is rapidly converted to sphinganine by an NADPH-dependent reductase, then ceramide syntase(s) acylate sphinganine to dihydroceramides using fatty acyl-CoA's varying in length from C16 to C30 (and usually saturated or mono-unsaturated) (Figure 2). Ceramide synthase is actually a family of enzymes, each of which appears to arise from a different gene and to utilize a particular subset of fatty acyl-CoA's (e.g., TRH4 utilizes palmitoyl-CoA whereas UOG1 uses stearoyl-CoA).

Ceramide synthase is activated by a number of stimuli, including cancer chemotherapeutic drugs and irradiation, and the increased production of ceramide is thought to mediate the toxicity of these treatments. Ceramide synthase is also the target of a number of mycotoxins (fumonisins), which are produced by fungi that grow on corn and, when consumed, result in spectrum of diseases that are important to agriculture (equine leukoencephalomalacia and porcine pulmonary edema) as well as human cancer and possibly birthdefects.

Dihydroceramide Desaturase

Insertion of double bond(s) into the sphingoid base backbones occurs mainly after formation of dihydroceramide(s) (Figure 2). For mammals, introduction of the

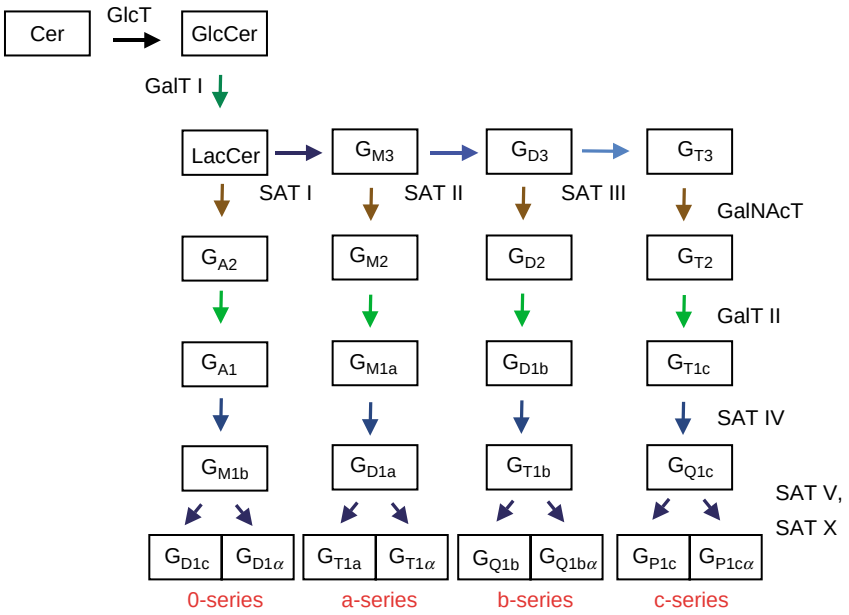

FIGURE 3 A representation of the combinatorial nature of glycosphingolipid biosynthesis. Shown are the reactions leading to the major ganglioside series and the enzymes involved. The abbreviations refer to ceramide (Cer), glucosylceramide (GlcCer), lactosylceramide (LacCer) and the different categories of gangliosides designated by "G" and subscripts for the number of sialic acids (M,D,T and Q representing 1,2,3 and 4, respectively) and other structural features. Abbreviations: GalNAcT, N-acetylgalactosaminetransferase; GalT, galactosyltransferase; GlcT, glucosyltransferase; and, SAT (sialyltransferase) with the Roman numerals reflecting the subtypes. (Modified from Kolter, T., Proia, R. L., and Sandhoff, K. (2002). Combinatorial ganglioside biosynthesis. *J. Biol. Chem.* **277**, 25859–25862.)

4,5-double bond is catalyzed by two pyridine nucleotide-dependent desaturases (DES1 and DES2), one of which may also be responsible for addition of the 4-hydroxyl-group of phytoceramides.

Synthesis of More Complex Sphingolipids

Ceramides in their various forms (i.e., ceramides, dihydroceramides, phytoceramides, etc.) are at a key branch point of complex sphingolipid biosynthesis where these intermediates are partitioned into either phosphosphingolipids or glycosphingolipids. For cells that produce more than one category of glycolipid (for example, mammalian epithelial cells, which have both GlcCer and GalCer), the glycolipid arm can have multiple branches. The fate of a given intermediate is governed by the relative activities and selectivity of the enzymes at this branch point as well as by the subcellular localization of the participants.

Sphingomyelin and Other Phosphosphingolipids

Sphingomyelins are synthesized by transfer of phosphorylcholine from phosphatidylcholine to ceramides (Figure 2). This reversible reaction links glycerolipid and sphingolipid metabolism and signaling, because ceramides and diacylglycerols both function as metabolic intermediates and as intracellular second messengers. This may explain why cells produce dihydroceramides as the initial products of *de novo* sphingolipid biosynthesis since that allows a relatively innocuous intermediate to accumulate if later steps in the pathway slow.

Relatively little is known about the biochemistry of sphingomyelin synthase, including whether the activities in the Golgi apparatus and plasma membranes represent a single enzyme, or several different enzymes (two mammalian sphingomyelin synthase genes have been identified, *SMS1* and *SMS2*). The regulation of sphingomyelin biosynthesis is also intriguing – with changes in development, neoplasia, and other normal and abnormal cell states.

Ceramide phosphorylethanolamines are synthesized from phosphatidylethanolamine and ceramides in a reaction analogous to sphingomyelin synthase (i.e., transesterification with phosphatidylethanolamine), and once formed can be methylated to sphingomyelins in some species. Inositolphosphoceramides are also formed by transesterification (from phosphatidylinositols).

Glycosphingolipids

A pathway that is responsible for the biosynthesis of hundreds (to thousands) of different glycosphingolipids is obviously complex, but these compounds are nonetheless produced using surprisingly few

glycosyltransferases. Efficiency is achieved by a "combinatorial" biosynthetic pathway that directs precursors and intermediates toward the desired products by modulating the activities of key combinations of enzymes (see Figure 3 for an illustration).

The addition of the carbohydrate headgroups is catalyzed by glycosyltransferases that transfer a specific sugar from the appropriate sugar nucleotide (e.g., UDP-Glc, UDP-Gal, etc.) to ceramide or the nonreducing end of the growing carbohydrate chain attached to ceramide. GlcCer and GalCer are synthesized by UDP-Glc(or Gal):ceramide glucosyltransferases, hence, a major determinate of the types of glycosphingolipids made by a given cell type will be whether it expresses one or both of these genes. Factors that regulate these enzymes include cell type, the nature of the ceramide substrate (ceramides with α-hydroxy fatty acids are mainly utilized for GalCer synthesis), and exposure of the cells to agonists such as endotoxin and acute phase response mediators. A number of inhibitors of these glycosyltransferases are being tested for efficacy in sphingolipid storage diseases (caused by inherited defects in glycosphingolipid hydrolyases), based on the rationale that slowing biosynthesis may counterbalance these defects.

Additional glycosyltransferases are responsible for subsequent addition of sugars to make dihexosylceramides, trihexosylceramides, etc. as well as for addition of neutral sugars to gangliosides (Figure 3). Likewise, gangliosides are synthesized by the stepwise transfer of neutral sugars and sialic acids. In general, the enzymes responsible for these reactions are located in the lumen of the Golgi apparatus, and the region corresponds to the order in which the sugars are added. For example, the sialyltransferase catalyzing the synthesis of a simple ganglioside (ganglioside G_{M3}) is in the *cis*-Golgi, whereas enzymes involved in terminal steps of more complex gangliosides are located in the more distal *trans*-Golgi network.

Regulation of complex glycosphingolipid biosynthesis involves both transcriptional and posttranscriptional factors. For example, developmentally regulated, tissue selective variations in ganglioside amounts and types in mammalian tissues are under transcriptional control, but the activities of glycosyltransferases can be fine tuned by posttranslational modification.

The biosynthesis of sulfatides (i.e., sulfated glycosphingolipids such as 3′-sulfo-GalCer) is catalyzed by sulfotransferases (in this example: 3′-phosphoadenylylsulfate:GalCer 3′-sulfotransferase), which utilize the activated sulfate donor 3′-phosphoadenosine-5′-phosphosulfate.

Other Species

Although once thought to be only intermediates of sphingolipid turnover, lysosphingolipids such as sphingosine 1-phosphate and sphingosylphosphocholine (lysosphingomyelin) are now known to be synthesized as important signaling molecules. Sphingosine 1-phosphate formation requires the release of sphingosine from ceramide (note that sphingosine is not a direct intermediate of *de novo* sphingolipid biosynthesis but first appears in ceramide) by ceramidase(s) followed by transfer of phosphate from ATP by sphingosine kinase(s) (Figure 2). Less is known about the origin of sphingosylphosphocholine, although it is plausible that this could be made by a phospholipase A_2-type cleavage of sphingomyelin, the transfer of phosphocholine to sphingosine, or both.

Sphingolipidomics

The large number and structural complexity of sphingolipids has made quantitative analysis of all of the molecular species technically difficult, and heretofore impossible with small samples such as cells in culture. However, it is now feasible to map the sphingolipid "metabolome" due to the relatively recent availability of tandem mass spectrometers of multiple configurations (e.g., tandem quadrupole, time-of-flight, and ion traps as well as hybrids of these technologies) and modes of ionization (such as electrospray and matrix-assisted laser-desorption ionization (MALDI)), especially when combined with high-performance liquid chromatography. When complemented by the tools of genomics and proteomics, the new field of "sphingolipidomics" will finally be able to answer the many riddles of how these molecules are made, and for what functions.

See Also the Following Articles

Glycolipid-Dependent Adhesion Processes • Lipid Bilayer Structure • Lysophospholipid Receptors • Protein Palmitoylation • Sphingolipid Catabolism

Glossary

ceramide An N-acyl-derivative of sphingosine that is both a metabolic intermediate and a cell signaling molecule. In some cases, the term is applied generically to any N-acyl-sphingoid base.

glycosphingolipid A compound with a carbohydrate bound to a sphingoid base (and most often, attached to position 1 of an N-acyl-sphingoid base).

glycosyltransferase An enzyme that transfers a carbohydrate from a donor (usually a UDP-sugar) to an acceptor which, in the case of sphingolipids, is either ceramide or a carbohydrate chain attached to ceramide.

phosphosphingolipid A compound with a phosphate or phosphodiester linked headgroup attached to a sphingoid base (or more often, to position 1 of an N-acyl-sphingoid base).

sphingoid base The backbone of more complex sphingolipids as well as a cell signaling molecule. Structurally, a long-chain alkane (or alkene) with an amino at position 2, and (usually) hydroxyl groups at positon 1 and 3 plus various alkyl chain lengths, degrees of unsaturation, and additional hydroxyl groups.

sphingosine 1-phosphate A bioactive metabolite that serves as an intracellular and an extracellular signal as well as an intermediate of sphingoid base catabolism.

Further Reading

Hannun, Y. A., and Obeid, L. M. (2002). The ceramide-centric universe of lipid-mediated cell regulation: Stress encounters of the lipid kind. *J. Biol. Chem.* **277**, 25847–25850.

IUPAC-IUB Joint Commission on Biochemical Nomenclature (JCBN) (1998). Nomenclature of glycolipids. Recommendations 1997. *Eur. J. Biochem.* **257**, 293–298.

Kolter, T., Proia, R. L., and Sandhoff, K. (2002). Combinatorial ganglioside biosynthesis. *J. Biol. Chem.* **277**, 25859–25862.

Merrill, A. H. Jr., (2002). *De novo* sphingolipid biosynthesis. A necessary, but dangerous, pathway. *J. Biol. Chem.* **277**, 25843–25846.

Merrill, A. H., Jr., and Sandhoff, K. (2002). Sphingolipids: Metabolism and cell signaling. In *New Comprehensive Biochemistry: Biochemistry of Lipids, Lipoproteins, and Membranes* (D. E. Vance and J. E. Vance, eds.) Chapter 14, Elsevier, Amsterdam.

Spiegel, S., and Milstien, S. (2003). Sphingosine-1-phosphate: An enigmatic signalling lipid. *Nat. Rev. Mol. Cell Biol.* **4**, 397–407.

Sullards, M. C., Wang, E., Peng, Q., and Merrill, A. H., Jr. (2003). Metabolomic profiling of sphingolipids in human glioma cell lines by liquid chromatography tandem mass spectrometry. *Cell Mol. Biol.* **49**, 789–797.

Thudichum, J. L. W. (1884). *A Treatise on the Chemical Constitution of Brain*. Bailliere, Tindall, and Cox, London.

Biography

Martina Leipelt holds a Doctorate in Genetics from the University of Hamburg, Germany. Her doctoral research with Professor E. Heinz provided a systematic functional analysis of the glucosylceramide synthase gene family with representatives of plants (*Gossypium arboreum*), animals (*Caenorhabditis elegans*), and fungi (*Magnaporthe grisea*, *Candida albicans*, and *Pichia pastoris*). She is currently a postdoctoral fellow with Dr. Merrill.

Al Merrill is the Smithgall Institute Chair in Molecular Cell Biology in the School of Biology and the Petit Institute for Bioengineering and Biosciences at Georgia Institute of Technology. Dr. Merrill's laboratory, in collaboration with Dr. Ron Riley at the USDA, discovered the inhibition of ceramide synthase by fumonisins and identified the first diseases caused by disruption of *de novo* sphingolipid biosynthesis His current research deals with sphingolipidomics (http://www.lipidmaps.org).

Sphingolipid Catabolism

Akira Abe and James A. Shayman
University of Michigan, Ann Arbor, Michigan, USA

Sphingolipids are composed of a variety of membrane-associated molecules that contain a long-chain sphingoid base. The base may be acylated, glycosylated, and phosphorylated to produce a variety of structures with important biological functions. The catabolic pathways responsible for the degradation of sphingolipids have been extensively studied. The constitutive degradation of sphingolipids occurs in lysosomes through a series of degradative enzymes known as sphingolipid-specific hydrolases. The inherited deficiencies of sphingolipid hydrolases may result in metabolic disorders that lead to the abnormal accumulation of sphingolipids within cells. Recently, some sphingolipid metabolites have been assigned functions as extracellular and intracellular signaling molecules. In particular, certain sphingomyelin metabolites such as ceramide, sphingosine, and sphingosine-1-phosphate, may play important roles in cellular processes such as cell growth, differentiation, apoptosis, stress, and inflammation. The degradation of sphingolipids involved in the response to extracellular stimuli occurs through both the lysosomal and nonlysosomal catabolic pathways.

Sphingomyelin Catabolism

Sphingomyelinase catalyzes the hydrolysis of sphingomyelin to form phosphorylcholine and ceramide. Ceramide may be further metabolized to form other sphingolipids or may function as a signaling molecule. Sphingomyelinases are categorized into four groups: acid sphingomyelinase (aSMase), secreted sphingomyelinase (sSMase), neutral sphingomyelinase (nSMase) and alkaline sphingomyelinase (bSMase).

Acidic Sphingomyelinase

aSMase is a well-characterized sphingomyelinase with an optimal pH of 5 and localized to lysosomes. The enzyme primarily functions in the degradation of sphingomyelin. In humans, a genetic deficiency of lysosomal aSMase results in Niemann-Pick types A and B, autosomal-recessive lipid storage disorders. The enzyme was purified from urine as a 72 kDa monomeric glycoprotein with a 61 kDa polypeptide core. The human aSMase cDNA encodes a 629 amino acid polypeptide. Metabolic labeling studies in cell-lines cells transfected with the human aSMase cDNA reveal that a 75 kDa aSMase precursor is processed by extensive posttranslational modification during sorting to the lysosome.

There is some evidence that aSMase plays an important role in ceramide formation after stimulation with TNFα or CD95, or treatment with UV-A irradiation. However, the requirement of aSMase in apoptosis and differentiation induced by TNFα and Fas ligand is still debated. The involvement of aSMase in ceramide-meditated signal transduction may depend on the cell and tissue type and vary with the stimulus.

Secreted Sphingomyelinase

sSMase is a secretory form of the aSMase gene product and is secreted via a Golgi-apparatus-dependent pathway into the extracellular space. The enzyme is activated in the presence of physiological concentrations of Zn^{2+} and demonstrates maximum activity under acidic conditions. However, the enzyme is able to hydrolyze sphingomyelin from atherogenic lipoproteins, LDL extracted from arteriosclerotic lesions, and oxidized at neutral pH. LDL treated with sSMase forms aggregates that are retained on extracellular matrix and stimulates macrophage foam cell formation. Thus, sSMase may serve a normal physiological function in lipoprotein metabolism and a pathological function in atherogenesis.

Neutral Sphingomyelinase (nSMase)

In mammalian cells, nSMase is a membrane-associated protein with an optimal neutral pH. Although the enzyme is expressed ubiquitously in mammalian tissues, the highest activity is predominantly found in brain. Mammalian tissues express two isoforms of nSMase. The enzyme activity of the higher molecular weight isoform form is Mg^{2+} dependent but that of the lower molecular weight isoform is Mg^{2+} independent. The low-molecular weight isoforms appear to be degradation products of the high-molecular isoforms. The purified enzyme is activated by phosphatidylserine,

Mg^{+2}, and Mn^{2+}, and inhibited by Cu^{2+}, Zn^{2+}, Ca^{2+}, Cd^{2+}, Hg^{2+}, glutathione, and asialo-ganglioside, GM3.

Recently, an nSMase candidate (nSMase 1) with molecular mass of 47.5 kDa was cloned from mouse and human based on multiple sequence alignments of bacterial nSMases. Bacterial nSMases are soluble proteins with an optimal pH between 4.2 and 8.0. They are Mg^{2+} dependent. The product of the nSMase 1 gene is localized in endoplasmic reticulum, Golgi, and/or the nuclear matrix of cells. The natural substrate of nSMase 1 is still not known and the enzyme appears to not be involved in ceramide formation after stimulation by TNFα. A second nSMase (nSMase 2) with a molecular mass of 71 kDa has been cloned using an improved database search method combined with phylogenetic analysis. nSMase 2 is a brain-specific nSMase with a different domain structure and only marginal sequence similarity to other SMases. nSMase 2 has the basic properties of rat and bovine brain nSMase and is activated in response to TNFα. nSMase 2 colocalizes with a Golgi apparatus marker in a number of cell lines. One more nSMase candidate that is a different gene from nSMase 1 and 2 was recently cloned by use of expression cloning. This nSMase cDNA encodes a 397 amino acid polypeptide. The enzyme is activated by Mg^{+2}, inhibited by Cu^{2+} and glutathione, and recognizes sphingomyelin as a preferred substrate. The deduced amino acid sequence indicates that the enzyme is a membrane-integrated protein and has a significant homology to the death domains of the TNF-α and Fas/AP-1 receptors. The overexpression of this recombinant nSMase in human aortic smooth muscle cells results in apoptosis and augmented oxidized LDL-induced apoptosis. The limited amino acid sequence information from purified nSMase from bovine brain shows no sequence homology to the nSMases cloned to date.

The activation of SMase by extracellular stimuli that induce differentiation, apoptosis, and stress and inflammation is associated with both aSMase and nSMase activities. Because nSMases are localized in the plasma membrane and cytosol, nSMases and not aSMase would appear to be, on topological grounds, the logical participants in sphingomyelin signaling pathways. Recently, an adaptor protein, FAN (factor associated to nSMase activation), was shown to link the TNF receptor to nSMase and act upstream of nSMase. In addition, several recent reports suggest that nSMase in lipid rafts contributes to TNFα signaling.

Alkaline Sphingomyelinase (bSMase)

The enzyme activity of this SMase was initially found in the small intestine. Recently, bSMase was purified from rat intestine and required bile salt for the enzyme activity. The purified bSMase is 58 kDa, has an alkaline pH optimum, is Mg^{2+} independent, and is not inhibited by glutathione. The expression of this enzyme is specific to the intestinal mucosa. Another type of bSMase has an 85 kDa molecular mass and is found in human bile. These enzymes appear to function in the catabolism of dietary sphingomyelin.

Ceramide Catabolism

Ceramidase (CDase) catalyzes the hydrolysis of ceramide to fatty acid and sphingosine. Three types of ceramidase have been described based on their pH optima for activity. These include acid ceramidase, neutral ceramidase, and alkaline ceramidase. Sphingosine and its phosphorylated metabolite, sphingosine-1-phosphate, act as potent inhibitors of protein kinase C and potent effectors of cell proliferation and differentiation. CDase may change the balance of ceramide, sphingosine, and sphingosine-1-phosphate within cells in response to various stimuli. CDase may therefore regulate sphingolipid mediated signaling events.

Acid Ceramidase

Acid ceramidase (aCDase) can be characterized as an *N*-acylsphingosine deacylase with an acidic pH optimum. The enzyme is localized in lysosomal and endosomal compartments. The enzyme functions primarily in the degradation of ceramide. In humans, a genetic deficiency of lysosomal aCDase results in the lyososomal lipid storage disorder known as Farber disease. The enzyme, purified from human urine, is a 55 kDa heterodimeric glycoprotein consisting of two disulfide-linked polypeptide chains of 13 kDa (α) and 40 kDa (β). The human aCDase cDNA encodes a protein of 395 amino acids. The 13 kDa (α) and 40 kDa (β) subunits are derived from a common 55 kDa precursor encoded by the full length of aCDase-cDNA. Only the β-subunit is posttranslationally glycosylated during transport to acidic cellular compartments. aCDase activity is enhanced by an activator protein known as saposin D.

aCDase responds to extracellular stimuli. In rat hepatocytes, aCDase activity is bimodally regulated by IL-1β and is activated by tyrosine phosphorylation. In renal mesangial cells, aCDase is activated by TNFα but inhibited by nitric oxide. Inhibition of aCDase sustains the accumulation of ceramide induced by TNFα. Overexpression of aCDase in L929 cells suppresses TNFα induced ceramide formation and cell death.

Neutral Ceramidase

In mammals, nCDase is present in a variety of tissues and cell types and its activity is mainly found in membrane fractions. nCDase has been purified from rat

brain, where the highest activity is found. nCDase is a 90 kDa membrane-bound, nonlysosomal protein. The enzyme has a broad pH optimum in the neutral to alkaline range and does not require divalent cations for activity. The enzyme is stimulated by phosphatidic acid and phosphatidylserine. Similar membrane-bound nCDases, purified from mouse liver and rat kidney, are 94 and 112 kDa monomeric glycoproteins, respectively. Partial amino acid sequences of each nCDase were used to clone the genes from mouse, rat, and human. The mouse, rat, and human nCDase cDNAs encode 761, 756, and 763 amino acid polypeptides, respectively. In rat kidney, nCDase is mainly localized to the apical membrane of the proximal tubules, distal tubules, and collecting duct. By contrast, liver nCDases are detected in endosome-like organelles within the hepatocytes. Human nCDase over expressed in HEK293 and MCF7 cells is found in mitochondria. nCDase activity is activated by IL-1β in rat hepatocytes, resulting in a decrease of ceramide concomitant with an increase of sphingosine. TNFα stimulates and nitric oxide inhibits nCDase activity in renal mesangial cells.

Alkaline Ceramidase

Alkaline ceramidase activity has been described in human, rat, and mouse tissues. Two forms of membrane-bound alkaline ceramidases (bCDases) with molecular masses of 60 kDa (CDase-I) and 148 kDa (CDase-II) are present in skin. CDase-I and CDase-II have alkaline pH optima. Both enzyme activities are inhibited by sphingosine. Based on sequence homology to the yeast bCDase, a novel human bCDase was cloned. This bCDase cDNA encodes a protein of 253 amino acids. The enzyme has a pH optimum of 9.5 and is activated by Ca^{2+}, but is inhibited by Zn^{2+} and sphingosine. The enzyme hydrolyzes phytoceramide preferentially and when over expressed in COS-1 cells is localized to both the endoplasmic reticulum and Golgi apparatus.

Sphingoid Base Catabolism

At the penultimate step of sphingolipid catabolism the primary hydroxyl group of the sphingoid base is phosphorylated by sphingosine kinase. The phosphorylated sphingoid base is then cleaved between the vicinal carbons with amino and hydroxyl groups by sphingosine-1-phosphate lyase (SPLase). The predominant sphingoid base in mammalian cells is sphingosine. Sphingosine produced from ceramide by ceramidase is phosphorylated by sphingosine kinase and then degraded to form phosphoethanolamine and hexadecanal by SPLase. The sphingosine-1-phosphate, generated during sphingosine catabolism, is not only a catabolic intermediate but also functions as an extracellular and intracellular messenger. Sphingosine-1-phosphate is mitogenic. The extracellular actions of sphingosine-1-phosphate are mediated through the EDG receptor family of G protein-coupled receptors.

Sphingosine-1-Phosphate Lyase

SPLase is a pyridoxal phosphate-dependent member of a class of enzymes known as aldehyde lyases and cleaves 1-phosphorylated sphingoid bases into aliphatic fatty aldehydes and phosphoethanolamine with a neutral pH optimum. SPLase is a ubiquitous enzyme present in multiple species and mammalian tissues. However, platelets lack SPLase activity, suggesting that platelets may be the primary source of circulating sphingosine-1-phosphate. The enzyme is a membrane-bound protein and in rat liver is localized in the endoplasmic reticulum. The catalytic site and other domains essential for SPLase activity face the cytosol. Recently, SPLase cDNAs were cloned from mouse and human based on sequence homology to the *Caenorhabditis elegans* and yeast SPLases. Both cDNAs encode proteins of 568 amino acids. Hydropathy analysis indicates the presence of one-transmembrane region near the N terminus.

Sphingosine-1-phosphate levels in cells during signaling processes seem to be regulated not only by sphingosine kinase and SPLase but also by a lipid phosphate phosphohydrolase. Several sphingosine-1-phosphate specific phosphohydrolases have been identified in yeast and mammalian cells.

Glycosphingolipid Catabolism

Glycosphingolipids are components of cellular membranes and are comprised of one or more sugars linked to ceramide. Glycosphingolipids are tissue and cell-type specific. They form patterns that vary with the cell type, stage of growth and differentiation, viral transformation, and ontogeny. The biosynthesis of glycosphingolipids occurs within the Golgi apparatus where carbohydrates are added by membrane-associated glycosyltranferases. Glycosphingolipids are subsequently transferred to the plasma membrane. At this site they interact with membrane associated receptors and enzymes as well as with bacterial toxins and adhesion molecules and viruses. Following endocytosis, glycosphingolipids are transported to acidic intracellular compartments where they are degraded from the nonreducing ends by a set of lysosomal exoglycosidases that catalyze the stepwise cleavage of their component carbohydrates.

Glycosphingolipid storage disorders are caused by the deficiency of a specific glycosidase that is

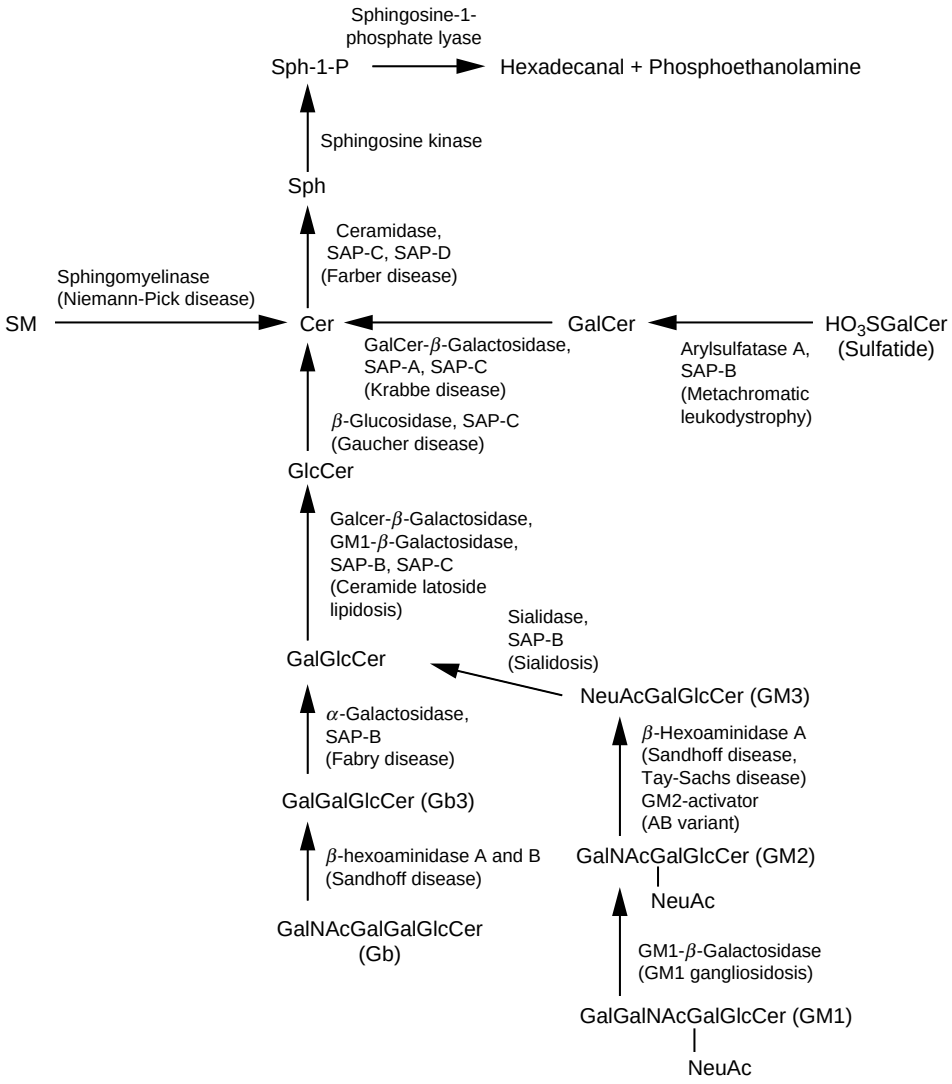

FIGURE 1 Degradation pathways of sphingolipids. The lysosomal diseases caused by genetic defects in a series of lysosomal enzymes and activator proteins for sphingolipid catabolism are indicated in parentheses. NeuAc, N-acetylneuramic acid; Cer, ceramide; Glc, glucose; Gal, galactose; GalNAc, *N*-acetylgalactosamine; Gb, globoside; Gb3, globotriaosyl ceramide; SM, sphingomyelin; $HO_3SGalCer$, sulfatide; Sph, sphingosine; Sph-1-P, spingosine-1-phosphate; SAP, sphingolipid activator protein.

involved in glycosphingolipid degradation (Figure 1). These deficiencies result in the abnormal accumulation of specific glycosphingolipids both in neural and nonneural tissues (Table I). These disorders vary in terms of their clinical presentations based on the affected organs.

The lysosomal hydrolases that degrade glycosphingolipids of the plasma membrane are water-soluble enzymes. Their activity is dependent on the presence of water-soluble activator proteins termed saposins. The four saposins (A through D) arise from a common precursor protein, prosaposin. Saposin B is an activator for arylsulfatase A, α-galactosidase A, and β-galactosidase. Saposin C is an activator of acid β-glucosidase. Saposin D is an activator of ceramidase. There is no assigned function for saposin A. Glycosphingolipid storage disorders may also arise from inherited deficiencies of the prosaposin as well as from individual saposins.

Arylsulfatase A

Arylsulfatase A catalyzes the desulfation of 3-*O*-sulfogalactosyl residues in glycosphingolipids. The enzyme activity requires the presence of saposin B as an activator. The arylsulfatase A gene encodes a 507 amino acid precursor protein that undergoes posttranslational processing. In addition to N-linked glycosylation required for lysosomal sorting through the mannose-6 phosphate receptor pathway, there is a

TABLE I

Major Sphingolipidoses

Disease	Sphingolipid stored	Defective enzyme	Clinical phenotype
Farber	Ceramide	Acid ceramidase	Painful and deformed joints, subcutaneous nodules, hoarseness
Niemann-Pick A and B	Sphingomyelin	Acid sphingomyelinase	Neurodegeneration, hepatosplenomegaly
Metachromatic leukodystrophy	Sulfatide	Arylsulfatase	Blindness, quadreparesis, seizures
Krabbe	Galactosylceramide	β-Galactocerebrosidase	Blindness, spastic paraparesis, dementia
Gaucher	Glucosylceramide	β-Glucocerebrosidase	Hepatosplenomegaly, bone infarctions and fractures
Fabry	Globotriaosylceramide	α-Galactosidase A	Parasthesias, renal failure, cerebrovascular disease
Sandhoff	Gangliosides GM2 and GA2, globoside	Hexosaminidase B	Neurodegeneration
Tay-Sachs	Ganglioside GM2	Hexosaminidase A	Neurodegeneration
GM1 gangliosidosis	Ganglioside GM1	GM1 β-galactosidase	Neurodegeneration, skeletal dysplasia, hepatosplenomegaly

unique oxidation that occurs for eukaryotic sulfatases. In human arylsulfatase A, a formylglycine residue is found in place of cysteine 69 and is due to the oxidation of a thiol group to an aldehyde. In addition to sulfatide, arylsulfatase A will cleave sulfate groups from other naturally occurring glycosphingolipids including lactosylceramide-3-sulfate and psychosine sulfate.

β-Galactosidases

β-Galactosidase catalyzes the degradation of galactosylceramide to galactose and ceramide within the lysosome. It also displays activity against galactosylsphingosine and lactosylceramide. The enzyme is more precisely referred to a galactocerebroside β-galactosidase because a second, genetically and enzymatically distinct β-galactosidase also exists with the lysosome, GM1 ganglioside β-galactosidase. GM1 ganglioside β-galactosidase catabolizes ganglioside GM1, GA1, lactosylceramide, and keratan sulfate. These enzymes have overlapping substrate specificities, but deficiencies in these enzymes result in distinct clinical disorders. Defects in the former enzyme cause Krabbe disease with the accumulation of galactosylceramide. Defects in the latter enzyme cause GM1 gangliosidosis.

Galactocerebroside β-galactosidase can be isolated as an 80 kDa polypeptide consisting of 50 and 30 kDa subunits. The pH optimum of the enzyme is acidic. The enzyme is active against galactosylceramides that vary in fatty acid chain length and α-hydroxylation. The enzyme is inhibited by sphingosine, ceramide, and galactose. The human gene for galactocerebroside β-galactosidase maps to chromosome 14q24.3.

GM1 ganglioside β-galactosidase has an acidic pH optimum. It is activated by chloride ions. The enzyme is isolated as a large-molecular weight multimer with monomeric units of 65 kDa. This enzyme is also activated in the presence of saposin B.

β-Glucocerebrosidase

Human acid β-glucocerebrosidase is a homomeric glycoprotein. The mature polypeptide is 497 amino acids in length. Both saposin A and saposin C activate the enzyme *in vitro*. However, only saposin C deficiency is associated with the clinical manifestations of Gaucher disease. Although saposin interacts directly with the enzyme, the association of glycosphingolipids and anionic phospholipids are required for its activity. The pH optimum for the glucocerebrosidase is 5.5. The enzyme is specific for D-glucosyl and not L-glucosyl forms of glucosylceramide. Activity is reduced by the absence of the C4–C5 *trans* double bond in sphingosine and is minimally affected by the acyl chain length of the ceramide moiety. The disease alleles in Gaucher disease are commonly missense mutations. This results in the synthesis of β-glucosidases with decreased catalytic activity or stability. These typically lead to the type I form of Gaucher disease that lacks central nervous system manifestations. The neuronopathic forms of Gaucher disease (types II and III) are more commonly associated with complete loss of catalytic activity.

α-Galactosidase A

α-Galactosidase A catabolizes glycosphingolipids with terminal α-galactosyl groups. These glycosphingolipids primarily include globotriaosylceramide, but are also present in galabiosylceramide and group B blood antigens. Initial studies on the enzyme activity suggested that there were two isozymes termed α-galactosidase A and B. Subsequent work demonstrated that these are two genetically distinct enzymes. α-Galactosidase B is an α-*N*-acetylgalactosaminidase. Deficiencies in α-galactosidase B are responsible for Schindler disease. Native α-galactosidase A has a molecular weight of 101 kDa and represents a homodimer with 49 kDa subunits. The enzyme is heavily glycosylated with asparagine-linked high mannose groups. The pH optimum for the glycosidase is acidic. The enzyme is activated in the presence of saposin B. The locus for human α-galactosidase A is found at Xq22.

Hexosaminidases A and B

Ganglioside GM2 is degraded in the lysosome by β-hexosaminidase A. This enzyme removes the terminal *N*-acetylgalactosaminyl residue. The enzyme requires the presence of an additional protein termed GM2 activator encoded by the *GM2A* gene. β-Hexosaminidase A is a heterodimer consisting of an α- and β-subunit. The α-subunit is a 55 kDa polypeptide encoded by the *HEXA* gene found on chromosome 15q23-24. The β-polypeptide varies between 22 and 30 kDa and is encoded by the *HEXB* gene found on chromosome 5q13. A second enzyme, β-hexosaminidase B is a homodimer consisting of two β-subunits. Thus *HEXA* gene mutations result in loss of β-hexosaminidase A activity and *HEXB* gene mutations result in loss of both β-hexosaminidase A and B activities. The β-hexosaminidase A and B enzymes are posttranslationally glycosylated for sorting to the lysosome through the mannose-6-phosphate receptor pathway. They display acidic pH optima as well.

Inherited mutations in *HEXA*, *HEXB*, and *GM2A* all result in the accumulation of ganglioside GM2 and are associated with Tay-Sachs, Sandhoff, and GM2 activator deficiency diseases respectively. β-Hexosaminidase B deficiencies are associated with the accumulation of GA2 as well.

See Also the Following Articles

Glycolipid-Dependent Adhesion Processes • Lipid Bilayer Structure • Lipid Rafts • Lysophospholipid Receptors • Protein Palmitoylation • Respiratory Chain and ATP Synthase • Sphingolipid Biosynthesis

Glossary

cerebroside A glycosphingolipid containing a single carbohydrate, most commonly glucosylceramide and galactosylceramide.

ganglioside An acidic glycosphingolipid containing one or more sialic acid groups.

glycosphingolipid A sphingolipid covalently linked with one or more carbohydrates.

lysosome An organelle bounded by a single membrane bilayer in the cytoplasm in eukaryotic cells and having an internal pH of 4–5. Lysosomes contain several hydrolytic enzymes and serve as the site for the degradation and recycling of cellular metabolites.

sphingolipid A lipid with a backbone containing a long chain sphingoid amine.

Further Reading

Goni, F. M., and Alonso, A. (2002). Sphingomyelinases: Enzymology and membrane activity. *FEBS Lett.* **531**, 38–46.

Huwiler, A., Kolter, T., Pfeilschifter, J., and Sandhoff, K. (2000). Physiology and pathophysiology of sphingolipid metabolism and signaling. *Biochim. Biophys. Acta* **1485**, 63–99.

Pettus, B. J., Chalfant, C. E., and Hannun, Y. A. (2002). Ceramide in apoptosis: An overview and current perspectives. *Biochim. Biophys. Acta* **1585**, 114–125.

Siegel, G. J., Agranoff, B. W., Albers, R. W., Fisher, S. K., and Uhler, M. D. (eds.) (1999). *Basic Neurochemistry.* Williams and Wilkins, Lippincott.

Biography

Akira Abe holds the position of Research Investigator in the Division of Nephrology, Department of Internal Medicine at the University of Michigan Medical School. He holds a Ph.D. in biochemistry from Hokkaido University and received his postdoctoral training in the laboratory of Norman Radin at the Mental Health Research Institute at the University of Michigan.

James A. Shayman is Professor of Internal Medicine and Pharmacology at the University of Michigan School of Medicine. He also holds the position of Associate Chair for Research Programs for the Department of Internal Medicine. He was awarded his M.D. from Washington University and received his postdoctoral training in the Department of Pharmacology at Washington University.

Spliceosome

Timothy W. Nilsen
Case Western Reserve University School of Medicine, Cleveland, Ohio, USA

The spliceosome (splicing body) is a massive ribonucleoprotein complex that catalyzes the removal of noncoding intervening sequences (introns) from nuclear pre-mRNAs in the process known as splicing. Essential components of the spliceosome include five small nuclear RNAs (snRNAs) which function as RNA/protein complexes (snRNPs), and more than 100 non-snRNP-associated proteins. Despite the large number of proteins required for splicing, it seems clear that the spliceosome, like the ribosome, is fundamentally an RNA enzyme (ribozyme).

Discovery and Initial Characterization of the Spliceosome

Early analyses, primarily the comparison of cDNA and genomic clones, demonstrated that introns were ubiquitous in higher eukaryotic genes. These analyses also revealed the presence of consensus sequences that marked intron boundaries (5′ and 3′ splice sites) as well as conserved sequences ~30 nucleotides upstream of the 3′ splice site called the branch point region. However, biochemical dissection of splicing awaited the development of cell-free systems (extracts prepared from cells) that were capable of catalyzing efficient and accurate splicing of synthetic pre-mRNAs. The availability of such systems quickly led to elucidation of the chemistry of splicing and permitted the identification of cellular components required for splicing.

A variety of experiments including sedimentation analysis showed that, when incubated with extract, pre-mRNAs become incorporated into complexes similar in size to that of the ribosome. Several lines of evidence indicated that these complexes (dubbed spliceosomes) were relevant to splicing. First, pre-mRNAs in which the consensus sequences at 5′ or 3′ splice sites were altered by mutation failed to assemble into the large particles. Second, splicing intermediates were found exclusively within spliceosomes and third, inactivation of factors essential for splicing inhibited both the formation of spliceosomes and concomitantly, splicing. The discovery of spliceosomes led to an intense effort that continues today to identify its constituents and to elucidate the function of each component. Before considering the factors that comprise the spliceosome, it is necessary to briefly consider the chemistry of the splicing reaction itself.

Splicing Takes Place via Consecutive Transesterification Reactions

As noted, introns are characterized by three conserved sequence elements, the 5′ and 3′ splice sites, and the branch point region. Intron removal occurs in two chemical steps, both of which involve the exchange of one phosphodiester bond for another (transesterification). In the first step, the 2′ hydroxyl of an adenosine residue located within the branch point region (the branch point adenosine) attacks the phosphodiester bond at the 5′ splice site, breaking that 3′5′ phosphodiester linkage and replacing it with a new 2′5′ bond that connects the branch point adenosine and the first base of the intron. Accordingly, the products of the first step of splicing are liberated 5′ exon and the intron (in the form of a lariat) still linked to the 3′ exon. The second step of splicing is also a transesterification reaction. Here, the 3′ hydroxyl of the 5′ exon attacks the phosphodiester bond at the 3′ splice site breaking that bond and creating a new 3′5′ phosphodiester linkage that precisely connects the 5′ and 3′ exons. Thus, the products of the second step of splicing are ligated exons and the intron released in the form of a lariat. Because of the remarkable similarities between this reaction pathway and the pathway by which certain introns (group II) excise themselves independently of proteins, it is widely suspected that the two steps of nuclear pre-mRNA splicing are catalyzed by RNA. In considering how the spliceosome performs its task, it is important to keep the reaction pathway of splicing in mind. In this regard, the spliceosome must juxtapose the branch point adenosine with the 5′ splice site prior to the first step, anchor the 5′ exon following the first transesterification reaction and properly position the 3′ hydroxyl of the 5′ exon such that the second step

can proceed. It is now clear that these functions are performed in large part by the spliceosomal small nuclear ribonuclear proteins (snRNPs).

Required Spliceosomal Constituents: The snRNPs

Well before it became possible to analyze splicing *in vitro*, a family of small abundant stable RNAs localized to the nucleus had been identified and the sequences of individual RNAs had been determined. Because these RNAs appeared to be ubiquitous and were, in general, uridine rich they became known as U small nuclear RNAs. As they were characterized, they were given numerical designations; accordingly, the most abundant U snRNAs are called U1, U2, U4, U5, and U6. As with all cellular RNAs, the U snRNAs are complexed with proteins and are thus U snRNPs. Some of these proteins are common to many snRNPs, while some are specific to individual RNPs. For example, U1 snRNP contains seven common proteins and three U1 specific proteins.

When consensus signals demarcating introns were identified, it became obvious that specific sequences within the U snRNPs could potentially interact via base pairing with those sequences. In particular, the 5′ end of U1 snRNA was predicted to base pair with 5′ splice sites and a region of U2 snRNA could base pair with the branch point region. These and other observations suggested that the U snRNPs might be involved in splicing. This hypothesis could be tested once cell free systems became available. Using a battery of specific depletion strategies, it was shown that U1, U2, U4, U5, and U6 snRNPs were all required for splicing and all were constituents of the spliceosome; accordingly these RNAs are now known as spliceosomal snRNAs. The specific function of each spliceosomal snRNP has been the subject of intense investigation for many years and our current understanding of their roles is discussed subsequently.

Spliceosomal Constituents—Non-snRNP Proteins

While much attention was focused on snRNPs, other approaches, primarily genetic analyses in budding yeast and biochemical fractionation of extracts prepared from mammalial cells, revealed that a plethora of factors were required for splicing. Several techniques, including specific immunoprecipitation, showed that these factors were *bona fide* spliceosomal constituents and that they were not intrinsic components of snRNPs. At one point, it was thought that there were 30–40 non-snRNP splicing factors. However, recent improvements in purification techniques coupled with dramatic advancements in the ability to determine the identity of proteins via mass spectrometry have revealed that the spliceosome contains at least 100 non-snRNP proteins and perhaps many more. Accordingly, the spliceosome contains, at a minimum, 200 distinct proteins and five distinct RNAs, making it among the most complex macromolecular machines in the cell. Some reasons for this remarkable complexity are discussed.

What are the non-snRNP splicing factors? While the role(s) of many non-snRNP proteins remain obscure, the functions of others have been elucidated at least in part. Among these are a group of enzymes known as RNA dependent ATPases (RNA helicases). At least six helicases are required for splicing and they are thought to catalyze the RNA/RNA rearrangements that occur during the splicing reaction. The only other known spliceosomal enzyme is a protein phosphatase, but a definitive substrate for this protein has not yet been identified. Other proteins with known functions are those involved in recognition of the pre-mRNA prior to assembly of the entire spliceosome; these proteins assist the snRNPs in engaging the intron.

Spliceosome Assembly and the Splicing Cycle

Unlike the ribosome, which is a stable preformed macromolecular complex, the spliceosome must assemble anew on each intron. An extensive variety of biochemical approaches has indicated that spliceosome assembly follows an ordered pathway (see Figure 1). First, U1 snRNP recognizes and binds to the 5′ splice site; this binding is mediated in part by base pairing between U1 snRNA and the pre-mRNA. Once U1 snRNP is bound, it promotes recognition of the branch point region by U2 snRNP, again this binding is mediated in part by base pairing. Once U1 and U2 snRNPs are bound, U4, U5, and U6 snRNPs join the growing spliceosome as a preformed unit (tri-snRNP). A host of non-snRNP associated proteins accompany tri-snRNP to the spliceosome. Upon completion of assembly, the spliceosome undergoes a dramatic conformational change which involves the release of proteins and the addition of new ones; it is not yet known what triggers this rearrangement. Most strikingly, during this first conformational change, U1 and U4 snRNPs are destabilized and released from the spliceosome; accordingly these snRNPs are not required for catalysis. After the precatalytic conformational changes are completed, the first chemical step of splicing occurs. Following this transesterification reaction, a second

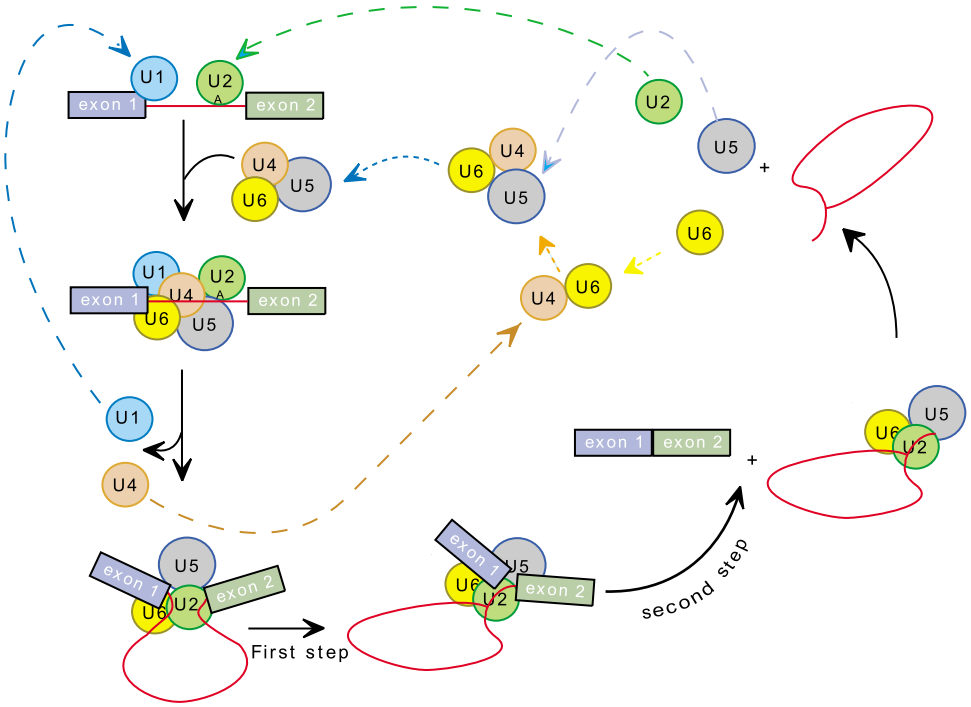

FIGURE 1 Schematic depiction of the splicing cycle (for details, see text).

conformational change ensues. Although not as well understood as the first, it is clear that this rearrangement also involves dramatic changes in spliceosomal composition; i.e., factors depart and new ones join. Subsequent to this conformational change, the second chemical step occurs and the spliceosome is disassembled. Disassembly is not well understood, but is it clear that the snRNPs and other splicing factors are recycled for subsequent rounds of assembly and catalysis (see Figure 1).

A Dynamic Network of RNA/RNA Interactions in the Spliceosome

While the precise role of many individual spliceosomal constituents remains to be determined, their main collective function is to orchestrate a complex series of snRNA/pre mRNA and snRNA/snRNA interactions that culminate in catalysis. Upon completion of spliceosome assembly, U1 snRNP is base paired to the 5′ splice site, U2 snRNP is base paired to the branch point region, U5 snRNP makes contact with the 5′ exon and U4 and U6 snRNPs are joined via extensive base pairing with each other. During the first rearrangement, the base pairing between U1 snRNP and the 5′ splice site is disrupted and replaced by base pairing interaction between U6 snRNA and the 5′splice site. Concomitantly, U4 and U6 are unwound and U6 snRNA forms extensive base pairing interactions with U2 snRNA. The net effect of these RNA/RNA arrangements is to juxtapose the reactants of the first step of splicing, the 5′ splice site and the branch point adenosine. Following the first step, U5 snRNP tethers the 5′ exon and positions it for attack at the 3′ splice site (see Figure 2). A large body of evidence indicates that catalysis is mediated by the snRNAs themselves. Indeed, fragments of U2 snRNA and U6 snRNA can catalyze a reaction analogous to the first step of splicing in the complete absence of protein cofactors. Accordingly, the spliceosome, like the ribosome, is fundamentally an RNA enzyme (ribozyme).

Why is the Spliceosome so Complex?

The overall complexity of the spliceosome is, at first glance, puzzling because the reaction it catalyzes is chemically straightforward; as noted above, certain introns can be excised without the assistance of any proteins. So, why so many proteins? At least four considerations help to explain the multitude of splicing factors.

First, the spliceosome must recognize a huge number of substrates; hundreds of thousands of introns are present in a higher eukaryotic genome. Introns vary greatly in length and in the degree of conservation of splicing signals. Thus the spliceosome must be able to adapt to many different sequence contexts. Indeed, several splicing factors are essential for the splicing of some introns but dispensable for the splicing of others.

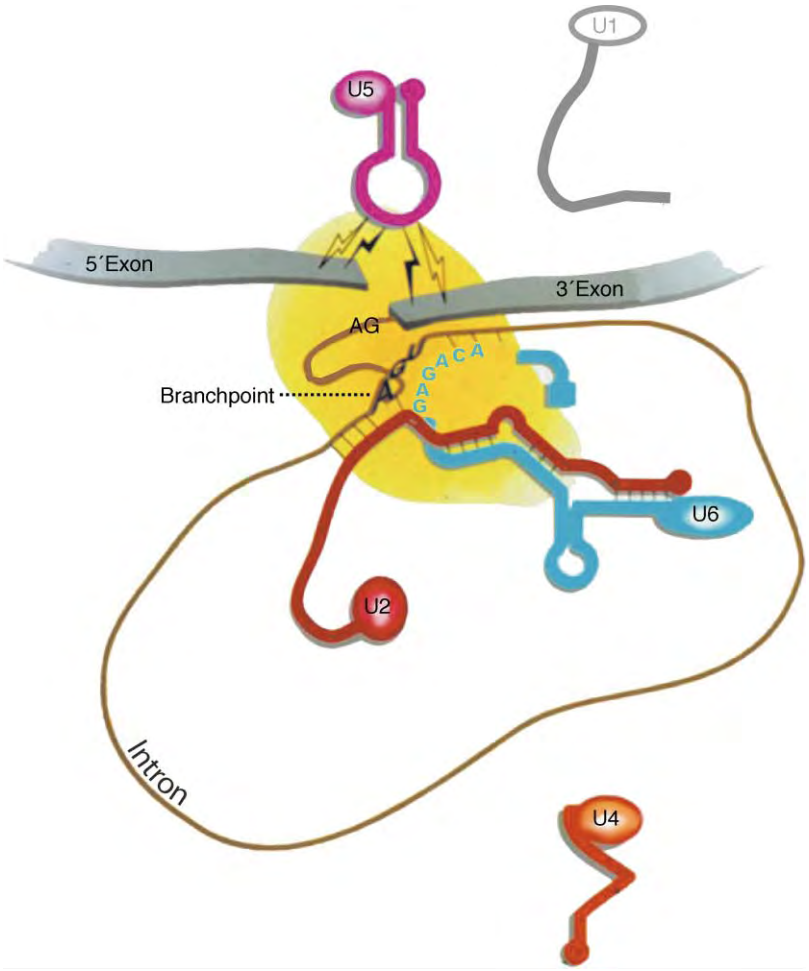

FIGURE 2 Schematic depiction of RNA/RNA interactions in the spliceosome after the first chemical step and prior to the second step (for details, see text).

Second, splicing must be extremely accurate. A mistake of only one base can lead to the production of a defective mRNA. The remarkable fidelity of splicing is achieved via the existence of multiple proofreading activities that monitor the correct alignment of each component prior to catalysis. For example, the 5′ splice site is inspected by at least four distinct activities during different steps in spliceosome assembly. The existence of "fidelity factors" was revealed by mutations in splicing components that led to high levels of mis-splicing.

Third, accumulating evidence indicates that splicing is intimately linked to other cellular processes such as transcription and 3′ end formation. It is now clear that many components of the spliceosome serve as molecular bridges between the transcription apparatus and the core splicing machinery.

Fourth, the spliceosome performs functions in addition to its catalytic role in splicing. Most strikingly in this regard, the process of splicing leaves a specific "mark" on spliced mRNAs. This "mark" known as the exon junction complex (EJC) is comprised of at least six proteins. While none of these proteins is essential for splicing itself, they serve multiple roles after splicing. The EJC facilitates transport of spliced mRNAs from the nucleus, is involved in mRNA surveillance (the process whereby defective mRNAs are identified and destroyed), and is important in the translation of spliced mRNAs.

These, and perhaps yet to be discovered activities, account in part for the remarkable complexity of the spliceosome. A major challenge in coming years will be the elucidation of the role(s) of many spliceosomal factors whose function is not yet known.

See Also the Following Articles

Pre-tRNA and Pre-rRNA Processing in Bacteria • Pre-tRNA and Pre-rRNA Processing in Eukaryotes • Ribozyme Structural Elements: Group I Introns • Ribozymes and Evolution

Glossary

branch point adenosine The intronic adenosine, whose 2′ hydroxyl forms a 2′5′ phosphodiester linkage with the 5′ base of an intron during the first chemical step of spicing.

exon Regions of pre-mRNAs that are retained in mature mRNAs following splicing.

exon junction complex A collection of proteins that are deposited on the mature mRNA as a consequence of splicing.

introns Noncoding regions of pre-mRNAs that are excised via splicing.

pre-mRNA The primary transcript of a gene synthesized by RNA polymerase. The primary transcript extends from the promoter to beyond the 3′ end of the mature mRNA and is subject to numerous processing events including splicing.

transesterification The chemical process in which one phosphodiester bond is broken and another is formed simultaneously.

Further Reading

Collins, C. A., and Guthrie, C. (2000). The question remains: Is the spliceosome a ribozyme? *Nat. Struct. Biol.* **7**, 850–854.

Hastings, M. L., and Krainer, A. R. (2001). Pre-mRNA splicing in the new millennium. *Curr. Opin. Cell Biol.* **13**(3), 302–309.

Jurica, M. S., and Moore, M. J. (2003). Pre-mRNA spicing: Awash in a sea of proteins. *Mol. Cell* **12**, 5–14.

Moore, M. J., Query, C. C., and Sharp, P. A. (1993). Splicing of precursors to mRNAs by the spliceosome. In *The RNA World* (R. F. Gesteland and J. F. Atkins, eds.) pp. 303–357. Cold Spring Harbor Laboratory Press, Cold Spring Harbor, New York.

Nilsen, T. W. (1998). RNA–RNA interactions in nuclear pre-mRNA splicing. In *RNA Structure and Function* (R. W. Simons and M. Grunberg-Manago, eds.) pp. 279–307. Cold Spring Harbor Laboratory Press, Cold Spring Harbor, NY.

Staley, J. P., and Guthrie, C. (1998). Mechanical devices of the spliceosome: Motors, clocks, springs, and things. *Cell* **92**, 315–326.

Will, C. L., and Lührmann, R. (2001). Spliceosomal U snRNP biogenesis, structure and function. *Curr. Opin. Cell Biol.* **13**, 290–301.

Biography

Timothy W. Nilsen is Professor and Director of the Center for RNA Molecular Biology at Case Western Reserve University School of Medicine. His principal research interest is in the mechanism of pre-mRNA splicing, with particular emphasis on the process of splice site recognition in higher eukaryotes and trans-splicing, an unusual splicing reaction that occurs in certain lower eukaryotes. He holds a Ph.D. from SUNY Albany and serves as Editor-in-Chief of the scientific journal, *RNA*.

Src Family of Protein Tyrosine Kinases

Jonathan A. Cooper
Fred Hutchinson Cancer Research Center, Seattle, Washington, USA

The Src (sarcoma) family is a group of protein tyrosine kinases closely related to Src. They are nonreceptor kinases, meaning that they lack a transmembrane domain and lie totally within the confines of the cell, although they are associated with cell membranes. Src family kinase activity is regulated by phosphorylation sites within the kinase domain activation loop and at the carboxy terminus, and by inhibitory interactions between the kinase domain and two other conserved domains, the SH2 and SH3 scaffolding domains. These latter domains can either inhibit the kinase domain or bind other cell proteins, thus helping localize Src to specific sub-cellular regions and protein complexes while simultaneously regulating Src kinase activity. There are eight Src family members in vertebrates, with different but overlapping expression patterns and, potentially, distinct functions within a given cell. However, there is also extensive genetic redundancy within the family, so inactivating mutations reveal only a subset of the potential cellular and developmental roles of family members. On the other hand, any of a number of different mutations can activate Src kinases, and the resulting deregulated kinase activity has profound effects on cell biology, including malignant transformation of some cell types and increased differentiation of others. At least one Src-like kinase gene is found in every metazoan, including sponges and Cnidarians, but is absent, like other tyrosine kinases, from yeasts, protists, plants, and non-eukaryotes. Src kinases are thus one of the ancestral tyrosine kinases and have basic, fundamental roles in cell biology.

History of Src

The history of Src is a story of firsts, and research on Src has spawned wider areas of research. Src was the first protein tyrosine kinase activity to be identified, as a consequence of its role in malignant transformation. In the early 20th century, P. Rous demonstrated that a chicken sarcoma could be transmitted from bird to bird by a particle smaller than a bacterium, and the field of tumor virus research was born. Rous's virus, RSV, was later shown to contain separable genetic elements for replication and for cell transformation. RSV also was one of the first viruses shown, by D. Baltimore and H. Temin, to contain RNA-dependent DNA polymerase (reverse transcriptase) activity, consistent with the idea that transformation was caused by a DNA copy of a viral gene for sarcoma (*src*). D. Stehelin, H. Varmus, and J. Bishop, using nucleic acid probes, showed that a gene related to the viral src gene was present in uninfected vertebrate cells and was conserved over evolution. This provided evidence for the cellular origin of viral oncogenes. The viral src gene is now generally called v-*src*, while the cellular proto-oncogene is called c-*src*, or just *src*. The role of cellular proto-oncogenes in viral and non-viral cancers of animals and humans is now widely accepted.

In 1977, J. Brugge and R. Erikson found that certain antisera from RSV-infected newborn rabbits precipitated a 60,000 M_r protein in addition to the virus structural proteins. The gene encoding this protein was shown to be v-*src*, and the protein was named pp60v-*src* or vSrc. It was soon found that this protein contained, or was associated with, a protein kinase activity that would transfer phosphate to antibody molecules or other model substrate proteins. While this kinase was first thought to phosphorylate threonine residues, T. Hunter and B. Sefton soon found that only tyrosine residues were phosphorylated. Indeed, the first tyrosine kinase to be identified was an activity, now known to be due to cellular Src family kinases, associated with the tumor-causing protein (middle T antigen) of polyoma virus (a DNA tumor virus). Both Src and vSrc are tyrosine kinases, but vSrc is 20+-fold more active than Src due to mutations that interfere with the negative autoregulatory interactions that restrain the activity of Src in normal cells. Different strains and derivatives of RSV have vSrc proteins with different numbers of such activating mutations, which have been very informative in understanding how Src is regulated.

The ability of vSrc to cause malignant transformation is thought to be due to unrestricted phosphorylation of substrate proteins that are normally phosphorylated, in a controlled fashion, by Src and other Src family kinases. In addition, the high kinase activity of vSrc

may lead to the phosphorylation of other cell proteins that are not normally phosphorylated by Src, but it seems unlikely that these additional substrates are involved in transformation. Similarly, transformation by polyoma virus involves the deregulation of Src, by physical association between middle T antigen and Src and several other proteins. The consequent unregulated activity of Src is critical for polyoma virus transformation.

While activated vSrc transforms fibroblasts, it causes other effects in other cell types. In some cases it can induce differentiation and in others increase cell migration or morphology changes. These dramatic effects of activated mutant Src or vSrc led to an expectation that endogenous Src would be vital for many fundamental cellular processes.

Functions of Src in Development

The unique functions of Src were revealed when P. Soriano knocked out the mouse *src* gene. Surprisingly, considering the profound effects of activated v-*src* on vertebrate cells, absence of *src* had remarkably mild effects on development *in utero*. However, some defects were detected after birth. Teeth failed to erupt through the gum, and the cranium grew to form a domed shape. Both of these phenotypes are due to increased bone density, attributable to altered osteoclasts, the macrophage-related blood cells that resorb and remodel bone. Detailed studies of *src* mutant osteoclasts indicate that they differentiate normally but have a reduced ability to form specialized adhesion contacts through which they stick to bone and initiate bone resorption. However, blood platelets and neurons, where Src is highly expressed, are not noticeably altered in *src* mutant mice.

Other Vertebrate Src Family Kinases: Redundant and Specific Functions

The mild effects of *src* deletion are partly due to redundancy with other *src* family genes. The *yes* and *fgr* genes were first identified, as with *src*, as oncogenes in various cancer-causing retroviruses. Upon sequencing, they were found to be related to *src*. *lck, hck, blk, lyn*, and *fyn* were cloned by homology. Of the Src family proteins, Src, Fyn, and Yes are widely expressed in many different cell types in the body, whereas Fgr, Lck, Hck, Blk, and Lyn are restricted to, and are more important in, hematopoietic cells. However, alternative splicing and alternative promoter usage (with different coding exons) creates additional diversity. For example, one splice form of Fyn is restricted to hematopoietic cells while another is more ubiquitous. All the Src family proteins contain canonical features of Src that are critical for regulation and localization: the SH3, SH2, and kinase domains, amino-terminal lipid modification sites, and carboxy-terminal and activation loop tyrosine phosphorylation sites. Other subfamilies of non-receptor protein tyrosine kinases include the Csk, Abl, Fes, Tec/Btk, JAK, Syk, and FAK families, which lack one or more features of Src or contain other distinctive domains. The common features of Src family members allow considerable overlap in function, as shown by targeted knockouts and characterization of multiple mutants.

Individual mutation of *fyn* and *yes*, like *src*, causes only mild effects. For example, *fyn* knockouts have several alterations in the brain, including misorientation of pyramidal neurons in cortex and hippocampus and reduced myelination. In addition, maturation of *fyn* mutant T lymphocytes is impaired. However, more phenotypes are manifested when *src, fyn*, and *yes* are mutated in combination. Double mutants have reduced perinatal survival, and triple knockouts survive poorly beyond mid-gestation (embryonic day 9 in the mouse). These triple mutant embryos resemble embryos mutant for the extracellular matrix protein fibronectin or some integrins, suggesting redundant roles for these three Src relatives in adhesive interactions between cells and the extracellular matrix.

The hematopoietic Src family kinases also have redundant and nonredundant functions. Consistent with their restricted expression, none of these kinases is needed for normal development: mice lacking *hck, fgr*, and *fyn* are moderately healthy and fertile, as are mice lacking *blk, fyn*, and *lyn*. However, some hematopoietic defects are detected. Mutation of *lck* alone blocks thymocyte development at a stage prior to a proliferative burst, with a resulting large decrease in T-cell numbers. Macrophages from *hck* mutant mice have impaired phagocytosis. Combined absence of *fyn* and *lyn* leads to autoimmune disease, absence of *blk, fyn*, and *lyn* inhibits late-stage B-cell development, and absence of *hck* and *fgr* leads to decreased resistance to bacterial infection. Blood platelets lacking *src, hck, fgr*, and *lyn* fail to spread on fibrinogen. Thus, important roles for Src kinases in signaling from immunoreceptors and integrins become evident when multiple Src kinases are absent.

The preceding examples indicate that there is considerable redundancy in the Src family (i.e., one kinase can take the place of another if one is missing). However, whether different family members have distinct functions in a given cell remains unknown, since one kinase may normally be dedicated to a specific function but may perform others if another family member is missing.

Cellular Functions of Src Family Kinases: Signaling Adhesion and Immune Responses

The Src family kinases present in hematopoietic cells are activated by a number of stimuli, including integrin ligands, cytokines, and, notably, stimuli that act via immunoreceptors, such as the T-cell antigen receptor on thymocytes and circulating T lymphocytes, B-cell antigen receptor on pre-B cells, and immunoglobulin (Fc) receptors on macrophages. Cell-based assays confirm essential (but redundant) roles for Src kinases in immunoreceptor responses. Current models envisage weak association of Src kinases with the cytoplasmic tails of subunits associated with the immunoreceptors. Clustering of the receptors, possibly associated with altered proximity to protein tyrosine phosphatases (PTPs) and movement into or out of lipid rafts, activates the Src kinase, allowing phosphorylation of tyrosine-containing activation motifs in the immunoreceptors and recruitment of other SH2 domain-containing nonreceptor tyrosine kinases of the Syk and Tec/Btk families. In this situation, the key Src substrate is the immunoreceptor, but Src also contributes to phosphorylation of downstream signaling molecules involved in calcium mobilization and gene expression.

Src, Fyn, and Yes are also activated by adhesive stimuli and by soluble ligands that act via transmembrane receptors of the tyrosine kinase, G protein-coupled, cytokine, and other classes. The substrates phosphorylated vary according to the type of stimulus and the other proteins recruited by the respective receptor. For example, integrin stimulation causes Src activation and phosphorylation of another tyrosine kinase, FAK. The exact relationship between FAK activation and Src activation is not clear, but probably FAK autophosphorylates and activates Src, which further phosphorylates FAK. Both proteins contribute to phosphorylation of other proteins associated with the integrin. Functionally, absence of Src kinases alters cytoskeletal dynamics, for example, reducing turnover of focal adhesion complexes and slowing cell migration. However, Src activation by integrins also contributes to tyrosine phosphorylation of signaling molecules responsible for stimulating mitogen-activated protein kinase cascades and regulating gene expression. Src kinase activity is also required for cell proliferation induced by soluble growth factors acting via tyrosine kinase receptors. Dissecting the effects of Src activation by the growth factor receptor from the effects of Src activation by integrins is complex, since many cell cycle events elicited by growth factors depend on cell adhesion via integrins. Src kinase activity can also regulate protein traffic to and from membranes. In relaying such diverse signals, Src family kinases probably have many important substrates, more than one of which may be necessary for an observed biological response. Src kinases thus represent branch points for activation of multiple signaling pathways.

Regulation of Src Kinase Activity

The combined results of mutational and crystallographic analysis have led to a picture of Src as a machine that integrates many different inputs to regulate its conformation and kinase activity (see Figure 1). There are at least two conformational states, simply thought of as on and off. In the off state, the kinase domain is relatively inactive, and the SH2 and SH3 domains are engaged in low-affinity intramolecular interactions. In the on state, the intramolecular interactions are absent, the kinase domain is at least partially active, and the SH2 and SH3 domains are completely accessible for binding other proteins. Thus, in its on state, Src can also potentially act as a scaffold, independent of its kinase activity. For example, Src may bind one protein through its SH3 domain and another through its SH2 domain, bringing the two proteins into a complex that conveys a signal to the cell. However, the extent to which Src kinases have kinase-independent functions *in vivo* when expressed at normal levels is not yet clear.

Src in the on state is only partially active as a kinase, and the kinase domain becomes fully active only when the activation loop is phosphorylated, a reaction that may be intramolecular but that can also be catalyzed by nearby tyrosine kinases, including other Src molecules. Clustering of partially activated molecules may thus increase activation loop phosphorylation and lead to full activity. Such clustering may be important in regulation of Src family kinases by integrins and immunoreceptors. Conversely, dephosphorylation of the activation loop would reduce Src activity in the cell.

The on and off states are not stable structures, however. Molecular motions at physiological temperature cause these states to be somewhat flexible, allowing the equilibrium to be disturbed by interactions with ligands for the SH2 and SH3 domains. Because the individual intramolecular interactions stabilizing the off state are each rather weak, reduction of any one interaction leads to a concerted transition to the on state. Thus, increasing the local concentration of either an SH2 or an SH3 ligand would be expected to shift the equilibrium toward the on state. This is thought to occur in some situations in which viral proteins (such as polyoma virus middle T antigen and human immunodeficiency virus Nef) are highly expressed. Particularly potent activators would have binding sites for both the SH2 and SH3 domains. Because phosphorylation of substrates by the Src kinase can create binding sites for

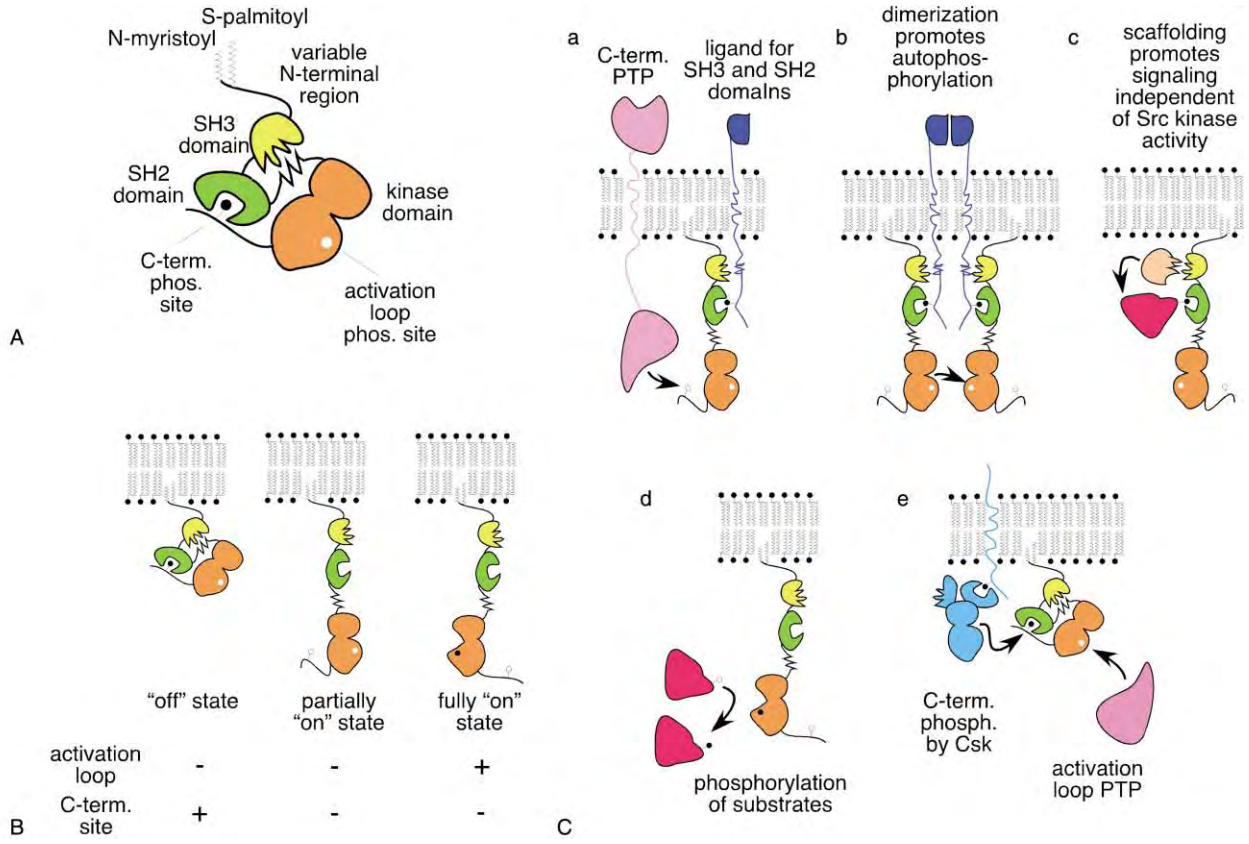

FIGURE 1 (A) Features of Src family kinases. The N terminus is modified by N-myristoylation and (for most but not all family members) by S-palmitoylation. Conserved structural domains are named SH3, SH2, and kinase (or SH1) domains, proceeding from N terminus to C terminus. In the off state conformation shown, the SH3 domain is engaged with a linker between the SH2 and kinase domains, and the SH2 domain is engaged with a phosphorylated tyrosine (black circle) near the C terminus. A tyrosine in the activation loop is not phosphorylated (white circle). (B) Different activity states of Src kinases. In both the partially and fully on states, the C-terminal phosphorylation site is dephosphorylated, and the molecule is opened into a flexible conformation with SH3, SH2, and kinase domains available for interactions with other proteins. In the fully on state, the activation loop phosphorylation site is phosphorylated, the kinase domain undergoes additional conformational changes, and substrates can be phosphorylated with high efficiency. (C) Regulatory interactions of Src kinases with other molecules in the cell. (a) Src can be partially activated by the combined or independent actions of PTPs that dephosphorylate the C-terminal site and protein ligands that can associate with the SH3 and/or SH2 domains. (b) Full activation may occur when partially activated molecules are brought together by clustering of a receptor or by decreased access to a PTP that dephosphorylates the activation loop (not shown). (c) Fully or partially active Src may also act as a scaffold, bringing proteins together but not phosphorylating them. (d) Active Src phosphorylates nearby cell proteins. Partially active Src may also phosphorylate substrates, but less efficiently. Substrates may be associated with the Src SH2 and/or SH3 domains. (e) Src is inactivated by the combined effects of Csk, which phosphorylates the C terminus, PTPs that dephosphorylate the activation loop, and inhibited access to SH2 and SH3 ligands (not shown). Csk may be recruited to Src by interactions with an anchor protein, such as Cbp/PAG. The PTP may also be specifically recruited (not shown). Interactions with regulatory molecules may be affected by movement of Src or the regulatory molecules between different microdomains in the lipid bilayer.

its SH2 domain, Src can be activated by the products of its own kinase activity. Clustering of Src with substrates containing SH3 domain-binding sites may thus activate Src under certain conditions. Removal of such ligands would allow Src to revert to the off state.

In addition to control by clustering and by phosphorylation of the activation loop, another control is provided by phosphorylation of a tyrosine residue in the carboxy terminus of Src. When phosphorylated, this tyrosine serves as a ligand for the Src SH2 domain, stabilizing the off state. Dephosphorylation of this site allows opening of the off state structure and hence activation. The carboxy-terminal region plays no apparent role when Src is active, and many mutationally activated forms of Src family kinases, found in various oncogenic retroviruses, have deleted or mutated this region. In the cell, a major source of Src regulation is provided by phosphatases that dephosphorylate the carboxy terminus and kinases that rephosphorylate this site. Genetic evidence suggests that the PTP CD45 is key to activating Lck in antigen-stimulated T cells, and that the PTPs RPTPα and Shp2 are involved in regulating Src in fibroblasts. However, to what extent these PTPs are regulated catalytically, and whether they provide a permissive environment in which Src family kinases can be activated by other means, is not clear.

Rephosphorylation of the carboxy terminus is catalyzed by a dedicated protein kinase, Csk, first identified by M. Okada and H. Nakagawa in brain extracts. Csk has few, if any, substrates other than the carboxy termini of Src family kinases. Genetic disruption of *csk* causes hyperactivation of Src family kinases, with consequent developmental abnormalities and death at mid-gestation stage. In *csk* mutant fibroblasts, Src family kinases are activated and the cells are transformed. A close Csk relative, Chk, may also be involved. In *Caenorhabditis elegans* and *Drosophila melanogaster*, Csk relatives can be recognized by sequence, and they are likely to function as Src inhibitors. Csk is structurally similar to Src family kinases but lacks the activation loop and carboxy-terminal tyrosine phosphorylation sites and an amino-terminal lipid modification site. It is thus not regulated like Src family kinases; its location inside cells, however, is regulated. Recent evidence indicates that Csk can bind to, and is activated by, one or more Src substrates (one named Cbp or PAG) that colocalize with activated Src family kinases in membrane subdomains. When these substrate molecules are phosphorylated, Csk is recruited by its SH2 domain, and the Csk is then brought close to the activated Src family kinases. Csk may also be associated, through its SH3 domain, with PTPs that target the activation loop tyrosine of Src. This mechanism would ensure that the Src family kinases are then turned back off by Csk-catalyzed phosphorylation of their carboxy termini and PTP-catalyzed dephosphorylation of the activation loop.

The activation state of an individual Src kinase molecule in the cell is thus the result of a balance between protein–protein interactions and phosphorylation and dephosphorylation of the activation loop and carboxy-terminal tyrosines. However, the activity state (on or off) also affects access by the modifying enzymes. Therefore, there is a complex balance of interactions that allows Src to integrate different inputs. In addition, Src molecules are subject to other post-translational modifications that regulate activity or localization. In mitosis, Src becomes phosphorylated by Cdk1/Cdc2-cyclin complexes. These serine phosphorylations partially activate Src by reducing the intramolecular interactions that stabilize the off state. In cells responding to agonists that increase cyclic AMP levels, the cAMP-dependent protein kinase phosphorylates Src and activates it.

Subcellular localization may also be regulated. All Src family kinases are associated with the plasma membrane and intracellular membranes by amino-terminal sequences. The amino-terminal methionine is removed and the next residue (glycine) is subject to N-myristoylation. This modification is cotranslational and not regulated, but the majority of Src family kinases are also subject to reversible, regulated lipid modification by palmitoylation. This modification affects one or more cysteine residues near the amino terminus. Palmitoylation ensures that most Src family kinases (with the exceptions of Src and Blk) are concentrated in microdomains within the plasma membrane that are enriched in phosphatidylinositol-4,5-bisphosphate, cholesterol, and glycosphingolipids, so-called lipid rafts. These microdomains are also enriched in many signaling molecules, placing the Src kinases close to potentially important substrates and effectors. Cbp/PAG, the aforementioned Csk-recruiting molecule, is also in the lipid rafts. Receptors bearing carboxy-terminal glycosylphosphatidylinositol anchors are localized in the outer leaflet of lipid rafts, and clustering these molecules activates Src family members associated with the inner leaflet. It seems probable that slight changes in protein distribution within lipid rafts will be very important for regulating Src kinase activity and directing phosphorylation activity to the appropriate substrates.

Nonvertebrate Src Kinases and their Functions

Genetic studies in the fruit fly *D. melanogaster* and nematode *C. elegans*, where there are fewer *src* genes (two in *D. melanogaster* and one in *C. elegans*), have not revealed distinctive mutant phenotypes. Thus, unlike several other signal transduction pathways, genetic analysis in these organisms has not led the way in understanding how Src is regulated and functions. It is possible that Src proteins in these organisms (as in vertebrates) serve as integrators of many different inputs, and mutations lead to pleiotropic phenotypes. However, one identified function of Src64B in *D. melanogaster* is to regulate cytoskeletal structures in the cells that nurse the developing oocyte, and it does so in concert with a Btk/Tec-related tyrosine kinase. In this regard, it resembles the role of Lck in activating Btk/Tec-related tyrosine kinases in mammalian lymphocytes. Src42A also regulates the actin cytoskeleton in the developing embryo. In *C. elegans*, Src is important in the early embryo for correct cell–cell interactions, which may implicate Src in cytoskeletal organization. Further study in these systems may provide insights into Src regulation and functions in vertebrates.

Summary: Integration of Many Inputs and Regulation of Many Outputs

The many ways to regulate Src family kinases, and the many substrates implicated in different downstream events, position Src family kinases as servants with many

masters. In the cell, Src kinases are regulated by the balance of kinases and phosphatases acting at both inhibitory and activating phosphorylation sites, and by proteins that bind to their SH2 and SH3 domains. The proteins phosphorylated depend on the subcellular localization and the protein complexes in which the active Src is found, and relay signals to regulate cytoskeletal, membrane, and nuclear events.

See Also the Following Articles

B-Cell Antigen Receptor • Glycosylphosphatidylinositol (GPI) Anchors • Immunoglobulin (Fc) Receptors • Integrin Signaling • Lipid Rafts • Mitogen-Activated Protein Kinase Family • Protein N-Myristoylated • Protein Palmitoylation • Reverse Transcriptase and Retroviral Replication • T-Cell Antigen Receptor

Glossary

C-terminal Src kinase (Csk) Kinase that phosphorylates the C-terminal tyrosine residue present on all Src-related kinases, thus inhibiting Src kinase activity.

protein tyrosine kinase A protein kinase that phosphorylates tyrosine residues in substrates.

SH2 domain A protein module that binds with high affinity to phosphotyrosine residues contained in a defined peptide sequence, with primary specificity usually being conferred to the three residues C-terminal to the phosphotyrosine.

SH3 domain A protein module that binds to sequences that adopt a left-handed type II polyproline helix, typically with a PXXP core.

Further Reading

Abram, C. L., and Courtneidge, S. A. (2000). Src family tyrosine kinases and growth factor signaling. *Exp. Cell Res.* **254**, 1–13.

Blume-Jensen, P., and Hunter, T. (2001). Oncogenic kinase signaling. *Nature* **411**, 355–365.

Lowell, C. A., and Soriano, P. (1996). Knockouts of Src-family kinases: Stiff bones, wimpy T cells, and bad memories. *Genes Dev.* **10**, 1845–1857.

Martin, G. S. (2001). The hunting of the Src. *Nat. Rev. Mol. Cell. Biol.* **2**, 467–475.

Sicheri, F., and Kuriyan, J. (1997). Structures of Src-family kinases. *Curr. Opin. Struct. Biol.* **7**, 777–785.

Thomas, S. M., and Brugge, J. S. (1997). Cellular functions regulated by Src family kinases. *Annu. Rev. Cell. Dev. Biol.* **13**, 513–609.

Weiss, A., and Littman, D. R. (1994). Signal transduction by lymphocyte antigen receptors. *Cell* **76**, 254–263.

Biography

Jonathan A. Cooper is a member of the Division of Basic Sciences at the Fred Hutchinson Cancer Research Center and an affiliate Professor in the Department of Biochemistry at the University of Washington in Seattle. He earned his Ph.D. at the University of Warwick and did postdoctoral work with Bernard Moss at the National Institutes of Health and with Tony Hunter at the Salk Institute. His principal research interests are the signaling pathways regulated by Src family kinases and the signaling and traffic functions of adaptor proteins.

Starvation

Oliver E. Owen and Richard W. Hanson
Case Western Reserve University School of Medicine, Cleveland, Ohio, USA

There is a paradoxical relationship between morbid obesity and starvation because most of the reproducible data regarding fasting metabolism were derived from obese people undergoing prolonged fasting periods to reduce their body weights. During starvation, blood glucose concentration falls and this decrease is paralleled by serum insulin concentrations. Proteolysis, lipolysis, gluconeogenesis, and ketogenesis ensue. During starvation there develops an orchestrated interplay among the organ systems to produce, select, and conserve fuels needed for body metabolism. Steady-state metabolic processes develop after ≃18 days of total starvation. Urinary excretion of nitrogen declines to 4–5 g day^{-1}, and ammonium becomes the primary nitrogenous excretory product. Blood substrates and hormones are near constant concentrations. Weight losses and energy requirements are comparable day after day. The brain derives the majority of its energy requirements by extracting β-hydroxybutyrate and acetoacetate from the blood. Glucose oxidation by the brain is suppressed. The liver supplies the large quantity of ketone bodies needed for brain metabolism. Muscle probably reduces acetoacetate to beta-hydroxybutyrate. The kidney permits a limited amount of ketone bodies to be excreted in the urine to maintain near-electrical neutrality with urinary ammonium. The kidney shares the essential but limited role of gluconeogenesis with the liver. Ketogenesis, gluconeogenesis, ammoniagenesis, ureagenesis, and ketonuria are tightly interrelated during prolonged starvation.

Starvation or hunger in humans is the deprivation of any or all of the elements necessary for their nutrition. Several extensive review chapters and books have been written about the physiological, biochemical, and psychological observations and measurements made during semi-starvation or total starvation. However, there is little reliable scientific information relating to weight loss, energy requirements, changes in the concentrations of hormones and substrate in the blood, and organ metabolism from healthy humans during or after prolonged periods of starvation. Nonetheless, reasonable conclusions regarding the metabolic effects of starvation can be made.

Food deprivation contrasts with conditions in most industrialized nations today, where obesity is epidemic and threatening the health of an increasing proportion of the population. There is a strange relationship between starvation and obesity in which overweight people often starve to lose weight.

The cells of the various organ systems require a continuous supply of energy to function. The biochemical mechanisms that maintain the constant availability of fuel to support metabolic functioning are part of a complex system of fuel homeostasis. All mammals store energy when food is available and mobilize the stored fuels during fasting.

This article focuses on the last century of metabolic studies that range from fasting overnight to prolonged starvation. It covers topics such as the loss of weight and energy requirements, the release of stored fuels, the conversion of free fatty acids (FFAs), glycerol, and amino acids into ketone bodies and glucose by the liver, the selective utilization of fuels by the brain and muscle, the conservation of fuels by the kidneys and their promotion of gluconeogenesis, and maintenance of acid–base balance.

Background

The resting metabolic rate (RMR) among humans varies widely. However, general principles of bioenergetics for adult humans, with body masses varying over a sixfold range, have been defined. First, the RMR increases as body weight increases; however, the energy requirement per unit weight decreases as body weight increases. Thus, as the weight of a human increases from 40 to 160 kg, the RMR per kg body weight decreases from 30 to 15 kcal per kg per 24 h. Second, based on total body weight, the RMR of men of a given weight is greater than it is for women. This difference disappears when the RMR is based on fat-free mass (FFM), measured by densitometry. Nonetheless, there is a broad range of energy requirements for people of identical gender and body weight, which is independent of body fat content. It is thus understandable why the quantity and nature of fuels oxidized under near-standard conditions among tens of thousands of human subjects show discrepancies for specific body sizes. However, there is general agreement when the fundamental rules of bioenergetics

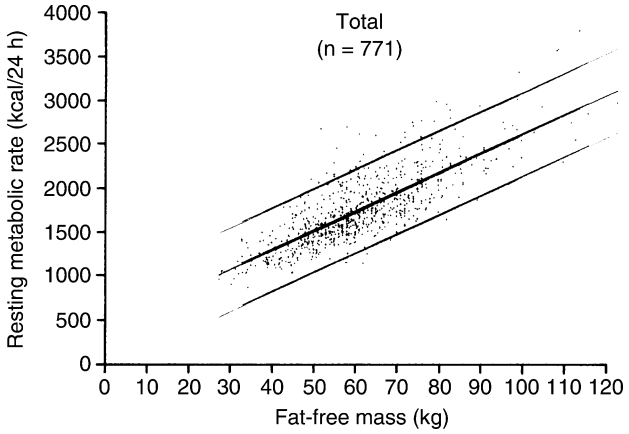

FIGURE 1 The relationship between fat-free mass, determined by hydrodensitometry, and the resting metabolic rate, as determined by indirect calorimetry, in 771 men and women.

are applied. This is illustrated in Figure 1 which shows the relationship between FFM and RMR in 771 men and women. It should be easier to understand why these data are diverse when the foregoing principles are applied to the analyses of the studies in Figure 1. A major advance in our understanding of the mechanisms of survival occurred with the advent of convenient and accurate methods for measuring β-hydroxybutyrate (β-OHB^-) and acetoacetate ($AcAc^-$). These two water-soluble, four-carbon compounds are synthesized from acetyl CoA derived from incomplete hepatic oxidation of long-chained fatty acids. Analytical techniques were developed in the laboratories of H.A. Krebs and coworkers in England. These fuels, along with acetone, are collectively referred to as ketone bodies and are immensely important for sustaining life during starvation.

Detailed, clinical studies of the biology of starvation began after 1965 when G.F. Cahill, Jr. and colleagues in the United States and elsewhere advanced the concept of fuel homeostasis in humans.

Obesity and Starvation, and Clinical Features of Starvation

It is somewhat paradoxical to note that mechanisms for maintaining the flux of fuels to provide the energy requirements to sustain life during starvation were derived primarily from normal and obese volunteers. These individuals were recruited from the general population or from hospitalized patients. Most of the volunteers and patients were housed in closely supervised, general clinical research units in hospitals. Those who underwent prolonged periods of starvation received water and, usually, salt tablets and multivitamins. All were studied after an overnight fast or during 3 to 63 days of total starvation.

A word about the courageous volunteers who made these important studies possible seems in order before we discuss the results. Prolonged starvation of the length mentioned above (up to 63 days) is a difficult physical and emotional experience and the volunteers required an enormous amount of support to complete these studies. Some developed headaches and postural hypotension during the first few days of total food deprivation. Everyone was preoccupied with hunger as starvation progressed. They did, however, usually develop a "team spirit" of trying to contribute the knowledge needed to understand what metabolic adaptations developed with weight loss during starvation. Understandably, some individuals became cantankerous and withdrew from the studies, and about one-half would manage to rarely sneak bits of food while under close observation, thus spoiling some of their data. Still, most of the volunteers struggled valiantly to comply with the research protocols. A sense of accomplishment pervaded the people working in facilities where these studies were conducted. We owe these individuals, whose names will never be known to us, a great debt of gratitude.

The compensated state of adult obese humans starving for experimental reasons is in sharp contrast to children, adults, and the elderly dying from inanition during famine or confinement in prisons. In the latter individuals, malnutrition is often complicated by other diseases. Understandably, their behavior varies from hostile selfishness to apathy and stupor. Superimposed bacterial, fungal, verminous, helminthic, and protozoal infections, with diarrhea, cough, and protuberant or contracted abdominal walls modify the clinical characteristics of starving people. Muscles can be "boggy or stringy." The loss of subcutaneous fat and muscle wasting accentuate the size of joints, especially the knees. The calf muscles are among the first to visibly shrink due to limited mobility, and the buttocks shows marked atrophy. Hair is broken and brittle and nails are split, pitted and spoon-shaped. The skin looks old and pale from anemia, but has regions of pressure hyperpigmentation, fistulae, and decubitus ulcers. Staring, sunken eyes search to identify anything, and the facial musculature is wasted and sometimes taut. Similar features are seen among patients hospitalized with severe malnutrition. Death occurs when about one-third to one-half of the lean body mass is lost in children, or lean and obese adults. In lean individuals practically all the body fat is mobilized before the irreversible state of malnutrition occurs.

The data from controlled starvation studies may not mimic many of the findings observed in patients from the harsh environments described above. Nonetheless, the data gathered from research centers provide the best available and reproducible data regarding starvation metabolism and fuel homeostasis. This data was collected largely over a period of about four decades.

As would be expected, the interpretation of some of the biomedical data changed with the accumulation of more information. An example of this is the changing attitude toward how the kidneys handle ketone bodies. As will be discussed in detail later, these ketone bodies play several metabolic roles and are essential for survival during prolonged starvation.

Metabolic Alteration Related to Starvation: Fed to Fasted to Fed

Fed State

When food is presented to an average hungry human who has undergone a mere 12 h overnight fast, he/she can readily eat at a rate of 150 times the individual's resting metabolic rate. Only minor perturbations occur in the concentrations of fuels in the blood but the postprandial concentration of insulin, the major anabolic hormone, can increase 50-fold in obese individuals. It may take several hours to digest, absorb, oxidize, and store the excessive caloric content of the food. Some of the nutrients that are consumed in overabundance are transiently stored as glycogen and intracellular amino acids or protein during the early postabsorptive period. However, the dominant storage form of energy in the body is triglyceride in adipose tissue. A human can consume about as much as 10 000–12 000 kcal per day for many days. If this excessive caloric intake continues over a long period of time, the adipose tissue mass can become huge, accounting for as much as 500 000–1 000 000 kcal of energy present as triglycerides. However, the maximum body fat content is usually limited to about one-half of the total body mass. Lean body mass also increases to support the fat mass. Thus, a 150 kg (330 lb) man or woman can have a triglyceride (fat) mass of $\simeq$75 kg (165 lb). The stored fat, along with some of the body protein and glycogen, is mobilized during semi-starvation or total fasting, usually when approximately 20–50 g of carbohydrate and 15–30 g of protein are eaten. However, during total, prolonged starvation among morbidly obese people, when amino acids are continuously mobilized from vital organs, (e.g. the heart), death may occur before the entire fat mass of the body is depleted. Thus, grossly obese humans subjected to prolonged starvation can die with body fat remaining.

Starved State

In going from the fed state to the starved state the body shifts from storing fuels to mobilizing fuels. The factors that control production and utilization of specific fuels change rapidly during this transition. In contrast, starving volunteers enter a near steady-state of metabolism after $\simeq$2–3 weeks of starvation, where day-to-day changes are minimal. During starvation, catabolism is tightly regulated and the supply of fuels from various depots adjusts to meet the body's energy requirements. Hepatic glycogen breakdown is brief (only 600 Kcal are available as hepatic glycogen in a 70 kg human), while proteolysis is continuous to supply gluconeogenic amino acid for energy and to maintain acid–base balance. The triglyceride present in adipose tissue is the major and persistent fuel reserve that supports metabolic process during starvation; it can account for as much as 90–93% of the body's energy needs during periods of prolonged starvation.

Refeeding

During a period of semi-starvation, a constant awareness of hunger dominates the thought processes of humans. During refeeding after periods of starvation or undernutrition, emaciated people may ingest as much food as possible, sometimes vomiting because of excessive intake. This craving for food persists until weight gain occurs largely from the deposition of fat in white adipose tissue. Eventually, weight gain plateaus and weight loss may occur until the body weight of an individual reaches an equilibrium that is at or near their weight before semi-starvation. On the other hand, after total starvation, the obese volunteers who become outpatients experience mild abdominal pain and may pass fecaliths. During the first 2–3 weeks of refeeding, these individuals routinely retain fluid and become edematous and are encouraged to maintain a low caloric intake until diuresis develops. However, the success rate for preventing the re-accumulation of body fat is low. Some clinical investigators hypothesize that the body possesses a "set-point" or has a body fat "lipostat." This is questionable because it is just as likely that individuals eat more than they need to replace body fat, and gain additional weight predominantly as adipose tissue.

Weight Loss, Body Composition, and Energy Requirements

The measurement of body weight is usually obtained accurately and easily. However, edema can complicate the interpretation of this simple measurement. Measuring body composition and energy requirements has several shortcomings. FFM or "active tissue" (lean body mass) is a conceptualized mass and difficult to measure accurately. This is because there are differences in the loss of mass among different organ systems in both the lean and obese individuals during starvation. The skeletal muscles and subcutaneous fat lose the greatest

quantity of weight. Among organs, the liver and spleen lose at least 50% of their usual mass. The gastrointestinal tract becomes atrophic; the diameter of the lumen of the small intestine becomes reduced to ≃50% of its normal diameter, and the villae become flattened. Gut motility also decreases. The heart decreases in size and the pulse rate and blood pressure decrease. The loss of bone mass is less than the loss of adipose tissue and skeletal muscle during experimental periods of starvation.

The energy needs of the body are determined by the sum of the metabolic requirements of various tissues (e.g. brain, liver, muscle, heart, adipose tissue, spleen, leucocytes, etc.) that depend on the mass and activity of individual organs. During the resting state, there is a 50- to 100-fold variation per unit mass for energy requirements among different tissue types (e.g. brain and adipose tissue). The energy requirements of skeletal muscles can change 12-fold in the transition from the resting state to strenuous exercise.

The proposed "metabolic efficiency" during starvation has long been claimed in lean people, but it has been difficult to demonstrate in starving, obese humans. Studies by Owen and colleagues differ from those of Leibel and associates in this regard. There is no question that as body size decreases in lean and obese humans; their metabolic requirements also decrease. Nonetheless, metabolic adaptation to starvation, where the energy requirements per unit of measurement decrease out of proportion to changes in unit of measurement, remains a perplexing issue. This is partly due to the method by which the data are calculated or expressed. The nonresting metabolic rate is more difficult to measure and is more inaccurate than estimates of the resting energy expenditure. Therefore, if there is an adaptive metabolic efficiency induced by food deprivation, it should be demonstrable by the (more) standardized RMR measurement. However, this has not been consistently demonstrated in all studies. Therefore, the increase in efficiency may be more apparent than real.

Thus, there remains an inadequately defined relationship between weight loss and metabolic rate. Contradictory data have been presented as to whether there is a decreased RMR per unit mass in adult men produced by prolonged semi-starvation. However, the normal RMR varies widely from low, normal or high values for humans of identical weight, gender and age. Therefore, it is not surprising that the literature on RMR for humans, based on the standard of measurement, is inconsistent. The differences among the various thyroid hormones, T_4, T_3, and rT_3, in lean and obese people subjected to protracted food deprivation may influence the RMR. It is well known that after about a week of total starvation, when the diuretic phase of starvation is completed, body weight loss was only ≃0.32% per day. Much later it was reported that the RMR of obese, starving volunteers, based on oxygen consumption per kg fat-free mass per day, and corrected for urinary nitrogen loss during starvation, is constant. This was truly disheartening for obese people who desperately wanted to lose body fat. It also showed clinical investigators how limited total starvation really is as a method for weight reduction for morbidly obese patients. Nonetheless, useful knowledge was gathered about starvation from these noble volunteers.

The Nature and Quantity of Fuels Oxidized during Starvation

Indirect calorimetry closely reflects the nature and quantity of the fuels oxidized. The results obtained using this method are influenced by dietary intake, total metabolic requirements, and state of physical activity. When lean individuals fast overnight, their nonprotein respiratory quotient (npRQ) is ≃0.84. This matches the previous day's intake of 12–20% protein, 40–45% fat, and 40–45% carbohydrate. When obese people eat the same balanced diet, but with a greater caloric intake to match their greater metabolic needs, the npRQ is significantly lower and decreases as body weight increases. Figure 2 shows the trend in the nature and quantity of fuels oxidized after an overnight fast in lean and obese humans. The data show that as weight and body fat increase, the npRQ falls. The greater the RMR, the greater the quantity of fat that is mobilized to meet the energy requirements of fasting humans. Due to body energy demands, obese humans shift into an accelerated rate of fat mobilization. However, this tendency to mobilize and oxidize stored fat becomes more obvious in

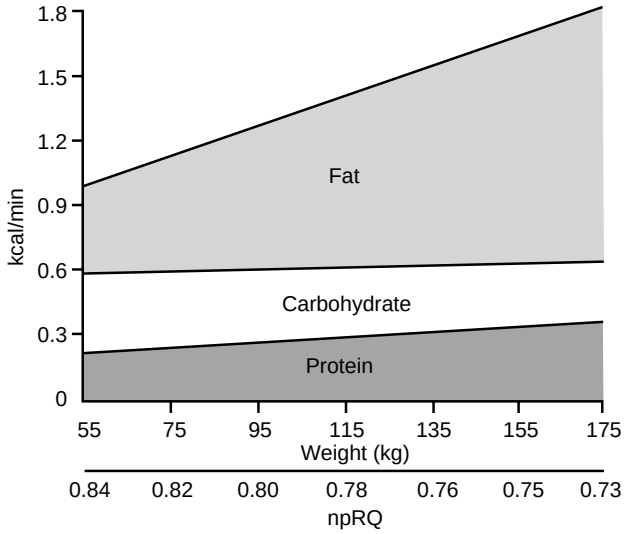

FIGURE 2 The nature and quantity of fuels oxidized by humans after a 12–14 h fast. Fat oxidation increases as body size increases.

both lean and obese people as fasting is prolonged. As starvation is extended to 2–3 days and beyond, lipids furnish 90–93% of the resting energy requirements in both lean and obese humans. These changes in the nature and quantities of fuels oxidized by tissues such as muscle and brain, spare carbohydrate (glucose) from oxidation; this provides the physiologic reasoning for insulin-resistance or insensitivity when carbohydrate oxidation must be curtailed for survival during food deprivation.

The absolute minimal rates for the major fuel utilization before death occurs have not been defined. The minimum requirement for fat and protein oxidation in grams/day/kg FFM has been approximated as follows: $\simeq 2.98 \pm 0.21$ g per kg per day FFM for fat; $\simeq 0.52 \pm 0.10$ g per kg per day FFM for protein. Glucose is derived from glyceride-glycerol, amino acid, and recycled lactate and pyruvate. About 1.91 ± 1.04 g per kg per day FFM are synthesized. However, most of the glucose that is synthesized during starvation is recycled from lactate and pyruvate (the Cori cycle), glycerol, alanine, and glutamine. The quantity of glucose that undergoes oxidation to CO_2 and H_2O is primarily determined by the catabolism of glucose in the central nervous system. This quantity is not closely related to the FFM because the size of the brain is unrelated to the FFM. The terminal oxidation of glucose is $\simeq 40–45$ g per day, which is derived primarily from gluconeogenesis from amino acids (alanine and glutamine) and glycerol.

In obese humans, during starvation there is no decrease in the metabolic requirement per unit mass, based on measurements of oxygen consumption. However, when the npRQ decreases below 0.7, the theoretical minimum for fat oxidation, there is a difficulty in extrapolating the respiratory exchange rates of O_2 and CO_2 and urinary nitrogen excretion into energy expenditure. The production of CO_2 falls disproportionately to O_2 consumption, creating a mysterious situation characterized by a calculated npRQ of 0.62–0.65. This unusual finding cannot be eliminated by correcting for ketonuria. However, it has been postulated that some of fatty acid released from triglyceride stores may undergo desaturation before being recycled to storage depots. The process of desaturation consumes oxygen and produces heat, but releases no carbon dioxide. Desaturated-FFAs in the blood have been identified in starving animals. If this process occurs in humans, the respiratory quotient (RQ) should rise before death, when unsaturated fatty acids are released and oxidized for energy. The RQ does rise in animals and humans during the pre-mortal period of starvation. This phenomenon has not been fully explained but is usually attributed to the mobilization and oxidation of amino acids. It is just as likely that it is due to oxidation of desaturated fatty acids.

Changes in the Concentration of Substrates and Hormones in the Blood

The concentration of glucose in the blood after an overnight fast is $\simeq 4.5$ mM; this value falls to $\simeq 3.6$ mM after 3 days of starvation. Thereafter, the concentration of glucose in the blood reaches a plateau. Anaerobic glycolysis in tissues such as muscle, brain, red blood cells, and kidney medulla converts glucose into lactate and pyruvate, and the liver extracts lactate and pyruvate to produce glucose. The concentration of lactate in the venous blood is less than 1.0 mM, while the concentration of pyruvate is less than 0.1 mM and is constant in the resting state. The concentration of FFA in the plasma rises from $\simeq 0.6$ mM, to $\simeq 1.4$ mM during the first few days of starvation. Thereafter, the concentrations of these fuels remain elevated and relatively constant. The rate of uptake and disposal of FFA is largely determined by its concentration in the blood. Insulin regulates the release of FFA from adipose tissue, primarily by influencing lipolysis, and thus the availability of FFA. The concentration of glycerol in the blood derived from lipolysis is less than 0.1 mM after an overnight fast and rises to 0.15 mM on the third day of starvation. Thereafter, glycerol remains constant because uptake, primarily by the liver, to synthesize glucose matches its release by adipose tissue. The concentration of triglycerides in the blood is less than 1.0 mM and remains constant during fasting.

A characteristic of fasting in humans is the presence of increased concentrations of ketone bodies in the blood (Figure 3) and urine. These water-soluble, short-chained compounds are synthesized primarily in the liver from the acetyl CoA derived from fatty-acid oxidation and serve as alternate fuels for tissues such as the brain. Ketone bodies replace glucose as the dominant energy source for the brain during starvation. Physical activity augments catabolism during starvation and promotes hyperketonemia. There are no other fuels in the blood that can change as markedly as the concentration of ketone bodies during starvation. This is partly due to the low concentration of ketone bodies in blood during the postprandial period, after a mixed meal containing adequate carbohydrate. After an overnight fast, lean people have blood $AcAc^-$ and β-OHB^- concentrations of $\simeq 0.05$ mM, while this value is slightly higher in obese individuals. Acetone is virtually absent after an overnight fast, unless the individual is regularly consuming a high-fat diet. There is an exponential rise in the concentration of $AcAc^-$ and β-OHB^- in the blood during starvation, until new steady levels develop. During the first 3 days of fasting, the $AcAc^-$ concentration in the blood increases to $\simeq 1.5$ mM, while β-OHB^- continues

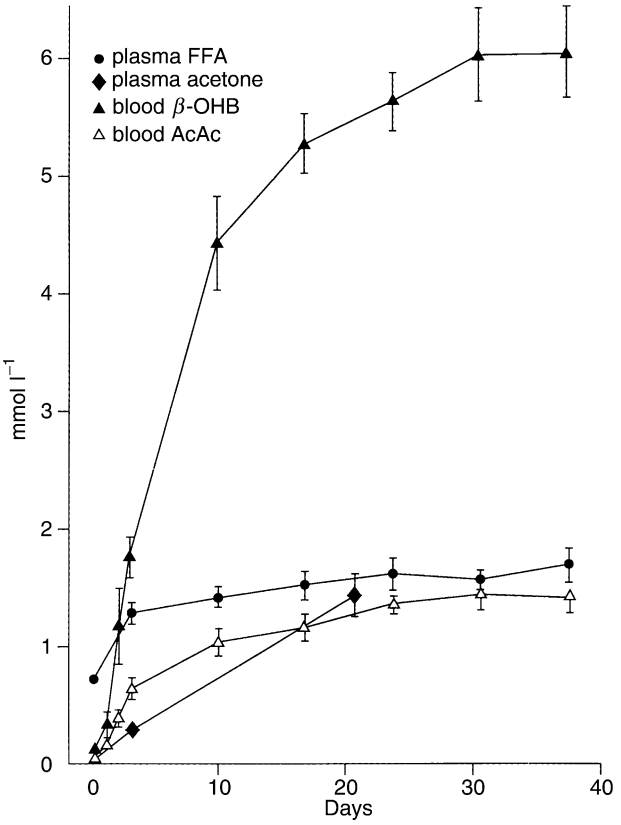

FIGURE 3 Changes in the concentration of ketone bodies and free fatty acids (FFA) during starvation.

to rise to ≃4.5 mM after day ten of starvation. $AcAc^-$ plus β-OHB^- reaches a plateau at ≃6–8 mM after 18 days of total starvation (water, salt, and vitamins were provided). The smell of acetone halitosis becomes evident after ≃2–3 days of starvation when the blood concentration is ≃0.25 mM. Acetone slowly increases to ≃0.35 mM after 21 days of starvation. A minimum estimate of the change in the concentration of ketone bodies in the blood from an overnight fast to 18 or more days of total starvation is 75–160 fold (0.1–0.2 mM to 15.0–16.0 mM). Blood $AcAc^-$ and β-OHB^- are anions and the hydrogen produced during ketogenesis combines with bicarbonate to form CO_2 and water. CO_2 is exhaled thus decreasing the concentration of bicarbonate in the blood; this creates the typical anion gap of ketonemia. Blood pH also falls appropriately (7.4 to 7.3), and a mild metabolic acidosis of starvation becomes evident.

The concentration of total amino acids in the plasma declines slowly from an overnight fasting value of ≃4.6 mM to ≃3.7 mM after 40 days of starvation. However, there are four basic patterns of change among the amino acids during total starvation, represented by alanine, glycine, valine, and glutamine. Alanine rapidly decreases to ≃30% of its overnight concentration. Glycine does the opposite; it rises nearly threefold, before reaching a plateau. The concentration of valine doubles in the plasma during the first 7–10 days of starvation, and then slowly and progressively falls to a value below its overnight fasting value. Venous glutamine, the predominant plasma amino acid, remains relatively stable during 5–6 weeks of fasting.

Blood urea nitrogen mimics the concentration of alanine in the blood. The concentration of creatinine in the blood slowly drifts downward, reflecting the decrease in muscle mass.

Hormonal Changes

Insulin is the main hormone that controls the anabolic processes that maintain fuel homeostasis in humans. Its secretion is primarily regulated by the blood glucose concentration, but the levels of amino acid, FFA and ketone bodies also modulate insulin release by the β-cells of the pancreas. The influence of insulin on the metabolism of the major organs is readily demonstrated in adipose tissue, skeletal muscle, liver, white blood cells, and other tissues. Insulin also inhibits glucagon secretion, a significant counter-balance catabolic hormone.

The concentration of insulin in the blood parallels the changes in the levels of glucose. The fall in the concentration of insulin diminishes some of its inhibitory effects on peripheral proteolysis and lipolysis. In the starved state, the concentration of insulin falls, resulting in a decrease in the rate of uptake of glucose, amino acids, and fatty acids in peripheral tissues and a subsequent increase in the rates of gluconeogenesis, lipolysis, and proteolysis. After an overnight fast, the concentration of insulin in the portal blood is 2–3 times greater than the peripheral venous concentration. After 2 to 3 days of starvation, the portal-peripheral insulin concentration gradient is small. During starvation, there is still a high enough concentration of insulin in the blood to limit the maximal rates of glycogenolysis, gluconeogenesis, and ketogenesis. In addition, insulin has at least two indirect effects on hepatic glucose and ketone body production. Insulin decreases the delivery of gluconeogenic precursors and FFA from the extrahepatic-tissue stores to the liver. As the concentration of insulin in the mesenteric blood decreases, the inhibitory effect of insulin on the β-cells of the pancreas curtails the secretion of glucagon. Thus, the low concentration of insulin in the blood promotes glucagon secretion.

Insulin has dual roles in controlling the release of glucose and ketone bodies from the liver (and kidney cortex), and the release of amino acid from muscle and FFA from adipose tissue. Glucagon has the opposite effect. It augments hepatic (and renal) gluconeogenesis and ketogenesis, and promotes peripheral lipolysis and proteolysis. A relatively low blood insulin concentration

and relatively high glucagon concentration creates a blood insulin/glucagon ratio that promotes fuel availability. These pancreatic hormones serve collectively to finely balance the fuel needs of various tissues. The catabolic role of glucagon is augmented by catecholamines, glucocorticoids, and growth hormones. Fuel homeostasis is critical for survival so there are multiple levels of hormonal control of this process.

Appetite Regulation

During starvation there are a number of factors that regulate the control of appetite. Ghrelin, an orexigenic hormone, primarily secreted by the stomach and duodenum, normally increases in the blood before meals and falls after meals. Ghrelin is thought to stimulate hunger, increase body weight, and decrease metabolic rate. Ghrelin rises with semi-starvation but its physiologic roles regarding hunger need further elucidation. Adipose tissue produces a satiety hormone, leptin, which suppresses appetite. The leptin concentration in the blood falls in parallel with insulin during the first three days of starvation. As body fat decreases during starvation, the blood leptin concentration decreases. A fall in the levels of leptin in the blood increases the hypothalamic concentration of neuropeptide Y, greatly stimulating appetite. However, the control of appetite is not a simple process, but rather involves the interaction of a number of neuroendocrine systems. There is no single hormonal neuropeptide that controls hunger in a starving human. Prolonged starvation causes exaggerated hunger, a psychosomatic state that dominates the conscious mind.

Insulin plays an important role in the regulation of appetite. Acting together with leptin, insulin circulates at concentrations proportional to the body fat content. Both hormones enter the CNS and bind to specific receptors in neurons involved in controlling food intake. The administration of leptin and insulin directly to the hypothalamus decreases appetite and suppresses food intake. It is probable that leptin is the more important of the two hormones since leptin deficiency, not a lack of insulin, results in obesity. The mechanism by which these hormones influence the CNS is the subject of intensive study. A detailed discussion of this area is beyond the scope of this article. However, it should be clear that during starvation, as the mass of adipose tissue decreases and the secretion of insulin by the pancreas is depressed due to a lack of food intake, the appetite centers of the brain would be stimulated by the lack of satiety signals such as leptin, insulin, and ghrelin.

Adipose tissue secretes a number of other regulatory peptides, besides leptin, that control fuel deposition. These include adiponectin, resistin, adipsin, acetylation-stimulating protein, angiotensinogen, and cytokines. The most abundant adipose specific hormone is adiponectin. The concentration of adiponectin in the blood is positively correlated with insulin sensitivity. Adiponectin promotes glucose uptake in muscle and fatty tissue. Its concentration in plasma is inversely related to adipose tissue mass, especially abdominal fat mass. The levels of adiponectin in the blood fall during semi- and total starvation, when glucose intolerance has been documented. Resistin is another protein secreted into the blood by adipose tissue, but it has an effect that is opposite to that of insulin. Its concentration in the blood of humans after prolonged starvation has not been defined. The behavior of adipose tissue cytokines in humans during weight reduction caused by semi-starvation is under investigation.

Biochemical Changes during Starvation

Starvation induces a number of specific biochemical changes that permit an individual to survive in the absence of food for a prolonged period of time. These include alterations in glucose synthesis, fatty acid utilization by specific tissues, and the preservation of nitrogen to insure the maintenance of lean body mass. Starvation is a catabolic state in which fuel reserves are mobilized to support metabolic needs. To understand the metabolic adaptations to starvation, it is first necessary to describe the available energy reserves of a human as starvation begins. It has been estimated that a 70 kg human contains 144 000 kcal as fat (largely as triglyceride), 24 000 kcal as protein (lean body mass), and only 900 kcal as carbohydrate (liver and muscle glycogen). The relatively low level of carbohydrate reserve in humans necessitates a number of biochemical adaptations to insure the appropriate energy supply to specific tissues. For example, the brain uses $\simeq$600 kcal of glucose each day; this means that the total carbohydrate reserve is depleted in about one day of starvation! It is clear that mechanisms must exist for the use of fuels other than glucose (fatty acids and ketone bodies) by tissues such as the muscle and the brain, to insure survival during starvation. This process is called "fuel sparing."

Control of Fatty Acid Release during Starvation

Since fat is the major caloric reserve in humans, the regulation of mobilization of FFA from adipose tissue during starvation is a critical factor for survival. The breakdown of triglyceride via lipolysis is under the control of a number of hormones, including

epinephrine, glucagon, glucocorticoids, and insulin. The concentration of insulin in the blood falls by $\simeq 50\%$ after 3 days of starvation. At the same time there is an increase in the concentration of glucagon. This change in the insulin to glucagon ratio is a critical factor in the increase in lipolysis and the enhanced rate of hepatic and renal gluconeogenesis that occurs during starvation. Insulin is the major antilipolytic hormone and its decrease is the major factor in insuring the increased availability of the fatty acids needed for energy metabolism during starvation.

Adipose tissue contains a hormone-sensitive lipase that is sensitive to the state of its phosphorylation. An increase in the concentration of cAMP in the tissue (caused by a rise in epinephrine, glucagon and growth hormone, and a drop in the level of insulin) activates protein kinase A (PKA) that in turn phosphorylates, and thus activates the hormone-sensitive lipase; this results in the breakdown of triglyceride and generation of FFA. Insulin counters this process, partly by decreasing the levels of cAMP in the adipose tissue, and by increasing the activity of a phosphoprotein phosphatase that dephosphorylates the hormone-sensitive lipase, thereby inactivating it. There is also evidence that insulin increases the activity of a phosphodiesterase in the adipocyte, causing a fall in the concentration of cAMP in the tissue. The net result of prolonged starvation is an enhanced rate of FFA release from adipose tissue that is used as a fuel by a number of tissues.

About 50% of the plasma FFA presented to the liver during starvation is extracted and $\simeq 50-80\%$ of the extracted fatty acids undergo partial oxidation to synthesize equal quantities of $AcAc^-$ and β-OHB^-. Most of the remaining quantity of FFA extracted by the liver is converted to triglycerides and recycled to adipose tissue as VLDL. It is interesting that such a large fraction of the FFA released by lipolysis is re-esterified back to triglyceride in adipose tissue or in the liver and other tissues, and returned to the adipose tissue for the resynthesis of triglyceride. Fatty acid recycling via this so-called triglyceride–fatty acid cycle can account for as much as 60% of the fatty acid released after 3 to 4 days of starvation in humans. The synthesis of triglyceride requires the generation of 3-phosphoglycerol, usually from glucose. During starvation, when glucose is at a premium, the 3-phosphoglycerol is generated from pyruvate, lactate, and amino acids via an abbreviated version of gluconeogenesis termed *glyceroneogenesis*. The triglyceride/fatty acid cycle is a "futile cycle" that uses energy for the synthesis of triglyceride (6 molecules of ATP per molecule of triglyceride synthesized), so it must have a role in preserving the FFA that was released by adipose tissue to be used later as a fuel by peripheral tissues.

Proteolysis and Amino Acid Metabolism

After a meal containing proteins, amino acids largely escape hepatic extraction and are carried by the blood to extrahepatic tissues. Insulin promotes the active transport of amino acids into cells, primarily skeletal muscle. Normally, amino acids are in a state of flux; they are precursors for protein synthesis and then appear as free amino acids after protein breakdown. Within the first day of starvation, however, protein catabolism dominates the metabolic flux. As starvation progresses, relatively more proteolysis occurs and amino acids are mobilized from protein depots. The dominant fate of the carbon skeletons and the amino and amide groups derived from the breakdown of amino acids in muscle, is conversion to alanine and glutamine that is mobilized from muscle and other depots and transported to liver and kidney to be utilized to synthesize glucose, urea, and ammonia.

Protein catabolism in the splanchnic tissues is somewhat less responsive to insulin than it is in skeletal muscles. In the periphery, the basal concentration of insulin that is present during starvation, limits proteolysis. Nonetheless, glucose must be continually synthesized from amino acids by the liver and kidney cortex during starvation; amino acids from muscle protein are a major source of carbon for gluconeogenesis. The first proteins degraded during starvation are the digestive enzymes secreted from the stomach, pancreas, and small intestine. The liver also loses various enzymes needed to process incoming nutrients into plasma protein, e.g., albumin. Thereafter, the largest protein mass of the body, striated muscle, begins to be drained, not only of intracellular proteins, such as enzymes, but also the contractile elements. The disintegrating muscles can easily be seen as skeletal muscle atrophy during prolonged starvation in humans.

The control of proteolysis in muscle is a complex process. Insulin retards proteolysis and enhances protein synthesis. In addition, metabolic acidosis promotes protein breakdown to insure the generation of ammonia to titrate the acidity of the tubular urine. The low plasma insulin concentration and mild metabolic acidosis of starvation are conducive to proteolysis. The best characterized pathway for protein catabolism is an ATP-independent system of acid proteases (cathepsin) and hydrolases contained in cellular lysosomes. In addition, there are calcium-dependent proteases, as well as cytosolic ATP-dependent and independent pathways. The most important muscle proteolytic system employs the ubiquitin proteasome pathways.

Amino acids generated from proteolysis undergo deamination and/or deamidation before entering the

tricarboxylic acid (TCA) cycle to participate in further transformations to alanine or glutamine which efflux from cells. Alanine plus glutamine account for ≃80% of the amino acids released from muscle after prolonged starvation, and are the principal vehicles for transporting nitrogen from peripheral tissues to liver and kidney. These two amino acids together account for only 10% of the composition of skeletal muscle protein, but they provide the majority of the carbon for the synthesis of glucose by the liver and kidney during starvation. Thus, there is a net conversion of other amino acids into alanine and glutamine in the muscle. Alanine is the major nitrogenous compound released from muscle and extracted by the liver for gluconeogenesis and ureagenesis. There is a "glucose–alanine" cycle between muscle and liver. Glutamine is the other amino acid released in high levels by muscle, but it is extracted from the blood by the kidney cortex to produce glucose and ammonia. During the catabolism of muscle, branched-chain amino acids provide the amino groups to α-ketoglutarate to form glutamate via glutamate dehydrogenase; glutamine is derived from glutamate and ammonia by the action of glutamine synthase.

The TCA cycle is the key metabolic pathway for energy production: acetyl CoA is oxidized to carbon dioxide. During starvation, the TCA cycle has another fundamental role in metabolism. Amino acids are catabolized to 4- (aspartate, asparagines, phenylalanine, tyrosine, methionine, isoleucine, and valine) and 5- (glutamine, glutamate, histidine, proline, and arginine) carbon intermediates that enter the TCA cycle by a process termed *anaplerosis*. The TCA cycle cannot serve as a carbon sink; therefore, the carbon atoms that enter the TCA cycle must leave the TCA cycle by a process called *cataplerosis*. Anaplerosis and cataplerosis are reciprocal reactions that must be balanced. These reactions have been reviewed in detail elsewhere in this volume.

During starvation, more fuels are released from storage depots or synthesized in liver and kidney than are oxidized to generate energy. About 60% of the fuels that enter the bloodstream are recycled, e.g., FFA, glucose and amino acids, especially alanine and glutamine.

Ketogenesis

The liver not only stores glucose as glycogen, it also converts fuels such as FFA, amino acids, lactate, pyruvate, and glycerol to glucose and ketone bodies; it also detoxifies the ammonia from amino acid breakdown by converting it to urea. After an overnight fast, hepatic glycogenolysis, gluconeogenesis, and ketogenesis provide ≃50% of the total energy-yielding fuels for the body in the resting state. Lipolysis of triglyceride in adipose tissue supplies FFA and glycerol; these substrates become precursors for ketone body (fatty acids) and glucose (glycerol) syntheses. Amino acids released primarily by skeletal muscles complement glycerol as gluconeogenic precursors. As fasting is prolonged, the kidney cortex also contributes to fuel homeostasis by conserving substrates and sharing the gluconeogenic role with the liver.

Ketone bodies are the only fuels synthesized in the body that do not recycle. Unlike FFA, amino acids and glucose, ketone bodies are either oxidized or excreted in the urine and/or the breath (acetone). A small amount of acetone can be converted to glucose. β-OHB^- and $AcAc^-$ are synthesized in the liver (and kidney) mitochondria by the following reactions. Two molecules of acetyl CoA condense head-to-tail to form acetoacetyl CoA; this reaction is catalyzed by acetoacetyl CoA thiolase. Another molecule of acetyl CoA is joined by β-hydroxy-β-methylglutaryl CoA (HMG CoA) synthase to form HMG CoA, also generating a hydronium ion (H^+). HMG CoA lyase cleaves HMG CoA into $AcAc^-$ and acetyl CoA. $AcAc^-$ is then reduced to β-OHB^- by β-hydroxybutyrate dehydrogenase. Acetone and CO_2 are formed from the degeneration of $AcAc^-$. Ketone bodies are synthesized from the acetyl CoA that is derived from the β-oxidation of fatty acids in the mitochondria. A small quantity can be synthesized from ketogenic amino acids during starvation. In addition, acetoacetyl CoA can be formed from FFA and cleaved to $AcAc^-$ in the kidneys. The hepatic production of β-OHB^- and $AcAc^-$ are about equal. During hyperketonemia, the concentration of β-OHB^- in the blood is ≃3 times greater than $AcAc^-$. This is due to the preferential removal of $AcAc^-$ or conversion of $AcAc^-$ to β-OHB^- by skeletal muscle. The brain removes β-OHB^- and $AcAc^-$ in a concentration-dependent manner.

The metabolism of ketone bodies during starvation is a critical element in the control of fuel homeostasis in humans. The demonstration that β-OHB^- and $AcAc^-$ could serve as major fuels for the metabolism of the brain during starvation provided the information needed to evaluate the roles of fatty acid oxidation, amino acid mobilization, glucose conservation, and urinary nitrogen excretion during prolonged starvation. From this research it became clear that the abundance of FFA stored in humans provides a substantial reserve for the synthesis of ketone bodies. The metabolism of ketones by the brain during starvation greatly limits the need to use amino acids to make glucose to support the metabolism of this tissue. This is an important example of "fuel sparing."

There are few synthetic processes that are quantitatively as large as the daily rate of ketogenesis during starvation. After an overnight fast, hepatic ketogenesis amounts to ≃10 g per day. After 2–3 days of starvation the liver synthesizes over 100–150 g per day of ketone bodies. Over this period, the average resting human

oxidizes a minimum of ≃3 g of fat per kg FFM per day. Thus, a large, but not obese adult man, weighing 80 kg, with a body composition of 80% FFM (64 kg) and 20% fat mass (16 kg) oxidizes a minimum of ≃192 g of fat per day. About 60 g of the FFA derived from the lipid stores undergo β-oxidation in the liver to yield an estimated 113 g per day of ketone bodies. Ninety percent of these water-soluble fuels undergo terminal oxidation, primarily by the brain and muscle. Most of the remainder is excreted in the urine. It is interesting to note that about half of the molecular weight of $AcAc^-$ and β-OHB^- is oxygen. Thus, if 10–12 g of ketone bodies are excreted in the urine, only 5–6 g of the carbon skeleton is derived from stored triglycerides. Since β-OHB^- and $AcAc^-$ are excreted with near equimolar quantities of NH_4^+, ketosis is an energetically cheap way to excrete nitrogen (the synthesis of urea requires 4 molecules of ATP per molecule of urea). Finally, for each gram of nitrogen lost in the urine ≃3.57 g of glucose is synthesized.

Gluconeogenesis

The *de novo* synthesis of glucose from nonhexose precursors (gluconeogenesis) occurs in the liver, kidney cortex, and perhaps to a minor extent in the small intestine. The precursor molecules for gluconeogenesis, and the organs involved in this process, change as starvation progresses. After an overnight fast, the liver is the primary, if not the sole, organ that makes a net contribution to glucose in the blood. The kidney extracts and releases glucose after an overnight fast but its overall contribution is minimal. After 3 days of starvation, renal gluconeogenesis increases and by 10–18 days of total starvation the kidney contributes ≃50% of the glucose added to the blood. However, during prolonged starvation, total glucose added to the blood from gluconeogenesis is only ≃50% of what it was after an overnight fast when gluconeogenesis is greatly complemented by hepatic glycogenolysis. In addition, during prolonged starvation only half of this glucose contributed to the blood is oxidized to CO_2 and H_2O. This is the result of the "sparing" of glucose by tissues that use more abundant fuels such as ketone bodies.

A schematic representation of the quantities of ketone bodies and glucose contributed to the blood by the liver and kidneys is shown in Figure 4. In general, glycogenolysis decreases as gluconeogenesis increases, and glucose production decreases as ketogenesis increases. An interesting aspect of gluconeogenesis during starvation is the relationship between renal gluconeogenesis and ammoniagenesis. Glutamine produced by the muscle is used by the kidney cortex as the major source of carbon for gluconeogenesis. The amino and amide groups are removed from glutamine to form α-ketoglutarate,

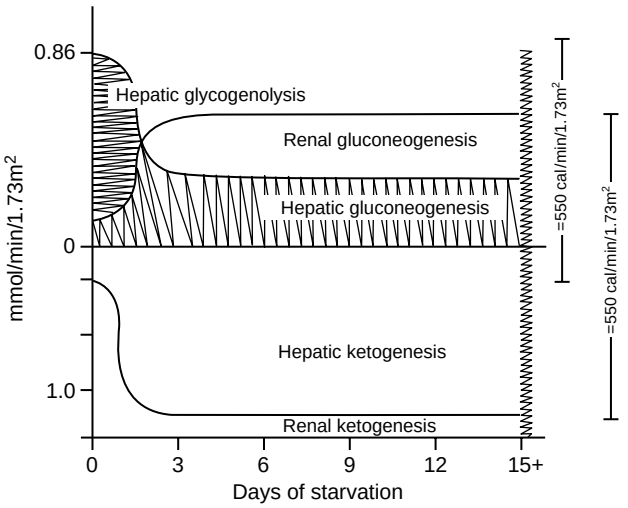

FIGURE 4 Schematic representation of fuel delivery by the liver and kidney during starvation. Hepatic gluconeogenesis, glycogenolysis and ketogenesis, and renal gluconeogenesis are expressed as mmol/min and converted to calories per 1.73m² body surface area. Hepatic glycogenolysis is rapidly dissipated during the first 1–3 days of fasting. The liver and kidney share the role of gluconeogenesis as starvation progresses. Hepatic ketogenesis becomes a dominant mechanism for supplying fuels to the blood after liver glycogenolysis is curtailed. Renal ketogenesis may contribute to ketonuria, but not to ketonemia.

which then enters the TCA cycle and is converted to glucose via renal gluconeogenesis. The kidney also has the ability to synthesize glucose from lactate, pyruvate, glycerol, amino acids and other precursors, but only glutamine has been closely associated with net renal gluconeogenesis.

The decreased rate of glucose production during starvation is linked to the increased ketone body production. Hyperketonemia is accompanied by ketonuria and ammoniagenesis. Renal NH_4 production is coupled to renal gluconeogenesis, while the release of NH_3 by the kidney is linked to hepatic urea production. In summary, gluconeogenesis, ketogenesis, ammoniagenesis, acid–base balance, and ureagenesis are all tightly interdependent during starvation.

Urinary Nitrogen Excretion

Total, daily urinary excretion undergoes an asymptotic, progressive decrease during starvation (Figure 5). Humans that consume a diet with 100 g protein (16.0 g nitrogen) excrete 15.5 g of nitrogen in the urine. Most of the nitrogen (85%) is excreted as urea. Ammonium, uric acid, and creatinine account for most of the remaining urinary nitrogen. Starvation initially induces an acute decrease in total nitrogen excretion. After 3–6 days of starvation, total urinary nitrogen decreases gradually, so that after 36 days of starvation

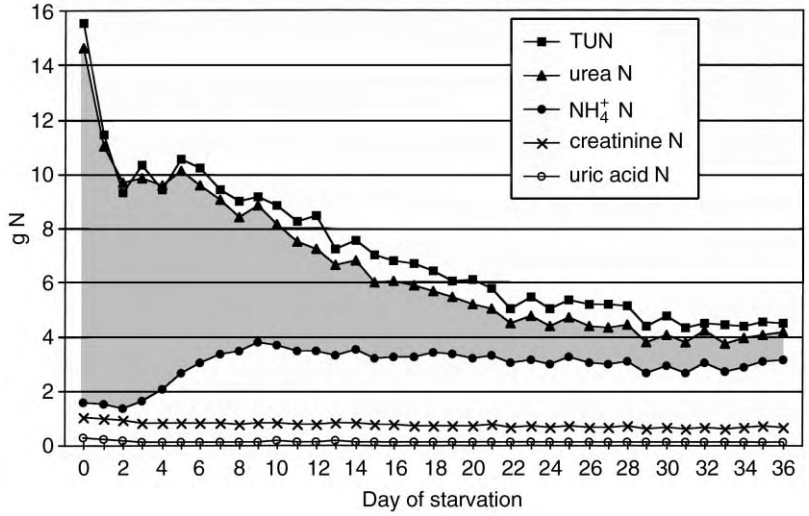

FIGURE 5 The total quantity and various components of urinary nitrogen excretion during prolonged starvation when five men and five women volunteers were given water, salt, and vitamins. TUN is an abbreviation for total urinary nitrogen. The nitrogen contents of urea, ammonium, creatinine, and uric acid are displayed.

the nitrogen excretion is $\simeq$4.6 g per day. The biggest decrease is in the exponential decay in urea nitrogen excretion. The excretion of ammonium ion (NH_4^+) parallels the excretion of $AcAc^-$ and β-OHB^-; it peaks at $\simeq$120–140 mmol per day at 6–9 days of starvation. After 15–18 days of drinking only water, NH_4^+ overtakes urea as the dominant urinary nitrogen compound. Urinary NH_4^+ gradually decreases as starvation is prolonged. NH_4^+, $AcAc^-$, and β-OHB^- urinary excretion rates are sensitive to small quantities of ingested glucose. In early studies of metabolism during starvation, subjects were allowed to drink beverages that contained carbohydrates. This distorted both urea and NH_4^+ urinary excretion. The excretion of creatinine decays in a linear manner that is dependent upon diminishing body muscle mass that occurs as starvation progresses. The output of uric acid in the urine drops acutely during the first 4 days of starvation as ketonuria rises. Thereafter uric acid nitrogen excretion plateaus at $\simeq$2 mmol per day (120 mg per day).

The rate of urea excretion provided the first clue that the concept that brain metabolized only glucose for energy had to be modified. Research in the first half of the twentieth century established that for each gram of urinary nitrogen excreted $\simeq$3.5 g of glucose could be synthesized from amino acids. Excluding the glycerol that is present in triglycerides, only trivial quantities of glucose could be derived from triglyceride. The brain requires $\simeq$100–125 g of glucose or equivalent energy sources daily. Plasma FFAs cannot pass the blood–brain barrier to provide a source of energy. In 1967 it was shown that $AcAc^-$ and β-OHB^- were the primary fuels for brain metabolism during starvation. Therefore, gluconeogenesis is clearly important during starvation, but the quantity of glucose formed is less than the quantity needed to provide energy for the brain. However, it should be pointed out that tissues such as the red blood cells, kidney medulla, and lens of the eye use glycolysis for energy production. The lactate and pyruvate generated by these tissues are recycled to the liver for the production of glucose.

Fuel Consumption during Starvation

While the liver and kidney release glucose into the blood during starvation, only the liver makes a net contribution of ketone bodies. However, more urinary excretion of $AcAc^-$ and β-OHB^- occurs than is extracted across the renal vascular beds, suggesting that the kidneys synthesize some of the ketone bodies excreted in the urine. Ketonuria augments ammoniagenesis. The deamination of glutamine to form α-ketoglutarate generates two molecules of NH_4^+, which are released into the tubular urine to maintain electroneutrality and acid–base balance. As mentioned above, the α-ketoglutarate produced in this process enters the TCA cycle via anaplerosis, and is subsequently converted to glucose that is released into the blood. The kidney can also convert lactate, pyruvate, other amino acids, and perhaps glycerol into glucose. Clearly the kidney shares the role of glucose production with the liver, but the kidneys make a net contribution to blood only after several days of starvation.

Early in starvation, the small intestine may provide gluconeogenic amino acids to the splanchnic (portal) system, but by 3 days of fasting there is no easily detected release of alanine or glutamine into the portal blood in fasting humans.

After $\simeq 3$ days of starvation skeletal muscles derive $\simeq 50\%$ of their energy requirements from ketone bodies and, as fasting progresses, muscle preferentially extracts a small quantity of $AcAc^-$ and may release β-OHB^-. At this time in starvation, FFA provides the great majority of fuels for muscle.

After an overnight fast the brain derives its energy from glucose, consuming $\simeq 100-125$ g per day. As starvation progresses and blood glucose concentration decreases and the concentration of $AcAc^-$ and β-OHB^- increases, ketone bodies become the major fuels for brain metabolism. These water-soluble fuels have access to neurons and can supply $\simeq 2/3$ of the total energy requirements during prolonged starvation.

Concluding Statement

Humans are capable of surviving long periods without food, but there are major limitations in this ability. When about one-half of lean body tissue is consumed to provide energy, death occurs. Morbidly obese people subjected to prolonged starvation can deplete the vital organs of structural proteins and die fat. The adaptations that permit humans to survive in the absence of food provide a fascinating look at the underlying biochemical adaptations to starvation. Much of what we know about the biological response to long-term starvation came from research with human volunteers who deserve our heartfelt thanks.

See Also the Following Articles

A-Kinase Anchoring Proteins • Amino Acid Metabolism • Fat Mobilization: Perilipin and Hormone-Sensitive Lipase • Fatty Acid Oxidation • Glycogen Metabolism • Insulin- and Glucagon-Secreting Cells of the Pancreas • Insulin Receptor Family • Ketogenesis • Leptin • Pyruvate Carboxylation, Transamination and Gluconeogenesis • Tricarboxylic Acid Cycle

Glossary

fuel homeostasis The steady-state maintenance of fuels.
gluconeogenesis The synthesis of glucose from nonhexose precursors.
glycogenolysis The breakdown of glycogen.
ketogenesis The synthesis of acetoacetate and β-hydroxybutyrate and the generation of acetone.
starvation The deprivation of any or all of the elements for nutrition.

Further Reading

Balasse, E. O. (1979). Kinetics of ketone body metabolism in fasting humans. *Metabolism* **28**(1), 41–50.

Cahill, G. F. Jr. (1970). Starvation in man. *N. Engl. J. Med.* **282**, 668–675.

Felig, P., and Bergman, M. (1995). The endocrine pancreas: Diabetes mellitus. In *Endocrinology and Metabolism* (P. Felig, J. D. Baxter and L. A. Frohman, eds.) 3rd edition, pp. 1107–1250. McGraw-Hill, New York.

Keys, A. J., Brozek, J., Henschel, A., Mickelsen, O., and Taylor, H. L. (1950). *The Biology of Human Starvation*, Vols I and II, University of Minnesota Press, Minneapolis.

Leibel, R. M., Rosenbaum, M., and Hirsch, J. (1995). Changes in energy expenditure resulting from altered body weight. *N. Engl. J. Med.* **332**, 621–628.

Owen, O. E., and Reichard, G. F. Jr. (1971). Human forearm metabolism during progressive starvation. *J. Clin. Invest.* **50**, 1536–1545.

Owen, O. E., Morgan, A. P., Kemp, H. G., Sullivan, J. M., Herrera, M. G., and Cahill, G. F. Jr. (1967). Brain metabolism during fasting. *J. Clin. Invest.* **46**, 1589–1595.

Owen, O. E., Licht, J. H., and Sapir, D. G. (1981). Renal function and effects of partial rehydration during diabetic ketoacidosis. *Diabetes* **30**, 510–518.

Owen, O. E., Smalley, K. J., D'Alessio, D. A., Mozzoli, M. A., Knerr, A. N., Kendrick, Z. V., Kavle, E. C., Donohoe, M., Tappy, L., and Boden, G. (1990). Resting metabolic rate and body composition of achondroplastic dwarfs. *Medicine* **69**(1), 56–67.

Owen, O. E., Kalhan, S. C., and Hanson, R. W. (2002). The key role of anaplerosis and cataplerosis for citric acid cycle function. *J. Biol. Chem.* **277**(34), 30409–30412.

Biography

Richard W. Hanson is Professor of biochemistry at Case Western Reserve University School of Medicine in Cleveland, Ohio. For many years he has been an Associate Editor of the *Journal of Biological Chemistry* and was the President of the American Society of Biochemistry and Molecular Biology. His research interests include the dietary and hormonal control of gene transcription and the regulation of gluconeogenesis and glyceroneogenesis in mammals.

Oliver E. Owen was previously Professor of medicine and Co-Principal Investigator and Program Director, General Clinical Research Center, Temple University School of Medicine and Hospital, and formerly Professor and Chair of medicine, Southern Illinois University School of Medicine.

Steroid/Thyroid Hormone Receptors

Ramesh Narayanan and Nancy L. Weigel
Baylor College of Medicine, Houston, Texas, USA

Steroid and thyroid hormones are important in regulating a wide variety of normal physiological processes, including development, metabolism, and reproduction. The receptors for these hormones are members of the nuclear receptor superfamily of ligand-activated transcription factors. For the most part, each hormone interacts with a unique receptor although the receptor may have multiple forms derived from the same gene by various mechanisms. Exceptions include estradiol, which activates two receptors derived from independent genes, estrogen receptor α (ERα) and the recently discovered estrogen receptor β (ERβ), thyroid hormone receptors (TRα and TRβ), and retinoic acids, which activate the retinoic acid receptors (α, β, and γ). In response to their cognate hormones, nuclear receptors bind to specific DNA sequences altering transcription. In addition to their best-characterized actions as DNA-binding transcription factors, the receptors also influence transcription and resulting cell function through direct interactions with other transcription factors, as well as through alterations in cell signaling. These functions and the structures of the receptors are described in this article.

Overview of Nuclear Receptor Ligands and Mechanism of Action

Figure 1 shows the structures of some of the ligands for members of the nuclear receptor family. Estradiol is the primary ligand for both estrogen receptors, ERα and ERβ. Testosterone, which is closely related to estradiol, is one of the two major ligands for the androgen receptor (AR). The ligands for the thyroid hormone receptor (T_3 and T_4) and the vitamin D receptor ($1,25(OH)_2D_3$) are also shown. The five major classes of steroids are synthesized from pregnenolone, which is derived from cholesterol through the actions of the cholesterol side-chain cleavage enzyme (P450scc). The synthesis of the hormones is complex, with a number of alternate pathways leading to the same hormone. Testosterone and estradiol are derived from 17α-hydroxy pregnenolone. Testosterone, the major circulating androgen, is synthesized in the testes of males and in the ovaries of females. It is important for development of the male reproductive tract, fertility, and secondary male characteristics. Estradiol, the major circulating estrogen, is produced in the ovaries of females. Estradiol is important in the female reproductive tract, playing roles in breast and uterine development, fertility, and also in bone and other tissues. Progesterone is synthesized directly from pregnenolone, and the major site of synthesis in females is the ovary. Progesterone, acting through the progesterone receptor, plays important roles in the breast and uterus and in the maintenance of pregnancy. Progesterone is a precursor of corticosterone and aldosterone, which are synthesized in the adrenal glands. The mineralocorticoid, aldosterone, is important for salt retention in the kidney. The glucocorticoid, cortisol, is produced in the adrenals from 17α-hydroxy pregnenolone and is important for regulation of carbohydrate metabolism; it also plays a role in suppressing immune responses. The secosteroid, $1,25(OH)_2D_3$, is derived from cholesterol through a UV-catalyzed reaction in the epidermis followed by sequential hydroxylations in the liver and kidney. The action of $1,25(OH)_2D_3$ is important for calcium homeostasis and also plays a role in the differentiation of a variety of tissues. Thyroid hormones are produced from tyrosines and iodide in the thyroid gland. Thyroid hormones have multiple actions in regulating metabolism, typically increasing oxidation rates. The hormones are transported through the blood to their sites of action.

Figure 2 depicts the general mechanism of action of nuclear receptors. The ligands are all lipophilic compounds, which enter the cells by passive diffusion. They bind to their cognate intracellular receptors located either in the cytoplasm or the nucleus. The receptors can be divided into two classes – those that do not bind DNA in the absence of hormone (Figure 2A) and those that bind to DNA in the absence of hormone (Figure 2B). The regulation of their activities differs somewhat. Classical steroid receptors such as AR, glucocorticoid receptor (GR), progesterone receptor (PR), mineralocorticoid receptor (MR), and

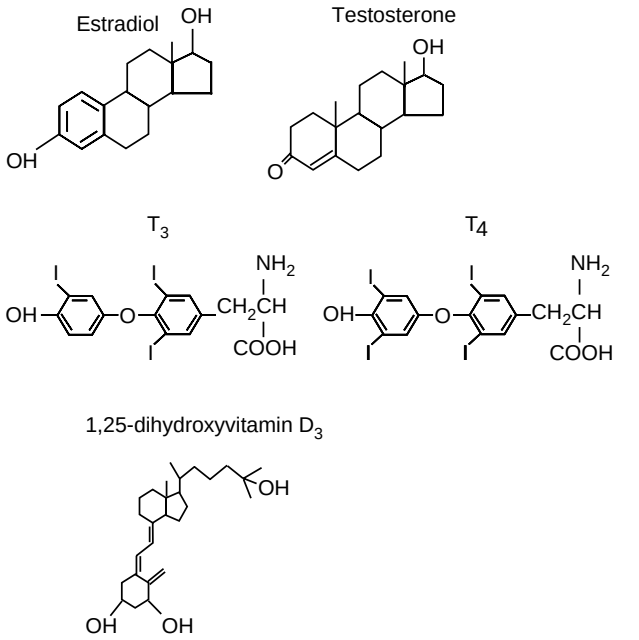

FIGURE 1 Structure of steroid and thyroid hormones. Estradiol is the ligand for estrogen receptor, testosterone is the ligand for androgen receptor, T_3-3,5,3-L-triiodothyronine, T_4-thyroxine are ligands for thyroid receptor, and 1,25-dihydroxyvitamin D_3 is the ligand for the vitamin D receptor.

ER belong to the first class; they are maintained in an inactive conformation capable of ligand binding by a complex of chaperone proteins including hsp90 and p23. Whether these complexes are nuclear or cytoplasmic depends upon the receptor. Upon ligand binding, the receptor changes its conformation, no longer binding to heat-shock proteins, homodimerizes and, if the unliganded receptor is localized in the cytoplasm, translocates to the nucleus. There, the receptor binds to DNA containing specific sequences called hormone response elements (HREs) that are most often found in the 5′ flanking region of target genes. The receptor recruits components of the basal transcription machinery, as well as proteins termed coactivators that perform a variety of functions including histone acetylation that enhance transcription. Unlike the receptors for classical steroids, thyroid receptors (TRs) are not bound to heat-shock proteins in the absence of hormone and, instead, are bound to the DNA as a heterodimer with the retinoid X receptor (RXR), another member of the steroid/thyroid hormone receptor superfamily (Figure 2B). In the absence of ligand, TR binds corepressors, which in turn bind histone deacetylases resulting in lower levels of histone acetylation and repression of target gene transcription. Hormone binding releases corepressors and promotes binding of coactivators, and subsequent transcription follows.

The Steroid/Thyroid Hormone Receptor Superfamily

The steroid/thyroid receptors are the largest family of ligand-activated transcription factors. In addition to the well-characterized steroid, thyroid, retinoid, and vitamin D receptors, the family contains receptors for numerous lipophilic metabolites and xenobiotics as well as receptors, termed orphans, for which ligands have not yet been identified.

Receptor Structure

Despite some evolutionary and functional differences, the steroid receptor family members have many similarities especially in their structure. As shown in Figure 3, there are multiple domains in the receptors, with all receptors containing domains A–E and only a subset containing the additional F domain.

The N Terminus

The N terminus or the A/B domain of the receptor is the least conserved domain among the family members. This region is the most variable in length ranging from a few amino acids to more than 500. This region has an activation function, AF-1, which contributes to the transcriptional activity of the receptor through binding of coactivators.

The DNA-Binding Domain (DBD)

The DNA-binding domain, region C, is important for the binding of receptor to the DNA and is the most highly conserved domain. This region has two type-2 zinc finger motifs, which are responsible for DNA recognition and dimerization (Figure 3B). Each finger is composed of four cysteines that coordinate with one zinc atom. Amino acids in this region also participate in receptor dimerization.

The Hinge Region

Downstream of the DBD is the hinge region (D), which contains a nuclear localization signal. This is a short lysine-rich region, with a high homology to the simian virus 40 T antigen nuclear localization signal. Additional functions of this region are receptor specific.

The Ligand-Binding Domain

The ligand-binding domain (E) is essential for the binding of ligand. The primary interaction site for the hsp complex is also in this domain. Also located in this region is the second activation function domain, AF-2,

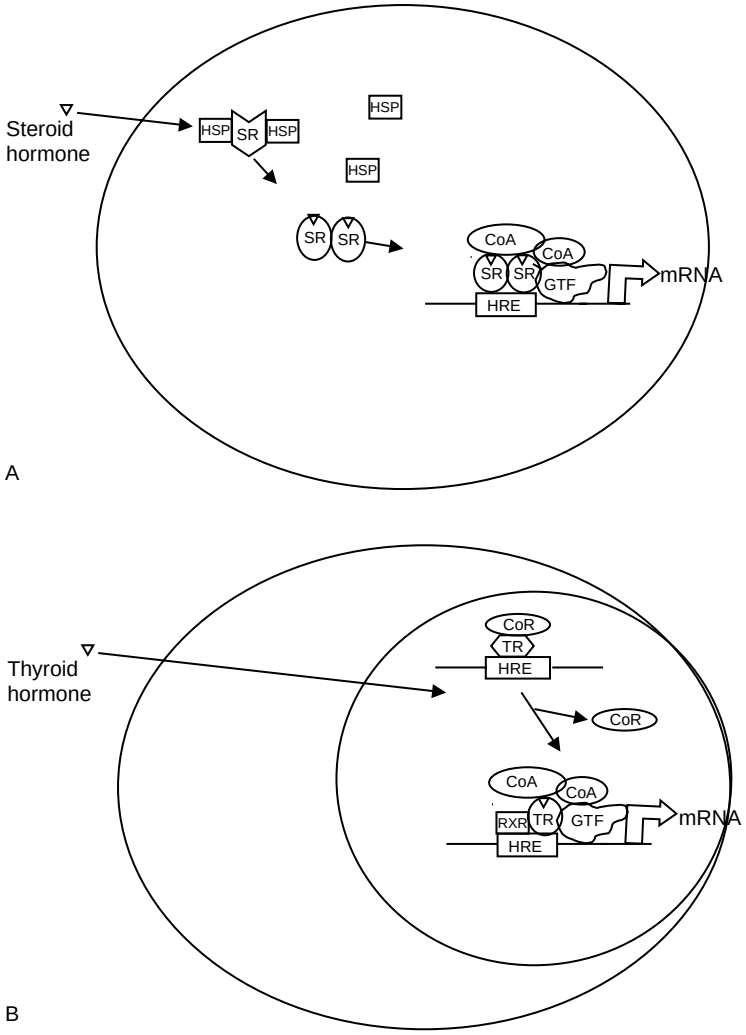

FIGURE 2 Mechanism of steroid (A) and thyroid (B) hormone action. The two classes are distinguished by whether they are associated with heat-shock proteins (A) like classical steroid receptors or are bound to DNA in the absence of hormone (B) like thyroid receptor. In both cases, binding of agonist causes dissociation of proteins that repress activity and promotes a conformation that induces recruitment of coactivators stimulating transcription of the target gene. SR, steroid receptor; HRE, hormone response element; GTF, general transcription factor; RXR, retinoid X receptor; TR, thyroid receptor; CoA, coactivator; CoR, corepressor.

which is responsible for ligand-mediated transcription of target genes. The relative importance of AF-2 and AF-1 in inducing transcription is receptor- and cell-type specific. The structures of the hormone-binding domains of several receptors have been determined using X-ray diffraction. The hormone-binding domain consists of a series of 12 α-helices. Binding of hormone causes a substantial conformational change in the receptor exposing AF-2 for interactions with coactivators. This domain also contains the strongest dimerization interface in most steroid receptors. The function of the F domain, located at the C terminus of some receptors such as the ER is not well defined.

Receptor Binding to DNA

All of the receptors bind to their cognate HREs as dimers. The consensus binding sequence for AR, PR, GR, and MR, shown in Figure 3C, contains two half-sites separated by three nucleotides with the sites oriented to form a palindrome. ER recognizes a related pair of half-sites with the same spacing and orientation. Each monomer binds to a half-site. The class-II receptors, including VDR and TR, bind to pairs of half-sites whose sequences are identical to the ER half-site, but whose orientation (direct or inverted repeats) and spacing (0–6 nucleotides) determines the specificity of binding. TR and VDR each heterodimerize with

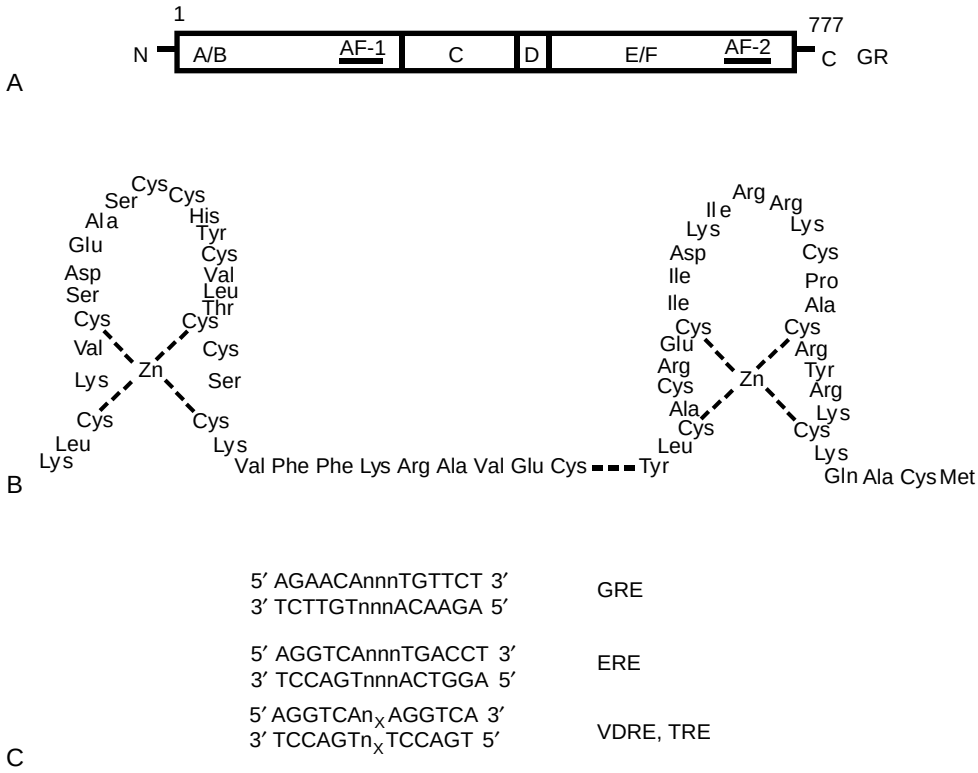

FIGURE 3 Receptor structure and DNA binding elements. Panel (A) shows the common structural features of nuclear receptors. The A/B region contains AF-1, a region important for transcriptional activation. C is the DNA-binding domain, the most conserved region in the nuclear receptors. D contains a nuclear localization sequence. E contains the hormone-binding domain and second activation function AF-2. Some receptors also contain a C terminal extension, termed the F domain, whose physiological function is not well described. Panel (B) shows the sequence of the DNA-binding domain of GR. Panel (C) shows sequences of consensus hormone response elements. The consensus sequence for a GRE (binds GR, AR, PR) and an ERE (binds ER) are shown. Vitamin D receptor and the thyroid hormone receptors bind to direct repeats separated by three and four nucleotides, respectively. Other receptors bind to direct or inverted repeats with a spacing of 0–6 (n_x indicates that the half-site may be separated by 0–6 nucleotides). GRE, glucocorticoid response element; ERE, estrogen response element; VDRE, vitamin D response element; TRE, thyroid response element; GR, glucocorticoid receptor; AF, activation function.

RXR and bind to the 3′ end (half of the HRE), whereas RXR binds to the 5′ end (half of the response element). Although these sequences represent the consensus binding sites, natural sequences may differ significantly and promoters may contain combinations of HREs as well as individual half-sites all of which contribute to the final activity.

Steroid Receptor Coregulators

When the receptor binds to the DNA, it recruits proteins in the basal transcription machinery such as TFIIB and RNA polymerase II. The receptors also bind additional proteins or protein complexes that modulate receptor activity; these are termed coactivators and corepressors. Coactivators are defined as proteins that interact with the receptors and increase their ability to transactivate the target gene. The mechanism by which individual coactivators achieve this can vary. More than 100 candidate coactivators have been identified. While some coactivators function only with steroid receptors and a small subset of other transcription factors, others are used by many transcription factors. The best characterized of the steroid receptor coactivators (SRCs) is the p160 family of coactivators: SRC-1, SRC-2 (GRIP1, TIF2), and SRC-3 (Rac3, AIB1). These bind to the receptor recruiting additional coactivators including CBP (CREB-binding protein), p/CAF (CBP-associated factor) and CARM-1 (coactivator-associated arginine methyltransferase). CBP/p300, p/CAF and some of the p160 proteins are histone acetyl transferases (HATs) and their binding increases local histone acetylation. Other coactivators include the DRIP/TRAP (D receptor interacting protein/thyroid hormone receptor-associated protein) complex. Many coactivators interact with AF-2 located in the LBD. In other cases, coactivators interact with the AF-1 region and some interact with both domains. Interactions with

AF-2 are typically mediated by LXXLL (L = Leucine and X = any amino acid) motifs in the coactivator.

Another class of proteins, termed corepressor, reduces the activation of target gene transcription through interaction with the receptors. The best-characterized nuclear receptor corepressors are nuclear receptor corepressor (NcoR) and silencing mediator of retinoid and thyroid (SMRT) receptors. These proteins bind histone deacetylase complexes and also interact with class II receptors in the absence of hormone resulting in local reductions in histone acetylation. Corepressors do not bind to unliganded steroid receptors. However, steroid receptor antagonists cause changes in the conformation of the hormone-binding domain that induce binding of the corepressors.

Steroid Receptor Agonists and Antagonists

Although steroid receptor family members are important for normal physiological processes, there are a number of instances in which it is desirable to block the actions of selected steroid receptors. These include breast cancer (ER) and prostate cancer (AR). Thus, although natural antagonists of steroid receptor action have not been identified, much effort has been devoted to identifying compounds that will antagonize hormone action. These compounds compete with the natural ligand for binding to the hormone-binding domain of the receptors. Although some antagonists block dissociation from heat-shock protein complexes or destabilize the receptor, most of the antagonists promote dissociation from heat-shock proteins and cause the receptors to bind to DNA. However, the conformation induced by the antagonist differs from that induced by agonist. This prevents recruitment of coactivators to AF-2 and, instead, promotes recruitment of corepressors. In some cases, it is desirable to maintain the activity of a receptor in some tissues while inhibiting activity in other tissues. The most common example of this is the need for tissue-specific regulation of ER activity. Estradiol is important for maintaining bone mass and postmenopausal women frequently develop osteoporosis. However, estradiol can promote uterine cancer and may also be detrimental in breast. Thus, a great deal of effort has been devoted to developing selective estrogen receptor modulators (SERMs) which have tissue-specific agonistic and antagonistic activities. Tamoxifen (a SERM) has been used in the treatment of breast cancer, but increases the risk of uterine cancer. A newer SERM, raloxifene, is an antagonist in both breast and uterus, but acts as an agonist in bone.

Crosstalk between Nuclear Receptors and Cell Signaling Pathways

Phosphorylation of Receptors and Coactivators

The nuclear receptors and their coactivators are phosphoproteins; phosphorylation regulates various functions of these proteins. In some cases, enhanced cell signaling is sufficient to induce the transcriptional activity of the receptor. The ability to be activated by cell signaling pathways alone is receptor specific, although changes in cell signaling modulate the activity of all of the receptors. Estrogen receptors are activated both by growth factor pathways and by activation of protein kinase A. Other receptors, such as GR, require hormone for activity.

Functional Interactions between Nuclear Receptors and Signal-Regulated Transcription Factors

In addition to altering transcription through direct binding to DNA, nuclear receptors alter transcription through interactions with other transcription factors. In some cases these protein–protein interactions prevent binding of the transcription factor to its DNA target site. In other cases, the receptor binds to the factors on their DNA target sites influencing (either + or −) the transcription of a target gene. Many of the anti-inflammatory actions of GR are a result of these protein–protein interactions. Figure 4 shows the

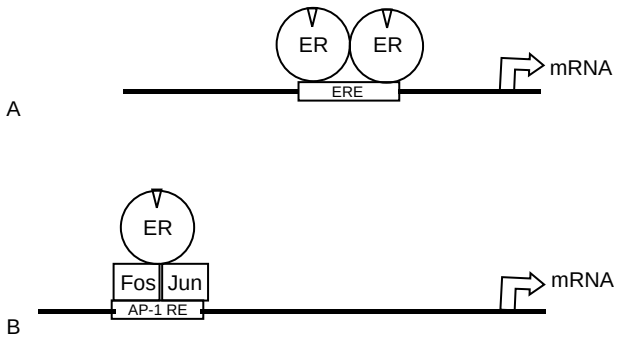

FIGURE 4 Mechanisms of transcriptional activation by nuclear receptors. Panel (A) shows the classical pathway for transcriptional activation with a steroid receptor dimer binding directly to a hormone response element. Panel (B) shows an alternative mode of activation. In this case, a receptor such as the estrogen receptor binds to another transcription factor and influences transcription through its interactions with the transcription factor and recruitment of coregulator proteins to the complex. ER, estrogen receptor; AP-1 RE, AP-1 response element; ERE, estrogen response element.

comparison between two of these pathways for ER. In the upper panel is the classical DNA-binding-dependent induction of transcription. We next depict the ability of ER to induce transcription through interactions with AP-1 complexes. In this instance, both estradiol as well as SERMs will stimulate the activity of AP-1.

Nuclear Receptor Stimulation of Cell Signaling Pathways

Both of the pathways above can be considered genomic pathways in that the nuclear receptor acts through altering transcription. Nuclear receptors can also act through stimulating kinase activity, although the final downstream target may be a change in transcription. These actions are rapid (minutes) and are termed non-genomic. The pathways are less well characterized, but there is evidence that activation of nuclear receptors can lead to downstream activation of mitogen-activated protein kinase (MAPK) In some cases, this is through activation of Src kinase and in others through generation of a ligand for a growth factor receptor. There are numerous other examples of these rapid actions. Induction by estradiol of nitric oxide synthase activity in endothelial cells is a rapid response that does not require transcription. Thus, steroid/thyroid hormones alter cellular activities through multiple mechanisms.

See Also the Following Articles

A-Kinase Anchoring Proteins • Mitogen-Activated Protein Kinase Family • Thyroid-Stimulating Hormone/Luteinizing Hormone/Follicle-Stimulating Hormone Receptors

Glossary

agonists Natural or synthetic ligands that bind to the hormone-binding domain of the receptor stimulating activity.

antagonists Ligands that compete with agonists for binding to the hormone-binding domain, but do not cause activation of the receptor.

nuclear receptors Ligand-activated transcription factors characterized by conserved zinc-finger motifs in their DNA-binding domains and smaller conserved regions in the hormone-binding domain.

phosphorylation A posttranslational modification of an amino acid in which a phosphate group is added by a kinase.

Further Reading

Falkenstein, E., Tillmann, H. C., Christ, M., Feuring, M., and Wehling, M. (2000). Multiple actions of steroid hormones—a focus on rapid, nongenomic effects. *Pharmacol. Rev.* **52**(4), 513–556.

McDonnell, D. P., Connor, C. E., Wijayaratne, A., Chang, C. Y., and Norris, J. D. (2002). Definition of the molecular and cellular mechanisms underlying the tissue selective agonist/antagonist activities of selective estrogen receptor modulators. *Recent Prog. Horm. Res.* **57**, 295–316.

McKenna, N. J., Lanz, R. B., and O'Malley, B. W. (1999). Nuclear receptor coregulators: Cellular and molecular biology. *Endocr. Rev.* **20**(3), 321–344.

Tsai, M. J., and O'Malley, B. W. (1994). Molecular mechanisms of action of steroid/thyroid receptor superfamily members. *Annu. Rev. Biochem.* **63**, 451–486.

Weigel, N. L., and Zhang, Y. (1998). Ligand-independent activation of steroid hormone receptors. *J. Mol. Med.* **76**(7), 469–479.

Whitfield, G. K., Jurutka, P. W., Haussler, C. A., and Haussler, M. R. (1999). Steroid hormone receptors: Evolution, ligands, and molecular basis of biologic function. *J. Cell Biochem.* **32–33**(suppl.), 110–122.

Biography

Nancy Weigel is a Professor of Molecular and Cellular Biology at Baylor College of Medicine. Her interests are in steroid receptor action and crosstalk with cell signaling pathways as well as the role of steroid receptors in prostate cancer. She received her Ph.D. from Johns Hopkins University and received her postdoctoral training at Baylor College of Medicine.

Ramesh Narayanan is a postdoctoral fellow in the Department of Molecular and Cellular Biology at Baylor College of Medicine. He studies steroid receptor action and crosstalk with cell signaling pathways. He received his Ph.D. from the University of Madras, India.

Store-Operated Membrane Channels: Calcium

Indu S. Ambudkar
National Institute Of Dental and Craniofacial Research, Bethesda, Maryland, USA

Ca^{2+} entry via plasma membrane Ca^{2+} influx channels regulates a wide array of physiological functions such as neurotransmission, muscle contraction, secretion, and gene expression. A number of different types of Ca^{2+} channels have been identified in excitable and nonexcitable cells, including voltage-gated Ca^{2+} channels, primarily found in neuronal and various types of muscle cells; receptor-operated channels that are activated by extracellular ligand; and second-messenger-activated channels that are activated by intracellular "ligands" such as cGMP. Over the last decade considerable interest has been focused on store-operated Ca^{2+} channels (SOCCs), which mediate store-operated Ca^{2+} entry (SOCE, also referred to as capacitative Ca^{2+} entry, CCE). SOCE is activated following stimulation of cell-surface receptors that lead to phosphatidylinositol bisphosphate (PIP_2) hydrolysis, generation of diacylglycerol (DAG) and inositol-1, 4, 5-trisphosphate (IP_3), and IP_3-mediated release of Ca^{2+} from internal Ca^{2+} stores via the inositol trisphosphate receptor (IP_3R). The concept of SOCE was proposed by Putney in 1986 according to which depletion of Ca^{2+} in intracellular Ca^{2+} store(s) acts as a trigger for activation of plasma membrane Ca^{2+} influx. Ca^{2+} entering the cells via this pathway not only achieves refilling of the intracellular Ca^{2+} stores but also provides a sustained elevation of cytosolic $[Ca^{2+}]$ ($[Ca^{2+}]_i$) that is critical in the regulation of a variety of cellular functions. Despite the large number of studies that have been directed towards SOCE, the molecular composition of these channels as well as the mechanisms that activate or inactivate them have not yet been elucidated.

Characteristics of SOCE

Store-operated Ca^{2+} entry (SOCE) was originally identified in nonexcitable cells, although it has now been shown to be present in excitable cells as well. Thus, our knowledge of the characteristics of SOCE is primarily based on studies with nonexcitable cells that span over two decades. Early studies using radioactive Ca^{2+} and subsequent studies using Ca^{2+}-sensitive fluorescent probes together demonstrate that neurotransmitter stimulation of cells leads to a biphasic increase in cytosolic Ca^{2+}. An immediate increase that is not substantially altered by the removal of external Ca^{2+} suggesting that it is due to internal Ca^{2+} release, primarily mediated by IP_3. This is followed by a relatively sustained elevation of Ca^{2+}, completely dependent on the presence of external Ca^{2+}, that is due to influx of Ca^{2+} from the external medium. Although other Ca^{2+} influx pathways might contribute to this sustained $[Ca^{2+}]_i$ elevation, SOCE accounts for a major part, or all, of this Ca^{2+} influx. Several key studies lead to the conclusion that this Ca^{2+} influx is triggered by the depletion of Ca^{2+} in the internal Ca^{2+} store. (1) Ca^{2+} influx is not activated by IP_3 or its metabolites. (2) Ca^{2+} influx remains active even after the receptor-coupled signaling is stopped by addition of the antagonist. (3) Ca^{2+} influx is inactivated after Ca^{2+} is reintroduced into the cell and allowed to refill the internal Ca^{2+} store. (4) The same type of Ca^{2+} influx is activated by treating cells with the SERCA inhibitors such as Tg which induce a rapid and specific block of Ca^{2+} uptake into the ER and unmask a "leak" of Ca^{2+} from the ER.

The first channel activity associated with SOCE was measured in RBL cells by Penner and co-workers in 1992. This channel CRAC has been extensively studied and has also been found in lymphocytes and megakaryotes. CRAC is characterized by a high Ca^{2+}/Na^{+} permeability ratio (>500), as well as a relatively rapid Ca^{2+}-dependent feedback inhibition. The channel displays strong anomalous mole fraction behavior suggesting that under normal physiological conditions external Ca^{2+} blocks the entry of Na^{+} via the channel, thus Ca^{2+} is the favored ion to permeate this channel. Since 1992, store-operated Ca^{2+} influx channels have been measured in many different cell types, including cell lines and primary cell cultures. It is now clear that, although store-operated Ca^{2+} channels are all activated by the same, presently unknown, mechanism associated with internal Ca^{2+} store depletion they are not homogeneous. They display distinct biophysical properties, e.g., selectivity to Ca^{2+}, which suggest possible molecular diversity in their composition as well as differences in their modulation. An interesting question

that arises from such data is whether these distinct properties of store-operated Ca^{2+} channels (SOCCs) reflect their cell-specific physiological functions.

Mechanism of SOCE

Although agonist-stimulation of Ca^{2+} influx was first recognized in secretory cells almost three decades ago by Douglas and Poisner, the molecular mechanisms that activate or inactivate this Ca^{2+} influx have not yet been established. Unraveling this mechanism has been a major challenge in the field of Ca^{2+} signaling. Since SOCE was first identified, several mechanisms have been proposed to describe how it is activated. The earliest model proposed that Ca^{2+} in the internal store negatively regulates Ca^{2+} influx. When the store Ca^{2+} content is decreased, Ca^{2+} influx is activated and external Ca^{2+} is somehow directly accumulated into the ER, bypassing the cytosol. This model was primarily based on experiments which revealed that during refilling of the internal Ca^{2+} store (e.g., after agonist stimulation and addition of antagonist) by Ca^{2+} entry via the SOCE pathway, there is no detectable increase in $[Ca^{2+}]_i$. This model was disproved by studies in which external Ca^{2+} was substituted by divalent cations such as Mn^{2+}, which enter the cell via SOCE but are not pumped into the ER by the SERCA. These studies lead to the proposal that Ca^{2+} first enters the cytosol from where it is rapidly taken up into the ER lumen by the SERCA activity, and thus does not produce any substantial increase in $[Ca^{2+}]_i$. This results in refilling of the internal Ca^{2+} stores which leads to inactivation of SOCE. Thus, there is reciprocal regulation of the ER Ca^{2+} store and plasma membrane Ca^{2+} channels.

Later models addressed the nature of the signal that conveys the status of the internal Ca^{2+} store to either activate or inactivate SOCE in the plasma membrane. While a number of different models have been proposed in an effort to explain this "ER–PM coupling," three major mechanisms have garnered the most attention; (1) conformational coupling, (2) a diffusible factor, and (3) regulated recruitment of channels by fusion of intracellular vesicles (Figure 1). Conclusive data are presently lacking to either support or rule out any of these proposed mechanisms for SOCE activation. A major hurdle in these efforts has been the lack of knowledge regarding the molecular identity of the SOCC channel.

Molecular Candidates for SOCC

The relatively recent discovery of mammalian homologues of the *Drosophila Trp* (transient receptor potential) gene has propelled the field of SOCE in a new direction. TRP proteins form a large functionally diverse

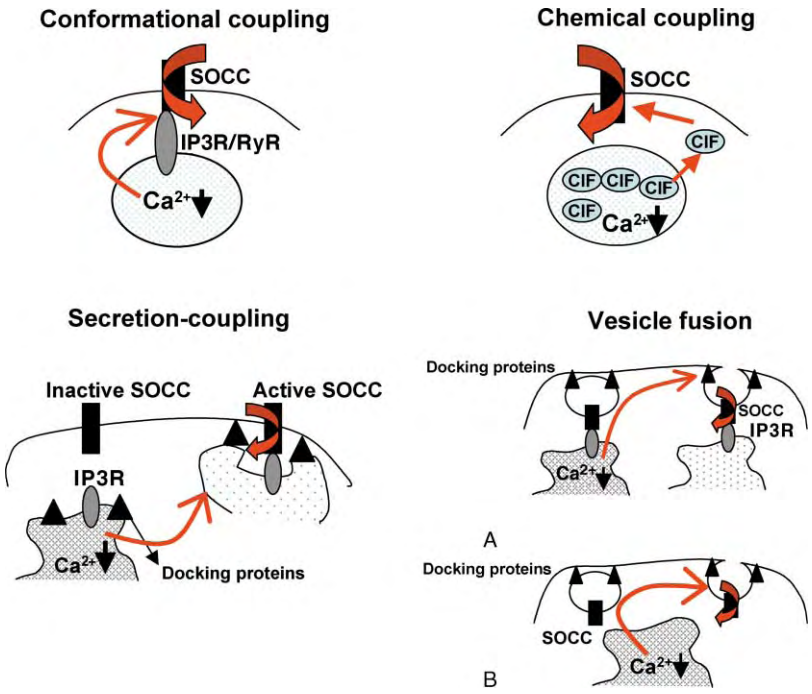

FIGURE 1 Proposed models for activation of SOCE. All components are labeled in the figures. See text for description. Two mechanisms are shown for the vesicle fusion model. (A) "Kiss and Run" model predicts that SOCC-containing vesicles might be docked to the ER and therefore sense depletion which initiates fusion to PM. Ion channel is retrieved during inactivation. (B) SOCC-containing vesicles are present in the subplasma membrane region and sense depletion of store that leads to vesicle fusion and channel insertion into the PM. Inactivation and retrieval could be independent events.

superfamily of ion channel proteins and are found in all excitable and nonexcitable tissues. Members of the TRPC subfamily and some members of the TRPV subfamily form channels that are activated in response to receptor-coupled Ca^{2+} signaling events (Figure 2 shows the proposed structure of TRPC1). TRP channels appear to fall into two general classes; nonstore operated such as TRPC3, TRPC6, TRPC7, which are activated by agonists and exogenous addition of diacylglycerol (DAG), but not by thapsigargin. Thus, it is suggested that this family forms channels that are activated by DAG generated in response to PIP_2 hydrolysis. The other group which includes TRPC1, TRPC4, TRPC5, TRPV6 has been shown to form store-operated channels. In this case, studies include heterologous expression, knockdown of endogenous proteins, and site-directed mutagenesis. However, there are exceptions. For example, TRPC3 has been shown to form SOCC and also to be regulated by the internal Ca^{2+} store via interaction with inositol trisphosphate receptor (IP_3R). Further, TRPCs have also been shown to interact to form heteromultimeric channels which display a wide range of biophysical characteristics. Thus, it is possible that TRPCs could be involved in the formation of a diverse range of SOCCs. Although further work is required to conclusively establish that TRP proteins are molecular components of SOCCs, presently they are the only viable candidates for these channels. Further, TRPs provide useful tools to test the validity of the models proposed for SOCC activation.

Signaling from ER to the Plasma Membrane

Conformational Coupling

This hypothesis was originally proposed by Irvine in 1990 and was based on functional analogy between IP_3R and ryanodine receptors (RyR) in muscle cells. RyR are Ca^{2+} release channels in the muscle sarcoplasmic reticulum (SR) and have been suggested to physically couple to the L-type Ca^{2+} channels in the T-tubule plasma membrane. During excitation–contraction coupling, Ca^{2+} inflow via the plasma membrane channels regulates Ca^{2+}-induced Ca^{2+} release via RyR in the SR. Although in the case of SOCE, the flow of information can be predicted to occur in the reverse direction, i.e., from ER to the plasma membrane, the homology between IP_3R and RyR channeled the hypothesis that regulation of SOCC could be mediated via a direct physical association between the IP_3R and the SOCC in the plasma membrane. The model proposes that there are preformed IP_3R–SOCC complexes and that store depletion is detected by the IP_3R, leading to a conformational change that results in activation of SOCC. A caveat to the IP_3R requirement in the regulation of SOCC is its activation by SERCA inhibitors or by depletion of Ca^{2+} stores by loading the cytosolic or ER with Ca^{2+} buffers. To explain this discrepancy, it was proposed that only a certain pool of IP_3R's interacts with SOCC, and that these are localized

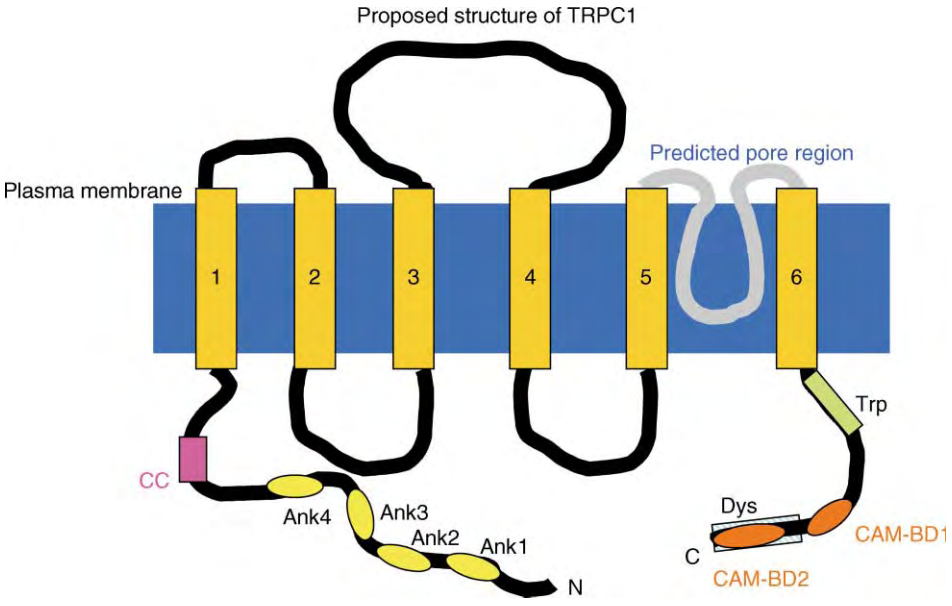

FIGURE 2 Proposed structure of transient receptor potential canonical 1 (TRPC1): The structure includes six-transmembrane domains (1–6), extracellular as well as intracellular domains (black lines) and a pore-domain between the fifth and sixth TMs (gray). The N terminus of the protein contains ankyrin repeats (ank) as well as a coil–coil domain (CC). The C terminus has the conserved TRP motif (Trp, EWKFAR), calmodulin-binding domains (CAMBD), and a dystrophin domain (Dys).

in ER membranes situated in close proximity to the PM. This also implied that this pool of IP_3R is not involved in internal Ca^{2+} release, but only in SOCC regulation. Currently, there are conflicting data regarding the role of IP_3R in the regulation of SOCC. Studies using a gene knockout approach have shown that IP_3Rs are not required for thapsigargin-stimulated Ca^{2+} entry, although they are clearly required for IP_3-mediated internal Ca^{2+} release. Other studies suggest that RyR, which are present in several nonmuscle cell types, can also couple with SOCC and regulate its function. Thus, it is possible that RyR could replace IP_3Rs in cells where IP_3R expression has been down-regulated or eliminated. However, further studies will be required to rule out or provide conclusive evidence for the conformational coupling hypothesis.

Secretion-Like Coupling/Vesicle Fusion

The activation of SOCE is a relatively slow process. A lag time of about 10 s has been detected between internal Ca^{2+} release and Ca^{2+} influx. Thus, it has been proposed that vesicle trafficking and fusion events could be involved in activation of SOCE. Two possible processes could occur. The first is a variation of the conformational coupling model and suggests that the ER–PM interaction is a dynamic, reversible, process and that the ER membrane moves towards and docks with the PM upon stimulation. The docking enables proteins in the PM and ER to interact, thus resulting in activation of SOCC. Although the ER protein is considered to be IP_3R or RyR, other proteins could also be involved in the ER–PM signaling. Since the ER and PM are apposed to each other at the site of interaction, there is no particular requirement that the ER or PM protein should have very long cytosolic domains. Support for the secretion-coupling hypothesis has been mainly provided by studies using reagents to disrupt the cytoskeleton and alter the spatial arrangement of cellular organelles. Further, TRPC1–IP_3R interaction was shown to be disrupted by reagents that induce cortical actin formation. However, several other studies have refuted this model as a possible activation mechanism for SOCC. The second mechanism that can be suggested involves vesicle trafficking and exocytotic insertion of the channel proteins. Here again, there are data to both support and refute the model. Experiments have shown that disruption of the SNARE proteins involved in exocytosis, inhibits activation of SOCE. However, in other studies, such maneuvers did not affect SOCC activation. An important point that needs to be considered when assessing the possible mechanisms for activation is whether the different SOCCs that have been detected in various cell types are activated by the same mechanism or does internal Ca^{2+} store-depletion induce a variety of cellular signals which can then activate different channel types. For example, if different TRP channels are involved in the SOCCs in the different cell types, can that account for differences in their regulation? Voltage-gated Ca^{2+} channels represent a family of proteins that are activated by various thresholds of membrane potential. They are also regulated differently, exhibit distinct characteristics and carry out specific physiological functions. Analogous to this, we might have to consider SOCC channels as a family of channels that sense the same fundamental signal, but are regulated by subtly distinct mechanisms. What these mechanisms are, presents a challenging question for future studies in this field.

Metabolic Coupling

Another hypothesis that has received sporadic attention is that an as yet unknown diffusible factor, referred to as CIF, is either released from the ER with Ca^{2+} or is generated during this process. CIF can reach the PM SOCC channels and either activate it directly or bind to a regulatory protein and enable channel activation. Evidence in support of this shows that extracts from stimulated cells can increase Ca^{2+} influx in unstimulated cells. However, these findings have not held up for all types of cells. Other metabolites that have been shown to regulate SOCC are of the cytochrome P450 epoxygenase pathway. Modifiers of the lipoxygenase pathway has been shown to affect I_{CRAC} in RBL cells. A role for arachidonic acid has also been suggested. Thus, further studies are needed to establish whether CIF is involved in SOCC activation. It should be noted that the requirement for CIF and secretion-like coupling need not be mutually exclusive, since dynamic trafficking of ER to the PM would decrease the diffusion restraints for CIF. In addition, reassembly of the cortical actin can also play a role in the access to the PM and diffusion of CIF. Interestingly, the status of the actin is controlled by the PIP_2 levels in the plasma membrane. Thus, the hydrolysis of PIP_2 not only initiates Ca^{2+} signaling but also remodeling of the actin cytoskeleton in order to facilitate the regulation of cellular function. In fact, modulation of PIP_2 metabolism, i.e., inhibition of PI-3 kinase has been shown to alter SOCE in some cells. Thus, it is becoming exceedingly evident that regulation SOCE is a highly orchestrated process with several orders of complexity that might be determined by the particular SOCC that is present, and the specific physiological function that it contributes to, in any given type of cell.

Ca^{2+} Signaling Microdomains

Recent studies have highlighted spatio-temporal aspects of Ca^{2+} signaling in cells. It has been demonstrated that agonist-stimulated Ca^{2+} influx occurs within specific

spatially restricted microdomains. During Ca^{2+} influx-dependent refill of internal Ca^{2+} stores there is minimal diffusion of Ca^{2+} in the subplasma membrane region due to rapid uptake into the ER by the SERCA pump, indicating close apposition between the ER and plasma membrane at the site of Ca^{2+} influx. SERCA, mitochondria, and PMCA together determine the efficiency of SOCC by removing Ca^{2+} from the vicinity of the channel, thereby decreasing Ca^{2+}-dependent feedback inhibition of the channel. PMCA, mitochondria, and SERCA have been functionally localized to the microdomain where SOCE is occurring. Furthermore, PMCA and SERCA have been shown to be immunoprecipitated with TRPC channels. Thus, the architecture of such Ca^{2+} signaling microdomains facilitates direct physical, or functional, coupling between the molecular components that are involved in regulating plasma membrane SOCC. Current models support the idea that SOCC and functionally associated proteins are strategically localized by the action of scaffolding proteins which allow dynamic regulation of cellular function (Figure 3).

A candidate for such a microdomain is caveolar lipid raft domains which have been shown to be involved in the regulation of SOCE in several cell types. These domains are functionally and biochemically distinct microdomains formed by the lateral packing of glycosphingolipids and cholesterol within the membrane bilayer. It has been proposed that arrangement of the lipids and scaffolding proteins within LRD forms a platform for the assembly of a number of proteins into signaling complexes. This compartmentalization of the signaling molecules can increase the rate of interactions and enhance crosstalk networks. Importantly, key protein and nonprotein molecules involved in the Ca^{2+} signaling cascade, such as PIP_2, $G_{\alpha q/11}$, PMCA, several TRPC proteins, and IP_3R-like protein, and Ca^{2+} signaling events such as receptor-mediated turnover of PIP_2 have been localized to caveolar microdomains in the plasma membrane. Studies have also revealed that (1) agonist-stimulated Ca^{2+} signal in endothelial cells originates in specific areas of the PM that are enriched in caveolin-1, and (2) intact lipid rafts are required for activation of SOCE. Thus, it has been proposed that caveolae might regulate the spatial organization of Ca^{2+} signaling by contributing to the localization of Ca^{2+} signaling complex as well as the site of Ca^{2+} entry.

It is now well recognized that Ca^{2+} signaling proteins are assembled in multiprotein complexes. This finding is again supported by studies carried out with TRP proteins. It was earlier shown that the well-studied TRP prototype, the *Drosophila* TRP, is assembled in a signaling complex by the scaffolding action of INAD, a multi-PDZ domain containing protein. Mammalian TRPC channels are also assembled in multimeric protein complexes that are associated with key Ca^{2+} signaling proteins such as $G_{\alpha q/11}$, IP_3R, PLCβ, PMCA, and SERCA as well as scaffolding proteins such as

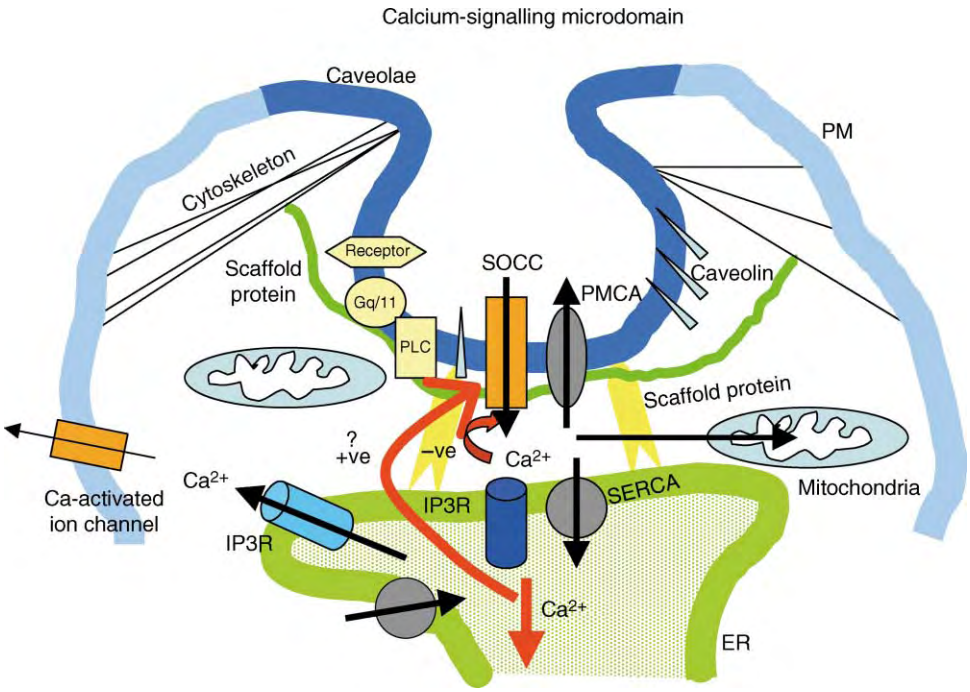

FIGURE 3 Proposed calcium-signaling microdomain: Functionally associated proteins are localized in distinct structures and assembled together by scaffolding proteins as well as cytoskeletal interactions. The architecture of the region enables the coupling between ER and PM that is involved in activation of SOCE. Protein components are labeled in the figure.

caveolin-1, homer, and NHERF. Accessory proteins have been identified not only for TRPC channels, but also for PMCA, SERCA, and IP_3Rs. These proteins encompass a variety of functions such as trafficking, phosphorylation, dephosphorylation, scaffolding, etc. Thus, further information regarding the protein components and assembly of the mammalian Ca^{2+}-signaling complex will provide a better understanding of SOCE. Such knowledge will impact several important areas of physiology and pathophysiology.

See Also the Following Articles

Calcium Signaling: Cell Cycle • Lipid Rafts • Plasma-Membrane Calcium Pump: Structure and Function • Voltage-Sensitive Ca^{2+} Channels

Glossary

Ca^{2+} channels Protein(s) that mediate passive, electrochemical gradient driven, flux of Ca^{2+}.

Ca^{2+} pump Protein(s) that utilize energy of ATP hydrolysis to drive Ca^{2+} flux against its gradient.

Ca^{2+} signaling Events that initiate elemental changes in cellular levels of Ca^{2+} which are then decoded into a physiological response.

cellular microdomains Morphological and functionally distinct subcellular domains.

neurotransmitter Chemical messengers secreted by nerve endings.

Further Reading

Berridge, M. J. (1995). Capacitative Ca^{2+} entry. *Biochem. J.* **312**, 1–11.

Isshiki, M., and Anderson, R. G. W. (2003). Function of caveolae in Ca^{2+} entry and Ca^{2+}-dependent signal transduction. *Traffic* **4**, 717–723.

Montell, C., Birnbaumer, L., and Flockerzi, V. (2002). The TRP channels, a remarkable functional family. *Cell* **108**, 595–598.

Muallem, S., and Wilkie, T. M. (1999). G-protein dependent Ca^{2+} signaling complexes in polarized cells. *Cell Ca^{2+}* **26**, 173–180.

Parekh, A. B. (2003). Store-operated Ca^{2+} entry: Dynamic interplay between endoplasmic reticulum, mitochondria, and plasma membrane. *J. Physiol.* **547**, 333–348.

Putney, J. W., Jr., Broad, L. M., Braun, F.-J., Lievremont, J.-P., and Bird, G. J., St. (2001). Mechanisms of capacitative Ca^{2+} entry. *J. Cell Sci.* **114**, 2223–2229.

Venkatachalam, K., von Rossum, D. B., Patterson, R. L., Ma, H.-T., and Gill, D. L. (2002). The cellular and molecular basis of store-operated Ca^{2+} influx. *Nat. Cell Biol.* **4**, 263–272.

Biography

Indu Ambudkar is Chief of Secretary Physiology Section at the National Institute of Dental and Craniofacial Research, NIH, in Bethesda, Maryland. She holds both Masters and Ph.D. degrees in Biochemistry from Lucknow and Madurai Kamaraj Universities in India and received postdoctoral training at the University of Maryland, School of Medicine. Her primary research interest is regulation of cellular Ca^{2+} homeostasis and more recently store-operated Ca^{2+} influx in salivary epithelial cells. Her work has contributed significantly to the understanding of SOCE, and the role of TRPC proteins in this process.

Substrate Binding, Catalysis, and Product Release

W. Wallace Cleland
University of Wisconsin, Madison, Wisconsin, USA

Enzymes catalyze reactions by forming complexes with their substrate(s), accelerating the chemical reaction by lowering the activation energy for the reaction, and then releasing the product(s). The enzyme has to have sufficient affinity for a substrate to form a complex with it at the physiological concentration of this molecule. Conversely, however, too great an affinity for the substrate usually results in too great an affinity for the product, so that product release becomes rate limiting. The maximum rate of an enzyme-catalyzed reaction is limited, in fact, by the relationship between the equilibrium constant and the kinetic constants called the Haldane relationship, and one element of this restriction is the affinity of the substrate.

The Haldane Relationship

As noted above, the Haldane relationship allows calculation of the maximum rate of an enzyme-catalyzed reaction. For the simple conversion of substrate A into product P, the initial rate of the forward reaction in the absence of P is

$$v_f = -d[A]/dt = V_1[A]/(K_a + [A]) \quad [1]$$

and that in the back reaction is

$$v_r = -d[P]/dt = V_2[P]/(K_p + [P]) \quad [2]$$

where V_1 and V_2 are maximum velocities in forward and reverse reaction, and K_a and K_p are Michaelis constants for A and P (i.e., apparent dissociation constants in the steady state).

The Haldane for this mechanism is the ratio of the V/K values in forward and reverse directions:

$$K_{eq} = [P]_{eq}/[A]_{eq} = (V_1/K_a)/(V_2/K_p)$$

$$= V_1K_p/(V_2K_a) \quad [3]$$

V/K, with units of reciprocal time, is the apparent first-order rate constant for reaction at low substrate concentration, so eqn. [3] is analogous to the one for a nonenzymatic reaction where K_{eq} would equal k_1/k_2, i.e., the ratio of rate constants in forward and reverse directions.

To optimize the turnover number of an enzyme (V_1/E_t) in this case, also known as k_{cat}, with units of reciprocal time, we can raise the two V/K values in constant ratio until one V/KE_t value (with units of $M^{-1}\,s^{-1}$) reaches the limit set by diffusion. V/KE_t (or k_{cat}/K) is a second-order rate constant for productive combination of enzyme and substrate and subsequent reaction to give product, and the combination of enzyme and substrate can only go as fast as these two can diffuse together. This limit is $\sim 10^9\,M^{-1}\,s^{-1}$ for small substrates, and somewhat less for larger ones like ATP.

Once the V_1/K_aE_t value in eqn. [3] is as high as it can go, the only way to increase V_1/E_t is to increase K_a as well. But K_a cannot exceed the physiological level of A, or the enzyme will not be at least half-saturated. Thus V_1/E_t has an upper limit, and enzymes that are part of metabolic pathways are optimized to operate at this limit. The actual turnover numbers vary, depending on K_{eq} and the physiological level of the substrate, but evolution has brought these enzymes to the limit set by the Haldane relationship. On the other hand, enzymes that are involved in control, as opposed to ones in metabolic pathways, often sacrifice speed for control characteristics, and do not have turnovers numbers at the Haldane limit.

Catalysis

The catalytic process on an enzyme starts once the substrate is bound. As noted above, the enzyme has to have sufficient affinity to bind the substrate at its physiological concentration. The enzyme then has to lower the activation energy of the reaction sufficiently for it to go at a rate approaching the maximum given by the Haldane relationship. It is commonly said that the enzyme accomplishes this by binding the transition state structure more tightly than the ground state of the substrate, but this is really a definition of catalysis. Molecules resembling the transition state structure are

often bound much more tightly than the substrate (see entry on transition state analogues). This is either because the geometry of the transition state is a better fit, or includes inherently tighter interactions (stronger hydrogen bonds, for example; see entry on low barrier hydrogen bonds). Alternatively, the differential binding results because the substrate is destabilized when it is bound (sterically deformed, placed in an unfavorable electrostatic environment, etc.), but this destabilization is relieved in the transition state. Of course, destabilization in one part of the substrate must be matched by tight binding in another part, or the substrate will not have sufficient affinity for the enzyme at its physiological level. OMP decarboxylase is a classic example, where a substrate analogue with $-COO^-$ replaced by $-O^-$ binds 10^5-fold more tightly to the enzyme. The difference is ascribed to charge repulsion between the carboxyl group of the substrate and an aspartate on the enzyme.

Free-Energy Profiles

The energetics of what happens during an enzymatic reaction is illustrated by a free-energy profile. Figure 1 shows the free-energy profile at equilibrium for the nonenzymatic reaction of A to P. The activation energy, $\Delta G^{\ddagger}$, corresponds to the height of the barrier, and ΔG for the reaction ($= -RT \ln K_{eq}$) is the difference between the levels marked A and P. For a corresponding enzymatic reaction, one must decide what levels of A and P to use. Figure 2 shows an equilibrium free-energy profile where the concentration of A is above its dissociation constant, so that formation of EA has an equilibrium constant greater than unity, but where P is less than its dissociation constant, so that EP dissociation is favorable. $\Delta G^{\ddagger}$ is given by the height of the barrier above the level of EA, not E + A. The turnover number (V/E_t or k_{cat}) is determined by $\Delta G^{\ddagger}$.

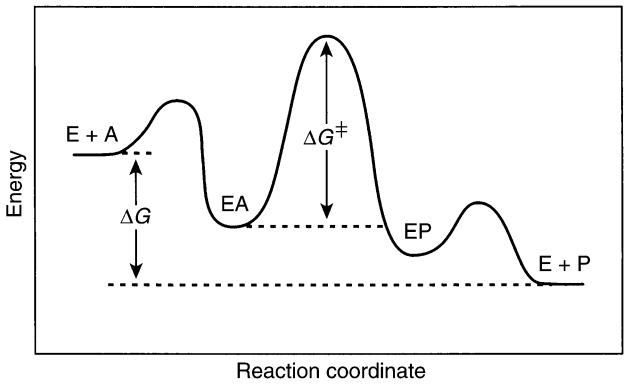

FIGURE 2 Free-energy profile at equilibrium for an enzymatic reaction. The symbols have the same meaning as in Figure 1.

If one picks different levels of A or P, the difference between E + A and EA, or E + P and EP, will differ as shown in Figure 3. The dissociation level of A (K_{ia}) is convenient, but then the level of P is determined by K_{eq} if an equilibrium free-energy profile is plotted, and will not usually match K_{ip}, its dissociation constant. Free-energy profiles may, of course, be plotted for nonequilibrium concentrations of reactants, but in any case it is critical to state the concentrations of reactions that are assumed in plotting the profile. When there are two or more substrates or products involved in the reaction, one must pick suitable levels of all reactants (and state them!) in order to plot a free-energy profile.

So far we have considered only simple free-energy profiles with a single transition state connecting

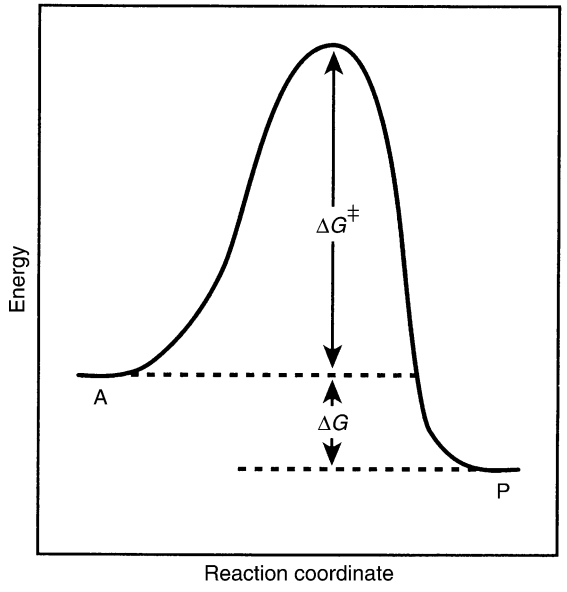

FIGURE 1 Free-energy profile at equilibrium for an uncatalyzed reaction. $\Delta G^{\ddagger}$ is the activation energy and $\Delta G = -RT \ln K_{eq}$, the energy difference between product and substrate.

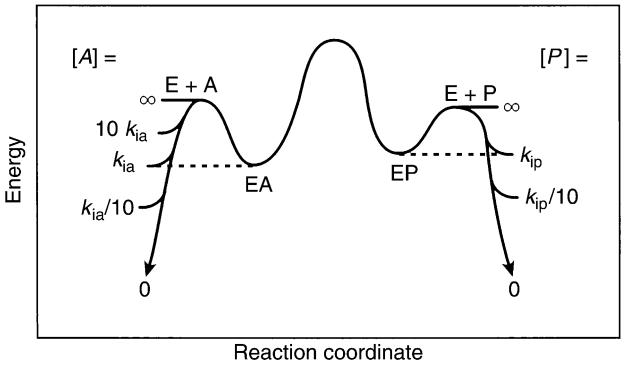

FIGURE 3 Free-energy profile showing the difference in the levels of (E + A) or (E + P) as the concentrations of A or P are changed. K_{ia} and K_{ip} are the dissociation constants of A from EA and of P from EP.

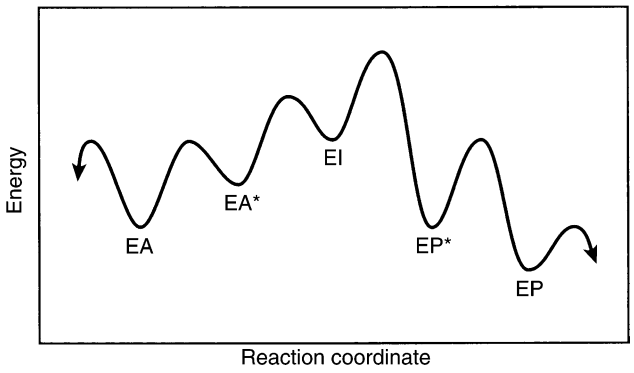

FIGURE 4 Free-energy profile showing conformation changes in the EA and EP complexes, as well as an intermediate between the two activated complexes. The levels of (E + A) and (E + P) are not shown.

EA and EP. In practice, enzymes have different conformations at the various stages of the catalytic cycle. Thus, they have open forms where the reactants are free to bind and dissociate, and closed forms in which catalysis takes place. The chemistry may also take place in more than one step, so that intermediates are present. Figure 4 shows a profile where a conformation change converts the open EA form to a closed, precatalytic EA* form. This undergoes a catalytic reaction to give an EI intermediate complex, which then is further converted to the closed EP* form. A final conformation change gives the open EP form, from which P can dissociate.

Rate-Limiting Step for *V/K*

The two independent kinetic constants for an enzymatic reaction are the maximum velocity, *V*, and the ratio of *V* and the Michaelis constant, *V/K*. There is a separate *V/K* for each substrate. Each of these parameters varies separately with pH, ionic strength, temperature, and the concentrations of other substrates, products, or inhibitors. The Michaelis constant, *K*, while it measures the apparent dissociation constant of the substrate in the steady state, is not an independent constant, but just the ratio of *V* and *V/K*. Thus when one speaks of "rate-limiting steps" one must specify whether one is referring to *V* or *V/K*.

The rate-limiting step for *V/K* is the one with the highest barrier in the free-energy profile. *V/K* involves the combination of enzyme and substrate and reaction through the first irreversible step, which normally is release of the first product. Later steps that involve further conformation changes in the enzyme and release of other products do not affect *V/K*. Thus the slow release of NADH from dehydrogenases, which often limits the maximum velocities of these enzymes, has no effect on *V/K*. As a result, the *V/K* value often is limited more by the chemistry of the reaction than *V*, and isotope effects on the chemistry are more fully expressed (see entry on kinetic isotope effects). Except for some slow mutants, full rate-limitation by the chemical reaction is unusual, however, and the conformation changes that precede and follow the chemical reaction are usually partly rate-limiting. The equation for an isotope effect on *V/K* is:

$$^{x}(V/K) = (^{x}k + c_f + {}^{x}K_{eq}c_r)/(1 + c_f + c_r) \qquad [4]$$

where *x* defines the isotope effect (D, T, 13, 15, 18 for deuterium, tritium, ^{13}C, ^{15}N, ^{18}O) and the leading superscript indicates the ratio of the parameters for light and heavy isotopes. ^{x}k is the intrinsic isotope effect on the chemical step, and $^{x}K_{eq}$ the equilibrium isotope effect on the reaction. The constants c_f and c_r are forward and reverse commitments to catalysis and are the ratio of the rate constant for the isotope sensitive step to the net rate constant for release from the enzyme of either the substrate (for c_f) or the first product (for c_r). For the simple mechanism

$$\mathrm{E + A} \underset{k_2}{\overset{k_1}{\rightleftharpoons}} \mathrm{EA} \underset{k_4}{\overset{k_3}{\rightleftharpoons}} \mathrm{EA^*} \underset{k_6}{\overset{k_5}{\rightleftharpoons}} \mathrm{EPQ^*} \underset{k_8}{\overset{k_7}{\rightleftharpoons}} \mathrm{EPQ}$$
$$\xrightarrow{k_9} \mathrm{EQ + P} \xrightarrow{k_{11}} \mathrm{E + P + Q} \qquad [5]$$

$$c_f = (k_5/k_4)(1 + k_3/k_2) \quad c_r = (k_6/k_7)(1 + k_8/k_9) \qquad [6]$$

The commitments thus consist of partition ratios of intermediates and these ratios correspond to the differences in barrier heights in a free-energy profile. In the profile shown in Figure 4, c_f and c_r will be small if the isotope effect measured involves reaction of EI to EP* because the barrier between EI and EP* is the highest one. But if the isotope effect measured is on reaction of EA* to EI, c_f will be small, but c_r will be large. Thus one will see largely the equilibrium isotope effect, as the EA* to EI step approaches equilibrium.

In the definition of c_f in eqn. [5], k_5/k_4 is the internal part of the commitment ($c_{f\text{-in}}$) and $k_3k_5/(k_2k_4)$ is the external part ($c_{f\text{-ex}}$). A sticky substrate is one where the net rate constant for reaction of the initial collision complex to give products is faster than the rate constant for dissociation (k_2). This ratio is called the stickiness ratio (S_r) and is given by $S_r = c_{f\text{-ex}}/(1 + c_{f\text{-in}} + c_r)$ in terms of the parameters of eqn. [5].

Rate-Limiting Steps for *V*

The rate-limiting step for the maximum velocity depends on the definition of rate limiting. One definition is the "slowest" step, or the one with the highest individual barrier in the forward direction. Another definition is the "least-conductive" step, which is the one that sees the highest total barrier to reach an irreversible step. A third definition is the "most-sensitive" step. This is the one

which causes the greatest percentage change in the turnover number for a given percent change in the forward rate constant. An isotope effect on this step is more fully expressed than one on any other step. The isotope effect on V for mechanism 3 is

$$^{x}V = (^{x}k + c_{v_f} + {}^{x}K_{eq}c_r)/(1 + c_{v_f} + c_r) \quad [7]$$

where ^{x}k, $^{x}K_{eq}$, and c_r have the same meaning as in eqn. [5], but

$$c_{v_f} = [k_3k_5/(k_3 + k_4)][1/k_3 + (1/k_7)(1 + k_8/k_9) + 1/k_9 + 1/k_{11}] \quad [8]$$

Note that c_{v_f}, unlike c_f, does not consist of partition ratios. Rather k_5, reduced by the factor $k_3/(k_3 + k_4)$, is compared to k_3, and to each of the net rate constants after the chemical step. A low value of k_{11}, for example, can result in a large value of c_{v_f}, and a greatly reduced expression of the isotope effect on V.

The "slowest," "least-conducting," and "most-sensitive" steps may be the same in an enzymatic reaction, but need not be, so one must define what one means when using the term "rate-limiting" for the maximum velocity.

See Also the Following Articles

Enzyme Inhibitors • Enzyme Kinetics • Enzyme Reaction Mechanisms: Stereochemistry • Kinetic Isotope Effects • Low Barrier Hydrogen Bonds • Metabolite Channeling: Creatine Kinase Microcompartments

Glossary

Haldane relationship An equation relating the equilibrium constant to the kinetic constants of an enzymatic reaction.

isotope effect The effect of isotopic substitution, expressed as the ratio of the parameter for the light isotope to that for the heavy one.

Michaelis constant The concentration of a substrate that gives half of the maximum velocity of an enzymatic reaction. It is the apparent dissociation constant in the steady state.

substrate A molecule that is converted to a product during an enzyme-catalyzed reaction.

turnover number The number of substrate molecules converted to product per enzyme molecule per unit time. The units are usually reciprocal seconds.

Further Reading

Cleland, W. W. (1982). An analysis of haldane relationships. *Meth. Enzymol.* **87**, 366–369.

Cleland, W. W. (1986). Enzyme kinetics as a tool for determination of enzyme mechanisms. In *Investigation of Rates and Mechanisms of Reactions* (C. F. Bernasconi, ed.) 4th edition, Part 1, pp. 791–870. John Wiley & Sons, New York.

Cleland, W. W., and Northrop, D. B. (1999). Energetics of substrate binding, catalysis, and product release. *Meth. Enzymol.* **308**, 3–27.

Biography

W. Wallace Cleland is M. J. Johnson Professor of Biochemistry at the University of Wisconsin and a co-director of the Institute for Enzyme Research. His research interest is in the use of kinetic methods for the determination of enzyme mechanisms, and in particular the use of isotope effects. He has a Ph.D. from the University of Wisconsin and was a postdoctoral Fellow at the University of Chicago. He is a member of the National Academy of Sciences and the American Academy of Arts and Sciences.

Sugar Nucleotide Transporters

Carlos B. Hirschberg
Boston University School of Dental Medicine, Boston, Massachusetts, USA

Sugar nucleotide transporters are proteins in the membrane of the Golgi apparatus. Their role is to translocate, from the cytosol into the Golgi lumen, nucleotide substrates for the glycosylation of proteins and lipids. Mutants in the above transporters have biochemical and developmental phenotypes, resulting in diseases such as leukocyte adhesion deficiency II.

A Requirement for Sugar Nucleotide Transport into the Golgi Apparatus Lumen

Approximately half of all proteins in eukaryotic cells are secreted or membrane-bound. These proteins are processed through the secretory pathway where 80% undergo post-translational modifications such as glycosylation, sulfation, and phosphorylation in the lumen of the Golgi apparatus. Intact nucleotide sugars, nucleotide–sulfate, and ATP, the substrates for these reactions, enter the lumen of the Golgi apparatus via specific transporter proteins (Figure 1). These are multi-transmembrane spanning proteins which function as antiporters with the corresponding nucleoside monophosphates and thereby concentrate the nucleotide derivatives in the Golgi lumen relative to their concentration in the cytosol (Figure 1). Evidence for this mechanism has been obtained through biochemical studies with rat liver-derived Golgi vesicles as well as with different species of yeast. In the latter, gene disruption of a Golgi lumenal GDPase, which generates GMP (the antiporter molecule coupled to entry of GDP-mannose into the yeast Golgi lumen), results in severe undermannosylation of proteins and lipids *in vivo*, reduced transport of the GDP-mannose into Golgi vesicles *in vitro*, as well as in a failure to make hyphae in *Candida albicans*.

Mutants in Nucleotide Sugar Transport—Biochemical and Developmental Phenotypes Including Diseases

Mutant mammalian cells grown in tissue culture have been described as having 95% reduced transport of specific nucleotide sugars into their Golgi apparatus, while their proteins and lipids have a drastic reduction in the specific sugar transported by the corresponding nucleotide derivative transporters. Multicellular organisms such as *C. elegans*, *Drosophila melanogaster*, plants, and humans that have mutations in the above proteins also have distinct morphological phenotypes affecting development of limbs, wings, brain, etc. Studies of these mutants have shown that some of the transporters can translocate more than one nucleotide sugar, whereas other transporters retain high substrate specificity such as differentiating between sugar epimers.

Mutants in nucleotide sugar transport have also been described in *Leishmania donovani* and in yeasts such as *S. cerevisiae*, *K. lactis*, and *C. albicans*.

Structure of Golgi Nucleotide Sugar Transporters

So far the primary amino acid sequence, together with the substrate specificity of approximately two dozen Golgi membrane nucleotide sugar transporters, has been determined. In most cases this was done by correcting the phenotypes of mutant cells or mutant multicellular organisms with libraries containing wild-type DNA or cDNA from homologous or heterologous organisms. In most cases after phenotypic correction, the specific DNA (or cDNA) was expressed in yeast or mammalian cells, Golgi vesicles were isolated, and transport of different nucleotide sugars assayed *in vitro*. Yeast is a particularly attractive system for

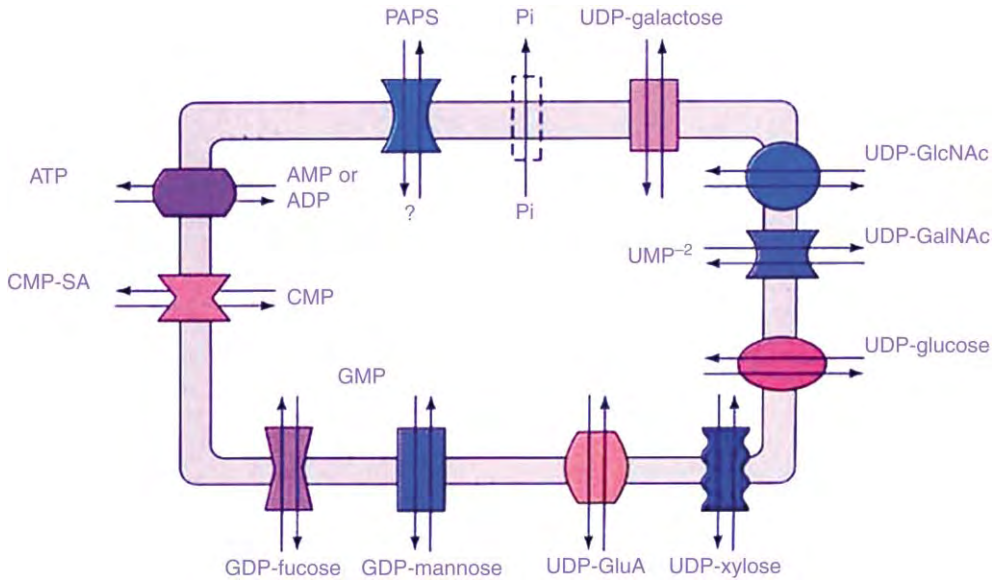

FIGURE 1 Golgi membrane nucleotide sugar, PAPS, and ATP transporters have been detected in mammals, yeast, protozoa, nematodes, insects, and plants. They are antiporters with the corresponding nucleoside monophosphate, except for PAPS, where the antiporter is not known, and for ATP, where it is either AMP or ADP or both.

heterologous expression of nucleotide sugar transporter genes, because it has few endogenous nucleotide sugar transport activities. This approach led to the identification of multisubstrate nucleotide sugar transporters from *C. elegans*. In some instances a particular cDNA was also tested for its ability to correct the phenotype of mutant cells where the substrate specificity of the defective nucleotide sugar is known.

The fact that the above approaches for determining the substrate specificity of particular transporters have worked is based on the following points:

1. the transporters DNA (or cDNA) can express the proteins in a heterologous system;
2. the targeting signals allowing the protein to localize to the Golgi apparatus are functional in different cell types; and
3. the targeted transporter is active once it reaches the Golgi apparatus of the recipient cell and can therefore affect phenotypic correction.

To date, the relationship of amino acid sequences and substrate specificities of nucleotide sugar transporters can be summarized as follows:

1. substrate specificities of nucleotides sugar transporters cannot be inferred even when amino acid sequences are ~50% identical;
2. only sequence identities of over 80% allow accurate predictions of substrate specificity; and
3. transporters from different organisms that have the same substrate specificity may have only 20% overall amino acid sequence identity.

Due to the above reasons the reader is cautioned that annotations about the identity (substrate specificity) of nucleotide sugar transporters in databases should be looked at very carefully!

Topography of Nucleotide Sugar Transporters in the Golgi Membrane

So far the only detailed topographic study of a nucleotide sugar transporter has been done with that for CMP-sialic acid in mammalian cells. Using a combination of tagged epitopes and immunocytochemistry, the transporter was found to have ten transmembrane domains and both its amino and carboxy termini facing the cytosol. A study on the topography of the *Kluyveromyces lactis* UDP-acetylglucosamine transporter using membrane accessibility of a peptide antibody and amino and carboxy termini epitope tags also found that both termini face the cytosol and that this transporter has either six or eight transmembrane domains. It is important to stress that none of the existing algorithms in the literature are designed specifically to address the issue of protein topography in the Golgi apparatus membrane which is somewhat thinner than the plasma membrane; most algorithms are designed for predicting topography in the plasma membrane.

Regulation of Macromolecular Glycosylation by Nucleotide Sugar Transporters

Studies with mutant mammalian cells in nucleotide sugar transporters grown in tissue culture as well as with fibroblasts and lymphoblasts from patients with leukocyte adhesion deficiency (LAD) syndrome II showed that decreased concentrations of nucleotide sugar in the Golgi lumen result in selective hypoglycosylation of proteins rather than across the board reduction. Thus, mutant MDCK cells which have a 95% reduction in transport of UDP-galactose into their Golgi lumen have a corresponding decrease in galactosylation of bulk glycoproteins, glycolipids, and keratan sulfate but not in heparan and chondroitin sulfates. LAD II patients appear to have normal O-fucosylation of Notch protein, whereas N-fucosylation of bulk proteins is drastically reduced. Although the detailed mechanism for these biochemical phenotypes is not understood, an attractive hypothesis is that when supply of nucleotide sugars is limited due to impairment in their transport, glycosylation reactions with lower K_ms would proceed, whereas those with higher K_ms would not.

See Also the Following Articles

Glycosylation, Congenital Disorders of • Golgi Complex • Protein Glycosylation, Overview

Glossary

glycosylation The covalent addition of sugars to each other or to proteins and lipids.

Golgi apparatus A membrane-enveloped organelle in the cytoplasm of all eukaryotes composed of several cisternae and vesicles; virtually all membrane-bound and secreted proteins of eukaryotes traverse through this organelle in route to their final location within or outside the cell.

nucleotide sugar Phosphodiesters, usually between nucleoside 5′ diphosphates and carbon 1 of the sugar.

phenotype The visual or physical characteristics of individual cells or a multicellular organism.

Further Reading

Abeijon, C., Mandon, E. C., and Hirschberg, C. B. (1997). Transporters of nucleotide sugars, nucleotide sulfate and ATP in the Golgi apparatus. *Trends Biochem. Sci.* **22**, 203–207.

Hirschberg, C. B., Robbins, P. W., and Abeijon, C. (1998). Transporters of nucleotide sugars, ATP and nucleotide sulfate in the endoplasmic reticulum and Golgi apparatus. *Ann. Rev. Biochem.* **67**, 49–69.

Lodish, H., Berk, A., Zipusky, S. L., Matsudaira, P., Baltimore, D., and Darnell, J. (2000). *Molecular Cell Biology.* W.H. Freeman, New York.

Varki, A., Cummings, R., Esko, J., Freeze, H., Hart, G., and Marth, J. (1999). *Essentials of Glycobiology.* Cold Spring Harbor Laboratory Press, New York.

Biography

Carlos B. Hirschberg is a Professor and Founding Chairperson of the Department of Molecular and Cell Biology at the Boston University Goldman School of Dental Medicine. He holds a Ph.D. in Chemistry from the University of Illinois at Urbana-Champaign and received his postdoctoral training at the Harvard Medical School and MIT. His principal research interests are mechanisms of posttranslational modifications in eukaryotes. His laboratory co-workers discovered the transport/antiport system for nucleotide derivatives in the Golgi apparatus and endoplasmic reticulum membranes and were the first to purify and clone proteoglycan sulfotransferases.

SUMO Modification

Frauke Melchior and Andrea Pichler
Max-Planck Institute of Biochemistry, Martinsried, Germany

Small ubiquitin-related modifier, SUMO-1, and its homologues are 10–12 kDa eukaryotic proteins that serve to regulate protein function. Like their relative ubiquitin, they are covalently coupled to many different target proteins in the cell. Specific enzymes required for the formation or cleavage of isopeptide bonds between SUMO and its targets ensure specificity and dynamics of this posttranslational modification. Functional consequences reach from changes in protein-protein or protein–DNA interactions, alteration in subcellular localization, or enhanced stability, to changes in biological activity.

The SUMO Family

Expression

Proteins of the *s*mall *u*biquitin-related *mo*difier (SUMO) family appear to exist in all eukaryotic cells. For nomenclature see Table I. The number of distinct family members varies from one (e.g., in baker's and fission yeasts, nematodes, and fruit fly) to several (three in mammals; eight in *Arabidopsis thaliana*).Where present, different family members appear to have at least partially distinct functions. Interestingly, mammalian SUMO1 is mainly conjugated to substrates, while mammalian SUMO2/3 primarily exists in its free form under normal growth conditions, but is conjugated rapidly after stress stimuli. Whether SUMO proteins are differentially expressed, and their expression levels are regulated, is currently unknown. Available knockout data suggest that reversible SUMO conjugation is essential for life in most organisms. Fission yeast grows without a functional SUMO gene, but the cells are severely impaired.

Structure

SUMO proteins are small acidic proteins with distant homology to ubiquitin. At primary amino acid sequence, they are 10–20% identical to ubiquitin. On a structural level, their relatedness is much more pronounced. As shown in Figure 1, ubiquitin and SUMO share the classical ubiquitin-superfold. Characteristic for all members of the SUMO family, and absent from ubiquitin or other ubiquitin-related proteins, is an N-terminal flexible extension of 10–30 amino acids. The function of this extension is however currently unknown.

All SUMO proteins are expressed as precursors that require trimming of their C-terminus. Proteolytic removal of several amino acids, which is accomplished by specific enzymes (SUMO isopeptidases), results in exposure of a C-terminal glycine–glycine motif. Maturation is rapid, and there is currently no evidence for regulation of this process.

Enzymology

Covalent interaction between SUMO and its targets is a reversible, often dynamic, process. This is accomplished by formation and subsequent cleavage of an isopeptide bond between the carboxy-terminus of mature SUMO and a lysine of the acceptor protein. Isopeptide bond formation requires ATP and involves several (two or three) distinct enzymes (see Figure 2). In contrast, cleavage is accomplished by a single enzyme and does not require energy.

Conjugation

Overview

The first step towards isopeptide bond formation is activation of the SUMO carboxy-terminus. This is accomplished by ATP-dependent thioester bond formation between a cysteine residue in the E1 activating enzyme and the C-terminal glycine residue in SUMO. Subsequently, SUMO is transferred to a cysteine residue in the E2 conjugating enzyme and again the resulting bond is a thioester. Finally, an isopeptide bond is formed by transferring SUMO to the ε-amino group in a lysine of the acceptor protein. Depending on the specific acceptor protein, this step can be carried out by the E2 conjugating enzyme alone, or it may require an additional component, a so-called E3 ligase.

TABLE I

Nomenclature for SUMO and its Conjugating Enzymes

	Human	Baker's yeast
SUMOs	**SUMO1**/PIC 1/Ubl1/sentrin1/GMP1/hSMT3	**Smt3**
	SUMO2/sentrin3/Smt3a	
	SUMO3/sentrin2/Smt3b	
E1 activating enzyme		
Subunit 1	**Aos1**/SAE1/Sua	**Aos1**
Subunit 2	**Uba2**/SAE2	**Uba2**
E2 conjugating enzyme	**Ubc9**/UBE2I	**Ubc9**
E3 ligating enzymes	**Pias1**/GBP/DEAD/H box-binding protein 1/ARIP	**Siz1**/UII 1
	Pias3	**Siz2**/Nfi1
	Piasx*α*/ARIP3	
	Piasx*β*/Miz1/Siz2	
	Piasy	
	RanBP2/Nup358	
	Pc2	

Known proteins involved in the SUMO conjugation pathway. Since most of them were independently identified by several groups, different names exist in literature.

SUMO Activating Enzyme (E1 Enzyme)

SUMO E1 activating enzyme is composed of two subunits, Aos1 and Uba2 (for alternative names see Table I), both of which are essential for the function. Aos1 and Uba2 share striking homology to the N- and C- terminal halves of ubiquitin E1 enzyme, respectively. SUMO E1 activating enzyme is present throughout the cell, with a strong enrichment in the nucleoplasm. A single SUMO E1 activating enzyme is expressed in most organisms, even those containing several distinct SUMO proteins. Current data suggest that mammalian SUMO E1 works with equal efficiency on each of the three mammalian SUMO proteins, although it has no affinity for other ubiquitin-related proteins.

SUMO Conjugating Enyzme (E2 Enzyme)

A single SUMO E2 conjugating enzyme, Ubc9, is expressed in cells (see Table I for alternative names). While it is strikingly similar to ubiquitin conjugating enzymes, it works exclusively on SUMO proteins. As for the E1 enzyme, Ubc9 does not appear to discriminate between different SUMO proteins expressed within a particular organism. Ubc9 localizes predominantly in the nucleus, but is also present in the cytoplasm and at nuclear pore complexes. A striking difference between the ubiquitin-conjugating and the SUMO-conjugating system is the ability of Ubc9 to directly bind to and modify SUMO targets. However, with a few exceptions, the efficiency of modification in the absence of E3 ligases is extremely poor.

SUMO Ligases (E3 Ligase)

Three types of SUMO E3 ligases are currently known (Table I). The first type is encoded by the

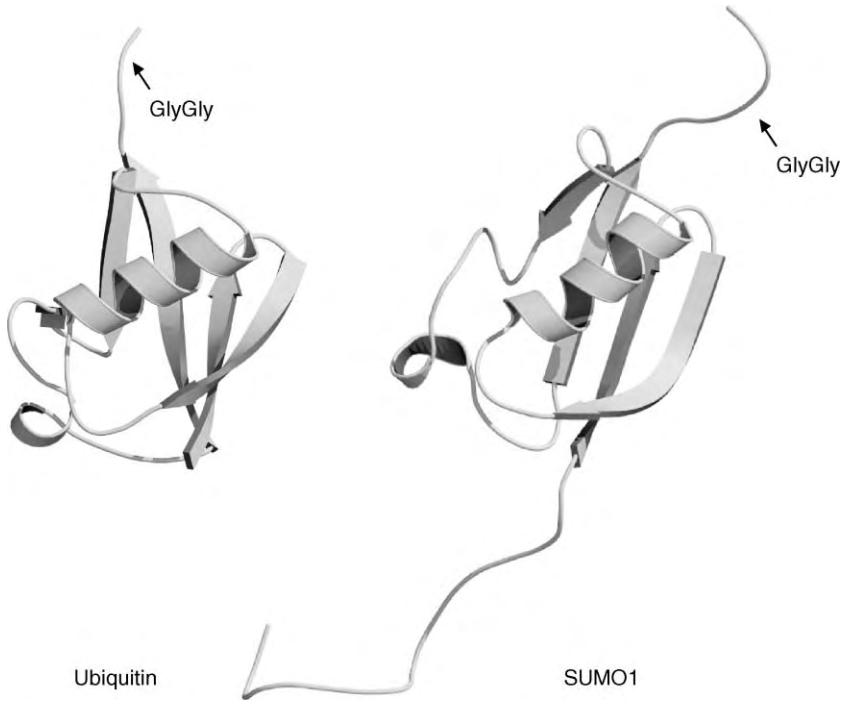

FIGURE 1 Ubiquitin and SUMO comparison. Although ubiquitin and SUMO1 share only 18% amino acid identity, the structural fold is very similar. The indicated C-terminal double glycine motif is the attachment site to substrates. The images (generated using Moscript 2.1.2 and Raster3D) were kindly provided by Dr. Peter Bayer.

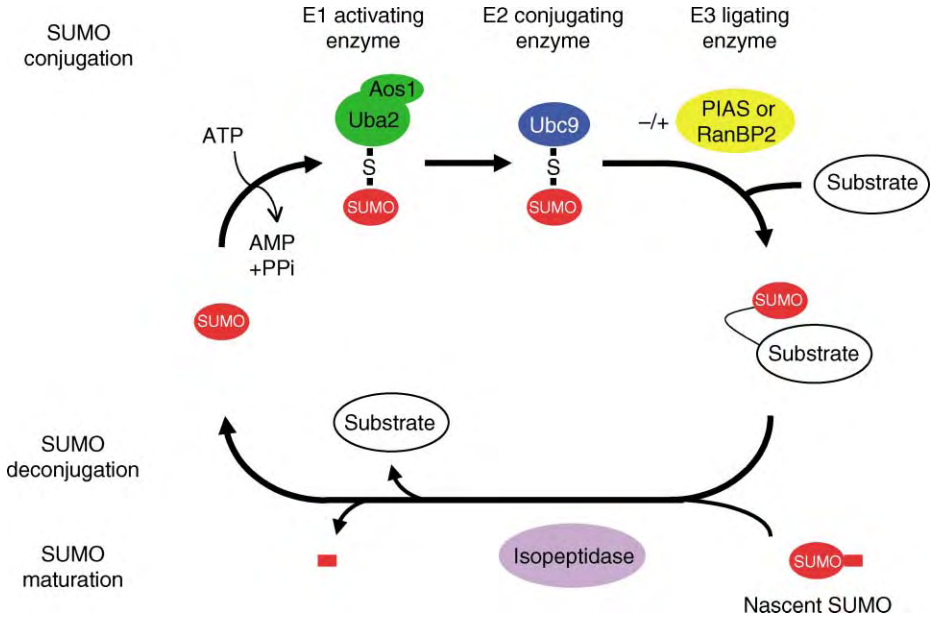

FIGURE 2 The SUMO modification pathway. SUMO is synthesized as a precursor that requires proteolytic processing. A C-terminal hydrolase/isopeptidase removes several C-terminal amino acids to expose the GlyGly motif essential for conjugation. SUMO conjugation involves an enzymatic cascade: In an ATP-dependent step, mature SUMO first forms a thioester with the E1 activating enzyme, the heterodimer Aos1/Uba2. Subsequently, it is transferred to the E2 conjugating enzyme, Ubc9. SUMO is then either directly or in an E3 ligase-dependent step conjugated to the substrate. SUMO de-modification is performed by isopeptidases.

"Protein inhibitor of activated STAT" (PIAS) family. These proteins contain a predicted RING finger-like structure that is essential for their function as E3 ligases. They bind directly to Ubc9 and to selected SUMO targets, and stimulate their modification both *in vivo* and *in vitro*. Baker's yeast contains two PIAS type E3 ligases, Siz1 and Siz2. These proteins seem to be responsible for most, but probably not for all, SUMO targets, and have partially overlapping target specificity. The second type is currently represented by a single (vertebrate specific) 358 kDa protein, RanBP2/Nup358 (Ran binding protein/nucleoporin). RanBP2 is a component of nuclear pore complexes, and thus may couple sumoylation and nucleocytoplasmic transport. Interestingly, the catalytic domain of RanBP2 does not contain a RING finger motif, and also shows no other homology to ubiquitin E3 ligases. The Polycomb group protein Pc2 appears to represent a third type of an E3 ligase, as it bears no similarity to other E3 ligases.

Deconjugation

Overview

Isopeptide bonds between ubiquitin-related proteins and their cellular targets are reversible in nature due to the presence of specific enzymes that recognize and cleave the bond. Currently, a single family of SUMO-specific isopeptidases is known (Table II). All members contain a 200 amino acid catalytic core that is distantly related to viral cysteine proteases but shows no similarity to ubiquitin-specific enzymes.

Interestingly, SUMO isopeptidases serve two physiological functions *in vivo*, cleavage of isopeptide bonds, but also maturation of nascent SUMO (C-terminal hydrolase activity). This distinguishes the SUMO system from the ubiquitin system, where two distinct enzyme families serve to fulfill these functions.

SUMO Isopeptidases

The founding member of this family is *S. cerevisiae* Ulp1 (*u*biquitin *l*ike *p*rotease). Bakers yeast contains

TABLE II

Nomenclature for SUMO Deconjugating Enzymes

Human	Mouse	Baker's yeast
Senp1	SuPr-2	**Ulp1**
Senp2/KIAA1331	Senp2/**Smt3IP2***/Axam2 and **Supr-1***	**Ulp2**/Smt4
Senp3/Susp3/SSP3	Senp3/**Smt3IP1**/SuPr-3	
Senp5		
Senp6/**Susp1**/SSP1/KIAA0797		
Senp7/Susp2/SSP2/KIAA1707		

SUMO isopeptidases share a 200 amino acid core domain. Known proteins containing this core domain are listed in this table. The proteins characterized as SUMO isopeptidases are indicated in bold.

*Indicates different isoforms or alternative splice products.

two enzymes of this family, Ulp1 and Ulp2. Ulp1 is required for viability in yeast, whereas Ulp2 is not essential. They localize to different intracellular compartments, with Ulp1 being enriched at nuclear pore complexes, and Ulp2 being diffusely distributed throughout the nucleus. Mammals on the other hand have at least six distinct genes for SUMO isopeptidases (see Table II). Due to alternative splicing, the number of enzymes expressed is probably much larger. Only a few of these proteins have been characterized in some detail. They vary significantly in size and intracellular localization. It is plausible to assume that different isopeptidases exert different target specificity in large part through their physical localization. Whether they also differ in enzymatic properties, such as substrate specificity or kinetics of cleavage, remains to be seen.

SUMO Target Proteins

Sumoylation as a means to regulate protein function appears to be quite a common mechanism. Modification has been documented for more than 70 different target proteins, and this number is expected to increase significantly. Based on current knowledge, some generalizations can be made about the nature of the targets, motifs required for modification, consequences of modification, and regulation.

Known Target Proteins

Based on immuno-fluorescence analysis, most targets for sumoylation are constitutively or transiently associated with the nuclear compartment. Consistent with this, most known targets can be associated with nuclear processes such as chromatin remodeling, DNA repair, transcription, or nucleocytoplasmic transport (amongst them are histone deacetylases, topoisomerases, thymine-DNA glycosylase, PCNA, p53, PML, heat shock factors, steroid hormone receptors, IκBα, RanGAP1, and many others). Other pathways to which SUMO has been linked are, e.g., progression through mitosis (mitotic arrest of yeast mutants defective in SUMO conjugation or deconjugation; yeast septins, topoisomerase II and Pds5 are modified specifically in mitosis), or infection with viruses (examples for viral SUMO targets are: cytomegalovirus immediate early proteins IE1 and IE2, adenovirus type 5 E1B-55 kDa, bovine papillomavirus E1).

Consensus Sites for Modification

In contrast to ubiquitinylation, for which a unifying motif has not been identified, sumoylation of most targets seems to be specified by a short consensus sequence in target proteins. This motif consists of just four amino acids, ΨK $\times$ E/D, and includes the lysine residue that forms an isopeptide bond with SUMO. Ψ stands for a bulky aliphatic amino acid residue. Additional structural features are probably required to ensure accessibility to the conjugation machinery. Some motifs are present at the very N- or C-terminal end of a protein, others are flanked by proline residues that may induce a loop structure. Consistent with this, RanGAP1, which is an extremely efficient SUMO target, presents its sumoylation motif in an accessible loop.

Functional Consequences for Modification

Similar to phosphorylation, sumoylation seems to have many different functional consequences that depend on the specific target protein. Considering SUMO's size, it is plausible to assume that conjugation can lead to masking of binding sites, generation of novel binding interphases, or conformational changes in the modified protein. Examples have been reported for changes in protein–protein or protein–DNA interactions, alteration in subcellular localization, enhanced stability through antagonizing ubiquitin/proteasome-mediated degradation, and changes in enzymatic activity.

Regulation

While some SUMO targets appear to be modified constitutively, others are sumoylated only during a specific period of the cell cycle, upon stress, or upon a specific extracellular signal. Examples are sumoylation of yeast septins during mitosis, sumoylation of topoisomerase upon treatment with DNA-damaging agents, or *Dictyostelium* MEK1 sumoylation in response to chemoattractant. While this suggests the existence of elaborate regulatory mechanisms, current knowledge is rather poor. Increased modification of a specific target may for example be due to changes in the target, activation of a specific E3 ligase, or relocalization of a specific isopeptidase. Evidence for cell-cycle-dependent regulation of E3 ligases and isopeptidases is currently only available in yeast: (1) fission yeast ulp1 resides at the NPC during interphase, but is nuclear during mitosis; (2) baker's yeast E3 ligase Siz1 is intranuclear during interphase, but partially relocalizes to the bud neck in mitosis.

See Also the Following Articles

Cysteine Proteases • JAK-STAT Signaling Paradigm • Nuclear Pores and Nuclear Import/Export • Ubiquitin System • Ubiquitin-Like Proteins • Zinc Fingers

Glossary

cysteine protease Protease that requires a cysteine for activity.

isopeptide bond Any amide bond formed between a carboxyl group of one amino acid and an amino group of another amino acid with the exception of the conventional peptide bond that is formed between amino- and carboxy- groups in α-position.

nuclear pore complex A large multiprotein complex embedded in the nuclear envelope that mediates both active transport of macromolecules and passive diffusion of small components to and from the nucleus.

RING finger proteins A family of structurally related zinc-binding proteins containing the RING consensus sequence: $CX_2CX_{(9\text{-}39)}CX_{(1\text{-}3)}HX_{(2\text{-}3)}C/HX_2CX_{(4\text{-}48)}CX_2C$. The cysteines and histidines represent the zinc-binding sites, whereby the first, second, fifth, and sixth of these complex the first zinc ion, and the third, fourth, seventh, and eighth complex the second.

Further Reading

Bernier-Villamor, V., Sampson, D. A., Matunis, M. J., and Lima, C. D. (2002). Structural basis for E2-mediated SUMO conjugation revealed by a complex between ubiquitin-conjugating enzyme Ubc9 and RanGAP1. *Cell* **108**, 345–356.

Freiman, R. N., and Tjian, R. (2003). Regulating the regulators: Lysine modifications make their mark. *Cell* **112**, 1–17.

Goettsch, S., and Bayer, P. (2002). Structural attributes in the conjugation of ubiquitin, SUMO and RUB to protein substrates. *Front Biosci.* **7**, a148–a162.

Johnson, E. S. (2002). Ubiquitin branches out. *Nat. Cell Biol.* **4**, E295–E298.

Kim, K. I., Baek, S. H., and Chung, C. H. (2002). Versatile protein tag, SUMO: Its enzymology and biological function. *J. Cell Physiol.* **191**, 257–268.

Kurepa, J., Walker, J. M., Smalle, J., Gosink, M. M., Davis, S. J., Durham, T. L., Sung, D. Y., and Vierstra, R. D. (2003). The small ubiquitin-like modifier (SUMO) protein modification system in Arabidopsis. Accumulation of SUMO1 and -2 conjugates is increased by stress. *J. Biol. Chem.* **278**, 6862–6872.

Melchior, F. (2000). SUMO – nonclassical ubiquitin. *Annu. Rev. Cell Develop. Biol.* **16**, 591–626.

Melchior, F., Schergaut, M., and Pichler, A. (2003). SUMO: ligases, isopeptidases and nuclear pores. *Trends Biochem. Sci.* **28**, 612–618.

Muller, S., Hoege, C., Pyrowolakis, G., and Jentsch, S. (2001). SUMO, ubiquitin's mysterious cousin. *Nat. Rev. Mol. Cell Biol.* **2**, 202–210.

Schwartz, D. C., and Hochstrasser, M. (2003). A superfamily of protein tags: ubiquitin, SUMO and related modifiers. *Trends Biochem. Sci.* **28**, 321–328.

Seeler, J. S., and Dejean, A. (2003). Nuclear and unclear functions of SUMO. *Nat. Rev. Mol. Cell Biol.* **4**, 690–699.

Wilson, V. G., and Rangasamy, D. (2001). Viral interaction with the host cell sumoylation system. *Virus Res.* **81**, 17–27.

Biography

Frauke Melchior is a group leader at the Max-Planck Institute for Biochemistry in Martinsried, Germany. Her principal research interests are nucleocytoplasmic transport, and ubiquitin-related proteins of the SUMO family. She holds a Ph.D. from the University of Marburg and received her postdoctoral training at the Max-Planck Institute for Biophysical Chemistry in Göttingen and the Scripps Research Institute in La Jolla. She participated in the discovery of SUMO during her postdoctoral time, and has since contributed to the field with her own group.

Andrea Pichler obtained her Ph.D. from the University of Vienna and received a postdoctoral training at the Novartis Forschungsinstitut of Vienna. Since 2000 she is a member of Dr. Frauke Melchior's group at the Max-Planck Institute of Biochemistry in Martinsried.

Superoxide Dismutase

Irwin Fridovich
Duke University Medical Center, Durham, North Carolina, USA

A small fraction of the O_2 consumed by living cells is converted to superoxide O_2^-. This free radical, and its progeny, can damage a variety of biomolecules. This is the cause of oxidation stress. Defenses are provided by the superoxide dismutases that catalytically eliminate O_2^- and by the catalases and peroxidases that do the same for hydroperoxides. The varieties, distributions, and mode of action of the superoxide dismutases are presented herein.

Introduction

Molecular oxygen (O_2), while essential for the life of aerobes, is potentially toxic. This toxicity is due to the propensity of O_2 for reduction by a univalent pathway. This facile univalent pathway of O_2 reduction generates intermediates that lie between one O_2 and its four electron reduction products – two molecules of water – and it is the reactivity of these intermediates that is responsible for the toxicity of O_2. In order of their production, these intermediates are the superoxide anion radical (O_2^-), hydrogen peroxide (H_2O_2), and the hydroxyl radical (HO·). Superoxide dismutases (SODs) catalyze the conversion of O_2^- into H_2O_2 plus O_2, i.e.,

$$O_2^- + O_2^- + 2H^+ \xrightarrow{\text{SOD}} H_2O_2 + O_2$$

and in so doing provide an important defense. H_2O_2, in turn, is eliminated by the catalases and peroxidases. The concerted action of the SODs with the catalases and peroxidases prevents the formation of the very reactive HO·. This is the case because HO· production *in vivo* requires both O_2^- and H_2O_2. O_2^- oxidizes the [4Fe–4S] clusters of dehydratases, such as the aconitases, causing release of Fe (II); the freed Fe (II) then reduces H_2O_2 to OH^- plus HO· in a reaction known as the Fenton reaction.

The SOD Family of Enzymes

The first truly photosynthetic organisms were the cyanobacteria and the oxygen they produced oxygenated a previously anaerobic biosphere. This imposed a common selection pressure on what must have been a varied anaerobic biota. It is not surprising that several different SODs were then evolved to deal with the toxicity of the accumulating O_2 and that these persist to this day. Thus, there are SODs based on Cu (II) plus Zn (II), Mn (III), Fe (III), and Ni (II). They all catalyze the dismutation of O_2^- into $H_2O_2 + O_2$.

All SODs work by a similar mechanism in which the metal at the active site is reduced by one O_2^- and then reoxidized by the next O_2^-. The active site metal thus acts as a mediator passing an electron from one O_2^- to the next. In this way the electrostatic repulsion, which would prevent close approach of one O_2^- to another, is bypassed by the SODs. All the SODs are very efficient catalysts and operate at close to the theoretical diffusion limit. Their rate constants for interaction with O_2^- are $\sim 3 \times 10^9\ M^{-1}s^{-1}$.

The Cu, Zn SODs

These SODs have been found in the cytosols of eukaryotic cells, the intermembrane space of mitochondria, the periplasm of gram-negative bacteria, and in chloroplasts. The Cu (II) is linked to the Zn (II) at the active site by the imidazolate moiety of a histidine residue and this bridging imidazolate functions as a proton supply during the catalytic cycle. Thus, when the Cu (II)) is reduced by O_2^-, the Cu (I) releases the imidazolate that then protonates to imidazole. When the Cu (I) is reoxidized to Cu (II), the imidazole provides a proton to the nascent $O_2^{=}$ converting it to HO_2^-, as the bridging to the Zn (II) is reestablished. The HO_2^- that leaves the active site protonates in the water to H_2O_2. This mechanism can be depicted as follows:

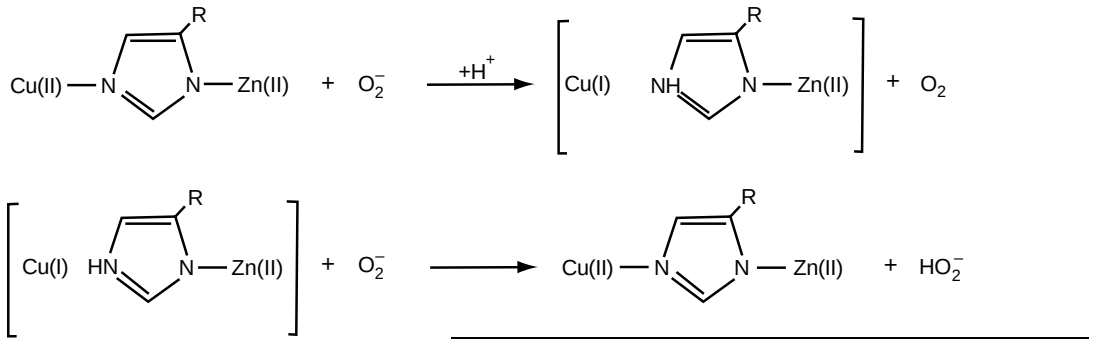

Both of these half-reactions of the catalytic cycle proceed with a rate constant of $\sim 3 \times 10^9\ M^{-1}s^{-1}$. The enzyme surface contains charged groups that provide an electrostatic funnel guiding the O_2^- toward the active site crevice. This electrostatic facilitation contributes to the efficiency of these enzymes.

The Cu, Zn SODs found in eukaryotic cytosols are homodimeric proteins with subunit weights ~16 kDa. The corresponding enzyme from the periplasm of *Escherichia coli* is monomeric. There is an extracellular Cu, Zn SOD found in higher animals. It is usually homotetrameric and glycosylated and has a subunit weight of ~23 kDa.

The Mn SODs

These enzymes, whether from the matrix of mitochondria or bacteria, exhibit marked sequence similarity, reflecting a close evolutionary history and supporting an endosymbiotic origin for mitochondria. The bacterial enzyme is usually a homodimer, whereas the mitochondrial enzyme is a homotetramer. The subunit weight is ~23 kDa. Some bacterial Mn SODs are tetrameric. This is the case in Cryptococcus neoformans. In *E. coli* the biosynthesis of Mn SOD is under the control of the soxRS regulon, which coordinately up-regulates the expression of a number of genes in response to O_2^-. The constitutively expressed SOX R protein is transcriptionally inactive in its reduced form. It can be oxidized by O_2^- and then activates the expression of the SOX S protein, which in turn activates all the genes in the regulon. Thus, Mn SOD is not measurable in extracts of anaerobically grown *E. coli*, but exposure of cultures to aerobic conditions elicits production of Mn SOD. Increasing production of O_2^-, by raising pO_2, or by adding compounds such as viologens, which can mediate enhanced production of O_2^-, increases the level of Mn SOD. It has been possible to force *E. coli* to produce Mn SOD to 7% of its soluble protein by aerobic exposure to the viologen paraquat.

The nectar of tobacco flowers has been found to contain a stable Mn-protein named nectarin that appears to be an Mn SOD.

The Fe SODs

These SODs, which are highly homologous to the Mn SODs, are found in bacteria and in plants. Although usually homodimeric, homotetrameric Fe SOD has been found in Rhodococcus bronchialis and Mycobacterum tuberculosis. The Fe SOD of *E. coli* is constitutive and thus is found even in anaerobically grown cells. It can thus be viewed as a standby defense against O_2^-, which is always maintained to protect in the event of a sudden exposure to O_2.

It is possible to reversibly remove the metals from SODs. The apo enzymes so prepared are inactive but can be reactivated by restoring the active site metal. It is striking, that in spite of sequence and structural homologies, the Fe SOD is inactive when made to contain Mn in place of Fe and the Mn SOD is inactive when similarly reconstituted with the non-native metal Fe. There are, however, SODs that are active with either Mn or Fe at their active sites. These SODs, termed cambialistic SODs, are usually found in anaerobes such as *Propionibacterium shermanii* or *Streptococcus mutans*. These organisms produce the SOD with iron when grown anaerobically but, when exposed to low levels of O_2, produce the same SOD but with Mn. It is clear that even anaerobes have need of a defense against the O_2^- during transient exposure to O_2. Ferrous salts are soluble, and thus available anaerobically, but become insoluble when oxidized to the ferric state by O_2. Manganous salts remain soluble under both conditions – hence the wisdom of a cambialistic SOD for an anaerobe. An iron SOD has also been reported in the protozoan *Tetrahymena pyriformis*.

Deletions and Consequences

E. coli

Mutants of *E. coli* lacking both the Mn SOD and the Fe SOD (SodA SodB) have been prepared. Anaerobically they grow as well as the parental strain. However, aerobically they grow slowly, exhibit a high rate of mutagenesis, and require branched-chain,

sulfur-containing, and aromatic amino acids. The null mutants are also hypersensitive towards paraquat. All of these phenotypic deficits disappear when a functional gene encoding any active SOD is inserted. The slow growth of the null mutant can be understood in terms of the energy devoted to repairing or replacing oxidatively damaged molecules and to the inactivation of such O_2^- sensitive enzymes as aconitase. The high rate of O_2-dependent mutagenesis reflects oxidative DNA damage, and repair, which is error-prone. The nutritional auxotrophies exhibited by the null mutant have several explanations. The need for branched amino acids arises because the penultimate step in the biosynthesis of these amino acids is catalyzed by a dihydroxy acid dehydratase that contains a [4Fe–4S] cluster that is rapidly oxidized, and inactivated, by O_2^-. The need for sulfur-containing amino acids evidently reflects leakiness of the cell envelope towards sulfite, which is an intermediate on the pathway from sulfate to cysteine. Finally, the aromatic amino acid auxotrophy reflects the inability to make erythrose-4-phosphate, which is one of the starting materials on the pathway leading to these amino acids. Erythrose-4-phosphate, in turn, depends on the sequential actions of transketolase and transaldolase, and the transketolase intermediate 1, 2-dihydroxyethylthiamine pyrophosphate is rapidly oxidized by O_2^-. The varied explanations for these phenotypic deficits reflect the variety of damage that can be caused by O_2^- and the multiple targets that are protected by the SODs.

Yeast

Mutants of the yeast *Saccharomyces cerevisia* lacking either the cytosolic Cu, Zn SOD or the mitochondrial Mn SOD have been prepared. Their phenotypic deficits, which are all oxygen-dependent, include slow growth, hypersensitivity towards paraquat or quinones, vacuolar fragmentation, sensitivity towards oxygen, and, in the case of the Cu, Zn SOD-null, lysine auxotrophy. All of these problems can be explained on the basis of O_2^- damage, as was the case for the *E. coli* SOD-null mutants.

Mice

Murine mutants lacking Mn SOD are severely affected and those that survive to term are low-birth-weight and only survive for 4–14 days. Their problems can be seen as a deficit of mitochondrial functions and that in turn can be explained on the basis of damage to mitochondrial components by O_2^-. The heterozygotes that have half the normal level of Mn SOD are viable but have been shown to be hypersensitive towards oxidative inactivation of aconitase and towards release of cytochrome *c* from mitochondria when challenged with tertiary butyl hydroperoxide. The deficit imposed by halving the Mn SOD was also seen as a greater susceptibility to reperfusion injury.

In contrast to the embryonic and neonatal fatality imposed by Mn SOD deletion, the homozygous Cu, Zn SOD-null mice were apparently normal under laboratory conditions. They are reported to be relatively intolerant of neuronal injury and prone to develop hepatoma at >9 months of age. It seems likely that there is some redundancy in scavenging O_2^- in the cytosol, so that the lack of Cu, Zn SOD may be compensated by up-regulation of another O_2^- scavenger, perhaps a superoxide reductase, such as has been found in anaerobes.

SOD and Amyotrophic Lateral Sclerosis

ALS or Lou Gherig's disease is a late onset, progressive, and fatal paralytic disease due to death of motor neurons. There are sporadic and familial types of ALS and these are not distinguishable on the basis of clinical symptoms. Approximately 20% of the familial cases of ALS have been associated with point mutations causing single amino acid replacements in Cu, Zn SOD. Transgenic mice expressing the wild-type human Cu, Zn SOD are normal, but those expressing one of the ALS-associated mutant Cu, Zn SODs develop progressive paralysis at ~ 3 months of age. Thus, the mutations in the SOD cause the death of motor neurons because of some as yet unknown gain of function, rather than because of a loss of SOD activity. This is certainly the case because: most of the mutant SODs retain full SOD activity; the transgenic mice retain the active murine Cu, Zn SOD; the disease is genetically dominant, i.e., heterozygotes develop the disease; and finally, Cu, Zn SOD knockout mice do not become paralyzed. The transgenic mice provide a useful model of the human disease and are being used to explore both the toxic gain of function of the mutant Cu, Zn SOD and treatment modalities.

Mimics

O_2^- has been found to play causative roles in numerous inflammatory diseases and reperfusion injuries. For this reason non-enzymic catalysts of the dismutation of O_2^- are being explored as pharmaceutical agents and appear to have promise.

See Also the Following Articles

DNA Oxidation • Free Radicals, Sources and Targets of: Mitochondria • Iron–Sulfur Proteins

Glossary

apo enzyme Enzyme whose prosthetic group has been removed.
Cu, Zn SOD Superoxide dismutases with copper and zinc at the active site.
Fe SOD Superoxide dismutases with iron at active site.
HO· The hydroxyl radical.
homodimer Protein composed of two identical subunits.
homotetramer Protein composed of four identical subunits.
Mn SOD Superoxide dismutases with manganese at an active site.
O_2^- The superoxide anion radical.

Further Reading

Hassan, H. M. (1997). Cytotoxicity by oxyRadicals and the evolution of superoxide dismutases. In *Lung Biology in Health and Disease* (L. B. Clerch and D. J. Massaro, eds.) Vol 105, pp. 27–47. Marcel Dekker, New York.

Maier, C. M., and Chan, R. H. (2002). Role of superoxide dismutases in oxidative damage and neurodegenerative disorders. *Neuroscientist* **8**, 323–334.

McCord, J. M. (2002). Superoxide dismutases in aging and disease. *Methods Enzymol.* **349**, 331–341.

Melov, S. (2002). Therapeutics against mitochondrial oxidative stress in animal models of aging. *Ann. N.Y. Acad. Sci.* **959**, 330–340.

Storz, G., and Imlay, J. A. (1999). Oxidative stress. *Curr. Opin. Microbiol.* **2**, 188–194.

Biography

Irwin Fridovich is a James B. Duke Professor of Biochemistry, Emeritus. He is a member of the National Academy of Science and of the National Academy of Arts and Sciences. He and his students discovered and characterized the superoxide dismutase.

Syk Family of Protein Tyrosine Kinases

Andrew C. Chan
Genentech, Inc., San Francisco, California, USA

The Syk (spleen tyrosine kinase) family of protein tyrosine kinases (PTKs) encode essential signaling components required for normal immunity. Their functions have been most intensely studied within mammalian immune cells. While not found within the *Caenorhabditis elegans* genome, this family of PTKs is represented earlier within the phylogenetic tree, in the hydra vulgaris, as a single gene product expressed in epithelial cells and plays an important function in the recognition of foreign cells. In mammalian systems, this family of PTKs appears to have evolved from a gene duplication event to give rise to its two family members – ZAP-70 and Syk in mammalian cells. Genetic studies in humans and mice have demonstrated their essential roles in the function and development of T cells, B cells, mast cells, monocytes/macrophages, and the lymphatic system. Studies further underscore their importance in T cell antigen receptor (TCR), B cell antigen receptor (BCR), IgG and IgE receptors (FcRs) and integrin receptor signaling. This review will discuss our current understanding of this family of PTKs in mammalian immune cell function.

Zeta-Chain-Associated Protein of 70K Mr (ZAP-70)

ZAP-70 was initially identified as a 70K Mr tyrosine phosphorylated protein that associates with the TCR following receptor activation. Biochemical and molecular characterization revealed that ZAP-70 is a PTK with the characteristic Syk-family signature of tandem Src-homology (tSH2) domains at its amino (N) terminus and a carboxy (C)-terminal catalytic domain. The domain between the two SH2 domains has been termed Interdomain A, while Interdomain B spans between the C-terminal SH2 and the C-terminal kinase domain (Figure 1).

Interaction of ZAP-70 with the TCR ITAM

Binding studies and, ultimately, the solution of the crystal structure encoding the tandem SH2 domains revealed that both SH2 domains of ZAP-70 cooperate to bind the doubly phosphorylated immunoreceptor tyrosine based activation (dP-ITAM) motifs (Figure 2). The ITAMs consist of the consensus sequence D/E x x Y x x L/I X_{6-8} Y x x L/I that is represented in the cytoplasmic domains of integrins as well as each of the signaling subunits of the TCR, BCR, and FcRs. Both tyrosine residues within the ITAM are phosphorylated by Src-family PTKs that, in turn, provide the high-avidity binding sites for the tSH2 domains of ZAP-70. While the C-terminal SH2 domain binds the N-terminal ITAM tyrosine, the C-terminal SH2 domain forms a portion of the pocket for the N-terminal SH2 domain that correspondingly binds the C-terminal ITAM tyrosine residue. This interdependence of the two SH2 domains explains the rigid requirements for the tandem SH2 domains of ZAP-70 as well as the little flexibility of spacing between the two tyrosine residues within the ITAM sequence in binding ZAP-70. Mutation of either SH2 domains or mutation of either ITAM tyrosine results in >100-fold decrease in binding avidities and, in turn, a non-functional TCR.

While ZAP-70 was initially found to be inducibly associated with the TCR in Jurkat T cells, subsequent studies in human and murine thymocytes and peripheral T cells revealed that the TCR ζ-subunit is already phosphorylated in its basal unactivated state, though the degree of phosphorylation is further augmented following TCR activation. In turn, in resting thymocytes and peripheral T cells, ZAP-70 is constitutively associated with the TCR, though the degree of association appears to be augmented concomitant with the degree of ζ-phosphorylation following receptor activation. A model of sequential phosphorylation of the ζ-chain was proposed based on observations in the 3.L2 T cell hybridoma, but this sequence does not appear to apply to thymocytes nor normal peripheral T cells. In addition to localizing ZAP-70 to the TCR complex, the tSH2:ITAM interaction has also been proposed to regulate ZAP-70 enzymatic activity. *In vitro* binding of ZAP-70 to a dpITAM peptide results in enhanced ZAP-70 activity. This model of ZAP-70 activation, however, is at odds with the pre-existing ZAP-70:ITAM interaction

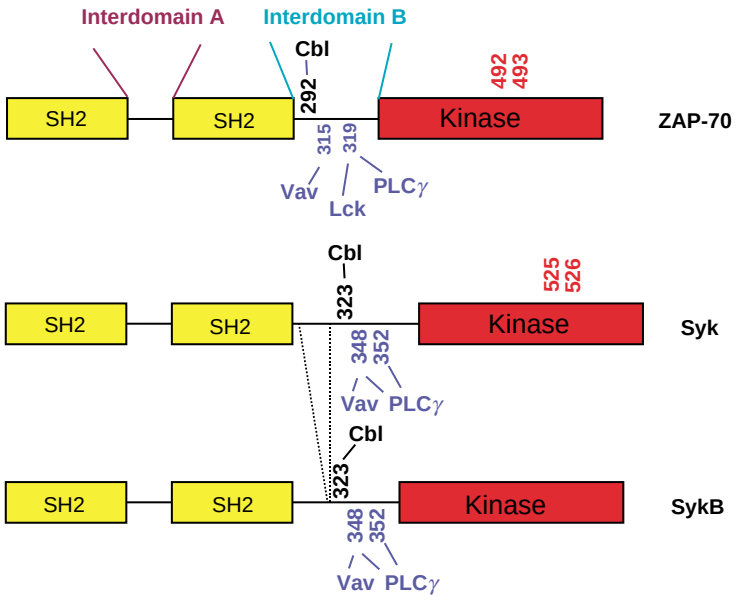

FIGURE 1 Schematic representation of ZAP-70 and Syk PTKs. Schematic structural representation of the structural domains within the Syk PTKs. T-loop tyrosine residues are represented in red; positive regulatory Interdomain B tyrosine residues are represented in blue; negative regulatory Interdomain B tyrosine residues are represented in black. Numbering utilizes the human protein sequences for both ZAP-70 and Syk.

described in normal human thymocytes, murine thymocytes, and peripheral T cells.

In contrast to the classical tSH2:dPITAM interaction, the crystal structure and NMR studies of the tSH2 domains in the absence of an ITAM peptide reveals two highly flexible independent SH2 domains. These additional forms of interaction may provide the structural basis for more non-classical interactions. For example, the N-terminal SH2 domain alone in conjunction with Interdomain A of both ZAP-70 and Syk bind the NXXY motifs within the cytoplasmic domain of the β3 integrin. Of note, tyrosine phosphorylation of the NXXY motif inhibits binding to the SH2 domain. These more non-classical interactions may, in part, explain immunofluorescence studies that demonstrate targeting of ZAP-70 to the T cell cortex independent of the tSH2 domains. In contrast, studies utilizing fluorescence imaging and immunofluorescence of green fluorescent protein-tagged ZAP-70 is more consistent with a cytosolic distribution of ZAP-70 in resting cells with redistribution to the plasma membrane following TCR engagement.

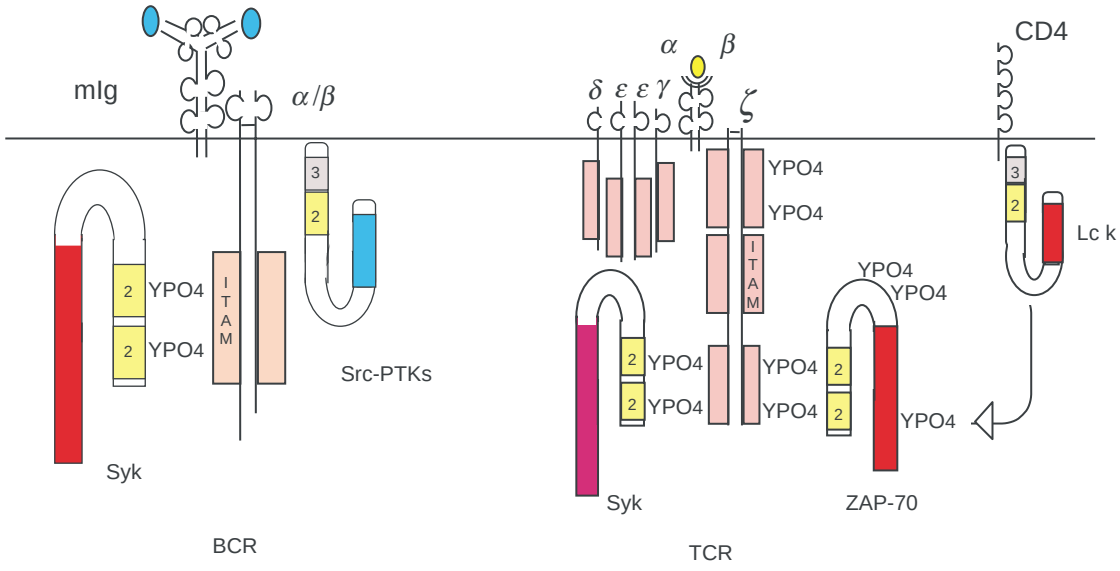

FIGURE 2 Schematic representation of T and B cell antigen receptors with Src- and Syk-PTKs.

Tyrosine Phosphorylation of ZAP-70

ZAP-70 undergoes a sequence of regulated phosphorylation events on multiple tyrosine residues that serve both positive and negative regulatory functions. The synergistic interactions between ZAP-70 and Src-PTKs was initially appreciated in overexpression studies in heterologous cell systems. While expression of ZAP-70, Lck or Fyn alone does not induce tyrosine phosphorylation of cellular proteins, co-expression of ZAP-70 with Lck or Fyn results in tyrosine phosphorylation of multiple cellular proteins. Studies in Jurkat T cells lacking either ZAP-70 or Lck further substantiate the requirement for both PTKs in efficient TCR function. Molecular dissection of the Lck/ZAP-70 interaction reveals multiple levels of regulation through phosphorylation of distinct tyrosines within ZAP-70.

Catalytic Domain: Tyr 492 and 493

Upon TCR engagement with major histocompatibility complex (MHC)-peptide complexes presented on antigen presenting cells (APCs), studies utilizing cellular fractionation, Forster resonance energy transfer analysis, chemical cross-linkers and microscopy have demonstrated the co-localization of CD4 and CD8 co-receptors with the TCR-centered "synapse". In this model, the synapse colocalizes a number of critical signaling molecules (e.g., TCR, ZAP-70, CD4 and Lck) to facilitate downstream signaling. As the cytoplasmic domains of both CD4 and CD8 interact with Lck, Lck is co-localized with ZAP-70 where it can transphosphorylate Tyr 493 within the trans-activation (T) loop of the ZAP-70 PTK (Figure 1). This initial phosphorylation results in the enzymatic activation of ZAP-70 and is required for the generation of second messengers (e.g., calcium mobilization and Ras activation). Within the T-loop, a hierarchy of phosphorylation occurs with the initial phosphorylation of Tyr 493, followed by phosphorylation of the neighboring Tyr 492. Mutation of Tyr 492 to Phe results in a hyperactive ZAP-70 PTK and heightened TCR functions and implicates a potential inhibitory function of Tyr 492 phosphorylation. Hence, the T-loop of ZAP-70 contains both positive and negative regulatory tyrosine residues that can finely modulate ZAP-70 enzymatic activity in a temporal fashion.

Interdomain B: Tyr 315 and 319

In addition to phosphorylation within ZAP-70's catalytic domain, ZAP-70 is phosphorylated on three tyrosine residues within its Interdomain B. Phosphorylation of Tyrs 315 and 319 serve scaffolding functions. The SH2 domains of Lck and PLCγ1 interact with Tyr 319 while the SH2 domain of Vav binds Tyr 315. Phosphorylation of these tyrosine residues is thought to serve scaffolding functions by which signaling complexes may be assembled and/or stabilized. Additionally, Tyr 315 may also have effects in determining the optimal tSH2 binding to the TCR ITAM sequences. Mutation of either tyrosine residues attenuates TCR-induced calcium and MAPK activation. Mice that express mutant ZAP-70 molecules in which Tyrs 315 or 319 are mutated to Phe demonstrate compromised T cell development. Given the homologous sequences surrounding these two tyrosines, it is likely that both tyrosine residues play overlapping functions.

Interdomain B: Tyr 292

Phosphorylation of Tyr 292 plays a negative regulatory function potentially through its interaction with the SH2-like (TKB) domain of the Cbl E3 ligase. Expression of a mutant ZAP-70 molecule in which Tyr 292 is mutated to Phe results in prolonged TCR signaling and is consistent with the inability of an activated and phosphorylated ZAP-70 to undergo ubiquitination and degradation. In turn, the TCR initiated signal lacks one of its normal extinguishing mechanisms and results in prolonged signaling. While Tyr 292 clearly plays a negative regulatory role in TCR activation, the mechanism through its interaction with Cbl has been called into question. The converse loss-of-function mutant in the Cbl TKB domain demonstrates altered activation of the Rac GTPase without any alteration to ZAP-70 enzymatic activity. Additional studies will be required to further define the molecular mechanism(s) by which Tyr 292 phosphorylation desensitizes TCR function.

Tyrs 474, 597, and 598

Given the precedent of the negative regulatory C-terminal tyrosine residues conserved within Src-PTKs, studies have also focused on a conserved series of tyrosine residues within the C-terminal of ZAP-70s catalytic domain (Tyrs 597 and 598). While these tyrosine residues have not been formally demonstrated to be phosphorylated *in vivo* following TCR engagement, mutation of either C-terminal tyrosine residues results in enhanced TCR-mediated IL-2 regulated promoter activity. In addition, Tyr 474 has been proposed to interact with the Shc adaptor protein. Likewise, expression of a mutant ZAP-70 with Tyr 474 mutated to Phe results in loss of IL-2 promoter activity without alterations in ZAP-70 activity or tyrosine phosphorylation of cellular proteins.

Posttranslational modification of ZAP-70 through tyrosine phosphorylation plays a major role in regulating ZAP-70 function. In addition to tyrosine phosphorylation, ZAP-70 is also phosphorylated on multiple

serine and threonine residues, the functions of which have not been well investigated. Hence, additional mechanisms likely exist to regulate ZAP-70 function.

Spleen Tyrosine Kinase (Syk)

Syk was initially identified as a 40K Mr (p40) peptide with intrinsic tyrosine kinase activity. Molecular characterization of Syk from a spleen cDNA library revealed that p40 represents a proteolytic fragment of a 72K Mr holoenzyme. While Syk is structurally homologous to ZAP-70 with tSH2 domains at its N terminus and a C-terminal catalytic domain, Syk has distinct regulatory mechanisms, when compared to ZAP-70, and has been implicated in a greater number of receptor signaling systems, in part, due to its more ubiquitous pattern of expression. Syk plays important functions in pre-TCR, BCR, FcR, IL-15R, and integrin signaling.

Interaction of Syk with the BCR ITAM

The tSH2 domains of Syk are similarly responsible for binding the dpITAM encoded within the Igα and Igβ signaling subunits of the BCR (Figure 2). Solution of the crystal structure of the Syk tSH2 domain complexed to a dpITAM revealed the lack of structural inter-dependence between the two SH2 domains. In fact, the two SH2 domains fold into independent SH2 domains that each bind a phosphorylated tyrosine residue within the dpITAM sequence. Moreover, a high degree of rotational flexibility was observed within Interdomain A, which may confer the ability of the Syk tSH2 domains to bind dpITAM sequences that have longer spacing between the two pY residues within the ITAM.

While ZAP-70 appears to be already associated with the dpITAMs within the TCR, Syk does not appear to be associated with the dpITAM in resting cells. In contrast, BCR or FcR engagement results in ITAM phosphorylation by Src-PTKs and the subsequent recruitment of Syk to the activated receptor. In addition to localizing Syk to the receptor, the dpITAM also plays an important role in Syk enzymatic activation. Hence, the tSH2 domains play both localizing and activation roles of the holoenzyme.

Alternative Splicing of Syk: Syk and SykB

Syk is expressed in two different forms, Syk and SykB, as a result of alternatively splicing (Figure 1). SykB lacks a 23 amino acid sequence within the interdomain B region. This shortened form has comparable enzymatic activity and tyrosine phosphorylation events as Syk, but altered ability to bind the dpITAMs. As such, interdomain B can regulate Syk function though the *in vivo* significance of the SykB splice form remains unclear.

Tyrosine Phosphorylation of Syk

Interdomain B: Tyrs 348 and 352

Three tyrosine residues within Interdomain B undergo phosphorylation following BCR engagement—Tyr 323, 348, and 352. Phosphorylation of Tyrs 348 and 352 are required for linking the BCR with PLCγ2 activation. Both sites can bind the SH2 domains of PLCγ while Tyr 348 can also bind the SH2 domain of Vav. These pTyr-SH2 interactions may contribute to signaling by localizing PLCγ and Vav effectors to the activated BCR complex, to facilitate the tyrosine phosphorylation and enzymatic activation of these effector molecules, and, in turn, facilitate membrane localization of these activated enzymes where their substrates (i.e., PIP2 and GTPases) normally reside. Mutation of these Interdomain B sites results in loss-of-function mutants of Syk. Hence phosphorylation of Tyrs 348 and 352 are thought to contribute a positive regulatory function for the Syk PTK.

Interdomain B: Tyr 323

While phosphorylation of Tyrs 348 and 352 results in gain of function, phosphorylation of Tyr 323 results in decreased receptor functions. Phosphorylation of Tyr 323 occurs in a Lyn-dependent fashion and facilitates the binding of Syk to the c-Cbl E3 ligase. Binding of c-Cbl to Syk initiates the ubiquitination pathway to down-regulate receptor-initiated signaling events including ubiquitination and degradation of Syk protein levels.

Catalytic Domain: Tyr 525 and 526

Similar to ZAP-70, Syk also has two tyrosine residues within the T-loop of its catalytic domain. However, unlike the hierarchy of phosphorylation within ZAP-70, both tyrosine residues within Syk are phosphorylated following receptor cross-linking and contribute to Syk enzymatic activation. Mutation of either tyrosine residues to phenylalanine results in attenuated activation of the resultant mutant enzyme. Also to be differentiated from ZAP-70 in which its activation results from trans-phosphorylation by the heterologous Src-PTKs, enzymatic activation of Syk appears to be mediated through trans-autophosphorylation. A recent study using a heterologous expression system suggests a slight variation in this model in which Syk functions as an allosteric enzyme that is positively regulated by ITAM phosphorylation. Within this model, Src-PTKs

phosphorylate the N-terminal ITAM tyrosine residue, while Syk can phosphorylate either ITAM tyrosine residues. Binding of Syk to the dpITAM induces a conformational change in the holoenzyme to induce amplification of its auto-activation and downstream signaling functions.

Tyrs 130, 629, 630, and 631

Tyrosine 130 within Interdomain A may play a role in regulating the release of Syk from the BCR. Mutation of Tyr 130 to Phe results in enhanced binding of Syk to the BCR; conversely, mutation of Tyr 130 to Glu reduced this interaction but results in enhanced Syk enzymatic activation. Finally, the C-terminal tyrosine residues 629, 630, and 631 of Syk, while also not having been demonstrated to be phosphorylated *in vivo*, can potentially serve as negative regulators of Syk function. Mutation of these C-terminal tyrosines results in an enhanced Syk PTK.

ZAP-70 and Syk PTKs in Hematopoietic Cell Function

The ubiquitous expression of the Syk PTKs amongst hematopoietic derived cells is consistent with the functional requirement for this family of PTKs in a multitude of receptor and cell type functions. While ZAP-70 has a more limited cellular expression, this PTK has been demonstrated to play important roles in $\alpha\beta$ TCR, $\gamma\delta$ TCR, integrin, and pre-BCR functions. The more ubiquitous expression of Syk is consistent with its demonstrated roles in pre-TCR, $\gamma\delta$ TCR, FcR, IL-15R, α2bβ3 integrin and collagen receptor-mediated functions.

T Lymphocyte Development

T cell development begins in the thymus where signaling through the pre-TCR promotes α-chain rearrangement and differentiation of $CD4^-CD8^-$ (double negative or DN) cells to immature $CD4^+CD8^+$ (double positive or DP) cells. Development of DP thymocytes into mature $CD4^+$ or $CD8^+$ single positive (SP) T cells is subsequently driven by selection events that require signals transduced through the $\alpha\beta$ TCR. A quantitative model of T cell selection has been proposed in which strong self-reactive T cells results in apoptosis through a process known as negative selection; T cells that do not recognize self-MHC have no signaling through the TCR and hence also undergo apoptosis through a process known as "death by neglect." Only T cells that recognize self-MHC in the absence of self-antigens are thought to have an "appropriate" level of TCR signal strength to promote DP thymocytes to differentiate to SP thymocytes.

ZAP-70 in $\alpha\beta$ T Cell Development

The functions of ZAP-70 during both pre-TCR and $\alpha\beta$ TCR signaling have been elucidated through an elegant series of genetic studies of lymphocyte development in mice and natural mutations in humans. Patients lacking ZAP-70 were described in the early 1990s that present with a selective $CD8^+$ T cell deficiency. While $CD4^+$ T cells are present in the peripheral blood of these immunodeficient patients, these cells are non-functional and lack the ability to proliferate to TCR induced signals. Thymic histology revealed the presence of DP thymocytes within the medulla, but the absence of $CD8^+$ thymocytes in the cortex. The molecular basis of these mutations are multiple and include missense mutations within the catalytic domain, truncation mutations, and altered splice acceptor sites that give rise to unstable proteins.

In contrast to the selective developmental defect in humans, mice engineered to be deficient in *zap-70* through homologous recombination demonstrate a block at the transition of DP to mature $CD4^+$ and $CD8^+$ cells. In turn, *zap-70* $^{-/-}$ mice accumulate DP thymocytes without SP thymocytes or peripheral $\alpha\beta$ T cells. Analysis of *zap-70* $^{-/-}$ mice that express a transgenic TCR reveal an essential role for ZAP-70 in both positive and negative selection.

A spontaneously arising mutation in the DLAARN motif within the mouse ZAP-70 catalytic domain that abrogates kinase activity similarly results in an arrest in thymocyte development at the DP T cell stage. An identical mutation has been described in a SCID infant with non-functional peripheral $CD4^+$ and absent peripheral $CD8^+$ T cells. Hence, the identical mutation within ZAP-70 results in distinct T cell developmental phenotypes in humans and mice. This difference may be due to differential expression and regulation of the Syk PTK during human and mouse thymic development.

Syk in $\alpha\beta$ T Cell Development

While *syk* $^{-/-}$ mice were initially thought to have normal T cell development and hence no role in T cell function, recent studies demonstrated overlapping and potentially independent functions of Syk and ZAP-70 during T cell ontogeny. In contrast to *zap-70* $^{-/-}$ mice that are blocked at the DP thymocyte stage, mice deficient in both *zap-70* and *syk* do not develop any DP T cells and accumulate DN thymocytes. Moreover, the pre-TCR expressed in *zap-70* $^{-/-}$ *syk* $^{-/-}$ DN thymocytes is non-functional. Hence, either ZAP-70 or Syk can mediate pre-TCR function while ZAP-70, in part due to the down-regulation of Syk following pre-TCR

signaling, plays a unique function in the transition from DP to SP T cells. Consistent with this quantitative explanation, forced expression of Syk in *zap-70* $^{-/-}$ mice restores T cell development to the SP T cell stage. Hence, both ZAP-70 and Syk play overlapping functions during T cell development.

While T cell development appears normal in *syk* $^{-/-}$ mice, studies using hematopoietic chimeras with *syk* $^{-/-}$ hematopoietic stem cells (FL-HSCs) suggest a unique function of Syk in early T cell development. *Syk* $^{-/-}$ FL-HSCs demonstrate compromised ability to reconstitute T cells in *rag2* $^{-/-}$ mice at the $CD44^{-}CD25^{+}$ stage – the stage in which pre-TCR signaling is important. In addition, ~50% decrease in T cell reconstitution is observed with *syk* $^{-/-}$ FL-HSCs. Together, these studies demonstrate a potential role of Syk during early T cell development. Additional studies will be required to ascertain the potential roles of ZAP-70 and Syk during other stages of T cell differentiation.

ZAP-70 and Syk PTKs in γδ T Cell Development

In addition to αβ T cells, γδ T cells also play critical roles in mucosal immunity. The Syk family of PTKs also play important roles in the development of various subsets of γδ T cells. Studies in *zap-70* $^{-/-}$ and *syk* $^{-/-}$ mice demonstrate important roles for both ZAP-70 and Syk in the development of skin dendritic epithelial (DETC) and intestinal epithelial (IEL) γδ T cells. Substantial reductions in these populations were observed in both strains of knockout mice. In addition, the remaining DETCs exhibited marked abnormalities in morphology in *zap-70* $^{-/-}$ mice. In contrast to the DETCs and IELs, lymph node and splenic γδ T cells were found in greater abundance in *zap-70* $^{-/-}$ and *syk* $^{-/-}$ mice. Hence, while murine αβ T cells demonstrate an absolute developmental requirement for ZAP-70, γδ T cells demonstrate variable dependence upon ZAP-70 and Syk.

Syk and ZAP-70 PTKs in B Cell Development

B cell development begins in the bone marrow through a program of developmental checkpoints regulated by signaling through the pre-BCR and subsequently the mature surface IgM (sIgM) receptor. In pro-B cells, heavy chain gene rearrangement begins through D_H to J_H genes followed by V_H to DJ_H genes. An in-frame rearranged heavy chain pairs with the λ5 and V-preB surrogate light chains to form the antigen-independent pre-BCR. Signaling through the pre-BCR expressed on pro-B cells induces cells to differentiate to pre-B cells. In pre-B cells, termination of heavy chain rearrangement (termed allelic exclusion), initiation of gene rearrangement of K or λ light chains, and pairing of these resultant heavy and light chains gives rise to the sIgM receptor expressed on immature B cells. Immature B cells leave the marrow to the spleen and other lymphoid organs where a small minority of cells is selected to differentiate to mature B cells that express both IgM and IgD, a selection process that requires signaling through sIgM on immature B cells.

Studies in *syk* $^{-/-}$ mice demonstrate a requirement for Syk in pre-BCR function. *Syk* $^{-/-}$ mice demonstrate a significant, but partial, block at the pro- to pre-B cell transition. While a small number of immature B cells develop *in syk* $^{-/-}$ mice, adoptive transfer experiments utilizing radiation chimeras demonstrate an additional requirement for Syk in the developmental transition from immature to mature recirculating B cells. Despite migrating from the bone marrow to the spleen, *syk* $^{-/-}$ immature B cells are unable to mature into recirculating mature B cells and accumulate in the outer splenic T cell zones. Hence, Syk plays important roles in both pre-BCR and sIgM receptor signaling.

Similar to the overlapping roles of ZAP-70 and Syk in pre-TCR function, mice deficient in both *zap-70* and *syk* demonstrate an absolute block in pre-BCR function and, in turn, a failure of heavy chain allelic exclusion. Hence, similar to the overlapping roles of these two PTKs in early T cell development, both ZAP-70 and Syk play overlapping roles during early B cell development.

Syk PTK in FcR Functions

While neither Syk nor ZAP-70 is required for monocyte or natural killer cell development, the functions of multiple receptors expressed on these cells are significantly compromised. While *syk* $^{-/-}$ macrophages form normal actin cups that oppose foreign particles, they are unable to phagocytose these particles. Additionally, *syk* $^{-/-}$ monocytes/macrophages exhibit defects in FcR-mediated antigen presentation and dendritic cell maturation.

In addition to FcRs, Syk is also required for signaling through the high affinity IgE receptor of mast cells. Mast cells derived from *syk* $^{-/-}$ bone marrow are unable to induce degranulation, synthesize leukotrienes, or screte cytokines when stimulated from the FcεRI receptor.

ZAP-70 and Syk in Integrin-Mediated Functions

A requirement for ZAP-70 has also been implicated in LFA-1-mediated functions. Inhibition of ZAP-70 through pharmacologic and genetic means demonstrate a role of ZAP-70 in LFA-1-dependent chemotaxis. An essential role of Syk has also been demonstrated for integrin-mediated functions in polymorphonuclear

(PMN) leukocytes. *Syk* $^{-/-}$ PMNs are unable to undergo degranulation, fail to generate a respiratory burst, and are unable to spread in response to β1, β2, or β3 signaling. Hence, in addition to the important roles of this family of PTKs in adaptive immunity, these PTKs also play important roles in innate immunity.

Syk PTK in Lymphatic Development and Platelet Function

Syk also plays requisite functions in collagen-mediated activation in platelets. *Syk* $^{-/-}$ platelets cannot induce increases in free cytoplasmic calcium in response to collagen or a collagen-related peptide. While *syk* $^{-/-}$ platelets are unable to function, bleeding times in *syk* $^{-/-}$ mice are normal. Hence, platelet dysfunction cannot account for the perinatal petechiae observed in these mice. *Syk* $^{-/-}$ mice develop peritoneal hemorrhage with chylous appearing ascites and the majority of mice die *in utero* or perinatally. This defect has been recently attributed to a critical function for Syk in a yet-to-be identified bone marrow derived endothelial cell required for separation of the lymphatic and vascular systems. Electron microscopy of the vasculature of *syk* $^{-/-}$ mice reveal not only decreased numbers of endothelial cells but also abnormal morphogenesis of these cells. Hence, Syk is required for a hematopoietic signaling pathway involved in the differentiation of the lymphatic from vascular systems.

Summary

Over the past decade, we have learned much about the regulation and functions of the Syk family of PTKs in mammalian immune cell function. While there is much to be still learned about the cell types and receptor systems that are regulated by these PTKs, there is emerging an interesting biology of these PTKs in a greater array of human diseases. Expression of Syk has been suggested to play a tumor-suppressive role in human breast cancer. The expression of ZAP-70 in human B cells has recently been identified as a marker for prognostication of survival in chronic lymphocytic leukemia. Clearly, much is still to be learned as to how aberrant expression of these PTKs may affect normal and abnormal immune and non-immune cell functions in health and disease.

See Also the Following Articles

Epidermal Growth Factor Receptor Family • Immunoglobulin (Fc) Receptors

Glossary

catalytic functions Enzymatic activity of a protein. In the case of protein tyrosine kinases, catalytic function measures the ability of the enzyme to phosphorylate itself or its substrates.

protein tyrosine phosphorylation Post-translational modification required of tyrosine residues that can modulate catalytic function as well as to mediate protein–protein interactions.

thymic ontogeny The process of T cell development from its immature stage in the thymus to differentiated T cells in circulation.

Further Reading

Chu, D. H., Morita, C. T., and Weiss, A. (1998). The Syk family of protein tyrosine kinases in T-cell activation and development. *Immunol. Rev.* **165**, 167.

Kurosaki, T. (2002). Regulation of B cell fates by BCR signaling components. *Curr. Opin. Immunol.* **14**, 341.

Singer, A. L., and Koretzky (2002). Control of T cell function by positive and negative regulators. *Science* **296**, 1639.

Turner, M., Schweighoffer, E., Colucci, F., and DiSanto, J. P. (2000). Tyrosine kinase SYK: essential functions for immunoreceptor signaling. *Immunol. Today* **21**, 148.

Van Leeuwen, J. E., and Samelson, L. E. (1999). T cell antigen-receptor signal transduction. *Curr. Opin. Immunol.* **11**, 242.

Biography

Andrew Chan is the Vice President of Research-Immunology at Genentech, Inc. His principal research interests are the signal transduction mechanisms in lymphocytes that regulate normal and aberrant immunity. He holds M.D. and Ph.D. from Washington University School of Medicine, St. Louis and received clinical training in Internal Medicine and Rheumatology.

T7 RNA Polymerase

Rui Sousa
University of Texas Health Science Center, San Antonio, Texas, USA

Upon infection of an *Escherichia coli* cell the T7 bacteriophage inactivates the host's transcriptional machinery and transcription of the phage genes is carried out by a phage encoded RNA polymerase. The T7 RNA polymerase is a single subunit protein with a molecular weight of 99 kDa and is therefore structurally simpler than the multisubunit cellular RNA polymerases which have molecular weights in excess of 500 kDa. This relative simplicity has facilitated study of this enzyme, so that T7 RNA polymerase is currently the best-understood RNA polymerase. T7 RNA polymerase exhibits structural similarity to DNA polymerases, reverse transcriptases, and RNA-directed RNA polymerases, and these structural similarities establish the existence of a vast polymerase superfamily that includes the majority of nucleic acid synthesizing enzymes. The high activity and stringent promoter specificity of T7 RNA polymerase have been used to develop systems for T7 RNA polymerase driven overexpression of heterologous genes *in vivo*, and to synthesize RNAs *in vitro* for a variety of purposes.

DNA-Directed RNA Polymerases

The enzymes which synthesize nucleic acids – the polymerases – are functionally defined on the basis of whether they use DNA or RNA as a template, and whether they synthesize RNA or DNA. The DNA directed RNA polymerases comprise two large families. One includes the large multi-subunit cellular RNA polymerases which synthesize the messenger and ribosomal RNAs of all cells. The other family includes the mitochondrial RNA polymerases and the RNA polymerases encoded by a variety of bacteriophage. These are simpler, typically single subunit, enzymes. The best-characterized representative of this family is the RNA polymerase of the T7 bacteriophage.

T7 RNA Polymerase

Structure

The three-dimensional structure of T7 RNA polymerase has been determined by X-ray crystallography (Figure 1A). This highly α-helical enzyme is comprised of an N-terminal domain (amino acids 1–312), and a C-terminal domain (amino acids 313–883). The C-terminal domain is further sub-divided into "thumb" (amino acids 330–410), "palm" (amino acids 411–448, 532–540, 788–838), and "fingers" (amino acids 541–737, 771–778) subdomains, which are so designated because together they form a structure similar in shape to a cupped right hand. Nucleic acids bind within the large cleft in this structure.

Structure–Function Relationships

The C-terminal domain contains the active site where RNA synthesis occurs. Phosphodiester bond formation is catalyzed by two Mg^{2+} ions complexed by two aspartates (D537, D812) of the palm subdomain (Figure 2). The thumb subdomain makes interactions with the RNA which stabilize the transcription complex, while the fingers subdomain binds the template strand and contains residues which bind the nucleotide triphosphate (NTP) and which discriminate ribo-NTPs from deoxyribo-NTPs. Residues 739–770 of the C-terminal domain form an extended "promoter recognition loop" which makes sequence specific interactions with the -7 to -11 base pairs (bp) of the promoter. The C-terminal domain also contains the binding site for the regulatory factor T7 lysozyme, and residues 839–883 form a "C-terminal loop" which functions in the allosteric mechanism by which T7 lysozyme regulates transcriptional activity. The N-terminal domain is involved in nascent RNA binding, in sequence specific binding to the promoter, and in separating (opening) the two strands of the promoter during initiation so as to expose one strand for templating RNA synthesis. Residues 93–101 of the N-terminal domain are rich in positively charged amino acids and make specific interactions with the AT-rich -13 to -17 bp of the T7 promoter, while residues 232–242 form an "intercalating hairpin" which inserts between the two DNA strands to open the promoter.

Similarities to Other Polymerases

T7 RNA polymerase shares extensive sequence similarity with mitochondrial RNA polymerases and with

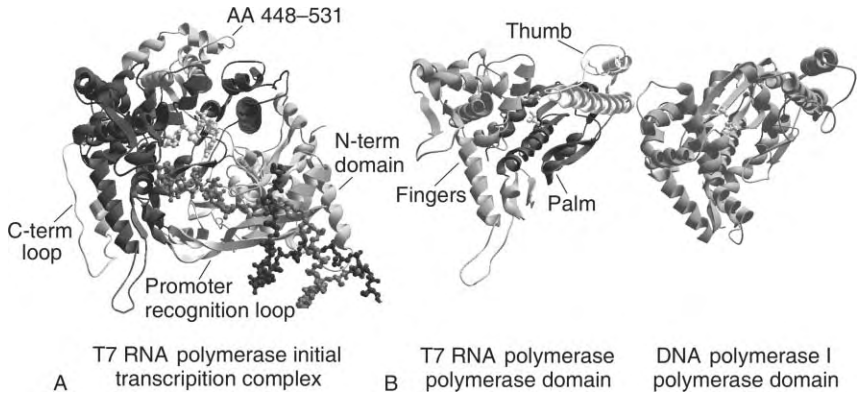

FIGURE 1 (A) Structure of a T7 RNA polymerase initial transcription complex. The template and nontemplate strands and the RNA are in medium, dark, and light gray, respectively. The core polymerase domain of the protein is in dark gray while the N-terminal domain, promoter recognition loop, C-terminal loop, and the subdomain formed by amino acids 439–531 are labeled and are colored light gray. (B) Comparison of the structures of the core polymerase domains of T7 RNA polymerase and DNA polymerase I. In the T7 RNA polymerase structure the thumb, palm, and fingers subdomains are in light, dark, and medium gray, respectively. Also shown are the side chains (colored light gray) of the pair of aspartic acids which bind the catalytic Mg^{2+} in the active site.

other bacteriophage-encoded RNA polymerases. T7 RNA polymerase is also structurally similar to the DNA-directed DNA polymerases of the pol I/pol α family, to the RNA-directed DNA polymerases (reverse transcriptases), and to the RNA-directed RNA polymerases. However, unlike the extensive sequence similarities within the mitochondrial and phage RNA polymerase family, the identifiable sequence similarities between T7 RNA polymerase and the DNA polymerases, reverse transcriptases, and RNA-directed RNA polymerases are limited to a few well-conserved amino acids in a small number of sequence motifs. Conservation of these motifs correlates with the template and product specificity of the polymerase as shown in Figure 3. The structural similarity suggested by this limited sequence similarity is confirmed by comparison of the three-dimensional structures of these enzymes (Figure 1B). This comparison reveals further that functions specific to particular classes of polymerase are incorporated by accretion of structurally dissimilar domains or "modules" onto a structurally conserved core. For example, DNA polymerase I and T7 RNA polymerase both exhibit structurally similar thumb, palm, and fingers subdomains which together form a polymerase domain with the core function of processive template-directed nucleic acid synthesis. Attached to this core domain are structural elements which are responsible for functions displayed by T7 RNA polymerase but not by DNA polymerase I (and vice versa). The "accessory modules" of T7 RNA polymerase have no structurally similar counterparts in DNA polymerase I. They include the N-terminal domain, which is involved in nascent RNA binding, transcription termination, and promoter opening; the promoter recognition loop which, together with the N-terminal domain, is responsible for sequence specific binding of the T7 promoter; the C-terminal loop, which is involved in regulation by T7 lysozyme, and residues 449–531, which form a subdomain of as yet undefined function.

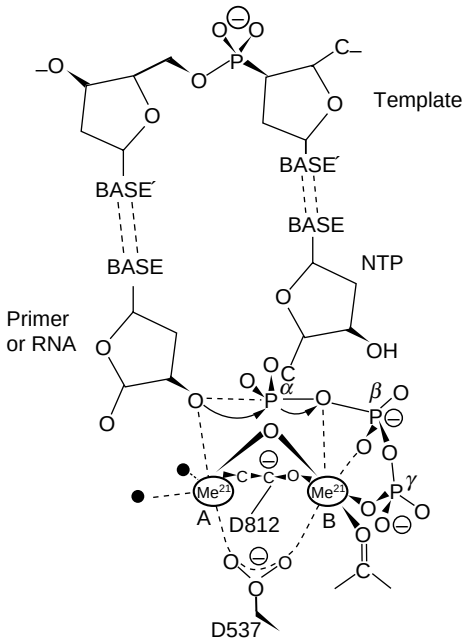

FIGURE 2 Bond formation in nucleic acid synthesis. The 3′-OH of the nucleotide at the end of the RNA or DNA primer attacks the α-phosphate of the NTP. A new bond is formed and the β- and γ-phosphates of the NTP are lost as pyrophosphate. The reaction is catalyzed by two metal ions which stabilize both the negative charge on the 3′-OH to enhance it nucleophilicity and the negatively charged pentacovalent α-phosphate intermediate which forms during the transition state. The two metal ions are bound by the side chains of two aspartic acids (D537 and D812 in T7 RNA polymerase) which are found in the active sites of all polymerases.

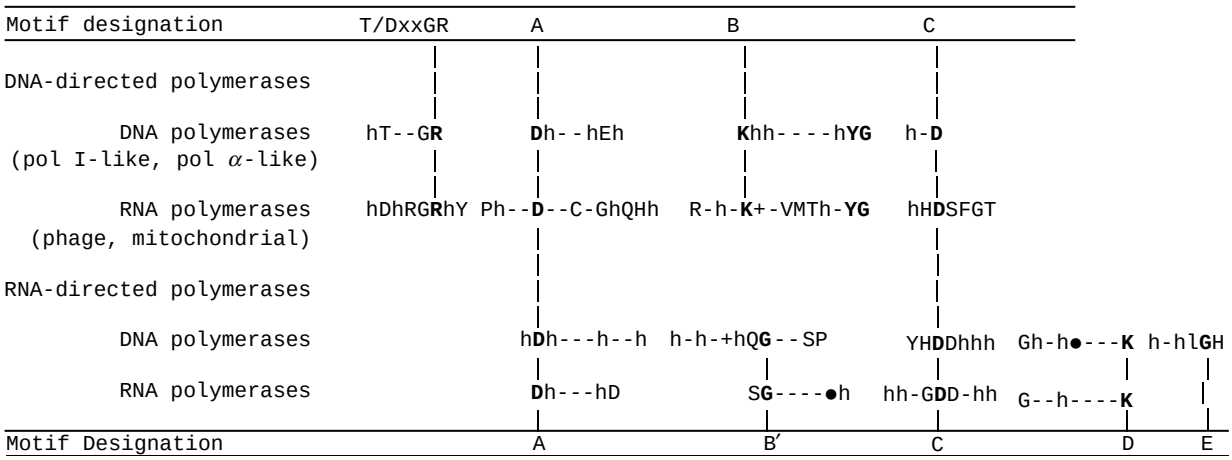

FIGURE 3 Patterns of sequence motif conservation in nucleic acid polymerases. h indicates a hydrophobic residue, + is a positively charged residue, – is any residue, and ● is a sequence gap. Invariant amino acids are in bold face. In T7 RNA polymerase the two invariant aspartic acids of motifs A and C correspond to D537 and D812, respectively, while the invariant arginine of motif T/DxxGR and the invariant lysine and tyrosine of motif B correspond to, respectively, R425, K631, and Y639.

T7 RNA Polymerase: Transcription Reaction

Promoter Structure, Recognition, and Opening

The T7 promoter is 23 bp in length and has a tri-partite structure (Figure 4). The −17 to −6 sequence is important for specific binding of the polymerase via interactions between residues 746, 748, 756, and 758 and the −7 to −11 bp, and between residues 93–101 and the −13 to −17 bp (bases are numbered relative to the transcription start site at +1). The −17 to −6 bp remain base paired during transcription initiation. The −4 to −1 "TATA" element facilitates promoter opening, which begins at the −4 bp and extends downstream, driven by imposition of a sharp (~50°) bend in the promoter when polymerase binds and by insertion of β-hairpin (formed by residues 231–242) between the DNA strands. The +1 to +6 initially transcribed sequence enhances the efficiency of the initial transcription reaction. Seven class III T7 promoters occur in the T7 genome and exhibit a perfect match to the sequence shown in Figure 4. There are also 16 class II T7 promoters in the T7 genome. The less active class II promoters typically exhibit a small number of base pair differences from the class III promoters.

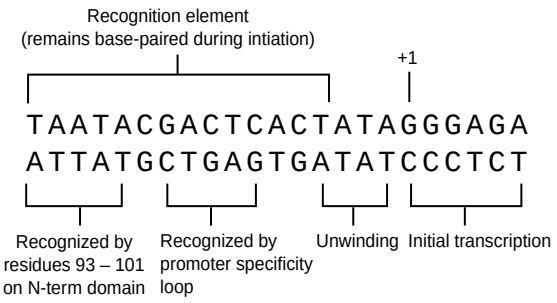

FIGURE 4 Structure of the T7 RNA polymerase class III promoter with the functions of different parts of the promoter indicated.

Initial Transcription

Following promoter binding and opening, the polymerase initiates RNA synthesis. While the nascent RNA is small (<9 nucleotides), the transcription complex is unstable and 2–8 nucleotide RNAs are frequently released from the complex. After an RNA is released, the polymerase reinitiates, usually without releasing the promoter. For this reason this initial phase of transcription, which is also characteristic of multi-subunit cellular RNAPs, is also referred to as "abortive" transcription. Throughout this initial phase of transcription the polymerase retains the specific promoter interactions made with the −17 to −6 bp in the initial binding step. Transcription to +8 is achieved by threading the template strand through the active site and by compacting (scrunching) it within the template-binding cleft, as well as by conformational changes in the polymerase that accommodate a growing RNA:DNA hybrid.

Promoter Release and Elongation

When the RNA reaches 9 nucleotides in length a large conformational change is triggered in the polymerase causing it to release the promoter. In addition to breaking up the promoter-binding surface created jointly by the promoter recognition loop and N-terminal domain, this conformational change reorganizes the N-terminal domain, leading to formation of a tunnel

through which the emerging RNA passes. The disposition of the DNA immediately upstream and downstream of the RNA:DNA hybrid is also changed. The result of all these changes is a stable "elongation complex" which can move along the template, synthesizing thousands of nucleotides of RNA without releasing either transcript or DNA.

Pausing and Termination

Certain sequences in the DNA can, however, act as pause or terminator sites and interrupt the progress of the elongation complex. Class I terminators cause the elongation complex to pause, and then to release the RNA. They contain a sequence which can form a G:C rich hairpin when transcribed into RNA (Figure 5). Immediately downstream of the hairpin is a U-rich sequence. It is believed that formation of a hairpin in the RNA may disrupt interactions normally made between the polymerase and single-stranded RNA 8–14 nucleotide away from the RNA 3′-end. It may also disrupt part of the RNA:DNA hybrid, which is usually ~7 bp in length in the elongation complex. Disruption of these interactions will weaken the association of the RNA with the elongation complex. The U-rich nature of the remaining RNA:DNA base pairs further weakens the RNA's association with the elongation complex, leading to release of the RNA and transcription termination. A class I terminator appears between genes 10 and 11 in the T7 genome, where it is important for attenuating transcription of downstream genes. Unlike class I terminators, class II terminators contain an invariant "ATCTGTT" sequence, which exhibits no obvious potential for forming secondary structure in the RNA. Termination at these sequences may involve a sequence-specific interaction with the RNA polymerase which alters the structure of the elongation complex. Encounter of the elongation complex with the class II terminator leads to a collapse in the size of the transcription bubble, from ~10 bases in the normal elongation complex, to ~5 bases in the complex which is paused at the class II site. A class II terminator occurs at the point at which T7 genomes are joined as concatemers before they are processed for packaging as mature phage particles, implying that pausing or termination of the polymerase at the concatemer junction is important for processing of the phage DNA.

Regulation

During the T7 life cycle the transcriptional activity of T7 RNA polymerase is regulated by T7 lysozyme, which binds to the polymerase and inhibits transcription initiation. Inhibition is allosteric: lysozyme binding changes the conformation of the C-terminal loop (amino acids 839–883) of the polymerase. This conformational change weakens the affinity of the polymerase for NTPs and short RNAs. This, in turn, reduces the rate

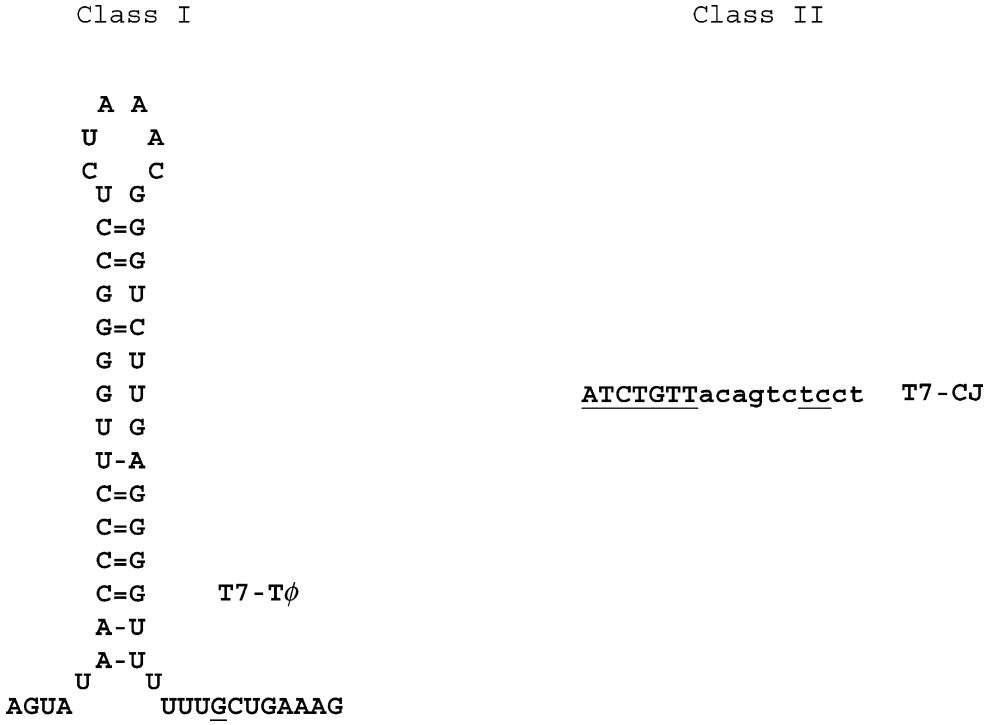

FIGURE 5 (Left) RNA structure of the T7 RNA polymerase Tϕ class I terminator. Termination occurs at the underlined nucleotide. (Right) Nontemplate strand DNA sequence of the class II T7 RNA polymerase concatemer junction terminator.

of transcription initiation at limiting NTP concentrations, and decreases the efficiency of progression through initial transcription by increasing the frequency at which short RNAs are released from the complex during abortive transcription. These inhibitory effects are greater for class II promoters, which, relative to class III promoters, display intrinsically higher rates of RNA release during initial transcription and require higher NTP concentrations to achieve high rates of initiation. Class III promoters drive transcription of genes which encode proteins, such as phage coat proteins, which are required late in infection, while class II promoters drive transcription of genes which encode proteins required during the early and middle stages of phage infection, such as proteins involved in replication of the phage DNA. Thus, in a T7 infected *E. coli*, the accumulation of T7 lysozyme late in the phage life cycle leads to a disproportionate decrease in transcription from class II promoters and to an increase in the production of the late phage proteins required for assembly of the mature phage particles. Since T7 lysozyme is itself encoded by a gene transcribed from a class II promoter, an auto-inhibitory feedback loop is created which ensures that repression by T7 lysozyme is kept within an appropriate range.

Priming DNA Replication

In addition to its primary function of transcribing the T7 phage genes, T7 RNA polymerase also primes rightward replication of T7 DNA. Priming occurs within an A–T rich region immediately downstream of two T7 promoters (dubbed 1.1a and 1.1b) which are located at the T7 origin of replication. The mechanism by which the RNA primer initiated at these promoters is transferred from T7 RNA polymerase to T7 DNA polymerase is not understood.

T7 RNA Polymerase: Applications

The stringent promoter specificity and robust transcriptional activity of T7 RNA polymerase has been taken advantage of to overexpress proteins *in vivo* and to synthesize RNAs *in vitro*. In the most widely used embodiment of the former application the gene encoding T7 RNA polymerase is placed under the control of an inducible promoter and is then stably integrated into the genome of an *E. coli* cell. A plasmid carrying the gene of interest under the control of a T7 promoter is then introduced into *E. coli*. When the gene encoding the T7 RNA polymerase is induced, the expressed T7 RNA polymerase transcribes the gene of interest at a very high level, resulting in a high degree of overproduction of the desired gene product. Similar approaches are used to overexpress proteins in eukaryotic cells. Synthesis of specific RNAs *in vitro* is done by using purified T7 RNA polymerase and templates in which a sequence of interest is placed downstream of a T7 promoter. The only other required reaction components are a buffering agent, Mg^{2+}, and NTPs. Such *in vitro* synthesized RNAs are used for a wide variety of research purposes, and are also being evaluated as diagnostic and therapeutic agents.

See Also the Following Articles

DNA Polymerase I, Bacterial • RNA Polymerase Reaction in Bacteria • RNA Polymerase Structure, Bacterial

Glossary

downstream The direction in which an RNA polymerase moves along the DNA during transcription.

primer A DNA or RNA molecule, typically short, that is extended by a DNA polymerase during DNA replication.

promoter A DNA from which an RNA polymerase initiates transcription.

template strand When a nucleic acid directs the synthesis of DNA or RNA, the template strand selects – by Watson–Crick base pairing – the nucleotides incorporated into the newly synthesized molecule.

transcription The synthesis of RNA using a DNA template.

Further Reading

Cheetham, G. M., and Steitz, T. A. (2000). Insights into transcription: Structure and function of single-subunit DNA-dependent RNA polymerases. *Curr. Opin. Struct. Biol.* **10**, 117–123.

McAllister, W. T. (1993). Structure and function of the bacteriophage T7 RNA polymerase (or, the virtues of simplicity). *Cell Mol. Biol. Res.* **39**, 385.

Milligan, J. F., Groebe, D. R., Witherell, G. W., and Uhlenbeck, O. C. (1987). Oligoribonucleotide synthesis using T7 RNA polymerase and synthetic DNA templates. *Nucleic Acids Res.* **15**, 8783–8798.

Mooney, R. A., Artsimovitch, I., and Landick, R. (1998). Information processing by RNA polymerase: Recognition of regulatory signals during RNA chain elongation. *J. Bacteriol.* **180**, 3265–3275.

Sousa, R. (1996). Structural and mechanistic relationships between nucleic acid polymerases. *Trends Biochem. Sci.* **21**, 186–190.

Studier, F. W., Rosenberg, A. H., Dunn, J. J., and Dubendorff, J. W. (1990). Use of T7 RNA polymerase to direct expression of cloned genes. *Methods Enzymol.* **185**, 60–89.

Biography

Rui Sousa is a Professor in the Department of Biochemistry of the University of Texas Health Science Center at San Antonio. He holds a B.A. from Harvard College and a Ph.D. from the University of Pittsburgh where he also received his postdoctoral training. His principal research interests are in transcription mechanisms and protein structural biology.

Tachykinin/Substance P Receptors

Mark D. Richardson and Madan M. Kwatra
Duke University Medical Center, Durham, North Carolina, USA

Tachykinins are small peptides, found in both vertebrates and invertebrates, which regulate many physiological processes. They are distributed mainly in the central nervous system (CNS), but are also important regulators of contractility in vascular smooth muscle and many areas of the gastrointestinal tract. Tachykinins (meaning "fast-acting") are characterized by an amidated C-terminus containing the amino acids F-X-G-L-M-NH_2, where X is a hydrophobic amino acid residue. Tachykinins act through receptors that are members of the G protein-coupled receptor (GPCR) superfamily. The best-known mammalian tachykinin is substance P (SP), a peptide of eleven amino acids. The preferred receptor for SP, substance P receptor (SPR), occurs as a full-length receptor and in a truncated form, which lacks the carboxyl-tail. The carboxyl-tail of SPR plays an important role in receptor desensitization, therefore the truncated form of SPR differs from full-length SPR in its interactions with proteins involved in receptor desensitization. Finally, SPR has an important role in pain and in several human disorders including depression, emesis, and glioblastoma.

Tachykinins

Tachykinins are peptides of 10–11 amino acids having the motif F-X-G-L-M-NH_2 at the C terminus; the $-NH_2$ group indicates that the C-terminal amino acid is amidated, a posttranslational modification necessary for biological activity.

There are currently four known mammalian tachykinins: SP, neurokinin A (NKA), neurokinin B (NKB), and hemokinin 1 (HK-1). As illustrated in Figure 1, these tachykinins are generated from three genes: preprotachykinin-A (PPT-A), preprotachykinin-B (PPT-B), and preprotachykinin-C (PPT-C). Alternative splicing of the PPT-A mRNA transcripts yields four products: α-PPT-A, β-PPT-A, γ-PPT-A, and δ-PPT-A. α-PPT-A and δ-PPT-A encode only SP, while β-PPT-A and γ-PPT-A encode both substance P (SP) and NKA. PPT-B yields only one product, NKB, and PPT-C encodes HK-1. The products of PPT-A transcripts (SP and NKA) are found in the central nervous system, CNS, and across a range of peripheral tissues, while a product of PPT-B (NKB) is found only in the CNS. PPT-C is widely distributed in many peripheral organ systems, but is not detected in the CNS.

The actions of mammalian tachykinins are mediated by three receptors: substance P receptor, SPR (also called NK1 receptor), neurokinin-2 (NK2) receptor, and neurokinin-3 (NK3) receptor. These receptors have the following binding preferences: SPR binds in the order SP > NKA > NKB; NK2 binds in the order NKA > NKB > SP; and NK3 binds in the order NKB > NKA > SP. Although SP, NKA, and NKB bind the tachykinin receptors with different affinities, they are all full agonists at all three receptors.

Mammalian Tachykinin Function

SP

SP is present in the outer laminae of the dorsal horn of spinal cord and in many areas of the brain, which is consistent with SP acting as a neurotransmitter. The hypothesis that SP has a role in pain transmission stems from its presence in primary afferent nerve fibers of the spinal cord such as C-fibers of laminae I and II of the dorsal horn. Efforts aimed at developing SPR antagonists to treat pain have met with limited success, leaving some doubt about the involvement of SP in pain transmission. However, recent experiments performed in genetically engineered mice, which lack expression of PPT-A have given new support for the role of SP in pain. While mice lacking PPT-A display normal responses to a variety of painful stimuli, their responses become blunted as the stimulus increases in intensity. However, above a certain pain threshold, mice lacking PPT-A seem to display responses that are similar to control mice. These results suggest that SP is indeed a pain neurotransmitter, and it functions within a discrete "window" of pain intensities. Other recent studies in mice lacking SPR also support the conclusion that SP plays a role in pain transmission.

SP also influences blood pressure. Intravenous injection of tachykinins in dogs and rabbits produces a strong hypotensive effect on mean arterial blood pressure, with SP showing much higher potency than NKA, NKB, or nonmammalian tachykinins. In human volunteers, intravenous SP causes a drop in diastolic, but not

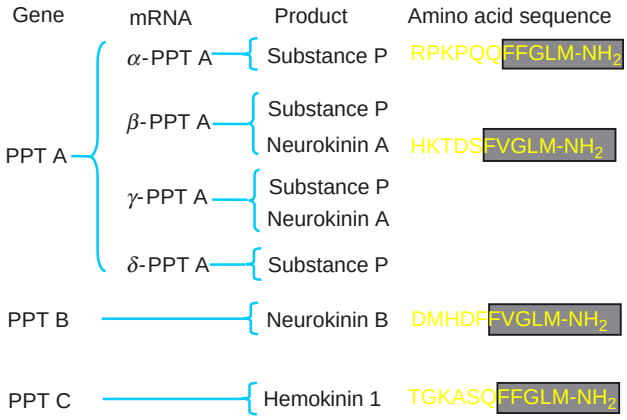

FIGURE 1 Synthesis of mammalian tachykinins. The mammalian tachykinins are generated from three genes (PPT-A, -B, and -C). Amino acid sequences of the human tachykinins are shown; shaded boxes highlight the F-X-G-L-M-NH2 motif.

systolic blood pressure, whereas NKA has no effect on either. Interestingly, the hypotensive effect is not diminished by autonomic blocking agents such as atropine, atenolol, or prazosin. This observation suggests that SP acts directly on vascular smooth muscle.

SP/NKA

The PPT-A mRNA transcripts which produce NKA (β- and γ-PPT-A) also produce SP (Figure 1); thus, SP and NKA are cosynthesized and coreleased from neurons. This suggests that NKA does not act alone, however, NKA can act as the primary signaling peptide in situations where the ratio of NKA to SP favors NKA, and where NK2 (the preferred receptor for NKA) is the predominant receptor in the target tissue. NKA is recognized as a very potent bronchoconstrictor, more potent than SP or NKB. Blockade of nerve-evoked bronchoconstriction by an antiserum having high affinity for NKA indicates that NKA has a more important role than SP in bronchoconstriction. Furthermore, experiments using NK2-selective antagonists indicate a predominance of NK2 over SPR in the mediation of noncholinergic bronchoconstriction responses. NKA is also more potent than SP in decreasing tracheal vascular resistance. Recent data indicate that NKA, like SP, binds to SPR with high affinity, thus, the effects of NKA may potentially be mediated by either SPR or NK2 receptor. In the CNS, which does not contain NK2 receptors, NKA produces biological effects similar to SP by interacting with SPR.

NKB

While SP and NKA frequently have overlapping tissue distribution, the distribution of NKB is distinct from that of SP and NKA. For example, in the spinal cord NKB is present in laminae III, while SP and NKA are abundant in laminae I and II but are not present in laminae III. NKB is most abundant in the hypothalamus and in the intestines. The physiological effects of NKB include contraction of rat portal vein and inhibition of gastric acid secretion. Interestingly, NKB potently decreases alcohol intake by a strain of alcohol-preferring rats. Also of potential clinical importance, NKB dilates the vasculature in human placenta and is thought to have an important role in the development of pre-eclampsia.

HK-1

Discovered in 2000, the tachykinin HK-1 is unique in that it is not of neuronal origin. HK-1 was first cloned from mouse B-lymphocytes, subsequent cloning of human HK-1 showed that it differs from mouse HK-1 in five out of eleven amino acid residues. Expression of human HK-1 has since been demonstrated in heart, skeletal muscle, thyroid, and skin. Weaker expression is detected in liver, lung, stomach, testes, placenta, and prostate. Receptor binding assays in cultured cells and tissues show that HK-1 has a strong binding preference for SPR over NK2 or NK3 receptors, and it is considered a full agonist of SPR.

HK-1 is similar to SP in many physiological effects, often with a potency that is very close to that of SP. Intravenous injection of HK-1 or SP into guinea pigs produces a dose-dependent hypotensive effect, with HK-1 and SP decreasing diastolic blood pressure at similar potencies of 0.2 nmol kg^{-1} and 0.1 nmol kg^{-1}, respectively. HK-1 and SP also induce salivary secretion in rats at essentially equal potencies. Studies are underway in several laboratories to develop a more complete understanding of the function of HK-1.

SPR, or NK1 Receptor

SPR and the other tachykinin receptors belong to the GPCR superfamily of receptors, which are characterized by the presence of seven hydrophobic transmembrane domains, designated TM1 through 7 (Figure 2). Cloning of human SPR from glioblastoma cells yields two forms of the receptor. One clone, with a stop codon after amino acid 407, encodes a full-length receptor and the other, with a stop codon after amino acid 311 (Δ311, Figure 2), encodes a truncated form of the receptor; the truncated form has also been cloned from guinea pig nervous system.

Full-Length SPR

SPR has three extracellular (EC) and three intracellular (IC) hydrophilic loops, a fourth IC loop formed by the palmitoylation of a cysteine residue, and in the case of the full-length receptor, a carboxyl-tail. The deduced

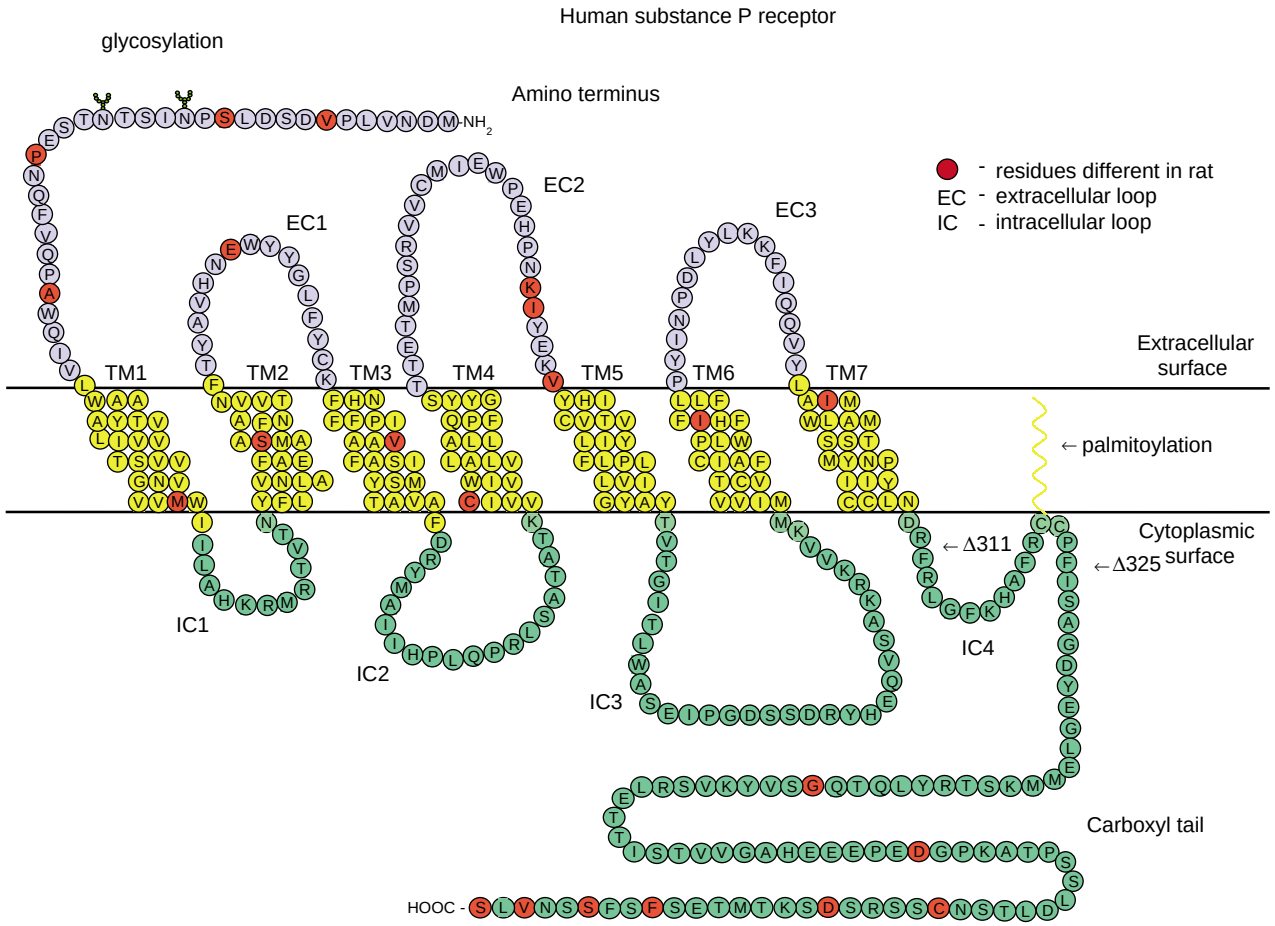

FIGURE 2 Two-dimensional representation of the human substance P receptor. The amino acid sequence of hSPR is shown. Seven putative transmembrane regions are labeled TM1–7, three extracellular loops are labeled EC1 through 3, and four intracellular loops are labeled IC1 through 4. Shaded circles show where amino acid residues in rat SPR differ from human SPR. Arrows indicate the termination site of the short form of SPR at Arg311, and truncation site of the mutant rat SPR at Phe325.

amino acid sequences of full-length rat and human SPR reveal that these receptors are 407 amino acids long, and share 95% amino acid identity; there are only 22 amino acids that differ between rat and human SPR (see shaded circles in Figure 2).

While rat and human SPR are very similar at the amino acid level, they interact differently with SP and several nonpeptide antagonists of SPR. For example, SP binds to rat SPR with a K_d of 3 nM whereas it binds to human SPR with a higher affinity characterized by a K_d of 0.7 nM. The difference between rat and human SPR pharmacology becomes even more striking for some of the nonpeptide antagonists. CP 96,345, the first nonpeptide antagonist of SPR to be synthesized, has 100-fold higher affinity for human SPR than for rat SPR, and the nonpeptide antagonist RP67580 has higher affinity for rat SPR than for human SPR.

Since rat and human SPR differ in only a few amino acid residues in the TM domains (a region believed to be involved in ligand binding), several groups have identified the amino acids responsible for differences in their pharmacology. These groups found that residue 290 in TM7 and the residues located on the second EC loop contribute to the selectivity of CP 96,345 for human SPR. Histidine 197 in TM5 is involved in binding of CP 96,345 whereas histidine 265 in TM6 is involved in RP67580 binding. These mutagenesis studies not only identify the residues involved in conferring species-dependent pharmacology to SPR, but also show that ligand binding to the receptor involves the TM domain as well as amino terminus and EC loops.

SPR activation in most cells stimulates phospholipase C, which hydrolyzes membrane phosphoinositides into two second messengers: inositol triphosphate (IP_3) and diacylglycerol. These molecules stimulate intracellular calcium release and protein kinase C (PKC) activation, respectively. More recent studies using U373 human glioblastoma cells, in which SPR occurs naturally, implicate several key molecules in SPR signaling including mitogen-activated protein kinases ERK1/2, mitogen-activated protein kinase p38, transcription factor NF-κB, and epidermal growth factor receptor. Of these molecules, ERK1/2 mediates SPR-stimulated proliferation of U373 MG cells.

Truncated SPR

Functional studies in which the truncated and full-length forms of SPR were expressed in *Xenopus* oocytes revealed that the truncated receptor is 100-fold less active than full-length SPR. Ligand binding analyses of the full-length and truncated forms of SPR expressed in COS cells reveal that the truncated form binds SP with much lower affinity. Tissue distribution of the truncated form of SPR differs from that of full-length SPR, with the truncated form showing lower expression in most regions of the brain. However, in peripheral tissues the truncated form is more prevalent than full-length SPR, with bone and spleen expressing solely the truncated form. Potentially, these two receptors could mediate SP signaling differently in different tissues due to the presence or absence of the carboxyl-tail; thus it is important to understand the function of the carboxyl-tail in SPR biology.

Role of the Carboxyl-Tail in SPR Function

One function of SPR in which the carboxyl-tail plays an important role is receptor desensitization. Like many other GPCRs, SPR undergoes agonist-induced desensitization, a phenomenon in which the responsiveness of the receptor diminishes in spite of the continued presence of the stimulus. Studies performed by Dr. Lefkowitz at Duke University Medical Center and by several other investigators have shown that agonist-specific or homologous desensitization of GPCRs proceeds through two cytosolic proteins, G protein-coupled receptor kinases (GRKs) and β-arrestins. GRKs phosphorylate agonist-occupied receptor at serine and threonine residues on the carboxyl-tail and IC loops, and this phosphorylation primes the receptor to bind β-arrestins. The binding of β-arrestin to the intracellular face of the receptor disrupts interactions between the receptor and G protein, resulting in a loss of signaling (Figure 3). β-arrestin binding also directs receptor internalization through clathrin-coated pits.

Since the carboxyl-tail plays a key role in GPCR desensitization, its absence would be expected to impair the ability of truncated SPR to desensitize. However, studies examining the role of the C terminus in rat SPR desensitization have yielded varying results. It has been reported that a C-terminally truncated mutant of rat SPR does not desensitize fully, while other studies have reported no loss of desensitization in the same truncation mutant. We have recently examined the effect of C-terminal truncation on the desensitization of human SPR. Full-length and truncated (Δ325) human SPR desensitize similarly, using two independent readouts of

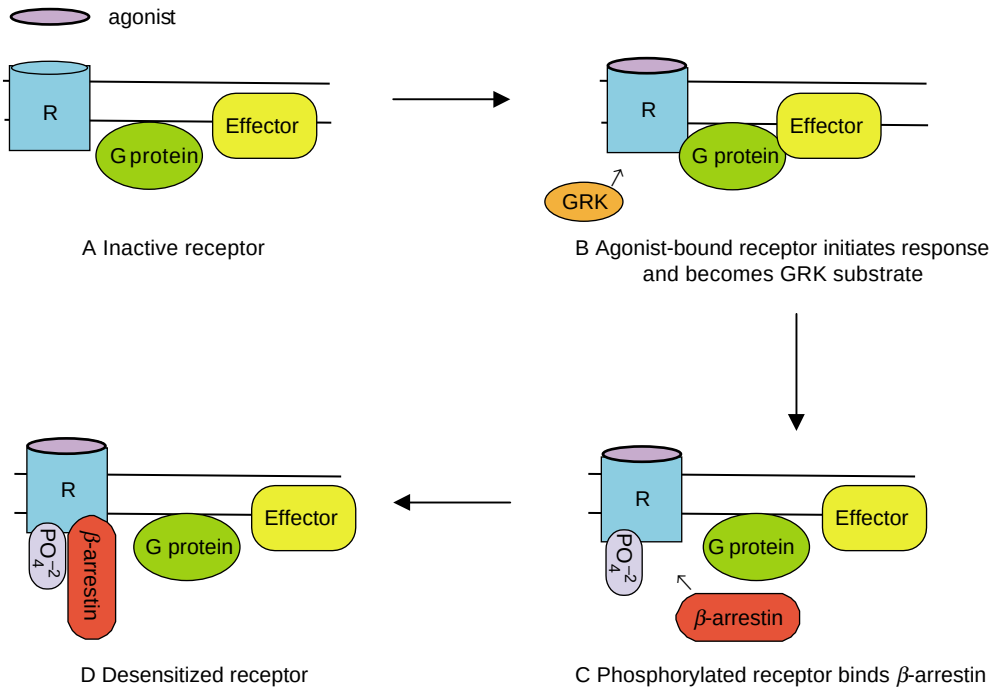

FIGURE 3 Model of homologous GPCR desensitization. (A) In the resting state, receptor, G protein and effector are inactive. (B) Occupancy of the receptor by agonist enables it to catalyze G protein activation, leading to activation of the effector by G protein. Receptor occupancy also makes it a target for phosphorylation by GRK. (C) Phosphorylation diminishes the ability of the receptor to activate G protein; the effector then reverts to the inactive state. Phosphorylation also facilitates the association of β-arrestin with the receptor. (D) Association of β-arrestin with phosphorylated receptor prevents any further G protein activations even though agonist is present.

receptor signaling, intracellular IP_3 accumulation and subcellular redistribution of fluorescently tagged PKC-βII in live cells. However, truncated and full-length SPR differ, in GRK-catalyzed phosphorylation and in their ability to form endocytic vesicles with two distinct β-arrestins, β-arrestin 1 and 2. Truncated SPR, unlike full-length SPR, does not undergo phosphorylation following exposure to SP. Also, full-length SPR forms endocytic vesicles equally well with either β-arrestin 1 or β-arrestin 2, while truncated SPR does not form any endocytic vesicles with β-arrestin 1 and forms fewer vesicles with β-arrestin 2. These data indicate that full-length and truncated SPR are likely to behave differently during endocytosis and receptor recycling.

The Role of SPR in Human Disease

While SP and SPR have been studied for several decades, renewed interest in SPR biology was generated following the report in 1998 that SPR antagonists have antidepressant activity. This discovery generated so much enthusiasm that a commentary entitled "Reward for Persistence in Substance P Research" by Claes Wahlestedt appeared in *Science* along with a timeline highlighting important events throughout the history of substance P research (Figure 4). While an SPR antagonist has not yet been introduced into clinical medicine as an antidepressant, there is no doubt that SPR plays a major role in the pathophysiology of several diseases including depression, emesis, and glioblastomas.

SPR in Depression

The distribution of SP and SPR in the brain is consistent with a role for these molecules in mood and depression. For instance, SP is the predominant tachykinin in human brain, and the expression of SP is particularly concentrated in areas of the brain that function in either affective behavior or stress responses, such as the hypothalamus, amygdala, habenula, periaqueductal gray, and dorsal raphe nucleus. Likewise, SPR is the most highly expressed tachykinin receptor in brain and is also concentrated in areas that are important for affective behavior.

The most convincing evidence of a role for SP in depression is found in a randomized, double-blind, placebo-controlled study of patients with moderate to severe major depression, which showed that the SPR antagonist, MK-869, has antidepressant activity equivalent to paroxetine, a current standard therapy. Importantly, MK-869 shows a significantly lower incidence of the side effects, which frequently cause patients to discontinue drug therapy. More recently, a second SPR antagonist, L759274, has shown similar results in clinical trials, further supporting a role for SPR in depression.

SPR in Emesis

An important role for SPR in emesis is indicated by clinical trials showing that the nonpeptide SPR antagonist, MK-869 (also called aprepitant), is effective against chemotherapy-induced nausea and vomiting (CINV). However, the molecular mechanism through which SPR influences emesis is not yet known. Clinical trial investigators noted that during the acute phase of CINV (the first 24 h), aprepitant was only effective in 37% of patients while the standard therapy, odansetron, was effective in 57% of patients. In contrast, during the delayed phase of CINV (the succeeding 6 days) aprepitant was effective in 72% of patients while odansetron was effective in only 7% of patients. This observation suggests that acute phase nausea and delayed phase nausea involve different molecular mechanisms and that SP is active in the delayed phase of CINV.

Another clinical trial tested a triple combination of aprepitant, granisetron, and dexamethasone for suppression of CINV. In this trial, 87% of patients receiving the triple combination reported that nausea did not affect their ability to perform daily functions, in comparison to 67% of patients receiving only granisetron and dexamethasone. Aprepitant has recently received Food and Drug Administration, FDA, approval for use in combination with other antinausea drugs to prevent CINV, which is a particular problem in high-dose cisplatin therapy. This result points to SPR as a promising target protein for future efforts to understand and control nausea.

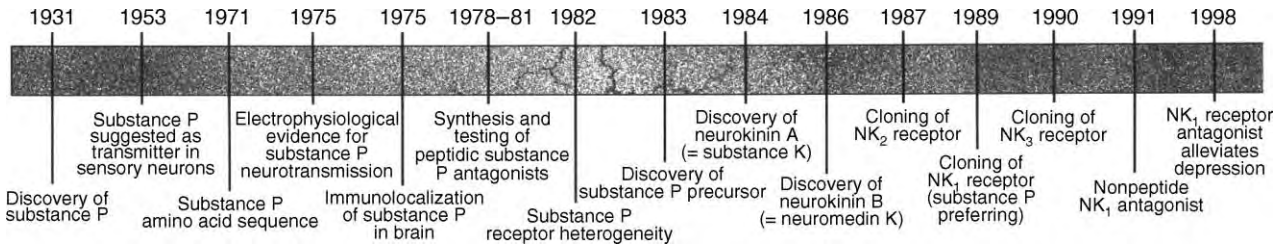

FIGURE 4 A timeline of landmark events in substance P research. (Reprinted from Wahlestedt, C. (1998). Substance P and related neuropeptides. *Science* **281**, 1624–1625, with permission of AAAS.)

SPR in Glioblastomas

Glioblastomas, classified as grade IV astrocytomas, are among the most aggressive and frequently occurring primary brain tumors in adults. Patients with glioblastomas have an extremely poor prognosis: with a 5-year survival rate of 1%, the currently available treatments of surgery, radiation therapy, and chemotherapy are inadequate. Current research focuses on understanding glioblastoma biology and identifying molecular targets for blocking tumor growth. SP has been observed to have a growth-promoting affect in a variety of cell types, and its role in glioblastoma growth is currently being studied. A recent study noted SPR expression in 9 out of 12 astrocytomas, and 10 out of 10 glioblastomas. Further, the density of SPR correlates with the degree of malignancy, with glioblastomas expressing more receptors than astrocytomas. At the molecular level, SPR stimulation in U373 MG human glioblastoma cells increases mitogenesis, cell proliferation, and release of interleukin-6 (IL-6). SPR-dependent release of IL-6 is noteworthy because IL-6 has been implicated in the progression of gliomas. Thus SPR likely plays an important role in the biology of glioblastomas. Consistent with this notion, SPR antagonists are reported to inhibit the growth of glioblastomas in nude mice.

See Also the Following Articles

G Protein-Coupled Receptor Kinases and Arrestins • Neurotransmitter Transporters • Phospholipase C

Glossary

carboxyl-tail The hydrophilic portion of a GPCR which follows the final transmembrane-spanning domain (TM7), extending from the cytosolic face of the plasma membrane and terminating in the cytosolic compartment of the cell.

G protein-coupled receptor (GPCR) Integral plasma membrane proteins having seven hydrophobic, transmembrane-spanning domains (designated TM1 through 7). GPCRs pass signals across the plasma membrane by transducing stimuli from extracellular signaling molecules to intracellular G proteins. G proteins, in turn, activate intracellular signaling cascades.

preprotachykinins The genes containing all the DNA sequence information needed to synthesize tachykinins. The actual production of tachykinins requires alternative splicing of mRNA transcripts derived from preprotachykinin, and post-translational modification of peptides generated from the mRNA transcripts.

phospholipase An enzyme that can hydrolyze the phosphodiester bond in phospholipids and produce soluble inositol lipids and membrane-bound diacylglycerol; type C phospholipases specifically use phosphoinositides as substrates.

tachykinin A peptide of 10-11 amino acids, having the amino acid sequence F-X-G-L-M-NH2 at the C-terminal end, where X is a hydrophobic amino acid residue. Tachykinins are released from neurons and act as neurotransmitters.

Further Reading

De Felipe, C., Herrero, J. F., O'Brien, J. A., Palmer, J. A., Doyle, C. A., Smith, A. J. H., Laird, J. M. A., Belmonte, C., Cervero, F., and Hunt, S. P. (1998). Altered nociception, analgesia and aggression in mice lacking the receptor for substance P. *Nature* **392**, 394–397.

Hökfelt, T., Pernow, B., and Wahren, J. (2001). Substance P: A pioneer amongst neuropeptides. *J. Intern. Med.* **249**, 27–40.

Holmes, A., Heilig, M., Rupniak, N. M. J., Steckler, T., and Griebel, G. (2003). Neuropeptide systems as novel therapeutic targets for depression and anxiety disorders. *Trends Pharmacol. Sci.* **24**, 580–588.

Kohout, T. A., and Lefkowitz, R. J. (2003). Regulation of G protein-coupled receptor kinases and arrestins during receptor desensitization. *Mol. Pharmacol.* **63**, 9–18.

Maggi, C. A. (2000). Principles of tachykininergic co-transmission in the peripheral and enteric nervous system. *Regulatory Peptides* **93**, 53–64.

Mantyh, P. W. (2002). Neurobiology of substance P and the NK1 receptor. *J. Clin. Psychiat.* **63**, 6–10.

Palma, C., and Maggi, C. A. (2000). The role of tachykinins via NK_1 receptors in progression of human gliomas. *Life Sci.* **67**, 985–1001.

Rittenberg, C. N. (2002). A new class of antiemetic agents on the horizon. *Clin. J. Oncol. Nurs.* **6**, 103–104.

Severini, C., Improta, G., Falconieri-Erspamer, G., Salvadori, S., and Erspamer, V. (2002). The tachykinin peptide family. *Pharmacol. Rev.* **54**, 286–322.

Wahlestedt, C. (1998). Substance P and related neuropeptides. *Science* **281**, 1624–1625.

Zimmer, A., Zimmer, A. M., Baffi, J., Usdin, T., Reynolds, K., Konig, M., Palkovits, M., and Mezey, E. (1998). Hypoalgesia in mice with a targeted deletion of the tachykinin 1 gene. *Proc. Natl. Acad. Sci. USA* **95**, 2630–2635.

Biography

Mark D. Richardson is a Research Associate in the Department of Anesthesiology, Duke University Medical Center. He is a protein biochemist with expertise in G proteins and his current focus is on signaling through substance P receptors. He holds a Ph.D. from the University of Texas (Houston).

Madan M. Kwatra is an Associate Professor in the Department of Anesthesiology and Assistant Professor in the Department of Pharmacology and Cancer Biology. His principal research interest is signaling through G protein-coupled receptors. His laboratory has been studying substance P receptor for the last 10 years and ongoing studies are directed toward understanding the role of substance P receptor and other G protein-coupled receptors in the biology of glioblastomas. He holds a Ph.D. from the University of Montreal, Canada.

Taste Receptors

John D. Boughter Jr.
University of Tennessee Health Science Center, Memphis, Tennessee, USA

Steven D. Munger
University of Maryland School of Medicine, Baltimore, Maryland, USA

Taste receptors are proteins that recognize taste stimuli of various types, thereby functioning as the initial component in the process of sensing and discriminating ingested material. Taste stimuli can be categorized as belonging to one of at least five classes, comprising qualities perceived by humans as sweet, salty, sour, bitter, and umami (the savory taste of L-amino acids such as glutamate). Recently, great progress has been made in the identification and functional characterization of mammalian taste receptors that respond to sweet, bitter, and umami (e.g., monosodium glutamate) stimuli. These receptors are expressed on the apical membranes of taste-receptor cells (TRCs) that extend into the oral cavity. The receptor–stimulus binding event initiates a transduction cascade in TRCs, leading to cell depolarization and neurotransmitter release onto afferent nerve fibers, and ultimately propagation of sensory information to taste processing areas in the central nervous system.

Taste-Receptor Cells

The initial events in taste processing occur in taste buds, structures found in the epithelia of the tongue, palate, larynx, and epiglottis of mammals, which contain ~50–100 cells of neuroepithelial origin (Figure 1). Taste buds contain morphologically distinct cell types including elongate, spindle-shaped cells that express a variety of identified transduction-related proteins (including taste receptors) and therefore likely function as TRCs. TRCs possess apical processes with microvilli that protrude into the oral cavity and interact with taste stimuli. These microvilli contain taste receptors and taste-responsive ion channels. Tight junctions between the cells in a taste bud restrict the access of most stimuli to the apical membranes of the cells. TRCs synapse with afferent special sensory fibers from one of three cranial nerves (VII, IX, X), and taste information is subsequently relayed through brainstem nuclei to forebrain taste areas, or to local circuits controlling oromotor reflexes.

Multiple signaling cascades in TRCs have been described, and there are fundamental differences in the transduction pathways associated with each stimulus quality. For example, salt and acid stimuli directly permeate or gate apical ion channels, causing TRC depolarization, while umami-, sweet-, and bitter-tasting stimuli are thought to predominantly activate taste receptors.

G Protein-Coupled Taste Receptors

The largest gene superfamily in the mammalian genome encodes the group of proteins known as G protein-coupled receptors (GPCRs). GPCRs play critical roles in a variety of cellular functions, including neurotransmitter and hormonal signaling and the detection of sensory stimuli. Although they are quite diverse in amino acid sequence, all GPCRs share common structural and functional features. Their most striking structural motif is their seven helical transmembrane domains, i.e., the GPCR polypeptide passes 7 times through the plasma membrane, leaving an extracellular amino terminus and intracellular carboxy terminus. GPCRs also share a common signaling mechanism, as is evidenced by their name: activation of a GPCR by its ligand initiates an intracellular signaling cascade via the stimulation of an associated heterotrimeric guanosine triphosphate (GTP)-binding protein (G protein). Most chemosensory receptors are GPCRs, including the olfactory receptors, vomeronasal receptors, and taste receptors. In the taste system, three families of GPCR-type taste receptors (T1Rs, T2Rs, and taste-mGluR4) are implicated in the detection of sweet- and bitter-tasting stimuli and of certain amino acids.

T1R Receptors

The first two members of the T1R taste-receptor family were identified only a few years ago by Nicholas Ryba, Charles Zuker, and colleagues. Now called T1R1 and T1R2, they were cloned through differential screening of taste and nontaste tissues from the tongue. The gene encoding a third family member, T1R3, was identified

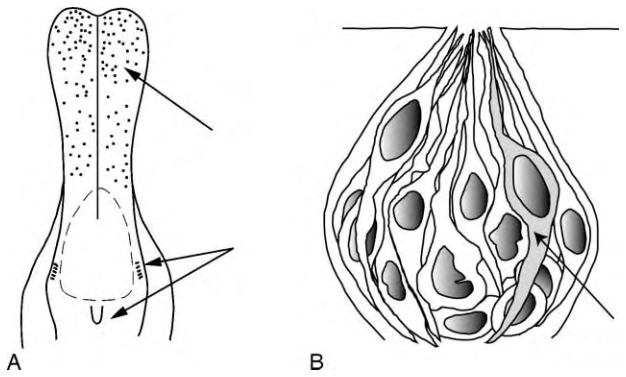

FIGURE 1 Taste-receptor cells. (A) Taste buds are specialized sensory structures located in the epithelia of the mammalian tongue (arrows indicate approximate locations of taste buds), as well as palate, larynx, and epiglottis (not shown). (B) Schematic of taste bud. Taste buds contain 50–100 cells of morphologically distinct types, including elongate, spindle-shaped cells (arrow) that express taste receptors.

by a number of investigators in a very different way: they determined that the *Tas1r3* gene corresponds to a genetic locus that confers taste sensitivity to saccharin and other sweeteners in mice. The T1Rs are class C GPCRs and share a large N-terminal extracellular domain, which comprises ~50% of the protein length, with other GPCRs of that class (Figure 2). The N-terminal domain contains the site of ligand binding in many class C GPCRs. However, it is unclear if the T1Rs interact with their ligands in a similar manner.

The mapping of the *Tas1r3* gene to a genomic locus conferring saccharin taste sensitivity suggested that T1Rs may play a role in the detection of sweet-tasting compounds. Further experimentation has supported this hypothesis. Experiments using either transgenic overexpression of T1R3 in mice or heterologous expression of various T1Rs in cultured mammalian cells have shown that the T1Rs are receptors for sugars, artificial sweeteners, sweet proteins, and amino acids. Additionally, heterologous expression studies suggest T1Rs function as heteromultimeric complexes. Specifically, T1R1 and T1R3 together form a functional receptor for umami-tasting stimuli (e.g., L-amino acids) but are unresponsive to sweet-tasting stimuli, while T1R2 and T1R3 together comprise a receptor for sugars, artificial sweeteners, sweet proteins, and D-amino acids. The native T1R1 and T1R2 subunits are coexpressed with T1R3 in different subsets of taste-receptor cells (TRCs): T1R3 and T1R1 are found in the same TRCs of the anterior tongue, while T1R3 and T1R2 are found in the same TRCs of the posterior tongue. These observations have several implications. First, no T1R subunit forms a functional receptor alone. Second, T1R3 is a common subunit for receptors with different ligand specificities. Third, these ligand specificities are largely dependent on whether the receptor complex contains T1R1 or T1R2.

However, more recent studies from Robert Margolskee and colleagues suggest that T1Rs are not the only receptors for these stimuli. Mice in which the gene encoding T1R3 has been deleted from the genome display a normal sensitivity to the taste of glucose, a reduced sensitivity to sucrose, and are indifferent to several artificial sweeteners that are normally preferred by mice. Additionally, the taste sensitivity of these mice to monosodium glutamate is reduced at low concentrations of the stimulus when compared to wild-type (i.e., normal) mice. While these findings suggest that mammals have other receptors for sweet and amino acid stimuli, an alternative interpretation, supported by the work of Zuker and colleagues, is that T1Rs can function *in vivo* as homomeric receptors.

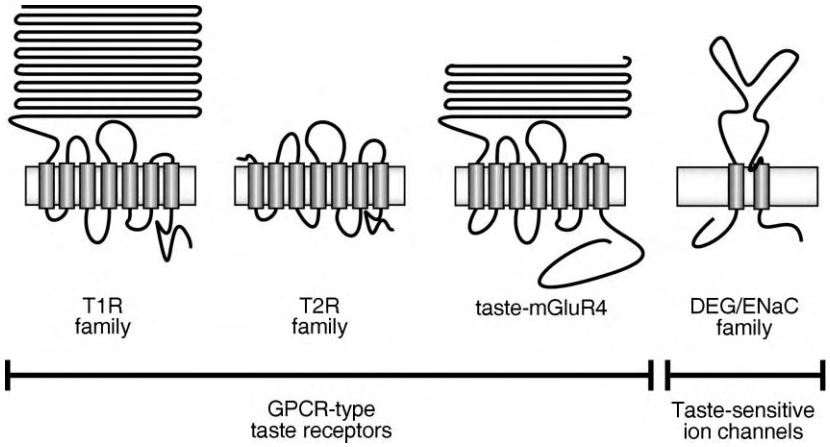

FIGURE 2 The proposed structures of taste-receptor proteins. Amino acid and sweet- and bitter-tasting stimuli are detected by GPCR-type taste receptors. Salt and acid stimuli activate TRCs through a GPCR-independent mechanism; they directly permeate or modulate ion channels, some of which may belong to the DEG/ENaC family.

T2R Receptors

A second class of taste receptors, the T2Rs, was identified by Ryba, Zuker, and colleagues, as well as by the laboratory of Linda Buck. They reasoned that genetic loci linked to bitter-taste sensitivities might contain genes encoding GPCRs involved in the detection of bitter tastants. Data mining of mouse and human genome databases bore out this hypothesis. To date, ~33 mouse and 25 human genes encoding T2Rs have been identified (each species also contains several apparent pseudogenes). T2Rs are class A GPCRs (the same class as olfactory receptors and rhodopsin), which are characterized by a short N terminus (Figure 2). Many class A GPCRs bind their ligands within a pocket defined by several of the transmembrane helices and/or the nearby extracellular loops; however, the site of ligand binding for T2Rs has not been determined.

To date, only a couple of T2Rs have been clearly linked to the detection of bitter-tasting compounds. The evidence implicating the mouse T2R5 receptor in the detection of cycloheximide is compelling: the genetic locus for cycloheximide taste sensitivity maps to a region of mouse chromosome 6 that contains the gene encoding T2R5; T2R5 specifically responds to cycloheximide in a heterologous expression assay; and polymorphisms in T2R5 that correlate with a reduced behavioral taste sensitivity to cycloheximide also confer a reduced sensitivity to this compound in an *in vitro* assay. In humans, the T2R38 receptor has been linked to phenylthiocarbamide (PTC) taste sensitivity. The gene encoding this receptor was recently mapped to a PTC-sensitivity locus in humans. Furthermore, polymorphisms in this gene correlate with variations in PTC-taste sensitivity between individuals in the sampled population.

As T2Rs display only a 30–70% sequence identity within the family, what is the evidence that other T2Rs are involved in bitter taste? First, many *Tas2r* genes are found in large clusters on one or two chromosomes where genetic loci for bitter-taste sensitivities have been mapped (two clusters are on mouse chr. 6 and one each on human chrs. 7 and 12). Second, localization studies have shown that numerous T2Rs are expressed in individual TRCs (primarily within bitter-responsive taste buds of the posterior tongue).

The Taste-mGluR4 Receptor

Another class C GPCR has been suggested to play a role in amino acid taste. Metabotropic glutamate receptors (mGluRs) are found throughout the nervous system, where glutamate serves as a major excitatory neurotransmitter. Nirupa Chaudhari and colleagues determined that one type of mGluR, mGluR4, is expressed in a subset of TRCs. Interestingly, the TRC-specific version of mGluR4 varies somewhat from the protein found in brain. The newly dubbed "taste-mGluR4", the product of an alternative transcript of the mGluR4 gene, displays a truncated N-terminal domain that is approximately half the length of other class C GPCRs. Heterologous expression of the taste-mGluR4 showed a glutamate dose-response curve to glutamate that is consistent with human taste thresholds, supporting a role for taste-mGluR4 in umami taste.

Ion Channels as Taste Receptors

Taste cells rely on the actions of a variety of ion channels to support stimulus-induced changes in membrane polarization and the synaptic release of neurotransmitter. However, several ion channel species can be thought of as receptors for taste stimuli: the channels interact directly with the taste stimulus and participate in the initial stage of taste transduction. Such channels play a central role in the detection of salty- and sour-tasting stimuli. A large portion of NaCl (salty) taste appears dependent on the influx of Na^+ through the epithelial sodium channel ENaC. The ENaCs, members of the degenerin (DEG)/ENaC superfamily of ion channels, are strongly Na^+ selective. DEG/ENaC family members display a common topology: they have two transmembrane domains, a large extracellular loop and a small pore-forming loop (Figure 2). They function as hetero-oligomeric complexes. Data implicating ENaCs in NaCl taste include: the presence of amiloride-blockable, Na^+-selective channels in TRCs that share a number of physiological properties with the ENaCs, and the expression of three homologous ENaC subunits, α, β, and γ, in TRCs.

Sour (acid) taste stimuli (i.e., H^+) depolarize TRCs either by activating cation channels or by directly permeating ion channels. As is the case for the transduction of Na^+, members of the DEG/ENaC channel family appear to play a major role in the transduction of acids: ENaC itself can conduct H^+, while ASIC-β acid-sensing ion channel-β (ASIC-β) and MDEG1/BNaC1 (mammalian degenerin-1/brain-type Na^+ channel-1), are activated directly by protons and are expressed in taste tissue.

Transduction Cascades

Unlike olfactory transduction, where a single intracellular pathway serves virtually all stimuli, the taste system appears to have a fairly diverse set of transduction mechanisms, both within and between stimulus classes. TRCs express many second-messenger components common to GPCR-coupled cascades such as cyclic nucleotide and phosphinositide signaling systems, and a transient receptor potential-related channel, TRPM5,

has also been implicated in taste transduction. TRPM5 appears to mediate capacitive calcium entry and is likely activated by the emptying of internal Ca^{2+} stores. The influx of calcium via TRPM5 may contribute to the receptor potential and/or mediate neurotransmitter secretion onto afferent fibers.

See Also the Following Articles

G Protein-Coupled Receptor Kinases and Arrestins • Glutamate Receptors, Metabotropic • Neurotransmitter Transporters • Olfactory Receptors

Glossary

taste quality The perceptual quality attributed to a taste stimulus, such as salty, sour, sweet, bitter, or umami.

taste receptor GPCR that binds sweet, bitter, or amino acid stimuli, leading to activation of a transduction cascade, receptor cell depolarization and transmitter release onto afferent nerve fibers.

taste-receptor cell Elongate, spindle shaped cell in taste buds that expresses taste receptors and/or transduction components.

transduction The process, often involving a biochemical cascade, by which one type of signal (e.g., a taste stimulus) is converted to another type (e.g., depolarization of the TRC).

Further Reading

Doty, R. L. (ed.) (2003). *Handbook of Olfaction and Gustation (Neurological Disease and Therapy)*, 2nd edition, Vol 57. Marcel Dekker, New York.

Gilbertson, T. A., and Boughter, Jr. J. D. (2003). Taste transduction: Appetizing times in gustation. *Neuroreport* **14**, 905–911.

Lindemann, B. (2001). Receptors and transduction in taste. *Nature* **413**, 219–225.

Margolskee, R. F. (2002). Molecular mechanisms of bitter and sweet taste transduction. *J. Biol. Chem.* **277**, 1–4.

Montmayeur, J. P., and Matsunami, H. (2002). Receptors for bitter and sweet taste. *Curr. Opin. Neurobiol.* **12**, 366–371.

Biography

John D. Boughter Jr. is an Assistant Professor of Anatomy and Neurobiology at the University of Tennessee Health Science Center. His principal research interests include the behavior genetics, physiology, and anatomy of the taste system. He holds a Ph.D. from Florida State University and received his postdoctoral training at the University of Maryland School of Medicine.

Steven D. Munger is an Assistant Professor of Anatomy and Neurobiology at the University of Maryland School of Medicine. His principal research interests include the molecular mechanisms of olfactory and taste transduction. He holds a Ph.D. from the University of Florida and received his postdoctoral training in the Howard Hughes Medical Institute at the Johns Hopkins Medical Institutes.

T-Cell Antigen Receptor

Andrea L. Szymczak and Dario A. A. Vignali
St. Jude Children's Research Hospital, Memphis, Tennessee, USA

The T-cell antigen receptor (TCR) is a highly organized, multimolecular complex found exclusively on T and NK T cells. The majority of TCRs are composed of TCRα and TCRβ chains, while a small percentage contain TCRγ and TCRδ chains. The TCR chains heterodimerize and are associated with the invariant chains of the CD3 complex, CD3$\varepsilon\gamma\delta$ and CD247 (often referred to as the zeta chain, TCRζ or CD3ζ). Each chain is essential for TCR surface expression and consequently T cell development and function. This complex mediates the development of T cells that are able to mount a specific immune response against a wide variety of foreign antigens and pathogenic organisms. This unique capability is due to the unusual genomic organization and rearrangement of TCR genes, which generates a vast number of TCRs that recognize almost any antigenic peptide in the context of major histocompatibility (MHC) molecules.

TCR:CD3 Complex: Genes, Proteins and the Receptor Complex

T Cell Antigen Receptor

T cells can only recognize and bind antigens when they are presented by major histocompatibility (MHC) molecules, a process called MHC restriction. Initially, the T cell antigen receptor (TCR) was difficult to study because it was membrane bound and could only recognize antigen in the context of MHC. The first TCR complexes isolated were composed of a disulfide-linked heterodimer of TCRα and TCRβ. Monoclonal antibodies against this complex were either specific for a particular T cell clone or nonspecific, indicating that the TCR chains were similar to the immunoglobulin (Ig) molecules, containing both variable (V) and constant (C) regions. While the vast majority ($>95\%$) of T cells had TCR$\alpha\beta$ heterodimers, another type of TCR containing a TCRγ and TCRδ heterodimer was later identified. The TCR chains, in particular the variable regions, are responsible for recognizing and binding to peptide–MHC molecules presented on the surface of antigen presenting cells (APC).

Genes: Organization and Rearrangement

As with antibody molecules, T cells must be able to recognize a wide variety of pathogens, therefore a diverse repertoire of TCR must be generated that recognize such antigens. Many similarities exist between the Igs and the TCR. The four TCR loci (α, β, γ, and δ) have a germ-line organization similar to that of Ig. The α- and γ-chains are produced by rearrangement of V and J segments, while the β- and δ-chains are produced by rearrangement of V, D, and J segments (Figure 1). The segments for TCRδ are located between the Vα and Jα segments. When the TCRα gene is rearranged, the TCRδ segments are deleted, thereby ensuring the T cell does not express TCR$\gamma\delta$ and TCR$\alpha\beta$ at the same time. The basic domain structure is evolutionarily conserved and is believed to have arisen through gene duplication. Organization of the TCR genes in the mouse and human is similar but vary in the numbers of segments (Table I).

The TCR genes encode areas of hypervariability similar to the complementarity determining regions (CDRs) of antibody molecules. Embedded within the V regions are CDR1 and CDR2. There is an additional area of hypervariability (HV4) that does not appear to interact with antigen and is therefore not considered a CDR (Figure 1). CDR3 is a result of VJ or VDJ joining. This intentionally imprecise process frequently results in the addition or deletion of nucleotides, adding significantly to the variability in this region (N region diversity). Occasionally, a nonproductive rearrangement of the first gene locus occurs due to an out-of-frame rearrangement or insertion of a stop codon. This induces the rearrangement of the TCR locus on the other chromosome.

Rearrangement occurs through the action of recombination-activating genes (RAGs) 1 and 2 during T cell development. Flanking each gene segment in the germ line DNA are conserved recognition signal sequences. The RAG enzymes recognize these heptamer and nonamer sequences and catalyze the VJ and VDJ joining with a mechanism analogous to that used to rearrange the Ig locus. In addition, secondary rearrangements termed receptor editing or revision can occur in both B and T cells. The role of receptor editing and revision in

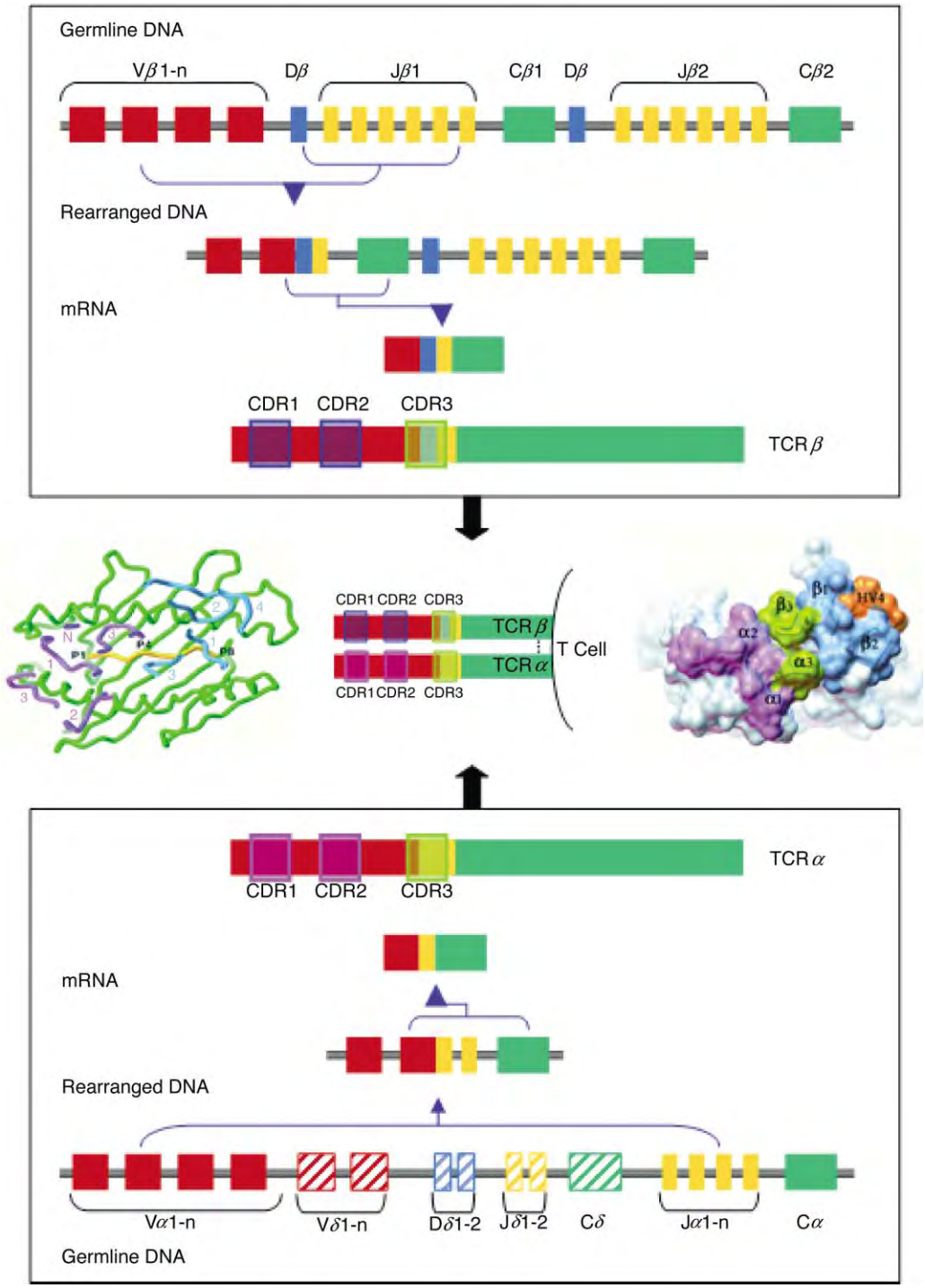

FIGURE 1 Rearrangement of TCR$\alpha\beta$ genes. Example of TCRα (bottom panel) and TCRβ (top panel) rearrangement. TCRα undergoes V to J rearrangement while TCRβ undergoes D to J followed by V to DJ rearrangement. Primary transcripts of rearranged DNA are processed to mRNA that encode the mature TCR$\alpha\beta$ chains expressed on the T cell surface (center panel, middle). Areas encoding the CDR regions are boxed. TCRδ segments in the TCRα locus are shown in stripes. The center left panel shows a view into the peptide–MHC combining site with peptide in yellow and MHC in green superimposed with the CDR regions (CDR1, 2 and 3; HV4) of TCRα (purple) and TCRβ (blue). CDR1 of Vα and Vβ and Vβ CDR3 are clearly positioned along the central axis of the peptide. N = the N-terminal residue of Vα. (Reprinted from Garcia, K. C., Degano, M., Pease, L. R., Huang, M., Peterson, P. A., Teyton, L., and Wilson, I. A. (1998). Structural basis of plasticity in T cell receptor recognition of a self peptide-MHC antigen. *Science* **279**, 1166–1172, with permission of AAAS.) The center right panel shows the surface of the TCR-binding site. The surface of the loop trace of the Vα CDRs 1 and 2 are purple; CDRs 1 and 2 of TCRβ are blue; Vα and Vβ CDR3s are green; and the hypervariable region of TCRβ (HV4) is orange. (Reprinted from Garcia, K. C., Degano, M., Stanfield, R. L., Brunmark, A., Jackson, M. R., Peterson, P. A., Teyton, L., and Wilson, I. A. (1996). An $\alpha\beta$ T cell receptor structure at 2.5Å and its orientation in the TCR-MHC complex. *Science* **274**, 209–219, with permission of AAAS.)

TABLE I

Chromosomal Location and Numbers of TCR Gene Segments

	Human				Mouse			
	TCRα (14)	TCRβ (7)	TCRγ (7)	TCRδ (14)	TCRα (14)	TCRβ (6)	TCRγ (13)	TCRδ (14)
V	40–50	30–57	11–14	3	50–100	20–50	7	10–11
D		2		3		2		2
J	60–70	13–14	5	3–4	60–100	12–14	4	2
C	1	2	2–3	1	1	2	4	1

Total number of gene segments for the human and mouse TCR. Numbers in parenthesis indicate the chromosome on which the gene is located. Reprinted from Allison, T. J., and Garboczi, D. N. (2001). Structure of $\gamma\delta$ T cell receptors and their recognition of non-peptide antigens. *Mol. Immunol.* **38**, 1051–1061, with permission from Elsevier.

T cells is still unclear, but it has been suggested to contribute to peripheral T cell tolerance.

While many similarities exist between Ig and TCR, there is one important distinction: TCR genes do not undergo somatic hypermutation and thus there is no affinity maturation. While the number of TCR V region segments is dramatically reduced compared to the Ig genes, the number of J region gene segments is greater, increasing the potential diversity at the V–J interface (Table II). This is likely due to differences in the nature of the antigen recognized by TCR and Ig.

TCR Structure and Recognition of Peptide–MHC Complexes

The TCR is a member of the Ig super family. Structural analysis has shown that the Vα and Vβ domains pair via a conserved hydrophobic core, while the Cα and Cβ domains pair via a highly polar interface, with a skewed distribution of acidic residues in Cα and basic residues in Cβ. The two chains also pair via a conserved disulfide bond close to the membrane (Figure 2). In addition, the C region contains a connecting peptide, a transmembrane region and short intracellular domain. The anchoring transmembrane domain is unusual as it contains several highly conserved basic amino acid residues (TCRα–Lys/and –Arg; TCRβ–Lys). These positively charged residues mediate interaction with the CD3 complex. The cytoplasmic domains are short, consisting of only 5–12 amino acids.

TCR specificity is mediated by the Vα and Vβ CDRs which interact with the peptide–MHC complex. MHC molecules are bound to the APC membrane and the antigenic peptide is bound in a groove between two α-helices (Figure 2). A number of TCR:peptide–MHC complexes have been crystallized. Although specific contact residues vary, all have a similar mode of binding in which the CDR2 regions contact the MHC surface and CDR1 and CDR3 contact both the peptide and MHC molecules (Figures 1 and 2). The V region of TCRα binds closer to the N-terminal region of the peptide while that of TCRβ is closer to the C terminus. The TCR binds in a diagonal orientation due to two peaks created by the MHC α-helices.

The binding properties for a number of TCR:peptide–MHC complexes have been described. In general, the on and off rate for TCR:peptide–MHC binding is fast and the affinity is low compared to other receptor –ligand interactions. These biophysical properties of the TCR contrast starkly with the generally high affinity of Ig:antigen interaction. However, in spite of these properties, TCR interaction is sufficiently stable to initiate signal transduction.

In most instances, only a very small fraction of MHC molecules on a cell contain the right antigenic peptide for an individual TCR. It has been proposed that T cells overcome this limited ligand supply by a process called serial ligation, where many TCRs (perhaps as many as 200) can be ligated by a single

TABLE II

Table Sequence Diversity in TCR and Ig Genes

	Ig		TCR$\alpha\beta$		TCR$\gamma\delta$	
	H	κ	α	β	γ	δ
V segments	250–1000	250	50	25	7	10
D segments	10	0	0	2	0	2
Ds read in all frames	Rarely			Often		Often
N-region addition	V–D, D–J	None	V–J	V–D, D–J	V–J	V–D1, D1–D2, D1–J
J segments	4	4	50	12	2	2
V region combinations	62 500–250 000		1250		70	
Junctional combinations	$\sim 10^{11}$		$\sim 10^{15}$		$\sim 10^{18}$	

(Reprinted from Davis, M. M. (1990). T cell receptor gene diversity and selection. *Annu. Rev. Biochem.* **59**, 475–496, with permission of Annual Reviews.)

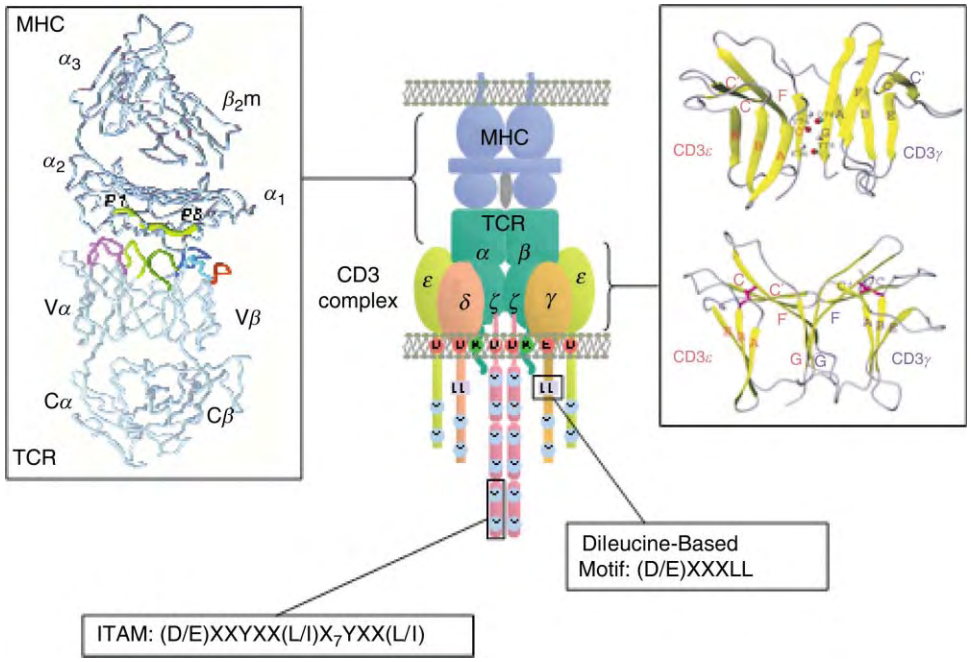

FIGURE 2 TCR:CD3 complex and its interaction with peptide–MHC. Schematic of the presumed stoichiometry of the TCR:CD3 complex. Highlighted are charged transmembrane residues, the ITAM sequence and the dileucine-based motif. In the upper left panel is a backbone structure of TCR:peptide–MHC complex. TCR is on the bottom and the MHC on top. The peptide (P1–8) is shown as a large tube in yellow. Vα CDRs 1 and 2 are in light and dark purple, respectively; αHV4 in white; Vβ CDRs 1 and 2, in light and dark blue, respectively; βHV4 in orange; and Vα and Vβ CDR3s in light and dark yellow, respectively. (Reprinted from Garcia, K. C., Degano, M., Stanfield, R. L., Brunmark, A., Jackson, M. R., Peterson, P. A., Teyton, L., and Wilson, I. A. (1996). An $\alpha\beta$ T cell receptor structure at 2.5Å and its orientation in the TCR-MHC complex. *Science* **274**, 209–219, with permission of AAAS.) In the upper right panel is a ribbon diagram of CD3$\varepsilon\gamma$. The beta strands are in yellow and the text colored red for CD3ε and blue for CD3γ. Three pairs of atoms involved in the hydrogen bond formation are designated with amide protons in gray and carbonyl oxygen atoms in red. Two disulfide-linked cysteine residues are shown. (Reproduced from Sun, Z. J., Kim, K. S., Wagner, G., and Reinherz, E. L. (2001). Mechanisms contributing to T cell receptor signaling and assembly revealed by the solution structure of an ectodomain fragment of the CD3γheterodimer. *Cell* **105**, 913–923, with permission from Elsevier.) In the lower left and right panels are the ITAM and dileucine-based consensus motifs, respectively.

peptide–MHC complex. It is thought that the low affinity and rapid off rate of TCR:peptide–MHC interaction may be instrumental in mediating this process.

Invariant Chains: CD3, CD247, and Pre-Tα

CD3 and CD247

The TCR is associated with the invariant chains of the CD3 complex.: CD3ε, CD3γ, and CD3δ are members of the Ig superfamily with one extracellular Ig domain followed by a transmembrane domain and cytoplasmic tail of ~40 amino acids in length. The zeta family of molecules are unique and have a short extracellular sequence and long cytoplasmic tail. This family consists of CD247 (otherwise known as CD3ζ or TCRζ), its splice variant η, and the γ-chain of the Fc receptor (FcRγ). The CD247 ζ- and η-chains are alternatively spliced gene products and are identical except for the carboxyl-terminal region of the cytoplasmic tail (113 and 155 amino acids long for ζ and η, respectively).

Analysis of CD3 and CD247 knockout mice demonstrates their importance in TCR expression and T cell development and function. Mice lacking CD247 (CD3ζ) and CD3γ exhibit a substantial block in early stages of T cell development, whereas mice lacking CD3δ develop a block at a later stage. CD3ε knockout mice display a complete arrest in T cell development, likely due to its requirement to form heterodimers with CD3$\gamma$and CD3δ.

The CD3 and CD247 chains contain a number of amino acid residues and motifs that are important for assembly, signal transduction, and regulation of cell surface expression (Figure 2). The transmembrane regions contain negatively charged amino acids that interact with the positively charged residues of TCR$\alpha\beta$ (CD3δ, CD3ε, and CD3ζ-Asp; CD3γ-Glu). The cytoplasmic tails contain immuno-receptor tyrosine-based activation motifs (ITAM) that when phosphorylated provide docking sites for SH2 domain-containing proteins, which are important for downstream signal transduction. Each CD3$\varepsilon\gamma\delta$ chain contains one ITAM while CD247 (CD3ζ) contains three. CD3δ and CD3γ also contain a dileucine-based motif. Both the YXXL sequence in the ITAM and the dileucine sequence have been shown to play a role in internalization and down-modulation of many types of receptors from the cell

surface. It has been suggested that these motifs are also utilized for TCR transport. A number of studies using T cell lines *in vitro* have shown a role for the CD3γ dileucine-based motif in TCR down-modulation, however its role *in vivo* remains to be defined.

Pre-Tα

During T cell development in the thymus, TCR$\alpha\beta$ precursors express a pre-TCR. The pre-TCR is formed by the functionally rearranged TCRβ chain, the CD3 complex and a surrogate TCRα chain, pre-TCRα (pTα). There are two notable differences between pTα and TCRα. First, pTα only has one invariant extracellular Ig domain. Second, the cytoplasmic tail of pTα is longer and contains two potential serine and threonine phosphorylation sites and a potential SH3 domain-binding motif. The requirements for surface expression of pTα are still unclear. However, it is clear that a number of signaling events are initiated through the pre-TCR. Pre-TCR signaling confirms the successful rearrangement TCRβ and induces the suppression of further TCRβ locus rearrangement, a process called allelic exclusion. Rearrangement of the TCRα locus then occurs leading to progression of T cell development.

TCR:CD3 Complex

Expression of the TCR on the cell surface requires all six chains of the complex. While the exact stoichiometry and make-up of the TCR:CD3 complex is unclear, it is generally accepted that the complex consists of four dimers: TCR$\alpha\beta$ or $\gamma\delta$, heterodimers of CD3$\varepsilon\gamma$ and CD3$\varepsilon\delta$, and a zeta family dimer. The majority of TCR:CD3 complexes (80–90%) contain a CD247 ζ homodimer. Heterodimers of ζ-η or ζ-FcRγ or homodimers of FcRγ have been observed in a small percentage of TCR complexes. An organizing principle has been proposed in which a single negatively charged amino acid in the TCR dimer interacts with two positively charged residues in the CD3$\varepsilon\gamma$, CD3$\varepsilon\delta$, and CD247 ζ dimers. In this model, the TCRα lysine interacts with the CD3$\varepsilon\delta$ dimer, the TCRβ lysine interacts with the CD3$\varepsilon\gamma$ dimer and the TCRα arginine interacts with the CD247 ζ dimer.

Role of the TCR in T Cell Biology and Signaling

T Cell Development

T cells that exit the thymus have been through a selection process based largely on TCR affinity. T cells with TCR that recognize self peptide–MHC too strongly are negatively selected and deleted. T cells that have too low an affinity to productively interact with self-MHC are ignored and ultimately die of neglect. However, T cells that display a moderate affinity for the self-MHC molecules are positively selected and allowed to exit into the periphery.

Cell Biology

It is known that each of the six protein chains is required for correct assembly and surface expression of the TCR:CD3 complex. Once expressed on the cell surface, the TCR:CD3 complex is constitutively internalized and recycled back to the cell surface via the endosomal network. Once ligated by peptide–MHC complexes, the TCR is down-modulated from the cell surface and diverted to lysosomes for degradation.

Assembly and Surface Expression of the TCR:CD3 Complex

Assembly of the complex is a highly ordered process that takes place in the ER. Most of the evidence for assembly order supports a model in which CD3$\varepsilon\gamma$ and CD3$\varepsilon\delta$ heterodimerize followed by sequential addition of TCRα and TCRβ chains and the ζ_2 homodimer (or heterodimer). Once the correct stoichiometry is achieved, the intact complex is transported from the ER. It has been shown that the ζ-chain can exit the ER independently of the rest of the receptor complex and remain in the Golgi complex. CD3γ and CD3ε have been reported to partly exist as heterodimers in association with calnexin while the TCRα and β-chains have been found to associate with calreticulin. It has been suggested that these molecules may serve as chaperones to prevent the transport of partial complexes. A number of residues are present within the chains that serve as ER retention signals or to target partial complexes to lysosomes for degradation, thereby ensuring that only complete TCR:CD3 complexes are expressed on the cell surface. The charged residues in the transmembrane regions increase their susceptibility to ER degradation. A number of additional residues have been described as possible ER retention or degradation signals, however a detailed mechanism of complex assembly, including specific interactions between individual chains, remains to be defined.

Internalization and Down-Modulation of the TCR:CD3 Complex

The TCR:CD3 complex is constitutively internalized and recycled back to the cell surface. Although the exact mechanism of this process has not yet been defined, it is likely to involve the interaction of the CD3/CD247 molecules with adaptor protein (AP) complexes that are associated with clathrin at the plasma membrane and intracellular recycling vesicles of the endosomal network. The dileucine-based motif in CD3γ has been

shown to be capable of binding to a member of the AP family of complexes, AP-2. In addition to dileucine based motifs, AP-2 can recognize YXXL-based sequences in a number of receptor systems. Given that the TCR:CD3 complex contains 20 such sequences, it is possible that one or more may be utilized for TCR internalization.

Upon ligation with peptide–MHC complexes, the TCR:CD3 complex is down-modulated from the cell surface and recycling is prevented. While the exact mechanism of this important process is unknown, it may involve two related E3 ubiquitin ligases, c-Cbl and Cbl-b, as T cells from mice lacking both proteins fail to down-modulate their TCR following ligation. While both internalization and down-modulation are hallmarks of TCR biology, their physiological importance and function remains to be determined.

Signaling Through the TCR

Initiation of T cell activation occurs when the TCR recognizes peptide–MHC complexes. TCR$\alpha\beta$ consists of the ligand-binding unit while the CD3 complex transduces signals into the T cell. Clustering of TCR:peptide–MHC complexes brings in the coreceptors CD8 or CD4 which bind to MHC class I and II molecules, respectively. Both coreceptors are associated with Src-related protein tyrosine kinase (PTK) p56^{lck}, while another PTK, p59^{fyn}, interacts with the CD3 complex. In resting T cells, these kinases are inactive due to the interaction of the C-terminal phosphotyrosine residues binding to the N-terminal SH2 domain. This intramolecular interaction prevents substrate access to the kinase (SH1) domain. T cell:APC interaction induces the removal of these inhibitory phosphates by the transmembrane phosphatase CD45. Cross phosphorylation of active site tyrosine residues further potentiates p56^{lck} and p59^{fyn} kinase activity and results in the phosphorylation of the ITAM tyrosine residues in the CD3/CD247 cytoplasmic tails. Phosphorylation of both ITAM tyrosine residues is required for docking of a specialized PTK, zeta associated protein-70 (ZAP-70), which has two tandem SH2 domains. ZAP-70 kinase activity is further potentiated through phosphorylation by p56^{lck} and p59^{fyn}.

Activated ZAP-70 initiates a number of signaling pathways. A key target of ZAP-70 is the raft-resident linker for activated T cells (LAT) which is heavily phosphorylated and recruits a wide variety of downstream signaling molecules. Phosphorylation of phospholipase Cγ_1 (PLCγ_1) leads to the production of potent second messengers, diacylglycerol (DAG) and inositol triphosphate (IP_3), whose actions lead to protein kinase C (PKC) activation and NFκB nuclear translocation as well as Ca^{2+} release and nuclear factor of activated T cells (NFAT) translocation. These events lead to the transcription of genes required for T cell proliferation and interleukin-2 (IL-2) production. Signaling through ZAP-70 also initiates activation of the Ras pathway and the MAPK signaling cascade which also results in up-regulation of genes required for proliferation. A wide array of additional signaling molecules and adaptor proteins have been shown to contribute to the signaling cascade initiated following TCR ligation and have been reviewed extensively elsewhere.

See Also the Following Articles

Immunoglobulin (Fc) Receptors • Mitogen-Activated Protein Kinase Family • Protein Kinase C Family • Src Family of Protein Tyrosine Kinases

Glossary

CD3 Complex of polypetides containing three dimers: $\varepsilon\gamma$ heterodimers, $\varepsilon\delta$ heterodimers and, most frequently, $\zeta\zeta$ homodimer (CD247). It is associated with the TCR through charged transmembrane residues and is involved in transducing signals into the T cell upon TCR:peptide–MHC interaction.

complementarity-determining region (CDR) Areas in the variable regions of antibody and TCR genes. In the TCR, the CDR regions contact the peptide and MHC molecule on antigen presenting cells.

immunoglobulin superfamily Group of proteins that contain immunoglobulin-fold domains of ~100 amino acids folded into two β-pleated sheets and stabilized by a central disulfide bond. Included in the family are MHC molecules, TCRs and a number of CD antigens.

major histocompatibility complex (MHC) A complex of polymorphic genes that encode histocompatibility antigens termed H2 in the mouse and HLA in humans. Two main classes of MHC antigens are found as surface glycoproteins on antigen presenting cells that bind and present peptides to T cells.

TCR Heterodimer of TCR$\alpha\beta$ or TCR$\gamma\delta$ expressed on the surface of T cells that is associated with the CD3 complex. The TCR binds to peptide–MHC molecules.

Further Reading

Allison, T. J., and Garboczi, D. N. (2001). Structure of $\gamma\delta$ T cell receptors and their recognition of non-peptide antigens. *Mol. Immunol.* **38**, 1051–1061.

Call, M. E., Pyrdol, J., Wiedmann, M., and Wucherpfennig, K. W. (2002). The organizing principle in the formation of the T cell receptor-CD3 complex. *Cell* **111**, 967–979.

Davis, M. M. (1990). T cell receptor gene diversity and selection. *Annu. Rev. Biochem.* **59**, 475–496.

Germain, R. N., and Stefanova, I. (1999). The dynamics of T cell receptor signaling: Complex orchestration and the key roles of tempo and cooperation. *Annu. Rev. Immunol.* **17**, 467–522.

Glusman, G., Rowen, L., Lee, I., Boysen, C., Roach, J. C., Smit, A. F. A., Wang, K., Koop, B. F., and Hood, L. (2001). Comparative genomic of the human and mouse T cell receptor loci. *Immunity* **15**, 337–349.

Goldsby, R. A., Kindt, T. J., and Osborne, B. A. (eds.) (2000). In *Kuby Immunology.* W. H. Freeman, New York.

Garcia, K. C., Degano, M., Stanfield, R. L., Brunmark, A., Jackson, M. R., Peterson, P. A., Teyton, L., and Wilson, I. A. (1996). An $\alpha\beta$ T cell receptor structure at 2.5Å and its orientation in the TCR-MHC complex. *Science* **274**, 209–219.

Garcia, K. C., Degano, M., Pease, L. R., Huang, M., Peterson, P. A., Teyton, L., and Wilson, I. A. (1998). Structural basis of plasticity in T cell receptor recognition of a self peptide-MHC antigen. *Science* **279**, 1166–1172.

Hennecke, J., and Wiley, D. C. (2001). T cell receptor-MHC interactions up close. *Cell* **104**, 1–4.

Kruisbeek, A. M., Haks, M. C., Carleton, M., Michie, A. M., Zuniga-Pflucker, J. C., and Wiest, D. L. (2000). Branching out to gain control: How the pre-TCR is linked to multiple functions. *Immunol. Today* **21**, 637–644.

Samelson, L. E., Harford, J. B., and Klausner, R. D. (1985). Identification of the components of the murine T cell antigen receptor complex. *Cell* **43**, 223–231.

Sun, Z. J., Kim, K. S., Wagner, G., and Reinherz, E. L. (2001). Mechanisms contributing to T cell receptor signaling and assembly revealed by the solution structure of an ectodomain fragment of the CD3γ heterodimer. *Cell* **105**, 913–923.

Valitutti, S., Muller, S., Cella, M., Padovan, E., and Lanzavecchia, A. (1995). Serial triggering of many T-cell receptors by a few peptide-MHC complexes. *Nature* **375**, 148–151.

Biography

Andrea Szymczak is a graduate student in the Department of Pathology at the University of Tennessee in Memphis, under the guidance of Dr. Dario Vignali at St. Jude Children's Research Hospital. She received her B.Sc. degree in biology at the University of Tennessee at Chattanooga. At present, her research interest is in T cell biology, specifically TCR:CD3 complex internalization and down-modulation.

Dario Vignali is an Associate Member in the Department of Immunology at St. Jude Children's Research Hospital. His research interests are the TCR:CD3 complex, regulation of T cell function and type 1 diabetes. He holds a Ph.D. from the London School of Hygiene and Tropical Medicine in England, and was a postdoctoral fellow at the German Cancer Research Center, Heidelberg, Germany, and Harvard University. His laboratory has made important contributions to the understanding of how the TCR recognizes MHC class II:peptide complexes and how T cells traffic TCR:CD3 complexes.

Tec/Btk Family Tyrosine Kinases

Shuling Guo and Owen N. Witte
Howard Hughes Medical Institute, University of California, Los Angeles, California, USA

Nonreceptor tyrosine kinases (NRTKs) are cytoplasmic enzymes that phosphorylate tyrosine residues when activated and thereby play critical roles in many signal transduction pathways in multicellular organisms. These kinases are grouped into families including Src, Syk, Abl, and Fak families, according to their protein sequence and structure similarities. In 1993, mutations in Bruton's tyrosine kinase (Btk) were demonstrated to cause human X-linked agammaglobulinemia (XLA) and murine X-linked immunodeficiency (xid). Since then, more proteins similar to Btk were discovered and Tec/Btk family tyrosine kinases became a new NRTK subfamily. This family is now the second largest nonreceptor tyrosine kinase family after the Src family.

Tec Family Kinase Members and Expression Pattern

The Tec family is composed of five mammalian members: Btk, Tec, Itk, Txk, and Bmx. These kinases are differentially expressed and most of them are found primarily in hematopoietic cells. This family is also expressed in other species, including *Drosophila melanogaster*, *skate*, and zebrafish. In addition, a Btk orthologue designated NRTK3 has been identified in the sea urchin *Anthocidaris crassispina*.

1. Btk is also known as Atk, Bpk, or Emb. Btk is expressed in all stages of B cell development except plasma cells. Btk is also expressed in myeloid and mast cells as well as early erythroid and megakaryocytic precursors, but Btk is not expressed in T cells. In tissues, Btk is found in bone marrow, spleen, lymph node, and fetal liver.

2. Tec (*t*yrosine kinase *e*xpressed in hepatocellular *c*arcinoma) is expressed in bone marrow, spleen, thymus, and liver. In cell lines, Tec is primarily found in T cells, myeloid cells, and hepatocarcinoma cells.

3. Itk (*i*nterleukin-2 inducible *T*-cell specific *k*inase, also known as Tsk or Emt) is primarily expressed in T cells, natural killer (NK) cells, and mast cells. The expression of Itk in T cells is developmentally regulated. Its expression begins at early fetal thymus and the expression level is higher in murine thymus than peripheral T cells.

4. Txk (*T* and *X* cell expressed *k*inase, also known as Rlk) is found in T cells, NK cells, as well as myeloid and mast cell lines.

5. Bmx (*b*one *m*arrow *k*inase gene on the X chromosome, also known as Etk) was originally identified from a bone marrow library and subsequently in prostate cancer cells. This kinase is the only member of the Tec family that is not primarily expressed in hematopoietic cells. Bmx is mainly found in endothelial, epithelial, fibroblast, neutrophil, and carcinoma cells.

Tec Family Kinase Domain Structure

The general domain structure for Tec family kinases is formed of the amino-terminal pleckstrin homology (PH) domain, a Tec homology (TH) domain, Src homology 3 (SH3) and Src homology 2 (SH2) domains, and the kinase domain which is adjacent to the SH2 domain through an SH2-kinase linker region. This differs from the Src family kinases that have a lipid modification motif in the amino terminus instead of a PH domain. Another difference between Src and Tec family kinases is that Src kinases contain a carboxyl-terminal tyrosine phosphorylation site as a negative regulation mechanism that the Tec kinases lack (Figure 1).

PH Domain

The core structure of PH domain is a 7-β-sheet structure that is mainly involved in protein-lipid interactions. For the PH domain of Btk, the high-affinity ligands are phosphatidylinositol 3,4,5-trisphosphate ($PI(3,4,5)P_3$) and inositol 1,3,4,5-tetrakisphosphate ($I(1,3,4,5)P_4$). $PI(3,4,5)P_3$ is the product of PI 3-kinase and acts as the second messenger to recruit cytoplasmic Btk to the plasma membrane. This recruitment is a critical step for the activation of Btk, so it is not surprising that many mutations are found in the PH domain in XLA patients.

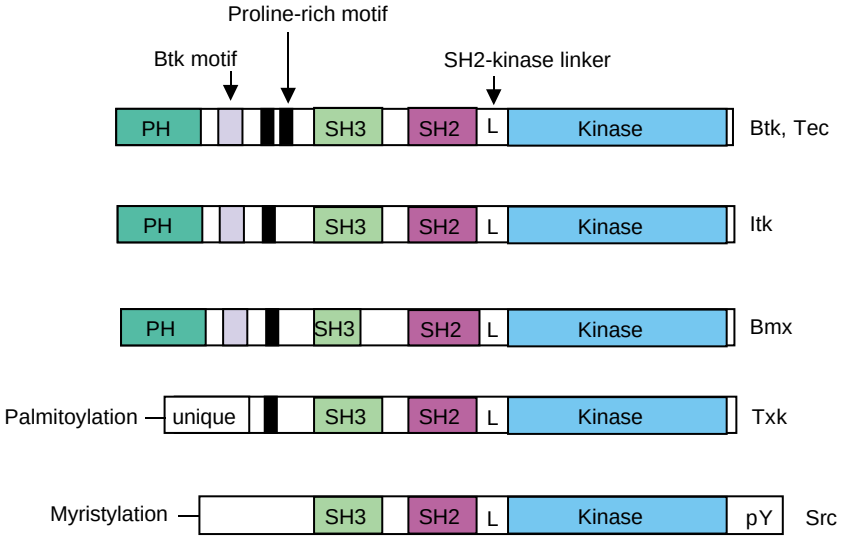

FIGURE 1 Domain structures of Tec family kinases. Src kinase is shown at the bottom for comparison.

The xid mutation (R28C) is also in the PH domain and the mutant PH domain has a greatly reduced ability to bind its ligand. On the other hand, a constitutively active mutant of Btk (E41K) showed improved membrane association capability. All Tec kinases contain the N-terminal PH domain except Txk. Txk has a unique region with a palmitoylated cysteine string, which serves a similar membrane-translocating function as the PH domain. As a result, Txk is not activated by PI 3-kinase.

TH Domain

The TH domains in Tec family kinases consist of a Btk motif (BM) and proline-rich region. The Btk motif is a 27-amino-acid stretch containing a zinc-binding fold formed by conserved cysteine and histidine residues homologous to Ras GTPase activating protein (GAP). This Btk motif is absent in Txk. Following Btk motif are two consecutive proline-rich motifs in Btk and Tec, while only one proline-rich motif is found in Itk, Txk, and Bmx. These proline-rich motifs are able to bind SH3 domain, so they may participate in intermolecular or intramolecular interactions.

SH3 and SH2 Domains

SH3 domains in Tec family kinases are adjacent to the proline-rich motif(s). The Itk SH3 domain has been crystallized with the N-terminal proline-rich motif and the intramolecular proline-rich motif binds to the SH3 domain, suggesting that this interaction may serve as a mechanism for the regulation of enzyme activity. In contrast, Bmx has a truncated SH3 domain. SH2 domain binds phosphotyrosine, providing a docking site for regulatory proteins or effector proteins. In the Itk SH2 domain, there is a proline residue that is not conserved in other Tec family kinases. This proline residue may undergo *cis–trans* conformational switch, possibly catalyzed by a peptidyl-prolyl isomerase cyclophilin A. This conformational change controls the orientation of the protein-binding surface of the SH2 domain and may affect the catalytic activity of Itk.

Kinase Domain

The kinase domains of Tec kinases are highly conserved. The Btk kinase domain contains a small lobe and a large lobe, with the active site in between. This structure is very similar to Src family kinases and other tyrosine kinases. However, the 30-amino acid linker region between SH2 domain and the kinase domain is less conserved in the Tec family kinases and very different between the Tec and Src family kinases. This linker region has been shown to regulate the intracellular interaction of Src family kinases, yet the function of this linker region in Tec family kinases is not yet known.

Although these kinases are primarily cytoplasmic kinases, there has been evidence that Btk, Itk, and Txk can also be shuttled into the nucleus. Itk is translocated into the nucleus through the interaction with a nuclear import chaperone karyopherin α. A shorter form of Txk originated from internal initiation of translation gets into the nucleus via nuclear localization sequence (NLS)-dependent mechanism, while Btk is found in the nucleus through an NLS-independent way.

Tec Family Kinase Functions

To date, Btk is the only Tec family kinase that is involved in human disease when mutated. However, the physiological importance of all these kinases has been investigated through the murine knockout models.

Btk is essential for B-cell development and function, as demonstrated by XLA. XLA patients lack mature B cells in the periphery and do not have immunoglobulins as a result. However, inactivating Btk in the mouse causes only a mild defect in B cell development and function. This mimics the phenotype of xid mice, caused by a spontaneous mutation (R28C) in the Btk PH domain. In these mouse models, mature B-cell number is reduced and these B cells have a defect in response to B-cell receptor (BCR) stimulation. A minor B-cell population, B-1 cells, is absent in these mice. Moreover, the serum immunoglobulins IgG3 and IgM levels are greatly reduced in these mice and they are not able to respond to T-independent type-II antigens. Interestingly, even though Tec-/- mice have no major phenotypic alterations of the immune system, Btk-/-Tec-/- mice showed a severe defect in B-cell development, similar to human XLA. This suggests that Tec may compensate partially for the lack of Btk in murine B-cell development.

In T cells, three Tec family members coexist: Itk, Txk, and Tec. Inactivating Itk results in slightly decreased number of mature thymocytes, especially $CD4^+$ cells, while inactivating Txk does not affect either T-cell development or activation. Double mutants, on the other hand, showed improved mature T-cell number, while still maintaining a decreased CD4/CD8 ratio, compared to Itk-/- mice. However, T cells in the double knockout mice have a severe defect in T-cell receptor (TCR) induced proliferation and cytokine production.

When the Bmx gene was replaced by the LacZ reporter gene, the homozygous mice lacking Bmx activity showed no obvious phenotype. But the expression of the reporter gene is strong in endothelial cells of large arteries and in the endocardium from embryogenesis to adult mice. Moreover, Bmx is activated through endothelial receptor tyrosine kinases Tie-2, vascular endothelial growth factor receptor 1 (VEGFR-1) and tumor necrosis factor (TNF) receptor. These data suggest a redundant role of Bmx in endothelial signal transduction.

Tec Family Kinases in Signal Transduction

Tec family kinases not only play a critical part in T-cell receptor or B-cell receptor signaling, but are also involved in cytokine receptor signaling as well as mast cell Fcepisilon receptor I (FcεRI) signaling. Here we will use Btk as an example to discuss the signaling functions of these kinases.

Each domain of Btk is essential for the function of the kinase, as suggested by mutation analysis in XLA patients. To date, over 400 Btk mutations (missense mutation, frameshift, truncation) from 556 XLA families have been reported and these mutations cover all the domains. However, missense mutations are found in each domain except the SH3 domain, suggesting that the SH3 domain may tolerate such alterations. Each domain has been shown to bind regulatory and/or effector proteins. In addition to $PI(3,4,5)P_3$, Btk PH domain can also bind protein kinase Cβ (PKCβ), Fas, F-actin and a transcription factor TFII-I. TH domain binds G protein subunits and Src family kinases as Lyn or Hck. SH3 domain interacts with proteins as Cbl, WASP, and Vav, while SH2 domain binds B-cell linker protein (BLNK) through interaction with phosphotyrosine. The catalytic domain has also been shown to bind G protein $\beta\gamma$-subunit, and the kinase activity is activated by this interaction. Although some of the interactions have been confirmed in cellular context, the physiological importance of many still needs to be carefully evaluated.

B-cell development and activation is a tightly regulated process and Btk plays an important role. It is involved in a number of signaling pathways that are activated when B cells are stimulated through the BCR, accessory molecules such as CD19 and CD38, or cytokine receptors such as IL-5R and IL-10R. In normal B cells, cross-linking of the BCR activates PI 3-kinase leading to the translocation of cytoplasmic Btk to the lipid raft on the plasma membrane. Src family tyrosine kinase Lyn, which is also activated upon BCR stimulation, phosphorylates Y551 in the Btk kinase domain and activates Btk kinase activity. These serial activations lead to the assembly of a B-cell signalosome and proteins like Btk, Lyn, PI 3-kinase, BLNK, PLCγ2, BCAP (B-cell adapter for PI 3-kinase), and PKC are among the players in the B-cell signalosome. Once activated, Btk transduces signals to a number of effectors, including phospholipase C gamma (PLCγ), calcium response, transcription factors such as TFII-I, genes involved in apoptosis (bcl-2 and bcl-xl), and cell cycle control (cyclins). Interestingly, the Btk-deficient and xid phenotype is phenocopied by the deficiency of PI 3-kinase regulatory subunit p85 or the catalytic subunit p110δ, BCAP, PKCβ, BLNK, or PLCγ2. These data indicate that these proteins are involved in the same signaling pathway and likely in the same B-cell signalosome (Figure 2).

There are several mechanisms to down-regulate Btk. Autophosphorylation at Y223 in the SH3 domain has been implicated to negatively regulate Btk function, and phosphorylation of S180 in the TH domain by PKCβ also serves to down-regulate the membrane association of Btk. Additionally, a recent study identified an inhibitor for Btk (IBtk). IBtk directly binds the PH domain of

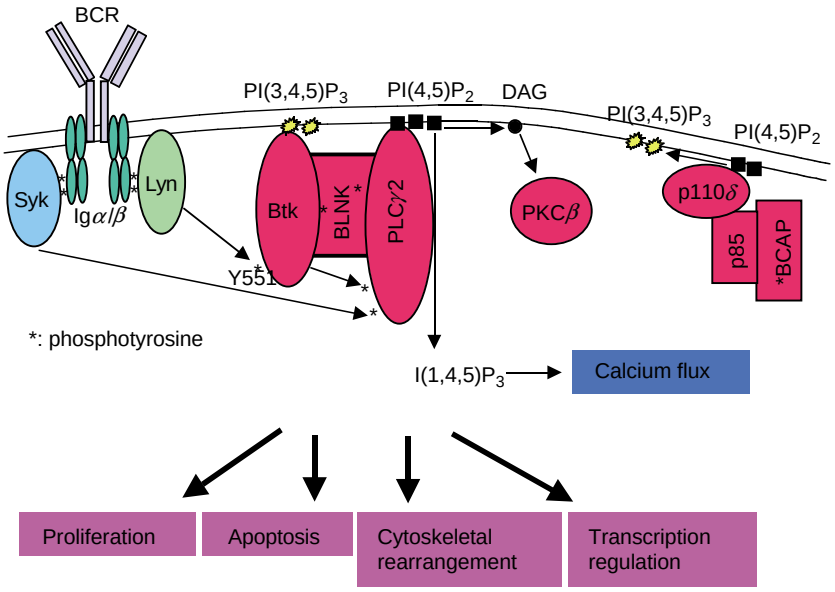

FIGURE 2 Signal transduction pathway after B cell receptor stimulation. Btk is activated through translocation to the plasma membrane through binding of $PI(3,4,5)P_3$ and phosphorylation at Y551 by Lyn. The B cell signalosome is assembled and downstream effectors will be sequentially activated. Proteins that have a xid-like phenotype when knocked out are shown in red. Adapted from Fruman, D. A., Satterthwaite, A. B., and Witte, O. N. (2000), Xid-like phenotypes: a B cell signalosome takes shape. *Immunity* **13**, 1–3.

Btk and down-regulates the kinase activity, calcium response and NF-κB-induced transcription.

In addition, Btk is involved in myeloid lineage cell signaling, including macrophages and mast cells. Although mast-cell development is normal in xid mice, Btk is phosphorylated and translocated to the plasma membrane after cross-linking of FcεRI in mast cells.

Future Directions

Extensive studies have been carried out on Tec family kinases since the 1990s, yet the detailed function of these kinases is far from resolved. In the coming years, further efforts will be put on the participation of these kinases in signalosome formation, the components of signalosome, and the regulation of the signal transduction. In addition, the complete structure of the proteins in this family will help the understanding of intramolecular domain–domain interaction as well as protein–protein interaction, and shed light on the regulation of kinase activity and function.

See Also the Following Articles

c-fes Proto-Oncogene • Epidermal Growth Factor Receptor Family • Phosphatidylinositol Bisphosphate and Trisphosphate • Phosphatidylinositol-3-Phosphate

Glossary

Bruton's tyrosine kinase (Btk) A member of the Tec/Btk tyrosine kinase family. Mutations of Btk cause X-linked agammaglobulinemia (XLA) in human and x-linked immunodeficiency (xid) in mouse. This protein was named after Dr. Ogden Bruton, who described XLA in 1950s.

signalosome Multiprotein signaling complex formed in the cell that is regulated both spatially and temporally.

Tec/Btk tyrosine kinase family A family of the non-receptor tyrosine kinases including Btk, Tec, Itk, Txk, and Bmx, which play important signaling roles primarily in hematopoietic cells.

X-linked agammaglobulinemia (XLA) A human genetic disease caused by the mutations in a proteins tyrosine kinase Btk. Patients lack mature B cells in the periphery and suffer from recurrent infections.

X-linked immunodeficiency (xid) An immunodeficiency found in CBA/N mice that is caused by a spontaneous point mutation in Btk (R28C). Xid mice have reduced mature B cells and defective B-cell response.

Further Reading

Fruman, D. A., Satterthwaite, A. B., and Witte, O. N. (2000). Xid-like phenotypes: a B cell signalosome takes shape. *Immunity* **13**, 1–3.

Lewis, C. M., Broussard, C., Czar, M. J., and Schwartzberg, P. L. (2001). Tec kinases: Modulators of lymphocyte signaling and development. *Curr. Opin. Immunol.* **13**, 317–325.

Miller, A. T., and Berg, L. J. (2002). New insights into the regulation and functions of Tec family tyrosine kinases in the immune system. *Curr. Opin. Immunol.* **14**, 331–340.

Pillai, S., and Moran, S. T. (2002). Tec kinase pathways in lymphocyte development and transformation. *Biochim. Biophys. Acta* **1602**, 162–167.

Qiu, Y., and Kung, H. J. (2000). Signaling network of the Btk family kinases. *Oncogene* **19**, 5651–5661.

Satterthwaite, A. B., and Witte, O. N. (2000). The role of Bruton's tyrosine kinase in B-cell development and function: A genetic perspective. *Immunol. Rev.* **175**, 120–127.

Smith, C. I., Islam, T. C., Mattsson, P. T., Mohamed, A. J., Nore, B. F., and Vihinen, M. (2001). The Tec family of cytoplasmic tyrosine kinases: Mammalian Btk, Bmx, Itk, Tec, Txk, and homologs in other species. *Bioessays* **23**, 436–446.

Vihinen, M., Kwan, S. P., Lester, T., Ochs, H. D., Resnick, I., Valiaho, J., Conley, M. E., and Smith, C. I. (1999). Mutations of the human BTK gene coding for bruton tyrosine kinase in X-linked agammaglobulinemia. *Hum. Mutat.* **13**, 280–285.

Biography

Owen N. Witte is an Investigator of Howard Hughes Medical Institute and a Professor at the University of California Los Angeles. His primary research interest is signal transduction in hematopoietic cells and related diseases. Dr. Witte is a pioneer in the study of tyrosine kinases. His group and others were the first to report Btk mutations cause Xid and XLA (Rawlings DJ *et al.*, Science 1993; Tsukada S *et al.*, Cell, 1993; Thomas JD *et al.*, Science 1993; Vetrie D *et al.*, Nature 1993).

Shuling Guo received her Ph.D. from Duke University and is currently a postdoctoral fellow in Dr. Witte's laboratory.

Telomeres: Maintenance and Replication

Alessandro Bianchi and David Shore
University of Geneva, Geneva, Switzerland

All linear eukaryotic chromosomes terminate in a specialized nucleoprotein structure, the telomere. Telomeres perform at least two essential functions: they provide a protective "cap" on chromosome ends that prevents their degradation or deleterious fusion, and they provide a special mechanism for replicating the DNA at chromosome ends. In most organisms, telomeres are composed of a tandem array of simple DNA repeats to which a large set of protein factors is bound. The telomeric DNA repeats are generated by a specialized reverse transcriptase, called telomerase that uses an endogenous RNA template. Defects in the maintenance of telomeric DNA, for example through inactivation of the telomerase enzyme, lead to the progressive loss of telomeric repeats and their bound factors, which eventually causes a catastrophic "uncapping" of telomeres that results in fusion of chromosome ends. The telomere complex is thus essential to ensure genome stability.

The Telomeric Complex, a Specialized Nucleoprotein Structure at Chromosome Ends

Pioneering studies in the fruit fly and in maize, carried out respectively by H. Muller and B. McClintock in the early 20th century, first identified the telomere as a special genetic entity that protects chromosome ends from degradation and fusion, a property absent in DNA ends that result from random chromosomal breakage. A wealth of subsequent genetic and biochemical studies have led to the understanding that telomeres are specialized nucleoprotein complexes composed of a large number of protein factors assembled onto telomeric DNA.

Telomeric DNA

In most eukaryotes, the terminal DNA sequences at each chromosome are composed of arrays of variable length of simple tandem repeats, as first recognized by Blackburn and Gall in the ciliate *Tetrahymena termophila*. These telomeric repeats are typically 5–8 nucleotides long, but can be up to 25 bp (Figure 1) and usually have a higher G content in the DNA strand that runs with a 5′ to 3′ polarity towards the end of the chromosome. In all species, the majority of the telomeric repeats appear to be in double-stranded form and their total length varies from a few nucleotides in some species of ciliates (28 bp of duplex telomeric repeats in *Euplotes*, for example) to tens of thousands of bp in some strains of laboratory mice. In both budding and fission yeasts, telomeres are ~300 bp in length, whereas in human cells telomeres are generally 6–12 kbp long. With the exception of several ciliate species in which the length of telomeric DNA is fixed, in most species the length of each telomere is variable from cell to cell, individual to individual, and during the life of the organism. In many species, it has been shown that telomeres terminate in a single-stranded overhang of the G-rich strand. This overhang can range from only a few nucleotides long (in some ciliates) to about 100–200 bases in mammals, and is believed to represent a general feature of telomeres. G-rich telomeric overhangs *in vitro* can adopt a variety of intra- and intermolecular paired structures involving most commonly four strands interacting through Hoogsteen-type G–G base-pairing (G-quartets), but the *in vivo* occurrence and significance of such structures remains unclear. In mammals, some ciliates, and Trypanosomes, telomeric DNA appears to fold back in a structure, the t-loop, where the single-stranded overhang is tucked into the duplex portion of the telomeric tract, by base pairing with the C-rich strand and thus displacing a short portion of the G-strand.

In most organisms, the short telomeric repeats described above are preceded by less conserved DNA elements, called subtelomeric repeats or telomere-associated sequences (TAS). These elements are of variable lengths but are generally at least a few hundred base pairs long and have been described in most studied organisms. In a particular species several classes of these repeats can be present, and elements of each class are associated with a particular chromosome with great variation in number and organization. The assembly of these subtelomeric repeats is highly dynamic and subject

Telomeric repeats	
Vertebrates	
Homo, Mus, Rattus, Gallus	TTAGGG
Arthropodes	
Insects	
Bombix mori	TTAGG
Nematodes	
Ascaris	TTAGGC
Caenorhabditis elegans	TTAGGC
Plants	
Arabidopsis thaliana	TTTAGGG
Green algae	
Chlamydomonas	TTTTAGGG
Fungi	
Ascomycota	
Hemiascomycetes	
Saccharomyces cerevisiae	$T(G)_{1–3}$
Kluyveromyces lactis	ACGGATTTGATTAGGTATGTGGTGT
Archeascomycetes	
Schizosaccharomyces pombe	$TTACAGG(G)_{0–4}$
Euascomycetes	
Neurospora	TTAGGG
Protists	
Alveolata	
Plasmodium	TT[T/C]AGGG
Ciliates	
Tetrahymena	TTGGGG
Oxytricha	TTTTGGGG
Euplotes	TTTTGGGG
Diplomonadida	
Giardia	TAGGG
Euglenozoa	
Trypanosoma	TTAGGG

FIGURE 1 Representative list of telomeric repeats in several eukaryotic organisms, including some of the most extensively studied ones with regard to telomere biology.

to active recombination, resulting in a large variation of subtelomeric regions between strains of yeast or between human individuals. TAS do not appear to carry out an essential telomeric function, as both human and yeast chromosomes that are devoid of them are replicated and segregated properly both through mitosis and meiosis.

Telomerase

DNA polymerases replicate DNA uniquely in a 5′ to 3′ direction. As a consequence, as the DNA replication "bubble" moves along the DNA, the two strands are replicated differently: one strand (the "leading" strand) is replicated in the same direction as the movement of the polymerase, while the other strand (the "lagging" strand) is replicated backwards in small installments, each one initiating from an RNA primer laid down by the primase enzyme (Figure 2A). Due to the requirement for an initiating RNA primer, which is later removed, replication of linear DNA molecules by the conventional DNA replication machinery would result in a terminal gap in the lagging strand end at the telomere (Figure 2A). The presence of overhangs at telomeres could in principle mask this problem at the lagging strand, but a terminal gap would then occur at the strand replicated by leading strand synthesis after processing of the end to generate the single-stranded overhang (Figure 2B). Thus, in the absence of a specialized mechanism to replicate the ends, loss of genetic material is expected to occur at each cell division. The most general solution to this problem in eukaryotes is represented by the specialized replication of telomeric repeats by the telomerase enzyme.

Telomerase was first identified by Greider and Blackburn in the ciliate *Tetrahymena termophila* based on its ability to add telomeric repeats in a terminal transferase-like fashion to a telomeric DNA primer in an *in vitro* reaction. The enzyme is in fact a ribonucleoprotein, composed of a protein and an RNA moiety, both of which are required for catalytic function (Figure 2C). Isolation of the protein component from the ciliate *Euplotes* by Lingner and Cech in 1997 has revealed that telomerase shares extensive homology with reverse transcriptases. Thus telomerase is a specialized reverse transcriptase that utilizes an endogenous RNA template for the synthesis of telomeric repeats. The enzyme appears to be capable of synthesizing several repeats on

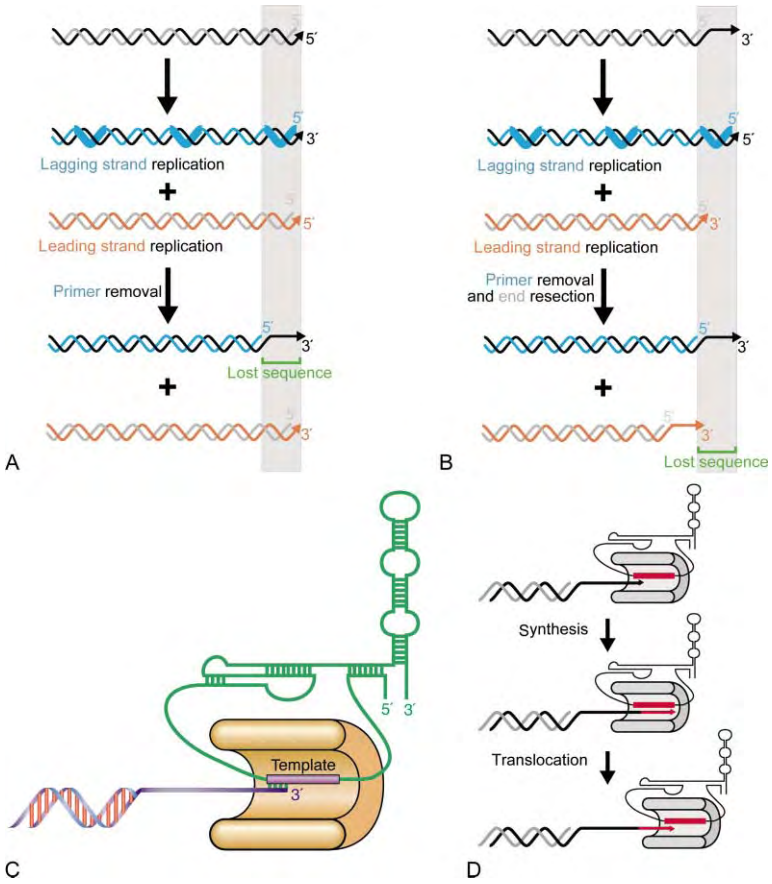

FIGURE 2 (A) Schematic view of the end replication problem of a linear DNA molecule. The RNA primers laid down by the primase enzyme for the synthesis of the so-called 'lagging' strand are indicated by thicker blue lines. After removal of the primers, replication of a double-stranded DNA molecule would result in a single-stranded terminal gap in the DNA strand replicated by lagging strand synthesis. (B) Schematic view of the end replication problem at a telomere terminating in a single-stranded overhang. Exonucleolytic resection of the ends is hypothesized to generate the overhangs after replication. In this scenario, a terminal gap would be created in the strand replicated by leading strand synthesis. (C) Representation of the structure of the core telomerase enzyme. The protein, based on its homology to known viral reverse transcriptases, is expected to be folded in a structure with a central cleft (palm) bearing the active site and flanked by two domains (thumb and fingers). The template region of the RNA is placed in this cleft, and the secondary structure of the RNA represented here is derived from ciliated Protozoa species and appears to be largely conserved in higher Eukaryotes. (D) Representation of the processive mechanism of action of telomerase, where a round of synthesis of telomeric repeats is followed by translocation of the enzyme on the DNA and a subsequent new round of synthesis.

a particular substrate through repeated steps of elongation and translocation (Figure 2D) and, like reverse transcriptases, appears to be a dimer.

Telomere Proteins

Telomeric repeats serve as binding sites for telomeric DNA-binding proteins, which act as a scaffold for the recruitment of additional protein factors to telomeres, including telomerase (Figure 3). The analysis of telomeric proteins in a wide range of organisms has revealed important similarities, though significant differences have also emerged.

The major double-stranded DNA-binding activity in budding yeast is Rap1, a protein also involved in transcriptional regulation at many other nontelomeric chromosomal sites. *S. cerevisiae* Rap1 binds directly to yeast telomeric repeats through two Myb-like DNA-binding domains. Rap1 is instrumental in recruiting to yeast telomeres a set of proteins involved in the regulation of telomere length (the Rap1 interacting factors 1 and 2, Rif1 and Rif2) and in the assembly of a complex (which includes the proteins Sir2, 3, and 4) that results in the transcriptional repression of genes positioned near telomeres (telomere position effect, or TPE). In contrast, mammalian and fission yeast Rap1 appears to be recruited to telomeres indirectly, through the binding to a different class of double-stranded DNA-binding factors, TRF1 and TRF2 in vertebrates and Taz1 in fission yeast. These proteins bind as dimers and contain a single Myb repeat that is essential for DNA binding. They share among themselves a large domain (TRFH, for TRF homology) that is responsible for homodimerization. Rap1 is recruited to mammalian and fission yeast telomeres through binding with TRF2 and Taz1, respectively. Human TRP2 also recruits the MRX

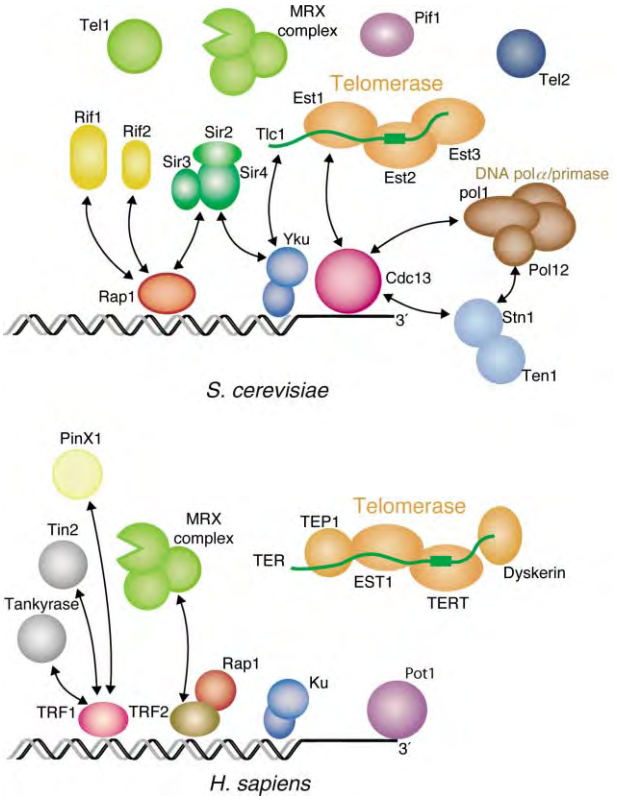

FIGURE 3 Representation of some of the characterized components of the budding yeast and human telomeric complexes. All proteins depicted have either been shown to affect telomere behavior and/or to interact with other telomere components.

complex to telomeres. TRF1 in mammals also is responsible for the recruitment of protein factors, including the telomere length regulators Tin2 and tankyrase, the telomerase inhibitor PinX1, and the single-stranded DNA-binding protein Pot1.

In addition to double-stranded DNA-binding activities, single-stranded DNA-binding factors also appear to be an essential and general feature of telomeres. Overhang-binding proteins were initially characterized in ciliates, where they form tenacious salt-resistant complexes with the single-stranded DNA termini. In budding yeast, the Cdc13 protein is bound to the single stranded overhangs created in S-phase in this organism and it carries out essential functions in telomere replication, through interaction with the telomerase and DNA replication complex, and in telomere protection, through interactions with the Stn1 and Ten1 proteins. In fission yeast and mammals, Pot1, an orthologue of the ciliate end factors, is involved in telomere protection in fission yeast and in telomere length regulation in mammals. Although Cdc13 does not share sequence homology with the ciliate, fission yeast and mammalian end factors, all these proteins bind DNA through an oligonucleotide/oligosaccharide-binding (OB) domain.

An additional factor, present at telomeres from yeast to humans, is the DNA repair protein Ku, which might bind to telomeres through its nonsequence-specific DNA end-binding activity. However protein–protein interactions between Ku and Sir4, and between Ku and TRF2 have been described in yeast and humans, respectively. Finally, the highly conserved telomere length regulator Tel2, has been shown (for the yeast protein) to be able to bind both single- and double-stranded telomeric repeats *in vitro*.

Telomere Replication

Telomeres are normally maintained through the action of the telomerase enzyme. Although telomerase activity in an *in vitro* assay requires only the reverse transcriptase-like protein motif and the RNA component, it is now clear that the action of the enzyme at telomeres is subject to complex regulation in *cis* at each individual telomere.

Positive Regulation of the Telomerase Enzyme

In budding yeast, a set of genes is required for telomerase activity *in vivo* in addition to the catalytic core components Est2 and Tlc1. These include Est1, which appears to bridge an interaction between telomerase and Cdc13 required to either recruit or activate the enzyme at the telomere, and telomerase-associated Est3, whose mode of action is unclear. The combined action of the DNA damage checkpoint kinases Tel1 and Mec1 is also necessary for telomerase activity in budding yeast, possibly by promoting a structural transition in the telomere complex from a "closed" to an "open" state that is accessible to telomerase. A similar requirement exists in fission yeast for the Tel1 and Mec1 homologues Tel1 and Rad3. In mammalian cells dyskerin binds the telomerase RNA and appears to affect *in vivo* telomerase activity by influencing accumulation of the RNA. Significantly, budding yeast telomerase action is strictly limited to the S-phase of the cell cycle and requires active DNA replication.

A Negative Regulatory Loop Stabilizes Telomere Length

In cells expressing telomerase, telomere length is maintained around a constant average value that is species specific, as mentioned above. Evidence from a variety of organisms, including the budding and fission yeasts, and human cells, has led to the proposal that telomere length is controlled by a protein-counting mechanism. In this

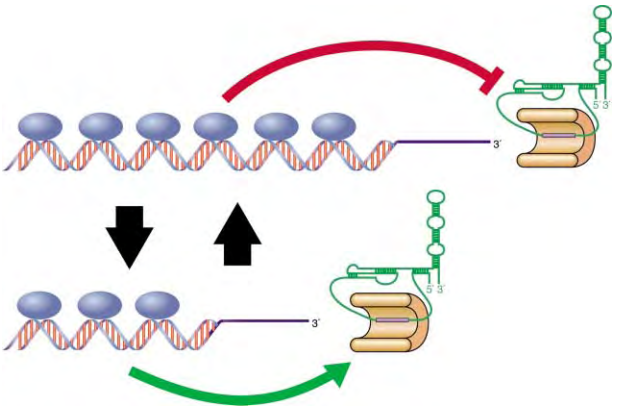

FIGURE 4 Depiction of the protein-counting mechanism for telomere length regulation. In this model, longer telomeres have higher numbers of inhibitory factors bound, resulting in repression of telomerase activity in *cis*. Diminished action by telomerase results in telomere shortening, loss of the bound inhibitor, and telomerase activation. In this manner telomeres are maintained in a state of dynamic equilibrium. The organism in which our understanding of the telomeric complex is the most complete, both with regard to the identification of protein components and to their function, is the budding yeast *Saccharomyces cerevisiae* (Figure 1).

scenario, the number of double-stranded DNA-binding factors that are associated with the telomere at any given time is somehow sensed by the telomere length regulation machinery. An increase in the number of these negative regulators results in the inhibition of telomerase activity in *cis* at the telomere (Figure 4). The inhibitory function of the DNA-binding factors (Rap1 in budding yeast, Taz1 in fission yeast, and TRF1 and 2 in mammals) is apparently mediated by a set of interacting factors (Rif1 and 2 in budding yeast, Pot1 in humans). The precise mechanism of the proposed *cis* inhibition of telomerase is unknown, but might, at least in some organisms, involve formation of the t-loop structure described previously.

Telomerase-Independent Maintenance of Telomeres

In the absence of telomerase, alternative pathways for the maintenance of telomeric repeats exists that are based on homologous recombination. In budding yeast, telomere-associated sequences can contribute to this recombinational process. In mammals, several tumor cell lines have been shown to maintain their telomeres without detectable telomerase activity through a mechanism named ALT, for alternative lengthening of telomeres. Finally, the fruit fly *Drosophila melanogaster* dispenses altogether with short telomeric repeats and forms telomeres through the repeated insertion of telomere-specific transposable elements (HeT-A and TART) onto the ends of its chromosomes.

Telomerase Repression in Somatic Cells: Implications for Replicative Senescence and Maintenance of Genome Integrity

Mice engineered to lack the gene encoding telomerase RNA (mTRT) exhibit a gradual (~sixth generation) loss of fertility, defects in cell proliferation, and an increase in the frequency of end-to-end chromosome fusions. These phenotypes result from telomere repeat erosion and consequent loss of telomere function. Since active telomerase enzyme is primarily detected in mouse germline cells, these data indicate that telomerase-dependent telomere length "resetting" in the germline is essential for long-term survival in the mouse, and by inference in all mammals. In humans, the gene encoding the catalytic subunit of telomerase is also repressed in most somatic cells, causing telomeres to undergo progressive shortening with each cell division. This process leads to cellular senescence in culture and can be reversed, at least in some primary cell lines, by the ectopic expression of an active telomerase gene in the senescing cells. These observations in cultured primary cells have led some researchers to propose that telomerase repression in humans, and consequent telomere erosion, acts as a kind of "mitotic clock" that determines aging of the whole organism.

An attractive alternative view is that the telomere "mitotic clock" in humans might instead represent a critical barrier against malignant transformation. Recent experiments suggest that either normal telomere erosion, or uncapping caused by mutational alteration of key telomere proteins, will induce a DNA damage checkpoint and apoptosis (programmed cell death). This mechanism may place a limit on continued cell proliferation, which is a prerequisite for tumor formation. However, telomere uncapping also leads to telomere-telomere fusions and rampant genomic instability, which is thought to be a driving force in oncogenesis. Telomere dysfunction might therefore represent an important step in the early stages of tumorigenesis, particularly in cells with compromised checkpoint (DNA damage surveillance) function. The proper regulation of telomerase and telomere capping thus appear to be remarkably critical cellular functions.

See Also the Following Articles

Chromosome Organization and Structure, Overview • DNA Replication: Eukaryotic Origins and the Origin Recognition Complex • Homologous Recombination in Meiosis • Meiosis • Mitosis

Glossary

telomerase A nuclear-encoded ribonucleoprotein complex homologous to viral reverse transcriptases that adds single-stranded telomeric repeats to the 3′ ends of duplex DNA using its own RNA template; responsible for telomere maintenance in most eukaryotic organisms.

telomere The DNA–protein complex at the extreme ends of linear eukaryotic chromosomes that orchestrates telomere replication and capping.

telomere associated sequence (TAS) The highly variable, often repeated DNA sequences found immediately internal to the terminal simple telomere repeat sequences.

telomere capping Refers to the ability of the telomere DNA–protein complex to prevent chromosome end degradation or fusion (DNA joining) reactions.

telomeric repeats Simple, short (usually 5–8, but as long as 25 nucleotides) DNA repeat sequences (T_2AG_3 in vertebrates and minor variants in many other eukaryotes) that constitute the DNA component of telomeres. Synthesized by the telomerase enzyme, with the TG-rich sequence extending towards the 3′ DNA end.

Further Reading

Blackburn, E. H., and Greider, C. W. (eds.) (1995). *Telomeres*. Vol 29, Cold Spring Harbor Monographs, Cold Spring Harbor Press, Plainview, NY.

Chakhparonian, M., and Wellinger, R. J. (2003). Telomere maintenance and DNA replication: How closely are these two connected? *Trends Genet.* **19**(8), 439–446.

de Lange, T. (2002). Protection of mammalian telomeres. *Oncogene* **21**(4), 532–540.

Evans, S. K., and Lundblad, V. (2000). Positive and negative regulation of telomerase access to the telomere. *J. Cell Sci.* **113**(Pt), 3357–3364.

Kass-Eisler, A., and Greider, C. W. (2000). Recombination in telomere-length maintenance. *Trends Biochem. Sci.* **25**(4), 200–204.

Lingner, J., and Cech, T. R. (1998). Telomerase and chromosome end maintenance. *Curr. Opin. Genet. Dev.* **8**(2), 226–232.

Lundblad, V. (2002). Telomere maintenance without telomerase. *Oncogene* **21**(4), 522–531.

Maser, R. S., and DePinho, R. A. (2002). Connecting chromosomes, crisis, and cancer. *Science* **297**(5581), 565–569.

McEachern, M. J., Krauskopf, A., and Blackburn, E. H. (2000). Telomeres and their control. *Annu. Rev. Genet.* **34**, 331–358.

Wright, W. E., and Shay, J. W. (2001). Cellular senescence as a tumor-protection mechanism: the essential role of counting. *Curr. Opin. Genet. Dev.* **11**(1), 98–103.

Zakian, V. A. (1996). Structure, function, and replication of Saccharomyces cerevisiae telomeres. *Annu. Rev. Genet.* **30**, 141–172.

Biography

David Shore is a Professor in the Department of Molecular Biology at the University of Geneva (Switzerland) and member of the NCCR program "Frontiers in Genetics." His principal research interests are in gene regulation, chromatin structure, and telomere biology. He holds a Ph.D. from the Department of Biochemistry at Stanford University Medical School and did postdoctoral work at the MRC Laboratory of Molecular Biology in Cambridge (UK).

Alessandro Bianchi received his Ph.D. at the Rockefeller University (New York) and is currently a postdoctoral fellow at the University of Geneva.

Thyroid-Stimulating Hormone/Luteinizing Hormone/Follicle-Stimulating Hormone Receptors

Deborah L. Segaloff, Dario Mizrachi and Mario Ascoli
The University of Iowa, Iowa City, Iowa, USA

The thyroid-stimulating hormone receptor (TSHR), luteinizing hormone receptor (LHR), and follicle-stimulating hormone receptor (FSHR) are collectively referred to as the glycoprotein hormone receptors because they bind the structurally similar glycoprotein hormones. The glycoprotein hormones consist of the pituitary hormones thyroid-stimulating hormone (thyrotropin, TSH), luteinizing hormone (lutropin, LH), and follicle-stimulating hormone (follitropin, FSH) as well as the placental hormone chorionic gonadotropin (choriogonadotropin, CG). They are each composed of two dissimilar subunits (α and β) that are noncovalently associated. Within a given species the α-subunit is identical, and the β-subunits are distinct but homologous. Due to the nearly identical nature of LH and CG, the LHR binds either LH or CG. However, the FSHR binds only FSH and the TSHR binds only TSH. Because the LHR and FSHR are localized primarily to the gonads, these two receptors are also referred to as the gonadotropin receptors. The glycoprotein hormone receptors are members of the superfamily of G protein-coupled receptors (GPCRs) and, despite their different physiological roles, share a similar structural organization and mechanism of action. In addition, the glycoprotein hormone receptors are also members of a subfamily of GPCRs known as the leucine-rich repeat-containing GPCRs (LGR). This subfamily of GPCRs is characterized by the presence of a large extracellular domain composed of several leucine-rich repeats.

Expression and Physiological Roles of the Glycoprotein Hormone Receptors

The Thyroid-Stimulating Hormone Receptor

TSHR is expressed primarily in the follicular cells of the thyroid. In more recent years, it has also been detected in lymphocytes, thymus, pituitary, testis, kidney, brain, adipose tissue and fibroblasts, heart, and bone.

In response to thyroid-stimulating hormone (TSH), the TSH receptor (TSHR) stimulates the synthesis and secretion of thyroid hormone by the follicular cells of the thyroid. Autoantibodies to the TSHR that are stimulatory are present in individuals with Grave's disease and stimulate the TSHR causing excessive and unregulated secretion of thyroid hormone. Conversely, inhibitory autoantibodies to the TSHR are found in individuals with Hashimoto's thyroiditis. These antibodies bind to the TSHR and inhibit the binding of TSH, thus blocking the synthesis and secretion of thyroid hormones.

The TSHR present in the adipose and connective tissue of the orbit of the eye is thought to play a role in the development of exopthalmos found in individuals with Grave's disease. The physiological roles of the TSHR in other nonthyroid tissues is not yet known.

The Luteinizing Hormone Receptor

The luteinizing hormone receptor (LHR) is expressed primarily in the ovaries and the testes. Within the ovary, the LHR is present on theca and interstitial cells and on mature granulosa cells. After ovulation, the granulosa and theca cells of the ruptured follicle differentiate into the luteal cells, and express higher levels of LHR. In males, the LHR is expressed on the Leydig cells. In both males and females, nongonadal expression of the LHR has also been reported in the reproductive tract and many other tissues.

In the nonpregnant postpubertal female, ovarian theca cells respond to luteinizing hormone (LH) with increased synthesis of androgens, which are used as substrates for estrogen production by follicle-stimulating hormone (FSH)-stimulated granulosa cells. Mature granulosa cells respond to LH with increased

progesterone production. In response to the ovulatory surge of LH, the ovarian LHR receptors mediate ovulation. If pregnancy ensues, then the LHR of the corpus luteum responds to placental chorionic gonadotropin (CG) with increased progesterone synthesis. As such, the LHR is essential for the maintenance of pregnancy, particularly during the first trimester.

In males, the testicular LHR plays an important physiological role during fetal development. Maternal hCG stimulates the fetal Leydig cells to synthesize testosterone, which is required for the differentiation of the external male genitalia and for the descent of the testes into the scrotum. Testosterone levels in boys decrease after birth (due to the absence of maternal LH) and the LHR remains unstimulated until the time of puberty. After puberty the testicular LHR responds to pituitary LH with increased testosterone synthesis.

The physiological roles of nongonadal LHR are not known. It should be pointed out, though, that the only functional consequences of loss-of-function or gain-of-function mutations of the LHR described in males or females have been restricted to abnormalities in reproductive physiology.

The Follicle-Stimulating Hormone Receptor

The follicle-stimulating hormone receptor (FSHR) is expressed in ovarian granulosa cells and in the Sertoli cells within the seminiferous tubules of the testes. In post-pubertal females, the FSHR mediates follicular growth and controls estrogen synthesis. In post-pubertal males, pituitary FSH facilitates spermatogenesis by stimulating the Sertoli cells that are adjacent to the developing sperm to synthesize and secrete components needed for spermatogenesis. Although it is accepted that optimal spermatogenesis requires the actions of FSH, it is controversial as to whether FSH is essential for this process.

Structural Organization of the Glycoprotein Hormone Receptors

Serpentine Regions

The glycoprotein hormone receptors are members of the rhodopsin-like family of GPCRs. As such, they all contain the seven membrane-spanning regions prototypical of the superfamily of GPCRs. Residues that are conserved within the transmembrane (TM) domains of the rhodopsin-like GPCRs are also generally conserved in the glycoprotein hormone receptors. The recent solving of a high resolution crystal structure of rhodopsin has provided a template for creating models of the TM regions of the glycoprotein hormone receptors and permitting investigators to envision the interhelical interactions maintaining the receptors in their inactive states. The crystal structure of rhodopsin also revealed the presence of an eighth α-helix that extends from TM7 and lies parallel to the inner face of the plasma membrane. In rhodopsin, helix 8 extends until a cysteine residue that is palimitoylated and serves to anchor the helix to the plasma membrane. This cysteine is conserved as a single residue or as a pair in the glycoprotein hormone receptors. An alignment of the human TSHR, LHR, and FSHR is shown in Figure 1. The amino acid identity is greatest between the glycoprotein hormone receptors in the transmembrane regions and helix VIII.

Extracellular Domains

A unique feature to the glycoprotein hormone receptors is their relatively large (i.e., 300–400 amino acids) extracellular domains. This is the receptor domain that is responsible for the selective recognition and high-affinity binding of each of the glycoprotein hormones. The extracellular domains are N-glycosylated and a fully conserved tyrosine residue has been shown to be sulfated in the TSHR. The TSHR has the largest extracellular domain which is clipped once the receptor is inserted at the plasma membrane. This proteolytic cleavage results in the formation of an α-subunit containing a portion of the N-terminal extracellular domain and a β-subunit containing the remaining of the N-terminal extracellular domain and the transmembrane and C-terminal domains. Although the α- and β-subunits are initially bound by disulfide bonds, these are reduced and the α-subunit is released from the membrane bound β-subunit.

The extracellular domains of the glycoprotein hormone receptors can be subdivided into a short, N-terminal cysteine-rich region which is followed by nine leucine rich repeats (LRR) and a C-terminal cysteine-rich region. LRR motifs are found in a variety of proteins and are composed of 20–30 amino acids. Based on the known three-dimensional structure of LRR motifs present in the ribonuclease inhibitor, each LRR is proposed to be formed by a β-strand and an α-helix joined by short loops and positioned in a nearly antiparallel orientation. Tandem arrays of these units are believed to form a horseshoe-like structure with consecutive β-strands forming a parallel β-sheet at the concave surface of the horseshoe. By analogy with the known structure of the ribonuclease–ribonuclease inhibitor complex, it is assumed that hormone binding occurs mostly through contact points with the β-sheets present at the concave surface.

Homology cloning and data mining have now uncovered additional GPCRs with large extracellular domain containing a variable number of LRRs. Four of these (designated LGR4–8) are found in mammals.

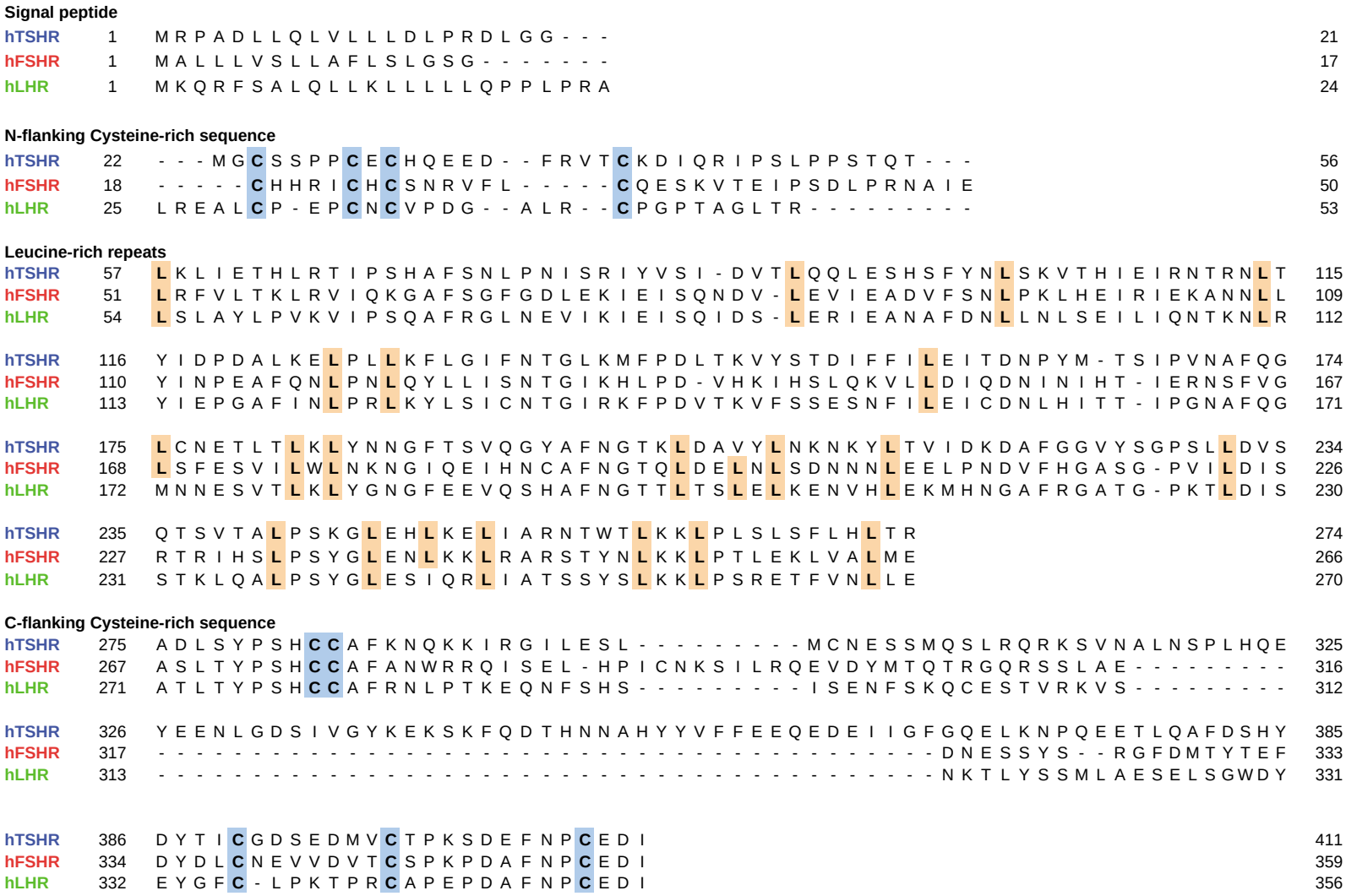

FIGURE 1 Alignments of the amino acid sequences of the human TSHR, FSHR, and LHR. The deduced amino acid sequences for each of the three glycoprotein hormone receptors of human origin are shown.

Transmembrane region

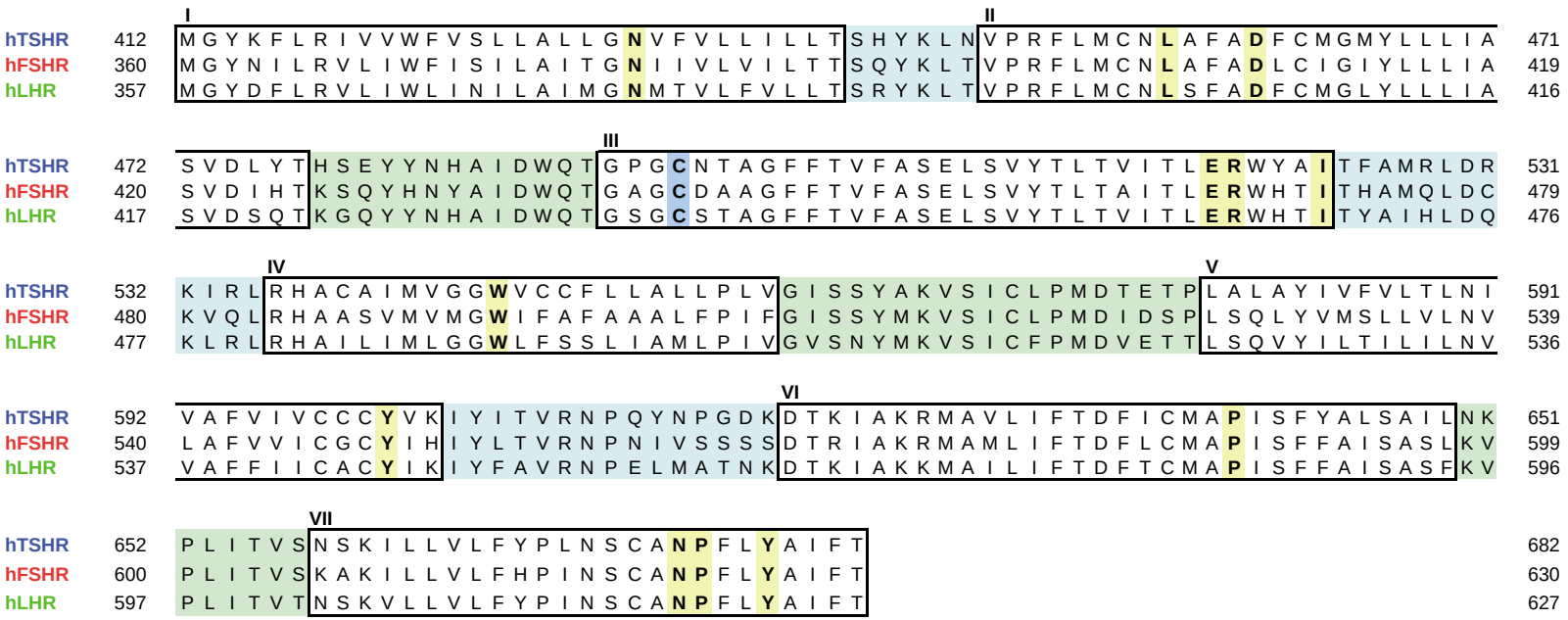

Helix VIII

C terminus

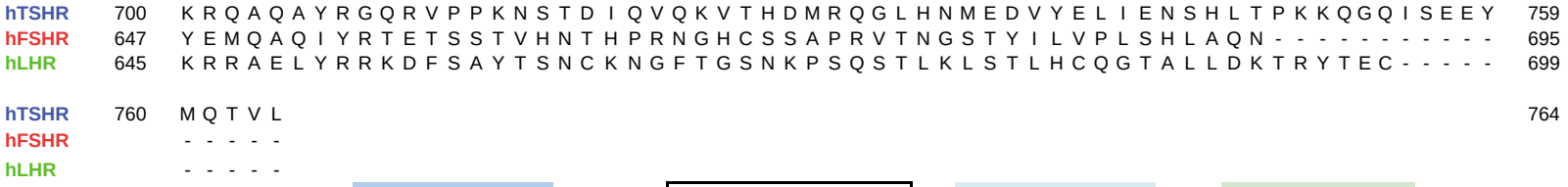

FIGURE 1 (*continued*)

Interestingly, the ligands for LGR7 and LGR8, relaxin and/or Leydig cell insulin-like peptide, are structurally homologous to insulin rather than to the glycoprotein hormones.

Genomic Organization of the Glycoprotein Hormone Receptors

The genes for these three receptors have a similar structure. The LHR gene has 11 exons and the TSHR and FSHR genes each have 10 exons. The last exon codes for a small portion of the N-terminal extracellular domain and all of the serpentine region, including the C-terminal cytoplasmic tail. The other exons are small and they are spliced together to form most of the N-terminal extracellular domain.

The TSHR, LHR, and FSHR genes map to human chromosomes 14q31, 2p21, and 2p21–16, respectively.

Activation of the Glycoprotein Hormone Receptors

G Proteins and Cellular Pathways Activated by the Glycoprotein Hormone Receptors

The identity of the G proteins activated by the FSHR has not been directly examined. The TSHR has been shown to activate all four families of G proteins and the LHR activates at least three or perhaps all four families as well. All of these receptors activate the cAMP and inositol phosphate/diacylglycerol signaling cascades. For each of the glycoprotein hormones, the EC_{50} for cAMP accumulation is lower than the EC_{50} for inositol phosphate accumulation. Moreover, activation of the cAMP pathway is detectable even at low receptor densities, whereas activation of the inositol phosphate/diacylglycerol pathway is generally detectable only at high receptor densities.

It is generally agreed that cyclic AMP is the principal mediator of the actions of the glycoprotein hormones on the differentiated functions of their target cells. The functional consequences of the activation of the inositol phosphate/diacylglycerol pathway are not fully understood. In addition to controlling the differentiated functions of target cells, the glycoprotein hormones also control their proliferation. The three glycoprotein hormones can each activate the extracellular regulated kinase 1/2 cascade (ERK1/2) in their target cells and, at least in the case of the LHR and the TSHR, this activation seems to be mediated by cAMP.

Mechanism of Activation

Although it is clear that binding specificity is provided by the large extracellular domains of the receptors and the β-subunits of the hormones, little else is known about how this event leads to receptor activation. Three models have been proposed. In one model the common α-subunit of the glycoprotein hormones is thought to directly interact with and activate the transmembrane region of the receptor. In another model hormone binding is thought to induce a conformational change in the extracellular domain of the receptor, thus allowing it to interact with and activate the transmembrane region. The last model proposes that the extracellular domain constrains a constitutive activity intrinsic to the transmembrane domain and that hormone binding to the extracellular domain relieves this inhibition. This latter model has received strong experimental support when tested with the TSHR.

Naturally Occurring Mutations of the Glycoprotein Hormone Receptors

Both activating (gain-of-function) and inactivating (loss-of-function) mutations of the glycoprotein hormone receptor genes have been identified in patients with particular endocrine disorders. Activating mutations of these receptors results in the constitutive activation and unregulated elevation of intracellular cAMP in the absence of bound agonist. Most activating mutations have been found in the serpentine regions of the receptors; however, activating mutations of the hTSHR have also been found in the extracellular domain. Germ-line mutations resulting in constitutive activation of the glycoprotein hormone receptors are inherited in an autosomal dominant manner.

Loss-of-function mutations refer to a number of different types of mutations that ultimately cause decreased target cell responsiveness to hormone. These include mutations that impair coupling to G protein, hormone binding, and/or cell surface expression. The majority of loss-of-function mutations of the glycoprotein hormone receptors result in decreased cell surface expression of the mutant receptor due to the intracellular retention of the misfolded mutant. Therefore, loss-of-function mutations have been identified in all regions of the glycoprotein hormone receptors. Mutations of the glycoprotein hormone receptors resulting in a loss-of-function are inherited in an autosomal recessive manner.

TSHR

A large number of activating mutations of the hTSHR have been identified in individuals with autonomously functioning thyroid adenomas (somatic mutations) or autosomal dominant nonautoimmune hyperthyroidism (germ-line mutations).

A number of loss-of-function hTSHR mutations have been identified in individuals with nonautoimmune congenital hypothyroidism, where the degree of hypothyroidism correlates with the extent of target cell unresponsiveness to TSH.

LHR

Numerous activating mutations of the hLHR have been identified in boys with gonadotropin-independent precocious puberty (testotoxicosis). In these cases, the constitutively active hLHRs inappropriately stimulate testosterone production in Leydig cells under conditions of prepubertal levels of LH. Only one hLHR mutation, D578H, has been found to also cause Leydig cell adenomas. Unlike the other hLHR activating mutations, D578H was somatic rather than germ-line in origin. Although it was initially postulated that D578H may activate a pathway(s) different from those activated by the other constitutively active hLHRs, such differences have not yet been observed. Therefore, as with the hTHSR, tumor formation by D578H may be due to its somatic origin.

Many different loss-of-function hLHR mutations have been identified in genetic males with micropenis (partial loss-of-function) or pseudohermaphroditism (severe loss-of-function). In the latter case, the individual presents with female external genitalia but fails to undergo breast development or menstruation at the time of puberty. Female siblings with homozygous or compound heterozygous loss-of-function LHR mutations are infertile.

FSHR

Only one naturally occurring activating mutation of the hFSHR has been reported. This mutation was found in a hypophysectomized male receiving testosterone supplementation who exhibited normal spermatogenesis. Studies of this mutant in cell culture, however, have led to disparate results on whether or not it is truly activating. Surprisingly, activating FSHR mutations have not been found in granulosa cell tumors examined thus far. The paucity of naturally occurring activating mutations of the hFSHR may reflect the lack of a readily detectable pathophysiological state in males or females arising from a constitutively active hFSHR and/or to the relative resistance of the hFSHR to mutation-induced constitutive activity.

The first loss-of-function hFSHR mutation was identified in a population of Finnish women with primary amenorrhea due to ovarian failure. Cells expressing the recombinant form of this hFSHR mutant display no responsiveness to FSH. Surprisingly, men homozygous for this mutation were not infertile, although their fertility may have been impaired somewhat. Therefore, although FSH plays an important role in spermatogenesis, these observations raised ongoing debates regarding its absolute requirement. Since then, other loss-of-function mutations of the hFSHR have been identified in women with varying degrees of FSH resistance.

See Also the Following Articles

G Protein-Coupled Receptor Kinases and Arrestins • Glycoproteins, N-linked

Glossary

chorionic gonadotropin (CG) A hormone secreted by the placenta that is nearly identical to the pituitary hormone LH and is, therefore, recognized by the LH receptor. Also, choriogonadotropin.

follicle-stimulating hormone (FSH) A pituitary hormone recognized by the FSH receptor. Also, follitropin.

glycoprotein hormones The structurally related hormones TSH, LH, CG, and FSH. The glycoprotein hormone receptors are the LH, FSH, and TSH receptors.

gonadotropins LH, CG, and FSH; members of the glycoprotein hormone family that act upon the gonads. The gonadotropin receptors are the LH and FSH receptors.

G protein-coupled receptors (GPCRs) A class of membrane receptors that contain seven transmembrane regions and mediate their actions through the activation of G proteins.

luteinizing hormone (LH) A pituitary hormone recognized by the LH receptor. Also, lutropin.

thyroid-stimulating hormone (TSH) A pituitary hormone recognized by the TSH receptor. Also, thyrotropin.

Further Reading

Ascoli, M., Fanelli, F., and Segaloff, D. L. (2002). The lutropin/choriogonadotropin receptor, a 2002 perspective. *Endocr. Rev.* **23**, 141–174.

Davies, T., Marians, R., and Latif, R. (2002). The TSH receptor reveals itself. *J. Clin. Invest.* **110**, 161–164.

Hsu, S. Y., and Hsueh, A. J. (2000). Discovering new hormones, receptors and signaling mediators in the genomic era. *Mol. Endocrinol.* **14**, 594–604.

Latronico, A., and Segaloff, D. L. (1999). Naturally occurring mutations of the luteinizing-hormone receptor: Lessons learned about reproductive physiology and G protein-coupled receptors. *Amer. J. Hum. Genet.* **65**, 949–958.

Paschke, R., and Ludgate, M. (1997). The thyrotropin receptor in thyroid diseases. *N. Engl. J. Med.* **337**, 1675–1681.

Rapoport, B., Chazenbalk, G. D., Jaume, J. C., and McLachlan, S. M. (1998). The thyrotropin (TSH) receptor: Interaction with TSH and autoantibodies. *Endocr. Rev.* **19**, 673–716.

Simoni, M., Gromoll, J., and Nieschlag, E. (1997). The follicle-stimulating hormone receptor: Biochemistry, molecular biology, physiology, and pathophysiology. *Endocr. Rev.* **18**, 739–773.

Themmen, A. P. N., and Huhtaniemi, I. T. (2000). Mutations of gonadotropins and gonadotropin receptors: Elucidating the physiology and pathophysiology of pituitary-gonadal function. *Endocr. Rev.* **21**, 551–583.

Biography

Deborah L. Segaloff is a Professor of Physiology and Biophysics and Mario Ascoli a Professor of Pharmacology in the Roy J. and Lucille A. Carver College of Medicine at the University of Iowa in Iowa City, Iowa Dr. Segaloff's laboratory cloned the cDNA for the rat LHR, the first glycoprotein hormone receptor to be cloned. Since then, Dr. Segaloff's and Dr. Ascoli's laboratories have performed extensive studies on the regulation and the mechanisms of activation and desensitization of the gonadotropin receptors.

Dario Mizrachi is a Postdoctoral Associate in Dr. Segaloff's laboratory. As a Lalor Fellow, Dr. Mizrachi developed homology models of the glycoprotein hormone receptors for use in predicting the structural arrangements of the receptors.

Tight Junctions

Shoichiro Tsukita
Kyoto University, Kyoto, Japan

The tight junction (TJ) or *zonula occludens* is one mode of cell-to-cell adhesion in vertebrate epithelial and endothelial cellular sheets, and is located at the most apical part of their lateral membranes. The existence of separate fluid compartments with different molecular compositions is of particular importance for the development and maintenance of multicellular organisms. These compartments are delineated by various cellular sheets, which function as barriers to maintain the distinct internal environment of each compartment. Within these sheets, individual cells are mechanically linked to each other to maintain the structural integrity of the sheet, and the intercellular space between adjacent cells is sealed to prevent the diffusion of solutes through the intercellular space. TJs are directly involved in this intercellular sealing.

Structure

Electron Microscopic Image

On ultrathin section electron microscopy, tight junctions (TJs) appear as a zone where plasma membranes of neighboring cells focally make complete contact (Figure 1D). On freeze-fracture electron microscopy, TJs are visualized as a continuous, anastomosing network of intramembranous particle strands (TJ strands or fibrils) and complementary grooves.

Three-Dimensional Image

Detailed electron microscopic observations led to our current understanding of the three-dimensional structure of TJs (Figure 1C); each TJ strand is associated laterally with another TJ strand in apposing membranes of adjacent cells to form "paired" TJ strands, where the intercellular space is completely obliterated.

Molecular Architecture

Integral Membrane Proteins

Three distinct types of integral membrane proteins are localized at TJs: claudin, occludin, and JAM (Figure 2). Claudin with a molecular mass of ~23 kDa is a major constituent of TJ strands, and bears four transmembrane domains. In mice and humans, claudins comprise a multigene family consisting of 24 members. When each claudin species is overexpressed in mouse fibroblasts, claudin molecules are polymerized within the plasma membranes to reconstitute paired TJ strands. As many distinct species of claudins are coexpressed in individual cells, heterogeneous claudin species are copolymerized to form individual TJ strands as heteropolymers, and between adjacent TJ strands claudin molecules adhere to each other in both homotypic and heterotypic manners, except in certain combinations.

Occludin, a ~65 kDa integral membrane protein, also bears four transmembrane domains, but does not show any sequence similarity to claudins. Occludin is incorporated in TJ strands *in situ*, but TJ strands can be formed without occludin. JAM with a single transmembrane domain associates laterally with TJ strands, while not constituting the strands *per se*. The physiological functions of occludin and JAM remain elusive.

Peripheral Membrane Proteins

Claudins are packed densely within the TJ strands. Therefore, their cytoplasmic surface appears similar to a brush consisting of numerous short carboxyl-terminal cytoplasmic tails of claudins. Interestingly, most of these tails end in valine at their carboxyl termini, suggesting that these carboxyl termini directly bind to PDZ domains. Therefore, the cytoplasmic surface of TJ strands can be regarded as a magnetic bar that strongly attracts and recruits many PDZ-containing proteins.

Indeed, three related PDZ-containing proteins, ZO-1 (~220 kDa), ZO-2 (~160 kDa), and ZO-3 (~130 kDa), are concentrated at TJs. These molecules all have three PDZ domains (PDZ1 to 3), one SH3 domain, and one GUK (guanylate kinase-like) domain in this order from their NH_2-termini indicating that they belong to membrane-associated guanylate kinase-like homologues (MAGUKs). Among these three PDZ domains, PDZ1 domain binds directly to the COOH termini of claudins.

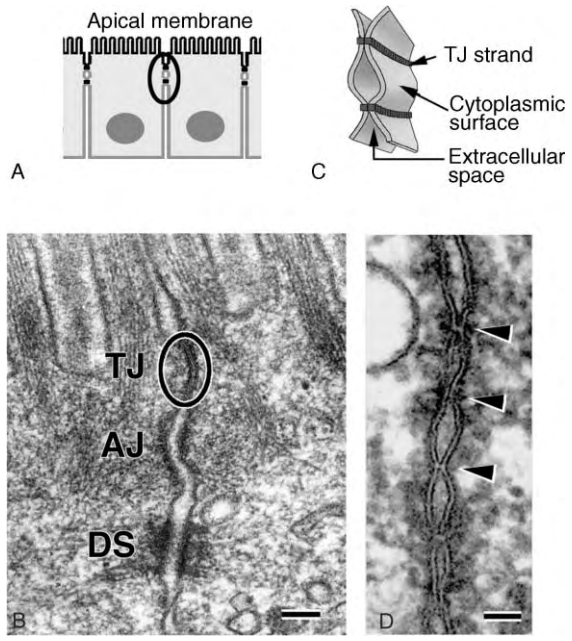

FIGURE 1 Structure of tight junctions. (A) Schematic drawing of simple epithelial cells. The junctional complex is located at the most apical part of lateral membranes (encircled). (B) Electron micrograph of the junctional complex in mouse intestinal epithelial cells. TJ, tight junction (encircled); AJ, adherens junction; DS, desmosome. (C) Schematic drawing of tight junctions. Individual tight junction strand within plasma membranes associates laterally with another strand in apposing membranes to form a paired strand. (D) Ultra-thin sectional view of tight junctions. At kissing points of TJs (arrowheads), the intercellular space is obliterated. Bars, 200 nm (b); 50 nm (d).

In addition to these three TJ-specific MAGUKs, several other PDZ-containing proteins are recruited to the cytoplasmic surface of TJ strands. These proteins are multidomain proteins, and may function as adapters at the cytoplasmic surface of TJs together with non-MAGUK proteins such as cingulin and symplekin, which recruit various proteins including cytoskeletal as well as signaling molecules.

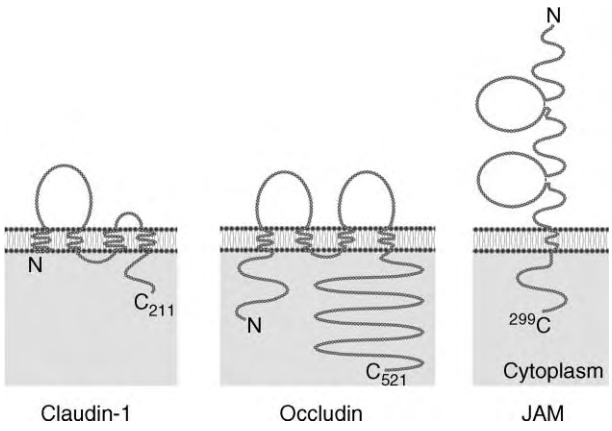

FIGURE 2 Integral membrane proteins localized at tight junctions. Membrane folding models of mouse claudin-1, occludin, and JAM.

Functions

Barrier Function

Claudins are directly involved not only in the formation of TJ strands but also in their barrier function in simple epithelia, not only for solutes but also for pathogens such as bacteria. Furthermore, TJs are not simple barriers; they show ion and size selectivity and their barrier function varies significantly in tightness depending on the cell-type and physiological requirements. Such regulated and diversified permeability of TJs is required for dynamically maintaining the environment of each compartment. To explain the material transport across TJs, aqueous pores (or paracellular channels) have been postulated to exist within paired TJ strands. It is now widely believed that the combination and mixing ratios of claudins within individual paired strands determine the tightness and selectivity of these aqueous pores.

Fence Function

TJ strands are heteropolymers of integral membrane proteins, claudins, within plasma membranes, and continuously encircle the top of individual epithelial/endothelial cells to delineate the border between the apical and basolateral membrane domains. Therefore, it is believed that TJ strands act as a "fence," limiting the lateral diffusion of lipids and proteins between the apical and basolateral membrane domains. Indeed, when fluorescently labeled lipids are inserted into the outer leaflet of the apical membrane of cultured epithelial cells, these lipids are retained on the apical surface. In contrast, the importance of TJs in the asymmetric distribution of integral membrane proteins remains controversial.

Other Possible Functions

As previously mentioned, various types of proteins including PDZ-containing proteins are recruited to the cytoplasmic surface of TJ strands to form a huge macromolecular complex. This macromolecular complex is expected to play central roles in the intracellular signaling of epithelial cells, being involved in the regulation of their proliferation and morphogenesis, i.e., contact inhibition of cell growth and epithelial cell polarization, respectively.

See Also the Following Article

MDR Membrane Proteins

Glossary

apical surface The free surface of epithelial cells facing the luminal space or external environment.

endothelial cells Thin, flattened cells of mesoblastic origin that are arranged in a single layer lining the blood vessels and some body cavities (e.g., those of the heart).

epithelial cells Closely packed cells, arranged in one or more layers, that cover the outer surfaces of the body or line any internal cavities or tubes (other than the blood vessels, heart, and serous cavities).

freeze-fracture replica electron microscopy An electron microscopic method that uses metal replicas to visualize the interior of cell membranes. This technique provides a convenient way of visualizing the distribution of large integral membrane proteins as intramembranous particles on the plane of a membrane.

PDZ domain Protein–protein interaction domain first described in proteins PSD-95, DLG, and ZO-1.

SH3 domain Src homology region 3, a protein domain present in various signaling proteins.

Further Reading

Alberts, B., Johnson, A., Lewis, J., Raff, M., Roberts, K., and Walter, P. (2002). *Molecular Biology of the Cell*. Garland Publishing, New York.

Cereijido, M., and Anderson, J. (2001). *Tight Junctions*. CRC Press, New York.

Gonzalez-Mariscal, L., Betanzos, A., Nava, P., and Jaramillo, B. E. (2003). Tight junction proteins. *Prog. Biophys. Mol. Biol.* **81**, 1–44.

Schneeberger, E. E., and Lynch, R. D. (1992). Structure, function, and regulation of cellular tight junctions. *Am. J. Physiol.* **262**, L647–L661.

Tsukita, Sh., Furuse, M., and Itoh, M. (2001). Multifunctional strands in tight junctions. *Nat. Rev. Mol. Cell. Biol.* **2**, 285–293.

Biography

Shoichiro Tsukita is a Professor in the Department of Cell Biology at Kyoto University, Kyoto, Japan. His principal research interests are in cell–cell adhesion and cytoskeletons. He holds M.D. and Ph.D. from the University of Tokyo. His group established a new isolation procedure for intercellular junctions and identified occludin and claudins.

Toll-Like Receptors

Himanshu Kumar, Kiyoshi Takeda and Shizuo Akira
Osaka University, Osaka, Japan

Toll-like receptors (TLRs) are the family of receptor molecules that recognizes microbe-specific conserved molecular motifs. Recognition of these molecular motifs by innate cells of innate immune system activates downstream signaling cascades to induce secretion of cytokines, chemokines, and expression of costimulatory molecules. These effects subsequently instruct the major component of adaptive immune system that is B and T cells to exhibit pathogen-specific antimicrobial activity. At the end of the twentieth century, this family of receptors has been discovered and till date ten TLR molecules are known.

Innate Immune System

Innate immunity acts as the first line of host defense against microbial pathogens. It is conserved from flies to mammals. Innate immunity is dependent on both cellular components such as monocytes, macrophages, neutrophils, dendritic cells, and endothelial cells, and humoral components such as C-reactive protein (CRP), lysozyme, and complements. The cellular component of innate immunity recognizes a wide range of pathogen-associated molecular motifs by virtue of pattern recognition receptors (PRR). There are two types of PRRs. One type of PRRs, such as CR3 and C-type lectins, facilitate receptor-mediated phagocytosis. Other PRRs, such as TLRs, trigger the activation of innate immunity. It has recently been shown that toll-like receptor (TLRs) are the most important PRRs in triggering the activation of innate immunity.

TLRs and their Ligands

Toll receptor was first described in context of the dorsoventral development of *Drosophila* embryo. Toll and its mammalian homologues (TLRs) are type I membrane proteins, harboring an ectodomain consisting of leucine-rich repeats (LRRs) and one or two cysteine rich regions. The intracellular domain of toll receptors is structurally similar to that of the IL-1 receptor. Therefore, it is called Toll/IL-1R (TIR) domain. This region of TLRs is required for homophilic and heterophilic interaction of TLRs. The TIR domain further interacts with several TIR domain-containing adaptors such as MyD88, TIRAP/Mal, and TRIF. To date, ten TLRs (TLR1–10) have been identified and shown to recognize different classes of pathogen-derived molecular motifs (Table I).

Distribution of TLRs

Distribution of these TLR molecules in different cells and tissue type is shown in Table II.

Intracellular Signal Transduction through TLR

The molecular mechanisms by which TLRs trigger activation of innate immunity have been elucidated through analysis of signaling pathways. Intracellular signal transduction initiates from the TIR domain of TLRs. The TIR domain of TLRs interacts with the TIR domain (present in the C terminus) of MyD88 adaptor protein. MyD88 contains a death domain at the N terminus. When ligands are bound to TLRs, MyD88 recruits IRAK to TLRs through the interaction of death domains and leads to phosphorylation of IRAK, which has serine/threonine kinase activity. IRAK then binds TRAF-6 to form the IRAK–TRAF6 complex. This complex activates the NFκB transactivator that induces transcription of inflammatory cytokine genes. This complex also activates the JNK pathway and generates the active AP-1 transactivator as shown in Figure 1. In addition to this MyD88-mediated component of signaling pathway, a MyD88-independent component leading to IFN-β production has been identified in TLR3 and TLR4 signaling pathways.

MyD88-Dependent Signaling Pathway

Stimulation of MyD88-deficient macrophages with known TLR ligands induced no production of inflammatory cytokines. This indicates that MyD88 plays a pivotal role in the TLR-mediated production of inflammatory

TABLE I

Description of Toll-Like Receptor

TLR	Gene (Human)	Functional receptor	Ligands of TLR	Immune response
TLR1	4p14	Heterodimers of TLR2-TLR1	Tri-acyl lipopeptides (bacteria, Mycobacteria), soluble factors, *Neisseria meningitis*	Induce secretion of inflammatory cytokine(s)
TLR2	4q32	Heterodimers of TLR2-TLR1 and heterodimer of TLR2-TLR6	Lipoprotein/lipopeptides (different pathogen), peptiodoglycan (gram-positive bacteria), lipoteichoic acid (gram-positive bacteria), lipoarabinomannan (Mycobacteria), a phenol soluble modulin (*Staphylococcus aureus*), glycoinositolphospholipids (*Trypanosoma cruzi*), glycolipid (*Treponema maltophilum*), porins (*Neisseria*), zymosan (fungi), HSP70 (host), atypical LPS (*Leptospira interrogans*), atypical LPS (*Porphyromonas gingivalis*)	Induce secretion of inflammatory cytokine(s)
TLR3	4q35	Not known	Double-stranded RNA (mainly from virus)	Induce type I interferon (IFN-α/IFN-β)
TLR4	9q32-33	LPS-LPS binding protein complex associate with CD14 and MD-2, in B-cell TLR4 associate with RP105 and MD-1	LPS (gram-negative bacteria, taxol (plant), HPS60 (host), HPS70 (host), fusion protein (RSV), HPS60 (*Chlamydia pneumoniae*), fibronectin (host), envelope proteins (MMTV), type III repeat extra domain A of fibronectin (host), oligosaccharides of hyaluronic acid (host), polysaccharides fragments of heparin sulfate (host) and fibrinogen (host)	Induce secretion of inflammatory cytokine(s) and chemokines
TLR5	1q33.3	Not known	55 kDa monomer obtained from bacteria flagella (flagellin)	Induce inflammatory cytokine(s)
TLR6	4p14	Heterodimer of TLR2-TLR6	Di-acyl lipopeptides (mycoplasma)	Induce secretion of inflammatory cytokine(s)
TLR7	Xp22	Not known	Synthetic compounds like imidazoquinoline (imquimod (R-848), resiquimod (R848)), loxoribine and bropirimine	Induce secretion of inflammatory cytokine(s)
TLR8	Xp22	Not known	Ligand(s) not known	Not known
TLR9	3p21.3	TLR9 (localized in endosomal compartment)	Unmethylated CpG DNA (Mycobacteria and Bacteria)	Activate Th1 type immune response, Induce proliferation of B-cell, activate macrophage and DCs
TLR10	Not known	Not known	Ligand(s) not known	Not known

TABLE II
Distribution of TLRs

		Types of Toll-like receptor									
	Cell/tissue type	TLR1	TLR2	TLR3	TLR4	TLR5	TLR6	TLR7	TLR8	TLR9	TLR10
1	Monocytes	+	+	−	+	+	+	+	+	+	+
2	Macrophage	+	+	−	+	+	+	+	+	+	+
3	Plasmacytoid dendritic cell	+	+	−	+	+	−	+	+/−	M(+) H(+)	NK
	Myeloid dendritic cell	NK	+	NK	+	NK	+	H(+/−) M(+)	+	M(+) H(−)	NK
4	Immature dendritic cell[a]	+	+	NK	+	+	NK	NK	NK	NK	NK
	Mature dendritic cell[a]	NK	NK	+	NK	NK	NK	NK	NK	NK	NK
5	Mast cell	NK	+	NK	+	−	+	NK	+	NK	NK
6	Intestinal cell (Apical side)	NK	NK	NK	+(low)	NK	NK	NK	NK	NK	NK
	Intestinal cell (Basolateral side)	NK	NK	NK	NK	+	NK	NK	NK	NK	NK
7	Renal epithelia	NK	+	NK	+	NK	NK	NK	NK	NK	NK
8	Pulmonary epithelia	NK	NK	NK	+	NK	NK	NK	NK	NK	NK
9	Corneal epithelia	NK	NK	NK	+	NK	NK	NK	NK	NK	NK

[a] Initially immature dendritic cells (DCs) express TLR1, 2, 4, and 5 as soon as immature DC encounter with antigen the expression of TLR1, 2, 4, and 5 regresses and expression of TLR progresses.
Abbreviations: M, mouse; H, human; NK, not known.

cytokines. Four family members of IRAK have been reported in mammals (IRAK-1, IRAK-2, IRAK-4, and IRAK-M). IRAK-1 and IRAK-4 are ubiquitously expressed active kinases, whereas IRAK-M is preferentially expressed in macrophage and monocytes. Stimulation of IRAK-4-deficient macrophages with ligands of TLR2, TLR3, and TLR4 induced almost no production of inflammatory cytokines. Inflammatory cytokine production was also significantly diminished in IRAK-1-deficient macrophages stimulated with LPS (the TLR4 ligand). Thus, IRAK-1 and IRAK-4 are involved in the TLR-mediated signaling pathways. On the other hand, IRAK-M-deficient macrophages showed overproduction of inflammatory cytokines in response to TLR ligands, indicating that this molecule is involved in the negative control of cytokine production. Stimulation of TRAF6-deficient macrophages with LPS led to impaired production of inflammatory cytokines, suggesting that TRAF6 is also important in the TLR-mediated signaling pathway.

In addition to MyD88, TIR domain-containing adaptor protein (TIRAP)/MyD88-adaptor-like (Mal) has been identified as the second TIR domain-containing molecule. Stimulation of TIRAP/Mal-deficient mice with LPS (the TLR4 ligand) and lipopeptide (the TLR2 ligand) induced no production of inflammatory cytokines. Thus, TIRAP/Mal is essential for the MyD88-dependent pathway of TLR2 and TLR4.

MyD88-Independent Signaling Pathway

As described, stimulation of MyD88-deficient macrophages with TLR ligands did not lead to inflammatory cytokine production. However stimulation with LPS induced delayed activation of JNK and NFκB in these cells, indicating that there is another bypass pathway which transduces signals in the absence of MyD88. Beside LPS, dsRNA (the TLR3 ligand) is also capable of activating NFκB in MyD88-deficient macrophages. In addition, it has been shown that LPS and dsRNA both induce the activation of IRF-3 transactivator and lead to the production of IFN-β in a MyD88-independent fashion.

Recently, a third TIR domain-containing adaptor protein called TIR domain-containing adaptor inducing IFN-β (TRIF) was identified. TRIF-deficient mice showed no activation of IRF-3 or production of IFN-β in response to the TLR3 and TLR4 ligands. Therefore, TRIF is an essential molecule for the activation of IRF-3 transactivator through TLR3 and TLR4. Furthermore, the lack of LPS-induced activation of NFκB and JNK in MyD88/TRIF double deficient cells indicates that TRIF is essential for the TLR4-mediated MyD88-independent pathway.

Structural and Functional Homologues of TLRs

RP105, a molecule containing an ectodomain with LRRs and one cysteine-rich region but lacking a cytoplasmic TIR domain, has been identified. RP105 is preferentially expressed in mature B cells. Mice deficient in RP105 or TLR4 does not show proliferation in

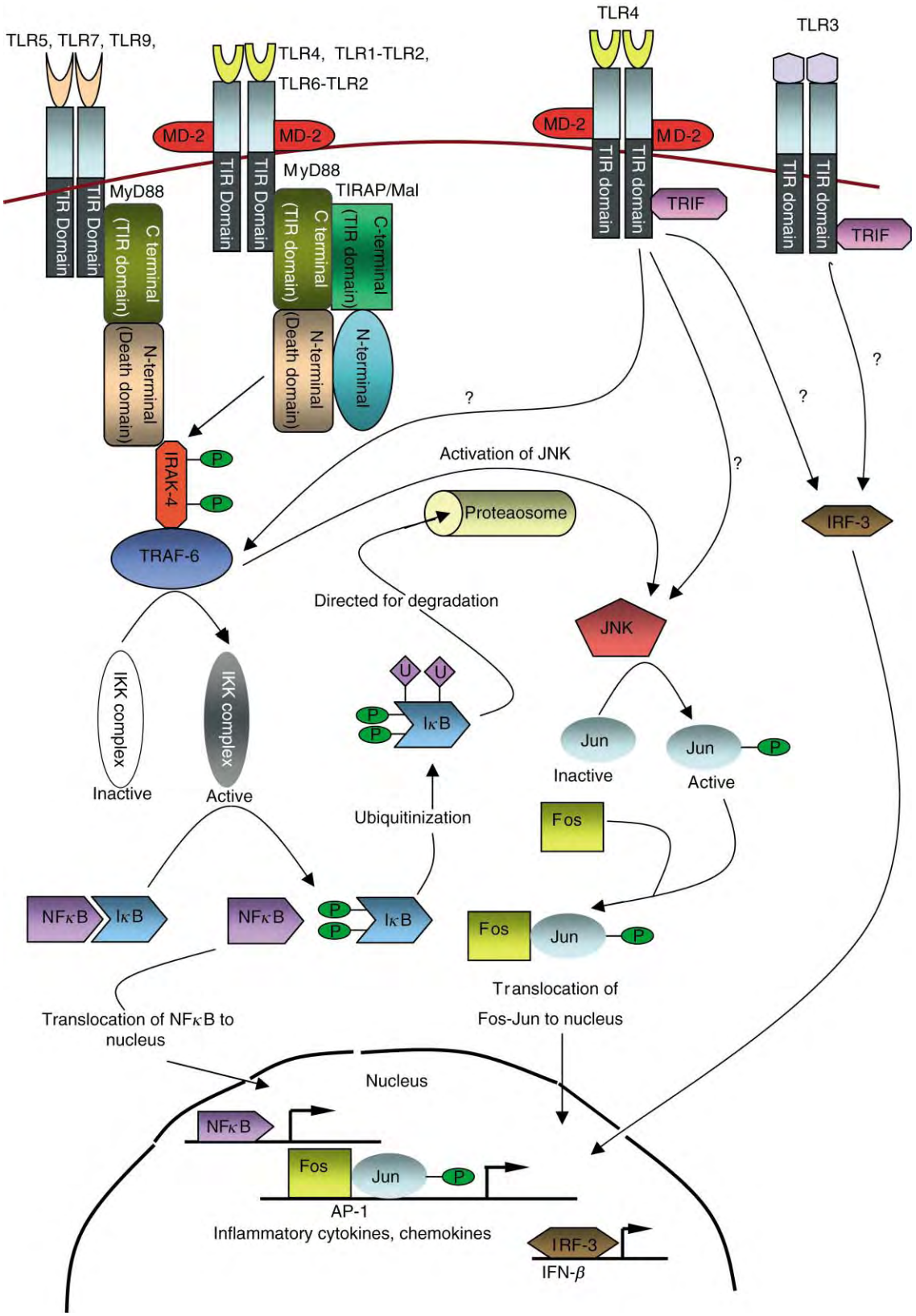

FIGURE 1 Intracellular signaling pathway through TLR. Binding of TLR ligands initiates TLR-mediated signaling pathways from the cytoplasmic TIR domain. The TIR domain-containing adaptor MyD88 is essential for the induction of inflammatory cytokines via all TLRs. Another TIR domain-containing adaptor TIRAP is involved in the MyD88-depdendent pathway of TLR2 and TLR4. In TLR3 and TLR4 signaling, the IRF-3 transcription factor is activated in a MyD88-independent fashion. The third TIR domain-containing adaptor TRIF mediates the MyD88-independent signaling, thereby inducing IFN-β.

response to LPS. This shows that RP105 is required for LPS-induced responses in B cells.

Besides mammals, plants also have more than 100 genes which encode proteins with the TIR domain. Some of these proteins also have LRRs and nucleotide-binding site (NBS). These proteins play an important role in defense against plant virus.

Future Perspective

Pathogens are dynamic entities, which contain many complex biomolecules such as LPS and lipoprotein. In recent years, intensive research has been conducted to elucidate the different TLR signaling pathways such as the MyD88-dependent and MyD88-independent pathway by using purified pathogen-derived biomolecules. However, it is still not known how all these pathogen-derived complex molecules interact with macrophages, what the net or final signals for clearance of pathogens are, or how different pathways communicate with each other *in vivo*. In the near future, all these questions will be clarified using several mutant mouse strains lacking the different components of TLR signaling pathways.

See Also the Following Articles

Chemotactic Peptide/Complement Receptors • Nuclear Factor kappaB

Glossary

adaptive immunity The response of antigen specific lymphocytes to an antigen, including the development of immunological memory. Adaptive immune responses are generated by clonal selection of lymphocytes.

complements The complement system is a set of plasma protein synthesized in the liver and act together on the surface of pathogens to form the membrane attack complex (MAC) in order to kill pathogens.

innate immunity The early phases of the host response to an infection, and is normally present in all individuals at all times. This immune system can discriminate between self and nonself (pathogen), but does not increase responses with repeated exposure to a given pathogen.

JNK A kinase that activates Jun by phosphorylation. Phosphorylated Jun associates with Fos and forms a complex known as AP-1, which transcribes many cytokine genes.

NFκB A transcription factor made up of 50 and a 65 kDa subunits. It is normally found in the cytosol, where it is bound to IκB, an inhibitor of NFκB. This transcription factor is involved in the transcription of many cytokine genes.

Further Reading

Akira, S. (2003). Mammalian toll-like receptors. *Curr. Opin. Immunol.* **15**, 5–11.

Akira, S., Takeda, K., and Kaisho, T. (2001). Toll-like receptor: Critical proteins linking innate and acquired immunity. *Nature* **2**, 675–680.

Medzhitov, R., and Kopp, E. B. (1999). The Toll receptor family and control of innate immunity. *Curr. Opin. Immunol.* **11**, 13–18.

Takeda, K., and Akira, S. (2003). Toll receptors and pathogen resistance. *Cell. Microbiol.* **5**, 143–153.

Takeda, K., Kaisho, T., and Akira, S. (2003). Toll-like receptors. *Annu. Rev. Immunol.* **21**, 335–376.

Yamamoto, M., Sato, S., Hemmi, H., Hoshino, K., Kaisho, T., Sanjo, H., Takeuchi, O., Sugiyama, M., Okabe, M., Takeda, K., and Akira, S. (2003). Role of adaptor TRIF in the MyD88-independent toll-like receptor signaling pathway. *Science* **301**, 640–642.

Biography

Shizuo Akira is a Professor in the Department of Host Defense at Research Institute for Microbial Diseases, Osaka University in Osaka, Japan. His principal research interests are in mammalian innate immunity. He holds a Ph.D. from Osaka University and has received postdoctoral training at the University of California, Berkeley. He analyzes the molecular mechanism by which the innate immunity senses microbial invasion in mammals through generation of knockout mice.

Kiyoshi Takeda was an Assistant Professor in the Department of Host Defense at Research Institute for Microbial Diseases, Osaka University in Osaka, Japan. He received Ph.D. from Osaka University. Presently, he is a Professor in Department of Molecular Genetics at Medical Institute of Bioregulation, Kyusha University in Fukuoka, Japan. His research focuses on the mechanism for regulation of macrophage activity and the involvement of innate immunity in inflammatory and infectious diseases.

Himanshu Kumar is a graduate student, pursuing research in the Department of Host Defense at Research Institute for Microbial Diseases, Osaka University in Osaka, Japan. His research interest is elucidation of new molecules involve in TLRs signaling.

Transcription Termination

Thomas J. Santangelo and Jeffrey W. Roberts
Cornell University, Ithaca, New York, USA

Transcription termination is the process by which RNA synthesis by RNA polymerase (RNAP) is stopped and both the RNA and enzyme are released from the DNA template. Since most regulation occurs at the initiation of RNA synthesis, failure to terminate transcription at the ends of operons would lead to bypass of downstream gene regulation due to rogue elongation complexes continuing transcription beyond the end of the upstream operon. Two types of transcription termination in bacteria have been characterized in both biochemical reactions with purified RNA polymerase and in genetic experiments: (1) "intrinsic termination," which requires only special template sequences, and (2) "factor-dependent termination," which requires an additional enzyme that interacts with RNA polymerase. The RNA polymerase transcription elongation complex is extremely stable – it must persist over time and distance in order for gene expression to succeed – but it also must be disrupted efficiently at termination sites.

Models of terminator function have been strongly informed by the recently determined atomic structures of RNAP and the transcription elongation complex, which reveal the molecular sources of stability that are overcome by termination mechanisms.

Figure 1 shows a general elongation complex, highlighting the major contacts that provide stabilizing energy to the complex. The RNAP enzyme surrounds an 8 or 9 bp DNA–RNA hybrid that is held within the main channel of the enzyme. The RNA emerges from the enzyme through an exit channel where additional contacts are made between single-stranded RNA (ssRNA) and the protein. By far, the greatest sources of stabilizing energy to the complex are the hydrogen-bonding within the hybrid itself and the interactions between the hybrid and the surrounding protein. Terminators function by weakening these contacts, leading to dissociation of the hybrid and disruption of the complex.

Intrinsic Termination

Intrinsic terminators are composed of two critical elements: a short region of dyad symmetry in the DNA which encodes an RNA sequence capable of forming an RNA–RNA duplex or RNA "hairpin," and a sequence encoding a uridine-rich sequence in the RNA that immediately follows the hairpin (Figure 1). Transcript release occurs 8–10 bp downstream of the base of the RNA hairpin. Correct base pairing within the stem of the hairpin, the presence of the uridine-rich segment, and the correct spacing of these elements are critical to termination efficiency. Terminator efficiency also can be modulated by the DNA sequence immediately upstream and downstream of the termination position.

Current research is focused on the way these sequences and structures facilitate release of the transcript. The complex has been weakened just by sequence context alone; the final 8 or 9 bases of a terminated transcript occupy the hybrid-binding site and a dA:rU hybrid is the weakest possible combination of nucleic acids. In the absence of a terminator hairpin structure, the weak hybrid alone is sufficient to induce RNAP to pause at the end of the uridine-rich sequence. The role of the uridine-rich sequence in termination is likely twofold: (1) to pause the elongation complex immediately downstream of the region capable of hairpin formation; and (2) to minimize the energetic contribution of the hybrid to the overall stability of the complex.

The role of the hairpin structure and its effects on the elongation complex remain debated. Although their details differ, most models predict that hairpin formation disrupts the upstream bases of the hybrid, triggering collapse of the elongation complex. One model proposes that hairpin formation immediately upstream of the complex pushes RNAP downstream in the absence of further synthesis. Forward translocation of several base pairs would reduce the length of the weak RNA/DNA hybrid, and the loss of hybrid interactions would result in transcript release. An alternative model of termination evokes a relatively large conformational change in the enzyme upon interaction of the hairpin with RNAP. The hairpin structure formed in the RNA could physically interact with the complex, opening the enzyme and freeing the RNA transcript from its enclosure within the elongation complex, a reaction that again would be promoted by the weak hybrid. It is also possible that a large conformational change accompanies a forward translocation to result in both transcript and enzyme release.

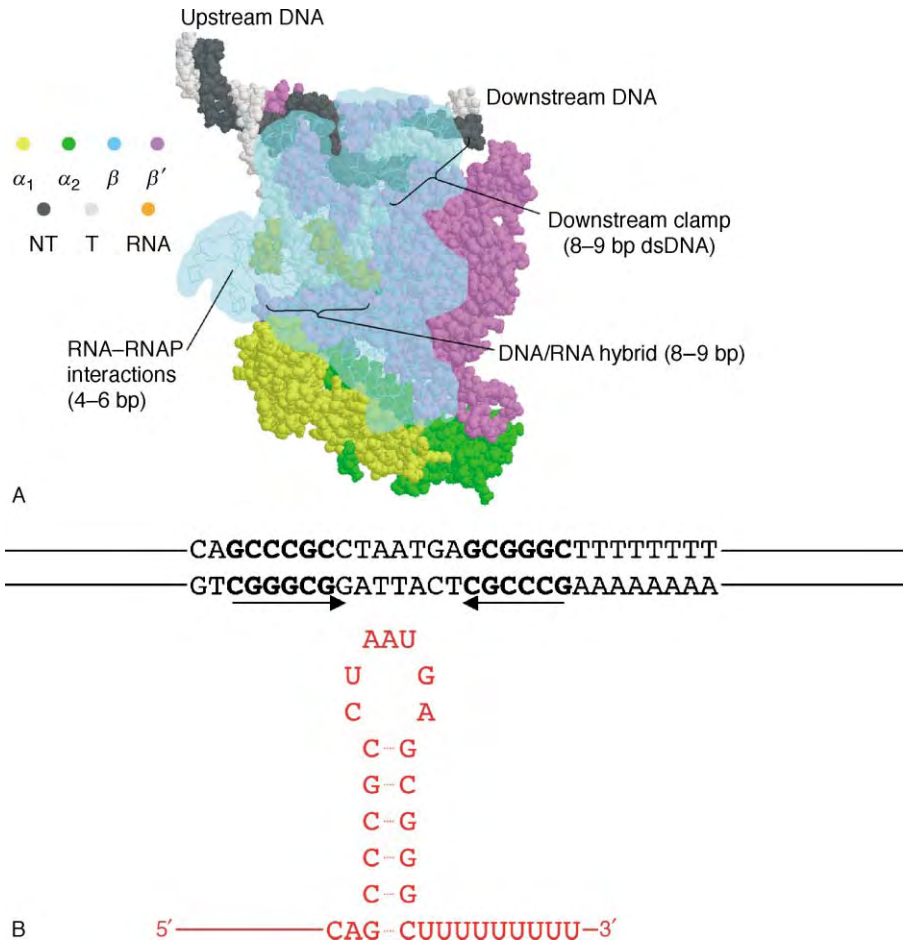

FIGURE 1 (A) The transcription elongation complex is shown, highlighting the protein–nucleic acid contacts that provide stabilizing energy to the complex. Subunits are colored according to the key at the left; β has been made partially transparent in order to reveal the main channel of RNA polymerase and the nucleic acid framework inside. NT, non-template DNA strand; T, template DNA strand. (B) Sequence of an intrinsic terminator (the *E. coli trpA* terminator) is shown in black with the corresponding RNA sequence and hairpin shown in red. The region of dyad symmetry in the DNA is shown in bold and is underlined and codes for the RNA hairpin.

All of the multisubunit RNAPs are predicted (and some are known) to share a common three-dimensional structure and thus are similar in terms of the contacts made between the enzyme and nucleic acid framework. Thus, termination of transcription by the specialized RNA polymerases in eukarya (RNA pol I, II, and III) and the archaeal RNAPs likely also involves mechanisms to initiate disruption of the RNA/DNA hybrid. Termination by pol I and pol III in eukarya, and the RNAP from archaea, does involve oligo-T tracts at or near the termination positions, although the mechanisms are unknown.

Factor-Dependent Termination

Rho-Mediated Termination

Rho factor is a hexameric RNA-dependent ATPase that is found in most eubacteria, but not in archaea or eukarya. Its general mechanism of action is to bind the nascent transcript of an elongation complex, wrapping ~60 nucleotides of RNA, translocating toward RNAP in an ATP-dependent reaction, and finally dissociating the complex by an unknown mechanism. An atomic structure of the Rho hexamer shows a hexameric ring of monomers, each with two domains. The structural model proposes that a ring of RNA-binding domains engages most of the RNA, which then projects through the center of the ring to contact the ATPase domains that effect translocation. A break in the hexameric ring ("lock-washer" model) is proposed to allow RNA to penetrate the hexamer.

Rho function is largely determined by the very tight coordination between transcription and translation, because it requires free RNA immediately upstream of RNA polymerase in order to act. Translation in bacteria occurs as the transcript is being made, and the ribosome travels immediately behind the elongation complex,

so that free RNA is generally unavailable to Rho. However, when the ribosome stalls are released, as at a translation stop codon, transcription and translation become uncoupled. As RNA polymerase continues to transcribe, more RNA is exposed to solution, allowing Rho access to the RNA. Since RNAP elongates at 50–100 nucleotides per second, Rho provides a rapid mechanism to ensure that RNAP does not transcribe much beyond the point of uncoupling.

Although a major function of Rho is to abort futile transcription as described above, Rho-dependent termination also is the natural mechanism at certain sites, likely serving as the sole mechanism to terminate transcription of many operons in *E. coli*. Well-characterized examples of such sites have properties that favor Rho action during transcription: absence of translation, the absence of any secondary structure that would prevent Rho wrapping RNA, and a cytidine-rich transcript that favors Rho binding; furthermore, natural Rho-dependent terminators are transcription pause sites, a property that presumably gives Rho time to translocate to RNAP and carry out release. It is likely that these characteristics are sufficiently common that Rho could generally act after translation fails in most operons.

Mfd and Transcription-Coupled DNA Repair

DNA damage is repaired more rapidly in actively transcribed than in rarely transcribed genes, and the template strand is preferentially repaired over the non-template strand. These facts led to the discovery that an RNAP molecule stalled at a DNA lesion can serve as a signal that the DNA is damaged and lead to its rapid repair. This activity contributes to an essential function, because a lesion in a single copy gene would block production of an essential protein. In bacteria, RNAP stalled at a template strand DNA lesion is the target of the Mfd protein, also termed the Transcription Repair Coupling Factor. Mfd is an ATPase and a DNA translocase that mediates both removal of RNAP stalled at the lesion and recruitment of the nucleotide excision repair machinery to the site of the lesion. Similar to Rho activity, Mfd can terminate transcription of almost any obstructed RNAP. Mfd binds to the DNA immediately upstream of the stalled elongation complex and makes direct contact with RNAP; using its two translocase domains, Mfd then pushes RNAP downstream along the DNA in an ATP-dependent reaction, collapsing the upstream edge of the transcription bubble as it moves. In the case where elongation is blocked by a template strand DNA lesion, the rewinding and forward translocation are proposed to force the RNA from the elongation complex and drive RNAP downstream to mediate termination. The rewinding of upstream sequences also can rescue complexes that are backtracked, forcing RNAP into an active, forward configuration in the case where continued elongation is possible.

General Elongation Factors – NusA and NusG

NusA and NusG are nearly universally conserved eubacterial proteins – both essential in *E. coli* – that affect the rate of elongation by RNA polymerase and modulate the efficiency of termination. Both NusA and NusG bind to the RNAP core enzyme and influence the activity of RNAP alone, in combination with each other, or in combination with specific regulatory factors. In a purified system, NusA generally slows elongation, enhances pausing, and increases intrinsic termination efficiency. NusA may interact with the RNA hairpin and enhance the proposed interactions between RNA hairpins and RNAP. NusG appears, in many ways, to function oppositely: in general, it enhances elongation and limits pausing. The molecular details of the interactions between these factors and RNAP are unknown.

Both NusA and NusG also influence Rho activity, and although strong Rho-dependent terminators are pause sites, the effects of NusA and NusG on Rho function are opposite to the prediction based on their effects on pausing: thus, NusA promotes pausing but inhibits Rho function, and NusG inhibits pausing and promotes Rho function. It has been suggested that the NusG effect may result from NusG inhibiting backtracking; this could stimulate Rho function if Rho is unable to release a backtracked complex. There may be a distinction between direct effects of the factors on RNA polymerase at a site where Rho-dependent termination occurs, and indirect effects due to NusA and NusG modulation of the overall rate of transcription. Thus, NusA inhibition could in fact favor termination by slowing RNAP so that Rho can catch it through translocation along the RNA. An important relation between the activities of NusA and Rho *in vivo* is shown by the ability of a NusA defective cell to survive if Rho is also defective, but not if Rho is normally functional.

Regulated Termination and Antitermination

Termination can serve as a means to regulate gene expression in two fundamentally different modes that involve antitermination. First, site-specific attenuator-based systems act at particular termination sites in operons to allow or disallow continued transcription, thus determining whether downstream genes are expressed. These terminators are usually intrinsic, but

are sometimes Rho-dependent. Second, generalized antiterminators modify RNA polymerase so that it ignores terminators that otherwise stop transcription, again allowing expression of downstream genes. Finally, a few examples are known of generalized modifications of RNA polymerase that cause termination.

Site-Specific Antitermination: Attenuators and Riboswitches

Intrinsic termination is used to control expression of many operons through devices that alternatively permit or prevent termination in a leader sequence or initially translated region of a set of genes. Such operons contain alternative RNA structures in the beginning of the transcribed region; competition between alternative folding patterns determines whether or not intrinsic terminators are formed, and in turn, whether transcription of the remaining portion of the operon or gene continues. The competition between structures in the leader sequence is influenced in different examples by coordinated translation and ribosome positioning on the RNA, or by small molecules, including tRNAs, that bind to the RNA transcript and affect global folding.

Regulation of the *trp* operon is the classic example of translation-coupled attenuation. Stalling of the ribosome at tryptophan codons, because of limitation in charged-aminoacyl tRNAs, determines which sequences of the transcript can fold, and thus whether a terminator hairpin can be formed. Attenuation can also be mediated by interactions between uncharged tRNAs and leader sequences containing binding sites for these tRNAs, termed T-boxes. Riboswitches consist of the leader and initially translated regions of regulated operons, which undergo alternative folding in response to small regulatory molecules; both positive and negative riboswitches have been described.

Termination and Antitermination Factors

Specific regulatory factors, such as the λN and Q proteins, the bacterial RfaH protein, and the HK022 Nun, regulate expression of specific genes or operons by changing the termination capacity of RNA polymerase. In general, the terminator/antiterminator is recruited to particular transcribing RNAPs via *cis*-acting nucleic acid sequences. Details of the exact modifications these factors make to the complex and the effects of these modifications on the stability of the elongation complex are just beginning to be understood at a molecular level.

λN binds a specific site (*nut*) in the nascent RNA, and in a complex with the general elongation factors NusA and NusG, and the bacterial proteins NusB and S10, interacts with RNAP to stimulate elongation through downstream terminators. Both λQ and RfaH require *cis*-acting DNA sequences to pause RNAP at discrete sites and present a novel complex for interaction. λQ protein interacts with RNAP at a σ-dependent promoter proximal pause and becomes a subunit of the elongating RNAP, modifying it to prevent recognition of downstream terminators. Q likely remodels the active site and strengthens interactions between the enzyme and the hybrid to resist the action of a terminator. RfaH regulates expression of particular operons by interacting with RNAP at a regulatory pause (*ops* sequence) to stimulate expression of distal genes. HK022 Nun protein stimulates transcription termination after binding the same RNA sequences that N protein binds, thus blocking superinfection of its host by another lambdoid phage that requires N function for growth. Elongation complexes are halted by the action of Nun but not disrupted. Thus, Nun is not a release factor; Nun-arrested complexes require the activity of the Mfd protein to efficiently release the transcript and disrupt the elongation complex.

See Also the Following Articles

Ribozyme Structural Elements: Hairpin Ribozyme • RNA Polymerase I and RNA Polymerase III in Eukaryotes • RNA Polymerase II and Basal Transcription Factors in Eukaryotes • RNA Polymerase II Elongation Control in Eukaryotes • RNA Polymerase II Structure in Eukaryotes • Transcription-Coupled DNA Repair, Overview

Glossary

backtracking Reverse translocation of RNA polymerase along the DNA template. The RNA is re-threaded through the complex as RNA polymerase moves backward.

core RNA polymerase and holoenzyme Core RNA polymerase is composed of five subunits ($\alpha_2\beta\beta'\omega$) and is sufficient for RNA synthesis, but not promoter recognition. Binding of an additional subunit, σ, results in formation of holoenzyme; σ is necessary for promoter recognition but is dispensable at latter stages of transcription.

RNA/DNA hybrid An RNA and a DNA strand paired in an A-form 8 or 9 bp double helix within the main channel of RNA polymerase.

termination Release of the nascent transcript from RNA polymerase; whether transcript release and enzyme dissociation from DNA occur simultaneously is unknown.

Further Reading

Burns, C. M., Richardson, L. V., and Richardson, J. P. (1998). Combinatorial effects of NusA and NusG on transcription elongation and Rho-dependent termination in *Escherichia coli*. *J. Mol. Biol.* **278**, 307–316.

Gusarov, I., and Nudler, E. (1999). The mechanism of intrinsic transcription termination. *Mol. Cell* **3**, 495–504.

Komissarova, N., Becker, J., Solter, S., Kireeva, M., and Kashlev, M. (2002). Shortening of RNA: DNA hybrid in the elongation

complex of RNA polymerase is a prerequisite for transcription termination. *Mol. Cell* **10**, 1151–1162.

Martin, F. H., and Tinoco, I. Jr. (1980). DNA–RNA hybrid duplexes containing oligo (dA:rU) sequences are exceptionally unstable and may facilitate termination of transcription. *Nucleic Acids Res.* **8**, 2295–2299.

Park, J. S., Marr, M. T., and Roberts, J. W. (2002). *E. coli* transcription repair coupling factor (Mfd protein) rescues arrested complexes by promoting forward translocation. *Cell* **109**, 757–767.

Selby, C. P., and Sancar, A. (1993). Transcription-repair coupling and mutation frequency decline. *J. Bacteriol.* **175**, 7509–7514.

Skordalakes, E., and Berger, J. M. (2003). Structure of the Rho transcription terminator: Mechanism of mRNA recognition and helicase loading. *Cell* **114**, 135–146.

Toulokhonov, I., Artsimovitch, I., and Landick, R. (2001). Allosteric control of RNA polymerase by a site that contacts nascent RNA hairpins. *Science* **292**, 730–733.

Weisberg, R. A., and Gottesman, M. E. (1999). Processive antitermination. *J. Bacteriol.* **181**, 359–367.

Yarnell, W. S., and Roberts, J. W. (1999). Mechanism of intrinsic transcription termination and antitermination. *Science* **284**, 611–615.

Biography

Jeffrey Roberts is the Robert J. Appel Professor of Molecular and Cell Biology in the Department of Molecular Biology and Genetics at Cornell University. His principal research interest is the mechanism of termination and antitermination in bacteria. He obtained his Ph.D. from Harvard University, and he is a member of the National Academy of Sciences and the American Academy of Arts and Sciences, and a Fellow of the American Society for the Advancement of Science.

Transcriptional Silencing

Ann Sutton and Rolf Sternglanz
Stony Brook University, Stony Brook, New York, USA

Transcriptional silencing is the process by which large regions of a eukaryotic genome are rendered transcriptionally inactive due to a change in chromatin structure. The role of chromatin structure in the regulation of gene expression has become an exciting area of study in recent years. In all eukaryotes, DNA is packaged into nucleosomes to form a protein-DNA structure called chromatin. Each nucleosome consists of 146 base pairs of DNA wrapped around a protein octamer consisting of the four core histones, H2A, H2B, H3, and H4. Linker DNA separates adjacent nucleosomes. Microscopic analysis of chromatin from higher eukaryotic cells has revealed the presence of two types of chromatin, a highly condensed form called heterochromatin, and a less condensed form called euchromatin. In general, genes within heterochromatin are transcriptionally silenced, while those within euchromatin are transcriptionally active. The transcriptional silencing results from the inaccessibility of the DNA to components of the transcriptional machinery or from an inability of RNA polymerase to elongate through heterochromatin. Silenced domains are also less accessible to recombination, replication, and repair machinery than are euchromatic regions. Silencing differs from gene-specific repression in a number of ways. For example, silenced domains extend over large regions of DNA, while gene repression is more local and results from protein interactions within the promoter of a single gene. Furthermore, silenced chromatin can be maintained through many generations. The mechanism of this inheritance is not yet well understood.

Heterochromatic or silenced chromatin domains exist in all eukaryotes examined to date. Regions of the DNA that are known to exist as heterochromatin include telomeres and centromeres in fission yeast and metazoans, chromosome 4 in *Drosophila*, and one of the X chromosomes in female mammals.

Transcriptional Silencing in Yeast

Transcriptional silencing is best understood in two genetically tractable organisms, the budding yeast, *Saccharomyces cerevisiae*, and the fission yeast, *Schizosaccharomyces pombe*.

Budding Yeast, *S. cerevisiae*

The mechanism and regulation of formation of silent chromatin domains have been studied most extensively in the budding yeast, *S. cerevisiae*, which has four major silenced regions: the two silent mating loci, telomeres, and ribosomal DNA (rDNA). Haploid budding yeast exists as one of two mating types, **a** or α, determined by whether **a**- or α-specific alleles are expressed at the *MAT* locus. Yeast also have identical **a** and α alleles at two additional loci, *HML* (which usually carries the α genes), and *HMR* (which usually carries the **a** genes). However, the genes at *HML* and *HMR* are not expressed because of transcriptional silencing. If silencing is lost at these loci as a consequence of a mutation in a silencing factor, cells express both **a** and α mating type information and lose the ability to mate. Largely through the use of genetic screens for mutants defective in mating, most of factors required for silencing at the *HM* loci have been identified.

Silencing requires *cis*-acting regions that flank the mating type genes as well as *trans*-acting factors, in particular the four silent information regulator proteins (Sir1–Sir4). The *cis*-acting regions, termed silencers, contain binding sites for at least two of the following three proteins: Rap1, Abf1, and the origin replication complex (ORC) (Figure 1). All three proteins have essential functions in yeast in addition to their roles in gene silencing; Rap1 and Abf1 are transcription factors, and ORC is required for DNA replication. On the other hand, at the silent mating loci, these proteins function to recruit the Sir proteins to the silencer. Orc1, one of the six subunits of the ORCs, binds Sir1, which then recruits Sir4, which most likely binds as a Sir4–Sir2 complex. Rap1 and Abf1 recruit Sir3 and Sir4. Once the Sir proteins are recruited to the silencer, multiple protein-protein interactions between Sir2, Sir3, and Sir4, and between Sir3 and Sir4 and the amino terminal tails of histone H3 and H4, cause the spreading of these Sir proteins, and consequently silenced chromatin, from the silencers to the regions to be silenced, in this case the *HM* loci (Figure 1). The extent of the repressed domains can be determined by monitoring the expression of a reporter gene placed at increasing distances from the silencer. Silencing at *HMR* spans about 3.5 kbp of DNA, and silencing at *HML* also extends over several kbp.

Sir3 and Sir4 are believed to play a structural role in silent chromatin. Sir2, on the other hand, has recently

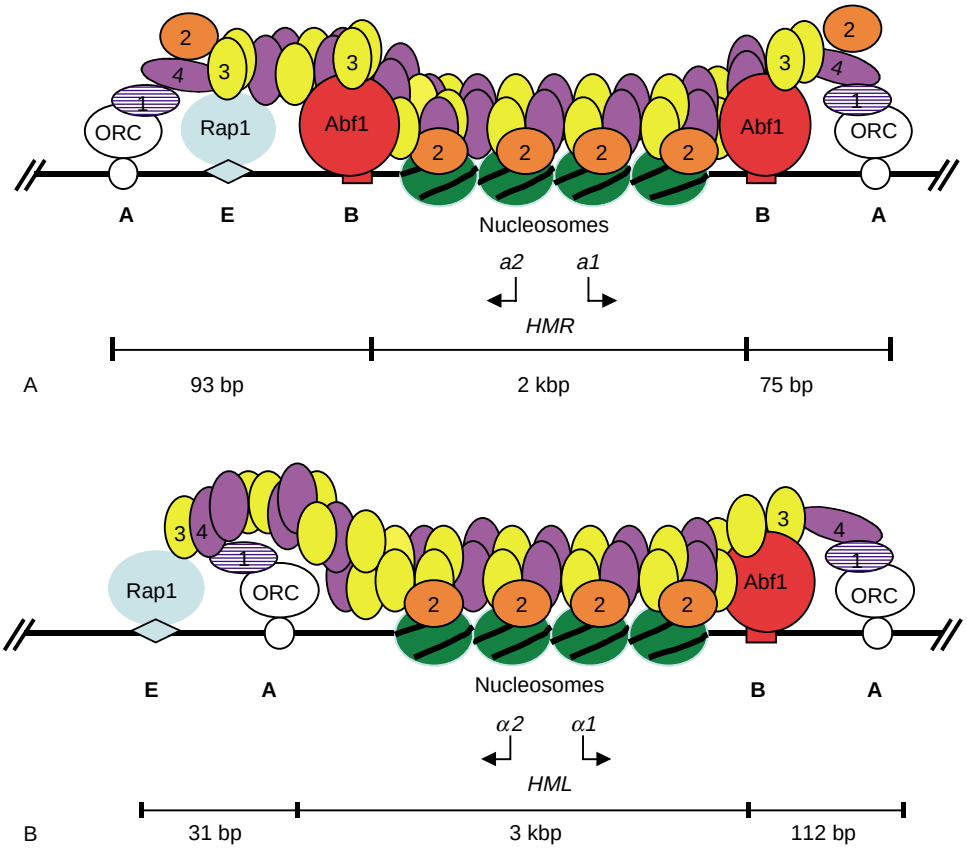

FIGURE 1 The silent mating loci in budding yeast, *S. cerevisiae*. The proteins that bind to the silencers are shown, as well as the four Sir proteins, Sir1 (cross hatched), Sir2 (orange), Sir3 (yellow), and Sir4 (purple). Nucleosomes are in green with diagonal hatch marks. Although the Sir proteins are depicted only between the two silencers, actually the proteins spread bidirectionally from the silencers. (A) The *HMR* locus. (B) The *HML* locus.

been shown to be an enzyme. It is an NAD^+-dependent histone deacetylase that removes acetyl groups from lysines in the amino terminal tails of histone H3 and H4. While this deacetylase activity is not required for the binding of the Sir proteins to the silencers, it is required for the spreading of the Sir proteins and the formation of silent chromatin. Hypoacetylation of the lysines in the histone tails has long been known to be a characteristic of heterochromatin and recent studies suggest that Sir3 preferentially binds to histone tails that are not acetylated. A model to explain the spreading of silent chromatin from the silencers is that Sir2, once recruited to a silencer, deacetylates the lysines on the tails of histones H3 and H4 on adjacent nucleosomes. Sir3 and Sir2–Sir4 complexes then bind to these histones, Sir2 deacetylates the histone tails on adjacent nucleosomes, Sir proteins then bind to them, and so on. The unusual NAD^+ requirement of Sir2 for its deacetylase activity may link silencing to cellular metabolism, and indeed, mutations in genes involved in a salvage pathway for NAD^+ biosynthesis have been shown to affect silencing.

The mechanism of transcriptional silencing at telomeres in *S. cerevisiae* is quite similar to that at the *HM* loci. Telomeres contain multiple binding sites for Rap1, the same protein found at the *HM* silencers. Rap1 is able to recruit Sir3 and Sir4–Sir2 and these proteins spread several kbp from the telomeres into adjacent nucleosomes, causing silencing of genes in these regions (Figure 2). Sir1 is not involved in telomeric silencing, because there are no ORC-binding sites at telomeres and Sir1 is recruited by ORC. Silencing within the rDNA genes requires Sir2, but none of the other Sir proteins. At these loci, Sir2 is a component of the RENT complex that also contains Net1 and Cdc14. The role of these proteins in the establishment and spreading of silencing at rDNA remains to be elucidated. Since Sir2 is the only Sir protein required for rDNA silencing, the mechanism of silencing at this locus is considered fundamentally different from that at the *HM* loci and telomeres. However, the deacetylation activity of Sir2 is required for rDNA silencing, and in that sense the mechanism is similar at all silent loci in budding yeast.

While silent chromatin can extend over several kbp of DNA, mechanisms exist to stop the spreading. Assays have been developed to look for sequences that can function as boundary elements between euchromatin and heterochromatin. In some cases, boundary elements appear to consist of strong transcriptional promoter

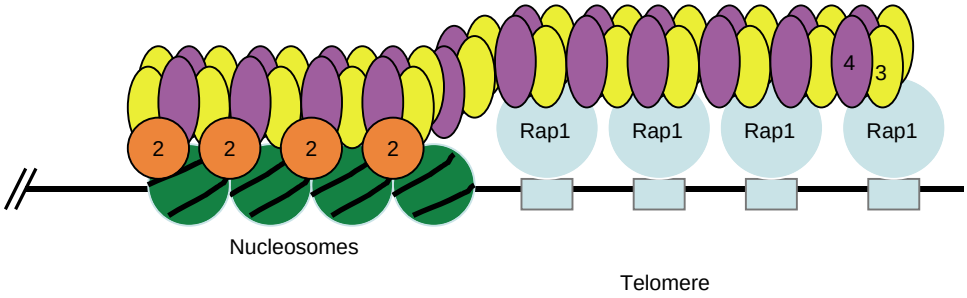

FIGURE 2 Silencing at a yeast telomere. A series of Rap1 proteins is shown binding to the repeated sequence at a telomere. Sir proteins and nucleosomes are designated and colored as in Figure 1.

elements. In these cases binding of transcription factors may sterically block the spread of the silencing proteins. The activity of histone acetyltransferases may also play a role in boundary function, perhaps by acetylating lysine residues on histone tails, and thus counteracting the Sir2-mediated deacetylation that is required for silencing. Mutations in the histone acetyltransferase Sas2 result in the spread of silencing and Sir proteins beyond the normal limits of silenced chromatin at telomeres, and tethering Sas2 to the DNA near *HMR* can limit the spread of silencing. Sas2 specifically acetylates lysine 16 of H4 and it is known that deacetylation of this residue, presumably by Sir2, is particularly important for the formation of silent chromatin.

A recently discovered histone modification that may also function to prevent heterochromatin formation in *S. cerevisiae* is methylation of lysine 79 of histone H3. The Dot1 protein is responsible for this methylation, and most of the H3 in yeast chromatin (but not that in silenced regions) is methylated. A current model is that Sir proteins do not bind well to nucleosomes with H3 methylated on lysine 79, and therefore this modification may function to restrict silencing to a few discrete regions of the genome. In summary, transcriptionally active (euchromatic) regions in yeast appear to be acetylated on H4 lysine 16 and methylated on H3 lysine 79, while silent regions (heterochromatin) lack these modifications.

Fission Yeast, *S. pombe*

Fission yeast also has silent mating type information, in this case within a 20 kbp region that is transcriptionally silent and completely devoid of recombination. There are significant differences between the two yeasts in the mechanism of silencing and the proteins involved. The most important difference involves a histone modification not found in budding yeast, namely, methylation of H3 lysine 9. This modification is also found in metazoan heterochromatin and is catalyzed by a conserved histone methylase called Clr4 in *S. pombe*, Su(var)3-9 in *Drosophila* and SUV39H1 in human. In order for H3 lysine 9 to be methylated, it must be deacetylated. The *S. pombe* homologue of Sir2 plays a crucial role in this deacetylation. Another conserved protein called Swi6 in *S. pombe* and HP1 in metazoans binds specifically to nucleosomes with H3 methylated on lysine 9. Again, this protein is not found in budding yeast. The combination of lysine 9 methylation and Swi6/HP1 binding to nucleosomes with this modification spreads on the chromatin to create the silent heterochromatic regions. The nucleation point from which silent chromatin initiates and spreads in fission yeast is still under active investigation, but seems to involve repetitive DNA sequences and targeting of noncoding RNAs to them.

The 20 kbp silent region is flanked by inverted repeats that serve as boundary elements that isolate the silent heterochromatic domain. Studies of the histone modifications in and around the silent domain show a sharp demarcation at the boundaries. Within the silent domain, H3 lysine 9 is methylated whereas in the euchromatic regions it is acetylated. Also, H3 lysine 4 is acetylated in the transcriptionally active regions outside the boundary elements whereas it lacks this modification in the 20 kbp silent region.

In contrast to *S. cerevisiae*, the centromeres in *S. pombe* are very large (more than 100 kbp) and consist largely of repetitive sequences that are also heterochromatic. Centromeric heterochromatin is methylated on H3 lysine 9 and has HP1 bound to it, just as is the case at the silent mating locus.

Metazoans

As mentioned above, heterochromatin is found in all eukaryotes examined to date. In metazoans, the mechanism for silencing appears to be quite similar to that in *S. pombe*. In fact, the heterochromatin protein HP1 was first identified in *Drosophila*, and three different isoforms are found in mammals. Just as in *S. pombe*, HP1 binds to H3 methylated on lysine 9 in metazoans and is the fundamental building block of

heterochromatin. Interestingly, HP1 in *Drosophila* also binds to the N terminus of Orc1, just as Sir1 binds to that domain of *S. cerevisiae* Orc1. This is the case even though there is no sequence similarity between HP1 and Sir1, and between the Orc1 N termini of the two species. Thus, the function appears to have been conserved even though the sequence is not.

In summary, silent heterochromatic domains in metazoans appear to have the same histone modification (H3 lysine 9 methylation) and the same protein that binds to it (HP1) as is found in fission yeast. The mechanism for initiating heterochromatin formation in metazoans is not known yet.

In all eukaryotes, including budding yeast, heterochromatin is less acetylated on the histone N-terminal tails than is euchromatin. Presumably, this deacetylation is catalyzed by Sir2 homologues and other histone deacetylases. A common theme for silent heterochromatin in all species is the presence of specifically modified histones and proteins that bind uniquely to them.

See Also the Following Articles

Chromatin: Physical Organization • DNA Replication: Eukaryotic Origins and the Origin Recognition Complex • Nuclear Organization, Chromatin Structure, and Gene Silencing • Telomeres: Maintenance and Replication

Glossary

euchromatin Transcriptionally active chromatin, with a different structure than heterochromatin.

heterochromatin A specialized form of chromatin that is transcriptionally silent.

nucleosomes The basic building block of chromosomes, consisting of an octamer of histones H2A, H2B, H3, and H4 plus 146 base pairs of DNA.

Sir proteins Silent information regulator proteins that are required for silencing in the budding yeast, *S. cerevisiae*.

transcription RNA synthesis.

Further Reading

Gasser, S. M., and Cockell, M. M. (2001). The molecular biology of the SIR proteins. *Gene* **279**, 1–16.

Grewal, S. I. S., and Moazed, D. (2003). Heterochromatin and epigenetic control of gene expression. *Science* **301**, 798–802.

Moazed, D. (2001). Common themes in mechanisms of gene silencing. *Mol. Cell* **8**, 489–498.

Rusche, L. N., Kirchmaier, A. L., and Rine, J. (2003). The establishment, inheritance, and function of silenced chromatin in *Saccharomyces cerevisiae*. *Annu. Rev. Biochem.* **72**, 481–516.

Biography

Ann Sutton is a Research Associate Professor and Rolf Sternglanz is a Distinguished Professor in the Department of Biochemistry and Cell Biology at Stony Brook University. Their research focuses on chromatin structure and function in yeast. Dr. Sutton received her Ph.D. in Molecular Biology from Stony Brook University and Dr. Sternglanz received his Ph.D. in Chemistry from Harvard University.

Transcription-Coupled DNA Repair, Overview

Isabel Mellon
University of Kentucky, Lexington, Kentucky, USA

Cells are continually exposed to a plethora of DNA-damaging agents formed within cells or present in the extracellular environment. To combat the harmful effects, cells possess an assortment of DNA repair pathways that recognize and remove damaged DNA. DNA can be structurally modified by the covalent addition of chemical adducts, the formation of crosslinks whereby two different bases on the same or opposite DNA strand become covalently linked, the introduction of UV light-induced photoproducts and an assortment of other alterations. Certain types of DNA damage inhibit transcription and pose blocks to RNA polymerase progression along the DNA template. Transcription-coupled repair (TCR) is a specialized feature of DNA repair that selectively removes transcription-blocking damage present in the transcribed strands of expressed genes.

Nucleotide Excision Repair

Nucleotide excision repair (NER) removes an assortment of different types of DNA damage. It removes chemical adducts introduced by exposure to chemical carcinogens and cyclobutane pyrimidine dimers (CPDs) and (6-4) photoproducts produced by UV light. Given that this pathway removes structurally different types of lesions, it is likely that it recognizes the distortion of the DNA helix produced by the lesion rather than the lesion itself. It involves damage recognition, unwinding of the DNA at the lesion, two incisions, one on each side of the lesion, removal (excision) of a stretch of DNA containing the lesion, DNA synthesis to replace the excised DNA, and ligation of the newly synthesized DNA to the parental DNA. The general strategy has been conserved in *Escherichia coli* (*E. coli*), yeast, and mammalian systems.

TCR has been clearly demonstrated to be a subpathway of NER. It is usually measured as more rapid or more efficient repair in the transcribed strand of an expressed gene compared with the nontranscribed strand. This was first demonstrated studying the removal of UV light-induced CPDs from each strand of the DHFR gene in hamster and human cell lines. TCR of CPDs was subsequently demonstrated in *E. coli* and yeast. In addition, certain bulky chemical lesions are substrates for TCR. Hence, this subpathway of NER has been conserved from bacteria to humans and operates on many different lesions. Repair in the nontranscribed strands of expressed genes and in unexpressed regions of the genome is referred to as global genome repair (GGR). Many of the same proteins are required for TCR and GGR. However, the two subpathways likely differ at the damage recognition step. For TCR, damage recognition is initiated by the stalling of RNA polymerase complexes at lesions in the transcribed strands of expressed genes. For GGR, damage recognition is initiated by other proteins.

E. coli

NER in *E. coli* is understood in detail and has served as a paradigm for the investigation of other organisms. Damage recognition and processing is carried out by the UvrABC system. UvrA dimerizes ($UvrA_2$) and binds UvrB and the $UvrA_2B$ complex binds DNA. The helicase activity of the complex may enable scanning for damage by translocation along the DNA and it unwinds DNA at the site of the lesion. $UvrA_2$ dissociates from the damaged site leaving an unwound preincision complex containing UvrB that is recognized and bound by UvrC. UvrBC produces an incision on each side of the lesion, both made by UvrC. UvrD unwinds and displaces the damaged oligonucleotide produced by the incisions. The resulting gap is filled in by DNA polymerase I and the repair patch is sealed by DNA ligase.

TCR in *E. coli* was first alluded to by studies of mutation frequency decline in tRNA operons. It was documented as more rapid removal of CPDs from the transcribed strand of the *lac* operon. Genetic and biochemical studies indicate that TCR and GGR require UvrA, B, C, and D. However, TCR also requires the mutation frequency decline (Mfd) protein. In addition, TCR in the *lac* operon requires transcription of the operon. CPDs in the transcribed strands of expressed genes pose blocks to RNA polymerase elongation while those in the nontranscribed strand are generally

bypassed. Hence, blockage of elongating RNA polymerase complexes at CPDs is an early step in TCR and the RNA polymerase complex and/or some feature of the transcription bubble likely play important roles.

Sancar and colleagues found that Mfd promotes the release of RNA polymerase complexes stalled at lesions in the transcribed strand of a gene expressed in a cell-free system. However, this provides somewhat of a conundrum in that, if the stalled polymerase complex or the transcription bubble is an important signal for TCR, presumably this signal is lost when the polymerase complex becomes displaced from the lesion. Recent studies have provided additional insights into possible mechanisms. First, certain lesions are bound more efficiently when present in "bubble" substrates and incision can occur in the absence of certain NER factors. In addition, bubble-like structures trigger the 3′ and 5′ endonuclease activities of UvrBC. Hence, it is likely that some aspect of the transcription bubble plays a key role in TCR. Second, a novel function for Mfd has been recently defined by Parks and colleagues; it has the ability to reverse "backtracked" RNA polymerase complexes. Backtracking involves translocation of the RNA polymerase complex and the transcription bubble backward from the site of blockage. In fact, Hanawalt and colleagues proposed that RNA polymerase complexes backtrack at CPDs.

A model for TCR in *E. coli* is described in Figure 1 that incorporates backtracking and loading of NER factors onto the transcription bubble. The model is as follows: After UV-irradiation, RNA polymerase complex elongates until it encounters a CPD on the transcribed strand and stalls. The polymerase then translocates backwards. Mfd recognizes the backtracked complex and induces forward translocation of the polymerase until it re-encounters and perhaps even bypasses the lesion for a short distance. $UvrA_2B$ or perhaps UvrB alone loads 5′ to the lesion (relative to the damaged strand). The loading of UvrB is facilitated by features of the transcription bubble brought about by

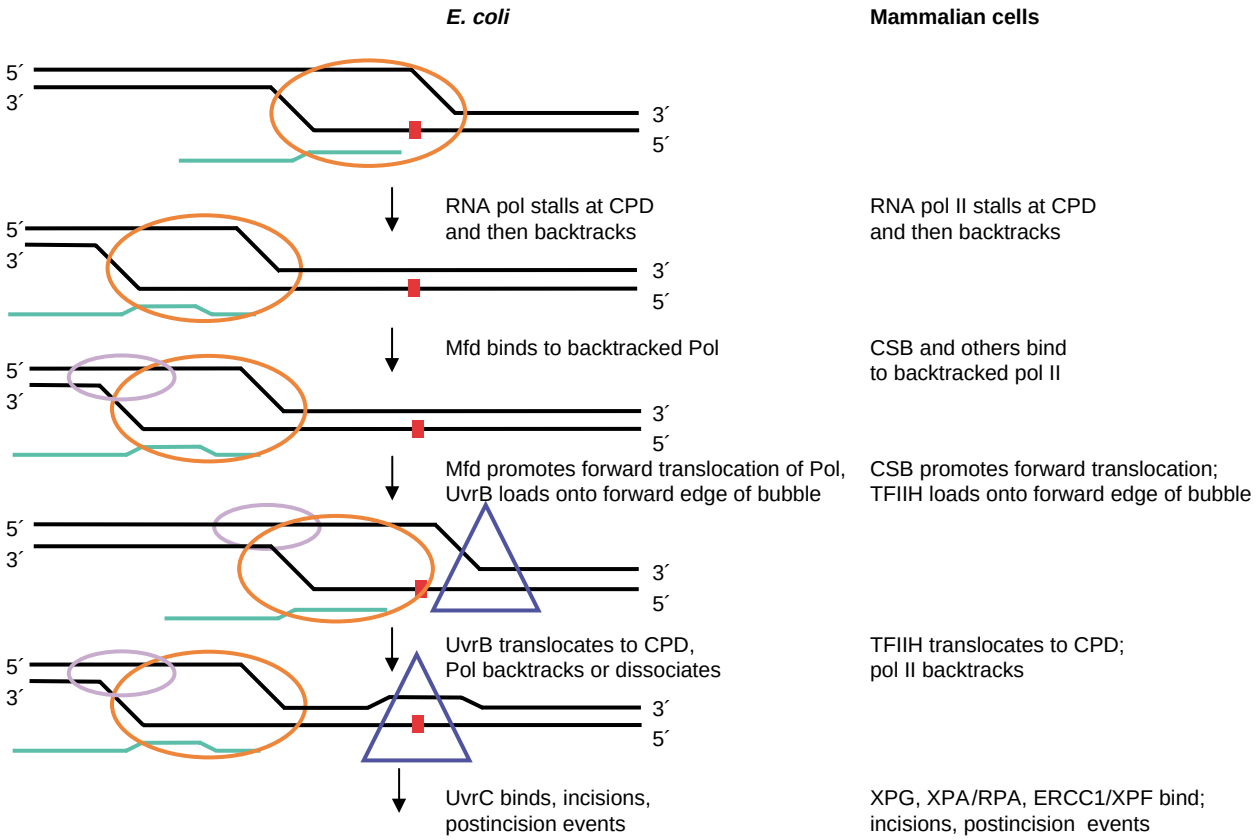

FIGURE 1 A model for TCR of CPDs. *E. coli*: Elongating RNA polymerase complex (orange oval) stalls at a CPD (small red square) in the transcribed strand. The polymerase complex, transcription bubble, and nascent RNA (green line) translocate backwards. Mfd (lavender oval) binds backtracked polymerase and DNA upstream of the bubble. Mfd promotes the forward translocation of the polymerase complex. UvrB (blue triangle) binds 5′ (relative to the damaged strand), loads onto the forward edge of the bubble, and translocates to the lesion. The polymerase complex backtracks or is dissociated by Mfd. Subsequent NER processing events continue as they would in nontranscribed DNA. Mammalian cells: Same as for *E. coli* except for the following: CSB (lavender oval) bind the backtracked polymerase complex and promote forward translocation. TFIIH (blue triangle) binds 5′ to the damage and loads onto the forward edge of the bubble. Subsequent NER events continue as they would in nontranscribed DNA.

the forward translocation induced by Mfd. At this point the polymerase may backtrack again or may be completely released by Mfd. UvrC then binds to the lesion-bound UvrB complex resulting in a stable preincision complex and this and subsequent downstream NER events continue as they would in nontranscribed DNA. The salient point is that the "coupling" of NER to transcription may be mediated by the correct positioning of the transcription bubble at the lesion. Mfd may serve two functions: one is to maintain the transcription bubble at the site of the lesion by reversing backtracked complexes and the other may be to ultimately displace the complex from the damaged site to allow incision and DNA synthesis.

Mammalian Cells

The general strategy of NER in mammalian systems closely parallels that of *E. coli*. However the repertoire of proteins required for mammalian NER is significantly more complex. There is considerable evidence that XPC/hHR23B complex is involved in an early step of damage recognition. TFIIH is then recruited which results in unwinding near the lesion by virtue of the helicase activities of XPB and XPD, components of TFIIH. XPG, XPA/RPA, and ERCC1/XPF assemble to form a stable preincision complex. Dual incisions are carried out; the 3′ incision by XPG and the 5′ incision by ERCC1/XPF, followed by postincision events. With the exception of XPC (and probably hHR23B) the same repertoire of proteins described above are required for TCR and GGR. It is likely that in TCR, the RNA polymerase complex replaces the function of XPC/hHR23B in damage recognition.

Genetic studies have indicated a requirement for additional genes in TCR. These include Cockayne syndrome group A and B (CSA and CSB) genes, genes involved in mismatch repair, UV-sensitive syndrome (UVSS), and XPA-binding protein (XAB2). Mutations in these genes result in a selective loss of TCR while repair in nontranscribed DNA is not effected or less effected. Biochemical studies have implicated the direct involvement of CSA, CSB, and XAB2 in TCR. As in *E. coli*, TCR in mammalian cells may be dependent upon the positioning of the transcription bubble at the lesion and not necessarily on direct interactions between NER proteins and transcription factors. CSA, CSB, TFIIH, and XAB2 may serve essential roles in remodeling the transcription bubble to facilitate TCR (Figure 1). Further investigation is required to determine their mechanism of action.

In mammalian cells TCR appears to be limited to genes transcribed by RNA pol II. The investigations of repair in genes transcribed by RNA polymerase I (pol I) and RNA polymerase III have found no evidence of TCR. However, the examination of ribosomal genes transcribed by pol I is complicated because only a subset of the genes are transcriptionally active. Recent studies by Smerdon and colleagues have fractionated active and inactive ribosomal genes in yeast and found TCR in the active fraction. Hence, TCR may not be limited to pol II genes in mammalian systems either and future studies are warranted to answer this important question.

Saccharomyces cerevisiae

The biochemical details of NER are not as well understood in *S. cerevisiae*. Genetic studies by several laboratories have demonstrated that *rad26* is required for TCR. More recent studies from the Smerdon laboratory have demonstrated that certain subunits of yeast RNA pol II, Rpb4, and Rpb9, also influence TCR. Deletion of the pol II subunit gene, *rpb9*, greatly reduces TCR of the GAL1 gene when cells are grown in log phase. Deletion of *rad26* greatly reduces TCR of GAL1 when cells are grown in stationary phase. In addition, deletion of a different pol II subunit gene, *rpb4*, restores TCR in the *rad26* mutant grown in stationary phase. Hence, in addition to providing novel information on the requirement of pol II in TCR, these studies also indicate that there are differences in TCR that depend on the growth state of the cell.

Base Excision Repair

Base excision repair (BER) represents a collection of repair pathways that operate on a variety of different lesions induced by oxidative damage, alkylation damage, and other types of damage. The broad substrate specificity is accomplished by a large number of different damage-specific glycosylases. Hence, this differs from NER where the broad substrate specificity is accomplished by assembling a multiprotein complex.

Alkylation Damage

Alkylating agents represent a broad class of DNA-damaging agents that are present in the environment, are used as chemotherapeutic agents and can be formed endogenously during cellular metabolism. N-methylpurines (NMPs) are the most abundant lesions produced by simple alkylating agents such as methyl methanesulfonate and dimethyl sulfate. 7-methylguaine and 3-methyladenine are the most abundant NMPs formed by these agents. NMPs are removed by BER in *E. coli*, yeast, and mammalian cells and repair is initiated by specific glycosylases. The removal of NMPs has been compared in the transcribed and nontranscribed strands of the DHFR gene in mammalian cells, the GAL1 gene in *S. cerevisiae*, and the lactose operon of *E. coli*. No significant difference was found in the repair of the transcribed and nontranscribed strands of these genes.

Hence, TCR does not appear to be a subpathway of methylation damage-specific BER.

Oxidative Damage

Oxidative damage is formed as a consequence of exposure to ionizing radiation and a variety of chemical agents and as byproducts of normal cellular metabolism. These agents introduce a large number of modifications to DNA including alterations of bases, the deoxyribose sugar, and cleavage of the phosphodiester backbone. Several studies have found more rapid removal of oxidative damage from the transcribed strands of expressed genes in yeast and mammalian cells. Hence, TCR operates on oxidative damage. It has been proposed that this finding indicates that TCR is also a subpathway of BER since many forms of oxidative damage are substrates for BER. However, there has been no direct genetic or biochemical demonstration of a role of BER in TCR. Ionizing radiation and other forms of oxidative agents produce a wide spectrum of different lesions, including some that are substrates for NER. Moreover, the Cooper, Clarkson and Leadon laboratories have found that TCR of oxidative damage is abolished or significantly reduced in human cell lines with certain mutations in the NER genes XPG, XPB, and

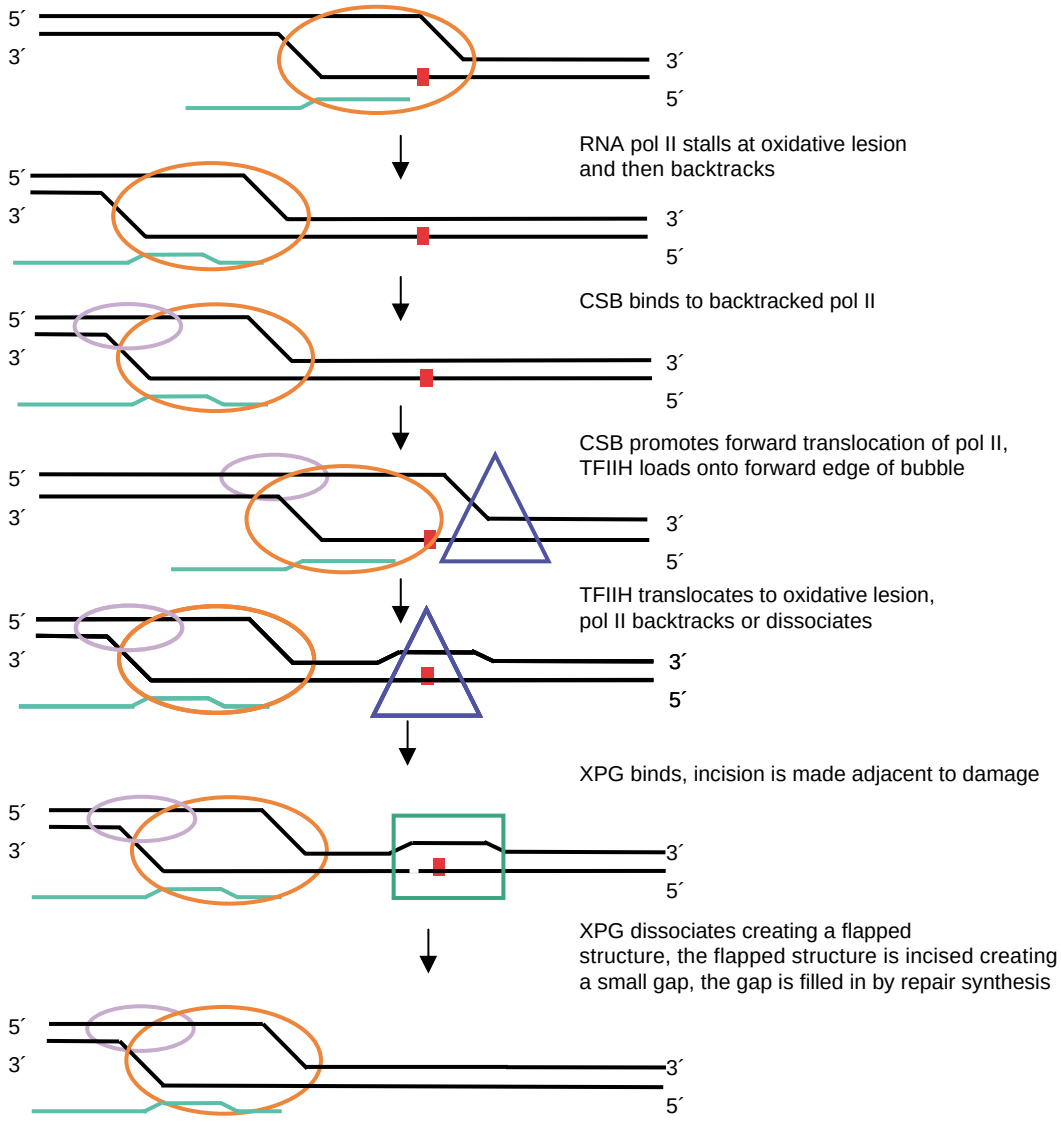

FIGURE 2 A model for TCR of oxidative damage. Elongating RNA pol II complex (orange oval) stalls at an oxidative lesion (small red square) in the transcribed strand. The pol II complex, transcription bubble, and nascent RNA (green line) translocate backwards. CSB (lavender oval) binds backtracked polymerase and promotes the forward translocation of the pol II complex. TFIIH (blue triangle) binds 5′ (relative to the damaged strand), loads onto the forward edge of the bubble, and translocates to the lesion. The polymerase complex backtracks. XPG binds (green square) and makes an incision at the oxidative lesion creating a flapped structure. The flapped structure is incised creating a small gap and the gap is filled in by repair synthesis.

XPD. XPG is involved in the incision process of NER and XPB, and XPD are components of TFIIH and unwind the helix at the site of damage. In addition, TCR of oxidative damage is abolished or reduced in human cell lines with mutations in CSA and CSB. The CSA and CSB genes are clearly required for TCR mediated by the NER pathway as described above.

A model for TCR of oxidative damage is described in Figure 2 that involves the RNA polymerase complex and components of the NER pathway. RNA polymerase II stalls at the oxidative lesion and then backtracks. CSB, the functional homologue of Mfd, promotes forward translocation of pol II. TFIIH translocates to the oxidative damage, unwinds the DNA as pol II backtracks. XPG incises the oxidative damage present in the unwound DNA creating a flapped structure. The flapped structure is incised 5′ to the damage creating a small gap that is filled in by DNA repair synthesis. As in the model for TCR of UV damage, the salient point is that the coupling of repair of oxidative damage to transcription may be mediated by the correct positioning of the transcription bubble at the lesion.

RNA Polymerase Turnover and Degradation

An interesting question from a teleologic viewpoint relates to why cells possess mechanisms that couple DNA repair and transcription. One reason may be that TCR serves to remove transcription-blocking lesions and hence, it facilitates a rapid recovery of transcription. However, transcription complexes are extremely stable when they are stalled at endogenous pause sites or at sites of damage. In the absence of a mechanism to specifically find transcription-blocking lesions, lesions would be shielded from the repair machinery by the RNA polymerase complex and hence, refractory to repair. Furthermore, stable arrested complexes would inhibit gene expression and perhaps interfere with or block the DNA replication machinery. Recent studies have found that RNA pol II complexes are degraded in response to DNA damage. Svejstrup has suggested that degradation of damage-stalled pol II complexes might be an alternative to TCR. Hence, the importance of removing stalled RNA polymerase complexes may be indicated by the development of specific repair mechanisms that remove transcription-blocking damage and if TCR fails to occur, then the RNA polymerase complex stalled at the damaged site may be actually degraded.

See Also the Following Articles

Cell Cycle: DNA Damage Checkpoints • DNA Base Excision Repair • DNA Damage: Alkylation • DNA Mismatch Repair and Homologous Recombination • DNA Mismatch Repair and the DNA Damage Response • DNA Mismatch Repair: *E. coli* Vsr and Eukaryotic G–T Systems • DNA Mismatch Repair in Mammals • Nucleotide Excision Repair and Human Disease • Nucleotide Excision Repair, Bacterial: The UvrABCD System • Nucleotide Excision Repair: Biology • Nucleotide Excision Repair in Eukaryotes • RNA Polymerase I and RNA Polymerase III in Eukaryotes

Glossary

cyclobutane pyrimidine dimer The covalent linkage of two adjacent pyrimidines in DNA produced by exposure to ultraviolet light.

glycosylase An enzyme that cleaves the N-glycosylic bond between a damaged base or inappropriate base and the deoxyribose sugar.

transcription bubble The unwound DNA structure produced by RNA polymerase in the elongation mode of RNA synthesis.

Further Reading

Batty, D. P., and Wood, R. D. (2000). Damage recognition in nucleotide excision repair of DNA. *Gene* **241**, 193–204.

Copper, P. K., Nouspikel, T., Clarkson, S. G., and Leadon, S. A. (1997). Defective transcription-coupled repair of oxidative base damage in Cockayne syndrome patients form XP group G. *Science* **275**, 990–993.

Li, S., and Smerdon, M. J. (2002). Rpb4 and Rpb9 mediate subpathways of transcription-coupled DNA repair in *Saccharomyces cerevisiae*. *EMBO* **21**, 5921–5929.

Moolenaar, G. F., Monaco, V., van der Marel, G. A., van Boom, J. H., Visse, R., and Goosen, N. (2000). The effect of the DNA flanking the lesion on formation of the UvrB-DNA preincision complex. *J. Biol. Chem.* **275**, 8038–8043.

Park, J.-S., Marr, M. T., and Roberts, J. W. (2002). *E. coli* transcription repair coupling factor (Mfd protein) rescues arrested complexes by promoting forward translocation. *Cell* **109**, 757–767.

Sugasawa, K., Ng, J. M. Y., Masutani, C. S. I., van der Spek, P. J., Eker, A. P. M., Hanaoka, F., Bootsma, D., and Hoeijmakers, J. H. J. (1998). Xeroderma pigmentosum group C protein complex is the initiator of global genome nucleotide excision repair. *Mol. Cell* **2**, 223–232.

Svejstrup, J. Q. (2002). Mechanisms of transcription coupled DNA repair. *Nat. Rev.* **3**, 21–29.

Tornaletti, S., Reines, D., and Hanawalt, P. C. (1999). Structural characterization of RNA polymerase II complexes arrested by a cyclobutane pyrimidine dimer in the transcribed strand of template DNA. *J. Biol. Chem.* **274**, 24124–24130.

Zou, Y., Luo, C., and Geacintov, N. E. (2001). Hierarchy of DNA damage recognition in *Escherichia coli* nucleotide excision repair. *Biochemistry* **40**, 2923–2931.

Biography

Isabel Mellon is an Associate Professor at the University of Kentucky, Lexington. Her principal research interests are in the field of DNA repair and include transcription-coupled repair and the roles of genetic alterations in DNA repair genes in the etiology of cancer. She holds a Ph.D. from the University of Illinois at Chicago. She was a postdoctoral fellow at Stanford University where she co-discovered transcription-coupled repair with Philip Hanawalt and colleagues.

Transforming Growth Factor-β Receptor Superfamily

Mark de Caestecker
Vanderbilt University, Nashville, Tennessee, USA

The transforming growth factor-β (TGF-β) superfamily consists of a large family of related growth factors. These can be divided into two main groups: the TGF-β/activin and bone morphogenetic protein (BMP)/growth and differentiation factor (GDF), and subdivided into several related subgroups based on their sequence similarity. Ligands are synthesized as precursor molecules that undergo cleavage, releasing the pro-domain from the active, receptor-binding, carboxy-terminal region of the molecule. The active, carboxy-terminal domains of these ligands have six intra-strand disulfide bonds that form a "cysteine knot" motif. A conserved seventh cysteine is required to form covalently linked dimeric structures that interact with their respective receptors. TGF-β is synthesized as an inactive precursor, cleaved into mature TGF-β and the latency associated peptide, LAP, which is then noncovalently linked to the mature TGF-β and prevents binding to the TGF-β receptors. Other members of the TGF-β superfamily are secreted as mature, active dimers that are inhibited locally through interactions with a variety of secreted antagonists including follistatin, noggin, chordin, and the DAN/cerberus family of proteins.

The TGF-β receptor superfamily have three-finger toxin folds in the ligand-binding extracellular domain, a single transmembrane and an intracellular serine–threonine kinase domain. These are divided into two main groups, the type I and type II receptors, based largely on sequence conservation within their kinase domains. In addition, the type I receptors have a conserved glycine-serine rich juxta-membrane domain (the GS box) that is critical for their activation. The nomenclature for the type I and II receptors is somewhat confusing. For simplicity I refer to the type I receptors by a common nomenclature, the activin-like kinases (Alks), and the type II receptors according to their dominant ligand interactions. Type I receptors are classified according to sequence similarities into three main groups: the Alk5 group which includes the TGF-β type I receptor Alk5, the activin receptor Alk4 and the nodal receptor Alk7; the Alk3 group comprising the BMP type I receptors Alk3 and 6; and the Alk1 group Alk1 and 2, which interact with different BMP/GDF and TGF-β/activin family ligands. Type II receptors include the TGF-β type II receptor, TGF-β RII, the activin and BMP/GDF receptors, activin RII and activin RIIB, the BMP/GDF receptor BMP RII, and the Mullerian inhibitory substance (MIS) receptor MIS RII. The purpose of this review is to describe the biochemical properties of the TGF-β superfamily receptors in mammalian cells, focusing specifically on receptor–ligand interactions, accessory receptors, and receptor activation. The reader is referred to a series of reviews for a more detailed description of the functional properties of this these events *in vivo*.

Receptor–Ligand Interactions

The basic paradigm by which TGF-β superfamily ligands (Figure 1) interact with and activate the receptors has been largely established from studies of TGF-β. TGF-β binds to the constitutively active TGF-β type II receptor, TGF-β RII, which then recruits the type I receptor, Alk5, resulting in transphosphorylation of the type I receptor and activation of downstream signals. A single dimeric ligand interacts with two, type I and two type II receptors to form heterotetrameric signaling complex. A similar mechanism occurs with activin binding to the type II receptor Act RII and recruiting the type I receptor Alk4, and the BMP-ligands BMP6 and 7 interacting with the type II receptors Act RII and IIB and recruiting the type I receptors Alk2, 3, and 6. In contrast, receptor-binding affinity is reversed with BMP2 and 4, which preferentially bind to the type I receptors Alk3 and 6 and recruit type II receptors into heteromeric signaling complexes. These ligand–receptor interactions are inhibited through direct interactions with secreted antagonists including noggin, chordin, follistatin, and the DAN/cerberus family of proteins (Figure 2). Overlapping receptor usage by different TGF-β family ligands adds to the complexity of this system. For example, TGF-β itself has the capacity to interact with and activate at least two additional type I receptors Alk1 and 2, in the presence of TGF-β RII, while the related BMP-ligands BMP2 and 4, have the capacity to interact with the type I receptors Alk3 and 6 and recruit type II receptors BMP RII/Act RII and Act RIIB into active receptor complexes. While the

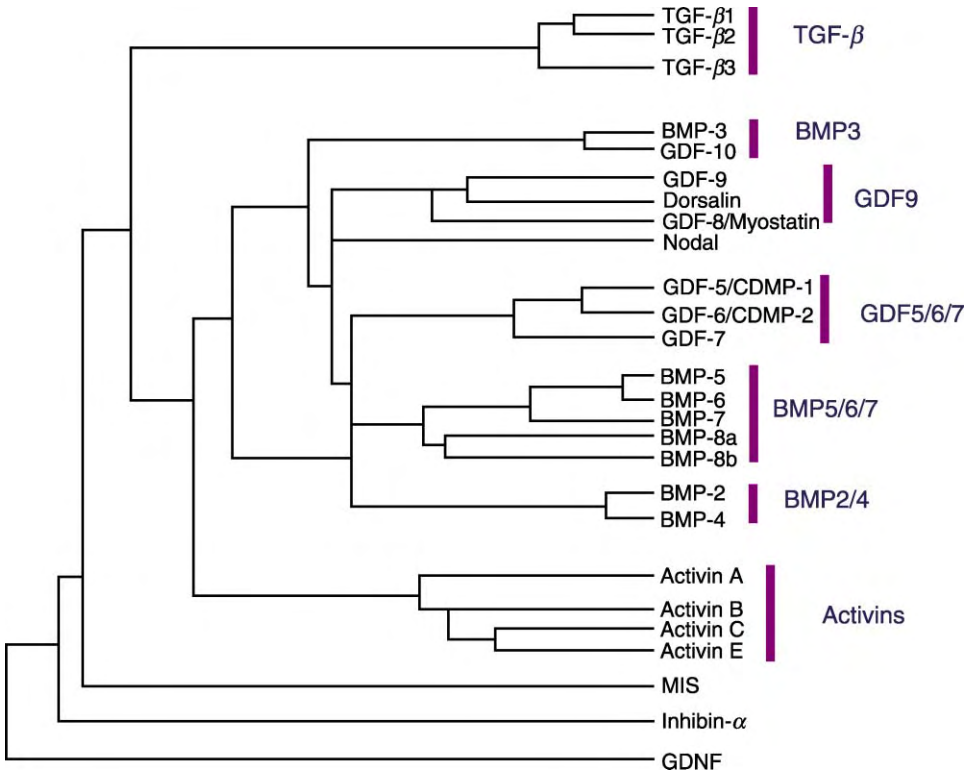

FIGURE 1 TGF-β superfamily of ligands.

functional significance of many different receptor–ligand combinations are poorly understood, the complexity of this combinatorial system is likely to explain the diversity of downstream responses that can be generated by engagement of these receptors in different cell types.

Accessory Receptors

Other cell surface proteins interact with and may be required for signaling. Some of these have been cloned and characterized and will be discussed in this article, while others have been identified from ligand–receptor cross-linking studies in certain cell types and are of uncertain significance. The first of these to be described in detail was the high-molecular-weight type III TGF-β receptor, TGF-β RIII or betaglycan. TGF-β RIII is a ubiquitous, highly glycosylated transmembrane protein with a large extracellular domain and short cytoplasmic tail lacking kinase activity. It was initially thought to function solely as a high-affinity TGF-β receptor, promoting TGF-β ligand binding to the signaling receptors, and is required for binding of TGFβ2 with TGF-β RII. However it is now known that TGF-β RIII is also a coreceptor for inhibin, promoting interactions between inhibin and other type II receptors, and giving rise to a functional inhibition of activin and BMP-dependent signaling. More recently it has been shown that the cytoplasmic tail of TGF-β RIII is required to support TGF-β2-signaling but is not required to promote binding of TGF-β2 to the signaling receptor complex. This suggests that it plays an additional role in regulation of TGF-β signaling. The mechanisms underlying these effects are uncertain, although it has been proposed that in the presence of ligand, the cytoplasmic tail of TGF-β RIII selectively interacts with activated, autophosphorylated TGF-β RII, enabling enrichment of active TGF-βRI/II complexes.

Endoglin is a related, membrane-associated disulfide-linked dimer that was originally identified as a TGF-β1 and β3-binding protein in endothelial cells. It is now known that endoglin interacts with diverse TGF-β family ligands including BMP2, 7, and activin, and that it is selectively expressed in other cell types. Unlike betaglycan, ligand binding occurs indirectly through association with the respective type I, and II receptors. Furthermore, while endoglin and betaglycan form heteromeric complexes in endothelial cells, comparison between endoglin and betaglycan overexpressing cells indicate that endoglin can inhibit while betaglycan enhances TGF-β responsiveness. This suggests that the two accessory receptors may have distinct functional properties.

Recently, another family of accessory receptors has been identified that are required for TGF-β superfamily signaling. Cripto and cryptic are two members of the EGF-CFC family of membrane-anchored proteins.

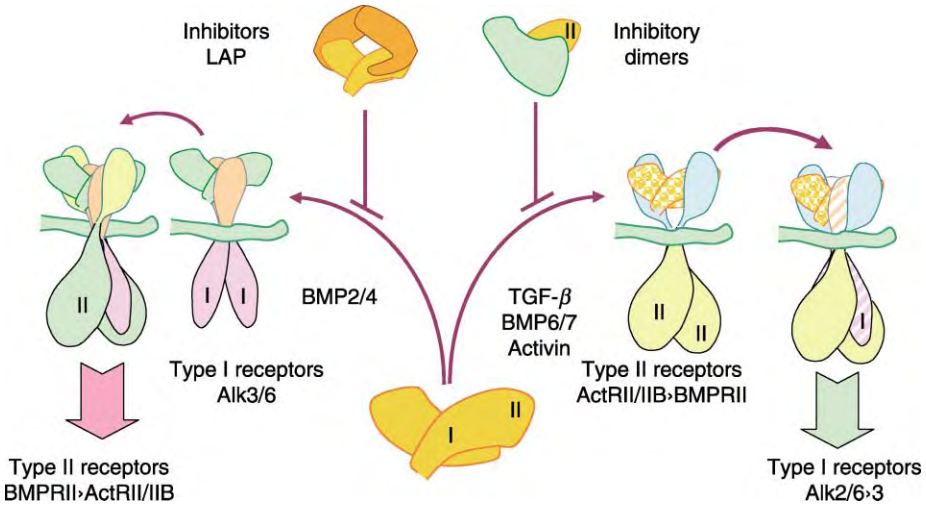

FIGURE 2 TGF-β superfamily receptor-ligand interactions. Ligands are secreted as disulfide-linked dimers, each presenting distinct hydrophobic type I and type II receptor interacting surfaces. Different ligands show variable affinities for type I and II receptors, promoting assembly of distinct hetero-tetrameric receptor–ligand complexes and downstream signals. These receptor interactions are inhibited through the formation of inhibitory complexes (e.g., LAP/TGF-β and noggin/BMP7), and/or heteromeric dimeric that block receptor–ligand interacting surfaces (e.g., inhibin-α/activin-βA subunits of inhibin A).

Genetic and biochemical evidence indicate that both proteins are required for signaling by the TGF-β family members, nodal and GDF1. These interact directly with nodal, GDF1, and the type I receptor, Alk4, and are required for the assembly of Alk4/activin type II receptor signaling complexes following engagement of these ligands. Interestingly, activin-dependent assembly of the ActRII and ActRIIB/Alk4 complexes are inhibited by overexpression of cripto, suggesting that EGF-CFC proteins may exert opposing effects on the assembly of different ligand-dependent TGF-β receptor complexes.

Receptor Activation

Activation of type I TGF-β receptors results from serine phosphorylation by the type II receptor kinase within the GS box immediately upstream of the catalytic domain. These phosphorylation events are associated with a conformational change in the GS box which forms an inhibitory wedge in the kinase domain of the inactive type I receptor, enabling ATP binding and phosphorylation of the downstream substrates, the receptor activated Smads (R-Smads). Basal activation of the type I receptor kinase domain is regulated through the interaction of a repressor protein, FKBP12, which binds to the unphosphorylated GS box, capping the type II receptor phosphorylation sites and stabilizing the receptor in an inactive conformation. In addition, ligand-dependent phosphorylation of the R-Smads is inhibited by direct competition for receptor binding by the inhibitory Smads 6 and 7, which are themselves transcriptionally regulated by diverse signaling pathways.

Phosphorylation of the R-Smads activates the Smad signaling pathway, resulting in the nuclear translocation of an R-Smad/Smad4 complex. This regulates transcriptional responses through direct interaction with both *cis*- and *trans*- activating elements associated with a variety of different gene targets. Two main groups of R-Smads are activated by different sets of type I receptors and activate distinct downstream responses. The BMP receptor activated Smads 1, 5, and 8, and the TGF-β/activin activated Smads, Smad2 and 3. A variety of proteins have been identified that interact with both the receptor complexes and the respective R-Smads, and are thought to function as Smad-anchors and/or chaperones involved in the recruitment of Smad proteins to and from the receptor complex. These include SARA, Hgs, Axin, ELF, Disabled-2, TRAP-1, FTLP, and SANE. The most extensively characterized of these is the FYVE domain protein, Smad anchor for receptor activation (SARA), which recruits Smad2 to the activated receptor complex and is required for receptor-mediated Smad phosphorylation.

Specificity of these responses is determined by a cluster of residues within the L45 loop of the type I receptor kinase domain which interact with a matching set of residues in the L3 loop in the carboxy-terminal domains of the R-Smads. The L45 loop sequence of the Alk5 group of receptors are compatible with L3 loop residues in TGF-β/activin activated Smads 2 and 3, while the Alk3 group sequence is compatible with BMP-activated Smads 1, 5, and 8. The Alk1 group of receptors, which are activated both by TGF-β and

BMP-ligands, carry a cluster of L45 loop sequences that are distinct from the Alk3 group of receptors but are compatible with the BMP-activated Smads 1, 5, and 8. As different ligands can recruit different type I receptors into the signaling complexes, differential activation of Smad substrates by Alk1 and 5 groups of receptors may account for the activation of distinct downstream signals by the same ligand under different conditions.

Endocytic trafficking of activated receptors plays an important role in regulating receptor-dependent signaling. This may result from the activation of signaling by promoting association between activated receptors and various signaling intermediates in the endosomal compartments, or by dampening receptor-dependent signaling through degradation of the activated receptor complexes. Recent data suggests both mechanisms can regulate TGF-β receptor-mediated signaling. In the presence of R-Smads, the FYVE domain protein SARA promotes uptake of the SARA/Smad/receptor complex to early endosomal membranes, promoting clathrin-dependent endocytosis, receptor-mediated phosphorylation and activation of the R-Smad. In contrast, Calveolin-dependent endocytosis and proteosomal degradation of the activated receptor complex is mediated by recruitment of the HECT domain E3 ligase SMURF to the activated type I receptor by the inhibitory Smad7. This results in the uptake of the SMURF/Smad7/receptor complex to Calveolin positive endosomes, and promotes SMURF-mediated ubiquitination and proteosomal degradation of the signaling complex.

In addition to the canonical Smad-signaling pathways, there is considerable evidence of cell-type-dependent regulation of alternative signaling pathways by different members of the TGF-β superfamily. These include activation of MAPK signaling pathways ERK, JNK and p38 MAPK, PI3 kinase, PKC, and inhibition of $p70^{S6K}$ signaling. These signals may be required to mediate and/or augment maximal Smad-dependent responses, or they may exert distinct downstream responses in different cell types. However, the precise mechanisms linking these noncanonical signaling pathways with the activated receptor complexes are incompletely understood. Some of these effects may be indirect, resulting from the induction of Smad-dependent target genes that themselves regulate these responses. For example, while JNK activation by TGF-β may result from activation of a rapid, Smad-independent response in a variety of cell types, a delayed Smad-dependent response has also been described. In other cell types, TGF-β signaling may repress p38 MAPK signaling through the induction of Smad-dependent MAPK phosphatases expression. In contrast, direct regulation of these alternative pathways may result from ligand-dependent protein interactions with the activated receptor complex. For example, interactions between the serine threonine phosphatase, PP2A and the activated TGF-β type I/II receptor complex, results in rapid, dephosphorylation-dependent inhibition of $p70^{S6K}$ activity. Other downstream intermediates may link receptor activation to these pathways. These include the Rho family of small GTPases and the MAPKKK TAK1 and its upstream kinase HPK1, that are involved in regulating TGF-β-dependent activation of JNK, Ras GTPase-dependent activation of ERK MAPK, and TAK1-dependent activation of p38 MAPK by TGF-β. Direct links between these pathways and the activated receptors are less clear.

In addition to these effects, activation of TGF-β family receptors gives rise actin polymerization and cytoskeletal re-organization in a variety of different cell types. While the long-term effects of TGF-β on these responses may be indirect, rapid changes in cytoskeletal organization can involve direct modification of small GTPase-dependent actin polymerization by TGF-β receptor signaling. More recently, LIM kinase 1 (LIMK1), which regulates actin polymerization through phosphorylation-dependent inactivation of Cofilin, has been shown to interact with the cytoplasmic tail of the BMP type II receptor. BMP4-treatment is associated with re-distribution of LIMK1 to the cell periphery, phosphorylation of Cofilin, and active re-organization of the actin cytoskeleton. This suggests that BMP RII-dependent activation of LIMK1 may regulate additional signaling pathways, and raises additional questions regarding the role of the C-terminal tails of TGF-β family receptors in the regulation of downstream signaling.

Conclusions

This review outlines the large number of TGF-β ligands, the plasticity of receptor usage and the diversity of downstream pathways that can be regulated by these receptors. However, while considerable advances have been made in our understanding over the last decade, many of these discoveries have raised many new questions about the complex biology of these receptor-signaling pathways. Important areas of research in the future will provide a more detailed understanding of the factors contributing to the diversity of cell-type-dependent responses and links to other signaling pathways.

See Also the Following Articles

Mitogen-Activated Protein Kinase Family • p70 S6 Kinase/mTOR • Protein Kinase C Family • Ras Family • Rho GTPases and Actin Cytoskeleton Dynamics

Glossary

activins and inhibins Proteins released from the gonads that stimulate and inhibit, respectively, the secretion of follicle-stimulating hormone, which is secreted by the pituitary and is a major regulator of reproductive function.

LIM kinase A protein serine kinase that phosphorylates and inactivates cofilin, a protein that regulates actin depolymerization and hence influences cytokinesis (cell division), endocytosis (uptake of molecules by cells), chemotaxis (directed cell movement) and morphogenesis (cell shape change).

Smads Proteins that are phosphorylated by transforming growth factor receptor family members and move as complexes into the nucleus to activate gene transcription.

transforming growth factors β A secreted protein that acts locally to either stimulate or inhibit cell proliferation or differentiation, and which plays a role in development and wound healing.

Further Reading

Balemans, W., and Van Hul, W. (2002). Extracellular regulation of BMP signaling in vertebrates: A cocktail of modulators. *Dev. Biol.* **250**(2), 231–250.

Chang, H., Lau, A. L., and Matzuk, H. H. (2001). Studying TGF-beta superfamily signaling by knockouts and knockins. *Mol. Cell Endocrinol.* **180**(1–2), 39–46.

de Caestecker, M. P., Piek, E., and Roberts, A. B. (2000). Role of transforming growth factor-beta signaling in cancer. *J. Natl. Cancer Inst.* **92**(17), 1388–1402.

Kawabata, M., and Miyazono, K. (2000). *Skeletal Growth Factors*. Lippincott Williams and Wilkins, Philadelphia.

Massague, J., Blain, S. W., and Lo, R. S. (2000). TGFbeta signaling in growth control, cancer, and heritable disorders. *Cell* **103**(2), 295–309.

Miyazono, K., Kusanagi, K., and Inoue, H. (2001). Divergence and convergence of TGF-beta/BMP signaling. *J. Cell. Physiol.* **187**(3), 265–276.

Pangas, S. A., and Woodruff, T. K. (2000). Activin signal transduction pathways. *Trends Endocrinol. Metab.* **11**(8), 309–314.

Piek, E., Heldin, C. H., and Ten Dijke, P. (1999). Specificity, diversity, and regulation in TGF-beta superfamily signaling. *Faseb J.* **13**(15), 2105–2124.

Shi, Y., and Massague, J. (2003). Mechanisms of TGF-beta signaling from cell membrane to the nucleus. *Cell* **113**(6), 685–700.

Zhao, G. Q. (2003). Consequences of knocking out BMP signaling in the mouse. *Genesis* **35**(1), 43–56.

Biography

Mark de Caestecker is an Associate Professor with the Departments of Medicine and Cell and Developmental Biology at Vanderbilt University. He graduated with a medical degree from the Universities of Cambridge and London, specializing in general internal medicine and nephrology, and Ph.D. from the University of Manchester in England. He began working on TGF-β signaling as a postdoctoral fellow with Anita Roberts in the Laboratory of Cell Regulation and Carcinogenesis at the NIH. His current research interests include the role of BMP-signaling in vascular remodeling and the regulation of epithelial cell fate in renal development and injury.

Translation Elongation in Bacteria

Oliver Vesper and Knud H. Nierhaus
Max-Planck-Institut für Molekulare Genetik, Berlin, Germany

Protein synthesis is one of the major processes in a living cell that translates the genetic information into protein structure and thus organizes and directs the life cycle and metabolism of a cell. The process of protein synthesis can be subdivided into four consecutive phases: (1) initiation, (2) elongation, (3) termination, and (4) ribosome recycling. All show features that are specific for each of the three main evolutionary domains, viz., bacteria, archaea, and eukarya, with only one exception, the elongation phase. This phase is at the heart of protein synthesis, where the codon sequence of an mRNA is translated into the corresponding amino acid sequence of proteins.

Introduction

Ribosomes translate the genetic information of mRNAs by using tRNA as adaptors. An acylated tRNA connects the decoding center on the small ribosomal subunit via the anticodon at the tip of the long arm of the L-shaped tRNA with the peptidyl-transferase (PTF) center on the large ribosomal subunit via its short arm, the amino-acid acceptor stem.

All ribosomes examined to date from all three evolutionary domains show three tRNA binding sites: (1) The A site, where the correct aminoacyl-tRNA is selected according to the codon present here. The A site tRNA binds in the form of a ternary complex (aa-tRNA·EF-Tu·GTP; aa, aminoacyl; EF-Tu, elongation factor Tu), thus providing the new amino acid for the growing peptide chain. (2) The P site, where the peptidyl-tRNA is located carrying the nascent peptide chain before peptide bond formation. And (3) the exit site (E site) that binds exclusively uncharged (deacylated) tRNAs. It is from this site that the tRNA is released from the ribosome. During the course of three elongation cycles a tRNA enters the ribosome at the A site, moves through the P site and leaves the ribosome from the E site. The only exception is the very first tRNA, termed initiator tRNA, which binds directly to the P site and selects the first codon to be translated thus determining the reading frame.

The Three Basic Reactions of Elongation

Elongation of the nascent peptide chain by one amino acid is performed in a cyclic manner, the sequence of reactions is termed elongation cycle. An overview of the elongation cycle is shown in Figure 1, where the three basic reactions are depicted: (1) A site occupation, (2) peptide bond formation, and (3) the translocation reaction.

A site occupation is separated into two subreactions: in the first step the correct (or cognate) ternary complex aa-tRNA·EF-Tu·GTP is selected via codon–anticodon interaction before the aa-tRNA fully occupies the A site. Successful decoding (decoding reaction) is sensed by the ribosome and leads to an as yet undefined conformational change within the ribosome that triggers hydrolysis of GTP to GDP by elongation factor Tu (EF-Tu). EF-Tu is a G protein, i.e., it can bind a GTP molecule and is now in its "on" conformation, where EF-Tu·GTP can bind an aa-tRNA thus forming the ternary complex. After the ternary complex has delivered its aa-tRNA to the ribosomal A site, the ribosome triggers the activation of the GTPase center on EF-Tu, the resulting EF-Tu·GDP snaps into the "off" conformation and falls from the ribosome.

In the second so-called accommodation step, the release of EF-Tu·GDP from the ribosome allows the tRNA to swing into the A site docking the aminoacyl-residue of the aa-tRNA into the PTF center of the 50S subunit. The aminoacyl-tRNA now occupies the A site and is ready to accept the peptidyl-moiety from the peptidyl-tRNA present at the adjacent P site. With A and P sites occupied with tRNAs the ribosome is in the so-called pretranslocational (PRE) state, although the ribosome is not yet ready for translocation. This is the case only after the next reaction.

In the second reaction peptidyl transfer occurs. The peptidyl residue from the donor (P site) is linked to the aminoacyl residue of the acceptor (A site) via a peptide bond, forming a peptidyl-tRNA at the A site (elongated by one amino acid) and leaving a deacylated tRNA at the P site. Note that the ribosome is still in the PRE state

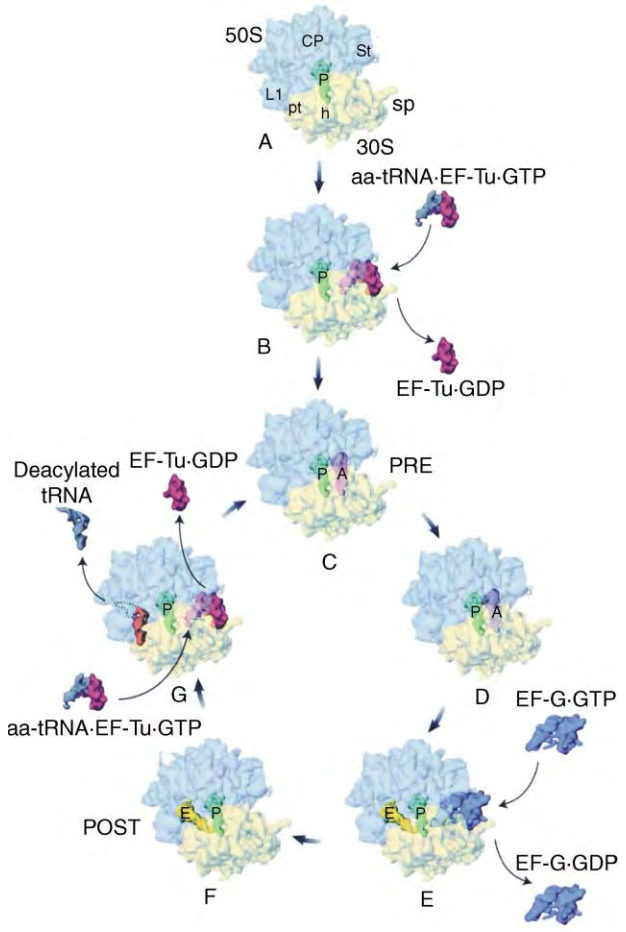

FIGURE 1 Overview of the translational elongation cycle. Multiple cryo-EM studies determined the tRNA and elongation factor binding positions on the 70S ribosome from *E. coli* during the different stages of the elongation cycle. The schematic view of the elongation cycle starts with an initiation complex (A) with the initiator fMet-tRNA in the P site that represents the last stage of initiation. A ternary complex aa-tRNA·EF-TU·GTP enters the vacant A site and after decoding and GTP hydrolysis the binary complex of EF-Tu·GDP leaves the ribosome (B). The A-site aa-tRNA is accommodated into the A site and a pretranslocation complex (PRE state) is formed that is characterized by occupied A and P sites (C). At this stage the peptidyl residue is linked to the aminoacyl-tRNA via a peptide bond. The result is a deacylated tRNA at the P site and a peptidyl-tRNA – prolonged by one aminoacyl-residue – at the A site. The tRNA positions do not change after peptide-bond formation (D). In the next step EF G·GTP binds to the PRE complex and facilitates the translocation of the A and P site tRNAs to the P and E sites, respectively (E). After hydrolysis of GTP EF-G·GDP dissociates from the ribosome, the ribosome is now in the posttranslocational state (POST state) (F). The POST complex is ready for the newly incoming aminoacyl-tRNA coming as ternary complex (aa-tRNA·EF-Tu·GTP). After decoding and GTP hydrolysis the binary complex of EF-Tu·GDP leaves the ribosome, the deacylated tRNA from the E-site is released via a reciprocal coupling between A and E sites and the PRE complex is formed (G → C). (Adapted from Agrawal, R. K., Spahn, C. M. T., Penczek, P., Grassucci, R. A., Nierhaus, K. H., and Frank, J. (2000). Visualization of tRNA movements on the *Escherichia coli* 70S ribosome during the elongation cycle. *J. Cell. Biol.*, **150**, 447–459.)

(A and P sites are occupied), and that the tRNAs have not changed their position after peptide-bond formation.

In the third reaction, the translocation reaction, tRNAs are moved from the A and P site to the P and E sites, respectively, shifting the ribosome into the post-translocational state (POST state, P, and E sites are occupied). The A site is vacant and ready for receiving the next incoming ternary complex. This movement of the $tRNA_2$·mRNA complex within the ribosome by one codon length is facilitated by elongation factor G (EF-G), which is also a G protein with its own GTPase center.

Functional Models of the Elongation Cycle

Various RNA modifying techniques have been used to probe the interactions of tRNAs within the ribosome and to identify tRNA-related functional centers on the ribosome. Distinct sets of rRNA bases have been assigned to contact tRNA in each of the classical binding site (A, P, or E site), which could be explained in the light of high-resolution structure as resulting from either direct contact between the tRNA and bases of rRNA or local conformational changes of the binding regions. In particular, the movement of tRNAs through functional sites during a single elongation was examined using foot-printing techniques. Two different approaches have been applied; interestingly both led to distinct models of the elongation cycle, although they are not mutually exclusive. The hybrid-site model proposed by Noller and colleagues is based on the protections of rRNA bases from chemical modification (kethoxal, dimethylsulfate (DMS) or hydroxyl radicals) by ribosome bound tRNA.

Nierhaus and co-workers applied the phoshorothioate technique for tRNA leading to the α–ε model of the elongation cycle. The latter model focuses not only on the path of tRNA through the ribosome but also on mechanistic features of the ribosome associated with decoding and maintenance of the reading frame.

The Hybrid Site Model

The essence of this model (Figure 2A) is a creeping movement of tRNAs through the ribosome. The diagnostic feature of this model is the movement of the tRNAs exclusively on the large subunit after peptide-bond formation and before translocation, while the 30S bound part of the tRNAs remain in the same site. This results in a hybrid site: The peptidyl tRNA moves after peptide-bond formation from an A/A site to an A/P site, and the deacylated tRNA from P/P site to P/E (the site before the slash indicates the site on the small subunit,

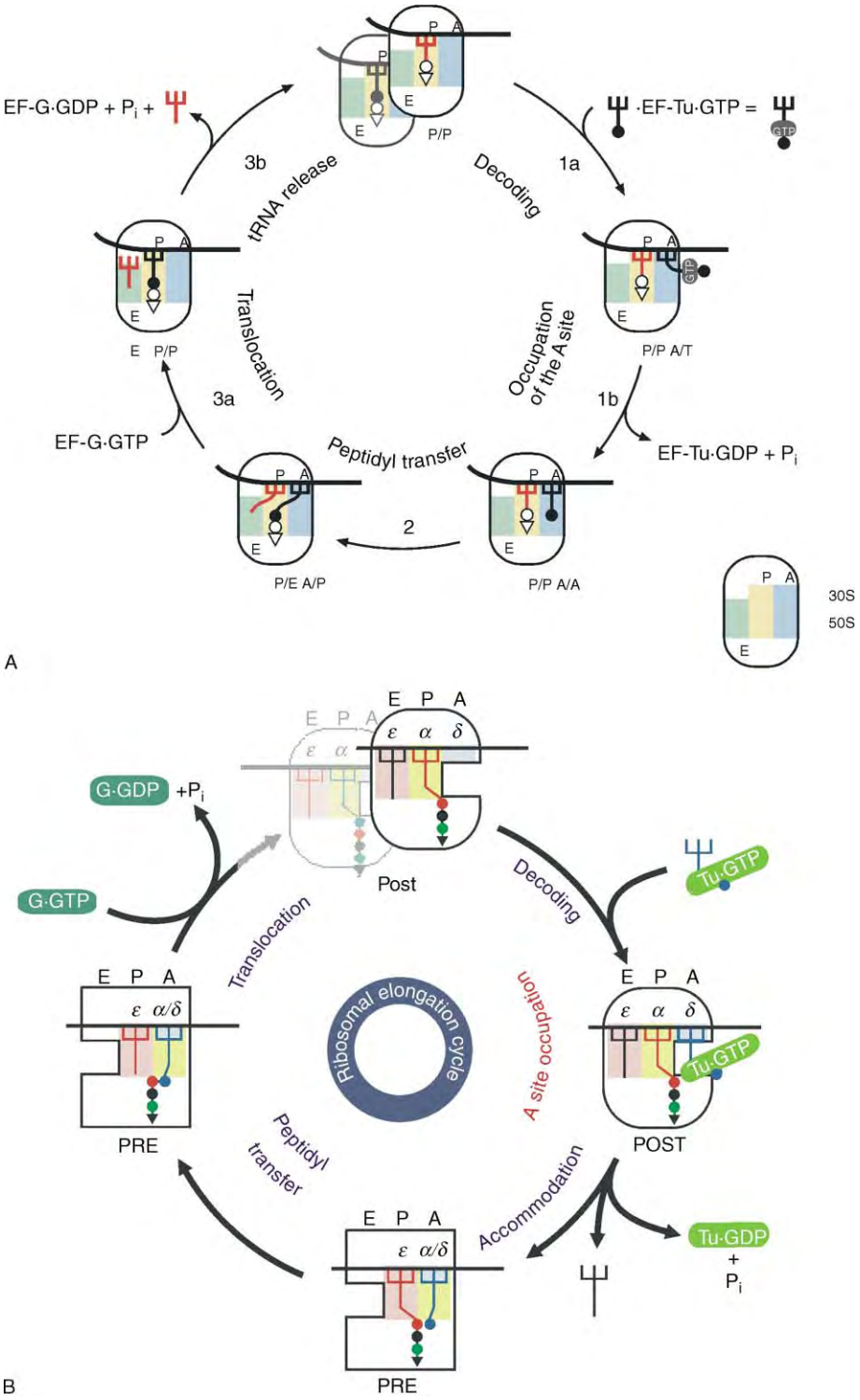

FIGURE 2 Models of the elongation cycle. (A) The hybrid-site model according to Moazed, D., and Noller, H. F. (1989). Intermediate states in the movement of transfer RNA in the ribosome. *Nature* **342**, 142–148; for explanation see text. The basic feature of this model is a creeping movement of tRNAs through the ribosome starting with a tRNA movement only on the 50S ribosome after peptide bond formation and before translocation. This movement is uncoupled from that on the 30S subunit. (B) The α–ε model of the elongation cycle according to Dabrowski, M., Spahn, C. M., Schafer, M. A., Patzke, S., and Nierhaus, K. H. (1998). Protection patterns of tRNAs do not change during ribosomal translocation. *J. Biol. Chem.* **273**, 32793–32800. The essential features are moveable ribosomal α- and ε-domains that connect both subunits through the intersubunit space, bind both tRNAs and carry them in concert from A and P sites to P and E sites, respectively, during the translocation step facilitated by EF-G. The model keeps all the features of the allosteric three side model (see text), but explains the reciprocal linkage between A and E sites by the fact that the moveable domain moves out of the A site during translocation leaving the decoding center alone at the A site in the POST state ribosome. The occupation of the E site generates a low-affinity A site, which is important for the selection of the newly incoming ternary complex at the A site. Yellow and pink, the two binding regions of the α–ε domain, blue the decoding center (δ) at the A site.

and after the slash that on the large subunit). In terms of the hybrid-site model, six different protection patterns were correlated to tRNA binding positions. The translocation reaction brings the peptidyl-tRNA from the A/P hybrid site to the P/P site and the deacylated tRNA from the P/E to the E/E site.

A number of criticisms can be raised, the most serious one is that a hybrid site was not observed when functional states of the elongating ribosome were systematically investigated by cryo-electron microscopy (cryo-EM). Note that a hybrid site can be easily detected, since 85% of a tRNA is in contact with the large subunit with the consequence that an even partial movement of a tRNA on the large subunit would result in a substantial change in the overall position of the tRNA. Even a movement of the CCA-ends of the tRNAs at the PTF center could not be observed in crystal structures of 50S complexes. This prompted a revision in the hybrid-site model so as to keep the tRNAs in the classical A/A and P/P sites after peptide-bond formation, and only after an undefined time span the tRNAs are then shifted to the hybrid sites A/P and P/E, respectively.

However, it seems likely that a peptidyl-tRNA at the A site moves via a transient hybrid position A/P into the P site and likewise a deacylated tRNA from P to E via hybrid position P/E during the translocation reaction, which has been resolved into a ratchet-like forth-and-back movement between the subunits. Analyses applying cryo-EM suggested indeed, that a tRNA moves from P to the E site via a hybrid P/E position during translocation.

The $\alpha-\varepsilon$ Model

The essential feature of the $\alpha-\varepsilon$ model of elongation cycle is a movable domain, called $\alpha-\varepsilon$ domain, which binds both tRNAs of an elongating ribosome and carries them from the A and P sites to the P and E sites, respectively, during translocation (see Figure 2B). But the model also includes the features of the previously described allosteric-three-site model.

1. The ribosome contains three tRNA-binding sites: A, P, and E site.

2. E and A site are coupled in a reciprocal manner: An occupied E site decreases the affinity at the A site and vice versa. The decreased affinity at the A site by an occupied E site might be important for preventing an interference of noncognate ternary complexes with the selection process of the cognate ternary complex from near cognate ternary complexes at the A site. During the accommodation of the aa-tRNA into the A site (stable A site occupation) the E site tRNA is released. The reciprocal interaction between the A and the E sites explains why statistically two tRNAs are found on polysomes that contain a mixture of both PRE and POST state ribosomes.

3. Both tRNAs on a ribosome are bound via codon–anticodon interactions in both the PRE and the POST states. Especially the codon–anticodon interaction at the E site seems to be essential for: first, establishing the POST state which is the proper substrate for the ternary complex, second, reducing the error rate of protein synthesis, and third, keeping the reading frame.

It is probable that the $\alpha-\varepsilon$ model will be modified as soon as higher resolution structures of the ribosomal PRE and POST states become available.

A comprehensive analysis of the translocation reaction by cryo-EM to date challenges an essential feature of the $\alpha-\varepsilon$ model: PRE states of ribosomes were analyzed by cryo-EM carrying an fMet-Phe-tRNA at the A site and a deacylated $tRNA^{Phe}$ at the P site. In these complexes a tRNA is also seen at the E site, although no tRNA was specifically bound to this site. The authors assume that the tRNA binds from the free pool of deacylated tRNA in solution to the "high affinity" E site. Either way the presence of well populated A and E site is at odds with the $\alpha-\varepsilon$ model. However, neither the origin of the E-site tRNA nor the tRNA:70S stoichiometry is known, therefore it would be premature to disregard carefully controlled experiments upon which the $\alpha-\varepsilon$ model is based.

Selection of the Ternary Complex: Decoding and A Site Occupation

In *Escherichia coli*, there are 45 different species of tRNAs, where a species is defined as a tRNA with a unique anticodon sequence. The tRNA species can be separated into three classes with respect to the codon displayed in the A site. The "cognate" class contains one aminoacyl-tRNA with an anticodon complementary to the A-site codon. The "near-cognate" class contains four to six aminoacyl-tRNA that carry anticodons similar to that of the cognate one (never more than one mismatch). The "noncognate" class contains the bulk of aminoacyl-tRNAs with a dissimilar anticodon (usually more than one mismatch). As the tertiary structure of tRNA is highly conserved the ribosome has to distinguish between tRNAs that hardly differ. The problem is compounded by the fact, that the substrate for the A site is not an isolated aa-tRNA but rather the much larger ternary complex aa-tRNA·EF-Tu·GTP, i.e., EF-Tu * GTP is twice as large as a tRNA. The ribosome must therefore discriminate between relatively large ternary complexes (72 kDa) that are extremely similar, on the basis of a small discriminatory region, namely the anticodon (1 kDa).

In view of the predominance of the nondiscriminatory fraction of free energy of binding over the discriminatory energy, protein synthesis must be either slow and accurate or fast and imprecise. This is not what

we see *in vivo*, where protein synthesis is fast and accurate, incorporating up to 10–20 amino acids per second with an accuracy of one misincorporation per 3000 amino acid incorporations. How is the ribosome solving this paradox?

A first hint gave the observation that the A site occupation occurs in two steps as already mentioned (see Figure 2B): a decoding step, where the selection of the cognate ternary complex takes place, is followed by an accommodation step. The α–ε model has integrated this observation in the following way: the decoding takes place at an A site with low affinity for tRNA, which reduces the binding energy of the ternary complex to mainly codon–anticodon interactions and excludes contacts of the tRNA outside the anticodon and of EF-Tu with the ribosome. In this state the free energy of binding is small, and since it is restricted to codon–anticodon interaction it is more or less identical with the discrimination energy. This feature explains why the majority of "noncognate" aa-tRNA (~90% of the aa-tRNA species) do not interfere with the decoding process: their anticodon is different from that of the cognate aa-tRNA, and interactions outside the anticodon are prevented by the low-affinity A site.

This fast initial step is followed by an accommodation step, where the aminoacyl-tRNA is tightly bound and accommodated into the A site. This step is accompanied by some gross conformational changes, since during this step the E-site tRNA is released and the A site switches into its high-affinity state. Therefore, the second step is probably slow in comparison to the decoding the step. The A site occupation is therefore a coupled system of two reactions, the first of which is fast and the second slow. An important consequence of this arrangement is that the first runs at equilibrium even under steady-state conditions and thus can exploit the discrimination potential of the decoding process.

The reciprocal linkage between A and E site seems to be a universal feature of ribosomes and has been demonstrated not only in bacteria but also in eukarya (yeast).

After considering the competition cognate versus noncognate aa-tRNAs, still a discussion on how the ribosome discriminates between cognate and near-cognate tRNAs arises. Two models have been proposed: (1) the kinetic proofreading model, and (2) the Potapov model.

In the late 1970s, stability measurements of anti-codon:anticodon interactions within a complex of two tRNAs have demonstrated that the corresponding energy cannot explain a selection accuracy of better than 1:10. Therefore, proofreading models have been developed according to which the stability energy is exploited several times in order to explain the observed accuracy of aa-tRNA selection at the ribosomal A site of about 1:3000. One proofreading event requires one EF-Tu dependent GTP hydrolysis, so that a measurement of the number of GTPs hydrolyzed by EF-Tu per incorporation of a near-cognate amino acid indicates the importance of proofreading for the selection process. Precise measurements revealed that the importance of proofreading is much less than originally thought, initial binding of the ternary complex gives a precision of about 1:300 up to 1:1000, whereas the corresponding proofreading factor is not better than 1:10.

How initial binding is able to achieve such an accuracy is explained by the Potapov model. This model suggests that the decoding center on the ribosome does not measure the stability of codon–anticodon interaction, but rather the stereochemical correctness of the three Watson–Crick base pairs, just as an enzyme recognizes its substrate. With this assumption the correct position of the sugar pucker contributes to the accuracy, and it could be demonstrated that indeed the 2′OH groups of the codon bases are of utmost importance for the accuracy of the selection process.

The detailed molecular mechanism could be unravelled by the Ramakrishnan group who determined the crystal structure of 30S subunits carrying either a cognate or near-cognate anticodon stem-loop structures. Indeed, the correct positions of the 2′OH groups of the codon–anticodon complex is checked by forming hydrogen bonds with universally conserved bases of the 16S rRNA (Figure 3). The first base pair of codon–anticodon interaction at the A site is analyzed via the so-called A-minor motif type I and the second by an A-minor motif type II (Figure 3B and 3C), whereas the third wobble position has more freedom to accommodate also non-Watson–Crick base pairs (Figure 3D). Furthermore, the head and shoulder of the 30S subunit move relative to each other defining an open and closed 30S configuration. In the "open" configuration binding of cognate (but not a near-cognate) substrate to the decoding center flips out the bases A1492 and A1493 from the helix 44, brings G530 from a "syn" into an "anti" conformation (Figure 3A), and shifts the subunit into a "closed" configuration providing a molecular basis for an understanding of mutations that increase or decrease accuracy. A molecular dynamic simulation agrees with the main conclusions and shows in addition that the kink between the A and P site codons of about 135° influences the accuracy pattern.

An Additional Role of EF-Tu

It is well known that EF-Tu binds an aa-tRNA at the amino acid acceptor stem thus shielding the labile ester bond between the aminoacyl residue and the tRNA, and delivers the aa-tRNA to the A site on the ribosome. However, a second function of EF-Tu was identified by Uhlenbeck and co-workers. Measuring the affinities of various cognate aa-tRNA (e.g., Val-tRNA^{Val}) and some mispairs (e.g., Ala-tRNA^{Val}) they recognized that either

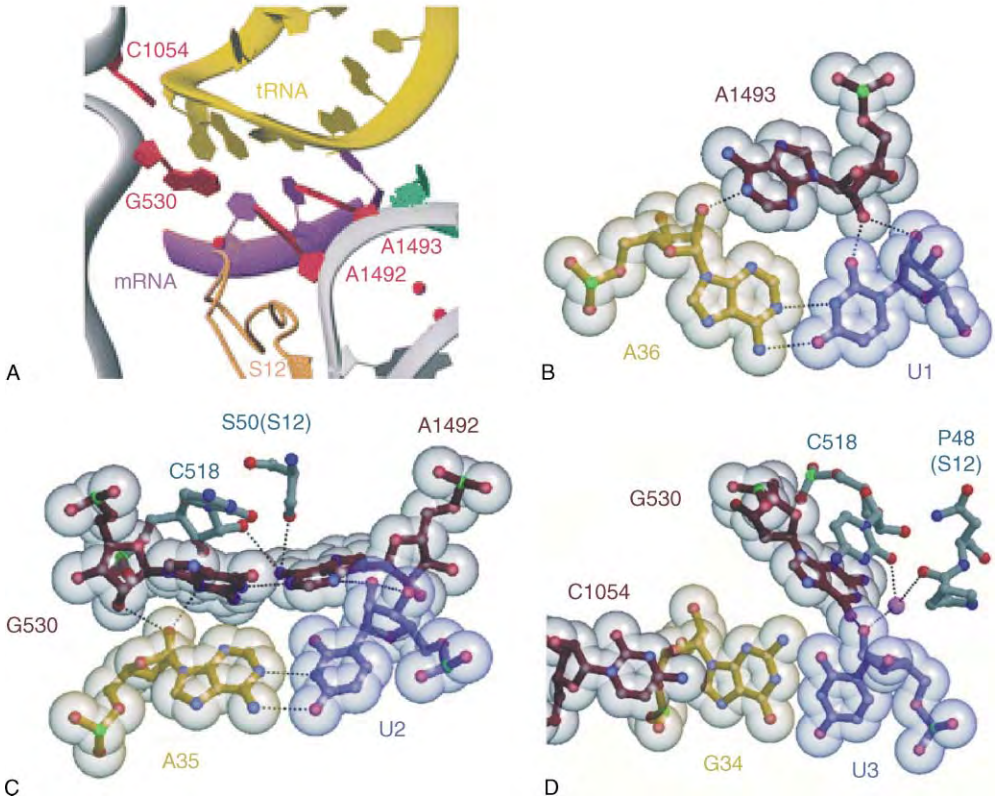

FIGURE 3 Molecular details of the decoding process, principles of decoding according to Ogle *et al.* 2001, *Science*, **292**, 897–902. (A) Conformational changes at the decoding center upon binding of a cognate anticodon-stem-loop (ASL) with permission. (B) Recognition of the Watson–Crick interaction at the first position of codon–anticodon by a type I A minor motive, A1493 is clinging into the minor groove of the first base pair of codon-anticodon interaction. (C) Recognition of the Watson–Crick interaction at the second position of codon–anticodon by type II A minor motive, A1492 and G530 are filling the minor groove at the second position, forming a hydrogen bond network to 2′OH groups, bases of codon–anticodon, and G518 and serine50 of S12. (D) The Watson–Crick geometry at position three is less restricted, G530, C518, and P48 are stabilizing the third codon position, but giving freedom, e.g., the G:U wobble base pair. Adapted from Ramakrishnan, 2002.

the amino acid or the tRNA should bind to EF-Tu with high affinity in order to form stable ternary complexes aa-tRNA·EF-Tu·GTP. For example, EF-Tu·GTP forms easily a ternary complex with Asp-tRNA^{Asp} (weak aa and strong tRNA) or Asn-tRNA^{Asn} (strong aa and weak tRNA), but not with Asp-tRNA^{Asn}, since in the latter case both moieties bind with low affinities. This observation explains an important case that was an enigma hitherto. In most organisms, there are not 20 different synthetases corresponding to the 20 natural amino acids, but only 19 or sometimes 18. For example, many organisms do not contain a synthetase specific for asparagine (Asn-RS). In this case the Asp-RS is charging also the tRNA^{Asn} with aspartic acid yielding Asp-tRNA^{Asn}, which is recognized by enzymes amidating Asp to Asn on the tRNA. The mis-charged Asp-tRNA^{Asn} does not form a stable ternary complex with EF-Tu·GTP and thus Asp is not incorporated at codons specifying Asn. This discrimination process via EF-Tu was termed thermodynamic compensation.

Peptide-Bond Formation

The PTF reaction, a central step in protein synthesis, is the catalytic activity of the large subunit. Even if the substrates are large, the reaction that occurs is quite simple–the aminolysis of an ester bond to form a peptide bond. The nucleophilic α-amino group of the amino acid moiety of the aminoacyl tRNA at the A site attacks the electrophilic carbonyl carbon atom of the ester-bonded peptide moiety of the P site tRNA. This forms an tetrahedral intermediate, which breaks down to an uncharged (deacylated) tRNA in the P site and a peptidyl-tRNA prolonged by one amino acid at the A site (Figure 4A). The PTF center of the 50S has been identified by using a transition state analogue of the PTF reaction, which was soaked into 50S crystals of the archaea *H. marismortui*. This analogue, CCdA-phosphate-puromycin (CCdApPmn), is a mimic of the CCA end of a tRNA in the P site attached to puromycin in the A site, where the

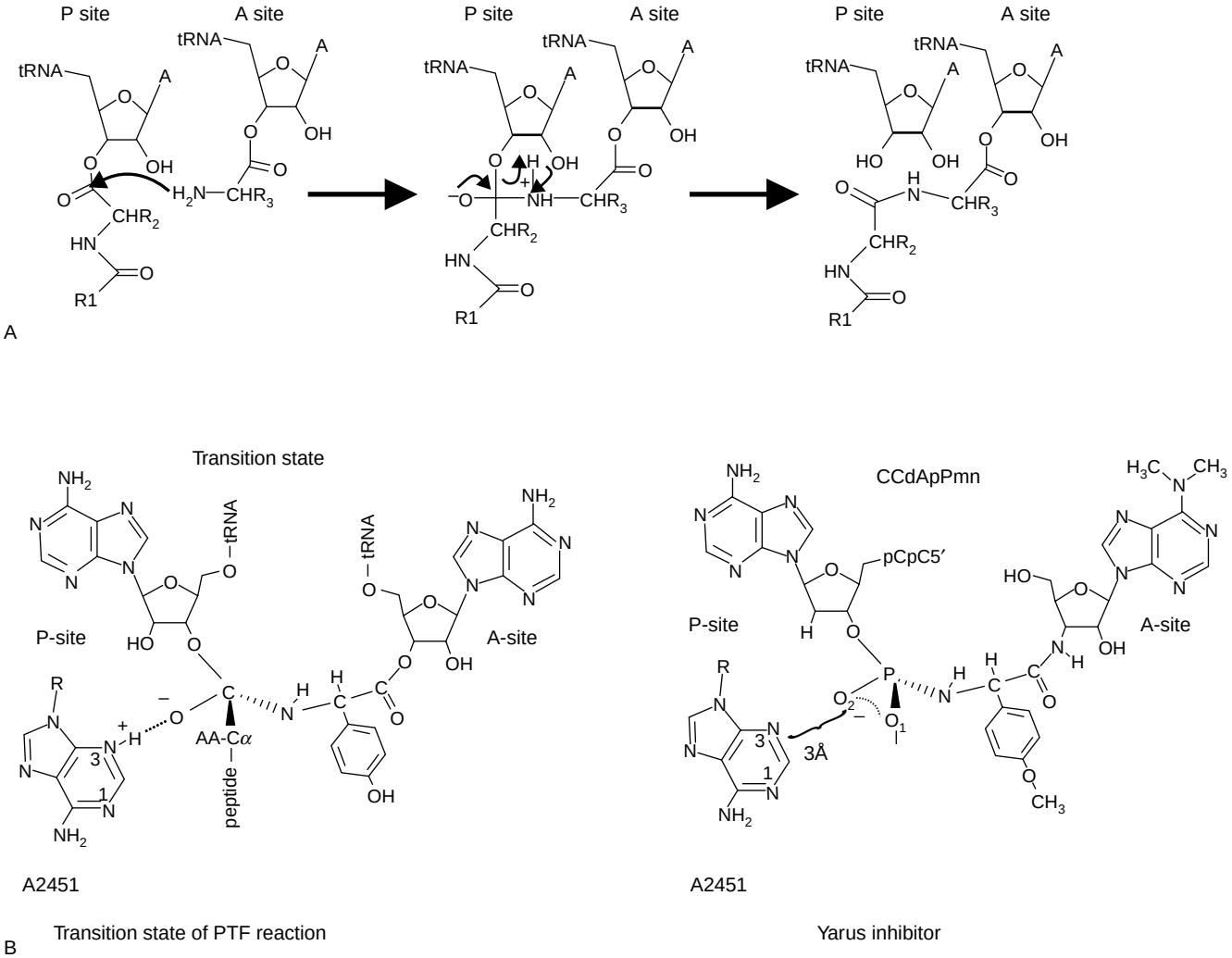

FIGURE 4 Mechanism of peptide bond formation. (A) PTF reaction: The α- amino group of the A site bond aa-tRNA attacks the electrophilic carbonyl carbon, which is attached via ester bond to the 3′OH of the adenosine residue of P site bond peptidyl-tRNA, forming a tetrahedral transition state that breaks down to a prolonged peptidyl-tRNA at the A site and a deacylated tRNA at the P site. (B) Comparison of the putative transition state of the PTF reaction with a possible transition-state analogue created by the Yarus group. From Parnell, K. M., Seila, A. C., and Strobel, S. A. (2002). Evidence against stabilization of the transition state oxyanion by a ρka-perturbed RNA base in the peptidyl transferase center. *Proc. Natl Acad. Sci. USA* **99**, 11658–11663.

3′-terminal deoxy-adenosine and the phosphate residue resemble the tetrahedral intermediate formed during peptidyl transfer (Figure 4B). It was shown previously by the Yarus group that this analogue is a strong inhibitor of the PTF reaction competitively inhibiting binding of the A-site substrate.

A long-standing discussion has been about the composition of the PTF center and the "players" involved in the PTF reaction, but now it is clear from the crystal structure – the ribosome is a ribozyme, i.e., no protein is directly involved in catalysis. The PTF center is tightly packed with rRNA, mainly derived from the domain V of 23S RNA (the so-called PTF ring), which are highly conserved over all domains of life. Although there are 15 proteins interacting with domain V, proteins are absent from the PTF within a distance of at least 18Å. The nearest proteins to the PTF in *H. marismortui* structure are L2, L3, L4, and L10e and interestingly, all four are also present in the vicinity of PTF in the eubacterial ribosome, when it is taken into account that eukaryotic L10e is evolutionary related to L16 in prokaryotes. These proteins have been identified previously, together with the 23S rRNA, as the major candidates for the PTF activity by single omission tests in a total reconstitution system of the large subunit. Although the structure reveals no direct involvement of protein in the catalysis, proteins might have a role in aligning the substrates and functioning as a "glue" to stabilize rRNA tertiary arrangement necessary for the peptide bond formation since complete removal of

proteins could only accomplished under conditions that unfolded the rRNA and totally abolished the PTF activity, whereas the removal of up to over 80% of proteins of the 50S subunit from *Thermus aquaticus* maintained activity. Detailed analysis of the neighborhood of the residues within close proximity to the CCA end analogues of tRNA led to the proposal for an acid-base catalysis mechanism for the PTF reaction involving the universal conserved A2451 in analogy to the back reaction of the mechanism used by serine proteases. This proposal was immediately under attack from a number of groups who presented biochemical and genetic data to the contrary.

Crystal structures of the 50S of *Deinococcus radiodurans* revealed some significant differences in the arrangement of nucleotides within the PTF center and the presence of a protein (L27), which is thought to play a role in placement of the CCA ends of both tRNAs. The debate on the mechanism of PTF reaction is on going. By re-examination of the transition state analogue it turned out that this analogue within the 50S structure can not answer all the mechanistic questions about the PTF reaction, since it is not a true mimic of the intermediate of the PTF reaction: modeling the missing oxygen atom at the 2′ position of the desoxy-adenosine caused a sterical clash with the phosphate group. Although the reaction seems to be quite simple, the kind of contribution of the ribosome in catalysis remains open.

Two main principles of enzymatic reactions can be distinguished and could be involved in PTF reaction. The first principle is the physical or template model, where the enzyme, here the ribosome, arranges the two substrates in optimal stereo-chemical positions for the reaction to proceed. Such an arrangement of substrates is sufficient to allow for a dramatic acceleration of the reaction rate by six to nine orders of magnitude. This strategy is certainly used by the ribosome, since there are binding sides for both tRNA substrates fixing the substrates in a defined position by interaction between 23S rRNA (A loop and P loop) and tRNAs (see Figure 5), placing the corresponding CCA ends into the PTF center.

In addition it is possible that a chemical concept is utilized by the ribosome, i.e., transiently covalent bonds are formed and broken between the enzyme and the substrates. There are three groups in close proximity to the reactive amino group within the PTF center in the *H. marismortui* crystal structure, that could form hydrogen bonds with it, namely (1) the 2′-OH of the peptidyl-tRNA, (2) the N3 of A2451 (*E. coli* nomenclature) of 23S rRNA, and (3) the 2′OH of A2451.

The hydrogen bonds these groups could form with the α-amino group of the aa-tRNA at the A site may help to fix and optimally align the reactive α-amino group within the PTF center. And if one of these groups have an elevated pK_a, its hydrogen bond would facilitate the nucleophilic attack from the α-amino group of the aminoacyl-tRNA at the A side to the carbon of the carbonyl group of peptidyl-tRNA at the P site. A major candidate for an enhancement of nucleophily of the α-amino group is N3 of A2451 (see Figure 6).

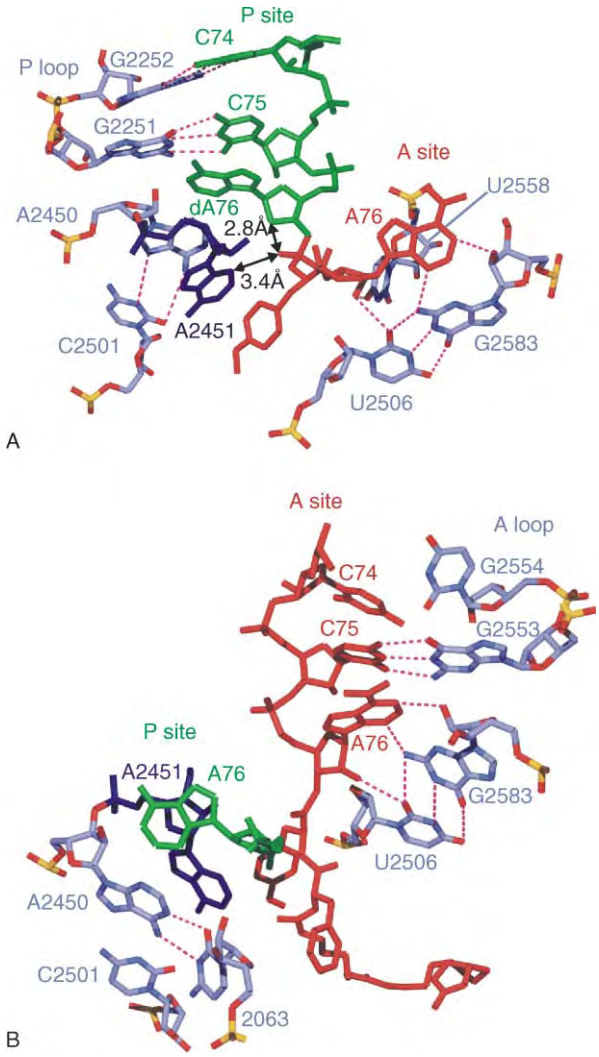

FIGURE 5 Tight fixation of the CCA ends of the P- and A-tRNAs observed in 50S subunit from *H. marismortui* in complex with (A) the Yarus inhibitor, and (B) the products following peptide bond formation. The CCA-ends of the tRNAs in the A and P sites are colored red and green, respectively. The N3 of A2451 (dark blue) is 3.4Å from the O2 of the Yarus inhibitor, while the same O2 is only 2.8Å from the 2′-deoxy of A76 (arrowed). Selected rRNA residues of domain V of the 23S rRNA are colored light blue, including the A- and P-loop bases that participate in A and P site CCA end fixation (*E. coli* numbering). In (B) the P site C74 and C75 have been omitted for clarity. Dashes indicate hydrogen bonding and rRNA nucleotides use the following color scheme: Oxygen, red; phosphorus, yellow; nitrogen, blue; carbon, dark blue. Adapted from Nissen, P., Hansen, J., Ban, N., Moore, P. B., and Steitz, T. A. (2000). The structural basis of ribosome activity in peptide bond synthesis. *Science* **289**, 920–930.

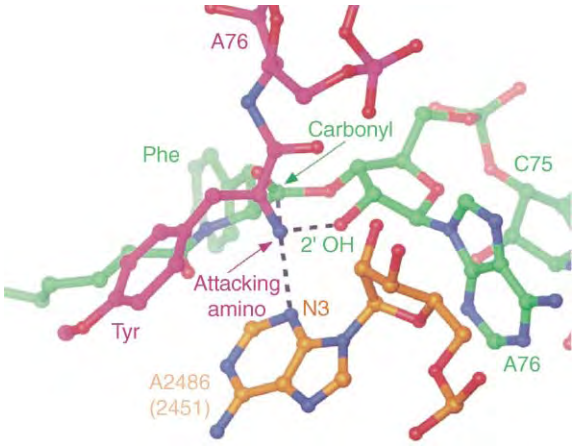

FIGURE 6 Putative arrangements of the residues involved in peptide-bond formation derived from crystal structures of the *H. marismortui* 50S with and without low-molecular weight substrate and transition state analogues. N3 of A2486 (A2451 in *E. coli*) and the 2′OH group of A76 of peptidyl-tRNA (green) forming hydrogen bonds to the α-amino group of the A site aa-tRNA (red) that may facilitate the nucleophilic attack of the α-amino group to the carbonyl carbon of peptidyl-tRNA at the P site. From Moore P. B., and Steitz, T. A. (2003). After the ribosome structures: how does peptidyl transferase work? *RNA* **9**, 155–159.

Translocation

The translocation step of elongation cycle is one of the most difficult to understand, since the ribosome must move two large molecules, the tRNAs (each ~25 kDa, ~ 75 × 50 × 30Å), and a mRNA in a concerted action through the ribosome precisely by one codon length (~10–15Å). Under certain *in vitro* conditions translation can occur spontaneously but with a rate that is three orders of magnitude slower than that in the presence of EF-G. Nevertheless, this indicates that the translocation reaction is a feature inherent in the ribosome itself. An impressive confirmation comes from the observation that the antibiotic sparsomycin that binds to the PTF center and blocks peptide-bond formation can trigger one round of translocation efficiently. Even EF-G dependent GTP hydrolysis is not needed in order to promote the translocation reaction, since EF-G·GDPNP, the noncleavable analogue of GTP, efficiently fosters translocation. Nevertheless, the proposal has been made that at least the energy of EF-G dependent GTP cleavage accelerates the translocation based on the observation that in the presence of the hardly cleavable GTP-γ-S analogue the translocation is somewhat slower than in the presence of GTP.

The most recent progress in the understanding of the translocation reaction comes from a detailed cryo-EM study of this reaction. EF-G induces a ratchet like movement between 30S and 50S subunits as first shown with empty ribosomes, but here the movement could be coupled to translocation of tRNAs at higher resolution yielding a more precise picture of this reaction:

1. After occupying the A site with an aa-tRNA and peptide bond formation, the peptidyl-tRNA is in the A site and a deacylated tRNA at the P site, no hybrid site is visible as was seen in cryo-EM studies.
2. EF-G·GTP binds and induces the first forth-movement of the ratchet motion of the 30S subunit, a turn of ~20°. During this movement the deacylated tRNA is shifted into a hybrid position P/E and it is hypothesized (although not yet observed) that the peptidyl-tRNA would also move in an analogous fashion to occupy a A/P hybrid position.
3. The ribosome triggers the EF-G dependent GTP hydrolysis and the authors postulate that the resulting EF-G conformational change into the GDP conformer completes the translocation reaction in that

- the 30S subunit moves back (second part of the ratchet movement),
- the tRNAs continue their movement to E and P sites, respectively, and
- EF-G·GDP dissociates from the ribosome.

A strong dislocation movement of domains 3-5 of EF-G·GDPPNP (a GTP analogue) on the ribosome was observed as compared to the crystal structure of EF-G·GDP. In particular, the tip of domain 4 moves ~35 Å away upon GTP cleavage. The authors speculate that this movement is responsible for the second half of the ratchet motion with the three consequences outlined in the preceding sentence. They also detect a substantial movement of the L1 protuberance during the translocation and postulate an active participation of this structure in the translocation of the deacylated tRNA from the P site to the E site. The translocational movement of the tRNAs from, e.g. , the A site to the P site via a A/P state can be well reconciled with the α–ε model of the elongation.

Note the difference to the hybrid-site model: this model postulates that after peptide-bond formation and before translocation the tRNAs move on the large subunit but stay on the 30S subunit, i.e., the peptidyl-tRNA at the A site moves from A/A site to the A/P site, and only the translocation movement brings the tRNA into the P/P site, whereas the cryo-EM study suggests that during translocation the peptidyl-tRNA moves from the A to the P site via a transient A/P position.

The ribosome research is an exciting upheaval phase where the structure begins to explain the function. For the first time it can be imagined how the ribosome is using its complicated structure to perform its yet more complicated function.

See Also the Following Articles

EF-G and EF-Tu Structures and Translation Elongation in Bacteria • Ribosome Assembly • Ribosome Structure • Translation Initiation in Bacteria: Factors and Mechanisms • Translation Termination and Ribosome Recycling

Glossary

A site Ribosomal tRNA binding site for aminoacyl-tRNA (A for aminoacyl-). At this site decoding of the displayed codon takes place; it is the entry site for aminoacyl-tRNA complexed with the elongation factor EF-Tu.

E site Ribosomal tRNA-binding site that exclusively binds deacylated tRNA before it dissociates from the ribosome.

EF-G An elongation factor that promotes translocation. It is a G protein that binds as binary complex EF-G·GTP to the ribosome. The homologue in eukaryotes and archaea is termed EF2.

EF-Tu An elongation factor that carries aminoacyl-tRNA to the ribosomal A site as a ternary complex aminoacyl-tRNA·EF-Tu·GTP. It is also a G protein. The homologue in eukaryotes and archaea is termed EF1.

P site Ribosomal tRNA-binding site for peptidyl-tRNA before peptide-bond formation (P for peptidyl-).

Further Reading

Agrawal, R. K., Spahn, C. M. T., Penczek, P., Grassucci, R. A., Nierhaus, K. H., and Frank, J. (2000). Visualization of tRNA movements on the *Escherichia coli* 70S ribosome during the elongation cycle. *J. Cell. Biol.* **150**, 447–459.

Fredrick, K., and Noller, H. F. (2003). Catalysis of ribosomal translocation by sparsomycin. *Science* **300**, 1159–1162.

Green, R., and Noller, H. F. (1997). Ribosomes and translation. *Annu. Rev. Biochem.* **66**, 679–716.

LaRiviere, F. J., Wolfson, A. D., and Ühlenbeck, O. C. (2001). Uniform binding of aminoacyl-tRNAs to elongation factor Tu by thermodynamic compensation. *Science* **294**, 165–168.

Moore, P. B., and Steitz, T. A. (2002). The involvement of RNA in ribosome function. *Nature* **418**, 229–235.

Noller, H. F., Yusupov, M. M., Yusupova, G. Z., Baucom, A., and Cate, J. H. D. (2002). Translocation of tRNA during protein synthesis. *FEBS Lett.* **514**, 11–16.

Ogle, J., Carter, A., and Ramakrishnan, V. (2003). Insights into the decoding mechanism from recent ribosome structures. *TIBS* **28**(5), 259–266.

Valle, M., Zavialov, A., Sengupta, J., Rawat, U., Ehrenberg, M., and Frank, J. (2003). Locking and unlocking of ribosomal motions. *Cell* **114**, 123–134.

Wilson, D. N., and Nierhaus, K. H. (2003). The ribosome through the looking glass. *Angew. Chemie* **42**(30), 3464–3486.

Biography

Oliver Vesper has studied biochemistry at the Free University in Berlin and is currently pursuing his Ph.D. studies in the Max-Planck-Institut für Molekulare Genetik in Berlin.

Knud H. Nierhaus has studied medicine in Tübingen and Vienna, is a Professor of Biochemistry at the Technical University in Berlin and Group Leader at the Max-Planck-Institut für Molekulare Genetik in Berlin.

Translation Elongation in Eukaryotes

William C. Merrick and Anton A. Komar
Case Western Reserve University School of Medicine, Cleveland, Ohio, USA

The process of translation is defined by three steps: initiation, which effects mRNA binding and correct match of the initiator tRNA with the AUG start codon; elongation, which effects the correct matching of all the remaining aminoacyl-tRNAs in a codon specific manner; and termination, which senses a stop codon and leads to the release of the completed peptide chain. Of these three steps, elongation is the most predominant one as it accounts for all but one of the amino acids that end up in the completed polypeptide chain. Elongation itself is composed of three traditionally defined steps: eEF1A-directed binding of the aminoacyl-tRNA to the A site (aminoacyl site) of the ribosome; peptide bond formation triggered by the one enzymatic activity of the ribosome (the peptidyl transferase center); and eEF2-mediated translocation which moves the peptidyl-tRNA from the A site to the P site (peptidyl site) by precisely one codon (three nucleotides). Although the matching of aminoacyl-tRNAs to codons in the A site is dictated by the genetic code, the accuracy and speed of the elongation process is driven by the hydrolysis of GTP in the binding and translocation steps.

Introduction

The purpose of this article is to provide a basic understanding of the process of protein synthesis elongation. While the focus will be on eukaryotic systems, the general mechanism of protein synthesis elongation is essentially the same in eukaryotes and prokaryotes (Table I). This is perhaps not surprising given the ease with which one can trace the evolution of the eukaryotic factors from their bacterial predecessors. At present, the best biochemical and structural data on the elongation cycle are from bacterial systems and includes crystallographic structures of the ribosomal subunits (30S and 50S), EF1A·GDP, EF2·GDP, and EF1A·GDPNP·Phe-tRNA. The regulation of the elongation cycle has been best studied in the eukaryotic system and there appear to be several posttranslational modifications that influence synthetic rate.

The Traditional Elongation Cycle: The A and P Sites

At the end of the initiation cycle, the final product is an 80S ribosome that has an mRNA (or AUG codon) bound to the initiator tRNA (Met-tRNA$_i$) correctly based paired with AUG start codon, and with the Met-tRNA$_i$ in the peptidyl or P site (Figure 1). This placement of the initiator tRNA in the P site sets the reading frame for all subsequent aminoacyl-tRNAs. The next event is the binding of the ternary complex (eEF1A·GTP·aminoacyl-tRNA) to the aminoacyl or A site (Figure 1). This binding is directed by the interaction of the anticodon of the tRNA and the three nucleotides in the A site. The specificity is such that perfect Watson–Crick base pairs are observed for the first two nucleotides in the codon (i.e., only A-U or G-C base pairs), but altered base pairing is possible at the third position (as originally proposed by Crick). The genetic code dictates which aminoacyl-tRNA will bind to the A site in response to the 61 possible triplet codons that specify an amino acid (note that three codons of the possible 64 are stop codons: UAA, UAG, and UGA). With the correct base pairing, a conformational change occurs that triggers the hydrolysis of GTP leading to the release of eEF1A·GDP from the ribosome.

The next step is peptide bond formation. The synthesis of the peptide bond is catalyzed by the peptidyl transferase center in the large ribosomal subunit (60S). *In vivo*, this step appears to occur instantaneously and is likely the most rapid step in the entire process. As should be noted in Figure 1, peptide bond formation leads to the movement of the upper halves of the two tRNAs such that the tRNA originally in the P site is now half in the exit or E site (aminoacyl end) (Figure 2) and half in the P site (the anticodon end). In a similar manner, the tRNA originally in the A site is now half in the P site (aminoacyl end) and half in the A site (the anticodon end).

The final step in the cycle is translocation. This is driven by the binding of eEF2·GTP to the A site of

TABLE I

Eukaryotic and Prokaryotic Components of the Elongation Cycle

Prokaryotes	Eukaryotes	Function
30S, 50S subunits	40S, 60S subunits	Peptide bond formation
EF1A	eEF1A	Binding of aa-tRNA to ribosomes
EF1B	eEF1B	Nucleotide exchange factor
EF2	eEF2	Translocation
aa-tRNA	aa-tRNA	Carrier of the activated amino acid, recognition of the codon in the A site

the ribosome. Hydrolysis of the GTP in the eEF2·GTP complex triggers the movement of the peptidyl-tRNA in the P/A site into the P/P site. During this movement, it is thought that an "arginine finger" in the ribosome stabilizes the interaction between the anticodon of the tRNA and the codon in the mRNA. By moving the anticodon of the peptidyl-tRNA fully into the P site (P/P), the mRNA is moved along the ribosome precisely by three nucleotides (or one codon). In this manner, the ribosome maintains the reading frame of the mRNA.

Although a complete elongation cycle has been completed, we are not back to the beginning. As noted above, eEF1A is released as an eEF1A·GDP complex. The binding affinity of eEF1A for GDP is $\sim 0.1\ \mu M$. Thus, in biological terms, this is a rather stable complex. To enhance the conversion of eEF1A·GDP into the biologically active eEF1A·GTP form, the eEF1A·GDP complex binds to eEF1B. This leads to the release of GDP and the formation of an eEF1A·1B complex. Subsequent binding of GTP yields eEF1A·GTP + eEF1B. This exchange cycle is very similar to that of most "standard G proteins." In contrast, eEF2 does not require an exchange factor as it has a much poorer affinity for GDP, and thus GDP is rapidly released from eEF2 following GTP hydrolysis.

A few notes on the elongation cycle: first, the energy cost would appear to be two high-energy phosphates per cycle; however, the actual value is four when one considers that two high-energy phosphates are required for the attachment of the amino acid to the tRNA, which was then placed in the A site. Second, on careful

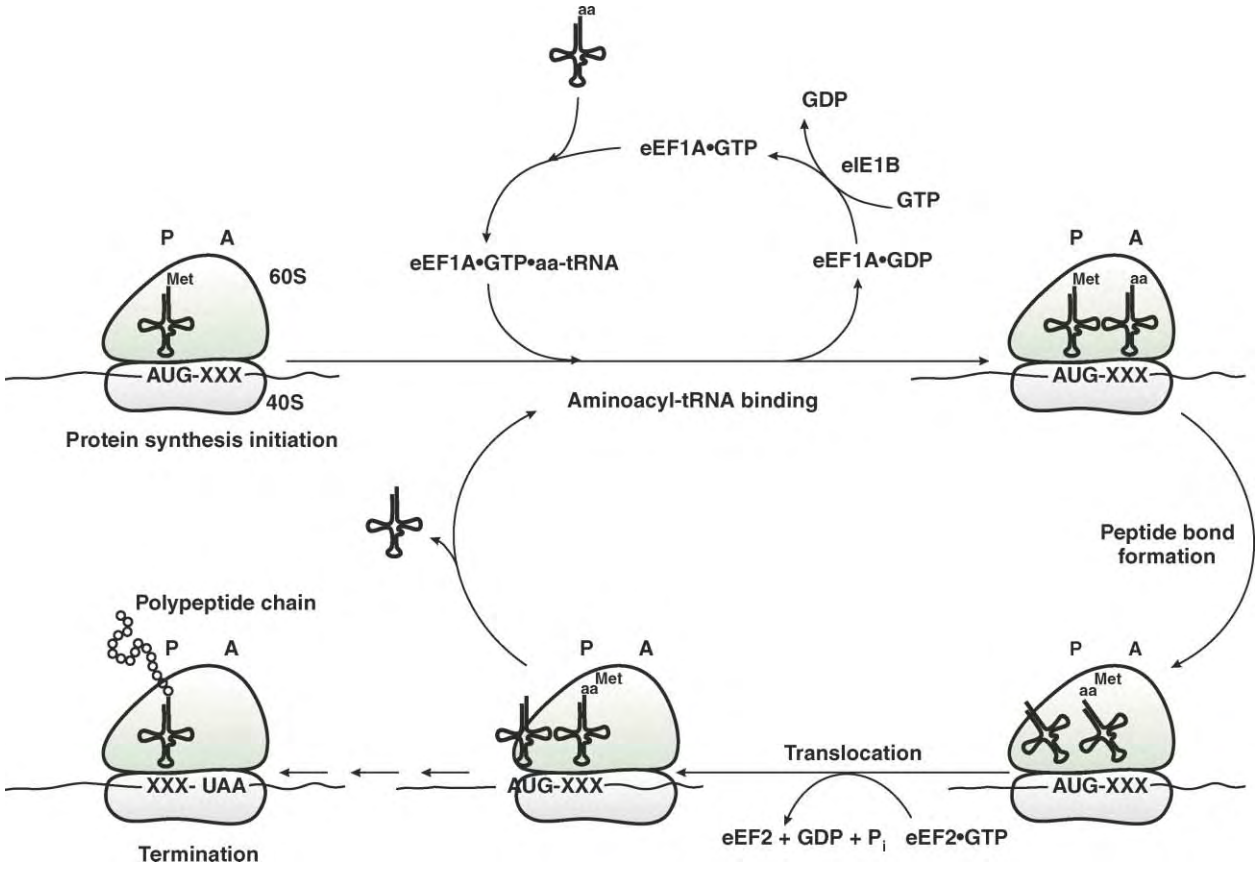

FIGURE 1 The traditional elongation cycle: The A and P sites. Shown above is the elongation cycle with the traditional A and P sites (aminoacyl and peptidyl sites, respectively). Following initiation, subsequent steps in the elongation cycle ensue with aminoacyl-tRNA binding, peptide bond formation, and then translocation. This process continues until a stop codon (UAA, UAG, or UGA) appears in the A site at which point termination occurs.

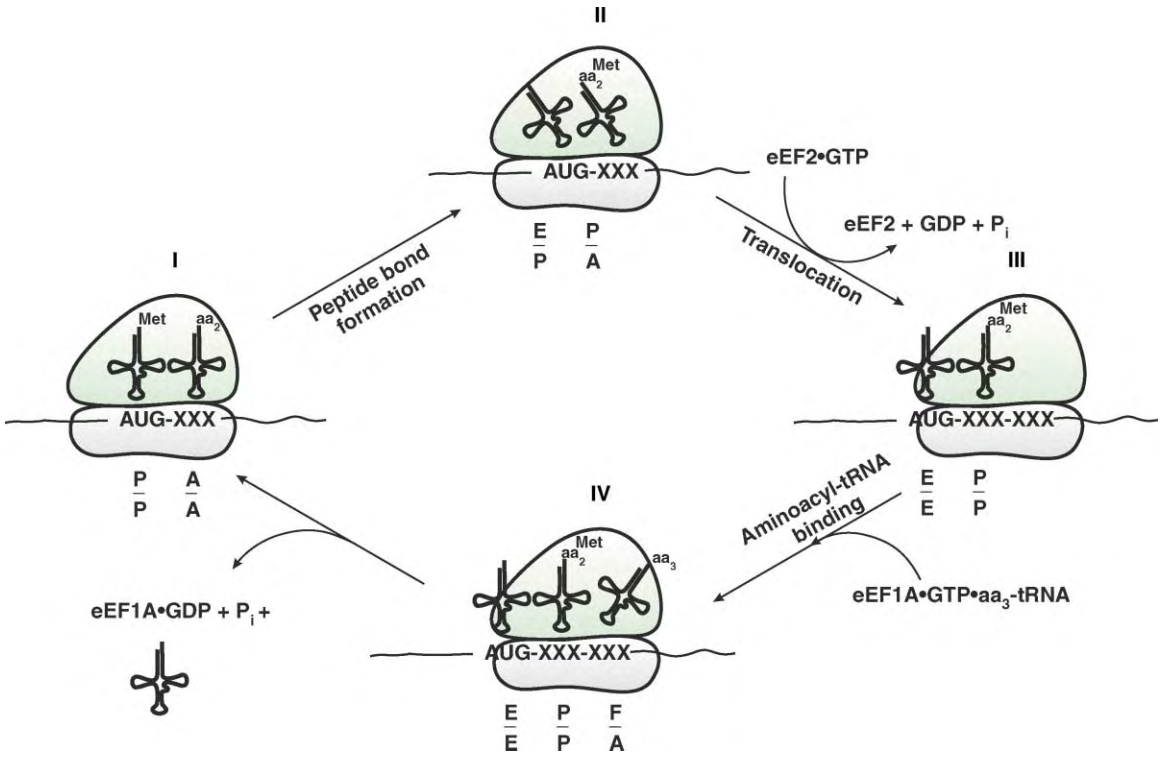

FIGURE 2 Influence of other sites. Illustrated in this figure are the four proposed sites in the eukaryotic ribosome. The A and P sites are the "traditional" tRNA binding sites on the ribosome (Figure 1). The E site (exit site) and the F site (entry site) are also shown. Note that a portion of each site is located on the small (40S) and the large (60S) ribosomal subunit. In the designation for the tRNA molecules, the upper letter indicates position on the 60S subunit and the lower letter indicates position on the 40S subunit.

examination, it should be apparent that the synthesis of the peptide/protein is from the amino terminus to the carboxy terminus while the mRNA codons are read in a 5′ to 3′ direction.

Elongation Cycle Chemistry

Figure 3 shows the "chemistry" that occurs with peptide bond formation. The initial step is the nucleophilic attack of the amino group of the second amino acid (R2) on the carbonyl of the initiating amino acid (methionine, R1) as is seen in Schiff's base formation (I). It is thought that the function of the peptidyl transferase center is to facilitate the abstraction of the H^+ in the intermediate (II) by providing a weak base (:B). With the release of this H^+ and a shift of electrons, the bond between the 3′ oxygen of the terminal adenosine in the tRNA in the P site and the methionine is cleaved, thus completing the transfer of the methionine to the amino group of the second amino acid and formation of the peptide bond (III). The cycle is then completed with the reacquisition of a proton at the 3′ position of the tRNA in the P site (IV). Finally, with eEF2-catalyzed translocation, the peptidyl-tRNA is moved completely into the P site (V). In the overall thermodynamics of the reaction, the resulting peptide bond is rather low energy while the original aminoacyl linkage is high energy (equivalent to that in ATP), and thus the net ΔG (change in the Gibb's free energy) is quite negative. While most primary amines would be expected to have a pK_a of ~9–10, that of the "α" amino groups is ~7.5 due to the inductive effects of the ester linkage of the amino acid to the tRNA (in a similar manner, the pK_a of the amino group at the amino terminus of the peptide/protein is also ~7.5). Thus, at physiologic pH values, the nucleophilic amino group is positively charged only about 50% of the time.

Molecular Mimicry

The crystallographic structures of bacterial homologues of eEF1A·GDPNP·Phe-tRNA and eEF2 have been determined. Comparison of these two structures indicated that to a first approximation they had a similar size, shape, and electronic distribution. While this might have been expected for the GTP-binding domain, EF2 has a unique protein finger that appears to mimic the anticodon stem and loop of a tRNA by overall size and charge (rich in aspartic and glutamic acid residues).

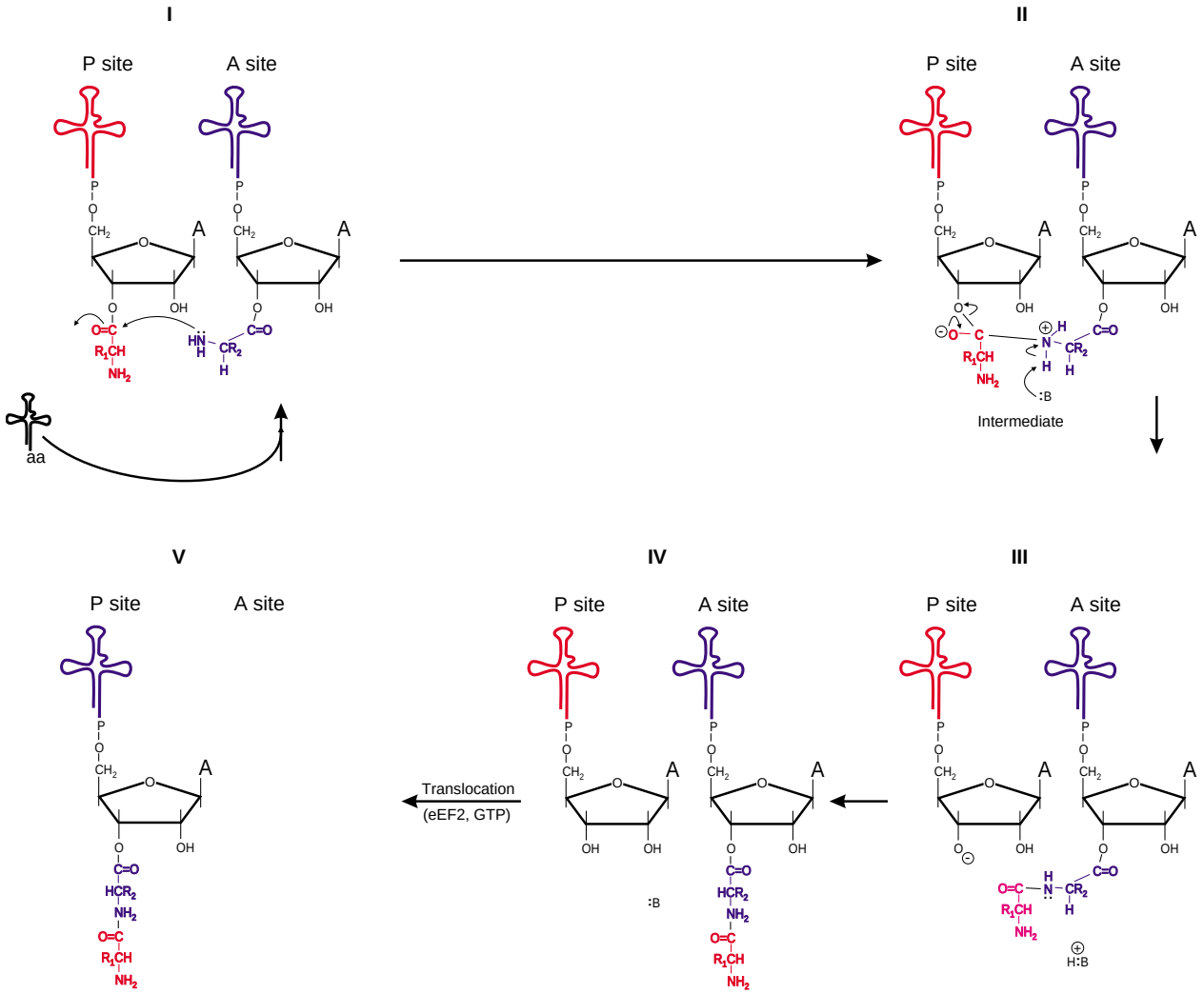

FIGURE 3 Elongation cycle chemistry. Shown above is the possible chemistry of the process of elongation. Nucleophilic attack by the amino group in the A site on the carbonyl bond of the amino acid in the P site leads to an amino-tetrahedral intermediate (II). The primary role of the ribosome in peptide bond formation is to facilitate the forward reaction by use of a general weak base (:B) although the group in the 60S subunit serving this function has not yet been identified. The chemistry is completed by subsequent cleavage of the ester bond to the tRNA in the P site (III). The cycle is then completed by the acquisition of a proton to the 3′ position, and the loss of the proton from the weak base (IV) followed by translocation (V). Binding of a new aminoacyl-tRNA (as an eEF1A·GTP·aminoacyl-tRNA complex) starts the beginning of a new cycle (I).

The ability of a protein domain to take on the apparent characteristics of RNA has been termed "molecular mimicry." Although not discussed here, it has been proposed that all factors (initiation factors, termination factors, stringent factor, etc.) that bind to this region of the ribosome are also molecular mimics and will probably yield structures that are similar to those of the ternary complex and EF2.

Influence of Other Sites

In the discussion above, reference was made to an E site (Figure 2). This site, to the 5′ side of the P site, has been visualized by cryoelectron microscopy and inferred by nuclease footprinting. The most important effect of the E site is that it appears to increase the stringency for the correct matching of the codon and anticodon in the A site of the ribosome. It should be noticed that, for the original binding of the first aminoacyl-tRNA, Met-tRNA$_i$, the E site was unoccupied. One might anticipate that this would allow for less stringent recognition of the initiating AUG codon; however, this strict recognition appears to result from the unique set of factors associated with the initiation process. A second proposed site is the F site or entry site which is just 3′ of the A site. The suggestion here is that this may be an initial test-binding site (a check of codon/anticodon match)

such that correctly matching complexes would be pulled into the A site, while incorrectly matching complexes would dissociate. The advantage of the F site is that it would be more accessible to ternary complexes of eEF1A·GTP·aminoacyl-tRNA, as both the A site and the P site appear to be partially occluded at the interface of the large and small ribosomal subunits. However, the biochemical evidence supporting the existence of the F site is weak compared to that for the E site.

Assuming that all four of the ribosomal sites exist and that they are functional, they can be characterized by positions of the tRNAs on either the large or small ribosomal subunits. Thus, following initiation, the Met-$tRNA_i$ may be described as being in the P/P position (both the aminoacyl end and the anticodon end of the tRNA correspond to the P site (Figure 2) I or III). In the next step, the initial binding of the aminoacyl-tRNA is to the F/A site where the anticodon is in the A site, but the aminoacyl end is in the F site, and this end of the aminoacyl-tRNA is still bound to eEF1A·GTP (Figure 3, IV). With correct codon/anticodon recognition, GTP is hydrolyzed and eEF1A·GDP is released from the ribosome, concomitant with the movement of the aminoacyl end of the tRNA into the A site (now in the A/A configuration; Figure 2, I). At the same time, any tRNA in the E site (as would be true for most elongation steps) would be released from the ribosome. Subsequent reactions would cyclically yield the other states of the ribosome (P/P A/A, E/P P/A, and then E/E P/P).

The Other Elongation Factor, eEF3

A translation elongation factor unique to yeast and fungi is eEF3. This protein, which contains two-nucleotide-binding sites, appears to be required for the nucleotide-dependent release of the nonacylated tRNA from the ribosomal E site. As this protein is an essential gene product in yeast, it is surprising that an equivalent activity has not been identified in other eukaryotes. However, it has been noted *in vitro* that only elongation reactions using yeast ribosomes demonstrate the eEF3 requirement, and thus this requirement for eEF3 would appear to reflect unusual properties of the yeast ribosome compared to other eukaryotic ribosomes.

Regulation of the Elongation Cycle

The major regulation of gene expression at the translational level occurs through the covalent modification of translation initiation factors or regulatory proteins that bind to the initiation factors. However, there is ample evidence that regulation of translation also occurs at the level of elongation although the degree of regulation (the fold change in the elongation rate) is not as great as seen with regulation of initiation. While eEF1A, eEF1B, and eEF2 are all phosphorylated under different conditions, eEF1A and eEF2 also contain unique posttranslational modifications. eEF1A contains methylated lysines (mono-, di-, or trimethyl lysine) and glycerylphosphorylethanolamine. eEF2 contains a hypermodified histidine residue (histidine #714 in mammalian eEF2's) that is found in all eukaryotic eEF2's called diphthamide. The diphthamide residue is a known inactivation site for ADP-ribosylation catalyzed by either *Diphtheria* or *Pseudomonas* A toxins with NAD serving as the donor of the ADP group. There is tentative evidence that this modification may be part of the normal cellular regulation of eEF2 activity as well.

The best-studied regulation of any of the elongation factors is via phosphorylation. In general, phosphorylation of eEF1A and eEF1B correlates well with increases in the rate of elongation noted *in vivo* with either insulin or phorbol ester treatment. Additionally, most phosphorylations of translation factors are associated with an increased rate of protein synthesis. In contrast, the phosphorylation of eEF2 leads to its inactivation. Under most circumstances, changes in the elongation rate due to changes in covalent modifications of eEF1A, eEF1B, or eEF2 are associated with a coordinate change in the rate of initiation of protein biosynthesis.

See Also the Following Articles

EF-G and EF-Tu Structures and Translation Elongation in Bacteria • Ribosome Structure • Translation Elongation in Bacteria • Translation Initiation in Bacteria: Factors and Mechanisms • Translation Initiation in Eukaryotes: Factors and Mechanisms • Translation Termination and Ribosome Recycling

Glossary

E, A, P, and F sites Physical locations on the surface of the ribosome that are occupied by aminoacyl- or peptidyl-tRNA.

elongation (of protein synthesis) The sequential steps that lead to the addition of one amino acid at a time to the growing polypeptide chain.

elongation factor (EF) A nonribosomal protein that facilitates the process of elongation only. (Note: eukaryotic elongation factors are designated eEF, where the lower case "e" signifies "eukaryotic.")

initiation (of protein synthesis) The required steps that lead to the placement of the initiator tRNA in the P site of the ribosome, correctly base paired with the initiating AUG codon.

protein synthesis The process of joining amino acids in a specific sequence through the a carbonyl and a amino groups via a peptide bond that is templated by an mRNA molecule.

termination (of protein synthesis) The codon-directed (UAA, UAG or UGA) process of cleavage (and therefore release) of the polypeptide chain from the tRNA in the P site of the ribosome.

Further Reading

Ban, N., Nissen, P., Hansen, J., Capel, M., Moore, P. B., and Steitz, T. A. (1999). Placement of a protein and RNA structures into a 5 Å-resolution map of the 50S ribosomal subunit. *Nature* **400**, 841–847.

Burkhardt, N., Junemann, R., Spahn, C. M. T., and Nierhaus, K. H. (1998). Ribosomal tRNA binding sites: Three-site models of translation. *Crit. Rev. Biochem. Mol. Biol.* **33**, 95–149.

Clark, B. F. C., Grunberg-Manago, M., Gupta, N., Hershey, J. W. B., Hinnebusch, A. G., Jackson, R. J., Maitra, U., Mathews, M. B., Merrick, W. C., Rhoads, R. E., Sonenberg, N., Spremulli, L. L., Trachsel, H., and Voorma, H. O. (1996). Prokaryotic and eukaryotic translation factors. *Biochimie* **78**, 1119–1122.

Clemons, W. M., Jr., May, J. L. C., Wimberly, B. T., McCutcheon, J. P., Capel, M. S., and Ramakrishnan, V. (1999). Structure of a bacterial 30S ribosomal subunit at 5.5 Å resolution. *Nature* **400**, 833–840.

Merrick, W. C., and Nyborg, J. (2000). The protein biosynthesis elongation cycle. In *Translational Control of Gene Expression* (N. Sonenberg, J. W. B. Hershey and M. B. Mathews, eds.) pp. 89–125. Cold Spring Harbor Laboratory Press, Cold Spring Harbor, New York.

Moazed, D., and Noller, H. F. (1989). Intermediate states in the movement of tRNA in the ribosome. *Nature* **342**, 142–148.

Nissen, P., Kjeldgaard, M., Thirup, S., Polekhina, G., Reshetnikova, L., Clark, B. F. C., and Nyborg, J. (1995). Crystal structure of the ternary complex of Phe-tRNA^{Phe}, EF-Tu, and a GTP analog. *Science* **270**, 1464–1472.

Proud, C. (2000). Control of the elongation phase of protein synthesis. In *Translational Control of Gene Expression* (N. Sonenberg, J. W. B. Hershey and M. B. Mathews, eds.) pp. 719–739. Cold Spring Harbor Laboratory Press, Cold Spring Harbor, New York.

Rodnina, M. V., and Wintermeyer, W. (2001). Fidelity of aminoacyl-tRNA selection on the ribosome: Kinetic and structural mechanisms. *Annu. Rev. Biochem.* **70**, 415–435.

Biography

William C. Merrick is a Professor in the Department of Biochemistry in the School of Medicine at Case Western Reserve University. For over 30 years he has studied the processes of protein synthesis initiation and elongation in eukaryotic systems. These studies have resulted in the identification, cloning, and characterization of approximately 15 different translation factors and have indicated a sequential utilization of these factors.

Anton A. Komar is a Senior Research Associate in Dr. Merrick's laboratory. Dr. Komar received his Ph.D. from Moscow State University. His research expertise is in molecular biology, yeast genetics, and protein chemistry. His efforts have led to the identification of an IRES (internal ribosome entry site) in the Ure2p mRNA, the first in yeast. He is continuing studies of the Ure2p mRNA, both as relates to IRES function and the ability of Ure2p to behave as a prion.

Translation Initiation in Bacteria: Factors and Mechanisms

Cynthia L. Pon and Claudio O. Gualerzi
University of Camerino, Camerino, Italy

Initiation of protein synthesis is a fundamental biological process which contributes greatly to fidelity, efficiency, and regulation of gene expression. Translation initiation is a multistep process in which start codon and consequently the reading frame of the mRNA are selected by the small ribosomal subunit (30S) through the decoding of initiator N-formyl-methionyl-tRNA (fMet-tRNA) by the initiation codon producing a "30S initiation complex" which subsequently either forms the "70S initiation complex" by its association with the 50S ribosomal subunit or—if incorrectly formed—dissociates into its individual components. The aminoacyl-tRNA encoded by the second codon of the mRNA is then bound, in a ternary complex with EF-Tu and GTP, to the A-site of the 70S initiation complex which bears fMet-tRNA in the P-site. The subsequent formation of the first peptide bond between N-formyl-methionine and the second aminoacyl-tRNA yields an "initiation dipeptidyl-tRNA" in the A-site. The first translocation event moves the dipeptidyl-tRNA to the P-site and the ribosome enters the elongation phase of translation. The entire translation initiation process is kinetically controlled by three proteins, the initiation factors IF1, IF2, and IF3.

Properties, Aminoacylation, and Formylation of the Initiator tRNA

In bacteria protein synthesis begins with a special brand of tRNA, the initiator $tRNA^{fmet}$. Apart from being recognized by the same Met-tRNA synthetase (the main recognition element being the CAU anticodon), the initiator tRNA is endowed with a number of structural and functional properties which make this particular RNA one of a kind. The main features distinguishing the initiator tRNA from elongator tRNAs is the extended G–C helix in its anticodon stem, which favors its interaction with the ribosomal P-site, and the unpaired 5′-end base which allows the recognition of Met-$tRNA^{fmet}$ by the transformylase. The recognition of fMet-tRNA by IF2 relies on the presence of a formyl group blocking the α-NH_2 group of the amino acid and requires just a few bases of the 3′ acceptor end of the molecule; indeed, fMet-ACCAAC has almost the same affinity for IF2 as the intact fMet-tRNA.

The Translation Initiation Region of Prokaryotic mRNAs

The "translation initiation region" (TIR) of the mRNAs invariably contains an initiation triplet from which the ribosomes begin to translate and which sets, at least provisionally, the reading frame of the template (a reading frameshift may occur during elongation). Whereas the most frequently used initiation triplet is AUG, ~10% of all known genes and open reading frames begin with rarer yet "canonical" codons such as GUG and UUG, and, even less frequently, with "non-canonical" triplets such as AUU, AUC, and AUA. However, regardless of its nature, the initiation triplet is always decoded by the initiator fMet-tRNA. The reason for this initiation codon degeneracy is not always clear but two facts should be recalled. First, AUG is the only triplet giving rise to a "best-fit" Watson–Crick base-pairing with the anticodon (CAU) of the initiator tRNA, while all other start codons are expected to yield either 3′ or 5′ wobbling interactions with the same anticodon. Second, if not resulting from neutral mutations, the rare initiation triplets must be considered (or suspected to be) important regulatory signals capable of controlling timing and/or efficiency of translation. It is not by chance that, as described below, initiation factor IF3 can discriminate against translation beginning at noncanonical start codons; the best known example of translation regulation based on the use of a rare codon is the translational autorepression of IF3 mRNA which begins with an AUU initiation codon.

Aside from some "leaderless" mRNAs, which are occasionally found in (mainly Gram-positive) bacteria, which begin with a 5′ AUG, the TIR of most mRNAs (Figure 1) contains, upstream of the initiation triplet a 5′ untranslated region (5′ UTR) of variable length

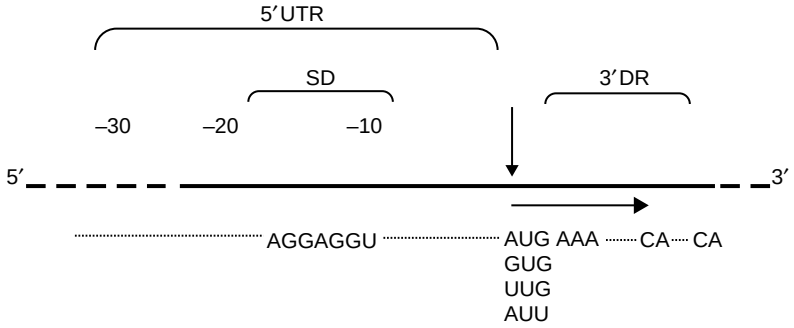

FIGURE 1 Schematic representation of the features characterizing a bacterial leader-containing mRNA translation initiation region (TIR). The arrows indicate the beginning of the coding region of the mRNA with four of the most common initiation triplets. To the left of the start point is the 5′ untranslated region (5′ UTR) with the approximate location of the Shine–Dalgarno sequence (SD) whose most extended consensus sequence is indicated below. To the right of the start point is the 3′ downstream region (3(DR)) with the most favorable second codon AAA and the repeated CA dinucleotides acting as translational enhancers in some mRNAs. Leaderless mRNA would start at the initiation codon.

and structure which generally includes a purine-rich Shine–Dalgarno sequence (SD sequence) complementary to the anti-SD sequence at the 3′-end of 16S rRNA. The SD sequence and the initiation triplet are separated by a spacer of variable length (optimally five nucleotides). Also the sequence at the 3′ side of the initiation triplet, the downstream region (DR), can have a strong influence on TIR selection. Highly expressed mRNAs seem to have a bias in favor of an AAA triplet as the second codon and a CA repeat sequence within the first 15 codons was shown to contribute to highly efficient initiation. Finally, important elements which contribute to the efficiency of translation initiation are also the secondary and tertiary RNA structures of the TIRs which may favor or disfavor formation of the 30S initiation complex and very often influence mRNA stability. In general, mRNAs whose TIRs are devoid of secondary structures tend to be translated with greater efficiency, although it is the optimal combinations of all the aforementioned TIR elements which can maximize translation of mRNA.

Initiation Complex Formation

Although the structural elements of the mRNA, such as the SD sequence of the TIRs, may contribute to the thermodynamic stability of the productive 30S–mRNA interaction, thereby favoring the selection of the correct start site of the mRNA, the initiation site is selected kinetically by the 30S ribosomal subunit with the aid of the initiator fMet-tRNA whose anticodon base pairs with the initiation codon of the mRNA forming a ternary complex (the "30S initiation complex") comprised of the 30S ribosomal subunit, fMet-tRNA and mRNA. Both conventional and fast kinetic analyses have contributed to the elucidation of the mechanistic aspects of the translation initiation process schematically illustrated in Figure 2, which summarizes the steps leading to the formation of the 30S and 70S initiation complexes and the late events of translation initiation. In this pathway the 30S ribosomal subunit with a full complement of initiation factors interacts (steps A and B′ or B and A′) with mRNA and fMet-tRNA in stochastic order forming first two "binary complexes" and then an unstable "pre-ternary complex" in which both mRNA and fMet-tRNA are 30S-bound without interacting with each other. A first-order isomerization of this pre-ternary complex kinetically controlled by the three initiation factors (step C) causes the mRNA start codon to base pair in the P-site of 30S with the anticodon of fMet-tRNA to yield a "30S initiation complex." The specific role played by the individual initiation factors in this as well as in other steps of initiation will be described below. The "70S initiation complex" is generated by the joining of the large (50S) ribosomal subunit (step D), a process which induces a conformational change in the 30S subunit and thereby causes the ejection of IF1 and IF3. The intrinsic GTPase activity of IF2 (step E) is also triggered in this step, generating an IF2–GDP complex and inorganic phosphate. The latter is then released from ribosome in a step (step F) which possibly entails also the dissociation of IF2–GDP. The dissociation of IF2 leaves fMet-tRNA in the ribosomal P-site with the acceptor end near the peptidyl transferase center of the 50S subunit. The binding and the adjustment of the cognate EF-Tu·GTP·aa-tRNA to the ribosomal A-site is a multistep and overall rapid process (steps G, H, I, J) which is followed by the formation of the initiation dipeptide (step K) with the P-site-bound fMet-tRNA. Formation of the initiation dipeptide is a fairly slow process compared to the rate of transpeptidation during elongation.

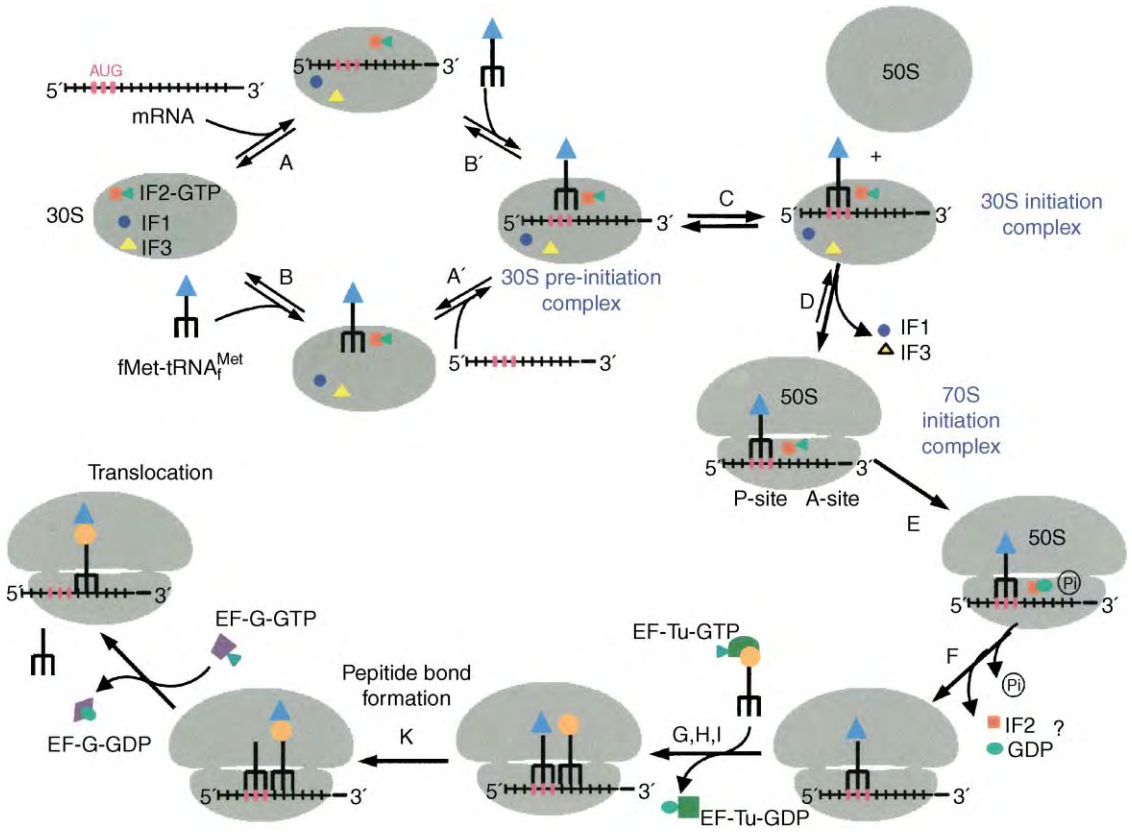

FIGURE 2 Initiation pathway. Scheme depicting the translation initiation pathway in bacteria as determined over the past two decades, mainly through traditional and fast kinetics analyses. Further details can be found in the text. The symbols and the denominations of the intermediate complexes are as indicated in the figure.

Structure and Function of the Initiation Factors

Overall, the three initiation factors ensure speed and accuracy in the initiation phase of protein synthesis. The properties and specific roles of these proteins are outlined below.

IF1

Structure

This protein (encoded by *infA*) consists of ~70 amino acids (71 in *Escherichia coli*) and is characterized by a rigid five-stranded β-barrel structure from which protrude the short disordered and highly flexible N- and C-terminal tails (Figure 3A). This structural motif, known as the "OB fold," is characteristic of a class of proteins that interact with oligonucleotides and RNA (like IF1) or with oligosaccharides.

Topographical Localization and Function

IF1 binds to the 30S ribosomal subunit mainly through electrostatic interactions involving the positively charged surface of the protein and the phosphate backbone of specific regions of 16S rRNA. Earlier topographical studies and more recent chemical probing and crystallographic data indicate that IF1 binds in the A-site of the 30S ribosomal subunit. More precisely, IF1 fits in the cleft between ribosomal protein S12, the 530 loop and helix 44 of 16S ribosomal RNA (rRNA) establishing contacts with two functionally important bases (A1492 and A1493) which belong to this rRNA helix. This ribosomal localization could cause IF1 to block the premature access of aminoacyl-tRNA to the A-site during 30S initiation complex formation and supports the premise that IF1 contributes to the fidelity of translation initiation. The existence of a mutual influence of IF1 and IF2 on their respective interactions with the 30S ribosomal subunit is well established so that IF1 is regarded as being a modulator of IF2 recycling on and off the ribosomes. IF1 also increases the rates of association/dissociation of ribosomal subunits and this activity is probably a decisive factor in favoring the otherwise inefficient ribosome dissociation activity of IF3. Finally, IF1 can also increase the rate of 30S initiation complex formation, probably through a conformational change of the small ribosomal subunit. Indeed, there is compelling evidence from the

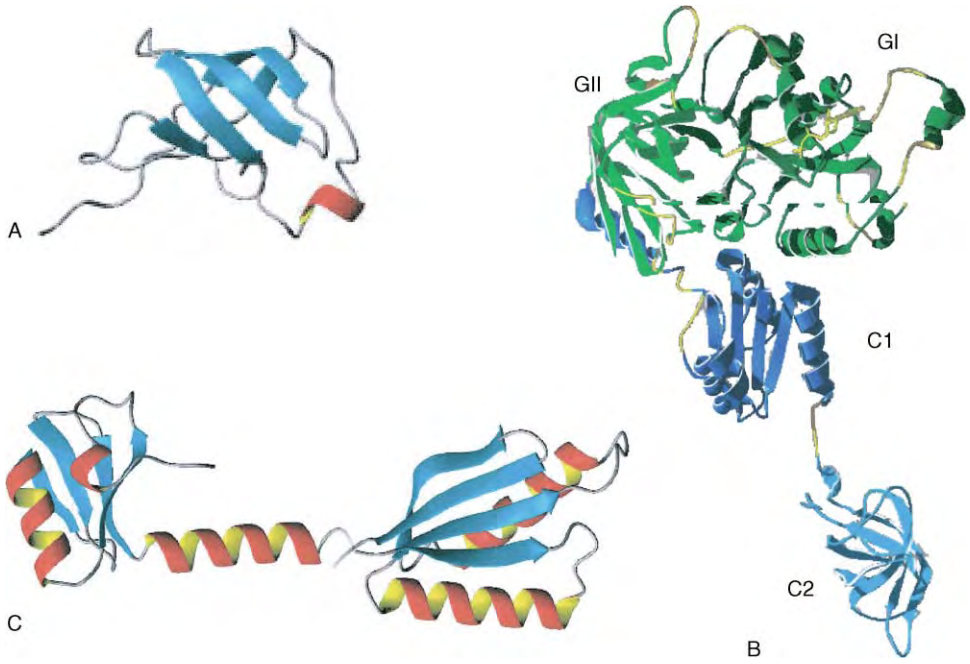

FIGURE 3 Three-dimensional structures of the three translation initiation factors. (A) β-Barrel structure of *E. coli* IF1 in solution as determined by NMR spectroscopy, (B) predicted structure of bacterial IF2 based on the crystal structure of archaeal eIF5b and on the solution structure of *Bacillus stearothermophilus* IF2C2 determined by NMR spectroscopy. The N-terminal domain is missing while the other domains are indicated with the following color patterns. Dark green, GI, light green GII, dark blue, C1, light blue, C2. (C) Crystallographic structure of *B. stearothermophilus* IF3 displaying the N domain (left), linker (center), and the multi-functional C-domain (right).

crystallographic data that IF1 binding induces several localized and long-range changes of the 30S structure. Overall, IF1 induces a rotation of head, platform and shoulder of the 30S subunit towards the A-site.

IF2

Structure

Bacterial IF2 (encoded by *infB*) is the largest initiation factor (890 residues in *E. coli*) and consists of three major parts: (i) a variable N-terminal region, (ii) a highly conserved 40 kDa region containing two domains, GI and GII, and (iii) the C-terminal region (25 kDa) which also consists of two domains, C1 and C2.

So far no three-dimensional (3D) structure has been directly determined for the whole bacterial IF2 molecule, and structural information concerning this factor relies on the NMR structure of the C2 domain of *Bacillus stearothermophilus* IF2 and on the crystal structure of *Methanobacterium thermoautotrophicum* eIF5B (Figure 3B), the archaeal homologue of IF2. However, although it is likely that the structures of the archaeal and bacterial factors are similar, it should be noted that the functions of these two proteins have very little in common. Overall, IF2 is an extended molecule containing four domains arranged in a unique architectural motif resembling a chalice whose cup is constituted by GI, GII, and N-terminal part of C1, the stem by the C-terminal part of the same domain and the foot by the C2 domain. No structural information is available for the hydrophilic, positively charged and likely flexible N-domain which is not present in the archaeal protein as well as in some bacterial IF2 molecules. The likely function of this domain, which is dispensable for translation both *in vitro* and *in vivo*, is that of anchoring the factor on the 30S ribosomal subunit in a more or less specific way until the acceptor end of an fMet-tRNA molecule is "captured" by the C2 domain of the factor. The GI-domain binds GTP/GDP and is highly homologous to small GTPases and to equivalent domains of other GTP/GDP binding proteins such as elongation factors EF-Tu and EF-G. The GI domain is also responsible for the interaction of IF2 with the 50S ribosomal subunit and probably contains the GTPase center of the protein which is naturally activated by the interaction with the ribosomes.

The structure of this domain consists of an eight-stranded β-sheet flanked by six α-helices and a 3_{10} helix. As mentioned above, this domain contains the four conserved sequence elements characteristic of GTP-binding proteins (G1/P loop, which participates in phosphate binding, the G3 and G4 loops, forming the walls of a hydrophobic pocket where the guanine moiety of GTP or GDP is bound and G4). The Switch 2 region

of the GI domain is centrally located in the cup of the chalice where it makes extensive contacts to domains GII and C1 and can therefore cause conformational changes resulting in profound global rearrangements of the molecule that can reach as far as 90Å to the C-terminal region of IF2. The GII domain, which together with C1 is responsible for the interaction of IF2 with the 30S ribosomal subunit, has a β-barrel structure very similar to that of the C2 domain. Three β-strands of this domain interact closely with the GI-domain in the vicinity of the Switch 2 region. The GII domain is connected by a 17 residue α-helix to the C1-domain which is characterized by a unique $\alpha-\beta-\alpha$ sandwich fold consisting of a four-stranded parallel β-sheet flanked on both sides by two α-helices. As mentioned above, the last 40Å long helix (H12) of the C1 domain extends from the cup to the C2 domain thus forming the "stem" of the chalice. The C2 domain of IF2, which is responsible for the specific recognition and binding of the acceptor end of fMet-tRNA is endowed with a structure which also consists of an eight-stranded β-barrel fold similar to that of GII and to domain II of EF-Tu and EF-G.

Topographical Localization and Function

IF2 is the only one of the three factors displaying a specific and fairly high affinity for both ribosomal subunits, and its interaction with the isolated 50S subunit is sufficient to elicit its GTPase activity. Recent experiments localize IF2 in a region of the 30S subunit topographically adjacent to the A-site, on a surface of the subunit's body facing the factor-binding region of the 50S subunit. With respect to the 50S subunit, IF2 was found to influence the chemical reactivity and/or the accessibility to nucleolytic cleavage of bases belonging to helix 89, to the sarcin-ricin domain (SRD) and to the L11/Thiostrepton-binding region of 23S rRNA leading to the conclusion that its topographical localization is on the right edge of the subunit interface site of the particle and at least partly overlaps that of elongation factors EF-G and EF-Tu.

The main function of IF2 is that of recognizing and binding (K_d in the μM range) the initiator fMet-tRNA and to stimulate (through an increase of the on-rate) its binding to the ribosomal P-site. Both specificity and thermodynamic stability of the IF2-fMet-tRNA interaction are properties of the C2 domain (~11 kDa). Additional IF2 functions include the stimulation of subunit association and the positioning of fMet-tRNA in the ribosomal P-site of the 70S initiation complex which favors the first transpeptidation. Furthermore, IF2 is a GTP/GDP-binding protein and a ribosome-dependent GTPase like EF-Tu and EF-G but, unlike these elongation factors, the function of the IF2-dependent GTP binding and hydrolysis is difficult to pin down. Thus, since neither GTP/GDP-binding nor GTPase activity seems to be mandatory for any translational function of IF2 and since the "metabolic alarmone" ppGpp can bind in place of GTP and inhibit the IF2-dependent 30S initiation complex formation and initiation dipeptide synthesis, it has been postulated that IF2 uses its GDP/GTP-binding site as a receptor for GTP (under optimal growth conditions) or for ppGpp (during nutritional stress) and accordingly behaves like a sensor of the metabolic state of the cell. This raises the interesting possibility that, in addition to and because of its roles in translation initiation, IF2 might function as a global regulator linking translational activity to the transcriptional control of stable RNA synthesis by adjusting the translational rate of the cell as a function of the allowable growth rate.

IF3

Structure

The structure of this medium-sized protein encoded by *infC* (180 amino acids in *E. coli*) is characterized by the presence of two domains of approximately equal mass connected by a long (~45Å) lysine-rich linker (Figure 3C). Whereas considerable controversy exists between crystallographic and NMR data as to whether this linker is a long and rigid α-helix or unstructured and flexible, the 3D structures of both N-terminal (IF3N) and C-terminal (IF3C) domains seem to be well established. IF3N contains a globular α/β fold consisting of a single α-helix, packed against a mixed four-stranded β-sheet. IF3C possesses a two-layered α/β sandwich fold, comprising a four-stranded β-sheet which is packed against two parallel α-helices in a $\beta\alpha\beta\alpha\beta\beta$ topology. The fold of IF3C is similar to that found in many eukaryotic RNA-binding proteins (such as U1A) and indeed IF3C interacts with the 30S subunit via a protein–RNA interaction involving primarily structural elements of this domain like strands β-7 and β-9 that contain consensus RNP motifs and two loops (L7 and L8). Regardless of the actual structure of the linker, several lines of evidence indicate that the two domains of IF3 do not interact with one another in the free or in the ribosome-bound protein and that they interact, independently of each other, with different sites of the 30S subunit.

Topographical Localization and Function

The main interaction of IF3 with the 30S subunit occurs via IF3C, the domain which encompasses all IF3 activities. Whereas there is good agreement that IF3C is localized on the platform of the 30S ribosomal subunit, the ribosomal localization of IF3N is more controversial, although it seems likely that its binding site is located somewhere on the head of the particle.

Binding of IF3 to the 30S ribosomal subunit interferes with subunit association thereby shifting to the left of the equilibrium 30S + 50S ⇌ 70S. In turn, this increases the pool of free 30S which are amenable to initiate a new round of translation. Furthermore, the presence of IF3 on the 30S increases the on-rate of "pre-ternary complex" isomerization which leads to 30S initiation complex formation (Figure 2) and thereby stimulates overall mRNA translation. However, since IF3 increases also the off-rate of the isomerization, in this context it can promote initiation fidelity favoring the dissociation from the 30S subunits of both tRNA and template. Indeed, the dissociation occurs with different rates depending on whether the 30S complex is a "canonical," a "noncanonical," a "leaderless," or a "pseudo" initiation complex and is in kinetic competition with the association of the same 30S initiation complex with the 50S ribosomal subunit which yields a "70S initiation complex" (Figure 2). The potential 30S initiation complexes recognized and accepted as "correct" by IF3 and those kinetically discriminated against as being "incorrect" are schematically represented in Figure 4. Contrary to earlier interpretations, IF3 is not required for mRNA binding to the ribosome but can promote a re-positioning of 30S-bound mRNA shifting it from the "stand by site" to the "P-decoding site" of the subunit. It is likely that this activity may be correlated to the kinetic selection of the correct initiation triplet by IF3. It is noteworthy that isolated IF3C not only binds to 30S subunit but is also capable of performing all the other known functions of the intact molecule while isolated IF3N has no autonomous function. Since the affinity of IF3C for the 30S subunits is approximately two orders of magnitude lower than that of the intact molecule and since secondary contacts established by IF3N stabilize the interaction, it has been suggested that the two-domain structure is required to modulate binding and release of IF3 to and from the 30S subunit.

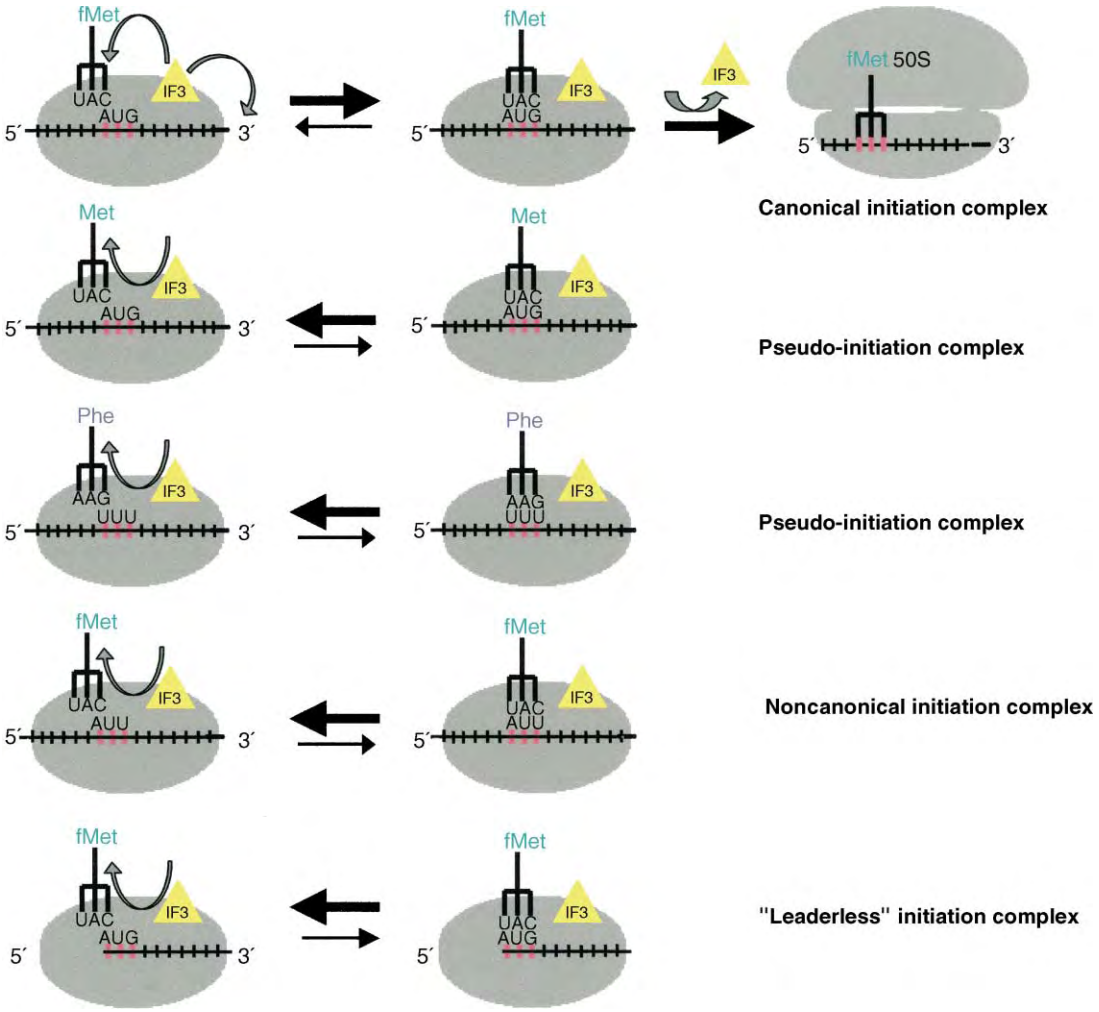

FIGURE 4 Initiation complexes recognized as "correct" and "incorrect" by IF3. The figure presents a scheme of the nature of the various types of complexes containing 30S ribosomal subunit, template and aminoacyl-tRNAs which are subjected to kinetic positive or negative discrimination by IF3. Further details may be found in the text.

The conformational change of the ribosome induced by subunit association would push platform and head of the 30S subunit away from each other thereby widening the gap between the IF3N- and the IF3C-binding sites. The loss of the stabilizing interaction established by IF3N would then facilitate the dissociation of IF3 from the 30S subunit.

See Also the Following Articles

EF-G and EF-Tu Structures and Translation Elongation in Bacteria • Ribosome Assembly • Ribosome Structure • Translation Elongation in Bacteria • Translation Termination and Ribosome Recycling

Glossary

A-site Aminoacyl-tRNA site, the binding site on the ribosome occupied by the tRNA carrying the next amino acid to be added to a growing polypeptide chain.

P-site Peptidyl-tRNA site, the binding site on a ribosome occupied by the tRNA carrying a growing peptide chain.

Watson–Crick base-pairing Association of two complementary nucleotides in a DNA or RNA molecule stabilized by hydrogen bonding between their base components.

wobbling interaction Ability of a tRNA to recognize more than one codon by unusual (non-G-C, non-A-U) pairing with the third base of a codon.

Further Reading

Boelens, R., and Gualerzi, C. O. (2002). Structure and function of bacterial initiation factors. *Curr. Protein Pep. Sci.* **3**, 107–119.

Gualerzi, C. O., Brandi, L., Caserta, E., Garofalo, C., Lammi, M., La Teana, A., Petrelli, D., Spurio, R., Tomsic, J., and Pon, C. L. (2001). Initiation factors in the early events of mRNA translation in bacteria. *Cold Spring Harbor Symp. Quant. Biol.* **66**, 363–376.

Ramakrishnan, V. (2002). Ribosome structure and the mechanism of translation. *Cell* **108**, 557–572.

Biography

Cynthia L. Pon is a Professor of Molecular Genetics at the University of Camerino, Italy. She holds a Ph.D. from Rutgers University and her current research interest concerns the regulation of gene expression during cold stress.

Claudio O. Gualerzi is a Professor of Molecular Biology in the Department of Biology at the University of Camerino, Italy. He holds a laurea degree from the University of Rome and his current research is directed toward the search for new antibiotics.

Translation Initiation in Eukaryotes: Factors and Mechanisms

Tatyana V. Pestova
Moscow State University, Moscow, Russia

Christopher U.T. Hellen
State University of New York Downstate Medical Center, Brooklyn, New York, USA

Translation initiation, the first stage in protein synthesis, is the process of assembly of large (60S) and small (40S) ribosomal subunits to form an 80S ribosome containing initiator tRNA (Met-tRNA$_i^{Met}$) that is base paired to the initiation codon of a mRNA in the ribosomal peptidyl (P) site. This process is mediated by at least 11 eukaryotic initiation factors (eIFs) and proceeds via the sequential formation of intermediate complexes. Initiation is the rate-limiting step of translation, and is a major focus for pathways that regulate gene expression.

The Structure of Eukaryotic mRNAs

Nearly all eukaryotic mRNAs have a 5′-terminal 7-methylguanosine (m^7G) "cap" and a 3′-terminal poly(A) tail that synergistically enhance the efficiency of translation initiation. Most eukaryotic mRNAs contain a single major open reading frame (ORF) that is translated into protein, and initiation usually begins at the first AUG triplet from the 5′-end of a mRNA, which follows a 5′ leader that is <100 nucleotide long. An AUG triplet can be bypassed if its context deviates from the optimal sequence GCC(**A/G**)CCAUG**G** (in which the initiation codon is underlined and the nucleotides in bold have the greatest influence), if it occurs very close to the 5′-end of an mRNA or if the 5′ leader has little secondary structure. Stable structures in the 5′ leader reduce initiation efficiency whereas stable structures downstream of an AUG codon can enhance initiation at it.

The Mechanism of Translation Initiation

Translation initiation on most eukaryotic mRNAs begins with binding of Met-tRNA$_i^{Met}$ to a 40S subunit, followed by ribosomal attachment at the 5′-end of a mRNA, scanning to the initiation codon and joining with a 60S subunit to form an 80S ribosome. Initiation is mediated by at least 11 eIFs (Table I), many of which act at multiple stages in this process (Figure 1). Initiation on a few mRNAs occurs by noncanonical mechanisms, of which the most common is 5′-end independent internal ribosomal entry.

Dissociation of Ribosomes into Free 40S and 60S Subunits

Initiator tRNA and mRNA initially bind to the 40S subunit rather than to the 80S ribosome. However, association of 40S and 60S subunits to form empty 80S ribosomes is favored under ionic conditions in the cytoplasm and a mechanism to maintain a pool of free subunits is therefore a prerequisite for initiation. eIF1A and eIF3 shift the equilibrium between ribosomes and their subunits towards dissociation. eIF3 dissociates 80S ribosomes and, with eIF1A, prevents subunit reassociation by binding directly to free 40S subunits.

Recruitment of Initiator tRNA to the 40S Ribosomal Subunit

The initiation codon is decoded by a unique initiator methionyl-tRNA. Its sequence and structural features distinguish it from the methionyl-tRNAs that decode AUG triplets during translation elongation. These features enable eIF2 to select Met-tRNA$_i^{Met}$ from the cytoplasmic pool of aminoacylated and deacylated initiator and elongator tRNAs, and also exclude Met-tRNA$_i^{Met}$ from translation elongation. eIF2 is a stable heterotrimeric protein consisting of α-, β- and γ-subunits that binds GTP and Met-tRNA$_i^{Met}$ to form a ternary complex. Binding of the ternary complex to a 40S subunit is strongly stabilized by eIF1A and eIF3 and yields a 43S preinitiation complex. eIF2′s activity in binding Met-tRNA$_i^{Met}$ is regulated; its affinity for Met-tRNA$_i^{Met}$ is enhanced by prior binding of GTP

TABLE I

Mammalian Initiation Factors

Factor	Subunits	Mass (kDa)[a]	Functions
eIF1		13	Promotes scanning and the fidelity of initiation codon recognition
eIF1A		17	Ribosome antiassociation; stabilizes Met-tRNA$_i$ binding to 40S subunit; promotes scanning
eIF2	α, β, γ	36, 39, 52	Binds GTP and Met-tRNA$_i$ to 40S subunit; GTPase
eIF2B	α, β, γ, δ, ε	34, 39, 50, 58, 80	Guanine-nucleotide exchange factor for eIF2
eIF3	a–l	167, 105, 99, 64, 52, 38, 35, 40, 37, 29, 25, 67	Ribosome dissociation and ribosome subunit antiassociation; stabilizes binding of the eIF2/GTP/Met-tRNA$_i$ complex to 40S subunit; required for ribosomal binding to mRNA and scanning on the 5′ leader
eIF4A		44	ATP-dependent RNA helicase/RNA-dependent ATPase
eIF4B		69	mRNA-binding cofactor for eIF4A
eIF4E		25	m^7 G "cap"-binding protein
eIF4F, eIF4E, eIF4A, eIF4G		25, 44, 176	Cap-binding complex comprising eIFs 4A, 4E, and 4G
eIF4G		176	Binds and coordinates the functions of mRNA, PABP, and eIFs 3, 4A, 4E
eIF4H		25	mRNA-binding cofactor for eIF4A
eIF5		49	GTPase-activating protein specific for eIF2
eIF5A		17	May enhance first cycle of translation elongation
eIF5B		139	GTPase; ribosome subunit joining
PABP		70	Binds the 3′ poly(A) tail and promotes ribosomal binding to mRNA

[a] Masses (kDa) correspond to those of human proteins, and where appropriate, to the largest isoform.

whereas hydrolysis of eIF2-bound GTP towards the end of each initiation cycle yields eIF2·GDP which dissociates from Met-tRNA$_i^{Met}$, leaving it in the peptidyl (P) site of the 40S subunit. Biochemical and genetic data suggest that eIF2′s γ-subunit binds Met-tRNA$_i^{Met}$ and GTP, but despite eIF2γ having the sequence motifs and structure characteristic of a conventional GTP-binding protein, eIF2 does not have an intrinsic GTPase activity. Hydrolysis of eIF2-bound GTP is induced by eIF5, a GTPase activating protein specific for eIF2.

Attachment of 43S Preinitiation Complexes to mRNA

Binding of initiator tRNA to form a 43S complex is an obligatory first step before a 40S subunit can bind mRNA, which for most mRNAs is a 5′ end-dependent process. Attachment of 43S complexes is enhanced synergistically by the 5′-terminal cap, the 3′ poly(A) tail and the factors that associate with these structures. The m^{7}G "cap" is bound by eIF4E, the cap-binding subunit of the heterotrimeric eIF4F, which also contains eIF4A and eIF4G subunits. eIF4A is an ATP-dependent RNA helicase that cycles in and out of the eIF4F complex. eIF4G is a large polypeptide that binds mRNA and eIF4E, eIF4A, and eIF3 and the cytoplasmic poly(A)-binding protein PABP, thereby coordinating and in some instances enhancing their activities. eIF4B and the less abundant eIF4H enhance the helicase activities of eIF4A and of eIF4F; eIF4B enhances but is not essential for ribosomal attachment to mRNA. The 3′ poly(A) tail's influence is dependent on PABP which binds to it, and synergism between the cap and the 3′ poly(A) tail depends on the bridging interaction of eIF4G with the m^{7}G cap/eIF4E and 3′ poly(A)/PABP complexes.

The eIF4F complex is required on most mRNAs to unwind the cap-proximal region to prepare it for attachment of 43S complexes. Recent studies have shown that 43S complexes can bind directly to a mRNA in the absence of eIF4F if the 5′-terminal region is completely unstructured. Ribosomal attachment likely involves protein–protein interactions between the eIF3 component of 43S complexes and both eIF4G and eIF4B as well as direct binding of eIF3, eIF4G, and the 40S subunit to the mRNA. ATP-dependent restructuring of mRNA and ribosomal attachment to the unwound region of the 5′ leader are probably coordinated by interaction of the eIF4G component of the eIF4F/PABP/mRNA complex with eIF3.

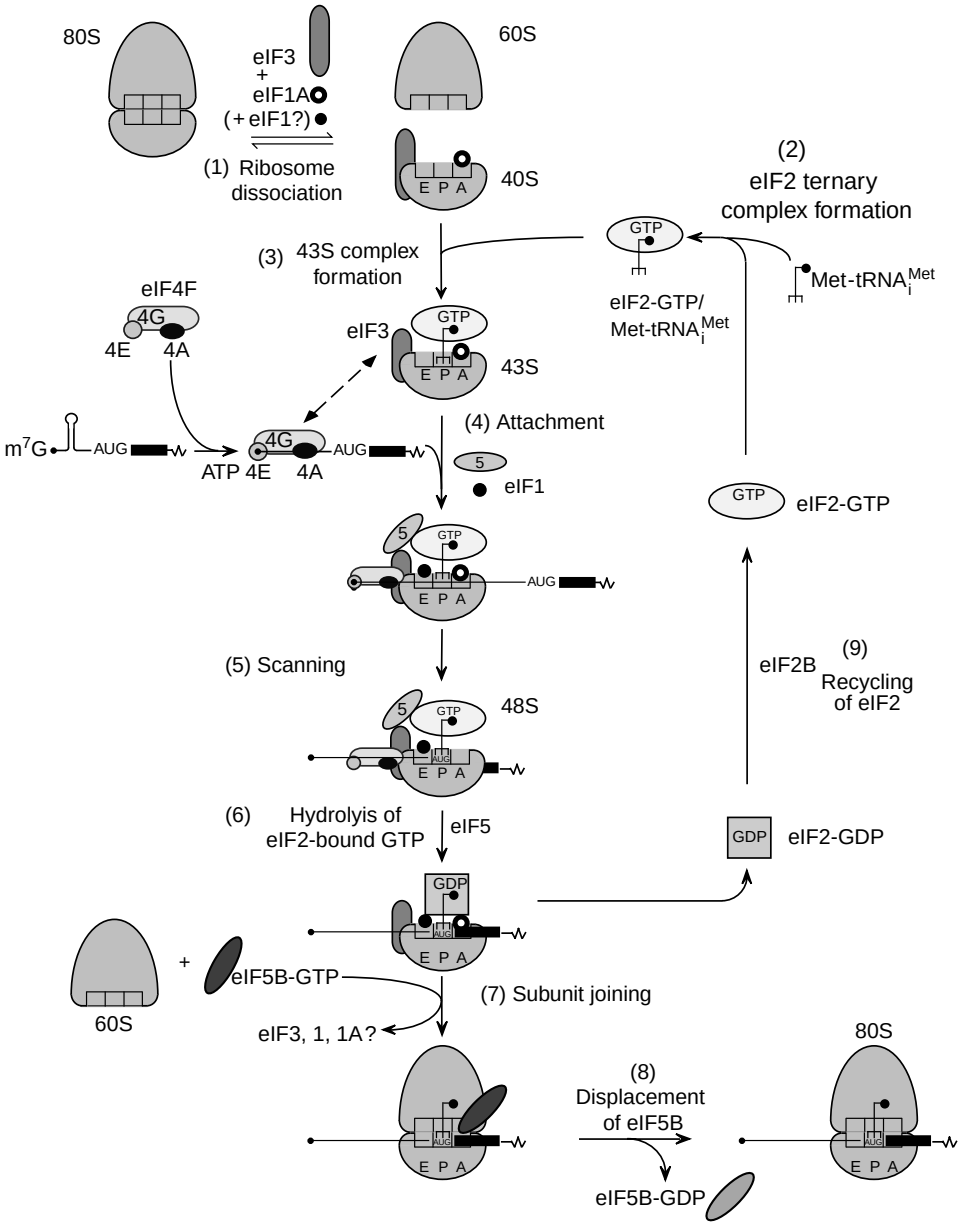

FIGURE 1 Schematic model of the pathway of 80S initiation complex formation on a model capped eukaryotic mRNA. eIF1A and eIF3 promote dissociation of the 80S ribosome into 40S and 60S subunits (Step 1). eIF2 binds aminoacylated initiator tRNA (Met-tRNA$_i^{Met}$) and GTP to form a ternary complex (Step 2). Binding of the ternary complex to a 40S subunit is stabilized by eIF1, eIF1A, and eIF3 to form a 43S complex (Step 3). The eIF4F complex binds to the 5′-terminal m^{7}G "cap" of an mRNA and with associated cofactors creates an unstructured cap-proximal site to which the 43S complex binds (Step 4). This step may be enhanced by the poly(A)-binding protein associated with the mRNA's 3′ poly(A) tail (not shown). The dashed, double-headed arrow indicates interactions that promote attachment of the 43S complex to mRNA, such as those of the eIF3 component of the 43S complex with the eIF4G subunit of cap-bound eIF4F and probably with the mRNA. The 43S complex scans downstream on the 5′-leader until it reaches the initiation codon (Step 5), which is base paired to the anticodon of Met-tRNA$_i^{Met}$ in the resulting 48S complex. Hydrolysis of eIF2-bound GTP is triggered by eIF5, and probably releases of eIF2-GDP (Step 6). The stages at which eIF5 joins and eIF1, eIF1A, and eIF3 are released from the 40S subunit are not known. The GTP-bound form of eIF5B mediates joining of a 60S subunit to the resulting complex (Step 7). eIF5B-GDP is released after hydrolysis of eIF5B-bound GTP, which is induced by both ribosomal subunits. The resulting 80S ribosome is then able to begin protein synthesis (Step 8). eIF2B recycles inactive eIF2-GDP to active eIF2-GTP, which can then bind Met-tRNA$_i^{Met}$ again (Step 9).

Ribosomal Scanning on the 5′-Leader

Following attachment to the 5′-terminal region of a mRNA, a 43S complex scans downstream until it locates the initiation codon, which is usually the first AUG triplet from the 5′-end. Scanning consists of ribosomal movement on the 5′-leader and inspection of it to identify the initiation codon. Recent studies have shown that ribosomal complexes containing only eIF1, eIF2, and eIF3 are intrinsically capable of ATP-independent movement on a 5′-leader if it is unstructured; eIFs 1, 1A, 4A, 4B, and 4F all contribute to the processivity of scanning. eIFs 4A, 4B and 4F, and ATP are involved in restructuring mRNA to permit scanning and are essential for scanning if the 5′-leader contains even weak-secondary structure. Many details of the mechanism of scanning remain poorly understood, including the identity of the set of factors associated with the scanning complex, the mechanism by which helicase-mediated unwinding of structured 5′-leaders is coupled to ribosomal movement, the stage at which eIF4F dissociates from the cap and from the 43S complex and the mechanism of action of eIF1 and eIF1A.

Selection of the Initiation Codon

The scanning 43S complex stops when it encounters an AUG triplet that it recognizes as an initiation codon. This is primarily determined by base pairing between it and the anticodon of initiator tRNA, but in higher eukaryotes the sequence flanking an AUG triplet also influences its selection. Genetic analyses in yeast of mutants that permit initiation at an UUG triplet have indicated that eIF1, eIF2, and eIF5 all influence start site selection. Recent studies have shown that eIF1 plays the principal role in maintaining the fidelity of initiation codon selection, for example, by destabilizing complexes aberrantly arrested at non-AUG triplets or assembled on AUG triplets that have a poor context.

Displacement of eIF2 from the 48S Complex

Establishment of base pairing between the initiation codon and the anticodon of Met-tRNA$_i^{Met}$ stimulates eIF5-induced hydrolysis of eIF2-bound GTP in ribosomal complexes. eIF2·GDP does not bind Met-tRNA$_i^{Met}$ or the 40S subunit and is released from the 48S complex, leaving Met-tRNA$_i^{Met}$ base paired to the initiation codon. eIF5-induced hydrolysis of eIF2-bound GTP is involved in conversion of the scanning ribosomal complex to a complex that is arrested at the initiation codon. Mutations in eIF5 or eIF2 that alter the rate of this reaction therefore influence selection of the initiation codon. eIF2 has a much higher affinity for GDP than GTP, and GDP has a slow off-rate from eIF2, so eIF2B, a guanine nucleotide exchange factor specific for eIF2 is required to regenerate active eIF2·GTP from inactive eIF2·GDP.

60S Subunit Joining to Form an 80S Ribosome

The release of eIF2·GDP from 48S complexes that is induced by eIF5 is not sufficient to permit 60S subunits to bind to the 40S subunit/Met-tRNA$_i^{Met}$/factor complex assembled at the initiation codon. Subunit joining also requires eIF5B, which is a homologue of the prokaryotic initiation factor 2, and like it has a GTPase activity that is maximally stimulated by large and small ribosomal subunits. Subunit joining leads to the release of all initiation factors from the 40S subunit and leaves Met-tRNA$_i^{Met}$ in the ribosomal P site. The GTP-bound form of eIF5B is active in promoting subunit joining but does not dissociate from the ribosome and instead blocks the ribosomal A site. GTP hydrolysis leads to the release of eIF5B·GDP from the 80S ribosome, so that it is able to begin polypeptide synthesis. Translation initiation therefore requires hydrolysis of two GTP molecules in reactions catalyzed by eIF2γ/eIF5 and eIF5B, respectively. The initial round of elongation may be enhanced by eIF5A.

Regulation of Translation Initiation

The intrinsic efficiency of translation initiation on a mRNA is determined by properties such as the degree of secondary structure in the 5′-leader and the sequence context of the initiation codon. Differences in these properties account for many of the differences in the relative levels of translation of different mRNAs. Translation initiation is also regulated either selectively on a single species or a small subset of mRNAs, or globally on all mRNAs, in order to integrate protein synthesis with physiological demands. Translation of a single species of mRNA or of a related group of mRNAs can be repressed by binding of a protein to a specific site on the mRNA in a manner that interferes with initiation. For example, the iron regulatory protein that binds to the 5′ leader of ferritin mRNA sterically prevents it from binding to the 43S complex. More commonly, translation is regulated at a more global level by alteration of the activities of initiation factors, either as a result of phosphorylation or by binding to regulatory proteins. Phosphorylation of eIF2α causes eIF2 to bind to and inhibit eIF2B, ultimately reducing formation of the eIF2/GTP/Met-tRNA$_i^{Met}$ complex and thus down-regulating initiation globally. Initiation on most mRNAs is cap-mediated and is down-regulated by

a reduction in the level of active eIF4F, which can occur either by proteolysis of eIF4G (for example, during some viral infections) or by disruption of eIF4E's interaction with eIF4G by eIF4E-binding proteins that compete with eIF4G for binding to eIF4E.

Initiation of Translation by Internal Ribosomal Entry

Translation on most eukaryotic mRNAs is initiated by end-dependent ribosomal scanning, but initiation on a few viral mRNAs is end-independent and is instead mediated by an internal ribosomal entry site (IRES) that promotes binding of the 40S subunit to an internal site in the mRNA without scanning from the 5′-end. IRESs are in general large and contain significant secondary structure. IRESs from a single virus family are similar, but the size and structure of IRESs from unrelated virus families differ greatly from each other. Three groups of IRESs have been characterized in detail; each mediates initiation by a different mechanism but all involve direct, noncanonical interactions of the IRES with canonical components of the translation apparatus. They all have simpler initiation factor requirements than cap-mediated initiation, and therefore escape some mechanisms that regulate that process. IRESs have been identified in several cellular mRNAs, but little is known of the mechanisms by which they promote initiation.

See Also the Following Articles

mRNA Polyadenylation in Eukaryotes • Pre-tRNA and Pre-rRNA Processing in Eukaryotes • Ribosome Assembly • Ribosome Structure

Glossary

eukaryotic initiation factor A protein that acts in one or more steps in the process of translation initiation.

initiator tRNA The anticodon of initiator transfer RNA is complementary to the AUG initiation codon and its structural properties differentiate it from tRNAs that decode AUG triplets during elongation. Initiator tRNA is activated by covalent linkage to methionine to form methionyl-tRNA, which is the substrate used by ribosomes to initiate protein synthesis.

mRNA The RNA template that is translated by ribosomes to synthesize a protein. Its coding sequence comprises consecutive triplet codons that are decoded by base pairing with the anticodon of aminoacylated tRNAs, and that therefore determine the amino acid sequence of the resulting protein.

ribosome The complex macromolecule that catalyzes mRNA template-directed protein synthesis. Its two subunits both consist of ribosomal RNA and proteins. The 40S subunit binds mRNA and the anticodon end of tRNA; the 60S subunit aligns the aminoacyl ends of tRNAs and catalyzes peptide bond formation.

Further Reading

Dever, T. E. (2002). Gene-specific regulation by general translation factors. *Cell* **108**, 545–556.

Gingras, A.-C., Raught, B., and Sonenberg, N. (1999). eIF4 initiation factors: Effectors of mRNA recruitment to ribosomes and regulators of translation. *Annu. Rev. Biochem.* **68**, 913–963.

Hellen, C. U. T., and Sarnow, P. (2001). Internal ribosomal entry sites in eukaryotic mRNA molecules. *Genes Develop.* **15**, 1593–1612.

Kozak, M. (1991). Structural features in eukaryotic mRNAs that modulate the initiation of translation. *J. Biol. Chem.* **266**, 19867–19870.

Pestova, T. V., and Kolupaeva, V. G. (2002). The roles of individual eukaryotic translation initiation factors in ribosomal scanning and initiation codon selection. *Genes Develop.* **16**, 2906–2922.

Sonenberg, N., Hershey, J. W. B., and Mathews, M. B. (eds.) (2000). *Translational Control of Gene Expression*. Cold Spring Harbor Laboratory Press, Cold Spring Harbor, New York.

Biography

Christopher U. T. Hellen is an Associate Professor in the Department of Microbiology and Immunology at the State University of New York Downstate Medical Center in New York. His principal research interests are in mechanisms of translation initiation by internal ribosomal entry. He holds a D.Phil. from Oxford University.

Tatyana V. Pestova is an Assistant Professor in the Department of Microbiology and Immunology at the State University of New York Downstate Medical Center in New York, and a senior research scientist in the A. N. Belozersky Laboratory of Physico-chemical Biology, Moscow State University, Moscow, Russia. Her principal research interests are in molecular mechanisms of translation initiation in eukaryotes. She holds a Ph.D. and a D.Sc. from Moscow State University.

Translation Termination and Ribosome Recycling

Nadja Koloteva-Levin and Mick F. Tuite
University of Kent, Canterbury, UK

The decoding of genetic information stored in an mRNA molecule is initiated by a ribosome locating the translation start codon AUG. The codons that define the encoded polypeptide chain are then read sequentially by the ribosome with the amino acids being delivered to the ribosome by tRNAs. The chain of amino acids is therefore assembled as directed by the order of codons in the mRNA which in turn are recognized by the anticodon sequence of the tRNA. Translation termination is the last stage in this process and results in the release of the completed polypeptide chain from the ribosome once the end of the coding sequence has been reached. The trigger for the termination process is the appearance of one of the three possible stop codons at the decoding center of the ribosome. Following termination the ribosome dissociates from the mRNA and is recycled to take part in a new protein synthesis cycle.

Translation Termination Apparatus in Prokaryotes and Eukaryotes

The facilitators of the final stage of the translation cycle are the protein release factors (RFs). Translation termination occurs when one or other of the three stop codons—UAA, UAG, or UGA—at the end of the mRNA's coding sequence are positioned at the ribosomal "acceptor" (A) site, i.e., at the decoding site within the small ribosomal subunit (Figure 1, step 1). The stop codon is recognized by an individual RF or by an RF complex that then triggers hydrolysis of peptidyl-tRNA from the nascent polypeptide chain positioned at the adjacent ribosomal "peptidyl" (P) site (Figure 1, step 2). This is mediated by the peptidyl-transferase center (PTC) of the large ribosomal subunit transferring the peptidyl group to water rather than to an amino-acyl tRNA.

RFs fall into one of two classes: class-I RFs recognize and bind to the stop codon while class-II RFs facilitate the release of the class-I factor after peptidyl-tRNA hydrolysis (Figure 1, step 3). In the final stage, a ribosome recycling factor (RRF) triggers the disassembly of the terminated ribosome from the mRNA and the release of the deacylated tRNA from the P ribosome (Figure 1, step 4). Table I summarizes the known protein factors involved in translation termination.

The ribosome also plays an active role in the process of termination: interaction of the small ribosomal subunit RNAs and ribosomal proteins with the stop codon and a class-I RF ensures that the stop codon is accurately decoded at the A site, whereas the interaction of large ribosomal subunit RNAs with the RF or the RF complex facilitates the catalysis of peptidyl-tRNA hydrolysis at the P site via the ribosomal PTC.

Release Factors

Prokaryotic Polypeptide Chain Release Factors

In bacteria, translation termination is controlled by three different RFs (Table I). Two class-I protein release factors, RF1 and RF2, each decode two of three stop codons, UAA or UAG (RF1) and UAA or UGA (RF2). Recognition of the stop codon by the RFs is mediated via a conserved tripeptide motif: Pro-Ala-Thr (PAT) in RF1 and Ser-Pro-Phe (SPF) in RF2. These tripeptides are referred to as peptide anticodons. The other important functional domain of class-I RFs contains the highly conserved amino acid motif Gly-Gly-Gln (GGQ) and it is this domain that triggers hydrolysis of the protein-tRNA bond. An understanding of how RFs trigger the release of the completed polypeptide from the tRNA at the P site has come from a study of RF2 and its interaction with the terminating ribosome. When RF2 binds to the ribosome with a stop codon positioned at the A site, RF2 changes its three-dimensional conformation such that the domain with the conserved "peptide anticodon" (SPF) interacts with the mRNA at the decoding center, and the GGQ-containing domain comes in the contact with the ribosomal PTC to trigger hydrolysis of the peptidyl-tRNA linkage (Figure 2).

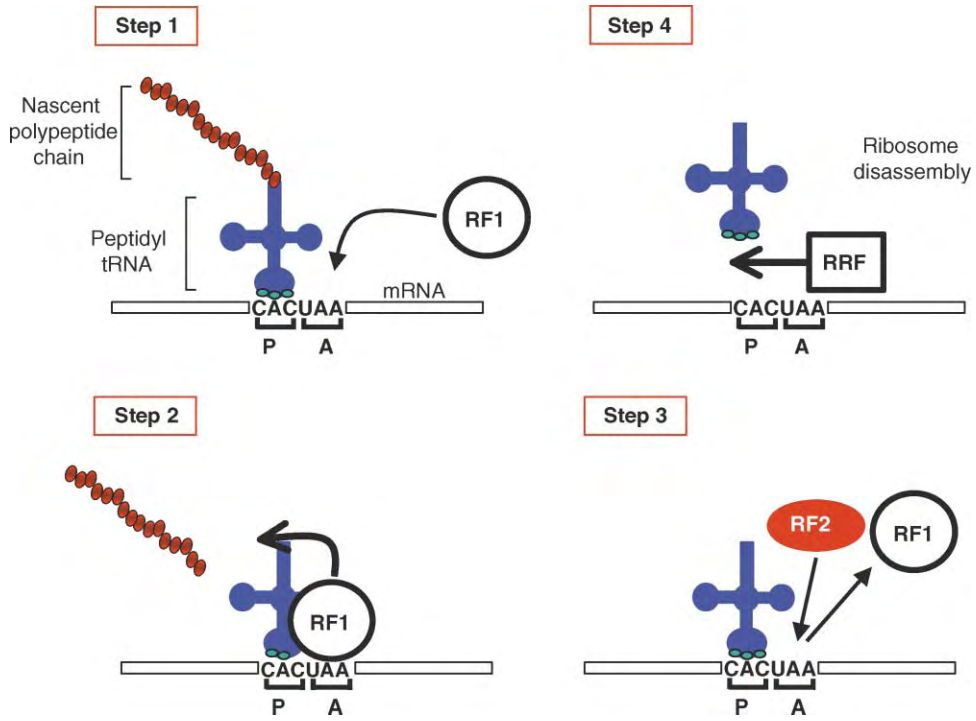

FIGURE 1 An overview of the mechanism of translation termination. The four key steps of the process triggered by the arrival of a stop codon at the ribosomal A site are shown. The peptidyl tRNA is positioned at the ribosomal peptidyl P site. The major protein factors associated with each step are indicated: RF1, class-I release factor; RF2, class-II release factor; RRF, ribosome recycling factor.

The single class-II RF in bacteria, namely RF3, is a GTP-binding protein that accelerates dissociation of either RF1 or RF2 from the ribosomal A-site after release of the completed polypeptide chain from the ribosome. RF3 bound to GDP accesses the ribosome which, in complex with RF1 or RF2, acts as guanine nucleotide exchange factors (GEFs) and triggers dissociation of GDP from RF3. This leads to the formation of a stable ribosome-RF1 (or RF2-) RF3 complex. Hydrolysis of the peptidyl-tRNA linkage triggered by RF1 or RF2 allows GTP binding to RF3. This induces an altered RF3 conformation with a high affinity for the ribosome and leads to rapid dissociation of RF1 or RF2 from the termination complex. To leave the ribosome, RF3 requires GTP hydrolysis, which converts it to the GDP-bound form of RF3 which has a lower affinity for the ribosome. Once RF3 leaves the ribosome, it is ready to enter the next translation cycle.

TABLE I

Protein Factors Involved in Translation Termination

Organisms	RF	Function
Archaebacteria		
	aRF1	Class-I RF, recognizes UAA/UAG/UGA
Prokaryotes		
	RF1	Class-I RF, recognizes UAA/UAG in mRNA
	RF2	Class-I RF, recognizes UAA/UGA in mRNA
	RF3	Class-II RF, GTPase, accelerates dissociation of termination complex from the ribosome
	RRF	Ribosome recycling factor
Eukaryotes[a]		
	eRF1	Class-I RF, recognizes UAA/UAG/UGA
	eRF3	Class-II RF, GTPase, increases termination efficiency, precise function unknown

[a] No RRF homologue has yet been described for eukaryotic cells other than a mitochondrially encoded homologue.

Eukaryotic Chain Release Factors

In contrast to bacteria, in eukaryotic cells translation is terminated by a single heterodimer consisting of two different RFs, eRF1 and eRF3. eRF1 is a class-I RF that decodes all three stop codons and triggers peptidyl-tRNA hydrolysis by the ribosome to release the nascent polypeptide. In eRF1, the stop codon recognition site is located close to the amino terminus of the protein molecule in a region that contains an evolutionarily conserved tetrapeptide sequence, Asn-Ile-Lys-Ser (NIKS). This sequence may be functionally equivalent to the bacterial RF peptide anticodon. The GGQ motif found in bacterial RF1 and RF2 is located in a

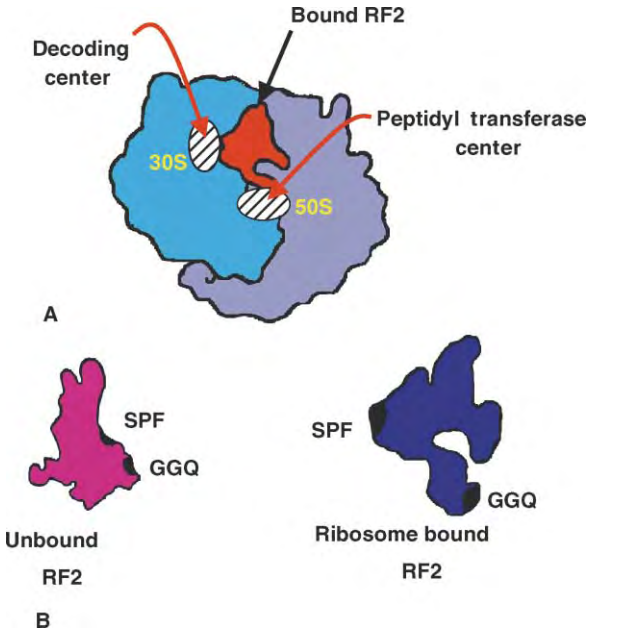

FIGURE 2 The three-dimensional conformation of a release factor changes once it is bound to the ribosome. (A) The RF2:bacterial ribosome complex indicating the points of contact between RF2 and the decoding center and the PTC of the ribosome. (B) The three-dimensional structures of the unbound and bound forms of bacterial RF2 indicating the location of the "peptide anticodon" sequence Ser-Pro-Phe (SPF) and the conserved Gly-Gly-Gln (GGQ) amino acid motif.

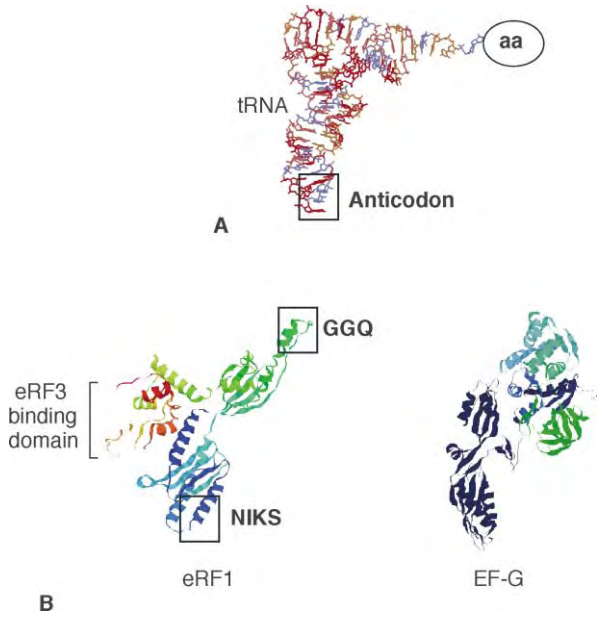

FIGURE 3 Many of the protein factors involved in translation elongation and termination have three-dimensional shapes that mimic a tRNA molecule. (A) Three-dimensional structure of a tRNA showing the location of the anticodon and the site to which the amino acid is covalently attached. (B) The three-dimensional structures of the mammalian RF eRF1 (left) and the bacterial translation elongation factor EF-G (right). The position of the conserved NIKS and GGQ amino acid motifs are indicated on eRF1, together with the domain to which the class-II factor eRF3 binds.

separate domain of the protein to the NIKS sequence. The carboxy-terminal part of the eRF1 binds eRF3. The crystal structure of human eRF1 shows that it is a Y-shaped molecule that resembles the structure of a tRNA (Figure 3). Since both bacterial and eukaryotic class-I RFs carry out essentially the same function, one would expect them to interact similarly with ribosomal A site. As with RF2 (see Figure 2), eRF1 must also undergo a conformational change after binding to the ribosome in order that it can interact with both the ribosomal decoding site and the ribosomal PTC.

The eukaryotic class-II RF, eRF3, forms a complex with eRF1, and via this interaction enhances the efficiency of the translation termination although its function remains to be fully defined. The GTPase activity of eRF3, which is triggered by stop codons, is both eRF1- and ribosome dependent. The carboxy-terminal half of the eRF3 molecule shows significant amino acid identity to the translation elongation factor eEF1A that is responsible for bringing the aminoacyl tRNAs to the ribosome during polypeptide chain elongation. This suggests that eRF3 may act in a manner analogous to eEF1A, a protein factor bringing the RF complex to the ribosome. A number of functions have been attributed to eRF3, e.g., it may displace eRF1 from the ribosome (i.e., the function assigned to prokaryotic RF3), or proofread the eRF1:stop codon interaction, or stimulate ribosome disassembly (i.e., the function assigned to prokaryotic RRF; see below), although direct experimental proof for any one specific function is lacking. In mammalian cells, eRF3 binds to the poly(A)-binding protein (PABP), a protein associated with the poly(A) tails located at the 3′ end of the majority of eukaryotic mRNAs. This interaction might be important for the regulation of both mRNA stability and translation initiation, since disruption of the eRF3::PABP interaction suppresses the recycling of the ribosome on the same mRNA.

In Bakers' yeast (*Saccharomyces cerevisiae*), the eRF3 protein (also known as Sup35p) has an additional remarkable property; it is a prion protein that acts as the protein determinant of a non-Mendelian genetic element called [*PSI*$^+$]. Like the mammalian prion protein PrP, eRF3 can exist in one of two different conformations with the aggregation-prone prion conformer catalyzing the conversion of the normal soluble form, to the prion form. In [*PSI*$^+$] cells the majority of eRF3 is found as an inactive, high molecular weight complex, and thus [*PSI*$^+$] cells have a defect in translation termination albeit without detriment to yeast cell growth. This mechanism may represent a novel means of regulating the efficiency of translation termination in yeast. There is no evidence that mammalian eRF3 is a prion.

In Archaebacteria, the single class-I RF found (aRF1) shares significant amino acid sequence and structural homology with eRF1, but not with either RF1 or RF2. Like eRF1, aRF1 is able to decode all three stop codons. No eRF3 homologue has been identified in any Archaebacterial genome.

Molecular Mimicry

RFs decode stop codons at the ribosomal A site and in that respect can functionally be compared to aminoacyl tRNAs which decode sense codons of the mRNA when positioned at the ribosomal A site during translation elongation. In so doing, RF1 and RF2 physically interact with the stop codons in the mRNA. That a common ribosomal binding site for tRNAs, translation elongation factors, and RFs exists has led to the suggestion that these protein and RNA molecules may also have similar three-dimensional structures, the so-called "molecular mimicry" model. The structural similarity—discovered by Clark, Nyborg, and colleagues in 1995—between bacterial elongation factor EF-G and the tRNA-EF-Tu-GTP complex provided direct evidence for this model. One of the structural domains of the EF-G protein strongly mimics the structure of the T-stem and anticodon loop of a tRNA (Figure 3). The "molecular mimicry" model can also be extended to include the RFs and confirmation of this came from the solution of the crystal structure of human eRF1, whose overall shape and dimensions resemble a tRNA molecule with the three clearly identifiable structural domains corresponding to the anticodon loop, the aminoacyl acceptor stem, and T-stem of a tRNA molecule (Figure 3). There is also significant amino acid sequence similarity between several RF domains and the carboxy-terminal portion of elongation factor EF-G, the region of the molecule that interacts with the ribosome.

Posttermination Events

Once the translation of an mRNA has been terminated and the completed polypeptide chain released, the ribosome must dissociate from the mRNA in order to be able to participate in a new round of protein synthesis. In bacteria, another protein factor, the RRF, is involved in this posttermination step together with the elongation factor that mediates ribosomal translocation, i.e., EF-G. The three-dimensional structure of RRF, like eRF1, also mimics a tRNA molecule which, in turn, is important for its activity in the dissociation of the posttermination ribosome. After RF3 catalyzes the release of RF1/RF2 from the ribosome, RRF enters the A-site of the ribosome, and it is then translocated by EF-G to the P site, similarly to the translocation of the peptidyl-tRNA during translation elongation (Figure 1, step 4). This releases the deacylated tRNA from the P site which then moves to the ribosomal exit (E) site from where it rapidly dissociates from the ribosome. The release of the mRNA from the ribosome is accompanied by the release of RRF and EF-G. The final step before the ribosome can re-enter the translation cycle is dissociation of the ribosome into its two subunits: an event that requires an additional protein factor, the translation initiation factor 3 (IF3).

In eukaryotes, the posttermination step still remains to be characterized. A gene encoding a eukaryotic RRF-like protein is found in most eukaryotic genomes but encodes an RRF that only participates in translation in the mitochondria. It is conceivable that eRF3 fulfills this function.

Bypassing Stop Codons: The Causes and Consequences

The accurate recognition of a stop codon as a termination signal is important for cell viability, although cells can tolerate a certain level of stop codon translation by nonsense suppressor tRNAs. However, the efficiency with which RFs mediate translation termination at a stop codon can be affected by several factors. These include the nucleotide context of the stop codons in the mRNA (i.e., the identity of the bases directly preceding or following the termination codon), the cellular concentration of RFs, and the presence of naturally occurring, nonmutant tRNAs, which are able to recognize a stop codon as well as their usual normal sense codon(s) albeit at much lower efficiency. For example, in yeast the tRNA that decodes the CAA codon as a glutamine residue can also recognize the related stop codon UAA at low efficiency.

A number of nonstandard translational events are known to compete with the termination machinery in order to facilitate the translational bypassing of specific stop codons. Such a bypass can extend the decoding properties of a single gene and is an event that can be regulated. For example, certain animal viruses can cause ribosomes to shift into a different reading frame just before a stop codon is reached thereby generating a second extended form of the translation product – which in this case is the viral gag-pol protein. In certain plant viruses, e.g., Tobacco Mosaic Virus (TMV), host-encoded tRNAs can decode a viral stop codon as a sense codon if that stop codon is present in the appropriate nucleotide context.

A further example where stop codons are treated as sense codons is in the translation of genes encoding certain selenoproteins, i.e., contains one or more

selenocysteine residues. In these mRNAs the UGA codon is used both as a signal for termination and as a signal for selenocysteine incorporation. How the UGA codon is read is defined by both a specific translation factor (e.g., the SelB protein in bacteria) and a structural element within the mRNA molecule that is being translated (e.g., the SECIS element in eukaryotic selenoprotein-encoding mRNAs).

See Also the Following Articles

Prions and Epigenetic Inheritance • Prions, Overview • Ribosome Structure

Glossary

aminoacyl tRNA A transfer RNA molecule that has an appropriate amino acid residue esterified to its 3′-terminal adenosine.

anticodon A contiguous sequence of three nucleotides in transfer RNA that are complementary to a specific codon in mRNA.

codon A contiguous sequence of three nucleotides in mRNA that are used to specify a particular amino acid, e.g., CAG is the codon specifying the amino acid glutamine.

nonsense suppressor tRNAs tRNAs that contain a mutation in their anticodon sequence such that they can recognize an mRNA stop codon positioned at the ribosomal A site by standard base pair interactions.

peptidyl-transferase center The region of the ribosome that is responsible for two reactions important for protein synthesis: peptide bond formation during translation elongation and nascent peptide chain release during termination.

prion A protein that can exist in a self-perpetuating conformationally altered isoform. Prions have been identified as infectious agents responsible for certain neurodegenerative diseases of animals and as epigenetic determinants in yeast.

reading frame Any one of three ways in which an mRNA sequence can be translated one codon at a time. The "open" reading frame encoding a gene product is set by the initiation codon AUG.

Further Reading

Bertram, G., Innes, S., Minella, O., Richardson, J., and Stansfield, I. (2001). Endless possibilities: Translation termination and stop codon recognition. *Microbiology UK* **147**, 255–269.

Ehrenberg, M., and Tenson, T. (2002). A new beginning of the end of translation. *Nat. Struct. Biol.* **9**, 85–87.

Kisselev, L., Ehrenberg, M., and Frolova, L. (2003). Termination of translation: Interplay of mRNA, rRNAs, and release factors? *Eur. Molecul. Biol. Orgn. J.* **22**, 175–182.

Klaholz, B. P., Pape, T., Zavialov, A. V., Myasnikov, A. G., Orlova, E. V., Vestergaard, B., Ehrenberg, M., and van Heel, M. (2003). Structure of the *Escherichia coli* ribosomal termination complex with release factor 2. *Nature* **421**, 90–94.

Nakamura, Y., and Ito, K. (2003). Making sense of mimic in translation termination. *Trends Biochem. Sci.* **28**, 99–105.

Nissen, P., Kjeldgaard, M., Thirup, S., Polekhina, G., Reshetnikova, L., Clark, B. F., and Nyborg, J. (1995). Crystal structure of the ternary complex of Phe-tRNAPhe, EF-Tu, and a GTP analog. *Science* **270**, 1464–1472.

Rawat, U. B., Zavialov, A. V., Sengupta, J., Valle, M., Grassucci, R. A., Linde, J., Vestergaard, B., Ehrenberg, M., and Frank, J. (2003). A cryo-electron microscopic study of ribosome-bound termination factor RF2. *Nature* **421**, 87–90.

Biography

Mick Tuite is a Professor of Molecular Biology at the University of Kent and the former Head of the Department of Biosciences at this institution. He has had a long-standing interest in the mechanism and regulation of translation termination using the yeast *S. cerevisiae* as a model system. This has recently led to a study of the prion-like properties of one of the release factors eRF3 (Sup35p). He has a D.Phil. from the University of Oxford and undertook postdoctoral research at both Oxford and the University of California, Irvine before joining the faculty at Kent. He has published over 150 research papers and reviews.

Nadja Koloteva-Levin is a Senior Postdoctoral Researcher in Mick Tuite's laboratory working on the prion behavior of eRF3 (Sup35p). She received her Ph.D. from University of Manchester Institute of Science and Technology (UMIST) in the United Kingdom and followed this with 4 years of postdoctoral research on posttranscriptional gene regulation at Tel Aviv University in Israel.

Translesion DNA Polymerases, Eukaryotic

Alexandra Vaisman and Roger Woodgate
National Institutes of Health, Bethesda, Maryland, USA

Translesion DNA polymerases are enzymes capable of copying templates containing DNA-distorting lesions. Unlike the highly processive and accurate replicative polymerases, translesion polymerases are relatively distributive and lack intrinsic 3′–5′-exonuclease activity and are, therefore, unable to proofread any errors made during replication. As a consequence, they have low base substitution and frameshift fidelity on undamaged DNA templates. Translesion DNA polymerases are also characterized by an ability to extend mismatched and misaligned primer termini.

Lesion bypass is believed to occur in two mechanistically discrete steps, both of which can be either relatively accurate or highly error-prone. The first step is nucleotide incorporation opposite the damaged base(s) itself, and the second step is extension of the nascent chain beyond the damage. For some lesions, translesion replication is facilitated by a single enzyme, but for certain lesions two polymerases are required; one enzyme for incorporation opposite the lesion and another for extension. The polymerase that gains access to the lesion terminus largely determines the fidelity of translesion synthesis, i.e., whether it is accurate or mutagenic. After lesion bypass is completed, the inherently distributive translesion polymerases dissociate from the DNA template so as to allow replicative polymerases to resume chromosomal duplication.

Y-Family DNA Polymerases: polη, polι, polκ and Rev1

Most of the enzymes implicated in replication of imperfect DNA belong to the Y-family of DNA polymerases. Phylogenetic analysis of this family suggests that it can be subdivided into several discrete branches consisting of UmuC-, DinB-, Rev1-, and Rad30-like proteins. The DinB subfamily is the most diverse and is found in prokaryotes, archaea, and eukaryotes. Members of the UmuC subfamily are found exclusively in bacteria, and proteins from the Rad30 and Rev1 branches are found only in eukaryotes. Multiple Y-family orthologues are often present in one organism. Humans, for example, have four Y-family DNA polymerases, two *RAD30* paralogues, polη and polι, a DinB homologue polκ, and Rev1.

Biochemical Properties

Enzymatic characterization of the Y-family DNA polymerases *in vitro* reveals that despite numerous similarities, each member of the family exhibits distinctive properties during DNA synthesis. For example, polη is truly unique among eukaryotic DNA polymerases in its efficiency and accuracy of replication past UV-induced cyclobutane pyrimidine dimers (CPDs). In contrast, Polι, a homologue of Rad30, differs from other Y-family DNA polymerases in that it has a 5′-deoxyribose phosphate lyase activity, similar to X-family pols β and λ. A most unusual biochemical feature of polι is, however, its sequence context fidelity when replicating undamaged DNA templates. Remarkably, Polι prefers making dGMP·T and dGMP·U wobble mispairs – three- to tenfold greater than the correct dAMP·T and dAMP·U base pairs. Yet at the same time, polι discriminates against certain other mismatches quite well. Thus, errors made by polι at template A occur up to 100-fold less frequently than that made by human pol η or κ. Polκ on the other hand, readily catalyzes extension of misaligned primer termini resulting in -1 frameshift mutations and is considerably more proficient at extending terminal mismatches compared to polη and polι. Finally, unlike other Y-family DNA polymerases that utilize all four deoxynucleotide triphosphates (dNTPs) in a template-dependent manner, *Saccharomyces cerevisiae* and human Rev1 proteins appear to be specialized deoxycytidyl transferases, since they utilize the three other dNTPs only very sparingly.

Structural Features

Sequence alignment of the Y-family DNA polymerases shows a high degree of conservation in the N-terminal region containing the catalytic domain, while the

C-terminal part is unique for each family member. Even though the amino acid sequences of these polymerases show no similarity to classical DNA polymerases, the general structure of polymerases from all families appears to be remarkably conserved. Crystallographic data have shown that like polymerases from the A-, B-, and X-families, the Y-family polymerases adopt a right-hand structure with characteristic finger, thumb, and palm domains. The Y-family polymerases differ, however, from classical polymerases in having a fourth small domain that has been termed the "little finger." DNA is held in a cleft between the thumb and the little finger domains (Figure 1). The active site of Y-family polymerases is more solvent accessible and, due to shorter fingers and thumb domains, forms a more open structure than that of replicative polymerases. Therefore, if the geometric constraints on the active site of Y-family polymerases are less stringent, DNA lesions and mispairs can be more readily accommodated within their active site. Such observations thereby help explain their proficiency at lesion bypass and a concomitant decrease in fidelity on undamaged DNA.

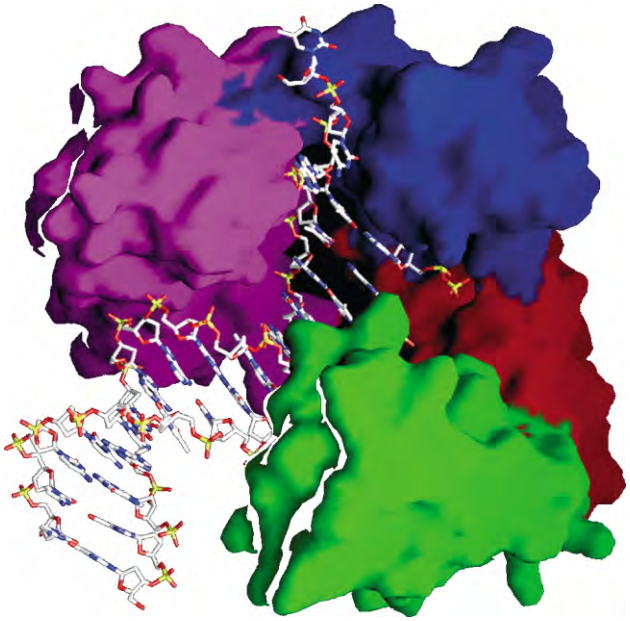

FIGURE 1 Crystal structure of Dpo4, an archaeal Y-family polymerase, in a ternary complex with a DNA template and an incoming nucleoside triphosphate. The surface of the enzyme is color-coded to indicate the four subdomains found in all Y-family polymerases. These consist of the palm (red), thumb (green), finger (blue), and little finger (purple) domains. The DNA molecule is drawn as sticks. Unlike replicative DNA polymerases, the catalytic cleft in Dpo4 is cavernous and solvent exposed, which explains in part why Y-family polymerases exhibit low-fidelity synthesis on undamaged DNA and can accommodate bulky DNA adducts/mismatched bases in their active sites.

B-Family DNA Polymerase: polζ

The ability to accommodate distorted DNA is not just limited to Y-family polymerases. Polζ, a eukaryotic B-family polymerase, is another important enzyme involved in the replication of damaged DNA. Catalytically active polζ comprises a heterodimer made from the REV3 and REV7 proteins. The fidelity of polζ on undamaged DNA is significantly higher than that of Y-family polymerases (Table I). However, polζ is extremely efficient at the extension of aberrant DNA primer ends, including lesion-containing sites and misaligned primer-template termini.

X-Family DNA Polymerases: polβ, polλ, and polμ

Although much attention in the last few years has focused on the Y-family polymerases, earlier studies raised the possibility that DNA polβ may play a role in translesion synthesis, even though its major function is in base excision repair. Polβ is a distributive enzyme in its mode of action, however, it is more processive than most Y-family DNA polymerases and the inherent ability of polβ to select correct rather than incorrect dNTPs for incorporation is considerably higher than that of the Y-family polymerases (Table I).

Lesion bypass with varying efficiencies can also be achieved *in vitro* by other X-family polymerases, such as the recently discovered pols λ and μ. Polμ is closely related to terminal deoxynucleotidyl transferase (TdT), but in contrast to TdT, it is a partially processive template-directed DNA polymerase. *In vitro*, polμ is highly error-prone and makes -1 frameshift errors in repetitive sequences. Polλ is a close homologue of polβ and like polβ is more accurate than polμ and possesses an intrinsic deoxyribophosphate lyase activity (Table I).

Lesion Bypass Specificity

DNA molecules are intrinsically unstable and are constantly subjected to the damaging effects of endogenous or exogenous agents. DNA synthesis past a wide variety of DNA lesions has been studied using both biological and biochemical approaches. Among the most common lesions that have been investigated are UV-induced *cis-syn* CPDs and the 6-4 pyrimidine-pyrimidone photoproducts (6-4PPs); abasic sites occurring spontaneously or from the action of DNA glycosylases; cisplatin adducts (CP) formed at adjacent guanines by anticancer drugs; and benzo[*a*]pyrene diol epoxide (BaP DE) adducts, a naturally occurring metabolite of carcinogens commonly found in cigarette

TABLE I

Eukaryotic DNA Polymerases Known to Participate in Translesion Replication

DNA polymerase	Gene or synonym	Family	Error rate on undamaged DNA	Additional proposed functions
β, beta	*POLB*	X	10^{-4}–10^{-6}	Base excision repair, double-strand break repair, synapsis and recombination, meiosis, neurogenesis
ζ, zeta	*POLZ (REV3L/REV7L)*	B	10^{-4}–10^{-5}	Somatic hypermutation, mismatch extension, developmental cell proliferation
η, eta	*POLH (RAD30A, XPV)*	Y	10^{-2}–10^{-3}	Somatic hypermutation
ι, iota	*POLI (RAD30B)*	Y	10^{1}–10^{-4}	Base excision repair, somatic hypermutation
κ, kappa	*POLK (DINB1)*	Y	10^{-3}–10^{-4}	Spontaneous mutagenesis
λ, lamda	*POLL (POL4)*	X	10^{-3}	Base excision repair, repair during meiosis
μ, mu	*POLM*	X	?	Nonhomologous end-joining pathway, lymphoid formation
Rev1	*REV1L*	Y		

smoke. The accuracy and efficiency of translesion replication varies not only on the chemical nature of the lesion and specific distortion that it imposes upon DNA, but also on the local sequence context within which the lesion is located and on the specific polymerase or combination of polymerases involved in a given translesion pathway. For example, in both *S. cerevisiae* and humans, polη is the most proficient and accurate enzyme at replicating past thymine–thymine CPDs. Pols ι, polμ and to a lesser extent polζ and polβ are also able to bypass the lesion but with a much lower efficiency and fidelity. By comparison, both polι and polη are proficient at incorporating a nucleotide opposite the 3′ base of a thymine-thymine 6-4PP, and polζ can readily extend the resulting primer termini. Similarly, translesion replication past an abasic site might involve pols $\eta, \iota, \kappa, \beta, \lambda$, or Rev1 to incorporate a base opposite the lesion and polζ for its subsequent extension. Polη and polβ are both very efficient and accurate when replicating past a CP lesion, whereas bypass by polμ is highly error-prone since it generally results in 2, 3, and 4 nucleotide deletions, polκ, polι, and polλ are completely blocked by CP adducts in template DNA.

The ability of the polymerase to facilitate lesion bypass also depends on the nucleotide at which a specific adduct is formed. For example, in human cells, efficient and accurate bypass of BaP DE adducts formed at deoxyadenosine (dA) can be achieved through the sequential action of polι and polκ, but not by polη or polβ. In contrast, the ability of translesion polymerases to bypass the same BaP DE adduct formed at deoxyguanosine (dG) base is quite different. Whereas human polη and polι bypass BaP DE dG adducts inefficiently and inaccurately, polκ bypasses the lesion with high efficiency and predominantly incorporates the correct base, dCMP, opposite the adducted dG.

Protein Partners

Despite extensive biochemical characterization of the polymerases involved in translesion synthesis, it is still unclear how the process physically occurs in living cells. It has been shown that at least three of the translesion polymerases, polη, polι, and Rev1 are associated with the replication machinery in an undamaged cell and that upon DNA damage the polymerase accumulates at sites of stalled replication forks.

The catalytic activity of pols η, ι, and κ on undamaged and lesion-containing DNA is substantially increased through protein–protein interactions with accessory proteins normally utilized by replicative polymerases. These include proliferating cell nuclear antigen (PCNA), which serves as a sliding clamp that helps recruit polymerases to their site of action, and a clamp loader, replication factor C (RFC). Given the sixfold symmetry of the PCNA complex, it is possible that multiple DNA polymerases connect simultaneously to a replicative single clamp. However, how a cell chooses between the various translesion polymerases it has at its disposal and how the switch from the replicative polymerase to a translesion polymerase and then back to the replicase occurs *in vivo* still remains to be determined.

Cellular Role(s)

Polη is clearly responsible for the accurate and robust replication of CPD-containing DNA *in vivo*. Although the lack of polη in human cells does not confer a substantial hypersensitivity to killing by UV light, humans with a defective polη do exhibit the *Xeroderma Pigmentosum Variant* (XP-V) syndrome and are predisposed to the manifestation of skin cancers.

To date, XP-V is the only known example of a human disorder caused by a defect in translesion replication. Apart from a clear role for polη in the bypass of CPDs, there is indirect evidence suggesting the participation of other enzymes in translesion replication *in vivo*. For example, cells with a reduced level of the deoxycytidyl transferase Rev1 show lower levels of UV-induced mutagenesis. *In vitro* assays suggest that polκ may play an important role in accurate bypass of certain lesions generated by polycyclic aromatic hydrocarbons and recent studies with transgenic mice devoid of polκ support such hypotheses.

Just as translesion replication often requires multiple DNA polymerases, so a particular translesion polymerase might have evolved to participate in one or more functional tasks in a cell. Indeed, various lines of evidence support a role for translesion polymerases η and ι in the somatic hypermutation of rearranged immunoglobulin genes. While *S. cerevisiae* strains with deletions in their *REV3* or *REV7* genes (encoding polζ) are viable, disruption of murine *REV3* unexpectedly leads to embryonic lethality in mice, suggesting that, in addition to lesion bypass, mammalian polζ may play additional role(s) in cellular development. Genetic and biochemical studies have shown that *S. cerevisiae* Rev1, in addition to participating in the bypass of UV-induced lesions and abasic sites, also has a second function that is independent of its dCMP transferase activity. Polβ whose primary function is in base excision repair, has also been implicated in double-strand-break repair, meiotic events associated with synapsis and recombination and in neurogenesis. On the other hand, owing to an associated 5′-deoxyribose phosphate lyase activity, it has been hypothesized that polι and polλ might possibly substitute for polβ in certain forms of specialized base excision repair. Finally, polμ's main cellular role may actually be to participate in a non-homologous end-joining pathway that repairs DNA double-strand breaks and its ability to traverse certain DNA lesions may, in fact, be rarely utilized *in vivo*.

See Also the Following Articles

DNA polymerase α, Eukaryotic • DNA polymerase β, Eukaryotic • DNA polymerase δ, Eukaryotic • DNA polymerase ε, Eukaryotic • DNA Polymerases: Kinetics and Mechanisms

Glossary

DNA polymerase families DNA polymerases have historically been classified into "families" based upon the phylogenetic relations of their primary amino acid sequence. A-family polymerases are related to *Escherichia coli* pol I; B-family polymerases to *E. coli* pol II; C-family polymerases to *E. coli* pol III; X-family polymerases to mammalian polβ; and Y-family polymerases to UmuC, DinB, Rad30, and Rev1 proteins.

fidelity The accuracy with which a polymerase replicates a DNA template.

polymerase processivity The number of nucleotides incorporated into a nascent DNA strand per polymerase–template binding event.

proofreading The removal of misincorporated nucleotides at a growing 3′ end by a 3′ exonuclease often associated with the polymerase.

replicative polymerases Enzymes involved in the accurate copying of genetic material. The active sites of these enzymes are usually much smaller and constrained than the translesion polymerases, so as to ensure that only the complementary "Watson and Crick" bases are incorporated into nascent DNA.

translesion replication Also referred to as lesion bypass or translesion synthesis (TLS), it is an inherently error-prone process that permits cells to tolerate the presence of persistent DNA damage and involves the direct replication through and beyond the DNA damaged site by DNA polymerases.

Further Reading

Friedberg, E. C., Wagner, R., and Radman, M. (2002). Specialized DNA polymerases, cellular survival, and the genesis of mutations. *Science* **296**, 1627–1630.

Goodman, M. F. (2002). Error-prone repair DNA polymerases in prokaryotes and eukaryotes. *Annu. Rev. Biochem.* **71**, 17–50.

Ohmori, H., Friedberg, E. C., Fuchs, R. P. P., Goodman, M. F., Hanaoka, F., Hinkle, D., Kunkel, T. A., Lawrence, C. W., Livneh, Z., Nohmi, T., Prakash, L., Prakash, S., Todo, T., Walker, G. C., Wang, Z., and Woodgate, R. (2001). The Y-family of DNA polymerases. *Molecul. Cell* **8**, 7–8.

Biography

Alexandra Vaisman is a Senior Research Fellow in the Laboratory of Genetic Integrity at the National Institute of Child Health and Human Development. Her principal research interests are in the field of mammalian DNA repair and replication. She holds a Ph.D. from the Moscow Institute of Fine Chemical Technology and received her postdoctoral training at the Russian Academy of Sciences and the University of North Carolina at Chapel Hill.

Roger Woodgate has devoted his scientific career to understanding the molecular mechanisms of damage-induced mutagenesis in prokaryotes and eukaryotes. He received his Ph.D. from the University of Sussex in Brighton, United Kingdom and for the past 15 years has worked at the National Institutes of Health in Bethesda, Maryland. At present, Dr. Woodgate is Chief of the Laboratory of Genomic Integrity in the National Institute of Child Health and Human Development.

Trehalose Metabolism

Alan D. Elbein
University of Arkansas for Medical Sciences, Little Rock, Arkansas, USA

Trehalose is a nonreducing disaccharide of glucose in which the two glucoses are linked in an α,α-1,1-linkage. This rather simple sugar is widespread throughout the biological kingdom, being found in bacteria, yeast, fungi, protozoa, nematodes, insects, plants, and so on. In these various organisms, this sugar can serve a number of key functions: as a storehouse of energy and carbon, as a protectant and stabilizer of cell membranes and proteins during stress, as a signaling molecule, and as a structural component of various glycolipids in bacterial cell walls. There are at least three different pathways for the synthesis of trehalose in various organisms, and several or all of these pathways may be present in the same organism. The fact that an organism may have multiple routes for the synthesis of trehalose strongly suggests that this sugar must be essential for the survival of the organism.

Pathways of Biosynthesis of Trehalose

The best-known and most-widely distributed pathway for synthesis of trehalose (Figure 1) involves two enzymes known as trehalose-phosphate synthase (TPS) and trehalose-phosphate phosphatase (TPP). The reactions catalyzed by these two enzymes are shown in Figure 2. TPS catalyzes the transfer of glucose from the sugar nucleotide, uridine diphosphate glucose (UDP-glucose), to glucose-6-phosphate to produce trehalose-6-phosphate and UDP. TPP then cleaves the phosphate from trehalose-6-P to give free trehalose and inorganic phosphate. These two enzymes have been isolated and characterized from the cytoplasm of many cells including bacteria, yeast, fungi, insects, and plants. The genes for these enzymes have been cloned from several different organisms and expressed in *Escherichia coli*. In several cases, the purified recombinant enzymes have been well characterized.

A more recently described pathway of trehalose formation, so far demonstrated in only a few bacteria, including *Mycobacterium tuberculosis*, involves the intramolecular rearrangement of maltose to convert the α1,4-glycosidic linkage of this disaccharide to the α,α1,1-glycosidic linkage of trehalose. This reaction is catalyzed by the enzyme trehalose synthase (TS) as shown in Figure 2. The gene for TS from *Pimelobacter* species was cloned to produce a 573 amino acid protein that had considerable homology to the glycosidase, maltase. The mechanism of action of TS is not known, but this enzyme can convert trehalose to maltose, or maltose to trehalose. Its physiological function in these cells is also not known.

A third pathway also only identified in a few bacteria involves several different enzymes, the first of which converts the glucose linked in an α1,4-bond at the reducing end of a malto-oligosaccharide to the α,α1,1-bond of trehalose. This enzyme is called malto-oligosyltrehalose synthase (TreY). The second enzyme then releases the trehalose to leave a malto-oligosaccharide i.e., two glucoses shorter (at the reducing end) than the starting oligosaccharide. This second enzyme is called malto-oligosyltrehalose trehalohydrolase (TreZ) (see Figure 2). These latter two pathways give rise to free trehalose without the involvement of the phosphorylated sugar, whereas the first pathway produces trehalose phosphate as the initial product. In some bacteria, at least two and possibly all three of these pathways may be present at the same time. The presence of these multiple pathways would suggest that trehalose is an essential component for these cells, and therefore alternate pathways have evolved to ensure that levels of trehalose are maintained.

Occurrence of Trehalose in the Biological World

The first report on the presence of trehalose in living cells was in 1832 when trehalose was tentatively identified in ergot of rye by Wiggers. Since that report, this sugar has been isolated from many different organisms, including yeast and fungi where it occurs in spores, fruiting bodies, and vegatative cells. In some of these organisms, such as the fungus, *Neurospora tetrasperma*, or the yeast, *Saccharomyces cerevesiae*, the amount of trehalose may be as high as 10% of the dry weight of the cells.

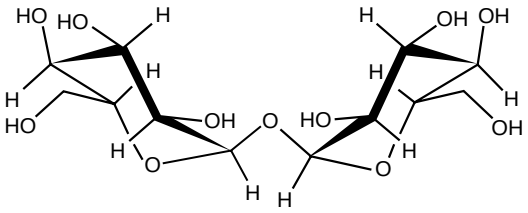

FIGURE 1 Structure of the naturally occurring isomer of trehalose, i.e., α,α1,1-D-glucopyranosyl-D-glucopyranoside.

Trehalose has also been isolated from lichens and algae, and is present in many higher plants, such as the resurrection plant (*Selaginella lepidophylla*), and *Arabidopsis thaliana*. It is also a component of the wound exudates of some plants, such as *Fraxsinus aras*. Many different species of bacteria, including *Streptomyces*, *Mycobacterium*, *Corynebacteria*, *Rhizobium*, *Arthrobacter*, and *Escherichia* have been shown to contain trehalose, and in most cases to also have the ability to synthesize this disaccharide. These many studies suggest that trehalose is probably present in many, if not most bacteria.

In the animal kingdom, trehalose was first reported in insects where it is present in hemolymph and also in larvae or pupae. In the adult insect, the levels of trehalose fall rapidly during certain energy-requiring activities such as flight, suggesting a role for this sugar as a source of glucose for producing ATP. In addition to insects, trehalose has also been identified in the eggs of the roundworm, *Ascaris lumbricoides*, where it may be present at levels as high as 8% of the dry weight. It is also found in a number of other invertebrates. On the other hand, trehalose has not been found in any mammals, although the enzyme trehalase is present in human intestine (intestinal villae membranes) and in human kidney (kidney brush border membranes). The intestinal enzyme is probably important in metabolizing ingested trehalose, since this sugar is present in various foods such as mushrooms which contain significant amounts of trehalose. On the other hand, the role of trehalase in human kidney remains a mystery.

Many lower organisms do contain the enzyme trehalase, and this activity may be important in maintaining physiological concentrations of trehalose in the cytoplasm. That is, as discussed below, trehalose plays a role as a protectant or stabilizer in some cells, and the levels of trehalose in these cells is significantly increased during times of stress. A high concentration of trehalose in the cytoplasm could upset the osmolar balance in the cell and cause serious problems. Thus, trehalase may be necessary to control such imbalances. This enzyme may also have an important function in the utilization of trehalose as an energy and carbon source for insect flight, for spore germination, and for other glucose-requiring processes.

In yeast, there are several different trehalases which apparently have different functions. The cytoplasmic trehalase, also referred to as the neutral trehalase because it has a pH optimum of 7.0, is a regulatory enzyme. This enzyme can exist in an inactive or zymogenic form, and this zymogen is converted by a cyclic-AMP-dependent phosphorylation to the active trehalase. Another trehalase in these cells is the acidic enzyme, which is found in the vacuoles and has a pH optimum of ~4.5. The acid enzyme may be involved in the utilization of trehalose as a carbon source by yeast since deletion of the gene for this protein leads to an inability of yeast to grow on trehalose. On the other hand, the trehalase that is regulated by phosphorylation might be involved in regulating the levels of trehalose in the cytoplasm, since trehalose levels can be significantly increased by various types of stress. However, the exact role of the various trehalase activities still remains to be determined.

Physiological Functions of Trehalose

Trehalose may have a number of different functions in nature, and its specific role may vary depending upon the system or organism being considered. The established functions of trehalose are outlined below.

As a Source of Energy and/or Carbon

Trehalose levels may vary greatly in certain cells depending on the stage of growth, the nutritional state of the organism, and the environmental conditions prevailing at the time of measurement. Trehalose is the major sugar in the hemolymph and thorax muscle of insects, and it is converted to glucose and consumed during flight. It is also an important source of energy and carbon in fungal spores and is utilized during the germination process.

As a Stabilizer and Protectant of Proteins and Membranes against Various Stresses

Various organisms, including plants, yeast, fungal spores, nematodes, brine shrimp, etc., can withstand dehydration and remain in this state (anhydrobiosis) for extended periods of time until water becomes available. These organisms generally contain high concentrations of trehalose. For example, when nematodes are slowly dehydrated, they convert as much as 20% of their dry weight into trehalose. Similar results have been

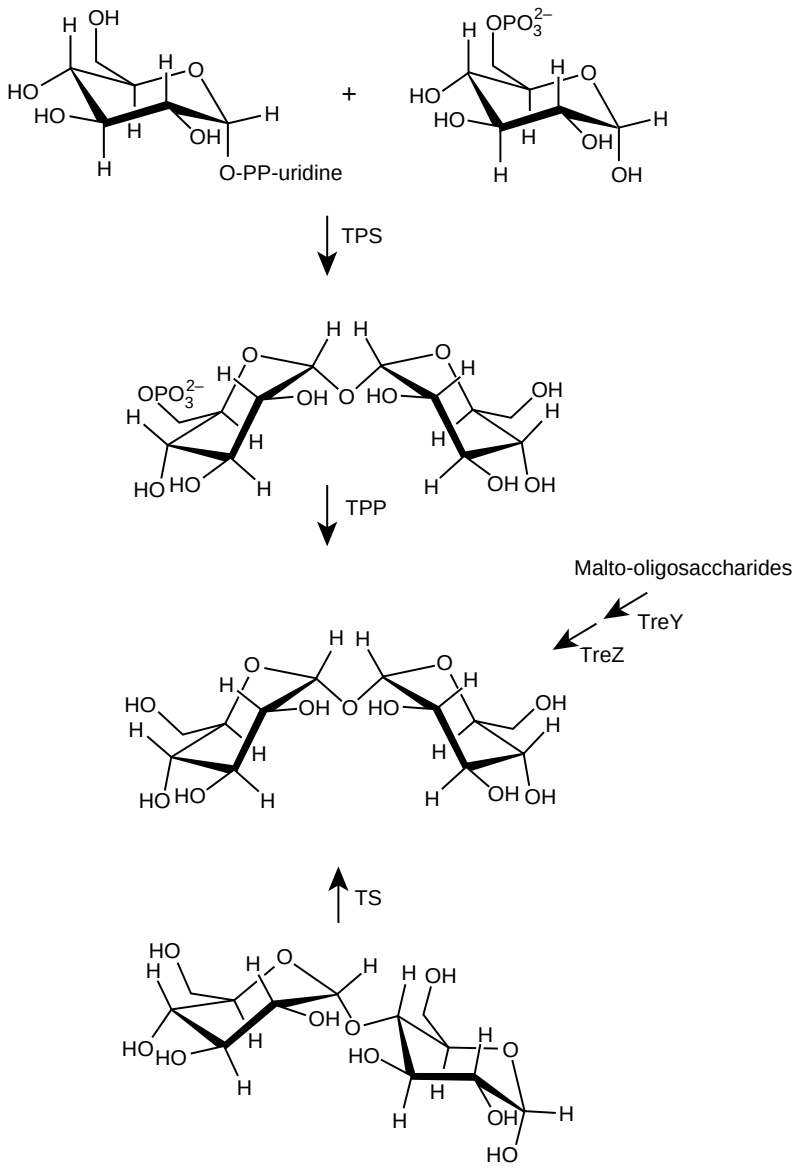

FIGURE 2 Pathways of biosynthesis of trehalose. The best-known pathway involves the transfer of glucose from UDP-glucose to glucose-6-phosphate to form trehalose-6-phosphate and UDP, catalyzed by trehalose-phosphate synthase (TPS). A second enzyme in this pathway, trehalose-phosphate phosphatase (TPP), removes the phosphate to give free trehalose. An alternate pathway involves the enzyme, trehalose synthase (TS) which catalyzes the interconversion of maltose and trehalose. Another alternate pathway involves two enzymes, TreY and TreZ, which catalyze the formation of trehalose at the reducing end of a malto-oligosaccharide (TreY) and then hydrolysis of this trehalose (TreZ) to give free trehalose.

demonstrated with other organisms. The use of trehalose to enable cells to survive dehydration may be an ancient adaptation since even *Archaebacteria* have been found to accumulate trehalose in response to stress.

Two primary changes are thought to cause destabilization of lipid bilayers during dehydration. These changes are fusion and lipid-phase transitions. Trehalose inhibits fusion and depresses the phase transition temperature of the dry lipids which maintains them in the liquid crystalline phase in the absence of water. This stabilizing effect of trehalose is a property of its structure and its stereochemistry. X-ray diffraction studies show that trehalose fits well between the polar head groups of the lipids with multiple sites of interaction. Its stereochemistry allows it to have the most favorable fit with the polar head groups of the phospholipids of cellular membranes.

This ability to withstand stress by increasing the levels of trehalose has been used by researchers to bioengineer more stable plant and animal cells. For example, introducing the genes that code for the biosynthetic trehalose enzymes (i.e., TPS and TPP) into human fibroblasts allowed these cells to be maintained in the dry state for up to 5 days, whereas control cells were

rapidly killed by this treatment. Similar technology has also been used to produce more stable transgenic plants.

As a Protectant against Heat

In yeast, stimuli that trigger the heat-shock response also cause an accumulation of trehalose. Two of the subunits of the trehalose-6-P synthase complex are actively synthesized when yeast cells are subjected to heat shock. Yeast mutants that are defective in either of the genes coding for TPS or TPP are not able to accumulate trehalose, and as a result, they are much more sensitive to heat shock than wild-type cells. Physiological concentrations of trehalose, up to 0.5 M, were found to protect enzymes of yeast and other organisms from heat inactivation, *in vitro*, and trehalose was a considerably better stabilizer than a number of other polyols, sugars, or amino acids. These data strongly implicate trehalose as playing a key role in thermotolerance, as well as in other stress conditions.

As a Free Radical Scavenger to Prevent Oxidative Stress

Another role for trehalose is in protecting cells against oxygen radicals. Exposure of yeast to a mild heat shock, or to a proteosome inhibitor, induced the accumulation of trehalose but also markedly increased the viability of these cells during exposure to a free radical-generating system (such as H_2O_2/iron). However, when the cells were returned to the normal growth temperature, both the trehalose content and the resistance to oxygen stress decreased rapidly and returned to the normal level. Mutants that were defective in the enzymes of trehalose metabolism were much more susceptible to oxygen stress than the wild-type organism, but adding exogenous trehalose to the medium enhanced the resistance of these mutant cells to the oxygen stress. The major effect of oxygen radicals on these cells was to damage amino acids in cellular proteins, and trehalose was able to prevent this damage, suggesting that this disaccharide functions as a free-radical scavanger.

As a Structural Component of the Bacterial Cell Wall

In mycobacteria and corynebacteria (and perhaps other organisms), trehalose is the basic component of a number of cell wall glycolipids. The best known and most completely studied of these trehalose lipids is cord factor, a cell wall component of the tubercle bacillus, that contains the unusual fatty acid called mycolic acid, esterified to the hydroxymethyl group of each glucose to give trehalose-dimycolate. This lipid is considered to be one of the major toxic components of the *Mycobacterium tuberculosis* cell wall, and is also largely responsible for the low permeability of this cell wall, which provides the organism with considerable resistance to many drugs. However, the function of this lipid, besides its obvious structural role, is still uncertain.

There are other antigenic glycolipids in the mycobacterial cell wall that also have trehalose as the basic structure. For example, there are a variety of acylated-trehalose compounds that contain any of three major types of fatty acids attached to the 2 and 3 hydroxyl groups of the two glucose moieties. These fatty acids are unusual and may be either C_{16-19} saturated fatty acids, C_{21-25} α-methyl branched fatty acids, or C_{24-28} α-methyl branched, β-hydroxy fatty acids. *M. tuberculosis* and other mycobacteria also have trehalose lipids that contain sulfate, such as 2,3,6,6′-tetra-acyl-2-sulfate-trehalose (sulfatide 1), or other types of fatty acids such as phthienoic acids. This great variation in the types of fatty acids found in these organisms and as cell wall components suggests specific functions, but thus far these have not been demonstrated.

Finally, some mycobacteria, such as *M. kansasii*, are characterized by the presence of seven species-specific neutral lipooligosaccharide antigens. These oligosccharide structures all have a common tetraglucose core which is distinguished by an α,α-trehalose substituent to which are attached various sugars, such as xylose, 3-0-methylrhamnose, fucose and a novel N-acylsugar. The exact structures of these complex polymers have not been established, but specific lipooligosaccharides are present in a number of "atypical" mycobacteria.

See Also the Following Articles

Free Radicals, Sources and Targets of: Mitochondria • Glucose/Sugar Transport in Bacteria • Oligosaccharide Chains: Free, *N*-Linked, *O*-Linked • Sugar Nucleotide Transporters

Glossary

enzymes Proteins that are necessary to catalyze specific chemical reactions at low temperature within the cell.

free-radicals Compounds that have an unpaired electron and are very reactive; free radicals can oxidize proteins or cell membranes and inactivate them.

free-radical scavanger Any substance that can react with and neutralize free radicals.

maltose A sugar (disaccharide) that is composed of two glucose molecules linked together in an α1,4-glycosidic bond; maltose differs from trehalose in that it is a reducing sugar and has a different glycosidic linkage.

stabilizer A chemical compound that prevents (i.e., protects) proteins or membranes from being inactivated or denatured.

sugar nucleotide The activated (or "high-energy") form of a sugar that is necessary for enzymatic formation of a glycosidic bond.

Further Reading

Banaroudj, N., Lee, D. H., and Goldberg, A. L. (2001). Trehalose accumulation during cellular stress protects cells and cellular proteins from damage by oxygen radicals. *J. Biol. Chem.* **276**, 24261–24267.

Birch, G. G. (1963). Trehaloses. *Adv. Carbohyd. Chem.* **18**, 201–224.

Brennan, P. J., and Nikaido, H. (1995). The envelope of mycobacteria. *Annu. Rev. Biochem.* **64**, 29–63.

Crowe, J., Crowe, L., and Chapman, D. (1984). Preservation of membranes in anhydrobiotic organisms. The role of trehalose. *Science* **223**, 209–217.

Elbein, A. D. (1967). Carbohydrate metabolism in *Streptomycetes*. Isolation and enzymatic synthesis of trehalose. *J. Bacteriol.* **94**, 1520–1524.

Elbein, A. D., Pan, Y. T., Pastuszak, I., and Carroll, J. D. (2003). New insights on trehalose: A multifunctional molecule. *Glycobiology* **13**, 17R–27R.

Lederer, E. (1976). Cord factor and related trehalose esters. *Chem. Phys. Lipids* **16**, 91–106.

Leopold, A. C. (1986). *Membranes, Metabolism and Dry Organisms*, pp. 377. Cornell University Press, Ithaca, NY.

Pan, Y. T., Carroll, J. D., and Elbein, A. D. (2002). Trehalose-phosphate synthase of *Mycobacterium tuberculosis*. *Eur. J. Biochem.* **269**, 6091–6100.

Thevelein, J. M. (1984). Regulation of trehalose metabolism in fungi. *Microbiol. Rev.* **48**, 42–59.

Biography

Alan Elbein is Professor and Chairman of the Department of Biochemistry and Molecular Biology at the University of Arkansas for Medical Sciences in Little Rock. He received his Ph.D. in microbial biochemistry from Purdue University and did postdoctoral research at the University of Michigan and the University of California at Berkeley. He joined the faculty as Assistant Professor of biology at Rice University and then moved to the Department of Biochemistry at the University of Texas Health Science Center at San Antonio as Professor. His research focuses on the role of complex carbohydrates in glycoprotein function, and on novel carbohydrate target sites in chemotherapy of microbiol diseases.

Tricarboxylic Acid Cycle

Richard L. Veech
National Institutes of Health, Rockville, Maryland, USA

The tricarboxylic acid cycle is the central pathway in intermediary metabolism, which accounts for the final combustion of foodstuffs into CO_2 and water while conserving the reducing equivalents produced for transmission up the mitochondrial electron transport system, to form the mitochondrial proton gradient responsible for ATP generation. The cycle occurs in nearly all life forms, even the archebacteria, suggesting that during the early evolution of life its function was anaplerotic and its direction reversed from that which exists in an oxygen-containing atmosphere.

The Discoverer of the Cycle

The tricarboxylic acid (TCA) cycle was first correctly formulated by Han Krebs, who was born on August 25, 1900 in Hildesheim. He was the son of a surgeon, Georg, and mother Alma, who was to die of depression when Krebs was 19. After completing gymnasium in Hildesheim in September 1918, Krebs joined the German army signal corps until the armistice of November 11, 1918. After completing his training in internal medicine at Gottingen, Freiburg, Munich, and Berlin in December 1925, Krebs looked for ways to obtain biochemical training. The time spent in the clinics had convinced him that it was necessary to pursue medical research. Through the influence of Bruno Mendel, who served with Krebs in theThird Medical Clinic in Berlin, and who was an acquaintance of Albert Einstein, Professor of Physics at the University of Berlin, who was in turn a frequent dinner guest at the home of Otto Warburg's father, Mendel heard that Warburg was looking for an assistant and recommended Krebs. This circle of influence allowed Krebs to obtain his first paid position as an assistant to Otto Warburg at the Kaiser Wilhelm Institut für Biologie at Berlin-Dahlem (see Figure 1). This stint was to change Krebs from a physician to a biochemist. Of Warburg, Krebs wrote (1981):

> *Otto Warburg was the most remarkable person I have ever been closely associated with. Remarkable as a scientific genius of the highest caliber, as a highly independent, penetrating thinker, as an eccentric who shaped his life with determination and without fear, according to his own ideas and ideals*

The Kaiser Wilhelm Institute was the leading scientific research facility of its time. In addition to Warburg, its faculty included Emil Fischer, Richard Willstater, Max von Laue, Fritz Haber, Otto Hahn, Lisa Meitner, Michael Polanyi. Otto Meyerhof, a former student of Warburg, was working in the same building and elucidated the glycolytic pathway responsible for the breakdown of glucose to lactate. Students of biochemistry who passed through Kaiser Wilhelm included, among others, Fritz Lipmann and Severo Ochoa, both of whom were to play a critical role in showing the role of coenzyme A in the TCA cycle. In addition to the discipline and rigor required for scientific research, Krebs learned from Warburg the techniques he had developed: use of tissue slices, spectrophotometry and manometry. These techniques, most notably manometry, were fundamentally important in leading Krebs to formulate the concept of a metabolic cycle, first the urea cycle and later the TCA cycle. It is important to recognize in understanding Krebs' work that the Warburg dictum "methods are everything" was dominant. There was no theoretical master plan. Only during his later work on the thermodynamics linking of cellular redox and phosphorylation states would Krebs remark in relation to that work, "This is the first time I ever thought you could predict in biology." In his early work, Krebs was a thorough empiricist. He could measure the rates of reaction. He added various potential participants in a metabolic pathway, and if they increased the overall rate, then he concluded they were part of the pathway. Krebs' training is of central importance to understand the cycle. As his biographer Holmes has pointed out, "Hans Krebs took 31 years to become a well-trained independent scientific investigator, and only 9 months to make one of the most significant discoveries of his generation in his chosen field."

History of the Discovery of the TCA Cycle

After leaving Warburg's lab in 1931, Krebs had obtained a position as chief medical resident in the university

FIGURE 1 Hans Krebs at age 68 in his laboratory at Oxford standing next to his beloved Warburg apparatus, which he learned to use in the laboratory of Otto Warburg and which was the major instrument used in his discovery of both the urea and the citric acid cycles. The square box in the background is a power supply for a Zeiss PMQ spectrophotomer. The spectrophotometer was first divised by Otto Warburg who also first discovered pyridine nucleotide and observed their spectral shift during oxidation/reduction. This spectral change formed the basis of many of the assays Krebs undertook in his later years. With these simple instruments and a devoted staff he worked happily in this building at the Radcliffe Infirmary until he was 81, when he died in a hospital ward in the same building in 1981 after a 2 week illness.

hospital at Freiburg, and was in charge of caring for 44 patients. With his Warburg manometer and the enzyme urease, he could measure the production of urea in liver slices. In his "off time" working by himself with the assistance of a medical student, Kurt Henseleit within 1 year he had formulated a salts solution to mimic the composition of plasma, "Krebs–Henseleit saline," the basis for modern tissue culture fluids, and had worked out the ornithine cycle responsible for the hepatic synthesis of urea from ammonia. This established for the first time that cyclic, not linear, pathways could play an important role in central metabolic processes. The process of this discovery is the subject of a detailed history dissecting the inventive processes entailed.

One of the great unsolved problems was to determine the reactions whereby foodstuffs undergo combustion to produce CO_2 and water. It was known that for glucose to undergo these reactions, it must first be broken down to pyruvate in the glycolytic pathway elucidated by Otto Meyerhof. Although in retrospect, it seems logical to assume that the idea of metabolic cycles would have been foremost in Krebs' mind when he began his

investigation into the oxidative combustion of foodstuffs, a careful analysis of his writing and notebooks gives no support for this idea. Rather his formulation of the TCA cycle was the result of the empirical methods learned in Warburg's lab. From Albert Szent-Gyorgyi, he had pigeon breast muscle minces which preserved intact, the then unknown mitochondria containing the enzymes of the TCA cycle, and could oxidatively decompose glucose to CO_2. From Warburg he had a manometer with which he could measure rates of CO_2 production. Again, he added possible intermediates and observed whether the rates of reactions increased. As he put it in his autobiography:

> *One way of tackling the problem of the intermediate steps of the combustion process is to test which substances, apart from carbohydrate and fat, burn most readily. The logic is that if a substance is an intermediate then it must readily undergo combustion: if it proves to be non-combustible, it cannot be an intermediate.*

In two sentences was his simple plan: the same as he had used in elucidating the urea cycle. There was no grand plan. In choosing the intermediates to be added, he was guided by others working on the same general problem. Earlier Szent-Gyorgyi had shown that addition of small amounts of succinate, fumarate, malate, or oxaloacetate could catalytically increase the rate of oxidation by pigeon breast muscle minces. Szent-Gyorgyi interpreted his findings as indicating that these compounds were not intermediates in a pathway, but rather that they served as hydrogen carriers transporting the H^+ and electrons from foodstuffs to cytochromes. By 1937, experiments by Martius and Knoop, Krebs' teacher at Freiburg, had shown in liver that citrate was converted to aconitate, then isocitrate and α-ketoglutarate, which in turn was known to be converted to succinate. It was also known from Thunberg's work that malonate could inhibit the conversion of succinate to fumarate. This presented a way for Krebs to separate the reactions of Carl Martius and Franz Knoop from those of Albert Szent-Gyorgyi. Krebs then hit on the crucial question:

> *So I asked myself whether perhaps oxaloacetate, together with a substance derived from foodstuffs, might combine to form citrate again, after the manner of a cycle.*

Krebs began his "Results" section on the discovery of the tricarboxcylic acid cycle with the experiments or data showing the catalytic effects of citrate on respiration in pigeon breast minces. His experimental results confirmed his hypothesis. In his mind this cycle could explain the complete combustion of foodstuffs to CO_2 and water.

Into the Wilderness and Back Again

After his triumph in discovering the urea cycle in 1932 and having been invited by Max Plank to discuss his findings, in the same year, on 19 June 1933, he was forced into exile from his own homeland, to which he and his father were devoted and whose army he had served, for reasons of racial identity which he had rejected. He found refuge in Hopkins Biochemistry Laboratory at Cambridge, dependent upon the kindness of strangers.

Triumph would again be followed by rejection, after Krebs formulation of the TCA cycle. This time, however, the rejection would not be by the Nazi's who took over his homeland, but rejection would come from his scientific colleagues. A revolutionary theory always has its critics. Krebs' tricarboxcylic acid cycle, published in 1937 after being rejected by *Nature*, was no exception. By 1940, Earl Evans, who had been trained in Krebs' lab at Sheffield, and Harland Wood, one of America's most distinguished biochemists then working at Iowa State, produced evidence that when C-labeled CO_2 condensed with pyruvate to form oxaloacetate it yielded α-ketoglutarate with the entire radioactivity confined to the carboxyl group adjacent to the carbonyl group. Wood suggested that this radioactive evidence was compatible with the condensation of pyruvate with oxaloacetate forming aconitate, then isocitrate and finally a-ketoglutarate at a rapid rate. If the formation of citrate from aconitate were only a slow side reaction, then this would account for the radioactive findings. For 7 years this reasoning was accepted and Krebs changed the name of his cycle from the more euphonious "citric acid cycle" (see Figure 2) to the more cumbersome TCA cycle, which it bears today to accommodate the generally accepted view in the biochemical community.

Krebs confined his work to practical nutritional problems for wartime Britain, which was literally starving from the depredations of Nazi submarine attacks. Then in 1948, Alexander Ogston published a short paper in Nature pointing out that the "three-point" attachment of the symmetrical citrate molecule to the citrate synthase enzyme would confer optical properties to the product of that chemically symmetrical molecule. The "citric acid cycle" was back in business as Krebs pointed out in his Harvey Lecture delivered on 17 March 1949. The final confirmation of the validity of Krebs' original postulate of the "citric acid cycle" came from Fritz Lipmann's study of the acetylation of sulfanilamides where he identified the so-called "active acetate" as acetyl coenzyme A. Soon thereafter, Stern, Ochoa, and Lynen showed that the intermediate through which pyruvate enters the TCA cycle was acetyl CoA which then combines with oxaloacetate to form citrate, confirming Krebs' original formulation of the cycle.

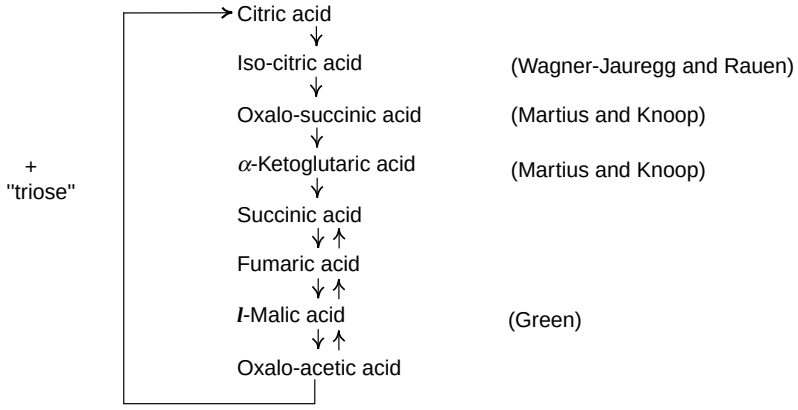

FIGURE 2 The original schematic of the citric acid cycle as it appeared in an article by Krebs and Johnson in 1937, after having been rejected by the editor of *Nature*. Krebs attempted to define the "reversible" and "irreversible" reactions of the cycle as he knew them at the time, but which would not be accepted as correct today. The nature of the "triose" combining with oxaloacetate was not known until the identification of acetyl CoA by Lipmann and Ochoa in the 1950s. The essential nature of the cycle as drawn in 1937 is however, correct to this day.

These workers also demonstrated that not only carbohydrate, but also fats and ketone bodies form acetyl CoA. This established that the Krebs citric acid cycle not only accounted for the complete conversion of carbohydrate to CO_2 and water, but that this cycle was the terminal pathway of the degradation of all foodstuffs, including fats and amino acids (see Figure 3). It may have been with some irony that Krebs entitled his Nobel prize speech of 11 December 1953, "the citric acid cycle" rather than the "TCA cycle" as it was called after the radioactive data were mistakenly interpreted to indicate that aconitate, and not citrate, was the condensation product of carbohydrate degradation. Subsequently, students of biochemistry would certainly have found the original name less fearsome than the "tricarboxcylic acid cycle," a name that evolved from erroneous interpretation of experimental results and was perpetuated by Krebs inherent modesty.

The TCA Cycle Today

It is now accepted that the TCA cycle is not only the metabolic pathway which accounts for the complete combustion of the product of glycolysis, pyruvate, to CO_2 and H_2O that is the pathway which accounts for the complete combustion of all foodstuffs, carbohydrates, fats, and amino acids in heterotrophic organisms. Much about the control of flux through the TCA cycle remains unknown even today. One persistent question is how cyclic pathways appear to defeat the laws of thermodynamics. It is easy to understand how a linear metabolic pathway, such as glycolysis, uses the chemical energy of the reactants to proceed from A to E. It is not so clear, however, how a pathway which goes from A to A accomplishes this feat in an apparent violation of thermodynamic imperatives.

The eight enzymes catalyzing the reactions of the TCA cycle and their equilibrium constants are listed in Table I.

The overall reaction of the TCA cycle is therefore:

$$\begin{aligned}\text{AcetylCoA} + 2\text{H}_2\text{O} + 3\text{NAD}^+ + \text{coenzymeQ} + \text{GDP} + \text{Pi} \\ \rightarrow 2\text{CO}_2 + \text{CoA} + 2H^+ + 3\text{NADH} \\ + \text{coenzymeQH}_2 + \text{GTP}\end{aligned}$$

with sum standard free energies, ΔG° at pH 7 of -11.7 kcal mol^{-1}. The sum of standard free energies of the reactions of the cycle is negative. While the sum of the standard free energies of the reactions of the cycle are negative in the direction of the cycle written, there is no complete information on the actual $\Delta G'$ of the cycle *in vivo*. The actual $\Delta G'$ of a reaction is of course, a sum of the standard free energy, ΔG°, and a term representing the actual ratio of the concentration of products over reactants.

Without knowledge of the ratio of concentrations in mitochondria of the products over the reactants of the various eight steps of the TCA cycle, no definitive statement about the reversibility of any step can be made, although most biochemical textbooks assign one or another TCA cycle as "irreversible."

The synthesis of citrate from acetyl CoA and oxaloacetate, by citrate synthase, has the largest standard free energy of any reaction within the cycle and might therefore qualify for the irreversible designation. However, the distinguished biochemist, Paul Srere, who spent much of his career in biochemistry studying the kinetics of citrate enzymes, argued forcefully that the citrate synthase reaction achieved near equilibrium *in vivo*. Krebs himself argued that both the NAD- and NADP-dependent mitochondrial isocitrate dehydrogenases were in near equilibrium with the free mitochondrial [NAD^+]/[NADH] pool. A near-equilibrium reaction is hardly compatible with irreversibility.

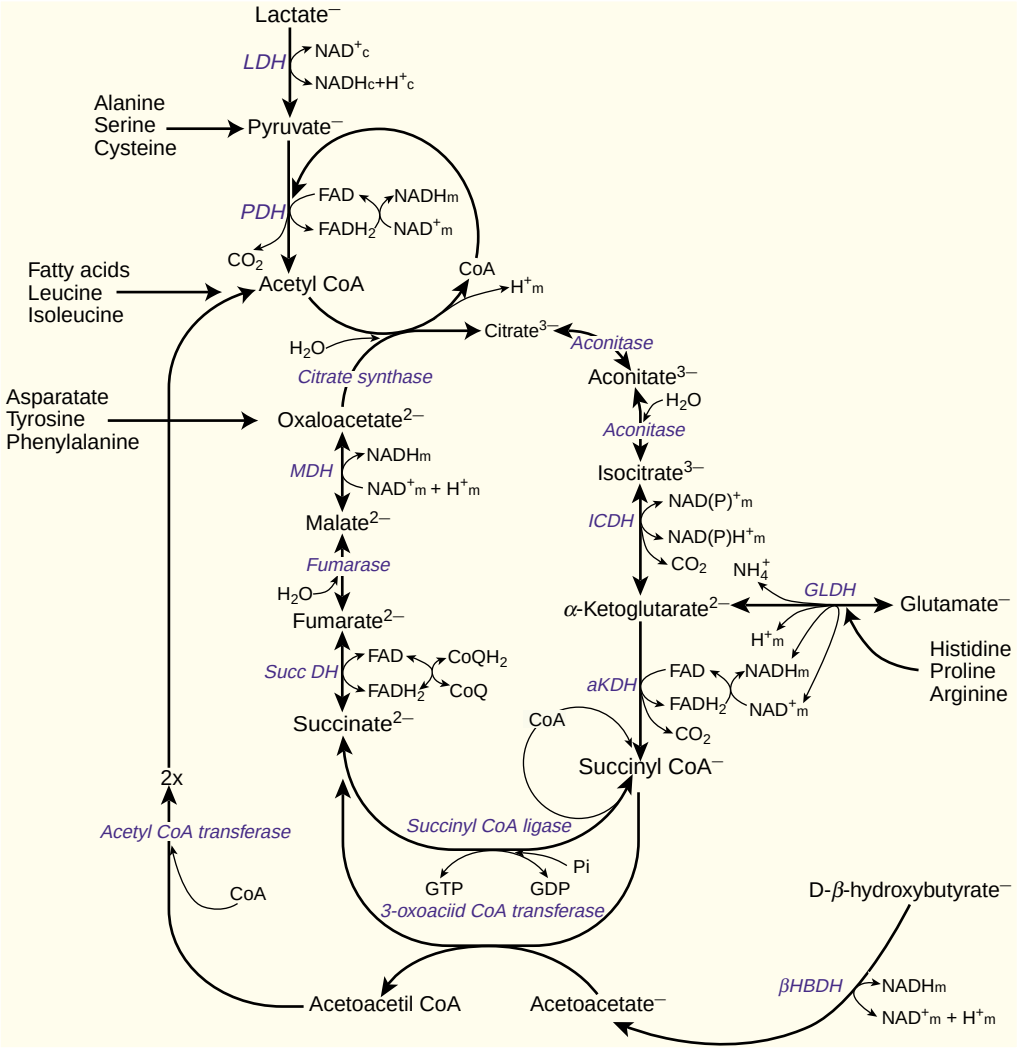

FIGURE 3 The TCA cycle is now recognized as the central pathway for the complete degradation of the major foodstuffs including carbohydrate, lipid, and proteins. It also captures the reducing equivalents which are then transferred to the electron transport system of mitochondria where the energy of their redox reactions generate the mitochondrial proton gradient used to power ATP synthesis.

The reaction catalyzed by the α-ketoglutarate dehydrogenase multienzyme complex could well be irreversible, but specific knowledge allowing one to come to a firm conclusion is lacking.

What is clear is that the disposal, of the reducing power produced in the reactions of the TCA cycle, mainly in the mitochondrial electron transport system critically affects the extent and possibly the direction of the reactions of the cycle. Within the last decade, it has been established that the TCA cycle exists in the earliest surviving life forms, the archebacteria which developed when Earth was covered in a reducing atmosphere of CO_2 and NH_3 and no O_2. Archebacteria contain a TCA cycle, which was proposed to serve as a primary anaplerotic source of metabolites and amino acids, not as the primary pathway for the degradation of foodstuffs in heterotrophs. When life forms were developing, in the absence of O_2, the direction of the TCA cycle would have been reversed.

Whether one accepts this speculation or not, it emphasizes the intimate relationship between the TCA cycle and the production of reducing power in the form of reduced pyridine nucleotide, which serves as the primary substrate for the electron transport system. When formulated in 1937, Krebs was primarily concerned with the stoichiometry of reactions accounting for the transformation of foodstuffs into CO_2. In 1936, Otto Warburg had just discovered NADP in red cells, so the central role of these essential cofactors was not appreciated until much later when Krebs played a crucial role in defining the redox potential of the mitochondrial $[NAD^+]/[NADH]$ ratio using principles first defined Holzer, Lynen, Bucher, and Klingenberg in defining the free cytoplasmic $[NAD^+]/[NADH]$. Krebs and his

TABLE I

The Eight Enzymes Catalyzing the Reactions of the TCA Cycle and their Equilibrium Constants

Enzyme	EC number	Reaction	Keq at pH 7.0	ΔG^{o} at pH 7 (kcal mol^{-1})
Citrate synthase	4.1.3.8	Acetyl CoA + oxaloacetate + $H_2O \rightarrow$ citrate + CoA	2.24×10^{6}	−9
Aconitase	4.2.1.3	Citrate ↔ isocitrate	18	−1.8
Isocitrate dehydrogenase	1.1.1.41	Isocitrate + $NAD(P)^{+}$ ↔ α-ketoglutarate + CO_2 + NAD(P)H	1.17 M	−0.01
α-Ketoglutarate dehydrogenase	Enzyme complex	α-Ketoglutarate + NAD^{+} + CoA → succinyl CoA + CO_2 + NADH	1.17×10^{3}	−4.4
Succinyl CoA ligase	6.2.1.4	Succinyl CoA + GDP + Pi ↔ succinate + GTP + CoA	3.5	−0.08
Succinate dehydrogenase	1.3.5.1	Succinate + ubiquinone ↔ fumarate + ubiquinol	6.5	−1.2
Fumarase	4.2.1.2	Fumarate + H_2O ↔ L-malate	4.4	−0.9
Malate dehydrogenase	1.1.1.37	Malate + NAD^{+} ↔ oxaloacetate + NADH	2.86×10^{-5}	6.5

colleagues then went on to show that the redox potentials of all of pyridine nucleotides were related to one another in a coherent manner. The free cytosolic NAD couple was about −0.19 V, and hence could accept reducing equivalents from glycolysis, the free mitochondrial NAD couple was a more negative −0.28 V, providing the energy necessary for mitochondrial ATP generation, while the free cytosolic NADP system was the most negative at −0.41 V, required for the completion of the reductive synthesis of fats. While it was recognized at the time that the pyridine nucleotides were related to the free [ATP]/[ADP][Pi] ratio, subtleties in the effects of free $[Mg^{2+}]$ complicated this relationship and it took another 10 years to accurately determine the equilibrium constants required to quantitatively define that relationship.

In addition to accounting for the chemical decomposition of foodstuffs, it is now recognized that the TCA cycle produces reducing power in the form of three reduced pyridine nucleotides and one reduced coenzyme Q within the mitochondria. Each of these cofactors contains two electrons. Those contained in NADH feed into the mitochondrial electron transport system at complex I, the NADH dehydrogenase multienzyme complex. The reducing equivalents contained in reduced coenzyme Q, generated in the conversion of succinate to fumarate feed into the electron transport chain at a site with a higher redox potential than that of the mitochondrial $[NAD^{+}]$/[NADH] couple. Approximately four protons are ejected from mitochondria at each site creating a ΔG $[H^{+}]$cytosol/mitochondria, which provides the energy approximately equivalent to that of the $\Delta G'$ of ATP hydrolysis in a near equilibrium reaction catalyzed by the F1 ATPase.

It was originally thought that the TCA cycle was so fundamental that any defects in the cycle would be fatal. It is now recognized that because of its central role, not only in the degradation of food stuffs, the TCA cycle plays a central role in generating the redox potentials not only of the mitochondrial NAD couple but also of the mitochondrial Q couple. The difference in the redox potential of these two couple, in turn, sets the magnitude of the energy of the proton gradient between the mitochondrial and cytosolic phases of the cell and thus determines the energy realized when the ATP formed by the mitochondria is hydrolyzed. The amount of realizable energy formed is a function of the amount and type of the substrate being utilized by mitochondrial TCA cycle.

See Also the Following Articles

Coenzyme A • Glycolysis, Overview • Pyruvate Carboxylation, Transamination and Gluconeogenesis • Urea Cycle, Inborn Defects of

Glossary

ΔG^{o} The standard free energy of a reaction, a constant where the products and reactants are 1 *M* in activity or more practically concentration.

$\Delta G'$ The free energy of a reaction, which is not constant but varies with the ratio of activity of concentration of products divided by reactions and is defined by the formalism

$$\Delta G' = \Delta G^{o} + RT \ln \frac{[\text{products}]}{[\text{reactants}]}$$

TCA cycle The tricarboxcylic acid cycle.

Further Reading

Holmes, F. L. (1991). *Hans Krebs, the Formation of a Scientific Life, 1900 to 1933*. Oxford University Press, Oxford.

Holmes, F. L. (1993). *Hans Krebs, Architect of Intermediary Metabolism, 1933 to 1937*. Oxford University Press, Oxford.

Krebs, H. A. (1954). The citric acid cycle. In *Les Prix Nobel en 1953*, pp. 139–150. Boktryckeriet P.A. Norstedt and Soner, Stockholm, Kungl.

Krebs, H. A. (1981). *Hans Krebs: Reminiscences and Reflections*. Clarendon Press, Oxford.

Krebs, H. A., and Henseleit, K. (1932). Untersuchungen über die Hamstoffbildung in Tierkörper. *Hope-Seyler's Z. Physiol. Chem.* **210**, 33–66.

Krebs, H. A., and Johnson, W. A. (1937). The role of citric acid in intermediate metabolism in animal tissue. *Enzymologia* **4**, 148–156.

Krebs, H. A., and Veech, R. L. (1969). Pyridine nucleotide interrelations. In *The Energy Level and Metabolic Control in Mitochondria* (S. Papa, J. M. Tager, E. Quagliariello and E. C. Slater, eds.) pp. 329–382. Adriatica Editrice, Bari.

Morowitz, H. J., Kostelnik, J. D., Yang, J., and Cody, G. D. (2000). The origin of intermediary metabolism. *Proc. Natl. Acad. Sci USA* **97**, 7704–7708.

Ogston, A. G. (1948). Mechanism of fixation of carbon dioxide in the Krebs cycle. *Nature* **162**, 963.

Wood, H. G., Werkman, C. H., Hemingway, A., and Nier, A. O. (1941). Interpretation of experiments on metabolic processes using isotopic tracer elements. *J. Biol. Chem.* **139**, 483.

Biography

Richard L. Veech is the Head of the Laboratory of Metabolic Control, NIAAA, NIH, DHHS, in Rockville, Maryland. He is an M.D. from Harvard Medical School, and has a D.Phil. in Biochemistry from Oxford University where his supervisor was Hans Krebs. He works on problems involving the control of the processes of intermediary metabolism, particularly in disease states.

tRNA Synthetases

Karla L. Ewalt and Paul Schimmel
Scripps Research Institute, La Jolla, California, USA

Protein biosynthesis is the culmination of the transfer of genetic information from DNA to proteins. It is a highly coordinated process that requires many cellular factors including RNAs, proteins, nucleotides, and amino acids. An essential component for the translation of genetic information from genes to proteins, is the group of enzymes known as aminoacyl-tRNA synthetases. These enzymes covalently link amino acids to transfer RNAs (tRNAs) and thereby establish the rules of the genetic code that pair amino acids to codons. The translation of codons on the messenger RNA into amino acids occurs at the ribosome – the center of protein biosynthesis.

Enzymatic Reaction

Accurate protein biosynthesis requires a collection of amino acids attached to tRNAs (aminoacyl-tRNAs), which are typically generated by 20 amino acid-specific enzymes called aminoacyl-tRNA synthetases. The aminoacylation reaction is carried out at the enzymes active sites in two-steps. In the first step, an amino acid (AA) is condensed with ATP yielding an aminoacyl-adenylate (AA-AMP) and pyrophosphate (PPi) (Scheme 1). In the second step, the aminoacyl group is transferred to either the 2′ or 3′-ribose hydroxyl on the terminal adenosine of tRNA (AA-tRNA). Certain tRNA synthetases contain a second active site (editing active site) for the hydrolysis of incorrectly paired amino acids and tRNAs. At this site, the tRNA synthetase corrects its errors.

Translational Accuracy

Aminoacyl-tRNA synthetases establish and determine the accuracy of the genetic code and of protein biosynthesis, as they pair amino acids with codons through selection of amino acids and tRNAs. Accuracy is achieved during selection of amino acids and tRNAs, as well as through editing reactions that correct errors.

Amino Acids

Each tRNA synthetase is specific for one of the 20 amino acids. A selective binding site for the amino acid accomplishes discrimination among the various amino acid substrates. However, amino acid substrates for a few enzymes are closely similar in size and functional groups to other amino acids. For example, isoleucyl-tRNA synthetase selects between isoleucine and valine, which are both β-branched aliphatic amino acids differing in length by only one methylene. The misactivation of valine to valyl-adenylate by isoleucyl-tRNA synthetase occurs at a low frequency. Threonyl-tRNA synthetase must select between threonine and serine, which differ by only a single methylene. The active site is a "course sieve" that allows the correct amino acid and occasionally similar, but slightly smaller amino acids to be transferred to tRNA.

tRNAs

tRNAs are adapters that covalently connect anticodons with amino acids. Sequences of tRNAs are 70–90 nucleotides (76 is most common) that form a common cloverleaf secondary structure with four major arms. This secondary structure in turn folds into an L-shaped tertiary structure made up of two domains (Figure 1). Amino acids are attached to tRNAs at the 3′-terminal adenosine at the end of a CCA trinucleotide sequence that is common to all tRNAs. In the second domain is a trinucleotide sequence known as the anticodon, located ~75Å from the amino acid attachment site. During protein synthesis, the anticodon triplet binds through complementary base pairing to a codon on mRNA and thereby delivers an amino acid to the growing polypeptide chain.

Since the genetic code is degenerate, more than one tRNA may exist for a single amino acid. The 61 sense codons of the code are recognized by a combination of distinct tRNAs (one tRNA specific for each codon) and tRNAs that employ wobble-base pairing (one tRNA that recognizes sets of related codons). (A notably reduced set of tRNAs is found in the mitochondria of eukaryotes, where 22 tRNAs read the codons.) Although, tryptophan and methionine each have a single tRNA, there are as many as five tRNAs specific for the six leucine codons. The multiple tRNAs specifying a single amino acid are termed isoacceptors, and are substrates for a single

$$E + AA + ATP \rightleftharpoons E\bullet(AA\text{–}AMP) + PPi$$

$$E\bullet(AA\text{–}AMP) + tRNA \rightleftharpoons E + AA\text{-}tRNA + AMP$$

SCHEME 1 Two-step aminoacylation reaction catalyzed by aminoacyl tRNA synthetases (E). Amino acid (AA) and ATP react to form an activated aminoacyl-adenylate (AA-AMP) and pyrophosphate (PPi). The aminoacyl group is transferred to either the 2′ or 3′ ribose hydroxyl of the terminal adenine on tRNA.

aminoacyl-tRNA synthetase. Specific recognition of tRNA is primarily through a nucleotide determinant located in the acceptor stem. Nucleotides at other positions including the anticodon stem are also important in many instances. The specific recognition of tRNAs by synthetases based on the nucleotides present in the acceptor stem, has led to the idea that these features constitute a second genetic code that may be left over from a smaller, historical RNA, which predated the current tRNA structure.

Editing

Several tRNA synthetases have an editing activity to ensure correct pairing of amino acids with tRNAs (Scheme 2). This editing, or proofreading, function prevents misincorporation of amino acids into proteins by hydrolyzing incorrectly aminoacylated tRNAs (post-transfer editing). The tRNA synthetases for isoleucine, leucine, valine, threonine, and alanine have been shown to have specific domains with editing active sites that are separate from the active site for aminoacylation. The editing site operates as a "fine sieve" to exclude the correct aminoacyl-tRNA while binding the smaller and incorrect aminoacyl-tRNA, which is then hydrolyzed. It is currently thought that tRNA synthetases can also hydrolyze misactivated amino acids prior to attachment to the tRNA (pre-transfer editing). Through the combination of proper substrate selection and editing, the general error rate for protein synthesis is estimated to be $\leq 1/3000$.

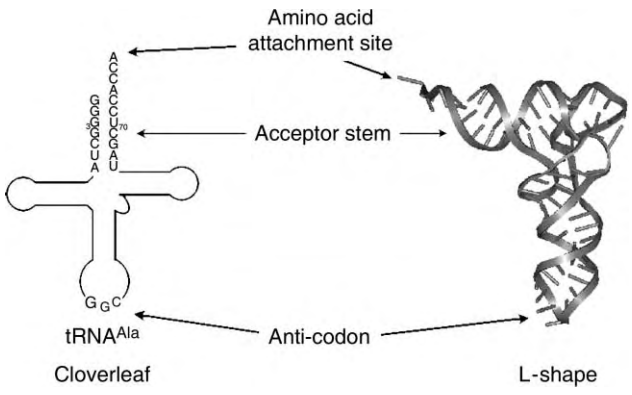

FIGURE 1 The cloverleaf secondary and L-shape tertiary structure of tRNA.

Two Classes of Enzymes

Structures

Aminoacyl-tRNA synthetases are divided into two groups of ten enzymes – class I and class II – based upon the sequences and structures of the active site domains. Ten different class I enzymes activate and transfer the amino acids Arg, Cys, Glu, Gln, Ile, Leu, Met, Tyr, Trp, and Val to tRNAs. All class I enzymes contain a Rossmann nucleotide-binding domain and an active site with two signature sequences, an 11 amino acid element that ends in HIGH and a KMSKS pentapeptide. The active site is interrupted by a polypeptide insertion called CP1 that encodes an editing domain. (Figure 2). Similarly, there are ten class II enzymes that activate and transfer the amino acids Ala, Asn, Asp, Gly, His, Lys, Phe, Pro, Ser, and Thr to tRNAs. These ten enzymes share an active site architecture formed by three conserved motifs (motif 1, 2, and 3) in an overall structure having a seven-stranded antiparallel β-sheet flanked by α-helices. Enzymes in both classes have additional motifs or domains that are idiosyncratic to each enzyme. Some of these domains provide RNA binding elements, while others have functions such as signaling in cytokine pathways.

Mechanisms

The enzymes in the two classes are distinguished by the orientation with which they bind tRNA. Class I enzymes generally bind tRNA on the minor groove side of the RNA helix and attach the amino acid to the 2′-ribose hydroxyl of the terminal adenosine. Most class II enzymes bind tRNA on the major-groove side and attach the amino acid to the 3′-ribose hydroxyl. While aminoacylation is specific to a particular hydroxyl, the amino acid rapidly migrates between the 2′- and 3′-ribose hydroxyl groups.

Alternative Pathways and Enzymes

In a few cases, amino acids are modified while attached to specific tRNAs in order to generate different aminoacyl-tRNA species. This type of mechanism has evolved as a biosynthetic pathway for glutamine, asparagine, and selenocysteine.

tRNA Dependent Amidation

Bacteria and archea have developed an alternate two-step route for producing aminoacylated tRNAs for glutamine and asparagine. In these organisms, glutamic acid is attached to the glutamine specific tRNA

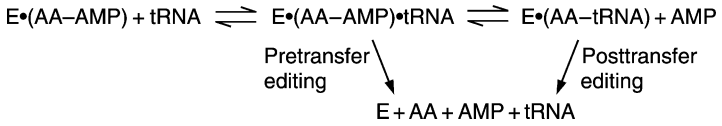

SCHEME 2 Pretransfer and post-transfer editing reactions catalyzed by aminoacyl-tRNA synthetases (E). Pretransfer editing occurs prior to the aminoacyl group transfer to tRNA. Posttransfer editing occurs after the aminoacyl group has been transferred to tRNA. The net result of both pathways is the enzymatic hydrolysis of the aminoacyl-group (AA-AMP or AA-tRNA) to the free amino acid (AA) with release of AMP and tRNA.

($tRNA^{Gln}$) by glutamyl-tRNA synthetase. This system requires that the glutamyl-tRNA synthetase have a relaxed specificity that permits the acylation of glutamic acid onto both $tRNA^{Glu}$ and $tRNA^{Gln}$. In the second step, glutamine is produced as Gln-$tRNA^{Gln}$ from Glu-$tRNA^{Gln}$, by the enzyme glutamyl-$tRNA^{Gln}$ amidotransferase. In these two kingdoms, this system is the predominant mechanism for producing Gln-$tRNA^{Gln}$. Although some bacteria and archea have the gene encoding asparaginyl-tRNA synthetase, an analogous system also exists for the amidation of Asp-$tRNA^{Asn}$ to produce Asn-$tRNA^{Asn}$.

Selenocysteine

Sometimes called the 21st amino acid, selenocysteine is incorporated into proteins at the UGA codon that normally is a stop codon. However, a special tRNA ($tRNA^{Sec}$) exists for the incorporation of selenocysteine at this position. Selenocysteyl-$tRNA^{Sec}$ is produced by modification of Ser-$tRNA^{Sec}$. Serine is attached to the $tRNA^{Sec}$ by seryl-tRNA synthetase, and is then modified by selenocysteine synthase. The enzyme incorporates selenide through a pyridoxal 5-phosphate-mediated reaction. Incorporation of selenocysteine into proteins at UGA is dependent on the presence of a selenocysteine-insertion-sequence in the mRNA that is immediately downstream of the codon.

Novel Functions of tRNA Synthetases

In addition to their essential role in protein biosynthesis, several tRNA synthetases are involved in other cellular processes. The novel functions that appear in tRNA synthetases are not common features to all of the enzymes for a particular amino acid, but rather are specialized features of the enzymes in selected organisms. For examples, mitochondrial leucyl- and tyrosyl-tRNA synthetase promote splicing in certain fungi. Bacterial threonyl-tRNA synthetase regulates its own translation by binding to an upstream region of the

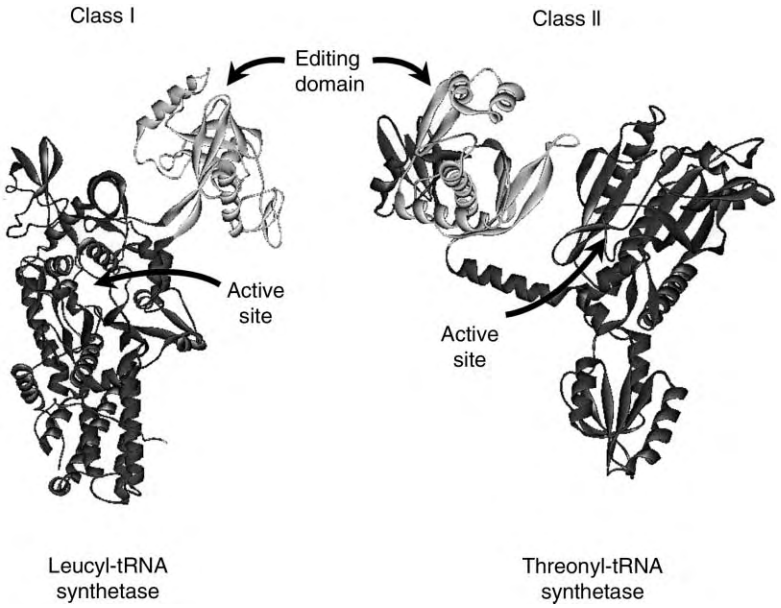

FIGURE 2 The crystallographic structure of a class I enzyme, leucyl-tRNA synthetase, and a class II enzyme, threonyl-tRNA synthetase, indicating the active sites and editing domains.

mRNA, and a histidyl-tRNA synthetase related protein called GCN2 regulates translation in eukaryotes. Increasingly, roles for tRNA synthetases as cell signaling factors are being discovered in higher eukaryotes. Fragments of tyrosyl- and tryptophanyl-tRNA synthetase are mediators of angiogenesis, while histidyl- and asparaginyl-tRNA synthetase specifically stimulate immune cells. These extra functions demonstrate how tRNA synthetases have been adapted and utilized for a wide variety of functions in addition to their enzymatic role in protein biosynthesis.

See Also the Following Articles

Amino Acid Metabolism • Pre-tRNA and Pre-rRNA Processing in Bacteria • Pre-tRNA and Pre-rRNA Processing in Eukaryotes • RNA Editing

Glossary

aminoacyl-tRNA synthetases A family of enzymes that attach each amino acid to its appropriate tRNA.

anticodon The three nucleotide sequence on tRNA that binds to the codon through complementary base pairing.

codon A three nucleotide RNA sequence that specifies a particular amino acid.

translation The process of protein biosynthesis from messenger RNA.

tRNA A small RNA molecule that carries an amino acid to the ribosome during protein biosynthesis, recognizes the codon specifying the amino acid and delivers it to the growing polypeptide chain.

Further Reading

Alberts, B., Bray, D., Lewis, J., Raff, M., Roberts, K., and Watson, J. D. (2002). *Molecular Biology of the Cell*. Garland Publishing, New York.

Schimmel, P., and Ribas de Pouplana, L. (2000). Footprints of aminoacyl-tRNA synthetases are everywhere. *Trends Biochem. Sci.* **25**(5), 207–209.

Soll, D., and RajBhandary, U. L. (1995). *tRNA Structure, Biosynthesis, and Function*. ASM Press, Washington, DC.

Voet, D., and Voet, J. G. (1995). *Biochemistry*. Wiley, New York.

Biography

Paul Schimmel is the Ernest and Jean Hahn Professor and member at the Skaggs Institute for Chemical Biology at the Scripps Research Institute. He holds a Ph.D. from the Massachusetts Institute of Technology, where he went on to become the John D. and Catherine T. MacArthur Professor of Biochemistry and Biophysics in the Department of Biology prior to joining the Scripps Research Institute. His major research activities have concentrated on the decoding of genetic information, with an emphasis on the rules of the universal genetic code established by aminoacyl-tRNA synthetases.

Karla L. Ewalt is a Staff Scientist in the Department of Molecular Biology at the Scripps Research Institute. She holds a Ph.D. from the University of California, San Diego. Her research focus is on the functional specializations found in components of eukaryotic protein translation machinery.

trp Operon and Attenuation

Paul Gollnick
State University of New York, Buffalo, New York, USA

Transcription attenuation can be defined as any mechanism that utilizes transcription pausing or termination to control expression of downstream genes. This mechanism of regulation is used to control expression of many genes in bacteria in responses to changes in their environment. Moreover, bacteria have evolved several elaborate and elegant variations on the attenuation theme, mainly based on the mechanism used to control formation the RNA structures that signal RNA polymerase to pause or terminate.

Attenuation

The first attenuation mechanism to be described was for the *Escherichia coli* tryptophan biosynthetic (*trpEDCBA*) operon. When Charles Yanofsky and his co-workers elucidated this mechanism, it was the first demonstration that organisms can utilize changes in RNA structure to regulate gene expression. Subsequently many other examples of transcription attenuation have been discovered. In each case the *cis*-acting genetic information is contained within a 150–300 bp region located after the start of transcription and prior to the start of the coding sequence for the first structural gene of the operon. This region is called the leader region. In this article, the features of transcription attenuation control of the *E. coli trp* operon are discussed, followed by the modifications in this classic system that allow it to be adapted to control other amino acid biosynthetic operons. Thereafter attenuation control of the *trp* operon in the gram-positive bacterium *Bacillus subtilis*, which involves a larger variation on the attenuation theme, is described. There are several recent reviews that cover the attenuation in more depth as well as describe attenuation control of other bacterial genes.

The *E. coli trp* Operon: Attenuation Based on Translation of a Leader Peptide

The *E. coli trpEDCBA* operon encodes the enzymes required to synthesize *L*-tryptophan from chorismic acid. Transcription of the *trp* operon is regulated in response to changes in intracellular tryptophan levels. When the cells contain adequate amounts of tryptophan, for example when it is present in the growth medium, transcription of the operon is down-regulated. In contrast, when tryptophan is limiting, the *trp* operon is actively transcribed in order to express the enzymes required for its synthesis. Initiation of transcription is regulated by the *trp* repressor, a DNA-binding protein encoded by the *trpR* gene. In addition, after transcription has initiated, the elongating transcription complex is subject to regulation by attenuation. Together, repression (80-fold) and attenuation (8-fold) serve to allow ~600-fold overall control of transcription of the *trp* operon in response to various levels of tryptophan availability.

Attenuation Control of the *E. coli trp* Operon

The *E. coli trp* operon contains a 162 bp leader region prior to the start of the *trpE* coding sequence. The *trp* leader transcript contains several inverted repeats, composed of the segments labeled 1–4 in Figure 1, that can form three different overlapping base-paired RNA secondary structures. These structures include an intrinsic transcription terminator (3:4), an overlapping antiterminator (2:3), and a pause structure (1:2). In addition, the leader transcription contains a small open reading frame (ORF) that encodes a 14-amino acid leader peptide, which contains two critical tandem UGG Trp codons. The cell's ability to efficiently translate these two Trp codons determines which RNA structure forms in the nascent leader transcript, which in turn controls whether transcription halts in the leader region or continues into the structure genes of the operon.

Shortly after transcription initiates from the *trp* promoter, the 1:2 pause hairpin forms (Figure 1). This structure signals RNA polymerase to pause transcription after nucleotide 92. This pausing of RNA polymerase is a critical feature of the attenuation mechanism because it allows time for a ribosome to

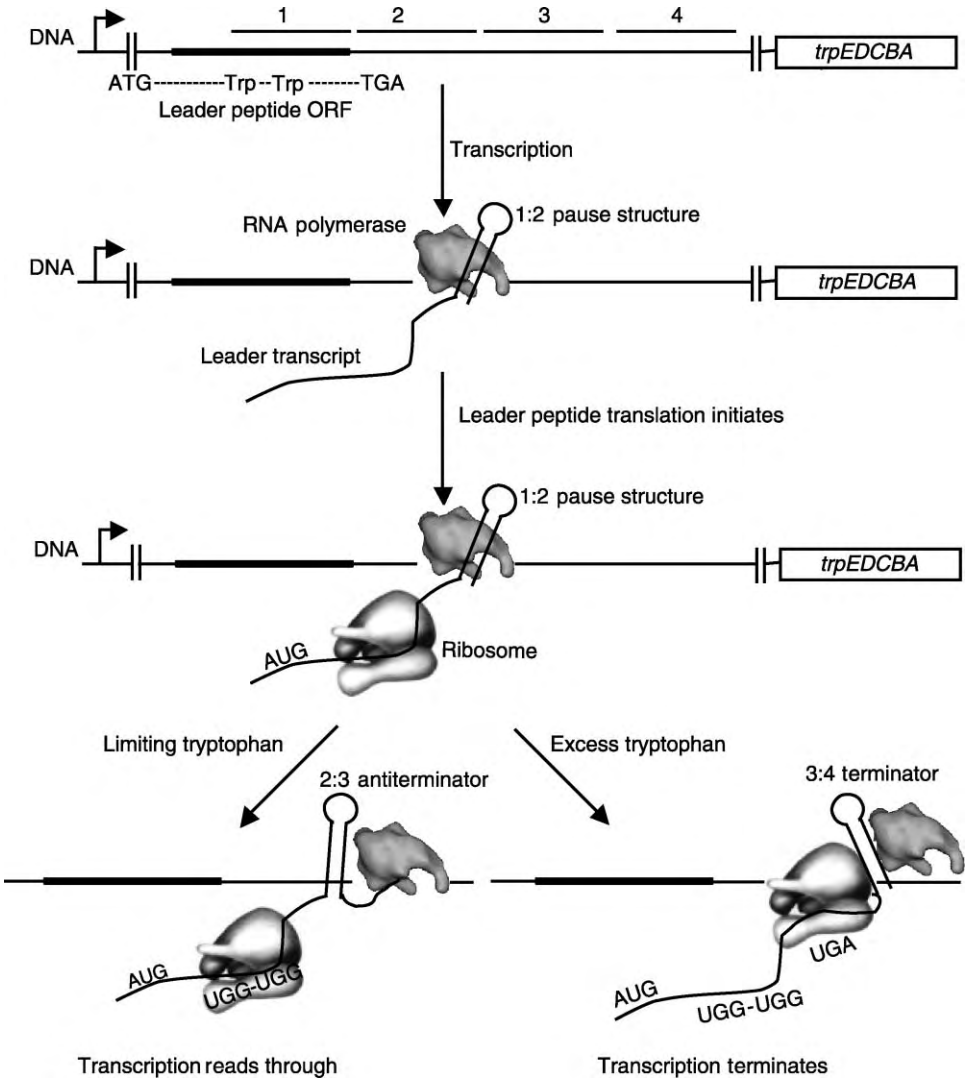

FIGURE 1 Model of transcription attenuation of the *E. coli trp* operon. RNA polymerase pauses following formation of the pause structure. This provides time for a ribosome to initiate translation of the leader peptide. Under tryptophan-limiting conditions the ribosome stalls at the tandem Trp codons, resulting in transcription read through. Under conditions of tryptophan excess the ribosome reaches the leader peptide stop codon. This ribosome position blocks formation of the antiterminator leading to terminator formation and transcription termination.

initiate translation of the leader peptide. When the ribosome begins translating the leader peptide this releases the paused RNA polymerase to resume transcription. Transcription and translation are now coupled, with the ribosome closely following RNA polymerase. This situation is essential to allow events involving the ribosome to affect transcription by the associated RNA polymerase.

At this point there are two possible pathways for the attenuation mechanism to follow depending on the level of tryptophan in the cell. The choice depends on how efficiently the tandem Trp codons in the leader peptide are translated. This efficiency reflects the availability of aminoacylated $tRNA^{Trp}$ in the cell. Under conditions where tryptophan is limiting, the amount of charged $tRNA^{Trp}$ is low. As a result of this low concentration of tryptophanyl-$tRNA^{Trp}$ translation of the tandem Trp codons is inefficient and the ribosome stalls at one of these two codons. The associated RNA polymerase continues to transcribe through the *trp* leader region and transcription and translation become uncoupled. As RNA polymerase proceeds through segments 2 and 3 of the leader region, the antiterminator structure (2:3) forms, which prevents formation of the overlapping intrinsic terminator (3:4) structure. Hence transcription continues through the leader region and into the *trp* structural genes.

When tryptophan is plentiful, the level of charged $tRNA^{Trp}$ in the cell is high. This allows efficient translation of the tandem Trp codons and hence the ribosome proceeds rapidly to the end of the leader peptide. When the ribosome reaches the leader peptide stop codon, it covers part of RNA segment 2 and thus prevents formation of the 2:3 antiterminator structure as transcription proceeds. This frees RNA segment 3 to base pair with segment 4 and form the terminator. Under these conditions transcription terminates in the leader region prior to the *trp* structural genes, which are therefore not expressed.

In this attenuation mechanism the regulatory signal is the level of charged $tRNA^{Trp}$ and the sensory event is the efficiency with which the ribosome can translate the tandem Trp codons in the leader peptide. This system can easily be adapted to regulate other bacterial amino acid biosynthetic operons. The only needed modification is to change the identity of the critical codons in the leader peptide, which controls the amino acid the system will respond to. There are numerous examples of such adaptations of this attenuation mechanism, particularly in enteric bacteria, including the *his, phe*, and *leu* operons, which contain seven His, seven Phe and four Leu codons in their respective leader peptides.

The *Bacillus subtilis trp* Operon: Attenuation Mediated by an RNA-Binding Protein

The transcription attenuation mechanism that regulates the *trp* operon in the gram-positive bacterium *Bacillus subtilis* differs more dramatically from that the *E. coli trp* operon than those described above for other amino acid biosynthetic operons in gram-negative bacteria. Most notably there is no leader peptide, and ribosomes are not involved in this attenuation mechanism. Instead an RNA-binding protein senses the level of tryptophan in the cell and determines whether transcription terminates in the leader region or continues into the structural genes.

The *B. subtilis trp* Leader

Expression of the *trpEDCFBA* operon in *B. subtilis* and several related bacilli is regulated by the *trp* RNA-binding Attenuation Protein (TRAP). Transcription of the operon initiates from the *trp* promoter 203 nucleotides upstream of the start codon of the first structural gene, *trpE* (Figure 2). There is no evidence for any regulation of initiation of transcription from this promoter. Hence there is no homologue, either

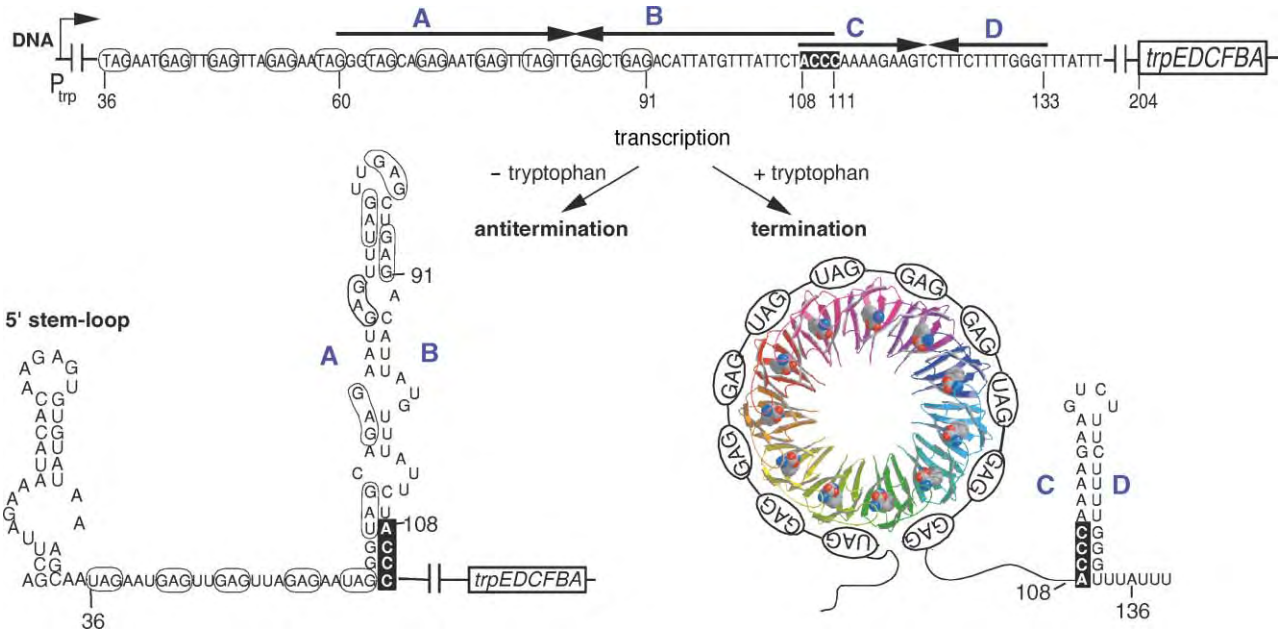

FIGURE 2 Model of transcription attenuation of the *B. subtilis trpEDCFBA* operon. The large blue letters indicate the complementary strands of the terminator and antiterminator RNA structures. The TRAP protein is shown as a ribbon diagram with each of the 11 subunits as a different color and the bound RNA is shown forming a matching circle upon binding to TRAP. The bound tryptophans are shown as space filling models. The GAG and UAG repeats involved in TRAP binding are shown in ovals and are also outlined in the sequence of the antiterminator structure. Numbers indicate the residue positions relative to the start of transcription. Nucleotides 108–111 overlap between the antiterminator and terminator structures and are shown as darkly outlined letters.

functional or based on amino acid sequence, of the *E. coli* DNA binding *trp* repressor in *B. subtilis*. The *B. subtilis trp* leader transcript also contains inverted repeats that can form an intrinsic transcription terminator (C:D) and an antiterminator (A:B) RNA secondary structure (Figure 2). These two structures overlap by four nucleotides and hence their formation is mutually exclusive.

In the presence of excess tryptophan, TRAP binds to a series of 11 trinucleotide repeats in the *trp* leader transcript consisting of seven GAGs and four UAGs (Figure 2). The (G/U)AG repeats are separated from each other by two or three "spacer" nucleotides, whose sequence is not conserved. These triplet repeats in part overlap the 5′ portion of the antiterminator structure and hence TRAP-binding interferes with formation of the antiterminator (A:B) thus favoring formation of the terminator (C:D) hairpin. Therefore under these conditions transcription halts in the leader region prior to the *trp* structural genes, which are not expressed.

When tryptophan is limiting, TRAP does not bind to the *trp* leader RNA transcript and formation of the A:B antiterminator is favored. This situation allows transcription to proceed into the *trp* operon structural genes, which can now be expressed to produce the enzymes to synthesize tryptophan.

The TRAP Protein

In this system the ability of TRAP to sense the levels of intracellular tryptophan and to then influence the structure of the nascent *trp* leader mRNA transcript is the basis for attenuation control of the *trp* operon. TRAP is a ring-shaped protein composed of 11 identical subunits (Figure 3). TRAP is activated to bind its RNA targets by binding 11 molecules of *L*-tryptophan in clefts between adjacent subunits. The detailed mechanism by which tryptophan binding activates TRAP to bind RNA is not known, however, recent studies suggest that tryptophan binding induces a conformational change in TRAP as well as reduces the flexibility of the protein. Upon activation by tryptophan, TRAP binds to its RNA target consisting of the 11 (G/U)AG repeats by wrapping the single-stranded RNA around the outer perimeter of the protein ring (Figure 3). The phosphodiester backbone is on the outside of the RNA ring and the bases point in toward the protein. The specificity of this interaction derives mainly from hydrogen bonds between several amino acids of each TRAP subunit including Glu36, Lys37, Lys56, and Arg58, and the bases on the (G/U)AG repeats. The spacer nucleotides do not contact the protein, and their identity is not crucial for TRAP recognition and binding. This mechanism of wrapping the RNA around the protein ring explains both the specificity of the TRAP–RNA interaction as well as how TRAP binding alters the structure of the *trp* leader RNA to regulate attenuation.

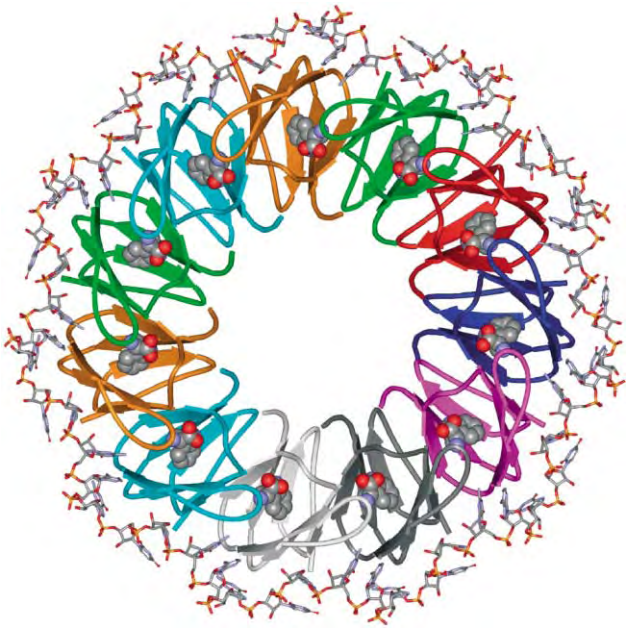

FIGURE 3 Ribbon diagram of TRAP complexed with an RNA containing 11 GAG repeats separated by AU spacers. The TRAP protein is shown in ribbon diagrams with each subunit depicted in a different color. The RNA is shown in stick models and the 11 molecules of bound *L*-tryptophan are shown in space-filling models.

The Role of Pausing in TRAP Mediated Attenuation

In addition to the terminator and antiterminator structures, there is an RNA hairpin at the 5′ end of the *trp* leader mRNA (Figure 2; 5′ stem-loop). Although this structure has been shown to be important for proper attenuation control of the *trp* operon, it is not a transcriptional pause signal analogous to the 1:2 structure of the *E. coli trp* attenuation system. The role of this 5′ stem-loop may be to enhance the rate of TRAP binding to the *trp* leader RNA. This is an important consideration because TRAP must bind to its target before RNA polymerase transcribes beyond the terminator structure, otherwise TRAP binding would not be able to influence attenuation. Recent studies published by Yakhnin and Babitzke indicate that RNA polymerase pauses at U107 (Figure 2) during transcription of the *trp* leader region, and that this pausing is dependent on the NusA transcription factor. This pause would provide additional time for TRAP to bind to the nascent *trp* leader RNA and promoter termination.

Anti-TRAP and the Role of $tRNA^{Trp}$ in Regulating the *B. subtilis trp* Genes

In this attenuation system the regulatory signal is the level of free tryptophan available to activate TRAP to bind RNA. In the previously described *E. coli trp* attenuation system, free tryptophan is sensed by the DNA binding *trp* repressor protein and the regulatory signal for attenuation is the availability of charged $tRNA^{Trp}$. The level of charged $tRNA^{Trp}$ also influences attenuation control of the *B. subtilis trp* operon, although by a very different mechanism than in the *E. coli* system. In *B. subtilis* the *rtpA* gene encodes a protein called anti-TRAP (AT). AT influences expression of the *trp* genes by binding to tryptophan-activated TRAP and preventing it from binding RNA, thus elevating expression of *trp* genes. Expression of *rtpA*, which is in a two-gene operon together with *ycbK* (unknown function), is regulated in response to changes in the level of uncharged $tRNA^{Trp}$ by a mechanism known as T-box antitermination. High levels of uncharged $tRNA^{Trp}$ induce expression of AT, which prevents TRAP from down-regulating expression of the *trp* genes. Hence even if free tryptophan levels are high enough to activate TRAP, if the level of charging of $tRNA^{Trp}$ is low, then the *trp* genes will be expressed. Thus while both *E. coli* and *B. subtilis* regulate expression of the *trp* genes in response to changes in levels of both free tryptophan and aminoacylated $tRNA^{Trp}$, they have evolved very different mechanisms to do so.

Occurrences of TRAP Mediated Attenuation in Bacteria

TRAP mediated attenuation control of the *trp* operon has till date been only observed in *B. subtilis* and several related bacilli including *B. pumilus, B. stearothermophilus, B. caldotenax*, and *B. halodurans*, as well as in *Clostridium thermocellum*. In contrast to the leader-peptide-dependent mechanism described previously, the RNA-binding protein-dependent attenuation mechanism has never been characterized for any other amino acid biosynthetic operons beside tryptophan even though it would seem to be easily adaptable by simply changing the amino acid that activates the protein to bind its RNA target. Perhaps with the explosion of bacterial genomic information currently becoming available we might soon discover such a system.

See Also the Following Articles

DNA Polymerase I, Bacterial • DNA Polymerase II, Bacterial • DNA Polymerase III, Bacterial • Ribosome Structure • RNA Polymerase Reaction in Bacteria • RNA Polymerase Structure, Bacterial • T7 RNA Polymerase

Glossary

intrinsic terminator A signal in the nascent RNA transcript that signals RNA polymerase to halt transcription and dissociate from the DNA template. Intrinsic terminators consist of a short base-paired stem-loop structure followed by a short stretch of U residues in the RNA. Also called factor-independent terminator or Rho-independent terminator.

ribosome The large RNA–protein complex that translated mRNA into protein. It consists of two subunits, termed small and large.

RNA polymerase The enzyme that transcribes DNA into RNA. In bacteria there is only one version of this enzyme.

transcriptional pausing In response to signals in the RNA, RNA polymerase will pause and discontinue transcription but not dissociate from the DNA template. Either after some period of time, or in response to a signal, a paused RNA polymerase will resume transcription.

tRNA The adaptor RNA molecule that reads the genetic code in the mRNA by base-pairing with the codon triplets. An amino acid is attached to the 3′ end of the last base in the tRNA by an enzyme called an aminoacyl tRNA synthetase in a process called aminoacylation or charging. There are tRNAs corresponding each of the 20 amino acids.

Further Reading

Antson, A. A., Otridge, J. B., Brzozowski, A. M., Dodson, E. J., Dodson, G. G., Wilson, K. S., Smith, T. M., Yang, M., Kurecki, T., and Gollnick, P. (1995). The three dimensional structure of *trp* RNA-binding attenuation protein. *Nature* **374**, 693–700.

Antson, A. A., Dodson, E. J., Dodson, G. G., Greaves, R. B., Chen, X.-P., and Gollnick, P. (1999). Structure of the trp RNA-binding attenuation protein, TRAP, bound to RNA. *Nature* **401**, 235–242.

Babitzke, P., and Gollnick, P. (2001). Posttranscriptional initiation control of tryptophan metabolism in *Bacillus subtilis* by the *trp* RNA-binding attenuation protein (TRAP), anti-TRAP, and RNA structure. *J. Bacteriol.* **183**, 5795–5802.

Valbuzzi, A., and Yanofsky, C. (2001). Inhibition of the B-subtilis regulatory protein TRAP by the TRAP-inhibitory protein, AT. *Science* **293**, 2057–2059.

Yakhnin, A. V., and Babitzke, P. (2002). NasA-stimulated RNA polymerase pausing and termination participates in the *Bacillus subtilis trp* operon attenuation mechanism *in vitro*. *Proc. Natl. Acad. Sci. USA* **99**, 11067–11072.

Yanofsky, C. (2000). Transcription attenuation: Once viewed as a novel regulatory strategy. *J. Bacteriol.* **182**, 1–8.

Yanofsky, C. (2001). Advancing our knowledge in biochemistry, genetics, and microbiology through studies on tryptophan metabolism. *Annu. Rev. Biochem.* **70**, 1–37.

Biography

Paul Gollnick is a Professor in the Department of Biological Sciences at the University of Buffalo, the State University of New York. His principal research interests are in RNA–protein interactions and regulation of gene expression. He holds a Ph.D. from Iowa State University and received postdoctoral training at Stanford University. He and his collaborator Dr. Alfred Antson at York University in England have determined the structure of TRAP and the TRAP:RNA complex.

Tubulin and its Isoforms

Eva Nogales
Howard Hughes Medical Institute, University of California, Berkeley, California, USA

Tubulin is an $\alpha\beta$ dimeric protein that self-assembles into microtubules and is present in all eukaryotes. Tubulin is highly conserved across species, reflecting the sequence constraints imposed by microtubule structure and function. Both α- and β-subunits exist in numerous isotypic forms and undergo a variety of posttranslational modifications. Tubulin assembly and disassembly, which are linked to GTP hydrolysis, make the microtubule network dynamic both in time and space to accommodate the needs of the cell during the cell cycle. Purified tubulin retains its self-assembling capabilities, allowing the biochemical and biophysical characterization of the microtubule polymerization and depolymerization processes. A variety of proteins interact with tubulin in the cell, affecting the stability of microtubules and their function. Numerous ligands bind to tubulin and influence its assembly properties, among them several drugs that have proven to have anticancer properties.

γ-tubulin is a rarer tubulin isoform involved in the nucleation of microtubules at microtubule organizing centers. Recently, additional tubulin isoforms of yet ill-defined function have been identified.

$\alpha\beta$-Tubulin

Physical Properties

General

Tubulin α- and β-subunits have molecular weights of $\sim$50 kDa and are 36–42% identical and 63% homologous. Both tubulin subunits bind guanine nucleotides. The binding to α-tubulin at the N-site is nonexchangeable, while the binding to β-tubulin at the E-site is exchangeable. Magnesium increases the affinity of the β-subunit for GTP with respect to GDP. Nucleotide in oligomeric tubulin or in microtubules does not exchange with the solution, except for terminal subunits at microtubule ends.

Neuronal cells are particularly rich sources of tubulin because microtubules are required for axonal transport. Neural tissue contains sufficient tubulin to allow tubulin purification by repeated cycles of 37°-induced assembly and 0°-induced disassembly, with intervening centrifugation to alternately pellet microtubules or impurities. The yield of tubulin from 1 kg of brain and yeast is $\sim$150 and $\sim$5 mg, respectively. The assembly of purified tubulin can be assayed by light scattering, X-ray scattering, centrifugation, and electron microscopy.

Isotypes and Posttranslational Modifications

Tubulin exists in different isotypic forms, the biological significance of which is still a matter of debate. The number of tubulin isotypes increases with the organism complexity. While yeast has only two α- and one β-isotypes, higher eukaryotes have up to seven β- and six α-tubulin isotypes. Certain isotypes have been found to be tissue specific, and differential expression of β-tubulin isotypes has been observed during the cell cycle. Some of these isotypes have been shown *in vitro* to have different relative stabilities, and such differences seem important for the response of the cell to antitubulin, anticancer drugs. The majority of differences between isotypes localize within the last 15 residues of the sequences, a region that has been identified as important in the interaction of microtubules with microtubule associated proteins (MAPs), pointing to a possible relevance for the functionality of microtubules in the cell.

Both tubulin subunits can be extensively altered by posttranslational modification, including detyrosination/tyrosination, acetylation/deacetylation, phosphorylation, polyglutamylation, and polyglycylation. All of these modifications, except for the acetylation of α-tubulin at Lys 40, occur at the divergent, highly charged C-terminal end of α- and β-tubulin. As for the different tubulin isotypes, the functionality of the posttranslational modifications is still a matter of debate. Certain modifications were initially identified as causing microtubule stability, and had been later described as the effect, not the cause of microtubule stability.

Structure

The structure of tubulin was solved by electron crystallography of zinc-induced two-dimensional tubulin sheets stabilized with the anticancer drug taxol. The α- and β-tubulin have basically the same secondary structure, each being made of a core of two β-sheets

surrounded by helices as shown in Figure 1. The N-terminal domain forms a Rossmann fold with the nucleotide-binding site at the C-terminal end of six parallel strands that are surrounded by five helices. An intermediate domain containing the binding site of taxol and colchicine is formed by a mixed β-sheet of four strands and five surrounding helices. The C-terminal domain contains two long helices that overlap the previous two domains and constitute the outside crest of the protofilaments in the microtubule to which motor molecules bind. The nucleotide sits at the interface between subunits along the protofilament. The N-site in α-tubulin is buried within the dimer, while the E-site in β-tubulin is partially exposed in the dimer but occluded in microtubules. FtsZ, a ubiquitous protein in eubacteria and archebacteria essential for cytokinesis, is the only known structural homologue of tubulin.

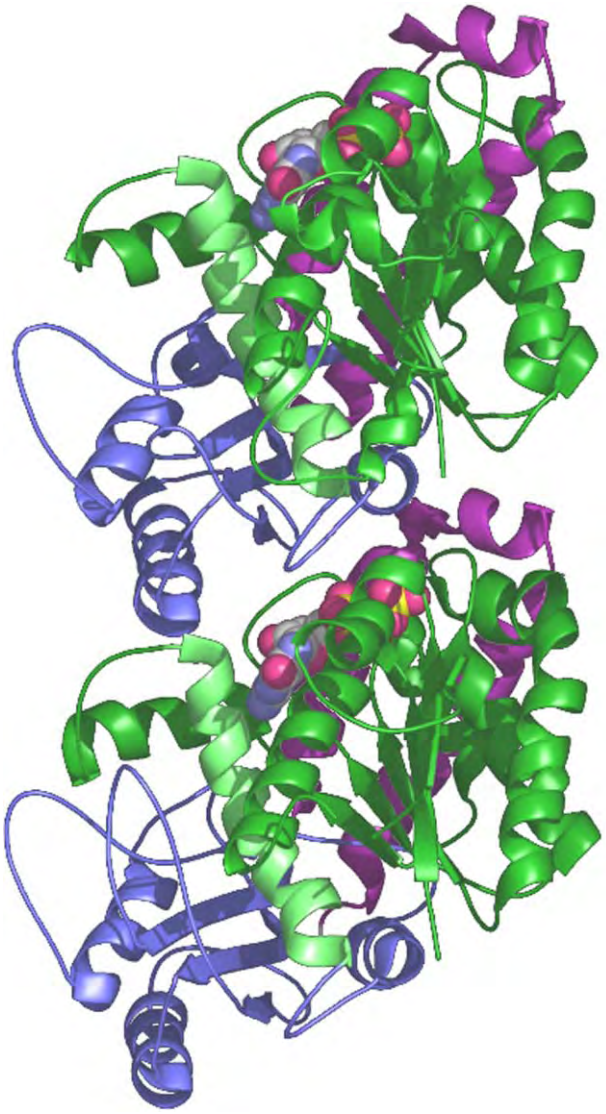

FIGURE 1 Ribbon diagram for the structure of $\alpha\beta$-tubulin corresponding to a view from the inside of the microtubule with the plus end at the top. β-Tubulin (top) is bound to GDP while α-tubulin (bottom) is bound to GTP. The color scheme highlights the three domains in the structure of each monomer: green for N-terminal, nucleotide-binding domain (helix H7 or core helix is shown in lime); second or intermediate domain in blue, C-terminal domain in purple.

Synthesis and Folding

Tubulin synthesis in cells is regulated by a process in which an increased subunit concentration leads to specific degradation of β-tubulin mRNA. In animal cells there is a mechanism to assure equivalent synthesis of α- and β-subunits. For its correct folding tubulin requires the citosolic chaperonin CCT (also referred to as TriC, TCP1, or Ct-cpn60), a hetero-oligomer formed by eight different subunits assembled into a hexadecamer of two double rings. Folding by CCT requires cycles of binding and full release, each cycle consuming one ATP by the chaperonin. In addition tubulin requires additional chaperonin cofactors that bind sequentially to α- and β-monomers and are necessary for the formation of the tubulin heterodimer. Folding cofactors are important also in regulating α/β tubulin ratios.

Tubulin Polymerization

Microtubule Assembly and Structure

The tubulin sequence and structure contains the information required for its self-assembly into polar, dynamic microtubules, which in turn interact with a variety of cellular factors. Tubulin dimers bind head to tail making linear protofilaments, which associate in a parallel fashion giving rise to a polar microtubule. In a cell the so-called minus-end of microtubule, capped by α-subunits, is attached to the centrosome where γ-tubulin and related proteins nucleate microtubules. The more dynamic plus-end, capped by β-subunits, binds the kinetochore in mitosis.

The orientation of the tubulin subunits in the microtubule is such that the C-terminal helices form the crest of the protofilaments on the outside surface, making them an essential part of the binding site for motor proteins (kinesins and dyneins) and MAPs. The taxol-binding site is on the inside surface of the microtubule, and close to lateral interactions. The lateral contact between protofilaments is dominated by the interaction of the so-called M-loop in the second domain with loop H1–S2 and helix H3 in the N-terminal, nucleotide-binding domain.

The plus end of the microtubule is crowned by β-tubulin subunits exposing their nucleotide end to the solution, while the minus end is crowned by α-subunits exposing their catalytic end. When a dimer is added to a plus end, its catalytic end contacts the E-site nucleotide of the previous subunit forming the interface that should bring about hydrolysis.

Dynamic Instability and GTP Cap Model

Microtubules are highly dynamic and can switch stochastically between growing and shrinking phases, both *in vivo* and *in vitro*. This nonequilibrium behavior, known as dynamic instability, is based on the binding and hydrolysis of GTP by tubulin subunits. Only dimers with GTP in their E-site can polymerize, but following polymerization this nucleotide is hydrolyzed by interactions with the previous tubulin dimer and then becomes nonexchangeable. In the GTP cap model the unstable body of the microtubule made of GDP–tubulin is stabilized by a layer of tubulin subunits at the ends that still retain their GTP. When this cap is stochastically lost, the microtubule rapidly depolymerizes. Depolymerization may occur by weakening of lateral contacts at the ends, and the consequent release of the constrained GDP subunits into a curved, lower energy, conformational state.

Microtubule assembly and stability are further modified in the cell by interaction with cellular factors that stabilize or destabilize microtubules at different points in the cell or at different stages in the cell cycle. Measurement of microtubule dynamics *in vitro* and *in vivo* by DIC or fluorescence microscopy yields the rate constants for addition of tubulin–GTP and loss of tubulin-GDP subunits at the two microtubule ends, as well as the rates of catastrophe (switch from growth to shrinkage) and rescue (switch from shrinkage to growth). A variety of drugs bind to tubulin and affect its polymerization. Microtubule-depolymerizing drugs, such as colchicine, nocodazole, vinca alkaloids, or podophyllotoxin, have a much higher affinity for the dimer than for tubulin in microtubules, so that disassembly is caused by their mass action effect. At substoichiometric concentrations tubulin-drug subunits bind to the microtubule ends and form caps that dramatically modify microtubule dynamics. Microtubule-stabilizing drugs such as taxoids, epothilones, or discodermolide act by binding preferentially to the polymerized form of tubulin.

An alternative microtubule behavior is treadmilling, a net flow of subunits from the plus to the minus end without a significant change in microtubule length.

Anti-Mitotic Tubulin Ligands

Recent years have seen the discovery of numerous tubulin ligands with anti-mitotic properties and anticancer potential. Concerning their binding site these agents can be classified into three main groups: those that bind tubulin at the colchicine binding site; those who bind it at the vinblastine site; and those who bind it at the taxol site. Functionally these antimitotic ligands can be separated into two classes: those that inhibit microtubule assembly (e.g., the colchicine and vinblastine families), and those that promote microtubule assembly and stabilization (e.g., the taxol family). In spite of these differences, the main action of all these agents seems to be to cause mitotic arrest by inhibiting normal dynamic instability at very low concentrations.

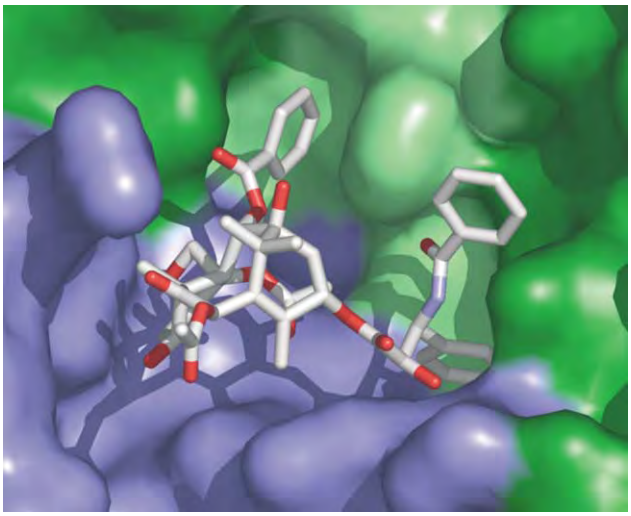

FIGURE 2 Anticancer drug taxol at its tubulin-binding site. Tubulin is shown on a surface representation with the same color scheme as in Figure 1. Both the N-terminal and second domain are part of the taxol-binding pocket.

The colchicine-binding site is located at the monomer–monomer interface within the dimer, in agreement with a model of colchicine action in which binding a distortion of the dimer structure that inhibits its polymerization. Vinblastine-like compounds are thought to bind at longitudinal polymerization contacts, resulting in a distorted protofilament structure. Finally, there is direct information on the binding site of taxol from the crystal structure of tubulin. Taxol binds to β-tubulin, near the M-loop and the site of lateral interactions, in a hydrophobic pocket that in α-tubulin is occupied by eight extra residues (see Figure 2). New microtubule-stabilizing agents with promise for cancer treatment, such as epothilones, discodermolide, eleutherobin, and the sarcodictins, while very different in structure, all seem to compete with taxol for the binding to a common site. It has been proposed that taxol stabilizes lateral contacts, or alternatively, that it acts as a bridge that holds the N-terminal and second domains in a relative orientation that favors longitudinal contacts between subunits.

γ-Tubulin and Microtubule Nucleation

Crucial to their dynamic behavior and function is the nucleation of microtubules in the cell at microtubule

organizing centers (MTOCs), to which they are attached by their minus ends. An essential role in microtubule nucleation is played by γ-tubulin, a protein with high homology to α/β-tubulins that localizes at MTOCs. γ-Tubulin forms ring structures that serve as templates for microtubule growth. The direct involvement of γ-tubulin in microtubule nucleation has been demonstrated *in vitro* using purified γ-tubulin-containing ring complex (γTuRC) containing at least seven different proteins. There are two main models in the literature. A model based on the shape and size of the γ-TuRC is that the ring forms the first helical turn of the growing microtubule, serving as a template for longitudinal interaction with the tubulin $\alpha\beta$ dimers. An alternative model, based on the similarity of rings structures formed by $\alpha\beta$-tubulin, γ-tubulin, and FtsZ, is that γ-tubulin forms a protofilament-like structure by longitudinal self-association that then serves as a template for lateral interaction with $\alpha\beta$-tubulin protofilaments.

Rarer Tubulin Isoforms: δ-, ε-, ζ-, and η-Tubulins

Four new tubulin isoforms have recently been discovered. The δ-tubulin was identified in *Chlamydomonas* mutants having abnormal basal bodies (these are microtubule structures at the base of cilia and flagella structurally similar to the centrioles in the centrosome at MTOCs). Human δ-tubulin was subsequently found in the human genome database, and shown to localize to the centrosome, where it partially colocalizes with γ-tubulin.

The ε-tubulin was identified from the human genome database on the basis of sequence similarity to other tubulins. Like δ-tubulin, ε-tubulin localizes to the centrosome, but in a cell-cycle-dependent manner: in cells with duplicated centrosomes ε-tubulin localizes only with the old centrosome.

Even rarer, ζ-tubulin has so far only been found on kinetoplastid protozoa where it localizes to the basal body, while η-tubulin has been found in paramecium where it may interact with γTuRC.

Tubulins and the Cell

The involvement of the microtubule cytoskeleton in a large number of essential and diverse functions requires both reliability and flexibility from the system at the expense of biochemical and structural complexity. Dynamic instability is an inherent property of microtubules, built into the $\alpha\beta$-tubulin structure. The spatial and temporal organization of the microtubule network in the cell is obtained through the regulation of dynamic instability by an increasing number of factors that fine-tune the behavior of the microtubule system to accommodate the requirements of the cell. Regulation may happen at many different stages, via transcription of different tubulin isotypes, the control of tubulin monomer folding, the formation of functional dimers, the posttranslational modification of tubulin subunits, the nucleation of microtubules, or the interaction of microtubules with numerous stabilizers and destabilizers. Tubulin-binding drugs can dramatically disrupt the finely tuned behavior of microtubules. Finally, while γ-tubulin is known to be essential for microtubule nucleation, additional tubulin isoforms, only recently discovered, have yet ill-defined functions.

See Also the Following Articles

Centrosomes and Microtubule Nucleation • Chaperonins • Kinesins as Microtubule Disassembly Enzymes • Microtubule-Associated Proteins

Glossary

$\alpha\beta$ tubulin dimer Essential, highly conserved protein dimer present in all eukaryotes that self-assembles forming microtubules. It is the target of antimitotic drugs with anticancer potential.

dynamic instability Nonequilibrium behavior of microtubules by which they can stochastically switch between phases of growth and shrinkage. It originates from the hydrolysis of GTP in β-tubulin and can be regulated by the interaction of tubulin/microtubules with cellular factors and antimitotic agents.

microtubules Cytoskeletal polymers made of $\alpha\beta$-tubulin essential for cell transport and cell division. They are polar, dynamic, and regulated through the cell cycle by their interaction with stabilizers and depolymerizers.

γ-tubulin Tubulin isoform most abundant at microtubule organizing centers where it is involved in microtubule nucleation. It forms higher-order complexes with associated proteins.

Further Reading

Desai, A., and Mitchison, T. J. (1997). Microtubule polymerization dynamics. *Ann. Rev. Dev. Biol.* **13**, 83–117.

Downing, K. H. (2000). Structural basis for the interaction of tubulin with proteins and drugs that affect microtubule dynamics. *Ann. Rev. Cell Dev. Biol.* **16**, 89–111.

Lewis, S. A., Tian, G. and Cowan, N. J. (1997). The α- and β-tubulin folding pathways. *Trend. Cell Biol.* **7**, 479–484.

Lowe, J., Li, H., Downing, K. H., and Nogales, E. (2001). Refined structure of alpha beta-tubulin at 3.5 A resolution. *J. Mol. Biol.* **313**, 1045–1057.

Mitchison, T., and Krischner, M. (1984). Dynamic instability of microtubule growth. *Nature* **312**, 237–242.

Nogales, E. (2000). Structural insights into microtubule function. *Ann. Rev. Biochem.* **69**, 277–302.

Nogales, E., Wolf, S. G., and Downing, K. H. (1998). Structure of the $\alpha\beta$ tubulin dimer by electron crystallography. *Nature* **391**, 199–203.

Nogales, E., Whittaker, M., Milligan, R. A., and Downing, K. H. (1999). High resolution structure of the microtuble. *Cell* **96**, 79–88.

Biography

Eva Nogales is an Assistant Professor in the Department of Molecular and Cell Biology at UC Berkeley, an Assistant Investigator at the Howard Hughes Medical Institute, and a Staff Scientist at Lawrence Berkeley National Laboratory. She was trained as a physicist in Spain, her country of origin, and obtained a Ph.D. in biophysics from Keele University for her work at the Synchrotron Radiation Source at Daresbury, UK. During her postdoctoral studies with Dr. Kenneth H. Downing at Lawrence Berkeley National Laboratory she obtained the structure of $\alpha\beta$-tubulin using electron crystallography. Her present research centers around the structural bases of microtubule dynamics and the structural characterization of protein complexes involved in eukaryotic transcription.

Tumor Necrosis Factor Receptors

Karen G. Potter and Carl F. Ware
La Jolla Institute for Allergy and Immunology, San Diego, California, USA

Tumor necrosis factor receptors (TNFRs) are a family of structurally similar cytokine receptors that act as transducers of cell death and induce the expression of genes involved in cellular differentiation and survival. Binding of specific ligands to their cognate TNFR initiates the recruitment of adaptor proteins, either death domain (DD)-containing or TNFR-associated factor (TRAF) family of adaptor proteins, to the cytosolic signaling domain of the receptor to initiate diverse effector functions. The most well-known function of the TNF superfamily is in immune regulation and development with specific roles in host defense, inflammation, cellular homeostasis, and lymphoid organogenesis. A critical role for TNFR in immunobiology is evidenced by the linkage of naturally occurring mutations in TNF family genes to human disease, as well as by the targeting of TNF family members by viruses as a mechanism of immune evasion. However, some TNF family members also act outside the immune system by regulating the development of hair follicles, sensory neurons, or bone-resorbing osteoclasts.

Features of Tumor Necrosis Factor Receptors

Structure

Tumor necrosis factor receptors (TNFRs) are identified by a highly conserved, cysteine-rich domain (CRD) in the extracellular portion of the protein that binds ligand (Figure 1). The CRD generally contains six cysteines that form three disulfide bonds typically recognized by the signature sequence motif CxxCxxC. Currently, there are 29 members of the cellular TNFR family in mammals, and several variants of TNFRs are found in herpesviruses and poxviruses. The cellular receptors are primarily type I transmembrane proteins (extracellular N terminus). Some receptors in this family lack transmembrane and cytoplasmic domains and are secreted, functioning as decoy receptors for the ligand. The TNFR family can be divided into two general groups – those that contain a death domain (DD) and those with a peptide motif that binds TNFR-associated factors (TRAF) adaptors – based on the structure of their cytoplasmic tails and the signaling adaptors they recruit to propagate signals to the cells.

Given the predominant role of the TNFR family in regulating immunity, this suggests that the evolution of the receptors in this family arose coincident with the evolution of adaptive immunity, also found exclusively in vertebrates. The size of the TNFR superfamily appears to have grown in a large part by gene duplication as many of the TNFR genes are linked to discrete loci reflecting their evolutionary derivation. Perhaps most obvious are those TNFRs found on chromosome (Ch) 12p13 (TNFR1, LTβR, and CD27), which likely underwent duplication and translocation events giving rise to the larger locus of TNFR on Ch 1p36 (TNFR2, HVEM, Ox40, CD30, AITR, 4-1BB, and DR3) (Figure 2A). Strikingly, NGFR is the only receptor that binds ligands structurally unrelated to TNF, representing a clear functional demarcation from the typical TNFR (Figure 2B). Another subtle branch in the TNFR family tree are those receptors that engage BAFF, the B cell survival factor, and related ligands APRIL and TWEAK (Figure 2C). These receptors have a single CRD and in the case of BAFFR only two disulfide bonds. Functional divergence is evident in the role some TNFRs play in bone (Osteoprotegerin-RANK-RANKL/TRANCE) and ectodermal (Ectodermal dysplasin EDA-EDAR), and angiogenesis (TWEAK-Fn14).

Expression

Expression patterns of the receptors are complex. Several members of the TNFR superfamily are expressed on cells of the immune system; for example, BAFFR expression is exclusive to B lymphocytes. Other receptors are found in hair follicles (e.g., EDAR and TROY) or the nervous system (e.g., NGFR), yet others have very broad tissue expression patterns, such as TNFR1. The expression of some TNFR is inducible and regulated and others are constitutive. For example, TNFR2 is absent on naïve T cells but is rapidly upregulated upon activation of T cells. In contrast, HVEM is highly expressed on naïve T cells, but shows diminished expression upon T-cell activation. Regulation of receptor expression can also be achieved through the

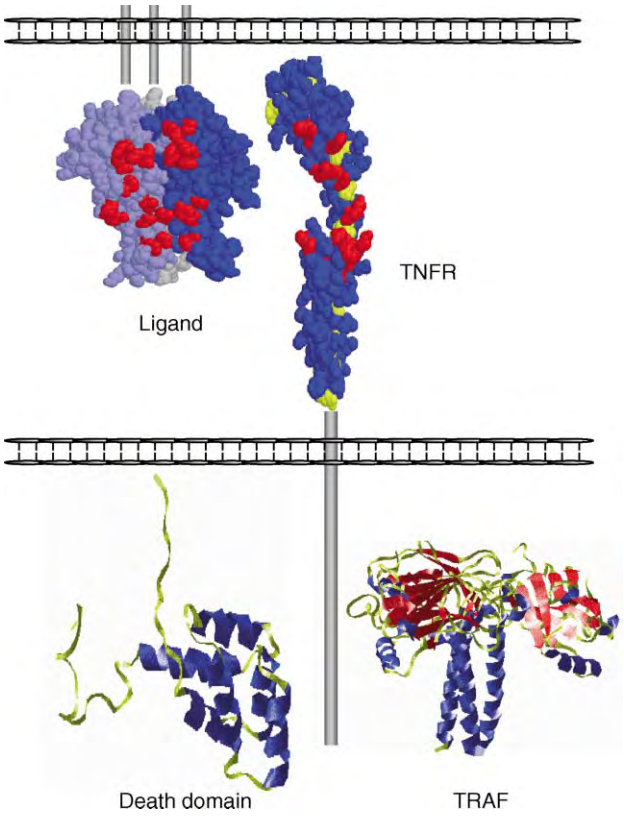

FIGURE 1 Structural features of TNFR family. Space filling model of a trimeric TNFR1 ligand, LTα, as it would exist as a membrane anchored ligand, and a single TNFR1 rotated 180° to reveal contact residues. Also shown are crystal structures of the cytoplasmic DD found in some TNFR and the TRAF that interacts with TNFR-containing TRAF binding sites.

generation of soluble receptors; soluble TNFRs can be generated by proteolytic processing (CD27, CD30, CD40, TNFR1, and TNFR2), alternative splicing of membrane forms (Fas, 4-1BB), or encoded in the genome without a transmembrane region (OPG, DcR3, TRAIL-R3).

Ligand Binding

TNF ligands are characterized as type II (intracellular N terminus) transmembrane proteins containing a "TNF homology domain" (THD) in their C terminus (Figure 1). The THDs of each ligand associate to form trimeric proteins; in most cases, the ligands form homotrimers, but LTα and LTβ form heterotrimers, and so do BAFF and APRIL, as has been shown recently. The TNF ligands are active in their membrane forms where cell-to-cell contact is required to initiate signaling; however, some ligands can be proteolytically cleaved from the surface creating soluble cytokines that affect cells distally.

The TNF ligand family currently includes 20 proteins that are able to pair off with one or more receptors. In fact, some ligands display overlapping receptor recognition; for example, LIGHT and LTα1β2 bind LTβR, and LTα and LIGHT bind HVEM. The ligand-receptor pairing seems promiscuous, although comparative studies using mice deficient in a specific TNF ligand or receptor suggest that each cytokine-receptor system has a unique role in immune physiology.

TNFR Signaling

Each TNF-related ligand has three receptor binding sites that can cluster together two or three cell surface receptors, juxtapositioning the cytoplasmic tails of the receptors to initiate signal transduction. Recruitment of specialized signaling molecules (adaptors) to the cytoplasmic domain occurs following receptor clustering. Propagation of TNFR signals occurs through two distinct classes of cytoplasmic adaptor proteins: TRAFs or DD molecules.

TRAF Signaling

TRAF adaptor proteins are a small family of RING finger proteins that play a critical role in propagating signal transduction leading to the activation of latent transcription factors (Figure 1). There are six numerically named TRAF proteins (TRAF1–6) that function predominantly in TNFR-induced signaling, although TRAF6 is also a key player in signal transduction initiated by the interleukin-1 receptor and the Toll-like receptor (TLR) superfamily. Several TRAFs can bind directly to the cytoplasmic tails of most of the TNFR. The binding site found in CD40 or the LTβR is a short peptide sequence, PXQXT/S or IPEEGD, respectively. The binding site in TRAF for receptor binding is flexible, thus accommodating a variety of motifs. TNFRs with a DD bind TRAFs indirectly via other adaptor proteins, such as TRADD (TNFR-associated DD). Each TRAF interacts with several different receptors such that TNFRs display distinct interaction patterns with multiple TRAFs. Since each TRAF is believed to have distinct biological effects, the variation in TRAF binding by the TNFR may be able to direct the signaling pathway to distinct biological outcomes.

Functionally, binding of TRAFs to TNFR culminates in the activation of transcription factors that act to regulate gene expression. For example, nuclear factor κB (NFκB) is a small family of latent transcription factors that induces the expression of a large variety of genes involved in inflammatory and immune responses (Figure 3). Two distinct forms of NFκB are recognized: NFκB1 (RelA, p65) and NFκB2 (p100/p52), and each pair with itself or other proteins (e.g., p50, RelB, and cRel) that form active transcription factors that bind

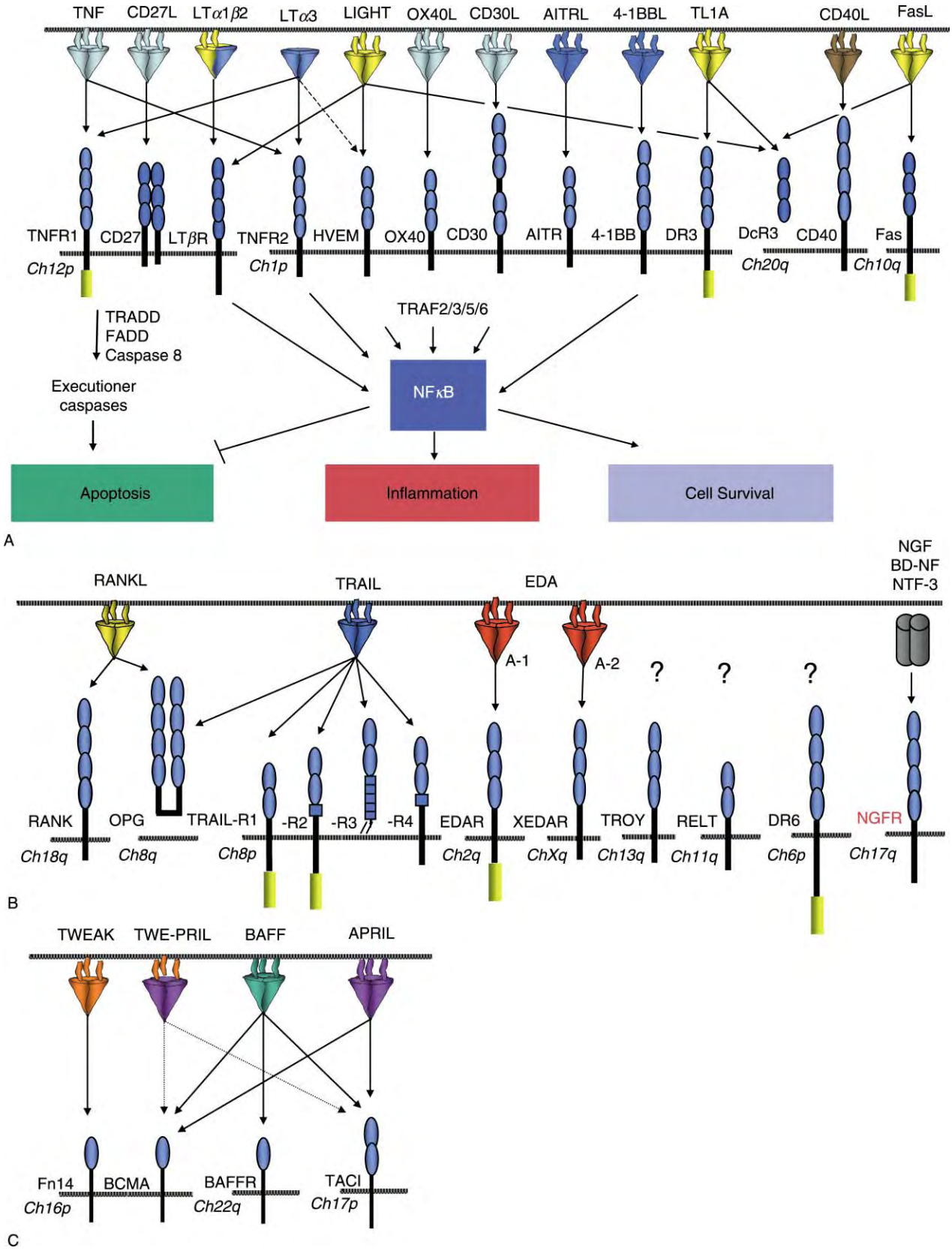

FIGURE 2 The TNF–TNFR superfamily grouped on the basis of chromosome (Ch) localization of TNFR. (A) TNFR and TNF ligands are shown with arrows connecting ligand–receptor pairs. CRDs are shown as small ovals. DD is denoted as a rectangular box in the cytoplasmic tail of appropriate receptors. The signaling and effector functions induced by either DD-containing or TRAF-binding TNFR is shown. (B and C) Same as (A), with remaining TNFR grouped on the basis of chromosome localization and ligand binding.

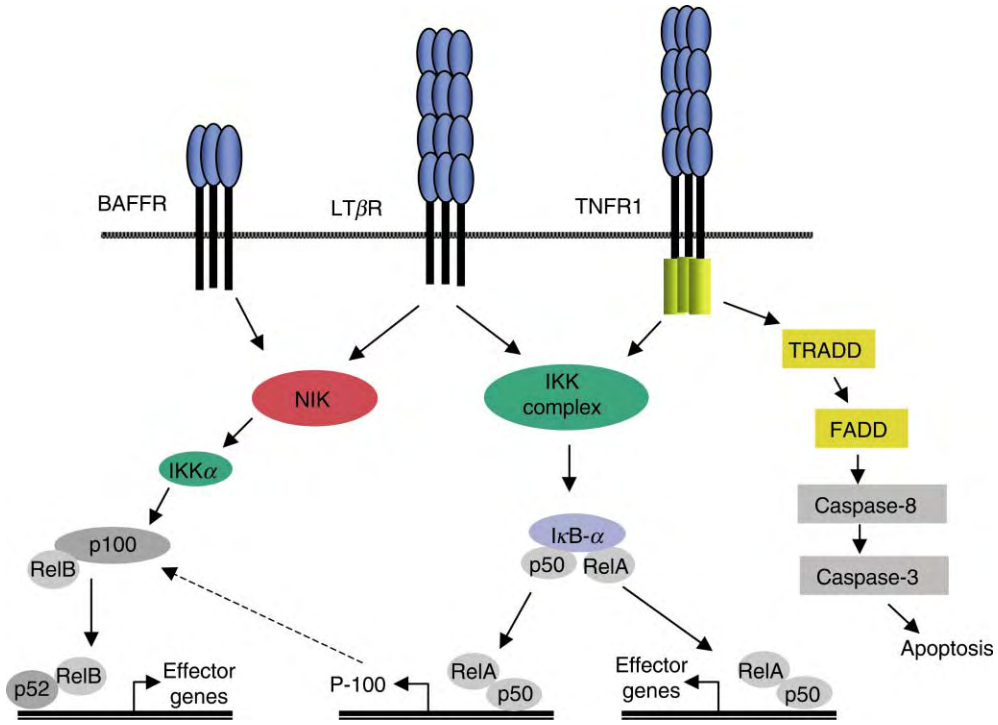

FIGURE 3 Mechanisms of signaling by TNFR. Upon ligation of LTβR, two NFκb pathways are induced. The first leads to induction of the NFκB1 pathway and the activation of IKKβ and RelA, which control expression of inflammatory genes. The second pathway results in the activation of NFκB2 and the processing of p100 to p52 following the activation of NIK and IKKα, leading to the transcription of genes implicated in secondary lymphoid organogenesis and homeostasis. BAFFR also activates the NFκB2 pathway, whereas TNFR1 only activates the NFκB1 pathway. TNFR1 also contains a DD to signal caspase activation and apoptosis.

DNA. NFκB1 is held in the cytosol by an inhibitor protein (IκB) while an inhibitory domain controls the cytosolic localization of NFκB2. The inhibitory proteins are phosphorylated and degraded in response to activation signals coming from diverse sources that all target the inhibitor κB protein kinase complex (IKK). Degradation of the inhibitor allows NFκB to localize to the nucleus and activate transcription. The NFκB1 and B2 pathways induce distinct sets of genes: NFκB1 regulates the expression of proinflammatory chemokines and adhesion molecules, while the NFκB2 pathway controls the expression of distinct chemokines and cytokines involved in lymphoid organogenesis. BAFFR is only able to activate the NFκB2 pathway, suggesting that this pathway is crucial for the expression of survival genes specifically important for B lymphocytes. By contrast, TNFR1 is unable to activate NFκB2, which may account for its strong proinflammatory action.

TRAF2 propagates signals to mitogen-activated protein (MAP) kinases, including JNKs/SAPKs, ERKs, and p38s, to activate the transcription factor AP-1 that plays roles in stress responses and cellular homeostasis. Like TRAF2, TRAF5 cooperates to activate NFκB and AP-1 transcription factors, while TRAF3 negatively regulates NFκB activation and thus may play a role in promoting cell death. TRAF6 also activates NFκB and AP1.

Death Receptor Signaling

A number of TNFR, including TNFR1 and Fas, are also termed "death" receptors because they regulate apoptotic cell death. Their cytoplasmic tails contain a region of ~80 amino acids that fold into six α-helices, termed the DD. The DD serves as a protein interaction motif to recruit signaling molecules to the inert cytoplasmic domain of TNFRs. As such, the DD of TNFR can self-associate or associate with other DD-containing adaptor proteins such as FADD, TRADD, and RIP.

In the simplest scheme known to activate the cell death machinery, the adaptor FADD is recruited to Fas initiating formation of the death-inducing signaling complex (DISC). Procaspase 8 is recruited to the DISC through a second interaction motif contained in FADD, termed the death effector domain (DED), activating downstream effector caspases (e.g., caspase 3) resulting in the cleavage of critical cellular substrates and the eventual collapse of the cells and death (apoptosis). Similarly, TNFR1 activates apoptosis although it requires the adaptor protein TRADD to facilitate

FADD recruitment, and is also able to recruit another adaptor protein RIP that also plays a role in procaspase 8 activation. The DISC is regulated by two forms of another protein known as FLIP, which can switch the DISC between activating caspases or NFκB, which in turn regulates genes that block apoptosis, such as the inhibitors of apoptosis (IAP) that promote cell survival.

Effector Functions of the TNFR Family

Despite similarities in structure and signaling mechanisms, TNFRs function in diverse, and often opposing, roles in immune physiology. As discussed above, several reasons that explain their functional diversity include differences in ligand binding, tissue and cellular expression, regulation of expression, and association with signaling adaptor proteins.

Inflammation

A role for TNF family members in host defense and inflammation was first appreciated when it was realized that TNF is identical to a factor termed cachectin, a protein known to cause fever and wasting. Inflammatory cells, such as macrophages, induce TNF when specialized innate immune receptors called TLRs recognize nonself patterns on microbial pathogens. Binding of TNF to its receptors, TNFR1 or TNFR2, induces a variety of molecules that are crucial for initiating the acute inflammatory response. For example, TNF signaling induces increased expression of adhesion molecules on endothelial cells and secretion of chemokines to promote inflammatory cell migration to the site of infection. TNF can also activate macrophages and neutrophils to increase their phagocytic capacity and their ability to secrete tissue-degrading enzymes into infected tissues. Although inflammation is crucial to prevent infection, it must also be minimized after the pathogenic challenge subsides in order to prevent uncontrolled damage to fragile host tissues. As such, uncontrolled TNF signaling can cause chronic inflammation and wasting, or acutely released, septic shock. Drugs that block TNF signaling, such as soluble TNFR decoy receptors, have been developed to prevent inflammatory diseases such as rheumatoid arthritis and inflammatory bowel disease.

Apoptosis

Cell death by apoptosis is one of the major functions of DD-containing TNFR. Fas, for example, mediates cell death for varied purposes. First, Fas, and its ligand FasL, cooperate as major effectors, along with the perforin/granzyme pathway, to trigger killing of pathogen-infected cells by cytotoxic T-lymphoctyes (CTLs) or by natural killer (NK) cells. In a second context, Fas is required to eliminate excessive CTLs and other effector cells. Fas is induced on long-term antigen-activated lymphocytes to elicit their removal and minimize the excessive expansion of T lymphocytes that can occur in response to T-cell activation in the space-restricted lymphoid environment. In fact, two naturally occurring mutations in mice encoding the gene *lymphoproliferative disorder (lpr)*, *lpr*, or *lpr^{cg}* that affect the expression or the biological activity of the Fas receptor, respectively, demonstrate the important role of Fas in lymphocyte homeostasis. Both of these mutant mice develop an autoimmune phenotype characterized by massive lymphadenopathy, splenomegaly, and autoantibody production.

Cell Survival

BAFFR, BCMA, and TACI are some of the most recently discovered members of the TNFR family that are predominantly expressed on B cells and represent a good example of TNFRs that play a role in cell survival. All three receptors bind the TNF-related ligand BAFF, produced by macrophages and dendritic cells, while BCMA and TACI can also bind the related ligand APRIL. BAFF is required in the maintenance and differentiation of mature B cells in peripheral tissues by supporting B-cell survival and maturation presumably through activation of anti-apoptotic genes. The mechanism for enhanced B-cell survival by BAFF may be partly due to the stimulation of the pro-survival protein bcl-2 and a decrease in the expression of the pro-apoptotic factors Bak and Blk. A crucial role for BAFFR in BAFF-mediated B-cell survival is evidenced by the fact that neither BCMA- nor TACI-deficient mice have defects in B-cell maturation, whereas A/WySnJ mice, containing a naturally occurring mutation in BAFFR, do show defects in B-cell maturation. Overexpression of BAFF in mice can result in autoimmune symptoms, and similarly patients with systemic lupus erythematosus (SLE), rheumatoid arthritis, and Sjogren's syndrome show elevated levels of BAFF in the blood. Other TNFRs also play roles in the survival and development of various tissues including the TRANCE system in bone, EDAR in ectodermal tissues, and NGFR in neurons.

Costimulation

T lymphocyte activation is also regulated by TNFRs where they act as costimulatory signals to positively or negatively influence the proliferation of antigen-stimulated T cells. OX40, CD27, 4-1BB, and HVEM, expressed on CD4$^+$ and CD8$^+$ T cells, promote T-cell

proliferation and cytokine production in response to their respective ligands expressed on dendritic cells. For example, mice deficient in the OX40–OX40L interaction show impaired T-cell proliferative capabilities and cytokine production in response to viruses such as lymphocytic choriomengiitis virus (LCMV) or influenza virus, and the ability to generate or sustain memory T cells is diminished. Additionally, some evidence indicates that several receptors such as CD30, Fas, or HVEM may play a role in positive and negative selection in thymocyte differentiation. Thus, TNFR family members can contribute to immune tolerance.

On B cells, CD40 is the most prominent costimulatory receptor where it interacts with its ligand, CD40L, on T cells to initiate T-cell-dependent B-cell antibody responses. Mutations in CD40 or its ligand affect a number of immune functions including immunoglobulin class switching; in humans, X-linked hyper-IgM syndrome is due to defects in CD40L structure and function manifesting as an inability to switch immunoglobulin M to IgG classes.

Organogenesis and Development

A number of TNFRs play roles in the organization of tissues. The lymphotoxin system mediated by LTβR, and its ligand LT$\alpha\beta$, play a critical role in lymph node development; mice deficient in either receptor or ligand completely lack lymph nodes and Peyer's patches. RANK and its ligand RANKL mediate osteoclast differentiation and therefore are important for maintaining normal bone homeostasis. Osteoporosis, a condition of bone thinning, can be caused by overexpression of the soluble RANKL decoy receptor, OPG, which is induced by estrogen and prevents normal bone formation. RANK-RANKL signaling also supports the development of mammary gland alveolar buds important for lactation, and consequently an absence of RANK induces accelerated apoptosis of mammary epithelial precursors. EDAR, XEDAR, and TROY, and the ligand EDA, regulate the development of ectodermal tissues including hair follicles. In fact, mice or humans with deficiencies in EDAR or EDA lack primary hair follicles and sweat glands. Finally, NGFR is important for the development of sensory neurons; acting alone it induces apoptosis, but upon association with other nerve growth factor receptors it mediates the differentiation and survival of neurons. NGFR-deficient mice develop cutaneous sensorineuronal defects.

Viral Targeting of TNFR

Since TNFRs and their ligands play a critical role in mediating immune defenses against invading pathogens, and control death and survival fates for cells, it is not surprising that viruses have evolved mechanisms that directly target the TNF family in order to subvert immune effector mechanisms. In fact, viruses when viewed collectively have targeted virtually every step of the TNFR signaling pathway, from ligand binding to activation of apoptosis. For example, infection by some viruses, including cytomegalovirus (CMV), herpes simplex virus (HSV), adenovirus, and HIV, induce the expression of FasL and/or TRAIL on the host cell resulting in the probable killing of recruited immune effector cells that express the cognate TNFR death receptor. In contrast, adenovirus down-regulates the proapoptotic receptors Fas and TRAILR from the surface of infected cells, thereby preventing the killing of the host cell harboring the virus. Another mechanism of immune evasion employed by poxviruses is the expression of soluble, secreted orthologs of TNFR2 or CD30 that inhibit the interaction of their respective ligands with their cellular receptors. In some cases, viruses and TNFR signaling have been adapted to function cooperatively. For instance, signaling through the LTβR or TNFR1 can prevent the replication of human CMV in fibroblasts without inducing death of the infected cell thereby allowing continued existence of CMV within the host. This molecular example of host–virus coexistence might provide a mechanism for CMV to persist latently in individuals with a strong host immune system, and reemerge to cause disease in individuals who are immunosuppressed.

See Also the Following Articles

Bax and Bcl2 Cell Death Enhancers and Inhibitors • Cell Death by Apoptosis and Necrosis • Chemokine Receptors • Mitogen-Activated Protein Kinase Family • Nuclear Factor kappaB • Toll-Like Receptors

Glossary

apoptosis An orderly process of programmed cell death whereby cellular machinery undergoes changes leading to death.

autoimmunity An immune response against self-antigens.

cytokine Proteins made by cells that affect the behavior of other cells.

signal transduction Term used to describe the processes inside cells used to respond to changes in their environment.

transcription factor A protein that binds DNA to control the transcription of genes involved in a large number of normal cellular and organismal processes.

Further Reading

Benedict, C. A., Banks, T. A., and Ware, C. F. (2003). Death and survival: Viral regulation of TNF signaling pathways. *Curr. Opin. Immunol.* **15**, 59–65.

Bodmer, J., Schneider, P., and Tschopp, J. (2002). The molecular architecture of the TNF superfamily. *Trends Biochem. Sci.* **27**, 19–26.

Chung, J. Y., Park, Y. C., Ye, H., and Wu, H. (2002). All TRAFs are not created equal: Common and distinct molecular mechanisms of TRAF-mediated signal transduction. *J. Cell Sci.* **115**, 679–688.

Dejardin, E., Droin, N. M., Dehase, M., Haas, E., Cao, Y., Makris, C., Li, Z. W., Karin, M., Ware, C. F., and Green, D. R. (2002). The lymphotoxin-β receptor induces different patterns of gene expression via two NFκB pathways. *Immunity* **17**, 1–11.

Locksley, R. M., Killeen, N., and Lenardo, M. J. (2001). The TNF and TNF receptor superfamilies: Integrating mammalian biology. *Cell* **104**, 487–501.

Orlinick, J. R., and Chao, M. V. (1998). TNF-related ligands and their receptors. *Cell. Signal.* **10**, 543–551.

Biography

Karen G. Potter is an NIH Postdoctoral Fellow in the lab of Dr. Carl F. Ware at the La Jolla Institute for Allergy and Immunology. She received her Ph.D. in Cell and Molecular Biology from Duke University in July 2002. Her research interests include the regulation and immunomodulatory functions of the TNFR HVEM.

Carl F. Ware is Head of Molecular Immunology at the La Jolla Institute for Allergy and Immunology, and a Professor of Biology at UCSD. His research program investigates the regulation of immunity by cytokines and viruses. He is an advisor for the National Institutes of Health and is an editor of scientific journals. Dr. Ware received his Ph.D. in Molecular Biology and Biochemistry from the University of California Irvine, and was an NIH Postdoctoral Fellow at the Harvard Medical School.

Two-Dimensional Gel Electrophoresis

Gerhard Schmid, Denis Hochstrasser and Jean-Charles Sanchez
Biomedical Proteomics Research Group, Geneva University Hospital, Geneva, Switzerland

Two-dimensional polyacrylamide gel electrophoresis (2D PAGE) is a high-resolution protein separation technique exploiting two independent physico-chemical properties (charge and size) of the protein components to be separated. During the first dimension, under the influence of an electrical field, charged proteins migrate in a pH gradient until each of them reaches a distinct pH value, which corresponds to its isoelectric point (*p*I). At its *p*I, a protein has zero net charge. This separation technique is called isoelectric focusing (IEF). In the second dimension, the protein mixture previously separated by IEF is sorted orthogonally by electrophoresis in the presence of sodium dodecyl sulfate (SDS). Migration of SDS-coated proteins in a sieving polyacrylamide gel results in a separation according to their relative molecular mass (M_r). Nowadays, 2D PAGE is a powerful and widely used tool for the analysis of complex soluble protein mixtures extracted from cells, tissues, or other biological samples.

Some Milestones in the Development of 2D PAGE

How it All Began

In 1975, three papers (Klose, O'Farrell, Scheele) introduced two-dimensional polyacrylamide gel electrophoresis (2D PAGE) using denaturing isoelectric focusing (IEF) and SDS-PAGE. At that time, IEF was carried out in cylindrical rod IEF gels cast in glass capillary tubes (1–1.5 mm inner diameter). The gels contained synthetic carrier ampholytes, which formed a continuous pH gradient under the influence of an electric current. After IEF the gel rods had to be removed from their tubes for second dimension separation by SDS-PAGE.

Technical Improvements

With the introduction of immobilized pH gradients (IPGs) by Bjellqvist *et al.* in 1982, problems associated with carrier ampholyte pH gradients such as gradient instability, low sample loading capacity, and difficulty to achieve reproducibility could be eliminated. In an IPG, a set of acidic and basic buffering groups is covalently incorporated into a polyacrylamide gel at the time it is cast. Precast IPG gel strips supported by a plastic film backing are commercially available in a variety of narrow and broad, linear and nonlinear pH ranges. This represents an important development and allowed 2D PAGE to become the tool of choice for high-resolution protein separation (Figure 1). Besides improvements in the 2D technique, critical developments in other fields greatly contributed to the more widespread use of 2D PAGE. In 1987, Matsudaira showed that classical N-terminal sequencing by Edman degradation can be applied to picomole quantities of proteins electro-transferred onto polyvinylidene difluoride (PVDF) membranes. In 1993, several groups independently showed that mass spectrometry allows the identification of proteins previously separated by 1D or 2D gel electrophoresis. Improvements on the level of the mass spectrometers as well as rapid access to genome sequence databases for various species from across the world nowadays allow the high-throughput identification of hundreds of proteins separated by 2D PAGE. More powerful, less expensive computers and appropriate software made computer-assisted evaluation of the highly complex 2D patterns possible.

2D Page in the Future

After more than 25 years, one can say that 2D PAGE finally became a routine protein separation method; however, its further development is a continuous process. A major interest, especially for the application of 2D PAGE in the clinical laboratory, lies in the field of miniaturized and automated 2D protein mapping. Recently, a fully automated 2D electrophoresis system (a2DE^{TM}) has been presented by NextGen Sciences. A microchip format that is based on 2D PAGE (digital ProteomeChip^{TM} from Protein Forest Inc.) allows protein separation, staining, and digital imaging in as little as 20 min, with a detection sensitivity below 1 pg of protein.

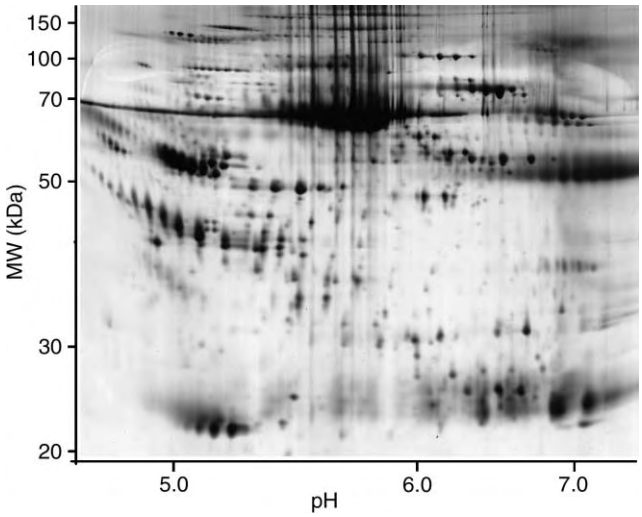

FIGURE 1 High-resolution protein separation of human plasma by 2D PAGE, silver staining.

The Current Protocol

The method described by O'Farrell back in 1975 already contained the magic bullets of 2D PAGE, i.e., urea, dithiothreitol (DTT), a nonionic or zwitterionic detergent for the first and SDS for the second dimension. The procedure of 2D PAGE using IPG gel strips in the first dimension is largely based on the work of Görg and co-workers.

Sample Solubilization

An ideal procedure results in the complete solubilization, disaggregation, denaturation, and reduction of all the proteins in the sample. However, dealing with several thousand different proteins with different physico-chemical properties makes complete solubilization practically impossible. In general, cells or tissues are disrupted by various techniques such as grinding in a liquid nitrogen cooled mortar, sonication, shearing-based methods, or homogenization. Proteins are then solubilized in a buffer containing 9 M urea, 4% 3-[(3-cholamidopropyl)dimethylammonio]-1-propanesulfonate (CHAPS), 50–100 mM DTT. Various minor modifications from this basic, IEF compatible solubilization buffer have been described over the years, trying to improve the solubilization of certain subclasses of proteins. DNA or RNA molecules, which can interfere with 2D PAGE, are removed by incubation with nucleases. Centrifugation is used to separate the solubilized proteins from nonsolubilized material. Prefractionation of complex samples is a good choice when only a subset of the proteins in a tissue or a cell is of interest or when abundant proteins dominate the sample as in the case of albumin in plasma.

First Dimension: IEF

IEF separates proteins according to their isoelectric point. Proteins diffusing away from their pI immediately gain charge and migrate back. This focusing effect allows proteins to be separated on the basis of very small charge differences. Simplified handling and improved performance made the commercially available precast IPG gel strips (from 7 to 24 cm in length) the method of choice for most applications. IPG strips with a pH range from 3 to 10 will display a wide range of proteins, whereas narrower pH ranges allow to zoom into a particular pH range. With a set of narrow range, overlapping pH gradients, a wide pH range can be covered at increased resolution. There are several ways to load the sample on the IPG gel strip. Efficient entry of the solubilized proteins, especially hydrophobic ones, into the gel is always a critical point. IPG dry strips need to be rehydrated before use in IEF. Traditionally, samples are applied on a discrete point via sample cups (Figure 2A). Cups are placed at either the acidic or basic pH extreme of the strip. Under these conditions, most of the proteins in the sample will be charged and immediately start migrating under the influence of an electric current, thereby minimizing sample loss through precipitation. Alternatively, the sample can be applied over the whole IPG gel surface during strip rehydration. This method is of special interest for more dilute samples since larger volumes can be loaded. For strip rehydration, a solution containing 8 M urea, 2% CHAPS, 10 mM DTT, 1% carrier ampholytes, traces of Bromophenol Blue (tracking dye) shows excellent results for most samples. As for the solubilization solution, various modifications were described. A general IEF protocol starts with the sample entry phase at low initial voltage (200 V). Voltage is then increased in a stepwise manner up to the desired final focusing voltage (up to 8000 V). Optimal focusing time depends on the nature of the sample. In general, overfocusing is not deleterious below a total of 100 kVh. State-of-the-art IEF systems allow simultaneous migration of up to 12 strips under temperature-controlled conditions.

Second Dimension: SDS-PAGE

Prior to the second dimension, the IPG gel strips are equilibrated in a solution containing SDS. This anionic detergent binds to the majority of proteins in a constant mass ratio (1.4 g SDS/g protein), such that the net charge per mass unit becomes approximately constant. This allows protein separation in a polyacrylamide gel according to their relative molecular mass. For an ideal transfer of the proteins separated in the IPG strip onto the second dimension gel, the equilibration step should result in the complete resolubilization of all proteins in the IPG gel. Again, the enormous chemical diversity

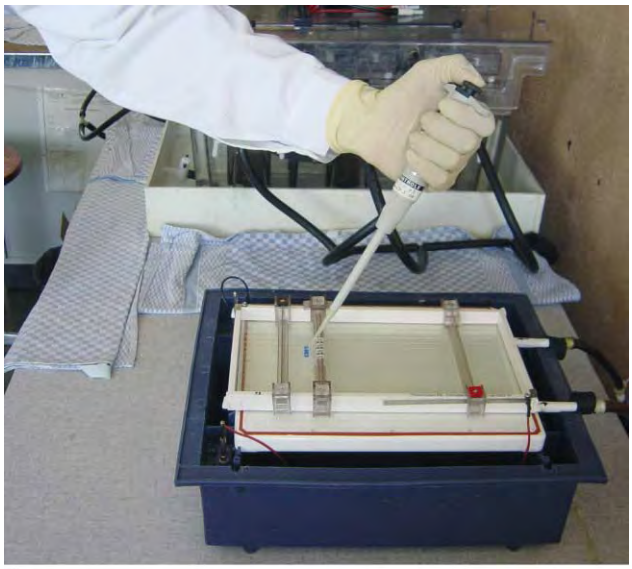

A

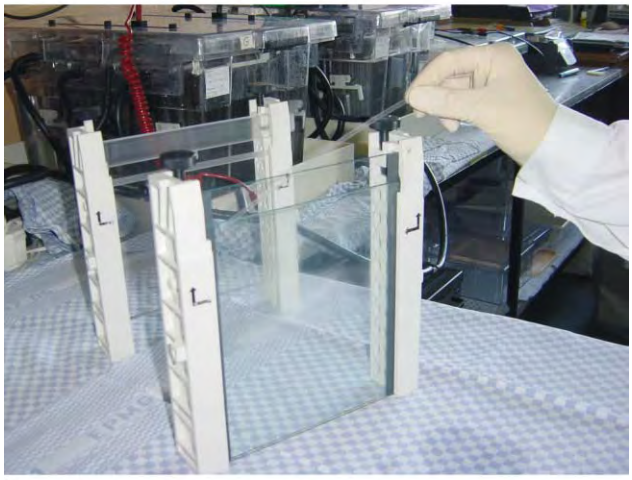

B

FIGURE 2 (A) Sample application for the first dimension of 2D PAGE – samples are loaded in cups at the cathodic end of the IPG strip. (B) Strip transfer to the second dimension of 2D PAGE – an equilibrated IPG strip is placed on the top of a large format polyacrylamide gel.

present within most samples makes it impossible to use ideal conditions for all its components. Composition of the equilibration solution and especially duration of the equilibration steps represent a compromise between accessing poorly soluble proteins with a tendency to adsorb to the gel matrix and diluting highly soluble proteins out of the gel strip. Equilibration in a buffer containing 6 M urea, 50 mM Tris–HCl buffer (pH 8.4), 2% w/v SDS, 30% w/v glycerol proved to be a good compromise. For protein reduction, IPG strips are first incubated in equilibration buffer containing 2% w/v DTT for 12 min. In a second step, proteins are alkylated by incubation in equilibration buffer containing 2.5% w/v iodoacetamide (IAA) and traces of bromophenol blue (tracking dye) for 5 min. In vertical SDS-PAGE, the equilibrated strip is placed on the surface of the second dimension gel and embedded in molten agarose (Figure 2B). Most commonly, the tris-glycine buffer system described by Laemmli is used. State-of-the-art 2D gel electrophoresis systems allow the simultaneous migration of up to 24 large format gels (20 by 24 cm) under temperature-controlled conditions.

Visualization

Most of the staining methods used for conventional 1D SDS-PAGE can be applied to 2D gels. Because of its very high sensitivity (down to 1 ng/spot), silver staining is probably most commonly used. However, the use of glutaraldehyde in the silver-staining procedure should be avoided for subsequent protein identification by mass spectrometry. Recently, MS-compatible, fluorescent stains with sensitivities comparable to silver became available. At the time being, application of this stains in large-scale and high-throughput 2D PAGE is hardly affordable. In addition, special imaging systems are required, whereas a simple desktop scanner can be sufficient for "visible" stains. This still leaves plenty of room for other MS-compatible, but less sensitive stains such as coomassie blue and zinc negative staining. Proteins labeled *in vivo* by the use of radioactive amino acids (metabolic labeling) can be visualized by exposing the dried 2D gel to an X-ray film or a storage phosphor screen for use with a PhosphorImager system. As for 1D SDS-PAGE, proteins from 2D gels can be electro-transferred on membranes, which are subsequently probed with antibodies. This so-called Western blot technique allows highly sensitive and specific visualization of a protein of interest.

Applications of 2D PAGE

The combination of a high-resolution protein separation tool (2D PAGE) with a highly sensitive protein identification tool (MS) offers an enormous potential. In 1994, on the occasion of the first Siena 2D Electrophoresis meeting, the expression "proteome" was proposed by Marc Wilkins for the description of the proteins expressed by a genome of a species, an organ, or a cell at a particular moment under particular conditions. Since then, the field of proteomics, i.e., the analysis of proteomes, is booming. The global approach taken with proteomics allows the massively parallel analysis of expressed proteins, including their isoforms originating from posttranslational modifications (PTMs). Global gene expression can also be studied at the level of mRNA. However, it needs to be emphasized that there is not a good correlation between mRNA abundance and protein amount in a cell at a given time and that PTMs

cannot be predicted from gene sequences. In general, applications of 2D PAGE can be divided into descriptive protein mapping without a need for protein quantification and differential analysis, where protein quantification is essential.

Protein Mapping and 2D PAGE Protein Databases

The classical approach, 2D PAGE coupled with MS, allows the establishment of 2D reference maps. One aims at identifying as many proteins as possible. A typical workflow is depicted in Figure 3. With the number of completely sequenced genomes increasing daily, protein identification became possible for a growing number of species. Over the last years, many 2D reference maps have been established using different tissues, body fluids, or cell lines as sample (for an overview see http://ch.expasy.org/ch2d/2d-index.html). Due to the enormous complexity of cells from higher eukaryotes, characterization of their complete proteome in a single step is still impossible. Isolation of subcellular fractions such as organelles, macromolecular structures, and multiprotein complexes represents a possibility to reduce the complexity of the entire cell.

Differential Analysis

Digitized 2D maps can serve more than just descriptive purposes. With specialized software packages, quantitative image analysis of the complex 2D patterns can be performed. This allows one to compare protein expression levels between different conditions for thousands of proteins in parallel. In general, one aims at identifying only the proteins showing differential expression in the samples under comparison. Since the early 1990s this approach has been used to tackle various biological questions. Comparison of proteomes from tissues or cells representing the healthy and the diseased state, respectively, allows the detection of putative molecular markers of the disease. Such a global approach is particularly useful in polygenic diseases such as cancer and cardiovascular diseases. Analysis of cell differentiation and monitoring therapy are other fields of application of differential analysis.

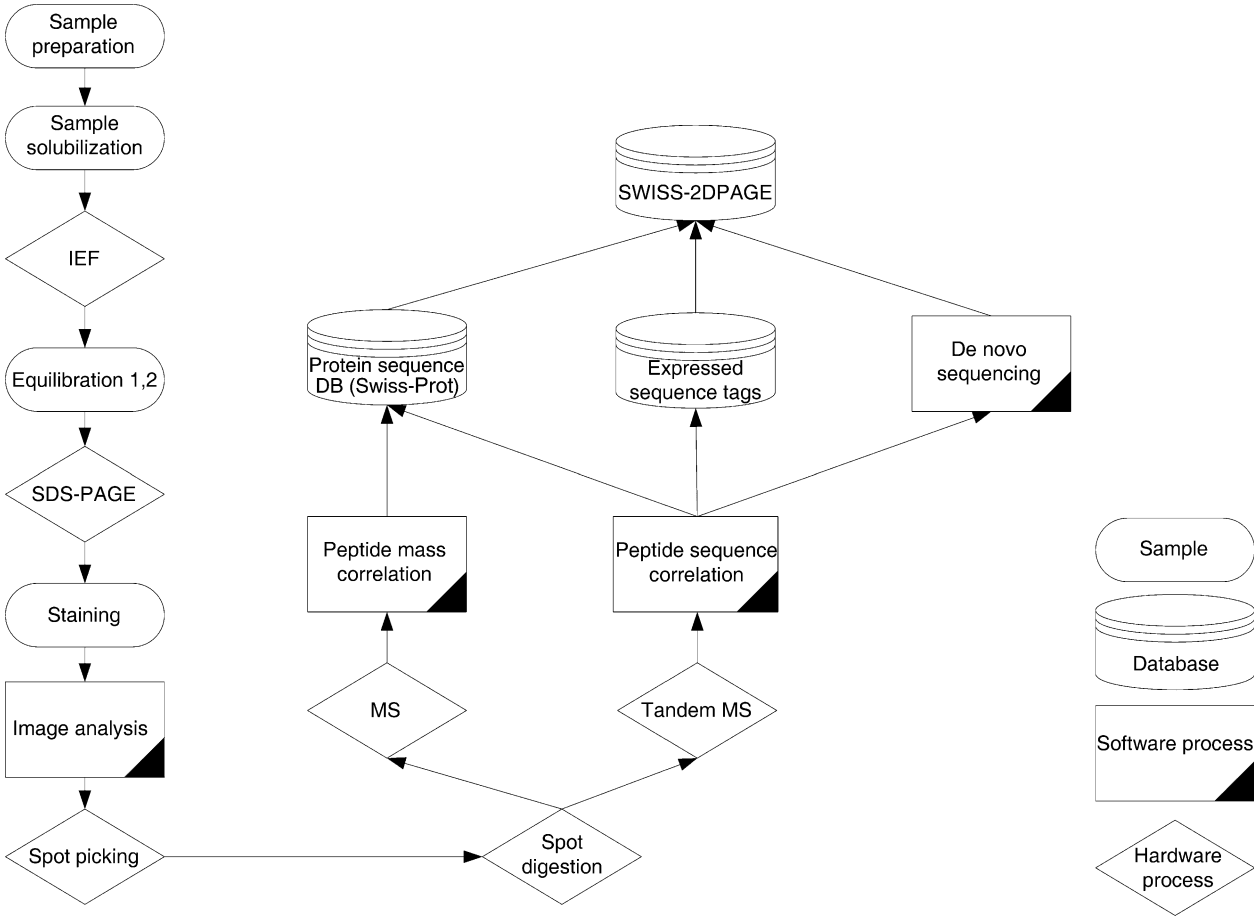

FIGURE 3 Typical proteomic workflow using 2D PAGE as protein separation tool.

Limitations and Perspectives of 2D PAGE

In spite of all benefits, 2D PAGE is not without limitations. On the one hand, there are intrinsic limitations of 2D PAGE and, on the other hand, there are general limitations encountered when dealing with complex protein mixtures.

Intrinsic Limitations of 2D PAGE

Hydrophobic Proteins

Very hydrophobic proteins such as integral membrane proteins and nuclear proteins were shown to be underrepresented in 2D gels. They have a tendency to stick to IPG gel matrix, and re-solubilization for the second dimension becomes a problem. Incorporation of thiourea, sulfobetaine surfactants, and organic solvents in the solubilization buffer showed some improvements. However, very hydrophobic proteins will probably remain a major limitation of IEF and therefore also of 2D PAGE.

Basic Proteins

Horizontal streaking on the 2D gel is usually observed in the region with pH > 7. This phenomenon is particularly prominent when basic narrow range pH gradients are used. The streaking is due to the disappearance of the reducing agent from the basic part of the strip. Oxidation of the protein thiol groups results in the formation of inter- and intra-chain disulfide bridges. Recently, oxidation of the protein thiol groups to mixed disulfides using hydroxyethyl disulfide (DeStreak^{TM}) has been introduced, showing massively improved focusing for the very basic proteins.

Automation and Miniaturization

For many years, the low degree in automation and miniaturization of 2D PAGE has hindered this labor-intense technique from becoming routinely used in clinical laboratories and in industry, where high throughput counts and sample amount is limited. Promising developments toward both automation and miniaturization can be observed and their availability seems to be very close.

General Limitations

A biological sample usually represents a complex protein mixture containing thousands of proteins with different physico-chemical properties and widely varying expression levels. In human cells the dynamic range exceeds 6 orders of magnitude and in human plasma it reaches more than 12 orders of magnitude. In contrast, 2D gels and silver staining offer a maximum of 4 orders of magnitude. Consequently, application of unfractionated samples allows one to see only the tip of the iceberg. In order to access the low abundance proteins, samples need to be prefractionated, using traditional biochemical separation techniques, for example.

Perspectives of 2D PAGE

For many years, 2D PAGE has been the core technology for protein separation in proteomics research. This dominant role is now being challenged by various non-gel-based approaches such as protein chips, serial liquid chromatography, or capillary electrophoresis. They can be very demanding in terms of data management and bioinformatic resources, which might be limited for most standard academic research institutions. In fact, these liquid-based techniques should be considered as complementary approaches to 2D PAGE, depending on the biological question one wants to answer. If one aims at identifying as many proteins as possible in a given sample, 2D PAGE coupled to MS no longer represents the method of choice. However, if one aims at differential analysis of protein expression, 2D gels remain very powerful. This is mainly due to the possibility to look at PTMs offered by 2D PAGE. PTMs such as phosphorylations, glycosylations, or proteolytic processing can be very important for the function of a protein.

See Also the Following Articles

Glycation • Protein Data Resources • Proteinase-Activated Receptors

Glossary

immobilized pH gradient (IPG) In an IPG gradient, a set of acidic and basic buffering groups is covalently incorporated into a polyacrylamide gel at the time it is cast. Precast IPG gel strips supported by a plastic film backing are commercially available in a variety of narrow and broad pH ranges.

isoelectric point (pI) The pH value at which the net electric charge of an elementary entity, here a protein, is zero. At a pH value below the pI of a protein, it is charged positively, and at a pH value above the pI it is charged negatively.

proteome Ensemble of proteins expressed by a genome of a species, an organ, or a cell at a particular moment under particular conditions.

proteomics Qualitative and quantitative comparison of proteomes under different conditions to further unravel biological processes.

Further Reading

Chambers, G., Lawrie, L., Cash, P., and Murray, G. I. (2000). Proteomics: A new approach to the study of disease. *J. Pathol.* **192**, 280–288.

Görg, A., Obermaier, C., Boguth, G., Harder, A., Scheibe, B., Wildgruber, R., and Weiss, W. (2000). The current state of two-dimensional electrophoresis with immobilized pH gradients. *Electrophoresis* **21**, 1037–1053.

Jung, E., Heller, M., Sanchez, J.-C., and Hochstrasser, D. F. (2000). Proteomics meets cell biology: The establishment of subcellular proteomes. *Electrophoresis* **21**, 3369–3377.

Rabilloud, T. (ed.) (2000). *Proteome Research: Two-Dimensional Gel Electrophoresis and Identification Methods*. Springer, Berlin, Heidelberg.

Rabilloud, T. (2002). Two-dimensional gel electrophoresis in proteomics: Old, old fashioned, but it still climbs up the mountains. *Proteomics* **2**, 3–10.

Swiss-2DPAGE on the Expasy Molecular Biology Server – http://ch.expasy.org/ch2d/.

Wilkins, M. R., Williams, K. L., Appel, R. D., and Hochstrasser, D. F. (eds.) (1997). *Proteome Research: New Frontiers in Functional Genomics*. Springer, Berlin, Heidelberg.

Biography

Gerhard Schmid is a Ph.D. student at the Biomedical Proteomics Research Group (BPRG) of the Clinical Pathology Department, Geneva University Hospital.

Denis Hochstrasser is the Director of the Clinical Pathology Department. At the academic level, he is a full Professor both to the Department of Pathology of the Medicine faculty and to the School of Pharmacy of the Science faculty. His innovations in the methodology of 2D gel electrophoresis have contributed decisively to the technique's becoming one of the main protein separation methods used in proteomics.

Jean-Charles Sanchez is the Head of the BPRG since 1995. Working in the field of proteomics since 1989, he contributed to the development of 2D gel electrophoresis and its application in biomedical research. He obtained Ph.D. in Biochemistry at the University of Buckingham (UK) in the field of proteomics and diabetes.

Two-Hybrid Protein–Protein Interactions

Ilya Serebriiskii and Erica A. Golemis
Fox Chase Cancer Center, Philadelphia, Pennsylvania, USA

The two-hybrid system is an artificially constructed genetic system intended to facilitate the detection and assessment of protein–protein interactions. In the two-hybrid system a host organism, typically yeast or bacteria, is so engineered as to contain three components. These are a first protein fused to a DNA-binding domain of known specificity (hybrid 1); a second protein fused to a transcriptional activation domain (hybrid 2), that can interact with the first protein, constituting a functional, albeit composite, transcription factor; and one or more reporter genes transcribed based on the binding of the composite transcription factor. Many permutations of the two-hybrid paradigm have been developed, and two-hybrid systems have become a mainstay of proteomic investigations.

The Yeast Two-Hybrid System

The purpose of the two-hybrid system is to provide a genetic system that is capable of scoring the degree of physical interaction between two proteins of interest. To this end, a simple organism such as yeast (*S. cerevisiae*) or bacteria (*E. coli*) is engineered such that the interaction of two proteins generates a scorable signal, that can be used either to gauge the interaction affinity of two defined proteins, or to identify interacting partners for one defined protein by screening an expression library.

The first working example of a two-hybrid system was described in 1989, by Fields and Song. A schematic showing the system paradigm is shown in Figure 1. There are three minimal components for a functioning two-hybrid system. The first component is an expression construct, which synthesizes a first protein of interest as a fusion with a DNA-binding domain (DBD) that binds a short DNA sequence of defined specificity (hybrid 1: frequently termed the "bait"). The second component is an expression construct that is used either to express a second defined protein, or random clones from a cDNA or genomic library, as a fusion with a transcriptional activation domain (AD) (hybrid 2: frequently termed the "prey"). The third component is a reporter cassette, which consists of the DNA-binding site for the first hybrid protein in the context of a minimal promoter, upstream of the coding sequence for an easily scored reporter gene.

For the yeast two-hybrid system to work, there are two preconditions. First, the bait must not be independently functional as a transcriptional activator, such that yeast containing only the bait and the reporter produce no reporter signal. Second, the bait and the prey must be capable of localizing to the cell nucleus; hence, proteins containing signal sequences that efficiently target them to the plasma membrane, or other non-nuclear compartments, are not generally acceptable as baits. However, for proteins that meet these preconditions, the interaction between the bait and the prey brings the transcriptional activation domain encoded in the prey to the promoter sequence bound by the bait, and activates the transcription of the reporter gene.

A number of groups have built systems that exploit this two-hybrid paradigm in yeast, with several of these systems in common use. The most common DBDs used in these yeast two-hybrid systems are derived from the yeast transcription factor Gal4p, or from the bacterial repressor protein LexA. A variety of different AD sequences have been used, and include the activation domain from Gal4p; the activation domain from the viral protein VP16; or "artificial" activation sequences encoded from selected fragments of the *E. coli* genome.

Two categories of reporter genes have been used. One category is colorimetric, exemplified by the bacterial *lacZ* gene. Activation of a *lacZ* reporter causes yeast colonies to turn blue when plated on medium containing an appropriate substrate, such as X-gal, or can be assessed quantitatively over a dynamic range in excess of 1000-fold in liquid assays using a spectrophotometer or luminometer. The second category of reporter provides an active selection for yeast growth based on the strength of interaction between two proteins. These reporters include genes encoding critical components of yeast metabolic pathways for amino acid synthesis, such that expression of the gene is required for yeast to grow on medium lacking the relevant amino acid (e.g., show

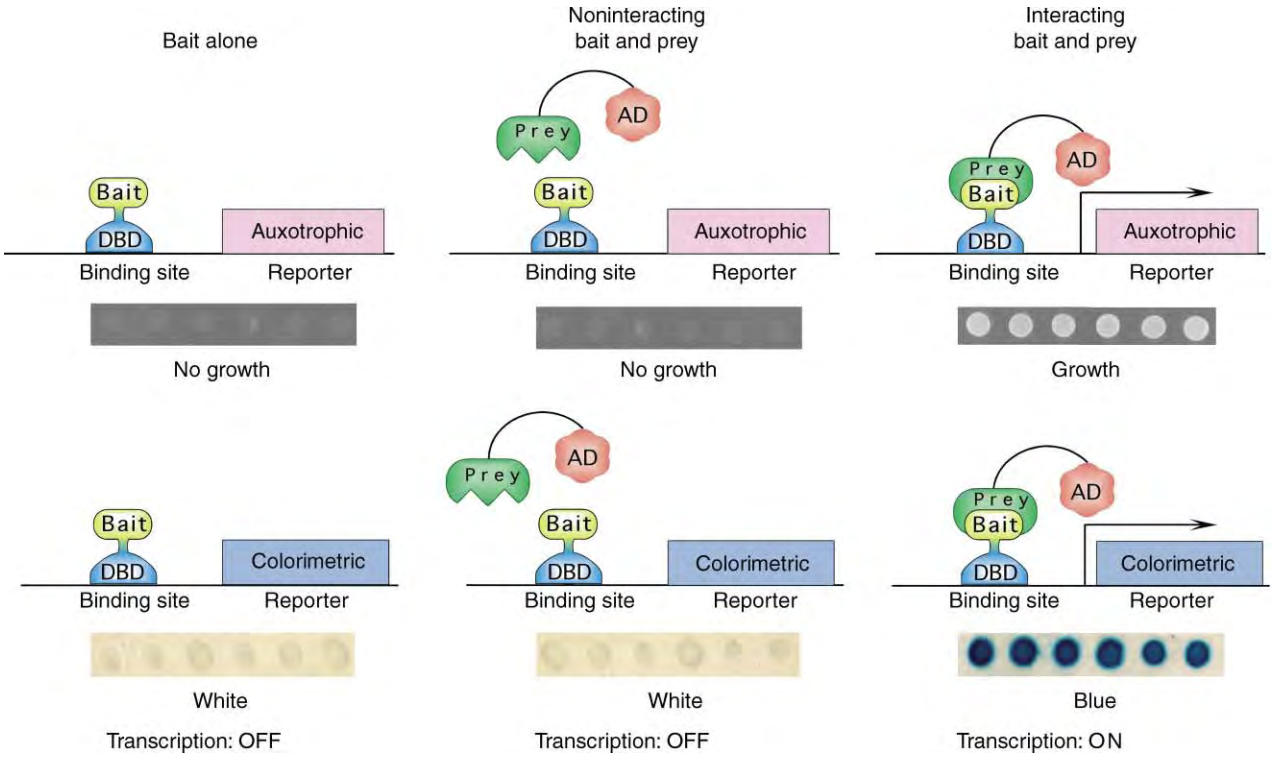

FIGURE 1 Schematic of yeast two-hybrid components, and profile of reporter activation. Details of system components are described in the text. Three situations are shown: (1) yeast containing only a bait and two reporters, left; (2) yeast containing bait, prey that does not interact with bait, and reporters, center; and (3) interacting bait and prey, and reporters, right. For each of these three situations, with a typical auxotrophic and colorimetric reporter, six independent colonies of yeast are dotted on plates with selective medium: expected results (growth/no growth, or color/no color) are shown as panel inserts below each schematic.

an auxotrophic requirement). *HIS3*, required for growth on medium lacking histidine, and *LEU2*, required for growth on medium lacking leucine, have been most commonly used. In general, two hybrid systems now generally incorporate one colorimetric and one auxotrophic selection, both responsive to the same bait. The use of two different reporter genes greatly minimizes the background of false positive and false negative interactions in the system, and is essential for library screening applications, where in excess of 10^6 clones must commonly be analyzed.

Because of the ease of manipulation provided by a genetic system, a yeast two-hybrid system provides a facile means of exploring the interaction of two known partner proteins. This can be done in a predetermined manner, by inserting targeted mutations or deletions into the AD-fused partner, or based on blind selection, for example, by using PCR mutagenesis or DNA sonication to develop a randomized library derived from the AD partner. Each mutant derivative can be readily screened for interaction phenotype. However, the most important use of the yeast two-hybrid system throughout the 1990s has clearly been for the purpose of screening libraries to identify novel interacting partners for proteins of interest. In contrast to other means of identifying interacting proteins, such as biochemical copurification, two-hybrid screening is extremely inexpensive, requiring only engineered strains of yeast and standard microbiological media. It is rapid, providing the potential of completing a screen from start to finish in less than a month. It is effective at yielding returns for a significant percentage of bait proteins (estimated at $>50\%$). Finally, following completion of a successful library screen, plasmids encoding the novel interacting preys can easily be isolated from yeast, avoiding the need for protein sequencing or mass spectrophotometric analysis required by biochemical methodologies. It is not an exaggeration to note that recent broad adaptation of two hybrid screening methodologies across the scientific community was a major contributing source of elucidation for key cell signaling pathways.

Advanced Applications

Following the validation of the basic two-hybrid system as a useful and reliable tool for study of protein–protein interactions, a number of investigators have explored the potential of the system to study interactions between proteins and partner proteins under additional selective constraints. A first step in this direction was the demonstration that it was possible to identify preys

that interacted with baits contingent upon the modification of the bait by a coexpressed kinase. A second point of interest was the feasibility of identifying proteins that interacted not with a single protein, but with a complex formed by a bait and one or more simultaneously expressed "co-baits." A number of investigators have used a two-hybrid approach to identify proteins that interact as constituents of ternary or even quarternary complexes.

Another application of interest has been to use the two-hybrid system to identify and characterize interactions between proteins and non-protein ligands. To date, two-hybrid derivative systems have been used to score interactions between proteins and small molecules/drugs, and proteins and RNAs. In each case, the derivative system has been shown to function at the level of library screening. While screening for RNAs has become relatively broadly adapted as a research tool, screening for drugs that regulate protein–protein interactions remains at an earlier stage of validation. Detailed description of the derivatization of the two-hybrid system required for the screening of non-protein ligands is beyond the scope of this review.

The two-hybrid system has been used by a number of investigators to identify peptide "aptamers" capable of binding and regulating the functions of specific bait proteins. Peptides isolated based on two-hybrid selection have been found capable of regulating diverse functions of their cognate baits, and may provide the basis for design of peptidomimetics or small molecule derivatives of therapeutic value. This is currently an area of active investigation.

Finally, a recent effort has been to refine the two-hybrid system so as to make it a more useful tool for evaluating the selectivity of protein interactions. In these approaches, the two-hybrid system is "parallelized," using two discrete sets of baits and reporters within a single strain of yeast. In one example, bait 1 (a fusion to LexA) directs the expression of the *lacZ* and *LEU2* reporters, while bait 2 (a fusion to cI) directs the expression of *gusA* (colorimetric) and *LYS2* (auxotrophic) reporters. In a situation where a prey initially interacts with both baits 1 and 2, turning on all four reporters, mutagenesis of the prey can be coupled with selective screening for activation of the *lacZ* and *LEU2*, versus the *gusA* and *LYS2*, reporters, providing a convenient means of identifying altered specificity mutants that can be used to deconvolute signal transduction pathways.

Alternative Two-Hybrid Systems

Although the yeast two-hybrid system has found many useful applications, it has not been appropriate in all cases. Toward the goal of identifying small molecules or mutations that disrupt, rather than permit, protein–protein interactions, a "reverse" two-hybrid system has been developed. In this system, activation of a reporter gene is toxic, providing selection pressure for clones that have lost protein–protein interactions. For proteins that strongly activate transcription in yeast, and hence cannot be used to create baits, one solution has been to move the two-hybrid components to an RNA polymerase III-based reporter system, eliminating transcriptional activity. Other investigators have generated two-hybrid-like systems in bacteria, where eukaryotic transcriptional activation sequences are generally ineffective. For proteins that are membrane associated, or cannot efficiently be nuclear localized, several methods for assessing protein interaction at membranes or in the cytoplasm have been developed. These include systems in which interaction of the bait and prey reconstitutes an intracellular signaling pathway (e.g., the SOS system), or generate an assayable enzymatic by-product, as in the ubiquitin-based split-protein sensor system (USPS). In one recent and promising development, the USPS system has been further modified such that interactions of a bait and prey at the cell membrane triggers the cleavage and release of a transcription factor that migrates to the nucleus and activates standard yeast two-hybrid colorimetric and auxotrophic reporters. This approach combines advantages of membrane-based interaction detection with the ability to use well-validated screening modalities.

Role in Proteomics

Two hybrid protein–protein interaction systems are an important element of strategies to analyze the complete protein–protein interactions of proteomes. To date, extensive protein interaction maps have been constructed for viruses and yeast, and large-scale screening efforts are underway in *Caenorhabditis elegans* (*C. elegans*), *Drosophila*, and humans. These efforts provide a useful complement to simultaneous efforts to analyze protein interactions by mass spectrometry: whereas mass spectrometry is of value in identifying proteins which bind with high affinity to an assembled complex, albeit potentially weakly to any single interactive partner, the yeast two-hybrid system excels at identifying proteins that interact with high affinity with single defined partners. Interactions being detected by these means are being integrated into datasets including transcriptional expression profiles, genetic interaction data, and protein localization data for the same proteins, providing a fundamental tool for the emerging field of systems biology. It is likely that continuing application of the two-hybrid protein–protein interaction will remain a source of scientific insights for many years to come.

See Also the Following Articles

LexA Regulatory System • Yeast GAL1–GAL10 System

Glossary

bait A term used to describe a DNA-binding domain–protein "X" fusion, used as a probe in the yeast two-hybrid system (e.g., to screen a library).

interaction map A schematic showing a network of protein–protein interactions involving one or more proteins of interest.

interactome A recently introduced term, proposed to describe the complete network of protein–protein interactions occurring within an organism.

prey A term used to describe a transcriptional activation domain–protein "Y" fusion, which interacts with a bait.

two-hybrid system A system in which the interaction of two "hybrid" proteins (created so that (1) one is a fusion between a DNA-binding domain and protein "X," and the second is a fusion between a transcriptional-activation domain and protein "Y"; and (2) X and Y normally interact) in a host organism such as yeast or bacteria causes the activation of one or more scorable reporter genes.

Further Reading

Bernstein, D. S., Buter, N., Stumpf, C., and Wickens, M. (2002). Analyzing mRNA–protein complexes using a yeast three-hybrid system. *Methods* **26**, 123–141.

Fashena, S. J., Serebriiskii, I. G., and Golemis, E. A. (2000). The continued evolution of hybrid screening approaches in yeast: How to outwit different baits with different preys. *Gene* **250**, 1–14.

Fields, S., and Song, O. (1989). A novel genetic system to detect protein–protein interaction. *Nature* **340**, 245–246.

Schwikowski, B., Ideker, T., and Uetz, P. (2002). Visualization and integration of protein–protein interactions. In *Protein Interactions* (E. A. Golemis, ed.) Cold Spring Harbor Laboratory Press, Cold Spring Harbor, NY.

Serebriiskii, I. G., Khazak, V., and Golemis, E. A. (2001). Redefinition of the yeast two-hybrid system in dialogue with changing priorities in biological research. *BioTechniques* **30**, 634–655.

Stagljar, I., and Fields, S. (2002). Analysis of membrane protein interactions using yeast-based technologies. *Trends Biochem. Sci.* **27**, 559–563.

Walhout, A. J., Reboul, J., Shtanko, O., Bertin, N., Vaglio, P., Ge, H., Lee, H., Doucette-Stamm, L., Gunsalus, K. C., Schetter, A. J., Morton, D. G., Kemphues, K. J., Reinke, V., Kim, S. K., Piano, F., and Vidal, M. (2002). Integrating interactome, phenome, and transcriptome mapping data for the *C. elegans* Germline. *Curr. Biol.* **12**, 1952–1958.

Zhu, H., and Snyder, M. (2002). "Omic" approaches for unraveling signaling networks. *Curr. Opin. Cell Biol.* **14**, 173–179.

Biography

Ilya Serebriiskii is a Staff Scientist in the Division of Basic Sciences at the Fox Chase Cancer Center in Philadelphia, PA. His research interests include bacterial and yeast genetics and proteomics. He has created and evaluated numerous advanced protein interaction screening tools based on two-hybrid paradigms. He holds a Ph.D. in Biology from VNIIGenetika, Moscow, Russia. He received his postdoctoral training with Prof. Gerard Leblon at The Institute of Genetics and Microbiology, University of Paris-Sud, France, and then with Dr. Erica Golemis at Fox Chase Cancer Center.

Erica Golemis is a Member of the Division of Basic Sciences at Fox Chase Cancer Center. Her interests include the study of protein interactions, and the intersection of cell attachment and cell cycle control signaling in mammalian cancer development. She performed research with Dr. Nancy Hopkins leading to a Ph. D. in Biology from the Massachusetts Institute of Technology in Cambridge, MA. Subsequent postdoctoral work with Dr. Roger Brent at Massachusetts General Hospital in Boston, MA, led to the development of an original LexA-based two-hybrid system. She has worked extensively in the area of yeast two-hybrid system reagent development.

Tyrosine Sulfation

Denis Corbeil and Wieland B. Huttner
Max Planck Institute of Molecular Cell Biology and Genetics, Dresden, Germany

The O-sulfation of tyrosine residues of membrane and secretory proteins that transit through the secretory pathway of eukaryotic cells is a ubiquitous posttranslational modification conserved in all multicellular organisms. Tyrosine sulfation is catalyzed by tyrosylprotein sulfotransferase (TPST) isoenzymes, which are integral membrane proteins of the trans-Golgi network. Tyrosine sulfation has been shown to be important for protein–protein interactions occurring in diverse biological processes, ranging from the receptor binding of regulatory peptides to the interaction of viral envelope proteins with the cell surface.

Tyrosine-Sulfated Proteins

Occurrence

Sulfation is one of the most abundant posttranslational modifications of tyrosine, since up to 1% of the tyrosine residues of total protein in an organism can be sulfated. Tyrosine is the only amino acid residue in proteins known to undergo sulfation. Following the first description of a sulfated-tyrosine residue in a peptide derived from fibrinogen by Bettelheim in 1954, it has been known since 1982 that tyrosine-sulfated proteins occur in all animals, from lower invertebrates up to humans. Tyrosine-sulfated proteins also exist in the plant kingdom, for example, in the green alga volvox, one of the earliest truly multicellular organisms, or in higher plants such as rice. While occurring throughout metazoan evolution, tyrosine-sulfated proteins appear to be absent in unicellular eukaryotes and prokaryotes, implicating this post translational modification in some aspect of multicellularity.

In a given animal, tyrosine-sulfated proteins have been observed in all tissues examined. Each tissue appears to contain a characteristic set of tyrosine-sulfated proteins, suggesting that proteins with tissue-specific expression are major targets for tyrosine sulfation. In cell culture, tyrosine sulfation of proteins has been detected in all primary cultures and cell lines investigated, including various secretory cells, epithelial cells, fibroblasts, neuronal cells, and cells of the immune system.

Tyrosine-sulfated proteins can be identified by various methods, including labeling using radioactive sulfate followed by tyrosine sulfate analysis of a given protein. In line with the intracellular localization of tyrosylprotein sulfotransferase (TPST) in the trans-Golgi network, all known tyrosine-sulfated proteins are either secretory or plasma membrane proteins. Reviews with comprehensive lists of tyrosine-sulfated proteins have been published, and several of these proteins have been shown to play important biological roles.

Structural Determinants of Tyrosine Sulfation

The recognition, by TPST, of the tyrosine residue to be sulfated in a secretory protein or the extracellular domain of a membrane protein requires the presence of certain structural features. These have been deduced from the comparison of identified tyrosine sulfation sites and the *in vitro* tyrosine sulfation of synthetic peptides. Although no strict consensus sequence for tyrosine sulfation exists, all sequences exhibit the presence of acidic amino acid residues in the vicinity, i.e., positions -5 (N-terminal) to $+5$ (C-terminal), of the sulfated tyrosine residue. A particularly critical position appears to be amino-terminal (-1) to the tyrosine. Turn-inducing amino acids (P, G) are also frequently present. The few examples of tyrosine sulfation sites lacking proline and glycine are located near the N- or C-terminus of the protein and/or contain several of the three other amino acid residues (D, S, N) with significant turn-conformational potential. Finally, another characteristic feature common to most identified tyrosine sulfation sites is the absence of cysteine residues or potential N-glycosylation sites (NXS or NXT) in the vicinity (positions -7 to $+7$). In either case, the presence of a disulfide-bridge or N-linked oligosaccharides is likely to prevent sulfation of nearby tyrosine residues due to steric hindrance.

Tyrosylprotein Sulfotransferase (EC 2.8.2.20)

The Tyrosine Sulfation Reaction

The sulfate transfer reaction to tyrosine residues is catalyzed by TPST, first described in 1983, and used as a

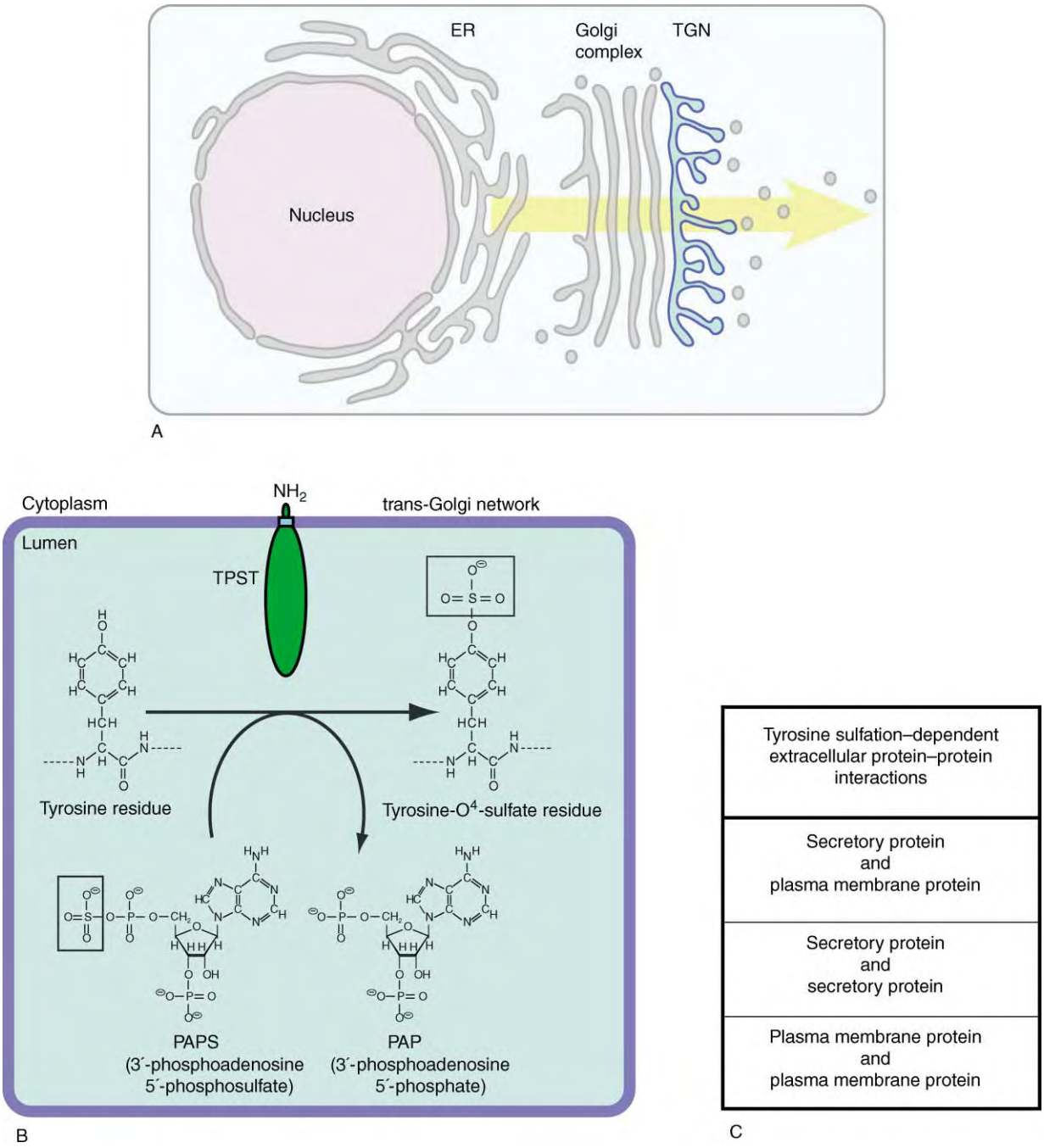

FIGURE 1 (A) Tyrosine sulfation occurs in the trans-Golgi network (TGN). (B) TPST, a type II transmembrane protein, catalyzes the transfer of the sulfate group (boxes) from the co-substrate PAPS to tyrosine residues of secretory proteins and ectodomains of membrane proteins passing through the lumen of the trans-Golgi network. (C) The three principal types of tyrosine sulfation-dependent protein–protein interactions.

sulfate donor, the cosubstrate 3′-phosphoadenosine 5′-phosphosulfate (PAPS) (Figure 1B). The transfer is thought to occur in an ordered reaction mechanism that involves the following sequential steps: (1) cosubstrate PAPS binding; (2) substrate binding; (3) sulfate transfer; (4) tyrosine-sulfated product release and, (5) PAP release. TPST activity can be detected by incubation of appropriate membrane preparations with [^{35}S]PAPS, using either endogenous or exogenous protein substrate. Biologically, tyrosine sulfation appears to be an irreversible event *in vivo* due to the lack of a sulfatase capable of catalyzing the desulfation of tyrosine-sulfated proteins under physiological conditions.

Properties of TPST

TPST is an integral membrane protein residing in the trans-Golgi network (Figure 1A). The TPST protein can

be identified in membrane preparations by MSC (*m*odification after *s*ubstrate *c*ross-linking) labeling, which is based on the cross-linking of a substrate peptide to TPST followed by intramolecular [^{35}S]sulfate transfer from the cosubstrate PAPS. Various nonionic detergents can be used to solubilize TPST from membranes.

TPST purified from bovine adrenal medulla is a 50–54 kDa sialoglycoprotein with an apparent S-value of 6. Its pH optimum is between 6.0 and 6.5, which is in line with the slightly acidic pH of the trans-Golgi network. The catalytic activity of the enzyme, towards endogenously as well as exogenously added proteins, is stimulated by divalent cations (Mg^{2+}, Mn^{2+}), and fluoride ions are required for maximal activity. The K_m for the cosubstrate PAPS is 1.4 μM. Like most sulfotransferases, TPST is inhibited by PAP. *In vitro*, the activity of the enzyme is also inhibited by certain lipids such as sphingosine, but the physiological relevance of this observation is unknown. Synthetic inhibitors of TPST (with IC_{50} values of 30–40 μM) have been generated by a combinatorial target-guided ligand assembly technique.

The K_m for most peptides (8–13 amino acid residues) with a single tyrosine sulfation site is in the range of 10–100 μM. It is likely that similar values hold true for individual tyrosine sulfation sites in proteins. Interestingly, K_m values for synthetic substrates containing multiple tyrosine sulfation sites are considerably lower. Given that several proteins exist with multiple adjacent sulfation sites, e.g., cionin, heparin cofactor, and prepro-cholecystokinin, the increased affinity of TPST for such substrates might be of physiological significance, e.g., by promoting stoichiometric sulfation. A remarkable example of the sequential sulfation of four tyrosine residues within a short stretch of amino acids is the N-terminal domain of the CC-chemokine receptor 5 (CCR5), which is a coreceptor for HIV.

Molecular Cloning and Membrane Topology of TPST

Distinct TPST isoenzymes, anticipated from the differential substrate specificities of various TPST preparations, exist in the human and mouse genome. Each contains two TPSTs, TPST-1 (see Swiss-Prot Database, Accession No. 060507) and TPST-2 (see Swiss-Prot Database, Accession No. 060704), which were first characterized at the molecular level in 1998. The human *TPST-1* (7q11) and *TPST-2* (22q12.1) genes encode for 370- and 377-amino acid proteins, respectively, that share an overall 65% identity. The murine *tpst* genes are located on chromosome 5, and the corresponding proteins show ~95% identity to their human counterpart. Both TPST isoenzymes are predicted to have a type II membrane topology, with a very short NH_2-terminal cytoplasmic domain (8 residues) and the bulk of the polypeptide, which is responsible for the catalytic activity, being located in the Golgi lumen (see Figures 1A and 1B). Although overall, TPST isoenzymes display a low degree of amino acid identity to other cytosolic and Golgi-associated sulfotransferases, most of the residues involved in PAPS binding, as deduced from comparison with the crystal structure of estrogen sulfotransferase, are conserved. The luminal domain of either isoenzyme also contains two potential N-glycosylation sites, consistent with presence of N-linked glycans in the TPST protein.

In agreement with the occurrence of tyrosine sulfation in all metazoan species, cDNAs that predict proteins obviously related to mammalian TPSTs are found in various vertebrates and invertebrates, including fish (GenBank Accession No. BI846282), frog (GenBank Accession No. BG815875), chicken (GenBank Accession Nos. BU142429, BU217098), fly (GenBank Accession No. AY124548), and worm.

TPST-1 Versus TPST-2

TPST-1 and TPST-2 transcripts are found in all tissues examined, e.g., brain, heart, skeletal muscle, gut, kidney, liver, lung, and leukocytes. Although ubiquitously expressed, the tissue distribution of TPST-1 and TPST-2 are not identical, recombinant TPST-1 and TPST-2 show similar, but not identical, activities toward certain small peptide substrates, consistent with some functional redundancy as well as a certain degree of differential substrate specificity.

TPST-1- and TPST-2-Deficient Mice

TPST-1- and TPST-2-deficient mice, generated by targeted disruption of the *tpst-1* and *tpst-2* genes, also point to functional redundancy between the two isoenzymes, as either line of knock-out mice is viable (K.L. Moore, personal communication). Although TPST-$1^{-/-}$ animals appear normal, their body weight is reduced about 5% and an increase in postimplantation fetal death is observed, suggesting that unidentified proteins involved in regulation of body weight and reproductive physiology require tyrosine sulfation for optimal function. TPST-2 deficient mice show a transient delay in growth during postnatal development. In addition, the males, but not females, appear to be infertile. Together, these observations are consistent with the idea that TPST-1 and TPST-2 have distinct, but partially overlapping, physiological roles.

Physiological Function and Medical Relevance

For most tyrosine-sulfated proteins, the physiological function of this posttranslational modification is presently unknown. With regard to the cases in which the biological role of tyrosine sulfation of a particular protein has been elucidated, the common denominator has emerged that tyrosine sulfation promotes extracellular protein–protein interactions. In line with the identification of numerous secretory and plasma membrane proteins that are tyrosine-sulfated, paradigmatic examples exist showing that tyrosine sulfation promotes the interaction between (1) a secretory and a plasma membrane protein, (2) two secretory proteins, or (3) two plasma membrane proteins (Figure 1C).

The regulatory peptide cholecystokinin is a classical example where tyrosine sulfation of a secretory protein dramatically promotes its interaction with a plasma membrane protein, i.e., its cell surface receptor. Thus, sulfated cholecystokinin is 260 times more potent than its unsulfated form. Of the several examples of tyrosine sulfation promoting the interaction between two secretory proteins, the case of the binding of the tyrosine-sulfated blood coagulation factor VIII to von-Willebrand-factor is particularly intriguing, as it also documents the medical relevance of this posttranslational modification. Humans with a mutation in the critical tyrosine residue of factor VIII that is sulfated and involved in its binding to von-Willebrand-factor are afflicted with hemophilia A.

An example of tyrosine sulfation promoting the interaction between two plasma membrane proteins is the important role of this posttranslational modification for the high-affinity binding of leukocyte-associated P-selectin glycoprotein ligand (PSGL)-1 to P-selectin on activated endothelial cells. This crucial interaction initiates adhesion of leukocytes to the vascular wall during inflammation. Tyrosine sulfation also occurs in seven-transmembrane-segment chemokine receptors, e.g., CCR5. Under physiological conditions, these plasma membrane proteins play a central role in chemokine signalling pathway through G proteins. Remarkably, human and simian immunodeficiency viruses use CCR5 as a co-receptor, together with CD4, to mediate their attachment to the host cell membrane. Specifically, sulfation of tyrosine residues in the CCR5 N-terminal domain has been shown to be critical for the interaction of this protein with HIV envelope glycoprotein gp120, leading to HIV infection. Thus, the design of tyrosine-sulfated peptide competitors – mimicking HIV gp120-binding sites – could turn out to be the basis for new therapeutic compounds that will block HIV cellular entry. These examples highlight the medical relevance of protein tyrosine sulfation.

See Also the Following Articles

Golgi Complex • Oligosaccharide Chains: Free, *N*-Linked, *O*-Linked • Secretory Pathway

Glossary

PAPS 3′-phosphoadenosine 5′-phosphosulfate, sulfate donor in the sulfate transfer reaction. PAPS has been known to be the activated form of sulfate and acts as cosubstrate for the sulfation of a wide variety of substances, including proteins.

trans-Golgi network The last station of the Golgi complex. This site is a major branching point of vesicular transport and the origin of two principal pathways of protein secretion: the regulated and constitutive pathways.

Further Reading

Bettelheim, F. R. (1954). Tyrosine-O-sulfate in a peptide from fibrinogen. *J. Am. Chem. Soc.* **76**, 2838–2839.

Huttner, W. B. (1982). Sulphation of tyrosine residues – a widespread modification of proteins. *Nature (London)* **299**, 273–276.

Huttner, W. B. (1984). Determination and occurrence of tyrosine O-sulfate in proteins. *Meth. Enzymol.* **107**, 200–223.

Huttner, W. B., and Baeuerle, P. A. (1988). Protein sulfation on tyrosine. *Mod. Cell Biol.* **6**, 97–140.

Huttner, W. B., Niehrs, C., and Vannier, C. (1991). Bind or bleed. *Curr. Biol.* **1**, 309–310.

Kehoe, J. W., and Bertozzi, C. R. (2000). Tyrosine sulfation: A modulator of extracellular protein–protein interactions. *Chem. Biol.* **7**, R57–R61.

Kehoe, J. W., Maly, D. J., Verdugo, D. E., Armstrong, J. I., Cook, B. N., Ouyang, Y. B., Moore, K. L., Ellman, J. A., and Bertozzi, C. R. (2002). Tyrosylprotein sulfotransferase inhibitors generated by combinatorial target-guided ligand assembly. *Bioorg. Med. Chem. Lett.* **12**, 329–332.

Moore, K. L. (2003). The biology and enzymology of protein tyrosine O-sulfation. *J. Biol. Chem.* **278**, 24243–24246.

Niehrs, C., Beisswanger, R., and Huttner, W. B. (1994). Protein tyrosine sulfation, 1993 – an update. *Chem. Biol. Interact.* **92**, 257–271.

Ouyang, Y.-B., Crawley, J. T. B., Aston, C. E., and Moore, K. L. (2002). Reduced body weight and increased postimplantation fetal death in tyrosylprotein sulfotransferase-1-deficient mice. *J. Biol. Chem.* **277**, 23781–23787.

Biography

Denis Corbeil is a Group Leader at the University of Dresden. His research interests are in the cell biology of stem cells, with a focus on prominin/CD133. He holds a Ph.D. from the University of Montreal and received postdoctoral training in the laboratory of W.B. Huttner, where he participated in the molecular cloning of TPST.

Wieland B. Huttner is a Professor of Neurobiology and Director at MPI-CBG in Dresden. His group made seminal contributions on protein tyrosine sulfation, including the identification, characterization, purification, and cloning of TPST. He holds an M.D. from the University of Hamburg, received postdoctoral training with Nobel Laureate Paul Greengard at Yale University, and has been pursuing research on neurosecretory vesicle biogenesis and neurogenesis in the mammalian central nervous system.

Ubiquitin System

Aaron Ciechanover and Michael H. Glickman
Technion – Israel Institute of Technology, Haifa, Israel

In the ubiquitin system, a target substrate is modified by ubiquitin or a ubiquitin-like protein. In most cases, proteins are modified by multiple moieties of ubiquitin, generating a polyubiquitin chain. This modification leads to their degradation by the 26S proteasome complex. Modification by a single moiety of ubiquitin can target proteins for degradation in the lysosome/vacuole. Modification by ubiquitin-like proteins serves nonproteolytic functions. Conjugation of ubiquitin is carried out by a modular cascade of enzymes, specific to each substrate. Ubiquitination of cellular proteins is a highly complex, temporally controlled, and tightly regulated process that targets in a specific manner thousands of cellular proteins and plays major roles in a variety of basic pathways, such as cell division, differentiation, and quality control. Not surprisingly, aberrations in the system underlie the pathogenesis of many diseases, certain malignancies, and neurodegenerative disorders. Mechanism-based drugs are currently being developed.

Mechanisms of Ubiquitination and Degradation

Ubiquitination

Degradation of a protein via the ubiquitin–proteasome pathway involves two discrete and successive steps: (1) tagging of the substrate by covalent attachment of multiple ubiquitin molecules, and (2) degradation of the tagged protein by the 26S proteasome complex with release of free and reusable ubiquitin. This last process is mediated by ubiquitin-recycling isopeptidases (deubiquitinating enzymes). Conjugation of ubiquitin, a highly evolutionarily conserved 76 residue polypeptide, to the protein substrate proceeds via a three-step cascade mechanism. Initially, the ubiquitin-activating enzyme, E1, activates ubiquitin in an ATP-requiring reaction to generate a high-energy thiol ester intermediate, E1-S~ubiquitin. One of several E2 enzymes (ubiquitin-carrier proteins or ubiquitin-conjugating enzymes (UBCs)) transfers the activated ubiquitin from E1, via an additional high-energy thiol ester intermediate, E2-S ~ ubiquitin, to the substrate that is specifically bound to a member of the ubiquitin-protein ligase family, E3. There are a number of different classes of E3 enzymes. For the homologous to the E6-AP C-terminus (HECT) domain E3s, the ubiquitin is transferred once again from the E2 enzyme to an active site Cys residue on the E3, to generate a third high-energy thiol ester intermediate, ubiquitin-S ~ E3, prior to its transfer to the ligase-bound substrate. RING finger-containing E3s catalyze direct transfer of the activated ubiquitin moiety to the E3-bound substrate.

E3s catalyze the last step in the conjugation process: covalent attachment of ubiquitin to the substrate. The ubiquitin molecule is generally transferred to an ε-NH_2 group of an internal lysine residue in the substrate to generate a covalent isopeptide bond. In some cases however, ubiquitin is conjugated to the N-terminal amino group of the substrate. By successively adding activated ubiquitin moieties to internal lysine residues on the previously conjugated ubiquitin molecule, a polyubiquitin chain is synthesized. The chain is recognized by the downstream 26S proteasome complex. Thus, E3s play a key role in the ubiquitin-mediated proteolytic cascade since they serve as the specific recognition factors of the system. In certain cases the first ubiquitin moiety is conjugated to the substrate by one E3, while chain elongation is catalyzed by a different ligase often termed E4. Modification by a single moiety of ubiquitin is catalyzed via an identical mechanism and set of enzymes. The specific enzymes that catalyze modification by ubiquitin-like proteins are somewhat different, though they utilize a similar mechanism.

Degradation

Degradation of polyubiquitinated substrates is carried out by a large protease complex, the 26S proteasome that does not recognize nonmodified substrates. In one established case, that of the polyamine synthesizing enzyme ornithine decarboxylase (ODC), the proteasome recognizes and degrades the substrate without prior ubiquitination. The proteasome is a multicatalytic protease that degrades polyubiquitinated proteins to short peptides. It is composed of two subcomplexes: a 20S core particle (CP) that carries the catalytic activity, and a regulatory 19S regulatory particle (RP). The 20S CP is a barrel-shaped structure composed of four

stacked rings, two identical outer α-rings and two identical inner β-rings. The eukaryotic α- and β-rings are composed each of seven distinct subunits, giving the 20S complex the general structure of $\alpha_{1-7}\beta_{1-7}\beta_{1-7}\alpha_{1-7}$. The catalytic sites are localized to some of the β-subunits. Each extremity of the 20S barrel can be capped by a 19S RP. One important function of the 19S RP is to recognize ubiquitinated proteins and other potential substrates of the proteasome. A ubiquitin-binding subunit of the 19S RP has indeed been identified; however, its importance and mode of action have not been discerned. A second function of the 19S RP is to open an orifice in the α-ring that will allow entry of the substrate into the proteolytic chamber. Also, since a folded protein would not be able to fit through the narrow proteasomal channel, it is assumed that the 19S particle unfolds substrates and inserts them into the 20S CP. Both the channel opening function and the unfolding of the substrate require metabolic energy, and indeed, the 19S RP contains six different ATPase subunits. Following degradation of the substrate, short peptides derived from the substrate are released, as well as reusable ubiquitin. Proteasomal degradation is not always complete. In some cases, the proteasome, rather than completely destroying its target, processes the ubiquitinated substrate precisely, releasing a truncated product. In the case of the NF-κB transcriptional regulator, an active subunit (p50 or p52) is thus released from a longer inactive precursor (p105 or p100). For a general scheme of the ubiquitin system and its multiple functions, see Figure 1.

Substrate Recognition

A major unresolved question is how does the system achieve its high specificity and selectivity. Why are certain proteins extremely stable in the cell, while others are extremely short-lived? Why are certain proteins degraded only at a particular time point during the cell cycle or only following specific extracellular stimuli, yet they are stable under most other conditions? It appears that specificity of the ubiquitin system is determined by two distinct and unrelated groups of proteins: E3s and ancillary proteins. First, within

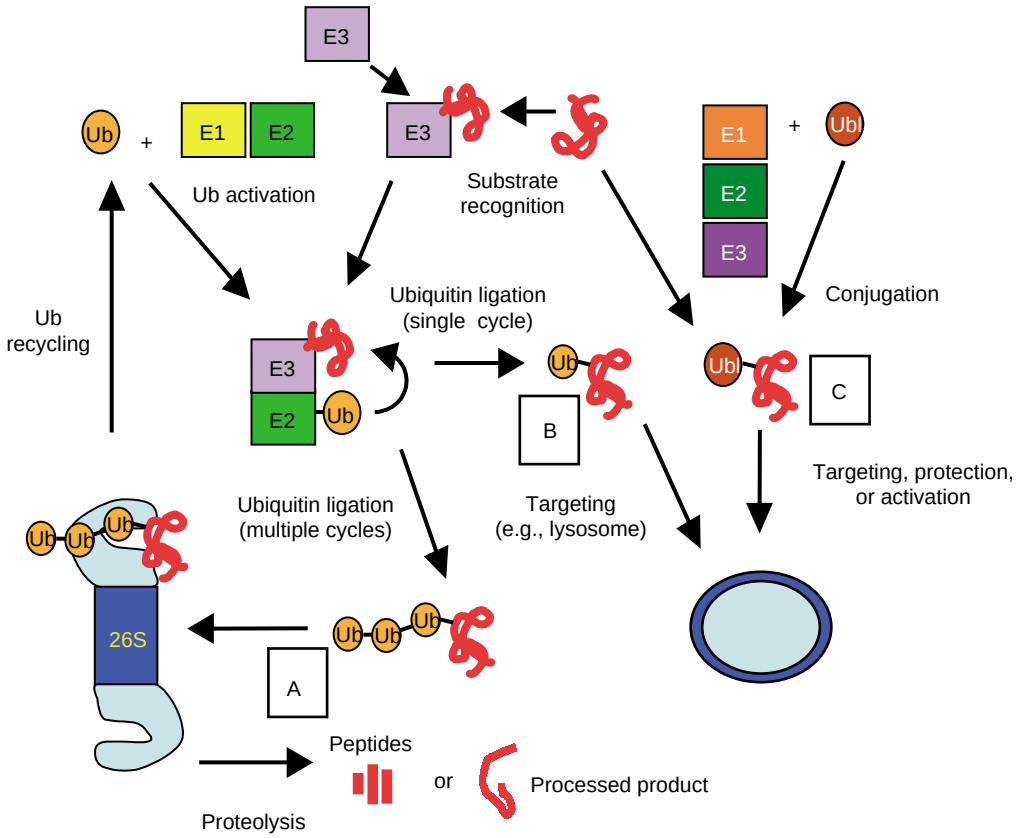

FIGURE 1 The ubiquitin system for protein modification. Ubiquitin (Ub) is activated by the three enzymes E1, E2, and E3, and the active ubiquitin moiety is transferred to the target substrate (red). Substrates can be either modified by a polyubiquitin chain (A) and targeted to the 26S proteasome complex for degradation (or processing), or modified by a single ubiquitin moiety, monoubiquitinated (B) and targeted to other organelles such as the lysosome (wherein it is degraded). Ubiquitin-like proteins (Ubl) are activated by E1, E2, and E3, which are similar but not identical to the enzymes that activate ubiquitin. Modification by Ubl (C) serves a variety of nonproteolytic functions such as routing of proteins to subcellular organelles (e.g., nucleus), protecting them from ubiquitination, or activating them.

the ubiquitin system, substrates must be specifically recognized by an appropriate E3 as a prerequisite to their ubiquitination. In most cases however, substrates are not recognized in a constitutive manner, and in some cases they are not recognized directly by the E3. In some instances, the E3 must "be switched on" by undergoing posttranslational modification in order to yield an active form that recognizes the substrate. In many other cases, it is the substrate that must undergo a certain change that renders it susceptible for recognition. The stability of additional proteins depends on association with ancillary proteins such as molecular chaperones that act as recognition elements in *trans* and serve as a link to the appropriate ligase. Others, such as certain transcription factors, have to dissociate from the specific DNA sequence to which they bind in order to be recognized by the system. Stability of yet other proteins depends on oligomerization. Thus, in addition to the E3s themselves, modifying enzymes (such as kinases), ancillary proteins, or DNA sequences to which substrates bind also play an important role in the recognition process.

Functions and Substrates of the Ubiquitin System

Ubiquitin-mediated proteolysis of a variety of cellular proteins plays an important role in many basic cellular processes. Among these are regulation of cell cycle and division, differentiation and development, involvement in the cellular response to stress and extracellular effectors, morphogenesis of neuronal networks, modulation of cell surface receptors, ion channels and the secretory pathway, DNA repair, transcriptional regulation, transcriptional silencing, long-term memory, circadian rhythms, regulation of the immune and inflammatory responses, and biogenesis of organelles. The list of cellular proteins that are targeted by ubiquitin is growing rapidly. Among them are cell-cycle regulators such as cyclins, cyclin-dependent kinase inhibitors, and proteins involved in sister chromatid separation, tumor suppressors, transcriptional activators, and their inhibitors. Cell surface receptors and endoplasmic reticulum (ER) proteins are also targeted by the system. Finally, mutated and denatured/misfolded proteins are recognized specifically and removed efficiently. In this capacity, the system is a key player in the cellular quality control and defense mechanisms. The products of the proteasome can play an important role in the immune response. In the case of degradation of foreign proteins – such as those of viral origin – the resulting short peptides are presented by MHC class I molecules to the cytotoxic T cell that lyse the presenting cell.

Regulation of the Ubiquitin System

The ubiquitin–proteasome pathway can be regulated at the level of ubiquitination or at the level of proteasome activity. Since conjugation and proteasomal degradation is required for multitude of cellular functions, regulation must be delicately and specifically tuned. In a few cases, general rather than specific, components of the pathway can be modulated by physiological signals. For example, up-regulation of the pathway is observed during massive degradation of skeletal muscle proteins that occurs under normal fasting, but also under pathological conditions such as cancer cachexia, severe sepsis, metabolic acidosis, or following denervation. In most cases however, regulation is specific and the target substrates are recognized by specific ligases that bind to defined motifs. The targeting motif can be a single amino acid residue (e.g., the N-terminal residue) or a sequence (the "destruction" box in cyclins) or a domain (such as a hydrophobic patch) that is not normally exposed. In other cases the motif is a posttranslational modification such as phosphorylation that is generated in response to cell needs or external signals. Phosphorylation can occur either on the substrate or on the ligase.

Ubiquitin-Like Proteins

Both enzymes and substrates of the ubiquitin system have been found to be modified by ubiquitin-like proteins. Modification by ubiquitin-like proteins occurs only once. In the case of enzymes, modification affects their activity. For example, the modification by the ubiquitin-like protein NEDD8 enhances the activity of a certain class of E3 ligases. Conjugation of NEDD8 to one of the components of the ligase complex (Cullin) increases its affinity to other components of the conjugation machinery. In the case of substrates, modification can affect their availability to the ubiquitination/degradation machinery and consequently cellular stability. For example, in the case of IκBα, the inhibitor of the transcriptional regulator NF-κB, modification by SUMO-1 was shown to protect the substrate from ubiquitination. In a completely different case, SUMOylation of RanGAP1 targets the protein to its final subcellular destination in the nuclear pore complex.

Ubiquitination and Pathogenesis of Human Diseases

Diseases

While inactivation of a major enzyme such as E1 is obviously lethal, mutations or acquired changes in

enzymes or in recognition motifs in substrates that do not affect vital pathways or that affect the involved process only partially, may result in a broad array of diseases. The pathological states associated with the ubiquitin system can be classified into two groups: those that result from (1) loss of function – mutation in a ubiquitin system enzyme or target substrate that result in stabilization of certain proteins, and (2) gain of function – abnormal or accelerated degradation of the protein target.

Alterations in ubiquitination and deubiquitination reactions have been directly implicated in the etiology of many malignancies. In general, cancers can result from "stabilization" of oncoproteins, or "destabilization" of tumor suppressor gene products. Some of the natural substrates for degradation by the proteasome are oncoproteins that, if not properly removed from the cell, can promote cancer. For instance, ubiquitin targets N-myc, c-myc, c-fos, c-jun, Src, and the adenovirus E1A proteins. Destabilization of tumor suppressor proteins such as p53 and p27 has also been implicated in the pathogenesis of malignancies.

In one fascinating case, that of uterine cervical carcinoma, the level of the tumor suppressor protein p53 is extremely low. Most of these malignancies are caused by high-risk strains of the human papillomavirus (HPV). Detailed studies have shown that the suppressor is targeted for ubiquitin-mediated degradation by the virally encoded oncoprotein E6. Degradation is mediated by the native HECT domain E3 enzyme E6-AP, where E6 serves as an ancillary protein that allows recognition of p53 in *trans*. E6-AP will not recognize p53 in the absence of E6. E6 associates with both the ubiquitin-ligase and the target substrate and brings them to the necessary proximity that is assumed to allow catalysis of conjugation to occur. Removal of the suppressor by the oncoprotein is probably an important mechanism used by the virus to transform cells.

Accumulation of ubiquitin conjugates and/or inclusion bodies associated with ubiquitin, proteasome, and certain disease-characteristic proteins have been reported in a broad array of chronic neurodegenerative diseases, such as the neurofibrillary tangles of Alzheimer's disease (AD), brainstem Lewy bodies (LBs) – the neuropathological hallmark in Parkinson's disease (PD), and nuclear inclusions in CAG repeat expansion (poly-glutamine expansion) disorders such as occurring Huntington's disease. However, in all these cases, a direct pathogenetic linkage to aberrations in the ubiquitin system has not been established. One factor that complicates the establishment of such linkage is the realization that many of these diseases, such as Alzheimer's and Parkinson's, are not defined clinical entities, but rather syndromes with different etiologies. Accumulation of ubiquitin conjugates in Lewy inclusion bodies in many of these cases may be secondary, and reflects unsuccessful attempts by the ubiquitin and proteasomal machineries to remove damaged/abnormal proteins. While the initial hypothesis was that inclusion bodies are generated because of the inherent tendency of the abnormal proteins to associate with one another and aggregate, it is now thought that the process may be more complex and involves active cellular machineries, including inhibition of the ubiquitin system by the aggregated proteins. This aggregation of brain proteins into defined lesions is emerging as a common, but poorly understood mechanistic theme in many sporadic and hereditary neurodegenerative disorders.

The case of Parkinson's disease highlights the complexity of the involvement of the ubiquitin system in the pathogenesis of neurodegeneration. Aberrations in several proteins such as mutations in α-synuclein, an important neuronal protein, or in the deubiquitinating enzyme UCH-L1, have been described that link the ubiquitin system to the pathogenesis of the disease. One important player in the pathogenesis of Parkinson's disease is Parkin which is a RING-finger E3. Mutations in the gene appear to be responsible for the pathogenesis of autosomal recessive juvenile parkinsonism (AR-JP), one of the most common familial forms of Parkinson's disease. Parkin ubiquitinates and promotes the degradation of several substrates. It is possible that aberration in the degradation of one of these substrates that leads to its accumulation is neurotoxic and underlies the pathogenesis of AR-JP.

The cystic fibrosis gene encodes the CF transmembrane regulator (CFTR) that is a chloride channel. Only a small fraction of the protein matures to the cell surface, whereas most of it is degraded from the ER by the ubiquitin system prior to its maturation. One frequent mutation in the channel is ΔF508. The mutation leads to an autosomal recessive inherited multisystem disorder characterized by chronic obstruction of airways and severe maldigestion due to exocrine pancreatic dysfunction. Despite normal ion channel function, $CFTR^{\Delta F508}$ does not reach the cell surface at all, and is retained in the ER from which it is degraded. It is possible that the rapid and efficient degradation results in complete lack of cell-surface expression of the ΔF508 protein, and therefore contributes to the pathogenesis of the disease.

Drug Development

Because of the central role the ubiquitin system plays in such a broad array of basic cellular processes, development of drugs that modulate the activity of the system may be difficult. Inhibition of enzymes common to the entire pathway, such as the proteasome, may affect many processes nonspecifically, although a narrow window between beneficial effects and toxicity can be identified

for a short-term treatment. Recent experimental evidence strongly suggests that such inhibitors may indeed be beneficial in certain pathologies, such as in multiple myeloma, a malignancy that affects the bone marrow.

A completely different approach to drug development can be the development of small molecules that interfere with the activity of specific E3s. For example, peptides that bind specifically to HPV-E6 can prevent its association with p53 and interfere with its targeting by E6-AP. Such peptides were able to induce p53 in HPV-transformed cells with subsequent reversal of certain malignant characteristics and induction of apoptosis.

See Also the Following Articles

26S Proteasome, Structure and Function • Ornithine Cycle • Proteasomes, Overview • Protein Degradation • SUMO Modification • Ubiquitin-Like Proteins

Glossary

proteolysis/degradation Hydrolysis of a protein which is a heteropolymer of amino acids to short peptides, which contain a few amino acids, and/or to single amino acids.

ubiquitination Covalent modification of a protein by the small protein ubiquitin.

Further Reading

Glickman, M. H., and Ciechanover, A. (2002). The ubiquitin–proteasome proteolytic pathway: Destruction for the sake of construction. *Physiol. Rev.* **82**, 373–428.

Goldberg, A. L., Elledge, S. J., and Wade, J. (2001). The cellular chamber of doom. *Sci. Am.* January, 68–73.

Hilt, W., and Wolf, D. H. (eds) (2000). *Proteasomes: The World of Regulatory Proteolysis*. Eurekah.com/LANDES BIOSCIENCE Publishing Company, Georgetown, Texas, USA.

Weissman, A. M. (2001). Themes and variations on ubiquitylation. *Nat. Rev. Cell Mol. Biol.* **2**, 169–179.

Biography

Aaron Ciechanover is a Distinguished Professor in the Cancer and Vascular Research Center in the Faculty of Medicine at the Technion, Haifa, Israel. His principal research interests are regulation of transcriptional factors by the ubiquitin system. He holds an M.D. from "Hadassah" Medical School of the Hebrew University in Jerusalem, and a Ph.D. in biochemistry from the Technion. While a graduate student of Dr. Avram Hershko, the two discovered the principles and machinery of ubiquitination as a degradation signal.

Michael Glickman is an Associate Professor in the Department of Biology at the Technion. His principal research interest is mechanisms of proteolysis by the proteasome, and proteasome composition. He holds a Ph.D. in chemistry from the University of California at Berkeley. As a research fellow with Dr. Dan Finley at Harvard Medical School, he uncovered the basic structure of the regulatory complex of the proteasome.

Ubiquitin-Like Proteins

Edward T. H. Yeh
The University of Texas, Houston, Texas, USA

Ubiquitin is a small polypeptide that covalently attaches to other proteins, which marks them for degradation by the proteasome. Ubiquitin regulates many important cellular processes, such as signal transduction, cell-cycle progression, and the transformation of normal to malignant cells. Several ubiquitin-like proteins, such as sentrin (also called SUMO) and NEDD8/Rub1 have also been discovered. Similar to ubiquitin, these ubiquitin-like proteins also modify other proteins. However, they do not trigger proteasomal degradation. Sentrin, in a process called sentrinization, usually produces a change of the target protein's cellular localization and function. NEDD8, with cullin as its substrate, is a key component of the ubiquitin ligase complex. Thus, NEDD8, in a process called neddylation, indirectly regulates the ubiquitin/proteasome system. Sentrinization and neddylation require unique enzymes – E1, E2, and E3 – that are distinct from those involved in the ubiquitin pathway. Furthermore, both sentrinization and neddylation can be regulated by proteases that specifically remove sentrin or NEDD8 from their cellular targets.

Sentrin

There are three sentrins. Sentrin-1 is a 101-amino-acid protein containing a ubiquitin homology domain (residues 22–97) that is 48% homologous to human ubiquitin (see Figure 1). Sentrin-2 is a 95-amino-acid polypeptide that is 66% similar to sentrin-1 in its ubiquitin homology domain. Sentrin-3 is a 103-amino-acid polypeptide that is 97% identical to sentrin-2 in its ubiquitin homology domain. All sentrins have distinct N-terminal amino-acid sequences and C-terminal extensions. In addition, the Gly–Gly residues required for sentrinization are conserved in all sentrins (Figure 1).

Activation, Conjugation, and Ligation of Sentrins

The amino acids following the conserved Gly–Gly residues in all sentrins are cleaved by C-terminal hydrolases. The resultant sentrin monomer is then transferred to a specific E1 complex (Figure 2). The activating enzyme (E1) for sentrin is composed of two subunits, AOS1 and UBA2. The human AOS1 protein is 56% similar to the N-terminal half of the ubiquitin E1. The human UBA2 protein, which is homologous to the C-terminal half of the ubiquitin E1, contains the active-site cysteine residue required for the formation of a thiol ester linkage with sentrins. The activated sentrin molecule attached to E1 is then transferred to a carrier protein, E2.

In contrast to the large number of E2s involved in ubiquitination, sentrin utilizes only UBC9 as the carrier protein. This exclusive usage of UBC9 is probably explained by the existence of a 5-residue insertion that forms an exposed tight β-hairpin and a 2-residue insertion that forms a bulge in a loop close to the active site of UBC9. The surface of UBC9 involved in sentrin-1 binding is positively charged, whereas the corresponding surface in sentrin-1 is negatively charged. Moreover, the face of UBC9 remote from the catalytic site possesses a distinct electrostatic potential that may account for the propensity of UBC9 to interact with other proteins.

There are at least three different E3 involved in sentrinization. RanBP2, a protein that has been localized in the nuclear pore complex, serves as the E3 for Sp100 and histone deacetylase 4. RanBP2 also binds to UBC9, suggesting that sentrinization could take place at the nuclear pore complex. Another E3, PIAS (protein inhibitor of activated STAT), promotes sentrinization of the androgen receptor, c-JUN, p53, and Sp3. Finally, the human polycomb group protein, Pc2, functions as an E3 for a generalized transcription repressor, CtBP.

Proteins Modified by Sentrin

The list of sentrinized proteins has been expanding rapidly. Three examples that have been characterized are discussed here, viz., PML, RanGAP1, and IκBα.

PML, a RING finger protein with tumor suppressor activity, has been implicated in the pathogenesis of acute promyelocytic leukemia, which arises following a reciprocal chromosomal translocation that fuses the PML gene with the retinoic acid receptor α (RARα) gene. PML can be modified by all sentrins, but not by ubiquitin or NEDD8. Two forms of PML-RARα fusion proteins have been found to be expressed in acute


```
Sentrin-1(1-50) MSD----QEAKPST  EDLGDKKEGE  -YIKLKVIGQD  SSEIHFKVKM  TTHLKKLKES
Sentrin-2(1-46) MAD-----E-KPK-  E--GVKTENN  DHINLKVAGQD  GSVVQFKIKR  HTPLSKLMKA
Sentrin-3(1-45) MSE-----E-KPK-  E--GVKTEN-  DHINLKVAGQD  GSVVQFKIKR  HTSLSKLMKA
NEDD8(1-29)                               MLIKVKTLT  GKEIEIDIEP  TDKVERIKER
Ubiquitin(1-29)                           MQIFVKTLT  GKTITLEVEP  SDTIENVKAK

Sentrin-1(51-101)    YCQRQGVPMN  SLRFLFEGQR  IADNHTPKEL  GMEEEDVIEV  YQEQTGGHSTV
Sentrin-2(47-95)     YCERQGLSMR  QIRFRFDGQP  INETDTPAQL  EMEDEDTIDV  FQQQTGGVY
Sentrin-3(46-103)    YCERQGLSMR  QIRFRFDGQP  INETDTPAQL  RMEDEDTIDV  FQQQTGGVPESSLAGHSF
NEDD8(30-81)         VEEKEGIPPQ  QQRLIYSGKQ  MNDEKTAADY  KILGGSVLHL  VLALRGGGGLRQ
Ubiquitin(30-76)     IQDKEGIPPD  QQRLIFAGKQ  LEDGRTLSDY  NIQKESTLHL  VLRLRGG
```

FIGURE 1 Alignment of sentrin-1, sentrin-2, sentrin-3, NEDD8, and ubiquitin. The conserved C-terminal glycine–glycine residues were printed in bold.

promyelocytic leukemia. Remarkably, neither can be sentrinized *in vivo*. Extensive mutational analysis of PML has shown that Lys65 in the RING finger domain, Lys160 in the B1 Box, and Lys490 in the nuclear localization signal constitute three major sentrinization sites. The PML mutant with Lys to Arg substitutions in all three sites is expressed normally but cannot be sentrinized. It also cannot recruit Daxx to the nuclear body. The lack of sentrinization of PML eliminates PML's transcriptional coactivator activity.

RanGAP1, a major regulator of the Ras-like GTPase Ran, which plays a critical role in the bidirectional transport of proteins and ribonucleoproteins across the nuclear pore complex was the first protein shown to be modified by sentrin-1. The 90 kDa sentrinized form of RanGAP1 associates with RanBP2 of the nuclear pore complex, whereas the 70 kDa unmodified form of RanGAP1 is exclusively cytoplasmic. Thus, sentrinization is critical for RanGAP1 to translocate to the nuclear pore. Interestingly, RanGAP1 cannot be modified by sentrin-2/3.

Although most sentrinized proteins are localized in the nucleus or associated with the nuclear envelope, a cytosolic protein, IκBα, can also be modified by sentrin-1.

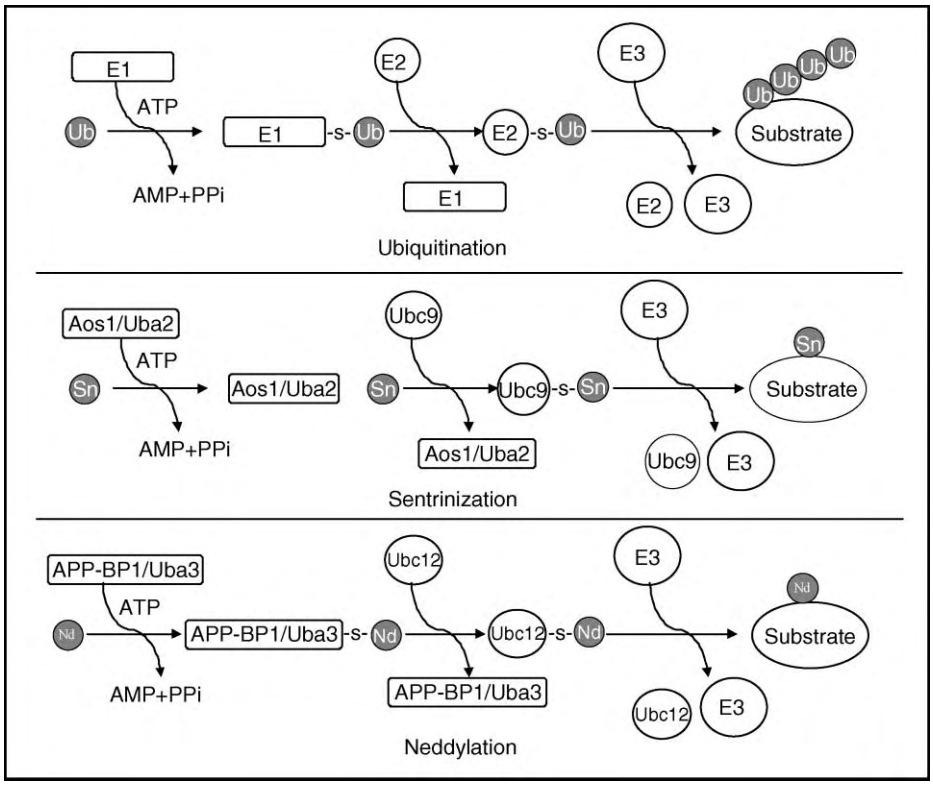

FIGURE 2 Schematic diagram of ubiquitination, sentrinization, and neddylation. E1: activating enzyme; E2: conjugating enzyme; E3: ligases. The E1 for the sentrinization pathway consists of Aos1 and Uba2, whereas the E1 for the neddylation pathway consists of APP-BP1 and Uba3. The E2 for the sentrinization pathway is Ubc9, whereas the E2 for the neddylation pathway is Ubc12. There are multiple E2s for the ubiquitination pathway. Ub: ubiquitin; Sn: sentrin: Nd: NEDD8.

IκBα is a cytosolic inhibitor of NFκB, a transcription factor involved in the induction of a large number of proteins involved in inflammation. IκBα is phosphorylated on serine residues 32 and 36 following tumor necrosis factor stimulation. The phosphorylated form of IκBα is then polyubiquitinated on lysine residues 21 and 22 and degraded by the proteasome. Unlike ubiquitination, sentrinization of IκBα on lysine residue 21 is inhibited by prior phosphorylation. Furthermore, sentrinized IκBα cannot be ubiquitinated and is resistant to proteasomal degradation. Thus, sentrinization can compete with ubiquitination for the same Lys residue on target proteins, effectively constitutes an antiubiquitin process.

By comparing the amino-acid sequences surrounding the acceptor lysine residues, a sentrinization consensus sequence can be formulated. It appears that the acceptor Lys residue is preceded by a hydrophobic amino acid (Ile or Leu) and followed by a polar amino acid, such as Gln, Thr, and a charged amino acid, Glu. The general consensus formula is (I/L)K(Q/T)E.

De-Sentrinization

In yeast, there are two sentrin-specific proteases (SENPs) that deconjugate sentrin from its substrate. Ulp1 possesses both isopeptidase and C-terminal hydrolase activity and is essential for the transition from G2 to the M phase of the cell cycle, the same phenotype observed for the Ubc9 mutation in yeast. These observations suggest that sentrinization and de-sentrinization are required for cell-cycle progression in yeast. Ulp2, on the other hand, is not essential for cell viability. The Ulp2 mutant exhibits a pleiotropic phenotype that includes temperature-sensitive growth, abnormal cell morphology, and decreased plasmid and chromosome stability. The mutant is also hypersensitive to DNA-damaging agents, such as hydroxyurea. Ulp1 is localized in the nuclear envelope, whereas Ulp2 is in the nucleus.

In humans, there are three well-characterized SENPs. All human SENPs have conserved C-terminal region, even though they vary in size. The similarity between yeast Ulp1, Ulp2, and human SENPs is confined primarily to the C-terminal region of ~200 amino acids, within which a ~90-residue segment forms a core structure common to cysteine proteases. It appears that the conserved C termini of the SENPs contain the catalytic domain, whereas the N termini regulate their cellular localization and substrate specificity. SENP1 is localized in the nucleus, excluding the nucleolus; SENP2 is localized in the nuclear envelope and also forms nuclear speckles; and SENP3 is localized predominantly in the nucleolus. Both SENP1 and SENP2 can deconjugate sentrinized PML but not RanGAP1. In addition, SENP1 and SENP2 can deconjugate many sentrinized nuclear proteins. However, SENP3 appears to have more restricted substrate specificity.

In summary, the sentrin system possesses its own E1, E2, E3, and deconjugating enzymes, which serve to regulate an increasingly recognized cellular processes.

NEDD8/Rub1

NEDD8 is a small protein consisting of 81 amino acids that is 80% homologous to ubiquitin (see Figure 1). The yeast and plant homologues of NEDD8 have been termed Rub1 (*r*elated to *ub*iquitin *1*) and are processed and conjugated to a small number of cellular proteins. The overall structures of NEDD8 and Rub1 are quite similar to those of ubiquitin. The major difference occurs in two surface regions with a different electrostatic surface potential. Thus, unlike sentrin-1, NEDD8 is structurally more closely related to ubiquitin.

Activation and Conjugation of NEDD8 and Rub1

UCH-L3, one of the ubiquitin C-terminal hydrolases, also binds to NEDD8 and functions as a NEDD8 C-terminal hydrolase. Following processing of its C terminus, NEDD8 is transferred to its E1.

The E1 for human NEDD8 is composed of two subunits, APP-BP1 and UBA3. The human APP-BP1 protein is 56% similar to the N-terminal half of ubiquitin's E1. The human UBA3 protein, which is homologous to the C-terminal half of ubiquitin's E1, contains the active-site cysteine residue required for the formation of thiol ester linkage with NEDD8. A similar E1 has also been identified in yeast and plants. The counterpart of APP-BP1 has been named AXR1 in plant. The importance of the Rub1 conjugation system is highlighted by the requirement of the AXR1 protein for the normal response to the plant hormone auxin in *Arabidopsis thaliana*. The specificity of NEDD8's E1 is due, in part, to the preferential binding of UBA3 to NEDD8, but not to ubiquitin or sentrin-1. The conjugating enzyme for NEDD8 or Rub1 is UBC12. A dominant-negative form of UBC12 could abolish NEDD-8 conjugation *in vivo* and inhibit cell growth.

Rub1/NEDD8 Modification of CDC53/Cullins

The major substrate for Rub1 in yeast is Cdc53 (also known as yeast cullin), a 94 kDa protein required for the G_1 to S phase of the cell-cycle progression. Cdc53 is a common subunit of the SCF complex, a ubiquitin ligase (E3) composed of *S*kp1, *C*dc53/cullin, and an *F* box

protein. There are many F-box proteins, which play a critical role in conferring substrate specificity to the SCF complex. For example, the F-box protein, Cdc4, forms a SCF^{Cdc4} complex with Skip1 and Cdc53/cullin that binds to phosphorylated Sic1 and catalyzes its ubiquitination.

In mammalian cells, NEDD8 modifies a limited number of human cellular proteins that primarily localized in the nucleus. Interestingly, all of the known NEDD8 targets in mammalian cells are cullins. Human Cul-1 is a major component of the SCF complex that is involved in the degradation of $I\kappa B\alpha$, β-catenin, and p27. The neddylation of Cul-1 dissociates CAND1, an inhibitor of Cul-1–SKP1 complex formation. The suppression of CAND1 therefore increases the level of the CuL-1–SKP1 complex. Thus, the neddylation of Cul-1 enhances the formation of the SCF complex, which in turn stimulates protein polyubiquitination. Human Cul-2 binds to the von Hippel-Lindau gene product through elongin B and elongin C to form a complex (Cul-2–VBC complex) that appears to have ubiquitin ligase activity. The VBC complex itself promotes, but is not essential for, NEDD8 conjugation to Cullin-2. Human Cul-3 was initially identified as a salicylate suppressible protein with unknown mechanism of activation, and was recently shown to be involved in the ubiquitination of cyclin E to control the S phase in mammalian cells. Human Cul-4A associates with UV-damaged DNA-binding protein and may play a role in DNA repair. Thus, the cullins may constitute a family of ubiquitin E3 ligases that have diverse biologic functions, with the neddylation of cullins playing a crucial role in ligase activity.

Regulation of NEDD8-Conjugates

There are several proteins that regulate NEDD8 conjugates. USP21 is a ubiquitin-deconjugating enzyme that is also capable of removing NEDD8 from NEDD8 conjugates. The overexpression of USP21 profoundly inhibits growth of U2OS cells. DEN1 is a specific protease for NEDD8 conjugates, as it has no activity against ubiquitin or sentrin conjugates. DEN1 can de-neddylate NEDD8 conjugated Cul-1. Interestingly, DEN1 is highly homologous to the catalytic domain of SENP. The COP9 signalosome (CSN) is an evolutionarily conserved multiprotein complex composed of eight subunits. It was first identified as an essential component in the repression of light-regulated development in *Arabidopsis*. CSN interacts with the SCF-type E3 ubiquitin ligases containing Cul1, which suggests that CSN and SCF-type E3 ubiquitin ligases are closely related. Indeed, CSN promotes the cleavage of NEDD8 from neddylated Cul1. The Jab1/MPN domain metalloenzyme motif in Csn5 subunit is responsible for the de-neddylation activity of CSN. Thus, CSN binds to SCF-type E3 ubiquitin ligases and probably regulates their activity through the de-neddylation of conjugated Cul-1. NUB1, an interferon-inducible protein, also regulates the neddylation system. The overexpression of NUB1 leads to the disappearance of most neddylated proteins. NUB1 appears to act by recruiting NEDD8 and its conjugates to the proteasome for degradation, further highlighting the close functional tie between neddylation and ubiquitination.

See Also the Following Articles

Proteasomes, Overview • SUMO Modification • Ubiquitin System

Glossary

neddylation The process of modifying a substrate with NEDD8.

proteasome A cellular organelle specialized in degrading ubiquitin-conjugated proteins.

sentrinization The process of modifying a substrate with sentrin/SUMO.

ubiquitination The process of modifying a substrate with ubiquitin.

Further Reading

Hay, R. T. (2001). Protein modification by SUMO. *Trends Biochem. Sci.* **26**, 332–333.

Melchior, F. (2000). SUMO – nonclassical ubiquitin. *Annu. Rev. Cell Dev. Biol.* **16**, 591–626.

Yeh, E. T. H., Gong, L., and Kamitani, T. (2000). Ubiquitin-like proteins: New wines in new bottles. *Gene* **248**, 1–14.

Biography

Edward T.H. Yeh is Chairman of the Department of Cardiology at the University of Texas M.D. Anderson Cancer Center and Director of the Research Center for Cardiovascular Diseases at the Institute of Molecular Medicine at the University of Texas-Houston Health Science Center. He holds an M.D. from the University of California, Davis and received his postdoctoral training at Harvard University. His laboratory was among the first to show that sentrin and NEDD8 can be covalently conjugated to other proteins.

UmuC, D Lesion Bypass DNA Polymerase V

Zvi Livneh
Weizmann Institute of Science, Rehovot, Israel

DNA polymerase V from the bacterium *Escherichia coli* (*E. coli*) is specialized to perform DNA synthesis across DNA lesions. The latter are sites in DNA that were chemically damaged by radiation or chemicals, and which usually block DNA replication. The reaction catalyzed by pol V is called translesion synthesis (TLS), translesion replication (TLR), or lesion bypass. It is usually mutagenic, since the coding properties of damaged nucleotides in DNA are often different from those of the original undamaged nucleotides. Pol V is a heterotrimer composed of one molecule of the UmuC protein (48 kDa), and two molecules of the UmuD′ protein (12 kDa each). UmuD′ is a proteolytic cleavage product of a larger protein, termed UmuD (15 kDa). The UmuD and UmuC proteins are encoded by an operon that is induced by DNA-damaging agents, under regulation of the SOS response. Pol V is a low-fidelity DNA polymerase, which does not have an exonuclease proofreading activity, and exhibits low processivity. Its lesion-bypass activity requires two additional proteins, RecA, which is also the main recombinase in *E. coli*, and single-strand DNA-binding protein (SSB), a protein essential for replication. In addition, pol V is stimulated by the processivity proteins of pol III, namely, the β-subunit DNA sliding clamp, and the γ-complex clamp loader. By virtue of its mutagenic lesion-bypass activity, pol V is responsible for the formation of mutations by a variety of DNA-damaging agents that cause replication blocks, such as UV radiation, methymethanesulphonate (MMS), and more. Pol V homologues were conserved in evolution from *E. coli* to humans, and comprise the Y family of DNA polymerases.

Pol V and the SOS Response

The SOS response is a global stress response in *E. coli*, induced by DNA damage that causes interruption of DNA replication. It involves the induction of 30–40 genes, which collectively act to increase cell survival under adverse environmental conditions. SOS genes comprise a regulon, whose members are negatively regulated at the transcriptional level by the LexA repressor. Induction involves autocleavage of free LexA repressor, promoted by an activated form of the RecA. This cleavage shifts the binding equilibrium of LexA, causing it to dissociate from its target genes, thereby causing induction. RecA is usually activated by forming a complex of multiple RecA molecules bound to a stretch of single-stranded DNA (ssDNA), which is formed as a result of exposure to damaging agents. This RecA nucleoprotein filament has multiple roles in cellular responses to DNA damage. In addition to the induction of the SOS regulon, it promotes homologous recombination repair, and it is essential for lesion bypass by pol V. The *umuD* and *umuC* genes, encoding the two subunits of pol V, are arranged in an operon that is part of the SOS regulon (namely, its transcription is regulated by LexA and RecA), and are therefore inducible by DNA-damaging agents such as UV radiation or MMS. Mutations that inactivate *umuC* or *umuD* cause a drastic decrease in UV- or MMS-mutagenesis, with a minor effect on cell survival. This demonstrated the surprising phenomenon that mutagenesis caused by DNA-damaging agents is an inducible process, which requires specific gene products. In other words, mutagenesis is not merely a by-product of replication, and the presence of lesions in DNA does not cause mutations without the activity of specific inducible proteins.

The Discovery of Pol V

It took nearly two decades from the time the *umuC* and *umuD* genes were cloned, until the discovery that they encode a specialized lesion-bypass DNA polymerase. This long period of time is attributed to the great difficulty in obtaining UmuC in soluble and active form, the lack of any amino acid homology to classical DNA polymerases, and the complexity of the *in vitro* lesion-bypass assay system. In addition, genetic experiments had indicated that the *polC (dnaE)*, encoding the α subunit of pol III, was required for lesion bypass *in vivo*. This led to the incorrect model that the UmuC and UmuD′ proteins were accessory proteins, which enabled pol III to bypass DNA lesions. Finally, UmuCD′-dependent lesion bypass systems were reconstituted

from purified components, and led to the finding that UmuC has DNA polymerase activity, and together with UmuD′ it forms pol V. This discovery was made simultaneously and independently in the laboratories of Myron Goodman (University of Southern California, Los Angeles) and Zvi Livneh (Weizmann Institute of Science, Rehovot, Israel).

Model for the Mechanism of Lesion Bypass by Pol V

Pol V is unable to bypass lesions on its own. It requires two additional proteins, RecA and SSB, known to be involved in other DNA transactions such as replication and recombination. In addition, pol V is stimulated by the processivity proteins, which are also required for DNA replication. The RecA protein is required as a nucleoprotein complex with ssDNA, in which multiple RecA monomers form a protective helical sleeve around the DNA (Figure 1, stage 1). The RecA filament prevents nonproductive binding of pol V to ssDNA regions remote to the primer terminus, and it targets pol V to the primer-template region (Figure 1, stage 2). Once targeted to the primer-terminus site, the RecA filament needs to locally dissociate, to allow productive binding of pol V. This requires, in addition to pol V, also the SSB protein. The pol V initiation complex is stabilized by RecA–UmuD′ interactions, UmuC–DNA interactions, and perhaps interactions with SSB. Once this pol V complex has formed an initiation complex, DNA synthesis can occur. However, to get full pol V holoenzyme activity, the processivity proteins are needed, including the β-subunit DNA sliding clamp, and the γ-complex clamp loader (Figure 1, stages 3, 4). These proteins are essential for highly processive DNA replication by DNA polymerase III; however, they also increase the processivity of DNA polymerases II, IV, and V, although to a much lesser extent than pol III. DNA synthesis by pol V holoenzyme causes dissociation of RecA monomers, as the polymerase progresses. Pol V is a major lesion-bypass machine, which can bypass a wide variety of DNA lesions. This includes abasic sites, and the two major lesions caused by UV light, a cyclobutyl thymine–thymine dimer, and a thymine–thymine 6–4 adduct. Most remarkably, pol V is able to bypass a stretch of 12 methylene residues inserted into the DNA. This artificial lesion is an extreme form of DNA damage, since it bears no resemblance to any of the regular DNA constitutents. Despite this remarkable bypass ability, pol V is poor in bypassing some DNA lesions, most notably benzo[a]pyrene–guanine adducts. The ability of pol V to bypass DNA lesions correlates with its low fidelity. However, low fidelity by itself is not sufficient to ensure effective lesion bypass, since there are enzymes with fidelity similar to pol V, which nevertheless are not lesion-bypass enzymes (e.g., mammalian DNA polymerase β). The crystal structure of pol V was not determined yet. However, based on several crystal structures of other homologous lesion-bypass DNA polymerases, a spacious and flexible active site is likely to be responsible, at least in part, for the ability to bypass DNA lesions.

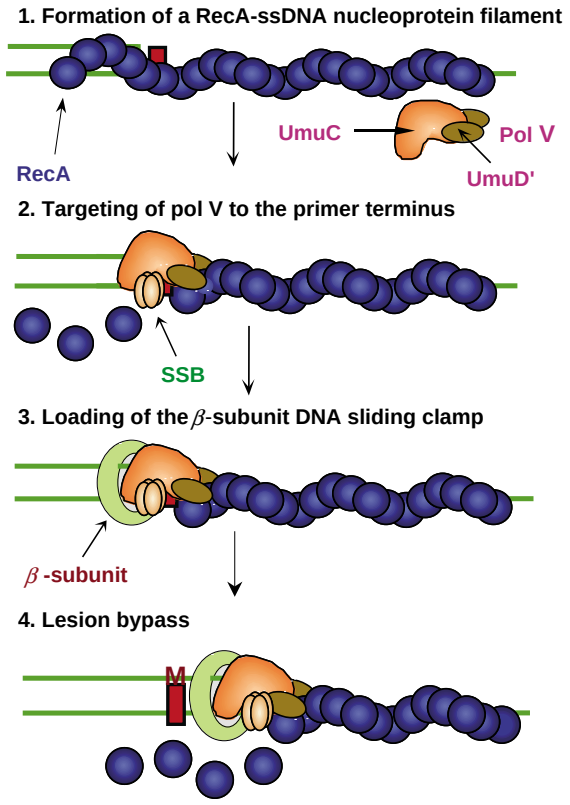

FIGURE 1 Outline of the mechanism of lesion bypass by pol V. The red square represents a blocking lesion. The "M" represents an incorrect insertion opposite the lesion. Reproduced from Livneh, Z. (2001). DNA damage control by novel DNA polymerases: Translesion replication and mutagenesis. *J. Biol. Chem.* **276**, 25639–25642, with permission of the American Society for Biochemistry and Molecular Biology.

The Fidelity of Pol V

The fidelity of DNA synthesis by pol V undamaged DNA templates is 10^{-3}–10^{-4} errors/nucleotide replicated. This is 100–1000-fold lower than the fidelity of the replicative pol III holoenzyme. DNA sequence analysis of pol V errors showed that pol V produces all types of errors, including frameshifts and base substitutions. However, it has a propensity to produce transversion mutations, namely, changing a pyrimidine into a purine, or vice versa. Pol V forms transversions at a frequency up to 300-fold higher than pol III holoenzyme (which tends to form transition mutations; Table I). It should be

TABLE I

Mutations Produced during *In Vitro* DNA Synthesis by Pol V and Pol III Holoenzyme

Mutation	Mismatch[a]	Mutation frequency × 10^{-5}/gene		
		Pol III	Pol V	Pol V/pol III
Transition				
T → C	T:G	<1.4	368.3	>263
Transversion				
A → C	A:G	2.8	161.1	58
A → T	A:A	<1.4	414.4	>296
C → A	C:T	<1.4	92.1	>66
T → A	T:T	2.8	230.2	82
T → G	T:C	<1.4	69.1	>49

[a] The mutations were formed in the *cro* repressor gene of phage λ during gap-filling DNA synthesis.

Reproduced from Maor-Shoshani, A., Reuven, N. B., Tomer, G., and Liuneb, Z. (2000). Highly mutagenic replication by DNA polymerase V (UmuC) provides a mechanistic basis for SOS untargeted mutagenesis. *Proc. Natl Acad. Sci. USA* **97**, 565–570, with permission of the National Academy of Sciences, U.S.A.

noted that base–base mismatches produced by DNA polymerases during synthesis on undamaged DNA are potential substrates for the mismatch repair system. This system primarily corrects mismatches that are precursors for transition mutations, namely, the types of mismatches that the replicative pol III holoenzyme tends to make. This significantly reduces mutations that can occur during DNA replication, and contributes to the high replication fidelity. The repair by the mismatch repair system of mismatches that are precursors of transversions, such as pol V tends to make, is 20-fold less effective than transition mismatches. This implies that pol V generates mismatches that are largely immune to mismatch repair and yield mutations. This provides the mechanistic basis for the phenomenon of untargeted SOS mutagenesis, also termed SOS mutator activity. In essence, this phenomenon involves the formation of mutations in undamaged regions of DNA in cells in which the SOS response was induced. This process is *umuDC*- and *recA*- dependent, and primarily yields transversion mutations. Based on the fidelity of pol V, untargeted mutagenesis can be explained by the activity of pol V under SOS conditions in undamaged regions of the *E. coli* chromosome. It should be noted that there is a second branch of untargeted mutagenesis that depends on pol IV rather than pol V.

Regulation of Pol V

The activity of pol V is tightly regulated at several levels, to ensure that this mutator polymerase acts only under situations, and at sites, when it is really needed. As described above, the *umuDC* operon is regulated at the transcriptional level by the LexA repressor and the RecA activator like other SOS genes. Within the timed expression of SOS genes, the *umuDC* operon is induced late, nearly an hour after the onset of induction. When SOS genes become repressed again, as the SOS response is shut down, the *umuDC* operon is repressed early. This late induction, early shutdown expression pattern provides an extra layer of regulation on pol V. It limits the activity of pol V to a stage after error-free repair mechanisms had a chance to repair DNA, and even at that late stage in SOS, the activity of pol V is limited in time, as it is shut off early. Additional regulation is at the posttranslational level. The $UmuD_2$ protein is cleaved to yield a shorter protein termed $UmuD'_2$, which is the active protein in pol V. The proteolytic processing occurs via the self-cleavage of the $UmuD_2$ protein, promoted by activated RecA, in a mechanism that is similar to the cleavage of the LexA repressor. Finally, there is regulation by turnover, as UmuD is degraded by the Lon and ClpXP proteases. The steady-state level of UmuC in noninduced cells is low and undetected by currently available antibodies. Upon SOS induction, UmuC accumulates to a level of ~200 molecules/cell. UmuD is present in higher amounts, starting with 200 molecules in the noninduced cell, and going up to 2400 molecules/cell after induction. Finally, pol V is regulated at the activity level, in its requirement for a RecA nucleoprotein filament. Such filaments are formed in DNA only when replication is arrested (e.g., at a lesion) and a persistent single-stranded region is generated.

In vivo Function of Pol V

The major phenotype of *E. coli* cells lacking pol V is a strong decrease in mutations caused by DNA-damaging agents such as UV radiation or MMS. Survival is decreased too, but to a lower degree compared to defects in other DNA repair pathways, such as excision repair. Based on these phenotypes, there are two views on the *in vivo* role of pol V. One is that pol V repairs replication gaps and this leads to increased survival. According to this model, the mutations formed by pol V are a by-product of the gap-filling activity, and can be viewed as the price paid for this gap repair (repair at the expense of mutations). The other view portrays the generation of mutations as the main role of pol V. According to this view, when a population of *E. coli* cells is under hostile environmental conditions, e.g., lack of nutrients, or presence of DNA-damaging agents such as UV light, it increases its mutations rate via pol V, to facilitate adaptation and increase fitness. Even one successful mutation in a cell (e.g., conferring higher resistance to sunlight) may have a great impact on the

entire population, since in time these cells, which have a selective advantage, may proliferate to a state where they take over the population. Consistent with such an idea is the finding that when mutator strains are grown for many generations along with nonmutator strains, the mutator strain takes over. Similarly, *umuDC*-deficient mutants suffer a severe reduction in fitness when competing against cells with normal pol V. Since mutations form randomly in relation to their functional outcome, a mutator acting long enough will start accumulating deleterious mutations, and will lose its adaptive advantage. The fact that the activity of pol V is transient (namely, as long as the SOS response is on) helps to preserve successful mutations from being neutralized by the formation of other mutations. It was also suggested that pol V initially evolved as a generic bypass DNA polymerse, which functioned to increase survival by overcoming replication blocks, but as more sophisticated DNA repair mechanisms evolved, the importance of the bypass function decreased, and what kept pol V during evolution was its mutator effect. Of course, the various hypotheses are not mutually exclusive, and the *in vivo* role of pol V may be both in survival and mutagenesis.

Bacterial Homologues of Pol V

E. coli contains a homologue of pol V, termed pol IV, which is the product of the SOS gene *dinB*. Like pol V, pol IV is an SOS-inducible, low-fidelity, and low-processivity DNA polymerase, which is able to bypass some DNA lesions. As in pol V, the processivity and lesion-bypass ability of pol IV are increased by the β-subunit clamp, and the γ-subunit clamp loader. However, unlike pol V, pol IV is a single subunit enzyme, and its bypass activity requires neither RecA nor SSB. On undamaged DNA, pol IV tends to form frameshifts, primarily minus-one deletions. The *in vivo* role of pol IV is not as clear as that of pol V. Pol IV is required for untargeted mutagenesis of phage λ. This mutagenic pathway is observed in nonirradiated phage λ when it infects a UV-irradiated *E. coli* host. In addition, pol IV is required for the bypass of a benzo[a]pyrene–G adducts. It is also required for stationary phase mutations.

Homologues of pol V exist in many, but not all bacteria. Pol V homologues were also found on native bacterial conjugative plasmids, such as R46. These are large plasmids, in the range of 100 kbp, with broad host-range specificity, which often carry multiple antibiotics-resistance markers. In the case of the R46 plasmid, the UmuD, UmuD′, and UmuC homologues are MucA, MucA′ and MucB, respectively. MucA′ and MucB were shown to form a lesion-bypass DNA polymerase, pol RI, with properties similar to those of pol V. Pol RI, like pol V, required both RecA and SSB for bypassing an abasic site. MucA and MucB are present on plasmid pKM101, a natural deletion derivative of plasmid R46. Plasmid pKM101 was introduced into the *Salmonella* strains that are used in the Ames test for mutagens, in order to improve its mutagenic sensitivity.

The emergence of pathogenic bacteria that are resistant to multiple types of antibiotics is associated in part of the cases with the presence of native conjugative plasmids. The fact that native plasmids, which have a limited genome size, and rely heavily on host factors, carry mutator lesion-bypass DNA polymerase genes indicates that the latter have a special role in the life cycle of such plasmid. One possibility is that the mutator activity of the polymerases is required when the plasmids enter a new foreign bacterial host, and need rapid adaptation to the new intracellular environment.

Eukaryotic Homologues of Pol V

Homologues of pol V were found to be conserved in evolution, and comprise the Y family of DNA polymerases. The yeast *S. cerevisiae* contains two homologues of UmuC, pol η (product of the *RAD30* gene), and REV1, a G-template specific DNA polymerase. Human cells contain no less than four homologues of pol V: pol η, pol ι, pol κ, and REV1. The DNA polymerases of the Y family were discovered in 1999 by several investigators, simultaneously and independently. The *S. cerevisiae* pol η was reported first, discovered by Satya Prakash and Louis Prakash (University of Texas Medical Branch, Galveston). Both the *S. cerevisiae* and the human pol η have the remarkable property that they replicate across an unmodified DNA TT sequence, with similar efficiency and specificity to that of a TT cyclobutyl dimer. In the absence of pol η in the cell, another polymerase takes over, but performs the reaction with a lower fidelity, leading to increased UV mutagenesis. This is the situation in the human hereditary disease Xeroderma Pigmentosum Variant (XP-V). Unlike other forms of XP, which are defective in components of the error-free nucleotide excision repair, XP-V patients are deficient in DNA pol η (the XP-V gene product). XP-V patients lacking this enzyme show extreme sensitivity to sunlight and a high susceptibility to skin cancer. This led to the unexpected conclusion that lesion bypass may be functionally nonmutagenic, and that lesion-bypass DNA polymerases may function to protect mammals from at least certain types of cancer.

S. cervisiae has an additional lesion-bypass polymerase, pol ζ, encoded by the REV3 and REV7 genes. It is homologous to the replicative pol δ, and not to the Y-family DNA polymerases. Historically, pol ζ was the first lesion-bypass DNA polymerase, discovered in 1996

by David Hinkle and Christopher Lawrence (Rochester University), followed soon thereafter by the discovery, in the same year, and by the same investigators, that REV1 has nucleotidyl transferase activity. Human cells also contain additional polymerases, which can bypass lesions *in vitro*. This includes pol μ and pol λ, and homologues of the yeast *REV3* and *REV7* genes, encoding a putative pol ζ. Overall this suggests that lesion bypass has an important role in the response to DNA damage in mammalian cells.

See Also the Following Articles

DNA Base Excision Repair • DNA Damage: Alkylation • DNA Polymerase I, Bacterial • DNA Polymerase II, Bacterial • DNA Polymerase III, Bacterial • Translesion DNA Polymerases, Eukaryotic

Glossary

base substitution mutation A mutation in which a particular DNA base is changed to another base (e.g., A → G).

benzo[*a*]pyrene–guanine adduct A DNA adduct formed between benzo[*a*]pyrene, a major tobacco smoke carcinogen, and a guanine base. Benzo[*a*]pyrene requires metabolic activation before it can react with DNA.

excision repair The major mechanism of DNA repair. It involves excision of the damaged site from DNA, followed by gapfilling DNA synthesis, based on the complementary intact strand and ligation.

frameshift mutation A mutation that changes the reading frame of a gene. Frameshifts involve either deletion or insertion of one or two nucleotides. Larger deletions or insertions may also cause frameshift mutations, when the number of deleted or added nucleotides is not a multiple integer of three.

operon A segment of the genome with two or more genes which are cotranscribed yielding a multicstronic mRNA.

processivity of DNA polymerase The number of nucleotides polymerized by a DNA polymerase per single binding event to the primer-template. Processivity of DNA polymerases varies from 1 (distributive DNA polymerase) up to 10 000 (highly processive DNA polymerase). Usually replicative polymerases have very high processivity, whereas DNA repair polymerases have lower processivity.

regulon A set of genes, residing at different locations in the chromosome, that are regulated by a common regulatory pathway. The genes regulated by the SOS response in *E. coli* comprise a regulon.

transition mutation A mutation in which a pyrimidine is changed to another pyrimidine, or a purine is changed to another purine. Changes of A → G or C → T are examples of transition mutations.

transversion mutation A mutation in which a purine changes to a pyrimidine, or a pyrimidine changes into a purine. Changes of A → C or T → A are examples of transversion mutations.

Further Reading

Baynton, K., and Fuchs, R. P. (2000). Lesions in DNA: Hurdles for polymerases. *Trends Biochem. Sci.* **25**, 74–79.

Goodman, M. F. (2000). Coping with replication 'train wrecks' in *Escherichia coli* using Pol V, Pol II, and RecA proteins. *Trends Biochem. Sci.* **25**, 189–195.

Livneh, Z. (2001). DNA damage control by novel DNA polymerases: Translesion replication and mutagenesis. *J. Biol. Chem.* **276**, 25639–25642.

Radman, M. (1999). Enzymes of evolutionary change. *Nature* **401**, 866–869.

Sutton, M. D., Smith, B. T., Godoy, V. G., and Walker, G. C. (2000). The SOS response: Recent insights into umuDC-dependent mutagenesis and DNA damage tolerance. *Annu. Rev. Genet.* **34**, 479–497.

Biography

Zvi Livneh received his Ph.D. from the Weizmann Institute of Science in Israel, and was a postdoctoral fellow at Stanford University School of Medicine in California. He is a Professor of biochemistry and molecular medicine, and Head of the Department of Biological Chemistry at the Weizmann Institute of Science in Israel. His main research interests are molecular mechanisms of DNA repair and mutagenesis in bacteria and in mammals, and the role of DNA repair in cancer risk.

Uncoupling Proteins

Daniel Ricquier and Frédéric Bouillaud
Centre National de la Recherche Scientifique, Paris, France

Uncoupling proteins (UCPs) are mitochondrial transporters present in the inner membrane of mitochondria. They belong to the family of anion mitochondrial carriers including adenine nucleotide transporters, phosphate carrier and other transporters. The term uncoupling protein was originally given to UCP1 which is uniquely present in mitochondria of brown adipocytes, the thermogenic cells devoted to maintenance of body temperature in mammals. In these cells, UCP1 acts as a proton carrier creating a shunt between complexes of respiratory chain and the ATP-synthase. Purine nucleotide inhibit UCP1 whereas fatty acids activate it. Activation of UCP1 stimulate respiration and the uncoupling process results in a futile cycle and dissipation of oxidation energy into heat. UCP2 is ubiquitous and highly expressed in lymphoid system and macrophages. UCP3 is mainly expressed in skeletal muscles. In comparison to the established uncoupling and thermogenic activities of UCP1, UCP2, and UCP3 rather appear to be involved in the limitation of free radicals levels in cells than in physiological uncoupling and thermogenesis. The mechanism of the protonophoric activity of the UCPs is still controversial since it has been proposed that the UCPs transport fatty acid anions and catalyse proton transport by fatty acid cycling. Quinones and superoxide ions may also activate the UCPs.

The Mitochondria and the Coupling of Respiration to ADP Phosphorylation

Cellular respiration, the reactions of the citric acid cycle, fatty acid oxidation, and several steps of urea synthesis and gluconeogenesis take place in specialized cellular organites, the mitochondria.

Mitochondria

In addition to oxidative phosphorylation and metabolic pathways, mitochondria are involved in thermogenesis, radical production, calcium homeostasis, apoptosis, and protein synthesis. Mitochondria contain two compartments bounded by inner and outer membranes. The outer membrane is permeable to many small metabolites whereas the permeability of the inner membrane is controlled in order to maintain the high electrochemical gradient created by the mitochondrial respiratory chain which is necessary for energy conservation and ATP synthesis in mitochondria. The inner membrane transports anion substrates such as ADP, ATP, phosphate, oxoglutarate, citrate, glutamate, and malate.

Coupling of Respiration to ATP Synthesis

It has long been known that respiration and mitochondrial ATP synthesis are coupled. The observation that respiration rate increased when mitochondria synthesized more ATP led to the concept of respiratory control by ADP phosphorylation. In fact, there is a link between mitochondrial ATP synthesis and cellular ATP demand by a feed-back mechanism. In agreement with Mitchell's theory, it was demonstrated that the mitochondrial electrochemical proton gradient, generated as electrons are passed down the respiratory chain, is the primary source for cellular ATP synthesis. In this way, several complexes of the respiratory chain pump protons outside of the inner membrane during reoxidation of coenzymes and generate a proton gradient which is consumed by the reactions of ATP synthesis. Proton leak represents another mechanism consuming the mitochondrial proton gradient. Mitchell's theory predicted that any proton leak non coupled to ATP synthesis would represent an uncoupling of respiration and result in thermogenesis. An excellent example of such an uncoupling of respiration to ADP phosphorylation is represented by the mitochondrial UCP of brown adipocytes (UCP1) which dissipates energy of substrate oxidation as heat.

Brown Adipose Tissue and UCP1: History of a True Respiration Uncoupling

Maintenance of body temperature in a cold environment or at birth requires thermogenesis. Another situation

requiring thermogenesis is arousal from hibernation. The two regulatory thermogenic processes are shivering and metabolic thermogenesis also referred to as nonshivering thermogenesis. The largest part of nonshivering thermogenesis in small mammals is achieved in the brown adipose tissue (BAT).

Brown Adipose Tissue (BAT)

BAT is found in all small mammals and in the newborn of larger mammals, such as humans. BAT is located in specific body areas near large blood vessels and consists of brown adipocytes which are distinct from white adipocytes. The brown adipocytes are characterized by numerous mitochondria containing a highly developed inner membrane (Figure 1). Activation of thermogenesis in BAT occurs in newborns, rodents exposed to cold, and in animals emerging from hibernation. It is commanded by the central nervous system and the orthosympathetic fibers innervating each brown adipocyte. The norepinephrine released by these fibers binds to adrenergic receptors on the surface of the brown adipocytes. The later steps of the activation of thermogenesis in brown adipocytes are production of cyclic AMP, activation of lipolysis, and oxidation of fatty acids by the numerous mitochondria. Released fatty acids stimulate brown adipocyte respiration and heat production.

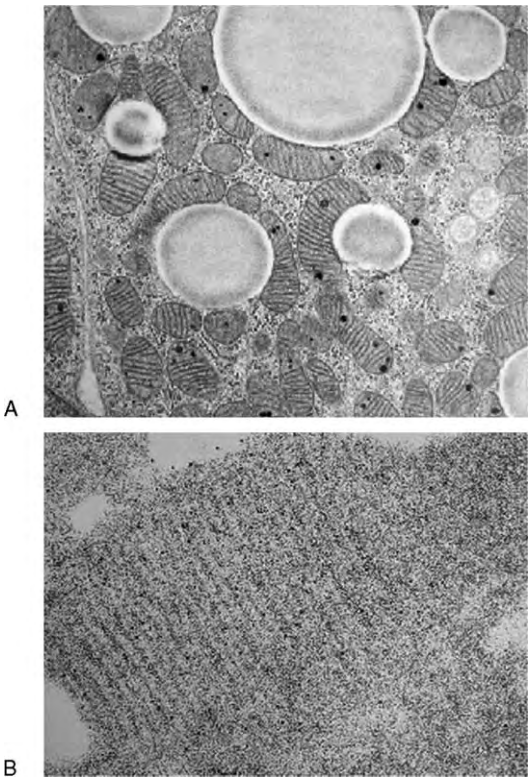

FIGURE 1 Histology of brown adipocyte. (A) The cytosol of brown adipocytes is characterized by numerous mitochondria and lipid droplets. (B) Magnification of a brown adipocyte mitochondrion showing parallel cristae and UCP1 detected using antibodies (black dots). (Figure kindly provided by Dr Saverio Cinti, University of Ancona.)

Respiration Uncoupling is the Thermogenic Mechanism in Brown Adipocytes

In most cell types such as muscular fibers, ATP utilization stimulates ADP phosphorylation and respiration (Figure 2). Original observations made in 1967 revealed that the high respiratory rate in brown adipocyte mitochondria was not controlled by mitochondrial ADP phosphorylation suggesting that energy from substrate oxidation was dissipated into heat instead of being converted in ATP (Figure 2). In line with Mitchell's chemiosmotic theory, if proton leakage is activated by a signal such as free fatty acids in the case of the mitochondria of brown adipocytes, the mitochondrial membrane potential is decreased and concomitantly, respiration is activated. Since, in addition, the activated proton leakage is not linked to ADP phosphorylation, respiration is uncoupled from ATP synthesis and oxidation energy is dissipated in the form of heat.

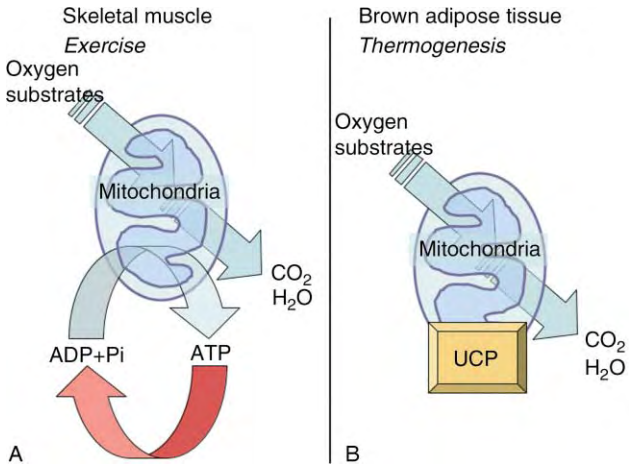

FIGURE 2 Comparison of skeletal muscle and brown adipose tissue mitochondria. (A) Mitochondria are cellular organelles converting the redox energy liberated during oxidation of organic substrates into ATP, a molecule containing energy under a form readily usable by most enzymes working to maintain cell structure and integrity or to perform work such as mechanical work in muscle. The cellular need for ATP controls oxidation rate by mitochondria. (B) In brown adipocyte, a specific uncoupling protein referred to as UCP (precisely UCP1) is present in a large amount in the inner membrane. UCP1 is able to fool mitochondria which accelerates their oxidation rate whereas no ATP is produced. UCP1 removes the control of energy expenditure by ATP demand and therefore oxidation rate and energy expenditure increase under the form of heat. This process is used in newborns, arousal from hibernation, and small mammals exposed to cold when muscle thermogenesis would not be sufficient.

The UCP of Brown Adipocyte Mitochondria

The protein responsible for proton leakage within the inner mitochondrial membrane and for respiratory uncoupling was identified in 1976–77, was purified, and its cDNA was cloned. It has an apparent molecular weight of 33 000 and was originally called UCP. This protein is known as UCP1 since the discovery of UCP2 in 1997. UCP1 is abundant in the inner membrane of the mitochondria of brown adipocytes and is specific to these cells. It short-circuits the proton circuit between complexes of the respiratory chain and the mitochondrial ATP-synthase which is the main consumer of the proton gradient (Figure 3). When there is no need for thermogenesis, purine nucleotides bound to UCP1 inhibit its activity. Upon activation of thermogenesis by the sympathetic nervous system, fatty acids overcome the inhibitory effect of nucleotides and activate UCP1. Heterologous expression of UCP1 in yeasts or mammalian cell lines induces respiration uncoupling. The protonophoric activity of UCP1 has been reconstituted in liposomes where it can be inhibited by nucleotides and activated by free fatty acids. The mechanism of action of UCP1 is still controversial: some scientists believe that it is a true proton transporter, whilst others assert that it returns anionic fatty acids to the intermembrane space, after they have crossed the membrane in protonated form. The observation that Ucp1−/− mice were unable to maintain body temperature in the cold proved that the UCP1-induced uncoupling of respiration was responsible for cold-activated nonshivering thermogenesis of rodents. In agreement with this observation, ectopic expression of UCP1 in skeletal muscles of transgenic mice promotes substrate oxidation in muscles and resistance to obesity and type 2 diabetes. UCP1 functions as a dimer and each monomer is made of six transmembrane fragments (Figure 4). Moreover, UCP1, the ADP/ATP translocator and other mitochondrial anion carriers derive from the same ancestral gene and probably share a similar structure. They all have a triplicated structure (Figure 4).

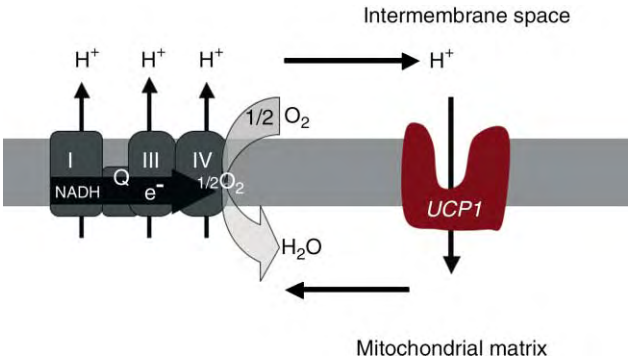

FIGURE 3 UCP1-induced proton cycling. Q (coenzyme Q) refers to complex II which is the succinate dehydrogenase. This enzyme directly reduces coenzyme Q but has no proton pumping activity contrary to complexes I, III and IV. UCP is inserted in the mitochondrial inner membrane where, also present, is a multienzymatic complex called the respiratory chain made of complexes I to IV. The respiratory chain reoxidize reduced coenzymes and electrons are driven to oxygen. This oxido-reduction step liberates energy which is used to generate an electrochemical gradient of protons across the inner membrane. This gradient is normally consumed by the ATP-synthase which phosphorylates ADP. UCP1 transports protons passively and makes possible a futile cycle of protons across the inner membrane leading to increased energy expenditure. This schema illustrates the situation encountered in brown adipocytes of mammals where a large amount of respiratory chains as well as a large amount of UCP1 are present. Activation of the futile cycling increases considerably energy expenditure and thus heat production in these thermogenic cells. In other cells where homologues of the UCP1 are expressed at much lower level, this pathway would represent a minor contributor to energy expenditure, but might be of importance to avoid oxidative damage.

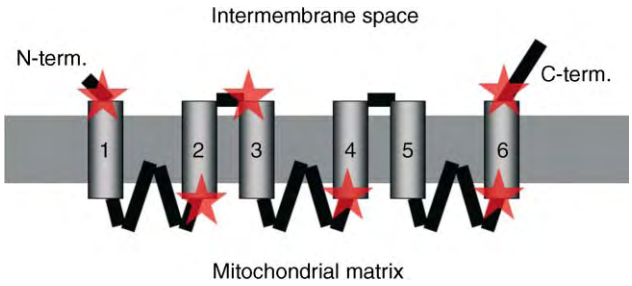

FIGURE 4 Model of insertion of UCP in the membrane. The determination of structure of the UCPs remains difficult because crystallization of such membrane proteins has not been successful yet. To modelize the organization of such proteins, indirect methods such as prediction of secondary structure by computers can be used. Experimentally, restricted domains of the protein in the membrane (indicated by stars) were explored using specific antibodies. The UCPs are made of six transmembraneous segments (probably alpha helices), and three hydrophilic loops stemming from the matricial side of the membrane. An internal repetition in the structural arrangement of the protein suggests that the protein (made of 300 amino acid residues) derived from the ancient triplication and divergence of a 100 amino acid domain (made of 2 helices and 1 loop).

The Novel UCPs

Given their specific role in thermogenesis, it has always seemed logical that brown adipocytes be equipped with an original mechanism, partial uncoupling of respiration, brought into play by a specific protein, UCP1, which induces proton leakage. In fact, it is known that mitochondrial respiration is always accompanied by heat production as it is imperfectly coupled to ADP phosphorylation in all types of cells. To explain this incomplete coupling of respiration and the energy loss mechanism, some authors have invoked slippage of the respiratory chains, while others referred to proton leaks. It has been estimated that proton leaks from the inner membrane of mitochondria of hepatocytes

and myocytes could explain about 20% of the body's basal metabolism.

UCP2: A Homologue of the Brown Fat UCP Present in Various Tissues

A clone corresponding to a protein with 59% sequence identity with the UCP of brown fat was isolated. This new UCP, called UCP2, was also identified in humans. In contrast with UCP1, the mRNA of UCP2 is present in almost all tissues and many cell types, such as spleen, thymus, digestive tract, lung, brain, adipose tissues, skeletal muscle, heart, adipocytes, myocytes, and macrophages (Figure 5). Expressed in yeasts, murine UCP2 decreased the potential of the mitochondrial membrane, raised the respiration rate and reduced sensitivity to uncouplers: UCP2 therefore was able to uncouple respiration and appeared to be a second mitochondrial UCP. The UCP2 gene is located on chromosome 7 of the mouse and chromosome 11 of humans, near a region linked to hyperinsulism and obesity. The expression of UCP2 mRNA was measured in obesity-prone and obesity-resistant mice given a lipid-rich diet: the obesity-resistant mice overexpressed UCP2 mRNA in their adipose tissue. These findings, together with the function of the protein and the chromosomal location of its gene, led to propose a role for UCP2 in diet-induced thermogenesis. However, this hypothesis was not validated in Ucp2−/− mice.

UCP3: Another UCP Homologue Predominantly Present in Skeletal Muscle

cDNAs corresponding to UCP3, a protein homologous to UCP1 and UCP2, were cloned soon after the discovery of UCP2. The amino acid sequence of UCP3 is 72% identical to that of UCP2 and 57% identical to that of UCP1. UCP3 mRNA is predominantly expressed in the skeletal muscles of humans, mice, and rats (Figure 5). Human and murine UCP2 and UCP3 genes are juxtaposed on the same chromosome.

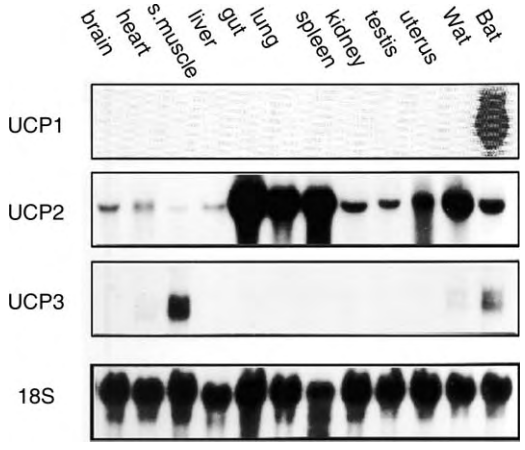

FIGURE 5 Tissular distribution of UCP1, UCP2, and UCP3 RNAs. The data correspond to mouse tissues. A very similar picture was obtained when analyzing human tissues. 18S refers to ribosomal RNA.

Plant and Bird UCPs

Functional studies of isolated plant mitochondria suggested that plants contain mitochondrial UCPs. Following this observation, a cDNA from a new UCP was isolated from a potato cDNA library. The sequence of the corresponding protein, called stUCP, is 44% identical to that of UCP1 and 47% identical to that of UCP2. The mRNA of stUCP is present in most plant organs. The most surprising result was that stUCP mRNA was markedly induced in the leaves of plants exposed to a temperature of 4°C. Cold, therefore, induced stUCP as it induces UCP1 in the brown adipose tissue of animals. However, plant and animal UCPs may have different functions. More recently, a chicken UCP termed avUCP was characterized. This gene is only expressed in skeletal muscles of birds and ducks and is induced upon exposure to the cold. Therefore avUCP seems to be involved in regulatory thermogenesis. Other proteins referred to as UCP4 and BMCP1/UCP5 were characterized. However their exact relationship to UCP1, UCP2, and UCP3 will require further work.

Role and Function of UCPs other than UCP1: A Role in Controlling the Level of Reactive Oxygen Species

Numerous questions remain unanswered, notably concerning the exact catalytic activity of each UCP, and the nature of the endogenous ligands of UCP2 and UCP3. These proteins may simply translocate protons. As said above for UCP1, it has been proposed that all the UCPs are active as fatty acid cycler through the membrane. According to this later hypothesis, protonated fatty acids cross the membrane and release a proton on the matricial side; then, the UCP facilitates the translocation of the anionic form of fatty acids. High loads of UCP2 or UCP3 can uncouple respiration in yeast or mammalian cell, but it is not certain whether the low physiological levels of these proteins may be sufficient to induce a net uncoupling of respiration *in vivo*. The divergent observations of the regulation of the activities of UCP2 or UCP3 by fatty acids or nucleotides will require further studies. Interestingly, it has been proposed that UCP2 and UCP3 could export fatty acid anion under conditions of elevated fatty acid oxidation.

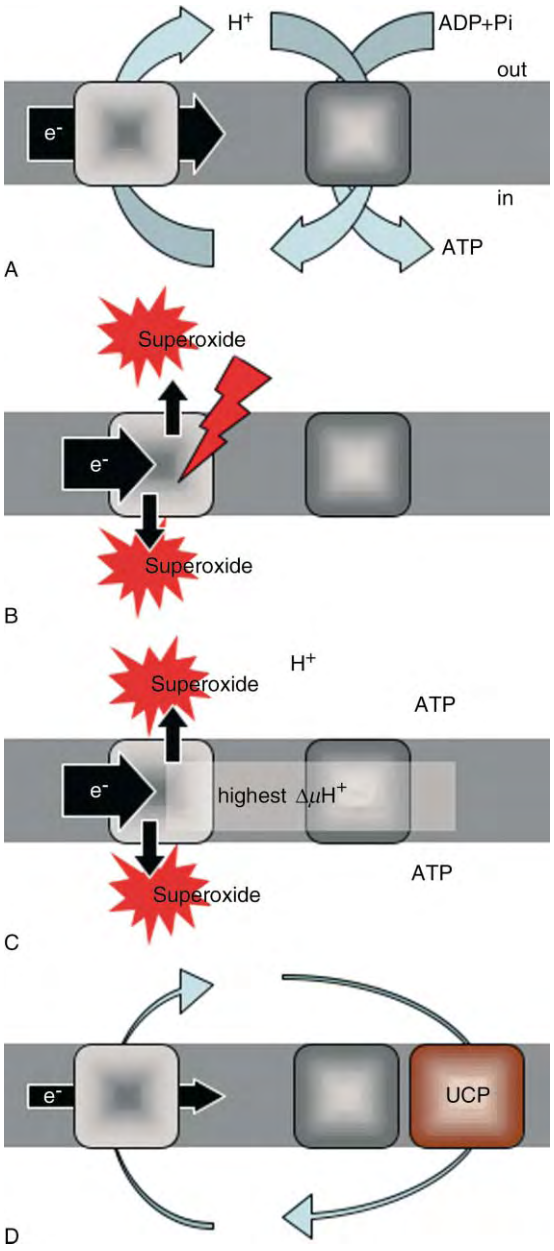

FIGURE 6 Role of UCP and superoxide generation by mitochondria. (A) mitochondria phosphorylating ATP: a proton gradient generator (the respiratory chain, left square) uses the energy liberated by the movement of electrons to pump protons through the membrane (grey zone) towards the intermembrane space. A proton gradient consumer (the ATP-synthase, right square) phosphorylates ADP coming from outside into ATP, that is exported afterwards. Therefore, a proton cycle across the inner membrane couples oxidation to ATP synthesis (and *vice versa*). (B) and (C) when oxidation is impaired (B) or slows down (C), an excess of electrons aiming to travel across the respiratory complexes cannot reach oxygen (to form water). Single electrons react with molecular oxygen and form superoxide anion ($O2^{\cdot -}$). It occurs either when the respiratory chain is poisoned (red arrow in panel B) or under physiological circumstances when the use of ATP by the cell is weak, ATP level rises, and ADP level decreases (panel C). In that case, the membrane potential rises to its highest value which impedes proton pumping, slows down reoxidation, and therefore increases superoxide production. (D) in tissues other than the thermogenic brown adipose tissue, the UCPs may induce a controlled leak of protons across the inner membrane that allows reoxidation to occur and maintain the membrane potential below the threshold inducing superoxide generation. The mechanism of proton transport (proton channeling or fatty acid cycling), as well as the identity of regulators of UCPs inside the cells are still controversial. Fatty acids would be cofactors of the proton transport whereas nucleotides are inhibitors. The membrane potential itself is a variable influencing heavily UCP1 activity. It has been proposed that superoxide anion and quinones directly activate proton transport by UCPs.

Metabolic Activity of UCP2 and UCP3

Conflicting data regarding the association of UCP2 or UCP3 genetic polymorphisms to body mass index, susceptibility to obesity, resting metabolic rate, metabolic efficiency, fat oxidation, insulin resistance, susceptibility to gain fat with age were obtained. However, UCP2 appears to act as a negative regulator of insulin secretion. Moreover, mice overexpressing a large amount of human UCP3 in skeletal muscle weigh less, have a decreased amount of adipose tissue, and an increased resting oxygen consumption.

Reactive Oxygen Species

Guided by the fact that UCP2 is expressed at high level in the immune system, a role for UCP2 in immunity was searched for. In fact, Ucp2 − /− mice are more resistant to infection by a parasite. This phenotype was explained by the fact that disruption of the Ucp2 gene provoked an elevation of ROS level that facilitated the killing of the pathogens. Mice lacking the Ucp3 gene also produced more oxygen radicals in myocytes. Therefore, it appears that UCP2 and UCP3 contribute to limit the level of reactive oxygen species in cells. Such an activity may be explained by a mild uncoupling activity of the proteins since a small decrease of the mitochondrial membrane potential opposes production of superoxide ion in mitochondria (Figure 6). The observation that UCP2 protects against atherosclerosis highlights its ability to counteract radical synthesis.

UCP1, UCP2, and UCP3, Conclusions and Perspectives

UCP1 has a well-demonstrated uncoupling activity and an essential role in maintenance of body temperature in small rodents exposed to the cold, but the exact biochemical and physiological roles of UCP2 and UCP3 remain to be further identified. Certain data support a true activity of these UCPs in respiration uncoupling and substrate oxidation, other data do not agree with a role for these UCPs in controlling adiposity. Several reports support a role for UCP2 and UCP3 in decreasing the level of reactive oxygen species in cells.

Whilst UCP1 is present at a high level, an open question is that of the exact amount of UCP2 and UCP3 in cells since whatever is the exact intrinsic ability of these proteins to uncouple respiration from ATP synthesis, a certain amount of the proteins will be required to achieve a physiological uncoupling. Finally, the possible contribution of a UCP to the hypermetabolic syndrome (known as Luft's disease) previously described in patients remains to be investigated.

See Also the Following Articles

ATP Synthesis in Plant Mitochondria: Substrates, Inhibitors, Uncouplers • Luft's Disease • Mitochondrial Membranes, Structural Organization • Quinones • Respiratory Chain and ATP Synthase

Glossary

mitochondria These organelles are the sites of respiration and oxidative phosphorylation in all animal and higher plant tissues as well as in protozoa, fungi, and aerobically grown yeasts. They are ~2–30 μm long and 0.5–10 μm wide.

respiration coupling/uncoupling In coupled mitochondria, respiration rate determines ADP phosphorylation rate and ATP synthesis determines respiration rate. When uncoupling occurs (due to chemical uncouplers or UCP), the respiration rate increases sharply since the control by ADP phosphorylation does not limit respiration. In such a situation, oxidation energy is dissipated as heat.

Further Reading

Boss, O., Hagen, T., and Lowell, B. B. (2000). Uncoupling proteins 2 and 3. Potential regulators of mitochondrial energy metabolism. *Diabetes* **49**, 143–156.

Cannon, B., and Nedergaard, J. (1985). The biochemistry of an inefficient tissue: Brown adipose tissue. *Essays Biochem.* **20**, 110–164.

Echtay, K. S., Winkler, E., and Klingenberg, M. (2000). Coenzyme Q is an obligatory cofactor for uncoupling protein function. *Nature* **408**, 609–613.

Enerbäck, S., Jacobsson, A., Simpson, E. M., Guerra, C., Yamashita, E. H., Harper, M. E., and Kozak, L. P. (1997). Mice lacking mitochondrial uncoupling protein are cold-sensitive but not obese. *Nature* **387**, 90–94.

Garlid, K. D., and Jaburek, M. (1998). The mechanism of proton transport mediated by mitochondrial uncoupling proteins. *FEBS Lett.* **438**, 10–14.

Himms-Hagen, J., and Ricquier, D. (1998). Brown adipose tissue. In *Handbook of Obesity* (G. Bray, C. Bouchard and W. P. T. James, eds.) pp. 415–441. Marcel Dekker, New York.

Ledesma, M., Garcià de Lacoba, M., and Rial, E. (2002). The mitochondrial uncoupling proteins. *Genome Biol.* **3** (on line November 29).

Nicholls, D. G., and Locke, R. M. (1984). Thermogenic mechanisms in brown fat. *Physiol. Rev.* **64**, 1–64.

Ricquier, D., and Bouillaud, F. (2000). The uncoupling protein homologues: UCP1, UCP2, UCP3, StUCP & AtUCP. *Biochem. J.* **345**(Pt 2), 161–719.

Skulachev, V. P. (1988). Uncoupling: New approaches to an old problem of bioenergetics. *Biochim. Biophys. Acta* **1363**, 100–124.

Stuart, J. A., Cadenas, S., Jekabsons, M. B., Roussel, D., and Brand, M. D. (2001). Mitochondrial proton leak and the uncoupling protein 1 homologues. *Biochim. Biophys. Acta* **1504**, 144–158.

Biography

Daniel Ricquier is Professor at Neckes-Enfants Malades Faculty of Medicine and Frédéric Bouillaud is Main Investigator at the Institut National de la Santé et de la Recherche Médicale. They work at CNRS Unit 9078 at Faculté de Médecine and Institut de Recherches Necker-Enfants Malades in Paris. They hold Ph.Ds from Pierre and Marie Curie University in Paris. Their laboratory first cloned UCP1, UCP2, BMCP1/UCP5, and avUCP. They also collaborated to the characterization of the first plant UCP. With their collaborators, they are authors of original reports dealing with biochemistry, physiology, and genetics of the UCP family.

Unfolded Protein Responses

David Ron
New York University School of Medicine, New York, USA

The unfolded protein response (UPR) is a transcriptional and translational response to the accumulation of unfolded proteins in the endoplasmic reticulum (ER). The UPR is mediated by highly conserved signaling pathways that are activated by imbalance between the load of unfolded (or malfolded) ER client proteins and the capacity of the organelle to process this load. Collectively these pathways restore equilibrium to the protein-folding environment in the organelle by increasing the expression of genes that enhance nearly all aspects of ER function and by transiently repressing the biosynthesis of new client proteins. Interest in the UPR has been stimulated by the realization that postsynthetic protein processing constitutes an important step in gene expression and that protein malfolding plays an important role in human disease.

ER Function and ER Stress

The ER, A Protein-Processing Machine

Proteins destined for secretion and membrane insertion are translocated across the ER membrane in an unfolded state. In the ER lumen they undergo chaperone-assisted folding, a variety of organelle-specific post-translational covalent modifications and often chaperone-assisted assembly into oligomeric structures. Once properly folded and assembled, most ER client proteins are packaged into vesicles that are transported to more distal sites in the secretory pathway. Proteins that fail to attain their proper folded and oligomeric conformation are retained in the ER by continued binding to chaperones and are ultimately translocated from the organelle to the cytoplasm for proteasomal degradation, in a process known as ER-associated protein degradation (ERAD).

To fulfill these various functions the ER is endowed with a unique complement of proteins. These include enzymes for post-translational covalent modifications (e.g., N-linked glycosylation, disulfide bond formation), chaperones that assist in folding and assembly steps, translocation channels and transporters involved in transmembrane traffic, and various components involved in the postassembly steps of client protein egress from the organelle. The build-up of these components defines the capacity of the organelle to handle its client proteins. In the late 1980s Sambrook, Gething, and their colleagues discovered that manipulations that interfere with the function of various aspects of the ER client protein-handling machinery, and thereby perturb protein folding in the ER, selectively up-regulate the expression of genes that encode components of that machinery. The extent of this transcriptional response was not fully appreciated at the time, however its selectivity was noted, hence its name: the ER unfolded protein response (or UPR).

It was imagined that the cell possessed means to monitor the load of client proteins presented to its ER and responded to an increase in such load by up-regulating the capacity of its ER to process unfolded client proteins. An additional clue to the workings of this response was provided by the seminal observation that forced overexpression of an ER chaperone, BiP (also known as GRP78) markedly suppressed the activity of the UPR. Thus, at least one target gene of the UPR (BiP) is able to exert negative feedback on the entire response. BiP overexpression does not restore function to a challenged ER; this requires the coordinate expression of numerous UPR target genes. However, BiP, which is a member of the highly conserved HSP70/DnaJ family of chaperones, promiscuously recognizes hydrophobic stretches of amino acids. These are normally incorporated into the cores of properly folded polypeptides and assembled oligomeric complexes, but remain exposed on the surface of unfolded, malfolded or unassembled proteins. The ability of BiP to suppress the UPR suggested that it might be doing so by masking a stress signal generated by many different unfolded and malfolded proteins. This phenomenon was assigned the heuristic term ER stress and its level reflects the balance between client protein load and the capacity of the organelle to process that load.

Physiological and Pathological ER Stress

To the extent that cell types vary in the load of secreted proteins that they are called upon to produce,

they are subject to widely different levels of physiological ER stress. This explains enhanced activity of the UPR in various professional secretory cells, such as pancreatic cells of vertebrates or intestinal cells of the nematode, *Caenorhabditis elegans*. ER stress also occurs when a mutation in an abundantly expressed ER client protein renders that protein especially difficult to fold. An example is provided by various degenerative diseases affecting myelinated neurons in which mutations in a component of the myelin sheath (an ER client protein) cause the protein to malfold and induce high levels of ER stress which, over time, destroys the myelin-producing cell. It is important to emphasize that most mutations that impede folding of ER client proteins do not cause measurable ER stress. However, because they diminish expression of the properly folded protein, such mutations may deprive the organism of the latter's beneficial actions. This genetic mechanism underlies such serious human diseases as cystic fibrosis, familial hypercholesterolemia, and hemophilia. Nonetheless, the level of expression of the mutant protein is not enough to globally challenge ER function in the cell that produces it and the phenotypic expression of the mutation reflects the lack of an important protein, rather than the production of a toxic one.

The above constitute client protein-driven ER stress, however ER stress may also initiate from impaired function of the organelle, which occurs in cells deprived of energy sources or oxygen, or in cells exposed to certain ER-specific toxins. We do not understand in detail how ER stress contributes to further organelle dysfunction and ultimately cell death. However a framework for thinking about this has recently emerged with the realization that unfolded and malfolded proteins present reactive interfaces that have not been vetted by evolution and may thus disrupt the cellular machinery by interacting promiscuously and illegitimately with essential cellular components. According to this theory, proteotoxicity is normally held in check by the chaperones that bind such potentially toxic protein interfaces and let go only once the latter have been buried in the hydrophobic cores of the properly folded client protein. ER stress (by definition) challenges the capacity of the chaperones and may permit illegitimate protein interfaces to emerge. The ability of chaperone overexpression to suppress ER stress signaling suggests that the need to prevent proteotoxicity is an important driving force in evolution of the UPR. The unifying feature of ER stress need not be the presence of toxic moieties on the surface of every unfolded or malfolded protein. The common feature of diseases of protein folding might instead be the exhaustion of a protective chaperone reserve, which normally suppresses the potential proteotoxicity of certain (possibly normal) folding intermediates of ER client proteins.

The Yeast Unfolded Protein Response

IRE1, A Prototype of Transmembrane Stress Signaling

Early studies on the UPR were carried out in the yeast, *Saccharomyces cerevisiae*, an organism that lends itself well to forward genetic screens. To screen for mutations affecting the UPR, the regulatory region of yeast BiP gene (KAR2) was fused to a reporter and mutant yeast with suppressed activity of this reporter were sought. The first gene thus identified was inositol requiring 1 (IRE1), so-called because its loss of function had been previously noted to result in inositol auxotrophy. IRE1 encodes a transmembrane ER resident protein with an N-terminal domain residing in the ER lumen and a C-terminal domain that is exposed on the cytoplasmic side. The membrane topology and subcellular localization of IRE1 immediately suggest a mechanism for transmitting information on the state of the ER (topologically equivalent to the extracellular space) to the cell's interior. The lumenal domain somehow senses ER stress, conveying the signal across the ER membrane to the cytoplasmic domain, which broadcasts it to the nucleus, turning "on" UPR target gene expression (Figure 1).

IRE1's C-terminal, cytoplasmic, effector-domain, is a protein kinase and undergoes autophosphorylation when activated by ER stress. This suggested that IRE1 might function like other transmembrane receptors that are also protein kinases and convey their signal by phosphorylating downstream targets, often through a kinase relay. However, other than IRE1 itself no substrates for the aforementioned kinase have been identified to date.

Unconventional Splicing of HAC1 mRNA

The clues to understanding propagation of the UPR signal, downstream of IRE1 again came from yeast genetics. Mutations in two additional genes were noted to block the yeast UPR. One of these, HAC1, encodes a transcription factor, which binds to and activates the promoters of the primary target genes of the yeast UPR, the second, more mysteriously turned out to be RLG1, which encodes for a multifunctional enzyme involved in tRNA splicing. ER stress promotes accumulation of HAC1 protein and this is blocked by mutations in IRE1 and RLG1.

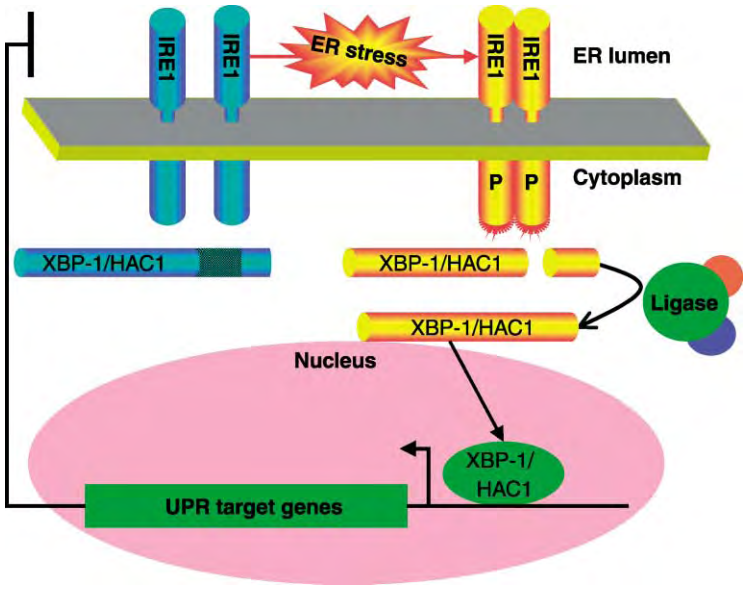

FIGURE 1 IRE1 and unconventional splicing of its target mRNA signal the unfolded protein response. ER stress leads to oligomerization and trans-autophosphorylation of IRE1 (indicated by the "P" on its cytoplasmic effector domain). Phosphorylation unmasks the effector function of IRE1 (cartooned by the red bristles on the cytoplasmic domain), which consists of the endoribonucleolytic processing of its target mRNA, XBP-1 in metazoans, and HAC1 in yeast. The two ends of the cleaved mRNA are joined together by a ligase. The unconventionally spliced XBP-1/HAC1 mRNA is more efficiently translated than the unprocessed mRNA and encodes a protein that is more stable and more effective at trans-activation of UPR target genes in the nucleus.

The underlying mechanisms, which turned out to be full of surprise, were revealed in a series of brilliant experiments carried out in the Walter and Mori laboratories.

The regulated step in HAC1 expression entails the removal of a 242 base internal segment at the 3′ end of the mature mRNA. The enzyme which precisely cuts the mRNA at the 5′ and 3′ ends of this segment turned out to be IRE1 itself, whose highly sequence-specific endoribonucleolytic activity appears to be subordinate to its kinase activity (though the molecular details remain to be worked out). The two ends of the severed HAC1 mRNA are held together by extensive base pairing and are subsequently religated by the protein product of RLG1. IRE1 is the master regulator of this unconventional mRNA splicing reaction, since its kinase and endoribonuclease are activated by ER stress. The removal of the aforementioned internal segment of the HAC1 mRNA de-represses HAC1 translation and the protein encoded by the processed mRNA is more stable and transactivates its target genes more potently than that encoded by the unprocessed mRNA.

Mutations in IRE1 and HAC1 similarly abolish most signaling in the yeast UPR. This was convincingly demonstrated by expression profiling which showed that the vast majority of the genes induced by exposing yeast to toxins that promote ER stress were no longer activated in IRE1 or HAC1 mutant strains. Thus the yeast UPR consists of a linear pathway in which HAC1 is an essential target of IRE1 and together the two proteins are required for the activation of most known UPR target genes.

Diversification in the Metazoan UPR

Conservation of the IRE1 Pathway

Systematic genomic sequencing of the metazoan *C. elegans* and random cDNA sequencing from several mammalian species, predicted proteins highly related to yeast IRE1 in higher eukaryotes. Their common membrane topology, localization to the ER, and conserved kinase and endoribonuclease domains suggested that they were indeed IRE1 homologues. However, HAC1 homologues could not be identified by simple sequence comparison to the yeast. Eventually, however, a combination of forward genetic screens in *C. elegans* and creative guesswork led to the identification of XBP-1 as a functional homologue of HAC1 in higher eukaryotes. It too encodes a transcription factor whose expression is tightly regulated by IRE1 through the processing of its mRNA.

Less conserved, however, is the role of the IRE1 pathway in the yeast and metazoan UPR. Whereas in the former, IRE1 and HAC1 are absolutely required for activating nearly all UPR target genes, in mammals, IRE1 and XBP-1 are dispensible for activation of

all but a very small set of UPR targets. This is all the more remarkable when one considers that most UPR target genes are conserved between yeast and mammals, it is just that the latter have found alternative means to couple their expression to ER stress. *C. elegans* occupies an intermediate position between yeast and mammals, in that most of its identifiable UPR targets are partially dependent on IRE1 and XBP-1, but can to some extent also be activated independently of that pathway.

Despite this redundancy in the mammalian UPR, both IRE1 and XBP-1 are essential for embryonic development (mammals have two IRE1 genes, a nonessential beta isoform restricted in its expression to the intestinal and bronchial epithelium and a broadly expressed alpha isoform which is essential). The reason(s) for the embryonic lethality of IRE1α and XBP-1 null animals are not fully understood, but it is hypothesized that in mammals the pathway may have diverted to specify the capacity for especially high levels of protein secretion. This hypothesis, which is clearly in need of further experimental support, suggests that specification of a secretory cell fate activates a conserved stress pathway that drives a developmental process, namely acquisition of an apparatus required by professional secretory cells for high-capacity protein secretion. This idea is further supported by the observation that many UPR target genes function far downstream in the secretory pathway rendering it unlikely that such genes merely relieve the stressed ER of its load of unfolded client proteins.

ATF6 and Intramembrane Proteolysis in the Metazoan UPR

The identification of ATF6 by Mori and colleagues confirmed the predicted redundancy in the metazoan UPR. Like IRE1, ATF6 is also an ER-localized transmembrane protein. However, its cytoplasmic effector domain consists of a transcription factor that activates UPR target genes directly. In its membrane-bound form, ATF6 is inert, as it cannot reach the nucleus. Activation involves regulated intramembrane proteolysis, which liberates the transcription factor part of ATF6 from the ER membrane under conditions of ER stress (Figure 2). The next surprise came when Brown, Goldstein, Prywes, and colleagues identified the proteases involved in this highly regulated event. These turned out to be the same proteases that process and activate the membrane-bound transcription factor, SREBP, which regulates genes involved in sterol and fatty acid biosynthesis and assimilation.

There are no mammalian gene knockouts reported for ATF6 (of which at least two isoforms exist). However, unlike cells lacking IRE1 or XBP-1, cells lacking the proteases required for ATF6 processing are severely impaired in UPR target gene expression. It seems likely therefore that mammalian ATF6 has picked up some of the role performed by IRE1 and XBP-1/HAC1 in simpler organisms. The similarities between ATF6 and the SREBPs highlight another remarkable feature of the UPR. IRE1 and HAC1 mutant yeast are unable to synthesize adequate amounts of the membrane phospholipid precursor, inositol. Though the details remain to be worked out, insufficiency of membrane lipid components also signals through the yeast UPR and enzymes involved in phospholipid metabolism are targets of IRE1 and HAC1. In metazoans this aspect of the UPR apparently has been split off and relegated to dedicated transcription factors, the SREBPs that are activated by insufficiency of lipid components. However the ancient link between the client protein-based UPR and membrane lipid insufficiency signaling has remained in the form of shared machinery for proteolytic activation of ATF6 and SREBP.

Translational Control in the UPR

PERK Couples ER Stress to eIF2α Phosphorylation and Translational Repression

In addition to activated gene expression ER stress results in a dramatic reduction in protein synthesis. Translational repression is an active process limiting the influx of client proteins into the stressed ER and thus serves as a counterpart to the gene expression program, which increases the organelle's capacity to process client proteins. Brostrom and colleagues and Kaufman and colleagues noted, early on, that translational repression by ER stress is associated with phosphorylation of the α-subunit of translation initiation factor 2 (eIF2α) on serine 51. This phosphorylation site is conserved in all eukaryotes and serves to regulate translation initiation in diverse stressful conditions. Trimeric eIF2, in complex with guanosine triphosphate (GTP), recruits the aminoacylated initiator methionyl–tRNA to the small ribosomal subunit, allowing translation initiation. Recognition of an AUG initiation codon on the mRNA leads to hydrolysis of GTP to GDP and dissociation of the ribosome–eIF2 complex. To participate in another round of translation initiation, the GDP bound to eIF2 must be exchanged to GTP. The enzyme catalyzing this exchange reaction (eIF2B) is inhibited by phosphorylated eIF2.

Distinct eIF2α kinases were known to be activated by distinct stress signals; PKR by double-stranded RNA

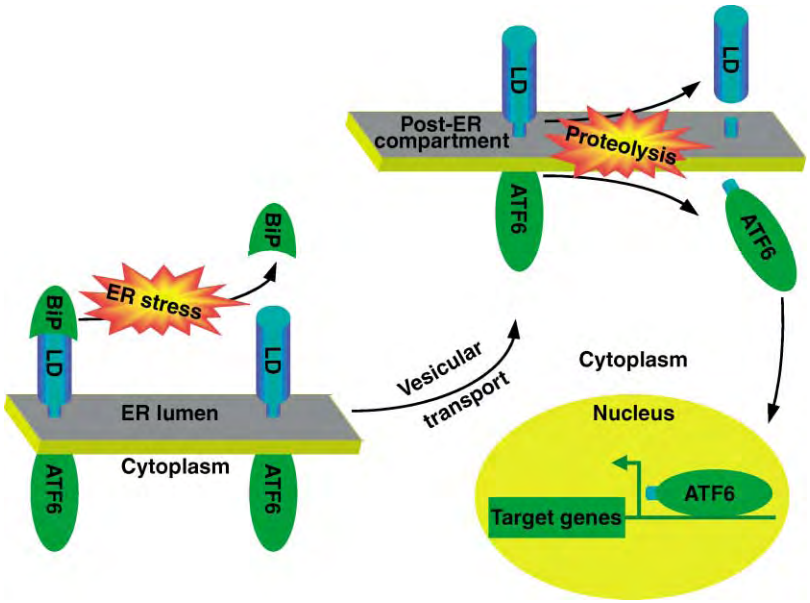

FIGURE 2 ATF6 activation by regulated intramembrane proteolysis. Membrane tethering inactivates the transcription factor ATF6, whose effector domain is prevented from accessing its target genes in the nucleus. BiP binding to the lumenal domain of ATF6 retains the protein in the ER compartment. However, under conditions of ER stress, BiP dissociates from ATF6, which then migrates (presumably by vesicular transport) to a post-ER compartment that contains the proteases that liberate the effector domain to signal in the UPR.

in viral infection and GCN2 by uncharged tRNAs in amino acid starvation. Our group noted the existence of a predicted transmembrane protein in the *C. elegans* genome, with an N-terminal "extracellular" domain similar to IRE1 and an intracellular domain similar to PKR and GCN2, known eIF2α kinases. This protein, which is conserved in metazoans (and absent from yeast) and to which we gave the name PERK (PKR-like ER Kinase), couples ER stress to eIF2α phosphorylation and is essential to translational regulation by ER stress. Cells lacking PERK are hypersensitive to ER stress and in mammals, PERK activity is especially important for preservation of cells engaged in high levels of secretion. Thus humans with PERK mutations and mice lacking the gene, develop diabetes mellitus and skeletal defects attributed to dysfunction of insulin- and collagen-secreting cells in the endocrine pancreas and bone, respectively.

Gene Expression, eIF2α Phosphorylation and Integration of Signals in the UPR, and Other Stress Pathways

In addition to limiting the load of client protein on the stressed ER (by inhibiting translation of most mRNA), eIF2α phosphorylation paradoxically activates the translation of the mRNA encoding the transcription factor ATF4 (and likely that of other regulatory proteins which remain to be discovered, Figure 3). PERK thus plays an important role in up-regulating target gene expression in the UPR. Expression profiling of ER stressed wild-type and PERK $-/-$ cells reveals a broad role for PERK in UPR-target gene expression, with mild impairment in most target genes and severe impairment in a smaller group. Among the UPR target genes that are strongly impaired in PERK $-/-$ cells are genes involved in amino acid transport and metabolism and a gene, *GADD34*, which encodes a phosphatase that dephosphorylates eIF2α and terminates signaling by PERK. The aforementioned strong PERK target genes play an important role in maintaining translation, by providing building blocks for secreted protein synthesis and by promoting eIF2α dephosphorylation. Thus, PERK and eIF2α phosphorylation appear to have a dual role in the UPR. Early in the response they protect the stressed cells from ER overload whereas later they promote conditions required for synthesis of secreted proteins.

A considerable overlap exists between genes activated by ER stress and genes activated by other stressful conditions that promote eIF2α phosphorylation. Thus, eIF2α phosphorylation integrates signaling in several stress pathways. The extent of this integrated stress response is not fully known, but it appears to control important aspects of cellular and organismal metabolism.

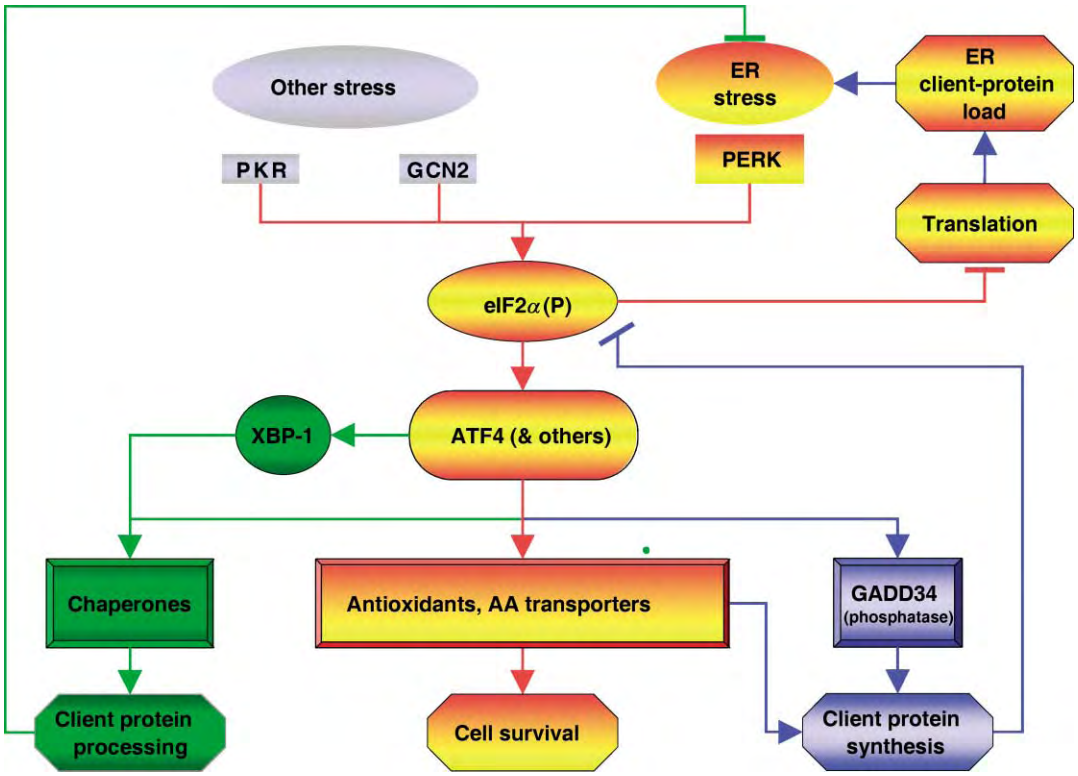

FIGURE 3 The eIF2α phosphorylation-dependent integrated stress response. ER stress and other stresses activate eIF2α kinases. Phosphorylated eIF2 inhibits translation initiation, alleviating ER client protein load, while at the same time activating the transcription factor ATF4 (and other, yet to be identified effectors). These activate a gene expression program with several components: The eIF2α phosphatase GADD34 promotes translational recovery and resumed client protein synthesis. Genes involved in antioxidant responses and amino acid import and assimilation, promote cell survival and client protein synthesis. PERK signaling also functions synergistically with other arms of the UPR (e.g., by transcriptional activation of the IRE1 target gene XBP-1) to enhance ER client protein processing.

A Common Mechanism for Sensing ER Stress

The identification of three different stress sensors in the UPR has allowed a comparison between their mode of activation. As mentioned earlier, overexpression of BiP and other ER chaperones had been noted to repress signaling in the UPR. In the equilibrated ER, all three stress transducers, IRE1, ATF6, and PERK, are found in a simple complex with BiP, which binds on the lumenal side to their stress-sensing domains. These complexes are rapidly dissociated under conditions of ER stress. Furthermore, dissociation precedes activation of the stress transducers. BiP dissociation promotes oligomerization of IRE1 and PERK, which in turns leads to transautophosphorylation and activation of downstream signaling. It seems likely that BiP-dissociation under conditions of ER stress unmasks a homo-oligomerization domain in the similarly structured lumenal domains of IRE1 and PERK.

The chain of events in the case of ATF6 activation is more complex, but conceptually similar. BiP binding retains ATF6 in the ER, segregated from the proteases that release its transcription factor portion, as these are localized to a post-ER compartment. BiP dissociation liberates ATF6 to migrate to the protease-containing compartment, a migration that presumably takes place by vesicular transport. Thus, dispensible molecules of BiP, which are not engaged in chaperoning ER client proteins actively repress signaling by all three known transducers of the UPR. It would thus appear that the recognition of unfolded and malfolded proteins is relegated to professional chaperones and the stress transducers passively monitor the degree to which the latter are engaged by their clients. This arrangement of the upstream steps of the UPR mirrors that of the cytoplasmic heat shock response in which unfolded proteins in the cytoplasm activate genes implicated in folding and degrading cytoplasmic proteins.

See Also the Following Articles

Chaperones for Metalloproteins • Chaperones, Molecular • Chaperonins • Endoplasmic Reticulum-Associated Protein Degradation • Regulated Intramembrane Proteolysis (Rip)

Glossary

chaperone A protein that assists folding and assembly of other proteins and prevents their aggregation in the unfolded state.

endoplasmic reticulum A membrane-bound organelle, present in all nucleated cells, which serves as the entry point for secreted proteins.

proteotoxicity A hypothetical property of unfolded and malfolded proteins, whereby peptide domains that are illegitimately exposed on the surface perturb cellular function.

Further Reading

Cox, J. S., and Walter, P. (1996). A novel mechanism for regulating activity of a transcription factor that controls the unfolded protein response. *Cell* **87**, 391–404.

Harding, H., Zhang, Y., and Ron, D. (1999). Translation and protein folding are coupled by an endoplasmic reticulum resident kinase. *Nature* **397**, 271–274.

Harding, H. P., Calfon, M., Urano, F., Novoa, I., and Ron, D. (2002). Transcriptional and translational control in the mammalian unfolded protein response. *Annu. Rev. Cell Dev. Biol.* **18**, 575–599.

Kaufman, R. J. (1999). Stress signaling from the lumen of the endoplasmic reticulum: Coordination of gene transcriptional and translational controls. *Genes Dev.* **13**, 1211–1233.

Sidrauski, C., and Walter, P. (1997). The transmembrane kinase Ire1p is a site-specific endonuclease that initiates mRNA splicing in the unfolded protein response. *Cell* **90**, 1031–1039.

Yoshida, H., Okada, T., Haze, K., Yanagi, H., Yura, T., Negishi, M., and Mori, K. (2000). ATF6 activated by proteolysis binds in the presence of NF-Y (CBF) directly to the cis-acting element responsible for the mammalian unfolded protein response. *Mol. Cell Biol.* **20**, 6755–6767.

Biography

David Ron obtained his Medical Doctorate at the Technion in Haifa, Israel. Following residencies in internal medicine and endocrinology at Mount Sinai Hospital and the Massachusetts General Hospital and a research fellowship at Harvard Medical School, he took a faculty position at New York University School of Medicine, where he is currently a Professor of Medicine and Cell Biology. His laboratory studies stress responses in eukaryotic cells, with a special emphasis on signaling between organelles and the nucleus.

Urea Cycle, Inborn Defects of

Marsha K. Fearing and Vivian E. Shih
Harvard Medical School, Boston, Massachusetts, USA

Surplus nitrogen generated by amino acid metabolism cannot be stored in mammals and must be excreted. The urea cycle is the primary pathway for the disposal of ammonium nitrogen by conversion of the toxic ammonia molecule into innocuous urea. Inborn errors of metabolism in the urea cycle can result in severe diseases in humans. An accumulation of ammonia can lead to severe morbidity, including brain damage and death.

Overview

The urea cycle is the major pathway for the disposal of nitrogen in humans (Figure 1). Ninety percent of ingested protein is metabolized to urea and excreted through the urine. Ammonia is derived from a variety of precursor protein sources. Part of the urea cycle resides in mitochondria where ammonia is converted to carbamoyl phosphate by carbamoyl phosphate synthetase (CPS) along with its allosteric activator, *N*-acetylglutamate. The next step involves carbamoyl phosphate forming citrulline when condensed with ornithine. This process is mediated by the enzyme ornithine transcarbamoylase (OTC). Citrulline exits the mitochondria and condenses with aspartate to produce argininosuccinate. This compound is then cleaved to arginine and fumarate by argininosuccinate lyase. Arginine is hydrolyzed by arginase, thus releasing urea and regenerating ornithine. Ornithine is then shuttled into mitochondria by its own transporter. Within the urea cycle ornithine is a conserved moiety, it is neither formed nor lost. One atom of waste nitrogen from ammonia and one from aspartate forms a molecule of urea.

Liver is the only organ that contains the complete urea cycle and is the major site of ureagenesis. Intestinal epithelial cells have CPS and OTC for citrulline synthesis and are the source of the circulating citrulline in plasma that serves as a precursor for synthesis of arginine, a semi-essential amino acid, in brain and kidney. These organs have negligible arginase activity, hence they do not produce urea.

Clinical Diseases

Urea Cycle Defects

Gene mutations resulting in urea cycle defects have been described for each of the five urea cycle enzymes. The individual disease states are N-acetylglutamate synthetase (NAGS) deficiency, carbamoyl phosphate synthetase (CPS) deficiency, ornithine transcarbamoylase (OTC) deficiency, argininosuccinate synthetase (AS) deficiency or citrullinemia, argininosuccinate lyase (AL) deficiency or argininosuccinic aciduria, and arginase (A1) deficiency.

The clinical features of the urea cycle disorders are similar. Depending on the enzyme involved and the residual enzyme activity, metabolic blocks in the urea cycle will cause a resultant elevation of the plasma ammonia level. Hyperammonemia is associated with many of the clinical features, which include respiratory alkalosis, seizures, acute encephalopathy, coma, and even death. Spasticity, resembling cerebral palsy can be a late complication. The most severe presentation is coma in the neonatal period, but symptoms can occur later in childhood as well. Metabolic stress, intercurrent illness, or fever can result in endogenous protein catabolism and precipitate a hyperammonemic crisis. In milder cases, abnormal neuropsychiatric behavior can be the only manifestation. Short, friable hair (trichorrhexis nodosa) and liver fibrosis are unique to argininosuccinate lyase deficiency.

The exact pathophysiology of hyperammonemia is not known and the etiology of brain edema is still unclear. Accumulation of ammonia and astrocytic glutamine are likely to be contributory to the brain damage.

Except for the X-linked ornithine transcarbamoylase deficiency, the enzyme defects of the urea cycle disorders are inherited as autosomal recessive traits.

The gene for OTC is located on chromosome Xp2.1. Thus, males with OTC deficiency are usually more severely affected with neonatal onset of hyperammonemia, whereas the clinical presentation in females with OTC deficiency can be quite variable, depending on random X-chromosome inactivation (Lyon hypothesis).

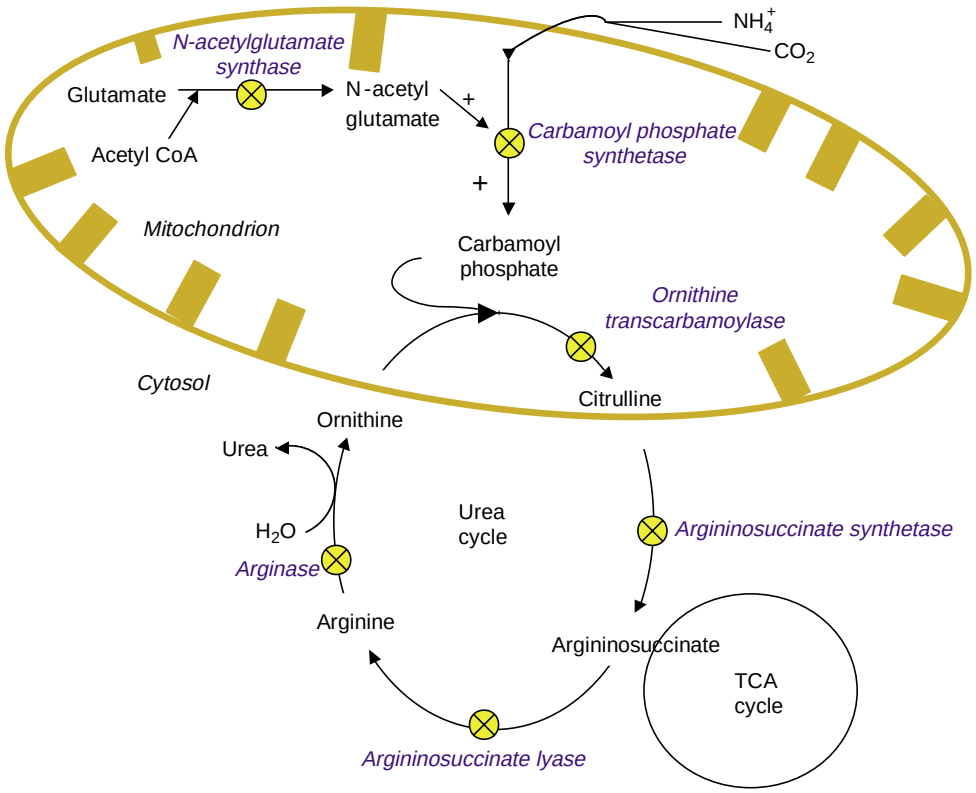

FIGURE 1 The urea cycle. (1) N-acetylglutamate synthetase, (2) carbamoyl phosphate synthetase, (3) ornithine transcarbamylase, (4) argininosuccinate synthetase, (5) argininosuccinate lyase, (6) arginase, (7) mitochondrial ornithine transporter, and (8) ornithine aminotransferase. NAG = N-acetylglutamate, an allosteric activator of carbamoyl phosphate synthetase.

Other Hyperammonemia States Due To Amino Acid Transporter Defects

Amino acid transporter defects are disorders of compartmentation. The urea cycle enzymes are available but the substrates are not transported to the proper site, resulting in a functional enzyme deficiency.

Triple H Syndrome (Hyperornithinemia, Hyperammonemia, Homocitrullinuria)

The HHH syndrome is a defect in ornithine mitochondrial transport, which prevents the recycling of ornithine as the substrate for OTC. The end result is a functional OTC deficiency and reduced urea synthesis. These children present with episodic hyperammonemia, ataxia, vomiting, irritability, lethargy, and coma. They often come to attention due to mental retardation and developmental delay, with occasional seizure activity. The diagnostic markers are a combination of high plasma ornithine, high blood ammonia, increased urine orotic acid, and high urine homocitrulline, the origin of which is unclear. The treatment is similar to that for OTC deficiency.

Lysinuric Protein Intolerance

Lysinuric protein intolerance (LPI), also known as hyperdibasic aminoaciduria, is an autosomal recessive disease with an extremely high prevalence in the Finnish population. The gene mutation has been identified on chromosome 14q12. LPI occurs from defects in the cellular basolateral membrane transporter of the dibasic amino acids, in renal tubules and the intestinal system. This results in excessive renal loss of lysine, arginine, and ornithine in the urine and poor gastrointestinal absorption of the same amino acids. Arginine and ornithine deficiency impairs the function of the urea cycle and results in hyperammonemia after protein intake. Symptoms of LPI include failure to thrive, vomiting, and chronic lysine deficiency, which causes growth failure with decreased bone density resulting in, osteoporosis. LPI patients also have recurrent autoimmune deficiency and infections due to low white and red blood cell counts. Other organ involvement includes interstitial lung disease and renal failure.

Citrin Deficiency (Citrullinemia Type II)

Citrullinemia type II was originally reported as an adult-onset citrullinemia, mainly in Japanese patients, with

TABLE I

Diagnostic Characteristics of Urea Cycle Disorders and Hyperammonemic Syndromes due to Amino Acid Transporter Defects

Disorder	Plasma Cit	Plasma Arg	Urine orotic acid	Other diagnostic amino acids	Genetic markers	Enzyme assay	Prenatal diagnosis
N-acetyl-glutamate synthetase deficiency	↓		N		AR; 17q21.31	Liver	DNA testing
Carbamoyl phosphate synthetase deficiency	↓	↓	N		AR; chromosome 2p	Liver	Linkage analysis; direct mutational analysis
Ornithine transcarbamoylase deficiency	↓	↓	↑		X linked; Xp2.1	Liver	Molecular diagnosis
Argininosuccinate synthetase deficiency	↑↑	↓	↑		AR; chromosome 9q34	Liver; fibroblasts; lymphoblasts, chorionic villi	Enzyme assay; direct mutational analysis; Metabolite measurement in amniotic fluid
Argininosuccinate lyase deficiency	↑	↓	↑	↑ Arginino-succinic acid (blood and urine)	AR; chromosome 7q	Liver; fibroblasts, red blood cells	Metabolite measurement in amniotic fluid
Arginase deficiency	N	↑	↑		AR; chromosome 6q23	Liver, red blood cells	Enzyme assay, DNA analysis
Lysinuric protein intolerance	↓	↓	↑	↑ arginine, lysine, ornithine (urine)	AR; chromosome 14q11.2		
Triple H syndrome	↓	↓	↑	↑ ornithine (blood) ↑ homocitrulline (urine)	AR; chromosome 13q14	Fibroblasts, Amniocytes	Enzyme assay in fetal blood, DNA analysis
Citrin deficiency	↑	↓	↑	↑ citrulline (blood and urine)	AR; chromosome 7q21.3	Liver	DNA analysis

a liver-specific argininosuccinate synthetase deficiency. The clinical presentation depends on the degree of hyperammonemia and includes a sudden disturbance of consciousness, restlessness, drowsiness, and coma with cerebral edema. Recent studies have identified a deficiency of the citrin protein, which is a mitochondrial transporter of aspartate and/glutamate, as the underlying cause. This has been confirmed by mutation analysis. Citrin deficiency has now been identified in citrullinemic patients of different ethnic backgrounds with neonatal intrahepatic cholestasis and other forms of severe hepatic dysfunction.

Diagnosis

All disorders have hyperammonemia. Plasma and urine amino acid analysis reveal the specific diagnostic patterns (Table I). The amino acids proximal to the enzyme block are increased and those distal to the block are decreased. When there is a blockage in the urea cycle beyond the step of CPS, the carbamoyl phosphate synthesized cannot be used for urea synthesis and is shunted to the biosynthetic pathway of pyrimidine to form orotic acid. Thus, orotic acid is increased in all urea cycle disorders except for NAGS deficiency and CPS deficiency. Diagnosis can be confirmed by enzyme assay in red blood cells (arginase deficiency) and cultured fibroblasts (AS deficiency, AL deficiency). Measurement of CPS and OTC activities can only be done in liver biopsy. Enzymatic details can be seen in Table II. Alternatively, molecular DNA mutation analysis can be useful for diagnosis as well as for future genetic counseling.

For all of the urea cycle defects, except NAGS, prenatal diagnosis is available. AS and AL deficiencies are noted by finding increased citrulline and increased ASA in amniotic fluid. Amniocytes do not have all of the urea cycle enzymes; only AS and AL are expressed. Fetal liver biopsy is required for prenatal diagnosis of CPS and OTC deficiencies, and fetal blood is needed for prenatal diagnosis of arginase deficiency. For prenatal diagnosis of HHH syndrome, the ornithine incorporation assay can be performed in cultured amniocytes. In cases of known mutations in a family, DNA analysis is the preferred procedure.

Treatment

Long-Term Management

Reduction in protein intake while maintaining nutritional needs to ensure growth and development remains the mainstay of therapy. The goal of therapy is to reduce the flow of nitrogen for disposal through the urea cycle. This can be achieved by restriction of dietary protein intake by providing an alternative pathway for nitrogen disposal.

Alternative pathway therapy for nitrogen excretion diverts ammonia clearance through compounds other than urea. Sodium benzoate is one of the drugs used for this purpose. When administered it conjugates with the amino acid glycine to form hippurate, which has high renal clearance. One mol of nitrogen is excreted per one mole of hippurate. Following the same principle but with greater efficiency, sodium phenylacetate conjugates with the amino acid glutamine to form phenylacetylglutamine, which eliminates two moles of nitrogen.

To maintain normal growth it is important to provide enough essential amino acids by supplementing the diet. In patients with a urea cycle defect, arginine synthesis is reduced and arginine becomes a semi-essential amino acid. Patients can be supplemented with citrulline, the precursor of arginine, to restore total body arginine pools or with arginine directly in patients with AS and AL deficiency.

In addition to medical management, liver transplantation has been used with some success for treatment of these disorders.

TABLE II

Urea Cycle Enzyme Characteristics and Locations

Enzyme	Cellular location	Relative activity in liver	pH optimum	Tissue distribution
NAGS	Mitochondrial matrix	0.01	8.5	L, I, (K)
CPS1	Mitochondrial matrix	3.1	6.8–7.6	L, I, (K)
OTC	Mitochondrial matrix	73	7.7	L, I, (K)
AS	Cytosol	1	8.7	L, K, F, (B)
AL	Cytosol	2.4	7.5	L, K, F, (B)
A1	Cytosol	962	9.5	L, RBC, (K), (B)

B = brain; I = small intestine; K = kidney; L = liver; RBC = red blood cells.

Acute Management

Hyperammonemic crisis is often precipitated by stressful situations such as fever, trauma, infection, surgery, and dietary indiscretion. The goal of treatment is to lower the blood ammonia levels to prevent brain edema. The most effective treatment is hemodialysis or peritoneal dialysis. Nitrogen scavenger medications, such as sodium phenylacetate and sodium benzoate, and arginine are also given intravenously. Protein intake is halted and an intravenous fluid with a high dextrose (10%) load is provided immediately to minimize catabolism and therefore the source of ammonia. Intercurrent infection should be treated appropriately.

Future Horizons

Future treatment modalities may include total or partial organ transplant, stem cell transplant, and enzyme replacement. Early diagnosis utilizing newborn screening and prenatal diagnosis will allow early treatment and improve the outcome.

See Also the Following Articles

Amino Acid Metabolism • Ornithine Cycle

Glossary

autosomal recessive A mode of genetic inheritance that describes a trait or disorder requiring the presence of two copies of a gene mutation on one of the 22 pairs of autosomes (nonsex chromosomes) at a particular locus in order to express observable phenotype.

enzyme Biological reactants that are protein catalysts, mediating reactions without themselves being changed in the overall process. They selectively channel substrates into pathways.

essential amino acids The amino acids that are synthesized by nonmammalian pathways and must be obtained in diet. They include histidine, isoleucine, leucine, lysine, methionine, phenylalanine, threonine, tryptophan, and valine. Arginine is considered a "semi-essential" amino acid because mammals synthesize arginine, but cleave most of it to form urea and require greater amounts than can be produced in mammalian biosynthesis.

Lyon hypothesis The X chromosome is randomly inactivated in early development in embryonic cells. This results in fixed inactivation in the female's descendant cells. The deactivated chromosome forms the Barr body.

non-essential amino acids Amino acids that can be produced by mammals from common intermediates and biosynthesis and are not strictly diet dependent. These include alanine, asparagine, aspartate, cysteine, glutamate, glutamine, glycine, proline, serine, and tyrosine.

X-linked disorder A mode of genetic inheritance that describes a gene mutation on the X chromosome that causes the phenotype to be expressed in males who are hemizygous for the gene mutation and in females who are homozygous for the gene mutation (meaning they must have a copy of the gene mutation on each of their two X chromosomes). Carrier females do not usually express the phenotype, although differences in X-chromosome inactivation can lead to varying degrees of clinical expression.

Further Reading

Berry, G., and Steiner, R. (2001). Long-term management of patients with urea cycle disorders. *J. Pediatrics* **138**(Suppl. 1), S56–S61.

Feillet, F., and Leonard, J. V. (1998). Alternative pathway therapy for urea cycle disorders. *J. Inher. Metab. Dis.* **21**(Suppl. 1), 101–111.

Fernandes, J., Saudubray, J. M., and Van den Berghe, G. (eds.) (2000). *Inborn Metabolic Diseases: Diagnosis and Treatment*, 3rd edition. Springer, Berlin.

Morizono, H., Caldovic, L., Shi, D., and Tuchmon, D. (2004). Mammalian N-acetylglutamate synthase. *Mol. Genet. Metab.* **81**, 4–11.

Nyhan, W. L., and Ozand, P. T. (eds.) (1998). *Atlas of Metabolic Diseases*. Chapman and Hall Medical, London.

Steiner, R., and Cederbaum, S. (2001). Laboratory evaluation of urea cycle disorders. *J. Pediatrics* **138**(Suppl. 1), S21–S29.

Summar, M., and Tuchman, M. (2001). Proceedings of a consensus conference for the management of patients with urea cycle disorders. *J. Pediatrics* **138**(Suppl. 1), S6–S10.

Biography

Marsha K. Fearing is a Clinical Fellow at the Harvard Medical School Genetics Training Program, specializing in Biochemical Genetics. She is a member of the Scholars in Clinical Science Program at Harvard Medical School. Her area of research is translational and public health research in metabolism. Dr. Fearing is a member of Alpha Omega Alpha, the American Academy of Pediatrics, and a candidate fellow of the American College of Medical Genetics.

Vivian E. Shih is Professor of Neurology at Harvard Medical School, Associate Neurologist and Pediatrician at Massachusetts General Hospital, and Director of the Clinical Neurochemistry and Amino Acid Disorders Laboratory at Massachusetts General Hospital. Her area of research is inborn errors of amino acid and organic acid metabolism.

Vacuoles

Christopher J. Stefan and Scott D. Emr
University of California, San Diego, La Jolla, California, USA

Vacuoles and their mammalian counterparts, lysosomes, are membrane-bound cytoplasmic organelles that contain an assortment of soluble acid-dependent hydrolases and a set of highly glycosylated integral membrane proteins. Most notably, this organelle is an important site for the degradation of cellular lipids, membrane-associated proteins, and cytoplasmic proteins. In addition to its degradative functions, the vacuole/lysosome plays an important role in pH and ion homeostasis and is a site for the generation/storage of nutrients, amino acids, antigens, and additional signaling factors.

Identification/Discovery of Vacuoles and Vacuolar Constituents

Vacuoles/lysosomes were first visualized by independent cell morphological studies undertaken in the 1950s by the Palade and Novikoff laboratories. These studies revealed that lysosomes appear as organelles with 0.5 μm diameter and a heterogeneous morphology, containing electron-dense cores and, in some cases, membrane vesicles. In the yeast *Saccharomyces cerevisiae*, vacuoles are larger with respect to cell size, but display similar characteristics in terms of electron density and intralumenal vesicles, when observed under certain conditions (Figures 1A and 1B).

Biochemical studies performed by de Duve and colleagues initially identified lysosomes as organelles of highly buoyant centrifugal properties that contained a number of hydrolytic activities. The hydrolases within this fraction demonstrated attenuated activity dependent on the integrity of their surrounding membrane. Specifically, hydrolase activity was retained within the limiting vacuole/lysosome membrane, restricted from the cell lysate unless the limiting membrane was disrupted. Since vacuoles/lysosomes are morphologically heterogeneous, biochemical studies have produced the current definition of vacuoles/lysosomes as membrane-bound acidic organelles that contain mature acid-dependent hydrolases and certain integral membrane-glycoproteins. Vacuoles lack other proteins that distinguish them from endosomes (compartments that deliver material to vacuoles), such as biosynthetic sorting receptors and recycling cell-surface receptors.

As already mentioned, vacuoles/lysosomes are membrane compartments that serve as a major degradative compartment in eukaryotic cells. Both endogenous and exogenous molecules can be delivered to vacuoles through biosynthetic and endocytic pathways. In addition, vacuoles can degrade proteins transported from the cytosol. The degradative function of these organelles is carried out by numerous acid-dependent hydrolases (e.g., proteases, lipases, glycosidases) contained within its lumen (Figure 2). The outer, limiting membrane of vacuoles also contains a set of highly glycosylated, vacuolar/lysosomal-associated membrane proteins. A subset exhibits known hydrolase activities (Figure 2), while the functions of many are still unclear. Additional vacuolar membrane proteins mediate transport of ions, amino acids, and other solutes across the vacuolar membrane and maintain an acidic lumenal pH in the range of 4.5–6.5 (Figure 2).

Vacuole Function in Yeast

The vacuole of the yeast *S. cerevisiae* plays an important role in protein degradation, pH regulation, ion homeostasis, and nutrient storage. The yeast vacuole contains a large number of hydrolases (proteases, lipases, glycosidases; see Figure 2) with various substrate specificities. Thus, it is a major site for degradation of cellular proteins, lipids, and even whole organelles.

A remarkable feature of vacuoles is their acidification. In yeast, a specific vacuolar proton pump ATPase (V-ATPase) mediates this process. Biochemical and genetic approaches have identified 14 subunits of the V-ATPase (encoded by the *VMA* genes for *v*acuolar *m*embrane *A*TPase). The V-ATPase subunit proteins form two complexes, the peripheral V_1 subcomplex, responsible for ATP hydrolysis, and the V_0 subcomplex, responsible for proton translocation across the membrane (Figure 2). Cells lacking a functional V-ATPase are viable, but require an intact endocytic pathway to the vacuole. Moreover, they fail to grow on media with neutral pH, indicating that vacuole acidification is an

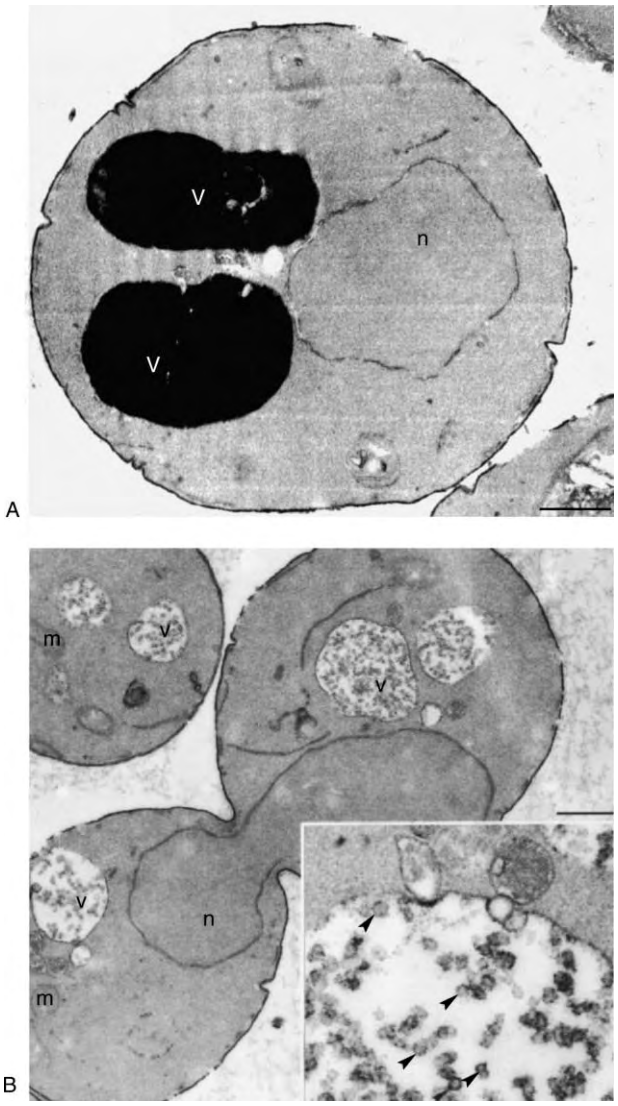

FIGURE 1 Ultrastructural analysis of vacuole morphology in wild type (A) and hydrolase deficient (B) yeast cells reveals electron dense cores and intralumenal membrane vesicles, respectively. (A) Wild type cells were grown to mid-log phase, fixed, and visualized by electron microscopy. Vacuoles appear as dark, electron dense organelles due to the accumulation of cellular proteins, lipids, and other molecules. (B) In cells lacking vacuolar ATPase activity (*vma4*Δ mutant cells), vacuoles appear translucent by electron microscopy and contain intralumenal vesicles. Inset: High magnification image of vacuolar vesicles (arrowheads) (v, vacuoles; n, nucleus; m, mitochondria; bars = 0.1 μm). (Reprinted with permission from Wurmser, A. E., and Emr, S. D. (1998). Phosphoinositide signaling and turnover: PtdIns(3)P, a regulator of membrane traffic, is transported to the vacuole and degraded by a process that requires lumenal vacuolar hydrolase activities. *The EMBO Journal* **17**, 4930–4942, copyright 1998 Oxford University Press.)

essential feature. Consistent with this, the electrochemical gradient generated by the V-ATPase is necessary to drive several other transport systems described in this article (Figure 2).

In addition to its hydrolytic functions, the vacuole serves as a storage compartment for several ions and

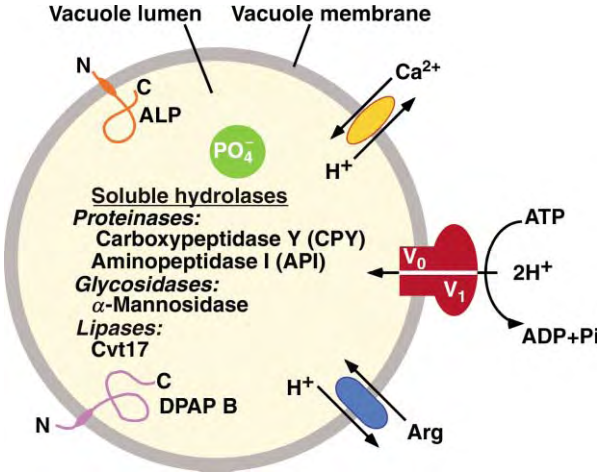

FIGURE 2 Schematic overview of vacuolar components. The vacuole lumen possesses several hydrolase activities and accumulates ions, such as phosphate (PO_4^-) and polyphosphates. The vacuolar membrane also contains known hydrolases, such as ALP, and proteases, such as dipeptidyl-aminopeptidase B (DPAP B). The vacuolar ATPase (V_0/V_1) functions as the primary proton pump that generates an electrochemical gradient used to drive other vacuole membrane transport systems, such as arginine (Arg) and divalent cation (Ca^{2+}) anti-transporters.

nutrients (Figure 2). For example, the Vcx1 protein acts as a high capacity H^+/Ca^{2+} exchanger *in vitro* and has been implicated in the regulation of vacuolar calcium flux *in vivo* (Figure 2). The vacuole also stores both phosphate and polyphosphate (Figure 2). Since hydrolysis of phosphate leads to the release of protons, a role for polyphosphate in pH homeostasis has been suggested. Polyphosphate is proposed to function as a cation counter ion as well. Some amino acids are also stored inside the vacuole at high concentrations. For example, arginine accumulates in vacuoles at concentrations nearly an order of magnitude greater than in the surrounding media (Figure 2). Consistent with this, several H^+/amino acid anti-porter systems have been identified in yeast. Pools of amino acids stored in the vacuole may be utilized during nitrogen starvation.

Vacuole Biogenesis and Transport Pathways to the Vacuole in Yeast

To carry out the numerous functions that vacuoles perform, several transport pathways have evolved that deliver cellular components to vacuoles. Model genetic systems such as the yeast *S. cerevisiae* have been instrumental in identifying both proteins and lipids that constitute components of vacuoles and the machinery involved in transport to vacuoles. Importantly, many of these factors and transport pathways are conserved in mammalian cells.

At least eight pathways have been identified in vacuole biogenesis and protein transport to vacuoles in

yeast: endocytosis from the cell-surface, two distinct biosynthetic pathways, the carboxypeptidase Y (CPY) and alkaline phosphatase (ALP) from the Golgi, multivesicular body (MVB) sorting, the cytoplasm to vacuole pathway (Cvt), macro-autophagy, micro-autophagy, and vacuole inheritance during cell division (Figure 3A). The endocytic pathway is essential for regulating levels of cell-surface proteins and intersects with the CPY pathway at a late endosomal compartment. Components of the CPY-sorting pathway are directly involved in vacuolar biogenesis, morphology, and function, as discussed here in greater detail. ALP travels from the Golgi to the vacuole along a pathway that is independent of the CPY and endocytic pathways. Proteins such as aminopeptidase I (API) are delivered from the cytoplasm to the vacuole through pathways involving products of the *CVT* and *APG* (autophagy) genes. In micro-autophagy, the vacuole membrane invaginates to engulf cytoplasmic material, including entire organelles such as peroxisomes. Vacuolar segregation into dividing daughter cells of budding yeast requires *VAC* (vacuolar inheritance) genes, some of which also participate in the CPY pathway. Previous studies have also identified several distinct factors involved in vacuolar inheritance.

The CPY Pathway

CPY is the prototype of a subset of proteins that traffics from the Golgi to the vacuole via an endosomal intermediate. This pathway depends on the function of over 60 *VPS* gene products, mutations in which result in the mis-sorting of CPY to the secretory pathway, abnormal vacuole morphology, and in some cases, abnormal endosome morphology. In a manner analogous to receptor-mediated sorting in mammalian cells, the CPY receptor Vps10 binds CPY at the Golgi via a targeting signal. Sorting of this receptor–ligand complex into vesicles bound to endosomes requires proteins such as clathrin and accessory factors such as the AP-1 clathrin adaptor complex and the Gga proteins. Next, the class D Vps proteins are involved in CPY vesicle targeting and fusion with endosomes, such as Vps21 (Rab5 homologue), Vps9 (Rab GEF), Vac1 (EEA1), Vps45 (Sec1 homologue), Pep12 (t-SNARE), and Sec18 (NSF). At the endosome, Vps10 dissociates from CPY and recycles to the Golgi in a process requiring the retromer complex (consisting of Vps29, Vps26, Vps35, Vps5, and Vps17). Mutants defective in retromer function mis-localize Vps10 to the vacuole membrane and secrete CPY, as Vps10 becomes limiting for subsequent sorting reactions at the Golgi.

Another set of Vps proteins (the class E Vps proteins) is necessary for efficient sorting at the endosome. Class E Vps mutant cells accumulate abnormal/aberrant endosomes containing both biosynthetic cargo such as CPY and endocytosed proteins. The class E proteins are also involved in the formation of multivesicular bodies (MVBs) at late endosomes. The abnormal/exaggerated endosomes observed in these mutant cells form in part due to impaired MVB vesicle budding into the lumen of the endosome.

Finally, fusion of late endosomes/MVBs with the vacuole requires another set of proteins including Ypt7 (Rab7 homologue) and SNARE proteins (Vti1, Ykt6, Nyv1, Vam7, and Vam3). The class C Vps protein complex (also termed HOPS) consisting of Vps18, Vps11, Vps16, and Vps33 (Sec1 homologue), Vps41, and Vps39 (Rab GEF) is required for this final fusion step as well (Figure 3B). The Vps34 PI 3-kinase also contributes to this fusion step by the generation of PI(3)P that recruits effector proteins such as the PX domain-containing protein Vam7. Mutants with defects in these gene products accumulate numerous endosomal intermediates and MVBs that fail to fuse with the vacuole. Accordingly, mutants defective in components of the vacuolar fusion machinery display highly fragmented vacuoles and can sometimes even lack vacuoles entirely.

The ALP Pathway

ALP is an integral membrane protein that travels from the Golgi to the vacuole independently of endosomal compartments that transport CPY and endocytic cargoes (Figure 3A). A specific adaptor complex, termed AP-3, mediates sorting of ALP into vesicles at the Golgi. However, following formation, fusion of ALP cargo vesicles with the vacuole is dependent on the class C Vps complex, Ypt7, Vam7, and Vam3. Thus, the ALP and CPY pathways converge upon common docking/fusion machinery at the vacuole (Figure 3B).

Cytoplasm to Vacuole Transport and Macro-Autophagy

Autophagy is a trafficking pathway to vacuoles regulated by changes in nutrient availability. In macro-autophagy, induced during starvation, cytoplasmic material is first sequestered in double-membrane vesicles called autophagosomes and then subsequently delivered to the vacuole (Figure 3A). While autophagy is induced, the Cvt pathway constitutively packages the hydrolases aminopeptidase I (API) and α-mannosidase into autophagosomes for delivery to vacuoles. Autophagosomes are targeted to, and fuse with, the vacuole by the same machinery that mediates endosome-vacuole fusion (Figure 3B). Inside the vacuole, the lipase Cvt17 is responsible for autophagosome turnover (Figure 2).

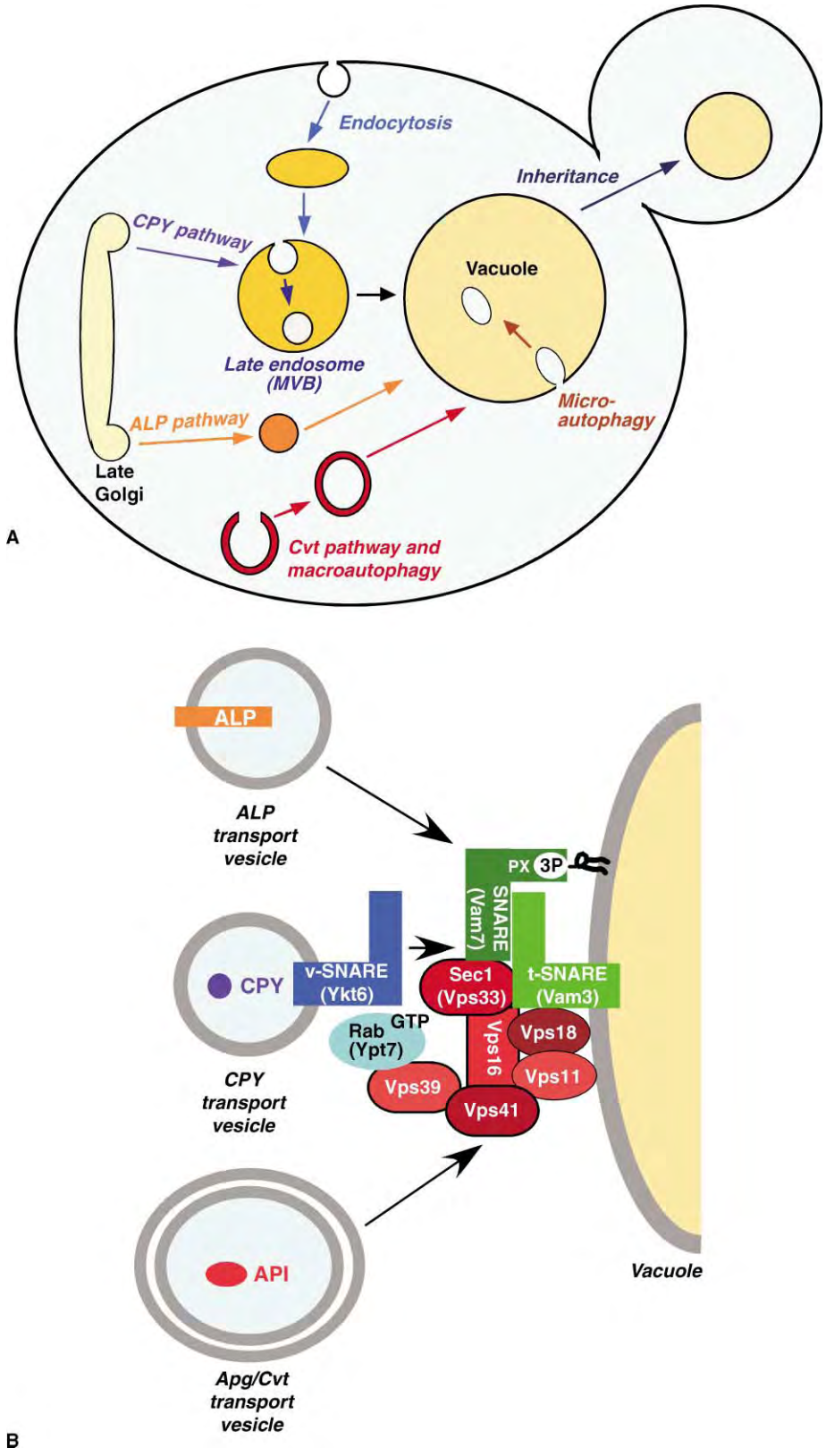

FIGURE 3 (A) Model representation of the transport pathways to the vacuole. Endocytosis of cell-surface proteins is followed by transport to early endosomes and then late endosomes. The CPY pathway sorts proteins from the late Golgi to the late endosome. At the late endosome, select cargo is sequestered into intralumenal vesicles to form multivesicular bodies (MVB) while other proteins, such as sorting receptors, are recycled to the Golgi. The ALP pathway functions as a Golgi to vacuole route that is independent of the late endosome/MVB. In the Cvt pathway, cytoplasmic proteins are enclosed within double membrane structures that subsequently fuse with and deliver their material into the

Vacuole/Lysosome Functions in Higher Eukaryotes

The Contractile Vacuole in Protozoa

Protozoa living in fresh water exist in a hypotonic environment. Water flows across their plasma membrane since their cytosol is hypertonic to the environment. To adapt, many protozoa have an organelle, the contractile vacuole complex (CVC), which collects and expels excess water. Previous work shows that CVCs are composed of a central vacuole with radial arm-like extensions. The extensions are often divided into separate bundles of tubules and contain proton-translocating V-ATPase enzymes that provide an electrochemical gradient necessary for fluid collection. The membrane of the central compartment lacks V-ATPases, but can expand into a reservoir for fluid storage, and is capable of fusing with the plasma membrane. It is then that the central compartment undergoes contraction, resulting in fluid expulsion.

Lysosome-Related Organelles

The mammalian vacuole-like lysosome also is a site for delivery of cellular materials targeted for degradation, as it is the terminal compartment of the endocytic, phagocytic, and biosynthetic pathways in mammalian cells. However, the idea that vacuoles/lysosomes are simply degradative sites has evolved, in part by the identification of lysosome-like compartments that perform additional cellular functions such as lysosomes that secrete their contents after fusion with the plasma membrane. Many properties of vacuoles/lysosomes are shared with this group of cell type-specific lysosome-related organelles, which include melanosomes (pigment granules), lytic granules, platelet-dense granules, basophil granules, nuetrophil granules, and dendrocyte MHC class II compartments (involved in antigen presentation). However, in addition to lysosomal proteins, these organelles contain cell type-specific components that are responsible for their specialized functions.

Pathogen-Containing Vacuoles

The uptake of foreign objects by macrophages often provides an important line of immune defense. To some intracellular pathogens (such as certain protozoa) however, phagocytosis represents an opportunity to gain protected access within a host cell. Other types of pathogens, including *Salmonella* and *Shigella*, actively invade host cells by delivering effectors into the host cell that leads to their direct uptake into intracellular vacuoles. Regardless of the mode of entry, the resulting intracellular vacuole that contains the parasite undergoes a maturation process, involving numerous membrane-trafficking events, as well as transmembrane transport of nutrients. Maturation of the vacuole yields a unique intracellular environment where the parasites are not only provided with essential nutrients, but are also protected from destruction by the host.

Diseases Associated with Lysosomal Disorders

Several human genetic disorders are associated with defects in vacuolar/lysosomal function and transport, such as I-Cell, Tay-Sachs', Pompe's, Galactosialdosis, and Gaucher's disease. I-Cell disease is manifested by the inappropriate targeting/transport of multiple lysosomal enzymes. Cells of these patients become highly vacuolated and contain numerous dense inclusion bodies. Patients with I-Cell disease display severe clinical defects including skeletal and neurological defects, delayed growth and psychomotor development, and often death before age five. Abnormalities in lysosome-related organelles have also been observed in human genetic diseases such as the Chediak-Higashi and Hermansky-Pudlak syndromes. The similarity of genes affected in these lysosomal diseases to genes involved in vacuolar transport in yeast further demonstrates the importance of understanding the molecular machinery involved in the biogenesis and function of vacuoles, lysosomes, and lysosome-related organelles. Further studies on vacuole biogenesis will likely shed light on additional aspects of vesicular transport in the endosomal, lysosomal, and secretory systems.

See Also the Following Articles

Endocytosis • V-ATPases

Glossary

active transport Use of energy to transport a substance, often across membranes from an area where it is in lower concentration to an

vacuole. Macro-autophagy is similar to the Cvt pathway but is induced primarily under starvation conditions. In micro-autophagy, the vacuole membrane invaginates to mediate the uptake of cytoplasmic material. (B) Schematic diagram of proteins that function in the final docking/fusion step of various cargo vesicles to the vacuole. SNARE proteins are represented by shaded rectangles (Vam3 and Vam7, green; Ykt6, blue). Components of the class C Vps complex (Vps11, 16, 18, 33, 39, and 41) that mediate SNARE pairing are shown in red. Tethering is also mediated by the Rab-like GTPase,Ypt7.

area where it is in higher concentration. Membrane proteins called transporters perform active transport.

endocytosis Ingestion of particulate matter or fluid by phagocytosis or pinocytosis; i.e., bringing material into a cell by invagination of its surface membrane and then pinching off the invaginated portion to form an endosome or vacuole.

hydrolases Enzymes that act as catalysts in the cleavage of covalent bonds with accompanying addition of water. Lipases are hydrolases that break down fatty acids and other lipids. Proteases specifically digest peptide bonds.

vacuole A large, membrane-bound cytoplasmic organelle that functions in ingestion, digestion, excretion, and storage of water, sugars, proteins, lipids, ions, and other materials. Vacuoles and vacuole-related organelles are found in fungal, plant, protozoan, and mammalian cells. Most plant cells have a single vacuole that takes up much of the cell and helps maintain the shape/turgor of the cell.

vesicular transport Trafficking of proteins and lipids from one cellular compartment to another by means of membrane-enclosed intermediates such as endosomes or organelle fragments.

Further Reading

Allen, R. D. (2000). The contractile vacuole and its membrane dynamics. *Bioessays* **22**, 1035–1042.

Bowers, W. E. (1998). Christian de Duve and the discovery of lysosomes and peroxisomes. *Trends Cell Biol.* **8**, 330–333.

Bryant, N. J., and Stevens, T. H. (1998). Vacuole biogenesis in *Saccharomyces cerevisiae*: Protein transport pathways to the yeast vacuole. *Microbiol. Mol. Biol. Rev.* **62**, 230–247.

Dell'Angelica, E. C., Mullins, C., Caplan, S., and Bonifacino, J. S. (2000). Lysosome-related organelles. *Faseb J.* **14**, 1265–1278.

Jones, E. W. (2002). Vacuolar proteases and proteolytic artifacts in *Saccharomyces cerevisiae*. *Methods Enzymol.* **351**, 127–150.

Knodler, L. A., and Steele-Mortimer, O. (2003). Taking possession: Biogenesis of the salmonella-containing vacuole. *Traffic* **4**, 587–599.

Klionsky, D. J., Herman, P. K., and Emr, S. D. (1990). The fungal vacuole: Composition, function, and biogenesis. *Microbiol. Rev.* **54**, 266–292.

Kornfeld, S., and Mellman, I. (1989). The biogenesis of lysosomes. *Annu. Rev. Cell Biol.* **5**, 483–525.

Mach, L. (2002). Biosynthesis of lysosomal proteinases in health and disease. *Biol. Chem.* **383**, 751–756.

Mullins, C., and Bonifacino, J. S. (2001). The molecular machinery for lysosome biogenesis. *Bioessays* **23**, 333–343.

Biography

Scott D. Emr is a Professor of Cellular and Molecular Medicine at the University of California, San Diego and an investigator of the Howard Hughes Medical Institute. His lab focuses on defining components of the core transport machinery as well as the regulatory apparatus that direct protein and membrane sorting to and from intracellular organelles, such as vacuoles.

Christopher J. Stefan is a Research Associate of the Howard Hughes Medical Institute.

Vascular Endothelial Growth Factor Receptors

Kenneth A. Thomas
Merck Research Laboratories, West Point, Pennsylvania, USA

Vascular endothelial growth factor receptors (VEGFRs) are a set of three homologous transmembrane receptor tyrosine kinases that bind vascular endothelial growth factors (VEGFs). VEGFRs are expressed primarily by endothelial cells lining the lumen of vascular and lymphatic vessels. VEGF-mediated activation of these receptors can induce endothelial cell migration and mitosis promoting the growth of blood vessels, denoted angiogenesis, and of lymphatic vessels, or lymphangiogenesis.

VEGFR Genes

Evolution

The three VEGFRs are denoted VEGFR-1, VEGFR-2, and VEGFR-3, or Flt-1, KDR/Flk-1 and Flt-4, respectively. Each VEGFR gene encodes a protein composed of seven extracellular immunoglobulin (Ig)-like domains, a short transmembrane-spanning polypeptide and an intracellular portion containing a tyrosine kinase. The VEGFRs are most closely related to the hematopoietic receptor tyrosine kinases c-kit, c-fms and Flt3 and to the platelet-derived growth factor receptor (PDGFR)-α and -β, each of which contain five extracellular Ig-like domains and an intracellular tyrosine kinase. The VEGFR-1, -2, and -3 genes are clustered with the hematopoietic receptors and PDGFRs on chromosomes 13, 4 and 5, respectively, consistent with divergence from a common ancestral receptor tyrosine kinase gene.

Structure

Each of the three VEGFRs is encoded by 30 exons (NCBI genomic database, http://www.ncbi.nlm.nih. gov/genome/guide/human). The corresponding exon-coding regions, in each gene, are of similar size although some of the introns that separate them vary substantially in length resulting in total genomic DNAs ranging from ~190 kb for VEGFR-1 to 47 kb and 46 kb for VEGFR-2 and -3, respectively. In all three genes, exon 1 encodes the secretory leader sequence, exons 2–15 span the extracellular region, exon 16 corresponds to the transmembrane-spanning polypeptide and exons 17–30 encode the cytoplasmic region including the tyrosine kinase containing a kinase–insert domain encoded by exon 21.

Gene Expression

Cellular differentiation status and responses to extracellular signals influence the expression of each of the VEGFR genes. Multiple transcription factor DNA-binding site consensus sequences are present within approximately the first 1 kb 5′ of the translational start site. Transcription factor binding sites within the first intron might also either augment or inhibit transcription.

VEGFR-1

Subsets of vascular endothelial cells, monocytes, dendritic cell precursors, and some types of smooth muscle cells express VEGFR-1. The basal promoter and 5′ sequences that control VEGFR-1 endothelial cell-selective expression contain Ets, Sp1, Egr-1, and CRE transcription factor binding site consensus sequences, several of which have been shown to be functional. In addition, a single hypoxic response element is located within the first 1 kb 5′ of the transcriptional start site, consistent with the observation that the transcription of VEGFR-1 is increased by hypoxia. Transcription is initiated downstream of a TATA box basal transcription factor binding site to generate a 7.5–8 kb mRNA.

VEGFR-2

VEGFR-2 is expressed primarily by vascular endothelial cells although a few other cell types can also express this receptor. Selective endothelial cell expression has been mapped to a region within the first 150 bp 5′ of the transcriptional start site that contains multiple Sp1, Ap-2, and NF-κB sites. *In vivo* expression of the corresponding murine VEGFR-2 gene has been studied using transgenic mice. Blood vessel targeted gene expression in developing mouse embryos is

controlled by sequences not only in the region 5′ of the translational start site but also within the first intron. The human gene, which does not contain a TATA box, is transcribed as a 7 kb mRNA.

VEGFR-3

Several consensus transcription factor sequences have also been recognized in the VEGFR-3 gene 5′ of the translational initiation site. A 1.6 kb 5′ region has been reported to drive lymphatic expression. Full-length VEGFR-3 mRNA is transcribed as a 5.8 kb mRNA.

Protein Structure

Extracellular Domains

The primary translation products of the VEGFR-1, -2, and -3 genes are 1338, 1356, and 1363 amino acid residue proteins, respectively. Each ~150 kDa protein is glycosylated at multiple sites on the extracellular Ig-like domains to generate mature proteins of 185–230 kDa. In addition, an alternatively spliced soluble 687 amino acid form of VEGFR-1, denoted sVEGFR-1 or sFlt-1, consists of the 6 N-terminal Ig-like domains. This 75 kDa protein is converted to 110 kDa by glycosylation. Partial proteolysis of VEGFR-3 generates an N-terminal 70 kDa polypeptide disulfide linked to the remaining 120–125 kDa transmembrane protein. A crystal structure of the VEGFR-1 Ig-like domain 2, composed of 5- and 3-stranded β-sheets, in complex with the dimeric VEGF-A ligand is shown in Figure 1.

Intracellular Domains

The structure of the VEGFR-2 tyrosine kinase, shown in Figure 2, contains N- and C-terminal domains consisting primarily of β-strands and α-helices, respectively. The catalytic site is located at the interface of these two domains denoted by the ADP modeled into the structure. It is flanked by the disordered activation-binding loop, the glycine-rich nucleotide-binding loop, the catalytic loop and that can participate in enzyme activation and substrate binding. The VEGFRs each contain a 65–70 amino acid kinase–insert domain within the N-terminal region of the C-terminal domain that is deleted in the crystallized VEGFR-2 kinase. A C-terminally truncated form of VEGFR-3, missing 65 amino residues, is also generated by alternative splicing.

Ligand Binding

VEGF Structure and Receptor Binding

The VEGFs are a family of five homologous dimeric glycoproteins. In addition, several VEGF homologues are expressed by the orf and pseudocowpox viruses, collectively denoted VEGF-E. HIV tat can also function as a VEGF. Each ligand binds with pM affinity either 1 or

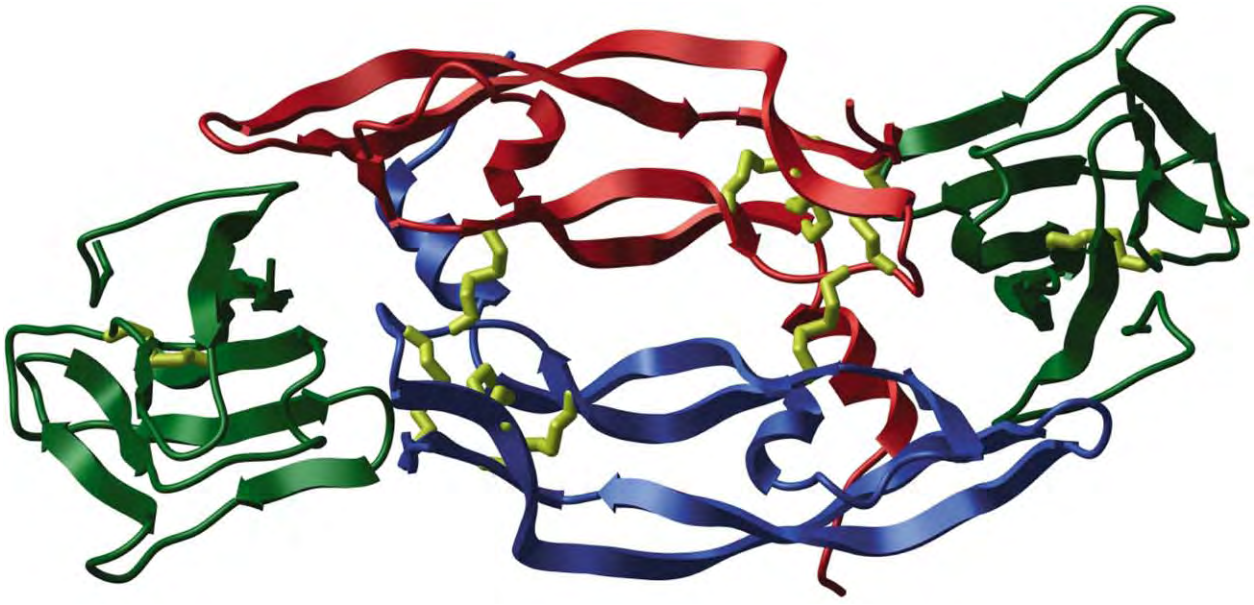

FIGURE 1 Structure of the complex between a VEGF-A dimer and domain 2 of VEGFR-1. The anti-parallel VEGF-A subunits are red and blue and the VEGFR-1 domains are green with disulfide bonds shown in yellow. Secondary structure is illustrated as arrows pointing toward the C-terminal ends. (Reproduced from Harada, S., and Thomas, K. A. (2002). Vascular endothelial growth factors. In *Principles of Bone Biology* (J. P. Bilezikian, L. G. Raisz and G. A. Rodan, eds.) 2nd edition, Vol 2, pp. 883–902. Academic Press, San Diego, with permission.)

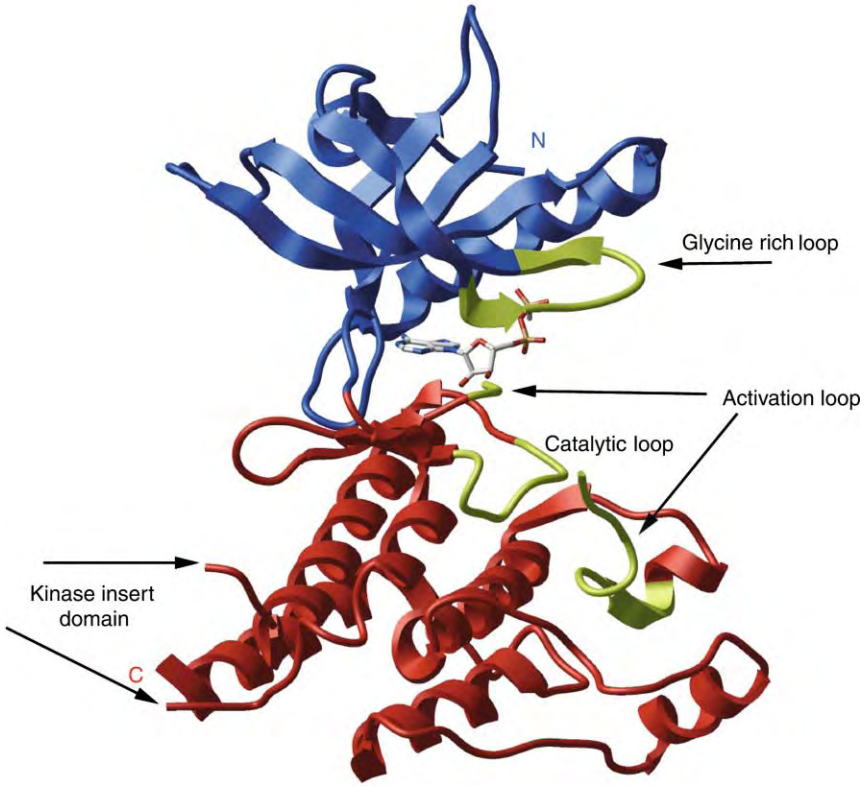

FIGURE 2 Structure of the VEGFR-2 tyrosine kinase. The N- and C-terminal lobes are blue and red, respectively. The active site region between these two domains is denoted by the location of ADP modeled into it. The glycine-rich, catalytic, and the ends of the disordered activation loops are shown in yellow. The ends of the largely deleted kinase-insert domain are also shown and labeled. (Reproduced from Harada, S., and Thomas, K. A. (2002). Vascular endothelial growth factors. In *Principles of Bone Biology* (J. P. Bilezikian, L. G. Raisz and G. A. Rodan, eds.) 2nd edition, Vol 2, pp. 883–902. Academic Press, San Diego, with permission.)

2 of the 3 receptors as shown in Figure 3. The core receptor-binding region of each subunit consists of ~120 amino acid residues. VEGF subunits, each composed of four β-strands and two short helices, dimerize in an anti-parallel arrangement as illustrated by VEGF-A in Figure 1. The loops between β-strands of both VEGF-A subunits interact with the second and third Ig-like domains of each of two receptor subunits through primarily hydrophobic interactions. Therefore, VEGF binding can promote receptor dimerization, which is additionally stabilized by interactions between the fourth Ig-like domains in VEGFR-1, as illustrated in Figure 4. VEGF-C and -D bind with highest affinity to VEGFR-3, mainly expressed on lymphatic endothelial cells and on the tips of some growing capillaries. Partial proteolysis, which removes sequences N- and C-terminal of the core-receptor-binding region, can increase the affinity of VEGF-C and -D for VEGFR-2 as indicated by the dashed lines in Figure 3.

Coreceptors

VEGF-A, VEGF-B, and PlGF are subject to alternative splicing that either incorporates or deletes C-terminal polycationic regions. These positively charged sequences can promote binding to negatively charged soluble heparin and heparin sulfate proteoglycans and to the membrane-anchored proteins neuropilin-1 and -2. Although these receptors do not appear to induce VEGF signal transduction, they might indirectly promote VEGF activity by partitioning the ligands to

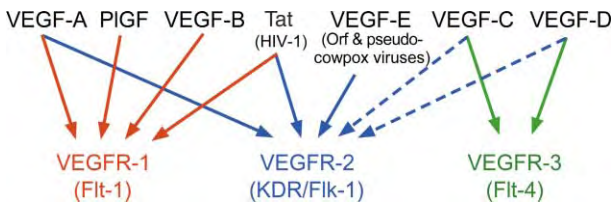

FIGURE 3 Receptor-ligand binding selectivity. VEGFs are listed in the top row with color-coded arrows pointing toward the high affinity VEGFRs that they bind. Tat and VEGF-E function as viral VEGFs. Dashed arrows from VEGF-C and -D to VEGFR-2 indicate high-affinity binding following full proteolytic processing to remove N- and C-terminal polypeptides. (Modified from Harada and Harada, S., and Thomas, K. A. (2002). Vascular endothelial growth factors. In *Principles of Bone Biology* (J. P. Bilezikian, L. G. Raisz and G. A. Rodan, eds.) 2nd edition, Vol 2, pp. 883–902. Academic Press, San Diego, with permission.)

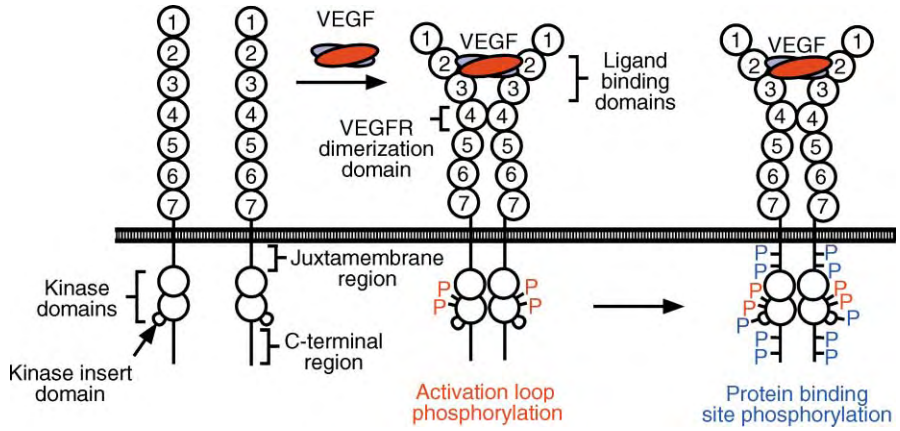

FIGURE 4 The structure of VEGFRs, containing seven extracellular Ig-like domains, a juxtamembrane region, the two domain tyrosine kinase containing a kinase-insert domain and a C-terminal tail, is shown on the left. Binding of dimeric VEGF to Ig domains 2 and 3 induce receptor dimerization, which can be aided by interactions between receptor domains 4. This promotes phosphorylation of two kinase activation loop tyrosines, denoted by the red "P" labels, and enzymatic activation in VEGFR-2 and probably in VEGFR-1 and -3. Additional tyrosines in the juxtamembrane region, kinase-insert loop and C-terminal tail are phosphorylated, as denoted by blue "P" labels, and bind signaling proteins that trigger several VEGF functions.

cellular surfaces, thereby increasing their local concentration in the vicinity of the high-affinity receptors, and by functioning as co-receptors that present the ligands to the high-affinity VEGFRs.

Signal Transduction

Receptor Activation

Intracellular signaling is initiated by VEGF-induced receptor dimerization that brings the intracellular tyrosine kinases into proximity where they are thought to phosphorylate each other as shown in Figure 4. The initial phosphorylation of tyrosine residues 1054 and 1059 on the tyrosine kinase activation loop of VEGFR-2 decreases the K_m of the enzyme for ATP and for peptide substrates without altering K_{cat}, the effective maximal rate of enzyme activity. This increased affinity for substrates could reflect the movement of the phosphorylated activation loop to provide better substrate access to their binding sites. Equivalent activation loop tyrosines exist on VEGFR-1 and -3 so that they might function in a similar manner.

Recruitment of Signaling Proteins

Additional tyrosines in the juxtamembrane region, the kinase–insert domain and the C-terminal tail can be phosphorylated, as shown schematically in Figure 4. Some of these phosphorylated tyrosine residues have been shown to serve as recognition sequences for binding by one or more signal transduction proteins. These include adapter proteins such as Grb2, Grap, Nck, Crk, Sck, Shc, and Vrap, which can bridge the receptors to other phosphorylated and non-phosphorylated proteins, and several enzymes such as phospholipase Cγ (PLCγ), phosphatidylinositol 3-kinase (PI3K), and the tyrosine phosphatase SHP-2. VEGF-induced phosphorylation is rapid, reaching maximal levels by 2-5 min, followed within 30 min by receptor internalization.

Some of these phosphorylated tyrosine residues have been linked with specific functions. For example, phosphorylation of VEGFR-2 Tyr_{1175} in the C-terminal tail is required for the efficient phosphorylation of PLCγ and mitogenic activity. The longer alternatively spliced form of VEGFR-3 contains tyrosines within the unique C-terminal 65 amino acid residues. At least one of these tyrosines, Tyr_{1337}, is required for transforming activity *in vitro* and upon phosphorylation can bind the adapter protein Shc.

Signal Transduction Cascades

The phosphorylation of VEGFR-2-associated PLCγ activates its enzymatic activity catalyzing the hydrolysis of membrane-anchored phosphatidylinositol 4,5-bisphosphate (PIP_2) to generate inositol 1,4,5-trisphosphate (IP_3) and diacylglycerol (DAG). Water soluble IP_3 activates an endoplasmic reticulum Ca^{2+} channel that releases Ca^{2+}, activating several enzymes including endothelial cell nitric oxide synthase (eNOS) and promoting the translocation of specific protein kinase C (PKC) isoforms to the membrane where it is activated by binding membrane-associated DAG. PKC appears to be able to activate the mitogen-activated protein kinase kinase (MAPKK) mitogenic pathway possibly involving Raf kinase. In addition, nitric oxide can activate protein kinase G (PKG) that subsequently activates Raf. MAPKK activates mitogen activated

kinase (MAPK), which can enter the nucleus to modulate transcription. Additional pathways, mediated through PI3K and the anti-apoptotic kinase Akt, promote cell adhesion, migration, and survival.

Biologic Activities

Development

The developmental activities of VEGFRs have been revealed by mouse gene knockouts, which are each embryonically lethal. Blood vessels exist in VEGFR-1 knockout mice but are disorganized, which appears to be a consequence of modified cell fate leading to increased numbers of endothelial cell progenitor hemangioblasts that altered vessel pattern formation. Surprisingly, knockout of the VEGFR-1 gene segment encoding the tyrosine kinase but retention of the extracellular and membrane-spanning regions leads to normal development of blood vessels and survival. This result is consistent with the possibility that one of the functions of VEGFR-1, which binds VEGF-A with ~10-fold higher affinity than VEGFR-2, might be to sequester low levels of VEGF, thereby "buffering" the VEGFR-2 receptor from inappropriate activation by low levels of VEGF. The VEGFR-1 cytoplasmic region might inhibit the VEGFR-2 mitogenic, but not migratory, activity by a mechanism involving VEGFR-1 juxtamembrane Tyr_{794}. The VEGFR-2 knockout is virtually devoid of vascular endothelial cells, consistent with its crucial role as a mediator of endothelial cell mitosis and survival. VEGFR-3 gene knockout mice exhibit vasculogenesis and angiogenesis in early developing embryos but large vessels appear abnormal with defective lumens leading to fluid accumulation in the pericardial cavity and cardiovascular failure. Therefore, at least during early embyrogenesis before lymphatic vessels develop from post-capillary venules, VEGFR-3 plays a critical role in vascular development.

Angiogenesis

In adults, VEGFR-2 is the primary angiogenic receptor family member. It can mediate the migration and mitosis of vascular endothelial cells culminating in neovascular growth. Ligands such as VEGF-A and the viral VEGFs that bind VEGFR-2 are sufficient to drive angiogenesis and the growth of some hematopoietic progenitor cells. Antibodies to VEGFR-2 and enzyme inhibitors of the VEGFR-2 tyrosine kinase inhibit angiogenesis and the resulting growth of tumors in mice.

Soluble VEGFR-1 (sVEGFR-1), which is expressed by cultured endothelial cells and has been detected *in vivo*, is the only identified naturally occurring specific VEGFR inhibitor. It retains the ligand-binding site and so recognizes the same VEGFs as full-length VEGFR-1. The soluble receptor can not only homodimerize but also heterodimerize with the extracellular regions of VEGFR-1 and VEGFR-2. Therefore, it can sequester ligands and perhaps inhibit activation of full-length membrane-spanning VEGFR-1 and VEGFR-2 by the formation of dominant negative heterodimers that contain a single tyrosine kinase so are incapable of kinase activation by trans-phosphorylation. Transfection experiments show that expression of sVEGFR-1 by tumor cells that express transfected sVEGFR-1 exhibit severely inhibited growth *in vivo* but not *in vitro*, consistent with an antiangiogenic mechanism.

Lymphangiogenesis

VEGFR-3 is expressed by lymphatic endothelial cells and also vascular endothelial cells at the tips of growing capillary shoots. The VEGFR-3 ligand VEGF-C is mitogenic for lymphatic endothelial cells in culture. Transgenic mice expressing elevated VEGF-C or -D in skin induce the growth of dermal lymphatic vessels but not blood vessels. However, inhibitory anti-VEGFR-3 antibodies can inhibit tumor angiogenesis. Naturally occurring human missense mutations with inactive tyrosine kinases are linked to lymphoedema, a genetic disease in which fluid accumulates in tissues as a consequence of deficient lymphatic function. Therefore, in adults VEGFR-3 appears to be active on lymphatic endothelial cells and at least some endothelial cells in actively growing capillaries.

Nonmitogenic Functions

In adults, activation of VEGFR-2 induces vascular permeability that can facilitate angiogenesis and promote edema. Although VEGFR-1 does not directly promote permeability, it might play a permissive role. Activation of VEGFR-1 by its selective ligands PlGF and VEGF-B does not appear to directly induce endothelial cell mitosis or angiogenesis under most conditions. However, it can induce vascular endothelial cell expression of specific proteins such as tissue factor, matrix metalloproteases, urokinase, plasminogen activator inhibitor-1, hepatocyte growth factor and pigment epithelium-derived factor. In addition, activation of monocyte and macrophage VEGFR-1 can drive expression of tissue factor, monocyte chemoattractant protein-1 and tumor necrosis factor-α. It can also induce the production of endothelial cell nitric oxide, and the migration of monocytes and some endothelial cells. Although the VEGFR-1 ligand PlGF is not a potent angiogenic agent, it does appear to promote the development of collateral blood vessels, a process involving the conversion of smaller to larger vessels.

Therefore, on the basis of the knockout and cell expression data, VEGFR-1 seems to modulate the expression of several genes associated with differentiated functions and the activity of VEGFR-2.

Summary

The homologous VEGFRs are critical mediators of the growth and function of blood and lymphatic vessels. These receptors and their ligands are intimately involved not only in development but also in the maintenance of normal differentiated functions. Their inappropriate activation or inhibition can have pathologic consequences so they also are potential targets for therapeutic intervention.

See Also the Following Articles

Mitogen-Activated Protein Kinase Family • Phosphatidylinositol Bisphosphate and Trisphosphate • Phospholipase C • Protein Kinase C Family

Glossary

angiogenesis Growth of new blood vessels from existing vessels.

lymphangiogenesis Growth of new lymphatic vessels.

vascular endothelial growth factor (VEGF) An extracellular soluble dimeric protein that binds and activates one or more VEGFRs.

vasculogenesis Embryonic *de novo* organization of blood vessels.

VEGFR Full-length membrane-spanning VEGF receptor containing an intracellular tyrosine kinase.

Further Reading

Claesson-Welsh, L. (2003). Signal transduction by vascular endothelial growth factor receptors. *Biochem. Soc. Trans.* **31**, 20–24.

Ferrara, N., Gerber, H.-P., and LeCouter, J. (2003). The biology of VEGF and its receptors. *Nat. Med.* **9**, 669–676.

Harada, S., and Thomas, K. A. (2002). Vascular endothelial growth factors. In *Principles of Bone Biology* (J. P. Bilezikian, L. G. Raisz and G. A. Rodan, eds.) 2nd edition, Vol 2, pp. 883–902. Academic Press, San Diego.

Larrivee, B., and Karsan, A. (2000). Signaling pathways induced by vascular endothelial growth factor (Review). *Int. J. Mol. Med.* **5**, 447–456.

McTigue, M. A., Wickersham, J. A., Pinko, C., Showalter, R. E., Parast, C. V., Tempczyk-Russell, A., Gehring, M. R., Mroczkowski, B., Kan, C.-C., Villafranca, J. E., and Appelt, K. (1999). Crystal structure of the kinase domain of human vascular endothelial growth factor receptor 2: A key enzyme in angiogenesis. *Structure* **7**, 319–330.

Robinson, C. J., and Stringer, S. E. (2001). The splice variants of vascular endothelial growth factor (VEGF) and their receptors. *J. Cell Sci.* **114**, 853–865.

Weismann, C., Fuh, G., Christinger, H. W., Eigenbrot, C., Wells, J. A., and de Vos, A. M. (1997). Crystal structure at 1.7Å resolution of VEGF in complex with domain 2 of the Flt-1 receptor. *Cell* **91**, 695–704.

Zachary, I., and Cliki, G. (2001). Signaling transduction mechanisms mediating actions of the vascular endothelial growth factor family. *Cardiovasc. Res.* **49**, 568–581.

Biography

Kenneth Thomas is Director of Growth Factor Research at the Merck Research Laboratories in West Point, PA. His general research interest is growth control in normal and pathologic conditions and he has led research efforts focused on the discovery and characterization of Fibroblast Growth Factors, VEGFs and their receptors. He holds a Ph.D. in biochemistry from Duke University and received postdoctoral training at the National Institutes of Health and Washington University School of Medicine in St. Louis. He is a member of the American Society for Biochemistry and Molecular Biology and the Association for the Advancement of Science.

Vasopressin/Oxytocin Receptor Family

Michael J. Brownstein
National Institute of Mental Health, National Institutes of Health, Bethesda, Maryland, USA

Large neurons at the base of the brain (the hypothalamus) of humans and other mammals send their axons through the median eminence to terminate in the posterior lobe (neurohypophysis) of the pituitary. Each of these "magnocellular" nerve cells typically synthesizes one of two neurohypophyseal hormones – vasopressin (VP) or oxytocin (OT). In fact, all vertebrates higher than jawless fish make vasopressin- and oxytocin-like hormones. Jawless fish and invertebrates, on the other hand, appear to produce only one VP/OT-like peptide per species.

The Structures of "Pressins" and "Tocins"

For the last billion years, the peptides in VP/OT family have retained certain structural features. With the exception of the hydrins – partially processed relatives of vasotocin, which are physiologically active in some amphibia – they all have nine amino acids and a C-terminal amide. Cysteine (C) is invariably present in positions 1 and 6, and the two cysteine residues form a cystine bridge, creating conformationally constrained, cyclic peptides. Except for seritocin (serine5, isoleucine8-oxytocin), which was reported in a single species, *Bufo regularis*, all family members have asparagines (N) in position 5, and proline (P) and glycine (G) in positions 7 and 9, respectively. VP-like peptides ("pressins") are characterized by the presence of arginine (R) or lysine (K) in position 8, while OT-like molecules ("tocins") have leucine (L), isoleucine (I), glutamine (Q), valine (V), or threonine (T) there. All of the invertebrate peptides except for the locust diuretic hormone, which has not been detected in other insect species, have an R instead of Q, N, or S in position 4. Thus, the primordial peptide that gave rise to the molecules we know today should have looked rather similar to one of the conopressins or to vasotocin, the likely ancestor of all of the vertebrate hormones. (The molecules detected in *Hydra* with antivasopressin antibodies share the C-terminal PRG-amide motif with VP, but are otherwise unrelated.)

In addition to the peptides shown in Table I and Figure 1, it is worth noting that the major metabolite of VP (pGlu4, Cystine6-AVP) mobilizes calcium in some cells in the central nervous system, and has been suggested to have a unique, but as yet unidentified, receptor of its own.

Peptide Biosynthesis

The peptides in the VP/OT family are synthesized as parts of precursor proteins. The vasopressin precursor has the following structural features:

signal peptide-CYFNQNCPRG***G***-K*R*neurophysin-copeptin

The signal peptide is removed cotranslationally in the endoplasmic reticulum, liberating the N terminus of the peptide. Then, after the precursor is packaged into vesicles by the Golgi apparatus, it is cleaved at the asterisked sites by a Lys-Arg calcium-dependent endoprotease. The remaining basic amino acids are removed by a carboxypeptidase B-like enzyme, leaving a glycine (***G***) on the carboxy terminus. This glycine serves as the donor of the amide group, which is generated by the sequential actions of a peptidyl-glycine monooxygenase and a peptidyl-hydroxyglycine lyase. Neurophysin is thought to serve as an internal chaperone, promoting proper folding and cystine-bridge formation. Copeptin, a glycosylated species, is part of the vasopressin, but not the oxytocin precursor. Its function is unknown. The genes encoding the VP and OT precursors are adjacent to one another on the same chromosome. In mammals, they are oriented tail-to-tail, and share regulatory elements.

The Functions of Vasopressin and Oxytocin

VP/OT-like peptides play different roles in the various species where they are found. They are very commonly involved in water homeostasis and/or

TABLE I

Vasopressin, Oxytocin, and Related Peptides

Oxytocin-like peptides (Tocins)		
Oxytocin (OT)	*C*YIQ*NCP*LG-amide	Mammals, Pacific ratfish
Mesotocin (MT)	*C*YIQ*NCP*IG-amide	Nonmammalian tetrapods, marsupials, lungfish
[Phe2]Mesotocin (FMT)	CFIQNCPIG-amide	Australian lungfish
Seritocin (ST)	*C*YIQS*CP*IG-amide	Dryness-resistant African toad
Isotocin (IT)	*C*YIS*NCP*IG-amide	Bony fish
Aspargtocin (AspT)	*C*YIN*NCP*LG-amide	Spiny dogfish
Asvatocin (AsvT)	*C*YIN*NCP*VG-amide	Spotted dogfish
Glumitocin (GT)	*C*YIS*NCP*QG-amide	Rays
Phasvatocin (PhT)	*C*YFN*NCP*VG-amide	Spotted dogfish
Valitocin (ValT)	*C*YIQ*NCP*VG-amide	Spiny dogfish
Annetocin (AnT)	*C*FVR*NCP*TG-amide	Earthworm
Cephalotocin (CT)	*C*YFR*NCP*IG-amide	Octopus
Vasopressin-like peptides (Pressins)		
A-Vasopressin (AVP)	*C*YFQ*NCP*RG-amide	Most mammals
L-Vasopressin (LVP)	*C*YFQ*NCP*KG-amide	Pig, marsupials
Phenypressin (PP)	*C*YFQ*NCP*RG-amide	Marsupials
Vasotocin (VT)	*C*YIQ*NCP*RG-amide	Non-mammalian vertebrates
Hydrin 2 (H2)	*C*YIQ*NCP*RGG	Frogs, toads
A-conopressin (ACP)	*C*IIR*NCP*RG-amide	Snail
L-conopressin (LCP)	*C*FIR*NCP*KG-amide	Snail, sea hare, leech
Locust diuretic hormone (LDH)	*C*LIT*NCP*RG-amide	Locust (but not fruitfly)
Putative Ancestor	*C*(F/Y)I(Q/R)*NCP*(R/K)*G*-amide	

Abbreviations: C (cysteine), F (phenylalanine), G (glycine), I (isoleucine), K (lysine), N (asparagine), P (proline), Q (glutamine), R (arginine), S (serine), T (threonine).

reproductive function. In humans vasopressin is an antidiuretic hormone. It is released from the posterior pituitary into the blood stream when the osmolarity (solute content) of the blood increases, and it acts on V2 receptors in the kidney to cause water retention. V2 receptors are Gs-coupled, and increase intracellular cyclic AMP. This, in turn, causes preformed aquaporin (AQP) 2 channels to be inserted into the luminal surfaces of cells in the collecting duct of the kidney. Water enters these channels, traverses the cells, exits through AQP 3 and 4 channels on their interstitial faces, and enters the bloodstream. Mutations in the genes encoding vasopressin, the V2 receptor, or AQP2 cause diabetes insipidus – an inability to concentrate urine, resulting in high urine volumes and a need to consume large amounts of fluid each day. Since the V2 receptor gene is on the X chromosome, female carriers pass X-linked nephrogenic diabetes insipidus along to their sons, but not their daughters.

Nonosmotic as well as osmotic stimuli can trigger vasopressin secretion. Osmoreceptors on cells in the anterior hypothalamus, and baroreceptors in the left ventricle of the heart, aortic arch, and carotid sinus monitor osmolarity and blood pressure, respectively, and participate in controlling the firing of VP-producing cells.

In addition to V2 receptors, vasopressin acts on V1a and V1b receptors. The former are found on blood vessels and are responsible for VP's pressor (blood pressure increasing) activity. The physiological importance of this is moot, but it is clear that certain vascular beds are especially sensitive to VP, including those in the skin and uterus. In fact, it has been suggested that V1a receptor antagonists might be useful for treating Raynaud's disease (excessive constriction of digital arteries) and dysmenorrhea (menstrual cramps which may be caused by dilation of vessels in the uterus).

V1b receptors are found on corticotrophs (adrenocorticotropic hormone or ACTH-producing cells) in the anterior pituitary. In addition to being made by magnocellular neurons, VP is also synthesized by small cells in the paraventricular nucleus of the hypothalamus. These same cells also make corticotropin releasing hormone (CRH), and their axons terminate on portal vessels in the external zone of the median eminence. VP and CRH are released into these vessels and transported to the anterior pituitary, where they act in concert to stimulate ACTH secretion. ACTH, in turn, causes the adrenal to release glucocorticoids. Thus, VP is important in mediating the body's response to stress.

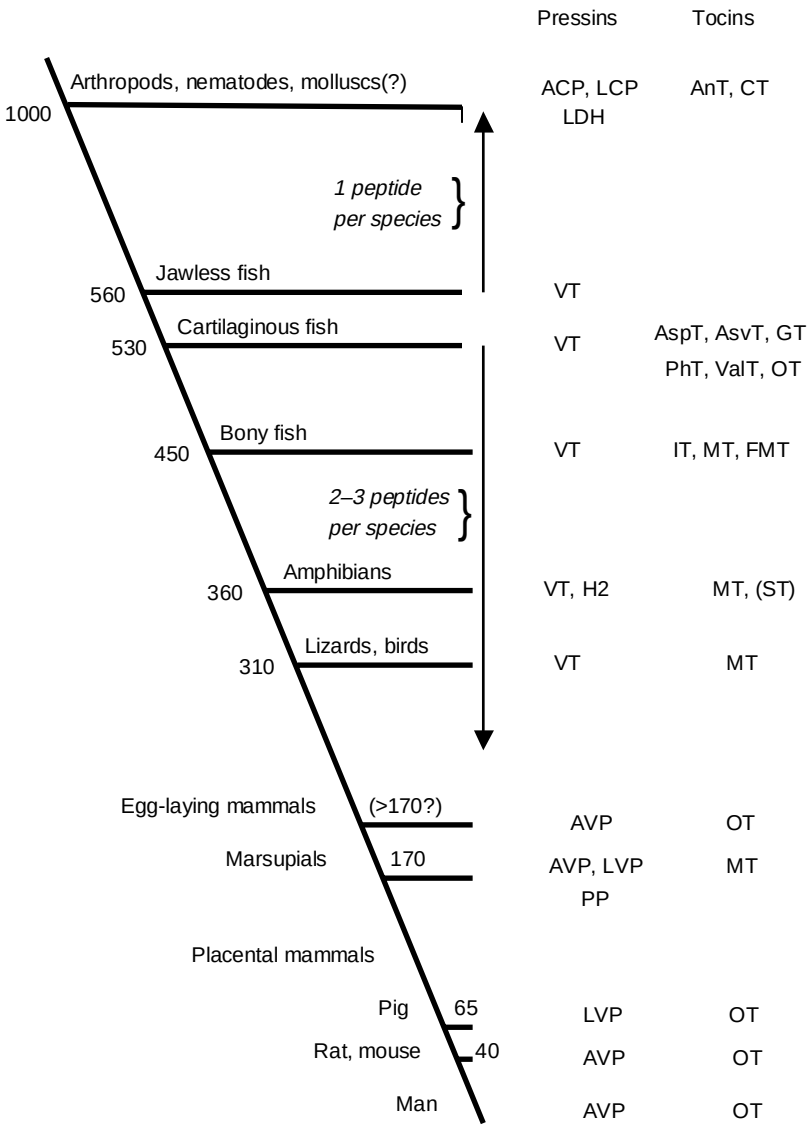

FIGURE 1 Evolution of vasopressin-related (pressins) and oxytocin-related (tocins) peptides. The timescale (millions of years ago) was taken from Hedges (2002). Note that invertebrates and jawless fish make a single pressin or tocin per species, and that vertebrates make two or, in the case of marsupials, three such peptides – one or two pressins and one tocin. It appears that vasotocin was the ancestor of the vertebrate hormones, and it continued to be synthesized by all vertebrates except mammals, in which it was replaced by arginine or lysine vasopressin. Tocins began to be produced in fish. It is not clear why cartilaginous fish make so many of these; lungfish make MT or FMT, and all of the remaining bony fish make IT. Based on the structures of the peptide precursors, it has been argued that lungfish are related to tetrapods (e.g., toads) and that bony fish form a separate lineage. Amphibians, lizards, birds, and marsupials make MT; egg-laying and placental mammals differ in the hormones they produce. Marsupials appear to have branched away as suggested by other analyses. The abbreviations used in this figure are defined in Table I.

V1a and V1b, but not V2, receptors are found in the brain. The central effects of vasopressin agonists and antagonists must be mediated by these receptors. These effects vary from species to species, and they are unknown in humans. It appears, however, that VP may mediate behavioral reactions to stress, aggressive and affiliative behavior, juvenile recognition, and parenting in rodents. In addition, V1a antagonists appear to block the vomiting associated with motion sickness in pigs and ferrets. This appears to be a central effect of the drugs, but could have a peripheral component.

Oxytocin-producing mammals make a single receptor for this peptide. Like the V1a and V1b receptors, it is Gq-coupled, and activates phospholipase C, increasing intracellular calcium. Oxytocin receptors increase dramatically in the pregnant uterus as term approaches. Despite the fact that it has been used for decades to induce uterine contractions, oxytocin is not essential for this process, and oxytocin receptor antagonists have not

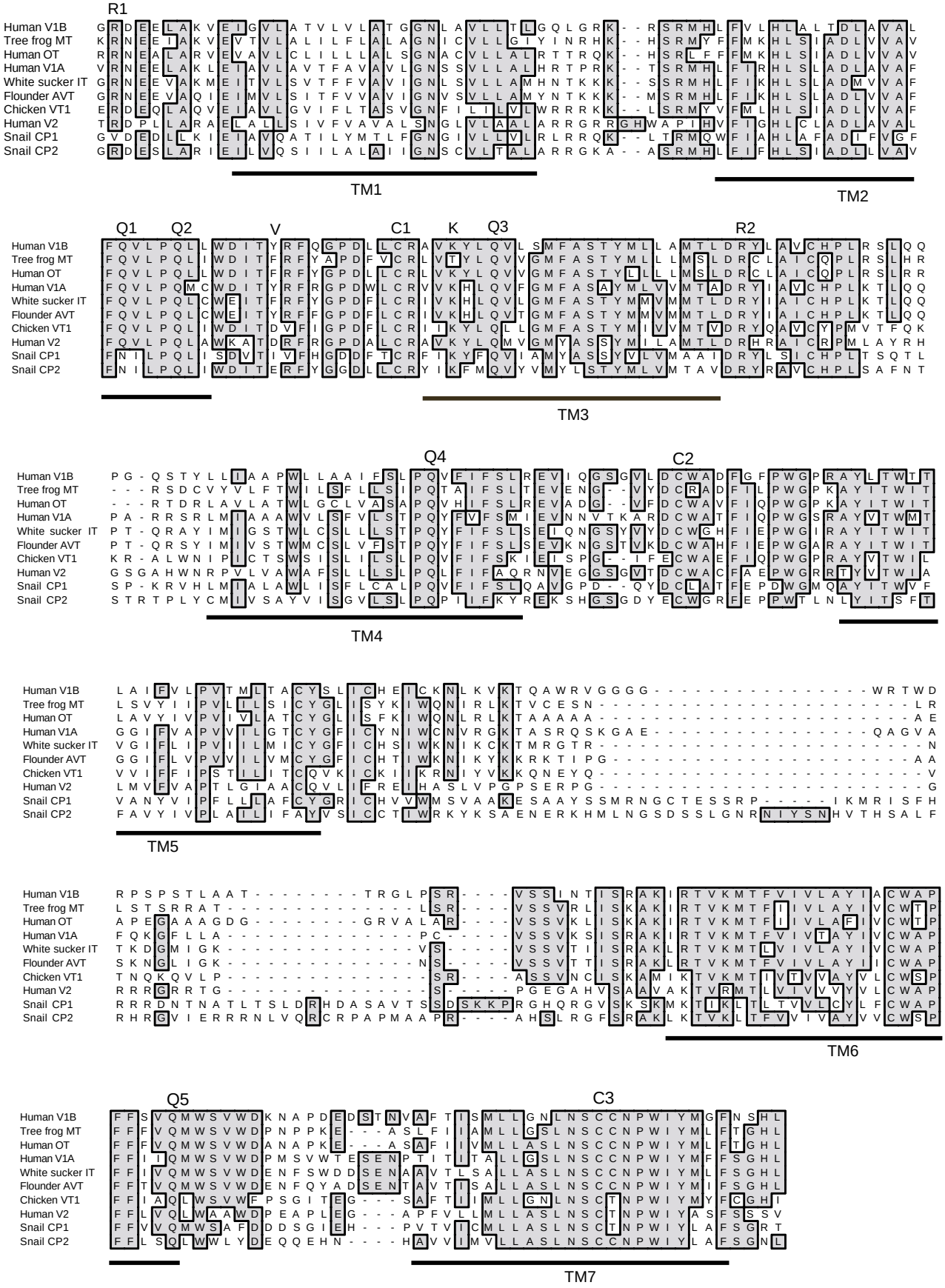
R1
Human V1B
Tree frog MT
Human OT
Human V1A
White sucker IT
Flounder AVT
Chicken VT1
Human V2
Snail CP1
Snail CP2
TM1
TM2
Q1
Q2
V
C1
K
Q3
R2
TM3
Q4
C2
TM4
TM5
TM6
Q5
C3
TM7

proven useful for treating preterm labor. There is no doubt, however, that the pulsatile release of OT from the pituitary in response to cervical dilation and vaginal stimulation, facilitates the expulsion of the fetus.

Oxytocin is required for milk ejection. Mechanical stimulation of pressure sensitive receptors in the nipple of the breast by the nursing infant results in activation of magnocellular neurons in the hypothalamus and release of pulses of OT into the bloodstream. The hormone causes breast myoepithelial cells to contract, increasing intramammary pressure and forcing milk into the ducts. In the absence of OT, milk cannot be let down, and the infant will starve if it is not provided an alternative source of food.

In addition to its roles in parturition and lactation, oxytocin appears to affect maternal and social behaviors, stimulate lipogenesis to compensate for lipid loss in the milk (via an action on insulin secretion), and possibly participate in regulating salt and water balance. While OT causes natriuresis in rats, it is not clear that this is the case in humans.

Vasopressin and Oxytocin Receptors

As expected from the fact that their ligands are similar, VP and OT receptors are structurally related. They are members of the rhodopsin superfamily, and have seven α-helical membrane-spanning domains connected to one another by intracellular and extracellular loops. The N terminus of each receptor faces the outside of the cell; the C terminus is cytoplasmic. The intracellular loops and C-terminal tail of the receptors interact with G proteins, coupling agonist binding to activation of second messenger systems. More than 40 VP/OT receptors found in species ranging from snails to humans have been cloned and sequenced. The primary sequences of some of these are shown in Figure 2. It is remarkable that from the beginning of its first transmembrane domain (TM1) to the end of its seventh one (TM7), the snail conopressin receptor 2 is 43% identical in amino acid sequence to the human V1a, V1b, and OT receptors and the white sucker fish vasotocin receptor. Unlike the vertebrate proteins, however, the conopressin receptor responds equally well to lysine8- and isoleucine8-conopressin (an OT-like synthetic analogue of lysine-conopressin). Duplication of a relatively promiscuous receptor of this sort might have permitted trial-and-error evolution of functionally distinct pressors and tocins in vertebrates.

A number of amino acids are conserved among all of the receptors in Figure 2. Some of these residues are found in most G-protein-coupled receptors. Among them, the arginine (R2) in the DRY motif, found just beneath TM3, is thought to dwell in a pocket formed by polar residues in TMs 1, 2, and 7 when the receptor is in its inactive state. Hormone binding dislodges this arginine from its polar pocket, exposing G-protein docking sites on the cytoplasmic loops.

The cysteines in extracellular loops 1 and 2 (C1 and C2, respectively) are also highly conserved among rhodopsin-like receptors. They form a cystine bridge that links these loops, stabilizing the conformation of the receptors. The pair of cysteines (C3 and its neighbor) located 15 aa's below TM7 in the cytoplasmic tails of most VP/OT receptors are likely to be palmitoylated and are thought to anchor their C termini to the plasma membrane. Like other members of the rhodopsin superfamily, VP and OT receptors appear to be glycosylated on their N termini, and regulated by phosphorylation of their intracellular domains.

A number of attempts have been made to model the binding of VP, OT, and vasotocin to their receptors. The models are fundamentally similar in the sense that they all predict that the peptide hormones fill a cleft located in the upper third of the barrel formed by the seven membrane-spanning α-helices. The hydrophobic amino acids that comprise the cyclic portion of the peptides (cysteine1, tyrosine2, isoleucine or phenylalanine3, and cystein6) appear to reside in a hydrophobic pocket formed by aromatic residues on helices 5 and 6 (and adjacent helices). The more polar amino acids (asparagine4, glutamine5), and the amidated C terminus of the hormones must occupy a hydrophilic region formed by residues on helices 2, 3, and 4. More specifically, residues that are conserved in the N-terminal domain and TMs 2, 3, 4, and 6 in most, if not all, of the VP/OT receptors (labeled R1, Q1, Q2, K, Q3, Q4, and Q5 in Figure 2) have been shown to be important for high-affinity binding, even though their predicted interactions with specific amino acids in the peptide hormones vary from model to model. Parsimony dictates that residues conserved among the various

FIGURE 2 Alignment of vasopressin and oxytocin receptors and selected relatives. To save space, the extracellular N termini and intracellular C termini have been removed. They are quite divergent, but it is remarkable that the transmembrane domains (TMs), the first two extracellular loops (linking TMs 2 and 3, and TMs 4 and 5), and portions of intracellular loops 2 and 3 (linking TMs 3 and 4, and TMs 5 and 6), have remained so similar throughout the course of their evolution. Specific residues in these domains are responsible for ligand binding and selectivity (see text), and other motifs are important for signal transduction. The variable intracellular portions of the receptors allow them to interact with specific G proteins.

VP/OT peptides should interact with conserved domains in the receptors, but perhaps things are not this simple.

One amino acid appears to be crucial for peptide agonist selectivity. This residue (marked with a V in Figure 2) is found in the first extracellular loop, and it interacts with the eighth amino acid of the peptide hormones (arginine and leucine in AVP and OT, respectively). The aspartic acid or tyrosine residues found at V in the human V2 and V1a/V1b receptors, respectively, are responsible for their marked preferences for AVP versus OT. The phenylalanine in this position in the OT receptor accounts for its modest preference for OT over AVP.

VP and OT antagonist-binding sites appear to be different from the ones where the peptide hormones bind.

See Also the Following Articles

Amino Acid Metabolism • Phospholipase C

Glossary

baroreceptor Receptor in the walls of the heart or blood vessels that is stimulated by alterations in pressure.

diuresis Increased urine excretion.

diuretic An agent that increases urine excretion.

hypothalamus The part of the brain that regulates the endocrine and autonomic and autonomic nervous systems, controlling water balance, blood pressure, body temperature, growth, and sexual function.

lipogenesis Formation of body fat.

magnocellular neurons Large neurons in the hypothalamus that manufacture vasopressin or oxytocin.

natriutesis Sodium excretion in the urine.

pressin An agent that increases blood pressure. In the context of this review, "pressins" are vasopressin-like peptides with nine amino acids, having a basic residue (arginine or lysine in the eighth position).

tocin An agent that promotes childbirth by causing uterine contractions; an oxytocin-like peptide lacking arginine or lysine in the eighth position.

Further Reading

Acher, R., and Chauvet, J. (1995). The neurohypophsial endocrine regulatory cascade: Precursors, mediators, receptors, and effectors. *Front. Neuroendocrinol.* **16**, 237–289.

Chini, B., and Fanelli, F. (2000). Molecular basis of ligand binding and receptor activation in the oxytocin and vasopressin receptor family. *Exp. Physiol.* **85S**, 59S–66S.

Hedges, B. S. (2002). The origin and evolution of model organisms. *Nature Rev. Genet.* **3**, 838–849.

Ivell, R., and Russell, J. A. (1995). *Oxytocin: Cellular and Molecular Approaches in Medicine and Research*. Kluwer Academic/Plenum, New York.

Zingg, H. H., Bourque, C. W., and Bichet, D. G. (1998). *Vasopressin and Oxytocin: Molecular Cellular, and Clinical Advances*. Kluwer Academic/Plenum, New York.

Biography

Michael J. Brownstein is Chief of the Laboratory of Genetics, National Institute of Mental Health, NIH, Bethesda, MD. He received his Ph.D. and M.D. degrees from the University of Chicago and did postdoctoral training with Julius Axelrod. His research has been in the areas of neurobiology, endocrinology, genetics, and genomics. He and his co-workers are known for their studies of vasopressin and oxytocin biosynthesis, and for cloning the vasopressin and oxytocin receptors.

V-ATPases

Michael Forgac
Tufts University School of Medicine, Boston, Massachusetts, USA

The V-ATPases (or vacuolar (H^+)-ATPases) are ATP-driven proton pumps whose primary function is to acidify intracellular compartments in eukaryotic cells, although they have also been identified in the plasma membrane of certain cells. V-ATPases have been shown to play a crucial role in a variety of normal cellular processes as well as a number of human diseases. The structure, mechanism, and regulation of these proton pumps have been the topics of intense study.

V-ATPase Function

Function of Intracellular V-ATPases

V-ATPases have been identified in many intracellular compartments, including endosomes, lysosomes, Golgi-derived vesicles and secretory vesicles. V-ATPases within endosomal compartments are important for the process of receptor-mediated endocytosis (Figure 1). During receptor-mediated endocytosis, cells take up ligands (such as the cholesterol carrying complex low density lipoprotein, or LDL) from their environment by binding them to receptors on the cell surface and clustering these receptors in specialized regions of the plasma membrane which then invaginate into the cell. Following this internalization, the ligand-receptor complexes are exposed to a low pH within the endosome that causes the internalized ligand to dissociate from its receptor. This dissociation allows the receptor to recycle to the plasma membrane (where it is reutilized) and the ligand to proceed to the lysosome, where it is degraded. The low pH within the endosome is generated by the V-ATPase.

Acidification of endosomes is also important in the formation of carrier vesicles that carry the released ligands from early to late endosomal compartments, and in the delivery of newly synthesized lysosomal enzymes from the Golgi to lysosomes. The latter process involves the binding of these enzymes to mannose-6-phosphate receptors in the trans-Golgi followed by their delivery to an endosomal compartment. Within this compartment, the low pH created by the V-ATPases causes dissociation of the lysosomal enzymes from their receptors, allowing delivery of the enzymes to the lysosome and recycling of the receptors to the trans-Golgi. Finally, endosomal acidification is involved in the entry of certain envelope viruses (such as influenza virus) into cells. These viruses bind to the surface of cells and are internalized by the process of endocytosis. Upon exposure to a low pH, the virus coat fuses with the endosomal membrane, releasing the viral nucleic acid into the cytoplasm of the host cell. Endosomal acidification is therefore essential in the process by which these viruses infect cells.

Lysosomes are the major compartment in which degradation of proteins and other macromolecules occurs in cells. The lysosomal enzymes responsible for this degradation all require an acidic environment to be active. This acidic environment is created by the V-ATPases. Secretory vesicles, such as synaptic vesicles, are also acidic compartments. Synaptic vesicles are located at the synaptic terminal of nerve cells and release neurotransmitters (that chemically trigger the next nerve cell) by fusion with the plasma membrane. Neurotransmitters become concentrated within synaptic vesicles by transport proteins within the synaptic vesicle membrane that utilize either the proton gradient or the membrane potential generated by the V-ATPases to drive uptake of the transmitter.

Function of Plasma Membrane V-ATPases

Plasma membrane V-ATPases play an important role in a number of normal and disease processes. In alpha-intercalated cells in the kidney, V-ATPases are located in the apical membrane where they pump protons into the urine, thus helping to control the pH of the blood. A genetic defect in this pump leads to a disease called renal tubule acidosis, in which the kidney is unable to secrete sufficient acid. V-ATPases are also present in the plasma membrane of osteoclasts, which are cells that function in degradation of bone. These cells are essential during development to facilitate bone remodeling. Plasma membrane V-ATPases in osteoclasts create an acidic extracellular environment that is necessary for bone degradation to occur. A genetic defect in the V-ATPase in osteoclasts leads to the human disease autosomal

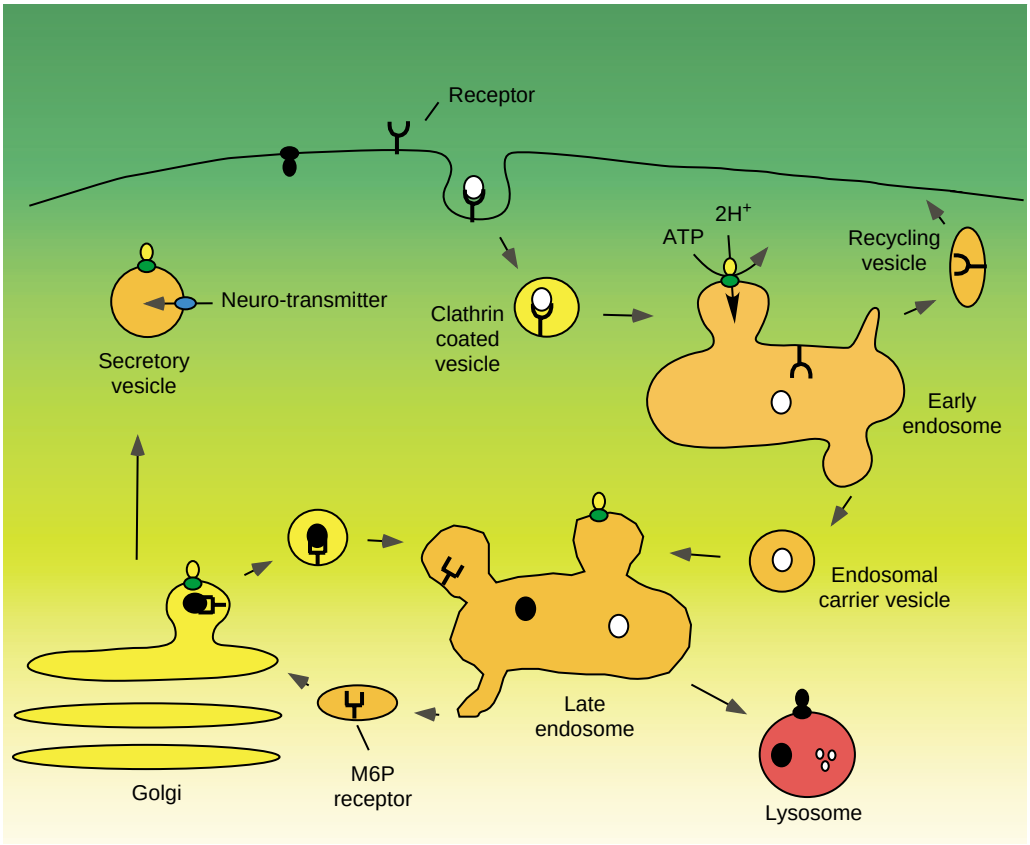

FIGURE 1 Function of intracellular V-ATPases. Acidification of early endosomes by the V-ATPase facilitates receptor recycling following endocytic uptake and formation of endosomal carrier vesicles. Recycling M6P receptors to the trans-Golgi is also low pH dependent. V-ATPase activity is also required to drive neurotransmitter uptake and facilitates protein degradation in lysosomes.

recessive osteopetrosis, in which the inability to degrade bone leads to severe skeletal defects and death.

Plasma membrane V-ATPases in macrophages and neutrophils have been shown to help maintain a neutral internal pH under conditions of severe acid load. In the vas deferens, V-ATPases create a low pH environment necessary for sperm development. V-ATPases in the plasma membrane of tumor cells have also been proposed to function in tumor invasion by providing an acidic extracellular environment necessary for secreted lysosomal enzymes to degrade extracellular matrix. Finally, V-ATPases in intestinal cells in insects create a membrane potential across the apical membrane that is used to drive potassium transport into the gut.

V-ATPase Structure

The V-ATPase is a large complex composed of 13 different subunits. These subunits are arranged into two separate domains termed V_1 and V_0 (Figure 2). The V_1 domain is made up entirely of subunits that are peripheral to the membrane (i.e., not membrane-embedded). This domain has a molecular mass of ~640 kDa and contains eight different subunits (subunits A–H) of molecular mass 70–13 kDa (Table I). The V_1 domain is responsible for hydolysis of ATP, which occurs on catalytic sites located on the three copies of subunit A. There are therefore three catalytic nucleotide binding sites per complex. The B subunits (which are also present in three copies per complex) can also bind nucleotides, but these sites are referred to as "non-catalytic" sites, since they do not actually hydrolyze ATP. The function of these sites is not known, but they may play a role in controlling the activity of the V-ATPase. The A and B subunits are arranged in a hexamer, like the segments of an orange, with alternating A and B subunits. ATP is hydrolyzed sequentially at each of the three catalytic sites. The other subunits in the V_1 domain (subunits C–H) function to connect the V_1 domain to the V_0 domain and are discussed here.

The V_0 domain is composed of five different subunits (subunits a, d, c, c′, and c″) of molecular mass 100–17 kDa. All of the subunits in the V_0 domain except subunit d are embedded in the membrane, and thus require detergent for solubilization. The V_0 complex has a molecular mass of 260 kDa and is responsible for transport of protons across the membrane.

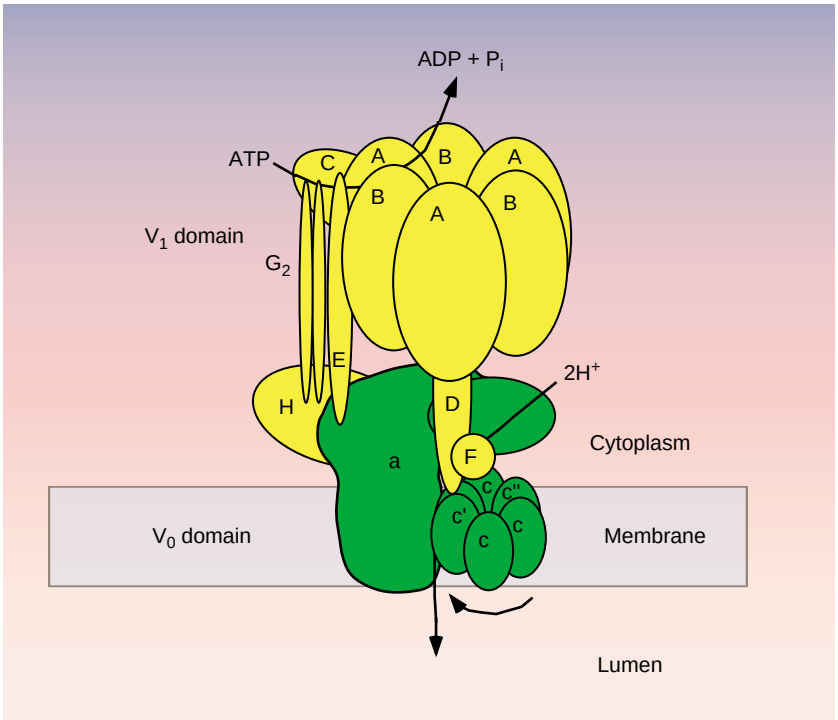

FIGURE 2 Structure of the V-ATPases. The V-ATPases contain two domains. The V_1 domain is responsible for ATP hydrolysis and the V_0 domain carries out proton transport across the membrane. Like the F-ATPases, the V-ATPases operate by a rotary mechanism in which ATP hydrolysis in V_1 drives rotation of a central stalk which is connected to a ring of proteolipid subunits in V_0. It is movement of the proteolipid ring relative to subunit a that drives proton transport (see text).

This proton transport only occurs when the V_1 domain is attached to V_0 and is driven by the hydrolysis of ATP in V_1. Three of the subunits in the V_0 domain are called proteolipid subunits (c, c′, and c″) because they are so hydrophobic that they can be extracted from the membrane using organic solvent mixtures, such as chloroform:methanol. These subunits are almost completely embedded in the membrane and the polypeptide chain of each one crosses the membrane four times (these are called transmembrane segments). Buried in the middle of one of the transmembrane segments of each of the proteolipid subunits is a single essential glutamic acid residue which is reversibly protonated and deprotonated during proton transport by the V-ATPases. Like the A and B subunits in the V_1 domain, the proteolipid subunits in the V_0 domain form a ring, with four copies of subunit c and one copy each of subunit c′ and c″. The specific V-ATPase inhibitor bafilomycin has been shown to bind to the proteolipid subunits of the V_0 domain.

In addition to the proteolipid subunits, the other V_0 subunit that is embedded in the membrane is the 100-kDa subunit a. This subunit is made up of two domains. The carboxyl-terminal half of the molecule contains nine transmembrane segments while the amino-terminal half is a hydrophilic domain that is present on the cytoplasmic side of the membrane. Like the proteolipid subunits, the subunit a also contains amino acid residues that are essential for proton transport. In particular, there is a positively charged arginine residue near the middle of the seventh transmembrane segment of subunit a that is absolutely required for proton transport

TABLE I

Subunit Composition of the V-ATPase

Domain	Subunit	Gene (yeast)	M_r (kDa)	Function/ location
V_1	A	*VMA1*	69	Catalytic ATP binding site
	B	*VMA2*	58	Noncatalytic ATP binding site
	C	*VMA5*	44	Peripheral stalk
	D	*VMA8*	29	Central stalk
	E	*VMA4*	26	Peripheral stalk
	F	*VMA7*	14	Central stalk
	G	*VMA10*	13	Peripheral stalk
	H	*VMA13*	54	Peripheral stalk
V_0	a	*VPH1/STV1*	100	Proton translocation, targeting
	d	*VMA6*	40	Cytoplasmic side
	c	*VMA3*	17	Proton translocation, bafilomycin-binding site
	c′	*VMA11*	17	Proton translocation
	c″	*VMA16*	23	Proton translocation

by the V-ATPases. The function of the remaining V_0 subunit d, which is tightly bound to the V_0 domain but is not embedded in the membrane, is not known.

The V_1 and V_0 domains are connected by two stalks. The central stalk is composed of the subunits D and F whereas the peripheral stalk is composed of subunits C, E, G, H, and the soluble domain of subunit a. The function of these stalks is described below.

Mechanism of ATP-Driven Proton Transport by the V-ATPases

The V-ATPases are believed to operate by a rotary mechanism, similar to that demonstrated for the F-ATPases (or ATP synthases), which are enzyme complexes present in mitochondria, chloroplasts, and bacteria that function in the reverse direction (that is in proton-driven ATP synthesis). For the V-ATPases, ATP hydrolysis in the V_1 domain drives rotation of the central stalk (containing subunits D and F), which in turn drives rotation of the ring of proteolipid subunits relative to subunit a in the V_0 domain. Subunit a is held fixed relative to the A_3B_3 hexamer of V_1 by the peripheral stalk (or stator), composed of subunits C, E, G, H, and the soluble domain of subunit a. It is rotation of the ring of proteolipid subunits relative to subunit a that drives active transport of protons from the cytoplasmic to the lumenal side of the membrane. A proton enters from the cytoplasmic side of the membrane via a cytoplasmic access channel in subunit a and protonates a buried carboxyl group on one of the proteolipid subunits. ATP hydrolysis in V_1 forces rotation of the proteolipid ring in the plane of the membrane such that the protonated carboxyl group on the proteolipid subunit reaches a second access channel in subunit a that leads to the lumenal side of the membrane. Interaction between this carboxyl group on the proteolipid subunit and the buried arginine residue of subunit a (which is positively charged) forces the proton off of the proteolipid subunit into the lumenal access channel, where it can be released to the lumenal side of the membrane, thus completing the transport cycle. In this way, the rotary motion driven by hydrolysis of ATP is converted into unidirectional transport of protons across the membrane.

Regulation of V-ATPase Activity *In Vivo*

The activity of V-ATPases in different membranes in the cell is known to be regulated such that the pH of different intracellular compartments and the degree of proton transport across the plasma membrane is carefully controlled, but the mechanisms employed in regulating V-ATPase activity in cells are still being elucidated. One important mechanism of regulation involves reversible dissociation of the V-ATPase complex into its component V_1 and V_0 domains. In yeast, dissociation occurs in response to removal of glucose from the media, probably as a way to preserve cellular energy stores. Dissociation has also been demonstrated to occur in insects and in mammalian cells. A second proposed regulatory mechanism involves the formation of a disulfide bond between two conserved cysteine residues located at the catalytic site on the subunit A.

Differential targeting of V-ATPases to different cellular membranes has also been proposed as a means of controlling proton transport. This has been shown to occur in intercalated cells in the kidney, where exposure to a low pH causes the fusion of intracellular vesicles containing the V-ATPase with the plasma membrane, thus increasing proton transport out of the cell into the renal fluid. Differential targeting of V-ATPases appears to be controlled by different isoforms of the subunit a. Thus the a3 isoform is able to target the V-ATPase to the plasma membrane in osteoclasts whereas the a4 isoform targets the V-ATPase to the intercalated cell plasma membrane. It is mutations in these isoforms that lead to the human diseases osteopetrosis and renal tubule acidosis mentioned earlier. Isoforms have now been identified in many of the V-ATPase subunits in mammalian cells, and these have been shown to be expressed in both tissue- and organelle-specific manner. This has led to the expectation that specific inhibitors can be identified that are selective in their ability to inhibit particular V-ATPase complexes, which may in turn lead to cures for diseases such as osteoporosis.

See Also the Following Article

Lipid Rafts

Glossary

access channel An aqueous channel that allows protons to reach buried carboxyl groups in the center of the membrane from one side of the membrane or the other.

osteopetrosis A genetic disease in humans associated with the inability to degrade bone, one cause of which is a defect in the V-ATPase of osteoclasts.

receptor-mediated endocytosis The process by which cells take up specific ligands from their environment (such as low density lipoprotein) via cell surface receptors.

V-ATPase Vacuolar proton translocating ATPase, which carries out active proton transport from the cytoplasmic to the non-cytoplasmic side of the membrane driven by energy released upon hydrolysis of ATP.

Further Reading

Arata, Y., Baleja, J. D., and Forgac, M. (2002). Localization of subunits D, E and G in the yeast V-ATPase complex using cysteine-mediated cross-linking to subunit B. *Biochemistry* **41**, 11301–11307.

Bowman, B. J., and Bowman, E. J. (2002). Mutations in subunit c of the V-ATPase confer resistance to bafilomycin and identify a conserved antibiotic binding site. *J. Biol. Chem.* **277**, 3965–3972.

Nishi, T., and Forgac, M. (2002). The vacuolar (H^+)-ATPases: Nature's most versatile proton pumps. *Nat. Rev. Mol. Cell Biol.* **3**, 94–103.

Smardon, A. M., Tarsio, M., and Kane, P. M. (2002). The RAVE complex is essential for stable assembly of the yeast V-ATPase. *J. Biol. Chem.* **277**, 13831–13839.

Toyomura, T., Oka, T., Yamaguchi, C., Wada, Y., and Futai, M. (2000). Three subunit a isoforms of mouse vacuolar (H^+)-ATPase. Preferential expression of the a3 isoform during osteoclast differentiation. *J. Biol. Chem.* **275**, 8760–8765.

Biography

Michael Forgac is a Professor in the Department of Physiology at Tufts University School of Medicine. His principal research interest is in the structure, mechanism, and regulation of the V-ATPases. He received his B.S. in biology and chemistry from Caltech in 1976 and his Ph.D. in Biochemistry and Molecular Biology from Harvard in 1981. He is author of over eighty publications and a recipient of a MERIT Award from the National Institutes of Health.

Vitamin A (Retinoids)

Joseph L. Napoli
University of California, Berkeley, CA, USA

Vertebrates require vitamin A, all-*trans*-retinol (atROH), for vision, fertility, embryogenesis, growth, and optimum neuro and immune function. atROH generates the visual pigment, 11-*cis*-retinal, and the humoral effector all-*trans*-retinoic acid (atRA). atROH transport and metabolism relies on serum and cellular chaperones (binding proteins) to maximize efficiency and impose specificity. Cleavage of carotenoids in the intestinal mucosa by carotenoid monooxygenase produces all-*trans*-retinal. CRBP(II) binds all-*trans*-retinal and dietary retinol, and allows only reduction and esterification into all-*trans*-retinyl esters (atRE). atRE storage occurs mostly in liver stellate cells. Liver only releases atROH bound with serum retinol binding protein, sRBP. In extra-intestinal tissues, cellular retinol binding-protein (CRBP) binds atROH and allows re-esterification. In the retinal pigment epithelium, the binding-protein RPE65 facilitates concerted atRE hydrolysis and conversion into 11-*cis*-retinol, catalyzed by an isomerohydrolase. Short-chain dehydrogenase/reductases (SDR) convert 11-*cis*-retinol into 11-*cis*-retinal. 11-C*is*-retinal crosses the interphotoreceptor matrix and enters the rod outer segments, where it binds covalently with opsin to form rhodopsin. Light isomerizes 11-*cis*-retinal into all-*trans*-retinal, changing the conformation of rhodopsin and generating a nerve impulse. The transporter ABCR aids leaching of all-*trans*-retinal from rhodopsin. Other SDR reduce all-*trans*-retinal into atROH. atROH crosses the interphotoreceptor space, rebinds with CRBP in the retinal pigment epithelium, and undergoes re-esterification. atRA biogeneration takes a different path. atROH, from hydrolysis of atRE by retinyl ester hydrolase or from serum, binds with CRBP and undergoes dehydrogenation by microsomal SDR. The all-*trans*-retinal produced undergoes dehydrogenation into atRA, catalyzed by retinal dehydrogenases. CRABP(II) delivers atRA to retinoic acid receptors, whereas the complex CRABP-atRA has higher enzymatic efficiency for atRA degradation than does free atRA. Cytochromes P-450 initiate atRA degradation through C4 and C18 hydroxylation and 5,6-epoxydation. Primary regulators of atROH homeostasis include apo-CRBP, which inhibits esterification of atROH and accelerates hydrolysis of atRE, and atRA, which induces its own catabolism.

Retinoids and their Functions

The term *retinoid* refers to compounds, both naturally occurring and synthetic, with vitamin A activity: vitamin A denotes the organic compound all-*trans*-retinol (atROH). All vertebrates require vitamin A/atROH for vision, fertility, embryogenesis, and growth. atROH does not support the physiological functions attributed to vitamin A; rather it acts as precursor for biosynthesis of retinoids directly responsible for producing "vitamin A activity". These atROH metabolites include 11-*cis*-retinal, the cofactor covalently bound with opsin to form the visual pigment rhodopsin, and all-*trans*-retinoic acid (atRA), the humoral effector of the non-visual, systemic functions attributed to vitamin A. These systemic functions include: controlling the differentiation programs of all epithelia, and of stem cells in the skin, nervous system, bone, immune system, hemopoietic system; acting as a tumor suppressor; and regulating apoptosis. Specific non-visual effects of retinoids include memory formation, immune responsivity, stress adaptation, and cell fate determination. atRA activates three nuclear receptors, RARα, β and γ, and thereby controls the expression of hundreds of genes. atRA, or perhaps other retinoids, may also function through non-genomic mechanisms, but the research is in its infancy.

The Chemistry of atROH Generation, Storage, and Metabolic Activation

Carotenoids with at least one β-ionone ring, especially β-carotene, provide the major retinoid precursors in most diets. Oxidative central cleavage by a plasma-membrane associated, but soluble, carotene 15,15′-monooxygenase (CMO) produces all-*trans*-retinal—a transient intermediate that occurs in very low concentrations outside of the neural retinal. Microsomal retinal reductases, RRD, members of the short-chain

dehydrogenase/reductase (SDR) gene family, catalyze reduction of all-*trans*-retinal into atROH, which then undergoes esterification into all-*trans*-retinyl esters (atRE), predominantly palmitate, by microsomal lecithin:retinol acyltransferase (LRAT). Chylomicrons carry atRE into circulation and chylomicron remnants deliver them to liver, where ultimately, most are stored in stellate cells.

In the visual cycle, atRE undergo concerted hydrolysis–isomerization into 11-*cis*-retinol by a microsomal isomerohydrolase (IMH), followed by dehydrogenation into 11-*cis*-retinal (SDR). 11-*Cis*-retinal forms a Schiff's base with a lysine residue in the protein opsin to form rhodopsin. When light strikes the neural retinal, 11-*cis*-retinal in rhodopsin undergoes *cis* to *trans*-isomerization, causing a conformation change that initiates nerve impulses and releases the newly formed all-*trans*-retinal. Reduction of all-*trans*-retinal into atROH (microsomal SDR) and re-esterification (LRAT) into atRE completes the visual cycle.

Activation of atROH into atRA uses the same intermediate used in the visual cycle, all-*trans*-retinal, but relies on a metabolically distinct route. atROH, either from blood or from hydrolysis of retinyl esters by microsomal retinyl ester hydrolase (REH), undergoes reversible dehydrogenation into all-*trans*-retinal, catalyzed primarily by microsomal retinol dehydrogenases, RDH, also members of the SDR gene family. In contrast to the comparatively high concentrations of retinals that allow the visual cycle to function, all-*trans*-retinal concentrations during atRA biosynthesis are kept low by reduction (back reaction of RDH and reduction by microsomal and peroxisomal reductases), and by irreversible dehydrogenation into atRA, catalyzed by soluble, ~54 kDa, high V_{max} retinal dehydrogenases (RALDH), members of the aldehyde dehydrogenase (ALDH) gene family. atRA isomers occur *in vivo*, such as 13-*cis*-RA and 9,13-di-*cis*-RA, but their significance and source(s) remain unclear.

These straightforward reactions offer complex opportunities for physiological regulation, owing to compartmentalization, distinct enzymes catalyzing each direction of chemically reversible reactions (*e.g.* dehydrogenation/reduction of retinol/retinal; esterification/hydrolysis of atROH/atRE), cell-distinct expression patterns, and multiple homologs/paralogs that catalyze several reactions. For example, at least four reductases have been identified, which belong to the SDR gene family, Rrd (peroxisomal) and RalR1 outside of the eye, and retSDR and prRDH, in the neural retina. At least three RDH, also SDR, have been identified in the rat: Rodh1, Rodh2 and Rodh3. Four Raldh have been identified in human, rat and mouse: Raldh1, 2, 3, 4 (aka ALDH 1A1, 1A2, 1A6 and 8A1). These constitute a complex enzyme system for absorbing and storing vitamin A, maintaining atRA homeostasis, and recycling vitamin A in the visual cycle.

Retinoid Binding-Proteins and their Contributions to Retinoid Homeostasis

Processing of dietary retinoids and retinoid precursors and biogeneration of active retinoids relies on serum and cellular chaperones for efficient and specific retinoid use, as demonstrated by studies *in vitro* and the consequences of gene knockouts and/or naturally occurring mutations.

Liver and other tissues synthesize a retinol binding-protein, sRBP, a member of the lipocalin gene family. atROH egress from liver requires sRBP, and sRBP-atROH represents the major form of vitamin A in serum. sRBP circulates as a complex with a tetramer of transthyretin, which protects the ~20 kDa sRBP from kidney filtration. The mechanism of atROH delivery from sRBP into cells has not been established. Some data suggest a membrane receptor, other data indicate that cellular retinol binding-protein(s) draw atROH from sRBP through the membrane. A third hypothesis would have a sRBP receptor mainly in eye, the major site of vitamin A consumption. The sRBP null mouse seems phenotypically normal, except for impaired vision after weaning. Feeding a vitamin A-adequate diet for months restores vision. Although the eye relies on sRBP for efficient atROH uptake, atROH obtained from postprandial lipoprotein delivery can substitute, at least under laboratory conditions. Interestingly, atRA serum levels increase in the sRBP null mouse, indicating that serum delivery of atRA to tissues helps compensate for impaired atROH delivery.

Binding-proteins channel retinoid intermediates through the series of reactions that constitute the visual cycle (Figure 1). Mice null in the retinal pigment protein (RPE) RPE65, for example, cannot produce 11-*cis*-retinoids, consistent with an RPE65 function of binding the hydrophobic atRE (K_d value ~20 pM), and accelerating their mobilization and delivery to the next step, acyl hydrolysis and C11 isomerization by the IMH. RPE65 belongs to the same gene family as the carotenoid-metabolizing enzyme CMO (the mouse proteins have only 37% amino acid identity, however), suggesting a gene family devoted to transport/metabolism of hydrophobic substances. The IMH product, 11-*cis*-retinol, undergoes sequestration in the RPE by the 36 kDa cytosolic cellular retinal binding-protein (CRALBP), a member of the gene family that includes the α-tocopherol transfer protein, TTP. CRALBP facilitates dehydrogenation of 11-*cis*-retinol into 11-*cis*-retinal, and drives forward the *trans* to *cis* isomerization.

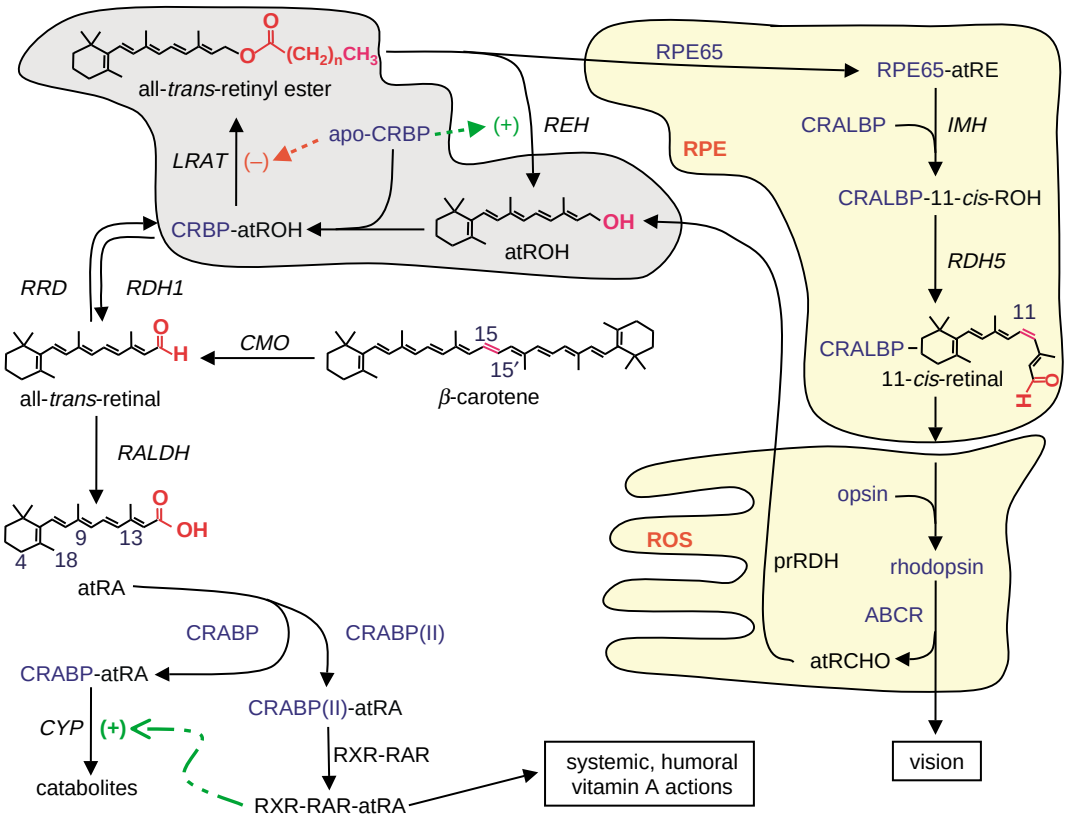

FIGURE 1 Major paths of retinoid metabolism. The white background designates reactions of retinol homeostasis and activation into atRA in the liver and extra-hepatic vitamin A target-tissues. The light gray background depicts reactions that occur both in extra-ocular tissues and in the retinal pigment epithelium (RPE) of the neural retina. The light yellow background designates reactions that occur in the RPE and in the rod outer segments (ROS). Numbers indicate the positions of *trans* to *cis* isomerization (C11), the positions of hydroxylations that occur during catabolism of atRA (C4 and C18), and the positions of atRA isomers of physiological interest (C9, C13). The dotted lines indicate the direct actions of apo-CRBP in regulating atRE hydrolysis and atROH esterification. The dashed-dotted line indicates transcriptional induction of cytochromes P-450 (CYP) by atRA. For simplicity, CRBP(II) is not shown.

Mutations in human CRALBP cause night blindness and photoreceptor degeneration. RDH4 and RDH5, respectively, represent the murine and human 11-*cis*-retinol dehydrogenase, which interacts with and/or accepts substrate from CRALBP. Mutations in RDH5 are associated with the rare, autosomal recessive disease fundus albipunctatus, i.e. night blindness from delayed photopigment regeneration. Lack of total blindness in the case of the RDH5 mutation, indicates that SDR in addition to RDH4/5 contribute to 11-*cis*-retinal biosynthesis. 11-*Cis*-retinal tranverses the interphotoreceptor matrix by an unknown mechanism and covalently binds with opsin to form rhodopsin in the rod outer segment (ROS). After the action of light, an ATP-dependent transporter, ABCR, facilitates release of all-*trans*-retinal from rhodopsin. prRDH then reduces the all-*trans*-retinal into atROH, which then travels back through the interphotoreceptor space to the RPE.

Several additional cellular retinoid binding-proteins occur. The four understood to be the most important, other than those mentioned above with respect to the visual cycle, include CRBP, CRBP(II), CRABP, and CRABP(II) (Table I). All vertebrates express all four, with well-conserved amino acid sequences among orthologs. All four are high-affinity, soluble, and specific for their ligands. CRBP binds atROH, and closely related compounds such as 3,4-didehydro-atROH, and all-*trans*-retinal to a lesser extent, and discriminate against *cis*-retinols and atRA. CRABP binds atRA, metabolites such as 4-OH-atRA, and discriminates against *cis*-RAs and atROH. These ~15 kDa globular proteins belong to the intracellular lipid binding-protein (iLBP) gene family, which includes the various fatty acid binding-proteins.

The cellular retinol/retinal binding-proteins enclose atROH and all-*trans*-retinal with the hydroxyl/aldehyde function, crucial to metabolic activation, sheltered inside. These two proteins apparently confer selective advantage to vertebrates by enhancing efficiency of sequestering, transporting and storing vitamin A, and limiting its catabolism. Vitamin A absorption and biosynthesis in the intestine relies on CRBP(II). CRBP(II)

TABLE I

Major Extra-ocular Retinoid Binding-Proteins

Retinoid binding-protein	Ligand(s)	K_d (nM)	Post-embryonic distribution
CRBP (cellular retinol binding-protein, type I)	atROH	~0.1	Nearly ubiquitous (low in intestine)
	All-*trans*-retinal	10–50	
CRBP(II) (cellular retinol binding-protein, type II)	atROH	10–50	Intestine, neonatal liver
	All-*trans*-retinal	10–50	
CRABP (cellular retinoic acid binding-protein, type I)	atRA	0.4	Widespread
CRABP(II) (cellular retinoic acid binding-protein, type II)	atRA	2	Limited (inducible?) (skin, uterus, ovary)

null mice pups die within 24 hours after birth, when delivered by dams fed a diet marginal in vitamin A content. CRBP(II) contributes ~1% of the soluble protein to the intestinal enterocyte—an indication of a mass-action function to sequester newly synthesized (from carotenoids) all-*trans*-retinal or newly absorbed dietary atROH. *In vitro*, all-*trans*-retinal bound with CRBP(II) undergoes reduction readily, but neither it nor bound atROH undergoes dehydrogenation. This would limit production of atRA, and other metabolism, from the bolus of all-*trans*-retinal produced during carotenoid metabolism. In the intestine, the esterifying enzyme LRAT recognizes atROH bound with CRBP(II) to produce atRE for incorporation into chylomicrons. Thus, CRBP(II) likely aids atROH uptake and chaperones the products of carotenoid metabolism down the pathway to atRE to enhance efficiency of retinoid recovery from the diet.

Extra-intestinal vitamin A uptake and storage relies on CRBP. CRBP-null mice seem morphologically normal, but eliminate atRE 6-fold faster than wild-type mice, and may sequester/esterify atROH less efficiently. Clearly, *efficient* use of atROH *in vivo* depends on the chaperone. Strikingly, CRBP has a K_d value for atROH far lower than the atROH concentration in tissues (1–30 μM), and CRBP concentrations exceed atROH concentrations, where measured. The law of mass action predicts from these data that non-esterified atROH would occur nearly exclusively in the CRBP-bound state, assuming no alternative high-affinity or very high-capacity acceptors. Alternatives to CRBP exert limited influence *in vivo*, because isolation of CRBP from animal tissues by traditional (time-consuming and containing membranes, lipids and lipid vesicles) biochemical techniques (tissue homogenization, centrifugation and several types of column chromatography) produces largely holo-protein. Evidently, the capacity of membranes and other potential acceptors to sequester atROH does not overwhelm the ability of CRBP to sequester atROH. Like CRBP(II), LRAT can access atROH bound with CRBP to produce atRE. Ultimately, liver stellate cells accumulate most of the atRE. CRBP seems necessary for retinoid transfer from hepatocytes to stellate cells, because the CRBP null mouse does not accumulate atRE in stellate cells.

atROH sequestering within CRBP, the need to store retinol as esters, and the need for atRA biosynthesis during specific times at specific loci, suggest that transfer of atROH for metabolism might depend on relationships between metabolizing enzymes and CRBP. Like CRBP(II), CRBP allows esterification of bound atROH, but in contrast to CRBP(II), CRBP also allows dehydrogenation of atROH. The CRBP–atROH complex shows Michaelis–Menton relationships with atRE formation by LRAT and atROH dehydrogenation by RDH. This relationship with the microsomal RDH is maintained even with changes in the CRBP/atROH ratio (provided the CRBP concentration exceeds the atROH concentration). This eliminates a "free diffusion" mechanism of transfer from the complex to select enzymes. Specific crosslinking of holo-CRBP with both RDH and LRAT confirms close proximity of CRBP and these two enzymes. Additionally, a single mutation in an exterior residue of CRBP (L35A) reduces the Vm of atROH dehydrogenation by microsomes, but does not alter the K_m, or the K_d of atROH binding to CRBP, consistent with conservation of exterior residues that aid transfer of atROH from CRBP to enzymes. Obviously, atRE and atRA biosynthesis *in vivo* occurs in the absence of CRBP, as indicated by the lack of morphological pathology in the CRBP null mouse, and their ability to sequester esters. This was predicted by the experiments *in vitro*, which showed that neither RDH nor LRAT require presentation of atROH by CRBP. Not surprisingly, the enzymes' active sites recognize their substrates in the absence of CRBP. CRBP operates as a chaperone, which restricts atROH metabolism to select enzymes, and seems required only for *efficient* atROH use *in vivo*. The ability of LRAT and RDH to access retinol from CRBP addresses the issue of how atROH would undergo efficient metabolism in the face of limited diffusion from the binding protein.

RALDH catalyze the irreversible conversion of atRCHO into atRA in the presence of CRBP, and also

can use atRCHO generated *in situ* from CRBP-atROH and RDH, or in cells presented with atROH and transfected with RDH and RALDH. In the rat, RALDH1 and RALDH2 have differing but overlaping expression patterns, and respond differently to changes in atROH status. This suggests a purpose for more than one—precise control over atROH use and atRA generation. The RALDH1 null mouse remains fertile and healthy, but may have decreased ability to produce atRA in the liver. The RALDH2 null mouse dies *in utero* at midgestation, demonstrating its unique contribution to atRA biosynthesis during embryogenesis. The situation may differ in the adult, as testes express RALDH2 strongly, but RALDH1 prevails outside of the testis. The RALDH3 null mouse dies during suckling from an obstruction in the nose. Apparently, RALDH can compensate for each other after critical developmental milestones.

A CRBP(III) has been detected in mouse heart and skeletal muscle, which express little or no CRBP or CRBP(II), but has not been detected in other retinoid target tissues, such as liver, kidney, brain, etc. CRBP(III) seems to bind about equally well with atROH, 9-*cis*-retinol and 13-*cis*-retinol, but with much lower affinity that either CRBP or CRBP(II) ($K_d \sim 80-110$ nM). Humans express yet another CRBP, originally referred to as CRBP(III), but distinct from mouse CRBP(III), and therefore CRBP(IV). CRBP(IV) mRNA is much more abundant in human liver and intestine than CRBP mRNA, but the mouse does not encode a complete CRBP(IV) gene. CRBP(IV) binds atROH with a K_d value of $\sim$60 nM, and does not bind *cis*-isomers. The precise functions of CRBP(III) and CRBP(IV) have not been clarified, and unlike CRBP and CRABP, their endogenous ligands have not been established.

The atRA binding-proteins, CRABP and CRABP(II), do not have well-defined functions. Doubly null mice have a $\sim$4-fold higher rate of death from unknown causes by 6 weeks after birth than wild-type, but the survivors appear normal, with one exception. The doubly null mouse, as well as the CRABP(II)-only null mouse, show 83% and 45%, respectively, incidence of a small outgrowth anomaly on the post-axial side of digit five, predominantly in the forelimbs. Mice doubly null in CRABP and CRABP(II) do not exhibit enhanced sensitivity to exogenous atRA, suggesting that the binding-proteins do not protect against atRA toxicity. In contrast to CRBP, both CRABP and CRABP(II) allow projection of the β-ionone ring of their ligand. Significantly, the first reactions of atRA degradation occur at these comparatively accessible sites, i.e. C4 and C18. Presenting atRA to microsomes bound with CRABP enhances kinetic efficiency (K_{cat}/K_m) of catabolism 7-fold. There seems to be little doubt that CRABP sequesters atRA: delivering the sequestered atRA for efficient catabolism seems a logical mechanism to discharge the ligand without releasing it back into the cell. Unfortunately, this insight doesn't reveal the primary purpose for CRABP impounding atRA in the first place, although CRABP tends to express in cells different from those that express CRBP and CRABP(II). CRABP(II), but not CRABP, seems to deliver atRA to RAR, via a transfer that does not require free diffusion. This would complete the chaperoning of atROH on its journey from atRE through atRA biogenesis to nuclear localization.

Many other enzymes, including medium-change alcohol dehydrogenases, and aldo-keto reductases, metabolize retinoids *in vitro*, which seems to confirm the need for evolution of CRBP to protect the sparse and valuable vitamin A from clearance as a "xenobiotic". These enzymes do not access atROH bound with CRBP. Neither the ADHI-null deermouse, a natural mutant, nor mice made null in ADHI, ADHIV, or ADHIII or doubly null in ADHI and ADHIV, present with vitamin A deficiency symptoms, revealing no inability to activate atROH. ADHI-null mice do show decreased ability to convert a very large dose (50 mg kg^{-1}) of atROH into atRA. Such a dose has no natural equivalent: the results indicate only that determination can overwhelm physiological chaperones.

Other Naturally Occurring Retinoids

Discrete loci, such as skin and the chick limb bud, synthesize 3,4-didehydro-atRA. 3,4-Didehydro-atRA binds retinoic acid receptors with affinity similar to that of atRA. The purpose has not been clarified of creating a signaling molecule that functions as atRA in specialized loci that also biosynthesize atRA. Although 9-*cis*-RA was reported as an activated retinoid, it is virtually undetectable *in vivo*: its putative function as a physiological ligand that controls RXR remains uncertain.

Control of Vitamin A Homeostasis

The primary regulators of retinoid homeostasis appear to be apo-CRBP and atRA. apo-CRBP inhibits LRAT and stimulates retinyl ester hydrolysis. Thus, the direction of flux into or out of atRE would reflect the ratio apo-CRBP/holo-CRBP, which would reflect the atROH status of the cell. atRA may serve as a signal to liver to release atROH into the serum. Little has been revealed about humoral regulation of atRA biosynthesis, but estrogen and PGE, increase and decrease, respectively, atRA biosynthesis in cultured cells. The metabolism of atRA limits its activity; conversely, inhibitors of atRA metabolism enhance atRA potency. atRA

induces its own oxidative metabolism into 5,6-epoxy-atRA, 18-hydroxy-atRA, and 4-hydroxy-atRA, through inducing cytochrome P-450 s (CYP). CYP26A1 and CYP2C39 appear to have major functions in the catalysis of atRA catabolism. CYP26A1 null mice die in mid to late gestation with serious morphological defects. Two other CYP, 26B1 and 26C1, also catabolize atRA, but their precise function has not been clarified. Many other CYP reportedly catabolize atRA (e.g. CYP1A1/2, CYP2A6, CYP2C8/9, CYP2E1, CYPP3A4/5), but atRA does not induce these isoforms and most have inefficient kinetics with atRA *in vitro*.

PPARβ induces transcription of CMO, CRBP, CRBP(II), LRAT, and RARβ, suggesting correlation between vitamin A homeostasis and general lipid metabolism, whereas LRAT and CRBP are among the numerous genes induced by atRA. This action of atRA may represent a "housekeeping" function, rather than acute control over retinoid homeostasis.

Several xenobiotics, including ethanol and polychlorinated aromatic hydrocarbons reduce atRE stores, possibly through enhancing atRA catabolism by inducing CYP: the polychlorinated hydrocarbons, such as dioxin, function through the AH receptor to decrease atRE stores.

Clinical Uses of Retinoids

Numerous studies have correlated vitamin A insufficiency in laboratory animals with increased incidence of spontaneous and carcinogen-induced cancer. Chemopreventive trials in humans show some promise for retinoids in actinic keratoses, oral premalignant lesions, laryngeal leukoplakia, and cervical dysplasia. The FDA has approved retinoids for acute promyelocytic leukemia and in non-life-threatening diseases such as cystic acne and psoriasis. Retinoids also provide the active ingredients in agents to treat sun-/age-damaged skin.

The WHO recognizes vitamin A-deficiency as a mortality factor for childhood measles. Two large doses (60,000 REQ each) of a water-soluble vitamin A formulation given to children on each of two days decreases the risk of death from measles 81% in areas of prevalent vitamin A-deficiency.

See Also the Following Articles

Retinoic Acid Receptors • Steroid/Thyroid Hormone Receptors

Glossary

K_{cat}/K_m A measure of the efficiency of an enzyme for its substrate from dividing the rate of turnover of the substrate by the enzyme by the Michaelis constant.

K_d (equilibrium dissociation constant) A measure of the affinity of a protein for its ligand. Lower numbers indicate higher affinity.

retinoid binding-protein Proteins that bind specific retinoids with high affinity, several with K_d values <10 nM.

short-chain dehydrogenase/reductase (SDR) A gene family consisting of ~ 50 mammalian members in the range of 25–35 kDa that uses pyridine nucleotide cofactors to dehydrogenate or reduce steroids, retinoids, prostanoids, and intermediates in lipid metabolism.

Further Reading

Blomhoff, R., Green, M. H., Green, J. B., Berg, T., and Norum, K. R. (1991). Vitamin A metabolism: new perspectives on absorption, transport, and storage. *Physiological Reviews* **71**, 951–990.

Harrison, E. H. (1998). Lipases and carboxyesterases: possible roles in the hepatic metabolism of retinol. *Annual Reviews of Nutrition* **18**, 259–276.

Maden, M. (2001). Role of retinoic acid in embryonic and post-embryonic development. *Proceedings of the Nutrition Society* **59**, 65–73.

Napoli, J. L. (2000). Retinoic acid: its biosynthesis and metabolism. *Progress in Nucleic Acids Research* **63**, 139–188.

Newcomer, M. E. (1995). Retinoid-binding proteins: structural determinants important for function. *FASEB Journal* **9**, 229–239.

Saari, J. C. (2000). Biochemistry of visual pigment regeneration: the Friedenwald lecture. *Investigative Ophthalmology and Visual Science* **41**, 337–348.

Stephensen, C. B. (2001). Vitamin A, infection, and immune function. *Annual Reviews of Nutrition* **21**, 167–192.

Sun, S. Y., and Lotan, R. (2002). Retinoids and their receptors in cancer development and chemoprevention. *Critical Reviews in Oncology and Hematology* **41**, 41–55.

Wolf, G. (1984). Multiple functions of vitamin A. *Physiological Reviews* **64**, 873–937.

Biography

Joseph L. Napoli is a Professor in the Department of Nutrition Sciences and Toxicology and a biochemist in the experimental station at UC-Berkeley. His main research interests are in the metabolism and functions of retinoids. He received his Ph.D. from the University of Michigan-Ann Arbor in medicinal chemistry and was a post-doctoral fellow in biochemistry at the University of Wisconsin-Madison.

Vitamin B_{12} and B_{12}-Proteins

Bernhard Kräutler
University of Innsbruck, Innsbruck, Austria

Vitamin B_{12} (CNCbl), the antipernicious anemia factor, is required for human and animal metabolism and was discovered in the late 1940s. The B_{12}-derivatives belong to the tetrapyrrolic natural compounds and are cobalt complexes of the unique and remarkably complex corrin ligand. The B_{12}-coenzymes are the cofactors in important organometallic enzymatic reactions and are particularly relevant in the metabolism of anaerobes. Indeed, the microorganisms are the only natural sources of the B_{12}-derivatives, whereas most living organisms (except for the higher plants) depend on these cobalt corrinoids. Vitamin B_{12} and its derivatives thus hold an important position in the life sciences and have attracted strong interest from medicine, biology, chemistry, and physics.

B_{12}: Structure and Reactivity

The red, cyanide-containing cobalt-complex vitamin B_{12} (cyanocobalamin, CNCbl) is a relatively inert and physiologically rather inactive Co(III)-corrin. The biologically relevant B_{12}-derivatives are the light sensitive and chemically more labile organometallic coenzyme forms, coenzyme B_{12} (5′-deoxy-5′-adenosylcobalamin, AdoCbl), and methylcobalamin (MeCbl, see Figure 1).

Structure of Vitamin B_{12}-Derivatives

The structures of vitamin B_{12} (CNCbl) and of coenzyme B_{12} (AdoCbl) were established by X-ray crystallographic studies from the laboratory of D. C. Hodgkin. This work helped clarify the nature of the corrin ligand and to discover the organometallic nature of the coenzyme AdoCbl (see Figure 1). CNCbl and other cobalamins, in which the cyanide ligand is replaced by another "upper" β-ligand (see Figure 1), represent the most common of the nucleotide containing (i.e., "complete") B_{12}-derivatives. The crystal structures of various (organometallic) Co(III)-corrins were analyzed, including MeCbl, to study the axial bonding at the corrin-bound cobalt center and the inherent "non-planar" nature of the corrin ligand (as opposed to the porphyrin ligand), as well as possible implications of this for B_{12}-catalyzed enzymatic reactions. An interesting structure is that of the oxygen-sensitive Co(II)-corrin cob(II)alamin (B_{12r}), the corrinoid moiety resulting from (Co–C)-bond homolysis of AdoCbl during the catalytic cycle of coenzyme B_{12}-dependent enzymes.

UV/vis- and circular dichroism (CD)-spectroscopy have been used to study the colored and chiral B_{12}-derivatives in solution. Nuclear magnetic resonance (NMR) spectroscopy and mass spectrometry helped to identify the corrinoids from anaerobes (methanogens, sulfur metabolizing, and acetogenic bacteria) and to characterize their solution structures. The Co(II)-forms, in turn, have been investigated by electron spin resonance (ESR) spectroscopy, a technique used increasingly to analyze for paramagnetic intermediates in B_{12}-catalyzed enzymatic reactions.

The natural B_{12}-derivatives are either "complete" or "incomplete" corrinoids (which lack the nucleotide function, see Figure 1). The natural "complete" corrinoids carry different functional β-axial ligands. In addition they may vary by the constitution of the "nucleotide base," a 5,6-dimethylbenzimidazole (DMB) in the cobalamins (such as CNCbl), but an adenine in pseudovitamin B_{12}. The "complete" corrinoids are also unique due to the unusual α-configuration of their (pseudo-)nucleotide appendage. The specific build-up of this function enables the heterocyclic base to bind in an intramolecular fashion to the "lower" α-axial coordination site of the corrin-bound cobalt center. In this way, the nucleotide function steers the organometallic reactivity at the cobalt center of "complete" B_{12}-derivatives and is also relevant for recognition and tight binding by the B_{12}-binding proteins.

B_{12}-Derivatives in Electron Transfer Reactions

Oxidation–reduction processes are of key importance for the chemistry and biology of B_{12}. Under physiological conditions B_{12}-derivatives may exist in three different oxidation states (Co(III), Co(II), or Co(I)), each possessing different coordination properties and reactivities: Axial coordination to the corrin-bound cobalt center depends primarily on the formal oxidation

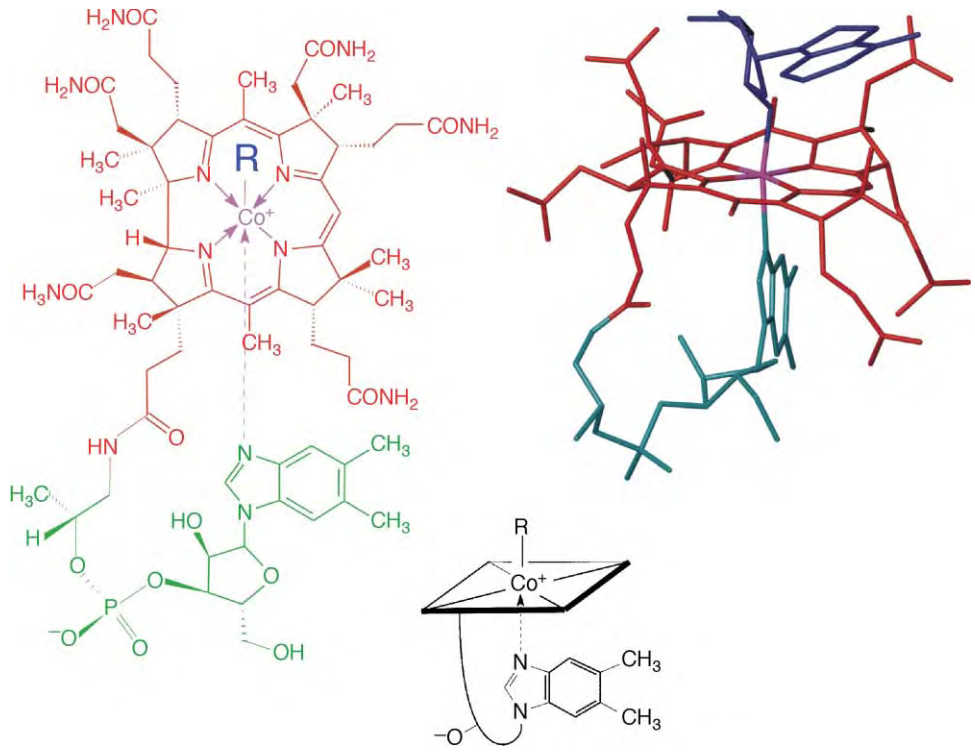

FIGURE 1 Left: structural formulas of vitamin B_{12} (R = CN, CNCbl), of coenzyme B_{12} (R = 5′-deoxy-5′-adenosyl, AdoCbl), methylcobalamin (R = methyl, MeCbl), cob(II)alamin (R = e^-, B_{12r}). Right/top: structure of coenzyme B_{12} (AdoCbl). Bottom: symbols used for vitamin B_{12} (R = CN: CNCbl) and other cobalamins.

state of the cobalt ion. As a rule, the number of axial ligands decreases in parallel with the cobalt oxidation state: In the thermodynamically predominating forms of cobalt corrins, two axial ligands are bound to the diamagnetic Co(III)-center, one axial ligand is bound to the paramagnetic Co(II)-center and axial ligands are assumed to be absent at the diamagnetic Co(I)-center. Electron transfer reactions involving B_{12}-derivatives, therefore, are accompanied by changes of the number of axial ligands and depend upon the nature of axial ligands. Axial coordination of the nucleotide base and of strongly coordinating ligands stabilizes the cobalt center against reduction and the reduction of alkyl-Co(III)-corrins typically occurs at potentials more negative than that of the Co(II)/Co(I)-redox-pair B_{12r}/B_{12s}.

Organometallic Reactions of B_{12}-Derivatives

The reactivity of B_{12}-derivatives in organometallic reactions holds the key to much of the biological activity of the B_{12}-dependent enzymes: formation and cleavage of the (Co–C)-bond in the B_{12}-cofactors are essential steps of the reactions catalyzed by B_{12}-dependent enzymes and are of particular interest.

In solution formation and cleavage of the (Co–C)-bond in organometallic B_{12}-derivatives were observed to occur on all oxidation levels of the cobalt center. Two of these reaction modes were also found to be relevant for B_{12}-dependent enzymatic reactions:

1. the homolytic mode of formation/cleavage of the organometallic axial bond at the cobalt center (formally a one-electron reduction/oxidation of the metal center, see Figure 2), is of particular importance for the role of AdoCbl as a cofactor AdoCbl is considered a "reversible carrier of an alkyl radical" (or a reversibly functioning "radical source"). The (Co–C)-bond of AdoCbl has been determined to be ~30 kcal mol^{-1} strong and to be affected only slightly by the nucleotide (in the "base-on" form). The (reverse) reactions of B_{12r} with alkyl radicals (such as the 5′-deoxy-5′-adenosyl radical) are remarkably fast. Indeed, the radicaloid B_{12r} is a highly efficient "radical trap" and its reactions with radicals can occur with minimal restructuring of the cobalt-corrin moiety.
2. the heterolytic, nucleophile induced (SN_2) mode of formation/cleavage of the (Co–C)-bond at the cobalt center (formally a two-electron oxidation/reduction of the metal ion) is accompanied by formation/cleavage of a second axial bond (Figure 2): Heterolytic formation/cleavage of the (Co–C)-bond is particularly important in enzyme-catalyzed methyl-transfer reactions (Figure 3). This mode is represented by the reaction of

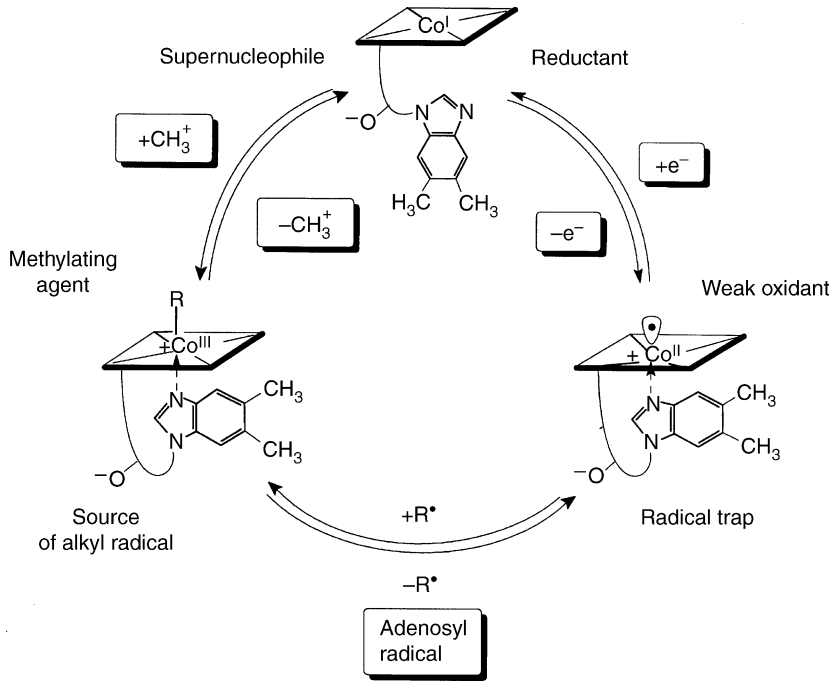

FIGURE 2 Elementary formal reaction steps of "complete" corrinoids characterizing their patterns of reactivity relevant for their cofactor function in B_{12}-dependent enzymes.

("supernucleophilic") Co(I)-corrins with alkylating agents and by the nucleophile-induced demethylation of methyl-Co(III)-corrins. Alkylation at the Co(I)-center usually occurs via "classical" bimolecular nucleophilic substitution (SN_2). The intramolecular coordination of the DMB-base in MeCbl has a notable thermodynamic effect on this type of reaction: e.g., it stabilizes "base-on" MeCbl by ~ 4 kcal mol^{-1}.

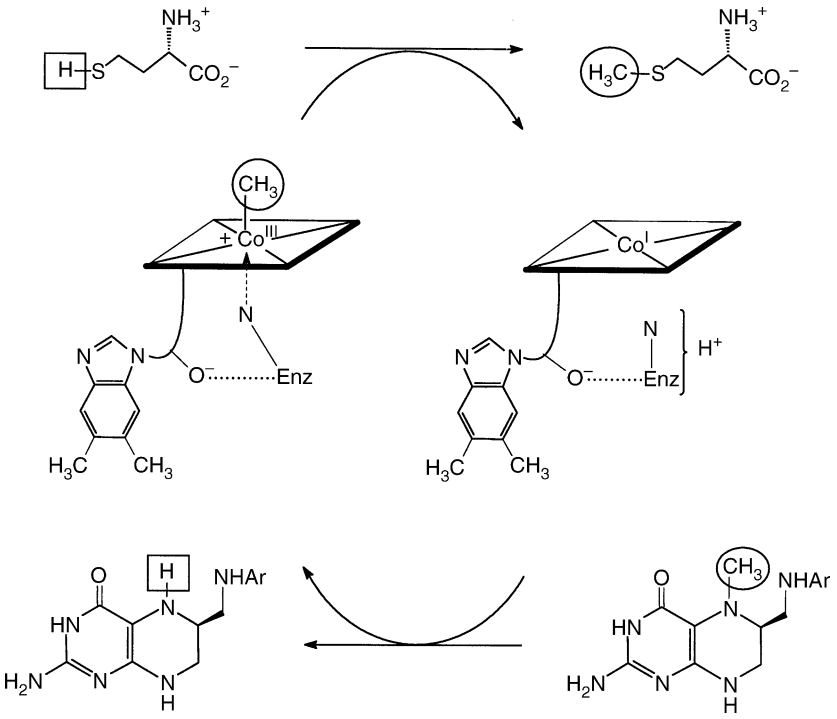

FIGURE 3 Biosynthesis of methionine by methylation of homocysteine is catalyzed by methionine synthase (MetH, Enz signifies the MetH-apoenzyme), where the bound corrinoid shuttles between MeCbl, in a "base-off/His-on" form, and cob(I)alamin.

Organometallic B_{12}-derivatives are rather resistant against proteolytic cleavage of the (Co–C)-bond under physiological conditions, crucial for the cofactor role of the B_{12}-coenzymes, but they are very sensitive to visible light, which induces the homolysis of the (Co–C)-bond.

B_{12}: Biosynthesis and Total Synthesis

The natural corrinoids are made exclusively by microorganisms, which are used for the industrial production of vitamin B_{12} (world output ~10 tons per year). A "last" common intermediate in the biosynthesis of the corrins and of other porphyrinoids is the tetra-pyrrole uroporphyrinogen III. The 'corrin pathway' separates off with the sequential incorporation of 'extra' methyl groups into the reduced ligand. A major difference of the two main biosynthetic paths in aerobic and in anaerobic microorganisms concerns the timing of the cobalt insertion on the way to cobalt-containing corrins. The nucleotide portion of the "complete" corrinoids is then built-up in the later phases of the B_{12}-biosynthesis, beginning at the stage of cobalt-adenosylated cobyric acid.

The total synthesis of vitamin B_{12} was achieved in the 1970s in the laboratories of Eschenmoser and Woodward. This conquest of the B_{12}-structure by abiotic synthesis led to the "incomplete" corrinoid cobyric acid first, to which the nucleotide part was attached in a specific way. The Co(II)-ion was incorporated easily into the corrin ligand, but attempts to remove cobalt from intact natural corrinoids have not been successful.

B_{12}-Dependent Enzymatic Reactions

B_{12}-Dependent Methyl Transferases

The reactivity of the "supernucleophilic" Co(I)-corrins and of methyl-Co(III)-corrins makes B_{12}-derivatives well-suited as cofactors in B_{12}-dependent enzymatic methyl group transfer reactions, which are widely relevant in many organisms. Anaerobic acetogenesis, methanogenesis and catabolism of acetic acid to methane and carbon dioxide make use of B_{12}-catalyzed enzymatic methyl transfer reactions. Various substrates act as sources of methyl groups, such as methanol, aromatic methyl ethers, methyl amines or N^5-methyltetrahydropterins (such as N^5-methyltetrahydrofolate). Thiols are the methyl group acceptors in methanogenesis and in methionine synthesis. In the anaerobic biosynthesis of acetyl-coenzyme A from one-carbon precursors the methyl group acceptor is suggested to be the nickel center of an Fe/Ni-cluster.

B_{12}-dependent methionine synthesis is one of the two essential roles of B_{12} in mammalian metabolism. In methionine synthase of *Escherichia coli* (MetH) B_{12}-dependent methyl transfer involves a sequential mechanism, in which tetrahydrofolate and methionine are formed and homocysteine and N^5-methyltetrahydrofolate act as methyl group acceptors and donors, respectively (see Figure 3). MetH is a modular protein, where the B_{12}-binding domain is bound to an N^5-methyltetrahydrofolate-binding module, the homo-cysteine-binding module and a reactivating module (that binds S-adenosyl-methionine). During turnover MetH catalyzes two methyl group transfer reactions which occur with an overall retention of configuration (consistent with two inversions). In a formal sense, these methyl-transfer reactions are SN_2 reactions with heterolytic cleavage/formation of the (Co–CH_3)-bond.

X-ray crystal analysis of the B_{12}-binding domain of MetH provided the first insight into the structure of a B_{12}-binding protein. This work revealed the cobalt-coordinating DMB-nucleotide tail of the bound cofactor MeCbl to be displaced by a histidine and to be anchored in a pocket of the protein. Accordingly, in MetH the corrinoid cofactor is bound in a "base-off/His-on" constitution. The crucial cobalt-ligating histidine residue is part of a Gly-X-X-His-X-Asp-sequence, which is conserved in a group of B_{12}-binding proteins.

Coenzyme B_{12}-Dependent Enzymes

About ten coenzyme B_{12}-dependent enzymes are now known. These enzymes are four carbon skeleton mutases, diol dehydratase, glycerol dehydratase, ethanolamine ammonia lyase, two amino mutases, and B_{12}-dependent ribonucleotide reductase. Of these AdoCbl-dependent enzymes, only methylmalonyl-CoA mutase is indispensable in human metabolism.

The coenzyme B_{12}-dependent enzymes perform transformations, that are difficult to achieve by typical "organic" reactions. With the exception of the enzymatic ribonucleotide reduction, the results of the coenzyme B_{12}-catalyzed enzymatic reactions formally correspond to isomerizations with vicinal exchange of a hydrogen atom and of a group with heavy atom centers. Homolytic cleavage of the (Co–C)-bond of the protein-bound AdoCbl to a 5′-deoxy-5′-adenosyl radical and cob(II)-alamin (B_{12r}) is the entry to H-abstraction reactions induced by the 5′-deoxy-5′-adenosyl radical. The AdoCbl-dependent enzymes rely upon the reactivity of bound organic radicals, which are formed (directly or indirectly) by a H-atom abstraction by the 5′-deoxy-5′-adenosyl radical. The substrate radicals rearrange rapidly to the product radicals in a (pseudo-)intramolecular rearrangement and without noticeable participation of the bound B_{12r} (i.e., the corrinoid is a "spectator").

The major tasks of the enzymes thus concern the enhancement of the critical radical reactions, the reversible generation of the radical intermediates and the protection of the proteins from nonspecific radical chemistry.

Coenzyme B_{12}-Dependent Carbon Skeleton Mutases

Methylmalonyl-CoA mutase interconverts *R*-methylmalonyl-CoA and succinyl-CoA. Binding of the substrate triggers the homolysis of the (Co–C)-bond of the bound AdoCbl. The radical carbon skeleton rearrangement reaction then proceeds, as outlined in Figure 4.

In all coenzyme B_{12}-dependent carbon skeleton mutases (methylmalonyl-CoA mutase (MMCM), glutamate mutase (GM), methyleneglutarate mutase, isobutyryl-CoA mutase) the B_{12}-binding motif (Gly-X-X-His-X-Asp) occurs. Consistent with this, the B_{12}-cofactor is bound "base-off/His-on" at the interface between the B_{12}-binding and the substrate-activating domains. The B_{12}-binding domain in MMCM, the B_{12}-binding subunit in GM and even the B_{12}-binding domain of MetH exhibit high sequence homology. Such a homology does not extend to the substrate-binding domains of these enzymes. The crystal structures of MMCM (from *Propionibacterium shermanii*) and GM (from *Clostridium cochlearium*) are available. The X-ray

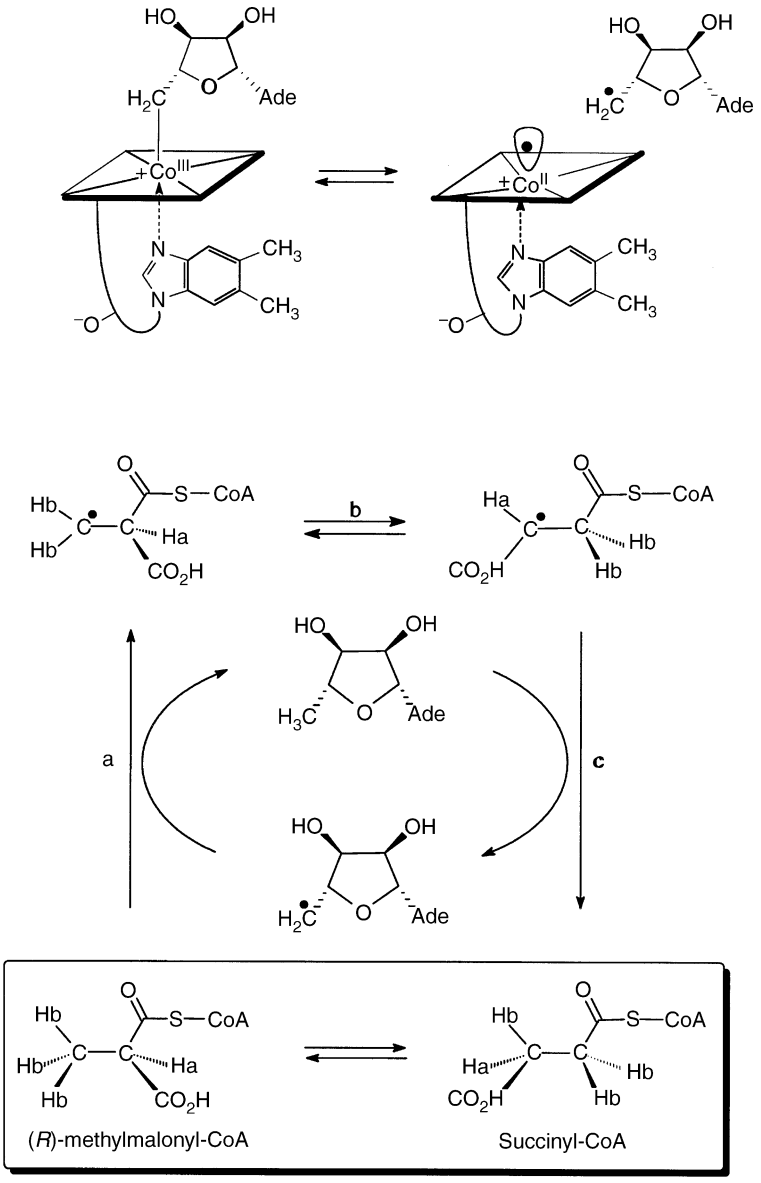

FIGURE 4 Top: coenzyme B_{12} (AdoCbl) is a reversible source of the 5′-deoxy-5′-adenosyl radical and cob(II)alamin (B_{12r}). Bottom: methylmalonyl-CoA mutase interconverts (*R*)-methylmalonyl-CoA and succinyl-CoA. This rearrangement is proposed to involve H-atom abstraction (step a), radical rearrangement (step b) and back transfer of H-atom (step c). (Formation of the 5′-deoxy-5′-adenosyl radical from protein bound AdoCbl is substrate triggered.)

analysis of MMCM provided the first crystal structure of a coenzyme B_{12}-dependent enzyme. Detailed crystallographic analysis of GM with bound AdoCbl revealed a likely structural basis for the operation of the radical mechanism in AdoCbl-dependent mutases: the ribose part of the 5′-deoxyadenosyl moiety is present in two conformations, related to each other by a pseudorotation of the furanose ring. The solution structure of the B_{12}-binding subunit of GM from *Clostridium tetanomorphum* (analyzed by heteronuclear NMR) provided a first structure of a cofactor-free B_{12}-binding protein and indicated it to be largely preorganized for B_{12}-binding.

In contrast to MMCM and GM, the crystal structure of the AdoCbl-dependent diol dehydratase from *Klebsiella oxytoca* showed the corrinoid to be bound "base-on" at the interface of the B_{12}-binding and of the substrate-binding subunits.

B_{12}-Dependent Ribonucleotide Reductase

In all organisms, ribonucleotide reductases (RNRs) play essential roles in the biosynthesis of DNA by catalyzing the reduction of nucleoside di- or triphosphates to the corresponding 2′-deoxynucleotides. The RNRs use various metal cofactors to initiate the nucleotide reduction by a radical reaction. The reductase from *Lactobacillus leichmanii* (RNR-*Ll*) uses AdoCbl as cofactor and nucleoside triphosphates as substrates, while 2′-deoxynucleoside triphosphates are allosteric effectors. In RNR-*Ll* the (Gly-X-X-His-X-Asp)-"B_{12}-binding motif" is absent and ESR-spectroscopy and crystallography showed "base-on" binding of the B_{12}-cofactor. In RNR-*Ll* homolysis of the bound AdoCbl generates a protein-centered thiyl-radical, which then induces the radical reactions that lead to the reductive removal of the 2′-OH group of the ribonucleotide.

Other B_{12}-Dependent Enzymatic Transformations

Methanogens and acetogens dechlorinate chloromethanes with reduced metal cofactors (corrinoids, in particular). Environmentally relevant microbiological dehalogenation reactions of chloroethenes were found recently. The anaerobe *Dehalospirillum multivorans* uses tetrachloroethene as the terminal electron acceptor, which is dechlorinated by a B_{12}-dependent tetrachloroethene reductive dehalogenase to trichloroethene and (then) *cis*-trichloroethene.

B_{12}: Medical Aspects

B_{12}-deficiency was found in the last century to be the cause for "pernicious anemia." Recently B_{12}-deficiency was recognized as a rather common condition with older persons. In most cases B_{12}-deficiency results from impaired uptake from the ingested food. A dose of about 3–4 μg per day of B_{12} are considered necessary for sustained physical well-being. In the human body B_{12} is metabolically active as MeCbl and as AdoCbl.

Three soluble B_{12}-binding proteins are known to be involved in the uptake and transport of cobalamins in humans: intrinsic factor (IF), transcobalamin (TC) and haptocorrin (HC). These three genetically related B_{12}-binders (apparent binding constants of $>10^{12}\,l\,mol^{-1}$) ensure that the needed amounts of B_{12} reach the two enzymes, methionine synthase (in the cytosol) and methylmalonyl-CoA mutase (in the mitochondria). IF is synthesized in the stomach and binds cobalamins in the small intestines. The IF-cobalamin complex is absorbed by specific receptors on the brush borders of the epithelial cells in the small intestines. Intracellular B_{12}-trafficking depends upon a complex interplay between the B_{12}-binders and cellular surface receptors that recognize complexes between B_{12} and the B_{12}-binding proteins IF, TC, and HC.

See Also the Following Articles

Giant Mitochondria (Megamitochondria) • Inorganic Biochemistry • Porphyrin Metabolism • Propionyl CoA–Succinyl CoA Pathway

Glossary

heteronuclear NMR Nuclear magnetic resonance (NMR) experiments that correlate nuclei of different elements (e.g., ^{1}H and ^{13}C) to obtain information on their mutual positions in a molecule (or a supramolecular complex).

organic radical Highly reactive organic molecules with unpaired electrons.

pernicious anemia Microscopic abnormalities of blood and bone marrow correlating with B_{12}-deficiency.

Further Reading

Banerjee, R. (1999). *Chemistry and Biochemistry of B_{12}*. Wiley, New York.

Buckel, W., and Golding, B. T. (1996). Glutamate and 2-methyleneglutarate mutase: From microbial curiosities to paradigms for coenzyme B_{12}-dependent enzymes. *Chem. Soc. Rev. (London)* **25**, 329–338.

Eschenmoser, A. (1988). Vitamin B_{12}: Experiments concerning the origin of its molecular structure. *Angew. Chem. Int. Ed. Engl.* **27**, 5–40.

Kratky, C., and Gruber, K. (2002). Coenzyme B_{12} dependent glutamate mutase. *Curr. Opin. Chem. Biol.* **6**, 598–603.

Kräutler, B., and Ostermann, S. (2003). Structure, reactions and functions of B_{12} and B_{12}-proteins. In *The Porphyrin Handbook*, Vol 11, pp. 227–274.

Kräutler, B., Arigoni, D., and Golding, B. T. (eds.) (1998). *Vitamin B_{12} and B_{12}-Proteins*. Wiley-VCH, Weinheim, Germany.

Matthews, R. G. (2001). Cobalamin-dependent methyltransferases. *Acc. Chem. Res.* **34**, 681–689.

Stubbe, J. (2000). Ribonucleotide reductases: The link between an RNA and a DNA World? *Curr. Opin. Struct. Biol.* **10**, 731–736.

Toraya, T. (2003). Radical catalysis in coenzyme B_{12}-dependent isomerization (eliminating) reactions. *Chem. Rev.* **103**, 2095–2127.

BIOGRAPHY

Bernhard Kräutler studied chemistry at the ETH (Zürich), where he did a dissertation with Prof. Albert Eschenmoser. He had postdoctoral association with Prof. Allen Bard (Austin, Texas) and Prof. Nick Turro (Columbia University). After return to the ETH he obtained his habilitation in organic chemistry (1985). Since 1991 he is a Professor of Organic Chemistry at the University of Innsbruck. His main research interests include bioorganic chemistry, porphyrinoid compounds, coenzyme B_{12}, chlorophyll, fullerenes, structure/function of biomacromolecules, and supramolecular chemistry.

Vitamin C

Robert B. Rucker and Francene Steinberg
University of California, Davis, California, USA

One of the most important redox cofactors in plant and animal systems is ascorbic acid or vitamin C. Although most animals make sufficient ascorbic acid, for some animals, ascorbic acid is a true vitamin because of their inability to carry out synthesis. For example, in humans, ascorbic acid deficiency can resulst in the nutritional disease scurvy, which causes a range of pathologic symptoms, because of defects in ascorbic-acid-specific enzymatic steps and processes.

In most plants and animals, ascorbic acid is derived as a product from the direct oxidation of glucose, galactose, and mannose (in plants), e.g., glucose or galactose → UDP-D-glucuronic acid → glucuronic acid/glucuronolactone → gulono-1, 4-lactone → ascorbic acid. In animals, a key enzyme in this process is L-gulonolactone oxidase (GLO, EC 1.1.3.8), which catalyzes the terminal step in ascorbic acid synthesis, i.e., gulono-1, 4-lactone is oxidized to ascorbic acid. L-gulonolactone oxidase resides in the kidney of most birds and reptiles, and during the course of evolution was transferred to the liver of mammals. For reasons that are not clear, the ability to express sufficient L-gulonolactone oxidase activity disappeared from the guinea pig, some fruit-eating bats, and most primates, including humans. Accordingly, a dietary source of ascorbic acid is needed in these animals. There is also a possibility that minor alternative pathways exist in plants and mammals for ascorbic acid synthesis.

Chemistry

The chemical designation for ascorbic acid is 2-oxo-L-theo-hexono-4-lactone-2, 3-enediol. Ascorbic acid is a near planar five-member ring with two chiral centers that resolves into the four stereoisomers. The oxidized form of ascorbic acid, dehydroascorbic acid, retains vitamin C activity and can exist as a hydrated hemiketal. Crystalline dehydro-L-ascorbic acid can exist as a dimer. The most important chemical property of ascorbic acid is the reversible oxidation of ascorbic acid to semidehydro-L-ascorbic acid and to dehydroascorbic acid (Figure 1).

In addition to facilitating reduction–oxidation reactions, ascorbic acid has the ability to form relatively stable free radical intermediates. Ascorbic acid can act as a free radical scavenger in reactions involving reactive oxidant species (ROS). In this regard, the rate constants for the generation of ascorbate radicals vary considerably, but often dictate rapid radical formation, e.g., 10^5–10^{10} $k_{obs}/M^{-1}\,s^{-1}$. Once formed, ascorbate (Asc) radicals decay relatively slowly by a process of disproportionation ($2\ Asc^{\cdot -} + H^+ \rightarrow AscH^- + DHA$). The ability to form free radical intermediates can significantly delay or prevent free radical-initiated oxidations. Ascorbic acid readily scavenges reactive oxygen and nitrogen species, such as superoxide, hydroperoxyl, peroxynitrite, and nitroxide radicals. Asc[H$^{-\cdot}$] donates a hydrogen atom ($H^{\cdot}$ or $H^+ + e^-$) to an oxidizing radical to produce the resonance-stabilized tricarbonyl ascorbate free radical. Asc[H$^{\cdot}$] has a pK_a of -0.86; thus, it is not protonated. Further, the unpaired electron of Asc [$-$] resides in the π-system that includes the tricarbonyl moiety of ascorbate. It is a weakly oxidizing and reducing radical. Due to its π-character, Asc [$-$] does not react with oxygen to form peroxyl radicals capable of damaging oxidations. It is relatively unreactive with a one-electron reduction potential of only $+282$ MV, and as such is considered a terminal, small-molecule antioxidant.

Ascorbic acid is often associated with the protection of lipid, DNA, and proteins from oxidants. As examples, when peroxyl radicals are generated in plasma, vitamin C is consumed faster than other antioxidants, e.g., uric acid, bilirubins, and vitamin E. Ascorbic acid is 10^3 times more reactive than a polyunsaturated fatty acid in reacting with peroxyl radicals. In contrast, ascorbic acid can be viewed as a pro-oxidant under aerobic condition when metals capable of redox ($Fe^{+2} \leftrightarrow Fe^{+3}$; $Cu^{+1} \leftrightarrow Cu^{+2}$) are also present. Metals, such as iron and copper in their reduced states, are effective Fenton catalysts.

With regard to other chemical properties, the acidity of ascorbic acid is due to the low pK_a of the proton on oxygen-3. In addition, ascorbic acid is not very stable in aqueous media, wherein it can decay within a few hours or even minutes at high pH (>10.0). In contrast, ascorbic acid is relatively stable in blood (a day or more), or if stored at acid pH (<3.0) or below -20°C (often weeks to months).

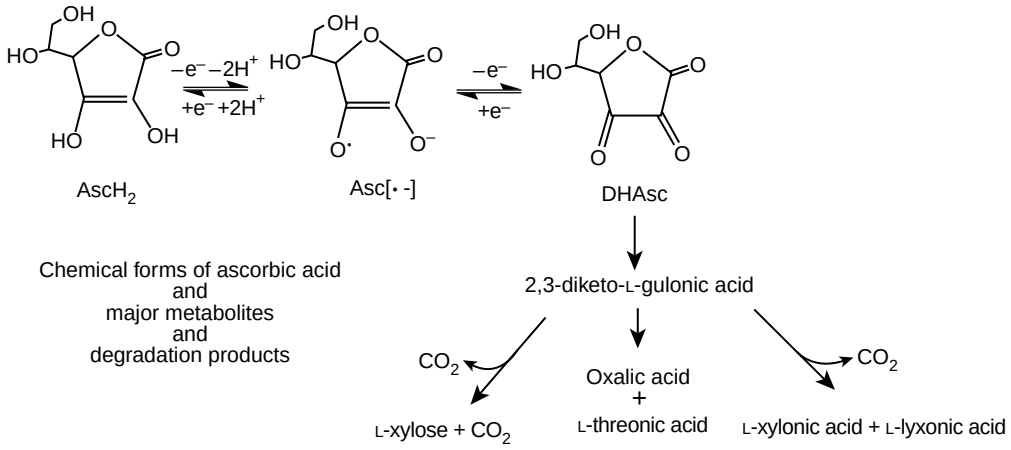

FIGURE 1 The major redox forms of ascorbic acid are shown in addition to products that result from both the chemical and enzymatic degradation of ascorbic acid. In alkaline solutions ascorbic acid is easily modified to 1 carbon (CO_2) and various 5-carbon compounds (e.g., xylonic acid, lyxonic acid) or the 2-carbon compound, oxalic acid and the 4-carbon compound, L-threonic acid. In addition, L-xylose and CO_2 may be formed *in vivo* following decarboxylation at the C-1 position of ascorbic acid followed by reduction.

Nutritional and Biochemical Importance

Ascorbic acid functions in many mono- and dioxygenases to maintain metals in a reduced state. For example, mono- and dioxygenases usually contain copper or iron as redox cofactors, respectively. As an additional characteristic, dioxygenases require α-ketoglutarate and O_2 as cosubstrates in reactions, while mono-oxygenases require only O_2. Important reactions and processes that require ascorbic acid include:

- Norepinephrine synthesis – dopamine-β-hydroxylase, EC 1.14.17.1, is the final and rate-limiting step in the synthesis of norepinephrine and requires copper and ascorbic acid for activity.
- Hormone activation – posttranslational steps involving α-amidations activate many hormones and hormone-releasing factors. Examples of hormone activation include melanotropins, calcitonin, releasing factors for growth hormone, corticotrophin and thyrotropin, pro-ACTH, vasopressin, oxytocin, cholecystokinin, and gastrin. Petidylglycine α-amidating monooxygenase (EC 1.14.17.3), the enzyme that carries out α-amidation is found in secretory granules of neuroendocrine cells.
- Carnitine Biosynthesis – ascorbate is a cofactor for two of the hydroxylation steps in the pathway of carnitine biosynthesis, gamma-butyrobetaine hydroxylase and epsilon-N-trimethyllysine hydroxylase. Ascorbate deficiency results in as much as 50% decrease in carnitine in heart and skeletal muscle in animals that require ascorbic acid.
- Prolyl and lysyl hydroxylations – ascorbic acid is an important cofactor in the hydroxylation of proline and lysine amino acid residues. In scurvy, poor wound healing, bruising, and osteopenic abnormalities can result from the under-hydroxylation of collagens. The various types of collagens are distinguished by their relative amounts of hydroxyproline and hydroxylysine. Hydroxylation of proline and lysine is important in collagen assembly and maturation into fibers. Because collagen is the principal connective tissue protein in the body, it is essential to all phases of normal growth, development, and repair. There are also other proteins that are not defined as collagens, which contain hydroxyproline, e.g., the subcomponent C1q of complement, acetylcholine esterase, pulmonary surfactant proteins, and proteins that function as cell surface receptors. In plants, prolyl hydroxylase hydroxylates proline residues in cell wall hydroxyproline-rich glycoproteins required for cell division and expansion. Approximately 50 hydroxyproline-containing proteins have been identified in viruses and bacteria, wherein ascorbic acid may also play a role as cofactor.

Along with glutathione, ascorbic acid is also an important nonenzymatic antioxidant/reductant in the water-soluble compartment of cells. Glutathione is L-(-glutamyl-L-cysteine-glycine (GSH). The antioxidant actions of glutathione and ascorbate are closely linked and involve mechanisms in which decreased glutathione may even stimulate ascorbic acid synthesis in those animals that can produce it. During postnatal development, a rapid change occurs as animals adapt, from a relatively hypoxic to a relatively hyperoxic environment. In this regard, one of glutathione's many functions is to keep ascorbic acid in a reduced form. In adult animals that can make ascorbic acid, a reduction in glutathione levels can lead to a rapid increase in liver dehydroascorbic acid. An adequate ascorbic acid intake is

particularly important in newborns and neonates, who do not yet have the potential to synthesize ascorbate. A deficiency of both ascorbic acid and glutathione can cause severe damage to liver and other organs.

With regard to plants, ascorbic acid reaches a concentration of over 20 mM in chloroplasts and occurs in all cell compartments, including the cell wall. It has a major role in photosynthesis, acting in the Mehler peroxidase reaction with ascorbate peroxidase to regulate the redox state of photosynthetic electron carriers and as a cofactor for violaxanthin de-epoxidase, an enzyme involved in xanthophyll cycle-mediated photoprotection. Ascorbic acid also serves as a cofactor in metabolic pathways important to ethylene, gibberellins, and anthocyanins. There is a rapid response of ascorbate peroxidase expression to (photo)-oxidative stress. Of interest, the ascorbate-deficient vtc 1 mutant of *Arabidopsis thaliana*, is very sensitive to ozone, ultraviolet-B radiation, and other forms of oxidant stress.

Cellular Regulation of Ascorbic Acid

Specific non-overlapping transport proteins mediate the transport of ascorbic acid across biological membranes. Dehydroascorbic acid uptake is via the facilitated-diffusion glucose transporters, (GLUT 1, 3, and 4), but under physiological conditions these transporters do not appear to play a major role in the uptake of dehydroascorbic acid due to the high concentrations of glucose that effectively block influx. L-ascorbic acid enters cells via Na^+-dependent systems. Two isoforms of these transporters have recently been cloned from human and rat sources, which differ in their tissue distribution. Cell accumulation of ascorbic acid occurs, because of cellular dehydroascorbate reduction systems that are capable of rapidly generating ascorbic acid.

In addition to cell regulation, ascorbate reduction systems are also important in reducing the ascorbic acid radical. As indicated, the ascorbic acid radical is relatively stable. An accessory enzymatic system is needed to reduce the potential of transient accumulation of the ascorbate radical. Excess ascorbate radicals may initiate free radical cascade reaction or nonspecific oxidations. In plants, NADH-monodehydroascorbate reductase (EC 1.6.5.4) has evolved to maintain ascorbic acid in its reduced form. NADH-monodehydroascorbate reductase plays a major role in stress-related responses in plants. In animal tissues, glutathione dehydroascorbate reductase (EC 1.8.5.1) serves this purpose.

Digestion, Absorption, and Nutritional Requirements

When ascorbic acid is consumed in the diet, the ileum and jejunum are major sites of ascorbic acid absorption. The bioavailability of vitamin C is dose dependent. In humans, saturation of transport occurs with dosages of 200–400 mg per day. Approximately 70% of a 500 mg dose is absorbed. However, much of the absorbed dose (>50%) is nonmetabolized and excreted in the urine. With a dose of 1250 mg, only 50% of the dose absorbed and most (>85%) of the absorbed dose is excreted. Vitamin C is not protein-bound and is eliminated with an elimination half-life of 10–12 hours. In Western populations plasma, vitamin C concentrations range from 54 to 91 $\mu mol\,l^{-1}$. Tissue concentrations range from μM to mM, i.e., high tissue levels of vitamin C are well tolerated in mammalian systems and lead to the conclusion that ascorbic acid is relatively nontoxic, although there is also some evidence that accelerated metabolism or disposal of ascorbic acid may occur after prolonged supplementation of high doses.

Sources and Detection

A number of approaches are available for ascorbic acid detection. Ascorbic acid absorbs strongly in UV light, the basis for some spectrophotometric assays. The redox properties of ascorbic acid allow for electrochemical detection or detection from interacting with redox-sensitive chromophores and dyes. Enzymatic methods (using ascorbate oxidase) and conventional and isotope ratio mass spectrometry are used for detection and quantitation of ascorbic acid following separation by means of ion exchange, absorption or partition chromatographic approaches. Typical food and tissue values are given in Table I.

Defining Ascorbic Acid Status

The requirements for vitamin C in humans (given as the range for female–male and expressed as the recommended dietary allowance, RDA or adequate uptake, AI) are as follows: infants, 40 mg per day (AI based on what is present in human milk); children (3–13 years), 15–45 mg per day (extrapolated from the RDA for adults); adolescence, 45–65 mg per day; adults (>19 years), 75–90 mg per day; lactating mothers, 115–120 mg per day. In keeping with these estimates, more recent clinical investigations have noted vitamin C deficiency in 2–6% of individuals surveyed (often defined as individuals meeting less than two-thirds of the RDA). With regard to marginal vitamin C status

TABLE I

Vitamin C in Selected Foods and Tissues

Sources of vitamin C	Mg of ascorbic acid per 100 g of wet weight or edible portion
Animal products	
Cow's milk	0.5–2
Human milk	3–6
Beef, pork, veal	2–10
Liver, chicken	15–20
Kidney, chicken	6–8
Heart, chicken	5
Crab muscle, lobster	1–4
Shrimp	2–4
Fruits	
Apple	3–30
Banana	8–16
Blackberry	8–10
Cherry	15–30
Currant, red	20–50
Currant, black	150–200
Grapefruit	30–70
Kiwi fruit	80–90
Lemon, orange	40–50
Melon	9–60
Strawberry	59–70
Pineapple	15–25
Rose hips	250–800
Vegetables	
Beans, various	10–15
Brussels sprouts	100–120
Cabbage	30–70
Carrot	5–10
Cucumber	6–8
Cauliflower	50–70
Eggplant	15–20
Chive	40–50
Kale	70–100
Onion	10–15
Peas	8–12
Potato	4–30
Pumpkin	15
Radishes	25
Spinach	35–40
Condiments	
Chicory	30–40
Coriander (spice)	90
Garlic	15–25
Horseradish	50
Lettuce, various	10–30
Leek	15
Parsley	200–300
Pepper, various	150–200

based on plasma ascorbic acid values, e.g., <20 μg/dL, the prevalence ranges from 17 to 24% US. In this regard, smokers are more likely to have marginal vitamin C status compared to nonsmoking adults. Several studies suggest that smokers require over 200 mg vitamin C daily to maintain plasma vitamin C concentrations at a level equivalent to that of nonsmokers.

Summary

Ascorbic acid usually carries out redox reactions by mechanisms dependent upon free-radical processes. Ascorbate metabolism is linked to the metabolism of glutathione. Ascorbic acid is also required in animals that lack or have mutations in the gene for L-gulonolactone oxidase. Ascorbic deficiency results in reduced mono- and dioxygenase activities. The consequences of severe deficiency are profound, since growth, extracellular matrix, and hormonal regulation are impaired. Recent data suggest optimal intakes of ascorbic acid, based on a range of criteria, should be as high as 75–90 mg per day for adult humans.

See Also the Following Articles

Carnitine and β-Oxidation • Peptide Amidation

Glossary

adequate intake (AI) One of the four terms used to define dietary reference intakes (DRIs), which are reference values that are quantitative estimates of nutrient intakes to be used for planning and assessing diets for healthy people. The AI is used when the RDA for a nutrient is not available. It is an RDI that is based on observed or experimentally determined approximations of nutrient intake by a group of healthy people.

amidation A complex reaction, which in some hormones results in a C-terminal protein modification. A C-terminus consensus sequence is required. The consensus is glycine, followed by two basic amino acids (Arg or Lys). The end product is an amide of glycine ($-NH-CH_2-CO-NH_2$) with loss of the basic amino acid residues.

anthocyanins Naturally occurring compounds that impart color to fruit, vegetables, and plants. They also have antioxidant and insecticidal properties.

carnitine Essential component of fatty acid transport into and out of mitochondria for their eventual oxidation. Carnitine is derived from the amino acid lysine following extensive modification.

complement A term originally used to refer to the heat labile factor in serum that causes immune cytolysis, the lysis of antibody-coated cells. The term now refers to the entire functionally related system comprising at least 20 distinct serum proteins that is the effector immune cytolysis and other biologic functions immune system related functions.

dioxygenase An oxidoreductase that incorporates two atoms of oxygen (from one molecule of O_2) into the (reduced) substrate.

Fenton reaction The formation of $OH^{\cdot}$, OH^-, and Fe^{3+} from the nonenzymatic reaction of Fe^{2+} with H_2O_2.

gibberellins Plant hormones that stimulate growth in the stem and leaves, and trigger the germination of the seed

Mehler reaction Describes the photoreduction of oxygen in chloroplasts by photosystem I in plants yielding $O_2^{\cdot -}$.

monooxygenase Oxidoreductases that induce the incorporation of one atom of oxygen from O_2 into the substance being oxidized.

recommended dietary allowance (RDA) The average daily dietary intake level that is sufficient to meet the nutrient requirement of nearly all (97–98%) healthy individuals in a group.

redox oxidation–reduction reactionary reaction in which electrons are removed from one molecule or atom and given to another molecule or atom.

transporter A class of transmembrane protein that allows substances to cross plasma membranes far faster than would be possible by diffusion alone. A major class of transport proteins that expend energy to move substances (called active transport) are the transport ATPases.

violaxanthin Photopigment involved in photoprotection in plants. When light energy absorbed by plants becomes excessive (relative to the capacity of photosynthesis), the xanthophyll (a chemical classification designation), violaxanthin is reversibly modified by violaxanthin de-epoxidase as a protective function in plants.

Further Reading

Frei, B. (ed.) (1994). *Natural Antioxidants in Human Health and Disease*. Academic Press, San Diego.

National Academy Press (2000). *Dietary Reference Intakes for Vitamin C, Vitamin E, Selenium, and Carotenoids*. A report of the Panel on Dietary Antioxidants and Related Compounds, Subcommittees on Upper Reference Levels of Nutrients and Interpretation and Uses of Dietary Reference Intakes, and the Standing Committee on the Scientific Evaluation of Dietary Reference Intakes, Food and Nutrition Board, Institute of Medicine, National Academy Press, Washington, DC.

Packer, L., and Fuchs, J. (eds.) (1997). *Vitamin C in Health and Disease*. Marcel Dekker, New York.

Simopoulos, A. P (Vol. Ed.) (1991). Selected vitamins, minerals, and functional consequences of maternal malnutrition. In *The Series World Review of Nutrition and Dietetics*,Vol. 64, Karger, Basel, New York.

Biography

Robert Rucker is a Professor of Nutrition and Internal Medicine at the University of California, Davis. Dr. Rucker's research interests are focused on extracellular matrix assembly, the role of micronutrients in early growth and development, and the physiological roles of quinone cofactors derived from tyrosine, such as pyrroloquinoline quinone. He holds a Ph.D. from Purdue University. Honors and appointments include serving as a past president of the *American Society for the Nutritional Sciences*, serving as an associate editor for the *American Journal of Clinical Nutrition*, receiving the Borden Research Award from the *American Society for Nutritional Sciences*, and recognition as a Fellow of the AAAS.

Francene Steinberg is an Associate Professor in the Department of Nutrition at UC Davis and Director of the Didactic Program in Dietetics. She received the Ph.D. in nutrition at UC Davis, received additional postdoctoral training in the Department of Endocrinology at the University of Washington. She is also a registered Dietitian. Dr. Steinberg's research area concerns the metabolism of lipids and lipoproteins, with an emphasis on the effects of nutrition on cardiovascular disease risk and the development of atherosclerosis. Areas of particular interest include dietary soy phytoestrogens, structured lipids, and antioxidant vitamins.

Vitamin D Receptor

Diane R. Dowd and Paul N. MacDonald
Case Western Reserve University, Cleveland, Ohio, USA

The vitamin D receptor is a member of the nuclear receptor/steroid hormone receptor superfamily. These receptors function as ligand-activated, transcriptional regulatory proteins. Thus, the vitamin D receptor selectively binds the 1,25-dihydroxyvitamin D_3 [1,25$(OH)_2D_3$] hormone and controls the expression of selected genes in target cells. The main actions of 1,25$(OH)_2D_3$, VDR, and the vitamin D endocrine system are to maintain overall calcium and mineral homeostasis. A fundamental physiological role is to maintain adequate absorption of dietary calcium at the level of the small intestine. Dietary deficiency of vitamin D or mutations in the vitamin D receptor result in human conditions of hypocalcemia and secondary skeletal undermineralization. The molecular details involved in vitamin D-regulated gene expression by the VDR in key mineral regulating tissues such as the intestine, kidney, and bone are revealing important insights into the manner in which our bodies maintain the structural integrity of skeletal tissue.

Introduction

Vitamin D_3, or cholecalciferol, was discovered nearly a century ago as a micronutrient that is essential for normal skeletal development and for maintaining bone integrity. 1,25$(OH)_2D_3$ is the bioactive, hormonal form of vitamin D. However, vitamin D_3 is more appropriately classified as a hormone since it is produced in the body in response to serum calcium levels and it functions through a mechanism that is analogous to other steroid hormones. It is generated by two sequential hydroxylations of vitamin D_3 in response to hypocalcemia and elevated parathyroid hormone. The predominant role of 1,25$(OH)_2D_3$ is to enhance the intestinal absorption of dietary calcium and phosphorus. 1,25$(OH)_2D_3$ also acts on mineral-regulating target tissues such as intestine, bone, kidney, and parathyroid glands to maintain normal calcium and mineral homeostasis. 1,25$(OH)_2D_3$ also directly affects skeletal bone remodeling by causing osteoblasts to terminally differentiate into osteocytes and deposit calcified matrix. 1,25$(OH)_2D_3$ also promotes the differentiation of precursor cells into mature osteoclasts which function to resorb bone and maintain appropriate bone remodeling. Thus, it is through an integrated series of diverse effects that vitamin D is thought to preserve and maintain the integrity of the bony tissues. To highlight this role, vitamin D_3 deficiency leads to rickets in children and osteomalacia in adults. The vitamin D endocrine system is also involved in a number of other important physiological processes including blood pressure regulation, immune function, mammary gland development, and hair follicle cycling.

The biological effects of 1,25$(OH)_2D_3$ are mediated through a soluble receptor protein termed the vitamin D receptor (VDR), a member of the steroid receptor or nuclear receptor (NR) superfamily. The VDR binds 1,25$(OH)_2D_3$ with high affinity and high selectivity. In the target cell, the interaction of the 1,25$(OH)_2D_3$ hormone with VDR initiates a complex cascade of molecular events culminating in alterations in the rate of transcription of specific genes or gene networks (Figure 1). Central to this mechanism, is the requisite interaction of VDR with retinoid X receptor (RXR) to form a heterodimeric complex that binds to specific DNA sequence elements (VDREs) in vitamin D-responsive target genes and ultimately influences the rate of RNA polymerase II-mediated transcription. An emerging concept in this mechanism is that protein–protein interactions between the VDR–RXR heterodimer, transcriptional comodulatory proteins and the transcription machinery are essential for the mechanism of vitamin D-mediated gene expression. This article discusses the molecular biology of the VDR with a focus on the macromolecular interactions that are required for the transcriptional regulatory activity of the VDR.

Functional Domains of the VDR

The N-Terminal DNA-Binding Domain (DBD)

Receptors in the nuclear receptor superfamily generally have two transcriptional activation domains, termed activation function (AF) 1 and 2, which are required for the receptor to function as a ligand-activated

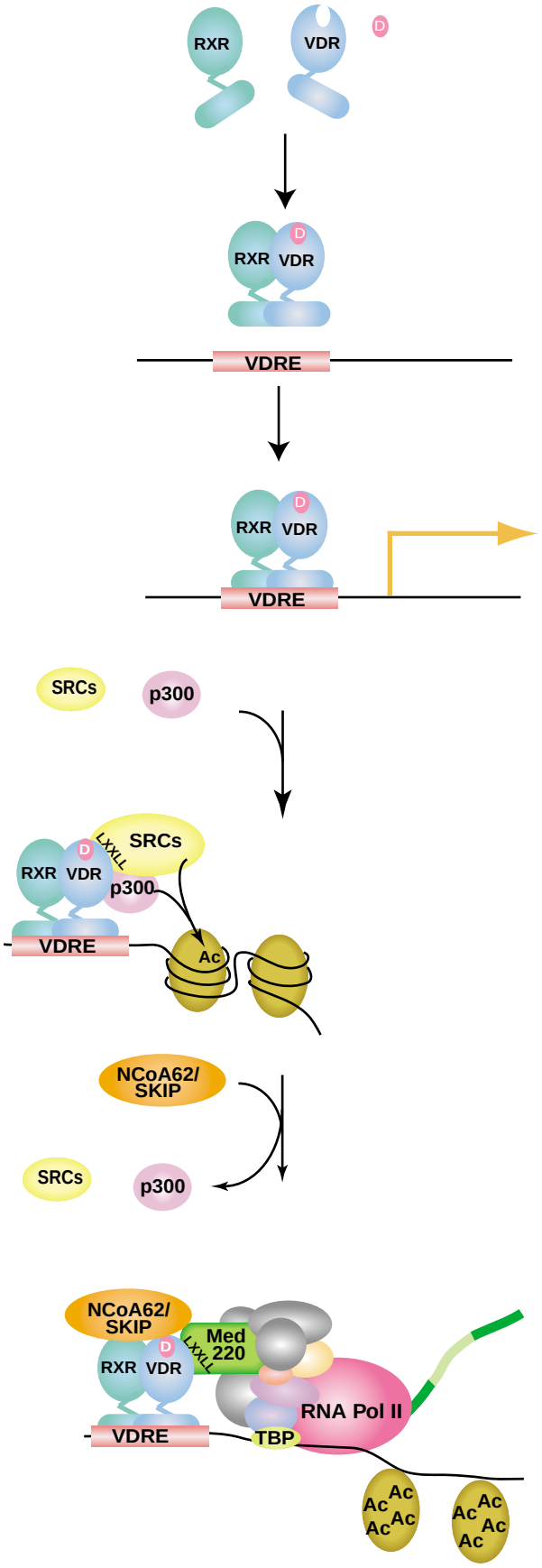

transcription factor. The AF-2 domain exists at the extreme COOH terminus while the AF-1 domain is located in the N-terminal region (or A/B domain) of the receptors (Figure 2). The AF-1 domain is a constitutive (i.e., hormone-independent) activation domain. In the VDR, the N-terminal A/B domain is truncated compared to other nuclear receptors and thus an analogous constitutive AF-1 domain is lacking in the VDR.

In order for VDR to regulate transcription of target genes, it must recognize and bind to DNA in the promoter regions of vitamin D-responsive genes. It does so through a specialized DNA-binding domain (DBD) located near the amino terminus of the receptor (Figure 3). This DBD is required for the VDR to bind selectively and with high affinity to specific DNA sequences termed vitamin D-responsive elements (VDREs). The minimal DBD of the VDR that mediates VDR–DNA interactions resides between amino acid residues 22 and 113 in the human sequence. There are nine cysteine residues within the DBD that are conserved throughout the family members. The first eight of these cysteines (counting from the N terminus) tetrahedrally coordinate two zinc atoms to form two zinc finger DNA-binding motifs. Mutation of the first eight of the nine cysteine residues to serines eliminates VDR binding to both nonspecific and specific DNA sequences and eliminates VDR-mediated transactivation. Indeed, inactivating mutations within the DBD of the human VDR are responsible for the rare inherited disorder termed vitamin D-resistant rickets type II. These patients express a nonfunctional VDR that cannot bind to DNA, and they exhibit classical symptoms of vitamin D deficiency that are not corrected by providing an external source of vitamin D.

Ligand-Binding Domain (LBD)

The large carboxyl-terminal ligand-binding domain (LBD) of VDR is organized into 12 α-helices. As the name suggests, the LBD is responsible for high-affinity binding of the 1,25$(OH)_2D_3$ ligand, exhibiting equilibrium binding constants of the order of 10^{-10} to

FIGURE 1 Mechanism of action of the vitamin D receptor. VDR binds to its ligand, 1,25$(OH)_2D_3$, heterodimerizes with RXR, and binds to a DR-3 type VDRE in the promoter of 1,25$(OH)_2D_3$-responsive genes. VDR occupies the proximal or 3′ half-site while RXR occupies the distal or 5′ half-site. VDR/RXR then recruits coactivators such as SRCs and p300/CBP. The HAT activity of these coactivators loosens the chromatin structure, allowing for a more transcriptionally permissive environment. SRCs and p300/CBP dissociate, allowing for binding of NCoA62/SKIP and the Mediator-D multimeric complex. This latter complex is thought to recruit RNA Pol II and the core transcriptional machinery to initiate active transcription of the target gene.

FIGURE 2 Functional domains of the VDR. A/B, amino terminal region; DBD, DNA- binding domain containing two zinc-finger motifs; LBD, ligand-binding domain; AF-2, activation function-2 domain encompassing helix 12.

10^{-11} M. Both the 1-hydroxyl and 25-hydroxyl moieties are crucial for efficient recognition by VDR, and the nonhydroxylated, inactive parent vitamin D_3 compound does not bind appreciably to the VDR.

In addition to hormone binding, the LBD is required for several other aspects of receptor function, particularly in mediating protein–protein interactions. One important protein–protein contact is the heterodimerization of VDR with the retinoid X receptor (RXR). As mentioned above, VDR–RXR heterodimer formation is generally required for high-affinity interaction of the receptor with VDREs and an extensive heterodimerization interface that coalesces around helices 10 and 11 in the LBD of VDR mediate protein–protein contacts with RXRs.

The LBD also mediates association of VDR with comodulatory proteins. Many of these interactions require at the extreme C-terminus of the receptor, where the AF-2 domain is located (Figure 2). The AF-2 domain is highly conserved throughout the hormone receptor superfamily and its main structural feature is that of an amphipathic α-helix. Removing 25 amino acids from the C-terminus of hVDR (Δ403–427), which contains the AF-2 domain, results in a complete loss of $1,25(OH)_2D_3$/VDR-activated transcription. This loss of function is not due to altered binding of RXR, VDRE, or hormone and the mutant receptor was appropriately targeted to the cell nucleus. Thus, the AF-2 domain of VDR, corresponding to helix 12, plays a central role in $1,25(OH)_2D_3$-activated transcription mediated by VDR.

Molecular Mechanism of Transcriptional Control by VDR

VDR Interaction with Vitamin D Responsive Elements

VDR modulates transcription by binding to specific VDREs, in the promoter regions of responsive genes. VDREs from a variety target genes have been identified and on this basis a consensus VDRE may be generally described as an imperfect direct repeat of a core hexanucleotide sequence,*G/AGGTG/CA*, with a spacer region of three nucleotides separating each half element (also termed DR-3 for direct repeat with a three nucleotide spacer). The mechanism of VDR binding to VDREs is reflected in the direct repeat nature of the element. For example, purified VDR alone does not bind to a VDRE with high affinity. Rather, RXR is required for high-affinity binding of VDR to VDREs. The asymmetry of the directly repeating motif causes the VDR–RXR heterodimer to bind to the VDRE with a defined polarity, with RXR occupying the 5′ half site and VDR occupying the 3′ half site.

The natural VDREs identified thus far provide only a snapshot of the DNA sequences that mediate the transcriptional effects of the VDR. Variations on the DR-3 motif for VDREs have been identified in the elements that mediate vitamin D responsiveness in the calbindin D_{9k} and calbindin D_{28k} genes. Moreover, several synthetic elements with large spacer regions and inverted arrangements can mediate vitamin D responsiveness under certain conditions. It is likely that the affinity of VDR for these atypical elements may vary from that of the classic DR-3 motif adding yet another level of regulatory complexity to the process of VDR-mediated gene expression.

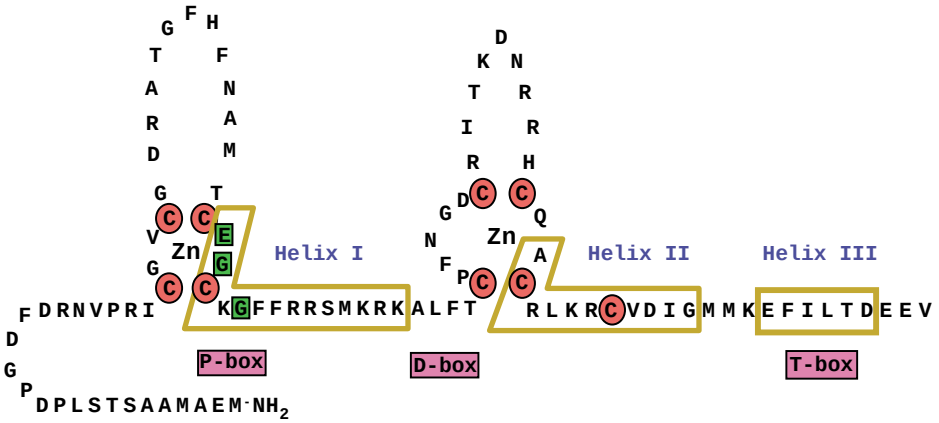

FIGURE 3 Schematic of the DNA-binding domain of the VDR. The cysteines responsible for coordinating the zinc atoms are shown in red.

One important role for the $1,25(OH)_2D_3$ ligand in the transactivation process is to dramatically enhance both the formation of the VDR–RXR heterodimer and the subsequent interaction of the heterodimer with the VDRE (Figure 1). Upon ligand binding, there is a clear $1,25(OH)_2D_3$-dependent decrease in the formation of VDR homodimers and a concomitant increase in VDR heterodimerization with RXR. These ligand-induced changes in VDR–RXR interactions are likely due to altered conformations of the VDR that disrupts weak homodimers of unliganded VDR and promotes liganded VDR heterodimerization with RXR. The interaction of VDR and RXR generates a heterodimeric complex that is highly competent to bind DR-3 like VDREs and subsequently affect the transcriptional process. Thus, the VDR–RXR heterodimer is the primary active complex involved in controlling DR-3 VDRE-driven promoters.

Communication between VDR and the Transcriptional Machinery

The regulation of VDR-mediated transcription involves a complex series of macromolecular interactions occurring in a temporally coordinated fashion (Figure 1). Other transcriptional components that associate with the liganded VDR/RXR heterodimer may be classified into two general categories: general transcription factors and the comodulatory proteins. The interaction of VDR with the first group results in direct contacts with the preinitiation complex (PIC), which may facilitate assembly or recruitment of the PIC and thereby stimulate transcription by RNA Pol II. Transactivator interaction with the PIC may occur via adapter proteins such as the TBP-associated factors (TAFs) or via direct interaction with other core transcription factors. In this regard, TFIIB may be a key target since it is known to interact directly with VDR and augment vitamin D-activated transcription in transient gene expression studies. Indeed, differences in the activities of NH_2-terminal VDR isoforms are attributed to differential interactions with TFIIB thus, supporting an important role for the VDR–TFIIB interaction in determining the overall transactivation potential of the liganded VDR.

In addition to direct contacts with the general transcription machinery, the liganded VDR is also linked to the transcriptional PIC by the NR comodulatory factors. The general functional properties of the NR comodulators are their ability to interact with nuclear receptors and control their transcriptional responsiveness to ligand. NR comodulators are classified either as coactivators or corepressors, and they aid in the induction or repression, respectively, of ligand/receptor-mediated transcription. NR coactivators may function as macromolecular bridges between the receptor and the transcriptional machinery that aid in the assembly or promote the stability of the preinitiation complex. Moreover, several coactivator proteins either possess intrinsic histone acetyltransferase (HAT) activities, or recruit other proteins that possess HAT activity (e.g., CBP/P300). Acetylation of histones near the promoter presumably results in a loosening of chromatin structure and greater accessibility of the promoter for the transcriptional machinery (Figure 1). The best-characterized coactivators are the steroid receptor coactivator (SRC) family of nuclear receptor coactivators that includes three members at present: SRC-1 (NCoA-1), SRC-2 (GRIP-1, TIF2, NCoA-2), and SRC-3 (pCIP, RAC3, ACTR, AIB-1, TRAM-1).

Structural studies of related receptors provide insight into the mechanism of ligand-induced interaction of VDR with SRC coactivators. It is hypothesized that the $1,25(OH)_2D_3$ ligand promotes coactivator interaction by inducing a repositioning of the AF-2 activation helix, or helix H12 (Figure 4). In the unliganded state, the AF-2 domain (helix H12) projects out away from the globular core of the LBD, while in the liganded state the AF-2 domain is folded over onto the LBD globular core domain. One outcome of helix H12 folding is the creation of a platform or protein interaction surface through which coactivator proteins such as SRCs effectively dock with the VDR. The domain in the coactivator proteins, which is responsible for this interaction is termed the nuclear receptor or NR box and is an amphipathic α-helix composed of the consensus core sequence LXXLL. This interaction is essential for transactivation mediated by the VDR.

A large multiprotein complex called Mediator D is another coactivator required for VDR-mediated transcription (Figure 1). Mediator D is also known as vitamin D receptor interacting protein (DRIP), thyroid receptor activating protein (TRAP) complex, and the mammalian mediator complex. The Mediator D complex is composed of at least ten different proteins anchored by Med220, which interacts directly with ligand-activated VDR/RXR heterodimers through one of two LXXLL motifs. DRIP is essential for *in vitro* VDR-mediated transcription from chromatinized templates. However, as the DRIP complex does not contain any SRCs and does not possess HAT activity, it appears to potentiate NR-mediated transcription through distinct mechanisms. In particular, DRIP directly recruits the RNA polymerase II holoenzyme to $1,25(OH)_2D_3$-activated VDR, indicating that DRIP may serve as a bridge between VDR and the core transcriptional machinery. Indeed, chromatin immuno-precipitation studies show that DRIPs enter transcriptional complexes at a later time than SRC coactivators, supporting the nonredundant roles of these coactivator classes in NR-mediated transactivation.

Another protein named NCoA62/SKIP was identified as a VDR and NR coactivator, and as such, it augments

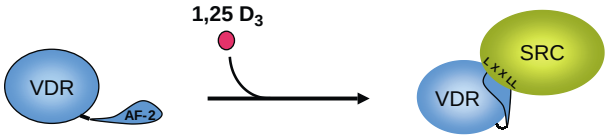

FIGURE 4 The vitamin D receptor undergoes a conformational change upon binding hormone. The VDR binds ligand and this induces a conformational change in the AF-2 domain to trap the ligand in the binding pocket. This change also creates a hydrophobic cleft or surface on VDR that LXXLL motifs in coactivator proteins use for docking to the VDR.

VDR- and other NR-activated transcriptional processes in transient reporter gene assays. On the basis of its primary amino acid sequence and its function, NCoA62/SKIP is a unique protein. One key difference is the lack of LXXLL motifs which are characteristic of a large variety of coactivators including the SRCs, CBP/P300 and the Mediator D coactivator complex. In addition, NCoA62 interacts with VDR in a ligand- and AF2-independent manner. Although NCoA62/SKIP does not interact directly with SRC coactivators, NCoA62/SKIP, VDR, and SRCs form a ligand-dependent ternary complex. NCoA62/SKIP also functions cooperatively with SRC coactivators to augment VDR-activated transcription and it is recruited to vitamin D responsive target genes in a distinct, temporal manner from the SRC coactivators. Presently, the mechanisms involved in this synergistic action of these two coactivator classes are unknown.

Summary

Research spanning the 1980s and 1990s reveals that $1,25(OH)_2D_3$-mediated transcription is more complex than the simple binding of the receptor to DNA and the recruitment of RNA Pol II to initiate transcription. VDR/RXR-activated transcription involves complex interactions that may occur in a spatially distinct and temporally coordinated fashion to increase the rate at which $1,25(OH)_2D_3$-responsive genes are transcribed and at which the resulting RNA transcript is processed. A model for VDR-mediated transcription is proposed which incorporates numerous properties of VDR that were discussed in this section (Figure 1). The initial event in this model is high-affinity binding of the $1,25(OH)_2D_3$ ligand to the VDR. Ligand binding induces VDR/RXR heterodimerization and the heterodimer specifically binds VDREs in the promoter regions of vitamin D responsive genes. The heterodimer then recruits coactivator molecules that acetylate core histones to make the DNA more accessible to the transcriptional machinery. Meanwhile, other coactivators and the PIC are recruited to the site and activated transcription proceeds. Understanding the complex interplay that occurs between these various factors is crucial to unraveling the complexities of activated or repressed transcription mediated by vitamin D and the VDR.

See Also the Following Articles

Calcium Buffering Proteins: Calbindin • Vitamin D • Zinc Fingers

Glossary

comodulatory proteins Proteins that interact directly with the nuclear receptor and alter the transcriptional regulatory activity of the receptor. Coactivators enhance the activity of the receptor, and corepressors attenuate the transcriptional regulatory activity of the receptor.

1,25-dihydroxyvitamin D_3 ($1,25(OH)_2D_3$) The active form of vitamin D in mammals.

histone acetyltransferase (HAT) Enzymes that add acetyl groups to the positively charged lysine residues on core histones, effectively negating the positive charge. Histone hyperacetylation is correlated with areas of active transcription, while hypoacetylation is correlated with nontranscribed promoters.

preinitiation complex (PIC) The complex of basic transcription factors that are necessary and sufficient for the initiation of transcription to occur. In addition to RNA Polymerase II, the PIC consists of transcription factor IIA (TFIIA), TFIIB, TFIIE, TFIIF, and TATA-binding protein or TBP.

retinoid X receptor (RXR) A member of the nuclear receptor superfamily of transcription factors that serves as a common heterodimeric partner for many of the class II nuclear receptors including retinoic acid receptor, vitamin D receptor, thyroid hormone receptor, and peroxisome proliferator-activating receptor.

vitamin D responsive elements (VDRE) Specific sequences of DNA that the VDR–RXR heterodimer selectively recognize and bind. This binding event is one of the initial steps in the mechanism through which 1,25-dihydroxyvitamin D_3 and the VDR regulate gene transcription.

Further Reading

Feldman, D., Glorieux, F. H., and Pike, J. W. (eds.) (1997). *Vitamin D*. Academic Press, San Diego.

Haussler, M. R., Whitfield, G. K., Haussler, C. A., Hsieh, J. C., Thompson, P. D., Selznick, S. H., Dominguez, C. E., and Jurutka, P. W. (1998). The nuclear vitamin D receptor: Biological and molecular regulatory properties revealed. *J. Bone Miner. Res.* **13**, 325–349.

Jones, G., Strugnell, S. A., and DeLuca, H. F. (1998). Current understanding of the molecular actions of vitamin D. *Physiol. Rev.* **78**, 1193–1231.

Jurutka, P. W, Whitfield, G. K., Hsieh, J. C., Thompson, P. D., Haussler, C. A., and Haussler, M. R. (2001). Molecular nature of the vitamin D receptor and its role in regulation of gene expression. *Rev Endocr. Metab. Disord.* **2**, 203–216.

Malloy, P. J., Pike, J. W., and Feldman, D. (1999). The vitamin D receptor and the syndrome of hereditary 1,25-dihydroxyvitamin D-resistant rickets. *Endocr. Rev.* **20**, 156–188.

McKenna, N. J., Lanz, R. B., and O'Malley, B. W. (1999). Nuclear receptor coregulators: Cellular and molecular biology. *Endocr. Rev.* **20**, 321–344.

Norman, A. W., Mizwicki, M. T., and Okamura, W. H. (2003). Ligand structure–function relationships in the vitamin D endocrine system from the perspective of drug development (including cancer treatment). *Recent Results Cancer Res.* **164**, 55–82.

Rachez, C., and Freedman, L. P. (2001). Mediator complexes and transcription. *Curr. Opin. Cell Biol.* **13**, 274–280.

Sutton, A. L., and MacDonald, P. N. (2003). Vitamin D: More than a "bone-a-fide" hormone. *Mol. Endocrinol.* **17**, 777–791.

Biography

Paul MacDonald and Diane Dowd are Faculty Members in the Department of Pharmacology at Case Western Reserve University. They are actively involved in basic research on the molecular, cellular, and physiological roles of the vitamin D receptor in normal and pathological states. Dr. MacDonald holds a Ph.D. in biochemistry from Vanderbilt University and received his postdoctoral training at the University of Arizona. Dr. Dowd received her Ph.D. in biochemistry from Vanderbilt University and her postdoctoral training at the Arizona Cancer Center and University of Arizona.

Vitamin D

Hector F. DeLuca and Margaret Clagett-Dame
University of Wisconsin, Madison, Wisconsin, USA

This article discusses the chemical identity and production of vitamin D. Its endocrine system, the nuclear receptor, and its mechanism of action are treated, along with the degradation of vitamin D hormone and its roles.

Chemical Identity, Natural Occurrence, and Production

The vitamin Ds are secosterols in which the B-ring of the steroid nucleus is replaced by a diene bridge. The two most common forms are vitamin D_2 (ergocalciferol) and vitamin D_3 (cholecalciferol). The structures of these two nutritionally important compounds are illustrated in Figure 1.

Although it is classified as a vitamin because of the nature of the discovery process, vitamin D in actual fact should not be considered a true vitamin for the following reasons. First and foremost, vitamin D utilized by higher organisms is manufactured in the epidermis of skin by photolysis of 7-dehydrocholesterol, a side reaction product of cholesterol synthesis. Secondly, vitamin D is nearly absent from the food supply for the most part. Vitamin D is found in fish liver oils and in egg yolk but is not found in virtually all plant materials, in skeletal meats, seeds, fruits, and vegetables. In fact, very little is found in an expected source, milk. We consider milk an important supply of vitamin D in many countries, primarily because it is fortified by the addition of vitamin D made artificially by man.

The chemical process whereby 7-dehydrocholesterol is converted to vitamin D_3 is well known. The 5,7-diene portion of either ergocalciferol or 7-dehydrocholesterol will absorb 280–310 nm ultraviolet light. This causes an isomerization to form a compound, previtamin D_3, which in itself is biologically inactive and remains in skin. Previtamin D is in equilibrium with vitamin D_3. The plant sterol, ergosterol, is converted to vitamin D_2 by an identical process. For many years, vitamin D_2 was the major synthetic form of vitamin D used in vitamin capsules, animal feeds, and in the fortification of foods. Because of improved synthetic methods, vitamin D_3 has become the major form used for both fortification and nutrition of domestic animals. The photolysis of 7-dehydrocholesterol is quite efficient in skin, and summer sun on hands and face and will in 10 minutes produce the daily requirement of vitamin D (currently believed to be 10–20 μg per day). Winter sun is unable to induce production of vitamin D because of the angle of the sunlight and the filtration of the critical wavelengths that cause vitamin D production. It is generally accepted that skin production of vitamin D_3 is quantitatively the most important source of the vitamin for human health.

Conversion of Vitamin D to its Hormonal Form

The vitamin D_3 that is produced in skin or that is absorbed from the intestine from vitamin pills or fortified foods is biologically inactive as such. The body must process vitamin D to form a final vitamin D hormone that is believed to carry out all of the known functions of vitamin D. Vitamin D_3 is first hydroxylated in the liver to form the circulating form of vitamin D_3, 25-hydroxyvitamin D_3 (25-OH-D_3). Interestingly, this compound is also biologically inactive and must be further modified before function. The second step occurs in the proximal convoluted tubule cells of the kidney where a 1 α-hydroxyl group is added to the molecule to produce the final vitamin D hormone, 1α,25-dihydroxyvitamin D_3 (1,25-$(OH)_2D_3$). The reaction steps that result in this transformation are shown in Figure 2. The first step in conversion of vitamin D to the circulating form occurs in the hepatocytes of liver but not exclusively so. At least two enzymes are known to make this conversion, a mitochondrial enzyme and a microsomal enzyme, both of which have been cloned. No natural human mutation blocking this initial step has yet been discovered. However, the second step occurring in the proximal convoluted tubule cells of the kidney is a highly regulated one. This 1α-hydroxylase, also known as CYP27B1, has also been cloned and natural human mutants of this enzyme are now well known. These mutations result in a disease called vitamin D-dependency rickets type I in which children present

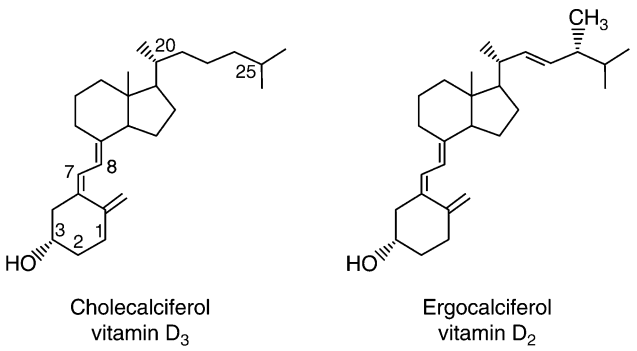

FIGURE 1 The nutritionally important forms of vitamin D. Vitamin D_3 is the form manufactured in skin and vitamin D_2 is the form produced by the irradiation of ergosterol. In mammals, both are equally active and both appear to be metabolized by almost identical routes.

vitamin D-deficiency diseases, i.e., rickets, hypocalcemia, and hypophosphatemia, even though they are naturally irradiated with sunlight or are provided vitamin D as a supplement. These children are cured by the administration of physiologic amounts of the natural vitamin D hormone, 1,25-$(OH)_2D_3$, establishing clearly the two-step activation process of vitamin D for man.

The Role of 1,25-$(OH)_2D_3$ in Calcium, Phosphorus, and Bone Metabolism

The basis for discovery of vitamin D in the first place is the disease rickets in children. This disease is also accompanied by hypocalcemia (low blood calcium) causing convulsive tetany. In adults, the deficiency of vitamin D causes the disease, osteomalacia. The diseases, rickets and osteomalacia, result from a failure to mineralize the organic matrix of newly synthesized bone. Early investigations to understand how vitamin D functions were, of course, directed toward the formation of mineralized bone. However, it is now abundantly clear that 1,25-$(OH)_2D_3$ does not act directly on the mineralization process in the healing of rickets or osteomalacia but rather acts on intestine, kidney, and bone to provide calcium and phosphorus in the plasma required for the mineralization of skeleton and prevention of the convulsive disease, hypocalcemic tetany. The essence of vitamin D action, therefore, in curing rickets and osteomalacia is the elevation of plasma calcium and phosphorus to supersaturating levels that are required for normal mineralization. The vitamin D hormone acts to provide this calcium by stimulating the enterocyte of the small intestine to absorb calcium as well as phosphate by an independent mechanism both of which require active metabolic energy.

Because of the constant need for calcium to support normal neuromuscular function, calcium must be available in the plasma even when it is not available in the diet. Thus, the vitamin D hormone, i.e., 1,25-$(OH)_2D_3$ acting together with parathyroid hormone will cause the mobilization of calcium from the skeletal fluid compartment into the plasma compartment. Thus, the skeleton serves not only a structural function but also as a source of calcium and phosphorus. A final point is that 1,25-$(OH)_2D_3$ works in concert with the parathyroid hormone to induce the distal nephron of the kidney to reabsorb the last 1% of the filtered load of calcium into the plasma compartment. These then work to maintain plasma calcium and phosphorus at levels that support both bone formation and prevent hypocalcemic tetany. A diagram representing these functions is shown in Figure 3.

The Vitamin D Endocrine System

One of the most elegantly regulated substances in the body is the plasma calcium level. The parathyroid glands continuously monitor serum calcium levels and a calcium receptor therein responds when calcium falls even slightly below the normal level. By a G protein

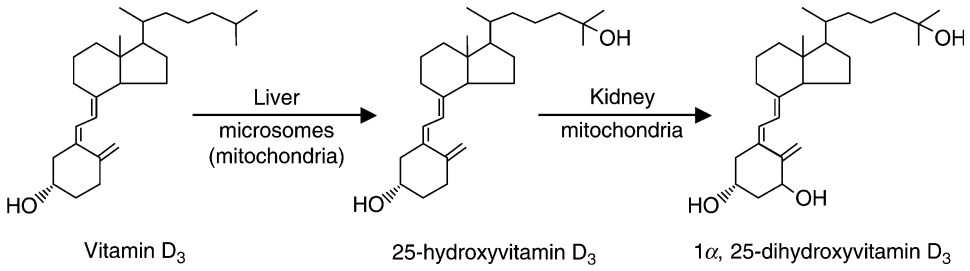

FIGURE 2 The required metabolism of vitamin D for function. Shown here is the metabolism of vitamin D_3 to the major blood form of vitamin D, 25-hydroxyvitamin D3 and its subsequent metabolism in the kidney to form the final vitamin D hormone, 1α,25-dihydroxyvitamin D_3. It is this form of vitamin D_3 that carries out all of the known functions of the vitamin. Vitamin D_2 not shown here is metabolized in an almost identical fashion to its active form, 1α,25-dihydroxyvitamin D_2.

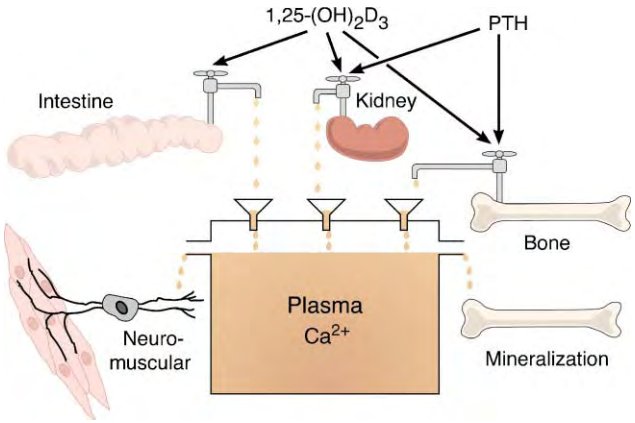

FIGURE 3 A diagrammatic representation of how the vitamin D hormone 1α,25-$(OH)_2D_3$) functions to maintain plasma calcium at supersaturating levels which are required for prevention of hypocalcemic tetany (neuromuscular) and for the prevention of rickets and osteomalacia (mineralization of bone).

mechanism, the calcium receptor stimulates the secretion of parathyroid hormone, a peptide hormone, that is the body's signal requesting calcium. It binds to the entire nephron of the kidney and to the osteoblasts of bone. Among its many functions in the kidney is to stimulate the 1α-hydroxylase (CYP27B1) to produce the vitamin D hormone in substantial quantities. The vitamin D hormone then acts on the bone, kidney, and intestine as described earlier to mobilize calcium as needed to raise blood calcium into the normal range, clearing the set-point of the parathyroids shutting down parathyroid secretion. Overshoot of calcium results in the C-cells of the thyroid secreting calcitonin, a 32 amino acid peptide hormone that blocks calcium mobilization from the skeleton. Calcitonin also has a stimulatory effect on the 1α-hydroxylase to produce the vitamin D hormone in small amounts to support its noncalcemic activities.

The Vitamin D Receptor

$1,25\text{-}(OH)_2D_3$ is a true steroid hormone that acts through a nuclear receptor called the vitamin D receptor (VDR). The human receptor is a 427 amino acid protein that serves as a ligand-dependent transcription factor. It is a member of the nuclear receptor superfamily of receptors. Other members of this superfamily include the retinoic acid, thyroid, estrogen, testosterone, glucocorticoid, and other steroid hormone receptors. VDR is the smallest of the steroid hormone receptors and largely acts in a fashion quite similar to other steroid hormone receptors. Unlike other nuclear receptors, there is only a single VDR in all tissues. No subtypes are known and it is this receptor through which all vitamin D actions occur. Natural mutants of the human VDR are known and produce a disease called vitamin D-dependency rickets type II. In this disease, high blood levels of $1,25\text{-}(OH)_2D_3$ occur in the face of severe rickets and severe hypocalcemia and hypophosphatemia. VDR null mutant mice have been produced and are available as experimental tools. The vitamin D-dependency rickets type II patients present a variety of diseases depending upon where the mutation has occurred. If there is a complete absence of a functional receptor, then very brittle vitamin D-resistant rickets occurs and can only be treated by the infusion of calcium and phosphorus into the blood stream to mineralize the skeleton but many of the other functions of vitamin D go unmet. The fact that VDR null mutant mice are normal at birth shows that vitamin D is not an embryonic developmental factor but functions primarily after parturition.

There are reports of nongenomic functions of vitamin D. These have been largely cellular-based observations, which have yet to be shown to occur *in vivo*. In fact, the administration of large amounts of $1,25\text{-}(OH)_2D_3$ to receptor null mutant mice produces no significant phenotype, suggesting that the only mechanism of action of vitamin D is through its receptor under physiologic circumstances.

Molecular Mechanism

Vitamin D-response elements (VDE) are found in the promoter region of target genes. These are hexameric repeats separated by three nonspecified bases. There can be as many as three repeat elements in a responsive element system. The VDR must heterodimerize with another transcription factor, the retinoid X receptor (RXR), in order to bind to the responsive elements. The RXR binds to the 5′ repeat and the VDR to the 3′ repeat. Figure 4 provides a cartoon to illustrate what is currently known about the mechanism of action of the vitamin D hormone working through its receptor to regulate expression or suppression of target genes. As with other steroid hormones, it is anticipated that the unliganded receptor may be retained in an inactive state by being bound to a corepressor. This has not been specifically shown for the VDR but is known for other class II nuclear receptors. There is increasing evidence that such a corepressor might be identified for the VDR. In this model, the corepressor that interacts directly with the VDR would be released upon binding of the ligand to the receptor probably because of a change in VDR conformation. The receptor would then be free to interact with a coactivator protein that is believed to be involved in chromatin remodeling and to link the complex bound at the hormone response element to the basal transcription machinery. Among the known coactivators believed to interact directly with the VDR

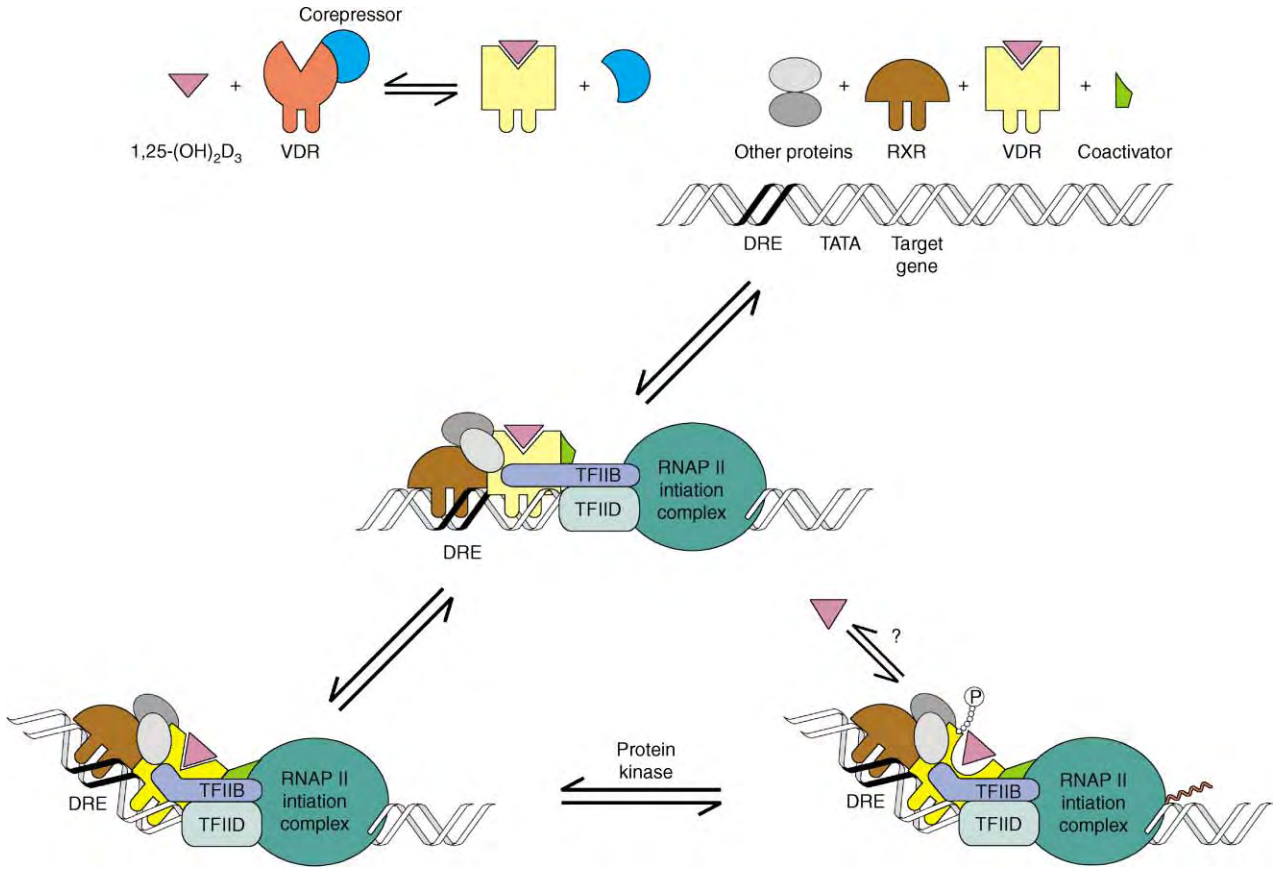

FIGURE 4 A cartoon representing the molecular mechanism of action of the vitamin D hormone ($1,25\text{-}(OH)_2D_3$) in regulating transcription of target genes in the target tissues. Binding of the ligand, i.e., $1,25\text{-}(OH)_2D_3$ to the VDR causes a conformational change and a rejection of the corepresssor. It also allows binding of a coactivator and formation of a heterodimer with RXR on the vitamin D responsive elements. Several proteins are required to form the transcription complex, all of which have not yet been identified. There is a bending of the DNA and a phosphorylation on serine 205 but their exact role in either suppression or activation of transcription remains unknown.

are SRC 1, 2, 3, and DRIP 205. Likely other participating coactivators will be discovered. A phosphorylation does occur on serine 205 of the VDR but whether this is of functional importance remains to be determined.

Metabolism and Degradation

The vitamin D hormone is degraded specifically by an enzyme it induces. That enzyme is the CYP24 (24-hydroxylase), which carries out a series of reactions on the side chain of the vitamin D hormone and its precursor, $25\text{-OH-}D_3$. It first causes hydroxylation in the 24R-position followed by oxidation of that same hydroxyl to a ketone. The next step again carried out by the same enzyme is a 23-hydroxylation followed by cleavage and oxidation giving rise to the biliary excretion product called calcitroic acid. Calcitroic acid is biologically inactive. Thus, the vitamin D hormone, an extremely potent biological substance, ensures its limited activity by inducing its own destruction. Other metabolism of vitamin D is known including the formation of the 26,23-lactone derivative, 26-hydroxylation, but quantitatively the most important reaction regulating the level of vitamin D hormone is the CYP24. The CYP24 is regulated in a negative fashion by the parathyroid hormone causing an instability of the mRNA encoding for that enzyme. Thus, the parathyroid hormone not only stimulates the 1 α-hydroxylase but also stimulates the destruction of the enzyme that destroys the hormone, thereby ensuring that large amounts of the vitamin D hormone are available to carry out its calcium functions.

New and Nonclassical Roles of the Vitamin D Hormone

With the discovery of the VDR came the observation that it is found in tissues not previously appreciated as target tissues of vitamin D action. The discovery of

the VDR in the intestine, kidney tubules, and osteoblasts was not unexpected. However, its presence in the parathyroid gland, the islet cells of the pancreas, the immune cells such as T-cells, macrophages, and keratinocytes made it possible that the vitamin D hormone had important functions besides raising blood calcium and phosphorus and mineralizing the skeleton. It is now clear that an important function of the vitamin D hormone is to suppress the growth of parathyroid glands and to suppress production of the parathyroid hormone. This basic function has been utilized by physicians using 1,25-$(OH)_2D_3$ and its analogues to treat secondary hyperparathyroidism in kidney failure patients.

Another important VDR site are the cells of the immune system and in the promyelocytes which are the precursors of the monocyte. The vitamin D hormone stimulates the formation of the monocyte by causing the production of RANKL by osteoblasts and stromal cells. This results in a coalescence of the monocytes to form giant osteoclasts which are further activated by RANKL. Thus, the formation of the giant osteoclast that causes bone turnover is a vitamin D function. Furthermore, vitamin D also functions to cause the formation of new bone, thus playing an important role in the bone remodeling and modeling systems.

The role of the vitamin D hormone in the keratinocyte has also become of importance therapeutically. The vitamin D hormone added to the keratinocytes in cultures or added topically will cause a cessation of proliferation of the keratinocyte and will cause its differentiation. Thus, 1,25-$(OH)_2D_3$ and analogues have been successfully used in the topical treatment of psoriasis.

Finally, attention must be focused on the immune system where the vitamin D hormone is now known to cause important immuno-modulatory effects. The vitamin D hormone can be used to block certain animal models of autoimmune disease. For example, it can be used to prevent experimental autoimmune encephalomyelitis (EAE), a model of multiple sclerosis in mice. However, in so doing, it does induce an abnormal rise in serum calcium. 1,25-$(OH)_2D_3$ can be used to prevent diabetes in the nonobese diabetic mouse model of type 1 diabetes. It can be used to prevent rheumatoid arthritis, systemic lupus, and inflammatory bowel disease. Thus, the immuno-modulatory role of the vitamin D hormone under normal circumstances is only now becoming realized.

Therapeutic Uses of 1α,25-$(OH)_2D_3$ and its Analogues

As discussed earlier, besides the treatment of vitamin D-dependency rickets and vitamin D-resistant rickets of many types, the vitamin D hormone and its analogues are certainly central actors in the treatment of bone disease secondary to kidney failure. This is primarily by suppression of parathyroid proliferation and by suppression of parathyroid hormone production. 1,25-$(OH)_2D_3$ and its analogue, 1α-OH-D_3 has been successfully used in certain parts of the world to treat postmenopausal and age-related osteoporosis, giving a modest rise in bone mass along with a clear reduction in fracture rate. The danger of hypercalcemia has limited its use in the treatment of this disease. However, newer vitamin D analogues with greater bone anabolic activity than 1,25-$(OH)_2D_3$ are currently under development and may make it possible to safely treat osteoporosis in the future.

An analogue of 1,25-$(OH)_2D_3$ called Dovonex is currently marketed for the topical treatment of the hyperproliferative skin disorder, psoriasis. Improved analogues will likely appear for treatment of psoriasis. There are potential new uses for the vitamin D analogues in the autoimmune diseases as described above or in the treatment of malignant cancer growth. The vitamin D hormone has been found to suppress growth of malignant cells *in vitro* and to cause their differentiation into functional cells. Thus, the use of vitamin D compounds as a potential treatment of metastatic neoplastic disease has been exciting but it has not yet yielded a therapeutic agent. The major problem with the use of 1,25-$(OH)_2D_3$ and many of its analogues for treatment of disease is that its primary purpose is to raise blood calcium and phosphorus which means that is a major side effect that must be dealt with before it can be used to treat noncalcemic diseases. One approach to this is the synthesis of analogues that retain the ability to suppress cancerous growth but do not raise blood calcium. New analogues with these desirable characteristics are currently under basic study, but are not yet available for pharmaceutical use.

See Also the Following Articles

Calcium Buffering Proteins: Calbindin • Cholesterol Synthesis • Cytochrome P-450 • Lipid Rafts • Parathyroid Hormone/Parathyroid Hormone-Related Protein Receptor • Vitamin D Receptor

Glossary

coactivator Protein(s) that enhance receptor activity in transcription.

convulsive tetany A disease precipitated by either low blood magnesium or low blood calcium resulting in a severe convulsive state. It is lethal unless immediately treated with calcium and/or magnesium.

corepressor A protein that silences transcription factors.

7-dehydrocholesterol The sterol precursor of vitamin D_3.

Dovonex A drug marketed by Leo Pharmaceuticals containing an analogue of 1,25-$(OH)_2D_3$ and used to treat psoriasis s by topical administration.

hepatocytes Cells comprising ~30% of the liver that carry out many of the liver's functions.

keratinocytes Cells of the skin that produce the keratin proteins and contribute to the skin barrier.

macrophages Cells of the immune system that are responsible for destroying foreign materials.

nongenomic Referring to or describing activities that are carried out not involving gene expression.

osteoblasts Cells of the skeleton that carry out synthesis of new bone and that mediate regulation of bone activities.

previtamin D An isomer of vitamin D formed during the irradiation process for producing vitamin D. It is in equilibrium with vitamin D.

proximal convoluted tubule cells Cells lining the proximal convoluted tubule of the kidney.

RANKL *R*eceptor *a*ctivator of *NF-K*appaβ *l*igand, a signal protein produced by osteoblasts and stromal cells in response to such stimulants as 1,25-$(OH)_2D_3$ and parathyroid hormone.

transcription factor A protein usually found in the nucleus that has a marked effect or role in the transcription of genes.

Further Reading

Darwish, H. M., and DeLuca, H. F. (1996). Recent advances in the molecular biology of vitamin D action. In *Progress in Nucleic Acid Research and Molecular Biology* (W. E. Cohn and K. Moldave, eds.) pp. 321–344. Academic Press, San Diego, CA.

DeLuca, H. F. (1974). Vitamin D: The vitamin and the hormone. *Fed. Proc.* **33**, 2211–2219.

DeLuca, H. F. (1997). Historical overview. In *Vitamin D* (D. Feldman, F. H. Glorieux and J. W. Pike, eds.) Vol 1, pp. 3–11. Academic Press, San Diego, CA.

Feldman, D., Glorieux, F. H., and Pike, J. W. (1997). *Vitamin D*. Academic Press, San Diego, CA, 1285pp.

Jones, G., Strugnell, S. A., and DeLuca, H. F. (1998). Current understanding of the molecular actions of vitamin D. *Physiol. Rev.* **78**, 1193–1231.

Biography

Hector F. DeLuca is Steenbock Research Professor and Chairman of the Department of Biochemistry at the University of Wisconsin-Madison. He has been a major contributor to the current understanding of the metabolism and mechanism of action of vitamin D. He has published over 2000 papers and patents. He has trained well over 250 students in vitamin D, vitamin A, bone and calcium fields. He is a member of the National Academy of Sciences, the American Academy of Arts and Sciences, a Fellow of the AAAS and has won many awards for his work on vitamin D.

Margaret Clagett-Dame is a Professor of Biochemistry and Pharmaceutical Sciences in the Department of Biochemistry at the University of Wisconsin-Madison and is best known for her work in the developmental role of the retinoids. She has published some 48 papers and 6 patents.

Vitamin E

Ute C. Obermuller-Jevic
BASF Aktiengesellschaft, Ludwigshafen, Germany

Lester Packer
University of Southern California, Los Angeles, California, USA

Vitamine E is the name for a group of biologically active substances including tocopherols and tocotrienols. Alpha-tocopherol shows the highest biological activity of all vitamin E forms and is the most common form found in the human body. Vitamin E was discovered in 1922 as essential micronutrient for reproduction. In the 1950s it was recognized that vitamin E is the body's major lipid-soluble antioxidant protecting lipoproteins and membranes against oxidative damage. The biological role of vitamin E goes, however, beyond its antioxidant function. Studies on the effects of vitamin E on gene expression have revealed many genes and signal transduction pathways which are influenced by vitamin E. All these actions of vitamin E help to explain the observed beneficial effects of vitamin E in chronic and degenerative diseases. A well-balanced diet rich in vitamin E seems a basic requirement for human health. Intake of supplementary vitamin E may be advisable for individuals who do not get adequate levels from diet, or who are at high risk for, or who are already suffering from, chronic and degenerative diseases.

Molecular Structure of Vitamin E

Vitamin E is the generic name for a group of eight plant-derived, lipid-soluble substances (tocols) including four tocopherols and four tocotrienols (Figure 1). The molecular structure of vitamin E is comprised of a chromanol ring with a side chain located at the C-2 position. Tocopherols have a saturated phytyl side chain and tocotrienols have an unsaturated isoprenoid side chain. The number and position of methyl groups located around the chromanol ring varies among the different tocopherols and tocotrienols, and accounts for the designation as alpha-, beta-, gamma-, or delta-forms. Natural and natural-source alpha-tocopherol occur in *RRR*-configuration only (formerly designated as d-alpha-tocopherol). In contrast, synthetic alpha-tocopherol consists of an equal racemic mixture of eight stereoisomers (*RRR*, *RSR*, *RRS*, *RSS*, *SRR*, *SSR*, *SRS*, *SSS*) arising from the three chiral centers of the molecule at positions C2, C4′ and C8′ and designated as *all-rac*-alpha-tocopherol (or dl-alpha-tocopherol).

Biological Activity of Vitamin E

The various forms of vitamin E differ in their biological activities. Alpha-tocopherol is the most common form of vitamin E occurring in human blood and tissues and it has the highest biological activity among all tocopherols and tocotrienols. Moreover, the human body preferentially accumulates the *RRR*- or 2*R*-forms of vitamin E. Thus natural *RRR*-alpha-tocopherol has a higher bioavailability and "biological activity" than synthetic *all rac*-alpha-tocopherol. According to the Food and Nutrition Board (FNB) of the US National Academy of Sciences, which publishes recommendations for dietary intake of vitamin E, only *RRR*-alpha-tocopherol itself, or the *RRR*- and 2*R*-stereoisomers of *all rac*-alpha-tocopherol meet the vitamin E requirements in humans. The FNB suggests a 2-fold higher potency of natural versus synthetic alpha-tocopherol sources, however, this value has been challenged. The biological activity of vitamin E in dietary supplements is usually expressed as international units (IU). As published in the United States Pharmacopeia (USP), 1 IU is defined as the biological activity of 1 mg *all rac*-alpha-tocopheryl acetate. Other biological activities of vitamin E are 1 mg *all rac*-alpha-tocopherol = 1.1 IU; 1 mg *RRR*-alpha-tocopherol = 1.49 IU; 1 mg gamma-tocopherol = 0.15 IU.

Dietary Sources and Recommended Intake of Vitamin E

Vegetable oils and lipid-rich plant products (e.g., nuts, seeds, grains) are the main dietary sources of vitamin E. In Western diets, vitamin E intake mainly derives from fats and oils as found in margarine, mayonnaise, salad dressing, and desserts, and increasingly also from fortified food (e.g., breakfast cereals, milk, fruit juices).

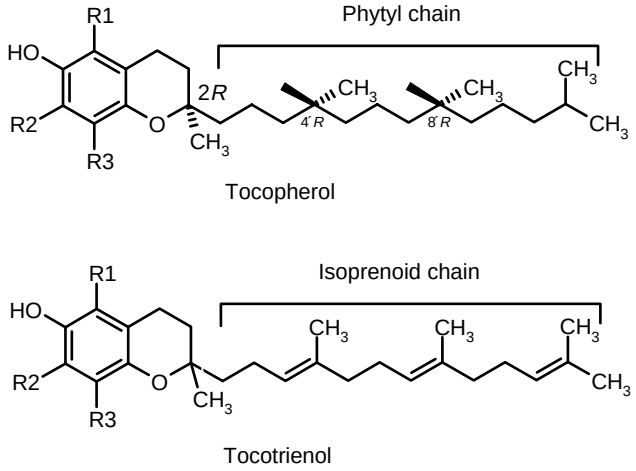

The four isoforms of tocopherols and tocotrienols:

α-:	$R_1 = CH_3$	$R_2 = CH_3$	$R_3 = CH_3$
β-:	$R_1 = CH_3$	$R_2 = H$	$R_3 = CH_3$
γ-:	$R_1 = H$	$R_2 = CH_3$	$R_3 = CH_3$
δ-:	$R_1 = H$	$R_2 = H$	$R_3 = CH_3$

FIGURE 1 The molecular structure of vitamin E. Tocopherols and Tocotrienols exist in four different isoforms (α-, β-, γ-, and δ-forms). Tocopherol is shown in its naturally occurring *RRR*-configuration. (Adapted from Food and Nutrition Board, 2000.)

Noteworthy, the diet of Americans contains large amounts of gamma-tocopherol when compared to populations in other Western countries, which is a result of the high consumption of soybean and corn oil containing more gamma- than alpha-tocopherol. Vitamin E used for food fortification or dietary supplements consists mainly of alpha-tocopherol, either derived from natural sources (i.e., methylated gamma-tocopherol from vegetable oil) or from synthetic production and it is usually esterified to increase stability.

The FNB recommends for adults a daily intake (recommended dietary allowance, or RDA) of 15 mg vitamin E including food, fortified food, and supplements. The recommendations are largely based on *in vitro* studies of M. Horwitt dating back to 1960, which are still considered the most adequate data for defining the physiological status and a health benefit of vitamin E in humans. In these studies, prevention of H_2O_2-induced erythrocyte hemolysis was used as test system. However, except when vitamin E is clearly deficient the erythrocyte hemolysis test is not a useful indicator of vitamin E functional status. Thus, the guidelines of the FNB were critically discussed in the literature and it was strongly agreed upon that other assays and new biomarkers need to be identified to define the physiologic role and beneficial potential of vitamin E in humans.

The recommended daily intake of 15 mg vitamin E is considered rather unlikely to be achieved by North Americans and other Western countries through diet alone. Although universal dietary supplementation has not been recommended, a dose of 200 mg/day vitamin E (alpha-tocopherol) has been suggested to saturate plasma levels and elevate tissue levels which may have possible health effects in the long term.

As an upper limit for supplemental vitamin E intake the FNB has published for adults a dose of 1 g/day alpha-tocopherol (i.e., 1 500 IU *RRR*- or 1 100 IU *all rac*-alpha-tocopherol) showing no apparent side effects, which is considered safe. In human intervention studies, various doses of vitamin E up to 3 600 IU/day have been used. Nevertheless, conclusive evidence from long-term studies regarding biological effects and safety of chronic intake of pharmacologic doses of vitamin E are lacking. In the Alpha-Tocopherol, Beta Carotene (ATBC) Cancer Prevention Study with Finnish smokers consuming 50 IU/day vitamin E for 6 years, an increase in mortality from hemorrhagic stroke was observed, however, other intervention studies did not report such an adverse effect. It was suggested that pharmacologic doses of vitamin E are contraindicated in persons with blood coagulation disorders as vitamin E might exacerbate defects in the blood coagulation system based on its inhibitory effects on platelet aggregation.

Uptake, Distribution, and Metabolism of Vitamin E

Together with dietary fat, alpha-tocopherol and all other forms of vitamin E are absorbed in the digestive tract, incorporated into chylomicrons and transported in the lymphatic system. Part of the absorbed stereoisomers are taken up into extrahepatic tissues by the action of lipoprotein lipase and the remainder is delivered in chylomicron remnants to the liver. Distribution of vitamin E into the circulation is regulated by a cytosolic alpha-tocopherol transfer protein (alpha-TTP) in the liver, which is selective for alpha-tocopherol in its *RRR*- or 2*R*-forms. The other stereoisomers of alpha-tocopherol as well as the other tocopherols and tocotrienols exert much less affinity for alpha-TTP. Alpha-TTP plays an important role in maintaining plasma levels of vitamin E.

In the liver, vitamin E is incorporated into very low density lipoproteins (VLDLs) and released to the systemic blood circulation. Excess amounts of alpha-tocopherol along with the other absorbed forms of tocopherols and tocotrienols are metabolized or eliminated by the biliary tract. VLDLs are converted into low-density lipoproteins (LDLs) and excess surface components including alpha-tocopherol are transferred

to high-density lipoproteins (HDLs). Delivery of alpha-tocopherol to peripheral tissues takes place via binding of LDL to LDL receptors and subsequent cellular uptake. Vitamin E preferably accumulates in adipose tissues. Cytosolic tocopherol-associated proteins (TAP) have been reported showing alpha-tocopherol-specific binding characteristics and also nuclear translocation and transcriptional activation in various mammalian cell types and organs. TAP seems to play an important role in vitamin E-induced gene expression, however, its biological functions are not widely known. A further cytosolic vitamin E regulatory protein, i.e., tocopherol-binding protein (TBP) has been reported whose functions are not fully understood.

The lowest acceptable vitamin E level in plasma is 11.6 μmol L^{-1} (0.5 mg dL^{-1}) and a ratio of vitamin E:cholesterol of 2.25 μmol $mmol^{-1}$. Serum levels of vitamin E correlate with cholesterol levels and hence do not necessarily correlate with vitamin E intake. Except for non- or poorly responding subjects, serum levels of vitamin E can usually be increased up to threefold by intake of dietary supplements reaching a saturation level.

Biological Importance of Vitamin E in Reproduction and Essentiality

Vitamin E was discovered in 1922 by H. Evans and K. Bishop as essential micronutrient needed to ensure normal reproduction in rats. It was named according to a consecutive alphabetical order preceded by the discovery of vitamins A to D. Later vitamin E was called alpha-tocopherol, according to the greek term "tokos" childbirth, "phero" to bear, and -ol, indicating an alcohol. Rats on a diet low in vitamin E showed reduced fertility and a high rate of fetal resorption. However, when animals were fed a lipophilic fraction from lettuce or, as later shown, wheat germ oil, their fertility was retained and a successful implantation of the fetus was observed. The biological activity of vitamin E is based on this so-called rat resorption-gestation assay. The family of natural vitamin E molecules as well as the stereoisomers of *all rac*-alpha-tocopherol all exhibit to varying degrees vitamin E activity in this bioassay. Unfortunately, this assay of reproductive activity in pregnant rats may bear limited relevance to human health.

Unique Role of Vitamin E as a Lipophilic Antioxidant in Lipoproteins and Cell Membranes

In the 1950s it was recognized under leadership of A. L. Tappel's group that vitamin E is the body's major lipid soluble antioxidant protecting lipoproteins and membranes where it resides against free radical-mediated lipid peroxidation which, if not prevented or interrupted by vitamin E, causes widespread oxidative molecular damage and pathology. All natural isoforms and synthetic stereoisomers of vitamin E exhibit to varying degrees the ability to inhibit lipid peroxidation as a "chain-breaking" antioxidant. Vitamin E primarily destroys peroxyl radicals and thus protects unsaturated fatty acids from oxidation. Additionally, vitamin E scavenges a variety of oxygen-derived free radicals including alkoxyl radicals, superoxide, and other reactive oxygen species (ROS) such as singlet oxygen and ozone, and it reacts with nitrogen species. Vitamin E participates in an *antioxidant network* (a concept advanced by L. Packer's group) and thus vitamin E radicals can be recycled or regenerated back to their native form, e.g., by vitamin C. The antioxidant network is strengthened by bioflavonoids (recycle vitamin C) and by carotenoids (free radical traps sparing vitamin E) (Figure 2).

Effects of Vitamin E on Cell Signaling and Gene Expression

In the early 1990s, inhibition of protein kinase C (PKC) activity by vitamin E was suggested by A. Azzi's group as the crucial factor for inhibition of cell proliferation in smooth muscle cells. PKC activity is an important factor contributing to disorders such as vascular disease, cancer, diabetes, and other age-related degenerative diseases. Vitamin E was found to inhibit PKC activity in many cell types including smooth muscle cells, monocytes, macrophages, neutrophils, fibroblasts, and mesangial cells and the effects were repeatedly confirmed in animal studies. Inhibition of PKC activity by vitamin E occurs indirectly via activation of a phosphatase that cleaves the active, phosphorylated form of PKC, or by modulating diacylglycerol kinase activity. What is novel, is that inhibition of PKC is apparently independent of antioxidant activity and rather is the result of inhibition due to the specific molecular structure of the RRR stereoisomer of alpha tocpopherol. Hence the biological role of vitamin E goes beyond its antioxidant function.

Recent advances in molecular biology and availability of microarray techniques for studying effects of vitamin E on gene expression have revealed novel vitamin E-sensitive genes and signal transduction pathways. Vitamin E regulates at the transcriptional level the expression of several genes including collagen alpha-1 and alpha-TTP in liver, collagenase in skin, adhesion molecules, and chemokines such as VCAM-1 and MCP-1 in endothelial cells, different integrins in erythroleukemia

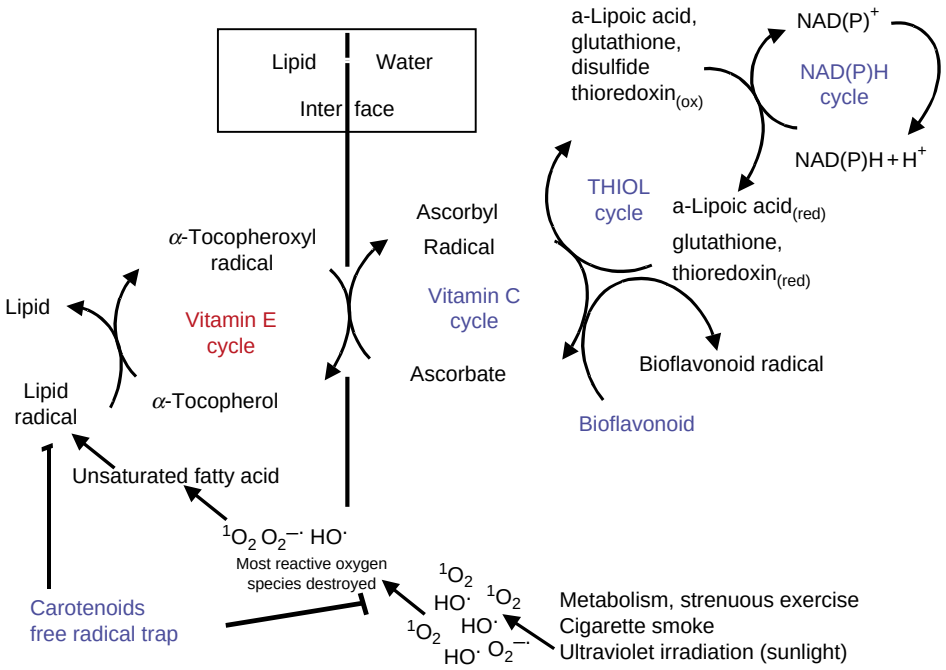

FIGURE 2 The antioxidant network concept.

cells, alpha-tropomyosin in smooth muscle cells, and scavenger receptors class A (SR-A) and CD 36 in macrophages and smooth muscle cells. At the posttranslational level, vitamin E regulates the expression of cyclooxygenase in monocytes leading to a decrease in prostaglandin E_2 levels. As this latter effect was also observed using other vitamin E homologues compatible with antioxidant activity this function of vitamin E may involve redox-signaling. In alpha-TTP knockout mice many genes associated with functions of liver or brain are remarkably modulated by deficiency in vitamin E, whereas the majority of genes over a broad range of expression levels show no change. This indicates that vitamin E regulates tissue-specific gene expression. These newly discovered actions of vitamin E help to explain the observed beneficial effects of vitamin E in chronic and degenerative diseases of aging.

Recognition of Vitamin E Deficiency Diseases and the Beneficial Effects of Vitamin E Supplements in Human Health and Disease Prevention

Clinically manifest vitamin E deficiency in humans is rare. Clear indications of vitamin E deficiency have been found in premature babies and in children suffering from an abnormal ability to absorb vitamin E as in abetalipoproteinemia, chronic cholestatic liver disease, cystic fibrosis, and in short-bowel syndrome.

A mutation in the alpha-TTP gene as found in "familial isolated vitamin E deficiency" results in a failure to deliver alpha-tocopherol to the systemic circulation. In these cases clinical vitamin E deficiency is recognized in babies showing symptoms of retrolental fiblasia and intraventricular hemorrhage, and in children suffering from muscular dystrophy, ataxia, and other disorders. High-dose vitamin E supplementation can reduce or eliminate clinical symptoms in these patients, however, to achieve amelioration of neurological symptoms early diagnosis and early start of treatment are crucial.

More frequently, a chronic sub-optimal supply in vitamin E (i.e., theoretically an intake below RDA levels) occurs population-wide and in all age groups. This may cause impaired defense against oxidative stress and increased susceptibility to oxidative injury and adverse health effects. In most diseases that have been examined with any degree of scrutiny, evidence for "oxidative stress" and oxidative damage has been observed in some stage of disease initiation or progression. Therefore it seems obvious that vitamin E like other antioxidants may prevent or delay disease progression. In numerous epidemiologic studies it has been observed that high intake of vitamin E is associated with a lower risk of age-related and chronic diseases, and experimental studies have suggested substantial

health benefits from vitamin E in disease prevention and therapy. Most large-scale human intervention trials on the prevention of cardiovascular disease, the main cause of morbidity and mortality in the Western world, however have failed to convincingly show that (relatively short-term) supplementation with vitamin E lowers the incidence of cardiovascular events or the rate of mortality from heart disease or stroke. Interestingly, a plethora of small clinical trials report a significant improvement of health status and/or retardation of disease progression by vitamin E supplementation in patients suffering from cardiovascular disease or other chronic and age-related diseases. Vitamin E appears to have important health benefits such as skin health, in reproductive diseases (pre-eclampsia), age-related eye diseases (cataract, AMD), metabolic disorders (Diabetes mellitus), neurodegenerative disorders (Alzheimer's and Parkinson's disease), skin aging (photoaging), and healthy aging.

Conclusion

An adequate dietary intake of vitamin E seems of crucial importance to guarantee throughout life normal function of physiologic processes in the body as well as adequate defense against oxidants generated by endogenous sources or from exposure to environmental stress. Vitamin E plays a unique role in the prevention of chronic and degenerative diseases, and thus in healthy aging. A well-balanced diet rich in vitamin E as part of a healthy lifestyle seems a basic requirement for human health. Moreover, intake of supplementary vitamin E may be advisable for individuals who are unable to sustain adequate levels, or who are at high risk for, or who are already suffering from chronic and degenerative diseases.

See Also the Following Articles

Lipoproteins, HDL/LDL • Protein Kinase C Family • Vitamin C

Glossary

α-tocopherol-binding protein A protein found mainly in liver, which discriminates between the different forms of vitamin E. It preferentially binds to RRR alpha-tocopherol leading to mainly retention of this vitamin E form in the human body whereas the other forms of vitamin E are mainly metabolized and excreted.

RRR-α-tocopherol The only stereoisomer of alpha-tocopherol occurring in nature. When alpha-tocopherol is made by chemical synthesis, it contains not only the RRR-stereoisomer, but a racemic mixture (called all-rac-alpha-tocopherol) of eight stereoisomers. Synthetic alpha-tocopherol is mainly used in dietary supplements and in fortified foods.

vitamin E The name for a group of eight substances of plant origin including four tocopherols and tocotrienols. Alpha-tocopherol is the most prominent form of vitamin E, which is considered essential in humans and animals. Besides its essentiality, alpha-tocopherol as well as the other forms of vitamin E are the major antioxidants in blood lipids and in cell membranes.

Further Reading

Brigelius-Flohe, R., and Traber, M. G. (1999). Vitamin E: Function and metabolism. *FASEB J.* **13**, 1145–1155.

Food and Nutrition Board (2000). *Dietary Reference Intakes for Vitamin C, Vitamin E, Selenium, and Carotenoids*, pp. 186–283. National Academy Press, Washington, DC.

Gordon, N. (2001). Hereditary vitamin-E deficiency. *Dev. Med. Child Neurol.* **43**, 133–135.

Hoppe, P., and Krennrich, G. (2000). Bioavailability and potency of natural-source and all-racemic alpha-tocopherol in the human: A dispute. *Eur. J. Nutr.* **39**, 183–193.

Packer, L., and Obermüller-Jevic, U. (2002). Vitamin E in disease prevention and therapy: Future perspectives. In *The Antioxidant Vitamins C and E* (L. Packer, M. G. Traber, K. Krämer and B. Frei, eds.) AOCS Press, Champaign.

Ricciarelli, R., Zingg, J. M., and Azzi, A. (2002). The 80th anniversary of vitamin E: Beyond its antioxidant properties. *Biol. Chem.* **383**, 457–465.

Rimbach, G., Minihane, A., Majewicz, J., Fischer, A., Pallauf, J., Virgli, F., and Weinberg, P. (2002). Regulation of cell signaling by vitamin E. *Prog. Nutr. Soc.* **61**, 415–425.

Biography

Ute Obermüller-Jevic Ph.D. is a Nutrition Scientist holding a doctoral degree in the field of antioxidant nutrients. Currently she is a scientific affairs manager for BASF Aktiengesellschaft, Ludwigshafen, focusing on the health benefits of vitamins and carotenoids.

Lester Packer received his Ph.D. from Yale University in 1956 and in 1961 joined the University of California at Berkeley where he was Professor of Molecular and Cell Biology and since 2000 is Adjunct Professor in the Department of Molecular Pharmacology and Toxicology, University of Southern California Health Sciences Center. Dr. Packer is a leading researcher on Antioxidants who has published over 800 articles, edited more than 90 books, is a member of numerous professional societies and editorial boards. He was Founder and Honorary President of The Oxygen Club of California, Past President of the Society for Free Radical Research International: he has received numerous awards including three Honorary Doctoral degrees.

Vitamin K: Biochemistry, Metabolism, and Nutritional Aspects

J. W. Suttie
University of Wisconsin-Madison, Wisconsin, USA

The term vitamin K refers to a number of compounds containing a 2-methyl-1,4-naphthoquinone ring with a hydrophobic side chain constituted at the 3-position (Figure 1). The biochemical role of the vitamin was not established until the mid-1970s, when it was shown that it was a substrate for a microsomal enzyme that converted protein bound glutamyl residues to γ-carboxyglutamyl (Gla) residues. This posttranslational modification has been found in relatively few proteins.

Vitamin K-Dependent Proteins

Prothrombin (clotting factor II), the zymogen of the plasma procoagulant thrombin, was the first protein shown to be dependent to vitamin K for its synthesis, and was also the first protein demonstrated to contain γ-carboxylglutamyl (Gla) residues. Plasma clotting factors VII, IX, and X were all initially identified in patients with hereditary bleeding disorders and were subsequently shown to be vitamin K dependent. Until the mid-1970s, these four vitamin K-dependent clotting factors were the only proteins known to require this vitamin for their synthesis. The amino-terminal, Gla domains of these four vitamin K-dependent procoagulants are very homologous, and the 10–13 Gla residues in each are in essentially the same position as in prothrombin.

Following the discovery of Gla, three more Gla-containing plasma proteins with similar homology were discovered. Protein C and protein S are involved in an anticoagulant rather than a procoagulant role in normal hemostasis, and the seventh Gla-containing plasma protein (protein Z) also has an anticoagulant function under some conditions. As these proteins play a critical role in hemostasis, they have been extensively studied, and the cDNA and genomic organization of each of them is well documented.

The discovery of Gla residues in the plasma vitamin K-dependent proteins led to a search for other proteins with this modification, and a 49 residue protein that contained three Gla residues, called osteocalcin (OC), was isolated from bone. It has little structural homology to the vitamin K-dependent plasma proteins. Although it is the second most abundant protein in bone, its function is not clearly defined. A second low-molecular-weight (79 residue) protein, matrix Gla protein (MGP), contains five Gla residues and was also first isolated from bone, but is also synthesized in cartilage and many other soft tissues. The function of these two proteins has not been clearly defined, but it has been shown that osteocalcin gene knockout mice develop more dense bones, and MGP knockout mice die from spontaneous calcification of arteries and cartilage. A limited number of other mammalian proteins have been found to contain Gla residues: Gas 6, a ligand for the tyrosine kinase Ax1, two proline rich integral membrane Gla proteins (PRGP-1, PRGP-2), and two additional Gla proteins (TMG-3 and TMG-4). A large number of Gla-containing toxic venom peptides are secreted by marine Conus snails and are found in some snake venoms. The vitamin K-dependent carboxylase has been cloned from a number of vertebrates, the Conus snail, a tunicate, and *Drosophila*, indicating the ancient evolutionary origin of this posttranslational modification.

Biochemical Role of Vitamin K

Beginning in the early 1960s, studies of prothrombin production in humans and experimental animals led to an understanding of the metabolic role of vitamin K. A biologically inactive form of prothrombin was demonstrated to be present in the plasma of patients treated with oral anticoagulants, and studies with hypoprothrombinemic rats were consistent with the presence of a hepatic precursor protein pool that was rapidly being synthesized and which could be converted to prothrombin by a posttranslational modification. Characterization of the abnormal prothrombin isolated from the plasma of cows fed the anticoagulant dicoumarol led directly to an understanding of the metabolic role of vitamin K. This protein lacked the specific calcium-binding sites present in normal prothrombin. Acidic peptides obtained by proteolytic enzyme digestion of prothrombin were shown to contain Gla

residues, but Gla residues could not be obtained by proteolysis of the abnormal prothrombin.

The Vitamin K-Dependent Carboxylase

In 1975, it was demonstrated that crude rat liver microsomal preparation contained an enzymatic activity (the vitamin K-dependent carboxylase) that promoted a vitamin K-dependent incorporation of $H^{14}CO_3^-$ into Gla residues of endogenous precursors of vitamin K-dependent proteins present in these preparations. Detergent-solubilized microsomal preparations retained this activity, and small peptides containing adjacent Glu–Glu sequences were found to be substrates for the enzyme. A general understanding of the properties of this unique enzyme was gained from studies utilizing this crude enzyme preparation, and these data have been adequately reviewed. The vitamin K-dependent carboxylation reaction does not require ATP, and the energy to drive this carboxylation reaction is derived from the oxidation of the reduced, hydronaphthoquinone, form of vitamin K (vitamin KH_2) by O_2 to form vitamin K-2,3-epoxide (Figure 2). The lack of a requirement for biotin and studies of the CO_2/HCO_3^- requirement indicate that carbon dioxide rather than HCO_3^- is the active species in the carboxylation reaction. Active substrates for the enzyme are 2-methyl-1,4-naphthoquinones substituted at the 3-position with a rather hydrophobic group. Although some differences in biological activity can be measured, phylloquinone, the plant form of the vitamin, and the predominant bacterial menaquinones are all effective substrates (Figure 1).

Only a small fraction of the proteins secreted by the liver to the plasma are vitamin K dependent, so an efficient mechanism for recognizing the precursors of the vitamin K-dependent proteins is essential. The primary gene products of the vitamin K-dependent proteins contain a very homologous domain between the amino terminus of the mature protein and the signal sequence. This propeptide region appears to be both a docking or recognition site for the enzyme and a modulator of the activity of the enzyme by decreasing the apparent K_m of the Glu site substrate. The role of vitamin K in the overall reaction catalyzed by the enzyme is to abstract the hydrogen on the γ-carbon of the glutamyl residue to allow attack of CO_2 at this position. A number of studies that utilized substrates tritiated at the γ-carbon of each Glu residue have been used to define the action and stoichiometry involved and have shown that it was an apparent equivalent stoichiometry between vitamin K-2,3-epoxide formation and Gla formation. The mechanism by which epoxide formation is coupled to γ-hydrogen abstraction is key to a complete understanding of the role of vitamin K. The association between epoxide formation, Gla formation, and γ-C–H bond cleavage has been studied, and the reaction efficiency defined as the ratio of Gla residues formed to γ-C–H bonds cleaved has been shown to be independent of Glu substrate concentrations, and to approach unity at high CO_2 concentrations. Identification of an intermediate chemical form of vitamin K which could be sufficiently basic to abstract the γ-hydrogen of the glutamyl residue has been a challenge. A possible candidate is that first proposed by Dowd, who suggested that an initial attack of O_2 at the naphthoquinone carbonyl carbon adjacent to the methyl group results in the formation of a dioxetane ring which generates an alkoxide intermediate. This intermediate is hypothesized to be the strong base that abstracts the γ-methylene hydrogen and leaves a carbanion that can interact with CO_2. This pathway leads to the possibility that a second atom of molecular oxygen can be incorporated into the carbonyl group of the epoxide product as well as the

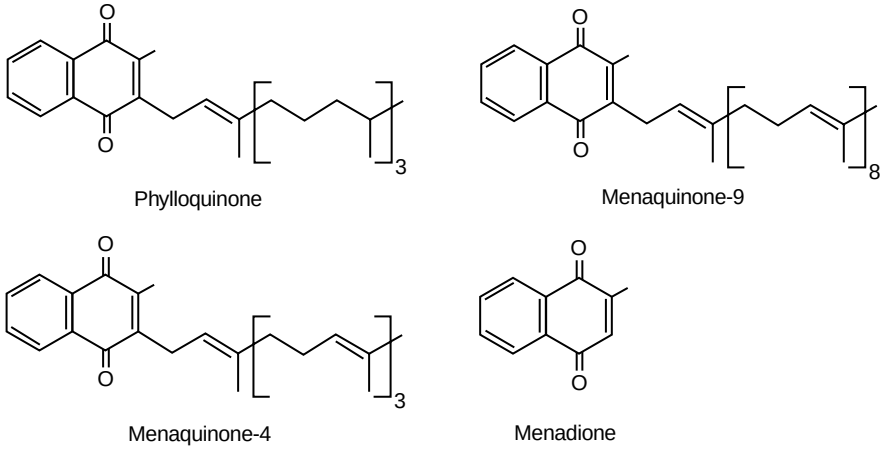

FIGURE 1 Structures of vitamin K active compounds. Phylloquinone (vitamin K_1) synthesized in plants is the main dietary form of vitamin K. Menaquinone-9 is a prominent member of a series of menaquinones (vitamin K_2) produced by intestinal bacteria, and menadione, vitamin K_3, is a synthetic compound that can be converted to menaquinone-4 by animal tissues.

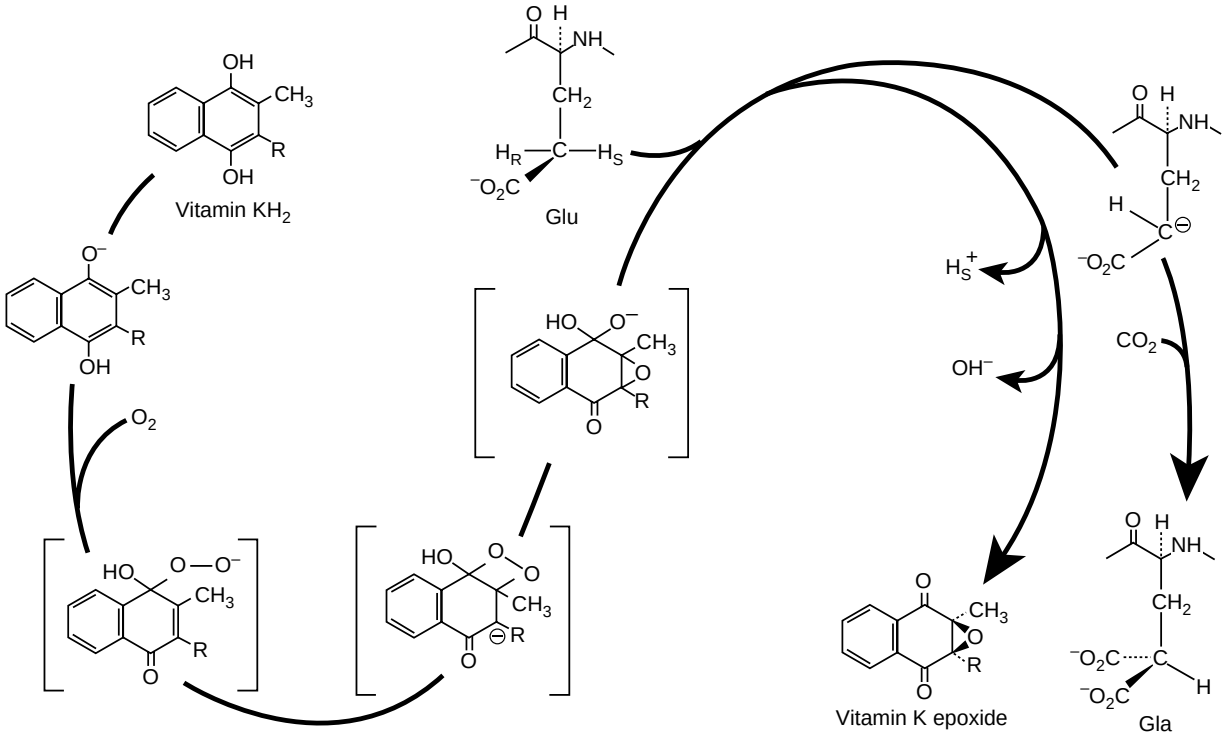

FIGURE 2 The vitamin K-dependent, γ-glutamyl carboxylase. The available data support an interaction of O_2 with vitamin KH_2, the reduced (hydronaphthoquinone) form of vitamin K, to form an oxygenated intermediate which is sufficiently basic to abstract the γ-hydrogen of the glutamyl residue. The products of this reaction are vitamin K-2,3-epoxide and a glutamyl carbanion. Attack of CO_2 on the carbanion leads to the formation of a Gla residue. The bracketed peroxy, dioxetane, and alkoxide intermediates have not been identified in the enzyme catalyzed reaction but are postulated based on model organic reactions, and the available data are consistent with their presence.

epoxide oxygen, and this partial dioxygenase activity has been demonstrated. Although the general scheme shown in Figure 2 is consistent with all of the available data, the mechanism remains a hypothesis at this time.

Progress in purifying this enzyme was slow. Utilization of bound propeptide as an affinity column aided progress in this field, and the enzyme was eventually purified to near homogeneity and cloned. The carboxylase is a unique 758 amino acid residue protein with a sequence suggestive of an integral membrane protein with a number of membrane-spanning domains in the N terminus, and a C-terminal domain located in the lumen of the endoplasmic reticulum. It has been demonstrated that the multiple Glu sites on the substrate for this enzyme are carboxylated processively as they are bound to the enzyme via their propeptide, while the Gla domain undergoes intramolecular movement to reposition each Glu for catalylsis, and that release of the carboxylated substrate is the rate-limiting step in the reaction.

Metabolic Interconversion of Vitamin K

Gla residues are not metabolized but are excreted in the urine. The amount of Gla excreted by an adult human is in the range of 50 μmol per day, so a similar amount must be formed each day. As the dietary requirement of vitamin K is only ~0.2 μmol per day, and tissue stores are very low, it is clear that the vitamin K 2,3-epoxide generated by the carboxylase can be actively recycled by the pathway shown in Figure 3. The vitamin K-epoxide reductase is capable of reducing both the epoxide to the naphthoquinone, and naphthoquinone to the hydronaphthoquinone, and this is the enzyme which is blocked by the common oral anticoagulant warfarin. In addition to the epoxide reductase, the quinone and hydronaphthoquinone forms of the vitamin can also be interconverted by a number of NAD(P)H-linked reductases including one that appears to be a microsomal-bound form of the extensively studied liver DT-diaphorase activity. The epoxide reductase utilizes a sulfhydryl compound as a reductant *in vitro*, but the physiological reductant has not been identified. Efforts to purify and characterize this enzyme have not yet been successful.

A second metabolic pathway utilizing phylloquinone has been discovered more recently. Chick liver contains a high concentration of menaquinone-4 (MK-4), and a number of extrahepatic tissues such as brain, salivary gland, and pancreas of rats and humans fed phylloquinone also contained a much higher

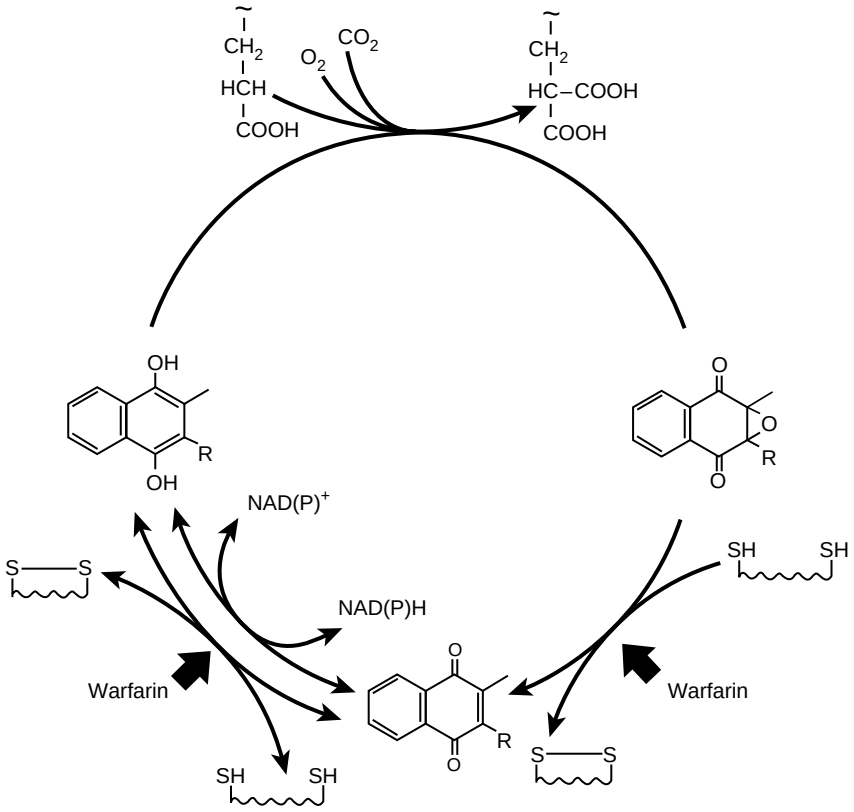

FIGURE 3 Tissue metabolism of vitamin K. Vitamin K epoxide formed in the carboxylation reaction is reduced to the quinone form of the vitamin by a warfarin-sensitive pathway, vitamin K epoxide reductase, that is driven by a reduced dithiol. The naphthoquinone form of the vitamin can be reduced to the hydronaphthoquinone form either by the same warfarin-sensitive dithiol-driven reductase or by one or more of the hepatic NADH or NADPH-lined quinone reductases which are less sensitive to warfarin.

concentration of MK-4 than of phylloquinone. Tissue formation of MK-4 from phylloquinone fed to germ-free rats and the observation that cultured kidney cells can convert phylloquinone to MK-4 have now demonstrated that bacterial action is not involved in the conversion and that numerous cell types have the ability to carry out this transformation. Details of the mechanism of this conversion are lacking, but it seems unlikely that a metabolic pathway leading to MK-4 has evolved unless there is some specific role for this vitamin. This role is unlikely to involve the vitamin K-dependent carboxylase, as phylloquinone and MK-4 have similar activity as a substrate for this enzymatic activity.

Nutritional Aspects of Vitamin K

Reports of uncomplicated adult deficiencies of vitamin K are extremely rare, and most diets contain an adequate amount (~100 mg per day) of vitamin K. Low lipid intake or the impaired lipid absorption resulting from the lack of bile salts will adversely affect vitamin K absorption, and depression of the vitamin K-dependent coagulation factors has frequently been reported in various malabsorption syndromes. This classic example of a human vitamin K deficiency is that of early vitamin K deficiency bleeding occurring during the first week of life in healthy appearing neonates. Low placental transfer of phylloquinone, low clotting factor levels, a sterile gut, and the low vitamin K content of breast milk all contribute to the disease. Although the incidence is low, the mortality rate from intracranial bleeding is high, and prevention by oral or parenteral administration of vitamin K immediately following birth is the standard cure. The presence of large amounts of osteocalcin in bone and reports that low vitamin K intake or increased amounts of circulating under-γ-carboxylated osteocalcin are correlated with low bone mineral density or fracture rate have focused significant attention on a possible role for vitamin K in bone health. A clear understanding of the significance of these reports is not yet available.

See Also the Following Articles

Quinones • Vitamin K: Blood Coagulation and Use in Therapy

Glossary

γ-carboxyglutamic acid An amino acid found in a limited number of proteins, formed by a posttranslational modification of Glu residues.

γ-glutamyl carboxylase The enzyme involved in the formation of Gla residues; also called vitamin K-dependent carboxylase.

Further Reading

Berkner, K. L. (2000). The vitamin K-dependent carboxylase. *J. Nutr.* **130**, 1877–1880.

Binkley, N. C., and Suttie, J. W. (1995). Vitamin K nutrition and osteoporosis. *J. Nutr.* **125**, 1812–1821.

Dowd, P., Ham, S.-W., Naganathan, S., and Hershline, R. (1995). The mechanism of action of vitamin K. *Annu. Rev. Nutr.* **15**, 419–440.

Furie, B., Bouchard, B. A., and Furie, B. C. (1999). Vitamin K-dependent biosynthesis of γ-carboxyglutamic acid. *Blood* **93**, 1798–1808.

Presnell, S. R., and Stafford, D. W. (2002). The vitamin K-dependent carboxylase. *Thromb. Haemost.* **87**, 937–946.

Suttie, J. W. (2001). Vitamin K. In *Handbook of Vitamins* (R. B. Rucker, J. W. Suttie, D. B. McCormick and L. J. Machlin, eds.) pp. 115–164. Marcel Dekker, New York.

Biography

John W. Suttie is Professor Emeritus of Biochemistry and Nutritional Sciences at the University of Wisconsin-Madison. He holds a Ph.D. from the University of Wisconsin-Madison. His research efforts have been directed toward an understanding of the biochemical and nutritional roles of vitamin K.

Vitamin K: Blood Coagulation and Use in Therapy

Matthew D. Stone and Gary L. Nelsestuen
University of Minnesota, Twin Cities, Minnesota, USA

Vitamin K is a fat soluble, quinone derivative (Figure 1) that is critical for healthy blood coagulation or hemostasis. It functions as a cofactor for a carboxylase in the post-translational production γ-carboxyglutamic acid (Gla), a unique amino acid that has calcium ion affinity. Henrik Dam first proposed the presence of this vitamin in the late 1920s and early 1930s in Germany through feeding chicks a strict organic solvent extracted diet. It was observed that these chicks died from uncontrolled bleeding. As a result, the vitamin was recognized as lipid soluble and named after the German word *koagulation*. Many proteins involved in blood coagulation contain Gla residues and these residues are essential for function.

Nomenclature

Vitamin K is defined as any molecule that contains the 2-methyl-1,4-naphthoquinone functional group (Figure 1A) and has biological function; i.e., it can reverse physiological effects of vitamin K deficiency. Two common forms are vitamin K_1 or phylloquinone (Figure 1B) and vitamin K_2 or menaquinone (Figure 1C). Vitamin K_1 has three repeating saturated prenyl groups adjoined to an initial unsaturated prenyl group at carbon 3 of the quinone. On the other hand, vitamin K_2 describes a class of compounds that contain multiple repeating unsaturated prenyl groups at carbon 3 of the quinone.

Biochemical Role of Vitamin K in Carboxylation

Vitamin K is a cofactor for a carboxylase that catalyzes the addition of CO_2 onto a peptidyl glutamic acid residue to produce γ-carboxyglutamic acid. Formation of a new carbon–carbon bond through carboxylation is energetically unfavorable. A more familiar method for biological carboxylation uses biotin as a cofactor and is coupled to adenosine triphosphate (ATP) hydrolysis to provide energy for product formation. In the vitamin K-dependent reaction, however, the energy to drive carboxylation is provided by vitamin K oxidation.

The reaction mechanism of the carboxylase is still under investigation. However, it is believed that the redox cycle (Figure 2) starts with the reduced form of vitamin K (KH_2). Molecular oxygen addition results in an epoxide, which is coupled to a concerted condensation of CO_2 and glutamic acid to form Gla. Within the concerted reaction, vitamin K oxidation has been proposed to result in a very strong base, which could abstract one of the γ protons of glutamic acid. The vitamin K epoxide is no longer active and must be reduced back to KH_2 in two stages by at least one reductase with concomitant disulfide oxidation.

The carboxylase is localized to the lumen of the endoplasmic reticulum from where it can modify newly synthesized peptides. Proteins to be carboxylated are recognized by a signal sequence near the amino terminus. The signal sequence is removed at a further processing event. The carboxylase only modifies specific glutamic acid residues.

Use of vitamin K as a biofactor appears to have evolved recently, since the vitamin K-dependent carboxylase has only been discovered in the animal kingdom. Naturally, it is expressed in all vertebrates with circulatory systems. However, it is also found in snails of the Conus genus, and the gene was recently identified in arthropods in *D. melanogaster*. High homology in sequence alignments suggests that the invertebrate carboxylase is an ancestor of the vertebrate form and that vitamin K function arose early in animal evolution.

Function of Vitamin K-Dependent Proteins

Blood Coagulation

The most well-understood biological process involving vitamin K-dependent proteins is blood coagulation. Blood coagulation is a complex pathway mediated by a

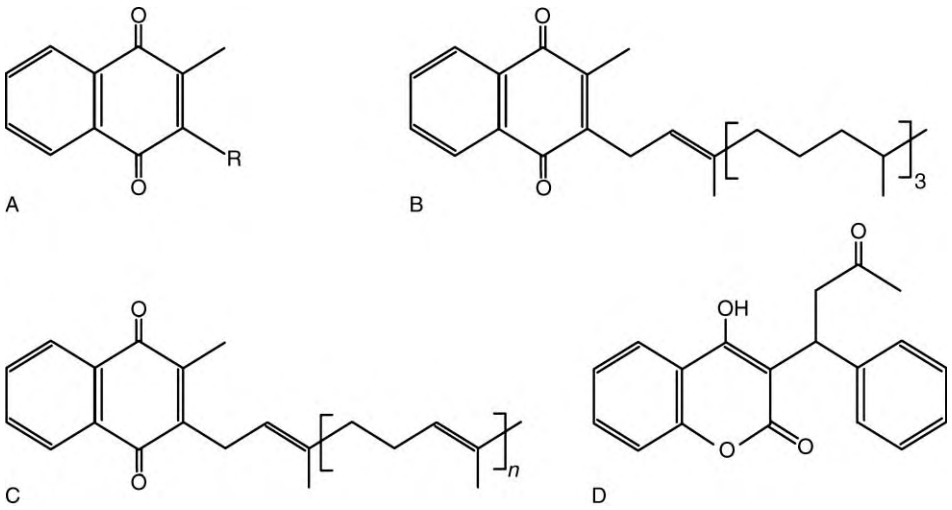

FIGURE 1 Vitamin K derivatives. (A) 2-methyl-1,4-napthoquinone, the functional group of vitamin K. (B) Phyloquinone or vitamin K_1. (C) Menaquinone or vitamin K_2. (D) Warfarin, a vitamin K antagonist.

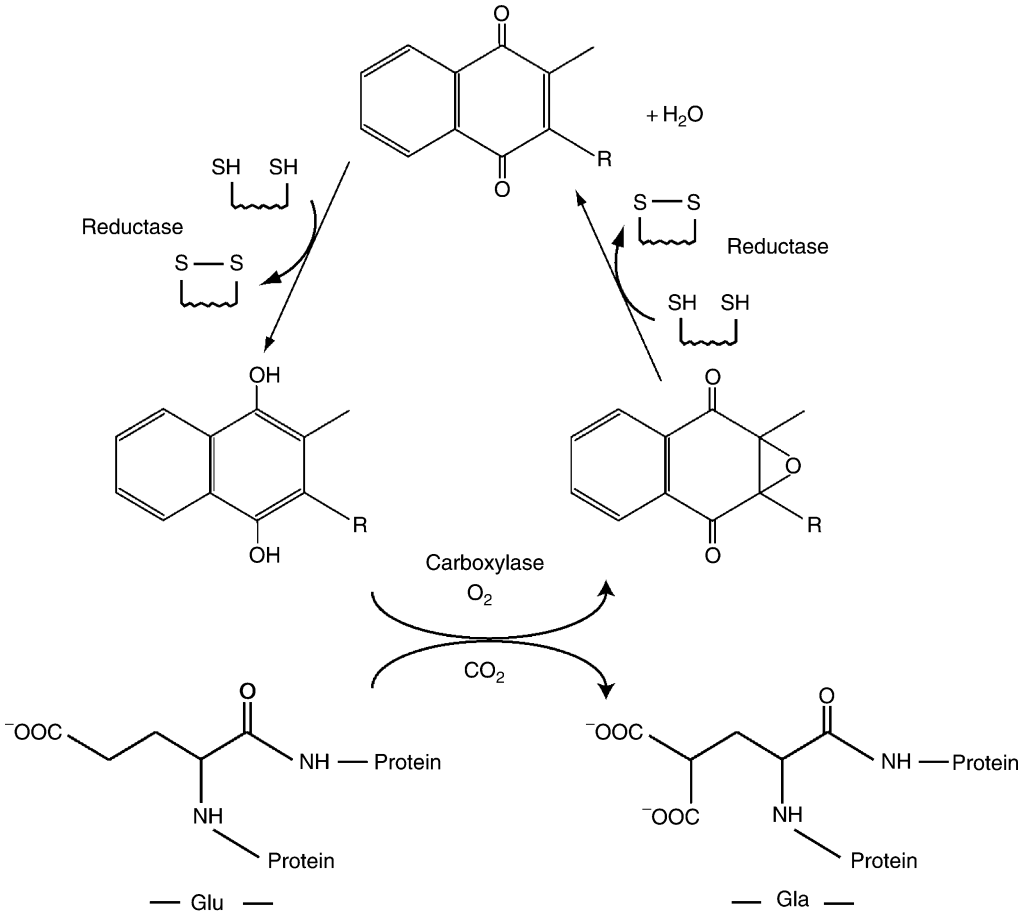

FIGURE 2 The vitamin K cycle. Oxidation of KH_2 to the epoxide provides sufficient energy for carboxylation and may participate in hydrogen abstraction. The cycle is completed by two reduction steps that regenerate KH_2.

series of proteolytic activation steps resulting in signal amplification (Figure 3). Many of the proteolytic reactions of the cascade depend on specific binding to membranes composed of acidic phospholipids such as phosphatidylserine. Binding to membrane aids the blood coagulation reactions by (1) directing the clotting factors to the site of injury and (2) increasing the concentration of clotting factors through localization to a restricted area.

The Procoagulation Pathway

Vitamin K-dependent plasma proteins within the procoagulant cascade include factor VII, factor IX, factor X, and prothrombin. The amino terminal 1–45 amino acids of each protein contain 9–12 Gla residues, which are not found elsewhere in the protein. As a result, this region is referred to as the Gla domain. The Gla residues bind calcium ions and the resulting conformational change shifts the Gla domain from a disordered structure to one that is able to bind to membranes. The exact membrane-binding site is still controversial.

Factor VII, factor IX, factor X, and prothrombin are zymogens containing a trypsin-like serine protease domain. The corresponding active enzymes are denoted with an "a" after the Roman numeral (e.g., factor VIIa). The exception is thrombin, the activated form of prothrombin (Table I).

Procoagulation is traditionally divided into two pathways, extrinsic and intrinsic, both leading to the production of factor Xa (Figure 3A). The extrinsic pathway is so-called because it relies on the expression of the cell surface receptor, tissue factor (TF), which is not found in plasma.

Blood coagulation is tightly regulated. Two important modes of regulation are (1) the above-mentioned selective membrane binding and (2) allosteric activation through cofactor protein binding. Initiation of the extrinsic pathway results from vascular injury. Injury disrupts cell membranes thereby exposing acidic

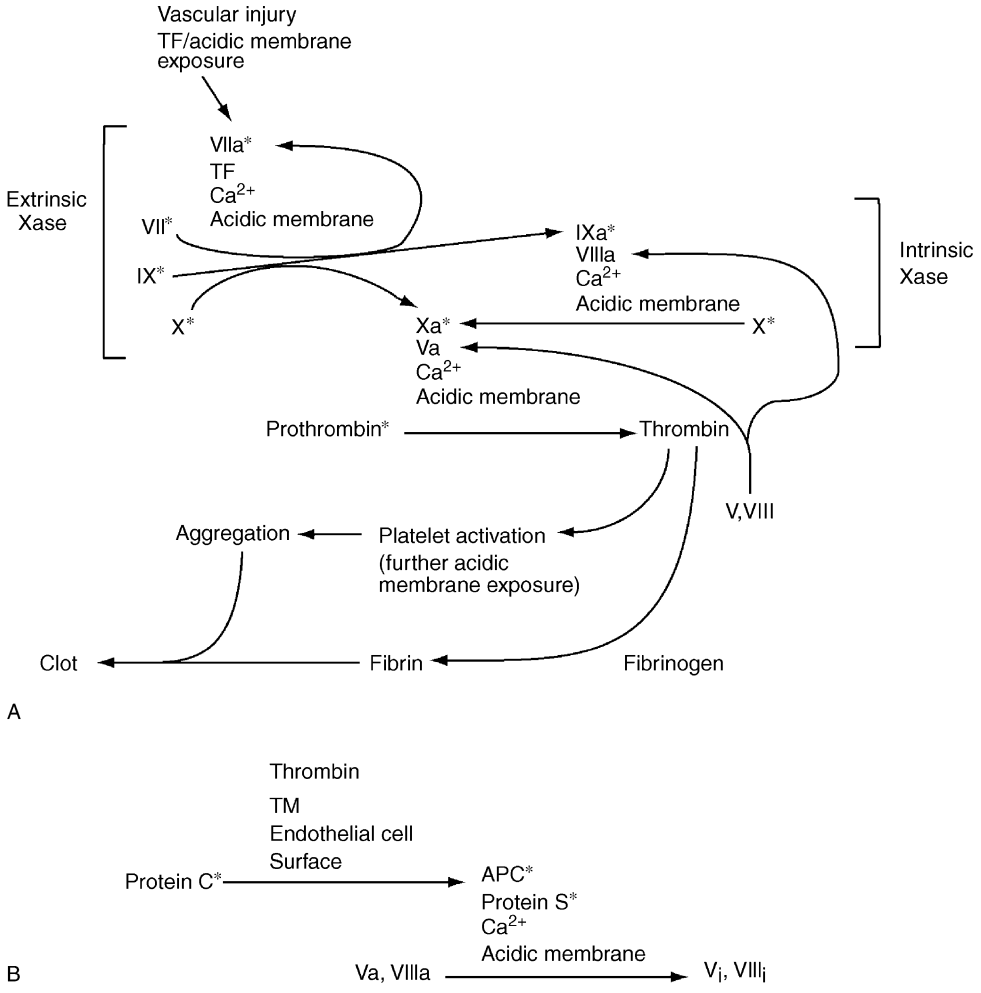

FIGURE 3 The coagulation cascade. (A) The procoagulation cascade is mediated by a series, a proteolytic activation steps with feedback activation for signal amplification. (B) The anticoagulant pathway inactivates factor Va and VIIIa. Enzyme complexes are depicted as vertical text columns with the proteolytic enzyme first, protein cofactors second, and calcium and membrane components last. The asterisk denotes a vitamin K-dependent protein.

TABLE I

List of Coagulation Factors

Factor	Active form	Alternative name	Alternative name of active form	Function
I	Ia	Fibrinogen	Fibrin	Clot forming protein
II[a]	IIa	Prothrombin	Thrombin	Enzyme
III		Membrane surface with tissue factor		Cofactor
IV		Calcium		Cofactor
V	Va	Proaccelerin	Accelerin	Protein cofactor
VII[a]	VIIa[a]	Proconvertin	Convertin	Enzyme
VIII	VIIIa	Anti-hemophilic factor		Protein cofactor
IX[a]	IXa[a]	Christmas factor		Enzyme
X[a]	Xa[a]	Stuart factor		Enzyme

[a] Denotes vitamin K-dependent protein.

phospholipids, such as phosphatidylserine, that are not normally exposed on healthy cell surfaces. Injury also exposes TF, the cofactor for factor VIIa, which is expressed in subendothelial layers. Protease activity of VIIa is greatly enhanced when bound in complex with membrane and TF allowing it to efficiently catalyze three reactions. It activates itself, factor VII to VIIa, factor IX to IXa, and factor X to Xa. Factor Xa similarly produces a small amount of thrombin, which initiates the intrinsic pathway through activation of factor VIII to factor VIIIa. Thrombin also activates factor V to factor Va and it activates platelets. Activation of platelets causes them to expose acidic membrane, thereby expanding the clotting reaction surface and to aggregate, thereby forming a plug at the site of injury.

The intrinsic pathway constitutes the second phase of the coagulation reaction and functions to amplify the clotting stimulus. Factor IXa, in complex with membrane and Factor VIIIa, catalyzes further conversion of factor X to factor Xa. Classic hemophilia is a result of deficiencies in either factor VIII or IX. Buildup of factor Xa and its cofactor, factor Va, leads to efficient large-scale production of thrombin. Finally, thrombin hydrolyzes fibrinogen to fibrin, which self-polymerizes into a macro-molecular protein net that, along with the platelet plug, comprises a clot.

The Anticoagulation Pathway

Of numerous anticoagulation pathways, one is comprised of two vitamin K-dependent plasma proteins, protein C and protein S (Figure 3B). This pathway is initiated when thrombin, in complex with the endothelial cell surface receptor thrombomodulin, catalyzes proteolytic activation of protein C to activated protein C (APC). Protein S, which is not an enzyme, acts as a cofactor for APC. Together these proteins inhibit amplification of the coagulation reaction through proteolytic inactivation of factor Va and factor VIIIa. Protein Z is another non-enzymatic vitamin K-dependent plasma protein involved in anticoagulation. It acts as a cofactor for a specific factor Xa inhibitor protein.

Other Vitamin K-Dependent Proteins

Vitamin K has diverse, although less characterized, roles outside of blood coagulation. One vitamin K-dependent protein, the product of the growth arrest specific 6 gene (Gas6), has high homology to protein S and appears to be involved in development. Skeletal tissues express two vitamin K-dependent proteins, bone matrix Gla protein, and osteocalcin. These proteins are rather small, contain only two Gla residues, and have little similarity to the plasma proteins. The bone matrix protein has been implicated in the prevention of vascular calcification.

Small unique peptide toxins called conantokins from snails of the Conus genus have also been identified as vitamin K dependent. These toxins function as neurotransmitter inhibitors that paralyze fish for these predatory snails.

The majority of vitamin K-dependent plasma proteins are expressed in the liver. However, virtually every cell type aside from muscle expresses the vitamin K-dependent carboxylase, implying that vitamin K is vital to many tissues. Some cell receptor proteins have been shown to contain Gla domains. However, the dominant symptom of vitamin K deficiency is a loss of blood coagulation potential.

Nutrition

Vitamin K_1 is found mainly in green leafy vegetables and to a lesser extent in cooking oils such as soybean and canola oil. The equally active vitamin K_2 molecules are synthesized by intestinal bacteria and absorbed with bile salts. However, the contribution of these derivatives toward the total vitamin K requirement has not been accurately determined. Nevertheless, the recommended daily amount of dietary vitamin K is 1 μg per kg of body weight.

Since the requirement is rather low and a typical adult human diet contains an excess of vitamin K, deficiencies are rare. Those that do occur are probably due to a variety of factors such as poor diet, liver disease or failure, low surface area for intestinal absorption, inadequate production of bile salts, or administration of antibiotics that could disturb bacterial vitamin K production.

Vitamin K deficiency leading to hemorrhagic disease in newborns is observed and is probably due to a lack of

established bacteria in the intestines of newborns, and a low vitamin K content in breast milk. As a result, newborns are given a 0.5–1.0 mg vitamin K injection upon birth and baby formula is typically fortified with vitamin K.

Use in Therapy

Vitamin K Antagonists as Anticoagulants

Several structural analogues of vitamin K, known as 4-hydroxycoumarins, have been synthesized and function as anticoagulants. The most common is warfarin (Figure 1D), also described by the term, coumadin. Warfarin functions as a vitamin K antagonist through inhibition of the epoxide reductase in the vitamin K reaction cycle (Figure 2). Treatment results in under-carboxylation of plasma proteins leading to loss of function and an anticoagulant state. Warfarin is typically used as a long-term anticoagulant and can be administered orally. However, therapy must be monitored, since overdose can lead to uncontrolled bleeding. Additionally, warfarin is an effective rodenticide and is the active ingredient in many pest traps.

Recombinant Vitamin K-Dependent Proteins as Anticoagulants

Advances in recombinant DNA technology have allowed the expression and purification of vitamin K-dependent proteins for use in factor replacement therapy. Recombinant proteins are more attractive than plasma concentrates because of the threat of viral contamination in donated blood.

Recombinant APC is useful for treatment of severe sepsis. Sepsis is caused by bacterial infection leading to a massive inflammatory response, which causes aberrant endothelial expression of TF as well as down-regulation in protein C levels. Severe sepsis leads to undesirable activation of the coagulation cascade inducing stroke or aneurysm and is often deadly. APC has proven to be an effective therapy of severe sepsis. Not only does it inhibit coagulation, but it also inhibits inflammation, and has been shown to significantly reduce associated fatalities.

Recombinant Vitamin K-Dependent Proteins as Procoagulants

Recombinant factor IX is used in replacement therapy for factor IX deficiency. Extreme cases of factor VIII or IX deficiency arise in hemophiliacs who develop antibodies to either factor VIII or IX that is administered through replacement therapy. In these patients, high dose recombinant factor VIIa can be used to treat bleeding episodes by a mechanism that bypasses the intrinsic pathway.

See Also the Following Articles

Proteases in Blood Clotting • Quinones • Vitamin K: Biochemistry, Metabolism, and Nutritional Aspects

Glossary

carboxylase An enzyme that catalyzes the addition of a carboxylic acid group onto a substrate.
coagulation The process of blood clot formation to stop bleeding.
cofactor Any agent (protein, metabolite, metal ion, etc.) that aids an enzyme during catalysis.
hemophilia A disease characterized by pronounced bleeding and a prolonged response to a coagulation stimulus.
warfarin or coumadin Orally administered vitamin K antagonists.

Further Reading

Booth, S., and Suttie, J. (1998). Dietary intake and adequacy of vitamin K. *J. Nutr.* **128**, 785–788.
Dowd, P., Ham, S., and Geib, S. (1995). The mechanism of action of vitamin K. *Annu. Rev. Nutr.* **15**, 419–440.
Hirsch, J., Ginsberg, J., and Marder, V. (1994). Anticoagulant therapy with coumarin agents. In *Hemostasis and Thrombosis: Basic Principles and Clinical Practice* (R. Colman, J. Hirsch, V. Marder and E. Salzman, eds.) pp. 1567–1583. J. B. Lippincott, Philadelphia.
McCoy, C., and Matthews, S. (2003). Drotrecogin alfa (recombinant human activated protein C) for the treatment of severe sepsis. *Clin. Ther.* **25**, 396–421.
Nelsestuen, G., Shah, A., and Harvey, S. (2000). Vitamin K-dependent proteins. *Vitam. Horm* **58**, 355–389.
Stenflo, J. (1999). Contributions of Gla and EGF-like domains to the function of vitamin K-dependent coagulation factors. *Crit. Rev. Eukayotic Gene Exp.* **9**, 59–88.
Suttie, J. (2001). Vitamin K. In *Handbook of Vitamins* (R. Rucker, J. Suttie, D. McCormick and L. Machlin, eds.) pp. 115–164. Marcel Dekker, New York.
Veldman, A., Hoffman, M., and Ehrenforth, S. (2003). New insights into the coagulation system and implications for new therapeutic options with recombinant factor VIIa. *Curr. Med. Chem.* **10**, 797–811.

Biography

Gary Nelsestuen is currently the Samuel Kirkwood Professor of Biochemistry, Molecular, and Biophysics at the University of Minnesota, Twin Cities. He was one of the investigators who discovered the relationship of vitamin K to Gla. He has also made numerous contributions in understanding the nature of interaction between calcium-binding proteins and membranes. He received his Ph.D. from the University of Minnesota in 1970 and was a postdoctoral fellow at the University of Wisconsin.

Matthew D. Stone currently holds the Thomas Reid Fellowship at the University of Minnesota, Twin Cities in the Department of Biochemistry, Molecular Biology, and Biophysics. He is a new researcher in the vitamin K field and currently studies functional consequences from the binding of vitamin K-dependent plasma proteins with membranes.

Voltage-Dependent K^+ Channels

Ramón Latorre and Francisco J. Morera
Centro de Estudios Científicos, Valdivia, Chile

Voltage-dependent K^+ channels are the intrinsic membrane proteins that by forming a conduction pathway, or pore, through which K^+ selectively diffuses down their electrochemical gradient across the membrane, draw the cell-resting potential toward the K^+ equilibrium potential. The voltage imposed across the cell membrane governs pore opening – hence the name voltage-dependent K^+ channels. By hyperpolarizing the cell membrane, these channels serve as the appropriate negative feedback to excitatory inputs on a cell when they are active. In general, voltage-dependent K^+ channels increase their activity on membrane depolarization and their activation dampens the excitatory events that elevate the cytosolic Ca^{2+} and/or depolarize the cell membrane. Voltage-dependent K^+ channels are widely distributed in mammalian tissues and play important physiological roles. Setting the duration of action potentials and the interspike interval during repetitive firing in neurons and in the heart, K^+ secretion in epithelia, setting the smooth muscle tone, and determining the resonance frequency in hair cells are some of the roles that voltage-dependent K^+ channels play. Voltage-dependent K^+ channels are made of subunits that assemble in the bilayer as tetramers to form highly selective K^+ channels. The large number of different genes, alternative splicing, auxiliary β-subunits, and metabolic regulation explain the tremendous diversity of voltage-dependent K^+ channels.

Voltage-Dependent K^+ Channel Structure and Diversity

Voltage-dependent K^+ (eag, AKT1, KAT1, hslo, KCNQ, K_v) channels are tetrameric assemblies, each subunit consisting of six hydrophobic segments, S1–S6. Hslo is an exception containing seven hydrophobic segments, S0–S6. In 2003, the group of Rod MacKinnon determined the crystal structure of the full-length K_v channel from the bacterium *Aeropyrum pernix* (K_vAP) at a resolution of 3.2Å. In the K_vAP channel, the linker between the S5 and S6 segment dips back down into membrane and participates in formation of the channel pore and determines ion selectivity (Figures 1(Aa) and 1(Ab)). This region is commonly referred to as the P region or the pore loop. Figures 1(Aa) and 1(Ab) show a comparison of the K_vAP pore (blue) with the KscA K^+ channel (green). The pore-lining, inner, S6-helices contain a conserved glycine (red dots in Figure 1(Aa)). This residue has been proposed to be a gating hinge that allows the inner helix bends 30° when the pore opens. In Figures 1(Aa) and 1(Ab), the K_vAP pore is in the open and the KcsA pore is in closed configuration. All K^+ channels have, inside the P region, a consensus amino acid sequence: TXXTVGYGD, dubbed the "signature sequence." The residues TVGYG line the selectivity filter (in some K^+ channels the tyrosine (Y) residue is replaced by phenylalanine (F), for example, in the eag channel). In the selectivity filter, carbonyl oxygen atoms are directed toward the pore to coordinate dehydrated K^+ ions and hydrophobic chains of valine and tyrosine directed toward the hydrophobic core surrounding the filter stabilize the main chain (Figure 1(Ac)).

Gating in the K^+ channels is conferred through the attachment of gating domains to the pore. The basic function of these gating domains is to perform mechanical work on the ion conduction pore to change its conformation between closed and open states. In voltage-dependent channels, a "voltage sensor" domain (S1–S4) is present on each subunit. Thus, a voltage sensor converts energy stored in the membrane electric field into mechanical work. There is evidence that the positive charges contained in S4 are the voltage-sensing elements. Thus, ion channel gating is essentially an electromechanical coupling between a gating unit and a pore unit.

K_vAP channels contain a central ion-conduction pore surrounded by the voltage sensor. Each S4 segment forms half of a "voltage-sensor paddle" (Figure 1(B)). Whether or not this is the structure involved in voltage-dependent activation is at present under heavy scrutiny.

Voltage-dependent K^+ channels are ubiquitously distributed in different cell and tissues and, therefore, K^+ channel diversity is of great importance in determining the variety of electrical responses of cells when subjected to stimuli. The possible mechanisms that originate the immense voltage-dependent K^+ channel diversity are: (1) multiple genes; (2) alternative splicing;

(3) formation of heteromultimeric channels; and (4) coexpression with regulatory β-subunits.

Voltage-dependent K^+ channel diversity seems to have accompanied animal cells through evolution, and some K^+ channels are the most conserved proteins in eukaryotes. Potassium channels became fundamental to animal cell physiology very early in evolution, and through voltage-dependent K^+ channel control of membrane potential they couple the cell inner dynamics to the outer environment. A differential expression of voltage-dependent K^+ channel mRNAs is found to accompany the events of animal development and this also occurs in adult animal tissues. This differential expression of voltage-dependent K^+ channels is particularly noteworthy in the brain where it has been documented from invertebrate to mammals.

Some idea of the diversity of voltage-dependent K^+ channel genes is indicated in the dendrogram shown in Figure 2. The dendrogram shows the major classes of voltage-dependent K^+ channels. The ramification of voltage-dependent K^+ channels was constructed by sorting the genes according to their similarity of amino acid sequence. In order to compare the amino acid sequences of the different voltage-dependent K^+ channels, the sequences were aligned using at least 300 amino acids from six hydrophobic segment (S1–S6) channels and their respective linkers. Branch lengths do not represent time, but the branching is expected to preserve evolutionary relationships.

Physiological Function of Voltage-Dependent K^+ Channels

Ether-a-go-go K^+ Channels

Mutant fruit flies which shook their legs like go-go dancing when anesthetized with ether were carriers of a mutated gene of a voltage-gated K^+. This gene was called ether-a-go-go or *eag*. A family of *eag*-like genes was isolated from *Drosophila*, known as aeg, erg, and elk. The human ether-a-go-go related gene (HERG) was cloned by homology from a human hippocampal cDNA library. HERG was strongly expressed in heart and LQT2, a mutation on this gene, impairs the

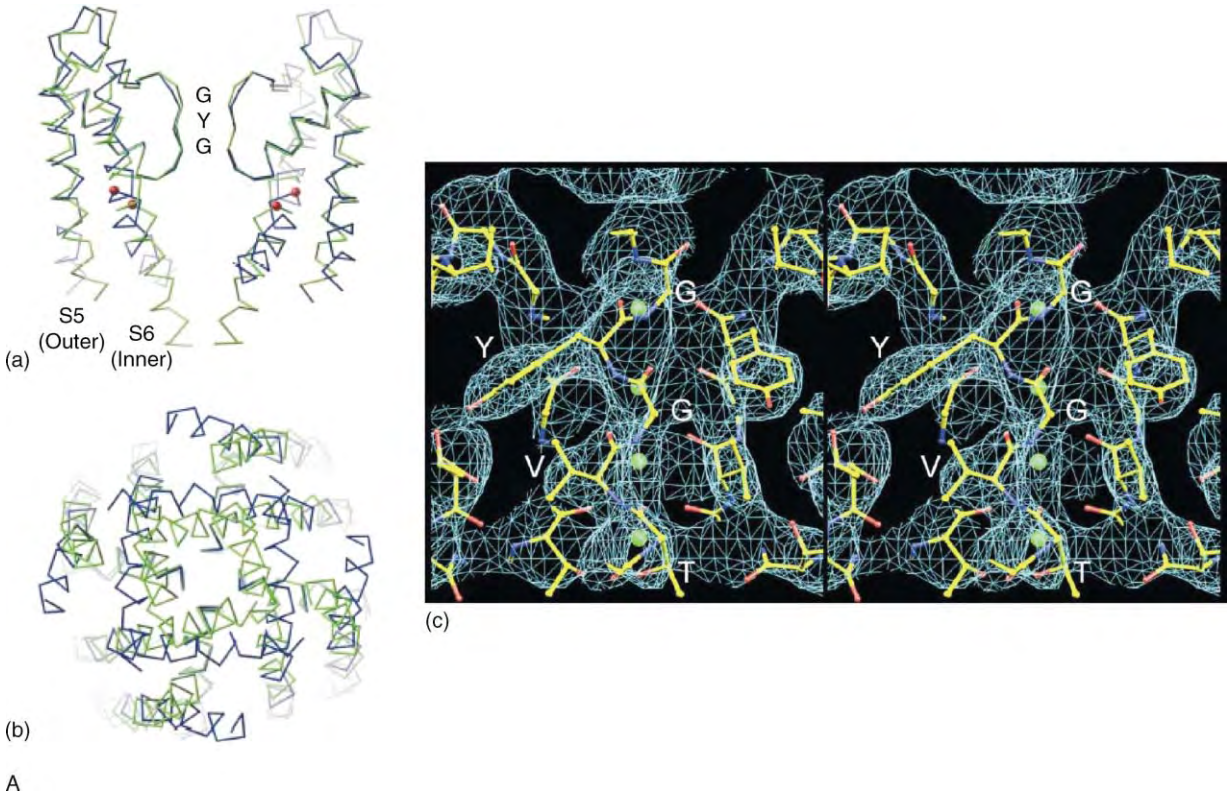

FIGURE 1 (A) The crystal structure of K_v channel from the bacterium *Aeropyrum pernix* (KvAP) (a); view from the side of the K_vAP pore (blue) and comparison with the KcsA channel (green) (b); and the α-carbon traces are shown from the intracellular solution (c). (B) Architecture of the K_vAP channel. Image of the K_vAP channel tetramer viewed from the intracellular side (a) of the membrane and from the side with the intracellular solution (b) below, and a single subunit viewed from the side (c and d). Each subunit has a different color. (Modifed from Jiang, Y., Lee, A., Chen, J., Ruta, V., Cadene, M., Chalt, B. T., and MacKinnon, R. (2003). X-ray structure of a voltage-dependent K^+ channel. *Nature* **423**, 33–41.)

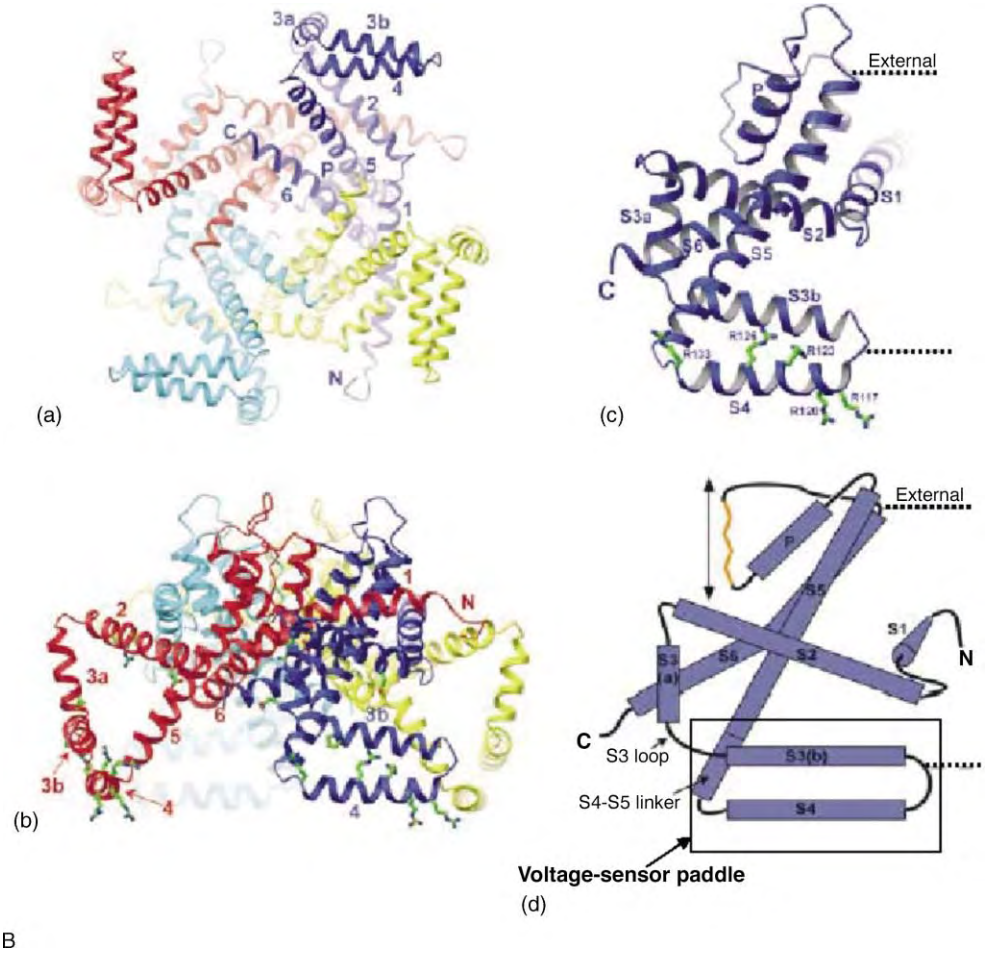

B

FIGURE 1 *(continued)*

repolarization of the cardiac action potential, causing a form of long QT syndrome.

Plant K^+ Channels: KAT1 and AKT1

In plants, voltage-dependent inward rectifiers mediate potassium uptake. KAT1 and AKT1 were the first inward rectifier K^+ channels cloned from the plant *Arabidopsis thaliana*. The KAT1 channel is expressed in guard cells and the vascular system of the stem. AKT1 is present in guard cells and in the root cortex and it plays an important role in K^+ uptake from the soil.

Calcium-Activated K^+ Channel

A change in the intracellular calcium concentration is a ubiquitous signaling mechanism that is frequently coupled with changes in membrane potential. These signals are integrated by the activation of a heterogeneous family of potassium channels, Ca^{2+}-activated potassium channels (K_{Ca}), whose open probability is increased by the elevation of cytosolic calcium to cause membrane hyperpolarization. They are found in a wide range of different tissues and in virtually all multicellular organisms. In nerve cells, they play a key role in controlling the action potential waveform and in regulating cell excitability. In secretory epithelia they are also involved in K^+ secretion. K_{Ca} channels contribute to the repolarization and after-hyperpolarization of vertebrate neurons. Since this article is related to a voltage-dependent K^+ channel only, in this section the importance of one K_{Ca} channel family code by a single gene called *slowpoke* (*slo*) will be discussed. Expression of *Slo* in mammalian cells or *Xenopus* oocytes induces the appearance of a highly K^+-selective, Ca^{2+}-activated and voltage-dependent channel also known as MaxiK or BK (big K) because of its large single-channel conductance (>200 pS in 100 mM symmetrical K^+). At difference of its other voltage-dependent K^+ channel congeners, the Slo protein has an extra hydrophobic segment at the NH2 terminus denominated S0. Thus, the NH2 terminus of the protein is placed in the extracellular side of the membrane. The intracellular COOH-terminal comprises about two-thirds of the protein containing four hydrophobic segments, several alternative splicing sites, and a stretch of negatively

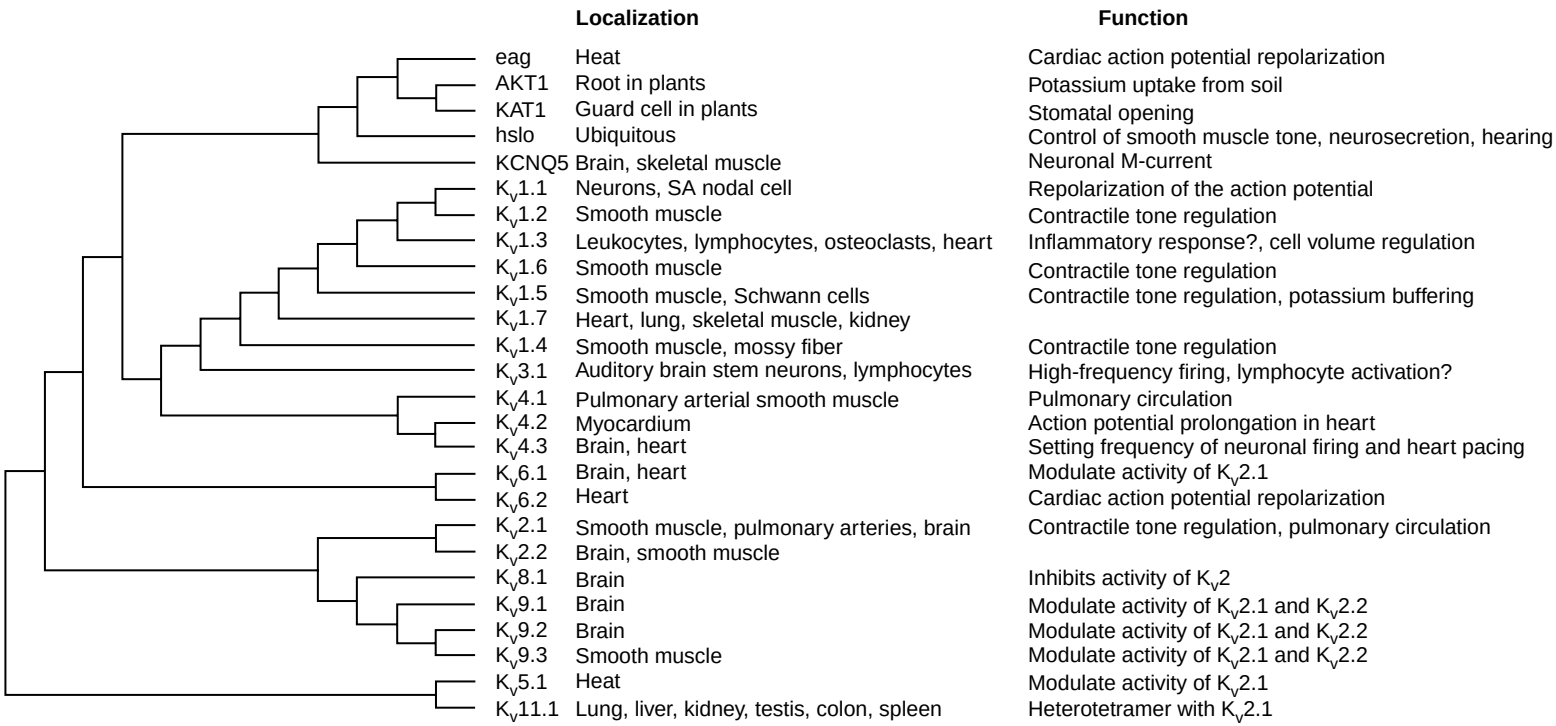

FIGURE 2 The major classes of voltage-dependent K^+channels, their tissue localization and function. Comparison of the amino acid sequences of the different α-subunits for voltage-dependent K^+ channels. The dendrogram was constructed using ClustalW and TreeView. The more similar the sequences for a pair of genes, the shorter the path connecting them.

charged amino acids (aspartates) denominated the "Ca^{2+} bowl." The Ca^{2+} bowl has emerged as a good candidate for the high-affinity Ca^{2+}-binding site.

Slo channels control a large variety of physiological processes, including smooth muscle tone, neurosecretion, and hearing. Despite being coded by a single gene, the diversity of Slo channels is great. Regulatory β-subunits, splicing, and metabolic regulation create this diversity fundamental to the adequate function of many tissues. Except in heart myocytes, Slo channels are almost ubiquitously expressed among mammalian tissues, and they play a variety of roles. In smooth muscle, local Ca^{2+} increases, called Ca^{2+} sparks, generate spontaneous transient outward currents, which are generated by Slo channels. This hyperpolarizes the membrane causing muscle relaxation. In chromaffin cells, Slo channels are important for rapid termination of the action potential. In the cochlea of turtles, frogs and chicks, gradients of spliced Slo channels, and β-subunits through an interplay with voltage-dependent Ca^{2+} channels, they are able to generate the different oscillatory responses in the hair cells.

KCNQ Channels

The first member of the KCNQ family to be cloned, *KCNQ1*, was isolated by virtue of the fact that mutations in this gene give rise to the most common form of long QT syndrome, LQT1. Exploiting their homology to KCNQ1, other members of this family were subsequently cloned. KCNQ1 encodes the major subunit of the cardiac I_{Ks} channel, which is involved in repolarization of the ventricular action potential. KCNQ1 mRNA is expressed strongly in the heart, with lower levels in pancreas, kidney, lung, placenta, and ear.

It has been suggested that KCNQ2 and KCNQ3 is a heteromer, an idea which is consistent with their overlapping tissue distribution and the fact that antibodies directed against KCNQ2 are able to coimmunoprecipitate KCNQ3, and vice versa. The heteromeric KCNQ2/KCNQ3 channel corresponds to neurone's M-channel. They are widely distributed throughout the brain, being expressed at high levels in hippocampus, chordate nucleus, and amygdala. Mutations in *KCNQ2* and *KCNQ3* rise to a form of idiopathic epilepsy known as benign familial neonatal convulsions.

K_v Channels

The vertebrate fast voltage-gated K^+ delayed rectifier channels fall into a variety of families (K_v1–K_v11) according to their amino acid sequence similarity (Figure 2). A channel from a fruit fly *Drosophila* was the first K^+ channel to be cloned (denominated in vertebrates as $K_v1.1$, the first number denoting subfamily and the second, order of discovery). The identification started with mutant flies called shakers, which shake their legs while under ether anesthesia. These flies lack a fast transient K^+ current in presynaptic terminals, so repolarization of the action potential is delayed and the evoked release of neurotransmitter from a single action potential becomes enormous.

K_v channels are found in a wide range of different tissues and they have many different functions. Some ideas of the diversity of roles of K_v channels are shown in Figure 2. For example, $K_v3.1$ channels are found in some neurons that are specialized to fire very short action potentials at high rates, such as those of the auditory system; $K_v1.3$ channels are found in leukocytes playing a role in inflammatory response; $K_v1.2$ channels are found in smooth muscle participating in contractil tone regulation; and $K_v4.2$ channels are expressed in myocardium and their function is action potential prolongation in heart.

Defects in K_v channels function therefore may have profound physiological effects. Linkage studies have identified the gene responsible for episodic ataxia type-1. This gene encoded for $K_v1.1$ channel, which is expressed in the synaptic terminals and dendrites in brain neurones.

See Also the Following Articles

Ion Channel Protein Superfamily • Voltage-Sensitive Ca^{2+} Channels

Glossary

delayed rectifier A K^+ channel that changes the membrane conductance with a delay after a depolarizing voltage step.

gating The opening or closing of a channel in response to some stimulus.

inward rectifier A K^+ channel that opens when the membrane is hyperpolarized.

long QT syndrome An inherited cardiac arrhythmia.

voltage sensor A channel structure able to detect changes in membrane potential. In voltage-dependent ion channels the voltage-sensing elements are located in the S4 segment.

Further Reading

Hille, B. (2001). *Ions Channels of Excitable Membranes*. Sinauer Associates, Sunderland, Massachusetts.

Jiang, Y., Lee, A., Chen, J., Ruta, V., Cadene, M., Chalt, B. T., and MacKinnon, R. (2003). X-ray structure of a voltage-dependent K^+ channel. *Nature* **423**, 33–41.

Lainé, M., Papazian, D. M., and Roux, B. (2004). Critical assessment of a proposed model of Shaker. *FEBS Lett.* **564**, 257–263.

Orio, P., Rojas, P., Ferreira, G., and Latorre, R. (2002). New disguises for and old channel: MaxiK channel β-subunits. *News Physiol. Sci.* **17**, 156–161.

Biography

Ramon Latorre is Professor and Chair of the Laboratory of Biophysics and Molecular Physiology, CECS. He holds a Ph.D. from the University of Chile and received his postdoctoral training at the Biophysics Laboratory in the National Institutes of Health, Maryland. He is a Foreign Associate of the National Academy of the United States of America. The main scientific interest of Dr. Latorre is the molecular workings of ion channels.

Francisco Morera holds a degree in biochemistry from the Catholic University, Chile and is at present a Ph.D. in the Austral University, Valdivia, Chile.

Voltage-Sensitive Ca^{2+} Channels

Harald Reuter
University of Bern, Bern, Switzerland

Ion channels are integral, pore-forming transmembrane proteins that serve to pass ions across biological membranes. The channels differ in their ion selectivity, i.e., each type allows certain ion species to permeate through the open channel pore. Conformational changes of the proteins leading to openings or closings of the channels are called "gating." It is achieved either by binding of ligands to special sites on the channels (ligand-gated ion channels), or by changes in membrane potential (voltage-gated ion channels). Calcium (Ca^{2+}) channels are voltage-gated and have a high selectivity for Ca^{2+} ions. Opening of these channels by membrane depolarization leads to an influx of Ca^{2+} ions into the cell. The resulting increase in the intracellular Ca^{2+} concentration initiates essential physiological functions, such as cardiac contraction, secretion of hormones and neurotransmitters, gene transcription, or repetitive electrical activity of neurons and the heart. Most of these functions result from binding of Ca^{2+} to specific intracellular proteins (e.g., calmodulin, troponin C) which subsequently mediate the Ca^{2+}-dependent cellular responses. The diversity of voltage-gated Ca^{2+} channels in surface membranes of different cells is important for initiation of specific signaling cascades within the cells. The various types of Ca^{2+} channels are encoded by different genes and show tissue-specific expression. They are targets for toxins and for drugs used for therapeutic purposes.

Molecular Properties

Structures

Voltage-gated Ca^{2+} channels are oligomeric protein complexes composed of the voltage-sensitive, pore-forming α_1-subunits, together with auxiliary disulfide-linked $\alpha_2\delta$-subunits and intracellular β-subunits (Figure 1). An additional transmembrane γ-subunit is associated with α_1S in skeletal muscles. The diversity of Ca^{2+} channel types not only results from different genes coding for the different channel subunits (10 for α_1, 4 for $\alpha_2\delta$, and 4 for β), but also from multiple splice variants of the subunits. The α_1-subunits consist of four homologous domains (I–IV), each being composed of six transmembrane α-helical segments (S1–S6). The N and C termini are located intracellularly, and the domains are linked together by intracellular loops. In the folded structures of α_1-subunits, hairpin loops between transmembrane segments S5 and S6 constitute the channel pore. Segments S4 contain highly conserved, positively charged amino acids that act as voltage-sensitive sensors during gating of the channels. The β-subunits are involved in the regulation of the channels' gating properties and, like $\alpha_2\delta$-subunits, play a role in the functional expression of the channels in cell surface membranes.

Selectivity

Ca^{2+} channels are selective pathways for the movement of Ca^{2+} ions down their electrochemical gradient into the cell. The pore-forming structures of the channel contain four negatively charged glutamate residues, each being in a homologous position on the four domains. The resulting ring of negative charges facing the pore coordinates binding of an entering Ca^{2+} ion. A second Ca^{2+} ion that enters the channel reduces the binding affinity of the first one by electrostatic repulsion, thus kicking it off from its binding site and letting it move down its electrochemical gradient. Thus, the selectivity of the channel for Ca^{2+} is critically dependent on the correctly placed negative charges of glutamate in the pore.

Calmodulin Binding

Two forms of autoregulation, Ca^{2+}-dependent inactivation and facilitation of $Ca_v1.2$ channels (Table I), involve calmodulin (CaM). The subunit α1C of $Ca_v1.2$ contains a consensus CaM-binding isoleucine-glutamine (IQ)-motif in its cytoplasmic C-terminal tail. The IQ-motif consists of 12 amino acids. Extensive mutations within this sequence revealed structural determinants for the two opposing forms of channel regulation. Two short stretches of aminoacids upstream of the IQ-motif seem to be sites for constitutive, Ca^{2+}-independent binding of apoCaM. The IQ-motif binds CaM only in the presence of Ca^{2+}. It represents the regulatory site for Ca^{2+} -dependent inactivation, while facilitation may require additional activation of Ca/CaMkinaseII.

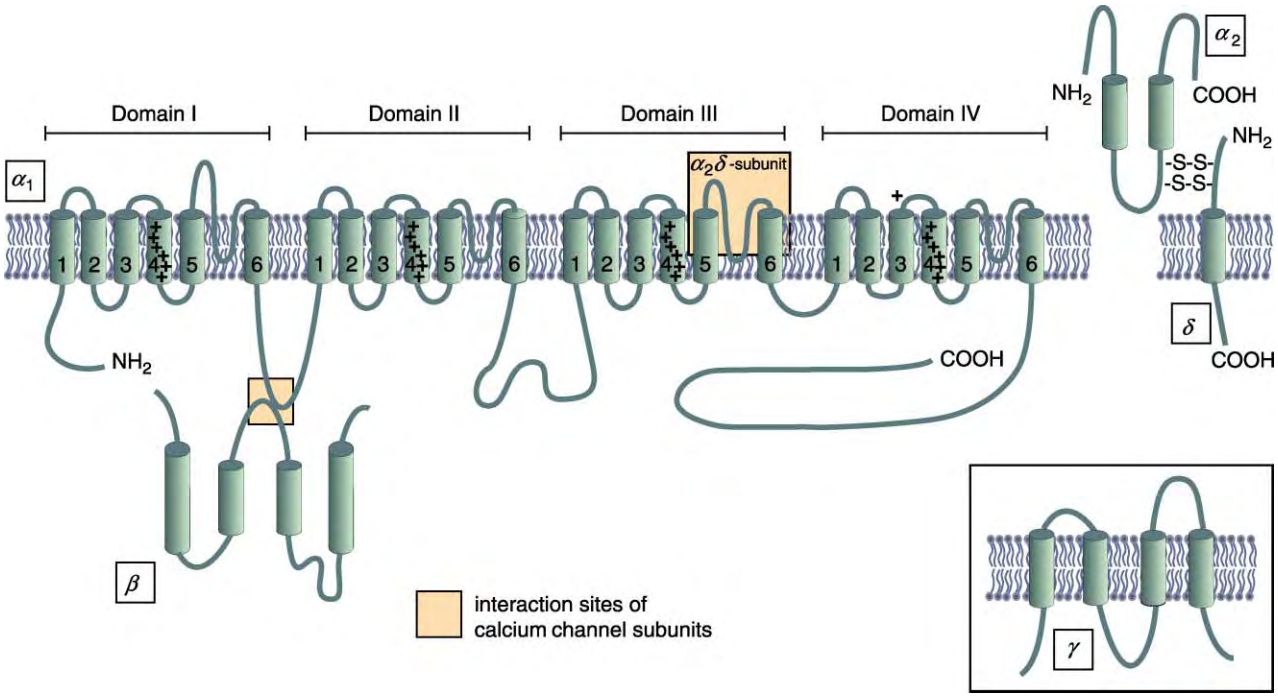

FIGURE 1 Oligomeric subunit complex of voltage-gated Ca^{2+} channels. The subunit composition consists of the pore-forming α1-subunit with its four homologous domains, the intracellular β-subunit, and the disulfide-linked α2-subunit. The sites of interaction between the subunits are indicated by the squares. An extra γ-subunit is present in skeletal muscle $Ca_v1.1$ complex (inset). Kindly prepared by Dr. R. D. Zuehlke, Bern.

Phosphorylation

Ca^{2+} channel function can be modulated by second messenger-activated protein kinases (PKs) such as cyclicAMP-dependent PKA, diacylglycerol-dependent PKC, or Ca/calmodulin-dependent kinases. Although the exact molecular mechanisms of these modulatory pathways are not yet fully understood, they do depend on phosphorylation by kinases of specific aminoacid residues of the Ca^{2+} channel protein. Multiple intracellular sites of phosphorylation have been identified on $\alpha 2_1$- and β-subunits. However, which phosphorylation sites are necessary and sufficient for different forms of modulation of Ca^{2+} channel function by the various protein kinases has not been clearly resolved.

G Proteins

Ca^{2+} channels of the Ca_v2 family (Table I) that are involved in neurotransmitter and hormone secretion are inhibited by G proteins. There is excellent evidence that the rapid inhibition of the channels results from direct binding of the $\beta\gamma$-subunits of G proteins to an identified segment of the intracellular loop between domains I and II (Figure 1), but other sequences in the C and N termini of the $\alpha 2_1$-subunits may also be important. Rapid inhibition of the channels by this mechanism does not require formation of soluble intracellular messengers. The inhibition results from a membrane-delimited pathway leading to the release of the $\beta\gamma$-subunit of the G-protein complex.

Ca^{2+}-Currents

Physiology

Depolarization of cell membranes during excitation leads to spontaneous openings (activation) and closings (inactivation) of Ca^{2+} channels. At a given voltage, stochastic openings of multiple channels produce a considerable flow of Ca^{2+} ions into a cell and can thus be measured as an electrical current. The currents are recorded by electrophysiological methods, at a level of resolution where even the current through an individual channel can be measured (patch-clamp method). This allows detailed quantitative analyses of the kinetic properties (gating) and selectivities of the channels. Currents through different types of Ca^{2+} channels have traditionally been classified as L-, P/Q-, N-, R-, and T-type (Table I). This classification resulted from functional and pharmacological analyses before the channels were cloned and sequenced. A general overview of the distribution of the channels in different tissues is summarized in Table I. The specific expression of different Ca^{2+} channel types in different tissues is of

TABLE I

Ca^{2+} Channels

Channel types[a]	Pore-forming α-subunits[b]	Tissue distribution	Pharmacology (blockers)
HVA			
$Ca_v1.1$ (L)	α1S	Skeletal muscle	DHPs
$Ca_v1.2$	α1C	Heart, smooth muscle, CNS	
$Ca_v1.3$	α1D	CNS, kidney, cochlea, glands	
$CA_v1.4$	α1F	Retina	
$Ca_v2.1$ (P/Q)	α1A	CNS	ω-Agatoxin
$Ca_v2.2$ (N)	α1B	CNS	ω-Conotox.GVIA
$Ca_v2.3$ (R)	α1E	CNS, heart, glands	
LVA			
$Ca_v3.1$ (T)	α1G	CNS, sinus node	Mibefradil
$Ca_v3.2$	α1H	CNS, heart, kidney, liver	
$Ca_v3.3$	α1I	CNS	

[a] Channel types: HVA = high-voltage-activated channels; LVA = low-voltage-activated channels; letters in brackets refer to the nomenclature of currents carried through the different channel types.

[b] Pore-forming α_1-subunits encoded by identified genes have multiple splice variants (not shown); CNS = central nervous system; DHPs = Dihydropyridines.

great physiological and pharmacological importance. The localization of individual channels in association with other cellular constituents governs specific signaling pathways. For example, P/Q-,and N-type channels are directly linked to the SNARE (Soluble *N*-ethylmaleimide sensitive fusion protein Attachment protein REceptor) protein complex in neural and endocrine cells that is essential for secretion of neurotransmitters and hormones. L-type channels that are predominant in cardiac cells, are in close proximity to intracellular Ca^{2+} stores. When Ca^{2+} ions move through the channels into these cells during excitation, they release more Ca^{2+} from the stores which eventually leads to contraction of the heart. Thus, changes in the intracellular Ca^{2+}-concentration are coding for important information of diverse cellular functions. Autoregulatory mechanisms, by which the channels inactivate in voltage- and Ca^{2+}-dependent manners, prevent Ca^{2+} overload of the cells. Ca^{2+}-dependent inactivation has been studied most extensively in L-type Ca^{2+} channels, but may also apply to other channel types. During the flow of Ca^{2+} ions through the pore, they bind to constitutively tethered apoCaM at the cytoplasmic C terminus of the channel. Occupancy of CaM by Ca^{2+} triggers binding of its C-terminal lobe to the nearby IQ-motif and accelerates inactivation of the channel, possibly by disinhibiting voltage-dependent inactivation (Figure 2).

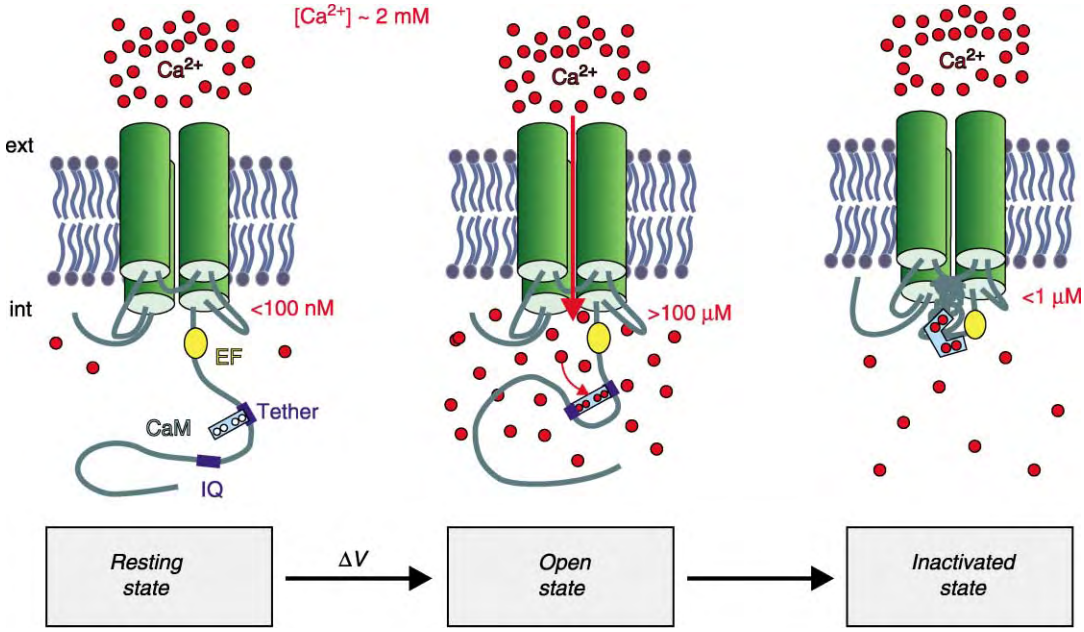

FIGURE 2 Model of voltage- and Ca^{2+} -dependent gating of a Ca^{2+} channel. The model shows a schematic folding of the α1-subunit in Figure 1. At membrane resting potential the pore is closed (resting state); upon depolarization (ΔV) the pore opens and Ca^{2+} ions move across the membrane down their electrochemical gradient (open state); when the intracellular Ca^{2+} -concentration increases, Ca^{2+} binds to tethered calmodulin (CaM) which then attaches itself to the regulatory IQ-motif and promotes closure of the pore (inactivated state). Kindly prepared by Dr. R. D. Zuehlke, Bern.

Modulation

Modulation of Ca^{2+} channel activity by neurotransmitters and hormones has become a major field of research. The up-regulation of cardiac Ca^{2+} current ($Ca_v1.2$) by epinephrine was the first example of modulation of an ion channel by a neurotransmitter. It has been shown to be the result of activation of the cyclicAMP pathway via β_1-adrenoceptors and subsequent phosphorylation by protein kinase A of aminoacid (serine) residues at intracellular sites of the channel. This causes enhanced probability of openings of the channels, resulting in largely increased Ca^{2+} currents. Other examples of modulation mainly concern N- and P/Q-type Ca^{2+} channels ($Ca_v2.1$ and $Ca_v2.2$; Table I). They are inhibited by neurotransmitters, such as norepinephrine. Release of G protein $\beta\gamma$-subunits by neurotransmitters shifts channel activation into a reluctant state, thus causing a reduction of Ca^{2+} currents during depolarization. These are just two examples of modulation of Ca^{2+} channel activities. There are several others that are not included under the scope of this article.

Pharmacology

Ca^{2+} channels are important targets for toxins and drugs. Although a full discussion of their effects is beyond the scope of this article, a few of them are listed in Table I. Dihydropyridines (e.g., nifedipine, nimodipine) are relatively specific inhibitors of the Ca_v1 channel family, mainly $Ca_v1.2$ type. Other drugs acting on these channels are the phenylalkyamines verapamil and the benzothiazepine diltiazem. They are grouped together as "Ca-channel blockers," and are therapeutically used for the treatment of cardiovascular diseases, notably hypertension and angina pectoris. The toxins have no, or very limited, therapeutic use. In some cases of otherwise untreatable pain, the N-type channel blocker ω-conotoxin GVIA has been successfully applied. Because of unwanted side effects, the T-type channel blocker mibefradil has been withdrawn from therapeutic use, although it was quite effective in the treatment of essential hypertension.

See Also the Following Articles

Calcium Oscillations • Calcium Transport in Mitochondria • Calcium/Calmodulin-Dependent Protein Kinase II • Intracellular Calcium Channels: $NAADP^+$-Modulated • Ion Channel Protein Superfamily • Store-Operated Membrane Channels: Calcium

Glossary

apoCaM Ca^{2+}-free calmodulin.
electrical activity Results from ion flow through channels in membranes.
electrochemical gradient Driving force for ions due to differences in concentrations and electrical potentials across membranes.
G proteins Small intracellur proteins involved in signaling pathways.
oligomeric proteins Composition of several protein subunits.
protein kinases Enzymes that catalyze phosphate transfer from ATP to proteins; protein kinases are activated by distinct second messengers.
second messengers Intracellular molecules formed after receptor activation and involved in signaling (e.g. cyclic-AMP, diacylglycerol).
signaling cascade Information transfer within a cell.

Further Reading

Catterall, W. A. (2000). Structure and regulation of voltage-gated Ca^{2+} channels. *Annu. Rev. Cell Dev. Biol.* **16**, 521–555.
Hille, B. (2001). *Ionic Channels of Excitable Membranes*. Sinauer, Sunderland, MA.
McDonald, T. F., Pelzer, S., Trautwein, W., and Pelzer, D. J. (1994). Regulation and modulation of calcium channels in cardiac, skeletal, and smooth muscle cells. *Physiol. Rev.* **74**, 365–507.
Perez-Reyes, E. (2003). Molecular physiology of low-voltage-activated T-type calcium channels. *Physiol. Rev.* **83**, 117–161.
Reuter, H. (1996). Diversity and function of presynaptic calcium channels in the brain. *Curr. Opin. Neurobiol.* **6**, 331–337.
Saimi, Y., and Kung, C. (2002). Calmodulin as an ion channel subunit. *Annu. Rev. Physiol.* **64**, 289–311.

Biography

Harald Reuter is Professor Emeritus and former Director of the Institute of Pharmacology at the University of Bern, Switzerland. He received his M.D. at the University of Mainz, Germany. Dr. Reuter first described Ca^{2+} currents and the sodium/calcium-exchange transport in the heart, and discovered regulation of Ca^{2+} channels by catecholamines and calmodulin. He is further interested in synaptic function in the brain. He has received many awards for his discoveries and has been elected a Foreign Associate of the National Academy of Sciences, USA.

Voltage-Sensitive Na^+ Channels

William J. Brammar
University of Leicester, Leicester, UK

Voltage-sensitive sodium channels are the transmembrane protein complexes that mediate the increased permeability to Na^+ ions during the initial rising phase of the action potential in most excitable cells. The channels are closed at resting membrane potentials, but open in response to membrane depolarization to become selectively permeable to Na^+ ions. The open or activated state is transitory: channels are inactivated and Na^+ permeability returns to the baseline level within about a millisecond, allowing the repolarization phase of the action potential that is controlled by K^+ channels.

A family of genes encoding multiple sodium channel isoforms has been revealed by molecular cloning. Mutations in genes encoding Na^+ channel subunits give rise to genetic diseases affecting the function of skeletal muscles, the heart or the brain. Sodium channel proteins include target-sites for the action of a number of neurotoxins, insecticides, and local anesthetics.

Isolation and Purification of Sodium Channel Proteins

The first biochemical identification of sodium channel proteins relied on specific covalent labeling of the proteins with a photoreactive derivative of the north African scorpion toxin. Denaturing polyacrylamide gel electrophoresis of proteins derived from rat brain synaptosomes revealed two labeled polypeptides of 260 and 36 kDa that were subsequently designated as the α- and β1-subunits of the sodium channel. Purification of the sodium channel solubilized from rat brain revealed three polypeptides, α of 260 kDa, β1 of 36 kDa and β2 of 33 kDa, in a 1:1:1 stoichiometry. The β1-subunit is non-covalently associated with the α-subunit, whereas the β2-subunit is covalently attached via disulfide bonds.

The sodium channels purified from rat skeletal muscle sarcolemma or transverse tubules consist of a 260 kDa subunit and one or two subunits of 38 kDa. In contrast, those purified from eel electroplax and chicken heart contain only the 260 kDa component. Reconstitution experiments, in which the purified proteins were incorporated into phospholipid vesicles to generate fully functional, neurotoxin-sensitive sodium channels, proved the validity of the protein purification methods based on neurotoxin-binding.

Primary Structures of Sodium Channel Proteins

The α-Subunits of Sodium Channels

Sequences encoding a complete Na^+ channel protein were first cloned as cDNAs derived from the mRNA of the electroplax of the electric eel. The deduced sequence of 1820 amino acids contains four internally homologous domains, each having six putative membrane-spanning α-helical segments (Figure 1). In each homology unit, five segments (S1, S2, S3, S5, and S6) are predicted to be hydrophobic, membrane-spanning helices. The interspersed S4 transmembrane segments contain positively charged amino acids located at every third position, forming an α-helix with a spiral of positive charges.

The suggestion that the four S4 segments act as voltage-sensors for the gating of the Na^+ channel has been confirmed by mutational alteration of the positively charged residues. The absence of an N-terminal signal sequence suggests that the N terminus is cytoplasmic.

The structural motif of four internally homologous domains, first promulgated for the sodium channel of the eel electroplax, is also evident in the voltage-gated calcium and potassium channels and in other channels within the large superfamily. Discernable sequence similarity ($\sim$32–37% identity) between the four homologous domains of the voltage-gated Na^+ channels and those of the voltage-gated Ca^{2+} channels reflects the common ancestry of these two channel types.

Sequences encoding mammalian sodium channel α-subunits have been isolated using segments of the eel electroplax Na^+ channel cDNA as hybridization probes and by screening expression libraries with antibodies prepared against purified components. DNA sequences encoding regions of brain Na^+ channels have been used in low stringency hybridizations to

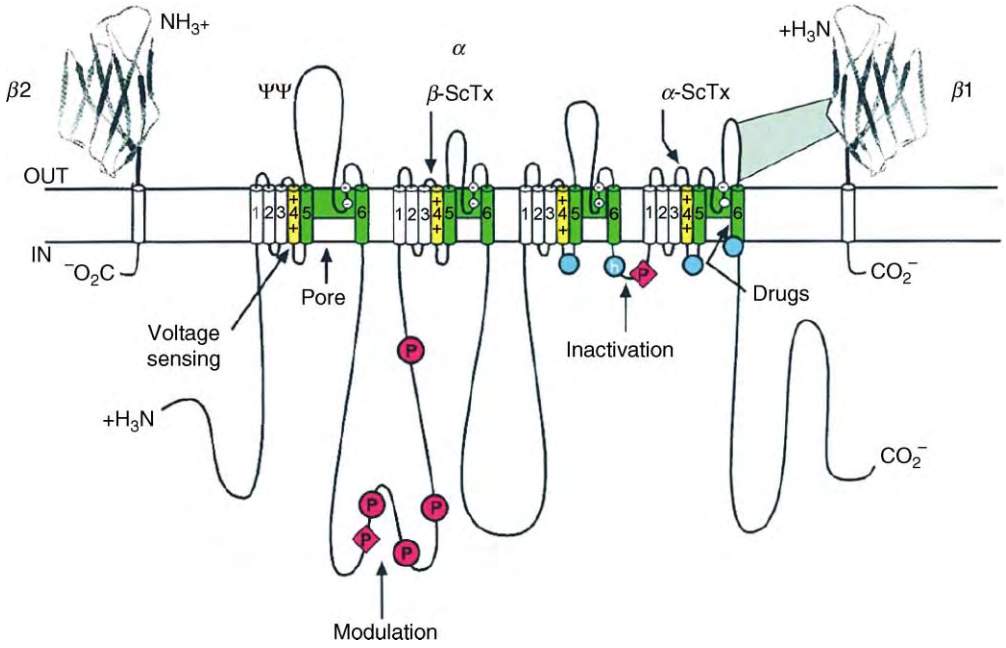

FIGURE 1 Primary structures of the subunits of the voltage-gated sodium channel. The α, $\beta 1$, and $\beta 2$ polypeptide chains are shown to illustrate their relationship to each other and to the cell membrane. The cylinders represent putative α-helices. The lengths of the intracellular and extracellular loops are roughly proportional to the number of amino acid residues in the brain sodium channel subtypes. The extracellular domains of the two β subunits are drawn as immunoglobulin-like folds. Ψ shows the site of probable N-linked glycosylation: P in red circles, sites of phosphorylation by (circles) and PKC (diamonds); the green regions are pore-lining segments; white circles represent the outer and inner rings of amino acid residues that form the ion selectivity filter and the tetrodotoxin-binding site: yellow shows the S4 voltage sensors; h in a blue circle represents the inactivation particle and blue circles the sites forming the receptor for the inactivation gate. Binding sites for α and β scorpion toxins (α-ScTx and β-ScTx) are shown by the downward arrows. (Reproduced from Catterall, W. A. (2000). From ionic currents to molecular mechanism: The structure and function of voltage-gated sodium channels. *Neuron* **26**, 13–25, with permission from Elsevier).

isolate cDNAs encoding α-subunits from other tissues such as skeletal muscle and heart. Although the different channel α-subunits vary slightly in length and sequence, they are clearly homologous and share fundamentally similar structures.

The β-Subunits of Sodium Channels

Both the $\beta 1$ and $\beta 2$ subunits of the voltage-sensitive Na^+ channel are predicted to contain a single transmembrane region, located near the intracellular C terminus, and an extracellular domain containing a single "immunoglobulin-like fold" (Figure 1). The latter consists of two superimposed β-sheets held together by hydrophobic interactions and is characteristic of the family of cell adhesion molecules that mediate cell–cell interactions. In such molecules, immunoglobin-like folds bind extracellular proteins and influence interactions with the extracellular matrix and with other cells to affect cell shape and mobility. Rat brain Na^+ channels and the $\beta 2$-subunit have been shown to bind to the extracellular matrix proteins tenascin-C and tenascin-R, leading to the suggestion that such interactions may influence the formation of specialized areas of high Na^+ channel density such as nodes of Ranvier.

Heterologous expression of cDNAs encoding Na^+ channel α and β subunits has shown that the $\beta 1$ and $\beta 2$ subunits modulate channel-gating behavior. Expression of the unaccompanied α-subunit of brain or skeletal muscle Na^+ channel in *Xenopus* oocytes produces channels that activate and inactivate more slowly than the native channels. Coexpression of $\beta 1$ and $\beta 2$ subunits with the α-subunit yields channels that gate normally, and the accelerating effect of the $\beta 1$-subunit is mediated by the immunoglobulin-like fold in the extracellular domain.

The Molecular Basis of Sodium Channel Function

The Outer Pore and Selectivity Filter

The guanidinium-containing compounds tetrodotoxin and saxitoxin, selective and reversible blockers of Na^+ channels at nanomolar concentrations, have been influential in allowing identification of the outer pore and selectivity filter of the channel. These toxins are membrane-impermeant and act only from the extracellular side of the membrane to plug the selectivity filter in the outer pore of the channel. Mutational studies have identified a pair of amino acids, mostly negatively charged, in analogous positions in all four domains of

the rat brain Na^+ channel α-subunit, that are important for binding tetrodotoxin and saxitoxin (Figure 1). These four pairs of amino acids were postulated to form outer and inner rings that acted as both the receptor-site for tetrodotoxin and saxitoxin and the selectivity filter in the outer pore of the channel. The concept is strongly supported by the finding that replacement of the four amino acid residues in the inner ring by four glutamic acid residues, their counterparts in voltage-gated Ca^{2+} channels, made the Na^+ channels calcium-selective.

Cardiac Na^+ channels bind tetrodotoxin with an affinity that is 200-fold lower than that of the brain or skeletal muscle channels, because of a replacement of an aromatic amino acid by a cysteine residue in the outer pore region of domain I. Cadmium is a high-affinity blocker of cardiac Na^+ channels because of its interaction with this same cysteine residue. Electrophysiological measurements of the voltage-dependence of the cadmium block of cardiac Na^+ channels place the target cysteine residue, and thus the selectivity filter, about 20% of the way through the membrane electric field.

The Inner Pore

Local anesthetics, such as lidocaine and procaine, are generally lipid-soluble tertiary amine compounds that inhibit propagated action potentials by blocking Na^+ channels. A quaternary amine analogue of lidocaine, QX-314, which is positively charged at all pHs and not lipid-soluble, blocks Na^+ channels only when applied to the inside of the membrane. Blockage requires prior opening of the channels by depolarization. Mutagenesis studies demonstrated that the binding-site for local anesthetics lies in the IVS6 transmembrane segment (Phe1764 and Tyr1771 in rat brain type IIA channels).

Similar amino acid residues in the S6 transmembrane segment of certain voltage-gated K^+ channels act as the targets for tetraethylammonium-based blockers. These amino acids are located in an aqueous cavity within the inner pore region of the K^+ channel, by extrapolation from a bacterial K^+ channel whose quaternary structure has been determined.

The Mechanism of Voltage-Dependent Activation

The voltage-dependent activation of sodium channels involves the net outward movement across the membrane electric field of $\sim$12 electronic charges in the channel protein. The S4 segments of the α-subunits, with positively charged amino acids at every third position, were predicted to act as the voltage-sensor and to undergo outward movement on depolarization of the membrane, initiating a conformational change associated with pore-opening.

Mutagenesis studies showed that neutralization of the positive charges in the S4 domains reduced the steepness of the potential-dependence of activation, equivalent to reducing the gating charge. Physical movement of the S4 segments has been demonstrated by substituting cysteine for the basic amino acids, then assessing the availability of the individual cysteine-SH groups to chemical modification by membrane-impermeant sulfhydryl reagents, before and after depolarization. Three successive basic amino acids in the S4 segment of domain IV (Arg1448, Arg1451, and R1454) move from being inaccessible within the membrane to being available for reaction from outside the membrane.

Similar outward movements of positively charged S4 segments have been demonstrated for voltage-sensitive K^+ channels. In this case it has been shown by mutagenesis that the positive charges in S4 are paired with negatively charged residues in either S2 or S3 segments, stabilizing the S4 segments in the membrane.

The Basis of Inactivation

Native sodium channels spontaneously inactivate within milliseconds of opening. The sensitivity of this rapid inactivation to limited cytoplasmic applications of proteases lead to the proposal of the 'ball and chain' hypothesis of inactivation, in which an intracellular inactivation gate ('the ball'), tethered by a flexible 'chain', was able to interact with the intracellular mouth of the pore and block the channel. The inactivation gate has been localized to a short intracellular loop connecting regions III and IV. Antipeptide antibodies directed against this sequence, cutting the loop in this region and mutagenesis of a hydrophobic triad of Ile, Phe, and Met in the region all prevent fast inactivation. Voltage-dependent movement of this segment has been detected by the depolarization-induced loss of accessibility to cytoplasmically applied reagents.

The receptor for the inactivation gate has been delineated by scanning mutagenesis experiments. Multiple amino acid residues at the intracellular end of transmembrane segment IVS6 and in intracellular loops IIIS4-S5 and IVS4-S5 contribute to the receptor for the inactivation the gate, allowing its binding to block the pore of the channel (Figure 1).

Modulation of Channel Activity

Sodium channels in neurons and skeletal muscle are susceptible to modulation by several protein kinases. Cyclic AMP-dependent protein kinase A (PKA) phosphorylates sodium channel α-subunits in brain synaptosomes and intact neurons on four sites in the intracellular loop between domains I and II. The consequence of phosphorylation by PKA is a reduction

in sodium conductance, with little effect on the voltage-dependence of activation and inactivation. Activation of adenylate cyclase via dopamine acting at D1-like receptors reduces action potential generation and peak sodium currents in hippocampal neurons. The presence of a protein kinase-anchoring protein, AKAP-15, which brings PKA close to the sodium channel, is essential for this regulation. Cocaine, which increases dopaminergic neurotransmission by inhibiting dopamine-uptake, also reduces sodium currents in nucleus accumbens neurons.

Protein kinase C (PKC) also acts on sodium channel α-subunits, slowing channel inactivation and reducing peak sodium currents. Phosphorylation of a site in the inactivation gate is responsible for the slowing of channel inactivation. The reduction in peak current is a consequence of phosphorylation at sites in the intracellular loop between domains I and II (see Figure 1).

The effects of PKA are enhanced by PKC-dependent phosphorylation and by steady membrane depolarization, so that the information from three distinct signaling pathways are integrated via the sodium channels in the hippocampus and CNS.

The Genetics of Sodium Channels

The Gene–Protein Family of Sodium Channels

A large family of sodium channel genes and proteins, containing at least ten members, has been recognized through molecular cloning and heterologous expression to make characterizable protein products. The nomenclature for sodium channels has been informal and inconsistent, but a standardized system has recently been proposed by a consortium of leading researchers (see Table I).

The nine isoforms of the sodium channel α-subunit that have been characterized are greater than 50% identical in the transmembrane and extracellular domains. The continuously variable pattern of sequences is consistent with their constituting a single family. The $Na_V1.1$, $Na_V1.2$, $Na_V1.3$, and $Na_V1.7$ α-subunits are the most closely related. These four channels are all highly tetrodotoxin-sensitive and expressed in the central and peripheral nervous system. The corresponding genes are all located on human chromosome 2q23–24. The $Na_V1.5$, $Na_V1.8$, and $Na_V1.9$ channel α-subunits, all forming tetrodotoxin-resistant sodium channels, are produced in heart and neurons of the dorsal root ganglia from genes located on chromosome 3p21–24. The skeletal muscle sodium channel isoform, $Na_V1.4$, formerly called type μ1, is at least 84% identical to the group of channels encoded on chromosome 2, but has a more distant phylogenetic relationship as determined by parsimony comparison.

Comparison across mammalian species shows that the chromosome segments containing sodium channel α-subunit genes are paralogous segments containing many sets of related genes, generated by large-scale duplication events during early vertebrate evolution.

Several sodium channel α-subunits have been recognized by molecular cloning and DNA sequencing, but have not yet been characterized by functional expression (Table I, Na_X). These sequences have more than 80% identity to each other and are phylogenetically closely related to the group of sodium channel subunits encoded on human chromosome 2q23–24, where the human SCN6A gene is located.

The genes encoding mammalian sodium channel α-subunits are complex, with more than 20 exons. Splice variants of several sodium channel proteins have been identified and more are likely to be found.

Genetic Defects Affecting Voltage-Gated Sodium Channels

Mutations in genes encoding sodium channel subunits are associated with several inherited human diseases characterized by hypersensitivity, including several monogenic epilepsy syndromes. Mutations in the human SCN1A gene have been associated with familial generalized epilepsy with febrile seizures plus (GEFS+), an autosomal dominant syndrome characterized by febrile seizures (FS) and a variety of afebrile generalized seizure types. *De novo* mutations in SCN1A are a major cause of severe myoclonic epilepsy of infancy (SMEI or Dravet syndrome). Benign familial neonatal-infantile seizures have been ascribed to mutations in the SCN2A gene.

Mutations in the SCN4A gene encoding the skeletal muscle sodium channel α-subunit are the cause of the hereditary disorders of sarcolemmal excitability, hyperkalemic periodic paralysis (HYPP or hyperPP) and paramyotonia congenita (PMC). Mutations have been shown to cause reduced rates of channel inactivation, altered voltage-sensitivity or slowed coupling between activation and inactivation. HYPP is a muscle disorder that is prevalent in American quarter horses, where selective breeding for muscular definition and hypertrophy has favored spread of the mutant SCN4A gene in the gene-pool.

One of the causes of long QT syndrome, an inherited cardiac arrhythmia, is mutation in the SCN5A gene, leading to non-inactivating sodium currents that prolong the plateau of the cardiac action potential. The result is an elongated interval between the QRS complex and the T wave in the electrocardiogram. The mutations usually affect amino acid residues in the inactivation gate or its receptor region, reducing the rate of inactivation.

TABLE I

Genes Encoding Mammalian Sodium Channel α-Subunits

Gene	Location	Channel type	Tissue specificity	Associated disease
SCN1A	2q24	$Na_v1.1$	CNS, PNS	Epilepsy
SCN2A	2q23–24	$Na_v1.2$	CNS	Neonatal-infantile seizures
SCN3A	2q24	$Na_v1.3$	CNS	
SCN4A	17q23–25	$Na_v1.4$	Sk.m.	Myotonia (HYPP, PMC)
SCN5A	3p21	$Na_v1.5$	Heart, Uninnervated sk.m.	Long QT syndrome
SCN8A	12q13	$Na_v1.6$	CNS,PNS	Cerebellar ataxia[a]
SCN9A	2q24	$Na_v1.7$	Schwann cells	
SCN10A	3p22–24	$Na_v1.8$	DRG	
SCN11A	3p21–24	$Na_v1.9$	PNS	
SCN6A[b]	2q21–23	Na_x	Heart, uterus, sk.m.	

[a] This condition is associated with mutations in the mouse SCN8A gene.
[b] This gene was originally designated SCN6A in human and SCN7A in mouse. The two genes represent homologues and the SCN6A symbol will probably be deleted. CNS = central nervous system; PNS = peripheral nervous system; sk.m. = skeletal muscle; DRG = dorsal root ganglion neurons.

Mutations in the SCN5A gene can also contribute to idiopathic ventricular fibrillation (IVF), a common cause of sudden cardiac death. A variant SCN5A gene segregating with IVF in an affected family contained two missense mutations, affecting amino acid residues in the extracellular loops between transmembrane segments S1 and S2 of domain III and between S3 and S4 of domain IV. The latter extracellular loop is involved in the coupling between channel activation and fast inactivation. The mutations affect the voltage dependence of steady-state inactivation of the sodium channels, shifting it more than 10 mV towards more positive potentials and accelerating rates of recovery from inactivation. Frameshift mutations and splice-site mutations in SCN5A have also been shown to be associated with IVF in affected families.

Mutations of the mouse *Scn8a* gene of the mouse have been shown to cause motor endplate disease, a lethal skeletal muscle atrophy. Less severe phenotypes involving 'jolting', a rhythmic tremor of the head and body and unsteady gait, are associated with missense mutations in the *Scn8a* gene.

A mutation affecting the sodium channel β1-subunit has been shown to be the cause of inherited febrile seizures. The mutation alters a cysteine residue involved in stabilizing the immunoglobulin-like fold in the extracellular domain of the β1-subunit that is involved in modulating sodium channel gating.

Toxins and Channel Modifiers

The voltage-gated sodium channels are subject to modification by a wide range of toxins produced by animals, for use in predation or defence, or by plants as protection against herbivores. Six distinguishable toxin-binding sites have been identified on sodium channels, as summarized in Table II. The groups of toxins have various effects on sodium channels, from complete block to prolongation of activation.

The guanidinium-containing compounds, tetrodotoxin, isolated from the internal organs of the puffer fish and its relatives in the family *Tetraodontidae*, and saxitoxin, from marine dinoflagellates, act as selective, reversible blockers at nanomolar concentrations. These membrane impermeant toxins bind at the extracellular opening of the channel pore and cause prolonged block of nerve and muscle action potentials. Sodium channels in heart and sensory neurons of dorsal root ganglia are relatively insensitive to tetrodotoxin and saxitoxin. The peptide μ-conotoxins, isolated from the venom of the fish-hunting cone snails of the *Conus* genus, also block muscle action potentials by binding to the extracellular opening of the pore of the skeletal muscle sodium channel. The venom, which is injected via a harpoon-like disposable tooth, rapidly results in paralysis and death of the prey.

A group of lipid-soluble alkaloids, including batrachotoxin, aconitine, veratridine, and grayanotoxin I, cause hyperexcitability and cardiac arrhythmias by promoting prolonged opening of sodium channels and long-lasting membrane depolarization. Batrachotoxin, secreted by the skin of Columbian frogs of the genus *Phyllobates*, is used by indigenous natives to make poison arrows for hunting. Brevetoxin, a fused cyclic ether produced by the marine dinoflagellate, *Ptychodiscus brevis*, the organism responsible for 'red tides', acts like the alkaloids, but via a different binding site on the sodium channel.

The peptide toxins of the scorpion α-toxin family, produced by north African genera *Androctinus*, *Buthus*, and *Leirus* and the American genus *Centruroides*, act to

TABLE II

Toxin-Binding Sites on Voltage-Gated Sodium Channels

Site	Toxin	Source	Chemical type	Effect
1	Tetrodotoxin	*Tetraodontidae* ("puffer fish")	Heterocyclic, Guanidinium	Channel block, via binding site at the extracellular opening of the pore of the channel. Result in blockade of nerve and muscle action potentials
	Saxitoxin	Marine dinoflagellates		
	μ-Conotoxins	Fish-hunting cone snails of the *Conus* genus	Small peptides (~17–22 aa)	
2	Veratridine	*Veratrum lilies*	Alkaloid	Slow inactivation, shift activation to more negative potentials and reduce selectivity. Result in hyperexcitability due to long-lasting membrane depolarization
	Batrachotoxin	*Phyllobates aurotaenia* (Columbian frog)		
	Aconitine	*Aconitum napellus* (monk's hood)		
	Grayanotoxins	Ericaceous plants	Diterpenoid	
3	Scorpion α-toxins	*Leiurus quinquestriatus*	Peptides, 64 aa	Slowing of inactivation and stabilization of the open state of the channel. Macroscopic effects include hyperexcitability and repetitive firing in motor units, accelerated respiration, convulsion, spastic paralysis, and eventual respiratory failure
	Sea anemone toxins	*Anemonia sulcata*	Peptides, 27–46 aa	
4	Scorpion β-toxins	*Centruroides* species	Peptides, 66 aa	Shift voltage-dependent activation in the positive direction. Toxin plus conditioning pre-pulse sift activation in the negative direction
				Hyperexcitability results, with heavy perspiration and tremor
5	Brevetoxins	Ptychodiscus brevis (marine dinoflagellate)	Cyclic polyethers	Inhibit inactivation and shift voltage-dependent activation to more negative potentials
	Ciguatoxins			
6	Pyrethrins	Chrysanthemums	Organic esters	Slow activation and inactivation, prolong channel open-time and promote membrane depolarization, leading to lethal paralysis in insects
	Pyrethroids	Synthetic		

Data based on *Trends in Neurosciences*, *Neurotoxins Supplement*, 1996.

prolong the action potential duration in muscle and nerves by inhibiting sodium channel inactivation. The nonhomologous sea anemone toxins act at the same site and produce similar effects.

A second group of peptide-based scorpion toxins, the β-toxins, slow both activation and inactivation of sodium channels in skeletal muscle. The consequence of this modulation is that channels close very slowly at rest. The resulting inward Na^+ currents support repetitive firing in response to minimal stimulation, producing hyperexcitability, with heavy perspiration and muscle tremor.

The pyrethrins, natural insecticides produced by flowers of the genus *Chrysanthemum*, and their synthetic analogues the pyrethroids, are organic esters that prolong sodium channel activation and inhibit inactivation in nerve axons. The consequence of this effect is repetitive firing and membrane depolarization, leading to lethal paralysis in insects. The synthetic insecticide dichlorodiphenyltrichloroethane (DDT) acts in a similar fashion.

Several local anesthetics, such as lidocaine and procaine, are lipid-soluble tertiary amines that block sodium channels in nerve axons to inhibit propagation of action potentials. Various sodium channel blockers, including local anesthetics and alkaloids, are being used clinically as neuroprotective agents in ischemic stroke patients and as antiarrhythmic agents in heart disease.

See Also the Following Articles

Ion Channel Protein Superfamily • Voltage-Dependent K^+ Channels • Voltage-Sensitive Ca^{2+} Channels

Glossary

action potential An electrical impulse arising from local changes in membrane permeability to Na^+ and K^+ ions that travels along nerve axons.

coexpression Expression of two or more coding sequences, usually following transfection, in the same host cell.

depolarization Change in membrane potential from the normal resting potential of −70 mV towards more positive potentials.

domain A compact, independently folded region of a polypeptide chain.

gating The process of opening or closing an ion channel.

heterologous expression Expression of a cloned coding sequence in a host cell that would not normally express it.

modulation Change in ion conductivity brought about by external influences, such as hormone-mediated intracellular signalling events.

pore The ion-permeable pathway created by the ion channel protein that provides the route through the cell membrane.

selectivity filter The region of an ion channel that imposes the selectivity for one ion over another.

Further Reading

Aidley, D. J., and Stanfield, P. R. (1996). *Ion Channels: Molecules in Action*. Cambridge University Press, Cambridge, UK.

Catterall, W. A. (2000). From ionic currents to molecular mechanisms: The structure and function of voltage-gated sodium channels. *Neuron* **26**, 13–25.

Goldin, A. L., Barchi, R. L., Caldwell, J. H., Hofmann, F., Howe, J. R., Hunter, J. C., Kallen, R. G., Mandel, G., Meisler, M. H., Netter, Y. B., Noda, M., Tamkun, M. M., Waxman, S. G., Wood, J. N., and Catterall, W. A. (2000). Nomenclature of voltage-gated sodium channels. *Neuron* **28**, 365–368.

Hille, B. (2001). *Ion Channels of Excitable Membranes*. 3rd edition, Sinauer Associates, Sunderland, Massachusetts.

Biography

William J. Brammar is a Professor of Biochemistry and Pro-Vice-Chancellor (Research) at the University of Leicester. He has a long-term interest in the regulation of expression of both prokaryotic and eukaryotic genes. He holds a Ph.D. from University College, London and was a postdoctoral fellow at Stanford University. He has written texts on molecular cloning and ion channels and is a member of the European Molecular Biology Organization.

Von Hippel-Lindau (VHL) Protein

Ronald C. Conaway and Joan Weliky Conaway
Stowers Institute for Medical Research, Kansas City, Missouri, USA

The Von Hippel-Lindau (VHL) protein is a tumor suppressor. Mutations in the VHL protein can give rise to tumors of multiple organ systems, including the central nervous system, the endocrine system, and the kidney. The VHL protein functions as a subunit of a multiprotein ubiquitin ligase that negatively regulates expression of a large collection of hypoxia-inducible genes controlled by hypoxia-inducible transcription factors (HIFs). The VHL ubiquitin ligase prevents inappropriate expression of these hypoxia-inducible genes when cells are grown in a plentiful supply of oxygen by targeting HIFs for rapid ubiquitylation and degradation by the proteasome.

Clinical Consequences of VHL Mutations

Mutations in the *VHL* gene are found in a variety of human diseases, including VHL disease, sporadic clear cell renal carcinoma, sporadic hemangioblastoma, and congenital polycythemia. VHL disease is an autosomal dominant familial cancer syndrome. In VHL kindreds, inactivation of both copies of the *VHL* gene can give rise to a variety of highly vascularized tumors, including clear cell renal carcinoma, cerebellar hemangioblastoma and hemangioma, retinal angioma, and pheochromocytoma. *VHL* mutations are also responsible for the majority of cases of sporadic clear cell renal carcinoma and for sporadic hemangioblastoma. In addition, *VHL* mutations are believed to give rise to some forms of polycythemia, a disorder characterized by elevated levels of expression of the hypoxia-inducible *erythropoietin* gene.

Function of the VHL Protein

The VHL protein is present in eukaryotes from worms to mammals, where it performs an evolutionarily conserved function as a subunit of a multiprotein ubiquitin ligase that negatively regulates expression of a large number of hypoxia-inducible genes controlled by hypoxia-inducible transcription factors (HIFs). The expression of these hypoxia-inducible genes is repressed in normal cells grown in a plentiful supply of oxygen (normoxic conditions), but is strongly induced in cells starved for oxygen (hypoxic conditions). The VHL ubiquitin ligase prevents the inappropriate expression of these hypoxia-inducible genes when cells are grown in normoxic conditions by targeting HIFs for rapid ubiquitylation and degradation by the proteasome. When cells are starved for oxygen, ubiquitylation of HIFs by the VHL ubiquitin ligase is blocked. Under these hypoxic conditions, cellular HIF levels rise, and HIFs enter the nucleus, bind to hypoxia response elements (HREs) in the promoters of hypoxia-inducible genes, and activate their transcription and expression.

The cellular levels of HIFs correlate well with the levels of expression of hypoxia-inducible genes in both normoxic and hypoxic conditions (Figure 1). In normal cells growing under normoxic conditions, HIFs are present in cells at low levels, and expression of hypoxic-inducible genes is barely detectable. Under hypoxic conditions, HIFs are present at relatively high levels, and expression of hypoxia-inducible genes is robust. Under both normoxic and hypoxic conditions in cells lacking a functional VHL protein, HIFs are present in cells at high levels, and maximal expression of hypoxia-inducible genes is observed. Inappropriate overexpression of hypoxia-inducible genes in cells lacking a functional VHL protein may contribute to the pathology of VHL-associated diseases. Among these are the genes encoding vascular endothelial growth factor (VEGF), transforming growth factor α (TGFα), and erythropoietin (EPO). VEGF is a secreted protein that appears to play a major role in the vascularization of VHL tumors by promoting ingrowth into tumors of blood vessels needed to carry oxygen and nutrients to the tumor cells. TGFα is also a secreted protein that appears to function as an autocrine growth factor for some types of VHL tumor cells and may be responsible for promoting their uncontrolled proliferation. An elevated EPO level in the serum of polycythemic patients is a hallmark of the disease.

Structure of the VHL Ubiquitin Ligase

Purification of the VHL ubiquitin ligase revealed that it is composed of multiple proteins. In addition to the VHL

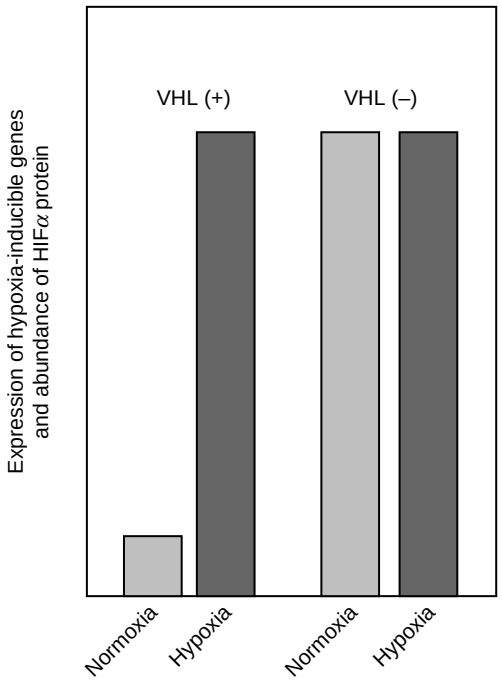

FIGURE 1 Regulation of expression of hypoxia-inducible genes and HIFα protein levels in normoxia and hypoxia. VHL (+), normal cells; VHL (−), cells lacking a functional VHL protein.

protein, the VHL ubiquitin ligase includes the elongin B and C proteins, cullin protein family member Cul2, and RING finger protein Rbx1 (Figure 2). In the VHL ubiquitin ligase, the VHL protein functions to recruit HIFs for ubiquitylation by interacting directly with them. The elongin B and C proteins bind stably to each other to form an adaptor that links the VHL protein to a Cul2-Rbx1 heterodimeric module. The Cul2-Rbx1 module functions to recruit the E2 ubiquitin conjugating enzyme Ubc5, which is responsible for ubiquitylation of HIFs. The VHL ubiquitin ligase is the founding member of a family of elongin BC-based ubiquitin ligases that include Cul2-Rbx1 or Cul5-Rbx1 modules. In the VHL ubiquitin ligase, the VHL protein binds directly to elongin BC through a conserved elongin BC-binding site motif (BC-box) with consensus sequence [(A,P,S,T)LXXXCXXX(A,I,L,V)]. In other elongin BC-based ubiquitin ligases, the VHL protein is replaced by one of many known BC-box proteins, including members of the family of more than thirty suppressors of cytokine signaling (SOCS) proteins, which play important roles in a variety of signal transduction pathways.

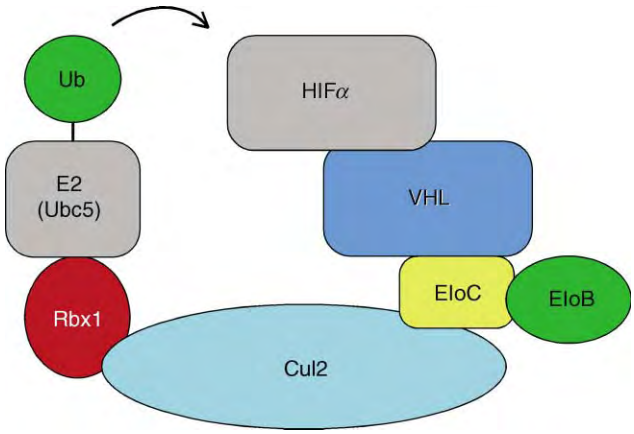

FIGURE 2 Architecture of the VHL ubiquitin ligase. Ub, ubiquitin; E2 (Ubc5), E2 ubiquitin conjugating enzyme Ubc5; EloB, elongin B; EloC, elongin C.

Regulation of HIF Ubiquitylation by the VHL Ubiquitin Ligase

To date, three members of the HIF family of transcription factors have been identified in mammalian cells and shown to be regulated by the VHL ubiquitin ligase. HIFs are heterodimeric DNA-binding transcription factors that bind to HREs in the promoters of hypoxia-inducible genes and activate their expression. In mammalian cells, HIF heterodimers are composed of one of three related HIFα proteins and a common subunit, the aryl hydrocarbon receptor nuclear translocator protein (ARNT). The HIFα and ARNT proteins are basic helix-loop-helix (bHLH) transcription factors that all contain an additional conserved domain, referred to as the PAS domain (PER-ARNT-SIM domain), of unknown function. The HIFα subunits, but not the ARNT subunits, of HIFs are targets of the VHL ubiquitin ligase. Whereas the ARNT subunit of HIFs is present in normoxic and hypoxic cells at similarly high levels, the HIFα subunits are continuously synthesized but rapidly ubiquitylated by the VHL ubiquitin ligase and degraded by the proteasome in normal cells grown under normoxic conditions. In hypoxic cells, ubiquitylation of HIFα subunits is attenuated. Under these conditions, cellular HIFα levels rise, and HIFα subunits heterodimerize with ARNT, enter the nucleus, and activate expression of hypoxia-inducible genes.

HIFα ubiquitylation by the VHL ubiquitin ligase is regulated by oxygen. Elegant studies have revealed that binding of HIFα subunits to the VHL protein and their recruitment to the VHL ubiquitin ligase depends on hydroxylation of a specific HIFα proline in a HIFα region referred to as the oxygen-dependent degradation domain (ODD). The HIFα ODD is an approximately 20 amino acid HIFα region that is essential for interaction of HIFα with the VHL protein and ubiquitylation of HIFα by the VHL ubiquitin ligase. The ODD is a portable domain capable of promoting oxygen-dependent degradation of a variety of ODD-containing fusion proteins. Binding of HIFα to the VHL protein depends on hydroxylation of a proline in the ODD by an iron- and oxoglutarate-dependent dioxygenase of the EGL-9 protein family. The EGL-9 proline hydroxylase uses O_2 as the oxygen donor for hydroxylation of HIFα

subunits in a reaction with kinetics proportional to the concentration of cellular O_2. In cells grown in hypoxic conditions, HIFα hydroxylation is significantly reduced, and the nonhydroxylated HIFα subunits are no longer substrates for ubiquitylation by the VHL ubiquitin ligase. Thus, oxygen-dependent hydroxylation of HIFα serves as a convenient molecular switch for regulation of expression of hypoxia-inducible genes.

See Also the Following Articles

Transforming Growth Factor-β Receptor Superfamily • Vascular Endothelial Growth Factor Receptors

Glossary

dioxygenase Enzyme that catalyzes the insertion of both oxygens of molecular oxygen, O_2, into substrate molecules.

erythropoietin An acidic glycoprotein hormone that regulates red cell production by promoting erythroid differentiation and the initiation of hemoglobin synthesis.

hemangioblastoma A highly vascularized tumor composed of capillaries and stromal cells.

hemangioma A benign lesion originating from blood vessels.

pheochromocytoma A tumor of the adrenal gland.

retinal angioma A benign lesion found in the retina that originates from blood vessels.

vascular endothelial growth factor A growth factor for vascular endothelial cells that promotes angiogenesis.

Further Reading

Conaway, R. C., and Conaway, J. W. (2002). The Von Hippel-Lindau tumor suppressor complex and regulation of hypoxia-inducible transcription. *Adv. Cancer Res.* **85**, 1–12.

Min, J. H., Yang, H., Ivan, M., Gertler, F., Kaelin, W. G., Jr., and Pavletich, N. P. (2002). Structure of an HIF-1alpha-pVHL complex: Hydroxyproline recognition in signaling. *Science* **296**, 1886–1889.

Pugh, C. W., and Ratcliffe, P. J. (2003). The Von Hippel-Lindau tumor suppressor, hypoxia-inducible factor-1 (HIF-1) degradation, and cancer pathogenesis. *Semin. Cancer Biol.* **13**, 83–89.

Semenza, G. L. (2001). Hypoxia-inducible factor 1: Oxygen homeostasis and disease pathophysiology. *Trends Mol. Med.* **8**, 345–350.

Stebbins, C. E., Kaelin, W. G., and Pavletich, N. P. (1999). Structure of the VHL-elongin C-elongin B complex: Implications for VHL tumor suppressor function. *Science* **284**, 455–461.

Biography

Ronald C. Conaway and Joan Weliky Conaway are Senior Scientists at the Stowers Institute for Medical Research. Research in their laboratory is aimed at contributing to an understanding of the molecular mechanisms governing the synthesis of eukaryotic messenger RNA. They hold Ph.D.s from the Stanford University School of Medicine.

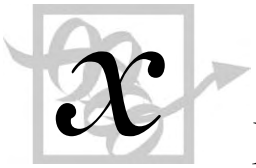

XPV DNA Polymerase and Ultraviolet Damage Bypass

Alan R. Lehmann
University of Sussex, Brighton, UK

DNA damage blocks the progress of the replication fork. In order to bypass the damage, cells have evolved special DNA polymerases, which are uniquely able to replicate damaged DNA. DNA polymerase η (eta) is the enzyme that carries out this bypass function for the major form of UV damage in DNA. A deficiency in this polymerase leads to a severe human condition, the variant form of xeroderma pigmentosum.

XP Variants

All cells sustain many kinds of DNA damage. This can be generated either endogenously from hydrolysis and oxidation reactions or exogenously from exposure to carcinogens. One of the most prevalent DNA damaging agents is UV radiation from the sun, which generates photoproducts in the DNA of cells in exposed areas of the skin. The most important photodimer, namely the cyclobutane pyrimidine dimer (CPD) and the pyrimidine 6-4 pyrimidone photodimer (6-4 PP) are removed from cellular DNA by the process of nucleotide excision repair (NER). The importance of this process can be seen from the features of patients with xeroderma pigmentosum (XP). XP patients show a wide variety of skin abnormalities on sun-exposed areas including freckling, hypo- and hyperpigmentation and ultimately multiple skin cancers. The incidence of skin cancer in XP individuals has been estimated to be 1000-fold higher than that in unaffected individuals. In the majority of XP patients this hypersensitivity to the effects of sunlight results from a genetic deficiency in NER. In ~20% of XP individuals however, NER is normal. These so-called XP variants (XPV) are deficient in their ability to produce intact daughter DNA strands during DNA replication after exposure of the cells to UV-irradiation. In other words, they are defective in their ability to replicate DNA damaged by ultraviolet light.

Polη and the Y-Family of DNA Polymerases

Although the cellular deficiency in XPV was identified in 1975, the molecular basis for the defect was not discovered until 1999. The gene defective in XPV cells was found to encode a new DNA polymerase designated DNA polymerase η or polη. Polη is a protein of 713 amino acids (aa) with no sequence similarity to previously discovered DNA polymerases, but it does share sequence similarity with several other DNA polymerases that were discovered at about the same time. This new group of polymerases was designated the "Y-family." They show sequence conservation over a region of ~400 aa, which contains the catalytic domain, and usually forms the N-terminal part of the protein. Y-family polymerases have a C-terminal extension, which is not conserved between family members.

Catalytic Activity

DNA polymerases that carry out the replication of undamaged DNA are very efficient and accurate, but they are blocked by most types of DNA damage including both major UV photoproducts. In contrast, polη is a rather poor polymerase on undamaged DNA. It dissociates after incorporating a few nucleotides and it is rather error-prone. However polη, in contrast to all other eukaryotic polymerases, is able to synthesize past a T-T CPD with the same efficiency as past undamaged T's. Furthermore in most instances the "correct" bases, namely two A's are inserted opposite the T's of the CPD. The reason for these properties became clear when the catalytic domains of several members of the Y-family (including yeast polη) were crystallized and their three-dimensional structures solved. Despite the lack of sequence similarity between classical and Y-family polymerases, the three-dimensional structures did have the three subdomains, designated finger, thumb and palm, found in all other DNA polymerases, with the Y-family having an extra subdomain designated

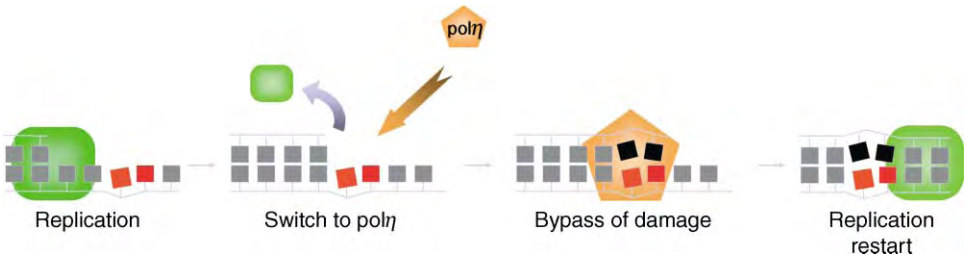

FIGURE 1 Translesion synthesis by polη. Replicative DNA synthesis is blocked by a CPD (indicated by red blocks). This leads to a switch to polη (step 1), which replicates past the CPD (step 2) and then dissociates, so that normal replication can restart (step 3).

pad or little finger. However the classical polymerases form a closed tight structure, which only permits normal bases into the active site. In contrast, polη has a much more open structure with two important consequences. Firstly, it has a relatively low stringency, so that incorrect bases can be incorporated rather easily. Secondly the open structure is able to accommodate the CPD in the template strand and the structure ensures that in general the correct bases are inserted opposite the bases in the CPD. Thus polη is tailor-made for replicating past CPDs. It can insert the appropriate bases opposite the damage and extend from these bases, but then it will soon dissociate from the template, so that the more accurate replicative polymerases can take over again. The ability to bypass DNA damage is termed translesion synthesis (TLS) and is shown schematically in Figure 1.

Apart from the CPD, polη is able to replicate past some other types of damage *in vitro*, but in most cases, it is much less efficient with other types of damaged templates than with undamaged or CPD-containing DNA. It is not yet known if it is involved in bypassing any of these other types of damage *in vivo*.

The importance of polη is seen in the severe clinical characteristics of XPV patients and in the very high UV-induced mutation frequency in XPV cells. The UV-mutability of XPV cells is several-fold higher than that of normal cells and the frequency of all types of mutations is increased. This is evidence that in the absence of polη, something else is able to do its job, but the replacement is less efficient and makes more mistakes.

Localization

The catalytic domain of polη is contained within the first 430 aa. What then is the function of the C-terminal 280 aa? DNA replication takes place during the S phase of the cell cycle in "replication factories" inside the cell nucleus. These factories can be visualized either by immuno-fluorescence with an antibody to a replication protein, or by tagging proteins involved in DNA replication with the green fluorescent protein (GFP). The factories appear as bright nuclear foci when viewed by fluorescence microscopy. Polη also localizes in replication factories during DNA replication, so that it is always on hand in case the replication machinery encounters DNA damage (Figure 2). It is the C-terminal 120 aa of polη (aa 595–713) that are responsible for this localization into replication factories. This C-terminal domain contains a nuclear localization sequence that is required for transporting polη into the nucleus, as well as a C_2H_2 zinc finger and a sequence found in proteins that bind to the replication accessory protein, PCNA. Both of these motifs are needed to localize polη in replication factories. The function of aa 430–595 in polη has not yet been determined but it is doubtless involved in interactions with other proteins. The domain structure of polη is summarized in Figure 3.

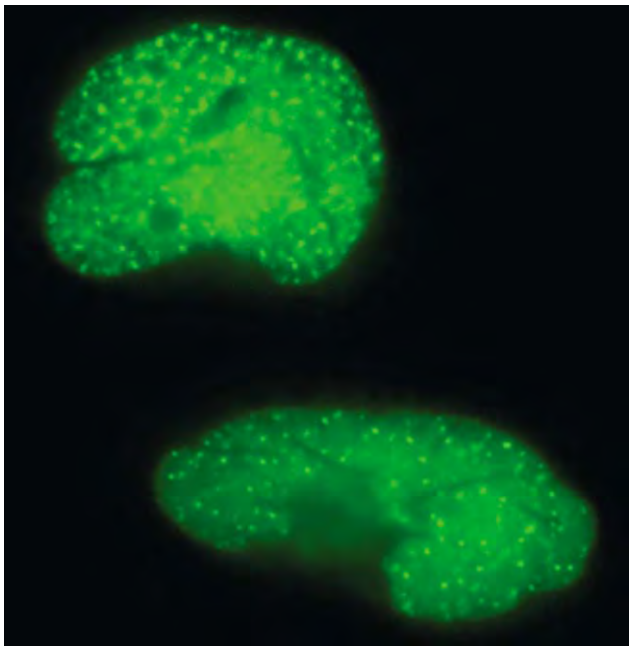

FIGURE 2 Localization of polη in replication foci. Polη, tagged with green fluorescent protein, localizes into nuclear foci during DNA replication.

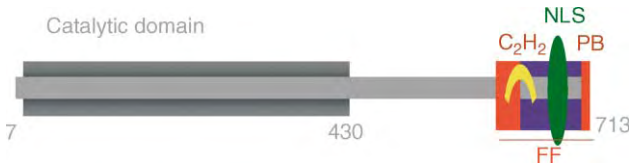

FIGURE 3 Domain structure of polη. C_2H_2, zinc finger; NLS, nuclear localization signal; PB, PCNA-binding motif; FF, foci formation.

Mutations in XPV Patients

Mutations have been identified in the polη gene in some 35 patients. The majority of the mutations result in truncations within the catalytic subunit and would not be expected to result in any functional polη. This suggests that polη is not an essential protein, since its absence is compatible with life. Several mis-sense mutations within the catalytic domain have also been identified and they are predicted either to inhibit binding to DNA or to interfere with the 3D structure of the protein. A small number of mutations do not affect the catalytic domain, but truncate the protein close to the C terminus. These mutant proteins would be expected to be fully active, but to lack the localization domain in the C terminus, which is required for transporting the polymerase into the nucleus. There is no clear relationship between the site or type of mutation and the severity of the clinical features, even though the severity of features differs widely between patients.

Replication Past Other Types of UV Damage

Although the CPD is the major UV photoproduct, the 6-4 PP is also formed in substantial quantities ($\sim$1/3 the frequency of the CPD). No single polymerase has been found that is able to carry out TLS past a 6-4 PP, which produces a much greater distortion in the DNA than a CPD. However two polymerases acting in concert are able to accomplish this. Insertion of the nucleotides opposite the 6-4 PP can be carried out either by polη or its paralogue, polι, but neither of these can extend further from the incorporated nucleotides. However once nucleotides have been inserted opposite the damaged bases, they can be extended by DNA polymerase ζ. So far, evidence for this dual polymerase mechanism has only been obtained *in vitro*. It is likely that this mechanism is also used *in vivo*, but as yet it is not known which polymerase carries out the insertion step.

See Also the Following Articles

DNA Damage: Alkylation • DNA Oxidation • DNA Polymerase α, Eukaryotic • DNA Polymerase β, Eukaryotic • DNA Polymerase δ, Eukaryotic • DNA Polymerase ε, Eukaryotic • Nucleotide Excision Repair in Eukaryotes • Translesion DNA Polymerases, Eukaryotic • Zinc Fingers

Glossary

DNA polymerase Enzymes which are able to synthesize new DNA molecules using a DNA template.

green fluorescent protein A highly stable intensely fluorescent protein, isolated from the jellyfish *Aequoria victoria*. It is widely used to "tag" other proteins to render them visible by fluorescence microscopy.

nuclear localization signal A sequence of amino acids in a protein that results in its localization in the nucleus.

nucleotide excision repair The enzymatic pathway by which many types of DNA damage are first recognized, then cut out of the DNA, and the excised region is replaced with new DNA.

zinc finger A sequence of amino acids which forms a finger-like structure and binds a zinc atom.

Further Reading

Goodman, M. F. (2002). Error-prone repair DNA polymerases in prokaryotes and eukaryotes. *Annu. Rev. Biochem.* **71**, 17–50.

Lehmann, A. R. (2002). Replication of damaged DNA in mammalian cells: New solutions to an old problem. *Mutat. Res.* **509**, 23–34.

Prakash, S., and Prakash, L. (2002). Translesion DNA synthesis in eukaryotes: A one- or two-polymerase affair. *Genes Dev.* **16**, 1872–1883.

Biography

Alan Lehmann is a Professor of Molecular Genetics and Chairman of the Genome Damage and Stability Centre at the University of Sussex, Brighton, UK. His research interests are in DNA repair and its relation to human health and disease, in particular the disorders xeroderma pigmentosum, Cockayne syndrome, and trichothiodystrophy. He identified the cellular defects in Cockayne syndrome, trichothiodystrophy and the variant form of xeroderma pigmentosum. Translesion synthesis polymerases are one of his current major interests. He obtained his Ph.D. from the Institute of Cancer Research, University of London, UK.

X-Ray Determination of 3-D Structure in Proteins

Martha L. Ludwig
University of Michigan, Ann Arbor, Michigan, USA

X-ray crystallography can decipher the three-dimensional arrangements of atoms in biological macromolecules. The primary data for such structure analyses are the intensities of diffracted X-rays (reflections). Determination of the positions and displacement parameters of the atoms requires assignment of the relative phases of these reflections, a task that can be accomplished by any of several strategies, including multiple isomorphous replacement, multiwavelength anomalous diffraction, and molecular replacement. Initial models are subsequently refined to optimize agreement with the diffraction data. Using X-ray crystallography, it has been possible to determine the structures of very large particles such as spherical viruses and of machines such as ATPase and the ribosome at near-atomic resolution. Because crystallographic studies of proteins and of their molecular complexes provide fundamental information about proteins and enzymes, it is important to consider both the scope and the limitations of X-ray structure determination.

Stages in an X-Ray Structure Analysis

Crystallization

Crystals of proteins and other biological macromolecules are remarkable. They form well-ordered three-dimensional arrays but nevertheless contain a significant fraction of mobile solvent that fills the interstices between the irregularly shaped molecules. Obtaining suitable crystals is the largest hurdle in the structure analysis of biomacromolecules. Most important among the criteria for suitability is that crystals must diffract X-rays to a resolution (Figure 1) that allows construction of a reliable atomic model. The requirements for resolution are somewhat flexible and depend on the problem. Most enzymologists would consider 3.0Å to be the lowest acceptable resolution for studies relating structure to mechanism. The crystal itself also must be of sufficient size to allow accurate measurement of scattered X-rays (enough photons for an adequate signal:noise ratio). This criterion has become less stringent as intense beams available at synchrotrons allow the use of crystals as small as 10 μm in thickness.

The parameters that affect nucleation and growth of crystals have been the subject of both theoretical and empirical studies. Finding appropriate buffers, precipitants, additives, and temperatures for crystallization has increasingly been made systematic, and sparse sampling of these variables has been incorporated in the design of several commercial crystallization kits. Robots can be deployed to mix protein samples with crystallization reagents and to disperse samples into sitting drops of sizes that vary from 5–10 μl to 50 nl or less. Mutations of individual residues and expression of domains, truncated sequences, or sequences with deletions often yield proteins that will crystallize when the full-length or wild-type counterparts resist all attempts at crystallization.

Diffraction Measurements

The intensities of diffracted X-ray beams (reflections) are the fundamental measurements in a crystallographic experiment. Thanks to the very bright X-ray sources at synchrotrons and the advent of area detectors (imaging plates or charge-coupled devices) that allow many reflections to be recorded simultaneously, data collection is no longer the rate-limiting step in a structure analysis. At modern synchrotron facilities, complete data sets for routine problems can be obtained on a timescale of minutes.

X-irradiation leads to loss of crystalline order and resolution by rupturing chemical bonds and by secondary reactions of the protein with radical species such as OH· that are generated by irradiation of the solvent. Immobilization of solvent by flash-cooling of crystals to about 100 K minimizes the radical reactions. Development of apparatus and reagents for cryoprotection and low-temperature data collection has helped to revolutionize structural biology. Cryotechniques are particularly important for measurements of anomalous diffraction effects (see below) because crystal lifetimes

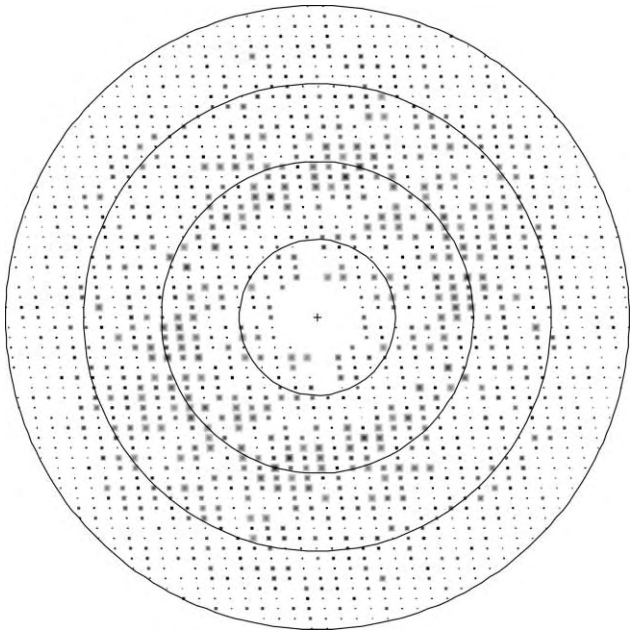

FIGURE 1 The definition of resolution in crystallography. This figure shows the relative intensities of diffracted X-rays (reflections) in a two-dimensional planar section through three-dimensional diffraction space. Each reflection occurs at a particular angle (2θ) determined by Bragg's law, $\lambda/d = 2\sin\theta$, where d is the distance between reflecting planes; reflections farther from the center have larger scattering angles and smaller d spacings. The superimposed circles are drawn with radii corresponding to resolutions of 7.2, 3.6, 2.4, and 1.8Å. All of the unique reflections within a sphere swept out by the 1.8Å circle will be used to calculate the electron density at a resolution of 1.8Å, whereas only the smaller number of reflections within the second sphere will be used for a 3.6Å electron density map. As the limiting d spacing becomes smaller, more data are incorporated in calculation of the electron density, and the resolution is said to be higher.

are extended sufficiently to permit all of the data required for structure determination to be collected from one crystal.

De novo Structure Determination

The result of a structure analysis is a 3-D electron density map, which is computed from the X-ray scattering by Fourier transformation. This calculation requires not only the measured amplitudes (square roots of the intensities) of the scattered X-rays but also the assignment of phases to all of the reflected waves. These phases are not determined by the X-ray experiments. Two strategies, multiple isomorphous replacement (MIR) and multiwavelength anomalous diffraction (MAD), are commonly employed to assign phases for structure analysis of a new or unknown protein fold. In both strategies, contributions of added heavy atoms or of incorporated selenomethionine are used to calculate the phases of the protein by triangulation. The first step in both methods is determination of the positions of the heavy atoms. MIR requires measurements from native crystals and from a series of derivative crystals modified by addition of heavy atoms. These derivatives are obtained by immersing preformed crystals in holding solutions containing heavy atom complexes, or less frequently, by co-crystallization. Typical reagents are mercurials or platinum complexes. The method assumes that X-ray scattering by the protein atoms is exactly the same in the derivative as it is in the native crystals so that all differences in the diffraction pattern can be attributed to the added heavy atoms. Perturbation of the protein induced by addition of heavy atoms (loss of isomorphism) is the most common source of errors in MIR.

Multiwavelength anomalous diffraction exploits scattering effects that occur at wavelengths near the X-ray absorption edges of elements such as Se, Br, and lanthanides. At the peak of the absorption edge of these elements, the imaginary anomalous component (f'') is large, producing differences between intensities of h,k,l and $-h,-k,-l$ reflections. The real anomalous component (f') is large (and negative) at the inflection point of an absorption edge, but is small at wavelengths remote from the edge. Effects of the real (dispersive) component appear as wavelength-dependent differences in intensities. Both f' and f'' vary with wavelength, and both components are used to determine phases. MAD experiments thus require X-rays that can be tuned to appropriate energies and are performed at synchrotron X-ray sources. Although the changes in intensities that arise from anomalous scattering effects are usually smaller than for MIR, MAD has the advantage that the requisite data are obtained from one crystal. Effects of nonisomorphism are thus circumvented. With precise measurements of the relevant intensity differences and algorithms based on direct methods, it is currently possible to locate ~100 Se atoms per asymmetric unit. Structures as large as 300 kDa have been determined from anomalous scattering by selenomethionine. Experience demonstrates that measurements of anomalous diffraction at the peak wavelength of lanthanides or even Se (single-wavelength anomalous diffraction, or SAD) can be sufficient to determine a structure.

In the determination of the phases that are used to calculate an initial experimental electron density map, it can be advantageous to combine data from isomorphous replacement and anomalous scattering. Requiring bulk solvent regions to have uniform electron densities (solvent flattening) is a useful restraint that improves the accuracy of phases. Computational suites such as CCP4, CNS, SHARP, or SOLVE/RESOLVE are designed to exploit all these and other sources of phase information.

Fitting Electron Density Maps

Atomic models are built into electron density maps using graphics displays that allow interactive and menu-driven manipulations of the models. Modern software for model fitting incorporates a number of features that

simplify and speed this process, including local optimization of models within the density and sampling of likely side chain rotamers.

Refinement

Initial atomic models that are constructed by interactive fitting of experimental electron density maps are usually incomplete and inaccurate. They serve as the starting point for refinement, a process in which the agreement between the observed and computed structure factors is improved by adjustment of the atomic positional and thermal parameters. Modified parameters are used in turn to compute phases and new maps that permit refitting of the model and addition of missing parts. This cyclic procedure is repeated until the fitting appears to have converged. It is a fortunate consequence of the physical and mathematical relationship between a crystal structure and its diffraction pattern that structures can be corrected or completed if most of the scattering has been accounted for in an atomic model. Missing and/or incorrectly placed atoms are detected in difference maps that subtract the computed from the observed structure. There are two fundamentally different approaches to optimization of molecular models: the first is straightforward minimization by algorithms such as conjugate gradient and the second is sampling of conformations, usually with molecular dynamics simulations. Molecular dynamics calculations that begin with atom velocities corresponding to elevated temperatures (simulated annealing) are a very efficient way to improve initial models. Standard minimizations are performed after the annealing cycles.

Minimizations are large, iterative least-squares computations whose convergence is hampered by small ratios of data to adjustable parameters. There are at least four parameters to be assigned to each atom: its position, *x, y, z,* and a temperature factor (or displacement parameter) that reports excursions of the atom about its equilibrium position. Even at 2.0Å resolution, a typical data:parameter ratio for this simplest set of parameters is about 2.5. To compensate for limitations in the data, most refinements are conducted with harmonic restraints that maintain standard polypeptide geometries and in effect increase the number of observations. Data:parameter ratios and robustness can also be increased by replacing Cartesian with torsional variables or by imposing strict constraints to maintain the identity of chains that are repeated in the asymmetric unit.

Various target functions can be chosen for minimization in least-squares refinement. The conventional target is the discrepancy between the observed amplitudes of reflections and the amplitudes calculated from the model. The corresponding reliability index, or *R*-factor, is defined as $\Sigma||F_{obs}| - |F_{calc}||/\Sigma|F_{obs}|$, where the sums are taken over all reflections. It thus resembles an average fractional error. Alternative targets substitute intensities for amplitudes or utilize correlation functions. R_{free}, an agreement index calculated with a subset of reflections that is never sampled in refinement, is an important monitor of refinement.

Structure Determination by Molecular Replacement

When the protein of interest is related to a known structure, coordinates for the known homologue may be employed to solve the unknown. The initial computation is usually carried out in two stages, referred to as rotation and translation searches. The model is oriented and then positioned in the unit cell of the unknown crystal by correlating observed intensities or structure factor amplitudes with those calculated from the oriented model. It is then subjected to refinement. There is no hard-and-fast rule about the level of sequence similarity that augurs success in molecular replacement (MRP), or about the fraction of the structure to be used in searches. A standard practice has been to truncate side chains that are not identical in the two proteins. For multidomain proteins it may be desirable to use individual domains, rather than the intact protein, as search models.

The principal hazard in MRP is bias from the model structure. Although incorrect features should appear at lower-than-average electron densities, they do not disappear completely. One effective strategy to minimize bias is the computation of "omit" maps, in which local regions of the model that need adjustment or verification are not included in the phase calculations.

Similarity of structures is exploited in another form of molecular replacement in which the electron densities corresponding to structural repeats are averaged to generate modified maps and modified phases. This approach assumes that the multiple copies of chains or subunits found in an asymmetric unit (the smallest motif from which the crystal can be generated by translation and rotation) adopt identical conformations. These copies are related by coordinate transformations that are local and do not obey crystallographic symmetry; hence they are referred to as non-crystallographic symmetry operations. Implementation of this mode of molecular replacement was the key to the pioneering structure analyses of spherical viruses.

Studies of Molecular Complexes and Conformational Changes

The classic comparisons of deoxy- with methemoglobin and the difference Fourier analyses that revealed azide

bound to myoglobin presaged the central role of crystallography in the descriptions of conformation changes and molecular interactions. Subsequent structures have firmly established the plasticity of proteins and have demonstrated that a surprising variety of conformational states can be accessed by a particular polypeptide.

Ligand Binding *in situ*

Myoglobin–azide and lyzozyme–tetrasaccharide complexes were the prototypes for experiments in which structures of molecular complexes have been determined from preformed crystals after immersion in holding solutions containing ligands. This approach is feasible because the extensive solvent-filled channels within the crystals allow small ligands or substrates to diffuse to their binding sites. Density corresponding to the ligands is found in maps computed with amplitudes measured from the complex and phases from the ligand-free protein. Subsequent refinement often reveals local changes in the protein, elicited by interactions with the ligands. If the binding sites are not saturated, the electron densities will include images of both the ligand-free and ligand-bound species, and it may be necessary to refine the occupancies of the ligands and to include alternate conformations for parts of the protein.

Large Conformation Changes

In contrast, major conformation changes such as those accompanying oxygenation of hemoglobin cannot be accommodated by the original crystal lattice and either are suppressed by competing crystal-packing forces or disrupt packing interactions and disorder the crystals. Descriptions of these larger structural changes therefore require analysis and comparison of different (non-isomorphous) crystals obtained under conditions that favor one or another conformation. Determination of the alternate conformation entails solution of a new structure by *de novo* or molecular replacement methods. Dramatic conformation changes are not uncommon and can include displacements of loops or flaps, swinging or pivoting of domains, and even remodeling of secondary structures. Numerous examples have been gathered in compendia of molecular motions.

Studies of Reaction Intermediates: Trapping Methods

Structures related to intermediates in enzyme-catalyzed reactions can be obtained from complexes with unreactive substrate analogues or transition-state analogues. More elegant experiments are also feasible, as many enzymes are active catalysts in the crystalline state. With sufficient knowledge of the reaction mechanism, it is possible to design experiments in which true intermediates accumulate in the crystal, or to trap structures of these intermediates at appropriate times by flash-cooling. In studies of isocitrate dehydrogenase, Stoddard and co-workers exploited mutations to favor accumulation of intermediates either prior to or following hydride transfer. The analysis of several intermediates in catalysis by P450-cam was accomplished by controlling addition of reactants. Data were collected from the ferrous enzyme–substrate complex after chemical reduction, and crystals were then allowed to react with oxygen to form the subsequent dioxygen intermediate, which was in turn reduced by X-irradiation to yield a putative activated-oxygen intermediate.

Time-Resolved Crystallography

The most challenging experiments are those that aim to determine structure as a function of time. They require a narrow time window for initiating reactions and very rapid data collection, usually by the Laue method, which employs broadband radiation to capture most of the reflections in a single image of the diffraction pattern. The mixtures of structures that are present vary with time and must be sorted out. Time-resolved structural studies of the photodissociation of CO from crystals of myoglobin have revealed non-heme binding sites for CO and established the nature of relaxations in the heme and globin that follow photolysis.

Accuracy of X-Ray Structures and Metrics of Reliability

The Importance of Resolution

The exact definition of resolution in crystallography is illustrated in Figure 1, which depicts a plane from the 3-D lattice in diffraction (reciprocal) space. Resolution is probably the most important parameter in any assessment of a structure determination. The dramatic effects of resolution on the appearance of electron density maps have been illustrated in several texts and reviews. The number of reflections included in a structure determination increases as $(1/d_{\min})^3$. Resolution thus controls the data:parameter ratios that are critical in refinement and is a primary determinant of positional accuracy. The choice of a resolution limit for a structure analysis is dictated by the completeness of the outermost shell of data and the agreement between measurements of symmetry-related reflections. These metrics are usually displayed in tables describing the structure determination.

Uncertainties in Coordinates

One would like to obtain estimates of the positional uncertainties for each atom and the derived uncertainties of bond lengths, bond angles, and torsions. The diagonal elements of the inverse matrix that is calculated in least-squares refinement provide these uncertainties in mathematically rigorous fashion. However, for proteins the size of the least-squares matrices (at least $3N$ by $3N$, where N is the number of atoms in the asymmetric unit) have generally precluded this computation. Approximations that derive global estimates of average coordinate errors from R-factors versus resolution are partly flawed because they assume the same temperature factors for all atoms. One compromise has been to invert large diagonal blocks taken from the full matrix. Evaluation of the estimated standard deviations arising from experimental errors is complicated by the inclusion of restraints in most refinements. The average errors in bond lengths are often dominated by the deviations chosen for restraints.

Refinements of a few structures have included inversion of the full matrix. Analysis of concanavalin A at 0.94Å resolution provided details of the geometry at the manganese- and calcium-binding sites with accurate estimates of the deviations of bond lengths and angles in the metal cluster, information that is critical for understanding the properties of the metal center. Comparison of rigorous with approximate error estimates for this and other ultra-high-resolution structures demonstrates, as might have been expected, that positional uncertainties depend strongly on the values of the temperature factor (displacement parameter). This dependence is especially pronounced in unrestrained refinements.

Solvent molecules (usually water) that occupy defined sites are included in archived coordinate lists (.pdb files). They are important for structure and function, and they contribute significantly to X-ray scattering even though their residence times may be short. Waters in buried or active sites may be very well-defined, but in general water oxygens are the least well-positioned atoms and the most subject to error. Some publications report refinement of both occupancy and isotropic B values for solvents, but because these parameters are highly correlated, others choose to allow only B to vary in refinement. It is customary to verify that waters are placed at canonical distances from neighbors and make reasonable interactions with protein atoms or other solvents.

Reliability Indices (R-Factors)

R-factors are widely cited criteria of the accuracy and reliability of a structure and are used to judge the progress and convergence of refinements. Readers of structure reports need to be aware of their shortcomings. The actual values will depend on the refinement algorithm, the choices of restraints or constraints, the omission or inclusion of weak reflections, and on the resolution (minimum d-spacing). The conventional R-factor, $\Sigma||F_{obs}|-|F_{calc}||/\Sigma|F_{obs}|$, can be decreased artificially by overfitting, e.g., by including many solvents with small scattering contributions or by using anisotropic temperature factors at too low a resolution.

The introduction of R_{free} in the early 1990s provided a better index of reliability and accuracy. R_{free} is calculated from a subset of data, randomly chosen with respect to intensity and resolution, that is never used in refinement. Acceptable refinement strategies such as inclusion of additional solvents should produce decreases not only in the conventional R but also in the R_{free} value.

Other Quality Indices: Structure Validation

Crystal structures are full of details, and models are built interactively and subjectively into the electron densities. It is useful to have objective methods to flag possible errors and regions that deserve further adjustment. Very occasionally, incorrect folds have been fit to electron densities, and wrong connections between pieces of the polypeptide have been introduced in maps at relatively low resolution. More common errors are mistaken registration of sequences and misoriented peptide planes. It is important to examine Ramachandran plots of Φ, Ψ angles for outliers with unusual (high-energy) backbone conformations; side-chain conformations should resemble one of the common rotamers. Comparisons of model density with experimental or omit maps identify residues that may be incorrectly modeled because they are mobile or adopt multiple conformations. The Protein Data Bank routinely subjects submitted coordinates to examination by PROCHECK, which analyzes the stereochemistry and other properties, flags possible errors, and assigns a quality index.

Structures at Very High Resolution

The library of structures at resolutions beyond 0.9Å is small but is growing steadily. Data:parameter ratios for these analyses allow unrestrained refinement and anisotropic modeling of the temperature factors, which requires specification of nine parameters per atom rather than four. In these structures it is possible to see what had to be surmised or inferred

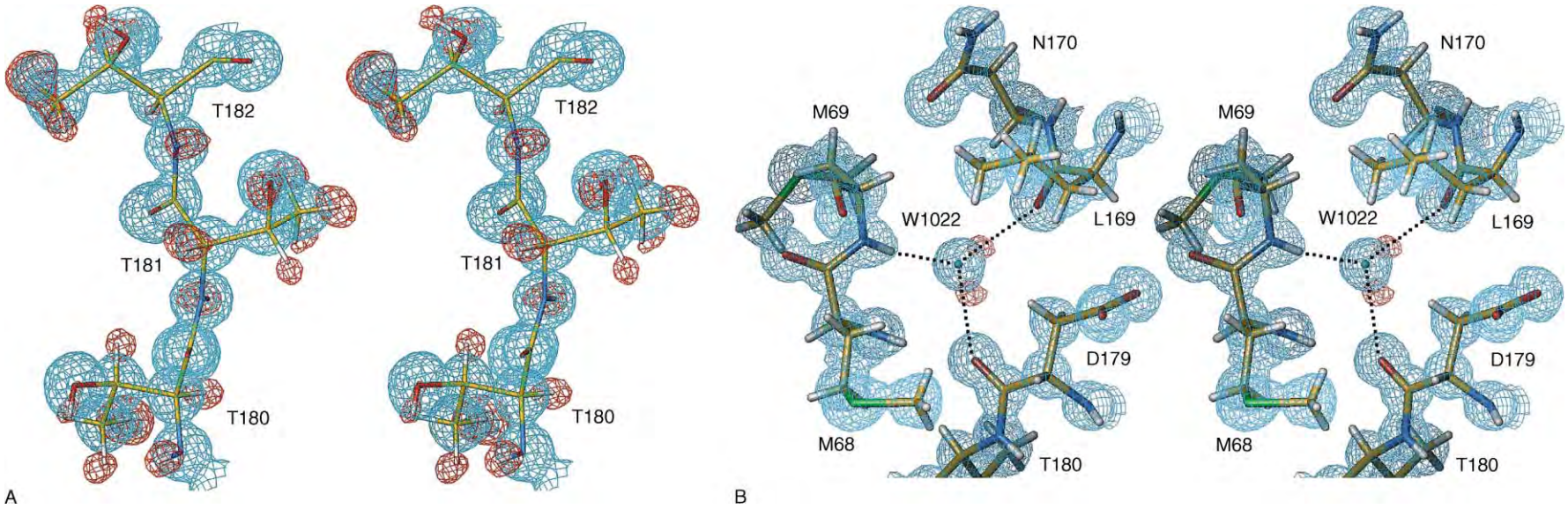

FIGURE 2 Stereoviews of electron density from the crystal structure determination of TEM-1 β-lactamase at 0.85Å resolution. At this resolution, densities corresponding to individual atoms are apparent (cyan), and difference densities (red) identify the positions of hydrogen atoms. The data:parameter ratio was 6:1 in refinement with anisotropic temperature factors; alternate conformations were included for 169 residues; R_{free} is 0.112. Reproduced from Minasov, G., Wang, X., and Shoichet, B. K. (2002). An ultrahigh resolution structure of TEM-1 beta-lactamase suggests a role for Glu 1 66 as the general base in acylation. *J. Am. Chem. Soc.* 124, 5333–5340.

from lower resolution structures—many of the hydrogen atoms, alternate conformations, and distinctions between oxygen and nitrogen atoms. Direct observation of hydrogen bonds is especially valuable for enzymologists, as is resolving ambiguities about the orientations of Asn, Gln, and His. As more high-resolution structures are completed, it should be possible to document true deviations of geometries from the canonical values embedded in restraint libraries. The example shown in Figure 2 illustrates the clear definition of densities corresponding to individual atoms and the assignments of hydrogens from difference maps.

Displaying and Comparing Structures

The computing power of current desktop machines allows the non-crystallographer to display and analyze structures that have been deposited in the Protein Data Bank. Particularly useful features of available programs are algorithms that align structures for comparisons of conformations, facile analysis of noncovalent interactions, routines for mutation and model building, and the capability to generate illustrations in a variety of styles.

See Also the Following Articles

Imaging Methods • Protein Data Resources • Secondary Structure in Protein Analysis

Glossary

asymmetric unit The smallest motif from which the crystal can be generated by translation and rotation operations. The unit cell that is repeated by translation to form the crystal may contain a number of asymmetric units.

isomorphism When addition of a ligand or heavy atom does not alter the scattering contribution (structure factor) of the protein atoms, the derivative and native crystals are said to be isomorphous. Cell dimensions are expected to be unchanged.

non-crystallographic symmetry (NCS) When the asymmetric unit includes more than one copy of a polypeptide, the multiple copies are related by local coordinate transformations that do not obey the symmetries that define the space group.

structure factor A vector **F** with phase $\alpha_{h,k,l}$ whose length |F| is the amplitude of the reflection *h*, *k*, *l*. The structure factor is the resultant of summing over scattering contributions from all the atoms in the asymmetric unit and can be calculated from the atom parameters. Fourier transformation of the structure factors yields the electron density.

temperature factor (displacement parameter) A measure of the motion of an atom about its equilibrium position. Temperature factors may be isotropic (B-values) or anisotropic. In the general anisotropic case, six parameters are required to describe the displacements.

Further Reading

Baldwin, J., and Chothia, C. (1979). Hemoglobin: the structural changes related to ligand binding and its allosteric mechanism. *J. Mol. Biol.* **129**, 183–191.

Brünger, A. T., Adams, P. D., and Rice, L. M. (1999). Annealing in crystallography: A powerful optimization tool. *Prog. Biophys. Mol. Biol.* **72**, 135–155.

Carter, C. W., Jr., and Sweet, R. M. (eds.) (1997). *Macromolecular Crystallography, Parts A and B. Methods in Enzymology*, Vols 276 and 277. Academic Press, San Diego.

Cruickshank, D. W. (1999). Remarks about protein structure precision. *Acta Crystallogr.* **D55**, 583–601.

Drenth, J. (1999). *Principles of Protein Crystallography.* Springer-Verlag, New York.

Garman, E. F., and Schneider, T. R. (1997). Macromolecular cryocrystallography. *J. Appl. Cryst.* **30**, 211–237.

Guex, N., and Peitsch, M. C. (1997). SWISS MODEL and the Swiss-PdbViewer: An environment for comparative protein modeling. *Electrophoresis* **18**, 2714–2723.

Kleywegt, G. J. (2000). Validation of protein crystal structures. *Acta Crystallogr.* **D56**, 249–265.

Moffat, K. (2001). Time-resolved biochemical crystallography: A mechanistic perspective. *Chem. Rev.* **101**, 1569–1581.

Rossmann, M. G., and Arnold, E. (eds.) (2001). *Crystallography of Biological Macromolecules, International Tables for Crystallography*, Vol F. Kluwer Academic Publishers, Dordrecht.

Schlichting, I., Berendzen, J., Chu, K., Stock, A. M., Maves, S. A., Benson, D. E., Sweet, R. M., Ringe, D., Petsko, G. A., and Sligar, S. G. (2000). The catalytic pathway of cytochrome P450cam at atomic resolution. *Science* **287**, 1615–1622.

Stoddard, B. L. (2001). Trapping reaction intermediates in macromolecular crystals for structural analyses. *Methods* **24**, 125–138.

Stryer, L., Kendrew, J. C., and Watson, H. C. (1964). The mode of attachment of the azide ion to sperm whole methemoglobin. *J. Mol. Biol.* **8**, 96–104.

Terwilliger, T. C., and Berendzen, J. (1999). Automated MAD and MIR structure solution. *Acta Crystallogr.* **D55**, 849–861.

Biography

Martha L. Ludwig is Professor of Biological Chemistry and Research Biophysicist at the University of Michigan in Ann Arbor. She is an X-ray crystallographer whose primary research interest is the structure and function of enzymes that require metal- and vitamin-based cofactors. She is a Fellow of the American Association for the Advancement of Science and a member of the National Academy of Sciences.

Yeast GAL1–GAL10 System

Dennis Lohr and Ralph Bash
Arizona State University, Tempe, Arizona, USA

The GAL1 and GAL10 genes in the budding yeast *S. cerevisiae* encode enzymes that help convert galactose to a glycolytic intermediate, thus allowing it to be used as a carbon source for cell growth. Genetic characterization of the GAL genes and dissection of their regulatory mechanisms by Douglas and Hawthorne in the 1960s provided a firm and crucial foundation for the molecular characterization of GAL1–10 regulation that began in the 1980s. Expression of GAL1 and GAL10 is strikingly carbon source-dependent. Transcription occurs at extremely high levels in galactose-grown cells but is undetectable in cells grown in other carbon sources. This clear-cut and efficient regulation plus the ability to couple genetic and biochemical studies in the analysis of single-copy genes have made GAL1–10 a very attractive model for eukaryotic gene regulation studies and a paradigm in which many general eukaryotic regulatory themes were first uncovered. The GAL1 promoter is also widely used to drive expression of heterologous genes, in various applications. The basic molecular aspects of GAL1–10 gene regulation are outlined below (genes referred to as GAL1, proteins as Gal1p).

The Elements Contributing to GAL1–10 Regulation

GAL1 and 10 share a common ~600 bp (base pair) intergenic region from which they are divergently transcribed (Figure 1). They are considered to be coexpressed and coregulated, mainly at the transcriptional level. Their regulation combines inputs from DNA sequence (promoter) elements, protein factors (gene-specific and general), and chromosome structure.

DNA Sequence Elements

The most important gene-specific promoter elements for GAL1–10 expression are the upstream activation sequence (UAS_G) elements. These ~17 bp motifs are necessary and sufficient for galactose-dependent gene expression because; they provide the binding sites for Gal4p, the specific activator of GAL gene transcription. GAL1–10 share four UAS_G asymmetrically located between the two genes (Figure 1). Each gene has its own TATA sequence for binding the general transcription factor TBP (TATA binding protein).

The Gene-Specific Regulatory Factors

Gal4p

As the required activator for GAL gene expression, Gal4p is a key player in GAL1–10 expression. In the presence of galactose, Gal4p activates transcription through a domain located near its carboxy terminus, residues 767–881, while bound to (UAS_G) DNA via a domain located near its amino terminus. It binds as a homodimer to individual UAS_G elements.

Gal80p

In carbon sources other than galactose, the negative regulator Gal80p binds specifically to the C-terminal activation domain of Gal4p such that it masks Gal4p activation activity and thus prevents GAL1–10 transcription. Gal80p binds Gal4p quite strongly (K_d ~ 5 nM).

Gal3p

In the presence of galactose, the Gal80p-mediated inhibition of Gal4p is relaxed by a Gal3p-dependent process, thus freeing the Gal4p activation domain to activate GAL1–10 transcription. Gal3p behaves like a signal transducer and appears to be located solely in the cytoplasm, which should facilitate its interaction with galactose. Gal3p can bind to Gal80p but how this (cytoplasmic) interaction might influence the nuclear Gal80p–Gal4p complex is unclear at this time. Interestingly, the product of the GAL1 gene contains a Gal3p-like activity that apparently makes it capable of fulfilling a similar function to Gal3p.

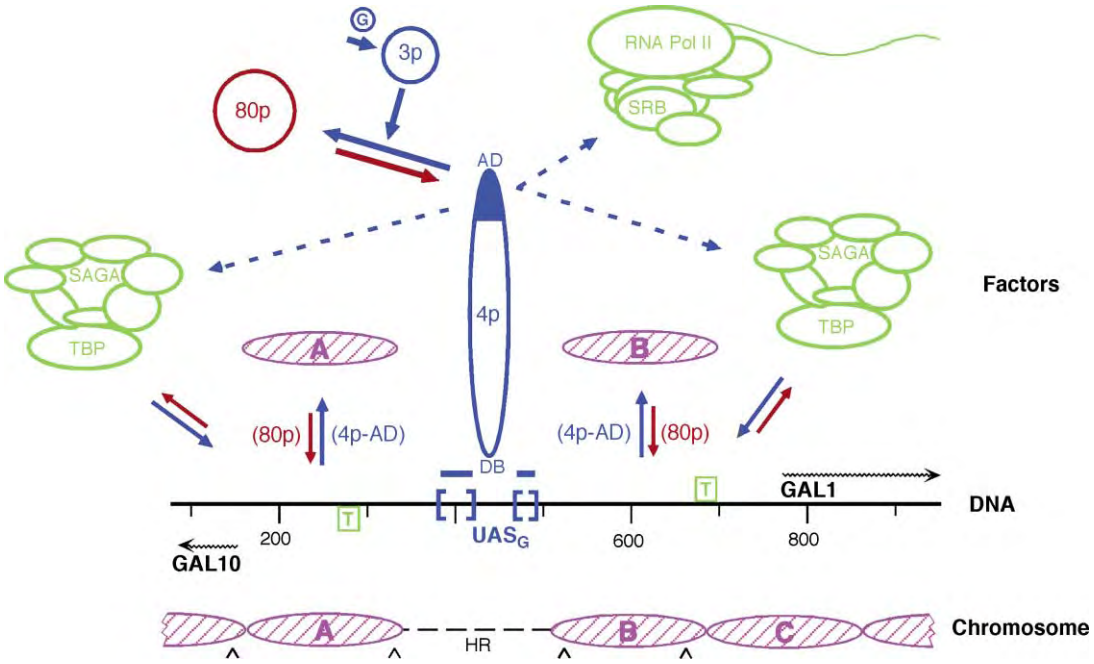

FIGURE 1 An outline of *GAL1–10* regulation. The DNA sequence organization of the yeast *GAL1–10* promoter region is shown in the center of the diagram ("*DNA*"), with UAS$_G$ (blue brackets) and TATA boxes (green, boxed "T") located to scale along the sequence (gray line). The numbers refer to base pairs from an EcoRI site in the *GAL10* gene. The transcription start sites are located at the origins of the two wavy arrows below (*GAL10*) or above (*GAL1*) the line. The chromosomal structure of this region in the inactive state of gene expression is shown at the bottom ("Chromosome") with nucleosomes A, B and C (pink) located to scale on the sequence and the nonnucleosomal, highly accessible region in the chromosome indicated by a dashed line ("HR"). The locations of intrinsic, sequence specific DNA bends are shown by " ∧ ". In the topmost portion of the Figure ("Factors"), various factors and complexes known or thought to be involved in regulating and implementing *GAL1–10* expression are shown. The *GAL*-specific factors ("3p", Gal3p; "4p", Gal4p) are shown in blue and the reactions that occur in, or are characteristic of, the active (galactose-induced, "G") state are designated by solid blue arrows. Dotted blue arrows indicate the suggested recruitment of complexes by Gal4p during gene activation, RNA polymerase II ("RNA pol II"), including SRB (*S*uppressor of *R*NA Polymerase *B* subunit) proteins and the SAGA (*S*pt-*A*da-*G*en5-*A*cetyltransferase) complex. The activation domain ("AD") of Gal4p is solid blue and the Gal4p DNA binding domain is identified ("DB"). The negative *GAL*-specific factor, Gal80p ("80p"), is shown in red and the reactions that occur in, or are characteristic of, the inactive state of expression are designated by red arrows. The association/dissociation of TBP with the *GAL1* and *GAL10* TATA and the disruption/redeposition equilibria of promoter nucleosomes A and B (pink) are also designated by solid blue/red arrows. The involvement of Gal4p and Gal80p in the promoter nucleosome disruption/redeposition equilibrium is indicated by their appearance in parentheses next to the appropriate arrow. Nucleosome C, which also undergoes disruption/redeposition, is not shown in this upper portion of the figure.

Other Factors

Global processes, such as the general glucose repression system, also participate in GAL1–10 regulation and elements of the RNA polymerase II transcription apparatus function in GAL1–10 transcription. Several other genes show galactose-sensitive and Gal4p-dependent expression, suggesting that their gene products may be part of the regulatory network: GAL6 (possible alternative regulator); GCY1 (oxido-reductase); PCL10 (cyclin); FUR4 (uracil permease); RPA; and YP53 (protein metabolism). Their precise roles are unknown.

Chromosomal Organization

The promoter region of GAL1–10 has a distinctive chromosomal organization that is an aspect of gene control. In all carbon sources, the UAS$_G$ elements reside within a sizable (at least 150 bp), highly accessible nucleosome-free region ("HR," Figure 1). Thus, the UAS$_G$ are always available to Gal4p; neither nucleosome removal nor competition with nucleosomes is required to expose these elements for Gal4p binding. The strategy of locating major promoter elements in a large, constitutively accessible region is not common on eukaryotic promoters and the features that maintain it have yet to be defined. In nongalactose carbon sources, nucleosomes bracket this highly accessible HR region, covering the TATA and transcription start sites ("A–C," Figure 1). The DNA near the termini of nucleosomes A and B contains intrinsic, sequence-dependent DNA bends (Figure 1) that may contribute to the preferential location of these promoter nucleosomes.

The (Three) States of GAL1–10 Gene Expression

The Active (Galactose-Induced) State

In galactose, GAL1–10 are transcribed at very high levels, indicating that the activation mechanisms for their expression are quite robust. Under these conditions, Gal4p is bound, via its N-terminal DNA-binding domain, to the UAS_G elements that lie between GAL1 and GAL10 while promoting transcription of the genes through its C-terminal activation domain. In this state, binding of TBP to the GAL1 and GAL10 TATA will be greatly aided by the apparent removal (disruption) of the promoter nucleosomes A–C, a process mediated directly or indirectly (through other factors) by the Gal4p activation domain. Transcription activation by Gal4p also involves the direct or indirect recruitment of cellular complexes (Figure 1). The UAS_G are >200 bp from the GAL1–10 transcription start sites suggesting that the three-dimensional structure of Gal4p and promoter chromatin architecture, both unknown, may also impact on the activation process. This variety of Gal4p activation depends upon the galactose-induced release of Gal80p inhibition that is mediated through Gal3p (and Gal1p?).

The Inactive States (Repressed or Poised)

There are two distinct types of inactive states, repressed (in glucose) or poised for expression (in nonfermentable carbon sources like glycerol/lactate). In both inactive states, Gal80p binds to the Gal4p activation domain, masking its activity, and nucleosomes A–C are present on the GAL1–10 promoter region, covering the TATA and transcription start sites.

The presence of glucose results in an additional negative feature, Gal4p absence from the UAS_G. This absence prevents GAL1–10 from being (rapidly) inducible in glucose. The UAS_G are still present in an open chromosomal region and should thus be available to Gal4p. Gal4p absence from the UAS_G is thought to result mainly from a decrease in Gal4p levels due to decreased expression of the *GAL4* gene, imposed by the global catabolite repression apparatus. The decrease in expression is fairly modest but Gal4p–UAS_G binding should be very sensitive to Gal4p levels due to its highly cooperative nature (multiple UAS_G/two Gal4p per UAS_G).

In carbon sources that are neither repressing nor inducing, such as glycerol lactate, the GAL1–10 genes are not expressed at all but they can be very rapidly (within minutes) induced to full expression by galactose. Rapid inducibility is due to the presence of Gal4p on the UAS_G in these carbon sources, strongly protecting these elements as in galactose-grown cells, and to the (low-level) presence of the signal transducer Gal3p. Elevated Gal4p levels (GAL4 is most actively expressed in these carbon sources) plus constitutive accessibility of the UAS_G elements probably account for the UAS_G occupation by Gal4p in this state. Thus, although inactive, GAL1–10 are poised for expression; only Gal80p inhibition of Gal4p (and the presence of nucleosomes A–C) prevents transcription. A poised state would probably have been a major advantage to wild yeast growing on poor carbon sources, by allowing them to utilize galactose even if it were only transiently available.

Key Themes in GAL1–10 Regulation

Gal4p: Completely Separable DNA Binding and Transcription Activation Functions

The ability of Gal4p to bind strongly to the UAS_G in the poised inactive state demonstrates that activator binding and transcription activation are separable aspects of GAL1–10 expression. As shown unambiguously by the Ptashne lab, this reflects the independence of the DNA binding and transcription activation functions of Gal4p. (This feature found an important general application in two-hybrid analysis.) These two functions of Gal4p are also differentially controlled: DNA binding by Gal4p levels, transcription activation by Gal80p.

How Gal4p Activates Transcription

As shown by Ptashne and co-workers, Gal4p can function throughout the eukaryotic kingdom, in microbes, animals, and plants. Thus, it must utilize basic and conserved mechanisms of transcriptional activation and target universal components of the transcription apparatus. TBP is a likely recruitment target of the Gal4p activation domain and recent work has suggested that the spt-ada-Gcn5-acetyltransferase (SAGA) complex mediates this recruitment. Gal4p has also been suggested to recruit RNA polymerase. Disruption of the promoter nucleosomes (A–C, Figure 1) in galactose is another explicit function of the Gal4p activation domain; this event is not simply an indirect consequence of transcription (as shown by the Majors lab). Exposing the DNA in these nucleosome-covered promoter regions is necessary to provide access for factors that initiate the transcription

process like TBP, which cannot bind to DNA that is nucleosome-covered. Surprisingly, the activation functions of Gal4p do not appear to depend on specific amino acids or protein structural motifs and sequence variations in the activation domain are exceptionally well tolerated as shown the labs of Johnston, Ptashne, and others.

The Central Role of the Negative Regulator Gal80p

In many respects, Gal80p may be viewed as the key regulator of GAL1–10 expression. It directly inhibits the activator Gal4p in nongalactose carbon sources, it responds to the Gal3p-dependent signal in galactose, thus mediating the activation response, and it even appears to temper GAL1–10 expression levels in galactose. The latter function may explain the surprising fact that expression of this negative regulator is significantly *increased* in galactose (up five- to tenfold), in a Gal4p/UAS_G-dependent transcription process. Gal80p also mediates, directly or indirectly, redeposition of the disrupted promoter nucleosomes A–C when conditions (activation signals, cellular energy levels) are unfavorable, as shown in the Lohr lab, and its effects on GAL1–10 expression in galactose, in particular, may reflect this activity.

The Importance of Protein–Protein Contacts in GAL1–10 Regulation

GAL1–10 regulation is implemented mainly through protein–protein interactions: Gal4p with Gal80p, Gal80p with Gal3p, Gal4p with transcription factors (TBP/SAGA/RNA pol II), and Gal4p/Gal80p with nucleosomes. The latter two may also involve other factors. The prominent role of protein–protein contacts might account for the importance of regulator (Gal4p, Gal80p, Gal3p) stoichiometries for proper regulation, which in turn are reflected in the levels and carbon source variations in regulatory gene expression.

The Role of Chromosome Structure in GAL1–10 Regulation

Chromatin structure is now seen as a major facet of eukaryotic gene regulation; studies of GAL1–10 chromatin as early as the mid 1980s in the Lohr lab provided indications of this feature. The advantages of maintaining the major promoter elements in an accessible chromosomal region, particularly for the poised state of expression, have been discussed previously. As shown by the Grunstein lab, the promoter nucleosomes A–C play regulatory roles in both the inactive and active states of GAL1–10 expression. These nucleosomes help inhibit transcription in nongalactose carbon sources; nucleosome depletion allows TATA-driven (Gal4p-independent) GAL1 expression, even in glucose. The N-terminal tails of histone H4 are needed for full levels of galactose-induced GAL1 expression and therefore play a positive role in this process; this role involves the nucleosome B region. In contrast, the removal of H3 histone tails results in an elevated level of induced GAL1 expression, in an effect that depends on the UAS_G region; therefore the H3 tails must normally function in a process that attenuates induced expression. Occupancy of the TATA regions on the GAL1–10 promoter probably involves a competition between TBP and the promoter region nucleosomes A and B/C (Figure 1). Galactose-inducing conditions favor TBP binding and thus transcription, as the nucleosomes are disrupted and the promoter region is exposed by a Gal4p-dependent process(es); under inactivating conditions, nucleosome binding to the regions is favored, and transcription is disfavored, by a process(es) that is dependent on Gal80p (Figure 1). Therefore, nucleosome presence on the promoter region (and thus transcriptional activity) is dependent on the state of a disruption/redeposition equilibrium, which is controlled by the gene-specific regulators Gal4p and Gal80p. The specific roles of the histone tails mentioned above may be linked to this regulator-dependent promoter region disruption/redeposition equilbrium. Only the promoter nucleosomes A–C show this behavior, not the GAL1 coding region nucleosomes, which is consistent with the suggested regulatory role of the promoter nucleosomes and their link to Gal4p/Gal80p action.

See Also the Following Articles

Chromatin: Physical Organization • Chromatin Remodeling • RNA Polymerase II and Basal Transcription Factors in Eukaryotes • RNA Polymerase II Elongation Control in Eukaryotes • RNA Polymerase II Structure in Eukaryotes • RNA Polymerase Reaction in Bacteria • RNA Polymerase Structure, Bacterial • T7 RNA Polymerase

Glossary

activator Proteins that enable or enhance transcription of genes.

gene-specific factors Proteins whose function is associated with expression of a specific gene(s).

nucleosome The complex of histone proteins wrapping up 147 bp of DNA that is the basic structural unit of eukaryotic chromosomes.

promoter DNA sequences that mediate gene expression.

Further Reading

Bash, R., and Lohr, D. (2001). Yeast chromatin structure and regulation of GAL gene expression. *Prog. Nucl. Acids Res. Mol. Biol.* **65**, 197–259.

Johnston, M. (1987). A model fungal gene regulatory mechanism: The GAL genes of *Saccharomyces cerevisiae*. *Microbiol. Rev.* **51**, 458–476.

Johnston, M., and Carlson, M. (1992). Regulation of carbon and phosphate utilization. In *The Molecular and Cellular Biology of the Yeast Saccharomyces* Vol. II, pp. 193–281. Cold Springs Harbor Laboratory Press, Cold Springs Harbor, New York.

Lohr, D. (1997). Nucleosome transactions on the promoters of the yeast *GAL* and PHO genes. *J. Biol. Chem.* **272**, 26795–26798.

Lohr, D., Venkov, P., and Zlatanova, J. (1995). Transcriptional regulation in the yeast GAL gene family: A complex genetic network. *FASEB J.* **9**, 777–787.

Reece, R., and Platt, A. (1997). Signalling activation and repression of RNA polymerase II transcription in yeast. *BioEssays* **19**, 1001–1010.

Biography

Dennis Lohr is a Professor in the Department of Chemistry and Biochemistry at Arizona State University, with principal interests in the relationships between chromatin structure and gene expression in eukaryotes. He holds a Ph.D. from the University of North Carolina (Chapel Hill) and was a postdoctoral associate in the Biochemistry and Biophysics Department at Oregon State University, in the lab of K. VanHolde. At Oregon State, he carried out most of the initial characterizations of yeast chromatin structure and in his own lab carried out the first detailed structural analyses of a single copy eukaryotic promoter, the GAL1–10 promoter, and its accompanying gene, GAL1.

Ralph Bash is a postdoctoral Research Associate at the Arizona Biodesign Institute and the Department of Physics and Astronomy at Arizona State University with interests in chromatin structure, chromatin function and molecular imaging. He holds a Masters from San Jose State University and a Ph.D. from Arizona State University, where he studied intrinsic DNA bending on GAL genes.

Zinc Fingers

Mark Isalan
European Molecular Biology Laboratory (EMBL), Heidelberg, Germany

Zinc fingers are small, compact protein subunits, with structured peptide chains folding around chelated zinc ions. Functionally, these subunits carry out a wide variety of tasks within cells by providing stable structural scaffolds and driving critical binding interactions, especially between proteins, DNA, and RNA. Zinc fingers are particularly important in gene regulation, where many proteins employ them to bind DNA in a sequence-specific manner, so as to activate or inhibit particular genes. Although many families of zinc fingers exist, each with a characteristic fold or structure, perhaps the best studied is the "classical" ("Cys_2–His_2" or "C2H2") type. Classical zinc fingers are extremely versatile, as can be seen by their abundance in nature: over 700 proteins contain such domains in the human genome alone, making them the second most common human protein motif. Zinc fingers may be seen as convenient molecular building blocks, often used in clusters, whose modular nature allows them to be conveniently duplicated, altered, and shuffled by evolution. In a biotechnology context, zinc fingers may be re-engineered to have novel binding properties with numerous applications in both research and medicine.

Zinc Finger Structures and Families

Classical Zinc Fingers

History

The zinc finger motif was discovered in 1985 by Miller, McLachlan, and Klug in a protein responsible for controlling gene expression: the *Xenopus* transcription factor IIIA (TFIIIA). Originally, nine novel consecutive repeats were found, each ~30 amino acids in length. Since every repeat had a conserved pair of cysteines and histidines at defined positions, Klug proposed that these residues could chelate a zinc ion, stabilizing an independent structural domain, the "zinc finger." Notably, the term "finger" was derived from the finger-like appearance of the sequences when drawn schematically around a zinc ion, as in Figure 1(A). The repeats found in TFIIIA are now used as a definition of the classical zinc finger, where individual fingers conform to the archetypal consensus sequence shown in Figure 2.

Secondary Structure and Hydrophobic Core

Structural studies revealed that the classical Cys_2–His_2 finger is a simple and compact unit based on an antiparallel β-hairpin packed against an α-helix (Figure 1(B)). In addition to chelating zinc, classical fingers are stabilized at the core by a hydrophobic cluster of residues, converging from three fixed positions (see Figures 1 and 2). Moreover, this hydrophobic triad is highly conserved, often consisting of tyrosine, phenylalanine, and leucine. By contrast, zinc fingers may withstand extensive amino acid substitutions at other positions, without significantly altering the overall structure.

The Role of Zinc

Small protein domains are inherently unstable and, even though the $\beta\beta\alpha$ fold found in zinc fingers can form around hydrophobic cores alone, the stability of the fold is dramatically improved by zinc chelation. Such stability cannot be obtained using the disulfide bridge – a common extracellular alternative – because of the highly reducing environment inside cells. Consequently, intracellular proteins have solved the problem of stabilizing small domains by utilizing metal-binding sites. Zinc is ideally suited for this purpose as it has a single oxidation state, a fixed and distinguishable ionic radius, and can accommodate both nitrogen and sulfur ligands.

Evolution

Zinc fingers may have evolved originally from peptides which maintained a simple $\beta\beta\alpha$ structure (similar to that shown in Figure 1(B)) independently of zinc. In any case, the $\beta\beta\alpha$ fold is one of the smallest possible units of protein tertiary structure, and may therefore be one of the oldest. Zinc fingers are very abundant in nature and the huge variety found in various organisms, from yeast to human, may in part be due to their modular nature.

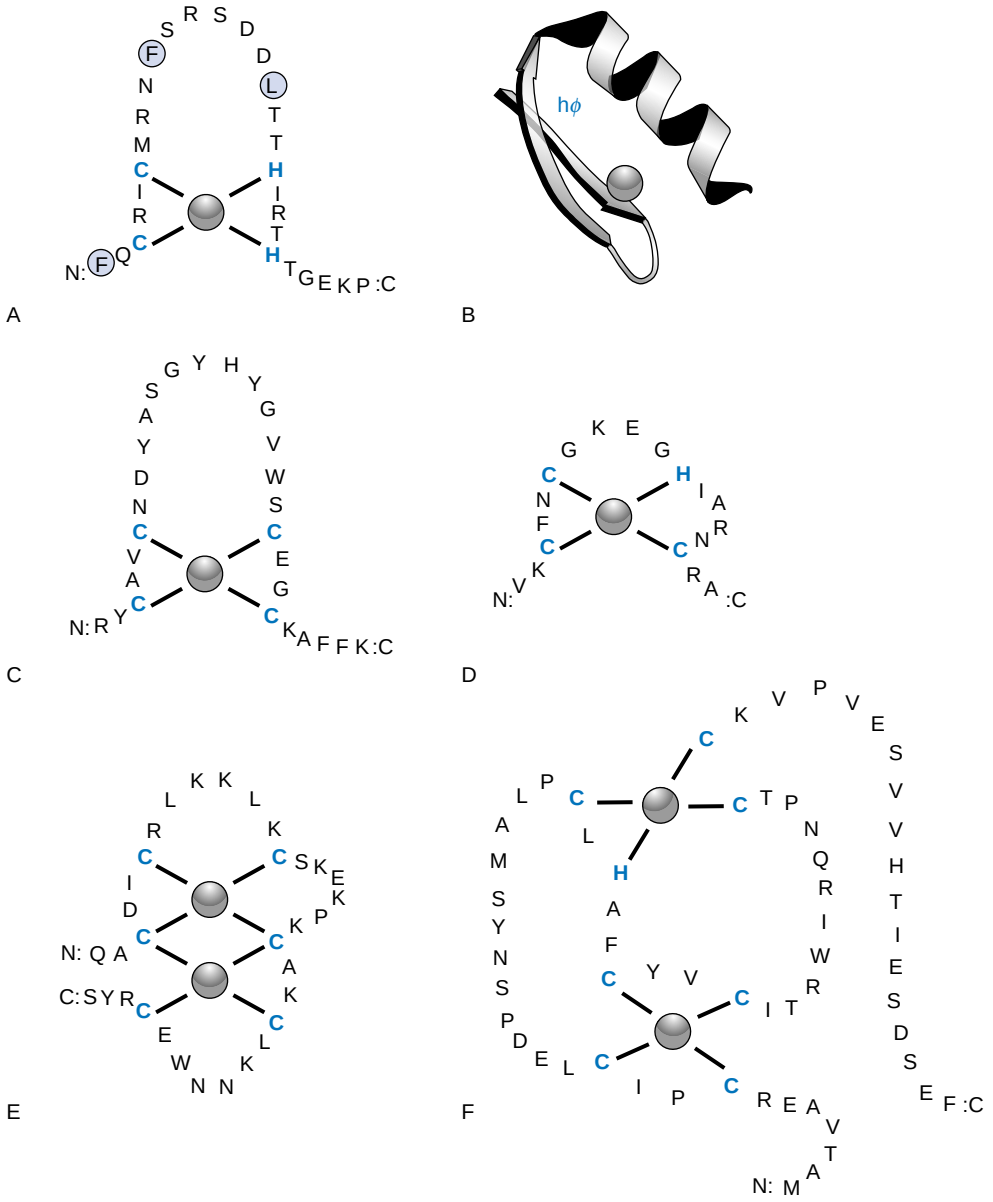

FIGURE 1 Examples of zinc finger families and folds. (A) A classical Cys_2–His_2 zinc finger is drawn schematically as a string of amino acids (1-letter abbreviations), with cysteine (C) and histidine (H) pairs chelating the central zinc ion. Three circled residues (F, F, L) come together in the structure to form a hydrophobic core. The finger shown is Finger 2 from the mouse transcription factor Zif268. (B) Representation of the actual $\beta\beta\alpha$ structure of a classical Cys_2–His_2 zinc finger. Note the position of the hydrophobic core (hϕ). (C) A Cys_4 steroid-receptor zinc finger from the estrogen receptor. Note that this protein actually contains two contiguous Cys_4 zinc finger repeats, forming a single structural unit. (D) A Cys_3–His zinc finger from a viral Nucleocapsid protein. (E) A yeast GAL4 domain. (F) The "ring" finger fold.

In this regard, not only are zinc fingers independently folding structural building blocks, but they are often encoded by single exons. Indeed, exon shuffling and gene duplication may account for why zinc fingers have spread so widely during evolution.

Genomic Abundance

The recent initial drafts of the human genome have revealed the extent to which classical zinc fingers are used by cells: there are 706 genes containing one or more classical zinc fingers in humans, totaling several thousand fingers, and making them the second most common human protein family. It is remarkable that only immunoglobulin domains are more abundant in humans, and indeed only slightly more so, being found in 765 genes. By contrast, the *Drosophila melanogaster* fly has 357 classical zinc finger genes, actually making these the most common protein family in this organism. Despite the fact that zinc finger usage varies from

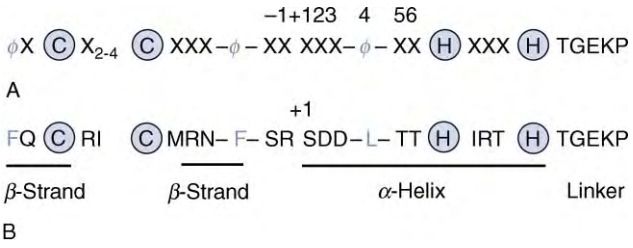

FIGURE 2 Zinc finger amino acid sequences. (A) Consensus sequence of a classical Cys_2–His_2 zinc finger, where X is any amino acid and ϕ represents hydrophobic residues (typically Y, F, and L). Zinc-chelating cysteine and histidine residues are circled. α-helical positions (numbered relative to position +1) are indicated above the sequence. (B) The sequence of Finger 2 of Zif268, showing conformity with the consensus sequence.

organism to organism, these motifs are clearly a widespread feature in all eukaryotic cells.

Non-Classical Zinc Fingers

Although zinc-binding proteins have been known for many years, the usual definition of zinc fingers maintains that they are distinct from other zinc-binding protein subregions by virtue of being autonomously folding, functional mini-domains. Following the discovery of the classical Cys_2–His_2 zinc finger, many other classes of "zinc finger" have emerged. Although these form a diverse collection, often with radically different folding topologies, these proteins are often referred to in the literature as zinc fingers. Therefore some well-studied examples are outlined here below.

Cys_4 Zinc Fingers

One of the best-characterized nonclassical zinc fingers is the Cys_4 type, including the steroid-hormone receptor family. The estrogen receptor (Figure 1(C)) was the first protein of this type to be elucidated structurally and the gene contains two Cys_4 zinc finger repeats, forming a single structural unit that is quite unlike the independent classical zinc fingers of TFIIIA. Functionally, the steroid receptors form dimers, that bind hormones like estrogen, and then mediate activation of gene expression through sequence-specific DNA-binding interactions in the promoter regions of target genes. Further examples of proteins containing Cys_4 finger motifs include other nuclear hormone receptors, such as the glucocorticoid and retinoic acid receptors. Many Cys_4 proteins function as transcription factors, such as the elongation factor TFIIS and the adenoviral E1A transactivator.

Cys_3–His Zinc Fingers

The Cys_3–His zinc finger is another variant defined by its characteristic combination of cysteine and histidine residues. For example, the nucleocapsid protein, found in certain viruses such as HIV, contains Cys_3–His fingers, with various nucleic acid binding properties that facilitate hybridization and the viral life-cycle (Figure 1(D)). Other examples of Cys_3–His proteins include MetRS and the first finger in the LIM domain.

Multi-Zinc Proteins

Moving beyond the simpler zinc finger domains, which fold around a single zinc ion, there exist larger more complex folds, each employing two or more zinc ions. Examples include the yeast GAL4 domain (Figure 1(E)) and the "ring" finger (Figure 1(F)). Note that although these larger domains are not quite as prevalent as the single-zinc modules, they nonetheless form quite abundant families. For example, the "ring" finger family ranks as the 15th most abundant domain in the human genome, with 210 members, while another fold, the "PHD" finger, ranks 34th with 84 members.

Zinc Finger Functions

Interactions with DNA and RNA

Since their discovery, zinc fingers have been associated with binding nucleic acids, namely, DNA and RNA. Indeed, the archetypal zinc finger protein, TFIIIA, is bi-functional, having distinct modes of binding which allow it to bind both to the DNA internal control region of 5S RNA genes and to the transcribed RNA gene product. In this sense, zinc fingers are master gene regulators, with the potential to influence both transcription and translation.

Structure of Zinc Finger Bound to DNA

The majority of our knowledge of zinc finger functions has focused on their ability to bind specific DNA sequences. The first structure of zinc fingers bound to DNA, that of the DNA-binding domain of the mouse transcription factor Zif268, was solved by Carl Pabo and colleagues in 1991. The structure revealed that each of the three classical zinc fingers occupies the major groove, wrapping around the DNA for almost one turn of the double helix (Figure 3A). Base specific contacts occur primarily from consecutive turns of the zinc finger α-helices to the guanine-rich strand of the DNA.

DNA Recognition Helix

Essentially, classical zinc fingers use the α-helix as a "reading head" to recognize specific DNA sequences. Contacts from amino acids consist primarily of electrostatic interactions and hydrogen bonds, although hydrophobic interactions also play a role. Conventionally, the amino acids in the α-helix are numbered

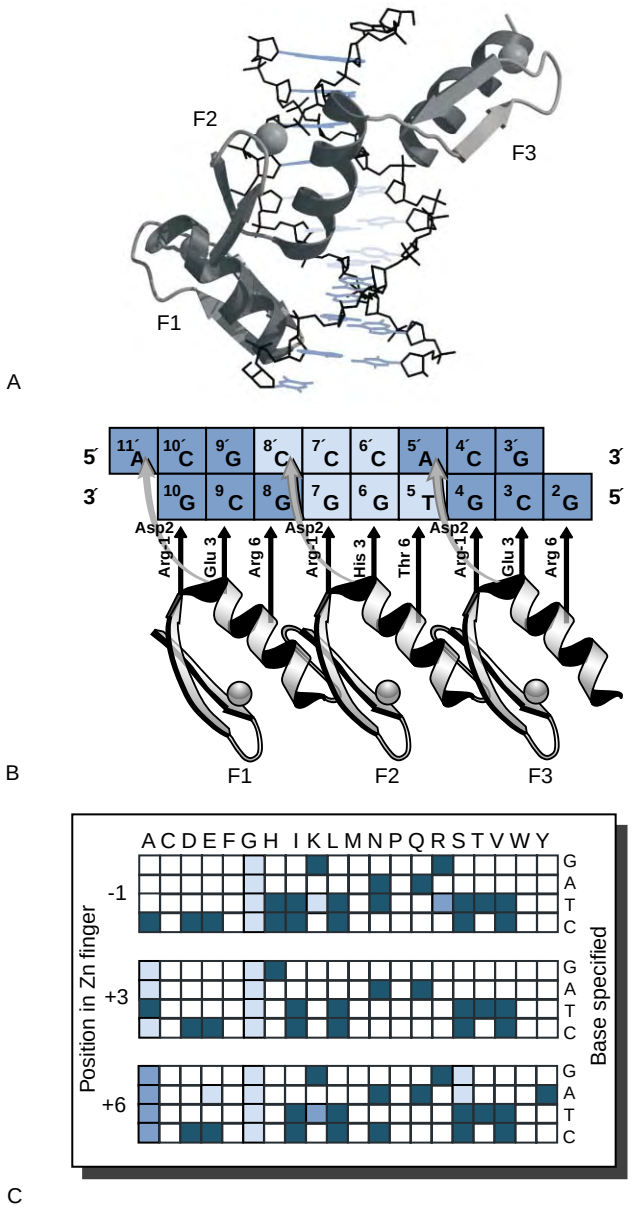

FIGURE 3 Interactions between zinc fingers and DNA. (A) Side view of Zif268 binding DNA (Pavletich and Pabo (1991). Zinc finger-DNA recognition: crystal structure of a Zif268-DNA complex at 2.1Å. *Science* **252**, 809–817. The three zinc fingers (F1–F3) bind the major groove of the DNA. (B) Schematic diagram of a simple model of recognition between the three zinc fingers of Zif268 and the triplet subsites of an optimized DNA-binding site. Arrows indicate contacts by recognition residues with bases in each DNA strand. Note that most contacts are to the G-rich strand. Since the N-terminal finger contacts the 3′ end of the DNA and the C-terminal finger the 5′ end, binding is said to be antiparallel. (C) Zinc finger DNA-recognition code. The grid summarizes common associations between amino acid residues (A–Y) and the bases they face in a classical zinc finger DNA-binding site. Darker shading of boxes indicates stronger associations. Note that contacts from overlapping C-terminal zinc fingers (especially from position 2) can significantly alter the coding specificity shown here for position +6.

relative to a defined first position, Position +1 (see Figures 2 and 3(B)). Since positions −1, +3, and +6 are all to be found on the external face of the helix, these can form a binding surface that is especially useful in DNA recognition because the spacing of the residues matches the register of the base pairs. It should be noted, however, that contacts from other positions, especially position +2, are also important in DNA recognition and that not all zinc finger–DNA interactions are as regular as the canonical structure of Zif268.

DNA Recognition "Code"

The most striking feature of the canonical Zif268 structure is the presence of regularly spaced one-to-one contacts between amino acids and DNA bases, from the same fixed helical positions in each finger (Figure 3B). By studying mutations at these positions, it has emerged that classical zinc fingers are a special case in terms of protein–DNA interactions. Unlike for most DNA-binding proteins, these positions do seem to fit a residue-base code-like pattern. Positions −1, +2, +3, and +6 in the α-helix are particularly important (Figure 3B), and some major residue-base associations are outlined in Figure 3C.

As a note of caution, it is important to mention that the code is not absolute, and is certainly an over-simplification of the interplay between different residues in the protein and between factors in the DNA structure, such as base stacking and unwinding. Nonetheless, thinking about zinc finger DNA interactions in this way can give a valuable approximation into the possible binding modes of a given zinc finger protein.

RNA Recognition

Unlike the double helical scaffold of DNA, RNA has much more complex folds, with every RNA presenting a unique binding surface. Nonetheless, zinc fingers have the versatility to accommodate such structures, with contacts from all over the finger framework. Like DNA recognition, electrostatic interactions and hydrogen bonding play a major role, with amino acids contacting either RNA bases or the phosphodiester backbone. Note that in RNA recognition there is a greater potential for hydrophobic interactions, with aromatic residues such as Tyr, Phe, and Trp stacking around extruding bases.

Non-Nucleic Acid Interactions

Protein–Protein Interactions

Zinc fingers are not limited to controlling gene expression, but also play an important cellular role in mediating specific protein–protein interactions.

Whereas nucleic acid recognition usually requires clusters of fingers, cytoplasmic proteins often contain only one or two fingers. This is possibly because a single protein-binding finger has sufficient affinity to bind effectively, given the more variable binding surface presented by other proteins.

Lipid Binding

Recently, the known binding repertoire of zinc fingers has been extended to include lipid recognition. This is exemplified by the FYVE zinc finger family, that is found in a wide range of eukaryotic cells. These nonclassical fingers have a complex structure consisting of multiple loops, two twin-stranded β-sheets and an α-helix stabilized by a pair of zinc ions. Functionally, the domains bind to phosphatidylinositol 3-phosphate (PI3P) in cellular membranes, commonly found on endosomes, and mediate further recruitment of a range of proteins.

Zinc Fingers in Biotechnology

Classical zinc fingers are the ideal scaffold for protein engineering. They are small and versatile, withstanding extensive mutations without destroying their basic structure. Moreover, individual finger modules may be linked in tandem repeats to allow recognition of extended target surfaces such as DNA grooves. Novel DNA-binding zinc fingers have been routinely engineered for nearly a decade and are beginning to demonstrate their utility in biotechnical applications. By fusing with suitable effector domains, effective transcription activators and repressors can be synthesized that recognize specific DNA sequences, typically 9–18 bp long. These constructs can up-regulate or down-regulate specific genes in a cell and have been used in a wide variety of contexts, including as antiviral agents and angiogenesis-promoting factors.

See Also the Following Articles

Aminopeptidases • Calpain • DNA Polymerase ε, Eukaryotic • DNA Sequence Recognition by Proteins • Inorganic Biochemistry • Nucleotide Excision Repair, Bacterial: The UvrABCD System • Opioid Receptors • Phosphatidylinositol Bisphosphate and Trisphosphate • Phosphatidylinositol-3-Phosphate • Retinoic Acid Receptors

Glossary

classical finger A zinc finger of the TFIIIA type, where a zinc ion is coordinated by two cysteines and two histidines ("Cys_2–His_2" or "C2H2").

protein motif A small structural element of a protein with a characteristic fold or shape.

TFIIIA A transcription factor protein from *Xenopus laevis*, in which zinc fingers were originally discovered.

transcription factor A protein involved in gene regulation that helps to activate or repress the expression of a particular gene.

zinc finger A small structural protein motif consisting of peptide chain folded around a central chelated (coordinated) zinc ion.

Further Reading

Beerli, R. R., and Barbas, C. F., III (2002). Engineering polydactyl zinc-finger transcription factors. *Nat. Biotechnol.* **20**, 135–141.

Berg, J. M., and Shi, Y. (1996). The galvanization of biology: A growing appreciation for the roles of zinc. *Science* **271**, 1081–1085.

Choo, Y., and Isalan, M. (2000). Advances in zinc finger engineering. *Curr. Opin. Struct. Biol.* **10**, 411–416.

Klug, A., and Schwabe, J. W. (1995). Protein motifs 5. Zinc fingers. *FASEB J.* **9**, 597–604.

Lander, E. S., *et al.* (2001). Initial sequencing and analysis of the human genome. *Nature* **409**, 860–921.

Mackay, J. P., and Crossley, M. (1998). Zinc fingers are sticking together. *Trends Biochem. Sci.* **23**, 1–4.

Pabo, C. O., Peisach, E., and Grant, R. A. (2001). Design and selection of novel Cys_2His_2 zinc finger proteins. *Annu. Rev. Biochem.* **70**, 313–340.

Biography

Mark Isalan is a fellow of the Wellcome Trust, UK, and is currently at the European Molecular Biology Laboratory (EMBL), Heidelberg. His principal research interests include combinatorial and design approaches to protein engineering, gene regulation, and gene networks. He holds a Ph.D. from the University of Cambridge, where he trained at the MRC Laboratory of Molecular Biology, developing methods to engineer novel DNA-binding zinc fingers.

Editors-in-Chief

William J. Lennarz

State University of New York at Stony Brook, Stony Brook, New York, USA

Section: Lipids, Carbohydrates, Membranes and Membrane Proteins

WILLIAM J. LENNARZ received his B.S. in Chemistry from Pennsylvania State University and a Ph.D. in Organic Chemistry from the University of Illinois. Subsequently he carried out postdoctoral work at Harvard with Konrad Bloch on fatty acid biosynthesis. In 1962 he was appointed Assistant Professor at Johns Hopkins in the Department of Physiological Chemistry. After promotion to Associate Professor in 1967, and full Professor in 1971, he remained at Hopkins until 1983. At that time, he was appointed Robert A. Welch Professor and Chair of the Department of Biochemistry and Molecular Biology at the University of Texas Cancer Center, M.D. Anderson Hospital. In 1989 he became a Leading Professor and Chair of the Department of Biochemistry and Cell Biology at SUNY at Stony Brook. In 1990 he founded and became Director of the Institute for Cell and Developmental Biology at Stony Brook.

Dr. Lennarz has served on many national and international committees. He has served as President of the Biochemistry Chairman's Organization, President of the American Society for Biochemistry and Molecular Biology and President of the Society for Glycobiology. He was a member of the Executive Committee of the International Union of Biochemistry and Molecular Biology for almost a decade.

He has presented special lectures at the University of Notre Dame, the NIH, the University of West Virginia, Johns Hopkins University, Florida State University, the University of California at San Diego, the University of Arkansas, Indiana University and the Medical College of Virginia.

He is a member of the National Academy of Sciences. The focus of his early work was on lipids and bacterial cell surfaces. More recent efforts have been in the structure, biosynthesis and function of cell surface glycoproteins. The biosynthesis studies initially were carried out in liver and oviduct, but these efforts now are focused in yeast. The functional studies have concentrated on the role of cell surface glycoproteins in fertilization and early development in the sea urchin and, more recently, the frog. For over 30 years Dr. Lennarz' research has been supported by federal sources, primarily the National Institutes of Health. Recently he was appointed Distinguished Professor and Chair of his department.

M. Daniel Lane

The Johns Hopkins University, School of Medicine, Baltimore, Maryland, USA

Section: Metabolism, Vitamins and Hormones

M. DANIEL LANE received B.S. and M.S. degrees in 1951 and 1953 from Iowa State University and a Ph.D. in 1956 from the University of Illinois. He was a Senior Postdoctoral Fellow with Professor Feodor Lynen at the Max-Planck Institute Fur Zellchemie in Munich. Following faculty positions at Virginia Polytechnic Institute and New York University School of Medicine, he joined the faculty at the Johns Hopkins University School of Medicine in 1969 and served as DeLamar Professor and Director of the Department of Biological Chemistry from 1978 to 1997. He is presently Distinguished Service Professor at Johns Hopkins. In 2002 he received an honorary degree, Doctor of Humane Letters, from Iowa State University.

Dr. Lane was elected to membership in the National Academy of Sciences (in 1987) and was elected as a Fellow of the American Academy of Arts and Sciences (in 1982) and of the American Society of Nutritional Sciences (in 1996). He received the Mead Johnson Award from the American Society for Nutritional Sciences in 1966 for his research on biotin-dependent enzymes and in 1981, the William C. Rose Award from the American Society for Biochemistry and Molecular Biology for his work on the insulin receptor. In 1990–1991 Lane served as President of the American Society of Biochemistry and Molecular Biology. He has presented many named lectureships (including the

Feodor Lynen Lecture in Germany in 1999) and served on numerous editorial boards including the Journal of Biological Chemistry and the Annual Reviews of Biochemistry. Currently he is Associate Editor for Biochemical and Biophysical Research Communications.

Dr. Lane has published 280 research papers in major scientific journals. His early work focused on various enzymatic CO_2 fixation reactions, notably the mechanisms by which the B-vitamin, biotin, functions in enzymes to catalyze carboxylation. Dr. Lane's work on the regulation of acetyl-CoA carboxylase, the key regulatory enzyme of fatty acid synthesis, led him to his present interests which are to understand the basic mechanisms of lipogenesis, adipogenesis and the consequence of aberrations in these processes, most notably obesity. Research currently underway in his laboratory focuses on: (1) the genes that signal stem cell "commitment" to the adipocyte lineage and subsequent differentiation into adipocytes, and (2) the mechanisms by which the region of the brain, known as the hypothalamus, monitors and controls the drive to eat.

Associate Editors

Ernesto Carafoli

Università degli Studi di Padova, Padova, Italy
Section: Bioenergetics

ERNESTO CARAFOLI earned his M.D. degree at the University of Modena in Italy in 1957. After postdoctoral studies in the Laboratory of Albert L. Lehninger at Johns Hopkins University in the mid 1960s he returned to his home institution in Italy where he worked until 1973, when he was appointed Professor of Biochemistry at the Swiss Federal Institute of Technology (ETH) in Zurich. He returned to Italy in 1998 as a Professor of Biochemistry at the University of Padova, where he now also directs the newly founded Venetian Institute of Molecular Medicine (VIMM).

Dr. Carafoli became interested in calcium as a signaling agent during his post-doctoral days at Johns Hopkins. When he arrived there his main interests were in mitochondrial bioenergetics and it was thus natural for him to expand them to the newly discovered area of mitochondrial calcium transport. He was involved in most of the early discoveries in the field, and he continued to work on mitochondria and calcium after his return to Italy and until he moved to the ETH. There his interests still remained focused on calcium, but the emphasis shifted to the proteins that transport it across membranes and to those that process its signal. His favorite object of study became the calcium pumps, especially that of the plasma membrane, an enzyme which is essential to the regulation of calcium homeostasis and thus to the well being of cells. His contributions on the enzyme, especially after he purified it in 1979, have helped establishing most of its properties and have clarified important problems of mechanism, regulation and structure.

Dr. Carafoli has authored or co-authored about 450 peer-reviewed articles and reviews, and has edited or co-edited about 20 books. He has served on the Editorial or Advisory Boards of several periodicals and has organized about 30 International Workshops and Symposia. He has been featured as a plenary or honorary lecturer at numerous events ranging from specialized Workshops to International Symposia and Congresses. Dr. Carafoli's honors and awards include several international prizes and medals, memberships in several Academies, and three honorary degrees.

Don W. Cleveland

University of California, San Diego, La Jolla, CA, USA
Section: Cell Architecture and Function

DON W. CLEVELAND has been a longstanding contributor to the elucidation of regulation of assembly of mitotic spindles and chromosome movement and how errors in these contribute to the chromosome loss characteristic of human tumors. He discovered the tubulin gene families encoding the major subunits of microtubules and the first mammalian example of control of gene expression through regulated RNA instability. He identified components required for microtubule nucleation and anchoring during spindle assembly. He identified the first human centromeric protein (CENP-B). He then discovered CENP-E, the centromere-associated, microtubule-motor that he showed to be essential for chromosome attachment and for activation and silencing of the mitotic checkpoint, the cell cycle control mechanism that prevents errors of chromosome segregation in mitosis.

Dr. Cleveland has also been a leading force in dissecting the disease mechanism for major human neurodegenerative disorders. He initially purified and characterized tau, the microtubule-associated protein that assembles aberrantly in human dementias including Alzheimer's disease and Pick's disease. He established that the extreme asymmetry of neurons acquired during development is achieved with a deformable array of interlinked neurofilaments, microtubules and actin. He showed that disorganization of neurofilament arrays caused selective death of motor neurons in mice and humans. He also demonstrated that neuronal death could also arise by a toxicity of mutant superoxide dismutase unrelated to its normal activity, thereby uncovering the mechanism underlying the major genetic form of amyotrophic lateral sclerosis. He showed that this toxicity could be

sharply ameliorated by lowering the content of neurofilaments.

Dr. Cleveland is currently Head, Laboratory for Cell Biology in the Ludwig Institute for Cancer Research and Professor of Medicine, Neurosciences and Cellular and Molecular Medicine at the University of California at San Diego. He is also the Editor of the Journal of Cell Biology and Current Opinion in Cell Biology.

Jack E. Dixon

University of California, San Diego School of Medicine,
La Jolla, CA, USA
Section: Protein/Enzyme Structure, Function, and Degradation

JACK E. DIXON earned his Ph.D. in Chemistry at the University of California, Santa Barbara in 1971 and did his postdoctoral training in Biochemistry at the University of California, San Diego.

Dr. Dixon is a pioneer and leader in the structure and function of the protein tyrosine phosphatases (PTPases). He demonstrated that the unique catalytic mechanism of the PTPases proceeds via a novel cysteine-phosphate intermediate. He discovered the first dual-specificity phosphatase, which led to the identification of the cell cycle protein, $p80^{cdc25}$, as a phosphatase. He also showed that the bacteria responsible for the plague or "black death" harbor the most active PTPase ever described. He and his colleagues went on to demonstrate that this PTPase gene product is essential for the pathogenesis of the bacteria. Dr. Dixon and his colleagues determined X-ray structures for both tyrosine and dual specificity phosphatases. Dr. Dixon also found that sequences outside of the PTPase catalytic domain could function to direct the subcellular localization of the PTPases and to restrict their substrate specificity. This is now a widely acknowledged regulatory paradigm for the PTPases. Recently, his laboratory demonstrated that the tumor suppressor gene, PTEN, which shares sequence identity with the PTPases, catalyzes the dephosphorylation of a lipid second messenger, phosphatidylinositol 3,4,5-trisphosphate (PIP3). This represents the first example of a PTPase dephosphorylating a lipid second messenger. PIP3 activates the protein kinase, AKT, which plays a critical role in controlling the balance between apoptosis and cell survival. The loss of the PTEN gene elevates PIP3 levels leading to constitutive activation by AKT and oncogenesis. Recently, Dr. Dixon in collaboration with Nikola Pavletich determined the X-ray structure of PTEN. Their structure–function studies explain the PIP3 substrate specificity of PTEN and also provide a rationale for many of the mutations seen in human cancers. Earlier in his career, Dr. Dixon adopted the tools of molecular biology as they became available in the 1970s, and his laboratory was among the first to use synthetic oligonucleotides to isolate and extensively characterize cDNAs encoding peptide hormones.

Dr. Dixon is Professor of Pharmacology, Cellular and Molecular Medicine and Chemistry and Biochemistry and Dean of Scientific Affairs at the University of California, San Diego. He is a member of the National Academy of Sciences, the Institute of Medicine and the American Academy of Arts and Sciences. Dr. Dixon was the recipient of the 2003 William C. Rose Award from the American Society for Biochemistry and Molecular Biology.

John H. Exton

Howard Hughes Medical Institute, Vanderbilt University School of Medicine, Nashvillie, TN, USA
Section: Signaling

JOHN H. EXTON was born and educated in New Zealand where he received his medical training and a Ph.D. in Biochemistry from the University of Otago in 1963. He did postdoctoral work at Vanderbilt University under Charles R. Park and Earl W. Sutherland, and became an Investigator of the Howard Hughes Medical Institute in 1968 and Professor of Physiology in 1970. He is presently Professor of Molecular Physiology and Biophysics, Professor of Pharmacology and a Hughes Investigator at Vanderbilt.

Dr. Exton's research initially focused on the changes in carbohydrate metabolism in liver during diabetes and treatment with various hormones using the perfused rat liver as the experimental system. His work concentrated on gluconeogenesis and identified the enzymatic reactions that were under control by insulin, epinephrine (adrenaline), glucagon and glucocorticoids, and demonstrated the importance of cyclic AMP in the regulation of these reactions. The role played by the supply of substrates, especially of alanine, was also shown.

Dr. Exton then turned his attention to the action of epinephrine (adrenaline) and demonstrated that many of its actions were not mediated by cyclic AMP but by calcium ions. This led to study of the breakdown of inositol phospholipids by phospholipase C that underlay the increase in calcium. Later this resulted in the discovery of G_q, a novel G protein that activated phospholipase C. Further studies demonstrated that agonists caused the breakdown of another phospholipid (phosphatidylcholine) by another phospholipase (phospholipase D). Current work is focused on the physiological role of phospholipase D.

Dr. Exton has authored over 350 scientific articles and is presently an Associate Editor of the Journal of Biological Chemistry. He has served on many scientific review groups and as a reviewer for many journals. He has won numerous awards, most notably the Lilly

Award of the American Diabetes Association, Fellow of the American Association for the Advancement of Science and election to membership in the National Academy of Sciences.

Paul Modrich

Duke University Medical Center, Durham, NC, USA
Section: Molecular Biology

PAUL MODRICH is an Investigator of the Howard Hughes Medical Institute and James B. Duke Professor of Biochemistry at Duke University Medical Center. He received his undergraduate degree from M.I.T. and his Ph.D. in Biochemistry from Stanford University. His current research addresses the mechanisms of DNA repair. He has served on the editorial boards of the Journal of Biological Chemistry, Biochemistry, Proceedings of the National Academy of Sciences, and DNA Repair. His honors include election to National Academy of Sciences and the Institute of Medicine, the Pfizer Award in Enzyme Chemistry, the General Motors Mott Prize in Cancer Research, and the Pasarow Foundation Award in Cancer Research.

Preface

Biological Chemistry is defined as the chemistry of the compounds and processes that constitute living organisms. The ultimate goal, of course, is to understand and define biology at a mechanistic level. This was aptly stated in an historical treatise on the founding of the *Journal of Biological Chemistry*, where John Edsall quoted a statement in a letter from J. L. Loeb (in Berkeley), "The future of biology lies with those who attack its problems from a chemical point of view." What was an emerging field in 1900 with its origins in physiology, nutrition and chemistry has broadened and expanded to include numerous other fields including mechanistic enzymology, molecular biology, structural biology, cell biology, genomics, proteomics, bioinformatics, metabolomics and others, that were not defined as discrete fields at that time.

Modern biochemistry (biological chemistry) began with the accidental discovery by Eduard Buchner in 1897 that a cell-free yeast extract could carry out fermentation of glucose to alcohol and CO_2 *in the absence of intact cells*. He named the dissolved substance responsible for this process zymase, the substance(s) we now refer to as enzymes. Importantly, Buchner recognized the significance of his discovery. This ended the dogma of the time, perpetuated by Pasteur, the concept of *vitalism*; i.e., that fermentation (and presumably other complex biological phenomena) required the action of intact cells. Thus, serendipity and a prepared mind ushered in a new era of discovery. Now it became possible to dissect complex physiological processes and to study them with preparations free of the constraints of intact cells. Once a metabolic pathway/process was established, it became possible to purify the enzymes, cofactors and substrates involved, to reconstitute the process with purified components and to characterize the components chemically. What followed was an information explosion in the field of biochemistry and progression through a series of trends, each "in vogue" in its time. The identification of the dietary essentials, the hunt for the vitamins/cofactors, the hormones, identification of metabolic pathways and the enzymes involved, oxidative phosphorylation, protein synthesis, molecular biology—each developed as a primary focus.

The need to associate chemistry with function came early and was evident in the naming of departments and journals. Over time names changed from Agricultural Chemistry to Physiological Chemistry to Biochemistry to Biological Chemistry. An example is the Department of Biochemistry at the University of Wisconsin, which began in 1883 as the Department of Agricultural Chemistry.

Where are we headed? We have reached the point where the borders of these areas have become blurred. What constitutes cell biology, molecular biology/genetics, developmental biology, physiology, immunology—ultimately reduces to chemistry. To understand these processes we must know what the molecules are and understand how they interact, i.e. the basic chemistry. That is what this encyclopedia is about.

The breadth of content of this encyclopedia aims to cover major topics of modern biochemistry, each authored by an expert in the area. We feel that the coverage is broad and we have been inclusive in choice of topics. The encyclopedia is a reference work encompassing four volumes containing over 500 articles with more than 750 authors or coauthors. Each article/topic covers an important area of the field which reflects the point of view of the authors. Together the articles cover virtually every aspect of biology for which we have "mechanistic" information. For those who wish to probe more deeply into a topic, references to further readings are included at the end of each article. The editorial board that made decisions on coverage consists of seven members, each an expert representing a major area in the field of biochemistry. A dedicated effort was made to provide coverage that is as complete as possible. The content is presented at a level that we hope will be interpretable to interested individuals with some background in chemistry and biology. It is intended for such individuals rather than specialists with extensive scientific backgrounds in specific areas. It is aimed at the generalist as opposed to the specialist.

Finally, we would like to single out Gail Rice and Dr. Noelle Gracy for their enormous contribution in putting this encyclopedia together. They, in fact, were a driving force that brought this major work to completion.

Notes on the Subject Index

Abbreviations used in subentries without explanation:

CoA	coenzyme A
DAG	diacylglycerol
ELISA	enzyme-linked immunosorbent assay
ERK	extracellular-signal regulated kinase
GlcNAC	N-Acetylglucosamine
HPLC	high-pressure liquid chromatography
IP_3	inositol 1,4,5-triphosphate
MAP	mitogen-activated protein
MMP	matrix metalloproteinase
mtDNA	mitochondrial DNA
NADPH	nicotinamide-adenine dinucleotide phosphate
PFK-2/ FBPase-2	6-phosphofructo-2-kinase/fructose-2,6-bisphosphatase
PI3K	phosphatidylinositol 3-kinase
PIP_2	phosphatidylinositol 4,5-bisphosphate
PIP_3	phosphatidylinositol-3,4,5-triphosphate
PPAR	peroxisome proliferator-activated receptor
RPLC	reversed-phase high-performance liquid chromatography

Volume 1

ABC Transporters, Pages 1-5, Andre Goffeau, Benoit De Hertogh and Philippe V. Baret

Abscisic Acid (ABA), Pages 6-11, Ramanjulu Sunkar and Jian-Kang Zhu

Actin Assembly/Disassembly, Pages 12-18, Henry N. Higgs

Actin-Capping and -Severing Proteins, Pages 19-26, Sankar Maiti and James R. Bamburg

Actin-Related Proteins, Pages 27-33, R. Dyche Mullins

Adenosine Receptors, Pages 34-39, Lauren J. Murphree and Joel Linden

Adenylyl Cyclases, Pages 40-45, Ronald Taussig

Adrenergic Receptors, Pages 46-50, David B. Bylund

Affinity Chromatography, Pages 51-56, Pedro Cuatrecasas and Meir Wilchek

Affinity Tags for Protein Purification, Pages 57-63, Joseph J. Falke and John A. Corbin

A-Kinase Anchoring Proteins, Pages 64-67, Lorene K. Langeberg and John D. Scott

Allosteric Regulation, Pages 68-73, Barry S. Cooperman

Alternative Splicing: Regulation of Fibroblast Growth Factor Receptor (FGFR), Pages 74-77, Mariano A. Garcia-Blanco

Alternative Splicing: Regulation of Sex Determination in Drosophila melanogaster, Pages 78-84, Jill K. M. Penn, Patricia Graham and Paul Schedl

Amine Oxidases, Pages 85-89, Giovanni Floris and Alessandro Finazzi Agro

Amino Acid Metabolism, Pages 90-95, Luc Cynober

Aminopeptidases, Pages 96-98, Ralph A. Bradshaw

Amyloid, Pages 99-104, Ronald Wetzel

Anaplerosis, Pages 105-110, Raymond R. Russell, III and Heinrich Taegtmeyer

Angiotensin Receptors, Pages 111-115, Tadashi Inagami

ara Operon, Pages 116-119, Robert F. Schleif

ARF Family, Pages 120-122, Gustavo Pacheco-Rodriguez, Joel Moss and Martha Vaughan

Aspartic Proteases, Pages 123-127, Ben M. Dunn

ATP Synthesis in Plant Mitochondria: Substrates, Inhibitors, Uncouplers, Pages 128-132, Kathleen L. Soole and R. Ian Menz

ATP Synthesis: Mitochondrial Cyanide-Resistant Terminal Oxidases, Pages 133-137, James N. Siedow

Autophagy in Fungi and Mammals, Pages 138-143, Daniel J. Klionsky and Ju Guan

B12-Containing Enzymes, Pages 145-151, Vahe Bandarian and Rowena G. Matthews

Bax and Bcl2 Cell Death Enhancers and Inhibitors, Pages 152-154, David L. Vaux

B-Cell Antigen Receptor, Pages 155-158, Thomas M. Yankee and Edward A. Clark

Bile Salts and their Metabolism, Pages 159-163, Ulrich Beuers and Thomas Pusl

Biliary Cirrhosis, Primary, Pages 164-169, Marshall M. Kaplan

Bioenergetics: General Definition of Principles, Pages 170-173, David G. Nicholls

Biotin, Pages 174-178, Steven W. Polyak and Anne Chapman-Smith

Biotinylation of Proteins, Pages 179-181, Ronald A. Kohanski

Bradykinin Receptors, Pages 182-185, Ronald M. Burch

Branched-Chain -Ketoacids, Pages 186-191, David T. Chuang

Brassinosteroids, Pages 192-197, Steven D. Clouse

Cadherin Signaling, Pages 199-204, David B. Sacks and Jonathan M. G. Higgins

Cadherin-Mediated Cell-Cell Adhesion, Pages 205-211, Frauke Drees and W. James Nelson

Calcitonin Gene-Related Peptide and Adrenomedullin Receptors, Pages 212-216, Debbie L. Hay, Alex C. Conner and David R. Poyner

Calcitonin Receptor, Pages 217-220, Samia I. Girgis, Niloufar Moradi-Bidhendi, Lucia Mancini and Iain MacIntyre

Calcium Buffering Proteins: Calbindin, Pages 221-225, Willi Hunziker and Igor Bendik

Calcium Buffering Proteins: ER Luminal Proteins, Pages 226-230, Jody Groenendyk and Marek Michalak

Calcium Oscillations, Pages 231-234, Marisa Brini

Calcium Sensing Receptor, Pages 235-240, Jacob Tfelt-Hansen and Edward M. Brown

Calcium Signaling: Calmodulin-Dependent Phosphatase, Pages 241-245, Claude Klee, Hao Ren and Shipeng Li

Calcium Signaling: Cell Cycle, Pages 246-249, Luigia Santella

Calcium Signaling: Motility (Actomyosin-Troponin System), Pages 250-255, Takeyuki Wakabayashi and Setsuro Ebashi

Calcium Signaling: NO Synthase, Pages 256-260, Zhi-Qiang Wang and Dennis J. Stuehr

Calcium Transport in Mitochondria, Pages 261-266, Rosario Rizzuto and Marisa Brini

Calcium Waves, Pages 267-269, Lionel F. Jaffe

Calcium, Biological Fitness of, Pages 270-273, Robert J. P. Williams

Calcium/Calmodulin-Dependent Protein Kinase II, Pages 274-280, Andy Hudmon and Howard Schulman

Calcium/Calmodulin-Dependent Protein Kinases, Pages 281-286, J. Robison and Roger J. Colbran

Calcium-Binding Proteins: Cytosolic (Annexins, Gelsolins, C2-Domain Proteins) , Pages 287-293, Joachim Krebs

Calcium-Modulated Proteins (EF-Hand), Pages 294-299, Robert H. Kretsinger

Calpain, Pages 300-306, Hiroyuki Sorimachi and Yasuko Ono

Carbohydrate Chains: Enzymatic and Chemical Synthesis, Pages 307-313, Thomas J. Tolbert and Chi-Huey Wong

Carnitine and -Oxidation, Pages 314-318, Janos Kerner and Charles L. Hoppel

Caspases and Cell Death, Pages 319-327, Don W. Nicholson, Pierluigi Nicotera and Gerry Melino

Cell Cycle Controls in G1 and G0, Pages 328-331, WengeShi and Steven F. Dowdy

Cell Cycle: Control of Entry and Progression Through S Phase, Pages 332-337, Susan L. Forsburg

Cell Cycle: DNA Damage Checkpoints, Pages 338-344, Jean Y. J. Wang

Cell Cycle: Mitotic Checkpoint, Pages 345-351, Tim J. Yen

Cell Death by Apoptosis and Necrosis, Pages 352-355, Pierluigi Nicotera

Cell Migration, Pages 356-361, J. Victor Small and Emmanuel Vignal

Cell-Matrix Interactions, Pages 362-366, Janet A. Askari and Martin J. Humphries

Centromeres, Pages 367-371, Beth A. Sullivan

Centrosomes and Microtubule Nucleation, Pages 372-376, Reiko Nakajima, Ming-Ying Tsai and Yixian Zheng

c-fes Proto-Oncogene, Pages 377-382, Thomas E. Smithgall and Robert I. Glazer

Chaperones for Metalloproteins, Pages 383-386, Valeria C. Culotta and Edward Luk

Chaperones, Molecular, Pages 387-392, Sue Wickner and Joel R. Hoskins

Chaperonins, Pages 393-398, Arthur L. Horwich, Wayne A. Fenton and George W. Farr

Chemiluminescence and Bioluminescence, Pages 399-404, Thomas O. Baldwin

Chemiosmotic Theory, Pages 405-412, Keith D. Garlid

Chemokine Receptors, Pages 413-418, Ann Richmond and Guo-Huang Fan

Chemolithotrophy, Pages 419-424, Alan B. Hooper

Chemotactic Peptide/Complement Receptors, Pages 425-429, Eric R. Prossnitz and Larry A. Sklar

Chlorophylls and Carotenoids, Pages 430-437, Hugo Scheer

Chloroplast Redox Poise and Signaling, Pages 438-445, John F. Allen

Chloroplasts, Pages 446-450, Nicoletta Rascio

Cholesterol Synthesis, Pages 451-455, Peter A. Edwards

Chromatin Remodeling, Pages 456-463, Eric Kallin and Yi Zhang

Chromatin: Physical Organization, Pages 464-468, Christopher L. Woodcock

Chromosome Organization and Structure, Overview, Pages 469-474, Elena Gracheva and Sarah C. R. Elgin

Coenzyme A, Pages 475-477, M. Daniel Lane

Collagenases, Pages 478-481, Kenn Holmbeck and Henning Birkedal-Hansen

Collagens, Pages 482-487, Darwin J. Prockop

Cyclic AMP Receptors of Dictyostelium, Pages 488-493, Dale Hereld and Peter N. Devreotes

Cyclic GMP Phosphodiesterases, Pages 494-500, Sharron H. Francis and Jackie D. Corbin

Cyclic Nucleotide Phosphodiesterases, Pages 501-505, Vincent C. Manganiello and Eva Degerman

Cyclic Nucleotide-Dependent Protein Kinases, Pages 506-511, Sharron H. Francis and Jackie D. Corbin

Cyclic Nucleotide-Regulated Cation Channels, Pages 512-515, Martin Biel and Franz Hofmann

Cysteine Proteases, Pages 516-520, David J. Buttle and John S. Mort

Cytochrome b6f Complex, Pages 521-527, Gunter A. Hauska and Thomas Schodl

Cytochrome bc1 Complex (Respiratory Chain Complex III), Pages 528-534, Bernard L. Trumpower

Cytochrome c, Pages 535-538, Hans Tuppy and Gunther Kreil

Cytochrome Oxidases, Bacterial, Pages 539-543, Peter Brzezinski and Pia Adelroth

Cytochrome P-450, Pages 544-549, Rita Bernhardt

Cytokines, Pages 550-555, Andrea L. Wurster and Michael J. Grusby

Cytokinesis, Pages 556-561, Masanori Mishima and Michael Glotzer

Cytokinin, Pages 562-567, Thomas Schmulling

Desmosomes and Hemidesmosomes, Pages 569-576, Rachel L. Dusek, Jonathan C. R. Jones and Kathleen J. Green

Detergent Properties, Pages 577-581, Darrell R. McCaslin

Diabetes, Pages 582-592, David W. Cooke

Diacylglycerol Kinases and Phosphatidic Acid Phosphatases, Pages 593-597, Stephen M. Prescott and Matthew K. Topham

Disulfide Bond Formation, Pages 598-602, Hiram F. Gilbert

DNA Base Excision Repair, Pages 603-608, Hilde Nilsen and Tomas Lindahl

DNA Damage: Alkylation, Pages 609-613, Anton B. Guliaev and B. Singer

DNA Glycosylases: Mechanisms, Pages 614-617, Daniel J. Krosky and James T. Stivers

DNA Helicases: Dimeric Enzyme Action, Pages 618-623, Timothy M. Lohman

DNA Helicases: HexamericEnzyme Action, Pages 624-631, Smita S. Patel

DNA Ligases: Mechanism and Functions, Pages 632-636, Alan E. Tomkinson and John B. Leppard

DNA Ligases: Structures, Pages 637-643, C. Kiong Ho, Mark Odell and Dimitar B. Nikolov

DNA Methyltransferases, Bacterial, Pages 644-651, Albert Jeltsch and Richard I. Gumport

DNA Methyltransferases, Structural Themes, Pages 652-659, Sanjay Kumar

DNA Methyltransferases: Eubacterial GATC, Pages 660-664, Martin G. Marinus

DNA Mismatch Repair and Homologous Recombination, Pages 665-670, Ivan Matic and Miroslav Radman

DNA Mismatch Repair and the DNA Damage Response, Pages 671-674, Guo-Min Li and Steven R. Presnell

DNA Mismatch Repair Defects and Cancer, Pages 675-681, Richard D. Kolodner

DNA Mismatch Repair in Bacteria, Pages 682-686, A-Lien Lu

DNA Mismatch Repair in Mammals, Pages 687-690, James T. Drummond

DNA Mismatch Repair: E. coli Vsr and Eukaryotic G-T Systems, Pages 691-693, Margaret Lieb

DNA Oxidation, Pages 694-697, Arthur P. Grollman and Dmitry O. Zharkov

DNA Photolyase, Pages 698-702, Carrie L. Partch and Aziz Sancar

DNA Polymerase, Eukaryotic α, Pages 703-707, Teresa S. -F. Wang

DNA Polymerase, Eukaryotic β, Pages 708-712, William A. Beard and Samuel H. Wilson

DNA Polymerase, Eukaryotic δ, Pages 713-715, Antero G. So and Kathleen M. Downey

DNA Polymerase, Eukaryotic ε, Pages 716-719, Yasuo Kawasaki and Akio Sugino

DNA Polymerase I, Bacterial, Pages 720-725, Catherine M. Joyce

DNA Polymerase II, Bacterial, Pages 726-728, Judith L. Campbell

DNA Polymerase III, Bacterial, Pages 729-733, Hisaji Maki

DNA Polymerases: Kinetics and Mechanism, Pages 734-739, Kenneth A. Johnson

DNA Replication Fork, Bacterial, Pages 740-744, Nancy G. Nossal

DNA Replication Fork, Eukaryotic, Pages 745-748, Lori M. Kelman, Jerard Hurwitz and Zvi Kelman

DNA Replication, Mitochondrial, Pages 749-752, David A. Clayton

DNA Replication: Eukaryotic Origins and the Origin Recognition Complex, Pages 753-760, Melvin L. DePamphilis and Cong-jun Li

DNA Replication: Initiation in Bacteria, Pages 761-766, Jon M. Kaguni

DNA Restriction and Modification: Type I Enzymes, Pages 767-771, David T. F. Dryden

DNA Restriction and Modification: Type II Enzymes, Pages 772-777, Darren M. Gowers and Stephen E. Halford

DNA Restriction and Modification: Type III Enzymes, Pages 778-781, Desirazu N. Rao and S. Srivani

DNA Secondary Structure, Pages 782-787, Albino Bacolla and Robert D. Wells

DNA Sequence Recognition by Proteins, Pages 788-793, Arabela A. Grigorescu and John M. Rosenberg

DNA Supercoiling, Pages 794-797, Tao-shih Hsieh

DNA Topoisomerases: Type I, Pages 798-805, James J. Champoux

DNA Topoisomerases: Type II, Pages 806-811, Renier Velez-Cruz and Neil Osheroff

DNA Topoisomerases: Type III-RecQ Helicase Systems, Pages 812-816, Rodney Rothstein and Erika Shor

Dopamine Receptors, Pages 817-822, Kim A. Neve

Dynactin, Pages 823-826, Trina A. Schroer

Dynein, Pages 827-831, K. Kevin Pfister

Volume 2

EF-G and EF-Tu Structures and Translation Elongation in Bacteria, Pages 1-5, Poul Nissen and Jens Nyborg

Eicosanoid Receptors, Pages 6-9, Richard M. Breyer and Matthew D. Breyer

Elastin, Pages 10-12, Judith Ann Foster

Endocannabinoids, Pages 13-15, Daniele Piomelli

Endocytosis, Pages 16-19, Julie G. Donaldson

Endoplasmic Reticulum-Associated Protein Degradation, Pages 20-23, Maurizio Molinari

Energy Transduction in Anaerobic Prokaryotes, Pages 24-30, Gottfried Unden

Enzyme Inhibitors, Pages 31-37, Vern L. Schramm

Enzyme Kinetics, Pages 38-44, Irwin H. Segel

Enzyme Reaction Mechanisms: Stereochemistry, Pages 45-50, Ming-Daw Tsai, Li Zhao and Brandon J. Lamarche

Epidermal Growth Factor Receptor Family, Pages 51-55, Denis Tvorogov and Graham Carpenter

ER/SR Calcium Pump: Function, Pages 56-60, Giuseppe Inesi

ER/SR Calcium Pump: Structure, Pages 61-65, Chikashi Toyoshima and Yuji Sugita

Exonucleases, Bacterial, Pages 66-72, Susan T. Lovett

F1-F0 ATP Synthase, Pages 73-79, Donata Branca

FAK Family, Pages 80-84, Steven K. Hanks

Fat Mobilization: Perilipin and Hormone-Sensitive Lipase, Pages 85-89, Constantine Londos and Alan R. Kimmel

Fatty Acid Oxidation, Pages 90-94, Horst Schulz

Fatty Acid Receptors, Pages 95-98, Christer Owman and Bjorn Olde

Fatty Acid Synthesis and its Regulation, Pages 99-103, Steven D. Clarke and Manabu T. Nakamura

Ferredoxin, Pages 104-106, Giuliana Zanetti and Vittorio Pandini

Ferredoxin-NADP+ Reductase, Pages 107-111, Giuliana Zanetti and Alessandro Aliverti

Fibroblast Growth Factor Receptors and Cancer-Associated Perturbations, Pages 112-117, Marko Kornmann and Murray Korc

Flavins, Pages 118-122, Barrie Entsch and David P. Ballou

Flippases, Pages 123-127, Charles J. Waechter

Focal Adhesions, Pages 128-133, Eli Zamir and Benjamin Geiger

Free Radicals, Sources and Targets of: Mitochondria, Pages 134-142, Alberto Boveris and Enrique Cadenas

Friedreich's Ataxia, Pages 143-145, Paul E. Hart and Anthony H. V. Schapira

G Protein Signaling Regulators, Pages 147-151, John H. Exton

G Protein-Coupled Receptor Kinases and Arrestins, Pages 152-157, Jeffrey L. Benovic

G12/G13 Family, Pages 158-161, Stefan Offermanns

GABAA Receptor, Pages 162-166, Richard W. Olsen and Gregory W. Sawyer

GABAB Receptor, Pages 167-170, S. J. Enna

Galectins, Pages 171-174, R. Colin Hughes

Genome-Wide Analysis of Gene Expression, Pages 175-180, Karine G. Le Roch and Elizabeth A. Winzeler

Gi Family of Heterotrimeric G Proteins, Pages 181-185, Maurine E. Linder

Giant Mitochondria (Megamitochondria), Pages 186-188, Bernard Tandler and Charles L. Hoppel

GlcNAc Biosynthesis and Function, O-Linked, Pages 189-192, Kaoru Sakabe and Gerald W. Hart

Glucagon Family of Peptides and their Receptors, Pages 193-196, Laurie L. Baggio and Daniel J. Drucker

Gluconeogenesis, Pages 197-203, Richard W. Hanson and Oliver E. Owen

Glucose/Sugar Transport in Bacteria, Pages 204-207, Lan Guan and H. Ronald Kaback

Glucose/Sugar Transport in Mammals, Pages 208-212, Silvia Mora and Jeffrey Pessin

Glutamate Receptors, Ionotropic, Pages 213-219, Derek B. Scott and Michael D. Ehlers

Glutamate Receptors, Metabotropic, Pages 220-223, P. Jeffrey Conn

Glutathione Peroxidases, Pages 224-228, Fulvio Ursini and Matilde Maiorino

Glycation, Pages 229-236, Suzanne R. Thorpe and John W. Baynes

Glycine Receptors, Pages 237-243, Bodo Laube and Heinrich Betz

Glycogen Metabolism, Pages 244-248, Peter J. Roach

Glycogen Storage Diseases, Pages 249-254, George H. Sack, Jr.

Glycogen Synthase Kinase-3, Pages 255-260, James R. Woodgett

Glycolipid-Dependent Adhesion Processes, Pages 261-265, Senitiroh Hakomori

Glycolysis, Overview, Pages 266-271, Robert A. Harris

Glycoprotein Folding and Processing Reactions, Pages 272-276, Armando J. Parodi

Glycoprotein-Mediated Cell Interactions, O-Linked, Pages 277-282, Robert S. Haltiwanger

Glycoproteins, N-Linked, Pages 283-292, Mark A. Lehrman

Glycoproteins, Plant, Pages 293-296, Carolyn J. Schultz

Glycosylation in Cystic Fibrosis, Pages 297-301, Andrew D. Rhim, Thomas F. Scanlin and Mary Catherine Glick

Glycosylation, Congenital Disorders of, Pages 302-307, Hudson H. Freeze

Glycosylphosphatidylinositol (GPI) Anchors, Pages 308-311, Anant K. Menon

Golgi Complex, Pages 312-315, Mark Stamnes

Gq Family, Pages 316-320, Wanling Yang and John D. Hildebrandt

Green Bacteria: Secondary Electron Donor (Cytochromes), Pages 321-324, Hirozo Oh-oka and Robert E. Blankenship

Green Bacteria: The Light-Harvesting Chlorosome, Pages 325-330, John M. Olson

Green Sulfur Bacteria: Reaction Center and Electron Transport, Pages 331-336, Gunter A. Hauska and Thomas Schodl

Gs Family of Heterotrimeric G Proteins, Pages 337-341, Susanne M. Mumby

Heat/Stress Responses, Pages 343-347, Davis T. W. Ng

Hematopoietin Receptors, Pages 348-353, Barbara A. Miller and Joseph Y. Cheung

Heme Proteins, Pages 354-361, Johannes Everse

Heme Synthesis, Pages 362-366, Gloria C. Ferreira

Hepatocyte Growth Factor/Scatter Factor Receptor, Pages 367-371, Selma Pennacchietti and Paolo M. Comoglio

Hexokinases/Glucokinases, Pages 372-377, Emile Van Schaftingen

Histamine Receptors, Pages 378-383, Stephen J. Hill and Jillian G. Baker

HIV Protease, Pages 384-387, Ben M. Dunn

HIV-1 Reverse Transcriptase Structure, Pages 388-392, Kalyan Das, Stefan G. Sarafianos, Eddy Arnold and Stephen H. Hughes

Homologous Recombination in Meiosis, Pages 393-397, Nancy M. Hollingsworth

HPLC Separation of Peptides, Pages 398-403, James D. Pearson

Imaging Methods, Pages 405-410, Gyorgy Szabadkai and Rosario Rizzuto

Immunoglobulin (Fc) Receptors, Pages 411-416, Mark Hogarth

Inorganic Biochemistry, Pages 417-420, Robert J. P. Williams

Inositol Lipid 3-Phosphatases, Pages 421-426, Gregory S. Taylor and Jack E. Dixon

Inositol Phosphate Kinases and Phosphatases, Pages 427-429, Stephen B. Shears

Insulin- and Glucagon-Secreting Cells of the Pancreas, Pages 430-435, Franz M. Matschinsky

Insulin Receptor Family, Pages 436-440, Paul F. Pilch and Jongsoon Lee

Integrin Signaling, Pages 441-445, Lawrence E. Goldfinger and Mark H. Ginsberg

Interferon Receptors, Pages 446-451, Christopher P. Elco and Ganes C. Sen

Intermediate Filament Linker Proteins: Plectin and BPAG1, Pages 452-457, Peter Fuchs and Gerhard Wiche

Intermediate Filaments, Pages 458-464, Kelsie M. Bernot and Pierre A. Coulombe

Intracellular Calcium Channels: cADPR-Modulated (Ryanodine Receptors), Pages 465-468, Antony Galione

Intracellular Calcium Channels: NAADP+-Modulated, Pages 469-472, Armando A. Genazzani and Marcella Debidda

Ion Channel Protein Superfamily, Pages 473-477, William A. Catterall

IP3 Receptors, Pages 478-481, Colin W. TaylorEdward Morris and Paula da Fonseca

Iron-Sulfur Proteins, Pages 482-489, Helmut Beinert

JAK-STAT Signaling Paradigm, Pages 491-496, Edward Cha and Christian Schindler

Keratins and the Skin, Pages 497-504, Pierre A. Coulombe and Kelsie M. Bernot

Ketogenesis, Pages 505-507, Janos Kerner and Charles L. Hoppel

Kinesin Superfamily Proteins, Pages 508-516, Nobutaka Hirokawa and Reiko Takemura

Kinesins as Microtubule Disassembly Enzymes, Pages 517-521, Susan L. Kline-Smith and Arshad Desai

Kinetic Isotope Effects, Pages 522-527, Justine P. Roth and Judith P. Klinman

lac Operon, Pages 529-534, Liskin Swint-Kruse and Kathleen S. Matthews

Lectins, Pages 535-540, Nathan Sharon and Halina Lis

Leptin, Pages 541-545, Thomas W. Gettys

LexA Regulatory System, Pages 546-550, Veronica G. Godoy, Penny J. Beuning and Graham C. Walker

Ligand-Operated Membrane Channels: Calcium (Glutamate), Pages 551-561, Elias K. Michaelis

Ligand-Operated Membrane Channels: GABA, Pages 562-566, F. Minier and Erwin Sigel

Light-Harvesting Complex (LHC) I and II: Pigments and Proteins, Pages 567-570, Stefan Jansson

Lipases, Pages 571-575, Howard L. Brockman

Lipid Bilayer Structure, Pages 576-579, Erwin London

Lipid Modification of Proteins: Targeting to Membranes, Pages 580-583, Marilyn D. Resh

Lipid Rafts, Pages 584-587, Deborah A. Brown

Lipoproteins, HDL/LDL, Pages 588-593, Fayanne E. Thorngate and David L. Williams

Low Barrier Hydrogen Bonds, Pages 594-598, Perry A. Frey

Luft's Disease, Pages 599-601, Salvatore DiMauro

Lysophospholipid Receptors, Pages 602-604, Gabor J. Tigyi

MDR Membrane Proteins, Pages 605-609, Nathan C. Rockwell

Meiosis, Pages 610-616, Neil Hunter

Melanocortin System, Pages 617-620, Roger D. Cone

Membrane Fusion, Pages 621-626, Joshua Zimmerberg and Leonid V. Chernomordik

Membrane Transport, General Concepts, Pages 627-630, Stanley G. Schultz

Membrane Transporters:Na+/Ca2+ Exchangers, Pages 631-636, Jonathan Lytton

Membrane-Associated Energy Transduction in Bacteria and Archaea, Pages 637-645, Gunter Schafer

Metabolite Channeling: Creatine Kinase Microcompartments, Pages 646-651, Uwe Schlattner and Theo Wallimann

Metalloproteases, Pages 652-656, David S. Auld

Metalloproteinases, Matrix, Pages 657-665, Hideaki Nagase and Gillian Murphy

Metaphase Chromosome, Pages 666-671, Sharron Vass and Margarete M. S. Heck

Methyl-CpG-Binding Proteins, Pages 672-675, David G. Skalnik

Microtubule-Associated Proteins, Pages 676-682, Nobutaka Hirokawa and Reiko Takemura

Mitochondrial Auto-Antibodies, Pages 683-688, Harold Baum

Mitochondrial Channels, Pages 689-692, M. Catia Sorgato and Alessandro Bertoli

Mitochondrial DNA, Pages 693-696, Gottfried Schatz

Mitochondrial Genes and their Expression: Yeast, Pages 697-702, Piotr P. Slonimski and Giovanna Carignani

Mitochondrial Genome, Evolution, Pages 703-708, B. Franz Lang, Dennis V. Lavrov and Gertraud Burger

Mitochondrial Genome, Overview, Pages 709-715, Douglas C. Wallace

Mitochondrial Inheritance, Pages 716-719, Eric A. Shoubridge

Mitochondrial Membranes, Structural Organization, Pages 720-724, Carmen A. Mannella

Mitochondrial Metabolite Transporter Family, Pages 725-732, Ferdinando Palmieri and Martin Klingenberg

Mitochondrial Outer Membrane and the VDAC Channel, Pages 733-736, Marco Colombini

Mitogen-Activated Protein Kinase Family, Pages 737-742, Hidemi Teramoto and J. Silvio Gutkind

Mitosis, Pages 743-747, Patricia Wadsworth and Nasser M. Rusan

mRNA Polyadenylation in Eukaryotes, Pages 748-752, Mary Edmonds

mRNA Processing and Degradation in Bacteria, Pages 753-757, Deborah A. Steege

Mucin Family of Glycoproteins, Pages 758-764, Juan Perez-Vilar and Robert L. Hill

Mucins in Embryo Implantation, Pages 765-769, Daniel D. Carson

Multiple Sequence Alignment and Phylogenetic Trees, Pages 770-774, Russell F. Doolittle

Muscarinic Acetylcholine Receptors, Pages 775-777, Neil M. Nathanson

Myosin Motors, Pages 778-781, Roy E. Larson

Volume 3

Natriuretic Peptides and their Receptors, Pages 1-5, Lincoln R. Potter

N-End Rule, Pages 6-10, Alexander Varshavsky

Neoglycoproteins, Pages 11-15, Y. C. Lee and Reiko T. Lee

Neuronal Calcium Signal, Pages 16-20, Hilmar Bading

Neuronal Intermediate Filaments, Pages 21-25, Ronald K. H. Liem

Neuropeptide Y Receptors, Pages 26-31, Eric M. Parker

Neurotensin Receptors, Pages 32-36, William Rostene, Patrick Kitabgi and Didier Pelaprat

Neurotransmitter Transporters, Pages 37-40, Aurelio Galli, Randy D. Blakely and Louis J. DeFelice

Neurotrophin Receptor Signaling, Pages 41-45, Jennifer J. Gentry and Bruce D. Carter

Nicotinamide Nucleotide Transhydrogenase, Pages 50-56, Jan Rydstrom

Nicotinic Acetylcholine Receptors, Pages 57-61, Nivalda O. Rodrigues-Pinguet and Henry A. Lester

Nitric Oxide Signaling, Pages 62-65, Michael A. Marletta

N-Linked Glycan Processing Glucosidases and Mannosidases, Pages 46-49, Linda O. Tremblay and Annette Herscovics

Non-Homologous End Joining, Pages 66-70, Penny A. Jeggo

Nonhomologous Recombination: Bacterial Transposons, Pages 71-79, Bao Ton Hoang and Michael G. Chandler

Nonhomologous Recombination: Retrotransposons, Pages 80-86, Siew Loon Ooi and Jef D. Boeke

Nuclear Compartmentalization, Pages 87-91, Kelly P. Smith and Jeanne B. Lawrence

Nuclear Envelope and Lamins, Pages 92-95, Bryce M. Paschal

Nuclear Factor kappaB, Pages 96-99, Thomas D. Gilmore

Nuclear Genes in Mitochondrial Function and Biogenesis, Pages 100-104, Alexander Tzagoloff and Carol L. Dieckmann

Nuclear Organization, Chromatin Structure, and Gene Silencing , Pages 105-108, Lori L. Wallrath, John R. Danzer, Oya Yazgan and Pamela K. Geyer

Nuclear Pores and Nuclear Import/Export, Pages 109-114, Anita H. Corbett

Nucleoid Organization of Bacterial Chromosomes, Pages 115-118, Charles J. Dorman

Nucleolus, Overview, Pages 119-122, Thoru Pederson

Nucleotide Excision Repair and Human Disease, Pages 123-129, James E. Cleaver

Nucleotide Excision Repair in Eukaryotes, Pages 130-133, Laura A. Lindsey-Boltz and Aziz Sancar

Nucleotide Excision Repair, Bacterial: The UvrABCD System, Pages 134-142, Bennett Van Houten and Lawrence Grossman

Nucleotide Excision Repair: Biology, Pages 143-147, Errol C. Friedberg

Olfactory Receptors, Pages 149-154, Sigrun I. Korsching

Oligosaccharide Analysis by Mass Spectrometry, Pages 155-160, Andrew J. Hanneman and Vernon N. Reinhold

Oligosaccharide Chains: Free, N-Linked, O-Linked, Pages 161-164, Tadashi Suzuki

Oncocytes, Pages 165-166, Bernard Tandler and Charles L. Hoppel

Opioid Receptors, Pages 167-171, P. Y. Law and Horace H. Loh

Ornithine Cycle, Pages 172-177, Malcolm Watford

Oxygenases, Pages 178-182, Osamu Hayaishi

P2X Purinergic Receptors, Pages 183-187, Annmarie Surprenant

P2Y Purinergic Receptors, Pages 188-191, George R. Dubyak

p53 Protein, Pages 192-195, Jamie Hearnes and Jennifer Pietenpol

p70 S6 Kinase/mTOR, Pages 196-200, Christopher G. Proud

Parathyroid Hormone/Parathyroid Hormone-Related Protein Receptor, Pages 201-207, Thomas J. Gardella

PCR (Polymerase Chain Reaction), Pages 208-210, Michael J. Brownstein

Pentose Phosphate (Hexose Mono Phosphate) Pathway, Pages 211-215, Bernard R. Landau

Pentose Phosphate Pathway, History of, Pages 216-225, John F. Williams

Peptide Amidation, Pages 226-230, Mark J. Niciu, Richard E. Mains and Betty A. Eipper

Periplasmic Electron Transport Systems in Bacteria, Pages 231-238, David J. Richardson, Gary Sawers and Rob J. M. Van Spanning

Peroxisome Proliferator-Activated Receptors, Pages 239-245, Mary C. Sugden, Edward A. Sugden and Mark J. Holness

Peroxisomes, Pages 246-250, Suresh Subramani

Phage Display for Protein Binding, Pages 251-255, Henry B. Lowman

Pheromone Receptors (Yeast), Pages 256-261, James B. Konopka and Jeremy W. Thorner

PHO Regulon, Pages 262-265, Bengt L. Persson

Phosphatidylinositol Bisphosphate and Trisphosphate, Pages 266-271, Alex Toker

Phosphatidylinositol-3-Phosphate, Pages 272-276, Joseph V. Virbasius and Michael P. Czech

Phosphofructokinase-2/Fructose Bisphosphatase-2, Pages 277-280, Daniel M. Raben

Phosphoinositide 3-Kinase, Pages 281-286, Khatereh Ahmadi and Michael Waterfield

Phosphoinositide 4- and 5-Kinases and Phosphatases, Pages 287-291, Shawn F. Bairstow, Matthew W. Bunce and Richard A. Anderson

Phosphoinositide-Dependent Protein Kinases, Pages 292-296, Nick R. Leslie and C. Peter Downes

Phospholipase A2, Pages 297-300, Timothy R. Smith and Edward A. Dennis

Phospholipase C, Pages 301-305, Fujio Sekiya, Yeun Ju Kim and Sue Goo Rhee

Phospholipase D, Pages 306-313, Mary M. LaLonde and Michael A. Frohman

Phospholipid Metabolism in Mammals, Pages 314-320, Claudia Kent

Phospholipid Synthesis in Yeast, Pages 321-325, Gil-Soo Han and George M. Carman

Photoreceptors, Pages 326-329, King-Wai Yau

Photosynthesis, Pages 330-335, Richard C. Leegood

Photosynthetic Carbon Dioxide Fixation, Pages 336-341, Matthew J. Paul

Photosystem I, Structure and Function, Pages 342-347, Petra Fromme

Photosystem I: FX, FA, and FB Iron-Sulfur Clusters, Pages 348-356, Mikhail L. Antonkine and John H. Golbeck

Photosystem II Light Harvesting System: Dynamic Behavior, Pages 357-362, Peter Horton and Alexander Ruban

Photosystem II: Assembly and Turnover of the D1 Protein, Pages 363-366, Eira Kanervo and Eva-Mari Aro

Photosystem II: Protein Components, Pages 367-374, James Barber

Photosystem II: Water Oxidation, Overview, Pages 375-380, Fabrice Rappaport and Pierre Joliot

Plant Signaling: Peptides, Pages 381-384, Clarence A. Ryan and Gregory Pearce

Plasma-Membrane Calcium Pump: Structure and Function, Pages 385-389, Emanuel E. Strehler

Plastocyanin, Pages 390-393, Elizabeth L. Gross

Platelet-Activating Factor Receptor, Pages 394-398, Katherine M. Howard and Merle S. Olson

Platelet-Derived Growth Factor Receptor Family, Pages 399-406, Marina Kovalenko and Andrius Kazlauskas

Polysialic Acid inMolecular Medicine, Pages 407-414, Frederic A. Troy, II

Porphyrin Metabolism, Pages 415-419, Mark Shepherd and Harry A. Dailey

Pre-tRNA and Pre-rRNA Processing in Bacteria, Pages 420-424, Sidney R. Kushner

Pre-tRNA and Pre-rRNA Processing in Eukaryotes, Pages 425-431, Hendrik A. Raue

Prions and Epigenetic Inheritance, Pages 432-436, Reed B. Wickner

Prions, Overview, Pages 437-440, Cedric Govaerts and Fred E. Cohen

Processivity Clamps in DNA Replication: Clamp Loading, Pages 441-446, Megan J. Davey and Mike O'Donnell

Propionyl CoA-Succinyl CoA Pathway, Pages 447-451, Wayne A. Fenton

Prostaglandins and Leukotrienes, Pages 452-456, William L. Smith and Robert C. Murphy

Proteases in Blood Clotting, Pages 457-463, John D. Kulman and Earl W. Davie

Proteasomes, Overview, Pages 464-468, Martin Rechsteiner

26S Proteasome, Structure and Function, Pages 469-473, Peter Zwickl and Wolfgang Baumeister

Protein Carboxyl Esterification, Pages 474-477, Shilpa G. Lalchandani and Jeffry B. Stock

Protein Data Resources, Pages 478-483, Philip E. Bourne

Protein Degradation, Pages 484-492, Tomo ari and Alfred L. Goldberg

Protein Folding and Assembly, Pages 493-499, David P. Goldenberg

Protein Glycosylation Inhibitors, Pages 500-503, Alan D. Elbein

Protein Glycosylation, Overview, Pages 504-509, Natasha E. Zachara and Gerald W. Hart

Protein Import into Mitochondria, Pages 510-515, Johannes M. Herrmann and Walter Neupert

Protein Kinase B, Pages 516-522, Bettina A. Dummler and Brian A. Hemmings

Protein Kinase C Family, Pages 523-526, Alexandra C. Newton

Protein N-Myristoylation, Pages 527-531, Erica Dutil Sonnenburg and Jeffrey I. Gordon

Protein Palmitoylation, Pages 532-535, Robert J. Deschenes

Protein Tyrosine Phosphatases, Pages 536-542, David J. Pagliarini, Fred L. Robinson and Jack E. Dixon

Proteinase-Activated Receptors, Pages 543-548, Kristina K. Hansen and Morley D. Hollenberg

Proteoglycans, Pages 549-555, Sara K. Olson and Jeffrey D. Esko

Pteridines, Pages 556-560, S. Colette Daubner and Paul F. Fitzpatrick

P-Type Pumps: Copper Pump, Pages 561-564, Ilia Voskoboinik and James Camakaris

P-Type Pumps: H+/K+ Pump, Pages 565-570, Jai Moo Shin and George Sachs

P-Type Pumps: Na+/K+ Pump, Pages 571-576, Peter L. Jorgensen

P-Type Pumps: Plasma-Membrane H+ Pump, Pages 577-581, A. Brett Mason and Carolyn W. Slayman

Purple Bacteria: Electron Acceptors and Donors, Pages 582-585, Evaldas Katilius and Neal W. Woodbury

Purple Bacteria: Photosynthetic Reaction Centers, Pages 586-594, C. Roy D. Lancaster

Pyridoxal Phosphate, Pages 595-599, David E. Metzler

Pyrimidine Biosynthesis, Pages 600-605, Monika Loffler and Elke Zameitat

Pyruvate Carboxylation, Transamination, and Gluconeogenesis, Pages 606-610, Sarawut Jitrapakdee and John C. Wallace

Pyruvate Dehydrogenase, Pages 611-615, Sam A. Johnson and James G. McCormack

Pyruvate Kinase, Pages 616-619, Kosaku Uyeda

Quinones, Pages 621-627, Giorgio Lenaz and Maria Luisa Genova

Rab Family, Pages 629-634, Mary W. McCaffrey and Andrew J. Lindsay

Ran GTPase, Pages 635-639, Mary Shannon Moore

Ras Family, Pages 640-644, Lawrence A. Quilliam

Recombination: Heteroduplexand Mismatch Repair in vitro, Pages 645-648, Leroy Worth

Recombination: Strand Transferases, Pages 649-653, Floyd R. Bryant

Recombination-Dependent DNA Replication, Pages 654-659, Kenneth N. Kreuzer

recQ DNA Helicase Family in Genetic Stability, Pages 660-664, Mary A. Risinger and Joanna Groden

Regulated Intramembrane Proteolysis (Rip), Pages 665-670, Jin Ye, Michael S. Brown and Joseph L. Goldstein

Respiratory Chain and ATP Synthase, Pages 671-675, David G. Whitehouse and Anthony L. Moore

Respiratory Chain Complex I, Pages 676-680, Ulrich Brandt

Respiratory Chain Complex II and Succinate: Quinone Oxidoreductases, Pages 681-687, C. Roy D. Lancaster

Respiratory Chain Complex IV, Pages 688-694, Hartmut Michel

Respiratory Processes in Anoxygenic and Oxygenic Phototrophs, Pages 695-699, Roberto Borghese and Davide Zannoni

Retinoblastoma Protein (pRB), Pages 700-703, Nicholas Dyson and Maxim Frolov

Retinoic Acid Receptors, Pages 704-707, Martin Petkovich

Reverse Transcriptase and Retroviral Replication, Pages 708-713, Laura Tarrago-Litvak, Marie-Line Andreola and Simon Litvak

Rho GTPases and Actin Cytoskeleton Dynamics, Pages 714-718, Priam Villalonga and Anne J. Ridley

Ribosome Assembly, Pages 719-724, John L. Woolford

Ribosome Structure, Pages 725-732, Brian T. Wimberly

Ribozyme Mechanisms, Pages 733-737, John Hsieh and Carol A. Fierke

Ribozyme Structural Elements: Group I Introns, Pages 738-742, Barbara L. Golden

Ribozyme Structural Elements: Hairpin Ribozyme, Pages 743-746, Adrian R. Ferre-D'Amare

Ribozymes and Evolution, Pages 747-752, Niles Lehman

RNA Editing, Pages 753-758, Charles E. Samuel

RNA Polymerase I and RNA Polymerase III in Eukaryotes, Pages 759-762, Robert J. White

RNA Polymerase II and Basal Transcription Factors in Eukaryotes, Pages 763-765, Joan Weliky Conaway and Ronald C. Conaway

RNA Polymerase II Elongation Control in Eukaryotes, Pages 766-769, David H. Price

RNA Polymerase II Structure in Eukaryotes, Pages 770-774, Patrick Cramer

RNA Polymerase Reaction in Bacteria, Pages 775-780, Arkady A. Mustaev and Alexander D. Goldfarb

RNA Polymerase Structure, Bacterial, Pages 781-784, Michael Anikin, Dmitri Temiakov and William T. McAllister

Volume 4

Secondary Structure in Protein Analysis, Pages 1-6, George D. Rose

Secretases, Pages 7-10, Robert L. Heinrikson

Secretory Pathway, Pages 11-16, Karen J. Colley

Selenoprotein Synthesis, Pages 17-21, August Bock

Septins and Cytokinesis, Pages 22-26, Makoto Kinoshita and Christine M. Field

Serine/Threonine Phosphatases, Pages 27-32, Thomas S. Ingebritsen

Serotonin Receptor Signaling, Pages 33-37, Paul J. Gresch and Elaine Sanders-Bush

Siglecs, Pages 38-40, Ajit Varki

Sigma Factors, Pages 41-44, John D. Helmann

Sliding Clamps in DNA Replication: E. coli -Clamp and PCNA Structure, Pages 45-47, Eric R. Goedken and John Kuriyan

Small GTPases, Pages 48-54, Adam Shutes and Channing J. Der

Somatostatin Receptors, Pages 55-60, Agnes Schonbrunn

Spastic Paraplegia, Pages 61-66, Elena Irene Rugarli and Andrea Ballabio

Spectrophotometric Assays, Pages 67-75, Britton Chance

Sphingolipid Biosynthesis, Pages 76-81, Martina Leipelt and Alfred H. Merrill

Sphingolipid Catabolism, Pages 82-87, Akira Abe and James A. Shayman

Spliceosome, Pages 88-92, Timothy W. Nilsen

Src Family of Protein Tyrosine Kinases, Pages 93-98, Jonathan A. Cooper

Starvation, Pages 99-110, Oliver E. Owen and Richard W. Hanson

Steroid/Thyroid Hormone Receptors, Pages 111-116, Ramesh Narayanan and Nancy L. Weigel

Store-Operated Membrane Channels: Calcium, Pages 117-122, Indu S. Ambudkar

Substrate Binding, Catalysis, and Product Release , Pages 123-126, W. Wallace Cleland

Sugar Nucleotide Transporters, Pages 127-129, Carlos B. Hirschberg

SUMO Modification, Pages 130-134, Frauke Melchior and Andrea Pichler

Superoxide Dismutase, Pages 135-138, Irwin Fridovich

Syk Family of Protein Tyrosine Kinases, Pages 139-145, Andrew C. Chan

T7 RNA Polymerase, Pages 147-151, Rui Sousa

Tachykinin/Substance P Receptors, Pages 152-157, Mark D. Richardson and Madan M. Kwatra

Taste Receptors, Pages 158-161, John D. Boughter, Jr. and Steven D. Munger

T-Cell Antigen Receptor, Pages 162-168, Andrea L. Szymczak and Dario A. A. Vignali

Tec/Btk Family Tyrosine Kinases, Pages 169-173, Shuling Guo and Owen N. Witte

Telomeres: Maintenance and Replication, Pages 174-179, Alessandro Bianchi and David Shore

Thyroid-Stimulating Hormone/Luteinizing Hormone/Follicle-Stimulating Hormone Receptors, Pages 180-186, Deborah L. Segaloff, Dario Mizrachi and Mario Ascoli

Tight Junctions, Pages 187-189, Shoichiro Tsukita

Title, Pages, Authors

Toll-Like Receptors, Pages 190-194, Himanshu Kumar, Kiyoshi Takeda and Shizuo Akira

Transcription Termination, Pages 195-199, Thomas J. Santangelo and Jeffrey W. Roberts

Transcriptional Silencing, Pages 200-203, Ann Sutton and Rolf Sternglanz

Transcription-Coupled DNA Repair, Overview, Pages 204-208, Isabel Mellon

Transforming Growth Factor-β Receptor Superfamily, Pages 209-213, Mark de Caestecker

Translation Elongation in Bacteria, Pages 214-223, Oliver Vesper and Knud H. Nierhaus

Translation Elongation in Eukaryotes, Pages 224-229, William C. Merrick and Anton A. Komar

Translation Initiation in Bacteria: Factors and Mechanisms, Pages 230-236, Cynthia L. Pon and Claudio O. Gualerzi

Translation Initiation in Eukaryotes: Factors and Mechanisms, Pages 237-241, Tatyana V. Pestova and Christopher U. T. Hellen

Translation Termination and Ribosome Recycling, Pages 242-246, Nadja Koloteva-Levin and Mick F. Tuite

Translesion DNA Polymerases, Eukaryotic, Pages 247-250, Alexandra Vaisman and Roger Woodgate

Trehalose Metabolism, Pages 251-255, Alan D. Elbein

Tricarboxylic Acid Cycle, Pages 256-262, Richard L. Veech

tRNA Synthetases, Pages 263-266, Karla L. Ewalt and Paul Schimmel

trp Operon and Attenuation, Pages 267-271, Paul Gollnick

Tubulin and its Isoforms, Pages 272-276, Eva Nogales

Tumor Necrosis Factor Receptors, Pages 277-283, Karen G. Potter and Carl F. Ware

Two-Dimensional Gel Electrophoresis, Pages 284-289, Gerhard Schmid, Denis Hochstrasser and Jean-Charles Sanchez

Two-Hybrid Protein-Protein Interactions, Pages 290-293, Ilya Serebriiskii and Erica A. Golemis

Tyrosine Sulfation, Pages 294-297, Denis Corbeil and Wieland B. Huttner

Ubiquitin System, Pages 299-303, Aaron Ciechanover and Michael H. Glickman

Ubiquitin-Like Proteins, Pages 304-307, Edward T. H. Yeh

UmuC, D Lesion Bypass DNA Polymerase V, Pages 308-312, Zvi Livneh

Uncoupling Proteins, Pages 313-318, Daniel Ricquier and Frederic Bouillaud

Unfolded Protein Responses, Pages 319-325, David Ron

Urea Cycle, Inborn Defects of, Pages 326-330, Marsha K. Fearing and Vivian E. Shih

Vacuoles, Pages 331-336, Christopher J. Stefan and Scott D. Emr

Vascular Endothelial Growth Factor Receptors, Pages 337-342, Kenneth A. Thomas

Vasopressin/Oxytocin Receptor Family, Pages 343-348, Michael J. Brownstein

V-ATPases, Pages 349-353, Michael Forgac

Vitamin A (Retinoids), Pages 354-359, Joseph L. Napoli

Vitamin B12 and B12-Proteins, Pages 360-366, Bernhard Krautler

Vitamin C, Pages 367-371, Robert B. Rucker and Francene Steinberg

Vitamin D, Pages 372-377, Hector F. DeLuca and Margaret Clagett-Dame

Vitamin D Receptor, Pages 378-383, Diane R. Dowd and Paul N. MacDonald

Vitamin E, Pages 384-388, Ute C. Obermuller-Jevic and Lester Packer

Vitamin K: Biochemistry, Metabolism, and Nutritional Aspects, Pages 389-393, J. W. Suttie

Vitamin K: Blood Coagulation and Use in Therapy, Pages 394-398, Matthew D. Stone and Gary L. Nelsestuen

Voltage-Dependent K+ Channels, Pages 399-404, Ramon Latorre and Francisco J. Morera

Voltage-Sensitive Ca2+ Channels, Pages 405-408, Harald Reuter

Voltage-Sensitive Na+ Channels, Pages 409-415, William J. Brammar

Von Hippel-Lindau (VHL) Protein, Pages 416-418, Ronald C. Conaway and Joan Weliky Conaway

XPV DNA Polymerase and Ultraviolet Damage Bypass, Pages 419-421, Alan R. Lehmann

X-Ray Determination of 3-D Structure in Proteins, Pages 422-428, Martha L. Ludwig

Yeast GAL1-GAL10 System, Pages 429-433, Dennis Lohr and Ralph Bash

Zinc Fingers, Pages 435-439, Mark Isalan

Lipids, Carbohydrates, Membranes and Membrane Proteins

Carbohydrate Chains: Enzymatic and Chemical Synthesis; Vol.1 - Pages 307-313, Thomas J. Tolbert and Chi-Huey Wong

Cell–Matrix Interactions; Vol.1 - Pages 362-366, Janet A. Askari and Martin J. Humphries

Detergent Properties; Vol.1 - Pages 577-581, Darrell R. McCaslin

Endocytosis; Vol.2 - Pages 16-19, Julie G. Donaldson

Flippases; Vol.2 - Pages 123-127, Charles J. Waechter

Galectins; Vol.2 - Pages 171-174, R. Colin Hughes

GlcNAc Biosynthesis and Function, O-Linked; Vol.2 - Pages 189-192, Kaoru Sakabe and Gerald W. Hart

Glycation; Vol.2 - Pages 229-236, Suzanne R. Thorpe and John W. Baynes

Glycolipid-Dependent Adhesion Processes; Vol.2 - Pages 261-265, Senitiroh Hakomori

Glycoprotein Folding and Processing Reactions; Vol.2 - Pages 272-276, Armando J. Parodi

Glycoprotein-Mediated Cell Interactions, O-Linked; Vol.2 - Pages 277-282, Robert S. Haltiwanger

Glycoproteins, N-Linked; Vol.2 - Pages 283-292, Mark A. Lehrman

Glycoproteins, Plant; Vol.2 - Pages 293-296, Carolyn J. Schultz

Glycosylation in Cystic Fibrosis; Vol.2 - Pages 297-301, Andrew D. Rhim, Thomas F. Scanlin and Mary Catherine Glick

Glycosylation, Congenital Disorders of; Vol.2 - Pages 302-307, Hudson H. Freeze

Glycosylphosphatidylinositol (GPI) Anchors; Vol.2 - Pages 308-311, Anant K. Menon

Ion Channel Protein Superfamily; Vol.2 - Pages 473-477, William A. Catterall

Lectins; Vol.2 - Pages 535-540, Nathan Sharon and Halina Lis

Lipases; Vol.2 - Pages 571-575, Howard L. Brockman

Lipid Bilayer Structure; Vol.2 - Pages 576-579, Erwin London

Lipid Rafts; Vol.2 - Pages 584-587, Deborah A. Brown

Lipoproteins, HDL/LDL; Vol.2 - Pages 588-593, Fayanne E. Thorngate and David L. Williams

MDR Membrane Proteins; Vol.2 - Pages 605-609, Nathan C. Rockwell

Membrane Fusion; Vol.2 - Pages 621-626, Joshua Zimmerberg and Leonid V. Chernomordik

Mucin Family of Glycoproteins; Vol.2 - Pages 758-764, Juan Perez-Vilar and Robert L. Hill

Mucins in Embryo Implantation; Vol.2 - Pages 765-769, Daniel D. Carson

Neoglycoproteins; Vol.3 - Pages 11-15, Y. C. Lee and Reiko T. Lee

N-Linked Glycan Processing Glucosidases and Mannosidases; Vol.3 - Pages 46-49, Linda O. Tremblay and Annette Herscovics

Oligosaccharide Chains: Free, N-Linked, O-Linked; Vol.3 - Pages 161-164, Tadashi Suzuki

Phospholipid Metabolism in Mammals; Vol.3 - Pages 314-320, Claudia Kent

Phospholipid Synthesis in Yeast; Vol.3 - Pages 321-325, Gil-Soo Han and George M. Carman

Prostaglandins and Leukotrienes; Vol.3 - Pages 452-456, William L. Smith and Robert C. Murphy

Protein Glycosylation Inhibitors; Vol.3 - Pages 500-503, Alan D. Elbein

Proteoglycans; Vol.3 - Pages 549-555, Sara K. Olson and Jeffrey D. Esko

Secretory Pathway; Vol.4 - Pages 11-16, Karen J. Colley

Siglecs; Vol.4 - Pages 38-40, Ajit Varki

Sphingolipid Biosynthesis; Vol.4 - Pages 76-81, Martina Leipelt and Alfred H. Merrill, Jr.

Sphingolipid Catabolism; Vol.4 - Pages 82-87, Akira Abe and James A. Shayman

Sugar Nucleotide Transporters; Vol.4 - Pages 127-129, Carlos B. Hirschberg

Trehalose Metabolism; Vol.4 - Pages 251-255, Alan D. Elbein

Metabolism, Vitamins and Hormones

Amino Acid Metabolism; Vol.1 - Pages 90-95, Luc Cynober

Anaplerosis; Vol.1 - Pages 105-110, Raymond R. Russell, III and Heinrich Taegtmeyer

Bile Salts and their Metabolism; Vol.1 - Pages 159-163, Ulrich Beuers and Thomas Pusl

Biliary Cirrhosis, Primary; Vol.1 - Pages 164-169, Marshall M. Kaplan

Branched-Chain -Ketoacids; Vol.1 - Pages 186-191, David T. Chuang

Carnitine and -Oxidation; Vol.1 - Pages 314-318, Janos Kerner and Charles L. Hoppel

Cholesterol Synthesis; Vol.1 - Pages 451-455, Peter A. Edwards

Diabetes; Vol.1 - Pages 582-592, David W. Cooke

Fat Mobilization: Perilipin and Hormone-Sensitive Lipase; Vol.2 - Pages 85-89, Constantine Londos and Alan R. Kimmel

Fatty Acid Oxidation; Vol.2 - Pages 90-94, Horst Schulz

Fatty Acid Synthesis and its Regulation; Vol.2 - Pages 99-103, Steven D. Clarke and Manabu T. Nakamura

Gluconeogenesis; Vol.2 - Pages 197-203, Richard W. Hanson and Oliver E. Owen

Glucose/Sugar Transport in Bacteria; Vol.2 - Pages 204-207, Lan Guan and H. Ronald Kaback

Glucose/Sugar Transport in Mammals; Vol.2 - Pages 208-212, Silvia Mora and Jeffrey Pessin

Glycogen Metabolism; Vol.2 - Pages 244-248, Peter J. Roach

Glycogen Storage Diseases; Vol.2 - Pages 249-254, George H. Sack, Jr.

Glycolysis, Overview; Vol.2 - Pages 266-271, Robert A. Harris

Hexokinases/Glucokinases; Vol.2 - Pages 372-377, Emile Van Schaftingen

Insulin- and Glucagon-Secreting Cells of the Pancreas; Vol.2 - Pages 430-435, Franz M. Matschinsky

Ketogenesis; Vol.2 - Pages 505-507, Janos Kerner and Charles L. Hoppel

Ornithine Cycle; Vol.3 - Pages 172-177, Malcolm Watford

Pentose Phosphate (Hexose Mono Phosphate) Pathway; Vol.3 - Pages 211-215, Bernard R. Landau

Pentose Phosphate Pathway, History of; Vol.3 - Pages 216-225, John F. Williams

Phosphofructokinase-2/Fructose Bisphosphatase-2; Vol.3 - Pages 277-280, Daniel M. Raben

Photosynthesis; Vol.3 - Pages 330-335, Richard C. Leegood

Photosynthetic Carbon Dioxide Fixation; Vol.3 - Pages 336-341, Matthew J. Paul

Porphyrin Metabolism; Vol.3 - Pages 415-419, Mark Shepherd and Harry A. Dailey

Propionyl CoA–Succinyl CoA Pathway; Vol.3 - Pages 447-451, Wayne A. Fenton

Pyruvate Carboxylation, Transamination, and Gluconeogenesis; Vol.3 - Pages 606-610, Sarawut Jitrapakdee and John C. Wallace

Pyruvate Dehydrogenase; Vol.3 - Pages 611-615, Sam A. Johnson and James G. McCormack

Pyruvate Kinase; Vol.3 - Pages 616-619, Kosaku Uyeda

Starvation; Vol.4 - Pages 99-110, Oliver E. Owen and Richard W. Hanson

Tricarboxylic Acid Cycle; Vol.4 - Pages 256-262, Richard L. Veech

Urea Cycle, Inborn Defects of; Vol.4 - Pages 326-330, Marsha K. Fearing and Vivian E. Shih

Vitamin A (Retinoids); Vol.4 - Pages 354-359, Joseph L. Napoli

Vitamin B12 and B12-Proteins; Vol.4 - Pages 360-366, Bernhard Krautler

Vitamin C; Vol.4 - Pages 367-371, Robert B. Rucker and Francene Steinberg

Vitamin D; Vol.4 - Pages 372-377, Hector F. DeLuca and Margaret Clagett-Dame

Vitamin E; Vol.4 - Pages 384-388, Ute C. Obermuller-Jevic and Lester Packer

Vitamin K: Biochemistry, Metabolism, and Nutritional Aspects; Vol.4 - Pages 389-393, J. W. Suttie

Vitamin K: Blood Coagulation and Use in Therapy; Vol.4 - Pages 394-398, Matthew D. Stone and Gary L. Nelsestuen

Cell Architecture and Function

Actin Assembly/Disassembly; Vol.1 - Pages 12-18, Henry N. Higgs

Actin-Capping and -Severing Proteins; Vol.1 - Pages 19-26, Sankar Maiti and James R. Bamburg

Actin-Related Proteins; Vol.1 - Pages 27-33, R. Dyche Mullins

Autophagy in Fungi and Mammals; Vol.1 - Pages 138-143, Daniel J. Klionsky and Ju Guan

Bax and Bcl2 Cell Death Enhancers and Inhibitors; Vol.1 - Pages 152-154, David L. Vaux

Cadherin-Mediated Cell–Cell Adhesion; Vol.1 - Pages 205-211, Frauke Drees and W. James Nelson

Caspases and Cell Death; Vol.1 - Pages 319-327, Don W. Nicholson, Pierluigi Nicotera and Gerry Melino

Cell Cycle Controls in G1 and G0; Vol.1 - Pages 328-331, WengeShi and Steven F. Dowdy

Cell Cycle: Control of Entry and Progression Through S Phase; Vol.1 - Pages 332-337, Susan L. Forsburg

Cell Cycle: DNA Damage Checkpoints; Vol.1 - Pages 338-344, Jean Y. J. Wang

Cell Cycle: Mitotic Checkpoint; Vol.1 - Pages 345-351, Tim J. Yen

Cell Migration; Vol.1 - Pages 356-361, J. Victor Small and Emmanuel Vignal

Centromeres; Vol.1 - Pages 367-371, Beth A. Sullivan

Centrosomes and Microtubule Nucleation; Vol.1 - Pages 372-376, Reiko Nakajima, Ming-Ying Tsai and Yixian Zheng

Chaperones for Metalloproteins; Vol.1 - Pages 383-386, Valeria C. Culotta and Edward Luk

Chaperones, Molecular; Vol.1 - Pages 387-392, Sue Wickner and Joel R. Hoskins

Chaperonins; Vol.1 - Pages 393-398, Arthur L. Horwich, Wayne A. Fenton and George W. Farr

Chromosome Organization and Structure, Overview; Vol.1 - Pages 469-474, Elena Gracheva and Sarah C. R. Elgin

Cytokinesis; Vol.1 - Pages 556-561, Masanori Mishima and Michael Glotzer

Desmosomes and Hemidesmosomes; Vol.1 - Pages 569-576, Rachel L. Dusek, Jonathan C. R. Jones and Kathleen J. Green

Dynactin; Vol.1 - Pages 823-826, Trina A. Schroer

Dynein; Vol.1 - Pages 827-831, K. Kevin Pfister

Endoplasmic Reticulum-Associated Protein Degradation; Vol.2 - Pages 20-23, Maurizio Molinari

Focal Adhesions; Vol.2 - Pages 128-133, Eli Zamir and Benjamin Geiger

Golgi Complex; Vol.2 - Pages 312-315, Mark Stamnes

Heat/Stress Responses; Vol.2 - Pages 343-347, Davis T. W. Ng

Inositol Lipid 3-Phosphatases; Vol.2 - Pages 421-426, Gregory S. Taylor and Jack E. Dixon

Intermediate Filament Linker Proteins: Plectin and BPAG1; Vol.2 - Pages 452-457, Peter Fuchs and Gerhard Wiche

Intermediate Filaments; Vol.2 - Pages 458-464, Kelsie M. Bernot and Pierre A. Coulombe

Keratins and the Skin; Vol.2 - Pages 497-504, Pierre A. Coulombe and Kelsie M. Bernot

Kinesin Superfamily Proteins; Vol.2 - Pages 508-516, Nobutaka Hirokawa and Reiko Takemura

Kinesins as Microtubule Disassembly Enzymes; Vol.2 - Pages 517-521, Susan L. Kline-Smith and Arshad Desai

Meiosis; Vol.2 - Pages 610-616, Neil Hunter

Metalloproteinases, Matrix; Vol.2 - Pages 657-665, Hideaki Nagase and Gillian Murphy

Microtubule-Associated Proteins; Vol.2 - Pages 676-682, Nobutaka Hirokawa and Reiko Takemura

Mitosis; Vol.2 - Pages 743-747, Patricia Wadsworth and Nasser M. Rusan

Myosin Motors; Vol.2 - Pages 778-781, Roy E. Larson

N-End Rule; Vol.3 - Pages 6-10, Alexander Varshavsky

Neuronal Intermediate Filaments; Vol.3 - Pages 21-25, Ronald K. H. Liem

Nuclear Compartmentalization; Vol.3 - Pages 87-91, Kelly P. Smith and Jeanne B. Lawrence

Nuclear Envelope and Lamins; Vol.3 - Pages 92-95, Bryce M. Paschal

Nuclear Pores and Nuclear Import/Export; Vol.3 - Pages 109-114, Anita H. Corbett

Peroxisomes; Vol.3 - Pages 246-250, Suresh Subramani

26S Proteasome, Structure and Function; Vol.3 - Pages 469-473, Peter Zwickl and Wolfgang Baumeister

Protein Glycosylation, Overview; Vol.3 - Pages 504-509, Natasha E. Zachara and Gerald W. Hart

Rho GTPases and Actin Cytoskeleton Dynamics; Vol.3 - Pages 714-718, Priam Villalonga and Anne J. Ridley

Septins and Cytokinesis; Vol.4 - Pages 22-26, Makoto Kinoshita and Christine M. Field

SUMO Modification; Vol.4 - Pages 130-134, Frauke Melchior and Andrea Pichler

Tight Junctions; Vol.4 - Pages 187-189, Shoichiro Tsukita

Transcriptional Silencing; Vol.4 - Pages 200-203, Ann Sutton and Rolf Sternglanz

Tubulin and its Isoforms; Vol.4 - Pages 272-276, Eva Nogales

Unfolded Protein Responses; Vol.4 - Pages 319-325, David Ron

Vacuoles; Vol.4 - Pages 331-336, Christopher J. Stefan and Scott D. Emr

Protein/Enzyme Structure Function and Degradation

Allosteric Regulation; Vol.1 - Pages 68-73, Barry S. Cooperman

Aminopeptidases; Vol.1 - Pages 96-98, Ralph A. Bradshaw

Amyloid; Vol.1 - Pages 99-104, Ronald Wetzel

Aspartic Proteases; Vol.1 - Pages 123-127, Ben M. Dunn

B12-Containing Enzymes; Vol.1 - Pages 145-151, Vahe Bandarian and Rowena G. Matthews

Biotin; Vol.1 - Pages 174-178, Steven W. Polyak and Anne Chapman-Smith

Biotinylation of Proteins; Vol.1 - Pages 179-181, Ronald A. Kohanski

Calpain; Vol.1 - Pages 300-306, Hiroyuki Sorimachi and Yasuko Ono

Chemiluminescence and Bioluminescence; Vol.1 - Pages 399-404, Thomas O. Baldwin

Coenzyme A; Vol.1 - Pages 475-477, M. Daniel Lane

Collagenases; Vol.1 - Pages 478-481, Kenn Holmbeck and Henning Birkedal-Hansen

Collagens; Vol.1 - Pages 482-487, Darwin J. Prockop

Cysteine Proteases; Vol.1 - Pages 516-520, David J. Buttle and John S. Mort

Disulfide Bond Formation; Vol.1 - Pages 598-602, Hiram F. Gilbert

Elastin; Vol.2 - Pages 10-12, Judith Ann Foster

Enzyme Inhibitors; Vol.2 - Pages 31-37, Vern L. Schramm

Enzyme Kinetics; Vol.2 - Pages 38-44, Irwin H. Segel

Enzyme Reaction Mechanisms: Stereochemistry; Vol.2 - Pages 45-50, Ming-Daw Tsai, Li Zhao and Brandon J. Lamarche

Flavins; Vol.2 - Pages 118-122, Barrie Entsch and David P. Ballou

Heme Proteins; Vol.2 - Pages 354-361, Johannes Everse

HIV Protease; Vol.2 - Pages 384-387, Ben M. Dunn

Kinetic Isotope Effects; Vol.2 - Pages 522-527, Justine P. Roth and Judith P. Klinman

Lipid Modification of Proteins: Targeting to Membranes; Vol.2 - Pages 580-583, Marilyn D. Resh

Low Barrier Hydrogen Bonds; Vol.2 - Pages 594-598, Perry A. Frey

Metalloproteases; Vol.2 - Pages 652-656, David S. Auld

Peptide Amidation; Vol.3 - Pages 226-230, Mark J. Niciu, Richard E. Mains and Betty A. Eipper

Phage Display for Protein Binding; Vol.3 - Pages 251-255, Henry B. Lowman

Prions, Overview; Vol.3 - Pages 437-440, Cedric Govaerts and Fred E. Cohen

Proteases in Blood Clotting; Vol.3 - Pages 457-463, John D. Kulman and Earl W. Davie

Proteasomes, Overview; Vol.3 - Pages 464-468, Martin Rechsteiner

Protein Carboxyl Esterification; Vol.3 - Pages 474-477, Shilpa G. Lalchandani and Jeffry B. Stock

Protein Degradation; Vol.3 - Pages 484-492, Tomo ari and Alfred L. Goldberg

Protein Folding and Assembly; Vol.3 - Pages 493-499, David P. Goldenberg

Protein N-Myristoylation; Vol.3 - Pages 527-531, Erica Dutil Sonnenburg and Jeffrey I. Gordon

Protein Palmitoylation; Vol.3 - Pages 532-535, Robert J. Deschenes

Pteridines; Vol.3 - Pages 556-560, S. Colette Daubner and Paul F. Fitzpatrick

Pyridoxal Phosphate; Vol.3 - Pages 595-599, David E. Metzler

Regulated Intramembrane Proteolysis (Rip); Vol.3 - Pages 665-670, Jin Ye, Michael S. Brown and Joseph L. Goldstein

Secretases; Vol.4 - Pages 7-10, Robert L. Heinrikson

Selenoprotein Synthesis; Vol.4 - Pages 17-21, August Bock

Substrate Binding, Catalysis, and Product Release; Vol.4 - Pages 123-126, W. Wallace Cleland

Two-Hybrid Protein–Protein Interactions; Vol.4 - Pages 290-293, Ilya Serebriiskii and Erica A. Golemis

Tyrosine Sulfation; Vol.4 - Pages 294-297, Denis Corbeil and Wieland B. Huttner

Ubiquitin System; Vol.4 - Pages 299-303, Aaron Ciechanover and Michael H. Glickman

Ubiquitin-Like Proteins; Vol.4 - Pages 304-307, Edward T. H. Yeh

Zinc Fingers; Vol.4 - Pages 435-439, Mark Isalan

Bioenergetics

ABC Transporters; Vol.1 - Pages 1-5, Andre Goffeau, Benoit De Hertogh and Philippe V. Baret

Amine Oxidases; Vol.1 - Pages 85-89, Giovanni Floris and Alessandro Finazzi Agro

ATP Synthesis in Plant Mitochondria: Substrates, Inhibitors, Uncouplers; Vol.1 - Pages 128-132, Kathleen L. Soole and R. Ian Menz

ATP Synthesis: Mitochondrial Cyanide-Resistant Terminal Oxidases; Vol.1 - Pages 133-137, James N. Siedow

Bioenergetics: General Definition of Principles; Vol.1 - Pages 170-173, David G. Nicholls

Calcium Buffering Proteins: Calbindin; Vol.1 - Pages 221-225, Willi Hunziker and Igor Bendik

Calcium Buffering Proteins: ER Luminal Proteins; Vol.1 - Pages 226-230, Jody Groenendyk and Marek Michalak

Calcium Oscillations; Vol.1 - Pages 231-234, Marisa Brini

Calcium Sensing Receptor; Vol.1 - Pages 235-240, Jacob Tfelt-Hansen and Edward M. Brown

Calcium Signaling: Calmodulin-Dependent Phosphatase; Vol.1 - Pages 241-245, Claude Klee, Hao Ren and Shipeng Li

Calcium Signaling: Cell Cycle; Vol.1 - Pages 246-249, Luigia Santella

Calcium Signaling: Motility (Actomyosin–Troponin System); Vol.1 - Pages 250-255, Takeyuki Wakabayashi and Setsuro Ebashi

Calcium Signaling: NO Synthase; Vol.1 - Pages 256-260, Zhi-Qiang Wang and Dennis J. Stuehr

Calcium Transport in Mitochondria; Vol.1 - Pages 261-266, Rosario Rizzuto and Marisa Brini

Calcium Waves; Vol.1 - Pages 267-269, Lionel F. Jaffe

Calcium, Biological Fitness of; Vol.1 - Pages 270-273, Robert J. P. Williams

Calcium/Calmodulin-Dependent Protein Kinase II; Vol.1 - Pages 274-280, Andy Hudmon and Howard Schulman

Calcium-Binding Proteins: Cytosolic (Annexins, Gelsolins, C2-Domain Proteins); Vol.1 - Pages 287-293, Joachim Krebs

Calcium-Modulated Proteins (EF-Hand); Vol.1 - Pages 294-299, Robert H. Kretsinger

Cell Death by Apoptosis and Necrosis; Vol.1 - Pages 352-355, Pierluigi Nicotera

Chemiosmotic Theory; Vol.1 - Pages 405-412, Keith D. Garlid

Chemolithotrophy; Vol.1 - Pages 419-424, Alan B. Hooper

Chlorophylls and Carotenoids; Vol.1 - Pages 430-437, Hugo Scheer

Chloroplast Redox Poise and Signaling; Vol.1 - Pages 438-445, John F. Allen

Chloroplasts; Vol.1 - Pages 446-450, Nicoletta Rascio

Cytochrome b6f Complex; Vol.1 - Pages 521-527, Gunter A. Hauska and Thomas Schodl

Cytochrome bc1 Complex (Respiratory Chain Complex III); Vol.1 - Pages 528-534, Bernard L. Trumpower

Cytochrome c; Vol.1 - Pages 535-538, Hans Tuppy and Gunther Kreil

Cytochrome Oxidases, Bacterial; Vol.1 - Pages 539-543, Peter Brzezinski and Pia Adelroth

Cytochrome P-450; Vol.1 - Pages 544-549, Rita Bernhardt

Energy Transduction in Anaerobic Prokaryotes; Vol.2 - Pages 24-30, Gottfried Unden

ER/SR Calcium Pump: Function; Vol.2 - Pages 56-60, Giuseppe Inesi

ER/SR Calcium Pump: Structure; Vol.2 - Pages 61-65, Chikashi Toyoshima and Yuji Sugita

F1–F0 ATP Synthase; Vol.2 - Pages 73-79, Donata Branca

Ferredoxin; Vol.2 - Pages 104-106, Giuliana Zanetti and Vittorio Pandini

Ferredoxin-NADP+ Reductase; Vol.2 - Pages 107-111, Giuliana Zanetti and Alessandro Aliverti

Free Radicals, Sources and Targets of: Mitochondria; Vol.2 - Pages 134-142, Alberto Boveris and Enrique Cadenas

Friedreich's Ataxia; Vol.2 - Pages 143-145, Paul E. Hart and Anthony H. V. Schapira

Giant Mitochondria (Megamitochondria); Vol.2 - Pages 186-188, Bernard Tandler and Charles L. Hoppel

Glutathione Peroxidases; Vol.2 - Pages 224-228, Fulvio Ursini and Matilde Maiorino

Green Bacteria: Secondary Electron Donor (Cytochromes); Vol.2 - Pages 321-324, Hirozo Oh-oka and Robert E. Blankenship

Green Bacteria: The Light-Harvesting Chlorosome; Vol.2 - Pages 325-330, John M. Olson

Green Sulfur Bacteria: Reaction Center and Electron Transport; Vol.2 - Pages 331-336, Gunter A. Hauska and Thomas Schodl

Heme Synthesis; Vol.2 - Pages 362-366, Gloria C. Ferreira

Intracellular Calcium Channels: cADPR-Modulated (Ryanodine Receptors); Vol.2 - Pages 465-468, Antony Galione

Intracellular Calcium Channels: NAADP+-Modulated; Vol.2 - Pages 469-472, Armando A. Genazzani and Marcella Debidda

IP3 Receptors; Vol.2 - Pages 478-481, Colin W. TaylorEdward Morris and Paula da Fonseca

Iron–Sulfur Proteins; Vol.2 - Pages 482-489, Helmut Beinert, Jacques Meyer and Roland Lill

Ligand-Operated Membrane Channels: Calcium (Glutamate); Vol.2 - Pages 551-561, Elias K. Michaelis

Ligand-Operated Membrane Channels: GABA; Vol.2 - Pages 562-566, F. Minier and Erwin Sigel

Light-Harvesting Complex (LHC) I and II: Pigments and Proteins; Vol.2 - Pages 567-570, Stefan Jansson

Luft's Disease; Vol.2 - Pages 599-601, Salvatore DiMauro

Membrane Transport, General Concepts; Vol.2 - Pages 627-630, Stanley G. Schultz

Membrane Transporters:Na+/Ca2+ Exchangers; Vol.2 - Pages 631-636, Jonathan Lytton

Membrane-Associated Energy Transduction in Bacteria and Archaea; Vol.2 - Pages 637-645, Gunter Schafer

Metabolite Channeling: Creatine Kinase Microcompartments; Vol.2 - Pages 646-651, Uwe Schlattner and Theo Wallimann

Mitochondrial Auto-Antibodies; Vol.2 - Pages 683-688, Harold Baum

Mitochondrial Channels; Vol.2 - Pages 689-692, M. Catia Sorgato and Alessandro Bertoli

Mitochondrial DNA; Vol.2 - Pages 693-696, Gottfried Schatz

Mitochondrial Genes and their Expression: Yeast; Vol.2 - Pages 697-702, Piotr P. Slonimski and Giovanna Carignani

Mitochondrial Genome, Evolution; Vol.2 - Pages 703-708, B. Franz Lang, Dennis V. Lavrov and Gertraud Burger

Mitochondrial Genome, Overview; Vol.2 - Pages 709-715, Douglas C. Wallace

Mitochondrial Inheritance; Vol.2 - Pages 716-719, Eric A. Shoubridge

Mitochondrial Membranes, Structural Organization; Vol.2 - Pages 720-724, Carmen A. Mannella

Mitochondrial Metabolite Transporter Family; Vol.2 - Pages 725-732, Ferdinando Palmieri and Martin Klingenberg

Mitochondrial Outer Membrane and the VDAC Channel; Vol.2 - Pages 733-736, Marco Colombini

Neuronal Calcium Signal; Vol.3 - Pages 16-20, Hilmar Bading

Nicotinamide Nucleotide Transhydrogenase; Vol.3 - Pages 50-56, Jan Rydstrom

Nuclear Genes in Mitochondrial Function and Biogenesis; Vol.3 - Pages 100-104, Alexander Tzagoloff and Carol L. Dieckmann

Oncocytes; Vol.3 - Pages 165-166, Bernard Tandler and Charles L. Hoppel

Oxygenases; Vol.3 - Pages 178-182, Osamu Hayaishi

Periplasmic Electron Transport Systems in Bacteria; Vol.3 - Pages 231-238, David J. Richardson, Gary Sawers and Rob J. M. Van Spanning

Phosphatidylinositol-3-Phosphate; Vol.3 - Pages 272-276, Joseph V. Virbasius and Michael P. Czech

Photosystem I, Structure and Function; Vol.3 - Pages 342-347, Petra Fromme

Photosystem I: FX, FA, and FB Iron–Sulfur Clusters; Vol.3 - Pages 348-356, Mikhail L. Antonkine and John H. Golbeck

Photosystem II Light Harvesting System: Dynamic Behavior; Vol.3 - Pages 357-362, Peter Horton and Alexander Ruban

Photosystem II: Assembly and Turnover of the D1 Protein; Vol.3 - Pages 363-366, Eira Kanervo and Eva-Mari Aro

Photosystem II: Protein Components; Vol.3 - Pages 367-374, James Barber

Photosystem II: Water Oxidation, Overview; Vol.3 - Pages 375-380, Fabrice Rappaport and Pierre Joliot

Plasma-Membrane Calcium Pump: Structure and Function; Vol.3 - Pages 385-389, Emanuel E. Strehler

Plastocyanin; Vol.3 - Pages 390-393, Elizabeth L. Gross

Protein Import into Mitochondria; Vol.3 - Pages 510-515, Johannes M. Herrmann and Walter Neupert

P-Type Pumps: Copper Pump; Vol.3 - Pages 561-564, Ilia Voskoboinik and James Camakaris

P-Type Pumps: H+/K+ Pump; Vol.3 - Pages 565-570, Jai Moo Shin and George Sachs

P-Type Pumps: Na+/K+ Pump; Vol.3 - Pages 571-576, Peter L. Jorgensen

P-Type Pumps: Plasma-Membrane H+ Pump; Vol.3 - Pages 577-581, A. Brett Mason and Carolyn W. Slayman

Purple Bacteria: Electron Acceptors and Donors; Vol.3 - Pages 582-585, Evaldas Katilius and Neal W. Woodbury

Purple Bacteria: Photosynthetic Reaction Centers; Vol.3 - Pages 586-594, C. Roy D. Lancaster

Pyrimidine Biosynthesis; Vol.3 - Pages 600-605, Monika Loffler and Elke Zameitat

Quinones; Vol.3 - Pages 621-627, Giorgio Lenaz and Maria Luisa Genova

Respiratory Chain and ATP Synthase; Vol.3 - Pages 671-675, David G. Whitehouse and Anthony L. Moore

Respiratory Chain Complex I; Vol.3 - Pages 676-680, Ulrich Brandt

Respiratory Chain Complex II and Succinate: Quinone Oxidoreductases; Vol.3 - Pages 681-687, C. Roy D. Lancaster

Respiratory Chain Complex IV; Vol.3 - Pages 688-694, Hartmut Michel

Respiratory Processes in Anoxygenic and Oxygenic Phototrophs; Vol.3 - Pages 695-699, Roberto Borghese and Davide Zannoni

Spastic Paraplegia; Vol.4 - Pages 61-66, Elena Irene Rugarli and Andrea Ballabio

Store-Operated Membrane Channels: Calcium; Vol.4 - Pages 117-122, Indu S. Ambudkar

Superoxide Dismutase; Vol.4 - Pages 135-138, Irwin Fridovich

Uncoupling Proteins; Vol.4 - Pages 313-318, Daniel Ricquier and Frederic Bouillaud

V-ATPases; Vol.4 - Pages 349-353, Michael Forgac

Voltage-Dependent K+ Channels; Vol.4 - Pages 399-404, Ramon Latorre and Francisco J. Morera

Voltage-Sensitive Ca2+ Channels; Vol.4 - Pages 405-408, Harald Reuter

Voltage-Sensitive Na+ Channels; Vol.4 - Pages 409-415, William J. Brammar

Molecular Biology

Alternative Splicing: Regulation of Fibroblast Growth Factor Receptor (FGFR); Vol.1 - Pages 74-77, Mariano A. Garcia-Blanco

Alternative Splicing: Regulation of Sex Determination in Drosophila melanogaster; Vol.1 - Pages 78-84, Jill K. M. Penn, Patricia Graham and Paul Schedl

ara Operon; Vol.1 - Pages 116-119, Robert F. Schleif

Chromatin Remodeling; Vol.1 - Pages 456-463, Eric Kallin and Yi Zhang

Chromatin: Physical Organization; Vol.1 - Pages 464-468, Christopher L. Woodcock

DNA Base Excision Repair; Vol.1 - Pages 603-608, Hilde Nilsen and Tomas Lindahl

DNA Damage: Alkylation; Vol.1 - Pages 609-613, Anton B. Guliaev and B. Singer

DNA Glycosylases: Mechanisms; Vol.1 - Pages 614-617, Daniel J. Krosky and James T. Stivers

DNA Helicases: Dimeric Enzyme Action; Vol.1 - Pages 618-623, Timothy M. Lohman

DNA Helicases: HexamericEnzyme Action; Vol.1 - Pages 624-631, Smita S. Patel

DNA Ligases: Mechanism and Functions; Vol.1 - Pages 632-636, Alan E. Tomkinson and John B. Leppard

DNA Ligases: Structures; Vol.1 - Pages 637-643, C. Kiong Ho, Mark Odell and Dimitar B. Nikolov

DNA Methyltransferases, Bacterial; Vol.1 - Pages 644-651, Albert Jeltsch and Richard I. Gumport

DNA Methyltransferases, Structural Themes; Vol.1 - Pages 652-659, Sanjay Kumar

DNA Methyltransferases: Eubacterial GATC; Vol.1 - Pages 660-664, Martin G. Marinus

DNA Mismatch Repair and Homologous Recombination; Vol.1 - Pages 665-670, Ivan Matic and Miroslav Radman

DNA Mismatch Repair and the DNA Damage Response; Vol.1 - Pages 671-674, Guo-Min Li and Steven R. Presnell

DNA Mismatch Repair Defects and Cancer; Vol.1 - Pages 675-681, Richard D. Kolodner

DNA Mismatch Repair in Bacteria; Vol.1 - Pages 682-686, A-Lien Lu

DNA Mismatch Repair in Mammals; Vol.1 - Pages 687-690, James T. Drummond

DNA Mismatch Repair: E. coli Vsr and Eukaryotic G–T Systems; Vol.1 - Pages 691-693, Margaret Lieb

DNA Oxidation; Vol.1 - Pages 694-697, Arthur P. Grollman and Dmitry O. Zharkov

DNA Photolyase; Vol.1 - Pages 698-702, Carrie L. Partch and Aziz Sancar

DNA Polymerase α, Eukaryotic; Vol.1 - Pages 703-707, Teresa S. -F. Wang

DNA Polymerase β, Eukaryotic; Vol.1 - Pages 708-712, William A. Beard and Samuel H. Wilson

DNA Polymerase δ, Eukaryotic; Vol.1 - Pages 713-715, Antero G. So and Kathleen M. Downey

DNA Polymerase ε, Eukaryotic; Vol.1 - Pages 716-719, Yasuo Kawasaki and Akio Sugino

DNA Polymerase I, Bacterial; Vol.1 - Pages 720-725, Catherine M. Joyce

DNA Polymerase II, Bacterial; Vol.1 - Pages 726-728, Judith L. Campbell

DNA Polymerase III, Bacterial; Vol.1 - Pages 729-733, Hisaji Maki

DNA Polymerases: Kinetics and Mechanism; Vol.1 - Pages 734-739, Kenneth A. Johnson

DNA Replication Fork, Bacterial; Vol.1 - Pages 740-744, Nancy G. Nossal

DNA Replication Fork, Eukaryotic; Vol.1 - Pages 745-748, Lori M. Kelman, Jerard Hurwitz and Zvi Kelman

DNA Replication, Mitochondrial; Vol.1 - Pages 749-752, David A. Clayton

DNA Replication: Eukaryotic Origins and the Origin Recognition Complex; Vol.1 - Pages 753-760, Melvin L. DePamphilis and Cong-jun Li

DNA Replication: Initiation in Bacteria; Vol.1 - Pages 761-766, Jon M. Kaguni

DNA Restriction and Modification: Type I Enzymes; Vol.1 - Pages 767-771, David T. F. Dryden

DNA Restriction and Modification: Type II Enzymes; Vol.1 - Pages 772-777, Darren M. Gowers and Stephen E. Halford

DNA Restriction and Modification: Type III Enzymes; Vol.1 - Pages 778-781, Desirazu N. Rao and S. Srivani

DNA Secondary Structure; Vol.1 - Pages 782-787, Albino Bacolla and Robert D. Wells

DNA Sequence Recognition by Proteins; Vol.1 - Pages 788-793, Arabela A. Grigorescu and John M. Rosenberg

DNA Supercoiling; Vol.1 - Pages 794-797, Tao-shih Hsieh

DNA Topoisomerases: Type I; Vol.1 - Pages 798-805, James J. Champoux

DNA Topoisomerases: Type II; Vol.1 - Pages 806-811, Renier Velez-Cruz and Neil Osheroff

DNA Topoisomerases: Type III–RecQ Helicase Systems; Vol.1 - Pages 812-816, Rodney Rothstein and Erika Shor

EF-G and EF-Tu Structures and Translation Elongation in Bacteria; Vol.2 - Pages 1-5, Poul Nissen and Jens Nyborg

Exonucleases, Bacterial; Vol.2 - Pages 66-72, Susan T. Lovett

HIV-1 Reverse Transcriptase Structure; Vol.2 - Pages 388-392, Kalyan Das, Stefan G. Sarafianos, Eddy Arnold and Stephen H. Hughes

Homologous Recombination in Meiosis; Vol.2 - Pages 393-397, Nancy M. Hollingsworth

lac Operon; Vol.2 - Pages 529-534, Liskin Swint-Kruse and Kathleen S. Matthews

LexA Regulatory System; Vol.2 - Pages 546-550, Veronica G. Godoy, Penny J. Beuning and Graham C. Walker

Metaphase Chromosome; Vol.2 - Pages 666-671, Sharron Vass and Margarete M. S. Heck

Methyl-CpG-Binding Proteins; Vol.2 - Pages 672-675, David G. Skalnik

mRNA Polyadenylation in Eukaryotes; Vol.2 - Pages 748-752, Mary Edmonds

mRNA Processing and Degradation in Bacteria; Vol.2 - Pages 753-757, Deborah A. Steege

Non-Homologous End Joining; Vol.3 - Pages 66-70, Penny A. Jeggo

Nonhomologous Recombination: Bacterial Transposons; Vol.3 - Pages 71-79, Bao Ton Hoang and Michael G. Chandler

Nonhomologous Recombination: Retrotransposons; Vol.3 - Pages 80-86, Siew Loon Ooi and Jef D. Boeke

Nuclear Organization, Chromatin Structure, and Gene Silencing; Vol.3 - Pages 105-108, Lori L. Wallrath, John R. Danzer, Oya Yazgan and Pamela K. Geyer

Nucleoid Organization of Bacterial Chromosomes; Vol.3 - Pages 115-118, Charles J. Dorman

Nucleolus, Overview; Vol.3 - Pages 119-122, Thoru Pederson

Nucleotide Excision Repair and Human Disease; Vol.3 - Pages 123-129, James E. Cleaver

Nucleotide Excision Repair in Eukaryotes; Vol.3 - Pages 130-133, Laura A. Lindsey-Boltz and Aziz Sancar

Nucleotide Excision Repair, Bacterial: The UvrABCD System; Vol.3 - Pages 134-142, Bennett Van Houten and Lawrence Grossman

Nucleotide Excision Repair: Biology; Vol.3 - Pages 143-147, Errol C. Friedberg

PHO Regulon; Vol.3 - Pages 262-265, Bengt L. Persson

Pre-tRNA and Pre-rRNA Processing in Bacteria; Vol.3 - Pages 420-424, Sidney R. Kushner

Pre-tRNA and Pre-rRNA Processing in Eukaryotes; Vol.3 - Pages 425-431, Hendrik A. Raue

Prions and Epigenetic Inheritance; Vol.3 - Pages 432-436, Reed B. Wickner

Processivity Clamps in DNA Replication: Clamp Loading; Vol.3 - Pages 441-446, Megan J. Davey and Mike O'Donnell

Recombination: Heteroduplexand Mismatch Repair in vitro; Vol.3 - Pages 645-648, Leroy Worth, Jr.

Recombination: Strand Transferases; Vol.3 - Pages 649-653, Floyd R. Bryant

Recombination-Dependent DNA Replication; Vol.3 - Pages 654-659, Kenneth N. Kreuzer

recQ DNA Helicase Family in Genetic Stability; Vol.3 - Pages 660-664, Mary A. Risinger and Joanna Groden

Reverse Transcriptase and Retroviral Replication; Vol.3 - Pages 708-713, Laura Tarrago-Litvak, Marie-Line Andreola and Simon Litvak

Ribosome Assembly; Vol.3 - Pages 719-724, John L. Woolford

Ribosome Structure; Vol.3 - Pages 725-732, Brian T. Wimberly

Ribozyme Mechanisms; Vol.3 - Pages 733-737, John Hsieh and Carol A. Fierke

Ribozyme Structural Elements: Group I Introns; Vol.3 - Pages 738-742, Barbara L. Golden

Ribozyme Structural Elements: Hairpin Ribozyme; Vol.3 - Pages 743-746, Adrian R. Ferre-D'Amare

Ribozymes and Evolution; Vol.3 - Pages 747-752, Niles Lehman

RNA Editing; Vol.3 - Pages 753-758, Charles E. Samuel

RNA Polymerase I and RNA Polymerase III in Eukaryotes; Vol.3 - Pages 759-762, Robert J. White

RNA Polymerase II and Basal Transcription Factors in Eukaryotes; Vol.3 - Pages 763-765, Joan Weliky Conaway and Ronald C. Conaway

RNA Polymerase II Elongation Control in Eukaryotes; Vol.3 - Pages 766-769, David H. Price

RNA Polymerase II Structure in Eukaryotes; Vol.3 - Pages 770-774, Patrick Cramer

RNA Polymerase Reaction in Bacteria; Vol.3 - Pages 775-780, Arkady A. Mustaev and Alexander D. Goldfarb

RNA Polymerase Structure, Bacterial; Vol.3 - Pages 781-784, Michael Anikin, Dmitri Temiakov and William T. McAllister

Sigma Factors; Vol.4 - Pages 41-44, John D. Helmann

Sliding Clamps in DNA Replication: E. coli -Clamp and PCNA Structure; Vol.4 - Pages 45-47, Eric R. Goedken and John Kuriyan

Spliceosome; Vol.4 - Pages 88-92, Timothy W. Nilsen

T7 RNA Polymerase; Vol.4 - Pages 147-151, Rui Sousa

Telomeres: Maintenance and Replication; Vol.4 - Pages 174-179, Alessandro Bianchi and David Shore

Transcription Termination; Vol.4 - Pages 195-199, Thomas J. Santangelo and Jeffrey W. Roberts

Transcription-Coupled DNA Repair, Overview; Vol.4 - Pages 204-208, Isabel Mellon

Translation Elongation in Bacteria; Vol.4 - Pages 214-223, Oliver Vesper and Knud H. Nierhaus

Translation Elongation in Eukaryotes; Vol.4 - Pages 224-229, William C. Merrick and Anton A. Komar

Translation Initiation in Bacteria: Factors and Mechanisms; Vol.4 - Pages 230-236, Cynthia L. Pon and Claudio O. Gualerzi

Translation Initiation in Eukaryotes: Factors and Mechanisms; Vol.4 - Pages 237-241, Tatyana V. Pestova and Christopher U. T. Hellen

Translation Termination and Ribosome Recycling; Vol.4 - Pages 242-246, Nadja Koloteva-Levin and Mick F. Tuite

Translesion DNA Polymerases, Eukaryotic; Vol.4 - Pages 247-250, Alexandra Vaisman and Roger Woodgate

tRNA Synthetases; Vol.4 - Pages 263-266, Karla L. Ewalt and Paul Schimmel

trp Operon and Attenuation; Vol.4 - Pages 267-271, Paul Gollnick

UmuC, D Lesion Bypass DNA Polymerase V; Vol.4 - Pages 308-312, Zvi Livneh

XPV DNA Polymerase and Ultraviolet Damage Bypass; Vol.4 - Pages 419-421, Alan R. Lehmann

Yeast GAL1–GAL10 System; Vol.4 - Pages 429-433, Dennis Lohr and Ralph Bash

Signaling

Abscisic Acid (ABA); Vol.1 - Pages 6-11, Ramanjulu Sunkar and Jian-Kang Zhu

Adenosine Receptors; Vol.1 - Pages 34-39, Lauren J. Murphree and Joel Linden

Adenylyl Cyclases; Vol.1 - Pages 40-45, Ronald Taussig

Adrenergic Receptors; Vol.1 - Pages 46-50, David B. Bylund

A-Kinase Anchoring Proteins; Vol.1 - Pages 64-67, Lorene K. Langeberg and John D. Scott

Angiotensin Receptors; Vol.1 - Pages 111-115, Tadashi Inagami

ARF Family; Vol.1 - Pages 120-122, Gustavo Pacheco-Rodriguez, Joel Moss and Martha Vaughan

B-Cell Antigen Receptor; Vol.1 - Pages 155-158, Thomas M. Yankee and Edward A. Clark

Bradykinin Receptors; Vol.1 - Pages 182-185, Ronald M. Burch

Brassinosteroids; Vol.1 - Pages 192-197, Steven D. Clouse

Cadherin Signaling; Vol.1 - Pages 199-204, David B. Sacks and Jonathan M. G. Higgins

Calcitonin Gene-Related Peptide and Adrenomedullin Receptors; Vol.1 - Pages 212-216, Debbie L. Hay, Alex C. Conner and David R. Poyner

Calcitonin Receptor; Vol.1 - Pages 217-220, Samia I. Girgis, Niloufar Moradi-Bidhendi, Lucia Mancini and Iain MacIntyre

Calcium/Calmodulin-Dependent Protein Kinases; Vol.1 - Pages 281-286, J. Robison and Roger J. Colbran

c-fes Proto-Oncogene; Vol.1 - Pages 377-382, Thomas E. Smithgall and Robert I. Glazer

Chemokine Receptors; Vol.1 - Pages 413-418, Ann Richmond and Guo-Huang Fan

Chemotactic Peptide/Complement Receptors; Vol.1 - Pages 425-429, Eric R. Prossnitz and Larry A. Sklar

Cyclic AMP Receptors of Dictyostelium; Vol.1 - Pages 488-493, Dale Hereld and Peter N. Devreotes

Cyclic GMP Phosphodiesterases; Vol.1 - Pages 494-500, Sharron H. Francis and Jackie D. Corbin

Cyclic Nucleotide Phosphodiesterases; Vol.1 - Pages 501-505, Vincent C. Manganiello and Eva Degerman

Cyclic Nucleotide-Dependent Protein Kinases; Vol.1 - Pages 506-511, Sharron H. Francis and Jackie D. Corbin

Cyclic Nucleotide-Regulated Cation Channels; Vol.1 - Pages 512-515, Martin Biel and Franz Hofmann

Cytokines; Vol.1 - Pages 550-555, Andrea L. Wurster and Michael J. Grusby

Cytokinin; Vol.1 - Pages 562-567, Thomas Schmulling

Diacylglycerol Kinases and Phosphatidic Acid Phosphatases; Vol.1 - Pages 593-597, Stephen M. Prescott and Matthew K. Topham

Dopamine Receptors; Vol.1 - Pages 817-822, Kim A. Neve

Eicosanoid Receptors; Vol.2 - Pages 6-9, Richard M. Breyer and Matthew D. Breyer

Endocannabinoids; Vol.2 - Pages 13-15, Daniele Piomelli

Epidermal Growth Factor Receptor Family; Vol.2 - Pages 51-55, Denis Tvorogov and Graham Carpenter

FAK Family; Vol.2 - Pages 80-84, Steven K. Hanks

Fatty Acid Receptors; Vol.2 - Pages 95-98, Christer Owman and Bjorn Olde

Fibroblast Growth Factor Receptors and Cancer-Associated Perturbations; Vol.2 - Pages 112-117, Marko Kornmann and Murray Korc

G Protein Signaling Regulators; Vol.2 - Pages 147-151, John H. Exton

G Protein-Coupled Receptor Kinases and Arrestins; Vol.2 - Pages 152-157, Jeffrey L. Benovic

G12/G13 Family; Vol.2 - Pages 158-161, Stefan Offermanns

GABAA Receptor; Vol.2 - Pages 162-166, Richard W. Olsen and Gregory W. Sawyer

GABAB Receptor; Vol.2 - Pages 167-170, S. J. Enna

Gi Family of Heterotrimeric G Proteins; Vol.2 - Pages 181-185, Maurine E. Linder

Glucagon Family of Peptides and their Receptors; Vol.2 - Pages 193-196, Laurie L. Baggio and Daniel J. Drucker

Glutamate Receptors, Ionotropic; Vol.2 - Pages 213-219, Derek B. Scott and Michael D. Ehlers

Glutamate Receptors, Metabotropic; Vol.2 - Pages 220-223, P. Jeffrey Conn

Glycine Receptors; Vol.2 - Pages 237-243, Bodo Laube and Heinrich Betz

Glycogen Synthase Kinase-3; Vol.2 - Pages 255-260, James R. Woodgett

Gq Family; Vol.2 - Pages 316-320, Wanling Yang and John D. Hildebrandt

Gs Family of Heterotrimeric G Proteins; Vol.2 - Pages 337-341, Susanne M. Mumby

Hematopoietin Receptors; Vol.2 - Pages 348-353, Barbara A. Miller and Joseph Y. Cheung

Hepatocyte Growth Factor/Scatter Factor Receptor; Vol.2 - Pages 367-371, Selma Pennacchietti and Paolo M. Comoglio

Histamine Receptors; Vol.2 - Pages 378-383, Stephen J. Hill and Jillian G. Baker

Immunoglobulin (Fc) Receptors; Vol.2 - Pages 411-416, Mark Hogarth

Inositol Phosphate Kinases and Phosphatases; Vol.2 - Pages 427-429, Stephen B. Shears

Insulin Receptor Family; Vol.2 - Pages 436-440, Paul F. Pilch and Jongsoon Lee

Integrin Signaling; Vol.2 - Pages 441-445, Lawrence E. Goldfinger and Mark H. Ginsberg

Interferon Receptors; Vol.2 - Pages 446-451, Christopher P. Elco and Ganes C. Sen

JAK-STAT Signaling Paradigm; Vol.2 - Pages 491-496, Edward Cha and Christian Schindler

Leptin; Vol.2 - Pages 541-545, Thomas W. Gettys

Lysophospholipid Receptors; Vol.2 - Pages 602-604, Gabor J. Tigyi

Melanocortin System; Vol.2 - Pages 617-620, Roger D. Cone

Mitogen-Activated Protein Kinase Family; Vol.2 - Pages 737-742, Hidemi Teramoto and J. Silvio Gutkind

Muscarinic Acetylcholine Receptors; Vol.2 - Pages 775-777, Neil M. Nathanson

Natriuretic Peptides and their Receptors; Vol.3 - Pages 1-5, Lincoln R. Potter

Neuropeptide Y Receptors; Vol.3 - Pages 26-31, Eric M. Parker

Neurotensin Receptors; Vol.3 - Pages 32-36, William Rostene, Patrick Kitabgi and Didier Pelaprat

Neurotransmitter Transporters; Vol.3 - Pages 37-40, Aurelio Galli, Randy D. Blakely and Louis J. DeFelice

Neurotrophin Receptor Signaling; Vol.3 - Pages 41-45, Jennifer J. Gentry and Bruce D. Carter

Nicotinic Acetylcholine Receptors; Vol.3 - Pages 57-61, Nivalda O. Rodrigues-Pinguet and Henry A. Lester

Nitric Oxide Signaling; Vol.3 - Pages 62-65, Michael A. Marletta

Nuclear Factor kappaB; Vol.3 - Pages 96-99, Thomas D. Gilmore

Olfactory Receptors; Vol.3 - Pages 149-154, Sigrun I. Korsching

Opioid Receptors; Vol.3 - Pages 167-171, P. Y. Law and Horace H. Loh

P2X Purinergic Receptors; Vol.3 - Pages 183-187, Annmarie Surprenant

P2Y Purinergic Receptors; Vol.3 - Pages 188-191, George R. Dubyak

p53 Protein; Vol.3 - Pages 192-195, Jamie Hearnes and Jennifer Pietenpol

p70 S6 Kinase/mTOR; Vol.3 - Pages 196-200, Christopher G. Proud

Parathyroid Hormone/Parathyroid Hormone-Related Protein Receptor; Vol.3 - Pages 201-207, Thomas J. Gardella

Peroxisome Proliferator-Activated Receptors; Vol.3 - Pages 239-245, Mary C. Sugden, Edward A. Sugden and Mark J. Holness

Pheromone Receptors (Yeast); Vol.3 - Pages 256-261, James B. Konopka and Jeremy W. Thorner

Phosphatidylinositol Bisphosphate and Trisphosphate; Vol.3 - Pages 266-271, Alex Toker

Phosphoinositide 3-Kinase; Vol.3 - Pages 281-286, Khatereh Ahmadi and Michael Waterfield

Phosphoinositide 4- and 5-Kinases and Phosphatases; Vol.3 - Pages 287-291, Shawn F. Bairstow, Matthew W. Bunce and Richard A. Anderson

Phosphoinositide-Dependent Protein Kinases; Vol.3 - Pages 292-296, Nick R. Leslie and C. Peter Downes

Phospholipase A2; Vol.3 - Pages 297-300, Timothy R. Smith and Edward A. Dennis

Phospholipase C; Vol.3 - Pages 301-305, Fujio Sekiya, Yeun Ju Kim and Sue Goo Rhee

Phospholipase D; Vol.3 - Pages 306-313, Mary M. LaLonde and Michael A. Frohman

Photoreceptors; Vol.3 - Pages 326-329, King-Wai Yau

Plant Signaling: Peptides; Vol.3 - Pages 381-384, Clarence A. Ryan and Gregory Pearce

Platelet-Activating Factor Receptor; Vol.3 - Pages 394-398, Katherine M. Howard and Merle S. Olson

Platelet-Derived Growth Factor Receptor Family; Vol.3 - Pages 399-406, Marina Kovalenko and Andrius Kazlauskas

Protein Kinase B; Vol.3 - Pages 516-522, Bettina A. Dummler and Brian A. Hemmings

Protein Kinase C Family; Vol.3 - Pages 523-526, Alexandra C. Newton

Protein Tyrosine Phosphatases; Vol.3 - Pages 536-542, David J. Pagliarini, Fred L. Robinson and Jack E. Dixon

Proteinase-Activated Receptors; Vol.3 - Pages 543-548, Kristina K. Hansen and Morley D. Hollenberg

Rab Family; Vol.3 - Pages 629-634, Mary W. McCaffrey and Andrew J. Lindsay

Ran GTPase; Vol.3 - Pages 635-639, Mary Shannon Moore

Ras Family; Vol.3 - Pages 640-644, Lawrence A. Quilliam

Retinoblastoma Protein (pRB); Vol.3 - Pages 700-703, Nicholas Dyson and Maxim Frolov

Retinoic Acid Receptors; Vol.3 - Pages 704-707, Martin Petkovich

Serine/Threonine Phosphatases; Vol.4 - Pages 27-32, Thomas S. Ingebritsen

Serotonin Receptor Signaling; Vol.4 - Pages 33-37, Paul J. Gresch and Elaine Sanders-Bush

Small GTPases; Vol.4 - Pages 48-54, Adam Shutes and Channing J. Der

Somatostatin Receptors; Vol.4 - Pages 55-60, Agnes Schonbrunn

Src Family of Protein Tyrosine Kinases; Vol.4 - Pages 93-98, Jonathan A. Cooper

Steroid/Thyroid Hormone Receptors; Vol.4 - Pages 111-116, Ramesh Narayanan and Nancy L. Weigel

Syk Family of Protein Tyrosine Kinases; Vol.4 - Pages 139-145, Andrew C. Chan

Tachykinin/Substance P Receptors; Vol.4 - Pages 152-157, Mark D. Richardson and Madan M. Kwatra

Taste Receptors; Vol.4 - Pages 158-161, John D. Boughter, Jr. and Steven D. Munger

T-Cell Antigen Receptor; Vol.4 - Pages 162-168, Andrea L. Szymczak and Dario A. A. Vignali

Tec/Btk Family Tyrosine Kinases; Vol.4 - Pages 169-173, Shuling Guo and Owen N. Witte

Thyroid-Stimulating Hormone/Luteinizing Hormone/Follicle-Stimulating Hormone Receptors; Vol.4 - Pages 180-186, Deborah L. Segaloff, Dario Mizrachi and Mario Ascoli

Toll-Like Receptors; Vol.4 - Pages 190-194, Himanshu Kumar, Kiyoshi Takeda and Shizuo Akira

Transforming Growth Factor-β Receptor Superfamily; Vol.4 - Pages 209-213, Mark de Caestecker

Tumor Necrosis Factor Receptors; Vol.4 - Pages 277-283, Karen G. Potter and Carl F. Ware

Vascular Endothelial Growth Factor Receptors; Vol.4 - Pages 337-342, Kenneth A. Thomas

Vasopressin/Oxytocin Receptor Family; Vol.4 - Pages 343-348, Michael J. Brownstein

Vitamin D Receptor; Vol.4 - Pages 378-383, Diane R. Dowd and Paul N. MacDonald

Von Hippel-Lindau (VHL) Protein; Vol.4 - Pages 416-418, Ronald C. Conaway and Joan Weliky Conaway

Techniques and Methodology

Affinity Chromatography; Vol.1 - Pages 51-56, Pedro Cuatrecasas and Meir Wilchek

Affinity Tags for Protein Purification; Vol.1 - Pages 57-63, Joseph J. Falke and John A. Corbin

Genome-Wide Analysis of Gene Expression; Vol.2 - Pages 175-180, Karine G. Le Roch and Elizabeth A. Winzeler

HPLC Separation of Peptides; Vol.2 - Pages 398-403, James D. Pearson

Imaging Methods; Vol.2 - Pages 405-410, Gyorgy Szabadkai and Rosario Rizzuto

Inorganic Biochemistry; Vol.2 - Pages 417-420, Robert J. P. Williams

Multiple Sequence Alignment and Phylogenetic Trees; Vol.2 - Pages 770-774, Russell F. Doolittle

Oligosaccharide Analysis by Mass Spectrometry; Vol.3 - Pages 155-160, Andrew J. Hanneman and Vernon N. Reinhold

PCR (Polymerase Chain Reaction); Vol.3 - Pages 208-210, Michael J. Brownstein

Polysialic Acid inMolecular Medicine; Vol.3 - Pages 407-414, Frederic A. Troy, II

Protein Data Resources; Vol.3 - Pages 478-483, Philip E. Bourne

Secondary Structure in Protein Analysis; Vol.4 - Pages 1-6, George D. Rose

Spectrophotometric Assays; Vol.4 - Pages 67-75, Britton Chance

Two-Dimensional Gel Electrophoresis; Vol.4 - Pages 284-289, Gerhard Schmid, Denis Hochstrasser and Jean-Charles Sanchez

X-Ray Determination of 3-D Structure in Proteins; Vol.4 - Pages 422-428, Martha L. Ludwig

ENCYCLOPEDIA OF
Biological Chemistry

Editors
William J. Lennarz
M. Daniel Lane